Groundwater recharge & discharge relations inferred from isotopes and hydrochemistry in Samail Catchment, Oman

OSMAN ABDALLA[1], TALAL AL-HOSNI[2], ABDULLH AL-RAWAHI[3]
[1]Sultan Qaboos University, Dept. of Earthsciences, P.O. Box 36, Oman osman@squ.edu.om (* presenting author)
[2]Sultan Qaboos University, Dept. of Earthsciences, P.O. Box 36, Oman
[3]Ministry of Regional Municipalities & Ware Resources, Alkhwair, Oman

Abstract

Groundwater recharge and discharge relation along the flow path in the regional catchment of Samail, Oman has been investigated using different isotopes and conventional hydrochemistry. The subsurface geology is complex and variable ranging from karstified carbonate rocks at the elevated areas of North Oman Mountains (NOM) to fractured ophiolitic sequence overlain by porous medium of Quaternary alluvium gravel at the top of the geologic section. The alluvium is thickening from elevated area downstream to exceed 300 m at the lower reaches of the catchment. The boundary between the carbonates and the ophiolites is controlled by a major thrust along which several springs are originating. Groundwater generally flows south-north with a hydraulic gradient decreasing to the south.

Groundwater samples (total 74) from deep and shallow wells as well as springs were analyzed for the isotopes C^{14}, ^{2}H, O^{18} and $^{87}Sr/^{86}Sr$ and major cations and anions. Carbon-14 dating (18.9 ka to modern), wells hydrograph analyses, $^{87}Sr/^{86}Sr$ data (0.70810 – 0.70895) and ^{2}H, O^{18} suggest two main sources of recharge: 1- direct infiltration through stream bed into alluvium and 2- recharge from carbonates lineaments and fissures into the alluvium and ophiolites. The recharge of the alluvium takes place across the entire catchment. The wells hydrograph analyses and $^{87}Sr/^{86}Sr$ data (0.70810 – 0.70895) show that the alluvium and Ophiolite are partly interconnected and recharged by the same water source with a delayed recharge response of 2-3 months. Groundwater in the southern part of the catchment is isotopically depleted water indicating a high altitude recharge source, whereas deviation from meteoric water line in the lower catchment indicates the effect of evaporation.

Spring discharge from the NOM down the gradient indicates local, intermediate and regional flow systems of a groundwater residence time ranging between a few years to a maximum of ca 10K years at the terminal end of flow. The Ca:Mg ratio varies in the different rock types indicating the influence of geology on the hydrochemistry.

Petrographic and geochemical characteristics of the Oman ophiolite lower crust

B. ABILY[1*], G. CEULENEER[1], M. GRÉGOIRE[1], M. PYTHON[2] AND M. BENOIT[1]

[1]CNRS, UMR 5563, Laboratoire Géosciences Environnement Toulouse, Observatoire Midi-Pyrénées, Toulouse, France (*presenting author: benedicte.abily@get.obs-mip.fr; georges.ceuleneer@get.obs-mip.fr; michel.gregoire@get.obs-mip.fr; mathieu.benoit@get.obs-mip.fr)

[2]Hokkaido University, Department of Natural History Science, Division of Earth and Planetary Systems Sciences, Sapporo, Japan (marie@mail.sci.hokudai.ac.jp)

Layered cumulates making up the lower crustal section of the Oman ophiolite are largely considered as the result of the fractional crystallization of normal mid-ocean ridge basaltic (N-MORB) melts at low pressure. A glance to former studies reveals however that layered cumulates have been explored only in some massifs and that no global petrological study of this unit has been performed at the ophiolite scale. Moreover, in the mantle section, melt migration structures are filled with cumulates from two contrasted parental melts: one with a N-MORB tholeiitic affinity and one with a depleted andesitic affinity, this latter being the most widespread [1].

In order to better constrain the origin of layered cumulates in the Oman ophiolite, we have conducted a petrographic and geochemical study (electron microprobe and LA-ICP-MS) on about 700 samples from the lower crustal section of seven major massifs. We discovered that abundant (~15%) primitive cumulates (XMg>80%) are characterized by the early crystallization of orthopyroxene implying parental melts significantly richer in SiO_2 than N-MORB. Moreover, at the same differentiation degree, plagioclases of the layered cumulates are richer in anorthite and clinopyroxenes (cpx) are more depleted in Al_2O_3, TiO_2 and Rare Earth Elements (REE) than N-MORB cumulates. These characteristics are reminiscent of boninitic-andesitic melts although layered cumulates do not present the extreme depletion in High Field Strengh Elements (HFSE) and the REE patterns typical of supra-subduction zone boninites. The simplest way to account for these observations is to invoke mixing between N-MORB melts extracted from an asthenospheric source and silica enriched melts produced by hydrated re-melting of a depleted lithospheric source, both melts migrating in mantle channels before feeding magma chambers.

We used TiO_2 in cpx to semi-quantitatively determine the contribution of both magmatic end-members to parental melts in selected stratigraphic cumulative sections distributed along the ophiolite. This quantification in a key massif displaying a diapiric structure [2] reveals that the relative contribution of both sources evolved during the upwelling of the asthenospheric diapir within the lithosphere, an observation in agreement with melt migration structures distribution in the mantle section of this massif.

[1] Python & Ceuleneer (2003) *Geochem. Geophys. Geosyst.* **4**. [2] Ceuleneer, Nicolas & Boudier (1988) *Tectonophysics* **151**, 1-26.

https://doi.org/10.1180/S0026461X00008434 Published online by Cambridge University Press

Geochemistry of upper mantle xenoliths and host basalts from NE Bavaria

LUKÁŠ ACKERMAN[1*], PETR ŠPAČEK[2], JAROMÍR ULRYCH[1]

[1]Institute of Geology v.v.i., Academy of Sciences of the Czech Republic, Rozvojová 269, 165 00, Praha 6, Czech Republic, ackerman@gli.cas.cz (* presenting author)

[2]Institute of Geophysics v.v.i., Academy of Sciences of the Czech Republic, Boční II, 141 34, Praha 4, Czech Republic

Introduction

The European Cenozoic Rift System (ECRIS) volcanics contain abundant upper mantle xenoliths. Their composition ranges from lherzolite to dunite with subordinate pyroxenite and they record complex histories including different partial melting degrees and basaltic/carbonatitic melt metasomatism [1,2,3]. We studied mantle xenoliths and their host lavas from Zinst, Hirschentanz and Teichelberg (NE Bavaria, Germany).

Host basalts

The host lavas have composition of basanites (based on TAS classification), have typical LREE-enriched patterns (La_N/Yb_N = 17-24) and show enrichment in trace elements (e.g., LILE, Nb), but depletion in K and Pb. Their Sr-Nd isotopic composition calculated at 30 Ma is similar ($^{87}Sr/^{86}Sr_{30Ma}$ = 0.7033-0.7035, ε_{Nd30Ma} = +4.0-4.6). However, Teichelberg basanite has more radiogenic $^{143}Nd/^{144}Nd$ (ε_{Nd} of +4.6), but less radiogenic $^{87}Sr/^{86}Sr$ (0.7033). Nevertheless, this Sr-Nd composition is similar to those of the European Astenospheric Reservoir. All these signatures suggest basanite derivation from garnet- and phlogopite/amphibole-bearing subcontinental lithospheric mantle.

Mantle xenoliths

The abundant xenoliths at Zinst, Hirschentanz and Teichelberg are mostly of spinel lherzolite composition with rare occurence of harzburgite. Coarse-granular types with strain-free grains predominate, however the textures are mostly non-equilibrated with olivine typically displaying non-unimodal grain-size and grain-shape distributions. Rare transitions to high-stress porphyroclastic textures suggest weak, late deformation. Spinel occurs as individual, mostly rounded grains or form sympletitic intergrowths with pyroxenes. In some xenoliths, symplectites recording complex multiphase garnet decomposition in presence of melts/fluids were identified. Spinel lherzolites with predominance of orthopyroxene over clinopyroxene were selected for analyses. They have fairly homogeneous equilibrium temperatures for the entire suite from 940 to 1040 °C. Variable Al_2O_3 contents and negative correlation between MgO and other major oxides likely suggest different partial melting degrees. On the other hand, the entire xenolith suite is significantly, but variably enriched in LREE (La_N/Yb_N = 3.5-23) and other trace elements (e.g., Rb, U, Sr, Pb), but depleted in Th and HFSE (Zr, Hf, Nb). This suggests cryptic metasomatic overprint by melt and/or fluid. Extremely variable CaO/Al_2O_3 ratios ranging from 0.5 to 1.6, the presence of common melt pockets containing carbonate and the negative HFSE anomalies may suggest metasomatism by alkaline and/or carbonatitic melts.

[1] Downes (2001) *Journal of Petrology* **42**, 233-250.
[2] Ackerman et al. (2007) *Journal of Petrology* **48**, 2235-2260.
[2] Matusiak-Malek et al. (2010) *Lithos* **45**, 99-102.

Experimental investigation of Ti in garnet at eclogite facies conditions

MICHAEL R. ACKERSON[1*], E. BRUCE WATSON[1], FRANK S. SPEAR[1]

[1]Department of Earth and Environmental Sciences, Rensselaer Polytechnic Institute, Troy, NY 12180, USA *ackerm3@rpi.edu (presenting author)

Garnet is a common mineral in metamorphic systems over a wide range of temperatures and pressures whose crystal chemistry has allowed for the calibration of several useful garnet-based geothermometers. Designing additional garnet-based thermometers could aid in the interpretation of metamorphic systems and deepen our understanding of the evolution of the crust. Developing such thermometers is dependent on our understanding of the nature of elemental substitutions within garnet. In this study we focused on understanding the nature of Ti incorporation into garnet and the possibility of Ti-based garnet geothermometers.

Garnets were grown in basalt, pelite and amphibolite bulk compositions. The bulk starting materials were doped with 5 wt. % TiO_2 to ensure saturation in either rutile or ilmenite. In addition, 1 wt. % ZrO_2 was added to saturate in zircon, and 10 wt. % H_2O to achieve water saturation. In some cases seed garnets were included in the experiments to facilitate new garnet growth. Experiments were conducted at temperatures ranging from 800-900ºC, pressures between 1.5-2.5 GPa, and they were buffered at QFM. The runs were preformed in silver capsules on a piston-cylinder apparatus. The compositions of minerals and the melt were analyzed by electron microprobe and LA-ICPMS. Accurate microprobe measurement of Ti content in garnets was complicated by secondary fluorescence from ilmenite and rutile crystals that occurred as inclusions in most garnets.

Typical phase assemblages from these experiments include garnet, clinopyroxene, ilmenite and melt ± rutile. Measured Ti concentrations in garnet range from ppm up to 2.5 wt % and these preliminary results show that the Ti concentration does not depend solely on temperature. Rather, a negative correlation between Ti and Al may indicate that the main mechanism for entry of Ti into the garnet lattice is a coupled substitution on the octahedral site ($Ti^{4+} + M^{2+} \leftrightarrow 2Al^{3+}$, where $M^{2+}=Mg^{2+}$, Fe^{2+}, or Mn^{2+}). If this mechanism is valid, then equilibria controlling the Ti concentration must include phase components other than those in garnet that will define the tschermak activity and application of Ti-based garnet geothermometers will require accurate activity models these components in the system.

https://doi.org/10.1180/S0026461X00008434 Published online by Cambridge University Press

Instantaneously developed crustal geochemical signatures in anatectic melts, and melt interconnection in the protolith

ANTONIO ACOSTA-VIGIL[1*], JÖRG HERMANN[2], DAVID LONDON[3] AND GEORGE B. MORGAN VI[3]

[1] CSIC-Universidad de Granada, IACT, aacosta@ugr.es (* presenting author)
[2]The Australian National University, RSES, joerg.hermann@anu.edu.au
[3]The University of Oklahoma, SGG, dlondon@ou.edu, gmorgan@ou.edu

One important issue to investigate in Earth Sciences is the rate of natural processes. Crustal anatexis and granite formation is key for understanding the generation and differentiation of the continental crust.

We have conducted an experimental program on the melting of solid rock cylinders of pelitic composition, 3-6 mm in diameter and 5-20 mm in length, at 690-800ºC, 200 and 700 MPa, under dry and wet conditions and for durations ranging from 1 hr to 60 days. The starting material is a schist with a mineral assemblage made of Ms+Bt+Crd+Pl+St+And, trace Kfs and accessories Gr+Ilm+Zrn+Mnz+Xen. All experiments produced variable proportions of melt that quenched to glass, and that was analyzed by electron microprobe and laser ablation ICP-MS.

Results show that granite melts can be generated, and likely interconnected throughout the entire protolith, in just hours to a few days, during anatexis at H_2O-saturated ($a_{H2O}\approx1$) but also H_2O-undersaturated ($a_{H2O}<<1$) conditions. Melting starts simultaneously along Qtz-Pl and Qtz-Ms interfaces and Qtz-Pl-Ms junctions distributed throughout the entire core, resulting in rapid melt interconnection. Microstructural observations indicate that residual Pl and Crd recrystallize even at low degrees of overstepping in temperature. Typically crustal geochemical signatures in the melt are developed extremely rapid in terms of both major and trace element compositions. For instance, melts from H_2O-undersaturated experiments at 730ºC and 700 MPa show, after 7 days, mean concentrations of ≈170 (s.d.=45) ppm Rb, ≈150 (65) ppm Sr, ≈6 (1) ppm Sc, ≈12 (9) ppm Zr and ≈25 (10) ppm ∑REE. Likewise, melts generated during H_2O-saturated anatexis at 730ºC and 700 MPa show, after only 4 days, mean concentrations of ≈110 (30) ppm Rb, ≈170 (60) ppm Sr, ≈5 (2) ppm Sc, ≈22 (8) ppm Zr and ≈60 (28) ppm ∑REE. Although heterogeneous, the compositions of these melts are similar to S-type leucogranites and glasses in anatectic metasedimentary enclaves.

This data implies that granitic melts loaded with trace elements can potentially be generated and extracted rapidly from the source. The results have implications for the transport mechanisms of certain trace elements (e.g. Zr, LREE) thoroughout granite melts, as well as for the calculation of melt residence times by using the measured concentrations of these trace elements in granites. However, the effect of the rate of heat supply (infinite, in these experiments) on the rate of melting and the composition of melt might represent a limitation for the general applicability of these results.

Five years of Keck OSIRIS observations of Titan: quantifying the transport of aerosol haze

MÁTÉ ÁDÁMKOVICS[1*] AND IMKE DE PATER[1]

[1]Astronomy Department, University of California, Berkeley, CA USA mate@berkeley.edu (* presenting author)

Abstract

We present spatially-resolved observations of Titan in the near-infrared obtained with the field integral spectrograph, OSIRIS, at the W. M. Keck Observatory. Datacubes were acquired in H (1.5 μm) and K (2 μm) bands from April 2006 to January 2012. Broadband spectra reveal the aerosol vertical structure from the surface through the stratosphere. We describe the temporal and spatial variation in aerosol distribution as constrained by our radiative transfer models, which include updates to methane opacity and aerosol scattering.

Observations

The OSIRIS imaging spectrograph is behind the adaptive optics system on the Keck II telescope. The instrument uses a 2048 × 2048 pixel Rockwell Hawaii-2 detector, which in our observing mode corresponds to at a spatial plate-scale of 0.020" and a spectral resolution (λ/δλ) of ~4000. We observe in both H- and K-bands when possible, covering 1.473–1.803 and 1.965–2.381 μm, respectively. The field of view is 0.32" × 1.28", such that four ~5min exposures are required to cover the entire ~1" diameter disk of Titan. We obtain datacubes on an approximately yearly basis between Apr 2006 and Jan 2012. Data are reduced using the OSIRIS data reduction pipeline, which includes flat-fielding, sky-subtraction, cosmic-ray rejection, wavelength calibration, spectral extraction and datacube assembly. Mosaicking of individual exposures is not performed with the pipeline due to spurious data near the edges of the field of view, likely caused by faulty lenslet masking. While individual exposures are nearly diffraction-limited in spatial resolution, assembling datacubes into mosaics is often limited by systematic offsets of up to a few pixels between exposures.

Aerosol Opacity Retrieval

Our models incorporate well-established numerical solutions to the radiative transfer equation and successfully simulate observations [1,2,3]. A discrete ordinates method is used with 16 pseudo-plane-parallel layers from 0 – 200 km altitude. The atmospheric vertical structure and aersol scattering measured by the Huygens probe is used as the default in the model. We explore several methods of scaling and varying the aersol structure for geographic locations and times when the Huygens probe measurements no longer apply.

Results

We describe an algorithm for navigating and reconstructing datacubes while selecting against lenslet masking artifacts. Mosaicked datacubes are used to retrieve the spatially-resolved atmospheric aerosol distribution on Titan with our radiative transfer model. We describe how the slow seasonal variation in the latitudinal haze gradient is punctuated by episodes of increased scattering.

[1] Ádámkovics et al. (2007) *Science* **318**, 962-965.
[2] Ádámkovics et al. (2010) *Icarus* **208**, 868-877.
[3] Mitchell et al. (2011) *Nature Geoscience* **4**, 589-592.

https://doi.org/10.1180/S0026461X00008434 Published online by Cambridge University Press

Applications of Raman XYZ mapping in the Earth sciences

FRAN ADAR[1], DAVID TUSCHEL[1] , AND ROBERT BODNAR[2,*]

[1]HORIBA Scientific, Edison, NJ, U.S.A., fran.adar@horiba.com; David.tuschel@horiba.com

[2]Virginia Tech, Blacksburg, VA, U.S.A., rjb@vt.edu

Introduction

Raman spectroscopy is a powerful tool that has been applied widely in the earth sciences to characterize a variety of fluid and solid materials. While microspot Raman analyses have been used with great success to identify and characterize materials, it has previously been less useful for characterizing minor components in samples and for characterizing sample heterogeneities. The recent development of high-speed, high resolution mapping capabilities using the SWIFT™ (Scanning With Incredibly Fast Times)[1] apparatus now makes it possible to obtain high spectral, high spatial resolution Raman maps quickly and easily.

Applications

One of the most successful applications of Raman spectroscopy in the earth sciences has been to analyze fluid (FI) and melt inclusions (MI). Many fluid phases that are common in FI, including H_2O, CO_2, CH_4, H_2S. etc., are easily recognized and in some cases quantified using their Raman band intensities and/or positions. Recently, there has been much interest in searching for small amounts of H_2O in FI that previously had been thought to contain only CO_2. Confirming the presence of even small amounts of water in FI is important in understanding some upper mantle processes in which, as a result of exposure to high temperatures and pressures, hydrated minerals lose water that may then occupy FI. At room temperature the liquid H_2O phase occurs as a thin, sub-microscopic rim on the walls of the inclusion, it has therefore been diffficult, if not impossible, to locate the H_2O film using spot analysis. Raman mapping, however, facilitates the search for H_2O in these inclusions and provides a rapid method to survey large numbers of FI to see which, if any contain H_2O.

Key to implementation of this method is the rapid mapping of many inclusions. This is achieved with SWIFT™ in which the sample is translated continuously and the detector readout is synchronized with that motion. Multivariate analysis methods are used to construct the Raman maps and indicate the presence, in this case, of the water. The same mapping technique has been used to examine the distribution of water in silicate melt inclusions, and to compare cathodoluminescence zones in zircon with the degree of metamictization of the sample based on Raman peak positions.

---

[1] HORIBA Scientific, Inc., Edison N.J.

The Ediacarian Nitrogen Isotope Conundrum

MAGALI ADER[1*], PIERRE SANSJOFRE[1], GALEN P. HALVERSON[2], RICARDO TRINDADE[3]

[1]IPGP, Paris, France, ader@ipgp.fr (* presenting author), sansjofre@ipgp.fr

[2]McGill University, Earth and Planetary Sciences, Monteral, Canada, galen.halverson@mcgill.ca

[3]AIG-USP, Sao Paulo, Brazil, rtrindad@iag.usp.br

Nitrate cycling and isotope composition ($\delta^{15}N$) in the oceans are strongly linked to the water column redox structure via its control on nitrogen speciation. The present-day nitrate $\delta^{15}N$ in the oceans results from the balance beween molecular nitrogen fixation, which yields nitrate close to 0‰, and water column denitrification which increases residual nitrate $\delta^{15}N$ [1]. In upwelling zones, where disoxic conditions result in partial denitrification, residual nitrate $\delta^{15}N$ are usually higher than +5‰. Since surface sediments most often record the $\delta^{15}N$ of the nitrogen source used by primary producers and changes minimally during diagenesis, sediment $\delta^{15}N$ can be used as a proxy for water column redox structure and nutrient influx [2]. During the Phanerozoic, sedimentary $\delta^{15}N$ values typically cluster close to 5‰, except during ocean anoxic events (OAEs), when values are close to 0‰ [3]. These low $\delta^{15}N$ values are attributed to a complete removal of fixed nitrogen species at the chemocline, which leaves nitrogen fixation as the dominant pathway of N assimilation.

The Ediacarian Period is expected to have seen a long-lived ocean redox stratification and the onset of deep ocean oxygenation. Hence significant variations in sedimentary $\delta^{15}N$ values are to be expected in Ediacarian succesions. Yet, hardly any $\delta^{15}N$ data have been published so far for this period. We present preliminary $\delta^{15}N$ data for 5 different Ediacarian platforms (South China, Svalbard, Canada, Brasil). Most of these platforms preserve separate evidence for redox stratification, but most of the data range between 3 and 6‰, with a few outliers reaching 1 or 9‰. These data suggest either a dominantly oxic Ediacaran ocean at odds with other proxies (geochemistry, sulfur isotopes and iron speciation), or an Ediacarian marine nitrogen cycle that operated very differently from Phanerozoic OAEs.

[1] Sigman et al. (2009) *Encyclopedia of Ocean Sciences*, 40-54. [2] Galbraith et al (2008) *Nitrogen in the marine environment* **chap 34**, 1497-1526. [3] Meyers (2006) *Pal. Pal. Pal.* **235**, 305-320.

https://doi.org/10.1180/S0026461X00008434 Published online by Cambridge University Press

Biomineralization in Corals and the The Hunt for New Tracers of the Past Ocean

JESS F. ADKINS[1]* AND ALEX GAGNON[2]

[1]Dept. of Geology and Planetary Sciences, Caltech, Pasadena, CA, USA, jess@gps.caltech.edu

[2]Earth Science Division, LBNL, Berkeley, CA, USA, acgagnon@lbnl.net

Geochemical records from biogenic carbonates are a mainstay of our understanding of past climates. Isotopic and elemental abundances are often correlated with aspects of the modern water column to 'calibrate' a tracer. Even in light of large offsets from chemical equilibrium, this approach has served the field very well. Emiliani demonstrated that there were donzens (not four) major glaciations in the past few million years. Yet the $\delta^{18}O$ tracer he used is still debated today for what part of its signal is climate and what part is 'vital effect'. In light of both these sucesses and challenges, it is our hope to show how the study of disequilibrium effects can lead to better paleo tracers.

We have been using deep-sea corals as a natural laboratory for studying these vital effects because they grow in modern seawater with relatively constant conditions. Our approach has been to first demonstrate that corals use seawater as the basis for their calcifying fluid which is then modified by specific biological processes before deposition in the skeleton. This direction was first outlined by McConnaughey over 20 years ago and while the details of his models have been challenged his basic approach is still important today. We will review work on the stable isotopes of carbon and oxygen, Mg/Ca, Sr/Ca, U/Ca, and several other tracers in an attempt to build a better understanding of how corals calcify and how this affects the record of past climate. Using a Rayleigh model of Me/Ca uptake into the skeletons we propose a new thermometer based on the trend of data from a single individual in Mg/Ca versus Sr/Ca space. In general, the use of simple models, while ignoring important concepts like organic membrane mediation of tracer incorporation, can both guide the development of new tracers and inform the variance already found for more established proxies.

Reduced Mixing Between Two Deep Ocean Cells During the LGM and a Theory for the Cold Phase of Glacials Cycles

JESS F. ADKINS[1]*

[1]Dept. of Geology and Planetary Sciences, Caltech, Pasadena, CA, USA, jess@gps.caltech.edu

In the mid-80s the three so called 'Harvarton Bears' box models emphasized the role of the Southern Ocean in setting past pCO_2 values. This seminal work has sparked a large data collection effort, many related theories of glacial CO_2 cycles, and intense debate. The core message is that a combination of lower Southern Ocean overturning and increased biological nutrient utilization efficiency (phrased at the time as increased biological production) in the polar Antarctic can lower pCO_2 to the LGM value. It is widely accepted that neither process on its own can give rise to the full glacial to interglacial change, and that carbonate compensation also plays an important role in any scenario of pCO_2 lowering. In this work I would like to explore the role of deep ocean mixing as another important process in setting the LGM pCO_2.

There is evidence from casting d18O as a conservative tracer that the ratio of transport to mixing in the deep Southern Ocean was much larger during the LGM. I interpret this measurement as indicating vertical mixing was lower during the glacial and explore two possible ways this could have come about. Both shoaling of the interface between northern and southern sourced deep waters to lie above the rough topography of the mid-ocean ridges, and the filling of the ocean with cold-salty bottom water can lead to much lower values of deep ocean mixing. With a simple box model I will explore the effects of reduced mixing on pCO_2 in the atmosphere and the carbonate ion content of the deep-sea. Finally, I will propose a hypothesis for how a deep ocean teleconnection around Antarctica, that mechanistically links the density contrast between the northern and southern deep ocean cells, can follow a northern high latitute summer time pace maker and lead from interglacials to glacials. The new theory, however, does not explicitly give rise to terminations.

https://doi.org/10.1180/S0026461X00008434 Published online by Cambridge University Press

Stability of garnets to chemical weathering: An experimental study

VALENTIN P. AFANASYEV*[1], OLEG V. SNEGIREV[1], NIKOLAY S. TYCHKOV[1] AND NIKOLAY P. POKHILENKO[1]

[1] V.S.Sobolev Institute of geology and mineralogy SB RAS, Novosibirsk, Russia,
avp-diamond@mail.ru (*presenting author)

Iintroduction

Garnets from kimberlites, mainly pyropes, are unstable to lateritic weathering and dissolve to produce distinct surface patterns [1]. Low-Cr orange garnets are less stable than Cr-rich violet varieties, this being a control for trends in placer pyrope assemblages changing away from the primary deposit. The naturally occurring patterns were reproduced in earlier HF etching experiments on pyropes with monitored weight loss. However, those experiments did not include analysis of composition changes in etched pyropes.

Methods and samples

The chemical stability of garnets from kimberlite has been studied in new experiments in which etching in HF was a good model of natural lateritic weathering. We used 226 pyrope grains of main kimberlite-hosted pyrope varieties. The work included weight loss monitoring and analysis of chemistry and parageneses of the output grains.

Results and Conclusion

The etching experiments demonstrated different degrees of chemical stability in garnets of different parageneses, as a function of Cr contents (Fig. 1).

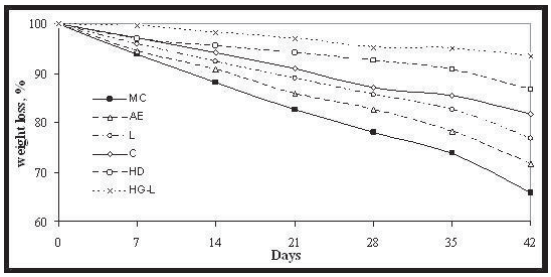

Fig. 1. Stability (weight loss) of garnets to etching in HF. The curves are coded according to assemblages of garnets: MC – megacrysts, AE – wehrlite, L – high-temperature depleted lherzolite, C – normal depleted lherzolite, HD – harzburgite-dunite, HG-L – TiO_2-rich harzburgite-dunite.

The experimental results are well consistent with data from natural pyrope assemblages, specifically, from unweathered pyropes of the Mir kimberlite compared to the weathered ones in the Vodorazdelnye Galechniki (Watershed pebble) placer derived from the same pipe.

References

[1] Afanasiev V.P., Zinchuk N.N., Pokhilenko N.P. (2010) *Mineralogy for Diamond Exploration*. GEO Publishers, Novosibirsk (in Russian), 650 p.

Clumped isotopes role in a multi-proxy paleoclimate reconstruction

AFFEK HP[1*], ZAARUR S[1], KLUGE T[1], DUBLYANSKY Y[2], SPÖTL C[2], DOUGLAS P[1], IVANY LC[3], SAENGER C[1], ZHANG YG[1]

[1]Yale University, New Haven, CT, USA, hagit.affek@yale.edu
[2]Universität Innsbruck, Innsbruck, Austria
[3]Syracuse University, Syracuse, NY, USA.

Carbonate clumped isotopes (Δ_{47}) is a temperature proxy that is based on the temperature-dependent preference of ^{13}C and ^{18}O to bind with each other. Δ_{47} of biogenic calcite and aragonite in aquatic organisms (with the exception of fast growing, shallow-water corals) is consistent with a calibration based on laboratory precipitation. Being a thermodynamically controlled proxy that does not depend, at equilibrium, on the composition of the solution in which the carbonate forms, Δ_{47}-based temperatures are better constrained than those from inorganic proxies such as $\delta^{18}O$ and Mg/Ca. It is also better understood than organic proxies such as TEX_{86} that rely on uncertain biological assumptions and unclear calibration. The main disadvantage is the large sample size required, preventing in most cases high-resolution Δ_{47} records. In a multi-proxy approach, clumped isotopes could play a role in high-resolution records, by providing absolute temperatures (and hence water compostions) that are required to constrain the assumptions in other proxies.

We applied clumped isotopes in bivalve shells in concert with the organic temperature proxy TEX_{86} during the Eocene in the Gulf of Mexico and in Seymour Island (Antarctica). Clumped isotope temperatures are consistent with TEX_{86} estimates, although the TEX_{86} calibration that provides the best fit with clumped isotope results varies between high and low latitude environments.

Being independent of the composition of water, Δ_{47} based temperatues can be used to reconstruct water $\delta^{18}O$, often using laboratory precipitation experiments for calibration [1]. However, such laboratory measurements involve relatively fast mineral growth, leading to potential disequilibrium. Calcite growing at an extremely slow rate in Devils Hole (Nevada) is likely to reflect formation under isotopic equilibrium, thus providing a test for the laboratory-based calibrations. Δ_{47} results from Devils Hole calcite yield a constant paleo-water temperature, during both glacial and interglacial periods over the last 180 Ky; it agrees with the modern-day groundwater temperature and confirms that the calcite precipitated at isotopic equilibrium. However, $\delta^{18}O$ is significantly enriched in Holocene calcite as compared to laboratory precipitation calibration [2]. We attribute this difference to the preferential incorporation of light oxygen isotopes during fast mineral growth in laboratory experiments (but not in slow growing Devils Hole calcite), without affecting the ^{13}C-^{18}O distribution that is reflected in Δ_{47}.

[1] Kim and O'Neil (1997) *Geochim. Cosmochim. Acta* **61**, 3461.
[2] Coplen (2007) *Geochim. Cosmochim. Acta* **71**, 3948.

https://doi.org/10.1180/S0026461X00008434 Published online by Cambridge University Press

LCA of Nanodrugs: Adding Constraints

B. AFFELTRANGER[1*]

[1]National Institute for Industrial Envionment and Risks (INERIS), Chronic Risks Division, BP2 Parc ALATA, 60550 Verneuil-en-Halatte, France, bastien.affeltranger@ineris.fr

Context

It is estimated that inflammatory diseases have now affected more than 80 million people worldwide, and counting. Studies have shown that disorder like rheumatoid arthritis (RA) shortens life span about 10 years. The treatment RA remains a challenge for the medical and scientific community. Vectorisation of active pharmaceutical ingredient(s) (API) is a promising option.

Project aim

NANOFOL proposes to develop a new diagnostic/therapy approach using folate based nanobiodevices (FBN) able to provide a new type of cost efficient treatment for chronic inflammatory diseases such as RA. The FBN is expected to generate low(er) side effects, possibly constituting a solution more advantageous than current therapies.

The concept

NANOFOL undertakes design, development and production of nanobiodevices (FBN) targeting directly effector cells.

Drug assessment issues

Establishing a proof of concept for one or several FBN, and testing it (pre-clinical) is a central aim of the project. However, other aspects of this new therapy shall be assessed – basically consisting in: occupational safety assessment; LCA; socio-economic analysis (SEA). Undertaking these combine difficulties typical of both pharmaceuticals and objects with nanometric caracteristics.

Work presented

This communication presents the key questions raised prior to developing the methodology for LCA and SEA , and how these have been answered. Available knowledge in LCA of nanos could be applied to some extent, as well as guidelines of REACH Regulation (EC). Working out the right hypotheses – a challenge in anticipation of clinical phase trials – did involve experts from the chemical, medical, engineering, social and economic sciences. Therapeutical strategies are introduced as scenarios for running LCA and SEA.

Acknowledgement

The research leading to these results has received funding from the European Union Seventh Framework Programme (FP7/2007-2013) under grant agreement NMP4-LA-2009-228827 NANOFOL"

Generating pore fluid isotope and solute profiles in exceptionally low permeability rocks

SARAH AGOSTA*, DALAL HANNA, IVY LIU AND IAN CLARK

Earth Sciences, University of Ottawa, Ottawa, Ontario, Canada, idclark@uottawa.ca, Ratan.Mohapatra@uOttawa.ca

Establishing geochemical and isotopic profiles for aquitard pore fluids is a critical, yet challenging, component of investigations of deep geological settings considered for nuclear waste isolation. A variety of advanced techniques have been developed internationally to extract and analyze pore waters and gases from sediments. However, the exceptionally low-permeability shales and limestones at the Bruce nuclear site, on the eastern margin of the Michigan Basin, demand innovative techniques for the extraction and analysis of pore fluids. Here we describe new methodologies, based on vacuum distillation and diffusive leaching developed to extract water, solutes and gases from rocks with hydraulic conductivities as low as 10^{-15} m s^{-1} and effective diffusion coefficients as low as 10^{-12} m s^{-2}.

Field investigations included the drilling of six cored boreholes to various depths through the ~860 m thick Paleozoic sedimentary sequence at the site. Samples of this high-quality, 76 mm diameter, core were broken to acquire inner material uncontaminated by drilling fluid, and were then crushed to 2-4 mm size to fill four 75 ml Pyrex flasks. Porewater and CO_2 were extracted for content and isotope analysis by heating under vacuum and condensing into 12 ml septum-fitted glass vials. Replicate testing of different rock types found optimum conditions to be 150°C for 6 hours. Solutes were analyzed after leaching with deionized water and normalized to the gravimetrically-measured recovered water content to produce molal concentrations.

The method is well suited to the illite-dominated shales (water contents of 6 to 8%) and for the exceptionally-low water content of the limestones (to less than 1%), as it uses a closed system for water extraction, and reduces error by normalization of solute mass to sample specific water contents. New developments to the method use a closed system ball-mill to crush and then heat smaller chip-samples. This offers greater control for investigating temperatures of release of mineral hydration waters and heterogeneities near permeable features.

https://doi.org/10.1180/S0026461X00008434 Published online by Cambridge University Press

Mantle source of back-arc Ecuador volcanoes: insights from B and radiogenic isotopes

SAMUELE AGOSTINI[1*], MATTEO PUERINI[2], ALBERTO RENZULLI[2], AND FILIPPO RIDOLFI[2]

[1]Istituto di Geoscienze e Georisorse, Pisa, Italy, s.agostini@igg.cnr.it (* presenting author)

[2]Dipartimento di Scienze della Terra, della Vita e dell'Ambiente, Urbino, Italy.

The Plio-Quaternary Ecuadorian volcanic arc belonging to the Northern Volcanic Zone (NVZ) of the Andes consists of the Western Cordillera (fore-arc), the Cordillera Real (main-arc) and scattered volcanoes in the rear-arc zone. The largest volcanoes of the rear arc zone are the Sumaco and El Reventador. These volcanoes, despite being located at the same distance from the trench, exhibit erupted magmas of different compositions.

The products of El Reventador are mainly represented by porphyritic lavas, ranging from basalt to rhyolite, with basaltic andesite and andesite being the most abundant. They belong to the medium-K to high-K calc-alkaline series. In contrast, the products of Sumaco are markedly SiO_2-undersaturated and vary from basanite to phonolite. Although both volcanoes show Nb-Ta-Ti negative anomalies typical of subduction-related environments, trace element concentrations are markedly different: modest enrichment in incompatible trace elements is typical of El Reventador lavas, whereas the Sumaco products are strongly enriched in all incompatible elements and show quite low LILE/HFSE ratios (i.e. Ba/Nb 35-105). In addition, El Reventador samples exhibit higher $^{87}Sr/^{86}Sr$ (0.7044-0.7046) and lower $^{143}Nd/^{144}Nd$ (0.51272-0.51280) with respect to Sumaco ($^{87}Sr/^{86}Sr \approx 0.7041$-0.7043, $^{143}Nd/^{144}Nd \approx 0.51284$-0.51297). It is worth noting that the Sr-Nd isotopic fields of the two back-arc volcanoes are well within the Ecuadorian NVZ variation range ($0.7035 < {}^{87}Sr/^{86}Sr < 0.7047$; $0.5126 < {}^{143}Nd/^{144}Nd < 0.5130$) [1]. Nevertheless, El Reventador Sr isotopic ratios are among the highest values of the Ecuadorian volcanic rocks from literature. The two volcanoes show similar and almost constant $^{207}Pb/^{204}Pb$ ratios. The other Sumaco Pb isotope ratios ($18.738 < {}^{206}Pb/^{204}Pb < 18.858$; $38.525 < {}^{208}Pb/^{204}Pb < 38.594$) are comparable with the overall Ecuadorian isotope variations ($18.700 < {}^{206}Pb/^{204}Pb < 19.150$; $38.450 < {}^{208}Pb/^{204}Pb < 38.950$[1]), whereas El Reventador lavas have the lowest $^{208}Pb/^{204}Pb$ and $^{206}Pb/^{204}Pb$ among all the other ecuadorian volcanoes (38.408-38.506 and 18.541-18.682, respectively). Even B isotopes are clearly distinct, with $\delta^{11}B$ ranging from -1.0 to -2.5 for El Reventador samples and -5.2 to -7.2 for the Sumaco samples.

All of this suggests that the erupted magmas of these rear-arc volcanoes represent two different mantle sources. The Sumaco product's source is consistent with very low degrees of partial melting due to the metasomatization of a supra-slab mantle wedge by small amounts of ^{11}B-depleted fluids released from subducted AOC and sediments. In contrast, under the El Reventador volcano a carbonatic sediment component (with low $^{206}Pb/^{204}Pb$ and high $\delta^{11}B$) is invoked as significant agent of mantle wedge metasomatization.

[1] Bourdon et al. (2003) *Earth Plan. Sci. Lett.* **205**, 123-138.

Carboxyl group $\delta^{13}C$ values of naphthenic acids: A novel approach to source discrimination

JASON M. E. AHAD[1*], HOOSHANG PAKDEL[2], MARTINE M. SAVARD[1], KERRY M. PERU[3], AND JOHN V. HEADLEY[3]

[1]Geological Survey of Canada, Natural Resources Canada, Québec City, Canada, Jason.Ahad@nrcan.gc.ca (* presenting author), MartineM.Savard@nrcan.gc.ca

[2]INRS Eau Terre Environnement, Québec City, Canada, Hooshang.Pakdel@ete.inrs.ca

[3]Water Science and Technology Division, Environment Canada, Saskatoon, Kerry.Peru@ec.gc.ca, John.Headley@ec.gc.ca

Naphthenic acids (NAs) are a complex mixture of alkyl-substituted acyclic and cycloaliphatic carboxylic acids naturally present in bitumen that become concentrated in oil sands process waters (OSPW). Difficult to characterize and quantify, NAs are highly toxic to aquatic organisms and thus pose a significant threat to the environment. Here we report a novel method to isolate and characterize NAs for use in source apportionment studies. NAs were extracted from a range of water samples and isolated into different mass fractions using preparative capillary gas chromatography (PCGC) prior to carboxyl group carbon $\delta^{13}C$ analysis ($\delta^{13}C_{carboxyl}$) by thermal conversion / elemental analysis – isotope ratio mass spectrometry. As the processes involved with bitumen recovery may result in a unique isotopic fingerprint in OSPW, our goal was to understand the variability in $\delta^{13}C_{carboxyl}$ of NAs in order to determine their potential to discriminate sources.

Results and Conclusion

The $\delta^{13}C_{carboxyl}$ ratio showed little variation within a given sample, demonstrating no significant isotopic differences between various mass fractions of NAs. The $\delta^{13}C_{carboxyl}$ value for unprocessed oil sand was -22.6‰ and did not vary considerably from that measured in OSPW (-21.8 ± 0.5‰). These results suggest that $\delta^{13}C_{carboxyl}$ of NAs cannot be used to distinguish between process-derived and natural background NAs. However, in samples taken along an OSPW-impacted groundwater transect, $\delta^{13}C_{carboxyl}$ values show a slight yet significant ^{13}C-depletion (~3‰) down-gradient away from the source. In conjunction with data from high-resolution Orbitrap mass spectrometry analyses used to identify NAs in these samples, the isotopic results point to a potential contribution from an additional source of "acid extractable" organic matter other than OSPW-derived NAs. This research highlights the need for accurate characterization of naphthenic acids in order to distinguish between anthropogenic and natural organic matter sources.

https://doi.org/10.1180/S0026461X00008434 Published online by Cambridge University Press

The Role of Microorganisms in the diversity and distribution of siderophores in Podzolic Forest Soil

ENGY AHMED*, SARA J. M. HOLMSTRÖM, VOLKER BRÜCHERT AND NILS G. HOLM
Department of Geological Sciences, Stockholm University, Stockholm, Sweden
(* Presenting author): engy.ahmed@geo.su.se

Iron is a key component of the chemical architecture of the biosphere. Due to the low bioavailability of iron in the environment, microorganisms have developed specific uptake strategies. The most important one is the production of siderophores, which are operationally defined as low-molecular-mass biogenic Fe (III)-binding compounds which may greatly increase bioavailability of Fe [1]. One of the primary biogeochemical functions of siderophores is therefore to increase Fe bioavailability by promoting the dissolution of iron-bearing minerals [2]. This study aims to understand the role of microorganisms in the chemical diversity and distribution of siderophores in podzol soil and how this diversity can contribute to the bioavailability of Fe in forest soil.

Soil samples were collected from an experimental site in the area of Bispgården in central Sweden (63°07′N, 16°70′E) from the O (organic), E (eluvial), B1 (upper illuvial), and C (mineral) horizons. Concentration and chemical composition of dissolved and adsorbed siderophores in the soil samples were determined using colorimetric assays and high-performance liquid chromatography.

The highest siderophore concentrations were found in the O layer and thereafter decreased by depth. Concentrations of dissolved hydroxamate, catecholate and carboxylate siderophores were up to 84, 17 and 0.2 nmol/ g soil, respectively. In contrast, concentrations of adsorbed hydroxamates, catecholates and carboxylates were only up to 1.8, 3 and 0.2 nmol/ g soil, respectively.

Siderophore-producing microorganisms were isolated from the same soil samples. Viable fungi, bacteria and actinomycete counts ranged from 7 to 300, from 300 to 1800, and from 0 to 5 cfu/gm, respectively. The highest counts were found in the O and E layers. Only the E layer contained the three types of siderophore-producing microorganisms investigated in this study. Siderophores were extracted from culture filtrates of the isolated microorganisms when grown under iron-limited conditions. These extracts varied considerably in siderophore composition. Fungal isolates produced up to 183 µM of hydroxamates, especially those isolated from the O layer, whereas bacteria and actinomycete isolated from the O and E layers of the soil produced high amounts of carboxylate, catecholate and hydroxamate siderophores. Actinomycete produced up to 93 µM of hydroxamates and 47 µM of catecholates, while bacteria produced up to 34 µM of carboxylates and up to 14 µM of catecholates.

The depth variability in concentration and chemical composition and the good correlation between abundance of siderophore-producing microorganisms and siderophore soil concentrations strongly suggest that these siderophore-producing microorganisms play an important role in the mobilization of iron in the podzol soil that may be important in iron availability to plants in forest environment.

[1] Clay *et al.* (1981) Biochemistry 20, 2432-2436. [2] Duckworth *et al.* (2009) ChemGeol 260, 149-158.

Adsorption of fecal microorganism on soils

HYANGSIG AHN[1*], CHANG HOON YOO[2], JEONG-HO LEE[1], HO YOUNG JO[1], SEONG-TAEK YUN[1], AND YONG SEOK JEONG[2]

[1]Korea University, Earth and Envionmental Sciences, Seoul, Republic of Korea, pl9ok8ij@korea.ac.kr (*presenting author)
[2]Kyunghee University, Biology, Seoul, Republic of Korea

Mobility of virus and microorganism through earth materials need to be investigated for evaluating soil and groundwater contamination. Surface charges of minerals or organic matters can vary with pH. When the surface charge polarity of soil particle is opposite to that of virus or microorganism, the virus or microorganism is adsorbed onto the soil particle by the electromagnetic attraction force [1]. Therefore, pH affects sorption characteristics of fecal virus or microorganism on the soil. This study investigated sorption characteristics of MS2 bacteriophage and E. coli on sorbents (i.e., quartz sand, iron oxide, and kaolinite) in aqueous solutions.

DI water was sterilized by filtering and then adjusted to pH 6~7 by adding the concentrated NaOH solution. Concentrated MS2 bacteriophage or E. coli was added to the pH adjusted solution. 1 g or 3.3 g of sorbent and the 10 ml of virus solution (10^3~10^8 PFU/ml) was reacted for 1~16 hours at 50 rpm and 15 ℃. After the reaction, the leachate was obtained by filtering the mixture of sorbent and virus solution using 0.22 ㎛ membrane filters. MS2 bacteriophage and E. coli concentrations of the leachate s were measured.

Sand and iron oxide adsorbed more MS2 bacteriophage than kaolinite. 1 g of sand or iron oxide removed almost completely MS2 bacteriophage from the 10 ml solution with 10^4~10^5 PFU/ml of MS2 bacteriophage. However, appromimately 20 % of MS2 bacteriophage was removed by kaolinite at the same condition. Iron oxide adsorbed more E. coli than sand and kaolinite. 1 g of iron oxide adsorbed 43~96 % of E. coli in the 10 ml solution with 10^3~10^5 PFU/ml for 1~16 hours, whereas no adsorption onto sand and kaolinite occurred. These results suggest that moblity of virus or mirooragnism can be affected by the soil constituents.

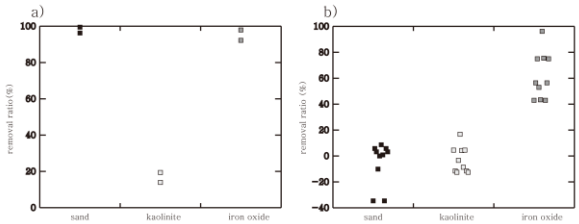

Figure 1: Removal ratio of a) MS2 bacteriophage and b) E. coli

[1] Redman et al (1997) *Environ. Sci. Technol.* **31,** 3378-3383.

https://doi.org/10.1180/S0026461X00008434 Published online by Cambridge University Press

The action of sulfur species and water on organic matter

WARD SAID-AHMAD[1,2], ALON AMRANI[2], ZEEV AIZENSHTAT[1*]

[1]Chemistry Institute The Hebrew University of Jerusalem, 91904 Israel, zeev@vms.huji.ac.il (* presenting author)

[2] Institute of Earth Sciences The Hebrew University of Jerusalem, 91904 Israel,wardsaid@gmail.com ;alon.amrani@mail.huji.ac.il

The incorporation of inorganic sulfur species into organic matter during early diagenesis stage has been studied and demonstrated by chemical analysis of sedimentary sulfurized organic matter (S-OM) and laboratory experiments. The importance of S-OM as one of the major quantitative and significant sinks of sulfur in sediments and its interaction with the global oxygen and carbon cycles is being recognized in recent years. Sedimentary OM reacts with S species (e.g. HS^-,S_x^{-2}, RS^-)in all stages of OM formation and thermal maturation. Recently, we have shown that elemental S is reactive even under mild temperatures (60-80ºC) and aquatic conditions. We have employed detailed chemical analyses and S-isotopic studies to decipher the mechanisms controlling these reactions. A variety of organosulfur compounds as well as oxidized compounds (non-S) such as ketones were formed by the reaction of elemental S and organic model compounds. The sulfurized and oxidized organic compounds seem to form in parallel. There is 5-13‰ isotopic fractionation; between elemental S and H_2S that decreases as a function of temperature. Organosulfur compounds and polysufides exhibit smaller fractionation relative to elemental S of 0-3‰. We suggest that the action of elemental S on organic matter is two folds: it activates water to produce hydroxyl radical that can oxidize organic compounds, and second, it reacts directly with organic matter to produce organosulfur compounds and H_2S. Similar effect was observed for polysulfides but not for H_2S or SO_2, suggesting that the catanated nature of S-S bonds has a decisive effect, probably through the formation of thyil radical ($SH^\cdot$) from the cleavage of these bonds. This in turn initiates a radical chain reaction that forms secondary radicals such as hydroxyl radicals. This species ($OH^\cdot$) was identified in our simulation experiments and are probably responsible for the ketones formation, demonstrating an important pathway for lowering the activation energy of water splitting and its subsequent reactions with OM. These findings improve our understanding of the intermediate temperature regime during OM thermal maturation that is mostly neglected in previous studies. It also provides new routes for hydrothermal processes such as thermochemical sulfate reduction. More importantly, this study shows the inherent connection of the carbon, hydrogen, oxygen and sulfur in the geosphere under much milder environmental conditions then previously thought.

Iron isotopic fractionation in tropical soils

A. AKERMAN[1,2*], F. POITRASSON[1,2], P. OLIVA[1], G. BOAVENTURA[2], L. C. VIEIRA[2], S. AUDRY[1] AND P. SEYLER[1]

[1]Laboratoire Géosciences Environnement Toulouse, IRD-CNRS, 14, av. E. Belin, 31400 Toulouse, France (* correspondence: alisson.akerman@get.obs-mip.fr)

[2]Instituto de Geociências, Universidade de Brasilia, Campus Universitario Darcy Ribeiro, 70904-970 Brasilia-DF, Brazil

Iron is the fourth most abundant element in the continental crust. It is particularly abundant in tropical environment due to the large amounts of poorly mobile oxidized Fe in lateritic soils. A better understanding of Fe biogeochemical cycle remains a major issue, particularly within the tricky problem of environmental change consequences (land use change, climate change, ...). This study focused on iron isotopic compositions of soils from three distinct toposequences in tropical environment: 1/ at the scale of the Nsimi experimental watershed in South Cameroon, 2 and 3/ in the Rio Capim's watershed in the northeast of the Brasilian Amazon, respectively in rainforest and pasture landscape. We worked both on ferralitic soils (i.e., the top of the hills), and on evolved/degraded soils present within the slopes and the bottom of the hills in connection with stream waters.

The objectives of this study were 1) to determine if significant isotopic differences in iron compositions exist between laterites and soils resulting from laterite degradation, 2) to investigate the processes responsible for these differences in isotope compositions, and 3) to evaluate to which extent Fe isotopes can be used as a proxy to understand metal cycling in the environment.

Iron isotope compositions were determined by MC-ICP-MS analysis after a complete microwave mineralization and iron purification.

Samples from evolved/degraded lateritic soils both in forest and pasture show important Fe loss compared to the reference feralitic soils (i.e., 30 to 90% estimated on the basis of a constant Zr concentration). Our first results on the Fe isotope compositions of these samples reveal that the δ^{57}Fe of the evolved/degraded soils ($\delta^{57}Fe = 0.6 \pm 0.1$‰ for soils at the bottom of the slope in forest and $\delta^{57}Fe = 0.4 \pm 0.1$‰ for soils under pasture) are isotopically heavier than the continental crust baseline and the reference lateritic soils (i.e; 0.1‰ in $\delta^{57}Fe_{IRMM-14}$). These results contrast with previous data published on the Fe isotopic compositions in lateritic soils showing no differences between soils and the continental crust [1]. Hence, our results suggest that chemical weathering and pedogenesis can significantly fractionate iron isotopes under tropical environments. This shows that Fe isotopes can be used as a new geochemical tool to study iron transfer during soil degradation and weathering processes in reponse to natural and anthopogenic processes.

[1] Poitrasson, F., et al. (2008) *Chemical Geology* **253**, 54-63.

https://doi.org/10.1180/S0026461X00008434 Published online by Cambridge University Press

Understanding the origin of porewater geochemical profiles in the Michigan Basin, southwest Ontario

TOM AL[1*], IAN CLARK[2], LAURA KENNELL[4], KEN RAVEN[3], MARK JENSEN[5]

[1]Earth Sciences, University of New Brunswick, Fredericton, New Brunswick, Canada, tal@unb.ca ([*]presenting author)
[2]Earth Sciences, University of Ottawa, Ottawa, Ontario, Canada
3Geofirma Engineering, Ottawa, Canada
[4]Nuclear Waste Management Organization, Toronto, Ontario, Canada

With a view toward establishing a deep geological repository for low- and intermediate-level radioactive waste, a geoscientific site characterization program has been conducted on the eastern margin of the Michigan Basin at the Bruce nuclear site. Drilling and collection of cores within an ~ 860 m near-horizontally layered Paleozoic sedimentary sequence, resting atop the Precambrian basement, has provided an opportunity for porewater and groundwater sampling and analysis with an unprecedented level of detail. Utilizing geochemical data from groundwater and porewater, this paper describes a natural analogue study in which the distribution of natural tracers within the sedimentary sequence is explored to develop insight regarding the timing and processes governing solute migration.

Depth profiles for the natural tracers $\delta^{18}O$, $\delta^{2}H$, Cl and Br in porewater and groundwater are presented and interpreted in terms of advection and diffusion processes that have caused them to evolve from initial conditions. Illustrative numerical simulations have been performed which support current interpretations of solute transport.

The tracer profiles are characterized by first-order trends that result from diffusive mixing near the top and bottom of the section over hundreds of millions of years. Near the top of the section, hypersaline evaporated seawater brine in the Silurian was in contact with porewater of normal marine salinity in the Ordovician. Contrasting chemical and isotopic compositions resulted in diffusive mixing across the Ordovician – Silurian boundary. Similarly, differences in isotopic composition between porewater in the Precambrian shield and the overlying Paleozoic sedimentary rocks resulted in diffusive mixing across the lower boundary of the basin.

These ancient first-order features in the tracer profiles have been disrupted by seemingly episodic events in the geologic past. The shallow groundwater system (<180 mBGS) shows evidence of a glacial meltwater component (decrease in $\delta^{18}O$ and $\delta^{2}H$), as does a thin, isolated, aquifer in the Salina A1 (~325-328 mBGS). The infiltration of fresh water in these intervals is manifest by dilution of salinity. At depth, in the Black River Group, the tracer profiles are deflected toward higher values that reach maxima in the Cambrian aquifer. The composition of porewater in the Cambrian is similar to deep groundwater from petroleum wells elsewhere in the Michigan and Appalachian basins and these deflections at the base of the tracer profiles are interpreted to represent fluids of deep basin origin. The results of numerical simulations conducted to date suggest that the disruptions at both the upper and lower boundaries could be explained as relatively recent events (e.g. during the Pleistocence). However, data evaluation is ongoing in efforts to advance understanding of the evolution of the profiles.

Indications of geochemical and C-O isotopic compositions in the origin of the UAE carbonatites

SULAIMAN A. ALAABED[1*] AND BAHAA EDDIN NAHMOUD[2]

[1]Department of Geology, FOS, United Arab Emirates University, AlAin, UAE, s.alaabed@uaeu.ac.ae (* presenting author)
[2] Department of Geology, FOS, United Arab Emirates University, AlAin, UAE, bahaa.mahmoud@uaeu.ac.ae

Carbonatite occurrences commonly associated with alkaline volcanic rocks in intracontinental rifting zones. In the UAE, few carbonatitic rocks occur as part of the metamorphic sole of the Semail ophiolite. They form pods, lenses and small layers within the deep sea meta-sediments and meta-volcanic rocks of Hawasina and Haybi Complexes at two different areas: Dibba and Hatta Zones. The previous little work attributed the UAE carbonatite existence to extrusive subaerial magmatic activities in an intra-oceanic setting associated with the Semail ophiolite emplacement. Although, they are internally undeformed, petrographic study reveals some metamorphic minerals in addition to the magmatic signatures. Geochemically, they show a significant enrichment in the REE and trace elements, close to but little above the average carbonatite composition. δ18O and δ13C analysis shows an increase in the isotopic composition of the studied rocks in array from the primary igneous carbonatite, indicating a heavier isotopic source affected these carbonatites. Combining field observation, petrographic study, geochemical and isotopic signatures, the UAE carbonatites might have formed in association with alkaline volcanic activities at the oceanic environment of the Semail ophiolite prior its obduction and final emplacement, and been affected by hydrothermal metasomatism .

https://doi.org/10.1180/S0026461X00008434 Published online by Cambridge University Press

Solar Nebulæ

FRANCIS ALBAREDE[1] AND FRÉDÉRIC MOYNIER [2]

[1] Ecole Normale Supérieure, Lyon, France, albarede@ens-lyon.fr
[2] Washington University in St Louis, MO, USA,

Lodders and Fegley [1] pointed out the necessarily multiple-component origin of the Solar System. Warren [2] argued for the bimodality in ^{50}Ti, ^{54}Cr, and O nucleosynthetic anomalies exhibited by planetary materials and suggested a division between carbonaceous and noncarbonaceous sources. Such a dichtomy is also visible in the Cu and Zn isotope compositions of the same material [3]. Using a novel presentation of oxygen isotope data, we show that all the analyzed material in the Solar Nebula can be accounted for by a component mixture not unlike Warren [2]'s two component mixture but involving three components. The new orthogonnal coordinates clearly separate mass-dependent from mass-independent fractionation and unveil well-defined mixing trends. Most of the accessible material in the Solar System may be accounted for by a mixture of a non-carbonaceous (L chondrite-like), a CV and a CI end-members. Similar components are also found when other nucleosynthetic anomalies (Ti, Cr, Ni) are plotted against water content of meteorites. It is arguable that the CV component is of solar origin. The most common proportions of CV and CI components in the mixture are reminiscent of a CM composition. We suggest the approximate contributions of the noncarbonaceous sources: 90% for L chondrites, 80% for H chondrites and Mars, 70% for E chondrites, the Earth, and Moon, and 20-40% for ureilites.

A first far-reaching consequence is that the Solar System is not well mixed and that accretion time scales are shorter than nebular mixing time scales. The Solar nebula does not represent the condensation of a homogeneous cloud of gas and dust, but the accretion of a number of genetically unrelated streaks, two of which (L-type and CI) having resisted full accretion to the central star.

In a session honoring Mike Drake's immense contribution, and more specifically to this issue [4], the origin of water in planets appears essentially pinned down on that of their CI component. Several correlation plots show that water is not a rogue component of the Solar System. It is remarkably well correlated with other gaseous (C, N) and lithophile (Zn) volatiles. Even if the history of water and of the CI component in terrestrial planets are intimately related, the timing of when the components discussed in this talk were mixed is still eluding final explanation.

[1] Lodders & Fegley (1997) *Icarus* **126**, 373-394. [2] Warren (2011) *EPSL* **311** 93-100 [3] Luck *et al.* (2005) *GCA* **69**, 5351-5363 [4] Drake & Righter (2002) *Nature* **416**, 39.

Multiple age components in individual molybdenite grains

JOHN ALEINIKOFF[1]*, ROBERT CREASER[2], HEATHER LOWERS[1], CHARLES MAGEE[3], AND RICHARD GRAUCH[1]

[1]US Geological Survey, Denver, Colorado, USA jaleinikoff@usgs.gov (* presenting author), hlowers@usgs.gov, rgrauch@usgs.gov
[2]University of Alberta, Earth & Atmospheric Sciences, Edmonton, Canada robert.creaser@ualberta.ca
[3]Australian Scientific Instruments, Canberra, Australia cwmagee@gmail.com

Molybdenite occurs within a pod of unusual monazite-xenotime gneiss (MXG) that is part of a granulite-facies paragneiss in the Hudson Highlands, NY. Whereas both the paragneiss and MXG contain detrital zircon older than about 1170 Ma, only MXG has a population of irregularly zoned prismatic zircon (U-Pb age of 1036±5). This age is thought to date the formation of MXG, probably by metasomatic/metamorphic processes, rather than as a paleo-placer. Subsequent events at about 1010, 985, and 920-880 Ma formed rims on zircon, xenotime, and monazite in MXG.

Re-Os geochronology of multi-grain fractions composed of unsized, coarse, and fine molybdenite yielded dates of 950.5 ± 2.5, 953.8 ± 2.6, and 941.2 ± 2.6 Ma, respectively. These dates are not recorded by co-existing zircon, xenotime, or monazite. SEM-BSE imagery of molybdenite in thin section and as separated grains reveals that most molybdenite grains are composed of core and rim plates that are approximately perpendicular. Rim material invaded cores, forming irregular contacts that probably reflect dissolution/reprecipitation.

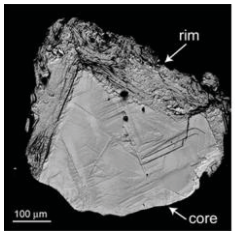

Figure 1: molybdenite grain showing core and rim.

Microanalysis for Re-Os geochronology of small volumes within individual grains was not attempted because parent ^{187}Re and daughter-product ^{187}Os can "decouple" [1, 2], yielding dates that can be too old or too young. However, EPMA and LA-ICP-MS analyses show that cores and rims have different trace element concentrations (for example, cores are richer in W). We conclude that the range of Re-Os dates on our multi-grain samples reflect mixing of at least two age components.

The discovery of cores and rims in individual molybdenite grains is analogous to multiple age components in U-Pb geochronometers such as zircon, monazite, and titanite. Thus, molybdenite, particularly of *metamorphic* origin, should be carefully examined prior to dating of multi-grain samples to ensure that the requirement of age homogeneity is fulfilled.

[1] Stein *et al.* (2003) *Geochim. Cosmochim. Acta* **67**, 3673-3686. [2] Selby & Creaser (2004) *Geochim. Cosmochim. Acta* **68**, 3897-3908.

https://doi.org/10.1180/S0026461X00008434 Published online by Cambridge University Press

Stability and transformations of monomeric U(IV) species at the Rifle, Colorado IFRC field site

DANIEL S. ALESSI[1,*], MALGORZATA STYLO[1], JUAN S. LEZAMA-PACHECO[2], JOANNE E. STUBBS[3], SARRAH M. DUNHAM-CHEATHAM[2], NOÉMIE JANOT[2], JOHN R. BARGAR[2], KATE M. CAMPBELL[4], PHILIP E. LONG[5], RIZLAN BERNIER-LATMANI[1]

[1]Ecole Polytechnique Fédérale de Lausanne, Switzerland, daniel.alessi@epfl.ch (* presenting author)
[2]Stanford Synchrotron Radiation Lightsource, Menlo Park, CA, USA, bargar@slac.stanford.edu
[3]University of Chicago, Chicago, IL, USA, stubbs@cars.uchicago.edu
[4]United States Geological Survey, Boulder, CO, USA, kcampbell@usgs.gov
[5]Lawrence Berkeley National Laboratory, Berkeley, CA, USA, pelong@lbl.gov

Strategies for the *in situ* immobilization of uranium aim to reduce oxidized and mobile U(VI) to relatively insoluble U(IV), a process long thought to result in the precipitation of the U(IV) mineral uraninite [$UO_{2(s)}$]. However, recent research indicates that non-crystalline products named monomeric U(IV) may form during the *in situ* reduction of U(VI)[1,2]. These products may form via uranium reduction by microbes, by Fe(II) minerals of biogenic origin[3], and in biostimulated natural sediments[4]. Monomeric U(IV) has garnered recent study because it is likely to be more susceptible to reoxidation and remobilization in the environment than uraninite.

To test its stability and possible transformations, two types of materials containing monomeric U(IV) were fixed in agarose gel pucks: (1) monomeric U(IV) produced via U(VI) reduction by *Shewanella sp.* CO-9, and (2) monomeric U(IV) produced by the reduction of U(VI) by phosphate-treated nanoparticulate magnetite of biogenic origin. These gel pucks were deployed in two groundwater wells at the Rifle, Colorado IFRC site for recovery after 1, 2, and 3 months. Digestions of the gels reveal that uranium is lost more rapidly from gels containing monomeric U(IV) than those containing biogenic uraninite. The monomeric U(IV) associated with biomass is more stable than that associated with magnetite. Uranium L_{III}-edge X-ray absorption spectroscopy (XAS) data point to a relative enrichment of uraninite in the gels as monomeric U(IV) species are selectively removed by the groundwater over time. Our results provide the first direct evidence of the *in situ* instability of monomeric U(IV) species relative to uraninite. Thus, the identification and quantification of these species at field remediation sites is likely to be critical in devising accurate uranium transport and fate models.

[1] Bernier-Latmani *et al.* (2010) *Environ. Sci. Technol.* **44**, 9456-9462.
[2] Fletcher *et al.* (2010) *Environ. Sci. Technol.* **44**, 4705-4709.
[3] Veeramani *et al.* (2011) *Geochim. Cosmochim. Acta*, **75**, 2512-2528.
[4] Sharp *et al.* (2011) *Geochim. Cosmochim. Acta*, **75**, 6497-6510.

The origin of water in asteroids and the terrestrial planets

CONEL M.O'D. ALEXANDER[1], ROXANE BOWDEN[2], MARILYN L. FOGEL[2], KIEREN T. HOWARD[3] AND CHRISTOPHER D.K HERD[4]

[1]DTM, Carnegie Institution of Washington, Washington DC, USA, alexander@dtm.ciw.edu (* presenting author)
[2]GL, Carnegie Institution of Washington, Washington DC, USA, rbowden@ciw.edu, m.fogel@gl.ciw.edu
[3]Natural History Museum, London, UK, kieren.howard@nhm.ac.uk
[4]Dept. Earth and Atmospheric Sciences, University of Alberta, Edmonton, herd@ualberta.ca

Introduction

Determining the source(s) of the volatile elements H, C and N in the terrestrial planet region is important not only for understanding the origin of life on Earth, as well as dynamical processes in the solar nebula and during planet formation. For instance, a massive influx of water ice from the outer Solar System is thought to have altered the O isotopic composition of the inner Solar System early in its history [1,2]. The bulk and secondary mineral O isotopic compositions of chondrites exhibit behavior that is at least consistent with this. It has also been proposed that C, D and P type asteroids, to which carbonaceous chondrites have been linked, were injected into the asteroid belt from the comet-forming regions prior to formation of Mars [3] and during the late heavy bombardment [4]. Equilibrium and kinetic factors should produce increasingly D-rich water with increasing radial distance from the Sun. In support of this, the water in all but one of the measured comets is significantly ($\delta D \approx 1000$ ‰) more D-rich than Earth. Here, we use the H, C and N elemental and isotopic compositions of chondritic water to determine its provenance(s).

Results

The bulk H abundances and isotopic compositions of CM and CR chondrites are produced by variable mixtures of a common organic component ($\delta D \approx 3500$ ‰) and water with δD values of about -450 ‰ and 100 ‰, respectively. After subtracting this common organic component from bulk analyses of the most primitive CIs, COs and CVs, as well as Tagish Lake, their estimated water δD values are in the same range as for the CMs. In contrast, the water in the ordinary chondrite Semarkona has a δD value of >800 ‰.

Discussion and Conclusions

The estimated H isotopic compositions of the water described above should all probably be regarded as upper limits since they may have been D enriched by oxidation of Fe by water during aqueous alteration [5]. Even the current estimates show that, with the possible exception of the CRs, the carbonaceous chondrites did not form in the same regions as known comets. This calls into question both the ice influx and dynamical models described above. Comparison of the H and N isotopic compositions of chondrites and Earth suggests that the Earth's composition is most simply explained as a mixture of CI and a small amount of solar material.

[1] Lyons & Young (2005), *Nature* **435**, 317 (2005). [2] Yurimoto & Kuramoto (2004), *Science* **305**, 1763. [3] Walsh, et al. (2011), *Nature* **475**, 206. [4] Levison et al. (2009), *Nature* **460**, 364. [5] Alexander et al. (2010), *Geochim. Cosmochim. Acta* **74**, 4417.

https://doi.org/10.1180/S0026461X00008434 Published online by Cambridge University Press

Grain size vs. multi-mineral $^{40}Ar/^{39}Ar$ thermochronology

PAUL ALEXANDRE[1*]

[1]Queen's University, Geological Sciences, Kingston, Canada, alexandre@geol.queensu.ca (* presenting author)

In the case of volume diffusion, the closure temperature of a mineral is function of, among other factors, the characteristic diffusion dimension, which can be approximated by the grain size of the mineral analysed for grains smaller than or similar in size to the diffusion domains. The theoretical possibility of single mineral grain size thermochronology had been demonstrated empirically in earlier studies, mostly using biotite. In order to examine the potential of this method, it was tested alongside the widely used multi-mineral $^{40}Ar/^{39}Ar$ thermochronology.

The sample comes from the granitic McLean pluton, in the south section of the Grenville orogeny. Seven grain size separates of biotite (ranging between 90 and 1000 μm), eight size fractions of amphibole (between 63 and 1000 μm), and three size fractions of K-feldspar (250 to 600 μm) were extracted and dated by the laser step-heating $^{40}Ar/^{39}Ar$ method. The total gas ages obtained behave as theoretically predicted, with increasing ages for increasing grain sizes, including for K-feldspar, but with the exception of the smallest and the largest grains for biotite and amphibole (Fig. 1). The calculated cooling rates are ca. 0.7 °C/Ma for K-feldspar, ca. 2.5 °C/Ma for biotite, and ca. 11 °C/Ma for amphibole, corresponding very well to a monotonic cooling of the McLean Pluton. A quick initial thermal re-equilibration with the cooler host-rocks is followed by a much slower cooling on a thermal path parallel to that of the Frontenac Terrain situated immediately to the southeast.

The validity of the single mineral grain size thermochronology is demonstrated by comparison with the thermal evolution of the adjacent units and with the cooling history derived from a multi-mineral thermochronology, suggesting that it can be routinely used. The application of this method can be hampered by insufficiently low analytical uncertainties.

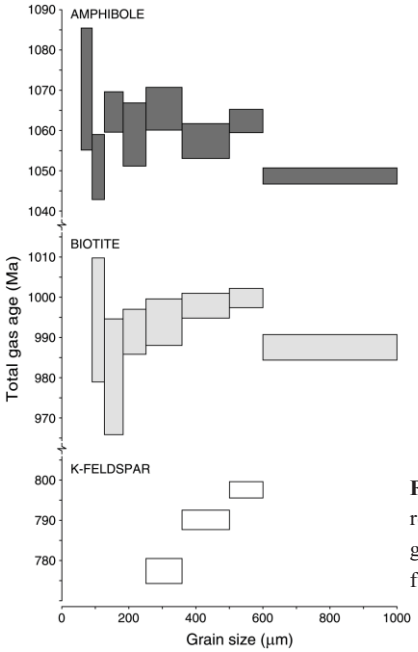

Figure 1: Analytical results, showing total gas $^{40}Ar/^{39}Ar$ ages as function of grain size.

Volcanic impact on the silicon isotope composition of natural waters during the 2010 Eyjafjallajökull eruption, S-Iceland

H. A. ALFREDSSON[1,3*], S. OPFERGELT[2,3], K. W. BURTON[3], F. MOKADEM[3], E. S. EIRIKSDOTTIR[1], AND S. R. GISLASON[1]

[1]Institute of Earth Sciences, University of Iceland, Reykjavik, Iceland, haa4@hi.is (* presenting author)

[2]Earth and Life Institute, Université catholique de Louvain, Louvain-la-Neuve, Belgium.

[3]Department of Earth Sciences, University of Oxford, Oxford, UK.

When Eyjafjallajökull volcano erupted in 2010, volcanic ash exploded through crater ice. The resulting fine grained ash and several *jökulhlaups* (glacial outburst floods), flushed volcanic material over the surrounding lowlands, towards the oceans and distributed atmospheric dust ash deposition over much of Europe. The ash and volcanic suspended matter, including dissolved solids and gases were incorporated into the surface waters surrounding the volcano and hence into the ocean. We collected natural water samples from the field, including *jökulhlaups* close to the vent south of the volcano (X), the big *jökulhlaups* in Markafljót river which is flowing from the north of the volcano, south towards the sea (Y), and ash contaminated surface waters (Z). In addition, flow-through plug experiments on pristine trachyandesitic ash samples, were performed in order to determine release rates of leachates from the ash [2].

The temperature of the natural waters ranged from 0.1 to 11°C and the pH from 5.86 to 7.95. The dissolved Si content ranged from 7 to 18 $mg \cdot l^{-1}$, with the highest value measured in the *jökulhlaups* during the first day of the eruption. The Si isotope composition ($\delta^{30}Si$) in the natural waters ranged from -0.45 to 1.38 ‰. Prior to the first flood, the Si isotope composition of the river (Y) was 0.84 ‰, very close to other surface waters in Iceland [1]. The lightest $\delta^{30}Si$ ratios were found in X. In contrast, waters from Y were isotopically heavier (0.35 – 1.17 ‰). The heaviest Si isotope signatures were measured in Z (0.51 to 1.38 ‰).

The ash experiments were conducted on single cell plug, with fixed flow rate of DI water. The experiment was run at ambient T/P. The pH in the collected leachates went up to 10.3 the first day, dropping to pH 9.2 after 1 week. The results showed higher release rates of most elements during dissolution of salt coatings found on the ash-grain surface [2]. The total Si release rate, normalized to the measured BET surface area, went from $10^{-7.6}$ mole Si $/m^2/sec$. at the beginning, reaching steady state at $10^{-8.6}$ mole Si $/m^2/sec$. The $\delta^{30}Si$ ratio measured was 0.28 ‰ in the first sample (after 13 min.) and then dropped down to -1.40 ‰ during dissolution of the salt coatings. It stabilazed at -0.60 ‰, closer to the isotope ratios of basalt [1].

These results show dramatic changes in the $\delta^{30}Si$ ratios of the surface waters and floods during the eruption. The waters directly linked to the erupting crater and pristine ash, had significally lighter ratios than recorded in waters accompanying basalt weathering [1]. The flooded rivers recovered quickly, within 11 days the Si isotopic composition was found to be similar to that prior to the eruption.

[1] Georg et. al. (2007) *Earth Planet. Sci. Lett.* **261**, 476-490. [2] Alfredsson et. al. (2011) *Min. Mag.* **75(3)**, 423.

https://doi.org/10.1180/S0026461X00008434 Published online by Cambridge University Press

Environmental controls on the reactivity of sedimentary organic matter in the St. Lawrence Estuary

MOHAMMAD ALKHATIB[1]*, CARSTEN J. SCHUBERT[2], PAUL A. DEL GIORGIO[3], YVES GELINAS[4] , MORITZ F. LEHMANN[5]

[1] GEOTOP, UQAM-GRIL, Département des Sciences Biologiques Montreal, Canada, alkhatib.mohammad@courrier.uqam.ca (* presenting author)
[2] Eawag, Kastanienbaum, Switzerland, Carsten.Schubert@eawag.ch
[3] UQAM-GRIL, Département des Sciences Biologiques, Montreal, Canada, del_giorgio.paul@uqam.ca
[4] Concordia University, Chemistry and Biochemistry, Montreal, Canada, ygelinas@alcor.concordia.ca
[5] Universität Basel, Department for Environmental Science, Basel, Switzerland, moritz.lehmann@unibas.ch

Abstract

We report multiple parameters used to describe the reactivity and diagenetic state of sediment organic matter (OM), including total hydrolysable amino acid (THAA), amino acid enantiomer, chlorin (CI) and amino acid degradation (DI) indices, along a transect between the Upper St. Lawrence Estuary and the Gulf of St. Lawrence, Canada. The study area is characterized by gradients in water oxygen concentration, water depth, OM source, primary productivity, and sedimentation rate. Both CI and DI indicate a decline in OM reactivity with the transition of a more terrestrial to a more marine-dominated sedimentation regime from the shallow Upper Estuary (23-95m) to the hypoxic, mid-depth Lower Estuary and to the deep (>400m), well-oxygenated Gulf. Systematic variations in the amino acid composition along the Laurentian Channel confirmed the increased diagenesis of OM with distance from the Upper St. Lawrence Estuary. The ratio of D/L stereoisomers of alanine increased along the transect, and the co-variation between DI and the D/L-Ala suggests a close coupling between the extent of diagenesis and the accumulation and selective preservation of bacterially-derived cell wall material in the sediments. The patterns observed along the estuarine transect were also present down-core in two sediment cores, confirming the robustness of our reactivity indices. Oxygen exposure time of the sediments appears to strongly determine sediment OM reactivity in the St. Lawrence Estuary. The sediment oxygen regime itself is related to the interplay between water column depth, vertical OM flux, and reactivity of settling OM.

Rare Earth Elements in the Misten peat bog (Belgium) as tracers of dust depositions and past environmental changes

MOHAMMED ALLAN*[1], GAËL LE ROUX[2, 3], NADINE MATTIELLI[4], NATALIA PIOTROWSKA[5] AND NATHALIE FAGEL[1]

[1] AGEs, Département de Géologie, Université de Liège, Allée du 6 Août, B18 Sart Tilman B-4000, Liège, Belgium, mallan@doct.ulg.ac.be; nathaliefagel@ulg.ac.be
[2] Université de Toulouse ; INP, UPS; EcoLab (Laboratoire Ecologie Fonctionnelle et Environnement) ; ENSAT, Avenue de l'Agrobiopole, 31326 Castanet Tolosan, France,
[3] CNRS; EcoLab; 31326 Castanet Tolosan, France, gael.leroux@ensat.fr
[4] Laboratoire G-Time, Université Libre de Bruxelles, Bruxelles, Belgium. nmattiel@ulb.ac.be
[5]Department of Radioisotopes, GADAM Centre of Excellence, Institute of Physics, Silesian University of Technology, Gliwice, Poland natalia.piotrowska@polsl.pl

The Misten peat bog representing 7.5 m of peat accumulation in the Hautes-Fagnes Plateau, Belgium, provides a record of Rare Earth Elements (REE) deposition since more than 7000 years. The analyses of REE and lithogenic element concentrations, as well as the Nd isotopes, were performed by HR-ICP-MS and MC-ICP-MS, respectively in peat layers previously dated by ^{210}Pb and ^{14}C. REE concentration variations in peat samples are correlated with Ti, Zr and Sc that are lithogenic conservative elements, suggesting that REE are immobile in the studied peat bogs [1] and can be used as tracers of dust deposition. Peat humification, C/N ratio, ash content and bulk density were used to evaluate hydroclimatic conditions. The εNd values show large variability, between +1 to –22, identifying three major sources of dusts falling into the peat: local soils, distal volcanic and desert particles. More recently, industrial emissions provide a fourth source of dusts [2], which is also clearly recorded in the last 200 years of the Misten peat profile.

[1] Aubert D., Le Roux G. *et al.* (2006) *Geochimica Cosmochimica Acta* 70, 2815-2826.

[2] Le Roux G., Fagel N. *et al.* (in press) *Geology* Volcano- and climate-driven changes in atmospheric dust sources and fluxes since the Late Glacial in Central Europe.

https://doi.org/10.1180/S0026461X00008434 Published online by Cambridge University Press

The matrix effect as alpha dose: improving LA-ICP-MS Pb/U ages

CHARLOTTE M. ALLEN[1]* AND IAN H. CAMPBELL[1]

[1]Research School of Earth Sciences, Australian National University, charlotte.allen@anu.edu.au (*presenting author)

[1]Research School of Earth Sciences, Australian National University, ian.campbell@anu.edu.au

The Matrix Effect, New Experiments, and Results

Matrix effects are purported to be the cause of offsets of ages from spot (*in situ*) dating techniques relative to TIMS work in which zircons are dissolved and U and Pb are isolated and concentrated through column chemistry. Moreover they are thought to contribute to Pb/U differences in zircon spot dating. Age offset is the measured age minus the accepted age all divided by the accepted age. Black et al. (2004) showed that there are age offsets among TIMS, SHRIMP and LA-ICP-MS $^{206}Pb/^{238}U$ ages for well characterized zircons and suggested that Nd was a monitor for degree of offset [1]. Klötzi et al. (2009) showed in a LA-ICP-MS experiment using each of 4 standard zircons to deduce the age of a fifth produced a minimum precision of 3-4%, prescision worse than that generally ascribed to the technique [2]. Klötzi's work (rastering not drilling) shows that understanding, minimizing and/or eradicating the matrix effect is vital for truly accurate and precise LA-ICP-MS $^{206}Pb/^{238}U$ ages.

We have shown by 2 different LA-ICP-MS round robin experiments on 6 well characterized zircon standards with TIMS ages (OG1, FC1, 91500, Temora, R33 Plesovice, and LP521) that the matrix effect is not chemical but physical in nature. We have expanded our database to include Miocene zircons with high precision $^{40}Ar/^{39}Ar$ ages (Cougar Point Tuff) as well as some other zircons [3]. Briefly our system consiststs of an Agilent ICP-MS and Excimer 193 nm wavelength laser with in-house ablation chamber. In a He atmosphere we drill 30 µm spots to 20 µm depths while measuring 18 masses. Of these only one variable showed a strong correlation with age offset, radiogenic Pb. The cause of the matrix effect is not the presence of the Pb itself, but what the Pb represents – the accumulated decay of U and Th since zircon crystallization. Our results show that if a zircon is substantially older and/or more radiogenic than the standard (Temora in this study) then the measured ICP-MS age is too old by up to 3%. More startlingly, if the unknown is substantially younger and/or less radiogenic than the standard then the age obtained is too young by up to 8%. We surmise that in grains that have had higher alpha particle doses, Pb escapes the ablation site with greater ease relative to U. The exponential fit of percent age offset vs alpha dose$*10^{-15}$ for 14 populations given below can be used to correct our existing work.

$$y=382.68e^{0.8331x} \quad r^2=0.96.$$

In experiment 2 we have demonstrated that annealing the same 6 standards to the same conditions (850°C for 48 hours) obliterates the matrix effect. Age offsets are then about the uncertainty expected from counting statistics (<1%). We highly recommend annealing standards and unknowns before LA-ICP-MS dating.

[1] Black *et al.* (2004) *Chem. Geol.* **205**, 115-140. [2] Klötzi *et al.* (2009) *Geostd. And Geoanal. Res.* **5,** 5-15. [3] Bonnichsen, *et al.* (2008) *Bull. Volcanol*. **70**, 315-342.

Influence of seawater carbonate chemistry on B/Ca in cultured planktic foraminifera

KATHERINE ALLEN[1*], BAERBEL HOENISCH[1], STEPHEN M. EGGINS[2] AND YAIR ROSENTHAL[3]

[1]Columbia University, Earth and Environmental Science, katallen@ldeo.columbia.edu (* presenting author) hoenisch@ldeo.columbia.edu

[2]The Australian National University, Research School of Earth Sciences, Stephen.Eggins@anu.edu.au

[3]Rutgers University, Institute of Marine and Coastal Science, rosentha@marine.rutgers.edu

The ratio of boron to calcium (B/Ca) in fossil calcite tests of planktic foraminifers has recently been used to investigate the carbonate chemistry of ancient oceans. The theoretical basis for this proxy is rooted in the pH-dependent concentration of dissolved borate ($B(OH)_4^-$) and its subsequent incorporation into foraminiferal calcite (Hemming and Hanson, 1992). Here, we present new insights into B incorporation from laboratory culture experiments with live specimens of *Globigerinoides ruber* (pink) and *G. sacculifer*. We find that in *G. sacculifer*, B/Ca increases with pH (higher $[CO_3^{2-}]$ and $[B(OH)_4^-]$, lower $[HCO_3^-]$), but decreases with total dissolved inorganic carbon (DIC) (higher $[CO_3^{2-}]$ and $[HCO_3^-]$, constant $[B(OH)_4^-]$). This suggests competition between aqueous boron and carbon species for inclusion into the calcite lattice. Similar to previous experiments with cultured *Orbulina universa*, B/Ca increases with salinity, but not with temperature. We evaluate possible control parameters, including $[B(OH)_4^-]/[HCO_3^-]$ and $[B(OH)_4^-]$/DIC. Our culture calibrations are broadly consistent with field data, including new core-tops from the Gulf of Mexico. Some discrepancies may indicate the presence of unidentified controls, and more work is needed to probe specific controls on B/Ca and to test culture calibrations in the open ocean.

[1] Hemming and Hansen (1992) *Geochim. et Cosmochim. Acta* **56**, 537-543.

https://doi.org/10.1180/S0026461X00008434 Published online by Cambridge University Press

Submarine weathering of detrital silicates simulated in the laboratory

G. ALOISI[1], C. ALBRECHT[2], M. HAECKEL[2], S. KUTTEROLF[2], C. DEUSNER[2*], K. WALLMANN[2]

[1]LOCEAN, CNRS UMR, Université Pierre et Marie Curie, Paris, France, galod@locean-ipsl.upmc.fr (* presenting author)
[2]GEOMAR Helmholtz Centre for Ocean Research Kiel, Kiel, Germany, calbrecht@geomar.de, mhaeckel@geomar.de, skutterolf@geomar.de, cdeusner@geomar.de, kwallmann@geomar.de

Silicate detritus is transported from the continents to the oceans by rivers. Although it is a major component of marine sediments, its reactivity in the oceanic environment has only been scarcely investigated. Wallmann et al. (2008) [1] propose that significant weathering of detrital silicates takes place in the anoxic sediments of the Sakhalin Slope, Sea of Okhotsk.

We carried out batch experiments with these sediments to further test this idea. In our experiment the sediments reacted with the artificial seawater in a matter of minutes to days, releasing dissolved compounds, such as TA (total alkalinity), Ca, K, Si, B, Sr, Li, Mn, Fe, and Ba. Applying a numerical biogeochemical model, we show that organic matter degradation and dissolution of carbonates can account for only a part of the observed TA increase. Detailed mineralogical analyses suggest that the only alternative source for TA is the weathering of primary silicates and clay minerals which are abundant in Sakhalin Slope sediments. Thermodynamic modeling of silicate solubilities shows that the experimental fluids are undersaturated with respect to a wide range of chemically diverse silicates which potentially contribute to the TA build-up. The weathering rate in our experiment is only one order of magnitude larger than in the natural setting, suggesting that in-situ dissolution of silicates takes place at a high degree of undersaturation.

Since the ocean is also highly undersaturated with respect to a wide variety of primary silicates and clay minerals, weathering of detrital silicates in oceanic and sedimentary environments could be a widespread process.

[1] Wallmann, Aloisi, Haeckel, Tishchenko, Pavlova, Greinert, Kutterolf, Eisenhauer (2008) *Geochim. Cosmochim. Acta* **72**, 3067-3090.

Methane biogeochemistry in anoxic marine sediments: insights from reaction-transport models applied to $\delta^{13}C\text{-}CH_4$ and $\delta^{13}C\text{-}\Sigma CO_2$ depth distributions

MARC J. ALPERIN

Department of Marine Sciences, Univeristy of North Carolina at Chapel Hill, Chapel Hill, NC 27599-3300, USA (correspondence: alperin@email.unc.edu)

Three fundamental questions regarding the methane cycle in anoxic marine sediments are: (1) what are the pathways of methane production; (2) how are methane production, methane oxidation, and sulfate reduction zoned within the sediment column; and (3) how much of the sulfate reduction is coupled to methane oxidation? Stable carbon isotopes in CH_4 and ΣCO_2 have been used to address each of these questions. However, simple isotope mass-balance calculations that ignore the effect diffusive transport on isotope distributions can be misleading. I will present an advection-diffusion-reaction model that is suited for quantitative interpretation of stable isotope depth distributions in marine sediments where molecular diffusion is the dominant transport process. The model is driven by organic matter remineralization via sulfate reduction and methane production and can reproduce the features in $\delta^{13}C\text{-}CH_4$ and $\delta^{13}C\text{-}\Sigma CO_2$ profiles that are characteristic of marine sediments. A detailed comparison of predicted stable isotope distributions with methane production pathways and rates of processes illustrates the insights into the sedimentary methane cycle that can be derived from $\delta^{13}C\text{-}CH_4$ and $\delta^{13}C\text{-}\Sigma CO_2$ profiles.

https://doi.org/10.1180/S0026461X00008434 Published online by Cambridge University Press

Approaching acid gas - fluid interactions

T. ALPERMANN[1]*, C. OSTERTAG- HENNING[1]

[1]Federal Institute for Geosciences and Natural Resources, Stilleweg 2, 30655 Hannover, Germany
(* correspondence: Theodor.Alpermann@bgr.de)

Acid gases like CO_2 and H_2S as well as organo-sulfur compounds are common components in natural gas and oil reservoirs originating from a variety of sulfate reduction processes. Depending on the composition of a hydrocarbon reservoir, significant amounts of these objectionable compounds might have to be removed from the hydrocarbons during the refinery process.

Therefore, new disposal practices for acid gases and organo-sulfur compounds are needed due to the projected exploitation of giant hydrocarbon reservoirs with exceptionally high amounts of sulfur-containing compounds. One option for the disposal may be the geological sequestration within suitable strata. Although mixtures of H_2S/CO_2 have been injected into deep geological formations in Canada for more than 20 years,[1] little is known about possibly occurring geochemical reactions in the underground.

In order to contribute to a better understanding of chemical processes under geological storage conditions, interactions of CO_2/H_2S, low-molecular organo-sulfur compounds and brines of different composition were investigated. Typically, experiments are conducted in sealed gold tubes at a temperature of 120°C and a pressure of 100 bar.

The experimental outcomes may provide a basis for a more detailed evaluation of the underground storage potential of organo-sulfur compounds and acid gases.

[1] Bachu & William (2004) *Geol. Soc. Special Publ.* **233**, 225-234.

Arsenic and old gold mines: mineralogy, speciation, and bioaccessibility

CHARLES N. ALPERS[1*], TAMSEN L. BURLAK[2], ANDREA L. FOSTER[3], NICHOLAS T. BASTA[4], AND VALERIE L. MITCHELL[5]

[1]U.S. Geological Survey, California Water Science Center, cnalpers@usgs.gov (* presenting author)
[2]Sacramento State University, Geology, tlb226@saclink.csus.edu
[3]U.S. Geological Survey, afoster@usgs.gov
[4]The Ohio State University, basta.4@osu.edu
[5]Calif. Dept. of Toxic Substances Control, vmitchel@dtsc.ca.gov

Understanding the behavior of arsenic (As) during weathering of sulfide-bearing mineral deposits and associated mine wastes is important with regard to minimizing the exposure of humans and wildlife to this carcinogenic element. In low-sulfide gold-quartz vein deposits of the Mother Lode region of California, As occurs predominantly in the primary sulfide minerals arsenopyrite (FeAsS) and arsenian pyrite ($Fe(S,As)_2$). Detailed characterization of As- and iron- (Fe-) bearing primary and secondary minerals in mine waste piles at the Empire Mine State Historic Park (EMSHP), Grass Valley, California, was done as part of a larger study designed to evaluate the influence of mineralogy and speciation of As on bioaccessibility in mineralized environments and abandoned mines.

On the basis of electron microprobe analysis, arsenian pyrite at Empire mine has 0 to 5 wt. % As and arsenopyrite has 41 to 43 % As; secondary weathering products include hydrous Fe oxides (HFO, ferrihydrite and goethite, 0 to 18 wt. % As), hydrous Fe arsenates (HFA, including scorodite, $FeAsO_4 \cdot 2H_2O$, and related phases, more than 20 wt. % As), As-bearing jarosite ($KFe_3(SO_4,AsO_4)(OH)_6$, 0.2 to 0.8 wt. % As) and unidentified Ca-Fe-arsenate minerals. The speciation of As in the seconary minerals is predominantly As(V) (at least 90%), based on x-ray absorption spectroscopy. The molar ratio As:Fe in HFO is about twice as high as that in arsenian pyrite grains in close spatial association; most likely, this reflects adsorption or coprecipitation of arsenate from solution on HFO. Based on electron microprobe analysis, HFO from Empire mine has a minimum of 1 wt.% SiO_2.

Bioaccessible As, measured using *in vitro* methods simulating conditions in the human stomach and small intestine, ranged from 1.4 % to 11% of total As in 25 samples of mine waste from the EMSHP area. In addition, a sequential extraction procedure [1] was applied to the 25 samples. The first two fractions (F1, 0.05 M ammonium sulfate; F2, 0.05 M ammonium phosphate) liberated sorbed As; the sum of F1+F2 concentrations was less than the *in vitro* test results for all samples. The third fraction (F3, 0.2 M oxalate at pH 3) liberated As associated with amorphous and poorly crystalline oxides of Fe and aluminum (Al). The sum of F1+F2+F3 concentrations was consistently higher than results from the *in vitro* tests, suggesting that some As associated with amorphous and poorly crystalline Fe and Al oxides is not bioaccessible. Adsorbed SiO_2 tends to lower the dissolution rate of HFO [2], reducing bioaccessibility.

[1] Wenzel *et al.* (2010) *Analytica Chimica Acta* **436**, 309-323.
[2] Eick *et al.* (2009) *Clays and Clay Minerals* **57**, 578-585.

https://doi.org/10.1180/S0026461X00008434 Published online by Cambridge University Press

He and Ar diffusivity in naturel MORB glasses

JULIEN AMALBERTI[1*], PETE BURNARD[1]

[1] CRPG-CNRS, Vandoeuvre-lès-Nancy, France, *
amalbert@crpg.cnrs-nancy.fr (* prensenting author)

Diffusion in glasses

Given the short timesacales implied for the creation and seperation of a volatile phase during magmatic degassing, it seems likely that disequilibrium processes could fractionate the noble gases as well as other volatiles [1, 2, 3]. In order to document the diffusivity of noble gases in basaltic systems, we present a study of He and Ar diffusion by stepwise degassing. He and Ar analyses were performed on natural fresh MORB glasses (*AMK 3375,* mid-Atlantic Ridge).

Results

The results produce linear trends in a plot of ln(D) vs. 10000/T (Fig. 1). We observe high Ar diffusivity at low temperature. This behaviour is not well understood but may reflect a specific diffusion path of Ar into MORB glass. Further work is planned to determine the origin of this behaviour. Nevertheless, there is a convergence of He and Ar diffusivities consitent with a 'compensation' temperature [4] where He and Ar diffusivities are equal.

Implications

The experimental data show a compensation temperature for He and Ar diffusion at ~750°C. The implications of this are that there will be no kinetic fractionnation during magmatic processes. From Fig. 1 Ea = 192,16 kJ.mol^{-1} and Do = 9,91E^{-4} cm².s^{-1} for He and 67.73 kJ.mol^{-1} and Do = 1.68E^{-4}cm².s^{-1} for Ar in natural MORB glasses. In order to apply these results to natural magmatic systems there are two important caveats to consider:- 1) In our samples, He and Ar were originally present predominantly as gases in vesicles, and therefore extraction consists of two steps: solubilisation of vesicle gases into the glass and then volume diffusion of dissolved He or Ar through the glass itself. The diffusivities measured (Fig. 1) will reflect the slowest of these processes, and it seems possible that this is the reason behind rapid Ar diffusion at low T. 2) Our experiments were carried out below the glass transition temperature and diffusivities may be different in true liquids. Further work is planned to constrain both of these issues.

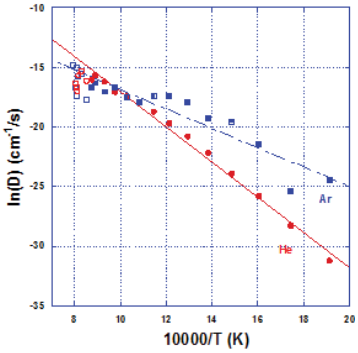

Figure 1 : He (circles) and Ar (squares) diffisivities in MORB glass which was heated between 150 and 950°C for 20 mins; diffusivities are for spherical geometry. The compensation temperature is estimated at ~1000K where ln(DHe) = lnD(Ar)

[1] A. Paonita (2006) *Earth Planet Sci. letts* **241** 138-158. [2] C. Aubaud (2004) *Earth Planet Sci. letts* **222** 391-406. [3] H.M Gonnermann (2003) *Earth Planet Sci. letts* **238** 1-16. [4] S.R. Hart (1981), G.C.A. **269**, 507 - 516

Cosmogenic ^{3}He in calcite: under what conditions is it useful?

WILLIAM AMIDON[1*], DANIEL HOBBS[1]

[1]Middlebury College, Middlebury, VT, USA
wamidon@middlebury.edu

Abstract

Spallation produced ^{3}He has recently been explored as a dating tool in a variety of non-traditional mineral phases, including apatite, garnet, hornblende, titanite, and zircon. Three problems limit the utility of these phases to differing degrees: 1) nucleogenic Li-produced ^{3}He, 2) redistribution of Li-produced ^{3}He between small crystals, and 3) presence of large amount of radiogenic ^{4}He. Calcite is less vulnerable to these problems because it is generally very low in Li, U, and Th, it has a very low He closure temperature, and it occurs in very large crystal sizes. Here we build on recent work[1] by exploring the apparent retentivity of calcite formed in different aqueous environments. Results comparing ^{36}Cl against ^{3}He in micritic limestones from the Dead Sea and Aegean regions show that ^{3}He is not quantitatively retained in calcite from these limestones over 10 kyr timescales. In contrast, results from hydrothermal vein calcite from multiple sites on the Pamir and Tibetan Plateaus suggests quantitative retention over at least 20 kyr timescales. Cross-calibration of ^{3}He against ^{36}Cl in these sample suggests reasonable ^{3}He production rates between 130-160 at g^{-1} yr^{-1}. Step-wise diffusion experiments of the same vein calcite reveals complex arrhenious relationships characterized by a decrease in diffusivity during successive degassing steps at the same temperature. This behavior is consistent with the presence of multiple diffusion domains, which may reflect the size of calcite growth pyramids or "hillocks." [1] Ongoing work seeks to establish whether diffusivity of ^{3}He depends on the size of calcite growth pyramids, which are in turn dependent on the CO_3 saturation level and the presence of impurities in the crystallizing fluid. Ultimately, we hope to define a set of growth conditions under which the resultant calcite crystal is likely to be retentive to ^{3}He over timescales and surface temperatures suitable for cosmogenic dating.

[1] Copeland et al., (2007) *Geochimica et Cosmochimica Acta* **71** 4488-4511

https://doi.org/10.1180/S0026461X00008434 Published online by Cambridge University Press

Modeling plastic deformation of minerals under mantle strain-rates

AMODEO J.[1], CARREZ PH.[2] AND CORDIER P.[3*]

[1]University of Lille, Villeneuve d'Ascq, France, jonathan.amodeo@yahoo.fr
[2] University of Lille, Villeneuve d'Ascq, France, philippe.carrez@univ-lille1.fr
[3] University of Lille, Villeneuve d'Ascq, France, patrick.cordier@univ-lille1.fr (* presenting author)

Mantle convection involves plastic deformation of minerals and rocks under extreme conditions that are very difficult to reproduce in the laboratory. In particular, experimental strain-rates are at least 6 orders of magnitude larger than in nature. Extrapolation to natural conditions of semi-empirical constitutive flow laws parameterized on laboratory data is thus very unsafe and leads to significant discrepencies with observations (e.g. post-seismic deformation). Here we describe a physically-based model able to describe the rheology of MgO (the magnesium end-member of the second most abundant phase of the lower mantle) under very low strain-rates representative of mantle convection. Our multiscale numerical model involves : (i) dislocation core modeling based on the Peierls-Nabarro-Galerkin model, (ii) thermal activation modeling of dislcoation glide based on the kink-pair theory, (iii) critical resolved shear stress modeling based on the Orowan equation (in ther thermally-activated regime) or on Dislocation Dynamics modeling (in the athermal regime). The kink-pair theory allows to describe the mobility of dislcoations under very low stresses without extrapolations. We show that decreasing the strain-rate counteract the influence of high-pressure and emphasizes the athermal regime for MgO in lower mantle conditions.

This approach will be further applied to other phases of the Earth's mantle within the ERC-funded *RheoMan* project (wwww.rheoman.eu)

Reactive Trasnsport Modelling of Gas Formation and Mineral Precipitation in a Granular Iron Column

RICHARD T. AMOS[1*], SUNG-WOOK JEEN[1,2], DAVID W. BLOWES[1]

[1]University of Waterloo, Waterloo, Ontario, Canada, ramos@uwaterloo.ca (* presenting author), blowes@uwaterloo.ca
[2]Atomic Energy of Canada Limited, Chalk River, Ontario, Canada jeens@aecl.ca

The (bio)geochemical reactions resulting in the degradation of contaminants in aquifers and remediation systems are often coupled to physical processes that can affect the rate of reaction or the rate of solute transport. In granular iron permeable reactive barriers (PRBs), the precipitation of secondary minerals can lead to armoring of the iron surfaces, reducing reactivity, and also reducing permeability due to the reduction in porosity [1-3]. The generation of hydrogen gas in granular iron PRBs can lead to the production of gas bubbles that can also reduce permeability due to pore blocking [3-5].

Processed-based reactive transport modelling was used to simulate the coupling of these proceses to the treatment of trichloroethene (TCE) with granular iron in a laboratory column experiment. This was carried out with the multi-component reactive transport model MIN3P [6], which was enhanced to couple gas formation and release, secondary mineral precipitation, and the effects of these processes on hydraulic properties and iron reactivity.

The simulation reproduced the observed temporal and spatial trends in gas formation, permeability changes, and TCE degradation. The simulation showed an initial sharp decrease in permeability due to hydrogen gas production and gas bubble formation throughout the column. Over time, as the reactivity of the granular iron decreased due to armoring by secondary minerals, the degree of gas saturation throughout the column decreased, but the porosity of the column also decreased as a result of the secondary mineral formation. The result is a steady decrease in permability. The simulation demonstrated that after 704 days, armoring by carbonate mineral precipitation resulted in TCE breakthrough at 473 days followed by a steady increase in TCE concentrations in the column effluent.

The enhanced MIN3P model effectively demonstrated the coupling of geochmical and physical processes in this system. The simulation results suggest that the spatial and temporal evolution of gas formation and secondary mineral precipitation are critical factors in determing the effectiveness and longevity of granular iron PRBs.

[1] Phillips *et al.* (2010) *Environ. Sci. Technol.* **44**, 3861–3869.
[2] Agrawal *et al.* (2002) *Environ. Sci. Technol.* **36**, 4326–4333.
[3] Zhang, Gillham (2005) *Ground Water* **43**, 113–121.
[4] Reardon (1995) *Environ. Sci. Technol.* **29**, 2936–2945.
[5] Reardon (2005) *Environ. Sci. Technol.* **39**, 7311–7317.
[6] Mayer *et al.* (2002) *Water Resour. Res.* **38**, 1174-1194.

https://doi.org/10.1180/S0026461X00008434 Published online by Cambridge University Press

Hg methylation and demethylation kinetics in aquatic environments: Role of biotic and abiotic pathways on Hg isotopic fractionation

VINCENT PERROT[1], MARIA JIMENEZ-MORENO[1,2], ROMAIN BRIDOU[1,3], REMY GUYONEAUD[3], MATHILDE MONPERRUS[1], AND DAVID AMOUROUX[1]*.

[1] Laboratoire de Chimie Analytique Bio-Inorganique et Environnement, IPREM, CNRS-UPPA-UMR-5254, Pau, France (*david.amouroux@univ-pau.fr)
[2] Department of Analytical Chemistry and Food Technology, Faculty of Environmental Sciences and Biochemistry, University of Castilla-La Mancha, Toledo, Spain
[3] Equipe Environnement et Microbiologie, IPREM, CNRS-UPPA-UMR-5254, IBEAS, Pau, France

Hg methylation and demethylation pathways in aquatic ecosystems are kinetically controlled mechanisms, which critically affect monomethylmercury (MMHg) occurrence and accumulation in food webs. Various biotic, chemical and physical parameters can thus influence the overall net methylation of inorganic Hg(II) in aquatic systems [1]. Because Hg isotopic composition in environmental samples may allow tracking Hg sources and cycling, laboratory experiments on Hg species kinetics and isotopes fractionation during the main Hg transformations are essential. The aim of this study was to investigate Hg reversible methylation/demethylation mechanisms via 1) metabolic pathways using sulphate-reducing bacteria (SRB) cultures and 2) chemical non-enzymatic pathways by naturally occurring methyl group donor methylcobalamin (MeCo). Kinetics of the transformations and related Hg compounds isotope fractionation were measured and compared between the different experimental conditions.

Abiotic methylation processes driven by MeCo showed production of both MMHg and DMHg (dimethylmercury). Successive and reversible kinetics of methylation and demethylation were identified. Hg(II) methylation rate constants were 10 to 100 times higher than dimethylation and demethylation ones. Under dark conditions DMHg isotopic composition varied significantly during the time course of the experiment (48 h), being progressively enriched in heavier isotopes (δ^{202}DMHg varied from -1.37 to +0.66‰). Demethylation of DMHg was then identified to promote Hg isotopes fractionation when compared to MMHg methylation. Presence of chloride (0.5M) avoided DMHg production but enhanced Hg species fractionation (δ^{202}Hg from -1.44 to 2.48‰ for inorganic Hg and MMHg, respectively). Pure cultures of SRB incubated with Hg(II) produced significant amounts of MMHg and were also capable of MMHg oxidative degradation. Rate constants were 100-times lower and to the same order of magnitude, for methylation and demethylation respectively, than in abiotic experiments. Physiologies and global metabolism of the bacteria (i.e. fermentative or sulphate-reducing activity) did not affect significantly Hg species production/degradation kinetics and isotope fractionation. At steady state, 20% of MMHg was produced by SRB activity, resulting in MMHg enriched in lighter isotopes (δ^{202}MMHg between -0.88 and -0.45‰) and inorganic Hg enriched in heavier isotopes (δ^{202}IHg between +0.32 to +0.62‰).

Overall, both abiotic / biotic pathways of methylation and demethylation induced Hg mass-dependent isotopic fractionation which was influenced by the respective kinetics of these reversible pathways. Our results exhibit that isotopic composition of Hg in aquatic natural samples (biota, sediments) should be interpreted with care since reversibility of main Hg transformations need to be taken into account.

[1] Ullrich et al. (2001). Critical Reviews in Environmental Science and Technology, **Volume 31**, pp241-293

Neptunium (V) adsorption to a halophilic bacterium at 2 and 4 M ionic strength: Surface complexation modeling in high ionic strength systems

DAVID A. AMS[1*], JULIET S. SWANSON[1], JENNIFER E. S. SZYMANOWSKI[2], JEREMY B. FEIN[2], MICHAEL M. RICHMANN[1]AND DONALD T. REED[1]

[1]Earth and Environmental Sciences Division, Los Alamos National Laboratory, Carlsbad, New Mexico, U.S.A., dams@lanl.gov (* presenting author)
[2]Department of Civil Engineering and Geological Science, University of Notre Dame, Notre Dame, Indiana, U.S.A.

Abstract

The mobility of neptunium (V) in high ionic strength aqueous environmental systems, such as in the vicinity of salt-based nuclear waste repositories and high ionic-strength groundwater at Department of Energy sites, may be strongly influenced by adsorption to the cell wall of halophilic bacteria. This is the first study to evaluate the adsorption of neptunium (V) to the surface of a halophilic bacterium as a function of pH at the relatively high ionic strengths of 2 and 4 M. The experimental adsorption data were incorporated into a surface complexation model that was adapted for high ionic strength conditions where traditional corrections for aqueous ion activity are invalid.

Adsorption was significant over the entire pH range evaluated for both ionic strength conditions and was shown to be dependent on the speciation of the sites on the bacterial surface and neptunium (V) in solution. Strong electrostatic attraction controlled the adsorption behavior of the positively charged neptunyl ion to the negatively charged bacterial surface at pH below circum-neutral. At pH above circum-neutral, the influence of negatively charged neptunium (V) carbonate complexes resulted in decreased, although still significant, adsorption. Adsorption in 4 M $NaClO_4$ was enhanced relative to adsorption in 2 M $NaClO_4$ over the majority of the pH range evaluated, apparently due to the effect of increasing aqueous ion activity at high ionic strength.

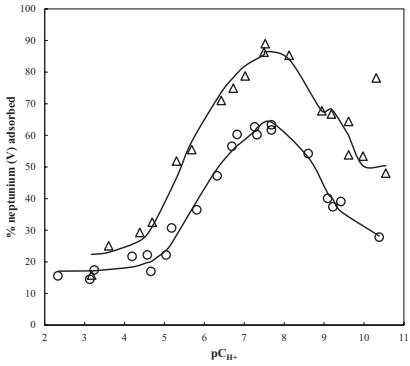

Figure 1: Experimental data for neptunium (V) adsorption onto *Chromohalobacter* sp. in 2 (open circles) and 4 (open triangles) M $NaClO_4$. Solid curves represent calculated surface complexation models. The adsorption data were modeled by testing likely reaction stoichiometries involving the adsorption of neptunium aqueous species (neptunyl: NpO_2^+, hydroxyl: NpO_2OH^0, $NpO_2(OH)_2^-$, and carbonate: $NpO_2CO_3^-$, $NpO_2(CO_3)_2^{3-}$, $NpO_2(CO_3)_2^{5-}$) to the four bacterial surface sites determined from bacteria titration modeling.

https://doi.org/10.1180/S0026461X00008434 Published online by Cambridge University Press

Salts and Water: Stable Isotope Evidence for the Direction of Solute Flow in Deserts

RONALD AMUNDSON[1]* AND STEPHANIE EWING[2]

[1] Department of Environmental Science, Policy and Management, University of California, Berkeley, CA 94720 USA, earthy@berkeley.edu (* presenting author)
[2]Department of Land Resources & Environmental Sciences, Montana State University, Bozeman MT 59717, USA, stephanie.ewing@montana.edu

Abstract

Soil is the epidermis of a planet, bearing chemical and physical properties that reflect the processes driven by its surroundings. Due to heat, gas, and water/solute transport between soil and the atmosphere, its properties are highly depth dependent. Soil forms with or without biology, and while life imparts unique characteristics to soils, its absence does not impinge on many geophysical processes that constitute soil formation. In that vein, soils found in the lifeless or nearly lifeless places on Earth are highly illuminating as analogs for the now dry and abiotic soils of Mars.

One of the key revelations of isotope research in arid and hyper-arid soils on Earth is that *stable isotopes in soils are rarely conservative tracers of elemental source*, and instead reflect complex post-depositional processes caused by aqueous or gaseous transport. Research in the past decade in both the warm and cold hyperarid regions of the world show distinctive depth trends in both the mass and the isotope composition of calcium and sulfates (Ewing et al., 2008), as well as chlorides (Amundson et al., in review). These profiles, resulting from aqueous transport, can be mimicked by physical models that describe the processes, and the direction of solute flow.

Based on our understanding from these dry environments, the exploration of the chemistry and isotope composition of salts on the Mars surface must rely on careful observation strategies to minimize ambiguities in interpretation. Chemical profiles of Mars soils record a history of aqueous processes that can be revealed through our better understanding of similar processes that occur here on Earth (Amundson et al., 2008).

[1] Ewing, S.A. et al. (2008) *Geochimica et Cosmochimica Acta* **72**, 1096-1110.
[2] Amundson, R. et al. (2008) *Geochimica et Cosmochimica Acta* **72**, 3845-3864.

Calibration of the B isotope paleo-pH proxy in the deep sea coral *Desmophyllum dianthus*; fine scale sampling and 2-D mapping

E. ANAGNOSTOU[1*], G. L. FOSTER[1], K.-F. HUANG[2], E. L. SIKES[3], C.-F. YOU[4] AND R. M. SHERRELL[5]

[1]Ocean and Earth Science, National Oceanography Centre, University of Southampton, Southampton, UK, e.anagnostou@noc.soton.ac.uk (* presenting author); Gavin.Foster@noc.soton.ac.uk
[2]Department of Geology and Geophysics, WHOI, USA, kfhuang05@gmail.com
[3]IMCS, Rutgers University, NJ, USA, sikes@marine.rutgers.edu
[4]ES and EDSRC, National Cheng Kung University, Tainan, Taiwan, cfy20@mail.ncku.edu.tw
[5]IMCS amd EPS, Rutgers University, NJ, USA, sherrell@marine.rutgers.edu

The boron isotope ratio ($\delta^{11}B$) of marine carbonate has been proposed to record seawater pH [1], and thus has the potential to provide information about the evolution of the ocean carbonate system and atmospheric pCO_2 [2]. Here we discuss calibrations based on distinct skeletal sampling strategies of this pH proxy in the deep sea coral *Desmophyllum dianthus* (*D. dianthus*). Ten modern corals from a depth range of 274-1470m in the Atlantic, Pacific, and Southern Oceans were analyzed using multi-collector ICP-MS (Neptune), and the measured $\delta^{11}B$ was regressed against ambient pH taken from hydrographic data sets (range pH 7.6 to 8.1) [3]. The array of $\delta^{11}B$ values for these corals plots above the seawater borate $\delta^{11}B$ vs. pH curve [4] by an apparently constant value of 11‰, well above the range of values seen in foraminifera and surface corals. This offset is attributed to physiological manipulation of the calcifying fluid to pH 8.7-9.0. The uncertainty in estimation of seawater pH from $\delta^{11}B$ currently limits the precision of absolute pH reconstructions to ±0.05-0.10pH units. To reduce potential uncertainty resulting from spatial heterogeneities among skeletal sub-structures, we compare $\delta^{11}B$ made on bulk septal skeleton to $\delta^{11}B$ of fibrous aragonite regions. Fibrous aragonite boron isotope data plot somewhat below those of bulk analyses and suggest a stronger dependence on ambient seawater pH. Finally, we discuss our findings with reference to 2-D maps of $\delta^{11}B$ across distinct skeletal features.

[1] Sanyal et al. (2001) *Paleoceanography* **16**, 515-519. [2] Hönisch et al. (2005) *EPSL* **236**, 305-314. [3] Anagnostou et al. (in review) *EPSL*. [4] Klochko et al. (2006) *EPSL* **248**, 276-285.

https://doi.org/10.1180/S0026461X00008434 Published online by Cambridge University Press

Accuracy of Lu-Hf and Sm-Nd garnet dating

ROBERT ANCZKIEWICZ[1*], SUMIT CHAKRABORTY[2], SOMNATH DASGUPTA[3], DILIP K MUKHOPADHYAY[4]

[1]Polish Academy of Sciences, Kraków, Poland, ndanczki@cyf-kr.edu.pl (* presenting author)
[2]Ruhr Universität, Bochum, Germany
[3]Indian Institute of Science Education & Research-Kolkata, India
[4]Indian Instituite of Technolohy Roorkee, Roorkee, India

Lu-Hf garnet dating provides high precision age information, which is competitive even for the most precise geochronometers. Accuracy of garnet geochronology, however, may suffer from several obstacles such as protracted garnet crystallization, resorption or different diffusivities of REE and Hf. In this study we demonstrate the potential of Lu-Hf system for high precision dating of metamorphism and deformation, and show the influence of the above mentioned obstacles on precision and accuracy of garnet geochronology. We compare bulk and high spatial resolution dating of metapelites from the inverted Barrovian metamorphic sequence of the Sikkim Himalaya in India, and migmatites from the Red River shear zone in Vietnam in the context of major and trace element distribution.

Lu-Hf bulk garnet dating of the inverted Barrovian sequence of the Lesser Himalaya in Sikkim yielded Lu-Hf dates from 10.6±0.2 to 14.6±0.1 Ma with uncertainty smaller than 2% achieved for all samples. Such high precision of bulk garnet dates may be significantly underestimated due to uncertainty about the duration of garnet growth. This was verified by chemically controlled, high spatial resolution dating of synkinematically grown garnet. Lu-Hf analyses did not show resolvable time difference between core and rim. Instead, all analysed fractions define an isochron age of 13.3±0.5 Ma, which points to fast crystallization and rather short lasting early deformation phase. Dating of the post-kinematic outer rim in the same crystal gave a 9.4±1.5 Ma age, which additionally brackets timing of deformation. All obtained ages reflect the time of prograde garnet crystallization, which is indicated by Rayleigh-like zonation profiles of Lu and Hf up to the silimanite zone.

Under migmatitic conditions garnets from the Red River shear zone display strongly disturbed Rayleigh zonation trends. Light REE, and to a lesser extent, heavy REE rim-to-rim zonation profiles show progressive flattening with the decreasing garnet size. Nd and Sm are completely homogenized in the smallest crystals, while Lu always preserves variable degree of core-to-rim concentration gradient. The observed REE patterns are interpreted as resulting from the combination of protracted garnet growth of progressively smaller crystals and intracrystalline diffusion. This had profound influence on Sm-Nd and Lu-Hf geochronology and resulted in a wide range of the obtained dates. The youngest age was obtained for a sample, where all garnet crystals are smaller than 2 mm and light REE profiles are completely or nearly completely homogenized. Very old apparent Lu-Hf ages are interpreted as being the consequence of variable degree of intracrystalline Lu diffusion and preservation of the original Hf distribution. Commonly observed back diffusion of Lu during resorption typically affected very narrow garnet rims and played subordinate role in modifying the isotope systematics.

The Influence of Recycling on Mantle 238U/235U?

M. B. ANDERSEN[1*], T. ELLIOTT[1]

[1]Bristol Isotope Group, School of Earth Sciences, University of Bristol, Wills Memorial Building, BS8 1RJ, United Kingdom (*morten.andersen@bristol.ac.uk)

The sub-chondritic Th/U (~2.5) of typical mid-ocean ridge basalts (MORB) is puzzling a much higher integrated Th/U (~3.8) evident from 208Pb/206Pb measurements [1,2]. A popular explanation of this problem has been to invoke recycling of U from the surface into the mantle since the Great Oxidation Event [e.g. 3]. It is intriguing that the lowering of Th/U seems concentrated in the upper mantle, such that MORB have lower Th/U than ocean island basalts (OIB), which are thought to be derived from deeper seated upwellings. This observation potentially informs on the style and vigour of mantle convection. Although an attractive hypothesis, it is uncertain if the recycled U fluxes over the last 2Ga are sufficient to lower the Th/U of MORB to 2.5 [4], despite recent improvements in estimates of modern recycling rates [5].

Mass-related variations in the natural 238U/235U ratio [6,7] offer a new means to test this model and we present new data that pertains to the problem. Variations in 238U/235U are related to low-temperature fractionation processes on Earth, with some of the largest variations observed in oceanic material (e.g. black shales). Thus, recycled material may have 238U/235U that deviates significantly from bulk Earth. We initially contrast the isotopic composition of seawater U, as might be quanitatively transferred to oceanic crust by high temperature alteration and Ocean Island basalts (OIB). Such measurements allow us to discern if we will be able to resolve 238U/235U differences between high Th/U OIB and low Th/U MORB as a result of recycling. We have measured the 238U/235U compositions of a suite of well-characterised OIB and related samples with high precision (±20, 2 SD). The measured OIBs include samples from La Palma, Azores and Iceland, spanning a wide range of U/Th compositions. The measured OIBs have identical 238U/235U compositions within ± 25 ppm (2 SD) and these are ~100 ppm heavier than modern seawater. Furthermore, preliminary measurements of hydrothermal altered MORB yields a weigthed 238U/235U mean simliar to seawater. This indicates that MORB should have 238U/235U ~50ppm ligther than the OIB if the recycling hypothesis is correct. We are currently undertaking the challenging task of making high precision 238U/235U measurements on MORB.

[1] Tatsumoto (1966) *Science* **153**, 1094-1101. [2] Galer and O'Nions (1986) *Chemical Geology* **56**, 45-61. [3] Zartman and Haynes (1988) *Geochimica Cosmochimica et Acta* **42**, 1327-1339 [4] Elliott *et al.* (1999) *Earth and Planetary Science Letters* **169**, 129-145 [5] Kelley *et al.* (2005) *Earth and Planetary Science Letters* **234**, 369-383 [6] Stirling *et al.* (2007) *Earth and Planetary Science Letters* **264,** 208-225. [7] Weyer *et al.* (2008) *Geochimica Cosmochimica et Acta* **72**, 345-359.

https://doi.org/10.1180/S0026461X00008434 Published online by Cambridge University Press

Are crystal-rich inclusions in spodumene crystallized aliquots of boundary-layer melt?

ALAN J. ANDERSON[1*]

[1] St. Francis Xavier University, Earth Sciences, Antigonish, Canada, aanderso@stfx.ca*

The constitutional zone-refining model for the crystallization of granitic pegmatites stipulates that a highly-fluxed and incompatible element-enriched boundary-layer liquid develops at rapidly advancing crystal growth fronts in undercooled granitic melts. It has been argued that crystal-rich inclusions in granitic pegmatites represent the products of entrapped boundary-layer melts and are thus not representative of the bulk-melt composition. A key example given in support of this claim is the crystal-rich inclusions in spodumene from the Tanco pegmatite, Manitoba. According to London [1], boundary layer melts are erratically variable and chemically more evolved than the bulk-melt, and this is precisely the characterization that describes the silicate-rich inclusion at Tanco. However, at Tanco, inclusions of the same character and composition occur in two types of spodumene: 1) primary magmatic spodumene laths, and 2) secondary spodumene, formed together with quartz by the isochemical breakdown of petalite. Although it is conceivable that a boundary-layer melt developed at the growth front of primary magmatic spodumene and petalite, it is unlikely that this ephemeral and spatially-restricted melt was available for entrapment in secondary spodumene during the transformation of petalite to spodumene + quartz.

Inclusions in both secondary and primary spodumene contain an assemblage of minerals (mainly quartz, cookeite and zabuyelite, with rare cesium analcime, albite, nacohlite, and Ca-Mn carbonates) that is essentially identical to the alteration assemblage in the lithium-rich zones at Tanco [2]. Image analysis measurements of 450 inclusions reveal a positive correlation between volume percent of solid phases in an inclusion and inclusion size, indicating extensive necking after precipitation of the solids. These observations suggest that the crystal-rich inclusions are not crystallized aliquots of boundary-layer melts but are instead samples of aqueous-carbonic fluid that had dissolved spodumene and precipitated quartz, cookeite and zabuyelite during and after entrapment.

[1] London (2008) *Canadian Mineralogist Special Publication* **10**. [2] Černý (1972) *Canadian Mineralogist* **11**, 714-726.

Dissolved $^{231}Pa/^{230}Th$ in the U. S. GEOTRACES North Atlantic Zonal Transect

ROBERT F. ANDERSON[1*], CHRISTOPHER T. HAYES[1], MARTIN Q. FLEISHER[1], LAURA F. ROBINSON[2], KUO-FANG HUANG[2], HAI CHENG[3,4], R. LAWERENCE EDWARDS[4], AND S. BRADLEY MORAN[5]

[1]Lamont-Doherty Earth Observatory of Columbia University, Palisades, NY, boba@ldeo.columbia.edu (* presenting author)
[2] Woods Hole Oceanographic Institution, Woods Hole, MA + University of Bristol, Bristol, United Kingdom, lrobinson@whoi.edu
[3] Institute of Global Environmental Change, Xi'an Jiaotong University, Xi'an, China cheng021@umn.edu
[4]University of Minnesota, Minneapolis, MN, edwar001@umn.edu
[5]University of Rhode Island, Narragansett, RI, moran@gso.uri.edu

The North Atlantic Ocean displays zonal gradients in many of its properties. The western basin has more recently ventillated deep waters [1] and also a greater standing crop of suspended particulate material [2]. Both of these factors have the potential to induce zonal concentration gradients in ^{231}Pa and ^{230}Th. These radionuclides are produced uniformly throughout the water column by the decay of U. The balance between their subsequent redistribution by adsorption onto sinking particles (scavenging) and ocean circulation is not well known and incites debate over the interpretation of sedimentary $^{231}Pa/^{230}Th$ ratios with significant paleoceanographic consequences.

New results from the U. S. GEOTRACES North Atlantic Zonal Transect, completed over two legs in 2010 and 2011, will be presented that highlight the contrast between east and west $^{231}Pa/^{230}Th$ distributions. Furthermore, the deconvolution of the influences of deep water ventillation and scavenging intensity on $^{231}Pa/^{230}Th$ distributions can be discussed in light of indicators of particle concentrations from transmissometry and indicators of ventilation such as chlorofluorocarbons and ^{14}C [3]. Nepheloid layers, or more turbid waters containing resuspended sediments near the seafloor, were sampled in both the eastern and westwern basins. The increased scavenging intensity associated with these layers in environments of contrasting circulation patterns further informs our deconvolution of the two effects. These observations contribute to a more complete understanding of the chemical cycling of ^{231}Pa and ^{230}Th in the modern ocean and may inspire new directions for the interpretation of sedimentary records.

[1] Broecker et al. (1991) *GRL* **18**, 1-3. [2] Biscaye and Eittreim (1977) *Mar. Geol.* **23**, 155-172. [3] Holzer et al. (2010) *JGR* **115**, C077005.

https://doi.org/10.1180/S0026461X00008434 Published online by Cambridge University Press

Hydrochemistry of a variably snow-covered catchment

SUZANNE PRESTRUD ANDERSON[1*], TAYLOR J. MILLS[1] AND RACHEL GABOR[1]

[1]INSTAAR, University of Colorado, Boulder, CO, USA, suzanne.anderson@colorado.edu (* presenting author)

Streamwater chemistry is useful for measuring contemporary weathering in a catchment. However, streamwater composition can vary seasonally, modulated by evapotranspiration, flow rate, flow paths, and biogeochemical processes within the watershed. We explore the seasonal dynamics of streamwater chemistry in a variably snow-covered catchment in the Boulder Creek Critical Zone Observatory as a foundation for understanding both hydrologic flowpaths and weathering in the catchment.

Gordon Gulch watershed

Gordon Gulch is a 2.7 km^2 forested catchment at ~2600 m a.s.l. in the Colorado Front Range, underlain by Precambrian gneiss and granodiorite. Mobile regolith depths are typically less than 1m, but bedrock tors dot the slopes; depth to fresh rock is ~8-10 m [1, 2]. Snowpack on N-facing slopes melts in spring, pushing groundwater levels up and fueling the annual discharge peak. Snow melts intermittently on S-facing slopes throughout fall, winter, and spring. Solute concentrations in streamwater vary by factors as high as 4 (Cl) to as little as 1.3 (Si), in seasonal patterns.

Cl concentrations shed light on the source of water discharging at different times in the year. Early fall and spring snowmelt produces high Cl concentrations in runoff, which appear to reflect throughfall traveling shallow paths to the stream. Cl peaks are accompanied by high dissolved organic matter (DOM) concentrations [3]. For more than a month after spring snowmelt, water sources are in transition. Cl dips to an annual minimum, approaching the low concentrations seen in precipitation, and lower than groundwater values. Only in very late summer (August) is Cl in streamwater the same as in groundwater. This suggests that late summer is the best time to analyze bedrock weathering from streamwater in this catchment. Perhaps not surprisingly, alkalinity, Ca and Na all rise to steady high concentrations during this time of groundwater fed baseflow.

Watershed dynamics

Streamflow, water-table heights, and water chemistry yield a picture of the watershed "breathing" on an annual basis. A "breath" begins with fall snow, which melts on S-facing slopes. This induces a small rise in water-table height and a dramatic streamwater flush of Cl and DOM. Early spring produces a more sustained rise in Cl, DOM, and the water table. Discharge and the water-table height rise to a dramatic peak during the sustained snowmelt from the N-facing slope. By the time of this crescendo, however, Cl and DOM are in precipitous decline. In midsummer minimally altered precipitation water is expelled during the long summer decline in discharge. The bottom of the breath is late summer, when only groundwater emerges. We will assess solute fluxes and mineral weathering variations during each stage of the annual watershed breath cycle.

[1] Befus (2011) *Vadose Zone Journal* **10**, 915-927. [2] Dethier (2006) *Geomorphology* **75**, 384-399. [3] Gabor (2009) *Eos, Trans. AGU* **90**, Abstract EP53C-0631.

Spectroscopic study of aluminum and gallium complexation by aquatic organic matter

K. ANDERSSON[1]*, P. PERSSON[1] AND T. KARLSSON[1]

[1]Department of Chemistry, Umeå University, 901 87 Umeå, Sweden *kristoffer.andersson@chem.umu.se (presenting author)

The fate and behavior of aluminum (Al) in aquatic systems is largely influenced by pH and interactions with natural organic matter (NOM). However, knowledge on the molecular structure and hydrolysis of Al species in presence of aquatic NOM is still limited. In this study Extended X-ray Absorption Fine Structure (EXAFS) and Infrared (IR) spectroscopy was used to characterize Al and gallium (Ga) interactions with organic matter from the Suwannee River at varying metal concentrations and pH. There are relatively few studies of Al interactions with NOM using these techniques [e.g. 1], one reason being the difficulty of analyzing Al in aqueous samples using EXAFS due to its low K-edge energy (1.5596 keV). Ga (K-edge at 10.367 keV), on the other hand, is readily accessible to EXAFS, and could serve as a model for Al because of the similar coordination chemistries of Al(III) and Ga(III). Indeed, previous studies of Al(III)- and Ga(III)-carboxylates have shown that these complexes can be considered analogous with respect to thermodynamic and spectroscopic properties [2, 3].

Our IR spectroscopic results showed that Al(III)- and Ga(III)-NOM interactions occur mainly via carboxylic functional groups, as indicated by characteristic shifts of the carboxyl stretching frequencies in presence of the metal ions. Overall, the behavior of the two systems was very similar, thus supporting our idea that Ga can be used as a model to study the complexation of Al by aquatic NOM.

The EXAFS results indicated that Ga formed chelate complexes in association with aquatic NOM. At low Ga concentrations (≤16 000 μg g^{-1}; pH 5) mononuclear Ga(III)-NOM complexes dominated the speciation while at higher pH values and high Ga concentrations (60 000 μg g^{-1}; pH 5-7) there was a mixture of mononuclear Ga(III)-NOM complexes and a polymeric Ga(III) (hydr)oxide phase. Thus, the organic Ga complexes formed were sufficiently strong to suppress hydrolytic polymerization even at pH 7.0 and high Ga concentrations. An additional finding was that the local structure of the Ga(III)-NOM complexes formed at the lowest concentration (100 μg Ga g^{-1}) clearly differed from those at higher Ga concentrations, which might indicate involvement from different functional groups.

Our combined EXAFS and IR results highlight the significant effects on metal ion speciation induced by the Al(III) and Ga(III)-NOM interactions. Accordingly, these interactions may exert a substantial control over the geochemistry of Al in aquatic systems, and the distribution between mononuclear complexes and polymeric species is likely to influence the toxicity and mobility of Al. Furthermore, the interactions with NOM may play a key role in determining the properties of the solid Al phases e.g. particle size.

[1] K. Elkins, D. Nelson (2002) *Coord. Chem. Rev.* **228**, 205-225.
[2] M. Clausén et al. (2005) *J. Inorg. Biochem.* **99**, 716-726.
[3] M. Clausén et al. (2003) *J. Mol. Struct.* **648**, 225-235.

https://doi.org/10.1180/S0026461X00008434 Published online by Cambridge University Press

Pb-Tl chronology of IIAB and IIIAB iron meteorites

RASMUS ANDREASEN[1,2*], MARK REHKÄMPER[1], GRETCHEN M. BENEDIX[3], KAREN J. THEIS[4], MARIA SCHÖNBÄCHLER[4], AND CAROLINE L. SMITH[3]

[1]Imperial College London, Earth Science and Engineering
[2]University of Houston, Earth and Atmospheric Sciences, randreas@central.uh.edu (* presenting author)
[3]Natural History Museum London, Department of Mineralogy
[4]University of Manchester, School of Earth, Atmospheric and Environmental Sciences

The short-lived ^{205}Pb-^{205}Tl system ($t_{½}$= 15.1 My) is the only decay system in which the parent nuclide is an s-process only nuclide, and thus the Solar System initial abundance of ^{205}Pb provides unique constraints on the amount of AGB star material injected into the Solar Nebula shortly before its collapse. The Pb-Tl system is furthermore one of few that can be used to date metal crystallization and hence provide independent age constraints on the core crystallization and thermal history of planetary bodies.

Measured Pb concentrations vary widely—from 0.5 ppb to more than 1 ppm due to terrestrial Pb contamination, which was not removed despite repeated leaching. The fraction of primordial Pb is calculated assuming deviation in the Pb isotope composition of the iron meteorites from primordial Pb is due to terrestrial Pb contamination. The concentration range of primordial Pb is very limited—from 0.1 ppb to 1.7 ppb. Concentrations of Tl range from 2 ppt to 485 ppt, with most samples below 20 ppt. This gives ^{204}Pb/^{203}Tl ratios for the IIABs from 0.05 to 5.8, and from 1.6 to 14 for the IIIABs, close to the chondritic ratio of 1.4. Values of ε^{205}Tl range from -18 to +23 and correlate with ^{204}Pb/^{203}Tl ratios, suggesting that the ε^{205}Tl variations are from the decay of ^{205}Pb at different Pb/Tl ratios. The IIAB isochron has an intercept, $\varepsilon^{205}Tl_0$ = -12±1 that is more negative than that of the carbonaceous chondrites, $\varepsilon^{205}Tl_0$ = -7.6±2.1.

This may imply that metal/silicate separation of the IIAB parent body was associated with mass-dependent Tl isotope fractionation of ~7 ε-units. However, experimental data suggest that a fractionation of this magnitude is not likely. Alternatively, if the carbonaceous chondrite isochron is recalculated rejecting samples suffering from large terrestrial Pb contamination, the slope of ε^{205}Tl vs. ^{204}Pb/^{203}Tl is steeper, with $\varepsilon^{205}Tl_0$ = -13±6. This gives Pb-Tl ages for the IIAB and IIIABs of around 15 Ma after carbonaceous chondrites.

The IIAB isochron intersects the carbonaceous chondrite isochron at ^{204}Pb/^{203}Tl = 0.15. This indicates that metal-silicate segregation took place around 2 Ma after carbonaceous chondrites, and that the metal portion of the IIAB parent body had a low Pb/Tl ratio. The latter conclusion is in agreement with previous work that inferred that IIAB irons had sulphur-rich metal compositions, and with existing experimental partitioning data suggesting that a sulphur-rich metal phase should be significantly enriched in Tl compared to Pb. The reinterpreted carbonaceous chondrite isochron gives a Solar System initial ^{205}Pb/^{204}Pb ratio of 2±1 x 10^{-3}.

Laboratory mesocosm experiments to quantify effects of elevated CO_2, plant evolution, and mycorrhizal status on carbon flux and weathering.

MEGAN Y. ANDREWS[1,2*], JONATHAN R. LEAKE[2], GABRIELLA KAKONYI[3], MARIA ROMERO-GONZÁLEZ[3], STEVEN A. BANWART[3], AND DAVID J. BEERLING[2]

[1]Department of Soil Science, North Carolina State University, Raleigh, USA, myandrew@ncsu.edu (* presenting author, current institution)
[2]Department of Animal and Plant Sciences, University of Sheffield, Sheffield, UK
[3]Cell-Mineral Research Centre, Kroto Research Institute, North Campus, University of Sheffield, Sheffield, UK

The evolution of vascular land plants in the Paleozoic is hypothesized to have enhanced weathering of Ca and Mg bearing silicate minerals (e.g. [1]). However, this plant-centric view neglects the co-evolution of plants and their associated mycorrhizal fungi. Indeed, many weathering processes usually ascribed to plants may actually be driven by the combined activities of roots and mycorrhizal fungi [2]. Here we present results from a novel mesocosm-scale laboratory experiment designed to allow investigation of plant-driven carbon flux and mineral weathering at different soil depths, and under ambient (400 ppm) and elevated (1500 ppm) atmospheric CO_2.

We selected plant species to quantify the effects of mycorrhizal type (arbuscular, AM, vs. ectomycorrhizal, EM), rooting depth, and angiosperms vs. gymnosperms on carbon flux and biological weathering. These species included the AM *Sequoia sempervirens, Osmunda regalia, Magnolia grandiflora*, and *Ginkgo biloba,* as well as two EM species, *Pinus sylvestris* and *Betula pendula*. Two long-term (7-13 months) experiments were conducted under similar environmental conditions with one exception: Experiment 1, focused on rooting depth, used a low nutrient substrate and Experiment 2, studying angiosperms vs. gymnosperms, used an organic-rich substrate.

Only under low nutrient conditions did we observe increased biomass in plants and bulk fungus grown under elevated CO_2. For the two species grown in both experiments, mineral core fungal biomass and the magnitude and timing of carbon flux from plant to belowground biomass seemed to be more correlated to soil organic content than CO_2. Fungal activity was related to plant carbon flux and was not proportional to fungal biomass, which may be important for biological weathering. Bulk and mineral core solution chemistries differ between plant-free controls, plant species, minerals, and CO_2 levels, potentially giving insight into mechanisms and degree of mineral weathering. Ongoing measurements will further assess mineral weathering and quantify biomass element uptake in these systems.

[1] Berner (1997) *Science*, **276**, 544-546. [2] Taylor et al. (2009) *Geobiology* **7**, 171-191

https://doi.org/10.1180/S0026461X00008434 Published online by Cambridge University Press

Anatexis in K-poor and Si-Rich migmatites

MICHAEL ANENBURG[1*] AND YARON KATZIR[1]

[1]Ben-Gurion University of the Negev, Geological and Environmental Sciences, Beer Sheva, Israel,
michaela@bgu.ac.il (* presenting author)
ykatzir@bgu.ac.il

K-poor and Si-rich pelites are potential protoliths of migmatites, but often lack clear mineralogical indicators for anatexis. This is due to the limited number of peritectic phases, and because the products of melting reactions tend to be erased by retrograde deformation and recrystallization. Thus the pre- and post-peak assemblages may be almost identical and evidence for migmatization is overlooked.

The Roded migmatites of southern Israel were previously thought to form by subsolidus metamorphic differentiation based on the lack of K-feldspar in leucosomes and similarity of plagioclase compositions in coupled leucosomes and melanosomes [1]. Geochemical analysis of carefully sampled palaeosomes shows that the protoliths of Roded migmatites were K-poor and Si-rich metapelites. Nonetheless relict textural evidence for melting is found in the Roded migmatites including quartz-filled embayments in plagioclase crystals, and newly formed euhedral crystals of plagioclase in leucosomes. Likewise lenticular K-felsdpar occurs within melanosome biotite indicating muscovite dehydration melting. Thermodynamic analysis of specific palaeosome compositions show that anatexis should have occurred at peak P-T conditions estimated for the Roded migmatites (Fig.1; 4.5 kbar; ~650ºC). Petrographic and microstructural observations suggest that potassium was mobilized from the leucosomes to the melanosomes during melt crystallization: Leucosome K-feldspar was replaced by myrmekite and melanosome sillimanite was replaced by symplectites of muscovite and quartz.

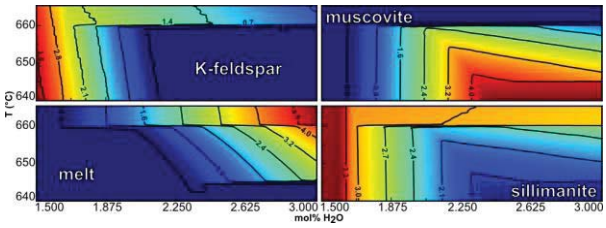

Figure 1: Modelled modes of key phases in melting reactions displayed on T vs. whole-rock H_2O content diagrams calculated for a specific rock composition of Roded migmatites. P=4.5 kbar.

Wider neosomes are characterized by diatexitic microstructures and by lower amount of myrmekite suggesting channeled influx of water resulting in higher degree of anatexis and dilution of potassium in the melt.

K-feldspar and muscovite+quartz symplectites in melanosomes, and myrmekite in leucosomes are established as criteria for inferring partial melting in heavily overprinted and retrogressively deformed K-poor, Si-rich migmatites.

[1] Gutkin & Eyal (1998) *Isr. J. Earth Sci.* **47**, 1-17.

Cation substitution in Iron Oxides in BIF-hosted Iron Ore: the Role of Inheritance and Fluids

THOMAS ANGERER[1*], STEFFEN HAGEMANN[1]

[1]Center for Exploration Targeting, University of Western Australia, thomas.angerer@uwa.edu.au (*presenting author)

Little is known about the chemisty of the often complex iron oxides paragenetic sequences in BIF-hosted high-grade iron ore, and its potential use for genetic modelling (e.g., iron oxide and fluid origin) and exploration (e.g., as chemical tracer towards ore). In order to investigate this, minor and trace elements (lithophile: Ti, V, Cr, Sc, Al, Ga, Mg, Mn, and chalcophile: Ni, Cu, Zn, As, Co) in magnetite, hematite, and goethite species in the Koolyanobbing and Windarling iron ore deposits located in the Yilgarn Craton, which are hosted in lithostratigraphic unit of same Age (3.0 Ga), but in different greenstone belts, were analysed by means of laser ablation ICPMS.

Early very-low to low metamorphic grade magnetite (M-1) in least-altered BIF have lithophile element contents between 1 and 1000 ppm (Mg>Al>Mn>Ti>V>Ga) and chalcophile element contents between 0.1 and 100 ppm (Zn≥Ni≥Cu>Co±As). Compared to other hydrothermal deposit classes, magnetite types in BIF-hosted iron ore are poor in most substituting cations, especially Cr, V, and chalcophile elements (up to three magnitudes). The analytical precision decreases with lower element concentration (<100 ppm), but due to these very low concentrations, laser ablation is the only method to measure indicative chemistry of BIF-related iron oxides.

Hydrothermal magnetite (M-2) types in hydrothermal carbonate- and quartz-altered BIF (both are most prolific protoliths to ore) show typically even lower concentrations of most lithophile elements (Mg, Al, Ga, ±V, ±Ti) than M-1, but higher concentrations of Mn and chalcophile elements, most prominently Co. This suggests that in both deposits M-2 precipitated from fluids of a common type, probably low T (limited element substitution), sulphide-rich, and with a redox condition in which Mn substitution was favored. A partial inheritance of M-2 from disolved M-1 may be concluded from similar immobile element (V, Ti, Al, Ga) ratios.

Both, hydrothermal and supergene-related martite (after M-1 and M-2) do not involve significant changes of the chemistry, except a Mg (±Zn) loss (due to the exclusion of solely II-valent elements from hematite). A mineral chemical differentiation between hypogene and supergene martite is presently difficult, mainly due to the inheritance.

Intermediate to late stage hydrothermal hematite types show commonly a decrease of Mg, Mn, Zn, Ni, Cu, Co. In Koolyanobbing a remarkably similar content of other lithophile elements with respect to M-1 and/or M-2 points to a chemistry inheritance from (proximal) dissolved or in-situ replaced BIF magnetite.

Supergene goethite chemistry is distinct when comparing different goethite types (goethite after siderite vs quartz). For example, goethite after siderite shows similar Ni, Cu, and Co concentrations when compared to the replaced siderite.

In conclusion, cation substitution of hydrothermal and supergene iron oxides in BIF-related iron ore systems of the Yilgarn craton show that iron oxides are capable of capturing chemical signatures that help deciphering geological/fluid regimes.

https://doi.org/10.1180/S0026461X00008434 Published online by Cambridge University Press

New Data on the Cenozoic Epithermal Uranium Concentrations at Nopal deposit, Mexico

SAMUEL ANGIBOUST[1,2], Mostafa Fayek[2], Ian M. Power[3], Alfredo Camacho[2], Georges Calas[4*], Gordon Southam[3]

[1] Institut des Sciences de la Terre de Paris, Université P&M Curie, 75252 Paris, France [samuel.angiboust@upmc.fr]
[2] Department of Geological Sciences, 240 Wallace Building, University of Manitoba, Winnipeg, MB, R3T 2N2, Canada
[3] Department of Earth Sciences, University of Western Ontario, London, ON, N6A 5B7, Canada
[4] Institut de Minéralogie et de Physique des Milieux Condensés, Université P&M Curie, 75252 Paris, France
([*] presenting author)

Epithermal uranium deposits of the Sierra Peña Blanca are classic examples of volcanic-hosted deposits and have been used as natural analogues for radionuclide migration in volcanic settings. We present a new genetic model that incorporates both geochemical and tectonic features of these deposits, including one of the few documented cases of a geochemical signature of biogenic reducing conditions favoring uranium mineralization in an epithermal deposit. Four tectono-magmatic faulting events affected the volcanic pile. Uranium occurrences are associated with breccia zones at the intersection of fault systems. Periodic reactivation of these structures associated with Basin and Range and Rio Grande tectonic events resulted in the mobilization of U and other elements by meteoric fluids heated by geothermal activity. Focused along breccia zones, these fluids precipitated under reducing conditions several generations of pyrite and uraninite together with kaolinite. Oxygen isotopic data indicate a low formation temperature of uraninite, 45–55°C for the uraninite from the ore body and ~20°C for late uraninite hosted by the underlying conglomerate. There is geochemical evidence for biological activity being at the origin of these reducing conditions, as shown by low δ34S values (~ -24.5 ‰) in pyrites and the presence of low δ13C (~ -24 ‰) values in microbial patches intimately associated with uraninite. These data show that tectonic activity coupled with microbial activity can play a major role in the formation of epithermal uranium deposits in unusual near surface environments.

(U)SANS analysis of experimental dissolution and formation of quartz overgrowths in St. Peter Sandstone

LAWRENE M. ANOVITZ[1], DAVID R. COLE[2], ANDREW JACKSON[3], GERNOT ROTHER[4], KEN LITTRELL[5] AND LAWRENCE F. ALLARD[6]

[1]Chemical Sciences Division, MS 6110, Oak Ridge National Laboratory, Oak Ridge, TN USA, anovitzlm@ornl.gov (* presenting author)
[2]Ohio State University, Columbus, OH cole.613@osu
[3]NIST Center for Neutron Research, Stop 8562, Gaithersburg, MD USA, ajj@nist.gov
[4]Chemical Sciences Division, MS 6110, Oak Ridge National Laboratory, Oak Ridge, TN USA, rotherg@ornl.gov
[5]Neutron Scattering Science Division, MS 6393, Oak Ridge National Laboratory, Oak Ridge, TN USA, littrellkc@ornl.gov
[6]Materials Science and Technology Division, MS 6064, Oak Ridge National Laboratory, Oak Ridge, TN USA, allardlfjr@ornl.gov

Introduction

The microstructure and evolution of porosity in time and space play a critical role in many geologic processes, including migration and retention of water, gas and hydrocarbons, the evolution of hydrothermal systems, weathering, diagenesis and metamorphism, as well as technological processes such as CO_2 sequestration, shale gas and secondary oil recovery. The size, distribution and connectivity of these confined geometries collectively dictate how fluids migrate into and through these micro- and nanoenvironments, wet and react with mineral surfaces. To interpret the time-temperature-pressure history of a geological system the physical and chemical "fingerprints" of this evolution in the rock should be interrogated from the nanoscale to the macroscale.

Description

We have performed a series of experiments to understand the effects of quartz overgrowths on nanometer to centimeter scale pore structures of sandstones. Blocks from two samples of St. Peter Sandstone with different initial porosities (5.8 and 18.3 %) were reacted from 3 days to 7.5 months at 100 and 200°C in aqueous solutions supersaturated with respect to quartz by reaction with amorphous silica. Porosity in the resultant samples was analyzed using small and ultrasmall angle neutron scattering and SEM/BSE-based image processing techniques.

Results and Conclusion

Significant changes were observed in the multiscale pore structures. By 3 days the overgrowths in the low-porosity sample dissolved away. The reason for this is uncertain, but the overgrowths can be clearly distinguished from the cores in the BSE images. At longer times the larger pores are observed to fill with needle-like precipitates. As with the unreacted sandstones, porosity is a step function of size. Grain boundaries are typically fractal, but no evidence of mass fractal or fuzzy interface behavior was observed [cf.1] suggesting a structural difference between chemical and clastic sediments. After the initial loss of the overgrowths image scale porosity (> ~ 1 μm) decreases with time, while submicron porosity (typically ~25 % of the total) is relatively constant or slightly decreasing, and the fraction of small pores increases.

[1] Anovitz et al. (2009) Geochimica et Cosmochimica Acta 73, 7303

Research sponsored by the Division of Chemical Sciences, Geosciences, and Biosciences, Office of Basic Energy Sciences, U.S. Department of Energy.

https://doi.org/10.1180/S0026461X00008434 Published online by Cambridge University Press

In vitro simulation of oscillatory redox conditions in intertidal sediments

PIERRE ANSCHUTZ[1*], GWENAEL ABRIL[1], JONATHAN DEBORDE[1], SYLVAIN BOUCHET[2], ROMAIN BRIDOU[2], EMMANUEL TESSIER[2] AND DAVID AMOUROUX[2]

[1]Université de Bordeaux, CNRS, UMR 5805 EPOC, Talence, France, *p.anschutz@epoc.u-bordeaux1.fr (* presenting author)
[2]LCABIE - IPREM UMR 5254 CNRS/UPPA, Pau, France, david.amouroux@univ-pau.fr

Experimental results that are environmentally relevant are needed to predict transient diagenetic processes. For that, we developed a designed reactor for the examination of diagenetic processes [1]. We present here the results from two independent experiments with sediment slurries collected the Arcachon bay and the macrotidal Adour estuary. Slurries and in-situ water were mixed to give a SPM concentration of 150 g/l. Sediments were submitted to redox oscillations at the tidal and neap-spring time scales to assess the diagenetic mechanisms that affect N, P, Fe, Mn and S species. The experiments started in anoxic conditions during one week. Then oxic conditions were obtained by purging with air. After one week of oxic conditions, anoxic conditions were recovered by purging with N2.

From anoxic to oxic conditions : We observed rapid oxidation of dissolved Fe(II). Dissolved phosphorus was trapped with new Fe-oxides. It was totally titrated in Arcachon sediments, but not in Adour sediments. Because of the strong control of P by Fe, the N/P ratio was never constant and did not reflect the N/P of the mineralized organic matter. Mn(II) was slowly oxidized. A major part of Mn(II) was rather adsorbed on new Fe-oxides. In Arcachon sediments, ammonium remained constant in oxic conditions. Nitrate was produced from organic-N mineralization. In Adour sediment nitrate was produced from ammonium nitrification.

From oxic to anoxic conditions : A part of newly precipitated Fe-oxides was reduced, another part was trapped with sulfides. Dissolved P concentrations were not recovered. P was probably trapped in an authigenic phase. In Adour sediments, high concentrations of Mn-oxides prevented Fe(II) accumulation. In Arcachon sediments, direct reduction of nitrate to ammonium, rather than denitrification occurred. Anammox probably occurred in anoxic conditions of Adour sediments. Anaerobic production of nitrate also occurred in Adour sediments, probably because the concentration of Mn-oxides was high

These experimental results show that nutrient dynamics in oscillatory redox enviromnents such as estuary turbidity zone, bioturbated sediment or tidal permeable sediments strongly depend on reactive Fe and Mn content.

[1] Abril *et al.*, (2010) Estuar. Coast. Shelf Sci. **88**, 279-291.

Foreland view of the extruding Himalayan metamorphic core, West Nepal

BORJA ANTOLÍN [1*], LAURENT GODIN [1], KLAUS WEMMER [2]AND CARL NAGY [1]

[1] Queen´s University, Department of Geological Sciences and Geological Engineering, Kingston, Canada, antolin@geol.queensu.ca (* presenting author)
[2] Georg-August University, Department Isotope Geology, Göttingen, Germany

We have studied the deformation, metamorphic, and cooling history of the Himalayan suprastructure (Tethyan sedimentary sequence – TSS) and infrastructure (Greater Himalayan sequence – GHS) preserved in the most southward and foreland part of the orogen in west Nepal, to better understand the relationship between hinterland and foreland deformation in a mid-crustal flowing orogen.

The studied N-S profile (28 km) transverses the Dadeldhura klippe. The klippe is characterised by an early to late Miocene syncline structure bound to the north and south by the folded Dadeldhura Thrust, regionally correlated to the Main Central thrust. The northern limb is characterised by medium metamorphic -grade rocks (mylonitic augen gneiss ± garnet, mica-schist ± garnet ± staurolite, muscovite bearing quartzite) with south-dipping foliation and down-dip elongation lineation. The southern limb exposes ca. 4 km-thick medium metamorphic-grade rocks, structurally overlain by ca. 9 km-thick meta-igneous rocks (augen gneiss) with north-dipping and down-dip elongation lineation. Rocks of both limbs are regionally correlated to the GHS and are characterized by pervasive S-C-C′ fabrics, σ and δ porphyroclasts, and mica-fish consistent with top-to-the-south shear. Close to the contact with the overlying TSS meta-pelites, the GHS displays top-to-the-north sense of shear, which is likely related to the southern extent of the South Tibetan Detachment system. Microstructural analyses of quartz-rich units suggest the GHS underwent non-coaxial top-to-the-south sense of shear at temperatures between 450 ºC and 550 ºC.

Meso and microstructural analyses performed on the TSS meta-pelites outcropping in the core of the syncline highlights a polyphase deformation history characterized by two main cleavage development phases. Illite crystallinity measured on <2 µm and <0.2 µm size fractions and the corresponding $^{40}K/^{40}Ar$ ages of the meta-pelites show that the samples are dominated by newly formed white mica. Illite crystallinity values range from Kübler Index 0.136 to 0.238 suggestive of epizonal conditions to lower greenschist facies (min. 350 ºC). Illite-muscovite $^{40}K/^{40}Ar$ ages are interpreted as cooling ages after peak metamorphic conditions and range between 18.2 ± 0.8 Ma close to the STDS to 26.6 ± 1.3 Ma in the core of the syncline.

Despite its structural similarity, the Dadeldhura GHS rocks differ from the GHS rocks described in the higher Himalaya 100 km to the north by the absence of migmatite and sillimanite-bearing rocks. This difference might be a field expression of telescoped and folded metamorphic isograds at the frontal part of the extruded GHS. Future work in the Dadeldhura GHS, including U-Pb in-situ dating of deformation fabrics and ^{40}Ar-^{39}Ar analyses, will assist in testing links between hinterland-style deformation (e.g. channel-flow) in the higher Himalaya with foreland-style deformation (e.g. critical-taper) in the external klippes of the Himalayan system.

https://doi.org/10.1180/S0026461X00008434 Published online by Cambridge University Press

Fate of groundwater-derived nutrients in tidally influenced coastal aquifers: numerical simulations

NAWRIN ANWAR[1*], AND CLARE ROBINSON[1]

[1]The University of Western Ontario, London, Canada, nanwar3@uwo.ca ; crobinson@eng.uwo.ca (* presenting author)

Introduction

The flow, transport and transformation processes in a subterranean estuary strongly control the exit conditions for groundwater-derived nutrients discharging to coastal waters. While several studies have examined the fate of nutrients in subterranean estuaries [e.g., 1, 2], the impact of oceanic fluctuations including tides is often neglected. These water level fluctuations however can induce a highly dynamic surficial mixing and reaction zone in the near-shore aquifer and significantly alter the subsurface flow paths for discharging nutrients. In this study the variable density groundwater flow model SEAWAT-2005 is used in combination with the reactive multi-component transport model PHT3Dv2.10 to examine the influences of tide on the transport and transformation of nutrients (ammonium, nitrate, and phosphate) in this dynamic zone. Reactions considered in the model include denitrification, nitrification, aerobic degradation of dissolved organic carbon, iron oxidation and reduction, and phosphate adsorption [1].

Results and Conclusion

SEAWAT combined with PHT3D provides a powerful modeling platform for simulation of the multi-component reactive transport processes occurring in a tidally-influenced subterranean estuary. Simulations reveal that tidal fluctuations significantly alter the transport pathways of the groundwater-derived nutrients and the mixing between the groundwater and recirculating seawater in the near-shore aquifer. This alters the biogeochemical reactions occurring in this region and thus impacts the nutrient transformations and subsequent loading rates to coastal waters (e.g., Figure 1). Tide-induced recirculation also leads to the precipitation of iron oxides around the upper mixing zone and this may act as an important geochemical barrier for accumulating chemicals including phosphate in the intertidal sediments. A sensitivity analysis is presented for the governing parameters.

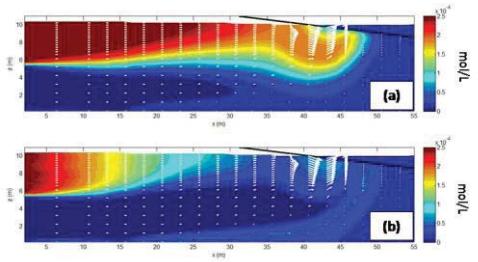

Figure 1: Nitrate concentrations ina nearshore aquifer exposed to tidal fluctuations (amplitude 0.5 m) (a) without, and (b) with reactions considered.

[1] Spiteri et al. (2008) *Water Resources Research* **44**, W02430.
[2] Kroeger et al. (2008) *Limnology and Oceanography* **53**, 1025-1039.

An *Ab Initio* and Raman Investigation of Aqueous Cu(I) and Cu(II) Chloride Complexes

L. M. S. G. A. APPLEGARTH[1*], C. C. PYE[2], J. S. COX[1] AND P. R. TREMAINE[1]

[1]Department of Chemistry, University of Guelph, Guelph, ON, Canada, lapplega@uoguelph.ca (* presenting author)
[2]Department of Chemistry, Saint Mary's University, Halifax, NS, Canada, cory.pye@smu.ca

Abstract

Thermodynamic properties of metals with common ligands under hydrothermal conditions are needed to model the geochemistry metal ore deposits and the chemistry of Generation IV super-critical water nuclear reactor designs. While the thermodynamic stability of copper (I) and copper (II) chloro complexes are quite well established over a wide temperature range [1,2], the structure of some of these species is a subject of active investigation [3].

This study uses Raman spectroscopy as a tool to identify the structure, speciation and thermodynamic properties of copper complexes. Briefly, polarized Raman spectra, collected parallel and perpedicular to the orientation of the exiting beam as a function of molality and temperature, relative to an internal standard (ClO_4^-), were used to determine reduced isotropic spectra [4]. The spectra are very weak, and this technique yields an accurate baseline correction. Ab initio calculations, using methods similar to those for Zn-Cl [5], have been used to predict the stability, structures and Raman spectra of all the possible chloro and aquo complexes with Cu^+ and Cu^{2+}. The Cu-Cl vibrational frequency for Cu^+ complexes was sensitive to the hydration number and the type of calculation (HF,MP2,B3LYP).

Based on these *ab initio* calculations, and the temperature dependent spectra in H_2O and D_2O, vibrational bands were assigned to the copper (II) species Cu^{2+}, $CuCl^+$, $CuCl_2^0$ and $CuCl_3^-$. While the spectra for copper (I) species were much less intense, there is strong evidence for $CuCl_2^-$ and $CuCl_3^{2-}$.

[1] Liu *et al*. (2005) *Chem. Geol.* **221**, 21-39.
[2] Trevani *et al*. (2009) *Int. J. Hydrogen Energy* **35**, 4893-4900.
[3] Brugger *et al*. (2007) *Geochim. Cosmochim. Acta.* **71**, 4920-4941.
[4] Rudolph, *et al.*, *J. Solution Chem.* 28, 625-635 (1999).
[5] Pye et al. (2006) *Phys. Chem. Chem. Phys.* **8**, 5428-5436.

https://doi.org/10.1180/S0026461X00008434 Published online by Cambridge University Press

Origin of Mississippi Valley-type deposits in the Ozark and Interior Low Plateaus, U.S. mid-continent: constraints from fluid inclusions

MARTIN S. APPOLD[1]*, ZACHARY J. WENZ[2] AND MICHAEL A. PELCH[1]

[1]Dept. of Geological Sciences, University of Missouri, Columbia, MO 65211, USA, appoldm@missouri.edu (* presenting author)
[2]Minnesota Dept. of Natural Resources, St. Paul, MN 55155, USA

Mississippi Valley-type (MVT) deposits have long been understood to be products of sedimentary basinal brines based on the bulk salinity, temperature, and major element composition of their fluid inclusions. Whether MVT mineralizing fluids resemble typical sedimentary brines with respect to ore metal content has until recently been far less certain and was a major concern of the present study. A further motivation for determining ore metal content in MVT mineralizing fluids is that ore metal content, together with pH, redox potential, and sulfur content, largely governs precipitation mechanism, which is also uncertain for many MVT deposits. Major element concentrations in MVT fluids reported in previous studies have largely been determined from bulk leachate analysis of fluid inclusions, where mixing of primary and secondary fluid inclusions and mineral matrix contributions are likely to have affected the reported results. Thus, another goal of the present study was to obtain improved measurements of major element concentrations, along with ore metal concentrations, through in situ analysis of individual fluid inclusions. These major element concentration data provide additional constraints on precipitation mechanism, fluid flow paths, and genetic relationships among deposits.

The focus of the present study was on fluid inclusions from the Southeast Missouri, Tri-State, Northern Arkansas, and Central Missouri districts of the Ozark Plateau, and the Illinois-Kentucky district of the Interior Low Plateau. A consistent feature found for these districts is that they contain populations of Pb-rich sphalerite-hosted fluid inclusions (containing 100's to 1000's of ppm Pb) that probably reflect the intermittent invasion of Pb-and possibly overall metal-rich ore fluid into the districts during sulfide mineralization. High methane concentrations in both sphalerite- and gangue-hosted fluid inclusions indicate that mineralizing conditions were predominantly reducing, such that sulfide mineralization was probably caused by mixing of Pb-rich ore fluid with a sulfide-rich fluid. Methane concentrations in fluid inclusions could be used to calculate minimum mineralization depths, which yielded a range from about 100 to 1500 m. Pb-rich ore fluids in all of the districts had dolomitizing Ca/Mg ratios, indicating that the the fluids did not travel very far through the predominantly limestone aquifers in which sulfide mineralization is presently hosted. The Pb –rich ore fluids in the districts differed from one another with respect to major element composition, indicating that although all of the districts may have been formed from the same physical flow system, this fluid was chemically heterogeneous. In the Illinois-Kentucky district, the compositional distinctives of the ore fluid are consistent with inputs expected from local igneous activity contemporaneous with MVT mineralization.

Pressure dependence of enthalpy, viscosity and diffusivity of olivine and its constituent minerals near melting

SAYYADUL ARAFIN*, RAM N. SINGH AND ABRAHAM K. GEORGE

Physics Department, College of Science, Sultan Qaboos University, P.O. Box: 36, Al-Khoudh 123, Sultanate of Oman, sayfin@squ.edu.om (*presenting author)

Introduction

Olivine, the major mineral of the Earth's upper mantle, plays a key role in the mineralogical models for the Earth's mantle. It is greatly appreciated that rheological properties of olivine are important ingredients in modeling the geodynamic processes in the upper mantle such as convective flows, evolution of subduction zones, deep seismicity patterns and post-seismic mantle relaxation. Our knowledge of crystallographic orientaion of olivine can help interpret the seismic anisotropy of the upper mantle in terms of mantle flow[1]. The physical and chemical conditions of deformation mechanisms control the crystallographic and shape preferred orientations of olivine.

We have derived a mathematical expression for the melting temperature, T_m and its pressure dependence by extending the Lindemann's melting law. Seismic p- and s-wave velocities and density data as a function of pressure were used as inputs to compute Debye temperature, Θ_D, which forms the important ingredient of the empirical relation for the melting temperature. We have applied the formalism to estimate T_m and its pressure dependence, which in turn has been used to estimate enthalpy, viscosity and diffusivity of olivine and its constituent minerals such as foresterite (Mg_2SiO_4) and fayalite ($Fe_2\ SiO_4$).

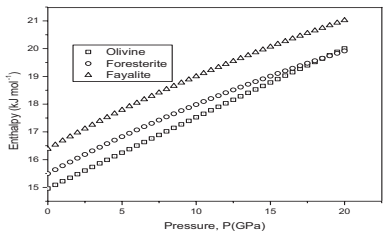

Figure 1: Enthalpy of olivine and its constituent minerals as a function of pressure

Results and discussions

We present here in Figure 1 only a part of the results. Our preliminary results show linear increase of enthalpy, viscosity and diffusivity for olivine and non-linear increase for foresterite and fayalite with increasing pressure. At room temperature and atmospheric pressure, the values of enthalpy, viscosity and diffusivity are found to be 14.96 kJ mol^{-1}, 2.58 mPa s and 1.69 x 10^{-4} m^2 s^{-1} for olivine , 15.50 kJ mol^{-1}, 2.58 mPa s and 1.75 x 10^{-4} m^2 s^{-1} for foresterite and 16.38 kJ mol^{-1}, 3.07 mPa s and 1.53 x 10^{-4} m^2 s^{-1} for fayalite respectively.

1] Kneller (2005) Earth Planet. Sci. Lett., 237, 781-797

https://doi.org/10.1180/S0026461X00008434 Published online by Cambridge University Press

Lithium isotope ratio of samples collected from salt lakes at Nevada, USA: Implication for lithium origin in salt lakes

DAISUKE ARAOKA[1*], YOSHIRO NISHIO[2], TETSUICHI TAKAGI[3], YASUSHI WATANABE[3] AND HODAKA KAWAHATA[4]

[1]Graduate School of Frontier Sciences and Atomosphere and Ocean Research Institute, The University of Tokyo, Kashiwa, Japan, araoka@aori.u-tokyo.ac.jp (* presenting author)

[2]Kochi Institute for Core Sample Research, Japan Agency for Marine-Earth Science and Technology, Nankoku, Japan, nishio@jamstec.go.jp

[3]Institute for Geo-Resources and Environment, National Institute of Advanced Industrial Science and Technology, Tsukuba, Japan, takagi-t@aist.go.jp, y-watanabe@aist.go.jp

[4]Atomosphere and Ocean Research Institute, The University of Tokyo, Kashiwa, Japan, kawahata@aori.u-tokyo.ac.jp

Lithium is a useful and worth element for industrially purposes. Lithium has unique characteristics such as lowest Oxidation-reduction potential among all elements and the third-lightest element after hydrogen and helium. These properties are valuable for lithium-ion secondary battery that is non-memory-effect, high-power and the highest energy density among batteries in practical use.

Salt lakes are the most major lithium resources on earth. Highly concentrated lithium resources were formed in salt lakes by repetition of water evaporation and inspissation with an arid climate. As a result of rising consumption of lithium carbonate, lithium-rich brine in salt lakes have been developed all over the world. Therefore, it is essential for revealing the origin of highly concentrated lithium in salt lakes for future exploration.

Lithium isotope ratio is known for newly useful tool understanding water-rock interaction. Moreover, lithium isotopic fractionation is dependent on temperature and its compositions are strongly affected by initial values of host rocks. We report lithium and strontium isotope ratio, as well as major and trace element compositions, of samples collected from some salt lakes at Nevada, USA. These lithium isotopic values (δ^7Li) of samples have a large variation among each sample, however all the values are much lower than the values of river water reported previously [1], and are close to values of upper continental crusts [2]. These results suggest that highly concentrated lithium in salt lakes were not formed during surface weathering processes, but were supplied by the result of water-rock interaction below the surface of the earth at high temperature.

We demonstrated that lithium isotope ratio has a potential for tracing lithium origin in salt lakes and further detailed studies must be required such as the values of host rocks.

[1] Huh *et al.* (1998) *Geochim. Cosmochim. Acta* **62**, 2039-2051.
[2] Teng *et al.* (2004) *Geochim. Cosmochim. Acta* **68**, 4167-4178.

Mg/Ca Paleothermometry in *G. ruber* (white): mechanisms and calibration

Jennifer A. Arbuszewski[1*], Peter B. deMenocal[2]

[1]Woods Hole Oceanographic Institute, Woods Hole, USA, [*]jarbuszewski@whoi.edu

[2]Lamont-Doherty Earth Observatory of Columbia University, Palisades, USA, peter@ldeo.columbia.edu

Abstract

Paired planktonic foraminiferal Mg/Ca and δ^{18}O analyses are frequently applied to jointly estimate sea surface temperature and $\delta^{18}O_{seawater}$, a proxy for ocean salinity. The relationship between shell Mg/Ca and temperature is rooted in thermodynamic theory; Mg/Ca increases as temperature increases as a result of the endothermic substitution of Mg^{2+} into the calcite lattice[1-2]. While temperature has previously been indicated as the main controlling factor in foraminifera, there is significant biological mediation[1,3-6].

Recent results suggest that ocean salinity may also be a significant influence on shell Mg/Ca ratios[7-9]. This influence was noted in our findings from an Atlantic meridional coretop sample transect, where we found that *G. ruber* (white) shell Mg/Ca values were significantly elevated in higher salinity gyre waters. This "excess Mg/Ca" (the residual between the observed and expected Mg/Ca composition at the δ^{18}O calcification temperature) is well correlated with surface salinity[7]. We investigated the nature of this "excess Mg/Ca" signal for the planktonic species, *G. ruber* (white). We employ multiple techniques including scanning electron microscope imaging, flow through ICP-MS, and electron microprobe elemental mapping, with a goal of separating potential mechanisms for the observed enhanced uptake of shell Mg/Ca at high salinity.

In addition, we will present our latest global calibration efforts. Our global database consists of 301 coretops, and is growing, composed of both new and published data for the surface-dwelling planktonic foraminifer, *G. ruber* (white). We use multivariate regression analyses to produce new global equations relating shell Mg/Ca, δ^{18}O, and bottom water ΔCO_3^{2-} to ocean temperature and salinity. Our goal is to better understand how environmental (and biological) conditions influence shell chemistry and to use this knowledge to improve calibration equations. We will discuss the validation of these new equations and their applicability to downcore paleoclimate reconstructions.

[1] Lea, D.W., Mashiotta, T.A. & Spero, H. J. (1999) *Geochem. Cosmochem. Acta* **63**, 2369-2379 .
[2] Oomori, T., Kaneshima, H., Maezato, Y., Kitano, Y. (1987) *Mar. Chem.* **20**, 327-336.
[3] Dekens, P. S., Lea, D.W., Pak, D.K., Spero, S.J. (2002) Geochem. Geophys. *Geosyst.* **3**, doi:10.1029/2001GC000200.
[4] Anand, P., Elderfield, H. & Conte, M. H. (2003) *Paleoceanography* **18**, doi:10.1029/2002PA000846.
[5] Kisakürek, B., Eisenhauer, A., Böhm, F., Garbe-Schönberg, D. & Erez, J. (2008) *EPSL* **273**, 260-269.
[6] Rosenthal, Y., Boyle, E. A. & Slowey, N. (1997) *Geochem. Cosmochem. Acta* **61**, 3633-3643.
[7] Arbuszewski, J., DeMenocal, P., Kaplan, A. & Farmer, E. C. (2010) *EPSL* **300**, 185-196.
[8] Mathien-Blard, E. & Bassinot, F. (2009) *Geochem. Geophys. Geosyst.* **10**, Doi 10.1029/2008gc002353.
[9] Ferguson, J. E., Henderson, G. M., Kucera, M. & Rickaby, R. E. M. (2007) *EPSL*, 10.1016/j.epsl.2007.1010.1011.

https://doi.org/10.1180/S0026461X00008434 Published online by Cambridge University Press

Mo and Ni isotope systematics in petroleum fluids across subsurface alteration gradients

COREY ARCHER[*1], TIM ELLIOTT[1], SANDER VAN DEN BOORN[2], PIM VAN BERGEN[3]

[1]Bristol Isotope Group, School of Earth Sciences, University of Bristol, BS8 1RJ, UK (*c.archer@bristol.ac.uk)
[2] Shell Projects and Technology , Rijswijk, The Netherlands
[3] Shell Upstream International Europe, Aberdeen, UK

The presence of trace metals in oils has long been of interest for both their beneficial and detrimental effects during hydrocarbon exploration and processing, respectively. For example, the diagnostic potential of trace metals incorporated in fluids and source rocks has been successfully applied in various fingerprinting studies. The majority of work to date has focussed on the two most abundant metals in oils, vanadium (V) and nickel (Ni), where abundances and elemental ratios have been used as tools in correlation and fingerprinting, and provide information on redox conditions during source rock deposition [1]. Here, we focus on the molybdenum (Mo) isotope system, well known to display a bi-polar redox chemistry [2], and similarly explore the potential of Ni isotopes, with the aim of developing valuable new tools to exploit in petroleum systems' studies.

We have developed techniques for the determination of Mo and Ni isotopes in hydrocarbon (HC) fluids. The analyte is extracted from its complex organic fluid matrix, through high pressure ashing, which renders the complete decomposition of the HC fluid, allowing the Mo and Ni from the same sample fraction to be purified via conventional ion-exchange methods. Data from replicate analyses of both samples and an NIST HC standard suggest a precision of better than 0.1‰ in both $\delta^{98/95}$Mo and $\delta^{60/58}$Ni. These techniques are applied to co-genetic oil samples from a well characterised petroleum system to investigate Mo and Ni isotope systematics across subsurface alteration gradients (e.g maturation, biodegradation and migration).

The co-genetic samples thus far analysed show remarkably invariable $\delta^{98/95}$Mo values along various alteration gradients, such as maturation. This is in contrast to many organic geochemistry proxies which are traditionallly employed to examine these changes in HCs, and an overall $\delta^{98/95}$Mo range of ~1.5‰ for the entire HC dataset (incl. samples from other petroleum systems). Ni is much more variable along the studied gradients, displaying a range in $\delta^{60/58}$Ni from -0.5‰ to +0.8‰, suggesting a different mechanistic behaviour to Mo. These results highlight the potential of Mo isotopes to be used as a new tool in oil-oil/source rock correlations on a basin-wide scale, whereas Ni isotopes may prove to be useful in the characterization of processes operating on more restricted spatial scales.

[1] Lewan, M.D. (1984). *Geochim. Cosmochim. Acta* **48**, 2231-2238. [2] Erikson, B.E. and Helz, G.R. (2000). *Geochim. Cosmochim. Acta* **64**, 1149-1158.

Stable isotope geochemistry and the optimization of hydraulic fracturing of petroleum wells – lessons from the Bakken Formation in Canada and the USA

SERGUEY ARKADAKSKIY[1*] AND BEN ROSTRON[2],

[1]Isobrine Solutions Inc., Edmonton, Canada, serguey@isobrine.com (*presenting author)
[2]University of Alberta, Earth and Atmospheric Sciences, Edmonton, Canada, ben.rostron@ualberta.ca

Hydraulic fracturing (a.k.a. fracing) is an established method for petroleum well stimulation used to enhance reservoir permeability through the creation of artificial fractures by injecting aqueous fluid under high pressure in the target zone. Recent developments of that technology have allowed petroleum production from low permeability reservoirs previously considered uneconomic. Hydraulic fracturing combined with precise horizontal drilling has provided access to tens, perhaps hundreds of Bbls of high quality light crude oil in the late Devonian/early Mississippian Bakken Formation in the Williston Basin [1]. The Bakken reservoir is a thin (13 m on average) dolomitic silt/sandstone horizon sandwiched between two organic-rich marine shales. Oil and gas generated in the shales migrated to and remained for the most part within the Middle Bakken reservoir [2], which close to the basin center (USA) is largely water unsaturated but exhibits various degrees of water saturation in the thermally immature parts near the edges of the basin (Canada). Unexpected and/or excessive water co-production following high volume multistage fracing of horizontal wells drilled throughout the basin has been of concern lately. Since both the overlying (i.e., the Mississippian Lodgepole) and the underlying (the Devonian Torquay and Nisku/Birdbear) formations are water-saturated, it has been hypothesized that fracing may have resulted in fracture propagation into these formations. Questions have also been raised about the presence and/or apportioning of fracing fluids and/or other service/maintenance fluids in the co-produced waters. While standard formation water identification techniques have been largely unable to provide unambiguous answers to those questions, stable isotope geochemistry and other geochemical techniques have met with greater success. In this presentation we will discuss the application of stable isotope geochemistry and other geochemical methods for identifying the source(s) of different fluids in waters co-produced from horizontal Bakken wells stimulated with hydraulic fracturing. We will also discuss the impact our findings have been having on petroleum producers in the basin and the changes these have made to their hydraulic fracturing practices in order to minimize unwanted water co-production.

[1] Flannery & Kraus (2006) *Am. Assoc. of Petrol. Geol. Search and Discovery Article* No.10105 [2]. Halabura, Buatois, Angulo and Piche (2007) in *Summary of Investigations 2007 vol. 1, Sask. Geol. Surv. Misc. Rep.* 2007-4.1 pp.8

https://doi.org/10.1180/S0026461X00008434 Published online by Cambridge University Press

Evaluating ocean acidification using stable isotope fractionation of fossil scallop shells

JILL ARRIOLA[1*], BRYANNA BROADAWAY[1]

[1]University of Massachusetts-Boston, Boston, USA, jill.arriola001@umb.edu (* presenting author)

As ocean pH declines, due to increased atmospheric carbon dioxide, the saturation states of carbonate polymorphs is expected to decline. Fractionation of oxygen, carbon, and sulfur stable isotopes in growing shells in response to these changes, whether direct or indirect, could provide a new tool for reconstruction of paleoenvironments. In the laboratory bay scallops were reared (*Argopecten irradians*) under low pH conditions induced by high CO_2 (pH = 7.8, 7.6, 7.4, and 7.2). Carbonate chemistry was measured/modeled as well as other water quality parameters. Animals were sacrificed over a 1 month period and growth (length, buoyant weight) was measured. New shell was excised and $\delta 1^3C$, $\delta^{18}O$, and $\delta^{34}S$ as well as total C and S were measured. Fractionation of C and O associated with pH was observed as was fractionation of S though, in the case of S, the fractionation was not significantly associated with pH. A C-O fractionation model was developed that predicted pH treatment. This model was then tested on Pliocene scallop fossils (*Carolinapecten eboreus*; Pinecrest Sand, Florida). The Pinecrest was deposited in the Late Pliocene as the final closure of the Central America Isthmus was occuring and ocean circulation patterns were changing as a result. Decline in pH associated with these changes has been suggested. Given the exceptional preservation of these fossils we tested our experimentally determined pH stable isotope model and evaluated the potential for this model to predict changes in pH in the Late Pliocene ocean.

Large Mo isotope variations before the Great Oxidation Event

D. ASAEL[1]*, O.J. ROUXEL[2], A. BEKKER[3] AND C.T. SCOTT[4]

[1]Université de Bretagne Occidentale, IUEM, UMR 6538, 29280 Plouzané, France (*dan.asael@univ-brest.fr)

[2]IFREMER, Département Géosciences Marines, 29280 Plouzané, France

[3]Department of Geological Sciences, University of Manitoba, Manitoba R3T 2N2, Canada

[4]Department of Earth and Planetary Sciences, McGill University, Montreal, Quebec H3A 2A7, Canada

Molybdenum (Mo) isotopes are efficiently removed under euxinic conditions and therefore may directly record contemporaneous seawater in ancient organic-rich shales. Removal of Mo in other environments (i.e., anoxic and oxic) is less efficient and accompanied by a significant negative isotope fractionation, where $\Delta^{98}Mo_{SW\text{-}SED}$ is typically 1 to 3 ‰ [1,2]. It is generally accepted that before the Great Oxidation Event (GOE) at ca. 2.3 Ga the transfer of Mo to the oceans was primarily in detrital form. This is in accordance with the available sedimentary data showing a narrow range of isotopic compositions corresponding to the crustal reservoir. As atmospheric oxygen started to rise, Mo was chemically weathered from continental sources and transported to the oceans as oxidized molybdate (MoO_4^{2-}). There, it was removed to sediments via several fractionating mechanisms, depending on the redox conditions. Consequently, Proterozoic and Phanerozoic black shales record a wide range of Mo isotopic values, reflecting variations in the isotopic composition of seawater as determined by the mass balance between the different sinks.

We measured Mo concentrations and isotopic compositions of black shales from several Neoarchean and Paleoproterozoic sections (2.7 Ga - Belingwe Fm., Zimbabwe; 2.63 Ga - Jeerinah Fm., Western Australia; 2.52 Ga - Gamohaan Fm., South Africa; 2.15 Ga - Sengoma Argillite Fm., Botswana; 2.06 Ga – Zaonega Fm., Karelia). The data show large isotopic variations and significantly elevated $\delta^{98}Mo$ values in sections dated up to 400 Myr before the GOE. Moreover, these pre-GOE sections show Mo concentrations which are higher than those typically found in older sections [3,4], but still lower than those found in post-GOE Proterozoic sections[5,6]. These observations imply a process of chemical weathering, transport and sedimentation of Mo, which was accompanied by significant isotope fractionation. We propose that such a process may be driven by either (a) low and fluctuating oxygen levels which led to episodes of continental Mo weathering, or (b) enhanced atmospheric sulfur levels after volcanic events which may initiate removal of Mo from the continental crust to the oceans.

[1] Barling et al. (2004) *Earth Planet. Sc. Lett.* **217**, 315-329.
[2] Goldberg et al. (2009) *Geochim. Cosmochim. Ac.* **73**, 6502-6516.
[3] Siebert et al. (2005) *Geochim. Cosmochim. Ac.* **69**, 1787-1801.
[4] Wille et al. (2007) *Geochim. Cosmochim. Ac.* **71**, 2417-2435.
[5] Kendall et al. (2011) *Earth Planet. Sc. Lett.* **307**, 450-460.
[6] Duan et al. (2010) *Geochim. Cosmochim. Ac.* **74**, 6655-6668.

https://doi.org/10.1180/S0026461X00008434 Published online by Cambridge University Press

Structural characterization of humic-like substances in atmospheric aerosols in Osaka, Japan

DAICHI ASAKAWA[1*] AND NOBUHIDE FUJITAKE[2]

[1]Osaka City Institute of Public Health and Environmental Sciences, Osaka, Japan, d-asakawa@city.osaka.lg.jp (* presenting author)
[2] Faculty of Agriculture, Kobe University, Kobe, Japan, fujitake@kobe-u.ac.jp

Macromolecular organic substances in atmospheric aerosols have been termed humic-like substances (HULIS) and it can influence functions of aerosols, such as cloud nucleation, absorption of solar radiation, and transportation of pollutant. However, despite its importance in environment, a comprehensive understanding of the structure of the HULIS remains elusive. We therefore studied the structural features of the HULIS in urban aerosols and compared it with those of soil and aquatic humic substances (HS).

Samples and Experiment

Water soluble HULIS (WS-HULIS) was obtained from aerosol sample, which was collected in Osaka city, Japan in summer and autumn 2010, and was analyzed using high-performance size-exclusion chromatography (HPSEC), pyrolysis gas chromatography (py-GC), and liquid-state ^{13}C NMR spectroscopy.

Results and Discussion

A weight-averaged molecular weight of the WS-HULIS was estimated 800–950 by HPSEC and molecular size distribution of the WS-HULIS was similar to that of the aquatic HS, particularly to fulvic acids. ^{13}C NMR spectroscopy showed lower aromatic (16–19% of total C) and higher aliphatic carbon content (35–45%) of the WS-HULIS (Fig.1) as compared to those of the soil HS. This result also suggests the structural similarities between the WS-HULIS and the aquatic HS. However, contrary to previous study [1], signals of lignin derived structure (55, 150ppm), which are generally detected in the soil and aquatic HS, were not observed in the NMR spectra of the WS-HULIS in both summer and autumn. This observation is supported by py-GC using tetramethylammonium hydroxide.

In conclusion, average chemical structure of the WS-HULIS in aerosols is relatively similar to that of the aquatic HS rather than soil HS. However, the WS-HULIS used in this study has no lignin derived component, indicating that the origin of the WS-HULIS may differ from that of the soil and aquatic HS. The structural features of alkaline extractable HULIS will also be presented.

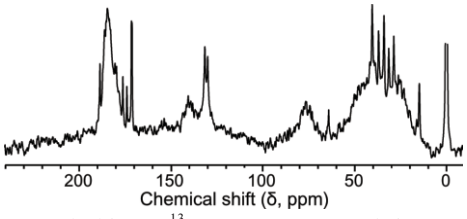

Figure 1: Liquid-state ^{13}C NMR spectrum of the water soluble humic-like substances in aerosols collected in summer 2010

This study was supported by Grant-in-Aid for Young Scientists (B) (23710037) from the JSPS.

[1] Duarte et al. (2007) *Atmos. Environ.* **41**, 8100-8113.

The role of contamination in the genesis of shoshonitic volcanism, central Pontide, Turkey

KÜRŞAD ASAN[1,2*], HÜSEYIN KURT[1], DON FRANCIS[2], AND GANERØD MORGAN[3]

[1]Selçuk University, Geological Engineering Department, Konya, TR kasan@selcuk.edu.tr (* presenting author), hkurt@selcuk.edu.tr
[2]McGill University, Earth and Planetary Sciences, Montreal, QC, CA donald.francis@mcgill.ca
[3]Geological Survey of Norway, Trondheim, NO morgan.ganerod@ngu.no

Late Cretaceous (~ 80 Ma) subduction-related volcanic rocks are widespread in the central Pontides of Turkey, both in the Sinop area to the North and in the Alaçam-Dikmen-Durağan areas to the South. There are two distinct groups of lava in both areas in terms of K_2O. The northern area rocks display high-K calcalkaline or shoshonitic affinities, whereas the southern area rocks have either medium-K calcalkaline or shoshonitic affinities. The shoshonites are younger than calcalkaline rocks in both areas, but the northern shoshonites are more potassium-rich than the southern shoshonites. The chondrite-normalized trace element patterns of all the lavas are characterised by strong enrichments in LILE (Rb, Ba, K and Sr) and LREE (La, Ce) and prominent negative Nb, Ta, and Ti anomalies, all typical of subduction-related lavas. There is a systematic increase in the REE fractionation from calcalkaline (La_N/Yb_N: 4-5) to high-K calcalkaline (La_N/Yb_N: 6-10) to shoshonitic (La_N/Yb_N: 4-19) lavas.

The calcalkaline rocks from the northern and southern areas have similar $^{87}Sr/^{86}Sr_{(i)}$ (0.705764-0.706959) and $^{143}Nd/^{144}Nd_{(i)}$ (0.512402-0.512531) isotopic ratios. The shoshonitic rocks from the two areas, however, have different Sr-Nd isotopic systematics. The shoshonites from the southern area have relatively low $^{87}Sr/^{86}Sr_{(i)}$ (0.704541-0.705022) and high $^{143}Nd/^{144}Nd_{(i)}$ (0.512589-0.512797) ratios that are independent of SiO_2 content and plot near Bulk Earth in a Sr-Nd correlation diagram. The shoshonites from the northern area, however, have high $^{87}Sr/^{86}Sr_{(i)}$ (0.706664-0.708340) and low $^{143}Nd/^{144}Nd_{(i)}$ (0.512266-0.512364) ratios plotting in enriched mantle quadrant of a Sr-Nd correlation diagram (Figure 1). Furthermore, $^{87}Sr/^{86}Sr$ increases and $^{143}Nd/^{144}Nd$ decreases with increasing SiO_2 content, suggesting progressive contamination with crystal fractionation. Thus, crustal contamination appears to have played an important role in the genesis of the northern shoshonites and was responsible for their higher K contents, but contamination was apparently not involved in the genesis of the southern shoshonites. This suggests that crustal contamination is not essential for the genesis of shoshonitic volcanism.

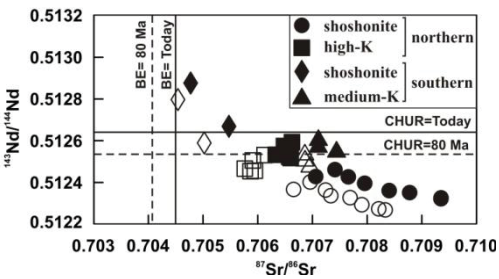

Figure 1: Sr-Nd correlation diagram of the volcanites (closed symbols: measured, open symbols: age corrected ratios for 80 Ma).

https://doi.org/10.1180/S0026461X00008434 Published online by Cambridge University Press

P-T-D Histories and Reequilibration of Ti in Quartz: Using the TitaniQ Thermobarometer in Poly-Deformed Tectonic Terranes

KYLE T. ASHLEY[1*], LAURA E. WEBB[2], FRANK S. SPEAR[3], AND JAY B. THOMAS[3]

[1]Dept. of Geosciences, Virginia Tech, Blacksburg, USA, ktashley@vt.edu (* presenting author)
[2]Dept. of Geology, University of Vermont, Burlington, USA, lewebb@uvm.edu
[3]Earth and Environmental Sciences, Renssaelaer Polytechnic Institute, Troy, USA, spearf@rpi.edu, thomaj2@rpi.edu

Constraining *P-T* conditions of deformation is essential in understanding lithospheric processes at all scales. The Ti-in-quartz ("TitaniQ") thermobarometer [1] has the potential to constrain either T or P if the other is known and if titania activity (a_{TiO2}) can be estimated. The extensive petrologic and structural framework previously established for the Strafford Dome, coupled with abundant quartz in various microstructural settings, provides and excellent case study for investigating use of the method in poly-deformed terranes. Two nappe emplacements (D_1 and D_2) and a following doming event (D_3) resulted in three schistositities (S_1-S_3) that provide a framework to investigate whether [Ti] of quartz in different microstrucural settings records *P-T* conditions of fabric formation. We conducted cathodoluminescence (CL) imaging to observe Ti-zoning in quartz grains and seconadry ionization mass spectrometry to determine [Ti].

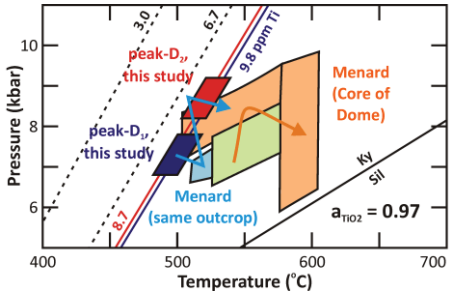

Figure 1: *P-T* paths calculated by TitaniQ from this study compared to proximal samples constrained in previous studies.

Results from these analyses coupled with previously established *P-T* paths [2] indicate that quartz preserves evidence for five recrystallization or reequilibration periods: 1) prograde (dark cores in CL, [Ti] = 2–3 ppm); 2) peak D_1 reequilibration (bright rims on quartz inclusions, [Ti] = 5.5 ppm); 3) dark rims on D_1 rims due a quartz-producing, kyanite-in reaction (sharp zonal sector contact); 4) peak D_2 in matrix quartz ([Ti] up to 9.8 ppm); and 5) retrograde reequilibration (darker rim in CL due to reduced T conditions). Rapid exhumation prevented extensive retrograde overprinting. This study has shown that TitaniQ coupled with microstructural analysis can provide insight into prograde conditions and reequilibration relative to deformation in poly-deformed terranes.

[1] Thomas *et al.* (2010) *Contrib Mineral Petrol* **160**, 743-759.
[2] Menard and Spear (1994) *J. Metamorphic Geol.* **12,** 811-826.

Equation of state for CaO-FeO-MgO-Al_2O_3-SiO_2 melts and evolution of a whole-mantle magma ocean

PAUL D. ASIMOW[1*], CLAIRE W. THOMAS[1], CARL B. AGEE[2], QIONG LIU[3] AND REBECCA A. LANGE[3]

[1]California Institute of Technology, Pasadena, CA, USA, asimow@gps.caltech.edu (* presenting author)
[2]Univ. of New Mexico, Albuquerque, NM, USA, agee@unm.edu
[3]Univ. of Michigan, Ann Arbor, MI, USA, becky@umich.edu

Understanding the consequences for Earth evolution of formation and crystallization of a magma ocean – plausibly involving the entire silicate earth, e.g. after a moon-forming impact – requires detailed knowledge of the physics and thermochemistry of multi-component silicate liquids at all mantle pressures (*P*), near-liquidus temperatures (*T*), and a range of candidate bulk silicate Earth compositions. Also, a grasp of deep mantle partial melting (e.g. at the core-mantle boundary (CMB)) requires simlar information for a wider range of liquids (with high volatile and incompatible concentrations) at near-solidus *T*.

There are sufficient constraints from shock wave data and first principles molecular dynamics to define the thermal equation of state (EOS) of end-members spanning the five oxides CaO-FeO-MgO-Al_2O_3-SiO_2. FeO-bearing compositions (Fe_2SiO_4 and $CaFeSi_2O_6$) have recently had their Hugoniots defined to CMB *P*; Fe_2SiO_4 results agree well with new simulations [1]. We still need to assume ideal mixing of volumes (except along MgO-SiO_2 [2]) to fill composition space, but two intermediate compositions that have been determined are consistent with this approximation. Hence, the data support construction of a liquid EOS able to describe density and compute isentropes for ultramafic to mafic liquids of varying composition.

The thermal EOS of each of five endmembers – $CaMgSi_2O_6$, $CaAl_2Si_2O_8$, $MgSiO_3$, Mg_2SiO_4, Fe_2SiO_4 – can be fit to one of several formalisms: (1) 4th order Birch-Murnaghan isentrope with Mie-Grüneisen (M-G) thermal pressure and constant heat capacity; (2) a linear shock wave EOS with M-G thermal offset; or (3) de Koker and Stixrude's fundamental relation [3]. Properties of other liquids are derived by assuming constant partial molar volume and heat capacity of the five endmembers at each *P* and *T*. Isentropes of intermediate compositions can be computed iteratively.

The liquidus curve for KLB-1 peridotite of [4] gives a critical isentrope with potential temperature 2800 K for onset of perovskite crystallization in the mid-lower mantle at ~80 GPa. But the steeper liquidus curve for model chondritic mantle by [5] gives a critical isentrope with potential temperature 2600 K for crystallization at the CMB. We find the neutrally buoyant liquids at the CMB as a function of Mg# and (Mg+Fe)/Si: at perovskite stoichiometry, liquid Mg# $\leq$ 0.55 is needed for liquid density to exceed that of $MgSiO_3$ perovskite, whereas at olivine stoichiometry only Mg# < ~0.9 is needed.

[1] Muñoz Ramo & Stixrude (submitted) *PRL*. [2] de Koker et al. (submitted) *Nature*. [3] de Koker & Stixrude (2009) *GJI* **178**, 162-179. [4] Fiquet et al. (2010) *Science* **329**, 1516-1518. [5] Andrault et al. (2011) *EPSL* **304**, 251-259.

https://doi.org/10.1180/S0026461X00008434 Published online by Cambridge University Press

A low flow desolvating nebulizer system as a tool for calibration in LA-ICP-MS

DHINESH ASOGAN[1*], DAVID CLARKE[1],

[1] CETAC Technologies, Omaha, NE, USA dasogan@cetac.com

Calibration for laser ablation inductively couple plasma mass spectrometry is a continuing challenge to analysts. Precise matrix matching is required to ensure ablation characteristics and subsequent plasma dynamics are consistent between calibrants and samples.

On-line additions of liquid standards to ablated aerosol streams has been shown to elminate the need for precise matrix matched standards and still provide good calibration.[1–4] In this paper, the authors present a technical overview of the technique of on-line additions and a comparison with traditional, matrix matched calibration for the analysis of Arkansas Womble Shale.

(1) Yang, C.-K.; Chi, P.-H.; Lin, Y.-C.; Sun, Y.-C.; Yang, M.-H. *Talanta* **2010**, *80*, 1222-7.

(2) O' Connor, C. J. P.; Sharp, B. L.; Evans, P. *Journal of Analytical Atomic Spectrometry* **2006**, *21*, 556.

(3) Gunther, D.; Cousin, H.; Magyar, B.; Leopold, I. *Journal of Analytical Atomic Spectrometry* **1997**, *12*, 165-170.

(4) Leach, J. J.; Allen, L. A.; Aeschliman, D. B.; Houk, R. S. *Analytical Chemistry* **1999**, *71*, 440-445.

Carbon isotope constraints on degassing of MORB from the Southwest Indian Ridge (32-50°E)

CYRIL AUBAUD[1*], EILEEN GÜTTLER[1], PIERRE CARTIGNY[1]

[1]Laboratoire de Geochimie des Isotopes Stables, Institut de Physique du Globe, Sorbonne-Paris Cité, Paris, France, aubaud@ipgp.fr (*), guttler@ipgp.fr, cartigny@ipgp.fr

The Southwest Indian ridge is remarkable for its slow spreading rate and large radiogenic isotope anomalies. It is therefore ideal to test possible carbon isotope variations in the mantle. However, due to its low solubility in basalts, CO_2 is affected by strong degassing processes which must be precisely characterised before investigating compositional variation of the mantle source. In this study, we analyzed 28 SWIR basaltic glasses for their vesicularity, CO_2 vesicle content, and $\delta^{13}C$ of CO_2 in vesicles. The samples were collected on the SWIR axis from 32 to 50°E and in a range of depths from 1320 to 3850 m.

These data are discussed in the light of an improved mass balance model that takes into account: (1) variable initial CO_2 contents, (2) a deep degassing step, (3) isobaric loss of vesicles at crustal level, (4) the depth of magma storage in the crust, (5) the effect of crystal fractionation on degassing, and (6) the full range of degassing regimes between the magma chamber and the eruption depth (closed vs. open system degassing and equilibrium to kinetic degassing regimes).

Vesicularities show a large range: from 0 to 9.15 vol%, most samples having less than 4% vesicles. Carbon isotopic compositions of CO_2 in vesicles extracted by crushing in vacuo show a relatively large range of $\delta^{13}C$-values from –1.26 to –13.36‰ with most values between –4 and –8‰. The measured $\delta^{13}C$-values are similar to those observed for other ridges (Atlantic and Pacific).

The computed results show that approximately half of the dataset can be explained by a shallow stage of degassing occurring as a closed system after total loss of the first generation of vesicles in axial magma chambers. The second half of the dataset requires that the shallow degassing stage occurred as an open-system degassing process. One sample requires the stage of open-system degassing to start much deeper than 6 km depth (below sea floor) or to be strongly kinetic. The few remaining samples are best explained by kinetic open-system degassing in order to fit their relatively high $\delta^{13}C$ values.

The model shows that the mode of the last degassing step and the extent of isobaric degassing at crustal level exert a strong control on the volatile characteristics of the erupted melts, the other processes having minor effects. If carbon content and/or carbon isotopic ratio anomalies exist below the SWIR, these are either small in magnitude or masked by degassing processes.

https://doi.org/10.1180/S0026461X00008434 Published online by Cambridge University Press

Yttrium and rare earth element composition of the Rapitan Iron Formation (Northwest Territories, Canada)

NATALIE R. AUBET[1]*, ERNESTO PECOITS[1], LUKE OOTES[2] AND KURT O. KONHAUSER[1]

[1]University of Alberta, Edmonton, Canada, aubet@ualberta.ca (* presenting author)
[2]Northwest Territories Geoscience Office, Yellowknife, Canada, Luke_Ootes@gov.nt.ca

The Neoproterozoic represents a time in Earth's history when significant environmental changes took place, including global glaciations that led to ocean stagnation and an apparent build-up of dissolved ferrous iron. As the ice receded and ocean circulation became re-established, the iron became oxidised and formed a suite of iron formations (IFs) in the oxic zone of upwelling areas. However, the ultimate source of iron is still a matter of intense debate.

Rare earth elements plus yttrium (REY) concentrations in IFs have been successfully used as proxies to study secular trends in Precambrian ocean chemistry. Despite a number of previous geochemical studies on Cryogenian IFs, complete REY datasets are virtually absent. Here we examine bulk and mineral phase trace-element geochemistry (REY) of the Rapitan Iron Formation, Northwest Territories, Canada. Samples for geochemical analysis were selected on the basis of extremely low, if any, Th, Zr, Hf and Sc concentrations and lack of co-variations between Zr vs. Y/Ho, Y/Ho vs. Ce/Ce* and Th vs. La/La*. The results show: (1) REY profiles with distinctive seawater-like signatures (i.e., LREE-depletion relative to HREE, superchondritic Y/Ho ratios and positive anomalies of both La and Gd); (2) precipitation under oxygen-deficient conditions (no to slightly positive Ce anomaly); and (3) iron being sourced from hydrothermal vents (positive Eu anomaly). Of particular interest, along with Ce, is the identification of an Eu anomaly in all of the samples analyzed. The latter might be explained either by precipitation in an open stratified ocean involving ferruginous deep waters -through which hydrothermally sourced Eu (and iron) could travel long distances- or by deposition taking place in a somewhat restricted basin where the Eu signature is more easily retained. In the first scenario, our results might confirm, as previously proposed, that ferruginous conditions dominated during the Sturtian "snowball glaciation". Alternatively, a semi-isolated basin should be considered for the deposition of the Rapitan IF.

Zinc sorption on carbonate reservoir system, implications on CO_2 geological storage.

BAPTISTE AUFFRAY[1A*], BRUNO GARCIA[1A], CHARLES-PHILIPPE LIENEMANN[1B] AND ADRIAN CEREPI[2]

[1A]IFP Energies nouvelles, Rueil-Malmaison, France, baptiste.auffray@ifpen.fr (* presenting author) bruno.garcia@ifpen.fr
[1B]IFP Energies nouvelles, Solaize, France, charles.lienemann@ifpen.fr
[2]EA 4592 G&E, ENSEGID, University of Bordeaux, Pessac, France, adrian.cerepi@egid.u-bordeaux3.fr

Geological storage is one of the solutions envisaged to reduce greenhouse gases concentration in atmosphere, and storage in underground saline aquifers is of major interest considering their high storage capacity. One of the main question still unanswered regards the consequences of the supercritical CO_2 injection on the metals mobility; from the storage formation to the sub-surface. Indeed, supercritical CO_2 injection (over 31 °C and 74 bar) acidifies the aquifer and induces metals release from rock matrix. In consequences, geochemistry (dissolution/precipitation phenomena, sorption of metals...) and petrophysical properties (porosity and permeability) of each compartment impacted will be changed.

In this study, two natural carbonates (from Lavoux and St-Emilion) were used to carry out zinc sorption experiments (initial concentration equal to 10^{-5} mol/L) at 40 °C and four different CO_2 pressures ($3.5e^{-4}$, 30, 60 and 90 bar) in saline solutions (100g/L NaCl) in batch reactors.

Results obtained for the different pressure conditions investigated on Lavoux carbonate show that: (i) in atmospheric conditions, the zinc adsorption phenomenon is clearly put in evidence and matches well with a Freundlich adsorption isotherm model [1]; (ii) at 30 bar of CO_2, the dissolution of Lavoux carbonate [2] induces a zinc release in the system, with no adsorption observed; (iii) at 60 bar, a strong decrease of zinc concentration is observed (factor 2) over 70 days and after, it goes back close to its initial value; (iv) with a CO_2 pressure of 90 bar, adsorption is observed but in lower proportions and slower kinetic than in atmospheric conditions. Comparative studies with St-Emilion carbonate are being carried out and will be discussed with these previous results obtained with the Lavoux carbonate.

Though more investigations have to be carried out to better understand the coupling and competition of rock dissolution and metals adsorption phenomenons, these results are very important in order to better understand the behavior of metals in the {carbonate/saline-solution/CO_2} system in a geological storage context. Indeed, the CO_2 pressure implies very different comportment on metals sorption, which will occur in natural context. These results will allow us to predict by reactive modelling the future behavior of metals in CO_2 geological storage sites, their potential mobilization up to surface aquifers and their impact on surface potable aquifers.

[1] Limousin et al. (2007) *Applied Geochemistry* **22**, 249-275.
[2] Pokrovsky et al. (2005) *Chemical Geology* **217**, 239-255

https://doi.org/10.1180/S0026461X00008434 Published online by Cambridge University Press

Hatiba to Port Sudan Deep (Red Sea) Imaging a growing Ocean

N. AUGUSTIN[1*], C.W. DEVEY[1], R. BANTAN[2], F. M. VAN DER ZWAN[1], P. FELDENS[1] AND T. KWASNITSCHKA[1]

[1]GEOMAR | Helmholtz Centre for Ocean Research Kiel, Germany, naugustin@geomar.de (* presenting author)
[2]King Abdulaziz University, Jeddah, Saudi Arabia

The current knowledge of the bathymetry of one of the youngest oceans on earth, the Red Sea, and its spreading centres is poor and mainly based on several low resolution maps of a few deeps of higher interest, like the Atlantis II Deep [e.g., 1, 2]. During the RV Poseidon cruise 408 we collected a continuous bathymetric dataset of Red Sea deeps from the Hatiba Deep via Atlantis II Deep to the Port Sudan Deep over a total N-S distance of 300 km between 22°28´N and 19°59´N along the Red Sea rift with a resolution of 25-30 m.

The bathymetric data visualize very well tectonic features (complex fault and rift structures) and related volcanic edifices, in Hatiba, Atlantis II as well as Port Sudan Deep. The position of the rift axis can be determined for the Hatiba Deep and Atlantis II Deep based on graben fault symmetry and slope angle calculations, together with the recovery of fresh basalts. The models demonstrate that especially the tectonic setting of the comparatively large Hatiba Deep is much more complex than previously thought and reveal evidence for a rift-axis-jump to the south. Basalts with characteristic flow textures and enclosed sediments, recovered from the southwestern Hatiba basin, give strong indications for rupturing in an environment, where possibly magma interacted with wet sediments. Thermobarometry calculations based on geochemical analyses (EMP, FTIR) of basalt glass from Hatiba deep reveal generally variable depths of last equilibration with a gabbroic mineral assemblage of about 6 to 14 km for samples from different locations in the deep, whereas samples from the assumed actual spreading center point to a crystalization depth of about 8 km at 1170°C.

Distinct tectonic features as visible in the Hatiba Deep become less prominent to the south. Therefore, the bathymetry of the Port Sudan Deep marks the changeover from the rifting in the northern Red Sea to the drifting in the southern Red Sea. For all mapped deeps, the bathymetric data show strong influence of salt/sediment flow as well as land slides into the deeps, which in some cases cover large parts of the graben structures. Due to sedimentation, indications of ridge offsets between the deeps are covered by sediments and the tectonics of ridge transition are not visible in the recently available dataset.

We present a unique collection of bathymetric models and volcanic/tectonic interpretations. Combined with data about ground truthing, geological mapping and geochemical data this work provides a detailed look into the structure, tectonics, magmatic centres and evolution of Red Sea deeps in larger detail than observed before.

[1] Laughton (1971) Philosophical transactions of the Royal Society of London, **267**, 21-22
[2] Bäcker and Richter (1973) Geologische Rundschau, **62**. 697-741

Siderophile element redistribution during mantle metasomatism

SONJA AULBACH[1*], LARRY HEAMAN[2], VLADIMIR MATJUSCHKIN[1], JOHANNES HOFMANN[1], THOMAS STACHEL[2] AND GERHARD BREY[1]

[1]Goethe-University, Facheinheit Mineralogie, Frankfurt, Germany, s.aulbach@em.uni-frankfurt.de
[2]University of Alberta, Department of Earth and Atmospheric Sciences, Edmonton AB, Canada

During subduction zone processing, highly siderophile elements (HSE) including Re-Os may be mobilised differentially from different parts of the slab, with consequences for their transfer into the mantle wedge and retention in deeply subducted residual eclogites [e.g. 1]. The Slave craton in northern Canada was affected by Paleoproterozoic subduction, leading to emplacement of gabbroic materials, eclogitisation during interaction with deserpentinisation fluids and associated diamond formation [2]. Pristine sulphide inclusions in these 1.9 Ga eclogitic diamonds have HSE and other trace metal concentrations attesting to conservative behaviour during dehydration-induced metasomatism and metamorphism of their subduction-related gabbroic source rocks. This is taken to indicate that the fluids involved were reducing and Cl-poor, and therefore unable to mobilise HSE from the gabbroic portion of the slab into the supra-subduction zone.

Contrary to sulphide included in diamond, sulphide of the same composition and inferred age in eclogite xenoliths have been exposed to mantle metasomatic processes since their 1.9 Ga emplacement into the cratonic lithosphere. Such metasomatism may lead to introduction and/or remobilisation of HSE, either as sulphide melts or dissolved along with oxidised S species in silicate or carbonate melts or related fluids [e.g. 3]. Earlier investigation of sulphide minerals in these eclogite xenoliths has revealed three of five samples to be too Ni-rich to be in equilibrium with a meta-basaltic source, and to have disturbed Re-Os isotope systematics. By contrast, the silicate portion of the eclogites does not show evidence for metasomatic overprint. This may indicate introduction of mobile Ni-rich sulphide melts derived from surrounding mantle peridotite [4].

We are in the process of measuring HSE and other trace metal contents of sulphide minerals in these rocks, and in a pyroxenite giving a 1.9 Ga sulphide-derived Re-Os isochron age. This will enable us to compare HSE signatures of sulphide in eclogite xenoliths with corrupted Re-Os isotope systematics to primary sulphide included in diamond and in the pyroxenite. We anticipate there will be differences in HSE abundances and/or ratios that will afford insights into the nature and effects of mantle metasomatic agents that lead to redistribution of HSE and disturbance of primary Re-Os isotope signatures.

[1] McInnes et al. (1999) *Science* **286**, 512-516. [2] Aulbach et al. (2011) *Lithos* **126**, 419-434. [3] Alard et al. (2011) *J. Petrol.* **52**, 2009-2045. [4] Aulbach et al. (2009) *Earth Planet. Sci. Lett.* **283**, 48-58.

https://doi.org/10.1180/S0026461X00008434 Published online by Cambridge University Press

Heterogeneous mantle source for the recent magmatism of Gran Canaria

MERITXELL AULINAS[1*], DOMINGO GIMENO[1], JOSE LUIS FERNANDEZ-TURIEL[2], LAURA FONT[3], FRANCISCO JOSE PEREZ-TORRADO[4], ALEJANDRO RODRIGUEZ-GONZALEZ[4], AND GEOFF NOWELL[3]

[1] Dpt. Geoquímica, Petrologia i Prospecció Geològica, Universitat de Barcelona, Spain, meritxellaulinas@ub.edu (* presenting author), domingo.gimeno@ub.edu

[2] Institute of Earth Science Jaume Almera, ICTJA-CSIC, Spain, jlfernandez@ictja.csic.es

[3] Dpt of Earth Sciences, Durham University, United Kingdom lfont@fawl.vu.nl, g.m.nowell@durham.ac.uk

[4] GEOVOL, Dpt de Física, Universidad de Las Palmas de Gran Canaria, Spain fperez@dfis.ulpgc.es arodriguez@proyinves.ulpgc.es

Chemical and Sr-Nd-Pb isotopic data of the Pliocene-Quaternary mafic lavas of Gran Canaria (Canary Islands, Spain) reported in Aulinas et al. (2010) are used to investigate the composition of their mantle source. The isotopic differences between the Plio-Quaternary (Post-Roque Nublo Group) and the older Pliocene (Roque Nublo Group) mafic parental magmas reflect small-scale mantle heterogeneities. Two distinct mantle components were involved in partial melting to form the Pliocene-Quaternary magmas of Gran Canaria, the first being isotopically more depleted and similar to the DMM type and the second being more radiogenic in Pb-isotope ratios comparable to an HIMU type. Geochemical variations show that the Pliocene-Quaternary mantle source is not only compositionally but also lithologically heterogeneous and supports the presence of a silica-deficient pyroxenite mantle component. Calculation of its contribution in the generation of the Pliocene-Quaternary magmas is estimated to be in the range from 50 to 70%. However, no significant differences between the Roque Nublo and the Post-Roque Nublo Groups are detected, suggesting that pyroxenite-derived melts played a similar role in both groups. Trace element ratios support mixing between the two mantle components (a silica deficient pyroxenite and a peridotite) which obscure the original chemical and isotopic compositions of these two end-members. The proposed scenario for the generation of the Pliocene-Quaternary magmas involves a lithologically heteorogenous mantle plume consisting of pyroxenite veins in a peridotite matrix which melted and mixed both mantle components during its ascent until the base of the lithosphere.

This research was funded by the Spanish projects CGL2004-04039BTE and CGL2011-28022 and it was carried out in the framework of the PEGEFA Research Group (SGR2009-972) and GEOVOL Research Group.

[1] Aulinas et al. (2010) *Lithos* **119**, 377-392.

Current regulatory limitations for the development of products containing nanomaterials with a life cycle perspective

CLAIRE A. AUPLAT[1*] AND AURELIE DELEMARLE[2]

[1]Novancia Business School, Paris, France, cauplat@novancia.fr (* presenting author)

[2]ESIEE , Noisy-le-Grand, France, a.delemarle@esiee.fr

The analysis of the specific properties of nanomaterials compared to bulk material has already received ample attention and generates research in a vast array of directions, including the design of new materials. One innovative approach is to introduce a life cycle perspective in the design of products containing nanomaterials. At the current stage of knowledge and scientific advancement, this approach includes examining the interactions between all sorts of nanomaterials and the surrounding biota during the entire life cycle of a product with an objective of designing new nanomaterials that minimize potential adverse effects.

The task of researchers is immense because of the absence of data concerning the life cycle of nanomaterials and their transformation over time. However, since the 1990s they have made significant progress in their understanding of microscopic design as well as of interactions at the nanoscale, notably concerning surface areas, and they can now envisage a true paradigm change in the management of innovation.

One important aspect of their work is that they operate in a regulatory context where the life cycle-based methodology has so far not been taken into account. After establishing a panorama of all mandatory regulatory options that frame the development of nanoproducts [1], our study aims to identify inconsistencies and gaps to fill in regulation in order to accompany this paradigm change. In other words, we seek to contribute to the development of a benchmark to foster new processes of nanomaterial design based on life cycle assessments.

[1] Claire Auplat (2012) *Global Policy* **Forthcoming.**

https://doi.org/10.1180/S0026461X00008434 Published online by Cambridge University Press

From partly serpentinized peridotite to continental crust through weathering and recycling processes

H. AUSTRHEIM[1*] A. PUTNIS[2], C.V. PUTNIS[2] AND B.GRGURIC[3]

[1] PGP, University of Oslo, Norway, h.o.austrheim@geo.uio.no (* presenting author)
[2]Institut für Mineralogie, University of Münster, Münster, Germany putnis@uni-muenster.de
[3]Norilsk Nickel Australia, Perth, Australia ben.grguric@nornik.com.au

Partial melting of peridotite is a fundamental process in forming continental crust. However ultramafic material are also added to the crust through obduction of ophiolites and extrusion of komatitic lavas. Such olivine rich rocks are highly reactive and so prone to weathering. In a tropical climate they are known to develop into a thick Ni-laterite zone, hosting some of the worlds largest Ni-deposits. In order to evaluate the role of weathered peridotites on the composition of both the continental crust and the oceans, we need to understand how weathering of peridotites can fractionate elements and how the various components involved are incorporated in continental sediments or alternatively transported to the oceans. That is, a knowledge of the mechanisms involved in weathering processes and element mobilization is essential for the understanding of the continuous redistribution of elements within the Earth.

We present microtextures and mineral and whole rock chemistry from a weathering profile through the Goliath laterite of the Archaean Agnew-Wiluna Greenstone belt of Western Australia, to show that the protolith was a strongly serpentinized peridotite and that weathering involved removal of Mg, leaving behind a 20 m thick residue of quartz hematite with high Ni/Mg and Cr/Mg ratios. Rocks with similar geochemical and textural signatures are also present in clast material from three studied Devonian sedimentary basins of S-Norway[1]. Weathering of peridotite to form quartz-hematite rocks may explain that the average Cr and Ni values of continental crust are higher than those of andesite and this deviation may be used to estimate that ca 5 % of the crust may have formed from weathered peridotite. Consequently the removed Mg may contribute to the Mg budget of the Oceans.

[1] Beinlich *et al*. (2010) *Geochim. Cosmochim Acta***. 74**, 6935-6964.

Zircon and baddeleyite solubility in alkaline aqueous fluids

J.C. AYERS [1*], L. ZHANG [1], Y. LUO[1], AND T. PETERS[1]

[1]Vanderbilt Univ., Nashville, TN, USA, john.c.ayers@vanderbilt.edu (* presenting author)

Field evidence and thermodynamic data at ambient conditions suggest that complexing of Zr with hydroxyl ions at high pH enhances the solubilities of Zr-bearing minerals. We tested this hypothesis by measuring the solubilities of baddeleyite (ZrO_2) and the assemblages zircon ($ZrSiO_4$) + baddeleyite (Z + B) and zircon + quartz (Z + Q) in neutral to alkaline fluids at 0.2 GPa. Measured solubilities expressed as molality (*m*) of Zr in the fluid are very low, close to procedure detection limits.

We measured the solubility of baddeleyite in alkaline fluid (0.1, 1*m* NaOH) at 600°C. Solubilities measured in 1*m* NaOH using the single crystal weight loss method were higher than double capsule values, possibly due to recrystallization in a temperature gradient. For double capsule measurements the average measured Zr concentration in equilibrium with baddeleyite was 1.8 x 10^{-5}*m* in 0.1*m* NaOH and 5.8 x 10^{-5}*m* in 1*m* NaOH, suggesting that baddeleyite solubility increases with increasing hydroxyl concentration in the fluid, presumably due to formation of the $Zr(OH)_5^-$ complex.

In neutral to alkaline fluids (0, 0.1, 1*m* NaOH) zircon dissolved incongruently in quartz-undersaturated fluids to form baddeleyite. At 450°C vlasovite ($Na_2ZrSi_4O_{11}$) also precipitated from fluids saturated and undersaturated in quartz. We observed no significant dependence of solubility on temperature. Ion microprobe analysis showed that the oxygen isotope compositions of zircon grains in the starting material and run products were similar, indicating that zircon dissolution-reprecipitation did not occur during the experiments.

The solubility of zircon increases with increasing fluid silica concentration, suggesting that zirconium complexes with silica in the fluid. At 600°C linear regression of experiment results yielded:

ln (Zr) = -3.9 + (1.9 * ln (Si))

where terms in parentheses represent molal concentrations. Zircon solubility also seems to increase with increasing hydroxyl concentration in the fluid.

At low silica activities the solubility of Zr-minerals is enhanced at high pH through complexing of zirconium with hydroxyl. Alkaline fluids may therefore dissolve zirconium minerals such as baddeleyite and zircon and mobilize Zr. At high silica activity zircon solubility is enhanced by complexing of zirconium with silica, suggesting that zirconium may also be mobile in silica-rich fluids. Fluids without high concentrations of hydroxyl or silica are not responsible for the rare observed occurrences of Zr metasomatism, but they may still catalyze recrystallization of zircon grains because recrystallization does not require high solubility.

https://doi.org/10.1180/S0026461X00008434 Published online by Cambridge University Press

Sources of Pb contamination in well water and soil at former orchards in the Mid-Atlantic, USA

ROBERT A. AYUSO[1]*
[1]U.S. Geological Survey, Reston, VA, 20192, USA,
rayuso@usgs.gov (*presenting author)

Lead and strontium isotopes, rare earth element, and trace metal compositions were measured to infer the sources of anomalously high concentrations of Pb in residential water wells and soils in former fruit orchards in Pennsylvania. The results were used to characterize potential anthropogenic and geogenic sources of lead, to evaluate specific contributions from various distinct sources, and to assess the geochemical relationship between water, soil, bedrock, and anthropogenic materials.

Groundwater from residential wells, in-line well water filters, surface water, Pb-arsenical pesticides, orchard and garden soils, the Ordovician carbonate-dominated bedrock, and coal deposits in the region display variable $^{206}Pb/^{207}Pb$ (1.16862-1.2236), $^{208}Pb/^{207}Pb$ (2.43551-2.46570) and $^{87}Sr/^{86}Sr$ (0.709030-0.730596) isotope signatures. Waters have variable Pb (up to 200 ppb) and As (up to 11 ppb) contents, and mostly low REE contents (La <0.096 ug/L; Yb ~ 0.027 ug/L). Soils are enriched in Pb (up to 2452 ppm) and As (up to 450 ppm), which might be caused by past use of lead arsenical pesticides applied to orchard crops. Rare earth element contents of soils resemble those of bedrock; however, the abundances of Pb and As in bedrock are much lower than in the soils. Pb isotope signatures of all ground and surface waters closely match, however, the waters do not match the Pb (or Sr) signatures of bedrocks, soils, or lead arsenical pesticides. Residential well waters show a broad linear trend in Pb isotope composition and match Pb isotope signatures of sediments captured in water filters. Surface water matches the Pb isotopic signature of the residential well waters. Depth-constrained water samples obtained from new monitor wells sited in bedrock (Martinsburg Fm., Jacksonburg Limestone, and the Epler Member of the Beekmantown Group) generally overlap the trend of the residential well waters, although some samples extend to lower Pb isotope ratios. Soils and well waters plot in broad fields along contrasting slopes in standard Pb isotope diagrams; the isotope fields do not overlap. Contributions of soil-Pb are apparently limited to wells having shallow water-bearing zones and significant sediment content. As a consequence, neither soils nor bedrock can be the exclusive or dominant source of Pb in the majority of the residential or monitor well waters.

Comparison of the Pb isotope data for the well waters, orchard soils, bedrock, and regional and local anthropogenic sources suggests the lasting impact of industrial lead from past leaded gasoline use, power plants, and various near-by metal manufacturing and processing facilities (e.g., smelters, lead-acid battery production), and waste disposal activities. Thus, the groundwaters are thought to have a regional industrial Pb isotope signature before arriving at the former orchard areas. The Pb in water is thought to be derived by mixing of lead from various industrial origins together with a contribution of labile lead from bedrock, rather than from historical application of pesticide in the region.

https://doi.org/10.1180/S0026461X00008434 Published online by Cambridge University Press

Rationalising nanoparticle sizes measured by AFM, FlFFF and DLS: sample preparation, polydispersity and particle structure

MOHAMMED BAALOUSHA* AND JAMIE LEAD

1 School of Geography, Earth and Environmental Sciences, College of Life and Environmental Sciences, University of Birmingham, Birmingham, United Kingdom, m.a.baalousha@bham.ac.uk (* presenting author)

8e.Towards the fundamentals of nanoparticle interactions with the living world: a life cycle perspective.

This presentation will discuss the sources of variability in the measured nanomaterial (NM) size by different analytical tools including atomic force microscopy (AFM), dynamic light scattering (DLS) and flow-field flow fractionation (FlFFF). The results suggest that differences in NM size measurements between different analytical tools can be rationalised by taking into consideration (i) sample preparation, (ii) sample polydispersity and (iii) structural properties of the NMs.

Appropriate sample preparation is a key to obtain representative particle size distributions (PSDs), and this may vary on a case by case basis. For AFM analysis, an ultracentrifugation method is the optimal method to prepare samples from diluted suspensions of NMs (<1 mg L-1). For FlFFF, the overloading effect, particle-particle and particle-membrane interactions as well as nature of the calibration standards are important determinants of the quality of data. For DLS, the quality of the fitting of the autocorrelation function is a key issue in obtaining correct estimates of particle size. Conversion of intensity PSD to number or volume PSD is promising for determination of number and volume PSD, but hampered by uncertainties in solving and optimizing the autocorrelation function fit.

The differences between the z-average hydrodynamic diameter by DLS and the particle height by AFM can be accounted for by sample polydispersity. The ratio of z-average hydrodynamic diameter: AFM particle height approaches 1.0 for monodisperse samples and increases with sample polydispersity. A polydispersity index of 0.1 is suggested as a suitable limit above which DLS data no longer remains accurate. Conversion of the volume PSD by FlFFF-UV to number PSD helps to rationalise for some of the variability in the measured sizes. The remaining variability in the measured sizes can be attributed to structural variability in the particles and in this case is mainly attributed to the thickness and permeability of the particles/surface coating. For citrate coated NMs, the dFlFFF/dAFM approaches 1 and the particles are described as hard spheres, whereas for PVP coated NMs, the dFlFFF/dAFM deviates toward values greater than one, indicating that these particles are either permeable or non-spherical.

Yttrium mobility during weathering: implications for riverine Y/Ho

MICHAEL G. BABECHUK[1*], BALZ S. KAMBER[2], MIKE WIDDOWSON[3]

[1]Laurentian University, Sudbury, ON, Canada (* presenting author)
[2]Trinity College Dublin, Dublin, Ireland
[3]The Open University, Milton Keynes, United Kingdom

Yttrium has similar geochemical properties to the lanthanides and closely mirrors the behaviour of its geochemical twin, Ho, in anhydrous magmatic systems. In the hydrosphere, however, Y is noteably less particle reactive than the lanthanides [1] and is more mobile during chemical weathering as a result [e.g., 2]. Here, this behaviour is further explored using chemical transects through two basaltic weathering profiles in India that are preserved in different stages of alteration: the Bidar laterite profile (~50 m) and an incipient to intermediately weathered profile developed across two lava flows (~5 m) near Chhindwara. Both profiles were characterized using major element and high-precision trace element data to establish the progressive compositional changes during chemical weathering.

The parent rock Deccan Traps basalt of both profiles is chemically similar with an average Y/Ho ratio of 25.2 ± 1.1 in the least-weathered samples. In the Chhindwara weathering profile, the enhanced mobility of Y relative to the lanthanides is observed already at the incipient stages of weathering. The preferential loss of Y continues during increasing weathering intensity in the profile as demonstrated by a strong anti-correlation between the chemical index of alteration (CIA; ranging from 35-80) and the Y/Ho ratio (ranging from ~25-23). Yttrium mobility is evident at the scale of the profile as well as across a corestone-saprolite interface (< 1 m). The Bidar laterite profile (CIA>90) has highly subchondritic Y/Ho ratios (19.4-14.7) with the exception of one sample in the mottled zone with highly enriched REE abundances and a superchondritic Y/Ho ratio of 30.1.

River waters have superchondritic Y/Ho ratios prior to reaching the estuary (where additional, much more extreme Y/Ho fractionation occurs due to the higher particle reactivity of the HREE), indicating that the greater mobility of Y relative to the HREE during weathering may be sufficient to affect mass balance. Care must be taken to correctly identify the Y/Ho ratio of river water due to the possibility of marine chemical sedimentary rocks in the drainage area and/or contamination from phosphate fertilizers. Using previously published Y/Ho data from eastern Australia rivers [3,4] screened based on P content and salinity to minimize the influence of these complications, a net superchondritic Y/Ho ratio remains. Thus, the weathering behaviour of Y may be more important to the interpretation of riverine Y/Ho ratios than previously considered.

[1] Nozaki et al. (1997) *EPSL* **148**, 329-340.
[2] Hill et al. (2000) *Geology* **28**, 923-926.
[3] Lawrence et al. (2006) *Marine & Freshwater Research* **57**, 725-736.
[4] Lawrence et al. (2006) *Aquatic Geochemistry* **12**, 39-72.

https://doi.org/10.1180/S0026461X00008434 Published online by Cambridge University Press

Multi-laboratory Comparison of Sequential Metals Extractions

CAROL BABYAK [1*], JENNIFER N. GABLE [2], KWOK-CHOI PATRICK LEE [3], WILLIAM J. ROGERS [4], ROCK J. VITALE [5], AND NEIL E. CARRIKER [6]

[1] Appalachian State University, Boone, North Carolina, United States, babyakcm@appstate.edu (* presenting author)
[2] Environmental Standards, Inc., Valley Forge, Pennsylvania, United States, jgable@envstd.com
[3] Tennessee Valley Authority, Muscle Shoals, Alabama, United States, plee@tva.gov
[4] Tennessee Valley Authority, Muscle Shoals, Alabama, United States, wjrogers@tva.gov
[5] Environmental Standards, Inc., Valley Forge, Pennsylvania, United States, rvitale@envstd.com
[6] Tennessee Valley Authority, Chattanooga, Tennessee, United States, necarriker@tva.gov

Abstract

Following the December 2008 rupture of a coal fly ash retaining pond at the Tennessee Valley Authority (TVA) Kingston Fossil Plant near Harriman, Tennessee, a comprehensive monitoring effort was intiated to evaluate impact of the release on the surrounding aquatic environment. The sequential extraction procedure developed by Querol et. al [1] was utilized by TVA's contracted laboratory and by Appalachian State University (ASU) researchers to evaluate bioavailability of ash-related trace metals in sediments impacted by the release.

Sediment samples collected in 2009 were split and submitted to ASU and to TVA's contracted laboratory for sequential extraction and subsequent metals analysis. This paper presents a comparison of the laboratories' data using the same method.

In 2011, several of the 2009 sediment sampling locations were revisited; these 2011 sediment samples were subjected to sequential extraction by ASU following the same procedure as used for the 2009 samples. This paper also includes comparisons of the data for the 2009 and 2011 sediment samples collected at similar locations.

In 2011, TVA collected and homogenized surface sediment samples in bulk quantities at several locations for several purposes. Sub-samples were submitted to ASU for sequential extraction; these samples were air-dried prior to extraction and between extraction steps. TVA also submitted these surface sediment samples to TVA's contracted labroatory for sequential extraction; these samples were not dried prior to or during the extraction process. A third part of this paper compares sequential extraction data generated with and without drying prior to and during extraction.

Conclusion

This paper evaluates interlaboratory precision for the Querol et al. sequential extraction method; presents temporal trends in bioavailability for several locations; and evaluates the impact of the sampling, handling, and extraction environments on metals leaching during the sequential extraction process.

References

[1] Querol, X., Juan, R., Lopez-Soler, A., Fernandez-Turiel, J.L., Ruiz, C.R. (1996). Fuel **75**, 821-838.

Electron transfer and atom exchange among Fe and Mn phases

JONATHAN E. BACHMAN[1]*, DREW E. LATTA[2], MICHELLE M. SCHERER[1], AND KEVIN M. ROSSO[3]

[1]The University of Iowa, Civil and Environmental Engineering (*jonathan-bachman@uiowa.edu)
[2]Argonne National Laboratory, Biosciences (dlatta@anl.gov)
[3]Pacific Northwest National Laboratory, Chemical and Material Sciences (Kevin.Rosso@pnnl.gov)

Fe and Mn are both common redox-active metals in environmental systems, and Fe-Mn redox chemistry is an important consideration when predicting fate and transport of contaminants. Recent work has shown that electron transfer and atom exchange occurs between aqueous Fe(II) and Fe(III) oxides and results in extensive recrystallization both with and without secondary mineral formation [1]. It is unclear, however, whether similar redox processes occur among Fe and Mn phases that might result in incorporation and release of Fe in Mn oxides, or conversely, incorporation and release of Mn in Fe oxides. Furthermore, it appears unknown whether the reaction of aqueous Mn(II) with Mn oxides leads to similar atom exchange and recrystallization as has been observed for the reaction of aqueous Fe(II) with Fe(III) oxides [2].

We are exploring the mechanisms driving the redox reactions of Mn(II)/Fe-oxides, Fe(II)/Mn-oxides, and Mn(II)/Mn-oxides using 57Fe Mossbauer spectroscopy and isotope tracer approaches. We have found that Mn-incorporated in goethite is released in the presence of aqueous Fe(II), similar to what has recently been demonstrated for Ni in goethite [3]. These experiments will provide a more fundamental understanding of the reactivity at mineral-water interfaces, in addition to providing a model for trace metal incorporation and release in Mn and Fe oxides.

. [1] Gorski and Scherer (2011) Aquatic Redox Chemistry, **1071,** 315-343. [2] Handler *et al.* (2009) *Environmental Science & Technology* **43**. 1102-1107. [3] Friedrich *et al.* (2011) *Geology* **39**. 1083-1086

https://doi.org/10.1180/S0026461X00008434 Published online by Cambridge University Press

The Marmion Shear Zone: A kinematic study of Archean terrane boundaries

N. R. Backeberg[1*], C. D. Rowe[1]

[1] McGill University, Earth and Planetary Science, Montreal, Canada, nils.backeberg@mail.mcgill.ca (* presenting author)

Introduction

The Marmion Shear zone marks the Archean terrane boundary between the ~3.003 Ga Marmion tonalite-trondhjemite-granodiorite (TTG) gneisses and the 2.931 – 3.003 Ga Finlayson Lake greenstone belt [1]. The shear zone is intruded by younger undeformed granites. They have not been dated, but petrologically similar units in the Eye Dashwa pluton have been dated at 2.665 Ga [1]. The low-grade (< 1 g/t) Hammond Reef gold deposit is hosted within a network of fractures and alteration zones parallel to the Marmion Shear within the Marmion gneiss and *not* in a major fault or shear zone at the boundary nor within the mafic greenstone belts as seen in most Archean gold deposits, for example in Abitibi [2,3].

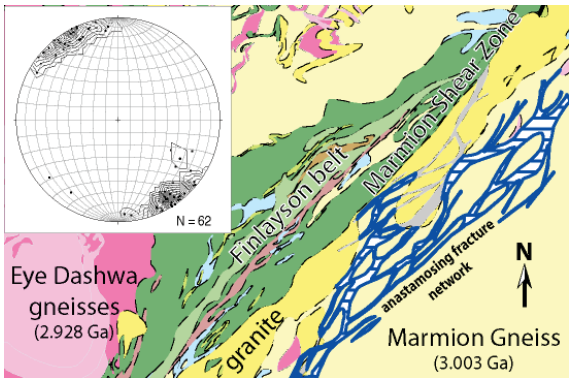

Figure 1: Geological map of the Marmion Shear area [1], showing the location of the anastamosing fracture and alteration zone (blue). The shear zone is intruded by a granite (yellow). Stereonet shows poles to flattening foliation (N = 62) across the Finlayson belt (green).

Preliminary Results and Observations

The Finlayson belt is divided into three parallel belts with different inherited ages (2.931 – 3.003 Ga [1]). At exposure level the belts are parallel to the northeast structural grain of the Marmion Shear (Figure 1). Penetrative flattening foliation is developed across the Finlayson belt (Figure 1). There are no spatial gradients in the strength of the foliation, which deforms all discontinuous lenticular lithologic units. Displaced lithologic unit boundaries demonstrate the presence of discrete faults.

The younger granite crosscuts the shear zone and ductile fabrics in the Marmion Gneiss, and has no penetrative deformation fabrics. It obscures the core of the shear zone. The deformation fabrics in both terranes bounding the Marmion Shear show a transition from ductile to discrete brittle structures, suggesting a common deformation path. The distinct anastamosing fracture network and zone of alteration which hosts the gold in the Marmion Gneiss is not seen in the Finlayson belt. This may be attributable to preferential fracturing and fluid migration within the gneiss during ore formation.

[1] Stone (2008) *Ontario Geological Survey Preliminary Map.* [2] Vearncombe (1998) *Geology* **26 (9)**, 855-858. [3] Wyman *et al.*, (1999) *Journal of Geology* **107**, 715-725

A cooling history for the Nicola Horst, British Columbia.

David Bacque[1*] and Bernard Guest[1]

[1]University of Calgary, Calgary, Canada, dpbacque@ucalgary.ca (* presenting author)

Introduction

The Nicola Horst (NH), is located in the Intermontane belt of British Columbia. It is bound along the east and west by steep post-Paleocene faults [1] (Fig 1). The faults are boundries between undeformed, low grade metamorphic rocks and deformed medium grade metamorphic rocks within the NH [2]. It has been suggested by some authors that the medium grade rocks are mid-crustal and are part of an antiformal thrust duplex [2,3]. The medium grade rocks, amphibolite facies, became exposed via unroofing along the steep post-Paleocene faults. This study aims to determine both the timing of the faults and model the isostatic response caused by the unroofing along the steep post-Paleocene faults using thermochronometry.

Thermochronology and geochronology

Most of the ages gathered in and around the NH have been for determining the absolute ages (geochronology) of the rocks. To understand how the NH formed, we are using thermochronometry, which records various closure temperatures depending on the mineral and system. Previous work done by Simon Fraser University produced four, unpublished, biotite Ar-Ar ages (50.3, 50.3, 56.5, 63.8 Ma, located in the northern, western, eastern, and southern areas respectively). Our samples (Fig 1) are located along a horizontal transect in the central area of the NH and along a vertical transect in the southern area of the NH. These samples are collected for purposes of producing a complete suite of ages, spanning temperatures from 900-60°C. By comparing cooling curves around the NH to ones within, we will determine a better age of the faults around the NH and model the response of the mid-crustal rocks exposed in the NH to the unroofing along the two post-Paleocene faults.

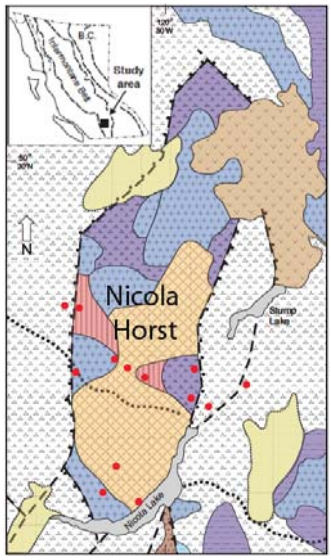

Figure 1: Nicola Horst is located in south central British Columbia. Blues, purples and red are Jurassic, Triassic and older, respectively. Browns, tans and yellows are Eocene, Tertiary and Quaternary, respectively. Red dots indicate locations of samples collected. Image modified from [2].

[1] Monger and McMillan (1989) *Geologic Survey of Canada* **Map 42-1989**. [2] Moore and Pettipas (1990a) *Ministry of Energy, Mines and Petroleum Resources* Open file **1990-29**, 3-13. [3] Erdmer, Moore, Heaman, Thompson, Daughtry, and Creaser (2001) *Canadian Journal of Earth Science* **39**, 1605-1623.

https://doi.org/10.1180/S0026461X00008434 Published online by Cambridge University Press

The importance of accurate and precise temperature reconstruction for alkenone paleobarometry

MARCUS P. S. BADGER[1*], RICH D. PANCOST[2]

[1]Department of Earth Sciences, University of Bristol, Wills Memorial Building, Queen's road, Bristol, BS8 1RJ, U.K., marcus.badger@bristol.ac.uk (* presenting author)

[2]Organic Geochemistry Unit, Bristol Biogeochemistry Research Centre, University of Bristol, Cantock's close, Bristol, BS8 1TS, U.K., r.d.pancost@bristol.ac.uk

By measuring the carbon isotope ratio of long chain ketones produced by haptophyte algae (alkenones) the isotope fractionation during photosynthesis (ε_p) can be determined. Fractionation is dependent on the concentration of carbon dioxide in surface waters, thus, past atmospheric CO_2 can be reconstructed. Recent studies have successfully applied this technique at across several intervals of rapid climatic change in the Cenozoic [1-4], and efforts have been made to use alkenone paleobarometry to constrain climate (or Earth system) sensitivity [2].

Several factors are important to the accurate and precise determination of atmospheric CO_2; for example, recent work has focussed on the effect of changes in algal cell size [5, 6]. However, reconstructions are also highly dependent on the accurate and precise determination of sea surface temperature (SST), as this effects both the determination of ε_p from alkenone $\delta^{13}C$ values, and the conversion of $[CO_2]_{(aq)}$ to atmospheric pCO_2. This has become of paticular importance given the multitude of proxies now applied to the reconstruction of SST, and uncertainty about exactly what each proxy represents.

Here we assess the sensitvity of alkenone pCO_2 estimates to innaccurate and/or inprecise SST reconstructions using new high resolution data from the Pliocene, and investigate the possible implications for previously published records. We highlight the importance of these results, especially the revised uncertainties of paleo-pCO_2 estimates, to understanding climates of the past and estimating climate sensitivity (or Earth system sensitivity) for models of the future.

[1] Bijl et al., (2010) *Science* **330,** 819-821. [2] Pagani et al., (2010) *Nature Geosciences* **3**, 27-30. [3] Seki et al., (2010) *EPSL* ***292,*** *201-211*. [4] Pagani et al., (2011) *Science* **334**, 1261-1264. [5] Henderiks and Pagani (2007) *Paleoceanography* **22**, PA3202. [6] Plancq et al., (2012) *Paleoceanography* **27,** PA1203.

The Major Element Composition of Earth's Core

JAMES BADRO[1*], JOHN BRODHOLT[2], ALEXANDER COTE[1,2]

[1]IPGP, Paris, France, badro@ipgp.fr (* presenting author)

[2]UCL, London, UK, j.brodholt@ucl.ac.uk

Earth's core formed as a results of a major chemical differentiation event; the melting of accretionary building blocks (meteorites, planetesimals, protoplanets) leads to a separation of the metal from the silicate, ensued by a gravitationally-driven segregation of a dense metal-rich core at the centre of the planet, with the lighter buoyant silicates remaining on top to form the mantle and crust. The bulk composition of the core depends on the path and conditions (pressure, temperature, redox) at which core formation took place; the process also leaves an imprint on the residual bulk silicate Earth, a record that is observable in present-day mantle rocks.

Constraining experimental and theoretical data with geophysical (core density and velocity profiles) observations provides a robust way to estimate the present day composition of the core, as well as the conditions under which it formed.

We will present results obtained from ab initio molecular dynamics calculations to estimate outer-core density and seismic velocity, and combine it with mineral physics on the inner core to define a range of possible compositions of the core that satisfies the observations. We will interpret these results and propose a consistent compositional model, and formulate plausible scenarios for core formation.

https://doi.org/10.1180/S0026461X00008434 Published online by Cambridge University Press

Lower crustal Archaean rocks in South-East Greenland

LEON BAGAS[1], TOMAS NÆRAA[2*], BARRY L. RENO[2,3], JOCHEN KOLB[2]

[1] Centre for Exploation Targeting, University of Western Australia Perth, Australia
[2] Geological Survey of Denmark and Greenland, Copenhagen, Denmark, tomn@geus.dk (*presenting author)
[3] Institute for Geography and Geology, University of Copenhagen, Denmark

The Skjoldungen region in South-East Greenland is characterised by felsic gneisses and granites that often contain abundant mafic and ultramafic inclusions (agmatitic) with only minor amounts of mainly mafic but also ultramafic gneisses occurring in narrow belts. The gneisses are commonly migmatitic and mafic gneisses often contain abundant intrusive felsic sheets. The gneissic basement is intruded by a ca. 2.7 Ga alkaline complex and preliminary age data suggest that regional migmatisation occurred during a period from 2.8 to 2.7 Ga [1].

The mafic gneisses group into calc-alkaline and tholeiitic suites, suggesting a heterogeneous mantle source. The felsic gneisses divide into a group with a adakite-like composition and a group characterised by large positive Eu anomalies and often depleted and fractionated HREE. Felsic gneisses formed during at least two stages: 1) an early phase of crustal differentiation of a mafic proto-crust possibly starting at ca. 2.86 Ga and, 2) a late stage related to crustal thickening and remelting which seems to relate to a prolonged stage of high grade metamorphism at ca. 2.8-2.7 Ga [1]. The regional crust is dominated by granites formed during the second stage. The early felsic gneisses have adakitic chemistry and aparrantly formed in the presence of residual garnet whereas the later felsic gneisses formed from an already differentiated lower crust with accumulated plagioclase. The tectonic setting during the early crust forming episode is envisaged to range from a magmatic-arc to the mid-ocean ridge setting. The later stage probably occurred during crustal thickening in a collision orogen involving the root zone of a magmatic arc at the base of the crust (Fig. 1).

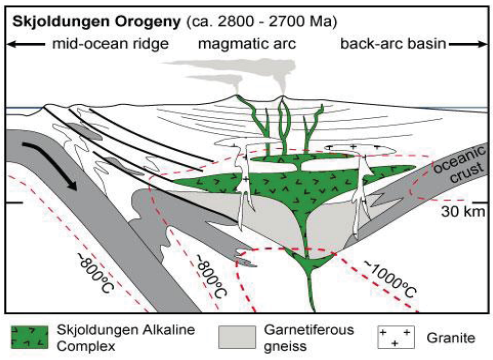

Figure 1: Model for the formation of the protoliths for gneisses in southeastern Greenland

[1] Kolb, J., Thane, K., Bagas, L., in review. Tectonometamorphic and magnetic evolution of high-grade Neo- to Mesoarcharan rocks of South-East Greenland. Gondwana Research.

Bacterial communities in drainage from waste-rock test piles

BRENDA L. BAILEY[1*], DAVID W. BLOWES[1], W. DOUGLAS GOULD[2], LESLIE SMITH[3] AND DAVID C. SEGO[4]

[1]University of Waterloo,Waterloo, Canada, blbailey@uwaterloo.ca
[2]Natural Resources Canada, Ottawa, Canada
[3]University of British Columbia, Vancouver, Canada
[4]University of Albert, Edmonton, Canada
(* presenting author)

Sulfide mineral oxidation is catalysed by microorganisms, increasing oxidation rates by orders of magnitude, releasing SO_4, Fe and H^+ [1]. Sulfide mineral oxidation rates decrease with decreasing temperature. Seasonal temperature fluctuations influence the rate of release of sulfide oxidation products from waste rock stockpiles over time [2]. Iron and sulfur oxidizing bacteria contribute to the oxidation of mine tailings in Arctic environments at temperatures as low as -11°C [2,3]. Yet, limited information exists on the importance of bacterially-catalysed oxidation of sulfide minerals in waste-rock stockpiles and their role in the generation of acid mine drainage in Arctic conditions.

Two large-scale waste-rock test piles, one with 0.035 wt. % S (Type I test pile) and another with 0.058 wt. % S (Type III test pile), located in the continuous permafrost region at the Diavik Diamond Mine were studied to examine the role of microoganisms in the biochemical evolution of test-pile drainage. Three groups of bacteria in test pile drainage were quantified using most probable number techniques [4] for neutrophilic and acidophilic sulfur oxidizers (SOBn and SOBa, respectively), and iron oxidizers (IOB). The media compositions, incubation conditions, and enumeration procedure are described in detail by Hulshof et al. [5]. The monitoring of populations present in test-pile drainage began in 2007 and a microbial succession was observed over time.

Drainage from the Type I test pile maintained a near neutral pH with low concentrations of SO_4 and Fe for the duration of this study. A population of SOBn was present from 2009 through 2010, with the exception of one sample in September 2010. Acidophilic sulfur oxidizers were only detected at very low numbers ($< 10^2$ bacteria/mL). IOB were detected in June 2009 and late 2010, but at low numbers ($< 10^3$ bacteria/mL).

Every year, the pH of the drainage from the Type III test pile decreased from near neutral in May to acidic conditions by October. Concentrations of SO_4 increased with decreasing pH. A population of SOBn were observed in the Type III test-pile drainage in 2008, however, population numbers decreased in late 2009 as the pH decreased. Acidophilic S oxidizers were only detected in 2009 after the drainage pH had decreased. In addition, the population of IOB increased with decreasing pH.

These results suggest bacteria populations evolved with changes in the drainage chemistry. Continued monitoring with more detailed analysis is required to better understand the biogeochemical evolution of these waste-rock test piles.

[1] Kirby et al. (1999) *Applied Geochemistry* **14**, 511-530.
[2] Elberling et al. (2000) *J. Contam. Hydrology* **41**, 225-238.
[3] Leduc et al. (1993) *FEMS Microbiology Letters* **108**, 189-194
[4] Cochran (1950) *Biometrics* **6**, 105-116.
[5] Hulshof (2006) *Water Research* **40**, 1816-1826.

https://doi.org/10.1180/S0026461X00008434 Published online by Cambridge University Press

Geodynamic regimes of intra-oceanic subduction: Thermomechanical modeling of geochemical signatures

B. BAITSCH GHIRARDELLO[1*], A. STRACKE[2], AND T.V. GERYA[1]

[1]ETHZ, Switzerland, Institut f. Geophysik (*), baitsch@erdw.ethz.ch

[2]Westfälische Wilhelms-Universität Münster, Institut f. Mineralogie, Germany, stracke.andreas@uni-muenster.de

The aim of this study is to investigate isotope signatures in different geodynamic regimes of intra-oceanic subduction processes with our 2D coupled geochemical-petrological-thermomechanical numerical model (I2ELVIS). We investigated systematically influences of fluid and melt weakening effects, which are responsible for the degree of plate coupling/decoupling and the mechanical strength of the overriding plate. Based on results of systematic experiments we distinguish the following three geodynamic regimes a) retreating regime, b) stable regime and c) advancing regime.

a) Retreating subduction regime is characterized by a strong rheological weakening of the overriding plate mantle by hydration/serpentinization and melt propagation processes. A necking of the (fore) arc causes the onset of decompression melting in the mantle wedge. Differently to the isotope signatures in the magmatic arc, decompression melting causes a MORB-like isotope signatures in the newly formed crust.

b) The volcanic rocks in a stable subduction regime are mainly produced from the subducted oceanic crust and molten hydrated mantle. Some of the stable subduction regimes are characterized by development of a broad area of subduction mélange in which subducted basaltic crust is strongly mechanically mixed with the serpentinized fore-arc mantle. These intense mixing is promoted by increased degree of fluid related weakening. The correspondent isotopic signature in the arc depends on the degree of fluid related weakening that controls intensity of flux melting.

c) Advancing subduction regime develops under condition of notably reduced fluid-related weakening that results in strong coupling between the plates in the fore-arc region. Strong coupling between plates produces large stresses that are able to overcome the mechanical resistance of the serpentinized fore-arc mantle that starts to subduct together with the plate. Large amount of new basaltic crust forms at the surface as the result of enhanced fluid-fluxed melting of the mantle wedge that coins the isotope signature of the arc.

Diffusion of water through quartz: a fluid inclusion study

RONALD J. BAKKER*, MIRIAM BAUMGARTNER, GERALD DOPPLER

Resource Mineralogy, University of Leoben, Austria, bakker@unileoben.ac.at (* presenting author)

Introduction

Diffusion of H_2O through minerals, such as quartz, that do not incorporate water at regular lattice positions is of major importance to understand fluid-rock interaction processes in deep rock, and to interpret fluid inclusion studies. The outcome of a variety of re-equilibration experiments with natural and synthetic fluid inclusions indicate that diffusion of H_2O plays an important role in these processes. Diffusion coefficients of H_2O in nominally anhydrous minerals were experimentally estimated from H_2O molecules (or part of these molecules) that replace oxygen at regular lattice positions in silicates, and which positions were detected in quenched samples after re-equilibration experiments.

Experiments

The properties of fluid inclusions in quartz can be relatively easily obtained from a variety of analytical techniques. Fluid inclusions can be regarded as constant volume containers inside a crystal lattice, which are more or less protected by the surrounding crystal from material exchange with rock pore volumes. Any change in fluid inclusion density and compositions is directly the result of diffusion processes. The exchange of fluid components in our experiments is provoked at high temperatures and pressures. Deoendent on experimental conditions, time, fluid inclusion size, and distance of fluid inclusions to the grain boundary, a variety of compositional changes are detected. similar effects are observed in assembalges of ynthetoc and natural fluid inclusions in quartz.

Conclusions

Concentration profiles based on fluid inclusion composition and density are not confirm diffusion coefficients obtained by altered isotopic compositions of quartz grains (i.e. the traditional technique to trace water in quartz). This illustrates that the mobility of H_2O in quartz must be a complex interaction of bulk diffusion and other processes suh as micro-crack enhanced or dislocation-enhanced diffusion. The reliability of natural fluid inclusions in metamorphic rock to determine rock-forming conditions can only be improved if these re-equilibration processes are fully understood.

https://doi.org/10.1180/S0026461X00008434 Published online by Cambridge University Press

Ice, but no fire: a new depositional age for the Rapitan Group, Canada

GEOFFREY J. BALDWIN[1*], ELIZABETH C. TURNER[1], AND BALZ S. KAMBER[2]

[1]Laurentian University, Department of Earth Sciences, Sudbury, ON, Canada, gj_baldwin@laurentian.ca (* presenting author), eturner@laurentian.ca

[2]Trinity College Dublin, Department of Geology, Dublin, Ireland, kamberbs@tcd.ie

The timing and causes of the glacial events associated with the 'Snowball Earth' hypothesis remain contentious. The earliest of these events, the Sturtian glaciation, has returned U-Pb zircon and Re-Os black shale ages from 740 Ma to as young as 660 Ma. Recently, strata correlated with the glaciogenic Rapitan Group of NW Canada have been dated at 716.47±0.24 Ma [1]. This supported a genetic correlation of the Sturtian glaciation and the Rapitan Group with the Franklin large igneous province (LIP), suggesting that the Sturtian glaciation may have been triggered by excessive CO_2 drawdown by weathering of this LIP – the 'fire and ice' model [1,2]. This model relies on penecontemporaneous emplacement of the LIP, its weathering, and Rapitan Group glacial onset at low latitudes. Here we present a new age for detrital zircon from the Rapitan Group itself. The sample was extracted from cross-bedded sandstone underlying the Rapitan iron formation by 75 m. A large number of zircon were pilot dated by LA-ICP-MS on double-sided tape and the youngest were then dated by high-precision ID-TIMS (see diagram). A coherent population of 8 grains defines a concordia age of 711.34±0.25 Ma. This is the new maximum age for deposition of the Rapitan Group and for the Sturtian glaciation in the region, and is consistent with Re-Os dates from shales overlying other Sturtian glacial deposits [3]. Significantly, it is a full 5 million years younger than the Franklin LIP, a span of time that is too long to support the 'fire and ice' model. The Rapitan Group may have been erroneously correlated with similar nearby strata. It is also possible that global 'Sturtian' glacial deposits were not the result of a single glacial episode.

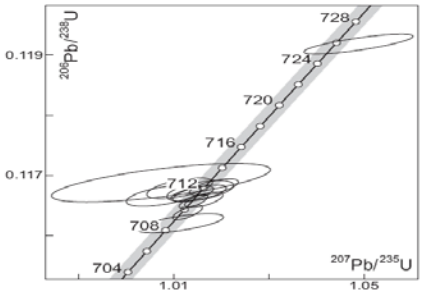

Figure 1: U-Pb concordia diagram for detrital zircon from the Rapitan Group, Canada. N=12, eight grains yielded a mean age of 711.34±0.25 Ma (MSWD = 2.0).

[1] Macdonald *et al.* (2010) *Science* **327**, 1241-1243. [2] Goddéris *et al.* (2003) *Earth Planet. Sci. Lett.* **211**, 1-12. [3] Rooney *et al.* (2011) *Precamb. Res.* **185**, 202-214.

Reconstruction of *P-T* paths in polymetamorphic rocks of the Clearwater core complex, northern Idaho

JULIA A. BALDWIN [1*] AND VICTOR E. GUEVARA[1]

[1]Dept. of Geosciences, University of Montana, Missoula, MT, 59812, USA, jbaldwin@mso.umt.edu (* presenting author), victor.guevara@umontana.edu

Understanding where, when, why, and how metamorphic core complexes form in settings of continental shortening is important because these features are part of the rock record of deformation. Moreover, core complexes provide the most direct observational information about the relationship between the middle and uppermost crust in the late stages of orogenesis, so offer a valuable opportunity to investigate crustal coupling and mass transfer within continental crust.

In the northern U.S. Rockies, core complexes show a prolonged metamorphic history, lie inboard of the $^{87}Sr/^{86}Sr$ 0.706 line, and are spatially associated with major Cordilleran batholiths. Peak metamorphic conditions are amphibolite facies, with maximum crustal depths of around 25-35 km in the most deeply exhumed complexes. Metamorphosed footwall rocks include units within Proterozoic crystalline basement as well as the sediments of the overlying Mesoproterozoic Belt Supergroup. Widespread extension occurred 59-40 Ma, with several core complexes recording an initial rapid phase of extension at *c.* 49-48 Ma followed by more protracted exhumation. The focus of this paper is on characterization of polymetamorphism in the Clearwater metamorphic core complex (CMCC) located in northern Idaho, which contains a history of both Proterozoic and Cretaceous-Eocene tectonometamophic events.

Metamorphic events in rocks within the CMCC range from Paleoproterozoic basement formation, Mesoproterozoic crustal thickening, and Cretaceous convergence, magmatism, and final exhumation in the Eocene. The samples focused on in this study are pelitic and unusual Mg-Al-rich schists from both within the high grade core of the complex, as well as schists that lie west and east of the bounding detachments. Previous work has indentified three major metamorphic events in the area [1]. The first has recently been correlated with Mesoproterozoic (1.3 Ga) crustal thickening based on Lu-Hf garnet dating [2]. Rocks also show evidence for a 1.1 Ga event. Zircon rims indicate Cretaceous to Eocene metamorphism in pulses from 82-80, 74-72, 64, and 59-55 Ma [3]. The younger dates likely correspond to fluid migration during exhumation of the complex. Here we present results of pseudosection modeling and garnet compositional isopleth thermometry to place contrainsts on the complex polymetamorphic history of these rocks. The Cretaceous to Eocene history is best preserved in multi-stage garnet microstructures with diffuse high Ca – low Mn rims, rutile converting to ilmenite, pre-kinematic staurolite, and abundant andalusite and sillimanite after kyanite, particularly in rocks within Eocene shear zones.

[1] Grover et al. (1992) *American Journal of Science*, **292**, 474-507. [2] Nesheim et al. (2012) *Lithos*, **134-135**, 91-107. [3] Doughty et al. (2007) *GSA Special Paper,* **434**, 211-241.

https://doi.org/10.1180/S0026461X00008434 Published online by Cambridge University Press

Coping with Oxygen: Peroxy defects in Rocks and the survival of bacteria

MELIKE BALK[1*], PAUL MASON[1], ALFONS J.M. STAMS[2], FRIEDEMANN FREUND[3,4], AND LYNN ROTHSCHILD[3]

[1] Department of Earth Sciences, Utrecht University, (m.balk@uu.nl, presenting author* and p.mason@uu.nl), [2]Laboratory of Microbiology, Wageningen University (fons.stams@wur.nl) [3]NASA Ames Research Center, Moffett Field, CA, (Lynn.J.Rothschild@nasa.gov), [4]SETI Institute, Mountain View, CA (friedemann.t.freund@nasa.gov).

An oxygen-rich atmosphere appears to have been a prerequisite for complex life to evolve on Earth and possibly elsewhere in the Universe. The question is still shrouded in uncertainty how free oxygen became available on the early Earth. Here we study processes that introduce peroxy defects into silicate minerals which, upon weathering, result in oxygen formation in an initially anoxic subsurface environment. Reactive Oxygen Species (ROS) are precursors to molecular oxygen during this process. Due to their toxicity they may have strongly influenced the evolution of life. ROS are generated during hydrolysis of peroxy defects, which consist of pairs of oxygen anions. A second pathway for formation occurs during (bio) transformations of iron sulphide minerals. ROS are produced and consumed by intracellular and extracellular reactions of Fe, Mn, C, N, and S species. We propose that despite an overall reducing or neutral oxidation state of the macroenvironment and the absence of free O_2 in the atmosphere, microorganisms on the early Earth had to cope with ROS in their microenvironments. They were thus under evolutionary pressure to develop enzymatic and other defences against the potentially dangerous, even lethal effects of ROS and oxygen.

We have investigated how oxygen might be released through weathering and test microorganisms in contact with rock surfaces and iron sulphides. Our results show how early Life might have adapted to oxygen. Early microorganisms must have "trained" to detoxify ROS prior to the evolution of aerobic metabolism and oxygenic photosynthesis. A possible way out of this dilemma comes from a study of igneous and high-grade metamorphic rocks, whose minerals contain a small but significant fraction of oxygen anions in the valence state 1- , forming peroxy links of the type $O_3Si\text{-}OO\text{-}SiO_3$ [1, 2]. As water hydrolyzes the peroxy links hydrogen peroxide, H_2O_2, forms. As a result, microorganisms attached to mineral grains will be exposed to a constant trickle of ROS from the H_2O_2 production. Many different groups of microorganisms are able to grow or survive in the presence of ROS.

[1] Balk et al. (2009) *Earth and Planetary Science Letters* **283,** 87-92. [2] Grant, R. A. *et al.* (2011) *Int. J. Environ. Res. Public Health* **8**, 1936-1956.

Impact of fungi and bacteria on the mobility of metals (Fe, Al) in podzolic soils

C. BALLAND-BOLOU-BI*, S. J. M. HOLMSTRÖM, N. G. HOLM

Stockholm University, Dept. of Geological Sciences, Stockholm, Sweden (*Clarissebolou-bi@geo.su.se)

Mineral weathering is a key process in soil leading to leaching and release of essential elements (Fe, Al), which sustain plant growth and determine the chemistry of soil solutions and exchange complex. Soil microorganisms (fungi and bacteria) play a major role in the availability of nutrients in soils. They participate in weathering of primary materials through the production of low-molecular organic molecules (siderophores and organic acids). Determination of their relative contribution and understanding their interaction with soil minerals through different mechanisms is a key step toward characterization of the mobility of metals and identification of the pedogenic processes in action.

Recent techniques of *in situ* dynamic sensor have been developed to assess bioavailable fractions of metal in soil according to different relevant time scales of environmental processes. Diffusive gradients in thin films (DGT) are one of these speciation analyses [1]. This technique allows to establish a permanent flux of labile metal through a gel and then to measure the labile concentration upon its deployment time (i.e. the labile fraction corresponds to free metals in solution and metals linked to inorganic and organic ligands). In order to identify different weathering agents implied on the mobility and speciation of metals (Fe and Al) in soil solutions both in field studies and laboratory experiments, we have deployed DGT and DET (Diffusive Equilibrium in Thin Film) in different horizons of a podzol (developed on granitic rocks) on Norunda Site (Sweden) in November 2011. In parallel, we lead several experiments of geological material (granite) bioweathering to investigate the impact of fungi and bacteria on the release of Fe and Al from granite. To characterize mechanisms of dissolution, we monitored low-molecular organic molecules produced by microorganisms, microbial biomass, pH, and free and labile iron and aluminium fraction released by combining DGT and DET techniques.

The comparison of the results between field studies and laboratory experiments will permit the improvement of our knowledge of the contribution of microorganisms on the bioavailability of metals in soils and also on the podzolisation process that remains still always debated.

[1] Zhang *et al.,* (2001) *Env. Sci. Technol.,* **35**, 2602-2607.

https://doi.org/10.1180/S0026461X00008434 Published online by Cambridge University Press

The oldest isolated life-bearing macrosystem on the planet?

C.J. BALLENTINE[1]*, G. HOLLAND[1,2], G.F. SLATER[3], L. LI[4], G. LACRAMPE-COULOUME[4] AND B. SHERWOOD LOLLAR[4]

[1]University of Manchester, UK, chris.ballentine@manchester.ac.uk
[2]University of Lancaster, UK, g.holland@lancaster.ac.uk
[3]McMaster University, Hamilton, Canada, gslater@mcmaster.ca
[4]University of Toronto, Toronto, Canada, bslollar@chem.utoronto.ca
(* presenting author)

Water bearing macrosystems that have been isolated from the surface, preserved on geological timescales (>10Ma) and capable of supporting life, are seemingly rare. The only study of its type is now established in the South African Precambrian Crystalline Shield [1, 2]. The Witwatersand Basin provides the case type study and a unique insight into the evolution of chemolithotrophic life, the ability of even the most nutrient poor environments to support life in extremis, and thus environments that may support life on other planets [2]. The stable isotopic composition of the water, showing a high degreee of water-rock interaction, allows the inference of isolation from surface waters and a long residence time. It is the in-situ buildup of radiogenic noble gases (e.g. ^{4}He, ^{21}Ne, ^{40}Ar, ^{136}Xe) that has provided the basis for quantifying how long this system may have been isolated from the surface [1]. An outstanding question is how rare are such systems?

We have determined the noble gas concentration and isotopic composition of 6 gas samples, co-produced with water, from deep exploratory boreholes in a producing mine in the Timmins region of the Canadian Precambrian Crystalline Shield. Neon isotopic compositions are similar to the Witwatersand study and used to validate the closed system assumption for the radiogenic noble gases [1]. Using a similar model to [1], modified for local conditions (2.8ppm U, 10.6ppm Th, 3.4% K and 1% porosity and 100% release efficiency), we calculate closed system noble gas ages of the free produced fluids to be between 650Ma to 1.5Ga. These are the oldest 'free water' yet found in a crustal system.

Multi-collector noble gas mass spectrometry provides an order of magnitude more precision in the isotope determination of some free fluids [3]. We also resolve in all samples a clear ^{129}Xe signal in excess of atmospheric values. We can discount mass fractionation mechanisms and need to identify the source of the ^{129}Xe enrichment, only ever observed before in mantle-derived terrestrial fluids. ^{3}He/^{4}He allows us to discount a significant magmatic fluid source. Similarly, U-fission Xe (e.g. $^{132\text{-}136}$Xe) are produced at a known rate with fission ^{129}I (^{129}I → ^{129}Xe, t½=15.7Ma). The excess U-fission ^{136}Xe precludes a simple U-fission source for the ^{129}I → ^{129}Xe.

The ^{129}Xe excess observed is nevertheless most likely due to a local source of ^{129}I. We are collecting data to resolve two possible sources: i) U-fission ^{129}I released at steady state into the porewater through an extreme CFF (Chemical Fractionation of Fission products) process. CFF is required to prevent the associated fission Xe products reaching the porefluid and in turn would impact our previous assumption of 100% release efficiency and require older ages yet; or ii) the possibility of organic rich sediments associated with the formation lithologies supplying either the ^{129}I or its decay product (^{129}Xe). The latter would require a fluid closure date related to the last major mineralising event at 2.670Ga.

While the age determinations undgergo refinement with the new Xe information, our results nevertheless suggest that ancient and isolated macrosystems that have the potential to support life [2] may yet be found in a substantial portion of the Earth's Precambrian Crystalline Shields.

[1] Lippmann-Pipke et al. (2011) *Chemical Geology* **283,** 287-296.
[2] Lin et al. (2006) *Science* **314,** 479-482.
[3] Holland et al. (2009) *Science* **326,** 1522-1525.

Biotite Weathering in Watersheds of the Slavkov Forest, Czech Republic

Z. BALOGH-BRUNSTAD[1,2*], L. SACCONE[3,4], M.M. SMITS[5], C. BERNER[6], H. WALLANDER[6], T.J. MCMASTER[4], S.L.S. STIPP[1]

[1]NanoGeoScience, University of Copenhagen, Denmark (*correspondence: balogh_brunz@hartwick.edu)
[2]Hartwick College, Oneonta, NY, USA
[3]Institute for Forest Products Research, Edinburgh Napier University, Scotland, UK
[4]H.H. Wills Physics Laboratory, University of Bristol, UK
[5]Environmental Biology, Hasselt University, Belgium
[6]Microbial Ecology, Lund University, Sweden

Introduction and Methods

Biotite is one of the primary sources of potassium and magnesium in soils and is easily weathered by microbes and plants to access these nutrients. It is shown that ectomycorrhizal fungi play a significant role in mineral dissolution and nutrient translocation to their host plant. Numerous controlled laboratory experiments have demonstrated physical and chemical interactions of ectomycorrhizal fungi with biotite, ranging in scale from individual grains to artificial mineral soils. However, whether ectomycorrhizal fungi have a significant contribution to soil mineral weathering under natural forest conditions, remains controversial.

In our study, mesh bags containing 1 wt% small biotite flakes and one large freshly cleaved flake in quartz sand, were buried in spruce forest soils for two years at three sites where the bedrocks were serpentinite (K limited), leucogranite (Mg limited) and amphibolite (no limitations). The 60 µm mesh size allowed fungal hyphae to grow in the bags, but excluded direct plant root contact with the minerals, allowing us to test the direct contribution of ectomycorrhizal fungi on biotite weathering under naturally occuring K and Mg limitations. Mineral surfaces were examined with scanning electron microscopy (SEM) and atomic force microscopy (AFM). The total ectomycorrhizal biomass was determined by Ergosterol analyses.

Results and Discussion

Microscopy documented 5% or less direct fungal attachment to basal planes of biotite from all sites, with the lowest occurrence found at the low Mg site. The ergosterol results support these observations, with the lowest colonization of the bags at the low Mg site. Potassium limitation does not influence ectomycorrhizal colonizations. Shallow etched channels, similar to hyphae in size and branching pattern, are seen by AFM and SEM. These channels show short, segmented sections, i.e. a pulsive growth pattern and at each "pulse," the channel deepens in the direction of growth. We propose that this morphology reflects both chemical dissolution and physical force at the hyphal-mineral interface. However, abiotic processes, such as wear from sand grains rolling over biotite surfaces can produce similar patterns that are nearly indistinguishable from channels formed by hyphal activity.

Our observations from these field experiments support laboratory results, i.e., that fungal hyphae exercise both chemical dissolution and physical force at the hyphal-mineral interface, but abiotic processes cannot be excluded as an explanation for the formation of shallow channels on the soft biotite surfaces.

https://doi.org/10.1180/S0026461X00008434 Published online by Cambridge University Press

Aragonite – calcite seas and the evolution of biocalcification

UWE BALTHASAR[1*] AND MAGGIE CUSACK[1]

[1]University of Glasgow, School of Geographical and Earth Sciences, Glasgow, UK, uwe.balthasar@glasgow.ac.uk (* presenting author), maggie.cusack@glasgow.ac.uk

The influence of aragonite-calcite sea conditions on the evolution of biocalcification remain poorly understood. While selection for the polymorph favored by the aragonite-calcite sea status is relatively strong for organisms that evolved shells for the first time [1], there is no statistically significant correlation between shifts in the aragonitic/calcitic proportions in calcareous skeletons through time and sea chemistry [2]. However, case studies suggest that changes in aragonite/calcite sea conditions can influence the mineralogy of individual calcifying lineages [3].

A particularly intriguing group in this context is trimerellids, the only known group of aragonitic brachiopods [4]. With shells up to 20cm wide, trimerellids were also the most prolific calcifiers amongst brachiopods of the Ordovician/Silurian calcite seas. The success of trimerellids as measured by their large shell size and cosmopolitan distribution in the Ordovician/Silurian palaeo-tropics suggests that the innovation of aragonite during a calcite sea interval was advantageous for this group.

This success is best explained by considering the role of temperature on $CaCO_3$ polymorph formation. While the switch between aragonite and calcite sea conditions is commonly attributed to the ratio of Mg/Ca or pCO_2 [5, 6], it is often ignored that Mg/Ca controls the formation of aragonite and calcite as a function of temperature [7], with warmer temperatures favoring aragonite. When combining the values of marine Mg/Ca through time [5] with the Mg/Ca – temperature curve that separates aragonite from calcite precipitation fields [7] it becomes apparent that aragonite was the favored polymorph in warm tropical surface waters even during calcite sea intervals (Fig. 1).

Based on the available data [5, 7], water temperatures above 25° C favored the formation of aragonite even during calcite sea intervals (Fig. 1). The conventional view of aragonite/calcite sea conditions as a globally homogenous model needs to be reconsidered in the light of latitudinal surface water temperature differences.

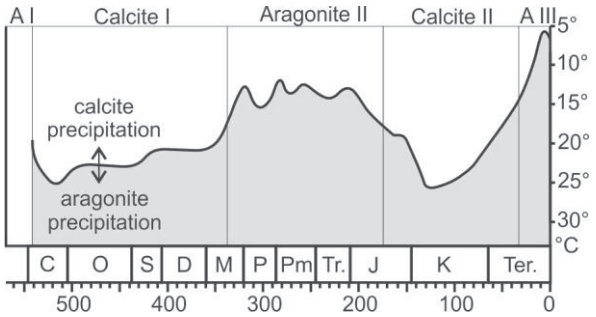

Figure 1: temperature separating the marine aragonite/calcite precipitation fields through time (from [4]; based on [5] and [7]).

[1] Porter (2010) *Geobiology* **8**, 256-277. [2] Kiessling et al (2008) *Nature Geoscience* **1**, 527-530. [3] Harper et al. (1997) *Geological Magazine* **134**, 403-407. [4] Balthasar et al. (2011) *Geology* **39**, 967–970. [5] Stanley & Hardy (1998) *Palaeogeography, Palaeoclimatology, Palaeoecology* **144**, 3-19. [6] Zhuravlev & Wood (2009) *Geology* **37**, 1123-1126. [7] Morse et al. (1997) *Geology* **25**, 85-87.

A transferable classical polarizable model for the water molecule

ANDRÁS BARANYAI[1*] AND PÉTER T. KISS[2]

[1]Eötvös University, Institute of Chemistry, Budapest, Hungary bajtony@chem.elte.hu (* presenting author)

[2]Eötvös University, Institute of Chemistry, Budapest, Hungary peter.kiss.20@gmail.com

The model

We developed a new model for the water molecule, which contains only three Gaussian charges. Using the gas-phase geometry, the dipole moment of the molecule matches, the quadrupole moment closely approximates the experimental values. Two positive charges are on the hydrogen atoms, while the negative charge is connected by a harmonic spring to its gas-phase position. This position is on the main axis of the molecule between the oxygen and the hydrogen atoms. The polarized state is established by the equality of the electrostatic forces and the spring force of the negative charge. In each time step the position of the massless negative charge is determined by iteration.Using the technique of Ewald summation, we derived expression for the energy, the forces, and the pressure for Gaussian charges. The dispersion interactions were fitted [1].

Tests of the new model

The model was tested and provided good results for the properties of gas-phase clusters up to 6 molecules, ambient water and hexagonal ice [1]. We calculated the properties of ice polymorphs under high pressure as well. In moderatly dense phases the closest O-O distances are very close to the same distances in hexagonal ice. In compressed phases, however, the number of neighboring molecules in the second shell is larger than in hexagonal ice. To use a repulsion suitable for hexagonal ice gives low density for the compressed ice phases. We calculated the "compressing force" for each particle and connected a variable "size" to this force. With this approach we obtained agreement from water clusters to ice VII up to 25 GPa [2]. Relying on earlier studies, we devised a reasonable form for an electric field dependent polarizability of the molecules. At low fields the polarizability starts from the experimental gas-phase value towards a treshold at high fields. The decline of this function was determined by the calculated dielectric constant of ambient water [3]. The model was tested for liquid-vapor behavior. The surface structure of the model was analysed. Its surface tension provides superior estimates of the experimental value than nonpolarizable models [4]. The algorithm of the program code is given for the model. Due to different numerical speeding up methods, it is only 2.6 times slower than the code of the well-known TIP4P nonpolarizable model [5].

[1] A. Baranyai, P.T. Kiss, J.Chem.Phys.,**133**, 144109 (2010)
[2] P.T. Kiss, A. Baranyai, J.Chem.Phys., **134**, 214111 (2011)
[3] A. Baranyai, P.T. Kiss, J.Chem. Phys.,**135**, 234110 (2011)
[4] P.T. Kiss, M. Darvas, A. Baranyai, and P. Jedlovszky, J.Chem.Phys., submitted
[5] P.T. Kiss, A. Baranyai, and A.A. Chialvo, J.Comput.Chem., submitted

Acknowledgement: Support for AB during this work was given by OTKA fund K84382..

https://doi.org/10.1180/S0026461X00008434 Published online by Cambridge University Press

Probing iron oxide interactions with organic matter by X-ray spectroscopy.

ANDREW BARBER[1*], ALESSANDRA LERI[2], KARINE LALONDE[3] AND YVES GÉLINAS[4]

[1]Concordia University, Montréal, Canada, andrew.jack.barber@gmail.com (* presenting author)
[2]Marymount Manhattan College, New York, USA , alessandra.leri@gmail.com
[3]Concordia University, Montréal, Canada, k_lalonde@hotmail.com
[4]Concordia University, Montréal, Canada, ygelinas@alcor.concordia.ca

Abstract

Iron oxides have been shown to promote the preservation of 1/5th of the total organic carbon pool in marine sediments (1). These iron-organic matter phases are formed within the oxic layer of marine sediments through oxidation of dissolved iron(II) produced during weathering and diagenetic recycling (2). However, it remains unclear what type of interaction (adsorption of organic matter onto the surface of oxides or co-precipitation to form iron-organic complexes) is formed between iron and organic matter in these systems. In this work, iron oxides were synthesized by oxidizing a solution of Fe(II) in seawater at constant, near circumneutral pH to closely mimic natural environmental conditions. Synchrotron X-ray absorption techniques (XANES and EXAFS) were used to probe the local environment of iron using beamline X26A at the Brookhaven National Laboratory. We determined that iron oxides precipitated in the presence of organic matter have a shifted iron Kα edge with respect to organic free iron oxide minerals, demonstrating that iron-OM co-precipitates are likely a prevalent form of iron in sedimentary environments. Using this shift in Kα edge the approximate contribution from organic free iron oxides and organic rich mononuclear iron compounds of our synthetic Fe(III)-OM precipitates were determined using linear combination fitting.

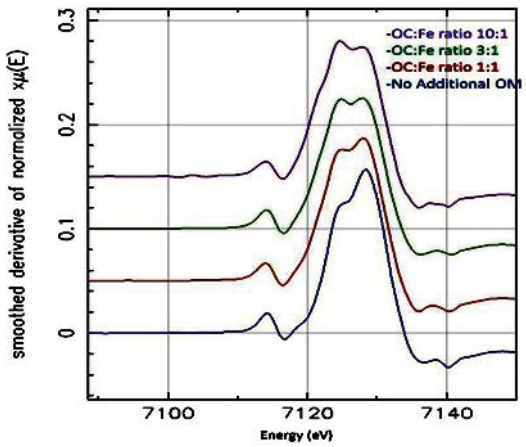

Figure 1: The first derivatives of stacked normalized iron Kα edge XANES spectra with OC:Fe ratios varying from 10:1 to 1:1.

[1] Lalonde et al. (in press) *Nature*. [2] Canfield, D. E. The geochemistry of river particulates from the continental USA: Major elements. (1997) *Geochim. Cosmochim. Acta* **61,** 3349–3365

Synchrotron radiation characterization of ferruginous bodies from human lung tissue

FABRIZIO BARDELLI[1*], ELENA BELLUSO[2], SILVANA CAPELLA[2], GIULIA VERONESI[3], AND LAURENT CHARLET[1]

[1]ISTerre, Grenoble, France, fabrizio.bardelli@gmail.com (* presenting author), charlet38@gmail.com
[2]Dipartimento di Scienze della Terra, Turin, Italy elena.belluso@unito.it silvana.capella@unito.it
[3]ESRF, Grenoble, France giulia.veronesi@esrf.fr

Introduction

Exposure to asbestos fibers is well known to be associated with respiratory diseases such, mesotheliomas and lung cancer. *FB* (**Figure 1**) are the result of a coating process, taking place in the host organism, of a variety of fibers such as asbestos (crocidolite, amosite, chrysotile) and phyllosilicate fibers (talc, mica, kaolinite), coal dust, oxalate, and fiberglass. This coating was generally accepted to be a protective mechanism produced by macrophages to segregate the cytotoxic fibers from the organic tissues [1]. However, more recently, other authors suggested that the coating material may enhance the cytotoxic properties of the asbestos fibers by increasing the production of free radicals [2,3,4,5,6]. In spite of the large attention devoted to this subject, the exact nature of the coating, along with the biological effect of *FB*, is still not clear. This is mainly due to the difficulty of sampling large enough amounts of *FB* using reliable isolation procedures, and to their microscopic dimensions (2-5 μm diameter, 20-90 μm length). The use of state of the art synchrotron radiation microprobe techniques gave the first direct characterization of single *FB*.

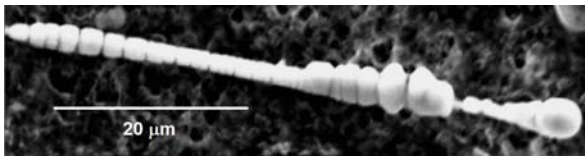

Figure 1: SEM image of a *FB* collected from human lung tissue.

Results and Conclusion

Human lung tissue rich in *FB*, owing to professional exposure, were collected from two subjects who were affected by lung cancer. μXRF high resolution elemental maps of *FB* (2 μm pixel size) were acquired on ID18F at ESRF, and μXANES spectra were recorded at selected points at the Fe edge on ID21. μXRF revealed that the external coating is mainly composed of Fe, Cu, Zn, and As (plus Ge and Ba in one subject) distributed in different areas of the *FB*, while μXANES gave the first direct confirmation that iron is mainly present as ferritine.

[1] Mace *et al.* (1980) *Cancer. Lett.*, **9**, 95. [2] Ghio *et al.* (2004) *Toxicologic Pathology*, **32**, 643. [3] Hardy *et al.* (1995) *Aust. Chem. Rev*, **90**, 97. [4] Lund *et al.* (1994) *Aust. Occup. Environ. Med.*, **51**, 200. [5] Pooley (1972) *Environ. Res.*, **5**, 363. [6] Pascolo *et al.* (2011) *Particle and Fibre Toxicology* **8**, 7.

https://doi.org/10.1180/S0026461X00008434 Published online by Cambridge University Press

Fe atom exchange between aqueous Fe^{2+} and hematite

MICHELLE BARGER[1*], KEVIN ROSSO[2], AND MICHELLE SCHERER[1]

[1]Civil and Environmental Engineering, University of Iowa, Iowa City, IA 52242(*correspondence: michelle-barger@uiowa.edu)
[2]Chemical and Materials Science Division, Pacific Northwest National Laboratory, Richland, Washington 99352

Recent work has revealed that Fe oxides are dynamic phases that will undergo significant Fe cycling in the presence of aqueous Fe(II) [1]. Complete exchange of Fe atoms between aqueous Fe(II) and goethite has been shown [2] and extensive exchange has also been observed for ferrihydrite and lepidocrocite [3]. Bulk electrical conduction linking oxidative adsorption of Fe(II) and reductive dissolution of the Fe(III) oxide at spatially separated sites has been suggested as a potential mechanism to explain the extensive exchange observed in the presence of Fe(II) [2; 4]. Interestingly, bulk electrical conduction linked to growth and dissolution has only been directly demonstrated in hematite, yet, ^{55}Fe isotope data indicate little exchange occurred between aqueous Fe(II) and hematite [3].

Here we are investigating atom exchange between aqueous isotope specific ^{57}Fe(II) and isotopically normal hematite to determine if exchange occurs between aqueous Fe(II) and hematite. Our working hypothesis is that the reaction of aqueous Fe(II) with hematite will result in significant Fe atom exchange and recyrstallization of hematite particles and that the rate of exchange will be influenced by particle size.

[1] Gorski and Scherer (2011) *Aquatic Redox Chemistry* **1071**, 315-343. [2] Handler *et al.* (2009) *Environ. Sci. Technol.* **43**, 1102-1107. [3] Pedersen *et al.* (2004)) *GCA* **43**, 3967-3977. [4] Yanina and Rosso (2008) *Science* **320**, 218-222. [5] Williams and Scherer (2004) *Environ. Sci. Technol.* **38**, 4782-4790.

Unravelling the crustal architecture of Cape Verde; the xenolith record

ABIGAIL K. BARKER[1*], DAVID NILSSON[1], VALENTIN R. TROLL[1], THOR H. HANSTEEN[2] AND ANDREAS KLÜGEL[3]

[1]CEMPEG, Department of Earth Sciences, Uppsala University, Uppsala, Sweden abigail.barker@geo.uu.se (* presenting author)
[2]IFM-GEOMAR, Dynamik des Ozeanbodens, Kiel, Germany
[3]Department of Earth Sciences, University of Bremen, Bremen, Germany

The Cape Verde submarine plateau was extensively sampled during the Meteor M80/3 research cruise in January 2010. The suite of sampled lavas are found to host a range of xenoliths. These xenoliths provide a spectrum of lithologies available to interact with magmas during transport through the lithospheric mantle and crust. Exploring the depths of origin of such xenoliths will complement the information we derive from the host lavas and thus the 3-D geochemical framework of magma-crust interaction in the Cape Verde magmatic plumbing systems. This will allow the development of a model for the crustal architecture beneath the Cape Verde oceanic plateau.

The host lavas are nephelinites containing clinopyroxene, nosean, nepheline, ± apatite, ± sanidine phenocrysts. The crustal xenoliths are mostly mafic plutonic assemblages with one sedimentary xenolith occurring. The mafic plutonic xenoliths are holocrystalline, and fine to medium grained. They contain plagioclase, clinopyroxene, olivine and/or amphibole. The sedimentary xenolith contains rounded grains of quartz, together with minor clay minerals, biotite and alkali feldspar.

Mafic plutonic xenoliths have developed reaction zones on contact with the host magma. The reaction zones are approximatley 50 to 100 microns and are observed petrographically by crystallisation of fine grained sericite, epidote and chlorite. Element mapping highlights the increase of Na and K and decrease in Ca and Al in the reaction zone compared to plagioclase of the xenolith.

REE profiles of clinopyroxenes in the host lavas are LREE enriched whereas clinopyoxenes from the plutonic xenoliths are LREE depleted. Modelling of REE melt compositions indicates the plutonic xenoliths are derived from MORB ocean crust opposed to intrusives of the Cape Verde plateau.

Mineral chemistry of the clinopyroxenes in the host lavas and xenoliths have been used to determine crystallization pressures. Thermobarometry indicates that clinopyroxenes in the host lavas formed at depths of 17 to 46 km[1], whereas those in the xenoliths formed at 5 to 15 km. This places the depth of origin of the plutonic xenoliths above the Cape Verde Moho and in the oceanic crust.

The xenoliths thus trace magma-crust interaction to the MORB oceanic crust and overlying sediments located beneath the Cape Verde submarine plateau. The spatial distribution and vertical representation provided by crustal xenoliths will help to develop a better idea of the 3-D architecture of the oceanic crust beneath the Cape Verde plateau.

[1] Barker et al., (2011) *Contrib. Mineral. Petrol.* doi: 10.1007/s00410-011-0708-2.

https://doi.org/10.1180/S0026461X00008434 Published online by Cambridge University Press

Laboratory CO_2 flow experiments to model hydrochemical and mineralogical changes in the Arbuckle aquifer during CO_2 storage

ROBINSON BARKER[1*], LYNN WATNEY[2], SAIBAL BHATTACHARYA[3], BRIAN STRAZISAR[4], LOGAN KELLY[1], SOPHIA FORD[1], SAUGATA DATTA[1]

[1]Kansas State University, Department of Geology, Manhattan, Kansas rbarker@ksu.edu (* presenting author)
[2] Kansas Geologic Survey, Lawrence, Kansas lwatney@kgsu.ku.edu
[3]Chesapeake Energy Corporation, Oklahoma City, Oklahoma saibal.bhattacharya@chk.com

[4]National Energy Technology Laboratory, Pittsburg, PA brian.strazisar@netl.doe.gov

The saline Arbuckle aquifer in south-central Kansas has been proposed for a pilot scale injection of CO_2 [1]. This paper presents characterization of Arbuckle mineralogy and hydrogeochemistry along with experimental flow cell data and geochemical modelling of CO_2 injection. Two wells (KGS 1-32 and 1-28) have been drilled to the basement to provide rock core and brine data for a site specific determination of the storage potential of the Arbuckle. Thin section and XRD data reveal dominant mineralogy in the injection zone to be dolomite with sporadic cherty nodules. Chert appears to replace dolomicrite and euhedral dolomite as well as infilling porosity. Porosity values range between 1.2 and 11.8% within the injection zone. Drill stem test water samples were collected from 8 depths (3677, 4182, 4335, 4520, 4876, 4927, 5036, 5183 ft) to describe the changing brine chemistry with depth. Sulfate peaks at 4876' and 4927' may be indicative of microbial action at these depths. Chemical analysis show a hyper saline brine (~50,000 - 190,000 TDS) dominated by Cl, Na and Ca. Elemental ratios of Cl:Br, Na:Cl and Ca:Sr are what is expected of a typical saline aquifer system [2]. Major and trace elemental chemistry suggest the brine originated from evaporated seawater that has been affected by digenetic processes.

Laboratory flow experiments carried out at the National Energy Technology Laboratory show increases in Ca, Mg, Na and Cl while Fe, S, P and SO_4 decrease within the first 15 hours while hours 15 through 24 show a reverse trend for these elements. Flow experiments at supercritical temperatures and pressures allow determination of the extent of mineral carbonation, mineral dissolution reactions and help constrain reaction rates determined through geochemical modelling [3].

[1] Carr *et al.* (2005) *AAPG Bulletin*. **89** 1607-1627. [2] Barker *et al.* (2011) Abstract, *American Geophysical Union*. [3] Kharaka *et al.* (2006) *J. Geochem. Explor.* **89** 183-183

A textural and mineralogical assessment of NWA 3118

G. C. BARLET[1*], D. W. DAVIS[1], D. MOSER[2], K. TAIT[1,3], I. BARKER[2] AND B. C. HYDE[3]

[1]Department of Geology, University of Toronto, Toronto, Canada barlet@geology.utoronto.ca
[2]Department of Earth Sciences, University of Western Ontario, London, Canada
[3]Department of Natural History, Royal Ontario Museum, Toronto, Canada

Northwest Africa (NWA) 3118 is a reduced CV3 chondrite, with large, irregularly shaped Calcium-Aluminum-rich Inclusions (CAIs) and Amoeboid Olivine Aggregates (AOAs) as well as dark inclusions [1]. Previous work by Ivanova [2,3,4] on NWA 3118 showed remarkable features such as compound CAIs with variable degrees of internal melting as well as unusual Zr-Y-Sc-rich mineral inclusion. NWA 3118, a relatively new addition to the list of chondrites, still contains numerous evidences about the early solar system. Initial textural observations were made by optical microscopy. EDS mapping and BSE imaging of uncoated slabs was carried out in variable pressure mode by FEG-SEM. In complement, we investigated the mineralogy of CAIs and AOAs using Raman Spectroscopy.

The surface distribution of chondritic components appears heterogeneous on our slabs where some areas are overpopulated by large inclusions, while other areas are composed of widespread small inclusions, and the rest is a mixture of both. Amorphous (fluffy) CAIs and AOAs are relatively common in NWA 3118 and appear very similar when observed optically. In some cases their shapes are controlled by compression between adjacent chondrules, although there does not seem to be any consistent axis of strain. Silicate chondrules themselves are rarely spherical and some of them appear to have responded to local strain, suggesting that they were partially molten when NWA 3118 was accreted.

Our specimen contains singular assemblages of fine-grained and coarse-grained amorphous CAIs. We also report the presence of compact (spherical) CAIs surrounded by Wark-Lovering rims embedded in fluffy CAIs. The largest compact CAI (400 micron) is associated with two significantly smaller distorted compact CAIs (50 micron) near the edge of its amorphous host.

Because amorphous CAIs and AOAs are nearly indistinguishable in texture, we presume that they were produced by similar physical processes in different reservoirs, or in the same reservoir with an evolving bulk chemistry. The presence of amorphous CAIs with different grain sizes supports the idea that the heat transfer and/or other factors that control crystal size (e.g. degree of undercooling) in the forming region were not uniform. In particular, the presence of compact CAIs included in amorphous CAIs suggests a variable non-uniform heat source where dusty CAI material may have been melted to form compact CAIs which subsequently accreted more dust in a process similar to that suggested for chondrules [5].

[1] Russell et al. (2005) *Meteoritical Bulletin* **89**, *MAPS* **40**, A201-A263. [2] Ivanova et al. (2010) *LPSC* **41**,1670. [3] Ivanova et al. (2011) *LPSC* **42**,1728. [4] Ivanova et al. (2011) *LPSC* **42**,1738. [5] Rubin (2010) *GCA* **74**, 4807–4828.

https://doi.org/10.1180/S0026461X00008434 Published online by Cambridge University Press

Links between tectonics and life, 4.0 to 2.3 Ga and the rise of oxygen

M.E. BARLEY[1*],

[1] School of Earth and Environment, The University of Western Australia, Crawley, Western Australia, 6009, Australia (correspondence: mark.barley@uwa.edu.au)

Earth is the only planet in our solar system with a bimodal topographic distribution crucial for the evolution of complex life. The tectonic records of the Archean to Paleoproterozoic (4.0 to 2.3 Ga) terranes indicate a link between evolving global tectonics with the formation of stable continents, increased subaerial volcanism and increased orogenic mountain building and the rise of atmospheric oxygen on Earth ~2.4 billion years ago. The first 2 stable cratons formed between 3.0 and 2.9 Ga after the first unambiguous evidence for plate tectonics. The Neoarchean record started at 2.8 Ga involving the possible break of a single pre-existing continent and the most prodigious period of generation and preservation of juvenile continental crust during a period of mantle plume breakout (2.72 to 2.65 Ga). During this period many cratons formed and aggregated into larger cratons and continents. Lower sea levels between 2.65 and 2.55 Ga were followed by a second (~2.51 to 2.45 Ga) period of plume breakout. Although oxygenic photosynthetic bacteria are thought to have evolved by 2.7 Ga or 2.5 Ga, the irreversible rise of atmospheric oxygen appears to have occured between 2.48 and 2.32 Ga suggesting a dynamic linkage and interaction of both sources and sinks of oxygen. Increased subaerial volcanism [1] and reduced temperature of magmatism (less komatiites) after 2.65 Ga helped cyanobacteria and also resulted in a decline of methane helping oxygen strat to rise [2]. There is growing evidence the long time the rise took involves interaction between cyanobacteria and oxygen using acid rock drainage bacteria from 2.48 Ga [3] as well as the rise of iron in the ocean using oxygen to form the bigest banded iron formations (BIFs). The 2.4 Ga break in tectonics and decline of BIFs helped the cyanobacteria and volcanic gasses with the rise of oxygen.

References.

[1] Kump and Barley (2007) Nature 448, 1033-1036.

[2] Konhauser at al. (2009) Nature 458, 750-753.

[3] Konhauser at al (2011) Nature 478, 369-373.

Chlorine isotope geochemistry of Icelandic geothermal waters

JAIME D. BARNES[1] AND ANDRI STEFÁNSSON[2]

[1]Department of Geological Sciences, University of Texas, Austin, Texas, USA jdbarnes@jsg.utexas.edu (* presenting author)

[2]Institute of Earth Sciences, University of Iceland, Reykajavik, Iceland, as@hi.is

The chlorine isotope composition of several geothermal systems in Iceland were determined in order to evaluate possible chlorine stable isotope fractionation in geothermal systems. The geothermal systems studied exhibit a range of temperatures (~38°C to >300°C) and pH (6 to 9.5). Chlorine concentrations range from ~5 to ~200 ppm. δ^{37}Cl values for all samples are near 0‰ (range = -0.3 to +0.3‰; error = +/- 0.2‰).

The source for the chlorine in the analyzed systems is commonly hypothesized to be from magmatic degassing or from leaching of host basalt during water-rock interaction. The δ^{37}Cl values are consistent with either of these hypotheses based on the near 0‰ value for the upper mantle and MORB glasses [1].

No large isotopic shifts due to fractionation are observed in these samples. These results are in agreement with previous experimental work on chlorine isotope fractionation between coexisting vapor and liquid in the system H2O–NaCl at 400°C and 450°C which show $\Delta^{37}Cl_{vapor-liquid}$ = 0 +/- 0.2‰ [2]. However, large Cl isotope fractionation has been observed in a few high-temperature (>100°C) and highly acidic volcanic fumaroles in Central America. ^{37}Cl preferentially partitions into the vapor phase as HCl resulting in extreme positive δ^{37}Cl values (~ +4 to +12‰) in acidic geothermal systems [3]. Further work will focus on acidic Icelandic geothermal systems in which Cl^- is hosted as HCl in order to explore the full range of δ^{37}Cl values in geothermal systems.

These results show that Cl stable isotopes act as a conservative tracer in neutral to slightly basic geothermal sytems regardless of phase separation; thereby, making Cl isotopes an excellent tracer of chloride sources in neutral systems.

[1] Sharp *et al.* (2007) *Nature* **446**, 1062-1065. [2] Liebscher *et al.* (2006) *Chemical Geology* **234**, 340-345. [3] Sharp *et al.* (2010) *GCA* **74**, 264-273.

https://doi.org/10.1180/S0026461X00008434 Published online by Cambridge University Press

The Composition of the Stillwater and Bushveld Parental Magmas.

SARAH-JANE BARNES [1]* AND PHILIPPE PAGE[2]

[1] Universite du Quebec a Chicoutimi, Canada sjbarnes@uqac.ca
[2] Universite du Quebec a Chicoutimi, Canada ppage@uqac.ca

The Bushveld and Stillwater Complexes contain most of the world's platinum-group element resources and it has long been recognized that their cumulate stratigraphies show similarites, which suggests that the magmas they formed from were similar with respect to major element compositions. At both localities a magma rich in SiO_2 and MgO is needed to produced the orthopyroxene rich lower parts of the intrusions. Chill margins with the composition of Mg-rich basaltic andesite are present at both localities (the B-1 and Gp-3 chills). To produce the gabbroic middle zones of the intrusions, melts close to tholetiitic basalt composition are required. Chills with these compositions are found at both intrusions (B-2 and Gp-1 chills). Recent studies on Bushveld have provided information on the trace element content of the Bushveld magmas and cumulates indicating that the magmas were strongly enriched in LILE and LREE (Fig. 1). We have determined the trace element content of the equivalent magmas from Stillwater and they are poorer in LILE and LREE. The Mg-rich andesite (Gp-3) are closer to boninite compositions than the Busheld B-1 rocks. The tholeiitic basalt (Gp-1) show some similarities to arc tholeiites.

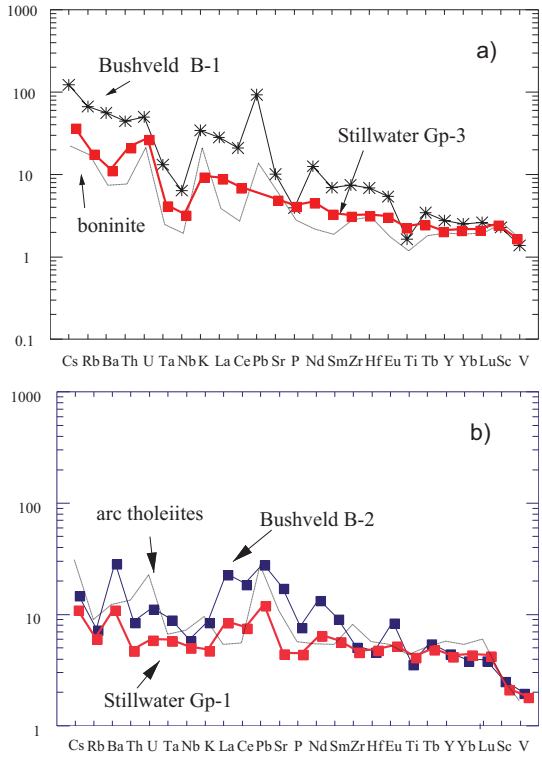

Fig. 1 Mantle normalized incompatible element plot of the marginal rocks of the Bushveld and Stillwater compared with modern magmas

Lead Isotopic bias during the *Chaîne Opératoire* of Non Ferrous metal: Implications for Provenance Studies

S. BARON[1*], C.G. TAMAS[2] AND B. CAUUET[3]

[1]CNRS, Toulouse, France, sbaron@univ-tlse2.fr (* presenting author)
[2]University Babes-Bolyai, calingtamas@yahoo.fr
[3]CNRS, Toulouse, France, cauuetb@aol.com

Introduction

The rise of the high resolution mass spectrometers (MC-ICP-MS) during the last ten years allows the analyses of traditional and non traditional isotopes to be more accurate, precise, relevant and consequently subtly interpretable [*e.g.* 1, 2]. The lead isotopic tracing, from mines/ore bodies to archaeological materials, constitutes the main tool of metal provenance studies. Despite the use of high-resolution isotopic measurements, the identification of the geographical ores source is difficult because of several factors. The most important factor is inherent to the ores themselves: *i)* the ores could have lead isotopic heterogeneity in a same ore body and *ii)* numerous different geographical mining districts could have same lead isotopic compositions. Furthermore, the ores are disconnected of any geological, archaeological and historical significance in respect with the metal provenance study. When the archaeological materials are well documented by mining archaeology and history, the provenance studies (coupled with high resolution measurements) are improved [3]. Another factor, rarely taken into account, is the possible lead isotopic bias during the metallurgical processes. Because the isotopic tracing is directly operated from ores to object at global scale, the consequence is that the *chaîne opératoire* is not taken into account. But, during the *chaîne opératoire*, numerous human operations occurred. Some archaeological experiments conducted on ores reduction have measured isotopic bias between ores / metal of slags and metal of slags / slags silicated matrix at furnace scale [4]. Through two regional studies, conducted on materials well documented by mining archaeology and history, we found isotopic bias due to the local *chaîne opératoire*. These results corroborate the previous experimental ones.

Results and discussions

We will present here the results from two *chaîne opératoire* well documented by mining archaeology: *i)* the lead-silver one in France for medieval time and ii) the gold-silver one in Romania for roman time. We will demonstrate here that the addings during the metallurgical processes produce lead isotopic bias. According the high-resolution isotopic measurement available today, it is necessary to take into account these biases in order to refine the tracing and understand the *chaîne opératoire* in its historical context. This approach will allow the understanding of regional management of ore sources in ancient times. It constitutes the first step before the beginning of a metal diffusion at global scale.

[1] Klein et al. (2010) *Archaeol. Anthropol. Sci.* **2**, 45-56. [2] Desaulty et al., (2011) PNAS **108**, 9002-9007. [3] Baron et al., **submitted** in *Archaeometry*. [4] Baron et al. (2009) *Appl. Geochem.* **24**, 2093-2101.

https://doi.org/10.1180/S0026461X00008434 Published online by Cambridge University Press

Mercury stable isotopes in fish tissue as indicators of photochemical transformations

GIDEON BARTOV[1*], THOMAS M. JOHNSON[1]

[1]University of Illinois Urbana-Champaign, Urbana, USA, (*gbartov2@illinois.edu)

During the 1950s and 1960s, the U.S Department of Energy (DOE) plant Y-12, near Oak Ridge, TN, was using Hg in the production of thermonuclear weapons. During normal plant operations, large amounts of Hg were discharged into the East Fork Poplar Creek (EFPC) and its floodplain [1]. Current research aims to better understand Hg transformations that control its mobility and bioavailability.

Hg isotopes have the potential to identify and perhaps quantify certain biogeochemical reactions. Photo-reduction and -demethylation have been shown to fractionate the odd isotopes of Hg (^{199}Hg and ^{201}Hg), independent of their mass, due to the magnetic isotope effect [2]. Fish are assumed to be good integrators of bioavailable Hg over space and time and do not change the mass independent fractionation signature of the odd Hg isotopes. As a result, it is possible to use fish as indicators of photochemical reactions occurring in the water column. According to Bergquist and Blum [2], photoreduction of $Hg(II)_{(aq)}$ creates a slope, on a Δ^{199}Hg vs. Δ^{201}Hg graph, of 1.00±0.02, methyl-Hg (MeHg) photoreduction has a slope of 1.36±0.02, and fish tissue plots on a 1.28±0.03.

Our study aims to detect and quantify Hg chemical transformations in the EFPC. Frozen fish tissues received from Oak Ridge National Laboratory were digested and analyzed on a Nu Instruments MC-ICP-MS using the Mead and Johnson [3] double-spike technique. The ^{202}Hg/^{198}Hg ratio (reported as δ^{202}Hg) was measured with a precision of ~0.11‰ relative to the NIST SRM 3133 Hg standard. Odd isotope deviations were measured with a precision of ~0.04‰ and are reported as Δ^{199}Hg and Δ^{201}Hg deviations from theoretical mass dependent fractionation values.

The δ^{202}Hg of the fish shows a weak increase increasing distance downstream from Y-12, from -0.57±0.08‰ (n=4) upstream to -0.29±0.15‰ (n=4) downstream. The odd isotope deviations also show a slight positive trend with increasing distance downstream from Y-12 (shifting Δ^{201}Hg from -0.05±0.04‰ to 0.05±0.04‰ and Δ^{199}Hg from -0.04±0.07‰ to 0.09±0.05‰). The slope of the data is 1.3, consistent with the slope obtained for photochemical demethylation by Bergquist and Blum [2]. Based on equations given by Bergquist and Blum [2], we can calculate, to first order, the amount of photoreduction of MeHg in the water between 4-11% using the Δ^{201}Hg values.

Fish are a good proxy for the extent of photoreduction of Hg in the water column; however, it would be beneficial to look directly at the Hg present in the water, the reactant pool. Therefore, water samples from the EFPC have been obtained and will be analyzed.

[1] Southworth *et al.* (2000) *Environmental Monitoring and Assessment* **63**, 481-494. [2] Bergquist and Blum (2007) *Science* **318**, 417-420. [3] Mead and Johnson (2010) *Analytical Bioanalytical Chemistry* **397**, 1529-1538.

Bottom Water Changes in the South Pacific Over the Last 30 ka Documented by Nd Isotopes

CHANDRANATH BASAK[1, 2]*, KATHARINA PAHNKE [1,2]

[1]Max Planck Institute for Marine Microbiology, Bremen, Germany *(cbasak@mpi-bremen.de)

[2]Institute for Chemistry and Biology of the Marine Environment (ICBM), Oldenburg, Germany

North Atlantic Deep water (NADW) and the Antarctic Bottom water (AABW) are the two central supporting pillars that control deep ocean ventilation and influence atmoshperic CO_2 concentrations on glacial-interglacial timescales. While much is known about past NADW changes, very little is known about variations in AABW formation and export from the Southern Ocean. Available paleo-records point at enhanced northward advection of southern sourced deep water during times of reduced NADW formation [1]. It is, however, not clear whether the observed presence of AABW in the North Atlantic is due to increased southern sourced deep water production or related to reduced NADW formation. In this study we used paleo seawater Nd isotope ratios to address the AABW formation history in the Pacific Southern Ocean for the last 30 ka.

Our study site is located in the eastern Pacific sector of the Southern Ocean [PS58/271-1; 61.24°S, 116.05°W, 5214m water depth; [2]]. Currently this site is bathed by AABW with contributions from Circumpolar Deep Water and Pacific Deep Water, and is located at the Polar Front. The Ross Sea is the nearest deep water formation area and the prsent-day northern limit of 'pure' Ross Sea bottom water (RSBW; defined by high salinity and density) reaches just south of our site. Thus, during times of enhanced deep water formation in the Ross Sea, RSBW would be expected to have reached the study site. Since RSBW carries the characteristic Nd isotope signal of Ross Sea sediments (ε_{Nd} = -7; [3]), any northward expansion of RSBW should be recorded in the sediments at our core site. The Late Holocene ε_{Nd} value (ε_{Nd} = - 6.2) at our study site is consistent with the influence of RSBW and CDW/PDW at the core site. The downcore ε_{Nd} record shows that the study site was bathed by a water mass with an Nd isotopic composition of (ε_{Nd} =) ~ -5.5 during the last glacial maximum (LGM). The ε_{Nd} value of the water mass gradaully started to change towards more Pacific deep water-like values (ε_{Nd} = -3) with the initiation of deglaciation around 18 ka BP. Strong Pacific deep water influence is observed at around 15.3 ka, followed by a gradaul decrease to the Late Holocene value (ε_{Nd} = -6.2). The time of maximum ε_{Nd} around 15.3 ka coincides with warming in the Southern Hemisphere and corresponding cooling and shut down of NADW in the Northern Hemispere. Our data do not support increased RSBW/AABW formation at this time, rather, we observe enhanced influence of Pacific deep water. If this holds true for the entire Southern Ocean, the observed presence of AABW in the deep North Atlantic has to be explained by reduced NADW production.

[1] Lynch-Stieglitz *et al.* (2007) *Science* **316**, 66-69. [2] Jacot Des Combes *et al.* (2008) *Paleoceanography* **23**, PA4209. [3] Pahnke *et al.* (2011) *Geophysical Research Abstracts*, 13, EGU General Assembly.

https://doi.org/10.1180/S0026461X00008434 Published online by Cambridge University Press

Toward an understanding of metal uptake in a methanogenic archaeon isolated from the Rancho La Brea Tar Pits

JENNA L. BASS[1], ELIZABETH L. EDWARDS[1], ALEXIS LLOYD[1], SARA J. WEAVER[1] AND JOHN S. MAGYAR[1*]

[1]Department of Chemistry, Barnard College, New York, NY 10027, USA jmagyar@barnard.edu (* presenting author)

Recalcitrant petroleum sources, such as heavy oil, oil sands, and asphalts, are an increasingly important part of the global petroleum supply. In situ conversion of these materials to methane would have significant environmental and economic advantages over current mining and extraction methods, but significant fundamental research on anaerobic methanogenic petroleum degradation is required before such approaches will become practical. Understanding the bioinorganic chemistry of such processes is essential to an overall understanding of methanogenesis, which requires a series of metallocofactors. Of these, several key proteins are nickel-binding proteins, including the hydrogenases. We are investigating mechanisms of nickel uptake in *Methanocorpusculum labreanum*, a methanogen isolated from natural asphalt sediments in the La Brea Tar Pits, Los Angeles. We have isolated a gene for a putative metalloregulatory protein from genomic DNA, cloned it into *E. coli*, and overexpressed and purified the resulting protein. Using a variety of spectroscopic methods, including UV-vis-NIR absorption, fluorescence, and circular dichroism spectroscopies, we are characterizing the coordination chemistry and structure of this protein. We have identified the presence of both flavins and iron-sulfur clusters, and work is currently underway to elucidate the structure and binding of these cofactors and the role they may play in regulating cellular nickel uptake.

Microbial uranium reduction monitoring: Linking isotopic fractionation factors with microbial metabolism

ANIRBAN BASU*, THOMAS M. JOHNSON, ROBERT SANFORD, AND CRAIG C. LUNDSTROM

Department of Geology, University of Illinois at Urbana-Champaign, Urbana, IL, USA, abasu3@illinois.edu (* presenting author), tmjohnsn@illinois.edu, rsanford@illinois.edu, lundstro@illinois.edu

Microbial reduction of soluble and mobile U(VI) to sparingly soluble U(IV) is a promising remediation strategy for uranium-contaminated aquifers. A wide range of microorganisms with diverse metabolic pathways can reduce U(VI) to U(IV). Microbial U(VI) reduction fractionates U isotopes; heavier isotopes partition in the solid U(IV) products. The remaining U(VI) pool becomes isotopically lighter with progressive reaction. The isotopic enrichment is quantified by measuring $^{238}U/^{235}U$ ratio in the remaining unreacted pool of U(VI) and the magnitude of the isotopic enrichment is expressed by the isotopic fractionation factor ε ($\varepsilon=1000*(\alpha-1)$; $\alpha = (^{238}U/^{235}U)_{Product}/(^{238}U/^{235}U)_{Reactant}$). The isotopic enrichment is related to the extent of reduction by the fractionation factor ε. $^{238}U/^{235}U$ ratios can be used to detect and possibly quantify U(VI) reduction, if the ε for the relevant microbial reductions are known.

Here we report ε values for U(VI) reduction by two strains of *Geobacter sulfurreducens* (PCA and Criddle), *Anaeromyxobacter dehalogenans* strain FRCW, *A. dehalogenans* strain FRC-R5, and *Desulfitobacterium* Viet1. For each bacterial species, we measured the ε values in duplicate batch incubation experiments with U(VI) and 0.5 mM electron-donor at 30 °C.

All strains tested in this study induced significant isotopic fractionation during U(VI) reduction. The ε yielded by *Geobacter sulfurreducens* strains PCA and Criddle were 0.68‰ and 0.95‰, respectively. The ε values for *A. dehalogenans* strain FRCW, *A. dehalogenans* strain FRC-R5, and *Desulfitobacterium* Viet1 were 0.75‰, 0.98‰, and 0.84‰, respectively. The results of this study indicate that the ε does vary with microbial metabolism. We observed an increasing trend in ε with decreasing cell-specific reduction rate. Our results suggest that cell-specific reduction rates are good indicators of the magnitude of microbial U isotopic fractionation. The ε tends to reach highest values (~1‰) under nutrient limited electron-donor poor conditions. Our results shed light on the fundamental relationship between metabolism and isotopic fractionation and will be useful to detect and possibly quantify U(VI) reductions in the sites undergoing active bioremediation.

https://doi.org/10.1180/S0026461X00008434 Published online by Cambridge University Press

Progress in detrital garnet Sm-Nd geochronology: the second point on the isochron

E.F. BAXTER , K.A. ECCLES, N.C. SULLIVAN

Boston University, Department of Earth Sciences, Boston, MA, 02215 U.S.A, (*correspondence: efb@bu.edu)

Detrital minerals in the sedimentary record provide valuable information about the tectonic evolution of the Earth. Detrital garnets also preserve a chemical record of tectonometamorphic processes, conditions and provenance [1] that may not necessarily be recorded by other commonly dated detrital minerals. Detrital garnets could therefore form a valuable and complimentary tool in detrital analysis of ancient tectonic processes and provenance. Here, we describe recent advances beyond previous attempts to date detrital garnets [2,3] and illuminate the current possibilities and limitations.

Two challenges must be overcome. First, is the sample size limitation which is solved through use of NdO^+ TIMS analysis with Ta_2O_5 activator [3,4]. This small sample capability provides an opportunity for geochronology on single >500 um grains or equivalent multi-grain separates. Second, a detrital garnet grain is no longer associated with the parent rock from which it crystallized. Thus there is no obvious second point to constrain an isochron. Here, detrital garnets may be crushed and treated with acids (including HF) to partially dissolve and analyze mineral inclusions which should in most cases adequately represent the original garnet host assemblage. But, well established methods for conventional garnet geochronology demonstrate that the garnet's inclusions often fall off the garnet-matrix isochron [5], and thus these inclusions are typically removed and discarded. Fortunately, in the detrital garnet application, the magnitude of the "age effect" related to the use of inclusions as the second point on the isochron (rather than the matrix) is small; generally less than a few million years which is an acceptable tolerance for most detrital geochronologic studies. Only if inherited zircons, which themselves can have high Sm/Nd ratios, represent a dominant part of the inclusion population could the detrital garnet age be skewed more significantly.

Test garnets extracted from New England (USA) sediments have been dated with this approach, yielding Acadian ages (as expected) with age uncertainty as low as ±4 Myrs on single grains as small as 3mg (or about 1.5mm diameter). $^{147}Sm/^{144}Nd$ ratios as high as 2.4 in cleansed garnet reflect success in separating inclusions from garnet via partial dissolution. Our data show a correlation with apparent isochron age and spread in $^{147}Sm/^{144}Nd$. The larger the spread between the two points in the isochron, the younger and more accurate the age. With our test samples, we have found that $^{147}Sm/^{144}Nd$ spread greater than 0.5 is necessary to produce accurate ages. Samples which yield less spread are too old, reflecting incomplete separation of garnet from inherited inclusions.

[1] Hutchinson AR & Oliver GJH 1998. J. Geol. Soc. Lond. 155, 541-550; [2] Oliver GJH et al. 2000. Geology, 28, 459-462; [3] Baxter EF et al. 2010. Goldschmidt; [4] Harvey J & Baxter EF 2009. Chem. Geol. 258, 251-257; [5] Pollington AD & Baxter EF 2011. Chem. Geol. 281, 270-282.

Hydrochemical and multiple isotopic approach to delineate the contamination of urban groundwater in Ulaanbaatar, Mongolia

BATSAIKHAN BAYARTUNGALAG[1*], SEONG-TAEK YUN[1], KYOUNG-HO KIM[1], BERNHARD MAYER[2], SANG-TAE KIM[3], BUYANKHISHIG NEMER[4], YOUNG-JOON LEE[5], AND EUN-SEON JANG[1]

[1]Korea University, Green School and the Department of Earth and Environmental Sciences, South Korea, bayartungalag@korea.ac.kr (* presenting author)
[2]University of Calgary, Geoscience, Canada
[3]McMaster University, Geography and Earth Sciences, Canada
[4]Mongolian University of Science and Technology, Hydrogeology and Environmental Geology, Mongolia
[5]Korea Environment Institute, South Korea

In Ulaanbaatar City (UB), Mongolia, significant population growth (currently, ~1.2 million) and rapid industrialization over the last two decades resulted in diverse environmental problems including a shortage and contamination of the water supply. Municipal water supply in UB depends on groundwater withdrawn from an alluvial aquifer located along the Tuul River. There are also many private wells completed in variable depths. Groundwater in UB has become increasingly polluted because of a deficient municipal sewer system, illegal waste dumping, air and soil pollution, and deforestation of surrounding areas. To our knowledge, there is no detailed survey that has assessed the status of groundwater quality in UB. Therefore, we have performed a hydrogeochemical survey including hydrochemical and multiple isotopic (i.e., $\delta^{13}C$ of dissolved inorganic carbon, $\delta^{15}N$ and $\delta^{18}O$ of nitrate, and $\delta^{34}S$ and $\delta^{18}O$ of sulfate) measurements on 45 groundwater, 4 surface water and 2 spring water samples collected in July 2011. The obtained data were interpreted in relation to land use patterns, which include the urban center, peripheral residential areas with dense traditional homes, grasslands, and forests.

Our results show the occurrence of three major hydrochemical types: 1) Ca-HCO_3 type, 2) Ca(-Na)-HCO_3-Cl(-NO_3) type, and 3) Ca-Na-HCO_3 type. The spatial distribution of different water types is controlled by land use. Types 1 and 3 occur under forest and grassland areas and are representative of unpolluted or less-contaminated groundwater. On the other hand, type 2 occurs predominantly in urbanized areas and shows progressive enrichments of groundwater with Cl+NO_3 (and NO_2)+SO_4 with increasing TDS, due to anthropogenic impact from latrines and domestic sewage. Nitrate contamination especially in the city center and peripheral residential areas is pervasive and severe resulting in NO_3^- concentrations of up to ~290 mg/L. The $\delta^{15}N$ and $\delta^{18}O$ values of nitrate suggest that in the city center and peripheral residential areas, latrines and domestic sewage are major sources of the severe nitrate contamination. Therefore, better management of latrines and sewage systems is urgently needed in UB. Our study also shows that groundwater contamination in UB is linked to the progressive population growth and city expansion.

https://doi.org/10.1180/S0026461X00008434 Published online by Cambridge University Press

Intensifying weathering and land-use in Iron Age Central Africa

GERMAIN BAYON[1]*, BERNARD DENNIELOU[1], JOËL ETOUBLEAU[1], EMMANUEL PONZEVERA[1], SAMUEL TOUCANNE[1], SYLVAIN BERMELL[1]

[1]IFREMER, Géosciences Marines, Plouzané, France gbayon@ifremer.fr (* presenting author)

A major vegetation change occurred in Central Africa during the third millennium before present, when mature evergreen trees were abruptly replaced by savannas and secondary grasslands [1-3]. The consensus is that the forest disturbance was caused by a regional climate change [1-3]. However, this episode of forest clearance occurred contemporaneously with the migration of Bantu-speaking peoples from near the modern Nigeria-Cameroon border [4-7]. The so-called Bantu expansion led to diffusion of agriculture and iron smelting technology across Central Africa, with potential impacts on the environment [10]. Whether the Bantu farmers played an active role in the Central African deforestation event remains an open question.

Here we present major element (Al/K ratios) and radiogenic isotope (Nd, Hf) records from a marine sediment core recovered in the Gulf of Guinea, that permit the reconstruction of chemical weathering intensity in Central Africa for about the last 40,000 years. The data indicate a pulse of intensified weathering centered around 2,500 years ago, contemporaneous with the rainforest crisis. Evidence that this weathering event departs significantly from the long-term weathering fluctuations related to the Late Quaternary climate suggests that it was not triggered by natural climatic factors solely. Instead, we propose that the settlement of Bantu-speaking farmers in Central Africa at that time had a more pronounced environmental impact than initially thought.

[1] Vincens *et al.* (1999) *J. Biogeog.* **26**, 879-885. [2] Maley & Brenac (1998) *Rev. Palaeobot. Palynol.* **99**, 157-187. [3] Ngomanda *et al.* (2009) *Quat. Res.* **71**, 307-318. [4] Diamond & Bellwood (2003) *Science* **300**, 597-603. [5] Huffman (1982) *A. Rev. Anthropol.* **11**, 133–150. [6] Vansisa (1984) *J. Afr. Hist.* **25**, 129–145. [7] Holden (2002) *Proc. R. Soc. Lond. B* **269**, 793-799. [10] Willis *et al.* (2004) *Science* **304**, 402-403.

Rock micro-structure controls regolith thickness

E. BAZILEVSKAYA[1]*, M. LEBEDEVA[1], G. ROTHER[2], M. PAVICH[3], D. PARKINSON[4], D. COLE[5] AND S.L. BRANTLEY[1]

[1]The Pennsylvania State University, University Park, PA 16802 USA (*correspondence: eab204@psu.edu)

[2]Oak Ridge National Laboratory, Oak Ridge, TN 37831 USA

[3]U.S. Geological Survey, Reston, VA 20192 USA

[4] Lawrence Berkeley National Laboratory, Berkeley, CA 94720, USA

[5] School of Earth Science, Ohio State University, Columbus, Ohio, 43219

As feldspar transforms to clay, a zone of residual weathered material, regolith, forms on ridges of diabase and granite in the Piedmont Province, Virginia. In spite of similar erosion rates and the fact that Ca-rich plagioclase in diabase is expected to dissolve 10x faster, weathering has advanced 20x deeper into the granite compared to the diabase. This result runs counter to conventional wisdom that would predict a deeper weathering profile on the diabase. We explained this enigma by studying the nano- to micro-structural features of these two rocks in plagioclase reaction zone. Nano-pores (1 nm < d < ~5 μm) and micro-pores (> 3 μm) were studied by neutron scattering (NS) and micro-computed tomography (μ-CT), respectively. We found that granite has a larger connected micron-sized pore network than diabase as well as abundant micro-fractures around oxidizing biotite. In contrast, the plagioclase reaction zone in diabase has some regions of low porosity due to smectite and calcite precipitation. Therefore, we concluded that the regolith is 20x thinner on diabase because it supports only minimal fluid advection, while advective transport in granite is significant.

We explored this hypothesis with numerical modelling of plagioclase dissolution in diabase and granite. For diabase, the diffusion-only model yields shallow regolith with a thin reaction front -- as observed in the field. However, we could not model a deeper and thicker reaction front in granite with diffusion only. With advection in the numerical model, the reaction front in granite is wide and the regolith is deep, as observed.

Our results show that the difference in regolith thicknesses in the Piedmont is largely explained by different regimes of reactive fluid transport. Minimal advection creates shallow regolith and a thin reaction front in the more massive diabase. In contrast, significant advection occurred in the relatively fractured granite, producing deep regolith and a thick reaction front. At the grain-scale, infiltration of advecting fluid is controlled by texture (e.g., grain size distribution, porosity) and reaction-induced permeability. The parent lithology is an important factor in this latter permeability because oxidation of biotite at depth apparently accelerated pervasive fluid infiltration into the granite. If micro-structure is important in controlling the factor of 20x, then it is possible that felsic rocks such as granites generally develop thicker regolith profiles than diabase, regardless of age or location, under comparable geomorphological regimes. Such observations may help predict and explain regolith thickness in localities in many places around the globe.

.

https://doi.org/10.1180/S0026461X00008434 Published online by Cambridge University Press

Identifying Key Controls on the Behavior of an Acidic-U(VI) Plume at the Savannah River Site using Reactive Transport Modeling

S.A. BEA[1*], H. WAINWRIGHT[1], N. SPYCHER[1], S. HUBBARD[1], AND J. DAVIS[1]

[1]Lawrence Berkeley National Lab., Berkeley, CA, 94720 USA, sabea@lbl.gov (*presenting author)

Acidic waste solutions containing low level radioactivity from numerous isotopes were discharged to a series of unlined seepage basins at the F-Area of the Savannah River Site, South Carolina, from 1955 through 1989. Although the site has gone through many years of active remediation, the groundwater remains acidic, and the concentrations of U(VI) and other radionuclides are still significant. Monitored Natural Attenuation (MNA) is a desired closure strategy for the site, based on the premise that clean background groundwater will eventually neutralize the groundwater acidity, causing an increase in pH and driving natural immobilization of U(VI) through sorption. The development of the understanding of the long-term pH and U(VI) sorption behavior at the site is critical to assess MNA and in-situ treatment over the long term.

We use reactive transport (RT) models and uncertainty quantification (UQ) to explore key controls on the U(VI)-plume evolution and long-term mobility at this site through considering U(VI) adsorption by sediments and key hydrodynamic processes. Two-dimensional RT simulations through the saturated and vadose zones were conducted by considering the dissolution and precipitation of Al and Fe minerals, as well as H^+ and U(VI) surface complexation. Simulations indicate that mineral dissolution and precipitation together with sorption reactions on goethite and kaolinite (primary minerals present with quartz) could buffer pH at the site for long periods of time.

UQ techniques were applied with RT modeling in order to: (1) identify the complex physical and geochemical processes that control the migration of the acidic-U(VI) plume in the pH range where it is highly mobile, (2) evaluate those physical and geochemical parameters that are most controlling, and 3) attempt to predict the future plume evolution constrained by historical chemical and hydrological data. UQ-RT results show that model results are most sensitive to the reactive surface area available for sorption, discharge rates, the relative rates of H^+ influx and kaolinite dissolution. The plume behaviour also appears to be sensitive to parameters controlling the amount of residual U(VI) in the vadose zone, which acts as a buffering zone in the modeled system.

Iron isotope fractionation during femtosecond laser ablation of magnetite determined by aerosol size sorting experiments

BRIAN L. BEARD[1,2*], ANDREW D. CZAJA[1,2], WEIQIANG LI[1,2], JAMES J. SCHAUER[3], MICHAEL OLSON[3], CLARK M. JOHNSON[1,2]

[1]Univ. Wisconsin, Dept. of Geoscicence, Madison WI, USA beardb@geology.wisc.edu (* presenting author)

[2]NASA Astrobiology Institute

[3] Univ. Wisconsin, Dept. of Civil and Environmental Engineering, Madison WI, USA, jjschauer@wisc.edu

Aerosol particles generated from femtosecond laser ablation (fs-LA; 198nm laser manufactured by Photon Machines) of natural magnetite were size sorted using a Micro-Orifice Uniform-Deposit Impactor (MOUDI). The MOUDI separates particles by size based on aerodynamic properites using 10 stages. Aerosols were collected using fluences of 1, 2, and 4 J/cm^2 and there is a positive correlation between total Fe collected per laser shot; 25, 50, and 100 picograms of Fe per laser shot were harvested from the impactor, respectively. The aerosol size distribution of the fs-LA generated particles were determined by analyzing Fe concentration for each stage of the impactor using ^{57}Fe isotope dilition mass spectrometry (~10^5 laser shots) or spectroscopically via the ferrozine technique (~10^6 laser shots). The size distribution of aerosol particles done at different fluences are the same; all are unimodal with a peak at an aerodynamic size between 180 to 320 nm.

Sized aerosol particles have been analyzed for their Fe isotope composition. The smallest sized particles have δ^{56}Fe values that are less than the magnetite substrate by 0.5‰, whereas larger sized particles (≥180–320 nm stage) have δ^{56}Fe values that were up to +0.7‰ greater than the magnetite substrate. There are no differences in isotope compositions as a function of fluence. In all experiments, the integrated Fe isotope composition of all the stages matches that of the magnetite substrate. This isotopic mass balance highlights that although the process of fs-LA produces Fe isotope fractionation, if the generated aerosol is quantitatively delivered and ionized, one can obtain accurate Fe isotope measurements. Indeed, for sample-standard comparisons, accuracy of Fe isotope compositions will hinge on having similar transport efficiencies spatially in the ablation cell. For example, if 12% of the particles ≥ 180–320 nm in aerodynamic size are not transported to the ICP source, and these particles consist of 70% of the total Fe mass with δ^{56}Fe values that are 0.7‰ greater than the bulk substrate, the measured Fe isotope composition would be inaccurate by -0.1‰. This can easily be monitored, however, by comparing Fe yields derived by total ion signal. Using the above example, there would be a ~9% decrease in the total Fe ion signal.

The correlation between Fe isotope composition and particle size may result from condensation wherein the first condensed particles from fs-LA generated vapor have low δ^{56}Fe values. As condensation continued and some particles coarsened, they inherited higher δ^{56}Fe values from the isotopically heavy vapor.

https://doi.org/10.1180/S0026461X00008434 Published online by Cambridge University Press

Clay-rock alteration experiments at 80°C in closed and open conditions: application to the waste storage

CATHERINE BEAUCAIRE[1*], EMMANUEL TERTRE[2], ERIC FERRAGE[2], BERNARD GRENUT[1], STEPHANE PRONIER[2] AND BENOIT MADÉ[3]

[1]CEA, DEN/DANS/DPC/SECR/L3MR, Gif-sur-Yvette, France, catherine.beaucaire@cea.fr

[2]Université de Poitiers-CNRS, IC2MP UMR 7285, Poitiers, France, emmanuel.tertre@univ-poitiers.fr

[3]ANDRA, Chatenay-Malabry, France, benoit.made@andra.fr

In the framework of radioactive waste storage in geological formations, many investigations were carried out to characterize chemical properties of pore water at the field temperature (*e.g.*, 20°C). However, few studies were devoted to the modifications that temperature could induce on the chemical composition of pore water in the host-rock. Among the chemical parameters which are sensitive to temperature, the pH and $CO_{2(g)}$ partial pressure (*i.e.*, $p_{CO2(g)}$) are likely the most sensitive. These latter parameters could also strongly impact the mobility of radionuclides in geosphere. Under thermal gradient, many reactions would occur such as minerals dissolution-recrystallisation or organic matter degradation. The knowledge of geothermal systems in sedimentary contexts tends to prove that whatever the mineral or/and organic contribution, $p_{CO2(g)}$ is likely constrained by a mineralogical buffer combining carbonate mineral (calcite, dolomite), quartz or chalcedony and alumina-silicate phases (kaolinite, illite or Mg-chlorite) [1]. Hydrothermal alteration experiments were carried out with Callovo-Oxfordian clay-rock with the aim of characterizing the ultimate step of thermal alteration at 80°C, which is the temperature expected in the waste storage.

The experiments were performed in both open and closed systems where initial $p_{CO2(g)}$ values were fixed (*e.g.*, $p_{CO2(g)}$=0.4 atm.). High solid/solution ratios (1 to 3 kg/L) are chosen in order to favour neoformation of secondary mineral phases. Aqueous and gas phases were regularly extracted at temperature and fully analyzed. The evolution of clay mineralogy was also characterized using X-ray diffraction profile modeling of experimental patterns and Transmission Electron Microscopy. Then, results obtained for solution as well as for solids were interpreted and discussed in term of thermodynamic equilibrium achievement.

After 15 months of alteration in closed conditions at 80°C, the $p_{CO2(g)}$ is stabilized at 1 atm. and final solution is equilibrated with respect to quartz, kaolinite, calcite and ordered-dolomite. Modeling of experimental X-ray diffraction patterns [2] evidenced a slight increase of the illitic layers content in mixed-layer minerals (*i.e.*, 5%). However, it is not possible to conclude to illite neoformation. Consequently, in absence of equilibrium with a secondary Al-Si mineral phase which would participate to the complete mineralogical buffer, the constrain on $CO_{2(g)}$ is not evidenced in these experimental conditions. Other experiments devoted for determining reaction pathways are currently in progress.

[1] Coudrain-Ribstein, Gouze & De Marsily (1998) *Chem. Geol.,* **145***, 73-89*. [2] Ferrage, Vidal, Mosser-Rück, Cathelineau & Cuadros (2011) *Am. Min.* **96,** 207-223.

Can submarine groundwater discharge balance the oceanic strontium isotope budget?

AARON J. BECK[1*], MATTHEW A. CHARETTE[2], J. KIRK COCHRAN[3], MEAGAN E. GONNEEA[2] AND BERNHARD PEUCKER-EHRENBRINK[2]

[1]Virginia Institute of Marine Science, College of William & Mary, Gloucester Point, VA, USA
abeck@vims.edu (* presenting author)

[2]Department of Marine Chemistry and Geochemistry, Woods Hole Oceanographic Institution, Woods Hole, MA, USA
mcharette@whoi.edu
mgonneea@whoi.edu
bpeucker@whoi.edu

[3]School of Marine and Atmospheric Sciences, Stony Brook University, Stony Brook, NY, USA
kcochran@notes.cc.sunysb.edu

It is not clear if the strontium (Sr) isotope budget of the modern ocean is at steady state [1]. It has been hypothesized that submarine groundwater discharge (SGD) is an important Sr source to the ocean [2], but few data exist for Sr in coastal groundwater or in the geochemically-dynamic subterranean estuary (STE). We examined Sr concentrations and isotope ratios from 9 globally-distributed coastal sites, and examined the behavior of Sr in the STE.

Dissolved Sr generally exhibited conservative mixing behavior in the STE, although large differences were observed in the meteoric groundwater endmember among sites (0.1 – 24 μM Sr). Differences in groundwater Sr concentrations and isotope ratios ($^{87/86}$Sr = 0.707-0.710) reflected aquifer lithology characteristics. In part, because groundwater Sr concentrations are orders of magnitude higher in less-radiogenic carbonate and volcanic island aquifers, the SGD endmember Sr ratio must be lower than modern seawater (i.e., less than 0.70916). A simple lithological model was used to estimate a global average groundwater endmember of 2.9 μM Sr with $^{87/86}$Sr = 0.7089, representing a meteoric-SGD-driven Sr input to the ocean of 0.7-2.8 × 10^{10} mol Sr a^{-1}. Meteoric SGD therefore accounts for 2-8% of the oceanic Sr isotope budget, comparable to other known source terms, but insufficient to balance the remaining budget.

Sr isotope exchange was observed in the STE at five of the sites studied, invariably favored the meteoric groundwater endmember signature, and reached up to 40% exchange at salinity 10. Using reported estimates for brackish SGD, the estimated volume discharge at salinity 10 (7-11 × 10^{15} L a^{-1}) was used to evaluate the impact of isotope exchange in the STE on the brackish SGD Sr flux. A moderate estimate of 25% isotope exchange in the STE gives a resultant SGD Sr endmember isotope composition of 0.7091. The brackish SGD Sr flux accounts for 12-25% of the marine Sr isotope budget, and does not appear sufficient to balance some 40% of the remainder.

Substantial uncertainties remain for estimating the SGD source of Sr to the global ocean, such as the volume flux of meteoric SGD, and lacking measurements of groundwater Sr isotope composition in major SGD regions such as Papua New Guinea, the South America west coast, and West Africa. Nevertheless, the combined sources of meteoric SGD and isotope exchange in the STE are a major component of the modern oceanic Sr isotope budget, and represent a Sr source to the ocean that may have contributed to documented fluctuations in the oceanic $^{87/86}$Sr ratio over geologic time.

[1] Davis *et al.* (2003) *EPSL* **211**, 173-187.
[2] Allègre *et al.* (2010) *EPSL* **292**, 51-56.

https://doi.org/10.1180/S0026461X00008434 Published online by Cambridge University Press

Primary origin *vs.* redistribution of trace elements by fluid flow in slope facies Ediacaran carbonate rocks from the Yangtze Platform (South China)

HARRY BECKER[1*], WIEBKE BAERO[1], MANUEL QUIRING[1], KONRAD HAMMERSCHMIDT[1], UWE WIECHERT[1] AND DOROTHEE HIPPLER[2]

[1]Freie Universitaet Berlin, Institut fuer Geologische Wissenschaften, Germany, hbecker@zedat.fu-berlin.de (* presenting author)

[2]Technische Universitaet Berlin, Institut fuer Angewandte Geowissenschaften, Germany

A major problem for the interpretation of the composition of ancient marine carbonates is the variable response of different elements to diagenesis and post-depositional fluid flow. We have studied this issue in Ediacaran dolostones, limestones and marlstones from members D1, D3 and D4 of the Doushantuo Formation (635-551 Ma) from the slope facies Panmen section (Songtao, Guizhou) on the Yangtze Platform. The carbonate rocks display a strong, but variable influence of secondary processes as indicated by $\delta^{18}O$ (-5 to -14) and $^{87}Sr/^{86}Sr$ (0.723 to 0.710) data in comparison to data of stratigraphically correlated samples from shallow platform settings [1]. Decreasing $^{87}Sr/^{86}Sr$ from bottom to top of the section and very low abundances of feldspar, illite and chlorite in some of these samples suggest that the radiogenic Sr in the carbonates was not introduced by closed-system diagenetic redistribution from silicates within the rock, but by open-system fluid flow and associated recrystallization of carbonates. In the D3 member, the overprint by fluid flow is indicated by a weak correlation of $\delta^{18}O$ with $^{87}Sr/^{86}Sr$ and correlation of $\delta^{18}O$ with $\delta^{13}C_{carb}$. Modeling of fluid-rock interaction shows that high and variable Sr abundances in water rich fluids (low-C/O) are consistent with the data trends in the D3 member, and may account for 1 to 2 ‰ of the variation in $\delta^{13}C_{carb}$. In spite of these secondary modifications, some carbonate rocks at different positions in the section display seawater signals in their acetic acid leachates, such as high Y/Ho and positive or negative Ce anomalies. Relatively high abundances of Th, REE and Pb in the acetic acid leachates and correlations of Th with Fe abundances, suggest that these elements were redistributed by fluid flow. They may have been originally hosted in Fe oxyhydroxide phases in the rock, released upon reduction and dissolution of Fe phases and incorporated into recrystallized carbonates. Further constraints were obtained from leaching experiments on cap dolostones of the section using stepwise digestion in 10% HAc, 6 M HCl and conc. HF-HNO_3. These results indicate the presence of HCl soluble Fe rich phases, presumably oxides or oxyhydroxides. The REE patterns of the HCl fraction are bell shaped and differ considerably from the patterns of acetic acid leachates. The data suggest that in many samples, fluid mobile elements, but also REE, Th and Fe have been redistributed into recrystallized carbonates. This is raising questions about the scale of postdepositional element redistribution in such sections.

[1] Sawaki *et al.* (2010) *Precambrian Research* **176**, 46-64.

Quantum-mechanical calculations on actinide sorption and reduction of sulfides and oxides

U. BECKER[1]* AND D. RENOCK[2]

[1] Dept. of Earth and Environmental Sciences, University of Michigan, Ann Arbor, MI., USA, ubecker@umich.edu (* presenting author)

[2] Dept. of Earth Sciences, Dartmouth College, Hanover, NH., USA, Devon.J.Renock@Dartmouth.edu

The results of several recent studies are challenging the way actinide geochemists consider redox processes in the near surface environment. Such studies include: the complex chemistry of electron and spin transitions between $U^{6+} \leftrightarrow U^{5+} \leftrightarrow U^{4+}$ aqueous complexes and solids, spatially separated redox processes linked over millimeter distances by complex networks of bacterial nanowires combined with pyrite, simultaneous oxidative growth and reductive dissolution on a single hematite crystal driven by potential differences between crystal faces, sulfide oxidation mechanisms that are rate-limited by the transition from high spin O_2 to low spin O.

In order to shed light on the electron transfer between reductants (*e.g.*, hydrogen sulfides, Fe^{2+}, hydroquinones as an organic/microbial analogue), oxidants (different actinyl complexes), catalytic mineral surfaces (periodic slabs and nano-clusters of hematite, pyrite, and mackinawite, and galena), and polarizing anions (*e.g.*, carbonate, sulfate).

An example calculation is the co-adsorption of a uranyl cation and a hydroquinone on the opposite sides of a pyrite nano-cube. The interaction of the hydroquinone with the uranyl complex through the pyrite nanoparticle can be quantified/visualized in different ways: (i) by the synergistic energy of the co-adsorption of uranyl and hydroquinone on pyrite, (ii) by the amount of electron transfer to the uranyl, and (iii) by visualization of the charge distribution in different adsorbate configurations.

During the co-adsorption/reduction process, the hydroquinone becomes positive (sum of Mulliken charges = 1.12) and the uranyl with an initial charge of +2 becomes almost neutral (+0.08), indicating electron transfer of about two elemental charges towards the uranyl. This is an indication that a neutral UO_2 unit is formed, which can serve as a nucleus of UO_2 formation. In contrast, if no hydroquinone is present, only about half an elemental charge is transferred from the pyrite nanoparticle. This is an example how the hydroquinone can be used as an analogue for electron shuttling by metal-reducing bacteria through the pyrite towards the uranyl.

Another example is the co-adsorption of hydroquinone and uranyl on a mackinawite nanoparticle. While the π orbitals of the quinone interact with the postitive Fe cations, the uranyl-O comes within bond distance with the Fe on the right. Electrons can be transferred within the same orbital of the entire system (e.g, the HOMO stretches over the entire system). Interestingly, even though mackinawite is a low-spin system as a bulk mineral, the co-attack by quinone and uranyl spin-polarizes the Fe atoms along the path in a down-up-up-down pattern. This is kinetically important to accommodate the spin transition on the right from U^{6+} (no spin) to U^{4+} (two unpaired spins).

https://doi.org/10.1180/S0026461X00008434 Published online by Cambridge University Press

Archaean cratonic mobilism and growth on a subductionless, stagnant lid Earth

BÉDARD, J.H.[1*], Harris, L.B.[2], THURSTON, P.[3]

[1]Geological Survey of Canada, Québec, Canada, jbedard@nrcan.gc.ca (*presenting author)

[2]Institut national de la recherche scientifique, Québec, Canada

[3]Laurentian University, Sudbury, Canada

Igneous rocks with geochemical signatures similar to those of Phanerozoic continental or oceanic arcs are rare in the Archaean and proposed Archaean ophiolites, Atlantic-style passive margins, overprinting thrust and fold belts, blueschists, ultra high-pressure rocks, paired metamorphic belts, orogenic andesites, and subduction-zone mélanges that typify Phanerozoic orogens are rare to absent. The archetypal Archaean granite-greenstone dome-and-keel architecture has no modern analogue. Most Archaean lavas have geochemical signatures that imply evolution by assimilation-fractional crystallization, rather than the source-metasomatic signatures of Phanerozoic arcs; and trace element models imply that the felsic contaminants were generated by anatexis of typical Archaean tholeiites. Mass balance calculations imply that melting of subducted crust or fractionation of basalt cannot generate requisite volumes of TTG in the available time, and a basal/delaminated oceanic plateau melting model is preferred.

Despite the absence of evidence for Archaean subduction, many Archaean cratons have shortening fabrics and cratons contain terranes with contrasting histories that were somehow assembled. What could be a plausible driving force for compression and terrane accretion on a subductionless Earth? Cratonic mobilism in response to mantle convection currents offers a possible solution to this paradox. Once a proto-craton develops a stiff mantle keel, it would become subject to pressure from mantle currents and would drift. Immature cratons or oceanic plateaux lack deep keels and so would be static. So, contrary to conventional wisdom, we consider that Archaean cratons are not immobile nucleii along whose margins 'mobile belts' form by subduction-zone accretion. Instead, we propose that Archaean cratons were active tectonic agents, accreting basaltic plateaux, other proto-cratons, and heterogeneous mantle domains as they migrated. Overridden oceanic plateau lithosphere would form subcretion complexes where the underthrust basalt would melt to generate syntectonic pulses of tonalite-trondhjemite-granodiorite (TTG), so contributing to craton growth and stabilisation. Garnet pyroxenite restites from anatexis would founder into the mantle and trigger new pulses of tholeiitic magmatism. The non-cratonic Earth would have been covered by a mosaic of shield volcanoes, with eruption and basal attrition being in a quasi steady-state in a stagnant lid régime, suggesting that mantle convection may have been layered in the Archaean.

The Neoproterozoic Franklin Large Igneous Province, geochemical and isotopic evidence for changing sources, and linkages between intrusive and extrusive components

BÉDARD, J.H.[1*], DELL'ORO, T.[2], WEIS, D.[2], SCOATES, J.S.[2], WILLIAMSON, N.[3], COUSENS, B.[3], NASLUND, H.R.[4], HAYES, B.[5], HRYCIUK, M.[6], WING, B.[6], BEARD, C.[2,7]

[1]Geol. Survey of Canada, Québec, Canada, jbedard@nrcan.gc.ca (* presenting author)

[2]PCIGR University of British Columbia, Vancouver, Canada

[3]Carleton University, Ottawa, Canada

[4]SUNY Binghamton, USA

[5]Cardiff University, UK

[6]McGill University, Montreal, Canada

[7]University of Bristol, UK

The Neoproterozoic (ca.716 Ma) Franklin Large Igneous Province formed during the breakup of Rodinia. The Natkusiak continental flood basalts (≤1 km thick, preserved as 2 lobes in a syncline) are the extrusive phase of the Franklin event, and erupted onto a shallow-water continental platform. An underlying fluvial sandstone, the Kuujjua Fm., pinches out towards the NE, suggesting pre-eruptive thermal doming, possibly associated with arrival of a mantle plume. The lowermost extrusive unit (ca 50-100 m thick) is a primitive basalt (7-11 wt% MgO), and is tentatively interpreted as agglutinate (welded fire fountain deposits) erupted from multiple vents. The unit is characterized by LREE-LILE-enrichment, high L/HREE, high $^{87/86}Sr_i$ (up to 0.70791), intermediate εNd (4.0-8.1) and εHf (0.03-6.7), high $^{208/204}Pb$ (up to 39.136), high $^{207/204}Pb$ (up to 15.686), and high $^{206/204}Pb$ (up to18.978) ratios; indicating either an enriched source, extensive crustal contamination, or influx of enriched fluids from the footwall. A hiatus in eruptive activity is marked by deposition of red-weathering volcaniclastic rocks that contain matrix-supported conglomerates (lahars or damburst deposits?) that fill palaeovalleys. Two differentiation cycles of laterally extensive basaltic (10-6% MgO) sheet flows were then deposited above the basal lavas and volcaniclastics. Both cycles show upward shifts in phenocryst populations, decreases in Mg#, Cr and Ni, and increases in incompatible element concentrations, consistent with up-section fractional crystallization. Only cycle 1 sheet flow basalts are exposed in the SW. These have higher εNd (7.7-9.6), lower $^{87/86}Sr_i$ (0.70251-0.70605), higher εHf (4.1-9.7), lower $^{208/204}Pb$ (36.196-37.623), lower $^{206/204}Pb$ (16.147-17. 787), and lower $^{207/204}Pb$ (15.383-15.605) than basal basalts. The cycle 1 sheet flow basalts in the NE have trace element and isotopic trends that differ from those in the SW (c.150km separation), indicating regional-scale isotopic heterogeneity in the source and/or contaminants of these lavas. Alternatively, isotopic heterogeneities may have been enhanced during ascent through the crust in a compartmentalized feeder system.

The plumbing system that fed the lavas is dominated by sills, with localized fault-guided dykes. Two magma populations have been identified: Younger diabasic sills with trace element signatures matching the sheet flow lavas, and older sills (based on cross-cutting relationships), commonly with olivine-enriched bases, that match the basal basalts. Field, geochemical and isotopic evidence imply that steep, dyke-like feeders were sites of preferential wall rock assimilation and allowed melt to ascend between sills. On the scale of the entire magmatic system, the secular decrease in incompatible trace element concentrations, L/HREE ratios, and radiogenic isotope signatures could be interpreted as a decrease in the degree of host contamination with time. Changing magma composition could also reflect a shift from a fertile mantle source to a less enriched source, possibly associated with upwelling of asthenospheric mantle during the separation of Siberia from Laurentia.

https://doi.org/10.1180/S0026461X00008434 Published online by Cambridge University Press

Reference materials mapping: spatial geochemical heterogeneity characterization

L.PAUL BÉDARD[1*], GABRIELLE ROCHEFORT[2], ALEXANDRE NÉRON[3], AND KIM H. ESBENSEN[4]

[1]Sciences de la Terre, Université du Québec à Chicoutimi, Chicoutimi, QC, Canada PBedard@uqac.ca (* presenting author)
[2]Sciences de la Terre, Université du Québec à Chicoutimi, Chicoutimi, QC, Canada gabrielle.rochefort@uqac.ca
[3]Sciences de la Terre, Université du Québec à Chicoutimi, Chicoutimi, QC, Canada alexandre.neron@uqac.ca
[4]Geological Survey of Denmark and Greenland, Copenhagen, Denmark, ke@geus.dk

Reference materials (RM) are mandatory to produce high quality analytical results, and therefore must be well characterized with respect to heterogeneity. Microbeam techniques use very small sample masses, which can make representativity a difficult goal to achieve. Characterization of RM has mainly been done by computing statistics on numerous replicate determinations (microbeam and bulk samples; mg to g). Such studies do not take into account the systematic spatial relationships between determinations and may hence not necesarily arrive at a representative heterogeneity estimate. In the case of glasses (NIST-600s, GSD-1, etc.) and some pressed pellets (MASS-1, MACS-1 and MASS-3), anomalous "hot pots" can sometimes be larger than beam size, and can be clustered or segregated along a spatial trend. Such information is critical to determine optimal beam size or for locating optimal transects for calibration. Improved heterogeneity characterisations will lead to improved constraints on precision and accuracy of RM in general and specifically for microbeam RM.

A set of systematic experiments has been carried out to map RM with LA-ICP-MS and microXRF, to determine concentration variations in the widest possible field of view regimen. The first step is instrumental optimization of mapping to control instrumental drift. MicroXRF mapping of pulverized RM (precious metal bearing: WMS-1, CHR-Pt+, MASS-1 and MASS-3) were used to delineate precious metals nuggets, which are indeed present in many instances. This has been used to demonstrate that large sample masses are often necessary for many sulfide RM. Precipitated materials (such as MASS-1) are devoid of nuggets while most powdered RM showed nuggets. LA-ICP-MS mapping of glasses typically used to calibrate analysis, e.g. NIST-600 series, also show heterogeneities, especially for precious metals. Elemental maps have been computed to show visually heterogeneities and their locations. Variographic analysis has been undertaken to visualize variability as a function of the spatial scales.

Spatial information is an important contribution in characterizing many RM (glass and powders). Such information was previously difficult or expensive to acquire. Now spatially resolved geochemical data for RM are rapidly becomming easily accessible; this type of characterisation is the next step in RM characterization.

Volatile transfer from magma sources in the Taupo Volcanic Zone

FLORENCE BÉGUÉ[1], CHAD DEERING[2*], DARREN GRAVLEY[1], BEN KENNEDY[1] AND ISABELLE CHAMBEFORT[3]

[1]University of Canterbury, Christchurch, New Zealand, florence.begue@pg.canterbury.ac.nz darren.gravley@canterbury.ac.nz ben.kennedy@canterbury.ac.nz
[2]University of Wisconsin-Oshkosh, Oshkosh, USA, deeringc@uwosh.edu (* presenting author)
[3]GNS Sciences, Wairakei Research Centre, Taupo, New Zealand, i.chambefort@gns.cri.nz

The Taupo Volcanic Zone (TVZ) is a rifted arc where dominantly silicic magmatism and volcanism has evolved intimately with tectonic. Two distinct rhyolite magma types (dry-reducing and wet-oxidizing) have erupted from the central TVZ over the past ~550kyrs [1]. We measured major, trace, and volatile element concentrations (including B isotopes) in quartz-hosted melt inclusions from several large, rhyolitic eruptions representing these distinct types in an effort to: 1) determine if the magma was vapour saturated, and 2) identify disparities in the volatile contributions to the overlying hydrothermal systems. Dry magma in the upper crust may not be volatile saturated and, therefore, would contribute very little to the overlying hydrothermal system.

Melt inclusions from the dry type Ohakuri and Mamaku eruptions (~240 ka) have high chlorine values ranging from 0.25 to 0.36wt%, and show a positive correlation between chlorine, fluorine, Rb/Sr ratio and other incompatible elements, suggesting that no vapour phase was exsolved prior to eruption. In comparison, volatile data from the wet type Kaharoa eruption (~1314AD) show vapour saturation and exsolution of a volatile phase during crystallisation [2].

The combination of boron and boron isotopes is an effective tracer of the volatile contribution from slab-derived fluids. Measured B and $\delta^{11}B$ in these two different types of systems, reveal distinct signatures. The isotopic composition of the Kaharoa is homogeneous, with $\delta^{11}B$ of + 4‰, and boron contents range from 20-30 ppm. Because the Kaharoa was saturated, the boron preferentially partitions into the fluid phase ($D_B^{fluid/melt} >> 1$), which requires that a much higher bulk content of boron existed prior to eruption. The Mamaku and Ohakuri melts, on the other hand, have homogeneous boron contents around 15 ppm, but isotopic ratios ranging from – 3 to + 3‰. These two different signatures can be linked to variable contributions of fluid from the subducting slab, and we attribute this to a decrease in slab-derived fluid flux across the TVZ.

Geochemical heterogeneities and the generation of wet vs. dry rhyolites in the TVZ can be directly linked to the input of slab-derived fluids. As such, boron could potentially be a very useful tracer for volatile transfer processes where magmas are saturated. Our methodology can determine if a magmatic system is volatile saturated, and hence, could help identify areas in the upper crust where there is a maximum potential for heat transfer to the overlying geothermal system.

[1] Deering (2008) *Journal of Petrology* **49**, 2245-2276. [2] Johnson (2011) *Geology* **39**, 311-314.

https://doi.org/10.1180/S0026461X00008434 Published online by Cambridge University Press

Great Oxidation Event: How quickly did it come and go?

A. BEKKER[1*], N. PLANAVSKY[2], C. SCOTT[3], C. PARTIN[1], B. RASMUSSEN[4]

[1]Department of Geological Sciences, University of Manitoba, Winnipeg, MB, R3T 2N2 Canada, bekker@cc.umanitoba.ca (* presenting author)
[2]Department of Earth Sciences, University of California, Riverside, CA 92521, USA, planavsky@gmail.com
[3]Department of Earth and Planetary Sciences, McGill University, Montreal, Canada, clinton.scott@mcgill.ca
[4]Department of Applied Geology, Curtin University, Kent Street, Bentley WA 6102, Australia, B.Rasmussen@curtin.edu.au

The loss of mass-independent fractionation of sulfur isotopes (MIF-S) defining the first appearance of oxygen in the atmosphere as a stable component, the so-called Great Oxidation Event (GOE), has been recently constrained between ~2.4 and 2.32 Ga. However, the texture of the pO_2 secular changes in the Late Archean to the Paleoproterozoic remains controversial and highly debated. Some authors favor a gradual rise in atmospheric oxygen starting at ca. 2.7 or 2.5 Ga and a peak at 2.1-2.0 Ga at the end of the Lomagundi positive carbon isotope excursion in seawater composition. Combining geological and geochemical constraints, we will discuss the history of atmospheric and oceanic redox conditions in the early Paleoproterozoic.

Detrital pyrite and uraninite in shallow-marine and terrestrial deposits persists until the loss of MIF-S at ca. 2.32 Ga, when sulfate evaporites first appear in the shallow-water marine record. This change indicates a rapid increase in the seawater sulfate content, at least 10 fold, to >>2 millimole level, associated with oxidation of the atmosphere-ocean system. Consistent with this rapid change, concentrations of redox-sensitive elements (e.g., Mo, Re, and U) in the ca. 2.32 Ga and younger GOE black shales are dramatically higher from those in the pre-GOE black shales. Although surface oxidation likely continued during the Lomagundi excursion, which was tied to high burial rates of organic carbon and high flux of oxygen to surface environments, evidence for this progressive rise is currently unrecognized, with the potential exception of the concentration of redox-sensitive elements in black shales.

The end of the Lomagundi excursion is associated with a sharp collapse in the surface oxidation state as reflected by an abrupt fall in seawater sulfate content, disappearance of sulfate evaporites from the rock record, and drop in concentrations of redox-sensitive elements in black shales. The surface oxidation state returned to the intermediate state between those before and during the GOE. In association with this collapse, methane flux from the ocean to the atmopshere and atmospheric methane concentrations increased, contributing to climatic stability during the Boring Billion. The end of the Lomagundi excursion at ca. 2.1-2.0 Ga and associated negative excursion in carbon isotope values of organic carbon in shales, the so-called Francevillian Event, thus reflects the collapse rather than a peak in the oxidation state of the atmosphere-ocean system.

Land use changes and mercury transfers to aquatic systems in the Brazilian Amazon

Bélanger[1*], Emilie; Lucotte[1], Marc; Oestreicher[1], Jordan; Moingt[1], Matthieu; Rozon, Christine[1]; Davidson[1,2], Robert; Grégoire[1], Benjamin,.

[1]Université du Québec à Montréal, GEOTOP
emilie.belan@gmail.com

[2]Biodôme de Montréal, Canada
robertdavids@gmail.com

In the Tapajos River region of the Brazilian Amazon, mercury (Hg) contamination has become a problem to human health trough fish consumption. Hg present in the water system rises into the trophic chain and affects riparian communities. Studies have shown that recent deforestation contributes to soil mercury release trough terrigenous organic matter fluxes to the aquatic environment. Changes in sedimentation patterns have also been observed, suggesting a large-scale modification of the natural organic matter dynamics in the drainage basins. Local small-scale farmers use slash-and-burn agricultural practices, which consist in slashing and burning a patch of forest to benefit from the soil fertility enrichment caused by fire. After one or two years, soil fertility drops and another patch is slashed and burned. This dynamics creates a mosaic of different land uses: agricultural lands, pastures, secondary forest fallows and forested areas. The aim of this study was to investigate the movements of organic matter and its associated Hg in the watershed and to relate it to land use characteristics. Three watersheds were characterized by geographical system analysis and sampled for vegetation (20 species), soils (33 cores), suspended particulate matter (6 stations) and sediment cores (3, one in each aquatic system). All samples were analyzed for total Hg, lignin biomarkers, C, N and Pb^{210} datation was performed on sediment cores. TOM signatures were elaborated for the different land uses and followed from the terrestrial environments to the aquatic systems. Our results show an increase of TOM and mercury concentrations in recent sediments, with maximum values ranging up to 310 ng/g, concomitant to land use changes and altered watershed characteristics. These findings on the newly colonized watersheds of the Amazon can help to establish the dynamic portrait of Hg movements, leading to the development of conservation measures adapted to this environment.

https://doi.org/10.1180/S0026461X00008434 Published online by Cambridge University Press

Influence of afforestation on soil : The case of mineral weathering

NICOLAS BÉLANGER[1*], BENOIT LAFLEUR[2], YVES CLAVEAU[2] AND DAVID PARÉ[3*]

[1]Université du Québec, Centre d'étude de la forêt
belanger.nicolas@teluq.ca (* presenting author)
[2]UQAM, Centre d'étude de la forêt
benoit.lafleur@uqat.ca
[2]UQAM, Centre d'étude de la forêt
y_claveau@sympatico.ca
[3]Canadian forest service, Laurentian forestry centre
david.pare@rncan-nrcan.gc.ca

Introduction

Planting fast growing trees on abandoned agricultural land (afforestation) is done all over the world as a means to satisfy increasing wood demand. However, similar to modern agriculture, increased nutrient uptake due to fast growth and nutrient export from harvest could lead to a decrease in soil nutrient availability and the increased use of fertilizer to maintain soil productivity. Recent research suggests that some tree species, notably late succession conifers, release acid exudates from their roots which attack the crystal lattice of minerals. This releases substantial amounts of base nutrients (Ca, Mg, K) which could sustain productivity over several rotations without fertilization. A sequential extraction/leaching procedure with diluted salt and weak acid solutions was therefore used to evaluate if available and structural base nutrients and other major cations (Na, Al, Fe) in soils were being depleted along a soil productivity (and age) gradient of hybrid *Populus*, a fast growing early succession deciduous tree genera used worldwide in an intensive plantation context, relative to abandoned agricultural fields.

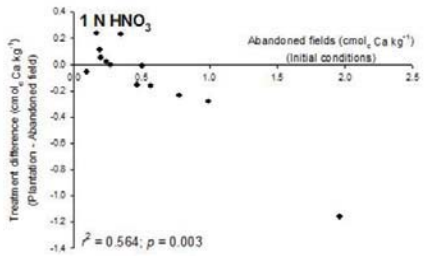

Figure 1. Relationship between abandoned fields and treatment difference for soil Ca following 1 N HNO_3 extraction.

Results and Conclusion

Soil structural Ca and Mg were lower under *Populus* at about half of the sites. The results suggest a greater capacity of the trees to promote soil mineral weathering than plants in abandoned fields. However, this ability appears to be linked to the initial chemical and mineralogical composition of the soils: the divergence between land use types was larger at sites with greater soil cation exchange capacity (more clay) and (or) structural Ca and Mg (more easily weathered Ca and Mg containing minerals) (Fig. 1). This means that fast growing *Populus* may only be capable of augmenting soil mineral weathering where soils are vulnerable to acid exudates. Hybrid *Populus* are not able to promote base nutrient release from minerals on coarse textured acidic soils where soil productivity is a real concern.

High-iron chamosite in bituminous coals in Xuanwei County, China: a possible contributing factor to a high lung cancer rate

HARVEY E. BELKIN[1*], AND JAMES C. HOWER[2]

[1]U.S. Geological Survey, Reston, USA, hbelkin@usgs.gov (* presenting author)
[2]University of Kentucky Center for Applied Energy Research, Lexington, USA, james.hower@uky.edu

Certain communes in Xuanwei County, eastern Yunnan Province, have some of the highest rates of lung cancer mortality in China. Nationwide, age-adjusted mortality rates (per 100,000) are 6.8 and 3.2 for Chinese males and females, respectively [1]. With rates for Yunnan Province 4.3 and 1.5. In Xuanwei County, the rates are 27.7 for males and 25.3 for females and in the three communes with the highest mortality, the rates are males 118.0 and females 125.6 [1]. This exceptionally high rate and the similarity between the male and female rates is unusual as the females in this locality are essentially non-smokers. Previous workers attributed the high incidence of Xuanwei County lung cancer to domestic combustion of locally mined coal in houses with non-vented stoves [2]; however, this practice occurs in many Provinces without the effect of a high lung cancer rate. Generation of polycyclic aromatic hydrocarbons (PAHs) by coal combustion was first thought to be the disease etiology [1]. Additional work on coal mineralogy and combustion models suggested that small (<10 μm) to nanometer-sized quartz played a significant role in the disease etiology and that the combined influence of silica-volatile (PAHs) interaction was more hazardous and causal than either component alone [3].

We have examined 12 smoky bituminous coals from mines in communes with various degrees of age-adjusted lung cancer death rate as well as smokeless anthracite coals from mines southwest of Xuanwei City. We find no significant relationship between overall coal characteristics and the lung cancer rate with the exception of the iron content of the coal (expressed as Fe_2O_3 on an ash-basis). The abundance of very iron-rich chamosite [(Fe/(Fe+Mg)) > 0.85] is the source of this iron enrichment (iron sulfides and oxides are rare).

Although iron is critical for normal cell function, because of its ability to reduce oxygen, iron is the most potent inducer of free radicals in most biological systems. Recent work on the cause of coal workers' pneumoconiosis suggests a strong correlation with the bioavailable iron content of coal [4]. We suggest that during domestic coal combustion, chamosite is thermally decomposed and may supply minute iron oxides to the coal smoke. Although our statistical basis is small (n = 12) the presence of this high-iron phase may add to the combined influence of PAHs and silica and should be considered as a potential contributing factor to the high lung cancer rate.

[1] Mumford *et al.* (1987) *Science*, **235,** 217-220. [2] Chapman *et al.* (1988) *Arch. Environ. Health*, **43**, 180-185. [3] Large *et al.* (2009) *Environ. Science & Tech*. **43**, 9016-9021. [4] Xi *et al.* (2005) *Environ. Health Persp*. **113**, 964-968.

https://doi.org/10.1180/S0026461X00008434 Published online by Cambridge University Press

The Effects of Dissolved Chloride on the $Fe^{3+}/\sum Fe$ of Rhyodacitic Melt

AARON S. BELL*[1], JAMES WEBSTER[2], & M. DARBY DYAR[3]

[1]American Museum of Natural History, New York, NY, USA, abell@amnh.org
[2]American Museum of Natural History, New York, NY, USA, jdw@amnh.org
[3]Mount Holyoke College South Hadley, MA, USA , mdyar@mounthoyoke.edu

We have conducted a series of experiments designed to evaluate intrinsic effects of the dissolved chlorine on the equilibrium $Fe^{3+}/\sum Fe$ in hydrous, chloride-rich rhyodacite liquids. Experiments were conducted at series of controlled fO_2 in an IHPV at 950°C and 130 MPa. The $Fe^{3+}/\sum Fe$ values of the run-product glasses were measured with synchrotron μ-XANES spectroscopy on beamline 13ID-D at the Advanced Photon Source, Argonne National Laboratory.

Data from experiments indicate that the addition of dissolved chloride increases the equilibrium $Fe^{3+}/\sum Fe$ of the melt relative to values predicted by several popular algorithms that equate $Fe^{3+}/\sum Fe$ with fO_2 and bulk melt composition. The deviation of the observed $Fe^{3+}/\sum Fe$ values from their predicted "equilibrium" values suggests that the interaction of dissolved chloride with Fe in the melt alters the activity-composition relationships for FeO and $FeO_{1.5}$ in the melt. Calculated G^{ex} associated with the $FeO_{1.5}$ and FeO components of the melt systematically vary as a function of the imposed experimental fO_2.

Data from these experiments imply that hydrous Fe-poor melts with intermediate silica and fairly modest chloride contents (i.e., ≤ 0.75 wt%) may display rather oxidized $Fe^{3+}/\sum Fe$ values despite possessing a relatively reduced equilibrium fO_2. The data further suggest that any empirical or thermodynamic model of the $Fe^{3+}/\sum Fe$ in silicate liquids must include terms to account for the non-ideal behaviour of $\gamma FeO_{1.5}/\gamma FeO$ that is associated with the presence of dissolved chlorine in the melt.

Jack Hills zircons record a thermal event coincident with the hypothesized Late Heavy Bombardment

*E. A. BELL, T. M. HARRISON

Dept. of Earth and Space Sciences, University of California Los Angeles, Los Angeles, CA, USA, ebell21@ucla.edu (* presenting author)

Introduction

The Late Heavy Bombardment (LHB) is a hypothesized period of intense bombardment of the inner solar system at ca. 3.9 Ga, inferred from disturbed lunar ages. Major thermal effects to the Earth's crust are expected from LHB-impact scenarios, but unambiguous terrestrial evidence of this event is unknown, probably owing to the sparse geologic record from this period. However, detrital zircons from Jack Hills, Western Australia span the period 4.3-3.0 Ga, including the time period of the LHB, and may record evidence for this event.

Results and Discussion

We investigated the trace element chemistry of the Jack Hills detrital zircon record for the period 4.0 – 3.8 Ga in search of apparent changes in thermal conditions consistent with the LHB. The Ti-in-zircon temperature (T^{xlln}) distribution is well established for Hadean detrital grains, clustering about an average value of ~680°C – likely indicating near water-saturated granitic melting conditions. The average T^{xlln} does not change appreciably through the period 4.0-3.8 Ga, but between 3.91-3.84 Ga, there is a notable group of low-Ti zircons with apparent T^{xlln} extending well below the granite solidus. Further investigation revealed that this period contains two groups of zircons with clearly distinguishable trace element signatures. Group I resembles the Hadean Jack Hills zircons in Ti, Hf, Ce, U, and Th/U, whereas Group II contains lower Ti, Ce, and Th/U along with higher Hf and U. Group II also displays a high degree of U-Pb concordance compared to the 4.0-3.8 Ga Jack Hills zircons as a whole, despite their high U contents. We interpret Group II as originating from the solid-state recrystallization of originally magmatic (perhaps even Group I-like) zircon during a thermal event ca. 3.9 Ga. This thermal excursion is also seen in epitaxial growths on Hadean zircon cores found in previous studies.

Conclusion

A group of Jack Hills zircons at ca. 3.9 Ga appear recrystallized, and likely record a significant thermal event in the source terrane. Although an endogenic cause for this thermal event cannot be definitively ruled out, these observations may constitute the first terrestrial evidence for the LHB.

https://doi.org/10.1180/S0026461X00008434 Published online by Cambridge University Press

Genome-enabled studies of anaerobic, nitrate-dependent U(IV) oxidation

HARRY R. BELLER[1]*, TINA C. LEGLER[2], STACI R. KANE[2], PEGGY O'DAY[3], PENG ZHOU[1,3]

[1]Lawrence Berkeley National Laboratory, HRBeller@lbl.gov (* presenting author)
[2] Lawrence Livermore National Laboratory
[3] University of California, Merced

Anaerobic, nitrate-dependent U(IV) oxidation has considerable relevance to the bioremediation of uranium-contaminated aquifers and also represents a novel bacterial metabolic capability of fundamental scientific interest. A favored process for U bioremediation is *in situ* reductive immobilization, a process by which anaerobic bacteria reduce water-soluble U(VI) complexes to poorly soluble U(IV) phases. The discovery that *Thiobacillus denitrificans* [1] and other bacteria can anaerobically re-oxidize, and thus, re-mobilize, uranium in groundwater highlights a process that could compromise the efficiency of this bioremediation approach. While microbial U(VI) reduction has been the subject of extensive research, far less is known about anaerobic U(IV) re-oxidation.

We will discuss our efforts to identify the genes/proteins that are key to nitrate-dependent U(IV) oxidation in *T. denitrificans*. These efforts included: (a) detailed analysis of the *T. denitrificans* genome [2], (b) whole-genome transcriptional analyses of *T. denitrificans* with high-density, oligonucleotide microarrays [3], (c) proteomic studies of membrane-associated, *c*-type cytochromes in *T. denitrificans* [4], and (d) development of a genetic system in *T. denitrificans* [5].

We identified two diheme, *c*-type cytochromes critical to anaerobic U(IV) oxidation in *T. denitrificans* (putatively c_4 and c_5 cytochromes, Tbd_0187 and Tbd_0146, respectively). Insertion mutations in each of the two genes encoding these cytochromes resulted in a greater than 50% decrease in nitrate-dependent U(IV) oxidation activity, and complementation *in trans* restored activity to wild-type levels. Sucrose-density-gradient ultracentrifugation confirmed that both cytochromes are membrane associated. Sequence-based evidence links the Tbd_0187 protein to the high midpoint reduction potentials that would be required to catalyze U(IV) oxidation. Insertion mutations in other membrane-associated *c*-type cytochromes in *T. denitrificans* did not diminish U(IV) oxidation. To date, Tbd_0146 and Tbd_0187 are the only genes identified as being associated with anaerobic U(IV) oxidation.

We are also investigating nitrate-dependent Fe(II) oxidation in *T. denitrificans*, a process that we observed to accelerate U(IV) oxidation. Notably, the two cytochromes involved in U(IV) oxidation in *T. denitrificans* do not appear to be involved in Fe(II) oxidation. Random transposon mutagenesis studies to further investigate Fe(II) oxidation in *T. denitrificans* are ongoing.

[1] Beller (2005) *Applied and Environmental Microbiology* **71**, 2170-2174. [2] Beller *et al.* (2006) *Journal of Bacteriology* **188**, 1473-1488. [3] Beller *et al.* (2006) *Journal of Bacteriology* **188**, 7005-7015. [4] Beller *et al.* (2009) *Biodegradation* **20**, 45-53. [5] Letain *et al.* (2007) *Applied and Environmental Microbiology* **73**, 3265-3271.

Stable Isotope and Isotopomeric Constraints on N_2O Production in Wastewater Treatment Plants

F. BELLUCCI[1*], M. GONZALEZ-MELER[2], N.C. STURCHIO[2], J.K. BÖHLKE[3], N. E. OSTROM[4], AND J. KOZAK[5]

[1]Argonne National Laboratory, Argonne, IL, USA, fbellucci@anl.gov (* presenting author)
[2]University of Illinois at Chicago, Chicago, IL, USA, mmeler@uic.edu; sturchio@uic.edu
[3]U.S. Geological Survey, Reston, VA, USA, jkbohlke@usgs.gov
[4]Michigan State University, E. Lansing, MI, USA ostromn@msu.edu
[5]Metropolitan Water Reclamation District of Greater Chicago, Chicago, IL, USA, joseph.kozak@mwrd.org

Wastewater treatment plants (WWTPs) constitute a substantial source of N_2O to the atmosphere, with a wide range of estimated emission factors, varying from 0.3 to 140 g N_2O/person/yr [1]. The majority of N_2O emissions occur in the aerobic reactors, where both incomplete nitrification and denitrification might contribute to the overall N_2O emissions. To better constrain production mechanisms and overall N_2O fluxes, we measured N and O isotope ratios of NH_4^+, NO_2^-/NO_3^-, and N_2O, and isotopomer ratios (N isotope site preference) of N_2O at two large-scale activated-sludge WWTPs in Chicago.

The average N2O concentration in the off-gas from the aerobic reactors was 34 and 56 ppmv for plants 1 and 2, respectively. At both plants the isotopic distribution of the major aqueous N-species (NO_3^- and NH_4^+) within the aerobic reactor can be approximated with a Rayleigh-type fractionation model determined by nitrification of ammonium along the wastewater flow path, accompanied by denitrification of about 5 % of the NO_3^- produced, with constant fractionation factors of about -15 ‰ and -20 ‰ for NH_4^+ nitrification and NO_3^- denitrification, respectively. The N isotope site preference in N_2O, averaging +2.7 ‰ and +3.9 ‰ at the two plants, suggests that N_2O was mainly produced by incomplete denitrification [2] in the portions of the tanks where dissolved oxygen was between 0.2 and 2.5 mg/L (fig. 1).

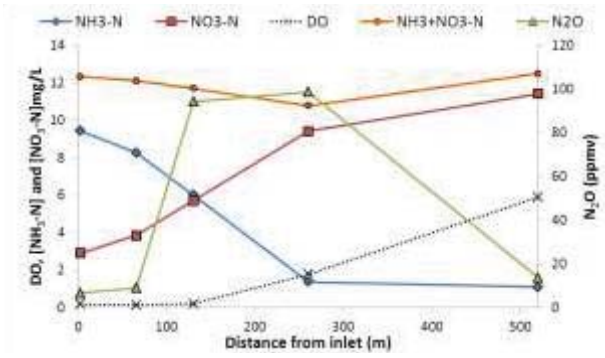

Figure 1. Average concentrations of dissolved oxygen (DO), N aqueous species, and off-gas N_2O along the wastewater flow path in a single tank of the aerobic reactor at plant 1.

[1] Ahn *et al.* (2010) *Environ. Sci. Technol.* **44**, 4505-4511.
[2] Sutka *et al.* (2006) *Appl. Environ. Microbiol.* **72**, 638-644.

https://doi.org/10.1180/S0026461X00008434 Published online by Cambridge University Press

The early formation of the continental crust: constraints from zircon Hf-isotope data

E.A. BELOUSOVA[1], W.L. GRIFFIN[1], Y.A. KOSTITSYN[2], N.J. PEARSON[1], G. BEGG[3] AND S.Y. O'REILLY[1]

[1]ARC Centre of Excellence for Core to Crust Fluid Systems, Department of Earth and Planetary Sciences, Macquarie University, Sydney, NSW 2109, Australia
elena.belousova@mq.edu.au (*presenting author); bill.griffin@mq.edu.au; norman.pearson@mq.edu.au; sue.oreilly@mq.edu.au
[2]GEOKHI RAS, Moscow, Russia, kostitsyn@geokhi.ru
[3]Minerals Targeting Intl., West Perth WA, 6005, Australia, graham@mineralstargeting.com

A worldwide database of >16,000 U–Pb and Hf-isotope analyses of zircon, largely from detrital sources, has been interogated to analyse the processes of crustal evolution on a global scale, and to test existing models for the growth of continental crust through time. At any timeslice, most zircons have ε_{Hf} well below the Depleted Mantle (DM) growth curve, reflecting later reworking of originally juvenile material. To quantitatively estimate the proportion of juvenile material added to the crust at any given time during its evolution, it is necessary to correct for this effect. "Crustal" model ages are calculated assuming the zircon-bearing magmas were generated from the average continental crust ($^{176}Lu/^{177}Hf = 0.015$); zircons with non-juvenile Hf are projected back to the DM growth curve using this ratio. Juvenile magmas are defined as having $\varepsilon_{Hf} \geq 0.75$ times the ε_{Hf} of the DM at the time of genesis. The distribution of corrected model ages can then be used to model the true crustal growth rate over the 4.56 Ga of Earth's history. The modelling shows that there was little episodicity in the production of new crust, as opposed to peaks in magmatic ages. The distribution of age-Hf isotope data from zircons worldwide implies that at least 60% of the existing continental crust separated from the mantle before 2.5 Ga, and has been variably reworked since then. However, taking into consideration new evidence coming from geophysical data, and correcting for the geographical biases in database, the formation of most continental crust still earlier in Earth's history (at least 70% before 2.5 Ga) is even more probable. Thus, crustal reworking has dominated over net juvenile additions to the continental crust, at least since the end of the Archean. Moreover, the juvenile proportion of newly formed crust in any timeslice decreases stepwise through time: it is about 70% in the 4.0–2.2 Ga time interval, about 50% in the 1.8–0.6 Ga time interval, and possibly less than 50% after 0.6 Ga. These changes may be related to the formation of supercontinents.

Applications of the Arctic sea ice proxy IP_{25}: Quantitative versus qualitative considerations

SIMON BELT[1*], PATRICIA CABEDO SANZ[1], ALBA NAVARRO RODRIGUEZ[1], JOCHEN KNIES[2], KATRINE HUSUM[3], AND JACQUES GIRAUDEAU[4]

[1]Plymouth University, Plymouth, UK, sbelt@plymouth.ac.uk (* presenting author)
[2]Geological Survey of Norway, Trondheim, Norway, Jochen.Knies@NGO.NO
[3]University of Tromsø, Tromsø, Norway, katrine.husum@uit.no
[4]Université Bordeaux, Bordeaux, France, J.Giraudeau@epoc.u-bordeaux.fr

Background

The presence of the sea ice diatom biomarker IP_{25} in Arctic marine sediments has been used in previous studies as a proxy for past spring sea ice occurrence and as an indicator of wider palaeoenvironmental conditions for different regions of the Arctic over various timescales [e.g. 1, 2]. Recent attempts have also been made to make the interpretations of the IP_{25} data more quantitative by comparison of IP_{25} (and other biomarker) concentrations with known sea ice conditions (3). However, the extent to which such calibrations can be extrapolated for longer timescales and for different Arctic regions remains unclear.

Current work

This presentation will focus on recent results, with particular emphasis on the importance of accurate analytical methods for the quantification of IP_{25} in marine sedments and a consideration of the factors that likely influence whether IP_{25}-based interpretations can be considered as qualitative or quantitative. Recent case studies to illustrate these points will be taken from different geological epochs (including modern times, the Holocene and the Younger Dryas) and from a diverse range of Arctic and sub-Arctic regions including the Canadian Arctic and the Nordic Seas. The outcomes of these analyses not only provide important information on past Arctic sea ice conditions, but also help identify areas of research that still require attention.

[1] Belt et al. (2007) *Org. Geochem.* **38**, 16-27. [2] Vare et al. (2009) *QSR* **28**, 1354-1366. [3] Müller et al. (2011) *EPSL* **306**, 137-148.

https://doi.org/10.1180/S0026461X00008434 Published online by Cambridge University Press

Geochemical proxies for changes in dust sources in Negev desert loess

MICHAL BEN-ISRAEL[1,2*], YIGAL EREL[1], YEHOUDA ENZEL[1], RIVKA AMIT[2]

[1]Hebrew University of Jerusalem, Institute of Earth Sciences, Israel, michal.benisrael@mail.huji.ac.il (* presenting author)
[2]Geological Survey of Israel, Jerusalem, Israel

The loess of the Negev desert of Israel, was deposited mainly during the late Pleistocene [1, 2]. It is characterized by a bimodal grain-size distribution with modes between 2-8 micrometer (fine silt) and 50-60 micrometer (coarse silt) that represent two different sources of dust, one distal and one proximal [3].

Here we investigate the carbonate-free samples of the two size fractions and search for a geochemical signature of the distal and proximal sources of the loess in three OSL-dated primary loess sequences along a climatic transect: Hura village (~250 mm/yr) and Ramat Beka (~150 mm/yr) in the northern Negev and Mt. Harif (~100 mm/yr) in the central Negev. The fractions are separated and analyzed for major and trace elements and for Sr and Nd isotopic composition. Preliminary results show differences between the fine and coarse fractions that agree with the observation of two different sources contributing to loess in the Negev. Sr-Nd isotopic ratios of both silt fractions suggest contribution from several distal (e.g. Sahara, Arabia) and local proximal sources (e.g. Sinai deserts, Nile delta sediments, and the Sinai-Negev sand dunes). Moreover, changes in loess sources over time were detected in shifts in Sr and Nd isotopic values of the fine fractions, these shifts acure at ~60-70 kyr in Mt. Harif and Ramat Beka sites and at ~20 kyr at Hura site.

These results support the formation model of primary desert loess by eolian abrasion of sand dunes and suggest that the loess chemical and isotopic composition reflect changes of dust sources over time.

[1] Crouvi *et al.* (2009) *Journal of Geophysical Research* **114 (F02017)**, 1-16.
[2] Amit *et al*. (2011) *Geological Society of America Bulletin* **123**, 873-889.
[3] Yaalon and Dan (1974), *Zeitschrift fur Geomorphologie Supplementband* **20**, 91–105.

CHARACTERIZATION OF HUMIC ACID REACTIVITY MODIFICATIONS DUE TO ADSORPTION ONTO α-AL_2O_3

M. F. BENEDETTI[1*], N. JANOT[1,2], X. ZHENG[3], J.P. CROUE[3], P. E. REILLER[2]

[1] Université Paris Diderot, Sorbonne Paris Cité, Institut de Physique du Globe de Paris, UMR 7154 CNRS, F-75013 Paris, France, benedetti@ipgp.fr (* presenting author)
[2] CEA/DEN/DANS/DPC/SECR, Laboratoire de Spéciation des Radionucléides et des Molécules, F-91191 Gif-sur-Yvette, France, Pascal.REILLER@cea.fr
[3] King Abdullah University of Science and Technology Thuwal, Water Desalination and Reuse Research Center, Kingdom of Saudi Arabia, jp.croue@kaust.edu.sa

Adsorption of purified Aldrich humic acid (PAHA) onto α-Al_2O_3 is studied by batch experiments at different pH, ionic strength and coverage ratios R (mg of PAHA by m² of mineral surface). After equilibration, samples are centrifuged and the concentration of PAHA in the supernatants is measured. The amount of adsorbed PAHA per m² of mineral surface is decreasing with increasing pH. At constant pH value, the amount of adsorbed PAHA increases with initial PAHA concentration until a constant pH-dependant value is reached.

UV/Visible specific parameters such as specific absorbance $SUVA_{254}$, ratio of absorbance values E_2/E_3 and width of the electron-transfer absorbance band Δ_{ET} are calculated for supernatant PAHA fractions of adsorption experiments at pH 6.8, to have an insight on the evolution of PAHA characteristics with varying coverage ratio. No modification is observed compared to original compound for $R \geq 20$ mg_{PAHA}/g. Below this ratio, aromaticity decreases with initial PAHA concentration. Size-exclusion chromatography - organic carbon detection measurements on these supernatants also show a preferential adsorption of more aromatic and higher size fractions.

Spectrophotometric titrations were done to estimate changes of reactivity of supernatants from adsorption experiments made at pH ≈ 6.8 and different PAHA concentrations. Evolutions of UV/Visible spectra with varying pH were treated to obtain titration curves that are interpreted within the NICA-Donnan framework. Protonation parameters of non-sorbed PAHA fractions are compared to those obtained for the PAHA before contact with the oxide. The amount of low-affinity type of sites and the value of their median affinity constant decrease after adsorption. From PAHA concentration in the supernatant and mass balance calculations, "titration curves" are obtained and fitted for the adsorbed fractions for the first time. These changes in reactivity to our opinion could explain the difficulty to model the behavior of ternary systems composed of pollutants/HS/mineral since additivity is not respected.

Figure 1: LC-OCD chromatograms of PAHA and of supernatants from adsorption experiments at 0.1M and pH ≈ 6.8 (R in mgPAHA/g α-Al_2O_3).

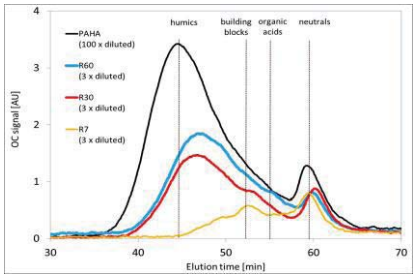

https://doi.org/10.1180/S0026461X00008434 Published online by Cambridge University Press

Stabilization and Assembly of Mineral Clusters Guided by Enamel Proteins.

PING-AN FANG[1], HENRY C. MARGOLIS[2], JAMES F. CONWAY[1], JAMES P. SIMMER[3], ELIA BENIASH[1*]

[1]University of Pittsburgh, Pittsburgh, PA, USA;
[2]The Forsyth Institute, Cambridge, MA, USA;
[3]University of Michigan, Ann Arbor, MI, USA;
*-presenting author ebeniash@pitt.edu

Dental enamel, being the most mineralized vertebrate tissue, is extremely well preserved in the paleontological record and thus a favorite subject for studies of vertebrate evolution, archeology and paleoclimate. Enamel is a structurally complex hierarchical nanomaterial. Although, mature enamel is 95% carbonate apaptite it starts as a network of nanocrystaline arrays suspended in a protein matrix, with the mineral phase comprising only 10% of its volume. Despite these differences in composition, the mineral organization in nascient and mature enamel is identical. While the organic matrix is believed to regulate mineral formation, the basic mechanisms of enamel mineralization are poorly understood. Here we present our recent studies of calcium phosphate mineralization *in vitro* in the presence of the major enamel matrix protein, amelogenin. These experiments were carried out on carbon-coated electron microscopy (EM) grids, and studied in conventional and cryo-EM. We found that amelogenin induces formation of parallel arrays of apatitic crystallites that are structurally similar to the basic building blocks of enamel, enamel rods. Importantly, these structures only formed when monomeric, rather than preassembled, amelogenin was introduced to the mineralization solutions. These results suggest that the mineralization occurs not on the preformed organic matrix as in other systems but instead via cooperative interactions between forming crystals and assembling proteins.[*1*] Our cryo-EM studies show that amelogeinin undergoes stepwise assembly via oligomers that then organize into higher order structures. Our results indicate that amelogenin oligomers stabilize calcium phosphate prenucleation clusters and organize them into linear chains. Subsequently, the clusters fuse together to form needle-shaped mineral particles which further organize into parallel arrays.[*2*] We find that the mechanism of enamel formation is very different from the templated mineralization that is observed in other biomineralization systems. Specifically our results indicate that amelogenin oligomers can stabilize prenucleation clusters and organize them into mesostructures prior to their crystallization. This mechanism in which protein assemblies fully control organization of the initial mineral phase enables formation of intricate structures that cannot be obtained via classical crystallization from supersaturated solutions. These studies supported by NIH grants R01DE016376 (to H.C.M.), R01DE016703 (to E.B.) and PA grant SAP 4100031302 (to J.F.C.)

[1] E. Beniash, J. P. Simmer, H. C. Margolis, (2005) *J. Struct. Biol.* **149**, 182. [2] P. A. Fang, J. F. Conway, H. C. Margolis, J. P. Simmer, E. Beniash, (2011) *PNAS* **108**, 14097.

Fluid inclusions give chemical, physical, biological, and climatic insights into acid saline lake and groundwater systems

KATHLEEN COUNTER BENISON
Dept. of Earth and Atmospheric Sciences, Central Michigan University, Mt. Pleasant, Michigan, 48859 USA, benis1kc@cmich.edu

Acid saline lakes and associated shallow groundwaters represent amongst the Earth's most extreme aqueous chemistries. Modern lakes and groundwaters in Western Australia and Chile have pHs as low as 1.5, total dissolved solids as high as 32%, unusually high concentrations of Al, Si, and Fe, and many other atypical chemical characteristics. Permian lake environments in the U.S. midcontinent had even more extreme water compositions.

Fluid inclusions in halite and gypsum from modern and Permian acid saline lakes record specific physical, chemical, and biological conditions of these environments. Primary inclusions in these chemical sediments trap shallow lake water, air bubbles, crystals of other minerals, and microorganisms. Isolated fluid inclusions in early diagenetic phases of halite are remnants of shallow groundwaters and yield their chemical compositions.

A variety of traditional methods, including petrography, freezing/melting microthermometry and laser Raman spectroscopy, and innovative variations, such as homogenization of artificially-nucleated vapor bubbles and UV-vis petrography, produce data detailing environmental conditions. Other traditionally used methods, such as laser ablation ICP-MS, are not effective due to the nature of the inclusions. Making synthetic solutions that match the complexity of natural acid saline inclusions is another challenge. Ongoing efforts include the analyses of modern and Permian air and documentation of microorganisms and organic compounds within these fluid inclusions (Fig. 1).

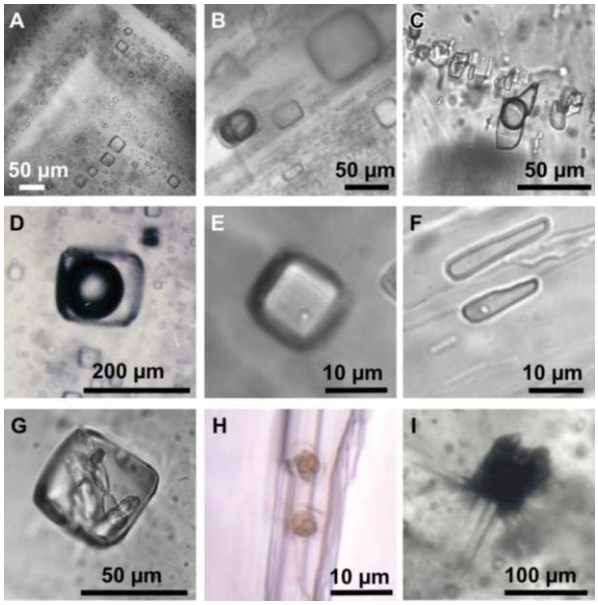

Figure 1: Primary fluid inclusions in acid saline halite and gypsum. A. Fluid inclusions along growth bands in Permian Nippewalla Group halite, Kansas. B. Air in inclusion in modern halite, Western Australia. C. Air in inclusion in modern gypsum, Western Australia. D. Air in inclusion in Permian halite, Nippewalla Group, Kansas. E. Cocci-shaped bacterium/archaeon suspect in Permian halite, Nippewalla Group, Kansas. F. Cocci-shaped bacterium/archaeon suspect in modern gypsum, Western Australia. G. Organic compounds and crystals in fluid inclusion, Permian Nippewalla Group halite, Kansas. H. Algal or pollen suspects in modern gypsum, Western Australia. I. Microbial community in inclusion, Permian Opeche Shale halite, North Dakota.

https://doi.org/10.1180/S0026461X00008434 Published online by Cambridge University Press

Equilibrium core formation loses it's lustre: High pressure & temperature partitioning of gold

NEIL BENNETT[1*] & JAMES BRENAN[1]

[1]The University of Toronto, Toronto, Canada, bennett@geology.utoronto.ca (* presenting author)

Experiments to determine the distribution of highly siderophile elements (HSE) between core-forming metal and the magma ocean suggest that the primitive upper mantle (PUM) should be highly depleted in most of these constituents relative to what is observed. This is not the case for Au. We have measured Au solubility at 2GPa and 1800-2315°C, at ~IW-IW+2.5, under both C-bearing and C-free conditions. Metal-silicate partition coefficients ($D_{Met/Sil}$) were then calculated using the relation of [1]. After combination with the low temperature results of [2], the following temperature dependence for $D_{Met/Sil}$ was found:

$$D_{Met/Sil} = 1.14(0.07)*10^4/T\,(\mathrm{K}) - 1.41(0.34)$$

$D_{Met/Sil}$ is essentially independent of fO_2 and the results from previous studies at 0.1MPa-23GPa [2], [3] agree well with our 2GPa data. Temperature therefore appears to be the primary factor controlling the affinity of Au for Fe-metal. Os isotope systematics and concentrations of the other HSEs in the PUM are best explained by a late veneer of LL-chondrite, comprising 0.5% of the bulk silicate earth [4]. $D_{Met/Sil}$ values for Au limit metal-silicate equilibration to ~2450°C if an over-abundance of Au in the PUM is to be avoided, placing the base of the magma ocean at ~400km. This is much shallower than the >800km depth required by the convergence of Ni-Co partitioning [5]. Low $D_{Met/Sil}$ values at high temperature also predict Au/Ir ratios much greater than estimated for the PUM. Metal-silicate equilibrium therefore appears unable to account for the Au content of the PUM. One solution to this discrepancy may be incomplete equilibration between the magma-ocean and the accreting cores of large, differentiated planetesimals [6]. In this scenario, Au may be transported to the Earth's proto-core deprived of communication with molten-silicate, thus imbuing the core with a Au content greater than predicted by metal-silicate partitioning.

[1] Borisov *et al* (1994) *GCA* **58**, 705-716. [2] Borisov & Palme (1996) *Min. & Pet.* **56**, 297-312. [3] Danielson *et al* (2005) *LPSC XXXVI*, 1955. [4] Brenan & McDonough (2009) *Nature* **2**, 798-801 [5] Bouhifd & Jephcoat (2011) *EPSL* **307**, 341-348. [6] Dahl & Stevenson (2010) *EPSL* **295**, 177-186.

Expanding early Earth frontiers: A new Eoarchean-Hadean(?) terrane in Southwestern Greenland

VICKIE C. BENNETT[1*], ALLEN P. NUTMAN[2], JOE HIESS[3] AND CLARK R.L. FRIEND[4]

[1]Australian National University, Canberra, Australia, vickie.bennett@anu.edu.au. (* presenting author)
[2]Universisty of Wollongong, allen.nutman@gmail.com
[3]NIGL, British Geological Survey, jies@bgs.ac.uk
[4]45 Stanway Road, Headington, Oxford, UK

The strongest controls on early Earth processes and environments are obtained through direct study of the rock record, which currently, with few exceptions, terminates at ca. 3.9 Ga. Although rare >4.0 Ga zircons and their inclusion suites preserved in Western Australian Mesoarchean metasediments provide a wealth of information about early Earth history and conditions, they are an incomplete and likely restricted record of early processes.

Here we present new geochemical observations from metagabbros and associated felsic rocks from a previously unstudied region of SW Greenland. Minimum age constraints on the metagabbros are provided by U-Pb zircon (SHRIMP) ages of cross-cutting granitoids; a dated tonalite has a dominant population of euhedral, oscillatory-zoned magmatic zircons with an age of 3889±5 Ma. Two adjacent relatively older gabbros yielded populations of small, oval zircons with only ca. 2.97 Ga ages, which are interpreted to have formed in a recognized regional metamorphic event. This event is not recorded at either Isua or on Akilia, demonstrating that this is a distinct block of ancient crust, rather than contiguous with previously documented Eoarchean domains. Initial εHf values of the ca. 3.89 Ga zircons are within error of estimated chondritic compositions, with no evidence for early Lu/Hf fractionation. This is in accord with Lu-Hf data from zircon populations extracted from >3.7 rocks worldwide.

Measured Hf isotopic compositions of the metagabbro Mesoarchean metamorphic zircons determined by LA-MC-ICPMS range from εHf= -79 to -83; initial compositions calculated at the metamorphic age are highly negative (-13 to -16). Two-stage chondritic mantle model ages calculated using plausible $^{176}Lu/^{177}Hf$ ratios for the pre-zircon first stage are >4.0 Ga. For example, using $^{176}Lu/^{177}Hf$ =0.018 as typifies Isua metabasaltic rocks, yields chondritic model ages of ca. 4.3 Ga. In contrast, similar-aged metamorphic zircons from a nearby Mesoarchean metasedimentary rock have positive initial εHf values =+8 with DM model ages equal to zircon crystallization age. The ancient Hf model ages combined with the minimum 3.89 Ga age provided by cross-cutting tonalites point to a ≥4.0 Ga age for the metagabbros. Continued investigations of these potential Hadean rocks are in progress.

The majority of rocks analysed from SW Greenland Eoarchean terranes have ^{142}Nd isotopic anomalies when compared with modern terrestrial rocks, with the magnitude of ^{142}Nd generally increasing with crystallization age as shown by Bennett et al, (*Science*, 2007). In the absence of igneous zircons in the ≥3.89 Ga metagabbros, ^{142}Nd compositions may provide confirmation of the Hadean age suggested by Hf isotopic modelling. These recently recognised earliest Eoarchean and possibly Hadean suites are a significant new laboratory for testing models of early Earth formation and evolution.

https://doi.org/10.1180/S0026461X00008434 Published online by Cambridge University Press

3D visualisation of core-forming melts

M. BERG*[1], I.BUTLER[1,2], S.REDFERN[3], G.D. BROMILEY[1,4]

[1]School of Geosciences, Grant Institute, University of Edinburgh, Edinburgh, UK M.Berg@sms.ed.ac.uk (*presenting author)
[2]ECOSSE (Edinburgh Collaborative of Subsurface and Engineering) Joint Research Institute of the Edinburgh Research Partnership in Engineering and Mathematics, UK
[3]Dept. Earth Sciences, University of Cambridge, Cambridge, UK
[4]Centre for Science at Extreme Conditions, Erskine Williamson Building, University of Edinburgh, Edinburgh, UK

The mechanism of metal-silicate segregation is key to constraining core formation processes in the early Earth. Experiments performed at conditions of core formation in terrestrial planets have generally found metallic melts to be immobile in a solid silicate matrix. This implies that a liquid silicate 'Magma Ocean' was required for efficient differentiation to occur. There is some doubt as to the applicability of this model to other planetary bodies, particularly those with smaller radii, which may not have been heated to silicate melting temperatures. Recent experimental work has found that deformation can enhance permeability of melt through a solid silicate system without the need to melt the surrounding silicate. We have conducted a series of deformation experiments in the rotational Paris-Edinburgh Cell (roPEC), which allows controlled deformation at simultaneous high pressures and temperatures over a large range of strain rates. Textural analysis confirms melt is interconnected at a grain scale. This implies core formation could have taken place earlier and more rapidly than previously believed, affecting inferred geochemistry of the core and mantle. We use 3D reconstructions of the sample interior from Computed Axial Tomography scans to characterise melt network geometry in order to constrain melt migration rates and permeability.

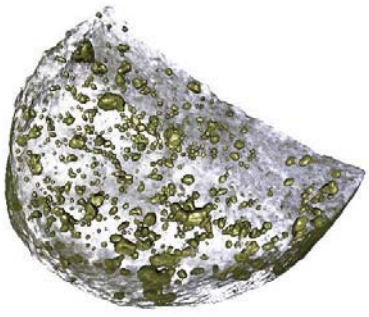

Figure 1: Preliminary tomographic reconstruction of undeformed sample. Sample diameter is 2mm. High density Fe_3S shown in gold, grey-transparent areas are olivine.

Petrogenesis of voluminous silicic magma in northeast Iceland

SYLVIA E. BERG[1, 2*], VALENTIN R. TROLL[2], MORTEN S. RIISHUUS[1] AND STEFFI BURCHARDT[2]

[1]Nordic Volcanological Center, Reykjavik, Iceland sylvia@hi.is (*presenting author)
[2]Dept. of Earth Science, CEMPEG, Uppsala University, Sweden

Neogene silicic volcanic complexes in the greater Borgarfjörður eystri area, NE-Iceland, are the focus of a petrological and geochemical investigation. The region contains the second-most voluminous occurrence of silicic rocks in Iceland, including caldera structures, inclined sheet swarms, extensive ignimbrite sheets, sub-volcanic rhyolites and silicic lava flows. Despite the relevance of these rocks to understand the generation of evolved magmas in Iceland, the area is geologically poorly studied [c.f. 1, 2, 3].

The voluminous occurrence of evolved rocks in Iceland (10-12 %) is very unusual for an ocean island or a mid-oceanic ridge, with a typical signal of magmatic bimodality, often called "Bunsen-Daly" compositional gap [e.g. 4, 5, 6]. The Bunsen-Daly Gap is a long-standing and fundamental issue in petrology and difficult to reconcile with continuous fractional crystallization as a dominant process in magmatic differentiation [7]. This implies that partial melting of hydrothermally altered crust may play a significant role. Our aim is to contribute to a solution to this issue by unravelling the origin, timing and evolution of voluminous evolved rhyolites in NE-Iceland.

We use a combined petrological, textural, experimental and in-situ isotope approach on a comprehensive sample suite of intrusive and extrusive rocks, ranging from basaltic to silicic compositions. We are performing major, trace element and Sr-Nd-Hf-Pb-He-O isotope geochemistry, as well as U-Pb geochronology and Ar/Ar geochronology on rocks and mineral separates. Zircon oxygen isotope analysis will be performed in conjuction with zircon U-Pb geochronology for further assessment of the role of processes such as partial melting of hydrated country rock and/or fractional crystallization in generating Icelandic rhyolites. In addition, high pressure-temperature partial melting experiments aim to reproduce and further constrain natural processes. Using the combined data set we intend to produce a comprehensive and quantitative analysis of rhyolite petrogenesis, and of the temporal, structural and geochemical evolution of silicic volcanism in NE-Iceland. The chosen field area serves as a good analogue for active central volcanoes in Iceland, such as Askja and Krafla, where interaction of basaltic and more evolved magma has led to explosive eruptions.

[1] Gústafsson (1992) PhD dissertation, Berlin University. [2] Martin & Sigmarsson (2010) Lithos **116**, 129–144. [3] Burchardt, Tanner, Troll, Krumbholz & Gustafsson (2011) G^3 **12** (7), Q0AB09. [4] Bunsen (1851) Annalen der Physik und Chemie **159** (6), 197-272. [5] Daly (1925) Proceedings of the American Academy of Arts and Sciences **60** (1), 3-80. [6] Barth, Correns & Eskola (1939) Die Entstehung der Gesteine. Springer Verlag, Berlin. [7] Bowen (1928) The evolution of the igneous rocks. Princeton University Press.

https://doi.org/10.1180/S0026461X00008434 Published online by Cambridge University Press

Petrology of two pre-orogenic granites, Damara Orogen, Namibia

CHRISTIAN BERGEMANN[1*], STEFAN JUNG[1], JASPER BERNDT[2] AND ANDREAS STRACKE[2]

[1] Mineralogisch-Petrographisches Institut, Universität Hamburg, Germany (*), christian_bergemann@yahoo.de

[2] Institut für Mineralogie, Universität Münster, Germany

The Damara Orogen sensu strictu of Namibia was formed during the late Archean/early Proterozoic Pan-African orogenic event. It is characterised by medium p/high T regional metamorphism and large-scale granitoid intrusion. The two plutons investigated in this study are part of the Damaran Northern Central Zone within the Okombahe district and can readily be distinguished by field criteria. LA-ICP-MS U-Pb geochronology on zircon yielded similar ages of 576±6 Ma and 571±5 Ma. This is the earliest date of granite intrusion discovered in the Central Damara Orogen. Both plutons consist of granodiorite and granite that are metaluminous to slightly peraluminous. Both rock types have high calculated zircon saturation temperatures up to 890°C, show only limited fractionation and exhibit no signs of shallow crustal contamination. Chemical and isotope data overlap almost completely in which the granodiorites and granites are characterized by a range in K_2O (3.1-5.9 wt.%) and moderate to high HFSE and LREE abundances (up to 620 ppm Zr and 250 ppm Ce) and a strong enrichment of LREE over HREE (La/Yb: 19-49) with variable negative Eu anomalies (Eu/Eu*: 0.82-0.19). Initial Sr and Nd isotopic compositions vary over a narrow range (init $^{87}Sr/^{86}Sr$: 0.704 - 0.706; init. ε Nd: -1.9 to -3.9). Relatively young Nd model ages (T_{DM}: 1.2-1.4 Ga) and 1.7 Ga-old restitic zircon suggest a derivation from a juvenile source rock of probably meta-igneous composition. As the intrusion ages precede the minimum age of high-grade regional metamorphism, crustal heating as the cause of granite formation can be ruled out. Previous studies have shown that the meta-igneous basement of the Damara orogen has an average heat production of 6.8 HGU (1 HGU=10^{-13} cal/cm^3*sec; Haack et al. 1983). This value is significantly higher than that of average continental crust (2.14 HGU; Rudnick & Gao 2004) hence, a major contribution from pre-existing continental crust is possible. In addition, intrusion of large scale mafic bodies in the lower crust could also potentially provide some extra heat for crustal melting, however, seismic refraction studies gave no evidence for the existence of large volumes of mafic rocks in the lower crust (Green 1983). We therefore suggest that emplacement of numerous sill-like intrusions (Petford & Gallagher 2001) may have provided the necessary heat for melt generation.

[1] Haack, Gohn & Hartmann (1983) Spec. Publ. geol. Soc. S. Afr. 11, 225-231. [2] Rudnick & Gao (2004) In: Treatise on Geochemistry, Elsevier. 3, 1-64. [3] Green (1983) Spec. Publ. geol. Soc. S. Afr. 11, 355-367. [4] Petford & Gallagher (2001) Earth and Planetary Science Letters 193, 483-499.

Mercury Isotopes in the Precambrian

BERGQUIST, B.A.[1]*, GHOSH, S.[2], ONO, S.[3], HAZEN, R.M.[4], SVERJENSKY, D.[5], PAPINEAU, D.[6], KAH, L.C.[7], BLUM, J.D.[8]

[1]University of Toronto, Toronto, Canada, bergquist@geology.utoronto.ca*

[2]Unveristy of Toronto, Toronto, Canada, sanghamitra.ghosh@utoronto.ca

[3]MIT, Boston, USA, sono@mit.edu

[4]CIW Geophysical Laboratory, Washington, DC, USA, rhazen@ciw.edu

[5]Johns Hopkins University, Baltimore, USA, sver@jhu.edu

[6]Boston College, Chestnut Hill, USA, dominic.papineau@bc.edu

[7]University of Tennessee, Knoxville, USA, lckah@utk.edu

[8]University of Michigan, Ann Arbor, USA, jdblum@umich.edu

Mercury (Hg) is an active redox-sensitive metal with a complex biogeochemical cycle that displays a wide range of stable Hg isotopic fractionation. In addition to mass-dependent fractionation (MDF), Hg isotopes also display large (up to 10‰) mass-independent fractionation (MIF). The large MIF in Hg isotopes is commonly expressed only for the odd isotopes (^{199}Hg, ^{201}Hg). To date, the large MIF in the odd Hg isotopes is thought to occur during kinetic photochemical reactions due to the magnetic isotope effect. In the first photochemical experiments (Bergquist and Blum, 2007), Hg(II) species were photo-reduced to Hg(0) in the presence of fulvic acid. It was found that the odd isotopes were preferentially enriched in the reactant in the aqueous reservoir. In these experiments, the Hg/DOM ratios were such that Hg was likely bound to carboxylic ligands. However, subsequent experiments show that the sign and ratio of MIF can be changed during photo-reduction in the presence of different organic ligands or in presence of UVC. In particular, Zheng et al. (2010) demonstrated that photoreduction of Hg bound to reduced S containing ligands results in the odd isotopes being depleted in the reactant in the aqueous phase.

The chemistry of the atmosphere and ocean changed drastically in the Precambrian due to the evolution of life and rise of oxygen. The large changes in the redox conditions and the sulfur cycle of the surface Earth along with changes in UV penenetration likely had large impacts on the biogeochemical cycle of Hg and on the Hg isotope system. It is also likely that the nature of the organic ligands binding Hg changed dramatically in response to evolution of different groups of organisms. The goal of this research was to study Hg isotopes preserved in the sedimentary and metasedimentary geologic record where major changes in either UV shielding or major changes in the nature of DOC may have occurred. Preliminary Hg isotope analyses show that the younger samples mostly show negative MIF with $\Delta^{199}Hg/\Delta^{201}Hg$ close to 1 whereas the older samples have positive MIF with $\Delta^{199}Hg/\Delta^{201}Hg$ greater than 2. The timing of the shift is consistent with the first major glaciation and suggestion of an organic fractal haze, which would have blocked higher energy UV. The timing is also consistant with a change in S isotopes that is thought to occur because of an increase in sulfate and sulfate reducing bacteria. Both possible explanations will be discussed in the context of experimental constraints. These are preliminary results, but they reveal the potential of Hg isotopes to add to our understanding of the eveolution of life and chemistry of the early Earth.

https://doi.org/10.1180/S0026461X00008434 Published online by Cambridge University Press

CO_2-rich fluids in the mantle: a comparative fluid inclusion study

MÁRTA BERKESI[1], CSABA SZABÓ[1*], TIBOR GUZMICS[1], ZSANETT PINTÉR[1], RÉKA KÁLDOS[1], JEAN DUBESSY[2], MUNJAE PARK[3] AND GYÖRGY CZUPPON[4]

[1]Lithosphere Fluid Research Lab, Eötvös University, Budapest, Hungary (*martaberkesi@caesar.elte.hu)
[2]G2R, Université de Lorraine, CNRS, CREGU, Nancy, France (jean.dubessy@g2r.uhp-nancy.fr)
[3]School of Earth and Environmental Sciences, Seoul National University, Seoul, Republic of Korea
[4]Institute for Geological and Geochemical Research, Budapest, Hungary

Negative crystal shaped fluid inclusions enclosed in spinel lherzolites from five different locations all around the world were the subject of a detailed fluid inclusion study. Samples were studied from: the Central Pannonian Basin (Hungary), Cameroon Volcanic Line (Cameroon), Jeju Island (S-Korea), Rio Grande Rift (New-Mexico, USA) and from Mt. Quincan (Australia). As a result, CO_2-rich fluids within the fluid inclusions could be studied and compared.

High resolution Raman spectroscopy at different temperatures revealed that fluids in inclusions are heterogeneous and contain small amounts of other species. We show that nitrogen (N_2) can be present in the dense fluid and is more common than was previously thought. H_2O is present in almost all of the inclusions, and was identified by the combination of stepwise heating experiments and Raman spectroscopy [1]. Our results show that, although H_2O is a minor component in mantle fluids, its relative amount varies between different locations, which has not been previously recognized.

Sulfur in the fluid at room temperature can be present either as H_2S or as SO_2, however these species never occur together at the same location. In addition, following fluid inclusion exposure by the FIB-SEM (Focused Ion Beam-Scanning Electron Microscopy) technique, a complexity of S-bearing solid phases has also been identified: sulfides and sulfates were also found within the fluid inclusion cavity. OH-bearing solids are also found in some cases within the fluid inclusions.

Combination of Raman spectroscopy and the FIB-SEM technique proved the presence of carbonates and quartz that are interpreted to be a reaction product of the trapped CO_2 and the host pyroxene. In addition, a common feature found on the inclusion walls is a thin glass film at a submicron scale that documents the ability of mantle fluids to dissolve and transport trace elements and cause cryptic metasomatism as has previously been inferred [2].

We can conclude that, similar to the solid phases involved in the construction of the subcontinental lithospheric mantle, the coexisting fluid can also be heterogeneous in the mantle, although the dominant component in each case is CO_2.

[1] Berkesi *et al.* (2009) *J. Raman Spectrosc.* **40**, 1461-1463.
[2] Hidas *et al.* (2010) *Chem. Geol.* **274**, 1-18.

Investigating the role of microbial processes in the weathering of rock-derived graphitic carbons

SABRINA BERLENDIS [1 *], OLIVIER BEYSSAC[1], KARIM BENZERARA[1], FERIEL SKOURI-PANET[1], CELINE FERARD[1]

[1] IMPMC, CNRS & Université Pierre et Marie Curie, Paris, France , sabrina.berlendis@impmc.upmc.fr, (* presenting author)
olivier.beyssac@impmc.upmc.fr,
karim.benzerara@impmc.upmc.fr

During erosion and chemical weathering, organic carbon contained in (meta)sedimentary rocks may be oxidized or recycled. Recent studies in the Himalaya[1] and Andes[2] orogenic systems have demonstrated that the fate of these carbonaceous phases is highly dependent on their graphitization degree: in such large-scale systems only graphite is finally preserved whereas poorly graphitic compounds are oxidized. This oxidation which happens in the bedrock or during fluvial transport is assisted, and most likely driven, by microbial processes. The present study investigates the effect of inorganic compounds commonly found in shale and coal (metals, sulphur and nitrogen compounds) on the bio-alteration of carbonaceous material by microbial populations. For that purpose, we sampled several carbon-bearing rocks which experienced varying metamorphic grades and have therefore various structural organizations for carbons (from kerogen/coal to graphite) following a strict protocol to minimize contamination. The sample set includes carboniferous coals (Graissessac and Briançon basins, France) and black shales as well as graphitic schists (Western Alps, France). The mineralogy and structure of organic carbon have been characterized by various techniques (XRD, Raman and IR, SEM). The high-grade metamorphic rocks contain highly crystalline carbonaceous phases (graphite) and a low mineral diversity (chlorite, muscovite and quartz). In addition, sulfate minerals such as jarosite and gypsum were detected in slightly less graphitized schist rock. By contrast, the coals contain turbostratic carbons and a wide variety of minerals (montmorillonite, feldspar, illite and kaolinite). Back to the lab, enrichment cultures were set up under both oxic and anoxic conditions using the rock-derived carbonaceous material as the sole carbon source. The effect of various inorganic electron donors and acceptors added in combination are tested. Microscopy and biomolecular studies show a low biomass content in microbial enrichments, but we have detected in some of them thin filamentous bacteria and short rod cells that are embedded in a biofilm deeply-incrusted inside carbonaceous particles and other minerals. The metabolic functions of enriched microbial populations are currently assessed by microscopy, hybridization techniques and spectroscopy techniques. Their possible influences on the alteration of rock-derived graphitic carbons will be discussed.

[1] Galy (2008) *Science* **322**, 943-945.
[2] Bouchez (2010) *Geology* , **38**, 255-258.

https://doi.org/10.1180/S0026461X00008434 Published online by Cambridge University Press

The halogen composition of hydrothermal fluids in the Taupo Volcanic Zone, New Zealand.

NELSON F. BERNAL[1*], SARAH A. GLEESON[1], PAUL HOSKIN[2]

[1]University of Alberta, Department of Earth and Atmospheric Sciences, Edmonton, Canada, T6G 2E3.
bernal@ualberta.ca (* presenting author)
sgleeson@ualberta.ca
[2]The University of Auckland, Geology, School of Environment, Auckland, New Zealand.
p.hoskin@auckland.ac.nz

9f. Innovative geochemical approaches to understanding geothermal systems

The halogen composition of seven geothermal fields and eight hot spring areas in the Taupo Volcanic Zone (TVZ), North Island New Zealand, were studied in order to constrain the origin of the geothermal fluids and to identify the effect of physico-chemical processes on the isotopic composition of these fluids. A set of 74 samples from well brines and hot springs were analyzed for Cl, Br, Li, $\delta^{37}Cl$, $\delta^{18}O$ and δD. In particular, this study offers a first approach to the application of the Cl/Br systematics in geothermal fluids to constrain the behaviour of stable chlorine isotopes.

The determination of the Cl/Br ratios in the set of samples analyzed, allowed the initial characterization of geothermal fields and hot spring areas in the TVZ. The highest Cl/Br ratios were found at Mokai (1,664), Orakeikorako (1,611), Rotokawa (1,478) and White Island (1,373). The chlorine isotopic composition of all the samples ranged from -0.97 to 0.67‰. With the exception of some samples from Orakeikorako and Rotokawa, most samples with high Cl/Br ratios had positive $\delta^{37}Cl$ values, the geothermal field Mokai was the most enriched in $\delta^{37}Cl$ (0.03 to 0.38‰). The sample from Broadlands Ohaaki had a negative $\delta^{37}Cl$ value (-0.57‰) and a Cl/Br ratio of 870. In the hot springs the Cl/Br ratios also correlate well with the $\delta^{37}Cl$ values. Waikite has the highest $\delta^{37}Cl$ values (0.47 to 0.67‰), followed by Taupo, White Island, Tokaanu and Waimangu.

The data suggest that in the central part of the TVZ, there is a deep fluid of magmatic origin with a Cl/Br ratio of at least 1,200, a positive $\delta^{37}Cl$ signature around 0.5‰, a Cl concentration above 3,200 ppm and a Li content of more than 29 ppm. Fluids with similar characteristics were found at Tokaanu, White Island, Mokai, Wairakei, Tauhara and Ngatamariki. A second fluid is characterized by negative $\delta^{37}Cl$ values (-0.02 to -0.97‰), Cl/Br ratios below 1,200 and Li concentrations around 10 ppm. The influence of this second fluid is more dominant towards the E and NE of the TVZ in hot spring areas and geothermal systems like Rotorua, Waiotapu, Rotokawa and Kawerau.

How citrate slows magnesite growth: a high temperature AFM study

ULF-NIKLAS BERNINGER[1*], QUENTIN GAUTIER[2], GUNTRAM JORDAN[1] AND JACQUES SCHOTT[2]

[1] Ludwig-Maximilians-Universität, Department für Geo- und Umweltwissenschaften, Munich, Germany,
ulf-niklas.berninger@campus.lmu.de (*presenting author)
[2]CNRS, Géosciences et Enviroment Toulouse, Toulouse, France,
quentin.gautier@get.obs-mip.fr

Preliminary work and experimental methods

Magnesite shows a high stability in natural enviroments and hence is of scientific interest due to its potential for long-term CO_2 sequestration. In a recent study we were investigating the inhibition of carboxylic ligands on magnesite growth and found out that among the investigated ligands citrate caused the highest degree of inhibition [1]. Besides the effect of complexation of Mg^{2+} in aqueous solution, a prominent surface effect of citrate was detected. This surface effect of citrate on magnesite growth at elevated temperatures, however, is still insufficiently understood.

In the present study, hydrothermal atomic force microscopy (HAFM) was used to investigate magnesite growth on the (104) surface as a function of citrate concentrations (0.1-10 mmol/kgw) and saturation state. Experiments were conducted at pressures up to 4 bars, temperatures of 100 °C and 120 °C and alkaline conditions (pH 7.5-8.5).

Results and outlook

HAFM experiments showed that spiral growth is the dominant growth mechanism over a wide range of saturation state in ligand-free solutions as well as in the presence of citrate. Accordingly, the determined growth rates follow an exponential dependency on supersaturation and are in close agreement with previous mixed-flow reactor experiments [1][2]. Furthermore, HAFM observations revealed that citrate interacts with steps on the (104) surface of magnesite producing growth islands elongated along the trajectory of the c-axis. This pronounced morphological change was taking place without an effect on obtuse step kinematics but with a reduced advancement rate of acute steps. These observations indicate specific blocking of acute kinks by citrate. For the rotation frequence of spirals and thus the growth rate, acute step advancement is essential. The rate of step generation via spiral growth in the presence of 1 mmol/kgw citrate was thereby decreased by a factor of more than 3.

Overall, this study confirms the control exerted by acute steps on magnesite growth rates. Therefore, numerical molecular simulations should preferentially focus on stereochemical effects between organic molecules and acute steps and kinks. This could help to better understand and predict the role of organic additives on magnesite growth.

[1] Gautier *et al.* (2012) in prep. [2] Saldi *et al.* (2009) *Geochim. Cosmochim. Acta* **73**, 5646-5657.

https://doi.org/10.1180/S0026461X00008434 Published online by Cambridge University Press

Controls on the Carbonation of Steel Slag

ELEANOR J. BERRYMAN[1*], ANTHONY E. WILLIAMS-JONES[1], ARTASCHES A. MIGDISOV[1], SIEGER VAN DER LAAN[2]

[1]McGill University, Montreal, Canada, berryman.eleanor@gmail.com(* presenting author)
[2]Tata Steel RD&T, IJmuiden, The Netherlands

Goals and Methodology

Mineral carbonation provides a robust method for permanent sequestration of CO_2 that is environmentally inert. Larnite (Ca_2SiO_4), the major constituent of steel slag, reacts readily with aqueous CO_2 [1]. Consequently, its carbonation offers an exciting opportunity to reduce CO_2 emissions at source [2]. A potential added benefit is that this treatment may render steel slag suitable for recycling. This study investigates the impact of temperature, fluid flux and reaction gradient on the dissolution and carbonation of steel slag, and is part of a larger study designed to determine the conditions under which conversion of larnite, and other calcium silicates, to calcite is optimized.

The experiments were conducted on 2 – 3 mm diameter steel slag grains supplied by Tata Steel RD&T. A CO_2-saturated aqueous fluid was pumped through a steel flow-through reactor containing these grains at a temperature between 120°C to 200°C; the fluid pressure was 250 bar. Fluid flux was varied between 0.8 and 6 mL/min/cm^2. The duration of experiments ranged from 3 to 7 days.

Results

The steel slag grains reacted with the CO_2-saturated aqueous fluid to form phosphorus-bearing Ca-carbonate phases. At high fluid flux, these phases dissolved at the edges of grains, leaving behind a porous aluminium and iron oxide rind. Increasing temperature increased the rate of this reaction. At low fluid flux, carbonates precipitated on the slag grain surface inhibiting further reaction. In contrast, at intermediate fluid flux, dissolution of the primary Ca-bearing minerals was balanced by precipitation of carbonate phases, thereby optimising carbonation of the steel slag.

Conclusions

These results of this study show that carbonation of steel slag by aqueous CO_2 is feasible using relatively large grains and that it can be optimised by varying fluid flux. Experiments of the type described above will contribute to the eventual global reduction of industrial CO_2 emissions.

[1] Santos et al. (2009) *Journal of Hazardous Materials* **168**, 1397-1403.
[2] Berryman et al. (2011) *Mineralogical Magazine* **73(3)**, 522.

CO_2 attack of a caprock-type argillite: From lab experiments to modeling

GUILLAUME BERTHE[1,2*], SEBASTIEN SAVOYE[3], CHARLESWITTEBROODT[1], JEAN-LUC MICHELOT[2]

[1]IRSN, DEI/SARG/LR2S,92260 Fontenay-aux-Roses, France
[2]IDES,CNRS-Université Paris-Sud F-91405 Orsay, France
[3]CEA, DEN/DANS/L3MR, F-91191 Gif-sur-Yvette, France
guillaume.berthe@cea.fr (*presenting author)

Introduction

In the case of a CO_2 storage in geological media, the understanding of the behavior of the caprock encountering an acid fluid is crucial. A set of twenty "dynamic" through-diffusion experiments was performed to investigate the changes in chemical and physical properties of a caprock-type argillite.

Methods

The "dynamic" through-diffusion setup enables, during the CO_2 attack, (i) a monitoring of the ion concentrations in the upstream and the downstream reservoirs and, (ii) an estimate of the transport property change, using HTO, HDO, ^{36}Cl and Br^- as tracers [1]. The impact of several parameters on the caprock behavior was studied, such as the amount of carbonate minerals, the sample thickness, the upstream volume, the presence or not of calcite-filled fracture and the bedding plane orientation regarding the diffusion.

Results and Discussion

The results showed that the extent of the reaction front, lowering the caprock confinement properties, would be more related to the initial rock transport properties and the calcite texture than the amount of carbonate minerals.

This large set of experimental data acquired, allowed us to identify from the chemistry-transport modeling some key parameters, such as the kinetic rate equations used for describing the dissolution/precipitation reactions (Figure 1).

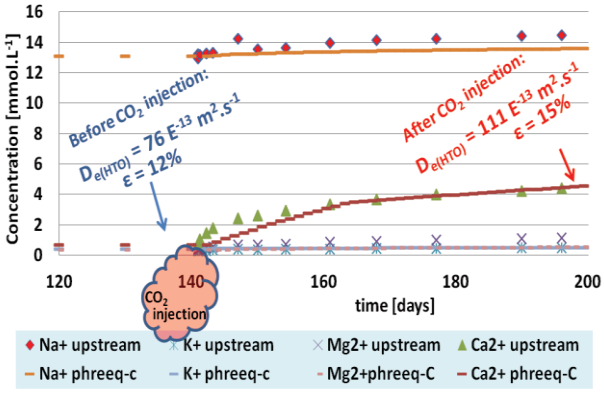

Figure 1: Comparison of experimental concentrations measured in the upstream reservoir with the simulated ones obtained by means of PHREEQC using rate equations from [2].

[1] Savoye *et.al.* (2010) *Environ. Sci. Techn.* **44**, 3698-3704.
[2] Palandri *et al* (2004) USGS, open file report 2004-1068, 64 pp.

https://doi.org/10.1180/S0026461X00008434 Published online by Cambridge University Press

Can we use ice sheet reconstructions to constrain meltwater for deglacial simulations?

INGO BETHKE[12]*, CAMILLE LI[12] AND KERIM H. NISANCIOGLU[12]

[1]Bjerknes Centre for Climate Research, Bergen, Norway, ingo.bethke@bjerknes.uib.no (* presenting author)
[2]Uni Research, Bergen, Norway

Abstract

Freshwater pulses from melting ice sheets are thought to be important for driving climate variability. This study investigates challenges in simulating and understanding deglacial climate evolution within this framework, with emphasis on uncertainties in the ocean overturning sensitivity to meltwater inputs. The response of the model used in this study to a single Northern Hemisphere (NH) meltwater pulse is familiar: a weakening of the overturning circulation, an expansion of NH sea ice cover and a meridional temperature seesaw. Nonlinear processes are vital in shaping this response, and are found to have a decisive influence when more complex scenarios with a history of pulses are involved. For this study, a meltwater history for the last deglaciation (21-9 ka) was computed from the ICE-5G ice sheet reconstruction, and the meltwater was routed into the ocean through idealized ice sheet drainages. Forced with this meltwater history, model configurations with different freshwater sensitivities produce a range of outcomes for the deglaciation. Theses outcomes are determined by the thresholds for collapse and resumption of the overturning circulation, as well as the dependence of the sensitivity on the changing background climate. For all sensitivity configurations, there is a mismatch between the simulated deglaciation and proxy records, indicating that uncertainties in the meltwater scenario play an important role as well. This study illustrates that current uncertainties in model sensitivity to freshwater and meltwater reconstructions are limiting in efforts to forward-model deglacial climate variability using data-constrained meltwater forcing scenarios.

Strata-specific bacterial diversity in aquifers of the Thuringian Basin/Germany

A. BEYER[1;2*], M. LONSCHINSKI[2], E. KOTHE[1], G. BÜCHEL[2],

[1] Friedrich Schiller University, Institute of Microbiology-Microbial Phytopathology, Jena, Germany
andrea-beyer@uni-jena.de (*presenting author)
erika.kothe@rz.uni-jena.de
[2] Friedrich Schiller University, Institute of Applied Geology, Jena, Germany
georg.buechel@uni-jena.de
martin.lonschinski@uni-jena.de

The INFLUINS (Integrated fluid dynamics in sedimentary basins) project investigates coupled dynamics of near surface and deep flow patterns of fluids, transported materials and component substances in the Thuringian Basin. The extensive basin landscape is located in eastern Germany and belongs to the Triassic period of Bunter sandstone (Buntsandstein), shell limestone (Muschelkalk) and Keuper, which crop out at the surface. Older sediments and Permian (Zechstein) can be found at the edges of the basin. With microbial investigations, we are analyzing the bacterial diversity of ground- and mineral water at different locations to see whether there are special patterns in bacterial distributions originating from the different rock strata. This will facilitate understanding fluid movement in the Thuringian Basin. We determined bacterial diversity from water samples out of two natural springs and ten groundwater wells by cultivation and subsequent morphological, physiological and molecular identification. To elucidate differences to other rock strata, we compared these samples to two brine springs (4.62 M and 1.03 M salt content), located in Permian aquifers. First results show that the largest proportions were found to be members of Bacilli and γ- proteobacteria, including the genera *Pseudomonas* and *Bacillus*. Next steps will be a comparison of cultivation-dependent and cultivation-independent methods to gain further information on bacterial strains which where uncultivable or suppressed by other bacteria strains.

https://doi.org/10.1180/S0026461X00008434 Published online by Cambridge University Press

Trends in Solute fluxes across a 3.8 km elevation transection from Narayani river system in central Himalaya

M.P. BHATT, J. HARTMANN

KlimaCampus, University of Hamburg, Hamburg, Germany, maya.bhatt@zmaw.de

Chemical weathering is an integral part of the rock and carbon cycles and rates vary largely. To study the variability of chemical weathering rates and controls within a mountainuous system, the hydrochemistry along the Narayani basin in central Himalaya region has been sampled including glacial meltwater samples of the upstream Langtang glacier.

Cation composition of the water was dominated by carbonate and silicate dissolution. Preliminary results based on samples of the first months show that concentration of measured chemical parameters such as the sum of base cations, dissolved silica and alkalinity decreased exponentially with elevation (from 169 m to 3989 m). Contribution of sea-salt appeared negligible to the total mass of solute along the drainage network except for the lowermost elevation site. The export of sea-salt corrected sulfate at the outlet point of the Narayani river suggests pyrite dissolution as its main source. Thus the oxidation of sulfide minerals might regulate significantly the dissolution of minerals within the basin. Export of nitrate from the Narayani basin appeared many fold higher than observed fluxes in the Langtang sub-basin, located upstream in the upper Himalaya.

First results suggest that area specific cationic and silica weathering fluxes were comparable with previous reports from the region but appeared to be increased at lower latitudes if compared to the upper Himalayan section of the basin and the world average. Human influence, primarily agricultural activities, may have increased the rate to some extent. Preliminary results of the weathering advance rate of the basin, at the terminus of the Himalaya, also appeared increased compared to large river systems of the world [1, 2, 3]. Influence of controlling factors like relief, physical erosion rates, temperature and precipitation will be discussed.

[1] Navarre-Sitchler & Brantley (2007) *EPSL* **261**, 321-334.
[2] Meybeck and Ragu (1997) *UNEP*, 245p.
[3] Gaillardet et al. (1999) *CG* **159**, 3-30.

Monitoring of Oxidation-Reduction Reactions between redox active Fe and Cysteine : Spectroscopic studies and Multiplet Calculations

AMRITA BHATTACHARYYA[1*], JOSEPH DVORAK[2], ELI STAVITSKI[2] AND CARMEN ENID MARTÍNEZ[1]

[1] The Pennsylvania State University, Department of Crop and Soil Sciences, University Park, USA, axb1000@psu.edu (* presenting author), cem17@psu.edu

[2] Brookhaven National Laboratory, National Synchrotron Light Source, Upton, USA, jdvorak@bnl.gov, istavitski@bnl.gov

Section Heading

Introduction This study aims to monitor the electron exchange interactions between the Fe(II,III) center and the different functional groups of cysteine (carboxylic, amine and thiol) with time using X-ray absorption spectroscopy. We present the XANES spectra of Fe(II,III)-cysteine complexes at all relevant absorption edges (Fe L-edge and C, N,O and S K-edges) collected at different times (0,2,10 and 12 months) after the initial synthesis of the complexes as well as the Fe K-edge EXAFS of Fe(II,III)-cysteine complexes, also as a function of time. The experimental results are compared with multiplet and quantum mechanical simulations, providing a detailed picture of the iron-ligand structure, co-ordination, and electron shuttling capabilities of the complex.

Results and Conclusion

The Fe L-edge XANES of Fe(III)-cysteine indicates an initial reduction of Fe(III) caused by an internal electron transfer reaction either from N of $-NH_2$ or S of -SH, both of which show oxidation in their respective spectral features. The N K-edge of Fe(II) cysteine at all time scales did not show much variation and is identical to the N spectrum of cysteine. The N of Fe(III) cysteine showed oxidation of N (to nitrate, a +5 oxidation state of N) at time scales 0, 10 and 12 months; however, at time=2 months the N spectral features resemble that of N in cysteine. The O K-edge spectra for Fe(II) cysteine shows a change in spectral pattern with passage of time whereas that for Fe(III) cysteine does not change much after the time of initial synthesis and had characteristics similar to that of O in cysteine. Oxidation of Fe(II) in Fe(II)-cysteine with time was accompanied by a simultaneous reduction of the C as revealed by the C K-edge features of Fe(II) cysteine. This is reflected in a reduction of the C which involves an electron exchange of the C within the unsaturated –COOH of cysteine. In contrast, the C K-edge features for Fe(III) cysteine show no variation with time. The S K-edge of Fe(II) cysteine show S oxidation states intermediate between sulfoxide and sulfate. Overall, spectral characteristics of Fe(II,III)-cysteine complexes suggest thiol/disulfide exchange, H-atom transfer, or electron transfer between Fe and cysteine. Our studies of the Fe(II,III)-cysteine system provide a mechanistic understanding of the electron shuttling that occurs between a redox active metal and a redox active ligand. In this particular case, cysteine represents an organic molecule with functionalities (O-, S-, N- functional groups) and a C backbone that may mimic the functional groups present in organic matter from terrestrial and aquatic environments.

https://doi.org/10.1180/S0026461X00008434 Published online by Cambridge University Press

High resolution rare earth element (REE) study on mussel shells, a proxy for the geochemical cycling at the coastal region?

NANXI BIAN[1*], PAMELA A. MARTIN [2], ALBERT COLMAN[1] AND CATHERINE PFISTER[3]

[1]Department of Geophysical Sciences, the University of Chicago, Chicago, IL, USA, nanxibian@uchicago.edu
[2]Department of Earth and Environmental Sciences, IUPUI, Indianapolis, IN, USA
[3]Department of Ecology and Evolution, University of Chicago, Chicago, IL, USA

Trace and minor element variations in biogenic calcium carbonate shells have been widely applied in reconstruction of past environmental conditions [1,2,3]. Successively deposited biogenic calcareous shells, such as mussel shells, may have the potential to provide high resolution records of temporally resolved variability to investigate changes in climatic configurations and/or geochemical cycling where instrumental records are non-existent. In our previous work, we developed a high precision analytical method, using laser ablation coupled with sector field inductively coupled plasma mass spectrometry (LA-ICP-MS), to obtain high resolution time series of a suite of element/Ca ratios for mussel shells [4]. Here, we investigate the potential of one species of mussels, *Mytilus californianus*, to provide high-resolution records of coastal geochemical changes.

Mussel shell samples used in this study are from Tatoosh Island, Washington, USA, a coastal upwelling region where 11 years of instrumental records are avaialble to calibrate shell chemistry on modern shells. Age models of the shells are anchored by stable isotope analysis on seasonally resolved micromilled shell material. An anti-correlated relationship between rare earth element (REE)/Ca and $\delta^{18}O$ is apparent upon comparison of the two records. A reliable shell age model is then constructed by combining both high resolution REE/Ca records and the seasonally resolved $\delta^{18}O$ records. Multi-Taper Method (MTM) spectral analysis was applied to identify significant quasi-periodic variability in shell REE/Ca records [5]. An intra-annual (3-5 cycles/year) periodic component has been identified in both modern and midden shells; similar periodic variability was also observed in the high resolution instrumental data for evironmental parameters, such as upwelling and temperature. Calculated Ce anormalies (Ce*), a proxy for redox state in the water column, show similar ranges of variations in modern and acient shells. Our results indicate REE/Ca ratios in mussel shells have the potential to serve as a proxy for the geochemical cycling at this coastal area and could possiblly offer hints for explaining the recent and dramatic pH declines at this location [6].

[1] Klein et al. (1996) *Geology* **24**, 415-418. [2] Lea et al. (1999) *GCA* **63**, 2369-2379. [3] Wyndham et al. (2004) *GCA* **68**, 2067-2080. [4] Bian et al. (2012) *GCA*, submitted. [5] Mann and Lees (1996) *Climate Change* ***33***, 409-445. [6] Wootton et al. (2008) *PNAS* ***105***, 18848-18853.

Molecular structure and acidity

BARRY BICKMORE[1]*, JOSHUA MAURER[1], AND KENDRICK SHEPHERD[1]

[1]Brigham Young University, Geological Sciences, Provo, UT, USA barry_bickmore@byu.edu (*presenting author), josh3996@gmail.com, kenear@gmail.com

Surface complexation models (SCMs) are often capable of fitting the same macroscopic data (e.g., titration data) by employing substantially different assumptions about molecular-scale reactions. This has been addressed by constraining SCMs with 1) more macroscopic data and information about molecular-scale processes obtained from 2) advanced spectroscopic techniques, 3) molecular modeling studies, and 4) quantitative structure-activity relationships (QSARs) like MUSIC [1]. All of these are reasonable, but even given the first three options, QSARs would still be necessary to provide a conceptual framework for interpreting the other types of results.

A problem with QSARs is that they assume only certain aspects of the molecular structure determine a particular type of reactivity. Sometimes, however, other structural features are important, but were roughly constant in the calibration set. E.g., MUSIC is calibrated on a certain set of (hydr)oxo-monomers, and assumes only the metal-oxygen bond valences and coordination numbers are important for determining functional group acidities. The model is then applied to the acidities of oxide surface functional groups, which are much more difficult to experimentally determine.

Are the MUSIC predictions always accurate for oxide surface functional group acidity, or are some important structural features missing from the model? Our previous work [2] used an expanded calibration set of solution monomers to show that in addition to bond valence and coordination number, the electronegativity of the metal atoms is also necessary to accurately predict acidity, but we provided no compelling structural explanation.

We are now assembling a complete potential energy model, based largely on the Bond-Valence Model (BVM), to guide development of QSARs based on the BVM. Our model combines the predictions of the VSEPR model of molecular geometry with the BVM, using the concept of bond valence vectors [3], along with van der Waals and electrostatic potentials to describe non-bonded interactions. So far, we have been able to show that changes in Me-H van der Waals potential energies due to structural relaxation are likely to be important for determining acidity in our calibration set of oxyacids, and that this effect is highly correlated with the electronegativity of the metal atoms. Thus, we have found a way to explain our previous results in structural terms, and a way to determine how an acidity QSAR based on bond valence, coordination number, and acidity might be successfully transferred to oxided surfaces. This kind of theoretical guidance for creating and transferring QSARs is essential for systems like mineral-water interfaces, where it is often difficult to check the veracity of model results at the molecular scale.

[1] Hiemstra *et al*. (1996) *J. Colloid Interface Sci*., **184,** 680–692. [2] Bickmore *et al.* (2006) *GCA* **70**, 4057-4071. [3] Harvey et al. (2006) *Acta Crstallographica*, B62, 1038-1042.

https://doi.org/10.1180/S0026461X00008434 Published online by Cambridge University Press

Very fast silicic magma genesis in caldera and rift environments based on isotope zoning in zircons, experiments, and thermal modeling

BINDEMAN IN[1]*, LUNDSTROM C.[2], SCHMITT AK[3], SIMAKIN[4] A., SELIGMAN A.[1] AND DREW D[1]

[1]Geol Sci, Univ of Oregon, Eugene, USA, bindeman@uoregon.edu (*presenting), [2]University of Illinois, Urbana-Champaign, IL, USA, [3]Earth Space Sci, UCLA, Los Angeles, CA, USA, [4]Inst Physics Earth, Moscow, Russia

Large-volume sub-liquidus silicic rocks are erupted in caldera environments with short repose time. Modern in situ isotopic methods have recently permitted analysis of isotopic and trace elemental abundances on micron to smaller scale and demonstrate strong crystalline heterogeneity. We review recent discoveries of isotopically (O, U-Pb) zircons in large volume ignimbrites (Snake River Plain, Kamchatka, and Iceland).

We report results from a long-duration isotope exchange experiment with natural zircon and rutile that was held for 4 months at 850°C and 0.3 kbars in a silica-rich solution doped with ^{18}O, ^{2}H, ^{7}Li and ^{10}B. The length-scales of in-diffusion were examined by depth profiling using time-of-flight (TOF) and Cameca 1270 high-sensitivity dynamic SIMS. Rutile and zircon developed ~2 μm and ≤0.13μm Fickian profiles, respectively, suggesting that rutile diffusion coefficients were at ~400 times greater than zircon's, and both are consistent with the wet diffusion coefficients for zircons and rutiles reported by Watson and Cherniak (1997) and Moore et al (1998). These results are relevant for interpreting timescales of magma evolution, in particular those related to controversial sharp intra-crystal zircon oxygen isotopic gradients. We instead consider sharp boundaries to be related to rapid episodes of solution-reprecipitation that outpace diffusive exchange, and generate concave-up zircon crystal size distributions (CSDs). Isotopic profiles in natural zircons will translate into 100-1000 yrs residence and characterize 100-1000 km^3 volumes of near-liquidus magmas.

Given diffusive-equilibration and recrystallization timescales, these new results call for very fast magma segregation from diverse in $\delta^{18}O$ hydrothermally-altered protoliths, occuring rapidly at shallow depths. As oxygen is a major component of silicates and oxides, isotopic variation of several permil reflect tens of percent of mass addition. Isotopic diversity in zircons spanning 2-7‰ $\delta^{18}O$ characterize near-liquidus magmas of 100-1000km^3 volume. Coexisting high, normal and low-$\delta^{18}O$ zircons indicate contributions from diverse protoliths, and convective mixing on 10^2-10^3 yr. timescales comparable to mineral-diffusive, solution-reprecipitation, and crystal size distribution timescales. Modeled convective rates of silicic magmas are fast enough to homogenize ~1000 km^3 magma over 10^4 yr. timescales.

Numerical experiments demonstrate the feasibility of rapid (10m/yr) convective melting rate which may translate into >10km^3/yr magma production rates over spatial dimensions of typical calderas. We suggest that neither conductive cooling nor hydrothermal refrigeration are capable of dissipating heat sufficiently fast to prevent catastrophic melting.

Evidence for a mid-crustal channel flow during the Sveconorwegian orogeny of Baltica ?

B. BINGEN [1*], G. VIOLA [1,2], K. YI [3] AND A.K. ENGVIK [1]

[1]Geological Survey of Norway, 7491 Trondheim, Norway, bernard.bingen@ngu.no (* presenting author)
[2]Norwegian University of Science and Technology, 7491 Trondheim, Norway, giulio.viola@ngu.no
[3]Korea Basic Science Institute, 363-883 Chungbuk, South Korea, kyi@kbsi.re.kr

New structural, petrological and SIMS U-Pb zircon data from SE Norway suggest that a mid-crustal channel flow may have developed during the main Sveconorwegian orogenic phase at the margin of Baltica. The 500 km wide Sveconorwegian orogen is interpreted as the product of a hot and long-lived, polyphase, bivergent orogeny, resulting from the collision of Baltica with another major plate (Amazonia, Laurentia) at the end of the Mesoproterozoic. The Sveconorwegian orogen is built on Mesoproterozoic crust that youngs toward the west. The orogeny followed a voluminous 1200-1130 Ma bimodal, within-plate magmatism in the west, more extensive than previously assumed. High-pressure (HP) metamorphic rocks are only recorded in the east of the orogen. These three observations suggest a warm lithosphere at the onset of orogeny, increasingly warmer toward the west. At around 1080 Ma, Bamble and Kongsberg were thrusted westwards on top of Telemark marking the onset of collisional tectonics. The main orogenic phase started at c. 1050 Ma. In the Idefjorden terrane, HP granulite-facies mafic boudins and kyanite gneisses locally record conditions of c. 930 °C - 1.3 GPa at c. 1050 Ma. This was followed by widespread LP amphibolite-facies partial melting. Leucosomes associated with top-to-the-west regional kinematics and resulting from muscovite-, biotite- and amphibole-dehydration melting of orthogneiss and paragneiss, range in age from 1039 ± 17 to 997 ± 16 Ma, as provided by low-U zircon rims. This partial melting episode was coeval with metamorphism along the Vardefjell shear zone bounding the Idefjorden terrane in the west, and coeval with widespread syn-collisional granitic plutonism and LP amphibolite- to granulite-facies metamorphism in the west of the orogen in Rogaland-Vest Agder. The reported long-lived high-grade conditions suggest development of a mid-crustal west-directed (?) channel flow activated after c. 1040 Ma, probably associated with a slowly eroding orogenic plateau. Lack of foreland basins to the east of the orogen is consistent with west directed flow. In this model, the low-grade Telemark supracrustals may belong to a shallow orogenic lid, covering a large area in the centre the orogen and characterized by deposition of immature sediments in grabens (Eidsborg Fm <1118 Ma, Kalhovde Fm <1065 Ma). At c. 980 Ma, the Sveconorwegian orogeny propagated eastwards in the footwall of the arcuate, southeast-verging, "Mylonite Zone" back-thrust, leading to eclogite-facies metamorphism in the Eastern Segment. Convergence was followed by gravitational collapse after c. 970 Ma. High-grade LP conditions were maintained in Rogaland-Vest Agder until c. 930 Ma and were associated with voluminous post-collisional plutonism, including anorthosites.

https://doi.org/10.1180/S0026461X00008434 Published online by Cambridge University Press

Isotopic fractionation between Cr^{3+} species in aqueous solutions

JEAN LOUIS BIRCK[1*], TU-HAN LUU[1,2], AND ROXANE JOURDAIN[1,3]

[1]IPGP, Paris, France, birck@ipgp.fr (*presenting author)
[2] luu@ipgp.fr
[3]roxanejourdain@gmail.com

When chromium is oxidized from the 3+ to the 6+ state, the 6+ species displays a δCr_{53-52} of up to 7 permil ($^{o}/_{oo}$) relative to the 3+ state [1-3]. Here we show that large fractionation predicted by theory [4] within the same oxidation state (3+) can also be evidenced. Cations are present in different species which result from the interaction with the anions present in the solution. Chromium has the property similar to only a few other elements (e.g. Os) that coexisting species do not re-equilibrate immediately when the medium changes (e.g. by dilution or by addition of an acid). In contrast to most cations which interact instantaneously with the aqueous solvent, Cr^{3+} requires several days at room temperature in HCl solution for the different species to reach equilibrium.

Procedure

This property which is usually a drawback for a clean separation of Cr from other elements [5] can be used for identification purposes as described in the following. A chromium III standard solution was made in HCl 6N to produce easily measurable amounts of chlorocomplexes and was left for several days to reach equilibrium. A chromatographic separation [5] was achieved in less than 30mn to avoid significant kinetic isotopic effects. The isotopic ratios of the different hydrated chlorocomplexes as well as the Cl free hydrated $[Cr(H_2O)_6]^{3+}$ cation were measured by high precicion MC-ICPMS at medium mass resolution (ca 4000) with a precision of $0.05^{o}/_{oo}$.

Results and conclusion

The $[Cr(H_2O)_6]^{3+}$ species shows an excess in δCr_{53-52} of 2.37 ± 0.05 $^{o}/_{oo}$ relative to the starting Cr solution. $[CrCl(H_2O)_5]^{2+}$ displays a deficit in δCr_{53-52} of -0.03 ± 0.05 $^{o}/_{oo}$. The higher complexes $[CrCl_x(H_2O)_{(6-x)}]^{(3-x)+}$ x>1 which have not yet been resolved in the chemical separation display alltogether a deficit of δCr_{53-52}: -0.39 ± 0.05 $^{o}/_{oo}$. HBr and H_2SO_4 media have also been investigated; they yield negative values for $[Cr(H_2O)_6]^{3+}$ which are interpreted as being dominated by kinetic effects during the hydrolysis of the anion-chromium complexes.

The results for the HCl media are in a first order agreement with the theoretical estimates of Schauble et al. [1]. Whether the significant fractionation that may occur in solutions within the Cr^{3+} oxidation state has an impact in natural samples has to be investigated.

[1] Johnson, Bullen (2004) Rev. Min. & Geochem. **55,** 289-319. [2] Ellis et al. (2002) Science 295, 2060-2062. [3] Frei *et al.* (2009) Nature **461**,250-253. [4] Schauble et *al.* (2004) Chem. Geol. **205**, 99-114. [5] Strelow (1973) in Ion exchange and solvent extraction Marcel Dekker. **5**, 121-206

The solubility of amorphous aluminous silica between 100 - 350°C: Implications for scaling in geothermal power stations

JULIA. K. BJÖRKE [1, 2 *]; BRUCE. W. MOUNTAIN [2]; TERRY. M. SEWARD[1]

[1]Victoria University, Wellington, New Zealand, j.bjorke@gns.cri.nz (*presenting author), terry.seward@vuw.ac.nz
[2]GNS Science, Wairakei Research Centre, Taupo, New Zealand, b.mountain@gns.cri.nz

Scaling is a common problem in geothermal power plants. In particular it occurs from brines where minerals become saturated and precipitate. To prevent scaling, geochemists use thermodynamic modelling to apply treatment methods, such as adjusting temperature or pH. Amorphous aluminous silica scaling has been reported in many geothermal power plants such as in New Zealand, Philippines, Salton Sea, Japan and Iceland [1]. Currently, the sole study on the solubility of amorphous aluminous silica was carried out by Gallup 1998 [2]. These were simple batch experiments in which there was no control on pH or Al concentration. A general reaction can be written for the precipitation of this phase as:

$$xH_4SiO_4 + yAl(OH)_4^- + yH^+ = xSiO_2.yAlO_{1.5} + (2x + 2.5y)H_2O.$$

Unlike amorphous silica precipitation, this reaction is pH and Al concentration dependent over a wide region of pH. Unfortunately, there have been no well-controlled experiments to determine thermodynamic data for this reaction.

Preliminary calculations, using the data of Gallup 1998 [2], were used to estimate the solubility of amorphous aluminous silica and compare it with the solubility of pure silica. These show that scaling, caused by amorphous aluminous silica, can occur at temperatures up to 50°C higher than for pure silica, based on the chemistry of a cooling, flashed Ohaaki brine.

Four samples of amorphous aluminous silica scale were collected from Wairakei and Ohaaki geothermal power plants. XRD, XRF and SEM analyses were carried out on the samples and to verify that Al was not present as a distinct Al phase from the amorphous silica. Results from the XRD analyses showed amorphous material with quartz peaks in all samples. XRF results show concentrations of SiO_2 ranging from 73.89-76.70%, Al_2O_3 from 8.38-10.46%, K_2O from 2.13-3.05%, Na_2O from 1.72-2.15%, CaO from 1.08-2.13% and MgO from 0.06-1.99%. Other oxides were less than 1% of the total sample. XRD results and EDX mapping by SEM verified that Al is present within the silica and is not in a distinct phase. Al concentration is zoned and correlates with increases in alkali concentration.

Experiments are planned to investigate the solubility of amorphous aluminous silica in the temperature range 100 - 350°C. These will be conducted at saturated vapor pressure and with varying pH using a continuous flow-through system and batch reactors.

[1] Gallup (1997) *Geothermics* **26**, 483-499. [2] Gallup (1998) *Geothermics* **27**, 485-501.

https://doi.org/10.1180/S0026461X00008434 Published online by Cambridge University Press

Oxygen consumption by granite samples under sterile glacial melt water conditions

EVA BJÖRKMAN[1], DAQING CUI[1,2], AND IGNASI PUIGDOMENECH[3*]

[1]Mat. & Env. Chem., Stockholm University, Stockholm, Sweden, eva.bjorkman@mmk.su.se (* presenting author)
[2]Studsvik, Nyköping, Sweden, daqing.cui@studsvik.se
[3]Swedish Nuclear Fuel and Waste Management Co (SKB), Stockholm, Sweden, ignasi@skb.se

Background

During future glacial periods in Fennoscandia it may not be excluded that, at least temporarily, increased groundwater recharge and flows may occur. The glacial melt water may have large amounts of dissolved O_2, and this might affect the stability of spent nuclear fuel canisters in the repositories planned in Sweden and Finland [1]. Several processes are able to remove dissolved oxygen: reactions with Fe(II) and sulphide minerals in the rock matrix and in fracture fillings and microbial processes consuming CH_4 or DOC [2].

As the availability of microbial substrates might be substantially reduced during glacial periods, there is a need to confirm the consumption of O_2 by abiotic reactions with Fe(II) minerals. The relative importance of inorganic and microbial processes is difficult to obtain unless special precautions are taken [3,4]

Experimental details

Batch experiments were performed at ~22°C under sterile conditions in serum bottles filled with minerals, MQ sterilized water and a gas phase containing N_2 at ~1.3 bar to which a known amount of air was added. The O_2 in the head-space gas was analyzed for up to 727 days by GC, using the Ar in the injected air as reference.

Two different rock types were used: a quartz monzodiorite and a fine-grained granite with several size fractions ranging between 0.25 and 10 mm. A chlorite sample was used as a Fe(II)-rich reference mineral, and quartz and pure water as un-reactive controls. The materials were characterized by BET, pore size distribution, Mösbauer, and chemical analysis.

Results and Conclusions

The quartz and water samples showed stable O_2 concentration within ±500 ppm while oxygen decreased to different degrees in the rock samples and it was completely exhausted in the chlorite experiments demonstrating oxygen consumption by Fe(II) under sterile conditions. The importance of the surface area is evidenced from the reaction rates expressed as "moles O_2 day^{-1} m^{-2}" which overall vary between -2.7×10^{-8} and -1.3×10^{-8} independent on mineral type, iron content or size fraction used.

The rates obtained are comparable to previous laboratory studies and support the long-term safety evaluation [1] of spent nuclear fuel repositories during glacial periods.

[1] Sidborn *et al* (2010) *Report SKB-TR-10-57*. [2] MacQuarrie et al (2010) *J. Contaminant Hydrol.* **112**, 64-76. [3] Puigdomenech *et al* (2000) *Scient. Basis Nucl. Waste Manag. XXIII*. (Smith & Shoesmith eds) 179-184. [4]Trotignon *et al* (2002) *Geochim. Cosmochim. Acta* **66**, 2583-2601.

A thermal and erosional history of cratonic lithosphere over billion-year time scales

TERRENCE BLACKBURN[1*], SAMUEL BOWRING[1], TAYLOR PERRON[1], KEVIN MAHAN[2], FRANCIS DUDAS[1]

[1]EAPS, MIT, Cambridge, MA, USA (*correspondance: terrence@mit.edu)
[2] Dept of Geol. Sci., Univ. of CU Boulder, CO, USA

The continental lithosphere contains the oldest and most stable structures on Earth, where fragments of ancient material have withstood destruction by tectonic and surface processes operating over billions of years. Though present-day erosion of in these remnants is slow, a record of how they have uplifted, eroded and cooled over Earth's history can provide insight into the composition and density of the continents and forces operating to exhume them over geologic time. Because the exhumation or burial of the Earth's surface has a direct effect on the rate of heat loss within the lithosphere, a continuous record of lithosphere exhumation can be reconstructed through the use of a temperature-sensitive radiometric dating technique known as thermochronology. The combination of thermochronologic data with thermal models for heat transfer in the lithosphere can be used to measure the processes operating to cool or heat the lithosphere in the geologic past. Thermochronologic systems sensitive to cooling at high temperatures is insensitive to the "noise" associated with near-surface cooling and therefore provides a measure of the background rate of erosion or burial associated with the vertical motions of a craton. The U-Pb thermochronologic system is sensitive to cooling at temperatures of ~400-650 °C, corresponding to lower crustal depths in cratonic regions of ~20-50 km. Here we utilize this technique to reconstruct an ancient and long-lived thermal history of volcanically exhumed lower crustal fragments, samples that resided at depth for billions of years before recent volcanism transported them to the surface as xenoliths. A high fidelity reconstruction of time-temperature paths for these samples is produced using the U-Pb system's dual decay scheme, where parent isotopes 238U and 235U decay at different rates to daughter isotopes 206Pb and 207Pb, respectively. Coupling this dual isotopic system with diffusion's length scale dependency, which causes different crystal sizes to retain Pb over different absolute time scales, results in a set of daughter isotopic compositions for a range of crystal sizes that is unique to the time-temperature history of the sample. Combining these measurements with thermal and Pb-diffusion models constrains the range of possible erosion histories. Measured U-Pb data are consistent with near zero erosion rates persisting over time scales approaching the age of the continents themselves. This indicates that the isostatic balance observed in the present-day continents has been largely maintained over geologic time, extending back at least to the onset of cooling within each terrane. Since this stability was first meet, the craton has experienced a balance between erosion and burial, with a corollary balance between the lithosphere's internal buoyancy forces and near zero isostatic uplift, further indicating a minimal change in the relative densities of the lithosphere and mantle over intervals lasting billions of years.

https://doi.org/10.1180/S0026461X00008434 Published online by Cambridge University Press

DATING FLUID FLOW EVENTS IN A SHALLOW SEDIMENTARY BASIN: THE KEY CONTRIBUTION OF K-Ar GEOCHRONOLOGY OF AUTHIGENIC ILLITE

THOMAS BLAISE[1,2,*], NORBERT CLAUER[3], MICHEL CATHELINEAU[1], PHILIPPE BOULVAIS[4], MARIE-CHRISTINE BOIRON[1], ISABELLE TECHER[5], ALEXANDRE TARANTOLA[1], PHILIPPE LANDREIN[2]

[1]G2R, Univ. Lorraine, France ; * thomas.blaise@G2R.uhp-nancy.fr
[2]ANDRA, Chatenay-Malabry, France
[3]LHyGES, Univ. Strasbourg, France
[4]Geosciences Rennes, France
[5]GIS, Univ. Nîmes, France

In shallow parts of sedimentary basins, low-temperature diagenetic processes (<90-100°C) produce discrete mineralogical changes on both the carbonates and clays. These processes are somehow challenging to investigate as most of the geothermometers are at their application limits. Furthermore, the low concentrations of trace elements in the newly-formed minerals (e.g., REE in fluorite, U in calcite) complicate the dating attempts. In this context, this study presents petrographic and geochemical data acquired on secondary minerals filling the fractures, vugs and primary porosity of three aquifers of the Mesozoic sedimentary sequence from Paris Basin, France.

The Oxfordian and Middle Jurassic limestone aquifers located respectively above and below Callovian-Oxfordian claystones are essentially cemented by successive stages of blocky calcite. Isotopic tracing ($\delta^{18}O$, $\delta^{13}C$ and $^{87}Sr/^{86}Sr$) and data acquired on hosted fluid inclusions (salinity, δD of paleo-fluids) reveal that the physical-chemical properties of calcite-forming waters were rather different for each of the aquifers and from present-day groundwaters. The aquifer located in Lower Triassic siliciclastic sedimentary rocks is buried at a 2000m depth and evidences a diagenetic alteration, among which quartz overgrowth, adularia precipitation and widespread illitization. Illite nanometric particles (<0.02 and 0.02-0.05 μm fractions) were separated, analyzed (DRX, EDS microprobe, $\delta^{18}O$, $^{87}Sr/^{86}Sr$) and K-Ar dated. Two ranges of K-Ar ages were obtained: 183 ± 2 Ma (2 samples), 150 ± 2 Ma (7 samples) and an additional age at 116 ± 2Ma. All ages are consistently younger than the Triassic sedimentation. They further strongly suggest that at least two mineralizing fluid flows occurred before the maximal burial of the sediments (Upper Cretaceous). These ages fit with the identified episodes of successive opening stages of the central Atlantic Ocean where increasing heat flows and associated fluid circulations have induced: (i) several Pb-Zn-F-Ba mineralizations along the margin of the basin, and (ii) extensive illitization in Triassic and Permian sandstones in many locations of Western Europe.

The study shows also that each studied aquifer underwent an individual and specific diagenetic history that highlights the role of the Callovian-Oxfordian claystones as an efficient hydrological barrier between the limestone units. This effective isolation is of major engineering importance as these claystones represent the currently studied target for a long-term geological disposal of radioactive waste.

Complementarity of computational molecular modelling and experimental techniques to study trace elements geochemistry

MARC BLANCHARD[1*]

[1]IMPMC, UPMC, CNRS, 4 place Jussieu, 75252 Paris Cedex 05, France, marc.blanchard@impmc.upmc.fr (* presenting author)

Chemical reactions at the interfaces between soils components and water play an important role in numerous natural processes, like in particular the fate and behaviour of potentially toxic trace metals. One efficient approach has recently emerged to address this question. It consists in the combination of X-ray absorption spectroscopy (XAS) and isotopic techniques. Besides this experimental approach, computational molecular modelling can also contribute significantly to improve our understanding of the atomic-scale processes that control the biogeochemical cycles of trace elements. This presentation will expose the complementarity of both experimental and theoretical approaches. Within the same theoretical framework, it is now possible (i) to calculate the local structural and electronic properties of any atom in the studied system and compare these properties with XAS data, (ii) to model XANES spectra, which allows a better interpretation of spectral features, and (iii) to determine the equilibrium fractionation factors of traditional as well as non-traditional isotopes, associated with any structural site of the system. Several applications will be presented, including the arsenic adsorption complexes at the hematite surface [1], the calculated XANES spectra of 3d transition metal compounds [2], and the isotopic properties of Al- and OH-bearing hematite [3].

[1] Blanchard *et al*. (submitted) *GCA*. [2] Cabaret *et al*. (2010) *PCCP* **12**, 5619-5633. [3] Blanchard *et al*. (2010) *GCA* **74**, 3948-3962.

https://doi.org/10.1180/S0026461X00008434 Published online by Cambridge University Press

Time-resolved SAXS study of nucleation and growth of iron(III) oxyhydroxides

MARK W. BLIGH[1*], ANDREW L. ROSE[2], RICHARD N. COLLINS[1], AND T. DAVID WAITE[1]

[1]University of New South Wales, Sydney, Australia, m.bligh@unsw.edu.au (*presenting author), d.waite@unsw.edu.au, richard.collins@unsw.edu.au

[2]Southern Cross University, Lismore, Australia, andrew.rose@scu.edu.au

Introduction.The process of hydrolysis and polymerization of Fe(III) oxyhydroxides plays an important role in the chemistry of natural waters. However, these transformations are rapid and occur over timescales that are much smaller than those typically studied. Time-resolved SAXS studies provide the capacity to investigate nucleation and the evolution of particle size distribution on a sub-second timescale. Different mechanisms of particle production have previously been identified, for example, a nucleation burst followed by monomer addition [1] and, nucleation followed by aggregation [2]. In this study we use TR-SAXS to examine polymerization of Fe(III) oxyhydroxides following rapid mixing, such that mixing times are less than reaction times. In this initial study, at [Fe] = 1 mM, required to produce sufficient scattering intensity, reaction times were sufficiently long only at pH 3 and 4. Investigation of higher pHs will require the optimization of a micro-fluidic device.

Results and Conclusions. The SAXS curves were analysed, both directly and by fitting a pair distance function, to produce values for the invariant Q, zero-angle scattering intensity $I(0)$, and radius of gyration R_g. Q is a measure of the total scattering mass while $I(0)$ is sensitive to particle size and number. At pH 3, with $[NO_3]$ = 6 mM, R_g stabilized at ~25 nm after only 30 s while both Q and $I(0)$ continued to increase till ~300 s. At times >300 s, Q was relatively stable while $I(0)$ decreased. In the same system at pH 4, R_g followed the same pattern as for pH 3, however maximum values for Q and $I(0)$ were attained after ~77 s, and decreased thereafter. These results show that at early times, small but increasing numbers of maximum sized particles coexisted with monomers or oligomers that were too small to scatter significantly in the q-range used to calculate Q. Such a system evolution implies that slow nucleation and relatively rapid particle growth proceeded concurrently until the maximum scattering mass was achieved. Particle growth appears to have occurred via a monomer addition mechanism ('monomers' here may be oligomers) since the stable R_g implies that significant aggregation is not occurring. The more rapid development of the maximum scattering mass at pH 4, compared to pH 3, is consistent with a higher rate of polymerisation of Fe(III) hydrolysis species and therefore more rapid production of stable nuclei. Whether the observed decreases of Q and $I(0)$ following attainment of maximum values are due to sedimentation or further transformation via dissolution and reprecipitation remains unclear and will be the subject of further investigation.

[1] Liu *et al.* (2010) *Langmuir* **26**, 17405-17412. [2] Polte *et al.* (2010) *ACS Nano* **4**, 1076-1082.

Determining garnet crystallization kinetics from growth zoning and Mn-calibrated Sm-Nd ages at Townshend Dam, VT

ROSE A. BLOOM[1*], DAVID M. HIRSCH[1], BESIM DRAGOVICH[2], MATT GATEWOOD[3], ETHAN BAXTER[2], HAROLD STOWELL[3]

[1]Western Washington University, Bellingham, WA USA, bloomr3@students.wwu.edu (* presenting author), hirschd@geol.wwu.edu

[2]Boston University, Boston, MA USA, dragovic@bu.edu, efb@bu.edu

[3]The University of Alabama, Tuscaloosa, AL, USA, matthewpgatewood@gmail.com, hstowell@geo.ua.edu

Introduction

Essential to an understanding of metamorphic rocks are the rates at which a metamorphic reaction can occur. Kinetics of porphyroblast crystallization includes rates of both growth and nucleation. Though some studies have been able to quantify growth rates, direct measurements of nucleation rates have remained enigmatic. We present a method to indirectly measure nucleation as well as growth rates of chemically zoned porphyroblasts by linking chemical and age data.

This project examined a garnet + muscovite + paragonite + biotite + chlorite + quartz + plagioclase schist from the Pinney Hollow formation at Townshend Dam, VT. Biotite-quartz-rich layers alternate with muscovite-paragonite-rich layers on a millimeter scale and define the foliation. Garnets are sub- to euhedral, vary in size from 5 to 30 mm in diameter, and display curved quartz inclusion trails continuous with foliation at the rims.

Method

The specimen was imaged in 3D using high-resolution X-ray computed tomography. Garnet porphyroblasts were extracted and portions of them with quantified Mn content underwent Sm-Nd geochronology methods to produce a Mn-age curve for the rock [1]. A subvolume from the interior of the specimen was separated and disaggregated, allowing extraction of 62 garnets. Morphological centers of each were exposed, polished, and chemically mapped (via SEM-EDS). The EDS characterization facilitated location of peak-Mn regions, from which core-rim linescans were performed via EPMA for quantitative zoning determination. Mn data were converted to ages via reference to the Mn-age curve [1], allowing determination of nucleation and growth kinetics.

Results

Townshend Dam garnets show concentric, smooth Mn zoning curves. Microprobe analyses yield central garnet MnO content ranging from 2.3 to 11 wt%, depending on the size of the garnet. Rims of garnets are Mn-poor with ca. 0.1 to 0.2 wt% MnO. Data collection is ongoing, but preliminary EPMA results indicate that among the analyzed garnets, the range of core X(Mn) is 0.047-0.249, corresponding (via the curve in [1]) to an age range of 384.8-378.1 Ma. Given this duration of nucleation (6.7 m.y.), the number of garnets (62), and the subvolume size (1210 mm^3), we calculate a nucleation rate of approximately 0.0076 nuclei per m.y. per mm^3.

[1] Gatewood et al. (2011) AGU Fall Mtg., Abstract #V13G-05.

https://doi.org/10.1180/S0026461X00008434 Published online by Cambridge University Press

Influence of alkalinity on the magnesium composition of amorphous calcium carbonate

CHRISTINA BLUE[1*], NIZHOU HAN[1], AND PATRICIA DOVE[1]

[1]Virginia Tech, Department of Geosciences, Blacksburg, USA cblue@vt.edu (*presenting author)

An increasing number of studies are showing that many calcifying organisms form skeletons by nonclassical growth. This biomineralization process begins with the accumulation of an amorphous precursor phase that subsequently transforms to an organic-mineral composite. Little is known about mineralization by this pathway because the last 50 years of research have focused almost entirely on traditional, step-growth processes.

To investigate the factors that influence the composition of amorphous calcium carbonate (ACC) and quantify their effects, we have developed a procedure for synthesizing this phase under controlled chemical conditions. The method uses a flow through reactor and high precision syringe pumps to prepare ACC from solutions that maintain a constant supersaturation and a well-characterized solution chemistry. This approach confers significant advantages over previous approaches such as the "Koga" method [1], that uses very high pH solutions (11.2–13.5), and the "ammonium carbonate" method [2], that produces highly variable supersaturation conditions and introduces significant amounts of ammonium ion to the mineralizing solution.

Using the new flow-through method, we are investigating the effect of alkalinity on the magnesium content of calcite that forms via the ACC intermediate phase. Previous studies have suggested that the magnesium levels in biogenic calcite may be correlated with the alkalinity of local growth environment [3]. The first phase of this project determined the effect of alkalinity on the magnesium content of the ACC at 24–25°C. The experiments were conducted by preparing two sets of syringes that contained solutions of 1) variable alkalinity using 40mM–150mM $NaHCO_3$ and 2) a 5:1 ratio of Mg:Ca (modern seawater) using $MgCl_2 \bullet 6H_2O$ and $CaCl_2 \bullet 2H_2O$. For the range of alkalinities used in this study, the effluent pH was 9.0–9.3. After achieving steady state output conditions, the ACC products were collected on 0.20 micron nylon mesh filter and characterized using SEM, Raman Spectroscopy, and ICP-OES. Future work will also determine the effect of alkalinity on the composition and structure of calcite that forms by the ACC pathway.

[1] Koga et al. (1998) *Thermochimica Acta,* **318**, 239-244. [2] Han & Aizenberg (2008) *Chem. Mater.,* **20**, 1064-1068. [3] Boyle & Erez (2004) *Eos Trans. AGU, **84(52)**,* Ocean Sci. Meet. Suppl.

Magmatic vs crustal volatiles: a reconnaisance tool for geothermal energy exploration

LARA S. BLYTHE[1*], VALENTIN R. TROLL[1], DAVID R. HILTON[2], FRANCES M. DEEGAN[3], ESTER M. JOLIS[1] AND JAMES STIMAC[4]

[1]Dept. of Earth Sciences, Uppsala University, Uppsala, Sweden. lara.blythe@geo.uu.se (* presenting author).

[2]Geosciences Research Division, Scripps Institution of Oceanography, La Jolla, California, USA.

[3]Laboratory for Isotope Geology, Swedish Museum of Natural History, Stockhom, Sweden.

[4] Geoglobal Energy LLC, Santa Rosa, California, USA.

Volcanically-hosted geothermal energy is an important resource in Indonesia of which Salak Geothermal Field in W Java is the largest developed one [1]. All 5 power-producing plants on Java are located in the western and central crustal sectors [1] and there appears to be a correlation between the location of commercially-viable geothermal systems, such as Salak Geothermal Field, and the thickness of the local upper crust and/or the volume of sediment on the downgoing plate [2]. This implies that crustal input from the subducting slab or from upper crust is central to the development of productive geothermal resources in this part of the world. Java's upper crust can be divided into three lateral segments: thick crust of continental affinity in the west [3], grading into arc-type and oceanic crust in central Java into increasingly oceanic affinity eastwards [3; 4].

Here we combine He isotope data from gas, fluids, pyroxene separates and whole rock Sr and Nd isotope values from volcanoes along the Sunda Arc (from Anak Krakatau to Bali, East of Java) with literature data to further understand sources to the crustal contamination signals and their influence on geothermal systems.

Helium isotope values (in R/R_A notation) are lower in both crystal and geothermal samples (down to $3.4R_A$ in pyroxene at Gede volcano) in the central and western crustal sectors, when compared to the eastern sector (7.46 R_A from fumaroles at Kawah Ijen volcano). Equally, Sr (as demonstrated by [5]) and Nd vary systematically eastwards along the arc, with values showing a significant crustal influence in central and western Java. East of the Progo-Muria fault, which delineates the central and eastern crustal sectors, volcanic rocks and geothermal samples give a more mantle-like signal (i.e. in eastern Java and Bali). The correlation between upper crustal type and crustal contamination is present in all three isotope systems (He-Sr-Nd). Together with the location of all commercially productive geothermal plants in west and central Java we propose that regional crustal influences may be highly relevant in understanding the development of geothermal systems with exploitation potential in Indonesia.

[1] Bertani, R. (2005) *Geothermics* **34**, 651-690.
[2] Stimac, J. *et al*. (2008) *Geothermics* **37**, 300-331.
[3] Hamilton, W. (1979) *U.S.G.S: Professional Paper* **1078**, 1-345.
[4] Smyth, H.R. *et al.* (2007) *Earth Planet Sc Lett* **258**, 269-282.
[5] Whitford, D.J. (1975) *Geochim Cosmochim Ac* **342**, 1287-1302.

https://doi.org/10.1180/S0026461X00008434 Published online by Cambridge University Press

Reconstruction of the North Atlantic Circulation back to the Last Interglacial by a combined proxy approach

E. BÖHM[1]*, J. LIPPOLD[1], M. GUTJAHR[2], J.GRÜTZNER[3], A. MANGINI[1]

[1] Heidelberg Academy of Sciences, INF 229, Heidelberg, Germany
*correspondence: eboehm@iup.uni-heidelberg.de
jlippold@iup.uni-heidelberg.de, amangini@iup.uni-heidelberg.de
[2] National Oceanography Centre Southampton, UK
m.gutjahr@soton.ac.uk
[3] Alfred Wegener Institute, Bremerhaven, Germany
Jens.Gruetzner@awi.de

Studies of past variations of the Atlantic Meridional Overturning Circulation (AMOC) are essential for evaluating possible future developments. In order to asses such past variations two new proxies (Nd isotopes and $^{231}Pa/^{230}Th$) have been applied frequently in recent years, but only two combined data sets are available to date [1,2]. The combined use of Fe-Mn oxyhydroxide-derived Nd isotopes (ε_{Nd}), a sensitive chemical water mass tag, and $^{231}Pa/^{230}Th_{xs}$, a kinematic circulation proxy, from identical sediment core samples allows to obtain information about both the rate of overturning circulation and water mass provenance.

Here we present neodymium isotope compositions of past seawater and $^{231}Pa/^{230}Th$ extracted from sediments from a high sedimentation rate location (< 10 cm/ka) in the western North Atlantic (ODP Site 1063, Bermuda Rise), back to the Last Interglacial (Eemian).

First measurements of ε_{Nd} have been accomplished for the time range from 53 to 150 ka with a temporal resolution averaging 3 ka. The Nd isotopic record suggests the presence of Southern Source Water during MIS 6 to MIS 6.4 as well as active deep water formation in the North Atlantic at the beginning of the Eemian Interglacial (MIS 5.5). The transition between these two different modes in AMOC is marked by a distinct drop in the ε_{Nd} values (-11.5 to -14). This is consistent with ε_{Nd} results from [1] and [2] at the transition from MIS 2 to MIS 1.1 which implies recurring millenial-scaled identical processes converting the AMOC from a Glacial mode into an Interglacial mode.

Numerous measurements of Pa/Th have been performed in the time range from 65 to 143 ka with a high temporal resolution (1 ka or less). Results show that the Pa/Th method reaches its detecting limit at 125 ka due to the short half life of ^{231}Pa ($T_{1/2}$=33 ka). The interval between 95 and 125 ka displays strong fluctuations (Pa/Th=0.046 to 0.079) with one pronounced peak at 119 ka (Pa/Th=0.095) indicative of a slowdown of the AMOC (no corresponding peak in opal). This is consistent with [3] who found a short cold event with near-glacial surface ocean summer temperatures in MIS 5.5.

[1] Gutjahr, M. and J. Lippold, 2011. Paleoceanography. 26(PA2101). [2] Roberts, N., A. Piotrowski, J. McManus and L. Keigwin, 2010. Science. 327(75). [3] Bauch, H., E. Kandiano, J. Helmke, N. Andersen, A. Rosell-Mele, H. Erlenkeuser, 2011. Quaternary Science Reviews, 30(15-16): 1813-1818.

Fe(II)-mediated reduction of Cr(VI) and U(VI) in the presence of Fe(III) oxyhydroxides

DANIEL D. BOLAND[1*], RICHARD N. COLLINS[1], CHRIS J. GLOVER[2], TIMOTHY E. PAYNE[1,3] AND T. DAVID WAITE[1]

[1]School of Civil and Environmental Engineering, The University of New South Wales, Sydney, Australia, daniel.boland@student.unsw.edu.au. (* presenting author)
[2]Australian Synchrotron Company Ltd, Clayton, Australia.
[3]Institute for Environmental Research, Australian Nuclear Science and Technology Organisation, Lucas Heights, Sydney, Australia.

Reduction of both Cr(VI) and U(VI) generally leads to the precipitation of insoluble phases and, thus, decreases the mobility of these toxic metals. In this study we examined the reduction of Cr(VI) during the Fe(II)-catalysed transformation of ferrihydrite to goethite, and compared the results to our previous experiments examining U(VI) reduction in the same system [1].

Cr(VI) was sorbed to ferrihydrite, silica-coprecipitated ferrihydrite (Si-ferrihydrite) and goethite in pH 6.5 buffered solutions in the form of CrO_4^{2-}, and Fe(II) added at 1mM. Cr K-edge X-ray absorption spectroscopy (XAS) analyses of the resultant solids showed that there was an immediate reduction of Cr(VI) to Cr(III) under all treatments (Figure 1), preceding any changes to the Fe(III) oxyhydroxide initially present. This contrasts to U(VI) in the same system, whose reduction is dependent upon the presence of goethite. Ferrihydrite continued to transform to goethite as expected, which has implications for the reactivity of this now Cr-bearing substrate.

These results are consistent with what may predicted by the relative positions of Cr and U in the "redox ladder". They emphasise the validity of using localised thermodynamic calculations to predict the redox state of trace species present during Fe(II)-catalysed Fe(III) oxyhydroxide transformations.

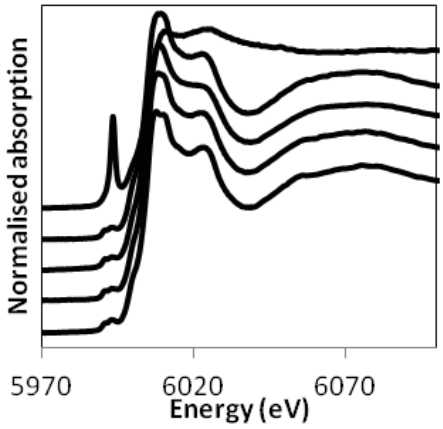

Figure 1: Cr K-edge XAS data. From top: Cr(VI) sorbed on ferrihydrite, following reaction with Fe(II) on ferrihydrite, Si-ferrihydrite and goethite, Cr (III)-substituted Fe(III) oxyhydroxide. Reduction is clear from the diminished pre-edge feature.

https://doi.org/10.1180/S0026461X00008434 Published online by Cambridge University Press

Chemistry of diatoms and coccoliths records carbon acquisition strategies during biomineralization

CLARA BOLTON[1], KIRSTEN ISENSEE[1],LUZ MARIA MEJIA-RAMIREZ[1], ANA MENDEZ-VICENTE[1], JORGE PISONERO[2], NOBUMICHI SHIMIZU[3], HEATHER STOLL[1]*

[1]Geology Dept., Univeristy of Oviedo, Oviedo, Spain , hstoll@geol.uniovi.es (* presenting author)

[2]Physics Dept., University of Oviedo, Oviedo, Spain

[3]Geology and Geophysis, Woods Hole Oceanographic Institute, Woods Hole, USA

Introduction

A strong biological control over trace element or stable isotopic composition of marine biominerals is frequently viewed as a liability in reconstructing past ocean chemistry and temperature, and the significance of reconstructing the biological processes themselves is often overlooked. We propose that the chemistry of opal, produced by diatoms, and calcite, produced by coccolithophorids, predominantly reflects key biological processes for cellular carbon acquisition. Reconstruction of these biological processes in the past will reveal how marine algae responded to changes in atmospheric CO2, key to both the past and future carbon cycle.

Biomineralization effects on stable isotopes in coccoliths

Coccolithophorids exhibit strong biological effects in carbon and oxygen isotopic composition. Previously we hypothesized that the size-correlated range of vital effects in carbonate liths produced by different coccolithophore species was due to variable significance of carbon concentrating mechanims in their C acquisition. Our new culture experiments with coccolithophorids reveal strong plasticity in the magnitude of stable carbon isotope vital effects in coccoliths of *Calcidiscus leptoporus* and *Emiliania huxleyi* with variable CO_2. At high CO_2 coccoliths of both species are more isotopically enriched, but the magnitude is greater in *C. leptoporus* leading to reduced interspecific offsets at high CO_2. In the case of *E. huxleyi*, higher CO_2 conditions resulted in significant reduction in the magnitude of DIC accumulation in the intracellular carbon pool, and more positive carbon isotopic values inside the particulate organic matter. A model of carbon acquisition incorporating both photosynthetic and carbonate production is used to assess mechanisms for these relationships. Stable isotope data from size-separated deep-sea sediments dominated by small, intermediate, and large coccoliths show a range of vital effects which is distinct during several major Cenozoic proxy-inferred climate-CO_2 transitions. Furthermore, where vital effects are significant their magnitude scales with coccolith size in the same sense as modern cultures.

Biomineralization effects on diatom B content

From two species of diatoms, *Thalassiosira weissflogii* and *T. pseudonana*, cultured at a range of pCO_2 from 200 to 2000 ppmv, B content of cleaned diatom opal was measured by Laser Ablation-ICP-MS and Secondary Ion Mass Spectrometry. Determination of growth rate, type of carbon acquired, and silicon and carbon quotas during diatom growth provides data on biomineralization process. B content in *T. pseudonana* is correlated with bicarbonate uptake rate and with normalized Si quotas. For *T. weissflogii*, which is a bicarbonate-restricted user at the pH studied, B content seems to be regulated primarily by the borate/bicarbonate seawater ratio, at pCO_2 <1000ppmv . We present a simple cellular model of B and Si uptake by diatoms to quantitatively explore the mechanisms for variable B content and its potential as a proxy.

Oceanic Material recycled within the Subpatagonian Lithospheric Mantle (Cerro del Fraile, Argentina)

B. FACCINI[1] , C. BONADIMAN[1*], M. COLTORTI[1], M. GREGOÌRE[2], AND F. SIENA [1]

[1] Department of Earth Sciences, Ferrara University, Ferrara, bdc@unife.it

[2] DTP, CNRS-UMR 5562 Observatoire Midi-Pyrenées, Toulouse, France

A detailed petrological study of mafic and ultramafic xenoliths from the Cerro del Fraile (Southern Patagonia, Argentina) was developed in order to highlight: I) the mineralogical and geochemical composition of the lithospheric mantle beneath the area, II) the nature of the metasomatising agents which infiltrate the mantle wedge above the Antarctic subducting Plate, III) the processes that allow the mantle to be refertilised and IV) the nature of the material dragged down in the subduction zone and recycled within the south patagonian sub-arc mantle.

Major and trace element analyses of clinopyroxene and orthopyroxene in peridotitic and pyroxenitic rocks suggest that a proto-adakite, deriving from the melting of the subducting Antarctic plate, was responsible for both the metasomatic features of the peridotitic rocks and the crystallisation of the pyroxenites. A few composite xenoliths bridge the two processes - peridotite enrichment and pyroxenite crystallization - indicating that the variously depleted mantle reacts with the incoming melt to generate a newly fertile mantle domain. HREE and Al2O3 and MgO contents in pyroxenes indicate a partial melting degree varying from 10 to 25 %. The peculiar enrichment in Zr (-Hf), Th and U of the pyroxenes speaks in favour of the melting of oceanic sediments, which are composed of a remarkable amount of manganese nodules and micronodules and, possibly, organic matter. Some geochemical analogies have been found between the calculated metasomatic melts and the Austral Volcanic Zone adakites. In this case, the amount of sediments involved in the genesis of the infiltrating melts is larger than that previously proposed for the genesis of the erupted Patagonian adakites. Chemical-physical conditions favouring the upward percolation through the mantle wedge of these SiO2-rich and viscous melts are also discussed.

https://doi.org/10.1180/S0026461X00008434 Published online by Cambridge University Press

U-Pb age zoning in titanite by SIMS: New criteria for preservation

CHLOË E. BONAMICI[1*], REINHARD KOZDON[1], C. MARK FANNING[2], JOHN W. VALLEY[1]

[1]WiscSIMS, University of Wisconsin-Madison, Madison, WI, 53706, USA, bonamici@wisc.edu (* presenting author)
[2]Research School of Earth Sciences, Australian National University, Canberra, Australia, Mark.Fanning@anu.edu.au

We report a set of thirty-two U-Pb SIMS ages measured in situ along two traverses of a single titanite porphyroclast from the Carthage-Colton mylonite zone in the Adirondack Mountains, New York, USA. Ages span ~140 m.y. from 1190 Ma to 1050 Ma and generally decrease from core to rim; however, ages within the interior of the grain fluctuate by as much as 50 m.y. over length scales < 100 μm. Electron microprobe element maps and Th/U spot analyses (SIMS) reveal distinct core and rim compositional domains. These do not correlate with the observed grain-interior age fluctuations and thus argue against trace element growth zoning as the source of U-Pb age variability. Light microscopy and EBSD mapping verify that the grain has not been recrystallized and show that more than 50% of the grain suffered deformation-related mechanical twinning. Ages in twinned areas of the grain are younger and more variable than ages in untwinned areas, suggesting that the presence of organized planar defects may have affected Pb mobility and abundance. SIMS $\delta^{18}O$ zoning along traverses parallel to U-Pb traverses, indicates volume diffusion of oxygen during cooling from peak T of 700°C. The strong positive correlation between $\delta^{18}O$ and U-Pb age (Figure) is consistent with the presence of first-order, core-to-rim age zonation similar in shape and extent to the zonation developed by diffusive exchange of oxygen, and it agrees with experimental studies that show similar diffusivities for oxygen and Pb in titanite over the temperature range 600-800°C.

We conclude that U-Pb age zoning within the Adirondack titanite grain reflects heterogeneous Pb redistribution by a combination of volume and intragrain fast-path diffusion. The oldest ages, preserved in untwinned areas, correlate with the 1164 ± 11 Ma intrusion age of the Diana metasyenite that hosts the grain. The youngest, ca. 1050 Ma ages near the grain rim are consistent with Pb loss and age resetting by volume diffusion during granulite-facies metamorphism accompanying the Ottawan phase (1090-1020 Ma) of the Grenville orogeny. We interpret the transitional and highly variable ages in twinned areas as reflecting segmentation of part of the grain into smaller diffusion domains between twin boundaries that behaved as diffusion fast paths. An integrated whole-grain age on this Adirondack grain would, at best, constrain the minimum age for syenite intrusion or the maximum age of high-T Ottawan metamorphism. Knowledge and careful characterization of the correlation between U-Pb age and $\delta^{18}O$ zoning in titanite will permit retrieval of more accurate ages for each event and may additionally allow for applications of coupled U-Pb-$\delta^{18}O$ titanite geospeedometry.

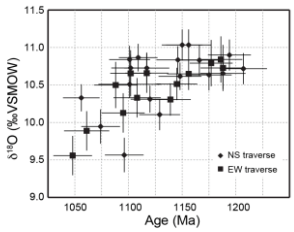

Microbial communities in low-permeability uranium mine tailings

V.F. BONDICI[1], J.E. HILL[2], N.H. KHAN[3], J.R. LAWRENCE[4], G.M. WOLFAARDT[5], T. KOTZER[6] D.R. KORBER[7*]

[1]Univ. of Saskatchewan, Saskatoon, Canada, vfb326@mail.usask.ca
[2]Univ. of Saskatchewan, Saskatoon, Canada, Janet.Hill@usask.ca
[3]Univ. of Saskatchewan, Saskatoon, Canada, mnk252@mail.usask.ca
[4]Environment Canada, Saskatoon, Canada, John.Lawrence@ec.gc.ca
[5]Ryerson Univ., Toronto, Canada, gwolfaar@ryerson.ca
[6]Cameco Corp., Saskatoon, Canada, Tom_Kotzer@cameco.com
[7]Univ. of Saskatchewan, Saskatoon, Canada, drk137@usask.ca
(*presenting author)

Uranium mine tailings management

The processing of uranium mine tailings at the Deilmann Tailings Management Facility (DTMF) at Key Lake was designed to stably co-precipitate ferrihydrite with various elements of concern (EOCs), such as As, Se, Ni, and Mo, present in the processed rock. During UO_2 extraction, tailings are milled to ≤100 μm diameter; on disposal in the DTMF, a saturated, diffusion-dominated matrix with restricted pore space (dry bulk density ~1.2 – 1.6 g/cm^3) results. The chemical stability of the DTMF relies upon maintenance of highly oxic, high pH conditions. However, microbes, given time and nutrients, have the potential to metabolically reduce the tailings which could result in the solubilization and subsequent mobilization of the EOCs. To date, the DTMF hasn't been studied from a microbiological perspective; it has been suggested that the high pH, radiation, and limiting nutrients in the DTMF would limit microbial growth and activity.

Characterization of the tailings microbial community

An in-depth analysis of microbial diversity, as well as their metabolic potential, within the tailings system has been undertaken using culture dependent and culture-independent analyses. A total of 60 tailings samples were obtained at 1 m intervals over a top 60 m of the tailings body and subjected to DNA extraction, as well as cultivation on a variety of microbiological media. A surprisingly high diversity (determined using 16s rRNA sequencing) of cultivatable bacteria under aerobic and anaerobic conditions were isolated over the tailings depth profile. These bacteria exhibited a range of characteristics reflective of being highly-adapated to life within the DTMF: of the 59 unique isolates, 69% were multiple metal resistant, 15% exhibited dual-metal hypertolerance, and a number were capable of reducing or oxidizing various metal elements.

Using extracted DNA from composited tailings samples from the upper, middle and lower 20 m layers of the DTMF profile, three *cpn60* clone libraries were assembled and sequenced. A total of 920, 952, and 693 sequences were generated for the upper, middle, and lower zones, respectively. Comparative phylogenetic analysis led to the classification of the different sequences from the three libraries into nine taxonomic groups: Gemmatimonadetes, Verrucomicrobia, Acidobacteria, Synergistetes, Planctomycetes, Actinobacteria, Bacteriodetes, Proteobacteria and Firmicutes. The prevalence of populations of metabolically-diverse, metal-resistant microorganisms capable of transforming metal elements suggests the potential for these organisms to influence the geochemical stability of the tailings. Integration of biological and geochemical data will aid in the construction of a predictive stability model that incorporates the role of organisms with unique metabolic activities.

https://doi.org/10.1180/S0026461X00008434 Published online by Cambridge University Press

Linking mackinawite (FeS) structure to redox activity

SHARON E. BONE[1*], KIDEOK KWON[2], JOHN R. BARGAR[3], GARRISON SPOSITO [1]

[1]Lawrence Berkeley National Laboratories, Berkeley, USA, SBone@lbl.gov (* presenting author), GSposito@lbl.gov
[2]Sandia National Laboratory, Albuquerque, USA, kkwon@sandia.gov
[3]Stanford Synchrotron Radiation Lightsource, Menlo Park, USA, bargar@slac.stanford.edu

The nanoparticulate tetragonal iron sulfide mineral mackinawite (FeS) is thought to be ubiquitous in wetlands, estuaries and groundwater where bacterially produced sulfide and ferrous iron mix. FeS has the potential to be used as a bioremediation tool because of its ability to reduce a range of contaminants including chlorinated organics, metals and metalloids.

The goal of our research is to link the molecular-scale structure of FeS to its reactivity towards environmental contaminants, in this case, the biomagnifying toxicant mercury. To this end, we have integrated X-ray spectroscopic, X-ray scattering, computational and wet chemical techniques to investigate FeS size and structure, and to identify which FeS moieties participate in reduction as well as what oxidized products result as a function of time, pH, and [Hg(II)] in batch reactors.

Using Hg L_{III}-edge extended X-ray absorption fine structure (EXAFS) spectroscopy we have found that Hg(II) forms a discrete Hg(0) phase after reaction with FeS. Density functional theory (DFT) computations show that surface Fe(II) in FeS preferentially binds Hg(II) relative to surface S(-II), suggesting a pathway by which electrons might be transferred to Hg(II) to produce Hg(0) and Fe(III). Using Fe K- and $L_{II,III}$-edge X-ray absorption spectroscopy, we have quantified Fe(III) formation in FeS suspensions. Fe(III) exists in octahedral coordination as a second, amorphous phase, possibly as a mixed Fe(II)-Fe(III) phase, which may be a pre-cursor to the Fe(II)-Fe(III) sulfide, greigite. Lastly, we used X-ray diffraction, electron microscopy and Fe K-edge EXAFS spectroscopy to derive a particle size distribution for FeS, and to determine FeS molecular-nanoscale structure before and after oxidation. We combined this information with thermodynamic modelling of equilibrium aqueous Fe(II) and S(-II) concentrations in order to identify the redox processes that occur in FeS suspensions.

Our research demonstrates that Fe(II) in FeS is key to FeS reactivity, dominating its surface chemistry and redox activity.

Timing the evolution of seawater chemistry during the Neoproterozoic: case study of the Svalbard succession.

P. BONNAND[1*], I. J. PARKINSON[1], I. J. FAIRCHILD[2], E. MCMILLAN[2], D. CONDON[3], G. P. HALVERSON[4].

[1]Department of Environment, Earth and Ecosystem, The Open University, Walton Hall, Milton Keynes, MK7 6AA, UK
[2]School of Geography, Earth and Environmental Sciences, University of Birmingham, Edgbaston, Birmingham, B15 2TT, UK.
[3]NERC Isotope Geosciences Laboratory, British Geological Survey, Keyworth, Nottinghamshire NG12 5GG, UK
[4]Department of Earth and Planetary Sciences, McGill University, 3450 University Street, Montreal, QC H3A 2A7, Canada
[*]p.bonnand@open.ac.uk

The Neoproterozoic Era (1000-542 Ma) is a key period in the evolution of the Earth system. This period is characterised by the widespread occurrence of glacigenic sediments and by large variations in carbon isotope compositions of seawater [1]. These excursions are among the largest described in the geological record, and together with global periods of glaciation, make the Neoproterozoic one of the most dramatic periods of change in surface processes on Earth. Another major change that occured during this period is a purported increase in oxygen concentration in the atmosphere and associated changes in ocean redox [2]. In order to unravel the global record of evolving Neoproterozoic ocean chemistry, several successions around the world have been studied [e. g. 3]. However, the lack of precise radiometric constraints on suitably preserved samples in most Neoproterozoic sedimentary successions hinders the interpretation and correlation of geochemical signals. The Polarisbreen Group in northeast Svalbard is one of the best preserved Neoproterozoic successions and has great potential to significantly improve the record of Neoproterozoic environmental evolution, but to date has yielded no direct radiometric age constraints

In this study, we investigate the potential of the Svalbard succession to represent a type succession to assess the climate and chemical variations that occured during the Neoproterozoic. The Svalbard succession is characterised by the presence of 2 distinct glaciation episods which have been correlated with the first and second Cryogenian glaciations [3, 4]. Here, we present new constraints on the depositional age of two discrete glacial intervals in the Polarisbreen Group based on U-Pb detrital zircon data from siliciclastic sediments. We also investigate Sr isotopes and REE concentration in well preserved carbonate rocks through the succession in order to correlate the variation in Sr isotopes to the proposed Neoproterozoic seawater Sr curve [3] and assess variation in marine redox conditions during this interval.

These new data will allow a better correlation of the Svalbard succession with other Neoproetrozoic successions and provide a framework to characterise the evolution of seawater during the Neorpoterozoic.

[1] Fairchild and Kennedy (2007) *Journal of the Geological Society.* [2] Holland (2006) *Philosophical Transactions of the royal Society.*[3] Halverson et al. (2010) *Precambrian Research*. [4] Fairchild and Hambrey (*1995) Precambrian Research.*

https://doi.org/10.1180/S0026461X00008434 Published online by Cambridge University Press

Assessing the use of $^{13}C\{^{1}H\}$ CPMAS NMR for comparisons of boreal watershed soil and dissolved organic matter compositions

JENNIFER BONNELL*, CELINE SCHNEIDER, CHRISTINA BOTTARO AND SUSAN ZIEGLER[1]

[1]Memorial University, St. John's, NL, Canada, jennifer.bonnell@mun.ca (*presenting author)

Understanding high latitude ecosystems and their links to global carbon cycling depends greatly on our study of the composition of both dissolved and soil organic matter (DOM and SOM, respectively) and their interactions. DOM plays a major role in aquatic carbon and nutrient cycling, but may also reveal changes in landscape biogeochemistry. Headwater streams are intimately connected to and strongly influenced by the terrestrial environment such that stream DOM likely provides important chemical clues relevant to change in the watershed.

^{13}C cross polarization magic angle spinning nuclear magnetic resonance spectroscopy (^{13}C $\{^{1}H\}$ CPMAS NMR, hereafter referred to as CP) has been used extensively in the study of both DOM and SOM. It allows assignment of types of carbon in relative proportions, which informs our understanding of the chemical composition, source, and diagenetic state. It is well known that CP introduces a matrix effect caused by the dependence of signal strength of different carbon groups on the hydrogen environment surrounding it, resulting in types of carbon being over- or underrepresented in terms of relative proportion. ^{13}C single pulse NMR (^{13}C SPMAS NMR, hereafter referred to as SP) can be performed to determine the actual proportions of carbon types. Samples from a boreal forest headwater stream were run using both CP and SP to determine if an average correction factor (CF) could be applied by carbon type across a larger suite of DOM samples taken from a large boreal watershed in western Newfoundland. Five carbon types (aliphatic, carbohydrate, aromatic, carboxylic, and carbonyl) were assessed across all samples. Amplification or under representation of carbon types via CP was consistent in both stream DOM samples, and CFs were calculated for each carbon type. CFs were tested and consistently predicted results within 5%, on average (ranging from 0.59% to 7.7%), of carbon type percentages obtained via SP. The greatest effect observed was the underrepresentation of aromatic carbon, while both carbohydrate and aliphatic carbon were the most amplified.

This same methodological comparison was applied to litter and organic and mineral horizon soils (from the same watershed), as well as DOM derived from these soil horizons (leachates) to determine if these corrections would be consistent across sample types. While some similar CP effects were observed across both soil and leachate samples, the magnitude of these differences was less than that observed in stream DOM samples, and varied between soil and leachate samples. The larger CFs required for stream DOM samples, perhaps due to the lower carbon abundance relative to other matrix components, are particularly important as we consider how the chemical composition of stream DOM relates to the landscape. Obtaining and applying CFs for a specific study area to enable comparisons of the chemical composition of DOM in both soil and aquatic environments should facilitate our understanding of terrestrial-aquatic biogeochemical linkages, allowing a more accurate comparison across sample types.

A model for copper isotopic fractionation during weathering and transport

DAVID M. BORROK[1*], JESICA U. NAVARRETE[1], FOTIOS CHRISTOS A. KAFANTARIS[1]

[1]University of Texas at El Paso, USA, dborrok@utep.edu (*presenting author), jnavarrete2@miners.utep.edu, fkafantaris@miners.utep.edu

A consensus appears to be forming that the fractionation of Cu isotopes in natural systems is underpinned by redox reactions (chiefly changes from Cu(I) to Cu(II) and vice-versa). The heavier Cu isotope, ^{65}Cu, is preferentially incorporated in the oxidizied Cu species relative to ^{63}Cu. This has been speculated for coexisting minerals, coexisting fluid/mineral systems, and for biological systems, including microorganisms, plants, and mammals. Although additional reactions such as adsorption, organic complexation, and diffusion add complexity, Cu isotopes may prove to be a powerful tool for understanding current and historical redox processes in nature. The problem, however, is that we don't yet have a full understanding of how this redox-related fractionation process is reflected in different environments and over different scales.

Using experimental and field data collected from new and previous Cu isotope investigations, we present a conceptual model for the fractionation of Cu isotopes during the aqueous and oxidative weathering of Cu(I) sulfide minerals. The model suggests that the Cu isotopic signature of the fluid phase (relative to the mineral) is controlled by the relative rates of oxidation and leaching/transport.

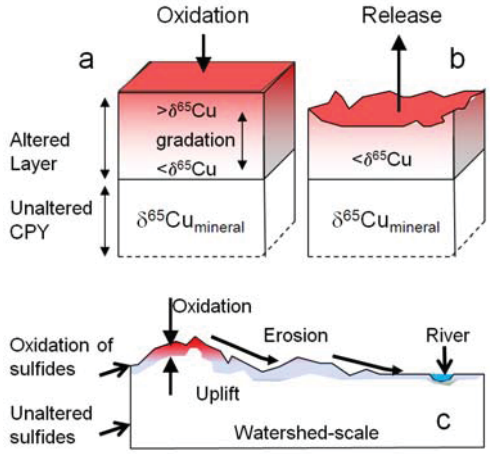

Figure 1: Conceptual model for Cu isotopic fractionation during chalcopyrite (CPY) oxidation, including (a) oxidation of Cu(I) to Cu(II) at the mineral surface followed by (b) the release of Cu into solution. Panel (c) is a cartoon watershed-scale version of this process.

We further examine how this model might be adapted from the molecular scale to watershed and continental scales, highlighting key knowledge gaps. Specifically, we address how Cu isotope controls might change from aqueous systems at low pH that are rich in dissolved Cu to higher pH systems where dissolved Cu is scarce and largely complexed by organic ligands.

https://doi.org/10.1180/S0026461X00008434 Published online by Cambridge University Press

The carbon dioxide mineral sequestration analogues: examples from Tuscany (Italy)

CHIARA BOSCHI[1*], LUIGI DALLAI[1], ANDREA DINI[1], ILARIA BANESCHI[1], ANTONIO LANGONE[2], ANDREA CAVALLO[3], GIOVANNI RUGGIERI[4],

[1]Institute of Geosciences and Earth Resources - CNR, Pisa, Italy, c.boschi@igg.cnr.it (* presenting author)
[2] Institute of Geosciences and Earth Resources - CNR, Pavia, Italy,
[3] Istituto Nazionale di Geofisica e Vulcanologia, Roma, Italy,
[4] Institute of Geosciences and Earth Resources - CNR, Firenze, Italy

The Southern area of Tuscany (Italy) provides clear examples of natural analogues of carbon dioxide mineral sequestration. Our studies focused on the geological and geochemical characterization of the different natural manifestations of CO_2-trapping processes. Widespread serpentinite-hosted magnesite deposits have been investigated in the Southern Tuscany (Monti Livornesi, Colline Metallifere, Elba Island), together with shallower deposits of hydromagnesite in Montecastelli area. The magnesite deposits are a consequence of a realtively shallow hydrothermal circulation of Si- and CO_2-rich fluids intensively affecting serpentinite lenses, hosted by argillites [1].

The hydromagnesite incrustations (Figure 1), with the typically white rounded shape and vein or fracture fillings, represent an ongoing carbonation process on a gangue materials dumped from a serpentinite-hosted copper mine, close to Pomarance (Tuscany, Italy).

The study of these natural analogues complements laboratory experiments and possibly provides opportunity to constrain the boundary conditions and the mechanisms for CO_2-bearing phases to form. Here, we report a review of our geological mapping, petrological observation, mineralogical and geochemical analyses together with isotopical studies (C, O, Sr) of different outcrops in order to address: 1) the carbon source (deep versus atmospheric); 2) the fluid path-way during the alteration in relationship with the induced/reactived fracturation; 3) the areal diffusion and the efficency of the carbonation process; and 4) the mass balance of major and trace element during the alteration.

Figure 1: Example of hydromagnesite incrustation at Montecastelli

[1] Boschi (2009) *Chemical Geology* **Volume 265**, 209–226.

Eating Iron and Loving it: Ferrous Iron Metabolism in *Rhodopseudomonas palustris* TIE-1

ARPITA BOSE[1*], DIANNE K. NEWMAN[2], AND PETER R. GIRGUIS[3]

[1]Harvard University, Department of Organismic and Evolutionary Biology, abose@fas.harvard.edu, (* presenting author)
[2]California Institute of Technology, Department of Biology, dkn@caltech.edu
[3]Harvard University, Department of Organismic and Evolutionary Biology, pgirguis@oeb.harvard.edu

Iron is an essential element in biological systems, and its transport is thus a prime concern to all life. Iron also serves as an electron donor and acceptor for microbial respiration. However, a lot remains to be understood about these processes and we believe that studying iron specialists will provide fresh insight. *Rhodopseudomonas palustris* TIE-1, is an α-proteobacterial iron specialist that uses energy from light and electrons from ferrous iron Fe(II) to support photoautotrophy (photoferrotrophy). *R. palustris* TIE-1 is the only genetically tractable photoferrotrophic microbe, and we are interested in employing molecular and geochemical analyses to better understand A) how it copes with high Fe(II) concentrations, and B) how electrons are transferred from Fe(II) to the photosynthetic reaction center.

Bioinformatics was used to interrogate the genome of *R. palustris* TIE-1 for putative Fe(II) transporters. The *pioABC* operon, the genetic locus essential for photoferrotrophy, was also included in this analysis. This locus might be responsible for both iron and electron transport. A combination of techniques such as heterologous complementation, mutant analysis, and immunofluorescence was used to confirm the role of the identified loci in Fe(II) transport. To assess the role of the Pio proteins in electron transfer from Fe(II) to the photosynthetic reaction center, novel bioelectrochemical reactors were devised. Our data indicate that *R. palustris* TIE-1 employs different membrane-bound Fe(II) transport systems under aerobic, anaerobic and photoferrotrophic conditions. Although the role of the Pio proteins in iron transport remains unclear, we demonstrate that they allow *R. palustris* TIE-1 to accept electrons from a poised electrode in the presence of light, supporting net carbon fixation and growth. We refer to this process as "photoelectrosynthesis" (PES).

This comprehensive study provides a better understanding of Fe(II) transport in α-proteobacteria. We also show that a pure phototrophic culture can perform PES, which has not been demonstrated previously. The role of the Pio proteins in PES brings to light the use of a common protein module to perform electron transfer reactions in unrelated bacteria. Ongoing studies are aimed at further understanding this process at the molecular level.

https://doi.org/10.1180/S0026461X00008434 Published online by Cambridge University Press

DISTRUBUTION OF FERRIHYDRITE IN SEDIMENTS AND ITS ROLE IN REGULATING GROUNDWATER ARSENIC EXPOSURE POTENTIAL

BENJAMIN BOSTICK[1*], JING SUN[2], IVAN MIHAJLOV[3], STEVE CHILLRUD[4] AND BRIAN MAILLOUX[5]

[1]Lamont-Doherty Earth Observatory of Columbia University, Palisades, U.S.A, chilli@ldeo.columbia.edu
[2]Columbia University, New York, U.S.A, jingsun@ldeo.columbia.edu
[3]Columbia University, New York, U.S.A, mihajlov@ldeo.columbia.edu
[4]Lamont-Doherty Earth Observatory, Palisades, U.S.A, chilli@ldeo.columbia.edu
[5]Barnard College, New York, U.S.A, bmaillou@barnard.edu

The environment plays a key role in regulating the concentation of environmental toxins such as arsenic. Minerals are the matrix on which contaminants are retained, affecting both their aqueous concentrations and the transport properties. In some cases, minerals serve as either electron acceptors and donors for a variety of biogeochemical processes that affect the mineral form, surface area, and reactivity of sediments. This critical role is well established, yet suprisingly little is known about the distribution of some of the most important minerals in regulating arsenic concentration. Here, we quantify the concentrations of ferrihydrite in a variety of settings, and study the relationship between its concentration and dissolved arsenic levels from a variety of arsenic-affected environments. Ferrihydrite is a metastable mineral that only somewhat crystalline, and is highly reactive for both adsorption and microbially-mediate reduction. Its presence is often controversial given this metastability, yet the retention of arsenic and other ions is often not easily modeled with low surface area Fe minerals. Using a combination of sequential extractions and X-ray absorption spectroscopy to identify these phases, we find that there is clear evidence for the persistence of ferrihyrite or other poorly crystalline Fe(III) phases even in tropical environments where rapid Fe cycling often is assumed to convert it to hematite and goethite. We attribute the stability of these nanoparticulate forms of Fe(III) to the presence of adsorbed silicate or phophate or other phases on the mineral surface in these environments. A critical factor in the identification of this phase involves the differentiation of crystalline minerals that have distinct, but variable spectral signatures depending on factors such as morphology and particle size. The distribution of ferrihydrite and Fe(III) in sediments also appears affect As speciation, possibly by affecting Fe reduction. While ferrihydrite is found, it often appears to be less effective at minimizing aqueous As levels than crystalline oxides.

A new look on the barium cycle: Stable barium isotope fractionation in ODP sediments and calibration experiments

BÖTTCHER M.E.[1,*], VON ALLMEN, K.[2], PAYTAN, A.[3], NEUBERT, N.[1,2], BRUMSACK, H.-J.[4], SAMANKASSOU, E.[5], AND NÄGLER, T.F.[2]

[1]Leibniz IOW, Warnemünde, FRG, michael.boettcher@io-warnemuende.de (* presenting author)
[2]University of Bern, Switzerland, naegler@geo.uibe.ch
[3]University of California, Santa Cruz, USA, apaytan@ucsc.edu
[4] ICBM, University of Oldenburg, FRG, brumsack@icbm.de
[5]University of Geneva,Switzerland, Elias.Samankassou@unige.ch
[6]Present address: University of Hannover, FRG

We show by the analysis of the stable barium isotope composition ($^{137}Ba/^{134}Ba$) of natural marine barite ($BaSO_4$), that significant isotope fractionation takes place in the marine biogeochemical barium cycle. We have combined previous measurements of the S and O isotopic composition with new Ba isotope ratio determinations. We find that biogenic marine barites separated from sediments collected in different parts of the world´s Ocean with ages up to about 55 million years fall within a close range and have isotope ratios comparable to recently reported value for continental barium-bearing minerals (von Allmen et al., 2010). Whereas, cold seep barites, show isotope values close to modern biogenic barite, marine hydrothermal samples are enriched in the lighter isotope. Highest ^{134}Ba-enrichments are found in authigenic barite minerals formed above black shales in the deep sediments of ODP Leg 207 that are depleted in sulfate due to AOM-triggered microbial sulfate reduction.

Laboratory experiments were conducted to investigate the potential of different low-temperature reactions to result in barium isotope discrimination. These reactions include adsorption of dissolved Ba on MnO_2 and kaolinite, and the precipitation of anhydrous $BaCO_3$ and $BaSO_4$ under different experimental conditions (reaction process and temperature). The Ba minerals were generally enriched in light Ba compared to the aqueous solution, to magnitudes depending on precipitation conditions.

As an important finding, we can conclude that diagenetic barites at ODP Leg 207 record coupled transport induced isotope discrimination, probably superimposed by desorption/adsorption processes in the sulfate-depleted part of the sediment column. Despite the relatively short residence time, the barium isotopic composition of primary barites seem to have been relatively constant through the past 55 m.y.

It should be noted that S and O measurements of a Cambrian barite sample from China showed the influence of microbial sulfate reduction and were accompanied by a depletion in the heavy Ba isotope comparable to our findings from ODP Leg 207.

[1] von Allmen et al. (2010) Chemical Geology **277**, 70-77.

https://doi.org/10.1180/S0026461X00008434 Published online by Cambridge University Press

Environmental impacts of nanomaterials: physico-chemical evolution, exposure mechanisms and mechanisms disturbing the biological activity in aqueous environment

JEAN-YVES BOTTERO[1,2*], MELANIE AUFFAN[1,2], JEROME LABILLE[1,2], ARMAND MASION[1,2], JEROME ROSE[1,2]

[1] CEREGE UMR 6635 CNRS-Université Aix-Marseille, France (bottero@cerege.fr)
[2] GDRI I-CEINT International Center for Enviromental Implications of Nanotechnology

The new properties of materials at the nanoscale are at the heart of current scientific advances such as drug vectorization, cancerous tumor targeting, replacement of silicon in microelectronics by carbon, or the manufacture of more resistant materials... The main cause for this change in properties is the very high surface to volume ratio of nanoparticles and stronger reactivity. It is therefore impossible to simply transfer the physical, chemical, and thermodynamic knowledges on reactions occurring at the solution/microparticles interface to those occurring at the solution/nanoparticles interface (<20-30 nm). Thanks to the unique properties of nanoparticles, nanotechnologies will considerably grow in the near future. However, this growth stirs up awareness that we cannot ignore. In particular, people wonder about the impact of mass-produced nanoparticles that could spread into the environment.

To date, scientists master the manufacture and use of nanomaterials, however we do not know what are the risks for humans and ecosystems. No database exists regarding the amounts released within the ecosystems. However, nanoparticles due to their reactivity, their surface atoms are labile, their redox states can change easily, they are highly reactive towards aqueous compounds and can change from hydrophobic to hydrophilic. Before contacting biota they interact with many objects such as natural organic matter, clays, oxides…. It is impossible to study and understand the environmental biological effects of nanomaterials without a good knowledge of the exposure, their physico-chemical properties changes. The properties of nanoparticles able to disturb the biological activity depend on their size, on their mineralogy, their crystallinity, and their surface reactivity. All these parameters affect the toxicity via their oxido-reductive potential, the generation of Reactive Oxygen Species (ROS), their dissolution into toxic or non ions (*e.g.* Cd^{2+}, Zn^{2+}, Ag^{+}), or also the retention of toxic molecules on their surface (*e.g.* As, Cd, Co). The exposure i.e interactions with components , transfer within the water column or/and sediments is a crucial problem which can be resolved through experiments in mesocosms, search and analysis of Nps in media and analysis of the transformation after alteration of "nano products".

Dating drinking water in eskers from Amos, Abitibi, Canada

CHRISTINE BOUCHER[1*], LAURELINE BERTHOT[2], MARIE LAROCQUE[3], MARTIN ROY[4], VINCENT CLOUTIER[5], DANIELE L. PINTI[6], MARIA CLARA CASTRO[7], CHRIS M. HALL[8]

[1,2,4,6] GEOTOP-UQAM, Montréal, QC, Canada
[1] christinebouc@hotmail.com (* presenting author)
[2] berthot.laureline@courrier.uqam.ca
[4] roy.martin@uqam.ca
[6] pinti.daniele@uqam.ca
[3] Département des Sciences de la Terre et de l'Atmosphère, UQAM, Montréal, QC, Canada
[3] larocque.marie@uqam.ca
[5] Groupe de recherche sur l'eau souterraine, UQAT, Amos QC, Canada
[5] vincent.cloutier@uqat.ca
[7,8] Dept. of Earth and Environmental Sciences, University of Michigan, Ann Arbor, MH, USA
[7] mccastro@umich.edu
[8] cmhall@umich.edu

In Abitibi-Témiscamingue (Québec), eskers, glaciofluvial landforms formed by accumulations of sand and gravel, were deposited during the last deglaciation. 8000 years BP, peatlands developed around the esker flanks by drainage of the Lake Barlow-Ojibway. The eskers are known to be aquifers containing drinking water of exceptional quality, yet little is known about their hydrologic regime. A better understanding of these systems is necessary to assess the vulnerability of these aquifers to potential contaminants and to implement a suitable management plan for water resources. With a such goal, a multi-isotopic study was initiated in eskers of Amos region (Saint-Mathieu-Berry, Baraute and Harricana Moraine) using stable noble gases and ^{222}Rn to date these waters and trace fluid flow within the eskers and into surrounding peatlands. $^{3}He/^{4}He$ ratios have been preliminarily used to identify water mixing and to estimate groundwater residence times through the ^{3}H-^{3}He method and, when possible, U-Th-^{4}He age model [1].

First results point to the occurrence of tritiogenic ^{3}He in groundwater flowing in the Saint-Mathieu-Berry esker that provide drinking water to the town of Amos and the bottled water Eska. Using tritium contents measured in 2004 [2] and in 2011, this study yields an age of 21-23 years. Groundwater from two deep wells (40 and 70 m) from the Harricana moraine gives ^{3}H-^{3}He ages of 7-9 yrs.

Interestingly, the Barraute esker, which is buried under Quaternary clay and the well of Landriennne which taps water at the interface with the Proterozoic basement show $^{3}He/^{4}He$ ratios (R) (normalized to that of atmosphere or Ra) of 0.930±0.022 Ra and 0.946±0.024 Ra, respectively. R/Ra below atmospheric ratio suggests a possible contribution of radiogenic ^{4}He and thus, older water ages. This finding is in agreement with the higher salinity measured in these two wells compared to the regional background.

Rocks samples from the Harricana Moraine were selected for measurements of U and Th contents and to estimate the ^{4}He release rate from the protoliths composing this aquifer [1] in order to calculate meaningful U-Th-^{4}He ages for Barraute and Landrienne groundwaters.

[1] Solomon (1996) *Water Resou. Res.* **32**, 1805-1813. [2] Riverin (2006) Msc Thesis, University Laval, pp.

https://doi.org/10.1180/S0026461X00008434 Published online by Cambridge University Press

Core differentiation of the IVA asteroid

R. A. BOUCHET[1*], J. BLICHERT-TOFT[1] AND F. ALBAREDE[1]

[1]ENS Lyon, LGLTPE, 69007 Lyon, FRANCE, romain.bouchet@ens-lyon.fr (* presenting author)

The group of IVA iron meteorites are regarded as magmatic cumulates that, together, have recorded most of the crystallization sequence of the core of a small planet (e.g. [1]). The main argument for a crystallization process rests on the chemical trends defined by the siderophile elements [2]. Using mathematical parameterization of element partition coefficients [3], we tested the hypothesis of fractional crystallization between a solid and a liquid by calculating the amount of sulfur in the liquid. Because the resulting sulfur concentrations did not follow a simple fractional crystallization law, we instead considered fractional crystallization between a solid and a mush. We calculated two key parameters from the trace element concentrations of the IVA irons [2]: the amount of sulfur in the liquid and the fraction of solid in the mush. The computed fraction of solid in the mush is very near unity during most of the differentiation history, implying that the underlying assumption of crystallization between a solid and a liquid suspension is invalid.

We therefore examined whether the chemical trends observed for siderophile elements in the IVA iron meteorites may record a compaction process rather than crystallization. Elements such as Au and Ni were progressively removed in the process, whereas compatible elements such as Ir and Pt became more concentrated in the residue. The correlation between cooling rates and Ni content in the IVA irons therefore signals a trend opposite to what is commonly admitted in the literature [4] and supports centrifugal solidification and cooling rates increasing as compaction proceeds. In addition, the calculated composition points to sulfur-saturated liquids. Upon compaction, these liquids rose in the solid metal where they were partially trapped as troilite inclusions, such as is observed in a number of IVA irons. The low Th/U ratio of these troilite inclusions [5] may reflect fractionation upon unmixing of minute amounts of silicate melts [6]. Although most of the silicates were subsequently lost, some occasionally survived as silicate inclusions [7].

[1] Chabot and Haack (2006) *Univ. of Arizona Press*, 741-771. [2] Wasson and Richardson (2001) *GCA* **65**, 951-970. [3] Chabot and Jones (2003) *MAPS* **38**, 1425-1436. [4] Rasmussen et al. (1995) *GCA* **59**, 3049-3059. [5] Blichert-Toft et al. (2010) *EPSL* **296**, 469-480. [6] Murrell and Burnett (1986) *JGR* **91**, 8126-8136. [7] Scott and Wasson (1975) *Rev. Geophys. Space Phys.* **13**, 527-546.

Modeling stable isotope ratios of metals in the weathering zone: mass-balance controls

J. BOUCHEZ[1*], F. VON BLANCKENBURG[1] AND J. A. SCHUESSLER[1]

[1]German Research Centre for Geosciences (GFZ), Potsdam, Germany (*presenting author; bouchez@gfz-potsdam.de)

During the last decade, the stable isotope composition of metals and metalloids (e.g. Li, B, Mg, Ca, Fe, Cu, Zn, Sr, Mo) in the weathering zone were mapped out. The overarching aim is to improve our understanding of the processes fractionating isotopes and generating elemental transfers between the main compartments (e.g. bedrock, soil, surface water and plants). However, a conceptual framework is still lacking for interpreting isotope data in terms of isotope fractionation factors, or in terms of elemental fluxes. Such a framework represents a prerequestite to identify biogeochemical processes from isotope ratios measured in river material or in the sedimentary record.

To this end, we design a simple steady-state model based on elemental mass-balance equations, and simulate, at first-order, a weathering system from the scale of a soil column to that of continents. The model links (1) isotope compositions of the main compartments of the weathering zone (expressed in the δ-unit) (2) isotope fractionation factors Δ_{prec} and Δ_{up} (associated with precipitation of secondary weathering products, and with plant uptake, respectively) (3) elemental fluxes to, within and out of the weathering zone. The fluxes are expressed relative to the supply rate of the considered element into the weathering zone which is, at steady-state, denudation rate times bedrock chemical composition.

Using this model, we show how soil water or river water isotope composition δ_{water} will be offset from the bedrock composition δ_{rock} by an amount that is not only (1) depending on the flux weighted-average of Δ_{prec} and Δ_{up}, but also (2) increasing with increasing elemental flux of combined net precipitation of secondary weathering products and net litter formation, and (3) increasing with decreasing elemental flux resulting from the dissolution of primary minerals. (2) and (3) represent strong mass balance effects that likely depend on the considered element (and on its biogeochemical properties such as solubility, affinity for clay minerals, or importance as a nutrient) and the geomorphic regime of the considered setting (e.g. supply versus kinetically limitated weathering). These mass-balance effects have to be taken into account when linking isotope ratios with isotope fractionation factors and biogeochemical processes in the weathering zone.

Furthermore, the model shows that δ_{water} will depend strongly on the intensity of biological uptake only if a significant proportion of the considered element is exported as plant litter, establishing a prerequisite to the use of metal stable isotope ratios in the sedimentary record as a tracer of terrestrial biological activity.

The model also has important implications in terms of sampling strategy: it can be shown in particular that the effects of Δ_{prec} and of Δ_{up} cannot be disentangled using isotope composition of river water or of bulk sediment alone. For this purpose, separates of organic and secondary phases from river particulate load or from topsoil, are needed.

https://doi.org/10.1180/S0026461X00008434 Published online by Cambridge University Press

No REE into the Earth's core

M.A. BOUHIFD[1*], M. BOYET[1], D. ANDRAULT[1], N. BOLFAN-CASANOVA[1] AND J.L. DEVIDAL[1]

[1]Laboratoire Magmas et Volcans, Université Blaise Pascal, CNRS UMR 6524, 5 Rue Kessler, 63000 Clermont-Ferrand, France

Introduction

The earliest history of the Earth was marked by accretion and core formation within about 100 Myr [1, for a review]. Short-lived radioisotope systems such as ^{146}Sm-^{142}Nd (composed by two refractory elements) are useful in determining how the silicate Earth, for example, evolved during and after accretion. Recent Sm-Nd data show that all terrestrial samples have on average 20 ppm ^{142}Nd excess relative to chondritic meteorites [2]. It is thus evident that an enriched Hadean reservoir has to exist, unless the bulk Earth accreted with a Sm/Nd ratio that was higher than the chondrite average. Within several hypothesis [3], the enriched Hadean reservoir maybe the core since rare earth elements (REE) are not strictly litophiles in more reducing conditions [4]. In order to test this hypothesis, experiments at core-forming conditions (P, T, f_{O2}, etc) are needed to assess whether or not the core plays an active role in the observed ^{142}Nd anomalies.

To simulate Earth's core formation under conditions of segregation from a deep magma ocean, we performed multi-anvil experiments between 3 and 8 GPa at various temperatures between 2073 and 2373 K, to determine the partition coefficients of REE between molten C1-chondrite model composition and various Fe-rich alloys (including $Fe_{90}Ni_{10}$, $Fe_{83}Si_{17}$, and $Fe_{80}Ni_{10}S_{10}$). The run products indicate that the oxygen fugacity (f_{O2}) ranges from 1.5 to 5 log units below the iron-wüstite (IW) buffer, and is in agreement with core-formation models in which metallic liquid equilibrates with molten silicate under reducing conditions. The chemical compositions of the run products were determined by laser ablation ICP-MS and electron microprobe. Our results show a low liquid metal-silicate melt partition coefficients of all REE that range between 10^{-3} and 10^{-5} (an increase of the partition coefficients with decreasing the f_{O2} is observed). More importantly, our experiments show that the metal-silicate partition coefficients of Sm and Nd are similar within the investigated conditions, meaning that the Sm/Nd ratio is not fractionated by metal-silicate segregation. Another line of support of this conclusion is found by an independent work on the cosmochemical and petrological study of enstatite chondrites [5].

Conclusion

If the bulk Earth has chondritic ^{142}Nd/^{144}Nd ratio, an enriched Hadean reservoir has to exist within the deep mantle. In contrast, if the bulk Earth has an Nd isotopic composition distinct from that of the chondrites, then there is no need to invoke a hidden reservoir. In any case the Earth's core is out of the equation concerning the ^{142}Nd anomalies.

[1] Kleine *et al*. (2009) *GCA* **73**, 5150-5188.
[2] Boyet and Carlson (2005) Science **309**, 576-581.
[3] Andreasen *et al*. (2008) *EPSL* **266**, 14-28.
[4] Lodders (1996) *Meteoritics & Planetary Science* **31**, 749-766.
[5] Gannoun *et al*. (2011) *GCA* **75**, 3269-3289.

Mg,Fe-rich carbonates stability at lower mantle conditions

E. BOULARD[1]*, W. MAO[1]

[1]Stanford University, Stanford, U.S.A., boulard@stanford.edu (*presenting author); wmao@stanford.edu

Only a small fraction of the total carbon budget of the Earth is found at the surface; with the mantle and core likely being the largest carbon (C) reservoirs in the planet [e.g. 1, 2]. Carbonates are the main C-bearing minerals that are recycled into the deep Earth. Previous studies, focusing on the stability of Ca and Mg rich carbonates in the upper mantle, demonstrated the possibility of C to be recycled into the lower part of the mantle [e.g. 3]. A few experimental studies have been conducted on the stability of magnesite ($MgCO_3$) in equilibrium with silicates at lower mantles pressure and temperature (P-T) conditions. The decarbonation reaction: $MgCO_3$(magnesite) + SiO_2 (stishovite) -> $MgSiO_3$ (perovskite) + CO_2 (solid) has been reported at lower mantle conditions limiting the carbon cycle to about the first 1200 km deep (about 45 GPa - 2200 K) [4]. On the other hand, Seto et al. [5] supports the possibility for a deeper recycling of carbon in the Earth in relatively cold slabs, as they observed decarbonation of magnesite in equilibrium with mid ocean ridge basalt (MORB) at higher temperature. However, several carbonate phase transitions have been reported at higher P-T [e.g. 6].

We conducted high P-T experiements on iron-bearing carbonates stability. We used both *in situ* and *ex situ* analyses including synchrotron based X-ray diffraction and transmission electron microscopy to characterize the structure and the chemistry of the different phases in the samples. Two new high P-T phases were observed for two compositions: (1) the $(Mg,Fe)CO_3$ system above 85 GPa – 2000 K [7] and (2) the $FeCO_3$ composition above 40 GPa – 1500 K [8]. In both of these new phases, the structures determined from *ex situ* analyses led us to propose a change in the C environment as the C formed $(CO_4)^{-4}$ tetrahedra instead of triangular $(CO_3)^{-2}$ groups as in carbonates. We will discuss the influence of such structural changes on carbonate stability and its solubility within mantle silicate phases.

[1] Javoy, M. et al. (1982) *Nature,* **300**, p. 171-173. [2] Dasgupta, R., and M.M. Hirschmann (2010) *Earth Planet. Sci. Lett.*, **298** (1-2), 1-13. [3] Poli et al. (2009) *Earth Planet. Sci. Lett.*, **278**(3-4), 350-360. [4] Takafuji et al. (2006) *Physics and Chemistry of Minerals*, **33**, p. 651-654. [5] Seto et al. (2008) *Physics and Chemistry of Minerals*, **35**, p. 223-229. [6] Isshiki et al. (2004) *Nature*, **427**, p. 60-63.[7] Boulard et al. (2011) *PNAS*, **108**, no 13, 5184-5187. [8] Boulard et al. (in press) *J. Geophys. Res.*

https://doi.org/10.1180/S0026461X00008434 Published online by Cambridge University Press

Upper crustal record of migmatites exhumation: the South Armorican Domain

PHILIPPE BOULVAIS[1*] ,ROMAIN TARTESE[1,2], MARIE-CHRISTINE BOIRON[3], MARC POUJOL[1], GILLES RUFFET[1],

[1]Université de Rennes 1,UMR CNRS 6118 Géosciences Rennes, 35042 Rennes, France - philippe.boulvais@univ-rennes1.fr (* presenting author)
[2]Open University, Planetary and Space Sciences, Milton Keynes, UK
[3]Université de Lorraine, UMR CNRS 7566 G2R, 54501 Vandoeuvre-lès-Nancy, France

The South Armorican Massif hosts a high-grade metamorphic domain mainly composed of medium to high-grade micaschists, migmatitic gneisses and anatectic granites [1]. At the end of the Carboniferous, these deep crustal units were exhumed rapidly during the extension associated with the collapse of the Hercynian chain [2]. To the North, this domain is limited by the listhospheric-scale South Armorican Shear Zone (SASZ). Giant quartz veins are associated with the SASZ and recorded important synmetamorphic fluid circulation [3]. Together with very low $\delta^{18}O$ values for some euhedral quartz, down to -2‰, low-salinity fluid inclusions argue for a contribution from meteoric fluids [3]. Corresponding $\delta^{18}O_{fluid}$ values estimated around -11‰ are probably related to the high palaeo-elevation of meteoric precipitation. Scarce, but significant, CO_2 fluid inclusions in euhedral quartz indicate also a metamorphic contribution. Metamorphic fluids were probably sourced from the exhumed metamorphic basement in the southern part of the Massif. Also, because of the synchronicity between the metamorphic event (exhumation) and the meteoric infiltration, it is proposed that the heat advected towards the surface by the exhumation of high-grade metamorphic rocks provided the driving force for meteoric fluid circulation on a regional scale.

The meteoric infiltration is recorded regionally by the mylonites which actually define the SASZ and by the syn-kinematic granites which emplaced along the SASZ. Low $\delta^{18}O$ values have been measured on some feldspar and zircon grains in the formers [4] while oxygen isotope disequilibirum was recorded by Qz-Fds pairs in the latters [5]. The muscovite Ar-Ar and monazite U-Th-Pb chronometers from these lithologies were highly disturbed [4,6]. In the Questembert granite, a classical example of a syn-kinematic granite, pervasive infiltration of oxydative meteoric water was facilitated by the penetrative character of the deformation (C/S planes are observed throughout the massif) and was probably responsible for the leaching of millions of tons of uranium while the granite was still at depth.

[1] Brown M. and Dallmeyer R.D. (1996) *Journal of metamorphic Geology* **14**, 361-379. [2] Gapais D. et al. (1993) *Comptes Rendus de l'Académie des Sciences* **316**, 1123-1129. [3] Lemarchand J. et al. (2012) *Journal of the Geological Society* **169**, 17-27. [4] Tartèse R. et al. (2012) *Journal of Geodynamics*, in press. [5] Tartèse R and Boulvais P (2010) *Lithos* **114**, 353-368. [6] Tartèse R. et al. (2011) *Terra Nova* **23**, 390-398.

Petrology, geochemistry and petrogenesis of the Beattie Syenite, Porcupine-Destor fault zone, Abitibi Subprovince, Québec

JULIE BOURDEAU[1]*, ANDRÉ E. LALONDE[1], JEAN GOUTIER[2]

[1]University of Ottawa, Ottawa, Canada, bourdeau.julie.e@gmail.com*, aelzr7@uottawa.ca
[2]Ministère des Ressources Naturelles et de la Faune, Rouyn-Noranda, Canada, jean.goutier@mrnf.gouv.qc.ca

Abstract

The Beattie Syenite is composed of five lenticular bodies of syenitic rocks that occur immediately north of the Porcupine-Destor fault zone in the town of Duparquet, approximately 32 km north of Rouyn-Noranda in the Abitibi Subprovince. The principal body is 3.3 km long and 425 m in width and is flanked by a series of smaller lenses to the south and northeast. The intrusion has yielded zircon ages of 2682 ±1 Ma and 2682.9 ±1.1 Ma and hosted the major part of the Au-mineralization of the now defunct Beattie mine; a major producer of gold in the area from 1933 to 1956 (9.66 Mt at 4.88 g/t Au). A total of 5 principal petrographic units are defined on the basis of field relationships, petrography, mineralogy, and textures:

1) The Beattie syenite porphyry unit is composed of 2-10% of tabular euhedral feldspar phenocrysts (2-10 mm) set in a red feldspathic and aphanitic matrix.
2) The unaltered syenite unit is composed of 2-10% of euhedral feldspar phenocrysts (2-10 mm) in a fine-grained matrix. It is characterized by unaltered phenocrysts of amphibole and titanite and is the only unit with relicts of pyroxene.
3) The Central Duparquet syenite porphyry containing between 2-25% of coarse equant euhedral feldspar phenocrysts (5-16 mm) in a red or sometimes grey aphanitic matrix.
4) The megaporphyritic syenite unit is composed of very coarse alkali feldspar phenocrysts, 1-6 cm across, in a red aphanitic matrix.
5) The feldspar lath dyke unit occurs as numerous thin dykes, on the order of a few meters in width, that cross-cut all other petrographic units. The lath dykes display a characteristic trachytoid texture defined by the preferential alignment of alkali feldspar laths (1-3 cm) in a grey or red aphanitic matrix.

From petrographic observations, there is evidence of a syenitic magma which is exhibited by the occurrence of syenite dykes with trachytoid flow textures. Detailed petrographical and mineralogical studies reveal a series of hydrothermal events including the precipitation of albite, sericite, chlorite and carbonate minerals. Initial geochemical results indicate that the Beattie Syenite is part of the alkaline series, as defined in the ($Na_2O + K_2O$) vs. SiO_2 diagram, and is feldspar normative. Whole-rock normalized REE patterns demonstrate that all the petrographic units are comagmatic. Furthermore, with selective trace elements, the tectonic setting of the syenite according to [1] would correspond to a volcanic-arc environment.

[1] Pearce, Harris and Tindle (1984) *Journal of Petrology* **25**, 956-983

https://doi.org/10.1180/S0026461X00008434 Published online by Cambridge University Press

Isotope fingerprints for the formation and the composition of the Earth

BERNARD BOURDON [1]*

[1]Laboratoire de Géologie de Lyon, ENS Lyon, UCBL and CNRS UMR 5276, Lyon France, bernard.bourdon@ens-lyon.fr

Building blocks

Most models for the formation and composition of the Earth usually focus on specific characteristics of its chemical or isotope composition. For example, since the formation of the Earth leads to substantial heating of planetary materials, volatile depletion and metal-silicate separation, it is sensible to consider only the refractory lithophile elements (RLE) to assess the potential building blocks of the Earth. In this context, the carbonaceous chondrites, notably the CI chondrites give the best match for RLE in the Earth's mantle and are often used as a starting material, although the processes mentioned above can affect the siderophile and volatile element concentrations in this starting material.

In contrast, when considering isotope observations, it appears that enstatite chondrites show an almost perfect match with many isotope systems, including oxygen, chromium, nickel and titanium. Then, if one considers the ^{146}Sm-^{142}Nd system, it appears that the terrestrial composition does not match with carbonaceous chondrites but could be better explained by ordinary or enstatite chondrites. However, the ^{146}Sm-^{142}Nd observations can also be explained by a non-chondritic Earth. Last, in the case of silicon isotopes, there is a clear offset between the terrestrial composition and that of chondrites. In summary, there seems to major issues in building the Earth from a single class of chondrites or from unprocessed chondritic material.

Processing of planetary materials

There are several processes that can modify the composition of the planetary materials that have formed the Earth, including thermal processing leading to volatile depletion (partial condensation or evaporation), grain sorting, impact-driven processes or metal segregation. In this presentation, I will examine the possible role of these processes in light of our recent isotope observations with a focus on Nd, Si, Mg, Mo and Sr isotopes and show how mixtures of various chondritic materials together with significant later processing is required to explain the composition of the Earth.

Molecular-scale basis of the ion exchange selectivity of clay minerals

IAN C. BOURG[1,*]

[1]Earth Sciences Division, Lawrence Berkeley National Laboratory, Berkeley, USA, icbourg@lbl.gov (* presenting author)

Ion exchange reactions on clay mineral surfaces play important roles in the aquatic geochemistry and mechanical properties of argillaceous media (soils, sediments, clayshales, engineered clay barriers). Despite more than a hundred years of investigation, fundamental aspects of the ion exchange selectivity of clay minerals, such as the activity coefficients of adsorbed species, the molecular-scale basis of ion exchange selectivity coefficients, and the structure of the electrical double layer (EDL), are poorly understood [1]. We report new molecular dynamics (MD) simulations elucidating the structure of the EDL on smectite surfaces contacting mixed NaCl-$CaCl_2$ electrolyte solutions at dilute concentrations ($\leq$ 0.1 mol_c dm^{-3}). Our simulations used methodologies known to correctly describe the structure and diffusion coefficients of water and solutes in smectite interlayer nanopores [2]. They complement our previous simulations of concentrated electrolyte solutions (0.34 to 1.83 mol_c dm^{-3}) on smectite surfaces [3]. Our results confirm the molecular-scale view of EDL stucture on phyllosilicate basal surfaces derived from X-ray reflectivity measurements of adsorption on mica surfaces [4]. They also provide insights into several fundamental aspects of the ion exchange selectivity of clays, such as the adequacy of the Gaines-Thomas or Vanselow conventions and the affinity of clay surfaces for $CaCl^+$ ion pairs [1].

[1] Bourg & Sposito (2011) *Ion-Exchange Phenomena*, In: *Handbook of Soil Science*, 2nd ed., Chapter 16. [2] Bourg & Sposito (2010) *Environ. Sci. Technol.* **44**, 2085. [3] Bourg & Sposito (2011) *J. Colloid Interface Sci.* **360**, 701. [4] Lee, Fenter, Park *et al.* (2010) *Langmuir* **26**, 16647.

https://doi.org/10.1180/S0026461X00008434 Published online by Cambridge University Press

Landscape-scale pedogenic relationships between soil carbon and secondary metal oxides in Hubbard Brook podzols, northeastern US

REBECCA R. BOURGAULT[1*], DONALD S. ROSS[1], SCOTT W. BAILEY[2], PATRICIA A. BROUSSEAU[3], JOHN P. GANNON[3], KEVIN J. MCGUIRE[3] AND THOMAS D. BULLEN[4]

[1]University of Vermont, Burlington, VT, USA, rbourgau@uvm.edu (* presenting author), dross@uvm.edu

[2]US Forest Service, North Woodstock, NH, USA, swbailey@fs.fed.us

[3]Virginia Tech, Blacksburg, VA, USA, patrb87@vt.edu, jpgannon@vt.edu, kevin.mcguire@vt.edu

[4]US Geological Survey, Menlo Park, CA, USA, tdbullen@usgs.gov

Abstract

Podzols are unique soils in which metals and carbon are intimately linked by the pedogenic process of podzolization. In this soil-forming process, organic matter (OM) chelated by Al, Fe and Mn leaches from the soil surface and accumulates in the subsurface spodic (B) horizon. Spodic materials (ill-defined associations of Al, Fe, Mn and C) in the B horizon are more resistant to decomposition than OM in the soil surface, in part due to the stabilizing effect of chelation and/ or sorption by Al, Fe and Mn. Podzols are found globally in a variety of environments, and therefore represent an important carbon sink. Research suggests that spatial variations in podzolization can result in part from hydrologic processes such as dominant flowpath direction, and reduction-oxidation processes driven by water table dynamics. These processes determine solubility, transport, and accumulation of Al, Fe, Mn and C. In this study, we document vertical and lateral distributions of total soil C in Watershed 3 (WS3), which is a forested, podzolized catchment in the Hubbard Brook Experimental Forest (HBEF), New Hampshire, in the Northeastern US. We will examine the relationships of C to total secondary Fe oxides and Mn oxides (extracted by citrate-dithionite), and poorly crystalline Al and Fe oxides (extracted by acid ammonium oxalate). Eighty pedons have been described, sampled, and extracted by horizon throughout WS3. In order to determine the role of hydrologic processes in determining soil chemistry in WS3, combined hydrometric monitoring and isotope tracers are used to document flowpaths, water table dynamics, and ground water chemistry and transport. Preliminary results indicate redistribution of spodic materials according to flowpaths. For example, where lateral flowpaths predominate, there is landscape-scale lateral podzolization: leaching/ loss of metals and C upslope, and accumulation of metals and C downslope. In contrast, pedon-scale vertical podzolization is more evident where flowpaths are dominantly vertical, such as on well-drained backslopes. As expected, the Mn:Fe ratio is higher in laterally deposited spodic materials as opposed to vertically deposited spodic materials, due to the fact that Mn is more sensitive to redox conditions and therefore more mobile than Fe. Understanding the spatial distributions of Al, Fe, Mn, and C at the landscape scale in WS3 may provide valuable information about the complex interactions between water and soils, metals and carbon in a forested, podzolized Northeastern US watershed.

An experimental study of the stability of the REE(III) in sulphate-bearing aqueous solutions

N. BOURQUE*, ART. MIGDISOV, AND A.E. WILLIAMS-JONES

McGill University, Earth & Planet. Sci., Montreal, QC, Canada (*correspondence: nicolas.bourque@mail.mcgill.ca)

During the past fifteen years, numerous studies of a variety of geological settings have demonstrated that the rare earth elements (REE) are mobilized by hydrothermal fluids [1, 2, 3]. As sulphate complexes of the REE are known to be among the most stable aqueous species at ambient temperature, it is therefore reasonable to propose that these species play an important role in REE transport in hydrothermal systems with high sulphate activity. However, published experimental data on the behaviour of REE sulphate species at elevated temperatures are limited to Nd, Sm, and Er [1] and therefore, evaluations of the mobility of the REE in hydrothermal sulphate-bearing solutions have been based mainly on the theoretical predictions of Haas et al. (1995). In view of this, we have systematically investigated the behaviour of the REE, including Y, in sulphate-bearing aqueous solutions and determined the properties of sulphate complexes of these elements at elevated temperature.

The technique employed in the experiments was identical to that described in Migdisov and Williams-Jones (2007). The experiments involved determining the solubility of REE oxides and fluorides in solutions with a range of sulphate concentrations, and were performed at temperatures up to 250 °C and saturated pressure of water vapour.

The data derived from the measured solubility of the REE solids show that the stability of REE sulphate species varies little with the atomic number of the REE. For example, the logarithm of the first formation constant of La (log β_1) at 200°C differs from that of Yb by less than 1 log unit. The same observation was made in earlier spectroscopic studies of Nd, Sm, and Er sulphate species [1]. This observation suggests that the REE are unlikely to fractionate in nature, if they are transported as sulphate species.

[1] Migdisov, A.E. Williams-Jones (2008) *Geochimica et Cosmochimica Acta* **72**, 5291–5303

[2] Migdisov, A.E. Williams-Jones (2007) *Geochimica et Cosmochimica Acta* **71**, 3056–3069.

[3] Haas et al. (2005), *Geochimica et Cosmochimima*. Acta **59**, 4329–4350.

https://doi.org/10.1180/S0026461X00008434 Published online by Cambridge University Press

Minor and trace element composition of iron oxides from IOCG deposits worldwide and its application to mineral exploration

EMILIE BOUTROY[1*], GEORGES BEAUDOIN[1], SARAH-JANE BARNES[2] AND LOUISE CORRIVEAU[3]

[1]Université Laval, Département de géologie et de génie géologique, emilie.boutroy.1@ulaval.ca (* presenting author) Georges.Beaudoin@ggl.ulaval.ca
[2]Université du Québec à Chicoutimi (UQAC), Sciences de la Terre, sjbarnes@uqac.ca
[3]Geological Survey of Canada, Natural Resources Canada louise.corriveau@rncan-nrcan.gc.ca

There are significant variations in the concentration of trace elements in magnetite and hematite depending on the metallogenic environment at the time of formation of the deposit. This makes iron oxides useful as indicator minerals for mineral exploration.

Iron oxides are a major component of Iron Oxide Copper-Gold deposits (IOCG) and of Iron Oxide-Apatite deposits (IOA). Magnetite and hematite in IOCG (n= 84 samples) and IOA deposits (n= 6), representative of 8 major IOCG and IOA deposits, worldwide, representing a range of geological environments and ages of formation, were analyzed by electron microprobe analysis (EMPA). A subset of IOCG (n = 30 samples) and IOA (n= 6) was analysed by LA-ICP-MS. The IOCG deposits samples are divided based on the principal iron oxide present: (1) Hematite (n = 10), (2) Magnetite (n = 37) and (3) Hematite ± Magnetite (n =8). Similarly, IOA deposits are divided: (1) Magnetite (n = 3) and (2) Magnetite ± Hematite. In these types of deposits, iron oxides are in mineralization and in host rock alteration assemblages, and there are typically multiple generations of iron oxides. Iron oxides are studied according to their paragenetic stage: (1) ore stage and (2) hydrothermal alteration of host rocks. Hydrothermal alteration iron oxides are grouped according to the type of alteration: (1) Ca-Fe alteration (Am-Ap-Mag), (2) Na(Fe) alteration (Ab-Scp-Mag/Hem), (3) High temperature K-Fe alteration (Bt-Kfs-Mag) and (4) Low temperature K-Fe (Ser-Kfs±Chl±Cb-Hem). Preliminary results show hematite in Hematite-group IOCG deposits is depleted in Zn, Ni, Mn, V and enriched in K, Ti, Al, Si compared to magnetite in Magnetite-group IOCG deposits. In Magnetite-IOA deposits, magnetite is enriched in V, Al and Mg compared to Magnetite-Hematite-IOA deposits, which is enriched in Ca.

Compared to primary magnetite in Ni-Cu-PGE deposits, ore-stage magnetite in IOCG deposits are depleted in Ni, Cu and Cr and enriched in Ti, Al and Si.

Functional gene pyrosequencing sheds light on the distribution and diversity of a key nitrogen cycle gene (*nirS*) in marine systems

JENNIFER L. BOWEN[*1], DAVID WEISMAN[1], AMAL JAYAKUMAR[2], MICHIE YASUDA[1] AND BESS B. WARD[2]

[1]University of Massachusetts Boston, MA, USA Department of Biology, jennifer.bowen@umb.edu (*presenting author), weisman@lydon.com, michie.yasuda@umb.edu

[2]Princeton University, Princeton, NJ, USA Department of Geosciences, ajayakum@princeton.edu, bbw@princeton.edu

Introduction

Denitrification, a critical pathway in the nitrogen cycle that converts dissolved inorganic nitrogen to its gaseous form, plays a central role in removing nitrogen from the environment. Denitrification in estuaries, continental shelves, and oxygen minimum zones accounts for nearly 60% of the global fixed nitrogen loss [1]. There are two genes, *nirS* and *nirK* that encode functionally similar nitrite reductase enzymes that facilitate the denitrification process. The two genes do not appear to co-occur within a given microorganism but both genes are present in most environments. In the marine environment *nirS* tends to be more abundant than *nirK* [2]. Examining the structure and abundance of denitrifiers represented by the *nirS* gene in a variety of marine environments will shed new light on biogeochemical ecology of this critically important ecosystem service.

Results and Conclusions

We used functional gene pyrosequencing to examine the abundance and diversity of denitrifying bacteria in all three major oceanic oxygen minimum zones as well as in coastal sediments from Chesapeake Bay and a New England salt marsh. To assess the role of sequencing error in inflating our diversity estimates we sequenced amplicons of four clones and show that our data analysis pipeline successfully identifies and removes the overwhelming majority of spurious sequences (Fig. 1). The data indicate an astonishing degree of diversity in the *nirS* gene, with over 3500 taxa (defined operationally as sharing 95% sequence identity), found in salt marsh sediments alone. Pyrosequencing detects distinct differences in the composition of nirS assemblages in water column and sediment environments.

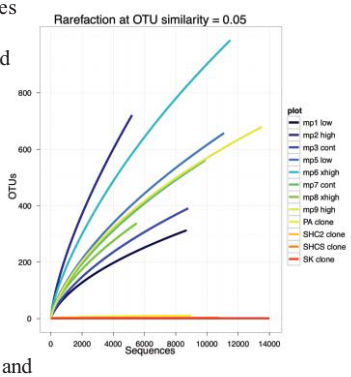

Figure 1: Rarefaction curves resulting from pyrosequencing of the nirS gene in salt marsh sediments and in control sequenced

[1] Seitzinger (2004) *Ecol. Appl.* **52**, 47-59. [2] Jones and Hallin (2010) *ISME J* **4**, 633-641.

https://doi.org/10.1180/S0026461X00008434 Published online by Cambridge University Press

Role of hydration energy on near-surface H_2O and ion molecular-scale dynamics: Comparing Na- and Ca-hectorites with NMR spectroscopy

GEOFFREY M. BOWERS[1,3*], R. JAMES KIRKPATRICK[2], JARED WESLEY SINGER[3]

[1]Alfred University, Division of Chemistry, Alfred, NY, USA, bowers@alfred.edu (* presenting author)
[2]Michigan State University, College of Natural Science, East Lansing, MI, USA, rjkirk@cns.msu.edu
[3]Alfred University, Kazuo Inamori School of Engineering, Alfred, NY, USA, jws4@alfred.edu

Solid-state NMR spectroscopy is uniquely equipped to study behavior at interfaces and in confinement within complex geochemical systems. The primary advantage of this technique is that it can simultaneously provide information on the molecular-scale structure and dynamic behavior over a broad range of rate scales difficult to probe via other methods (kHz to MHz) and on a site-specific basis. In this work, we share recent results from our ongoing variable temperature NMR studies of phyllosilicate/H_2O interfaces [1-4] by focusing on the influence that metal charge and hydration energy have on H_2O and metal ion structure and dynamics in the interlayer of Na- and Ca-hectorites between -120°C and 50°C. We find that near-surface ^2H_2O in 2-layer hydrates of Na- and Ca-hectorites are well modeled by simultaneous C2/C3 reorientation of a slightly compressed or extended hydration shell (with respect to an ideal octahedral hydration shell) at a rate in excess of 200 kHz between -50°C and 40°C [1]. Though our model and ^2H VT NMR show the hydration shell compression/extension varies slightly over the temperature range in each type of hectorite, the Ca^{2+} hydration shell geometry deviates less from the ideal case at all temperatures, consistent with the higher hydration energy of Ca^{2+} vs. Na^+. Associated ^2H T_1 relaxation experiments at several temperatures shows nearly identical reductions in T_1 with respect to temperature, though the ^2H nuclei in Ca-hectorite relax more quickly at all temperatures, suggesting a higher intensity of motion in the power spectrum at 45.6 MHz and that the power spectrum intensity increases with decreasing temperature for Na- and Ca-hectorite. With respect to the associated metal dynamics, both Na^+ and Ca^{2+} in 2-layer hectorite hydrates are dominated by rapid diffusion in 2 or 3 dimensions, though comparison of the ^{23}Na and ^{43}Ca VT NMR shows that Ca^{2+} experiences very rapid diffusion at much lower temperatures than Na^+ (-120°C vs. -20°C, respectively). These results are consistent with our recently published general principle that rapid diffusion becomes the dominant mode of metal cation motion for near-surface water and ions in smectites at lower temperatures as the metal hydration energy increases if the ionic radii are similar [1].

[1] Bowers et al. (2011) *Journal of Physical Chemistry C* **115**, 23395-23407. [2] Bowers et al. (2008) *Journal of Physical Chemistry C* **112**, 6430-6438. [3] Weiss et al. (1990) *Geochimica et Cosmochimica Acta* **54**, 1655-1669. [4] Bowers et al. (2012) in preparation.

Characterization of naphthenic acids in oil sands tailings ponds by two-dimensional gas chromatography time-of-flight mass spectrometry (GCxGC-TOF-MS)

DAVID BOWMAN*, B. E. MCCARRY

[1]McMaster University, Department of Chemistry and Chemical Biology, Hamilton, Ontario
bowmand@mcmaster.ca (* presenting author)
mccarry@mcmaster.ca

Naphthenic acids are a complex mixture of aliphatic and polyalicyclic organic acids found naturally in hydrocarbon deposits. Oilsand ore is refined using the Clark hot water extraction procedure; naphthenic acids are extracted and end up in the process water. These waters are sent to large tailing ponds where particulate materials settle out slowly. Naphthenic acids are of environmental concern due to their toxicities in various mammals and fish; these concerns have lead to a zero discharge policy for oil sands tailings.[1] Naphthenic acids are known to be utilized by plants.[2] We have proposed that these compounds may be utilized by soil bacteria in the tailings ponds which may serve as a source for the generation of H_2S.

In this study, we are using two-dimensional gas chromatography time-of-flight mass spectrometry (GCxGC-TOF-MS) to provide profiles of complex mixtures of naphthenic acids (see Figure 1). Using this method it is possible to resolve over 8000 components in this sample. We hypothesize that the profiles of naphthenic acids will be altered by bacterial biodegradation and that these changes will be detectable using GCxGC. The extraordinary peak capacity and resolving power of two-dimensional gas chromatography makes it a suitable tool for the comparison of profiles of naphthenic acid mixtures.

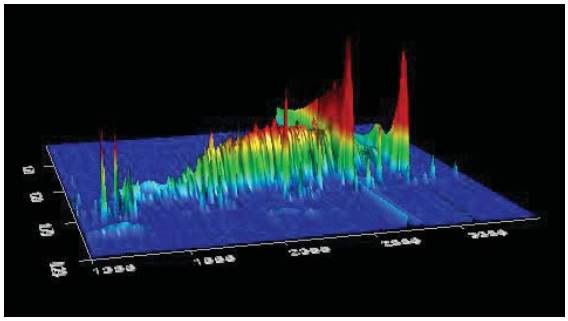

Figure 1: Two-dimensional total ion chromatogram (TIC) plot of naphthenic acids in oil sand process water sample (sample provided by Syncrude).

[1] Hao, C.; Headley, J.; Peru, K.; Frank, R.; Yang, P.; Solomon, K. (2005) *Journal of Chromatography A* **1067**, 277-284.
[2] Headley, J. V.; Armstrong, S. A.; Han, X.; Martin, J. W.; Mapolelo, M. M.; Smith, D. F.; Rogers, R. P.; Marshall, A. G (2009) *Rapid Communications in Mass Spectrometry* **4**, 515-522.

https://doi.org/10.1180/S0026461X00008434 Published online by Cambridge University Press

Mercury species and thiols from GEOTRACES cruises in the North and South Atlantic Ocean

K.M. BOWMAN[1], T. KADING[2], G.S. SWARR[2], C.H. LAMBORG[2]*, C.R. HAMMERSCHMIDT[1] AND M. RIJKENBERG[3]

[1]Wright State University, Earth and Environmental Science, Dayton OH USA (correspondence: bowman.49@wright.edu)
[2]Woods Hole Oceanographic Institution, Marine Chemistry and Geochemistry, Woods Hole, MA USA (*presenting: clamborg@whoi.edu)
[3]Royal Netherlands Institute for Sea Research, Marine Geology, The Netherlands

As part of GEOTRACES research activities, we have measured dissolved and particulate mercury (Hg) species, aerosol and rainwater total Hg and dissolved thiols from a US zonal transect in the North Atlantic Ocean as well as total Hg from a meridional transect in the South Atlantic Ocean from a Dutch/UK sponsored cruise. This is currently the largest database of its kind. Findings include: 1) total Hg profiles are nutrient-like in the upper 1000 m, but show a mixture of qualities in deep water that appeared to be controlled by water mass transport; 2) surface total Hg concentrations were strongly affected by rain inputs, productivity and the Amazon River plume; 3) dissolved elemental Hg frequently followed nitrate distributions; 4) monomethyl- and dimethyl-Hg showed distinctive peaks in the oxygen minimum zones; 5) methylated Hg concentrations showed a lower response to organic carbon remineralization rates than those recently reported for the Pacific and Indian Oceans; 6) thiols appear to be important complexing agents for Hg (and other metals) in surface waters; 7) thiol concentration distributions are similar to chlorophyll, and therefore do not predict methylated Hg concentrations well.

Transformations of aqueous U(VI) during redox cycling of Fe phases

MAXIM I. BOYANOV[1]*, DREW E. LATTA[1], MICHELLE M. SCHERER[2], EDWARD J. O'LOUGHLIN[1], AND KENNETH M.. KEMNER[1]

[1]Argonne National Laboratory, Argonne, IL, USA, mboyanov@anl.gov (* presenting author)
[2]The University of Iowa, Iowa City, IA, USA

The activity of dissimilatory iron-reducing bacteria or the corrosion of waste containers often result in the presence of Fe^{II} and Fe^{III} species in subsurface environments. Recent work has shown that dissolved Fe^{II} exchanges atoms with Fe^{III}-containing solids in a dissolution-reprecipitation equilibrium, which likely proceeds via formation of minor but highly reactive Fe^{II}/Fe^{III} species at the surface. The fate of dissolved or adsorbed U^{VI} during such transformations will depend on the reactivity and transformations of both major and minor Fe phases, with possible outcomes including reduction and precipitation of $U^{IV}O_2$ (uraninite), reduction and incorporation of U^{IV} atoms in other phases, and non-reductive solid-phase incorporation of U^{VI}. We examined the reaction of dissolved U^{VI} with a host of Fe^{II}-containing phases, including dissolved and carboxyl-adsorbed Fe^{II}, green rusts with different interlayer anions, magnetite, and NAu-2 nontronite clay, as well as with oxidized analogues such as maghemite and pyroaurite. The goal was to establish the uptake mechanisms and to characterize the molecular structure of the solid-associated U species.

Experimental Methodology

We used x-ray absorption fine-structure spectroscopy (EXAFS and XANES) at the U L_{III}- and Fe K-edge to probe the speciation of U and Fe in the hydrated solid phases after reaction. Samples were reacted under geochemical conditions relevant to the subsurface, including the presence of carbonate and/or phosphate.

Discussion of Results

U^{VI} was reduced to U^{IV} by sulfate, chloride, and carbonate green rusts; the speciation of reduced U^{IV} varied between that in uraninite and a non-uraninite, adsorbed/incorporated U^{IV} species. Pyroaurite sequestered U^{VI} as a U^{VI}-carbonate complex, presumably by interlayer ion exchange. Magnetite reduced U^{VI} to nanoparticulate uraninite when its Fe^{II}/Fe^{III} content exceeded 0.38. Reactions with more oxidized magnetite ($Fe^{II}/Fe^{III}<0.38$) resulted in oxidized U species. The latter had less uranyl character than U^{VI} adsorbed to maghemite, suggesting U uptake in a distinct phase. Reactions between U^{VI}, nontronite, and Fe^{II} also resulted in oxidized, non-uranyl U species that were distinct from nontronite-adsorbed U^{VI}. Carboxyl-adsorbed U^{VI} and Fe^{II} reacted only when Fe^{II}-OH-Fe^{II} bonds formed, resulting in a combination of uraninite and U^{IV} atoms coordinated to Fe atoms in the nucleated mineral. The presence of dissolved phosphate (U:P=1:1) in the same system inhibited uraninite formation and resulted in U^{IV} atoms in phosphate-coordinated sites. The diversity of U incorporation modes in these model systems highlights the complexity in predicting U fate in subsurface environments — non-uraninite U^{IV} and non-uranyl oxidized U were also significant species in biostiumulated sediments from a contaminated field site (Oak Ridge, TN), and in naturally reduced soil from Hedrick, IA, reacted with U^{VI}.

https://doi.org/10.1180/S0026461X00008434 Published online by Cambridge University Press

Nucleosynthetic Nd isotope anomalies in primitive enstatite chondrites

M. BOYET[1]* AND A. GANNOUN[1]

[1] Laboratoire Magmas et Volcans, Université Blaise Pascal, CNRS UMR 6524, 5 rue Kessler, 63038 Clermont-Ferrand, France Boyet@opgc.univ-bpclermont.fr

Introduction

The first high precision measurements of $^{142}Nd/^{144}Nd$ ratios in chondrites have revealed that different groups of chondrites are characterized by different ratios [1, 2]. In order to interpret properly the deviation of $^{142}Nd/^{144}Nd$ ratio measured between terrestrial samples and chondrite material, it is crucial to understand the cause of the ^{142}Nd deviation in the different groups of chondrites. Enstatite chondrites (EC) present similar isotope compositions to terrestrial samples for a large number of elements (O, N, Mo, Cr, Ti) and have also the smallest ^{142}Nd offset (-10±12 ppm, [3]). We have selected primitive EC belonging to the EH subgroup for further Sm-Nd isotope investigations using a step-wise acid disolution method. The goal of this study is to better characterize the carrier phase of Nd nucleosynthetic anomalies and define their isotope composition.

Methods and Results

Sample powders were subjected to the following sequential leaching procedure: (1) H_2O then acetic acid, (2) EDTA, (3) 6M HCl, (4) Aqua regia and concentrated HF-HNO_3 mixture.. The major and trace element compositions of each fraction have been measured by ICP-AES and ICP-MS, respectively. Sm and Nd were separated using a 3 steps chemistry procedure and isotopes were measured on the Thermo-Fischer thermal ionization mass spectrometer at Laboratoire Magmas et Volcan, Clermont-Ferrand.

Most of the REE (50 to 80%) are contained in the first two leachate fractions mostly derived from the dissolution of oldhamite and ninigerite as deduced from the major element compositions. The last fraction have small REE contents (5-20%) which is mostly derived from the dissolution of enstatite and djerfisherite. Nd isotopes anomalies (ratios normalized to $^{146}Nd/^{144}Nd=0.7219$) are always positive for ^{145}Nd, ^{148}Nd and ^{150}Nd and negative in ^{142}Nd in fraction (1) to (3). The largest isotope anomalies are always measured in the last fraction (residu) with ^{142}Nd excess ranging from +200 to +600 ppm. The largest effects are measured in ALH77295, which is the most primitive EC analysed in this study.

Discussion

The residues obtained after leaching treatment are strongly enriched in s-process nuclides. The different Nd isotopes plot along the same correlation lines defined for leachates and residues of carbonaceous and odinary chondrites [4] suggesting that all residues contain s-process rich presolar grains. The amount of Sm in each fraction was too small to allow precise measurement of the $^{144}Sm/^{152}Sm$ ratios, however the p-process variability seems to be relatively small.

[1] Boyet and Carlson M. (2005) Science 309, 576-581. [2] Carlson et al. (2007) Science 316, 1175-1178. [3] Gannoun et al. (2011) PNAS 108, 7693-7697. [4] Qin et al. (2011) GCA 75, 7806-7828.

Aerosol release of Fe into the ocean: the extreme cases

EDWARD BOYLE[1*] AND JESSICA FITZSIMMONS[1,2]

[1]Massachusetts Institute of Technology, Cambridge MA 02139 USA, eaboyle@mit.edu

[2]MIT/WHOI Joint Program in Oceanography, jessfitz@mit.edu

By now it is well-known that partial dissolution of Fe from atmospheric aerosols is a major source of iron for oceanic phytoplankton and nitrogen fixers. But many of the details of the process are only partially understood: (1) What regulates the degree of Fe dissolution? (mineralogy of the source and chemical processing within the atmosphere are believed to be important, with anthropogenic aerosols releasing more Fe either because of the source or processing from anthropogenic acidity and photochemical processing), (2) What determines the form that iron takes upon release into seawater? (it appears that most of the aerosol-released Fe is converted into organic or inorganic colloidal form in high-dust regions, although there is an expectation that soluble organic complexes should also be important), (3) How does the dust flux influence the biota? (both phytoplankton and nitrogen fixers).

In order to learn more about these issues, we will discuss the contrasting oceanic iron distributions under a high-dust region (tropical North Atlantic) and a low-dust region (southeast Pacific between Chile and Easter Island). Under the high-dust region, most of the surface water Fe is colloidal and is removed to low concentrations near the chlorophyll maximum. Phosphorus is depleted to extremely low concentrations, as any excess over Redfield N:P ratios is compensated by nitrogen fixation. Below that, iron increases in step with increasing AOU, and the C:Fe ratio is low (~100,000). Under the low-dust environment, Fe is relatively low (0.10-0.15 nM) and uniform in the upper few hundred meters (despite increasing AOU below the chlorophyll maximum) and then increases to much higher C:Fe ratios (~500,000). Dissolved inorganic phosphorus remains at fairly high concentrations (~0.20 uM) because insufficient Fe prevents nitrogen fixers from compensating for the low N:P ratio in the upwelling deep waters.

https://doi.org/10.1180/S0026461X00008434 Published online by Cambridge University Press

Evolution of bioturbation buffered Neoproterozoic oxygenation

RICHARD A. BOYLE[1*] & TIMOTHY M. LENTON [1]

[1]University of Exeter, UK, r.a.boyle@exeter.ac.uk (*presenting author)

A range of geochemical evidence suggests a major oxygenation of the ocean (and by implication atmosphere) at the end of the Neoproterozoic – a change that may well have been necessary (although not sufficient) for the proliferation of the earliest animal life. However, indications of a localised reversion to more anoxic (and sulphidic) ocean conditions during the Cambrian raise the possibility of a subsequent drop in atmospheric oxygen. Furthermore, an explanation for why oxygen stopped rising during the Neoproterozoic remains elusive. Here we hypothesize that the efficiency of phosphorous removal from the ocean was significantly increased by the onset of large-scale sediment bioturbation and resultant ventilation - caused by the proliferation of macroscopic animals. This was due to (a) increased microbial P sequestration under oxic sedimentary conditions, and (b) greater net organic carbon oxidation reducing the C:P burial ratio[1,2]. The resulting reduction in the concentration of phosphorus in the ocean suppressed new production and organic carbon burial, reducing the long-term source of atmospheric oxygen and thereby buffering its concentration on a multi-million year timescale. We suggest that a plausible scenario for the integrated evolution of the Earth system at the end of the Neoproterozoic is therefore "increased marine P concentration via weathering of the land surface following terrestrial colonisation $\longrightarrow$ increased marine production and organic carbon burial $\longrightarrow$ increased atmospheric oxygen $\longrightarrow$ drastic increase in biomass and motility of the (already multi-cellular and differentiated) animal biosphere $\longrightarrow$ increased bioturbation $\longrightarrow$ reduction in marine P reservoir size and stabilisation of global phosphate and oxygen cycles"[3,4]. We argue that these feedbacks and a trajectory along these lines can help explain why atmospheric O_2 and marine PO_4 fluctuations have been well buffered during the Phanerozoic.

References

[1] Ingall, Bustin & Van Capellen. 1993. Geochim Cosmochim Act.**57**(2). 303-316.

[2] Krom & Berner. 1980. Limnol. Oceanog.**25**(5). 797-806.

[3] Lenton & Watson 2004. Geophy. Res. Lett. **31**(5) L05202.1-L05202.5.

[4] Boyle, 2008. Phd Thesis. University of East Anglia.

Lead-isotope geochemistry of the Bagirkacdere lead– zinc deposit, Biga Peninsula, NW Turkey

BOZKAYA, GULCAN

Cumhuriyet University, Department of Geological Engineering, Sivas, Turkey, gbozkaya@cumhuriyet.edu.tr

The Biga Peninsula contains several base-metal skarn deposits associated with Oligo-Miocene age granitic intrusions. The Bagirkacdere lead-zinc deposit is a typical example of the skarn-type deposits occurring in the northern section of the Biga Peninsula (5.2 Mt at 3.8 % Pb, 2.18 % Zn). The mineralization developed within the Paleozoic meta-sedimentary (Torasan metamorphics) and meta-granitic rocks (Camlik meta-granitoids) as stratabound disseminations and thin veins in schists, marble and meta-granitoids of the skarn zone. Pyrite, sphalerite and galena are the main sulphide minerals and they are accompained by minor amounts of chalcopyrite, arsenopyrite and hematite. Limonite, malachite, smithsonite, anglesite and cerrusite are secondary alteration products. The skarn is dominated by garnet, calc-silicates, epidote, actinolite, diopsite, feldspar and quartz.

Lead isotope ratios for galena have mean values of $^{206}Pb/^{204}Pb$ 18.758, $^{207}Pb/^{204}Pb$ 15.698, and $^{208}Pb/^{204}Pb$ 38.958. . When the data are plotted on the model curves for average crustal Pb-isotope evolution [1], $^{207}Pb/^{204}Pb$ and $^{208}Pb/^{204}Pb$ ratios are close to or above the evolution curves and clearly indicate a crustal source. Possible Pb sources have been investigated using the plumbo-tectonic diagrams [2] and the $^{208}Pb/^{204}Pb$ vs. $^{206}Pb/^{204}Pb$ data points are distributed along a trend between the representative curves for the Lower and Upper Crust, but they are closer to the Orogenic and Upper Crustal curves. The isotope data has higher $^{206}Pb/^{204}Pb$ ratios that are close to the 0-age suggesting young (Cenozoic) Pb-model ages [1]. The Pb data for Bagirkacdere is similar to mineralization at Arapucandere and Koru, which are close to Bagirkacdere in the north part of peninsula, indicating that similar processes were operatring over a wide area.

The $\delta^{34}S$ values of galena and sphalerite from the Bagirkacdere deposit, which are close to 0 ‰, are consistant with dominantly magmatic sulphur reservoir [3]. The combined lead and sulfur isotope data indicate that the source of lead and other metals in the skarn is primarily derived from Tertiary granites.

[1] Stacey and Kramers (1975) Earth Planetary Science Letters **26**, 207–221. [2] Zartman and Haines (1988) Geochimica et Cosmochimica Acta **52**, 1327–1339. [3] Bozkaya (2011) Goldschmidt, Abstract Volume, 571.

https://doi.org/10.1180/S0026461X00008434 Published online by Cambridge University Press

Source, transport, and matrix controls on metal bioavailability in floodplain soils

DANIEL J. BRABANDER[1,2*], EMILY R. ESTES[1], YONGMEI SHEN[1], AND JAMES P. SHINE[1]

[1]Harvard School of Public Health, Boston, USA, , eestes@fas.harvard.edu, yshen@hsph.harvard.edu, jshine@hsph.harvard.edu

[2]Wellesley College, Wellesley, USA dbraband@wellesley.edu (*presenting author)

With the deposition of metal-bearing sediments from upstream sources, floodplains have the potential to serve as an exposure vector for heavy metals. Not only are floodplains frequently located proximate to population centers, transported metals may also be present in more bioavailable forms (adsorbed or in secondary mineral phases) than in source material. Thus, a complex set of transport and biogeochemical transformation processes determines the spatio-temporal distribution of metal-bearing phases. Given that complexity, which variables (source, transport, matrix, aging) control metal speciation and the fraction of metals that are bioavailable by ingestion and inhalation pathways?

We examine this question for lead-, zinc-, and cadmium-bearing soils in the Neosho-Tar Creek floodplain system in Miami, Oklahoma, USA. To identify the source of metals within floodplain soils we have combined major and trace element geochemistry with multivariable statistical analysis (PCA) to develop fingerprints for distinct metal sources (Figure 1). By combining this approach with X-ray diffraction (XRD) to broadly characterize soil mineralogy we have developed endmembers for mixing models that apportion the relative contribution of various metal-bearing phases (detrital primary ore minerals versus secondary iron oxides and hydroxides (FeOx) minerals).

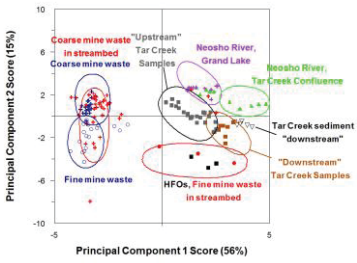

Figure 1: PCA of bulk element concentrations from floodplain soil and river sediment samples that demonstrate endmember sources and mixing relationships

Floodplain soil and sediment coring additionally allow us to reconstruct historic flood events and the temporal changes in metal flux, distribution, and speciation. We examine the role that shallow burial plays on the aging and in-situ weathering processes that result in FeOx mineral transformations. This combined approach will aid in estimating current and future risks associated with this evolving pool of bioavailable metals.

Calcite ($CaCO_3$) growth as a function of calcium-to-carbonate ratio in the presence of strontium: implications for the mechanism of inhibition

JACQUELYN N. BRACCO[1*], MEG C. GRANTHAM[1], ANDREW G. STACK[2]

[1]Georgia Institute of Technology, Earth and Atmospheric Sciences, Atlanta, USA, jbracco3@mail.gatech.edu (* presenting author)

[2]Oak Ridge National Laboratory, Chemical Sciences Division, Oak Ridge, USA, stackag@ornl.gov

One potential remediation method for toxic contaminants that has been proposed is to sequester the contaminant as an impurity in the crystal lattice of a mineral which incorporates the impurity. For example, radioactive strontium is present as a contaminant in a number of U.S. DOE sites and it may be possible to sequester it *in situ* through the engineered growth of calcium carbonate.[1] To enable targeted precipitation without porosity clogging and scale formation, separate injection wells of calcium and carbonate containing solutions have been proposed.

To understand this phenomenon, here we use atomic force microscopy (AFM) to examine the effect of strontium on calcite growth rates under solutions containing variable ratios of aqueous calcium-to-carbonate. Growth rates of the obtuse and acute step orientations on calcite were measured at two saturation indices as a function of the aqueous calcium-to-carbonate ratio and various aqueous strontium concentrations ranging from $0 - 9 \times 10^{-3}$ M. It was found that the amount of strontium necessary to inhibit growth correlated with the aqueous calcium concentration, but no correlation or inverse correlation was observed for carbonate. This suggests strontium is inhibiting attachment of calcium but not carbonate attachment or detachment.

At an average strontium-to-calcium ratio of 1.1 for the obtuse step orienation and 1.4 for the acute step orientation, the average step velcocity decreases to half of the maximum step velocity, which corresponds to the ratio where the concentration of strontium and calcium on the step at kink propagation sites is the same.[2] We propose that this corresponds to the cation exchange coefficent for calcium and strontium bound to precursor sites on the step.

The implications of this study are two-fold. Firstly, to ensure calcite growth is not inhibited by strontium, the concentration of calcium should be kept approximately higher than the cation exchange coefficient. Secondly, extensions of existing analytical models are unable to capture all the salient features of observed growth rates, indicating that improvement in analytical expressions can still be made.

This research was sponsored by the Division of Chemical Sciences, Geosciences, and Biosciences, Office of Basic Energy Sciences, U.S. Department of Energy.

[1] Tartakovsky, A. M. et al. (2008) *Wat. Resour. Res.*, **44**, W06S04.
[2] De Yoreo, J. J. et al. (2009) *Cryst. Growth Des.* **9**, 5135-5144.

https://doi.org/10.1180/S0026461X00008434 Published online by Cambridge University Press

Volcanogenic massive sulfide deposits host the evidence for sulfate-rich Archean oceans

JAMIE BRAINARD[1], ANDREW CHORNEY[1], AND HIROSHI OHMOTO[1]

[1]Penn State Astrobiology Center and Department of Geosciences, Penn State University, University Park, USA, JLB5156@psu.edu; APC5060@psu.edu; HQO@psu.edu

Recent researchers have suggested that the Archean oceans were sulfate poor (<0.1 mM SO_4^{2-}, compared to 28 mM today), because the atmosphere was supposedly poor in O_2 ($pO_2 < 10^{-6}$ atm) to completely oxidize the sulfur-bearing volcanic gases (H_2S and SO_2) and sulfide minerals in soils to SO_4^{2-}. However, such a scenario cannot explain the abundance of pyrite of Archean ages, much like those of younger ages, because these pyrites most likely formed by bacterial (or thermochemical) reduction of seawater SO_4^{2-}-.

One of the strongest lines of evidence for SO_4^{2-} rich Archean oceans comes from volcanogenic massive sulfide (VMS) deposits and alteration zones in their host rocks. VMS deposits, such as the black smoker deposits on MORs, formed on and beneath the seafloor by reactions between submarine hydrothermal fluids (typically ~50° to ~450°C) and the local seawater. The hydrothermal fluids evolved mostly through reactions between the underlying volcanic rocks and deep-circulating seawater, rather than derived directly from magmas. Therefore, the mineralogy and geochemistry of VMS deposits and their alteration zones reflect the chemistry of the contemporaneous ocean water. Phanerozoic VMS deposits are characterized by the abundance of pyrite and sulfate minerals, and by increased Fe^{3+}/Fe^{2+} ratios in the alteration zones due to the involvement of sulfate-rich seawater: some of the H_2S used to form the pyrite was generated by reduction of seawater sulfate by FeO components in rocks, resulting in the increases of Fe^{3+}/Fe^{2+} ratios. The ~3.2 Ga Panorama Formation of Western Australia hosts many VMS deposits with mineralogy, geochemistry, and associated alteration zones that are essentially identical to those of Phanerozoic ages, suggesting that the processes of submarine mineralization and the sulfate content of the seawater at 3.2 Ga were essentially the same as today.

Many other Archean VMS deposits and their alteration zones host barite ($BaSO_4$), such as the ~3.46 Ga Big Stubby deposits in Western Australia, the 3.26 Ga Fig Tree deposite in South Africa, the 2.6 Ga Geco deposit in Canada, and the 2.7 Ga Hemlo deposits in Ontario, Canada, suggesting that the Archean oceans remained sulfate-rich. The only major difference between the sulfate in the Archean oceans and that in the Phanerozoic oceans was the $\delta^{34}S$ values, between +2 and +5‰ during the Archean, but between +10 and +35‰ for the Phanerozoic. This difference has caused the $\delta^{34}S$ values of sulfides in Archean VMS deposits to be less than +5‰, where as those of Phanerozoic ages could be higher than +5‰, because the H_2S in the hydrothermal solutions came from the leaching of sulfides in igneous rocks ($\delta^{34}S \approx 0$‰) and from the partial reduction of seawater sulfate. These data suggest that the Archean oceans were as sulfate-rich as today's oceans due to the weathering of pyrite in rocks under an O_2-rich atmosphere.

Oxygen isotopes & Mg content in brachiopod calcite: equilibrium fractionation and a new paleotemperature equation

UWE BRAND[1*], K. AZMY[2], A. LOGAN[3], A. M. BITNER[4], B. DURZI[5], T. DURZI[6], M. ZUSCHIN[7]

[1]Department of Earth Sciences, Brock University, St. Catharines, Canada, uwe.brand@brocku.ca (* presenting author)
[2]Memorial University, St. Johns, Canada, kazmy@mun.ca
[3]University of New Brunswick, Saint John, Canada, logan@unbsi.ca
[4]Polish Academy of Sciences, Warsaw, Poland, bitner@twarda.pan.pl
[5]18 Paradise Close, Grand Harbour, Cayman Islands
[6]University of Guelph, Guelph, Canada, tdurzi@uoguelph.ca
[7]University of Vienna, Vienna, Austria, martin.zuschin@univie.at

Modern brachiopods and ambient seawater were collected at fourteen localities from the Arctic to the Antarctic. The brachiopods were analysesd for Mg, $\delta^{13}C$ and $\delta^{18}O$, and their ambient seawater was measured for temperature, salinity and $\delta^{18}O$. Our materials were supplemented by those of Lowenstam [1]. $\delta^{18}O$ values of marine carbonates increase by about 0.06 or 0.17 ‰ per mol% $MgCO_3$ [2,3], and failing to adjustment for this 'Mg-effect" has a profound impact on water temperatures determined with standard paleotemperature equations. This Mg-effect on $\delta^{18}O$ values applies to all marine invertebrates secreting shells or tests made of calcite with variable amounts of $MgCO_3$, such as articulated brachiopods, foraminifera and enchinoderms. The Mg content of our brachiopods varies from a low of 250 to a high of 30,660 ppm, which needs to be accounted for by the oxygen isotope impact of the Mg-effect. We propose a new paleotemperature equation that considers the pristine biogenic calcite (δc) and accounts for both the Mg-effect as well as the established seawater oxygen isotope (δw) correction:

$$T°C=14.5-3.5((\delta c\text{-Mg effect})-\delta w)+0.13((\delta c\text{-Mg effect})-\delta w)^2$$

The 'Mg effect' is defined as the $MgCO_3$ content of brachiopod calcite*0.17 ‰ (per mol% $MgCO_3$, accepting the latest study results [3]). Without adjustment for the Mg-effect, paleo seawater temperatures and compositions may be different than actual ones.

Without considering the effect of $MgCO_3$ on the oxygen isotopic composition, most modern brachiopods were found to precipitate shell carbonate in equilibrium with ambient seawater [4,5]. To re-evaluate the exceptions, *Thecidellina* and *Hemithiris* were collected from several localities. After making allowance for the Mg-effect on their $\delta^{18}O$ compositions and water-$\delta^{18}O$ corrected, calculated seawater temperatures were significantly similar to measured ones. $\delta^{18}O$ values of other modern brachiopods deemed problematic, after adjustment for the Mg-effect also offered up equilibrium water temperatures. Thus, we can state that modern, calcitic, articulated brachiopods incorporate oxygen isotopes into shell calcite in equilibrium with ambient seawater, and this will be of critical importance to other modern and fossil calcitic carbonates.

[1] Lowenstam (1961) *Journal of Geology* **69**, 241-260.
[2] Tarutani et al. (1969) *GCA* **33**, 987-996.
[3] Jiménez-López et al. (2004) *GCA* **68**, 3367-3377.
[4] Brand et al. (2003) *Chemical Geology* **198**, 305-334.
[5] Parkinson et al. (2005) *Chemical Geology* **219**, 193-235.

https://doi.org/10.1180/S0026461X00008434 Published online by Cambridge University Press

X-ray Spectromicroscopy: Illuminating the biogeochemical cycles of elements in the marine environment

JAY A. BRANDES[1*], ELLERY D. INGALL[2], AND JULIA M. DIAZ[3],

[1]1Skidaway Institute of Oceanography, 10 Ocean Science Circle, Savannah, GA 31411 USA,jay.brandes@skio.usg.edu (* presenting author)

[2]Georgia Tech, Atlanta, GA, USA, ellery.ingall@eas.gatech.edu

[3]Harvard University, Cambridge, MA, USA, jdiaz@seas.harvard.edu

The geochemical cycling of elements on Earth's surface is intrinsically linked to biological processes. These links include biologically-mediated formation/solution of minerals, sorption/desorption onto surfaces modified by organic matter, and biological activity. All such processes begin at the nanoscale. Therefore the ability to examine biologically generated or modified sediments, soils and other particulates at nanoscales provides a fundamental view into the cycling of elements. Unexpected insights are often generated using instruments capable of examining the nanoscale composition, speciation, redox state and co-association of elements within particulates. For example, in the marine environment, one can consider the generation and sequestration of carbon by phytoplankton as being limited by the availability of necessary nutrients, such as phosphorus (P) and iron (Fe). X-ray spectromicroscopy of P within planktonic organisms, sinking particulates, and underlying sediments has revealed a wide array of P types, including organic P compounds, polyphosphates, apatites and other P-containing minerals. Further examination of the associations of P, Fe and other elements also shows a variety of nutrient removal mechanisms. The results begin to show how P is sequestered in the environment, first through the preservation and burial of poorly organized but relatively pure biogenic polyphosphates and calcium phosphates, then through transformation into more ordered, and substituted mineral phases. Overall the picture of P chemistry at sub-micron scales reveals a complex system interacting both with biologically produced particulate P and terrestrially- or aeolian-derived P mineral phases.

Mesozoic MORB

P. A. BRANDL[1*], M. REGELOUS[1], C. BEIER[1] AND K. M. HAASE[1]

[1]GeoZentrum Nordbayern, Friedrich-Alexander Universiät Erlangen-Nürnberg, Erlangen, Germany, philipp.brandl@gzn.uni-erlangen.de (* presenting author)

Formation of the oceanic crust at mid-ocean ridge spreading centres and its subsequent evolution has an important influence on sea-level, the carbon cycle and seawater chemistry over timescales of 10-100 Ma. Previous geochemical studies of ancient MORB (e.g. [1, 2, 3]) reported chemical differences between Mesozoic and young mid-ocean ridge basalt (MORB) that were interpreted as the result of a 50-60°C higher upper mantle temperature [1, 2]. Higher mantle temperature on average would cause shallower depth of mid-ocean ridges, rising sea-levels and global warming by increased CO_2 emission.

We present new major and trace element data, measured using electron microprobe and LA-ICPMS techniques, for more than 360 glasses from 30 DSDP-ODP-IODP drill sites. The age of the oceanic crust at these sites ranges from 6 Ma up to 160-170 Ma, and all sites were drilled into normal oceanic crust far from hotspots. We have analysed exclusively fresh volcanic glasses, since whole-rock samples may be compromised by alteration and accumulation of phenocrysts.

We find that there are small but significant differences between fractionation corrected major element compositions of old (drilled) and zero-age (dredged) samples, e.g. for Na_{72}, Fe_{72}, Ca_{72}, and Al_{72}. We can exclude any analytical bias, alteration effects or uncertainties in fractionation correction for these differences. For both, Pacific and Atlantic, there is no clear systematic change in fractionation corrected major element composition of drilled MORB with time, as would be expected for a change in mantle temperature [1]. Some of these differences between zero-age and drilled MORB samples could arise if the oceanic crust is compositionally layered. MORB drilled from off-axis represent younger flows erupted further from the ridge axis. In contrast, most samples in the zero-age MORB dataset were dredged from the ridge axis, which eventually make up the lowermost section of the oceanic crust [4].

Lavas erupted off-axis may sample different parts of the melting region and/or undergo different fractional crystallisation histories to lavas erupted at the ridge axis. This effect could mean that average MORB compositions calculated using only samples dredged from the ridge axis are not completely representative of the extrusive section of the oceanic crust.

[1] Humler et al. (1999) *Earth Planet. Sci. Lett.* **173**, 7-23. [2] Fisk and Kelley (2002) *Earth Planet. Sci. Lett.* **202**, 741-752. [3] Janney and Castillo (2001) *Earth Planet. Sci. Lett.* **192**, 291-302. [4] Hooft et al. (1996) *Earth Planet. Sci. Lett.* **142**, 289-309.

https://doi.org/10.1180/S0026461X00008434 Published online by Cambridge University Press

The Shergottite Chronology Debate: In Support of Young Igneous Crystallization Ages

ALAN BRANDON[1]*

[1]University of Houston, Department of Earth and Atmospheric Sciences, Houston, TX, 77204, USA, abrandon@uh.edu

The shergottite meteorites provide powerful constraints on early differentiation in Mars ([1,2] and references therein). These constraints depend on having well determined igneous crystallization ages for the rocks, from which initial ratios for radiogenic isotope systems are calculated. Shergottite ages interpreted to be igneous, ranging from 474 to 166 Ma have been obtained from internal isochrons using the Lu-Hf, Sm-Nd, and Rb-Sr systems (e.g. [1,3]). Recently, these young igneous crystallization ages have been called into question [4,5,6]. Secondary Pb-Pb isochrons for different shergottites give purportedly circa 4.1 Ga ages and have been interpreted to be the true igneous ages while the younger ages represent resetting from shock or fluid-rock interaction [4,5,6].

This issue is examined here by first presenting the petrological, mineralogical, and lithophile isotope evidence that supports the young ages as being igneous. Second, these relationships are evaluated using Re-Os isotopes [7]. One strong piece of supporting evidence for young ages is the EETA 79001 Re-Os isochron (Figure 1). The two lithologies sampled come from portions of the meteorite several centimeters apart, give an isochron age of 164±12

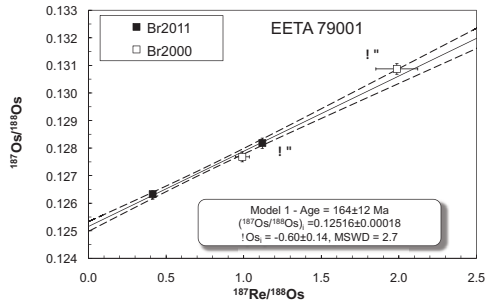

Figure 1: Re-Os isotope systematics of EETA 79001, modified from [7]. A and B designate fractions analyzed from litholigies A and B, respectively. Data from [7] – Br2011, from [8] – Br2000.

Ma (±2σ), concordant to internal mineral isochron ages for ^{87}Rb-^{87}Sr of 173±10, 177±12, and 174±3 Ma, for ^{147}Sm-^{143}Nd of 169±23 Ma, for ^{238}U- ^{206}Pb of 150±15 Ma, and for ^{232}Th-^{208}Pb of 170±36 Ma [9,10,11]. It is not likely possible to generate such systematics from shock unless diffusion rates are orders of magnitude faster than expected. Additional evidence will be presented that examines this issue.

[1] Nyquist et al. 2001, *Rev. Chronol. Evolut. Mars* **96**, 105–164. [2] Debaille et al. 2007, *Nature* **450**, 525-528. [3] Shafer et al. 2010, *GCA* **74**, 7307–7328. [4] Bouvier et al. 2005, *EPSL* **240**, 221-233. [5] Bouvier et al. 2008, *EPSL* **266**, 105-124. [6] Bouvier et al. 2009, *EPSL* **280**, 285-295. [7] Brandon et al., 2011. [8] Brandon et al. 2000, *GCA* **64**, 4083-4095. [9] Chen & Wasserburg 1986, *GCA* **50**, 955-968. [10] Nyquist et al. 2001, *LPS* **XXXII**, #1407. [11] Wooden et al., 1982, *LPS* **XIII**, 879-880.

Replacement of Barite by Radiobarite at close to equilibrium conditions and room temperature

FELIX BRANDT[1*], MARTINA KLINKENBERG[1], KONSTANTIN ROZOV[1], GUISEPPE MODOLO[1], DIRK BOSBACH[1]

[1]Forschungszentrum Juelich, IEK-6, Juelich, Germany, f.brandt@fz-juelich.de (*presenting author); m.klinkenberg@fz-juelich.de; k.rozov@fz-juelich.de, g.modolo@fz-juelich.de, d.bosbach@fz-juelich.de

The solubility control of Ra by coprecipitation of a $Ra_xBa_{1-x}SO_4$ solid solution has been demonstrated in many cases and can be modeled reliably (Doerner & Hoskins, 1925). However, an open question is whether a Ra containing solution will equilibrate with solid $BaSO_4$ under repository relevant conditions. Here, Radium enters a system in which barite is in equilibrium with the aqueous solution. Previous studies have indicated that Ra uptake is not limited by pure adsorption but involves a significant fraction of the bulk solid, i.e. barite partially or fully recrystallizes to radiobarite (Bosbach et al., 2010; Curti et al., 2010). Here, we present experimental data from batch recrystallization experiments at room temperature in which a pure barite solid was put into contact with an aqueous solution with an initial Ra/Ba ratio of 0.3 ($5 \cdot 10^{-6}$ mol/L Ra) at neutral pH. Two barites of different morphology and surface area were used during the recrystallization experiments at close to equilibrium conditions and with variation of solid to liquid ratio.

The experimental results show a decrease of the Ra concentration to $3.5 \cdot 10^{-9}$ to $7 \cdot 10^{-9}$ mol/L within the first 70 days of the experiment at a solid/liquid ratio of 5 g/L. At a solid/liquid ratio of 0.5 g/L a slower decrease of the Ra concentration to $2 \cdot 10^{-8}$ mol/L is observed after 180 days. The decrease of the Ra concentration is apparently not related to the specific surface area of the barite crystals. The final radium concentrations are in the range as can be expected from thermodynamic calculations assuming full reequilibration of the barite to a $Ra_xBa_{1-x}SO_4$ solid. Different thermodynamic models describing the mechanism of Ra incorporation into barite are discussed: (1) Ba – Ra exchange into the crystal volume, combining the Ra – Ba exchange with the Ba – Ba recrystallization rate at equilibrium conditions (Curti et al, 2010);

(2) the formation of a Ra-Ba-Phase on barite surfaces. The formation of a Ra-Ba phase on the barite surfaces could be possible because all experiments are already slightly supersaturated with regard to $Ra_xBa_{1-x}SO_4$ after about one day. Crystallization rates calculated according to this model are in a similar range for all experiments when normalized to the barite surface area.

The results of this study will provide the basis for further spectroscopic and microscopic investigations in order to obtain a molecular-level understanding of the Ra incorporation into barite.

[1] Doerner, H. A. & Hoskins, W. M. (1925) *Journal of the American Chemical Society*, **47**, 662-675

[2] Bosbach, D.; Böttle, M. & Metz, V. (2010) *Waste Management, Svensk Kärnbränslehantering AB*

[3] Curti, E.; Fujiwara, K.; Iijima, K.; Tits, J.; Cuesta, C.; Kitamura, A.; Glaus, M. & Müller, W. (2010) *Geochimica et Cosmochimica Acta*, **74**, 3553-3570

https://doi.org/10.1180/S0026461X00008434 Published online by Cambridge University Press

Back to the Future: The Art of Weathering

SUSAN BRANTLEY[1*] HEATHER BUSS[2] MARJORIE SCHULZ[3]

[1]The Pennsylvania State University, Earth and Environmental Systems Institute, University Park, PA, USA, sxb7@psu.edu (*presenting author)
[2]University of Bristol, School of Earth Sciences, Bristol, UK, h.buss@bristol.ac.uk
[3]U.S. Geological Survey, 345 Middlefield Road, Menlo Park, CA, USA, mschulz@usgs.gov

Geologists and soil scientists attempt to go back to the future to read the geochemical record written in regolith. If we could do this, we could use earthcasting models to project the surface earth in the future just as we use forecasting models to project the weather. But going back into geological time to read the record in soil profiles is both a science and an art due to the interdependence of chemistry, physics, and biology at the earth's surface. The art of earthcasting is also hard because such models must have the capacity to span timescales ranging from seconds for hydrogeochemical effects up to tens of millions of years or longer for tectonic processes.

We discuss the contributions of one scientist, Art White (recently retired from the U.S. Geological Survey, Menlo Park, CA, USA), who spent a career investigating geochemical processes and how they affect mineral-water reactions in pursuit of understanding the surface Earth. Art recognized that soil profiles are records of biogeochemistry that can be interpreted using kinetics and thermodynamics. With the use of geochemical, physical, hydrological and biological measurements, regolith formation rates can be constrained and geochemical descriptions can be made quantitative. Art's work in the laboratory – including a 16 year experiment – and at several field sites as part of the USGS WEBB program, including Panola, Georgia; the Luquillo Mountains, Puerto Rico; and the Santa Cruz terraces, CA; resulted in a series of papers that have greatly influenced our understanding of the earth's surface. Today, much of this work is termed Critical Zone science: Art was one of the originators of the Critical Zone Exploration Network and is therefore one of the original CZEN masters. His contributions helped lead to the big programs in Critical Zone science in the U.S.A. and elsewhere. Art and the many scientists before him (back to even the 16th century when soil profiles were first studied) set the stage for today's "artists of weathering". Now, new field opportunities, theoretical models, analytical tools, microbiological observations and sensors are elucidating the beauty and art of the Critical Zone.

Low temperature alkaline pH hydrolysis of oxygen-free Titan tholins

CORALIE BRASSE[1]*, FRANCOIS RAULIN[2], PATRICE COLL[3], OLIVIER POCH[4], AND ARNAUD BUCH[5]

[1] Laboratoire Inter-universitaire des Systèmes Atmosphériques, Créteil, France, coralie.brasse@lisa.u-pec.fr (* presenting author)
[1] Laboratoire Inter-universitaire des Systèmes Atmosphériques, Créteil, France, francois.raulin@lisa.u-pec.fr
[3] Laboratoire Inter-universitaire des Systèmes Atmosphériques, Créteil, France, patrice.coll@lisa.u-pec.fr
[4] Laboratoire Inter-universitaire des Systèmes Atmosphériques, Créteil, France, olivier.poch@lisa.u-pec.fr
[5] Centro de Investigaciones Quimicas, Cuernavaca, Mexico, ramirez_sandra@ciq.uaem.mx
[6]Ecole Centrale Paris, Laboratoire de Génie des Procédés et Matériaux, bucha@ecp.fr

The largest moon of Saturn, Titan, is known for its dense, nitrogen-rich atmosphere. The organic aerosols which are produced in Titan's atmosphere are of great astrobiological interest. particularly because of their potential evolution when they reach the surface and may interact with putative ammonia-water cryomagma[1].

In this context we have followed the evolution of alkaline pH hydrolysis (13wt% ammonia-water) of Titan tholins (produced by an experimental setup using a plasma DC discharge named PLASMA) at low temperature. Our group identified urea as the main product of tholins hydrolysis along with several amino acids (alanine, glycine and aspartic acid). However, those molecules have also been detected in non-hydrolyzed tholins meaning that oxygen gets in the PLASMA reactor during the tholins synthesis[2]. So the synthesis system has been improved by isolating the whole device in a specially designed glove box which protects the PLASMA experiment from the terrestrial atmosphere.

After confirming the non-presence of oxygen in tholins produced with this new experimental setup, it is necessary to perform alkaline pH hydrolysis in oxygen-free tholins in order to verify that organic molecules cited above are still produced or not... Moreover, a recent study shows that the subsurface ocean may contain lower fraction of ammonia (about 5wt% or lower[3]), than previously used. Thus new hydrolysis experiments will take this lower value into account. Additionally, a new report [4] provides upper and lower limits for the bulk content of Titan's interior for various gas species. It also shows that most of them are likely stored and dissolved in the subsurface water ocean. But considering the plausible acido-alkaline properties of the ammonia-water ocean, additional species could be dissolved in the ocean and present in the magma. They could also be included in our hydrolysis experiments.

The preliminary results of those experiments will be presented.

[1] Mitri et al. (2008) *Icarus* **196**, 216-224. [2] Poch et al.(2011) *Planetary and Space Science* **61**, 114-123. [3] Beghin et al. (2012) *Icarus* **submitted**. [4] Tobie et al. (2011) EPSC-DPS2011 **6**.

https://doi.org/10.1180/S0026461X00008434 Published online by Cambridge University Press

Comparison of methods and results in recent studies of direct groundwater discharge to the Atlantic coast and Great Lakes

JOHN F. BRATTON[1*], KEVIN D. KROEGER[2], STEVEN A. RUBERG[3], HOLLY A. MICHAEL[4], AND DAVID E. KRANTZ[5]

[1]NOAA Great Lakes Environmental Research Lab, Ann Arbor, Michigan, USA, john.bratton@noaa.gov (* presenting author)
[2]USGS, Woods Hole, Mass., USA, kkroeger@usgs.gov
[3]NOAA-GLERL, Ann Arbor, Mich., USA, steve.ruberg@noaa.gov
[4]Univ. of Delaware, Newark, Del., USA, hmichael@udel.edu
[5]Univ. of Toledo, Toledo, Ohio, USA, david.krantz@utoledo.edu

Submarine and Sublacustrine Groundwater Discharge

Groundwater/surface water interaction has been the subject of intense investigation in both marine and freshwater settings in recent years. Although many study methods can be used interchangeably in these systems (e.g., seeepage meters), those that rely on salinity contrasts to distinguish surface water from groundwater (e.g., electrical resistivity profiling) cannot. A schematic spatial framework that was recently developed for dividing submarine groundwater discharge (SGD) phenomena [1] can also be applied to large lakes with some modifications. Some natural radioisotopic tracers of SGD developed in marine systems can be used in freshwater settings [2]. Conversely, a regional approach to examining groundwater occurrence and flow in a watershed containing large lakes, as has been undertaken for the Great Lakes [3], might be productively applied to a coastal ocean region.

In addition to the salinity contrasts, one major geochemical difference between discharge of groundwater to fresh or saline surface water is the influence on eutrophication. Because nitrogen is typically the limiting nutrient in marine systems, whereas phosphorus limits productivity in most freshwater systems [4], SGD plays a much larger role in eutrophication of marine systems than in freshwater systems. Dissolved nitrogen species tend to be concentrated in coastal groundwater, but phosphorus is particle reactive and unlikely to be delivered to surface water in large quantities from groundwater in most lakes. Most phosphorus comes from runoff and sediment recycling in freshwater systems.

Unusual groundwater vent features have been documented in both marine and lake settings, especially along carbonate-dominated coasts. Among the most spectacular are brackish sinkhole springs in Florida and Lake Huron, the latter of which include extensive purple cyanobacterial mat communities [5].

Conclusion

Significant opportunities exist for advancing understanding of elemental cycling and other features of groundwater/surface water interaction in large water bodies with more exchange of methods and results among scientists that work in marine and freshwater settings.

[1] Bratton (2010) *J. Geol.* **210**, 565-575. [2] Moore (2008) *Mar. Chem.* **109**, 188-197. [3] Granneman *et al.* (2000) *USGS WRIR* **00-408**. [4] Howarth and Marino (2006) *Limnol. Oceanogr.* **51**, 364-376. [5] Biddanda *et al.* (2009) *Eos* **90**, 61-62.

Contemporary saprolite production rates and aggressiveness of pore waters: Comparison between Nsimi and Mule Hole small experimental watersheds

JEAN JACQUES BRAUN[1]*, JEAN-CHRISTOPHE MARECHAL[2], JEAN RIOTTE[1,3], MUDDU SEKHAR[1,4]

[1]IFCWS IISc-IRD joint laboratory, Bangalore, India, jjbraun1@gmail.com (* presenting author)
[2]BRGM, Montpellier, France, jc.marechal@brgm.fr
[3]GET, Toulouse, France, jeanriotte1@hotmail.com
[4]Dept. of Civil Engg., IISc., Bangalore, India, sekhar.muddu@gmail.com

Introduction

Thanks to geochemical, mineralogical and hydrological studies and using Chloride Mass Balance approach, we compare two ridge top weathering profiles (WP) developed on granodioritic basement from Mule Hole (South India) and Nsimi (South Cameroon) small experimental watersheds (SEW). The objective is to get deeper insight into (i) the contemporary saprolite production rates and (ii) the combined effect of precipitation and evapotranspiration on the aggressiveness of the draining solutions.

Field settings

The Nsimi SEW presents the contemporary weathering conditions for a 36 meter deep, mature weathering cover under humid climate (Mean Annual Rainfall = 1660 mm/yr, Actual EvapoTranspiration (AET) = 1270 mm/yr) with a Recharge (R) = 332 mm/yr out of which 90% of the solutes are discharged into the springs/brook and 10 % through the groundwater[1][2]. The Mule Hole SEW presents the contemporary weathering conditions for a 17 meter deep, immature weathering cover under sub-humid climate (MAR = 1280 mm/y, AET = 1100 mm/yr) with R = 45 mm/yr out of which 100% of the solutes are discharged through the groundwater as underflow from the watershed[3][4][5]. Moreover, the Nsimi groundwater saturates the entire saprolite whilst the Mule Hole groundwater saturates the fractured bedrock only.

Results and conclusions

Considering (i) Na as representative of the dissolution of plagioclase crystals and conservative during saprolitization processes and (ii) steady state of the inter-annual recharge for a 10 years period, the current saprolite production rates (SPR) are of 22 mm/kyr for Mule Hole and 2 mm/kyr for Nsimi, respectively.

Even with a very low R/MAR ratio (0.04) compared to Nsimi, the chemical weathering at Mule Hole is active and related to the groundwater exports. However, the high Nsimi R/MAR ratio (0.2) allows the solution to be still aggressive with respect to the plagioclase at the bedrock interface leading to their complete breakdown in a few centimeters. For Mule Hole, plagioclase are still present in the saprolite and the soil cover.

[1] Braun (2005) *Geochimica Cosmochimica Acta* **73,** 935-961. [2] Maréchal (2011) *Hydrological Processes* **25**, 2246–2260. [3] Maréchal (2011) *Applied Geochemistry* **26,** S94-S96. [4] Maréchal (2009) *J. of Hydrology* **361,** 272-284 [5] Ruiz (2010) *J. of Hydrology* **380,** 460-472.

https://doi.org/10.1180/S0026461X00008434 Published online by Cambridge University Press

The source of carbon in cave air CO_2 under mixed woodland and grassland vegetation

DANIEL O. BREECKER[1*], ASHLEY E. PAYNE[1], JAY QUADE[2], JAY L. BANNER[1], CAROLYN E. BALL[3], AND KYLE W. MEYER[1]

[1]The University of Texas at Austin, Austin, USA, breecker@jsg.utexas.edu (* presenting author)
[2]The University of Arizona, Tucson, USA
[3]The University of Florida, Gainesville, USA

We measured concentrations and stable carbon isotope compositions of CO_2 in the atmospheres of several caves in central Texas and southern Arizona in order to identify the sources of CO_2 -carbon. The vegetation above all of the caves studied is a mixture of grasslands (C_3 and C_4 vegetation) and woodlands (dominantly C_3 juniper and oak trees). We tested the hypothesis that the deepest rooting plants have a dominant influence of the $\delta^{13}C$ value of CO_2 in the caves. Within caves, we monitored CO_2 at individual locations on monthly and daily time-scales. We also measured CO_2 in the pore spaces of soils dominated by different vegetation types above each cave. The $\delta^{13}C$ value of respired CO_2 ($\delta^{13}C_r$) was calculated for all gas samples from the measured $\delta^{13}C$ values and CO_2 concentrations by rearranging equations derived by Davidson[1]. The sources of cave CO_2 were then identified by comparing soil and cave air $\delta^{13}C_r$ values. In three of the caves, mean cave air CO_2 $\delta^{13}C_r$ values were within 0.5 ‰ of mean $\delta^{13}C_r$ values in woodland soils (-23 to -24‰ vs VPDB), even when measured $\delta^{13}C$ values of cave and soil CO_2 were different by up to 2.5‰. The $\delta^{13}C_r$ values in grassland soils above these three caves were 3-5 ‰ higher than cave and woodland soil values. In one cave covered primarily by grassland and roads, the cave $\delta^{13}C_r$ values were intermediate between grassland and woodland values. When cave-air CO_2 concentrations were below 1000 ppmV, cave $\delta^{13}C_r$ values were more negative than woodland soil values by 20‰ or more, likely the result of preferential degassing of $^{12}CO_2$ from CO_2-supersatured drip water[2]. The consistent agreement between soil and cave air $\delta^{13}C_r$ values indicate that the same mixing and diffusion equations, which are used to calculate $\delta^{13}C_r$ and have been previously applied to soils, also apply to cave atmospheres. Our results suggest that unless cave CO_2 concentrations are <1000 ppm the majority of CO_2 advects or diffuses into these caves from soils as a gas rather than being transported in aqueous solution. Calculated $\delta^{13}C_r$ values suggest that juniper and/or oak trees supply most of the carbon to CO_2 in the atmospheres of these caves, likely because these trees have deeper roots than the other plants in these ecosystems. A one-dimensional numerical model of CO_2 production and diffusion that uses depth-dependent $\delta^{13}C_r$ values as input supports our empirical results and our hypothesis that deeply rooted trees control the $\delta^{13}C_r$ values of cave air CO_2, even if deep respiration rates are small compared with those in the shallow subsurface. We further suggest that if a vegetation signal is archived in the carbon isotope composition of speleothem calcite, then it may be biased toward deep-rooted plants.

[1] Davidson (1995) *Geochimica et Cosmochimica Acta* **59**, 2485-2489. [2] Spötl et al. (2005) *Geochimica et Cosmochimica Acta* **59**, 2451-2468.

Sulfide-silicate partitioning of PGEs (and Au): Implications for noble metal behaviour in magmatic systems

JAMES M. BRENAN[1*]

[1]University of Toronto, Toronto, Canada, brenan@geology.utoronto.,ca (* presenting author)

There is considerable variation in sulfide-silicate melt partition coefficients for the noble metals (PGEs and Au), with most direct measurements (analysed by bulk methods) yielding values of 10^4 or less [e.g., 1]. More recent estimates, which combine separate metal solubility measurements in sulfide and silicate, have suggested partition coefficients exceeding 10^7 [2,3]. Resolving this discrepancy is essential for developing accurate models of noble metal behaviour during melting, and validating metal concentration mechanisms in magmatic systems.

In this study, sulfide and silicate were equilibrated at known fO2-fS2 conditions, with run-products analysed by LA-ICPMS to ensure exclusion of sulfide contamination from the silicate melt analysis. Experiments were done at 1200 deg. C and 1 atm with fS2 controlled using the Pt-PtS buffer and fO2 estimated to be FMQ-1. Three different synthetic basalts were employed, differing in their FeO content (5-15 wt%), with the added sulfide melt composition having FeS stoichiometry + 1 wt% each of Cu and Ni. Glass + sulfide were packed in crucibles made from natural chromite, then loaded, along with the sulfide buffer, in silica ampoules, which were evacuated, then sealed. Samples were held for 1 to 4 days at temperature, then quenched in cold water. Run-product glasses were free of obvious sulfide contamination, as evidenced by uniform, and low time-resolved signals for the PGE and Au.

Concentrations of Ru and Os in run-product glasses were always below detection (approx 20 and 5 ppb, respectively), yielding minimum sulfide/silicate partition coefficients of >10^5 (Ru) and >10^6 (Os). Measurable, but low, abundances for other PGE and Au were determined, with calculated sulfide/silicate partition coefficients of >10^5 (Pd, Rh, Ir, Pt) and 4000-11000 (Au). Partition coefficients for Pd, Rh, Ir and Pt were found to increase with increasing concentrations of these elements added to the sulfide melt, with little or no change in the silicate melt concentration. This is interpreted to reflect a low level of sulfide contamination in the silicate melt, and argues for even higher partition coefficients for these elements. Thus, results are in line with the large partition coefficients estimated from combined sulfide and silicate PGE solubility data. Application of these data to sulfide-saturated partial melting models yields levels of PGE and Au in calculated melts which are much lower than observed for MORB or OIB; only at the point of near complete sulfide exhaustion are calculated and observed abundances similar. An alternative to residual sulfide, such as a combination of olivine, chromite along with an alloy phase, may be required to account for levels of these elements in oceanic basalts.

[1] Fleet *et al* (1999) Lithos **47**, 127–142. [2] Andrews & Brenan (2002) *Chem Geol* **192**, 163-181. [3] Fonseca et al (2009) *GCA* **73**, 5764–5777.

https://doi.org/10.1180/S0026461X00008434 Published online by Cambridge University Press

Concentrations and isotope ratios of He and other noble gases in the atmosphere during 1978–2011

M.S. BRENNWALD[1*], M.K. VOLLMER[2], N. VOGEL[1,3], S. FIGURA[1,4], R.P. NORTH[1,4], R. LANGENFELDS[5], L.P. STEELE[5], R. KIPFER[1,3,4]

[1] Eawag, Swiss Federal Institute of Aquatic Science and Technology, Dübendorf, Switzerland (*matthias.brennwald@eawag.ch)

[2] Laboratory for Air Pollution and Environmental Technology, Empa, Swiss Federal Laboratories for Materials Science and Technology, Dübendorf, Switzerland

[3] Institute of Geochemistry and Petrology, Swiss Federal Institute of Technology, Zurich, Switzerland

[4] Institute of Biogeochemistry and Pollutant Dynamics, Swiss Federal Institute of Technology, Zurich, Switzerland

[5] Centre for Australian Weather and Climate Research/CSIRO Marine and Atmospheric Research, Aspendale, Victoria, Australia

The concentration of He in the atmosphere (residence time ~10^6 years) is governed by the balance between its release from the solid earth and its loss into space. Due to the burning of fossil fuels, which is known to be rich in He, an increase of the atmospheric He concentration over the past decades has been predicted. However, the predicted increase is small, and the precision of currently available measurement techniques is insufficient to verify this potential increase.

An alternative approach to study this possible increase in the atmospheric He concentration is to analyse the $^3He/^4He$ ratio in historic air samples. The $^3He/^4He$ ratio in fossil fuels is commonly one to two orders of magnitude lower than in the atmosphere. An increase of the He concentration in the atmosphere due to burning of fossil fuel would therefore correspond to a decrease of the atmospheric $^3He/^4He$ ratio that might be detectable with currently available measurement techniques. However, while some studies claim to have found evidence for a decrease in the $^3He/^4He$ ratio in the atmosphere during the last few decades, other studies were not able to confirm this observation.

In an attempt to resolve this long-standing controversy, we conducted isotopic analyses of *all* the atmospheric noble gases (He, Ne, Ar, Kr and Xe) in air samples from a well-defined archive of marine boundary layer air in the southern hemisphere (Cape Grim Air Archive, Australian Bureau of Meteorology and CSIRO). In our presentation we will report the results of these analyses and discuss them in terms of a possible change in the atmospheric He concentration. The $^4He/^{20}Ne$ ratio in particular turned out to be a very sensitive proxy for this purpose. Because the $^4He/^{20}Ne$ ratio in fossil fuels is about 8 orders of magnitude lower than in the atmosphere, the addition of noble gases from fossil fuels to the atmosphere has a much stronger effect on the $^4He/^{20}Ne$ ratio than on the $^3He/^4He$ ratio. At the same time, if He and Ne are not separated from each other before analysis in the mass spectrometer, the $^4He/^{20}Ne$ ratio can be quantified with a better precision than the $^3He/^4He$ ratio. Broadening the atmospheric He analysis to include other noble gas isotopes therefore allows us to put much firmer constraints on possible changes in the atmospheric He concentration that may have resulted from the burning of fossil fuels during the last few decades.

Improving ^{182}Hf-^{182}W ages in altered CR chondrites

T. BRETON*, G. QUITTÉ AND F. ALBARÈDE

CNRS UMR 5276, ENS de Lyon, Université Lyon 1, Lyon, France, thomas.breton@ens-lyon.fr (* presenting author)

Introduction

Despite their high content of segregated metal and their diverse degrees of alteration, CR chondrites are considered among the most primitive meteorites in the solar system. Applying the ^{182}Hf-^{182}W chronometer to these samples therefore seems interesting to better constrain the earliest stages of metal segregation. While NWA 721 and NWA 801 yield ^{182}Hf-^{182}W ages of ~5 Ma after CAIs, Renazzo is surprisingly ~50 Ma younger [1], which suggests that the ^{182}Hf-^{182}W chronometer may have been disturbed in this particular sample.

Hf and W behavior in natural processes

Although the ^{182}Hf-^{182}W chronometer may have been reset by thermal metamorphism [2], Renazzo seems free of thermal overprinting. However, this meteorite shows evidence of strong aqueous alteration [3] and Pourbaix (Eh-pH) diagrams indicate that tungsten is affected by this process [4]. $\varepsilon^{182}W$ values, which are corrected for mass dependent fractionation, will not be harmed, whereas the Hf/W (parent/daughter) ratios will. Hafnium is indeed far less mobile than W that, in neutral to high-pH fluids, are most likely lost as tungstate. The internal isochron is thus disturbed and the apparent age is younger.

A simple single-stage model suggests that aqueous alteration rotates the isochron around the y-intercept. Thus, the y-intercept seems suited to determine the timing of metal-silicate segregation, even in altered samples. This model reduces the time interval between NWA 701 / NWA 801 and Renazzo to 14 ± 14 Ma.

Tafassasset: an old unaltered CR chondrite

Tafassasset, an anomalous CR chondrite [5, 6] is metamorphosed but not aqueously altered. If alteration affects the Hf-W isochron, this meteorite is of particular interest to experimentally infer the timing of metal-silicate segregation in the CR parent body(ies). Seven different mineral phases (pure metal, several magnetic phases, silicate phases and two bulks) have been separated and analyzed. The W concentrations are 800 ppb and 15 ppb in metal and silicates, respectively. MC-ICPMS and N-TIMS measurements were performed, depending on the amount of W available in each fraction. Both techniques yield the same results within uncertainties. Data plot on a well defined line in an isochron diagram. Ages calculated from the slope or from the initial of this isochron relative to CAIs [7, 8] are consistent with each other: metal-silicate equilibration in Tafassasset occurred less than 2 Ma after Allende CAIs. This meteorite is thus older than the other CR2 chondrites analyzed so far, and among the oldest known chondrites.

[1] Quitté et al. (2010) *MAPS* **45**, A167. [2] Kleine et al. (2005) *EPSL* **231**, 41-52. [3] Schrader et al. (2008) *GCA* **72**, 6124-6140. [4] Lillard et al. (1998) *J. Electrochem. Soc.* **145**, 2718-2725. [5] Bourot-Denise et al. (2002) *LPSC 33rd* Abstr. #**1611** [6] Göpel et al. (2011) *Mineral. Mag.* **75**, 936. [7] Kleine et al. (2005) *GCA* **69**, 5805-5818. [8] Burkhardt et al. (2008) *GCA* **72**, 6177-6197.

https://doi.org/10.1180/S0026461X00008434 Published online by Cambridge University Press

Interaction of selenite with iron sulphide minerals: a new perspective

ERIC BREYNAERT[1,*], DIRK DOM[1], ANDREAS C. SCHEINOST[2], CHRISTINE E.A. KIRSCHHOCK[1], ANDRÉ MAES[1]

[1] KULeuven, Center for Surface Chemistry and Catalysis, kasteelpark arenberg 23, bus 2461, B-3001 Leuven, Belgium eric.breynaert@biw.kuleuven.be (* presenting author)

[2] HZDR, Inst. of Resource Ecology, Bautzener Landstrasse 400, 01314 Dresden, Germany

The geochemistry of selenium, exhibiting valence states from +VI to –II, is of key importance due to its role as a highly toxic essential micronutrient and as a significant component of high level radioactive waste (HLRW). XAS studies conducted at circum-neutral pH have shown that pyrite (FeS_2), the most relevant redox-active mineral in Boom clay, reduces selenite to a solid-state Se(0) phase. This observation raises several questions. First, why does an Fe-free Se(0) phase form in presence of pyrite, while selenite is reduced to $FeSe_x$ by troilite and mackinawite (FeS)?[1-4]. What is the exact identity of this Se(0) phase, which has been observed by several authors? Why is a dissolved, low oxidation-state selenium species encountered in association with the Se(0) phase; and what is its identity? Correlating selenium redox chemistry with sulphide mineral oxidation pathways allowed to link these observations to the different oxidation behaviour of acid-soluble and acid-insoluble metal sulphides [5].

Acid insoluble metal sulphides such as pyrite, molybdenite or tungstenite exhibit oxidative dissolution only. Upon six consequent one-electron oxidation steps, a thiosulphate anion is liberated (thiosulphate pathway). In contrast, acid soluble metal sulphides (troilite, mackinawite, sphalerite, etc.) exhibit also non-oxidative dissolution thereby liberating sulphide species (H_2S, HS^-,S^{2-}). Under oxidative dissolution in presence of Fe^{III}, they release sulphide cations (e.g. H_2S^+). The latter can spontaneously dimerize into disulphide species, which may further react to polysulphide (polysulphide pathway) and finally elemental sulphur.

The end products of Se(IV) reduction by acid-soluble iron sulphur minerals are fairly well known, but the solid and liquid phase species present during interaction of SeO_3^{2-} with pyrite are poorly characterized. The solid phase reaction product could not yet be assigned as a specific phase, but clearly identified as a Se^0 compound. Trigonal (grey) selenium could be excluded as a canditate.[4]

The presence of an unexpected high concentration of reduced, dissolved species in presence of pyrite, led to a new pyrite-centered reduction mechanism. Based on this mechanism, a hypothesis about the identity of the unknown dissolved species was put forward. In addition, the new mechanism explains all current experimental observations, especially the presence of the currently non-identified dissolved species and the unexpected relation between Se(IV) reduction and pH.[6]

[1] Breynaert, *et al.* (2008) ES&T. **42**(10): 3595-3601.

[2] Scheinost and Charlet, L. (2008) ES&T. **42**(6): 1984-1989.

[3] Scheinost, *et al.* (2008) J. Contam. Hydrol. **102**(3-4): 228-245.

[4] Breynaert, *et al.* (2010) ES&T. **44**(17): 6649-6655.

[5] Rohwerder and Sand (2007) in *Microbial Processing of Metal Sulfides.p* 35-58.

[6] Kang, *et al.* (2011) ES&T. **45**: 2704-2710.

Numerical modelling of nano-scale mineral dissolution and simulation of mycelial growth dynamics to couple observations of mycorrhizal weathering at single-hypha and whole-plant scales

JONATHAN W BRIDGE[1*], STEEVE BONNEVILLE[2], LIANE G. BENNING[3], JONATHAN LEAKE[4], LYLA TAYLOR[4], STEVEN A BANWART[1] AND THE WEATHERING SCIENCE CONSORTIUM TEAM

[1] Kroto Research Institute, The University of Sheffield, Sheffield, UK (* presenting author: j.bridge@sheffield.ac.uk)

[2] Université Libre de Bruxelles, Departement de Science de la Terre et d'Environnement, Brussels, Belgium

[3] School of Earth and Environmental Sciences, The University of Leeds, UK

[4] Department of Animal and Plant Sciences, The University of Sheffield, Sheffield, UK.

Soil mycorrhizal fungi act through biochemical interactions at nanometre scale to dissolve minerals and transport weathering products to plant symbionts through metre-scale mycelial networks. This symbiosis has profound consequences for rates of carbon sequestration from the atmosphere to soil, and rates of nutrient mobilisation from soils, that are apparent on global and geological time scales [1]. Previous research within our consortium has shown convincingly the nanoscale weathering of minerals by hyphae in direct contact with minerals [2], and at the same time the transport and redistribution of mineral- and plant-derived nutrients (carbon, phosphorus) within the rhizosphere and the plant itself [3].

A key factor in this biologically-driven weathering system is the relationship between the energy supplied from the plant to the mycorrhiza, and the rate of weathering of minerals. Critically, what is the nature of the feedback between the plant root and the distal hyphae that controls allocation of photosynthate within the mycelial network in response to nutrient uptake? Here, we present the results of numerical modelling and simulation of hypha-mineral weathering and hyphal network growth which couples a mechanistic model of element release from minerals with fluxes of carbon and mineral nutrients between the plant root and the whole mycelium. Our models indicate that the efficiency of mycorrhizal weathering is sensitive to both geochemical and biological parameters and is time-dependent. We hypothesize that pore-scale variations in weathering efficiency as mycorrhizae progressively spread through soil provide a mechanism to drive hyphal growth behaviour (e.g., exploratory vs. exploitative) and direct photosynthate demand.

References

[1] Taylor (2011) *American Journal of Science* **311(5)**, 369-403

[2] Bonneville (2011) *Geochimica et Cosmochimica Acta* **75**, 6988–7005.

[3] Leake (2008) *Mineralogical Magazine*. **72**, 85–89.

https://doi.org/10.1180/S0026461X00008434 Published online by Cambridge University Press

Unlocking the Zinc Isotope Systematics of Iron Meteorites

L.J. BRIDGESTOCK[1], M. REHKÄMPER[1,2]*, F. LARNER[1], M. GISCARD[1,2], R. ANDREASEN[1,3], B. COLES[1], G. BENEDIX[2], K.J. THEIS[4], M. SCHÖNBÄCHLER[4], C. SMITH[2]

[1] Dept. of Earth Science & Engineering, Imperial College, London, UK; luke.bridgestock07@imperial.ac.uk (* presenting author)
[2] Dept. of Mineralogy, The Natural History Museum, London, UK
[3] Department of Earth and Atmospheric Science, University of Houston, 312 SR1, Houston TX 77204, USA
[4] School of Earth, Atmospheric and Environmental Sciences, University of Manchester, Manchester M13 9PL, UK

High precision Zn concentration and stable isotope composition data were acquired for 21 metal samples of 15 different iron meteorites of groups IAB, IIAB and IIIAB. Troilite nodules were also analyzed, in addition to leachates and leachate residues of troilites separated from the IAB iron Toluca. All results were obtained by MC-ICP-MS using a Zn double spike technique for correction of instrumental mass bias.

The metal samples of each group display a discrete range of Zn concentrations – about 80 to 250 ppb for IIABs, 1 to 3 ppm for IIIABs and 10 to 35 ppm for IABs – at similar and overlapping $\delta^{66/64}$Zn values. These results are in accord with earlier studies [e.g., 1], which inferred that IAB irons are derived from a volatile rich parent body, whilst IIABs and IIIABs are from more volatile depleted precursors. They furthermore support previous stable isotope work, which concluded that volatile element depletion in the solar nebula was not associated with significant isotope fractionation because it did not involve partial Rayleigh evaporation or condensation [e.g.,2].

The Zn isotope compositions of the metal samples are ubiquitously heavy with $\delta^{66/64}$Zn of between about 0‰ and +2.5‰. In comparison, both the silicate Earth, which contains the bulk of the Earth's Zn budget, and most chondritic meteorites are characterised by $\delta^{66/64}$Zn values of about 0.0±0.5‰ [3,4]. Considered together, this suggests that metal–silicate segregation during planetary differentiation is associated with minor but resolvable Zn isotope fractionation, whereby isotopically heavy Zn is enriched in the metal phase.

Furthermore, distinct negative trends of decreasing $\delta^{66/64}$Zn with increasing Zn content were observed for each meteorite group. Such systematic variations were also seen for four sub-samples of the IIAB iron meteorite Sikhote – Alin. Hence it is likely that the trends are caused by small-scale heterogeneities in the distribution of Zn within the meteorites. Furthermore, our analyses and previous work [e.g., 5] suggest that the correlations reflect the variable occurance of isotopically light and Zn-rich phases, most likely chromite and/or daubreelite associated with troilite inclusions, within a metal matrix characterised by low Zn contents and high $\delta^{66/64}$Zn values.

[1] Palme, H., Larimer, J.W., Lipschutz, M.E. (1988) in: *Meteorites and the early Solar System*, 436-461. [2] Wombacher, F., Rehkämper, M., Mezger, K., Bischoff, A., Münker, C. (2008) *Geochim. Cosmochim. Acta* **72**, 646-667. [3] Luck, J.-M., Ben Othman, D., Albarède, F. (2005) *Geochim. Cosmochim. Acta* **69**, 5351-5363. [4] Moynier, F., Blichert-Toft, J., Telouk, P., Luck, J.-M., Albarède, F., (2007) *Geochim. Cosmochim. Acta* **71**, 4365-4379. [5] Keil, K., (1968) *Amer. Mineral.* **53**, 491-495.

Constraints on seawater sulfate concentrations through examination of temporal trends in δ^{13}C of methane seep carbonates

THOMAS F. BRISTOW[1*], JOHN P. GROTZINGER[2],

[1]NASA Ames Research Center, Moffett Field, USA, (thomas.f.bristow@nasa.gov)
[2]California Institute of Technology, Pasadena, USA, grotz@gps.caltech.edu

Since the relatively recent discovery of ecosystems based on energy derived from anaeorobic methane oxidation (AMO) more than 50 ancient examples have been recognized in the geological record [1]. Ancient methane seeps are recognized by endemic seep fauna and/or lithological, textural evidence of the passage and metabolism of methane bearing fluids. Highly ^{13}C-depleted carbonates (<-30‰ PDB) that precipitate from carbonate alkalinity generated by AMO provide an additional diagnostic indicator of ancient seeps; no other biogeochemical process is known to produce carbonates with such isotopic signatures at Earth-surface conditions.

Examination of the temporal occurance of seep deposits reveals that the majority of examples are reported from the Phanerzoic. Furthermore, δ^{13}C depletion to <-30‰ PDB in seep carbonates is not observed until the Early Carboniferous [2]. Because the main oxidant utlized in AMO at modern methane seeps is sulfate, it has been hypothesized that the temporal and isotopic trends of seep carbonates may reflect the influence of changing oceanic sulfate concentrations on AMO rates [3]. This hypothesis was investigated using 1D reaction-transport model that simulates the δ^{13}C of porewaters and precipitation of carbonates in a porous sedimentary profile where AMO is the main biogeochemical process.

AMO rates and controls on rates at modern methane seeps are well documented [4]. The model was tuned using porewater data collected from cores taken at Hydrate Ridge – a site with one of the highest integrated AMO rates observed in recent seeps. With these parameters we are able to estimate minimum threshold ocean [SO_4^{2-}] required to produce the levels of δ^{13}C depletion in seep carbonates observed in the geological record. Preliminary results show that low ocean [SO_4^{2-}], thought to characteristize much the Proterozoic and Archean, provides a plausible explanation for the absence of geochemical evidence for seeps in this period. Although the Paleozoic record of seeps is sparse, model calculations support S-isotope and fluid inclusion data indicating mM [SO_4^{2-}] in the early Paleozoic oceans, with a rise to >10 mM levels in the Late Devonian/Early Carboniferous, corresponding with the rise of land plants [5,6]. Implications for Ediacaran ocean [SO_4^{2-}] will also be discussed. Our investigation shows that secular variations in ocean [SO_4^{2-}] provide a plausible explanation for the temporal distribution and δ^{13}C of seep carbonates and highlight the need to refine criteria for recognizing ancient methane seep ecosystems.

[1] Campbell (2006) *Palaeogeo. Palaeoclim. Palaeoecol.* **232,** 362-407. [2] Peckmann (2001) *Geology* **29**, 271-274. [3] Bristow (2011) *Nature* **474,** 68-71. [4] Regnier (2011) *Earth Science Reviews* **106,** 105-130. [5] Gill (2007) *Palaeogeo. Palaeoclim. Palaeoecol.* **256,** 156-173. [6] Gill (2011) *Nature* **469,** 80-83.

https://doi.org/10.1180/S0026461X00008434 Published online by Cambridge University Press

The unusual nature of the Proterozoic biomarker record and the Mat-Seal hypothesis

JOCHEN J. BROCKS[1*], MARIA M. PAWLOWSKA[2], AND NICHOLAS J. BUTTERFIELD[2]

[1] The Australian National University, Research School of Earth Sciences, jochen.brocks@anu.edu.au

[2] University of Cambridge, Earth Sciences, mmp30@cam.ac.uk and njb1005@cam.ac.uk

Petroleum and bitumens are concentrates of hydrocarbon fossils of biological lipids (biomarkers). These biomarkers often contain significant biological and environmental information and can remain stable over hundreds of millions of years. However, bitumens of pre-Ediacaran age (>635 Ma) are scarce in the geological record and frequently adulterated by younger contaminants [1].

In this study, we re-analysed most known pre-Ediacaran bituminous deposits and determined 10 basins that contain clearly indigenous biomarkers dating back to 1,640 Ma [2, 3]. After exclusion of allochthonous hydrocarbons, the molecular fossils detected in these Precambrian sequences are distinct from their Phanerozoic counterparts. The pre-Ediacaran bitumens show significantly higher concentrations of 'unresolved complex mixture' (UCM), low concentrations or absence of eukaryotic steranes, the presence of putative bacterial aromatic steroids, high relative concentrations of mono- and dimethyl alkanes, and a conspicuous carbon isotopic enrichment of straight-chain lipids relative to acyclic isoprenoids and total organic carbon. Here we propose that these unusual characteristics primarily derive from non-actualistic taphonomic processes based on the pervasive presence of microbial mats in the Precambrian. This 'mat-seal effect' was broken with the onset of bioturbation in the Ediacaran when the primary source of fossil biomarkers switched from the benthos to the plankton.

The disturbance of soft sediments and associated microbial mat cover by infaunal burrowing was one of the most important geobiological innovations in the Neoproterozoic-Phanerozoic transition. This "Cambrian substrate revolution" [3] had profound effects on contemporaneous ecology [4], sedimentology [5] and sulphur geochemistry [6]. We argue that it also fundamentally altered the way in which organic matter was incorporated and preserved in the sedimentary record, giving rise to typical Ediacaran and Phanerozoic petroleum reserves, and potentially contributing to increasing atmospheric oxygen levels.

[1] Brocks (2011) *GCA* **75**, 3196-3213. Brocks *et al.* (2008) *GCA* **72**, 871-888. [2] Brocks *et al.* (2005) *Nature* **437**, 866-870. Summons *et al.* (1988) *GCA* **52**, 1747-1763. [3] Indigenous hydrocarbons occur as far back as ~2,500 Ma (Brocks *et al.* (2003) *Org. Geochem.* **34**, 1161-1175). However, these bitumens exclusively consist of PAH and diamondoids with little biological information. [3] Bottjer *et al.* (2000) *GSA Today* **10**, 1-7. [4] Seilacher (1999) *PALAIOS* **14**, 86-93. [5] Droser *et al.* (2002) *PALAIOS* **17**, 3. [6] Canfield and Farquhar (2009) *PNAS* **106**, 8123-8127.

What cooled the Earth during the last 20 million years?

WALLACE S. BROECKER[1*]

[1]Lamont-Doherty Earth Observatory of Columbia University, Palisades, New York, USA, broecker@ldeo.columbia.edu (*presenting author)

Abstract

During the last 20 million years earth temperature decreased but the CO_2 content of the atmosphere appears to have remained constant. Further, large changes in the Mg to Ca ratio and in the isotopic content of lithium in sea water also took place during this time interval. Explaining the lack of a CO_2 change constitutes a dilemma.

https://doi.org/10.1180/S0026461X00008434 Published online by Cambridge University Press

Capabilities of LA-ETV-MC-ICPMS for the measurement of Sr isotope ratios in Rb-rich samples

R. BROGIOLI, L. DORTA, B. HATTENDORF* AND D. GÜNTHER

[1]Laboratory of Inorganic Chemistry, ETH Zurich, Wolfgang-Pauli Strasse 10, 8093, Zürich, Switzerland

The successful use of LA-MC-ICPMS for the determination of Sr isotope ratio in the field of geochronology has been demonstrated for samples with relatively low Rb concentration [1, 2]. Its applicability for samples with higher Rb content is however still a challenge, mainly because mathematical correction of the isobaric interference of ^{87}Rb on ^{87}Sr affects the accuracy of the method [3, 4].

In an earlier study we investigated the effect of heating laser generated aerosols within an Electrothemal Vaporizer (HGA600 MS, Perkin Elmer, CAN) prior to the introduction into the ICPMS. Passing the laser generated aerosol through a commercial electrothermal vaporizer heated to 2000°C before the ICP allowed to attenuate the Rb interference by almost two orders of magnitude [6] for a silicate glass reference standard (NIST SRM610, Rb/Sr ~1). This same approach was now used for the measurement of Sr isotope ratios by LA-MC-ICPMS. To benchmark the Rb removal efficiency and the accuracy of Sr isotope ratio, a wide range of reference standard material were tested: NIST SRM610 (Silicate glass, Rb/Sr = 1), MPI-DING ATHO-G (rhyolite glass, Rb/Sr = 0.54), MPI-DING T1G (diorite glass, Rb/Sr = 0.28), USGS BCR-2G (basalt glass, Rb/Sr = 0.14) and $Li_2B_4O_7$ fused disks of NIST 607 (potassium feldspar, Rb/Sr = 8) . Depending on crater size adopted for the analysis and the ETV heating temperature, Rb signal was decreased by factor ~5 (for NIST SRM 607) to 100 (for NIST 610 and BCR-2G) resulting in an improved accuracy for the measured ^{87}Sr/^{86}Sr ratio.

Rb is not the only element interfering with Sr isotope analysis, doubly charged rare earth elements, metal oxides or calcium polyatomic ions are known to affect results accuracy [3]. For this reason $Li_2B_4O_7$ fused disks of NIST SRM987 (Sr carbonate) were spiked with Er, Yb, Hf, Ca, Fe, Ga, Zn to investigate the formation of potential interferences and the applicability of mathematical corrections. This study will show that he use of electrothermal vaporization coupled to LA sampling has the potential to widen the range of samples suitable for accurate *in-situ* determination of Sr isotope ratio.

[1] Yang Z.P. (2011) *J. Anal. Atom. Spectrom.* **26**, 241-351. [2] Fietzke J. (2009) *J. Anal. Atom. Spectrom.* **23**, 955-961. [3] Ramos F.C. (2004) *Chem. Geol.***211**, 135-158. [4] Jackson M.G. (2006) *Earth Planet. SC Lett.*, **245**, 260-277 [5] Rowlan A. (2008) *J. Anal. Atom . Spectrom* **23**, 167-172. [6] Brogioli R. (2011) *Anal. Bioanal. Chem.* **399**, 2201-2209

Biogeochemistry of mercury in contaminated sediments of East Fork Poplar Creek

SCOTT C. BROOKS[1*], DAVID KOCMAN[2], CARRIE MILLER[1], XIANGPING YIN[1], AMI RISCASSI[1]

[1]Oak Ridge National Laboratory, Oak Ridge, TN, USA, brookssc@ornl.gov (* presenting author)

[2] Jožef Stefan Institute, Ljubljana, Slovenia, david.kocman@ijs.si

Mercury use at the Oak Ridge Y-12 National Security Complex (Y-12 NSC) between 1950 - 1963 resulted in contamination of the East Fork Poplar Creek (EFPC) ecosystem. Hg continues to be released from point sources and diffuse contaminated soil and groundwater sources within the Y-12 NSC and outside the facility boundary. In general, methylmercury (MeHg) concentrations in water and in fish have not declined in response to improvements in water quality and exhibit trends of increasing concentration in some cases.

Therefore, our study focuses on identifying ecosystem compartments and/or characteristics that favor the production, as well as degradation, of MeHg in EFPC. Detailed geochemical characterization of the surface water, interstitial pore water, and creek sediments were performed during quarterly sampling campaigns in 2010 and 2011 at two locations. One site is 3.7 km (NOAA) and the other 20 km (NH) downstream of the headwaters and source of the point discharges. Vertical profiles of interstitial pore water collected from fine-grained deposits at the creek margin showed decreases in nitrate, sulfate, and oxidation-reduction potential (ORP) with depth as well as increases in dissolved manganese, iron, and small increases in sulfide. The results indicate the progression of terminal electron accepting processes with depth in the upper 30 cm of these fine grained sediments. Dissolved (passing 0.2 μm pore) MeHg concentration was positively correlated with depth suggesting these areas served as a source of MeHg. MeHg in the surface water is associated with phases small enough to pass a 3 kiloDalton filter. In contrast, interstitial water collected from the cobbly center channel of the creek did not exhibit these redox gradients. The observed constant or decreasing MeHg concentrations with depth suggest that the interstitial water in the fast flowing sections of the creek is rapidly exchanging with the surface water and these sections do not serve as MeHg sources. Total Hg concentration in sediment cores from the creek margin was variable, 0.057-24 mg/kg and 0.02-155 mg/kg, at NH and NOAA respectively. MeHg measured on a subset of these sectioned cores ranged from 0.71-17.5 μg/kg at NH and 1.08-46.7 μg/kg at NOAA. Large intra- and inter-site variability of Hg distribution in these samples is partly attributed to the very heterogeneous sediment texture that ranged from coarse- to fine-grained. Methylation potential, measured using enriched stable isotopes of Hg on intact sediment cores, was significantly correlated with ambient MeHg concentration at both sites.

https://doi.org/10.1180/S0026461X00008434 Published online by Cambridge University Press

Enhanced radionuclide capture by bioreduced biotite and chlorite

DIANA R. BROOKSHAW[1]*, KATHERINE MORRIS[1], JONATHAN R. LLOYD[1], RICHARD A.D. PATTRICK[1] GARETH T. LAW[1/2], AND DAVID J. VAUGHAN[1]

[1]Williamson Research Centre and Research Centre for Radwaste and Decommissioning, SEAES, The University of Manchester, Manchester, M13 9PL. diana.brookshaw@postgrad.manchester.ac.uk (*presenting author)

[2]Centre for Radiochemistry Research The University of Manchester, Manchester, M13 9PL. gareth.law@manchester.ac.uk

Background and methodology

Management and geological disposal of our nuclear waste legacy requires an in-depth understanding of biogeochemical processes that occur in the subsurface and their influence on radionuclide speciation and mobility. Here, we explore molecular-scale processes involved in radionuclide immobilisation at the solution-mineral interface and the indirect, but potentially crucial role which microorganisms play in such reactions. The research focuses on two common rock-forming minerals, biotite and chlorite that contain both ferric (Fe(III)) and ferrous (Fe(II)) iron within their octahedral layers. The experimental systems were focussed around "unaltered" or as-sampled biotite and chlorite, and "bioreduced" biotite and chlorite. For the bioreduced minerals, biotite and chlorite were exposed to the model Fe(III)-reducing subsurface microorganism *Geobacter sulfurreducens* in the presence of an electron shuttle (AQDS) to promote reduction of bioavailable Fe(III) within the mineral moeity to Fe(II). After this, unaltered or bioreduced biotite and chlorite were suspended in solutions containing undersaturated Tc(VII), U(VI) or Np(V). The solubility of the redox active radionuclides was then monitored and the variations in the solid phase speciation of the radionuclides was characterised by X-ray absorption spectroscopy (XAS).

Results and implications

G. sulfurreducens was able to reduce Fe(III) associated with biotite and chlorite thus priming the minerals with Fe(II) for "indirect" reductive transformations. However, the interactions of the different radionuclides with the mineral systems differed. There was evidence for reductive transformation of Tc(VII) to Tc(IV) in the bioreduced biotite and chlorite, presumably mediated by labile Fe(II) associated with the bioreduced minerals [1,2]. By contrast, there was poor reactivity towards Tc(VII) in the unaltered samples. Ongoing work with the actinides shows some selectivity for the different mineral surfaces with both sorption and potentially reductive precipitation pathways possible.

Overall, these results show that relatively small increases in Fe(II) content (up to 0.12 mmoles per gram) in the bioreduced minerals can have a profound effect on mineral reactivity and radionuclide behaviour compared to bacterial-free systems. This suggests that indirect reduction of microbially reduced minerals may be an important pathway to immobilisation in rock environments typical of geological disposal sites for radioactive wastes.

[1] Lloyd et al (2000) *Appl. Environ. Microbiol* **66,** 3740-3749, [2] Morris et al (2008) *App. Geochem.* **23**, 603-617.

Effects of pore fluid chemistry on diagenesis.

J. BROUWER*, A. PUTNIS

Institut für Mineralogie, Westf. Wilhelms Univ. Münster, Germany, brouwer.janneke@gmail.com

Sediment compaction by dissolution – precipitation creep

Sediment compaction occurs largely through dissolution-precipitation creep, also called pressure solution, a process that is driven by gradients in stress. Grains dissolve at grain contacts that support the load of overlying sediments, and solutes precipitate at pore walls, leading to a decrease in permeability. Pore fluid chemistry can be expected to significantly affect sediment compaction behavior and therefore how permeability changes with time. However, not much research has been done to study such chemical effects. Recently, [1] studied the effect of additives on calcite compaction. We investigate the influence of trace elements in solution that affect dissolution and precipitation rates, and the effect of mineral replacement on compaction behavior.

Experiments

We present results of uniaxial compaction experiments on cylindrical (10 mm. length, ø 2.3 mm.) aggregates of various alkali halides. A stress of 1.2 MPa is applied and compaction monitored using a simple set-up after [2]. We show that certain trace metals in solution may affect compaction rates of NaCl, but not of KCl. We investigate the effect of mineral replacement during compaction in the solid-solution system $K(Br_xCl_{1-x})$. A reservoir containing a saturated solution of KCl or KBr is placed on top of the cylindrical aggregate of KBr resp. KCl. The results show that reaction leads to enhancement and localization of compaction, leading to fast reduction in permeability. The change in permeability with time, and therefore fluid infiltration and reaction progress, is not only influenced by the compaction rate, but also by solid volume changes related to the reaction.

Conclusion

Mineral and pore fluid chemistry is an important factor in sediment compaction behavior. Chemical disequilibrium leading to mineral reaction during compaction leads to enhancement and localization of compaction.

[1] Zhang et al. (2011) *Geofluids* **11**, 108-122. [2] De Meer and Spiers (1997) *J. Geophys. Res.* **102**, B1 875-891.

https://doi.org/10.1180/S0026461X00008434 Published online by Cambridge University Press

Impact of radiation on the microbial reduction of iron oxides

ASHLEY R. BROWN[1*], PAUL WINCOTT[1], DAVID J. VAUGHAN[1], SIMON M. PIMBLOTT[2], ROYSTON GOODACRE[3] AND JONATHAN R. LLOYD[1]

[1]Williamson Research Centre for Molecular Environmental Science, School of Earth, Atmospheric and Environmental Sciences, University of Manchester, Manchester, UK, ashley.r.brown@postgrad.manchester.ac.uk (* presenting author)

[2]Dalton Nuclear Institute and School of Chemistry, University of Manchester, Manchester, UK

[3]Manchester Interdiscplinary Biocentre and School of Chemistry, University of Manchester, Manchester, UK

The microbial reduction of Fe(III) in geodisposed nuclear waste or radwaste contaminated land can play a significant role in controlling the mobility of a range of long-lived radionuclides, including U(VI), Np(V) and Tc(VII). As such environments are likely to receive large radiation doses, radiation induced changes to the iron mineralogy may impact upon microbial respiration and subsequently alter the stability of the radionuclide inventory. Hence, characterization of radiation damage to Fe(III) mineralogy and the resultant impact upon microbial respiratory processes is essential in the preparation of a geological waste disposal safety case. In this study aerobic irradiation (1 MGy gamma) of hematite and ferrihydrite led to an increase in the rate of Fe(III) reduction by the Fe(III)-reducing bacterium *Shewanella oneidensis* MR-1 in the presence of an electron shuttle, riboflavin. Sequential extractions of iron in microbial cultures containing irradiated ferrihydrite suggested a 10% increase in ferrous iron partitioned into an operationally defined iron carbonate phase. A 15% increase in microbially reduced iron in irradiated hematite systems was incorporated into a combination of a putative carbonate phase, an easily reducible fraction and also increased dissolved Fe(II). Mossbauer spectroscopy of irradiated ferrihydrite suggests conversion to a more crystalline phase similar to akaganeite, whilst anoxically irradiated hematite appears to show a decrease in Fe coordination. This study suggests that structural changes in the mineralogy by irradiation lead to an increase in bioavailabilty of ferric iron. This may have positive implications to the geological disposal of nuclear waste, as reducing conditions may be accelerated by radiation-induced microbial iron reduction, potentially mediating the enhanced stability of key radionuclides.

Geochemical insights from accessory phases in a sanukitoid-like suite: Towards understanding temporal changes in subduction style

E. BRUAND[1*], C. STOREY[1], M. FOWLER[1]

[1]School of Earth and Environmental Sciences, Portsmouth, United Kingdom, emilie.bruand@port.ac.uk (* presenting author)

Crustal evolution is governed by plate tectonics and it has been shown that between the Archean and the Phanerozoic major changes in subduction style occured. Among others, the chemistry of different plutonic rocks through time and the understanding of their petrogeneses have helped to define different stages in the evolution of plate tectonics on Earth. Although TTG, the direct product of melted oceanic lithosphere, were the main plutonic rocks generated during the Archean, an important change around 2.7 Ga led to the genesis of rocks that are the result of melting of a metasomatized mantle wedge: the sanukitoids. This observation is often interpreted as the result of a change from shallow to steep subduction. Modern plate tectonics generally generates calc-alkaline suites but exceptions can occur such as the Caledonian (Paleozoic) high Ba-Sr plutons in Northern Scotland. The latter have been interpreted as a "modern" analogue of sanukitoids [1].

In this contribution, we present a study of accessory minerals from this Caledonian sanukitoid-like suite (ultrabasic to acidic). Whole-rock chemistry (trace elements, radiogenic and stable isotopes) is well constrained [1] but the study of accessory phases reveals additional petrogenetic constraints [2]. Indeed, accessory phases are important beyond their modal proportion because they commonly contain elements that are not incorporated easily into major rock forming minerals. The incorporation of trace elements and more particularly rare earth element (REE) in their structures make them ideal to delineate petrogenetic processes. In particular, the study of apatite, titanite and zircon will test the ability of accessory phases to retain the signature of their tectonic affinity. We present a detailed petrographic study and the systematic analysis of trace elements and O isotopes of these phases in a range of fractionated plutonic rocks from appinitic (ultrabasic) to granitoid composition. These results have an important impact in the understanding of accessory phases saturation during the magma genesis and thus offer another way to study the petrogenesis of these sanukitoid-like rocks. This approach will be extended to other magma compositions to further our insight into petrogenetic processes and tectonic affinity that may be available from accessory phase studies.

[1] Fowler et al. (2008) *Lithos* **105**, 129-148. [2] Hoskin et al. (2000) *Journal of Petrology* **41**, 1365-1396.

https://doi.org/10.1180/S0026461X00008434 Published online by Cambridge University Press

Mineralogical and geochemical evidence for syngenetic precious metal enrichment in a deformed volcanogenic massive sulfide (VMS) system

STEFANIE M. BRUCKNER[1*], STEPHEN J. PIERCEY[1], PAUL J. SYLVESTER[1], STEPHANIE MALONEY[2], LARRY PILGRIM[2]

[1]Memorial University, Dept. of Earth Sciences s.brueckner@mun.ca (* presenting author)
[2]Rambler Metals & Mining Canada Ltd., Baie Verte, NL, Canada

Introduction

The early Ordovician Ming Mine (487 Ma; total resource 12.5 Mt ore @ 1.52 wt% Cu, 1.69 ppm Au, 8.11 ppm Ag, and 0.45 wt% Zn), NW Newfoundland, Canada, is a type example of a precious metal-enriched VMS deposit. Moderate deformation and metamorphism makes deciphering the origin of Au-Ag-enrichment (e.g., syngenetic vs. epigenetic) difficult. However, mineralogic and geochemical evidence support a syngenetic origin with Au-Ag coming via a magmtic contribution to the primary VMS hydrothermal fluid [1, 2, 3]. Mineralogical observations show a complex sulfide mineral assemblage in stringer and massive sulfide mineralization. Besides base metal sulfides (e.g., pyrite, chalcopyrite, sphalerite, galena, pyrrhotite), sulfosalts rich in magmatic suite elements (e.g., arsenopyrite, tetrahedrite-tennantite, stannite, boulangerite, loellingite), Te-bearing phases (e.g., BiTe, coloradoite), Ag-phases (e.g., miargyrite, unnamed AgCuFeS phase, argentotetrahedrite, AgHg alloy), and electrum occur throughout the deposit, but are slightly more enriched in the upper part of the deposit. Main, minor and trace element analysis by electron microprobe (EPMA) show the emrichment of magmatic suite elements (e.g., As, Bi, Hg, Sb, Sn, Te) as major, minor and trace constituent in base metal and other sulfides phases.

Results and Conclusions

Electrum and Ag-phases occur as: (1) free phases in gangue or on pyrite/chalcopyrite margins; (2) as inclusions in pyrite, arsenopyrite, pyrrhotite, and galena; (3) along veinlets in and on grain boundaries of pyrite and arsenopyrite; (4) in odd myrmekitic-like textures; and (5) in close proximity to each other and tetrahedrite-tennantite. EPMA data on 17 elements in sulfide and precious metal phases reveal: (1) no invisible gold in any phase; (2) a high Hg-content (12 – 17 wt%) in electrum; and (3) sphalerite with a varying Fe-content (2 – 9 wt%). The mineralogical and geochemical features of the ores favor a syngenetic, magmatic origin for precious metal enrichment. However, later deformation remobilized some metals, especially Au and Ag, as evidenced by textural relationships and the absence of invisible gold.

[1] Sillitoe et al. (1996) *Economic Geology* **91**, 204-212. [2] Hannington et al. (1999) *Reviews in Economic Geology* **8**, 325-351. [3] Huston (2000) *Reviews in Economic Geology* **13**, 401-426.

From aqueous to solid solutions: A process understanding of trace metal incorporation into solid structures

JORDI BRUNO[1,2*]

[1]Amphos 21 Group Barcelona, Catalunya, jordi.bruno@amphos21.com (* presenting author)
[2]UPC BarcelonaTech, Barcelona, Catalunya, jordi.bruno@upc.edu

Introduction

Aqueous-solid solution systems are ubiquitous in natural and anthropogenic systems and they influence the fate and mobility of heavy metals and radionuclides.

The process understanding of the structural incorporation of trace components into existing or forming solid phases is essential to the assessment of the potential environmental consequences.

Objective of the presentation

In my presentation I will introduce some of the key concepts involved in the suite of processes that are involved in the transition of a trace component from the aqueous to the solid solution both from the kinetic and thermodynamic points of view.

I will devote particular attention to recent solution chemical and spectroscopic data that has been recently acquired in the frame of the EC Funmig project[1] and I will frame it to the conceptual developments presented in [2]

I will also propose some ways forward to integrate the experimental information on the structural incorporation of trace elements into the current models used in current environmental assessments.

[1] Bruno, J. and Montoya, V. (2012 *Applied Geochemistry*, **27, 444–452**
[2] Bruno, J., Bosbach, D., Kulik, D. Navrotsky, A., (2007) *Chemical Thermodynamics of Solid Solutions of Interest in Nuclear Waste Management* **Chemical Thermodynamics Volume 10. OCDE-NEA**.

https://doi.org/10.1180/S0026461X00008434 Published online by Cambridge University Press

On the use of hydrochemical mixing models to conceptualize hydrogeology in fractured rocks

JORGE MOLINERO[1], JORDI BRUNO[1] (*)PAOLO TRINCHERO[1], AND LUIS MANUEL DE VRIES[1]

[1]Amphos 21 Consulting SL, Barcelona, Spain, jordi.bruno@amphos21.com (* presenting author)

Abstract

Mixing models are broadly used in hydrogeology as a tool to understand groundwater systems. Simple mixing models are based on inferring the relative abundance of assumed end-member waters from measured concentrations of conservative species in the mixture. However, simple mixing methodologies present clear limitations for complex systems with the influence of several initial and boundary waters. For these cases, more sophisticated mixing models have to be used by using statistical multivariate techniques such as Principal Component Analysis.

On the other hand it is also known that mixing modeling presents practical limitations, basically derived from the uncertainties in the definition of the end-members, as well as mixing artifacts associated to groundwater sampling procedures by drilling and pumping, that use to magnify the apparent mixing in the system.

In addition to the abovementioned practical limitations, we claim in this work that mixing models are also subjected to conceptual limitations that can lead to serious misuses, especially when applied to fractured rocks. This is due to the fact that matrix diffusion phenomena introduce a "memory" effect in the system previously affected by the influence of different waters. This fact could make mixing modelers to misunderstand the real groundwater behavior.

We present a series of synthetic numerical simulations to illustrate that hydrogeological models based on computed mixing models, of known end-member waters, are unable to properly conceptualize the real hydrogeological behavior of a fractured rock aquifer.

Mechanisms governing nanoparticle transport in porous media

STEVEN BRYANT*[,1], HAIYANG YU[2], MICHAEL MURPHY[2], TIANTIAN ZHANG[2], ANDREW WORTHEN[3], KI YOUL YOON[3], KEITH JOHNSTON[3], CHUN HUH[2]

[1]Dept. of Petroleum and Geosystems Engineering, The University of Texas at Austin, Austin, USA, steven_bryant@mail.utexas.edu (* presenting author)

[2] Dept. of Petroleum and Geosystems Engineering, The University of Texas at Austin, Austin, USA

[3] Dept. of Chemical Engineering, The University of Texas at Austin, Austin, USA

Abstract

The prospect of using engineered nanoparticles for subsurface applications raises practical questions. How far can nanoparticles be transported through porous media? If multiple fluid phases are present, does this affect the transport distance? Do the nanoparticles travel at their injected concentration and at the velocity of the carrier phase? The science needed to answer these questions raises its own set of interesting problems. Can nanoparticle transport be treated like solute transport, or must the nanoparticles be treated like colloids? If the latter, what forces govern the interaction between nanoparticle and the solid surface of the porous medium? If nanoparticles attach or adhere to the solid, can they detach? Is the nanoparticles/solid interaction reversible? In this talk we review a large set of transport experiments conducted in our laboratory. The data provide some insight into key mechanisms of nanoparticle transport and retention. For example, we typically observe small amounts (much less than a monolayer) of irreversible adsorption, and even smaller amounts of reversible adsorption. Experiments with variable flow velocities indicate that nanoparticle adsorption capacity is a dynamic, hysteretic property. For suitably engineered particle coatings, particle adhesion at fluid/fluid interfaces is the same magnitude as adhesion on the solid surface. We discuss a framework for modeling these phenomena.

https://doi.org/10.1180/S0026461X00008434 Published online by Cambridge University Press

Progress of weathering reactions in ultramafic rocks

KURT BUCHER

[1]Institute of Geosciences. University of Freiburg. Albertstr. 23b. D-79102 Freiburg. Germany. bucher@uni-freiburg.de

Section 7a: The Art of weathering

Chemical weathering results from a complex interaction between geochemistry, hydrology, biology, and physical erosion and is therefore site specifie [1].

Chemical weathering of dark green massive ultramafic rocks produces a distinct and remarkable yellow weathering rind when exposed to the atmosphere long enough. Crust formation on rocks from three European climates have been studied: a) Ronda Peridotite, Spain, b) Seiland Complex, Norway, c) Zermatt Ophiolite, Switzerland). Rinds from the three areas vary mineralogically and have very different thicknesses. The rind thickness depends on the mineralogy of the bedrock, atmospheric parameters and on the details of transport and kinetics of the chemical reactions.

Fig. Weathering rinds on dunite (Reinfjorden, N Norway)

The fundamental reaction "peridotite (serpentinite) + rainwater = weathering rind + runoff water" describes the crust forming process. This hydration reaction depends on the water supply from the rock surface to the reaction front. The transport mechanism is grain boundary diffusion. At the reaction front, kinetics controls the progress of the weathering reactions. The competing kinetics-diffusion control determines the rate of rind growth. The alteration zone must be wetted after a dry period and the reaction resumed at the front. The wetting-drying cycles may contribute significantly to the hydraulic properties of the weathering rind. Reaction details of the rind forming process are saved in the subtle structures of the crusts.

The propagation of the reaction front and the internal structure of the rinds have strong similarities to hydrothermal reaction veins [2]. It is evident that rind thickness development is not related to pervasive advective fluid flow.

[1] White A. F. 2008, Quantitative Approaches to Characterizing Natural Chemical Weathering Rates. In *Kinetics of Water-Rock Interaction* (ed. S. L. Brantley, J. D. Kubicki, and A. F. White), pp. 151-210. Springer.
[2] Bucher K. 1998, Growth mechanisms of metasomatic reaction veins in dolomite marbles from the Bergell Alps. Mineralogy and Petrology, 63, 151-171.

Biomineralization of selenium: proteins as the reason for altered colloidal stability of nanoparticle suspensions

BENJAMIN BUCHS[1], MICHAEL W.H. EVANGELOU[2], PHILIPPE F.X CORVINI[1,3], MARKUS LENZ[1,4*]

[1] University of Applied Sciences and Arts Northwestern Switzerland (FHNW), Institute for Ecopreneurship
[2] ETH Zürich , Institute of Terrestrial Ecosystems
[3] School of the Environment, Nanjing University, 22# Hankou Rd., Nanjing, 210093, P.R.China com
[4] Wageningen University, Sub-Department of Environmental Technology, markus.lenz@fhnw.ch (* presenting author)

Although biomineralization of selenium has been investigated in the frame of bioremediation for decades, the molecular principles behind it remain largely unknown. Despite of its microbial origin, biogenic elemental selenium typically consists of nanosized spherical particles (Figure 1), stabilized against gravitational settling. These particular properties were suspected to be mediated by organic molecules associated to the selenium particles. In this study, organic molecules associated with high-affinity to selenium bionanominerals were isolated from such molecules with low-affinity by density-based centrifugation. The proteic fraction was characterized via capillary liquid chromatography-electrospray ionization-tandem mass spectrometry (LC-ESI-MS/MS). A plenitude of proteins was found to strongly associate to biomineralized selenium formed by physiologically different microorganisms [1]. Interestingly, one protein - a metalloid reductase - did associate strongly to both biogenic nanoselenium and synthetically produced selenium surfaces, indicating some specific recognition properties. By means of electrophoretic measurements (zeta –potential) and settling experiments it was demonstrated that, indeed, the proteic fraction considerably alters the colloidal stability of selenium bionanominerals. Furthermore, it could be demonstrated that the aqueous transport will be considerably influenced by the environmental media composition (i.e. acidic vs. neutral waters; sea vs. surface waters; waters differing in dissolved organic matter content, etc.).

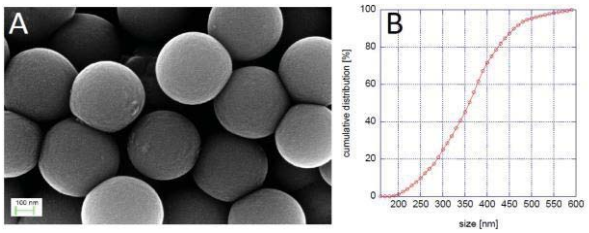

Figure 1: SEM images of purified biomineralized selenium produced by *Bacillus selenatarsenatis* (A) and corresponding cummulative particle size distribution (B)

[1] Lenz, M. et al. (2011). *Applied and Environmental Microbiology*, **77 (13)**, 4676-4680.

https://doi.org/10.1180/S0026461X00008434 Published online by Cambridge University Press

Buoyant asthenosphere affects mid-ocean ridge depths and melt patterns

W. ROGER BUCK[1*], CHRISTOPHER SMALL[2], AND WILLIAN B. F. RYAN[3]

[1]Lamont-Doherty Earth Observatory, buck@ldeo.columbia.edu (*presenting author)
[2]Lamont-Doherty Earth Observatory, small@ldeo.columbia.edu
[3]Lamont-Doherty Earth Observatory, ryan@ldeo.columbia.edu

The East Pacific Rise (EPR) is the fastest spreading ridge yet it is deeper that most other spreading centers. Along the 5000 km of the EPR the depth averages 400 m greater than the adjacent Pacific-Antarctic Ridge [1]. The other very deep section of ridge is the Australian-Antarctic Discordance (AAD). Analytic and numerical models show that dynamic thinning of asthenosphere with a lower density than the underlying mantle can explain the magnitude and wavelength of the depth anomalies along the EPR and the AAD [2]. At the EPR, fast plate divergence thins the asthenosphere by both sequestering it into diverging lithosphere and dragging it with the plates in contrast to the slower spreading, but faster migrating PAR [1]. The AAD asthenosphere is greatly thinned because of the restriction of asthenospheric flow due to nearby thick continental lithospheric roots combined with a moderately fast spreading rate [2]. The ADD is a major isotopic boundary. This can be explained if there is efficient mixing within the low-viscosity asthenosphere of the Indian and Pacific Ocean basins. Low-viscosity, low-density asthenosphere that is thinned beneath a spreading center should accentuate the asymmetry in melting related to migration of a spreading center as illustrated in Figure 1. This may help explain the observed pattern of oceanic crustal thickness variations as a function of ridge offsets and spreading directions [3].

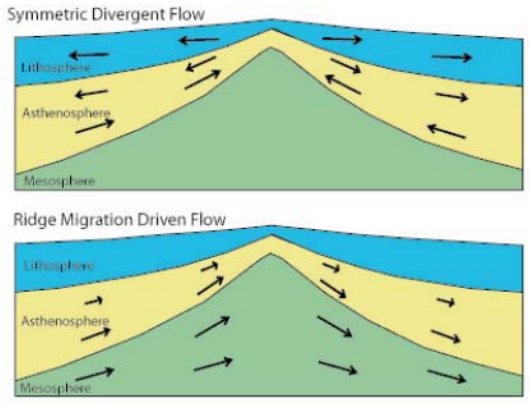

Figure 1: Flow under a migrating ridge should combine the effect of divergent and migration driven flow, but the asymmetry of upwelling and melting is accentuated due to relief on the base of the buoyant asthenosphere.

[1] Small, and Danyushevsky (2003) *Geology* **31**, 399-402. [2] Buck, Small and Ryan (2009) *Geochemistry, Geophysics, Geosystems* **10**, doi:10.1029/2009GC002373. [3] Carbotte, Small and Donnelly (2004), The influence of ridge migration on the magmatic segmentation of mid-ocean ridges, *Nature* **429**, 743-746.

Using automated mineralogy to evaluate bioaccessibility of Pb-bearing mine waste

MARTHA BUCKWALTER-DAVIS[1*], HEATHER JAGGARD[1], SUZETTE MORMAN[2], GEOFFREY PLUMLEE[2], AND HEATHER JAMIESON[1]

[1]Queen's University, Kingston Ontario, Canada mbuckwalterdavis@gmail.com (*presenting author)
[2]U. S. Geological Survey, gplumlee@usgs.gov, smorman@usgs.gov

The toxic effects of Pb, especially on children, are well known. The concentration of Pb in waters draining mine tailings tends to be low due to the relative insolubility of galena (PbS) and weathering products such as anglesite ($PbSO_4$). A more hazardous route of exposure is the direct ingestion of windblown dust or contaminated soil, particularly if the ingested material contains the Pb carbonate mineral cerussite ($PbCO_3$), a highly bioaccessible form of Pb.

Detailed mineralogical examination of mine tailings from the New Calumet Pb-Zn mine in Quebec has shown that after decades of subaerial exposure, almost all Pb is hosted in primary galena and secondary cerussite ($PbCO_3$), with only trace amounts of anglesite and massicot (PbO). Some of the goethite formed from alteration of pyrrhotite contains detectable Pb.

Simulated gastric fluids (pH=1.5) were used to evaluate Pb bioaccessibility in the <250 micron fraction of six near-surface tailings samples (Pb_{total} =1740-4730 $mgkg^{-1}$). The percent of Pb that is bioaccessible ranges from 23% to 69% and is not correlated with total Pb. The bioaccessible Pb for some samples is below industrial soil clean-up criteria.

Automated SEM-based mineralogy provides the opportunity to rapidly characterize thousands of Pb-bearing particles in terms of mineralogy, grain size and degree of liberation from armouring silicates, all features which control bioaccessibility. We have used a FEG-SEM instrument with the Mineral Liberation Analyzer (MLA) software suite to characterize and quantify the Calumet tailings samples. MLA was developed for the metallurgical industry but has increasing environmental applications due to its ability to characterize fine grained sediments including tailings. Some difficulties were presented in distinguishing galena (low bioaccessibility) and cerussite (high bioaccessibility), due to overlapping peaks between S and Pb but these issues have been largely resolved with careful development of a standard reference library within the MLA software and use of X-ray mapping of Pb-bearing grains.

Sample GD-nonVEG (bioaccessibility = 38% Pb) is more fine grained with respect to all particles than sample MS-nonVEG (bioaccessibility = 23% Pb). The ratio (by analyzed area) of cerussite to galena is higher in MS-nonVEG than sample GD-nonVEG, which is contrary to what is expected based on the relative bioaccessibilites of these two minerals, but particle size analysis indicates that cerussite grains are larger in sample MS-nonVEG. Smaller particles have a larger surface area and are more leachable and bioaccessible, which may explain why GD-nonVEG is more bioaccessible while having relatively less cerussite. Research is continuing with efforts to improve the distinction of galena and cerussite and to better characterize very fine grained material.

https://doi.org/10.1180/S0026461X00008434 Published online by Cambridge University Press

Reconstructing the Toba magmatic system: insights from stable isotope geochemistry

DAVID A. BUDD[1*], VALENTIN R. TROLL[1,5], ESTER M. JOLIS[1], FRANCES M. DEEGAN[1,3], VICTORIA C. SMITH[2], MARTIN J. WHITEHOUSE[3], CHRIS HARRIS[4], CARMELA FREDA[5], DAVID R. HILTON[6] AND SAEMUNDUR A. HALLDORSSON[6]

[1]CEMPEG, Uppsala University, Sweden
david.budd@geo.uu.se (* presenting author)
[2]Research Lab. for Archaeology, University of Oxford, UK
[3]Swedish Museum of Natural History, Sweden
[4]Dept. Geological Sciences, University of Cape Town, South Africa
[5]Istituto Nazionale di Geofisica e Vulcanologia, Italy
[6]Scripps Institution of Oceanography, UCSD, USA

The Toba caldera located in Sumatra (Indonesia) is the result of the four successive eruptions at 1.2, 0.84, 0.5 and 0.074 Ma [1]. This study presents oxygen isotope data for a suite of whole rocks and quartz crystals erupted as part of the Young Toba Tuff (YTT), an eruption event producing 2,800 km^3 of material some 74 ka ago [1, 2]. Oxygen isotope data have been obtained from whole rock (conventional fluorination), single mineral grains (laser fluorination-LF) and *in-situ* (SIMS) in combination with cathodoluminescence (CL) imaging in order to establish the relative roles of magmatic fractionation, magma-crust interaction and crystal recycling occurring in the Toba magmatic system. The CL images of quartz crystals exhibit defined patterns of zoning that often coincide with fluctuations in $\delta^{18}O$ values, allowing correlation of textural and compositional information. Measured $\delta^{18}O_{quartz}$ values from SIMS and LF range from 6.7 to 9.4 ‰, independent of their position on the crystal. Whole rock values, in turn, range from 8.2 to 9.9 ‰. The $\delta^{18}O_{magma}$ values calculated from quartz (assuming $\delta^{18}O_{quartz\text{-}magma}$ = 0.7 ‰), suggest a minimum value of 6.0 ‰, similar to that expected from a mantle derived magma [3], and a maximum value of 8.7 ‰. Several quartz crystals, however, have rims with lower $\delta^{18}O$ values, suggesting a late, low-$\delta^{18}O$ contaminant. This indicates multiple sources to the Toba system, including at least two crustal components, one with high- and one with low-$\delta^{18}O$. Helium isotope data obtained from pyroxenes from the oldest Toba eruption (R/R_A = 0.7 and 1.8) are consistent with a significant crustal contribution.

Barometry calculations from feldspar and amphibole suggest the magma chamber system resided at similar depth (~10 km) for all four Toba eruptions. The system probably persisted as a crystal mush, which was repeatedly re-mobilised by fresh magma injections. Crystal recycling, consistent with compositional and textural features in most of the YTT quartz crystals, seems an integral part of how super-eruptions are assembled. Therefore, large volumes of isotopically heterogeneous sources were mixed to make the final YTT cocktail, including a late low-$\delta^{18}O$ contaminant, substantial high-$\delta^{18}O$ crustal contributions, and considerable amounts of recycled antecrysts from the three previous eruptive episodes of the Toba system.

[1] Rose & Chesner (1987) *Geology* **15**, 913-917. [2] Aldiss & Ghazali (1984) *J Geol. Soc. London* **141,** 487-500. [3] Taylor & Sheppard (1986) *Rev. Min.* **16,** 227-271.

A mesocosm study of fate and effects of CuO nanoparticles on endobenthic species (*Scrobicularia plana*, *Nereis diversicolor*)

PIERRE EMMANUEL BUFFET[1], MARION RICHARD[2], FANNY CAUPOS[2], AURORE VERGNOUX[1*], HANANE PERREIN-ETTAJANI[1], HELENE THOMAS-GUYON[2], ANDREA LUNA-ACOSTA[2], CLAUDE AMIARD-TRIQUET[1], JEAN-CLAUDE AMIARD[1], CHRISTINE RISSO[3], MARIELLE GUIBBOLINI[3], PAUL REIP[4], EUGENIA VALSAMI-JONES[5], AND CATHERINE MOUNEYRAC[1]

[1] Groupe Mer, Molécules, Santé (MMS), Université de Nantes et Université Catholique de l'Ouest (Angers), France, aurore.vergnoux@univ-nantes.fr (* presenting author)
[2] Littoral Environnement et Sociétés (LIENSs), Université de La Rochelle, France, helene.thomas@univ-lr.fr
[3] ECOMERS, Université de Nice Sophia-Antipolis, France, christine.risso@unice.fr
[4] Intrinsiq Materials Ltd., Hants, UK, paulreip@intrinsiqmaterials.com
[5] Department of Mineralogy, Natural History Museum London, UK, e.valsami-jones@nhm.ac.uk

Introduction. To investigate the transfer of CuO nanoparticles (CuONPs) from the medium to endobenthic species (*S. plana*, *N. diversicolor*), under environmentally realistic conditions, animals were exposed in field mesocosms to Cu (10 µg.L^{-1}) added either as CuONPs or as soluble Cu in comparison with controls for 21 days. The fraction of Cu under labile form was determined in water and sediment by using Diffusive Gradient in Thin film (DGT). Bioaccumulation of Cu was measured in the whole soft tissues of both species. Behavioural and biochemical biomarkers were determined in organisms.

Figure 1: Experimental intertidal mesocosms deployed in natural environment.

Results. No release of labile Cu from CuONPs was observed at days 7, 14 and 21. Cu bioaccumulation was shown in both species with CuONPs and with soluble Cu for clams. Impairments of behaviour (feeding and burrowing) were observed in both species. Antioxidant activities (CAT, GST) increased in both species for both chemical forms except for GST in worms exposed to soluble Cu. In clams exposed to both Cu forms, detoxification protein (MT) induction was observed and an apoptosis effect only under CuONP exposure. Concerning other biomarkers of defense (SOD, LDH, Laccase) and damage (TBARS, AChE, acid phosphatase) no significant effects were detected.

Conclusion. This experiment shows the suitability of mesocosms for studying the environmental effects of nanoparticles. Behavioral biomarkers and antioxidant defenses are the most sensitive tools to highlight the effect of soluble or nanoparticulate Cu forms.

https://doi.org/10.1180/S0026461X00008434 Published online by Cambridge University Press

Soil salinity: a driver in macroevolutionary processes?

ELISABETH BUI[1*], JOE MILLER[2]

[1]CSIRO Land and Water, GPO Box 1666, Canberra ACT 2601, Australia, elisabeth.bui@csiro.au (* presenting author)
[2]Centre for Australian National Biodiversity Research, GPO Box 1600, CSIRO Plant Industry, Canberra, ACT 2601, Australia

Recent evidence from Australia, one of the most biologically diverse areas of the world, with one of the most extensive arid zones and widespread natural salinity, suggests a role for soil salinity in biogeography and ecology. The distribution of plant species in Queensland responds strongly to a geochemical gradient as expressed by soil salinity and pH, starting at levels of salinity much lower than those for saline soil [1]. Statistical modelling shows that adding soil salinity to climatic and other soil variables in a Generalized Additive Model to account for site scores from a correspondence analysis of site by species data improved the results dramatically (Mean Squared Error decreased from 0.89 to 0.65 and R^2 improved from 0.41 to 0.57) [1]. Three *Acacia* species (*Acacia harpophylla* (commonly called 'brigalow'), *A. cambagei and A. argyrodendron)* that exhibit high salt tolerance are closely related species of microneurous *Plurinerves* as indicated by *Acacia* systematics [2].

Parallel investigations of thrips systematics and their behavioral ecology have shown that: 1) there are specific host-plant relationships of elongate and round gall thrips (*Kladothrips* spp.) on the *A. harpophylla* clade of Plurinerves; 2) phyllode-glueing thrips also show host specificity; and 3) thrips on *A. harpophylla* and *A. cambagei* display high species richness [2, 3]. Chronological phylogenetic analyses indicate that the approximate age of origin of gall thrips (*Kladothrips* spp.) is Miocene and that their subsequent diversification is closely linked to host-plant evolution [3]. Host affiliation with *Plurinerves* has been estimated to date from 7.5 My with a pronounced diversification episode for gall-thrips lineages affiliated with *Plurinerves* hosts between 3 and 6 My [3]. Aridity developed across Australia in the late Miocene [4]. The *A. harpophylla* clade of Plurinerves with host-specific gall-inducing *Kladothrips* occurs on alkaline and/or saline substrate throughout Australia. Other *Plurinerves* occur in a range of different habitats. Thus congruence between plant and insect phylogenies and co-speciation are apparent. While adaptive radiation may be a response to climatic change, more proximal environmental drivers include aridity, alkalinity, and salinity.

Independent lines of evidence—phytogeography, plant and insect systematics, and insect behavioral ecology—point to a potentially important role for soil salinity in macroevolutionary processes for the genus *Acacia*. The potential role of substrate chemistry in macroevolutionary processes should be investigated for other genera found in arid environments.

[1] Bui & Henderson (2003) *Austral Ecology* **28**, 539-552. [2] Crespi, Morris & Mound (2004) *Evolution of ecological and behavioural diversity: Australian Acacia thrips as model organisms*. CSIRO, Canberra. [3] McLeish et al. (2007) *BMC Biology* **5**, 3. doi:10.1186/1741-7007-5-3. [4] Martin (2006) *Journal of Arid Environments* **66**, 533–563.

Sulphur and carbon isotope records across the terrestrial Permian-Triassic (P-T) boundary

THI HAO BUI[1*], JEAN-FRANCOIS HELIE[2], AND BOSWELL WING[1]

[1] McGill University, Earth and Planetary Sciences, thi.h.bui@mail.mcgill.ca (* presenting author)
boswell.wing@mcgill.ca
[2] Département des sciences de la Terre et de l'atmosphère, UQAM, PK-7720
helie.jean-francois@uqam.ca

The end Permian mass extinction (~ 252 Ma [1]) is known as the greatest biotic crisis in earth history with the disappearance of more than 90% of marine species and 70% of terrestrial vertebrate families [2]. To better understand the interaction of the carbon and sulphur cycles across the terrestrial P-T boundary, we collected 27 sedimentary rock samples at average resolution of 35 cm and 9 carbonate nodules along a section of ~10 meters in Karoo Basin, South Africa. We determined carbon and sulphur contents as well as carbon and sulphur isotope records of above samples.

The organic carbon contents of sedimentary rocks are quite low, less than 0.04 wt %. The average $\delta^{13}C$ value of organic carbon is around -25‰ throughout the section, but at 59 cm before the P-T boundary, this value increases to -23.8‰ and drops sharply to -26.5‰ over a distance of 110 cm. The background value of -25‰ is recovered within 19 cm. The $\delta^{13}C$ values of carbonate nodules in the ≈3 m preceding the boundary are around -8.5‰, while those found n the ≈5 m after the boundary are around -11.5‰. Total sulphur contents of sedimentary rocks are generally less than 0.01 wt%, with the exception of a sharp peak of ≈0.45 wt % at 5 cm above the boundary. Although their full pattern is noisier than that seen in the $\delta^{13}C$ record, the $\delta^{34}S$ values of Cr(II)-reducible sulphides and different sulphate species (water-soluble, acid-soluble, and acid-insoluble sulphates) all decrease by at least 8‰ within the 100 cm after the boundary.

The negative shifts of both $\delta^{13}C_{carbonate}$ and $\delta^{13}C_{organic}$ (≈ -3‰) at the boundary indicate a decrease in the ^{13}C content of carbon input into the P-T terrestrial system. Likewise, the sharp peak of total sulphur content coinciding with the boundary suggests a rapid addition of sulphur into the terrestrial environment. The shared initial decreases in $\delta^{34}S$ values suggest that this sulphur was depleted in ^{34}S. Multiple sulphur isotope compositions ($\delta^{34}S$ and $\Delta^{33}S$) of the different sulphate species are generally equivalent, indicating a shared sulphate source throughout the section. While the $\delta^{34}S$ values of the Cr(II)-reducible sulphides are compatible with bacterial sulphate reduction, the associated $\Delta^{33}S$ values are more negative than those typically associated with this process. Although the $\delta^{13}C$ and $\delta^{34}S$ records imply the coherent transfer of ^{13}C- and ^{34}S-depleted material to the PT terrestrial environment, the $\Delta^{33}S$ values complicate a straightforward identification of the source of this material.

[1] Shen *et al.* (2011) *Science* **334**, 1367-1372.
[2] Erwin (1994) *Nature* **367**, 231-235.

https://doi.org/10.1180/S0026461X00008434 Published online by Cambridge University Press

Determining solute sources and water flowpaths in catchments using the Ca-Sr-Ba multi-tracer

THOMAS BULLEN[1*], SCOTT BAILEY[2] AND KEVIN MCGUIRE[3]

[1]U.S. Geological Survey, Menlo Park, CA, USA, tdbullen@usgs.gov (* presenting author)
[2]U.S.Forest Service, N. Woodstock, NH, USA, swbailey@fs.fed.us
[3]Virginia Tech, Blacksburg, VA, USA, kevin09@vt.edu

Determining solute sources and water flowpaths in catchments is essential for understanding how catchments function. For example, stream water chemistry is determined by multiple factors including delivery of water from different portions of the catchment and from different depths along hillslopes and processes such as mineral weathering, ion exchange and biological cycling. As part of a larger study aimed at understanding the inter-relationships of these factors, we are using a hydropedologic approach to interpret concentration and isotope ratios of the alkaline earth elements Ca, Sr and Ba in stream water, groundwater, the soil exchange pool and plants from a catchment at the Hubbard Brook Experimental Forest, New Hampshire, USA. This 41 hectare forested headwater catchment supports a beech-birch-maple-spruce forest growing on vertically- and laterally-developed Spodosols and Inceptisols formed on granitoid glacial till that mantles Paleozoic metamorphic bedrock. Across the watershed in terms of the soil exchange pool, the forest floor has high Sr/Ba and Ca/Sr ratios, weathered mineral soil has intermediate Sr/Ba and low Ca/Sr ratios, and relatively unweathered till has low Sr/Ba and high Ca/Sr ratios. Waters moving through these various soil compartments obtain Sr/Ba and Ca/Sr ratios reflecting these characteristics, and thus variations of Sr/Ba and Ca/Sr ratios of streamwater provide evidence of the depth of water flowpaths feeding the streams. $^{87}Sr/^{86}Sr$ of soil exchangeable Sr spans a broad range from 0.715 to 0.725, with highest values along the mid- to upper flanks of the catchment and lowest values in a broad zone along the central axis of the catchment associated with groundwater seeps. Thus, variations of $^{87}Sr/^{86}Sr$ in streamwater provide evidence of the spatial distribution of water flowpaths feeding the streams. In addition, we are using Ca, Sr and Ba stable isotope ratios ($^{44}Ca/^{40}Ca$, $^{88}Sr/^{86}Sr$, $^{138}Ba/^{134}Ba$) as novel tracers of Ca, Sr and Ba sources and transport pathways in catchments. Initial results indicate that: 1) Sr and Ba stable isotopes are fractionated by plants similarly to patterns observed globally for Ca stable isotopes; 2) organic soils have the lightest values and weathered mineral soils have the heaviest values of exchangeable Ca, Sr and Ba, with particularly heavy Sr and Ba associated with accumulation of humic materials (i.e., in Bh horizons); and 3) the total range of isotope ratios observed for the exchange pool on a mass percent basis increases unexpectedly in the order Ca<Sr<Ba, suggesting an important role for Ca-oxalate that contains lighter Ca than that sampled in the exchange pool. We hypothesize that while biologically-cycled Ca is efficiently retained in the organic soil-plant system (e.g. as Ca-oxalate), biologically-cycled Sr and especially Ba will be more easily leached by soil waters and delivered to the streams and thus their stable isotope ratios may provide an additional means to distinguish between shallow and deep water flowpaths.

XRF archaeometry for lithic characterization and provenance.

ADRIAN L. BURKE[1*], GILLES GAUTHIER[2]

[1]Université de Montréal, Anthropologie, Montréal, Canada, adrian.burke@umontreal.ca (* presenting author)
[2]Université de Montréal, Chimie, Montréal, Canada, gilles.gauthier@umontreal.ca

The use of XRF over the last forty years to determine whole-rock geochemistry and establish an internationally approved chemical nomenclature for igneous rocks [1] has proven to be vital for the geological community. Its use as an archeometric tool specifically for lithic materials has been limited and historically overshadowed by INAA. This is in part due to the lower amount of material required to perform the latter, which is more in line with archaeological conservation guidelines.

If one considers the silicate nature of lithic materials used in the fabrication of sharp-edged tools one is immediately confronted by the inability of INAA to determine the major component of such materials: silica. This precludes the use of rock type based chemical classifications which for aphanitic materials have proven to be crucial, and unbiased, when compared to macroscopic ones (mineralogy based). A complete set of major element oxide determinations, compatible with data found in geological publications, is essential to determine the rock type and in turn narrow possible geological sources . Most importantly, for igneous types, it permits the use of an internationally approved and established chemical rock nomenclature (basalt, andesite, rhyolite, etc.) [1].

Non-destructive methods were developed [2, 3] in order to comply fully with archaeological conservation rules, and in order to profit from the many advantages of XRF when characterizing archaeological lithic materials, such as relative cost, throughput, and the immediate reuse of samples (non-radioactive) for other specific archaeological and geochemical assays.

Concentration data for major and trace elements produced with a specific non-destructive method using long counting times, calibrations using certified rock reference materials, and a geochemical data treatment approach [4] – notwithstanding the caveats imposed by unprocessed samples (slabs versus fused beads and powder pellets) such as surface irregularities, inhomogeneities and varying thicknesses – will be shown here to be quite useful for 1) the correction of macroscopic misclassifications in archaeological collections, 2) the assessment of chemical variations among chert types (nodular, bedded, chemically precipitated, etc.), 3) the determination of specific chemical markers, 4) the evaluation of the geochemical effects of weathering, and finally 5) the determination of provenance.

[1] Le Maître (2002) Second ed., *Cambridge University Press, New York*, 236p. [2] Hermes (1997) *Geoarchaeology* **12**, 31-40. [3] Lundblad & Mills (2008) *Archaeometry* **50**, 1-11. [4] Gauthier & Burke (2011) *Geoarchaeology* **26**, 269-291.

https://doi.org/10.1180/S0026461X00008434 Published online by Cambridge University Press

Modern and deglacial radiocarbon depth profiles from the Southern Ocean

ANDREA BURKE[1*] AND LAURA F. ROBINSON[1,2]

[1]Dept. of Marine Chemistry and Geochemistry, Woods Hole Oceanographic Institution, Woods Hole, USA, aburke@whoi.edu (* presenting author)

[2]Dept. Earth Sciences, University of Bristol, Bristol, UK, laura.robinson@bristol.ac.uk

Mixing and upwelling in the Southern Ocean is thought to be an important driver of glacial-interglacial atmospheric CO_2 change, but paleoceanographic records from this region are sparse. Radiocarbon is a useful tool for reconstructing past circulation change because it is produced in the atmopshere, enters the ocean through air-sea gas exchange at the surface, and then decays away as it is isolated from the atmosphere. Here we present twenty-two new radiocarbon measurements of U-Th dated deep-sea corals from the Drake Passage and combine them with forty previously published deep-sea coral radiocarbon data from this region [1]. Measured $\delta^{234}U$ values from these corals are within error of modern seawater values, consistent with closed-system behavior of the uranium series isotopes. These new corals come from twelve new dredge sites ranging from 328 to 1710 m water depth, and grew between 9.9 and 27.2 thousand years ago. These additional corals provide an increased depth resolution which allows us to reconstruct radiocarbon depth profiles within the Drake Passage at important time intervals during the deglaciation, such as the Younger Dryas, Antarctic Cold Reversal, and Heinrich Stadial 1. We compare these depth profiles to modern radiocarbon profiles from seawater dissolved inorganic carbon. Millenial scale changes in the vertical structure of radiocarbon in the Drake Passage suggest variation in the mixing and exchange of carbon between different water masses and the atmosphere over the deglaciation.

[1] Burke, A. and Robinson, L. F. (2011) *Science Express* 10.1126/science.1208163.

"Bubble-less" degassing of MORB magmas

PETE BURNARD[1*], AURELIA COLIN[2]

[1]CRPG-CNRS, Vandoeuvre-lès-Nancy, France, peteb@crpg.cnrs-nancy.fr

[2]Faculty of Earth and Life Sciences, VU University, Amsterdam, The Netherlands

Noble gas and major volatile systematics indicate that MOR magmas lose volatiles via open system distillation. However, given the low Stokes velocity of bubbles within basaltic magmas (~10 cm h^{-1} for a 300 μm vesicle), it is not possible to efficiently separate bubbles from their enclosing liquids and hence it is difficult to see how open system degassing can physically occur. However, if the magma – crust interface is sufficiently permeable, then volatile loss could be achieved via degassing directly into the crust, without necessarily passing through the vesicle phase. This "bubble-less" degassing could potentially be efficient because the partial pressure of volatiles in the enclosing crust should be very low in contrast to the partial pressure of volatiles within vesicles which is limited by their solubility at the pressure of the degassing magma.

In order that degassing directly into the crust can be efficient, three conditions need to be met: 1) the surface area of the magma-crust interface needs to be similar to or greater than the surface area of the sum of the vesicles; 2) the magma crust interface needs to be permeable; 3) the magma needs to be sufficiently convective to ensure that a significant fraction of the magma passes within the characteristic diffusion distance of the magma-crust interface.

We asses here condition #1. The surface area of bubbles in a magma depends on the bubble size distribution, the total vesicularity and magma pressure during degassing; typically specifc surface areas of magmas will be in the range 1 – 10 $mm^2\ g^{-1}$ for most MORBs (up to a maximum of ~50 $mm^2\ g^{-1}$ for the "popping rock"). Sill-like magmas have surface/volume ratios of between $1x10^{-2}$ and $1x10^{-5}$ (corresponding approximately to sills between 0.15 and 150 m) thick. Figure 1 shows that the total vesicle surface area of a magma is the same as or slightly higher than the surface area of the magma/crust interface. Given the uncertainties involved, it is possible that "bubble-less" degassing may be a potential mechanism through which magmas lose their volatiles. Further modelling will investigate conditions 2) and 3).

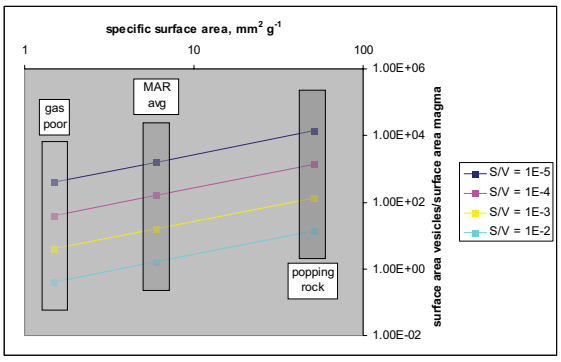

Figure 1: Variation of (vesicle surface area)/(magma-crust interface area) as a function of vesicle specific surface area ($mm^2\ g^{-1}$) for different magma geometries (different Surface/Volume ratios).

https://doi.org/10.1180/S0026461X00008434 Published online by Cambridge University Press

Diffusion compensation and application of Graham's law to noble gas diffusivities

PETE BURNARD[1*]

[1]CRPG-CNRS, Vandoeuvre-lès-Nancy, France, *peteb@crpg.cnrs-nancy.fr (* presenting author)

Diffusion Compensation

The temperature dependence (E_a) of slow-diffusing species tends to be greater than that of faster diffusing species, resulting in an interdependence between D_0 and E_a [1, 2, 3]. The net result is that the difference in diffusivity between two species in a given matrix will reduce with temperature, converging at a particular "compensation" or "isokinetic" temperature where the two (or more) species have the same diffusivities.

Graham's Law of effusion on the other hand states that, as far as gases are concerned, the relative diffusivity of two species is equal to the inverse of the square root of their masses:

$D_1/D_2 = \sqrt{(M_2/M_1)}$

In situations where experimental data are lacking, this relationship is often used to calculate the relative diffusivities of noble gas pairs. However, Graham's Law and "Compensation Temperature" relationships are mutually exclusive: according to Graham's Law, two noble gases should have the same Ea and differ only in D_0 (which should be constrained by $\sqrt{(M_2/M_1)}$). There cannot be compensation of diffusion with temperature for species following Graham's Law.

Non-Graham's Law behaviour

Recent results (Amalberti et al, this volume) show that He and Ar diffusivities in silicate glasses do infact differ in Ea: Graham's Law does not apply to diffusion of noble gases in silicate glasses (i.e. it is not possible to assume that $D_{He}/D_{Ar} = \sqrt{(M_{Ar}/M_{He})}$). The predicted isokinetic temperature for He and Ar diffusion in basaltic glasses is ~1000 K. The lack of conformity to Graham's law is easily understood: The Graham's Law relation is based on the two gas species of interest having the same kinetic energy (for example, for gases diffusing through a pinhole in the classic experiments by Graham in the 19th century). Volatile species diffusing through solid matrices are not expected to be isokinetic (they are not free gases) and Graham's law likely does not apply to diffusion of gases dissolved in solid matrices.

Implications

As a result, kinetic fractionation of different noble gases will only occur at "low" temperatures (the lower the temperature, the greater the potential for kinetic fractionation). Thus it does not appear likely that diffusion during magmatic processes (mantle melting or degassing of magmas) will be able to kinetically fractionate the noble gases. However, post-deposition (low temperature) processes out of equilibrium will create large He-Ar (and by extension, Ne-Ar, Kr-Ar etc) fractionation. The geological implications of these observations will be discussed.

[1] Winchell (1969) *High Temp. Sci.* **1**, 200 - 215. [2] Hart (1980) *Earth Planet Sci. letts* **269**, 507 - 516. [3] Zhao (2007) *Am. Mineral.* **92**, 289-308.

Identification of chromitite and kimberlite occurences in the James Bay lowland using statistical analysis of detrital chromite compositions

MARCUS BURNHAM[1*], DAVE CRABTREE[1] & RIKU METSARANTA[2]

[1]Geoscience Laboratories, Ontario Geological Survey, Sudbury, Canada. marcus.burnham@ontario.ca

[2]Precambrian Geoscience Section, Ontario Geological Survey, Sudbury, Canada. riku.metsaranta@ontario.ca

Introduction

In 2001, under the Operation Treasure Hunt (OTH) program [1], the Ontario Geological Survey carried out a stream sediment sampling program in the James Bay lowland during which over 1000 stream sediment samples were collected and processed for kimberlite and metamorphic/magmatic massive sulphide indicator minerals and gold grains. Because the primary objective of this survey was to evaluate the potential of the region to host additional kimberlite pipes, an emphasis was placed on the compositions of the garnet fraction. However, with the recent discoveries of chromite, Cu-Ni-PGE-sulphide and Ti-V mineralisation in the McFaulds Lake or "Ring of Fire" area, the chemistry of the detrital chromite grains is being re-investigated through statistical analysis of the original OTH dataset (>5500 electron probe microanalyses [2]) supplemented by analyses of chromites from the bed rock (in particular lithologies associated with the McFaulds Lake area mineralisation and Attawapiskat kimberlite diatremes).

Statistical Analysis

Initial statistical analysis of the major and minor element contents of the chromites, using agglomerative hierarchical clustering (AHC) after log-ratio transformation of the data to remove the constant-sum problem [3], suggests that at least nine compositional groups can be recognised. These groups show spatial associations with the bedrock geology, most notably in their Ti, Fe^{3+}, Fe^{2+}, and V contents (Figure 1).

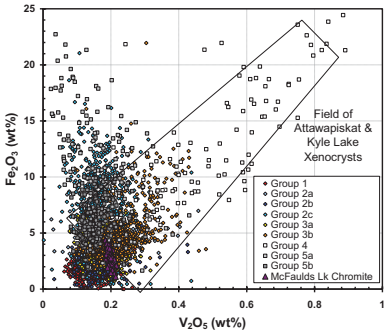

Figure 1: Compositions of detrital chromites from the James Bay lowlands. Field of Attawapiskat and Kyle Lake xenocrysts from [4].

[1] Crabtree (2003) *OGS Open File Report* **6108**, 115p. [2] Crabtree & Felix (2005) *OGS Misc. Release Data* **161**. [3] Aitchison (1986) The Statistical Analysis of Compositional Data, 416 pp. [4] Sage (2000) *OGS Open File Report* **6019**, 341p.

https://doi.org/10.1180/S0026461X00008434 Published online by Cambridge University Press

Plastic Deformation in Olivine Polycrystals:In-situ diffraction and EPSC models

PAMELA C. BURNLEY[1*]

[1]University of Nevada Las Vegas, Department of Geoscience, Burnley@physics.unlv.edu

Introduction

An important problem in rock deformation studies is the so-called meso-scale problem; understanding how the behaviour of individual mineral grains deforming via grain-scale processes interact to produce the bulk behaviour of the aggregate. A number of models for thinking about this problem exist, ranging from various averages of isolated grain behaviour to those that are dominated by grain configuration, for example stress percolation (as observed in granular materials). It is likely that the degree to which any given model is useful for a particular material depends on the degree of mechanical heterogeneity and anisotropy of the material. We are investigating the deformation of polycrystalline olivine in this light.

Methods

We report on in-situ synchrotron x-ray diffraction from high pressure deformation experiments conducted using olivine in the D-DIA apparatus at beamline X17b2 at the NSLS. We observe the diffraction behaviour of x-ray reflections for lattice planes oriented nearly perpendicular to compression and at several other orientations including the transverse orientation. Sample strain is measured using radiograph of the sample (which is bounded by metal foils). We used elastic plastic self-consistent (EPSC) modelling[1] to analyse diffract-tion from the sample during deformation. The models assume that rheology of the bulk is controlled by the critical resolved shear stress of the slip systems and the orientation of the grains in the polycrystal.

Results and Discussion

The failure of the known olivine slip systems to meet the von Mesis criteria for arbitrary shape change causes the EPSC models to exhibit very strong work hardening and nearly elastic behaviour for many grain populations. This is in stark contrast to our experimental data which consistently shows little or no work hardening after yield.

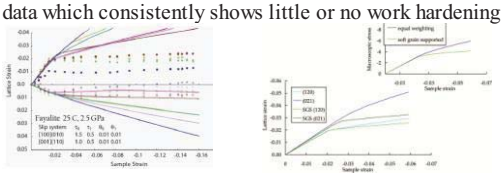

Figure 1: a) (left) Experimental diffraction results (points) for the (021), (010), (120), (002), (131) and (112) lattice planes in compression (above axis) and transverse directions (below axis). EPSC model is shown with matching coloured lines. **b)** (right) Modified EPSC model in which weakest grains dominate.

One possible reason that the deformation behaviour of polycrystalline olivine cannot be predicted with the EPSC model is that grains in the polycrystal that are well oriented for slip (soft grains) dominate the deformation behaviour or the aggregate, with grains that are not well oriented for slip passively "riding along" and not contributing to the aggregate strength. To test this, we assign a weighting factor to each grain depending on the degree of plastic strain that accumulates in the grain during deformation. Using this strategy the EPSC model more closely mimics the lack of work hardening as well as smaller difference in lattice strain between the (120) and (021) reflections.

[1] Turner and Tome (1994) *Acta Metallurgica Materialia* **42**(12) 4143-4153

Integrated 3D multimodal CARS microscopy, Raman spectroscopy, and microthermometry of gas-rich inclusions in the Marcellus shale-gas system

R. C. BURRUSS[1*], M. EVANS[2], A. D. SLEPKOV[3], A. F. PEGORARO[4] AND A. STOLOW[4]

[1]USGS, Reston, USA, burruss@usgs.gov (* presenting author)
[2]Central Connecticut State University, New Britain, USA, evansmaa@mail.ccsu.edu
[3]Trent University, Peterborough, Canada, aaronslepkov@trentu.ca
[4]National Research Council of Canada, Ottawa, Canada Adrian.Pegoraro@nrc-cnrc.gc.ca; Albert.Stolow@nrc-cnrc.gc.ca)

Gas-rich inclusions in fracture filling cements in the Marcellus Shale and younger Devonian age formations in the Appalachian basin record a complex history of gas generation, migration, and alteration during evolution of the Alleghenian orogen[1]. Quartz and calcite cements contain multiple overlapping fluid inclusion assemblages (FIAs) formed during crystal growth and deformation. To resolve the complex sequences of gas generation and migration recorded by FIAs we applied a nonlinear optical microscopy method capable of 3D, molecule-specific imaging with sub-micrometer resolution: multimodal coherent anti-Stokes Raman scattering (CARS) microscopy. Our implementation of CARS microscopy[2] produces molecule-specific images in the range of 2100 to 4000 cm^{-1} (N_2, CH_4, H_2O) and simultaneously creates second harmonic generation (SHG) images of inclusions with associated quartz microstructures, and two-photon excitation fluorescence (TPEF) images of higher hydrocarbons. The CARS images show the distribution of methane-rich and aqueous phases in inclusions and the TPEF images show the distribution of gas-rich inclusions that contain trace levels of higher hydrocarbons. Individual gas-rich inclusions within distinct 3D FIAs identified with multimodal CARS were analyzed by conventional confocal Raman spectroscopy for minor components (C_2H_6, CO_2, H_2S, N_2) and internal pressure[3]. 2D maps of inclusions with microthermometric measurements were correlated with 2D projections of 3D SHG images. Integration of measurements on individual inclusions with 3D images allows identification of FIAs with distinct spatial orientation and differences in composition (C_2H_6, CO_2, higher hydrocarbons) and density. 3D imaging with CARS microscopy is a major advance in our ability to assign FIAs with distinct compositions to distinct orientations of microstructures formed during kinematic evolution of the orogen. These observations provide new insight to the temporal evolution of hydrocarbon gas generation and migration during evolution of the Marcellus shale-gas system.

[1] Evans (2010) *Geol. Soc. Am. Mem.* 206. [2] Pegoraro *et al.* (2010) *App. Phys.* 49, F10–F17. [3] Lu *et al.* (2007) *GCA* 71, 3969–3978.

https://doi.org/10.1180/S0026461X00008434 Published online by Cambridge University Press

Pore-water diffusive fluxes of ^{224}Ra and CO_2 in Bedford Basin, Nova Scotia.

WILLIAM BURT[1*], HELMUTH THOMAS[1], KATJA FENNEL[1], JOHN N. SMITH[2], AND EDWARD HORNE[2]

[1]Dalhousie University, Department of Oceanography, Halifax, NS, Canada willburt@dal.ca, helmuth.thomas@dal.ca, katja.fennel@dal.ca, (*presenting author)

[2]Bedford Institute of Oceanography, Fisheries & Oceans Canada, Dartmouth, NS, Canada John.Smith@dfo-mpo.gc.ca, Ed.Horne@dfo-mpo.gc.ca

Introduction and aim of the study

On the seafloor, chemical processes occurring within sediments create pore-waters highly enriched in various chemical constituents. Many of these processes are fuelled by particulate organic matter (POM), generated during primary production in the euphotic zone and settled onto the surface sediments. Biological transformations of POM in the surface sediments, aerobic or anaerobic, eventually increase pore-water concentrations of dissolved inorganic carbon (DIC), and depending on redox conditions, also alkalinity (A_T). Furthermore, the decay of radioactive elements in the sediments constitutes a further source of chemical species enriched in pore-waters, such as the decay of sediment-bound ^{228}Th ($t_{1/2}$=1.91y), which yields high concentrations of its shorter-lived daughter ^{224}Ra ($t_{1/2}$=3.66 d). We investigate the diffusive flux of three such constituents, the short-lived radium isotope ^{224}Ra, DIC and A_T, from pore-waters into the deep waters of Bedford basin (Nova Scotia, Canada), in order to shed light on both the biogeochemical behaviour of ^{224}Ra and on the return flow of DIC and A_T into the water column from POM respiration on the surface sediments.

Results and Discussion

We apply a 1-D diffusive mixing model (Moore, 2000) to near-bottom profiles of excess ^{224}Ra activity. The recurrence of sharp Ra gradients supports the assumption of a diffusion-dominated mixing regime. We yield vertical eddy-diffusion coefficients (K_Z), along with estimates of ^{224}Ra activity at the sediment-water interface, from which we derive ^{224}Ra fluxes per unit area of sediment. Subsequently, we apply K_Z values to the near-bottom gradients of DIC and A_T, in order to estimate benthic DIC and A_T fluxes from Bedford Basin sediments into the overlaying water column.

Integrating our findings over a full annual cycle, the benthic return flux of DIC constitutes as much as 50% of the annual primary production [2], suggesting substantial additional delivery of organic carbon to deep sediments in the basin. Input from nearby sewage outfalls, re-suspension and transport of sediments at shallower depths [3], and high retention levels within the basin [4] may provide the mechanisms required for this enhanced carbon delivery. Finally, we do not observe any significant release of A_T from the surface sediments to the overlaying water column, which can be seen as an indicator of primarily aerobic respiration of the settled POM, fuelled by sufficiently high dissolved oxygen levels. [5]

[1] Moore (2000) *Cont. Shel. Res.* **20**, 1993-2007. [2] Irwin (1981) *Mar. Ecol. Prog. Ser.* **71**, 97-102. [3] Taguchi and Hargrave (1978) *J. Fish. Res. Board. Can* **35**, 1604-1613. [4] Shan et al. (2011) *Ocean Dynamics* **61**, 951-976. [5] Hargrave et al. (1976) *Tech. Rep. Fish. Mar. Serv., Envir. Can.* **608**, 1-129.

Assessing global N cycling in subduction zones from data on metamorphic rocks: Implications for the evolution of N in Earth's reservoirs

VINCENT BUSIGNY*, PIERRE CARTIGNY, PASCAL PHILIPPOT

IPG-Paris and Univ. Paris Diderot, Sorbone Paris Cité, France, busigny@ipgp.fr (* presenting author), cartigny@ipgp.fr, philippot@ipgp.fr

In order to evaluate the budget of nitrogen buried to the mantle in subduction environments, we performed quantitative and N isotopic analyses of Alpine metamorphic rocks subducted to different depths, and on their non-metamorphic analogues. The samples investigated represent a complete section of the oceanic lithosphere including from bottom to top, serpentinized peridotites, metagabbros, metabasalts and overlying metasediments.

A global annual flux of N subducted by metagabbros has been estimated at about 4.2 ($\pm$ 2.0) $\times 10^{11}$ g/yr with an average δ^{15}N-value of 1.8 $\pm$ 0.8 ‰ (1σ). This flux is about half that of sedimentary rocks, which indicates that gabbros carry a significant portion of the subducted nitrogen. The net budget between subducted N and that outgassed at volcanic arcs indicates that ~80% of the subducted N is not recycled to the surface.

On a global scale, the total amount of N buried to the mantle via subduction zones is estimated to be 3 times higher (13.2 $\times 10^{11}$ g/yr) than that released from the mantle via mid-ocean ridges, arc and intraplate volcanoes and back-arc basins. This implies that N contained in Earth surface reservoirs, mainly in the atmosphere, has been progressively transferred and sequestered into the mantle, with a net flux of ~9.6 $\times 10^{11}$ g/yr. Assuming a constant flux of subducted N over the Earth's history suggests that an amount equivalent to the present atmospheric N may have been sequestered into the silicate Earth over a period of 4 billion years.

Considering a present day mantle value of ~ -5‰, an average δ^{15}N value of subducted nitrogen of about 3.4 ±1.4 ‰ implies that the secular evolution of the mantle δ^{15}N value should have increased through time, whereas that of the crust and atmosphere should have decreased.

https://doi.org/10.1180/S0026461X00008434 Published online by Cambridge University Press

Probing the deep critical zone beneath the Luquillo Experimental Forest, Puerto Rico

H.L. BUSS[1*], S.L. BRANTLEY[2], F.N. SCATENA[3], M. SCHULZ[4], A.F. WHITE[4], A.E. BLUM[5], AND R. JIMINEZ[3]

[1]School of Earth Sciences, University of Bristol, Bristol, UK, h.buss@bristol.ac.uk (* presenting author)
[2]Earth and Environmental Systems Institute, The Pennsylvania State University, University Park, PA, USA, brantley@eesi.psu.edu
[3]Department of Earth and Environmental Science, University of Pennsylvania, Philadelphia, PA, USA, fns@sas.upenn.edu
[4]US Geological Survey, Menlo Park, CA, USA, mschulz@usgs.gov, afwhite@usgs.gov
[5]US Geological Survey, Boulder, CO, USA, aeblum@usgs.gov

The interfaces where intact bedrock weathers to disaggregated material, such as saprolite and soil, are often hidden deep within the critical zone. The majority of weathering studies in the field focus on the shallow critical zone: soils, sediments, regolith, saprolite, and outcrops. However, weathering of primary minerals along bedrock fractures located in the groundwater or deep vadose zones may supply significant weathering products to streams and oceans.

We investigated the deep critical zone in the Bisley watershed in the Luquillo Critical Zone Observatory from two 9.6 cm diameter boreholes drilled with a hydraulic rotary drill to 37.2 and 27.0 m depth. Continuous core samples through coherent rock were taken using an HQ-wireline barrel. Bulk solid-state chemical analysis and powdered XRD were performed on rock and saprock samples. Thin sections were examined by optical microscopy and SEM. A history of low- to moderate-grade metamorphism is reflected by the presence of epidote, prehnite, pyrite, and tourmaline. Fresh rock contains abundant plagioclase and chlorite, with lesser quartz, K-spar, and pyroxene.Weathering rinds developed on fracture surfaces are porous and contain abundant secondary Fe(III)-oxides.

Drilled cores revealed repeated zones of highly fractured rock, identified as corestones, embedded within layers of regolith. Some corestones are massive and others are highly fractured. Subsurface corestones are larger and less fractured in the borehole drilled along the spine of a ridge, compared to the borehole drilled near a stream channel. As corestone size is thought to be a function of fracture spacing, the location of the valleys and ridges in the watershed may be controlled by the fracture spacing of the underlying bedrock.

Drilling terminated in coherent rock, thought to be bedrock based on a model that hypothesized a thickness for the corestone zone [1]. The 2 drilled boreholes and a resistivity profile [2] are only 20-50m apart and of similar elevation. However, all 3 have different profiles demonstrating that this is a complex landscape that needs both geophysics and drilling to understand. Even so, all of the profiles indicate that the weathering zone is well below the stream channel; thus weathering depth is not controlled by local base level. Furthermore, weathering rinds on fracture surfaces at depth indicate that water and oxygen are transported below the stream channel; thus not all of the water in the watershed is discharged to the stream.

[1] Fletcher and Brantley (2010) *Amer. J. Sci* **310**, 131-164.
[2] Schellekens et al. (2004) *Hydrological Processes* **18**, 505-530.

Efficiency of covers made of low sulphide tailings to control AMD from surface impoundments

BRUNO BUSSIÈRE[1*], MICHEL AUBERTIN[2]

[1]Université du Québec en Abitibi-Témiscamingue, Institut de recherche Mines et Environnement, (*presenting author), Bruno.bussière@uqat.ca
[2]École Polytechnique de Montréal, Département de génie civil, géologique et des mines, Michel.Aubertin@polymtl.ca

Introduction

It is now recognized that one of the best options to reclaim acid-generating tailings impondments is to use an oxygen barrier. Water contamination can be controlled by limiting the oxygen flux reaching the reactive tailings. Different types of oxygen barriers can be used, including engineered covers that rely on a high moisture content in one of its layers to prevent oxygen migration [1,2]. The authors work has shown that when appropriate soils are not available close to the mine site, low sulphide tailings can advantageously be used as a component of layered covers.

Main results

Different laboratory and *in situ* tests were performed over the last 20 years or so by the authors and collaborators to evaluate the response and performance of covers made with low sulphide tailings to limit water contamination. The initial series of tests used «naturally» low sulphide tailings as the moisture retaining layer in covers with capillary barrier effects (CCBE). Results showed that it was possible to maintain the water quality below the regulation criteria with such type of CCBE placed over reactive tailings. The control tests on exposed acid-generating tailings (without the cover) showed that the pH of the leachates droped below 3, with concentrations in dissolved metals in the hundreds of mg/l [3]. Another series of tests were performed in the laboratory to evaluate the feasibility of artificially producing the low sulphide tailings by a flotation process, and to use the desulphurized tailings as moisture-retaining layer in a CCBE. When the tailings are properly desulphurized, testing results showed that water contamination was effectively prevented, producing a leachate that meets water quality criteria [4]. An additional series of experiments were performed to evaluate the performance of monolayer covers made of low sulphide tailings, in combination with the elevated water table technique [5]. These column tests results show that the water table level is the most important parameter affecting the monolayer cover performance to control acid generation. The water table must be located at a minimum depth below the cover to prevent water contamination.

Conclusion

Results from different experiments at different scales showed that low sulphide tailings can be an efficient material to be used in engineered covers designed to control acid production from reactive tailings. In adddition, the use of low sulphide tailings valorises a mining waste and reduces the borrowing of natural soils and the related pertubations.

[1] Nicholson et al. (1989), *Can.Geot.J.* **26**, 1-8. [2] Bussière et al. (2003), *Can.Geot.J.* **40**, 512-535. [3] Molson et al. (2008), *Appl. Geochem.* **23**, 1-24. [4] Bussière et al. (2004), *Env. Geol.* **45**, 609-622. [5] Ouangrawa et al. (2009) *Appl. Geochem.* **24**, 1312-1323.

https://doi.org/10.1180/S0026461X00008434 Published online by Cambridge University Press

Shear-Induced Melt Bands with Anisotropic Viscosity and Implications for Melt Extraction at Mid-Ocean Ridges

SAMUEL BUTLER[1*]

[1]University of Saskatchewan, Department of Geological Sciences, Saskatoon, Canada, sam.butler@usask.ca (* presenting author)

Introduction

Melt at mid-ocean ridges is produced over a broad lateral area but is mostly extracted in a narrow region in the vicinity of the ridge crest. Geochemical evidence also indicates that it is extracted rapidly, necessitating a mechanism to focus melt towards the ridge axis. When systems of partial melt are subjected to an externally driven strain-rate, melt segregates into bands of low and high porosity provided that the viscosity of the solid matrix decreases with increasing porosity and that the system is larger than the material compaction length. These bands have been suggested as candidates for focusing melt flow towards the ridge axis[1]. Experimental investigations of these systems have shown that the bands form at roughly 25° to the direction of maximum compression, regardless of the degree of strain-rate dependence of the matrix viscosity. In contrast, numerical and theoretical investigations show that bands should grow fastest if they are oriented parallel to the direction of maximum compression of the background flow if the viscosity is strain-rate independent and isotropic. Recently, it has been suggested that the matrix viscosity should be anisotropic because of the anisotropic arangement of melt at the grain scale caused by stress and that this anisotropy could result in low angle bands as observed in the experiments[2]. In this contribution, I will present numerical simulations of melt bands with anisotropic viscosity.

Results

When matrix viscosity is anisotropic with orientation appropriate for the orientation of grain-scale melt seen in experiments at low strain, the bands do form at angles that are consistent with those seen in experiments. However, in experiments at high strain, the melt in seen to reorient and the resulting viscosity anisotropy results in simulated bands that are not consistent with those seen in experiments.

The effects of buoyant interstitial fluid are also investigated and it is found that a large degree of buoyancy results in two sets of band orientations and short wavelength bands.

[1] Katz R.F., Spiegelman M., Holtzman B., (2006) , *Nature*, 442, 676-679.
[2] Takei Y, Holtzman B., (2009), *J. Geophys. Res*., 114, doi:10.1029 /2008JB005852.

https://doi.org/10.1180/S0026461X00008434 Published online by Cambridge University Press

The Mayon Volcano (Philippines) plumbing system: Insights from crystal zoning patterns and volatile contents

JOAN CABATO[1*], FIDEL COSTA[2], CHRIS NEWHALL[3]

[1]Earth Observatory of Singapore, joan.cabato@ntu.edu.sg (* presenting author)

[2]Earth Observatory of Singapore, fcosta@ntu.edu.sg

[3]Earth Observatory of Singapore, cnewhall@ntu.edu.sg

Mayon is a persistently degassing volcano, producing vulcanian-strombolian eruptions every few years, and perhaps a plinian eruption every century. We investigate the plumbing system beneath Mayon using phenocrysts, microlites and melt inclusions, which record processes in the magma chamber and conduit. We also inspect matrix glass composition to relate the magmatic history all the way to the last stages of cooling during an eruption.

Eruptive products of Mayon are consistently basaltic andesite in composition. Petrological data for this study are derived mostly from bread-crust bombs of the 2000 eruption, which have inclusions of up to 40cm in size. These inclusions have the same bulk composition and phenocryst populations as the host rock, the difference lies only in their more crystalline matrix. The coarse microlites in the inclusions imply relatively slow degassing rates, revealing an upward magma movement slower than that of an eruption, as would occur during convection in the conduit.

Similarity in the phenocrysts of the host and inclusions indicate the same magma at depth. Plagioclase phenocrysts show complex patterns, from oscillatory zoning to pervasive sieve textures that may occur multiple times in a single crystal. The most calcic end member resorbs more sodic zones, forming geometrically complex zones rich in glass that result to the sieve texture. Clinopyroxene and orthopyroxene phenocrysts are also zoned, but show less complexity than the plagioclase. In many cases, pyroxene cores are more iron-rich than the rims, although iron-rich outermost rims are also common. These textures and zonations can be explained by the mixing of at least two end-members in the reservoir, one more primitive (An80, Mg#75) and probably more volatile-rich than the other (An60, Mg#65). The extent to which these patterns reflect a single – versus multiple – replenishment, is unclear.

Fe-Mg diffusion modelling in pyroxenes suggests timescales of less than 10 years between mafic injection and subsequent eruption. Preliminary volatile data from melt inclusions in tephra fall deposits of the 2000 eruption yield source depths of about 9km. Additional volatile analyses of different Mayon eruption deposits are underway to further characterise the inner workings of the volcano.

Titan tholins: A synopsis of our current understanding of simulated Titan aerosols

MORGAN L. CABLE[1*], SARAH M. HÖRST[2], ROBERT HODYSS[1], PATRICIA M. BEAUCHAMP[1], MARK A. SMITH[3] AND PETER A. WILLIS[1]

[1]NASA Jet Propulsion Laboratory, California Institute of Technology, Pasadena, USA, morgan.l.cable@jpl.nasa.gov (* presenting author)

[2] University of Colorado, Boulder, USA, sarah.horst@colorado.edu

[3]Universty of Houston, Houston, USA, markasmith@nsm.uh.edu

What Are Tholins?

Since the term 'tholin' was first applied by Carl Sagan to the dark organic residue formed from gas phase activation of cosmically relevant mixtures, [1] many hundreds of papers have been published on the generation and/or analysis of this material. In particular, the similarity of tholin optical properties to those of the Titan haze has caused new investigations into laboratory simulation of these aerosols. Much has changed both in terms of our abilities to simulate conditions of the Titan atmosphere and to analyze the samples produced.

We will summarize work involving laboratory analogues of Titan complex organic material (tholins) in the context of recent discoveries. Our current understanding of Titan as a prebiotic system is constantly evolving, and recent data from the Cassini-Huygens mission has greatly improved physical and chemical constraints on models of the atmosphere. However, laboratory experiments are still necessary to provide critical insight for defining the next series of *in situ* experiments to perform on Titan, which will better elucidate processes occurring in the atmosphere and on the surface.

Are Any Tholins Titan-Like?

A variety of complex organic aerosols produced using gas phase activation techniques (cold plasma/corona discharge, hot plasma/spark discharge, UV irradiation, etc.) have all been labeled 'tholins', despite the fact that their physical and chemical properties can be enormously different. This variability begs the question: which, if any, of these tholins are truly Titan-like?

We examine various tholin generation methods and compare the organic material produced to the expected composition of the aerosols in Titan's haze and precipitates settled onto the surface. Tholins are assessed in terms of their optical properties, physical characteristics and chemical composition. We also investigate the possibility of additional chemistry occurring on the surface of Titan, and examine potential *in situ* analysis techniques that could be used on future landed missions to search for evidence of this chemistry. Finally, we develop a metric to classify tholins based on how effectively the relevant properties of the Titan atmosphere (temperature, pressure, energy density, etc.) are replicated during tholin formation. This metric should also help inform the next generation of chemical protocols and instrumentation for use on the surface or in the atmosphere of future Titan *in situ* missions.

[1] Sagan (1979) *Nature* **277**, 102-107.

https://doi.org/10.1180/S0026461X00008434 Published online by Cambridge University Press

Oceanic gabbro signature in Mangaia melt inclusions

R.A. CABRAL[1]*, M.G. JACKSON[1], E.F. ROSE-KOGA[2], J.M.D. DAY[3], K.T. KOGA[2], N. SHIMIZU[4], M.J. WHITEHOUSE[5], A. PRICE[1]

[1]Boston University, Dept. Earth Sciences, Boston, MA 02215 (*correspondence: racabral@bu.edu)
[2]Universite Blaise Pascal, Laboratoire Magmas et Volcans, CNRS, UMR 6524, Clermont-Ferrand, France
[3]Scripps Institution of Oceanography, La Jolla, CA 92093-0244
[4]Woods Hole Oceanographic Institution, Woods Hole, MA 02543
[5]Swedish Museum of Natural History, Laboratory for Isotope Geology, SE-104 05, Stockholm, Sweden

Lavas from Mangaia exhibit an extreme HIMU (high-μ, or high $^{238}U/^{204}Pb$) signature that has been attributed to melting of ancient recycled oceanic crust within ocean island basalt (OIB) mantle sources [1]. In a landmark study, Saal *et al.* [2], measured extreme lead isotopic diversity in melt inclusions (MI) from Mangaia, spanning half of the global range observed in OIBs. In Pb-isotopic space, these MI display a trend towards an unradiogenic end member similar to MORB. However, the origin of Pb isotope diversity and the identity of the unradiogenic end member could not be resolved due to lack of coupled major-trace-volatile element abundances for the MI.

This study examines homogenized olivine-hosted MI in Mangaia lavas. We present the first coupled measurements of major-trace-volatile element abundances and Pb-isotopic measurements on the same MI. Critically, we identify Pb-isotopic variability in our MI, and Pb-isotopic ratios correlate with ratios of major, trace, and volatile elements. For example, the anomalous MI with MORB-like Pb-isotopic ratios exhibit geochemical signatures associated with oceanic gabbro, including elevated Sr/Nd, Ca/Al, Cl/La, and K/La.

It is difficult to constrain the origin—modern plate or ancient recycled lithosphere—of the gabbroic signature. One hypothesis is that the gabbroic signature in the MI derives from melting of the gabbroic section of ancient, recycled oceanic crust [3]. Alternatively, Saal *et al.* [4] suggested that a gabbroic signature in OIB lavas derive from shallow assimilation of gabbros during magmatic ascent. The primary difference between these two hypotheses is that the former requires gabbros processed in a subduction zone, and the latter does not. The elevated Cl/La and K/La in the anomalous melt inclusions is not consistent with subduction zone processing, as Cl and K are fluid mobile and should be lost from the down-going slab. By contrast, altered oceanic gabbros have elevated (Cl, K)/La. Based on the current dataset, we favor the hypothesis that the anomalous gabbro signature (and Pb-isotopic diversity) in Mangaia MI owes to assimilation of Pacific oceanic crust during magmatic ascent.

[1] Hofmann & White (1982) *EPSL* 57, 421-436. [2] Saal *et al.* (1998) *Science* 282, 1481-1484. [3] Sobolev *et al.* (2000) *Nature* 404, 986-990. [4] Saal *et al.* (2007) *EPSL* 257, 391-406.

Petrologic evidence for rapid exhumation of Alpine UHP rocks from > 100 km depth

MARK J. CADDICK[1*], ROBERT J. TRACY[1], NANCY L. ROSS[1]

[1]Department of Geosciences, Virginia Tech, Blacksburg, Virginia, United States, caddick@vt.edu (* presenting author)

We report on a whiteschist from the Brossasco Zone in the Dora Maira UHP Alpine massif – a sample that preserves a remarkably well-constrained record of its late-prograde to peak pressure history, and allows exploration of the processes, mechanisms and timescales of burial and exhumation in rocks reaching ultra-high pressure conditions. Thermodynamic modeling suggests that the abundance and composition of the major phases (garnet, kyanite, Mg-phengite, phlogopite, Na-phlogopite, quartz/coesite, talc and rutile) are consistent with equilibration at ~ 3.5 GPa, 775 ˚C. Well-preserved palisades-textured quartz around large coesite inclusions in garnet attests to this high-pressure phase of the rock's history, whilst complete coe-qtz inversion during exhumation is reflected in the matrix. Unusual evidence of the path taken to reach maximum *P* and *T* can be inferred from asymmetric, high-Ca bands within pyrope-rich (~ prp_{92}) garnet. These bands, which mimic their host crystal's shape and contain ~ 3 times higher X_{gro} than the host, are sharply defined at their inner margin (towards the crystal core) but decay gradually to a low-Ca rim. We interpret this as fractionation of Ca from a finite matrix source during garnet growth. Thermodynamic constraints strongly indicate that the precursor host for this Ca was lawsonite, which is now entirely absent from the sample but helps to constrain the early heating history.

Indicators such as retained strain in matrix quartz crystals and sharp boundaries in garnet zoning profiles suggest that exhumation and cooling were very rapid. Diffusion modeling of garnet zoning yields best-fit timescales of ~ 5 Myrs, consistent with exhumation timescales previously inferred from isotope geochronology [e.g. 1]. This is corroborated by preliminary EMP dating of two monazite populations, which can be characterized as low-Y and high-Y bearing. High-Y rims are common on low-Y cores of matrix monazite but are absent from crystals present as inclusions in garnet, and are interpreted as representing growth during decompression-driven garnet breakdown. Initial results suggest that this rim growth occurred < 10 Myrs (and possibly closer to 5 Myrs) after prograde growth of the low-Y monazite cores.

The constrained pressure-temperature history, including rapid exhumation and an almost complete lack of retrogressive reaction (other than slight garnet breakdown to Mg-rich talc and kyanite) indicates possible mechanisms for burial, heating and exhumation. Likely exhumation rates approach rapid plate tectonic velocities, indicating that erosion was not a major controlling factor. Furthermore, thermodynamic models suggest that the Dora Maira sample had a density of ~ 3.2 g/cm^3 at 110 km depth, implying that despite the relatively small volume of preserved whiteschist material, buoyant exhumation back along a subduction channel remains a feasible mechanism.

[1] Rubatto & Hermann (2001) *Geology* **29**, 3-6.

https://doi.org/10.1180/S0026461X00008434 Published online by Cambridge University Press

Storage conditions of the silicic magmas preceding major plinian eruptions of Santorini volcano

ANITA CADOUX[1*], BRUNO SCAILLET[1], ETIENNE DELOULE[2] AND TIM DRUITT[3]

[1]Institut des Sciences de la Terre d'Orléans, UMR 7327, Orléans, France, acadoux@cnrs-orleans.fr (* presenting author), bscaille@cnrs-orleans.fr

[2]Centre de Recherches Pétrographiques et Géochimiques, Vandoeuvre-les -Nancy, France, deloule@crpg.cnrs-nancy.fr

[3]Laboratoire Magmas et Volcans, UMR 6524, Clermont-Ferrand, France, T.Druitt@opgc.univ-bpclermont.fr

Magma storage conditions can dramatically change over time at a single volcano and might be in close relationships with stress variations imposed on the crustal plumbing system by the overlying edifice as well as changes in eruptive dynamism. The Santorini volcano (Greece) is an ideal target to unravel these potential relationships. We focused on the silicic products of the four major plinian eruptions of Santorini which occurred since the last 200 ka: the Lower Pumice 1 and 2 rhyodacites, the Cape Riva dacite and the Minoan rhyodacite. In order to precisely define the P, T, fO_2 and volatiles pre-eruptive storage conditions of these silicic magmas, we combined a micro-petrological and geochemical study on natural and experimental products. This study is of particular interest in the context of caldera unrest ongoing at Santorini since July 2011.

Our results indicate pre-eruptive temperatures ranging from ca. 850 to 900°C, and a fO_2 along the FMQ buffer curve (log fO_2 = -12.9 to -13.5) except for the Minoan rhyodacite which displays more oxidizing conditions near the NNO buffer (fO_2 = $10^{-12.8}$). The rhyolitic melt inclusions (MI) of plagioclase and pyroxene phenocrysts are mostly H_2O-rich (~3 to > 6 wt.%). The MI and the matrix glasses are both Cl-rich (~3000-4000 ppm) while F (< 1000 ppm) and S (< 100 ppm) represent minor species. Phase equilibria from crystallization experiments for the four eruptions were established at T = 850-900°C, P = 2-4 kbar, fO_2 ~ FMQ, and XH_2O [= moles of H_2O/ (H_2O+CO_2)] between 1 (i.e., H_2O saturated) and 0.6. Significantly, phase relationships show marked differences between eruptions, outlining the need to establish phase equilibria specific to each composition. While the petrological attributes are broadly reproduced at 2 kbar in the temperature range explored, additional experiments are in progress to explore more oxidizing (~NNO +1) and shallower storage conditions (1 kbar).

Hydro-geochemical impact of CO_2 leakage from CCS on shallow potable aquifers: batch, tank and field scale experiments.

AARON CAHILL[1*], AND RASMUS JAKOBSEN[1]

[1]Technical University of Denmark, Department of Environmental Engineering, aarc@env.dtu.dk (* presenting author)

Investigations regarding the environmental implications resulting from leakage of CO_2 from a geological sequestration site into overlying shallow potable aquifers include; simple laboratory batch experiments [1], reactive transport models [2] and field based studies [3]. However, the value of the methods has not been evaluated in detail and the application of several methods to a single field site has not been made. A 6 month field release experiment will commence in spring 2012 at Vrøgum plantation, Western Denmark and preliminary work has been conducted to aid design. First batch experiments exposing field site sediment to CO_2, followed by a sediment flow tank experiment injecting CO_2 continuously were conducted. Finally, in a pilot field injection 45 kg of food grade CO_2 was injected at 10 m depth over 48 hours and the effects on water chemistry observed. The results from each method are compared to assess suitability and relevance to geochemical process understanding and risk assessment.

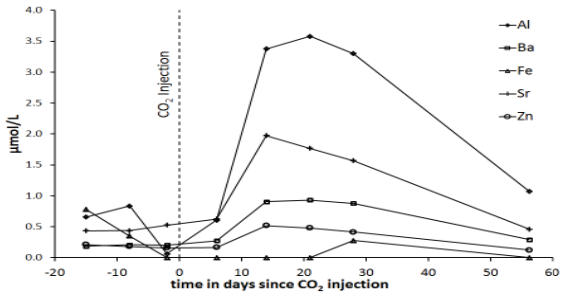

Figure 1: Trace metal concentrations measured 1.0 m down flow of injection point in field pilot experiment.

Results and Conclusion

Batch, tank and pilot injection results all indicate a release of sorbed major and trace elements as well as a release from dissolving silicate minerals. Results also indicate that the risks to water resources from a short term leak from CCS into shallow, overlying, silicate based aquifers (such as the Vrøgum site) are minimal. Some elements approach or exceed guideline values but none of these are particularly toxic or beyond the scope of normal water treatment. Sorption of released elements and accumulation of other elements was observed in the tank and field injections, inferring that a large scale, long lasting leak may develop a CO_2 charged plume or front carrying elements exceeding guideline values for major and trace elements. Differrences in the results from batch and flow based experiments were observed (both for element concentrations and physico chemical parameters) indicating that batch experiments do not accurately indicate the risks to water resources from CCS leakage.

[1] Lu *et al.* (2010) Enviro Earth Sci 60, 335–348. [2] Apps *et al.* (2010) Transp Porous Med 82, 215–246. [2] Kharaka *et al.* (2010) Enviro Earth Sci 60, 273–284.

https://doi.org/10.1180/S0026461X00008434 Published online by Cambridge University Press

Spatial variability in ocean redox conditions during early Cambrian

CHUNFANG CAI[1*], LEI XIANG[1], YUYANG YUAN[1], LIANQI JIA[1] AND TIANKAI WANG[1]

[1]Institute of Geology and Geophysics, CAS, Beijing, P R China, cai_cf@mail.iggcas.ac.cn (* presenting author)

Lower Cambrian black shales have extensively been considered as euxinic sediments. However, recent studies suggest that euxinic conditions may have been over-estimated and ferruginous-dominated deep water and a statified redox stucture may have occurred from 742 to 542Ma [1, 2]. Interestingly, small amounts of samples from the Lower Cambrian in the Songtao section, South China show deposition in a Fe-rich as well as a euxinic enviroment [1]. However, spacial variation for the ocean chemistry during the period is unclear. Here, we analyzed about 300 samples for the total Fe content (FeT) and the abundance of Fe in highly reactive mineral species (FeHR): pyrite, Fe(III) oxides, magnetite and carbonate minerals, using the standard method [1]. These samples were collected from Lower Cambrian black shales of age about 526 to 510Ma [3] and chert and samll amounts of limestones of age about 542 to 526Ma from eight sections in South China with depositional environments ranging from inner shelf, outer shelf, slope and basin.

The results show that all the anlyzed samples except one have FeHR/FeT>0.22, indicating all deposition in an anoxic enviorment. All the chert and limestone and most of the black shale samples have FePy/FeHR<0.7, suggestive of an anoxic, Fe-rich enviorment. Only a few black shales from inner shelf at Shatan section, out shelf at Muyangxiang section and isolated topographic highs within the basin facies at Zhalagou and Tianzhu sections have FePy/FeHR>0.8, a product of a euxinic condition. Black shales and cherts from basin facies at Lijiatuo and Siduping sections show a characteristic of a ferruginous condition, however, a few euxinic sediments were found in the basin facies from Songtao section. Thus, it is very likely for a statified redox ocean to occur during early Cambrian, similar to Ediacaran ocean, as proposed by Li et al. (2010) [2].

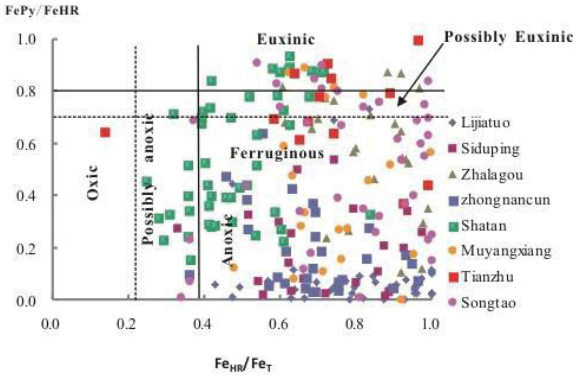

Figure 1: Relationship between FePy/FeHR and FeHR/FeT ratio

[1] Canfield et al (2008) *Science* **321**, 949-952. [2] Li et al (2010) *Science* **328**, 80-83. [3] Jiang et al (2012) *EPSL* **317-318**, 96-110.

Geochemistry of mafic to felsic sequences in the SW border of Ossa-Morena-Zone (OMZ), Portugal

RITA CALDEIRA[1,2*] AND LUISA RIBEIRO[1,3]

[1] LNEG – UGCG, National Laboratory of Energy and Geology, Dept. Geology and Geol. Mapping, Portugal, rita.caldeira@lneg.pt (* presenting author)
[2]CeGul – Geology Center, Faculty of Science,Lisbon University, Portugal.
[3]Geoscience Center, Coimbra University, Portugal

The Beja Igneous Complex (Portugal), located at the SW margin of the Ossa-Morena-Zone (OMZ) in the SW Iberian Variscides, comprises three main units: the LGS - Beja Layered Gabbroic Sequence (gabbros and anorthosites), the CAC - Cuba-Alvito Complex (gabros, diorites and quartzodiorites) and the BPC - Baleizão Porphyry Complex (rhyolites, dacites and granophyries). This Carboniferous Complex has been attributed to a volcanic continental arc related to the closure of a back-arc basin. We studied mafic to felsic outcrops occuring at the Torrão - Alvito – Alcáçovas regions, that have been included by some authors in the CAC and in the BPC.

From the geochemical and mineralogical points of view the studied rocks are sub-alkaline ranging from tholeiitic (Torrão) to calc-alkaline (Alvito - Alcáçovas). The most relevant geochemical features (e.g. TiO2 < 1.9 %, Nb/Y < 0.31, La/Nb > 2, LILE/HFSE enrichment patterns and Nb, Ta, Ti, P negative anomalies) are distinctive of orogenic signature, typical of a subduction zone related continental arc. Beside the tholeitic character of Torrão samples, evidenced by trace element ratios and clionopyroxene composition disciminative plots, they show some other distinctive features i.e. they don't fall in the same liquid line of descend as the others and their normalized REE patterns show lower LREE/MREE than MREE/HREE [$(La/Sm)_N$ = 1.36 and $(Sm/Yb)_N$ = 2.31) while the Alvito – Alcaçovas samples have $(La/Sm)_N$ = 2.41 and 3.39 $(Sm/Yb)_N$ = 1.80 and 1.47. The Alvito – Alcaçovas observed compositional variations are consistent with fractional crystallization + crustal contamination/assimilation evolution from intermediate magmas to the acid magmas that originated the dacites and rhyolites. The integration of these results with other already published for the units of the Beja Massif, geographic information and known stratigraphic/geochronologic information suggest that the Torrão gabbros cannot be included in the same geodynamic stage as those of the CAC. Instead, given their geochemical afinity, they are closer to a earlier stage attributed to Beja Layered Gabbroic Sequence. The Alvito gabbrodiorites and Alcaçovas porphyries are respectively associated with the CAC and the BPC, resulting from a latter period of the Ossa-Morena southwest margin evolution related to a subduction zone linked to the closure of an open basin (South-Portuguese Zone)

https://doi.org/10.1180/S0026461X00008434 Published online by Cambridge University Press

Zinc isotopic fractionation in *Phragmites australis* in response to toxic levels of zinc

CRISTINA CALDELAS[1,*], SHUOFEI DONG[2], JOSÉ L. ARAUS[1] AND DOMINIK J. WEISS[3]

1 Unitat de Fisiologia Vegetal, Facultat de Biologia, Universitat de Barcelona, Barcelona, Spain, jaraus@ub.edu, criscaldelas@ub.edu (* presenting author)

2 Earth Science and Engineering, Imperial College London, London SW7 2AZ, UK, shuofei.dong08@imperial.ac.uk, d.weiss@imperial.ac.uk

3 The Natural History Museum, London SW7 5PD, UK, d.weiss@imperial.ac.uk

Abstract

Stable isotope signatures of Zn have shown great promise in elucidating changes in uptake and translocation mechanisms of this metal in plants during environmental changes [1] [2]. Here this potential was tested by investigating the effect of high Zn concentrations on the isotopic fractionation patterns of *Phragmites australis* (Cav.) Trin. ex Steud [3]. Plants were grown for 40 d in a nutritive solution containing 3.2 mM (sufficient) or 2 mM (toxic) Zn. The Zn isotopic composition of roots, rhizomes, shoots, and leaves was analysed. Stems and leaves were sampled at different heights to evaluate the effect of long-distance transport on Zn fractionation. During Zn sufficiency, roots, rhizomes, and shoots were isotopically heavy ($\delta^{66}Zn_{JMCLyon}$ = 0.2‰) while the youngest leaves were isotopically light (–0.5‰). During Zn excess, roots were still isotopically heavier ($\delta^{66}Zn$ = 0.5‰) and the rest of the plant was isotopically light (up to –0.5‰).

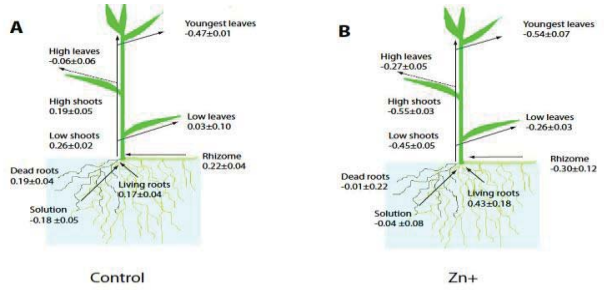

Figure: Isotopic signature of the studied plant sections compared to solutions.

Conclusion

The enrichment of heavy isotopes at the roots was attributed to Zn uptake mediated by transporter proteins under Zn-sufficient conditions and to chelation and compartmentation in Zn excess. The isotopically lighter Zn in shoots and leaves is consistent with long-distance root to shoot transport. The tolerance response of *P. australis* increased the range of Zn fractionation within the plant and with respect to the environment

[1] Weiss et al. (2005) *New Phytol* **165**, 703–710. [2] Arnold et al. (2010) *Plant Cell Environ* **33**, 370–381. [3] Caldelas et al. (2011) *J Exp Bot* **62**, 2169-2178.

Interaction of Pb with calcite (104) surface in the presence of EDTA

E. CALLAGON[1*], S.S. LEE[2], P. FENTER[2], K.L. NAGY[1] AND N.C. STURCHIO[1]

[1]University of Illinois at Chicago, Earth and Environmental Sciences, Chicago, Illinois 60607, ecalla4@uic.edu (* presenting author); klnagy@uic.edu; sturchio@uic.edu

[2]Argonne National Laboratory, Chemical Sciences and Engineering, Argonne, Illinois 60439 fenter@anl.gov; sslee@anl.gov

The incorporation of metals in calcite is important for understanding many geological and environmental processes but is still incompletely understood. Calcite (104) cleavage surfaces were reacted with Pb-EDTA aqueous solution (0.09 mM Pb, 0.11 mM EDTA, 0.5 mM Ca, pH 8.35) at room temperature for times ranging from minutes to hours. Freshly cleaved calcite was placed in a flow-through cell, and reacted first with calcite-saturated solution and then Pb-EDTA solution, both at 0.3 mL/min. In situ synchrotron XR measurements revealed evidence for incorporation of Pb into the calcite lattice as well as the formation of cerrusite ($PbCO_3$) with its (021) plane oriented parallel to calcite (104). The reacted calcite was further studied ex situ by atomic force microscopy (AFM) and optical microscopy. AFM imaging of the reacted surface outside the X-ray beam footprint showed narrow overgrowths atop steps and sparse precipitates on terraces (Fig. 1a). Different behavior was seen within the X-ray beam footprint; it contained abundant trapezoidal-and hexagonal-shaped precipitates oriented mainly along a single crystallographic direction, which is consistent with heteroepitaxial cerussite (021) overgrowths (Figs. 1b and 2). X-ray microfluorescence spectroscopy showed that the trapezoidal growth islands are Pb-rich. Features similar to those in Fig. 1a were observed by AFM in separate ex situ experiments without exposure to X-rays. These observations suggest that the X-ray beam enhanced precipitation even at bulk-undersaturated conditions with respect to cerussite (log SI = -2.3), possibly by photolytic destabilization of the Pb-$EDTA^{2-}$ solution complex.

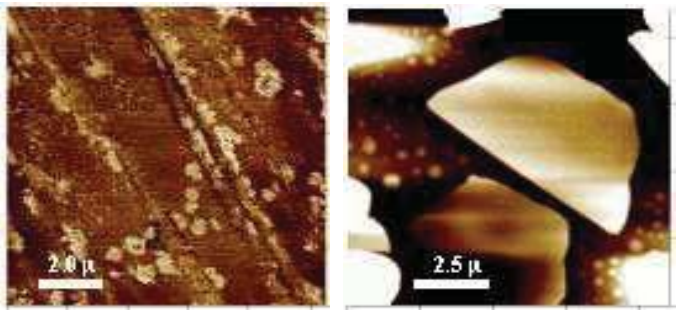

Figure 1: AFM images of the reacted calcite surface. (a) phase contrast image outside the X-ray beam footprint; (b) height image of an area within the X-ray beam footprint (*z*-scale: 100 nm).

Figure 2: The reacted calcite surface imaged within the X-ray beam footprint, observed under reflected light microscopy. Cerussite occurs as trapezoidal precipitates showing euhedral (021) growth face.

https://doi.org/10.1180/S0026461X00008434 Published online by Cambridge University Press

Mobility of isotopes in deformed and undeformed rocks

ALFREDO CAMACHO[1]*, DON DAVIS[2], W.J. DAVIS[3], RICHARD ARMSTRONG[4]

[1]Univ. of Manitoba, Dept. Geological Sciences, Winnipeg, Canada.
camacho@cc.umanitoba.ca (* presenting author)
[2]Univ. of Toronto, Dept. Geology, Toronto, Canada.
dond@geology.utoronto.ca
[3]Geological Survey of Canada, Ottawa, Canada.
Bill.Davis@NRCan-RNCan.gc.ca
[4]The Australian National Univ., RSES, Canberra, Australia.
Richard.Armstrong@anu.edu.au

Understanding the mechanisms that govern the mobility of elements in rocks and minerals is critical to unravelling the tectonothermal evolution of orogenic belts. The redistribution by diffusion of elements in a system is considered to be extremely sluggish under dry, static conditions, such that reequilibration will not take place even though temperatures far exceed commonly assumed closure temperatures over long periods of time. Here we consider the general question of what physicochemical factors (such as dry vs wet and deformed vs undeformed) control mobility of isotopes in a system (i.e., rock-scale, mineral-scale).

In the Musgrave Block, central Australia the Nulchara charnockite outcrops as a low angle sheet over the Michell Nob Granite. Mutally intrusive relationships and indistinguishable U/Pb ages on zircon of ~1070 Ma in both rock-types indicates that the two magmas crystallized at the same time. Consequently, both rock types have experienced exactly the same thermal and deformational events. The region was subsequently deformed at upper-greenschist to amphibolite facies conditions during the Petermann Orogeny (~550 Ma). The Michell Nob granite is foliated and shows recrystallization/neocrystallization/mylonitic textures. The charnockite does not have a foliation, but exhibits recrystallization/neocrystallization textures that may have formed during cooling.

In the Michell Nob granite, zircon and titanite did not respond to deformation and metamorphism, and the U/Pb analyses yield the emplacement age. ^{147}Sm/^{143}Nd ratios on metamorphic garnet and whole rock suggest that this isotopic system did not equilibrate under these conditions. The apparent ^{40}Ar/^{39}Ar ages of hornblende and biotite are older than the emplacement age, suggesting the presence of excess Ar. This excess Ar is attributed to a relatively high partial pressure of Ar owing to release of radiogenic Ar during recrystallisation of K-feldspar. The Rb/Sr system is partially equilibrated, with the outcome on the age dependent on the biotite. In the charnockite, magmatic amphibole gives a ^{40}Ar/^{39}Ar age that is similar to the U/Pb zircon age and records the age of crystallization. Biotite and K-feldspar give ages that are considerably younger but older than the age of the Petermann Orogeny.

The isotopic results suggest that high-strain deformation at upper-greenschist to amphibolite facies conditions will not necessarily equilibrate the different isotopic systems to give a consistent age. In addition, we show that Ar is mobile in rocks that are relatively dry and undeformed, which has implications for diffusion rates and for determining the duration of thermal events.

Lu-Hf isotope study of mafic and ultra mafic plutonic rocks, Grenville province

Erwan Cambrai[1,2*], Marc Constantin[2] and Christophe Hémond[1]

[1] Laboratoire Domaines Océaniques, UMR6538 UBO-CNRS, Université de Brest, Brest, France.
erwan.cambrai@univ-brest.fr (* presenting author)
[2] Dept. Géologie et Génie Géologique, Université Laval, Québec, QC, Canada

Proterozoic anorthosite suites are common features occurring along the Grenville Province. Still debated, the genesis of these suites is commonly assumed to be linked to lithospheric delamination [1] during or post to collisional and contractional orogenies. A new possible origin that has been proposed is the recycling of juvenile crust [2] in the long-lasting Laurentian convergent margin during the Mesoproterozoic. This crust could be buried into the mantle and/or lower crust, due to subduction processes and later recycled into partial melts that generates AMCG magmatism.

In order to test these hypotheses and to study the magma sources, we determined Lu-Hf, Sm-Nd isotopic ratios, coupled with trace element contents from six sites of anorthosites suites and mafic-ultramafic plutons from the Grenville Province of Québec that range from 1.45 to 1.069 Ga. We also look at plutonic mafic to ultra mafic rocks as possible candidates to represent juvenile crust.

Following the method described by Blichert-Toft [3] we obtained Hf and Lu concentrations using isotope dilution on MC-ICP-MS and TIMS; they range from 0.037 to 14.56 ppm and from 0.003 to 0.989 ppm respectively. We also measured ^{176}Hf/^{177}Hf ratios ranging from 0.282123 to 0.282936, displaying various trends from apparently mantle derived material, to possible crustal contamination with less radiogenic materials. Anorthosite ^{176}Hf/^{177}Hf ratios range from 0.282373 to 0.282490. For these samples, εHf(t) values are between +9.77 and +1.48, what shows possible crustal contamination for anorthosite genesis. Plutonic mafic and ultramafic rocks ^{176}Hf/^{177}Hf ratios range from 0.282123 to 0.282942 and present εHf(t) values between +10.21 and +2.76. They display different trends for each sites, from mantle derived material to possible mixing with crustal-like source. Model ages were calculated for each samples. Except for one case, anorthosites model ages tend to be older than known crystallisation ages by nearly four hundred million years. For plutonic mafic to ultramafic rocks, some samples present juvenile crust characteristic with calculated model ages close to crystallisation age by nearly one or two hundred million years. These results could be explained by incorporation of a less radiogenic component such as melting of the inferior crust by hot asthenosphere in the case of lithospheric delamination, or burying of juvenile crust in a subduction-like environment.

[1] McLelland, Daly & McLelland (1996) *Tectonophysics* **265**, 1-28. [2] Chiarenzelli *et al.* (2010) *Geology* **38**, 151-154. [3] Blichert-Toft (2001) *Geostandards Newsletter* **25**, 41-56.

https://doi.org/10.1180/S0026461X00008434 Published online by Cambridge University Press

Clumped isotope calibration using modern brachiopods: Implications for reconstructions of temperature and the oxygen isotopic composition of seawater

ROSEMARIE E. CAME[1*], ALEXANDER M. BEACH[1], UWE BRAND[2], AND HAGIT P. AFFEK[3]

[1]Department of Earth Sciences, The University of New Hampshire, Durham, New Hampshire, 03824-3589 U.S.A., Rosemarie.Came@unh.edu (* presenting author)
[2]Department of Earth Sciences, Brock University, St. Catharines, Ontario L2S 3A1 Canada, uwe.brand@brocku.ca
[3]Department of Geology and Geophysics, Yale University, New Haven, Connecticut 06520-8109 U.S.A., hagit.affek@yale.edu

Reconstructions using the isotopic compositions ($^{87}Sr/^{86}Sr$, $\delta^{13}C$, $\delta^{18}O$) of fossil brachiopods have provided fundamental insights into the evolution of the Earth's seawater over the course of the Phanerozoic (e.g. Veizer *et al*. [1]). However, the interpretation of oxygen isotopic reconstructions is complicated by the fact that the $\delta^{18}O$ of carbonate is a function of both temperature and the oxygen isotopic composition of the water ($\delta^{18}O_{sw}$) in which the carbonate grew. The carbonate clumped isotope (Δ_{47}) paleothermometer, which is based on the temperature-dependent ordering of ^{13}C and ^{18}O atoms into bonds with each other in the carbonate mineral lattice, provides a means to isolate the temperature and $\delta^{18}O_{sw}$ signals because Δ_{47} is independent of the isotopic composition of the water in which the carbonate grew [2].

Our clumped isotope calibration is based on 7 specimens of modern brachiopods spanning a temperature range of 1-29°C. Sample locations and depths were carefully selected in order to minimize the effects of seasonal temperature variability. Three replicate analyses were preformed for each sample. Our results indicate that brachiopod carbonate shows a relationship of Δ_{47} to temperature that is similar to the previously published inorganic calcite relationship [2]. However, the new brachiopod calibration does yield different temperatures at the extremes of the calibration temperature range, and may be more consistent with the inorganic calcite relationship of Zaarur *et al.* [3].

In addition, the results of our ongoing investigation into the isotopic heterogeneities within single brachiopod shells (primary versus secondary calcite layers) will be presented and discussed.

[1] Veizer *et al*. (1999) *Chem. Geol*. **161**, 59-88. [2] Ghosh *et al.* (2006) *Geochim. Cosmochim. Acta* **70**, 1439–1456. [3] Zaarur *et al.* unpublished data.

WHAT DETRITAL ZIRCONS TELL US ABOUT GROWTH OF THE CONTINENTAL CRUST

IAN CAMPBELL[1*], JAMES GILL[2], TSUYOSHI IIZUKA[3] and CHALOTTE ALLEN[4]

[1]The Australian National University, Canberra, Australia, Ian.Campbell@anu.edu.au (* presenting author)
[2]University of California, Santa Cruz, USA, gillord@ucsc.edu
[3]University of Tokyo, Tokyo, Japan, iizuka@eps.s.u-tokyo.ac.jp
[4]The Australian National University, Canberra, Australia, Charlotte.Allen@anu.edu.au

Zircons provide the only evidence for Earth having a crust older than 4.0 Ga but how extensive was that crust? If it was not extensive when did the continental crust start to form, what was its rate of growth, was growth continuous or episodic and what was time interval between formation of primitive continental crust and remelting of that primitive crust to form stable, cratonic crust? To answer these questions we have analyzed 1500 detrital zircons from the World's major rivers for Lu-Hf, U-Th-Pb and O isotopes. The Lu-Hf system gives a model age for the time at which continental crust that melted to form the granitic magma from which the zircon crystallized separated from the mantle, the U-Th-Pb system dates the crustal melting event and O isotopes can be used to determine whether the crustal source region included a significant sedimentary component. Continents that have been covered include Europe, Russia, North America, Africa and Australia. If we confine our discussion to 500 zircons with mantle-like O isotopic values (between 4.25 and 6.25) to eliminate zircons that cystallized from a hybrid source (e.g. zircons from S-type granites) the maximum model age observed is 4150 Ma and there is little evidence of growth of the continental crust starting before 4.0 Ga. This conclusion is in agreement with Nd model ages for Earth's oldest sediments, and with observation that there in no known preserved continental crust older than that age. However six of the eight model ages that exceed 4.0 Ga have been extrapolated over two billion years from their U/Pb age and uncertainty in the Lu/Hf ratio used in the calculations make the reliability of these ages questionable. We conclude that there is no unambiguous evidence in our data for growth of the continental crust prior to 4.0 Ga and that significant growth of the continental crust was delayed until 3.5 Ga. Distinct peaks can be recognized in the Hf model age histogram at 400-1100 Ma, 1600-2500 Ma and 3000-3500 Ma but we caution against interpreting this as proof of episodic growth because the peaks differ between continents and because we have yet to analyze zircons from South America, SE Asia and Antarctica for Hf and O isotopes. The U-Pb ages how five distinct peaks that correspond to the five known supercontinent-forming events suggesting that continent-continent collisions are periods of enhanced crustal melting. The time difference between the formation of primitive continental crust, as recorded by the Hf model ages, and remelting of that crust to form cratonic crust, as recorded by the U-Pb age, varies between 0 and 3.8 Gyr and averages 780 Myr.]

https://doi.org/10.1180/S0026461X00008434 Published online by Cambridge University Press

Kinetic modeling of microbial Fe(II) oxidation, Fe(III) hydrolysis, and As(III) oxidation in acid waters

KATE M. CAMPBELL [1,*], MICHAEL B. HAY[2], AND D. KIRK NORDSTROM[3]

[1]U.S. Geological Survey, Boulder, CO, USA, kcampbell@usgs.gov (* presenting author)
[2]ARCADIS U.S., Inc., Highlands Ranch, CO, USA, Michael.Hay@arcadis-us.com
[3]U.S. Geological Survey, Boulder, CO, USA., dkn@usgs.gov

Abiotic oxidation of Fe(II) in acidic natural water is slow, but acidophillic Fe(II) oxidizing microorganisms, such as *Acidithiobacillus ferrooxidans*, can rapidly oxidize Fe(II). These organisms play an important role in the oxidative dissolution of pyrite and the mobility of many trace elements, including As, realeased from sulfide mineral deposits. The mobility of As depends on the rates of microbial Fe(II) oxidation, abiotic Fe(III) hydrolysis, mineral precipitation, sorption, and photochemical Fe(III) reduction causing As(III) oxidation. Biogeochemical predictions for acidic, Fe(II)-rich natural waters require a coupled biotic-abiotic model that can capture these processes.

A series of batch experiments were conducted at four inital Fe(II) concentrations (10-159 mM) and four inital pH values (1.5-3.0) in the absence of As. A strain of *A. ferrooxidans* isolated from acid rock drainage was used. At least three main reactions can be delineated: microbial Fe(II) oxidation with pH increase, Fe(III) hydrolysis with a pH decrease, and mineral precipitation with pH decrease. Mineral precipitation and Fe(III) hydrolysis were constrained in separate batch experiemnts. Dissolved Fe(II) data were fit with a Monod expression, using parameters optimized by coupling the geochemical modeling code PHREEQC to UCODE, a least squares fitting code. PHREEQC was then used to incorporate microbial Fe(II) oxidation kinetics, Fe(III) hydrolysis kinetics, and mineral precipitation into a simulation of the batch experiments. The Monod expression captures the kinetics of Fe(II) oxidation over the range of pH and inital Fe conentrations. Even in a relatively simple system, the model requires a complex interplay of kinetic and equilibiurm geochemistry.

Rates of abiotic As(III) oxidation were measured as a function of Fe(III) to As molar ratio (0.1-10,000) under a simulated natural light source in the absecence of microorganisms. This reaction is driven by the photoreduction of Fe(III) causing oxidation of As(III) [1 and references therein]. The effect of pH and concentration on reaction rate was also measured. As(III) oxidation proceeds faster at higher Fe(III) concentrations, in an approximately log-linear manner with respect to Fe:As ratio, and is faster at higher pH values.

Microbial Fe(II) oxidation experiments were conducted in the presence of As(III) and light, and the experimental results were modeled using the PHREEQC code. The model was used to evaluate our understanding of coupled biotic/abiotic processes, especially the ability to incorporate kinetic expressions into biogeogeochemical models.

[1] Asta (2012) *Applied Geochemistry* **27**, 281-291.

Does Tl/Pb in basalts record low pressure degassing behaviour?

DANTE CANIL [1*]

[1]University of Victoria, Victoria, Canada, dcanil@uvic.ca (* presenting author)

Abstract

Thallium and lead are both incompatible in crystals involved in melting and crystallization of basalts but are fluid-compatible during low pressure degassing of magmas, and occur in considerable concentrations in volcanic aerosols. A compilation of crystalline and glassy basalts (n=628) from mid-ocean riddges (MORs), ocean islands (OIBs), arcs (ARCs) and continental (CONs) settings show sub-parallel but offset arrays of Tl-Pb covariation as a function of eruptive style, irrespective of geologic setting. Specifically, at a given Tl content, all subaqeously erupted basalts, whether from the OIB or ARC settings, glassy or crystalline, contain 5 to 10 times less Pb compared to subaerially equivalents.

Both Tl and Pb have a Kd fluid/melt of between 5 and 10, and Kd Tl/Pb descreases with Cl in the fluid, with Pb preferring Cl-rich fluids. Preferential Pb loss observed in subaqeous rocks could be due to degassing of Cl-rich fluids compared to subaerially erupted magmas, but the variability in Cl in natural basalts is not large enough to affect the change in Tl/Pb observed. Another possibility is that the lower pressure of degassing of subaerial magmas relative to subaqueous examples, leads to lower H_2S/SO_2 in the fluid and causes much higher compatibility of Tl relative to Pb in the fluid, and decreased Tl/Pb in a degassed magma. If fluid-melt partitioning for Tl and Pb can be experimentally calibrated at presures below 2000 bars, the Tl/Pb ratio of basalts could potentially serve as a record of their degassing pressure.

Conclusion

Both Tl and Pb are geochemically similar but the ratio of these metals in erupted basalts differs with eruption mode, and is potentially a record of degassing pressure and fluid composition.

https://doi.org/10.1180/S0026461X00008434 Published online by Cambridge University Press

Psychrophiles at the Seafloor: Temperature Response of the Microbial N Cycle in Arctic Fjord Sediments

ANDY CANION[1*], JOEL E. KOSTKA[2], AND PATRICK CHANTON[2]

[1]Earth,Ocean, and Atmos. Science Dept., Florida State University, Tallahassee, FL, acanion@fsu.edu (* presenting author)
[2]Department of Biology, Georgia Institute of Technology, Atlanta, GA, joel.kostka@biology.gatech.edu

The response of the microbial N cycle in polar environments to climate change will depend on the metabolic potential of microbial communities. This research addresses the temperature response of nitrate/nitrite respiration activity and the coupling of the C and N cycles in Arctic fjord (Svalbard) sediments at two sites, Kongsfjorden and Smeerenbergfjorden, with contrasting organic carbon contents of 0.3% and 1.45%, respectively. Rates of denitrification and anammox were determined in anaerobic slurries from -1°C to 40°C with and without the addition of organic carbon substrates. Kongsfjorden sediments showed a lower temperature optimum for anammox (10-20°C) than denitrification (25°C). Smeerenbergfjorden showed similar potential rates of denitrification across a temperature range from 5°C to 30°C, and anammox rates were highest at 26°C. A long term (weeks) temperature shift experiment was performed with Kongsfjorden sediment at 4°C and 25°C to determine structure-function relationships of the microbial communities. Sediments maintained at 4°C exhibited decreased rates of denitrification and increased anammox rates. Sediments exposed to warming (25°C) showed a shift in the optimal denitrification rate to 35°C, a loss of anammox activity, and a change in microbial community composition. Cold sediments amended with carbon substrates maintained the same temperature optima for NO_3^- respiration but showed a pronounced increase in microbial community diversity. Our results indicate a tight interaction between temperature and organic carbon in controlling rates of microbial N cycling that is linked to shifts in microbial community structure in permanently cold environments.

^{17}O anomaly of tropospheric CO_2 fluxes from soil, leaf and ocean

XIAOBIN CAO[1*], YUN LIU[1]

[1]STATE KEY LABORATORY OF ORE DEPOSIT GEOCHEMISTRY, INSTITUTE OF GEOCHEMISTRY, CHINESE ACADEMY OF SCIENCES, GUIYANG, CHINA, LIUYUN@VIP.GYIG.AC.CN (* presenting author)

^{17}O anomaly, a new potential tracer, may supply additional information about the sources and sinks of CO_2. Previous works focused on troposphere-stratosphere CO_2 exchange, which were resulted from the limited understanding of ^{17}O anomaly mechanisms and the lack of precise analytical methods. Recently, a new analytical technique can precisely determine $\Delta^{17}O$ of CO_2,[1] which may change the scenario of this field. It has been expected for a long time that the study of ^{17}O anomaly of CO_2 can be just like those of small ^{17}O anomaly of meteoric waters.(eg, [2]) In this work, we will present theoretical estimates of $\Delta^{17}O$ of CO_2 fluxes from soil, leaf and ocean.

To estimate $\Delta^{17}O$ of CO_2 fluxes from soil and leaf, previous models are used.([3], [4]) Equilibrium theta value (i.e., $\ln^{17}\alpha/\ln^{18}\alpha$) for CO_2-H_2O exchange is taken from [5]. Kinetic theta value for the CO_2 diffusion process is calculated from kinetic theory of gases.(e.g., [6]) CO_2 flux from ocean is assumed to be in equilibrium. The results show that $\Delta^{17}O$ of CO_2 fluxes from different sources are different and the differences are on the order of 0.1 per mil, in the scope that recent techniques can precisely distinguish. Using $\Delta^{17}O$ of tropospheric CO_2, a lot of information could be obtained. The ^{17}O anomalies are temperature and other properties dependent, which could be used to refine or re-check previous models, providing new chance to build more reasonable CO_2 flux models.

[1] Hofmann and Pack (2010) *Anal. Chem.* 82, 4357-4361. [2] Luz and Barkan (2010) *GCA* 74, 6276-6286. [3] Tans (1998) *Tellus* 50B, 163-178. [4] Cernusak, et al. (2004) *Plant Physiol.* 136, 3350-3363. [5] Cao and Liu (2011) *GCA* 75, 7435-7445. [6] Barkan and Luz (2007) *RCMS* 21, 2999-3005.

https://doi.org/10.1180/S0026461X00008434 Published online by Cambridge University Press

Ionization of H_2O – saturated CO_2 at PT conditions relevant to CCS

RYAN M. CAPOBIANCO[1*], MIROSLAW S. GRUSZKIEWICZ[2], ROBERT J. BODNAR[1], J. DONALD RIMSTIDT[1]

[1]Department of Geosciences, Virginia Tech, Blacksburg, USA, rcapobi@vt.edu (* presenting author)

[2]Oak Ridge National Laboratory, Oak Ridge, USA, gruszkiewicz@ornl.gov

Recent studies have shown that mineral carbonation reactions proceed rapidly in the presence of CO_2 – rich ("supercritical") H_2O – CO_2 fluids at temperatures and pressures relevant to Carbon Capture and Storage (CCS) [1][2]. These earlier studies suggest that reactions are occurring on the mineral surface (or in a thin film of aqueous fluid), rather than as dissolution – precipitation mediated by the bulk fluid, as is the case in aqueous geochemistry. This has important implications for CCS in saline aquifers, as the CO_2 – rich phase is positively buoyant with respect to existing brine and will be the fluid in contact with cap rock. Reactions between the CO_2 – rich phase and the cap rock can enhance storage security (if carbonate minerals form) or degrade security (if the fluid corrodes the cap rock). It is well known that in aqueous solutions, H_2O and CO_2 react to form H_2CO_3 which ionizes and promotes dissolution – precipitation reactions. If significant ionization occurs in CO_2 – rich fluids under geologically relevant conditions, understanding reactions between H_2O – saturated CO_2 and mineral phases present in the aquifer will be important when assessing risk associated with CCS.

When ionization occurs in a fluid, such as due to dissociation of H_2CO_3, it allows the fluid to conduct electricity. The conductivity of the fluid is related to the concentration of ions, their charge, solvation, and the physical properties of the fluid. In this study we measure the conductivity of H_2O – saturated CO_2 solutions from 25 to 200°C and 7.39 to 20 MPa using a flow-through conductivity cell. Flow conductivity experiments reduce error associated with sorption to the walls of the cell and accumulation of impurities. Combined with a low cell constant (0.03/cm) we are able to detect conductivity on the order of pS to nS/cm.

In this study we show that conductivity of H_2O – saturated CO_2 does not exceed 3nS/cm from 25-200°C and 7.39 to 20MPa. These conductivity values are comparable to "dry" CO_2 (< 3ppmw H_2O), and indicate that little or no ionization is occurring. In addition, we show that there is no detectable relationship between H_2O content and conductivity from < 1ppmw H_2O to saturation. We conclude that at these conditions "wet" CO_2 has no significant ability to ionize.

[1] Schaef et al. (2011) *Geochimica et Cosmochimica Acta* **75**, 7458-7471. [2] Kwak et al. (2010) *J. Phys. Chem. C* **114**, 4126-4134.

Seasonal and inter-annual variations in emerging groundwater mine pollution: Essential background information for acid mine drainage management and remediation

MANUEL A. CARABALLO[1,2*], FRANCISCO MACÍAS[2], JOSÉ MIGUEL NIETO[2], CARLOS AYORA[3] AND MICHAEL F. HOCHELLA, JR.[1]

[1] Department of Geosciences, Virginia Tech, Blacksburg, VA 24061, U.S.A., manuelac@vt.edu (*presenting author)

[2] Geology Department, University of Huelva, Campus "El Carmen", E-21071 Huelva, Spain.

[3] Institute of Environmental Assessment and Water Research, CSIC, Jordi Girona 18, E-08034 Barcelona, Spain.

Design and development of water resources management and restoration strategies requires a deep understanding not only of the specific characteristic of the pollution affecting the water environment but specially of the possible short and long term cycles affecting the intensity of the pollution. The acid mine drainage (AMD) emerging from the adit of Mina Esperanza (Iberian Pyrite Belt, SW Spain) was selected as a typical AMD groundwater effluent from a sulfide mining district influenced by a dry (Mediterranean) climate. This point AMD discharge was monitored for more than four years to reveal the effect of seasonal and inter-annual weather changes in the water flow rate and pollutant concentration. Three well differentiated polluting stages were observed corresponding to: 1) stable low flow rate and high metals concentration, 2) increasing-decreasing cycle of both high to extreme metals concentration and flow rate, and 3) increasing-decreasing cycle of flow rate but steady high metals concentration. The specific processes and mechanism involved in the generation of these three stages (pyrite dissolution, evaporitic salts precipitation-redisolution and pluviometric inter-annual fluctuations) can be understood on the basis of the water chemistry and statistical analyses performed. Despite the almost negligible seasonal variations observed in the AMD pollution, the important variability observed in the inter-annual periods strongly recommends long-period AMD monitoring as essential background information for water resources management. This knowledge is being shown to be critical to efficiently perform environmental impact studies in these specific areas (sulfide mining and dry climates) and subsequently to design efficacious remediation strategies.

https://doi.org/10.1180/S0026461X00008434 Published online by Cambridge University Press

Urban soil-dust interactions: improving urban risk models

RAQUEL CARDOSO[1*], KEVIN TAYLOR[2], JIANQUAN CHENG[1], AND NEIL BREWARD[3]

[1]Manchester Metropolitan University, School of Science and the Environment, raquel.cardoso@stu.mmu.ac.uk (* presenting author), j.cheng@mmu.ac.uk

[2]University of Manchester, School of Earth, Atmospheric and Environmental Sciences, kevin.taylor@manchester.ac.uk

[3]British Geological Survey, nbr@bgs.ac.uk.

Introduction

Road deposited sediments (RDS) carry a high loading of potentially harmful elements (PHE). Another environmental media that is a likely source of PHE in urban areas is soil. PHE present in these media may cause deleterious human health effects due to close proximity to the receptors; furthermore, urban agglomerations tend to grow exponentially and so does the importance of RDS and soil characterization and monitoring. The aim of this research is to explore the spatial, geochemical and mineralogical linkages, and produce novel mineralogical data on the PHE/particulate relationships within and between soils and RDS.

Results and Conclusion(s)

Geochemical datasets are composed of 144 RDS and 300 soil samples, collected across 75 Km^2 of Manchester urban centre. PHE maximum and average concentrations, determined by XRF, are generally higher in soils than in RDS. Geographic information systems (GIS) allowed the spatial detection of contamination hotspots for these media, where PHE concentrations (namely for Cr, Ni, Cu, Zn, Pb and Cd) were in excess of the regional 90th percentile. Spatial analysis pointed to localised contamination sources as main influences on RDS composition, which vary considerably over short distances. However, spatial distribution of PHE in soil highlighted four broader areas with systematically high concentrations. Principal component analysis (PCA) has evidenced important PHE associations both for soils and RDS. PCA of grain size data obtained by laser diffractometry revealed that, in RDS, the 63-125µm fraction might act as hosts for PHE. SEM-EDS analysis supported this observation, but the source(s) of these grains still needs further investigation - they have also been observed in soil samples from the same area.

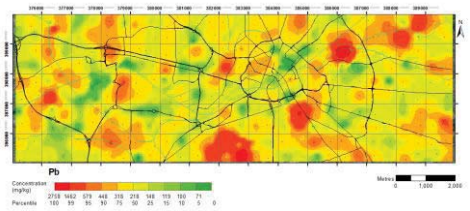

Figure 1: Interpolated surface for lead in Manchester soils.

This detailed geochemical and mineralogical characterization of both soil and RDS, as well as their spatial associations, allow a better understanding of PHE dynamics in urban systems and add vital knowledge on the risks posed to human populations by PHE exposure.

Icelandic zircon: Illuminating juvenile silicic crust construction

T.L. CARLEY[1*], C.F. MILLER[1], A.J. PADILLA[1], J.L.WOODEN[2], I. BINDEMAN[3], A.K. SCHMITT[4], R.C. ECONOMOS[4], C.M. FISHER[5], J.M. HANCHAR[5]

[1] Vanderbilt U., Earth and Environmental Sciences, Nashville, TN, USA, tamara.l.carley@vanderbilt.edu (*presenting author), calvin.miller@vanderbilt.edu, a.padilla@vanderbilt.edu

[2] Stanford U., USGS-SUMAC SHRIMP Lab, Stanford, CA, USA, jwooden@stanford.edu

[3] U. of Oregon, Geological Sciences, Eugene, OR, USA, bindeman@uoregon.edu

[4] U. of California Los Angeles, Earth and Space Sciences, Los Angeles, CA, USA, axel@oro.ucla.edu, economos@ucla.edu

[5] Memorial U., Earth Sciences, St. John's, NL, Canada, c.fisher@mun.ca, jhanchar@mun.ca

Iceland's crust (thick, juvenile, silicic and mafic, zircon bearing, with an elevated geothermal gradient) resembles what is visualized for the early (Hadean-Archean) crust, whose physical record exists only in detrital zircon. It is tempting to postulate that Icelandic crust construction is an analogue for early-Earth processes. We explore this hypothesis using trace elements (SHRIMP) and O (SIMS) and Hf (LA-MC-ICPMS) isotopes to characterize zircon from 15 samples (active and ancient volcanoes, intrusions, sandstones, river sands) spanning Iceland's range of ages and tectonic settings.

Our Icelandic "protocontinental" zircons exhibit setting-specific variability, but together share elemental and isotopic characteristics that clarify silicic petrogenesis in this type of environment. They define a narrow range of compositions, overlapping with zircon from ocean islands and, notably, Alid Volcanic Center (continental-oceanic transitional rift, Eritrea); their compositions are largely distinct from continental, MORB, arc, and Hadean zircon (e.g., on plots of U/Yb vs Y, Yb/Nb vs U/Yb). Icelandic zircons are typically ~3x richer (~15 vs 5 ppm) and more variable in Ti than Hadean-Archean zircons, suggesting higher crystallization temperatures. Their range of $\delta^{18}O$ (~0 to +3‰ on-rift, ~+3 to +5‰ off-rift, to -6‰ hydrothermal-like) is very low by global standards, and significantly lower than reported Hadean-Archean values (~4.5-7.5‰). Icelandic zircon ε_{Hf} typically ranges from +10 to +17 (lowest off-rift, highest on), spanning reported values for Icelandic basalt. Extremely low ε_{Hf} of +5 for zircon from Askja 1875 AD pumice (host pumice ε_{Hf} +14) suggests that Icelandic rhyolite might not all be truly juvenile; ancient crust may influence petrogenesis, in discrete locations.

Our data set, while not precluding petrogenetic similarities between Icelandic and early-Earth silicic magmas, demonstrates differences in zircon that call into question a closely similar origin.

https://doi.org/10.1180/S0026461X00008434 Published online by Cambridge University Press

Wiring the cell wall: Surface multiheme *c*-type cytochromes from *Thermincola potens* and implications for dissimilatory metal reduction by Gram-positive bacteria

HANS K. CARLSON[1,2], ANTHONY T. IAVARONE[3], AMITA GORUR[7], BOON SIANG YEO[6], ROSALIE TRAN[4,8], RYAN A. MELNYK[1], RICHARD A. MATHIES[4,8], MANFRED AUER[2,7] AND JOHN D. COATES[1,2,5]

Department of Plant and Microbial Biology[1], Energy Biosciences Institute[2], QB3/Chemistry Mass Spectrometry Facility[3], and Department of Chemistry[4], University of California, Berkeley; Earth Sciences Division[5], Chemical Sciences[6], Life Sciences Division[7] and Physical Biosciences Division[8], Lawrence Berkeley National Laboratory, Berkeley, CA 94720

Background

Almost nothing is known about the mechanisms of dissimilatory metal reduction by Gram-positive bacteria, although they have been shown to be the dominant species in some environments. Thermincola potens strain JR was isolated from the anode of a microbial fuel cell inoculated with anaerobic digester sludge and operated at 55 °C. Preliminary characterization revealed that T. potens coupled acetate oxidation to the reduction of hydrous ferric oxides (HFO) or an analog of the redox active components of humic substances, anthraquinone-2,6-disulfonate (AQDS). The genome of T. potens was recently sequenced, and the abundance of multiheme c-type cytochromes (MHCs) is unusual for a Gram-positive bacterium.

Results and Conclusions

We present evidence from trypsin shaving LC-MS/MS experiments and surface-enhanced Raman spectroscopy (SERS) that indicates the expression of a number of MHCs during T. potens growth on either HFO or AQDS and that several MHCs are localized to the cell wall or cell surface of T. potens. Furthermore, one of the MHCs can be extracted from cells with low pH or denaturants suggesting a loose association with the cell wall or cell surface. Electron microscopy does not reveal an S-layer, and the precipitation of silver metal on the cell surface is inhibited by cyanide, supporting the involvement of surface-localized redox-active heme proteins in dissimilatory metal reduction. These results are the first direct evidence for cell-wall associated cytochromes and MHC involvement in conducting electrons across the cell envelope of a Gram-positive bacterium.

Early Earth differentiation: Before and after Earth formation

R.W. CARLSON[1*], M. BOYET[2], , M. JACKSON[3], J. O'NEIL[2], L. QIN[4]

[1]Carnegie Institution of Washington, USA, rcarlson@ciw.edu (* presenting author)
[2]Laboratoire Magmas et Volcans, Clermont-Ferrand, France, m.boyet@opgc.univ-bpclermont.fr, j.oneil@opgc.univ-bpclermont.fr
[3]Boston University, USA, jacksonm@bu.edu
[4]Lawrence Berkeley National Laboratory, USA, lqin@lbl.gov

An increasingly long list of isotopic differences between Earth and most types of chondritic meteorites is straining the traditional model of a bulk Earth composition that has chondritic abundances of the refractory lithophile elements. Some isotopic differences (e.g. Cr, Mo, Ba) reflect an imperfect mix of the various nucleosynthetic contributions to the Solar nebula. Oxygen isotope differences between Earth and meteorites appear to reflect photochemically induced isotope variation in the nebula with differential sampling of volatile and refractory components by meteorites and terrestrial planets. Both causes of isotope variation point to chemical variability in the Solar nebula that was inherited by the terrestrial planets. The composition of the bulk-silicate-Earth predicted from the difference in $^{142}Nd/^{144}Nd$ between Earth and chondrites is most consistent with the loss of a component produced by low-pressure melting. Compared to chondritic Earth models, the calculated non-chondritic Earth composition has 30-35% lower concentrations of heat producing elements (U, Th, K), eliminating the need for ^{40}Ar retention in the mantle, and implying that incompatible element depleted material is the volumetrically dominant mantle component.

Variability in the relative abundance of daughter products (^{142}Nd, ^{182}W) of short-lived nuclides in Archean/Hadean rocks points to preservation of chemical heterogeneity within Earth's interior that was created by differentiation events occurring prior to 4.3-4.4 Ga. The declining ^{142}Nd variability between 3.8 and 3.5 Ga must reflect mixing within the silicate mantle. While this explanation might also apply to the recent discovery of ^{182}W variability, another option is that the W isotopic variability reflects addition of siderophile elements to Earth's mantle by continued late accretion. The composition of Hadean crust exposed in the Nuvvuagittuq greenstone belt and the inferred composition of the host rocks of the western Australia Hadean zircons point to the beginning of crust forming processes similar to those acting through the Archean within 100-200 Ma of Earth formation.

https://doi.org/10.1180/S0026461X00008434 Published online by Cambridge University Press

Kinetics of garnet nucleation: Inferences from natural occurrences

WILLIAM D. CARLSON[1*], ERIC D. KELLY[1], RICHARD A. KETCHAM[1]

[1]Department of Geological Sciences, University of Texas at Austin, Austin, Texas 78712 USA, wcarlson@mail.utexas.edu (* presenting author)

Recent assessments of nucleation and growth of garnet in metamorphic rocks [1-3] invoke divergent controlling mechanisms, and make widely contrasting predictions for nucleation kinetics that are sharply differentiated by the sizes of the thermal intervals over which nucleation is envisioned to extend. Tests of these predictions against chemical and textural features in natural occurrences favor a mechanism in which diffusive impediments to equilibration produce protracted nucleation that extends across a large fraction of the crystallization history.

A set of 371 centered radial concentration profiles on central sections (located by HRXCT) and 468 central compositions for individual garnet crystals in a single sample from the Picuris Range (New Mexico, USA) [4] can be explained only if nucleation of new crystals continued throughout nearly the entire period of garnet crystallization. Mutual consistency among Fe, Mg, and Mn concentrations documents establishment of rock-wide chemical equilibrium for these elements, which allows one to use, for example, Mn content as a proxy for time. A strong correlation exists between crystal size and central Mn content, and central Mn contents in progressively smaller crystals match Mn concentrations in progressively more rimward portions of larger crystals. In these and other rocks, further evidence of protracted nucleation arises when quantitative textural analysis reveals spatial ordering of crystal centers, consistent with suppression of nucleation in diffusionally depleted zones surrounding pre-existing crystals. Such effects have been documented in a suite of 13 garnetiferous pelitic and mafic rocks spanning a wide range of metamorphic conditions.

These chemical and textural observations require that nucleation of garnet is commonly essentially continuous throughout nearly all of its crystallization history: nucleation commonly spans a broad thermal interval (several tens of degrees) and is thus characterized by substantial thermal overstepping and significant departures from chemical equilibrium. The observations are consistent with numerical models of diffusion-controlled nucleation and growth [3] that replicate measured size-composition-isolation correlations, plus spatial ordering and other key textural features; such models require that nucleation intervals span 50-100 °C or more. The observations run strongly counter to the predictions of models that invoke interface-limited precipitation control [2] or reactant-dissolution-limited control [1], for which thermal intervals of nucleation are calculated to be very narrow, ~1 °C or < ~6 °C respectively.

In one exceptional case, chemical data indicate that nucleation was restricted to a short period near the beginning of garnet crystallization [5], but textural measures show that early site-saturation — rather than non-diffusional controls — was responsible.

[1] Schwarz *et al.* (2011) *J Meta Geol* **29**, 497-512. [2] Gaidies *et al.* (2011) *Contrib Mineral Petrol* **162**, 975-993. [3] Ketcham & Carlson (in press) *J Meta Geol*. [4] Chernoff & Carlson (1997) *J Meta Geol* **15**, 421-438. [5] Meth & Carlson (2005) *Can Mineral* **43**, 157-182.

Biological controls on Mn oxide ore formation in east Tennessee, USA

SARAH K. CARMICHAEL*, CRYSTAL G. WILSON, MICHAEL RASH, AND JOSHUA FEIERSTEIN

Appalachian State University, Boone, NC, USA, carmichaelsk@appstate.edu (* presenting author)

Field Relationships

Mn oxide ore deposits are commonly found as discrete and disseminated deposits below the middle Ordovician unconformity throughout the Valley and Ridge from GA to VA. Deposits in the Cambrian Erwin, Shady, and Rome Formations in northeast TN are associated with brecciated jasperoid and residual clays of the Shady dolomite and are exposed in the hanging wall of northeast trending thrust faults juxtaposed atop Erwin Formation quartzites. Ore formation postdates jasperoid replacement and occurs primarily as matrix material in jasperoid breccias and as vug infillings with minor occurrences along faults and bedding planes.

Mineralogy and Crystal Morphology

Mn oxides in these ores exhibit a variety of morphologies: loose pellets enclosed in geodes, botryoidal nodules, dendrites and shrubs, drusy coatings on geode interiors, and massive porous and laminated ore with interbedded laminae of Mn oxides and Fe oxyhydroxides. X-ray diffraction (XRD), and scanning and transmission electron microscopy (SEM, TEM) indicate that the shrubs, pellets, and laminae are composed of columnar crystals of a cryptomelane-hollandite solid solution, and are associated with filaments of goethite nodules that form a draped net-like structure. Botryoidal nodules are composed of sheets of romanechite exhibiting stromatolitic layering. The dendritic and drusy Mn oxides are composed of nanoscale acicular cryptomelane needles radiating from irregular chains and interconnected clumps of clay spheres. The dendrites and drusy are microporous with imprints of gas bubbles. The shrubs and laminae resemble stalactites with crystals radiating out from nucleation sites in increasing sizes, and are partially encased by ropes of gravity-draped goethite filaments. Nucleation sites consist of irregular sheets, encrusted ropes, and networked filament structures. TEM and XRD analysis indicate that individual Mn and Fe oxide crystals around the nucleation sites are highly ordered, yet on the μm scale they exhibit unusual morphologies commonly associated with biological mineralization [1,2,3]. Fluid inclusion observations in the jasperoid matrix indicate fluid temperatures < 120°C for the region, which does not rule out biological associations.

Conclusions and Continuing Work

Due to the scale and shape of of the nucleation sites, it is likely that small Mn oxide crystals nucleated on negatively charged biological particles (such as extracellular polymeric substances), allowing for abiotic crystal growth, and were not deposited directly on cell surfaces as primary, poorly crystalline biominerals. $^{40}Ar/^{39}Ar$ dating of cryptomelane will constrain the timing of ore emplacement and allow paleoreconstruction of regional sources of ore fluids.

[1] Hofmann and Farmer (2000) *Planet. Space Sci.* **48**, 1077–1086
[2] Chafetz and Guidry (1999) *Sedimentary Geology* **126**, 57-74
[3] Parenteau and Cady (2010) *PALAIOS* **25**, 97-111

https://doi.org/10.1180/S0026461X00008434 Published online by Cambridge University Press

Structural changing control of potassium saturated smectite at high pressures and high temperatures: application for subduction zones

L.C.CARNIEL[1], R.V.CONCEIÇÃO[1,2], N.DANI[1], V.F.STEFANI[2]

[1]Instituto de Geociências, UFRGS, Porto Alegre – RS, Brasil.
larissa.colombo@ufrgs.br
rommulo.conceicao@ufrgs.br
norberto.dani@ufrgs.br
[2]PGCIMAT, UFRGS, Porto Alegre – RS, Brasil.
vicentestefani@hotmail.com

The lithospheric mantle is characterized by pressure ranges from ~ 2.0 and ~ 7.7 GPa and a specific mineralogy and composition. This region can be re-hydrated and re-enriched in incompatible elements (*e.g.* potassium) through subduction processes that bring pelagic material, composed of clay minerals and other phyllosilicates, together with the hydrated subducted oceanic slab. A mass transfer from the subducted slab plus sediments into the mantle wedge occurs primarily through the release of aqueous fluids produced by devolatilization of hydrated minerals. In this context, smectite stands out as one of the most important minerals responsible for re-enriching the lithospheric mantle with water and incompatible elements when its structure is destabilized. By pressure and temperature increasing smectite can lose its interlayer water, at the same time that it transforms into a mixed-layer Illite-Smectite, followed by illite crystallization. In this condition of dehydration, and with increasing burial, reactions evolve in transforming illite to phengite, a variety of muscovite which plays an important role as host of potassium in subducted oceanic crust. In this work, we verified the structural and compositional behavior of K saturated smectite under pressure from 2.5 to 4.0 GPa and at different temperatures (400ºC to 700ºC). . X-ray diffraction, scanning electron microscopy (SEM), infrared spectroscopy (FTIR) and transmission electron microscopy (TEM) results suggest that under the pressure of 2.5GPa, which is about 75km depth in the mantle, and at around 500ºC smectite transforms into phengite, while under the pressure of 4.0GPa, equivalent to 120km depth, the same transformation occurs at 400ºC. These results contribute significantly to understanding how pelagic sediment dehydration occurs in a subduction process, as well as the behavior of smectite under the influence of increasing pressure and temperature.

Structural evolution of the retrowedge, SE Canadian Cordillera

SHARON D. CARR[1*] & PHILIP S. SIMONY[2]

[1]Carleton University, Ottawa Carleton Geoscience Centre, Department of Earth Sciences, scarr@earthsci.carleton.ca
[2] University of Calgary Department of Geoscience, pssimony@ucalgary.ca

In the southern Canadian segment of the Cordilleran orogen, a Middle Jurassic "small cold accretionary orogen [1]" evolved into a doubly vergent, "warm medium-sized orogen [1]" during Cretaceous to Eocene oblique convergence. In some orogens (e.g. Appalachians, Caledonides, Himalaya) a megathrust sheet or crystalline sheet with basal shear zone overrode the foreland obscuring the relationships between coeval Internal and External structures. However, in the ~400 km wide, east-verging, retrowedge of the southern Canadian Cordillera, the Internal zone is situated to the rear of the External zone preserving evidence of structural and kinematic linkages. The External Rocky Mountains and Foothills comprise three major east-verging, Late Cretaceous to Eocene, thin-skinned, piggyback thrust and fold systems, with ~180 km of shortening, that root westward into a basal décollement. The Western Internal zone is characterized by tracts of metamorphic rocks and metamorphic core complexes (e.g. Kettle, Okanagan, Priest River and Valhalla), some of which are basement-cored domes (e.g. Frenchman Cap, Thor-Odin, and Spokane). They have a downward-younging progression of Late Cretaceous to Eocene metamorphism and deformation in infrastructural flow zones characterized by transposition foliation, migmatites, flow folds and 1-7 km thick shear zones. Nested between the External and Western Internal zones is a relict ~100-200 km wide Early Cretaceous orogen, that predated emplacement of ca. 100 Ma plutons. The geology and architecture of the Western Internal and External zones can be explained by progressive development of major Late Cretaceous to Eocene shear zone systems in the Internal zone that can be directly linked with coeval thrust and fold systems in the External zone. The linkage was via Late Cretaceous activation and Late Cretaceous to Early Eocene reactivation of the 150-200 km-wide central portion of the Rocky Mountain basal décollement that lies beneath and translated the intervening Early Cretaceous orogen. During orogenesis, the craton was progressively underthrusting the developing retrowedge. Thickening in the retrowedge insulated the underlying rocks of the incipient Internal zone, thus resulting in a mechanism of progressive heating, weakening and localization of the basal shear zone. At the base of the wedge, cooler stiffer rocks lay to the east of the Internal zone, at each stage, acting as an indentor. Thus, the development of a basal shear zone was coupled with flow of the hot mass of the Internal zone up and over an indentor, strain softening of it, and incorporation of it into the wedge in successive stages. Our general model is consistent with those of Beaumont et al. (2010) demonstrating the lateral transition from stiff cool crust to hotter weaker crust where the stiff cool crust acted as an indentor, with development of a ramp at the edge of the indentor, and flow up and over the ramp. In the latest stages of Early Eocene shortening, extensional shear zone systems were localized on the margins of tectonothermal culminations. Motion of deep-seated décollements beneath some of these culminations may have contributed to their doming. Crustal shortening ended at ca. 52 Ma due to a change in tectonic setting to that of a transtensional tectonic regime, coinciding with the end of thrusting in the External thrust belt and with crustal-scale extension in the Western Internal zone.

[1] Beaumont *et al.* (2010) *CJES* **47,** 485-515.

https://doi.org/10.1180/S0026461X00008434 Published online by Cambridge University Press

Geochemical evidence for complex preeruption configuration of a silicic magma chamber associated with Los Humeros caldera, Mexico

GERARDO CARRASCO-NÚÑEZ [1*], MICHAEL BRANNEY[2], MICHAEL MCCURRY[3], AND MICHAEL NORRY[2]

[1] *Centro de Geociencias, Universidad Nacional Autónoma de México, Querétaro, Mexico.* gerardoc@geociencias.unam.mx
[2] *Department of Geology, University of Leicester, Leicester, U.K.* mjb26@leicester.ac.uk
[3] *Department of Geology, Idaho State University, Pocatello, ID, USA.* mccumich@isu.edu

The >15 km^3 late Pleistocene Zaragoza ignimbrite from Los Humeros caldera volcano in central Mexico shows complex (rhyodacite-andesite-rhyodacite) compositional zoning, including mingled and rare mixed pumice (dacite-D). Petrographic and microprobe analyses of coexisting glass and phenocrysts provides evidence of crystal-liquid equilibrium and disequilibrium conditions in multiple types of magmas at the time of eruption. Highly resorbed calcic plagiocase (to An_{82}) mantled by more sodic plagioclase suggests that pre-eruptive mixing between andesitic and plagioclase-bearing basaltic magma was followed by equilibrium crystallization within the resultant hybrid magma. A broad co-genetic relationship between the rhyodacite and basaltic andesite-trachyandesite magmas is indicated by overlapping Nd-, Sr- and Pb-isotopes, major- and trace-element covariation patterns, and the association in space and time. Differences in phenocryst chemistries indicate that the andesite-trachyandesite (A-TA) magma was at least 80˚C hotter than the rhyodacite (RD) magma at the time of the eruption. We propose a model (Fig. 1) where the ignimbrite eruption started tapping rhyodacite and then andesite from a zoned magma chamber. This was followed by a complex syn-eruptive mechanical mixing between a fairly uniform reservoir of rhyodacite, with a pre-eruptive heterogeneous (hybridized) mafic reservoir formed from andesites and andesite-trachyandesites, possibly in the form of semi-connected high-melt lenses within a partially consolidated crystal mush. Episodic replenishment of basaltic magmas occurs periodically.

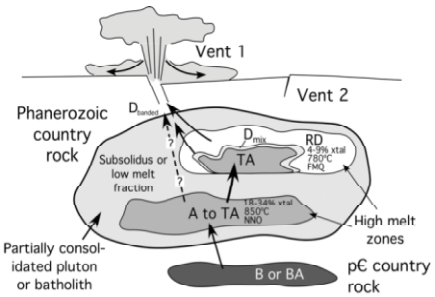

Figure 1: This shows our preferred pre-eruption magma reservoir model for the Zaragoza ignimbrite.

Lead, Cadmium and Copper concentrations and Lead isotopic distribution in seawater, sediments and coral reefs in Kuwait

CARRASCO, G. [1*], BOYLE, E.A.[1], NURHATI, I.[2], GEVAO, B.[3], AL-MATROUK, K. [3] AND AL-GHADBAN, A.N.[3]

[1]Earth, Atmospheric and Planetary Sciences Department, Massachusetts Institute of Technology, Cambridge, USA, gcarrasc@mit.edu (* presenting author)
[2]Singapore-MIT Alliance for Research and Technology, Singapore, intan@smart.mit.edu
[3]Kuwait Institute for Scientific Research, Kuwait City, Kuwait, aghadban@kisr.edu.kw

Objective and Methods

The objective of this study was to reconstruct detailed input chronologies of trace metals in the Kuwaiti marine environment, influenced by the Shatt al-Arab River's load, using water, sediment cores and corals. Pb, Cd and Cu concentrations in seawater and sediments were determined by plasma mass spectrometry using isotope dilution for seawater and Indium internal standardization for "Graney leach" sediment extracts. Pb isotopic distributions in seawater and sediments were determined using multicollector magnetic sector plasma mass spectrometry after anion exchange purification of Pb.

Results and Discussion

Pb, Cd and Cu concentrations in seawater are high in the northern stations, including Kuwait Bay, Awhah and south of Bubiyan Island. They show combined anthropogenic and riverine sources, while waters near two coral reefs near Kubar and Qaruh islands show high Pb, but low Cd and Cu. Surface sediment samples show metal enrichments in Kuwait Bay as expected for elements with anthropogenic enhancements; the 206/207Pb isotope data shows a large range, hinting to a mix of natural and leaded gasoline sources, or other sources, with a negative correlation of 206/207Pb in sediments vs. Pb in seawater and a decreasing trend into Kuwait Bay.

Analyses of the concentration and isotope distribution of Pb in the upper ~60-cm sediment strata and on porite corals are in progress.

https://doi.org/10.1180/S0026461X00008434 Published online by Cambridge University Press

Environmental Geochemistry of some Ore Deposits in the "Sierra Gorda" nature preserve, east-central Mexico

ALEJANDRO CARRILLO-CHAVEZ[1*], NORMA CRUZ-ORTIZ[2], ALICIA I. AUDIFRED-VALDEZ[3], ERIK SALAS[2], ELIHU AYALA[3], GILLES LEVRESSE[1], TAMMIE GERKE[4]

[1]Centro de Geociencias-UNAM, Juriquilla, Queretaro, 76230, Mexico, ambiente@geociencias.unam.mx (* presenting author), glevresse@geociencias.unam.mx

[2]Posgrado Ciencias de la Tierra UNAM, Juriquilla, Queretaro, 76230, Mexico, lunanueva@hotmail.com, turtlefsm@gmail.com

[3]Facultad de Quimica, Univ. Autonoma de Queretaro, Queretaro 76200, Mexico, audifred@uaq.mx, elihuayala@gmail.com

[4] University of Cincinnati, OH, USA, tammie.gerke@uc.edu

General Geology and Mineralization

Sierra Gorda nature reserve is the central part of the East Sierra Madre (Mother Range) of east Mexico. The Sierra Gorda is mostly composed by a highly deformed sequence of Mesozoic Carbonate sedimentary rocks. The Zuluaga Jurrassic formation host various hydrothermal deposits, which include Sn mantos, polymetallic sulfide veins and other irregular bodies [1]. There have been reconigzed some Eocene to Oligocene igneous intrusive bodies (granitoides stocks), crosscuting all the sedimentary sequence and developing mineralized metamorphic halos and hydrothermal veins, mantos, snd skarn bodies (stibine, cinabar, realgar, chalcopyrite, galena, sphalerite, Ag minerals with some Au and As) [2]. Exploitation of these mineralized bodies have left behind millions of tons of mine waste materials scattered in the nature preserve. These waste materials have released to the environemnt (soil and water) heavy metals (Cd, Cr, Co, Cu, Ni, Pb, Hg and Zn), and metalloids (As and Sb).

Environmental Geochemistry

We select three mining zones in the Sierra Gorda nature preserve for chemical analisis on the mine waste material, sediments, soil, water and some plants to assess the mobility, dispersion and geochemical controls of heavy metals and metalloids in the environment. Preliminary results show that mine tailings have up to 7 gr/Kg of As, 1 gr/Kg of Cu, 5 gr/Kg of Zn and 3 gr/Kg of Pb. River sediments concentrations of As and metals (maximum) are as follow: As = 2.5 gr/kg, Cu = 0.146 g/Kg, Zn = 1 g/Kg, and Pb = 0.117 g/Kg. For agricultural soils (small patches of land along river terraces) the As and metals concentrations are: As = 0.117 g/kg, Cu = 0.022 g/kg, Zn = 0.087 g/kg, and Pb = 0.037 g/kg. For surface water (seasonal mountain creeks) the As and metals concentrations are: As = 0.05 mg/l; Cu = 0.01 mg/l; Pb <0.017 mg/l, and Zn = 0.01 mg/l. We are processing different vegetation to determine bioacumulation of As and metals in different parts of the plants and in different zones of the mining area (affected by mine tailings, and no-affected by mine tailings). The ultimate goal is to understand the geochemical controls of As and heavy metals in this environemnet.

[1] Mascuñano et al., (2011) *Simple Sb Deposits in Mexico, in Barra, F. et al. (eds,) Proceedings, SGA Meeting, Chile Sept, 2011.*

[2] Vassallo, L.F., et al., (2001) *Mineralogy, age and control setting of La Negra and Zimapan skarn ore deposits, central part of Mexico. GEOS, Unión Geofísica Mexicana*, **Volume** 21, No. 3, p. 192.

Uranium concentration processes in Archaean batholiths, sources of the oldest uranium deposits

Simon Carrouée[1*], Jean-François Moyen[1], and Michel Cuney[2]

[1]Université Jean Monnet, Laboratoire de Transferts Lithosphériques, Saint-Etienne, France.
simon.carrouee@univ-st-etienne.fr (* presenting author)
jean.francois.moyen@univ-st-etienne.fr

[2]Université de Nancy, UMR G2R 7566 CNRS-CREGU, Nancy, France.
michel.cuney@g2r.uhp-nancy.fr

Session 9e : from a durable ressource to its environmental impact

The oldest economic uranium deposits on Earth are the quartz pebble conglomerate containing detrical uraninite from the Dominion Group (3074 ± 6 Ma) and the Witwatersrand Supergroup (2970 to 2714 Ma) on the Kaapvaal craton in South Africa. A reducing atmosphere before 2.2 Ga allowed uraninite to be stable on Earth's surface. We investigte the magmatic source of the uraninite; the ubiquitous Archaean TTG suite (trondhjemite-totalite-granodiorite) having uranium concentrations (about 2 ppm) insufficient to permit uraninite cristallization, the only posible source is ca. 3.1 Ga, incompatible elements-enriched, granitic batholiths such as the Mpuluzi and Heerenveen batholiths located to the South of the Barberton Greenstone Belt of South Africa

The Heerenveen and Mpuluzi batholith belong to the 3105 Ma granodiorite-monzogranite-syenogranite GMS suite intruding paleoarchaean TTG plutons. These two batholiths are made of different facies belonging to different phases of emplacement. Early sheeted leucogranites are followed by the intrusion of a large core of porphyritic granite, then by the intrusion of diverse facies in the border shear zones of both batholiths.

Although the average U composition of either batholiths is low (3 and 6 ppm for Heerenveen and Mpuluzi resp.), late phases emplacing in shear zones are significantly richer. However, they show a similar U/Th ratio than the bulk of the intrusions. On the other hand, a few samples show uranium concentrations up to 25 ppm, with Th/U ratios below 1, compatible with uraninite cristallization. Radiometric maps and analysis show that all these samples are located inside the shear zones; however in details the distribution of these spots is independant of lithologies. The size of these high uranium concentration zones is about 100 meters and can be located in later phases of intrusion as well as in earlier phases. This suggests that redistribution of incompatible elements and fractionation of U relative to Th occurred after emplacement of the granitoids and independantly of it.

Microscopic studies confirm that the primary uranium-bearing minerals such as monazite, xenotime and thorite are partially or totally altered, uranium-rich phases being secondary minerals such as brannerite and uraninite. Primary monazite have been altered by calcic fluids, and replaced by apatite and thorite; REE from the monazite form allanite and residual thorite, while uranium is partially incorporated into secondary thorite and partially liberated into the fluid. In ilmenite, uranium is concentrated in altered crystals (up to 6% wt UO_2), showing that ilmenite was altered by uranium-enriched fluids.

Conclusion

Two different processes seem to explain the uranium concentrations: (1) a magmatic process which concentrate uranium and thorium in the later intrusion phases and (2) a second process, calcic fluids associated to the shear-zones which alter primary accessory minerals and preferentially concentrate uranium in small zones independent of the different intrusion lithologies.

https://doi.org/10.1180/S0026461X00008434 Published online by Cambridge University Press

Distribution and Speciation of Arsenic in Poultry Particulate Emissions

SHANNON E CARTER[1*], DONALD L SPARKS[2], ANA MARIA RULE[3], RYAN TAPPERO[4] AND ERIC BENSON[5]

[1]University of Delaware, Newark, United States, Shanncar @udel.edu (* presenting author)
[2]University of Delaware, Newark, United States, dlsparks@udel.edu
[3]Johns Hopkins Bloomberg School of Public Health, Baltimore, United States, arule@jhsph.edu
[4]National Synchrotron Light Source, Upton, United States, rtappero@bnl.gov
[5]University of Delaware, Newark, United States, ebenson@udel.edu

The use of organo-arsenicals such as roxarsone in poultry production is quite common. These compounds are primarily used as anticoccidials, as growth promoters, and to increase feed efficiency. Such usage has raised a variety of environmental concerns such as the accumulation of arsenic in poultry excrement and the release of arsenic into air, soil and water resources. Confined animal feeding operations (CAFOs), such as broiler poultry houses, are sources for airborne particulate matter (PM) emissions and have become major environmental and human health concerns. Many growers and their families are the primary operators of these CAFO facilities, and can spend anywhere from 25-45 hours per week working on the farm. Farm workers who average as little as two hours per day inside of a CAFO may develop acute and chronic respiratory diseases associated with the long term exposure to the particulate matter. Studies have indicated that there is a presence of toxic metals and metalloids, such as arsenic found in the poultry litter; however, it is not well known whether the re-suspended PM from these poultry houses carries such toxic contaminants, which could be harmful to human health. This presentation will focus on the chemistry and metal(loid) speciation of airborne emissions of both $PM_{2.5}$ and PM_{10} from confined broiler operations. The samples were analyzed using traditional wet chemistry techniques, such as inductively coupled plasma-mass spectrometry (ICP-MS) to determine total heavy metal and metalloid concentrations. More advanced, state-of-the-art, synchrotron-based spectroscopic and microscopic techniques, such as SEM-EDX were applied to determine arsenic and other metal speciation and distribution, and thus shed light on the potential toxicity. The results of this research suggest that arsenic concentrations vary depending upon location, size fraction, and period of growout cycle. In addition, u-XANES results suggest that the arsenic present in both PM_{10} and $PM_{2.5}$ fractions can be in organic and inorganic forms, and is widely distributed across the filtered samples of the particulate matter.

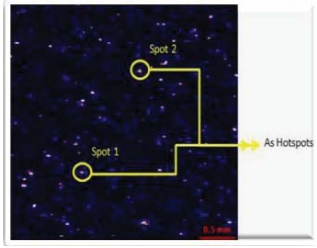

Figure: 3mm x 3mm micro X-ray fluorescence (m-XRF) map of As from a PM10 sample. The bright "hot" spots indicate an area where there is higher intensity of As present.

On overview of the deep carbon cycle and its isotope heterogeneity

P. CARTIGNY[1*], M. PALOT[2,1], M. CLOG[3,1], J. LABIDI[1], E. THOMASSOT[4], C. AUBAUD[1], V. BUSIGNY[1], J.W. HARRIS[5]

[1] IPG-Paris, Stable Isotope Laboratory, France (cartigny@ipgp.fr).
[2] Earth and Atmospheric Sciences, University of Alberta, Canada.
[3] Division of Geological and Planetary Sciences, Caltech, Pasadena, California, USA.
[4] CRPG-Nancy, Vandoeuvre-Les-Nancy, France.
[5] Dept of Geographical and Earth Sciences, University of Glasgow, Glasgow.

Carbon is massively exchanged between the Earth's surface and the deepest part of the mantle so that, on billion years time-scales, is at, or close to, steady state (= amounts and isotope compositions of C being degassed and subducted being balanced). This is best evidenced by constant C-isotope compositions, over nearly 3.5 Gy, in both sediments (typically 20% organic matter, 80% carbonates with δ^{13}C-values of -25 and 0‰ respectively) and mantle-derived samples (MORB, OIB, diamonds, carbonatites, carbonates from kimberlite) averaging $\delta^{13}C \sim -4\pm1$‰. This can also be inferred from the short modern residence time of surface carbon, close to 1.5 Gy. The implication is that modern recycled carbon flux equals degassed carbon flux at about 2×10^{12} mol/y.

Owing to mantle carbon steady-state, it is unlikely that mantle (= *cycled*) and primordial (= *uncycled yet)* carbon would display distinct isotopic, although longer residence time of mantle carbon, ca. 4-6 Gy, suggests that such a primordial C-reservoir might exist. Our best estimate, based upon diamonds having the most primordial (= *lowest*) N-isotope compositions, indicates a primordial C-isotope composition close to -3.5‰. The size of the primordial carbon reservoir remains however elusive.

If subducted carbon has a $\delta^{13}C_{average}$~-4‰, it is originally both chemically and isotopically heterogeneous; so there is some chance that some deep mantle domains would record a subduction-related heterogeneity. Such a heterogeneity cannot however be inferred from mid-ocean ridge or ocean island basalts; the C-isotope variability mostly reflect degassing processes (= lowering residual δ^{13}C). This is best illustrated by relationships with degassing proxies (e.g. $^{40}He/^{40}Ar^{*}$) but not with those tracing mantle volatile heterogeneity (e.g. H_2O/Ce, D/H or δ^{34}S-ratios). So, if any, mid-ocean ridge or ocean-island basalts bear very small C-isotope heterogeneity.

Many authors ascribe low δ^{13}C-diamonds (typically in the range of -15 to -25‰) to mantle carbon isotopic *heterogeneity* related either to subduction or to be primordial. Coupled ^{34,33}S, N and C-isotope systematics suggest however that most relate to high-temperature fractionation, occurring at depths (typically 250-150 km), prior to diamond precipitation.

Yet, several diamond populations (from komatiites in French Guyana and from Jericho kimberlite in Northern Slave with δ^{13}C-modes ~-28 ‰ and -38‰ respectively) are unique and difficult to interpret in the light of heterogeneity being either primordial, subducted or mantle-related (i.e. there are only rare sediments with δ^{13}C as low as -40‰). Together with diamonds from the transition-zone (from 300 to 660 km depth), there is still the possibility that mantle domains with odd C-isotope characteristics indeed exist. If correct, this would have very strong implications when considering sedimentary C-isotope excursions associated with the emplacement of large igneous provinces: their C-budget would not need to be close to the *canonical* mantle δ^{13}C of -4‰.

https://doi.org/10.1180/S0026461X00008434 Published online by Cambridge University Press

GEOCHEMICAL AND TEXTURAL CHARACTERIZATION OF FRESH WATER MICROBIALITES OF LAGUNA, BACALAR, MEXICO

SET CASTRO-CONTRERAS[1*], ERNESTO PECOITS[1], NATALIE R. AUBET[1], DANIEL PETRASH[1], MURRAY K. GINGRAS[1], KURT O. KONHAUSER[1]

[1]University of Alberta, Edmonton, Canada, sicastro@ualberta.ca (* presenting author)

Microbialites are amongst the oldest direct evidence of life [1]. Understanding how they are formed and the biosignatures they may disclose is important in understanding the evolution of early life on Earth. Microbialites reached their peak during the Proterozoic (>542 Ma) and drastically declined thereafter. The cause of which has been attributed to either grazing and/or burrowing by metazoans [2], or to changes in ocean chemistry leading to a drop in [CO_3^{2-}] [3]. The recent discovery of rare, freshwater endolithic microbialites in Laguna Bacalar, Mexico offers a unique opportunity to test the interaction between burrowing and grazing organisms, calcium carbonate precipitation, and microbialite growth. The Bacalar microbialites vary from centimetre- to metre-sized structures. The larger of these show two distinct layer types: (a) stromatolitic layers composed of millimetre-thick laminae of cyanobacterial cells encrusted in a low Mg-calcite matrix, and (b) thrombolitic, centimetre-thick layers of rounded micritic peloids, randomly distributed in microsparite cement. In contrast, the smaller microbialites are always laminated with a stromatolitic fabric. We observe that unlike stromatolitic layers, thrombolitic layers occur during a period of higher sediment and contain a lower abundance of biolimiting trace elements (e.g., Mn, Mg, Fe). This suggests that the rapidity of such migration (due to cementation) leads to an increase in binding/trapping and the resulting thrombolitic texture. Additionally, microbialites and sediment have a similar C- and O-isotopic signature, unlike those of associated gastropods and bivalves, suggesting no vital effect and the preservation of an environmental signature. In conclusion, while the rate of microbialite growth is largely a function of CO_3^{2-} ion saturation, the texture is especially dependant on accretion rate. Furthermore, the variability of the trace element concentrations is highly dependant on texture dependant. The very coexistence of these thriving microbialites with grazing and burrowing organisms implies that these do not inhibit growth and, therefore, suggest that the decline in microbialite abundance and diversity during the Phanerozoic was likely due to other factors.

[1]Lowe (1980) *Nature* **284**, 441-443. [2] Garrett (1970) *Science* **169**, 171-173. [3] Grotzinger (1e990) *Am J Sci* **290A**, 80-103

Deep water coral reefs as important sites of benthic mineralization?

CÉCILE CATHALOT [1,*], PIERRE POLSENAERE [2], TOM COX [1], DICK VAN OEVELEN [1], MARC LAVALEYE [1], GERARD DUINEVELD [1], TINA KUTTI [3] AND FILIP MEYSMAN [1,2]

[1]Nederlands Instituut voor Onderzoek der Zee (NIOZ), Yerseke/Texel, Netherlands,
Cecile.Cathalot@nioz.nl ([*]presenting author)
Tom.Cox@nioz.nl
Dick.van.Oevelen@nioz.nl
Marc.Lavaleye@nioz.nl
Gerard.Duineveld@nioz.nl
Filip.Meysman@nioz.nl
[2]Vrije Universiteit Brussel (VUB), Brussels, Belgium
Pierre.Polsenaere@nioz.nl
[3]Institute of Marine Research, Bergen, Norway
tina.kutti@imr.no

Benthic Oxygen Uptake rates measured on deep-water coral reef by Eddy Covariance (EC)

Deep-water coral reefs are unique biodiversity hotspots that are vulnerable to future environmental changes in response to climate change or fishing activities [1]. Accurately assessing the coral reef community metabolism is needed to ensure a suitable monitoring and management of these areas, but traditional methods are inadequate to map the complex 3D structure of these reefs.

Therefore the non-invasive EC technique has been used to measure in situ benthic respiration rates of a deep-water coral reef ecosystem and surrounding sponge-beds in the Træna Deep (Norway). EC measurements were contrasted with on-board oxygen incubations of living coral and bare sediments.

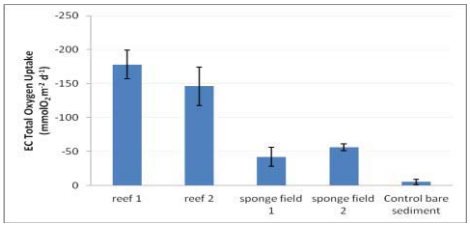

Figure 1: EC Total Oxygen Uptake rates (TOU, $mmolO_2\ m^{-2}\ d^{-1}$) at the Traena Deep site in June 2011.

Deep-water coral reefs: active benthic ecosystems

The Traena deep-water coral reefs have benthic oxygen consumption rates that are comparable to coastal benthic systems (TOU > 50 $mmolO_2\ m^{-2}\ d^{-1}$) and 35 times higher than bare sediments at comparable depth. If such high consumption rates are a common feature, deep water coral reefs are likely to play an important role in regional carbon cycles and need to be accounted for in global carbon budgets.

[1] Van Oevelen (2009) *Limnol. Oceanogr.*, **54(6)**, 1829–1844

https://doi.org/10.1180/S0026461X00008434 Published online by Cambridge University Press

What caused the 2.4 Ga rise of oxygen?

DAVID C. CATLING[1*], KEVIN J. ZAHNLE[2], MARK W. CLAIRE[3]

[1]University of Washington, Seattle, USA, dcatling@uw.edu (*presenting author)
[2]NASA Ames Research Center, Moffett Field, CA, USA, kevin.j.zahnle@nasa.gov
[3]University of East Anglia, Norwich, UK, M.Claire@uea.ac.uk

The Great Oxidiation Event (GOE) was an increase in O_2 levels from <1 ppm to 0.2-2% at ~2.45-2.22 Ga. How it happened is still debatable. One idea is that the GOE ensued when oxygenic photosynthesis originated [1]. But evidence suggests that oxygenic photosynthesis considerably predates the GOE, e.g., from redox-sensitive metals, stromatolites, organic carbon derived from methanotrophs, and biomarkers [2]. Instead, reductants plausibly cleared the late Archean air of O_2. Most hypotheses explain the delay by suggesting that O_2 sources took time to overwhelm O_2 sinks.

The O_2 source, organic carbon (C_{org}) burial, may have slowly increased to cause the GOE [3]. But the noisy $\delta^{13}C$ record may not allow for such a change [4], while the decomposition of C_{org} in the ~10^8 yr geologic cycle destroys O_2 gains from C_{org} burial. Also, inventories show that continents have excess oxygen, not excess C_{org} [5]. An alternative is that O_2 could have risen if the sink from volcanic reducing gases declined. Many ideas have focused on a shift in mantle or seafloor reductant fluxes [4], including appeals to changes in subaerial vs. submarine gases [6, 7]. But for this idea to work, the surface still has to export net reductant to the mantle, which is itself initially reduced.

Oxidation of *other* planetary or satellite surfaces is universally attributed to the escape of hydrogen. This accounts for Mars' redness and tenuous O_2 atmospheres on Europa, Ganymede, and Rhea. Earth's pre-GOE atmosphere was enriched in CH_4 and H_2 and prone to hydrogen escape at rates that must have produced large irreversible oxidation. If continents grew until ~3-2 Ga, they would have accumulated excess oxygen in minerals. Atmospheric O_2 would have become more stable by application of Le Chatelier's principle to the surface environment of the whole Earth.

Conclusions: Overall, rapid escape of hydrogen to space from the pre-GOE atmosphere should have gradually oxidized the Earth, accompanied by falling atmospheric CH_4 levels. The disappearance of S isotope mass independent fractionation at 2.4 Ga is best explained by the collapse of CH_4 as marine sulfate levels grew and methanotrophy kicked in [8]. The "tipping point" for flooding the atmosphere with O_2 was when the flux of O_2 from the burial of organic carbon exceeded O_2 losses. Glaciations during 2.45-2.22 Ga suggest oscillations in atmospheric composition until a new O_2 balance with oxidative weathering was established.

[1] Kirschvink J. L., Kopp R. E. (2008) *Phil. Trans. R. Soc.* 363, 2755. [2] Buick R. (2008) *Phil. Trans. R. Soc. B.* 363, 2731. [3] Bjerrum C. J., Canfield D. E. (2004) *Geochem. Geophys. Geosys.* 5, 8. [4] Holland H. D. (2002) *Geochim. Cosmochim. Acta* 66, 3811. [5] Catling D. C. et al. (2001) *Science* 293, 839. [6] Kump L. R., Barley M. E. (2007) *Nature* 448, 1033. [7] Gaillard F. et al. (2011) *Nature* 478, 229. [8] Zahnle K. et al. (2006) *Geobiology* 4, 271.

Reconstructing impact basins from *ex situ* shocked zircon

AARON J. CAVOSIE[1,*], HENRI A. RADOVAN[1], DESMOND E. MOSER[2], IVAN BARKER[2], JOE WOODEN[3], KOUKI KITAJIMA[4], JOHN W. VALLEY[4]

[1]Univ. Puerto Rico, aaron.cavosie@upr.edu (* presenting author)
[2]Univ. Western Ontario, [3]Stanford University, [4]Univ. Wisconsin

Meteorite impacts have played a critical role in the evolution of Earth and the terrestrial planets. Large impacts cause profound geomorphic changes of the crust, the concentration of economic metals, and have been correlated to climate change and biological extinctions. Despite the importance of impact cratering to a variety of disciplines, the terrestrial impact record is poorly known. On Earth, most impact structures have been removed by erosion or burial; only 180 impact structures have been confirmed, and none from the Archean when impact rates were higher. To locate Earth's missing impact record, and to build a tool for extraterrestrial impact chronology, we present a method to identify evidence of eroded impact craters through the identification of detrital (*ex situ*) shocked minerals.

We describe a detrital shocked zircon collected in modern sediment in the Vaal River basin at the Vredefort Dome in South Africa, one of Earth's largest known impact structures. Detailed isotopic, elemental (U-Th-Pb, $\delta^{18}O$, REE), and microstructural (CL, BSE, EBSD) analysis reveals that the detrital grain comprises a single mineral record of the giant impact basin. Multiple shock microstructures, including planar fractures (PFs) and granular texture, occur in different domains distinguished by CL zoning and U-Pb age, and allow the determination of the age of the source terrain and timing of impact. EBSD analysis documents the presence of shock-induced microtwins in one PF orientation. Oxygen isotopes ($\delta^{18}O$) and trace elements (REE, Th, U, Pb) record the variable response of an evolved granitoid zircon to extreme conditions during and after impact.

Modeling the source of this zircon yields the following impact basin reconstruction. The target rocks were comprised of 3161±71 Ma felsic granitoid; the impact crater thus formed on an Archean craton. U-Pb ages of granules record a Proterozoic impact at 1974±74 Ma. The impact created a >5 km diameter complex crater, as evidenced by the presence of PFs. PFs and microtwins require pressures >20 GPa; granular texture requires higher pressure, ~50 GPa. The two billion year time lag indicated by the presence of a detrital shocked zircon from a ca. 2 Gyr old impact in modern sediments suggests either that the impact structure may have been considerably larger than 5 km and eroded, or that the structure escaped early erosion due to burial and was later exposed. Thus with the exception of original crater size, many significant aspects of the Vredefort impact are accurately recorded in this grain. This method of impact basin reconstruction from single grains is well-suited for studies of lunar impacts, and also for other sample return missions where the quantity of sample is limited.

https://doi.org/10.1180/S0026461X00008434 Published online by Cambridge University Press

An early Ediacaran cap carbonate sequence in east central Brazil

FABRÍCIO CAXITO[1*], GALEN P. HALVERSON[2], ROSS STEVENSON[3], ALEXANDRE UHLEIN[1]

[1]UFMG, Belo Horizonte, Brazil, boni@ufmg.br (*presenting author)
[2]McGill University, Earth and Planetary Sciences and GEOTOP, Montréal, Canada, galen.halverson@mcgill.ca
[3]UQAM, Sciences de la terre et de l'atmosphère and GEOTOP, Montréal, Canada, stevenson.ross@uqam.ca

Introduction

The Sete Lagoas Formation is a 200 m thick carbonate unit sitting atop glacially-related diamictites (Jequitaí Formation) at the São Francisco craton, east central Brazil. It is currently recognized as a typical Neoproterozoic cap carbonate, and most authors prefer a mid-Cryogenian (post-Sturtian) age for it, based mainly on Pb-Pb data. Recently, however, Ediacaran zircons have been recovered from the middle portion of the Sete Lagoas Formation, constraining the deposition of its upper half to be younger than 610 Ma[1]. These conflicting results underline the need for further research on the assignment of a relative age for the Sete Lagoas cap carbonate.

Materials and Methods

We present lithostratigraphic and C, O and Sr isotopic data from a 127-m section of the Sete Lagoas Formation near Correntina, Bahia. In addition, sixty-five carbonate clasts from four separate diamictite occurences were sampled for C and O isotopic analysis.

Results and Conclusions

A 1.5 m thick layer of pink laminated dolomite marks the base of the Sete Lagoas Formation at Correntina ($\delta^{13}C$: -3.8 to -4.2‰; $\delta^{18}O$: -4.5 to -5.1‰). It is overlain by 55 meters of reddish laminated limestone with $\delta^{13}C$ values of about -5‰, jumping abruptly to around -0.5‰ at the middle of the section and remaining nearly constant upwards. The thin pink dolostone unit at the base of the section, preserving decreasing-upwards $\delta^{13}C$, is nearly identical to basal Ediacaran cap dolostones globally. The $^{87}Sr/^{86}Sr$ values obtained from high Sr carbonates (above 1000 ppm), around 0.7076, are also consistent with deposition during the early Ediacaran. The carbonate clasts display similar ranges of $\delta^{13}C$ (-6.7 to +2.6‰), except for the meter thick Carrancas Formation, which yielded pale dolostone clasts with $\delta^{13}C$ in a small range between -4.2 and -3.4‰, and $\delta^{18}O$ around -6.5‰. These could be derived from the cap dolostone unit itself, in which case the Carrancas Formation would represent resedimented basal Sete Lagoas Formation, implying that cap carbonate sections sitting atop it are incomplete. The base-truncated sections have confused previous attempts to assign a relative age for the Sete Lagoas cap carbonate. The combination of available lithostratigraphic, isotopic and geochronological data strongly supports the interpretation of an early Ediacaran age for the Sete Lagoas Formation. This new interpretation profoundly impacts the current views of Neoproterozoic history and sedimentation within the São Francisco craton.

[1] Rodrigues (2008) *Unpublished PhD Thesis, UnB, Brasília, Brazil,* **128 p.**

An absorption method for porewater characterization in low permeability sedimentary rocks

MAGDA CELEJEWSKI[1*], TOM AL[1], IAN CLARK[2], AND JENNIFER MCKELVIE[3]

[1]Earth Sciences, University of New Brunswick, Fredericton, New Brunswick, Canada, m.celejewski@unb.ca, tal@unb.ca (*presenting author)
[2]Earth Sciences, University of Ottawa, Ottawa, Ontario, Canada, idclark@uottawa.ca
[3]Nuclear Waste Management Organization, Toronto, Ontario, Canada, jmckelvie@nwmo.ca

Determination of porewater geochemistry in low-permeability, low-porosity rocks is problematic given small fluid volumes and difficulty associated with extracting representative samples. Several techniques are available including crush and leach, vacuum distillation and forced advective displacement. However, these methods are not always successful and can be subject to error arising from the estimate of matrix porosities. The purpose of this study is to explore a new innovative method for characterization of representative pore fluids in clay rich rocks. The method involves the extraction of pore fluids using absorption into hydrophyllic membranes. From preliminary experiments, scanning electron microscope (SEM) images and energy-dispersive x-ray spectroscopy (EDS) analyses confirm that the method successfully extracts porewater and associated solutes. Absorbed water was determined gravimetrically and the solute masses were quantified by x-ray fluorescence (XRF).

Interim experimental results have been compared with porewater compositions derived using the crush and leach technique. The gravimetric water-content analyses are subject to large errors, which carry through to porewater concentrations. However, when the extracted solute masses for major elements (Na, Mg, K, Ca, Br and Sr) are normalized to Cl mass, data from the absorption method display higher precision than data from the crush and leach technique. The Cl normalized elemental masses from the two extraction methods compare well for Sr and Ca, but K:Cl and Mg:Cl ratios obtained with the crush and leach method are higher than from the absorption method, while Br:Cl and Na:Cl ratios are lower.

Continuing research and development aims to refine the technique by investigating preferential ion sorption and reversibility of ion leaching, improving water-content measurements using near-infrared spectroscopy, and testing other analytical methods such as neutron activation analysis. With refinement of the water-content and solute analytical methods, the technique holds promise for characterizing porewater geochemistry occurring in low-permeability, low porosity rocks.

https://doi.org/10.1180/S0026461X00008434 Published online by Cambridge University Press

Heavy metal sequestration in nanoporous minerals

AARON J. CELESTIAN[1*], MICHAEL POWERS[1], AND SHELBY RADER[1]

[1]Advanced Materials Institute, Dept. of Geography & Geology, Western Kentucky University, USA aaron.celestian@wku.edu (* presenting author), michael.powers509@topper.wku.edu, and shelby.rader684@topper.wku.edu

Introduction

The nanoporous minerals sitinakite (sodium titanium silicate hydrate) and umbite (potassium zirconium silicate hydrate) are a pair of highly selective, fast ion conductor that are being tested for targeted removal of cesium and strontium from high level waste solutions [1]. In addition to their environmental applications, titanium silicates, and similar zirconium and yttrium silicates, have many technological uses including battery materials, hydrogen storage, and rare earth and transition element catalysts for gasses and petrochemicals [2]. Sitinakite and umbite are stable under a wide range of pressure, temperature, and chemical conditions making them potential host materials to perform selective chemistries in extreme environments. We are determining the fundamental structural properties governing ion selectivity in these unique minerals with emphasis toward understanding their energy related applications.

Results and Discussion

The studied materials exhibit multiple ion exchange steps that serve to enhance ion selectivity, and these steps are controlled by the host crystalline framework as well as the chemistry and hydration state of the native and ion exchanged compounds. To determine the exchange mechanisms, we collected high resolution in situ Raman spectroscopy, X-ray diffraction and computational data to capture the ion exchange processes from the natural forms, to the enhanced hydrogen form, and finally to the heavy metal exchanged structure.

The results from these ion exchange studies (using Y, Eu, Gd, Cu, Ni, Cs, Sr) indicates that a range of exchange dynamics exsist within a single host mineral. Specifically in sitinakite the exchange dynamics are sigificanly different for each REE tested (Y, Gd, Eu). This was somewhat suprising as all three elements possess the same valance charge, similar ionic radii (±0.05Å), and similar hydration states in aqeous solutions (CN=8-9). TGA/DSC curves for before and after exchange states showed significant variation in nanopore H_2O capacities, indicating that the hydration states of the element and valence electron conduction have an effect on the sequestion mechansims and pathways through the porous host structure. The selectivity hypothesis concerning the effects of internal hydration and valence electron conduction has been previously proposed [3,4], however the mechanisms of framework conformational changes, presence of intermediate structural states, and diffusion pathways have only been reported for a handful of materials and is the main area of focus for this study.

[1] Wilmarth (2011) *Solvent Extraction and Ion Exchange* **29**, 1-48. [2] Rocha (2000) *European Journal of Inorganic Chemistry* **5**, 801-818. [3] Clearfield (2006) *Journal of Materials Science* **41**, 1325-1333. [4] Celestian (2008) *Journal of the American Chemical Society* **130**, 11689-11694.

Implementing Stable Isotope Fractionation of Two Elements in Reactive Transport Models to Validate Novel Assessment Methods for Biodegradation in Aquifers

FLORIAN CENTLER*AND MARTIN THULLNER

Helmholtz Centre for Environmental Research - UFZ, Leipzig, Germany, florian.centler@ufz.de (* presenting author), martin.thullner@ufz.de

Compound-specific stable isotope analysis has been established as a viable method to detect and quantify *in situ* biodegradation. Even the identification of dominant degradation pathways is possible if stable isotope data of two elements are combined in the so-called two-dimensional isotope analysis. These assessment methods can be applied at field sites where degradation occurs via a single dominating pathway that does not change qualitatively over space. If spatially varying redox conditions lead to multiple degradation pathways, each associated with a different zone along a groundwater flow path, the application of current stable isotope based methods is not straigth forward. For such conditions, novel analytically derived concepts are presented which allow the use of two-dimensional isotope analysis for estimating the share of two competeing degradation pathways on overall degradation at a specific location as well as along a given flow path interval. In order to test these novel estimates, reactive transport simulations implementing a generic benzene plume/degradation scenario with aerobic and anaerobic degradation as exemplary degradation pathways were performed using the numerical model GeoSysBRNS [1]. Simulations considered besides biochemical reactions also the associated concurrent fractionation of both carbon and hydrogen isotopes. Resulting isotope signatures were used to estimate pathway contributions which were then compared to actual contributions calculated from simulated reaction rates. Estimates were very accurate for one-dimensional plume scenarios. For two-dimensional plume scenarios, estimates for pathway specific contributions to overall biodegradation were most accurate along the center of the plume, but lost accuracy towards the fringe, where transversal mixing processes were shown not only to affect contaminant concentration but also associated stable isotope signatures [2]. Total estimates could be significantly improved if additional observation points were taken into account along the flow path. Reactive transport models that incorporate the concurrent fractionation of two elements are helpful in validating and testing novel assessment methods based on two-dimensional stable isotope data and can also be applied to field sites where two-dimensional isotope data are available, improving the expressive power of the model by considering the concurrent fractionation of two elements as an additional process parameter.

[1] Centler (2010) *Computers & Geosciences* **36**, 397-405. [2] Thullner (2012) *Organic Geochemistry* **42**, 1440-1460.

https://doi.org/10.1180/S0026461X00008434 Published online by Cambridge University Press

Nanogranites in anatectic metapelites: building up the database

BERNARDO CESARE[1*], SILVIO FERRERO[1], OMAR BARTOLI[2], ANTONIO ACOSTA-VIGIL[3], ALICE TURINA[1], STEFANO POLI[4], TANYA EWING[5] AND ROBERT BODNAR[6]

[1]Department of Geosciences, University of Padova, Italy, Email bernardo.cesare@unipd.it (* presenting author)
[2]Department of Geosciences, University of Parma, Italy; omar.bartoli@libero.it
[3]IACT-CSIC, Granada, Spain; email: aacosta@ugr.es
[4]Department of Geosciences, University of Milano, Italy; email: stefano.poli@unimi.it
[5]RSES-ANU, Canberra, Australia; email: tanya.ewing@anu.edu.au
[6]Dept of Geosciences, Virginia Tech, Blacksburg, VA, USA; email: rjb@vt.edu

Nanogranites are inclusions of former anatectic melt trapped within peritectic minerals, particularly garnet, and crystallized to a cryptocrystalline aggregate of quartz, feldspars and micas. After their recent discovery[1] in the khondalites of the KKB (India), nanogranites have been found in numerous localities worldwide and, with their appropriate characterization and analysis can provide the missing information on the composition of natural anatectic melts before they undergo modification processes. We report the main results of the study of *nanogranites* in the Ronda migmatites, and preliminary results from migmatites in the Ivrea Zone (Italy) and Kaligandaki (Himalaya). Successful experimental rehomogenization of the inclusions to a glass allows the analysis of major elements and H_2O contents of the natural anatectic melts. Despite being all leucogranitic, the compositions generally plot away from those of *minimum melts*. Systematic differences occur among samples, particularly concerning Qtz-Ab-Or relationships. The analysis of H2O in the rehomogenized inclusions demonstrates that nanogranites preserve the primary fluid contents and that melts produced at Ronda were mainly H_2O-undersaturated even at low degree of melting. Since H_2O is one of the main parameters determining melt viscosities and, in turn, the strength of partially melted rocks, the characterization of the fluid contents of *nanogranites* will allow more realistic constraints to the rheological behaviour of the deep crust, and to the timescales of melt extraction from it.

[1] Cesare *et al.* (2009) *Geology*, **37**, 627-630.

C and Sr-isotope Stratigraphy, Ce and Eu Anomalies in Neoproterozoic Carbonates the Serra do Paraíso (Rio Pardo Basin) and São Desiderio (Rio Preto Belt) formations, Bahia, Brazil

W. S. CEZARIO[1*], A. N. SIAL[1], V. P. FERREIRA[1], L. D. LACERDA[2], M. M. PIMENTEL[3], A. MISI[4] AND A. J. PEDREIRA[5]

[1]NEG-LABISE, Dep. Geol. UFPE, Recife, Brazil, wilker_cezario@yahoo.com.br (* presenting author)
[2]LABOMAR, UFC, Fortaleza, Ceará, Brazil, ldrude@pq.cnpq.br
[3]UFRGS, Rio Grande do Sul, Brazil, marcio.pimentel@ufrgs.br
[4]UFBA, Salvador, Bahia, Brazil, misi@ufba.br
[5]CPRM, Salvador, Bahia, Brazil, augusto.pedreira@terra.com.br

Introduction. The Rio Pardo Basin and Rio Preto Belt surround, respectively, the southeastern and northwestern portions of the São Francisco Craton, eastern Brazil. We examined the possibility that carbonates of the Serra do Paraíso Formation (Rio Pardo Basin) that overly diamictite/arkose of Panelinha Formation or basement, and those of the São Desiderio Formation (Rio Preto Belt) that covers the Canabravinha Formation, represent Neoproterozoic cap carbonates.

In the Serra do Paraíso Formation, the $\delta^{13}C$ values for carbonates with stromatolites at Serra do Paraíso Farm are ~ -5‰ and upsection values jump to around +9‰ towards the top of this formation.

In the Rio Preto Belt, representative sections of São Desiderio Formation have the following $\delta^{13}C$ values: at the Mineração do Oeste Quarry, limestones show $\delta^{13}C$ values from +1.2 to +2.2‰ in the first 16m changing abruptly upsection to values between +10 and +12‰ in organic matter-rich limestones. At Sítio Rio Grande, limestones show values from +13.5 to +15‰ in the first 30m, and from +14 to +16‰ upsection, in organic matter-rich limestones.

Carbonates from Serra do Paraíso Formation display negative Ce anomaly values in the base of the formation and positive values upsection, as an indication that the depoitional environment passed from anoxic into oxic conditions. Their positive Eu anomalies roby resulted from influence of hot exhalation of hydrothermal fluids. Carbonates from the São Desidério Formation exhibit just positive Ce anomaly values, indicating an anoxic environment, and display negative Eu anomaly values that suggest reducer environment.

Hg values have been used as a proxy of volcanism intensity and CO_2 buildup during Snowball Earth events. Hg contents in cap carbonates are usually over 10 times higher than background values (<1 $ng.g^{-1}$) [1], in Serra do Paraíso Formation Hg values is 0.92 in the base changing upsection to 10.64$ng.g^{-1}$.suporting the idea of mantle-origin for the CO_2 in cap carbonates, transferred to the atmosphere by volcanism.The values of $^{87}Sr/^{86}Sr$ for carbonates of both formations vary from 0.707584 to 0.708061, compatible with a depositional age bracketing the end of Cryogenian (Marinoan) glaciation.

Conclusions. Our current data set is compatible with the hypothesis that Serra do Paraíso and São Desidério formations represent two cap carbonates.

[1] Sial *et al.* (2010) Precambrian Research **182**, 351-372.

https://doi.org/10.1180/S0026461X00008434 Published online by Cambridge University Press

Biogeochemical Mn cycling and its influence on the water column Mn concentrations in the Southwestern East/Japan Sea

CHA, HYUN JU[1*], AND CHOI MAN SIK[2]

[1]Chungnam National University/Research Institute of Marine Sciences, , Daejeon, Republic Of Korea hcha80@chol.com (* presenting author)

[2]Chungnam National University/Department of Oceanography/Graduate School of Analytical Science and Technology, Daejeon, Republic Of Korea, mschoi@cnu.ac.kr

Abstract

Biogeochemical cycling of Mn was studied for the southwestern East/Japan Sea for the upper part of sediments collected from 1995 through 2007. The sites cover continental shelf, continental slope and deep basin areas (the Ulleung Basin ~ 2300 meter deep). From the profiles of dissolved Mn concentrations in porewater, we found that intensive redox-cycling of Mn occurring in the upper layer of sediments over the study area. From the vertical profiles of dissolved Mn in porewater and particulate Mn in iron-oxyhydroxide phase of sediment, we calculated benthic fluxes of dissolved Mn and accumulation rates of particulate Mn in sediment that varied significantly between sedimentological settings. Accumulation rates of particulate Mn in the oxyhydroxide phase increased with water depth of sampling site. On the contrary benthic fluxes of dissolved Mn decreased with water depth of each site despite of the high sediment accumulation rate and high organic carbon concentrations of the continental margin areas. The authors related this phenomena to the concentrations of water column Mn concentrations showing downward increase below 1000m water depths and concluded that there may be a horizontal transport of dissolved and/or colloidal Mn from the continental slope to the basin.

Modelling of U-series nuclides in regoliths and the recovering of weathering propagation rates

F. CHABAUX[1]*, E. PELT[1], E. BLAES[1], R. DI CHIARA-ROUPERT[1]

[1]LHYGES, Université de Strasbourg/EOST, CNRS, France (*correspondence: fchabaux@unistra.fr)

The interest of U-series nuclides as tracers and chronometers of weathering processes results from the dual property of the nuclides to be fractionated during water-rock interactions and to have radioactive periods of the same order of magnitude as the time constants of many weathering processes. The development of U-series nuclides for investigating weathering processes is quite recent, and was significantly stimulated by the analytical improvement made over the last decades in measuring the ^{238}U series nuclides with intermediate half-lives (i.e., ^{234}U-^{230}Th-^{226}Ra) (1-5).

Here it is proposed to present some recent results obtained with the analysis of U-series nuclides in weathering profiles to determine rates of soils processes. We will especially highlight how a simple modelling of u-series nuclides based on mathematical formalism assuming a continuous gain and loss of the different U-series nuclides within a weathering profile allow ones to recover propagation rates of weathering front within the regolith. The limitations of this approach and the future developments required to progress in this topic will be also discussed.

[1] Pelt et al. (2008) *Earth and Planet. Sci. Let.,* **276,** 98-105. [2]Chabaux et al., (2008) , Radioactivity in the Environment, 13, 49-104. [3] Chabaux et al. (2011) *Applied Geochemistry*, **26**, S20-S23. [4] Ma et al. (2010), Earth and Plant. Sci. Lett., **297**, 211-225. [5] Ma et al. (2012) *Geochimica et Cosmochimica Acta*, **80**, 92-107.

https://doi.org/10.1180/S0026461X00008434 Published online by Cambridge University Press

Intrinsic and Extrinsic Factors Governing Development of Time-Dependant Leaching/Depth Thresholds in Hawaiian Soils

OLIVER A. CHADWICK[1]

[1]University of California, Santa Barbara, USA, oac@geog.ucsb.edu

Sampling and Methods

Soils have been sampled across the Hawaiian Islands guided by state factor theory which dictate sampling along near orthogonal gradients of climate and time. Hawaii has strong gradients of both and due to the intersection of island topography and the dominant NE tradewinds, climate patterns have been quite stable over the last 4 my. In particular, climate gradients ranging from <500 mm to >3000 mm have been sampled on 10 ky, 150 ky, 400 ky, and 4000 ky lava flows. Soils were sampled to depth of backhoe and/or auger refusal and analysed for total element composition, soil physico-chemical exchange, mineralogical and plant nutrient properties.

Results and Conclusions

We observed distinct thersholds in soil depth and soil chemical properties that become more strongly expressed over time and that are expressed at rainfall values that decline from about 1800 mm at 10 ky, to 1300 mm at 150 ky, 1000 mm at 400 ky and 800 mm at 4000 ky. Below the threshold soil depth is a meter or less on the yonger flows and increases to between 3 and 4 m on the oldest flow. Above the threshold soil depth is between 1 and 2 m on the youngest flows increasing to about > 5 m on the intermediate age flows and to as much as 20 m on the oldest flow. Nutrient status as indexed by the fraction of non-hydrolizing cations sorbed to soil exchange complex changes strongly across the threshold but the difference varies according to flow age. Young and intermediate age flows show very strong differences whereas the oldest flows are quite depleted in cations even below the threshold. The observed thresholds are very sharp occurring over spatial distance of a km or less and over a rainfall distance of a few hundred mm. Although they are strongly expressed, the processes associated with formation of the thresholds are complex and are a response to both intrinsic and extrinsic variables. The dominant control of threshold location is related to the balance of rainfall and evapotranspiration. Where the latter predominates leaching and weathering depths are limited. Increasing amounts of rainfall lead to increased pore volumes of water which enhances both weathering depth and cation removal. However even at low rainfall occasional extreme wetting events serve to slowly deepen weathering depths and remove ions. Thus over time the threshold is expressed at lower rainfall values. On Hawaiiain shield surface erosion is quite low which allows these thresholds to be expressed in ways that might not occur in most landscapes.

Element impurities as time scale in otoliths of wild Prussian carp (*Carassius gibelio*): Implications for past environmental reconstructions

XINNA CHAI[1*], MING LI[2], SHENGHONG HU[1], ZHAOCHU HU[2] AND LANLAN JIN[1]

[1] State Key Laboratory of Biogeology and Environmental Geology, China University of Geosciences, Wuhan 430074, China, chaixinna@gmail.com (* presenting author)

[2] State Key Laboratory of Geological Processes and Mineral Resources, China University of Geosciences, Wuhan 430074, China, liming19820426@163.com

Otoliths are paired structures composed of biogenic calcium carbonate in teleost fish inner ears [1]. Otoliths accrete new crystalline and protein material on to their exterior surface daily throughout fish's life, incorporating minor and trace elements, and are not re-metabolized once deposited [2]. These element impurities, which represent less than 1% of the otolith weight, provide a chemical chronology over the entire life of a fish. The combination of laser ablation with inductively coupled plasma mass spectroscopy (LA-ICPMS) is a powerful tool for determination of trace elements or elemental ratios and has wide applications in otolith section analysis providing message in a specific life-history period or changes in long periods of time. Otolith annuli, opaque and translucent zones in otolith, relate to fish age due to seasonal variation in the diurnal process of the deposition of the calcareous, crystalline structure and protein matrix. Hence spatial otolith chemistry usually is match to fish age using otolith annuli as temporal references. From the combination of optical and chemical characteristics of fish otoliths, it have been used to reconstruct the sequence of environmental changes experienced by a fish throughout its life and to relate these changes to when they occurred [3]. Here, we analyzed concentration profiles of element impurities in wild Prussian carp otoliths by LA-ICPMS. The periodic distribution of normalized ratios of Mg, Sr, Mn to Ca were appeared along the otolith growth axes. The high value of ratios were corresponding to the opaque zones and the low value corresponding to the translucent ones. A series of experiments were undertaken to verify the consistency of the elemental vibration and otolith annuli with a pair of otolith, different sampling strategy with antero-posterior and dorso-ventral direction, and different otolith with the visible or invisible annuli. These element impurities, distributing in otoliths with periodical fluctuations, can be used for fish age determination and time scale for past environmental reconstructions.

[1] Elsdon *et al.* (2008) *Oceanogr. Mar. Biol. Ann. Rev.* **46**, 297-330. [2] Campana (1999) *Mar. Ecol. Prog. Ser.* **188**, 263-297. [3] Fowler *et al.* (2005) *Mar. Freshwater Res.* **56**, 661-676.

https://doi.org/10.1180/S0026461X00008434 Published online by Cambridge University Press

Effect of abiotic environment on biogeochemical response of arctic sediments : a multivariate analysis

GWÉNAËLLE CHAILLOU[1], HEIKE LINK[2] AND PHILIPPE ARCHAMBAULT[3]

[1] Canada Research Chair in the Geochemistry of Coastal Hydrogeosystems Department of biology, Chimistry, Geography, Université du Québec à Rimouski, Rimouski, Canada, gwenaelle_chaillou@uqar.ca

[2]Institut des Sciences de la Mer, Université du Québec à Rimouski, Rimouski, Canada, heike.link@uqar.ca

[3]Institut des Sciences de la Mer, Université du Québec à Rimouski, Rimouski, Canada, philippe_archmbault@uqar.ca

The effects of global changes on Arctic Ocean biogeochemical cycles are difficult to predict given the complex web of physical, biological and chemical interactions that act in this system. It is clear, however, that the flux of organic matter to coastal Arctic sediment will be considerably altered. In this context, understanding how the benthic biogeochemical fluxes of arctic sediment are controlled by organic carbon fluxes is essential.

To examine the effect of abiotic environment on benthic nutrient and metabolite exchanges, we measured fluxes of dissolved oxygen, nitrate, nitrite, ammonia, soluble reactive phosphate and silicate at the sediment-water interface of nine stations located in the souheastern Beaufort Sea in water depth from 45m to 580m. We focussed on abiotic parameters that characterize the quality of the organic matter that reaches the seafloor (e.g. Chla, phaeopigment, $\delta^{13}C_{org}$, C/N_{tot}, $\delta^{13}C$ on lipids, particulate organic carbon fluxes) and others that characterize the surficial sedimentary environment (e.g. overlying dissolved oxygen concentration, salinity, temperature, surficial Fe and Mn concentrations, surficial porosity). In this communication, after a presentation of the spatial distribution of the measured fluxes, we will use a multivariate approach enabling simultaneous evaluation of several variables. The biogeochemical response pattern will be evaluated with ordination by non-metric multidimensional scaling (nMDS) and principal components (PCA). The relationship between multivariate biogeochemical fluxes and abiotic parameters will also examine using distance-based multivariate multiple regression using the DISTLM routine. The model will be built using a forward selection of abiotic parameters tested on individual fluxes using a mutiple regression analysis. Most of these tests are still in progress.

We will show that multivariate approach is efficiant to reveal hidden relationships between samples and that it can be used to improve our knowledge on coastal environments.

Mass-independent sulfur isotopic fractionation in VUV photodissociation of H_2S: implications for meteorite data

SUBRATA CHAKRABORTY[1*], RYAN DAVIS[1], TERESA L. JACKSON[1], MUSAHID AHMED[2], AND M. H. THIEMENS[1]

[1]Department of Chemistry and Biochemistry, University of California, San Diego, La Jolla, California 92093-0356, subrata@ucsd.edu (* presenting author)

[2]Lawrence Berkeley National Laboratory, 1 Cyclotron Road, Berkeley, CA 94720, mahmed@lbl.gov

Introduction

Mass-independent sulfur isotopic compositions have been observed in chondritic chondrules and organics [1-2] and bulk achondritic meteorites [3-4]. Sulfonic acid extracts from Murchison also displayed a significant ^{33}S anomaly and it was suggested that methanesulfonic acid could have resulted from gas-phase ultraviolet irradiation of a precursor, carbon disulfide [2]. Stellar nucleosynthesis and cosmic ray spallation have been ruled out as the cause of the observed $\Delta^{33}S$ anomaly [3]. Photochemical reactions in the early solar nebula was inferred to be a leading process to generate mass independent sulfur composition.

UV photolysis of SO_2, H_2S and CS_2 with $\geq$ 180 nm photons have been carried out in the laboratory to understand the isotope effect in photolysis of sulfur bearing molecules [5-7]. Here we present S-isotope data from VUV photodissociation (using Chemical Dynamics Beamline at the ALS synchrotron) of H_2S.

Results and Discussion

H_2S photolysis was carried out at four different synchrotron bands centred at 90, 121.6, 139.1, and 157.6 nm at various pressures in a differentially pumped chamber. Elemental sulfur produced in all these experiments was collected and converted to SF_6 to measure the isotope ratios (e.g., $^{33}S/^{32}S$, $^{34}S/^{32}S$, and $^{36}S/^{32}S$). Among four different synchrotron bands used, 121.6 nm photolysis products show significant mass-independent fractionations both in $\Delta^{33}S$ and $\Delta^{36}S$ with a $\Delta^{36}S/\Delta^{33}S$ ratio of -3 ‰.

H_2S is one of the major sulfur-bearing species in the gas-phase of the solar nebula. Photodissociation of H_2S by Lyman-alpha (121 nm) lines from solar radiation could change the isotopic composition of this major sulfur reservoir. The observed meteoritic sulfur isotopic anomaly, especially those measured in organics may be due to the isotope shift of this precursor sulfur reservoir due to photochemistry. The complete results and a full discussion will be presented at the conference.

MA and the ALS are supported by the Director, Office of Energy Res., U. S. Dept. of Energy (Contract No. DE-AC02-05CH11231).

[1] Rai & Thiemens (2007) *Geochimica Et Cosmochimica Acta* ***71***, 1341-1354. [2] Cooper et al. (1997) *Science* ***277***, 1072-1074. [3] Rai et al. (2005) *Science* ***309***, 1062-1065. [4] Farquhar et al. (2000) *Geochimica Et Cosmochimica Acta* ***64***, 1819-1825. [5] Farquhar et al. (2001) *Journal of Geophysical Research-Planets* ***106***, 32829-32839. [6] Farquhar et al. (2000) *Nature* ***404***, 50-52. [7] Colman et al. (1996) *Science* ***273***, 774-776.

https://doi.org/10.1180/S0026461X00008434 Published online by Cambridge University Press

Glacial-Interglacial boron isotope changes in the deep North Atlantic

THOMAS B. CHALK[1*], GAVIN L. FOSTER[1], AND PAUL A. WILSON[1]

[1]Ocean and Earth Sciences, National Oceanography Centre Southampton, University of Southampton Waterfront Campus, Southampton, United Kingdom, (* presenting author) t.chalk@noc.soton.ac.uk

Despite many decades of research, the causes of the well documented pCO_2 changes that accompany, and partly drive, glacial-interglacial climate cycles remains elusive. The speed with which these changes take place points to the importance of changes in storage of carbon in the deep ocean , but the mechanisms involved remain uncertain. Recent modelling studies have suggested the volume of bottom water of southern origin that bathes the abyss may play a crucial role ("the standing volume effect"; Brovkin et al. 2011[1]; Skinner et al. 2009[2]).

Here we investigate this phenomenon by producing boron isotope records of epibenthic foraminifera, *Cibicidoides wuellerstorfi,* at three North Atlantic sites ([I]ODP 980, 1308 and 1313) from Marine Isotope stage six to the Holocene. These sites effectively form a depth profile from 2100 to 3900m. At these northern latitude sites, changes in the ocean storage of carbon, and in particularly northerly excursions of corrosive southern sourced water, are expected to be seen as changes in water column profile of the carbonate system parameters pH and $CO_3^=$ which can be reconstructed by changes in $\delta^{11}B$ and B/Ca in epibenthic foraminifera (Rae et al. 2011[3], Yu and Elderfield 2008[4]). Our chosen sites therefore are a sensitive monitor of the "standing volume effect" and by comparing our results to records of atmospheric CO_2 we will gain new insight into the role of this phenomenon in driving glacial-interglacial CO_2 change.

[1] Brovkin *et al*. (2011) Clim. Past Discuss., 7, 1767–1795 [2] Skinner *et al*. (2009) Science 328, 1147- [3] Rae *et al*. (2011) Earth and Planetary Science Letters 302 (2011) 403–413. [4] Yu and Elderfield (2008) Earth and Planetary Science Letters 258 (2007) 73–86

Direct magmatic input in geothermal systems of the Taupo Volcanic Zone

ISABELLE CHAMBEFORT[1*], ANDREW RAE[1] AND GREG BIGNALL[1]

[1]GNS Science, Wairakei Research Centre, Private Bag 2000, Taupo, New Zealand, i.chambefort@gns.cri.nz (* presenting author).

In the last 20 years, insights on the content and behaviour of volatile constituents in magmas, particularly from melt inclusion studies, have enhanced our understanding of hydrothermal fluid-magma interactions, and volatile transfer from magma to active hydrothermal systems. Exsolved fluids from magmatic sources contribute to the evolution of geothermal systems, by influencing fluid (reservoir) chemistry and associated hydrothermal alteration.

Geothermal systems of the Taupo Volcanic Zone (TVZ), New Zealand, are large convective cells of heated, primarily meteoric-derived waters. CO_2, Cl, B and N contents in TVZ well discharges indicate magmatic fluids are present in small proportion, but until now no direct, unequivocal evidence of magmatic fluid input or magmatic-derived hydrothermal minerals have been identified.

Secondary (alteration) minerals can point to magmatic, meteoric or mixed fluid origins, and processes (e.g. boiling, fluid mixing) within active geothermal systems. In the future, tracking a magmatic fluid signature in geothermal systems is expected to be an important consideration for establishing the spatial distribution of deep-seated magma bodies in the TVZ and for potential delineation of green-field geothermal systems with resource potential. New oxygen and sulphur stable isotope analyses of anhydrite in drillcore from ~2000 mVD (vertical depth) within the Rotokawa Geothermal Field exhibit an arc-related magmatic-hydrothermal signature, similar to anhydrite from the Ladolam epithermal gold depost (Lihir, Papua New Guinea, [1]) or Butte porphyry-copper deposit (Montana, USA [2]). Isotopic compositions of the Rotokawa anhydrite are $\delta^{18}O_{anh}$ = +13.9 to +17.9 (± 0.5‰, with one anhydrite of $\delta^{18}O$= 0.4‰), and $\delta^{34}S_{anh}$ +10.1 to +13.0 (± 0.5‰). The calculated sulphur isotopic composition of H_2S in equilibrium with the Rotokawa anhydrite are -4 to -9‰, whilst $\delta^{34}S_{H2Sg}$ in well discharges range between +4.1 and +4.8‰. The trace element composition of the Rotokawa anhydrite (e.g. Sr content up to 5000 ppm) also show similarities with inferred magmatic-derived anhydrite seen elsehwere (e.g. at Ladolam).

The trace element and isotopic compositions of Rotokawa anhydrite both point to sulphate in the hydrothermal system having a magmatic origin. In contrast, chemical analysis of discharge Rotokawa well fluids cannot have precipitated the anhydrite seen in core samples from >2000 mVD in several Rotokawa wells. We suggest that the anhydrite observed in Rotokawa core samples formed in equilibrium with magmatic-derived, low pH, sulphate-rich fluids, at some time during the the evolution of the hydrothermal-magmatic system, as a result of magmatic degassing. This study provides the first direct evidence of magmatic fluid input to the otherwise dilute, meteoric-dominated, low-salinity geothermal systems of the TVZ, and is expected to impact future deep geothermal exploration strategies.

[1] Gemmell, Sharpe, Jonasson & Herzig (2004) *Economic Geology* **99**, 1711-1725. [2] Field, Zhang, Dilles, Rye & Reed *Chemical Geology* **215**, 61-93.

https://doi.org/10.1180/S0026461X00008434 Published online by Cambridge University Press

SIMS in-situ micro-baddeleyite U-Pb method for dating mafic rocks

K.R. CHAMBERLAIN[1*], A.K. SCHMITT[2], S.M. SWAPP[1], N.G. SWOBODA-COLBERG[1], D.E. MOSER[3], J.E. WRIGHT[4], W. BLEEKER[5], A.K. KHUDOLEY[6]

[1]University of Wyoming, Laramie, U.S.A., kchamber@uwyo.edu (*presenting author); swapp@uwyo.edu; SwobCol@uwyo.edu
[2]University of California, Los Angeles, Los Angeles, U.S.A., axel@oro.ess.ucla.edu
[3]Western University, London, Canada, desmond.moser@uwo.ca
[4]University of Georgia, Athens, U.S.A., jwright@gly.uga.edu
[5]Geological Survey Canada, Ottawa, Canada, Wouter.Bleeker@NRCan-RNCan.gc.ca
[6]St. Petersburg State University, St. Petersburg, Russia, khudoley@AH3549.spb.edu

We report an *in-situ* method to date micro-baddeleyite grains whose exposed dimensions are less than 20 μm in length using secondary ion mass spectrometry (SIMS) U-Pb isotopic analysis [1,2]. We've successfully dated grains as small as 3 microns using the CAMECA *ims*1270 at UCLA. The method is ideal for samples that contain baddeleyite crystals that are too small to separate physically, such as fine-grained tholeiitic dikes and lavas, or samples that are too rare and precious to crush for mineral separation, such as meteorites, drill cores and samples from remote regions. Baddeleyite is common as a magmatic phase in tholeiitic and (less commonly) alkaline mafic rocks where it is not known to nucleate metamorphically, thus baddeleyite dates can generally be regarded as magmatic ages. We have occasionally documented zircon overgrowths on baddeleyite, however. The method requires only portions of polished thin sections and is relatively non-destructive, as it preserves the analyzed sections largely intact and still suitable for additional types of analyses. X-ray mapping, energy-dispersive spectrometry and backscattered electron imaging (BSE) are used to locate and image the grains and have added benefits of identifying alteration-free grains, armoring relationships, and mineral growth mechanisms. Coexisting zircons can also be dated in the same sections, if present, and often yield metamorphic ages. Analytical precision is practically limited by presence of common Pb (e.g., present at grain boundaries or crystal imperfections), and can be enhanced by averaging multiple crystal analyses. From our experience, precisions obtained by averaging 8 to 10 spot analyses range from 0.5 to 1% for $^{207}Pb/^{206}Pb$ dates from rocks that are >1000 Ma, and 3 to 8% for $^{238}U/^{206}Pb$ dates from Paleozoic to Mesozoic rocks. Recent case studies include lunar, Martian and eucritic meteorites, tholeiitic dikes and sills from 2.7 Ga to 0.4 Ga, Mesoproterozoic volcanic rocks and Caribbean intrusive rocks.

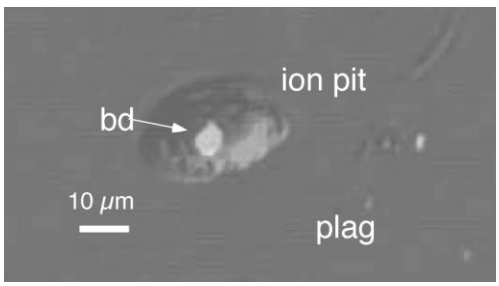

Figure 1: Post-analysis BSE image of micro-baddeleyite (bd).

[1] Schmitt et al. (2010) *Chemical Geology* **269**, 386-395. [2] Chamberlain et al. (2010) *Precambrian Research* **183**, 379-387.

CHALLENGES OF CELL-MINERAL CONTACT DURING MINERAL FORMATION AND DISSOLUTION BY FE AND S-OXIDIZING BACTERIA

CLARA S. CHAN[1*], THOMAS E. HANSON[2], JENNIFER HIRAS[2], KEVIN A. CABANISS[2] AND JEFFREY BRODZINSKI[3]

[1]Dept. of Geological Sciences, University of Delaware, Newark, DE, USA, cschan@udel.edu (* presenting author)
[2]School of Marine Science and Policy, University of Delaware, Newark, DE, USA, tehanson@udel.edu

Microbial Fe and S redox transformations commonly involve mineral formation and dissolution, which presents challenges due to spatial issues. During mineralization, cell-mineral contact is ideally minimized to prevent encrustation. During dissolution, cell access to mineral surfaces can be limiting. We are studying mineral dynamics and cell-mineral interfaces in chemolithotrophic Fe oxidizers and phototrophic S-oxidizers. The Fe-oxidizers cultured from Rifle, CO groundwater produce Fe oxyhydroxides; the phototroph *Chlorobaculum tepidum*, a well-characterized model organism with a genetic system, oxidizes sulfide to solid elemental S(0) and once sulfide is exhausted, oxidizes the S(0) to sulfate. Real time dynamics of cell-mineral interactions are observed by time lapse light microscopy of live cultures. Higher resolution images are obtained by scanning and transmission electron microscopy, including cryo-techniques to preserve delicate cell-mineral spatial relationships. *C. tepidum* appears to require biogenic S(0) for growth and direct cell contact with S(0) during dissolution, but only a subset of cells appear to be firmly attached. Current efforts are aimed at dissecting the molecular components mediating cell-S(0) interactions in *C. tepidum* using a variety of microscopic, proteomic, and analytical chemistry tools.

https://doi.org/10.1180/S0026461X00008434 Published online by Cambridge University Press

Global Mercury Pollution and Seafood Safety

LAURIE H.M. CHAN

University of Ottawa, CAREG, Biology, Ottawa, Canada, laurie.chan@uottawa.ca

Mercury is a global pollutant and there is strong evidence that the emission will increase by 50% in 2050. The major source of mercury is from the emission of fuel fossil burning power plants. Mercury accumulates along the aquatic food chain and can reach high levels in fish and shellfish. Mercury is a known neurotoxicant that is particularly harmful to fetal brain development. However, fish and shellfish are widely available food that provides many nutrients, particularly the n-3 polyunsaturated fatty acids (n-3 PUFAs), to many populations globally and there are benefits linked to brain and visual system development in infants and reduced risk for certain forms of heart disease. In this talk, we will review the current state of knowledge including results of our ongoing research in this area. We will also discuss the national and international efforts on regulation policy and public health messages on benefits and risks associated with fish consumption (1).

[1] Mahaffey KR, Sunderland EM, Chan HM, et al. (2011). Balancing the benefits of n-3 polyunsaturated fatty acids and the risks of methylmercury exposure from fish consumption. Nutr Rev. **69(9):**493-508.

Fate, Transport, and Deposition of Gold Nanoparticles in Porous Media

MATTHEW Y. CHAN[1*], MATTHEW S. HULL[1], JASON C. JONES[2], AND PETER J. VIKESLAND[1]

[1]Department of Civil and Environmental Engineering, Virginia Tech, Blacksburg VA 24061, USA, mychan@vt.edu (* presenting author)

[2]Department of Materials Science and Engineering, Virginia Tech, Blacksburg VA 24061, USA

Over the past two decades, there has been a steady increase in the application of nanomaterials and nanotechnology.[1] Gold-nanoparticles (AuNP) show significant potential in cancer treatment, drug delivery, self-assembling constructs, chemical analytical techniques and many more.[2] As the utilization and manufacture of AuNP increase it is important to understand the fate of these materials once they are released to the environment. In this work, we sought to investigate the fate, transport and stability of AuNP discharged to groundwater environments.

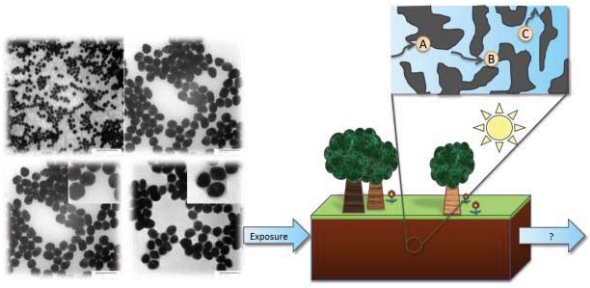

Figure 1: Exposure of AuNP to groundwater environment. There can be many possibilities for the fate of AuNP once released. For example: A) Adsorped by sediment; B) Fitrated and retained by pores; C) Unhindered transport.

AuNP transport in groundwater is heavily influenced by the intrinsic properties of the nanoparticles and the external parameters of the environment. Batch experimental data indicated that 15 nm AuNP coated by bovine serum albumin (BSA-AuNP) was more stable under high ionic strength conditions compared to citrate-coated AuNP (Cit-AuNP) of similar size. It was expected that the stability of these AuNP would be replicated in column studies. Column experiments with varying monovalent and divalent ion concentrations using both types of AuNP yielded breakthrough curves that both adhere and deviate from this hypothesis. BSA-AuNP was found to be more stable relative to Cit-AuNP during flow in the presence of increasing concentrations of $CaCl_2$, but the opposite occurred with an increase in NaCl concentration. Colloidal filtration theory (CFT) fails to predict and explain this discrepancy.

[1] Mueller, N. C.; Nowack, B. Environ. Sci. Techno. 2008, 42:4447-4453.
[2] Halvorson, R. A.; Vikesland, P. J. Environ. Sci. Techno. 2010, 44:7749-7755.

https://doi.org/10.1180/S0026461X00008434 Published online by Cambridge University Press

Mercury isotope fractionation during aqueous photo-reduction of methylmercury in presence of dissolved organic matter

PRIYANKA CHANDAN[1] , SANGHAMITRA GHOSH[1] AND BRIDGET A. BERGQUIST[1*]

[1]Department of Geology, University of Toronto, 22 Russell Street, Toronto, Ontario, M5S 3B1, Canada
(*correspondence: bergquist@geology.utoronto.ca)

Monomethylmercury (MMHg) is a globally persistent toxin that bioaccumulates in aquatic ecosystems. The photo-degradation of MMHg in freshwater systems is a significant pathway for the destruction of MMHg from surface waters and is considered an important sink in aqueous systems, which limits MMHg availability to biota. Quantifying this sink for MMHg is challenging, and it was suggested that natural fractionation of Hg isotopes might be useful in both understanding and quantifying this pathway [1]. In order to use this new tool, the isotopic fractionation factors associated with MMHg photo-degradation need to be characterized along with the variability that might be induced by environmental factors (i.e. type and amount of organic matter, light intensity and wavelength).

In a previous study, aqueous photo-reduction of MMHg in the presence of dissolved organic matter (DOM) was shown to display both mass dependent (MDF) and mass-independent (MIF) fractionation of Hg isotopes with the odd isotopes (^{199}Hg and ^{201}Hg) being preferentially retained in the reactant [1]. The observation of large MIF signatures (>0.5‰) is likely due to magnetic isotope effect (MIE), which is expressed during radical pair photochemistry. It was also observed that the magnitude and extent of MIF was different for two concentrations of DOM. Since these experiments were carried out on different days in natural sunlight, which likely had different solar intensity and frequency, it was unclear whether the variability in MIF was due to varying DOM concentrations or the variability in solar radiation.

We investigated the effects of different types and amounts of DOM on the isotope fractionation of Hg isotopes during aqueous photo-reduction of MMHg to assess if MIF signatures can be used to track photo-degradation of MMHg in natural waters. From experiments conducted with different amounts of reduced organic sulfur (S_{red}-DOM), it appears that MIF during photo-reduction may be dependent on whether MMHg is dominantly bound to S_{red}-DOM. Similar fractionation factors were observed for experiments where S_{red}-DOM was in far excess of MMHg, while significantly lower fractionation factors were observed with lower S_{red}-DOM. We also characterized the signature of MIF (i.e. $\Delta^{199}Hg/\Delta^{201}Hg$) during MMHg photo-degradation to assess if it was similar in different matrices. The experimental $\Delta^{199}Hg/\Delta^{201}Hg$ ratio for all the MMHg-DOM experiments was 1.39±0.06 (2SE). However, we observed that the experimental slope is slightly but statistically different than the slope observed in freshwater fish.

[1] Bergquist & Blum (2007) *Science* **318**, 417-420.

Anomalous zircon Ce^{4+}/Ce^{3+} ratios from early Jurassic plutons in Yukon: implications for porphyry exploration

JOHN B. CHAPMAN[1*], SIMON E. JACKSON[1] AND JAMES J. RYAN[2]

[1]Geological Survey of Canada, Ottawa, Ontario, Canada, john.chapman@nrcan-rncan.gc.ca (* presenting author); simon.jackson@nrcan-rncan.gc.ca
[2]Geological Survey of Canada, Vancouver, British Columbia, Canada, jim.ryan@nrcan-rncan.gc.ca

Studies suggest that a genetic link exists between oxidized magmas and porphyry-style Cu (±Au±Mo) mineralization.[1] However, many indicators of magmatic redox state – such as whole-rock Fe^{3+}/Fe^{2+} ratio – can be reset during both hydrothermal alteration and surficial weathering. Zircon ($ZrSiO_4$) is an abundant accessory mineral in granitoids, and is both refractory and resistant to alteration. Cerium commonly shows anomalously high concentrations within zircon, due to its stable +4 oxidation state and preferential incorporation of the Ce^{4+} ion over Ce^{3+}. The magnitude of this substitution should correlate with the Ce^{4+}/Ce^{3+} ratio in the parent magma, and as such can be used as a qualitative proxy for oxidation state.[2] In this study, we determined zircon Ce^{4+}/Ce^{3+} ratios for a suite of late Triassic to Jurassic granitoid intrusions from southern and western Yukon, Canada, including mineralised and host rocks of the Minto Cu-Au mine, and for mid- to late-Cretaceous intrusive phases associated with the Casino Cu-Mo-Au deposit.

Results for the Casino samples show that the major mineralising intrusive breccia phases have average zircon Ce^{4+}/Ce^{3+} values of 200-350, and peak values approaching 500, in contrast to mid-Cretaceous host granitoid rocks which have average values of 50-100 and peak values <250. Both sets of observations fit previously published models for the identification of Cu prospective intrusive rocks.[2,3] Hence, it appears possible to use zircon Ce^{4+}/Ce^{3+} ratios for exploration fingerprinting within the Cretaceous of the Yukon.

The 'Carmacks Copper Belt' (CCB) of western central Yukon includes the Minto Cu-Au mine, the Carmacks Copper deposit, and several smaller Cu±Au occurrences and showings. Both the Minto and Carmacks Copper deposits are hosted within the Triassic-Jurassic plutonic rocks of the Granite Mountain batholith, part of a regionally extensive suite of plutonic rocks of similar age and composition. The Triassic-Jurassic samples appear to fall into two distinct groupings: those with modal zircon Ce^{4+}/Ce^{3+} values >700, and those with values <600. The regionally extensive nature of these elevated Ce^{4+}/Ce^{3+} values may reflect the petrogenesis of these plutonic rocks, and as such need to be better understood before reliable prospectivity indicators can be defined. In contrast to the Cretaceous suite, all early CCB samples analysed have zircon Ce^{4+}/Ce^{3+} ratios greater than the previously published prospectivity threshold values.[2,3] However, Granite Mountain samples have higher apparent oxidation state, so the broad relationship to mineralisation established for the Cretaceous suite is maintained.

[1] Richards (2011) *Economic Geology* **106**, 1075-1081. [2] Ballard et al. (2002) *Contributions to Mineralogy and Petrology* **144**, 347-364. [3] Liang et al. (2006) *Mineralium Deposita* **41(2)**, 152-159.

https://doi.org/10.1180/S0026461X00008434 Published online by Cambridge University Press

MOLYBDENUM SEQUESTRATION IN SULFIDIC SEDIMENTS: XAFS EVIDENCE FOR MO REDUCTION

ANTHONY CHAPPAZ[1,*], TAIS W. DAHL[2], JEFFREY P. FITTS[3] AND TIMOTHY W. LYONS[4]

[1] Institute for Great Lakes Research, Dept. of Chemistry and Dept. of Earth and Atmospheric Sciences, Central Michigan University, Mount Pleasant, MI 48859, USA

[2] NordCEE and Institute of Biology, University of Southern Denmark, Odense, Denmark.

[3] Dept. of Civil & Environmental Engineering, Princeton University, Princeton, New Jersey 08540, USA

[4] Dept. of Earth Sciences, University of California – Riverside, CA 92521, USA

Molybdenum (Mo) has attracted attention as a paleoredox proxy particular because of its isotopic behavior and concentration relationships in sediments [1,2]. Much of this strength lies with the specifics of Mo redox behavior. In oxygenated water, Mo occurs dominantly as unreactive molybdate ($Mo^{VI}O_4^{2-}$). When sulfide appears under in the sediments or water column, sulfur substitutes progressively for oxygen in MoO_4^{2-}, leading to reactive tetrathiomolybdate ($Mo^{VI}S_4^{2-}$) by way of transient intermediates ($Mo^{VI}O_xS_{4-x}^{2-}$) [3]. However, the post-thiomolybdate steps and the ultimate Mo host in sulfidic sediments remain unclear and thus compromise its strength as a redox proxy.

We used x-ray absorption fine structure spectroscopy (XAFS) to determine the oxidation state and molecular coordination environment of solid phase Mo in sediments deposited under a permanently sulfidic (euxinic) water column. Samples were taken from a 9 meter drill core from Lake Cadagno representing the last ten thousand years of deposition.

Our data provide unequivocal evidence for Mo reduction in the sulfidic water column and/or in the sediments. We identified two types of spectral patterns. Type 1 samples contain primarily Mo^{IV} bonded exclusively to sulfur atoms; Type 2 samples contain mainly Mo^{VI} bonded to both oxygen and sulfur atoms.

Based on experiments, we argue that Mo^{VI}-O-S compounds have been oxidized after collection. These Type 2 compounds compare to spectra previously reported for black shales and thiomolybdate adsorption experiments on Fe-sulfides [4,5] and suggest that oxygen exposure might have altered these samples too.

Mo^{IV}-S compounds are found in both modern and ancient sediments indicating that Mo has not experienced diagenetic alteration over the last ~10,000 years. These Type 1compounds show many similarities with the Mo-Fe-S cubane structure. Finally, our results support a model involving post-thiomolybdate reactions wherein the Mo^{VI} reduction proceeds via reactions with with zero-valent sulfur (S_8) [6].

We conclude that Mo-XAFS is a powerful way to study the geochemical details of the Mo burial pathway and enhance our ability to infer ancient environmental conditions from the sedimentary rock record. Further, the post-thiomolybdate reduction may exert isotope fractionation that could affect the Mo isotope composition in euxinic sediments.

[1] Scott et al. (2008) *Nature* **452** *456-459* [2] Dahl et al. (2011) EPSL, **311** *264-274* [3] Erickkson & Helz (2000) *GCA* **64** *1149-1158,* [4] Helz et al. (1996) *GCA* **60** *3631-3662,* [5] Bostick et al. (2003) ES&T **37** *285-291* [6] Vorlicek et al. (2004) *GCA* **68** *547-556.*

Number density considerations in the dispersion-dissolution behavior of engineered silver nanomaterials

MARK A. CHAPPELL[1*], LESLEY F. MILLER[1], CYNTHIA L. PRICE[1], MATTHEW MIDDLETON[2], GAIL S. BLAUSTEIN[3], LATOYA J. JACKSON[2] ANTHONY J. BEDNAR[1], ALAN J. KENNEDY[1], AND JEFFERY A. STEEVENS[1]

[1]Environmental Laboratory, U.S. Army Engineer Research and Development Center (ERDC), Vicksburg, MS, USA, mark.a.chappell@usace.army.mil (*presenting author), Lesley.f.miller@usace.army.mil, cynthia.l.price@usace.army.mil, Anthony.j.bednar@usace.army.mil, alan.j.kennedy@usace.army.mil, jeffery.a.steevens@usace.army.mil

[2]Badger Technical Services, Anchorage, AK, matthew.a.middleton@usace.army.mil, Latoya.j.jackson@usace.army.mil

[3]West Liberty University, West Liberty, WV, gail.blaustein@westliberty.edu

Background

With the acquisition of new technologies, the U.S. Army is now required to consider the environmental implications of fielding new nanomaterial-based technologies in theater and as part of warfighter training. To this end, the U.S. Army Engineer Research & Development Center (ERDC) has expended considerable effort and resources into quantifying the environmental fate of nanomaterials. Here is presented our work on the dispersion-dissolution processes associated with silver nanoparticle dispersions under simulated environmental conditions.

Methods

Long-term dispersion studies were conducted either by shaking or stirring nanomaterial suspensions under laboratory-controlled conditions. Systems were sampled periodically with time and analyzed for multiple dispersion and dissolution endpoints.

Results & Discussion

Our results demonstrate that the dissolution processes were coupled to the solid-phase dispersion characteristics. We note that such linkages are often apparent in the scientific literature yet not explicitly explained because this behavior is almost invariably considered in terms of particle mass concentrations. Instead, these relationships are preferably viewed through considering the change in the suspension number density. The number density parameter is (i) inversely related to the size distribution of the dispersion and (ii) shifts by several orders of magnitude with small changes in particle size at the nano-scale. Experimental results show that an increase in dissolved Ag concentration observed over a two-week period correlated with the increase in the number density of silver nanoparticle dispersions. This relationship was only apparent as long as the suspension remained in a sub-saturation mode. This latter observation is important as at the nanoscale, where the nearly two-order magnitude length difference in our current analytical technologies blurs the classical definitions between particles and dissolved solutes. We reason that the relationship to nanoparticle dissolution and particle surface area commonly portrayed in the scientific literature is mathematically fortuitous but mechanistically inaccurate. Here, we discuss number density in terms of implications for ecosystem effects described in eco-toxicology literature.

https://doi.org/10.1180/S0026461X00008434 Published online by Cambridge University Press

In situ monitoring for studying the seasonal pattern of dissolved oxygen in a sandy beach of the Aquitaine coast (France)

CELINE CHARBONNIER[1*], PIERRE ANSCHUTZ[1], BRUNO DEFLANDRE[1], DOMINIQUE POIRIER[1], STEPHANE BUJAN[1] AND PASCAL LECROART[1]

[1]Université de Bordeaux, CNRS, UMR 5805 EPOC, Talence, France, *c.charbonnier@epoc.u-bordeaux1.fr

Despite low concentrations of organic matter and associated reactive compounds, sandy sediments of tidal beaches are now considered as biogeochemical bioreactor [1]. Tidal beaches are affected by an intense advective transport of seawater during each tide: during floods, seawater penetrates sandy sediments, bringing dissolved oxygen and marine organic matter in the pore space. The aim of this study is to determine how dissolved oxygen evolves in pore waters along the year and how this evolution is linked to physical forcing such as tide and swell. Autonomous sensors were buried into sediment during 3 to 14 days on the Truc Vert beach (Aquitaine, France) every 3 months. Dissolved oxygen concentration (measured with Aanderaa optodes and NKE data loggers), temperature, salinity and pressure were recorded with a high frequency (from 2 to 10 minutes) at the top of the water table (30-50 cm below sediment surface). The data showed that dissolved oxygen depletions occurred in pore waters and that the intensity of these depletions varied seasonally. Indeed, dissolved oxygen concentration was influenced by the intensity of coastal planktonic primary production. Plankton from the near coastal ocean is the main source of organic matter entering sands. Degradation of this organic matter by respiration processes in the sediment significantly decreased the dissolved oxygen concentration in the pore waters. Strong depletions of dissolved oxygen were observed during spring, with some anoxic events. Furthermore, high frequency recordings highlighted the strong influence of tidal forcing on the benthic dynamic of dissolved oxygen in sands. Swell breaking generated episodic rises in the dissolved oxygen concentration during ebb tides. This in situ study demonstrated how physical (tide and swell) and biogeochemical (respiration) processes may control dissolved oxygen dynamics in intertidal sandy beaches.

[1] Anschutz et al. (2009) Estuar. Coast. Shelf Sci. **84**, 84-90.

Evaluating meteorites using LA-ICPMS: 'Lovina' test case

CHRISTOPHER R.J. CHARLES[1*], PHIL J.A. MCCAUSLAND[2], ROBERTA L. FLEMMING[2] AND DONALD W. DAVIS[1].

[1]Jack Satterly Geochronology Laboratory Dept. Geology, Univ. of Toronto, Toronto, Canada (*christopher.charles@utoronto.ca).
[2]Dept. Earth Sciences, Univ. of Western Ontario, London, Canada.

'Lovina' was found on a beach in Bali, Indonesia in January, 1981 appearing as a football-sized 8.2 kg weathered iron. Lovina was originally classified as an ungrouped ataxite on the basis of petrography and geochemistry [1,2] but was found to have virtually no record of exposure to cosmic rays [3] so its meteoritic status was in question. Here we measure the Pb isotopic composition (IC) of troilite nodules in Lovina in an effort to determine its source.

Pb and U isotopes were analyzed in 10 randomly chosen troilite nodules on a Lovina polished thin-section, by a VG PQ ExCell ICP-MS and UP-213 laser ablation system. Data were acquired on 100 um spots at 70% power and 10Hz. Surface Pb was ablated off each nodule by rastering 4x over an area larger than the spots (raster 4-5 'lines' spaced 30 um apart at 70%, 10 Hz at 120 um/sec speed). Mass fractionation for Pb (~1%) was corrected based on NIST-610.

No U was detected in any of the trolite nodules. 207Pb/206Pb ratios (Figure 1) for all 10 analyses fall in the range expected for modern terrestrial Pb [4-7] and are distinctly below the primordial CDT Pb composition of meteoritic troilite [8]. We conclude that the Pb in Lovina troilite is consistent with a terrestrial source. Lovina's origin remains unclear, but it does not appear to be a meteorite. Despite the relatively poor precision of LA-ICPMS, this rapid and cheap technique may also be useful for identifying meteoritic phases most amenable to U-Pb geochronology.

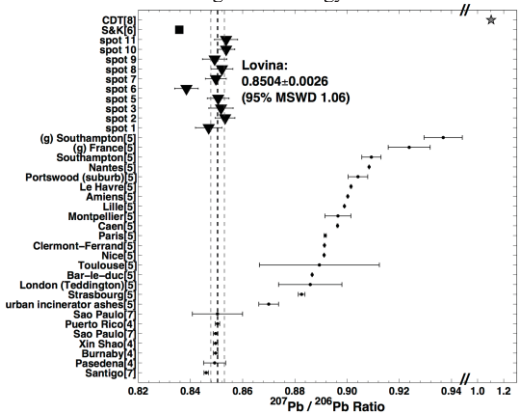

Figure 1: Pb IC of Lovina troilite nodules (triangles) compared to [6], terrestrial airborne particulates and gasoline (g) Pb sources [4,5,7] and Canyon Diablo Troilite (CDT) [8]. Note the break and change in $^{207}Pb/^{206}Pb$ axis scale for plotted CDT.

[1] Met. Bulletin 93 (2008) *MAPS* **43**, 571-642. [2] Flemming et al (2008) *LPSC* **39**, 2412. [3] Nishiizumi & Caffee (2011) *MetSoc* **74**, 5485. [4] Bollhofer & Rosman (2001) *GCA* **65**, 1727-1740. [5] Monna et al (1997) *Env.Sci.Tech.* **31**, 2277-2286. [6] Stacey & Kramers (1975) *EPSL* **26**, 207-221. [7] Bollhofer & Rosman (2000) *GCA* **64**, 3251-3262. [8] Tatsumoto et al (1973) *Science* **180**, 1279.

https://doi.org/10.1180/S0026461X00008434 Published online by Cambridge University Press

Redox oscillation impact on natural and engineered biogeochemical systems

L. CHARLET[1,2].

[1]ISTerre, University of Grenoble, B. P. 53, 38041 Grenoble, France.
[2]Institut Universitaire de France, Paris, France

Many systems fluctuate from oxic to anoxic conditions, in an oscillatory way. Systems becoming seasonally anoxic include irrigated, phreatic- or engineered-flooded soils, seasonally stratified lakes, urban waste sewage pipe and floodplain, macrophyte water treatment plant, and engineered low activity nuclear waste disposal. Conversely, lake "sediments", swamp and peat-bog become oxic "soils" upon urbanization, desertification or agriculture expansion, while anoxic sedimentary formation and aquifers turn oxic upon groundwater over-abstraction or fracking fluid intrusion.

Many reactions in these systems do not reach thermodynamic equilibrium and physical/chemical diffusion, electron transfer kinetics, and solid (e.g. carbonate, sulphide, metallic) phase nucleation control, together with microorganisms, the transitory states of these system. To conduct field work and experimental, analytical or spectroscopic investigation on these systems is a challenge which will be discussed, together with the "natural attenuation"- or release - of toxic elements (such as As, Hg, Se, U..) [1, 2]. (Bio)chemical models of redox oscillatory systems must include a combination of fast reversible reactions (e.g. aqueous and surface complexation equilibria), surface- or microbially- mediated redox kinetic reactions and slow irreversible adsorption/co-precipitation [3]. They should be included in risk assessment and system management of former military or mine sites, waste storage facilities, "green" waste water treatment, floodplains and urban development [4].

[1] Crancon, et al. (2010) *Sci. Tot. Environ*. 408, 2118-2128 [2] Winkel, et al. (2012) *Environ. Sci. Technol (in press)* [3] Burnol *et al.* (2007) *Geochemical Transactions*, **8**:12. [4] Guedron, et al. (2011) *Water research* 45, 2659-2669.

Hydrogen and methane fluxes from the ultramafic-hosted hydrothermal systems on the Mid-Atlantic Ridge

J. L. CHARLOU[1*], C. KONN[1], J.P. DONVAL[1], V. GUYADER[1], F. PEREZ[2], C. MUGLER[2], P. JEAN-BAPTISTE[2], E. FOURRE[2]

[1]Ifremer, Centre deBrest, Département Géosciences Marines, Plouzané, France (*correspondence: charlou@ifremer)
[2]IPSL/LSCE-CEA-Saclay, Gif-sur-Yvette, France (philippe.jean-baptiste@cea.fr)

Mantle-seawater exchanges contribute significantly to the hydrothermal fluxes at slow-spreading ridges. The emplacement of serpentinized mantle at all ultramafic-hosted hydrothermal systems discovered along the slow-spreading Mid-Atlantic Ridge (MAR) where tectonic extension dominates over magmatic construction is a common feature leading to the production of hydrogen and hydrocarbons. To understand the processes controlling the gas generation in ultramafic-hosted active fields, field data including the chemical composition of plumes and fluids are necessary to constraint experimental studies and modeling. The chemical composition of fluids from ultramafic-hosted hydrothermal fields (Rainbow, 36°14'N, Lost City, 30°N, Logatchev I and II, 14°45'N; Ashadze I and II, 12°58'N), all located along the MAR [1] is compared here. Like basalt-hosted fluids, the ultramafic-hosted fluids are controlled by phase-separation. But everywhere H_2 content is extraordinarily enriched in low or high chlorinity phases, demonstrating that the serpentinization process is mainly responsible for hydrogen production. As a consequence of the high reducing power of these systems, isotopic measurements of light hydrocarbons (C_1 to C_4) show that abiogenic hydrocarbons are generated by catalytic Fischer-Tropsch type reaction, considering their isotopic pattern, which is opposite to that for thermogenically-produced hydrocarbons. From plume and fluid data, H_2 and CH_4 fluxes may be calculated. For example, the total hydrogen discharge Φ_{H2} is found to be between 2.5 to 7.5 millions standard cubic meters per year for the Rainbow single site. Based on Rainbow $H_2/^3He$ and ^3He/heat ratios, the global H_2 and CH_4 fluxes for slow-spreading ridges are estimated to be 89 x 10^9 and 8 x 10^9 mol/year, respectively.

[1] Charlou et al. (2010) *AGU Monograph Series* **188**, 265-296.

https://doi.org/10.1180/S0026461X00008434 Published online by Cambridge University Press

Noble gases and halogens in the oceanic crust

D. CHAVRIT[1]*, R. BURGESS[1], B. WESTON[1], L. ABBOTT[1], D. TEAGLE[2], C.J. BALLENTINE[1]

[1]S.E.A.E.S., University of Manchester, Manchester, UK (*deborah.chavrit@manchester.ac.uk)

[2]National Oceanography Centre, University of Southampton, Southampton, UK

Recent studies showed that seawater-derived noble gases and halogens can be recycled into the mantle during the subduction of the oceanic crust [1, 2, 3]. To better understand how this signature is acquired and thus can be preserved, we determined the heavy noble gas (^{36}Ar, ^{84}Kr, ^{130}Xe) and halogen (Cl, Br, I) concentrations in the pre-subducted materiel represented by altered MORB (IODP sites 504, 896, 1256 in the Pacific ocean). The measurements were obtained from samples irradiated via neutron activation, by the release of noble gases in vacuo step crushing (N=18) and followed by in vacuo step heating (N=11).

The ^{130}Xe/^{36}Ar ratios are on average 2 times higher for the heating data (13±5.10^{-4}) than for the crushing data (5.0±4.8.10^{-4}) for similar ^{84}Kr/^{36}Ar (0.05±0.01 and 0.04±0.02 respectively). Thus, the fluid phase is interpreted to be a mixture of air and seawater (± sediments) whereas the solid phases contain an additional altered MORB noble gas component.

An average of ~90% of the halogens are contained in the solid phases and are comparable to the levels present in unaltered MORB glasses. The bulk rock Br/Cl ratio is ~constant (1.05±0.45.10^{-3}) but is 30% lower than in unaltered MORB. In more detail, the Br/Cl ratios of the fluid phases are higher than the seawater's ratio (1.54.10^{-3}) and lower than seawater in the solid phases. The I/Cl ratios vary by 4 orders of magnitude for both the fluid and the solid phases (from 5.5.10^{-7} to 9.03.10^{-3}). The halogen ratios of the fluid phases can thus be explained by a mixing of seawater and sediment or marine pore fluid components. In contrast, the lower Br/Cl value of the altered oceanic crust is mainly attributed to the addition of Cl during the alteration process on the seafloor.

For both halogens and heavy noble gases, we observe different partitioning between the fluid phase and the solid phase. While the fluid phases are more likely a mixing between seawater and a sediment/marine pore fluid signature component, the solid phases define an altered MORB signature. Halogens seem to be a powerful tool to trace the seawater and marine pore fluid signature in rocks and the budget of these elements that is potentially available to be delivered to mantle during subduction.

[1] Holland & Ballentine (2006), Nature 441, 186-191.
[2] Sumino et al. (2010), EPSL 294, 163-172.
[3] Kendrick et al. (2011), Nature Geosciences 4, 807-812.

Zircon as a probe of oxygen fugacity: observations and limitations from natural samples

CYRIL CHELLE-MICHOU[1*], MASSIMO CHIARADIA[1], KALIN KOUZMANOV[1] AND JÖRN F. WOTZLAW[1]

[1]Section of Earth and Environmental Sciences, University of Geneva, 1205 Geneva, Switzerland, cyril.chelle-michou@unige.ch (*presenting author)

Ongoing experiments on zircon crystallization confirm the idea that Ce, Eu and Th/U in zircon are sensitive to the oxygen fugacity (fO_2) of the melt from which it crystalizes [1]. At high oxidation states zircons will display a prominent positive Ce anomaly and none or only a weak negative Eu anomaly that are attributed to the predominance of Ce^{4+} over Ce^{3+} and Eu^{3+} over Eu^{2+}, respectively.

The accurate determination of the Ce anomaly is often problematic due to the low La and Pr concentrations in zircon and possible contamination of the signal during LA-ICP-MS analyses by small LREE-rich mineral inclusions. Alternatively, the Ce^{4+}/Ce^{3+} ratio can be calculated by using the more enriched REEs, from Nd to Lu, together with Zr, Hf and Th [2]. This ratio can be used to infer the relative oxidation state of magmas if a representative population of zircons for each sample is available.. The method is based on the assumption that zircons are in equilibrium with their host rock. If xenocrystic and/or antecrystic zircons are present, the calculated Ce^{4+}/Ce^{3+} ratio may then be inaccurate. Xenocrysts will alter the trace element budget of the whole rock that had never been available in the magma and then affect the calculated Ce^{4+}/Ce^{3+} value of the neoformed zircons. Antecrystic zircons (that cannot be differentiated from autocrysts unless high-precision dating can be done) may have crystallized in a magma of different composition from the rock they are found in. Their relative effect was investigated by numerical simulations on a dataset from dated zircons (by LA-ICP-MS) of the Eocene-Oligocene calc-alkaline Coroccohuayco magmatic suite in southern Peru, associated with porphyry and skarn copper mineralization.

Results show that the effect of xenocrystic zircons on the calculated Ce^{4+}/Ce^{3+} is very limited. Values obtained on antecrystic zircons can be inaccurate if the melt from which they crystallized has a significantly more fractionated REE pattern than the rock they are finally found in. The absolute zircon Ce^{4+}/Ce^{3+} ratio was also found to be very sensitive, by almost one order of magnitude, to the number of REEs used for its calculation. The Ce anomaly does not necessarily correlate with Ce^{4+}/Ce^{3+}. Nevertheless, the interpretations of the Ce^{4+}/Ce^{3+} ratio calculated using different REEs and of the Ce anomaly are very similar, if a representative number of zircons per sample is available. In our dataset, the zircon Eu anomaly was found to correlate with the bulk rock Eu anomaly and not with the zircon Ce^{4+}/Ce^{3+}, suggesting a first order control by the primary melt composition. The zircon/rock partition coefficient of the Th/U ratio decreases systematically with increasing zircon Ce^{4+}/Ce^{3+} values (i.e., fO_2). This supports the idea that U can also occur as U^{5+} and/or U^{6+} in magmas, altering the relative partitioning of Th and U.

[1] Burnham & Berry (2011) *Mineral. Mag.* **75**, 600.
[2] Ballard *et al.* (2002) *Contrib. Mineral. Petrol.* **144**, 347-364.

https://doi.org/10.1180/S0026461X00008434 Published online by Cambridge University Press

Unusual fractionation of both odd and even Hg isotopes in precipitation

JIUBIN CHEN[1,2*], HOLGER HINTELMANN[2], XINBIN FENG[1] AND BRIAN DIMOCK[2]

[1]State Key Laboratory of Environmental Geochemistry, Institute of Geochemistry, Chinese Academy of Science, Guiyang, China. jiubinchen@vip.gyig.ac.cn (* presenting author)

[2]Chemistry Department, Trent University, 1600 West Bank Drive, Peterborough, Ontario, K9J7B8, Canada.

Preliminary studies have demonstrated both mass-dependent fractionation (MDF) and mass-independent fractionation (MIF) of Hg isotopes in the environment and the potential for their application in biochemistry and geochemistry. Though atmospheric deposition is a primary pathway by which Hg enters earth surface ecosystem, little has been reported on Hg isotopes in precipitation.

In order to examine Hg isotopic composition in precipitation, rainwater and snow samples were collected in Peterborough (Ontario, Canada) in 2010. Hg isotopic compositions were determined after Hg pre-concentration using the method developed by Chen et al. (2010). All precipitation samples displayed significant MDF (δ^{202}Hg between -0.02‰ and -1.48‰) and MIF of odd isotopes (Δ^{199}Hg varying from -0.29‰ to 1.13‰). We reported here, for the first time, a seasonal variation of even Hg isotope MIF (Δ^{200}Hg). Our results suggest that photo-reduction in droplets or on the surface layer of snow crystals induce odd Hg isotope anomalies determined in precipitation samples, while mass independent fractionation of even Hg isotopes is likely triggered by elemental Hg oxidation occurring on aerosol or solid surface in the tropopause. Though more research is required to fully understand the behaviour of Hg isotopes in the atmosphere, the striking seasonal variation of even Hg MIF (and with temperature) may provide useful information for meteorological research and related climate studies and help in monitoring atmospheric Hg transportation.

[1] Chen et al., (2010) *JAAS* **25**, 1402-1409.

The analysis of solution-ICP-MS of rare earth elements of carbonate minerals in carbonate rocks

LINYING CHEN, CHONGYING LI AND DUOFU CHEN*

CAS Key Laboratory of Marginal Sea Geology, South China Sea Institute of Oceanology, Chinese Academy of Sciences, Guangzhou, China, cdf@gig.ac.cn

The trace elements of carbonate minerals in carbonate rocks, especially rare earth elements (REEs), are the best parameters to trace the redox conditions of the sedimentary environment. However, because the REE contents of carbonate minerals are much lower than that of terrigenous clays, a small quantity of clays dissolved will affect true redox implication. Therefore, to conduct an analytical method to get the true REE contents of carbonate minerals deposited in marine environment without the contamination from terrigenous clays is very important.

At the present time, the analytical methods of REEs of carbonate minerals in carbonate rocks mainly are solution-ICP-MS and LA-ICP-MS. In solution-ICP-MS method, hydrochloric acid, nitric acid and acetic acid are usually used. Hydrochloric acid and nitric acid could dissolve all carbonate minerals in carbonate rocks and also possibly parts of non-carbonate minerals, which disturb the analysis results. Although using acetic acid can avoid the interference of non-carbonate minerals, it probably could not completely dissolve the carbonate minerals in carbonate rocks, the results also could not be true. In LA-ICP-MS analysis, carbonate minerals was ablated by laser beam firstly, and then evaporation was directly carried into ICP-MS, which could be the most effective method for REE analysis of carbonate minerals without clays. But, because the diameter of laser beam is too large to avoid tiny clays which usually occur in carbonate minerals, LA-ICP-MS also has uncertainty.

Here we use 5% CH_3COOH, 5% HCl, 2% and 5% HNO_3 to dissolve powder samples split from one carbonate rock for 0.5, 1, 2, 3, 6 and 24 hours, respectively. The XRD analysis results show that there is no calcite in insoluble residues after acid dissolution suggesting that calcite was completely dissolved. The ICP-AES analysis results of acid dissolved solution indicate that small quantities of clays were dissolved. These dissolved clays result in an increase of REE contents, but do not affect Eu/Eu*, LaN/YbN and Gd/Gd*. The obvious positive relation between Al_2O_3 and Ce/Ce* in acid dissolved solutions suggests that the dissolved clays did affect the Ce/Ce* values of carbonate minerals to a certain degree.

Comparing results under different acid dissolution, we could conclude that the appropriate conditions for REE analysis of carbonate minerals in carbonate rocks is 0.5-1g samples reacting with 5% CH_3COOH for 1 hour, which decrease the influence of clays on Ce/Ce* values to the lowest. As for HNO_3 dissolution, the acid with concentration <2% should be used to react with 0.2g power sample for <30 min. And for 5% HCl dissolution, the reacting time should be <30 min with 0.2-1g sample. The Ce/Ce* values obtained from HCl and HNO_3 dissolutions could still be used to trace sedimentary environment, but will be higher about 0.1 than that from CH_3COOH dissolution.

This work was supported by CAS Key Lab. Of Marinal Sea Geology (MSGL11-01), and CAS (KZCX2-YW-GJ03).

https://doi.org/10.1180/S0026461X00008434 Published online by Cambridge University Press

Investigating biogeochemical alteration of oil sand tailings: Field vs. laboratory studies

M. CHEN[1], M. GOETZ[1], N. LOICK[1] AND C. WEISENER[1]

[1]Great Lakes Environmental Research Institute, University of Windsor, Windsor, Canada, weisener@uwindsor.ca

Introduction

The oil sands deposits in Northern Alberta are one of the largest oil reserves in the world, containing an estimated 2.5 trillion barrels of recoverable bitumen held in a mineral matrix consisting of sand, clay and water. The current practice is to store the tailings in large settling basins, to allow the solids to settle out by gravity forming a denser unconsolidated mass termed fluid fine tailings (FFT). FFT is transferred from settling basins into the mined-out pits, being proposed for a series of end pit lakes, a strategy for sustainable environments being evaluated in the Fort McMurray region. As these end pit lakes (EPL) evolve, significant changes in the physicochemical properties, microbiology and geochemistry can occur affecting both the volume and quality of the intended water cap. To date little information exists on the biogeochemical nature (redox mediated reactions) of the FFT product prior to deposition. Our research program is investigating both the chemistry and the microbial community structure within core samples collected from oil sands tailings basins. To compliment and confirm predictive models there is a need for detailed systematic studies bridging the physical (mineralogy) and chemical (redox chemistry abiotic vs. biotic; cycling of Fe and S) gradients observed for samples collected.

Results/Conclusions

Detailed studies in our group have shown that chemical and biological mechanisms play a role in controlling diffusivity, O_2, HS^-, NO_x gradients which may be linked to sulfur and Fe (II/III) cycling during initial settling under aerobic and anaerobic conditions [1, 2]. To validate these assumptions further investigations have assessed the chemical and secondary mineralization mechanisms that occur in REDOX sensitive microaerophilic zones in both laboratory studies and collected field samples from the settling basins. Data will be presented which support these assumptions from the EPL materials by looking at temporal chages of the materials as well as comparing results from bioreactor-studies and field-samples.

[1] Chi Fru (2012) *Bioreactor studies predict whole microbial population dynamics in oil sands tailings ponds, Environmental Science and technology,* in review.
[2] Chen (2012) *Bioreactor assessment of the biogeochemical evolution of sulfur and oxygen in oil sands fluid fine tailings, Science and the total environment*, in review.

Early diagenesis of redox-sensitive elements in the Estuary and Gulf of St. Lawrence

QIANG CHEN[1*], ALFONSO MUCCI[1], BJORN SUNDBY[1, 2], AND WILLIAM MINARIK[1]

[1]GEOTOP & McGill University, Earth and Planetary Sciences, Montreal, Canada
qiang.chen@mail.mcgill.ca (*presenting author), alfonso.mucci@mcgill.ca, william.minarik@mcgill.ca
[2]Université du Québec à Rimouski, Institut des Sciences de la Mer de Rimouski (ISMER), Rimouski, Canada
bjorn_sundby@uqar.qc.ca

Redox-sensitive elements (RSEs) are potentially powerful paleo-redox tracers [1]. To realize this potential requires an improved understanding on their geochemical properties and the chemical reactions they participate in during early diagenesis.

We measured the distributions of Fe, Mn, U, Mo, Re, and Cd in solid phase sediment and their porewaters in six cores collected along the Laurentian Trough of the Estuary and Gulf of St. Lawrence and the Eastern Canadian continental shelf. The data were obtained via ICP-MS analysis of porewaters and buffered-ascorbate and 1 N HCl extractible solid phase components. The results are consistent with the conclusions of a previous investigation that the accumulation rates of U, Mo, Re, and Cd are controlled by slow precipitation kinetics [2]. At the most landward station, where the sedimentation rate is highest (~4 mm/yr) and the bottom water dissolved oxygen concentration is lowest (~60 μM), the porewater U, Mo and Re concentrations decrease gradually with depth, supporting diffusion from the bottom water into the sediment. In contrast, porewater U, Mo and Re profiles show little variation with depth in the Gulf and on the continental shelf where the sedimentation rates are lower (0.5-1.5 mm/yr) and the bottom water oxygen concentration is higher (~150 μM). At all stations, the porewater Cd concentration is variable with depth. The extractible solid phase concentrations of Mo, U, Re and Cd increase with depth in all cores. These findings provide a useful test of how RSEs respond to variable overlying water oxygenation and sediment accumulation rates and how their vertical distributions are modified by early diagenetic processes.

[1] Tribovillard *et al*. (2006) *Chem. Geol.* **232**, 12-32.
[2] Sundby *et al.* (2004) *GCA* **68**, 2485-2493.

https://doi.org/10.1180/S0026461X00008434 Published online by Cambridge University Press

Nd & Hf concentrations and isotopic compositions in the Baltic Sea

TIANYU CHEN[1], MARTIN FRANK[1], AND ROLAND STUMPF[1*]

[1] GEOMAR | Helmholtz Centre for Ocean Research Kiel, Wischhofstr.1-3, Kiel, Germany, rstumpf@geomar.de (*presenting author)

Abstract

Within a process study in the framework of the international GEOTRACES program and led by the Institute of Oceanology of the Polish Academy of Sciences (IOPAN) a two-week cruise on the R/V Oceania sailed in November 2011 to investigate the distribution of trace elements and their isotopes in the Baltic Sea. The scientific goals were particularly focused on compiling trace element budgets for the Baltic Sea including in- and outflow, as well as to investigate elemental behavior and isotopic fractionation associated with the redox gradients of the Baltic Sea water column and the permanently anoxic conditions within its deep basins (i.e. Gotland Deep, Landsort Deep).

The Baltic Sea is a shallow, brackish inland sea with an average salinity of ~7 psu in the mixed layer. It is fed by the Bothnian Sea in the north, by the Finland Sea in the east, as well as by numerous rivers from Scandinavia and the Baltic states, and it is drained through the Danish Strait into the North Sea. In the opposite direction, a denser bottom water mass enters the Baltic Sea through deeper channels from the Danish Strait successively filling the deep basins northward. Below 130 m water depth, the water column is permanently anoxic.

Here we present the first combined data set of Nd and Hf concentrations and isotopic compositions for the Baltic Sea. A total of 21 water samples (60L volume per sample) including two water column profiles from the deeper basins were filtered (0.45 μm) and Nd and Hf were extracted and analysed following the accepted GEOTRACES protocols. The distribution patterns of the two elements and their isotopic compositions are compared to hydrographic data and oxygen measurements and provide information on sources and mixing of water masses, as well as on exchange processes with the underlying sediments, which are influenced by the prevailing redox gradients.

Acknowledgements

Very special thanks go to the Institute of Oceanology of the Polish Academy of Sciences (IOPAN) as well as to the crew and science party of the R/V Oceania for making this cruise possible.

Stability of engineered nanoparticles in aqueous environments: measurements and modeling

YONGSHENG CHEN*, WEN ZHANG AND KUNGANG LI

School of Civil and Environmental Engineering, Georgia Institute of Technology, Atlanta, Georgia, 30332; e-mail: yongsheng.chen@ce.gatech.edu

Aqueous stability of engineered nanoparticles (ENPs) plays a crucial role in their environmental fate, transport, bioavailability and biological consequences. ENPs, once disposed into aqueous enviornments, may undergo aggregation and dissolution or ion release. In this study, we systematically investigated aggregation kinetics of serval selected ENPs through assessment of the environmental effects (e.g., ionic strength) and modeling approaches. Particularly, CeO_2, due to its broad industrial applications, was chosen as a model ENP to study the aggregation kinetics under different concentraions and species of electrolyte (K^+ and Ca^{2+}) [1] and natural organic matter (NOM) [2] using time resolved-dynamic light scattering (TR-DLS). Expeirmental results were further evaluated by theoretical models developed on the basis of Extended Derjaguin−Landau−Verwey−Overbeek (EDLVO) theory. Based on the EDLVO theory and the von Smoluchowski's population balance equation, a model accounting for diffusion-limited aggregation (DLA) kinetics was established. Furthermore, a new approach was presented for assessing the attachment efficiency (a measure of relative aggregation kinetics) of ENP aggregation based on the Maxwell-Boltzmann distribution coupled with the DLVO theory [3], which is a first attempt to the best of our knowledge. The modified attachment efficiency equation was proposed and the equation successfully interpreted the effects of ionic strength, NOM, and temperature on aggregation kinetics [3], showing the balanced consideration of interfacial energy and Brownian motion in evaluating the aggregation kinetics of NP dispersions. For chemically reactive ENPs, silver NPs (or AgNPs) was selected to investigate the disolution kinetics and effects of particle size and concentration, and other factors (e.g., aggregation) [4]. An Arrhenius-based equation was developed for the first time to describe and simulate the Ag^+ release kinetics. Oxidative dissolution of AgNPs was accompanied by particle aggregation, which differed in kinetics with or wihtout the presence of disssolved oxygen [5]. The knowledge gained from this research proivdes insight into the aqueous stability of ENPs and using expeirmental and modeling approaches, allowing us to better undertand and predict environmental fate of ENPs at nanoscale.

[1] Li, *et al*., *J. Nanopart. Res.* 2011, 13, 6483-6491.
[2] Li, *et al*.,*J. Hazard. Mater.* 2012, Accepted.
[3] Zhang, *et al*., *Environ. Sci. & Technol.* 2012, Accepted.
[4] Zhang, *et al*., *Environ. Sci.Technol.* 2011, 45, 4422–4428.
[5] Zhang, *et al*., *Environ. Pollut.* 2011, 159, 3757-3762.

https://doi.org/10.1180/S0026461X00008434 Published online by Cambridge University Press

The Formation and Evolution on the Central Asian Orogenic Belt

YUELONG CHEN[1*], DAPENG LI[1], ZHONG WANG[2], JINBAO LIU[2], CHANGZHENG LIU[3]

[1] China University of Geosciences (Beijing), Faculty of Earth Sciences and Mineral Resources, Beijing, China, chyl@cugb.edu.cn (*presenting author); ldpzhuanyong@163.com

[2] Geological Survey of Inner Mongolia Autonomous Region, Hohhot, China, wzhong61@126.com; nmgljb@126.com

[3] The Fifth Geological Survey of Qinghai Province, Xining, China

Geological Setting

The Central Asian Orogenic Belt (CAOB), one of the largest orogens on the Earth, has attracted numerous geologists and geochemists around the world[1]. It is surrounded by the Siberian craton in the north and by the North China and Tarim cratons in the south and extends from the Ural Mountains in the west to the Pacific coast in the east. The CAOB is considered as an accretion orogen through arc/backarc systems, ophiolites, and microcontinental fragments[2,3]. Although there are many achievements on geodynamic models, accretion rates, Precambrian microcontinents etc., general characters of the CAOB have not been summarized yet.

Methodology

Due to rapid development of SHRIMP and LA-(MC)-ICP-MS techniques, a lot of precise and accurate U-Pb dating and Hf isotopic data of zircons in the CAOB have been accumulated during recent 10 years. We compiled the comprehensive histograms and probability density curves of U-Pb ages and Hf model ages on zircons as well as Nd depleted mantle model ages of whole rocks on the basis of our results and published data.

Results and Conclusions

Although the Hf isotope of a zircon grain represents its composition in a micro-domain, averaged Hf model age (1.39Ga) is almost consistent with that (1.28Ga) of Nd model ages，which are much older than that (571Ma) of zircon U-Pb ages. Collectively, the most intensive magmatic and crustal growth event took place during the Early Palaeozoic and Neoproterozoic periods according to consistent peaks among U-Pb ages and Hf model ages of zircons and Nd model ages. The earliest history can be tracked to ~3.2Ga by U-Pb ages of zircons and Nd model ages, whereas the oldest Hf model age is ~4.3Ga, which indicates that the crustal components of older than 3.2Ga have only been recorded in some zircon grains. The zircons of older than 1.0Ga derived from reworked Precambrian basements of the CAOB, which account for <10% in populations of all zircon U-Pb ages, in contrast to cumulative probability of over 60% in those of Hf and Nd model ages. Therefore, the Mesoproterozoic juvenile crustal components constitute dominant part of CAOB's Precambrain basements, most of which have involved in subsequent intra-crustal magmatisms. The Neoproterozoic is a transition period initiating intensive magmatism in the CAOB. Magmatism arrived at the climax in Palaeozoic, whose cumulative probability possesses 76% in whole range of ages.

[1] Rojas-Agramonte (2011) *Gondwana Res*.**19,**751-763.
[2] Rytsk et al. (2007) *Geotectonics* **41**, 440-460.
[3] Windley et al.(2007) *PJ uJ.Geol. Soc. London* **164**,31-47.

Local spatial and scaling modelling for geochemical heterogeneity and anomaly detection

ZHIJUN CHEN[1*] AND QIUMING CHENG[1, 2]

[1]State Key Lab of Geological Processes and Mineral Resources, Faculty of Earth Resources, China University of Geosciences (Wuhan), Wuhan, China, chenzhijuncs@163.com (*presenting author)

[2]Department of Earth and Space Science and Engineering, York University, Toronto, Canada, qiuming@yorku.ca

Regional geochemical mapping with stream sediments provides information on weathering and transport processes and on the presence of contaminants and mineral deposits. Various quantitative methods have been developed in geochemical exploration to separate anomalies associated with mineralization from background reflecting regional geological processes. However, geochemical datasets often show strong heterogeneity in geomorphologically and geologically complex settings. Therefore, anomaly detection methods based on the assumption of homogeneity and stationary are inappropriate. A key change in separating anomalies from background has been from a focus on local singularities rather than the search for global regularities and production of local mappable statistics rather than global summaries. The local spatial and scaling model that combines local singularity analysis and spatial U-statistics introduced is a potential powerful method for geochemical heterogeneity and anomaly detection.

The study area is in the northern part of the Lanping basin, Yunnan province, China. A total of 1172 stream sediment samples were collected at 2 km intervals. Many Pb-Zn-Ag deposits including the Jinding super large Pb-Zn deposit exist in this area.

The scale-invariant property has been observed not only in many geochemical maps but has also proved useful for characterizing variability in maps. Local singularity analysis based on multifractal theory is a powerful tool for characterizing local structural properties of spatial patterns. It uses the local singularity index α to indicate background or anomaly, where $\alpha(x)$ close to 2 represents background with homogeneity, $\alpha(x) > 2$ corresponds to local depletion, and $\alpha(x) < 2$ to anomalous enrichment at the neighborhood $\Omega(x)$. Locally-adaptive detection of the geometrical properties of $\Omega(x)$ (size, shape, and orientation) will obtain better $\alpha(x)$ if patterns are heterogenous at the scale of measurement. A spatial U-statistic can be used not only for geochemical anomaly separation but also for searching anisotropic parameters at arbitrary sample location. Thus, it useful for anisotropic local singularity modelling.

The combined local singularity analysis and spatial U-statistics considers not only concentration values, frequency distributions and spatial correlation, but also geometrical properties of anomalies and scale independence characteristics, which are effective to reveal multi-scale anisotropy and heterogeneity in geochemical exploration data. It can be a useful tool to discover weak anomalies related to buried mineral deposits.

This research was supported by NCFC(40802081), 863 Plan(2009AA06Z110), and the Special Fund for Basic Scientific Research of Central Colleges at China University of Geosciences (Wuhan).

[1] Cheng (1999) *Journal of Geochemical Exploration* **65**, 175-194. [2] Chen et al. (2007) *Journal of China University of Geosciences* **18**, 348-350.

https://doi.org/10.1180/S0026461X00008434 Published online by Cambridge University Press

Identification of Transport Pathway and Geographical Source Location of Light Absorbing Species and Co-Pollutants

MENG-DAWN CHENG[1*] AND JOHN M.E. STOREY[1]

[1]Energy and Environmental Directorate, Environmental Sciences Divison, Oak Ridge National Laboratory, Oak Ridge, TN, USA, chengmd@ornl.gov (* Presenting author)

Ground observations of light absorption and aerosol-borne species are analysed and digested in a hybrid receptor-modelling framework called the Potential Source Contribution Function (PSCF)[1]. The analytic method establishes the relevant events based on observations using a number of time-series techniques to separate various frequency components; then the PSCF algorithm computes the probability of the overloading probability of identifiable polluting events for each grid cell in the modelling domain. The calculated probability is then an indication of a grid cell being an emission source of a particular pollutant under investigation. Multiple pollutants and or co-pollutants are used in the combined / joint probability analysis to enhance the identification power. We have analyzed the assembled time-series observations made at Barrow, Alaska for the past 15 years. Similar to many previous data taken at other site such as Alert, NWT, periodic pattern of light absorption, CNC, and other ground aerosol species concentrations were observed. Many data from Barrow are ran off by low-freqency compoent in the timer-series analysis. For those detectable, the correlation between light absorption and black carbon measurements were analyzed to show that there are other light absorption components existing in the Arctic particles. Backward trajectories segregated by season show different transport pathways to the two receptor sites suggesting alternative control strategies. Ongoing PSCF modeling will identify the geographical locations of various pollutants modeled and show the uncertainty of the identification, which will be presented in the conference.

[1] Cheng, M.D., Schroeder, W.H., 2000. J. Atmos. Chem. 35, 101-107.

Diffusion in Minerals Relevant to Geochronology

D.J. CHERNIAK[1]*, E.B. WATSON[1]

[1]Department of Earth and Environmental Sciences, Rensselaer Polytechnic Institute, Troy, NY, USA, *chernd@rpi.edu (presenting author)

Understanding diffusion processes in minerals of geochronologic interest is important in interpreting results from geochronological studies and in refinement of thermal histories. Much progress has been made in characterizing diffusion in various systems, and work continues. Diffusivities in minerals may depend on many factors, including the presence of fluids. There is abundant evidence [1] that the presence of water or other hydrous species affects oxygen diffusion in minerals. However, studies of cation diffusion generally indicate little influence of the presence of hydrous species. Hence, while fluids can play a significant role in geochronological systems in facilitating dissolution/precipitation reactions which can result in the resetting of isotopic and chemical signatures, it appears that fluids will have little additional effect on resetting due to volume diffusion within mineral grains at crustal conditions. A summary of relevant diffusion studies will be presented, along with implications of these findings with regard to transport in fluid-present systems.

Diffusion data have long found application in geochronologic studies through the concept of diffusive closure advanced by Dodson [2] and its subsequent refinements [e.g., 3,4]. When considering geologic temperature-time paths, the most important limitation of Dodson's [2] expressions is that they apply strictly to cooling regimes, since many geological processes involve heating of mineral grains that are initially diffusively closed. Thus, in a prograde thermal regime, it is not a question of when closure "sets in" but when a mineral grain "opens up" diffusively. Despite its original intent, Dodson's equation has been used frequently to address closure conditions of minerals during heating, perhaps because simple alternatives are lacking. Sophisticated approaches have been developed to address diffusive loss during heating, but mainly for specific applications; however, Gardes and Montel [5] have recently more generally examined conditions for "opening" and "resetting" in prograde temperature regimes.

In a complementary study, we take a somewhat different approach, using a combination of numerical simulations and mathematics to obtain simple equations with parameters equivalent to those in used in Dodson's equation [2], to evaluate conditions for opening and resetting in prograde T-t regimes. Tests of these equations demonstrate accuracy to within 5°C for the vast majority of measured diffusivities, and within 1° in most cases. In addition, there are essentially no restrictions on grain size or heating rate (up to 2000°C/Myr) that can be used without loss of accuracy. These findings will be presented, with discussion of various parameters considered in the modelling, including linear heating vs. other prograde paths, and the production of radiogenic species.

[1] Farver (2010) *Rev. Mineral. Geochem.* **72**, 447-507. [2] Dodson (1973) *CMP* **40**, 259-274. [3] Dodson (1986) *Mat. Sci. Forum* **7**, 145-154. [4] Ganguly & Tirone (1999) *EPSL* **170**, 131–140. [5] Gardes & Montel (2009) *CMP* **158**, 185–195.

https://doi.org/10.1180/S0026461X00008434 Published online by Cambridge University Press

Diffusion of Neon in Olivine and Quartz

D.J. CHERNIAK[1]*, J.B. THOMAS[1], E.B. WATSON[1]

[1]Department of Earth and Environmental Sciences, Rensselaer Polytechnic Institute, Troy, NY, USA, *chernd@rpi.edu (presenting author)

Diffusion of neon has been characterized in olivine and quartz. Polished, oriented slabs of olivine (synthetic forsterite and natural Fe-bearing olivine) and synthetic quartz were implanted with ^{22}Ne at 100 keV with a dose of $5x10^{15}/cm^2$. Experiments on the implanted olivine and quartz were run in 1-atm furnaces, with ^{22}Ne distributions in samples following diffusion anneals measured by Nuclear Reaction Analysis using the reaction $^{22}Ne(p,\gamma)^{23}Na$.

For diffusion in synthetic forsterite, for transport parallel to the b-axis, we obtain the following Arrhenius relation over the temperature range 500-1000°C:

$D_{forst} = 2.4x10^{-12}exp(-155 \pm 12 \text{ kJ mol}^{-1}/RT) \text{ m}^2\text{sec}^{-1}$.

Diffusion parallel to the c-axis appears similar over the temperature range investigated. Data from "soaking" experiments on forsterite, in which ^{20}Ne was diffused into samples during anneals in cold-seal vessels pressurized with neon, are in generally good agreement with results from the ^{22}Ne implantation experiments. Work is currently underway on measurements of Ne diffusion in a natural Fe-bearing olivine.

The Ne diffusivities for olivine measured in this work are roughly two orders of magnitude slower than those obtained by Futagami et al. [1], who measured Ne diffusion in synthetic forsterite by outgassing ^{20}Ne implanted samples.

Activation energies for Ne diffusion are comparable to those recently measured for helium diffusion in olivine [2], but diffusion of Ne is about 5 orders of magnitude slower than He diffusion.

For quartz, we obtain the following Arrhenius relation over the temperature range 450-1000°C for Ne diffusion parallel to the c-axis:

$D_{qtz} = 1.3x10^{-14}exp(-112 \pm 15 \text{ kJ mol}^{-1}/RT) \text{ m}^2\text{sec}^{-1}$.

Ne diffusion normal to the c-axis appears similar. As with olivine, data from "soaking" experiments using pressurized ^{20}Ne are in generally good agreement with the ion implantation results. However, these diffusivities are about 10 orders of magnitude slower than the values for diffusion of ^{21}Ne in quartz from outgassing experiments reported by Shuster and Farley [3].

Our data suggest that both quartz and olivine may be moderately retentive of neon; for example, 500 micron radius grains of quartz and olivine would experience only 5% loss of Ne in 1 Myr at 320°C and 395°C, respectively, and negligible Ne losses at surface temperatures over times on order of the age of the earth.

[1] Futagami et al. (1993) *Geochim. Cosmochim. Acta* **57**, 3177-3194. [2] Cherniak & Watson (2011) *2011 AGU Fall Mtg.* [3] Shuster & Farley (2005) *Geochim. Cosmochim. Acta* **69**, 2349-2359.

The transient rheology of crystallizing magmas

MAGDALENA ORYAËLLE CHEVREL[1*], LEA J. DE BIASI[1], JONATHAN B. HANSON[1, 2], CORRADO CIMARELLI[1], YAN LAVALLÉE[1], DONALD B. DINGWELL[1]

[1] Ludwig-Maximilians-University, Department of Earth and Environmental Sciences, Munich, Germany, chevrel@min.uni-muenchen.de (*presenting author)

[2] University of Bristol, Department of Earth Sciences, Bristol, United-Kingdom

Introduction

The viscosity of magmas is a key parameter in magma transport processes and volcanic eruptions. In nature, magmas are transient. Changes in P-T conditions force the magma to chemically and physically evolve, resolving a transient viscosity of the melt (e.g., 10^{-1} to 10^{14} Pa s), overprinted by the complex rheological effects of the suspended fraction (crystals and bubbles). Such a dynamic understanding of transient rheology escapes our ability to fully assess the extent of volcanic hazards (e.g., lava flow reach out). To date, rheological studies provide a static view on individual contributions (e.g., chemical composition of the interstitial liquid [1] vs physical effects of the suspended phases [2,3]), without consideration of the feedback involved in the thermodynamic process underlying the evolution of the magmatic system. Alternatively, thermodynamic calculators (e.g., MELTS [4]) provide a static view of mineral assemblage equilibrium, disregarding kinetic information on the physical evolution of the system during crystallization. Here, we assess the adequacy of combining rheological, petrologic and thermodynamic models in a transient system (such as lava flow dynamics) by comparing their outcome to dynamic rheological experiments on crystallizing and flowing natural melts with various (andesitic to basaltic) compositions.

Methodology and results

We optimized previous experimental methods [5,6] for the concentric cylinder apparatus to measure the dynamic apparent viscosity of a magmatic suspension undergoing cooling and crystallization. The spindle is left in situ during quenching of the experimental products, to preserve the complete developed texture of the sample. Experiments are carried out in air or under controlled oxygen fugacity in order to avoid extensive oxide crystallization. Below the liquidus we record a transient evolution of the system; when crystals nucleate and when crystals grow. Thermodynamic equilibration is then reached after some hours. With each further cooling increment equally complex rheological response (overprint by non-Newtonian behavior) is observed. Quantification of the evolving mineralogical assemblage as well as the crystal fraction and distribution reveal that the steady state flow conditions are reached upon completion of crystallization at equilibrium (under a given T increments). Comparatively, the apparent viscosity at each investigated temperature is calculated as a function of the crystallization sequences (via MELTS), the residual liquid composition (via GRD calculator [1]) and the characteristics of the solid fraction [2,3], presenting the discrepancies of employing static models in a dynamic system. Our findings suggest that dynamic models will need to be developed to improve the description of magma transport in our assessment of volcanic hazards.

[1] Giordano et al., (2008) *Earth Planet. Sci. Lett.* **271**, 123– 134. [2] Mueller et al., (2010) *Philos. Trans. R. Soc. Lond.* **A 466**, 1201–1228. [3] Cimarelli et al., (2011) *Geochem. Geophys. Geosyst.* **12**, Q07024, 14 PP. [4] Ghiorso et al., (1995) *Contributions to Mineralogy and Petrology*, **119**, 197-212. [5] Ishibashi and Sato, (2007) J. Volcanol. Geoth. Res. **160**, 223–238. [6] Vona, et al., (2011). *Geochim. Cosmochim. Acta*, **75**, 3214-3236.

https://doi.org/10.1180/S0026461X00008434 Published online by Cambridge University Press

Hydrodynamic constraints on relationships between different types of U deposits in southern China

GUOXIANG CHI[1], YONGZHANG ZHOU[2]

[1]University of Regina, Department of Geology, Regina, Canada, guoxiang.chi@uregina.ca (* presenting author)
[2]Sun Yat-sen University, Guangdong Provincial Key Lab of Mineral Resources and Geological Processes, zhouyz@mail.sysu.edu.cn

Four types of U deposits (granite-, volcanic-, carbonaceous-siliceous-pelitic-, and sandstone-type) have been documented in southern China [1, 2]. The majority of them were formed in late Cretaceous-Tertiary (K-E) [2, 3], much younger than the host rocks, suggesting that most of them did not form from magmatic (Triassic-Jurassic) fluids [2]. Based on their association with K-E red-bed basins, it was proposed that the U deposits are genetically related to basinal fluids, like Proterozoic unconformity-type [3]. Alternatively, mantle-derived CO_2-rich fluids, in relation to crustal extention during K-E, were held responsible [4]. It remains poorly understood why U deposits were not well developed before Cretaceous.

It is proposed here that the paucity of U mineralization in Jurassic and Triassic is related to the compressional tectonic environment, which resulted in impermeable basement and dominantly upward fluid flow in sedimentary basins (Fig. 1a). Such a hydrodynamic regime limited oxidizing fluids near the surface and reduced the opportunity for them to extract U from granites at depth. In contrast, the extentional tectonic environment in K-E increased the permeability of the basement, resulting in "leaky" basins and infiltration of oxidizing fluids into the basement (Fig. 1b), forming U deposits in various basement rocks including granites.

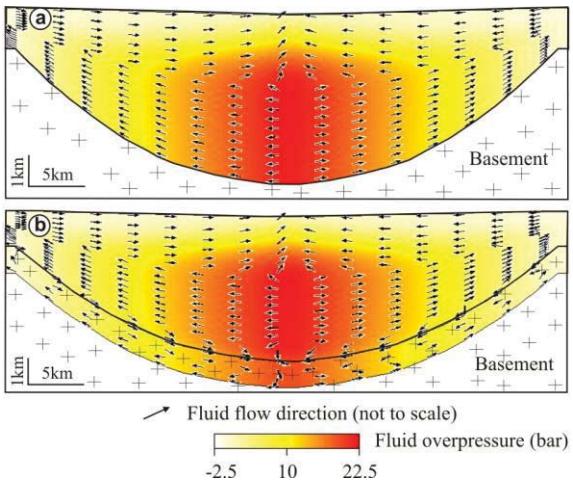

Figure 1: Fluid flow patterns of generic basins in southern China. (a) Triassic-Jurassic model with impermeable basement; (b) Cretaceous-Tertiary model with permeable (upper 1km) basement. Basin 50km wide, 5km deep, duration 100 Ma, 50% sand + 50% shale, topographic relief 250 m, computed with *Basin2*.

[1] Du and Wang (1984) *Radioactive Geology* **3**, 1-10.
[2] Zhang (1989) *Nuclear Science and Engineering* **9**, 162-169.
[3] Wang et al. (2002) *Geological Review* **48**, 365-371.
[4] Hu et al. (2008) *Economic Geology* **103**, 583-598.

CO_2 rich environments under silica confinement

ARIEL A. CHIALVO[1*] , LUKAS VLCEK[2], AND DAVID R. COLE[3]

[1] Oak Ridge National Laboratory, Oak Ridge, TN 37631, U.S.A., chialvoaa@ornl.gov, (* presenting author)
[2] Oak Ridge National Laboratory, Oak Ridge, TN 37631, U.S.A., vlcekl1@ornl.gov
[3] Ohio State University, Columbus, OH 43210, U.S.A., cole.618@osu.edu

A potential approach toward the mitigation of the greenhouse effects of CO_2 release into the atmosphere is based on its geological capture and sequestration, a process that relies on the low hydraulic permeability of caprocks resulting from fluid-substrate interfacial and confinement behaviour. Current studies have mainly focused on the interactions of either water-rich CO_2 or pure CO_2 environments with representative caprock substrates, and the concomitant modeling is based on that assumption, *i.e.*, the impact of the CO_2-contaminants has rarely been addressed. In fact, due to its source, CO_2 always carries small quantities of 'contaminants' including SO_2, N_2, NO_x whose impact in terms of fluid-rock interactions must be considered.

Obviously, the presence of SO_2 in aqueous solution may trigger the formation of sulfurous/sulfuric acids [1], whose immediate consequence is the increase in acidity and the potential for dissolution/precipitation of secondary mineral phases that results in significant changes in substrate porosity and permeability [2]. Unfortunately, thermophysical properties for these mixtures at reservoir conditions are scarce or nonexistent [3], and our microscopic understanding of their interaction with caprock is extremely limited.

For that reason, we carried out a molecular-based study of the behavior of CO_2-rich environments containing common contaminants when in contact with and under severe confinement of silica surfaces, to address fundamental issues, including (a) how the degree of surface hydrophobicity affects the interfacial structure and dynamics, (b) how the overlap of interfacial structures affects the confined fluid composition, and (c) how contaminants affect the preferential adsorption and composition of the interfacial fluid layers.

[1] Crandell, L.E., *et al.*, Environmental Science & Technology, 2010. **44**(1): p. 349-355; [2] Knauss, K.G., *et al.*, Chemical Geology, 2005. **217**(3-4): p. 339-350; [3] Jacquemet, N., *et al.*, *Greenhouse Gas Control Technologies 9*, Gale, Herzog, and Braitsch, Eds. 2009. p. 3739-3746.

Acknowledgements. Support for this work comes from the US Department of Energy through the LBNL "Center for Nanoscale Control of Geologic CO_2" (FWP ERKCC67) under contract DE-AC05-00OR22725 to Oak Ridge National Laboratory, managed and operated by UT-Battelle, LLC.

https://doi.org/10.1180/S0026461X00008434 Published online by Cambridge University Press

Adsorption of Humic Acid onto Alumina: Conformational Changes

G. CHILOM[1*], M.M.R. KHALAF[1] AND J. A. RICE [1]
[1]Dept. Chemistry & Biochemistry, South Dakota State University, Brookings, SD 57007, USA, moustafa.khalaf@sdstate.edu, gabriela.chilom@sdstate.edu (* presenting author), james.rice@sdstate.edu

Natural organic matter is a key component of both soils and sediments that is likely to be associated with mineral matter. Natural organic matter - mineral complexes typically represent more than 50% of the organic carbon in a soil and typically more than 70% of the OC in unlithified sediments. The behavior of NOM in the environment is affected by their interactions with minerals due to their possible fractionation and conformational changes. The objective of this study was to investigate these conformational changes and the mechanisms that produce them. The adsorption isotherms of a humic acid as well as its non-amphiphilic and amphiphilic components, onto alumina were determined. The adsorbed and remaining humic acid in solution at both low and high concentration was characterized by solid state NMR and UV spectroscopy. Data suggested that preferential sorption and changes in the mobility of aromatic carbon occur upon adsorption and these changes vary with concentration. Analysis of the data for the amphiphilic fraction of humic acid suggested that surfactant character plays an important role in the adsorption selectivity and conformational changes that occur upon adsorption onto alumina.

Electrochemical study of pyrite oxidation in oxygen-bearing solutions

PAUL CHIRITA[1]*, CRISTINA A. CONSTANTIN[1] AND MICHEL L. SCHLEGEL[2]
[1]University of Craiova, Department of Chemistry, Calea Bucuresti 107I, Craiova Romania, paulxchirita@gmail.com (* presenting author) and cristina_a_constantin@yahoo.com
[2]CEA, DEN/DANS/DPC/SEARS//Laboratory for the Engineering of Surfaces and Lasers, F-91191 Gif-sur-Yvette, France, michel.schlegel@cea.fr

Pyrite (FeS_2) is the most common disulfide mineral. [1,2] Oxidation of FeS_2 in presence of dissolved oxygen results in the release of sulfuric acid and toxic trace metals in acid mine drainage, which is one of the most serious environmental problems. Inspite of this importance, the kinetics and mechanism of electron transfer from pyrite to oxidants are poorly understood. The aim of this study was to investigate the kinetics of FeS_2 interaction with dissolved oxygen using electrochemical techniques.

Electrochemical experiments were performed in a conventional three-electrodes electrochemical cell with a Pt counter electrode and saturated calomel reference electrode. The electrochemical parameters (exchange currents densities, charge transfer resistances, etc) of pyrite oxidation in air-saturated HCl solutions were measured as a function of pH (1.0 to 5.0) at temperatures from 25 to 40°C.

Preliminary analysis of the experimental data indicated that temperature has a notable effect on the rate of pyrite oxidation by dissolved O_2. The values obtained for activation energy decrease from 69 kJ mol^{-1} (at pH 5.0) to 33 kJ mol^{-1} (at pH 1.0), suggesting that pyrite oxidation is controlled by surface reaction at high initial pH, with diffusion of reactants and reaction products between surface and solutions gradually becoming rate-limiting at lower initial pH. The reaction order with respect to $[H^+]$ shows a small decrease from 0.15 at 25°C to 0.09 at 40°C. This variation can be attributed to the decrease of oxygen solubility at greater temperature.

Another important observation is that for oxidation by dissolved oxygen under similar experimental conditions (initial pH and temperature) the exchange currents densities (i_0) measured for pyrite are lower than those measured for iron monosulfide (FeS). For example, at initial pH 3.5 and 30°C temperature, i_0 of FeS oxidation is $1.19 \cdot 10^{-5}$ cm^{-1}, and i_0 of FeS_2 oxidation is $1.48 \cdot 10^{-6}$ cm^{-1}.

The authors greatly appreciate support from IFA-CEA Program (Project C1-04), and Cr.A.C-tin support from the strategic grant POSDRU/CPP107/DMI1.5/S/78421, Project ID 78421 (2010).

References

[1] Holmes & Crundwell (2000) *Geochim. Cosmochim. Acta* **64**, 263-274. [2] Rimstidt & Vaughan (2003) *Geochim. Cosmochim. Acta* **67**, 873-880.

https://doi.org/10.1180/S0026461X00008434 Published online by Cambridge University Press

Tracers of pollutant sources and transport pathways using stable Cd and Pb isotopes in Ulsan Bay sediments

JUNG-SUN CHAE · MAN SIK CHOI*

Chungnam National University, GRAST, Daejeon, Korea
Kbsi2987@nate.com
mschoi@cnu.ac.kr (*presenting author)

Abstract

Metal sources have been traced by exclusively Pb isotopes in the previous studies. Although Pb isotopes were successfully used for the identification of Pb sources and mixing processes, the explanation for other metals with different geochemical behaviour was restricted. Cd isotopes become a candidate to trace Cd sources and transport pathways because Cd isotopic ratios could be fractionated by high-T processes such as smelting and refinery processes. Evaporated Cd showed depleted isotopic composition while Cd in slags from refinery has heavy isotope enriched composition [1]. This study aimed to apply stable Cd and Pb isotope ratios in Ulsan bay sediments to identify their sources and transport pathways. To do this, firstly we setup the analytical procedures for precise and accurate Cd isotope ratios including chemical separation and instrument measurement steps [2]. And we presented stable Cd and Pb isotope ratios in real sediment samples.

Surface and core sediments were collected at the Ulsan Bay, Korea. After the chemical separation of matrix and interferent metals using AGMP-1 and TRU-spec, Cd and Pb isotope ratios were measured by MC ICP/MS equipped with APEX desolvation system

Cd concentrations in surface sediments ranged from 0.15 ppm to 1.6 ppm, and were the maximum at station close to Onsan industrial complexes and at station close to Jangsaengpo harbor. Offshore stations showed the lowest concentration of Cd. $\epsilon^{114/112}_{NIST}Cd$ in surface sediments showed a little variation and ranged from –4.5 to 0.6. Sediments with the highest concentrations of Cd showed the most depleted (St. 30), non-fractionated (St. 4) and slightly enriched (St. 17). Sediments with the lowest concentration of Cd showed slightly depleted $\epsilon^{114/112}_{NIST}Cd$ values (St. 36 and 7). Although isotopic composition of Cd did not show systematic aerial distribution, it might be suggested that most Cd in Ulsan bay sediments were negatively fractionated except for harbor and ship building plant, which indicates that atmospheric transport are important pathway for Cd in sediments.

Pb concentration in surface sediments ranged from 10 ppm to 215 ppm and was the maximum at station close to Onsan industrial complexes and was the minimum at offshore station. Pb contamination was focused at stations in the southern part of the Ulsan Bay but sediments in the northern parts showed also slightly enriched Pb concentration. 207Pb/206Pb showed the wide range of variation from 0.844 to 0.90. Combining isotope ratio and the inverse of Pb concentration (Fe/Pb), three end-members of Pb sources were identified; that is, the first one is high concentration and highly un-radiogenic Pb which has similar to those in Broken Hill ores, the second is high concentration and radiogenic Pb isotope similar to background value, and the last is background concentration and Pb isotope. In other words, imported ores and local ores were two major pollutant sources.

References

[1] Wombacher et al., (2004). GCA, 68(10): 2349-2357
[2] Gao et al. (2008). ACA, 612: 114-120.

Characteristic and Leaching behavior of Cd-, Pb-substituted goethite under CO_2

SUNKYUNG CHOI [1*] AND RICK WILKIN[2]

[1]National Research Council Resident Research Associate at the USEPA, National Risk Management Research Laboratory, Ada, USA, choi.sunkyung@epa.gov (*presenting author)
[2]USEPA, National Risk Management Research Laboratory, Ada, USA, wilkin.rick@epa.gov

Introduction and Methods

Transport of CO_2 from deep geological formations to shallow ground-water aquifers may threaten the long-term quality of drinking water resources in locations adjacent to sites of carbon sequestration. Metal transport resulting from potential CO_2 leakage into freshwater aquifers is a major concern accompanying carbon sequestration operations. Acidity resulting from dissolution of leaked CO_2 into aquifer waters may result in release of metals from aquifer minerals. Goethite (α-FeOOH) is one of the most abundant and reactive iron oxides in soils and sediments. Goethite plays an important role in nature controlling the mobility of heavy metals cations as well as certain anions as it possesses a strong affinity to a variety of contaminants in subsurface environments. Natural goethite is usually associated with a number of metals. Heavy metals such as Pb(II) and Cd(II) are common in surface water and groundwater and their transport, toxicity, and bioavailability are mostly impacted by interactions with water and oxide and (oxy)hydroxide surfaces. In this study, we synthesized and characterized metal-substituted (Cd, Pb) goethite[1]. Dissolution experiments were performed with or in the absence of CO_2 and $CaCO_3$ at two different temperatures (room and 60°C). This study provides data from small-scale, short-term tests involving direct release of CO_2 in a system in order to provide constraints on potential migration of metals under CO_2 leaking carbon storage areas.

[1] Kaur *et al.* (2009) *Clays and Clay Minerals* **57**, 234-250.

https://doi.org/10.1180/S0026461X00008434 Published online by Cambridge University Press

Petrogenesis of Cenozoic plateau lavas from the Pali Aile Volcanic Filed and Morro Chico Volcano, southern Patagonia in South America

MI KYUNG CHOO[1,2*], MI JUNG LEE[1], JONG IK LEE[1], KYU HAN KIM[2] AND KYE-HUN PARK[3]

[1]Korea Polar Research Institute (KOPRI), Incheon, Korea, mkchoo@kopri.re.kr (* presenting author), mjlee@kopri.re.kr and jilee@kopri.re.kr

[2]Ewha Womans University, Seoul, Korea, kyuhan@ewha.ac.kr

[3]Pukyong National University, Busan, Korea, khpark@pknu.ac.kr

Geochemical and Sr-Nd-Pb isotopic analyses of late Miocene to Quaternary plateau lavas from the Pali Aike Volcanic Field (PAVF) and Morro Chico Volcano (MCV) (52°S) were undertaken to constrain the melting processes and mantle sources that contributed to magma generation and the geodynamic evolution of southernmost Patagonia, South America. The PAVF and MCV lavas are alkaline (PAVF, 45–49 wt% SiO_2; 4.3–5.9 wt% Na_2O+K_2O) and subalkaline (MCV, 50.5–50.8 wt% SiO_2; 4.0–4.4 wt% Na_2O+K_2O), relatively primitive mafic volcanic rocks that have typical intraplate ocean island basalt-like signatures. Incompatible trace element ratios and isotopic ratios of the PAVF and MCV lavas differ from those of the majority of Neogene southern Patagonian slab window lavas in showing more enriched characteristics and are similar to high-μ (HIMU) end-member basalt. The REE melting model suggests that these lavas were produced by low degrees of partial melting of a garnet lherzolite mantle source. The major systematic variations of Sr-Nd-Pb isotopes in southern Patagonian lavas are related to geographic location. The PAVF and MCV lavas from the southernmost part of Patagonia have lower $^{87}Sr/^{86}Sr$ and higher $^{143}Nd/^{144}Nd$ and $^{206}Pb/^{204}Pb$ ratios, relative to most of the southern Patagonian lavas erupted north of 49.5°S, pointing to a HIMU-like signature. An isotopically depleted and HIMU-like asthenospheric domain may have been the main source of magmas in the southernmost part of Patagonia, suggesting the presence of a major discontinuity in the isotopic composition of the asthenosphere in southern Patagonia. On the basis of geochemical and isotope data and the available geological and geotectonic reconstructions, a link between the HIMU asthenospheric mantle domain beneath southernmost Patagonia and the HIMU mega-province of the southwestern Pacific Ocean is proposed.

Organic matter effects on xenobiotic sorption at critical zone interfaces

JON CHOROVER

School of Earth and Environmental Sciences, University of Arizona, Tucson, Arizona US. chorover@cals.arizona.edu

Processes ranging from rhizosphere exudation to anthropogenic wastewater discharge result in infusion of reduced carbon compounds into the upper critical zone. This drives incongruent (bio)weathering reactions toward products that include neo-formed secondary minerals and their nanoparticulate complexes with natural organic matter. Mobility of these colloids in soil pore water depends on system hydrochemistry and microbial response. Increasingly thrust into the mix are organic micropollutants (OMPs) from human activity. Several research groups have been documenting a widespread distribution of OMPs in watersheds worldwide. These include endocrine disrupting compounds that exhibit biological effect even at trace concentration We hypothesize that the fate of these micropollutants is coupled to their interfacial reactivity with bio-inorganic products of critical zone weathering.

Since many OMPs released to the environment are polar and/or ionic, their fate is often controlled by interfacial reactions that are highly sensitive to OMP and surface functional group composition and charge, with strong dependence on solution chemistry of contaminant sorptive partitioning. Such reactions are also affected by aqueous phase OMP complexation with solutes including dissolved organic matter (DOM). Ternary OMP-DOM-surface reactions may be particularly important in microbially-active pore waters where DOM enters and exits the aqueous phase, and where mineral surfaces are often masked by biomolecular coatings resulting from DOM sorptive fractionation.

Given the known capability of OM constituents to form aggregated “supramolecular” structures, we postulate that OMPs may enter into DOM aggregates by similar modes of association. Many OMPs possess polar, ionic and/or hydropobic functional groups like those of DOM components, and so processes such as H-bonding, cation bridging, and hydrophobic interaction that promote DOM aggregation are likely to also sequester OMPs. This should, in turn, affect OMP reactivity toward surfaces and, by extension, environmental transport. For example, we have shown via aqueous infusion experiments that effective separation and quantification of OMPs via LC-MS/MS methodologies are diminished in DOM-containing solutions (Wickramasekara et al., 2012). Additional model systems experiments under controlled laboratory conditions show that various DOM fractions differently affect the partitioning of OMPs in aqueous solutions monitoried by LC-MS/MS. To help identify the DOM components involved in OMP interaction, we measured OMP-induced quenching of bulk and DOM fraction fluorescence (Hernandez-Ruiz et al., 2012). Results of several types of experiments indicate a strong role of hydrophilic acid DOM fractions in complexing the target analytes. The effect of DOM on OMP reaction at mineral surfaces is being investigated, to assess its impact on sorptive uptake and release of OMPs in natural systems.

[1] Wickramasekara et al. (2012) *Anal. Chim. Acta* doi:10.1016/j.aca.2011.12.019

[2] Hernandez-Ruiz et al. (2012) *Water Res.* **46**, 943-954.

https://doi.org/10.1180/S0026461X00008434 Published online by Cambridge University Press

In situ observations on the crystallization of spodumene from aqueous solutions in a hydrothermal diamond-anvil cell

I-Ming Chou[1]*, Jiankang Li[2], Shunda Yuan[2], and Robert C. Burruss[1]

[1]US Geological Survey, Reston, Virginia, U.S.A.
imchou@usgs.gov (*I-Ming Chou); burruss@usgs.gov
[2]Chinese Academy of Geological Sciences, Beijing, China
Li9968@126.com; sdyuan011981@yahoo.com.cn

Crystallization experiments were conducted in a new type of hydrothermal diamond-anvil cell (HDAC; type V) using $LiAlSi_2O_6$ (S) gel and H_2O (W) as starting materials. The sample chamber is a hole (0.1 mm diameter) at the center of a Re gasket (0.3 mm diameter and 0.25 mm thick), sealed by compressing the gasket with two parallel diamond anvil faces. A total of 21 experiments were performed at temperatures up to 950 °C and pressures up to 788 MPa. In the samples with relatively high S/W ratios, many small crystals formed in the melt phase during cooling. Those with low S/W ratios, only few crystals with smooth surfaces crystallized from the aqueous fluid in the presence of melt droplets, which were gradually consumed during the growth of the crystals, indicating rapid transfer of material from the melt to the crystals through the aqueous fluid. The nucleation of crystals started at 710 (±70) °C and 520 (±80) MPa, and crystal growth ended at 570 (±40) °C and 320 (±90) MPa, with the cooling *P-T* path within the stability field of spodumene + quartz in the S-W system. The observed linear crystal-growth rates in the aqueous phase, calculated by dividing the maximum length of a single crystal by the duration of the entire growth step [1, 2], were 4.7×10^{-6} and 5.7×10^{-6} cm/s for the cooling rates of 0.5 and 1°C/min, respectively.

Our results show that when crystals nucleate in the aqueous instead of the melt phase, there are fewer nuclei formed, and they grow much faster due to low viscosity of the aqueous fluid, which accelerates diffusion of components for the growth of crystals. Therefore, the large crystals in pegmatite most likely crystallized from aqueous fluids instead of hydrosilicate melt. This conclusion was further supported by our homogenization experiments in HDAC for crystal-rich inclusions in spodumene from Jiajika lithium pegmatite deposit in China. During heating, decrepitation of the fluid inclusions was prevented by applying external pressures (2.7 to 5.6 MPa) to the inclusions in the sample chamber of HDAC. In these inclusions, the H_2O-CO_2-NaCl fluid phase homogenized at ~290 ℃, followed by the melting of zabuyelite and other daughter minerals (i.e., quartz, calcite, spodumene, and unidentified minerals) during heating. Finally, the melt dissolved totally into the H_2O-CO_2-NaCl fluid, which represents the "boundary-layer liquid" [3, 4] from which the host spodumene crystallized. In other words, the spodumene crystals in the Jiajika pegmatite deposit crystallized from flux-rich aqueous fluids instead of hydrosilicate melt.

[1] Fenn (1977) *Can. Mineral.* **15**, 135-161. [2] Swanson & Fenn (1992) *Can. Mineral.* **30**, 549-559. [3] London (2008) *Can. Mineral. Spec. Pub.* **10**. [4] London (2009) *Can. Mineral.* **47**, 697-724.

On using natural chemical and isotopic tracers to monitor fracture surface area evolution in enhanced geothermal systems

John N. Christensen[1*], Giuseppe D. Saldi[1], Nicolas F. Spycher[1], Kevin G. Knauss[1], and B. Mack Kennedy[1]

[1]Lawrence Berkeley National Laboratroy, Berkeley, CA;
JNChristensen@lbl.gov; GDSaldi@lbl.gov; NSpycher@lbl.gov;
KGKnauss@lbl.gov; BMKennedy@lbl.gov (* presenting author)

It has been proposed, and various trials are taking place, to inject fluids into geothermal systems to stimulate fracturing and hence increase fluid flow and heat-exchange efficiency in such enhanced geothermal systems (EGS). We are investigating a new approach to detect increases in fracture surface area in reponse to geothermal well stimulation using natural chemical and isotopic tracers. Our working hypothesis is that freshly-created fracture surfaces are out of chemical and isotopic equilibrium with newly flowing fluids, and thus subsequent mineral dissolution and precipitation generate transient chemical and isotopic signals that can be monitored in production wells. Such signals in turn could be interpreted through reactive transport modeling to infer induced changes and the temporal evolution of reservoir fracture reactive surface and permeability.

To test this hypothesis, a series of laboratory hydrothermal experiments were conducted using altered rhyolitic tuff from core taken at the Desert Peak geothermal field in Nevada, an EGS site. Two kinds of reactivity experiments were conducted at differing water-to-solid ratios: crushed tuff of variably sized fractions (600-710, 150-180 and 63-75 μm) and a solid rock wafer. These experiments were conducted in flexible Au bag autoclaves that allow multiple acquisitions of fluid/gas samples during experiments without perturbations of temperature and pressure conditions. Experiments were run from 15 to 60 days at 220˚C and 100 bars to maintain a single fluid phase. The initial fluid was high purity water, spiked with NaCl (0.1 M). Periodically during the experiments, fluid samples were drawn off and anlyzed for chemical and isotopic (e.g. $^{87}Sr/^{86}Sr$) composition. In batch experiments with 600-710 μm sized rock fragments, $^{87}Sr/^{86}Sr$ rose over the first several days then subsequently declined, followed by several reversals in trend over the next 6 days. Overall, $^{87}Sr/^{86}Sr$ roughly follows the Rb/Sr trend. In contrast, with the rock wafer experiment, after initially falling, $^{87}Sr/^{86}Sr$ increased along with Rb/Sr for sixty days. In the case of both experiments, the Sr concentration of the fluid fell or held steady despite changing $^{87}Sr/^{86}Sr$, suggesting the precipitation of Sr bearing phases concomitant with dissolution of primamy rock minerals (e.g., plagioclase, k-spar) and/or their alteration products (e.g., carbonates) with a range of $^{87}Sr/^{86}Sr$. A flow-through experiment with 600-710 μm material exhibited similar behavior. Simulations of the experiments using geochemical and reactive transport models are being conducted to investigate the types of reactions taking place and their dependence on solid-to-water ratios. Preliminary results indicate that plagioclase dissolution is accompanied by precipitation of Al hydroxides, zeolites/clays, secondary feldspars and calcite, yielding fluid composition trends that are sensitive to initial water/rock ratios.

https://doi.org/10.1180/S0026461X00008434 Published online by Cambridge University Press

Review of issues associated with evaluation of Pitzer interaction parameters

CHRISTOMIR CHRISTOV[1], MIN ZHANG[2*], STEPHEN TALMAN[2], ERIC REARDON[3], TAMMY YANG[4]

[1]GeoEco Consulting, San Marcos, USA, hristovi@sbcglobal.net
[2]Alberta Innovates – Technology Futures, Edmonton, Canada, min.zhang@albertainnovates.ca (* presenting author)
[3]Unversity of Waterloo, Waterloo, Canada, ejreardo@uwaterloo.ca
[4]Nuclear Waste Management Organization, Toronto, Canada, TYang@nwmo.ca

Aqueous geochemical models that predict solid and gas equilibria over a broad range of water compositions and temperatures are powerful tools for studying the geochemistry of natural waters, solving environmental problems and optimizing industrial processes. The Pitzer ion interaction model has been widely accepted as the most effective approach to predict chemical behaviour in concentrated solutions; however, the description of natural waters requires a large compilation of interaction parameters. These parameters are derived from experimental data such as isopiestic, electrochemical, and solubility measurements on simpler systems.

In this study, a large number of binary systems have been evaluated to understand issues which could potentially compromise the representation of more complex solutions. The results revealed that the concentration range within which Pitzer parameters are derived, together with the aqueous species that are included in the model, and the accuracy of temperature coefficients are of most importance.

For a system that is parameterized over a limited concentration range, model predictions may deviate substantially from the experimental data outside this range, as shown in many binary salt systems of interest in environmental studies such as CaI_2, CsF, $NiCl_2$, $CuCl_2$, $ZnCl_2$, and $Th(NO_3)_2$. Further evaluations of parameters within a chemical system will be hampered if any of the data points used in evaluating new parameters fall outside this concentration range. In particular, the new introduced parameters may be biased to compensate for inaccuracies in the original model rather than real chemical effects. It is possible to reduce the potential for introducing such systematic errors into an analysis by ensuring that the parameterization is valid up to the saturation limit of binary solids, and even to supersaturated conditions, if possible.

The standard Pitzer approach treats electrolytes as being completely dissociated. In some instances ionic species can be incorporated into the model; however, the addition of ion pairs and complexes into the solution model requires the determination of interaction parameters between these new species and each of the other species in solution. In addition, inclusion of ion pairs and complexes may compromise the model when moving away from the concentration range at which the model was derived. The ideal approach is to rely on the additional parameter $\beta^{(2)}$ to account for the effect of ion pairing or complexing in solution but this may not always be possible. However, it has been successfully demonstrated for the $NdCl_3$-H_2O system, where the new model was able to eliminate $NdCl^{2+}$ and $NdCl_2^{+}$ species used in early development.

Os-Hf-Nd-Sr isotopic constraints on the origin of highly potassic basalts in northeast China

Z.-Y. CHU[1]*, F.-Y. WU[1], J.-H. GUO[1], Y.-H. YANG[1], Y.-L ZHANG[2] AND C.-Z. LIU[1]

[1]State Key Laboratory of Lithospheric Evolution, Institute of Geology and Geophysics, Chinese Academy of Sciences, P. O. Box 9825, Beijing 100029, P. R. China, e-mail: zhychu@mail.iggcas.ac.cn (* presenting author)
[2]College of Earth Sciences, Jilin University, Changchun 130026, China

The very young (about 0.6Ma-1721AD) Wudalianchi (WDLC) and Erkeshan (EKS) basalts in northeast (NE) China are characterized by high K_2O contents ($K_2O/Na_2O>1$) and strong enrichment in incompatible elements, especially the large ion lithophile elements (LILEs) and light rare earth elements (LREE) and are isotopically similar to EM-I, which differ from the basalts in eastern China elsewhere. The origin of these WDLC and EKS potassic lavas is still under debate. Here, we present new Re-Os isotopic data, together with Sr-Nd-Hf isotopic and traditional elemental data to further constrain the origin of the WDLC and EKS potassic lavas. The $^{187}Os/^{188}Os$ ratios of the WDLC and EKS basalts range from 0.1187 to ~0.17. In general, samples with low Os concentrations have high $^{187}Os/^{188}Os$ ratios while samples with high Os concentrations have relatively low $^{187}Os/^{188}Os$ ratios. Since minor amounts of crustal contamination will alter significantly the Os isotopic composition of a basaltic magma with low Os concentrations, it is possible that the WDLC and EKS basalts were contaminated by minor crustal materials during magma ascent. The suprachondritic Os of some WDLC and EKS basalts may also possibly result from preferential melting of a metasomatized mantle peridotites which contain interstitial sulfides that are characterized by low Os concentrations and suprachondritic $^{187}Os/^{188}Os$. Nonetheless, since the WDLC and EKS basalts generally have relatively low $^{187}Os/^{188}Os$ ratios compared to the Cenozoic continental basalts in other localities such as Hannuoba, Columbia River, SE Australia and Central European, we think that the crustal contamination did not play an important role for formation of the WDLC and EKS basalts.

The WDLC and EKS basalts have unradiogenic Hf-Nd and radiogenic Sr isotopic compositions, with εHf range of -3.9 to -9.2, εNd values between -5.8 and -3.2 and $^{87}Sr/^{86}Sr$ ratios between 0.7051 and 0.7057, indicating the contribution of a metasomatized sub-continental lithospheric mantle (SCLM). In term of Os isotopes, the most unradiogenic sample has Os isotopic compositions as low as 0.1187, also confirming the contribution of an ancient SCLM for generation of the WDLC and EKS magmas. This sample gives a T_{RD} model age as old as 1.2Ga, indicating that the SCLM underlying the WDLC and EKS area could be at least as old as Proterozoic.

Consistent with previous reports, these lines of evidences together suggest the WDLC and EKS mainly originated from an anicent metasomatized SCLM.

Acknowledgment
This study was supported by NSFC Grant (No. 40873008).

https://doi.org/10.1180/S0026461X00008434 Published online by Cambridge University Press

CO_2 rich springs of the Far East Russia. Composition and Origin

CHUDAEV OLEG[1*] AND KHARITONOVA NATALY[1]

[1]Far East Geological Institute FEB RAS, Vladivostok, Russia
chudaev@fegi.ru*

Introduction

CO_2-rich cold springs are widespread in the Far East Russia. The measured temperatures vary from 5°C up to 10°C. In most cases dissolved oxygen (DO) is close to 0%, which means that the system is isolated from the atmosphere. pH values are in the range of 5.22-6.3. They are mainly of the Ca-Mg-HCO_3 type with high amount of CO_2. Content of elements depends on residence time, type of bedrocks and dissolved CO_2 gas. Over 90% of the cationic species occur as free ion and less than 10% as ion-pairs with HCO_3. Waters of springs are over-saturated with the clay minerals (smectite, illite, kaolinite), low temperature zeolites (heulandites, mordenite, clinoptilolite), and dolomite. Using tritium isotope study we previously showed the young age of these ground waters and the hydrogen and oxygen isotopic ratio suggested meteoric origin. Yet, the origin of CO_2 remained uncertain and is a subject of the present study.

Results and Conclusion

In studied springs dissolved CO_2 ranged from 94% to 99% and the maximum calculated CO_2 partial pressure is 1.7 bar. We hypothesized that the carbon was of magmatic origin. Geological data and young volcanic activities in some areas of location springs support this hypothesis. $\delta^{13}C$ and $^3He/^4He$ data also suggests magmatic origin (up to 70%) for the CO_2 in Primorye (Maritime region of the Russia) springs [1,2]. $\delta^{13}C$ for most studies springs ranged from -4.19‰ to -8.19‰. These values are too high for the CO_2 to have an organic source and too low to be carbon of limestone. They are, however, close to magmatic carbon, but it is difficult to assert that this, because some processes cause fractionation of these carbon isotopes. To solve the problem we sleeked an alternative method to identify carbon source. The ratio of carbon to mantle helium ($C/^3He$) had been used by others in similar situation. [3]. Using this method mantle carbon and atmosphere carbon had ratios of about $2*10^7$ - $2*10^9$ and 10^{12}, respectively. The studied springs had a value close to $2*10^9$, suggesting that most of the carbon in the studied CO_2-rich waters has magmatic origin. Similar deep origin of CO_2 in spring waters had been previously shown in other springs around the world, for example in the Malki CO_2-rich cold springs in Kamchatka [2], in Wudalianchi springs in N-E China [2] and in the springs of San-Andreas fault in California. [4].

This work was supported by grant RFBR 10-05-00658 , grants of the Far Eastern Branch RAS 12-1-0-08-018 and 12-3-A-08-143

[1] Shand et al (1995). *Proceedings of the 8th WRI:* 393-396. Rotterdam: Balkema. [2] Chudaev et al (2007). *Proceedings of the 12th WRI:* .489-492. Rotterdam: Balkema. [3] Marthy & Jambon (1987). *Earth and Planetary Science Letters* **83**: 16-26. [4] Kharaka et al (1999). *Geochemistry of Earth's Surface:* 515-518. Rotterdam: Balkema.

.

Structure and surface reactivity of Al-, Si- and organic matter-rich naturally occurring ferrihydrite

A. C. CISMASU[1*], F.M. MICHEL[2], A.P. TCACIUC[3] AND G.E. BROWN, JR.[1,2,4]

[1] Department of Geological and Environmental Sciences, Stanford University, Stanford, CA 94305, USA, cismasu@stanford.edu (* presenting author)
[2] Stanford Synchrotron Radiation Lightsource, SLAC National Accelerator Laboratory, 2575 Sand Hill Rd, MS 69, Menlo Park, CA 94025, USA
[3]Woods Hole Oceanographic Institution, Massachusetts Institute of Technology, Cambridge, MA, 02139, USA
[4] Department of Photon Science, SLAC National Accelerator Laboratory, 2575 Sand Hill Rd, MS 69, Menlo Park, CA 94025, USA

Ferrihydrite is a poorly crystalline iron oxide nanomineral (2-7 nm) found in a variety of natural surface environments. Its occurrence is documented at near-neutral pH conditions in a variety of redox-active environments, such as soils and sediments, as well as freshwater and marine settings. As a result of its high surface area and its chemical reactivity, it is an important environmental sorbent, and plays an essential role in the geochemical cycling of pollutant (in)organic species. Under natural aqueous conditions, ferrihydrite precipitates in the presence of several inorganic species such as aluminum, silica, phosphate, etc., or in the presence of organic matter (OM). These impurities can affect the domain size, composition, and molecular-level structure of ferrihydrite, thus modifying fundamental properties that are directly correlated with solid-phase stability and surface reactivity. In this study we have characterized a series of ferrihydrite samples of variable Al, Si, and OM content by laboratory (TEM, chemical extractions, electrophoresis) and synchrotron-based techniques (high energy x-ray total scattering and pair distribution function analysis, scanning transmission x-ray microscopy) in order to place constraints on their short- and intermediate-range structure, their composition, their surface chemistry and association with organic matter. A significant decrease in crystallinity occurred with increasing impurity content. We attribute these changes primarily to the presence of strong binding ligands such as silica and organic matter, both of which are known to affect Fe polymerization and poison particle growth. It is expected that the presence of these ligands at the ferrihydrite surface will alter significantly its surface composition and reactivity in the environment.

https://doi.org/10.1180/S0026461X00008434 Published online by Cambridge University Press

The bi-stability of organic haze in the Archean atmosphere

MARK W. CLAIRE[1*], AUBREY L. ZERKLE[2], SHAWN D. DOMAGAL-GOLDMAN[3], JAMES FARQUHAR[4] AND SIMON W. POULTON[2]

[1]School of Environmental Sciences, University of East Anglia, Norwich, England, UK, M.Claire@uea.ac.uk (*presenting author)
[2]School of Civil Engineering and Geosciences, Newcastle University, Newcastle upon Tyne, England, UK
[3]Fellow of the NASA Postdoctoral Program, administered by Oak Ridge Associate Universities, in residence at NASA Headquarters, Washington, D.C., USA
[4]Department of Geology and ESSIC, University of Maryland, College Park, MD, USA

Methane has long been a postulated component of the Archean atmosphere, but very little direct evidence exists for this contention. Ecosystem models predict that modest fluxes of methane into reducing atmospheres would result in high concentrations[1], while models of the evolution of atmospheric redox on the early Earth suggest important roles for methane associated with the rise of oxygen[2, 3]. Here, we expand previous photochemical modeling efforts[3, 4] by linking changes in methane concentration to observable geochemical signatures. In a suite of reducing model atmospheres, we increase concentrations of methane until an organic haze forms. Using particles which scatter using both classical Mie physics as well as newly postulated fractal scattering behavior [5], we find that the Archean atmosphere would exhibit bi-stability between a "clear skies" case and one with a thin organic haze. The photochemical modeling further demonstrates that the presence of the thin organic haze would significantly affect the fractionation of minor isotopes of sulfur (mass-independent fractionation of sulfur or S-MIF) by both UV opacity effects and by changing the redox chemistry of S species in the atmosphere. The prediction of an Earth system with correlated changes in methane concentration and variations in S-MIF is evident in new data from the Campbellrand-Malmani platform of South Africa [6], which indicate multiple appearances of organic haze due to a methanogen-driven high CH_4:CO_2 ratios [4] in the late Neoarchean. These combined results provide stronger evidence for a role for methane in the Neoarchean atmosphere, and support arguments that the Great Oxidation Event may have been related to the the disappearance of a large biological flux of methane [3].

[1] Kasting et al. (2001) *Origins of Life and Evolution of the Biosphere* **31**, 271-285. [2] Catling et al. (2001) *Science* **293**, 839-843. [3] Zahnle et al. (2006) *Geobiology* **4**, 271-283. [4] Domagal-Goldman et al. (2008) *Earth and Planetary Science Letters* **269**, 29-40. [5] Wolf and Toon, (2010) *Science* **328**, 1266-1268. [6] Zerkle et al. (2012) *Nature Geosciences* (in press).

How does the continental crust get really hot?

CHRIS CLARK[1*], IAN C.W. FITZSIMONS[1] AND DAVID HEALY[2] AND

[1] *Department of Applied Geology, Curtin University, Perth WA, Australia*, c.clark@curtin.edu.au (* presenting author)
[2] *School of Geosciences, King's College, University of Aberdeen, United Kingdom*

Evidence for the physical conditions under which the Earth's crust can generate large volumes of magma is provided by metamorphic rocks that represent the solid residue of partial melting and chemical differentiation. Many of these rocks preserve mineral assemblages stabilised at very high-temperature and moderate pressure conditions that lie above the dry solidus for most crustal rock types. These ultra-high temperature (UHT) metamorphic rocks can only be formed after substantial degrees of partial melting and, although originally regarded as isolated thermal anomalies, there is increasing evidence that continental crust has attained UHT conditions repeatedly in time and space. Our ability to quantify this metamorphic record as absolute temperature-depth information has increased dramatically over the last 40 years with improved thermodynamic constraints on the pressure-temperature stability of mineral assemblages. At the same time, development of mathematical models for the thermal behaviour of continental crust has allowed us to compare pressure-temperature data from real metamorphic rocks with geothermal gradients predicted for simple tectonic settings, and identify possible causes of elevated metamorphic temperatures. While these thermal models can reproduce conditions recorded by the majority of metamorphic rocks, UHT metamorphism remains difficult to replicate with standard numerical models for orogenesis. In this contribution, we examine a number of heat sources that might account for these extreme temperatures and investigate the link between UHT metamorphism and magma generation.

https://doi.org/10.1180/S0026461X00008434 Published online by Cambridge University Press

Erosion of organic matter in a tropical mountain catchment: Implications for carbon delivery from the Andes to the Amazon River

K.E. CLARK[1*], R. G. HILTON[2], A.J. WEST[3], Y. MALHI[1], D.R. GROCKE[4], C. BRYANT[5], A. ROBLES[6], Y. RAO[4], AND M. NEW[1]

[1] Department of Geography and the Environment, University of Oxford, UK. (* correspondance: kathryn.clark@ouce.ox.ac.uk)
[2] Department of Geography, Durham University, Durham, DH1 3LE, UK (r.g.hilton@durham.ac.uk)
[3] Department of Earth Sciences, University of Southern California, Los Angeles, USA. joshwest@usc.edu
[4] Department of Earth Sciences, Durham University, DH1 3LE, UK (d.r.grocke@durham.ac.uk)
[5] NERC Radiocarbon Facility, East Kilbride, Scotland, G75 OQF, UK (c.bryant@nercrcl.gla.ac.uk).
[6] Universidad Nacional de San Antonio Abad del Cusco, Cusco, Peru

Mountain rivers play a key role delivering carbon in particulate organic matter (POM) to large fluvial systems and the coastal ocean. In the case of the Amazon, one of Earth's most important biogeochemical systems, ~40% of the POM transported by the main river is thought to be derived from the Andes [1]. Nonetheless, we have poor constraint on POM sources delivered by tropical mountain rivers, particularly in sediment-laden flood waters. POM derived from vegetation and soil contains recently sequestered atmospheric CO_2 and exports nutrients downstream. In contrast, POM derived from bedrock may be a CO_2 source and supply nutrients downstream.

Here, we address these issues in the Peruvian Andes. We combine hydrometric measurements (water discharge) and frequent sampling of suspended sediments (every 3 hrs) during flood events in 2010, at two gauging stations (2250 masl and 1350 masl) on the Kosñipata River. We use elemental ($\%C_{org}$, %N) and stable isotope composition and radiocarbon content of the organic carbon ($\delta^{13}C_{org}$, $\delta^{15}N$, $\Delta^{14}C_{org}$) to quantify POM sources [2]. $\delta^{13}C_{org}$ vs. N/C and $\Delta^{14}C_{org}$ demonstrate binary mixing of POM derived from fossil and non-fossil (soil and vegetation) sources. Mixing analysis allows us to quantify the proportion of fossil particulate organic carbon (POC_{fossil}) and bedrock-derived nitrogen ($PN_{bedrock}$), and allows us to identify the $\delta^{13}C_{org}$ and $\delta^{15}N$ of POM derived from the terrestrial biosphere.

We find that POC_{fossil} contributes ~40% of the total river POC. We also show, for the first time, that $PN_{bedrock}$ completely dominates the riverine particulate nitrogen load, comprising over 70%. Until now, the bedrock contribution to Andean river POM has been overlooked, and our findings provide impetus for further investigation. In addition, our measurements allow the contributions of POM from vegetation and soil to be isolated. They demonstrate that during the rising limb and peak discharge of floods, POM was mobilised predominately from upper (O_H) soil horizons, with important additional input from live vegetation. The results suggest an important climatic control on the erosion and export of carbon derived recently from atmospheric CO_2.

[1] Hedges et al. (2000) *Limnol Oceanogr* **45**, 1449-1466. [2] Hilton et al. (2010) *Geochim Cosmochim Ac* **74**, 3164–3181.

Igneous and metamorphic garnet-clinopyroxene assemblages in eclogite and granulite, Breaksea Orthogneiss, New Zealand: major and rare earth element characteristics

CLARKE, G.L.[1],*, DACZKO, N.R.[2] AND MIESCHER, D.[2]

[1]School of Geosciences, FO9, University of Sydney, Sydney, NSW, 2006, Australia, geoffrey.clarke(at)sydney.edu.au (* presenting author)
[2] GEMOC ARC National Key Centre, Department of Earth and Planetary Sciences, Macquarie University, NSW 2109, Australia

Eclogite and omphacite granulite, interlayered on cm- to decameter-scale, form most of the Cretaceous Breaksea Orthogneiss, which experienced peak conditions of P≈1.8 GPa and T≈850°C. It is the highest grade part of the c. 125–115 Ma Western Fiordland Orthogneiss. A gneissic fabric in the host orthogneiss truncates igneous layering in coarsely layered, decametre-scale clinopyroxenite and garnetite inclusions. Field and microstructural relationships, together with rare earth element (REE) characteristics across a broad range of rock types permits the conclusion that most garnet is of igneous origin; geochemical data alone are ambiguous. Igneous diopside persists in coarse-grained, weakly deformed samples. Garnet cores in garnetite, and late-formed garnet rims in garnetite and clinopyroxenite have a range of REE contents interpreted to reflect cumulate processes involving continued grain growth isolated from the parent magma. Clear rims on inclusion- and Ca-Tschemakite-rich diopside in clinopyroxenite of composition distinct to grain cores are interpreted as recrystallization features. Garnet in granulite occurs in three textural settings, the most common Type 1 garnet having REE characteristics identical to garnet in eclogite, but depleted in heavy REE relative to garnet in garnetite. Type 2 garnet in granulite forming metamorphic coronae on omphacite has a pronounced positive Eu anomaly and is depleted in heavy REE compared with Type 1 garnet. Type 3 garnet in granulite migmatite is indistinguishable from Type 1 garnet, consistent with formation through magma injection.

https://doi.org/10.1180/S0026461X00008434 Published online by Cambridge University Press

Kinetics of $CO_{2(g)}$-$H_2O_{(l)}$ isotopic exchange, including $^{13}C^{18}O^{16}O$

MATTHIEU CLOG[1*], JOHN EILER[1]

[1]California Institute of Technology, Pasadena CA, USA, eiler@gps.caltech.edu (* presenting author)

The analysis of mass 47 isotopologues of CO_2 (mainly $^{13}C^{18}O^{16}O$) is established as a constraint on sources and sinks of environmental CO_2, complementary to $\delta^{13}C$ and $\delta^{18}O$ constraints, and forms the basis of the carbonate 'clumped isotope' thermometer. This measurement is commonly reported using the Δ_{47} value — a measure of the enrichment of doubly substituted CO_2 relative to a stochastic isotopic distribution. Values of Δ_{47} approach 0 (a random distribution) at high temperatures (≥ several hundred degrees C), and increase with decreasing temperature, to ~1 ‰ at 25 ˚C.

While the thermodynamic properties of doubly substituted isotopologues of CO_2 (and, similarly, carbonate species) are relatively well understood, there are few published constraints on their kinetics of isotopic exchange. This issue is relevant to understanding both natural processes (e.g., photosynthesis, respiration, air-sea or air-groundwater exchange, CO_2 degassing from aqueous solutions, and possibly gas-sorbate exchange on cold planetary surfaces like Mars), and laboratory handling of CO_2 samples for Δ_{47} analysis (e.g., re-equilibration in the presence of liquid water, water ice or water adsorbed on glass or metal surfaces).

We present the results of an experimental study of the kinetics of isotopic exchange, including changes in Δ47 value, of CO_2 exposed to liquid water between 5 and 37 ˚C. Aliquots of CO_2 gas were first heated to reach a random distribution of its isotopologues and then exposed at low pressure for controlled periods of time to large excesses of liquid water in sealed glass containers. Containers were held at 5, 25 and 37°C and durations of exchange ranging from 5 minutes to 7 days. To avoid the formation of a boundary layer that might slow exchange, the tubes were vigorously shaken during the period of exchange. At the end of each experiment, CO_2 gas was recovered from the head space of the reaction vessel, purified and analyzed for its Δ_{47}, $\delta^{13}C$ and $\delta^{18}O$ by gas source isotope ratio mass spectrometry.

Equilibrium was reached for both $\delta^{18}O$ and Δ_{47} after durations of few tens of hours. $\delta^{18}O$ values at equilibrium were consistent with known fractionation factors for the CO_2-H_2O system. The evolution of $\delta^{18}O$ and Δ_{47} with experiment duration was fitted with an exponential rate law, yielding rate constants equal to each other (within error), averaging 0.18 h^{-1} at 5°C and 0.29 h^{-1} at 25°C. We calculate an activation energy for this isotopic exchange reaction of 16kJ/mol. By comparison, Mills and Urey (1940) measured the rate of ^{18}O exchange between CO_2(aq) and water to have a rate of 11 h^{-1} at 25 ˚C and an activation energy of 71.7 kJ/mol. Our finding of a slower rate and lower activation energy is consistent with the rate limiting step of our experiment being the CO_2(g)—CO_2(aq) exchange. Our experiments also define the path through $\delta^{13}C$— $\delta^{18}O$— R^{47} composition space (where R^{47} is the ratio of mass 47 to 44 isotopologues) followed by CO_2 gas during exchange with water. The stochastic distribution is a curved surface in composition space, hence changes in composition of CO_2 during exchange with water may, in some circumstances, yield distinctive co-variations in Δ_{47} and $\delta^{18}O$. This may be relevant for the study of vital effects and other natural processes in which CO_2 and DIC species depart from local isotopic equilibrium.

Unravelling the paragenesis at one of Australia's highest-grade gold deposits

J. CLOUTIER[1*], J.L. WALSHE[1], R. HOUGH[1], A. BATH[1] AND R. HUTCHISON[2]

[1]CSIRO Earth Science and Resource Engineering Australian Resources Research Centre, 26 Dick Perry Avenue, Kensington, Western Australia 6151, Australia. (*correspondence: Jonathan.Cloutier@csiro.au)

[2]Ramelius Resource, Level 1, 130 Royal Street, East Perth WA 6004

Australia's currently producing highest-grade gold deposit, (ave. 19.7g/t Au), the Archean Wattle Dam deposit, is located in the Yilgarn Craton of Western Australia. Despite its obvious importance, very little is understood about its formation. In the current study we report on a paragenetic framework for the deposit, mineral zoning, conventional optical petrography, SEM and stable isotope data of carbon, oxygen and sulphur. These data record important characteristics of ore-forming fluids and aid with the development of accurate genetic and exploration models.

The Wattle Dam deposit is hosted within a 350m thick amphibolite grade ultramafic unit which is bounded by a 400m thick metasedimentary unit to the west [1]. The alteration envelope surrounding the main lode is gradational and extends up to 10m. The Wattle Dam deposit is atypical as it lacks quartz veining and a low gold-grade envelope surrounding the main mineralisation normally associated with other Archean gold deposits [1].

A paragenetic study of the ultramafic rocks reveals a peak metamorphism assemblage consisting of actinolite, hornblende and plagioclase followed by a patchy calcite overprint of the peak metamorphism assemblage and by retrograde metamorphism clinochlore. These assemblages were overprinted during the main alteration event which culminated with the creation of the Wattle Dam gold deposit. The main alteration event consists of the precipitation of early calcite ± pyrite veins followed by tschermakitic amphiboles, biotite, clinochlore (possibly enriched in Fe3+) and by late coarse-grained gold nuggets (quartz-free), pyrrhotite, pentlandite and breithauptite (NiSb) in veins. Dolomitisation of calcite veins and serpentinisation and talcification of the ultramafic rock were observed post-mineralisation.

Stable isotope values vary between -5.5 to -2.7‰ (VPDB) for $\delta^{13}C_{Cal2}$, +10.7 to +15.0‰ (VSMOW) for $\delta^{18}O_{Cal2}$ and +3.85 to +5.23‰ (VCTD) for $\delta^{34}S_{Py}$ distal to the deposit while elevated $\delta^{13}C_{Cal2}$ (-0.3‰) and $\delta^{18}O_{Cal2}$ (+18.1‰) were observed proximal to the deposit within the main lode. These elevated values combined with the presence of pyrrhotite, the lack of clear alteration selvages around gold nuggets and the lack of quartz within the main lode are consistent with a reduced vapour-rich, relatively water-poor environment in which $CO_{2(g)}$ is partially reduced to $CH_{4(g)}$ during the main-stage of alteration.

[1] Hutchison (2010) *Gravity Gold Conference,* Bellarat 22-23 Sept.

https://doi.org/10.1180/S0026461X00008434 Published online by Cambridge University Press

Tracing land use controls on silica dynamics in the soil-vegetation continuum

WIM CLYMANS[1,*], GERARD GOVERS[1], ELISABETH FROT [2], BENEDICTA RONCHI[1], BAS VAN WESEMAEL[2], ERIC STRUYF[3] AND DANIEL J. CONLEY[4*]

[1]University of Leuven, Earth and Environmental Sciences, wim.clymans@ees.kuleuven.be
[2]Université Catholique de Louvain, Earth and Life Institute,
[3]University Antwerp, Ecosystem Management research Group
[4] Lund University, Department of Geology

Bio-available silica (Si) is a key element in global biogeochemical cycling. In terrestrial ecosystems plants take-up dissolved silica (DSi), and form plant Si-bodies called phytoliths [1]. Upon die-off these return to the soil as amorphous silica (ASi), which dissolves far more easily than mineral silica. This dissolved Si is prone to recycling by vegetation, biological (e.g. bio-mineralisation) and/or pedogenic processes (e.g. precipitation or adsorption), but part of it is lost to aquatic systems [2]. Changes in the biological component of the Si cycle may lead to more rapid variations in the land-ocean Si transfer than previously thought [3].

The objective of this study is to contribute to understanding of the controls on temporal Si dynamics in terrestrial ecosystems, by studying Si budgets (fluxes and pools) from a small forested catchment and human disturbed catchments in central Belgium. Si is used as a tracer to determine pathways, and to assess land use control. Detailed concentrations and load patterns (2008-2010) of bio-available Si in pore-water, streams and soils made it possible to determine the different processes causing variation in kinetic equilibrium of DSi with land-use.

For the forested catchment, which is used as a reference, discharge-concentration relationships made it possible to distinguish the main processes responsible for Si dynamics during runoff events: (1) within-channel mobilization controls ASi-delivery, and (2) a dilution-flushing effect controls DSi-delivery. End-member mixing analysis showed that at up-stream catchments base-flow delivers 92.5±10% of the water, and a chemostatic behavior confirms the existence of an important kinetic equilibrium at the catchment scale.

In contrast, disturbed catchment tend to be less chemostatic, and had a significant lower kinetic Si equilibrium and bio-available Si pool (up to three times). This is explained by a perturbation of the interactions in the critical zone: a reduced Si restitution, increased Si leaching, reduced chemical weathering and conversion to less labile Si forms in severely disturbed catchments. Lower final bio-available Si delivery from disturbed catchments indicate a lower importance of subsurface delivery which is not compensated by increased overland sources. Land-use controls on Si pathways together with biological and pedological interactions were conceptualized. We show that deforestation of the catchment, as has historically taken place elsewhere in temperate regions, would drastically alter the the Si dynamics of the catchment.

[1] Watteau and Villemin (2001) *Eur. J. Soil Sci.* **52**,385-396. [2] Cornelis *et al*. (2006) *Biogeosciences* **8,** 89-112. [3] Conley. (2002) *Global Biogeochem Cy* **16**, 11-21.

Metal evolution during differentiation of calc-alkaline magmas (Hunter Ridge, SW Pacific)

GISELA COBENAS[1]*, LEONID DANYUSHEVSKY[1], TREVOR FALLOON[1]

[1]CODES, ARC, Centre of Excellence in Ore Deposits, University of Tasmania, Hobart, Australia,
gcobenas@utas.edu.au(* presenting author)
l.dan@utas.edu.au
trevor.falloon@utas.edu.au

Understanding the behaviour of metals during magmatic differentiation processes helps constrain the important of parental magma composition for the potential fertility of a particular magma series, i.e. whether the association of an ore deposit with a specific magma type is due to the metal-rich parental magma, or is a consequence of later processes.

Rock samples collected from the Hunter Ridge (North Fiji Basin) include a typical island-arc calc-alkaline suite that covers a very broad range of rock MgO contents (1-14 wt.%) (Fig. 1). Phenocrysts in these samples have highly variable compositions (i.e. olivine Fo 79-95, clinopyroxene Mg# from 70-92, plagioclase An 22-92). Magnesian olivine and clinopyroxene record early, pre-eruptive stages of fractionation.

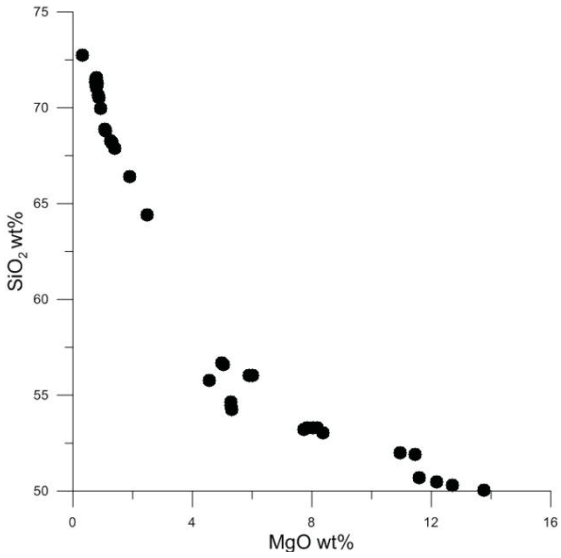

Figure1: SiO_2 wt% vs MgO wt% contents of calc-alkaline lavas from the Hunter Ridge.

In order to constrain the behaviour of metals (Cu, Zn, Pb, Co, Ni, and others) during magma fractionation, we have analysed their content in phenocrysts formed at various stages of magmatic fractionation using LA-ICPMS. A comparison of their behaviour with a wide range of lithophile elements allows for 1) a better constraint on the relative incompatibility of various metals during crystallisation processes and 2) on their distribution between immiscible phases such as fluids and sulphide melts at different stages of magma evolution.

Our results indicate that partitioning between silicate melts and water-rich fluids can affect the concentration of some metals from the earliest stages of magma evolution at crustal levels.

https://doi.org/10.1180/S0026461X00008434 Published online by Cambridge University Press

APATITE U-PB THERMOCHRONOLOGY: AN ID-TIMS AND LA-ICP-MS STUDY FROM SOUTHERN ECUADOR

RYAN COCHRANE[1]*, RICHARD SPIKINGS[1], DAVID CHEW[2] AND JÖRN WOTZLAW [1]

[1] Department of Mineralogy, University of Geneva, Switzerland, ryan.cochrane@unige.ch (* presenting author)

[2] Department of Geology, School of Natural Sciences, Trinity College Dublin, Ireland

Introduction

A combination of U-Pb LA-ICP-MS and ID-TIMS analyses of apatite has been used to investigate the high temperature (>450°C) thermal history of the Ecuadorian Andean margin. The rocks of the Eastern Cordillera of Ecuador evolved via Mesozoic terrane collision and accretion events, and intermittent active margin magmatism since the Early Ordovician. Our approach is novel because i) previous U-Pb thermochronological studies [1, 2] focused on the construction and stabilization of Precambrian cratons, whereas our study tests the applicability of U-Pb apatite thermochronology to relatively young rocks, and ii) we apply an inverse modeling technique to search for thermal history solutions to the data.

Apatite LA-ICP-MS and ID-TIMS U-Pb data have been acquired from a Triassic (247.2±4.3 Ma; U-Pb zircon) rift-related granite from southern Ecuador. ID-TIMS data were obtained from fifteen, euhedral apatite size-fractions, with grain radii ranging between 45-175 um, representing a theoretical Tc range of 450–510 °C at cooling rates of 10°C/my. Concordant $^{238}U/^{206}Pb$ dates range between 81.9±0.21 and 137.87±0.27 Ma, and positively correlate with grain size, supporting our hypothesis that Pb loss has occurred via volume diffusion. LA-ICP-MS ^{207}Pb corrected dates have been obtained from apatite size fractions that were fixed to a single epoxy mount. Primary and secondary standard apatites were: i) 92.5 Ma Emerald Lake with a measured weighted mean age of 91.5 ± 1.3 Ma, 2σ (N = 12), and ii) ~523 Ma McClure Mountain Syenite, with a measured weighted mean age of 519.9 ± 4.4 Ma, 2σ (N = 47). The apatite ^{207}Pb corrected dates range from 196.9 ± 11.4 to 69.1 ± 12.1, 2σ (N = 43), with a majority of ages that cluster between 90-100 Ma.

Time (t)-temperature (T) solutions for the data have been generated using a controlled random search procedure provided by the HeFTy software (version 1.7.0; Ketcham, 2011), using the diffusion parameters of Cherniak et al. (1991) [3]. The thermal history solutions simultaneously satisfy apatite ID-TIMS U-Pb ages obtained from six size aliquots. The best fit t-T solutions (Kolmogorov-Smirnoff goodness of fit >0.5) reveal periods of: i) rapid cooling (~240-220 Ma) through the Pb Partial Retention Zone (PRZ) shortly after crystallization, ii) residence at temperatures lower than the PRZ throughout the Jurassic, iii) reheating during 140-90 Ma, and iv) rapid cooling starting at 80-70 Ma. These solutions corroborate conclusions based on geochronological and sedimentological data. Additional in-situ age transects of apatite are scheduled to further determine the concentration and mechanisms for the distribution of radiogenic lead in the apatites.

[1] Blackburn *et al.* (2012) *Science* **335**, 73.
[2] Schoene & Bowring (2007) *GCA* **71**, 165-185.
[3] Cherniak *et al.* (1991) *GCA* **55**, 1663–1673.

A Plausible relationship between D/H in primitive Solar System organic solids, their origin, and their associated water

G. D. CODY[1*], Y. WANG[1], Y. KEBUKAWA[1], M. L. FOGEL[1], C. M. O'D. ALEXANDER[2].

[1]Geophysical Laboratory, Carnegie Institution of Washington, Washington, USA gcody@ciw.edu

[2]Department of Terrestrial Magnetism, Carnegie Institution of Washington, USA, email@association.net

Primitive extraterrestrial organic solids such as are present in type 1 and 2 chondrites (Insoluble Organic Matter, IOM, and Interplanetary Dust Particles (IDPs) are typically enriched in deuterium relative to terrestrial water, in some cases as much a 4 or more times so. The origin of such enrichment has predominantly been accepted to be a signature of a very low temperature origin of organic solids and/or their lower molecular weight precursors. Analyses of a wide range of pure IOM isolated from many different meteorites reveals no systematic relationship between IOM structure and D/H. Whether one plots D/H against H/C or the fraction of aromatic carbon, no obvious trends emerge [1]. A recent exception to this is observed with the Tagish Lake Clasts that reveal a very systematic variation in D/H with H/C [2]. We have been integrating materials characterization and laboratory based experimentation to address both the origins of primitive organic solids and gain improved understanding of the molecular nature of D/H abundances in context with gaining insight on fate of volatiles during early Solar System evolution. Towards this end we have proposed and demonstrated a likely route from interstellar formaldehyde to organic solids in comets, IDPs, and primitive chondrites [3]. We have also developed the capacity to detect deuterium speciation amongst different organic functional groups within organic solids. We find that comparison of D speciation with H speciation reveals a characteristic (apparent) intra-molecular fractionation that informs us how initial D/H enrichment reflects the environment of formation of organic solids. Finally, laboratory experiments investigating D-H exchange kinetics provide an essential understanding of why D/H in organic solids is what it is and may explain D/H variation in cometary water. It is clear that the early evolution of IOM sets the initial D/H, whereas subsequent evolution during hydrothermal processing in the parent body may affect a secondary evolution in D/H.

[1] Alexander C. M. O'D. et al. (2010) *GCA* **74**, 4417-4437. [2] Herd et al. (2011) *Science* **332**, 1304-1307. [3] Cody G. D. et al. (2011) *PNAS* **108**, 19171-19176.

https://doi.org/10.1180/S0026461X00008434 Published online by Cambridge University Press

Revealing the signature of ancient biochemistry with Soft X-rays

G. D. CODY[1]

[1]Geophysical Laboratory, Carnegie Institution of Washington, Washington, DC

The preservation of organic fossils extends back to the dawn of the Cambrian. Notwithstanding such an extent of preservation, the preservation of intact or molecularly identifiable biological molecules extends only a much shorter interval of time, 10's of millions of years. The preservation potential of organic fossils is related to the emergence of recalcitrant biopolymers, e.g. polysaccharides and in the case of vascular plants, lignin. The disappearance of a molecular signal of discrete biopolymers results from diagenetic molecular transformation, either through thermogenic and/or microbial processes. Over the past decade we have been developing the use of Scanning Transmission X-ray microscopy (STXM) and micro-spectroscopy utilizing the fine absorption fine structure on carbon's, nitrogen, and oxygen K-edges, i.e. X-ray Absorption Near Edge Structure (XANES) spectroscopy. Exploiting the high-energy resolution of the STXM monochromator (5000 ΔE/E) and the spatially resolving power of the soft X-ray optics (25 nm) has allowed us to explore sub-micron biochemical complexity that is preserved in ancient organic fossils. Our goal has been to use the signature of sub-micron chemical differentiation to address issues related to biochemical evolution; e.g. searching for the evolutionary emergence of lignin by studying the fossil record of extinct plants near the phylogenetic root of plants [1]. Most organic fossils, either derived from arthropod cuticle or vascular plant tissue have been subjected to considerable molecular modification, yet with a judicious choice of absorption energy, remnant chemical differentiation can be still observed. Chemical differentiation is a hallmark of tissue that was originally composed of two or more biopolymeric material. For example, lignin and cellulose in the case of vascular plant tissue. Traditionally, the loss of characteristic spectroscopic and/or molecular features associated with polysaccharide was interpreted to suggest that all carbon associated with polysaccharide had been removed from the organic fossil. Thus, distorting understanding of the nature of the actual molecular transformation chemistry. Studies employing STXM and micro-XANES now reveal a more complex story in which the presence and retention of a substantial amount of polysaccharide derived carbon is an essential aspect of organic matter preservation in ancient organic fossils [2].

[1] Boyce K. C., et al *Geology* 30, 1039-1042.
[2] Cody G. D., et al (2011) *Geology* 39, 255-258.

Objective mapping of the geographical distribution of εNd in seawater and outlook for past and present Nd budget in the oceans

ANTOINE COGEZ[1*], GAEL FORGET[2], CLAUDE ALLÈGRE[1], LAURE MEYNADIER[1] AND CARL WUNSCH[2]

[1]Equipe de Géochimie et Cosmochimie, Institut de Physique du Globe de Paris, Sorbonne Paris Cité, Univ Paris Diderot, UMR 7154 CNRS, F-75005 Paris, France, cogez@ipgp.fr (* presenting author)

[2]Department of Earth Atmospheric and Planetary Sciences, Massachusetts Institute of Technlogy, Cambridge MA02139, USA

Neodymium (Nd) isotope composition (expressed in εNd notation, in per 10 000) in sediment cores are commonly used in paleoceanography and paleoclimatology to reconstruct changes in ocean circulation and/or continental weathering over the last thousands to tens of millions of years. A good understanding of the present processes affecting the transport of Nd in the oceans, the different sources and their relative influence is a prerequisite for its use in paleoceanography.

We compiled all the present data available for direct seawater measurements and authigenic fractions of core-top sediments in order to plot up-to-date interpolated maps displaying a depth averaged as well as a the deep distributions of present seawater εNd, using optimization methods. We observe clear patterns of Nd injections in the different basins, especially the clearly distinct isotopic signature of the different basins, the deep Atlantic circulation, the deep circum Antarctic water masses penetrating Pacific ocean, the Indonesian througflow into the Indian ocean, the Iceland local influence, the Himalayan rivers discharge, the East Pacific Rise local contribution… We also compared this distribution to an interpolated map of detrital εNd data, which show similar patterns. The misfits obtained help us to discuss what both types of data (sediments and seawater measurements) really tell us in such an approach.

All these observations lead us to distinguish different geographical groups consistent with εNd distribution, and to conclude on the major role of the rivers as source of Nd in seawater, the important vertical transfer in the water column from the superficial layers to the bottom and the limited exchange of Nd between the different ocean basins, due to a short residence time. These conclusions lead to conceptualize a model on Nd cycling in the oceans that will be presented in a joint paper by C.J. Allègre. Simulations on a coarse box model and on a matricial form of the MIT GCM are still in progress and will be helpful to put this model to the test.

https://doi.org/10.1180/S0026461X00008434 Published online by Cambridge University Press

Dating Early Archean partial melting events: whole-rock versus single grain Re-Os ages in 3.81 Ga chromitites from West Greenland

JUDITH A. COGGON[1*], AMBRE LUGUET[1], PETER W. U. APPEL[2]

[1]Steinmann Institut, Universität Bonn, Bonn, Germany, jude@uni-bonn.de (* presenting author), ambre.luguet@uni-bonn.de

[2]Geological Survey of Denmark and Greenland, Copenhagen, Denmark, pa@geus.dk

Abstract

Large melt depletion events in the mantle are recorded in refractory phases and lithologies by the ^{187}Re-^{187}Os isotope system as rhenium-depletion model ages (T_{RD}). Numerous studies have shown that the peaked distribution of these ages coincides with crustal U-Pb zircon ages providing a record of periodic episodes of significant crustal growth over the last ~3 Ga. However, the frequency of T_{RD} ages preserved decreases with time. In order to detect older events it is necessary to analyse samples that were extracted from the mantle before later events were able to dilute or overprint more ancient signals. A >3.81 Ga chromitite-ultramafic layered body from the Ujaragssuit nunât area of western Greenland provides an ideal target for this study. Peridotites (0.303 – 4.02 ppb Os) display U-shaped PGE patterns (Fig. 1) atypical of partial melt depletion, while chromitites exhibit a gentle decrease in chondrite normalised PGE concentration with increasing incompatibility. Both lithologies show anomalously high Re contents, illustrating significant re-enrichment by one or more post-magmatic events (two late Archean metamorphic events have been suggested [1]). T_{RD} ages for whole-rock peridotites and chromitites are artificially low (483 – 2926 Ma and 2666 – 3250 Ma respectively), a result of the aforementioned Re addition, hence whole-rock model ages are unreliable. We will present a comparison of data from whole-rock samples, leached chromite separates and single grains of Os-bearing minerals. This combined approach will allow us to further constrain the history of the earliest Archean genesis of continental crust, providing information that has so far been inaccessible when considering only whole-rock Re-Os analyses.

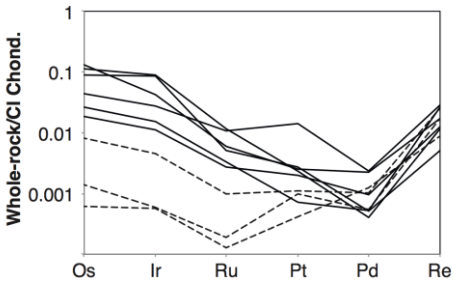

Figure 1: Chondrite [2,3] normalised PGE & Re contents of Ujaragssuit nunât peridotites (dashed) and chromitites (solid).

[1] Rollinson et al. (2002) *Journal of Petrology* **43**, 2143-2170. [2] Anders & Grevesse (1989) *Geochimica et Cosmochimica Acta* **53**, 197-214. [3] Horan et al. (2009) *Geochimica et Cosmochimica Acta* **73**, 6984-6997.

The CO_2-Vadose project: Numerical simulations coupled with geochemical and geophysical monitoring of CO_2 in the vadose zone

G. COHEN[1], B. GARCIA[2*], C. LOISY[1], P. DELAPLACE[2], F. LARROQUE[1], C. LAVEUF[1], C. MAGNIER[2], V. ROUCHON[2], O. LE ROUX[1], M. FRANCESCHI[1], A. CEREPI[1]

[1]EA 4592 "Géoressources et Environnement",ENSEGID, University of Bordeaux, France, adrian.cerepi@egid-u.bordeaux3.fr

[2]IFP New Energy, Rueil-Malmaison, France, bruno.garcia@ifpen.fr (* presenting author)

The CO_2-Vadose project aims at developing a facility around a cavity, in a former underground limestone quarry, to perform experimental releases of CO_2 under controlled conditions in order to study its migration along the vadose zone and to test near-surface detection techniques. Preliminary modelling carried out with the research code COORES^{TM} permitted to model the extend of the CO_2 plume, at a chosen release rate, the concentrations and flow rates expected at a specific depth, the timing of the migration and of the sampling strategy [1].

Based on the results provided by the preliminary modelling, an array of detection and monitoring tools was deployed. These tools allow the regular surveillance of water and gas compositions and fluxes as well as their samplings, all monitored. Micro-climatic parameters were also recorded by a weather station at the site surface. Geochemical signatures of carbon isotopes, and natural noble gases were also determined after samplings. A baseline, a tracers injection and also a CO_2 migration were performed in this project.

Results show that the natural CO_2 concentration at soil surface is depending of the season but rather homogenous (2.0±1.0% in october 2009 and 1.0±0.7 % in march 2010), and its carbon isotopic signature is constant ($\delta^{13}C_{CO2}$= -18.5±1.0 ‰). Natural noble gases composition at soil surface is equal to atmospheric composition. CO_2 flux is considered as a "normal" flux. Around and in the cavity, same trends were observed [2].

For the tracers injection, modelling results allow us to determine at which time the maximum concentration of Helium and Argon would arrived at soil surface. Experimental results are in good accordance with these previous modelling ones, specially around the cavity but not at soil surface by the fact of the presence of a clay zone just above the top of the cavity.

CO_2 experimental injection was realised in december 2011 with a flow of 2m^3 per hour during 9 hours (18m^3 of CO_2 injected for a cavity with a volume of 9m^3) in order to have a concentration of CO_2 at the top of the cavity equal to the injected CO_2 amount. Monitoring of CO_2 was realised with success from the cavity to the limestone around the cavity and is in good accordance with modelling results considering the clay zone.

[1] C. Laveuf et al. (2010) *International Journal of Greenhouse Gas Control,* submitted.
[2] C. Loisy (2011) *International Journal of Greenhouse Gas Control,* submitted.

https://doi.org/10.1180/S0026461X00008434 Published online by Cambridge University Press

Scaling up production of biogenic magnetite for industrial use

VICTORIA S. COKER[1*], JAMES M. BYRNE[1], HOWBEER MUHAMAD-ALI[1], CHRISTOPHER HAINSWORTH[2], JERRY COOPER[2] & JONATHAN R. LLOYD[1]

[1]SEAES, University of Manchester, Manchester, M13 9PL, UK vicky.coker@manchester.ac.uk (* presenting author) james.byrne@postgrad.manchester.ac.uk, jon.lloyd@manchester.ac.uk howbeer.muhamadali@postgrad.manchester.ac.uk

[2]Centre for Process Innovation, Wilton, UK jerry.cooper@uk-cpi.com, christopher.hainsworth@uk-cpi.com

Magnetite nanoparticles have a high surface to volume ratio and magnetic properties that can be exploited for a wide range of applications including targeted cancer therapies [1], magnetic data storage devices [2] and bioremediation [3-4]. Fe(III)-reducing bacteria produce nanoscale magnetite through the reductive transformation of low crystallinity Fe(III)-bearing oxides [5]. However, the commercial applicability of biogenic nanoparticles depends critically upon the ability to generate kg to tonne quantities of the nanoparticles. Therefore this technology relies upon the upscaling of laboratory biotransformation experiments which are commonly performed at 10 to 100 ml volumes. The goal of this study was to develop a batch fermentation of *Geobacter sulfurreducens* which could then be used to generate large quantities of biogenic magnetite that match the performance of the biomaterials made at small scale in the laboratory.

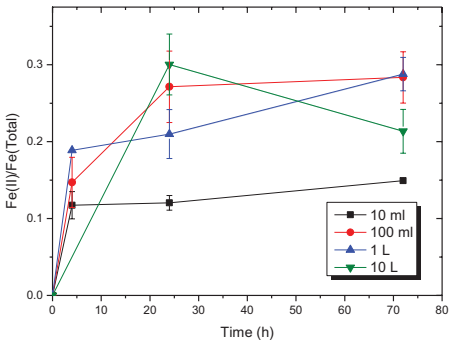

Figure 1: Fe(III) reduction (monitored by Fe(II) measurements by ferrozine) for bioreduction of Fe(III)oxyhydroxides during scale up of biomagnetite production.

Fermentation was carried out at 50 L scale and this led to production of biogenic magnetite via the reduction of Fe(III) oxyhydroxide in vessels from 10 ml to 10 L in size, containing 50 mmoles/L of Fe (Fig. 1). Spectroscopy (XAS/XMCD), microscopy (ESEM/TEM) and testing of the material against model contaminants, such as Cr(VI), was carried out to determine the quality and performance of the materials produced from the industrial scale fermentation.

[1] Goya et al. (2008) *Current Nanoscience* **4**, 1-16. [2] Zeng et al. (2006) *Phys Rev B* **73**, 4. [3] Hencl et al. (1995) *Water Res* **29**, 383-385. [4] Cutting et al. (2010) *Environ Sci Technol* **44**, 2577-2584 [5] Lovley et al. (1987) *Nature* **330,** 252-254.

Isotopic composition of volcanic sulfate aerosols

JIHONG COLE-DAI[1*], JOËL SAVARINO[2], ALYSON L. LANCIKI[1], AND MARK H. THIEMENS[3]

[1]South Dakota State University, Chemistry and Biochemistry, Brookings, SD, USA, jihong.cole-dai@sdstate.edu (* presenting author)

[2]Laboratoire de Glaciologie et Géophysique de l'Environnement, Grenoble, France, jsavarino@lgge.obs.ujf-grenoble.fr

[3] University of California, Chemistry and Biochemistry, San Diego, CA, USA, mht@chem.ucsd.edu

Volcanic sulfur dioxide is oxidized in the atmosphere to sulfate aerosols. Volcanic aerosols present in the stratosphere, by altering the atmospheric albedo and energy balance, can impact the global climate significantly. Records of past volcanic eruptions are needed tp determine the role of volcanism in climate change.

Polar ice cores provide some of the most valuable volcanic records constructed from time series of sulfate in snow. The time coverage of such records can be as long as tens of thousdands of years. However, many of the sulfate signals in these records may be from relatively small tropospheric eruptions with no significant climatic impact and therefore should be excluded from consideration when investigating the volcano-climate connection.

We have found that the sulfate converted from volcanic sulfur dioxide in the stratosphere contains unique isotopic signatures [1,2]. Mass independent fractionation (MIF) of sulfur isotopes in sulfate indicate photolysis-based conversion reactions in the stratosphere and therefore can be used to identify climate-impacting stratospheric eruptions in the ice core records [3,4]. We present here sulfur isotope measurement of volcanic sulfate in Greenland and Antarctica ice cores. In addition to sulfur-33 data discussed in preivous work, we present data of sulfur-36 MIF excess in the sulfate of several volcanic eruptions in the last 1,000 years and discuss the possible interpretation of the new data in terms of the reaction mechanism of the oxidation of sulfur dioxide to sulfate.

[1] Savarino *et al*. (2003) *Geophys. Res. Lett.* **30**, 2131. [2] Baroni *et al*. (2008) *J. Geophys. Res.-Atmos.* **113**, D20112. [3] Cole-Dai *et al*. (2009) *Geophys. Res. Lett.* **36**, L22703. [4] Lanciki *et al*. (2011) *Geophys. Res. Lett.* **39**, L01806.

https://doi.org/10.1180/S0026461X00008434 Published online by Cambridge University Press

Bacterial H_2S Generation in Oil Sands Process Wastes: Where Does it Begin?

TARA COLENBRANDER NELSON[1*], STEVEN P. HOLLAND[1], KATHRYN KENDRA[1], KATE STEPHENSON[1], TARA PENNER[2] AND LESLEY A. WARREN[1]

[1]School of Geography and Earth Sciences, McMaster University, Hamilton, Canada, warrenl@mcmaster.ca (* presenting author)
[2]Syncrude Environmental Research, Edmonton, Canada, penner.tara@syncrude.com

Reclamation of tailings, wastewater, and afflicted land represents one of the largest challenges facing the Alberta Oil Sands industry. Syncrude Canada Ltd., one of the largest producers in the Alberta Oil Sands, is assessing a novel reclamation strategy involving the establishment of a freshwater fen overlying a sand-cap topped, gypsum ($CaSO4{\cdot}2H_2O$)-amended, composite tailings (CT) waste material. However, a recent phenomenon resulting in the unpredicted generation of H_2S gas in CT dewatering wells has indicated the importance of constraining microbial S dynamics in the tailings system. On-going work is establishing the occurrence of microbially-linked S cycling in CT undergoing reclamation. However, this research will investigate Fe and S biogeochemistry and the hypothesized connections with porewater H_2S generation from fluid fine tailings (FFT), the gypsum-free precursor to CT, via a series of microcosm experiments. FFT is microbially rich and contains iron-rich clays; both constituents could be involved in S biogeochemical cycling within CT. Thus, in order to establish the relative roles of microbial and geochemical factors in FFT that may contribute to observed CT H_2S generation in situ, experimental microcosms were established to assess: i) microbial links to tailings porewater H_2S generation, and ii) the implications of gypsum amendment on porewater H_2S generation in variably microbially amended FFT treatments. Results of these experiments establishing the linkages between FFT and microbial S cycling prior to the amendment of gypsum and reclamation activities will be discussed.

Unraveling the Genetic Basis of an Ancient Geochemical Biomarker

R.E. COLLINS[1*], B. WING[2]

[1]Origins Institute, McMaster University, Hamilton, ON, Canada, rec3141@mcmaster.ca (* presenting author)
[2]Earth & Planetary Sciences, McGill University, Montreal, QC, Canada, boswell.wing@mcgill.ca

Abstract

Based on phylogenetic and geochemical evidence, the cycling of inorganic sulfur compounds was likely among the first metabolisms used by life. Sulfur isotope fractionation is a geochemical biomarker which has been observed in marine sediments dating back more than 2.5 billion years, but the cellular-level processes responsible for the fractionation effect are not well understood. Utilizing bioinformatic approaches in combination with measurements of sulfur isotope fractionation in pure cultures we seek to make quantitative links between SRB and their geochemical biomarkers.

The intrinsic sulfur isotope fractionation effect, ε, is essentially a measure of the preferential use of ^{32}S-substituted sulfate over ^{34}S-substituted sulfate expressed in parts per thousand, usually measured on pure cultures grown under optimal conditions. Much effort has gone into expanding the range of measured values of ε by subjecting SRB to a wide range of physiological stress, but this approach has failed to elucidate the underlying genetic basis of sulfur isotope fractionation. The mechanism is thought to involve kinetic limitation at the reaction sites of critical enzymes or the uptake of sulfur species, but there also appears to be an overarching energetic association such that SRB that completely oxidize their electron donors to CO_2 tend to have larger ε. However, this relationship is confounded by a phylogenetic split between two major Orders of SRB: within the Desulfobacterales, complete oxidation is the norm; within the Desulfovibrionales, complete oxidation is the exception. The interaction between the evolutionary history of SRB, their mode of metabolism, and their intrinsic fraction effect points towards the need for a genomic approach to unravel the basis of sulfur isotope fractionation.

Analyses of a set of genomes from 24 sulfur-metabolizing and 37 non-sulfur-metabolizing Bacteria and Archaea have identified gene families which may play a role in setting the magnitude of sulfur isotope fractionation effects. Though the members are phylogenetically divergent, genomes of SRB with moderate ε (10–20 per mille) and small ε (<10 per mille) each contain conserved gene clusters not found in the other genomes, including regulatory proteins and conserved hypothetical proteins. Unfortunately, a dearth of genome sequences from high-ε species (>20 per mille) limits our ability to further investigate the genetic basis of these large fractionation effects. The Desulfobacteraceae is a major lineage of SRB that is under-represented in genome sequences but which includes 90% of known SRB with ε >20. Presently we are expanding the representation of complete genomes by sequencing *Desulfobacula phenolica*, *Desulfospira joergensenii*, and *Desulfotignum balticum*, which have large ε values of 37, 26, and 21, respectively. Our ongoing biogeochemical measurements continue to expand the range of known fractionation effects, and sequencing of these SRB will increase the phylogenetic coverage of fractionation effects observed in vitro.

https://doi.org/10.1180/S0026461X00008434 Published online by Cambridge University Press

How to measure the pure dissolution kinetics of a soft mineral?

JEAN COLOMBANI[1*], AGNES PIEDNOIR[1], EDGAR A. PACHON-RODRIGUEZ[1]

[1]Laboratoire de Physique de la Matière Condensée et Nanostructures, Université de Lyon, Université Claude Bernard Lyon 1, CNRS, Villeurbanne, France, Jean.Colombani@univ-lyon1.fr (* presenting author)

Among interfacial processes, dissolution of minerals is present in countless problems: durability of mineral materials, management of nuclear wastes, sequestration of atmospheric CO2, pollution of drinking water … The modelling of all these situations requires the knowledge of the mineral dissolution kinetics, which in turn necessitates, to be reliable, a precise understanding of all the basic mechanisms intervening in the reaction.

The understanding of these fundamental mechanisms has progressed during the last decade. For instance, the use of molecular simulations and atomic-scale microscopy has enabled to understand the weak role of etch pit density on the dissolution kinetics, or the role of the surface history on this kinetics. But beside these successes, the measurement of the pure dissolution kinetics, and accordingly the identification of the basic processes driving the kinetics, is often a delicate experimental task.

We present here two situations of apparently inconsistent dissolution kinetics results of a soft mineral in the literature. In the two cases, a detailed data analysis and the identification of external phenomena blurring the results have permitted to gain the pure dissolution kinetics and then determine the basic processes:

- The dissolution rate constants of gypsum in water measured by various bulk methods are inconsistent. We have shown that the removal of the contribution of mass transport to these dissolution rates enables to obtain the pure chemical reaction rate constant of gypsum in water, coherent with all the measurements.

- The dissolution of gypsum proceeds via the migration of atomic steps. The step velocities, measured by Atomic Force Microscopy, show a large dispersion. We have shown that this dispersion stems from the influence of the AFM tip. The force applied by the lever increases locally the solid elastic energy, which promotes dissolution, and hence the step velocity.

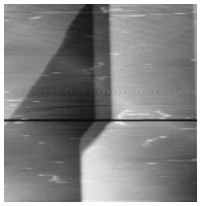

Figure 1: AFM picture of the cleavage plane of gypsum during dissolution. The black line shows the AFM tip path during a step velocity measurement performed just before the picture.

Microbial production of methylmercury from Hg(0)

MATTHEW COLOMBO*, JUYOUNG HA, JOHN R. REINFELDER, TAMAR BARKAY AND NATHAN YEE

School of Environmental and Biological Sciences, Rutgers University, New Brunswick, NJ, USA, mcolombo@eden.rutgers.edu (* presenting author)

Introduction

Mercury [Hg] is a global pollutant and its accumulation in food as methylmercury [MeHg] has caused serious public health crises this past century. In order to predict the fate and deleterious effects of Hg in the environment, a mechanistic understanding of MeHg production in aquatic ecosystems is required. Previous studies have elucidated the mercuric [Hg(II)] species that are bioavailable to methylating microbes [1,2]. Although it is generally assumed that elemental Hg [Hg(0)] is unavailable for biologic methylation [3], the uptake and transformation of Hg(0) by anaerobic Hg-methylating bacteria have never been tested. Here we demonstrate that Desulfovibrio desulfuricans ND132 produces MeHg when provided with dissolved Hg(0) as its sole mercury source.

Materials and Methods

D. desulfuricans ND132 was grown to exponential phase and subsequently exposed to a constant source of dissolved Hg(0) under anaerobic conditions in the dark. At periodic intervals, samples were collected for total non-purgeable Hg analysis. These samples were purged with N_2 gas, digested with BrCl, and analyzed for Hg by cold vapor atomic absorption spectroscopy. Cell suspensions containing non-purgeable Hg were filtered (0.2 µm filter) to determine the amounts of dissolved and cell-associated Hg. To examine the chemical speciation of cell-associated Hg, cells were collected and examined using X-ray absorption near edge structure (XANES) spectroscopy. Finally, ND132 cultures were analyzed for MeHg production by distillation, ethylation-gas chromatography, and cold vapor atomic fluorescence spectroscopy.

Results and Discussion

We observed a rapid transformation of Hg(0), with bacterial cultures producing ~40 µg/L of non-purgeable Hg within 30 min. Examination of the Hg L_{III}-edge position in the XANES spectra revealed that Hg oxidation to Hg(II) had occurred. After 24 h of incubation, D. desulfuricans ND132 produced up to 700 µg/L of non-purgeable Hg and 50 µg/L of MeHg. Similarity between the XANES spectra of bacterial samples at 30 min. and 24 h and a Hg-$(cysteine)_3$ reference compound suggested that most of the Hg(II) was associated with cells via coordination with thiol functional groups. The formation of Hg-thiol structures is consistent with Hg(II) uptake into the cell, since Hg(II) transfter into and within bacterial cells is governed by thiol-containing protiens [3]. The results of this study demonstrate a previously unrecognized source of MeHg in the environment.

[1] Benoit et al. (1999) Appl. Environ. Microbiol. 67, 51-58. [2] Schaefer & Morel (2009) Nature Geosci. 2, 123-126 [3] Fitzgerald et al. (1991) Water, Air, Soil Poll. 56, 745-67. [4] Barkay et al. (2003) FEMS Microbiol. Rev. 27, 355-84.

https://doi.org/10.1180/S0026461X00008434 Published online by Cambridge University Press

The HP stability of Bloedite ($Na_2Mg(SO_4)_2\ 4H_2O$: a contribution to the knowledge of asteroids and icy satellites

PAOLA COMODI[1]*, SABRINA NAZZARENI[1], TONCI BALIC-ZUNIC[2], AZZURRA ZUCCHINI [1], MICHAEL HANFLAND[3]

[1] Dipartimento Scienze della Terra, Università di Perugia, Italy; comodip@unipg.it (* presenting author)

[2]Natural History Museum of Denmark, University of Copenahgen, Denmark, TonciB@snm.ku.dk

[3] ESRF, Grenoble, France, hanfland@esrf.fr

Bloedite, $Na_2Mg(SO_4)_2H_2O$ is a common mineral in evaporitic marine sediments. Being one of the phases in the system H_2O-$MgSO_4$-$NaSO_4$ it has a large planetological interest. In fact volatiles of icy satellites are considered to contain brines with sulphates, as well as carbonates and chlorides. To understand their internal structure and to evaluate the presence of a deep internal ocean, it is important to know the phase relation between water and brine mixtures [1]. Bloedite crystal structure consists of parallel layers of $MgO_2(H_2O)_4$ and $NaO_4(H_2O)_2$ octahedra, interconnected through SO_4 tetrahedra and hydrogen bonds [2]. This paper intends to investigate the high-pressure behavior of bloedite to determine the equation of state, the density evolution, as well as the dehydration conditions. Data were collected at ID-09 beamline, at ESRF (Grenoble, France). We used a diamond anvil cell with 300 micron diamond culet, Neon gas as pressure transmitting medium and ruby chip as pressure calibrant. The very large image-plate detector, Mar555, allowed to collect data of high quality from single crystals. Lattice parameters and reflections intensities were obtained by Crysalis software. SHELXL software was used to refine the structure at different pressures up to 12 GPa. Equation of state (EoS) of bloedite was determined with data collected up to 12 GPa and EOS-Fit program [2]. A second order Birch-Murnaghan EoS fit yields V_0 = 495.6(9) Å^3 and K_0 = 40.5(7) GPa, whereas a third order Birch-Murnaghan EoS fit yields V_0 = 497.6(4) Å^3 , K_0 = 34(1) GPa and K' = 5.8 (4) GPa^{-1}. The lattice parameters compressibilities are β_a = -0.0074 (4) GPa^{-1}; β_b= -0.0069 (4)GPa^{-1}; β_c = -0.0054 (2) GPa^{-1} with an anisotropic ratio of 1: 1.07: 1.37. The structure is more incompressible along the direction perpendicular to open sheet, than the other directions. The SO_4 tetrahedra are incompressible, K_{MgO6} octahedra is 90 GPa and K_{NaO6} octahedra is 42 GPa. No phase transitions were observed in the bloedite structure up to 12 GPa, who remained stable at very HP. Hydrogen bonds evolution were followed through the O_{donor}-$O_{acceptor}$ distance, whose configuration explained the large compressibility of *a* and *b* parameters with respect to *c* lattice parameter. The lack of strong structural rearrangement, essential to compensate the dehydration process, suggested that water remaineds in the structure of bloedite in the investigated P range.

[1] Nokamura, Othani (2011) *Icarus*, 211, 648-656, [2] Hawthorne (1985) *Canadian Mineralogist*, 23, 669-674, [3] Angel (2000) Reviews in Mineralogy and Geochemistry 41.

Syenitic Provinces in the São Francisco Craton, Brazil

HERBET CONCEIÇÃO[1*], MARIA LOURDES SILVA ROSA[1], DÉBORA CORREIA RIOS[2]

[1]Sergipe Federal University, Núcleo de Geologia, Aracaju, Brazil, herbet@ufs.br

[2]Bahia Federal University, Instituto de Geociências, Salvador, Brazil, dcrios@ufba.br

The Paleoproterozoic in the Bahia State, Brazil, is characterized by the generation and emplacement of varius syenite bodies. The mainly occour in two mobile belts that represent parte of the basemente of the São Francisco Craton. These mobile belts are: (i) the Salvador-Curaçá mobile belt (SCMB), located in te eastern parte of the state, and (ii) the Urantdi-Paratinga mobile belt (UPMB), in the western part. Both are characterized by the emplacement of alcali-syenitic, potassic to ultrapotassic rocks, during the late stages of the stabilitaztion of these mobile belts, which occurred between 2.1 and 2.0 Ga. However, in the east parte the syenite is placed as tabular bodies and shows gneissic texture, while in the west parte they are related to pull-part system and developt only magmatic textures. The UMPB syeinte occur as wide single batholith (6,000 km^2), the Guanambi Batholith (GB), dated 2.05±0.02 Ga (U-Pb age). In the GB two main domins were recognized; (i) multipe intrusions (about 92% of the batholith), and (ii) late intrusions. Both have composiiton from syenite to mafic syenite towards monzonite. The U-Pb data show that the difference between the empacement of late intrusions was less them 5 Ma. The Eastern Bahia State, the SCMB syenite consist mainly of four massifs, discontinuously disposed. From north to south occur the following bodies: Itiúba (1800 km^2, 2.00±0.03 Ga, Pb/Pb age), Santanápolis (180 km^2, 2.10±0.04 Ga, U-Pb age), São Felix (32 km^2, 2.09±0.01 Ga, Pb-Pb age) and Anuri (70 km^2, 2.10±0.020 Ga U-Pb age). All intrude both gneiss-migmatitic and granulitic terrains. These syenite, despite the mobile belt in which they occur, show the same petrographic characteristics. They are leucocratic, porphyritic, mainly composed of perthitic alkali-feldspar, diopside, hornblend, phlogopite and biotite, ilmenite anda magnetite. In the syenites was found lamprophiric dykes (minette). Geochemical data indicate theat all these syenites are SiO_2-sturated to oversatured, alkalic to sub-alkalic and metaluminous. The K_2O/Na_2O ratios is always greater tham the unity, being higher in mafic terms. In some cases, these mafic terms can be classified as ultrapotassic. Ba (up to 8,0000 ppm), Sr (up to 6,000 ppm) and Rb (up to 940 ppm) are strongly enriched in these rocks. Cr (from 50 to 700 ppm), Ni (from 80 to 270) and Mg# (form 0.20 to 0.77) are reltively high form common syentic rocks. Chrondite-normalised REE patterns show strongely fractionated LREE with a small negative Eu anomaly, $\varepsilon_{Nd(t)}$ range from -10 to 0 (SCMB), and -11 to -7 (UPMB) and Sr_i values are around 0.705. From those data, we can concluded that the Paleoproterozoic was a propicius time form the generation of syenitic rocks in these two mobile belts of the Bahia State, independely from the tectonic regime. The syenitic result probably from fractionated crystallizaton of a lamprophiric magma, the later gernerated buy melting of Paleoproterozoic enriche mantle.

Acknowledgments: This work was supported by CNPq, CBPM and FAPITEC.

https://doi.org/10.1180/S0026461X00008434 Published online by Cambridge University Press

Zircon age gaps in the Great Proterozoic Accretionary Orogen: a possible connection between the 1.5-1.3 Ga granite-rhyolite province and subduction erosion

KENT C. CONDIE[1*], DAVID W. SCHOLL[2]

[1]Department of Earth & Environmental Science, New Mexico Tech, Socorro, NM, USA, kcondie@nmt.edu (* presenting author)
[2]Department of Geology & Geophysics, University of Alaska, Fairbanks, AK, USA, dscholl@usgs.gov

Collisional zircon ages record the assembly of Nuna between 2100-1900 Ma (early phase) and 1900-1800 Ma (main phase). During this time collisional convergent margins shifted to the perimeter of Nuna forming the possibly contiguous Great Proterozoic Accretionary Orogen (GPAO) in Laurentia-Baltica-Amazonia (1900-1300 Ma). Accompanying this shift is an increase in the proportion of juvenile crust as reflected by eHf values in detrital zircons. Major gaps in both *in situ* and detrital zircon age spectra occur at 1750-1700 (Baltica, Amazonia), 1600-1500 (Laurentia), and 1300-1200 (all three cratons). The two oldest age gaps in the GPAO may be due to subduction erosion related to initial rifting of Siberia from Baltica and of Amazonia from West Africa (1750-1700 Ma) and Laurentia from Siberia (1600-1500 Ma). The 1300-1200-Ma gap may record major breakup and limited dispersal of the supercontinent. Depending on how much Paleoproterozoic crust is buried beneath the margin of the Grenville orogen, as much as 30% of the original crustal volume of the GPAO may have been lost by subduction erosion. Subduction of 1600-1500-Ma continental crust along the coast of Laurentia may have resulted in enrichment of the mantle wedge above a low-dip subduction zone between 1500 and 1300 Ma as the convergent margin migrated inwards towards the center of the supercontinent. This may have given rise through multi-stage melting of the mantle wedge and its mafic melting products to the extensive 1500-1300 Ma granite-rhyolite province in south-central and southwestern Laurentia.

Integrated Sr-Pb-S-O-Cu Isotopes of Sulfide and Mn-oxide Mineralization of the Boléo Cu-Co-Zn-Mn District, Baja California Sur, Mexico

ANDREW G. CONLY[1*] AND RYAN MATHUR[2]

[1]Department of Geology, Lakehead University, Thunder Bay, Canada, andrew.conly@lakeheadu.ca
[2]Department of Geology, Juniata College, Huntingdon, USA, MATHUR@juniata.edu

Introduction

Stable and radiogenic isotope composition of stratiform Cu-Co-Zn-Mn mineralization from the Boléo district of the Miocene Santa Rosalía basin, Baja California Sur, are used to constrain the source and evolution of fluids and the mechanisms responsible for sulphide and oxide deposition. Mineralization consists of finely disseminated sulfides and Mn-Fe-Cu-oxides within claystones and tectonically triggered debris flows that occur near the base of five cyclical fan-delta sequences of the Boléo Formation, which developed in response to development of the Proto-Gulf of California.

Results

Newly acquired isotope data and data compliled from [1,2] are provide in Table 1. Results from this study are compariable to those recently reported by [3].

Table 1: Range in radiogenic isotope compositions of Boléo manto Mn oxides and sulphides.

Phase	$^{87}Sr/^{86}Sr$	$^{208}Pb/^{204}Pb$	$^{207}Pb/^{204}Pb$	$^{206}Pb/^{204}Pb$
Mn-ox	0.70750 to 0.70584	38.70 to 38.40	15.67 to 15.57	18.80 to 18.70
Sulfide	n/a	38.49 to 38.41	15.60 to 15.57	18.80 to 18.72
	$\delta^{18}O$ (‰)	$\delta^{34}S$ (‰)	$\delta^{65}Cu$ (‰)	
Mn-ox	12.5 to -2.9	n/a	1.86 to 0.50	
Sulfide	n/a	1.8 to -13.7	-0.39 to -2.72	

Discussion and Conclusions

Strontium and Pb isotopes indicate that the ore-forming brines originated as basin seawater that interacted with basement volcanic and plutonic rocks and the evaporite sequence that underlies the Boléo Formation. $\delta^{34}S$ values of pyrite-Cu-sulfide-bearing mineralization show that sulfur originated from bacterial sulfate reduction, with more enriched $\delta^{34}S$ values indicating sulfate reduction at higher temperatures during the infiltration of the metal-bearing brines. The $\delta^{65}Cu$ composition of sulfides is consistent with reaction of Cu-rich fluids ($\delta^{65}Cu \approx 0‰$) with a framboidal pyrite reductant [e.g., 4]. Higher $\delta^{65}Cu$ values for Mn oxides are the product of abiotic oxidative leaching of chalcocite-covellite mineralization [e.g. 5], during the wanning stages of discrete hydrotheral episodes.

[1] Conly et al. (2006), Miner. Dep. **41**, p. 127-151. [2] Conly et al. (2011), Econ Geol. **106**, p. 1173-1196. [3] Del Rio Salas (2011), PhD Thesis Univ. Arizona, 259p. [4] Asael et al. (2006), Geochim Cosmochim Acta **70**, A23–A23. [5] Mathur et al. (2005), Geochim Cosmochim Acta **69**, p. 5233–5246.

https://doi.org/10.1180/S0026461X00008434 Published online by Cambridge University Press

Evaluating the robustness of Pb-Pb ages of meteorites

JAMES N. CONNELLY* AND MARTIN BIZZARRO

Centre for Star and Planet Formation, Copenhagen University, Øster Voldgade 5-7, 1350 Copenhagen K, Denmark. connelly@snm.ku.dk (* presenting author)

A variety of methods for acquiring Pb-Pb data to constrain the ages of meteorites and their components exist today, all capable of yielding ages with varying levels of complexity. Regardless of the method employed, basic measures exist to evaluate the degree of confidence in a calculated age, including:

1. The analyses should yield sufficient spread in Pb-Pb space (courtesy of either stepwise dissolution methods and/or analyzing separate mineral concentrates from a single sample) to yield an internal isochron free of any model or presumed initial Pb isotopic composition that cannot be independently verified,
2. The array defining an isochron must represent mixtures of in situ radiogenic Pb and only one other source of common Pb, most typically initial Pb or, less typically, secondary contaminant Pb. At least one analysis that is more radiogenic than modern terrestrial contaminant Pb assures that the resulting array does not reflect a binary mix of initial Pb and terrestrial contaminant Pb,
3. Back projection of the isochron should yield a permissible isotopic composition for an initial Pb component given the context of the object being dated (except atypical cases where it is presumed that only contaminant common Pb exists as the non-radiogenic component),
4. The U isotopic composition of the object being dated must be known by direct measurement,
5. All U and Pb isotopic analyses must be corrected using an internal measure of instrumental isotopic mass fractionation,
6. All errors on final ages should reflect errors for the Pb and U isotopic measurements and assumptions therein,
7. Analyses of accepted, appropriate standards run concurrently with the samples and using the same protocols should be reported with the geochronological results,
8. When stepwise dissolution is employed, at least the acid type and concentration, exposure time and temperature should be reported in the data table,
9. When feasible, critical ages should be verified by an independent research group in a second laboratory.

While these criteria may be obvious, there is presently no standardization of data presentation or consistent culture of critical evaluation of the confidence level of ages for meteorites that would include exploring alternative interpretations where appropriate. Where the listed criteria are not fulfilled, practitioners of Pb-Pb geochronology of meteorites have the obligation to make clear the assumptions and/or shortcomings of each data set. Only through such an open dialogue regarding the true robustness of each age will we publish results that can be used confidently by the meteoritics community at large. Towards this end, we are working to erect an absolute Pb-Pb chronological framework for the early solar system based on FUN and normal CAIs, chondrules and differentiated bodies that will be evaluated by these criteria.

The role of ArxA in photosynthesis-linked arsenite oxidation by bacteria from extreme environments

ALISON CONRAD[1*], SHELLEY HOEFT[2], LAURENCE MILLER[2], RONALD OREMLAND[2], MICHAEL ROSEN[3], AND CHAD SALTIKOV[1]

[1]University of California, Santa Cruz, CA, USA, atconrad@ucsc.edu[+]
[2]United States Geological Survey, Menlo Park, CA, USA
[3]United States Geological Survey, Carson City, NV, USA

Background

The metabolic process of photosynthesis-linked arsenite oxidation (arsenophototrophy) has likely existed on earth since 2.7 - 3.5 billion years ago [1]. However, it is poorly understood and has only been identified in thermal springs on Paoha Island of Mono Lake, CA [2]. As this metabolism utilizes solar energy to convert the more toxic arsenite to the less toxic arsenate, it has implications for bioremediation. The arsenite oxidase ArxA is thought to be responsible for the oxidation of arsenite in arsenophototrophy. However, the first and only isolated arsenophototroph, *Ectothiorhodospira sp.* str. PHS-1, has not proven amenable to genetic manipulations. This makes genetic confirmation through gene disruption or deletion of the *arxA*-like gene in the organism impossible, leaving the hypothesis unconfirmed. The first aim of this work is to study the microbial ecology of anoxygenic arsenophototrophs in arsenic-rich environments other than Mono Lake and secondly, to isolate and develop an arsenophototroph which can serve as a genetic model for arsenophototrophy.

Materials

Water, sediment, microbial mat and tufa collected from Big Soda Lake (Churchill County, NV), Mono Lake and various hot springs in the Mammoth Lakes (CA) area were used for enrichment culturing and functional gene analyses.

Results

Currently *arxA*-specific primers have successfully amplified products from 15 out of 18 environmental samples, and all products so far cloned and sequenced show high homology to existing *arxA*-like sequences. Additionally, strains containing *arxA*-like sequences and capable of arsenite oxidation belonging to the genera *Ectothiorhodospira* and *Halomonas* have been isolated. One strain in particular, *Ectothiorhodospira* sp. str. BSL-9 is aerotolerant, grows well on plates, and is susceptible to common antibiotics, making it a potential model for arsenophototrophy.

Conclusions

This work demonstrates that ArxA is unlikely limited to the Mono Lake area and may be widespread in arsenic-rich environments. It is also a necessary stepping-stone in actualizing a genetic model for photosynthesis-linked arsenite oxidation.

[1] Oremland et al. (2009) *Geomicrobiology Journal* **26**, 522-536
[2] Kulp et al. (2008) *Science* **321**, 967-970

https://doi.org/10.1180/S0026461X00008434 Published online by Cambridge University Press

Highly depleted Colorado Plateau gypsum deposits attributed to multiple episodes of redox cycling

MARK E. CONRAD[1*], KENNETH H. WILLIAMS[1], JENNIFER L. DRUHAN[1,2] AND WAYNE W. LUKENS[1]

[1]Lawrence Berkeley National Laboratory, Berkeley, CA, USA, msconrad@lbl.gov (* presenting author)
[2]Earth and Planetary Science Department, University of California, Berkeley, CA, USA

Introduction

The Department of Energy's Old Rifle site is a former uranium mill site situated along a floodplain of the Colorado River in western Colorado. The aquifer underlying the site consists of 6-7 m of Quaternary alluvium overlying the Tertiary Wasatch Formation. Sulfate concentrations in Old Rifle groundwater are elevated (8-10 mM), with unusually low sulfur isotope ratios ($\delta^{34}S$ values from -6 to -10‰). The source of the low $\delta^{34}S$ sulfate in groundwater appears to be gypsum veins within the Wasatch Formation, which outcrops above the site and through which regional groundwater recharges the Old Rifle aquifer. Veins of gypsum sampled from the upper Wasatch have $\delta^{34}S$ values lower than any previously reported in the literature (as low as -56‰). The veins are associated with Fe-oxide minerals and visible iron staining and are in close proximity to fossilized plant material within the Wasatch sediments (Figure 1). The low $\delta^{34}S$ gypsum is inferred to result from oxidation of ^{34}S-depleted sulfide minerals that formed in reducing zones associated with organic matter. Subsequent oxidation of the isotopically light sulfides mobilized low $\delta^{34}S$ sulfate that precipitated as gypsum infillings within high permeability fractures. Modern analogs of such naturally reduced zones occur within the alluvial sediments at Old Rifle, which are characterized by lignitic organic carbon and framboidal pyrites having low $\delta^{34}S$ values (as low as -70‰). Associated with these pyrites are greatly elevated concentrations of uranium [1]. Oxidation of such reduced zones within the alluvium and Wasatch Formation could lead to mobilization of reduced metals, such as uranium, that may explain the high background concentrations of metals in the Rifle groundwater outside of the tailings-impacted area.

Figure 1: Petrified branch or root in upper Wasatch Formation replaced with quartz, Fe-oxides and gypsum ($\delta^{34}S$ = -55.4‰).

[1] Qafoku *et al.* (2009) *Environmental Science & Technology* **43**, 8528-8534.

Recycling of crust in Proterozoic convergent margins : evidences from Sm-Nd isotopes and trace elements of mafic-ultramafic plutonic rocks from the Grenville Province

MARC CONSTANTIN [1*], CHRISTOPHE HÉMOND[2], ANNE-A. SAPPIN[1], JEAN-F. MONTREUIL[1,3], RAPHAEL PIK[4],

[1]Dépt géologie et génie géologique, Université Laval, Québec, Canada, marc.constantin@ggl.ulaval.ca (* presenting author)
[2]UMR6538 Domaines Océaniques, IUEM, Brest, France
[3]INRS-ETE, Québec, Canada
[4]CRPG-CNRS, Vandoeuvre-Les-Nancy, France

Nearly 50 mafic and ultramafic rocks were sampled for a Sm-Nd isotopes study in 6 plutons coeval to the La Bostonnais complex, each <1 to 3 km^2 of surface and spread over 100 km within a north-south belt called the Portneuf-Mauricie Domain (PMD). Results show Nd T_{DM} ages that range from 1400 to 1970 Ma and $\varepsilon_{Nd}(t)$ mostly between +2.5 and +4.3. Trace element patterns of these 6 plutons normalized to the primitive mantle show strong negative Ta anomaly and moderate to strong negative Zr, Hf, and Ti anomalies. Two mafic lithologies within two plutons from the PMD (Lac Nadeau, Rochette West) with TIMS U-Pb zircon ages respectively of 1.396 and 1.386 Ga that are interpreted to represent crystallization ages [1]. A regression of 18 samples from the Nadeau and Lac-à-la-Vase plutons provide a Sm-Nd isochron age of 1423 ±28 Ma (MSWD=4), similar within error to the U-Pb ages. The Lac-à-la-Vase pluton is compatible with derivation from a near-depleted mantle reservoir whereas the other plutons suggest a mantle separation time of 100 to 400 millions years earlier than 1.39 Ga. Pyroxenites hosting the Lac Edouard Ni-Cu deposit show the lowest ε_{Nd} of the 6 PMD plutons with values between +0.85 and +2.6.

A second region of interest is the Renzy Terrane (RT), identified over an area covering at least 50 km^2, where sub-kilometric pyroxenites lenses have REE and HFSE ~1x to 10x primitive mantle contents with strong negative Ta anomaly and moderate to strong negative Zr, Hf (±Ti) anomalies. Coeval mafic gneisses have REE and HFSE ~5x to 50x primitive mantle contents and were divided in 3 distinct groups, although a majority have trace element signatures akin to subduction zone processes [2]. Both RT and PMD ultramafic rocks have 15-30 ppm Zr rendering them difficult to date by U-Pb zircon methods. A regression of 14 pyroxenites and 4 mafic gneisses samples from the RT provided a Sm-Nd isochron age of 1504 ±67 Ma (MSWD = 2.5) in agreement with U-Pb zircon ages of 1457 ±15 Ma obtained by ion microprobe on 3 different mafic to intermediate rocks. A Sm-Nd isochron including pyroxenites, mafic gneisses and felsic gneisses yields an age of 1508 ±47 Ma, and these rocks have a range of $\varepsilon_{Nd}(t)$ between +1.7 and +3.9, an average Nd T_{DM} age of 1.77 ±0.14 Ga (n=32) and therefore ~300 millions years older that their crystallization age.

Most of the trace element chemistry of the DMP and RT mafic and ultramafic rocks indicate that they probably originated from arc and back-arc magmatic activity. The RT was probably accreted to Laurentia as a thrust sheet over the Paleoproterozoic belt of the Grenville Province.

[1] Sappin et al. (2009) *Can. J. Earth Sci.* **46**, 331-353.
[2] Montreuil, Constantin (2010) *Prec. Res.* **181**, 150-166.

https://doi.org/10.1180/S0026461X00008434 Published online by Cambridge University Press

A composite speleothem paleoclimate record for the last 400 ka from Romania

SILVIU CONSTANTIN[1*]

[1]"Emil Racovita" Institute of Speleology, Bucharest, Romania, silviu.constantin@iser.ro

Paleoclimate studies based on speleothem records from Romania have seen a constant increase in the last 15 years. Hence, an increasing number of speleothem isotope records have become available form the karst regions of both SW and NW Romania. Here we review the available data and present a composite speleothem $\delta^{18}O$ record that spans roughly over the last 400,000 years. The record is based on several high resolution dated speleothems from the SW Carpathians and is correlated with coeval samples from the NW Carpathians. The record (Figure 1) shows a higher variability for the SW Carpathians when compared with the NW Carpathians. This is considered as a direct effect of the Mediterranean climate influence as opposed to the distal-NAO influence on the climate from the inner part of the Carpathian arch, i.e. the NW Romania. Probability density function graphs based on dated speleothems were constructed for both regions and they too show a much higher response during warming periods for regions located in the southern part of the Carpathians. The record is compared with known composite records from the Eastern Europe and Eastern Mediterranean and potential biasing factors when comparing other $\delta^{18}O$ records are discussed.

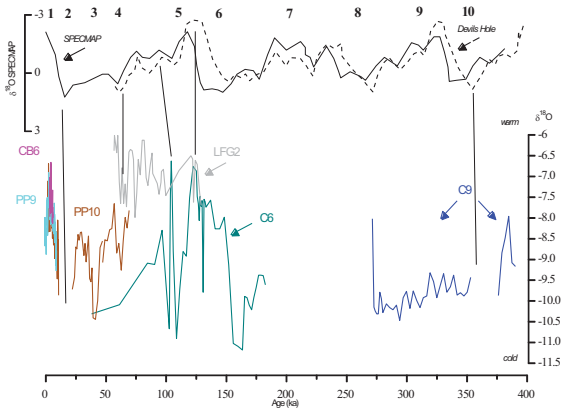

Figure 1: A cumulative speleothem record from Romania showing higher variance of the $\delta^{18}O$ values for the Mediterranean-influenced SW Romania when compared with the NW Romania.

Petrogenesis of recent trachytic eruptions from Sete Cidades volcano, São Miguel, Azores (Portugal)

E. CONTE[1]*, E. WIDOM[1] AND Z. FRANCA[2]

[1]Dept. of Geology & Environmental Earth Science, Miami University, Oxford, Ohio, USA, conteer@muohio.edu (*presenting author)

[2]Departamento de Geociências, Universidade dos Açores, Ponta Delgada, São Miguel, Açores, Portugal, zfranca@uac.pt

Sete Cidades has produced 12 intracaldera, trachytic eruptions (Sete A-L) within the last ~4-5 ka [1,2]. We have completed detailed petrographic, major and trace element, Sr, Nd and Pb isotope and U-series disequilibria studies of whole rock samples from the Sete A-L deposits to constrain petrogenetic processes, eruptive ages and repose intervals associated with the Sete Cidades magmatic system [3]. Major and trace element analyses were performed on a suite of 16 samples representing all of the deposits from Sete A-L. The data show limited major element variation (~63% SiO_2) but highly variable trace element abundances (e.g. >1.6-fold variations in Zr and ~4-fold variations in Sr). Trace element abundances show a complex relationship with stratigraphy that we interpret to reflect a 3-stage evolutionary process. Stage 1 (Sete A-B), characterized by an increase in Zr concentration with stratigraphic height, reflects evolution of a trachytic magma via 35% fractionation of the observed mineral assemblage including sanidine>biotite>clinopyroxene>Fe-Ti oxides>apatite. Stage 2 (Sete B-F) is characterized by decreasing Zr concentrations with stratigraphic height, suggesting injection of a less evolved trachytic magma into the Sete Cidades magma chamber. Stage 3 (Sete F-L) is recorded by an increase in Zr with stratigraphic height, and is consistent with 54% crystallization of the observed mineral assemblage. Sr isotopic variation in leached whole rock samples ($^{87}Sr/^{86}Sr$=0.70375-0.70439) further requires assimilation of hydrothermally altered syenite wall-rock [4,5]. Nd and Pb isotopic compositions are essentially invariant ($^{143}Nd/^{144}Nd$=0.51287; $^{206}Pb/^{204}Pb$=19.52-19.56) and within the range of local basalts, consistent with trachytic magma evolution from parental basalts derived from a single mantle source over the past ~4-5 ka. Six samples have also been analyzed for U-series disequilibria, and all are Th-enriched and Ra-depleted. With one exception, $^{238}U/^{232}Th$ and $^{230}Th/^{232}Th$ activity ratios are constant with ($^{238}U/^{232}Th$)≈0.88 and ($^{230}Th/^{232}Th$)≈0.96, similar to basalts from the Sete Cidades region, and consistent with the trachytes deriving from parental basalts that evolved rapidly (within ~10 ka) to produce the Sete A-L trachytic magmas. Present-day $^{226}Ra/^{230}Th$ activity ratios range from 0.32-0.75, consistent with recent and extensive sanidine fractionation during trachyte magma evolution, and further allowing constraints on the maximum eruptive ages. Preliminary data indicate a maximum eruptive age of 912 years B.P. for Sete B, which suggests that the recent recurrence interval of Sete Cidades may be only ~42 years, much shorter than the recurrence intervals of 200 and 1200 years at neighboring Furnas and Fogo volcanoes [6].

[1] Booth et al. (1978) *Roy. Soc. Lon.* **288**, 271-319. [2] Queiroz (1997) *Universidade dos Açores* **226p.** [3] Conte et al. (2010) *Geochim. Cosmochim. Ac.* **74**, A188. [4] Snyder et al. (2007) *Chem. Geo* **239,** 138-155. [5] Snyder et al. (2004) *J. Petrol.* **45**, 723-738. [6] Rowland-Smith (2007) *Miami University.*

https://doi.org/10.1180/S0026461X00008434 Published online by Cambridge University Press

Iron isotopes in the eastern North Atlantic

TIM M. CONWAY[1*], SETH G. JOHN[1] AND ANGELA D. ROSENBERG[1]

[1]Dept. Earth and Ocean Sciences, University of South Carolina, USA
[*]Presenting author (correspondence tconway@geol.sc.edu)

Iron (Fe) is a crucial nutrient for phytoplankton and the marine food chain, and low dissolved Fe concentrations limit growth in many regions of the oceans. Knowledge of the sources, sinks and cycling of Fe in the ocean is vital to our understanding of marine biogeochemical cycles; however, concentration measurements alone are often unable to discriminate between different fluxes and processes. Fe isotope ratios address this limitation, and provide us with the unique opportunity to discriminate between biological utilization of Fe, Fe from continental shelf sediments or aerosols, and Fe from hydrothermal activity. Fe isotope values also allow investigation of internal cycling of Fe, and provide an insight into the relative importance of kinetic and equilibrium controls on dissolved Fe concentrations in the oceans.

This study presents new methodology for the simultaneous extraction of dissolved Fe, Cd and Zn from seawater using a chelating resin, followed by ion-exchange column purification and isotopic analysis by Neptune multi-collector ICP-MS. This method has been developed in order to make determinations of multiple isotope systems in the same sample as part of the GEOTRACES program, and generates a lower blank than previous methods [1].

We present the first Fe isotope (δ^{56}Fe) depth profiles from the GEOTRACES A10 (North Atlantic) Transect. This work focuses on A10 stations along 17.4° N (North Africa to Cape Verde), where multiple sources of dissolved Fe, a pronounced oxygen minimum zone at depth, and internal cycling of Fe complicate the dissolved Fe picture. δ^{56}Fe values indicate surface input of isotopically heavy Fe, biological utilisation at the surface and input of isotopically light Fe from the sediments. Relatively little variation in δ^{56}Fe through the intermediate ocean adds support to the hypothesis that rapid exchange between the dissolved and particulate Fe pools may be important in controlling dissolved Fe concentrations and δ^{56}Fe in the North Atlantic.

[1] Seth G. John and Jess. F. Adkins, 2010. Marine Chemistry 116, 65-76.

Mantle thermal anomalies associated with large igneous provinces

LAURENCE A. COOGAN,[1*], ANDREW D. SAUNDERS[2] & ROBERT N. WILSON[2]

[1]School of Earth and Ocean Science, University of Victoria, Victoria, Canada, lacoogan@uvic.ca
[2]Department of Geology, University of Leicester, Leicester, LE1 7RH, UK, ads@le.ac.uk, rnw@le.ac.uk

The classical mantle plume model involves heat transport across the core-mantle boundary, heating the lowermost mantle, leading to a thermally buoyant mantle upwelling; melting of the upwelling material in the upper-mantle can generate large volumes of mantle-derived melt in geological short time periods such as large igneous provinces (LIPs). If correct, this is of fundamental importance for the thermal evolution of our planet. A key prediction of the thermal plume model is that some melts generated by the plume should show evidence of having been generated from mantle with a higher potential temperature than the ambient upper mantle.

Testing the 'hot mantle' prediction has proved controversial. Olivine-melt thermometry has been the most popular approach but has been used to argue for both large and negligible temperature anomalies in the mantle in regions of intraplate volcanism [e.g. 1,2]. This approach invariably involves the back-calculation of an observed lava composition, via olivine addition, to a melt composition thought to be in equilibrium with an observed primitive olivine composition. Since the primitive olivine and its host basalt are not in equilibrium, it is unclear if *any* form of recalculation will produce a melt composition that ever existed. In particular, because Mg-Fe diffusion in olivine is rapid at high-temperatures [3], primitive olivine are unlikely to simply be 'early crystallization products' from the parent to the host melt. Differentiation to produce an evolved residual magma occurs much more slowly than diffusive Mg-Fe exchange will change the olivine composition.

In an attempt to overcome these problems we have applied the Al-in-olivine thermometer [4] to primitive olivine-spinel pairs from several LIPs as well as primitive MORB. This thermometer is based on the exchange of Al between olivine and spinel and requires no back-calculation of initial compositions. Also, as Al diffusion in olivine is much slower than Mg-Fe diffusion this thermometer has a better chance of preserving the temperature of initial crystal growth. However, the thermometer can only record the temperature at co-saturation of these two phases and will not (directly) recover mantle temperatures. Application to primitive MORB from several locations, containing primitive olivine (Fo up to 91.3), gives maximum olivine-spinel co-precipitation temperatures of 1300°C. Applying the same approach to LIPs (N. Atlantic igneous province, Gorgona, Madagascar) gives higher temperatures in all locations of up to 1450°C. Relative temperature differences between MORBs and LIPs suggest that LIPs are generated by melting hotter than average mantle. The absolute temperatures for MORB are consistent with the thickness of oceanic crust.

[1] Putirka K.D., et al. (2007) *Chemical Geology* **241**, 177-206. [2] Falloon T.F., et al. (2007) *Chemical Geology* **241**, 207-233. [3] Dohmen R., et al. (2007) *Physics and Chemistry of Minerals* **34**, 389-407. [4] Wan Z., et al. (2008) *American Mineralogist* **93**, 1142-1147.

https://doi.org/10.1180/S0026461X00008434 Published online by Cambridge University Press

PLIOCENE EAST ANTARCTIC ICE SHEET INSTABILITY

C. COOK[1]*, T. VAN DE FLIERDT[1], T. WILLIAMS[2], S. HEMMING[2], E. L. PIERCE[2] AND IODP EXPEDITION 318 SCEINCE PARTY

[1]Imperial College London, London, UK, SW7 2AZ (*correspondance: c.cook09@imperial.ac.uk)

[2]Lamont-Doherty Earth Observatory, Palisades, NY 10964-1000 USA

Warm climatic intervals during the Pliocene Epoch (5.33-2.58 Ma) are apt analogues with which to compare future climate scenarios, but there are currently no direct constraints on the dynamics of the East Antarctic Ice Sheet (EAIS) in potentially vulnerable low-lying regions during these times. Analyses of the isotopic provenance of multiple detrital marine sediment components can offer novel insights into the spatial and temporal response of the EAIS to climatic change, on both glacial-interglacial and longer-term timescales.

Here we present results of neodymium and strontium isotopic analyses of clay and silt sediment fractions (<63um), and argon isotope ages of individual hornblende grains from ice-rafted detritus (IRD) (>150um), from ODP Site 1165 (64˚22-77S, 67˚13-14E), Prydz Bay, and IODP Site U1361 (64˚24-57S, 143˚53-19E), Adelie Land. Both sites are ideally located to receive terrigenous sediments sourced from the Wilkes and Aurora Subglacial Basins, where large areas of the EAIS lie below sea level in direct contact with the Southern Ocean.

Pliocene clay and silt sediments from IODP U1361 reveal two distinct ε_{Nd} and $^{87}Sr/^{86}Sr$ endmembers – the first matches Early Paleozoic terranes found to the east (ε_{Nd}:- -11 to -16 and $^{87}Sr/^{86}Sr$ values of 0.721 to 0.730), and the second displays a mixed signature between these same terranes and the Jurassic-Triassic Ferrar Large Igneous Province (FLIP) (ε_{Nd}: -4 to -7; $^{87}Sr/^{86}Sr$: 0.712 to 0.719). Sediments characterised as the latter endmember are consistently found during high productivity (warm) intervals as revealed by physical property and bulk geochemistry measurements in U1361, at 4.8-4.6, 4.3-4.2 and 4.05-3.9 Ma. These time intervals additionally appear to correspond to maxima in modelled solar insolation. In fact, FLIP strata have been inferred within the Wilkes Subglacial Basin by aero-geophysical surveys as far as 74.3°S, suggesting this area may be the most likely source for the endmember approaching FLIP composition identified in U1361, and implies that the Wilkes Subglacial Basin may be a source of EAIS destabilisation during warm intervals in the Pliocene.

Late Pliocene sediments (3.3-2.8 Ma) from ODP Site 1165 display an increase in IRD hornblende $^{40}Ar/^{39}Ar$ ages of 1100-1300 Ma during interglacial intervals. This signature has not been identified on-land proximal to the study site, but matches very well hornblende argon isotope ages in modern marine sediments offshore of the Aurora Subglacial Basin, some 2000 km away from Site 1165. A Wilkes Land IRD provenance signal is positively correlated to detrital $^{87}Sr/^{86}Sr$ and εNd signatures in the <63um fractions, implying that ice sheet destabilisation of the Aurora Subglacial Basin played an important control on bulk sediment composition in the Prydz Bay area in the Late Pliocene.

Overall, the radiogenic isotope compositions of multiple detrital marine sediment components at two locations in the Southern Ocean suggest significant destabilisation events of the EAIS in the vicinity of the Wilkes and Aurora Subglacial Basins in response to Pliocene climatic warmth, with significant implications for future sea level estimates.

W isotopic composition of IVB iron meteorites

DAVID L. COOK[1*], THOMAS S. KRUIJER[1,2], THORSTEN KLEINE[1]

[1] Institut f r Planetologie, Westf lische Wilhelms-Universit t, M nster, Germany, d.cook@uni-muenster.de (* presenting author)

[2] Institut of Geochemistry and Petrology, ETH, Z rich, Switzerland

Introduction

The investigation of W isotope anomalies in meteorites is of interest because of the former presence of the short-lived isotope ^{182}Hf, which decays to ^{182}W. Thus, variations in ^{182}W can be used to infer timescales of early solar system processes [e.g., 1] However, the application of Hf-W chronometry relies on the assumption that W isotopes were homogeneously distributed in the solar nebula. This assumption appears to be valid for most meteoritic samples, but small deficits in s-process W isotopes have been observed in group IVB irons [2] and CAIs [3]. More recently, excesses in ^{180}W have been measured in several magmatic iron groups [4]. These data seem to imply heterogeneity of W isotopes in the early nebula, but these results have been questioned [5]. We report new isotopic measurements for several IVB irons to examine the extent of nucleosynthetic W isotope anomalies in this group.

Samples and Analytical Methods

We analyzed three IVB irons, and we processed two aliquots of the NIST W solution standard (SRM 3163) and one aliquot of a NIST Fe-Ni steel (SRM 361) using our chemical separation protocol for W. Isotopic measurements were made with a ThermoScientific Neptune Plus MC-ICPMS in low resolution mode. Signal intensities for both ^{180}W and ^{178}Hf were measured using 10^{12} Ohm resistors. The interference correction on ^{180}W from ^{180}Hf was tested by analyzing several aliquots of SRM 3163 doped with Hf.

Results and Discussion

All three of the NIST samples of terrestrial W have $\varepsilon^{180}W$ values within uncertainty of zero. These results demonstrate the accuracy of the method and do not suggest the presence of analytical artefacts on the W masses in low-resolution mode, which was recently suggested [5] to explain a previous report [4] of ^{180}W excesses in magmatic iron meteorites. Furhermore, the results for SRM 3163 doped with Hf show that the interference correction on ^{180}W is accurate for the range of Hf/W ratios of the samples. The $\varepsilon^{180}W$ values for all three IVB irons agree within uncertainty; the data hint at a slight $\varepsilon^{180}W$ excess, but this excess is not unambiguously resolvable at the current level of precision. All three IVBs exhibit small $\varepsilon^{184}W$ deficits, consistent with previous results [2]. The $\varepsilon^{182}W$ values of all three IVBs are below the CAI initial [3], indicating neutron-capture induced shifts in the W isotope abundances caused by cosmic rays. This process may also lower $\varepsilon^{180}W$ values, but the magnitude of the effect is currently unknown. Efforts are underway to improve the precision of the measurements as well to perform analysis of additional samples.

[1] Kleine et al. (2009) GCA 73, 5150-5188. [2] Qin et al. (2008) ApJ 674, 1234-1241. [3] Burkhardt et al. (2008) GCA 72, 6177-6197. [4] Schultz & M nker (2010) 73rd Met. Soc. #5116. [5] Holst, Paton & Bizzarro (2011) Workshop on Formation of the First Solids in the Solar System #9065.

https://doi.org/10.1180/S0026461X00008434 Published online by Cambridge University Press

Hg deposition in the tropics during the Younger Dryas

COLIN A. COOKE[1*] AND NATHAN D. STANSELL[2]

[1]Yale University, Department of Geology & Geophysics, New Haven, CT, 06511, USA, colin.cooke@yale.edu (* presenting author)

[2]The Ohio State University, Byrd Polar Research Center, Columbus, OH, 43210, USA

Mercury (Hg) loadings to even the most remote aquatic ecosystems have increased by 3-fold or greater since the 20th century, greatly accelerating human exposure to this toxic trace metal. The rise in environmental Hg has been documented from a range of natural archives, including ice cores, snow deposits, peat cores, and (most frequently) lake sediment cores. A majority of these study sites are from to high- and mid-latitude locations; considerably less is known about trends in Hg deposition from low latitudes. In addition, few studies have investigated long-term variability in natural (i.e., pre-industrial) Hg deposition rates, despite evidence for changes in Hg cycling associated with environmental change. Long-term sedimentary archives of past climatic and environmental variability therefore offer a unique opportunity to asses how natural processes serve to influence natural Hg cycling in the environment. Here, we present new Hg geochemical data from a low-latitude lacustrine sediment core collected from Laguna de los Anteojos, a high-altitude (3920 m a.s.l.) cirque lake located in the Mérida Andes of Venezuela. This ^{14}C-dated sediment core spans 14,680 to 9,350 years before present (BP), and includes multi-proxy evidence for large paleoclimatic and paleoecological shifts associated with the Bølling-Allerød, Older Dryas, and Younger Dryas climatic intervals [1].

There are two clear end-member sediment facies within the Anteojos core: clastic-rich sediments high in titanium (Ti) and low in organic matter (OM), and the opposite. Sediment [Hg] spans an order of magnitude (12-124 ng g^{-1}), and is, to some degree, associated with OM (r^2=0.38). [Hg] and Hg flux are lowest during the Younger Dryas, which was not only cold but also arid. Southerly migration of the intertropical convergence zone (ITCZ) during the initial stages of the Younger Dryas chronozone [2] likely decreased regional precipitation and thus Hg deposition to the lake. The return of the ITCZ and a warmer and wetter climate ~12,200 BP appears to have initiated a rapid increase in [Hg] within Anteojos sediment, as both [Hg] and Hg flux rise by >4-fold in less than a century. Alternatively, the demise of regional snowfields and glaciers, which expanded during the Younger Dryas, may have released legacy Hg into the lake. The Anteojos sediment record presented here offers a well-dated and multi-proxy archive of past environmental change through a period of rapid climatic transitions.

[1] Stansell, *et al.* (2010) *EPSL* **293**, 154-163. [2] Haug, *et al.* (2001) *Science* **293**, 1304-1308.

Isotopic evidence for preindustrial mercury emissions to the atmosphere

COLIN A. COOKE[1*], HOLGER HINTELMANN[2], HARALD BIESTER[3], AND JAY J. AGUE[1]

[1]Yale University, Department of Geology & Geophysics, New Haven, CT, USA, colin.cooke@yale.edu (* presenting author)

[2]Trent University, Department of Chemistry, Peterborough, ON, Canada

[2]Technische Universität Braunschweig, Institut für Umweltgeologie, Pockelsstraße 3, 38106 Braunschweig, Germany

Lake sediment cores from the South American Andes record anthropogenic Hg emissions to the atmosphere extending as far back as 1400 BC [1]. Early Hg pollution resulted from a range of activities including cinnabar (HgS) mining [1], Hg amalgamation [2], and the smelting of non-ferrous ores [3]. While Hg may spend centuries or even millennia circulating in the environment, it remains unclear just how far early these Hg emissions were transported and to what degree they influenced the global biogeochemical cycle of Hg. Here, we present new Hg stable isotopic data from two lake sediment cores that offer insight into the magnitude and geographic extent of early anthropogenic Hg emissions. One of the cores is from the Peruvian Andes, and records clear increases in Hg associated with Andean cinnabar mining and Hg amalgamation [1]. The other sediment core is from a crater lake on San Cristobal Island (Galápagos archipelago), and thus is far removed Hg emission sources, both past and present.

Concentrations of Hg in both sediment cores increase above stable background values after ~1500 AD, signaling the onset of intensive Hg emissions and subsequent deposition resulting from Colonial cinnabar mining and Hg amalgamation. In addition, both mass dependent (MDF; δ^{202}Hg) and mass-independent fractionation (MIF; Δ^{201}Hg) of sedimentary Hg is evident in both sediment cores (Fig. 1). Pre-pollution sediments (uncontaminated by even the earliest metallurgical activities) consistently record negative MDF (-2‰) and MIF (-0.2‰). However, early increases in Hg concentration are matched by a positive shift in sediment δ^{202}Hg of nearly 2‰; Δ^{201}Hg values, in contrast, remain stable across this transition. The same trends are present in both sediment cores, suggesting they record hemispheric scale processes. Moreover, the Hg stable isotopic signature of preindustrial Hg pollution overlaps with new determinations of MDF and MIF in Peruvian cinnabar, which strongly suggests that early Hg emissions can be isotopically linked to their primary mineralogical sources.

The rise of global Hg pollution during the 20th century is also recorded in both sediment cores. However, while MDF values remain constant across the preindustrial-industrial transition, MIF values shift from negative to positive. This suggests either a difference in the MIF signature of preindustrial and industrial Hg sources, or a change in the direction of photochemically-induced MIF since ~1900 AD. Collectively, these results suggest Hg stable isotopic ratios can offer insight into Hg emissions associated with both preindustrial and industrial anthropogenic activities.

[1] Cooke, *et al.* (2009) *Proc. Nat. Aca. Sci.* **106**, 8830-8834. [2] Cooke, *et al.* (2009) *Geology* **37**, 1019-1022. [3] Cooke *et al.* (2011) *Ambio* **40**, 18-25.

https://doi.org/10.1180/S0026461X00008434 Published online by Cambridge University Press

Insights into magmatic processes from combined crystal age and compositional data

KARI M. COOPER[1]*, GARY R. EPPICH[2], ERIK W. KLEMETTI[3], PHILIPP RUPRECHT[4], MARK E. STELTEN[1]

[1]Department of Geology, University of California Davis, Davis, CA, USA, kmcooper@ucdavis.edu (*presenting author)
[2]Lawrence Livermore National Laboratory, Livermore, CA, USA, eppich1@llnl.gov
[3]Department of Geosciences, Denison University, Granville, OH, USA, klemettie@denison.edu
[4]Lamont-Doherty Earth Observatory of Columbia University, Palisades, NY, USA, ruprecht@ldeo.columbia.edu

Many, if not most, crystals in volcanic rocks preserve chemical records of subvolcanic processes (such as growth in multiple magmas and storage in a mush or plutonic body) that extend well beyond the life time of the liquids that brought them to the surface. Uranium-series disequilibria represent one of few methods of measuring absolute crystal ages in young volcanic systems, thereby placing chemical, textural, and/or isotopic data in a temporal framework. We present here a synthesis of our recent work [1-5] combining U-series crystal ages with other types of information, which provides new insights into magmatic processes.

Intermediate magmas erupted at Volcán Quizapu, Chile, and Mt. Hood, USA, are the result of mixing of silicic and mafic magmas. We used U-series ages of plagioclase in combination with crystal size distributions, trace-element zoning, and diffusion modeling to constrain both the pre-mixing and post-mixing storage times of crystals [3-5]. Plagioclase in both systems have U-series ages of ka to tens of ka, representing the total average storage time of the crystals. In contrast, diffusion modeling permits a maximum of days to weeks of crystal storage in the host magmas post-mixing. These data suggest that crystals remain in the 'active' (i.e., eruptible) part of the reservoir for thousands of years yet eruption follows quickly on mixing.

Studies of crystals in rhyolitic systems of different volumes may provide insights into processes that are common in silicic melt generation yet may be obscured in larger systems. We have analyzed zircon and plagioclase in three rhyolitic systems ranging from small (South Sister, USA [2]) to intermediate (Okataina Caldera Complex, New Zealand [1]) to large (Yellowstone, USA). Combinations of age data with trace-element and Hf isotopic compositions show the coeval presence of chemically-distinct magma or mush bodies in all three systems; only Yellowstone shows evidence for effective homogenization of the liquid fraction of the magma prior to eruption. If these results generally hold for other systems, it would imply that (only) the largest silicic eruptions are preceded by accumulation of a significant body of liquid that remains in the subsurface long enough to homogenize. Such bodies would likely be detectable by seismic imaging prior to eruption.

[1] Klemetti et al. (2011) *EPSL* **305,** 185-194. [2] Stelten and Cooper (2012) *EPSL* **313-314**, 1-11. [3] Eppich et al. (2012) *EPSL* **317-318**, 319-330. [4] Ruprecht and Cooper (in press) *J. Petrology*. [5] Ruprecht et al. (in press) *J. Petrology*.

Discrimation between biotic and abiotic rates of stabilization of Se(VI) in soil

F.COPPIN[1*], N. LOFFREDO[1], S. MOUNIER[2],Y. THIRY[3] AND L. GARCIA-SANCHEZ[1]

[1] IRSN, PRP-ENV/SERIS/L2BT, Saint paul lez Durance, France, frederic.coppin@irsn.fr (* presenting author)
[2] Universitée du Sud Toulon Var, laboratoire PROTEE-CAPTE, La garde, France
[3] ANDRA, R&D Division, Chatenay Malabry, France

Selenium (Se) is an essential micronutrient for organisms, with a narrow range of concentrations lying between deficiency and toxicity. ^{79}Se is a long-lived fission product generated by the nuclear industry and in the context of risks assessment studies from nuclear waste repository, it is one of the main potential contributor to the dose to population [1]. Selenium is present in the soil under different oxidation states (+VI; +IV; 0 and–II), that controlled its behaviour. Selenate (Se(VI)) which may preferentially form highly mobile complexes on the surface of numerous solids, is considered to be potentially the most mobile form in the environment[2]. However, biotic or abiotic reduction processes could transform selenate into lower Se oxidation state promoting its stabilization in soil [3], [4].

To discriminate between the impacts of biotic and abiotic processes on Se(VI) stabilization in soils, stirred flow through reactor (SFTR) experiments were realised. A regenerated cellulose dialysis tubing containing a sterilised (abiotic modality) or a raw (biotic modality) silty clay loam soil suspension was placed in SFTR containing a $3x10^{-3}$ mol.L^{-1} NaCl solution. A 10^{-8} mol.L^{-1} radiolabelled ^{75}Se(VI) solution was injected in SFTR during 3 to 20 days (flow rate between 2 to 30 ml.h^{-1}) and then flushed by a NaCl solution (6 days). Se interactions with soil were followed by analyses on the outlet solution.

The results obtained showed that a simple equilibrium model based on reversible exchange reactions can not be applied to fit the experimental data as, for both biotic and abiotic conditions a fraction of Se(VI) was stabilised in soil. The use of a simple kinetic model that involves a fraction of selenate sorbed on the solid surface sites accessible for water lixiviation, and another fraction stabilized resulting in biotic or abiotic reduction was shown to better describe experimental results. (Figure 1).

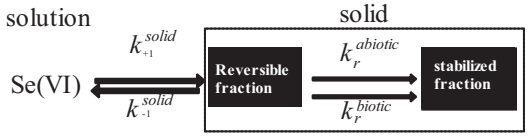

Figure 1 : Kinetic model describing Se(VI) stabilisation in soil under biotic or abiotic conditions

The kinetic parameters of the model were adjusted in two steps : (1) on abiotic experiments for k_{+1}^{solid}, k_{-1}^{solid}, $k_r^{abiotic}$ (with $k_r^{biotic} = 0$) and (2) on the biotic conditions, for k_r^{biotic},by considering that abiotic parameters remain constant.

[1] Aguerre & Frechou (2006) *Talanta* **69**, 565-571. [2] Séby *et al.* (1998) *Analusis* **26**, 193-198. [3] Siddique *et al.* (2006) *Bioresource. Technol.* **97**, 1041-1049. [4] Olegario *et al.* (2010) *J. Nanopart. Res.* **12**, 2057-2068.

https://doi.org/10.1180/S0026461X00008434 Published online by Cambridge University Press

Reducing the uncertainty of spent nuclear fuel dissoluon: an investigation of UO_2 analogue CeO_2

CLAIRE L. CORKHILL[1*], DANIEL J. BAILEY [1], MARTIN C. STENNETT[1], AND NEIL C. HYATT[1]

[1]The Immobilisation Science Laboratory, Department of Materials Science and Engineering, The University of Sheffield, UK (* c.corkhill@sheffield.ac.uk)

In the safety case for the geological disposal of nuclear waste, the release of radioactivity from the repository is controlled by the dissolution of the spent fuel in groundwater. Therefore, to assess the performance of the repository after infiltration of groundwater and contact with spent fuel, the dissolution characteristics must be determined. In spent nuclear fuel, high energy sites occur at grain boundaries and within the material as naturally occurring surface defects. Current studies of spent nuclear fuel dissolution have not considered the effect of high energy surface sites within the material structure.

In this investigation, CeO_2 analogues, which approximate as closely as possible the characteristics of fuel-grade UO_2, were characterised after dissolution under a wide range of conditions. Samples were powdered to three different size fractions to investigate high energy surface site density on dissolution rates, while monolith samples were monitored for development of surface defects as pores, steps and dissolution pits. These samples were subject to a range of aggressive and environmentally relevant alteration media with different solubility controls, including 2M HCl, a simplified groundwater of dilute NaCl (10mM) buffered to pH 7.5 by $NaHCO_3$ (2mM) and 0.01M NaOH, and reacted at a range of temperatures from 90°C to 150°C. Dissolution was monitored through analysis of the coexisting aqueous solution, and morphological changes at the surface using atomic force microscopy, confocal profilometry and scanning electron microscopy. Dissolution rates were found to be greater in high pH solutions, and at higher temperatures, and greatest for samples with the highest reactive surface area. Chemical analysis of additional monolith samples reacted in ^{18}O-enriched aqueous solutions was conducted using TOF-SIMS. The data demonstrate re-precipitation of Ce-hydroxide species on the sample surface, which may form a passivating barrier to dissolution.

Nanometer scale characterization of fossil bacteria in an Eocene phoshorite sample

JULIE COSMIDIS[1*], KARIM BENZERARA[2], IMÈNE ESTÈVE[3] AND EMMANUEL GHEERBRANT[4]

[1]IMPMC & IPGP, Paris, France, Julie.Cosmidis@impmc.upmc.fr (* presenting author)
[2]IMPMC, CNRS & Univ. PMC, Paris, France, Karim.Benzerara@impmc.upmc.fr
[3]IMPMC, Paris, France, Imene.Esteve@impmc.upmc.fr
[4]CR2P, CNRS & MNHN, Paris, France, Gheerbra@mnhn.fr

A great number of microstructures described as fossilized microbial bodies have been described in phosphorites of all ages in the past years (e.g., [1]). Most of these putative fossils have been identified based on their morphology (sizes and shapes) using SEM observations only. However, this approach might be misleading since micrometer-sized calcium phosphate globules ressembling bacteria can also be produced by abiotic processes, as we will show here.

Here, we will present the study of an Eocene phosphatic coprolite from Morocco containing numerous purported bacterial fossils. We characterized the mineralogical structure and chemical composition of these objects down to the nano-meter scale using a combination of FIB-SEM, TEM dans STXM .

The fossils are composed exclusively of francolite ($Ca_{10}(PO_4,CO_3)_6(F,OH)_2$). However, some variations in electron density outlining these fossils could be evidenced. Based on TEM and STXM analyses, we interpret them as variations of mineralogical texture and chemical composition, resulting from the precipitation of francolite in the cell wall of the bacteria during their fossilization.

We compare these fossils with modern bacteria calcified in the laboratory on the one hand, and with bacteria-free and enzymatically-produced hydroxyapatite globules on the other hand. We will show that although they present great morphological similaritires at the SEM scale (Figure 1), theses different objects can be discriminated unambigously at greater spatial resolution.

This study provides new signatures for identifying microbial activity in past and present phosphorites and illustrates the importance of using high resolution analytical tools for the search of biosignatures in terrestrial and extraterrestrial rocks.

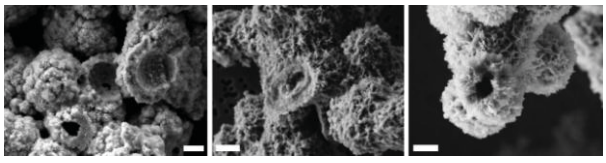

Figure 1: SEM images of the fossils in the Eocene phosphorite (left), bacteria calcified in the laboratory (middle) and bacteria-free, enzymatically-precipitated hydroxyapatite globules (rigth). Scale bars: 1 µm.

[1] Zanin & Zamirailova (2011) *Russian Geology and Geophysics* **52**, 1134-1139.

https://doi.org/10.1180/S0026461X00008434 Published online by Cambridge University Press

Total Mercury and Methylmercury Accumulation in Aquatic Sediments

DANIEL COSSA[1,*], CÉDRIC GARNIER[2], CHARLES GOBEIL[3], FRANCOISE ELBAZ-POULICHET[4], NEVENKA MIKAC[5], NATHALIE PATEL-SORRENTINO[2], AND ERWAN TESSIER[2]

[1]Ifremer, BP 330, 83507 La Seyne-sur-Mer, France, dcossa@ifremer.fr (* presenting author)
[2]Laboratoire PROTEE, Université du Sud Toulon-Var, BP 20132, 83957 La Garde, France, cedric.garnier@univ-tln.fr
[3]INRS-ETE, Université du Québec, 490 de la Couronne, Québec (Qué.), Canada G1K9A9, gobeilch@ete.inrs.ca
[4]Laboratoire Hydrosciences, Université de Montpellier, 34095 Montpellier cedex 5, France, felbaz@univ-montp2.fr
[5]Center for Marine and Environmental Research, Ruđer Bošković Institute, PO Box 1016, 10000 Zagreb, Croatia, mikac@irb.hr

Methylation of Hg in sediments is a crucial process that controls Hg accumulation in biota. Several studies have reported a significant positive correlation between methylmercury (MeHg) and total Hg in aquatic sediments. However, these relationships differ among studied systems due to geochemical and biological controls. We show here, by compilling published and unpublished HgT-MeHg couples from riverine, estuarine and marine sediments covering various environmental conditions, from deep pristine abyssal to heavily contaminated river sediments, that a general relationship relies the two parameters. The net methylation, i.e. methylation/demethylation equilibrium, governs the position of the points within the drawing. This global equation suggests that most of the variability in the MeHg concentration is explained by the inorganic Hg availability, a proxy of which is HgT in the sediment. The position of the points on both sides of the equation line are discussed in terms of redox and sedimentation conditions, with surface sediment points above the line.

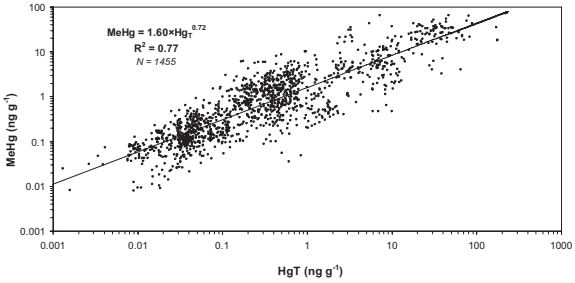

Figure 1: The unpublished results are from abyssal plains of the Arctic Ocean and the Mediterranean Sea, and continental shelf and bays of the Mediterranean Sea. Published results are from references 1 to 15.

[1] Abi-Ghanem et al (2011) *Arch Env Cont Tox* **60**,394-405;[2] Benoit et al (1998) *Biogeochem* **40**,249–265;[3] Benoit et al (2002) ACS Symp. Ser. 835, Chap 19, Y. Cai & O. Bairds eds., 262-297;[4] Drott et al (2008) *ES&T* **42**,153-158;[5] Guedron et al (2012) *Mar Chem* **130**,1-11;[6] Hammerschmidt et al (2004) *ES&T* **38**,1487-1495;[7] Hammerschmidt et al (2006) *GCA* **70**,918-930;[8] Hintelmann et al (1995) *STOTEN* **166**,l-10;[9] Hollweg et al (2010) *L&O* **55**,2703–2722;[10] Kwokal et al (2002) *Mar Poll Bull* **44**,1152–1169;[11] Mikac et al (1999) *Appl Org Chem* **13**,715-725;[12] Muhaya et al (1997) *WASP* **94**,109–123;[13] Muresan et al (2007) *Est Ctsl Shelf Sci* **72**,472-84;[14] Seunghee et al (2007) *Env Tox Chem* **26**,655-663;[15] Sunderland et al (2006) *Mar Chem* **102**,111-123.

Time scales of magmatic processes and volcanic unrest at caldera systems

FIDEL COSTA[1*], TIM DRUITT[2], ETIENNE DELOULE[3], MICHAEL DUNGAN[4], AND BRUNO SCAILLET[5]

[1]Earth Observatory of Singapore, Nanyang Technological University, Singapore, fcosta@ntu.edu.sg
[2]Blaise Pascal University-CNRS, Clermont-Ferrand, France, T.Druitt@opgc.univ-bpclermont-Ferrand.fr
[3]CRPG-CNRS, Vandoevre Les Nancy, France, deloule@crpg.cnrs-nancy.fr
[4]Departement de Mineralogie, Universite de Geneve, Switzerland, Michael.Dungan@unige.ch
[5]ISTO-CNRS, Universite d'Orleans, Orleans, France, bscaille@cnrs-orleans.fr

Calderas are capable of producing the largest and most explosive eruptions on Earth. The type of unrest in many caldera systems consists of long periods (years or decades) of deformation and earthquake activity (e.g. Campi Flegrei - Italy, Yellowstone or Long Valley – USA); however not all periods of unrest culminate in a volcanic eruption and not all eruptions are related to a caldera collapse. Despite the importance of properly interpreting the caldera unrest signals as magmatic proceses, there are few historical caldera eruptions that have been well monitored. We have taken a complementary approach to understanding the dynamics of magmatic processes at calderas by studying crystal zoning styles from the Minoan eruption of Santorini. Modeling the zoning patterns of the crystals can provide the times involved in destabilization of the magmatic system, and allows first order comparisons with the time scales of unrest signals. We investigated more than 300 plagioclase crystals with the electron microscope. A subset of these were investigated with the electron microprobe, and from these the trace element zoning of six crystals were measured by SIMS.

We distinguished two main types of plagioclase; a dominant one with cores at about An $_{43\text{-}58}$ and another, very rare, type with cores at An$_{30\text{-}36}$. Both types have similar rims at about An $_{36\text{-}43}$, and also rare high An cores (58-88). We think that these crystals record at least two mixing events. A first involved a basaltic-andesitic magma with an dacitic one at relatively deep levels, and later on these two magmas mixed with a rhyolitic magma located much closer to the surface. We have modeled the Mg and Sr zoning profiles across the different zones of the crystals using a diffusion model. We find two time scales associated with the different mixing events. A few decades occurred since the first and deeper mixing event and eruption, whereas the last transfer of the mixed dacite into the shallow rhyolite only occurred a few months prior to eruption. Mass balance constraints indicate that the dacitic magma that intruded in the upper reservoir accounted for at least 15 % of the total hybrid magma erupted, or about 5-9 km^3 of replenishment. The two time scales we have found are analogous with the three decades of deformation and seismic unrest that occurred at Rabaul caldera during 1973-1994, and which culminated in eruption in 1994 after an increased seismicity and deformation only about 5 months before eruption.

https://doi.org/10.1180/S0026461X00008434 Published online by Cambridge University Press

Monazite petrochronology by laser ablation split stream inductively coupled plasma mass spectrometry (LASS-ICPMS)

JOHN M. COTTLE[1*], ANDREW KYLANDER-CLARK[1] AND BRADLEY R. HACKER[1]

[1] Department of Earth Science, University of California Santa Barbara, CA 93106-9630, USA, cottle@geol.ucsb.edu (* presenting author)

Because monazite readily incorporates actinide and lanthanide elements and is reactive across a broad range of pressure, temperature, and fluid conditions, it is an ideal recorder of the nature and rates of a wide variety of diagenetic, metamorphic, magmatic and fluid-flow processes. It is common for monazite to preserve multiple episodes of growth, dissolution and re-precipitation within distinct intra-crystal compositional domains that are typically at, or below, the tens of micron scale. Development of measurement protocols to obtain age and petrologic information at high spatial resolution is therefore crucial to advancing monazite petrochronology.

This contribution details a new analytical configuration that enables simultaneous collection of both isotope and trace-element data. The laser ablation split stream inductively coupled plasma mass spectrometry (LASS-ICPMS) system at the University of California, Santa Barbara, uses two mass spectrometers (a Nu Plasma HR and an AttoM) coupled to a 193 nm ArF excimer laser ablation system to rapidly determine simultaneous *in-situ* U/Th-Pb dates, Sm-Nd isotopic compositions and trace-element concentrations. Hardware innovations include i) a modified collector configuration that enables simultaneous determination of Th-Pb and U-Pb dates by LA-MC-ICPMS using either Faraday cups or ion counters for Pb isotopes, and ii) increased instrument sensitivity and signal transmission resulting in a spatial resolution of 5 μm for U-Th-Pb dates and 9 μm for U-Th-Pb + Sm-Nd + trace-element determinations on Tertiary monazite; these allow the ability to directly tie measured dates to specific petrologic processes via Sm-Nd ratios, and/or trace-element abundances and ratios. Long-term accuracy and precision for Th-Pb and U-Pb dates is ~2% (2σ). Individual Nd ratio measurements have precisions of 20–30‰ and are accurate to within 5‰. Trace-element concentrations are accurate to within 3–5%.

The utility of the LASS approach—combining U-Th-Pb dates, isotopic compositions and trace-element abundances and ratios—will be illustrated with a broad range of geologic examples ranging from new insight into detrital monazite provenance, resolving fine-scale timing and duration of ultrahigh-pressure tectonics and unraveling the pressure–temperature history of Himalayan metamorphic rocks.

δ^{66}Zn profiles in five highly Zn-contaminated soils

E. COUDER[1,2*], E. SMOLDERS[3], B. DELVAUX[1], C. CAMBIER[1] & N. MATTIELLI[2]

[1] Earth and Life Institute, Université catholique de Louvain, 1348 Louvain-la-Neuve, Belgium - Eleonore.Couder@uclouvain.be (*presenting author)

[2] Laboratoire G-TIME, Université Libre de Bruxelles, 1050 Brussels, Belgium - nmattiel@ulb.ac.be

[3] Division of Soil and Water Management, Katholieke Universiteit Leuven, 3001 Heverlee, Belgium

Metalurgical industry, through emission and slag dumping, has strongly modified metal biogeochemical cycling. The soil-plant system is crucial for the understanding of metal transfer between terrestrial pools. In Belgian soils, zinc (Zn) is a main inorganic pollutant.

Variations in δ^{66}Zn between compartments of the plant-soil system are indicative of abiotic and biotic processes. Our previous data indicate that Zn isotopic compositions (δ^{66}Zn) of topsoils reflect the Zn isotopic signature of the main Zn-emitter. The main goal of the present study consists to examine the δ^{66}Zn profiles in five contrasted soils covered by various plant species.

Two natural soils, a calcareous soil (CS) and a shale-derived soil (SS), both contaminated by Zn aerial fallouts, and three soils developed on a slag heap were chosen. Throughout the soil profiles, the soils have been characterized: (i) the total Zn concentrations in bulk soil (Zn_{tot}), which vary from 0.2 up to 74.8 g kg^{-1}, and (ii) the oxidizable Zn fractions (Zn_{ox}, i.e. proportion of Zn-bearing organic matter *vs* Zn_{tot}) ranging between 3.5 and 34.7 % of Zn_{tot}. High precision δ^{66}Zn data measured by MC-ICP-MS are reported (relative to the JMC Zn standard solution) for bulk soils, gravity soil solutions, surrogate soil solutions obtained by 0.01M $CaCl_2$-extraction and shoots from plants growing on-site.

Relative to the bulk soils (δ^{66}Zn from -0.7±0.03‰ to +0.56±0.03‰), enrichment in light Zn isotopes is observed both in the gravity and surrogate solutions (δ^{66}Zn varies from -0.25±0.01‰ to +0.25±0.01‰ (±2SD)) as well as in shoots (δ^{66}Zn from -0.05±0.02 to +0.14±0.02‰). As a result of Zn uptake by plants or Zn leaching, the residual topsoils will be comparatively enriched in heavy isotopes.

Throughout the soil profiles (CS and SS), an increase in δ^{66}Zn values with depth is observed and is negatively correlated with Zn_{ox}. This trend reflects transport of Zn-bearing organic matter, coming from the dead plant material and enriched in light Zn isotopes, from the topsoil to the depth via bioturbation and/or mass movement processes.

In summary, the δ^{66}Zn profiles in the five contaminated soils reflect the combined processes: (i) soil leaching, (ii) dead plant return to soil, and (iii) organic matter transfer to depth.

https://doi.org/10.1180/S0026461X00008434 Published online by Cambridge University Press

An early-branching microbialite cyanobacterium forms intracellular carbonates

ESTELLE COURADEAU[1,2,3*], KARIM BENZERARA[1], EMMANUELLE GERARD [3], DAVID MOREIRA[2], SYLVAIN BERNARD[4], GORDON E. BROWN, JR.[5] AND PURIFICACION LOPEZ-GARCIA[2]

[1]IMPMC, CNRS UMR 7590, Université Pierre et Marie Curie, Paris, France. estelle.couradeau@impmc.upmc.fr (* presenting author)
[2]ESE, CNRS UMR 8079, Université Paris-Sud, Orsay, France
[3]IPGP, CNRS UMR 7154, Université Paris Diderot, Paris, France
[4]LMCM - MNHN, CNRS UMR 7202, Paris, France
[5] Department of Geological and Environmental Sciences, Stanford University, Stanford, CA 94305-2115, USA

Abstract

The evolution of Earth environments has been deeply linked with that of Cyanobacteria for billions of years. Cyanobacteria have impacted major geochemical cycles (C, N & O) through Earth history. They have played a major role in the carbon cycle by converting CO_2 into organic carbon and carbonates and by enriching the atmosphere in oxygen. They have been looked for in the geological record in the form of fossil encrusted cells based on the assumption that cyanobacterial calcification is always an extracellular process. Here, we report the discovery of a cyanobacterium found in microbialites from Lake Alchichica (Mexico) [1,2] that forms intracellular carbonate phase inclusions, revealing an unexplored pathway for calcification. Electron diffraction shows that these phases are amorphous although XANES nanospectroscopy reveals local ordering consistent with the structure of benstonite, a Mg-Ca-Sr-Ba carbonate. Phylogenetic analyses place this cyanobacterium within the deeply divergent order Gloeobacterales. Accordingly, we tentatively name it *Candidatus* Gloeomargarita lithophora. This discovery opens the possibility that ancestral calcifying cyanobacteria may have biomineralized carbonates intracellularly, and thus are not prone to encrustation in extracellular precipitates. This lack of encrustation provides an alternative explanation for the absence of cyanobacterial microfossils in the oldest fossil stromatolites and opens questions about the evolution of calcification in cyanobacteria.

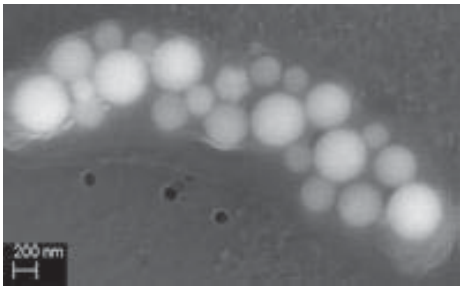

Figure: SEM picture (secondary electron mode) of a cell of *Ca.* G.lithophora. Intracellular carbonate inclusions filling the cell are visible.

[1] Couradeau *et al.,* (2011) *PLoS ONE* **6(12)**: e28767
[2] Couradeau *et al.*, *Science,* under review

Diminished S isotope fractionation accompanies internal sulfate accumulation by sulfate-reducing bacteria

M.L. COUSINEAU[1]*, D. FORTIN[1], AND B.A. WING[2]

[1]Earth Sciences, University of Ottawa, Ottawa, Ontario, Canada, mlcousineau@gmail.com (*presenting author)
[2]Earth and Planetary Sciences, McGill University, Montréal, Québec, Canada, boswell.wing@mcgill.ca

Microbial sulfate reduction (MSR), one of the earliest metabolisms to appear on Earth, is a process by which some prokaryotes use sulfate as an electron donor to obtain energy for metabolic processes. BSR results in the fractionation of sulfur isotopes, with the reactant sulfate enriched in ^{34}S, and the product sulfide depleted in ^{34}S. As studies have shown that MSR in low sulfate conditions results in small S isotope fractionations, limited variability in S isotope fractionation in ancient biogenic sulfides has been interpreted to indicate sulfate-poor conditions in early oceans.

We conducted closed-system experiments using two pure strains of acid-tolerant sulfate-reducing bacteria (M1, optimum pH 4; and GBSRB4.2, pH 4.2) in non-sulfate-limiting conditions. We identified two distinct fractionation regimes during the growth cycle: 1) low (<5‰) fractionation in the beginning lag phase, when sulfate reduction and growth are negligible, and 2) higher fractionation (≈11-24‰) during the exponential phase, when cell growth and sulfate reduction are occurring rapidly. The low fractionation during the lag phase apparently results from initial sulfate uptake by the cells, which leads to internal sulfate accumulation prior to the initiation of sulfate reduction.

The small S isotope fractionations that we have identified are consistent with rare experiments that have been designed to specifically investigate sulfate uptake during MSR. Isotopic calibration of the first link in the MSR processing chain contributes to our understanding of the multi-step process of MSR and may help in developing a mechanistic interpretation of S isotope compositions in modern and ancient biogenic sulfides.

https://doi.org/10.1180/S0026461X00008434 Published online by Cambridge University Press

Physico-chemical and structural controls on copper isotope fractionation during its sorption by benthic algae and a phototrophic biofilm

AUDE COUTAUD[1,2*], OLEG S. POKROVSKY[1], PIETER GLATZEL[3], GLEB S. POKROVSKI[1], JÉRÔME VIERS[1] AND JEAN-LUC ROLS[2]

[1]GET, Toulouse, France , aude.coutaud@get.obs-mip.fr (* presenting author)
[2]EcoLab, Toulouse, France
[3] ESRF, Grenoble, France, pieter.glatzel@esrf.fr

The interaction of one of the most phyto-toxic but also essential metals, copper, with different phototrophic microorganisms as a function of exposure time was studied via physico-chemical characterization of metal adsorption on and incorporation into cells under controlled laboratory conditions. The novelty of the present study is to combine two different approaches, the "macroscopic" stable-isotope techniques with the "microscopic" molecular-level observations using X-ray absorption spectroscopy (XAS) of the complexes formed on the surface and inside the cells. The isotopic study included batch and flow-through experiments which allowed to distinguish among assimilation, excretion and adsorption processes within the mature biofilm dominated by cyanobacteria. Moreover, relationships between the fractionation of Cu stable isotopes and the biofilm growth cycle in a Taylor Couette flow-through reactor was quantified. To investigate the local atomic environment of Cu in peryphytic biofilms and benthic algae, freeze-dried samples with 1 to 5000 ppm Cu were examined by XAS at beamline ID26 (ESRF). The high-resolution mode, for the first time used for Cu in biological matrices, allowed establishing specific features of the Cu pre-edge and quantifying the oxidation state, the nature and the number of neighbours around Cu. Results show that the degree of isotope fractionnation depends on the metal concentration in the biomass, the degree of Cu reduction and the structural environment of Cu. For instance, heavy Cu isotopes are preferentially adsorbed on the surface whereas the intracellular incorporation favours light Cu isotopes. Theses trends may be linked to the drastic changes in the local chemical environment of copper occured upon its adsorption onto or incorporation in the cells, similarly to Zn and Cd [1-3]. However, in contrast to other heavy metals, Cu undergoes Cu(II) to Cu(I) reduction during its uptake by our biomodels. Thus, low-concentrated samples (1-20 ppm), demonstrate the presence of sulfur in the nearest atomic shell of Cu(I), whereas in concentrated samples, the carboxylic complexes of Cu(II) predominate. These findings help to establish the interaction mechanism of autotrophic photosynthetic microorganims with copper both at trace and toxic level of metal concentration. The results of this integrated study can be useful for tracing the environmental effects of copper - biofilm interactions, and allow to identify the factors exerting the direct control on the mechanisms of Cu stable isotope fractionation in biological systems.

[1] Guiné *et al.* (2006) *Environ. Sci. Technol.* **40**, 1806-1813. [2] Pokrovsky *et al.* (2005) *Environ. Sci. Technol.* **39**, 4490-4498. [3] Pokrovsky *et al.* (2008) *Geochim. Cosmochim. Acta* **72**, 1742-1757.

Arsenic sequestration during early diagenetic sulfur redistribution

RAOUL-MARIE COUTURE[1,*], JÉROME ROSE[2], DIRK WALLSCHLÄGER[3] AND PHILIPPE VAN CAPPELLEN[4]

[1]University of Waterloo, Waterloo, Canada, raoul.couture@uwaterloo.ca (*presenting author)
[2]CEREGE, Aix-en-Provence, France, rose@cerege.fr
[3]Trent University, Peterborough, Canada, dwallsch@trentu.ca
[4]University of Waterloo, Waterloo, Canada, pvc@uwaterloo.ca

Despite accumulating evidence that thiolated arsenic (As) species play a major role As cycling, the pathways leading to the formation of these elusive species in freshwater environments, as well as their sorption affinity in redox-active sediments, remain poorly studied. We used flow-through reactors (FTRs) to look at the fate of As species during the degradation of sedimentary organic carbon (C_{org}) and iron (Fe) oxyhydroxides under sulfate (SO_4^{2-}) reducing conditions. Sediment samples from Lake Tantaré, a well studied oligotrophic lake whose surface sediments are supplied with both labile C_{org} (C_{org} oxidation rates, R_C, up to 400 µmol cm^{-3} yr^{-1}) and reactive ferric Fe (Fe ≥ 1 mmol g^{-1}), were incubated for 8 weeks in reactors supplied with SO_4^{2-} and soluble As (Fig. 1). Lactate was added to the inflowing solutions after depletion of the labile sedimentary C_{org} pool, witch occured after 21 days. As and sulfur (S) solid phase speciation was investigated using X-ray absorption spectroscopy (XAS), and aqueous speciation using a combination of ion chromatography, voltammetry, spectro-photometry.

Figure 1. Sample selection based on the Fe (symbols, triplicate) and R_C values (line) measured in the sediments of Lake Tantaré [1].

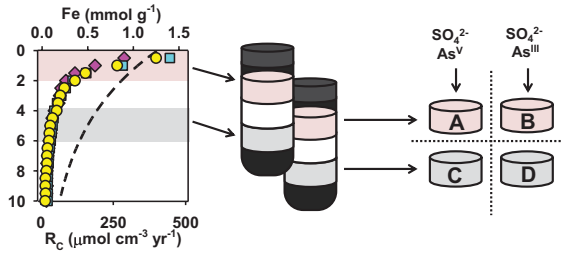

Aqueous S speciation throughout the experiment was dominated by (poly)sulfides, while As speciation was dominated first by arsenite and then, in FTR A (Figure 1), by mono-thioarsenate. The availability of labile C_{org} exerted the following dual control on the fate of S during the incubations: i) higher SO_4^{2-} reduction rates were observed in FTRs A-B than in FTRs C-D, and ii) evolving sulfides were sequestered as organic-S^{-II} in FTRs A-B and as FeS_2 and $\alpha S_{8(s)}$ in FTRs C-D. Similarly, As removal proceeded through either realgar (FTR A-B) or orpiment (FTR C-D) formation, confirming the key influence of free S^{-II} on the mechanisms of As sequestration [2]. XAS data also show that solid-phase tetra-thioarsenate was present, probably as a sorbed complex, representing up to 35% of total As in FTR C. While current geochemical models are able to reasonably predict As speciation in the aqueous phase, they fail to predict the prevalent form of As in the solid phase.

[1] Couture et al. (2010) *ES&T* **44**, 197-203.
[2] O'Day et al. (2004) *PNAS* **101**, 13703-13708.

https://doi.org/10.1180/S0026461X00008434 Published online by Cambridge University Press

The critical role of hydrothermal activity in forming hyperenriched deposits of metals in black shales

RAYMOND M. COVENEY, JR.*; JAMES B. MUROWCHICK

Department of Geosciences, University of Missouri-Kansas City, Kansas City MO 64110 U.S.A.
coveneyr@umkc.edu ; murowchickj@umkc.edu
* presenting author

Introduction

Certain black shale-hosted deposits contain exceptional metal values that are several orders of magnitude greater than average black shale (which typically contains, for example, 300 ppm Zn; 10 ppm Mo)[1,2]. In Illinois and Indiana, for example, bed B of the Carboniferous Mecca Quarry Shale Member[3,4] contains an average of 1100 ppm Mo as well as erratic values for Zn that average 3000 ppm but in some cases even exceed 10,000 ppm. Elsewhere, the Ni-Mo sulphide beds in Cambrian shales of southern China contain more than four weight per cent Mo and nearly as much Ni[5,6]. We suggest that mineralized beds containing such highly concentrated deposits of metals be called "hyperenriched". Known examples of such deposits are all located in exceptionally metal-rich geological environments (i.e. in the Mississippi Valley of North America, the rich ancient mining areas of southern China in Guizhou and Hunan or are adjacent to *bona fide* sedex deposits[7]).

Origins of Hyperenriched Deposits

Although hyperenriched deposits of metals in black shales have been studied since the days of Goldschmidt's early 20th Century work on the Kupferschiefer, a consensus on the mode (or modes) of origin has yet to emerge. Workers have variously attributed black shale-hosted deposits to a wide range of agents including syngenetic or epigenetic hydrothermal activity, bolide impact, or accumulation from sea water.We note, however, that the hyperenriched deposits in black shales that we cite are associated regionally with coeval hydrothermal ore systems that have left evidence in the form of hot saline fluid inclusions found in association with the shales. For these reasons, we infer that the metalliferous black shale deposits, such the Late Paleozoic American black shales, and the unusual Ni-Mo deposits of China, primarily owe their origins to hydrothermal processes.

Conclusions

Besides the evidence cited above, we and others[8] note the absence of a clear modern analog for deposition of hyperenriched enriched deposits directly from sea water as has been proposed by some other workers. We conclude, therefore, that hyperenriched deposits result from hydrothermal sources.

[1] Turekian & Wedepohl (1961) *Geol Soc. Amer. Bull.* 72, 175-192
[2] Vine & Tourtelot (1970) *Econ. Geol.* 65, 253-272
[3] Coveney & Martin (1983) *Econ. Geol.* 78, 132-149
[4] Schultz & Coveney (1992) *Chem. Geol.* 99, 83-100
[5] Fan (1983) in The Significance of Trace Elements in Solving Petrogenetic Problems and Controversies, Theophrastus Publ., 447-474
[6] Lott et al., 1999. *Econ. Geol.,* 94, 1051-1066
[7] Dumolin et al., 2011, *USGS Prof. Paper 1776C*, 64 p.
[8] Emsbo & Breit (2011) *Mineral. Mag.* 75, 810

Influence of salinity on methanogenesis in the Alberta oil sands region

BENJAMIN R. COWIE[1], LISA M. GIEG[1], AND BERNHARD MAYER[1].

[1]University of Calgary, Calgary, Alberta, Canada.
brcowie@ucalgary.ca

This study examined the relationship between water chemistry and methanogenic microbial activity in the Alberta oil sands using a bench-scale experiment. The terminal redox process, methanogenesis, is common in many shallow hydrocarbon reservoir systems and is thought to be a central process in the geological history of Alberta's oil sands. The biodegradation of light oil over geological time via methanogenesis has been proposed to be a primary formation process of the oil sands reserves in western Canada [1]. Shallow hydrocarbon reservoir environments are favourable to methanogenic communities that require moderate temperature, pH and reducing geochemical conditions to conduct their metabolic processes. In the McMurray formation, the predominant Athabasca oil sands reservoir, formation water geochemistry is variable and salinities vary from fresh to brine. Furthermore, quaternary-aged glacial channels have brought fresh groundwater into contact with oil sands deposits since the last glaciation [2], possibly stimulating increased methanogenic activity in the sedimentary basin [3]. Therefore the relationship between microbial processes and aqueous geochemistry requires investigation to gain insight into potential biodegradation mechanisms and rates of oil sands.

Laboratory cultures of methanogenic communities grown on an oil sands substrate were prepared using waters with three different geochemical compositions and salinities ranging from fresh to saline. Methane generation rates, microbial community composition and stable isotope geochemistry of carbon and sulphur systems were determined over eight months to assess the influence of variable salinity on biodegradation of oil sands via methanogenesis.

Microbial methane generation was variable among replicates with similar chemical water compositions. However, mean methane generation rates were higher in brackish and freshwater cultures than in saline cultures. Carbon isotope measurements indicated that neither CO_2 reducing, nor acetoclastic methanogens were dominant, and that a mixed methanogenic community was most likely active in all three geochemical variants. Sulphur isotope data suggested that bacterial sulphate reduction (BSR) is a likely process in the saline cultures where sulphate concentrations were elevated. However, in the cultures with active BSR, methanogenesis was not inhibited. Increasing concentrations of acetate in all cultures suggest syntrophic fermenting bacteria play a dominant role in the microbial ecosystem under all geochemical conditions tested.

These preliminary results indicate that both CO_2 reduction and acetoclastic methanogenesis are potential processes for oil sands biodegradation under laboratory conditions, and may also be active in modern oil sands reservoirs.

[1] Jones et al. (2008) *Nature* **451**, 176-180.
[2] Lemay (2002) *Alberta EUB/AGS Geo-Note 2002-03*.
[3] Fomolo et al. (2008) *Geology* 36 (2), 139-142.

https://doi.org/10.1180/S0026461X00008434 Published online by Cambridge University Press

Geochemistry of Cryogenian Ironstones – the link to N-MORB and its implications

GRANT COX[1*], GALEN HALVERSON[1], WILLIAM MINARIK[1], ROSS STEVENSON[2], DANIEL LE HERON[3], FRANCIS MACDONALD[4], JUSTIN STRAUSS[4], PAOLO SOSSI[5], ERIC BELLEFROID[1].

[1] McGill University, Montreal, Canada, grant.cox@mail.mcgill.ca[*]
[2] GEOTOP/UQAM, Montreal, Canada.
[3] Royal Holloway University of London, Surrey, U.K.
[4] Harvard University, Cambridge, U.S.A.
[5] Australian National University, Canberra, Australia.

The reappearance in the geological record of sedimentary iron formations after a ~1 Ga hiatus [1,2] is a geologically unique feature of the Cryogenian (~850 Ma to 625 Ma). Whereas their close association with globally distributed glacial deposits invites interpretation that they are the product of snowball glaciation, they have also been interpreted to be a local product of rifting, similar to modern Red Sea metalliferous sediments. Based on major element, REE, and $^{143}Nd/^{144}Nd$ data from stratigraphically-constrained samples from South Australia (Holowilena), NW Canada (Tindir and Rapitan) and southern Namibia (Numees), Cryogenian iron formations can be characterized as a mixture between a hydrothermal source and mid ocean ridge basalt (N-MORB), with very little contribution from the continental crust. Similar positive-upward iron isotope profiles in each of these basins suggest a common depositional process for the iron formation. These data indicate that both snowball glaciation and local rifting are prerequisites to Cryogenian iron formation. Notably, the Cryogenian IF patterns are distinct from both Archean-Paleoproterozoic banded iron formation and Phanerozoic ironstones.

[1] Isley, A. E. & Abbott, D. H. (1999) Journal of Geophysical Research, 104, 461-477.
[2] Klein, C. (2005) American Mineralogist, 90, 1473-1499.

Stable Isotopes of Platinum: A New Geochemical and Cosmochemical Tracer?

JOHN CREECH[1*], MONICA HANDLER[1], JOEL BAKER[1], LORETTA CORCORAN[1], VICTORIA BENNETT[2]

[1] School of Geography, Environment and Earth Sciences, Victoria University of Wellington, P.O. Box 600, Wellington, New Zealand, john.creech@vuw.ac.nz (* presenting author)
[2] Research School of Earth Sciences, Australian National University, Canberra, ACT 0200, Australia

Platinum is a highly siderophile transition metal with 6 naturally occuring isotopes (^{190}Pt, ^{192}Pt, ^{194}Pt, ^{195}Pt, ^{196}Pt, ^{198}Pt). The platinum stable isotope system is of cosmochemical and geochemical interest due to its strong sequestration into planetary cores during planetary differentiation and its range of oxidation states which are found in planetary environments from core to crust (Pt^0, Pt^{2+}, Pt^{4+}). As with other non-traditional stable isotope systems, the ability to make precise and accurate measurements of Pt isotope compositions in natural samples may provide possibilites to trace a range of natural processes. Potential examples include planetary core formation under different redox conditions, Pt mineralisation in ore deposits, and redox controlled behaviour of Pt in the oceans and marine sediments where it potentially exists in the 2+ and 4+ state.

We have developed, for the first time, mass spectrometric methods for the precise determination of platinum stable isotopes. Pt stable isotopes have been measured with a Nu Plasma multiple collector ICPMS using a ^{192}Pt-^{198}Pt double-spike to correct for instrumental mass bias. Samples are introduced to the MC-ICPMS with a DSN-100 desolvating nebuliser. Repeated measurements of standards consuming ca. 50 ng of Pt show that an external reproducibility of < 25 ppm/amu (2σ) can be obtained on double-spike corrected ratios using this technique. Three commercially available Pt standards have been measured to high precision, and show resolvable differences in isotopic composition.

A method for the chemical separation of Pt from geological materials (silicates, metals, Fe-Mn oxyhydroxides) has also been developed using anion exchange techniques. This method yields ≥ 85% of Pt, with > 90% purity. Analytical tests of Pt doped with a range of elements show that this degree of separation does not compromise the accuracy of the double-spike corrected Pt isotope ratios. We will also present Pt stable isotope data for a range of international reference materials, where samples have been double-spiked prior to chemistry.

https://doi.org/10.1180/S0026461X00008434 Published online by Cambridge University Press

Alkali and alkaline earth metal adsorption to goethite

LOUISE J CRISCENTI[1]*, DAVID HART[2], AND KIDEOK KWON[3]

[1]Sandia National Laboratories, Geochemistry, ljcrisc@sandia.gov (*presenting author)
[2]Sandia National Laboratories, National Security Applications, dbhart@sandia.gov
[3]Sandia National Laboratories, Geochemistry, kkwon@sandia.gov

The adsorption of metals to Fe-hydroxides such as goethite influences contaminant migration in the subsurface environment. Many surface complexes have been proposed for cation adsorption to goethite. In this study, we use classical molecular dynamics (MD) simulations to investigate the specific location of surface species with respect to both the mineral surface and to the structured water at the interface. Simulations are conducted for a range of NaCl, $MgCl_2$ and $BaCl_2$ concentrations to evaluate the impact of ion adsorption on the interfacial water structure, and to evaluate how surface speciation might change with increased surface loading.

Figure 1 illustrates preliminary results for the (100) and (101) surfaces of goethite in a 5 M NaCl solution. Interfacial water at the (100) surface exhibits more ordered arrangements of interfacial water and more hydrogen bonding with surface hydroxyl groups than at the (101) surface. The overall water structure is not affected by Na^+ and Cl^- adsorption. Sodium binds as an inner-sphere complex in 1 M NaCl solutions, but in a 5 M NaCl solution, it adsorbs both as inner and outer-sphere complexes. In 1M – 5 M NaCl solutions, the Cl^- ion adsorbs strictly as an outer-sphere complex.

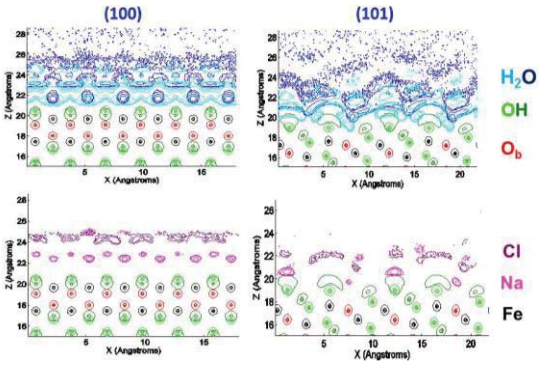

Figure 1: Water, Na^+, and Cl^- adsorption on goethite surfaces.

Comparisons will be made between the adsorption of Na^+, Mg^{2+}, Ba^{2+} from NaCl, $MgCl_2$ and $BaCl_2$ solutions of different concentrations. Atomic density profiles, partition coefficients, statistics on the types of species formed on the surfaces (i.e., inner- vs. outer-sphere, ion-pairs), and water dipole orientation data will be presented. Differences in the electric double layer formed at the (100) and (101) surfaces will be discussed.

This research is supported by the U.S. Department of Energy, Office of Basic Energy Sciences, Division of Chemical Sciences, Geosciences, and Biosciences. Sandia is a multiprogram laboratory operated by Sandia Corporation, a Lockheed Martin Company, for the United States Department of Energy's National Nuclear Security Administration contract DE-AC04-94AL85000.

Negative C-isotope excursion in carbonates during 2.0 Ga Shunga Event

ALENKA E. ČRNE[1*], VICTOR A. MELEZHIK[1], AIVO LEPLAND[1], ANTHONY E. FALLICK[2], ANTHONY R. PRAVE[3], AND ALEXANDER T. BRASIER[2]

[1]Geological Survey of Norway, Trondheim, Norway, alenka.crne@ngu.no (* presenting author), victor.melezhik@ngu.no, aivo.lepland@ngu.no
[2]Scottish Universities Environmental Research Centre, East Kilbride, UK, t.fallick@suerc.gla.ac.uk, alex.brasier@glasgow.ac.uk
[3]University of St. Andrews, St. Andrews, UK, ap13@st-andrews.ac.uk

The ~2.0 Ga Shunga Event (SE), characterized by worldwide accumulation of extraordinary amounts of organic material, was among several global Paleoproterozoic events associated with the rise of atmospheric oxygen that were targeted by ICDP Fennoscandia Arctic Russia – Drilling Early Earth Project (FAR-DEEP). The SE appears to be linked to major disturbances in the C-cycle during the Paleoproterozoic, and follows or transitionally overlaps with the Lomagundi-Jatuli positive isotopic excursion of carbonate carbon at ~2.3-2.1 Ga. Four FAR-DEEP drillholes intersecting 670 m of sedimentary and volcanic rocks of the Zaonega Formation (ZF) offer a unique opportunity to study the C-cycle during the SE. Compositionally heterogeneous carbonate phases with $\delta^{13}C$ values ranging from -22 to +8 ‰ indicate a complex, multistage formation and alteration of sedimentary carbonates. In order to make a distinction between primary and secondary phases and their compositional signatures, a suite of samples was characterized by SEM-BSE imaging and geochemical investigations (major and trace elements, C- and O-isotopes).

The lowermost part of the drilled succession, where sedimentary rocks are sandwiched between mafic lavas and sills, contains one carbonate phase. This is patchy calcite, with relatively constant, low $\delta^{13}C$ values around -10 ‰. As the calcite is overgrowing previous mineral phases (e.g. pyrite), it is interpreted as a seconday carbonate phase unrelated to depositional or early diagenetic environmental conditions. The middle part of the drilled succession contains carbonate beds consisting of dolomite in the middle and calcite associated with talc in the outer parts of the beds. The talc-calcite association, which overgrows dolomite, indicates a metamorphic origin of the calcite through dolomite-silica reaction in marginal parts of the carbonate beds. Samples containing nearly pure dolomite, which is the earliest preserved carbonate phase, have highest $\delta^{13}C$ values, between +3 and +8 ‰. Samples with a mixture of calcite and dolomite have $\delta^{13}C$ values as low as -10 ‰ depending on the relative amount of the two mineral phases. Dolomite-dominated samples in the upper part of the succession are isotopically lighter with values from -2 to -5 ‰.

Even though the C-isotope composition of the carbonates of the ZF has been affected by post-depositional alteration, a negative C-isotope shift of 10 ‰ is recognized in best preserved dolomite samples with $\delta^{13}C$ values from +8 to -2 ‰ over a 260-m thick stratigraphic interval. This shift may reflect a global change in isotopic composition of atmospheric/oceanic CO_2 [1], but local factors related to petroleum generation and spilling together with volcanic activity might have also influenced $\delta^{13}C$ of the ambient sea-water.

[1] Kump et al. (2011) *Science* **334**, 1694-1696.

https://doi.org/10.1180/S0026461X00008434 Published online by Cambridge University Press

Changes in the deglacial NW Atlantic from deep sea coral ε_{Nd}

KIRSTY C. CROCKET[1*], TINA VAN DE FLIERDT[1], LAURA F. ROBINSON[2], AND JESS F. ADKINS[3]

[1]Earth Science and Engineering, Imperial College London, UK (*k.crocket@imperial.ac.uk; tina.vandeflierdt@imperial.ac.uk).

[2]Department of Earth Sciences, University of Bristol, UK (Laura.Robinson@bristol.ac.uk).

[3]Californian Institute of Technology, Pasadena, USA (jess@gps.caltech.edu)

Carbon storage in the deep ocean during glacials and its subsequent release during deglaciation undoubtedly played a role in glacial/interglacial variation of atmospheric CO_2, with the Southern Ocean a strong candidate for both glacial storage and deglacial venting to the atmosphere. While radiocarbon records support this hypothesis [1], they cannot unambiguously identify the water masses involved. To do so requires pairing the radiocarbon data to a conservative water mass tracer, such as the Nd isotope composition (ε_{Nd}).

We describe the use of deep sea corals as an archive material providing same-sample U/Th ages, radiocarbon, and Nd isotope compositions. The majority of corals in this study are deglacial in age and span intermediate water depths of 1000 to 2600 m on the New England Seamounts (NW Atlantic), where pronounced changes in water column radiocarbon across the last glacial/interglacial cycle have already been identified [2, 3].

In the modern ocean, North Atlantic Deep Water has an offset to atmospheric radiocarbon of ~-65‰ ($\Delta^{14}C$), whereas Antarctic Bottom Water has a larger offset of ~-165‰ due to longer storage time in the deep ocean. During the last glacial maximum, this storage time probably increased, leading to offsets of perhaps as much as -300‰ or greater for Southern source water [1, 4]. Circulation of these waters in the Atlantic should be identifiable from Nd isotope compositions due to their distinct compositional source regions, resulting in unradiogenic North Atlantic Deep Water (~-13.5 ε_{Nd}; [5]) and more radiogenic Antarctic Bottom Water (~-9 ε_{Nd}; [6]). These are not thought to have changed significantly over the last glacial/interglacial cycle [7].

Shifts in coral radiocarbon are most pronounced between 15 and 17 ka, demonstrating incursion of radiocarbon-depleted water masses (i.e. -150 to -200‰ $\Delta^{14}C$) up to depths of ~1700 m in the NW Atlantic [3]. The corresponding Nd isotope compositions are -13 to -14.5 ε_{Nd}, typical of Northern source waters. Overlying this are comparatively well ventilated waters (-100 to -150 ‰ $\Delta^{14}C$) with ε_{Nd} compositions in the range of -11 to -12 ε_{Nd}, suggestive of mixing between Northern and Southern source waters. It is emphasised that these Nd isotope data are contrary to expectations, where shifts to more radiogenic compositions were forecast to reflect incursion of Southern source water against the less radiogenic background of the North Atlantic. These data raise several questions concerning our current understanding of ocean circulation changes during the deglaciation as well as the Nd isotope proxy as a tracer of ocean circulation, which will be discussed in this presentation.

[1] A. Burke, L.F. Robinson (2011), *Science*, doi: 10.1126/science.1208163.
[2] J.F. Adkins, et al. (1998), *Science* 280, 725-728.
[3] L.F. Robinson, et al. (2005), *Science* 310, 1469-1473.
[4] L.F. Robinson, T. van de Flierdt (2009), *Geology* 37, 195-198.
[5] D.J. Piepgras, G.J. Wasserburg (1987), *GCA* 51, 1257-1271.
[6] C. Jeandel (1993), *EPSL* 117, 581-591.
[7] G.L. Foster, et al. (2007), *Geology* 35, 37-40.

Chloride: the Unexpected Poison in the Growth of Crystalline Iron Oxides

NYSSA CROMPTON[1*], SATISH MYNENI[2]

[1]Princeton University, Chemistry Dept., Princeton, USA, crompton@princeton.edu (* presenting author)

[2] Princeton University, Geoscience Dept., Princeton, USA, smyneni@princeton.edu

Introduction

Iron is one of the essential elements to life on Earth, existing primarily in various insoluble ferric (Fe^{III}) iron oxide and oxyhydroxide phases. These phases exhibit varying degrees of solubility and bioavailbility: the amorphous Fe-oxide and ferrihydrite being the most soluble, and hematite and goethite being the least soluble and most stable phases. Different cations and anions substitute into or interact with these phases, modifying their growth and solubility. If ligands bind strongly to the freshly precipitated iron oxide phase or ferrihydrite, they block polymerization reactions and slow the transformation to more stable Fe-oxide phases. This is expected for strongly complexing ligands, such as sulfate, phosphate, and carbonate. Ligands such as chloride are not expected to play a large role; however, this study found that chloride deters iron oxyhydroxide growth.

Freshly precipitated iron hydroxides and their transformation to crystalline phases were monitored by IR and X-ray absorption spectroscopy (XAS) methods. The structural information about Cl, S, and Fe was found using XAS techniques at the National Synchrotron Light Source (Brookhaven National Laboratory, NY, USA). Studies were conducted at room temperature and at pH values of 5.5 and 8.1.

Results & Discussion

At pH 5.5, IR spectroscopy shows that transformation from freshly prepared ferric hydroxide to goethite was found to be hindered to the greatest extent by the presence of chloride. Spectral features corresponding to goethite (bending vibrations of OH) arose out of a broad band corresponding to the amorphous iron hydroxide. Even after 250 days, chloride containing samples showed no evidence of goethite. In contrast, the sulfate containing samples showed evidence of transformation into goethite before 120 days. The XANES spectra at the chlorine K-edge exhibit a clear pre-edge feature, which is indicative of a chlorine-iron bond. Additionally, Cl-EXAFS data on these samples indicate a Cl-Fe bond, supporting the XANES observations. At pH 8.1, the spectral features of goethite start appearing after just 70 days, and the Cl-Fe pre-edge feature is missing from the Cl-XANES spectra, indicating that the Cl-Fe bonds are not forming at the higher pH and the transformation is proceeding unhindered.

These results indicate that amorphous iron hydroxides and ferrihydrite can be stable for a long time, and could be the most prevalent phase when chloride is present in reacting solutions at slightly acid pHs. Additionally, chloride's direct role in the growth of iron oxides indicates that it is not simply an inert electrolyte in these systems, and its role cannot be ignored.

https://doi.org/10.1180/S0026461X00008434 Published online by Cambridge University Press

O_2 controls the Biogeochemical cycling of Cd, Fe and Mn along 85˚50´ W in the Oxygen Minimum Zone of the Eastern Tropical South Pacific

P. CROOT[1], F MALIEN[2], L STRAMMA[3] P STREU[4] AND K. WUTTIG[5]

[1] National University of Ireland Galway, Galway, Ireland (croot.peter@gmail.com)
[2] Geomar, Kiel, Germany (fmalien@geomar.de)
[3] Geomar, Kiel, Germany (lstramma@geomar.de)
[4] Geomar, Kiel, Germany (pstreu@geomar.de)
[5] Geomar, Kiel, Germany (kwuttig@geomar.de)

Oxygen Minimum Zones (OMZs) in the Eastern Tropical South Pacific (ETSP) is formed via a complex interplay of weak ocean ventilation (oxygen supply) and biological resipration (oxygen consumption). Dissolved oxygen (O_2) concentrations are a critical controlling parameter for the partitioning between redox states for a number of bio-essential metals such as Fe and Mn. Under low O_2 conditions (< 10 μM) the more soluble lower oxidation states are stabilized leading to longer residence times for these elements in the water column with implications for the distribution of these elements in these waters. Potential feedbacks may also occur whereby enhanced Fe concentrations, fuel surface water productivity resulting in higher fluxes of sinking organic matter which when respired further decreases O_2 in the OMZ.

In early 2009 we undertook a meridional transect across the ETSP OMZ from 14° S to the equator along 85˚ 50´ W using the German research vessel Meteor (Expedition M77-4). During this expedition we focused on the relationships between the location of the OMZ, the absolute O_2 concentrations and the concentrations and distributions of the redox sensitive metals Fe and Mn in order to assess the current state of this OMZ with regard to redox sensitive metals. We also estimate here fluxes for Fe and Mn to the 85˚ 50´W transect supplied by upwelling, aeolian deposition or via the transport of Fe and Mn rich waters from the Peruvian shelf to the study area.

In this work we also observed that OMZs can influence the biogeochemistry of non-redox sensitive elements. Most notably for Cd, as our data suggested changes in the remineralization length for Cd was most likely linked to changes in Zooplankton diel migration due to the depth of the OMZ.

Organic Geochemistry and Toxicology of Fluids from Shale Gas Wells

LYNN CROSBY[1*], MATTHEW VARONKA[1] and WILLIAM OREM[1]

[1*]U.S. Geological Survey, Reston, VA, USA, lcrosby@usgs.gov

Background

Hydraulic fracturing frees energy resources previously thought uneconomical to produce, allowing contemporary industrial and societal needs to be met. Fluids resulting from this process (frac fluid and produced water) are complex chemical mixtures that contain various additives used for hydrofracing and naturally-occurring substances extracted from the shale. A list of hydrofracing additives used can be found in publically available registries such as FracFocus, www.fracfocus.org and additives are disclosed in a growing number of states. However, scientific research on this issue is still lacking and few studies have been published regarding the geochemistry of these fluids or their possible effects on human cell lines.

Results and Conclusion

In the present work we quantified and identified the dichloromethane-extractable organic constituents in the fluids (frac and produced waters) using gas chromatography/mass spectrometry. We also used short term *in vitro* bioassays with human lung (A549) and liver (HepG2) cells to assess the toxicity of fluids (frac and produced waters) from several hydraulic fracturing wells (HFX) at dilutions ranging from full strength to 1:1000 and exposure times from 36 hr - 2 weeks. Major organic constituents included: C10-C17 branched alkanes, ethylene glycol monododecyl ethers, di-n-octyl-phthalate, and 2,2,4-trimethyl-1,3-pentanediol. Using the fluids at full strength 50-75% of cells were killed after 36-60 hr. After 72 hr 4 of 8 HFX samples killed ≥92% of HepG2 cells ($p<0.05$) and the other 4 killed 50-80% of the cells. After two weeks, 100% of A549 cells initially plated in HFX at full strength were dead. We also examined HFX waters collected from 1 - 10 days following hydraulic fracturing in order to assess whether toxicity would abate. Toxicity in HFX waters remained significantly higher than in laboratory pure water ($p<0.05$) without a clear trend. Future studies will determine whether the observed toxicity was due to these organic compounds, inorganic constituents, hypersalinity or a combined effect.

https://doi.org/10.1180/S0026461X00008434 Published online by Cambridge University Press

A stable isotope methodology to trace nanoparticles fates in biota

MARIE-NOËLE CROTEAU[1]*, AGNIESZKA DYBOWSKA[2], SUPERB MISRA[3], SAMUEL LUOMA[4] AND EUGENIA VALSAMI-JONES[5]

[1]USGS, Menlo Park, USA, mcroteau@usgs.gov (* presenting author)
[2]Natural History Museum, London, UK, a.dybowska@nhm.ac.uk
[3]Natural History Museum, London, UK, s.misra@nhm.ac.uk
[4]Univeristy of California, Davis, USA, snluoma@ucdavis.edu
[5]University of Birmingham, Birmingham, UK, e.valsamijones@bham.ac.uk

Introduction

One challenge in understanding the environmental implications of nanotechnology lies in tracing nanoparticles in organisms during controlled experimental studies as well as in the environment. Stable isotope methodologies offer great potential to address this challenge. Metallo-nanoparticles can be synthesized from a metal enriched with a rare stable isotope [1,2]. Here we quantify the bioavailability of metal nanoparticles (NPs) from food and water under conditions that might be typical of nature, and develop links to toxicity. Metal oxides NPs (CuO, ZnO) as well as Ag NPs were synthesized with an enriched stable isotope. We use a tracing technique that allows us to determine uptake and loss rates in freshwater snails exposed to NPs dispersed in water or mixed with food. The rate constants developed in these experiments were used to model bioaccumulation from both routes under environmentally realistic conditions. The isotope tracer was also used to quantitatively evaluate physiological processes like feeding rates and assimilation efficiency that might be adversely affected by exposure to metal NPs in diet.

Results and Conclusion

We demonstrate that isotopically modified ^{67}ZnO and ^{65}CuO NPs are required in uptake experiments because the high natural background metal concentrations limit the ability to detect bioaccumulation at environmentally relevant exposures. A tracer is also required when studying uptake of Ag NPs at environmentally relevant concentrations. For example, we demonstrate that Ag concentrations as low as 0.005 nmol g^{-1} can be detected in freshwater snails exposed to 0.1 nM of dissolved Ag enriched with ^{109}Ag (Fig.1). Exposures more than 20-times higher would be required to detect Ag uptake if no tracer were used. Without a tracer, uptake rates can only be determined at concentrations typical of extreme contamination.

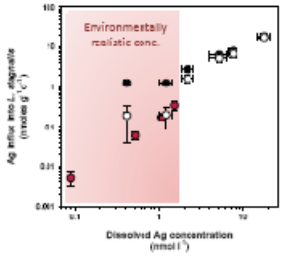

Figure 1. Silver uptake rates in snails after exposure to $AgNO_3$ (solid circles) or enriched ^{109}Ag (red circles). Open circles show uptake rates when Ag background is removed with a mathematical correction.

[1] Dybowska et al. (2011) *Environ. Pollut.* **159**, 266-273.
[2] Misra et al. (2012) *Environ. Sci. Technol.* **46**, 1216-1222.

Cr isotopes in a ferruginous lake

S.A. CROWE[1]*, A. BASU[2], L.N. DØSSING[1], A. ELLIS[3], D.A. FOWLE[4], A. MUCCI[5], T.M. JOHNSON[2], AND CANFIELD D.E[1].

[1]Nordic Center for Earth Evolution, Odesne, Denmark sacrowe@biology.sdu.dk, ldoessing@gmail.com, dec@biology.sdu.dk
[2]Dept. of Geol., Univ. of Illinois, Urbana, USA mailanirban@gmail.com, tmjohnsn@illinois.edu
[3]GeoSci. & Env., California State Univ. Los Angeles, USA aellis3@exchange.calstatela.edu
[4]Dept. of Geol., Univ. of Kansas, Lawrence, USA fowle@ku.edu
[5]GEOTOP & McGill Univ., Montreal, Canada alm@eps.mcgill.ca

Cr isotope signatures have recently been introduced as a robust paleo-redox proxy and Cr isotopes in banded iron formations (BIFs) broadly track Earth's oxygenation history as revealed by other proxies [1]. Cr isotopes, however, appear to reveal additional structure in the evolution of atmospheric oxygen not exposed by other proxies. Notably, Cr isotopes indicate an oxygen pulse nearly 400 Ma prior to the widespread oxygenation of the atmosphere at the 2.3 Ga Great Oxidation Event (GOE). To better constrain the behaviour of Cr isotopes and their record of paleo-redox conditions, we examined the Cr cycle and its accompanying isotope fractionation in Lake Matano—a modern analogue for the iron-rich oceans from which BIFs were deposited [2]. Cr speciation in Lake Matano's oxic surface waters and inflowing streams is dominated by Cr(VI). This Cr(VI) is quantitatively reduced in the lake's ~100m deep chemocline. With δ^{53}Cr values between +2.2 and +3.3 ‰ (δ^{53}Cr ‰ = $[(^{53}Cr/^{52}Cr)_{sample} - (^{53}Cr/^{52}Cr)_{NIST\ SRM\ 979}] / (^{53}Cr/^{52}Cr)_{NIST\ SRM\ 979} \bullet 1000$), this Cr(VI) is isotopically heavy relative to mantle inventories, and the catchment bedrock and soils. Cr(III) in the lake's anoxic bottom waters is also isotopically heavy (δ^{53}Cr = +2.22 to +2.61 ‰), suggesting that Cr(III) records the heavy composition of Cr(VI) from the lake's surface waters and inflowing streams. Our observations are thus consistent with the mechanisms proposed to explain the δ^{53}Cr record in BIFs.

[1] Frei et al. (2009), *Nature*, **461**, 250-254, [2] Crowe et al. (2008), *PNAS*, **105**, 5938–15943

https://doi.org/10.1180/S0026461X00008434 Published online by Cambridge University Press

Pearls as Biomineralization Models for Layered Growth and Crystallization

JEAN-PIERRE CUIF[1*], YANNICKE DAUPHIN[2], JULIUS NOUET[3]

[1] University Paris-Sud Orsay, Geology, jean-pierre.cuif@u-psud.fr (* presenting author)
[2] University P. and M. Curie, Paris yannicke.dauphin @upmc.fr
[3] University Paris-Sud Orsay, Geology , julius.nouet@u-psud.fr

Cultivated pearls are produced by introducing a *graft* (a fragment of the mantle cut from the nacre producing area of the *Pinctada*) in the body of a "receiver" pearl oyster. The mineralizing side of the graft (the outer cell layer) is placed against the surface of a *nucleus* (a sphere of Ca-carbonate acting as substrate). After a recovery period during which the nucleus is completely wrapped by the graft spreading on the nucleus surface, resulting in formation of the *pearl-sac*, the mineralizing epithelium regains activity. But in contrast to what can be expected, minerals deposited by the newly formed tissue exhibit a great diversity in structures, correlated to an equivalent diversity in the associated biochemical compounds.

Taking advantage of an on-going research program (ADEQUA) granted by the Polynesian Office for Marine Resources, several tens of pearls grafted and grown in controlled similar conditions have been submitted to different physical methods allowing correlated mineralogical and biochemical data to be collected.

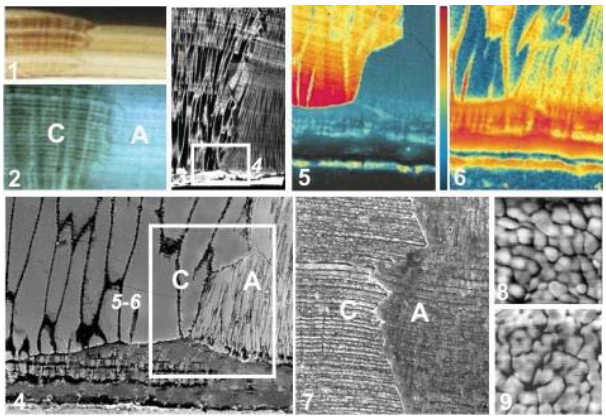

Figure 1: Example of a composite (calcite aragonite) pearl layer early developmental stage. 1: optical; 2: UV-fluo; 3: Laser conf.; 4: BSE; 5: XANES S-polysaccharides; 6: XANES S-protein; 7: SEM; 8-9: AFM.

Physical *in-situ* characterizations (Fig. 1) illustrate the strict correlation between organic secretions and mineralogical properties of distinct areas of the pearl bed [1]. AFM data show that whatever the biochemical composition of the organic phase, mineralized material exhibit a reticulate pattern without any crystalline growth faces. Extensive investigation [2] suggests that this layered mode of growth and crystallization is a widely shared process.

[1] Cuif *et al.* (2011) *Aquat. Liv. Res*. **24**, 411-424. [2] Cuif *et al.* (2011) Biominerals and Fossils through Time. Cambridge Univ. Press, 490 pp.

Durability of the Uranium resources

MICHEL CUNEY

UMR7566-CNRS CREGU-Université de Lorraine, FRANCE
michel.cuney@g2r.hup-nancy.fr

Introduction

Uranium is a major mineral resource for the production of energy. Primary resources (conventional and unconventional) derived from mining, can be supplemented by secondary resources [1]. However, only a small fraction of the U from the primary resources is presently used in nuclear reactors and a small part of the various materials issued from nuclear fuel cycle (secondary resources) are reprocessed to be re-used as a nuclear fuel.

Conventional uranium Resources

U deposit types are extremely diverse and form at all steps of the geological cycle [2], but three types: Olympic Dam, diagenetic-hydrothermal and deposits related to meteoric water infiltration represent over 75% of identified world U resources [3]. Identified resources recoverable at less than $260US /kg U ($118US/pd) reach 6.306 Mt U [1], and can last for 100 years at the present rate of consumption by the nuclear reactors.

Unconventional uranium Resources

The durability of the U resources can be greatly increased by the recovery of U as minor by-product of the mining of phosphorites, carbonatites, black shales, lignite, seawater. A variety of other non-conventional U resources are being or may be developed in a near future: production from the cleaning of waters deriving from former U mines and tailings, reprocessing of tailings produced by previous U or other metal extraction, recovery from Ni-Zn black shale ores by bio-heapleaching (Talvivaara, Finland), recovery from lignite-coal ash, from porphyry copper operations, from monazite of sand placers if REE recovery from this resource restart.

Secondary uranium Resources

The durability of the U resources can be further increased by developing the use of secondary resources. Only ^{235}U (1/140 of the natural U) is burned in most nuclear reactors. In fact, 0.25 to 0.30% ^{235}U remains in depleted U after enrichment, and 0.8 to1% remains in the spent nuclear fuel. The production of 1 t U enriched at 3.5% ^{235}U leaves 6.7 t of depleted U. Burning of ^{235}U produces a series of nuclides, among which about 1% of ^{238}U is transformed to ^{239}Pu, with a world production of 70t Pu /year (www.worldnuclear.org). Several processes have been or are being developed for a sustainable use of these secondary resources: dilution of military highly enriched U (HEU), re-enrichment of depleted U or spent fuel after preprocessing, use of Pu for MOX production, the burning of ^{238}U with Pu or HEU in the 4th generation reactors increasing about 60 times the durability of the U resources.

Conclusion

Beside conventional U resources large amounts of nuclear fuel can be recovered from unconventional and secondary resources. A sustainable development of nuclear energy requires a wider development of existing technologies and the development of new ones to use more thoroughly these differents types of U resources.

[1] IAEA (2009) Uranium 2009, Paris, [2] Cuney (2009) *Mineral. Dep.* **44**, 3-9, [3] Cuney (2012) *in Non-renewable resources Geoscientific & Societal Challenges, Springer*.

https://doi.org/10.1180/S0026461X00008434 Published online by Cambridge University Press

Brachiopods recording seawater temperature – grow up and be a good proxy

M. CUSACK[1]* AND A. PÉREZ-HUERTA[2]

[1] School of Geographical & Earth Sciences, University of Glasgow, UK. Maggie.Cusack@glasgow.ac.uk

[2] Dept. of Geological Sciences, The University of Alabama, Tuscaloosa AL 35487, USA. aphuerta@as.ua.edu

Brachiopods are attractive proxies

The stable, low- magnesium shells of brachiopods and their long geological record means that they are an attractive source of past seawater temperature data. Although brachiopod shells appear simple, analysis of their crystallography e.g. [1-2] or shell punctae (perforations) [3], reveals the extent of the biological control that is exerted as these shells form. This biological control makes it all the more impressive that the calcite fibres of the secondary (inner) layer of low magnesium-calcite brachiopod shells are in oxygen isotope equilibrium with ambient seawater [4-5].

Maturation or class?

In *Terebratalia transversa*, micromilling and conventional mass spectrometry revealed that oxygen isotope equilibrium is not achieved instantly with the abrupt switch from primary (outer) to secondary (inner) layer secretion but rather that oxygen isotope equilibrium is attained towards the innermost shell [6]. Thus, the first formed calcite fibres of the secondary layer of *T. transversa* are not in isotopic equilibrium while the later fibres of mature valves are in oxygen isotope equilibrium with seawater.

This study exploits the high spatial resolution of secondary ion mass spectrometry (SIMS) to investigate this oxygen isotope trend in *Terebratalia transversa* as investigated by Auclair [6] as well as *Terebratulina retusa* and *Notosaria nigricans*. Thus, three species of brachiopod from two Orders and two sub-orders are investigated by high resolution SIMS. This will help us understand whether only mature valves can be relied upon in proxy measurements or whether this caveat is restricited to *T. transversa*.

[1] Schmahl, W.W., et al., (2004). *European Journal of Mineralogy*. **16**, 693-697.

[2] Cusack, M., et al., (2008). *Journal of Structural Biology*. **164**, 96-100.

[3] Pérez-Huerta, A., et al., (2009). *Journal of Structural Biology*. **167**, 62-67.

[4] Carpenter, S.J., et al., (1995). *Geochimica et Cosmochimica Acta*. **59**, 3749-3764.

[5] Parkinson, D., et al., (2005). *Chemical Geology*. **219**, 193-235.

[6] Auclair, A.C., et al., (2003). *Chemical Geology*. **202**, 59-78.

Arsenic and phosphate cycling in surface waters of the North Atlantic

GREGORY CUTTER[1*], OLIVER WURL[2], LOUISE ZIMMER[3], AND MELISSA PHILLIPS[4]

[1]Old Dominion University, Ocean, Earth, and Atmospheric Sciences, Norfolk, Virginia, USA, gcutter@odu.edu (* presenting author)

[2]Old Dominion University, Ocean, Earth, and Atmospheric Sciences, Norfolk, Virginia, USA, owurl@odu.edu

[3]Old Dominion University, Ocean, Earth, and Atmospheric Sciences, Norfolk, Virginia, USA, lzimmer@odu.edu

[4]Old Dominion University, Ocean, Earth, and Atmospheric Sciences, Norfolk, Virginia, USA, mmphilli@odu.edu

Introduction

It is well known that As(V), arsenate, is toxic to marine phytoplankton when phosphate concentrations drop to the 10-15 nM levels of arsenate found in oligotrophic surface waters. This toxicity is due to the chemical and biochemical similarities of the two. Interestingly, many phytoplankton have evolved arsenic detoxification mechanisms that include reducing arsenate to arsenite (AsIII) and/or methylating it to monomethyl (MMAs) and dimethyl arsenic (DMAs); these species are not taken up by phytoplankton. Thus, phytoplankton in oligotrophic, low P waters have a two-fold problem: first phosphate stress and then arsenate toxicity. Existing methods to assay phosphate stress via measurements of the enzyme alkaline phosphatase's activity (APA) have no associated time clock to establish how long the stress has occurred. Depending on their residence times, the As detoxification products could provide this missing temporal information.

The coupled biogeochemistries of As and P were examined on the US GEOTRACES cruises from Lisbon, Portugal to Cape Verde and then Charleston, South Carolina USA in 2010, and Woods Hole, Massachusetts USA to Cape Verde in 2011. Surface samples were acquired with a trace metal-clean towed "fish" at two hour intervals, 0.2 μm filtered, immediately refrigerated, and analyzed within 24 hours. Additional samples for APA were unfiltered and passed through an 80 μm mesh to remove zooplankton; assays were begun within 4 hours. Nanomolar reactive phosphate was determined using a modified molybdenum blue method and liquid core waveguides. Arsenic speciation was determined using selective hydride generation coupled to gas chromatography with photoionization detection.

Results and Discussion

On the two transects, phosphate varied from 3-20 nM (except near the coasts). AP activities were highest in the oligotrophic central gyre with the lowest phosphate concentrations. Arsenite varied between 0.2-5 nM, the highest values in the gyre. Arsenite has an surface residence time of ca. 3d and showed a significant correlation with APA (r=0.6), suggesting it may be a good short term indicator of P-stress. MMAs was relatively uniform in its distribution, while DMAs varied more, 0-4 nM. Neither methyl species correlated with APA, but if their residence times (to be determined) are longer, then no direct relationship would be expected. Overall, it does appear that As speciation may be a useful integrator of P-stress.

https://doi.org/10.1180/S0026461X00008434 Published online by Cambridge University Press

Early Archean Fe oxidation revealed by meso- and micron-scale Fe isotope analyses of the 3.7–3.8 Ga Isua BIFs

ANDREW D. CZAJA[1,2*], CLARK M. JOHNSON[1,2], BRIAN L. BEARD[1,2], STEPHEN MOORBATH[3]

[1]Department of Geoscience, University of Wisconsin, Madison, WI, USA, aczaja@geology.wisc.edu (* presenting author)
[2]NASA Astrobiology Institute
[3]Department of Earth Sciences, University of Oxford, Oxford, GBR

Iron isotopes are increasingly used to constrain the conditions of Earth's paleoenvironments and even suggest the influence of biological activity. Interpretations of Fe isotope fractionations in Archean and Paleoproterozoic banded iron formations (BIFs), shales, and carbonates suggest a role for biological processes (bacterial dissimilatory iron reduction (DIR) and anoxygenic photosynthetic iron oxidation (APIO)] and abiological processes (oxidation by free O_2). Measurements of rock powders micromilled from individual magnetite layers and of individual magnetite grains analyzed by femtosecond laser ablation ICP-MS (fs-LA-ICP-MS) from BIFs of the 3.7–3.8 Ga Isua Greenstone Belt reveal a consistently narrow range of non-zero δ^{56}Fe values. Analyses by fs-LA-ICP-MS allow for precise and accurate micron-scale analyses without the orientation effects associated with secondary ion mass spectrometry analyses of magnetite [1]. Magnetite δ^{56}Fe values range from +0.4‰ to +1.1‰ among different bands, but within individual layers magnetites are homogenous. In buld samples, δ^{56}Fe and SiO_2 concentration are negatively correlated, whereas δ^{56}Fe and total Fe concentrations are positively correlated, reflecting mixtures between magnetite and Fe silicate. A simple mixing model between a low-δ^{56}Fe component (Fe silicate) and a high-δ^{56}Fe component (magnetite) can explain the range in Fe isotope compositions of the micromilled rock powders. Although these BIFs have been metamorphosed to greenschist- to amphibolite-facies, the isotopic heterogeneity observed on both scales suggests that the Fe isotope compositions reflect primary, low-temperature sedimentary values.

The positive δ^{56}Fe values measured from the Isua magnetites are best explained by deposition of Fe-oxides produced by partial oxidation of Fe(II)-rich ocean water either by free O_2 or APIO. Comparison of the Fe isotope data from the Isua BIFs with those from the 2.5 Ga BIFs from the Hamersley and Transvaal basins suggests a striking difference in Fe sources and pathways. The Neoarchean magnetite facies BIFs of Australia and South Africa have δ^{56}Fe values that range from -1.2 to +1.2 ‰ [2] and are on average significantly lower than those reported here from the Isua BIFs. Such a range suggests a role for DIR, the most likely means by which to produce large masses of negatively fractionated Fe. The absence of low δ^{56}Fe values in the Isua BIFs may indicate formation prior to the evolution of DIR or in an environment that excluded this metabolism.

Acknowledgements

We thank Morgan Herrick, Robert Dymek, Cornelius Klein for provision of samples, assistance with analyses, and discussions.

[1] Kita (2010) *Surf. Interface Anal.* **43**, 427-431. [2] Johnson (2008) *Annu. Rev. Earth Planet. Sci.* **36**, 457-493.

https://doi.org/10.1180/S0026461X00008434 Published online by Cambridge University Press

X-ray microspectroscopic investigations of Ni(II) uptake by argillaceous rocks of the Boda Claystone Formation in Hungary

RAINER DÄHN[1*], JÁNOS OSÁN[2], DÁNIEL BREITNER[2], ISTVÁN SAJÓ[3], MARIA MARQUES[1], BART BAEYENS[1] AND SZABINA TÖRÖK[2]

[1]Paul Scherrer Institut, Villigen, Switzerland (*rainer.daehn@psi.ch)
[2]Centre for Energy Research, Hungarian Academy of Sciences, Budapest, Hungary
[3]Chemical Research Centre, Hungarian Academy of Sciences, Budapest, Hungary

One of the main aspects for evaluating the safety case of a potential radioactive waste repository in a deep geological formation is to understand and quantify the geochemical and physical processes that influence the mobility of the radionuclides in the geochemical environment imposed by the host rock. This information is needed to make reliable predictions of the long-term retardation behaviour of radionuclides. The present study focuses on the interaction of a key radionuclide with the Boda Claystone Formation (BCF) of the planned high level radioactive waste repository in Hungary. BCF is rich in illite and hematite. The aim is to identify the mineral phases responsible for the uptake of Ni by BCF, and to investigate the uptake mechanisms of radionuclides on clays and other minerals present in the host rock.

Small pieces of selected BCF core hole samples from a depth of 540 m were prepared as thins sections and equilibrated with $NiCl_2$ solutions at pH = 7.05 in a 0.1 M NaCl background electrolyte. Combined µ-XRF/XAS/XRD measurements were performed at HASYLAB Beamline L (Hamburg, Germany) and µ-XRF/XRD at the ANKA FLUO Beamline (Karlsruhe, Germany). µ-XRF maps were recorded from pre-selected areas of the samples, using a step size comparable to the beam size (20 µm at HASYLAB and 5 µm at ANKA) and 1 s counting time per pixel. The elemental maps served as a basis for selection of small areas of interest where µ-XRD images were collected by a CCD detector. The µ-EXAFS measurements were measured in fluorescence mode at HASYLAB Beamline L, at 20 µm lateral resolution for certain points of interest.

The distribution maps indicate that Ni is mainly associated to K- and Fe-rich phases. µ-XRD analyses with a 5 µm beam diameter indicate that the composition of the argillaceous rock matrix on the micro-scale agree well with the mineral composition of the clay rich areas obtained by bulk-XRD measurements. The good correlation of Fe with K is mainly caused by the high K content in illite (a K-rich 2:1 clay mineral). Micro-EXAFS investigations demonstrated that inner-sphere complexation of Ni occurred to clay minerals. At higher Ni concentrations (10^{-3} M Ni) surface precipitation processes prevailed. The formation of Ni precipitated phases such as Ni-phyllosilicates has important geochemical implications because layered silicates are stable minerals in mildly acidic to basic pH conditions and can irreversibly bind metals in waste and soil matrices. The uptake of contaminants on mineral surfaces forming inner-sphere complexes strongly reduces the mobility of metals in the geosphere. The results of the analyses demonstrated that for Ni(II) the clay mineral illite is an effective sinks in the BCF sample.

Tracing Euxinia in Ancient Oceans with molybdenum

TAIS W. DAHL[1,*] AND DONALD E. CANFIELD[1]

[1] Nordic Center for Earth Evolution and University of Southern Denmark, Odense, Denmark, tdahl@biology.sdu.dk

Elevated molybdenum (Mo) concentrations in organic-rich sediments are a characteristic feature of deposition in sulfidic waters. A comparative study of modern sediment cores from more than 200 marine sites worldwide show that all euxinic basins display >25 ppm Mo [1]. Conversely, all organic-rich sediments with >25 ppm Mo are deposited from a permanently or intermittently sulfidic water column. We show that this last observation can now be determined in <30 seconds using handheld X-Ray absorption Fluorescence spectroscopy (HH-XRF). The new tool enables euxinic classification in the field.

The Mo enrichment process in euxinic settings is expected based on the critical role that aqueous H_2S plays in breaking Mo=O double bonds when soluble MoO_4^{2-} forms reactive Mo sulfides [2]. However, we have identified Neoproterozoic euxinic settings based on Fe-speciation indicators [3] with only small sedimentary Mo enrichments [4]. The Fe speciation technique is unlikely to give false-positive identifications of euxinia, and the question remains what controlling factors could have obstructed the Mo enrichment process at that time.

First, we speculate that the Mo supply to the basins was particularly slow. However, the Mo enrichment process takes place today even in settings with low Mo supply, whether limited by basinal restriction and a slow deepwater renewal rate (e.g. Black Sea) or low Mo load in the source waters of only (e.g. 10 nM in Lake Cadagno).

We have established a one-box model for the oceanic Mo cycle, where Mo burial rates are linked 1st order with respect to ambient Mo reservoir. It shows that seawater Mo concentrations, today 105 nM, never decreased below modern riverine values (~6 nM). Hence, a low seawater inventory is insufficient to obstruct the Mo enrichment process in settings with supply comparable to Lake Cadagno, but a combination of both widespread euxinia (lowering seawater Mo inventory) and basinal restriction (lowering basinal Mo relative to open ocean) could potentially compromise Mo enrichment in the Neoproterozoic sediments.

This illustrates how expansion of oceanic euxinia derived from our models rests on a rigorous understanding of the key factors involved in the removal pathway of Mo from oxic surface waters to euxinic sediments. We discuss how laboratory and field-based studies elucidate which factors, other than H_2S, could influence the Mo burial pathway in the past. Overall, we illustrate the linkage between studies of modern euxinic systems and reconstructions of global-scale ocean conditions of the past.

[1] Lyons et al. (2009) *Annu. Rev. Earth Planet Sci.* **37** *507-534* [2] Erickson and Helz (2000) *GCA*, **64** *1149-1158*; Dahl et al. (2012) *in prep.* [3] Canfield et al. (2008) *Science*, **321** (5891) *949-952,* [4] Dahl et al. (2011) EPSL, **311** (3-4), *264-274*

https://doi.org/10.1180/S0026461X00008434 Published online by Cambridge University Press

The nature of orogenic lithospheric mantle: constraints from geochemistry of postcollisional mafic-ultramafic rocks in the Dabie orogen

LI-QUN DAI*, ZI-FU ZHAO, YONG-FEI ZHENG

CAS Key Laboratory of Crust-Mantle Materials and Environments, School of Earth and Space Sciences, University of Science and Technology of China, Hefei 230026, China, lqdai@mail.ustc.edu.cn

Oceanic and continental arc volcanic rocks are a window into crust-mantle interaction in oceanic subduction zones, with involvement of the asthenospheric mantle. They are assumed to originate from partial melting of altered peridotite in the overlying mantle wedge, with trace element geochemical signature inherited from aqueous fluids released from subducting oceanic crust. While this process-product link has been a common percept in geochemistry, it is intriguing whether there is the similar relationship in continental subduction zones. Ultrahigh-pressure (UHP) metamorphic rocks are a typical product of continental deep subduction to mantle depths, but arc magmatism is absent above continental subduction zones. While the subducted continental crust can be reworked as postcollisional granitoids, it is unclear whether the overlying subcontinental lithospheric mantle (SCLM) was involved in postcollisional mafic magmatism.

Postcollisional mafic-ultramafic rocks from the Dabie orogen were studied for their zircon U-Pb ages and Lu-Hf isotopes, whole-rock major-trace elements and Sr-Nd-Pb isotopes as well as whole-rock and mineral O isotopes. The results provide insights into the nature of orogenic lithospheric mantle in the continental collisional orogen. The zircon U-Pb dating gave consistent ages of 125 ± 3 to 129 ± 1 Ma for magma crystallization. Few residual zircon cores have U-Pb ages of 234 ± 5 Ma and 739 ± 9 Ma, respectively, in agreement with tectonothermal events for UHP metamorphism and protolith formation in the Dabie orogen. The mafic-ultramafic rocks have high contents of MgO (up to 18.0 wt.%), Cr (up to 1546 ppm) and Ni (up to 349 ppm), but low contents of SiO_2 (41.0-51.9 wt.%), and show the arc-like patterns of trace elements distribution and the enriched signature of Sr-Nd-Pb-Hf isotopes. These geochemical features indicate their derivation from partial melting of the orogenic lithospheric mantle that is fertile in lithochemistry and enriched not only in LILE and LREE but also in radiogenic isotopes. The orogenic lithospheric mantle is suggested to be generated by metasomatic reaction of the overlying SCLM-wedge peridotite with hydrous felsic melts derived from the subducted continental crust during the Triassic continental collision, with the enriched signatures imparted by the felsic melts. In this regard, the crust-mantle interaction is implicated during the continental deep subduction, with the postcollisional mafic-ultramafic rocks as its derivatives. On the other hand, significant differences in elemental and isotopic compositions between different mafic-ultramafic intrusions suggest that the orogenic lithospheric mantle is geochemically heterogeneous, with the possible presence of hornblende-rich and pyroxene-rich lithologies in mantle sources. This difference is attributed to differences in the compositions of subducted crustal-derived melts with a tectonic affinity to the South China Block, but the same SCLM wedge of the North China Block was involved in the crustal metasomatism. Therefore, the compositional variations in the orogenic lithospheric mantle are recorded by the geochemical compositions of postcollisional mafic-ultramafic intrusions.

A spatially-structured model for Proterozoic ocean biogeochemistry

STUART DAINES[1*], ANDY RIDGWELL[2] AND TIM LENTON[1]

[1]University of Exeter, UK, s.daines@exeter.ac.uk (* presenting author). [2]University of Bristol, UK.

The picture for Proterozoic ocean biogeochemistry from marine proxy data and simple box models has been of an anoxic and ferruginous ocean prior to 1.85 Ga, with a switch to either oxic or euxinic conditions then responsible for removing iron from the deep ocean and halting Banded Iron Formations ~1.85 Ga [1]. However, recently-gathered geochemical data from what remains of the Proterozoic ocean margins reveal a more complex picture with some euxinic intervals prior to 1.85 Ga, and a largely ferruginous ocean with only some sulphidic intervals and/or sulphidic waters at intermediate depths post-1.85 Ga [2],[3].

Here we use a spatially-structured biogeochemical model GENIE to propose a scenario consistent with proxy data, and also consistent with constraints from both oxygen demand and ventilation, and ocean mixing and Fe, S residence timescales. A robust feature of scenarios that avoid global euxinia is a vertical redox gradient from an oxygenic mixed layer, through euxinic mid-depths in shelf or upwelling regions, to a suboxic deep ocean. A suboxic (rather than fully anoxic and ferruginous) deep ocean is consistent with evidence from hematitic cherts [4]. This model makes two testable predictions: (i) that the "ferruginous" water column state inferred from iron-speciation proxy data arises from iron transport in a marginally suboxic or anoxic region underlying euxinic region, and (ii) that feedback processes must exist to balance the deep ocean on the edge of anoxia.

Nitrogen cycling in the mixed aerobic/anaerobic surface/mid-depth regions results in relatively high levels of denitrification and nitrification with small marine nitrogen reservoirs and short residence times.

[1] Canfield (1998) *Nature* **396**, 450-453. [2] Kendall (2010) *Nature Geoscience* **3**, 647-652. [3] Poulton (2010) *Nature Geoscience* **3**, 486-490. [4] Slack (2007) *EPSL* **255**, 243-256.

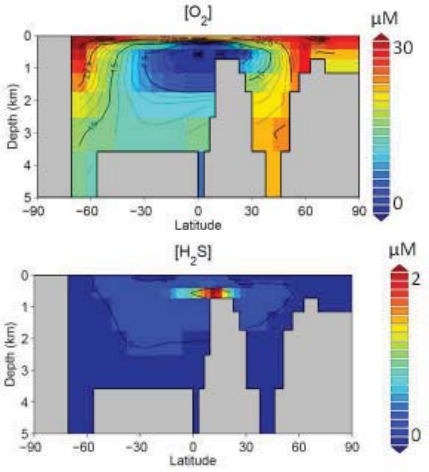

Figure 1: Meridional sections for $[O_2]$ and $[H_2S]$ with localized euxinia and suboxic deep ocean.

https://doi.org/10.1180/S0026461X00008434 Published online by Cambridge University Press

Selection for Gaia at multiple scales

STUART DAINES, RICHARD BOYLE, JAMES CLARK, HYWEL WILLIAMS AND TIM LENTON*

University of Exeter, UK, s.daines@exeter.ac.uk (*presenting author)

Biological regulation of the environment is present at scales from individuals, to ecosystems, to the global biosphere. However, the emergence of regulation at scales which cannot have been units of natural selection is a very different problem from the Darwinian evolution of organism-level homeostasis. Nevertheless, at local ecosystem level, regulation is beginning to be understood as a consequence of "niche construction" [1]. Recent work [2] has also demonstrated the evolutionary emergence of global regulation from local selection in spatially structured environments that tend to distribute the benefits from regulation preferentially to regulators (and not free-riders or organisms with a destabilising effect). At global scales, biosphere regulation must in addition be reconciled with geochemical feedbacks, often involving well-mixed global reservoirs such as the atmosphere, or geological time delays. This temporal and/or spatial decoupling of effects from actors make evolutionary explanations problematic.

Here we investigate mechanisms by which global regulation might emerge by a non-evolutionary process of self-organisation. We argue that the global biota is assembled over time by a process analogous to ecological community assembly [3], but operating at global scale over geological and macroevolutionary timescales and perturbed by macroevolutionary innovations [4] and geological events. By a process of "sequential selection" [5], fragile systems, or those that destabilise their environment, are then short-lived, and result in extinctions and reorganisations until a relatively stable (but possibly lifeless) state is temporarily reached. We employ simple conceptual models for community assembly, evolutionary innovation, life-environment interaction, and anthropic bias to test three hypotheses for the implications of this mechanism for the stability and regulation of an observed biosphere. The limited information input and the "satisficing" (rather than optimising) nature of the sequential selection mechanism make it probable that: (i) regulation at the global level involves only simple configurations of multiple (individually local and Darwinian) physiologically limited "biotic plunder" mechanisms [7],[8] combined with abiotic feedbacks, and (ii) regulation of the environment is strongest at limits, rather than at optimal conditions for life. Anthropic bias [6] applies a further filter to the distribution of biosphere properties such that (iii) our observed biosphere need be only sufficiently stable for the evolution of complex life.

[1] Odling-Smee (1996) *Am. Nat.* **147**, 641-648. [2] Williams (2008), *PNAS* **105**, 10432-7. [3] Post (1983), *Math. Biosci.* 64,169-92. [4] Williams (2010) *Oikos* **119**, 1887-99. [5] Betts (2007) *Gaia Circ.***2007**, 4-6. [6] Watson (2008) *Astrobiology* **8**, 175-85. [7] Tyrell (2004) *Scientists Debate Gaia, Schneider ed*, 137-47. [8] Lenton (2000). *J Th. Biol.* **206**, 109-14.

A bottom-up perspective on N and P cycling in low oxygen environments: the Baltic Sea versus the Peruvian shelf

ANDY W. DALE[1]*, LISA BOHLEN[2], ANNA NOFFKE[3], STEFAN SOMMER[4], CHRISTIAN HENSEN[5], AND KLAUS WALLMANN[6]

[1]Geomar | Helmholtz-Zentrum für Ozeanforschung Kiel, Kiel, Germany, adale@geomar.de (* presenting author)

[2]Geomar | Helmholtz-Zentrum für Ozeanforschung Kiel, Kiel, Germany, lbohlen@geomar.de

[3]Geomar | Helmholtz-Zentrum für Ozeanforschung Kiel, Kiel, Germany, anoffke@geomar.de

[4]Geomar | Helmholtz-Zentrum für Ozeanforschung Kiel, Kiel, Germany, ssommer@geomar.de

[5]Geomar | Helmholtz-Zentrum für Ozeanforschung Kiel, Kiel, Germany, chensen@geomar.de

[6]Geomar | Helmholtz-Zentrum für Ozeanforschung Kiel, Kiel, Germany, kwallmann@geomar.de

This study presents a combination of field measurements and state-of-the-art modeling to investigate N and P cycling in sediments of two contrasting oxygen stressed systems. Boknis Eck is a 28 m deep channel in the southwest Baltic Sea which experiences severe hypoxia (< 2 μM O_2) in boreal summer lasting until October [1]. A time series analysis of benthic nutrient analyses based on monthly samplings from February to December 2010 revealed that N and P fluxes were elevated in winter due to porewater pumping by bioirrigating organisms which efficiently flushed the upper 10 cm of sediment. During hypoxia, no bioirrigation was measurable, macrofauna were absent and phosphate accumulated to concentrations exceeding 400 μM, resulting in a large diffusive flux to the water column. At the same time, denitrification rates were elevated yet dissimilatory nitrate reduction to ammonium (DNRA) by sulfide oxidizing bacteria (*Beggiatoa* spp) played a much larger role in recycling N between the water column and sediments, thus conserving reactive N in the system. By January 2011, typical winter conditions were once again established.

In the Peruvian OMZ, anoxia is more permanent and ventilation events are less predictable. Benthic N and P cycling investigated at six stations along 11 °S using landers revealed very high rates of ammonium and phosphate fluxes on the shelf and upper slope (80 – 250 m water depth) where extensive areas of mats of *Beggiatoa* were present [2]. DNRA dominated total N turnover (≤ 2.9 mmol N m^{-2} d^{-1}) and accounted for ≥ 65 % of nitrate uptake by the sediments from the bottom water. Only at greater water depths within the OMZ (300 – 1000 m) were the sediments a net sink for reactive N due to denitrification. Overall, our findings in Peru and the Baltic Sea show that high measured benthic uptake rates of oxidized N within OMZs do not necessarily indicate a loss of fixed N from the marine environment, but are instead recycling sites converting nitrate into ammonium. Phosphate release is elevated in both environments, which altogether indicate that similar processes occur in sediments underlying seasonal and more permanent OMZs. Due to the high rates of benthic N and P turnover in OMZs, pelagic models ought to incorporate benthic dynamics in their calculations.

[1] Bohlen et al. (2011) *Geochim. Cosmochim. Acta* **75**, 6094-6111. [2] Dale et al. (2011) *Estuar. Coast. Shelf Sci*. **95**, 14-28.

https://doi.org/10.1180/S0026461X00008434 Published online by Cambridge University Press

Osmium and oxygen isotopes in Etendeka picrites and their olivines: mantle melts and crustal interaction

CHRISTOPHER W. DALE [1*], R. N. THOMPSON [1], D. G. PEARSON[2], A. J. V. RICHES[2], D. P. MATTEY[3]

[1]Dept. of Earth Sciences, Durham University, UK christopher.dale@durham.ac.uk (*presenting author)
[2]Dept. Earth & Atm. Sciences, University of Alberta, Edmonton, Canada
[3]Dept. Earth Sciences, Royal Holloway, University of London, UK

The existence of basal picrites and picritic dykes in the Etendeka large igneous province (LIP) provides the opportunity to study high-degree, relatively unfractionated melt products from a hot plume head and hence gain the best insight into the source composition. Moreover, highly magnesian olivine phenocrysts (occasionally up to Fo 93.3), which reflect crystallisation from melts with up to 24 wt% MgO [1], provide particularly primitive isotopic information. Such high MgO melts require mantle potential temperatures up to 1700°C [1], amongst the highest known for the Phanerozoic. At the same time, the eruption of the picrites through continental crust allows the role of assimilation, in imparting an isotopic signature, to be investigated.

Here we present major and trace elements and Sr, Nd, Pb and Os isotopes for whole rocks, and combine these with major elements and osmium and oxygen isotopes for olivine phenocrysts. Highly siderophile element abundances are also presented.

The Pb isotopic compositions of whole rocks covary with Pb content and are clearly controlled by a local crustal sedimentary input, and give little information on the source. Strontium and Nd isotopes in the Horingbaai dykes covary negatively, indicating variable contributions from depleted and slightly enriched endmembers, the latter likely local crust.

The $^{187}Os/^{188}Os$ compositions of the primitive Horingbaai and more evolved Spitzkoppe picrites (0.128-0.131) are in the same range as some other high-T plume melts (e.g. North Atlantic Igneous Province picrites: 0.127-0.134 [2]). The least radiogenic values support a predominantly mildly-depleted peridotite source for the highest temperature volcanism in the region, which is also consistent with MORB-like REE patterns. The Os data exclude the possibility of a long-term strongly Re-depleted source input, such as old lithosphere. The more radiogenic values could reflect a contribution from an isotopically enriched mantle component. Olivines from the Horingbaai and Spitzkoppe picrites, however, have similar or slightly lower isotopic compositions than their respective whole rocks, suggesting that, at least in part, the more radiogenic Os isotope values are a result of crustal assimilation after olivine crystallisation, even in these Os-rich picritic melts.

Oxygen isotope compositions in olivines ($\delta^{18}O$ up to 6.5‰) extend higher than typical mantle, and are associated with more radiogenic $^{187}Os/^{188}Os$. Although it is difficult to rule out a mantle eclogite component as a source of coupled O-Os enrichment, a crustal input is the likely cause of this effect, and is supported by the combined isotopic and elemental data.

[1] Thompson & Gibson (2000) *Nature* **407**, 502-506.
[2] Dale et al. (2009) *EPSL* **278**, 267-277.

Fe(III) reduction by the Gram-positive bacterium *Desulfotomaculum reducens*

ELENA DALLA VECCHIA[1], PAUL SHAO[1], ELENA SUVOROVA BUFFAT[1], JULIEN MAILLARD[2], RIZLAN BERNIER-LATMANI[1,*]

[1] Environmental Microbiology Laboratory, Ecole Polytechnique Federale de Lausanne, EPFL, Lausanne, Switzerland, rizlan.bernier-latmani@epfl.ch (* presenting author)
[2] Environmental Biotechnology Laboratory, EPFL, Lausanne, Switzerland, julien.maillard@epfl.ch

Microbial Fe(III) reduction, specifically that of solid phase Fe(III), presents a challenge to bacteria as electrons must be transported to an extracellular electron acceptor. This process has been studied extensively for Gram-negative bacteria such as *Shewanella oneidensis* and *Geobacter sulfurreducens*. Several strategies have been documented in these microbes: (a) the secretion of endogenous redox mediators that are reduced by cells following oxidation by Fe(III); (b) direct contact of outer-membrane multi-heme cytochromes with the solid-phase substrate or (c) the extension of micron-long electroconductive pili that can transport electrons away from the cell. The transfer of electrons in the latter two cases was dependent on several multi-heme cytochromes located in the cytoplasmic and outer membranes as well as in the periplasmic space.

In the case of Gram-positive bacteria, there is evidence either for the involvement of redox mediators [1] or the requirement for direct contact with the electron-receiving surface [2]. In both cases, the mechanism remains unknown. In this study, we probe the reduction of soluble Fe(III) [as Fe(III)-citrate] and of solid-phase Fe(III) [as hydrous ferric oxide, HFO] by the Gram-positive bacterium *Desulfotomaculum reducens*. The best growth was obtained with pyruvate due to fermentation but some growth was detected with lactate as an electron donor. In the presence of HFO, pyruvate was rapidly (~3 days) converted to acetate and Fe(III) slowly reduced over 25 days. Tests with spent medium from pyruvate- and HFO-grown cells indicate the presence of an endogenous redox mediator able to reduce anthraquinone disulfonate (AQDS). In contrast, HFO reduction occurred concomitantly with lactate oxidation to acetate and there was no evidence for a redox mediator. Experiments with HFO enclosed in glass beads (and thus only accessible to diffusable redox mediators) confirmed those findings as reduction of Fe(III) was observed in the pyruvate case but not detectable in the lactate case.

The *D. reducens* genome harbors a sole multi-heme *c*-type cytochrome complex (NrfHA) with homology to the nitrite reductase in *Desulfovibrio vulgaris*. Quantitative reverse transcription PCR (qRT-PCR) showed that while *nrf*HA was expressed during fermentation, there is no evidence for expression during Fe(III) reduction. Hence, we conclude that (a) HFO reduction occurs via a redox mediator with pyruvate while it is mediator-independent in the presence of lactate; (b) the sole *c*-type cytochrome complex present in the genome of *D. reducens is* not involved in Fe(III) reduction. Ongoing work focuses on the characterization of the mechanism of lactate-dependent HFO reduction and aims at providing a mechanistic understanding of electron transfer across the Gram-positive cell wall.

[1] Pham et al. (2008) *Appl. Microbiol. Biotechnol.* **77**, 1119-1129.
[2] Wrighton et al. (2011) *Appl. Environ. Microbiol.* **77**, 7633-7639.

https://doi.org/10.1180/S0026461X00008434 Published online by Cambridge University Press

Continental surface temperatures inferred from the investigation of fossil hydrothermal systems

LUIGI DALLAI [1*] AND RAY BURGESS[2]

[1]Institute of Geosciences and Earth Resources - CNR, Pisa, Italy dallai@igg.cnr.it (* presenting author)

[2] SEAES, University of Manchester, UK ray.burgess@manchester.ac.uk

Plutonic and sub-volcanic igneous rocks have been shown to be a promising source of data relevant to paleo-temperature reconstruction. A first Antarctic terrestrial record of climate variations through the Cenozoic has been recently published, based on the hydrogen isotope composition of hydrothermally altered minerals of intrusive rocks from the coastal areas of the Wilson Terrane, Northern Victoria Land, Antarctica (Dallai & Burgess, 2011). Cenozoic land surface temperature data for this remote area located at 73-74°S latitude are poorly known but may be crucial to understand how and possibly why, the climate changed in continental Antarctica before and during the Eocene-Oligocene transition. In this investigation, the variations of hydrogen isotope composition of hydrothermal waters have been studied in detail. By dating the minerals formed upon hydrothermal alteration, a record of meteoric-hydrothermal water compositions has been reconstructed, enabling the atmospheric conditions during the Cenozoic era to be inferred. This continental record of polar climates in Antarctica is in reasonable agreement with the global climatic records derived from oceanic deep cores and with the model curve for atmospheric pCO_2. These observations give insights into the climatic evolution of continental areas in an important region over a critical time interval suggesting that temperature fluctuations as large as 20°C occurred repeatedly during the Eocene. The aim is to determine continental paleo-temperatures for different periods of the Cenozoic and to merge data from hydrothermal systems from high latitude regions of both hemispheres to define bi-polar climatic conditions through geological time. Preliminary data of hydrothermal systems from high latitude regions of the Northern Hemisphere fit the hydrogen based paleo-temperature curve, thereby implying that extending this study to other Cenozoic (and older) intrusive bodies may better constrain continental paleo-temperature records both in space and in deeper times.

References

Dallai L., & Burgess R., 2011. A record of Antarctic surface temperature between 25 and 50 million years ago. Geology **39**, 423–426.

Evolution of silicic magmas and the origin of the Daly Gap at Santa Barbara volcano, Terceira, Azores

G. E. DALY[1*], E. WIDOM[1] AND Z. FRANÇA[2]

[1]Department of Geology, Miami University, Oxford, Ohio, USA, dalyge@muohio.edu (*presenting author)

[2]Departamento de Geociências, Universidade dos Açores, Ponta Delgada, São Miguel, Açores, Portugal, zfranca@uac.pt

The origin of compositional gaps (e.g. the Daly Gap) and high volumes of silicic rocks among volcanic deposits in ocean islands have remained controversial subjects. Although silicic magmas can be produced by fractional crystallization of parental basalts, the paucity of intermediate compositions and the relatively large volumes of silicic compositions amongst erupted materials are difficult to explain by this mechanism. Several hypotheses have been proposed for the scarcity of erupted intermediate rocks, including development of physical/chemical properties (density, viscosity and/or volatile content) that may inhibit them from erupting [1]. Alternatively, melting of altered mafic crust may produce bimodal volcanism without formation of intermediate magma compositions, and can potentially explain large volumes of silicic deposits [2].

Santa Barbara volcano (Terceira, Azores) is an ideal locality for investigating these problems. Terceira has an uncommonly high percentage (~50%) of silicic volcanic rocks relative to mafic compositions [1], and Santa Barbara exhibits a well defined Daly Gap from 54 to 64 wt.% SiO_2 amongst eruptive products, including flank basalts and trachytes erupted from the central vent [3]. However, we show that the compositional gap closes if plutonic nodules contained in air fall deposits from Santa Barbara are considered.

We have performed petrographic, major and trace element, and Sr–Nd-Pb isotopic analyses on eruptive products from the relatively recent (<2ka) Santa Barbara-G trachyte deposit [4], as well as flank basalts [5] and plutonic nodules collected from older trachytic air fall deposits from Santa Barbara. These data demonstrate an essentially continuous compositional variation from 45 to 69% SiO_2, with the plutonic nodules ranging from 45 to 65 wt% SiO_2, and thus effectively filling in the compositional gap defined by the bimodal basaltic-tracyhtic volcanic products. Trace element systematics indicate that the plutonic nodules are genetically related to the basalts and trachytes, following a common fractional crystallization path. The plutonic nodules exhibit large (~4- to 10-fold) variations in concentrations of trace elements including highly incompatible elements (Hf, Nb, and Zr) and compatible elements (Ba and Sr). Most significantly, some of the plutonic nodules have incompatible element concentrations equal to those in the Santa Barbara G trachytes. Together, these data suggest that the plutonic nodules represent liquid rather than cumulate compositions, as inferred for syenites from Fogo volcano (Sao Miguel, Azores; [6]).

These results indicate that intermediate magma compositions are produced during fractional crystallization from parental basalts to trachytes, and that these intermediate magma compositions generally fail to erupt as volcanic products. Ongoing Sr-Nd-Pb and planned U-series isotopic analyses of the plutonic nodules will further constrain their genetic relationship to the Santa Barbara basalts and trachytes, and potentially allow evaluation of their crystallization ages.

[1] Mungall & Martin (1995) *Contrib. Mineral. Petrol.* **119(1)**, 43-55 [2] Bindeman et al. (2006) *Earth and Planet. Sci. Lett.* **245**(3-4), 245-259 [3] Self (1976) *J. Geol. Soc. of London* **132**(6), 645-666 [4] Daly et al. (2010) Goldschmidt [abs.] A204 [5] Yu & Widom (2010) Goldschmidt [abs.] A1191 [6] Widom et al. (1993) *J. Pet.* **34,** 929-953

https://doi.org/10.1180/S0026461X00008434 Published online by Cambridge University Press

Analysis and modelling of arsenic dynamics in coastal sediments

DUC HUY DANG[1*], ERWAN TESSIER[1], VÉRONIQUE LENOBLE[1], GAËL DURRIEU[1], CHRISTOPHE LE POUPON[1], JEAN-ULRICH MULLOT[2], STÉPHANE MOUNIER[1] AND CÉDRIC GARNIER[1]

[1]Laboratoire PROTEE, Université du Sud Toulon Var, BP20132, 83957 La Garde, France, duc-huy.dang@univ-tln.fr

[2]LASEM-Toulon, Base Navale de Toulon, BP 61, 83800 Toulon, France

Sediments of the Toulon bay (SE, France) are significantly polluted by trace metals, metalloids and organic contaminants, due to historical events (2nd World War...). Contaminants behavior in sediments and transfer to the water column should be investigated to evaluate the risks linked to such pollution. This work focused on As dynamics in the Toulon Bay by studying two major processes: effect of early diagenesis and subsequent diffusive flux.

Interface sediment cores were sampled at contrasted locations and seasons, followed by porewater analysis of physico-chemical parameters (pH, Eh, DOC), diagenesis tracers (Fe, Mn, S, Ca, DIC, …) and As species. The obtained sediment depth profiles showed a significant variation of Eh, SO_4^{2-}, DOC and arsenic in porewaters between the campaigns. Such observation could result from different diagenesis activities, linked to inputs of labile organic matter (e.g. plankton bloom). Additionally, in the deepest layer (> 15 cm), As appeared to be significantly correlated (R^2 0.89) to the DOC content, indicating a possible association between As and organic matter.

Based on the measured phyco-chemical parameters and the dissolved species concentration (majors, diagenesis tracers, arsenic,...), PHREEQC was used to calculate As chemical speciation [1]. Then, PROFILE fitting of diagenesis tracers and As depth profiles allowed the evaluation of their diffusive fluxes at the sediment/water column interface [2]. Finally, As depth profiles were successively simulated by PHREEQC, taking account of solid As concentration, dissolved organic matter, carrier solid phases (clays, calcite, iron oxy(hydroxide), iron (mono)sulfide), and the affinity of these components for each As species.

The As dynamics in Toulon coastal sediment appears to be mainly controled by its chemical speciation in porewater, immobilization on carrier phase, and interaction with dissolved organic matter (as AsV but also as AsIII). Association of analysis and modelling tools (thermodynamic calculation, reactive transport fitting and sorption simulation) is suitable to better understand trace elements behavior at the sediment/water interface.

[1] Couture et al. (2010) *Geochim. Cosmochim. Acta* **74**, 1238-1255.
[2] Berg et al. (1998) *Limnol. Oceanogr.* **43**, 1500-1510.

Colloidal stability of TiO_2 nanoparticles in the presence of phenolic carboxylic compounds

KARIN DANIELSSON*, JENNY PEREZ HOLMBERG, JULIÁN GALLEGO-URREA, ELISABET AHLBERG, ZAREEN ABBAS, MARTIN HASSELLÖV, AND CAROLINE M. JONSSON

University of Gothenburg, Department of Chemistry and Molecular Biology, Gothenburg, Sweden
karin.danielsson@chem.gu.se (* presenting author), perezj@chem.gu.se, julian.gallego@chem.gu.se, ela@chem.gu.se, zareen@chem.gu.se, martin.hassellov@chem.gu.se, caroline.jonsson@chem.gu.se

Nanotechnology is a rapidly growing industry, which leads to an increased amount of synthetic nanoparticles released into the environment. Nanoparticles generally have higher reactivity than larger particles of the same material. As the particle size is decreased to the nanometer size range (1-100nm), the surface chemistry changes and this might influence the surface charging and aggregation behavior. Further, nanoparticles can interact with natural organic material (NOM), such as humic and fulvic acids, which is present in most natural waters. Adsorption of NOM affects the surface speciation and net charge of the nanoparticles and is therefore of great importance for their colloidal stability. This might alter the mobility of nanoparticles in surface waters and in soils, thus determing their bioavailability and toxicity.

The focus of the present study was to investigate the aggregation behavior of nanoparticles in aqueous solution as a function of pH, ionic strength, and in the presence of NOM. Well-characterized TiO_2 nanoparticles obtained from hydrolytic synthesis were used as test nanoparticles, and selected phenolic carboxylic compounds were used as model substances to mimic the interactions of nanoparticles with NOM. The selection of organic compounds was based on the possibility of determining the influence of various types, numbers, and positions of functional groups on the surface charging and colloidal stability of the TiO_2 nanoparticles. The aggregation and surface charging of the particles were studied by simultaneously monitoring the changes in particle size and zeta potential during the reactions.

https://doi.org/10.1180/S0026461X00008434 Published online by Cambridge University Press

Testing efficacy of zircon ($^{238}U/^{230}Th$) + (U-Th)/He and radiocarbon dating methods on the New Zealand late Quaternary tephras

MARTIN DANIŠÍK[1,2*], PHIL SHANE[3], AXEL K. SCHMITT[4], ALAN HOGG[5], GUACIARA M. SANTOS[6], NOREEN J. EVANS[2,7], SONJA STORM[3], KEITH FIFIELD[8], JAN LINDSAY[3]

[1]The University of Waikato, Hamilton, New Zealand, m.danisik@waikato.ac.nz (* presenting author)
[2]John de Laeter Centre for Isotope Research, Curtin University, Perth, Australia
[3]University of Auckland, Auckland, New Zealand, pa.shane@auckland.ac.nz, s.storm@auckland.ac.nz, j.lindsay@auckland.ac.nz
[4]University of California Los Angeles, Los Angeles, USA, axel@oro.ess.ucla.edu
[5]Radiocarbon Laboratory, University of Waikato, Hamilton, New Zealand, alanh@waikato.ac.nz
[6]University of California, Irvine, USA, gdossant@uci.edu
[7]CSIRO, Perth, Australia, Noreen.Evans@csiro.au
[8]Australian National University, Canberra, Australia, Keith.Fifield@anu.edu.au

Combined $^{238}U/^{230}Th$ disequilibrium and (U-Th)/He dating of zircon [1] is a novel approach for dating young (<350 ka) volcanic eruptions. This method with great potential for the Quaternary geochronology has been successfully applied in various settings [e.g. 2,3], however its accuracy and limitations has not been rigorously tested and validated by independent methods. New Zealand's record of late Quaternary tephras provides an excellent natural laboratory for conducting such inter-calibration experiments.

In this study we apply the combined $^{238}U/^{230}Th$ disequilibrium and (U-Th)/He zircon dating to the deposits of the coeval Rotoiti and Earthquake Flat eruptions in the Taupo Volcanic Zone to investigate consistency of the method. In addition, wood sampled below and above the Rotoiti tephra is dated by high-precision radiocarbon method to provide independent constraints on the accuracy of the zircon eruption ages.

Results and Conclusion

The two independent methods revealed concordant ages, which are also in accord with the stratigraphic position of the samples. Based on these results we assign new ages of ~45 ka to the Rotoiti and Earthquake Flat eruptions. This is by ~16 kyr younger than the currently accepted age, which has implications for paleoclimatic reconstructions and volcanic hazards assessment in the Taupo Volcanic Zone. This study proves the combined $^{238}U/^{230}Th$ disequilibrium and (U-Th)/He dating of zircon reliable at late Quaternary time scale and also demonstrates demonstrates reliability of the radiocarbon dating method at higher end of its sensititvity at ~50 ka.

[1] Schmitt *et al.* (2006) *J. Volcanol. Geoth. Res.* **158** (3-4), 281-295. [2] Schmitt *et al.* (2010) *Earth Planet. Sci. Lett.* **295** (1-2), 91-103. [3] Schmitt *et al.* (2011) *Contrib. Mineral. Petrol.* **162** (6), 1215-1231.

The Pantelleria shallow plumbing system: extreme differentiation processes and dynamics in an intraplate volcanic field

MASSIMO D'ANTONIO [1,2*], ROBERTO MORETTI[3,2], LUCIA CIVETTA[1,2], AND GIOVANNI ORSI[2]

[1]Università di Napoli "Federico II", Napoli, Italy, masdanto@unina.it (* presenting author)
[2]Istituto Nazionale di Geofisica e Vulcanologia, Sezione Osservatorio Vesuviano, Napoli, Italy
[3]Seconda Università di Napoli, Napoli, Italy

The island of Pantelleria, the type locality for pantelleritic rocks, is an active volcanic field located in the Sicily Channel Rift Zone, an intraplate setting affected by transtensional tectonics related to the complex geodynamics of the Western Mediterranean area. The island, dominated by a nested, resurgent caldera, has been affected by regional tectonism and volcano-tectonism that controlled both evolution of the magmatic system and distribution of eruption vents. The eruptions were fed through time by magmas of variable composition, typically bi-modal, both mafic and silicic. The island is divided into two sectors by a NE-SW fault system, which likely represents a crustal discontinuity along the axial ridge of the rift. The north-western sector, affected only by NW-SE crustal structures, includes most of the exposed transitional to alkaline basaltic rocks. The south-eastern sector includes silicic peralkaline rocks, variable from comenditic trachyte to rhyolite (pantellerite). Eruption of differentiated magmas and occurrence of the nested caldera, suggest that crustal magma chambers were established in this sector, probably at the intersection of the main tectonic lineaments. On the other hand, eruption of abundant mafic magmas in the north-western sector of the island suggests a deeper plumbing system linked to the mantle source region. The geochemistry of volcanics representative of the younger-than-15 ka activity has been investigated with the aim of better understand the magmatic processes governing the behaviour of the Pantelleria shallow plumbing system. The investigated volcanic rocks, products of both explosive and effusive activity, range in composition from comenditic trachyte to pantellerite, matching the typical range of evolved peralkaline composition of Pantelleria. Alkali-feldspar-rich enclaves are common in these rocks, testifying to diffuse mingling phenomena. Electron microprobe and micro-Raman analyses of interstitial glass of enclaves has revealed unusual compositions even more evolved than the host rocks. These data, integrated with recent experimental petrology results on peralkaline silicic magmas, allowed us to put forward hypotheses on the extreme differentiation processes and dynamics occurred within the Pantelleria shallow plumbing system in the past 15 ka.

https://doi.org/10.1180/S0026461X00008434 Published online by Cambridge University Press

Olivine record of crystal residence times and the internal dynamics of magmatic plumbing systems

LEONID DANYUSHEVSKY[1]*, ALEXEY ARISKIN[2]

[1]CODES, an ARC Centre of Excellence in Ore Deposits, Hobart, Australia, L.dan@ utas.edu.au (* presenting author)
[2]Vernadsky Institute of Geochemistry, Moscow, Russia, ariskin@rambler.ru

Analysis of the kinetics of post-entrapment re-equilibration of melt inclusions in high-Fo olivine phenocrysts in lavas suggests their common short residence times (< 6-12 months). This implies that if eruption does not happen within a few months after a primitive magma begins cooling and crystallisation within the plumbing system, early formed olivines are unlikely to be erupted as phenocrysts, being efficiently separated from the melt, and rapidly incorporated into the cumulate layers within the plumbing system.

These results suggest that in most cases erupted high-Fo olivine phenocrysts retain their original composition, which explains commonly observed large compositional variations between olivine phenocryst cores in a single sample. Short residence times imply that large unzoned cores of high-Fo phenocrysts cannot reflect diffusive re-equilibration of originally zoned phenocrysts. The unzoned cores are a result of fast efficient accumulation of olivines from the crystallising magma, i.e., olivines are separated from the magma faster than melt changes its composition. Thus, the main source of high-Fo crystals in the erupted magmas is the mush zone of the plumbing system. Olivine-phyric rocks represent mixtures of an evolved transporting magma (which forms the groundmass of the rock) with crystals that were formed during crystallisation of more primitive melt(s). Unlike high-Fo olivine phenocrysts, the evolved magma may reside in the magmatic system for a long time. This reconciles long magma residence times estimated from the compositions of rocks with short residence times of high-Fo olivine phenocrysts.

Olivines incorporated in the cumulate layers are sometimes erupted in gabbroic/ultramafic xenolith. Unlike phenocrysts in lavas, olivines in xenoliths commonly have uniform compositions, reflecting diffusive re-equilibration during long residence times.

Slow cooling rates and extensive re-equilibration within the plumbing systems results in complete re-equilibration of the cumulate crystals at near solidus temperatures. In parts of these systems where cumulate compaction and intercumulus melt migration were minimal, correlations between compositions of olivine and the bulk samples can be used to estimate the compositions of the parental magmas and the amount and composition of phenocrysts they carry. Having established the composition of parental magmas, comparing them to the bulk compositions of different parts of the plumbing system can indicate their open or closed behaviour.

Using the Dovyren magmatic system (Northern Baikal region, Siberia, Russia) as an example, we show that the parental magmas were phenocryst rich, the supplying conduits were thermally and compositionally zoned, and the large layered intrusive body of the complex represented an open plumbing system feeding the associated volcanic centres.

Are the "magnetite lava flows" of El Laco (Chile) magmatic? Comparison of trace elements in magnetite with other magmatic Fe-oxide deposits

S.A.S. DARE[1*], S.-J. BARNES[1], G. BEAUDOIN[2] AND J. MERIC[1]

[1] Université du Québec à Chicoutimi, Québec, Canada, sasdare@hotmail.com (*presenting author)
[2] Université Laval, Québec City, Québec, Canada

Magnetite forms under a wide variety of conditions, crystallizing at high temperature from silicate magmas or precipitating at low temperature from hydrothermal fluids or seawater. Trace element content of magnetite may reflect the differences in these conditions. Therefore as part of a larger project examining the trace element content of magnetite, by laser ablation ICP-MS, we have characterized magnetite in magmatic massive Fe-oxide deposits (magnetite-ilmenite, ± apatite) from layered intrusions (Bushveld and Sept Iles Complexes) and a massif anorthosite (Lac St. Jean) in order to study how magmatic processes affect the trace element compositions. We have also collected trace element data from the enigmatic "magnetite lava flows" from El Laco, Chile, in order to consider whether these magnetites are indeed of igneous origin.

Magnetite from the layered intrusions record the evolution of the fractionating silicate liquid (Fig. 1a), with those found lower in the sequence (more primitive) being richer in Cr, Mg, V and Ni whereas those found higher (more evolved) being richer in Ti, Nb and Ta. Magnetite layers from the uppermost parts of the intrusions contain apatite and this magnetite shows the most evolved composition (Fig. 1a). Magnetite from the anorthosite shows similar compositions to those of the layered intrusions. However, magnetite from the El Laco lava flow are much richer in Si (0.4 wt.%), Ca and P and poorer in Ti (<0.1 wt%), Al (<0.2 wt%) and Ga than magnetite from any magmatic Fe-oxide deposit (Fig. 1b) which raises doubts about the El Laco "magnetite lava flow" having formed by igneous processses.

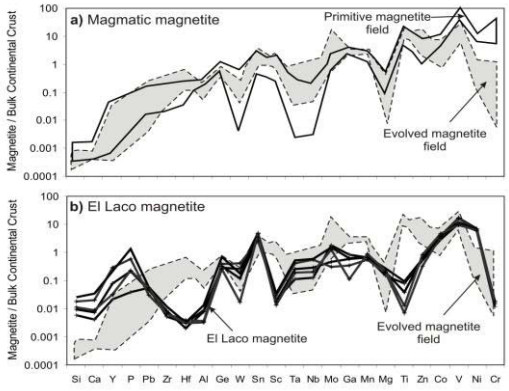

Figure 1: Trace element patterns for (a) magmatic magnetite and (b) El Laco magnetite compared to evolved magmatic magnetite. Order of elements: increasing compatibility into magnetite to the right.

https://doi.org/10.1180/S0026461X00008434 Published online by Cambridge University Press

Zircon U-Pb geochronology of the Nuvvuagittuq Greenstone Belt

J. DARLING[1*], D. MOSER[1], L. HEAMAN[2], W. DAVIS[3], R. STERN[2], J. O'NEIL[4], R. CARLSON[4], D. FRANCIS[5]

[1]Uni. of Western Ontario, London, Canada ([*]jdarli5@uwo.ca)
[2]University of Alberta, Edmonton, Canada
[3]Geological Survey of Canada, Ottawa, Ontario, Canada
[4]Department of Terrestrial Magnetism, Washington, DC, USA
[5]McGill University, Montreal, Quebec, Canada

The Nuvvuagittuq Greenstone Belt in northern Québec is a rare ~10 km^2 fragment of the Earth's early crust. The belt contains metamorphosed supracrustal rocks that are at least 3.77 billion years old [1,2], and amphibolites (the Ujaraaluk Unit) that may have protoliths as old as 4.3 Ga [3]. Primary contacts and relative age relationships have been obscured by multiple episodes of intensive ductile deformation, however the geological history of the belt is beginning to be unraveled via geochronology and geochemistry.

In this study we have undertaken SHRIMP U-Pb analysis of zircons from key meta-igneous and meta-sedimentary units of the belt. The analysed samples fall into three categories: (a) felsic bands (0.5 to 1 m in width) and tonalitic orthogneiss interlayered with the Ujaraaluk Unit; (b) fuchsite-bearing quartz-rich bands and a newly identified metasedimentary unit; (c) garnet-biotite amphibolite from the Ujaraaluk Unit and a meta-gabbro.

The felsic lithologies place contraints on the minimum age of the supracrustal assemblage. Oscillatory zoned zircons separated from a plag-qtz-bt schist form a discordant array with an upper intercept of 3774 ± 32 Ma, consistent with previous analyses of similar lithologies [1,2]. The tonalitic orthogneiss yields concordant zircon ages between 3740 and 3800 Ma, consistent with the observation of oscillatory zoned cores and rims from CL imaging.

Zircons from the fuchsite-bearing quartz band are subrounded and have oscillatory zonation textures very similar to the orthogneiss zircons, with little textural variation, and concordant ages of between 3750 and 3800 Ma, similar to the orthogneiss. In contrast, a quartz-albite-clinozoisite dominated metasediment identified within a lower strain domain, interfolded with amphibolites, has highly variable zircon CL textures. The zircons are dominated by concordant ages of 3630 to 3680 Ma, similar to the age of nearby tonalites [2], with minor concordant populations at ca. 3800 and 3500 Ma. Accordingly, the belt must have been exhumed following intrusion of the ca. 3660 Ma tonalite [2], and prior to high-T metamorphism and deformation.

Electron microscopy of polished thin sections was used to locate zircons within 4 samples of the Ujaraaluk Unit mafic amphibolites. Large (≤ 500 μm) zircons separated from a gt-bt rich sample, together with those from the meta-gabbro sample, are sector zoned and yield metamorphic ages of ca. 2700 Ma.

Although unequivocal constraints on the primary age of the Ujaraaluk Unit amphibolites remain elusive for now, continued geochronological studies are revealing that the belt contains a detailed record of Eoarchaean to Paleoarchaean crustal processes.

[1] Cates and Mojzsis (2007) *EPSL* **255**, 9-21
[2] David et al. (2009) *GSA Bulletin* **121**, 150-163
[3] O'Neil et al. (2008) *Science* **321**, 1828-1840

Zircon-adhering, crystallized melt inclusions in peritectic garnet from the western Adirondack Mountains, New York State, USA.

ROBERT DARLING [1*]

[1]Geology Department, SUNY Cortland, Cortland, NY, 13045, USA
robert.darling@cortland.edu (* presenting author)

Micrometer-scale, multiple-solid inclusions occur in garnet from metapelitic gneiss extracted from the hydroelectric plant on the Black River at Port Leyden, NY (western Adirondack Highlands). The garnet host grains are small (0.5-1.0 mm diameter), euhedral neoblasts that formed peritectically during biotite dehydration melting accompanying the Ottawan phase of the Grenville Orogeny (ca. 1040 Ma; [1]). Partial melting conditions of 4 to 6.4 kbar and 735°C, and a peritectic reaction of bio + sil + vapor = gar + melt, or bio + sil + qtz = gar + melt ± K-feldspar have been proposed for these rocks [1].

The inclusions are typically 10-20 μm in diameter and occur randomly in garnet. Both negative crystal and irregular inclusion morphologies are present. Many, if not all, of the inclusions contain a large (5-8 μm), often euhedral, zircon grain surrounded by finer-grained (some less than 1 μm) phases with EDX spectra consistent with biotite, K-feldspar, quartz, and albite. The inclusions are similar in size and composition to those described in garnet from other migmatites (e.g. [2], [3], [4]) and are similarly interpreted as anatectic melt inclusions.

Low Zr solubility in silicate melts [5] indicates the large zircon grain in each inclusion is a trapped phase. Therefore, it appears that micrometer-scale droplets of anatectic melt adhered to refractory zircon grains while peritectic garnet grew around them.

[1] Florence et al., 1995, CMP, v. 121, p. 424-436. [2] Hartel, et al., 1990, GAC-MAC Program Abs. v. 15, p. A54-A55. [3] Cesare et al., 2009, Geology, v. 37, p. 627-630. [4] Ferrero et al., 2012, J. Meta. Geology, (in press). [5] Watson and Harrison, 1983, EPSL, v. 64, p. 295-304.

https://doi.org/10.1180/S0026461X00008434 Published online by Cambridge University Press

Spectrophotometric determination of alkalinity and pH in freshwaters

YACINE DARMOUL[1*], GIL MICHARD[1], MARC F. BENEDETTI[1], ALEXIS GROLEAU[1] AND FRANÇOIS PREVOT[1]

[1]Univ. Paris Diderot, Sorbonne Paris Cité, IPGP, Paris, France darmoul@ipgp.fr (* presenting author), michargf@noos.fr, benedetti@ipgp.fr, groleau@ipgp.fr, prevot@ipgp.fr

The different compartments of the hydrosphere are major sinks or sources of CO_2 and the role of freshwaters in the global carbon cycle has been recently reevaluated as substantial [1]. Freshwaters show variations of the carbonate system variables at hourly time scales and in a large range. A key limitation for the carbonate system studies is the necessity of accurate, *in-situ* and high frequency measurements that would provide data with suitable spatial and temporal resolutions to enlighten the processes affecting the carbonate system.

With the aim of *in-situ* and high frequency sensor development to assess the freshwaters whole carbonate system with the simultaneous measurement of the pH-Alkalinity couple [2], spectrophotometric measurement of these parameters is developped. Spectrophotometric pH measurements already exist [3] this work focuses mainly on the alkalinity (Alk) measurement, which is an original contribution. This new method, based on [4], consists to neutralize all the basic species taken into account in the Alk by a weak acid mixed with a pH sensitive dye to measure accurately the pH end point value and thus deduce the alkalinity of the sample.

The performance of spectrophotometric methods is assessed in low pH buffer solutions for pH, commercial mineral and spring waters for Alk and natural freshwaters for both, by a comparison to conventional potentiometric measurements and theoretical calculations.

pH measurements show a precision of ±0.005 and an accuracy of 0.01 pH unit; Alk measurements show a precision of ±8µM and an accuracy ranging from 19 to 2 µM. The best accuracy is obtained by downplaying the excess acid term and thus its associed uncertainty. Additionnaly, accuracy relies upon the performance of the spectrophotometer, carefully prepared and defined indicator solution and all very controlled and reliable thermodynamic constants with their temperature and ionic strength dependence. The somewhat poorer precision reported might be ascribed in a larger part to the totally handmade procedure steps that introduce more errors than an automatic device. Tests on our pH and Alk *in-situ* sensor (still in development), shows that a precision better than ±0.001 unit on pH and better than ±2 µM on Alk are expected.

This work provide a strong theoretical basis for its future use as an *in-situ* high frequency sensor, which precision and accuracy meet the requirements of scientist working on freshwaters systems.

[1] Prairie (2008) *Can. J.Fish.Aquat. Sci.* **65**, 543-548.
[2] Park (1969) *Limnol. Oceanogr.* **14** (2), 179-186.
[3] Clayton (1993) *Deep-Sea Res. I* 40 (10), 2115-2129
[4] Podda (1994) *Compt. R Acad. Sci.,* **319** (2), 651-657

Using Noble Geochemistry to Identify the Genetic Fingerprint of Natural and "Fugitive Gases" in the Marcellus Play of Northern Appalachian Basin

THOMAS H. DARRAH[1,*], NATHANIEL WARNER[1], AVNER VENGOSH[1], ROBERT B. JACKSON[1] AND ROBERT POREDA[2]

[1] Division of Earth and Ocean Sciences, Nicholas School of the Environment; Duke University, Durham NC 27708 USA *thomas.darrah@duke.edu

[2]Department of Earth and Environmental Sciences, University of Rochester, Rochester NY 14627 USA

Abstract

Osborn et al [1] recently reported 17-times higher concentrations of thermally mature methane (CH_4), consistent with production gases from the Marcellus shale, in drinking water wells within 1km of hydraulically fractured horizontal drilling sites producing from the Marcellus Shale in northeastern Pennsylvania. We employ a combination of hydrologic (groundwater age dating [^{3}H-^{3}He and fluid flow modeling]), noble gas geochemistry, and carbon isotopic composition to distinguish the potential sources of gases present in drinking water aquifers within the region. These techniques simultaneously distinguish Marcellus/Devonian gas from deeper Trenton Group/Ordovician gases and other potential sources (e.g. shallow biogenic methane, stray landfill gases, other organic-rich lithologies, and natural gas that has migrated naturally over geologic time) providing a powerful technique for delineating the source and potential for fugitive gas migration in areas active or targeted for drilling. We will present preliminary results of noble gas and isotope geochemistry for Pennsylvania and New York areas of the Marcellus fairway.

[1] Osborn SG, Vengosh A, Warner NR, & Jackson RB (2011) Methane contamination of drinking water accompanying gas-well drilling and hydraulic fracturing. *Proceedings of the National Academy of Sciences* 108:8172-8176.

https://doi.org/10.1180/S0026461X00008434 Published online by Cambridge University Press

Precise Pb-Pb dating of Precambrian zircon using thermal extraction-condensation (TEC) and ^{202,205}Pb double spike

ABIN DAS[1] AND DONALD W. DAVIS[1*]

[1]Department of Geology, University of Toronto,22 Russell St., Toronto M5S 3B1 , Canada, das@geology.utoronto.ca[1], dond@geology.utoronto.ca[1*]

Method

Demonstrating reproducibility of Pb isotopic ratios in zircon is sufficient for accurate dating of Precambrian samples without the need for isotope dilution and U analysis, which require total dissolution of sample and chemical processing to remove Zr. The Kober [1,2] and Davis [3] methods of thermal extraction of Pb are simple but both provide relatively inefficient ionization and neither is amenable to double Pb isotope spiking, which limits the accuracy of ages that they can provide. We have experimented with a modification of Kober method that overcomes these limitations. Zircon is folded into a 0.03 in x 0.0005 in Re filament and thermally pre-treated at about 1450C for 30-45 min in vacuum to evaporate disturbed Pb from chemically altered domains. A condensation surface is then exposed to the sample and the zircon is heated at 1600C over 15 min to totally evaporate Pb. The condensation surface consists of either a 0.25 in wide Re ribbon (thermally cleaned using high current in a carbon coating chamber) or the inside of a 3 ml Savillex vial. Condensation of common Pb from the posts of the filament is prevented by the use of blinders welded to the posts of the evaporation filament. Operations are carried out inside a bell jar normally used for filament outgassing. Deposited silica from the zircon is subsequently removed using HF, by swabbing the Re surface using a pipette or open fluxing in the vial. The recovered Pb in the solution is dried, converted to HCl and spiked with ET2535 ^{202,205}Pb-^{233,235}U spike, then loaded onto a conventional Re filament with phosphoric acid and silica gel for conventional TIMS analysis. The vial condensator is more convenient than the wide filament but it produces relatively high blanks probably because of partial melting of a thin teflon surface layer by the hot silica. The Re condensator gives negligible blank but is less efficient for collecting Pb.

Results

The TEC method has been tested on two Precambrian zircon populations from northwest Ontario previously dated by conventional methods. One of them is from the Marmion tonalite which has a conventional U-Pb age of 3002.6 ± 1.5 Ma [4]. Four fractions of it gave an average TEC age with 2 standard deviation of 3001.9 ± 0.6 Ma. The other one consists of two zircon fractions from a rhyolite at Nevison Lake (conventional age of 2998.6 ± 0.8 Ma) with a TEC age of 2998.5 ± 0.4 Ma.

[1] Kober (1986) *Contrib. Min.& Petr.* **Vol. 93**, 482-490. [2] Kober (1987) *Contrib. Min.& Petr.* **Vol. 96**, 63-71.[3] Davis (2008) *Geol.* **Vol. 36**, 383-386.[4] Tomlinson et al. (2003) *Contrib. Min.& Petr.* **Vol. 144,** 684–702.

Noble gas and radionulcides study of chondrules from Dhajala and Bjurbole chondrites

J. P. DAS[1*], G. E. BRICKER[2], A. MESHIK[1], O. PRAVDIVTSEVA[1], M. W. CAFFEE[3], C. M. HOHENBERG[1], K. NISHIIZUMI[4].

[1]Dept. of Physics, Washington University, St. Louis, MO 63130, USA., jdas@physics.wustl.edu

[2]Dept. of Physics, Purdue University, Westville, IN 46391, USA.

[3]Primelab, Dept. of Physics, Purdue University, West Lafayette, IN 47907, USA.

[4]Space Sciences Lab, University of California, Berkeley, CA 94720, USA.

Chondrules were formed ~ 2-3 Myr after the formation of CAIs (the first solid condensates of solar system) and then accreted into large bodies with fine-grain matrix material [e.g.,1]. Chondrules might experience excess exposure to energetic solar particles and cosmic rays before their compaction. To investigate such pre-compaction exposure, cosmogenic noble gas isotopes and radionuclides were studied for individual chondrules from Dhajala and Bjurböle.

Separated individual chondrules from Bjurböle (L/LL4) and Dhajala (H3.8) meteorites were crushed to small and uniform grain size and then divided into three aliquots for composition, radionuclide and noble gas analyses. To calculate production rates of cosmogenic nuclides, major element compositions of the samples were determined by a Thermo Electron Corporation iCAP 6000 series mass spectrometer. Measurements of ^{10}Be, ^{26}Al, and ^{36}Cl were performed by AMS at Primelab, Purdue University. He, Ne and Ar measurements were carried out using noble gas mass spectrometry at Washington University in St. Louis. The cosmic ray exposure age of Bjurböle (> 8 Myr, [2]) is greater than five half-lives for all the radionuclides measured, indicating that the production rate is equal to the activity of the sample. The production rates of ^{10}Be, ^{26}Al, and ^{36}Cl were calculated based on irradiation depth using the model suggested by [3]. Estimates for the pre-atmospheric size of Bjurböle are ~ 400kg with a density of 2.28 g cm^{-3} [4]. Assuming a spherical shape, the pre-atmospheric radius of Bjurböle is ~ 35 cm. From radionuclide analysis, we find the Bjurböle samples were located from 2-5 cm inside the parent body. For Dhajala (CRE age ~ 4 Myr, [5]), ^{36}Cl and ^{26}Al activity is at the saturation point. Based on ^{26}Al, the most likely size and location of the sample is 70 cm inside a 120 cm body. At this depth, the ^{10}Be activity is saturated and the minimum CRE age is 6.8 Myr. The noble gases in chondrules are dominated by cosmogenic component however a detectable amount of trapped gases are also present. We are initially using the ^{22}Ne/^{21}Ne as a depth indicator, allowing us to calculate production rates of ^{3}He, ^{21}Ne and ^{38}Ar [6]. An alternative method is to deduce the irradiation depth based on radionuclide activity [3]. ^{3}He, ^{21}Ne and ^{38}Ar CRE ages suggest that chondrule D#10C from Dhajala and chondrule BC06C from Bjurböle were exposed to cosmic rays longer than the host matrix. The remainder of the chondrules show CRE ages similar to matrix. The excess exposure duration is within the range of earlier reports [2, 5]. Radionuclide data in this study were used to find size and depth profile of the samples; future radionuclide data will be used to quantify recent exposure history with the goal of elucidating pre-compaction exposure from the total exposure history.

[1] Kita et al. (2005) Chondrites & the protoplanet. Disk, ASP conf. series, 341, 558-587. [2] Polnau et al. (2001) *Geochim. Cosmochim. Acta* **65,** 1849-1866. [3] Leya et al. (2001) *Meteor. Planet. Sci* **36,** 1547-1561. [4] Flynn (2004) Earth Moon and Planets **95,** 361-374. [5] Eugster et al. (2007) *Meteor. Planet. Sci* **42,** 1351-1371. [6] Eugster and Michel (1995) *Geochim. Cosmochim. Acta* **59,** 177-199.

https://doi.org/10.1180/S0026461X00008434 Published online by Cambridge University Press

Phase transformation of two-line ferrihydrite: Effects of pH, temperature, and adsorbed arsenate and molybdate

SOUMYA DAS[1*], M. JIM HENDRY[1], JOSEPH ESSILFIE-DUGHAN[1]

[1]University of Saskatchewan, Geological Sciences
sod671@mail.usask.ca (* presenting author)
jim.hendry@usask.ca
joe377@mail.usask.ca

Introduction

A dominant control on the mobility and speciation of many toxic elements from mining and milling operations is their adsorption onto the surface of iron oxy-hydroxides, of which two-line ferrihydrite (hereafter called ferrihydrite) is one of the most common and reactive. For example, tailings generated from uranium (U) mining and metallurgical operations are a potential source of As, Mo, Se, and Ra^{226} (termed Elements of Concern; EOCs) to the geosphere and biosphere. Generally, these elements are removed from oxic, acidic leach solutions (pH ~1.5) in the U mill via neutralization with lime and co-precipitation with ferric iron. Ferrihydrite starts to precipitate at pH ~3.5-4 during this neutralization process, which ultimately increases the pH to ~9.5 in the tailings prior to discharge. The EOCs subsequently adsorb onto the ferrihydrite, which thus controls their mobility in the pore waters. Because ferrihydrite is metastable and can transform to more structurally ordered oxy-hydroxide phases such as goethite and, under certain geochemical conditions, hematite, this study was conducted to assess the ability of ferrihydrite to act as a long-term sink for As and Mo in U tailings bodies. The results will also be useful in determining the long-term stability of ferrihydrite in other mine environments.

Materials and Methods

A comprehensive study was carried out to determine the rate of transformation of pure ferrihydrite (i.e., no adsorbed As or Mo) to goethite and hematite as a function of temperature (25, 50, 75, and 100°C) and pH (2, 7, and 10) via batch experiments. Subsequently, the impact of adsorbed arsenate and molybdate on the rate of ferrihydrite transformation was determined based on As/Fe (0.500-0.010) and Mo/Fe (1.000-0.010) molar ratios (to approximate elemental concentrations measured in the tailings) at pH ~10 and 75°C. These rates were extrapolated to the environmental conditions measured in the tailings (i.e., 1°C and pH=10) at Cameco Corporation's Deilmann Tailings Management Facility, Saskatchewan, Canada. Pure and transformed phases were characterized and quantified using XRD, XANES, AFM, SEM, BET, and Raman spectroscopy.

Results and Discussion

The rate of transformation of pure ferrihydrite to hematite increased with increasing temperature at all pH values considered and followed first order reaction kinetics. In the case of As adsorbed to ferrihydrite, the rate of ferrihydrite transformation decreased by two orders of magnitude as the As/Fe ratio increased from 0.010 to 0.018. No transformation was observed at higher As/Fe ratios (0.050, 0.100, and 0.500). Calculations show that the rate of ferrihydrite transformation under *in situ* conditions (~1°C; pH ~10; As/Fe ratio >0.250) is negligible and thus the ferrihydrite should continue to act as a sink for As for at least 10,000 years. Results of the ferrihydrite-molybdate testing remain to be analyzed.

Carbon solution and partitioning between metallic and silicate melts in a shallow magma ocean: implications for the origin and distribution of terrestrial carbon

RAJDEEP DASGUPTA[1*], HAN CHI[1], NOBUMICHI SHIMIZU[2], ANTONIO BUONO[3,4] AND DAVID WALKER[3]

[1]Rice University,Houston, TX, USA, (*Rajdeep.Dasgupta@rice.edu)
[2]Woods Hole Oceanographic Institution, Woods Hole, MA, USA
[3]Columbia University, Palisades, NY, USA
[4]Massachusetts Institute of Technology, Cambridge, MA, USA

Carbon in the Earth's mantle has critical influence on planetary geodynamics, chemical differentiation, long-term climate, and habitability. But how early did the bulk silicate Earth acquire its current inventory of carbon? Is the mantle carbon mostly recycled or primordial? Answering these questions requires knowledge of the element's fate during magma ocean processes and parameters such as carbon solubility and partitioning between metal and silicate during core formation are key.

Experiments were performed at 2-7 GPa, 2000-2100 °C on mixtures of silicates (tholeiitic basalt/ komatiite/ fertile peridotite) and Fe-Ni-Co-C-S mix contained in graphite or MgO capsules. All the runs produced immiscible Fe-rich metallic and silicate melts at fO_2 between IW-1.0 and IW-2.2. Carbon concentrations of basaltic glasses and non-glassy quenched silicate melts were determined using secondary ionization mass spectrometry (SIMS) and speciation of dissolved C-O-H volatiles in silicate glasses was constrained using Raman spectroscopy. Carbon contents of metallic melts were determined using both electron microprobe and SIMS. Our experiments indicate, that at reduced, core-forming, conditions, carbon in mafic-ultramafic magmas dissolves primarily as a hydrogenated species and its storage capacity remains low. The total C content in our reduced melts at graphite saturation increases with increasing melt depolymerization (NBO/T), consistent with a recent spectroscopic study [1]. Carbon behaves as a metal-loving element during core-mantle separation and D_C (metallic melt/ silicate melt) varies between ~3500 and ≥100 and increases with increasing pressure and decreases with increasing melt NBO/T.

Our data suggest that if only a trace amount of carbon (~730 ppm C; [2]) was available to participate in the early differentiation of Earth, most of it was partitioned to the core and no more than ~10-30% of the present-day mantle carbon budget (50-200 ppm CO_2) can be derived from a magma ocean residual to core formation. With core formation removing most of the carbon initially retained in the terrestrial magma ocean, explanation of the modern Earth carbon inventory requires a later replenishment mechanism. Addition of volatile-rich, late veneer and inefficient core formation both remain viable mechanisms. Alternatively, carbon ingassing by magma ocean-atmosphere interaction, soon after core formation, may also make the Earth's primordial carbon inventory similar to that of the present-day budget.

[1] Mysen et al. (2009) *Geochimica et Cosmochimica Acta* **73**, 1696-1710. [2] McDonough (2003) *Treatise on Geochemistry* **2**, 547-568.

https://doi.org/10.1180/S0026461X00008434 Published online by Cambridge University Press

Insights on the Late-Stage Evolution of Glacial Lake Ojibway

VIRGINE DAUBOIS[1], MAXIME MÉNARD[2], MARTIN ROY[3], AND JEAN J. VEILLETTE[4]

[1,2,3] Dép. des Sciences de la Terre et de l'Atmosphère – GEOTOP, Université du Québec à Montréal, Montréal, QC, Canada
[1] virg_do@hotmail.com (*presenting author)
[2] max-menard@hotmail.com
[3] roy.martin@uqam.ca
[4] Geological Survey of Canada, Ottawa, ON, Canada
[4] Jean.Veillette@NRCan-RNCan.gc.ca

Meltwater released at the southern margin of the Laurentide ice sheet during the last deglaciation led to the development of Lake Ojibway in NE Ontario and NW Quebec. The late-stage evolution of Lake Ojibway was marked by ice (Cochrane) readvances, while recent mapping of low-elevation lakeshores indicate abrupt drawdowns of Ojibway lake level prior to its final discharge into Hudson Bay ~8200 cal yr BP. Additional late-stage events are also suggested by the presence of thick (10-15 cm) bands of massive silt that truncate Ojibway rhythmites. This silt band is in turn overlain by ~1 m of rhythmites. Although this sequence suggests the occurrence of drainage episode(s), the late-stage history of Lake Ojibway remains inadequatly documented. Here we report results from the study of 12 Ojibway sediment sequences that contain the silt band.

Grain-size analyses of bulk Ojibway rhythmites (winter and summer beds) show a textural composition consisting of 73% clay (<2 μm) and 25 % of fine silt (2–8 μm), with the remaining material being composed of medium silt (8–16 μm). This contrasts with the thick silt band that consist primarily of ~54–86% of fine to coarse silt (2–63 μm), with the clay fraction typically representing < 20%. The detrital carbonate content of rhythmites samples shows values ranging from 0.72 to 2.02%, while silt band samples commonly show a slight increase with respect to the bounding rhythmites, going from 1.85 to 3.34%. Ostracods were extracted from specific sediment intervals for oxygen isotope ($\delta^{18}O$) measurements. Preliminary results indicate that ostracods from the silt band and underlying rhythmites have $\delta^{18}O$ values ranging from –23.26 to –25.04 ‰ (vs VPDB), typical of glacial metltwater. In contrast, the rhythmites overlying the silt band show $\delta^{18}O$ ranging from 10.03 to 16.62 ‰.

Interpretation of the results is still limited at this stage of the study. Nonetheless, the textural changes reported could be associated with a drainage episode(s) that was followed by a deepwater phase(s). Alternatively, this *drainage varve* (?) could represent a drastic change in the sediment supply (or source) to the lake. This appears to be supported by the increase in detrital carbonate of the silt band. Because the Ojibway basin lies primarily on crystalline bedrock, the presence of detrital carbonate in Ojibway sediments is commonly attributed to the late-glacial dynamics (metlwater runoff or ice readvances) of the decaying ice in Hudson Bay, which is underlain by carbonate rocks. Any explanation for the origin of this silt band and associated compositional changes must also take into account the sharp change in $\delta^{18}O$ composition obtained for the sediments overlying the silt band, which shows an evolution towards post-glacial values. Upcoming ^{14}C ages from the ostracods extracted from the silt bands and bounding rhythmites should also help refining our understanding of these events.

A surface complexation model for the copper-bacteria-iron oxide system

CHRISTOPHER J. DAUGHNEY[1*], PETER J. SWEDLUND[2], MAGALI MOREAU-FOURNIER[3], SARAH L. HARMER[4], BERNT JOHANNESSEN[5], AND CHRISTOPHER G. WEISENER[6]

[1]GNS Science, Lower Hutt, New Zealand, c.daughney@gns.cri.nz (* presenting author)
[2]University of Auckland, Auckland, New Zealand, p.swedlund@auckland.ac.nz
[3]GNS Science, Wairakei, New Zealand, m.moreau-fournier@gns.cri.nz
[4]University of South Australia, Adelaide, Australia, sarah.harmer@unisa.edu.au
[5]Australian Synchrotron, Clayton, Australia, bernt.johannessen@synchrotron.org.au
[6]University of Windsor, Windsor, Canada, weisener@uwindsor.ca

Laboratory experiments were performed to track the fate of dissolved Cu and Fe at a fixed pH of 5.2 during the gradual, incremental oxidation of dissolved Fe(II) and precipitation of iron oxide in the presence of *Anoxybacillus flavithermus* cells. The experimental data reveal significant and complex controls on Cu immobilization, related to progressive changes in 1) ratio of Cu to dissolved Fe(II) concentration, inferred to result from competition for bacterial sorption sites; 2) ratio of precipitated iron oxide to bacteria, inferred to result from desorption of Fe(II) initally associated with the bacterial surface; and 3) reaction time, inferred to result from Cu complexation by increasing quantities of biogenic dissolved organic matter. Surface complexation models were developed to describe the experimental data, with constraints on reaction mechanims provided by polarography and X-ray absorption spectroscopy. Differential pulse polarography demonstrated that Cu complexes form with dissolved organic ligands in filtered bacterial suspensions. The concentration and Cu complexation capacity of these bacterial exudates could be quantified and related to the conditions and history of the suspensions. The bacterial exudates significantly inhibited Cu adsorption onto the bacterial cells but slightly enhanced adsorption onto the iron oxide under the experimental conditions. X-ray absorption spectra were collected at the Cu K-edge on the bacterial exudates and wet pastes of the bacteria, the iron oxide, and the bacteria-iron oxide composites. The EXAFS data suggest that Cu complexation by the bacterial exudates involves binding by carboxyl or phosphate sites. The EXAFS data also show that under the experimental conditions Cu in the solid phase is associated predominantly with carboxyl structures on the bacterial cell walls, not with bacterial phophoryl structures or with binding sites on the iron oxide. This study demonstrates that the immobilization of metal cations in bacteria-bearing settings should not be examined independently of progressive oxidation, hydrolysis and precipitation of iron.

https://doi.org/10.1180/S0026461X00008434 Published online by Cambridge University Press

Iron isotope geochemistry with a synchrotron light beam

NICOLAS DAUPHAS[1*], MATHIEU ROSKOSZ[2], ESEN E. ALP[3], CORLISS K. SIO[1], FRANÇOIS L.H. TISSOT[1], DANIEL NEUVILLE[4], MICHAEL HU[3], JIYONG ZHAO[3], LAURENT TISSANDIER[5] AND ETIENNE MÉDARD[6]

[1]Origins Laboratory, The University of Chicago, Department of the Geophysical Sciences and Enrico Fermi Institute, Chicago, USA, dauphas@uchicago.edu (* presenting author)
[2]Unité Matériaux et Transormations, Université de Lille
[3]Advanced Photon Source, Argonne National Laboratory
[4]Institut de Physique du Globe de Paris
[5]Centre de Recherches Pétrographiques et Géochimiques-CNRS, Nancy
[6]Laboratoire Magmas et Volcans, Université de Clermont-Ferrand

Previous studies have suggested that iron isotopes could be good tracers of redox conditions during melting [*e.g.*, 1]. However, we lack a reliable database of equilibrium fractionation factors between melts and igneous minerals such as olivine to interpret the rock record [2]. Iron equilibrium fractionation factors (or more specifically reduced partition function ratios, β) can be derived from Nuclear Resonant Inelastic X-ray Scattering (NRIXS) experiments at a synchrotron facility [3,4]. We have developed a new method (*i.e.*, the *general moment* approach), based on a Bernoulli expansion of the reduced partition function ratio, to calculate β-factors from the moments of raw NRIXS spectra [4]. The first term in this expansion corresponds to the mean force constant of the iron bonds [5], a quantity that is readily measured and often reported in NRIXS studies [6]. We have used this technique to determine the β-factors of olivine and geologically relevant silicate glasses.

At a given Fe^{3+}/Fe^{2+} ratio, the force constants of basaltic, andesitic, and dacitic glasses are almost identical. However, the force constant of rhyolitic glass is higher. For all samples, the force constant increases with the Fe^{3+} content. Thus, for mafic melts, there is little structural control on iron isotopic fractionation; redox effects seem to dominate. The relationship between force constant and Fe^{3+}/Fe_{tot} for basalt, andesite, and dacite is approximately linear. We can estimate the force constants of Fe^{2+} and Fe^{3+} in basalt by interpolating the data to $Fe^{3+}/Fe_{tot}=0$ and $Fe^{3+}/Fe_{tot}=1$. At 1,100 °C, we calculate an equilibrium $\delta^{56}Fe$ fractionation of +0.25 ‰ between the two oxidation states of iron in magmas. The olivine-melt and melt Fe^{2+}-Fe^{3+} iron isotopic fractionations derived from NRIXS data may explain the heavy iron isotopic compositions measured in MORBs.

This study provides a solid reference for interpreting Fe isotopic variations in igneous rocks. Specifically, it reveals the potential of using Fe isotopes to trace redox variations and magmatic differentiation processes in planets.

References: [1] Dauphas N. et al. (2009) EPSL 288, 255-267. [2] Teng F.-Z., Dauphas N., & Helz R.T. (2008) Science 320, 1620-1622. [3] Polyakov V.B. (2009) Science 323, 912-914. [4] Dauphas N. et al. (submitted) Geochimica et Cosmochimica Acta. [5] Bigeleisen J. & Goeppert Mayer M. (1947) Journal of Chemical Physics 15, 261. [6] Lipkin H.J. (1995) Phys. Rev. B 52, 10073-10079.

Cyclic growth layers in calcareous biominerals

YANNICKE DAUPHIN[1*], C. TERRY WILLIAMS[2], AND JEAN-PIERRE CUIF[3]

[1]Université P. et M. Curie, Paris, France yannicke.dauphin@upmc.fr (* presenting author)
[2]Natural History Museum, London, UK, ctw@nhm.ac.uk
[3]Université Paris Sud, Orsay, France, jean-pierre.cuif@u-psud.fr

Mollusc shells are among the best known calcareous biominerals. The calcitic prisms of *Pinna* and *Atrina* are often used because of their large size and simple geometry. As other biominerals, they are organo-mineral composites [1,2]. Thin sections observed in polarized light show they behave as monocrystals [3]. However, polished and etched sections show they are composed of growth zonations. Thickness of a growth line is about 1-3 µm. Moreover, the distribution of chemical elements is not uniform. Outer organic walls have low Mg and high S contents. Within the prisms, more or less intense zonations are visible. In both structural and chemical images, zonations are synchronous across adjacent prisms, showing the strict physiological control of the biomineralization processes. The comparison of chemical maps show that the rhythm and intensity differ according to the element.

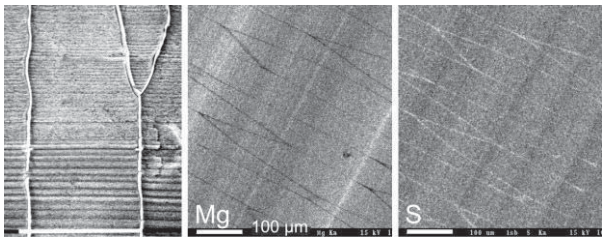

Figure: structural growth lines and chemical zonations in the calcitic prisms of *Pinna*

AFM images show that prisms are made of granules surrounded by a cortex. TEM data show that in distinct regions of a prism, granules are amorphous, while others are crystallized as subunits of a large single crystal. At the boundary of the two regions, granules display a crystallized core and an amorphous rim [4]. Such a limit probably marks out an arrested crystallization front having propagated through a previously biocontrolled architecture of the piling of amorphous micro-domains.

Such a crystallization process, developed within the organic matrix, differs from the usual model occurring within a fluid, the composition of which is assumed to be close to sea water. Such a model, used in the palaeo-climate/ geochemical areas, cannot account for any species-specific property of the calcification process. A matrix-driven crystallization within the spheroids of the growth layers provides us a reasonable way to explain the black-box of the "vital effect".

[1] Grégoire (1961) *Bull. Inst. R. Sci. Nat. Belg.* **37**, 1–34. [2] Dauphin (2003) *J. Biol. Chem.* **278**, 15168-15177. [3] Dauphin et al. (2003) *J. Struct. Biol.* **142**, 272-280. [4] Baronnet *et al.* (2008) Miner. Mag. **72**, 617-626.

https://doi.org/10.1180/S0026461X00008434 Published online by Cambridge University Press

Does diopside dissolve like glass? Insights from measurements of nano- to macroscale dissolution rates

DAMIEN DAVAL[1,2*], GIUSEPPE D. SALDI[2], ROLAND HELLMANN[3] AND KEVIN G. KNAUSS[2]

[1]LHyGeS, Université de Strasbourg – CNRS UMR 7517, Strasbourg, France; ddaval@unistra.fr (* presenting author)
[2]ESD, LBNL, Berkeley, USA; kgknauss@lbl.gov, gdsaldi@lbl.gov
[3]ISTerre, Université Grenoble 1 – CNRS, Grenoble, France; roland.hellmann@obs.ujf-grenoble.fr

Whereas the dissolution rate of silicate minerals has been extensively studied at far-from-equilibrium conditions, extrapolating such rates over a broad range of solution compositions has proven challenging. In particular, a growing amount of studies have pointed out that the simplest TST-based rate-affinity dependence commonly implemented into most of geochemical codes was the source of dramatic overestimations of the actual fluid-rock interaction rates [1, 2]. Such limitations acted as a driving force for developing alternative dissolution models of solids over the past 10 years [3, 4].

Diopside was shown to belong to that category of minerals for which rate-affinity relationships do not follow a simple TST-like model, since an unexpected drop of the rate was evidenced at ΔG_r(diopside) as low as –76 kJ.mol^{-1} [5]. An examination of these data led us to envisage that two different, non-exclusive aspects were worth investigating: (i) the possible passivating ability of interfacial, nm-thick Si-rich layers developed on weathered silicate surface, and (ii) the stop of etch pits formation on crystal surface, which were found to be responsible for drops of olivine [2] and albite [3] dissolution rates, respectively. The former mechanism should be evidenced by the dependence of diopside dissolution rate on [SiO_2(aq)], whereas the latter should verify a strong anisotropy of diopside dissolution, with (h k l≠0) faces dissolving noticeably faster than (h k l=0) faces. Both of these models were tested by running either classical flow-through experiments with controlled [SiO_2(aq)], and face specific dissolution experiments. In this latter case, single crystals were immersed in solution. The dissolution features were monitored by AFM imaging and the dissolution rates were calculated by measuring the global surface retreat between masked and unmasked regions using VSI [1].

Our results show that the dissolution rate of diopside drops as SiO_2(aq) is added to the solution, consistently with a dissolution mechanism controlled by the stabilization of a passivating, interfacial Si-rich layer, as already suggested for glass [6]. On the other hand, our preliminary results on the face-specific dissolution of diopside show that the dissolution rate of faces varies following: (021) >> (110) ~ $(1\bar{1}0)$>> (010) ~ (100), which does not invalidate the etch pit nucleation control of diopside dissolution kinetics. The results of the ongoing experiment on (001) face, as well as upcoming investigations of the interfacial layers by TEM, will help to make a final decision between the two proposed models.

[1] Beig (2006) *Geochim. Cosmochim. Ac.* **70**, 1402-1420. [2] Daval (2011) *Chem. Geol.* **284**, 193-209. [3] Arvidson (2010) *Chem. Geol.* **269**, 79-88. [4] Cailleteau (2008) *Nat. Mater.* **7**, 978-983. [5] Daval (2010) *Geochim. Cosmochim. Ac.* **70**, 2615-2633. [6] Daux (1997) *Chem. Geol.* **142**, 109-126.

Differentiation and source controls along the Lesser Antilles arc

JON P. DAVIDSON[1*] AND MARJORIE WILSON[2]

[1] Department of Earth Sciences, Durham University, Durham DH1 3LE, UK, j.p.davidson@durham.ac.uk (* presenting author)
[2] School of Earth & Environment, the University of Leeds, Leeds LS2 9JT, UK, B.M.Wilson@leeds.ac.uk

The fluxes of elements into, and out of, subduction zones dictate both the composition of the crust and the heterogeneity of the mantle. Most flux estimates are predicated on the basis of the compositions of magmas erupted from arc volcanoes. However, volcanic rocks represet only 10-20% of the total magma flux from the mantle at arcs, and these magmas have undergone the maximum amount of filtering, having passed through the entire thickness of the upper plate lithosphere. In order, therefore, to realistically determine the contributions from the mantle wedge and slab (sediments and fluids) to arc magmas, it is critical to account for the effects of differentiation.

We have done this at the Lesser Antilles arc for two volcanoes; The Quill (Statia) in the north and Mt Pelee (Martinique) in the central part of the arc. An evaluation of the volcanic rocks, their constituent minerals and associated cumulate blocks allows us to show that 1) differentiation was controlled by an amphibole-plagioclase-dominated assemblage, as reflected in the cumulate blocks, and 2) differentiation was open system, involving assimilation of the arc crust.

Even though amphibole is not present in the phenocryst assemblage of the volcanic rocks, it is common in the cumulate xenoliths. Thus fractionation control is cryptic, with compositions determined largely by mineral assemblages not represented in the erupted fractionates. Indeed amphibole may be more common as a fractionating phase at arcs than has previously been appreciated [1]: By increasing SiO_2 and generating LREE enrichment, amphibole might have an important role in generating crust-like differentiates at arcs. The inferred assimilation of the arc crust modifies Pb and Sr isotope compositions in the magmas, suggesting that even at intra-oceanic arcs the isotopic compositions of erupted magmas cannot a priori be taken as indicative of their mantle source.

Once differentiation trends are established they can be back-extrapolated. When this is done, differentiation trends for The Quill and Mt Pelee do not converge on a common primitive/ parental composition, suggesting that mantle source compositions vary along the arc. The mantle sources of both volcanoes can be modlled by addition of <5% sediment or <1% sediment melt, along with LILE-bearing fluid. The differences between the sources of the two volcanoes can be explained by different sediment compositions delivered along the arc, or a slightly greater sediment contribution at Mt Pelee [2].

References

[1] Davidson, J., Turner, S., Handley, H., Macpherson, C., and Dosseto, A., (2007) *Geology* **35**, 787-790. [2] Turner, S., Hawkesworth, C., Macdonald, R., Black, S. and van Calsteren, P., (1996) *Earth Planet. Sci. Lett.,* **142**, 191-207.

https://doi.org/10.1180/S0026461X00008434 Published online by Cambridge University Press

A Particle-Based Approach to Modelling Water Flow and Residence Times in a Small Catchment

JESSICA DAVIES[1]*, KEITH BEVEN[1,2], LARS NYBERG[3], ALLAN RODHE[2]

[1]Lancaster University, Lancaster, United Kingdom, j.davies4@lancaster.ac.uk (* presenting author) k.beven@lancaster.ac.uk
[2]Uppsala University, Uppsala, Sweden, allan.rodhe@hyd.uu.se
[3]Karlstad University, Karlstad, Sweden, lars.nyberg@kau.se

Introduction

Understanding water flow processes in the near-surface environment is crucial in determining movement of nutrients and pollutants. The majority of hydrological models used employ continuum-based expressions to derive mass flow linked with advective dispersive equations (ADEs) if transport is also considered. The appliability of these approaches to real soils which contain structural heterogeneities is questionable. Continuum-based models requires sub-grid equilibrium of potentials and fluxes, leading to impracticably fine grid-scales if the heterogeneities are to be represented, and the assumption of Brownian motion in ADEs is not representative of preferential flow features that allow solute movement at velocities much in excess of the wave celerities.

Multiple Interacting Pathways Model

The Multiple Interacting Pathways (MIPs) concept is an alternative approach to modelling transport and flow that directly acknowledges the presence of preferential flow pathways. Water in the slope or catchment is represented as a set of discrete particles, the movement of which is simulated through random particle tracking. Velocity distributions are applied to the particles, which attempt to characterise the range of pathways available to the water. These pathways are interacting as movement between them is simulated with exchange probabilities, which may also be used to simulate evapotranspiration or bedrock losses.

This concept provides unified simulation of transport and flow, allowing analysis of input/output/storage residence times and water origin, with the potential of adding chemistry to the particle interactions.

Application to Hydrometric and Isotopic Data

The MIPs model has previously been applied to simulating plot scale hydrometric and artificial tracer data at a site in Gårdsjön, Sweden with some success [1]. This modelling has been extended to simulate a catchment-scale step-change in isotopic input that occurred at the site on construction of a roof. Hypotheses are sought which provide consistent results across both spatial scales and temporal scales of transport. Having found a behavioural model, a fuller analysis is made of the input/output/storage residence time distributions suggested by the model.

[1] Davies (2011) Hydrological Processes **25**, 3602-3612.

Geochemical and isotopic insights into the origin of the 'Scourie' Dykes

JOSHUA H. F. L. DAVIES*, LARRY M. HEAMAN, S. ANDREW DUFRANE, KARLIS MUEHLENBACHS AND ROBERT A. CREASER.

University of Alberta, 1-26 Earth Sciences Building, Edmonton Alberta Canada. (jdavies1@ualberta.ca Presenting author)

The 'Scourie' dykes are a NNW trending dyke swarm in the Lewisian gneiss terrain of Northwest Scotland. They represent important time markers in the evolution of the Lewisian as the majority were intruded between two regional high-grade metamorphic events – the Inverian (~2.5 Ga) and the Laxfordian (~1.7 Ga). Importantly, the area around Loch Assynt was variably affected by the Laxfordian event leaving some of the dykes un-metamorphosed with primary igneous textures and minerals. The dykes therefore are perfectly placed to distinguish between the metamorphic events and provide information on the Paleoproterozoic history of the Lewisian terrain. Numerous field, geochemical and geophysical studies have been conducted on the Scourie dykes over the past 30 years, despite this the age and origin of the dykes is still poorly known.

Field relationships and geochronology indicate that there are at least four separate Paleoproterozoic dyking events intruding the Lewisian crust spanning a period of more than 400 m.y. The majority of dated dykes using high precision U-Pb zircon/baddeleyite geochronology were emplaced between 2420 and 2380 Ma, which is the time period focus of this study. Whole rock and clinopyroxene oxygen isotopic analyses have shown that some of the dykes have low $\delta^{18}O$ signatures (~2‰) whereas other dykes have normal mantle values (~5.5‰). Geochemical studies of the dykes indicate that there maybe at least two mantle sources involved in dyke genesis that are variably enriched in trace elements.

Here we combine new Sm-Nd, Rb-Sr, $\delta^{18}O$, geochronological and trace element data on the dykes to suggest a new model for the origin of the 'Scourie' dykes. Preliminary results indicate that the initial pulse of dyke emplacement (~2420-2400 Ma) was characterized by normal mantle oxygen isotope signatures and mantle source enrichment. A second period of dyke emplacement occurred subsequently (~2400-2380 Ma) in which the dykes are less geochemically enriched and contain low $\delta^{18}O$ signatures possibly indicating the involvement of subducted oceanic crust. Using the new geochemical and geochronological classifications we define the 'Scourie dyke suite' senso stricto as those emplaced between ~2420 and 2380 Ma with a concentration of these dykes in geographic proximity to the town of Scourie.

https://doi.org/10.1180/S0026461X00008434 Published online by Cambridge University Press

Effective mixing and reaction front kinetics in porous media

PIETRO DE ANNA[1], TANGUY LE BORGNE[1*], MARCO DENTZ[2], ALEXANDRE TARTAKOVSKY[3]

[1]Géosciences Rennes, Université de Rennes, Rennes, France, tanguy.le-borgne@univ-rennes1.fr (* presenting author)
[2] Spanish National Research Council (IDAEA-CSIC), Barcelona, Spain, marco.dentz@idaea.csic.es
[3]Pacific Northwest National Laboratory, Richland, Washington, USA, alexandre.tartakovsky@pnl.gov

The effective reaction kinetics of chemical species transported in solution in the subsurface depends on the probability of reactants to mix. While chemical reactions ultimately occur by diffusive mixing at the molecular scale, the effective reaction kinetics can be greatly enhanced by the shear and stretching action of the flow field, which increases the surface available for diffusive mass transfer [1]. Understanding and quantifying the effect the flow field heterogeneity on the upscaled mixing and reaction rates is thus a key issue for the prediction reactive transport in the subsurface.

We use pore scale Smooth Particle Hydrodymanic (SPH) simulations to investigate effective mixing and reaction kinetics for reaction fronts where an initially resident reactant is displaced by an incoming reactant. The reaction kinetics is found to be faster than that of homogeneous diffusion-reaction fronts, for which the mass of product grows like the square root of time. At early time, the effective reaction rate is controlled by the formation of fingers of incoming reactant, which invade the porous media, rapidly increasing the reaction front area. At late time, the reaction kinetics is governed by the longitudinal dispersive growth of the mixing area and by the spatial distribution of concentration gradients in the mixing zone, which characterize a persistent state of incomplete mixing [2.3]. We discuss the effect of changing the relative contribution of advective and diffusive motions (quantified by the Peclet number) on the temporal evolution of effective mixing and reaction rates.

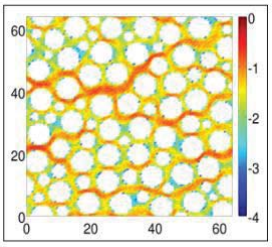

Pore scale flow field

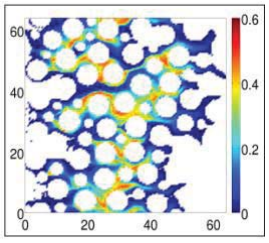

Distribution of product concentration within the reaction front

[1] Dentz M., T. Le Borgne, A. Englert, B. Bijeljic (2011) Review Article J. of Cont. Hydrol., **120-121**, 1–17
[2] Le Borgne T., Dentz M., Davy P., Bolster D., de Dreuzy, J. R. and Bour O. (2011) Phys. Rev. E, **84**, 1
[3] de Anna, P., T. Le Borgne, M. Dentz, D. Bolster and P. Davy (2011) J. of Chem. Phys., **135**, 174104

Contrasting Biogeochemical Cycling of Iron and Aluminium along the GEOTRACES West Atlantic section

H.J.W. DE BAAR[1,2]*, M.J.A. RIJKENBERG[1], L.J.A. GERRINGA[1], R. MIDDAG[1,3], M.M.P. VAN HULTEN[4], P. LAAN[1], V. SCHOEMANN[1], J.T.M. DE JONG[1], A. STERL[4] AND H.M. VAN AKEN[1]

[1] Royal Netherlands Institute for Sea Research, P.O. Box 59, 1790 AB Den Burg, The Netherlands (*correspondence: Hein.de.Baar@nioz.nl)
[2]Department Ocean Ecosystems, University of Groningen, P.O. Box 11103, 9700 CC Groningen, The Netherlands
[3]Department of Ocean Sciences & Institute of Marine Sciences, University of California Santa Cruz, CA 95064, USA
[4]Royal Netherlands Meteorological Institute, P.O. Box 201 3730 AE De Bilt, The Netherlands

The thus far longest (13,000 km) complete deep ocean section of iron (Fe), aluminium (Al) and a suite of other trace elements and isotopes was realized in 2010-2011 in the West Atlantic Ocean. The more than 1200 data values reveal the major sources and processes controling Fe and Al in the oceans. Overall Fe is decoupled from Al except in the uppermost surface layer of dust input. Overall the Al shows an amazing inverse relationship with Si.

The background concentrations of Fe are quite uniform around 0.5 nM but there are several major enhancements. In the 10-30 ºN region the uppermost samples (10m depth) have maximum concentrations of Fe exceeding 2nM and Al exceeding 40 nM, respectively, due to partial dissolution of dust supply from the Sahara. This extra Fe supports N_2 fixation by diazotrophs in the Sargasso Sea, that upon sinking of plankton debris and mineralization causes a high anomaly of the nitrate/phosphate ratio in the 200-800m depth zone. The Amazon River plume provides a signal of high Fe and Mn but Al is not enhanced. Underlying the equator the strong oxygen minimum zone contains higher Fe concentrations, that by upward mixing may well be the major source of Fe to surface waters supporting plankton growth. The Confluence zone (~30 ºS) of the Brazil and Malvinas Current is a well known region of high biological productivity and chlorophyll biomass. We now find this is supported by very high dissolved Fe from below at ~3 nM or more, the supply of which may also be due to influence of the Rio de la Plata or submarine groundwater discharge. The North Atlantic Deep Water shows a very strong correlation of Al and silicate (Si) in the subArctic Gyre, yet going southwards the NADW content of Al decreases and of Si increases and far south no relationship exists anymore. This is consistent with ocean simulation modeling of steady remineralization of Si versus continuous loss of Al due to adsorptive scavenging. An enhanced Fe pool at 2000-3000m depth below and south of the equator (4ºN - 15ºS) is consistent with hydrothermal input, confirmed by higher Mn but no extra Al.

https://doi.org/10.1180/S0026461X00008434 Published online by Cambridge University Press

Dissolved Iron in the Arctic and Antarctic Oceans

H.J.W. De Baar[1,2]*, M.B. Klunder[1], C.-E. Thuroczy[1], P. Laan[1], L.J.A. Gerringa[1], A.-C. Alderkamp[2,3], R. Middag[1,4] and K.R. Arrigo[3]

[1] Royal Netherlands Institute for Sea Research, P.O. Box 59, 1790 AB Den Burg, The Netherlands (*correspondence: Hein.de.Baar@nioz.nl)

[2]Department Ocean Ecosystems, University of Groningen, P.O. Box 11103, 9700 CC Groningen, The Netherlands

[3]Department of Environmental Earth Systems Sciences, Stanford University, Stanford, CA 94305-4216, USA

[4]Department of Ocean Sciences & Institute of Marine Sciences, University of California Santa Cruz, CA 95064, USA

Iron (Fe) is an essential trace element for all biota but the dissolved Fe in ocean waters is extremely low and limiting for phytoplankton growth in over 40% of world ocean surface waters. Indeed in the Southern Ocean extremely low dissolved Fe was found in surface waters along the Greenwich meridian, both in the Antarctic Circumpolar Current and in the most southerly Weddell Gyre adjacent to the ice-covered Antarctic continent [1]. The low dissolved Fe is maintained in solution by organic complexation [2]. The extending continental ice-sheet floating over the continental shelf is unique in largely preventing biological processes and cycling. As a consequence Antarctica is the only continent that does not supply Fe [1] and Mn [3] from shelf sediment sources into adjacent surface and intermediate waters. In contrast the shelves at both sides of the Antarctic Peninsula are a source for dissolved Fe, Mn and Al into the western Weddell Sea and southern Drake Passage, respectively. Otherwise dissolved Fe concentrations are extremely low in the entire water column of the Weddell Sea and Drake Passage. In West Antarctica the local Pine Island Glacier is a source of dissolved Fe [4] fueling intensive phytoplankton blooms [5] in the Amundsen Sea where organic complexation [6] of Fe plays a key role. In deep waters there is a significant hydrothermal plume of Fe and Mn over the Bouvet Triple Junction region. One water mass in Drake Passage also shows hydrothermal Fe and Mn associated with δ^3He anomalies originating from the Pacific Ocean [7]. In the Arctic Ocean a very strong hydrothermal Fe and Mn plume was found over the Gakkel Ridge [8, 9]. The large spatial extent of Fe of hydrothermal origin is ascribed to its stabilization in solution by organic complexation [10]. Surface waters in the central Arctic Ocean have fairly high dissolved Fe concentrations due to the Transpolar Drift bringing along coastal waters, mainly of Siberian riverine origin with high dissolved Fe contents [11]. As a result the Arctic Ocean has fairly adequate Fe abundance for phytoplankton growth, this in contrast to the very low and bio-limiting dissolved Fe in large areas of the Antarctic Ocean.

[1] Klunder et al. (2011) Deep-Sea Res. II, 56, 2678. [2] Thuroczy et al. (2011) Deep-Sea Res. II, 56, 2695. [3] Middag et al. (2011) Deep-Sea Res. II, 56, 2661. [4] Gerringa et al. (2012) Deep-Sea Res. II, in press. [5] Alderkamp et al. (2012) Deep-Sea Res. II, in press. [6] Thuroczy et al. (2012) Deep-Sea Res. II, in press. [7] Middag et al. (2012) J. Geophys. Res. Oceans, in press. [8] Middag et al. (2011) Geochim. Cosmochim. Acta, 75, 2393. [9] Klunder et al. (2012a) J.Geophys. Res. Oceans, in press. [10] Thuroczy et al. (2011) J. Geophys. Res. Oceans, 116, C10009, doi:10.1029/2010JC006835. [11] Klunder et al. (2012b) J. Geophys. Res. Oceans, in press.

Atmospheric gases: the archaeological glasses memory

Aurore de Bigault de granrut[1*], Eric Humler[1]

[1]Laboratoire de Planétologie et Géodynamique - Université de Nantes, Nantes, France, (*aurore.de-bigault-de-granrut@univ-nantes.fr)

The atmospheric components of past climatic changes are often constrained from ice records of polar ice sheets. In temperate areas, this kind of study is more difficult to apply due to the low spatial and temporal resolution of the iced records.

In this study, we propose an alternative method based on analyses of atmospheric gases trapped in bubbles of archaeological glasses from the Western Europe and dated between the Ist century BC to the present. Indeed, during the shaping of ancient glasses, bubbles are created in glass paste, from the melting of raw materials inside furnace and glass-paste degassing, or from the step of glass working in open air. In this second case, the surrounding atmosphere could be trapped, particularly during the glass-making of ancient and medieval stained windows.

While the study of Vesicule Size Distribution (VSD) [1] of archaeological flat glasses show a bimodal size bubbles distribution in flat glasses, the distribution of the other kind of glasses (blown cup or vessel, and raw glasses) are unimodal. Geochemical analyses of major gases included in bubbles in flat glasses, show a chemical dichotomy between two groups of bubbles, independent of chemical composition of glass paste. The smallest bubbles (Ø<100-500 μm) are exclusively composed of CO_2. In contrast, the largest bubbles (Ø>250-500 μm) are N_2 rich (~80%), CO_2 poor and contained Ar (~1%), and sometimes O_2. So, the origins of the two populations of bubbles are obviously different and the largest vesicles seem to have an atmospheric origin (the Ar/N_2 ratios of these large bubbles are closed to the modern atmosphere).

Despite these gases look like an atmospheric composition, the CO_2 contents are too high and the oxygen contents are too low. The carbon excess could have different origins (mixing between atmosphere and furnace/combustion gases, and/or chemical reactions between trapped gases and particular soots). SEM analyses have shown some deposits in the inner wall of the largest bubbles (graphite, carbon oxides etc.), supporting the idea of a catch of elements as alien to glass and in-situ chemical reactions.

We need to take care of these soot-reactions and the gases diffusion rates through the glass, to estimate the initial compositions of gases included in vesicles, and to extract the atmospheric contribution from the bubbles gases set using mixing models. Finally, we suggest that the archaeological glasses could appear like a new but complex source of archeo-climatic recording.

[1] Sarda & Graham (1990), EPSL 97, 268-289.

https://doi.org/10.1180/S0026461X00008434 Published online by Cambridge University Press

Mixing of Contrasting Silicate Melts: preliminary Raman Spectra

CRISTINA P. DE CAMPOS[1]*, DIEGO PERUGINI[1,2], DANIEL R. NEUVILLE[3], KAI-UWE HESS[1], WERNER ERTEL-INGRISCH[1], AND DONALD B. DINGWELL[1]

[1]Dept. of Earth and Environmental Sc., Univ. of Munich, Munich, Germany campos@min.uni-muenchen.de (*presenting author)
[2]Dept. of Geosciences, Univ. of Perugia, Perugia, Italy. diegop@unip.it
[3]CNRS, IPGP, Sorbonne Paris Cité neuville@ipgp.fr

Glasses melts and magmas

A widely debated question in Geosciences is how viscous magmas with extreme viscosity contrast mix under natural conditions. In order to study how chaotic dynamics may control chemical interactions, and therefore timescales of hybridization during magma mixing, we developed a modified Journal Bearing System device [1] for experiments on chaotic mixing silicate melts at high temperature [2]. In this work we focus on preliminary Raman spectra of mixed glasses obtained by mixing two end-members at 1,673K: (i) a peralkaline haplogranite melt (HPG8N5K5), and (2) a haplobasaltic melt corresponding to the 1-atm eutectic composition of the Anorthite-Diopside (An-Di) binary system. These two compositions are intended to act as analogues for natural dry granitic and basaltic magmas. Raman spectra were obtained along two transects along filaments from the resultant glasses, next to the same points analysed for major and trace elements (microprobe and Laser Ablation ICP-MS) [3]. Experimental conditions were kept 'extreme', since most of melt fraction consisted of a high-viscosity melt (95%) and small amounts of lower viscosity mafic melt (5%).

Figure 1: Raman spectra along two transects crossing filaments of mixed haplogranite and An-Di

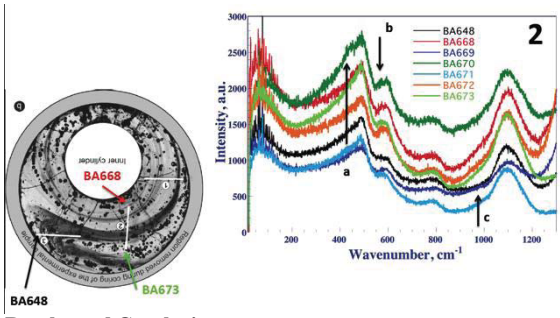

Results and Conclusion

We observe some changes, in particular the arrows a, b and c show changes in the Raman spectra, and they can link at changes in the polymerization network. Spectra 648 is probably more polymerized than spectra 666 (not shown in Figure 1). This observation is also confirmed for the spectra 670, consisting of the more polymerized melt. Although the changes are still subtle, these point towards changes in the polymerization degree, which are due to differential hybridization of the two stating compositions. For the preliminary results peak-changes vary with the geometry and interaction degree among filaments. Results are consistent with those obtained from microchemical studies along the same lines [3].

[1] Ottino etal. (1988) *Nature* **333**, 419-425; [2] De Campos et al. (2011) *Contrib. Mineral Petrol* **161**, 863-881; [3] Perugini et al. (*in prep.).*

Case study of an abandoned Zn-Pb mine: Ingurtosu (Sardinia, Italy).

GIOVANNI. DE GIUDICI[1]*, FRANCESCA PODDA[1], DANIELA MEDAS[1], ROSA CIDU[1], PIERFRANCO LATTANZI[1], BRIANT KIMBALL[2], RICHARD WANTY[3], KATARZYNA TURNAU[4], CHIARA ALISI[5], ANNA ROSA SPROCATI[5]

[1]University of Cagliari, Cagliari, Italy, gbgiudic@unica.it
[2]US Geological Survey, Salt Lake City, USA
[3]US Geological Survey, Denver Federal Center, Colorado, USA
[4]Jajiellonian University, Kracow, Poland
[5]ENEA, Casaccia, Italy

Ingurtosu mine characterization

The Ingurtosu Pb-Zn mine (S-W Sardinia) was in production for about a century until 1968. Huge amounts of tailings were abandoned, resulting in long-term heavy metal dispersion in both stream sediments and waters. Downstream from the mine wastes, the Naracauli waters discharge directly into the Mediterranean Sea. At least two biomineralization processes (Fig. 1) are known to be effective in the abatement of Zn and other heavy metals transported in solution.

In this work, many different techniques were used to study the mineralogy and geochemistry controlling the biomineralization processes. Microbial consortia within biofilm associated with seasonal precipitation of an amorphous mineral made of Si, Zn and O were examined. In addition, the load of metal dissolved in the Naracauli waters was measured using hydrologic tracers with synoptic sampling.

The results presented in this work show that a) the consortium of bacteria changes along the river, creating a cascade of processes that results in biologically mediated formation of different Zn-bearing minerals [1]; b) the changes in water chemistry along the river are moderate for the major constituents, but large changes in trace-element concentrations are observed [2]; c) the heavy metals load derives from the interaction between mine wastes and Naracauli water, and about half of the metal load comes from tributaries with high water flow but relatively low heavy metal concentrations.

Figure 1. SEM images of Naracauli biominerals: hydrozincite on the left, and Zn-Si-O phase on the right.

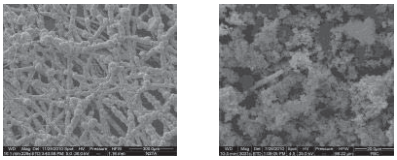

Conclusion

This work indicates that any remediation plan for the Ingurtosu abandoned mine must take into account the whole Naracauli basin, and water treatment is needed before river water is allowed to discharge to the sea. Finally, biomineralization processes could offer a way for a natural abatement of Zn and some other heavy metals.

[1] De Giudici et al. (2009) *American Mineralogist* **94**, 1698-1706. [2] Medas et al. (2011) in Soil Biology- Kothe and Warma eds. **31**, pp-pp.113-130.

https://doi.org/10.1180/S0026461X00008434 Published online by Cambridge University Press

Modelling the nucleation of hydroxyapatite at a collagen template

NORA H. DE LEEUW[1]*, N. ALMORA-BARRIOS[1]
[1]University College London, Department of Chemistry, London, UK
n.h.deleeuw@ucl.ac.uk (presenting author)

The biomineral hydroxyapatite nucleates at an organic collagen matrix, which controls the growth process and eventual morphology of the apatite crystallites. An important but largely unresolved issue is the way in which nature controls the nucleation, growth and morphology of the inorganic crystallites and the function of the templating biomolecules, here collagen, in these reactions. However, as it is not yet possible to study directly, by experiment alone, the molecular mechanisms of biomineralisation processes, we have employed a combination of *ab initio* and classical Molecular Dynamics simulations to investigate the early processes of the nucleation of hydroxyapatite at a collagen template, by immersing a triple-helical collagen molecule in a stoichiometric solution of Ca^{2+}, PO_4^{3-} and OH^- ions.

The average number of water molecules in the first hydration shells of the Ca ions and PO_4 groups from the classical MD simulations are all in excellent agreement between with the *ab initio* MD and experiment. Very quickly, a number of stable calcium phosphate (CaP) clusters form in solution, although preferential CaP formation occurs at the collagen matrix.

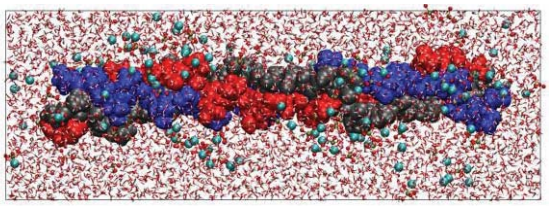

Figure 1: Graphical representation of the collagen triple helix in stoichiometric hydroxyapatite solution.

Electrostatic attractions are prevalent between calcium ions and oxygen atoms of the glycine and hydroxyproline residues, which were the starting point for the formation of the calcium phosphate clusters. At body temperature, calcium ions interact with water molecules to form stable complexes, but attracted by electrostatic forces, they coordinate to PO_4 ions and start forming clusters. Some phosphate ions form hydrogen-bonds with the hydroxy groups of hydroxyproline residues, whereas due to strong water-OH interactions most of the hydroxy ions stay in solution, although some become attached to calcium phosphate clusters. These results agree with suggestions that HA growth follows initial amorphous CaP formation.

Comparison of our results[1] with those of Kawska et al.[2] shows that fluoride ions inhibit calcium phosphate formation by competitively binding the Ca ions into calcium fluoride clusters.

[1] Almora-Barrios (2012) Cryst. Growth Des. DOI: 10.1021/cg201092s. [2] Kawska (2008) Angew. Chem. Int. Ed. **47**, 4982.

Geochemical modelling of long-term mineral alteration induced by the injection of CO_2 in a saline aquifer: the Ketzin site

MARCO DE LUCIA*, ELISA KLEIN, MICHAEL KÜHN
AND THE KETZIN TEAM
Helmholtz Centre Potsdam, German Research Center for Geosciences - GFZ, delucia@gfz-potsdam.de (* presenting author)

The assessment of expected long-term CO_2-induced mineral alterations of reservoir and cap rock is crucial to ensure the long-term stability of the storage project, and to evaluate the potential carbon trapping provided by mineralization. In the first european on-shore pilot site at Ketzin, nearby Potsdam, Germany, about 60,000 t of CO_2 were injected (as of February, 2012) in a saline aquifer in a Triassic sandstone at about 650 m depth. A rich set of analyses of pristine formation fluids [1] as well as mineralogical and geochemical composition of the reservoir rock [2] made possible a precise parametrization of the reference geochemical model.

Batch 0-D simulations including reaction kinetics were run using the speciation code PHREEQC under the assumption of a constant CO_2 pressure over the simulation time of 5,000 y. The pore pressure itself was found to have a negligible impact on mineral alterations, at least in the considered range of approximately 50 to 80 bar expected for the site. The reference simulation predicts the precipitation of kaolinite, K-feldspar, and plagioclase (represented by the end-member albite) which greatly compensate the partial dissolution of illite, Fe-rich chlorite, and anhydrite cement. Of all carbonate minerals included in the model (siderite, magnesite, calcite, and dolomite), siderite is the only one which precipitates in significant amounts, and thus contributes to mineral trapping. However, the precipitation of carbonates always starts after several hundreds years in the models.

To investigate the robustness of these results, different scenarios were run, each representing a different choice for primary and secondary minerals and different hypothesis for the parametrization of mineral reactive surfaces with respect to the reference model. The simulated results are quite variable, but the simulated total relative change in pore volume after 5,000 years was always below 2%. This can be considered irrelevant in terms of influence on the hydrodynamic properties of the rock. These results are confirmed by the observations from laboratory experiments on core samples exposed to CO_2.

[1] Würdemann et al. (2010) *CO_2SINK—From site characterisation and risk assessment to monitoring and verification: One year of operational experience with the field laboratory for CO_2 storage at Ketzin, Germany* **International Journal of Greenhouse Gas Control** 4(6), pp 938-951
[2] Förster et al. (2010) *Reservoir characterization of a CO_2 storage aquifer: The Upper Triassic Stuttgart Formation in the Northeast German Basin*, **Marine and Petroleum Geology** 27, 2156-2172.

https://doi.org/10.1180/S0026461X00008434 Published online by Cambridge University Press

Sulfur Isotope Fractionation During Basaltic Degassing

J. MAARTEN DE MOOR[1*], TOBIAS P. FISCHER[1], PENELOPE L. KING[2], ZACHARY D. SHARP[1], MATTHEW MARCUS[3], MICHAEL N. SPILDE[4], BERNARD MARTY[5]

[1]Dept. of Earth & Planetary Sciences, UNM, Albuquerque, USA mdemoor@unm.edu*
[2]Research School of Earth Sciences, ANU, Canberra, Australia
[3]Advanced Light Source, LBNL, Berkeley, USA
[4]Institute of Meteoritics, UNM, Albuquerque, USA
[5]Centre de Récherche Petrographique et Géochimique, Nancy, France

We examine S degassing and S isotope fractionation at basaltic volcanoes using S isotope compositions of scoria and magmatic gases from three active basaltic volcanoes in contrasting tectonic settings: Masaya and Cerro Negro (Central American Arc), and Erta Ale (East African Rift). We present S contents and S speciation of gases and melt inclusions to constrain degassing conditions. An equilibrium isotope fractionation degassing model is used to assess the S systematics considering oxygen fugacity, temperature, and pressure of degassing.

Erta Ale is a reduced system at Δ QFM ~0 [1]. Pristine scoria from Erta Ale have an average $\delta^{34}S$ value of + 0.9 ± 0.3 ‰ (n = 5) and gas samples have $\delta^{34}S$ values of + 0.7 ‰ to -1.9 ‰, spanning the MORB range of + 0.3 ± 0.5 ‰ [2] and extending to lighter values. Synchrotron micro-X-ray Absorption Near Edge Spectroscopy (XANES) analysis of an olivine-hosted melt inclusion from Erta Ale indicates that S^{2-} is the dominant S species in the melt (rather than S^{6+}). High temperature (1086°C) fumarolic gas samples have SO_2 as the dominant S species. Significantly, the scoria are isotopically heavier than the gases, which is the opposite of that expected for equilibrium conditions between S^{2-} in the melt and SO_2 gas because at equilibrium the more oxidized S species retains the heavy isotope. We interpret the low $\delta^{34}S$ values of the gas to reflect a kinetic effect that occurs as S diffuses from the melt into the gas phase (on the bubble scale) that favours the transfer of the light isotope into the gas.

Gas and scoria samples from the oxidized arc volcanoes (Cerro Negro and Masaya; ~ΔQFM +2 [3]) have a range of $\delta^{34}S$ values from + 2.2 ‰ to + 9.3 ‰. Scoria are isotopically heavier than the gases by ~3 ‰ at Masaya and by ~5 ‰ at Cerro Negro. XANES analysis of an olivine hosted melt inclusion from Cerro Negro shows that S^{6+} is the dominant S species in the melt. The negative $\Delta^{34}S_{gas\text{-}melt}$ relationship observed at Masaya and Cerro Negro is consistent with degassing of SO_2 or H_2S from a melt containing S^{6+}. However, equilibrium modelling predicts that the gas should be isotopically lighter than the melt by only 1‰ to 1.7‰ for degassing between 1 bar and 4 kbar (higher degassing pressure favours H_2S over SO_2, resulting in larger fractionation between gas and S^{6+} in the melt). The large $\Delta^{34}S_{gas\text{-}melt}$ observed at Masaya and Cerro Negro can be explained by equilibrium fractionation in addition to a kinetic effect as observed at Erta Ale. In all three cases the compositions of the gases are isotopically lighter than predicted by equilibrium modelling by 2 ‰ to 4 ‰, suggesting a common kinetic effect that favours the transfer of the light isotope into the gas phase.

[1] Giggenbach and Le Guern (1976) *GCA* **40**, 25-30. [2] Sakai et al. (1984) *GCA* **48**, 2433-2441. [3] Mather et al. (2006) *JGR* **111**, D18.

Ex situ carbonate mineralization: a novel way to sequester CO_2 at the expense of saline wastewater

CATERINA DE VITO[1], SILVANO MIGNARDI[1], VINCENZO FERRINI[1] AND ROBERT F. MARTIN[2]*

[1]Sapienza University, Earth Sciences Department, Rome, Italy, cdevito@uniromal.it
[2] McGill University, Earth and Planetary Sciences, Montreal, Canada, robert.martin@mcgill.ca (* presenting author)

In situ and ex situ technologies based on carbonate mineralization offer ways to insure the permanent and safe storage of this greenhouse gas. In our opinion, both anthropogenically produced CO_2, at a cement plant, for example, and saline wastewaters can be utilized as valuable resources. The brines recovered from desalination operations and produced water associated with oil and gas exploitation are promising sources of alkalis and alkaline earths needed in the carbonation process. Our ex situ approach involves the formation of hydrated carbonate minerals (e.g., nesquehonite, $MgCO_3 \cdot 3H_2O$) at room temperature through the reaction of gaseous CO_2 bubbling in Mg (7 g L^{-1}) wastewater, similar to what is commonly available industrially [1]. The reaction rate is rapid, with carbonate deposition in about ten minutes. We have demonstrated that the method can be efficiently applied to more concentrated solutions, up to 32 g L^{-1} of Mg. The efficiency of the carbonate mineralization process ranges between 65 and 80%, depending on the salinity of the solution [2]. The thermal behavior and structural stability of the nesquehonite precipitate suggest that it will remain stable at the temperature conditions that prevail at the Earth's surface, i.e., below 600 K, the threshold of periclase nucleation [3]. Moreover, our results indicate that if this mineral is left in contact with the simulated brine or heated, it can be expected to transform to other carbonates thermodynamically more stable, up to about 650 K, e.g., dypingite $[Mg_5(CO_3)_4(OH)_2 \cdot 5H_2O]$ and hydromagnesite $[Mg_5(CO_3)_4(OH)_2 \cdot 4H_2O]$. These experimental results also provide information about the fate of secondary carbonates that form in a CO_2 injection environment.

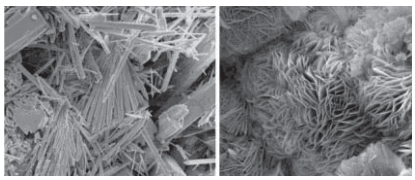

Figure 1: Nesquehonite (left), obtained by direct synthesis, and dypingite (right), obtained by transformation of early-formed carbonate.

The resulting carbonate precipitates formed in our approach can profitably be used in many applications, for example in the production of building materials. Our approach offers a complementary solution to CO_2 abatement in countries where the production of saline waste is significant.

[1] Ferrini *et al.* (2009) *Journal of Hazardous Materials* **168**, 832-837.

[2] Mignardi *et al.* (2011) *Journal of Hazardous Materials* **191**, 49-55.

[3] Ballirano *et al.* (2010) *Journal of Hazardous Materials* **178**, 522-528.

https://doi.org/10.1180/S0026461X00008434 Published online by Cambridge University Press

Peat bog Records of Atmospheric Dust fluxes - Holocene palaeoenvironmental and paleoclimatic implications for South America

FRANÇOIS DE VLEESCHOUWER[1,2*], HELEEN VANNESTE[1,2], SEBASTIEN BERTRAND[3], ANDREA CORONATO[4], DIEGO GAIERO[5], GAËL LE ROUX[1,2] AND THE PARAD TEAM[6].

[1] Université de Toulouse, INP, UPS, EcoLab (Laboratoire Ecologie Fonctionnelle et Environnement), ENSAT, Avenue de l'Agrobiopole, 31326 Castanet Tolosan, France (francois.devleeschouwer@ensat.fr)
[2] CNRS, EcoLab, 31326 Castanet Tolosan, France
[3] RCMG, Gent, Belgium
[4] CADIC-CONICET, Ushuaia, Argentina,
[5] CICTERRA-CONICET, Cordoba, Argentina
[6] PARAD team are: Maarten Blaauw (QUB, Belfast, Ireland), C. Jeandel (LEGOS, Toulouse, France), Malin Kylander (Univ. Stockholm, Sweden), Antonio Martinez-Cortizas (Univ. Sandiago de Compostella, Spain), D. Mauquoy (Univ. Aberdeen, UK), Anna Pazdur (GADAM, Gliwice, Poland), Natalia Piotrowska (GADAM, Gliwice, Poland), Frederico Ponce (CADIC-CONICET, Ushuaia, Argentina), Jean-Luc Probst (ECOLAB, Toulouse, France) and William Shotyk (Univ. Alberta, Edmonton, Canada).

Abstract

Few attention has been given to pre-anthropogenic signals recorded in peat bogs, especially in the Southern Hemisphere. Yet they are important to 1/ better understand the different particle sources during the Holocene and 2/ to tackle the linkage between atmospheric dust loads and climate change and 3/ to better understand the impact of dust on Holocene palaeoclimate and palaeoenvironments in a critical area for ocean productivity.

In this poster, we will present the preliminary results and the main objectives of the PARAD project, which are: 1) to provide high-resolution continuous records of natural atmospheric dust using the elemental and isotopic signature of peat cores from Tierra del Fuego, and 2) to assess the linkage between dust inputs and climate.In this project, we will explore the use of a broad range of trace elements as dust proxies (soil particles, volcanism, cosmogenic dusts, marine aerosols). Radiogenic isotopes (Pb, Nd, Hf) will be used as tracers for fingerprinting predominant sources. Coupling these findings with biological proxies (plant macrofossils, pollen) and detailed age-depth modeling, we expect not only to identify and interpret new links between atmospheric dust chemistry and climate change but also to significantly improve our understanding of peat bogs as archives of climate change, and the role of dust in both palaeoenvironmental and palaeoclimatic changes.

Non-classical pathways of mineralization: Pre-nucleation clusters and oriented attachment

JAMES J. DE YOREO[1]*, ADAM WALLACE[1], DONGSHENG LI[1], MICHAEL H. NIELSEN[2], JONATHAN R. LEE[3], ,JILLIAN BANFIELD[4], AND CATHRINE FRANDSEN[5]

[1]Materials Science Division, Lawrence Berkeley National Laboratory, Berkeley, CA, USA jjdeyoreo@lbl.gov (* presenting author), dongshengli@lbl.gov, afwallace@lbl.gov
[2]Department of Materials Science and Engineering, University of California, Berkeley, CA, USA, mhnielsen@lbl.gov
[3]Physical Sciences Directorate, Lawrence Livermore National Laboratory, Livermore, CA, USA, lee204@llnl.gov
[4]Department of Earth and Planetary Science, University of California, Berkeley, CA, USA, jbanfield@berkeley.edu
[5]Department of Physics, Technical University of Denmark, Kongens Lyngby, Denmark, fraca@fysik.dtu.dk

Introduction

Recent investigations of crystallization in the calcium carbonate and phosphate systems have conclusded that classical concepts of crystal growth fail to predict observed pathways of nucleation. These pathways appear to start with pre-nucleation clusters and depend upon particle mediated growth processes that involve amorphous precursors. These conclusions follow upon a body of research documenting aggregation-based growth mechanisms in which primary crystalline particles are found to be co-aligned in the final crystal structure. However, little is known about the formation, structure and energetics of pre-nucleation clusters, and the mechanism by which co-alignment of primary particles occurs has not been established. Here we report results of novel simulations and experiments exploring these phenomena.

Results and Conclusion

Using replica-exchange molecular dynamics techniques previously applied to protein folding, we investigate initial formation and onset of order within hydrated calcium carbonate clusters. The clusters initiate as short linear chains that rapidly evolve into 2D and 3D structures with continued growth. Establishment of order is hindered by incomplete ion desolvation. However, in ~1 nm diameter particles, ordered motifs emerge that resemble the local order within crystalline carbonate phases. The free energy along the simulated growth pathways is currently being calculated to determine whether the clusters are thermodynamically stable or metastable with respect to ions in solution and to predict the free energy barrier that separates the cluster species from supercritical nuclei.

We investigated mechanism of oriented attachment (OA) of iron oxyhydroxide nanoparticles using high-resolution fluid cell TEM. The particles undergo continuous rotation and interaction until they find a perfect lattice match. A sudden "jump to contact" then occurs over < 1nm, followed by lateral atom-by-atom addition at the contact point. Interface elimination proceeds at a rate consistent with the curvature-dependence of the chemical potential. Translational and rotational accelerations show that strong, highly-

https://doi.org/10.1180/S0026461X00008434 Published online by Cambridge University Press

Vegetation uptake controlling groundwater solute evolution on a southeast Australian granite

JOSHUA F. DEAN[1,2*], JOHN A. WEBB[1,2], GERALDINE JACOBSEN[3], ROBERT CHISARI[3] AND P. EVAN DRESEL[4]

[1]La Trobe University, Agricultural Sciences, Australia, jf3dean@students.latrobe.edu.au (* presenting author)
[2]National Centre for Groundwater Research and Training, Australia
[3]Institute for Environmental Research, ANSTO, Australia
[4]Department of Primary Industries Victoria, Australia

Groundwater geochemical signatures are typically considered derived from rock-water dissolution and weathering interactions. However, many major ions (Ca^{2+}, K^{+}, HCO_3^{-}, Mg^{2+}, S, and Si) are essential plant nutrients, and are removed from rainfall, soil-water and groundwater, where soils are depleted in these species. This in turn affects the solute composition of infiltrating water.

Conventional methods [1] of determining relative groundwater solute contributions from specific rock weathering reactions were carried out for a pair of sub-catchments in the Dwyer Granite, southwest Victoria, Australia. This method was adapted for semi-arid, southwest Victoria by standardising all ions to rainfall Cl^{-} to remove the effects of evapotranspiration. While this step is commonly omitted in high rainfall, northern hemisphere studies [2], it is important for the Australian setting, where groundwater solutes are primarily derived from the concentration of rainfall by evapotranspiration [3,4].

In a few groundwater samples in the study area, enrichment with respect to rainfall of Na^{2+} and H_4SiO_4 is ascribed to plagioclase weathering, while SO_4^{2-} enrichment is ascribed to pyrite oxidation, indicating that rock weathering reactions play a role in this setting. However, in most samples, after subtracting rainfall input (as per [1]), there is wholesale depletion of all measured ions. This prevents the use of the plagioclase, biotite and k-feldspar chemical weathering reactions in the mass-balance, as these release cations (Na^{2+}, K^{+}, Mg^{2+} and Ca^{2+}), all of which are depleted in the groundwater with respect to rainfall.

This ion depletion is not due to mineral precipitation as neither geochemical modelling nor X-ray diffraction analyses show evidence of this occuring. Nor is it due to ion exchange as there is no balancing import of ions or significant acidification of the groundwater. Having already ruled out evapotranspiration effects through Cl^{-} standardisation, the depletion is instead attributed to vegetation uptake, which has been identified as a significant process elsewhere in the region [5], causing depletion of recharge solutes.

[1] Garrels and Mackenzie (1967) *Equilibrium Concepts in Natural Water Systems* **Advances in Chemistry Series**, 222-242. [2] Velbel and Price (2007) *Appl. Geochem.* **22**, 1682-1700. [3] Herczeg *et al*. (2001) *Mar. Freshwater Res*. **52**, 41-52. [4] Bennetts *et al*. (2006) *J. Hydrol*. **323**, 178-192. [5] Edwards and Webb (2009) *Hydrogeol. J.* **17**, 1359-1374.

Equilibrium Partitioning of Li between Olivine and Clinopyroxene at Mantle Conditions

JAMES A. DEANE JR.[1*], MAUREEN D. FEINEMAN[1], JESSICA L. YAKOB[1], DAVID H. EGGLER[1], SARAH C. PENNISTON-DORLAND[2]

[1]Pennsylvania State University, University Park, PA, USA, jad5678@psu.edu (*presenting author)
[2]University of Maryland, College Park, MD, USA

Abstract

The lithium isotope system holds great allure as a tracer of recycled subducted materials in the Earth's interior, owing to the striking isotopic contrast between lithium at the Earth's surface and that in the mantle, combined with the presence of Li at measurable quantities in mantle minerals. Unfortunately, measurements of lithium isotope ratios in mantle xenoliths have proven difficult to interpret. Mantle xenolith data compiled from samples worldwide have revealed that lithium elemental and isotopic distribution between olivine and clinopyroxene is highly variable. At high temperatures such as those found in the mantle, the isotopic fractionation factor $\alpha_{ol/cpx}$ $[=(^7Li/^6Li)_{ol}/(^7Li/^6Li)_{cpx}]$ is expected to approach 1, and experimental constraints on equilibrium partitioning show that the partition coefficient ($D^{Li}_{ol/cpx}$) is between 1.5-2. Many xenolith samples exhibit equilibrium behavior with respect to both isotopic fractionation and equilibrium partitioning, but some samples do not. Xenoliths with apparent $D^{Li}_{ol/cpx} < 1$ trend toward isotopically lighter Li in clinopyroxene relative to olivine, with $\Delta^7Li_{ol\text{-}cpx}$ $[=\delta^7Li_{ol} - \delta^7L_{cpx}]$ ranging from 3 - 25‰. A physical process explaining this relatively extreme isotopic fractionation between co-existing mantle phases has yet to be satisfactorily demonstrated. One proposed hypothesis to explain the apparent Li isotopic disequilibrium in mantle xenoliths is that upon exhumation, closed system redistribution of Li between mantle minerals occurs as a function of cooling, meaning the partition coefficient is temperature dependent. Richter et al. (2003) have shown potential for considerable kinetic isotopic fractionation of Li during diffusion. Thus if Li is redistributed under dynamic conditions preceding or concurrent with eruption, kinetically driven isotopic fractionation might be "locked in" to the mantle minerals upon reaching closure conditions. We have conducted a series of piston cylinder experiments at 1.5 GPa and 700-1100 ˚C, the results of which show that $D^{Li}_{ol/cpx}$ is 2.0 ± 0.2 regardless of temperature over this range. It seems that a new explanation is needed to explain the Li signature in mantle xenoliths. Mantle olivine contains some amount of iron (~10% FeO*), and the ambient $fO2$ controls the relative amount of Fe^{+2}/Fe^{+3}. Variation in the amount of Fe^{+3} could potentially influence the incorporation of Li^{+} into the octahedral site of olivine by providing a charge-balancing mechanism. This could allow for a redistribution and isotopic fractionation of Li in response to changing fO_2. Experiments at 900°C and 1.5 GPa with solid state fO_2 buffers of Re-ReO, Ni-NiO, and Mo-MoO are currently underway to determine whether oxygen fugacity plays a role in controlling Li partitioning.

[1] Richter et al. (2003) *Geochimica et Cosmochimica Acta* **67**, 20, 3905–3923.

https://doi.org/10.1180/S0026461X00008434 Published online by Cambridge University Press

Stagnant-lid tectonics in early Earth revealed by ^{142}Nd variations in late Archean rocks

V. DEBAILLE[1*], C. O'NEILL[2], A. D. BRANDON[3], P. HAENECOUR[4], Q.-Z. YIN[5], N. MATTIELLI[1], A. H. TREIMAN[6]

[1] Laboratoire G-Time, Université Libre de Bruxelles, CP 160/02, 50 Avenue F. D. Roosevelt, 1050 Brussels, Belgium. (vinciane.debaille@ulb.ac.be) (* presenting author)
[2] GEMOC ARC National Key Centre, Earth and Planetary Science, Macquarie University, New South Wales 2109, Australia.
[3] Department of Earth and Atmospheric Sciences, University of Houston, Houston TX 77204, USA
[4] Laboratory for Space Sciences and Earth and Planetary Sciences Department, Washington University, St. Louis MO 63130-4899, USA
[5] Department of Geology, University of California Davis, One Shields Avenue, Davis, CA 95616, USA.
[6] Lunar and Planetary Institute, 3600 Bay Area Boulevard, Houston TX 77058, USA

The progressive μ^{142}Nd decrease in early Archean rocks from +20 to 0 between 3.9 to 3.6 billions years (Gyr), with rocks younger than 3.5 Gyr showing no μ^{142}Nd anomalies, is thought to indicate the efficient remixing of the first primitive crust into the Archaean convecting mantle that ultimately produce a well-mixed present-day convecting mantle with μ^{142}Nd = 0 [1]. The implied long mixing time of ~1 Gyr from the Hadean to Archaean for the whole mantle is paradoxical on several levels. This is much longer than the rapid mixing time (<100 Myr) inferred for the Archean due to vigorous mantle convection related to Earth's hotter thermal regime [2], and similar to the mixing time inferred for the present-day Earth's mantle [3].

Here we report a resolvable positive ^{142}Nd anomaly of μ^{142}Nd = +7 ± 3 ppm relative to the modern convecting mantle in a 2.7 Gyr old tholeiitic lava flow from the Abitibi Greenstone Belt in the Canadian Craton. Our result effectively extends the early Archean convective mixing time to ~1.8 Gyr, i.e. even longer than present-day mantle mixing timescale [3], despite a more vigorous convection expected in the Archean. Different hypotheses have been examined to explain such a protracted mixing in the Archean, such as mantle overturn, two-layer convection or the existence of a dense layer at the bottom of the mantle. We postulate that the requirement of a delayed mixing in a strongly convective mantle is best explained by long periods of stasis in the global plate system, with scarce episodes of subduction throughout the Hadean and Archean [4].

Our numerical model confirms that in absence of continuous plate tectonics, the convective mantle mixing is relatively inefficient in erasing the chemical heterogeneities inherited from the primordial differentiation of the early Earth. This constrains the tectonic regime of the Hadean and Archean to a stagnant-lid regime with episodic subduction. In this case, the timing for the onset of continuous modern plate tectonics can only occur shortly before or after 2.7 Gyr.

[1] Bennett et al. (2007) *Science* **318**: 1907-1910. [2] Coltice and Schmalzl (2006) *GRL* **33**: L23304. [3] Kellogg and Turcotte (1990) *JGR* **95**: 421-432. [4] O'Neill et al. (2007) *EPSL* **262**: 552-562.

The effect of aqueous organic ligands on forsterite dissolution rates

JULIEN DECLERCQ[1*], OLIVIER BOSC[2], ERIC H. OELKERS[2]

[1]Geoscience environnement Toulouse (GET), Toulouse, France, declercq@get.obs-mip.fr (* presenting author)
[2]GET, Toulouse, France, bosc@get.obs-mip.fr
[3]GET, Toulouse, France, oelkers@get.obs-mip.fr

Forsterite is an abundant mineral which reacts exothermically with CO2 to form secondary minerals including carbonates. As such it is viewed as the most promising source material for the divalent metals required for mineral carbonation [1]. Mineral carbonation could potentially be accelerated if catalyses that accelerate forsterite dissolution can be identified. This study was initiated to determine if common aqueous organic ligands can accelerate forsterite dissolution rates. Aqueous organic species have long been considered as potential catalyses for enhancing silicate mineral dissolution rates (e.g. [2], [3]).

Forsterite dissolution rates were measured at 25 ºC in 10-2 M NaCl using mixed-flow reactors as a function of pH and concentration of 13 organic ligands (acetate, alginate, oxalate, Na-glutamate, citrate, EDTA, L-glutamic, humic, malic, malonic salicylic, tartaric and L-aspartic). Stoichiometric dissolution was observed. Selected measured dissolution rates as a function of organic ligand concentration is presented in figure 1.

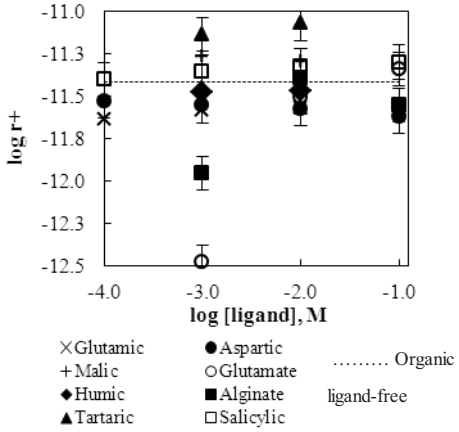

Figure 1: Summary of pH 3 olivine steady-state dissolution rates as a function of ligand concentration.

As depicted in Fig. 1, aqueous organic ligands in general have weak effects on pH 3 forsterite dissolution rates. Humic, salicylic and aspartic acid have no detectable effect on these rates, while the tartaric and malic acid decreases these rates.

Overall, results of this study demonstrate that organic ligand do not affect sufficiently forsterite dissolution rates at mildly acidic conditions. As these pH conditions likely to be characteristic of the fluids at carbon storage sites due high CO2 pressure carbon storage, it seems likely that organic additives will not accelerate substantially forsterite carbonation.

[1] Oelkers et al. (2008) *Elements,* **4,** 333-337.
[3] Pokrovsky et al. (2009) *Am. J. Sci.* **309**, 731-772.
[4] Wolff-Boenisch et al. (2011) *Geochim. Cosmochim. Act.* **75**, 5510-5525.

https://doi.org/10.1180/S0026461X00008434 Published online by Cambridge University Press

Crustal versus source processes on the Northeast volcanic rift zone of Tenerife, Canary Islands

DEEGAN, F.M.[1*], TROLL, V.R.[2], BARKER, A.K.[2], HARRIS, C.[3], CHADWICK, J.P.[4], CARRACEDO, J.C.[5], AND DELCAMP, A.[6]

[1]Laboratory for Isotope Geology, Swedish Museum of Natural History, Stockholm, Sweden. Frances.Deegan@nrm.se
[2]Dept. Earth Sciences (CEMPEG), Uppsala University, Sweden
[3]Dept. Geological Sceinces, University of Cape Town, South Africa
[4]Dept. Petrology, Vrije Universiteit Amsterdam, Netherlands
[5]Dept. de Física, Universidad de Las Palmas de Gran Canaria, Spain
[6]Dept. Geography, Vrije Universiteit Brussels, Belgium

The Miocene-Pliocene Northeast Rift Zone (NERZ) on Tenerife is a well exposed example of a major ocean island volcanic rift. We present elemental and O-Sr-Nd-Pb isotope data for dykes of the NERZ with the aim of unravelling the petrological evolution of the rift and ultimately defining the mantle source contributions.

Fractional crystallisation is found to be the principal control on major and trace element variability in the dykes. Differing degrees of low temperature alteration and assimilation of hydrothermally altered island edifice and/or sediments elevated the primary $\delta^{18}O$ and the Sr isotope composition of many of the dykes, but had little to no discernible effect on Pb isotopes. Minor degrees of sediment contamination, however, may be reflected in the Pb isotope composition of a few samples that plot to slightly higher $^{207}Pb/^{204}Pb$ values.

Once the data are screened for alteration and shallow level contamination, the underlying isotope variations of the NERZ reflect a mixture essentially of Depleted Mid-Ocean Ridge-type Mantle (DMM) and young High-μ (HIMU, where $\mu = {}^{238}U/{}^{204}Pb$)-type mantle components. Furthermore, the Pb isotope data of the NERZ rocks ($^{206}Pb/^{204}Pb$ and $^{207}Pb/^{204}Pb$ range from 19.591-19.838 and 15.603-15.635, respectively) support a model of initiation and growth of the rift from the Central Shield volcano (Roque del Conde), consistent with latest geochronology results [1]. The similar isotope signature of the NERZ to both the Miocene Central Shield volcano and the Pliocene Las Cañadas central edifice suggests that the central part of Tenerife Island was derived from a mantle source of semi-constant composition through the Miocene to the Pliocene. This can be explained by the presence of a discrete "blob" of HIMU material, ≤ 100 km in vertical extent, occupying the melting zone beneath central Tenerife throughout this period. The most recent central magmatism on Tenerife appears to reflect greater entrainment of DMM material, perhaps due to waning of the blob with time.

[1] Carracedo *et al.* (2011) *Bull. Geol. Soc. America,* **123,** 562-584.

Uranium mineralogy and factors of stability in the mill tailings of the COMINAK mine at Akouta (Niger)

ADRIEN DEJEANT[1,2*], LAURENCE GALOISY[1,2], GEORGES CALAS[1], NICOLAS MENGUY[1], VANNAPHA PHROMMAVANH[3] AND MICHAEL DESCOSTES[3]

[1]Institut de Minéralogie et de Physique des Milieux Condensés, Université Pierre et Marie Curie, Paris, France, dejeant@impmc.upmc.fr ([*]presenting author), calas@impmc.upmc.fr, menguy@impmc.upmc.fr
[2]Université Paris-Diderot, Paris, France, galoisy@impmc.upmc.fr
[3]AREVA, BG Mines, R&D, Paris la Défense, France, vannapha.phrommavanh@areva.com, michael.descostes@areva.com

The world's largest uranium underground mine, at Akouta (Niger), has been mined for more than 30 years. Since that time, around 14 million tons of mill tailings were accumulated on site. After the processing of the ore, with an extraction process efficiency reaching ~95%, some U is left within the mill tailings. Some U reconcentrations may be observed in the storage heap, pointing out potential migrations. This study aims at an assessment of U mobility for revaluating/rehabilitating mill tailings stored in heaps and preventing any U releases in the environment.

The ore deposit occurs in continental lower Carboniferous sandstones, containing quartz and feldspar with detrical clays and organic matter. Pitchblende is associated with minor coffinite, U-Ti and U-Mo oxides, with an average U concentration of 4‰ associated to trace metals (V, Zr, Mo…). Ore processing is based on an oxidative dissolution in sulfuric acid. As a result, a gypsum-indurated duricrust is formed at the upper surface of the tailings heap, referred to as a gypscrete crust.

Gypscrete samples were analyzed using different mineralogical methods: SEM, TEM, electron microprobe, XRD and cathodoluminescence. Micrometer-size U-bearing phases are observed: UO_2, U-Ti oxides (brannerite-type) and secondary phases such as uranyl phosphates. At the nanometer scale, supposedly neoformed U phases are associated with clay minerals, together with evidence of U sorption.

Brannerite-type minerals are most likely inherited from the ore, as they are more resistant than uraninite to the process. Such as UO_2 included in quartz grains, they appear as stable hosts for U. The main source of U^{VI} may rather come from more accessible U-rich phases which have suffered from oxidation and solubilization. The formation of secondary U minerals, in association with U sorption on clay minerals, may delay U^{VI} transport. The comparison of ore samples with their associated tailings sampled before their storage, provides complementary data on the processes governing U mobility.

https://doi.org/10.1180/S0026461X00008434 Published online by Cambridge University Press

Monitoring dynamics of species and adsorption reactions at the corundum-oxalate-solution interface by *in situ* ATR-FTIR spectroscopy

MIRELLA DEL NERO[1*], CATHERINE GALINDO[1], GUILLAUME BUCHER[1] AND REMI BARILLON[1]

[1]Institut Pluridisciplinaire Hubert Curien, UMR 7178 UdS/CNRS, Strasbourg, France
mireille.delnero@iphc.cnrs.fr (* presenting author)

Introduction

We addressed the molecular level description of the interactions occurring at low pH between oxalate ions and the surface of corundum colloids, for oxalate in the low concentration range relevant to freshwater (1-50µM). We monitored the dynamics of species at the corundum- solution interface during the oxalate sorption process by using a highly sensitive technique, namely Attenuated Total Reflectance – FTIR spectroscopy, joint to a method of layer deposition of corundum particles on the ATR crystal [1-3].

Results and conclusion

Examining changes in IR spectra during the oxalate sorption process, for frequency regions characteristics of oxalate, surface hydroxyls and ClO_4^- electrolyte ions, has revealed the existence of two types of sorption mechanisms dependent on the oxalate concentration.

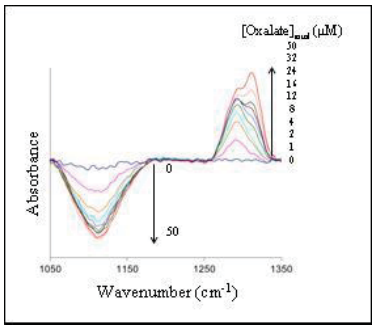

Figure 1: In situ ATR-FTIR monitoring of the corundum-solution interface during gradual increase of $[Ox]_T$ at pH 4.7, 0.01M $NaClO_4$.

In the trace level concentration range, the uptake of oxalate is accompanied by removal of ionisable surface hydroxyls and weakly adsorbed ClO_4^-. This is direct spectroscopic evidence that a reaction of surface ligand exchange controls the oxalate sorption. The other sorption reaction involves no surface hydroxyls or counter-ions and it exists in a wider range of oxalate concentration, indicating weak sorption of hydrated oxalate via H-bonds. Our study suggests that the sorption of oxalate at the trace level influences surface reactivity and charge of oxides in soils, as well as colloid aggregation and mobility.

[1] Del Nero *et al.* (2010) *J. Colloid Interf. Sci.* **342**, 437-444. [2] Galindo *et al.* (2010) *J. Colloid Interf. Sci.* **347**, 282-289. [3] Halter *et al.* (2010) *Applied Surf. Sci.* **256**, 6144-6152.

Laser spectrometry for tracing evaporation in a Mediterranean wetland (Rhône delta, France)

HÉLÈNE DELATTRE[1], CHRISTINE VALLET-COULOMB[1*], AND CORINNE SONZOGNI[1]

[1]CEREGE, CNRS, Aix-Marseille Université, Aix en Provence, France,
delattre@cerege.fr,
vallet@cerege.fr (* presenting author),
sonzogni@cerege.fr

Context

Evaporation from wetlands may contribute significantly to local atmospheric moisture, and may thus provide an additional water source to regional precipitation. In the context of global change, the distribution of wetlands is expected to vary, making necessary to better understand the influence of wetlands on climate. Isotopic tracing ($\delta^{18}O$, δD) is an efficient tool for detecting the contribution of local vapor to the atmospheric component of the water cycle, because the fractionation that occurs during evaporation induces a modification of the deuterium excess [1].

Results and conclusions

We performed continuous measurements of the isotopic composition of the atmospheric vapor during summer 2011, near a lagoon located in the Rhône delta, using wavelength-scanned cavity ring-down spectrometer (WS-CRDS). Calibrations were regularly performed with 3 different water compositions, and for mixing ratio varying between 4 to 33 g/kg. Linear calibration results were obtained, except for mixing ratio higher than 25 g/kg. Laser spectrometer measurements were compared to atmospheric vapor samples collected by cryogenic trapping (65 samples). The difference between results from the two methods was acceptable for $\delta^{18}O$ (±0.36‰ on average), while the laser spectrometer slightly overestimated δD, by 4.3‰ on average. Based on hourly-averaged time series, we evidenced a clear difference in deuterium excess between day-time and night-time data (Figure 1), resulting from the influence of local evaporation. Further work is under way to elucidate the shift in deuterium measurements. Preliminary attempts for a quantitative interpretation of deuterium excess variations in terms of evaporation fluxes [2] will be discussed at the meeting.

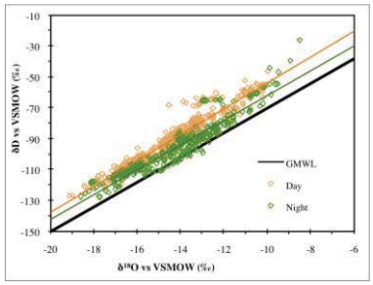

Figure 1: Isotopic composition of atmospheric water vapour between 2011/07/19 and 2011/08/13. Data are hourly averaged. Solid lines represent linear regressions (orange: $\delta^2H=8.3x\delta^{18}O+30.1$; green: $\delta^2H=8.0x\delta^{18}O+18.5$), with the Global Meteoric Water line in black.

[1] Gat & Airey (2006) *Global and planetary change* **51**, 25-33. [2] Lai & Ehleringer (2011) *Oecologia* **165,** 213–223.

https://doi.org/10.1180/S0026461X00008434 Published online by Cambridge University Press

Events control of karst aquifer recharge

CELESTINE DELBART[1*], FLORENT BARBECOT[2], DANIÈLE VALDÈS[3], ANTONE TOGNELLI[4] AND ROLAND PURTSCHERT[5]

[1,4]CEA, DAM, DIF, F-91297 Arpajon, France, [1]celestine.delbart@cea.fr (* presenting author), [4] antoine.tognelli@cea.fr

[2]Univ Paris-Sud, Laboratoire IDES, UMR8148, Orsay, F-91405, CNRS, France, florent.barbecot@u-pusd.fr

[3]UPMC Univ Paris 06, UMR 7619 Sisyphe, F-75005, Paris, France, daniele.valdes_lao@upmc.fr

[5]Climate and Enviromental Physics, University of Bern, Switzerland, purtschert @climate.unibe.ch

Fissured karst aquifers are vulnerable resources that react very sensitive to the dynamics of recharge events

The description of water and tracer flow in fissured aquifers and recharge event integration are generaly roughly depicted. In fact, there are characterized by multiple water transit velocities ranging from fast flow through fissured network to slow water infiltration in porous media.

An experimental field site located in French Burgundy under a topographic hill with well recognized boundaries has been monitored in-situ (head, temperature, conductivity, discharge flow), continously sampled for stable isotopes and major ion analyses on several sites (springs and boreholes) since two years. This long time monitoring allow us both to define baselines and discuss the impact of recharge events on groundwater dynamics.

The tracers $\delta^{13}C$, ^{14}C, $\delta^{2}H$, $\delta^{18}O$ and major chemical constituents have been used to describe the temporal response of the water flow through the unsaturated zone. The geochemical signals have been monitored at different levels of the system (precipitation, boreholes and springs) during several rainfall events. The preliminary results highlight a wide distribution of transit velocities during a recharge event.

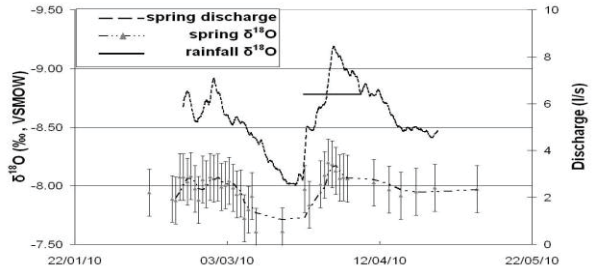

Figure 1: Times series of discharge and $\delta^{18}O$ at R14 spring.

Specific velocities or residence times of the different reservoirs as determined by recharge event characterisation, can be supported by tracers as ^{85} Kr, ^{39}Ar, ^{3}H, ^{3}He, CFCs, SF6 [1]. A recharge event will be monitoring (February 2012) on 2 springs and 1 boreholes. Tracers will allow to realize a geochemical deconvolution and to obtain the water residence times in the fractures and the matrix of this fissured aquifer.

[1] Corcho (2007) *Water Resources Research* **43**, 16pp.

Biogeochemical dynamics related to seasonal changes and biomass-density patterns in rhyzosphere sediments of a *Zostera noltii* meadow

MARIE LISE DELGARD[1*], BRUNO DEFLANDRE[1], EMERIK KOCHONI[1], FLORIAN CESBRON[2], GUILLAUME BERNARD[1], CELINE CHARBONNIER[1], DOMINIQUE POIRIER[1], SABRINA BICHON[1], EDOUARD METZGER[2], JONATHAN DEBORDE[1], AND PIERRE ANSCHUTZ[1]

[1] Univ. Bordeaux, EPOC, UMR 5805, Talence, France, m.delgard@epoc.u-bordeaux1.fr (* presenting author)

[2] Univ. d'Angers, UPRES EA 2644, BIAF, Angers, France

This study was conducted in the Arcachon bay that shelters the largest *Zostera noltii* meadow in Europe [1]. A severe but non-homogeneous decline of this meadow coverage has been recently observed. In this context, we investigated seasonal changes and short-scale spatial variability of sediment biogeochemistry in a tidal mudflat of this lagoon colonized by a stable eelgrass meadow. Cores were collected at low tide on vegetated and unvegetated sediment over an annual cycle from autumn 2010 to summer 2011. Additional sediment cores were collected along a density-biomass gradient of seagrass in autumn and summer. Concentrations of major redox species were measured in sediment porewaters. In sediment solid-phase, two reactive fractions of Fe and P were extracted. Total oxygen fluxes were determined under light and dark conditions and used to calculate the benthic gross primary productivity (GPP).

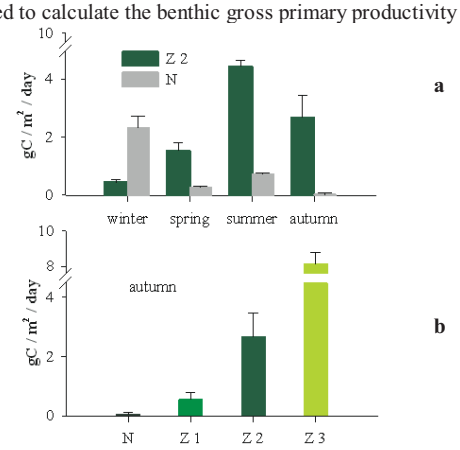

Figure 1: Daily GPP calculated for vegetated (Z) and unvegetated sediments (N) over an annual cycle (**a),** and in autumn 2010 (**b**) along a density-biomass gradient of *Z. noltii* (Z1 to Z3) (*n=4 - 6*).

Some redox species such as dissolved iron did not show significant seasonal changes and along the biomass gradient. For other parameters, e.g. DIP or GPP, the variability observed along the biomass gradient was higher than the one observed between seasons (Fig.1). Results suggest that the effect of seagrass on sediment biogeochemistry can be strongly dependent on the plant biomass, which highly vary with seasons but also on short and large space scales. Hypothesis to explain how this component influences the biogeochemistry of superficial sediments are proposed.

[1] Plus *et al.* (2010) *Estuar. Coast. Shelf Sci.* **87**, *357-366.*

https://doi.org/10.1180/S0026461X00008434 Published online by Cambridge University Press

The record of human impact in the sedimentary record at *Portus*, the harbor of ancient Rome

H. DELILE[1, 2]*, J. BLICHERT-TOFT[2], J.-P. GOIRAN[3], J.-P. BRAVARD[1] AND F. ALBAREDE[2]

[1]Université Lumière Lyon 2, 69676 Bron, France
(*correspondence: hdelile@gmail.com)
[2]Ecole Normale Supérieure de Lyon, 69007 Lyon, France
[3]CNRS – UMR 5133 Archéorient, 69365 Lyon, France

The present study focuses on the analysis of palaeo-pollutions and the sedimentary environments in which they were trapped in the Roman *Portus* harbor. *Portus* received heavy-metals pollution both from local foundries, fulling, and tanning and from distal upstream development in Rome. Rome wastewaters, which accounted for up to 3 percent of the total Tiber discharge, were forwarded to *Portus* through a network of canals (*Canale Romano* and *Canale Trasverso*) connecting the river to the sea. In this manner, harbor basins accumulated both allochthonous and autochthonous heavy metals.

We determined major and trace element concentrations as well as Pb isotope compositions in a high-resolution set of samples from sediment cores recovered in the *Portus* area. Principal component analysis of elements that are less prone to the influence of human activities, such as Ca, Mg, Mn, Zr, K, Al, Ti, Na, Sr, and Mn, was used in conjunction with metallic elements to break down the sedimentary load into local and regional components.

The record of Pb concentrations and isotopic compositions reveals an overall general trend on which other signatures are superimposed. The geochemical background of the Tiber catchment (24.7-26.2 ppm Pb and $^{206}Pb/^{207}Pb$ ~ 1.198) represents geologically young (model age T_m <50 Ma) Pb derived from natural runoff over young sediments and volcanics in the Latium. From the 1st century AD to the end of the roman period, the harbor regime evolved from a dominant fluvial (enriched in Al, Ti, Mg, K, and Zr) to a more marine influence (high Ca/Mg, Na/Al, Sr, and $CaCO_3$) in the upper part of the harbor unit. "Imperial" Pb (90.5-35.4 ppm Pb and $^{206}Pb/^{207}Pb$ ~ 1.187-1.192) requiring the prevalence of Hercynian (T_m >200 Ma) Pb, probably imported from central or northern Europe, gets progressively diluted with time. The transition from the roman to the medieval period is characterized by a closed environment (high Ca/Mg, Na/Al, Sr, and $CaCO_3$) with a spike of unradiogenic $^{206}Pb/^{207}Pb$ (~ 1.184). Either an alluvial plug formed, which blocked fresh water entry into the harbor from the *Canale Trasverso*, or the harbor burned, causing melting of the ancient waterworks. Finally, the upper part of the sediment cores consists of overflow deposits enriched in Al, Ti, K, Mg, and Mn associated with the return of the pre-anthropogenic geological background (18.9-28.2 ppm Pb and $^{206}Pb/^{207}Pb$ ~ 1.196-1.201). In this post-roman sedimentary unit pollution signatures shift to a mix of heavy metals dominated by Co, Cr, Ni, and Zn, whereas during the roman period elements such as Pb, As, Fe, Cu, and Sn were predominant.

The fractionation of Lithium isotopes during continental weathering: clues from the Amazon and Mackenzie rivers

M. DELLINGER[1*], J. GAILLARDET[1], V. GALY[2], P. LOUVAT[1], J.-L. BIRCK[1], J. BOUCHEZ[3]

[1]IPGP- Géochimie et Cosmochimie, 75238 Paris, France
(*correspondence: dellinger@ipgp.fr)
[2]Woods Hole Oceanographic Inst., Woods Hole, MA 02543, USA
[3]GFZ (German Centre for Geosciences), 14473 Potsdam, Germany

Numerous studies on river systems have shown that Lithium isotopes are fractionated during chemical weathering as ^6Li is preferentially retained in solid secondary phases whereas dissolved fractions are enriched in ^7Li. In this study we investigate the Li isotope composition of Suspended Particulate Matter (SPM) and bedload transported in two of the largest world river systems having drastically differing climate conditions: Amazon and Mackenzie rivers. In order to separate the effects of hydrodynamic sorting and chemical weathering, Li isotope were measured along river depth profiles to capture all the SPM grain size variability.

We find that Li content and isotope composition display a strong variability in relation with grain size within a single water column in both Amazon and Mackenzie Rivers. Li content in SPM increases by a factor up to 3 from coarse (river bed) to fine (channel surface) particles, ranging from 30 to 90 ppm. All bedloads and SPM samples have Li/Al molar ratios higher that of the mean Upper Continental Crust (UCC), despite the fact that 10 to 20% of total Li in both rivers is transported in the dissolved load.

River sediments Li isotopic composition (δ^7Li) ranges between -3.5 to 5‰ and displays an inverse relationship with grain size. δ^7Li is also well correlated (R^2>0.9) to the weathering index Na/Al, further illustrating the fact that weathering products are isotopically fractionated toward low light δ^7Li values. Amazon river-sediments δ^7Li values are more than 1‰ lower than those of the Mackenzie for a given Na/Al value. We interpret these relationships between Li content, δ^7Li, Na/Al and grain size as a binary mixing between a coarse-grained, relatively Li-poor, high δ^7Li component (δ^7Li~5‰) and a fine end-member having low δ^7Li and high Li concentrations. The low δ^7Li value of the fine component could be the result of either present day light-Li co-precipitation/adsorption into secondary minerals or of the recycling of fine-grained silicate sedimentary rocks or a combination of both processes. These results have important implications for establishing global mass budgets of erosion and for using lithium concentrations and isotopes as a tracer of sedimentary recycling.

https://doi.org/10.1180/S0026461X00008434 Published online by Cambridge University Press

Li isotopes fractionation during lower crustal magmatic segragation.

E. DELOULE[1], I. ETTORI[1], J. INGRIN[2], M. GRÉGOIRE[3].

[1]CRPG-CNRS, BP20, 54500 Vandoeuvre les Nancy, France. deloule@crpg.cnrs-nancy.fr, isabelle-ettori@wanadoo.fr

[2] UMR CNRS 8207, Univ. Lille 1, 59655 Villeneuve d'Ascq, France. jannick.ingrin@univ-lille1.fr

[3]*GET, UMR CNRS 5563, OMP, Univ. Toulouse III, 31400, Toulouse, France*. gregoire@get.obs-mip.fr

Introduction

Kerguelen basalts contain abundant mantle xenoliths, including mantle peridotites and deep magmatic segregates equilibrated in the granulite facies [1]. Lithium chemical and isotopic distribution were measured in two-pyroxene granulites in using the Cameca IMS 1270 Ion probe at CRPG, in order to define their signature and describe the Li behavior during the lower crust formation process.

Samples description

The studied xenoliths display close mineralogical compositions, bearing Mg81-92 Al-diopside, Mg-78-93 enstatite and labradorite or bytownite. Spinel and garnet are observed in 2 of them, and they all are type II xenoliths [1,2]. The xenoliths range along a regular magmatic cristallisation trend, with decreasing Mg content.

Li and δ^7Li distribution

On the whole rock scale the Li contents increase from 1,5 up to 9 ppm, following the cristallisation trend with the Li content increasing during the cristallisation. At the sample scale Li contents is higher in Cpx compared to Opx and to plag, with a ratio Opx/Cpx of 0.8-0.9 and a ratio Plag/Cpx of 0.2-1. At the grain scale, Li displays an homogeneous distribution in most minerals, at the exception of few depleted or enriched Cpx rims.

The δ^7Li values measured on Cpx and Opx range in between -9 and +20, normalized to lsvec . The Cpx Li depleted rims display enriched δ^7Li values, associated to Li diffusion isotopic fractionation. Most xenoliths display relatively homogenous δ^7Li distibution, with only few per mil scatters, and only one Li poor xenolith display δ^7Li values scattered on a large range, from -9 to +14. A general observation is that Cpx display higher δ^7Li values than Opx (+2 to +3 ‰), and that the values are more scattered in Opx than in Cpx. There is positive correlation between the Li contents and the δ^7Li values, both at the mineral and whole rock scales, pointing out a melt-mineral isotopic fractionation for Li, with the melt being enriched in ^{7}Li compared to the residue.

Conclusions

The bulk value for these granulite samples is in agreement with a direct derivation from the mantle (5-8 ppm, d^7Li≈+5), but at the sample scale, Li content and Li isotopic composition is strongly dependent on the melt-solid fractionation during crystallization in the granulite facies. The large scatter observed on the Li poor sample could result from the partial re-equilibration of this early formed granulite with late enriched fluid.

[1] Gregoire et al. (1998) Contrib Mineral Petrol 133, 259-283. [2] Gregoire (1994) PhD thesis.

Understanding Archean weathering using silicon isotopes and Ge/Si ratios

C. DELVIGNE[1,2*], S. OPFERGELT[3], A. HOFMANN[4], D. CARDINAL[2,5] AND L. ANDRÉ[2]

[1]Department of Earth Sciences and Environment, Université Libre de Bruxelles, Brussels, Belgium (* cdelvign@ulb.ac.be)

[2]Department of Geology and Mineralogy, Royal Museum of Central Africa, Tervuren, Belgium

[3]Earth and Life Institute, Université Catholique de Louvain, Louvain-la-Neuve, Belgium

[4]Department of Geology, University of Johannesburg, South Africa

[5]LOCEAN, University Pierre and Marie Curie, Paris, France

Weathering conditions in the Mesoarchean are poorly constrained. Recent studies have shown that neoformation of secondary clay minerals are associated with large Si isotope and Ge/Si fractionation in response to desilication processes and the weathering degree [1, 2, 3, 4]. Here, we present the first application of these weathering proxies on a 2.95 Ga paleosol profile and coeval shales. The paleosol is developed on andesite and shows a well defined mineralogical and chemical differentiation. δ^{30}Si values are lighter (down to -0.44‰) and Ge/Si values higher (up to 3.2µmol/mol) than parental andesite values (-0.14‰ and 2.1µmol/mol, respectively). Such trends support the formation of secondary minerals that preferentially incorporate light Si isotopes and Ge relative to Si, as observed during modern weathering [1, 2, 3, 4, 5]. However, less pronounced fractionation relative to modern soils with neoformation of kaolinite can be potentially explained by mineralogical control on δ^{30}Si with the formation of Fe-rich smectite, reported with heavier Si isotope composition than kaolinite [6]. In contrast, the top of the paleoprofile shows a return to heavier δ^{30}Si values (up to -0.11‰) and lower Ge/Si ratios (down to 1.1µmol/mol). This may be explained by a preferential release of light Si isotopes and Ge during partial dissolution of Fe-rich smectite to form kaolinite. This transformation is thought to have been governed by drainage conditions with fast drainage favoring kaolinite, implying moderate rainfall and/or poor-drainage conditions during weathering. In addition, we demonstrate that the combination of δ^{30}Si and Ge/Si tracers in 2.95 Ga Archean shales can reflect the relative proportions of primary rocks and secondary minerals. Moreover, a kaolin-rich or -poor nature of secondary clays can be evaluated. Therefore, combining δ^{30}Si and Ge/Si ratio as paleoweathering tracers opens new perspectives in quantifying Archean superficial weathering dynamics with potentially important paleoclimatic implications.

[1] Kurtz et al., (2002) *Geochim. Cosmochim. Acta* **66**, 1525-1537

[2] Ziegler et al., (2005) *Geochim. Cosmochim. Acta* **69**, 4597-4610.

[3] Opfergelt et al., (2010) *Geochim. Cosmochim. Acta* **74**, 225-240.

[4] Steinhoefel et al., (2011) *Chem. Geol.* **286**, 280-289.

[5] Lugolobi et al., (2010) *Geochim. Cosmochim. Acta* **74**, 1294-1308.

[6] Georg et al., (2009) *Geochim. Cosmochim. Acta,* **73**, 2229-2241.

https://doi.org/10.1180/S0026461X00008434 Published online by Cambridge University Press

Late Cretaceous rapid arc growth in the Arequipa area of southern Peru

SOPHIE DEMOUY[1*], MATHIEU BENOIT[1], MICHEL DE SAINT-BLANQUAT[1], THIERRY SEMPERE[2], JEAN-LOUIS PAQUETTE[3]

[1]GET, Toulouse, France, sophie.demouy@get.obs-mip.fr (*presenting author), mathieu.benoit@get.obs-mip.fr, michel.desaintblanquat@get.obs-mip.fr
[2]ISTerre, Grenoble, France, thierry.sempere@ird.fr
[3]LMV, Clermont-Ferrand, France, J.L.paquette@opgc.univ-bpclermont.fr

During the Late Cretaceous and Paleocene, intense magmatic activity along the Toquepala arc resulted in the building of a continuous relief along the Peruvian margin. This arc growth coincided with the only known significant uplift along coastal southern Peru [1] and can thus be considered to have been a major factor in this uplift.

Our study has focused on a batholith segment extending in the Arequipa area over 60x40 km for a ≥7 km thickness. We confirm that granitoids were emplaced mainly between 90 and 60 Ma, into the Proterozoic basement, a dominantly mafic Liassic (200-175 Ma) plutonic suite, and Jurassic strata. The Late Cretaceous–Paleocene suite consists of numerous plutons, dykes and sills with compositions varying from gabbro to granite.

We analysed trace elements, and Sr and Nd isotopic ratios on a collection of 100 samples principally located along 3 cross-sections of the batholith. The obtained geochemical compositions are in good agreement with data available from the literature [2]. Given the large lithological range, covering a wide spectrum of chemical compositions, Rb-Sr systematics was used to identify two magmatic suites. Samples represent either the Liassic or the Late Cretaceous-Paleocene suite, which are easily distinguished in a Rb-Sr isochron plot. Samples plotting along the 60 Ma isochron were separated and their measured $^{87}Sr/^{86}Sr$ isotopic ratios were used to determine LLD (liquid lines of descent) for gabbro-granite series within the batholith. Using $^{87}Sr/^{86}Sr_m$ as an indirect proxy for fractional crystallization, we propose a simple but powerful method to estimate the nature and compositions of primitive magmas in a plutonic environment.

These results are critical to estimating crustal growth and thickening in the Arequipa area. They will also be analysed in terms of magmatic flux for a better understanding of the mantle vs. crustal contribution to Andean arc magmatism.

[1] Wipf, M. (2006) ETH Zurich PhD n°16383. [2] Boily, M., et al. (1989) JGR **94** n°B9, 12483-12498.

Unravelling glacial sediment provenance through soil chemistry in the north of Ireland.

MICHAEL DEMPSTER[1*], PAUL DUNLOP[1], ANDREAS SCHEIB[2], AND MARK COOPER[3]

[1]School of Environmental Sciences, University of Ulster, Coleraine, Northern Ireland, dempster-ml@email.ulster.ac.uk (* presenting author)
[2]British Geological Survey, Keyworth, England, ascheib@bgs.ac.uk
[3]Geological Survey of Northern Ireland, Belfast, Northern Ireland, mark.cooper@detni.gov.uk

Background and method.

Reconstructing palaeo-ice sheets provides important information on how they respond to and drive climatic changes over long timescales. Traditional approaches to reconstructing palaeo-ice sheets rely heavily on geomorphological evidence. However, recent work on ribbed moraines [1] and drumlins [2], which are used to reconstruct ice flow direction, major ice flow pathways and drainage conduits, indicates that using geomorphology alone can potentially produce misleading results if small areas are investigated. Furthermore, ascertaining ice flow direction in regions where no bedforming events have occurred can present difficulties. An alternative approach to investigating former ice flow direction is to use geochemistry to determine glacial sediment provenance, from which transport direction can then be established.

This study presents results from the first regional geochemical investigation of glacial sediment provenance in Ireland using soils developed in areas of till superficial geology. The soil samples were gathered as part of Geological Survey of Northern Ireland's Tellus survey [3] which collected soil samples at a density of 1 sample per $2km^2$ accross all of Northern Ireland. The Tellus samples were supplemented by an additional 81 samples taken at a density of approximately 1 sample per $4km^2$ around the margins of the Tellus survey where no previous sampling had occurred. Bulk geochemistry was determined by X-ray Fluorescence from which 28 lithophile and rare earth elements were selected. Principal Component Analysis (PCA) was then applied to these elements using 3917 soil samples from across the entire region. PCA is a variable reduction procedure that allows groups of elements to be identified, and is used here to infer underlying till geochemistry. Since till geochemistry is a product of its parent materials, the PCA groupings can aid identification of the original bedrock source and thus the sediment provenance and ice transport direction.

Results and conclusion.

The results show that most till deposits in the study area are closely related to local bedrock, with changes of geochemical composition occurring across lithological boundaries. This suggests that the majority of tills have been locally derived and that till transport in this sector of the British-Irish Ice Sheet was low, with rapid comminution and low evacuation rates of entrained debris.

[1] Dunlop & Clark (2006) *Quaternary Science Reviews* **25**, 1668-1691. [2] Spagnolo *et al*. (2010) *Sedimentary Geology* **232**, 119-129. [3] http://www.detini.gov.uk/deti-energy-index/tellus-project/introduction-to-the-tellus-project.htm

https://doi.org/10.1180/S0026461X00008434 Published online by Cambridge University Press

Controls on seawater ^{231}Pa, ^{230}Th and ^{232}Th concentrations along the flow path of major deep-water masses in the Southwest Atlantic

FEIFEI DENG[1*], ALEX L. THOMAS[1], GIDEON M. HENDERSON[1] AND MICHA J.A. RIJKENBERG[2]

[1]Department of Earth Sciences, University of Oxford, Oxford, OX1 3AN, United Kingdom (*feifei.deng@earth.ox.ac.uk)

[2]Royal Netherlands Institute for Sea Research (Royal NIOZ), 1790 AB Den Burg, The Netherlands, micha.rijkenberg@nioz.nl

12b. Pa and Th distributions in the ocean: controlling mechanisms

Pa-231 and ^{230}Th are naturally occurring radionuclides in the ocean, produced through the α-decay of dissolved U. Once produced, the two radionuclides are adsorbed onto particles and removed from seawater as the particles settle to the sediment. Due to its higher particle reactivity, ^{230}Th is readily removed from seawater once produced, while less particle-reactive ^{231}Pa can be advected by deep ocean circulation to high-productivity areas to be subsequently removed. Therefore, a fractionation between ^{231}Pa and ^{230}Th takes place in seawater, making the ^{231}Pa/^{230}Th ratio a potential water-mass proxy to reconstruct past ocean circulation. However, factors such as particle flux and composition also play a part in the oceanic distribution of ^{231}Pa and ^{230}Th. To make use of ^{231}Pa/^{230}Th as a paleo-circulation tracer therefore requires a thorough understanding of the controls on the distribution of the two nuclides in seawater. Despite a growing knowledge of water-column ^{231}Pa and ^{230}Th concentrations, rather little is known about the distribution of the nuclides in the South Atlantic Ocean. This basin has recently been the focus of down-core ^{231}Pa/^{230}Th records [1], but is characterised by a more complex pattern of deep-water circulation than the North Atlantic, with multiple water masses flowing in different directions.

In this study, we present high-resolution dissolved ^{231}Pa, ^{230}Th and ^{232}Th data for twelve profiles in the Southwest Atlantic collected during GEOTRACES cruise GA02s (JC057) in March, 2011. The data capture all the main Atlantic water masses along their meridional flow paths and cross a gradient of productivity and dust input. Concentrations of dissolved ^{230}Th range from 0.0060~1.27 dpm/1000l and show a nearly linear increase with increasing water depth as a result of reversible scavenging process [2]. Concentrations of dissolved ^{231}Pa range from 0.0094~0.37 dpm/1000l and show an increase with depth in the upper water column with more variable concentrations at depth. ^{231}Pa/^{230}Th ratios characterise the three deep water-masses (AAIW, NADW, AABW) and show an evolution along flow paths. There is, however, also an obvious decrease in ^{231}Pa/^{230}Th near the equator, potentially due to higher productivity in this region. We will discuss the impact of these observations on the use of ^{231}Pa/^{230}Th to assess past ocean circulation. Concentrations of ^{232}Th are low but appear to provide information about detrital inputs to the region from dust and from the Rio Plata.

[1] Negre et al. (2010) *Nature* **468** 84-88. [2] Nozaki, Tsubota (1981) *EPSL* **54**, 203-216.

Applications of XRF analysis in lithogeochemical anomaly prospecting

HUI DENG[1], XIUHONG PENG[2, 3*], HAI YANG[1], CHENGSHI QING[1] AND JIANGSU ZHANG[2, 4]

[1]State Key Laboratory of Geohazard Prevention and Geoenvironment Protection, Chengdu University of Technology, China

[2]Geochemistry Dep., Chengdu University of Technology , China, (*correspondence author: pengxh@cdut.edu.cn)

[3]Key Laboratory of Nuclear Techniques in Geosciences, China

[4]Third Geology and Mineral Resources Exploration Academy of Gansu Province, Lanzhou, China

X-ray fluorescence (XRF) can be used directly to analyze contents of ore-forming elements in a gold mine and other characteristic indicator elements such as Zn, Cu, Pb, As, Sb, Fe, etc. in the field. It will make contributes to delineate the favorable areas for mineralization of gold mine, and quickly obtain the location and distributional pattern of gold mine geochemical halo.

Due to the polytropism of geological samples and the differences of analytical methods, the results of chemical analysis are quite different from the results of XRF analysis. As a result, specific standard samples corresponding to each kind of elements are requested in different lithology for each mine. And then the standard curve of best sample linear can be made.

Dashui Gold Deposit in Maqu, Gansu, which was found in west Qinling mountain area, is a type of gold deposits with unique mineralization. On the basis of geochemical exploration and actual situation of the deposit, the representative 3530 m and 3490 m middle sections of No.103 exploration line of Dashui Gold Deposit were selected for measuring. The measuring device is CIT-3000SMP. The design spacing is 3 m, and the analyzing time is 120 seconds per point. Five limestone and six diorite porphyrite samples with chemical analysis results had been used to fit standard curves and establish standard database respectively by the linear fit of the peak area and contents combining with the inverse computation of software. Then multi-element analyses had been down on the survey middle sections to delicate the favorable areas for mineralization of gold mine, and quickly obtain the location and distributional pattern of gold mine geochemical halo. The results demonstrate that:

1. Au, As, Cu, Fe, Mn, Ag, Sb, Ti, Sr, etc. appear high strength anomalies on the known middle sections, meaning that they can be treated as the indicating elements for Dashui Gold Deposit.

2. There is a high anomaly area in and near the contact zones of diorite porphyrite and hematite limestone of known ore body in 3490 m middle section. The width of the anomaly is about 33m. Combining with the geological situations of other middle sections, this area is delineated as level one prospective area. This area might be formed by the combination of two narrow gold veins, and it connects with other ore veins of the higher and lower middle sections.

The authors acknowledge the support of the National Nature Science Foundation of China (No.41103025) and Cultivating Programme of Middle-aged Backbone Teachers of Chengdu University of Technology.

https://doi.org/10.1180/S0026461X00008434 Published online by Cambridge University Press

CALCIUM ISOTOPES: KEYSTONE FOR UNDERSTANDING ISOTOPIC FRACTIONATION AND PLANETARY MATERIAL PROCESSES

DONALD J. DEPAOLO

Earth Sciences Division, Lawrence Berkeley National Laboratory, Berkeley, CA 94720, djdepaolo@lbl.gov

Non-traditional elements like Ca, Mg, Li, Fe, Mo and others have proven to be valuable for assessing the mechanisms and magnitude of non-equilibrium isotopic fractionation processes. These so-called kinetic effects are important not only for low-temperature processes, but also for hydrothermal and magmatic conditions. Theory and experiments are progressing rapidly and are leading to a new level of understanding and a roadmap for further experimental work. This presentation will focus mainly on Ca isotopes, but the principles and effects are applicable to other elements. With respect to mineral growth from aqueous solution, the essential insight is that equilibrium growth can occur only if the molecular exchange fluxes at the mineral-solution interface are large in comparison to the rate of growth. For typical minerals growing at Earth surface temperature, this is unlikely to be the case, the consequence being that the kinetics of the forward reaction strongly influence isotopic fractionation, causing precipitated solids to be enriched in light isotopes. A rough estimate of surface exchange fluxes can be derived from mineral dissolution rates, but more detailed ion-by-ion growth models can be used to develop a more comprehensive description of the forward and backward reaction rates. For calcite, not only solution oversaturation, but also the Ca:CO3 ion ratio in solution can strongly affect both growth rate and Ca isotopic fractionation. Ionic strength and other aspects of solution composition also modify isotopic fractionation, and analogous models can account for trace element partitioning as well. Preliminary data suggest that Ca isotopic fractionation in calcite and epidote also occurs at hydrothermal temperatures of 150 to 400C, with fractionation factors similar in magnitude to those for calcite at 25C. In magmatic systems, isotopic fractionation can be deduced by both chemical diffusion and thermal gradients in silicate liquids. The magnitude of Ca isotopic fractionation due to chemical diffusion has been shown to be dependent on silicate liquid composition, with high-Si, high-viscosity liquids producing larger fractionations than low-Si liquids. Diffusion in the solar nebula is probably responsible for some Ca isotopic variations observed in carbonaceous chondrites. Both phenocrysts in magmas and nebular condensates are likely to have kinetic fractionation effects if they grow under transport-limited or high oversaturation conditions. Current efforts are directed at experimental testing of model predictions, and modeling the coupling between growth inhibition/catalysis and isotopic fractionation.

A comparison of shale weathering rates inferred from catchment solute mass balance versus soil profile chemistry at Plynlimon, Wales

ASHLEE L. DERE[1]*, BRIAN REYNOLDS[2], TIMOTHY S. WHITE[3] AND SUSAN L. BRANTLEY[4]

[1]Penn State University, University Park, USA, ald271@psu.edu*

[2]Centre for Ecology and Hydrology, Bangor, Wales, UK, br@ceh.ac.uk

[3]Penn State University, University Park, USA, tsw113@psu.edu

[4]Penn State University, University Park, USA, sxb7@psu.edu

In an effort to quantify the influence of climate on shale weathering rates, a transect of study sites has been established on Silurian shales along a climatic gradient in the northern hemisphere as part of the Susquehana Shale Hills Critical Zone Observatory, PA (USA). The coldest and most northerly site of this transect is the Hafren watershed in the headwaters of the River Severn, at Plynlimon, Wales, UK. The watershed, which is approximately 24 km from the west Wales coast, has an area of 357 ha and is 70% covered by Sitka spruce plantation forestry. The watershed has been extensively studied with continuous measurements of precipitation and runoff since 1968 and weekly monitoring of rain and stream water chemistry since 1983. These data provide an ideal opportunity to compare weathering rates derived from watershed mass balance to those derived from soil geochemical profiles. Annual solute mass balances over the past 25 years were determined by subtracting stream output fluxes from precipitation input fluxes using Cl as a conservative tracer. Annual mass balance estimates for dissolved elements such as Si are relatively consistent over time (mean value 23.2 ± 0.7 kg Si ha^{-1} yr^{-1}) while those of Na are more variable (mean value 2.69 ± 1.2 kg Na ha^{-1} yr^{-1}) and show influence of variations in sea salt input. Area-weighted release rates of Mg (mean value 5.36 ± 0.3 kg ha^{-1} yr^{-1}) are indicative of weathering rates of the dominant shale minerals illite and chlorite. Weathering rates were also estimated from soil geochemical profiles, where elemental depletions relative to parent shale chemistry were used to calculate a weathering rate over the last 10 ka. Mg release estimates from soil ridgetop samples (5.16 kg Mg ha^{-1} yr^{-1}) are in close agreement with the watershed mass balance calculations. Conversely, the estimated Si weathering flux derived from soil profiles of 6.6 kg ha^{-1} yr^{-1} is much smaller than the watershed mass balance flux estimate. This may imply that the watershed mass balance estimates for Si are influenced not only by weathering processes in the augerable regolith but also in the fragmented shale bedrock underlying the soil profile. Si cycling through the Sitka spruce trees must also be evaluated. The weathering rates obtained from the two methods at Plynlimon will be placed in context with our observations for the overall shale climosequence, where weathering rate estimates at the other locations are restricted to geochemical profiles alone.

https://doi.org/10.1180/S0026461X00008434 Published online by Cambridge University Press

Distribution of GDGTs in tropical sediments from Guadeloupe (French West Indies): implications for application of MBT/CBT and TEX_{86} proxies

S. DERENNE[1*], A.HUGUET[1], I. BELMAHDI[1], C. FOSSE[2], AND V. GROSSI[3]

[1] BioEMCo, CNRS/UPMC UMR 7618, Paris, France, sylvie.derenne@upmc.fr (* presenting author)
[2] Chimie ParisTech (ENSCP), Paris, France
[3] PEPS, UMR 5125 CNRS–Univ. Lyon 1, Lyon France

Glycerol dialkyl glycerol tetraethers (GDGTs) are lipids of high molecular weight present in membranes of Archaea and some bacteria. Archaeal membranes are composed predominantly of isoprenoid GDGTs, with acyclic or ring-containg biphytanyl chains. The amount of isoprenoid GDGTs with cyclopentyl moieties was shown to increase with water temperature and variations in surface water temperature can be determined via the TEX_{86} proxy. Recently, another type of GDGTs, with branched instead of isoprenoid alkyl chains, has been discovered in peat. Branched GDGTs were suggested to be produced in soils by still unknown bacteria. The degree of methylation of branched GDGTs, expressed in the MBT, was shown to depend on air temperature and to a lesser extent on soil pH, whereas the relative abundance of cyclopentyl rings of branched GDGTs, expressed in the CBT, was related to soil pH. The MBT/CBT proxies are increasingly used as paleoclimate proxies. The aim of this study was to investigate the distribution of GDGTs in tropical sediments from Guadeloupe (French West Indies). Surficial sediment samples were collected in four coastal water ponds: two located in Grande-Terre and two in a smaller island named La Désirade, 10 km east from Grande-Terre. GDGTs either present as core lipids (CLs; presumed of fossil origin) or derived from intact polar lipids (IPLs; markers for living cells) were analysed. Interestingly, the distribution of archaeal and bacterial GDGTs differed between the four sites, as shown by the higher values of the TEX_{86} and MBT in sediments from La Désirade than in those from Grande-Terre. These differences were also reflected in the TEX_{86}- and MBT/CBT-derived temperatures. Temperature estimates derived from GDGTs present in La Désirade sediments were consistent with temperature recorded in the area (annual air temperature 26 °C), whereas temperature estimates derived from Grande-Terre sediments were much lower than expected values. The variability in archaeal GDGT distribution between the four water ponds might be due to different archaeal communities between Grande-Terre and La Désirade. Bacterial GDGTs seem to be essentially derived from surrounding soils in La Désirade. In contrast, in Grande-Terre, a substantial proportion of bacterial GDGTs might be produced in the water pond in addition to being produced in surrounding soils, as revealed by the high relative abundance of bacterial IPLs vs. CLs downcore. Our results suggest that caution should be exercised when interpreting MBT/CBT-derived temperatures in aquatic environments, as they might be largely biased by in situ microbial production.

Weathering of voclanics and the geological carbon cycle

LOUIS DERRY

Cornell Uninversity, Dept. of Earth & Atmospheirc Sciences, Ithaca, NY, USA, derry@cornell.edu

Weathering and volcanic rocks

Weathering rates in granitic and cratonic terranes have been well studied, yet information on weathering in volcanic terranes remains sparse. Available data suggest that mafic – intermediate volcanic terranes play a disproportionately large role in the carbon cycle. They have high abundances of Ca and Mg silicates, the weathering of which results in much greater CO_2 consumption rates than the weathering of the alkali silicates typical of continental crust, which is an inefficient CO_2 sink. They also have mineralogy and texture that weather much faster than those typical of most cratonic terranes. Additionally, most active volcanic centers are associated with arcs and hotspots that are adjacent to oceans where marine moisture and orographic effects can lead to high runoff and erosion rates, and many of the active island arcs today are located in the wet tropics. All of these features suggest that weathering and CO_2 consumption rates of volcanics should be high. While there are relatively few published data from streams draining active arcs that permit estimation of CO2 consumption rates, there is growing evidence to support the hypothesis that arc weathering is an important CO2 sink [1, 2]

The contribution of arc terranes to global weathering budgets is poorly known in part because rivers in these settings tend to be small and have not been sampled systematically (or in most cases at all) for geochemical purposes. Unlike major continental regions, where a single large river can give information about a large fraction of both the continental surface and total runoff, island arcs are a type of "non-point source" problem. Many smaller streams deliver large loads per unit basin area, and the aggregate flux can be quite large, but no one stream samples a large region.

The srtontium isotope ratios of arc and hot spot weathering is low, reversing the common relationship beteen silicate weathreing and changes in seawater 87Sr/86Sr. Changes in the rates of arc weatheirng can be important drivers of the long term carbon cycle

[1] Rad et al. (2006) *J. Geochem. Exp* **88#**, 308-312. [2] Shopka et al. (2011) *Geochim. Cosmochim. Acta* **75**, 978-1002.

https://doi.org/10.1180/S0026461X00008434 Published online by Cambridge University Press

Open-system behavior of U-series in carbonates: what we can learn from old limestones

P. DESCHAMPS[1*], C. HILLAIRE-MARCEL[2], B. HAMELIN[1], B. GHALEB[2]

[1]CEREGE, UMR Aix-Marseille Univ. - CNRS - IRD, Aix-en-Provence, France, deschamps@cerege.fr
[2]GEOTOP, Montreal, CANADA, hillaire-marcel.claude@uqam.ca

Conventional U/Th age determination assumes closed-system behavior. This criterion is violated in most Pleistocene fossil corals as evidenced by unreliable ages, ^{226}Ra offsets with respect to radioactive equilibrium with parent ^{234}U, as well as variable initial coral ^{234}U/^{238}U ratio, that are in most case substantially higher than that of modern seawater. The source of excess ^{234}U (and ^{230}Th) in fossil corals and its relationship to U-series age determinations remains an open issue in U-Th geochronology. Many investigators [2,3] consider that open-system behavior results from an enhanced alpha-recoil mobility of U-series nuclides (^{230}Th, ^{234}Th and consequently ^{234}U).

The premise of this study is that alpha-recoil-related processes evoked for open-system behavior of fossil corals, should also be active in "old" carbonates. Here we illustrate this issue with precise and accurate measurements of ^{234}U/^{238}U ratios in borehole core samples from deep, low-permeability Mesozoic formations of the Paris basin, France [3]. The initial objective of the study was to investigate the behavior of naturally occurring uranium isotopes as a means to assess the long-term safety of radioactive waste disposal in a clayey formation of Callovo-Oxfordian age targeted by the French Agency for nuclear waste management (ANDRA). Special attention was paid to U-series disequilibria within over- and underlying Mesozoic carbonate formations. All samples associated with pressure-dissolution features (stylolites) depicted systematic ^{234}U/^{238}U disequilibria at the centimetric scale, thus illustrating some uranium mobility during the last 2 Ma. This finding illustrates an unusual and unexpected mechanism of uranium remobilisation implying relocation and fractionation processes, since U was supposed to be practically immobile under the reducing conditions and low porosity and permeability characterizing the host sedimentary formations. We intend to discuss here the mechanisms responsible for uranium mobility in such deep sedimentary rocks and will make a comparison with mechanisms that have been proposed to drive U mobility in fossil corals.

[1] Thompson et al. (2003). *EPSL*, **210(1-2)**: 365-381.
[2] Villemant et al. (2003). *EPSL*, **210(1-2)**: 105-118.
[3] Deschamps et al. (2004). *HESS*, **8(1)**: 35-46.

Impact of remediation design on arsenic leaching from historic gold mine tailings

S.L. DESISTO[1*], M.B. PARSONS[2], J.L. KAVALENCH[3] AND H.E. JAMIESON[1]

[1]Department of Geological Sciences and Geological Engineering, Queen's University, Kingston, Ontario, Canada, desisto@geoladm.geol.queensu.ca (* presenting author), jamieson@geol.queensu.ca
[2]Natural Resources Canada, Geological Survey of Canada (Atlantic), Dartmouth, Nova Scotia, Canada, Michael.Parsons@nrcan-rncan.gc.ca
[3]AMEC Earth and Environmental, London, Ontario, Canada, Jennifer.Kavalench@amec.com

Secondary As minerals can reduce metal(loid) mobility in mine wastes, but may dissolve under changing geochemical conditions during or after remediation. The objective of this study is to optimize remediation strategies for As-bearing tailings from abandoned gold mines in Nova Scotia. A logical clean up plan at these publicly accessible sites would be to place a cover on the tailings, a method often successful at limiting sulphide oxidation and thus, preventing acid production and metal(loid) release. However, due to the heterogeneous nature of these strongly weathered mine wastes, this may lead to dissolution of some As-bearing minerals and an influx of As to local waters. The challenge of remediating such tailings lies in the different Eh-pH niches in which Fe-arsenates (oxidizing, acidic), Ca-Fe-arsenates (oxidizing, alkaline), and sulfides (reducing) are stable. Since these mine wastes are mineralogically complex and associated with variable pH and redox conditions, a one-size-fits-all remediation approach will be difficult to achieve.

To assess the geochemical changes induced by various remediation scenarios, the following options have been tested: (1) unremediated tailings in the field, (2) unremediated tailings in the lab, (3) a simulated limestone cover, (4) a simulated vegetative cover, and (5) a soil cover. For scenario 1, four field bins were filled with one of each tailings end member (hardpan tailings, oxic surface tailings, wetland tailings, or high Ca/As tailings). Leachate from the bins was sampled bi-weekly for two years. Scenarios 2-4 involved a set of three columns per tailings end member that were leached weekly with one of three input solutions: synthetic rainwater, synthetic rainwater equilibrated with $CaCO_3$, or a weak organic acid solution, respectively. Scenario 5 consisted of one column of each tailings end member topped with a 30-cm-thick soil cover that was leached with synthetic rainwater.

Results from Scenarios 1-4 show the As mineralogy in the tailings is the primary control on As mobility. Under field conditions, both hardpan and wetland tailings produced acidic, metal(loid)-rich drainage over time, and only the high Ca/As tailings remained near-neutral throughout the tests. In the lab, column leachates for a given tailings end member showed similar pH values and concentrations of sulphate, As and Fe despite the range in input solution pH (from 4.6 to 10). The scenarios tested so far have not proven to be effective mitigation strategies against As leaching. Reducing water and oxygen availability may be the best way to minimize As release and prevent acid generation.

https://doi.org/10.1180/S0026461X00008434 Published online by Cambridge University Press

Stablization of mercury in riverbank sediments of the South River, Virginia (U.S.A.)

KRISTA DESROCHERS [1*], CAROL PTACEK [1], DAVID BLOWES[1] RICHARD LANDIS [2], JAMES DYER[2], WILLIAM BERTI[2], NANCY GROSSO[2]

[1]Earth and Environmental Sciences, University of Waterloo, Waterloo, ON, CA
k2desroc@uwaterloo.ca (* presenting author)
[2]E.I du Pont de Nemours and Company, Wilmington, DE, USA

Metal-bearing sediment particles from eroding riverbanks can be an ongoing source of bioavailable mercury (Hg) to aquatic ecosystems. Hyporheic zones in particular can be important sources of both inorganic and organic-complexed Hg, which can be rapidly transported to adjacent surface waters. The objective of this study was to investigate the release and treatment of dissolved and particle-bound Hg in water derived from the riverbank sediments of the South River, Virginia. A profile of sediment was collected along a riverbank. Samples were characterized to assess the potential for Hg release as both dissolved and particulate forms. A series of resuspension experiments was conducted to simulate erosion of the riverbanks into the river. Mechanisms controlling transport of Hg during a riverbank inundation event were evaluated through column leaching experiments, which were conducted under variable flow conditions. Carbon-based amendments were applied in batch experiments to limit the release of Hg from sediment containing either 70 mg kg^{-1} or 280 mg kg^{-1} of Hg. Continuous flow-through column experiments were conducted to evaluate the potential for treatment of both dissolved and particulate Hg under transport conditions.

Elevated concentrations of Hg were observed in the river water during the resuspension experiments. The highest concentrations of Hg released (up to 80 μg L^{-1}) were observed for sediment samples collected from near the top of the riverbank profile. Mercury release during the resuspension experiments showed a non-linear response as the mass of sediment was increased, suggesting a possible solubility control on aqueous Hg concentrations. In column experiments, Hg concentrations in the in the 0.45 μm-filtered fraction of the effluent varied from 0.15 μg L^{-1} for samples collected from the base of the riverbank to 8 μg L^{-1} for samples collected from the top of the riverbank. Filter size-fractionation of water column effluent suggested approximately 50% of the leached Hg was present in the dissolved phase, with the remainder in particulate form.

Results from batch and column experiments indicated that the addition of reactive media resulted in lower aqueous concentrations of Hg. The co-blending of carbon-based adsorbent to sediments resulted in decreases in aqueous Hg ranging from 43 to 89% in the South River water. The adsorption of Hg ranged from 32 to 202 ng Hg per g reactive material. Decreases of 98% of Hg in column effluent were observed following 35 pore volumes of flow, and 91% after 100 pore volumes of flow. Results from laboratory-based experiments indicated that the addition of reactive media resulted in lower concentrations of both dissolved and particulate Hg in the river water. The potential application of carbon-based amendments to the riverbank sediment may be an alternative approach to reduce Hg flux in the South River.

Use of stable (HOCN) and radiogenic (Sr) isotopes to determine the geographic provenance and traceability of artisanal cheeses of Quebec, Canada.

S. DESROCHERS*, R. K. STEVENSON, J-F. HÉLIE, A. POIRIER

GEOTOP et, Science de la Terre et de l'Atmosphère, Université du Québec à Montréal, P.O. Box 8888, Station Centre-Ville, Montreal, Qc, Canada, H3C 3P8
(*correspondence:ldesrochers.steph@gmail.com)

Analysis of stable isotopes has often been used to determine the traceability of different food products [1]. The light stable isotope ratios in dairy products such as cheese can provide information for tracing geographical origin [4]. The province of Quebec is Canada's largest cheese producer and artisanal cheeses are becoming a larger part of this market. In this context, we selected artisanal cheeses from six different regions of the province of Quebec to study the applicability of light stables isotopes and radiogenic isotope (Sr) ratios as descriminants to provide geographic traceability.

The cheese samples were analysed for light stable isotope ratios (HOCN) which are mainly influenced by altitude, distance from the sea, use of fertilizer, rainfall, food type, temperature, longitude and latitude [2,3,6]. The Sr isotope analyses are indicative of the geology of the type of substrate of the grazing areas [5]. Prelininary results yeild $^{87}Sr/^{86}Sr$ ratios that vary from 0.70978 to 0.71347 for both winter and summer cheeses. These values reflect soils composed largely of glacial tills derived from either the Canadian Shield or Appalachain Orogen. Furthermore, we observed a direct correlation of the $^{87}Sr/^{86}Sr$ ratios of cheese, milk and soil from the grazing area. Stable isotope δD values vary beteween -107.57‰ to -56.38‰, and $\delta^{18}O$ beteween -18,64 ‰ to -6,45‰ for both winter and summer cheeses. Water and milk δD and $\delta^{18}O$ results are similar to chesse results but with and enrichment in $\delta^{18}O$ values. Stable isotope $\delta^{13}C$ values vary between -27.12‰ to -21.40‰ and $\delta^{15}N$ beteween 4.66‰ and 6.21‰ wich is representative of C_3 plant CO_2 fixation. These results allow us to conclude that the use of stable and radiogenic isotopes can provide geographical provenance and traceability of the artisanal cheese of Quebec.

[1]Kelly, Heaton & Hoogewerff (2005) Food Science and Technology 16, 555-567.
[2]Mariotti et al (1981) Plant soil, 62, 413-430.
[3]Moser & Rauert (1980) Berlin: Bornträger.
[4]Pillonel & al (2003) Lebensm. Wiss. u. Technol. 36, 615-623.
[5]Rossmann et al (2000) European Food and Research Technology, 211, 32-40.
[6]Smith & Epstein (1971) Plant physiology, 47, 380-384.

https://doi.org/10.1180/S0026461X00008434 Published online by Cambridge University Press

The climate sensitivity of oceanic oxygen

CURTIS DEUTSCH*[1], TAKA ITO[2]

[1]University of California Los Angeles, Los Angeles, USA, cdeutsch@atmos.ucla.edu (* presenting author)
[2]Georgia Institute of Technology, Atlanta, USA, taka.ito@eas.gatech.edu

The warming of Earth's climate is expected to lead to a widespread loss of oxygen from the ocean, exacerbating the localized effects of coastal eutrophication. The mechanisms responsible for climate-forced deoxygenation – changes in gas solubility, ventilation of the ocean interior, and respiration of organic matter – are spatially heterogeneous, so the susceptibility to oxygen loss varies greatly among water masses. Moreover, the wide range of time scales involved in the adjustment of the oceanic oxygen distribution, coupled with the presence of strong internally generated variability greatly complicate the detection and attribution of trends. This talk will synthesize the current evidence for and understanding of changes in oceanic oxygen from model simulations, modern ocean observations, and the geologic record. A central conclusion is that the low latitude ocean, where the biological constraints from low oxygen are most profound, are also intrinsically most sensitive to climatic perturbations. Given the long transit times from thermocline outcrops to the tropical oxygen minimum zones, the response of oxygen in those regions to climate warming must either be slow to arrive, or else driven by local rather than remote climate trends. This suggests that if an expansion of the tropical oxygen minimum is already underway, its climatic origin is likely to be found in tropical winds rather than high latitude stratification. The major uncertainties and implications for ecosystems and biogeochemical cycles will also be discussed.

Benthic nitrogen fluxes and denitrification in Bering Sea shelf sediments.

ALLAN DEVOL[1*], RAHCHEL HORAK[1], DAVID SHULL[2], CALVIN MORDY3 AND HEATHER WHITNEY[1]

[1]University of Washington, Oceanography, Seattle, WA, USA, devol@u.washington.edu(* presenting author), rahorak@uw.edu,hwhitney@uw.edu
[2]Western Washington University, Bellingham, WA USA, david.shull@wwu.edu
[3]University of Washington, JSIAO, Seattle WA, USA, Calvin.W.Mordy@noaa.gov

Abstract

Benthic-pelagic coupling is hypothesized to be quite strong in the in the highly Bering Sea shelf ecosystem and primary production of the system is thought to be nitrogen limited[1]. Nevertheless, sedimentary denitrification and benthic nutrient fluxes and their seasonal trends are poorly characterized. Through the Bering Sea Ecosystem Study (BEST) program, we measured benthic fluxes of N_2 and dissolved inorganic nitrogen species, the extent of coupled nitrification/denitrification, and the water column nitrate deficit (using N**[2]) on the Bering Sea shelf in the spring and summer 2009 – 2010. We found that sedimentary denitrification is widespread over the shelf and is fuelled mostly through coupled nitrification/denitrification, the net balance of sedimentary DIN flux is negligible over the shelf, and that water column N** varies widely according to season and year. In the summer, N** appeared to be strongly affected by non-Redfieldian uptake of inorganic nutrients by phytoplankton in the spring bloom; in the winter, N** was strongly affected by sedimentary denitrification. Our findings indicate that the estimate of total N loss in the Bering Sea shelf should be revised upwards by at least 50% to 5.2 – 6.2 Tg N y^{-1}. In addition sediments appear not to be a large source of remineralized nutrients for primary production over the shelf, hence sedimentary denitrification exacerbates N-limitation of the ecosystem.

[1] Grebmeier et al. (2006) *Nature* **311**,1461-1464
[2] Mordy, et al (2010) *Mar.Chem.***121,** 157-166

https://doi.org/10.1180/S0026461X00008434 Published online by Cambridge University Press

Kinetic Monte-Carlo: a tool to investigate the corrosion of glasses

FRANÇOIS DEVREUX[1*], CÉLINE CAILLETEAU[1,3], OLIVIER SPALLA[2] AND FRÉDÉRIC ANGELI[3]

[1]Ecole Polytechnique-CNRS, PMC, 91128 Palaiseau, France
francois.devreux@polytechnique.fr
celine.cailleteau@polytechnique.edu
[2]CEA, DSM, LIONS, 91191 Gif-sur-Yvette, France
olivier.spalla@cea.fr
[3]CEA, DEN, LCLT, 30207 Bagnols-sur-Cèze, France
frederic.angeli@cea.fr

Monte-Carlo modeling

The Monte-Carlo modeling of the corrosion of glasses by water makes it possible taking into account both the chemical reactivity at the atomic level and the morphology of the altered surface film at the mesoscopic scale. The method was mainly applied to borosilicates in relation to the durability of the nuclear waste confinement glasses. The effect of substituting silica for more (B, Na) or less (Al, Zr) oxides was studied [1, 2].

The model leads to three major predictions. First, the initial dissolution rate is controlled by the surface area of the porous layer produced by the departure of the most soluble oxides. Second, the corrosion blocking that frequently occurs in static conditions is due to the restructuring of the altered film, which leads to the densification of the external layers and to the closure of the pores (Fig 1). Third, the presence of insoluble oxides in the glass composition paradoxically increases the degree of corrosion, since it prevents the layer reconstruction.

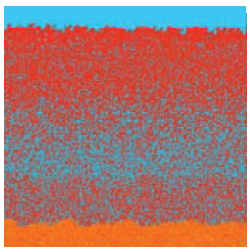

Figure 1: Cross section of the reorganized gel showing the densification of the external layers and the closure of the pores [3].

Experimental studies

All these predictions were broadly confirmed by experimental studies of the kinetics of corrosion and by the characterization of the corroded films by various techniques including NMR, gas adsorption and spatially resolved mass spectroscopy [3, 4]. Especially, the gel reconstruction was probed by small angle X-ray scattering and the porosity closure was evidenced by neutron scattering with solvent index matching. An inverse correlation between the initial dissolution rate and the final degree of corrosion was demonstrated both as a function of pH, and glass composition when silica is replaced by zirconia, or Na_2O by CaO [4].

[1] Devreux (2001) *J. Mater. Sci.*, **36**, 1331-1341 [2] Devreux (2004) *J. Non Cryst. Solids*, **343**, 13-25 [3] Cailleteau (2008) *Nature Mater.*, **7**, 978-983. [4] Cailleteau (2011) *J. Phys. Chem. C*, **115**, 5846-5855.

Continental growth through the sedimentary reservoir: Hf in zircon & Nd in shales records

BRUNO DHUIME[1,2*], CHRIS HAWKESWORTH[1], PETER CAWOOD[1]

[1]University of St Andrews, Department of Earth Sciences, St Andrews, UK, b.dhuime@bristol.ac.uk (* presenting author)
[2]University of Bristol, Department of Earth Sciences, Bristol, UK

~7% of the present-day exposed crust consists of rocks of Archean age, yet models of continental growth suggest that 20-100% of the present-day volume of the continental crust had formed by 2.5 Ga ago [e.g. 1]. These models rely on understanding the balance between the generation of new crust and the reworking of old crust, and how these have changed with time. For that purpose, the variations in radiogenic isotope ratios in detrital rocks and minerals are a key archive.

We considered two different approaches to model the growth of the continental crust: (i) the variation of Nd isotopes in continental shales with various deposition ages, which requires a correction of the bias induced by preferential erosion of younger rocks through an erosion parameter 'K' [2-3]; and (ii) the variations in U-Pb, Hf and O isotopes in detrital zircons sampled worldwide. These two approaches independently suggest that the continental crust appears to have been generated continuously, but with a marked decrease in the continental growth rate at ~3 Ga. The >4 Ga to ~3 Ga period is characterised by relatively high net rates of continental growth (~3.0 $km^3.a^{-1}$), which are similar to the rates at which new crust is generated, and destroyed, at the present time [4]. Net growth rates are much lower since 3 Ga (~0.8 $km^3.a^{-1}$), which may be attributed to higher rates of destruction of continental crust. The inflexion in the continental growth curve at ~3 Ga indicates a change in the way the crust was generated and preserved. This change may be linked to onset of subduction-driven plate tectonics and discrete subduction zones.

[1] Hawkesworth *et al.* (2010) *JGSL* **167**, 229-248. [2] Allègre & Rousseau (1984) *EPSL* **67**, 19-34. [3] Dhuime *et al.* (2011) *Geology* **39**, 407-410. [4] Scholl & von Huene (2009) *Geol. Soc. London Sp. Pub.* **318**, 105-125.

https://doi.org/10.1180/S0026461X00008434 Published online by Cambridge University Press

Improved analytical method for determination of Mg isotopes: Application to seawater and natural carbonates

ANGELA DIAL[1*], C. RIDGEWELL[2], B. KILGORE[1], D. TREMAINE[1], S. MISRA[3] AND V. J. M. SALTERS[1]

[1]Florida State University; NHMFL – Geochemistry; Tallahassee, FL, USA; (presenting author: dial@magnet.fsu.edu)
[2]Vanderbilt University, Nashville, TN, USA
[3]University of Cambridge; Dept. of Earth Sciences; Cambridge, UK

Magnesium isotopes are a powerful tracer of low temperature geochemical processes [1, 2]. However, widespread application of Mg isotopes in geochemical studies is limited due to the relative amount of Mg required for high precision measurements, high procedural blanks, artificial fractionation induced by chromatographic methods, and low matrix tolerance [1, 2]. The improved method for Mg isotope ratio (δ^{25}Mg & δ^{26}Mg) determination has low mass consumption (5 ng-Mg) with high precision (± 0.1‰, 2s) and high matrix tolerance using Neptune® MC-ICP-MS. A single step chromatographic method is used to quantitatively (100.0% ± 0.2%) separate Mg from matrix elements with low blanks and no column induced fractionations. Quantitative separation of other matrix elements (Li, Na, Ca, and Sr) was also achieved with > 99% recovery (Fig. 1). This procedure is optimal for natural carbonates and seawater samples with high matrix loads.

Preliminary MC-ICP-MS analyses of CAM1, DSM3, and seawater fall in the published range ($\Delta^{25}Mg_{Cam1}$ and $\Delta^{26}Mg_{Cam1}$ relative to DSM3 are 1.47‰ and 2.67‰, respectively) (Fig. 2). Internal reproducibility ranges from 0.029‰ to 0.144‰ / AMU (1σ, n=105), while external reproducibility obtained on pure Mg solutions is 0.009‰ / AMU (1σ). These new analytical methods will be used to investigate relationships between $^{7/6}$Li, $^{(26/25)/24}$Mg, and $^{(88/87)/86}$Sr ratios in natural carbonates to asses their viability as indicators of weathering and endmember mixing in carbonate systems.

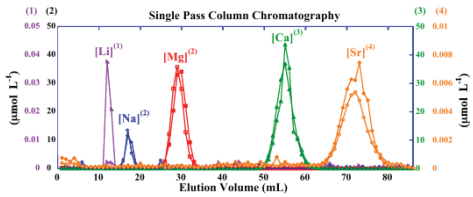

Figure 1: Quantitative separation of alkali and alkaline earth elements.

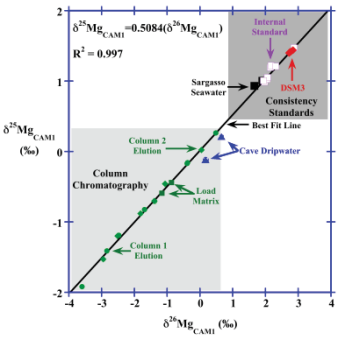

Figure 2: δ^{25}Mg vs. δ^{26}Mg for elution matrices, seawater, cave dripwater, DSM3, and internal isotope standards. Error bars (2σ) are contained within data symbols. The slope of the best-fit line through all data is δ^{25}Mg = 0.5084 (δ^{26}Mg) R^2 = 0.997.

[1] Galy et al. (2001) *Int. J. Mass Spectrom.* **208**, 89-98. [2] Galy et al. (2003) *J. Anal. At. Spectrom.* **18**, 1352–1356.

Effect of Nanoparticles on the Displacement Pattern of CO_2 Injection in Porous Media

D. A. DICARLO[1*], B. AMINZADEH[1], D. H. CHUNG[1], M. ROBERTS[1], C. HUH[1], AND S. L. BRYANT[1]

[1]The University of Texas at Austin, Department of Petroleum and Geosystem Engineering (* DiCarlo@mail.utexas.edu]

Introduction

The patterns that emerge from a displacement process depend greatly on the mobility ratio between displaced and displacing phases. When a less viscous fluid (e.g. CO_2) displaces a more viscous fluid (e.g. brine) the displacing fluid fingers through the porous media, causing it to travel faster and longer distances. Spontaneous formation of foam during the displacement may be an effective solution to stabilize the displacement. Surface treated nanoparticles have been shown to stabilize CO_2 in water foam by adhering to the surface of CO_2 bubbles and preventing their coalescence [1]. However, the large adhesion energy suggests that mechanical work must be applied to bring the nanoparticles from bulk phases to the CO_2-water interface [2]; Co-injection of CO_2 and nanoparticle solution at high rates is known to provide sufficient energy. Here, we study the foam formation during a fluid/fluid displacement at low shear rate.

Methodology

In order to capture the efficiency of the nanoparticle foam flood, we inject CO_2 and CO_2 analogue fluids into sandstone cores preloaded with either brine or brine with suspended nanoparticles. We use CT scanning to measure the saturation profile and flow pattern during a displacement, and pressure transducers to measure the overall mobility.

Results and Conclusion

Even at small flow rates (low shear rate) the presence of nanoparticles acts to control the CO_2 mobility. The displacement front is more spatially uniform and breaks through later in the presence of nanoparticles compared to displacements without nanoparticles (Fig. 1). Pressure measurements during the displacement are consistent with generation of a viscous phase such as an emulsion. These observations suggest that nanoparticle stabilized emulsion is formed during the displacement which acts to suppress the viscous instability. We argue that generation of droplets of CO_2 occurs at the leading edge of all drainage displacements; however, the droplets are preserved only in the presence of nanoparticles.

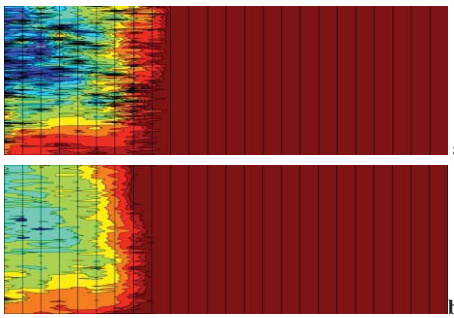

Figure1. Side view of the Boise sandstone core after injection of 0.10 PV of octane, a) without nanoparticle, b) with nanoparticle

[1] Zhang, et al. (2010), Paper SPE 129885. [2] Binks (2002), *Current Opinion in Colloids interface sciences, 7*, 21- 41

https://doi.org/10.1180/S0026461X00008434 Published online by Cambridge University Press

MELT ROCK REACTION IN THE MANTLE AND ACCRETION OF THE LOWER CRUST AT SLOW SPREADING RIDGES

HENRY DICK[1], ALESSIO SANFILIPPO[2], AND JOHANNES LISSENBERG[3], YASUHIKO OHARA[4]

[1]Woods Hole Oceanographic Institution, hdick@whoi.edu (* presenting author)

[2] Università degli Studi di Pavia, alessio.sanfilippo@unipv.it

[3] Cardiff University, lissenbergcj@cardiff.ac.uk

Introduction

Primitive olivine cumulates; dunite, troctolite, and olivine gabbro associated with mantle peridotite are common features of oceanic core complexes away from fracture zones. They are broadly interpreted as from the crust-mantle transition zone, formed where melt transport focused beneath a 2nd order ridge segment. Mapping at Kane Megamullion on the MAR shows local magmatic centers may form anywhere beneath a ridge segment: existing for several hundred thousand years before magmatism focused elsewhere [1].

Olivine-rich troctolites form by melt-rock reaction with the mantle, in a sequential reaction between peridotite and migrating melt, forming first dunite, then troctolite, then olivine gabbro. This occurs due to solidification-by-reaction between melt and the mantle [2]. Such reactions may continue in the lower crust until olivine is eliminated. Ol-rich troctolites in IODP Hole U1309D appear to have this origin [3-5]. Rafting of troctolites to higher levels likely due to tectonic rollover wgeb the lower crust supports a shear stress at low magmatic budgets. Thus a portion of the lower crust may be hybridized mantle.

Ol-rich troctolites also occur within a mantle section at Godzilla Megamullion in the Parece Vela Basin [3]. They include both Ol-rich (Ol > 60 vol.%) and plagioclase-rich (Pl > 60 vol.%) troctolites. The latter likely formed by local dissolution of a plagioclase matrix, and crystallization of olivine, Cpx and new plagioclase by melt produced by mixing high-MgO melt residual to Ol-troctolites formation with melt crystallizing cumulus plagioclase in a melt transport conduit.

We find olivine nickel contents can constrain the formation environment of Ol-rich rocks in the lower crust and mantle, the nature of the formation process, and the magma budget. Comparison to the nickel contents of other troctolite and gabbro occurrences in oceanic and ophiolite settings reveals a set of relationships generally consistent with our interpretations. Notably, the olivine gabbros from the 1500-m Hole 735B Atlantis Bank gabbro section have low nickel contents, while those from the 1400-m Hole U1309D Atlantis Massif gabbro section have high nickel. This is consistent with less-reacted infiltrating melt at the latter, strongly supporting the idea that U1309D represents a deeper section of the lower crust near the crust-mantle transition, while the former have been shown to represent the dike-gabbro transition and underlying gabbros.

Godzilla troctolites and gabbros have clear similarities to EPR troctolites and gabbro segregations drilled in dunites crosscutting mantle peridotites at Site 895 at Hess Deep. These represent multi-stage crystallization of stagnant melts in conduits beneath the EPR. Thus, it appears that the processes that formed the Godzilla troctolites occur beneath ocean rises across the spreading rate spectrum.

[1] Dick et al. (2010). J. Petr. 51, 425-467. [2] Lissenberg & Dick (2008) EPSL 271, 311-325. [3] Drouin et al. (2007) Eos 88 (52), T53B-1300. [4] Drouin et al. (2009) Chem. Geol. 264, 71-88. [5] Suhr (2008) G3 9, 31 pp.

THIN CRUST OVER THE MARION RISE: MELTING A HETEROGENOUS MANTLE FROM BENEATH GONDWANA

HENRY DICK[1*], HUAIYANG ZHOU[2]

[1*]Woods Hole Oceanographic Institution, hdick@whoi.edu (* presenting author)

[2]Tongji University, State Key Laboratory of Marine Geology, zhouhy@tongji.edu.cn

The Marion Rise stretches ~ 3100 km along the SWIR from its shoalest point at 850 m, 250-km north of Marion Island, to 5600-m just west of the Rodriguez TJ. By any measure it has essentially the same relief as the Icelandic/Reykjanes Rise, but is twice as long. Cut by numerous large-offset transforms, which would likely dam sub-axial asthenospheric flow, it is unlikely that the rise can be supported by a mantle plume beneath the Marion Hotspot. The hotspot, however, traces back to the Karoo volcanic event at 185 Ma near the time of the breakup of Gondwana, and formation of the SWIR. Hence the mantle substrate beneath the SWIR likely comes from beneath southern Africa, representing the residue of the Karoo event.

We compiled new and existing data on SWIR dredge and dive samples, and find that large peridotite exposures occur throughout, including the Marion Rise crest. In the absence of significant gabbro representative of a lower crustal section, and the presence of near-amagmatic spreading segments along the rise, we conclude that the crust over the Marion Rise, in sharp contrast to the Reykjanes Ridge, is relatively thin and discontinuous. At the same time, analysis of peridotite spinel shows a systematic increase in mantle depletion up the Marion Rise correlating to the composition of spatially associated basalts and ridge depth. Hence the degree of mantle depletion increases towards the rise crest. In the absence of significantly thicker crust, this must be in large part the consequence of an earlier mantle melting event – presumably coinciding with the Karoo volcanism – but possibly including a yet earlier mantle depletion.

This, then, provides an explanation for the Marion Rise other than a simple thermal anomaly attributable to sub-axial asthenospheric flow fed from a mantle plume beneath the Marion Hotspot. Harzburgite in the garnet stability field is significantly less dense than lherzolite, and hence the systematically higher degree of mantle melting required by the Marion Rise basalts and peridotites likely reflects a major density anomaly beneath the SWIR centered on Marion Island 250 km to the south. Thus the Marion Rise may exist due to an isostatic response to an earlier mantle depletion event predating the present day volcanism.

Basalts isotopic compositions along the Marion Rise are highly variable, reflecting a heterogenous mantle consistent with interactions and entrainment of a heterogeneous continental lithosphere and crust in the asthenosphere as Africa migrated northward during the opening of the SW Indiaan Ridge [1-3].

[1] Escrig, S., Capmas, F., Dupre, B., Allegre, C.J., 2004.Nature 431, 59-63. [2] Mahoney (1992) JGR 97, 19,771-19,790. [3] Meyzen et al. (2005) 6, 34 pp.

https://doi.org/10.1180/S0026461X00008434 Published online by Cambridge University Press

Thermodynamic properties of aqueous phenanthrene and isomers of methylphenanthrene at high temperature

JEFFREY DICK[1*], KATY EVANS[2], ALEX HOLMAN[1], CAROLINE JARAULA[1] AND KLITI GRICE[1]

[1]WA Organic and Isotope Geochemistry Centre, Department of Chemistry, and [2]Department of Applied Geology, Curtin University, Bentley WA, Australia, Jeffrey.Dick@curtin.edu.au (* presenting author)

Polycyclic aromatic hydrocarbons, including monomethylated phenanthrenes (MP), are common components of bitumen associated with sediment-hosted ore deposits. Their relative abundances are often interpreted as indicators of thermal maturity and hence may help constrain models for the transport and deposition of metals sharing a genetic history with the organic compounds. A high degree of thermal maturation yields products in chemical equilibrium [1], but a lack of thermodynamic data for aqueous MP at high temperature has precluded a quantitative interpretation of their origin in hydrothermal settings. Values for the standard molal Gibbs energy and enthalpy, entropy, and heat capacity were generated for aqueous phenanthrene and the MP isomers methylated at the 1-, 2-, 3-, 4- and 9-positions on the phenanthrene structure. These values were derived from reported thermodynamic properties of the crystalline compounds [2], their solubilities and enthalpies of solution, and relative properties of the MP isomers from quantum chemical simulations [3] at 25 °C. Preliminary extrapolations to higher temperature were carried out using a constant heat capacity difference between the isomers. At 25 °C, 2-MP is highly favored over 1-MP. With increasing temperature, however, the difference in stability between the two diminishes, eventually crossing over to higher stability of 1-MP at temperatures greater than ~400 °C. The calculated equilibrium ratios of 2-MP to 1-MP (MPR) are consistent with two independent constraints: (1) maximum reported values for mature source rocks (~160 °C), and (2) MPR observed in Archaean rocks exposed to temperatures of 200–300 °C [4].

These comparisons indicate that relative abundances of methylphenanthrenes can be used to infer thermal conditions and sources of bitumen found in ores and host rock. At the Here's Your Chance (HYC) Pb-Zn-Ag deposit (McArthur River, Northern Territory, Australia) bitumen in the ore zones has a lower MPR than unmineralized shale samples. The range of values in the bitumen associated with the ore is consistent with temperatures of isomeric equilibration of ~350–400 °C. The source of MP, therefore, could reasonably have been a hot brine that cooled as it reached the ore zone. The offset in the relative abundances of MP between the ore and shale layers suggests a different degree of interaction of the brine with these layers. Since phenanthrene has a higher average oxidation state of carbon than its methylated counterparts, consideration of their relative abundances in a thermodynamic framework could place constraints on redox conditions in the ore-forming system.

[1] Mackenzie, A. S. (1984) *Advances in Petroleum Geochemistry* **2**, 115-214. [2] Richard, L. and Helgeson, H. C. (1998) *Geochim. Cosmochim. Acta* **62**, 3591-3636. [3] Szczerba, M. and Rospondek, M. J. (2010) *Org. Geochem.* **41**, 1297-1311. [4] Brocks, J. J. et al. (2003) *Geochim. Cosmochim. Acta* **67**, 4289-4319.

The possible role of crystal conduction and inter-particle electron transfer in Fe-oxide phase transformation and growth

K. DIDERIKSEN[1]*, B. GILBERT[2], C. FRANDSEN[3], M. ZHU[2], S.L.S. STIPP[1], J.F. BANFIELD[4]

[1]University of Copenhagen, Nano-Science Center, Dept. of Chemistry, knud@nano.ku.dk (*presenting author); stipp@nano.ku.dk

[2]Lawrence Berkeley National Laboratory, Earth Science Division, BGilbert@lbl.gov; mzhu@lbl.gov

[3]Technical University of Denmark, Dept. of Physics, fraca@fysik.dtu.dk

[4]University of California, Berkeley, Dept. of Earth & Planetary Science, jbanfield@berkeley.edu

A series of anerobic experiments have been conducted to study the mechanism of Fe^{2+}-mediated ferrihydrite transformation. At pH 6.5 and 7 and in the presence of 5 mM dissolved $Fe(II)Cl_2$, freshly formed, 2-line ferrihydrite rapidly exchanges isotopes with Fe^{2+} in solution (75% equilibration within 10 minutes). During the first 2-3 hours of reaction, X-ray pair distribution function (PDF) analysis and transmission electron microscopy shows evidence of increasing size of ferrihydrite particles and coherent scattering domains, but minor or no mineral transformation. After this lag phase, more rapid transformation commences to major end-phases lepidocrocite (pH 6.5) and magnetite (pH 7).

Extensive isotope exchange for ferrihydrite without significant phase transformation indicates that interfacial electron transfer and crystal conduction leads to oxidation of adsorbed Fe(II), resulting in Fe(III)-oxide growth, and reductive dissolution of Fe(III) at a different site, similar to what was initially observed for hematite [1]. In contrast to the lag phase observed for 2-line ferrihydrite, transformation of 6-line ferrihydrite to magnetite commences immediately at pH 7. More rapid conversion of larger and presumably less soluble ferrihydrite is inconsistent with recrystallisation by classical dissolution/reprecipitation. Rather, it suggests solid state transformation with magnetite nuclei forming either inside the ferrihydrite or at its surface.

With X-ray diffraction, materials subjected to ultrasonification during reaction display much weaker Bragg peaks from goethite, lepidocrocite and magnetite than those observed from material synthesised in regular experiments and the coherent scattering domains of the phases are smaller in PDF. This indicates that particle contact enhances crystal growth. Such a feature could reflect growth by 1) oriented attachment, which has been observed for ferrihydrite conversion to goethite [e.g. 2], or 2) electronic coupling between crystals, leading to Fe^{2+} electron donation and crystal growth on one particle, then transfer of the electron to an adjacent particle where interfacial reduction and dissolution occur.

[1] Yanina et al. (2008) *Science* **320**, 218-220. [2] Banfield et al. (2000) *Science* **289**, 751-754.

https://doi.org/10.1180/S0026461X00008434 Published online by Cambridge University Press

The role of fluids in the monazite record during successive partial melting events: a textural, chemical and in situ dating study in Grt-Ky gneisses of the Central Rhodope (Bulgaria, Greece)

AMELIE DIDIER[1*], VALERIE BOSSE[1], ZLATKA CHERNEVA[2], MILENA GEORGIEVA[2], PIERRE GAUTIER[3], JEAN LOUIS PAQUETTE[1], IANKO GERDJIKOV [2]

[1] Clermont Université, Université Blaise Pascal, Laboratoire Magmas et Volcans, BP 10448, 63000 Clermont-Ferrrand, France, a.didier@opgc.univ-bpclermont.fr (*presenting author)
[2] Sofia University "St Kliment Ohridski", 15 Tzar Osvoboditel Blvd, 1504 Sofia, Bulgaria
[3] Géosciences Rennes, Université de Rennes 1, UMR 6118 CNRS, Observatoire des Sciences de l'Univers de Rennes, 35042 Rennes Cedex, France

Monazite is considered to be resistant to diffusive Pb loss at high temperatures and thus, it is particularly adapted to record various stages during a sequence of high-temperature geological events. This study focuses on Grt-Ky gneisses from the lower part of the metamorphic pile in the central part of the Rhodope Metamorphic Complex, in the areas of Chepelare (Bulgaria) and Sidironero (Greece). The outcrops of both regions have experienced a polycyclic evolution during Alpine times, with at least two stages of high temperature metamorphism. According to P-T estimates, the first event involved granulite facies dehydration melting that produced peritectic garnet and kyanite together with a K-rich melt. The second event relates to widespread fluid-assisted partial melting. The latter is well known in adjacent rocks, where it is dated at ~36-50 Ma, but is poorly expressed in our samples, which well preserve the early granulite facies assemblages. Monazite is present in all samples, included in early porphyroblasts such as garnet and kyanite or in the matrix. Matrix monazites are associated with white mica, rutile and biotite (Greek part) and sillimanite and biotite (Bulgarian part). Matrix monazite grains show fluid-assisted dissolution-recrystallisation features with pronounced Y-zoning correlated to age domains. Y-poor domains, dated by LA-ICPMS method ($^{208}Pb/^{232}Th$ ages) between 130 and 155 Ma, represent the largest part of each grain, while Y-rich domains, dated between 40 and 50 Ma, occur either as thin discontinuous rims (< 15 µm) or as small single grains surrounding the Mesozoic grains or filling white mica cleavages. The low P and REE-content of the surrounding minerals suggests that the Cenozoic domains essentially crystallized at the expense of the Mesozoic domains. In addition, garnet being the Y-richest mineral in the samples, its fluid-assisted resorption is the most likely mean to provide Y involved in the Cenozoic domains. The origin of the fluid is not clearly defined: external fluid infiltration or fluid produced by the recrystallisation of H_2O-bearing minerals. Regardless, this fluid interaction was responsible for the partial dissolution of Mesozoic monazite grains, as well as for garnet resorption, and the precipitation of newly-formed Y-rich monazite during mid-Cenozoic times.

Low-*P*, clockwise metamorphism of the Aus granulite terrane, Namibia

JOHANN F.A. DIENER[1*] AND RICHARD W. WHITE[2]

[1]Geological Sciences, University of Cape Town, South Africa, johann.diener@uct.ac.za (* presenting author)
[2]Institute of Geoscience, University of Mainz, Germany, rwhite@uni-mainz.de

Introduction

Intermediate *P-T* metamorphism has been inferred to indicate the initiation and operation of collisional orogenesis from the Palaeoproterozoic to the present [1]. However, the Precambrian also preserves examples of anomalously hot, likely collisional, orogenies that do not occur in the Phanerozoic. These orogenies are characterised by low-*P*, high-*T* metamorphism, high apparent geotherms and clockwise or anticlockwise *P-T* paths [2], and have been suggested to form during continental back-arc inversion involving juvenile and weak crust [1].

Regional Geology

The Aus granulite terrane of southern Namibia forms part of the Namaqua metamorphic complex that has been metamorphosed and migmatised in a hot orogenic environment during the Kibaran. The terrane consists of older TTG basement gneisses, a high-grade metamorphic supracrustal sequence, and syn-tectonic garnet leucogranite gneisses formed through anatexis of the surrounding rocks. Residual metapelitic rocks preserve assemblages of g-sill-cd-bi-ksp-pl-q-ilm that equilibrated in the presence of silicate melt. Sillimanite mats occur as large, blocky prisms interpreted as pseudomorphs after prograde andalusite. Sillimanite is included in garnet and rimmed by cordierite, indicating consumption of sillimanite to form garnet and cordierite at prograde to near-peak metamorphic conditions.

Results and Conclusions

Pseudosection modelling of metapelitic and metapsammitic residuum compositions constrain peak *P-T* conditions to 825°C and 5.5 kbar. The replacement of sillimanite by garnet-cordierite suggests that the rocks experienced heating with minor decompression to peak metamorphic conditions. The retrograde path likely involved decompression-cooling, as isothermal decompression would have led to the introduction of orthopyroxene, whereas isobaric cooling would have re-introduced sillimanite, neither of which occurred in these rocks. Pseudosections for melt-reintegrated estimates of the protolith composition show that andalusite stability along the prograde path is restricted to *P* below 4 kbar at 550-600°C. This indicates that prograde metamorphism occurred along a high apparent geotherm of 40°C/km, yet the textures suggest that the rocks evolved along a clockwise path at peak *P-T*. Retrogression occurred along a similar geotherm, suggesting that exhumation was slow, and dominantly occurred through erosion, rather than tectonic processes, and that elevated crustal temperatures outlasted the duration of orogeny.

The origin of such a long-lived heat source is enigmatic, particularly as direct evidence for mantle involvement, such as contemporaneous mafic magmatism, is absent. Metamorphism could have involved initial magmatic underplating that led to widespread crustal melting and the redistribution of melt and heat producing elements to higher crustal levels, thereby maintaining an elevated geotherm during the latter stages of orogeny.

[1] Brown (2006) *Geology*, **34**, 961-964.

[2] Cagnard *et al.* (2007) *Precambrian Res.* **154**, 125-141.

https://doi.org/10.1180/S0026461X00008434 Published online by Cambridge University Press

Melt Rheology and Glass Formation

DONALD BRUCE DINGWELL [1]

[1] Earth and Environment, LMU – University of Munich, Theresienstr. 41/III, 80333 Munich, Germany, dingwell@lmu.de

Melt Rheology

The rheology of molten silicates has been the subject of a century of investigation. Current empirical models for Newtonian melt viscosity are adequate for many applications in petrological and volcanological modelling. Structure-based models have been proposed but no one has delivered yet a complete validation of any of these models.

In detail - potentially in petrologically important detail - the rheology of silicate melts contains a number of features that are not yet sufficiently well modelled. In particular, the high viscosity – high pressure regime of silicate melts will require detailed mapping before the grand conclusions of silicate melt viscosities can be developed.

Glass Formation

The departure of molten silicate from the viscous state forms the central event of explosive volcanism. The glassy products of all eruptions can shed light on the conditions of eruptions themselves. Tracking the path of glass formation in molten silicates has revealed a wide range of phenomena in the petrogenesis of these rocks and many new frontiers await exploration.

Some of the currently identifiable areas of progress in both areas will be reviewed. Some potential next steps will be presented.

Dynamics of organic carbon sedimentation and bottom oxygen and their impact on phosphorus retention in Lake Simcoe: reactive-transport modeling and experimental study.

M. DITTRICH[1*], A. CHESNYUK[1], J. MCCULLOCH[1], A. GUDIMOV[1], G. ARHONDITSIS[1], J. YOUNG[2], J. WINTER[2], AND E. STAINSBY[2]

[1]Department of Physical and Environmental Sciences, University of Toronto Scarborough, 1265 Military Trail, Toronto, Canada, M1C 1A4, mdittrich@utsc.utoronto. ca (* presenting author)
[2]Ontario Ministry of the Environment, 125 Resources Road, Toronto, Ontario, Canada M9P 3V6, joelle.young@ontario.ca, jennifer.winter@ontario.ca, eleanor.stainsby@ontario.ca

Introduction

Lake Simcoe experiences cultural eutrophication associated with point and non-point loading sources. Efforts to reduce total phosphorus (P) inputs to Lake Simcoe since the 1990s, have resulted in significant annual load reductions to the lake [1]. This lake still suffers from excessive growth of filamentous algae, macrophytes, and low hypolymnetic oxygen concentration. Despite a good understanding of the total P budget, our knowledge about the potential for bioavailable P loading from the sediments is limited. The impact of dynamic conditions at sediment–water interface, such as organic carbon flux and oxygen concentration, on phosphorus retention remains unknown. In this study, phosphorus sediment retention in three basins, that experienced distinct sedimentation dynamics, has been investigated experimentally and theoretically. Using diagenetic reaction-transport modeling and sediment core analysis, we investigated the effects that variations in the organic carbon loadings and oxygen bottom concentration, had on the availability of sediment P.

Methods and Results

We performed phosphorus sequential fractionations of sediments during summer stratification and under ice-cover. Phosphorus binding forms have been divided into four operational groups: apatite-bound-P, organic P, inorganic redox-sensitive P (iron-hydro-oxides-bounded) and loosely-bound P, that is in equilibrium with P dissolved in pore water.

The following rank was determined for the P in the sediment apatite-P > organic-P > redox-sensitive-P > loosely bound-P. It was found that the largest amount of P is bound in the sediment as apatite-P, essentially stable in respect to redox conditions. The model results are in agreement with the measured flux of total phosphate to the system and the fractionation data of phosphorus binding forms. A sensitivity analysis was undertaken to identify the most significant parameters, demonstrating that variations in sedimentation rate, and bottom water oxygen concentration, have the largest impact on P diagenesis.

[1] Hiriart-Baer et al. (2011) *Temporal trends in phosphorus and lacustrine productivity in Lake Simcoe inferred from lake sediment, Journal of Great Lake Research,* **37**, 764-771.

https://doi.org/10.1180/S0026461X00008434 Published online by Cambridge University Press

Chromium isotope fractionation during mobilization and transport in Sukinda Valley, India

L. N. DØSSING[1,*], K. DIDERIKSEN[2], S. A. CROWE[3], S. K. MONDAL[4], N. BOVET[2] AND R. FREI[1]

[1]University of Copenhagen and Nordic Center for Earth Evolution (NordCEE), Denmark, ldoessing@gmail.com (* presenting author) and robertf@geo.ku.dk

[2]University of Copenhagen, Nano-Science Center, Denmark, knud@nano.ku.dk and bovet@nano.ku.dk

[3]University of Southern Denmark and NordCEE, Denmark, sacrowe1@gmail.com

[4]Jadavpur University, India, sisir.mondal@gmail.com

Abstract

The potential of stable chromium (Cr) isotopes as a tracer for the biogeochemical Cr cycle depends on understanding the fractionation Cr isotopes experience. Here we present Cr isotope analyses of different Cr reservoirs to elucidate the Cr isotope fractionation occurring during oxidative weathering in a natural system from Sukinda Valley, India.

Pristine chromite seams show Cr isotope composition similar to mantle inventory rocks [1]. Weathered chromites, highly weathered ultramafic rocks and soils consistently display light Cr isotope composition, indicating that oxidative weathering have preferentially leached and mobilized heavier Cr isotopes. The surface waters display variable Cr isotope signature. However, total dissolved Cr concentration correlate with Cr isotope composition so that high Cr concentration waters (<2.6 mg L^{-1} Cr) show lighter Cr isotope values, possibly reflecting the presence of Cr in colloids, while low Cr concentration waters (>17 µg L^{-1} Cr) have heavier Cr isotope values, reflecting dissolved Cr(VI).

These results show that heavy Cr isotopes are preferentially leached during oxidative weathering. The overall consistency between data indicate that oxidation of Cr(III) to Cr(VI) and subsequent mobilization leads to considerable Cr isotope fractionation, enriching the waters in the heavier isotopes. Contrary, reduction of Cr(VI) during transport enriches the produced solid phases in the lighter isotopes and the remaining solution, in heavier isotopes [2]. The variability of the Cr isotopic composition of natural samples including soil, rock and water samples demonstrates that significant fractionation is associated with Cr biogeochemistry in the environment.

[1] Schoenberg et al. (2008), *Chemical Geology* **249**, 294-306.

[2] Ellis et al. (2002), *Science* **295**, 2060-2062.

Pre-eruptive volatile contents of silicate melt inclusions hosted in the Grey Porri Tuffs of Monte dei Porri Volcano, Island of Salina, Aeolian Islands, southern Italy.

A.L. DOHERTY[123*], R.J. BODNAR[2], B. DE VIVO[3], R. ESPOSITO[2] AND A. MESSINA[1]

[1]Università degli Studi di Messina, Messina, Italy, ilovevolcanoes@gmail.com (* presenting author)

[2]Virginia Tech, Blacksburg, USA, rjb@vt.edu; rosario@vt.edu

[3]Università degli Studi di Napoli (Federico II), Naples, Italy, bdevivo@uninia.it

The Aeolian Islands are an arcuate chain of submarine seamounts and volcanic islands, lying just north of Sicily in southern Italy. The eruptive products on the second largest of the islands, Salina, exhibit a wide compositional range, from basaltic lavas to rhyolitic pumice. The eruptions that produced the Grey Porri Tuffs (GPT) during the opening stages of the Monte dei Porri eruption cycle were among the most explosive in the history of the Aeolian Islands. Recent advances in microanalytical techniques permit quantification of the pre-eruptive volatile contents of magmas through analysis of silicate melt inclusions (MI). These data, in turn, provide valuable insights into magma dynamics and evolution, including the role of volatiles in controlling the style of eruption. To this end, lapilli pumice and scoria fragments were collected from the GPT and analyzed to determine the pre-eruptive volatile contents of the magmas as well as their compositional evolution.

Electron Microprobe Analysis (EMPA) of 38 naturally quenched (glassy) MI hosted in olivine, plagioclase and pyroxene define a complicated evolutionary history. Bulk-rock analyses identify the GPT host units as andesitic pumice (SiO_2 59.9 wt %) and high-silica basaltic scoria (SiO_2 53.4 wt%). MI hosted in the GPT pumice unit have basaltic compositions (SiO_2 46.2 wt%) and MI hosted in the scoria unit have basaltic andesite (SiO_2 56 wt%) compositions.

Secondary Ion Mass Spectrometric (SIMS) analysis of 23 inclusions reveals a similar bimodal distribution in volatile contents between the GPT scoria and pumice units. Olivine-hosted MI from the GPT pumice unit have higher average H_2O and S contents (4.53 wt % and 3790 ppm, respectively) compared to olivine-hosted MI from GPT scoria unit (2.7 wt % and 1772 ppm, respectively) but slightly lower F contents (659 ppm in pumice-hosted MI and 875 ppm in scoria-hosted MI). Cl contents are fairly uniform, averaging 3339 ppm in scoria-hosted MI and 3559 ppm in pumice-hosted MI. The higher H_2O contents of MI from the pumices compared to scorias is consistent with more explosive nature of eruptions that produced the pumices, compared to the less-explosive scoria eruptions.

Analysis of several spots within individual, large olivine-hosted MI shows CO_2 abundances of approximately 187-492 ppm in the GPT pumice unit and 233-576 ppm in the scoria unit. If the melt was saturated in CO_2 at the time of MI entrapment, CO_2/H_2O ratios indicate that the olivine in the pumices crystallized at approximately 6.5 km, whereas those in the scorias formed at 4.8-6.2 km.

https://doi.org/10.1180/S0026461X00008434 Published online by Cambridge University Press

Black carbon in Arctic snow and sea ice: The big picture through the details

SARAH J. DOHERTY[1*]

[1]JISAO, Univ. of Washington, Seattle, WA, USA, sarahd@atmos.washington.edu (* presenting author)

Overview

Model studies have indicated that black carbon (BC) in snow and sea ice may be producing significant warming in the Arctic and contributing to accelerated sea ice loss. All of these studies indicate that even small concentrations of BC may lead to large climate forcing because positive feedbacks, such as the snow albedo feedback, amplify the initial forcing. However, the magnitude of the forcing reported by different studies varies.

This talk will review our current state of knowledge regarding climate forcing by BC in Arctic snow and sea ice. The range of modeled estimates to date will be presented and reasons for differences between them explored. A recent Arctic-wide measurement study of snow and ice (BC) concentrations and sources will also be presented. This data set can be used to test modeled transport, deposition and in-snow concentration changes. However, the climate impact of BC in the cryosphere also depends strongly other factors such as snow cover, baseline snowpack radiative properties, cloud cover, in-snow redistribution of black carbon, and the presence of other light absorbing constituents. I will review what we know and what we still need to explore in order to understand whether black carbon is making a significant contribution to recent Arctic warming.

Benthic $\delta^{18}O$ signature of dense brine from sea ice formation in the North Atlantic

TROND M. DOKKEN[1,2*], ABDIRAHMAN OMAR[1,2], CAMILLE LI[1,2]

[1]Bjerknes Centre for Climate Research, Bergen, Norway, trond.dokken@uni.no (* presenting author)

[2]Uni Bjerknes Centre, Uni Research, Bergen, Norway

Abstract

Sea ice is thought to be an important factor for explaining abrupt North Atlantic climate changes during the last ice age. Reconstructing past variations in sea ice cover remains a challenge, in large part because of the complicated and indirect relationships between sea ice proxy indicators and actual sea ice conditions. One approach is to use the idea that the isotopic signature of dense brines produced via salt rejection during the formation of sea ice may be detected in benthic foraminifera records [1]. Brine formation is an active process in the Arctic and Antarctic shelf regions today [2], [3], [4]. In the Southern Ocean in particular, large quantities of dense brines are generated in polynyas and contribute an isotopically light $d^{18}O$ signature to Antarctic Bottom Water [5]. To date, it has been unclear whether North Atlantic and Arctic brines formed from isotopically light surface waters can become dense enough to penetrate to the depth habitats of benthic foraminifera. Storfjorden, located in the southeastern Svalbard Archipelago, is a site of active winter brine formation due to a recurrent polynya. Each winter, dense, brine-enriched waters fill the depressions of the fjord to its sill level and subsequently descend as a gravity current following the bathymetry towards the shelf break [6]. Observations from a September 2000 cruise reveal the presence of cold, salty, brine-enriched seawater sitting in the deepest channels (> 100 m depths) of Storfjorden, with isotopically light $d^{18}O$ values corresponding to the $d^{18}O$ values of the surface water in the region. These results are useful in better characterizing the signature of brine-enriched seawater and brine formation processes, and suggest a way forward for reconstructing sea ice variability from paleoclimate records.

[1] Dokken and Jansen (1999) *Nature* **401**, 458-461. [2] Warren (1981) *Evolution of Physical Oceanography. Scientific Surveys in Honor of Henry Stommel*, 6-41. [3] Fer et al. (2003) *Deep Sea Research I* **50**, 1283-1303. [4] Omar et al. (2005) *The Nordic Seas: An integrated Perspective oceanography, climatology, and modelling* **158**, 177-187. [5] Mackensen (2001)) *Deep Sea Research I* **48**, 1401-1422. [6] Skogseth et al. (2005) *The Nordic Seas: An integrated Perspective oceanography, climatology, and modelling* **158**, 73-88.

https://doi.org/10.1180/S0026461X00008434 Published online by Cambridge University Press

Fixation and remediation of trace elements associated with coal fly ash

RONA J. DONAHOE[1*], SIDHARTHA BHATTACHARYYA[1], GHANASHYAM NEUPANE[1], KENNETH E. LADWIG[2], AND DAN V. PATEL[3]

[1]University of Alabama, Geological Sciences, Tuscaloosa, AL rdonahoe@geo.ua.edu
[2]Electric Power Research Institute, Palo Alto, CA keladwig@epri.com
[3]Southern Company Services, Birmingham, AL dvpatel@southernco.com

Introduction

Fly ash is the dominant component of solid waste produced by coal combustion. Only 38% of the total fly ash generated in 2010 was used for beneficial purposes, primarily due to concerns about potential leaching of trace elements to the environment [1]. In this study, bench-scale batch and column experiments were performed to test treatment methods aimed at reducing the mobility of trace elements associated with coal fly ash.

Results and Conclusions

Chemical fixation of fly ash using a ferrous sulfate (FS) treatment was tested at various solid:liquid ratios for a range of fly ash compositions. The best results were obtained for the 1:30 FS treatment, which successfully reduced the mobility of oxyanion trace elements in all of the fly ash samples studied. Sequential chemical extractions of treated and untreated coal fly ash showed that much of the As, Cr, Mo, Se and V associated with the acidic (Class F) fly ash samples was transferred from mobile to more stable, reducible fractions. Although reduction in trace element mobility was similar for alkaline (Class C) fly ash, FS treatment was less effective in reducing the mobility of As and Se. These elements showed significant reductions in mobility during long-term leaching, suggesting that this treatment method could increase the beneficial use of fly ash.

Older, unlined disposal facilities may serve as sources of trace elements to the environment if meteoric water interacts with the fly ash, creating leachate. Surfactant-modified zeolite (SMZ) has the potential to adsorb both cationic and anionic trace elements from aqueous solutions, but has not previously been tested for remediation of trace elements in fly ash leachate. Bench-scale batch and column experiments were performed to test the ability of SMZ to remediate trace elements in fly ash leachate. Batch experiments showed SMZ affected modest decreases in the concentrations of all oxyanion trace elements in leachate generated from both Class F and Class C fly ash, but was more effective for removal of Cr. Column experiments designed to simulate the use of SMZ as a permeable reactive barrier (PRB) at a CCP disposal facility showed large reductions in leachate trace element concentrations, but indicate that the effective lifetime of a SMZ PRB in the ash disposal environment would be relatively short.

[1] Adams, Thomas H. (2011) *ACAA Press Release*, **Dec. 13, 2011,** 4 pp.

An isotopic record of mercury in San Francisco Bay

PATRICK M. DONOVAN[1]*, JOEL D. BLUM[1], DONALD YEE[2], GRETCHEN E. GEHRKE[1]

[1]Department of Earth and Environmental Sciences, University of Michigan, Ann Arbor, MI, USA (*presenting author: pmdon@umich.edu)
[2]San Francisco Estuary Institute, Richmond, CA, USA, donald@sfei.org

San Francisco (SF) Bay is an urban estuary that has been subjected to extensive pollutant inputs over the past 150 years. Potentially important sources of mercury (Hg) to SF Bay include Hg mining, placer gold mining, agriculture and industrial activity[1]. A previous study of Hg stable isotopes from intertidal surface sediment showed a geographic gradient in δ^{202}Hg from south (higher δ^{202}Hg) to north (lower δ^{202}Hg)[2]. To constrain background Hg isotopic composition and understand possible changes in Hg sources to SF Bay through time, we analyzed samples from eight dated sediment cores from SF Bay for total Hg concentration (HgT) and Hg isotopic composition. Sediment cores were collected at six open water sites (water depth: 2.3 to 7.8 m) and two wetland locations. At least three sediment intervals (pre-anthropogenic, ~1960, surface) were analyzed from each core. Sediment was also collected downstream of placer gold mines in the Yuba River, CA. HgT was measured by CV-AAS and Hg isotopic composition was determined by CV-MC-ICP-MS.

In all cores analyzed, HgT in pre-anthropogenic sediment is between 39 and 73 ng/g, which is within the range of expected background HgT[3]. In 1960-dated sediment, HgT varies from 239 to 532 ng/g in SF Bay open water cores and is significantly higher in wetland cores (3657 and 4777 ng/g). Surface sediment HgT in the eight cores range from 200 to 640 ng/g. HgT in the sediment derived from gold mine tailings is between 3180 and 6821 ng/g.

In all of the SF Bay cores, the pre-anthropogenic isotopic composition of Hg is similar: δ^{202}Hg = -1.00‰ (2SD = 0.14, n=6), Δ^{201}Hg = 0.09‰ (2SD = 0.08, n = 6) and Δ^{199}Hg = 0.18‰ (2SD = 0.07, n = 6). The 1960-dated sediment in the open water cores show a geographic trend similar to that reported by [2] for intertidal surface sediments: the southernmost location has the highest δ^{202}Hg (-0.32‰), the south-central locations have lower δ^{202}Hg (-0.40‰) while further north in San Pablo Bay δ^{202}Hg is lowest (-0.62‰). In surface sediment, δ^{202}Hg shows little geographic variation [δ^{202}Hg = -0.52‰ (2SD = 0.07, n = 6)]. In the sediment derived from gold mine tailings δ^{202}Hg = -0.57‰ (2SD = 0.21, n=2).

The results demonstrate that the isotopic composition of pre-anthropogenic Hg in SF Bay is different than Hg input from anthropogenic sources. A geographic trend in δ^{202}Hg is observed in sediment from ~1960, but δ^{202}Hg of SF Bay open water surface sediment does not vary geographically. It appears that intertidal surface sediments retain an isotopic memory of distinct Hg sources to SF Bay, whereas open water surface sediments have been homogenized, obscuring distinct signals of Hg source.

[1] Conaway *et al.* (2008) *Rev. of Environmental Contamination and Toxicology* **194,** 29-54. [2] Gehrke *et al.* (2011) *Geochimica Et Cosmochimica Acta* **75,** 691-705. [3] Conaway *et al.* (2004) *Marine Chemistry* **90,** 175-184.

https://doi.org/10.1180/S0026461X00008434 Published online by Cambridge University Press

Fluid inclusion size, depth and shape: aspects of re-equilibration

GERALD DOPPLER*, MIRIAM BAUMGARTNER AND RONALD J. BAKKER

University of Leoben, Resource Mineralogy, Austria
gerald.doppler@unileoben.ac.at (* presenting author)

Introduction

In recent decades of fluid inclusion research potential evidences of post-entrapment changes of fluid inclusions have been increasingly noticed. Several studies of re-equilibration experiments have already been published with complex multi-component fluid mixtures. This series lacks experiments with relative simple one-component fluid systems, where the result of alteration processes, such as diffusion, can be directly related to the activity of one fluid component. Specific re-equilibration experiments are currently performed by using pure H_2O and pure D_2O. The interaction of distinct fluid inclusions attributes such as the inclusion depth below the crystal surface, the inclusion size and the inclusion shape appear to be essential for post-entrapment compositional changes.

Performing re-equilibration experiments

For this study pure H_2O fluid inclusions are synthesized in Brazilian quartz crystals which are then exposed to pure D_2O during the re-equilibration process. Fluid properties of D_2O and H_2O are approximately similar, as evidenced with specific equations of state at our experimental conditions. However, diffusion coefficients through quartz will be slightly higher for H_2O than D_2O. Both, synthesis and re-equilibration are carried out under hydrothermal conditions without a pressure gradient. The initial synthesis and the subsequent re-equilibration are performed each at the same experimental conditions.

To clarify the emphases of the above mentioned fluid inclusions attributes two different series of re-equilibration experiments are performed, as examined: **1)** time-dependent series, i.e. different experimental running-times; **2)** temperature-dependent series, i.e. different formation and re-equilibration temperatures.

Results

The gradient in the chemical potential of the entraped H_2O and the external D_2O is a driving force for diffusion of these species through the quartz crystal at constant *P-T* conditions. Fluid inclusion size and depth play an important role in relative short experiments. Fluid inclusion shapes change from irregular to regular and equant in all experiments. The diffusion of H_2O and D_2O increases rapidly between 400 and 500 ˚C at 337 MPa. At a geological time scale, fluid inclusions in deep rock should re-equilibrate instantanously to new pore-fluid conditions, if the grain that contains these inclusions is completely enclosed by the pore-fluid.

High resolution reservoir age reconstructions from cold-water corals in the North-eastern Atlantic during the Holocene (~ 1700 – 4800 cal yr BP)

MELANIE DOUARIN[1(*)], MARY ELLIOT[1], DANIEL SINCLAIR[2], STEVEN G. MORETON[3], STEPHEN R. NOBLE[4], DAVID LONG[5], J. MURRAY ROBERTS[6]

[1]School of Geosciences, Edinburgh University, Edinburgh, Scotland, UK, M.A.L.Douarin@sms.ed.ac.uk (*), mary.elliot@ed.ac.uk
[2]Institute of Marine and Coastal Sciences, Rutgers University, USA
[3]NERC Radiocarbon Facility (Environment), East Kilbride, Scotland, UK, Steven.Moreton@glasgow.ac.uk
[4]NERC Isotope Geosciences Laboratory, British Geological Survey, Keyworth, England, UK, srn@nigl.nerc.ac.uk
[5]British Geological Survey, Edinburgh, Scotland, UK dal@bgs.ac.uk
[6]School of Life Sciences, Heriot-Watt University, Edinburgh, Scotland, UK J.M.Roberts@hw.ac.uk

Coupled U-series and radiocarbon dating were performed on cold-water corals (*Lophelia pertusa*) from the North-eastern Atlantic. The coral fragments come from 2 sediment cores (+56-08/929VE and +56-08/930VE with 3.61 m and 5.25 m recovery, respectively) retrieved from shallow inshore coral reefs from the Mingulay Reef Complex (~56°N, 7°W and 120-190 m water depth).

The 40 U-series dates show that coral fragments within the cores are in chronological order and span the mid-late Holocene (1700 - 4800 yr BP). The sediment cores show exceptionally high accumulation rates around 5 - 6 mm yr^{-1} which is higher than those estimated for reefs along the Norwegian shelf (2 - 3 mm yr^{-1}) and an order of magnitude greater than from the coral carbonate mounds of the European continental margin (~ 0.2 mm yr^{-1} for the Holocene).

Reservoir ages were reconstructed from 18 paired U-series and ^{14}C dates measured on the same coral fragments. This high resolution dating, about one analysis every 150 yrs, allows reconstructions of high frequency changes in ventilation and ocean circulation patterns in this region. The reservoir ages estimated range from 240 yrs to 700 yrs with a mean value around 400 years. Our results also suggest cyclic circulation changes in the North-eastern Atlantic: 3 periods, around 2800, 3300 and 3700 yr BP, are characterized by lower values 240, 260 and 290 yr, respectively. One prominent increase of reservoir age is observed at about 3250 yr BP with values reaching 700 yr. The lower reservoir ages are relatively well correlated with lower $\delta^{18}O$ values recorded by planktonic foraminifer *G. bulloides* and reduced coral reef accumulation rates within the Mingulay Reef Complex.

This study suggests that cyclic circulation changes occurred in the North-eastern Atlantic during the mid-late Holocene every 400 - 500 yrs. Further studies with records of similar resolutions would be needed to determine if these changes in reservoir ages are related to local and/or global environmental changes. This study demonstrates that cold-water corals constitute a powerful alternative to provide accurate reservoir ages with unprecedented temporal resolutions.

https://doi.org/10.1180/S0026461X00008434 Published online by Cambridge University Press

A clumped isotopes perspective on sea surface temperatures in the Eocene southern high latitudes

PETER M. DOUGLAS[1*], LINDA C. IVANY[2], ALAN G. BEU[3], CHRISTOPHER J. HOLLIS[3], ALEXANDER J. P. HOUBEN[4], APPY SLUIJS[4] AND HAGIT P. AFFEK[1]

[1]Yale University, New Haven, CT, USA, (*peter.douglas@yale.edu)
[2]Syracuse University, Syracuse, NY, USA
[3]GNS, Lower Hutt, New Zealand
[4]Utrecht University, Utrecht, The Netherlands

Recent studies of high southern latitude sea surface temperatures during the Eocene Epoch have suggested that very warm temperatures, possibly exceeding 30° C, extended to the Antarctic margin[1,2]. These results could have profound implications for understanding polar amplification of greenhouse warming. However, there are large uncertainties associated with the temperature proxies applied in these studies, due either to unconstrained seawater chemistry (in $\delta^{18}O$ or Mg/Ca) or ambiguity in selecting the appropriate TEX_{86} calibration. Clumped isotopes paleothermomtery is a thermodynamically controlled temperature proxy that does not depend on the isotopic compositions of seawater, and presents a novel opportunity to reduce uncertainties in Eocene SST estimates.

We measured clumped isotopes in Eocene bivalves from two southern high latitude localities: Seymour Island, Antarctica (~65° S paleolatitude) and the South Island of New Zealand (~55° S). Middle to late Eocene (45 to 35 Ma) paleotemperatures at Seymour Island range from 18 to 11°C. Analyses of New Zealand bivalves indicate a temperature decrease from ~26°C to ~20°C between the early and middle Eocene (49 to 40 Ma). These temperature estimates are most consistent with TEX_{86} paleotemperatures from New Zealand and the East Tasman Plateau calculated using the $TEX_{86}L$ calibration[3], supporting the use of this calibration in the Eocene southwest Pacific and possibly other high latitude regions.

Clumped isotope paleotemperatures suggest that New Zealand was approximately 7°C warmer than Seymour Island during the middle Eocene. This difference points either to a sharp meridional temperature gradient or to zonal heterogeneity in southern high latitude SSTs related to different paleocurrent systems influencing the southwest Pacific and southern Atlantic. Paleotemperatures from the East Tasman Plateau suggest that this temperature difference persisted into the late Eocene.[1]

Coupled clumped isotope and $\delta^{18}O$ measurements in bivalves also provide an estimate of the oxygen isotope composition of coastal seawater. At Seymour Island $\delta^{18}O_w$ values are generally within error of the ice free latitude-corrected value of -1.2‰[4]. However a marked decrease to values less than -3‰ around 41 Ma suggests a pronounced hydrologic change. In New Zealand, mean $\delta^{18}O_w$ estimates increase from -1.4‰ in the early Eocene to -0.8‰ in the late Eocene. This shift could suggest an increase in coastal salinity to normal marine conditions, either due to decreased continental runoff or a change in surface paleocurrents.

[1] Bijl et al., (2009) *Nature* **461,** 776-779.
[2] Hollis et al., (submitted) *Earth and Planet. Sci. Lett.*
[3] Kim et al., (2010) *Geochim. Cosmochim. Acta* **74**, 4639-4674.
[4] Zachos et al., (1994) *Paleooceanography* **9**, 353-387

Refertilisation of the Hawaiian oceanic lithospheric mantle

JASON DOULL[1*], GREGORY YAXLEY[1], MARC NORMAN[1], HUGH, O'NEILL[1], PAOLO SOSSI[1], IAN SMITH[2]

[1] Research School of Earth Sciences, Australian National University, Canberra, Australia, jason.doull@anu.edu.au, (* presenting author)
[2] School of Environment, Auckland University, Auckland, New Zealand

A suite of fresh spinel peridotite xenoliths from the Island of Kaula, Hawaii erupted ~3 Ma ago and offer the opportunity to characterise the composition of the oceanic lithosphere and its metasomatic history. Peridotite xenoliths from continental and oceanic lithosphere often indicate early partial melting in which "basaltic" components were removed from the system, followed by varying degrees of metasomatic enrichment in incompatible trace elements.

Depletion of basaltic components in the Kaula samples is well demonstrated by the whole rock major element chemistry. Whole rock MgO wt% ranges from 40.52-45.24 and has strong negative correlations with basaltic components such as Na_2O (0.10-0.33 wt%), CaO (0.69 – 2.41 wt%) and Al_2O_3 (0.78-2.46 wt%) and a positive correlation with Ni (2129-2454 ppm). In particular, the low CaO and Al_2O_3 (<2.5 wt%) indicate relatively refractory compositions, compared with fertile peridotite.

In contrast, trace elements in clinopyroxenes show strong positive correlations between HFSE such as Ti and the HREE. Samples that depart from this trend have elevated LILE contents, in particular Ba (>1 ppm *vs.* an average of 180 ppb) and Pb (>1 ppm *vs* an average of 300 ppb).

The enrichment in trace elements and the relationships between them suggest two distinct types of mantle metasomatism that are possibly related to localised refertilisation of the lithosphere by low degree partial melts of crustal components, within a broader scale metasomatic overprint linked with plume magmatism.

https://doi.org/10.1180/S0026461X00008434 Published online by Cambridge University Press

"Natural toxicant" is not an oxymoron. Earth and health scientists need to meet.

STEPHANIE L. DOUMA [1*], R.A. KLASSEN[2],

[1]Associate of Nova Tox Inc.,Population Health Risk Assessment and Management , Geochemistry, Ottawa, Canada, douma@novatox.ca; stdouma@gmail.com

[2]Retired NRCan Geological Survey of Canada, Ottawa, Canada r.klassen@sympatico.ca

Large parts of Canada may be characterized by natural enrichments in toxicants having a potential to harm health. Originating in bedrock and environmentally re-distributed in air, water, and soil, such toxicants include metals (e.g., Cr, Ni, Cd, Hg), metalloids (e.g.,As), radioactive elements (e.g., Rn, U) and organic compounds (e.g., coal, PACs). Large areas in Alberta, Ontario, New Brunswick, Nova Scotia and Newfoundland with elevated natural arsenic in lake sediments and water. Fluorite elevated in Waterloo, Ontario. Sporatically across Canada areas underlain by chromium and nickel bearing rocks enriching soils and drinking water. Arsenic and uranium in lake sediments (water) on Melville Peninsula in Inuit hunting grounds.

Far from trivial, these naturally occurring toxicants have the potential to cause morbidity (carcinogenic and non-carcinogenic disease) that exceed those that would develop from 'a pack a day' smoking habit.

Despite its potential to inform on the nature and extent of natural toxicants, and their health costs, the earth sciences remain poorly integrated with current approaches to environmental, ecological and human health protection.

All of these toxicants are naturally occurring, present in the environment at levels that will cause harm to human health and despite each toxicant being listed Health Canada's Priority Substance List 1, there is little research in their occurrence. Health officials are not aware they exist, earth scientists are unaware of the implications of their existence. It is time for earth and health scientists to meet.

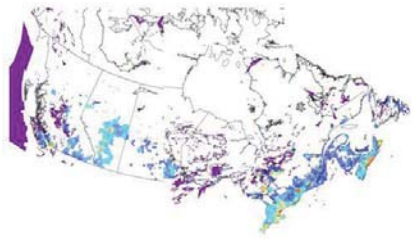

Figure #1: Risk of exposure to nickel and chronium in soil, water, food. Population (2006) of Canada living on rocks that contain chromium and nickel (mafic, ultramafic rocks) . Rocks based on Wheeler's (1997) Scale: 1:7,600,000. Blue, yellow, range polygons delineate census areas (Statistics Canada, 2006).

1. **Wheeler,G.M.,** ***1997*** *Geological Map of. Canada. Geological Survey of Canada*, Map D1860A.
2. **Statistics Canada,** 2006. *Statistics Canada Website*. Census http://www12.statcan.ca/english/census06/reference/dictionary/tables/table1-dictionary.htm Accessed November 20, 2008.

Evidence of ocean acidification viewed by boron isotopes and B/Ca in scleractinian corals

ERIC DOUVILLE[1*], CECILE GONZALEZ-ROUBAUD[1], PASCALE LOUVAT[2], JEROME GAILLARDET[2], GUY CABIOCH[3] PAOLO MONTAGNA[1], NORBERT FRANK[1], MARION GEHLEN[1]

[1] LSCE/IPSL, UMR 8212 UVSQ-CNRS-CEA, F-91198 Gif/Yvette *Eric.Douville@lsce.ipsl.fr; Cecile.Gonzalez@lsce.ipsl.fr Norbert.Frank@lsce.ipsl.fr; Marion Gehlen@lsce.ipsl.fr; Paolo.Montagna@lsce.ipsl.fr

[2] IPG-Paris, Département de Géochimie et Cosmochimie, F-75274 louvat@ipgp.fr; gaillardet@ipgp.fr

[3] IRD, Nouméa in New Caledonia and Bondy in France

The monitoring of ocean acidification (seawater pH fall due to rising anthropogenic CO_2 in the atmosphere) is mainly based on three 20-30 years long pH records: ALOHA at Hawaii in the central North Pacific, BATS at Bermuda in the west North Pacific and ESTOC at Canary Islands in the eastern North Atlantic. The current acidification rate of the surface waters deduced from these records is well established at -0.018 ± 0.001 pH-units/yr [1]. This trend is in good agreement with model projections. However the impact of ocean acidification on marine biology and ecosystems, in particular on key marine species such as foraminifera, corals, pteropods, bryozoan and molluscs still remains poorly constrained and further quantification of pH fall and its impact is needed for the high latitudes and the deep environments. While ocean acidification, since the start of the industrial era, was estimated at around -0.07 pH-units for tropical surface waters, the pH decrease since 1870 could reach values higher than 0.15 pH-units at high northern and southern latitudes.

It has been suggested that the isotopic composition of boron trapped in marine biogenic carbonates can be used to infer the pH of the ambient seawater [2]. Since the publication of this pioneering paper, a number of studies have 1) investigated the existing relationship between boron isotopic composition of carbonates (foraminifera, corals) and seawater pH in order to "calibrate" boron isotopes as pH-proxy and 2) used boron isotopes to reconstruct paleo pCO_2 over the Quaternary and further, for the whole Cenozoic. With the development of analytical techniques to measure precisely B-isotopes by MC-ICPMS, intense studies become feasible to precisely quantify ocean acidification over the industrial era using corals.

With the aim to reconstruct the major carbonate chemistry changes of the ocean, we analyzed the B-isotopic composition of long-lived sub-equatorial Pacific surface corals (*Porites* sp.) and Atlantic mid-depth dwelling cold-water corals (*Lophelia pertusa* and *Madrepora oculata*). Boron isotopes were here measured using MC-ICPMS. Our results demonstrate that boron isotopes in scleractinian corals are sensitive to small ambient seawater pH changes and can thus be reliably used to quantify past ocean acidification. The B-isotope results will be discussed together with B/Ca ratios to enlighten the crucial role of temperature in the paleo-pH reconstructions. Finally, a few examples of quantification of the anthropogenic pH fall during the twentieth century will be presented and compared to expected trends for the surface waters of the Pacific Ocean and for the intermediate waters of the North Atlantic. This research was supported by the European integrated project EPOCA and the French INSU/LEFE/CYBER project PHARE.

[1] Dore (2009) *PNAS* **106,** 12235-40.
[2] Hemming & Hanson (1992) *GCA* **56,** 537–543.

https://doi.org/10.1180/S0026461X00008434 Published online by Cambridge University Press

The influence of mineralization pathway on composition and isotope signatures in calcite

PATRICIA M. DOVE[1*], ANTHONY J. GIUFFRE[1], NIZHOU HAN[1], JAMES J. DE YOREO[2], ALEX C. GAGNON[2]

[1]Department of Geosciences, Virginia Tech, Blacksburg, USA, dove@vt.edu (* presenting author);
[2] Earth Sciences Division, LBNL, Berkeley, CA, USA.

Chemical proxy models are based upon the assumption that isotopic signatures and concentrations of minor and trace elements reflect equilibrium fractionation processes that occurred during mineralization. This picture is rooted in the fundamental assumptions of BCF crystal growth theory— a thermodynamic-based model that was derived for step growth at very near equilibrium conditions. However, the applicability of these assumptions are being called into question with the realization that many carbonate biominerals form by non-classical processes. Here, mineralization begins with accumulation of amorphous calcium carbonate (ACC) in a localized environment that subsequently transforms to the crystal/organic composites we know as skeletal structures. It is not yet known 1) if the transformation involves classical microscopic dissolution-reprecipitation or an altogether different type of process and 2) the consequences of this process for composition and isotopic signatures.

This study investigates the influence of the ACC to calcite pathway on the Mg content and isotopic signature of calcites. For low solution levels of Mg/Ca, Mg content is insufficient to inhibit step growth and ACC transforms into crystallites of Mg calcites that exhibit the expected linear fractionation with Mg/Ca of initial solutions (0-20 mol% $MgCO_3$). In contrast, when initial Mg levels are above the threshold for step growth, ACC transforms to nanoparticle aggregates of very high Mg calcite (30-50 mol% $MgCO_3$). The Mg content of calcites formed by this process is independent of solution chemistry, without evidence of fractionation. The data suggest mineralization is biased to the alternative pathway when the Mg level in the local environment is too high for significant calcite growth beyond nanoparticle sizes. This pathway is allowed because high levels of supersaturation render thermodynamic barriers to nucleation less significant than the larger kinetic barriers. Thus, the alternative pathway is a consequence of interplays between kinetic and thermodynamic factors.

Parallel experiments used enriched isotope labels (43Ca and 25Mg) to distinguish dissolution-reprecipitation from direct conversion during the ACC to calcite transformation. When solution Mg/Ca is low calcite assumes the isotopic label of the growth media consistent with a dissolution-repreciptiation pathway. In contrast, very high Mg calcites that grow from high Mg solutions retain a portion of the ACC isotope signature. This suggests the transformation of high Mg ACC occurs by an alternative pathway that involves a substantial fraction of direct transformation. Collectively our data show that mineralization pathway dramatically affects composition. This type of mechanistic understanding of mineralization processes will be necessary to explain proxy behavior and more accurately reconstruct past environental conditions.

Constraining dehydration rates during regional metamorphism, Townshend Dam, Vermont, U.S.A.

BESIM DRAGOVIC[1*], MATTHEW GATEWOOD[2], ETHAN F. BAXTER[1], HAROLD STOWELL[2], DAVID M. HIRSCH[3] AND ROSE BLOOM[3]

[1]Boston University, Deparrtment of Earth Sciences, Boston, MA, U.S.A, dragovic@bu.edu (* presenting author), efb@bu.edu
[2]University of Alabama, Department of Geological Sciences, Tuscaloosa, AL, U.S.A, matthewpgatewood@gmail.com, hstowell@geo.ua.edu
[3]Western Washington University, Department of Geology, Bellingham, WA, U.S.A., hirschd@geol.wwu.edu, bloomr3@students.wwu.edu

Progressive dehydration during regional metamorphism can result in pervasive or channelized fluid flow. Given sufficient fluxes, fluid flow may have profound effects on rheological properties of the rock, bulk rock composition, stable and radiogenic isotope compositions, mineralogy, and the kinetics of mineral reactions. Many published studies have used petrologic and stable isotopic data to constrain time-integrated syn-metamorphic fluid fluxes. Here, an integrated geochronologic and thermodynamic anaylsis is used to estimate the dehydration rate and flux during metmorphism of a pelitic schist from Townshend Dam, Vermont.

Microdrilling based on Mn growth zoning, from large (1-3 cm) garnets from one sample, provides information on the rate and duration of garnet growth. Three to six concentric zones (depending on crystal size) of garnet, were sampled for ID-TIMS Sm-Nd geochronology. A partial dissolution procedure was utilized in order to remove inclusion phases from garnet fractions which were analyzed as NdO+ with Ta_2O_5 activation. This yielded clean garnet, with $^{147}Sm/^{144}Nd \leq 3.18$. Garnet-matrix isochron ages of individual garnet zones have been previously reported [1], with the duration of garnet growth across the sample ranging from 5.5 to 11.7 Ma, and an average duration of 7.8 Ma.

Garnet growth may be linked directly to dehydration during regional metamorphism. Thermodynamic analysis of this reaction allows calculation of the stoichiometric ratio between garnet formation and water release. The garnet:water ratio depends on the growth reaction, and the P-T path during growth. In our sample, the average water:garnet molar production ratio is 3.3:1 over the duration of garnet growth. Early garnet growth involves the consumption of chlorite, resulting in initially higher water:garnet ratio. Both thermodynamic and textural analysis have determined that ~ 5.5 vol% garnet was formed during the age span stated above. This equates to a release of 1 wt% (or 2.8 vol%) water during garnet formation, similar to water volumes estimated in previous studies from southeastern Vermont [2]. Using the duration of growth (5.5 to 11.7 Ma), a time-averaged dehydration rate of 1.3 to 2.8 x 10^{-10} moles of water/ cm^3 of rock/ year can be calculated.

[1] Gatewood et al. (2011) AGU Fall Mtg., Abstract #V13G-05.
[2] Kohn, M.J. & Valley, J.W. (1994) *GCA* **58**, 5551-5566.

https://doi.org/10.1180/S0026461X00008434 Published online by Cambridge University Press

Global-scale changes in Hg cycling during glacial-interglacial transitions

PAUL DREVNICK[1*], CARL LAMBORG[2], AND GRETCHEN SWARR[2]

[1]INRS-ETE, Université du Québec, Quebec City, Canada, paul.drevnick@ete.inrs.ca (* presenting author)
[2]Woods Hole Oceanographic Institution, Woods Hole, USA, clamborg@whoi.edu

Abstract

Records of Hg in ice cores from Dome C indicate elevated Hg deposition to Antarctica during cold periods (glacials, stadials) of the Late Quaternary [1, 2]. Hypotheses to explain this phenomenon ultimately center on coincident increases in deposition of soil dust (of South American origin). Vandal et al. [1] suggested dust-driven increases in productivity of the Southern Ocean resulted in increased oceanic Hg^0 evasion, whereas Jitaru et al. [2] argued cold conditions facilitated efficient scavenging of atmospheric Hg onto dust particles. We will present data from additional geologic archives (sediments, ice) that challenge these hypotheses and, further, indicate glacial-interglacial transitions resulted in global-scale changes in Hg cycling. A 40,000-year sediment record from Lake Titicaca (Bolivia/Peru) (corrected for detrital Hg inputs) shows elevated Hg deposition during the Last Glacial Maximum – in remarkable agreement with the extent and timing of the Dome C record. However, there is not enough Hg in the atmosphere and surface ocean even today that could be redistributed to account for the absolute increase in deposition to Lake Titicaca. An additional source of Hg to the system is required, and one possibility is the massive reservoir of Hg in the solid earth. Volcanism was initially dismissed as a source of Hg to Dome C, based on an inadequate amount of non-seasalt sulfate in glacial ice to explain Hg increases [1, 2]. During the Last Glacial Maximum, however, lowered sea level could have acted to depressurize shallow volcanic and hydrothermal systems, encouraging greater activity [3]. Submarine volcanism would add Hg to the ocean, which could later be mobilized to the atmosphere, decoupling it from sulfate and other non-volatile tracers of volcanic activity. We will explore this hypothesis by constraining Hg fluxes from submarine volcanism during glacial and interglacial periods, as well as by comparing the records from Dome C/Lake Titicaca to other Late Quaternary records (reconstructions in progress for GISP-2, Cariaco Basin, Lake Baikal). This work may provide the basis for using Hg as a paleo-proxy of large-scale geophysical/climate change.

[1] Vandal et al. (1993) *Nature* **362**, 621-623. [2] Jitaru et al. (2009) *Nature Geoscience* **2**, 505-508. [3] Huybers and Langmuir (2009) *EPSL* **286**, 479-491.

Construction of a Fully Searchable Soils Database Integrating Soil Characterization Data and Whole-Soil Geochemical Data

S.G. DRIESE[1], L.C. NORDT[1], G.E. STINCHCOMB[1], K. KUIJPER[1]

[1]Department of Geology, Baylor University, One Bear Place 397354, Waco, TX 76798 USA
*Correspondance: Gary_Stinchcomb@baylor.edu

Paleopedological studies rely heavily on the use of contemporary soil characterization and whole-soil geochemical data [1, 2, 3]. These soil science resources serve the needs of paleopedologists who reconstruct ancient climate and soil systems using models to relate modern physical/chemical soil characterization data, whole-soil geochemical data, and climate parameters [3, 4, 5]. The (paleo)pedologist currently faces a "data overload" problem due to a number of global and continental-based soil geochemical databases becoming widely available. The overwhelming nature of the available data makes model construction difficult and time-consuming. The emerging field of data analytics addresses the overload problem by providing a systematic process for data acquisition, cleaning, initial analysis and main analysis. We used a data analytics approach to construct the Baylor Paleosol Informatics Cloud (BU-PIC). The BU-PIC uniquely combines: (1) USDA-NRCS pedon data, (2) PRISM-based climate parameters, (3) NLCD land-cover attributes, and (4) published paleosol data. This aggregation of data will allow paleopedologists to upload standardized geochemical data and test and refine soil-derived paleoclimate proxies and paleopedotransfer functions. Although BU-PIC development is in the initial stages of data cleaning, preliminary analysis shows promising results. For example, variations in whole-soil weight % Fe_2O_3 explain approximately 76% of the variance in % Fe_d (pedogenic iron) in all soil horizons spanning 4000 pedons, and variations in whole-soil weight % CaO explain approximately 86% of the variance in $CaCO_3$% in 865 pedons (A and B horizons only, no gypsum). This may be useful for paleopedologists interested in determining the amount of pedogenic iron and pedogenic carbonate within a lithified paleosol. Binning by specific soil orders and soil textural classes suggests that proxies can be improved by separation rather than aggregation seeking "universal" proxies. We believe the success of BU-PIC will rely on building rapport with modern soil scientists while seeking their consultation during the developmental stages. [1] Sheldon, Retallack & Tanaka (2002), *Journal of Geology* 110, 687-696. [2] Driese et al. (2005*) Journal of Sedimentary Research* 75, 339-349. [3] Nordt & Driese (2010), *Geology* 38, 407-410. [4] Nordt & Driese (2010), *American Journal of Science* 310, 37-64. [5] Nordt, Dworkin & Ashley (2011) *GSA Bulletin* 123, 1745-1762.

https://doi.org/10.1180/S0026461X00008434 Published online by Cambridge University Press

Towards reconstructing climate and ecosystem for paleoVertisols using bulk geochemistry

S.G. DRIESE[1], L.C. NORDT[1], G.E. STINCHCOMB[1], K. KUIJPER[1]

[1]Department of Geology, Baylor University, One Bear Place 397354, Waco, TX 76798 USA
*Correspondance: Steven_Driese@baylor.edu

Whole-rock molecular oxides, especially the Chemical Index of Alteration Minus Potassium (CIA-K) have been popularly used in the paleosol community for reconstructing climate, especially mean annual precipitation (MAP) [1, 2]. Initial approaches were universal, aggregating soil geochemical data from widely disparate soil types (e.g., soil orders, soil textural classes, soil ages, etc.). Because CIA-K ($Al_2O_3/(Al_2O_3+CaO+Na_2O)*100$) is fundamentally an index of clay formation and base loss related to feldspar weathering, it is inappropriate for one soil order that is especially well-represented in the rock record as paleosols, namely, the Vertisols, which are high clay-content soils (typically smectite mineralogy) that have a high shrink-swell potential, and commonly form from alluvium that has been "pre-weathered". Recent advances in developing MAP proxies specific for paleo-Vertisols, such as the new CALMAG index ($Al_2O_3/(Al_2O_3+CaO+MgO)*100$), have not only improved MAP estimates [3, 4], but have lead to understanding potential use of bulk geochemistry and modern soil characterization data to develop pedotransfer functions for reconstructions of colloidal soil properties such as pH, CEC, Base Saturation, etc. [5]. Carrying this a step further are ecosystem reconstructions of paleosols that evaluate soil conditions influencing net primary productivity using geochemical proxies [6]. Noteworthy is reconstruction of organic C and N in paleo-Vertisols using pedotransfer functions developed using ppm Pb in modern Vertisols [7]. The limits of application of bulk geochemistry to paleosols are as yet unknown, but it is clear that our approach for analyzing separate soil types has merit. We are currently developing a soil database that contains over 1500 US pedon and 6000 soil horizon records that can be queried using different soil wet-chemical and geochemical (whole-soil) parameters to predict specific conditions. Our initial attempts with circa 40 US Vertisol pedons to develop several new proxies specific to paleoVertisols provide more uniform MAP estimates than using CIA-K, as demonstrated by specific examples from Mississippian, Triassic, and K/T boundary paleosols. [1] Sheldon, Retallack & Tanaka (2002), *Journal of Geology* 110, 687-696. [2] Driese et al. (2005*) Journal of Sedimentary Research* 75, 339-349. [3] Nordt & Driese (2010), *Geology* 38, 407-410. [4] Adams, Kraus & Wing (2011) *Palaeo*[3] 309, 358-366. [5] Nordt & Driese (2010), *American Journal of Science* 310, 37-64. [6] Nordt, Dworkin & Ashley (2011) *GSA Bulletin* 123, 1745-1762. [7] Nordt et al. (2012) *Geochimica et Cosmochimica Acta* (accepted).

Wind-driven diurnal variability in freshwater surface microlayer biogeochemistry

CHRISTOPHER DRUDGE[1*] AND LESLEY WARREN[1]

[1]McMaster University, School of Geography and Earth Sciences, Hamilton, Canada, drudgecn@mcmaster.ca (* presenting author), warrenl@mcmaster.ca

Introduction

Understanding the compositional dynamics of the surface microlayer (SML) at the air-water interface of surface waters is critical because of its role in regulating the exchange of matter between the atmosphere and hydrosphere [1,2]. Temporal variability in SML biogeochemistry is poorly understood, particularly with respect to changing physico-chemical conditions. The objective of this study was to examine the geochemical and microbial composition of the SML and underlying water column (0.5 m depth) in two contrasting freshwater environments (Sunnyside Beach, Lake Ontario, a littoral hard water environment heavily impacted by anthropogenic inputs; Coldspring Lake, a pelagic environment in a small (<1 km^2) and relatively pristine soft water lake) over a diurnal timeframe during the summers of 2010 and 2011.

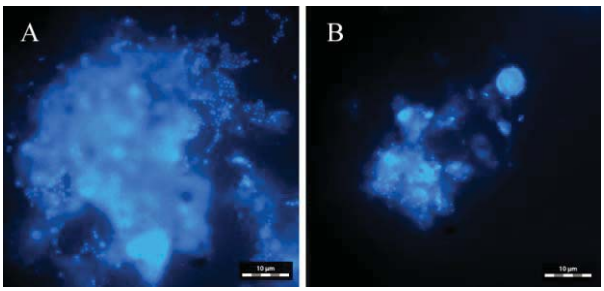

Figure 1: Fragmentation of SML microbial aggregates with increasing wind speed (from A to B, DAPI stained).

Results and Conclusion

Diurnal variability in SML biogeochemistry was closely linked to wind speed in both environments. The visual fragmentation of microbial aggregates (Fig. 1), a reduction in prokaryotic cell numbers, and an increase in dissolved organic carbon accompanied the diurnal transition from relatively quiescent to windy conditions. These changes were not observed at 0.5 m. In both environments, SML enrichment in total particulate matter and particulate iron was negatively correlated with wind speed. Particulate iron decreased in the SML and increased at 0.5m from morning to afternoon with increasing wind speed.

Collectively, these results suggest that particulate matter, including organic carbon and iron, is enriched in the SML under quiescent conditions and undergoes fragmentation over the course of a day in concert with increased wind speed. Further, wind-driven diurnal changes in SML biogeochemistry appear to be (a) conserved between contrasting freshwater environments, and (b) distinct from changes occurring at a depth of 0.5m, highlighting the unique characteristics of the SML.

[1] Cunliffe *et al.* (2011) *FEMS Microbiol. Rev.* **35**, 233-246.
[2] Hardy (1982) *Prog. Oceanogr.* **11**, 307-328.

https://doi.org/10.1180/S0026461X00008434 Published online by Cambridge University Press

Calcium isotope fractionation as a function of solution stoichiometry in groundwater

JENNIFER L. DRUHAN[1,2*], CARL I. STEEFEL[2], KENNETH H. WILLIAMS[2], LAURA C. NIELSEN[1,2], AND DONALD J. DEPAOLO[1,2]

[1]University of California Berkeley, Earth and Planetary Science, jennydruhan@berkeley.edu (* presenting author)
[2]Lawrence Berkeley National Laboratory, Earth Science Division,

While modeling predictions have suggested fluid calcium to carbonate ratio may influence the calcium isotope fractionaton factor as well as the net rate constant during calcite growth, field evidence of the macroscopic effects of solution stochiometry on precipitation rate and isotopic fractionation has been difficult to observe. Here we present some of the first evidence of solution stoichiometry influencing the fractionation in $\delta^{44}Ca$ of groundwater in a series of clogged well bores during organic carbon ammended uranium bioremediation of a contaminated aquifer in western Colorado. Secondary mineral formation induced by carbonate alkalinity generated during the bioremediation process lead to substantial permeability reduction in multiple electron-donor injection wells at the field site. These conditions resulted in removal of aqueous calcium from a backrgound concentration of 6mM to >1mM while $\delta^{44}Ca$ enrichment ranged from 1‰ to greater than 2.5‰ [Figure 1].

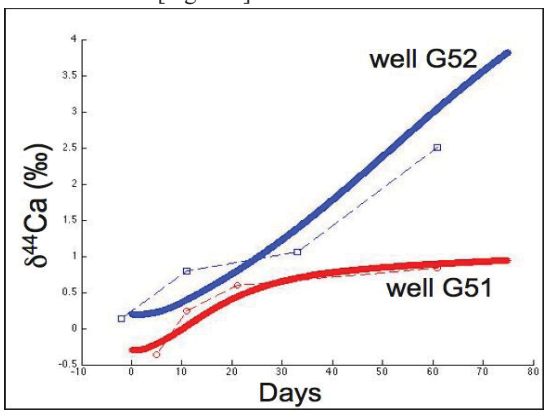

Figure 1: Data and models of $\delta^{44}Ca$ fractionation in clogged well bores as a function of time.

The variation observed in $\delta^{44}Ca$ between wells is attributed to the difference in carbonate alkalinity generated in each well bore, presenting some of the first field evidence supporting theoretical models of calcium isotope fractionation as a function of fluid Ca^{2+}:CO_3^{2-} ratio. Where the Ca^{2+}:CO_3^{2-} ratio remains >30 the $\delta^{44}Ca$ fractionation is accurately modeled by precipitating Ca-40 and Ca-44 as independent species in a TST-style model with carbonate formation calculated as a solid solution [Figure 1 red line]. However reproducing the observed $\delta^{44}Ca$ trend where Ca^{2+}:CO_3^{2-} <30 is only accomplished by utilizing a newly developed analytical model for calcium isotope fractionation as a function of solution stochiometry [Figure 1 blue line].

Constraining late Miocene seawater composition: a multiproxy approach

ANNA JOY DRURY[1*], CÉDRIC M. JOHN[1], ANNE-LISE JOURDAN[1]

[1]Department of Earth Science and Engineering, Imperial College London, London SW7 2AZ, United Kingdom.
a.j.drury10@imperial.ac.uk (* presenting author), cedric.john@imperial.ac.uk, a.jourdan@imperial.ac.uk

The late Miocene (11.61–5.33 Ma) was one of the most climatically stable periods of the past 60 Myr. However, superimposed on the stable long-term trend, short-term, 40 kyr high-amplitude changes in $\delta^{18}O$ are observed that suggest Milankovitch forcing of seawater $\delta^{18}O$ composition, temperature, or both. Understanding seawater composition evolution during this time could offer insight into the natural variation of important climate parameters, such as ice volume and sea surface temperatures.

The goal of our study is to reconstruct seawater $\delta^{18}O$ composition at different levels in the water column across the late Miocene (3.50-8.50 Ma). The study site is located in the Eastern Equatorial Pacific (Site U1338), and samples were collected during IODP Expediton 321. Understanding temporal changes in Equatorial Pacific seawater temperature and compostion is critical due to the importance of the low-latitude regions for global ocean circulation. Reconstructing $\delta^{18}O_{seawater}$ will be achieved by combining multiple geochemical proxies on benthic and planktic foraminifera. Here we present preliminary $\delta^{18}O$ and $\delta^{13}C$ data from the benthic foraminifera *Cibicidoides mundulus*. The data's long-term trends reflect global patterns, which implies the site is suitable for a high-resolution seawater composition study. Our ultimate target resolution is 3-4 kyr, which allows resolution of ~20 kyr orbital cycles. As $\delta^{18}O_{calcite}$ from benthic foraminifera is a function of both $\delta^{18}O_{seawater}$ and calcification temperature, the $\delta^{18}O_{calcite}$ will be combined with Mg/Ca and Li/Ca measurements, both temperature proxies, to reconstruct $\delta^{18}O_{seawater}$.

A second component of future work is to reconstruct temporal changes in surface water $\delta^{18}O$ and Mg/Ca by combining traditional stable isotope and trace element measurements with a novel proxy called clumped isotopes. The 'clumped isotope themometer' Δ^{47} reflects the amount of rare, heavy stable isotopes ^{13}C and ^{18}O bound together in the carbonate crystal lattice. Δ^{47} shows an inverse relationship with temperature, as more ^{13}C-^{18}O bonding occurs at lower temperature. The initial T-Δ^{47} calibration was based on inorganic calcite, however a recent study has shown that foraminiferal and coccolithophore calcite shows the same T-Δ^{47} relationship and is not affected by 'vital effects'.

We will present initial data comparing Δ^{47} measurements on the fine fraction (predominantly consisting of coccolithophores) to Mg/Ca and $\delta^{18}O$ measurements on planktic foraminifera (*Globigerinoides sacculifer*). By measuring Δ^{47} on samples consisting mainly of planktic material, we will be able to deconvolve sea surface temperature from secular changes in Mg/Ca and $\delta^{18}O$ seawater values measured in planktic foraminiferal calcite.

https://doi.org/10.1180/S0026461X00008434 Published online by Cambridge University Press

Geochemical modeling of lung fluid-mineral interactions: Highlighting fundamental knowledge gaps

GREG K. DRUSCHEL[1*], MICKEY E. GUNTER[2], AND ANNE E. TAUNTON[2]

[1] Indiana University-Purdue University Indianapolis, Indianapolis, Indiana,USA, gdrusche@iupui.edu (* presenting author)
[2] University of Idaho, Moscow, Idaho, USA, mgunter@uidaho.edu

Minerals respired into lungs are known, from a number of epidemiological studies and historical accounts, to have significant human health effects when the dose is high. These health effects often have latency periods of tens of years before symptoms manifest. Geochemists and mineralogists can contribute towards an understanding of how these diseases work in considering mineral interactions in the lung as a fluid-mineral interaction problem. We have performed a series of fluid-mineral interaction models utilizing the Geochemist's Workbench modeling platform, considering thermodynamic, kinetic, and fluid flow parameters towards the dissolution of a set of commonly encountered minerals. Employing rate laws from the literature, we calculated possible residence times of minerals in the lung and found that those times and possible mineral reactions products were sensitive to dose, particle size, lung fluid composiiton, and the flushing rates of fluid across particles in the lung [1].

These calculations bring into light some fundamental parameters that are poorly defined but are important in our ability to define how minerals behave in human lungs over decadal scales. While some reaction rates for minerals are defined in fluids of similar composition to lung fluids [2], many mineral rate laws are not well defined for these conditions. The composition of lung fluid itself is also not well defined with respect to some fundamental chemical speciation, noteably the speciation of phosphorus, and the organic speciation of many key cations for whose activity these calculations of mineral reactivity need to be defined. Additionally the physiological role of fluids flushing past minerals is largely undefinined in the human lung, and may have a significant role in the biodurability of minerals.

Within this context as well we can consider how mineral reactivity may be linked to cellular damage and the initiation of fibrotic diseases and cancers. Mineral reactivity can affect cells directly or can affect the biochemical environment cells function in through possible surface reactions that generate reactive molecules (often readicals), sorption of key biomolecules, or changes in the surrounding pysicochemical environment these cells reside in. Some of these reactions may be quite different if we consider the immediate reactivity of a mineral when it enters the lung and becomes whetted by lung fluid v. the reactivity of a mineral and potential secondary minerals forming on dissolution of that mineral over decades. We will discuss the results of our modeling study and what they have brought us to consider about the future state of mineral reactivity and lung fluid interactions.

[1] Taunton et al. (2010) American Mineralogist 95, 1624-1635. [2] Jurinski and Rimstidt (2001) American Mineralogist 86, 392-399.

Effect of fertilizing soil with Selenium on trace element uptake by kenaf (*Hibiscus cannabinus*)

GIJS DU LAING[1*], RAMA VENKATA SRIKANTH LAVU[1] AND FILIP M.G. TACK[1]

[1]Laboratory of Analytical Chemistry and Applied Ecochemistry, Ghent University, Ghent, Belgium, Gijs.DuLaing@UGent.be (* presenting author)

Fertilizing food and feed crops with Selenium (Se) fertilizers can result in an increased uptake of Se by the crops, which may be beneficial for humans and animals consuming these crops. However, assessing nutritional quality of Se-enriched crops includes not only studying uptake of Se by the crops, but also how the uptake of other trace elements is affected by fertilizing the soil with Se fertilizer. Therefore, we fertilized three types of soils with two types of Se (Selenate and Selenite, 1 mg Se kg^{-1} added to the soil) and studied the uptake of Se, Cd, Cu, Mn, Ni, Pb, Al, Fe, and Zn by kenaf (*Hibiscus cannabinus*), an indicator plant species for Se, grown on these soils. The three soils were clayey, loamy and sandy, and originally contained 0.50, 0.28 and 0.29 mg Se kg^{-1} dry mass, respectively. Afterwards, we conducted this experiment again on loamy soil using different application doses (0.5, 1, 2 and 4 mg Se kg^{-1} added to the soil).

Applying Selenate resulted in the highest increase of Se concentrations in the crop, with the highest accumulation being obtained on sandy (477 ± 77 mg kg^{-1}) and loamy (518 ± 97 mg kg^{-1}) soil, whereas Selenite performed best on a sandy (107 ± 17 mg kg^{-1}) and a clayey (122 ± 23 mg kg^{-1}) soil. Applying Selenate affects also significantly the concentrations of the other metals in crops grown on the loamy soil, but not in crops grown on the clayey and the sandy soil. When the Se application dose is varied on the loamy soil, Zn is already affected from an application dose of 0.5 mg Se kg^{-1}. The concentration of Al starts to be also affected from 1 mg Se kg^{-1}, and the concentrations of Fe, Mn and Pb also from 2 mg Se kg^{-1}. The Cu concentration is affected from a dose of 4 mg Se kg^{-1} onwards. The Al concentration clearly decreases with increasing application dose of selenite, whereas changes are less clear upon application of selenate. Zn, Pb and Fe concentrations are always reduced when applying selenite. Upon application of selenate, they are also lower than the control concentrations at the lower application doses (until 2 mg Se kg^{-1}), but they are elevated at the highest application dose (from 4 mg Se kg^{-1}). This may be related to reduced plant growth observed when selenate is used at its highest application dose. Mn concentrations are not affected when applying selenite, but they are reduced when applying selenate. Our findings illustrate that different metals respond to Se application in a different way.

Experiments with other crops and other Se fertilizers, including Se nanoparticles, that also focus on effects on Se mobility in the soil and the effects of ageing, are still ongoing. Results of these experiments will also be presented.

https://doi.org/10.1180/S0026461X00008434 Published online by Cambridge University Press

EXAFS analysis of crystal chemistry of Ni in a lateritic weathering profile from New Caledonia

G. DUBLET*[1], F. JUILLOT[1], G. MORIN[1], E. FRITSCH[1], D. FANDEUR[1], G. ONA-NGUEMA[1] AND G. BROWN JR.[2,3]

[1]Institut de Minéralogie et de Physique des Milieux Condenses (IMPMC), UMR CNRS 7590, UMR IRD 206, Université Pierre et Marie Curie, Université Paris Diderot, IPGP, 2 Place Jussieu, 75005 Paris, France, (* presenting author)
gabrielle.dublet@impmc.upmc.fr

[2]Stanford Synchrotron Radiation Laboratory, 2575 Sand Hill Road, Menlo Park, California, 94025, USA

[3]Department of Geological & Environmental Sciences, Stanford University, Stanford CA 94305-2115, USA

Weathering of ultramafic rocks under tropical conditions in New Caledonia yield lateritic profiles where metals, mainly Ni, are concentrated to economically valuable contents. The vertical distribution of Ni in these lateritic ores was investigated by analysing Ni K-edge EXAFS data along a 64 m depth lateritic weathering profile, to determine the quantitative role of the various minerals on the crystal-chemical behaviour of Ni upon weathering of ultramafic rocks. Three main units were identified from the bottom to the top of the weathering profile, i.e. the bedrock, the saprolite and the laterite. Our results show that Ni is mainly hosted by primary silicate minerals (olivine and serpentine) in the bedrock, while it is mainly incorporated in secondary phyllosilicates and Fe-oxides (goethite) in the saprolite unit, and in goethite within the upper laterite unit. A small part of Ni is also hosted by Mn-oxides at the bottom part of the laterite unit (transition laterite) which is rich in Mn-oxides. Actual modes of association of Ni with all these mineral species yield interesting information about the behaviour of this element during the lateriric differentiation. Ni content and distribution change within the phyllosilicates from the bedrock to the overlying saprolite, suggesting that several generations of these minerals have formed under different weathering conditions. Moreover, the ubiquitous occurrence of Ni-bearing goethite along the studied lateritic regolith emphasizes the major role of this mineral species on Ni speciation at the different weathering stages. This result suggests that Fe-oxides represent the ultimate host for Ni upon tropical weathering of ultramafic rocks in New Caledonia.

Trace metal complexation and dissolution by the triscatecholate siderophore protochelin

OWEN W. DUCKWORTH[1,*], JAMES M. HARRINGTON[1,2], MARTIN M. AKAFIA[1], JOHN R. BARGAR[3], ANDRZEJ A. JARZECKI[4], JAMES G. ROBERTS[5], LESLIE A. SOMBERS[5]

[1]Soil Science Department, North Carolina State University, Raleigh, NC 27695-7619, USA , owen_duckworth@ncsu.edu (* presenting author)
[2] U.S. Environmental Protection Agency, National Exposure Research Laboratory, Research Triangle Park, NC 27711
[3]Stanford Synchrotron Radiation Lightsource, 2575 Sand Hill Rd, Bldg 137, MS 69, Menlo Park, CA, 94025 USA
[4]Chemistry Department, the Brooklyn College and the Graduate School of the City University of New York, Brooklyn, NY 11210, USA
[5]Chemistry Department, North Carolina State University, Raleigh, NC 27695-8204, USA

Recent evidence has shown that siderophores, biogenic agents generally viewed as iron uptake agents, may play significant roles in the biogeochemical cycling and biological uptake of metals other than iron. For example, the triscatecholate siderophore protochelin, which is produced by the diazotrophic bacteria *Azotobacter vinelandii*, has been implicated in the uptake of non-ferrous metals [1]. To better understand the effect of catechol siderophores on metal cycling and uptake, we examined the solution chemistry of protochelin, its ability to promote the dissolution of metal oxides, and structure and stability of complexes with environmentally relevant trace metals.

Free protochelin was found to be unstable, decomposing in solution on the timescale of hours to days. Additionally, it is sparingly soluble at pH < 7.5. Electrochemical measurements of protochelin and metal-protochelin complexes revealed a ligand half-wave potential of 200 mV, but no electrochemical activity was observed for the metal centers. These results help to explain patterns in the rates and products of protochelin-promoted dissolution of metal hydroxides.

The structure and reactivity of metal-protochelin complexes was probed by spectroscopic, computational, and chemical methods. The Fe(III)Proto^{3-} complex exhibits a shift in coordination mode at circumneutral to acidic pH, as has been observed for structurally related siderophores [2]. The Mn(III)Proto^{3-} complex was found to have a stability constant approximately three orders of magnitude lower than for Fe(III)Proto^{3-}. Cobalt-protochelin complexes undergo redox cycling of Co with concommital siderophore degradation. Structural parameters derived from compuational and spectroscopic methods provide insights into the stability of the metal-protochelin complexes. These results suggest that common metals may affect the biological uptake of metals by protochelin, and that unique properties of the siderophore may affect its dissolution reactivity and the mechanisms of intracellular metal release.

[1] Kraepiel (2009) Biometals **22**, 573-581. [2] Abergel (2006) J. Am. Chem. Soc. **128**, 8920-8931.

https://doi.org/10.1180/S0026461X00008434 Published online by Cambridge University Press

Multi-scale segmentation of global continental and coastal waters: typological analysis and application to the carbon budget

HANS H. DÜRR[1*], GOULVEN G. LARUELLE[2], RONNY LAUERWALD[3], JENS HARTMANN[3], PIERRE REGNIER[2], AND CAROLINE P. SLOMP[4]

[1]Ecohydrology Research Group, Earth and Environmental Sciences, University of Waterloo, Canada, hhduerr@gmail.com (* presenting author)

[2]Biogeochemical Modelling of the Earth System, Dept. of Earth & Environmental Scences, Université Libre de Bruxelles, Belgium Goulven.Gildas.Laruelle@ulb.ac.be, pregnier@ulb.ac.be

[3] Institute for Biogeochemistry and Marine Chemistry, KlimaCampus, Universität Hamburg, Germany, geo@hattes.de, ronny.lauerwald@zmaw.de

[4]Faculty of Geosciences, Utrecht University, The Netherlands, c.p.slomp@uu.nl

Abstract

The coastline of the Earth is over 400 000 km long and about 40% of the world's population lives within 100 km of the coast. Segmentations of the global coastline and their classification into various coastal settings can be derived from a continental perspective based on an analysis of river basin properties (COSCATS) [1], from an estuarine point of view (typology of estuarine systems) [2] or from an oceanic perspective, constructed around a regionalization of the near-shore and distal continental margins (LME) [3]. Here, we present an overview of recent efforts to characterize the whole aquatic continuum using comprehensive geographical units which retain the most important physical characteristics of the land/river, near-shore, and shelf areas.

Geographic and hydrologic parameters such as the surface area, volume and fresh water residence time are calculated for each coastal unit. Next, a multi-scale typological analysis is used to classify river basins, estuaries and continental shelf seas according to climatic, lithologic, morphologic and hydrodynamic criteria of both land and sea.

We combine the different approaches with global databases (GLORICH, GlobalNEWS, SOCAT) to extend the quantification of lateral carbon and nutrient fluxes and establish regional carbon budgets. Applications relate to coastal sciences at local, regional or global scales (e.g., budget calculations, model parameterisations, scaling of local estimates) such as i) GIS-based modeling of carbon routing showing e.g., that 2/3 of the organic carbon delivered by rivers transit through estuarine filters where further processing occurs while the remaining 1/3 directly reaches continental shelf seas, ii) regionalized estimates of the contribution of estuarine systems (small deltas, tidal systems, lagoons, fjords) and continental shelf seas to atmospheric CO_2 exchanges, iii) first steps towards a regionalization of the coastal CH_4 fluxes to the atmosphere.

[1] Meybeck *et al.* (2006) *GBC* **20**. [2] Dürr *et al.* (2011) *ESCO* **34**, 441-458. [3] Liu *et al.* (2010) *IGBP Series*, 515-527.

Using garnet to record mineralization in a BIF hosted orogenic Au deposit

JASON DUFF[1*], KEIKO HATTORI[1], DAVID A. SCHNEIDER[1], ÉLISE COSSETTE[1], SIMON JACKSON[2], AND JOHN BICZOK[3]

[1]Department of Earth Sciences, University of Ottawa, (jduff018@uottawa.ca (* presenting author), khattori@uottawa.ca, david.schneider@uottawa.ca, ecoss075@uottawa.ca)

[2]Geological Survey of Canada, Ottawa Simon. Jackson@NRCan-RNCan.gc.ca

[3]Goldcorp Inc., Musselwhite Mine John.Biczok@golcorp.com

The origin of Archean banded-iron formation (BIF) hosted Au deposits are enigmatic and remain highly controversial. Although they are classified as an orogenic Au deposits, the origin of the fluids (magmatic vs. metamorphic) is still in discussion. In an attempt resolve this debate, we present major and minor element compositions of garnet determined by LA-ICP MS and EPMA, from the Musselwhite deposit in the North Caribou greenstone belt, Western Superior Province. The deposit occurs within meta-(chemical) sedimentary rocks, which are enveloped by amphibolite grade mafic to ultramafic rocks. Samples were collected from auriferous garnet -grunerite schist, footwall and hanging wall schist in the mine, as well as auriferous schist from north of Opapimiskan Lake. A sample was also collected from the non-mineralized chemical sedimentary bed that is continuous 24 km from the deposit. Major elements of garnet from mineralized rock show Mn-rich cores (18-25 % Sps component) and Mg (8-15 % Pyp component) and CaO rich rims. The latter is atypical for normal growth zoning in garnet. Mineralized samples show high Eu/Eu* values ranging from 6.34-1.26 in the ore zone in the mine to ~1 to 2.98 from north of Opapimiskan Lake. Low Eu anomalies occur in the non-mineralized sample (Eu/Eu*= 0.706-2.19). The majority of garnet grains show high HREE concentrations with a mean $(Sm/Lu)_{CN}$ value of 1.6 and low LREE (ΣHREE/ΣLREE = 41). Rims of garnet from mineralized samples show large variation in Ni/MgO from ~ 0.14 to 15.5, and Y concentrations from ~ 0.89 to 198 ppm. The high Ni and low MgO are recorded in the core of these grains from the ore zone, whereas their rims show low Ni. Trace element zonation in garnet from the non-mineralized rocks is minor compared to the auriferous samples. The data suggest that garnet growth was contemporaneous with the precipitation of pyrrhotite and chalcopyrite; both sulfides are closely associated with the introduction of Au. Gold-bearing fluid was derived from rocks during metamorphism or extensive alteration of mafic rocks as reflected by variably high Eu/Eu* values and calcic rich rims in the garnet crystals in the mineralized rocks. Results presented here indicate that garnet effectively records the history of hydrothermal activity associated with Au deposits and the data are consistent metamorphic fluid as the principle transporter of Au at Musselwhite.

https://doi.org/10.1180/S0026461X00008434 Published online by Cambridge University Press

Linear trend of mid-continent alkaline volcanism, USA: slab-edge focus

GENET I. DUKE[1*], RICHARD W. CARLSON[2], AND CAROL D. FROST[3]

1 Northeastern Illinois University, Earth Science, g-duke@neiu.edu (*presenting author)
2 Carnegie Institution of Washington, Terrestrial Magnetism, rcarlson@dtm.ciw.edu
3 University of Wyoming, Geology and Geophysics, frost@uwyo.edu

Alkaline volcanism in the mid-continent USA includes a linear zone of Cretaceous-Tertiary kimberlite-carbonatite magmatism. Magmatism along the N40°W linear trend from Louisiana to Alberta occurs at 109-85, 67-64, 55-52, and less than 50 Ma. Magmatism along the southern part of the trend occurred at 109-85 and 67-64 Ma, and magmatism in the north occurred during the last three pulses. In Arkansas, initial Sr-Nd-Hf-Pb isotopic compositions indicate that there were at least two distinct melt sources for alkaline rocks. One end member is characterized by low $^{87}Sr/^{86}Sr$ and high $^{143}Nd/^{144}Nd$ and $^{176}Hf/^{177}Hf$, similar to values of oceanic intraplate basalts interpreted as originating by melting of convecting mantle sources. The other end of the isotopic arrays extends to higher $^{87}Sr/^{86}Sr$, but most clearly lower $^{143}Nd/^{144}Nd$ and $^{176}Hf/^{177}Hf$ than seen in most intraplate oceanic basalts. In the north, there are three Sr-Nd isotopic groupings, with latest kimberlite-carbonatite volcanism having the lowest initial $^{87}Sr/^{86}Sr$ and highest initial $^{143}Nd/^{144}Nd$ ratios.

The position of the magmatic track roughly parallel to the western subduction margin of the North American plate, the lack of spatial age progressions of the magmatism that would be consistent with motion of North America over a fixed hot spot, and the presence of Sr-Nd-Hf-Pb isotopic and trace-element compositions that show a temporal evolution from lithospheric to asthenospheric melt-sources, suggest that this linear zone is the surface expression of mantle melting somehow connected to the behavior of the subduction system ~2000 km to the west. We propose that fragmentation of the Farallon and Kula plates, as imaged by tomography beneath North America, opened slab windows parallel to the trench, but well to the east of the convergent margin. These induced sheet-like mantle upwelling along their margins, resulting in small-degree decompression melting that produced highly alkaline magmas.

Tin sorption to magnetite nanoparticles under anoxic conditions

S. DULNEE[1*], D. BANERJEE[1,2], A. ROSSBERG[1,2], AND A.C. SCHEINOST[1,2]

[1]Institute of Resource Ecology, Helmholtz Zentrum Dresden Rossendorf, D-01314, Germany (*correspondance s.dulnee@hzdr.de)
[2]The Rossendorf Beamline at ESRF, F-38043 Grenoble, France

The long-lived fission product ^{126}Sn is of substantial interest in the context of nuclear waste disposal in deep underground repositories. However, the redox state (di- or tetravalent) under the expected anoxic conditions is still a matter of debate. We therefore investigated sorption and oxidation of Sn(II) in the presence of a typical corrosion product, magnetite ($Fe^{II}Fe^{III}_2O_4$), with a mean particle size of 9.4 nm. In order to simulate waste disposal conditions, the experiments were performed under strictly anoxic conditions in a glovebox at <2 ppm O_2. Macroscopic parameters (pH, Eh, [Sn], [Fe]) were monitored along with redox state and local structure of Sn (X-ray absorption spectroscopy) and Fe (XPS) as a function of time, pH, and surface loading.

Magnetite rapidly sorbed Sn(II), reducing Sn concentration within 0.5 h from 10 to 0.0084 µM. Tin was strongly sorbed by magnetite across a wide pH range from 3 to 9. Reduced sorption at pH <3 is in line with electrostatic repulsion between the positively charged surface of the magnetite nanoparticles (IEP ~6.7) and cationic Sn^{2+} or Sn^{4+} complexes. The reduced sorption at pH > 9 is in line with the transition from $Sn(OH)_2^0$ to the anionic $Sn(OH)_3^-$ which occurs at pH 9. Across the pH range 3-9 and reaction periods ≥1 h, EXAFS-derived sixfold oxygen coordination and XANES edge energy positions of ~29207 eV both indicate the presence of Sn(IV) at the magnetite surface. EXAFS shell fitting as well as Monte Carlo simulations showed formation of edge-sharing complexes of Sn(IV) with FeO_6 octahedra (Sn-Fe distance of 3.15 Å), and formation of corner-sharing complexes with FeO_4 tetrahedra (Sn-Fe distances of 3.60 Å). Even after the longest reaction periods of 1 month, we did not observe incorporation of Sn(IV) into the (compatible) magnetite structure. Also, precipitation of SnO_2 was not observed in spite of supersaturation.

In order to elucidate the reaction pathway, we also studied Fe in solution and at the surface (XPS). Starting with the PZC and increasing with $[H^+]$, the magnetite surface released Fe(II) into solution (0.11 g/L at pH 2). After addition of Sn(II), however, [Fe] in solution decreased as a function of Sn loading, in spite of the expected increase of structural Fe(II) due to the coupling to Sn(II) oxidation. This suggests a re-adsorption and possible re-precipitation of Fe(II) at the magnetite surface. Nevertheless, Fe(II) again re-dissolved as a function of time at low pH. With XPS we were not able to detect an adequate increase of the Fe(II)/Fe(III) ratio at the surface, supporting an electron redistribution between bulk and surface Fe centers.

In conclusion, our study demonstrates that Sn is strongly retained by magnetite across a wide pH range, forming stable surfaces complexes and stabilising the magnetite surface against dissolution.

https://doi.org/10.1180/S0026461X00008434 Published online by Cambridge University Press

Development of (U-Th)/He geochronology of columbite ores

István Dunkl [1*], Frank Melcher[2], Friedhelm Henjes-Kunst[2] and Hilmar von Eynatten[1]

[1]University of Göttingen, GZG-Sedimentology, Göttingen, Germany, istvan.dunkl@geo.uni-goettingen.de (* presenting author) hilmar.von.eynatten@geo.uni-goettingen.de

[2]Geozentrum Hannover, BGR, Hannover, Germany, frank.melcher@bgr.de, henjes-kunst@bgr.de

Goal

Columbite-tantalite (called also as 'coltan') belongs to the most important source minerals of high-tech elements [1]. Its genesis is mainly connected to granitic pegmatites ranging from the Archean to the Cenozoic. The major- and trace element pattern, and the formation age (typically determined by different techniques of U-Pb geochronology) [2] are used for understanding the development of the deposits, and also as diagnostic tools in provenance studies of ores. We aim to develop a double-dating procedure combining columbite U/Pb geochronology with (U-Th)/He thermochronology.

First He measurements - indications of high closure temperature

In order to avoid effects from zoning of the samples we used air-abraded multi-grain aliquots for dating. Our experiments support that the crystal lattice of columbite is tight, i.e. He is not leaking. The degassing tests were performed in an IR-laser-heated full-metal helium extraction line at the GÖochronology Laboratory. The duration and temperature needed for the complete gas release indicate that the closure temperature of columbite is higher than 250 °C. This temperature is considerably higher than the He closure temperatures of commonly used minerals like apatite (~ 60-70 °C; e.g. [3]), however, considerably lower than the closure temperature of the U-Pb geochronometer in zircon or in other oxides. Consequently, He-thermochronology of columbite can provide constraints to the post-emplacement thermal evolution and erosion history of the deposits. In consequence, the double-dating of columbite is thought to provide useful fingerprints for the provenance studies of ores.

Digestion technique

After degassing it is necessary to perform a complete dissolution of the crystals to measure precisely the U, Th and Sm by ICP-MS. In case of Ta, Nb, Fe and Mn rich solutions the precipitation and the adsorptive loss of U is a common problem. By a series of experiments on synthetic and natural columbite solutions we developed a chloride-based digestion technique that keeps the uranium and thorium quantitatively in low acid concentration solutions.

The first columbite (U-Th)/He ages

A well studied columbite specimen from Madagascar yielded a He age of 450 ± 27 Ma, which is slightly younger than its U-Pb TIMS age of 505.4 ± 1.0 Ma. In other pilot samples from African districts, the lag-times between the U-Pb formation and He cooling ages are considerably longer.

[1] Melcher (2008) *SGA News* **23**, 1-14. [2] Smith (2004) *Contrib Mineral Petrol* **147**, 549–564. [3] Farley (2002) *Rev Mineral Geochem* **47**, 819-844.

Enhanced calibration of a new natural gamma radiation technique for quantifying U, Th, and K concentrations in marine sediments

Ann G. Dunlea[1*], Robert N. Harris[2], Richard W. Murray[1], Maxim A. Vasilyev[3], Helen Evans[4], Steven D'Hondt [5] and Arthur J. Spivack [5]

[1] Boston University, Boston, MA, USA, adunlea@bu.edu*; rickm@bu.edu

[2] Oregon State University, Corvallis, OR, USA, rharris@coas.oregonstate.edu

[3] Texas A&M University, Integrated Ocean Drilling Program, College Station, TX, USA, vasilyeva@iodp.tamu.edu

[4] Lamont-Doherty Earth Observatory, Palisades, NY, USA, helen@ldeo.columbia.edu

[5] Graduate School of Oceanography, URI, Narragansett, RI, USA, dhondt@gso.uri.edu; spivack@gso.uri.edu.

Determining accurate concentrations of U, Th, and K in marine sediments and rocks is critical for a variety of oceanographic fields such as subseafloor microbiology, paleoceanography, sedimentology and mineralogy, and marine biogeochemistry. Rapid elemental characterization of marine cores will also enhance correlation with downhole geochemical logging. A newly developed natural gamma radiation (NGR) system aboard the Integrated Ocean Drilling Program's (IODP's) *JOIDES Resolution* research vessel provides improved measurement efficiency and lowered background signals to significantly increase the statistical reliability and quality of NGR data [1]. We are developing a combined analytical and modelling technique that converts these high-resolution energy spectra to concentrations with the use of core standards and U/K and Th/K ratios estimated from comparisons to Monte Carlo simulated and experimental spectra.

To further refine the Monte Carlo inversion technique it is critical to calibrate it by comparison to quantitatively measured concentrations of U, Th, and K in the core material. We present results based on the analysis of 38 marine sediment samples from four sites in the South Pacific Gyre recovered during IODP Expedition 329. We analyzed these sediments by ICP-ES and ICP-MS to provide a highly precise and accurate comparative data set. The ICP-ES (for K) and ICP-MS (for U, Th) data were themselves calibrated against international Standard Reference Materials and are both precise and accurate.

Our preliminary results indicate that the NGR technique captured the variability of K concentrations with depth, but systematically underestimated the absolute K concentrations by approximately a factor of two. U and Th NGR concentrations are also seen to deviate from the ICP concentrations, but much of the disparity may be driven by the offset in K concentrations. Since the NGR method calculates U and Th concentrations from U/K and Th/K ratios that are determined from Monte Carlo simulations and experimental data, an improper calibration of K can impact the accuracy of U and Th estimates. Continued improvements of the NGR K concentration calculation are likely to result in more accurate estimates of U and Th concentrations.

Additionally, inconsistencies between the data sets for sediments younger than ~1.5 Myr may arise because the NGR analysis infers U and Th concentrations from the radiation of their daughter products, which can have contrasting chemical behaviour (e.g. adsorptive character) between the different isotopes. We will present our strategies to address these effects, and discuss our efforts to continue development of this evolving new technique.

[1] Vasiliev et al., (2011) *J. of Applied Geophysics* **75**, 455-463.

https://doi.org/10.1180/S0026461X00008434 Published online by Cambridge University Press

Microbialite formation in two hypersaline lakes (Bahamas): Insights into organomineralization

CHRISTOPHE DUPRAZ[1*], ALEXANDRE FOWLER[1], CHRISTINA GLUNK[2], OLIVIER BRAISSANT[3], KIMBERLEY L. GALLAGHER[1], NATALIE J. STORK[1] AND PIETER T. VISSCHER[1]

[1]University of Connecticut, Marine Sciences, Storrs, USA christophe.dupraz@uconn.edu (* presenting author)
[2]University of Lausanne, Geology and Paleontology, Switzerland
[3]University of Basel, Laboratory of Biomechanics, Switzerland

The precipitation of carbonate minerals within a microbial mat (microbialite) results from complex interactions between the microbial communities and the surrounding geochemical environment. This process is referred to as 'organomineralization', and differs from 'biomineralization' (*e.g.*, shells and bones) by lacking genetic control on the mineral product. Organomineralization can be '*active*', when microbial metabolic reactions are responsible for the precipitation through actively changing the saturation index (*"biologically-induced" mineralization*) or '*passive*', when mineralization takes place within a microbial organic matrix, but is induced by environmental reactions (*e.g.*, through degassing or evaporation; *"biologically-influenced" mineralization*). Microbial metabolism can changed the carbonate mineral saturation by acting as an 'alkalinity engine' (changing the total alkalinity and/or the distribution of carbonate species within the total alkalinity) as well as the calcium availability (through Ca-binding capacity of the organic matrix).

Here two cyanobacteria-dominated microbialites that develop in hypersaline environments (Eleuthera and San Salvador Bahamas) are compared with respect to precipitation mechanism. In both lakes, the microbial metabolic activity, the characteristics and turnover of the extracellular organic matter (EOM), and the physicochemical conditions in the water column and sediments were determined to identify the driving forces in microbialite formation. Geochemical modeling indicated an oversaturation with respect to carbonates (including calcite, aragonite and dolomite) in both systems, but these minerals were never found to precipitate at the mat-water interface. This is attributed to the capacity to bind calcium by the EOM in the water column and the upper layer of the microbial mat, inhibiting crystal formation. Therefore, organomineralization within the microbial mat is the consequence of local oversaturation of the EOM binding capacity and/or EOM degradation.

Both microbialites in this study exhibit tight coupling of element cycling and display a stromatolitic lamination, but differ in some mineral features. Notably, isotopic measurements ($\partial^{13}C$ and $\partial^{18}O$) performed on the top carbonate layer (the microbially most active zone) indicate that the precipitate, although resulting from a complex interaction of metabolisms, indicate two opposite isotopic signatures (autotrophic vs. heterotrophic). However, in both systems the early diagenesis of the mineral product (through burial) suggests an increasing influence of heterotophic processes in the mineral precipitation. In the both systems studied here, the organic matrix (EOM) plays a key role in the shaping of the mineral product.

Iron oxide compositional variations in tills along ice-flow paths: Case studies from Sue-Dianne IOCG, and Thompson Ni-Cu deposits, Canada

CÉLINE DUPUIS[1*], ANNE-AURÉLIE SAPPIN[1], MARGOT POZZA[1], GEORGES BEAUDOIN[1], ISABELLE MCMARTIN[2], AND M. BETH MCCLENAGHAN[2]

[1]Université Laval, Géologie et génie géologique, celine.dupuis.1@ulaval.ca
[2] Geological Survey of Canada, Isabelle.McMartin@NRCan-RNCan.gc.ca

Sue-Dianne IOCG deposit

The composition of iron oxides contained in 8 till samples, 0.25-1 mm in size, and five bedrock samples, were selected along a cross-section from up-ice, proximal to, and down-ice from the Cu-Ag-(Au) Sue-Dianne IOCG deposit, Great Bear Magmatic Zone, Northwest Territories, Canada. Iron oxides in tills show the same, but weaker, compositional variations related to the proximity of the deposit than bedrock samples. At and immediately down-ice of the deposit, hematite is the dominant oxide and shows dominant BIF and IOCG chemical signatures in the Ca+Al+Mn vs. Ti+V discriminant diagram. Up-ice and farther down-ice of the deposit, magnetite and titano-magnetite are the dominant oxides and show dominant Kiruna and IOCG signatures (Fig. 1).

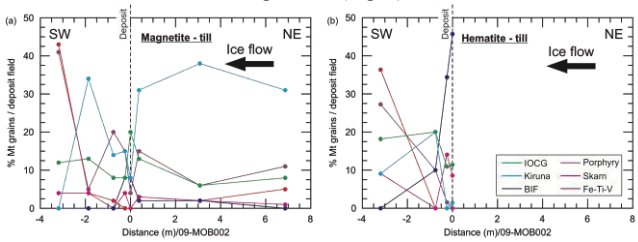

Figure 1: Magnetite and hematite proportion of grains falling in different deposit fields relative to the distance from the Sue-Dianne deposit.

Thompson Ni-Cu deposits

The 0.25-1 mm ferromagnetic fractions of 7 till samples are along a N-S profile along the first direction of ice-flow. In addition, 11 till samples were selected to document a 180 km-long cross-section from the Pikwitonei domain (East) across the Thompson Nickel Belt, Manitoba, Canada, and into the Kisseynew domain (West) along the direction of the last major ice flow movement. The proportions of magnetite having a Ni-Cu deposit signature in the Ni+Cr vs. Si+Mg discriminant diagram increase for at least 2 km to the south of the Pipe Mine along the direction of the first glacial movement, whereas the dispersion of the deposit-derived magnetite to the west is limited during the second glacial movement (Fig. 2)

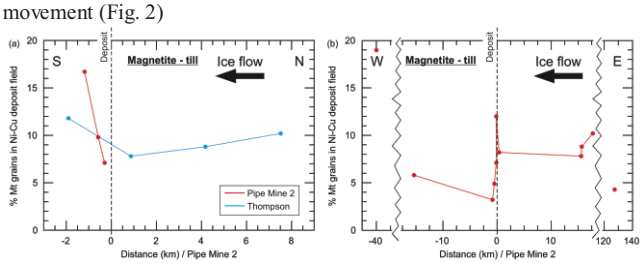

Figure 2: Magnetite proportion of grains falling in the Ni-Cu deposit field relative to the distance from Pipe Mine 2 deposit, Thompson Nickel Belt.

https://doi.org/10.1180/S0026461X00008434 Published online by Cambridge University Press

U distribution and speciation in Fe-bearing alteration minerals at the McArthur River U-deposit

JENNIFER DUROCHER[1*], MICHAEL SCHINDLER[1], MOSTAFA FAYEK[2], RONALD NG[3], KURT KYSER[3] & DAN JIRICKA[4]

[1]Laurentian University, Department of Earth Sciences
jl_durocher@laurentian.ca (* presenting author);
mschindler@laurentian.ca
[2]University of Manitoba, Geological Sciences
fayek@cc.umanitoba.ca
[3]Queens University, Geological Sciences
ng@geoladm.geol.queensu.ca; kyser@geol.queensu.ca
[4]Cameco Corporation, Exploration Division
dan_jiricka@cameco.com

The unconformity-related U-deposits of the Athabasca Basin represent an increasingly important energy resource (18% world's U-reserves) [1] and have been used as natural analogues for the deep geological disposal of radioactive waste products [2]. Since these deposits serve as large-scale natural records of U redox reactions, understanding their formation will contribute to reducing U mobility around contaminated environments. Multiple alteration and uranium mineralization events occurred throughout the basin's history [3] however the role of authigenic, diagenetic and hydrothermal alteration minerals in the reduction of uranium and subsequent precipitation of uraninite is not well understood. Graphite and various other organic compounds have been proposed as possible solid phase reductants [4] but more recent studies suggest the oxidation of Fe in alteration minerals may have played a role in the reduction of U in the Athabasca Basin [5]. In order to better understand the relationship between Fe and U, synchrotron based μXRF and μXAS experiments were conducted on altered and relatively unaltered samples from the McArthur River deposit using the VESPERS beamline at the Canadian Light Source. The distribution of Fe and U as well as other trace elements were determined by collecting μXRF element distribution maps on specific Fe-bearing alteration minerals. XANES and EXAFS spectra were measured on Fe-bearing clay and sulfide minerals, which were selected on the basis of their paragenesis, U concentrations and their proximity to the ore zone. The oxidation states of Fe and U were determined by measuring U LIII and Fe Kα absorption edges and in some cases EXAFS was used to further determine the speciation of U. Results indicate the distribution of U is closely related to that of Fe in proximity to the ore zone but become inversely related with increasing distance away from the ore zone. Variations in the shape of the Fe Kα pre-edge as well as the edge location, measured on similar phases, were attributed to changes in oxidation states. Least altered samples contained abundant reduced Fe and negligible U whereas higher uranium concentrations, and mixed Fe and U oxidation states were observed in altered samples. This study further suggests that Fe-bearing minerals played an important role in the redox processes involved in the formation of the McArthur River U deposit.

[1] Thomas *et al.* (2000) *Geol.Soc.Nevada Symp Proc.,* **1,** 103-126 [2] Burns (1999) *Rev.in Min.*, **38**, 23-90 [3] Alexandre *et al.* (2009) *Mineral. Dep.*, **44**, 41-59 & ref. therein. [4] Kyser *et al.* (1989) *Can.Jour.Earth Sci.,* **26**, 490-498 [5] Alexandre *et al.* (2004) *Tectonics,* **23(5)**

Proton and metal adsorption onto oxidized graphene

THOMAS DUSTER[1*], CHONGZHENG NA[1], HAITAO WANG[1], AND JEREMY FEIN[1]

[1]Department of Civil Engineering and Geological Sciences, University of Notre Dame, Notre Dame, IN, USA, tduster@nd.edu (* presenting author)

Oxidized graphene is produced from the chemical or mechanical exfoliation of oxidized graphite, and the resulting particles exhibit distinct physical, electrical, and thermal properties ideal for use in advanced materials, sensors, and transistors. The increasing utility of these materials suggests a strong likelihood for current and future environmental releases, and it will be important to understand the interactions between these particles and other environmental constituents. For example, due to a relatively high surface area to mass ratio and the presence of a variety of proton-active function groups, oxidized graphene may significantly influence the partitioning of metals via adsorption in environments where they exist. However, the surface chemistry and reactivity of oxidized graphene are poorly characterized. In order to construct quantitative surface complexation models of the effects of oxidized graphene adsorption on the distribution of metals in geologic systems, stability constants for the important oxidized graphene surface complexes must be determined. Hence, the objective of this study was to evaluate the capacity of oxidized graphene to adsorb protons and metals via potentiometric titrations and batch adsorption studies, respectively. Target metals included Cd, Pb, Ca, and U, and all adsorption studies were conducted over a wide pH range of approximately 2 to 10 in 0.1 M $NaClO_4$ solutions to buffer ionic strength. The potentiometric titration data indicate that oxidized graphene exhibits proton adsorption over a wide range of pH, and the data constrain the pKa values and site concentrations of the binding sites on the oxidized graphene surface. The batch metal adsorption measurements indicated extensive and strong adsorption of metals by oxidized graphene particles, with increasing adsorption with increasing pH. The pH dependence is consistent with measurements of electrochemical surface properties that indicate a more negative ζ-potential at higher pH values. Using the proton-active site concentrations determined from the potentiometric titrations, the metal adsorption data enable us to determine the thermodynamic stability constants for each of the important surface complexes. Through comparison of these stability constants to those for other environmental surfaces, we consider the propensity of oxidized graphene to influence the distribution of metals in natural and engineered systems.

https://doi.org/10.1180/S0026461X00008434 Published online by Cambridge University Press

Modeling Nd oceanic cycle in present and past climate, with a focus on the closure of the Panama isthmus during the Miocene.

DUTAY JEAN-CLAUDE [(1)*] , P SEPULCHRE[(1)], T ARSOUZE[(1)] , C JARAMILLO[(2)]

AUTHOR1 A. NAME[1*], AUTHOR 2 NAME[2], AUTHOR3 B. NAME[2], AUTHOR4 NAME[2] AND AUTHOR5 C. NAME[3]

[1]OrLSCE, Gif Sur Yvette, Jean-Claude.dutay@lsce.ipsl.fr[2]Organization2, City, Country, email@association.net

[3]STRI, PANAMA, JaramilloC@si.edu

The international GEOTRACES program has been organized to study the oceanic processes that control the oceanic distribution of trace elements in the ocean. Nd isotopes measurements represent a promising tracer to study past and present ocean circulation. However the processes that control the distribution of this tracer in the ocean are still not perfectly understood. Modeling represents a unique tool to improve our understanding on this trace element in the ocean. We will present some modeling studies where we have explicitly implemented this tracer in the General circulation model NEMO. The modeling studies has allowed us to progress in our understanding of Nd cycle in the ocean and to investigate the fluxes that dominate the Nd Input in the ocean, and to apprehend the relevant processes that control the internal oceanic cycle. We then show some results from past climate, focusing on the closure of the Panama Isthmus and its impact on the climate and the oceanic circulation during the Miocene.

Using Bulk Paleosol Organic Matter to Reconstruct Atmospheric $\delta^{13}C_{CO2}$

S.I. DWORKIN[1], L.C. NORDT[1], S.ATCHLEY[1]

[1]Department of Geology, Baylor University, One Bear Place 97354, Waco, TX 76798 USA

*Correspondance: Steve_Dworkin@Baylor.edu

The carbon isotopic composition of dispersed organic matter in paleosols has the potential to provide two of the input parameters into Cerling's [1] atmospheric pCO_2 paleobarometer equation. These variables are the $\delta^{13}C_{CO2}$ of the atmosphere and the $\delta^{13}C$ of soil respired CO_2. The isotopic composition of marine carbonates has often been used as a proxy for the composition of the atmosphere however, tenuous correlations between marine and terrestrial rocks limits the resolution of resulting atmospheric pCO_2 reconstructions. Additionally, bulk paleosols provide a terrestrial continuum of values for the paleosol barometer as opposed to the sporadic occurrence of coals or charcoal. Therefore, this study investigates the use of dispersed organic matter in paleosols as a record of atmospheric $\delta^{13}CO_2$.

Modern soils have not provided much insight into the likelihood that an atmospheric signal will be preserved in paleosol organic matter. Soil organic matter (SOM) in modern soils typically displays an increase in $\delta^{13}C$ with depth casting doubt on its isotopic reliabily in the rock record. The multitude of conflicting theories that have been proposed to explain modern depth trends in $\delta^{13}C$ of SOM [2] may indicate that the modern is not an appropriate analogue for ancient soils. We therefore turn to the rock record for evidence of a preserved atmospheric signal in bulk paleosol organic matter. Only pre-Miocene paleosols are considered in this study to avoid the confounding presence of C_4 plant material which would add an additonal pool of organic matter with its own distinct atmospheric signal. Additionally, none of the studied paleosols exhibit macroscopic evidence of extreme drought conditions, an environmental stress that significantly alters the atmospheric carbon isotope signal preserved in fossil plants.

The successions of stacked paleosols that we have studied (Late Cretaceous/EarlyTertiary in west Texas and Late Triassic in eastern Arizona) have the following characteristics: 1.) Low organic carbon contents (<0.05 wt. %), 2.) No correlation between organic matter abundance and carbon isotopic composition 3.) Carbon isotopic compositions that are similar to modern C_3 plants, 4.) No consistent relationship beween soil depth and $\delta^{13}C$ of SOM, 5.) Presence of temporal trends in the $\delta^{13}C$ of SOM that can be correlated to $\delta^{13}C$ trends in coeval marine carbonates, and 6.) Carbon isotopic compositions that are similar to terrestrial organic matter of the same age from different geographic locations.

Based on these observations, it appears that dispersed organic matter in bulk paleosol samples has the potential to preserve a carbon isotope ratio that reflects the composition of the ancient atmosphere and may be used for quantitative atmospheric reconstructions.

[1] Cerling T.E. (1991) *Science* **291**, 377-400. [2] Ehlringer J.R., Buchmann R.N., Flannagan L.B. (2000) *Ecological Applications* **10**, 412-422.

https://doi.org/10.1180/S0026461X00008434 Published online by Cambridge University Press

Constraining tropical climate sensitivity: the need for improved Mg/Ca calibrations

KELSEY A. DYEZ[1]*, A. CHRISTINA RAVELO[2]

[1]Earth and Planetary Sciences Dept., UC Santa Cruz, Santa Cruz, CA, USA, kelseydyez@gmail.com

[2]Ocean Sciences, UC Santa Cruz, Santa Cruz, CA, USA, acr@ucsc.edu

Abstract

One way to estimate how Earth's average surface temperature will increase with rising greenhouse gas concentrations (Earth system climate sensitivity) is to compare contemporaneous temperature and greenhouse gas concentration data from paleoclimate records. Since numerical models indicate that the tropical climate sensitivity is lower and more tightly constrained than global or high-latitude climate sensitivity, measurements of tropical climate sensitivity can be considered as a lower bound for global climate sensitivity estimates. Here we measure Mg/Ca of surface foraminifera *G. ruber* from ODP Site 871 from the past 800 kyr in the western Pacific warm pool to estimate tropical Pacific equilibrium climate sensitivity to a doubling of greenhouse gas concentrations to be ~4ºC. This tropical SST sensitivity to greenhouse gas forcing is ~1-2 Cº higher than that predicted by climate models of past glacial periods or future warming for the tropical Pacific.

Further, this record of past sea-surface temperature (SST) makes use of the relationship between the Mg/Ca ratio of surface foraminifera and mean annual temperature to estimate past SST. Since high-Mg calcite in modern core-top material preferentially dissolves at water depths as shallow as 1.6 km, well above the lysocline, a correction for such dissolution is necessary. Here we present a new type of dissolution correction for Mg/Ca-based paleotemperature estimation based on a regional core-top calibration from the tropical Pacific [data from 1]. We correct the Mg/Ca data for the loss due to dissolution and then apply the corrected value to the accepted Anand equation [2], since dissolution directly affects the Mg/Ca content of the tests. When applied to existing SST records the new correction decreases the observed glacial-interglacial range of SST. Such a depth-based dissolution equation is especially important for estimating the sensitivity of surface temperatures to changes in radiative forcing, such as atmospheric greenhouse gas concentrations. We recommend such a dissolution correction for all Mg/Ca-based temperature records from open ocean, low productivity sites.

[1] Dekens (2002) *G3*, **3**. [2] Anand (2003) *Paleoceanography*, **18**.

New U-series isotope data from the Andean backarc indicate shallow melting in the Payún Matrú complex

CHARLOTTE T. DYHR[1*], PAUL M. HOLM[1] AND THOMAS F. KOKFELT[2]

[1]Department of Geography and Geology, University of Copenhagen, Øster Voldgade 10, 1350 Copenhagen K, Denmark ctd@geo.ku.dk (*presenting author) paulmh@geo.ku.dk

[2]The National Geological Survey of Denmark and Greenland, Øster Voldgade 10, 1350 Copenhagen K, Denmark tfk@geus.dk

Essential differences between magmas in subduction zones and magmas in intraplate or MORB type settings have become apparent with an increasing number of ^{238}U-^{230}Th disequilibria data on recent volcanic rocks. Mid-ocean ridge and ocean island magmas are characterized by enrichment of thorium relative to uranium, whereas magmas related to subduction zones have been shown to vary from ^{230}Th-excess to ^{238}U-excess. In fact, radioactive equilibrium of ^{238}U and ^{230}Th (activity ratios = 1) seems to be a typical feature of many arc magmas, particular in continental arcs. We investigate three volcanic centers located in the main Andean arc and into the backarc system in order to constrain the influence induced by fluids in subduction zones.

The new U-series disequilibria analyses from the Andean backarc system support the OIB-character of the Payún Matru volcano, and the more fluid influenced arc-like character of the Infernillo volcano. Results from Maipo show radioactive equilibrium. For all samples the ($^{234}U/^{238}U$) ratios are within 1% of secular equilibrium, supporting evidence for the samples being unaffected by significant alteration.

The Infernillo samples plot beneath the equiline with 5-10% excess of ^{238}U. This feature is characteristic of those arcs deviating from equilibrium and is best ascribed a slab-derived fluid enrichment of the mantle source beneath Infernillo. The excess of ^{238}U also requires that the fluid addition occurred within the last 300 ka. In contrast data from the Payún Matru volcano show 5% excess of ^{230}Th, and plot within the ocean island basalt field as defined by literature data. In the case of OIB, partial melting is the main process fractionating Th/U and thus producing the $^{230}Th/^{238}U$ disequilibria. Analyzed samples are of Holocene age and the relatively low disequilibrium could indicate that melting induced fractionation between U and Th was limited due to shallow melting above the garnet stability field. This is supported by evidence from trace elements (e.g. low Dy/Yb).

https://doi.org/10.1180/S0026461X00008434 Published online by Cambridge University Press

Determination of soil organic C species using soft X-ray XANES: normalization & matrix effects

JAMES J. DYNES[1*], TOM REGIER[1], DAVID CHEVRIER[1], ADAM W. GILLESPIE[2], AND DEREK PEAK[3]

[1]Canadian Light Source, Saskatoon, Canada, james.dynes@lightsource.ca (* presenting author) tom.regier@lightsource.ca david.chevrier@lightsource.ca
[2]Agriculture & Agri-Food Canada, Ottawa, Canada adam.gillespie@agr.gc.ca
[3]University of Saskatchewan, Dept. of Soil Science, Saskatoon, Canada derek.peak@usask.ca

Soil organic matter (SOM) storage and turnover are affected by the chemical nature and properties of its constituents, particularly the chemical forms of organic C. Synchrotron-based soft X-ray absorption near edge spectroscopy (XANES), probing the atomic and molecular structures of materials, is being used to provide information on the types of C functional groups (e.g., C=O, C-OH, R-COOH) in SOM [1]. This type of information is required to fully understand the global C cycle.

Normalization of C K-edge TEY and TFY data has always been a challenge due to the C contamination in soft X-ray beamlines, imparting features into the incident x-ray flux (i.e., Io). The mineral fraction of the soil also contributes to the TEY and TFY signal, in ways not fully understood. Hence, there is concerns that artefacts such as erroneous peaks and/or spectral distortions may be introduced into the C K-edge total electron yield (TEY) and total fluorescent yield (TFY) spectra during the normalization of the raw data and/or into the raw data from the matrix itself (e.g., adsorption saturation), particularly at low soil C content. Both of these could result in incorrect conclusions being reached. To date, no fundamental studies have been conducted that address normalization issues and matric effects in known systems as a function of organic C content, organic functionality and in different matrices.

At the SGM beamline, at the Canadian Light Source, we are studying model systems consisting of varying amounts (50 to <1% (w/w)) of an organic compound with different function groups (e.g., citric acid, phthalic acid, glucose, tannic acid) mixed with a soil constituent (e.g., Al hydroxide, kaolinite, montmorillonite, Fe hydroxide). The organic-matrix mixtures are deposited onto various substrates (e.g., Au coated Si wafers) and TEY and TFY spectra are collected under a variety of conditions such as in the presence and absence of a Ti filter and/or reducing radiation dose rates (C is susceptible to radiation damage at high radiation doze rates and/or in the presence of certain elements such as Cu [2]) by conducting fast scans (20sec) versus normal scans (1500sec). Determination of the appropriate Io using different detection methods such a photodiodes and the collection of TEY and TFY of a variety of substrates such as Au coated Si wafers and C-free matrixes are being explored to normalize the data. From this fundamental approach it is expected that a protocol will be developed that reduces the possibly that artefacts are introduced during the normalization process and/or during the collection of the raw data due to matric effects. Also, the study will provide insight into factors that affect the C detection limit of the soft X-ray. Moreover, this project is part of an initiative to make the SGM beamline a center for Soil Science studies.

[1] Gillespie (2011) Soil Biol. Biochem. **43**, 766-777.
[2] Yang (2011) Anal. Chem. **83**, 7856-7862.

Surface Complexation Models and their Practical Application

DAVID DZOMBAK[1]

[1]Carnegie Mellon University, Dept of Civil and Environmental Engineering, Pittsburgh, PA 15213, USA. dzombak@cmu.edu

Abstract

While surface complexation theory and models for the description of inorganic ion sorption on mineral surfaces have advanced continuously since the introduction and initial development of these models in the 1970s and 1980s (reviewed in [1]), so too has the practical application of the models. Deployment of surface complexation models to interpret and predict water-mineral partitioning of ions in geochemistry and engineering applications is challenging because of the complexity of these systems, the limitations of the models, the lack of surface complexation databases for all of the minerals of interest, and other factors. The substantial progress in application of surface spectroscopy methods and molecular modeling to increase understanding of the properties of mineral surfaces and the nature of their reactions with ions has been of limited usefulness in constraining surface complexation models [2,3] and has done little to advance their practical application. Of necessity, there is still widespread use of empirical isotherms and distribution coefficients (K_d) to describe and simulate ion sorption processes in field systems. However, surface complexation models have been applied in a variety of contexts to gain insight into the role of sorption reactions in governing the fate and transport of particular ions, and in governing overall system chemistry.

This talk will provide an overview of the development of surface complexation models, and the history of their practical application. Examples from modeling of ion transport in geochemical systems and from contaminant treatment and remediation will be described. The strengths and limitations of the models for practical applications will be examined. Some thoughts about developments needed to advance the practical application of surface complexation models will be offered. The divergence yet complementarity of surface complexation research focused on advancement of basic scientific understanding of mineral-water surface phenomena, and research motivated by practical applications will be discussed.

[1] Dzombak and Morel (1990). *Surface Complexation Modeling: Hydrous Ferric Oxide*, Wiley, New York.
[2] Lutzenkirchen (2006). *Surface Complexation Modeling*, Academic Press, Amsterdam (especially pp v-x).
[3] Karamalidis and Dzombak (2010) *Surface Complexation Modeling: Gibbsite*, Wiley, New York.

https://doi.org/10.1180/S0026461X00008434 Published online by Cambridge University Press

Primordial Delivery of Potassium to Mercury and Enstatite Chondrites

DENTON S. EBEL[1,2,3*], CONEL M. O'D. ALEXANDER[4], AND RICHARD O. SACK[3]

[1]American Museum of Natural History, New York, NY USA, debel@amnh.org (* presenting author)
[2]Columbia University, New York, USA
[3]OFM Research, Redmond, WA, USA. rosack@ofm-research.org
[4]Carnegie Institution of Washington, Washington, DC, USA alexander@dtm.ciw.edu

In orbit around Mercury, gamma and x-ray spectrometers on the MESSENGER spacecraft return data indicating terrestrial K/Th [1] and high S/Si ratios [2] in the Mercurian mantle. Sulfur behaves as a refractory element in a vapor of solar composition that is enriched in a dust of anhydrous chondritic interplanetary dust particle (C-IDP) composition [3]. This scenario allows for accretion of Mercury from primordial disk solids in equilibrium with vapor at high temperatures, and suggests a similar origin for the highly reduced enstatite chondrites. Potassium, however, should be strongly depleted in such a scenario. But current equilibrium condensation calculations [3] do not include the refractory phase djerfisherite, ~$K_6(Fe,Ni,Cu)_{25}S_{26}Cl$, an important carrier of K in EH enstatite chondrites [4].

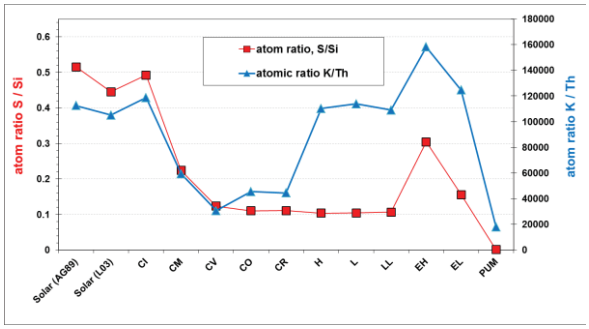

Figure 1: K/Th and S/Si ratios in solar compositions [5,6], carbonaceous chondrites (CI, CM, CV, CO [7] CR [8]), ordinary chondrites (H, L, LL [7]), enstatite chondrites (EH, EL [7]), and primitive upper mantle (PUM [9]).

It was shown by [3] that CaS, FeS and MgS are stable solids above 1100 K in vapor enriched above ~700x (atoms) in C-IDP dust. Little is known of the thermodynamic properties of djerfisherite. To first order, the free energy of djerfisherite may not differ substantially from that of FeS. If so, the abundance of K in both enstatite chondrites and Mercury may be consistent with their accretion from solides formed in equilibrium with highly reduced, C-IDP dust-enriched vapor at high temperature.

[1] Peplowski et al. (2011) *Science* 333, 1850-1852. [2] Nittler et al. (2011) *Science* 333, 1847, 1850. [3] Ebel & Alexander (2011) *Planet. Space Sci.* 59, 1888-1894. [4] El Goresy et al. (1988) *Proc. NIPR Symp. ANtarct. Meteorites* 1, 65-101. [5]Anders & Grevesse (1980) *Geochim. Cosmochim. Acta* 53, 197-214. [6] Lodders (2003) Ap. J. 591, 1220-1247. [7] Wasson & Kellemeyn (1988) Phil. Trans. R. Soc. A 325, 535-544. [8] Lodders & Fegley (1998) Planetary Scientist's Companion. [9] McDonough & Sun (1995) Chem. Geol. 120, 223-253.

Metal fractionation in the water column of a former U open pit mine

FRIDA EDBERG[1*], TERESIA WÄLLSTEDT[2], HANS BORG[1] AND SARA. J. M. HOLMSTRÖM[2]

[1]ITM, Stockholm University, SE-106 91, Stockholm, Sweden
Frida.edberg@itm.su.se (* presenting author)
[2]IGV, Stockholm University, SE-106 91, Stockholm, Sweden

Objectives, background and methods

Lake Tranebärssjön, a former open pit mine in Ranstad in Sweden has an interesting geochemistry; slightly alkaline, groundwater fed, stratified with high sulphate and metal concentrations and with an anoxic hypolimnion. The aim of this study was to investigate the partitioning of metals in the water column by (i) different size fractions: 0.45 µm filters, and ultrafiltration (10 kDa, 3 kDa and 1 kDa) and (ii) compare the analytical results with chemical equilibrium modeling calculations using Visual MINTEQ including Stockholm Humic Model (SHM). The hypothesis was that a more thorough examination of the distribution of metals in the water column would reveal that the size fractions of metals differs strongly between water layers with deviating geochemical conditions. The findings of the study could be relevant for restoration and remediation of mining sites.

Results and conclusions

The chemical analyses showed a stratified lake with an anoxic hypolimnion and high total concentrations of metals including Fe, Ca, Mn and U as well as sulfate and carbonate anions. The extremely high Fe concentration increased with depth and was dominated by particulate and colloidal fractions (>1 kDa) in the epilimnion, whereas in the hypolimnion the dissolved fraction (<1 kDa) held the major part. This was confirmed by analysis of Fe(II) which showed that in the epilimnion Fe(II) constituted less than 1% of the total Fe in contrast to the hypolimnion where Fe(II) made up 95% of the total Fe. For Mn, U, Ca, Co, As and Mo, the dominating fraction in both the epilimnion and the hypolimnion was the dissolved fraction. This is supported by the equilibrium model that suggests soluble inorganic complexes as the dominant species, with the exception of As where the model suggests that the major part is adsorbed to ferrihydrite and U in the hypolimnion for which the model suggests oversaturation with respect to uraninite. For U this partly agrees with the fractionation results as the particulate and colloidal fractions (>1 kDa) where about 30% in the hypolimnion.

Our study shows that the results of the size fractionations agreed well with the models using chemical equilibrium calculations for the water in Lake Tranebärssjön. However there are limitations in the models in the speciation of, e.g. U and of As in waters with high concentrations of Ca and carbonate, which need further investigation. High metal concentrations are still an environmental problem in Lake Tranebärssjön. The fractionation study indicates that a major part of many metals exist in the dissolved form in the anoxic hypolimnion and/or the epilimnion, and can thus be transported to downstream waters during lake turnover.

https://doi.org/10.1180/S0026461X00008434 Published online by Cambridge University Press

Highly Swellable Glass Composite Materials For *In Situ* Groundwater Remediation and Organic Vapor Permeable Proppants

PAUL L. EDMISTON[1,2*], DEANNA C. PICKETT[2], JEAN QUENNEVILLE[1]

[1]College of Wooster, Ohio, USA pedmiston@wooster.edu (* presenting author)

[2]ABSMaterials, Wooster, Ohio, USA, d.pickett@absmaterials.com

Abstract

Osorb is an organosilica material that swells in contact with organic compounds, but is impermeable to water. Swelling is substantial leading to absorption of up to 8 times the dry mass of the initial material with concomitant generation of mechanical forces in excess of 500 N/g [1]. The unique properties lead to a wide variety of sub-surface applications. Iron-Osorb® is a solid composite material of swellable organosilica with embedded nanoscale zero-valent iron that was formulated to extract and dechlorinate solvents in groundwater. The unique feature of the highly porous organosilica is strong affinity for chlorinated solvents, such as trichloroethylene (TCE), while being impervious to dissolved solids. The swellable matrix is able to release ethane after dechlorination and return to the initial state. Iron-Osorb was determined to be effective in reducing TCE concentrations in bench-scale experiments. A series of three pilot scale tests for *in situ* remediation of TCE in conjunction was completd in conjunction with the Ohio Environmental Protection Agency at a site in central Ohio [2]. In addition, Osorb has wide ranging uses in the oil and gas industry. The material has been evaluated for use as an proppant additive for selective and enhanced flow rates of hydrocarbons in wet environments, water management, and down-hole tooling.

[1] Burkett, C. M.; Underwood, L. A., Volzer, R. S.; Baughman, J. A.; Edmiston, P. L. (2008) *Chemistry of Materials* **20**, 1312-1321.
[2] Edmiston, P.L.; Osborne, C.; Reinbold, K.P.; Pickett, D.C.; Underwood, L.A. *Remediation Journal*, **22**, 105-121.

From tectonic gateways to diatoms: the build-up to Antarctic glaciation

KATHERINE E. EGAN[1*], ROSALIND E.M. RICKABY[1], KATHARINE R. HENDRY[2], ALEX N. HALLIDAY[1]

[1]University of Oxford, Oxford, UK, katherine.egan@exeter.ox.ac.uk (* presenting author)

[2] School of Earth and Ocean Sciences, Cardiff University, Cardiff, UK, (HendryKR@cardiff.ac.uk)

The Eocene-Oligocene boundary witnessed an end to the Earth's greenhouse climate and the abrupt initiation of modern icehouse conditions. Understanding the mechanisms which drove this fundamental shift is essential to a better comprehension of rapid climate response to gradual forcing. It has been suggested that enhanced marine organic carbon export and burial contributed to a drawdown of atmospheric CO_2 which triggered Antarctic Glaciation. We investigate this theory using the novel combination of sponge $\delta^{30}Si$ (a proxy for deep water silicic acid concentration, results from this study and [1]) and diatom $\delta^{30}Si$ (indicating diatom nutrient utilisation) at ODP sites 689 (sponge) and 1090 (diatom) in the Southern Ocean.

Our records, spanning 38-31Ma, document a dramatic increase in Southern Ocean intermediate/deepwater silicic acid concentration between ~35.5Ma and 34.5Ma. A build up of diatom production and global carbon export from 35.5Ma to the Eocene-Oligocene boundary is also implied. We hypothesise that prior to 35.5Ma ocean circulation was sluggish and driven by sinking at high southern latitudes. This drew down surface waters advected from the equatorial regions, bathing the seafloor in a low nutrient (and silicic acid) water mass, in a similar fashion to modern North Atlantic Deepwater. With ongoing subsidence of the Drake Passage and Tasman Gateway, a proto-Antarctic Circumpolar Current became established. From around 35.5Ma, this wind driven current increased the rate of ocean overturning and nutrient re-supply to surface waters, stimulating diatom productivity and increasing global organic carbon export. Thus, the gradual deepening of tectonic gateways prior to the establishment of permanent ice sheets on Antarctica may have driven organic carbon burial and contributed to the CO_2 drawdown that initiated glaciation.

[1] De La Rocha (2003) *Geology* **31**, 423-426

https://doi.org/10.1180/S0026461X00008434 Published online by Cambridge University Press

Determining historic extent of seagrass (*Zostera marina*) cover in Virginia's coastal bays

NOAH E. EGGE[1*] AND STEPHEN A. MACKO[1]

[1]Department of Environmental Sciences, Univeristy of Virginia, Charlottesville, Virginia, 22904 USA
noah@virginia.edu (* presenting author)

The environmental degradation of the Chesapeake Bay and its neighboring coastal areas has been linked with explosive population growth and subsequent increases in agriculture and urbanization of the region. In the coastal bays of Virginia, numerous efforts have been made to restore seagrass (*Zostera marina*) meadows. As a result of large-scale, seed-based restorations in South Bay (2001) and Hog Island Bay (2007), *Z. marina* has come to dominate portions of these bays.

In this study geochemical proxies are used to determine the historic extent of seagrass within Virginia's coastal bays. Sedimentary cores were collected from sites with different historical records of seagrass cover, including areas with no seagrass, reseeded seagrass, or naturally occurring seagrass. Carbon and nitrogen isotope analyses were conducted on freeze-dried, acidified samples and used as proxies of the sources of the organic matter; sediments dominated by seagrass contained organic matter more enriched in ^{13}C relative to autochthonous algal and plaktonic marine materials. Peak ^{137}Cs activity and overall inventory were used to infer the relative age of sediments.

Several features are apparent from the preliminary characterization of marine sediments from these locations. The reseeded areas of South Bay and Hog Island Bay have a similar antithetical relationship between TOC (total organic carbon) and $\delta^{13}C$ values in the topmost 15 cm of the sediment core; as the TOC increases the $\delta^{13}C$ values become more depleted, suggesting that in those samples, seagrass provides only a minimal contribution to the preserved organic matter. Additionally there are large sections of the cores, at approximately 20 cm depth within the cores taken from South Bay, that have significantly lower TOC; this could be a result of the period without seagrass cover. The site with a natural seagrass meadow in Hog Island Bay is unlike any of the other sites analyzed: TOC increases from 0.2% at the surface to 1.2% at the bottom of the core, while $\delta^{13}C$ values range from -17.7‰ at the surface to -24.3‰ at depth. This pattern suggests an increased accumulation of ^{13}C depleted organic material in areas with prolonged seagrass cover. Results from this study may be able to be used to infer the spatial extent of the historic seagrass and guide future restoration projects.

Iron Oxidizing Bacteria: Influence of Calcium and Magnesium on Growth Rates

T. EGGERICHS*, S. JEROFKE, T. OTTE, O. OPEL AND W. RUCK

Leuphana University of Lueneburg, Lueneburg, Germany,
(*correspondence: eggerichs@leuphana.de)

Occurring in wells, pipework, and in natural groundwaters, the oxidation of ferrous iron is a partly abiotic-, partly biotic-induced process.

Whilst chemolithoautotrophic bacteria, such as *Gallionella* spp. rely solely on ferrous iron oxidation as energy source, other heterotrophic organisms, *Lepthothrix* spp. for example, can apply their ability to catalyze ferrous iron oxidation. Furthermore, their ability to oxidize iron is nearly all of what is known about these bacteria, save for some findings made by studies concerning their requirements (carbon metabolism [1, 2], Mn oxidation [3], O_2, pH [4]). But knowledge regarding other their nutritional or habitat needs or other requirements is still scant.

The study established that calcium and magnesium concentrations influence *Gallionella* sp. and *Lepthothrix discophora* growth, as concentrations of these two cations vary over a wide range in natural groundwaters and are routinely analyzed. Therefore, the results from the kinetic approach based on laboratory experiments can be compared with Ca and Mg concentrations in waters. A large data base of literature values, combined with own measurements of waters with high ferric iron precipitation rates, where these organisms have been detected, has been used.

Ca and Mg concentrations in culture media were made to undergo variations over a range covering typical natural groundwaters values (Ca: 0.6-150 mgL^{-1}, Mg: 0.12-24 mgL^{-1}). Using optical density and TOC measurements as well as light microscopy, growth rates and maximum cell densities of the model organisms were determined in batch culture. Lowering the two cations corresponding to values in soft natural groundwater reduced both the growth rates and maximum cell densities. Growth occurred even at low nutrient concentrations.

The two organisms used in this study grow more slowly under natural conditions than in artificial culture medium, even at sufficient Ca and Mg concentrations.

Other factors evidently inhibit the growth of the two model organisms more than Ca and Mg do. In very soft groundwaters though, Ca and Mg concentrations, among other factors, may lead to reduced growth rates of *Gallionella* sp. and *Leptothrix discophora*.

[1] Kämpfer et al. (1995) *Water Res* **29**, pp 1585–1588
[2] Hallbeck, Pedersen (1991) *J Gen Microbiol* **137**, pp 2657–2661
[3] El Gheriany et al. (2009) *Appl Environ Microb* **75**, pp 1229-1235
[4] Eggerichs et al. (2011) *20th Int. Symp. on Environ. Biogeochemistry. Conference Proceedings* p. O72

https://doi.org/10.1180/S0026461X00008434 Published online by Cambridge University Press

Natural solar cells on Earth and Mars

CARRICK M. EGGLESTON[1*], BRUCE A. PARKINSON[2]

[1]Geology and Geophysics, [2]Chemistry, University of Wyoming, Laramie, USA, carrick@uwyo.edu (*presenting author), bparkin1@uwyo.edu

Introduction

There are a range of natural settings in which semiconducting minerals can play a role in driving photochemical reactions that generally involve interfacial electron transfer. Surface, bulk, and defect states of the minerals interact. We present 3 examples of naturally-occurring semiconductor systems that may help drive chemical processes to a degree not previously appreciated.

Example 1: Rock Varnish

There is renewed interest in rock varnishes because they may be biogenic. Some varnishes are rich in iron and manganese oxides, and can produce photovoltages. Hypothetically, sunlit varnishes can oxidize water and other materials, driving a redox cycle that supports the varnish-associated bacteria in a hybrid inorganic-biological system.

Example 2: Perchlorate in Mars polar soil

The Wet Chemical Laboratory on the Mars Phoenix Lander found that perchlorate is remarkably concentrated in the sampled soils, rivaling chloride as the most abundant anion [1]. We have shown that chloride in solutions exposed to TiO_2 (anatase and rutile) surfaces and sunlight can be readily oxidized to perchlorate (20% initial current efficiency, decaying with time). The lowest perchlorate production rates we record, if operating on <0.1% of the Mars surface, are still 2000 times faster than the current atmospheric deposition rates in the Atacama [2].

Example 3: Natural tandem cells for solar hydrogen

The products of sulfide mineral surface oxidation include soluble sulfates and, often, insoluble metal ions. Fe(III) or Mn(IV)-rich oxides and oxyhydroxides often form thin surface layers on sulfides during the incipient oxidation of the sulfides. This constitutes a natural two-semiconductor "tandem cell". Sunlight on the outer oxide layer can produce valence band holes that readily oxidize many species including water; light transmitted by the oxide layer can be absorbed by the underlying narrower bandgap sulfide. Sulfide valence band holes receive electrons from the oxide conduction band, leaving sulfide conduction band electrons available as reductants (e.g., form H_2 from H^+). We show that Fe-based tandem cells can oxidize water and produce H_2 at rates ~10^4 times higher than needed to explain all water loss from Mars, and intriguingly, at about the same rate that iron deposition in Banded Iron Formations has been estimated to occur. We therefore suggest that mineral semiconductor photochemistry could have played a role in widespread redox processes on Earth, as well as on Mars.

[1] Hecht M.S., Kounaves S.P., Quinn R.C., et al. (2009) *Science* **325,** 64-67.

[2] Schuttlefield J.D., Sambur J.B., Gelwicks M., Eggleston C.M., Parkinson B.A. (2011) *J. Am. Chem. Soc. Comm.* **133**, 17521-17523.

Deciphering the processes of crustal reworking during the formation of the Neoproterozoic Lufilian belt, NW Zambia

Aurélien Eglinger[1*], Olivier Vanderhaeghe[1], Anne-Sylvie André-Mayer[1], Armin Zeh[2], Philippe Goncalves[3], Julien Mercadier[1], Etienne Deloule[5]

[1]G2R, Université de Lorraine, aurelien.eglinger@univ-lorraine.fr
[2]Goethe Universität, Frankfurt
[3]Chrono-environnemt, Université de Franche-Comté
[4]GRPG, Université de Lorraine

Introduction

Deciphering the source and *P-T-t* history of high grade metamorphic rocks exposed in the core of polycyclic orogenic blets is not an easy task. In this study, we combine structural analysis, metamorphic petrology and isotopic analyses of monazite and zircon to address these questions on the Lufilian Panafrican belt in Zambia.

Geological setting

The Lufilian belt formed between the Congo and Kalahari cratons during the evolution of the Gondwana supercontinent [2]. The classical interpretation is that this belt is comprised by a Paleo- to Neo-Proterozoic sedimentary cover deposited on an Archean to Paleoproterozoic crystalline basement and that its formation results from tectonic inversion of a continental rift [3]. Alternatively, the identification of a nappe structure with HP mineral relics led other authors to propose that the formation of the Lufilian belt implies closure of an oceanic basin by subduction and development of an orogenic wedge in a way similar to Phanerozoic orogens [4]. It is to note that both models consider that gneisses exposed at the lowest structural level represent a continental basement.

Results

Our field investigation across the Solwezi dome reveals that the transition from the metasedimentary cover to the gneissic basement actually corresponds to a metamorphic gradient reaching partial melting as evidenced by migmatites developed to the expense of metasedimentary protolith. U/Pb dating of zircon grains from the migmatite yields two clusters, one with a weighted mean $^{207}Pb/^{206}Pb$ age of 2032±46 Ma and a second with a weighted mean $^{207}Pb/^{206}Pb$ age of 1342±60 Ma. Zircon grains from paragneisses yield a weighted mean $^{207}Pb/^{206}Pb$ age of 2010±15 Ma. In turn, U-Th-Pb chemical dating of monazite grains from high grade micaschist (P=10±4 kbar, T=630±40°C) give an age of 571±29 Ma.

Discussion

Based on these data, we propose that the migmatite exposed at the lowest structural level of the Lufilian belt were developped to the expense of metasedimentary protolith containing zircon grains attesting for both Paleoproterozoic and Mesoproterozoic sources. This working hypothesis will be tested by new O and Lu-Hf isotpoic analyses on zircon grains coupled with U-Pb geochronology and geothermobarometry in order to reconstruct a P-T-t path for the metasedimentary rocks and for the migmatites. We will discuss their significance in terms of crustal growth and orogenic evolution during the Neoproterozoic.

[1] Hawkesworth and Kemp (2006) *Chemical Geology* **226**, 144-162. [2] Unrug (1996) *Episodes* **19**, 11-20. [3] Porada and Berhorst (2000) [4] John (2001) *PhD Thesis* 75pp.

https://doi.org/10.1180/S0026461X00008434 Published online by Cambridge University Press

Se cycling in the critical zone in a seleniferous area in Punjab, India.

E. EICHE[1*], A. NOTHSTEIN[1], T. NEUMANN[1], U. SADANA[2], K. DHILLON[2]

[1]Institute for Mineralogy and Geochemistry, KIT, 76131 Karlsruhe, Germany (*elisabeth.eiche@kit.edu)

[2]Department of Soil Science, PAU, 141004 Ludhiana, India

Elevated selenium concentrations of up to 12 mg/kg occur in top soils from agricultural sites of Jainpur and Barwa in the state of Punjab, North-West India. Selenium concentrations of corresponding groundwaters are higly variable showing maximum concentrations up to 340 µg/L and, therefore, clearly exceeding current guideline values of 40 µg/L [1].

The depth distribution of Se in the soil with highest contents in the top 15 cm (Fig. 1a) suggests that this element is mainly introduced by irrigation with Se rich groundwater. Recent studies indicate that the enrichment of Se in soils and, consequently, in plants has been increasing over the years. This could be explained either by a general increase of Se in the irrigation water and/or by a recent change in agricultural land use practice from wheat-maize to wheat-rice rotation out of which the second is more water intensive.

Considerable percentages of Se in soils seem to be bioavailable as indicated by sequential extraction studies and X-ray absorption measurements. However, the change in agricultural practice probably has an influence on the mobility of Se. Temporary occurence of stagnant and reducing conditions during rice cultivation may lead to immobilization of parts of Se in soils. This assumption is supported by the detection of Se(0) in the top soil. Furthermore, the Fe, As and Mn content in soils below 15 cm is condsiderably higher compared to the top soils (Fig 1b/c) indicating a redox-influenced downward translocation of these elements. Volatilization and/or uptake of Se by plants also seem to be important processes which determine Se cycling in the critical zone as lowest Se concentrations in topsoils occur in the upper 2 cm (Fig. 1a).

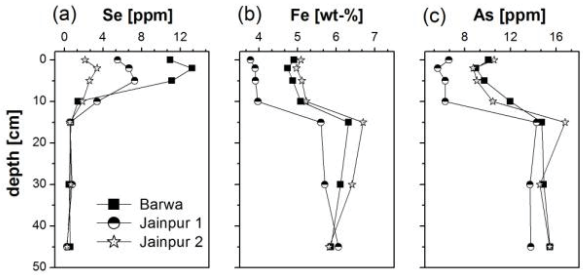

Figure 1: Depth distribution of Se (a), Fe (b) and As (c) in soil profiles from Barwa and Jainpur, Punjab, India.

[1] WHO, 2011. Guidelines for drinking-water quality, 4th edition.

Origin and evolution of reactive and noble gases dissolved in porewater of low-permeable crystalline rocks

FLORIAN EICHINGER[1,2], H. NIKLAUS WABER[2] AND JOHN A.T. SMELLIE[3]

[1]Hydroisotop GmbH, Schweitenkirchen, Germany, fe@hydroisotop.de

[2]Rock-Water-Interaction, Institute of Geological Sciences, University of Bern, Bern, Switzerland, waber@geo.unibe.ch (* presenting author)

[3]Conterra AB, Stockholm, Sweden, smellie@conterra.se

Reactive and noble gases dissolved in matrix porewater of low permeable crystalline bedrock were successfully extracted and characterized for the fist time based on drillcore samples from the Olkiluoto investigation site (SW Finland).

In crystalline bedrock systems, gases occur dissolved in fracture groundwater, matrix porewater and in fluid inclusions of rock forming minerals such as quartz and feldspars. Fracture groundwater and porewater, the latter being present in the inter- and intragranular connected pore space of the rock matrix, interact with each other predominately via diffusion. In contrast, mineral fluid inclusions represent isolated reservoirs without exchange for most gases under ambient conditions.

Reactive and noble gases dissolved in porewater and their isotope signatures carry valuable information about the evolution of a hydrogeological system. Information about origin and fluxes of dissolved gases is also important within the context of the safety assessment of a nuclear waste repository. For example, owing to their ability to buffer surface-derived dissolved oxygen, the occurrence of small amounts of hydrocarbons in fracture groundwater might be beneficial to safety assessment. In contrast, large amounts of hydrocarbons (mainly CH_4) in fracture groundwaters combined with dissolved sulphate may affect safety assessment adversely.

Changes in the chemical and isotopic composition of gases dissolved in fracture groundwater are transmitted and preserved in the porewater, which forms an archive for hydrogeochemical changes in the past. At Olkiluoto, core samples were collected along a continuos profile from a horizontal borehole that intersects with a major water-conducting fracture zone.. Porewater and present-day fracture groundwater are in transient state with respect to dissolved CH_4 and He concentration as well as the hydrocarbon mass ratio. Concen-trations of CH_4 and He are higher in the porewater and approach those of the fracture groundwater towards the water-conducting zone. For the encountered fracture system this indicates that the circulation of present-day low CH_4 and low He fracture groundwater has been to short to achieve equilibrium between the two reservoirs and CH_4 as well as He is now transferred along chemical gradients from the porewater into the fracture groundwater. Hydrocarbon mass ratios and $\delta^{13}C$-CH_4 values suggest the preservation of a small component of bacterially formed hydro-carbons in some parts of the pore water profile, whereas in fracture groundwater and porewater furthest away from the water-conducting zone only evidences for thermogenic formed hydrocarbons could be detected.

https://doi.org/10.1180/S0026461X00008434 Published online by Cambridge University Press

Preservation of lipid biomarkers of Fe(III)-reducers and anoxygenic phototrophic Fe(II)-oxidizers during exposure to high pressure and temperature (P/T)

MERLE EICKHOFF[1*], DANIEL BIRGEL[2], JÖRN PECKMANN[2], AND ANDREAS KAPPLER[1]

[1]University of Tuebingen, Center for Applied Geosciences, Geomicrobiology Group, Tuebingen, Germany merle.eickhoff@uni-tuebingen.de (* presenting author); andreas.kappler@uni-tuebingen.de

[2]University of Vienna, Department of Geodynamics and Sedimentology, Vienna, Austria daniel.birgel@univie.ac.at; joern.peckmann@univie.ac.at

Background

The rock record is analyzed to search for traces of ancient life on Earth. The fractionation of carbon, sulfur and iron stable isotopes, sedimentary structures, microfossils, as well as molecular fossils (lipid biomarkers), are important indicators for past life. Molecular fossils are persistent compounds that often derive from membrane lipids, recording biological activity in ancient rocks. They provide information on past environmental conditions as well as dominant microbial metabolisms and have been found in sediments as old as 1.6 Ga [1] and 2.5 Ga [2].

So far, molecular fossils have not been detected in Archean Banded Iron Formations (BIFs). The formation of these sediments is still controversial. Most likely, the earliest BIFs were deposited in the absence of significant amounts of oxygen [3,4]. Anoxygenic phototrophic Fe(II)-oxidizing bacteria were suggested being the most plausible mechanism for the deposition of the Fe(III) minerals under anoxic conditions [5]. Moreover, Fe(III)-reducing bacteria might have been involved in iron mineral transformation after deposition, as suggested by Fe and C isotope analyses [6].

Hence, Fe(II)-oxidizing and Fe(III)-reducing bacterial strains were chosen for a systematic biomarker study focusing on the fate of molecules during exposure to high pressure and temperature (P/T).

Current Research and Outlook

We present a new approach investigating the preservation of organic biomolecules of anoxygenic phototrophic Fe(II)-oxidizing and anaerobic Fe(III)-reducing bacterial cells during exposure to diagenetic conditions (P/T) in inert gold capsules. Analysis of fatty acids, alcohols and hydrocarbons was done before and after P/T exposure, with a focus on fatty acids and cyclic terpenoids. We determined how these lipid compounds are affected at increasing temperatures in the absence and presence of iron minerals. In particular, the close association of the iron minerals with the cells appears to have an influence on the stability and preservation of biomarkers. Moreover, in the future we are planning to extend this method to identify carotenoid pigments in the phototrophic Fe(II)-oxidizers and study their preservation.

In summary, the approach of simulating diagenetic and late-stage alteration will help identify stable and source-specific molecular fossils, and elucidate the likelihood of finding diagnostic biomarkers (and thereby evidence) for Fe-cycling bacteria in BIFs and other Fe-rich sediments.

[1] Brocks *et al.* (2005) *Nature* **437**, 866-870. [2] Summons *et al.* (1999) *Nature* **400**, 554-557. [3] Canfield *et al.* (2000) *Science* **288**, 658-661. [4] Bekker *et al.* (2004) *Nature* **427**, 117-120. [5] Kappler *et al.* (2005) *Geology* **33**, 865-868. [6] Johnson *et al.* (2008*) Annu. Rev. Earth Planet. Sci.* **36**, 457-493.

The MAT-253 Ultra — a novel high-resolution, multi-collector gas source mass spectrometer

JOHN EILER[1*], MATTHIEU CLOG[1], MICHAEL DEERBERG[2], PAUL MAGYAR[1], ALISON PIASECKI[1], HANS-JUERGEN SCHLUETER[2], JOHANNES SCHWIETERS[2], ALEX SESSIONS[1], DANIEL STOLPER[1], NITHYA THIAGARAJAN[1]

[1]California Institute of Technology, Pasadena CA, USA, eiler@gps.caltech.edu (* presenting author)

[2]Thermo Fisher Scientific, Bremen, Germany, johannes.schwieters@thermofisher.com

We present the design, performance and representative applications of the MAT 253 Ultra – the first prototype of a new class of high-resolution gas source isotope ratio mass spectrometers.

The MAT-253 Ultra is a forward geometry double focusing sector mass spectrometer with a Nier-type gas source. Samples are introduced through capilary bleeds from any of 4 automated flexible bellows and/or a carrier-gas port. Ions enter the analyzer through an adjustable entrance slit (5 to 250 μm). The analyzer has a 23 cm radius magnet and is similar in scale and design to the Neptune Plus MC-ICPMS. The detector array consists of 1 fixed position and 7 moveable positions on 6 trolleys. An RPQ lens is positioned before the central detector position. Each detector position contains both an SEM and faraday cup detector; each faraday can be registered through any of 10 amplifiers varying in gain from 10^7 to 10^{12}.

Ion beams from m/z 1 to ~300 can be collected, with a ~15 % mass range for simultaneous collection. Useful ion yield is ~1 ion per 1200 molecules for CO_2 under standard analytical conditions and using a 250 μm entrance slit. The dynamic range in simultaneously measurable ion currents is ~10^{14}. Backgrounds are negligible in the central detector position when the RPQ is in use, permiting quantitative analysis of low intensity ion beams even with high source pressures. Mass resolving power (M/ΔM, 5%/95% definition) has been measured up to 26,000 and is routinely as good as ~22-24,000 — sufficient to separate most isobaric interferences among isotopologues of H-C-N-O-S molecular species; in particular, it permits separation of ^{13}C from D isotopologues and both from H adducts in alkanes and related organics. Analyzer system stability is routinely < 2ppm/hour, permitting precise analysis of small features on complex peaks. External precision for isotope ratio measurements of relatively intense ion beams are routinely 10's of ppm, relative; measurements of weaker ion beam using SEM detectors reach counting statistics limits down to external precisions of ~0.1 ‰.

The MAT 253 Ultra enables many previously impossible isotopic analyses of gases and volatile organics and their fragment and adduct ions. Demonstrated examples include: $\delta^{13}C$, δD and $^{13}CH_3D$ of methane; $\delta^{13}C$ of propane and many of its fragments (enabling position-specific ^{13}C determination); direct analysis of $\delta^{17}O$ $\delta^{18}O$, $\delta^{15}N$ and ^{15}N-^{18}O 'clumping' in N_2O and its NO fragment; $^{18}O^{17}O$ and $^{18}O_2$ in O_2; and clumped isotope analysis of CO_2 free of contaminant isobaric interferences.

https://doi.org/10.1180/S0026461X00008434 Published online by Cambridge University Press

Modeling groundwater recharge and seawater intrusion in the Quaternary coastal plain aquifer of the Wadi Watir Delta, Sinai, Egypt

MUSTAFA A. EISSA[1,2*], JAMES M. THOMAS[2], GREG POHLL[2] ORFAN SHOUAKAR-STASH[3], RONALD L. HERSHEY[2], MAHER I. DAWOUD[4], KAMAL A. DAHAB[4], AND MOHAMED A. GOMAA[1]

[1]Desert Research Center, Hydrogeochemistry Dept. Matariya, Cairo, Egypt

[2]Desert Research Institute, Division of Hydrologic Sciences, Reno, Nevada, USA, Mustafa.Eissa@dri.edu

[3]University of Waterloo, Department of Earth Sciences, Waterloo, Ont., Canada

[4]Menoufiya University, Faculty of Science, Geology Dept., Shebein El Kom, El MenoufiyaEgypt

Abstract

The Wadi Watir Delta in Sinai, Egypt consists of an alluvial and sandy clay aquifer underlain by impermeable Precambrian basement. The scarcity of rainfall during the last decade and high pumping rates has increased salinity and degraded water quality in the main water-supply wells along the mountain front and along the coast. This degradation has required a reduction in groundwater production.

The main factors controlling groundwater salinity in the delta are water-rock interaction, seawater intrusion, and mixing with deep saline water. Water chemistry and stable isotopes in groundwater including $^{87}Sr/^{86}Sr$, $\delta^{37}Cl$ and $\delta^{81}Br$, were utilized to evaluate the groundwater geochemical evolution, sources of groundwater mixing, and the amount of seawater intrusion along the coast. Also, $^{87}Sr/^{86}Sr$, $\delta^{37}Cl$ and $\delta^{81}Br$ of various aquifer rocks were determined to assist in understanding the groundwater flow system.

Inverse geochemical modeling was used to identify possible geochemical processes that account for the chemical and isotopic changes in groundwater. Possible models are presented that quantify the amount of water-rock interactions, mixing and evaporation.

The isotopic results were utilized to develop a three-dimensional, variable-density, flow and transport model using the SEAWAT modeling environment. The models were calibrated using groundwater level changes and salinity variation. The models estimate average annual groundwater recharge and simulate annual groundwater pumping, upwelling of saline water from beneath the well field, and seawater intrusion along the coast for different pumping scenarios.

Keywords: groundwater sustainability, groundwater modeling, seawater intrusion, water chemistry, isotopes, Wadi Watir Egypt.

MICROBIAL BIOMINERALIZATION AS A TECHNIQUE FOR GROUTING FINE APERTURE ROCK FRACTURES

GRÁINNE EL MOUNTASSIR[1*], DOMINIQUE J. TOBLER[2], REBECCA J. LUNN[1], HEATHER MOIR[1], AND VERNON R. PHOENIX[2]

[1]Department of Civil and Environmental Engineering, University of Strathclyde, Glasgow, UK grainne.elmountassir@strath.ac.uk (* presenting author), rebecca.lunn@strath.ac.uk, heather.moir@strath.ac.uk

[2]School of Geographical and Earth Sciences, University of Glasgow, Glasgow, UK Dominique.Tobler@glasgow.ac.uk, Vernon.Phoenix@ges.gla.ac.uk

Abstract

For many engineering applications, such as sealing tunnels, shafts and boreholes, it is necessary to limit fluid flow through fractures. The particle size of conventional cementitious grouts limits the size of fractures into which they can penetrate. To address this issue increasingly microfine and ultrafine cement grouts are becoming commercially available. Despite this the radius of penetration remains dependent on the grout viscosity alongside injection pressure, pumping rate, grout setting time and grout cohesion: lower viscosity aqueous solutions potentially have a greater radius of penetration. In addition cementitious grouts typically undergo volumetric shrinkage during setting. In many applications this change in volume may not be of particular importance but in others where a very low hydraulic conductivity is a critical design criterion, such as borehole sealing for carbon storage reservoirs and tunnel sealing for nuclear waste repositories, this reduction in volume may be significant.

This study investigates the use of microbially induced carbonate precipitation (MCP) as a technique for grouting fine aperture rock fractures. Two types of laboratory experiment have been conducted: sealing fractures at the 10cm-1m scale between transparent polycarbonate plates; and sealing artificial fractures within granite cores. We investigate both the hydraulic and mechanical properties of the MCP grout. We show that the grout has the potential to seal fractures with apertures less than 100 microns, that it can 'biologically re-heal' when damaged and that the shear strength can be greater than traditional cementitious grouts.

https://doi.org/10.1180/S0026461X00008434 Published online by Cambridge University Press

Multiple Sulfur Isotope Effects During Sulfite and Bisulfite Oxidation in Aqueous Solution

DANIEL L. ELDRIDGE[1*], SANG-TAE KIM[2], AND J. FARQUHAR[1]

[1]Dept. of Geology and ESSIC, University of Maryland, College Park, MD 20742 USA (*correspondence: eldridge@umd.edu)

[2]School of Geography and Earth Sciences, McMaster University, Hamilton Ontario, Canada, L8S 4K1.

The multiple sulfur isotope fractionations accompanying the oxidation of sulfite (SO_3^{2-}) and bisulfite (HSO_3^-) to sulfate via oxygen (O_2) have been investigated, revealing both normal (-) and inverse (+) fractionations depending on pH. These compounds are important reaction intermediates in the oxidation of biogenic and volcanogenic hydrogen sulfide (e.g., [1]) and can be used by a variety of prokaryotes for dissimilatory metabolism, including the processes of oxidation, reduction, and disproportionation (e.g., [2]). Reactions involving these compounds are also relevant to the sulfur cycle in a variety of environments, including hydrothermal hot springs (e.g., Yellowstone NP), the chemocline in euxinic water bodies, marine sediments, and the atmosphere (forming acid rain).

Buffered sulfite and bisulfite solutions were prepared in batch reaction vessels from sulfur dioxide (99.9+%, Sigma Aldrich) at a pH of 12.5 (corresponding to ~99.9% SO_3^{2-}) and 4.6 (corresponding to ~99.5% HSO_3^-) using a custom built glass vacuum line. Oxidation of sulfite/bisulfite was initiated after placing vessels in a temperature controlled water bath (stability of 0.01 ˚C) and introducing ultrapure oxygen (Airgas), enough to oxidize a fraction of the bisulfite/sulfite in solution. Residual sulfite/bisulfite was separated from product sulfate via acidification and cryogenic trapping of evolved SO_2, and both product and residual reactant were processed for isotopic analysis using standard techniques.

Table 1 shows the preliminary results of sulfite and bisulfite oxidation experiments conducted at 5.00±0.01˚C. At relatively low pH where bisulfite is dominant, product sulfate is isotopically *light* relative to reactant bisulfite by about 5.32 ‰ based on $^{34}S/^{32}S$. In contrast, at high pH where sulfite is dominant, product sulfate is isotopically *heavy* by about 4.48 ‰ relative to reactant sulfite. Variations in the $\Delta^{33}S$ and $\Delta^{36}S$ values approach the limits of detection, although small positive shifts in $\Delta^{33}S$ may accompany these reactions. The change in the direction of the fractionation based on speciation appears to be a new observation. It is clear that the isotope effects associated with these reactions are more complex than previously recognized.

pH	$10^3\ln(^{34}\alpha)$ (‰)	$\Delta^{33}S$ (‰)	$\Delta^{36}S$ (‰)
4.6 (2 exp.)	-5.32±0.10	0.018 ± 0.010	-0.1 ± 0.2
12.5 (4 exp.)	4.48±0.29	0.011 ± 0.040	-0.1 ± 0.1

Table 1: Fractionations ($^{34}\alpha=^{34}R_{product}/^{34}R_{reactant}$) determined for bisulfite (pH=4.6) and sulfite (pH=12.5) oxidation experiments at 5.00±0.01˚C. Uncertainties are 2σ standard deviations of repeat experiments (duplicate or quadruplicate).

[1] J-Z. Zhang & F.J. Millero (1993) *GCA* **V. 57**, 1705-1718.
[2] D.E. Canfield (2001) *Rev. in Min. & Geochem.* **V.43** 607-636.

Microbial-mineral-metal interactions in suspended aquatic floc

ELLIOTT, A.V.[1*]; PLACH, J.M.[1]; DROPPO, I.G.[2,1]; AND WARREN, L.A.[1]

[1]McMaster University, Hamilton, Canada, elliotav@mcmaster.ca (* presenting author)

[2]National Water Research Institute, Environment Canada, Burlington, Canada

Characterization of suspended floc trace element (TE) abundance and partitioning for Ag, As, Cu, Ni and Co across 6 variably impacted aquatic ecosystems identify floc to be a key trace element sequestration phase, concentrating TEs ~55x above that of surfical bed sediments. Further, floc TE geochemical partitoning patterns were highly conserved across systems, with amorphous Fe oxyhydroxides (FeOOH) consistently the most important sorbent phase for TE retention, regardless of physico-chemical conditions or elements involved. In contrast, surfical (0-0.5cm) bed sediment TE partitioning was more classically reflective of both system geochemical parameters and element-specific reactivity, indicating differing controls on TE sequestration by suspended versus bed sediment system compartments. Results indicate that floc TE uptake is biologically linked to floc microbial components. Imaging analysis of floc architecture reveals bacterial extracellular polymeric substances (EPS) as the major constituent of floc organics and physical bridging mechanism between floc-associated organic and inorganic constituents. Moreover, floc organic concentrations (live cells, EPS) directly predict floc-FeOOH concentrations. Thus while floc-FeOOH are the dominant TE sequestration phase, floc-associated organic and microbial constituents provide the critical foundation underpinning enhanced floc TE uptake through their structure role in the nucleation, precipitation and/or trapping of TE-reactive FeOOH; ultimately creating a distinctly different solid than surfical sediments in close proximity with differing controls on trace element uptake.

.

[1] Author Last Name (Year) *Publication Name* **Volume#**, pp-pp.
[2] Author Last Name (Year) *Publication Name* **Volume#**, pp-pp.

https://doi.org/10.1180/S0026461X00008434 Published online by Cambridge University Press

Kinetics of Rb isotope equilibration in Savannah River Site soils

J. M. WAMPLER[1], W. CRAWFORD ELLIOTT[1]*, EIRIK J. KROGSTAD[2], BERND KAHN[3], LAURA ZAUNBRECHER[1], AND DANIEL I. KAPLAN[4]

[1]Georgia State University, Atlanta, GA, USA, claylab@gsu.edu (* presenting author)
[2]Pacific Northwest National Laboratory, Richland, WA, USA Eirik.Krogstad@pnnl.gov
[3]Georgia Institute of Technology, Atlanta, GA USA, Bernd.Kahn@gtri.gatech.edu
[4]Savannah River National Laboratory, Aiken, SC, USA daniel.kaplan@srnl.gov

Most of the Rb and nearly all of the Cs in near-surface soils of the Savannah River Site (SRS) appear to be fixed in interlayer wedge zones within hydroxy-interlayered vermiculite (HIV) particles [1]. To further investigate this idea, we studied the equilibration of added, highly enriched ^{85}Rb with natural soil Rb under mildly acidic and mildly basic conditions. Consistent results from four soil samples in acidic suspension show equilibration of the added ^{85}Rb with from 4% to 6% of the soil Rb in one day, followed by continued slow equilibration until after two months about twice as much of the soil Rb had equilibrated with the added ^{85}Rb. Equilibration was faster and continued to greater extent when soil was suspended in $NaHCO_3$ solution, on average by a factor of about 2 in rate and extent. We attribute the faster and more extensive equilibration in basic suspensions to slight expansion of the vermiculite interlayers, and of the adjoining interlayer wedges, as hydrated Na ions replaced the natural exchangeable acidity and as hydroxy-Al polymers were neutralized.

Data obtained earlier by Goto *et al.* [2] show that equilibration of natural soil Cs with ^{137}Cs proceeds more rapidly and is more extensive than what we observed for Rb. Up to 20% of the soil Cs equilibrated with the added ^{137}Cs under mildly acidic conditions, and up to about 50% under mildly basic conditions, in just four days. We interpret the more rapid and more extensive equilibration of Cs than Rb with an added isotope to indicate that Rb is more deeply entrenched in interlayer wedges of HIV than is Cs, because Rb ions are smaller than Cs ions. This interpretation is in accord with results of another experiment in which we found that added Mg, whose hydrated ions keep vermiculite interlayers expanded, strongly enhances the rate of acid extraction of Cs from SRS soils but has little effect on the rate of extraction of Rb.

[1] Wampler *et al.* (Submitted 2012) *ES&T* [2] Goto *et al.* (2008) *Health Physics* **94**, 18-32.

Interaction of Volatile Organic Compounds with Magnetite Nanoparticles: Fundamentals and Implications for Air Remediation

NERMIN ELTOUNY[1*], PARISA A. ARIYA[1]

McGill University, Chemistry, Montreal, Canada, nermin.eltouny@mail.mcgill.ca[1*]
McGill University, Chemistry and Atmospheric and Oceanic Sciences, Montreal, Canada parisa.ariya@mcgill.ca [1]

Introduction

Nanoparticles have become one of the most researched topics in the recent years as they are of interest to many fields. We are interested in the fundamental processes between organic vapours and iron oxide nanoparticle for their application in the remediation of polluted air.

Experimental Methods

We show the efficiency of iron oxide nanoparticles for the removal of organic vapours (BTEX) from air. We use various techniques including GC-FID, GC-MS, XRD, XPS and UV-VIS absorption spectroscopy to understand the interaction between gaseous organic molecules and iron oxide nanoparticles.

Results and Conclusion

We will discuss the role of the iron oxide nanoparticle heterogeneity in the interaction with aromatics vapours and the effect of organic vapours on the oxidation state of the iron oxide [1].

Determining the fundamental processes can yield information on the properties that dictate how iron oxide nanoparticles behave in the presence of organic vapours, which allows for improved designs of adsorption media as well better understanding of potential reactions in the environment.

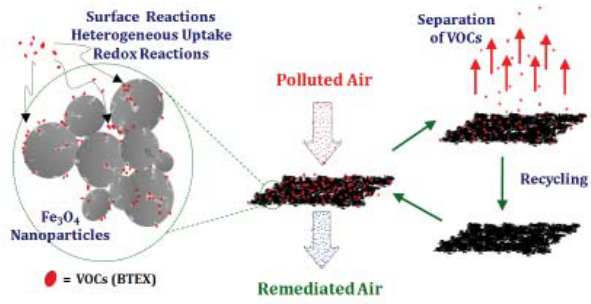

Figure 1. Overview of the removal of BTEX in the gas phase by iron oxide nanoparticles

[1] Eltouny and Ariya (2012) *Submitted* to Industrial Chemistry and Engineering Research (ie-2012-001524)

https://doi.org/10.1180/S0026461X00008434 Published online by Cambridge University Press

Gas clathrate hydrate thermodynamics and kinetics: limits on near-surface volatile fluxes for cold terrestrial planetary systems through deep time.

MEGAN ELWOOD MADDEN[1*], MARGARET ROOT[1], SETH GAINEY[2] AND JOHN LEEMAN[1]

[1]University of Oklahoma, School of Geology and Geophysics, melwood@ou.edu (*presenting author),
[2]University of Nevada,Las Vegas, Department of Geosciences

Gas clathrate hydrates (a gas molecule such as CO_2, CH_4, H_2S, etc. trapped within a cage of water molecules) are thermodynamically stable at low-moderate temperatures and moderate-high pressures, conditions found near the surface of many terrestrial planetary bodies in our solar system, including Earth, Mars, Europa, Titan, Enceladus, and other icy moons. While gas hydrates are often thought of as ephemeral phases in Earth's ocean and permafrost sediments, they can serve as reservoirs for water, carbon, and other volatile phases over millions to billions of years. Hydrate stability zones (HSZ- the depth at which gas hydrates are thermodynamically stable given the P-T conditions) can extend to significant depths [1]. In addition, gas hydrate formation and dissociation rates below the freezing point of water are transport limited, relying on solid-state diffusion of gas to or from the ice-hydrate interface [2]. Slow gas diffusion rates through ice and hydrate at low temperatures result in geologically long-lived metastable gas hydrate reservoirs in the near subsurface.

Geologic models of gas hydrates in planetary systems must thefore consider both thermodynamic and kinetic constraints on clathrate reservoirs to better understand long-term volatile fluxes in the near subsurface. Gas diffusion as well as hydrate formation and dissociation rates are needed to effectively model these complex systems. Using gas hydrate formation and dissociation rates measured in our laboratory, we have developed a coupled thermodynamic and kinetic model of obliquity-driven changes in HSZs on Mars. This model suggests that gas hydrates may provide a significant reservoir for carbon and water within the crust over 10s of km depth. In addition, these hydrate reservoirs may remain thermodynamically stable over geologic timescales, and even when preturbed, may persist as metastable bodies for thousands to millions of years, resulting in significant long-term volatile fluxes. Similar geologic models of gas hydrate reservoirs on Europa, Titan, and Enceladus are underway.

[1] Root and Elwood Madden (2012) *Icarus* doi:10.1016/j.icarus.2011.12.024
[2] Gainey and Elwood Madden (2012) *Icarus* doi:10.1016/j.icarus.2011.12.019

Control of aqueous Mn(II) on Mn(III, IV)-oxide mineralogy and structure

EVERT J. ELZINGA[1*]

[1]Rutgers University, Newark, New Jersey, USA, elzinga@andromeda.rutgers.edu (* presenting author)

Mn oxides are among the most reactive mineral phases found in the environment, exerting strong control on the aqueous and solid phase chemistry of soils and sediments through adsorption and redox reactions. Natural Mn oxides are believed to be of predominantly biological origin, representing either primary products of biological Mn(II) oxidation, or secondary products resulting from alteration of primary bio-oxides [1]. Oxidation of Mn(II) by bacteria and fungi has been shown to produce poorly crystalline and highly reactive hexagonal birnessite-type Mn-oxide products [2-5], which readily engage in (abiotic) secondary redox and sorption reactions that may impact their structure and reactivity.

Recent work [3,6] has shown that aqueous Mn(II) may act as a reductant of hexagonal birnessite (which typifies the phyllomanganates that dominate in natural aquatic environments), causing reductive transformation of birnessite (nominally Mn(IV)O2) into the feitknechtite and manganite polymorphs of Mn(III)OOH through interfacial electron transfer from adsorbed Mn(II) to structural Mn(IV) atoms and arrangement of product Mn(III) into Mn(III)OOH, summarized by the comproportionation reaction $Mn(II) + Mn(IV)O_2 + 2\,H_2O \rightarrow 2Mn(III)OOH + 2H^+$. The transformation reaction is time-dependent, involving formation of feitknechtite as the initial metastable transformation product which is catalytically converted into the more stable manganite polymorph during ongoing reaction with Mn(II) [6]. An important finding from this work is that thermodynamic predictions of occurring reactions and transformation have limited merit in these systems due to uncertainty in thermodynamic data of the Mn oxides involved (due to size and composition effects), which necessitates experimental work to assess the occurrence and importance of specific transformation pathways.

The work presented here focuses on the impacts of pH and Mn(II) concentration on occurring transformation reactions, reporting notable changes in system reactivity as a function of these variables. The results point to a potentially major role of aqueous Mn(II) as a control on the mineralogy and structure of environmental Mn-oxides, and as a moderator of the reductive arm of Mn-oxide redox cycling.

[1] Tebo *et al.* (2004) *Annual Rev. Earth Planet. Sci*. **32**, 287-328. [2] Villalobos *et al.* (2003) *Geochim. Cosmochim. Acta* **67**, 2649-2662. [3] Bargar *et al.* (2005) *Am. Mineral.* **90**, 143-154. [4] Webb *et al.* (2005) *Am. Mineral.* **90**, 1342-1357; [5] Santelli *et al*. (2011) *Geochim. Cosmochim. Acta* **75**, 2762-2776. [6] Elzinga (2011) *Env. Sci. Technol.* **45**, 6366-6372.

https://doi.org/10.1180/S0026461X00008434 Published online by Cambridge University Press

Iron isotope signatures in magnetite formed by marine invertebrates

SIMON EMMANUEL[1], JAKOB VINTHER[2], JAN A. SCHUESSLER[3]*, FRIEDHELM VON BLANCKENBURG[3], ALAN MATTHEWS[1]

[1] Institute of Earth Sciences, The Hebrew University of Jerusalem
[2] Jackson School of Earth Sciences, University of Texas at Austin
[3] German Research Centre for Geosciences GFZ, Section 3.4, Earth Surface Geochemistry, Potsdam, Germany, jan.schuessler@gfz-potsdam.de (* presenting author)

Marine organisms can be powerful recorders of past environmental conditions. Fe isotopic signatures in marine organisms might be used to infer paleoenvironmental conditions and/or biological processes. Chitons - a type of marine mollusk - are a remarkable group of marine invertebrates that accumulate significant amounts of Fe. They produce radula (teeth) that are coated in biomineralized magnetite, enabling them to graze on algae living on the surface of rocks [1]. As a result, their Fe isotopic signatures might be expected to provide an efficient tracer of ambient oceanic conditions and biogeochemical cycling.

Here, we examine Fe isotopes in modern marine chitons collected from different locations in the Atlantic and Pacific oceans to assess the range of isotopic values that might be encountered, and whether or not the isotopic signatures reflect seawater values. Furthermore, by comparing two species that have very different feeding habits but collected from the same location, we attempt to isolate the possible impact of diet on isotopic signatures.

The Fe isotopic analyses were performed on a total sample set of 17 individual chitons using a *Neptune* MC-ICP-MS at GFZ Potsdam. δ^{56}Fe values (relative to IRMM-014) cover a range from -1.89 to +0.12 (±0.03‰ external reproducibility in δ^{56}Fe). All analysed teeth show negative δ^{56}Fe values, some even more negative than reported for oceanic Fe(II). Strikingly, two different species from Port Orchard (Washington, USA) have distinct isotopic signatures. The teeth of the species feeding on red algae (*Tonicella lineata*) show a tight range in δ^{56}Fe of -0.58±0.12(1σ), while *Mopalia muscosa*, which feeds primarily on green algae, cover a range in δ^{56}Fe from -1.89 to -0.92.

The results suggest that although chitons do not record the ambient seawater Fe isotope signature, they could provide a potential tracer of Fe biogeochemical cycling. The distinct Fe isotope signatures of the two species from the same locality might be a result of the different ways in which magnetite is biomineralized (presumably Fe is being taken up as Fe(II) in the organisms); alternatively, the chitons may simply be inheriting the signatures from the different algal food sources.

[1] Lowenstam and Weiner (1989) *On Biomineralization. Oxford University Press.*

Mineral reactions in a porous world: calcite dissolution experiments revisited

SIMON EMMANUEL[1*] AND YAEL LEVENSON[1]

[1]The Hebrew University of Jerusalem, Jerusalem, Israel, simonem@cc.huji.ac.il (* presenting author)

The dissolution of calcite influences processes as diverse as the evolution of karst landscapes and the response of carbonate-hosted oil reservoirs to enhanced recovery techniques. Although much research has focused on determining the reaction kinetics of calcite dissolution from individual crystals, it is often assumed that the empirical rate laws derived in such studies can be used in a straightforward manner to describe calcite dissolution in porous and fractured rocks. In this study we challenge this assumption by using atomic force microscopy (AFM) to study the dissolution of natural porous carbonate substrates. We demonstrate how AFM can be used to estimate in situ reaction rates and identify dissolution mechanisms during reactive transport in porous media. Critically, in advective systems we observe a high degree of spatial heterogeneity that can be directly related to the porous structure. The precise mechanism behind pore-scale heterogeneous reaction rates is discussed, and we present a 3D numerical model that accurately reproduces the observed dissolution patterns on a porous surface. We also discuss the implications for current continuum descriptions of reactive transport, and how they might be modified to incorporate pore-scale heterogeneity.

https://doi.org/10.1180/S0026461X00008434 Published online by Cambridge University Press

Experimental study of S-MIF by SO_2 photolysis under CO atmosphere

YOSHIAKI ENDO[1]*, SEBASTIAN DANIELACHE[1], YUICHIRO UENO[1]

[1]Department of Earth & Planetary Sciences, Tokyo Institute of Technology, Tokyo, Japan. endo.y.ac@m.titech.ac.jp

Sulfur mass independent fractionation (S-MIF) of Archean sediment is regarded as a proxy of the atmosphere at that time. S-MIF is produced by photolysis of SO_2 in oxygen-free environment. However, the elementary reaction and the mechanisms of fractionation in the atmosphere are not fully understood. We present here a newly developed experimental setup to reveal the atmospheric photochemistry observed in the geological record. The photochemical system consists of a D_2 light-source, two gas chambers attached to a monochrometer and a UV detector designed to operate with no interference of atmospheric air. Here we present the first round of experiments of SO_2 photolysis conducted under SO_2 at low partial pressure (<5 Pa) and high amount of CO. The purpose of this experiment is to test a different experimental conditions from previously reported results where the environment of high pressure SO_2 is oxidative and optically thick, which may be significantly different from Archean atmosphere. Thus, our experiment condition hinders these problems. Additionally, this setting allow us to test the hypothesis that reducing atmosphere with a large amount of CO produces an stable amount of OCS [1]. In order to cut-off the large emission band of the deuterium lamp at 168 nm the chamber previous to the photochemical chamber was filled with CO_2. Analysis of reactions products confirms the production of OCS under CO atmosphere. The product OCS shows clear MIF signature. We calculated fractionation factors of SO_2 photolysis (185-220 nm) and also the chemistry associated with SO_2 photoexcitation (250-320 nm) as an additional source of MIF. We discuss a source of MIF involving not only SO_2 photodissiaction but also the chemistry associated to the photoexited SO_2* species in relation to the MIF signal meaured on the geological record.

[1] Ueno *et al.* (2009) *PNAS* **106**, 14784-14789.

Barite precipitation in submarine hydrothermal vents: Insights from Sr-isotope ratios

MARGARET S. ENGELBERT[1*], JOHN W. JAMIESON[2], BRIAN L. COUSENS[1], NICOLE M-B. WILLIAMSON[1] AND MARK D. HANNINGTON[2]

[1]Carleton University, Ottawa, Canada, (*mengelbe@connect.carleton.ca)

[2]University of Ottawa, Ottawa, Canada

At submarine hydrothermal vents, barite precipitates within vent chimney walls as hot hydrothermal fluid comes into contact and mixes with cold seawater. The formation of barite is dependent upon temperature and the availability of Ba^{2+} and SO_4^{2-}, from the hydrothermal fluid and local seawater, respectively. Fluid temperatures and ion availability are both intimately linked to the source fluids with respect to their amounts and degree of mixing. Thus, barite precipitation records the physical and chemical conditions of fluid mixing within the porous chimney walls. Here, we use $^{87}Sr/^{86}Sr$ values recorded in barite from hydrothermal vents along the intermediate-rate spreading Endeavour Segment of the Juan de Fuca Ridge, along with detailed petrography and electron microprobe analysis, in order to investigate the conditions of barite precipitation and fluid interactions within chimney walls.

The $^{87}Sr/^{86}Sr$ ratio in seawater differs from the $^{87}Sr/^{86}Sr$ ratio in hydrothermal fluid, making it possible to use the $^{87}Sr/^{86}Sr$ ratio in barite as a measure of the relative amount of local mixing between seawater and the hydrothermal fluids. The $^{87}Sr/^{86}Sr$ isotope ratios in a suite of 16 hydrothermal barite samples from the Endeavour Segment have been measured. The results demonstrate a broad scale of mixing, with the percent hydrothermal fluid component ranging from 25% to 90%. This variation in relative mixing suggests that barite can form under a variety of conditions. Petrographic examination of barite crystals show that barite in chimney walls can precipitate as a variety of different crystal habits, from dendritic to acicular and blocky. Variations in the relative amount of mixing are linked to barite crystal morphologies, providing further insights into the controls of ion availability on barite precipitation.

Electron microprobe analysis of barite crystals from the Endeavour vents reveals well-defined zones, characterized by varying Sr-concentrations within individual crystals. Two possible mechanisms for the formation of these zones are: 1) The relative contributions of seawater and hydrothermal fluid changes during the formation of the barite crystals; 2) The concentration of strontium in the seawater-fluid mixture changes as the crystals form. LA-MC-ICP-MS is used to determine the $^{87}Sr/^{86}Sr$ ratios of individual zones within the crystals, in order to evaluate the relative importance of these two processes.

The relationships between fluid mixing, barite crystal morphology, Sr content and $^{87}Sr/^{86}Sr$ ratios provide insights into the degree of conductive cooling relative to fluid mixing and into temporal variations in fluid chemistry as a control on mineral precipitation within vent chimney walls at Endeavour.

https://doi.org/10.1180/S0026461X00008434 Published online by Cambridge University Press

The Eh and pH of Fracking

DR. TERRY ENGELDER

[1]Department of Geoscience, The Pennsylvania State University (USA),

The extraction of natural gas from shale is now routine using massive slickwater hydraulic fractures. Along with its obvious economic advantages, this extraction technique comes with a number of well publicized risks, foremost of which is the migration of methane in the subsurface. Subsurface migration is a consequence of drilling into exhumed gas fields such as the Appalachian Basin where the areal extent of the Marcellus makes this gas reservoir one of the world's largest. During thermal maturation of the Marcellus between 300 Ma and 265 Ma gas was distributed throughout the Catskill Delta complex by natural hydraulic fractures (NHF). Migration of reducing fluids within redbeds of the delta complex accompanied NHF. Reduction halos allow the mapping of these pathways. While NHF was gas-driven as indicated by a cyclic plume pattern on fracture surfaces, high permeability NHF allowed the modern distribution of gas in these exhumed gas fields.

Peat land records of atmospheric mercury deposition in the French Pyrenees

ENRICO, MAXIME [1,2,3*], HEIMBÜRGER, LARS-ERIC[1], LE ROUX, GAEL[2,3], SONKE, JEROEN E.[1]

[1]CNRS; Geosciences Environment Toulouse, 31400, Toulouse, France, maxime.enrico@get.obs-mip.fr (* presenting author)
[2] Université de Toulouse; INP, UPS; EcoLab (Laboratoire Ecologie Fonctionnelle et Environnement); ENSAT, Avenue de l'Agrobiopole, 31326 Castanet Tolosan, France, gael.leroux@ensat.fr
[3] CNRS; EcoLab; 31326 Castanet Tolosan, France

Abstract

Mercury (Hg) has a long residence time in the atmosphere, which suggests that Hg recorded in peat lands derives partly from long-range transport. However, Hg accumulation rates (Hg AR) reconstructed from peat cores in European bogs do not show exactly the same spatiotemporal evolution. The question remains to which extent local point sources, climate and site specific processes might influence Hg AR.

We present here results of three peat lands in the French Pyrenees: 1) Pinet (42°51'N, 1°58'E), 2) Orri de Théo (OT: 42°45'N, 1°24'E), and 3) Estibere (42°50'N, 0°10'E). The three sites cover a 150 km East-West transect along the French Pyrenees. The peat cores were cut at 1cm resolution according to the protocol of Le Roux *et al.* [1], Hg AR were determined for the last 2,000 years in OT and Estibere, and for the last 10,000 years for Pinet. A multi-coring protocol was used to investigate local-spatial variability of Hg AR. Pre-anthropogenic Hg AR obtained at Pinet show natural variations during the Holocene (between 0.2 and 13µg.m^{-2}.y^{-1} with an average of 1.5µg.m^{-2}.y^{-1}), which could be related to climate change. Since the beginning of the Anthropocene, Hg AR increased by a factor 25 and are similar within and between the three peat lands.

In the upper part of the peat cores, three peaks are well-defined and recorded similarly at OT and Pinet, corresponding to the periods 1950-1955 (Hg AR at around 25µg.m^{-2}.y^{-1} at OT and 42µg.m^{-2}.y^{-1} at Pinet), the 1970's (38µg.m^{-2}.y^{-1} at OT and 52µg.m^{-2}.y^{-1} at Pinet) and 1994-95 (55µg.m^{-2}.y^{-1} at OT and 62µg.m^{-2}.y^{-1} at Pinet). The similar evolution of Hg AR in these two peat lands, which are spread out over 50km, suggest that they do not reflect Hg deposition from different local sources but more likely common regional or global source(s).

In addition to these similarities, we also observe some differences in Hg AR, reflecting local emission sources. For example, high Hg AR (around 12µg.m^{-2}.y^{-1}) are found around 1500AD at OT, probably the result of local Fe-Pb-Ag mining activities and related to coal burning, and a peak (100µg.m^{-2}.y^{-1}) is found at Pinet in 2001.

[1] Le Roux *et al.* (2010), *Mires and peat* **7**, 4.

https://doi.org/10.1180/S0026461X00008434 Published online by Cambridge University Press

Calcification mechanisms explain why proxies in foraminifera and corals are good recorders of their environment

JONATHAN EREZ *

The Institute of Earth Sciences, The Hebrew University, Jerusalem, Israel . erez@vms.huji.ac.il

Current thinking on biologically controlled calcification involves active and passive transport of calcium from the environment across cell membranes to form cellular storge [1]. The formation of the mineral phase may be intracellular (e.g. coccolithophores) or extracellular, within a delimited space. Calcium is transported from the cellular stores as an free ion or in vesicles, under tight cellular control to the delimited space. The carbonate supply is usually ignored or assumed simple: CO_2 may diffuse freely from the environment, or respiratory CO_2 may provide an internal source for DIC. Given the complete cellular control on the ions supply, it is surprising that trace elements and isotopes are incorporated into marine biogenic carbonates with meaningful relations to the seawater. Furtheremore, despite some deviations from thermodynamic equilibrium, geochemists and paleoceanographers have utilized various proxies in biogenic carbonates (mainly foraminifera, corals, sponges and mollusks) very successfully to reconstruct past oceanic conditions. The current biological thinking (described above) is incorrect. The ions (Ca, Mg, Sr, Ba, DIC, B, Li, and others) and their isotopes are supplied to the delimited calcification space by **direct trasport of ambient seawater** (slightly modified). This has been demonstrated unequivocally in foraminifera [2,3], and more recently has been shown for corals [4]. The pathway of seawater transport to the site of biomineralization is by vacuolization in foramoinifera, and apparently by paracellular leakage in corals. In other marine invertebrates seawater is present at the biomineralization delimited space, but it remains to be shown how this is achieved. Seawater is rich in Ca (~10.5 mM, as opposed to 0.1 µM in live cells), however the DIC concentration (~ 2mM), is much lower.. High Mg concentration (~ 55 mM) inhibits calcite precipitation and hence high supersaturation is needed in order to precipitate the $CaCO_3$ shells. The most common mechanism to increase saturation is elevation of pH at the calcification site. This pH elevation helps to supply DIC both from seawater and from respiration as observed in corals and foraminifera.. The composition of various isotopic and elemental proxies in both groups (e.g. O, C, B, Li, Mg, Sr and others) are best explained using this novel calcification mechanism. Direct seawater transport (DST) explains the usefulnes of paleoceanographic proxies in biogenic carbonates.

[1] Weiner and Dove, (2003) Rev. Mineral. & Geochem. **54**:1-29
[2] Erez, (2003), Rev. Mineral.& Geochem. **54**:115-149.
[3] Bentov, Erez, & Brownlee, (2009), PNAS **106**(51) 21500-21504
[4] Tambutté E, Tambutté S. Segonds, Zoccola, Venn, Erez, Allemand, (2011), Proc., Roy. Soc. London doi: 10.1098/ 2011.0733

Coupled Ge/Si and Ge isotope ratios as new geochemical tracers of seafloor hydrothermal systems: A case study at Loihi Seamount

ESCOUBE R. [1,2,3*], ROUXEL O.J.[2,3*], DONARD O.F.X.[4]

[1] Departement of earth sciences, University of Oxford, Oxford, UK, raphaele@earth.ox.ac.uk (*)
[2] IFREMER, Centre de Brest, DRO-GM, Plouzané, France
[3] Marine Chemistry & Geochemistry, Woods Hole Oceanographic Institution, Woods Hole, MA02543, USA
[4] LCABIE, CNRS UMR 525, Hélioparc, 64053 Pau, France

Germanium isotope and Ge/Si ratio systematics were investigated in low temperature hydrothermal vents from Loihi Seamount (Hawaii, USA) and results were compared to high-temperature vents from East Pacific Rise at 9-10°N. Loihi offers the opportunity to understand a low temperature basalt leach system with surface deposits mainely composed of iron oxyhydroxides. The results show that both Ge/Si and $\delta^{74/70}$Ge in hydrothermal fluids are fractionated relative to the host basaltic rock with Ge/Si ~ 30 and 5.7 µmol/mol and δ^{74}Ge ~ 1.9 and 1.55‰ for Loihi and EPR (Bio9) respectively vs. Ge/Si ~ 2.2 µmol/mol; δ^{74}Ge ~ 0.56‰ for basalt[1]. The relative enrichment in Ge vs. Si together with Ge isotope fractionation can be explained by quartz precipitation in the reaction zone at depth. Using Ge mass balance between hydrothermal fluids and fresh basalts, we calculated a $\Delta^{74}Ge_{quartz\text{-}fluid}$ of about -5.0‰. Although the fractionation of Ge isotopes in quartz is presently unknown, such apparent large Ge isotope fractionation at elevated temperature suggests concomitant loss of Ge and Si during fluid upflow resulting in Rayleigh-type effect and/or a fractionation during the basalt dissolution. The study of microbial mats at Loihi Seamount, composed essentially of Fe-oxyhydroxide with minor phases of amorphous silica and volcanic materials, also suggest that Ge isotopes are fractionated upon precipitation at the seafloor during seawater - hydrothermal fluids mixing. We obtained a maximum Ge isotope fractionation between Fe-oxyhydroxide (ferrihydrite) and dissolved Ge in the fluid of about -2.74‰. Isotopic variations observed in the different mats have being interpreted as reflecting the percentage of Ge sequestration in microbial mats; the lower values corresponding with the highest Ge trapping. This result is consistent with recent experimental estimation[2]. This study shows that combining Ge/Si and δ^{74}Ge systematics provide a useful tool to trace hydrothermal Ge and Si sources in marine environments and to understand formation processes of seafloor hydrothermal deposits. Preliminary mass balance of germanium isotope in seawater reveals that the missing Ge sink may correspond to Ge sequestration into Fe-oxyhydroxides within marine sediments.

[1] Escoube et al. (2011) *GGR*; [2] Galy et al. (2002) *GCA* **66**, A259

https://doi.org/10.1180/S0026461X00008434 Published online by Cambridge University Press

Do melt inclusions record the pre-eruptive volatile content of magmas?

ROSARIO ESPOSITO[1]*, JAMES SCHIFFBAUER[2], JERRY HUNTER[2] AND ROBERT J. BODNAR[1]

[1]Virginia Polytechnic Institute & State University, Department of Geosciences, Blacksburg, VA 24061 USA rosario@vt.edu (*presenting author)

[2]Nanoscale Characterization and Fabrication Labs, Virginia Tech, Blacksburg, VA 24061 USA

In the last several decades the number of publications describing the use of melt inclusions (MI) to determine the pre-eruptive volatile contents of magmas has significantly increased. However, in most MI studies, the volatile contents of the MI vary widely within phenocrysts from the same volcanic sample. It is common for MI hosted in the same phenocryst to show significant variations in volatile concentrations, especially for CO_2. In fluid inclusion (FI) studies, workers have developed a protocol to test that the inclusions in a sample record the original trapping conditions by studying groups of FI trapped at the same time (Fluid Inclusion Assemblage, FIA), and which obey Roedder's (Sorby's) Rules. Specifically, (i) the FI must have trapped a single homogeneous phase, (ii) the volume of the FI must remain constant after trapping, and (iii) nothing can be added or lost from the FI after trapping. While this approach has worked successfully in FI staudies and should be successful in MI studies, there are two main reasons why MI studies rarely apply this methodology. The first is related to the lower probability, relative to fluid inclusions (FI), of finding Melt Inclusion Assemblages (MIA) in a phenocryst. The second is related to the necessity of exposing MI at the crystal surface in order to obtain chemical analyses, and this is particularly true for volatile analyses. In this study, the MIA approach has been used to assess if MI provide reliable information of pre-eruptive volatile contents. Groups of MI within well-defined MIAs hosted in phenocrysts from White Island (New Zealand) and from Solchiaro (Italy) were analyzed by Secondary Ion Mass Spectrometry (SIMS). We have studied 39 MIA and 144 MI were analyzed for CO_2, H_2O, F, S, and Cl.

In most MIA, H_2O, F, and Cl abundances are consistent, indicating that MI in these MIA represent the pre-eruptive abundance of these three volatile species. CO_2 and S abundances were consistent in some MIA, but especially CO_2 showed a wide variation in others. The wide range in CO_2 content could reflect the presence of a CO_2-rich boundary layer at the MI/host interface controlled by post-entrapment crystallization of the MI, and may also be a function of the MI morphology. Thus, MI may appear to be highly heterogeneous in volatiles such as CO_2 and S that are the less soluble in melts of this composition. The wide range in S is restricted to MIA hosted in Fe-bearing phenocrysts, suggesting that the variability may be due to post-entrapment processes. Although working with MIAs is time consuming and tedious, we recommend the MIA approach to study pre-eruptive volatile contents in order to recognize MI whose volatile abundances do not accurately reflect pre-eruptive volatile concentrations in the magma.

Bulk and Micro Mineralogical Characterization of As in Uranium Mine Tailings

JOSEPH ESSILFIE – DUGHAN[1]*, M. JIM HENDRY [2], JEFF WARNER[3], AND TOM KOTZER[4]

[1]University of Saskatchewan, Geological Sciences, Saskatoon, Canada, joe377@mail.usask.ca (* presenting author)

[2]University of Saskatchewan, Geological Sciences, Saskatoon, Canada, jim.hendry@usask.ca

[3]Canadian Light Source Inc., Saskatoon, Canada, Jeff.Warner@lightsource.ca

[4] Cameco Corporation, Saskatoon, Canada, Tom_Kotzer@cameco.com

Introduction

In northern Saskatchewan, Canada, high-grade uranium ores and the resulting processed tailings can contain high levels of arsenic (As). The potential mobilization of As from the tailings management facilities (TMFs) to contaminate regional groundwater systems is an environmental concern in the uranium mining industry.

Knowledge regarding the speciation of As in natural systems is critical for determining its long-term environmental fate. Specifically, characterization of As-bearing mineral phases and complexes within the processed U tailings is required to evaluate their potential transformation, solubility, and long-term stability within the tailings mass. Synchrotron-based bulk X-ray absorption spectroscopy (XAS) was used to study the redox and molecular speciation of As in tailings samples obtained from the Deilmann TMF at Key Lake, Saskatchewan. Electron microprobe analysis (EMPA) and synchrotron-based micro-focussing X-ray fluorescence mapping and absorption spectroscopy (μXRF; μXAS) were employed to study the spatial distribution and speciation of As at the micron scale.

Results and Conclusion

Comparisons of K-edge XAS spectra of tailings samples and reference compounds indicate As in the tailings samples primarily exists in the +5 oxidation state; this reflects the generation of the tailings in a highly oxic mill process, their deposition in an oxidized environment, and complexation within stable oxic phases. Extended X-ray absorption fine structure (EXAFS) analysis of As K-edge spectra indicates that As^{+5} (arsenate) present in the tailings samples is adsorbed to ferrihydrite though an inner-sphere bidentate linkage. Backscattered electron (BSE) images of the tailings from the electron microprobe show the presence of nodule-like features with bright rims. Data from elemental mapping indicate the nodules are largely composed of Ca and S (i.e., gypsum), with the surrounding rims mainly consisting of As and Fe. μXRF elemental mapping confirms the EPMA results. μXAS data collected at various points on the rims surrounding the gypsum nodules suggest that Fe is present as ferrihydrite with adsorbed As.

These findings will facilitate the accurate characterization and quantification of the potential for long-term migration of As from TMF porewaters to adjacent groundwater systems.

https://doi.org/10.1180/S0026461X00008434 Published online by Cambridge University Press

Influence of ion coprecipitation and adsorption on iron (hydr)oxide structure and aggregate morphology

EMILY R. ESTES[1,2*], YONGMEI SHEN[2], M. DARBY DYAR[3], DANIEL J. BRABANDER[2,4] AND JAMES P. SHINE[2]

[1]Harvard University Earth and Planetary Sciences, Cambridge, USA, eestes@fas.harvard.edu (*presenting author)
[2]Harvard School of Public Health, Boston, USA, yshen@hsph.harvard.edu, jshine@hsph.harvard.edu
[3]Mount Holyoke College, South Hadley, USA, mdyar@mtholyoke.edu
[4]Wellesley College, Wellesley, USA, dbraband@wellesley.edu

Introduction

Due to their ubiquity in the environment, high surface area, and affinity for both inorganic and organic molecules, iron oxides and hydroxides (FeOx) play an important role in mediating contaminant mobility. Coprecipitation and adsorption of ions influence the reactivity and long-term stability of FeOx minerals by altering their crystal structure, grain size and morphology, and extent of particle aggregation. Al, Si, phosphate, and organic matter, for example, may coprecipitate at stoichiometric ratios up to 50%. TThese ions, along with heavy metals and other less common elements, may produce changes in reactivity and structure even at significantly lower concentrations. While numerous lab-based studies have parameterized the influence of individual variables, the difficulty inherent in characterizing naturally-precipitated FeOx minerals in a complicated matrix has limited the extrapolation of results to field systems.

Methods

We analyze natural samples collected from the Pb-, Zn-, and Cd-contaminated Tar Creek Superfund Site through a combination of sequential chemical extractions targeting iron phases and Mössbauer spectroscopy to monitor how heavy metal speciation varies during reactive transport and whether FeOx structural parameters obtained via Mössbauer correlate with sample bulk chemistry. We also show results of small angle X-ray scattering (SAXS) on synthetic ferrihydrite samples to investigate how ion coprecipitation and sorption affect aggregate morphology.

Results

Si and organic matter content covary most significantly with Mössbauer parameters, although extraction of P and Al by the sequential extraction steps targeting more crystalline FeOx phases suggests that they may also be an important determinant. Of the ions tested, phosphate produced the largest effect on aggregate structure, increasing mean particle radius and aggregate fractal dimension. This combination of techniques ultimately provides insight into how the matrix may alter iron reactivity and thus control contaminant speciation.

Probing the interactions between glutamic acid and diopside

CHARLENE F. ESTRADA[1,2*], EHOW H. CHEN[3], FRANZ M. GEIGER[3], DIMITRI A. SVERJENSKY[1,2], ROBERT M. HAZEN[2]

[1]Johns Hopkins University, Earth & Planetary Sciences, cestrada@jhu.edu (*presenting author), sver@jhu.edu
[2]Geophysical Laboratory, Carnegie Institution of Washington
[3]Northwestern University, Chemistry, geigerf@chem.northwestern.edu

Abstract

The manner in which organic molecules adsorb onto the mineral/water interface may hold implications for the origin of life. Chiral amino acids may have selectively adsorbed onto the chiral growth faces of silicate minerals by three or more non-colinear points of attachment, which may have led to the evolution of homochirality. Diopside is a common clinopyroxene mineral with the chiral growth faces (110) and (1-10), which are also the principal cleavage planes prominent in powdered samples. We demonstrated with batch adsorption experiments that up to 30% of L-glutamic acid (initially 20 μM) adsorbs onto crushed natural diopside at pH=10. We investigated the enantioselective potential of diopside by probing the interactions between glutamic acid and the chiral growth faces (110) and (1-10) with vibrational sum frequency generation (SFG) spectroscopy. Prior to our experiment, we prepared two 0.63 mm thick (1-10) diopside sections of approximately 500 mm^2, which were cleaned with a plasma cleaner. One diopside section was submerged in 100 μM L-glutamic acid for 2h and dried under nitrogen, whereas the other section served as a blank. The SFG spectra we collected for the diopside section with L-glutamic acid significantly differed from those of the blank. As a preliminary analysis, we assigned asymmetric and symmetric stretching modes for the β-methylene group and a symmetric stretching mode for the γ-methylene group of L-glutamic acid. We obtained SFG spectra of adsorbed L-glutamic acid under two experimental mutually perpendicular polarization combinations. In principle, spectra such as these can establish the configuration of the adsorbed molecule. A comparison of the ratio of SFG signal intensity for the methylene vibrational modes between the two polarization combinations will determine the dipole orientation of the methylene stretches relative to the diopside surface. This technique may be useful for establishing an enantioselective trend in glutamic acid adsorption.

https://doi.org/10.1180/S0026461X00008434 Published online by Cambridge University Press

Structural controls on fluid evolution in the Devonian Marcellus shale during deformation of the central Appalachians

MARK A. EVANS*

Central Connecticut State University, New Britain, CT 06050 USA
(Correspondence: evansmaa@ccsu.edu)

Fluid inclusion microthermometry of temporally controlled vein minerals is used to evaluate the fluid conditions of the Middle Devonian Marcellus shale during the Alleghenian orogeny. Samples from folded rocks in the Pennsylvania salient and in less deformed rocks of the Plateau province indicate that fluid pressure – temperature — composition (PTX) does not remain static during orogenesis, but varies significantly both in time and between structural settings.

Regionally, the earliest trapped fluids are in dolomite, calcite, and/or barite and consist of degraded liquid hydrocarbons, liquid hydrocarbons and condensate-type fluids. These fluids are interpreted to have been trapped during peak oil generation and migration, probably during basin filling and before folding. Fluid trapping occurred at temperatures of 60° - 118°C and at depths of less than 3.8 km.

Within the Valley & Ridge province, however, samples from folded rocks additionally contain later quartz and calcite with multiple fluid trapping events reflecting a dynamic vein opening history related to changes in fluid connectivity associated with syn-folding fracturing that allows for increased fluid mobility. The fluid trapping events are characterized by diferent fluid salinities (ranging from 10 to 25 wt. % equiv.) and CH_4:CO_2 ratios. This increased connectivity is occurring during 1) burial associated with overthrusting and/or syntectonic depositional loading and/or 2) syn-folding uplift and erosion. Importantly, the PTX history of sites in synclines is different from sites on anticlines, and reflects the different structural history of each location. The influx of fluids is indicated by the concurrent dissolution of vein calcite and precipitation of quartz, and that brine inclusions in the quartz consistently increase in T_h from early to late quartz. Interestingly, this late quartz is suprisingly methane-rich, and contains abundant, large CH_4±CO_2 inclusions, while aqueous inclusions are exceedingly rare.

Along the boundary between the subhorizontal rocks of the Plateau province and the folded rocks of the Valley and Ridge, the PTX conditions determined for the Marcellus veins indicate a significant variation along strike. To the northeast, the lack of quartz and the presence of only liquid hydrocarbon and CH_4±HHC inclusions in calcite and barite suggests little fluid mobility. On the other hand, to the southwest, late quartz contains more mature CH_4±CO_2 inclusions and the presence of corroded early calcite suggests a fluid influx. The sites containing the later quartz are adjacent to an area of the Plateau with increased thermal maturation based on vitrinite relectance, suggesting that 'warm' fluids passing through the Marcellus may be responsible for the increased maturation.

Yellowstone hot spring microbial communites fed with hydrogen and bicarbonate as a metabolically active analogue for early Earth environments

HALLGERD EYDAL[1,2*], LISE ØVREÅS[2], JOHN R SPEAR[1]

[1]Colorado School of Mines, Golden, USA, heydal@mines.edu*
[2]University of Bergen, Bergen, Norway, lise.ovreas@bio.uib.no

Obsidian Pool in Yellowstone National Park

Microbial ecosystems independent of sunlight and supported by hydrogenotrophic primary production have been shown in subsurface environments such as basaltic rock aquifers and volcanic rock [1,2]. The presence and activity of such ecosystems in Obsidian Pool sediments in Yellowstone National Park (YNP) was the focus of this study, as microorganisms in these environments include groups branching deeply in the phylogenetic tree of life.

Obsidian Pool is known to have diverse microbial communities of hydrogen-oxidizing bacteria and archaea [3, 4] and the water in the pool contains 46 nM H_2. The H_2 to support miro-organisms can be generated from magmatic gases [5]. Using molecular techniques, hydrogen oxidizing aerobic bacteria have been shown to be the most abundant microorganisms present at Obsidian Pool. By contrast, the sediment in Obsidian Pool is anoxic and hydrogen utilizing methanogens have been shown elsewhere in YNP [6].

Experimental

To study active hydrogenotrophic methanogens anaerobic *in situ* incubation microcosms fed with H_2 and $NaHCO_3$ were set up. Changes in H_2 and CH_4 concentrations were followed using gas chromatography. Additionally, copy number changes of a metabolic gene for methanogenesis (methyl coenzyme M reductase α-subunit; mcrA) was studied using quantitative PCR. The microbial community structure was studied with 16S rRNA gene sequence diversity via 454 pyrosequencing.

Results and conclusion

When the diversity of the 16S rRNA gene was followed using 454 pyrosequencing, Obsidian Pool was found to be dominated by Aquificales. Quantitative PCR of archaeal 16S rRNA and mcrA genes, consumption of H_2 and production of CH_4, as well as relative abundances of 16S rRNA sequences confirmed active populations of the hydrogenotrophic *Methanothermobacter* with a generation time of 6.4 h. Hydrogenotrophic organisms in turn sustained growth of heterotrophic organisms such as Thermotogales and Nitrospira. Our study supports the exsistence of a hydrogen driven subsurface ecosystems which in the 16S rRNA gene phylogeny have deeply branching microorganisms, potentially similar to the early life on Earth. This highly active and accessable early Earth analogue, will allow studies of microbial interaction in a natural environment.

[1] Stevens (1995) *Science* **270**, 450-454. [2] Chapelle (2002) *Nature* **415,** 312-5. [3] Hugenholtz (1998) *J Bacteriol* **180,** 366-76. [4] Spear (2005), *P Natl Acad Sci USA* **102**, 2555-60. [5] Fournier (1989) *Annu Rev Earth Pl Sc*, **17,** 13-53. [6] Zeikus (1980), *J Bacteriol* **143**, 432-40.

https://doi.org/10.1180/S0026461X00008434 Published online by Cambridge University Press

Melt movement by dilation-assisted compaction, Damara Belt, Namibia

CARLY FABER[1*], JOHANN F.A. DIENER[1], ALEX F.M. KISTERS[2]

[1]Department of Geological Sciences, University of Cape Town, South Africa, carlyfaber1@gmail.com (* presenting author), johann.diener@uct.ac.za

[2]Department of Earth Sciences, University of Stellenbosch, South Africa, akisters@sun.ac.za

Melt migration through the crust is the main mechanism that facilitates upward movement of heat and mass and the chemical differentiation of the continental crust. Crustal-scale melt movement is divided into three phases; segregation from the source, migration and ascent, and emplacement[1]. Whereas the processes of segregation and emplacement are relatively well understood, melt ascent mechanisms are more speculative.

We document an example of long-lived syn-deformational melt migration through an 80m-thick upper-amphibolite facies, subsolidus metasedimentary sequence in the southern Central Zone of the Damara Belt, Namibia. The package is shallowly-dipping and structurally bound by migmatitic gneisses at the top and bottom. The metasediments have not experienced extensive anatexis, and preserved leucosome represents migration and emplacement from the underlying migmatitic gneisses (melt source) into the metasediments.

The position and orientation of the leucogranites is structurally and lithologically controlled, and defines a composite 3D network of intersecting sheets and stringers on the metre to decametre-scale. Structures that comprise the networks include fabric-concordant sheets, sheets and dykes within conjugate shear zone planes, and leucogranite-bearing boudin necks, tensile fractures and leucogranite-cemented breccias. The deformation along the conjugate shears indicates that melt migration occurred during tectonic compaction of the sequence. The presence of at least five compositionally and texturally distinct leucogranite phases of different volume shows that structures within the network were repeatedly utilized by separate melt batches over a protracted period of time.

Low-volume melts achieved ascent through stepwise pervasive migration, controlled by the rate at which structures were able to dilate and create permeability during progressive deformation. High-volume melts ascended rapidly and in a single pulse along 10-25m diameter pipes that crosscut the entire supracrustal sequence. These pipes contain leucogranite-cemented breccias consisting of 5-10m angular and rotated wall-rock fragments. This suggests rapid opening of the fractures followed by implosion of the country rocks.

The different leucogranite phases indicate a repeated and long-lived utilization of networked structures formed during regional deformation. However, low melt volumes exploited these networks passively as the rate of tectonic dilation was sufficient to accommodate the low melt volumes. In contrast, high melt volumes contributed additional permeability to the network through fracturing and brecciation, driven by melt embrittlement and overpressure as melt supply exceeded the rate of tectonic dilation.

[1] Brown (2007) *Journal of the Geological Society* **164**, 709-730.

How do oceanic biotic components influence the production mechanism of organic aerosol in Marine Boundary Layer (MBL)?

M.C. FACCHINI[1]*, C. O'DOWD [2]

R. DANOVARO[3]

[1] Institute of Atmospheric Sciences and Climate, National Research Council ,Italy(*correspondence:mc.facchini@isac.cnr.it)

[2] Department of Experimental Physics & Environmental Change Institute, National University of Ireland Galway, Galway, Ireland

[3] Department of Life and Environmental Sciences Polytechnic University of Marche, Ancona, Italy

Studies performed during the past years strongly suggest that biogenic organic compounds play an important role in submicron marine aerosol chemical composition over biologically productive, high latitude, marine regions, in both hemispheres and new biogenic oceanic sources of primary and secondary origin of OA were revealed. We discuss on the global importance of biogenic OA marine sources and their high spatial and temporal variability and the complex interaction with gaseous biogenic precursors and oceanic biotic components (Phytoplankton, viruses and bacteria). Submicron marine organic aerosol are a complex mixture of biogenic materials transferred from the ocean surface by the sea spray or by oxidative gas to particle conversion of volatile organics emitted by decomposition processes of oceanic dissolved organic carbon. The role of marine biota on the evolution of plankton bloom and on the partitioning of oceanic organic carbon in POC and DOC or gaseous species and on transfer mechanisms into MBL will be discussed.

https://doi.org/10.1180/S0026461X00008434 Published online by Cambridge University Press

Opening-mode fracturing and cementation during hydrocarbon generation in mudrocks: an example from the Barnett Shale, West Texas

ANDRÁS FALL[1*], JULIA F. W. GALE[1], PETER EICHHUBL[1], WALAA A. ALI[1], STEPHEN E. LAUBACH[1], ROBERT J. BODNAR[2]

[1]Bureau of Economic Geology, Jackson School of Geosciences, The University of Texas at Austin, Austin, TX, USA, (* presenting author: andras.fall@beg.utexas.edu)

[2]Department of Geosciences, Virginia Tech, Blacksburg, VA, USA

Natural fractures in mudrocks are common and develop due to different mechanisms operating at different times during the burial history. Knowledge on the mechanisms and timing of fracture opening and cementation is desirable because natural fractures can contribute to permeability if open, and can interact with hydraulic fracture treatments of shale hydrocarbon reservoirs whether open or sealed.

Analysis of fracture-filling cements in three fracture sets in core from the Barnett Shale in the Delaware Basin, West Texas is combined with a burial history model and data from fluid inclusion microthermometry and Raman spectroscopy to determine fracture timing, and to obtain insights into the mechanism of fracture formation. An early fracture set that was folded during shale compaction is mostly sealed with dolomite cement, but retains small pores lined with barite. A second set includes horizontal (bedding-parallel), low angle, and irregular subvertical fractures that are sealed with fibrous barite. The barite contains coexisting primary, liquid-rich hydrocarbon (oil) and aqueous fluid inclusions trapped at temperature and pressure (P-T) conditions of ~110°C, and ~55 MPa, respectively. We interpret the primary inclusions as forming during rapid burial when compaction disequilibrium combined with cracking of type II kerogen to oil caused an overpressure, thus providing a mechanism for fracturing. In addition, this set of fractures contains secondary, vapor-rich hydrocarbon (methane dominated) inclusions with condensate rims, trapped along planes that cross-cut the barite fibers. We interpret these secondary inclusions as having formed during secondary gas generation from oil (bitumen). A third set of fractures, which are partly open, contains quartz cement bridges with crack-seal structure indicative of quartz cementation during episodic fracture opening. Quartz cementation continued after opening had ceased, overgrowing the crack-seal structure. Methane saturated aqueous inclusions in the quartz bridges formed at P-T conditions of ~110°C and 35-45 MPa in the crack-seal quartz, and ~128°C and ~35 MPa in quartz overgrowths. Correlation with a burial history model suggests this set opened concurrently with, or soon after, the fractures with fibrous barite, but prior to secondary gas generation. The heterogeneous distribution of inclusions may reflect heterogeneous trapping of the two-phase hydrocarbon/aqueous fluid system in the reservoir. All three fracture events may have formed during the burial phase, although elements of the third set may have developed during the first uplift event associated with Laramide deformation.

Evaluating the provenance study methodology of using detrital zircon U-Pb ages in the Changjiang drainage basin

DAIDU FAN*, YANGYANG WANG

Tongji University, State Key Lab of Marine Geology, ddfan@tongji.edu.cn

High-resolution provenance study has been highly expected since the availability of single-grain dating methods, especially after the wide application of LA-ICPMS on the microanalyses of zircon grains. Large volumes of zircon dating data have been published in the last two decades in China. Data of crystalline zircon U-Pb ages and εHf(t) values have been extensively collected in the Changjiang drainage basin from over 100 journal papers, which were majorly published in the last decade. They were systematically analyzed, together with statistics on the outcropped area of igneous rocks, to explore the possibility to fingerprint provenance in such a wide and complex drainage basin.

Some major findings are summarized. (1) Some vast tectonic provinces, like the Yangtze Block extending from the upper reach to the lower reach, should be subdivided into several parts for the high spatial resolution of provenance study. (2) Only a few groups of zircon ages, including <50 Ma, 250~270 Ma and >3000 Ma, can be used directly to fingerprint their source from the Changdu Block, the northern and the western subdivisions of the Yangtze Block, respectively. (3) Some zircon ages are indicative of their specified sources based on the different peak ages of single individual tectonic events in the varied tectonic blocks (subdivisions). (4) The effectiveness of provenance distinguishing can be significantly improved by application of the scatter plotting of zircon U-Pb ages and εHf(t) values, while some groups of zircon ages are still unable to assign to any certain source. (5) The intrusion of the recycled zircons cannot be excluded, and sometimes they make a significant contribution to the fluvial zircons, like those from the widely distributed Triassic turbidites in the Songpan-Garze Massif. (6) The frequency based on counting the available dated zircon grains in each tectonic units are not necessarily the abundance of different aged zircons, usually quite different from the area statistics of the outcropped igneous rocks of the corresponding ages, so the high-resolution provenance study should take both into consideration.

https://doi.org/10.1180/S0026461X00008434 Published online by Cambridge University Press

Evaluating pore fluid Mg isotopic and elemental constraints on seawater Mg chemistry in the Cenozoic

MATTHEW S. FANTLE[1,*] AND FANG-ZHEN TENG[2]

[1] Department of Geosciences, Penn State University, University Park, PA, USA, mfantle@psu.edu (* presenting author)
[2] Department of Geosciences, University of Arkansas, Fayetteville, AR, USA, fteng@uark.edu

Interpreting Cenozoic climate and environment accurately using marine geochemical proxies requires high fidelity proxies that are resistant to diagenetic alteration over tens of millions of years. For mineral-based proxies that do not passively sample seawater, such as Mg/Ca and stable isotopic proxies, it is also necessary to place limits on the chemistry of seawater (i.e, the solution from which the minerals precipitate). The latter is predominantly true for Cenozoic proxies over time scales longer than elemental residence times (τ) in the ocean (τ_{Mg}~10 Ma; τ_{Ca}~1 Ma).

This study utilizes depositional reactive transport models of carbonate diagenesis to simulate measured pore fluid and solid Mg isotopic and elemental data from ODP Site 807A (ave. $CaCO_3$ ~92 wt%). The ultimate goal of the iterative modeling approach taken is to (1) evaluate the extent to which pore fluid chemistry can be used to elucidate the Mg chemistry of the Cenozoic ocean and (2) estimate the degree to which diagenesis alters the Mg isotope and Mg/Ca proxies. Previously published recrystallization rates, based on Ca and Sr isotopic and elemental data, constrain the models [1-2].

The Mg isotopic composition ($\delta^{26}Mg_{DSM3}$) of 807A pore fluids varies systematically from -0.79 to -0.25‰ between the shallowest (13.4 mbsf) and deepest (738 mbsf) fluids. There is notable structure in pore fluid $\delta^{26}Mg$ as a function of depth that is not well explained by diffusion, either of an initial seawater signal or between boundaries that reflect modern seawater (upper) and basement basaltic Mg (lower). Accordingly, reaction must be considered.

In the current study, endmember model scenarios are used to evaluate the applicability (and uncertainty) of pore fluid chemical data for constraining past seawater chemistry. The modeling assumes that carbonate recrystallization is the dominant reaction controlling the alteration of Mg pore fluid chemistry in the sedimentary column. The first endmember scenario generates seawater Mg concentration and $\delta^{26}Mg$ curves for a range of partition coefficients (K_{Mg}) assuming a constant value for the diagenetic fractionation factor. A second set of simulations assumes seawater Mg concentrations consistent with evaporite fluid inclusion data and constrains K_{Mg} and the Mg isotopic evolution of the ocean accordingly.

The model results are subsequently used to assess the potential for diagenetic alteration of bulk carbonate. Given low Mg concentrations, reactions rates on the order of <2%/Ma, and an assumed equilibrium fractionation factor and partition coefficient that are different at depth than in the surface ocean, there is considerable leverage to change both the Mg isotopic composition and Mg/Ca of bulk carbonates over tens of millions of years.

[1] Fantle and DePaolo (2006) GCA, 70, 3883-3904.
[2] Fantle and DePaolo (2007), GCA, 71, 2524-2546.

Mineral-scale $^{87}Sr/^{86}Sr$ heterogeneities in the Elba Island intrusive complex: a consequence of prograde disequilibrium melting of the source

FEDERICO FARINA[1]*, ANDREA DINI[2], SERGIO ROCCHI[3] AND GARY STEVENS[1]

[1]Stellenbosch University, department of Earth Sciences, Stellenbosch, South Africa, farina@sun.ac.za (* presenting author); gs@sun.ac.za
[2] Istituto di Geoscienze e Georisorse, CNR, Pisa, Italia, a.dini@igg.cnr.it
[3]Universita' di Pisa, Dipartimento di Scienze della Terra, Pisa, Italia, rocchi@dst.unipi.it

Session- Evolution and differentiation of the continental crust: A celebration of the contributions by Michael Brown

Large $^{87}Sr/^{86}Sr$ variations are preserved at the mineral-scale within igneous units forming the late Miocene Elba Island intrusive complex (Italy), namely the San Martino granite porphyry laccolith (7.4 Ma), the Monte Capanne granite pluton and the Cotoncello felsic dyke (6.9 Ma). Decimetric K-feldspar megacrysts from the three units record a similar large core to rim decrease of $^{87}Sr/^{86}Sr_i$ ratios (from ≈ 0.719 to 0.715) while biotites included within feldspar cores, interpreted as an early crystallized magmatic phase formed from an early magma batch, have diverse initial Sr isotope ratios. Biotite inclusions from the pluton and the dyke have extremely high $^{87}Sr/^{86}Sr_i$ (≈0.733), while those in the porphyry record the lowest ratio in the intrusive system (≈0.712). It is noteworthy that reliable initial Sr isotope ratios for biotites included in the megacrysts have been determined as a consequence of the exceptional young emplacement age of the Elba Island intrusive complex.

The record of isotopic variations preserved at the mineral-scale in the different megacryst-bearing units of the Elba Island intrusive complex, reflects episodic recharge and mixing between crustally-derived magma batches having contrasting $^{87}Sr/^{86}Sr$ signatures. Intrusion of basaltic magmas in the crust causes high heating rates (>100 °C/Ma), preventing complete equilibration within rock-forming phases in the protolith prior to anatexis, as well as between the residuum and the melt during anatexis and magma segregation. Therefore, phases with $^{87}Rb/^{86}Sr$ ratios that are high (i.e. biotite), intermediate (i.e. muscovite) and low (i.e. hornblende and plagioclase) develop contrasting $^{87}Sr/^{86}Sr$ through time. Consequently, a range of isotopically distinct magma batches arise from disequilibrium melting of individual sources that are able to undergo melting through different reactions.

The increase in $^{87}Sr/^{86}Sr_i$ recorded by the San Martino system reflects mixing between magmas produced by the progression from muscovite- to biotite fluid absent melting within a metapelitic source. At higher temperatures, the progression from biotite to hornblende-dominated fluid absent melting within a layered, compositionally intermediate source generates the decrease in Sr isotope ratios recorded by the pluton-dyke magmatic system.

https://doi.org/10.1180/S0026461X00008434 Published online by Cambridge University Press

High-resolution ontogenic distribution of Mg/Ca ratios and Mg isotopes in modern brachiopods

JURAJ FARKAŠ[1*], ADAM TOMAŠOVÝCH[2], VLADISLAV CHRASTNÝ [1], DORRIT JACOB[3], MICHAELA FRANCOVÁ[4], FLORIAN BÖHM[5] AND HAUKE VOLLSTAEDT[5]

[1]Czech Geological Survey, Prague, Czech Republic, juraj.farkas@geology.cz (* presenting author)
[2]University of Chicago, Chicago, USA, tomasovych@uchicago.edu
[3]Johannes Gutenberg-Uni., Mainz, Germany, jacobd@uni-mainz.de
[4]Charles University, Prague, Czech Republic, francova@geology.cz
[5]Geomar | Helmholz Centre for Ocean Research, Kiel, Germany.

Shells of articulate brachiopods composed of low-Mg calcite provide valuable archives of temporal changes in trace element and isotope composition of past ocean water [1, 2]. However, in order to faithfully reconstruct the paleo-seawater signatures from geochemical data encoded in fossil brachiopods, one must have a full understanding of trace element incorporation, and the accompanying isotope fractionation during shell formation, in modern brachiopod species. Here we present high-resolution ontogenetic profiles of trace element distribution (i.e. Mg/Ca ratios) and Mg isotope variation ($\delta^{26/24}$Mg) in species of modern articulate brachiopods, *Terebratalia transversa* and *Terebratella sanguinea*, collected from the northeast (San Juan Island, Friday Harbor) and the southwest Pacific Ocean (New Zealand, Doubtful Sound), respectively. Results from LA-ICP-MS (Agilent 7500ce) and wet chemistry (Thermo X-Series II) elemental analysis indicate that Mg/Ca ratios (mmol/mol) in the secondary-layer composed of low-Mg calcite range between 5 and 10, whereas a thin primary layer composed of high-Mg calcite yielded significantly higher Mg/Ca ranging from 25 up to 50. Results of the isotope analysis, done on MC-ICP-MS (Thermo Neptune), show that for low-Mg calcite of modern brachiopods there is no significant species-dependent fractionation of stable Mg isotopes, as $\delta^{26/24}$Mg (DSM3) signatures of secondary shell layers of *T. transversa* and *T. sanguinea* yielded identical values of -2.225 ±0.055 and -2.241 ±0.187 per mil, respectively. Moreover, these values are also identical with those from modern *Terebratulina retusa* with published $\delta^{26/24}$Mg signatures of -2.075 ±0.097 [3] and -2.290 ±0.060 [4]. Hence, our preliminary data seem to support an existence of a common taxon-specific control of Mg isotope fractionation during biocalcification of low-Mg calcite of brachiopod shells from ambient seawater. In addition, we found no resolvable temperature-dependent Mg isotope fractionation for samples representing habitat temperatures ranging from 8.8 to 13.7 °C. However, a single sample with an estimated 8 to 15% contribution of Mg from primary high-Mg calcite layer (calculated based on Mg/Ca mass-balance) yielded significantly lower $\delta^{26/24}$Mg of -2.819 ±0.099, suggesting that an extra caution has to be exercised during sampling of brachiopod shell material for $\delta^{26/24}$Mg analysis. We plan to present new Mg/Ca and $\delta^{26/24}$Mg data from several other modern brachiopod species, and discuss their implications for paleo-seawater $\delta^{26/24}$Mg reconstructions.

[1] Lee et al. (2004) *Chemical Geology* **209**, 49-65. [2] Veizer et al. (1999) *Chemical Geology* **161**, 59-88. [3] Wombacher et al. (2011) *Geochimica et Cosmochimica Acta*, **75**, 5797-5818. [4] Hippler et al. (2009) *Geochimica et Cosmochimica Acta*, **73**, 6134-6146.

Boron isotopes in deep-sea bamboo corals

JESSE R. FARMER[1]*, BÄRBEL HÖNISCH[1], LAURA ROBINSON[2], TESSA HILL[3] AND MICHÉLE LAVIGNE[3]

[1]Lamont-Doherty Earth Observatory of Columbia University, Palisades, NY, USA, jfarmer@ldeo.columbia.edu (* presenting author)
[2]Woods Hole Oceanographic Institution, Woods Hole, MA, USA lrobinson@whoi.edu
[3]Bodega Marine Laboratory, University of California-Davis, Bodega Bay, CA, USA, mglavigne@ucdavis.edu

Background

Deep-sea corals represent an intriguing archive for application of the boron isotope-pH proxy because of their potential for subdecadal-scale reconstructions [1] during present and past carbon system perturbations [2]. However, previous studies of boron isotopes in aragonitic deep-sea scleractinian corals showed evidence for systematic skeletal variations in δ^{11}B that could not be attributed to environmental factors [3]. In contrast to scleractinians, deep-sea gorgonian bamboo corals secrete high-magnesium calcite and may not be expected to exhibit similar δ^{11}B heterogeneity, but the boron isotopic composition of bamboo corals has not been investigated in detail. Here we present an evaluation of δ^{11}B variability from the genus *Keratoisis*, a cosmopolitan deep-sea calcitic bamboo coral.

Results

Initial results from four modern *Keratoisis* specimens collected between 500 and 2500m depth in the North Atlantic and North Pacific Oceans show that coral surface δ^{11}B positively correlates with ambient seawater pH and is consistent with borate incorporation from seawater. Samples taken at 1mm spacing across the width of individual corals shows that intra-sample δ^{11}B does not exceed 2-3 per mil. An increase in δ^{11}B toward the central growth axis of our North Pacific *Keratoisis* specimen is associated with lighter carbon and oxygen isotopes [4]. Two North Atlantic corals show increased δ^{11}B toward the surface of the outer growth surface, a result that is in contrast to the expected increased contribution of anthropogenic carbon in the deep sea. We seek to constrain the observed boron isotopic variability and coral growth rates using trace metal (B/Ca, U/Ca, Sr/Ca, Mg/Ca), stable isotope (δ^{18}O, δ^{13}C), and radiocarbon analyses within our *Keratoisis* corals.

[1] Roark et al. (2005) *Geophys. Res. Lett.* **32**, L04606. [2] Robinson et al. (2005) *Science* **310**, 1469-1473. [3] Blamart et al. (2006) *Chemical Geology* **225**, 61-76. [4] Hill et al. (2011) *Geochem. Geophys. Geosys.* **12**, Q04008.

https://doi.org/10.1180/S0026461X00008434 Published online by Cambridge University Press

Origin of the bilateral structure of Pacific plume conduits

CINZIA G. FARNETANI[1 (*)], ALBRECHT W. HOFMANN[2,3], AND CORNELIA CLASS[2]

[1] Institut de Physique du Globe de Paris, France, cinzia@ipgp.fr (* presenting author)

[2] Lamont Doherty Earth Observatory, Palisades, N.Y. 10964, USA class@ldeo.columbia.edu

[3] Max-Planck-Institut für Chemie, 55020 Mainz, Germany. albrecht.hofmann@mpic.de

Hotspots with double volcanic chains provide a unique opportunity to map the distribution of isotopic heterogeneities in the deep mantle. Recently, Weis et al., [1] proposed that the isotopic enrichment of the southern (Loa-trend) Hawaiian volcanoes is due to sampling of deep material coming from the edge of the 'large low-shear-velocity province'. By studying several Pacific hotspots with double volcanic chains (i.e., Hawaii, Samoa, Marquesas) Huang et al., [2] showed that the southern chain is always isotopically enriched with respect to the northern one. Such a large scale, systematic geochemical zonation may be caused by the progressive involvement of a more enriched (DUPAL) component toward the southern latitudes.

Here we take a geodynamics perspective and model a north-south increase in the radiogenic lead isotope ratio ($^{208}Pb^*/^{206}Pb^*$) across the thermal boundary layer (TBL) source region of plumes. Our numerical simulations show that the resulting conduit structure has a novel `lobate' zonation. By mapping $^{208}Pb^*/^{206}Pb^*$ distribution within the melting zone of the Hawaiian plume we predict that Loa-trend volcanoes should have higher $^{208}Pb^*/^{206}Pb^*$ than Kea-trend ones. Moreover, the calculated $^{208}Pb^*/^{206}Pb^*$ time evolution is distinct, namely, in a Loa-trend volcano, shield-stage lavas are expected to have higher $^{208}Pb^*/^{206}Pb^*$ than pre- and post-shield lavas. In contrast, in a Kea-trend volcano, $^{208}Pb^*/^{206}Pb^*$ should progressively decrease from pre- to post-shield stages. Our simulations show that any large-scale north-south $^{208}Pb^*/^{206}Pb^*$ increase in the TBL causes bilateral zonation of plumes sheared in the direction of the Pacific plate motion.

[1] Weis, D., Garcia, M.O., Rhodes, J.M., Jellinek, M., Scoates, J.S.,(2011) *Nature Geoscience, DOI:10.1038/NGEO1328.* [2] Huang, S., Hall, P.S., Jackson, M.G., (2011). *Nature Geoscience, DOI:10.1038/NGEO1263.*

Effect of redox oscillations on iron and manganese behavior in a bank filtration setting

CLAIRE FARNSWORTH[1,2*]

[1]California Institute of Technology, Pasadena, CA, USA, claire.farnsworth@gmail.com (* presenting author)

[2]EAWAG, Swiss Federal Institute of Aquatic Science and Technology, Duebendorf, Switzerland

In bank filtration, groundwater is extracted from a well adjacent to a river or lake, thereby inducing infiltration from the surface water body into the shallow groundwater. The infiltrate is exposed to variable redox conditions along the flow path, from oxic surface water to reducing shallow sediments, followed by the re-introduction of oxygen in the vicinty of the production well as it cycles on and off. The natural processes along the infiltration flow path lead to nutrient, organic carbon, and pathogen removal, thereby improving the quality of the water recovered. However, manganese (Mn) and iron (Fe) can be released into bank filtrate along its flow path to the production well to an extent that necessitates drinking water treatment after extraction, as observed at various well fields in Canada, Germany, and the Netherlands.

The behavior of Mn and Fe were investigated at a lake bank filtration site (Lake Tegel, Berlin, Germany) subject to water table fluctuations and seasonal organic carbon loads, resulting in transient redox oscillations in the shallow groundwater. Field data will be compared with the potential of Mn and Fe for release in the reducing shallow sediments and for sequestration in the aquifer adjacent to the production well. The conditions under which transient redox oscillations in shallow groundwater can drive the release and sequestration processes in alluvial sediments will be presented.

https://doi.org/10.1180/S0026461X00008434 Published online by Cambridge University Press

Preservation of fossil bones of small mammals from El Harhoura 2 cave (Morocco, Pleistocene – Holocene)

YANNICKE DAUPHIN[1], AND BASTIEN FARRE[2*]

[1]UMR IDES, Université Paris Sud, France, yannicke.dauphin@u-psud.fr

[2]GEGENA2 Université de Reims, Champagne Ardennes, Bastien.farre@univ-reims.fr (* presenting author)

Introduction. Studying the Hominid installation in Maghreb is an outstanding question due to the fact that early *Homo sapiens sapiens* originated from Africa and some of the earliest remains has been found in North Africa. Numerous archaeological sites have revealed large mammals. However, only few Pleistocene sites from Atlantic Morocco have yielded microvertebrates. Did the 6th extinction start as modern humans settled? Biodiversity is based on the abundance of taxa. However, fossilisation induces substantial preservational bias in the fossil record. Thus, we study the preservation of fossil bones to estimate the impact of fossilisation on past biodiversity (ANR MOHMIE project [1]).

Results and Conclusion

Eleven layers have been identified in the Late Pleistocene - Middle Holocene series [2]. Sands represent more than 80% of the sediment. From SEM observations [2], rodent bones are well preserved, showing the main histological features (Fig.). Secondary deposits are rare. Nevertheless, FTIR analyses have evidenced differences between modern and fossil samples. The primary mineralogy (apatite) is preserved. All fossils show a decrease in CO_3/PO_4 ratio, but no regular trend from the top to the bottom of the excavation. Crystallinity is variable. All bones are strongly depleted in organic matrices, but again no regular trend has been detected through the stratigraphic levels.

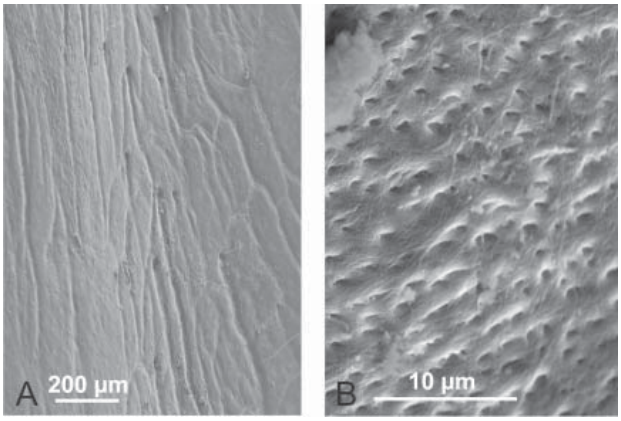

Figure: External surface (A) and fracture (B) of a femur of *Meriones*

Preliminary extractions yield very few quantities of soluble and insoluble organic components, and insoluble extracts contain residual minerals. There is no correlation between the external aspect and the preservation of histology and composition. Additional data are needed to answer the question about biases and changes in biodiversity in this site.

[1] MOHMIE was supported by ANR Grant 2009 PEXT 004 04. [2] Stoetzel *et al.* (2010) *Hist. Biol.* **22**, 303-319. [3] Farre (2011) AIR archéométrie, CNRS, abstract and poster.

The Buffering Nature of Iron Slag in Ironville, Adirondacks, NY, USA—a Preliminary Study

DORI J. FARTHING[1*]

[1]The State University of New York at Geneseo, Geneseo, NY, USA, farthing@geneseo.edu (* presenting author)

For years, acid rain has been an issue for the Adirondack region of the United States. Extremely low pH values have impacted the hydrosphere and the health of many local ecosystems (e.g., [1, 2]). This preliminary study indicates that, in Ironville, NY, the presence of iron slag might buffer these extreme conditions.

Iron smelting in Ironville, NY took place from 1828 through 1886. Today, all that remains of the operations are the foundations of worker buildings, part of the furnace and a ~362 square meter slag pile. The pile is a loosely consolidated mixture of slag and other debris including bricks and modern tree roots. The slag is highly glassy, variegated in color, and often has a vesicular and ropey appearance. Iron prills are common and are often in an oxidized state. Some samples also contain visible areas of crystalline material. SiO_2, FeO, and CaO predominate the major element chemistry for Ironville slag. Slag is not confined to the pile and can be found littering the ground adjacent to the pile, around the smelter remains, and also in Putnam Creek which borders the pile.

More than 50 soil samples from the slag pile and its vicinity were collected and analyzed on site using a Hellige-Truog Soil pH test kit. GPS data was collected in coordination with each soil sample so that a detailed map could be generated. The soils of the area are typically a fine sandy loam and the analyzed samples came from predominantly the O and A horizons (the upper 13 cm of soil). A pit was dug into the slag pile and soil-like material from the pit was also analyzed for pH. Soils from the pile and adjacent to it have an average pH of 8.0. Even close to the furnace, pH values continue to be mildly basic in nature. Moving beyond the pile, the basic pH persists and even 0.8 km downstream from the pile, pH's of 8 were still found. However, when soil samples were tested approximately 13 Km away, the soil pH dropped down to a value of 2.

[1] Sullivan, et al. (2006) *Soil Science Society of America Journal* ***Vol 70-1*** p. 141-152**.** [2] Lawrence, et al. (2009) *U.S. Geological Survey Fact Sheet* **3075**, p 1-6.

https://doi.org/10.1180/S0026461X00008434 Published online by Cambridge University Press

Partitioning and mobility of trace elements in brine impacted fly ash residues

O.O. FATOBA[1*], L.F. PETRIK[1], R.O. AKINYEYE[1] AND W.M. GITARI[2]

[1]Environmnetal and Nano sciences Resaerch Group, Chemistry Department, University of the Western Cape, Private Bag X17, Bellville, 7535, South Africa. (*Correspondence: ofatoba@uwc.ac.za)

[2]Department of Ecology and Resourses Management, University of Venda, Thohoyandou, Limpopo, South Africa

Fly ash and brine are waste materials generated from the combustion of coal and wastewater treatment respectively. Apart from the major elements, these waste materials contain trace elements such as As, Zn, Cu, Pb, Mo and Cr. The need to safely dispose fly ash and brine, in order to avoid contaminating the surrounding soils and groundwater, has led to the co-disposal of fly ash and brine by some power utilities in South Africa. Chemical speciation reveals the availability and mobility of metals in solid materials in order to understand their chemical behaviour and fate [1]. To evaluate the availability and mobility of metals from solid materials such as fly ash, some extraction tests such as sequential chemical extraction have often been applied. This study aims at determining the partitioning of the trace elements and their mobility in the brine impacted fly ash residue. The brine impacted fly ash residue was exposed to sequential chemical extractions [2]. The filtrates from each of the sequential extraction steps were analysed for trace elements using ICP-MS. The results of the tests showed that trace elements were partitioned into different physicochemical forms in the residue. Apart from the bulk of the Co, Cu, Ni, Pb and Zn that are contained in the residual fraction, high concentrations of these elements in the carbonate fraction showed their existence as co-precipitates with carbonate minerals which are not easily mobile under natural environmental conditions except when the pH is very low.

[1] Kalembkiewicz et al., (2008) *Microchemical Journal* **90**, 37-43.
[2] Nurmesniemi et al., (2008) *Waste Management and Research* **26**, 389-399.

Geochemical investigations of fjord surface sediments as basis for Holocence climate change studies in the Trondheimsfjord area

JOHAN C. FAUST[1*], JOCHEN KNIES[1], JACQUES GIRAUDEAU[2] AND GESA MILZER[2]

[1]Geological Survey of Norway, Trondheim, Norway, Johan.Faust@ngu.no (* presenting author), Jochen.Knies@ngu.no

[2]EPOC, University of Bordeaux - CNRS, Talence, France, j.giraudeau@epoc.u-bordeaux1.fr, g.milzer@epoc.u-bordeaux1.fr

High sedimentation rates in fjords provide excellent possibilities for high resolution sedimentary and geochemical records over the Holocene. To increase the understanding of these records the aim of this study is to investigate (a) recent factors controlling the inorganic/organic geochemistry of surface sediments, (b) to identify geochemical proxies for terrestrial input/river discharge and (C) compare these findings with Holocence records from three sediment cores.

In April 2011 sixty evenly distributed surface sediment samples were collected around the entire Trondheimsfjord, one of the largest fjords in Norway. All samples were analysed with regard to elemental composition, total organic carbon (TOC) and total nitrogen content (N), organic and inorganic carbon and nitrogen stable isotopes ($\delta^{13}C$, $\delta^{15}N$), bulk mineral composition and grain size distribution.

The TOC:N ratio of all samples varies between 8 and 16. However, excluding 7 samples collected in river deltas the ratio decreases to 8-10 corresponding to a high correlation between TOC and N (r^2=0.95) indicating a marine source. The fraction of $CaCO_3$ decreases gradually from 24% at the entrance to 1.4% at the inner fjord. The ratios of Fe/Al, Zr/Al and Sr/Ca show the opposite pattern. They are highest at river deltas and at the inner part of the fjord. Anthropogenic influences are identified by elevated heavy metal concentrations around Trondheim and heavy industries near the city of Orkdal in the south. The highest amount of total nitrogen (0.21%) and TOC (1.87%) are found at the fjord entrance in the Stjørnfjord. We assume that the TOC and N values are high in the Stjørnfjord due to a local upwelling. The Atlantic water entering the fjord is topographically steered towards the surface and induces an area of high primary production.

Our findings show that three main factors control the elemental distribution in Trondheimsfjord surface sediments: the inflow of ocean waters, the inflow of river waters and anthropogenic contributions. Therefore, we propose that Trondheimsfjord sediments provide an excellent geochemical record reflecting the intensity of river discharge and the impact of the North Atlantic Current on local climate and environmental changes since the last deglaciation. The application of these findings to Holocence sequences will provide insights into climate vulnerability of the Trondheimsfjord region.

https://doi.org/10.1180/S0026461X00008434 Published online by Cambridge University Press

Using surface complexation modeling to quantify bioavailability of metals to bacteria

JEREMY B. FEIN

University of Notre Dame, Civil Engineering and Geological Sciences, Notre Dame, IN 46556 USA; fein@nd.edu

Determining the controls on metal bioavailability is crucial in order to understand the geomicrobiology of geologic systems with high metal concentrations, such as acid mine systems or contaminated soils, and in order to optimize bioremediation strategies aimed at remediating those types of systems. In addition, the controls on the rates of several environmentally significant metabolic processes, such as mercury methylation or bacterial reduction/oxidation of metals, are poorly understood. The key to improved models of all of these geomicrobiological processes is the ability to quantitatively model bacterial metal bioavailability. Metal adsorption onto bacterial cell walls represents the first interaction of a metal with the cell, and for this reason we hypothesize that accessibility of the metal to the cell is directly related to, and can be predicted by, cell wall metal speciation.

In the research that will be discussed, we test the hypothesis that bacterial surface speciation and concentration of heavy metals controls the bioavailability of those metals. Previous models of metal bioavailability (e.g., the Biotic Ligand Model) characterize metal binding onto a wide range of organisms using a generic, unspecified metal-binding biotic ligand that does not account for the many complexities of metal adsorption reactions onto biological surfaces. These models often fail because of these overlooked complexities in adsorption reactions. Over the past 15 years, we have learned much about the mechanisms involved in metal binding onto bacterial cell walls, and have developed quantitative surface complexation models based primarily on x-ray absorption spectroscopy and bulk adsorption measurements.

In this presentation, I will review my group's work to improve surface complexation models of bacterial metal binding, and to use those models to quantify the controls on the bioavailability of aqueous metals to bacteria. We have shown that bacterial chemotactic response and the enzymatic reduction of U(VI) are two examples of adsorption-controlled processes. The extent and rate of both of these processes can be directly related to the concentration of metal adsorbed onto the bacterial cell wall. Therefore, improving the sophistication and accuracy of surface complexation models of metal adsorption onto bacteria will lead to improved quantitative models of bacterial processes in realistic complex systems.

"Normal" Southern Volcanic Zone basalts behind the arc at 34˚15′-34˚45′ S

MAUREEN FEINEMAN[1*], TIMOTHY MURRAY[1], DANA DREW[2], PATRICIA SRUOGA[3]

[1]Pennsylvania State University, University Park, PA, USA, mdf12@psu.edu (* presenting author)
[2]University of Oregon, Eugene, OR, USA
[3]CONICET/SEGEMAR, Buenos Aires, Argentina

The section of the Southern Volcanic Zone (SVZ) between ~33˚S and 34.5˚S is distinguished from the more southerly SVZ by its distinct geochemical signature – namely, $^{87}Sr/^{86}Sr$ > ~0.7045, Sr/Y > 35, La/Yb > 12, and major element characteristics typical of the High-K andesite series. Also charactieristic of the northernmost segment of the SVZ is a lack of basaltic lavas on the volcanic front (basaltic andesites are common). The distintive geochemical characteristics of the Northern SVZ magmas suggest a unique source, either in a lower crustal hot zone [1] / MASH zone [2], where mantle melts are hybridized by extensive partial melts of deep lower crust, or by incorporation of eroded crustal materials into the mantle source itself [3,4]. The lack of primitive basaltic materials in the NSVZ makes it difficult to directly assess the nature of the subarc mantle in this region. We have sampled seven olivine basalt lava flows, tephra rings, maars, and cinder cones from just behind the volcanic front (~50 km from the arc axis) between 34˚15′ and 34˚45′ S. Although these basalts do not necessarily represent the mantle source beneath the arc front, they do provide some constraints on the mantle composition at this latitude. The Sr isotopic composition of these primitive basalts is $^{87}Sr/^{86}Sr = 0.7040 \pm 0.0004$ (2σ), which is statistically different from the basaltic andesites and andesites located on the arc front at the same latitude, which have $^{87}Sr/^{86}Sr = 0.7050 \pm 0.0004$ (2σ). Neodymium isotopes show the same trend, with less overall varibility.

The basalts from behind the arc at 34˚15′ to 34˚45′ S have isotopic compositions essentially identical to those found in arc front lavas from the SVZ south of 35˚. It is certainly possible to imagine scenarios in which the mantle directly behind the arc could be compositionally decoupled from the mantle directly beneath the arc. Nonetheless, the existence of typical SVZ mantle in the atypical NSVZ region suggests that mantle source contamination by eroded crustal materials is not a pervasive feature at these latitudes. The strong contrast in source composition over 50 km E-W can be compared to the relative homogeneity of the NSVZ (radiogenic Sr) signature over ~150 km N-S at the arc front. Alternatively, the arc front lavas in the SVZ may be sourced in a hybridized lower crustal hot zone, while the behind-arc samples are sourced from the mantle itself with little crustal interaction. The lack of crustal interaction is consistent with thinner crust behind the arc, as well as the occurrence of these monogenetic basaltic features along lineations, suggesting that the low-volume melts have exploited planes of weakness in the overlying crust.

[1] Annen et al. (2006) *J. Pet.* **47**, 505-539.
[2] Hildreth and Moorbath (1988) *CMP* **98**, 455-489.
[3] Stern (1991) *Geology* **19**, 78-81.
[4] Kay et al. (2005) *GSA Bull.* **117**, 67-88.

https://doi.org/10.1180/S0026461X00008434 Published online by Cambridge University Press

The Cu Conundrum: Cu Budget During Partial Melting of Earth's Upper Mantle

STEVE A. FELLOWS[1*] AND DANTE CANIL[2]

[1]University of Victoria, Victoria, Canada, sfellows@uvic.ca (* presenting author)
[2]University of Victoria, Victoria, Canada, dcanil@uvic.ca

Abstract

Primitive basaltic glasses from mid-ocean ridges (MORB), ocean islands (OIB) and arcs contain three to five times the Cu as the currently accepted primitive upper mantle (PUM) value, suggesting a bulk partition coefficient $D_{Cu}^{mantle/melt}$ of ~0.20. Sulfide, with a $D_{Cu}^{sulfide/melt}$ of > 250 is presumed to be ubiquitous in the mantle, but its presence during melting is not commensurate with the Cu abundances in most basalts. To address this conundrum we determined D_{Cu} in olivine and orthopyroxene at 1250–1525 °C and 1.0 GPa in a hydrous basalt and KLB1 peridotite, at fO_2 near to melting conditions of the upper mantle. The measured $D_{Cu}^{ol/liq}$ of 0.06-0.21 and $D_{Cu}^{opx/liq}$ 0.15-0.82 do not vary with melt fraction, nor significantly with fO_2, and can be combined with estimates for D_{Cu} for clinopyroxene into melting models to examine the Cu contents of mantle-derived melts. The Cu abundances for MORB, OIB, and arc glasses are all explicable by the melting (up to 15%) of the silicate-only portion of the mantle in which Cu behaves as a mildly incompatible element $D_{Cu}^{mantle/melt}$ of ~0.26. For Cu to be enriched in basaltic melts in the presence of sulfide, the melt/sulfide ratio, or the oxidation state of the mantle during melting, must be significantly high to diminish the potential of sulfide to sequester any Cu.

Conclusion

Our results suggest the role of sulfide during mantle melting may be insignificant in regards to controlling the concentration of moderately chalcophile elements like Cu, and confirm that the previously estimated Cu content for PUM of 20 ppm is correct.

The dynamic nature of iron oxyhydroxides on modes of ion retention

SCOTT FENDORF[1*]

[1]Stanford University, Stanford, CA, USA, fendorf@stanford.edu (* presenting author)

Introduction

Iron oxyhdyroxides exert a dominant control on the fate and transport of numerous elements ranging from arsenic to phosphate to uranium. Owing, in part, to the redox active metal center, iron oxyhydroxides are dynamic solids within soils and sediments. As a consequence, iron retention is not strictly an adsorption phenomena but rather commonly also entails uptake into the mineral structure.

Conclusions

The iron oxide ferrihydrite is particularly prone to Fe(II) induced transformation to thermodynamically more stable phases such as goethite. Upon formation of the secondary phases, elements such as arsenic and uranium can be incorporated into the surface structure or adsorbed on the mineral surface; in the case of uranium, we also see reduction and secondary precipitation of UO_2 as a common retention mechanisms. However, competing ions such as phosphate as well and structural dopants (e.g., Al) modify the transformation pathway of ferrihydrite and may therefore limit formation of secondary phases that can host arsenic and uranium. The mode of retention is, however, often not singula, with multiple mechanisms in operation. Further, geochemical gradients, and in particular redox gradients resulting from variations in oxygen egress, lead to progressive changes in retention mechanisms. As an example, uranium retention often occurs via adsorption at high oxygen concentrations and progresses through a coprecipitated phase to a heterogeneously nucleated uranannite phase with successfully lower oxygen partial pressures. Here, variation in retention mechanisms and their spatial distribution within soil/sediment assemblages are illustrated.

https://doi.org/10.1180/S0026461X00008434 Published online by Cambridge University Press

The impact of on mineral surfaces metal-contaminant redox cycles

SCOTT FENDORF[1]*, AND PETER S. NICO[2]

[1]Stanford University, Stanford, CA, USA, fendorf@stanford.edu (* presenting author)
[2]Lawrence Berkeley National Laboratory, Berkeley, CA, USA, psnico@lbl.gov

Introduction

Redox reactions have a controlling influence on the cycling of numerous elements within surface and subsurface environments. Mineral surfaces are particularly critical conduits for redox reactions that both invoke and catalyze electron transfer processes, and which do so at rates that often rival (or even exceed) biologically mediate reactions. Here we examine the role metal (hydr)oxides play in the oxidation-reduction of elements ranging from arsenic to nitrogen to uranium within surface and near-surface environments.

Results and Conclusions

Of the various oxidizers in soils and sediments, Mn(III/IV) oxides are classically the strongest oxidant present; they serve as facial oxidants of most redox active metals and metalloids. While we generally do not consider solid-solid electron transfer processes, the rapid rates of oxidation imposed by Mn oxides for species such as Cr(III) allow even sparingly soluble solids (e.g., chromite) to undergo oxidation through a solubility minimum. In contrast to Mn, Fe can serve as a potent reductant as Fe(II) or an oxidant as Fe(III). For metals with close redox couples to Fe(III)-Fe(II), such as U(VI)-U(IV), the specific form of the Fe(III) mineral along with reaction conditions determine whether Fe serves as a reductant or oxidant. In other cases, such as with Cr(VI), Fe(II)-bearing solids and surfaces serve as dominant reductants. Collectively, metal (hydr)oxides have a critical impact on the redox state of a wide-range of elements within soils and sediments.

A reevaluation of early Cambrian ocean redox conditions through the iron geochemical studies of the lower Hetang black shales in South China

LIAN-JUN FENG[1*], CHAO LI[2], JING HUANG[1], HUA-JIN CHANG[3], CHAO-FENG LI[1], QI-RUI ZHANG[1], XUE-LEI CHU[1]

[1] Institute of Geology and Geophysics, Chinese Academy of Sciences, Beijing 100029, China
feng.lian.jun@gmail.com (* presenting author)
[2] State Key Laboratory of Biogeology and Environmental Geology, China University of Geosciences, Wuhan 430074, China
chaoli@ucr.edu
[3] School of Life and Geography Sciences, Qinghai normal university, Xining 810008, China
changhuajin@163.com

The widespread organic-rich shales during the early Cambrian in South China were always regarded to be deposited in persistent euxinic conditions suggested by the enrichment of redox-sensitive trace elements and narrow distribution of small-size pyrite framboids [e.g. 1].

In this study, iron speciation and ratios, widely applied redox proxies, clearly reveal that the black shales of the lower Hetang Formation were predominantly deposited under anoxic and ferrous iron-rich (ferruginous) water columns with some intermittent intervals of euxinia in contrast the previous interpretation of persistent euxinia. These observations suggest that the anoxic and ferruginous conditions during early Cambrian may have been more prevalent than generally recognized.

[1] *Zhou and Jiang.* (2009) *Palaeogeography, Palaeoclimatology, Palaeoecology 271, 279-286.*

https://doi.org/10.1180/S0026461X00008434 Published online by Cambridge University Press

Mercury contamiation to the environment and health impacts by small and large scale Hg mining activties in China

XINBIN FENG[1,*], GUANGLE QIU[1], PING LI[1], HUA ZHANG[1], THORJORN LARSSEN [2]

[1]State Key Laboratory of Environmental Geochemistry, Institute of Geochemsitry, Chinese Academy of Scineces, Guiyang 550002, China, fengxinbin@vip.skleg.cn

[2]Norweigian Water Research Institute, Oslo, Norway, thorjorn.larssen@niva.no

China currently is one of the largest mercury (Hg) consumers and Hg producers worldwide. From the perspective of the global plate tectonics, Guizhou province is situated in the center of the circum-Pacific mercuriferous belt [1]. Therefore, Guizhou was one of the world's important Hg production centers. So far, at least 12 large and super-large Hg mines have been discovered in the province. Currently all large scale Hg mining activites in Guizhou were completely stopped, but small scale Hg mining activites are still on-going. The Xunyang Hg mine situated in Shaanxi Province is presently the largest active Hg mining district in China[2]. We have conducted detailed studies to investigate Hg contamiantion to the envirnment and health impacts to local inhibitants at both large scale Hg mining and small scale (artisanal) Hg mining areas.

Our study revealed a significant contamination of Hg in soil, sediment, water, and rice in both Hg mining areas in Guizhou and the Xunyang Hg mining district. The highest concentrations of Hg in riparian soil, sediment, water and rice were found at the areas in the vicinity of the Hg retorting and mining sites. Moreover, GEM concentrations in ambient air exhibits a local spatial pattern indicating Hg^0 emission during the process of cinnabar ores retorting. Elevated concentrations of MeHg in rice also were found. The sources of MeHg in rice mainly derived from the soil MeHg, which is likely related to the deposition of GEM [3]. High concentrations of THg in surface water and stream sediment are mainly constrained by the calcines introduced during the retorting activity, which represents the major source of Hg contamination to the local ecosystems in the region. The mining waste piles in the study region must be appropriately disposed of and the mine runoff from those calcine piles should be properly treated and not be used as irrigating water to the paddy field. Our study showed that artisanal Hg miners exposed to high levels of Hg vapor and urine Hg concnetrations in Hg miners were two to three magnitudes higher than the control groups. Our data showed a serious adverse effect on renal system for the smelting workers. The workers were exposed to mercury vapor through inhalation, and the exposure route of Me-Hg was through intake of rice. Meanwhile, rice consumption is the primary MeHg exposure route for the local population in Hg mining areas.

[1] Feng X, Qiu G (2008) *Sci. Total Environ*. **400,** 227-237.
[2] Qiu G, Feng X, Meng B, Wang X (2012) *Pure Applied Chem.*, **84**, 281-289.
[3] Meng B, Feng X, Qiu G, Liang P, Li P, Chen C, Shang L (2011) *Environ. Sci. Technol*. **45**, 2711-2717.

Zircons in the T-Zone, Thor Lake rare element deposit: implications for deposit genesis

YONGGANG FENG[1*], AND IAIN SAMSON[2]

[1]University of Windsor, Department of Earth and Environmetal Sciences, fengl@uwindsor.ca*

[2]University of Windsor, Department of Earth and Environmetal Sciences, ims@uwindsor.ca

The Thor Lake Y-REE-Nb-Ta-Zr-Be deposit, NWT, Canada, one of the largest known rare-element deposits hosted by alkaline-peralkaline igneous complexes, comprises two main mineralized zones: the Nechalacho deposit and the T-Zone. The T-Zone is hosted by granite and syenite, and is a pegmatite that has a significant hydrothermal overprint. It is zoned, comprising, from rim to core, a Wall Zone, Lower Intermediate Zone (LIZ), Upper Intermediate Zone (UIZ), and Quartz Core Zone.

We have investigated the morphology, internal textures and chemistry of hydrothermal zircon from the UIZ and magmatic zircon from the host granite and syenite, combining LA-ICP-MS analysis with petrography, CL imaging, SEM-EDS and EMPA. Based on the morphology and associated mineral assemblages, zircon can be broadly classified into three types. Type 1 is fine grained (< 50 μm), euhedral, well-zoned, hydrothermal zircon and mainly occurs in pseudomorphs that have a prismatic to rhombic habit. Type 1 zircon can be subdivided into two subtypes: 1a, which is hosted by massive quartz, and 1b, which is associated with fluorite and sulfides. Type 2 zircon is anhedral, unzoned, and fine-grained, and is associated with rutile, quartz, magnetite, and hematite in the LIZ. Type 3 is magmatic zircon from the host igneous rocks, that is coarser grained and (50 ~ 300 μm) and also exhibits oscillatory growth zoning.

Type 1 zircon was affected by Ca metasomatism that altered the zircon and precipitated REE-bearing minerals, such as xenotime. Ti and REE concentrations in Type 1 and 3 zircons were obtained by LA-ICP-MS (Type 3 zircon was also analyzed by EPMA). The Ti in the unaltered magmatic zircon yields apparent Ti-in-zircon temperatures of ~ 614 to 860°C. In contrast, hydrothermal zircon has unreasonably high Ti concentrations and therefore calculated temperatures. This type of zircon contains high concentrations of REE and other HFSE, such that the coupled substitutions involving Ti may be affected to such an extent to invalidate the established geothermometric calibrations. Alternatively, the assumptions regarding Ti activity are invalid under hydrothermal conditions [1]. Both magmatic and hydrothermal zircon are generally HREE-enriched and exhibit negative Eu anomalies, however, the former is distinguished by a pronounced positive Ce anomaly. In addition, significant tetrad effects observed in the REE patterns of Type 1a zircon, but not Type 1b zircon, suggest that the nature of coprecipitated minerals play an important role in controlling zircon REE chemistry.

[1] Fu et al. (2009) *Chem. Geol* **259**, 131-142.

https://doi.org/10.1180/S0026461X00008434 Published online by Cambridge University Press

Structure of the calcite (104)-Water interface: direct comparison of x-ray reflectivity data with computational results

PAUL FENTER[1*], SANG SOO LEE[1], NEIL C. STURCHIO[2], AND SEBASTIEN N. KERISIT[3]

[1]Argonne National Laboratory, Chemical Sciences & Engineering, Argonne, IL, USA. fenter@anl.gov
[2]University of Illinois at Chicago, Earth and Environmental Sciences, Chicago, IL, USA.
[3]Pacific Northwest National Laboratory, Chemical & Materials Sciences Division, Richland WA, USA.

Understanding the calcite-water interface structure is important because of its abundance in natural systems, relatively high reactivity (e.g., rates of growth and dissolution), and ability to incorporate trace impurities. Previous studies have probed the structure of the calcite-water interface by X-ray reflectivity (XR) [1] and computational approaches [2]. These different approaches have led to a qualitatively similar picture of the molecular-scale structure at this interface, including displacements of the surface lattice and organization of the fluid water adjacent to the surface, but without a full quantitative agreement in the derived structures. It is unclear if these differences are significant (i.e., if there is a conflict between the XR measurement and the simulation) or whether the apparent discrepancy between the XR data and the simulation reflect a deficiency in the model used to described the XR data (e.g., due to a potential non-uniqueness of the model).

Substanial improvements in XR reflectivity data quality due to advances in detectors over the past ~10 years suggest that a reassessment of this system may be warranted. New XR measurements of the calcite-water interface were made at the Advanced Photon Source following previously described procedures [1] and care was taken to avoid X-ray-induced perturbations to the interfacial structure. The XR results show clear modulations of the specular reflectivity signal, which are associated with the presence of a small but significant oscillatory relaxation profile of the calcite surface layers, which has not been previously observed. Also observed is an organized interfacial water layer, similar to previous results.

A further test of these new results is to compare these XR data *directly* to computational results without any intevening model-dependent assumptions using a recent conceptual advance [3]. Comparison with a molecular-dynamics simulation shows that the simulated structure provides a qualitative description of the XR data, but with a poorer quality of agreement than that obtained using the model-dependent fitting approach.

[1] P. Fenter et al., *Geochimica et Cosmochimica Acta* **64**, 1221-1228 (2000).
[2] Kerisit and Parker (2004) *J. Am. Chem. Soc.* **126**, 10152-10161.
[3] P. Fenter et al., *J. Synchrotron Radiation*, **18**, 257-265 (2011).

Oxidation of black shales as a source of Re-Os ratios in epigenetic pyrite: A case study from MacMillan Pass, Yukon, Canada

NEIL.A. FERNANDES[1,2], SARAH A. GLEESON[2*], AND ROBERT A. CREASER[2]

[1] Exploraciones, Cía. Minera Barrick Chile, Santiago, Chile
nfernandes@barrick.com
[2] University of Alberta, Dept. of Earth and Atmospheric Sciences, Edmonton, Alberta, Canada
sgleeson@ualberta.ca (* presenting author)
rcreaser@ualberta.ca

High Os in late Devonian, shale hosted epigenetic pyrite

The Devonian - Mississippian Earn Group in the Selwyn Basin contains a number of sediment-hosted barite sequences which outcrop in the Mackenzie Mountains, NWT and Yukon. The Hess occurrence (middle Devonian) contains epigenetic pyrite with textures suggesting that it was formed post-lithification, but predating barium mineral formation.

Re-Os isotopic composition of Hess pyrite give values of 16.51 to 93.8 for $^{187}Re/^{188}Os$, and 0.8253 to 1.6001 for $^{187}Os/^{188}Os$ respectively. Most calculated initial $^{187}Os/^{188}Os$ ratios (at 390 Ma) range from 0.6 to 0.9, substantially higher than that of the $^{187}Os/^{188}Os$ value for seawater at the Frasnian-Fammenian boundary (0.42) [1].

Oxidation of organic matter as a source of Os

We suggest, therefore, the fluid that precipitated pyrite had acquired substantial radiogenic Os before pyrite formation. It is likely that organic matter in the underlying lower Earn Group shales was the source for the high Os and low Re values in the fluid. Oxidizing fluids migrating through the stratigraphy would be necessary in order to degrade the organic matter in the host shale and solubilize Os.

If we assume the Os is derived from the host shales, then modeling the data suggests that it would take 25 to 75 Myr to generate the high initial $^{187}Os/^{188}Os$ ratios observed. This supports an epigenetic source for the pyrite and suggests that the Re-Os isotopic system is a powerful tool in understanding the evolution of black shales and shale-hosted mineralization.

[1] Selby & Creaser (2005), *Geology*, **v. 33**, 545-548.

https://doi.org/10.1180/S0026461X00008434 Published online by Cambridge University Press

Uranium mobility in the process waste of a conversion facility (France): static experiments

T. FERNANDES[1,2*], L. DURO[1], P. MASQUÉ[2], A. DELOS[3], J.S. FLINOIS[4], G. VIDEAU[4]

[1]Amphos 21, Barcelona, Spain (*correspondence: teresa.fernandes@amphos21.com)

[2]Departament de Física & Institut de Ciència i Tecnologia Ambientals. Universitat Autònoma de Barcelona, Bellaterra. Spain

[3]Arcadis, Villeurbanne, France

[4]Comurhex Malvési, Narbonne, France

The COMURHEX Malvési industrial site is the first step in the treatment of uranium mining concentrate. Since 1959, the process waste, resulting from the conversion of yellowcake into uranium tetrafluoride (UF_4) has been managed in settling ponds. These ponds have been constructed on mine tailings and waste resulting from the flotation process of a former sulphur mine.

The settling waste, i.e. the resulting sludge, contains a variety of chemicals (nitrates, carbonates, fluorides and sulphates) and radioactive elements (the alpha activity in the solid phase is attributable to uranium (34%) and thorium-230 (64%)).

Previous studies of the source term suggest that the mine tailings act as an efficient buffer that minimises migration to the underlying ground. However, the actual mechanisms by which this control is active are not well understood.

This contribution focuses on the mobility of uranium in the waste based on the results of static experiments (batch studies) of leaching of solid samples. We aim to examine the desorption mechanisms that may account for release of contaminants from the waste and compare the results to field conditions.

In situ GISAXS studies of carbonate mineral nucleation on mineral surfaces

ALEJANDRO FERNANDEZ-MARTINEZ[1,*], YANDI HU[2], YOUNG-SHIN JUN[2], GLENN A. WAYCHUNAS[1]

[1]Earth Sciences Division, Lawrence Berkeley National Laboratory, Berkeley, CA, USA, AFernandez-Martinez@lbl.gov (* presenting author)

[2]Department of Energy, Environmental and Chemical Engineering, Washington University, St. Louis, MO, USA

The precipitation of carbonate minerals –mineral trapping– is considered the safest CO_2 sequestration mechanisms. However, the high pressure and temperatures and the high salinity of the fluids present in many geological reservoirs play important roles in modifying the properties of the mineral faces exposed to the solution, adding more uncertainties to the factors controlling nucleation in these environments. The goal of the present study is to determine the thermodynamic factors controlling heterogeneous nucleation of carbonate minerals on mineral surfaces representative of both reservoir and cap rocks. The quartz (100) and a mica (001) faces have been selected as representative of a sandstone reservoir and as a mineral face characteristic of cap-rocks, respectively.

A technique based on Grazing-Incidence Small-Angle X-ray Scattering, previously developed in our group [1], has been used to follow mineral nucleation of the carbonate minerals on quartz (100) and K-muscovite (001). By measuring nucleation rates at different saturation indexes, effective interfacial energies (α') can be determined. Effective interfacial energies result as the combination of different interfacial energies involved in the process: α_{ls} (liquid-substrate), α_{lc} (liquid-crystal) and α_{sc} (substrate-crystal). Literature values for α_{ls} and α_{lc} allow determining α_{sc}, a quantity very difficult to measure using other techniques.

The first experiments have been performed nucleating $CaCO_3$ on quartz (100) at ambient pressure and room temperature. The results show that heterogeneous nucleation of calcium carbonate is favored on quartz (100), even though the obtained substrate-crystal interfacial energies are higher than the typical values for liquid-crystal interfaces (*e.g.*, ~100 mJ/m^2 for calcite-water interfaces). This fact highlights the interplay existing between the different interfacial energies at play, and the 'competition' between water and the nucleated crystals for the substrate. From a thermodynamic point of view, and as a general rule of thumb, high substrate hydrophobicity and low surface mismatch are found to favor heterogeneous nucleation. In addition, a crystal growth mechanism based on aggregation of nuclei has been identified to be the dominant mechanism at the circum-neutral pH solution values used in this study.

Other mineral substrates currently under study include the edge-faces of phlogopite, a mica mineral, and olivine. These *in situ* and *ex situ* observations yield important quantitative parameters readily usable in reactive transport models of nucleation at the reservoir scale.

[1] Jun, Y.-S., Lee, B, Waychunas, G.A. (2010) Environmental Science & Technology **44**, 8182-8189

https://doi.org/10.1180/S0026461X00008434 Published online by Cambridge University Press

Mercury as a proxy for volcanogenic CO_2 buildup in Neoproterozoic snowball Earth and Volcanism in the K-T Transition

V.P FERREIRA[1], A.N. SIAL[1], L. D. LACERDA[2], R. FREI[3], C. GAUCHER[4], R. A. MARQUILLAS[5]

[1] NEG-LABISE, Dept. Geol. UFPE, Recife, Brazil (*correspondence sial@ufpe.br)

[2] LABOMAR, UFC, Fortaleza, Ceará, Brazil

[3] Inst. Geogr. Geol., Geol. Section, Univ. Copenhagen, Denmark

[4] Fac. Ciencias, Univ. Republica, Montevideo, Uruguay

[5] Universidad Nacional de Salta, Salta, Argentina

Introduction. Mercury tends to concentrate in sediments deposited right after major glacial events [1] as a result from leaching of volcanogenic Hg from land surface and accumulation along argillaceous sediments. Wherever geological background of Hg is negligible, its concentration in sediments may be useful for investigation of climatic changes.

Volcanism is assumed to be responsible for CO_2 build up in the atmosphere during Snownall Earth event with subsequent greenhouse effect, ice melting and cap carbonate deposition [2]. Intense volcanism witnessed the Cretaceous-Paleogene transition [3] and was, perhaps, responsible for dramatic climatic change.

Results. We have used Hg as a proxy of volcanism intensity and CO_2 buildup during snowball events in Neoproterozoic cap carbonates in NE Brazil. Localities where carbonates are in sharp – but not erosional – contact with basal diamictites (earliest stages of aftermath of glacial events) and show $\delta^{13}C$ values ~ −5‰ were analyzed. Hg contents are usually over 10 times higher than background values (<1 ngg^{-1}), occasionally reaching values > 200 ng g^{-1}. Hg contents in cap carbonates of the Sergipano Belt and Ubajara Basin are similar to those in carbonates deposited coevally to volcanic activity elsewhere. This study supports mantle-origin for the CO_2 in cap carbonates, transferred to the atmosphere by volcanism.

Across the the K-T transition (KTB) in the Yacoraite Formation, Argentina, Hg contents reach ~ 20 ngg^{-1}. In three drill cores in carbonate rocks across the KTB in the Paraiba Basin, northeastern Brazil, Hg increases (4 ngg^{-1}) in the early Danian right above the KTB. Hg spikes predating immediately the KTB suggest volcanism before this transition. At Stevns Klint, Denmark, Hg contents reach almost 300 ngg^{-1} within a 5 cm-clay layer (Fish Clay) that registers the KTB, and where a $^{87}Sr/^{86}Sr$ positive excursion and negative excursions of $^{206}Pb/^{204}Pb$ (T=65 Ma) and $^{187}Os/^{188}Os$ (T=65Ma) have been observed [4].

Hg content and Al_2O_3 show stratigraphically co-variation in all of the studied sections of Neoproterozoic cap carbonates or across the KTB, suggesting that Hg is probably adsorbed onto clays.

Conclusions. This study supports Hg stratigraphy as possible tracer of dramatic climatic changes as those in Neoproterozoic snowball Earth events and in the KTB.

[1] Santos et al., (2001). Radiocarbon **43**, 801-808. [2] Hoffman & Schrag (2002).Terra Nova**14**, 129–155. [3] Sheth (2005). Gondwana Research **8**, 109-127. [4] Frei and Frei, (2002). Earth Planetary Science Letters **203**, 6091-708.

Hydrothermal hydrocarbon gases: geothermometry and origins

JENS FIEBIG[1]*, FRANCO TASSI[2], WALTER D'ALESSANDRO[3], ORLANDO VASELLI[2] AND ALAN B. WOODLAND[1]

[1]Goethe University Frankfurt, Earth Sciences, Jens.Fiebig@em.uni-frankfurt.de (* presenting author)

[2]University of Florence, Earth Sciences, Franco.Tassi@unifi.it

[3]INGV Palermo, w.dalessandro@pa.ingv.it

Upon their ascent through the crust, volcanic gases often interact with externally and internally derived fluids. For reasons of energy exploitation and surveillance of volcanic activity it is of great interest to determine hydrothermal temperatures at depth. Methane discharging from these systems has been ascribed a hydrothermal origin, with the magnitude of carbon isotope fractionation between CH_4 and CO_2 reflecting the formation temperature of CH_4 [1]. For most volcanic-hydrothermal discharges, however, apparent carbon isotopic temperatures cannot be confirmed by common gas concentration geothermometers involving redox pairs such as H_2/H_2O and CO/CO_2. In these cases, the geological significance of the carbon isotope geothermometer remains open.

We have addressed the genetic relationship between H_2, H_2O, CO, CO_2, n-alkanes and n-alkenes in volcanic-hydrothermal gases emitted from Nisyros (Greece), Vesuvio, Campi Flegrei and Pantelleria (all Italy). Our results imply that the isotopic CH_4-CO_2 geothermometer records temperatures of CO_2-water interaction at depth. In any case, apparent carbon isotopic temperatures are confirmed by measured propene/propane concentration ratios. Apparent temperatures are close to the critical conditions of pure and saline waters, i.e. ~360°C at Nisyros, 420-460°C at Vesuvio, ~450°C at Campi Flegrei and ~540°C at Pantelleria. For temperatures >400°C, apparent carbon isotopic temperatures are additionally confirmed by ethene/ethane ratios. At least in some systems, CH_4-CO_2 and propene-propane equilibration takes place in different water phases, implying that boiling in high-enthalpy hydrothermal systems may occur isothermally. Among the redox pairs investigated, CO/CO_2 is most prone to secondary vapor phase reequilibration reactions occurring after hydrothermal interaction at depth. Redox conditions during these reactions are homogeneously buffered by H_2/H_2O ratios of the vapor.

Methane most likely derives from an abiogenic source (Sabatier-type reduction of CO_2). In contrast to CO_2, the C_{2+}-n-alkanes are not in equilibrium with CH_4. They derive either from the thermogenic decomposition of organic matter or from abiogenic methane polymerization.

[1] Fiebig et al. (2004) Geochim. Cosmochim. Acta **68**, 2321-2334.

https://doi.org/10.1180/S0026461X00008434 Published online by Cambridge University Press

Extreme magmatic differentiation at Dabbahu Volcano, Afar, Ethiopia

L. FIELD[1], J. BLUNDY[1*], A. CALVERT[2], G. YIRGU[3],

[1]School of Earth Sciences, University of Bristol, UK
jon.blundy@bris.ac.uk
[2]USGS, Menlo Park, USA
[3]Department of Earth Sciences, Addis Ababa University, Ethiopia

Dabbahu is a composite volcano at the north end of the Manda-Hararo segment of the Afar Rift, Ethiopia, which has experienced multiple dyking events since 2005. Dabbahu has erupted magmas ranging in composition from mildly alkaline basalt through trachyandesite to peralkaline rhyolites (comendites and pantellerites). Effusive eruptions predominate. On the basis of a new geological map, 93 new whole rock major and trace element data, mineral analyses from 65 samples, and 9 new ^{40}Ar / ^{39}Ar dates we show that Dabbahu has been active for a little over 70,000 yrs. Samples are aphyric or phenocryst-poor with olivine + clinopyroxene + feldpsar present in all rock types; minor Fe-Ti oxides and aenigmatite occur in some more evolved rocks. Continuous variations in whole rock chemistry, mineral compositions, e.g. Fo_{88-0} olivine, and calculated eruption temperatures support earlier findings [1] that the magma types are related through protracted (~90%) fractional crystallisation from a basaltic parent. Field evidence indicates that magmas were not erupted in fractionation sequence. Some magma mixing between cogenetic magmas is observed in intermediate rocks, but was not a primary cause of chemical varaitaion in the suite as a whole.

Geochemical modelling indicates recently erupted transitional basalts from the Manda-Hararo rift constitute plausible parents. MELTS modelling of differentiation provides an optimal match to rock and mineral chemistries with crystallisation at 100-300 MPa pressure and fO_2 ~1 log unit below FMQ buffer to suppress saturation with orthopyroxene, which is not observed in any samples. Melt inclusions from pantelleritic obsidians and pumices contains up to 6 wt% H_2O and ≤500 ppm CO_2, consistent with ~0.5 wt% H_2O in the parent basalt. Volatile saturation pressures are in the range 30-250 MPa, although solubilities in pantelleritic liquids are not well constrained experimentally. The CO_2-H_2O systematics are consistent with cooling-driven crystallisation of small magma batches over a range of depths, probably in a complex of stacked sills.

We propose that differentiation from basalt to rhyolite occurs in sills (or dykes) at relatively shallow depths (5-10 km) beneath the volcano, although some prior differentiation of mantle-derived basalts is likely to have occurred at greater depths. The sub-volcanic plumbing system must be configured in such a way that cogenetic magmas of different composition can be stored separately prior to eruption, rather than in a single large sub-volcanic reservoir. It is likely that the volcanic load facilitated focussing of magmas through a single summit fissure or vent.

[1] Barberi *et al*, 1974, A transitional basalt - pantellerite sequence of fractional crystallisation, the Boina centre, (Afar Rift, Ethiopia). *Jour Petrol*, **16**, 22-56.

Characterization of Microbial Communities Associated with Powder River Basin Coals, United States

ELLIOTT BARNHART[1], JOHN WHEATON[2], ALFRED B. CUNNINGHAM[3] AND MATTHEW W. FIELDS[*4]

[1]Montana State University, Bozeman, USA, elliott.barnhart@biofilm.montana.edu
[2]Montana Bureau of Mines and Geology, Butte, USA, JWheaton@mtech.edu
[3]Montana State University, Bozeman, USA, al_c@erc.montana.edu
[4]Montana State University, Bozeman, USA, matthew.fields@biofilm.montana.edu (*presenting author)

Introduction. A better understanding of the ecology and physiology of the methane-producing communities associated with coal-beds may promote new techniques that can improve coal-bed methane (CBM) production and enhance the sustainability of the wells. We have conducted initial phylogenetic diversity studies using inoculated coal and *in situ* samples from methane-producing wells in the Powder River Basin (PRB) (southeastern Montana and northeastern Wyoming). Advances in subsurface sampling and molecular techniques have provided a route to capture active microbial consortia from coal beds, but methods need to be refined in order to deal with the unique attributes of coal. We used coal-filled Diffusive Microbial Samplers (DMS) that were lowered into three wells in the PRB along a hydrogeochemical gradient and microbial communities were allowed to develop *in situ*.

Results and Conclusion. Coal slurry associated with the DMS had 100-fold more microbial cells as determined via epifluorescent direct counts. Coal slurry was immediately removed from the DMS in the field and fixed for FISH analysis. *Archaea* and *Bacteria* were detected and bacteria appeared to outnumber archaea within the *in situ* sample. Microorganisms appeared to be concentrated in the proximity of coal particles, and aggregates around coal particles contained both *Bacteria* and *Archaea*. Incubated materials from the DMS were used to inoculate enrichment cultures for the assessment of methane-production under different conditions, and archaeal diversity was low based upon both SSU rRNA and *mcr*A gene sequences. Sequences indicative of both hydrogentrophic and acetoclastic methanogens were detected. In addition, a coal-only enrichment contained higher bacterial diversity than an acetate-amended enrichment, and sequences indicative of presumptive fermenters and acetogens were observed. Nucleic acids were extracted from *in situ* material (DMS-coal and well-water), and 454 pyrosequencing libraries were used to characterize community composition and structure of *in situ* materials. Multivariate statistical methods were used to relate community composition and structure to hydrogeochemical parameters. The low sulfate well had low bacterial diversity compared to a well with intermediate sulfate levels while the archaeal diversity was higher in the low sulfate well compared to wells with higher sulfate levels. The described study aims to identify the relationships between populations of bacteria and archaea associated with CBM with the intent of identifying strategies for enhancement of *in situ* CBM production in terms of microbial structure-function relationships.

https://doi.org/10.1180/S0026461X00008434 Published online by Cambridge University Press

Coralline algae as pH-recorders on seasonal to centennial timescales

J. FIETZKE[1*], F. RAGAZZOLA[1,2], J. HALFAR[3], H. DIETZE[1], L.F. FOSTER[2], T.H. HANSTEEN[1], A. EISENHAUER[1]

[1]GEOMAR, Helmholtz Centre for Ocean ResearchKiel, Germany, * jfietzke@geomar.de
[2]Bristol University, Bristol, UK
[3]University of Toronto, Toronto, Canada

Both ocean warming and acidification caused by the antropogenic emission of carbon dioxide (CO_2)are the major challenges to marine ecosystems. In particular marine calcifiers are expecteded to be affected in their ability to produce skeletal hard parts when facing an environment with continuously decreasing calcium carbonate ($CaCO_3$) saturation state.

To evaluate the performance and possible strategies of acclimatisation/adaptation of marine calcifying organisms the reconstruction of ambient seawater pH is essential. This reconstruction is in particular important for the last decades and centuries as it allows for a comparsion of natural and antropogenic pH variability.

Boron stable isotopes ($\delta^{11}B$) revealed from carbonates have been used as a proxy for seawater pH for many years. Using a recently published LA-MC-ICP-MS method [1] we analysed the spatial distribution of boron isotopes in a specimen of *Clathomorphum nereostratum* a long-lived crustose coralline alga that exhibits annual growth increments. Crustose coralline algae have recently been introduced as climate (SST) recorders in high-latitude shallow-water habitats.[2] The particular specimen used in this study was collected alieve off the coast of Attu island (Aleutian Islands) in summer 2004.[2] With an annual growth of 400-500µm the 6cm long profile covers more than the entire 20th century.

Here we present the first high-resolution 2D-images of boron isotopes providing a precision and accuracy close to analytical bulk techniques for a spatial resolution of 100µm. The combination of electron microprobe elemental mappings and LA-MC-ICP-MS isotopic images now allows for a detailed reconstruction of two seawater key parameters: SST from Mg/Ca and pH from $\delta^{11}B$, respectively.

Our data show that long-term pH-decrease is recorded in the skeleton of our sample specimen. Between 1900 and the 1990's boron isotopes indicate a drop of ~0.08(1) pH units which is in accord with the value expected from atmospheric CO_2 time-series data.

A seasonal cycle of pH-variability (up to 0.1 pH units) is recorded too with highest values during late spring/early summer. His is most likely a result of the CO_2 consumption during the spring microalgal bloom. The latter is in agreement with instrumental data from a nearby location. During the spring bloom in May a rapid pH increase of up to 0.15 units was measured.[3]

[1] Fietzke et al. (2010) *J. Anal. Atom. Spectrom.* **25**, 1953-1957.
[2] Halfar et al. (2007) *Geophys. Res. Lett.* **34**, L07702.
[3] Codispoti et al. (1986) *Cont. Shelf Res.***5**, 133-160.

High Pressure and High Temperature Effect on the Smectite Saturated with Lanthanum

V. F. STEFANI[1*], R. V. CONCEIÇÃO[1,2], L. C. CARNIEL[2]

[1]PGCIMAT, UFRGS, Porto Alegre – RS, Brasil
Vicente.stefani@ufrgs.br
[2]Instituto de Geociências, UFRGS, Porto Alegre – RS, Brasil.
rommulo.conceicao@ufrgs.br
larissa.colombo@ufrgs.br

Smectites are phyllosilicates with high cation exchange capacity (CEC) in the interlayers. For these and other features, smectites have been used in various parts of the world as secondary barriers for possible leak of liquids that contain radioactive elements in definitive deposits of nuclear waste disposal [1]. In such case, radioactive cation could be captured by smectite through cationic exchanges. However, very little is known about the stability of smectite under high pressures and high temperatures (HPHT). Preliminary studies developed by our group in dioctahedral calcium smectites showed that the smectite structure is stable, remaining dioctahedric after processing up to 7.7 GPa and at room temperature [2]. This work replaced the calcium of the smectite for La^{+3}, an analogous of the actinide nuclear waste elements, with the difference that those elements are harmless [3]. We submitted this smectite doped with La to different range of pressure (2.5GPa and 7.7GPa) and temperature (400°C, 500ºC, 650°C and 700ºC), using a hydraulic presses with toroidal board, and we obtained a new La-rich muscovite-like structure. Moreover analyses of x-ray diffraction with Rietveld refinement, fourier transform infrared (FTIR) and transmission electron microscopy (TEM) were performed. Image of smectite doped with La from TEM shows layers of smectite with heavier elements due to the contrast of the image (Fig. 1) and also the effect of lattice fringe. Further images will be achieved in the coming days.

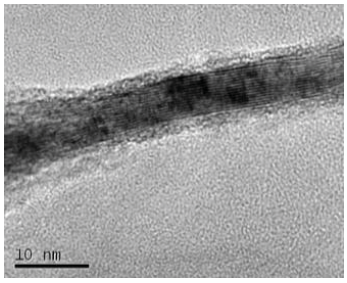

Figure 1: Image of smectite doped with La using TEM

[1] Pusch, R. (1998) *Transport of radionuclides in Smectite Clay.* Environmental Interactions of Clay – Clays and environment. Parker, A., Rae, J.E. Ed. Springer, Berlin.

[2] Alabarse, Frederico Gil. (2009). *Análise da estabilidade estrutural da esmectita sob altas pressões e altas temperaturas.* Master's Thesis – Programa de pós graduação em Ciências dos Materiais. UFRGS. Porto Alegre, Brasil.

[3] Krauskopg, KB (1986) *Thorium and rare-earth metals as analogs for actinide elements.* Chemical Geology, **Vol.** 55, pp. 323-335

https://doi.org/10.1180/S0026461X00008434 Published online by Cambridge University Press

Does reservoir rock integrity change during geological CO_2 storage in a saline aquifer?

SEBASTIAN FISCHER [1,2,*], AXEL LIEBSCHER[1], MARCO DE LUCIA[1], AND THE KETZIN-TEAM

[1]GFZ German Research Centre for Geosciences, Potsdam, Germany, fischer@gfz-potsdam.de ([*]presenting author)
[2]Berlin Institute of Technology, School VI, Department of Applied Geosciences, Chair of Mineralogy-Petrology, Berlin, Germany

At Ketzin in the federal state of Brandenburg, Germany, CO_2 is injected into a saline aquifer of the Upper Triassic Stuttgart Formation, since June 2008. Ketzin is the first European onshore pilot site for the geological storage of CO_2. To evaluate CO_2-fluid-rock interactions, two sets of long-term CO_2-exposure experiments were carried out. One set on reservoir rock (described here), the other on cap rock (data in process). Core samples of Ketzin reservoir sandstone were exposed to pure CO_2 and synthetic reservoir brine at simulated in-situ P-T conditions of 5 MPa and 40 °C. Mineralogical and geochemical analyses were performed on rock and fluid samples taken after 15, 21, 24, and 40 months, respectively. Over time, XRD data with Rietveld refinement show decreasing proportions of analcime, chlorite, hematite and illite, and increasing proportions of quartz. On freshly broken rock fragments, CO_2-treated samples display corrosion textures on plagioclase, K-feldspar and anhydrite surfaces. EMPA data exhibit a change in plagioclase composition from intermediate to Na-rich and albite endmember compositions. Compared to the synthetic reservoir brine, Na^+, Mg^{2+} and Cl^- concentrations increased slightly, while K^+, Ca^{2+} and SO_4^{2-} concentrations increased significantly. Reactive geochemical modeling using PHREEQC-2 code was performed to reproduce experimental observations.

The mineralogical and geochemical measurements imply preferred dissolution of Ca^{2+} out of plagioclase next to dissolution of K-feldspar and anhydrite. Petrophysical data show tendentially increasing porosities and permeabilities [1] also suggesting mineral dissolution during the experiments. Due to the heterogeneous character of the Stuttgart Formation, which formed in a fluvial environment [2], it is often difficult to distinguish between natural, lithostratigraphic variability and CO_2-related changes. Assuming thermodynamic equilibrium, preliminary reactive geochemical modeling of the observed CO_2-fluid-rock interactions shows that the measured evolution of fluid composition is consistent with precipitation of albite and dissolution of anhydrite and illite, respectively. Based on experimental data, the integrity of the Ketzin reservoir is not significantly affected by CO_2.

[1] Zemke et al. (2010) *Petrophysical analysis to investigate the effects of carbon dioxide storage in a saline aquifer at Ketzin, Germany (CO_2SINK).* Int J Greenhouse Gas Control; doi: 10.1016/j.ijggc.2010.04.008.
[2] Förster et al. (2006) *Baseline characterization of the CO_2SINK geological storage site at Ketzin, Germany.* Environ Geoscience, 13, 3, 145-161; doi:10.1306/eg.02080605016.

Ru isotope anomalies in meteorites

MARIO FISCHER-GÖDDE[1]*, CHRISTOPH BURKHARDT[2] AND THORSTEN KLEINE[1]

[1]Institut für Planetologie, Westfälische Wilhelms-Universität Münster, Wilhelm-Klemm-Str. 10, 48149 Münster, Germany, m.fischer-goedde@uni-muenster.de (*presenting author)
[2]Institut of Geochemistry and Petrology, ETH Zürich, Clausiusstrasse 25, 8092 Zürich, Switzerland

Nucleosynthetic isotope anomalies in bulk meteorites have been documented for some siderophile elements (e.g., Ni, Ru, Mo) [1-4] but seem to be absent for others (e.g. Os) [5]. The contrasting isotope systematics of these chemically similar elements may place important constraints on the extent and efficiency of mixing processes as well as pathways of material transport within the early solar nebula. So far, only a limited number of samples have been investigated for Ru and nucleosynthetic anomalies have been mainly reported for magmatic iron meteorites [3]. These Ru isotope anomalies correlate with those in Mo exactly as predicted from s-process nucleosynthesis, supporting evidence for a heterogeneous distribution of s-process carrier phases [1,4]. To further investigate the extent of Ru isotope anomalies in meteorites and to evaluate the significance of the cosmic Mo-Ru correlation we developed new analytical techniques for precise Ru isotope measurements by multicollector inductively coupled mass spectrometry (MC-ICPMS). We present new Ru isotope data for IVB iron meteorites, the ungrouped iron Chinga, and the CB chondrite Gujba. Ruthenium isotope compositions were measured using the ThermoScientific Neptune Plus at the University of Münster and are reported in ε^iRu-deviation from terrestrial Ru. For mass bias correction relative to $^{99}Ru/^{101}Ru$ all samples show a well resolved negative anomaly in $\varepsilon^{100}Ru$, consistent with previous data for IVB irons [3]. There are also hints for positive anomalies in $\varepsilon^{96}Ru$ and $\varepsilon^{98}Ru$ and negative anomlies in $\varepsilon^{102}Ru$ but these are not yet clearly resolved. When normalized to $^{99}Ru/^{100}Ru$ all samples show resolvable deficits in $\varepsilon^{96}Ru$ and large enrichments in $\varepsilon^{101}Ru$, $\varepsilon^{102}Ru$ and $\varepsilon^{104}Ru$. Small deficits in $\varepsilon^{98}Ru$ seem to be present as well but are currently not well resolved. The observed Ru isotope patterns are in excellent agreement with anomalies predicted for a deficit in s-process isotopes according to the stellar model of nucleosynthesis [6], consistent with previuosly reported data [3]. The CB chondrite Gujba plots on the Mo-Ru correlation line for a s-process deficit, indicating that the cosmic Mo-Ru correlation also extends to relatively young carbonaceous chondrites. However, more high-precision Ru isotope data for chondrites are needed to further evaluate the correlated behaviour of Mo and Ru anomalies in case of carbonaceous chondrites. A companion study on the same IVB irons did not find evidence for nucleosynthetic Pt isotope anomalies [7], indicating that in contrast to Ru and Mo, the solar nebula was well mixed with regard to Pt (and Os [5]) isotopes. The contrasting isotope systematics of Os, Ru and Pt may thus be related to thermal processes within the nebula, rather than reflecting a primordial heterogeneity in the distribution of presolar dust.

[1] Dauphas et al. (2002) *ApJ* **565**, 640-644. [2] Regelous et al. (2008) *EPSL* **272**, 330-338. [3] Chen et al. (2010) *GCA* **74**, 3851-3862. [4] Burkhardt et al. (2011) *EPSL* **312**, 390-400. [5] Yokoyama et al. (2007) *EPSL* **259**, 567-580. [6] Arlandini et al. (1999) *ApJ* **525**, 886-900. [7] Kruijer et al. (2012) *LPSC* **XLIII**, #1529.

https://doi.org/10.1180/S0026461X00008434 Published online by Cambridge University Press

A Sr isotope survey of a marine terrace chronosequence: equilibrium interrupted.

JOHN A. FITZPATRICK*[1], MARJORIE SCHULZ[1], DAN BAIN[2], THOMAS D. BULLEN[1], AND ART WHITE[1].

[1]United States Geological Survey, Menlo Park, CA jfitzpat@usgs.gov (* presenting author)
[2]University of Pittsburg, Pittsburg, PA

A well studied marine terrace chronosequence north of Santa Cruz, CA affords an ideal natural laboratory for the investigation of established cation pool equilibrium dynamics. The soils mantling the 5 terraces have developed in sediments derived locally from the Miocene Santa Margarita sandstone, the Purisima formation, and Salinian granites. Each of the terraces were extensively instrumented and sampled. Soils, vegetation, surface and soil pore waters, and precipitation have been sampled at various intervals. Sr isotopes ($^{87}Sr/^{86}Sr$) and cation chemistry have been utilized to investigate sources, cycling and behaviour of Sr and other base cations within each terrace soil horizon. Measured values of $^{87}Sr/^{86}Sr$ in the samples range from 0.706 in deep soil water and soil exchange extracts to 0.710 in surface waters and soil digests. Analysis of precipitation samples average 0.7095. Previous work has demonstrated establishment of similar Sr isotope trends with depth at terraces 1,2,3 and 5. $^{87}Sr/^{86}Sr$ ranges from 0.709 at the top of the profile toward 0.706 at 6 meter depth. Decreasing $^{87}Sr/^{86}Sr$ values with depth imply a precipitation influence at the top of the profile and an increasing mineral weathering signal at depth. Also evident in the depth profiles at these sites is apparent isotopic ($^{87}Sr/^{86}Sr$) equilibrium between ammonium-acetate exchangeable Sr and soil water Sr at equivalent depths. Sr isotope measurements at terrace 4, however, have demonstrated neither trend nor equilibrium. The contrast between behaviour at terrace 4 and the remaining terraces is the subject of this study. $^{87}Sr/^{86}Sr$ measurements of soil pore water at terrace 4 show an essentially fixed value (avg. 0.7088) from the top of the profile to >6 meter depth. Preliminary work on ammonium-acetate exchangeable Sr have yielded $^{87}Sr/^{86}Sr$ values averaging 0.7095. Comparatively, bulk water and soil chemistry are not unusual at terrace 4. Evidence for anthropogenic activity at the terrace 4 sampling site was not obvious at time of site selection. Absence of an A horizon at the site and nearby charcoal bearing mounds suggest small scale charcoal manufacture. Stripping of the Sr exchange pool may have been accomplished by pyroligneous acids interacting with terrace 4 minerals and the subsequent reset to precipitation like values (0.7091).

Dissolved iron in the Southeast Pacific Ocean: OMZ to the gyre

JESSICA N. FITZSIMMONS[1,2*], JONG-MI LEE[1,2], RICHARD A. KAYSER[2], AND EDWARD A. BOYLE[2]

[1]MIT/WHOI Joint Program in Chemical Oceanography, Cambridge MA, USA, jessfitz@mit.edu (* presenting author)
[2]Massachusetts Institute of Technology, Cambridge MA, USA, eaboyle@mit.edu

Dissolved iron (dFe, <0.4µm) samples were collected in the Southeast Pacific Ocean during the C-MORE Big RAPA cruise aboard the *R/V Melville* in December 2010, which sailed from Arica, Chile, to Easter Island. Full depth profiles are presented from three stations: one near the Chilean coast in the oxygen minimum zone (OMZ), one in the subtropical gyre, and one halfway between these two points. Four additional profiles to 1000m are also presented, two between each of the full depth stations, in order to provide higher geographic resolution of surface dFe dynamics.

This dataset provides a unique opportunity to examine dissolved Fe cycling in a transect with a wide biogeochemical range. Conncentrations of dFe were in excess of 3nmol/kg in the OMZ where oxygen concentrations fell below 3µM. In contrast, in the oligotrophic gyre where atmospheric deposition of Fe is very low, dFe is over an order of magnitude lower, near 0.1nmol/kg at the surface and throughout the upper ocean. In this transect are also recorded the first deep ocean dFe concentrations ever measured in the southeast Pacific Ocean.

This dFe distribution provides insight into the major sources of dFe to this understudied region, Fe:nutrient relationships, and the scavenging behavior of dFe from the OMZ into the gyre. This transect will also be of particular interest to participants in the upcoming US Pacific GEOTRACES cruise, which will occupy a similar biogeochemical regime along a nearby transect.

https://doi.org/10.1180/S0026461X00008434 Published online by Cambridge University Press

Thermodynamic stability of U60 nanoclusters based on solubility measurements

SHANNON L. FLYNN*, JENNIFER E. S. SZYMANOWSKI, PETER C. BURNS, AND JEREMY B. FEIN

Dept. Civil Eng. and Geological Sci., University of Notre Dame, Notre Dame, IN 46556, USA (Correspondence: *sflynn4@nd.edu)

U60 nanoclusters are uranyl peroxide based spherical phases that are approximately 2 nm in diameter, with a stoichiometry of $K_{18}Li_{42}[(UO_2)(O_2)OH]_{60}$. Although U60 nanoclusters remain intact in alkaline solutions for at least a year, their thermodynamic stability has not been determined. Of particular interest is whether the nanoclusters behave thermodynamically as a solid phase or as an aqueous species. In this study, we measured the dissolution of U60 nanoclusters under several pH conditions in order to determine their thermodynamic stability. We used the experimental results, in conjunction with aqueous speciation modelling, to calculate an ion activity product (IAP) for each condition studied using two approaches: 1) assuming unit activity for the U60 'solid', and 2) treating the U60 as an 'aqueous' ion.

U60 crystals were made in a mother solution of uranyl nitrate, potassium chloride, hydrogen peroxide and lithium hydroxide. Crystals were harvested by vacuum filtration and then disaggregated in nanopure water, creating a suspension of U60 nanoclusters of known concentration. Batch U60 dissolution experiments were conducted in Teflon reaction vessels at pH 7.5, 8.0 and 8.5, with approximate nanocluster concentrations of 1.4, 2.8 and 6.0 g/L. Samples were extracted periodically for 14 days. Each sample aliquot was divided into two portions: an unfiltered portion for total K, Li and U analysis, and a portion that was filtered through a 10 k Da molecular weight sieve to determine the aqueous concentrations of K, Li and U in each sample. All metal concentrations were determined using ICP-OES. The presence of U60 nanoclusters was verified using electrospray mass spectroscopy at the beginning and end of each dissolution experiment and no other phases were created during the course of the experiments.

Aqueous concentrations achieved steady-state values within 24 hours in each experiment. IAP values, calculated from the experimental measurements assuming unit activity for the U60 nanoclusters and accounting for the aqueous speciation of K, Li, and U, were found not to vary significantly with pH, but to vary as a function of nanocluster concentration, with the calculated IAP value increasing with increasing nanocluster concentration. The variation in the calculated IAP as a function of nanocluster concentration suggests that the assumption of unit activity for the nanocluster is invalid. Models with non-unit activity for the nanocluster yield significantly less variation in the calculated IAP values as a function of nanocluster concentration. Our results suggest that the U60 nanoclusters behave more like aqueous species than a solid phase, and our calculated stability constant for the U60 nanoclusters can be used to estimate the solubility of the nanoclusters under a range of aqueous conditions. Our results underscore the importance of characterizing the charging behavior of these nanoclusters in order to better constrain their activity coefficients and hence their solubility behavior.

Resilience of bacterial communities in a pristine aquifer despite changes in the availability of sulfate

THEODORE M. FLYNN[1,2*], ROBERT A. SANFORD[1], JORGE W. SANTO DOMINGO[3], NICHOLAS J. ASHBOLT[3], AUDREY D. LEVINE[3], AND CRAIG M. BETHKE[1]

[1]University of Illinois at Urbana-Champaign, Department of Geology Urbana, IL, USA

[2]Argonne National Laboratory, Bioscience Division, Argonne, IL, USA, tflynn@anl.gov (* presenting author)

[3]U.S. Environmental Protection Agency, Office of Research and Development, Cincinnati, OH, USA

We test how bacterial communities in a pristine aquifer respond to geochemical changes by incubating initially-sterile sediment traps in groundwater with a relatively high (1.5 mM) or low (0.04 mM) concentration of sulfate for one year, then transferring each trap to the opposite well. We sequenced 16S rRNA genes and created terminal restriction fragment length polymorphism (T-RFLP) profiles of the bacterial community from these switched traps, then used multivariate statistics to compare them with control traps which had remained in the same well for the duration of the experiment. These analyses showed that despite the 12 month incubation in a well with a 40-fold difference in the availability of sulfate, the bacterial communities attached to the switched traps retained a characteristic structure more similar to the well in which each trap was initially incubated than to the control community where they were subsequently placed. Although the relative abundance of many populations on the switched traps remained unchanged by this change in the availability of sulfate, the relative abundance of certain phyla associated with sulfate reduction (*Desulfobacter* and *Desulfobulbus*) was found to increase or decrease along with the corresponding change in the availability of sulfate. Other functional groups whose abundance has also been linked to the amount of sulfate in groundwater, however, such as the iron reducers *Geobacter* and *Desulfuromonas*, appeared unaffected by the switch between high and low sulfate wells. These results indicate that many bacterial populations present in an aquifer community do not simply represent the taxa are most favored by current geochemical conditions. Rather, the biogeographical and geological history of the area play a significant role in determining the composition of the bacterial community. Predicting its response to external perturbations, whether naturally-occurring or anthropogenic, would therefore require a more holistic understanding of the environment being studied than can be provided by a survey of bacterial populations alone.

https://doi.org/10.1180/S0026461X00008434 Published online by Cambridge University Press

Fe-isotopes of arc basalts indicate a variably oxidised mantle source?

JOHN FODEN[1*], PAOLO SOSSI [2,1], AND GALEN HALVERSON [3,1]
[1]University of Adelaide, Geology and Geophysics,
john.foden@adelaide.edu.au (*presenting author)
[2]Research School of Earth Sciences, ANU,
paolo.sossi@anu.edu.au
[3]McGill University, Earth and Planetary Sciences,
galen.halverson@mcgill.ca

New Fe-isotope data on (> 60) primitive basalt samples from the global network of arcs is used to investigate if Fe isotopic compositions reflect differing oxidation and water content of arc sources due to tectonic factors (rate of subduction, age of subducting plate) [1]. Subduction magmas are wetter than those of from other tectonic settings [2]. Melt-inclusion studies using XANES have established good positive correlations between water content of primitive melts and their oxidation state ($Fe^{3+}/\Sigma Fe$) [2]. Arc magmas have elevated $Fe^{3+}/\Sigma Fe$ (>0.1 to 0.5), compared to MORB (0.1-0.2) [3,4], and studies of peridotite from the sub-arc mantle [5] also reveal elevated oxidation states compared to non-arc mantle. Still, the site of oxidation of arc magmas is controversial. Redox-sensitive element ratios (V/Sc or Zn/Fe_T) imply oxidation is imposed after magmas leave the mantle wedge [3,6].

Our $\delta^{57}Fe$ data range from -0.2‰ to +0.2‰ (± 0.04), with $Fe^{3+}/\Sigma Fe$ in the range 0.2 to 0.5. $\delta^{57}Fe$ correlates positively with Pb- or Sr-isotope ratios and $Fe^{3+}/\Sigma Fe$ and weakly with age of subducting crust. The trend to heavier iron is not coupled to any correlation with MgO so not driven by olivine or pyroxene crystallisation. A two-fold increase in $Fe^{3+}/\Sigma Fe$ requires >50% olivine crystallization [3] and will only increase $\delta^{57}Fe$ by ~0.06 ‰. As magnetite $\Delta^{57}Fe_{mag\text{-}melt}$ values are ~ +0.30 ‰, they record pre-magnetite conditions.

Results and Conclusions

Our data may reflect differences in oxidation state of the mantle of different arcs. As Fe^{3+} mineral sites tend to have heavier Fe-isotopic compositions [7] and as Fe^{3+} is more incompatible than Fe^{2+}during mantle melting, partial melting of more a oxidized wedge will yield melts with heavier iron isotopes (as will smaller % melting) [7]. Positive correlations with Pb- and Sr-isotopes may be a measure of slab input to the wedge, and that with slab age may indicate that colder, older slab subduction delivers more oxidation capacity to that part of the mantle wedge that yields arc basalt magmas.

[1] Syracuse, *et al.* (2010) *Phys Earth & Planet. Int* **183**, 73-90. [2] Kelley & Cottrell (2009) *Science* **325**, 605–607. [3] Lee *et al*., (2010) *Nature* **468**, 681-685. [4] Bezos & Humler (2005) *Geochim. Cosmochim. Acta* **69**, 711–725. [5] Parkinson & Arculus (1999) *Chem Geol* **160**, 409-423. [6] Lee et al. (2005 *J. Petrol*. **46**, 2313–2336. [7] Dauphas *et al*. (2009) *Earth & Planet. Sci Let* **288**, 255-267.

Microbes at work: Biogeochemistry in oil sands tailings ponds

JULIA FOGHT*

[1]University of Alberta, Biological Sciences, Edmonton, Canada,
julia.foght@ualberta.ca (* presenting author)

Extraction of surface-mined oil sands ores yields bitumen for upgrading, plus tailings: a slurry of water, sand, silt, clay, unrecovered bitumen and hydrocarbon solvent. These extraction wastes are deposited into enormous tailings ponds where they de-water as the fine particles consolidate very slowly by gravity. After several years the tailings may reach >25% solids, becoming 'mature fine tailings' (MFT). Complex communities of diverse microbes have developed in the ponds (enumerated at 10*6 to 10*8 cells/ml MFT) where they anaerobically degrade labile aliphatic and aromatic hydrocarbons in the solvent (and perhaps low molecular weight components of the bitumen) to produce methane, CO_2 and organic metabolites. This activity has environmental and industrial significance because it affects physical properties of the MFT through unresolved mechanisms, promoting consolidation and de-watering of the MFT ('biodensification'), and generating copious volumes of greenhouse gases, a proportion of which is emitted from the ponds through ebullition. The microbial communities determined using 454 pyrosequencing of 16S rRNA genes comprise hundreds of bacterial genera, many of which represent uncultivated taxa, but only a few methanogenic euryarchaeal lineages. Laboratory enrichment cultures derived from MFT demonstrate methanogenic degradation of short-chain ($<C_{10}$) and long-chain ($>C_{14}$) *n*-alkanes, *iso*- and *cyclo*-alkanes, mono-aromatics (BTEX) and a few polyaromatics. Biodegradation is also observed under sulfate-reducing conditions by amending MFT with sulfate; the community structure shifts in response to C source and electron acceptor availability. However, often the communities are reluctant to 'go to work', sometimes with lag times of 1–2 years in laboratory cultures before biodegradation is apparent. Pure cultures isolated from enrichment cultures are now being studied to infer their roles in situ. Sequencing of functional gene families associated with anaerobic hydrocarbon activation is contributing to understanding biogeochemical potential in the tailings ponds, and full community metagenomic sequencing has provided additional context. Results from this work are contributing to models for predicting the consequences of microbial activity in situ and providing guidance for tailings management and reclamation strategies.

https://doi.org/10.1180/S0026461X00008434 Published online by Cambridge University Press

Constraining changes in ocean circulation modes and ^{14}C reservoir ages in the NW Atlantic between 35 and 15 ka BP

J. FOHLMEISTER[1*], J. LIPPOLD[1], M. KUCERA[2], L. WACKER[3], M. BAYER[2]

[1]Heidelberg Academy of Sciences, Institute of Environmental Physics, Germany, jens.fohlmeister@iup.uni-heidelberg.de, (* presenting author),
[2]Department of Geosciences, University Tübingen, Germany,
[3]ETH Zurich, Institute for Particle Physics, Switzerland

The Atlantic Meridional Overturning Circulation plays a key role in the climatic system by redistributing heat and carbon throughout the ocean. Reconstructions of ^{14}C concentrations revealed that large changes in the partitioning of radiocarbon among the main reservoirs on earth must have occurred in the past. Thus, significant effort went into the reconstruction of past ocean circulation and its control on the storage and release of CO_2 as well as its heat supply to higher Northern latitudes.

In our study we focus on a deep sea core from the North-West Atlantic (ODP Site 1063, Bermuda Rise). This core displays very high sedimentation rates (in general > 20 cm/ka), which minimizes bioturbation effects, allowing extraordinaryly high time resolution. For the last glacial the $CaCO_3$ content of this core preserved Heinrich and Dansgaard/Oeschger events. Linking the ODP Site 1063 $CaCO_3$ content to Greenland ice core $\delta^{18}O$ allows constructing a ^{14}C independent age model [1]. We compared sample ages derived from this model with the ^{14}C content of monospecific planktonic foraminifers measured in 35 sub-samples between 15 and 35 ka BP.

The resulting ocean surface reservoir age (R) shows almost constant values (~ 1200 years) during the Last Glacial, while during Heinrich Events (1, 2, 3), R varied between 0 and 2500 years. Additionally, we compare the surface water reservoir age with $^{231}Pa/^{230}Th$ and ε_{Nd} values available for this core [2,3]. In this way, we provide for the first time a data set of three distinct proxies of ocean circulation co-registered from the same sediment core. Comparison of these proxies give evidence of highly variable patterns of ocean circulation during Heinrich Events, characetrised by differences in circulation strength, water mass age and water mass provenance during different times of melt-water hosing in to the North Atlantic.

[1] Grützner, J. et al. (2002) Marine Geology, Volume 189, 2-23.
[2] Lippold, J. et al. (2009) Geophysical Research Letters, Volume 36, LI2601.
[3] Gutjahr and Lippold (2011) Paleoceanography, Volume 26, PA2101.

Behavior of REE in high-alumina alteration zones formed by weathering of felsic volcanic rocks

NORA K. FOLEY[1*]

[1]U.S. Geological Survey, MS 954, Reston, Virginia 20192 USA, nfoley@usgs.gov (* presenting author)

Variation in mineralogy and whole rock chemistry of kaolinite deposits of the Carolina slate belt, USA, are used to study processes leading to remobilization, transport, and concentration of REE and other elements (e.g., Ti, Al, As, Se, Ga, Hf, Zr) during weathering. High-alumina alteration zones are hosted by felsic volcanic rocks of the Persimmon Fork Formation (PFF). The largest deposits (Haile and Brewer, SC) contain reserves of >650,000 metric tons of clay formed by saprolitic weathering of crystal tuff (1). The 554 Ma tuffs have associated feldspar and sericitic alteration and contain epithermal, hot-springs-style deposits of Fe, Au, and other metals produced by acidic hydrothermal fluids that reacted with host volcanic rocks. Chemical weathering of the PFF since the mid-Paleozoic has strongly modified the major and trace element abundances and resulted in a high-quality white clay resource (~35% kaolinite, ~45% quartz, ~20% sericite) with accessory phases including reaction products of the original Ti, Al, and Fe-minerals, a distinctive trace element signature (e.g., Ga~4-36, Se~0-230, As~0-541, ΣREE~30-200 ppm) and diverse secondary minerals formed primarily by weathering of crystal tuff and siliceous-ferruginous sinter, including concretions (layered goethite-Al and kaolinite), Al-REE phosphates, gibbsite, hematite, lepidicrosite, and quartz.

Geochemical traverses across bedrock, saprolite, and clay bodies show that most of the alkali elements and Fe were removed from tuffs during weathering. In contrast, Th, Hf, and Zr contents were generally preserved. Chondrite-normalized REE patterns for variably altered volcanics fall into mineralogically distinct groups. The resultant clay rocks are LREE-enriched at ~50-100x chondrite and have Ce/Yb_N of ~2.0 to 6.6 and La/Sm_N = 1.99 to 5.6. The HREE portion of the pattern is typically flat and ~10-30x chondrite with Tb/Yb_N of ~0.71-1.05. In general, negative Eu/Eu* anomalies of 0.62 to 0.75 characterize the clay rocks. Fe-concretions in clay rocks are enriched by factors of 50 in Se and 25 in As (60-230 ppm Se and 11-511 ppm As) and have ΣREE~150-200. REE mobility did occur in the hydrothermally altered and weathered volcanic rocks; as a group the altered clay rocks and Fe-concretions (normalized to the mean value for unaltered PFF) show depletions in LREE, and slight enrichments in HREE. The changes in the bulk patterns can be explained by the presence of LREE-enriched and HREE-enriched minerals and reflect adsorption onto Fe-oxyhydroides and secondary clay minerals, rather than precipitation of secondary phosphate. Behavior of other trace elements (As, Se, Ga), relative to the parent rock, is also predictable based on the dominant mineralogy of the residual host (clay rock, silicastone, iron oxide concretions and crusts). Elements such as Ga, Hf, and Zr are retained under a combination of acidic hydrothermal and saprolitic alteration processes that result in subtle REE mobility.

[1] Foley (2007) *23rd International Applied Geochemistry Symposium*, 50.

https://doi.org/10.1180/S0026461X00008434 Published online by Cambridge University Press

Investigating the structural characterization of amorphous mineral precursors for enhanced understanding of contaminant adsorption and incorporation.

SAMANGI ABEYSINGHE AND TORI Z. FORBES*

Department of Chemistry, University of Iowa, Iowa City, IA, USA
tori-forbes@uiowa.edu

Metal oxyhydroxide mineral phases, particularly those containing Fe(III) or Al(III), play an important role in determining the long fate and transport of heavy metals and radionuclides in environmental systems. During rapid hydrolysis of the metal in solution, an amorphous or poorly crystalline precipitate initial forms, which can further transform into a thermodynamically stable mineral phase. During aggregation and flocculation processes, contaminants can adsorb to the surface of the particles, leading to co-precipitation and incorporation. Therefore, understanding the relationship between the soluble molecular precursor species present in solution and the amorphous precipitate is vital for gaining a molecular-level understanding of contaminant uptake by mineral species.

To investigate the structural relationship between the soluble precursors and the amorphous phase, we have begun synthesizing geochemical model compounds to compare to X-ray scattering of the amorphous phase. These model phases are metal oxyhydroxide nanoclusters that are 1-2 nm in diameter that can be packed into an ordered lattice for structure determination via single-crystal X-ray diffraction. The Pair Distribution Function (PDF) analysis of the module compounds can be calculated and compared to experimentally derived spectra. In this presentation we will focus on the relationship between aluminum based nanoclusters and amorphous aluminum hydroxide. In addition, geochemical model compounds with adsorbed contaminants will also be discussed that may provide information regarding possible adsorptions sites within amorphous materials.

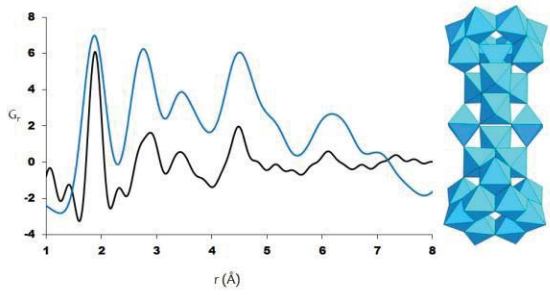

Figure 1. Comparision of the PDF spectra of amorphous metal oxyhydroxide material and the structurally characterized geochemical model compound.

Methane and dissolved inorganic carbon biogeochemistry in the Argentine Basin

M.FORMOLO[1*], N. RIEDINGER[2], J.M. MOGOLLÓN [3], S. HENKEL[4], J. TOMASINI[5], M. STRASSER[6], A. VOßMEYER[7], AND S.KASTEN[3]

[1]Dept. of Geosciences, University of Tulsa, Tulsa, OK 74104, USA, michael-formolo@utulsa.edu (* presenting author)
[2]Dept. of Earth Sciences, Univ. of California, Riverside, CA 92521, USA
[3]Alfred Wegener Institute for Polar and Marine Research, Bremerhaven, Germany
[4]Instit. Geology and Mineralogy, Univ. of Cologne, Cologne, Germany
[5]ANCAP, Montevideo, Uruguay
[6]Geological Institute, ETH, Zürich, Switzerland
[7]Center for Geomicrobiology, Aarhus Univ., Aarhus, Denmark

The Argentine Basin, located on the continental margin and slope of Uruguay and Argentina, has been well documented as a region susceptible to mass sediment transport processes and high sedimentation rates. These dynamic conditions impact the pore water and dissolved methane biogeochemistry. During Expedition M78/3 (May - June 2009) aboard the RV Meteor sediment and corresponding pore water samples were collected. The methane and pore water constituents provide a unique opportunity to address how sensitive methane and dissolved inorganic carbon (DIC) biogeochemistry are to environmental perturbations in these dynamic continental margin settings.

Adopting the definitions from Hensen et al. [1], for pore water profiles from this region, we have subdivided the sample locations into four profile categories; linear, concave-up, kink, and s-type. Comparisons among these categories allow us to address how methane biogeochemistry responds to sediment movements and variable methane fluxes. Within the Argentine Basin the observed sulfate and methane geochemistry are transitory in nature following mass-flow deposition or variations in methane fluxes. Over time the pore water profiles are constantly returning to a more steady-state situation and information regarding these transient periods can be lost. However, these end member steady-state, transient and non-steady conditions provide an opportunity to model the biogeochemical conditions during these phases. This will provide more detailed information regarding natural biogeochemical response to similar events in marine systems. Integrating pore water CH_4, DIC, and SO_4^{2-} concentrations with $\delta^{13}C$-CH_4 and $\delta^{13}C$-DIC into isotope and reactive-transport models will allow us to address what are the naturally occurring dominant biogeochemical pathways in these sediments and how they respond to perturbations from variable methane fluxes or sediment mass transport events.

[1] Hensen et al. (2003) *Geochim. Cosmochim. Acta* **67(14)**, 2631-2647.

https://doi.org/10.1180/S0026461X00008434 Published online by Cambridge University Press

Methods for the determination of Te isotope compositions of minerals in the system Au-Ag-Te by MC-ICP-MS

ANDREW P. FORNADEL[1*], PAUL G. SPRY[1], RYAN D. MATHUR[2], SIMON E.JACKSON[3], JOHN B. CHAPMAN[3] AND ISABELLE GIRARD[3]

[1]Iowa State University, Ames, IA, USA, fornadel@iastate.edu (* presenting author); pgspry@iastate.edu
[2]Juniata College, Huntingdon, PA, USA, mathur@juniata.edu
[3]Geological Survey of Canada, Ottawa, Ontario, Canada, Simon.Jackson@nrcan-rncan.gc.ca; John.Chapman@nrcan-rncan.gc.ca; Isabelle.Girard@nrcan-rncan.gc.ca

The high precision of multicollector ICP-MS (MC-ICP-MS) analyses has led to the investigation of stable isotope variability of increasingly heavy elements (e.g., Cu, Se, Hg) found in ore-forming systems. Tellurium is commonly associated with Au and Ag in epithermal and orogenic ore systems. To date, there have been no high-precision studies of the natural variability of tellurium isotopes in ore-forming systems.

Using a micromill, a sufficient mass of telluride or native Te sample can be isolated and extracted from coexisting ore and gangue minerals from ~50 μm wide by ~50 μm deep drilled holes. Dissolution of those samples and subsequent ion exchange chromatography isolates Te from matrix metals, with a tellurium yield of ≥ 95%. The chromatography procedure causes no net fractionation of Te.

MC-ICP-MS analyses were completed using two techniques, both of which employ the doping of samples using Cd to correct for drift in instrumental mass bias. The first method was the introduction of 100 ppb Te bearing solutions (with 100 ppb Cd) using a desolvating nebulizer (DSN). The second method was direct introduction of 2 ppm solutions of Te (with 1 ppm Cd) into the MC-ICP-MS. The average precision using the DSN is ±0.17 ‰, whereas that for the wet method is ±0.08 ‰.

Natural, hypogene tellurides (n = 17) and native Te have shown an isotopic range of $^{130/125}$Te of ~1.9 ‰, demonstrating resolvable disparate isotope ratios between samples, including in samples from the same locality (i.e., Cripple Creek).

The understanding of isotope systematics for Te will lead to a better understanding of the geochemistry of Te, as well as its transport and deposition mechanisms. Systematic spatial variation of Te isotopes within an orebody may serve as an exploration vector for associated Au (as Au only has one stable isotope) and other precious metals.

The relationship between CO_2 and ice-volume on geological timescales

GAVIN L. FOSTER[1*] AND EELCO J. ROHLING[1]

[1]Ocean and Earth Science, National Oceanography Centre Southampton, University of Southampton Waterfront Campus, Southampton, SO14 3ZH (* presenting author); Gavin.Foster@noc.soton.ac.uk; e.rohling@noc.soton.ac.uk

Sea-level is arguably the most serious impact of anthropogenic climage change [1]. Unfortunately, changes in sea-level cannot simply be predicted by numerical climate models because they do not physically describe the dynamics of processes associated with the volume reduction of continental ice sheets. This compounds the issue of long range prediction as retreat of these ice masses will increasingly contribute to sea-level rise as the 21st century progresses. Consequently, the likely magnitude of future sea-level change remains uncertain [1]. One way in which the uncertainty in future sea-level predications can be reduced is to study the behaviour of the ice sheets and sea-level in the past in relation to greenhouse gas forcing.

Here we compile several recent records of pCO_2 and ice-volume from the last 40 million years. A consistent pattern emerges that clearly demonstrates a non-linear relationship between these variables, largely consitent with our understanding based on ice sheet modelling [2]. Given an estimate of the current climate forcing by CO_2 we use the relationship we observe on geological timescales to provide an estimate of the modern long-term equilibrium sea-level. This treatment supports the notion of significantly elevated long-term sea level response to anthropogenic CO_2 forcing even if CO_2 levels are stablised at current levels [3].

[1] Vermeer and Rahmstorf (2009) *PNAS* **106**, 21527-21535. [2] Deconto et al. (2008) *Nature* **455**, 652-656. [3] Rohling et al. (2009) *Nature Geoscience*, **2**, 500-504.

https://doi.org/10.1180/S0026461X00008434 Published online by Cambridge University Press

Metastable equilibrium in the C-H-O system: Graphite deposition in crustal fluids

DIONYSIS I. FOUSTOUKOS

Geophysical Laboratory, Carnegie Institution of Washington, Washington, DC 20015, United States

The presence of graphite in natural environments is governed by the redox and thermal conditions of C-H-O fluid/mineral equilibrium in hydrothermal veins and metasomatic contacts. The majority of experimental and theroetical studies on the C-H-O system are focused on deriving the thermodynamic properties of species, and on modeling phase relationships under equilibrium conditions. The distribution of C-H-O species in natural systems, however, may also be controlled by metastable equilibria that involves disequilibrium volatile concentrations and deposition of graphitic carbon with different degrees of crystallinity.

Hydothermal experiments were performed to investigate the graphite undersaturated C-H-O system at 600°C – 1 GPa and at supercritical water conditions. Aqueous solutions were reacted in the presence of $Si_5C_{12}H_{36}$ (tetrakis(trimethylsilyl) silane) to generate C-H-O volatiles (e.g. CO_2, CH_4, H_2) in a piston cylinder apparatus. Phase equilibrium relationships were placed along a continuum from highly reducing (iron-wustite) to highly oxidizing (Pt/PtO_2) redox gradient that rendered $CH_{4(aq)}$ and $CO_{2(aq)}$ as dominant species.

Time-series measurements of the dissolved volatile concentrations and mass balance constraints indicate the formation of a metastable non-volatile carbon phase, that attained significant concentrations (up to 0.62 of total carbon) especially during methane oxidation to $CO_{2(aq)}$. The intermediate occurrence of this phase is short-lived and is linked to the precipitation of amorphous graphitic carbon. Indeed, Raman spectroscopic measurements performed on the solid reaction products revealed the presence of poorly-ordered graphite under all the redox conditions investigated. However, the thermometric empirical expressions using the distribution and the shape (FWHH) of the G and D bands in the Raman spectra of graphite failed to accurately estimate the experimental temperature. Thus, the existing Raman geothermometers appear inadequate to address graphite formation under metastable equilibrium conditions and to account for kinetic effects that could greatly affect the degree of crystallinity.

Formation of poorly ordered graphite suggests that the disordered structure of the mineral is more readily deposited than crystalline graphite, and thus it may attain a broader thermodynamic stability field. Exposing this metastable graphitic carbon to high temperatures and pressures could function as a precursor and substrate for the deposition of the well-ordered phase. Such metastable graphite, therefore, may provide an intermediate state that facilitates subduction of carbonaceous material other than crystalline carbonate minerals. This might also have important implications for the formation mechanisms and the carbon isotope systematics of deep seated carbonaceous fluids and minerals such as diamonds.

Steep Rock carbonate platform: an early marine oxygen oasis

PHILIP FRALICK[1] AND ROBERT RIDING[2*]

[1]Lakehead University, Thunder Bay, Canada
pfralick@lakeheadu.ca
[2]University of Tennessee, Knoxville, USA
rriding@utk.edu (*presenting author)

Limestones of Mesoarchean-Neoarchean (~2.8 Ga) age at Steep Rock Lake, Ontario, Canada, are up to 500 m thick and at least 35 km in extent. We suggest that this early example of a thick and relatively well-preserved carbonate platform represents an 'oxygen oasis' that formed in shallow-water adjacent to deeper-water iron oxide and iron carbonate sediments. Anoxic Archean seawater rich in dissolved iron and bicarbonate is expected to have precipitated iron carbonate minerals such as siderite, which is common in banded iron formation (BIF). Dominance of Ca-carbonates over Fe-carbonates at Steep Rock is consistent with relatively low levels of ferrous iron in a suboxic/oxic shallow-water zone above a chemocline. The most likely source of dissolved O_2 to sustain these conditions is oxygenic photosynthesis by cyanobacteria.

Our rare earth element (REE) analyses confirm that oxygen was present in the seawater from which the Ca-carbonate minerals at Steep Rock precipitated. A distinct negative cerium anomaly is present in the limestone and absent in the laterally and vertically adjacent iron formations. Cerium is the only REE with a 4+ valence state, in which it forms an insoluble oxide and is removed from solution. The negative anomaly indicates that seawater at Steep Rock locally encountered sufficient oxygen to remove cerium. Direct evidence for the source of the oxygen is lacking, but two features are consistent with a cyanobacterial origin. First, stromatolites are common in the Steep Rock limestone and cyanobacteria could have been included in their microbial communities. Second, black shales in the basinal iron formation contain up to 30 weight percent organic carbon suggesting the presence of phytoplankton and this community also could have included cyanobacteria.

We conclude that the Archean origin of marine carbonate platforms was closely linked to the transient development of shallow-water 'oxygen oases' at the margins of otherwise anoxic iron-rich seas, and that these were present locally in the mid-Archean, as exemplified at Steep Rock.

https://doi.org/10.1180/S0026461X00008434 Published online by Cambridge University Press

Origin and fluxes of dissolved sulphate in the Himalayan system : evaluation and implication

CHRISTIAN FRANCE-LANORD[1*], ANANTA P. GAJUREL[2], VALIER GALY[3], MAARTEN LUPKER[1], GUILLAUME MORIN[1]

[1]CRPG-CNRS U. Lorraine, BP 20 54501 Vandœuvre France cfl@crpg.cnrs-nancy.fr
[2] Tribuhvan U., Kathmandu, Nepal, apgajurel@gmail.com
[3] WHOI, Woods Hole, USA, vgaly@whoi.edu

Continental weathering budget requires careful analysis of dissolved sulphate origin as sulphide oxidation may represent a source of acid auxiliary to CO_2 [1]. In Himalayan rivers the concentration of sulphate is about 10 meq% that of HCO_3^- and previous studies underline the importance of sulphide oxidation processes [2-3]. We present isotopic compositions of dissolved sulphates from various Himalayan basins in Nepal, India and Bangladesh. More detailed data come from the Central Nepal Narayani basin. Isotopic data reveal that $\delta^{34}S$ are low between +6 and -15‰ and $\delta^{18}O$ are between +3 and -10‰. In addition there is a clear correlation between oxygen isotopic compositions of the river water and those of dissolved sulphate. These data confirm that the large majority of dissolved sulphate is derived from sulphide oxidation reactions occurring during erosion. Such reactions appear to be widespread over the Himalayan basin and can be sometime observed in winter as efflorescence of gypsum at the surface of sulphide bearing rocks such as black shale.

The analysis of rivers draining different lithologies in Nepal reveal that while sulphide oxidation is the prevalent source of sulphate it's intensity is highly variable. Assuming that all dissolved sulphate derive from pyrite, chemical erosion of pyrite vary between 10 and 60 t/yr/km^2 in High Himalayan gneisses and in Tethyan Sedimentary Series respectively. Among primary Himalayan basins, the Narayani Gandak and the Siang-Tsangpo rivers are the major sources of dissolved sulphate. Ganga and Brahmaputra in Bangladesh have isotopic compositions comparable to their Himalayan tributaries. The fluxes recorded in Bangladesh suggest that anthropogenic input to the river flux is not dominant in spite of the dense agricultural and industrial activity in the floodplain.

Overall sulphide oxidation processes represent a source of acid for weathering reactions during Himalayan erosion. It's association with Tethyan sediments suggest that sulphuric acid will mostly dissolve carbonates acting on the long term as a net source of CO_2 to the atmosphere.

[1] Calmels et al. (2007) Geology **35** 1003-6 [2]A. Galy & France-Lanord (1999) Chem. Geol. **159**, 31-60. [3] Karim & Veizer (2000) Chem. Geol.**170**, 153-177.

Particle size dependence on arsenic concentration and bioaccessibility in mine tailings from the Empire Mine, CA

JESSICA M. FRANCIES[1*], NATALIE E. KIWAN[1], CHRISTOPHER S. KIM[1]

[1] School of Earth and Environmental Sciences, Chapman University, Orange, CA, USA, jfranc@chapman.edu

As a result of the historic mining of gold and silver in California, an estimated 47,000 abandoned mine sites exist statewide. Since the halt of mining operations, communities have developed near and around abandoned mine wastes at these locations. This is of great concern because the waste material left over from the processing and extraction of precious metals contains associated toxic metal(loid)s, including arsenic (As), which can be mobilized into surrounding communities, contaminate surface and rain water, and be incidentally ingested by humans. The Empire Mine in the Sierra Nevada mountain range contains areas of varying As contamination. Prelimary studies have discovered a range of As bioaccessibility relative to initial As concentration, indicating that trends in arsenic concentration and bioaccessibility may be a function of particle size, correlations between arsenic and iron, and/or arsenic speciation.

Bulk samples were collected from six different locations at the Empire Mine and separated by particle size through a dry sieving method to generate eleven distinct size fractions. BET surface area analysis and EXAFS spectroscopy was conducted to determine the reactive surface area and arsenic speciation of selected size fractions. Acid digestion and ICP-AES analysis were then conducted to determine the initial concentrations of As and a host of other metals present in each size fraction. Finally, the bioaccessibility of As as a function of particle size was examined by conducting a physiologically based extraction test (PBET) utilizing a simulated gastric fluid (SGF).

The majority of samples collected displayed an inverse relationship between particle size and total arsenic concentration; these same samples also typically showed a strong As-Fe correlation. Conversely, samples without an inverse size-concentration relationship tend to have both low total As concentrations and poor As-Fe correlations. In addition, As concentrations were found to increase by over an order of magnitude as size decreases. In relation to the bioaccessibility tests, 7-10% As was consistently released into the simulated gastric fluid media, suggesting that bioaccessibility is linked with the initial As concitentration of the sample. However, when the percent As released is normalized for surface area in comparison to particle size, a decreasing trend in As as particle size decreased resulted. This indicates surface area also plays a significant role in As bioaccessibility. Furthermore, bulk (unsieved) samples that undergo PBET can underestimate bioaccessibility in fine-grained size fractions, also supporting the possible effect that surface area and particle size play in the degree of arsenic bioaccessibility in mine wastes. These results demonstrate that particle size is an important criterion in determining arsenic transport, concentration, exposure, and future remediation efforts.

https://doi.org/10.1180/S0026461X00008434 Published online by Cambridge University Press

Microbial dissolution of Se-jarosite by *Shewanella putrefaciens* CN32

RACHEL FRANZBLAU[1*], NADINE LOICK[1], CHRISTOPHER WEISENER[1]

[1]Great Lakes Environmental Institute for Research, University of Windsor, Windsor, Canada, franzbl@uwindsor.ca*

Introduction

Jarosites form in acidic, low temperature, sulfate-rich environments. Jarosite minerals scavenge trace elements, and are involved in trace metal cycling. Selenium (Se) is a trace element in human and microbial metabolism, but is chronically and actuely toxic in higher doses [1]. In jarosites, Se can completely substitute for the sulfate group ($MFe_3(SO_4)_x(SeO_4)_{2-x}(OH)_6$) [2]. Prior studies have focused on microbial interactions with the two aqueous Se oxyanions, selenate (SeO_4^{2-})and selenite (SeO_3^{2-}) but therie has been limited investigations pertaining to bacterial-mineral chemical pathways [3,4,5]. In this study, the circumneutral dissolution of jarosites with a range of Se-substitution for tetrahedral coordianted sulfate in the presence of *Shewanella putrefaciens* CN32 was examined under anaerobic conditions.

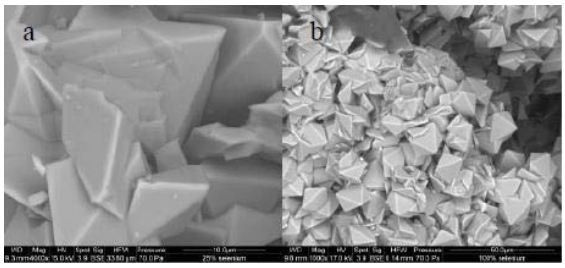

Figure 1: BSE-SEM images of Se-jarosites a) 25% Se substitution b) 100% Se substitution for sulfate

Results and Conclusion

Microbial biomass, ATP, SEM, [Se] and solution chemistry were considered during the experiment to evaluate the influence *Shewanella putrefaciens* CN32 on Se-jarosite dissolution. The reduction and fate of Se will be discussed to provide a better understanding of the interaction of bacteria and Se-minerals in reducing environments.

[1] Winkel (2011) *Environmental Science &Technology* **46**, 571-579. [2] Dutrizac (1981) *Hydrometallurgy* **6**, 327-337. [3] Kenward (2006) *Environmental Science & Technology* **40**, 3782-3786. [4] Ma (2007) *Environmental Science & Technology* **41**, 7795-7801. [5] Oremland (2004) *Applied and Environmental Microbiology* **70**, 52-60.

Yucatán hydroclimate during the Maya 'megadroughts': Speleothem records of multiple hazards and a test of the hurricane masking effect

AMY BENOIT FRAPPIER[1*], AURORA D. PINKEY-DROBNIS[1]

[1]Skidmore College, Department of Geosciences, Saratoga Springs, NY, 12866 USA, afrappie@skidmore.edu (* presenting author)

Severe and persistent megadroughts in the Yucatan peninsula have been associated with the so-called 'collapse' of the Maya high civilization in the Terminal Classic Period (TCP) around 900-1000 C.E. [1] An annual stable isotope record from the Chaac speleothem showed that TCP 'megadrought' was rather a series of 8 severe droughts lasting 3-18 years in the interval betweel 800 and 950 C.E., punctuated by brief moist periods characterized by low $\delta^{18}O$ values[2]. We present a nearby annually-dated multiproxy stalagmite record (CH-1), and compare it to the Chaac stable isotope record as a replication test for a coherent regional climate signal.

The CH-1 stalagmite also contains a conservative record of severe tropical cyclone flooding events, as mud layers embedded within the calcite laminae from cave flooding events [3]. In the 20th century historical period, all flooding events in this low-lying cave are associated with years of local hurricane rain events and associated temporarily high levels of the regional water table. Mud layers in CH-1 thus indicate some years with hurricane rainfall. In the 20th century historical period, the threshold for CH-1 mud layer emplacement varies with pre-existing hydrologic conditions; i.e. mud layers are less likely to be emplaced, even by severe storms, when the pre-existing water table was low due to persistent drought. Likewise, mud layers in CH-1 are more likely when the water table is elevated due to wet conditions and/or repeated hurricane events. Historical hurricanes and droughts are associated with other hazards such as wildfire. We combine stable isotope, stratigraphic, and trace element records from CH-1 to track multiple hazards.

In comparing the two local stalagmite records, we note a curious relation during the TCP between tropical cyclone activity (CH-1 mud layers) and breaks in the megadrought sequence (Chaac $\delta^{18}O$ values). Infiltrating hurricane rainwater, which has an anomalously low stable isotopic composition [6], can depress the $\delta^{18}O$ value of speleothem calcite for months to years after the storm event [5]. If this masking effect from hurricane rainfall has altered the speleothem isotopic record during the TCP, then we would expect that years with high hurricane rainfall would be correlated with years with low calcite $\delta^{18}O$ values. Furthermore, we would expect that during peristent drought, years with low hurricane activity would correlate to times with high speleothem $\delta^{18}O$ values. We present a test of the hurricane masking effect in Yucatan speleothems during the Terminal Classic 'megadroughts', and discuss the implications for tropical speleothem paleoclimatology, and for understanding complex patterns of human-climate interactions during this event.

[1] Haug *et al.* (2003) *Science* **299**, 1731–1735. [2] Medina-Elizalde *et al.* (2010) *EPSL* **298**, 255-262, [3] Pyburn (2010), MS Thesis, Boston College [4] Lawrence and Gedzelman (1996), *Geophys. Re.s Lett.* **23**, 527-530. [5] Frappier (2008) *Geochim. Cosmochim. Acta* **72**, A282.

https://doi.org/10.1180/S0026461X00008434 Published online by Cambridge University Press

Understanding Biomarker Records of Terrestrial Paleoecolgy

KATHERINE H. FREEMAN,*[1] HEATHER GRAHAM[2], ANNA HENDERSON[3], CLAY MAGILL[4]

Dept. of Geosciences, The Pennsylvania State University, University Park, PA, USA, 16802, [1]khf4@psu.edu; [2]geozilla@psu.edu; [3]ahenderson@gmail.com; [4]clayton.magill@gmail.com

The terrestrial biosphere is fundamental to the global climate system, influencing albedo, circulation, the water cycle, carbon sequestration and weathering. Paleobotanical records offer detailed insights to plant communities and their changes in response to climate perturbations. Leaf fossils do not lend themselves to high-resolution and continuous records through time, and although continous pollen records can be well preserved, they do not offer physiological insights such as those gained from leaf margins or stomata densities, for example. Plant biomarkers reflect plant phylogeny and functionality, and are well preserved in ancient soils and sediments. Both distributions and isotopic signatures of plant lipids are increasingly used in terrestrial paleoclimate studies.

Recent work on both modern and ancient plant biomarkers offers new ways to understand molecular records of terrestrial paleoecology. Lipid biomarker abundance and distribution patterns within modern plants are influenced both by plant phylogeneic affiliation as well as by functional properties, most notably leaf lifespan. Biomarker carbon-isotope signatures reflect both plant type and environmental factors such as seasonality, water availability, light exposure, and canopy closure. In modern leaves, these factors influence *n*-alkane $\delta^{13}C$ values, chain length distributions of homologs and total abundances in leaf tissue. Such data provide frameworks for interpreting plant-wax carbon-isotope signatures in terms of biome type and ecosystem structure, and provide constraints that aid interpretations of lipid δD signatures.

Understanding how growth environment and phylogenetic relationships influence waxes in modern plants engenders new proxies for past communities. Yet, to be useful to paleoclimate applications, biomarker and isotopic proxies based on modern plants must consider the role of litter flux that can both integrate and filter plant signatures in sedimentary archives. We extend observational data from modern flora with a statistical resampling (bootstrap) analysis to evaluate how variability in plant signatures are integrated by soil and sediment geochemical records.

We will present insights from lipid, leaf, biome and catchment-scale studies that inform our understanding of molecular record of the terrestrial biosphere. These insghts will be illustrated using examples from our studies of Cenozoic terrestrial paleoecology.

CHROMIUM ISOTOPES AS PROXY FOR SURFACE OXYGENATION – RESULTS FROM A ~1.9 GA PALEOSOL DEVELOPED ON OCEANIC CRUST (SCHREIBER BEACH, ONTARIO, CANDADA)

ROBERT FREI[1,2,*] ALI POLAT[3]

[1]Institute of Geography and Geology, University of Copenhagen, Denmark, robertf@geo.ku.dk(* presenting author)
[2]Nordic Center for Earth Evolution (NordCEE)
[3]Department of Earth and Environmental Sciences, University of Windsor, ON, Canada, polat@uwindsor.ca

The chromium isotope proxy is based on isotopic fractionation believed to accompany the oxidative weathering of Cr(III) minerals in soils. At equilibrium, oxidized Cr (Cr(VI) is predicted to be enriched in heavy isotopes, and consequently, one would expect this heavy and mobile Cr to be liberated to solution leaving an isotopically light soil behind.

In order to explore Cr isotope fractionation during soil formation, we investigated a ~ 1.9 Ga subaerial weathering profile at Schreiber Beach, Ontario, Canada. The section developed on Neoarchean (~2.8 Ga) pillow basalts and is unconformably overlain by the Paleoproterozoic (~1.88 Ga) Gunflint Chert and basal conglomerates. There are gradual textural, mineralogical and geochemical changes from unweathered basalts to strongly weathered hematite-bearing basalts with stratigraphic height.

The $\delta^{53}Cr$ value of unweathered basalts (-0.16 +/- 0.05 ‰) is within the range of mantle inventory values [1], whereas weathered brown to green basalts (soils), exhibiting up to 30% lower Cr concentrations compared to unaltered pillow cores, are isotopically lighter ($\delta^{53}Cr$ = -0.35 +/- 0.11 ‰). Red, hematite-rich (lateritic) basalts and hyaloclastites underlying the brown to green basaltic soils, instead are isotopically heavier ($\delta^{53}Cr$ = +0.05 +/- 0.15 ‰). These results speak for a process whereby ferrous Fe and likewise, Cr(VI), was leached from Fe-bearing minerals in upper soil horizons (mostly now eroded), and transported by oxygenated ground waters to lower portions of the profile where it precipitated as iron oxyhydroxides (later transformed to hematite during greenschist metamorphism after the deposition of the Gunflint Cherts) together with back-reduced isotopically heavy Cr(III) originally mobilized as Cr(VI) during surface weathering. An oxidative atmosphere at ~1.9 Ga, as implied by the results from the Schreiber profile, is furthermore supported by positively fractioned Cr isotopes ($\delta^{53}Cr$ = +0.2 +/- 0.05 ‰) recorded in the iron-rich Gunflint Cherts directly above the palaeo-weathered horizons at Schreiber Bay. These values are interpreted to reflect a positively fractionated shallow seawater chromium composition at ~1.88 Ga, a finding which is in accordance with the results of [2].

The potential of the Cr isotope system in ancient paleosols to untangle the presence of oxidative weathering processes makes this system a viable and important tracer for the reconstruction of surface oxygenation in Earth's history.

[1] Schoenberg et al. (2008) *Chemical Geology* **249**, 294-.306
[2] Frei et al. (2009) *Nature* **461**, 250-253.

https://doi.org/10.1180/S0026461X00008434 Published online by Cambridge University Press

Reverse weathering in the Okavango Delta, northern Botswana

PATRICK FRINGS[1*], DANIEL J. CONLEY[1], ERIC STRUYF[2] AND MIKE MURRAY-HUDSON[3]

[1]Lund University, 223-62 Lund, Sweden, patrick.frings@geol.lu.se (*presenting author), daniel.conley@geol.lu.se
[2]Antwerp Univeristy, 2610 Antwerp, Belgium, eric.struyf@ua.ac.be
[3]University of Botswana, Maun, mmurray-hudson@ori.ub.bw

Introduction

Reverse weathering was first proposed to balance elemental budgets in the oceans [1]. The suggestion was thermodynamically possible, but lacked direct observational evidence. Recent field and lab incubations unambiguously show rapid formation of authigenic clay minerals is plausible under certain conditions [2,3]. We present direct and indirect evidence for mineral authigenesis in the Okavango Delta, a shallow, freshwater, tropical wetland bounded by the southern extension of the East African rift valley. Water and sediment samples were collected after peak flood in 2011 along a hydrological gradient from riverine to seasonal floodplain. The watershed hydrodynamics and biogeochemical processing regulate elemental cycling and maintain the Delta as a freshwater system [4].

Evidence for new mineral formation

Direct evidence for rapid mineral authigenesis comes from microscopic, spectroscopic and geochemical analysis of floodplain sediments. Special attention is paid to biogenic silica particles that are known to provide viable substrates for clay precipitation.

Indirect evidence comes from downstream changes in dissolved element concentrations and Ge/Si ratios. PCA of elemental concentrations assessed by ICP-AES or -MS indicates a strong hydro-chemical concentration gradient. Boron acts conservatively and is interpreted as representing the expected enrichment (~12x inflowing concentration) if evapotranspiration was the only process occurring. Other elements show lesser or even negative enrichment (4 – 0.1x inflowing concentrations), suggesting biotic or abiotic removal. A simple mixing model suggests that for many elements involved in clay authigenesis (e.g. Fe, Mn, Mg, K) biotic uptake cannot explain the relative lack of enrichment.

The ratio of Ge to Si (Ge/Si, µmol/mol) is commonly used as a tracer of critical zone weathering processes. A downstream decrease in Ge/Si from ~1 to ~0.2 is interpreted here in terms of in-stream processing. Uptake of Ge relative to Si during biological production is poorly defined but thought to be either unbiased or slightly negative [5]. The observed decrease in Ge/Si ratios must therefore be explained by preferential abiotic Ge removal.

We suggest rapid formation of new mineral phases in floodplain sediments is an important process. Our results show biotic and abiotic processes control element cycling in the Delta and highlight the possibility of reverse weathering in freshwater systems.

References

[1] Mackenzie and Garrels (1966) *Am J Sci* **264**, 507-525. [2] Loucaides et al. (2010) *Chem Geol* **270**, 68-79. [3] Michalopoulos and Aller (1995) *Science* **270**, 614-617. [4] Ramberg and Wolski (2008) *Plant Ecol* **196** 215-231. [5] Delvigne et al. (2009) *J Geophys. Res.* **114** GB2013.

Nitrate ($\delta^{15}N$) isotopic distribution in Antarctic Sea Ice,

FRANÇOIS FRIPIAT[1-2*], DANIEL M. SIGMAN[2], JEAN-LOUIS TISON[1]

[1]Université Libre de Bruxelles, Department of Earth and Environmental Sciences, Brussels, Belgium, ffripiat@ulb.ac.be (* presenting author) jtison@ulb.ac.be
[2]Princeton University, Department of Geosciences, Princeton, USA, sigman@princeton.edu

The only study reporting nitrogen isotopic composition ($\delta^{15}N$ vs. Air N_2) in Antarctic Sea Ice pointed out an isotopic distribution for particulate nitrogen (PN) significantly different from the marine counterpart[1-2], respectively 2 to 41‰ vs. -6 ot 6‰. Antarctic sediments from the last ice age are characterized by heavier PN $\delta^{15}N$ (including diatom bound nitrogen)[3]. Since an equatorward sea ice expansion is expected during glacial periods, the potentially higher contribution of sea ice PN in glacial sediment may explain or accentuate such variation.

We have measured $\delta^{15}N$ of nitrate in Antarctic Sea Ice, as a first step toward developing a mechanistic understanding of the processes driving such isotopic difference (sea ice vs. marine realm). The nitrate $\delta^{15}N$ was measured in the brine network both in spring and summer Antarctic pack ice, respectively, in the Bellinghausen Sea (SIMBA, October 2007) and Weddell Sea (ISPOL, December 2005).

The $\delta^{15}N$ range for nitrate measured so far, 2.7 to 13.2‰, falls in the range of previously measured values. The mean $\delta^{15}N$ (± 1sd) is heavier in summer (9.4 ± 2.8‰) than in spring (4.1 ± 1.2‰), in agreement with the seasonal nitrate depletion together with a preferential assimilation of light nitrate into organic matter. An unexpected outcome is that some samples show a $\delta^{15}N$ lower than that of lower circumpolar deep water which is typically 4.7-4.8‰ [2], implying processes in addition of nitrate assimilation. Possible nitrogen source to the nitrate pool include the organic matter and ammonium (NH_4) inside the brine network[4], the nitrification of which could yield low $\delta^{15}N$ nitrate. Indeed, nitrification has been observed to occur in Antarctic Sea Ice[5], implying a regeneration of nitrate inside the brine network. Presumably, the generation of low $\delta^{15}N$ nitrate also causes the ammonium pool to be elevated in $\delta^{15}N$, an inference that we will test with measurements. The implication for the $\delta^{15}N$ of sea ice PN will then be investigated.

[1] Rau et al. (1991) *Mar. Chem.* **35**, 355-369. [2] DiFiore et al. (2009) *Geochem. Geophys. Geosyst.* **10(11)**, Q11016, doi:10.1026/2009GC002468. [3] Robinson & Sigman (2009) *Quaternary Sci. Rev.* **27**, 1076-1090.[4] Dumont et al. (2009) *Polar Biol.* **32**, 733-750. [5] Priscu et al. (1990) *Mar. Ecol. Prog. Ser.* ***62***, 37-46.

https://doi.org/10.1180/S0026461X00008434 Published online by Cambridge University Press

Lithium Isotope History of Cenozoic Seawater: Changes in Silicate Weathering and Reverse Weathering

PHILIP N. FROELICH[1,*], SAMBUDDHA MISRA[2]

[1]Froelich Education Services, 3402 Cameron Chase Dr., Tallahassee, FL, 32309. USA. (*correspondence: pfroelich@comcast.net)
[2]Dept. of Earth Sciences; University of Cambridge; Cambridge, UK

A stepwise nine per mil rise in lithium isotope ratios in seawater (^{7}Li / ^{6}Li, δ^7Li_{SW}) over the past 60 million years requires large changes in continental chemical weathering and cation fluxes through the sea, implying episodes of tectonic uplift and CO_2 drawdown. Weathering of uplifted continental rocks plays a central role in controlling both climate and seawater chemistry by consuming CO_2 and releasing cations to the ocean. Lithium isotopes provide a unique record of these changes because lithium, unlike other tracers of ocean chemistry change, is hosted entirely in silicates. This new 68 Ma record of seawater chemical change reveals shifts in global tectonic forces connecting Earth-ocean-climate processes. From the Paleocene (60 Ma) to the Present, δ^7Li_{SW} rose 9‰, requiring large changes in continental forward weathering and seafloor reverse weathering consistent with pulsed tectonic uplift, more rapid continental denudation, increasingly incongruent continental weathering (lower chemical weathering intensity) and more rapid CO_2 drawdown.

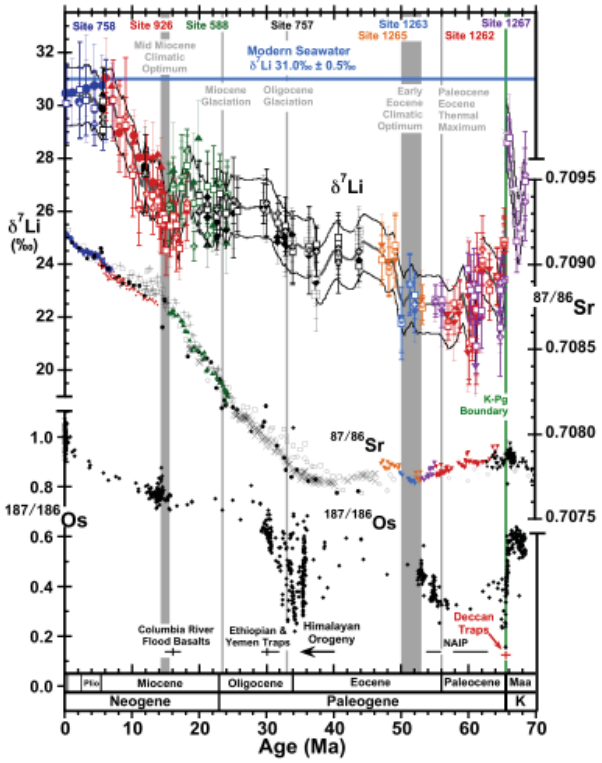

Figure: Li-, Sr-, and Os-isotope records over the past 68 Ma. The Li and Sr isotope records were reconstructed from forams in the same DSDP and ODP drill cores [1]. The Os-isotope data are from Peucker-Ehrenbrink & Ravizza (GTS 2012).

[1] Misra and Froelich (2012) *Science* (in press) (DOI: 10.1126/science.1214697).

Seawater Lithium Isotope Excursion Across the K-Pg Boundary: Chicxulub Impact vs. Deccan Traps

SAMBUDDHA MISRA[1], PHILIP N. FROELICH[2*]

[1]Dept. of Earth Sciences; University of Cambridge; Cambridge, UK
[2]Froelich Education Services, 3402 Cameron Chase Dr., Tallahassee, FL, 32309. USA. (*correspondence: pfroelich@comcast.net)

A 4‰ drop in the ^{7}Li/^{6}Li ratio of seawater (δ^7Li_{SW}), from about 29‰ in the Late Cretaceous to 25‰ in the Early Paleocene, occurs within less than 0.5 Ma across the Cretaceous-Paleogene boundary (K-PgB, 65.68 Ma). Because δ^7Li_{SW} is sensitive to both very large Li-isotope fractionation factors and to changes in silicate sources and sinks on time scales of the Li residence time in seawater (τ_{Li} ~1.2 Ma) [1], this negative excursion must reflect a large and fast influx of ^{6}Li to the ocean, presumably from continental or seafloor silicates, the primary Li-reservoirs in the Earth's crust. It can not be due to rapid addition of isotopically light Li from (a) the Chicxulub bolide itself nor its impact crater, even if pulverized and instantaneously dissolved in the ocean, or from (b) congruent weathering of the simultaneously erupted Deccan Traps Large Igneous Province (δ^7Li_{Basalt} ~3.4‰). One possibility is that estimates of the volume of Deccan basaltic lavas 'missing" in the Geologic Record is an order of magnitude too low. Another possibility is that the conflagration from the Chicxulub impact deforested large portions of the continents and induced rapid acid-rain chemical weathering of incinerated continental soils that then washed into the ocean. In any event, the cause of this large fast δ^7Li_{SW} drop across the K-Pg boundary remains enigmatic.

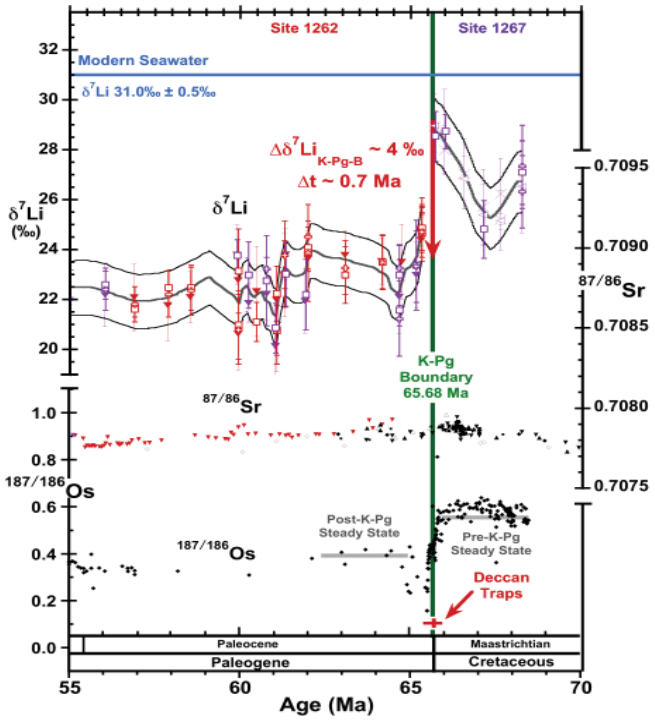

Figure: Li-, Sr-, and Os-isotope records across K-PgB. The lithium and strontium isotope records were recovered from forams in the same drill cores at ODP sites 1262 and 1267 [1]. Osmium isotope data are from Peucker-Ehrenbrink & Ravizza (GTS 2012)

[1] Misra and Froelich (2012) *Science* (in press). DOI: 10.1126/science.1214697

https://doi.org/10.1180/S0026461X00008434 Published online by Cambridge University Press

The composition of the lower mantle constrained by experiments on the elasticity of magnesium silicate perovskite

Daniel J. Frost*[1], Julien Chantel[2], Alexander Kurnosov[1], Dmytro Trots[1], Tiziana Boffa Ballaran[1], Yanbin Wang[3]

[1]Bayerisches Geoinstitut, Bayreuth, Germany, dan.frost@uni-bayreuth.de (* presenting author)
[2]ESRF, Grenoble, France, chantel@esrf.fr
[3]GSECARS, APS, Argonne, Il , USA , wang@cars.uchicago.edu

Comparison between seismic estimates for S and P wave velocities and similar experimental estimates for appropriate rock compositions is the only rigorous method for determining the composition of the Earth's lower mantle. Magnesium-silicate perovskite is the dominant mineral of the Earth's lower mantle. The composition of silicate perovskite forming within a typical Bulk Silicate Earth composition is dominated by the $MgSiO_3$ component but will also contain sub equal proportions of Al and Fe. The lower mantle may also contain a significant proportion of remnant subducted basaltic crust, from which more Al and Fe-rich silicate perovskite would form. Fe and Al substitution in perovskite will therefore be a significant source of chemical variability in the lower mantle and potentially the main cause of observed seismic heterogeneity in this region.

Using Brillouin spectroscopy we have studied the elasticity of $MgSiO_3$ perovsktie single crystals in the diamond anvil cell to lower mantle pressures. In addition we have examined the elasticity of polycrystalline $MgSiO_3$ perovskite plus samples of the same phase containing Fe and Fe and Al using ultrasonic interferometry in the multianvil. These measurements were performed at the APS synchrotron x-ray source to enable pressure and sample length measurements and were performed up to 25 GPa and 1200 K. The results allow models for seismic wave velocities in the lower mantle to be tested against seismic models and for variations in velocity in the lower mantle to be understood in terms of temperature and composition.

Simulating Arctic Black Carbon with GEOS-Chem/CMAQ Modelling System

JOSHUA S. FU*[1], XINYI DONG[1], KAN HUANG[1], MENGDAWN CHENG[2], AND JOHN STOREY[2]

[1]University of Tennessee at Knoxville, Knoxville, USA, jsfu@utk.edu (* presenting author)
[1]University of Tennessee at Knoxville, Knoxville, USA, xdong1@utk.edu
[1]University of Tennessee at Knoxville, Knoxville, USA, khuang7@utk.edu
[2]Oak Ridge National Laboratory, Oak Ridge, USA, chengmd@ornl.gov
[2]Oak Ridge National Laboratory, Oak Ridge, USA, storeyjm@ornl.gov

Introduction

Arctic black carbon (BC) is of special interest because it makes a 10-100 times larger climate forcing impact thant a midlatitude source of equal strength[1]. To fully understand the impacts of Arctic BC on both air quality and climate forcing, it is necessary to identify the transport, distribution, and concentrations of Arctic BC within modeling work. However, currently very limited infromation of BC emission inventory over Arctic region is available except for biomass burning which takes about 35% of total BC emission. In this study, GEOS-Chem has been applied to investigate Arctic BC with EDGAR emission inventory for year 2006-2008 with grid resolution of 2x2.5°. With initial and boundary conditions dynamically downscaled from GEOS-Chem[2], Hemispheric-CMAQ is also applied with the same emission inventory but at finer resolutions as 108km and 36km to eiliminate the model discrepancy and uncertainties caused by grid resolutions. Model performances are evaluated against surface network observations from AERONET for 2 sites in US and 2 sites in Russia. GEOS-Chem is found to be able to reproduce BC over US domain generally well with NMB as 4.5% and 7.9% for US sites, and underestimate BC over Russia greatly with NMB of -81.36% and -81.71%. Modelling results from Hemispheric CMAQ will be able to provide more detailed BC information including spatial distributiona and temporal variations, and also the cross-Arctic transport of BC.

Preliminary Summary

Based on our preliminary results, Arctic black carbon emission inventory is underestimated by 285 ~ 2500% over noth Eurasia area in the EDGAR HTAP emission inventory.

[1] Stohl (2011) *The Arctic as a Messenger for Global Processes, conference presentation, May4 th*, Copenhagen
[2] Lam and Fu (2009) *Atmos. Chem. Phys* 9, 9169-9185

https://doi.org/10.1180/S0026461X00008434 Published online by Cambridge University Press

Study on Activation Characteristics of Trace Elements in Black Soil Region of Central Jilin Province

Q.FU[1*], D.Y.WANG[1], Y.Y.YANG[1], C. WU[1] AND F.FEI[1]

[1] Jilin University, College of Earth Sciences, Changchun, China, fly19881118@yahoo.com.cn*, wang_dy@jlu.edu.cn, yangyuan52415241@163.com, 178275048@qq.com, flyindance313@hotmail.com

Introduction

Studying available contents of trace elements is the basis of making rational utilization of the land resources and improving soil quality as the effective state of soil elements is the available part in the process of crop utilization and absorption. In recent years, effects of soil trace elements on crop growth and quality have caught more attention, and the previous studies indicate that the consumption of trace elements in soil will increase with the improvement of crop yields, therefore, studying the activation characteristics of soil trace elements and the influence factors is of great significance.

Material, Method, Results and Discussion

This paper analyzes and determines the total contents and available contents of 10 trace elements (As, B, Cr, Cd, Cu, Mo, Mn, Ni, Se, Zn), collected from 62 surface soil samples in black soil region of central Jilin province, NE China, and correlation analyses are done by SPSS both between the total and available contents of trace elements, and between soil pH value and activation indexes of 10 soil trace elements, respectively. Statistics results show that the activation indexes (available contents of elements in soil accounting for total contents) of different trace elements in black soil region of central Jilin province make a great difference and activation index of Mo is 26.19%, reaching the highest while that of Cd is only 0.03% —the lowest. The total and available contents of Cu and Mn exhibit extremely significantly positive correlations while these of As have extremely remarkable negative correlations, and there are no significant correlations between the total and available contents of B, Cd, Cr, Mo, Ni, Se and Zn, respectively. Additionally, the activation indexes of Cr, Cd, Mn, Mo, Ni, Se and Zn have extremely significantly positive correlations with soil pH value, respectively.

Conclusion

Taken together, the above analysis indicates that the total contents of soil trace elements are not the only control factor effecting on the available contents, but soil physical and chemical properties also have some degree influence on activation characteristics of trace elements.

Thus, taking reasonable measures of soil management according to soil characteristics in study area is of vital importance to trace elements management during the agricultural production process.

[1] R L&J C (1979) Philosophical transactions of the Royal Society of London. Series B, Biological sciences **288**, 15-24. [2] Tu,He&Liu (2011) Plant and Soil **349**, 241-251.

Mg isotope variation in a ferromanganese crust from Line Seamount in the Central Pacific Ocean

YAZHOU FU[1] AND ZHENGRONG WANG[2*]

[1]State Key Laboratory of Ore Deposit Geochemistry, Institute of Geochemistry, Chinese Academy of Sciences, Guiyang, China, fuyazhoucas@gmail.com

[2]Department of Geology and Geophysics, Yale University, New Haven, USA, zhengrong.wang@yale.edu

Marine hydrogenous ferromanganese crusts grow slowly (a few mm/Ma) and contain distinctive laminar growth layers which have potential to document the long term evolution of ocean chemistry and/or deep ocean temperatures. In this study, we explored the evolution of Sr and Mg isotope variation in successive layers of a marine hydrogenous ferromanganese crust, MP2D06, from Line Seamount in Central Pacific Ocean.

Eighteen layers from this sample were subjected to a series of incremental leaching steps, using various concentrations of ammonium acetate, acetic acid, hydroxylamine hydrochloride-acetic acid, and hydrochloric acid, to leach out metals from different phases (including surface adsorbed metals, and those associated with carbonate, Fe-Mn oxides, silicates and phosphate phases). Leachates from each independent step were passed through three chromatographic columns to remove interfering metals prior to analysis (particularly Fe, Mn, and Ti). The high-precision isotopic compositions of Sr and Mg for each leachate at every layer were determined by MC-ICP-MS (Neptune) at Yale University.

Preliminary results show that hydroxylamine hydrochloride-acetic acid can dissolve Fe-Mn oxides and leachates after three serial leaching steps contain Sr and Mg associated with predominantly Fe-Mn oxides. Strontium isotopic ratios for leachates from this leaching portion are consistent with seawater $^{87}Sr/^{86}Sr$ ratios, indicating this manganese crust started to grow at about 40 Ma years ago when compared to the standard seawater Sr isotope record. Mg isotope compositions of the leachates are all greater than the contemporary sea water value-the surface layer, for example, is highly enriched in ^{26}Mg compared with contemporary sea water (+1.7 versus -0.82‰ relative to DSM). The $\delta^{26}Mg$ decreases gradually with increasing age. This decrease implies either an increases in ocean bottom temperature and/or decrease of $\delta^{26}Mg$ values of seawater in the last 40-50 Ma years.

https://doi.org/10.1180/S0026461X00008434 Published online by Cambridge University Press

Size effect in the adsorption of gold nanoparticles on pyrite surfaces

YUHONG FU, ZONGHUA QIN, SHANSHAN LI, JINKAI XIAO, YI XIAO AND QUAN WAN*

Institute of Geochemistry, Chinese Academy of Sciences, Guiyang, Guizhou, 550002, P.R. China, wanquan@vip.gyig.ac.cn (* presenting author)

Size effect is essential to perhaps all aspects of nanogeoscience. The metal adsorption by minerals is thought to be one important ore-depositing mechanism. Gold nanoparticles (<100 nm) have been ubiquitously found in the Carlin-type deposits, although how they were formed remains elusive. We hypothesize that nanosized gold may be involved in the pathway of ore transportation and enrichment, and therefore have carried out experimental study on adsorption of gold nanoparticles on pyrite surfaces.

Batches of gold nanoparticles in the size range of 10~80 nm were synthesized using the classic Frens method [1]. The monodisperse size of gold particles were controlled through changing the molar ratio of chloroauric acid to sodium citrate. Natural pyrite mineral powders with particle size of tens of microns were obtained through grinding/sieving, and were cleaned with deionized water. Aqueous nano-gold sols (10 ml) of varying gold particle size were mixed (with adequate stirring) at calculated proportions with pyrite powders of varying particle size for 20 hours. Transmission electron microscopy (TEM) was used to characterize the size of the gold nanoparticles as well as their distribution on pyrite surface. Atomic absorption spectroscopy (AAS) was used to monitor the gold concentration in the liquid phase.

We have found that pyrite can strongly adsorb gold nanoparticles. In some cases where sufficient amount of pyrite was present (e.g., 10% of gold coverage on pyrite surface), gold (original concentration ~50 μg/ml) was completely adsorbed from the gold sol to pyrite surface (i.e., zero gold absorbance on AAS after adsorption). This is consistent with the fact that pyrite exists as a major gold-bearing mineral in many gold deposits. Smaller pyrite particle (200~400 mesh) showed higher ability to adsorb gold nanoparticles than larger pyrite particles (100~160 mesh), i.e., more gold (mg) was adsorbed on unit mass of pyrite (g) of smaller particle size. This seems to readily explain the observation that higher concentration of gold was normally found on pyrite of smaller size, however does not necessarily support that gold travelled in either nanoparticle or ionic/complex state. Our data also indicate that more quantity (mg) of gold was adsorbed on pyrite when the size of the gold nanoparticle was larger. While appearing counter-intuitive, this along with other aforementioned results supports a simplified adsorption mechanism that gold nanospheres pack and cover the pyrite surface. Our ongoing work aims to elucidate the detailed thermodynamics and kinetics of gold nanoparticle adsorption on pyrite. It is also worth noting that nanoparticle adsorption by minerals has wider implication beyond the field of ore deposit.

[1] Frens (1973) *Nature-Physical Science* **241**(105), 20-22.

Mineralogy of lacustrine sediment from Darhad basin records the past lake level changes of the paleo-lake.

MADOKA FUCHIZAKI[1*], TAKAAKI YABE[1], HITOMI ABE[1], KEISUKE FUKUSHI[2], NORIKO HASEBE[2] AND KENJI KASHIWAYA[2]

[1]Division of Earth and Environmental Sciences, Graduate School of Natural Science and Technology, Kanazawa University, Ishikawa, Japan (*madoka14@stu.kanazawa-u.ac.jp)

[2]Institute of Nature and Environmental Technology, Kanazawa University, Ishikawa, Japan

Darhad basin in northern Mongolia is located in the continent where is sensitive to the climate change. It has been reported that several hydrologic events with climate changes occurred in this area. Ice dam lake had been formed in Darhad basin by Pleistocene glaciers. There had been several flooded events during warm periods. Darhad basin has many inflows and one outflow (Shishhid Gol river). Limestone is present in southeastrn rim of basin. Granitic rocks are distributed in northern part. There are basalt flows near the valley of the Shishhid Gol[1].

164 m of long drilling core (DDP10-3 core) were obtained from Hodon site (51˚20'11.20" N , 99˚30'04.40" E) in Darhad basin at April 2010. The core was cut into 3 cm. Top 100 m of the sediments were analyzed by X-ray diffraction in order to identify the constituent minerals. Selected samples were observed by scanning electron microscope. Water of several rivers were collected at August 2011. The water quality (pH, electric conductivities, ORP and alkalinities) were measured on site. The concentrations of chloride and sulfate were measured by high-performance liquid chromatography. Those of major cationic species were measured by inductively coupled plasma acrostic emission spectroscopy.

The mineralogical analyses showed that there are the intervals of presence of carbonate minerals and absence of the minerals. In the Some samples during the carbonates absence intervals, the formations of gypsum were observed. The water chemistry of the river samples showed that there are large variations of alkalinities among the inflows. The two inflows came from the southeast carbonate area on the basin have high Ca^{2+} and HCO_3^-. The pH of the rivers ranges from 7.39 to 8.86. The inflow came from northwest has lowest pH and dissolved solid.

The lake must be contacted with southeast limestone area if the lake level was high. The high Ca^{2+} and HCO_3^- of inflows from southeast area were evidence that clastic carbonates were entered in paleo-lake from this region. Therefore, the intervals of presence of carbonate minerals indicate the high lake level of the paleo-lake. In contrast, carbonates must be absent if lake got away from the limestone area. The formation of gypsum found in the carbonates absence intervals indicate the concentration of dissolved solid must be very high because the mineral possesses high solubility. Therefore, the intervals of absence carbonate indicate the periods of low lake level due to the evaporation.

[1] Gillespie.A.R et al. (2008) *Quaternary Research* **69**, 169-187

https://doi.org/10.1180/S0026461X00008434 Published online by Cambridge University Press

Electrochemical precipitation of gold from a hydrothermal fluid in the Black and Kimberley Reefs, South Africa

SEBASTIAN FUCHS[1*], ANTHONY WILLIAMS-JONES[2] AND WOJCIECH PRZYBYLOWICZ[3]

[1]McGill University, Earth and Planetary Sciences, Montreal, Canada, sebastian.fuchs@mail.mcgill.ca (* presenting author)
[2]McGill University, Earth and Planetary Sciences, Montreal, Canada,
[3]iThemba, Laboratory for Accelerator Based Sciences, Somerset West, South Africa

The Witwatersrand hosts the largest known gold resource on Earth, however, the genesis of the gold mineralization is still a matter of considerable debate (opinion is divided over the relative importance of detrital sedimentary and hydrothermal processes). In the Kimberley Reef (Upper Witwatersrand Supergroup) and the Black Reef (Lowermost Transvaal Supergroup), gold is locally enriched in areas proximal to underlying gold-bearing Witwatersrand reefs. Gold concentration in the Kimberly and Black reefs correlates strongly with hydrocarbon content. The gold occurs as angular to sub-angular, native gold particles in the interstitial space between pyrite and arsenic-bearing sulphides, in fractures cutting pyrite, in irregularly shaped pores within pyrite and in hydrocarbon nodules.

Particle-induced X-ray emmision (PIXE) analyses were performed on native gold grains and nearby grains of pyrite and other minerals. Quantitative element maps prepared from these analyses show that pyrite adjacent to gold grains is invariably zoned in respect to As (unless there is also an adjacent arsenic-bearing mineral) with the highest concentrations occurring adjacent to gold grains. The concentration of As varies from 86 ppm (+/- 20) to 7850 ppm (+/- 130). The chemical zoning of As is interpreted to correspond to a change from n-type (low As) to p-type (high As) conduction. This behaviour leads to large differences in the electric potential of the surfaces of growing pyrite crystals [1].

The evidence presented above suggests strongly that the gold grains discussed here are hydrothermal in origin. Assuming this to be the case, and based on data suggesting that temperature did not exceed 350 ºC and pH was < 5 [2], gold would have been transported mainly as $AuHS^0$ and $Au(HS)_2^-$ [3]. We propose that the close spatial association of gold with As-bearing pyrite reflects the electrochemical precipitation of gold onto the p-type pyrite because of the transfer of electrons from its surface to the gold species, thereby reducing Au^+ to Au^o and releasing HS^-. A similar interpretation is proposed for gold grains in contact with other arsenic-bearing minerals. In view of the strong evidence for the hydrothermal origin of the gold and its spatial association with underlying Witwatersrand gold reefs, we conclude that the gold in the Kimberly and Black reefs was hydrothermally remobilized from Witwatersrand gold reefs.

[1] Moeller & Kersten (1994) *Mineralium Deposita* **29(5)**, 404-413. [2] Meyer et al. (1994) Exploration and Mining Geology **3(3)**, 207-217.
[3] Williams-Jones et al. (2009) Elements 5(5), 281-287

Ab initio study of Zn isotope fractionation in aqueous compounds

TOSHIYUKI FUJII[1]*, FRÉDÉRIC MOYNIER[2], MARIE-LAURE PONS[3], AND FRANCIS ALBARÈDE[3]

[1]Research Reactor Institute, Kyoto University, Osaka, Japan, tosiyuki@rri.kyoto-u.ac.jp
[2]Department of Earth and Planetary Sciences, Washington University in St. Louis, St. Louis, USA
[3]Ecole Normale Supérieure de Lyon, Lyon, France

Isotopic variability of Zn in natural samples has been well documented by multi-collector ICP-MS [1]. The interpretation of these data is limited by our knowledge of isotope fractionation during chemical reactions. Intramolecular vibration of isotopologues is the major origin of chemical isotope effect for non-heavy elements [2]. Analysis of model molecules by *ab initio* methods is helpful to estimate magnitude of isotope fractionation. In the present study, isotope fractionation factor of various Zn species was calculated. Orbital geometries and vibrational frequencies of Zn(II) species were computed using density functional theory (DFT) as implemented by the Gaussian03,09 codes (Gaussian Inc.). The DFT method and basis set employed here are B3LYP and 6-311+G(d,p).

Isotope fractionation factor ln β (‰) for $^{66}Zn/^{64}Zn$ was estimated from the calculated vibrational frequencies of isotopologues for hydrated Zn ion, chlorides, sulfides, sulphates, carbonates, phosphates, citrates, and malates [3,4]. For the common species, our results are consistent with those of Black *et al*. [5]. With a site-averaged ln β value of 3.43‰ at 298 K, citrates are enriched in heavy isotopes with respect to the hydrated Zn^{2+} aqua ion $Zn(H_2O)_6^{2+}$, the dominant form of Zn in natural water. ln β was found to be 0.2-1‰ larger than that of Zn^{2+} for carbonates, phosphates, and sulphates, and 0.1-1‰ smaller for chlorides and sulfides. This suggests that strong oxygen donor ligands, notably phosphates and carbonates, are enriched in heavy Zn isotopes.

The present results provide a consistent framework for the interpretation of Zn isotope data in plants [6,7], with Zn phosphates in the root system being isotopically heavier than Zn malate and phosphate in the aerial parts. They also explain the heavy Zn isotope compositions of human and animal bones. The role of phosphates explains the isotopically light Zn in residual soils and isotopically heavy Zn in FeMn-nodules. It is anticipated that potential threats of aquifer pollutions by heavy metals and phosphates upon pH variations could also be monitored by Zn isotopes.

[1] Albarède (2004) *Rev. Mineral. Geochem.* **55**, 409-427. [2] Bigeleisen & Mayer (1947) *J. Chem. Phys*. **15**, 261-267. [3] Fujii *et al*. (2011) *Geochim. Cosmochim. Acta* **75**, 7632-7643. [4] Fujii & Albarède (in press) *PLoS ONE* http://dx.plos.org/10.1371/journal.pone.0030726. [5] Black *et al*. (2011) *Geochim. Cosmochim. Acta* **75**, 769-783. [6] Weiss *et al*. (2005) *New Phytologist* **165**, 703-710. [7] Moynier *et al*. (2009) *Chem. Geol*. **267**, 125-130.

https://doi.org/10.1180/S0026461X00008434 Published online by Cambridge University Press

Catchment-wide denudation rates from the Murrumbidgee River, Murray-Darling Basin, SE Australia, using *in situ* cosmogenic ^{10}Be

TOSHIYUKI FUJIOKA[1*], ANTHONY DOSSETO[2], PAUL HESSE[3] AND CHARLES MIFSUD[1]

[1]Australian Nuclear Science and Technology Organisation, Sydney, Australia, toshiyuki.fujioka@ansto.gov.au (* presenting author), charles.mifsud@ansto.gov.au

[2]School of Earth and Environmental Sciences, University of Wollongong, Wollongong, Australia, tonyd@uow.edu.au

[3]Department of Environment and Geography, Macquarie University, Sydney, Australia, paul.hesse@mq.edu.au

Abstract

The Murray-Darling Basin (MDB) is a large inland basin in southeast Australia (draining one seventh of the continent), and is by far the most important agricultural centre of the country. Sustainable use of the basin resources is a significant national agenda where the balance between two contrasting aspects - ecological preservation and industrial/agricultural development - has been long-debated. To evaluate the impact of human land use, it is required to understand the natural response of the basin to various external forcing such as climate and CO_2 fluctuation. This study is the first part of a larger investigation on the behavior of different river systems within MDB in response to past climate changes. Here, we present a study of the Murrumbidgee River catchment for the estimate of catchment-wide denudation rates using *in situ* cosmogenic-nuclide measurement in sediments. The Murrumbidgee River is among the longest (length ~1485 km) of the MDB rivers. Four stages of paleo-channel systems were identified and dated previously by thermoluminescence [1]. The paleo-denudation rates were calculated from the measured ^{10}Be corrected for post-depositional nuclide production. Results show remarkably constant nature of catchment-wide denudation rate (12-15 m/Ma) for the last 100 ka. The average rate of 14 ± 1 m/Ma (n = 8) is much slower than the global mean ^{10}Be-based basin denudation rate of 218 ± 35 m/Ma (n = 1149) [2]. At such low rate, time-averaging of denudation rate estimate is c. 50-70 ka, and our data integrate over the entire glacial or interglacial period. Overall, our results suggest that catchment-wide denudation in the Murrumbidgee River catchment has not been changed dramatically for the last two glacial-interglacial cycles. The result here is somewhat in contrast to U-series comminution ages of the same deposits, where interglacial sediments exhibit relatively longer residence time (c. 100-500 ka) over sediments deposited during the glacial periods (<50 ka) [3], which implies changes in weathering or erosion regimes between the two periods. Finally, response to certain climatic conditions may have been significantly different between rivers within the MDB, and our ongoing project will address this issue by comparing temporal variations in fluvial activity, denudation rates, and sediment residence times between different catchments within the basin.

[1] Page *et al*. (1996) *Journal of Quaternary Science* **11**, 311-326. [2] Portenga and Bierman (2011) *GSA Today* **21**, 4-10. [3] Dosseto *et al*. (2010) *Geology* **38**, 395-398.

Monitoring microbially induced calcite precipitation in the subsurface

YOSHIKO FUJITA[1*], TSIGABU GEBREHIWET[2], JAMES R. HENRIKSEN[1], JOANNA L. TAYLOR[2], BAPTISTE DAFFLON[3], SUSAN S. HUBBARD[3] AND ROBERT W. SMITH[2]

[1]Idaho National Laboratory, Idaho Falls, ID, USA, yoshiko.fujita@inl.gov (* presenting author), james.henriksen@inl.gov

[2]University of Idaho-Idaho Falls, Idaho Falls, ID, USA, tgebrehiwet@uidaho.edu, tayljl@if.uidaho.edu, smithbob@uidaho.edu

[3]Lawrence Berkeley National Laboratory, Berkeley, CA, USA bdafflon@lbl.gov, sshubbard@lbl.gov

Microbially induced calcite precipitation (MICP) has gained interest for a number of subsurface applications, such as contaminant remediation, flowpath modification for energy resource recovery and management, and improvement of soil shear strength. A specific example is the immobilization of the radionuclide ^{90}Sr by co-precipitation in calcite, where calcite precipitation is accelerated by microbial ureolysis. Previous work has shown that ureolytically driven calcite precipitation can be mediated by indigeneous subsurface microorganisms at numerous sites, and that nutrient addition can accelerate the process and thereby increase Sr partitioning. A critical need for the further development of this approach into a field-ready technology is the ability to verify and track the progress of the relevant biogeochemical processes.

Recently we have been conducting field experiments of MICP and testing various approaches for monitoring the effects of our perturbations of the subsurface biogeochemical environment. In an experiment at the Integrated Field Research Challenge site in Rifle, Colorado, USA, we injected urea and molasses into groundwater for 12 days, with a continuous recirculation system between two wells located approximately 4 meters apart. During the recirculation, water samples were withdrawn at various locations within and outside of the recirculation zone for analysis of chemical and isotopic (^{13}C) composition and of microbial ureolytic potential (cell counts, urease gene quantitation, and/or ureolysis rate estimations), and incubated solids were sampled for evaluation of the attached microbial community. Cross borehole geophysical data were collected prior, during, and after the amendment addition. Followup water sampling occurred periodically for almost a year after active recirculation. Ten months after the cessation of nutrient injection, core was collected from within the recirculation zone.

The urea and molasses treatment enhanced *in situ* ureolytic activity as evidenced by increases in *ureC* gene copies and estimated urea hydrolysis rates, as well as long-term observations of ammonium in the injection, extraction and downgradient monitoring wells. Isotopic analyses showed a decrease in the δ^{13}C of the dissolved inorganic carbon in the recirculated water, consistent with hydrolysis of the isotopically light urea. Permeability changes and increases in the calcite saturation indexes in the well field suggest that mineral precipitation occurred; core samples are being examined for evidence. Joint interpretation of radar, seismic and electrical data suggest that these techniques can track the spatiotemporal progress of the urea hydrolysis and calcite precipitation processes.

https://doi.org/10.1180/S0026461X00008434 Published online by Cambridge University Press

Chemical processes of zinc in aerosols inferred from the speciation and isotopic analyses

MASATOMO FUJIWARA,[1] MASAHARU TANIMIZU,[2,1] AND YOSHIO TAKAHASHI[1*]

[1]Hiroshima University, ytakaha@hiroshima-u.ac.jp; [2]Japan Agency for Marine-Earth Science and Technology (JAMSTEC);

Supply of Zn from atmosphere to earth's surface is important considering possible deficiency of zinc (Zn) for phytoplanktons in open oceans and also toxic effects of excess Zn to various organisms in surface environment. Relative concentration of zinc (Zn) in aerosols is very high compared with the crustal abundances normalized by aluminum for other elements, showing that Zn in aerosols is originated exclusively from anthropogenic sources. In addition, Zn is largely found in finer particle fractions, since the main process of the emission is combustion in refinery factories etc. Another possible source of Zn is its emission as particles by the ablation of polyorganic materials containing zinc such as tire wears.

When Zn is provided by gaseous species into the atmosphere, finer particle of Zn in aerosol is finally formed by condensation of vapor released by the combustion, the fraction of which exhibits lighter Zn isotopic ratio enriched feature [1]. For this reason, Zn isotopic analyses may be able to quantify the contribution of Zn emitted by the volatlization. On the other hand, Zn speciation is changed in the atmosphere during long-range transport due to the reactions with water and other ligands such as sulfate and oxalate in the atmosphere. Thus, the speciation of Zn in the aerosol by X-ray absorption fine structure (XAFS) can reflect the source and behavior of Zn in the atmosphere. However, there have been no studies conducted based on both speciation and isotopic analysis for Zn in the aerosols.

In this study, aerosol samples were collected at Tsukuba, Japan. We applied XAFS to identify the speciation in the aerosols coupled with ICP-AES or ICP-MS to determine total concentration of each Zn species at each particle size. In addition, we also measured isotopic ratio of Zn using multi-collector inductively-coupled plasma mass spectrometer (MC-ICPMS; Neptune) to examine the relationship between Zn species and their isotopic ratios.

For the particles larger than 3.3 μm, ZnO and ZnS were mainly observed, which may be released from tire wear and other materials emitted originally as particles into the atmosphere. Zinc isotopic ratios in the particles are not fractionated because there is no process to induce isotopic fractionation such as volatilization for Zn when they are prduced originally as particles.

For the finer particles, main zinc species were $ZnCl_2$, Zn sulfate, and Zn oxalate. A negative correlation between zinc concentration in the atmosphere and its isotopic ratios was observed. This result suggested that most of zinc in the finer particles is anthropogenic, and that most of zinc has been emitted by the vaporization during combustion.

References

[1] N. Mattielli et al., 2009. Atmos. Environ. 43, 1265-1272.

[2] T. Furukawa and Y. Takahashi, 2011. Atom. Chem. Phys., 11, 4289-4301.

Tellurium Isotope Analysis in Sequential Acid Leachates of Carbonaceous Chondrites

YUSUKE FUKAMI[1*] AND TETSUYA YOKOYAMA[1]

[1] Department of Earth and Planetary Sciences, Tokyo Institute of Technology, fukami.y.aa@m.titech.ac.jp (* presenting author)

Nucleosynthetic isotope anomalies found in primitive chondrites give us clues for understanding the origin of materials from which our solar system has formed. Precise determination of isotopic compositions for various trace elements in meteorites now suggests heterogeneous isotopic distribution in the protosolar nebula (e.g. Cr, Ti, Mo, Ru, Sm [1-3]), yet some limited elements support isotopic homogeneity in the early solar system (e.g. Zr, Te, Os [4-6]). The inconsistent isotopic signatures would be the result of incomplete mixing and/or destruction of some "selected" presolar materials in the early solar system. To investigate this, it is important to determine the main presolar phases for individual elements that have contributed to the solar system. However, it is difficult to directly measure isotope ratios in individual presolar grains for trace elements where concentrations are at ppm level. In contrast, sequential acid leaching of bulk chondirtes enables chemical mineral separation, and it has been commonly used for detecting isotope anomalies of trace elements. Tellurium is one of the intriguing elements for the study of nucleosynthetic isotope anomalies in meteorites. It has eight stable nuclides produced by nucleosynthesis of p-process (^{120}Te), s-process ($^{122, 123, 124, 125, 126}$Te) and r-process ($^{125, 126, 128, 130}$Te). The isotopic composition of Te is also affected by the extinct nuclide of ^{126}Sn that decays to ^{126}Te with a half-life of 234.5 kyr [7]. In this study, we present preliminary data of Te isotopic compositions in acid leachates of Murchison meteorite (CM2) and Tagish Lake meteorite (C2-ung), which were subjected to the sequential acid leaching procedure described in [8] that was used for Os isotope analysis.

Te isotope analysis was performed by using thermal ionization mass spectrometry in negative mode (N-TIMS). The typical analytical reproducibility was 310 ppm for ^{126}Te/^{124}Te ratios when measured by using Faraday cups. The Te isotopic compositions in all the acid leacahtes from Murchison and Tagish Lake were not resolvable from terrestlial standard within analytical uncertainties. This is contrasting to Os isotopic results which showed larage nucleosynthetic anomalies in acid leachates of Murchison, while bulk chondrites possess no Os isotope anomalies [6, 8]. This inconsistency might indicate that dominant presolar phases carrying Te were thermally or aqueously unstable compared to those containing Os. The difference of volatility might have acted to produce not only planetary but also minral-scale isotopic homogeneity for Te, which was not the case for Os and other elements.

[1] Trinquier *et al.* (2009) *Science* **324**, 374-376. [2] Burkhardt *et al.* (2011) *EPSL* **312**, 390-400. [3] Chen *et al.* (2010) *GCA* **74**, 3851-3862. [4] Schönbächler *et al.* (2003) *EPSL* **216**, 467-481. [5] Fehr *et al.* (2006) *GCA* **70,** 3436-3448. [6] Yokoyama *et al.* (2010) *EPSL* **291**, 48-59. [7] Oberli *et al.* (1999) *Int. J. Mass. Spectrom.* **184**, 145-152. [8] Reisberg *et al.* (2009) *EPSL.* **277**, 334-344.

https://doi.org/10.1180/S0026461X00008434 Published online by Cambridge University Press

^{230}Th-normalized fluxes of biogenic components from the central-southernmost Chilean margin during the last deglaciation and the Holocene

MIHO FUKUDA[1, 2], NAOMI HARADA[2*], MIYAKO SATO[3], CARINA B. LANGE[4], HAJIME KAWAKAMI[5], SILVIO PANTOJA[6] TAKESHI MATSUMOTO[7] AND ISAO MOTOYAMA[8]

[1]Univ. of Tsukuba, Tsukuba, Japan, fukudam@jamstec.go.jp
[2] JAMSTEC, Yokosuka, Japan, haradan@jamstec.go.jp (* presenting author)
[3]JAMSTEC, Yokosuka, Japan, satom@jamstec.go.jp
[4]Universidad de Concepcion, Concepcion, Chile, clange@copas.cl
[5]JAMSTEC, Mutsu, Japan, kawakami@jamstec.go.jp
[6]Univ. de Concepcion, Concepcion, Chile, spantoja@copas.cl
[7]Univ. of the Ryukyu, Nishihara-cho, Japan, tak@sci.u-ryukyu.ac.jp
[8]Yamagata Univ., Yamagata, Japan, i-motoyama@sci.kj.yamagata-u.ac.jp

Background and abstract

Throughout geologic time, variations in carbon fixation by photosynthesis have been associated with climate changes. During glacial periods, strengthened productivity and an efficient biological pump in the North Pacific, equatorial Pacific, and Southern Oceans may have contributed to low pCO_2 [1-4]. However, there is still some controversy as to whether marine productivity was high everywhere during glacial periods, and whether intensification (or weakening) of marine productivity contributed to a decrease (or increase) of atmospheric pCO_2 during the last deglaciation. Resolving this controversy requires more data from many regions regarding temporal changes in past export fluxes of biogenic materials.

Thorium 230 (^{230}Th) normalized fluxes of biogenic components from sediment cores collected at 36ºS off central Chilean covering the past 22 kilo years (ka) (PC-1) and at 52ºS near the mouth of Strait of Magellan, Pacific side over the past 13 ka (PC-3). The ^{230}Th-normalized fluxes of TOC at the PC-1 site was relatively low between 22 and 15 calendar ka (cal ka), and a substantial increase was observed after ~13 cal kyr BP. The ^{230}Th-normalized flux of TOC at the PC-3 site was relatively low from 13 to 6 cal kyr BP, thereafter increased during the late Holocene. Our ^{230}Th normalized fluxes suggested that biological pump would not have fully worked throughout 22–14 kyr BP and the early Holocene in the central–south Chilean and from 13 to 6 kyr BP at southern most Patagonia. Therefore, biological pump in the eastern South Pacific including this study area, may have not contributed to low pCO_2 during the last glacial and deglacial periods, and intensification of marine productivity occurred after 6 kyr BP at southern most Patagonia. We will also present the ^{230}Th-normalized fluxes of biogenic components recorded in the sediment core collected from the Drake Passage.

[1] Broecker (1982) *Geochim. Cosmochim. Acta* **46**, 1689–1705. [2] Kohfeld et al. (2005) *Science* **308**, 74–78. [3] Martin (1990) *Paleoceanography* **5**, 1–13. [4] McElroy, (1983) *Nature* **302**, 328–329.

Origin of the jadeite-quartzite from Yorii area, the Kanto Mountains, Japan

MAYUKO FUKUYAMA[1*], MASATSUGU OGASAWARA[2], KENJI HORIE[2], AND DER-CHUEN LEE[4]

[1]Akita University, Akita, Japan, mayuko@gipc.akita-u.ac.jp (* presenting author)
[2]Geological Survey of Japan, National Institute of Advanced Industrial Science and Technology, Tsukuba, Japan, masa.ogasawara@aist.go.jp
[3]National Institute of Polar Research, Tokyo, Japan, horie.kenji@nipr.ac.jp
[4]Institute of Earth Sciences, Academia Sinica, Taipei, Taiwan, dclee@earth.sinica.edu.tw

The petrological, chemical, and isotopic characteristics for the jadeite-quartzite in the serpentinite mélanges [1] from Yorii, Kanto Mountains, Japan have been examined in order to study the tectonic link between jadeite-quartzite and the Jurassic accretionary complex in Japan. The mineral assemblage of the jadeite-quartzite is mainly of jadeite, albite, and quartz, with minor aegirine-augite, zircon, and titanite. Mineral texture shows that the jadeite-quartzite has recorded the reaction: albite = jadeite + quartz. Zircon crystals exhibit two distinct characteristics (Type I and II), based on their morphology and REE abundance. Type I zircon is prismatic, and has REE pattern similar to that of the magmatic zircon, but with higher total REE contents. Thus, Type I zircon is considered to be formed with the influence of fluid. In contrast, Type II zircon is porous and with REE pattern of typical hydrothermal origin. The U-Pb age for both types of the zircon is 162.2±0.6 Ma (MSWD=1.4), and at this time, Japan was still a part of the eastern margin of the Asian continent. In the Jurassic, the Pacific oceanic plate subducted and formed a Jurassic accretionary complex, the Mino-Tanba-Chichibu complex, in Japan. The age suggests that the jadeite-quartzite was formed in a deep subduction zone contemporaneous to the formation of the Jurassic accretionary complex near the trench. Whole rock elemental data show that the jadeite-quartzite contains high concentrations of Zr and Nb and low LILE (large ion lithophile elements) contents. This indicates that the jadeite-quartzite may have acquired the HFSE (high field strength element) before the fluid moved up to the mantle wedge. Typical arc volcanic rocks are depleted in HFSE. Therefore, the high HFSE found in the jadeite-bearing rock is consistent with the fluid was stripped with HFSE before it got involved in the formation of arc magma. Although the occurrence of the jadeite-bearing rock is rare, it could be quite abundant in the subducted slab. [1] Hirajima (1983) *J. Japan. Assoc. Min. Petr. Econ. Geol.***78**, 77-83.

https://doi.org/10.1180/S0026461X00008434 Published online by Cambridge University Press

Solution chemistry controls multisite sorption of ^{137}Cs on micaceous soils

ADAM J. FULLER[1*], SAMUEL SHAW[1], CAROLINE L. PEACOCK[1], DIVYESH TRIVEDI[2], AND IAN T. BURKE[1]

[1]School of Earth & Environment, University of Leeds, UK eeajf@leeds.ac.uk (*presenting author)
[2]National Nuclear Laboratory, UK

Accidental releases of radioactive material have led to elevated levels of the hazardous radionuclide ^{137}Cs at a number of sites, notably: Fukushima, Japan; Chernobyl, Ukraine; Hanford, USA and Sellafield, UK. Once present in soils the mobility and bioavailability of ^{137}Cs is governed by its sorption to clay minerals [1]. This behaviour is influenced by the soil's mineralogy, solution pH, nature of competing cations, and the Cs concentration. We investigated the multi-site sorption behaviour of Cs on micaceous soils, as a function of Cs concentration and solution chemistry (pH and ionic strength).

This work used batch experiments to investgate sorption of Cs onto bulk 1 mm sieved micaceous soils from near Sellafield, W. Cumbria, UK. The amphoteric sorption behaviour of Cs is strongly controlled by its solution concentration (Fig. 1). At very low concentrations (10^{-11} M) Cs sorption is unaffected by pH. However as the concentration of Cs is increased pH becomes an important controlling factor on sorption.

At low concentrations, where sorption is pH independant, Cs selectively sorbs to the highly specific Frayed Edge Sites (FES) of illite. At increased concentrations (10^{-4} M) the FES become saturated and the excess sorbs to the basal plane [2]. This is a cation exchange process and is controlled by solution pH. At excessive Cs concentrations (10^{-1} M) the clay's sorption sites are saturated and any amphoteric behaviour is masked.

This study shows the complexity of the Cs sorption process on micaceous soils. It is governed by an interrelationship between solution chemistry and the availability of multiple sorption sites, as controlled by Cs solution concentration. It is important therefore to ensure that experiments are conducted at environmentally relevant Cs concentrations and that chemical variables are carefully controlled.

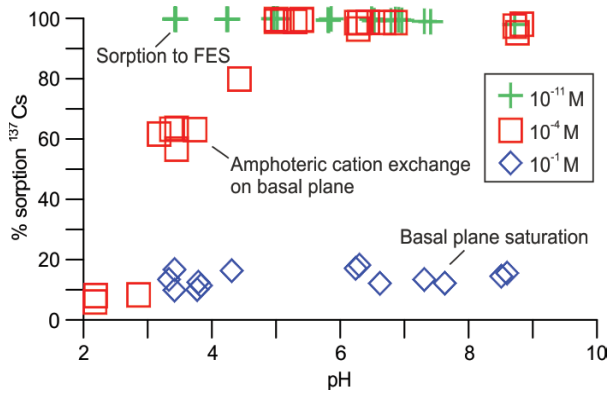

Figure 1 Sorption of Cs as a function of pH and Cs concentration

[1] Cornell (1993) *J. Radioanal. Nuclear Chem.* **171**, 483-500. [2] Poinssot, et al. (1999) *Geochim. Cosmochim. Acta*. **63**, 3217-3227

Isotope dilution analysis of Se and Te in chondritic meteorites

CLAUDIA FUNK[1*], FRANK WOMBACHER[1], HARRY BECKER[2], AND ADDI BISCHOFF[3]

[1]Institut für Geologie und Mineralogie, Universität zu Köln, Germany. cfunk0@uni-koeln.de (*presenting author)
[2]Institut für Geologische Wissenschaften, Freie Universität Berlin, Germany
[3]Institut für Planetologie, Westfälische Wilhelms Universität Münster, Germany

Introduction

The moderately volatile elements Se and Te have similar equilibrium (50%) condensation temperatures (697 and 709 K, respectively) at 10^{-4} bar for a gas of solar-system composition [1]. While the purely chalcophile element Se is exclusively hosted in sulfides [e.g. 2], the siderophile element Te can be incorporated in alloys, but also in sulfides due to its strong chalcophile affinity [1]. In CK and R chondrites and refractory inclusions in CV chondrites Te additionally forms noble metal-rich tellurides such as chengbolite ($PtTe_2$) and moncheite ($PtTe_2$) [e.g. 3, 4]. To further constrain early cosmochemical processes that led to (primary) depletion and fractionation processes affecting these two elements, precise Se and Te abundences were determined for different groups of primitive chondrites.

Analytical approach

^{77}Se and ^{125}Te enriched spikes were added to typically 50 mg of meteorite sample powder which was subsequently dissolved by HF-HNO_3 acid digestion. Chemical separation of Se and Te followed by using thiol cotton fiber (TCF). Mass spectrometric measurements were performed by multi collector ICP-MS, hydride generation and background substraction.

First Results

The presented method provides accurate and precise Se and Te abundances for chondritic samples. Concentrations were so far determined for a number of bulk carbonaceous chondrites (CI, C2 ungr., CM1, CM2, CO3, CV3, CR2, CH2), enstatite chondrites (EL3), ordinary chondrites (H3.3, L3.0), and Rumuruti chondrites (R3). Selenium and tellurium abundances are in general agreement with literature values [e.g. 2, 5]. Uniform Se/Te ratios were found for CI, C2 ungr. (Tagish Lake), CR2, CM1, and in one of the CM2 chondrites (Nogoya), whereas other CM2s, CV3, CO3.2 and CH2 chondrites show slightly lower Se/Te ratios. Ordinary, enstatite, and Rumuruti chondrites have consistently higher Se/Te ratios than carbonaceous chondrites. The data suggests that the CI chondrite Se/Te ratio is slightly higher than previously estimated by [1], and that Se/Te ratios discriminate ordinary, enstatite and Rumuruti chondrites from carbonaceous chondrites. Furthermore a weathered piece of Allende appears to confirm the suggestion that Se in chondrites is easily affected by terrestrial weathering [e.g. 2, 4].

[1] Lodders (2003) Astrophys. J. 591, 1220-1247. [2] Dreibus et al. (1995) Meteoritics 30, 439-445. [3] Geiger and Bischoff (1995) Planet. Space Sci. 43, 485-498. [4] Bischoff et al. (2011) Chemie der Erde 71, 101-133. [5] Brown et al. (2000) Science 290, 320-325.

https://doi.org/10.1180/S0026461X00008434 Published online by Cambridge University Press

Growth rate effect on oxygen isotope fractionation between aragonite and fluid at 24°C by *in situ* analysis

RINAT I. GABITOV[1*]

[1]University of California, Los Angeles, USA, gabitr@ucla.edu (* presenting author)

Introduction and Methodology

Oxygen isotope compositions ($\delta^{18}O$) of biogenic and inorganically precipitated calcium carbonate minerals are being used to reveal marine and terrestrial temperatures from the past. However, experimental and natural observations show that factors other than temperature control $\delta^{18}O$ in $CaCO_3$ via disequilibrium fractionation [1,2, etc.]. Among these factors are crystallization rate, solution pH, and saturation state of the fluid with respect to $CaCO_3$ phase (Ω). Previous experimental assessments of disequilibrium effects for $\delta^{18}O$ were focused on controlling pH and Ω of the experimental solution, followed by bulk analysis of $\delta^{18}O$ in multicrystalline precipitates. The precipitation rates in those works are usually being reported as amount of precipitated $CaCO_3$ per surface area and time (or simply amount per time) [3,4]. Because of this, inter- and intra-crystal isotopic variability has remained unknown.

In this work, I used the alternative approach of *in situ* Secondary Ion Mass Spectrometry (SIMS) at lateral spatial resolution of ~10 μm to determine isotopic and chemical variability of precipitated aragonite. The standard deviation of ten SIMS analyses of clear-beige natural aragonite (Belice, Bohemia) was 0.3 ‰ (1σ); the bulk $\delta^{18}O_{VPDB}$ in this reference aragonite was determined by stable isotope mass spectrometry as -7.79 ‰. Hemispherical bundles of aragonite crystals (spherulites) were precipitated by diffusion of CO_2 from ammonium carbonate into NH_4Cl-$MgCl_2$-$CaCl_2$ solution at 24°C. Spherulite growth (extention) rate (V) was monitored by sequentally spiking the growth medium with rare earth element (REE) dopants. After performing $\delta^{18}O$ analyses with a Cs^+ primary beam the same spots were revisited to determine their REE/Ca using an O^- beam. pH was measured in periodically sub-sampled fluids where aragonite nucleated and crystallized between starting and terminal pH of 8.3±0.1 and 8.63±0.02, respectively.

Results

SIMS spot analyses demontrate that nucleation centers of aragonite spherulites are depleted in $\delta^{18}O$ relative to their edges by as much as 4 ‰. REE/Ca profiles show decreasing V in the spherulites with time (i.e., spherulites edges advanced at slower rates than centers). $\delta^{18}O$ increases by 2.4 ‰ with decreasing V between 3 and 0.1 μm/hr. Because of a large fluid to crystal molar ratio (~4000) $\delta^{18}O$ of the fluid unlikely changed significantly during aragonite crystallization. Analysis of fluid sub-samples for $\delta^{18}O$ is ongoing and will permit to accurately calculate the dependence of the fractionation factor ($\alpha^{18}O$) on aragonite growth rate.

[1] McConnaughey (1989) *Geochim. Cosmochim. Acta* **53**, 151-162. [2] Rollion-Bard et al. (2003) *Coral Reefs* **22**, 405–415.
[3] Kim et al. (2006) *Geochim. Cosmochim. Acta* **70**, 5790–5801.
[4] Dietzel et al. (2009) *Chem. Geol.* **268**, 107–115.

Phase equilibrium constraints on the genesis of wehrlite cumulates at mid-ocean ridges and the origin of the clinopyroxene paradox

GLENN A GAETANI[1*], JOHN MACLENNAN[2]

[1]Department of Geology and Geophysics, Woods Hole Oceanographic Institution, Woods Hole, MA, 02543, USA (ggaetani@whoi.edu)

[2]Department of Earth Sciences, University of Cambridge, Downing Street, Cambridge, CB2 3EQ, UK (jcm1004@cam.ac.uk)

A longstanding gap in our understanding of ocean crust accretion is the occurence of pyroxene-bearing ultramafic cumulates near the base of the crust in ophiolites [1]. A similarly unresolved issue in the evolution of mid-ocean ridge basalts (MORB) is a compositional signature for clinopyroxene crystallization in abyssal tholeiites that are pyroxene saturated only at upper mantle conditions (the clinopyroxene paradox) [2]. Melting experiments conducted on lava from the Borgarhraun flow in the Theistareykir segment of Iceland's Northern Volcanic Zone provide new insights into both of these issues. Our results, combined with those of Winpenny and Maclennan [3], indicate that wehrlites nodules in the Borgarhraun flow crystallized at moderate pressures and relatively low temperatures from highly depleted magmas. This is consistent with an origin for wehrlite cumulates by crystallization of late-stage melts generated in the upper portions of the ascending mantle. The eventual mixing of these magmas with melts formed deeper the melting column imparts a clinopyroxene crystallization signature on erupted MORB.

Experiments were carried out on primitive (Mg# ~0.72) Borgarhraun lava at 1 bar and 1190 to 1320ºC by suspending rock powder from Re loops in a vertical gas-mixing furnace, with oxygen fugacity controlled at ~1.5 log units below the fayalite-magnetite-quartz buffer. Experiments were also conducted at 1.0 to 1.4 GPa and 1260 to 1370ºC, in graphite capsules, using a solid-medium piston-cylinder device. All run products were analyzed for major elements by electron microprobe. Trace elements were analyzed in a subset of the experiments by secondary ion mass spectrometry.

The 0.1 MPa liquid line of descent for Borgarhraun lava is typical of MORB, with olivine on the liquidus at ~1310°C, followed by olivine + plagioclase at ~1220°C. Clinopyroxene appears at ~1205°C. At 1.2 GPa Olivine + clinopyroxene crystallize together on the liquidus at ~1360°C. Clinopyroxenes in the wehrlite nodules studied by Winpenny and Maclennan [3] are compositionally distinct from those in our high-pressure experiments. The former are characterized by higher Mg# and CaO, and are strongly depleted in incompatible elements. A likley parent magma for the wehrlite cumulates is, therefore, a late-stage partial melt formed at relatively shallow depths. Dantas et al. [4] proposed a similar origin for pyroxenite cumulates from the Southwest Indian Ridge, suggesting that this process may be common at mid-ocean ridges.

References:

[1] Elthon et al. (1982) *J Geophys Res* **87** 8717-8734.
[2] Francis (1986) *Nature* **319** 586-589.
[3] Winpenny and Maclennan (2011) *J Petrology* **52** 1791-1812.
[4] Dantas et al. (2007) J Petrology **48** 647-660.

https://doi.org/10.1180/S0026461X00008434 Published online by Cambridge University Press

Me/Ca Proxies and Foram Biomineralization: The Role of Cation Transport

ALEXANDER GAGNON[1,2*], JAMES DEYOREO[2], DONALD DEPAOLO[1], HOWARD SPERO[3], ANN RUSSELL[3] AND ANTHONY GIUFFRE[4]

[1]Earth Science Division and [2]The Molecular Foundry, LBNL, Berkeley, USA, acgagnon@lbl.gov
[3]Department of Geology, UC Davis, Davis, USA
[4]Department of Geosciences, Virginia Tech, Blacksburg, USA

The Mg/Ca paleothermometer is a widely used technique and a powerful tool to reconstruct past sea surface temperatures from the tests of planktic foraminifera. However, the presence of unexplained diurnal Mg/Ca bands in these same tests [1] stands as a reminder of how little we know regarding the mechanistic details of biomineralization. During skeletal growth Mg/Ca and other proxies are controlled by a host of biological and physical factors including ion transport, aquatic speciation, surface chemistry, thermodynamic partitioning, crystal growth kinetics, and mineralization pathways. To build accurate environmental reconstructions we need to separate the impact of each parameter and use these data to build a chemical-scale understanding of biomineralization. In this study we isolate and characterize cation transport in cultured planktic foraminifera using stable isotope spikes and microanalysis. We then test if ion transport can explain diurnal Mg/Ca banding and develop a general model for the impact of ion dynamics on skeletal composition.

Living planktic foraminifera (*O. universa*) were placed in seawater enriched with stable isotopes of Mg, Ca, and Li. After 48 hours the forams were returned to natural abundance seawater. Imaged using NanoSIMS, the skeletal records of isotope uptake and efflux during this experiment reflect ion transport rates. We found that the calcium pool used for skeletal growth exchanges with the surrounding seawater with a turnover time of less than two hours. Furthermore, we observed no evidence for distinct day or night cation pools. Finally, magnesium, calcium, and lithium all showed identical dynamics suggesting direct and rapid seawater transport to the site of calcification rather than ion specific pathways. Thus selective calcium or magnesium pumping into the site of calcification cannot be used to explain diurnal Mg/Ca banding. Specific pumping of magnesium out from the site of calcification is still consistent with our data, however, and may explain banding. Combining ion transport rates and skeletal growth rate measurements from the same forams, we build a general analytical model to quantify the impact of ion dynamics on test composition. This transport model complements ongoing work on mineral growth rate effects in calcite and contributes towards a holistic and chemical-scale understanding of proxy behavior in foraminifera.

[1] Eggins, Sadekov, & De Decker (2004) *EPSL* **255**, 411-419.

Toward a quantitative model of metamorphic nucleation

FRED GAIDIES

Department of Earth Sciences, Carleton University, Ottawa, ON, K1S5B6, Canada

Mineral reactions in rocks take place as the result of a complex interplay between various atomic scale processes including dissolution, chemical diffusion, nucleation, and crystal growth. It is generally assumed that the product of a mineral reaction forms if the formation of that phase lowers the Gibbs free energy of the effective chemical system. However, even when that phase is part of the thermodynamically stable mineral assemblage, it may not necessarily nucleate. A certain departure from equilibrium is required to gain energy for the formation of the interface between reactants and products. This energy is referred to as interfacial energy, and only little is known about its magnitude during rock formation. In addition to this energy that has to be provided to initiate crystallization in rocks, chemical elements have to be transported between the sites of reactant dissolution and product nucleation, and attachment and detachment processes at the interfaces have to be efficient for crystallization to proceed. Knowledge of chemical transport and interface reaction rates in rocks are scarce but it is known that their interplay controls the microstructure and texture of rocks with important implications for the derivation of the conditions of rock formation relevant for the interpretation of past and future tectonic processes of Earth.

In this talk, a simple numerical model will be presented that accounts for the departure from equilibrium required for interface-controlled mineral nucleation [1]. The model simulates interface processes during metamorphic mineral reactions by which nuclei and crystals form on a molecular level based on classical nucleation and reaction rate theory and Gibbs free energy dissipation in a multi-component model system. Modeling results will be shown that allow to explore the interplay of several key parameters that impact on crystallization kinetics during petrogenesis such as the relative influences of interfacial energy and interface mobility on mineral content, mineral chemistry, and texture of rocks accounting for different rates of pressure – temperature changes during crystallization.

The comparison of nucleation simulations of contact-metamorphic garnet with analytical data obtained through XR-CT and EPMA provides first estimates of the order of magnitude of interfacial energies during metamorphic crystallization. It suggests furthermore that the interfacial energy has a first-order control on the departure from equilibrium required for mineral reactions if attachment and detachment processes at the surface of the product phase limit the overall crystallization rate. The influence of the heating rate on thermal overstepping is found to be negligible. A significant feedback is predicted between chemical fractionation associated with garnet formation and the kinetics of nucleation and crystal growth of garnet giving rise to its commonly lognormal – shaped crystal size distribution.

[1] Gaidies *et al.* (2011) CMP **155**, 657-671.

https://doi.org/10.1180/S0026461X00008434 Published online by Cambridge University Press

Chronic toxicity of metals/metalloids in mammals is mediated by their effect on Se-metabolism

JŰRGEN GAILER[1], GRAHAM N. GEORGE[2], AND INGRID J. PICKERING[2]

[1]University of Calgary, Calgary, Canada, jgailer@ucalgary.ca (* presenting author)

[2]University of Saskatchewan, Saskatoon, Canada, g.george@usask.ca; ingrid.pickering@usask.ca

The etiology of numerous human diseases, including autism and type 2 diabetes, the incidences of which are rising globally, is not well understood. Conversely, the concentration of toxic metals and metalloids, such as As, Cd, Hg and Pb in human blood of the average population is well established, but strikingly little is known about the role that these inorganic pollutants might play in the etiology of human disease processes [1]. Hence, the establishment of functional connections between the chronic exposure to inorganic pollutants and the etiology of certain diseases remains one of the great challenges in the post-genomic era. This requires us to uncover hitherto unknown biomolecular mechanisms which must explain how exceedingly small doses of a toxic metal/metalloid compound (low µg per day) – or mixtures thereof – may eventually result in a particular human disease. The biological complexity that is associated with mammalian organisms, however, makes the discovery of relevant mechanisms a monumental challenge. Recent findings suggest that a better understanding of the bioinorganic chemistry of inorganic pollutants in the bloodstream represents one fruitful strategy to unravel pertinent biomolecular mechanisms [1, 2]. In particular, the adverse effect(s) that toxic metals/metalloid compounds exert on the transport of the essential ultratrace element selenium to organs has emerged as highly relevant [3, 4]. An overview of the effect that As^{III} and Hg^{2+} exert on the mammalian metabolism of selenite will be presented and the health relevance of these findings will be discussed.

[1] Gailer (2012) *J. Inorg. Biochem.* in press. [2] Gailer (2009) *Biochimie* **91**, 1268-1272. [3] Jahromi *et al*. (2010) *Dalton Trans*. **39**, 329-336. [4] Gómez-Ariza, *et al.* (2011) *Metallomics*, **3**, 566-577.

The igneous contribution to atmosphere chemistry

FABRICE GAILLARD[1]*, BRUNO SCAILLET[1]

[1] CNRS-INSU, Université d'Orléans, ISTO, UMR 7327, 45071, Orléans, France, gaillard@cnrs-orleans.fr; bscaille@cnrs-orleans.fr (* presenting author).

We intend here to discuss the relationships between volcanic degassing and atmosphere chemistry in a (comparative) planetary perspective, with a particular emphasis on the atmospheric oxygenation that occurred on Earth, at the Archean-Proterozoic transition [1].

Igneous rocks and volcanic exhalations are moderately reduced [1]. For several reasons, secular variations in their redox state have been proposed [2] but so far no evidence of this has been found [3]. The only clear large scale modification of mantle redox state occurred at the end of the core formation at about 4.45 Ga. But it is only two billions years later that Earth's atmosphere became oxidized. This timelag between the mantle and the atmosphere great oxidation events [4] may possibly reflect changes in the conditions of volcanic degassing [5,6] that, in turn, may have been conditioned by large scale geodynamic modifications [7]. We will pursue here this analysis by evaluating alternative scenarii leading to changes in volcanic gas compositions. This includes changes in the intrusive/extrusive ratios and variations of the depth of melting. We will also discuss wether the great oxidation event (GOE) is unique to Earth or a common planetary process. The fact that Mars atmosphere is oxidized with an oxygen content comparable to that of the Earth's atmosphere after the GEO must be considered in the light of a possible GOE on Mars. The observation that Martian basalts show redox conditions much more reducing than that on Earth should also be incorporated in our contemplation on the role of igneous input to atmosphere chemistry. The fact that Venus atmosphere is reduced and may be comparable to that of Earth before the great oxidation event is also intriguing.

Because sulfur is an important component in volcanic processes and because of the diversity of its possible redox states, sulfur plays a dominant role in redox processes impacting oxygen abundance in planetary atmospheres [5,8]. We suggest that the efficiency of sulfur transfer from planetary interiors to their atmospheres is playing a major role in atmospheric oxygenation on Earth, and elsewhere.

[1] Holland (2002) *Cosmochimica Acta* **66,** 3811-3826. [2] Kasting, Eggler & Raeburn (1993) *Journal of Geology* **101**, 245–257. [3] Canil (2002) *Earth and Planetary Science Letters* **195**, 75-90. [4] Scaillet & Gaillard (2011), *Nature* **480**, 48-49. [5] Gaillard, Scaillet & Arndt (2011) *Nature* **478**, 229-232. [6] Kump, & Barley (2007) *Nature* **448**, 1033-1036. [7] Sleep & Windley (1982) *Journal of Geology* **90**, 363-379. [8] Lyons, Gill, (2010) *Elements* **6**, 93-99.

https://doi.org/10.1180/S0026461X00008434 Published online by Cambridge University Press

Denudation of the Lesser Antilles

JÉRÔME GAILLARDET[1*], ERIC LAJEUNESSE[1], SETAREH RAD[2], . CELINE DESSERT[1], PASCALE LOUVAT[1], KARINE RIVÉ[1], PIERRE AGRNIER[1], ELIMIE LLORET[3] ET MARC BENEDETTI[1]

[1]Institut de Physique du Globe de Paris, Paris, France, gaillardet@ipgp.fr (* presenting author)

[2] BRGM, Av. Guillemin, 45600 Orléans, cedex 05, France

[3] now at University of Alberta, Edmonton, Canada

We report in this paper the results of a multidisciplinary project aiming at determining the rates of chemical and physical denudation in the Lesser Antilles and the carbon fluxes exported to the ocean in a volcanic arc setting (Guadeloupe, Martinique, Dominica). Chemical denudation rates, determined by using river dissolved load range from 30 to 600 t/km2/yr, are extremely variable as a result of highly variable runoff and of the variable input of groundwaters influenced by volcanic acids [1], [2]. Physical denudation was estimated using different methods. Temporal monitoring of selected watershed gives a first estimate over a relatively short observation period. Based on the chemistry of the bottom sands transported in rivers, we calculated the physical denudation rates expected for a weathering system at steady state by solving a mass budget between source rocks and erosion products. Results show that the volcanic relief of Guadeloupe is eroding both chemically and physically at rates ranging between 100 mm/kr and more than 1000 mm/yr from the northern (and older) part of the Island to the southern (and younger) part respectively. These rates are important at a global scale and show that volcanic arc islands are "hot spots" of chemical and physical denudation on Earth. The denudation of the Lesser Antilles Arc is 2-3 higher that the eruptive rate, or island construction rate, meaning that volcanic arc islands have a limited lifetime (of typically 1 to a couple of million years) at a geological time scale. In addition to be a locus of intense sediment production to the ocean, the Lesser Antilles have a significant role of carbon export to the ocean. In terms of atmospheric carbon sequestration, first results show that the sequestration of organic carbon (in both dissolved and suspended load) may be about the same order of magnitude than inorganic sequestration [3]. Hydrology, and particularly orographic precipitation are proposed to be the main drivers of the weathering and denudation of tropical volcanic islands. Progresses have to be done primarily to establish proper water budgets of volcanic island to separate the effect of surface waters from groundwaters and to monitor over long periods of time the exportation of solids and particulate carbon.

[1] Gaillardet et al., (2012) *Am. J. of Sci.* in press. [2] Rivé et al., 2012, submitted to Earth Pl. Sci. Let. [3] Lloret et al. (2010) Chem. Geol. doi: 10.1016/j.chemgeo.2010.10.016, 2901-2910.

.

Non-traditional isotope variations in the Cordillera del Paine pluton

N. GAJOS[1*], C.C. LUNDSTROM[1] AND P.J. MICHAEL[2]

[1]Dept. of Geology, Univ of Illinois, Urbana, Il 61801 lundstro@uiuc.edu

[2]Dept. Geosciences, Univ of Tulsa, Tulsa, OK 74104 pjm@utulsa.edu

Non-traditional isotope systems provide unique insight into magma differentiation processes. We present new Fe and U isotope analyses (along with traditional Sr and Pb isotope data) on samples from the Cordillera del Paine igneous complex to assess relationships with differentiation. The Cordillera del Paine complex consists of a 1 km vertical exposure of relatively homogenous granite overlying a nearly contemporaneous and possibly cogenetic 0.5 km mafic gabbro suite. The mafic suite includes a small zone of diorites underlain by hornblende gabbros at the base of the exposure.

Samples previously characterized by Michael (1984, 1991) [1,2] were analyzed by MCICPMS. Fe isotope data shows a hyperbolic trend of increasing δ^{56}Fe with increasing SiO_2 in the pluton. Results show a strong correlation between $^{87}Sr/^{86}Sr$ and silica. Ten mafic suite samples average $^{87}Sr/^{86}Sr$ 0.7043(±)0.0004 and eleven granites average $^{87}Sr/^{86}Sr$ 0.70527(±)0.0004. In contrast, Pb isotopes are remarkably constant hovering ~ $^{208}Pb/^{204}Pb$ 38.72, $^{207}Pb/^{204}Pb$ 15.64 and $^{206}Pb/^{204}Pb$ 18.83. Finally, preliminary U isotope data show a trend of increasing $^{238}U/^{235}U$ with increasing SiO_2 (ranging from -0.37 to -0.26) although these data are only marginally outside of analytical error.

We assess four possible processes responsible for fractionating Fe isotopes during magma differentiation: 1) thermal migration and thermal gradients [3]; 2) crustal contamination, 3) fractional crystallization and 4) late stage fluid removal [4]. Quantitative assessment of #3 & #4 awaits results of experiments in progress to measure mineral-melt fractionation factors. The correlation of $^{87}Sr/^{86}Sr$ with silica as well as δ^{56}Fe suggests crustal contamination could be important to all isotope systems. This is reinforced by the Pb isotope data which fall very close to nearby Chile trench values [5]. On the other hand, fractionation of the heavy Fe and U isotope ratios with differentiation is also consistent with thermal migration and thermal gradient laboratory experiments. Further tests of other non-traditional stable isotope systems, such as Si, will help to assess the plausibility of this mechanism.

[1] Michael (1984) *Cont. Min, Petrol.***87**, 179-195. [2] Michael (1991) *Cont. Min. Petrol.* **108**, 396-418. [3] Lundstrom (2009) *GCA* **73,** 5709-5729. [4] Heimann A. et al. (2008) *GCA* **72**, 4379-4396. [5] Kilian R. and Berhmann J.H. (2003) *JGS* **160**, 57–70.

https://doi.org/10.1180/S0026461X00008434 Published online by Cambridge University Press

Upper ocean deoxygenation and denitrification at the end of the last ice age

ERIC GALBRAITH[1*] AND SAMUEL JACCARD[3]

[1]McGill University, Montreal, Canada, eric.galbraith@mcgill.ca (* presenting author)
[2]ETHZ, Zurich, Switzerland, samuel.jaccard@erdw.ethz.ch

The solubility of gases in the ocean decreased at the end of the last ice age, as ocean temperatures gradually rose, which would be expected to have increased water column denitrification rates. However, proxy records from marine sediments have shown that changes in oceanic oxygen contrations across this interval were not globally uniform, implying an important role for accumulated changes in oxygen consumption through the respiration of settling organic matter. A global compilation of marine sediment proxy records reveals that the upper ocean generally deoxygenated, but this included pauses and even reversals, consistent with changes in both temperature and oxygen consumption. [1] A new global nitrogen isotope compilation is consistent with a doubling of the rate of denitrification in the anoxic cores of oxygen-minimum zones across the deglaciation. This compilation is also consistent with a deglacial increase of nutrient supply via leakage from nitrate-rich upwelling regions, most notably the Southern Ocean, as previously suggested [2]. It seems likely that this increased nitrate supply contributed to the deglacial de-oxygenation by enhancing export and oxygen consumption, while also intensifying denitrification in anoxic waters. This analysis suggests that the nutrient flux across the thermocline is a key determinant of oxygenation and denitrification, in addition to temperature-driven solubility changes.

[1] Jaccard and Galbraith (2012) *Nature Geoscience* **5**, 151-156. [2] Robinson et. al. (2007) *Quat. Sci. Rev.* **26**, 201-212.

Computing the thermodynamics and reactivity of carbonates from solid state to speciation

RAFFAELLA DEMICHELIS[1], PAOLO RAITERI[1], JULIAN D. GALE[1*], DAVID QUIGLEY[2], DENIS GEBAUER[3], ANDREW G. STACK,[4] ROBERTO DOVESI,[5] VICTOR VINOGRAD[6] AND BJÖRN WINKLER[6]

[1]Curtin University, Chemistry, Perth, WA, Australia, J.Gale@curtin.edu.au (* presenting author)
[2]University of Warwick, Physics, Coventry, UK, D.Quigley@warwick.ac.uk
[3]University of Konstanz, Physical Chemistry, Konstanz, Germany, Australia, Denis.Gebauer@uni-konstanz.de
[4]Oak Ridge National Laboratory, Chemical Sciences Division, Oak Ridge, USA, stackag@ornl.gov
[5]Università degli Studi di Torino, Dipartimento di Chimica IFM, Torino, Italy, roberto.dovesi@unito.it
[6]Goethe Universität Frankfurt, Institut für Geowissenschaften, Frankfurt, Germany, B.Winkler@kristall.uni-frankfurt.de

Being able to compute the thermodynamics and reactivity of carbonate minerals and their solution species from atomistic simulation has long been a goal of geochemical modelling. The objective of this presentation is to address the question of how far can we go towards achieving this with present models and resources? Here a number of problems in carbonate geochemistry will be examined to demonstrate to what extend we can reproduce experimental data for the solid state and therefore be predictive for more complex environments, such as those for solution speciation.

A first test for any theoretical method is the polymorphism of crystalline calcium carbonate where the thermodynamics is well known. Examination of the performance of various first principles methods shows that reproducing the relative stabilities of calcite, aragonite and vaterite is sensitive to the choice of functional. Beside the quantitative thermodynamics, such methods offer new insights into the disorder within vaterite [1]. While there are also many force field models for carbonate minerals in the literature, most also fail to yield accurate thermodynamics unless explicitly considered during fitting [2]. If care is taken, force field models are found to provide a good description of cation-mixing in carbonate solid solutions.

More challenging than the bulk is the interface between carbonates and solution, including the influence of pH. Here the thermodynamics and reactivity of calcium carbonate in solution can be accurately predicted by atomistic methods. Computed free energies for ion pairing and formation of stable pre-nucleation clusters [3] are found to agree well with data from experimental speciation models [4]. Furthermore, simulations predict that nanoparticles of amorphous calcium carbonate are more stable than their crystalline counterparts below a critical size, depending on the degree of water incorporation [5]. The final challenge is to be able to compute rates of growth and dissolution for carbonates; this is now feasible with the use of enhanced sampling techniques [6].

[1] Demichelis, Raiteri, Gale and Dovesi (2012) *CrystEngComm*, **14**, 44-47. [2] Raiteri, Gale, Quigley and Rodger (2010) *J. Phys. Chem. C*, **114**, 5997-6010. [3] Demichelis et al (2011) *Nat. Commun.* **2**, 590. [4] Gebauer *et al.* (2008) *Science.* **322**, 1819-1822. [5] Raiteri and Gale (2010) *J. Am. Chem. Soc.*, **132**, 17623-17634. [6] Stack, Raiteri and Gale (2012) *J. Am. Chem. Soc.*, **134**, 11-14.

https://doi.org/10.1180/S0026461X00008434 Published online by Cambridge University Press

Simulation of non-classical crystallization of carbonate minerals

RAFFAELLA DEMICHELIS[1], PAOLO RAITERI[1], JULIAN D. GALE[1*], DAVID QUIGLEY[2] AND DENIS GEBAUER[3]

[1]Curtin University, Chemistry, Perth, WA, Australia, J.Gale@curtin.edu.au (* presenting author)
[2]University of Warwick, Physics, Coventry, UK, D.Quigley@warwick.ac.uk
[3]University of Konstanz, Physical Chemistry, Konstanz, Germany, Australia, Denis.Gebauer@uni-konstanz.de

The crystallization mechanisms of carbonate minerals have long attracted significant interest and none more so than calcium carbonate. Ion pairs have long been known to exist in carbonate solutions [1], while the existence of a range of $CaCO_3^0{}_{(aq)}$ species of varying hydration was proposed [2]. Recently, the demonstration that these pre-nucleation species are actually stable has sparked considerable interest in the non-classical nucleation of carbonates [3,4]. How this relates to the observation of amorphous states, such as Polymer Induced Liquid Precursors (PILP) [5] and Liquid Amorphous Calcium Carbonate (LACC) remains an open to debate [6].

In the present work we have utilized molecular dynamics simulation, based on both reactive [7] and conventional atomistic force fields, to identify the nature of the stable pre-nucleation clusters as being rapidly varying hydrated supramolecular polymers labelled as Dynamically Ordered Liquid-Like Oxyanion Polymers (DOLLOP) [8]. These DOLLOPs consist primarily of 1, 2 and 3-coordinate calcium and carbonate ions, leading to linear or branched polymer chains. However, ions remain in equilibrium with the solution through rapid exchange. The evolution and lifetime of the DOLLOP species depends on the size of the cluster; once a critical size is reached the properties are found to alter while remaining distinct from ACC. A preliminary examination of the influence of the presence of species other than calcium, carbonate and bicarbonate on the behaviour of DOLLOP has also been carried out.

[1] Greenwald (1941) *J. Biol. Chem.* **141**, 789-796. [2] Gal *et al.* (1996) *Talanta*, **43**, 1497-1509. [3] Gebauer *et al.* (2008) *Science.* **322**, 1819-1822. [4] Pouget *et al.* (2009) *Science*, **323**, 1455-1458. [5] Gower and Odom (2000) *J. Cryst. Growth*, **210**, 719-734. [6] Wolf *et al.* (2011) *Nanoscale*, **3**, 1158-1165. [7] Gale, Raiteri and van Duin (2011) *PCCP*, **13**, 16666-16679. [8] Demichelis, Raiteri, Gale, Quigley and Gebauer (2011) *Nat. Commun.* **2**, 590.

U(VI)-organic phosphate complex formation studied by ESI-FTMS

CATHERINE GALINDO[1], MIRELLA DEL NERO[1*], OLIVIER COURSON [1] AND SYLVIA GEORG[1]

[1]Institut Pluridisciplinaire Hubert Curien, UMR 7178 UdS/CNRS, Strasbourg, France
mireille.delnero@iphc.cnrs.fr (* presenting author)

Introduction

Complexation studies using model molecules with P=O and P-OH functionalities are highly required to assess to which extent organic phosphorus, present in the humic fraction of natural organic matter as derivatives of phospholipids, phosphonic acids, phosphoric esters, is involved in the binding of uranyl ions by humic acids. Electrospray ionization-Fourier transform mass spectrometry (ESI-FTMS) was used to investigate the formation of uranyl complexes in native solutions containing phenylphosphonic acid (H_2L) or phenylphosphoric acid and U(VI) at trace concentration level (µmolar range). Positive identification of the species was achieved, thanks to the high resolving power, high mass accuracy and reliability in ion abundance of the linear ion trap/orbitrap hybrid mass spectrometer.

Results and conclusion

Two types of complexes of stoechiometry of 1:1 (UO_2HL^+) and 1:2 ($UO_2(HL)_2$) were identified in native solutions at pH 3 containing U and phenylphosphonic acid, and the stability constants were evaluated. The technique was also successfully applied to elucidate the interactions between U(VI) and phenylphosphoric acid in native solutions with pH values favouring the hydrolysis of the organic ligand. Evidence was given for the presence of U(VI)-phenylphosphate complexes and for the formation of uranyl complexes with the degradation by-products of the ligand, with the relative contributions of species varying with time.

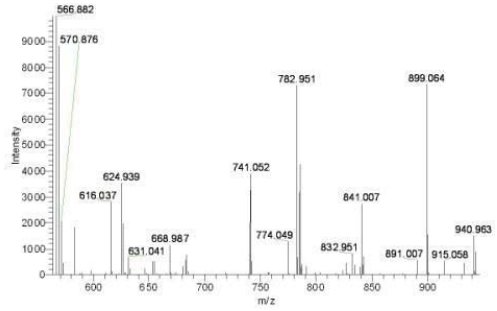

Figure 1: Negative ion mode ESI-FTMS spectrum showing presence of uranyl-phenylphosphonate complexes (detected as clusters formed with ClO_4^- electrolyte ions during ionization).

Studies of native solutions by means of ESI-FTMS has provided structural and quantitative information on the complexes formed between U(VI) and model molecules with P=O and P-OH functionalities. A complete speciation model was obtained for the uranyl - phenylphosphonic acid system, which is useful to model the binding of U by humic acids. The study was performed for trace level concentration of U, which is important for the applicability of the model to the speciation of uranyl in soil systems.

https://doi.org/10.1180/S0026461X00008434 Published online by Cambridge University Press

Tracing processes in the deep mantle by nickel stable isotopes

LOUISE GALL[1*], HELEN WILLIAMS[2], ALEX N. HALLIDAY[1]

[1]University of Oxford, Department of Earth Sciences, Oxford, UK louiseg@earth.ox.ac.uk (*presenting author)
[2]Durham University, Department of Earth Sciences, Durham, UK

The isotope system of nickel (Ni) has recently achieved some attention as a possible tracer for low-temperature processes [1]. However, although Ni is a ubiquitous element in the mantle the behaviour of Ni isotopes in high-temperature environments is yet to be investigated. In this study we have measured the mass-dependant isotope composition of Ni ($\delta^{60/58}$Ni, relative to the Ni metal standard NIST-SRM986) in a variety of mantle derived rock samples by MC-ICPMS using double-spike correction (long-term external reproducibility on silicate samples < 0.07‰) [2].

MORB glasses from different ocean ridges (Mid-Atlantic Ridge, Indian Ocean Ridge, and East Pacific Rise) and of different spreading rates were analysed for their Ni isotope compositions. The samples from the faster-spreading East Pacific Rise are heavier on average than those from the slower Mid-Atlantic and Indian Ocean Ridges, although all samples are significantly lighter (up to –0.4‰, δ^{60}Ni) in their isotope composition relative to peridotite samples. It is therefore possible that partial melting of the upper mantle cause fractionation of Ni isotopes, with the lighter isotopes being preferably extracted into the melt.

The Ni isotopic compositions of intraplate basalt (OIB) samples from widely different locations were also measured. Although the δ^{60}Ni-values for these basalt samples were spread over ~0.2‰, the values are within error of the isotopic composition of peridotites and Tertiary komatiites, which indicates that there is essentially no isotopic fractionation between mantle rocks and intraplate basalts. These preliminary results suggest that basalts may have small differences in their Ni isotopic composition depending on their origin, with MORBs appearing lighter than intraplate basalts.

Whether these results depend on differences in degree of partial melting between the MORB and OIB samples, or if their differences are due to the source's original chemical composition is difficult to say without further analyses. However, if partial melting causes fractionation of Ni isotopes between solid and melt in the mantle to the same extent in both OIBs and MORBs, resulting in the melt being slightly lighter than the residual solid, then the deep mantle may contain an undepleted reservoir of heavier δ^{60}Ni than measured in peridotite and komatiite samples.

[1] Cameron et. al. (2009) ***PNAS*** 106, 10944-10948.
[2] Gall et. al. (2012) ***JAAS*** 27, 137-145.

Supergene Evolution of Granitic Waste Rock Piles around U-mines in the Saint-Sylvestre Area (French Massif Central)

MARTINE GERARD[1,2], TANGUY POQUET[1,3], LAURENCE GALOISY[1,4*], GEORGES CALAS[1], VANNAPHA PHROMMAVANH[3] AND MICHAEL DESCOSTES[3]

[1]Institut de Minéralogie et de Physique des Milieux Condensés, Université P.&M Curie, France, martine.gerard@impmc.upmc.fr, calas@impmc.upmc.fr
[2] Institut de Recherche pour le Développement, Bondy, France
[3] AREVA, BG Mines, R&D, Paris la Défense, France vannapha.phrommavanh@areva.com, michael.descostes@areva.com
[4] Université Paris Diderot, Paris, France, galoisy@impmc.upmc.fr (*presenting author)

The French National Plan on the Management of Radioactive Materials and Waste launched a survey of some former uranium mines, worked in France between 1948 and 2001 to detect potential effects on the environment. We present preliminary data on the supergene evolution of waste rock piles generated during mining operations in the Saint-Sylvestre leucogranite complex (northwestern Limousin, French Massif Central) a granite intruded at 324 ± 4 Ma. This two-mica granite hosts an important U-ore mineralization deposited at 270-280 Ma, due to sustained hydrothermal circulation. In the Bellezane area, later lamprophyre dykes also cut the granite and suffered extensive low-T alteration. Mining operations have generated waste rock piles of granitic rocks, exposed to meteoritical weathering since the mining time. Biotites are a useful indicator of the type and intensity of alteration, showing chloritic or kaolinitic evolution. Low-T weathering is indicate by the presence of smectites. Fe-migration gives rise to the formation of Fe3+-phosphates and sulphates. Primary U-minerals mostly consist of pechblende and coffinite. Primary and secondary phosphates consist of monazite and crandalite, sometimes intergrown. is frequently observed. Secondary phases such as autunite of U-bearing smectite contribute to decrease U-mobility during meteoritic weathering.

https://doi.org/10.1180/S0026461X00008434 Published online by Cambridge University Press

Isotopic and petrologic evidence for graphite formation by carbonate reduction in blueschist metamorphic rocks

MATTHIEU E. GALVEZ[1,2,3*], ISABELLE MARTINEZ[2], OLIVIER BEYSSAC[1], KARIM BENZERARA[1], BENJAMIN MALVOISIN[3], CHRISTIAN CHOPIN[3], AND JACQUES MALAVIEILLE[4]

[1]IMPMC, Paris, France, galvez@ipgp.fr (* presenting author)
[2]IPGP, Géochimie des isotopes stables, Paris, France, martinez@ipgp.fr
[3]Ecole Normale Supérieure, Paris, France, chopin@ens.fr; malvoisin @ens.fr
[4]Géosciences Montpellier, Montpellier, France, malavie@gm.univ-montp2.fr

The formation of carbonaceous material by abiotic processes is an important standing issue. This process depends on redox conditions and fluid/rock interactions. Subduction zones are major interfaces between the surficial and the deep Earth carbon reservoirs where complex processes affecting carbon transfers are still poorly known.

Here, we studied the geochemistry of carbon (reduced and oxidized) in siliceous-marbles at the direct contact with serpentinites in the Alpine eclogitic meta-ophiolithic units of northern Corsica (France). We applied spectroscopic (Raman) and isotopic techniques to characterize the carbonaceous and carbonate reservoirs in the rocks across a reaction front where the reaction $CaCO_3+SiO_2+2H_2=CaSiO_3+C+2H_2O$ is evidenced.

The reaction zone consists in a centimeter-thick pale nephrite layer lying at the contact with serpentinites, overlaid by a thin wollastonite layer and a 5 to 20 cm thick dark zone composed of wollastonite, carbonaceous material (CM) and quartz. No carbonate could be evidenced in that reaction zone. There is a sharp (<0.5cm) transition between this reaction zone and the overlying "primary" metasediment, which is composed of calcite+quartz and contains significantly less CM. Raman spectroscopy shows that CM is much more graphitic in the reaction zone than in the "primary" metasediment. Significant isotopic differences are observed between the reaction zone and the overlying "primary" metasediment: $\delta^{13}C$ values are around -15‰ and 1.3‰ for CM and calcite respectively in the "primary" metasediment far from the reaction zone, whereas $\delta^{13}C$ (CM) is around -1‰ in the reaction zone.

We interpret the graphitic CM in the reaction zone as formed by the destabilization and reduction of calcite subsequently to the diffusion of reducing fluids from the underlying serpentinite unit. Mass balance calculations support this hypothesis and shows that a complete reduction of carbonates may have occurred. The timing of the formation of this abiotic macromolecular and graphitic C, and the possible role of catalysts is discussed. The geological importance of this process in the subduction zone carbon cycling will be critically assessed.

Constraints on the Mg initial isotopic composition of the solar system from CM & CR chondrite

A. GALY[1,*], C. GÖPEL[2], J.-L. BIRCK[2,3]

[1]Department of Earth Sciences, University of Cambridge, UK, albert00@esc.cam.ac.uk (* presenting author)
[2]Institut de Physique du Globe de Paris, France, gopel@ipgp.fr
[3]birck@ipgp.fr

The recent evaluation of the Al-Mg systematic in undifferentiated and differentiated meteorites at high precision using MC-SIMS or MC-ICPMS has returned conflicting information about the heterogeneity in the initial abundance of short-lived ^{26}Al (half-life of 0.73Ma) and in the Mg isotopic composition of the solar nebula (SN) [1-4]. Heterogeneity in the initial abundance of ^{26}Mg ($\delta^{26}Mg^*_0$) would prevent the use of olivine for dating the last thermal event [4] while $^{26}Al/^{27}Al$ heterogeneity would preclude any dating with Al-Mg.

Here, we report data, on the DSM3 scale, for Tafassasset, an equilibrated CR chondrite and for Paris, a well preserved CM chondrite. Sequential dissolution steps of bulk rock powder were performed but also separated minerals of olivine (Forsterite and Fayalite?) in Paris, accessory chromite (Tafassasset) and an aliquot of the bulk rock were analyzed for Al/Mg systematic. These fractions correspond to aliquots from the detailed Mn/Cr systematic study that suggested an age of 4.8±0.4 and 7.8±0.6 Ma older than the angrite LEW Cliff 86010 for the CR and the CM, respectively [5]. In Tafassasset, the Mg isotopic composition is homogeneous with $\delta^{26}Mg$= - 0.30±0.05‰ and $\delta^{26}Mg^*$= - 0.002±0.015‰ ($2\sigma_{mean}$, N=5) except for the chromite with a $\delta^{26}Mg$= 0.24±0.07‰ and a $\delta^{26}Mg^*_{Bulk\ CR}$<0.038‰ at 95% confidence level. This would suggest a $^{26}Al/^{27}Al \leq 2\times10^{-6}$ at the time of the thermal equilibration of the chromite with the rest of the chondrite. The difference in the $\delta^{26}Mg$ suggests an Mg equilibrium temperature of 1180-1450°K [6]. Assuming a homogeneous and initial $^{26}Al/^{27}Al$ of 5.23×10^{-5} for the SN, a $^{26}Al/^{27}Al \leq 2\times10^{-6}$ would only be compatible with the Mn-Cr age if the difference in age was > 9.5Ma between LEW Cliff 86010 and CAIs. Such an old age for the CAIs is also required from Hf-W systematic [7] and the chronological agreement between CAIs, CR and LEW Cliff 86010 for Al-Mg, Mn-Cr and Hf-W would support a homogeneous SN with respect to ^{26}Al [1-2]. In that case, the measured value implies $\delta^{26}Mg^*_0$= - 0.040±0.015‰ assuming a chondritic Al/Mg ratio for this CR. In Paris, the olivine fractions returned different Mg isotopic compositions. Their $\delta^{26}Mg^*$ are different by 0.064‰ just outside the $2\sigma_{mean}$. Given the old Mn/Cr age of this CM chondrite, the $\delta^{26}Mg^*_0$ is estimated to be - 0.006±0.039‰ ($2\sigma_{mean}$, for 4 objects defining the Mn-Cr isochron [5]). Altogether these data are more suggestive of small (~0.05‰) heterogeneity in the initial abundance of ^{26}Mg than of ^{26}Al in the SN. Attempt of detailed Al-Mg will be discussed but the small measured range of $\delta^{26}Mg^*$ (<0.15‰ at 95% confidence) is likely to prevent accurate determination of the $^{26}Al/^{27}Al$ for this CM.

[1] Villeneuve (2009) *Science* **325**, 985-988. [2] Schiller (2010) *EPSL* **297**, 165-173. [3] Larsen (2010) *AJL* **735:L37**, (7pp). [4] Villeneuve (2011) *EPSL* **301**, 107-116. [5] Göpel (2011) *Min.Mag.* **75(3)**, 936. [6] Schauble (2011) *GCA* **75**, 844-869. [7] Burkhardt (2008) *GCA* **72**, 6177-6197.

https://doi.org/10.1180/S0026461X00008434 Published online by Cambridge University Press

Metal contaminant emissions to waters surrounding a large tailings pond: Athabasca Oil Sands, Alberta.

PAUL GAMMON*[1], A. CALDERHEAD[2], M. SAVARD[2], R. LEFEBVRE[3], J. VAIVE[1], I. GIRARD[1]

[1] Geological Survey of Canada, Ottawa, Canada. pgammon@nrcan.gc.ca; jvaive@nrcan.gc.ca; igirard@nrcan.gc.ca (* presenting author)

[2] Geological Survey of Canada, Québec, Canada. acalderh@nrcan.gc.ca; msavard@nrcan.gc.ca

[3] Institut national de recherche scientifique, Centre Eau Terre Environment, Québec, Canada. rene.lefebvre@ete.inrs.ca

Reactive Transport Model

Alberta Oil Sands mining has introduced intensive petrochemical processing into an environmentally sensitive boreal landscape. The resulting tailings ponds are considered an environmental risk for contaminant emissions to surrounding environments. A reactive transport model has been developed along two transects of wells in order to quantify the fluxes of metal and organic contaminant emissions from a large tailings pond into surrounding ground and surface waters, including the Athabasca River. Here we report the results of the inorganic portion of that study, including lead and zinc isotopic signatures as a method for discriminating natural from anthropogenic contaminant emissions.

Metal concentrations in both ground and surface waters surrounding the tailings pond are lower than current environmental guidelines. Dissolved metal contaminant concentrations demonstrate a strong attenuation profile down gradient from the tailings pond. PHREEQC modelling, SEM observations, and precipitate monitoring all indicate groundwaters are strongly supersaturated in iron and manganese oxyhydroxides throughout the well profiles. Sorption of metals by actively precipiting oxyhydroxides can account for the subsurface attenuation profiles. Modelling suggests that the rate of subsurface metal sequestration along the groundwater flow path are ~10 µg/L Zn, ~0.5 µg/L As; ~1 µg/L Pb; ~20 µg/L Ni. These are calculated from a temporally limited suite of samples that may not represent long-term averages.

The metal isotopic dataset is from Athabasca River water, McMurray Formation, and groundwaters downflow of the active area of metal sequestration. The data fall on a mixing line between Athabasca River and McMurray Formation end-member signatures, suggesting that this technique has significant potential for discriminating natural from anthropogenic sources. However, there is minor scatter in the groundwater data that suggests further research is required to better characterise other potential end-member isotopic signatures (e.g. Clearwater and Waterways formations).

Conclusions

The flux of metal contaminants from the tailings pond reaching the Athabasca River is low due to the active sequestration process. Hydrogeological modelling to be completed shortly will determine the flux of subsurface metal sequestration, and will help assess the utility of metal isotopic analyses for monitoring metal contaminant emissions in this area.

Stable isotopes reveal biogeochemical processes in a shallow, eutrophic lake

C. H. GAMMONS[1*], WILLIAM HENNE[1], AND S. R. POULSON[2]

[1]Montana Tech, Geological Engineering, cgammons@mtech.edu (* presenting author), whenne@mtech.edu

[2]University of Nevada-Reno, Geological Sciences and Engineering, poulson@mines.unr.edu

Recent research has shown how the isotopic compositions of dissolved inorganic carbon (δ^{13}C-DIC) and dissolved oxygen (δ^{18}O-DO) can be used to track biogeochemical processes in rivers [1] and shallow groundwater [2]. This study uses the same approach to examine processes occurring under ice cover in Georgetown Lake, a shallow, eutrophic lake in western Montana, USA. The results have implications for survival of fish during winter hypoxia.

After the onset of ice (Nov-2010), DO concentrations decreased sharply with depth and time at two monitoring sites, while δ^{18}O-DO increased (Fig. 1B, Trends III, IV). Conversely, DIC concentrations increased with depth and time, while δ^{13}C-DIC initially decreased (Fig. 1A, Trend I). These trends are consistent with a respiration: photosynthesis ratio > 1. The lower slope of Trend IV vs. Trend III indicates a higher rate of photosynthesis (which produces isotopically light DO) at Site 2, which partly counteracts the effects of respiration (which preferentially consumes light DO). Photosynthesis in the top 1-2 m of the water column provides enough DO for trout and land-locked salmon to survive the 6-month winter.

Late in the winter, the deeper waters at both sampling sites (especially Site 2) saw a continued increase in DIC concentration and an increase in δ^{13}C-DIC (Fig. 1A, Trend II). Trend II is best explained by a shift in the dominant microbial pathway in the deeper water column and underlying sediment from organic-C oxidation to organic-C disproportionation, the latter yielding a mixture of isotopically heavy CO_2 and isotopically-light CH_4 [3]. Work is in progress to measure CH_4 and dissolved organic carbon concentrations and isotopic compositions to confirm this hypothesis.

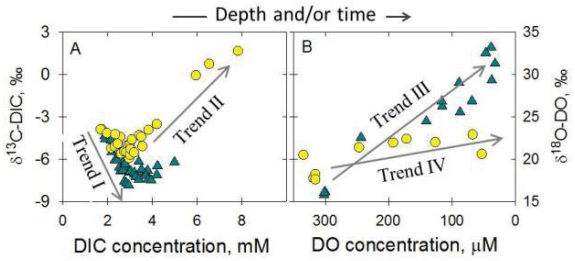

Figure 1: Seasonal changes in the concentration and isotopic compositions of (A) DIC and (B) DO between Nov-2010 and May-2011. Triangles are Site 1 (max. depth = 9 m); circles are Site 2 (max. depth = 6 m). Depth in the water column and elapsed time increase from left to right in both diagrams.

[1] Parker *et al.* (2010) *Chem. Geol.* **269,** 22-32. [2] Smith *et al.* (2012) *Geochim. Cosmochim. Acta* **75**. 5971-5986. [3] Whiticar (1999) *Chem. Geol*. **161**, 291-314.

https://doi.org/10.1180/S0026461X00008434 Published online by Cambridge University Press

Intrinsic Proton Activity of Surface Hydroxyl Groups of Single-crystal (Hydr)oxide Minerals: Insights from Recent AFM Studies

YANG GAN*

Harbin Institute of Technology, Chemical Engineering, China, ygan@hit.edu.cn (* presenting author)

Regardless of intensive interests in the surface chemistry of (hydr)oxide minerals, the surface charging behavior in aqueous solution is still not well understood. Using skillfully both AFM high-resolution imaging [1] and reliable colloidal probe technique [2, 3], we showed unambiguously that the basal plane of gibbsite developed significant net positive charge in the acidic pH range (Fig. 1) [4], and that the PZC of polished corundum single-crystals was sensitive to the change in off-cut angle of samples [5]. These results demonstrated that using samples with well-defined structures was essential towards a better understanding of the charging properties of gibbsite and corundum, particularly the intrinsic proton activity of surface hydroxyl groups like Al_2OH and AlOH [6].

Preparation contaminant-free surface of single-crystal corundum substrates, without resorting to vacuum annealing, is the prerequisite for studying the charging properties of corundum/water interface; however, after critical evaluation we found that existing wet/UV/plasma cleaning methods were not valid in terms of removing both organic and particulate contaminants. We proposed a modified RCA method which is reliable for producing contaminant-free surface with well-defined surface structures [7,8].

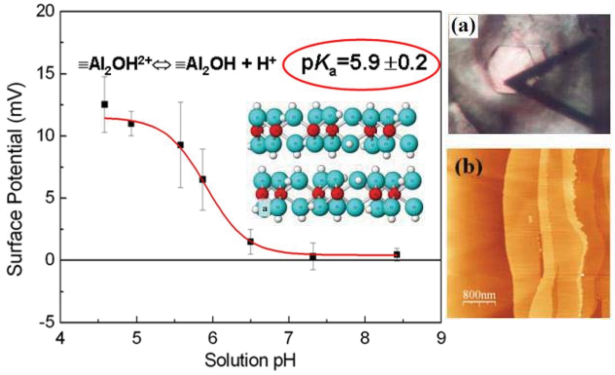

Figure 1: Diffuse layer potential of gibbsite (001) basal plane (the sample and an AFM image are shown on the right) in 1 mM NaCl at various pH obtained from fitting the AFM force curves. The red solid line is the fitting result based on a single-pKa protonation model shown in the inset (pKa=5.9). Also shown in the inset is the structural mode of gibbsite.

[1] Gan (2009), *Surf. Sci. Rep.*, **64**, 99. [2] Gan (2007), *Rev. Sci. Instru.*, **78**, 081101. [3] Gan & Franks (2009), *Ultramicroscopy*, **109**, 1061. [4] Gan & Franks (2006), *Langmuir*, **22**, 6087. [5] Zhang, Wang & Gan (2012), to be submitted. [6] Franks & Gan (2007), *J. Am. Ceram. Soc.,* **90**, 3373. [7] Gan & Franks (2005), *J. Phys. Chem. B,* **109**, 12474. [8] Zhang & Gan (2012), to be submitted.

Determination of trace mercury in geological samples by photo induced chemical vapour generation with isotope dilution inductively coupled plasma mass spectrometry determination

XIAFENG XIA[1], YING GAO[1*], AND FURONG YUE[1]

[1]College of Nuclear Technology and Automation Engineering, Chengdu University of Technology, Sichuan 610059, China, ying.gaoy@gmail.com

Abstract

Mercury is ubiquitous in the environment. Anthropogenic activities take the major responsibility for the significantly elevated mercury emission as a result of more and more human activities[1]. Much concern has been attracted to the determination of mercury due to their high toxicity and biomagnification[2]. The increasing mercury emission directly resulted in sediment and soil Hg contamination. To assess the toxicity and health risks of mercury, the accurate determination of Hg in sediment and soil is of great importance. However, the extremely low concentration of mercury and the complex sample matrix of soil and sediment samples make the accurate mercury determination troublesome. Furthermore, the severe memory effect of mercury determination by ICP MS is a rather difficult problem to overcome.

A simple, rapid and selective method was developed for the accurate determination of trace mercury in soil and sediment samples by photo induced chemical vapor generation (PVG) with isotope dilution inductively coupled plasma mass spectrometry determination (ID ICPMS). After microwave assisted acid digestion, sample solution was subjected to UV irradiation in the presence of formic acid. Mercury was thus efficiently converted into Hg^0 without the addition of any other reductants. Subsequently, the generated mercury vapor was rapidly separated from the matrix by an argon flow and swept into ICPMS for quantification. Under the optimal experimental conditions, the limit of detection of 0.6 ng L^{-1} was obtained. Compared to traditional CVG, the PVG systems have superior detection sensitivity and tolerance ability to transition metal ions. Up to 5000 folds of Cu^{2+}, Co^{2+}, Ni^{2+}, Mn^{2+}, Fe^{3+}, and Zn^{2+} have no significant interferences for mercury determination. The method was applied to the determination of mercury in geological samples with satisfactory results.

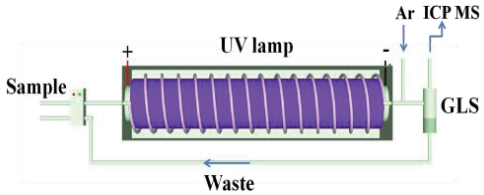

Fig. 1 Schematic diagram of the experimental set-up, gas/liquid separator (GLS).

[1] Lin et al., (2010), Applied Geochemistry, **25**, 60-68. [2] Lubick et al., (2009), Nature, **459**, 620-621.

https://doi.org/10.1180/S0026461X00008434 Published online by Cambridge University Press

Elemental sulfur nanoparticle coarsening kinetics and changes in Raman and voltammetric signals

ANGEL A. GARCIA[1*] AND GREG K. DRUSCHEL[1,2]

[1]University of Vermont, Burlington, Vermont, angel.garcia@uvm.edu (* presenting author)

[2]Indiana University-Purdue University Indianapolis, Indianapolis, Indiana, gdrusche@iupui.edu

Elemental sulfur exists is a variety of forms in natural systems, from dissolved forms (noted as S^0, or in ring form as in $S_{8\ (rings)}$) to bulk elemental sulfur (most stable as α-S_8, but existing in at least 180 different allotropes and polymorphs). Elemental sulfur can form via a number of biotic and abiotic processes, many of which would begin with single S^0 molecules that aggregate into larger and larger forms; this process is explained by the following pathway: $S^0 \rightarrow S_{8\ (rings)} \rightarrow S_{8\ (nano)} \rightarrow S_{8\ (\alpha\text{-}S_8)\ (bulk)}$. Formation of elemental sulfur has been done in the lab via two primary techniques to create an emulsion of liquid sulfur in water called sulfur sols that approximate some mechanisms of possible elemental sulfur formation in natural systems. These techniques produce Wiemarn (hydrophobic) and Raffo (hydrophilic) sols [1]. These sols begin as single S molecules, but quickly become nanoparticulate and coarsen into micron sized particles via a combination of Ostwald ripening and aggregation processes. In an effort to investigate fundamental questions related to elemental sulfur particle size in natural systems, we conducted a series of experiments to study the rate of elemental sulfur particle coarsening using dynamic light scattering analysis under different physical and chemical conditions. Results showed that coarsening of $S_{8(nano)}$ is partly pH dependent (with faster coarsening at pH 3 than at pH 7 or 10), and strongly temperature dependent (Figure 1). The addition of surfactants to emulate biotic mechanisms to transport elemental sulphur inside the cell shows a significant reduction in the rate of aggregation, in addition to known effects of these molecules on elemental sulphur solubility [2]. Initial cryo-SEM results additionally suggest coarsening is largely a product of ripening processes rather than particle aggregation. Raman spectroscopy and voltammetry (using Au-amalgam and mercury drop electrodes) signals change as a function of size and surfactant use..

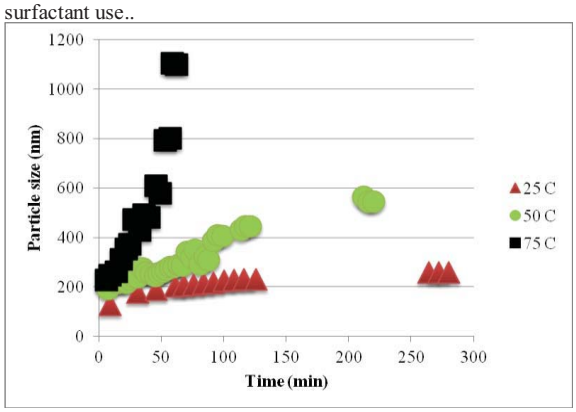

Figure 1: Elemental sulfur particle coarsening. Nanoparticles form from S^0 and $S_{8(rings)}$ in seconds, followed by coarsening (ripening and aggregation) that is strongly T-dependent.

[1] Steudel (2003) *Aqueous Sulfur Sols* **230,** 153-166.

[2] Steudel and Holdt (1988) *Angew. Chem. Int. Ed. Engl*. 27, 1358-1359.

Large magnesite vein and fracture formation in peridotite rocks

PABLO GARCÍA DEL REAL[1]*, KATE MAHER[1], DENNIS K. BIRD[1], AND GORDON E. BROWN, JR.[1,2,3]

[1]Department of Geological & Environmental Sciences, Stanford University, Stanford, CA 94305, USA. gdelreal@stanford.edu (* presenting auhor)

[2] Department of Photon Science and Stanford Synchrotron Radiation Lightsource, SLAC National Accelerator Laboratory, Menlo Park, CA 94025, USA

[3]Department of Chemical Engineering, Stanford University, Stanford, CA 94305, USA

Large monomineralic cryptocrystalline magnesite ($MgCO_3$) vein deposits hosted in ophiolitic peridotite provide insights into the chemical, structural, and temporal constraints on subsurface carbonation processes. The magnesite veins record the upward migration of deep mineralizing solutions to shallow crustal depths, which bear relevance to two fundamental problems important to industrial geologic sequestration of CO_2 in peridotite rocks: (1) the kinetics of magnesite formation—the target carbonate for CO_2 mineralization and (2) the generation of permeability required for modally abundant carbonate formation. Our field site, the Red Mountain Magnesite Mining District in the Diablo Mountain Range, California, provides information about these processes and a framework for comparison with the results of experimental and modeling studies of carbonation of Mg-silicates.

Mines at the Red Mountain Magnesite District, California, reveal more than 20 homogenous magnesite veins up to 40 m thick and >100s of m in length hosted in the variably serpentinized peridotite lithology of the Del Puerto ophiolite. The carbonate mineralization occurs primarily as cryptocrystalline magnesite veins with sharp mineralogic or structurally sheared/brecciated contacts with the host peridotite rock. Rapid, low-temperature mineralization is inferred from chemical, isotopic, and textural homogeneity of magnesite, and the lack of metasomatic reaction zones along the peridotite-magnesite interface. Opaline silica occurs as relatively small late-stage veins paragenetically distinct from the magnesite mineralization and the peridotite host rock. Silica expected from extensive peridotite dissolution and relic textures of peridotite in the carbonate are absent in the observed exposures, indicating that Mg was supplied from dissolution of Mg-bearing rocks below the mineralization zone and that silica did not inhibit magnesite precipitation. This suggests that the rates of Mg-silicate dissolution are decoupled from the rates of magnesite precipitation. At Red Mountain, magnesite precipitation was both effective and pervasive, implying that the experimental problems in magnesite formation (primarily slow nucleation kinetics) have been overcome in nature. These observations highlight both the complexity of natural analogues and the limitations in the chemical and temporal scope of dissolution-carbonation experiments in replicating natural systems. The magnesite veins evidence a structurally and paragenetically different carbonation mechanism than that proposed for carbon sequestration (direct Mg-silicate dissolution and creation of permeability via carbonate growth). Geochemical and geochronological work on the magnesite, silica, and peridotite rocks further constrain models of fracture-vein initiation and closure related to the carbonation at Red Mountain.

https://doi.org/10.1180/S0026461X00008434 Published online by Cambridge University Press

Evaluation of ^{224}Ra as a SGD tracer in Long Island Sound

GARCIA-ORELLANA, J.[1*], COCHRAN J.K.[2], DANIEL J.W.R.[2], RODELLAS V.,[1] BOKUNIEWICZ H.[2] AND HEILBRUN C.[2]

[1]Departament de Física – ICTA, Unversitat Autònoma de Barcelona, Bellaterra, Spain, jordi.garcia@uab.cat, valenti.rodellas@uab.cat

[2]School of Marine and Atmospheric Sciences - SUNY, Stony Brook, NY - US, kcochran@notes.cc.sunysb.edu, jwrdaniel@gmail.com, hbokuniewicz@notes.cc.sunysb.edu, cheilbrun@notes.cc.sunysb.edu

Introduction

In this work we present the Ra mass balance used to evaluate the importance of the submarine groundwater discharge (SGD) in Long Island Sound (NY, US). Long Island Sound is a large estuary on the east coast of the U.S. located between Long Island and Connecticut. It has a mean depth of 20m and tidal ranges up to 2 m with mud deposits that cover 67% of the western basin. In summertime, it is affected by hypoxia in the western basin. Three surveys were conducted between April 2009 and August 2010 where 25 water stations were sampled for Ra isotopes, oxygen concentration and Mn. Stations were oriented along 4 transects: one axial extending from the western to eastern Sound and three longitudinal transects in the western, central and eastern Sound.

Results and Conclusion

The inventory of ^{224}Ra in the water column in summer was two times higher than in winter pointing out an increased ^{224}Ra flux to the Sound in summer. A mass balance for ^{224}Ra was constructed considering tidal exchange and the inputs from rivers, desorption from particles, diffusive fluxes (including bioirrigation) and the loss due to radioactive decay. Diffusive fluxes of ^{224}Ra from bottom sediments have been measured by incubating cores in a continuous flow mode such that the overlying water was circulated through a Mn-oxide fiber to maintain a constant activity of ^{224}Ra. Diffusive fluxes from muddy sediments are about five times greater than those from sandy sediments. The Ra balance shows a net input of Ra to the Sound that could be attributed to fresh SGD, tidal recirculation through the beach sands or seasonal difference in the diffusive flux from sediments. ^{224}Ra values within 100 m of the shore were ten times those in the open sound. Radium concentrations were elevated in the pore water of the coarse beach sand along the Long Island and Connecticut coasts, suggesting that tidal recirculation through the beach face is an important source of Ra to the Sound. Seasonal variation in this source seems unlikely and we conclude that the variations seen in the ^{224}Ra inventories are probably produced by variations in sediment fluxes due to seasonal changes in bioirrigation and/or redox cycling of Mn.

Tourmalinites of the Brusque Group in the São João Batista-Tijucas area, Santa Catarina State – Brazil

MIGUEL A.S. BASEI[1], GIANNA M. GARDA[1*], FABIO BRENTAN[1]

[1]Instituto de Geociências da Universidade de São Paulo, São Paulo, Brazil, giagarda@usp.br (* presenting author)

Introduction

The Dom Feliciano Belt is the most important geotectonic unit of the southern portion of the Mantiqueira Province in southern Brazil. In eastern Santa Catarina State, it is represented by the Itajaí and Brusque groups and the Florianópolis Batholith.[1] The basal Rio do Oliveira Formation of the Brusque Group is constituted from top to bottom by metapsammitic, metapelitic, metavolcanic-exhalative and metabasic/calc-silicate units. Within the metavolcanic-exhalative unit, a discontinuous tourmalinite sequence stretches out for approximately 14 km, from São João Batista to Tijucas.

The tourmalinites of the São João Batista-Tijucas area

Two types of tourmalinites are distinguished in the São João Batista-Tijucas area. Those cropping out along the Oliveira River are banded, very fine-grained, and are composed of greenish yellow tourmalines. In contrast, those cropping out in the Morro do Carneiro are coarse-grained and massive to slightly foliated. The tourmalines are typically zoned, with a transparent core, a darker intermediate zone, and a greenish rim.

Electron probe microanalyses showed that the tourmalines of the Oliveira River tourmalinites are Al- and alkalis-rich, whereas those of the Morro do Carneiro tourmalinites are Mg- and Ca-rich. The Morro do Carneiro tourmaline color zoning corresponds to an increase in Mg# and decrease in Al, alkalis and Fe contents from the light core to the greenish rim. The sharp increase in Ca contents from core to rim may be explained by Ca input from the surrounding calc-silicate rocks. On the other hand, the Oliveira River tourmalines are Ca-poor and Al-rich.

Geochronological studies by LA-ICPMS helped distinguish four zircon age groups.[2] Detrital zircons from the Rio do Oliveira Formation basal rocks yielded ages in the 2101-2150 Ma interval, interpreted as those of the source rocks for the Brusque Group metasediments. A second zircon population yielded 1090 ± 230 Ma, age characteristic of the 'adjacent' Namaqua Metamorphic Complex (in Western Gondwana). The zircon age obtained for the Rio do Oliveira Formation basal amphibolites is 639 ± 11 Ma, which is considered the maximum age of the overlying banded tourmalinites. Younger ages, between 608 and 581 Ma, correspond to the thermal event associated with the Neoproterozoic granitic magmatism. These ages may correspond to the age of formation of the Morro do Carneiro massive tourmalinites.

Conclusions

The Rio do Oliveira tourmalinites formed by selective substitution caused by B-rich exhalative fluids affecting the sediments of the metavolcanic-exhalative unit, whereas metasomatic/igneous fluids led to the formation of the Morro do Carneiro massive tourmalinites. Zircon dating showed that the Rio do Oliveira tourmalinites are somewhat older than the Morro do Carneiro massive tourmalinites.

[1] Basei et al. (2011) *Journal of South American Earth Sciences* **32**, 324–350. [2] Brentan (2011) *Unidades turmaliníferas do Grupo Brusque, Rio do Oliveira, Tijucas, SC* (unpublished Graduation Monograph).

https://doi.org/10.1180/S0026461X00008434 Published online by Cambridge University Press

Hydrogen abundance in carbonaceous chondrites from thermogravimetric analysis

ALEXANDRE GARENNE[1*], P. BECK[1], G. MONTES-HERNANDEZ[2], R. CHIRIAC[3], F. TOCHE[3], E.QUIRICO[1], L. BONAL[1], B.. SCHMITT[1]

[1]UJF-Grenoble 1 / CNRS-INSU, Institut de Planetologie et d'Astrophysique de Grenoble (IPAG), France. (*alexandre.garenne@obs.ujf-grenoble.fr)

[2]Institut des Sciences de la Terre (ISTerre), OSUG/CNRS, UJF, BP 53X, 38041 Grenoble, France.

[3]Université de Lyon, Université Lyon 1, Laboratoire des Multimatériaux et Interfaces UMR CNRS 5615, France.

Abstract

Carbonaceous chondrites are considered as amongst the most primitive Solar System samples available, because of their enrichment in volatile elements. The mineralogy of CM and CI chondrites is dominated by serpentines and montmorillonite type clays, respectively but mineralogy of CR chondrites is poorly constrained so far. Here, in order to characterize and quantify the abundance of hydrous minerals in carbonaceous chondrites, we performed thermogravimetric analysis (TGA) of fragments of Tagish Lake (TL, UCC), Murchison (CM2.5), Orgueil (CI) and EET 92159 (CR2).

Chunks of meteorites were extracted for TGA analysis following [1]. In the case of the CR chondrite, a matrix-enriched fraction of the sample was prepared and compared to a bulk rock fragment. TGA experiments were performed with TGA/SDTA 851^e Mettler Toledo under the following conditions: sample mass of about 15 mg, platinum crucible of 150 μl, heating rate of 10 °C min^{-1}, and inert N_2 atmosphere of 50 ml min^{-1}. About 15 reference minerals were analyzed as standards.

All meteorites studied show significant endothermic mass loss below 200°C. Two distinct peaks are present on the first derivative curve corresponding to adsorbed H_20 (peak at 70°C) and water molecules trapped in mesopores (peak at 130°C), in agreement with IR study [2]. The total amount of this "exchangeable" water is 2.8, 6.0, 7.8 and 3.9 wt % for Murchison, TL, Orgueil and the matrix of the CR, respectively.

In the case of Orgueil, a significant amount of mass loss is centered at 250°C, likely related to the decomposition of ferrihydrite, confirming previous studies [3]. In addition, mass releases are observed at 570°C and 730°C, attributed to Fe and Mg-rich phyllosilicates. In the case of Murchison, the occurrence of Mg-rich serpentine is suggested by the presence of a mass loss at 730°C, together with cronstedtite (mass loss at 380°C and 545°C). TL shows a particular behaviour since Mg-serpentine appears to be absent and the first derivative curve shows a mass loss occuring at 570°C with a shoulder at 520°C. In the case of EET 92159, a significant mass loss occurs between 200° and 900°C (7,5 wt %) indicating that the matrix is hydrated. The amount of hydration of the matrix suggests a very high proportion of phyllosilicates. Numerous peaks are present in the derivative curve indicating a complex hydrated mineralogy dominated by phyllosilicates

[1] Montes-Hernandez et al., *submitted.* [2] Beck, P. et al., *Geochim. Cosmochim. Acta* **74**, 4881-4892 [3] Tomeoka K. and Buseck P.R. 1988, *Geochim. Cosmochim. Acta* 52, 1627-164

Hydrothermal vents as a source of pyrite and trace metal- containing mineral nanoparticles to the oceans

AMY GARTMAN [1*], MUSTAFA YÜCEL [2], GEORGE W. LUTHER, III[1]

[1]School of Marine Science and Policy, College of Earth, Ocean and Environment, The University of Delaware, Lewes, DE 19958, USA (*agartman@udel.edu)

[2] Université Pierre et Marie Curie, Banyuls—sur--mer, France, yucel@obs-banyuls.fr

The mechanisms by which metals from hydrothermal vents may be transported through the ocean are still largely unknown. We demonstrate that pyrite nanoparticles as small as 4nm, and aggregated into clusters of 50-350nm, are emitted from high temperature black smokers at Lau Basin. These nanoparticles, which contain other metals, are characterized via chemical methods as well as by using a combination of physical chemical techniques (TEM, SEM-EDS and EELS). Laboratory experiments show that synthesized pyrite nanoparticles are stable in oxic seawater for months, and thus provide a potential transport mechanism for iron far from vent sources. All these nanoparticles as well as others including iron silicates, which are present, likely influence the transport of iron and other elements from the hydrothermal environment to the ocean. Hydrothermal vents may serve as nanoparticle 'factories' that fertilize the ocean.

https://doi.org/10.1180/S0026461X00008434 Published online by Cambridge University Press

Isotopes and geochemistry of rock-water interaction, Chalk River, Ontario

MEL GASCOYNE [1]* , KAREN KING-SHARP[2], LEONID NEYMARK[3], ZELL PETERMAN[3] AND SHAUN FRAPE[4]

[1]GGP Inc ., Pinawa, Manitoba, Canada, gascoyne@granite.mb.ca (*presenting author)
[2]AECL, Chalk River Laboratories, Chalk River, Ontario, Canada
[3]USGS, Denver, CO, USA
[4]University of Waterloo, Waterloo, ON, Canada

A five-year pre-project study under the Nuclear Legacy Liabilities Program was undertaken to assess the suitability of the bedrock at the Chalk River Laboratories (CRL) site to safely host a proposed Geologic Waste Management Facility (GWMF) for Atomic Energy of Canada Limited's low- and intermediate-level radioactive waste (LILW) at CRL. The site investigations involved the disciplines of geology, hydrogeology, geochemistry, geomechanics and microbiology.

The authors have investigated certain geochemical parameters in the groundwater (e.g. redox, pH, Fe, U, isotopic data) and the mineralogy of the host rock. The geochemical composition of the groundwater and rock pore water at repository depth may affect the performance of the repository barrier system and ideally should be favourable to retarding radionuclide movement. Characterization of the groundwater was also identified as important in determining its residence time ('age') and origin.

This talk will summarize isotopic data (^{3}H, ^{18}O, ^{13}C, ^{14}C, ^{36}Cl, $^{87}Sr/^{86}Sr$ ratio, U-series) from CRL crystalline rocks, porewaters, groundwaters and fracture minerals. The application of heavy element isotope systematics (Rb-Sr, U-Pb and U-series) was also studied in selected bulk-rock samples from CRL. Currently, information is being obtained from isotope systematics based on past fluid chemistry, isotopic composition, and pressure and temperature conditions during paleohydrogeological events (such as metamorphic and glacial episodes). Other data for examination include age dates of rocks and groundwater that may indicate recent U mobility and transitions from oxidizing to reducing groundwaters effects of rock-water interactions.

The geochemical composition of the groundwater and the rock pore water is consistent with low hydraulic conductivity of rocks. It further indicates limited fracture-matrix interaction and implies that solute movement in the rock matrix in this area is diffusion controlled. The Rb-Sr & U-Pb isotope systematics indicate no geologically recent U mobility (<100 Ma) and most U isotopic data show secular equilibrium, and, therefore, no U loss/gain in the last 1 Ma.

Ureolytic $CaCO_3$ Precipitation in the Presence of Non-ureolytic Bacteria

DANIELLA GAT [1*], MICHAEL TSESARSKY [2,1] AND ZEEV RONEN [3]

[1]Ben-Gurion University of the Negev, Geological and Environmental Sciences, Beer-Sheva, Israel, mizdani@bgu.ac.il (* presenting author)
[2]Ben-Gurion University of the Negev, Structural Engineering, Beer-Sheva, Israel, michatse@bgu.ac.il
[3]The Zuckerberg Institute for Water Research, the J. Blaustein Institute for Desert Research, Ben-Gurion University of the Negev, Sede-Boqer, Israel, zeevrone@bgu.ac.il

Microbially induced $CaCO_3$ precipitation (MICP) is recently being studied due to its various potential applications, such as: sequestration of soil contaminants [1]; and mitigation of seismic liquefaction [2], among others. Some of these applications involve *in-situ* treatment of soils, and therefore require a better understanding of the interactions between microbial ecology and aquatic geochemistry.

Hydrolysis of urea, catalyzed by the enzyme *urease*, is one of the most common pathways for MICP [3]. Hydrolysis of urea produces ammonium and carbonate: $CO(NH_2)_2+2H_2O \rightarrow 2NH_4^+ + CO_3^{2-}$, thus increasing surrounding alkalinity. In the presence of dissolved calcium this process will result in the precipitation of $CaCO_3$: $Ca^{2+} + CO_3^{2-} \rightarrow CaCO_3$.

In order to study the interactions between ureolytic and non-ureolytic bacteria we performed a MICP experiment in artificial groundwater medium, inoculated with two model bacteria: *S. pasteurii* (ureolytic bacteria) and *B. subtilis* (non-ureolytic bacteria), and supplemented with Nutrient Broth and urea. Control was inoculated with *S. pasteurii* alone. The experiment lasted 10 days, during which NH_4^+, Ca^{2+}, pH, dissolved inorganic carbon and optical density (OD) were measured.

Results are summarized in Table 1. Most of the $CaCO_3$ precipitation took place until the 80th hour of the experiment. During which time, pH values and carbonate ion concentrations in the presence of non-ureolytic bacteria were lower than in their absence. However, measured Ca^{2+} concentrations indicates that $CaCO_3$ precipitation was accelerated in the presence of non-ureolytic bacteria, despite less favorable chemical conditions. Bacterial growth, as infferred from OD measurements was significantly higher in samples containing non-ureolytic bacteria. Therefore, we suggest that $CaCO_3$ precipitation in the presence of non-urealytic bacteria was accelerated due to addition of nucleation sites in the form of bacterial cells.

	Control	Both Bacteria
pH	**7.49-8.45**	**7.50-8.21**
CO_3^{2-} (mM)	**0.005-0.132**	**0.005-0.087**
OD	**20 hr. lag phase**	**6 hr. lag phase**
$CaCO_3$ precipitation	**100% in 123 hours**	**100% in 80 hours**

Table 1: Results summary.

[1] Fujita, Taylor, Gresham, Delwiche, Colwell, McLing, Petzke, Smith, (2008) *Enviro. Sci. Technol.* **42**, 3025-3032.
[2] DeJong, Fritzges, Nüsslein, (2006) *J. Geotech.Geoenviron. Eng.* **132**, 1381-1392.
[3] Ferris, Phoenix, Fujita, Smith, (2003) *Geochim. Cosmochim. Acta* **67**, 1701-1722.

https://doi.org/10.1180/S0026461X00008434 Published online by Cambridge University Press

Submarine groundwater discharge at an active margin: NE Taiwan coast

J.C. GATTACCECA[1,*], N. HOVIUS[1], A. J. WEST[2], A. GALY[1], D. HAMMOND[2], J. T. LIU[3], S-J. KAO[4]

[1]Department of Earth Sciences, University of Cambridge, UK, jcg54@esc.cam.ac.uk (* presenting author), ajbg2@cam.ac.uk, nhovius@esc.cam.ac.uk

[2]Department of Earth Sciences, University of Southern California, Los Angeles, USA, joshwest@usc.edu, dhammond@usc.edu

[3]Institute of Marine Geology and Chemistry, National Sun Yat-sen University, Kaohsiung, Taiwan, james@mail.nsysu.edu.tw

[4]Research Center for Environmental Changes, Academia Sinica, Nankan Taipei, Taiwan, sjkao@gate.sinica.edu.tw

Studies of submarine groundwater discharge (SGD) have been focused on passive margins with large floodplains [1]. SGD from active margins without substantial sediment cover remains unknown, but it is in the rapidly eroding highlands along these margins that the feedback between climate and weathering is most effective [2].

In Taiwan, measured erosion and silicate weathering rates are amongst the highest in the world. In a representative section of the northeast coast of Taiwan, at the outlet of the Liwu river, we have explored the possible magnitude and pattern of SGD, and its implications for weathering budgets. The river drains 4 km of emergent mountain relief, with a further 5 km of submarine relief above the Pacific abyssal plain. In the Liwu catchment, 16±1% of the river discharge (averaged over 37 years of record) comes from a deep groundwater reservoir, and deep seated chemical weathering of silicates accounts for 38% of the riverine silicate weathering flux [3]. It is likely that the large inland hydraulic head drives submarine discharge from this deep groundwater reservoir and weathering reactor.

We have used the radium quartet (^{228}Ra, ^{226}Ra, ^{224}Ra, ^{223}Ra) along with Temperature-Salinity (T-S) profiles on two 50 km West-East marine transects off the NE coast of Taiwan (<2000m water depth) to search for SGD. Stable isotopes, major elements, and Ra isotopes in water samples were analyzed to constrain the hydrogeology of rivers and two types of groundwater: sandy shallow aquifers (<200 m deep) and a deep bedrock aquifer (~400m deep).

Radium activities were measured using RaDeCC. Preliminray results show that the ^{224}Ra and ^{228}Ra activities at the sea surface exceed those in the average deep coastal water column. ^{228}Ra activities are also slightly elevated in some stations at 400-600m depth, below the Kuroshio current. These stations have anomalously low salinity, when compared to regional hydrographic profiles. Given the strong density barrier presented by the Kuroshio current, these Ra and salinity excursions at depth are not likely to result from downward mixing of surface seawater. They may be related to groundwater discharge from submerged mountain bedrock.

The T-S and Ra-isotopes data suggest that there may be active SGD across the structural dip of the active margin of East Taiwan. Using both transects and the deep groundwater characteristics, we will add constraints on sediment/water interactions and the occurrence and spatial extent of SGD in the area.

[1] Moore (1996) *Nature* **380**, 612-614. [2] West (2005) *EPSL* **235**, 211-228. [3] Calmels (2011) *EPSL* **303**, 48-58.

Mid- and far-infrared absorption spectroscopy of Titan's tholins

T. GAUTIER[1*], N. CARRASCO[1], A. MAHJOUB[1], S. VINATIER[2], A. GIULIANI[3] , C. SZOPA[1] , C. M. ANDERSON[4], J.- J. CORREIA[1], P. DUMAS[3] AND G. CERNOGORA[1]

[1] LATMOS, Université Versailles St Quentin, Guyancourt, France, thomas.gautier@latmos.ipsl.fr (*presenting author)

[2] LESIA, Observatoire de Paris, Meudon, France

[3] Synchrotron SOLEIL, Gif sur Yvette, France

[4] NASA GSFC, Solar System Exploration Division, Greenbelt, USA

In this work [1] we present mid- and far-Infrared absorption spectra of Titan's aerosol analogues produced in the PAMPRE experimental setup.

We provide a complete dataset regarding the influence that the concentration of methane vapor in the gas mixture has on the tholins spectra. Among other effects, the intensity of the 2900 cm^{-1} pattern (attributed to methyl stretching modes) increases whith the methane concentration. On the opposite, tholins produced with low methane concentrations seem to be more amine based polymers (see Fig. 1).

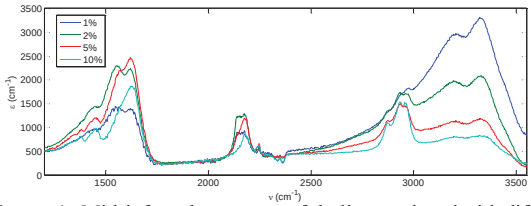

Figure 1: Mid-infrared spectrum of tholins produced with different methane concentrations

Moreover, we compare tholins spectrum with observation of Titan's atmosphere (see Fig. 2).

It is shown that the position of the bands around 2900 cm^{-1} depends on the chemical environment of the methyl functional group. We conclude that the presence of these absorption bands in Titan's atmosphere, as measured with the VIMS instrument onboard Cassini [2] is in agreement with an aerosol contribution.

In the far-infrared, tholins spectrum presents many similarities with the spectra of Titan's aerosols derived from recent Cassini-CIRS observations [3].

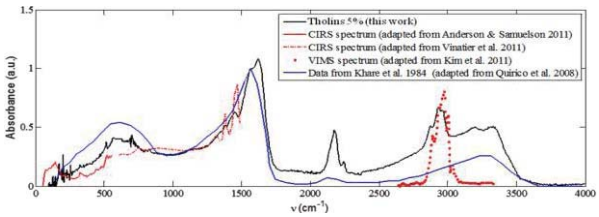

Figure 2: Far- and mid-infrared spectrum of tholins (black) compared to Cassini VIMS and CIRS observations (red)

[1] Gautier et al. (2012) *Mid- and far-infrared absorption spectroscopy of Titan's aerosols analogues* **Submitted to Icarus.**
[2] Rannou et al. (2010) *Titan haze distribution and optical properties retrieved from recent observations."* **Icarus 208(2)**, *850-867.*
[3] Anderson & Samuelson (2011) *Titan's aerosol and stratospheric ice opacities between 18 and 500 μm: Vertical and spectral characteristics from Cassini CIRS* **Icarus 212(2)**, *762-778.*

https://doi.org/10.1180/S0026461X00008434 Published online by Cambridge University Press

HSE and Os isotope systematics of mantle pyroxenites from the Lherz and Lanzo ultramafic massifs.

T. GAWRONSKI[1]*, H. BECKER[2]

[1*]Institut für Geologische Wissenschaften, Freie Universität Berlin, Germany, gawronsk@zedat.fu-berlin.de

[2]Institut für Geologische Wissenschaften, Freie Universität Berlin, Germany, hbecker@zedat.fu-berlin.de

Mantle pyroxenites provide direct evidence for mantle heterogeneity and magma transport in the mantle. These rocks may form by crystal accumulation at high pressures from mantle derived magmas, melt-peridotite reaction or partial melting of basic rocks in the mantle [1]. Pyroxenites are also useful to study fluxes and fractionation of highly siderophile elements (HSE) during transport in the mantle and to assess the influence of pyroxenites in magma genesis.

The peridotite massifs at Lanzo (northern Italy) and Lherz (southern France) provide the opportunity to study pyroxenites that have equilibrated at different P-T-conditions. The spinel facies Lherz peridotite contains spinel websterites, orthopyroxenites, garnet-clinopyroxenites.The plagioclase facies Lanzo peridotite massif includes spinel and plagioclase websterites, clino- and orthopyroxenites up to several dm in thickness. Aluminum poor websterites at Lherz and Lanzo display highly siderophile elment (HSE: Os, Ir, Ru, Rh, Pt, Pd, Au and Re) patterns similar to fertile lherzolite. In contrast, Lherz clinopyroxenites show more strongly frationated HSE patterns compared to Lanzo clinopyroxenites. with a stronger depletion in Os, Ir, Ru, Rh and Pt relative to Pd, Au and Re. These differences likely reflect different extent of reaction of parental melts with peridotite or different compositions of precursor materials (e.g. recycled oceanic crust). Re-Os data for pyroxenites from Lherz scatter around a 1.7 Ga reference line. This data is consistent with the Re-Os model ages obtained on peridotites [2] and hints that the refertilization of the Lherz body may have occurred in the Proterozoic. These results support the view that the Lherz body is indeed a fragment of Proterozoic continental lithospheric mantle and not Mesozoic oceanic mantle that contains ancient heterogeneities.

[1] Downes, H. (2007), *Lithos* ***99****, 1-24*

[2] Reisberg and Lorand (1995), *Nature* **376**, 159–16

Calibration of thermobarometry (TP) estimates with H_2O and fO_2 data from melt inclusions: Results from the Big Pine Volcanic Field, Western USA.

EATEBAN GAZEL[1,2]*, TERRY PLANK[2], DONALD W. FORSYTH[3], CLAIRE BENDERSKY[2], CIN-TY A. LEE[4], ERICK H. HAURI[5].

[1]Dep. of Geosciences, Virginia Tech, Blacksburg, VA, USA egazel@vt.edu (* presenting author)

[2]Lamont-Doherty Earth Observatory of Columbia University, Palisades, USA.

[3]Dep. of Geological Sciences, Brown University, Providence, USA

[4]Dep. of Earth Science, Rice,University, Houston, USA

[5]Dep. of Terrestrial Magnetism, Carnegie Institution, Washington, USA.

The Big Pine Volcanic Field (BPVF) is an ideal location for constraining the mantle melting conditions westernmost region of the Basin and Range. This work is the first to report H_2O and CO_2 concentrations in Big Pine magmas and fO_2, which are necessary for accurate estimates of the melting conditions. Melt inclusions trapped in primitive olivines (Fo_{82-90}) record surprisingly high H_2O contents (1.5 to 3.0 wt.%) for a location not currently above active subduction. The combined H_2O-CO_2 data are consistent with closed-system degassing from >5 kb (~ 20 km) to the surface. Estimates of the oxidation state of BPVF magmas are also surprisingly high (FMQ +1.0 to +1.5), based on constraints from V partitioning between melt and olivine and melt inclusion S contents (up to 5000 ppm), yielding Fe^{3+}/Fe_T ratios of 23 - 30%. While lithospheric mantle xenoliths from BPVF record low H_2O concentrations (whole rock <75 ppm). Pressures and temperatures of melt equilibration of the BPVF magmas indicate a shift over time, from higher melting temperatures (~1320 °C) and pressures (~2 GPa) for magmas that are >500 ka, to cooler (~1220 °C) and shallower melting (~1 GPa) conditions in younger magmas. The depth of melting also correlates strongly with some trace element ratios in the magmas, with deeper melts having higher Ce/Pb (14-21) and Ba/La (20), closer to typical upper mantle asthenosphere values, and shallower melts having lower Ce/Pb (<14) and variable Ba/La (20-30), more typical of subduction zone magmas, and within the range of the available lithospheric mantle xenolith data from BPVF. The correlated melting conditions and geochemical stratification of the mantle melts are consistent with seismic observations of a shallow lithosphere-asthenosphere boundary (~55 km depth). Combined trace element and cryoscopic melting models yield self-consistent estimates for the degree of melting (~5%) and source H_2O concentration (~1000 ppm). We suggest two possible geodynamic models to explain small convection necessary for magma generation. The first related with the Isabella seismic anomaly, either as a remnant of the Farrallon Plate or lithospheric foundering. The second scenario is related to slow extension of the lithosphere.

https://doi.org/10.1180/S0026461X00008434 Published online by Cambridge University Press

Towards an understanding of the non-classical nucleation of $CaCO_3$

DENIS GEBAUER

University of Konstanz, Physical Chemistry, denis.gebauer@uni-konstanz.de

Introduction

Nucleation of calcium carbonate from aqueous solution can proceed via an alternative pathway that involves stable pre-nucleation clusters [1] and results in the initial precipitation of amorphous calcium carbonate (ACC) nanoparticles, which may subsequently transform into crystalline species. This pathway is referred to as "non-classical nucleation", because it challenges the major concepts and assumptions made by classical nucleation theories [2]. Additive-free ACC formed in this manner exhibits distinct short-range structural features, which (depending on pH) can relate to the long-range order of different crystalline $CaCO_3$ polymorphs [3]. The presence of such proto-structures in ACC is well-known from biogenic, though additive-containing specimens [4], and may be the clue to a novel understanding of polymorph selection and control.

The atomistic background underlying non-classical nucleation of calcium carbonate should thus offer an explanation for at least three major experimental observations; (i) the thermodynamic stability of pre-nucleation clusters, (ii) the existence of a distinct barrier for nucleation separating solution (pre-nucleation) and solution/solid (post-nucleation) states, and (iii) the possibility of different structures in precipitated ACC.

Results and Conclusions

The non-classical pre-nucleation behavior of calcium carbonate can be rationalized by means of results obtained from computer simulation in combination with re-evaluations of experimental data [5], which show that stable pre-nucleation clusters are highly dynamic, liquid- and chain-like structures of $CaCO_3$ ion pairs. Various experimental observations [6–9] are put into context with this theoretical speciation, eventually allowing for speculations about what happens at the point of nucleation.

It appears that solid calcium carbonate can only be nucleated from homogeneous solutions if pre-nucleation clusters aggregate and coalesce to build larger entities above ca. 20 nm in size [8]. In turn, these considerations suggest that the classical pathway via ion-by-ion growth of un- and metastable nuclei may indeed be blocked under the conditions that have been investigated so far. Finally, implications of these findings for additive-controlled crystallization of calcium carbonate are outlined.

[1] Gebauer, Völkel & Cölfen (2008), *Science* **322**, 1819-1822. [2] Gebauer & Cölfen (2011), *Nano Today* **6**, 564-584. [3] Gebauer *et al.* (2010), *Angew. Chem. Int. Ed.* **49**, 8889-8891. [4] Addadi, Raz & Weiner (2003), *Adv. Mater.* **15**, 959-970. [5] Demichelis, Raiteri, Gale, Quigley & Gebauer (2011), *Nat. Commun.* **2**, 590. [6] Gebauer, Cölfen, Verch & Antonietti (2009), *Adv. Mater.* **21**, 435-439. [7] Gebauer, Verch, Börner & Cölfen (2009), *Cryst. Growth Des.* **9**, 2398-2403. [8] Kellermeier *et al.* (2012), *Adv. Funct. Mater.* **submitted**. [9] Verch, Gebauer, Antonietti & Cölfen (2011), *Phys. Chem. Chem. Phys.* **13**, 16811-16820.

Eruption and crystallization ages for Breccia Museo plutonic ejecta

SAMANTHA GEBAUER[1], AXEL K. SCHMITT[1*], DANIEL F. STOCKLI[2], ROMAN KISLITSYN[2], LUCIA PAPPALARDO[3]

[1]University of California, Los Angeles, USA, skg949@ucla.edu, axel@oro.ess.ucla.edu (*presenting author)

[2]University of Texas, Austin, USA, stockli@jsg.utexas.edu, roman.kislitsyn@jsg.utexas.edu

[3]Istituto Nazionale di Geofisica e Vulcanologia Sezione di Napoli - Osservatorio Vesuviano, Naples, Italy, lucia.pappalardo@ov.ingv.it

The Campi Flegrei volcanic district (Naples region, Italy) is a 12 km wide, restless caldera system that has erupted at least six voluminous ignimbrites throughout the late Pleistocene, including the >300 km^3 Campanian Ignimbrite (CI), originated by the largest known volcanic event of the Mediterranean region. One of these deposits, the Breccia Museo (BM), a petrologically heterogeneous and stratigraphically complex volcanic deposit extending over 200 km^2 in close proximity to Campi Flegrei [1], has long remained contentious regarding its age and stratigraphic relation to the CI. Here, we present crystallization and eruption ages for BM plutonic ejecta clasts that were determined via uranium decay series and (U-Th)/He dating of zircon, respectively. Plutonic clasts were examined by scanning electron microscopy, and zircon crystals were extracted for geochronologic analysis. Despite mineralogical and textural heterogeneity of these syenitic clasts, their U-Th zircon crystallization ages are indistinguishable with an average age of 49.2±3.0 ka (2σ errors; mean square of weighted deviates MSWD = 1.2; n = 34). Disequilibrium-corrected (U-Th)/He zircon ages for three plutonic clasts average 42.2±2.6 ka; MSWD = 0.7; n = 10). One exception is a single clast where zircon crystals yielded older (U-Th)/He ages of 50.6±3.9 ka (MSWD = 1.6, n = 6) that overlap with the U-Th zircon crystallization ages. The limited range in U-Th zircon ages indicates rapid crystallization within the plutonic margins of the pre-CI magma system. For most clasts, the limited range of (U-Th)/He ages suggests complete resetting during the eruption, or lack of pre-eruptive ^{4}He accumulation due to high ambient temperatures. Only in one instance we suspect that the explosive eruption that ejected the BM plutonic clasts may not have heated zircon sufficiently to completely degas pre-eruptive ^{4}He. There, the close overlap between crystallization and (U-Th)/He ages would imply very rapid cooling within the shallow intrusive complex. Our (U-Th)/He zircon eruption age overlaps with published ^{40}Ar/^{39}Ar sanidine ages for BM which, however, display considerable variation (i.e., plateau ages ranging between 34.2 and 41.0 ka; [1]). It is marginally older than the commonly cited ^{40}Ar/^{39}Ar CI eruption age (39.5±0.1 ka; [2]), but significantly pre-dates published ^{14}C ages for BM (17.9 ka [3]) and CI (between 42 and 27 ka reported in [4]). These results underscore the potential of combined U-Th and (U-Th)/He zircon geochronology for high-accuracy chronostratigraphy, and reconstruction of the thermal history of the magmatic feeder systems of supereruptions.

[1] Fedele *et al.* (2008) *Bul. Volcanol.* **70**, 1189-1219. [2] De Vivo *et al.* (2001) *Mineral. Petrol.* **73**, 47-65. [3] Lirer et al. (1991). *J. Volcanol. Geotherm. Res.* **48**, 223-227. [4] Scandone *et al.* (1991). *J. Volcanol. Geotherm. Res.* **48**, 1-31.

https://doi.org/10.1180/S0026461X00008434 Published online by Cambridge University Press

Synthesis and isotopic characterization of high-pure ^{12}C nano-calcite

ANTOINE GEHIN[1*], GERMAN MONTES-HERNANDEZ[1] AND LAURENT CHARLET[1]

[1] ISTerre, Maison des Geosciences, 38041 Grenoble, France, (correspondence antoine.gehin@ujf-grenoble.fr, german.montes-hernandez@ujf-grenoble.fr and charlet38@gmail.com)

In the present study, we report a simple and innovative synthesis route for high-pure ^{12}C nanosized calcite particles. Herein, $Ca(OH)_2$ nanoparticles portlandite were directly carbonated with high-pure $^{12}CO_2$ (99,99% ICP-MS certfified) gas using a static bed reactor under anisobaric conditions (initial $^{12}CO_2$ gas pressure = 20 bars and T = 303 K).

Calcite nature and particle size (including its morphology) were controlled by X-ray diffraction (XRD) and field emission gun scanning electron microscopy (FESEM), respectively. Its isotopic characterization by isotopic CO_2 Cavity Ring-Down Spectroscopy (CRDS from Picarro) analyzer has confirmed the very low negative delta of the ^{13}C (**Figure 1**), i.e. higher content in ^{12}C with respect to standard (measured against Vienna Pee Dee Belemnite *VPDB*).

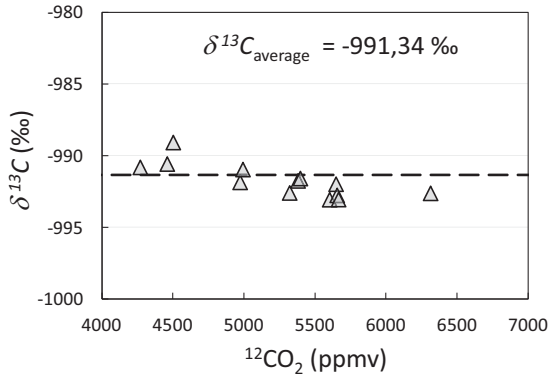

Figure 1: $\delta^{13}C$ value of $Ca^{12}CO_3$ as a funtion of $^{12}CO_2$ (in ppmv). The dashed line shows an average value of $\delta^{13}C$ = -991,34 ‰.

To the best of our knowledge, this is the first time ever that such $\delta^{13}C$ measurement is reported for a synthetic material. Remarking that $\delta^{13}C$ are expressed in permil and are typically in the range from -100 to +100. This new high-pure ^{12}C nano-calcite opens new possibilities to investigate on the carbon ^{12}C-^{13}C dynamic exchange at the calcite-fluid interfaces with relevance in natural and artificial systems.

Si isotope fractionation during silica precipitation in flow-through experiments

SONJA GEILERT[1*], MANFRED VAN BERGEN[1], PIETER VROON[2], PHILIPPE VAN CAPPELLEN[3]

[1]Department of Earth Science, Utrecht University, Utrecht, The Netherlands, s.geilert@uu.nl (* presenting author), m.j.vanbergen@uu.nl

[2]Department of Petrology, VU University, Amsterdam, The Netherlands, p.z.vroon@vu.nl

[3]Department of Earth and Environmental Sciences, University of Waterloo, Waterloo, Canada, pvc@uwaterloo.ca

Silicon isotopes are a promising proxy for (near-) surface processes and conditions. However, an unequivocal interpretation of isotope signatures in natural silica deposits is often hampered by the lack of quantitative constraints on isotopic fractionation for the environment of interest. To help alleviate these limitations, we performed precipitation experiments using flow-through reactors wherein silica precipitated from a saturated solution in the 10-60°C temperature range. Principal objective was to determine the sign and magnitude of silicon isotope fractionation during controlled precipitation of amorphous silica induced by a temperature drop.

A starting solution, brought to saturation in amorphous silica at 90°C, was forced to pass flow-through reactors containing seeds of amorphous silica powder. The reactors were placed in a water bath with a pre-set cooler temperature. Time-series results, obtained through monitoring the Si concentration in output solutions, were used to optimize the experimental conditions under which steady-state deposition could be achieved. This comprehensive set of test runs exposed strong effects from flow-rate, surface area of the seeding material and degree of supersaturation in the reactors.

Silicon isotope ratios ($^{30}Si/^{28}Si$ and $^{29}Si/^{28}Si$), measured in input and output solutions using a Thermo Neptune MC-ICPMS, showed a systematic time-dependent behaviour as well. Isotope shifts in initial run products, expressed as $\Delta^{30}Si_{out\text{-}in}$ ($\delta^{30}Si_{output}$ - $\delta^{30}Si_{input}$), ranged between -2.0 and +0.1‰, mainly depending on temperature and surface area of the silica seeds. Long-term runs (up to 2 month) were required to approach a steady isotopic signal in the output solution, which is taken to reflect equilibrium. In these cases, the output results are consistent with preferential incorporation of the light isotope in the precipitating silica, in qualitative agreement with expected fractionation behaviour. Our experimental results obtained so far yielded a maximum $\Delta^{30}Si_{out\text{-}in}$ value of +1.4‰, which was found when the precipitation temperature was lowest. The magnitude of fractionation tended to increase with decreasing temperature.

Our experimental set-up mimics a submarine hydrothermal vent system where silica deposition is associated with a steep temperature gradient. The results corroborate the potential of $\delta^{30}Si$ signatures of (precursors of) cherts as a paleo-proxy for ambient conditions, but question their robustness as indicator of paleo-temperatures alone.

https://doi.org/10.1180/S0026461X00008434 Published online by Cambridge University Press

Carbonatite extraction and seismic anomalies in the Galápagos plume

D. GEIST[1*], D.R. TOOMEY[2], D. VILLAGOMEZ[3], AND E. HOOFT[4]

[1]*University of Idaho, Moscow ID USA, dgeist@uidaho.edu
[2] University of Oregon, Eugene OR USA, drt@uoregon.edu
[3] University of Oregon, Eugene OR USA, emilie@uoregon.edu
[4]University of Oregon, Eugene OR USA, darwin7@gmail.com

Conventional models of plume-ridge action call on plume material (either melt or solid mantle) flowing along the base of the lithosphere toward the ridge. This model is inconsistent with a number of seismic and geochemical paradoxes in the Galápagos Archipelago. Although the Galápagos Spreading Center is contaminated with plume Sr, Nd, and Pb, there is no plume He in GSC lavas. Many of the northern Galapagos volcanoes have less of a plume isotopic signal than any GSC lava from within 400 km of the Galapagos hotspot. GSC magmas contain water from the Galapagos plume; there are no data bearing on whether the plume is richer in CO_2 than the GSC or whether plume CO_2 contaminates the GSC.

Combined surface and S-wave tomography reveals 4 velocity zones in the Galapagos plume: a 1 to 2% slow zone extending from 400 to 100 km, a normal velocity zone from 100 to 80 km, a zone 2% slow zone from 80 to 15 km, and the crust. The deep slow zone is unlikely to be due to hydrogen in olivine or temperature, owing to the magnitude of the velocity anomaly. Instead, we propose that it is due to a carbonatite melt that is produced at depths >400 km. A reasonable estimate of the carbon concentration of the Galapagos mantle is 500 ppm (as CO_2), which could yield a ~0.1% carbonatite melt. This melt is likely to extract the noble gases from the rock and ascend vertically to Fernandina's magmatic system. The zone with normal seismic velocity at 100 to 80 km may represent the intersection of the plume with the water-bearing solidus, as the removal of water from olivine is likely to result in an increased seismic velocity. For example, 150 ppm H_2O would depress the anhydrous solidus by about 55 km (Hirschmann, 2006). The shallower slow zone is likely caused by more extensive partial melting of the silicate phases in the garnet facies, producing a basaltic melt. Fernadina's high $^3He/^4He$ magmas result from mixing of the carbonatite and silicate melts above the plume axis, and trace element models are consistent with this hypothesis.

We propose that plume material is carried to the GSC by deep return flow of the asthenosphere toward the GSC (>100 km depth), not along the base of the lithosphere. Flow at this depth will incorporate plume material that is depleted in He and carbon, accounting for the lack of these signals in GSC lavas. Also, the shallow asthenosphere might be flowing with the plate, away from the GSC. Magmas from the northern Galapagos then are created by melting of mantle that has already had melt extracted at the GSC, accounting for their more depleted compositions. Carbonatite may be the cause of deep (>100 km) seismic anomalies in plume provinces on a worldwide basis.

Engineered nanoparticle sorption onto mineral surfaces

A. GÉLABERT[1,*], Y. SIVRY[1], C. SOARES PEREIRA[1], C. AUBRY[2], N. MENGUY[3], J.-P. CROUÉ[2] AND M.F. BENEDETTI[1]

[1] Université Paris Diderot - Sorbonne Paris Cité, IPGP, Paris, France, gelabert@ipgp.fr (* presenting author), Sivry@ipgp.fr, soarespereiracaroline@gmail.com, Benedetti@ipgp.fr
[2] Water Desalination and Reuse Research Center, King Abdullah University of Science and Technology, Thuwal, Saudi Arabia, jp.croue@kaust.edu.sa, Cyril.Aubry@kaust.edu.sa
[3]IMPMC, Université Pierre et Marie Curie, UMR 7590, Paris, France, Nicolas.Menguy@impmc.jussieu.fr

The strong increase in the use of engineered nanoparticles (NPs) during the last decade may ultimately result in their release in environmental settings as predicted for different types of NPs by Gottshalk et al.[1]. As part of previous modeling works, it has been showed that soils and sediments were able to accumulate high amounts of NPs while waters were acting as a dispersion agent. Thus, in order to be able to predict the fate of NPs in natural systems, an accurate understanding of the interactions involving the mineral surfaces is highly required. This study aims to estimate the NPs sorption properties onto model mineral substrates, to depict the molecular scale processes at work, and to assess the impact of the NPs physico-chemical properties, such as the NPs agregation state.

For this study, the bulk structure of commercial ZnO NPs have been investigated using XRD analysis in combination with high-resolution TEM observations. The physico-chemical properties of the NPs surface were estimated from zeta potential measurements and XPS spectrocopy. And the NPs agregation state was measured using DLS and cryo-TEM techniques. The sorption kinetics of ZnO NPs on mica surfaces and Al_2O_3 (1-102) oriented single crystals have been measured using atomic force microscopy (AFM) in 0.01M $NaNO_3$ solution. This revealed a fast sorption, in the order of minutes, followed by a slower evolution of the system during few hours. Furthermore, sorption studies on synthetic microsized goethite and alumina have been conducted at pH 7.0 in 0.01M $NaNO_3$ solutions. The time of exposure has been fixed at three hours and various mineral/NPs ratio have been tested. The obtained sorption isotherms could only be described using the Temkin equation, thus revealing a decrease in NPs affinity for the mineral surface with an increase in the total NPs sorption rate. This trend can be partly explained by TEM and cryo-TEM observations that showed a preferential sorption of agregated NPs on the mineral surfaces compared to individual NPs. Finally, the NPs aggregation state appears to be one of the major controls of the NPs sorbing properties.

This study constitutes an essential step to understand the fate of NPs in soils, and demonstrates the importance of the NPs physico-chemical properties during their interaction with mineral surfaces.

[1] Gottshalk F., Sonderer T., Scholz R.W., and Nowack B., Environmental Science and Technology, 2009, 43, 9216-9222

https://doi.org/10.1180/S0026461X00008434 Published online by Cambridge University Press

The Rusty Sink: Iron Promotes the Preservation of Organic Matter in Sediments

YVES GÉLINAS[1]*, KARINE LALONDE[2], ALFONSO MUCCI[3], ALEXANDRE OUELLET[4]

[1]Concordia University, Montréal, Canada, ygelinas@alcor.concordia.ca (* presenting author)
[2]Concordia University, Montréal, Canada, k_lalonde@hotmail.com
[3]McGill University, Montréal, Canada, alm@eps.mcgill.ca
[4]Concordia University, Montréal, Canada, axouellet@hotmail.com

The biogeochemical cycles of iron (Fe) and organic carbon (OC) are strongly interlinked. In oceanic waters, organic ligands have been shown to control the concentration of dissolved Fe [1]. In soils, solid Fe phases provide a sheltering and preservative effect for organic matter [2], but the role of iron in the preservation of OC in sediments has not been clearly established. Here, we determine the amount of organic carbon, associated with reactive iron phases in sediments of various mineralogies collected from a wide range of depositional environments, using an iron reduction method previously applied to soils [3]. Our findings suggest that 21.5 ± 8.6 per cent of the organic carbon in sediments is directly bound to reactive iron phases, representing a global mass of 19 to 45 × 10^{15} g of organic carbon in surface marine sediments [4]. This pool of OC is different from the rest of sedimentary OC, with ^{13}C and nitrogen-enriched organic matter preferentially bound to Fe which suggests that biochemical fractionation occurs with OC-Fe binding. We propose that these organic carbon-iron associations, formed primarily through co-precipitation and/or direct chelation, promote the preservation of organic carbon in sediments. Since reactive iron phases are metastable over geological timescales, they serve as an efficient "rusty sink" for OC, a key factor in the long-term storage of organic carbon and thus contributing to the global cycles of carbon, oxygen and sulphur [5]. New data showing Fe-OC interactions in water column suspended particles will also be presented.

[1] Johnson et al. (1997) *Marine Chemistry* **57**, 137-161.
[2] Kaiser at al. (2000) *Organic Geochemistry* **31**, 711-725.
[3] Wagai et al. (2006) *Geochimica Cosmochimica Acta* **71**, 25-35.
[4] Lalonde et al. (in press) *Nature.*
[5] Berner (2003) *Nature* **426**, 323-326.

O isotopes in the Azores: mantle melting versus AFC

FELIX S. GENSKE[1,2]*, CHRISTOPH BEIER[1,2], STEFAN KRUMM[1], KARSTEN M. HAASE[1], SIMON P. TURNER[2]

[1]GeoZentrum Nordbayern, Universität Erlangen-Nürnberg, Schlossgarten 5, D-91054 Erlangen, Germany
[2]CCFS, GEMOC, Department of Earth and Planetary Sciences, Macquarie University, Sydney NSW 2109, Australia (*correspondence: felix.genske@mq.edu.au)

The Azores archipelago in the central North Atlantic has been studied wideley over the last few decades, one reason being its formation history that is related to a slow-upwelling mantle plume. The plume sources identified in these ocean islands are predominantly inferred from Sr-Nd-Pb-(Hf) radiogenic isotope data along with major and trace element geochemistry. Contrastingly, few studies have dealt with the variability in stable isotopic composition. Here, we present a detailed isotopic study of oxygen isotope ratios ($^{18}O/^{16}O$) in olivines, clinopyroxenes and plagioclases that allow to infer on the quantiative and qualitativey involvement of altered oceanic crust (AOC) during ascent of the magmas. This is particularly important when aiming to place constraints on the primary O isotopic composition of the mantle plume source. Furthermore, such estimates can be combined with other newly availabe isotope data of boron (B) and Lithium (Li) of the Azores lavas.

We provide a comprehensive data set of phenocryst O isotope data obtained by laser fluorination along with their individual mineral chemistry measured by electron microprobe on the same grain. The phenocrysts originate from lavas from the entire archipelago, namely Faial and Pico (central Azores) and São Miguel (east Azores), and, for the first time, include data for the two islands west of the mid-Atlantic ridge (MAR), Flores and Corvo. The samples were selected from geochemically well characterised host lavas such that the newly obtained O data are placed in a tight geochemical and petrological background.

Our data indicate that the eastern Azores lavas are characterized by O ratios (i.e. $\delta^{18}O_{(ol)}$ 4.7-5.2 ‰) slightly lighter than the primitive mantle range ($\delta^{18}O_{(ol)}$ ~ 5.2±0.2 ‰), while the western lavas fall within the latter range. However, we find that decreasing forsterite contents in olivines are tightly correlated with decreasing $\delta^{18}O$. Such systematic is also observed in Hawaii', which is explained by assimilation of hydrothermally altered material during the crystallization-differentiation process [1]. We test whether assimilation fractional crystallization (AFC) models sufficiently describe the $\delta^{18}O$ systematic of the Azores lavas, and if the highest forsterite olivines can be used to distinguish the $\delta^{18}O$ signal of the plume source. Our data are also compared with those of the MAR [2] to better evaluate the nature and distribution of enriched components in the north Atlantic mantle.

[1] Wang, Z. & Eiler, J. M. (2008) *EPSL* **269** (3-4), 377-387.
[2] Cooper, K. M., Eiler, J. M., Asimow, P. D. & Langmuir, C. H. (2004) *EPSL* **220** (3-4), 297-316.

https://doi.org/10.1180/S0026461X00008434 Published online by Cambridge University Press

Acid mine drainage multi-step passive treatment system: the Lorraine case study

THOMAS GENTY[1]*, BRUNO BUSSIÈRE[1], CARMEN NECULITA[1], MOSTAFA BENZAAZOUA[1], AND GÉRALD J. ZAGURY[2]

[1]Université du Québec en Abitibi-Témiscamingue, Institut de recherche Mines et Environnement, Thomas.genty@uqat.ca (*presenting author), Bruno.bussière@uqat.ca, Carmen.neculita@uqat.ca, Mostafa.benzaazoua@uqat.ca

[2]École Polytechnique de Montréal, Département de génie civil, géologique et des mines, gerald.zagury@polymtl.ca

Introduction

At the closure stage of a mine site, passive treatment systems are an interesting alternative to reduce environmental impacts of acid mine drainage (AMD) [1] because they require low investments and maintenance, and natural organic materials (like manure and compost) or by-products (like wood ashes) can be used to build them. However, passive treatment of AMD with high iron concentrations is still a major challenge for system efficiency.

The Lorraine site is an AMD generating site in Quebec province reclaimed in 1999. Although the reclamation strategy is effective to limit the generation of new AMD, contaminated water (especially characterized by a high iron loading of 2020 mg/L) in the tailings pores will take time before being leached out. Laboratory studies have shown that a system composed of only one unit passive treatment system, such as sulfate-reducing passive biofilter (SRPB) or anoxic limestone drain, is not efficient to treat this type of AMD [2,3]. Therefore, a multi-step treatment system was designed and built [3]. The first step is a SRPB (containing 50%wt limestone and 50%wt mixture of chicken manure, vegetable compost, wood chips, and sand), which allows pH increasing and a partial dissolved metal removal. The second step is a wood ash filter, for iron removal, mainly. The third step consists of a second SRPB, which allows the removal of sulfates and residual metals.

A 120 m^3system (40 m long x 3 m wide x 1 m high) was built in August 2011 and allows treating 1L/min (Figure 1).

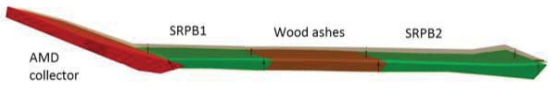

Figure 1: Multi-step treatment system design

Preliminary results

Results from the first four months of operation (see Table 1) showed a promising removal percentage for iron and sulfates (respectively 93% and 59% on average).

Parameter	pH	Fe (mg/L)	SO_4^{2-} (mg/L)
AMD	5.5	2020	4784
After treatment	6.4	150	1992

Table 1: Average water quality after treatment

[1] Neculita *et al.* (2007) *J. Env. Qual.* **36**, 1-16. [2] Potvin (2009) *PhD thesis*, 335 pp. [3] Genty (2011) *PhD thesis*, 252 pp.

Silicon Isotopes – A Global Weathering Proxy?

R.B. GEORG

Water Quality Centre, Trent University, Peterborough, Ontario, K9J 7B8 (rgeorg@trentu.ca)

Silicon stable isotopes are one example of the large group of so called "novel stable isotope tools" that became routinely available over the past decade. Advances in mass-spectrometry, especially ICP-MS and gas source mass-spectrometry, provided the technical means for determining Si isotope ratios with unprecedented precision and accuracy. These technical advances opened up new ways to study low-temperature processes, such as weathering reactions, in greater detail. Silicon is ubiquitous in the environment and the isotope system is therefore predestined to be a useful tracer for processes controlling the Si budget in the weathering zone.

Two major fractionation pathways have been identified; (1) biological uptake of Si and (2) the formation of secondary weathering products. Both of these fractionation processes discriminate against the heavier isotopes and produce dissolved Si in surface waters that is usually enriched in heavy Si isotopes. The global runoff has a δ^{30}Si of about +1.1‰ (De La Rocha et al 2005, Georg et al 2009), which reflects isotope fractionation due to a combination of biological processes and weathering processes. The interesting questions would be: which of the two major fractionation pathways dominates and produces the positive isotope composition of the global runoff?

The biological part of the continental Si cycle is often being perceived as the dominant one resulting in large biogenic Si fluxes. A fast turnover of biogenic silica, however, mitigates larger fractionation effects on the dissolved Si load in rivers. The formation of secondary clays represents a more effective way of removing Si from the weathering zone and therefore causing a much greater net fractionation.

I will present a fractionation model of the continental Si cycle that takes into account the interactions between various Si pools and isotopic evolution as a function of the two major fractionation processes. Results show that the formation of secondary minerals is the main driver behind the positive isotope composition in rivers. Although more Si is cycling through the biosphere, the fast turnover means that the biological Si cycle is mostly self-supporting and does not require larger inputs of fresh Si from weathering. Hence the net isotope fractionation is mitigated when biogenic silica is returned to the soil system. The biological cycle has a larger net effect only when significant amounts of biogenic silica are stored in long-term sinks (phytoliths). The typical positive Si isotope composition can only be achieved when significant proportions of Si are being locked-up in clays. In other words, the positive isotope composition of the global runoff reflects a slightly dominating inorganic Si cycle, e.g. dissolution of crustal material and formation of secondary weathering products. There appears to be some systematic change in the isotope composition of the runoff with weathering rates and intensities and in periods with extensive recycling of previously weathered materials, the Si isotope composition of the global runoff can be expected to be lighter than the modern value.

Silicon isotopes could potentially be used to track changes in continental weathering over time, providing a suitable archive exists, such as marine shales (see Savage et al – session 12c).

References:
De La Rocha et al (2005) – Marine Geology 215, pp 267
Georg et al (2009) – EPSL 283, pp 67

https://doi.org/10.1180/S0026461X00008434 Published online by Cambridge University Press

Re-Os shale ages constrain onset and duration of Late Jurassic anoxia, Barents Shelf

S. GEORGIEV[1,2], H.J. STEIN[1,2,3], J.L. HANNAH[1,2,3], B. BINGEN[1], H.M. WEISS[4]

[1] Geological Survey of Norway, 7491 Trondheim, Norway, georgiev@colostate.edu (* presenting author)
[2] AIRIE Program, Colorado State University, Fort Collins, CO, USA
[3] Physics of Geological Processes, University of Oslo, Norway
[4] SINTEF Petroleum Research, 7465 Trondheim, Norway

Organic-rich marine shales with excellent oil-generation potential were deposited in abundance during the Late Jurassic. These include the Kimmeridge Clay Formation, the main source rock for North Sea oils, and areally extensive black shales in North Alaska, Arctic Canada, the Barents Shelf and Northern Siberia [1]. One of them, the Hekkingen Formation, is the most widespread, though variably mature, hydrocarbon source rock on the Barents Shelf. We report high precision Re-Os isotopic data and geochemical data for three intervals from a condensed section of Hekkingen Formation in the Nordkapp Basin, southwestern Barents Sea.

We sampled shales of the Hekkingen Formation from two shallow drillcores [2], previously subject to detailed biostratigrahpic studies [3]. Shales at the base of the lower Alge Member yield a Re-Os age of ~158 Ma with an initial $^{187}Os/^{188}Os$ ratio of ~0.45. Up section, shales of the overlying Krill Member yield a Re-Os age of ~147 Ma and initial $^{187}Os/^{188}Os$ ratio of ~0.63.

Rock-Eval pyrolysis shows that the organic matter is thermally immature (T_{max} ~400 to 410 °C) and of mixed marine-terrestrial origin (kerogen type II/III predominates). The high total organic carbon (9-19 wt%) and lack of bioturbation, combined with unusually high enrichment in redox-sensitive trace elements Re, Os, Mo, U, Se and V, indicate deposition of the Hekkingen shales under oxygen-free bottom water conditions. Extreme enrichment in Ag, Zn, Ni, Cr, Cu, Cd, Sb, As and Tl, even for black shales, may stem from a high degree of anoxia combined with slow sedimentation in a distal setting with minimal clastic input.

The Re-Os ages provide time pins for the onset (~158 Ma) and duration (at least 11 m.y.) of Late Jurassic anoxia in the Barents Shelf, and for sedimentation rates of organic-rich muds with extreme trace metal concentrations. Additionally, comparison of Re-Os ages with detailed biostratigraphy provides new radiometric constraints for the age of the Kimmeridgian-Tithonian boundary. Rising initial Os isotope ratios from the Oxfordian to the Kimmeridgian shales mirror rising seawater Sr isotope ratios throughout the latest Jurassic [4]. These parallel trends suggest that the initial $^{187}Os/^{188}Os$ of shales records the $^{187}Os/^{188}Os$ of contemporaneous Late Jurassic seawater. The trend toward more radiogenic Sr isotope ratios may reflect decreasing mid-ocean ridge production [4], rather than changes in continental weathering rates.

Funding: NFR Petromaks project 180015/S30

[1] Leith et al. (1992) *NPF Spec. Publ.* **2**, 1-25. [2] Bugge et al. (2002) *Mar. Petr. Geol.* **19**, 13-37. [3] Wierzbowski and Smelror (1993) *Acta Geol. Pol.* **43**, 229-249. [4] Jones et al. (1994) *GCA* **58**, 3061-3074.

Intrabasaltic Regoliths in the Deccan (India) and Karoo traps (Lesotho): witnesses of volcanic quiescence and environmental links.

MARTINE GERARD[1*], FREDERIC FLUTEAU[2], VINCENT COURTILLOT[2] AND MAUD MOULIN[3]

[1] IMPMC, IRD, Université Pierre et Marie Curie, Paris, France, martine.gerard@impmc.upmc.fr (* presenting author)
[2] IPGP, Université Paris Diderot, Paris, France
[3] Dpmt de Géologie, Université Jean Monnet, Saint Etienne, France

Large igneous provinces (LIP) are often synchronous with major mass extinctions. Intertrappean layers ("red boles") correspond to periods of volcanic quiescence. Their study complements other methods, and may help to quantify how volcanic activity translates into major environmental perturbations. Geomagnetic secular variation recorded by lavas can be used as a relative time proxy (1,2), providing an estimate of the time needed to generate these regoliths. We have studied a 1200m thick stack of flows in the Deccan and Karoo LIPs. In the Deccan, 22 red boles occur between volcanic flows. Most consist in 5-10cm thick red clayey material filling joints and diaclases at flow contact, located in the frontal part of flow lobes. Only 5 red boles are thicker, but their lateral extent (less than 1km) prevents a stratigraphic reconstruction. The more mature regoliths (a few meters thick) correspond to weathering profiles of massive basalts. Red compact silty clay with relics of feldspars and voids grades into orange silty clay with friable vesicular relics of blocks of basalts, overlaying brown clay jointed lava and massive altered lava. Mineralogical parageneses and micromorphological observations indicate strong hydrolysis and also (deuteric or metasomatic) hydrothermal alteration. No organic relics were found. The duration of formation is likely much less than 10000 years for the more evolved regoliths, when compared to similar paleosols affected by hydrothermalism. Most red boles we observed in the top part of the Deccan lava pile were probably formed in less than 1000 years, consistent with the magnetostratigraphic study [1].The Karoo intra-basaltic regoliths are much less developed and numerous [2]. The red weathered horizons and hydrothermalized contacts always occur within lava lobes, more easily affected by alteration and topographic irregularities. At the base of the section, more or less baked sandstone interbeds have recorded a minor mineralogical signature of weathering from the surrounding lava flows. The altered bases of the overlying lava flows and the baked sediments suggest humid lacustrine conditions. The weathering profiles in the upper part of the section are basaltic saprolites with a summital horizon of smectites-hematites. Within a few profiles, silty quartz may also suggest colluvial paleosols. As is the case for the Deccan regoliths, zeolitic parageneses suggest a strong impact of hydrothermalism. Compared to the Deccan, the Karoo intertrappean layers suggest much more arid climatic conditions that would have drastically limited the occurence of weathering.

[1] CHENET et al. (2009), *JGR,* **114**, doi:10.1029/2008JB005644.
[2] MOULIN et al. (2011), *JGR,* **116,** doi:10.1029/2011JB008210.

https://doi.org/10.1180/S0026461X00008434 Published online by Cambridge University Press

Apparent crustal growth due to disequilibration of the Lu-Hf isotope system during crustal melting

AXEL GERDES[1]

[1]Goethe University, Frankfurt am Main, Germany, gerdes@em.uni-frankfurt.de

The combined U-Pb-Hf analysis of zircon is a powerful, widely-used tool for studying the evolution of the continental crust though time. It allows for estimates of the proportions of new, primitive crust relative to the recycled, older continental crust for separate time slices from the Hadean through to the present.

While the general concept appears clear and straight forward, individual data sets generally need careful evaluation before interpretation. Various issues have an important influence on the isotopic data, such as the complexity of natural zircon grains, demanding careful spot selection and high spatial resolution during isotope analyses. Other analytical problems are the possible disturbance of the U-Pb system and the substantial interference correction during Hf isotope analyses.

This study will discuss the possibility that many crustal melts do not reflect the isotopic composition of their source. Most granitic rocks contain inherited zircon in their zircon population commonly preserved as cores overgrown by newly crystallized rims. The Hf isotope composition of the rims usually represents that of the magma, which is either a mixture between mantle magma and crustal components or of pure crustal origin. Even in the latter case, the $^{176}Hf/^{177}Hf$ of the melt, as reflected by the zircon rim composition, will be more radiogenic than that of their average crustal source, as unradiogenic Hf is stored in the inherited cores. The effect will increase with the percentage of inherited, non-dissolved zircon and with the time since last isotope equilibration of the crustal source. This is because new ^{176}Hf formed from Lu-decay usually readily enters the melt, as Lu is incorporated in phases other than zircon that are reactants in the melting process, while only a fraction of the Hf stored in zircon will be dissolved. Assuming a time span of 0.5-1.0 Ga since the last isotopic equilibration and that 40-60% of zircon from the source dissolve in the melt, the Hf isotope composition of the melt will be about 3-11 εHf(t) (t= time of melting) units lower than that of the source. Using 4 different examples from the recent literature, inherited zircon cores have at time of granite generation a mean εHf(t) of -3±3, -13±20, -22±19, and -21±20, which is in average about 6-20 εHf units lower than that of their magmatic rims. This correlates well with the mean age of the cores, which are about 0.46 to 1.5 Ga older than that of their rims. Notably is also that the overall isotopic variation of the inherited cores is about 5-40times higher than that in the magmatic rims (e.g., ±0.5, SD).

As a consequence, estimation of the average crustal residence time (e.g. T_{DM} ages) based on the composition of the magmatic zircon will be too young and will thus overestimate the contribution of juvenile magmas to the system. Although granite magmas probably do not fully equilibrate with their sources, the data imply that crustal melting stimulates isotopic and chemical homogenisation of the crust.

Protracted tectonometamophic history at the base of an orogenic channel in the southeastern Canadian Cordillera

F. GERVAIS[1]*, J. L. CROWLEY[2], A. HYNES[3], E. GHENT[4]

[1] École Polytechnique, Montreal, Canada, felix.gervais@polymtl.ca*
[2]Boise State University, Boise, USA, jimcrowley@boisestate.edu
[3]McGill University, Montreal, Canada, andrew.hynes@mcgill.ca
[4]University of Calgary, Calgary, Canada, ghent@ucalgary.ca

We tested the recently proposed model of channel flow[1] by mapping key outcrops in the northern Monashee Mountains of the southeastern Canadian Cordillera. The structural and metamorphic continuity of this area constitute the main challenges for this controversial model. Our fieldwork revealed the existence of a major SE-striking, reverse-sense shear zone, named Hellroar Creek Shear Zone (HCSZ). It is characterized by a large volume (>60%) of highly sheared leucogranite and leucosome, whereas leucogranite in its footwall, although locally as abundant, forms a heterogeneous mesh of highly discordant intrusions. The HCSZ separates a low-strain domain with preserved stratigraphic polarity and dominated by SW- to W-verging structures in its footwall, from a high-strain domain with rocks recording complete transposition by top-to-the-NNE to top-to-the-E shearing in its hanging wall.

One migmatitic pelitic schist, one prekinematic, and one synkinematic leucogranite dykes from the hanging wall of the HCSZ, as well as one postkinematic leucogranite dykes from its immediate footwall were dated for U-(Th)-Pb monazite and zircon geochronology. Collectively, the near continuous record of monazite and zircon growth from 104 to 57 Ma in these samples indicates an exceptionally long tectonometamorphic history for this reverse-sense shear zone.

The presence of a major shear zone with a protracted history of ductile deformation in an area previously mapped as continuous supports the channel flow model. In addition, the timeframe of shearing coincides with the timing of flow derived from the pattern of younger cooling ages recorded from the front to the rear of the proposed channel.[1] The HCSZ is thus interpreted as the base of a channel flow system that was active for >40 Myr in the Late Cretaceous.

[1] Gervais & Brown (2011) *Lithosphere* **3**, 55-75.

https://doi.org/10.1180/S0026461X00008434 Published online by Cambridge University Press

Vapour phase oxidation of trichloroethylene, ethanol and toluene by solid potassium permanganate: Kinetic study

MOJTABA GHAREH MAHMOODLU [1*], NIELS HARTOG [2], S. MAJID HASSANIZADEH [3]

[1] Utrecht University, Department of Earth Sciences, The Netherlands, mahmodlu@geo.uu.nl (* presenting author)
[2]Utrecht University, Department of Earth Sciences, The Netherlands,n.hartog@uu.nl
[3]Utrecht University, Department of Earth Sciences, The Netherlands, hassanizadeh@geo.uu.nl

21g. Process-based reactive transport modelling of aquifer remediation and natural attenuation

Volatile organic compounds may cause major contamination problems in groundwater and soil. Their presence in air can create a hazard to public health. However, limited remedial options exist in controlling the vapour transport of these compounds in the unsaturated zone.

In this study, batch experiments were carried out to investigate the oxidation of TCE, ethanol, and toluene vapour in air by potassium permanganate. For each compound, three experiments with different combinations of vapour concentration and mass of potassium permanganate grains were performed. The objectives of these batch tests were (1) to evaluate the ability of solid potassium permanganate to transform contaminants in the gas phase to harmless compounds and (2) to determine the kinetic parameters. Experimental results have revealed that solid potassium permanganate is able to remove these harmful compounds from the vapour phase. We found that the removal efficiency for TCE and ethanol oxidation is higher than for toluene.

To obtain kinetic parameters, the reaction rate was assumed to be related nonlinearly to the concentration of the targets compounds and the amount of permanganate:

$$\frac{dC}{dt} = kA C^{\alpha} M^{\beta}$$

where k denotes the rate constant ($mol^{1-\alpha}\ L^{3\alpha+3\beta-5}\ M^{-\beta+1}\ T^{-1}$), A is the specific surface area of potassium permanganate ($L^2\ M^{-1}$), C is the vapour concentration of the compound (mol L^{-1}), M is the mass of potassium permanganate per volume of gas (M L^{-3}), α and β are constant parameters. We made sure that $KMnO_4$ was abundantly present so it was assumed that its consumption did not affect the reaction rate. This equation was fitted to experimental data in order to determine k, α, β for each compound. Results of the simulations are given in table1.

Compound	α	β	k($mol^{1-\alpha}\ L^{3\alpha+3\beta-5}\ M^{\beta+1}\ T^{-1}$)	R^2
TCE	0.9	1	6.92×10^{-7}	0.99
Ethanol	1.09	1	5.68×10^{-7}	0.99
Toluene	0.94	1	2.99×10^{-8}	0.99

Table1: kinetic parameters for target compounds

Conclusion

This study shows that TCE and ethanol in vapour phase can be rapidly oxidized by solid potassium permanganate. Toluene, however, is degraded much slower. A nonlinear reaction formula simulates results of experiment satisfactory. While, potassium permanganate shows promise for the remediation of TCE and ethanol vapour, further investigation of its applicability for toluene is needed.

Evaluation of Zr in rutile geothermometry for pelitic rocks from the Mica Creek area, British Columbia.

EDWARD D. GHENT[1] DOUGLAS K. TINKHAM[2]

[1]Department of Earth Science, University of Calgary, Calgary, Canada T2N 1N4

ghent@ucalgary.ca *

[2]Department of Earth Sciences, Laurentian University, Sudbury, Canada P3E 2P6

dtinkham1@gmail.com

ABSTRACT

Rutile occurs both as inclusions in garnet crystals and in the matrices of Late Precambrian metapelitic rocks in the Mica Creek area, British Columbia. Zr contents of these rutile crystals have been analyzed by electron microprobe. The Zr detection limit is 25 ppm (20 samples). Metamorphic grade ranges from staurolite-kyanite zone to K-feldspar-sillimanite zone. Temperatures are based upon experimental calibrations. Temperature (T) estimates for rutile inclusions in garnet range from 555 to 705°C (calculated at 7 kbar). T's for groundmass rutile range from <475 to 700°C. There is no apparent correlation of T with the metamorphic grade. In most samples there is no statistical difference between T's from inclusions and T's from matrix rutile. Many of these inclusion T's are simlar to those obtained from garnet-biotite geothermometry. Isopleths for garnet in isochemical phase diagram sections when compared to core garnet compositions yield T's which are much lower than those from Zr geothermometry. The isochemical phase diagram sections also suggest that garnet and rutile are not stable together except at high P-T. T's based upon Zr geothermometry for inclusions appear to be too high for the equilibrium growth of garnet at lower metamorphic grade. A study of Ti in quartz geothermometry for four samples (inclusions in garnet) yielded T's ranging from 417 to 553°C. Zr in rutile has been analyzed on two different microprobes and by laser ablation ICP-MS with consistent results. Other workers have found reasonable correlation between Zr T's and those based upon other methods. For the Mica Creek samples disequilibrium is a possibility but would require metastable growth of rutile with higher Zr contents. Most scenarios would predict T's which are too low rather than too high. Exchange of Zr between garnet and rutile inclusions during subsequent heating does not appear to be plausible. We suggest equilibrium at higher P-T between garnet and rutile inclusions than those suggested from garnet isopleths.

https://doi.org/10.1180/S0026461X00008434 Published online by Cambridge University Press

Fluid-absent melting of Phase D and the role of hydrous melts in the deep mantle

Sujoy Ghosh*[1], Max Schmidt[1]

[1]Dep. Earth Sciences, ETH Zurich, Switzerland, sujoy.ghosh@erdw.ethz.ch; max.schmidt@erdw.ethz.ch

The degree of hydration of and the amount of H_2O released from subducting slabs constrains the recycling and circulation of water in the Earth's interior. Water is transported into the Earth's interior via hydrous phases in descending slabs. Numerous high-pressure studies have determined the stabilities and role of several dense hydrous magnesium silicates (DHMS) at mantle conditions and H_2O-saturated conditions, mostly in MSH-model compositions. Among the DHMS, phase D is the one principally hosting water in the lower part of the transition zone (where slabs may travel along the upper/lower mantle boundary) and carrying H_2O from the upper to the lower mantle. The most likely state of a hydrated slab undergoing prograde metamorphism is that of fluid-absent but H_2O-present conditions at which hydrous phases destabilize through fluid-absent melting at their maximum temperature stability. In the present study, we constrain the fluid-absent melting relations of phase D and of phase D + olivine + enstatite in (i) MgO-SiO_2-H_2O system (ii) with Al_2O_3 and (iii) with Al_2O_3 + FeO added in proportions appropriate for the mantle. Stochiometric oxide mixtures of brucite and quartz of phase D composition were used as starting material. Multianvil experiments were carried out at 22-24 GPa and 1000-1800 ºC using 10/3.5 pressure assemblies.

Our data show that phase D decomposes to MgSi-ilmenite + stishovite + melt or MgSi-perovskite + stishovite + melt and indicate that phase D is stable along a slab geotherm to the top of the lower mantle for a range of H_2O contents. Melting temperatures are ~1400 ºC in the MSH system, 150 ºC higher with Al_2O_3 only, but similar to the MSH system with Al_2O_3+FeO. In all 3 systems, the melting temperature is almost constant with pressure. Melt compositions are strongly magnesian with Mg:Si ratio of 1.5-3.2. Furthermore, mass balance calculations of phase D composition experiments (with Al, Fe) suggest that the unquenchable melts contains ~ 23-32 wt% H_2O at the phase D-out, which fits well with EPMA analysis (difference of total to 100%). The data are used to determine the stability of phase D, the proportions of melt formed during melting, the composition of the partial melts and the variation in the melt composition at different pressure temperature conditions. Most interestingly, thermal relaxation to adiabatic temperatures of a slab traveling along the 660 km discontinuity, would lead to fluid-absent melting of phase D, thus producing a H_2O-rich magnesian melt.

THE PLAGIOCLASE AS ARCHIVE OF MAGMA ASCENT DYNAMICS: THE 2001-2006 ERUPTIVE PERIOD AT MOUNT ETNA

P.P. GIACOMOMI [1*], M. COLTORTI [1], C. FERLITO [2].

[1] Dipertimento di Scienze della Terra, Università di Ferrrara, Italy, pierpaolo.giacomoni@unife.it (* presenting author)

[2]Dipartimento di Scienze Geologiche, Università di Catania, Catania, cferlito@unict.it

ABSTRACT

Several studies are focused on textural and compositional features of plagioclase as an usefull tool to investigate magma chamber processes, ascent dynamics, and physico-chemical conditions. In particular water content, which plays a fundamental role in volcanic process, strongly affects plagioclase stability and, by conseguence, textural and compositional features. However, such reconstruction are usually biased by too many assumptions; particularly when dealing with past eruptions or remote volcanoes. Only few volcanoes provide an array of instrumental monitoring to constrain timing and modality of eruptive events. In this respect Mount Etna probably represents one of the most controlled volcano in the world and a great wealth of seismological and ground deformations data are available. In this work we present a textural and compositional study of plagioclases from lavas emitted during the 2001-2006 eruptive period on Mount Etna. Textural classification has been done on over 130 thin sections taking into account different portion of the crystals. This allow to recognize different types of core (ehuedral and rounded) and rims (dusty or with melt inclusion alignment) separated by oscillatory zoned overgrowth.

Oxygen fugacity in magmas has been calculated using the method of [1] and results has been used to reequilibrate the melts to mantle equilibrium, adding back the appropriate quantity of fractionated material. Water content of the melt has been estimated using the hygrometer of [2]. These data were used in the MELT model to estimate the plagioclase stability field and to calculate theoretic composition at different water content. Results were integrated with monitoring data acquired during the entire period under study with the aim to reconstruct magma ascent and storage conditions, as well as the mechanism of eruption triggering. Results indicate the 2001-2006 eruptive period involved magmas with quite similar major element composition but different dissolved H_2O. Complex zoning such as dusty areas and alignments of melt inclusions in outer portion of the phenocrysts suggest two different trigger mechanism respectively: i) magma input and mixing with a more basic and volatile-rich magma; ii) fracture migration that induce decompression of shallow magma batches.

[1] France et a., (2010) *A new method to estimate the oxidation state of basaltic series from microprobe analyses* **Journal of Volcanology and Geothermal Research 189**, 340-346.
[2] Lange et al., (2009) *A thermodynamic model for the plagioclase-liquid hygrometer/thermometer* **American Mineralogist 94**, 494-506.

https://doi.org/10.1180/S0026461X00008434 Published online by Cambridge University Press

Rates and mechanisms of lead(IV) oxide reductive dissolution

DANIEL E. GIAMMAR* AND YIN WANGAUTHOR

Washington University, Department of Energy, Environmental and Chemical Engineering, St. Louis, MO, USA, giammar@wustl.edu (* presenting author), yinwang@go.wustl.edu

The Pb(IV) oxides plattnerite (β-PbO_2) and scrutinyite (α-PbO_2) have very low solubility, but they can undergo reductive dissolution and release more soluble Pb(II). While PbO_2 solids are not common in nature, they can form in the presence of oxidants used for water disinfection and play a significant role in controlling lead concentrations in drinking water conveyed through lead pipes. Because PbO_2 is not stable in the absence of a strong oxidant, the dissolved Pb(II) concentrations achieved are governed by the kinectics and not the equilibrium of the dissolution reaction. The reductive dissolution of PbO_2 can be interpreted as a coupled process involving chemical reduction of Pb(IV) to Pb(II) at the PbO_2 surface followed by detachment of Pb(II) to solution.

The dissolution rates of plattnerite were measured as a function of water chemistry in continuously-stirred tank reactors that prevented the accumulation of reaction products and formation of secondary Pb(II) solids. Reaction rates were measured as functions of pH, a strong oxidant (hypochlorite) that might inhibit reductive dissolution, a reductant (iodide) that could accelerate the reduction of Pb(IV) to Pb(II), and a ligand (carbonate) with a high affinity for the Pb(II) formed during reduction.

PbO_2 is such a strong oxidant that soluble Pb(II) is produced even when water is the only possible reducant. The presence of hypochlorite at concentrations used in drinking water distribution systems strongly inhibited Pb release. The addition of iodide dramatically accelerated the dissolution of PbO_2 by driving the reduction of Pb(IV) to Pb(II) at the solid-water interface. The addition of dissolved inorganic carbon (DIC) to previously carbonate-free systems increased dissolution rates by facilitating the desorption of Pb(II) from the PbO_2 surface; however, once some DIC was present the dissolution rate was insensitive to further increases. The dissolution rate was higher at low pH, which could have been cuased by its effect on the overall electrochemical driving force for PbO_2 dissolution, impact on the kinetics of a rate limiting step, and control of iodide adsorption and Pb(II) desorption. A kinetic model similar to those used for the reductive dissolution of other metal oxides (i.e., iron and manganese oxides) was successfully fit to the experimental data. The data suggest that chemical reduction is the rate-limiting step for PbO_2 dissolution in the presence of iodide.

The reductive dissolution of PbO_2 present as a corrosion product on lead pipes can produce lead concentrations that exceed drinking water standards. Such reductive dissolution can occur for drinking water systems that switch their secondary disinfectant from hypochlorite to a weaker oxidant such as chloramines. While iodide was chosen in the present study as a model reductant, the reductive dissolution mechanism will likely be similar for natural organic matter, Fe(II), and Mn(II), which are more common reductants found in drinking water.

Isotopic evidence for sea ice and brine formation in the northern Labrador Sea at the terminations of Heinrich Events 1 and 2.

O. GIBB[1*], C. HILLAIRE-MARCEL[1], A. DE VERNAL

[1]GEOTOP-UQAM, Montreal, Canada, oliviagibb@gmail.com*

Reconstructions of sea surface conditions in the Northern Labrador Sea (HU2008-029-004PC) have been created using dinoflagellate cyst assemblages for the last ~35 cal ka BP. They demonstrate that the temperatures were near freezing, the salinity below 31, and the area was under close to permanent ice cover. There were however occurrences of the planktonic foraminifera *Neogloboquadrina pachyderma* sinistral (Npl). Since Npl requires salinity above 34 (e.g., [1]), its growth had to occur either deeper in the water column, if suitable salinities prevailed, or more likely, in brine canals in the sea-ice itself, as it does in modern sea-ice environments [2]. Similarly to previous studies (e.g., [3]), an isotopic shift of -2.5‰ occurs between the beginning and end of Heinrich Event 1 (H1), and a less dramatic -1‰ shift during H2. These light isotope excursions would typically be acknowledged as low-salinity pulses and higher sea surface temperatures. However the dinocyst data indicates this was not the case. As demonstrated by Hillaire-Marcel and de Vernal [4], the light $\delta^{18}O$ excursions are an effect of the foraminifera forming in isotopically light brines during sea ice formation. Perennial sea ice cover inferred from particularly low production of dinocysts occurred toward the end of the Heinrich events, concurrently with high abundance of ice rafted debris and Npl.

[1] Hilbrecht, H., 1996. Technischen Hochschule und der Universität Zürich, Neue Folge, p. 300 (93 pp., Zürich).
[2] Spindler, M., (1996). *Polar Biology* **9**, 85-91.
[3] Hillaire-Marcel, C. and de Vernal, A. (2008). *Earth and Planetary Science Letters* **268**, 143-150.
[4] Hillaire-Marcel, C., de Vernal, A., Bilodeau, G., Wu, G. (1994). *Canadian Journal of Earth Sciences* **31**, 63-89.

https://doi.org/10.1180/S0026461X00008434 Published online by Cambridge University Press

Application of X-ray absorption spectroscopy to characterize metal(loid) removal in passive treatment systems

BLAIR D. GIBSON[1*], MATTHEW B.J. LINDSAY[2], CAROL J. PTACEK[1], AND DAVID W. BLOWES[1]

[1]Earth and Environmental Sciences, University of Waterloo, Waterloo, ON, Canada, bgibson@uwaterloo.ca (* presenting author), ptacek@uwaterloo.ca, blowes@uwaterloo.ca

[2]Present Address: Earth and Ocean Sciences, University of British Columbia, Vancouver, BC, Canada, mlindsay@eos.ubc.ca

Introduction

Monitoring of the relative changes in dissolved metal concentrations and aqueous speciation modeling frequently are employed to evaluate the effectiveness of passive treatment systems for metal(loid) removal in mining environments. However, these methods do not provide mechanistic information on metal(loid) removal. Synchrotron-based X-ray absorption spectroscopy can provide information regarding the oxidation state and local coordination environment of the metal(loid) of interest on the reactive media, which can be used to determine if the metal(loid) removal mechanism involves sorption, oxidation/reduction, or precipitation reactions. This information is important for assessing treatment efficacy and the long-term stability of reaction products.

In this study, batch experiments were employed to evaluate the efficacy of different types of reactive media to induce removal of aqueous Se and Hg. For the Se experiments, 300 mg L^{-1} aqueous Se(VI) (from Na_2SeO_4) was allowed to react with granular Fe filings (GIF) and an organic carbon (OC) mixture consisting of a 1:1 (w/w) ratio of wood chips and crushed leaf mulch. For Hg, 4 mg L^{-1} aqueous Hg(II) (from $HgCl_2$) was allowed to react with GIF, granular activated carbon (GAC), attapulgite clay, and attapulgite clay pre-treated with two types of thiadiazole compounds [1]. Dissolved concentrations of Se and Hg were monitored over time, and X-ray absorption near edge structure (XANES) and extended X-ray absorption fine structure (EXAFS) spectroscopy methods were used to characterize the forms of metal(loid)s on the reactive media.

Results and Conclusion

After 5 days of reaction, Se(VI) removal was observed to be >90% in the presence of GIF and 15% with OC. Analysis with XANES spectroscopy suggested that removal in the presence of GIF was due to reduction of Se(VI) to insoluble Se(0), whereas removal with OC was due primarily to sorption of Se(VI). For Hg, treatment efficiency varied between the reactive media, ranging from 25% removal on untreated clay after 8 days of reaction to >99% removal on clay treated with 2,5-dimercapto-1,3,4-thiadiazole. Analysis with EXAFS spectroscopy indicated the presence of Hg-O bonding on GIF and GAC, suggesting Hg removal was due to binding with Fe corrosion products or to water sorbed to the surface of activated carbon. The presence of Hg-S bonding was observed in the presence of thiadiazole compounds, suggesting Hg was bound to thiol-functional groups on these compounds.

[1] Gibson *et al.* (2011), *Environ. Sci. Technol.* **45**, 10415-10421.

The mid-Cretaceous Canadian Cordillera: Paired orogenic belts or an Altiplano-esque Plateau deflated by deep crustal flow?

GIBSON, H.D.[1]*

[1]Simon Fraser University, Dept. Earth Sciences, Burnaby, Canada, hdgibson@sfu.ca (* presenting author)

The current configuration of the central and southern Canadian Cordillera clearly shows a pairing of highstanding orogenic welts, the Coast belt to the west and the Omineca belt to the east, separated by the intervening subdued topography of the Intermontane belt. How closely this reflects the Meoszoic orogenic architecture for the southern Canadian Cordillera is debatable, but it does bring to mind some important questions regarding the orogenic processes that shaped the southern Canadian Cordillera.

The last major orogen-wide compressional event within the southern Canadian Cordillera occurred in the mid- to Late Cretaceous time, coinciding with the final closure of a marginal basin and attendant accretion of the Insular terranes. Plutons, contractional deformation and high-grade metamorphism that attest to this orogenic event are most obviously manifest in the southern Coast and Omineca belts, and provide evidence for crustal thicknesses on the order of 55-65 km, similar to the average thickness of the Altiplano plateau. So, was there a continuous, high-standing (~4-5 km above sea level) plateau across the width of the southern Canadian Cordillera, or was there an intervening low-lying area of subdued topography much like there is today, which might suggest a paired-system of orogenic belts inherited from Mesozoic orogeny? If so, how would such a system operate?

The displacement along Paleogene strike-slip faults needs to be restored in order to assess the mid- to Late Cretaceous crustal architecture of the southern Canadian Cordillera. This places the Bowser basin in the intervening region with subdued topography whose crustal thickness was on the order of 40-45 km, compared to the flanking 55-65 km welts on either side of it. This implies that the crustal architecture for the mid- to Late Cretaceous time was dumb-bell shaped in cross-section, akin to lithospheric-scale boudinage. The flanking welts would represent paired-orogenic belts characterized by thick-skinned deformation, high-grade metamorphism, anatectic melting and plutonism that were separated by the Bowser basin with its classic thin-skinned Skeena fold and thrust belt. How did the stress that was driving the Coast belt orogen nearest the convergent margin transfer to the east across the width of the orogen to drive the thick-skinned deformation and substantial crustal thickening within the Omineca belt without similarly affecting the intervening crust within the Intermontane belt?

Alternatively, could there have been an Altiplano-style plateau spanning the width of the southern Canadian Cordillera? If so, could the apparent thinning of the crust within the central part of the plateau have been the result of deflation related to general non-coaxial flow within its deepest levels? In this scenario, the general non-coaxial flow, which would include a significant flattening component, effectively evacuated material out from beneath the plateau, perhaps accentuating thickening on its flanks, leaving the appearance of the paired-orogenic belts we see today.

https://doi.org/10.1180/S0026461X00008434 Published online by Cambridge University Press

Hydrogeochemical setting of the Northern Athabasca Oil Sands area

J.J. GIBSON[1,2*], Y. YI[1,2], S.J. BIRKS[1,2], M.C. MONCUR[1], J.W. FENNELL[3], K.TATTRIE[1]

[1]Integrated Water Management, Alberta Innovates-Technology Futures, Victoria & Calgary, Canada, john.gibson@albertainnovates.ca (*presenting author)
[2]University of Victoria, Victoria, Canada, jjgibson@uvic.ca.
[3]Worley Parsons, Calgary, Canada, jon.fennell@worleyparsons.com.

Introduction

The oil sands of Northern Alberta represents an important oil reserve for Canada and the world. These vast hydrocarbon deposits have been exposed to the surface via long-term erosion by the Athabasca River and its tributaries. This geological evolution has led to a complex hydrogeological system, which features numerous pathways connecting the surface and subsurface hydrologic systems. Here, we present a study based on data and information collected from several river sampling campaigns along the main channel of the Athabasca River, including geochemical and isotopic signatures in formation water, that shed light on the natural hydrogeological setting of the Northern Athabaca Oil Sands Area.

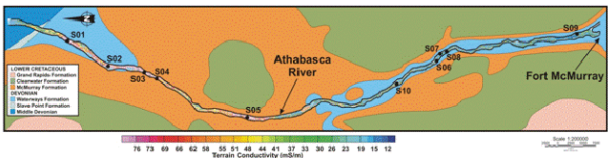

Figure 1: Terrain electrical conductivity of a 125-km reach of the Athabasca River from Fort McMurray to the Firebag River overlain on a map of bedrock geology. Zones of elevated terrain conductivities indicate potential connections between surface water and groundwater, and these areas were targeted for groundwater sampling for a full suite of geochemical and isotopic analyses to characterize and trace the origin and evolution of groundwater discharging to the river.

Results and Discussion

Electrical conductivity surveys reveal large areas with elevated conductivity, reflecting both variation in geologic substrate (e.g. evaporites), as well as variable salinity of inflowing waters in seeps and an array of groundwater springs. The geochemical and isotopic composition of these groundwater inflows are similar to those found in the McMurray Formation and Devonian Formation waters. The distribution of the seep geochemistry and some of the bulk river chemistry are related to changes in geology along the reach of the Athabasca River studied. The results of this investigation provide insight into the geochemical and isotopic evolution of riverine water quality, specifically the significant influence of natural groundwater sources of salinity and organics to the Athabasca River.

Assessing the health effects of atmospheric particulate matter

RETO GIERÉ[1]

[1] Universität Freiburg, Geowissenschaften, 79104 Freiburg, Germany (giere@uni-freiburg.de)

Atmospheric particulate matter (PM) is ubiquitous in the atmosphere and is generated in various environments through natural processes and human activity. Individual particles display a wide range of physical, chemical, structural and surface properties, which depend on source, chemical reactions, and transport under variable atmospheric conditions [1]. Several epidemiological and toxicological investigations have linked airborne PM with adverse effects on human health, both acute and chronic. Effects associated with PM exposure include chronic obstructive pulmonary disease (COPD), exacerbation of asthma, fibrosis, slower lung development in children, and lung cancer, but also an increase in cardiovascular diseases [2]. The inhaled fine particles ($PM_{2.5}$) can migrate to the alveoli in the deep lung, where they remain for long periods of time and interact with lung fluid and tissue. The deepest part of the lungs, thus, acts a special type of active sampler for atmospheric dust. The finest PM fraction may translocate to epithelial and interstitial sites and possibly to extrapulmonary organs. Inhaled coarse particles, on the other hand, are retained in the upper part of the respiratory tract, but there is increasing evidence that coarse particles may also produce adverse health effects [3].

Within the lung, the inhaled PM interacts with lung fluid and tissue, stimulating various types of biological and biochemical responses (e.g., immune defense reactions, inflammation, cytokine release). These reactions to external stimuli are still poorly investigated, and their relationship with, and dependence on, specific PM properties are largely unknown. To improve our knowledge on the health effects of PM, a close collaboration between diverse scientific disciplines is crucial. Moreover, it is essential to characterize single particles in detail in order to perform meaningful experiments designed to improve our currently poor knowledge on the interaction between atmospheric PM and the respiratory tract.

This presentation will discuss various approaches to assessing the health impacts of PM. It will describe experimental results obtained from *in-vitro* stimulation of lung cells with diverse types of PM, which have been found to be present in ambient air (magnetite, black toner dust, various metal sulfates, and tire-wear particles). This presentation will also report results from investigations on lung tissue samples and brochoalveolar lavage (BAL) fluids.

[1] Gieré & Querol (2010) *Elements* **6**, 215-222. [2] Pope et al. (2009) *New Engl J Med* **360**, 376-386. [3] Brunekreef & Frosberg (2005) *Eur Resp J* **26**, 309-318.

https://doi.org/10.1180/S0026461X00008434 Published online by Cambridge University Press

Schwertmannite formation in acid mine drainage in NE Viet Nam

RETO GIERÉ[1*], THI BICH HOÀNG-HÒA[1], RAUL E. MARTINEZ[1], AND RICHARD WIRTH[2]

[1] Universität Freiburg, Geowissenschaften, 79104 Freiburg, Germany (giere@uni-freiburg.de)

[2] GeoForschungsZentrum Potsdam, Section 4.1, Telegrafenberg C120, 14473 Potsdam, Germany

The province of Quang Ninh in northeastern Viet Nam is one of the largest coal mining districts of the country, hosting reserves estimated at 10 Gt. The coal is mostly anthracite and is mined both in open pits and underground. This study focuses on acid mine drainage from the Coc Sau open-pit mine near the town of Cam Pha. The mine is approximately 3 km in diameter and has an orange-colored lake in the center, which drains through a tunnel into a creek. After flowing for ~4 km through the densely populated town, the acid mine waters discharge into the ocean.

The drainage waters have a pH of 2.4±0.4, a temperature of 30.3 ºC, and an Eh of 0.63±0.02 V under normal conditions, but after major rain storms the pH may be as high as 7.2±0.1, with an associated Eh of 0.29±0.05 V. The low-pH water contains the following major components (in mg/L): Fe = 46±18, SO_4^{2-} = 850±100, Al = 7±2, Mg = 76±3, and Ca = 66±18.

The creek bed and the contained pebbles are covered by a bright orange crust. This crust consists primarily of schwertmannite, quartz and sheet silicates (mostly kaolinite and illite) in the outer, highly porous part, whereas the inner part, directly on the substrate, consists of mostly ferrihydrite and sheet silicates. Scanning electron microscopy revealed the typical appearance of schwertmannite, i.e. small (usually <1µm across), spherical to ellipsoidal aggregates resembling sea urchins, and further suggested that schwertmannite also forms crusts on, and is intergrown with, sheet silicates. This suggestion was corroborated by transmission electron microscopy, which has shown that the schwertmannite aggregates in many cases contain a core of sheet silicate. Selected area electron diffraction allowed for unequivocal identification of schwertmannite, but the typical needle-like features (~200 nm long) are in many cases amorphous and therefore not whiskers.

In order to construct an Eh-pH diagram showing the stability fields for schwertmannite and ferrihydrite, we calculated the activity of the major chemical components using the extended Debye-Hückel equation. The ionic strength of the system (I = 0.016 M) was computed from the water conductivity [1]. Based on the available thermodynamic data, including a logK_{sp} value of 1.2±0.5 for schwertmannite with the ideal formula $FeO(OH)_{3/4}(SO_4)_{1/8}$ [2], a plot of Eh *vs.* pH was generated showing a schwertmannite field that is consistent with the observed conditions of our low-pH water samples. The diagram also coincides with an Eh-pH diagram constructed with a logK_{sp} of 0.88±0.01 for schwertmannite with the formula corresponding to $FeO(OH)_{0.738}(SO_4)_{0.131}$ [3].

At present, we do not understand yet, why the innermost part of the crust, directly on the substrate, consists mostly of ferrihydrite.

[1] Dittrich *et al.* (2004) *Geomicrobiol J* **21**, 45-53, 2004. [2] Majzlan *et al.* (2004) *Geochim Cosmochim Acta* **68**, 1049-1059. [3] Kawano and Tomita (2001) *Am Mineral* **86**, 1156-1165.

Structural and chemical studies of the pyrite (001) surface

B. GILBERT[1,*], P. J. ENG[2], D. SINGER[1], J. F. BANFIELD[3] AND G. A. WAYCHUNAS[1]

[1]Lawrence Berkeley National Laboratory, Earth Sciences Division, Berkeley, USA, bgilbert@lbl.gov, gawaychunas@lbl.gov. (* presenting author)

[2]University of Chicago, Chicago, USA, eng@cars.uchicago.edu

[3]University of California – Berkeley, Dept. Earth & Planetary Science, Berkeley, USA, jbanfield@berkeley.edu.

Pyrite, FeS_2, is a widespread and important sulfide mineral. Pyrite is thermodynamically stable under reducing conditions and in saturated sediments provides surfaces for the adsorption of aqueous species. When exposed to oxidizing environments, for example through mining activities, pyrite oxidation leads to the generation of low pH solutions termed acid mine drainage (AMD). The impact of AMD on environmental health is a global concern.

Detailed understanding of the reactivity of pyrite surfaces requires knowledge of their atomic structure under relevant conditions. Many groups have studied the surface chemistry of pristine and oxidized pyrite surfaces but the structure of a hydrated surface has never been experimentally determined. We have employed the crystal truncation rod (CTR) method and complementary surface-sensitive techniques in order to determine the structure of the water—pyrite (001) interface and to establish how adsorbates interact with this surface.

We developed an anaerobic chemical–mechanical polishing method that creates low-roughness pyrite (001) surfaces shown by atomic force microscopy (AFM) to be dominated by irregularly shaped (001) terraces. We studied the structure of the hydrated pyrite (001) surface using the CTR method, obtaining reproducible results from three crystals. Optimal fitting of the CTR data requires the incorporation of two structurally distinct termination surfaces that differ in the coverage, and likely the chemical speciation, of surface sulfur atoms. In each case, surface iron atoms and disulfur groups are significantly displaced from bulk positions.

The adsorption of aqueous metal ions provides a complementary approach for assessing the chemical speciation of sites on the (001) surface. We observed modulation in the CTR scattering patterns following exposure to Fe^{3+} and Pb^{2+} ions, confirming that the termination surface is accessible and chemically reactive. Grazing incidence extended X-ray absorption fine structure (EXAFS) studies of surface-adsorbed Pb^{2+} revealed at least two near-neighbor distances consistent with a fraction of lead atoms adsorbing via inner-shell interactions with surface sulfur sites.

https://doi.org/10.1180/S0026461X00008434 Published online by Cambridge University Press

Sorption of Cr(VI) on Mineral Assemblages of Goethite with Clays and Al-Oxides

ANN M.GILCHRIST[1*], CARLA M. KORETSKY[1]

[1]Western Michigan University, Kalamazoo, MI, USA
ann.m.gilchrist@wmich.edu (* presenting author)

Anthropogenic activities have caused toxic Cr(VI) contamination of many natural systems. Cr(VI) travels readily in aqueous solution but can be impeded by sorption by reactions with Fe-bearing solids. Subsurfaces are not homogeneous, yet most surface complexation models (SCM) are developed for simple, single substrate systems, and do not account for mineral-mineral interactions. The goal of this study is to measure sorption of Cr(VI) on mineral assemblages of goethite, kaolinite, montmorillonite, γ-alumina, hydrous manganese oxide (HMO), and hydrous ferric oxide (HFO) as a function of pH and pCO_2, and to compare measurements to predictions from SCMs developed for single solid systems.

Goethite was synthesized by heating a mixture of KOH and $Fe(NO_3)_3 \cdot 9$ H2O at 70°C for 60 hours [1]; montmorillonite (SWy-2) and kaolinite (KGa-1b) were obtained from the Clay Minerals Society; γ-alumina (γ-Al_2O_3) was purchased from Inframat Advanced Materials; HMO was synthesized by alkametric titration [2] and 2-line HFO was synthesized according to [1]. Synthesized solids were confirmed by XRD and surface area measurements of all solids were completed using 11-point N_2BET analysis.

Adsorption edges were measured over a pH of 3.5 to 10, in open atmosphere or under 0% pCO_2. Binary mixtures of solids were used based on equal surface area (~5 g/L total solid) with 10^{-5} M Cr(VI) and 0.01 M $NaNO_3$. Batch slurries of Cr(VI), $NaNO_3$, and solids were equilibrated for ~1 hr at circumneutral pH. The pH was then lowered to 3.5 by addition of HNO_3, and then titrated upward with removal of ~60 mL aliquots of slurry at each ~0.5 pH increment. After 24 hr, 48 hr, 1 week and 2 weeks of mixing, ~15 mL of slurry was removed from each aliquot and the pH rechecked. Each slurry sample was centrifuged, the supernatant syringe-filtered (0.45 μm) and tested for Cr(VI) using the diphenylcarbazide method.

In all systems containing goethite sorption is near 100% below pH ~6. The sorption edge spans from 6-9 pH with <10% Cr(VI) sorbed at pH >9. The pH at which 50% of Cr(VI) is sorbed is ~6.8 for goethite-montmorillonite and increases to ~7.1 for goethite-kaolinite and ~7.7 for goethite-γ-alumina. Edges for the goethite-clay mixtures appear to be dominated by sorption on goethite, whereas mixtures of goethite and γ-alumina result in edges that are intermediate between those obtained for the pure end-member solids; this will also be assessed using component additivity surface complexation modeling.

Adsorption is rapid for goethite-montmorillonite, goethite-γ-alumina and goethite-kaolinite combinations with little change in sorption with increasing aging from 24 hrs to 2 weeks. All systems exhibit little variation in sorption under atmospheric compared to 0% pCO_2 conditions.

[1] Schwertmann & Cornell (1991) *Iron Oxides in the Laboratory,* Wiley-VCH, 604 pp.

[2] Stroes-Gascoyne, Kramer & Snodgrass (1987) Applied Geochemistry 2, 217-226.

Noble gas and C stable isotopes quash fears over CO_2 storage leaks at Weyburn

STUART GILFILLAN[1*], R. STUART HASZELDINE[1], GEORGE SHERK[2], AND ROBERT POREDA[3]

[1]Scottish Carbon Capture and Storage, University of Edinburgh, UK. stuart.gilfillan@ed.ac.uk (*presenting author:)
[2]International Performance Assessment Centre for Geologic Storage of CO_2 (IPAC-CO_2), Regina, Saskatchewan, Canada.
[3]Department of Earth and Environmental Sciences, University of Rochester, New York, USA.

In January 2011 it was extensively reported that the Kerr family had been forced to move from their property located above the Weyburn-Midale Monitoring and Storage Project in Saskatchewan, Canada. A geochemical consultant from Petro-Find GeoChem Ltd., who was hired on behalf of the Kerr's, reported measurements of $\delta^{13}C$ (CO_2) isotope values in soil gases rich in CO_2 which were similar to those of the CO_2 injected into the deep oil reservoir. The Petroleum Technology Research Centre (PTRC), who are responsible for the environmental monitoring of the Weyburn CO_2-EOR and storage operation, published a detailed response correctly stating that Petrofind had not taken the similar baseline $\delta^{13}C$ (CO_2) isotope measurements conducted prior to the injection into account. Also as $\delta^{13}C$ (CO_2) is not a unique tracer, there were several other natural sources that could account for the measured values. Whilst this response went some way to addressing the public perception fears raised by the alleged CO_2 leakage claims, it was clear that more research was required to re-establish confidence in the safety and security of CO_2 stored at Weyburn. This was imperative for both the project itself and the future of CO_2 storage. IPAC-CO_2 undertook a detailed independent incident response protocol focused on the near surface soil gases, the noble gas composition of the shallow groundwaters and a hydrogeological analysis.

Noble gases are extremely powerful tracers of source and the subsurface processes that act on CO_2. They have recently proved to be effective at tracing the migration of natural mantle derived deep CO_2 up a fault above the St. Johns Dome-Springerville CO_2 reservoir in Arizona [1]. A clear component of the helium fingerprint observed in the gaseous CO_2 contained in the deep reservoir could be traced in waters from both the groundwater wells and the springs emerging at the surface above the reservoir.

Here we use similar methodology to investigate the alleged leakage and we report noble gas and carbon stable isotope measurements from four groundwater wells surrounding the Kerr quarter, near Goodwater in Saskatchewan. We compare these to the noble gas and carbon isotope composition measured from fluids sampled from a production well and CO_2 and water from enhanced oil recovery injection wells associated with the Weyburn-Midale oil field, located near to the Kerr quarter. To determine if migration of dissolved CO_2 from the Weyburn oil field is responsible for the alleged CO_2 anomaly, we compare the noble gas and carbon stable isotope tracers in the water and CO_2 injected into the oil field, and the fluids produced from the field, with those measured in the groundwater well waters.

We find no evidence in any of the noble gas data that there is any presence of deep crustal derived noble gases within the groundwaters surrounding the Kerr quarter. The absence of crustal derived noble gases derived from depth means that there is no evidence of the migration of CO_2 from the Weyburn oil field into the groundwater on the Kerr quarter or surrounding area.

[1] Gilfillan et al., (2011) *IJGCC*, **Volume 5**, Issue 6, p 1507-1516

https://doi.org/10.1180/S0026461X00008434 Published online by Cambridge University Press

Sulfur cycling in shallow-sea hydrothermal vents, Milos Greece

WILLIAM P. GILHOOLY III[1*], DAVID FIKE[2], JAN AMEND[3], GREG DRUSCHEL[1] AND ROY PRICE[3]

[1]Dept. of Earth Sciences, Indiana University-Purdue University Indianapolis, Indianapolis, USA, wgilhool@iupui.edu (* presenting author); gdrusche@iupui.edu

[2]Dept. of Earth and Planetary Sciences, Washington University in St. Louis, St. Louis, USA, dfike@levee.wustl.edu

[3]Earth Sciences and Biological Sciences, University of Southern California, Los Angeles, USA, janamend@usc.edu; royprice@usc.edu

Milos is a volcanic island positioned along the Southern Aegean Volcanic Arc. Shallow-sea (5 m) hydrothermal venting is extensive throughout our study area, Paleochori Bay. Pore fluids exibit elevated temperatures (115°C), acidic conditions (pH 5), dissolved sulfide (3 mM), and either dilute or elevated chloride (1.5x Mediterranean seawater). The shallow hydrothermal vents offered an ideal opportunity to target microbial processes that presumably transition from sulfide delivered with volcanic gases to sulfide produced by dissimilatory sulfate reduction in background sediments. Seafloor vent features include large (> 1 m^2) white biofilms containing elemental sulfur and orange/yellow patches of arsenic-sulfides. We investigated three patches of colored seafloor, a non-vent area as a control site, and a brine. Pore waters, push-cores, surface films, and water column samples were collected by SCUBA from seafloor patches and background sediments. One goal of the study was to measure $\delta^{34}S$ spatial variability along environmental gradients that included volcanic vents and 'normal' ocean bottom.

We observed strong geochemical spatial patterns across each patch of colored seafloor. Temperature profiles within the upper 20 cm of the sediments ranged 35 to 111°C. Pore water sulfate concentrations (ranging 8 to 25 mM) and $\delta^{34}S$ values (ranging +17.5‰ to +21.4‰), show a clear decrease toward the center of each hydrothermal feature that coincided with maximum measured temperatures. We interpret the inverse relationship between temperature and sulfate $\delta^{34}S$ as a mixing process between oxic seawater and anoxic magmatic inputs. To better constrain this relationship, we collected endmember samples of seawater and vent gas sulfide. The $\delta^{34}S$ values of pore water sulfate extracted from low temperature (< 60°C) sediments along the fringe of the patches were identical to seawater ($\delta^{34}S$ = +21‰). In contrast, hydrogen sulfide in the free gas sampled from all study sites had uniform values, $\delta^{34}S$ = +2.5 ± 0.28‰ (n = 4) that were nearly identical to pore water sulfide, $\delta^{34}S$ = +2.7 ± 0.36‰ (n = 21). The relationship between the isotopic composition of dissolved sulfur species suggests the oxidation of dissolved sulfide by the entrainment of oxic seawater potentially mixed an isotopically light pool of secondary sulfate with the ambient pore water sulfate pool. An isotopic mass balance model demonstrates that the data plot along a conservative mixing array between seawater and a chloride rich, sulfidic fluid. Any biological sulfur cycling potentially operating within these hydrothermal systems is masked by abiotic chemical reactions.

INTERPRETING THE TRACE METAL RECORDS OF ANCIENT EPEIRIC SEAWAYS: LESSONS FROM THE TOARCIAN (JURASSIC) BLACK SHALES OF EUROPE

BENJAMIN C. GILL[1]*, TIMOTHY W. LYONS[2], JEREMY D. OWENS[2], STEVEN BATES[2], HANS-JÜRGEN BRUMSACK[3], HUGH C. JENKYNS[4]

[1]Department of Geosciences,Virginia Polytechnic Institute and State University, VA, USA, bcgill@vt.edu (* presenting author)

[2]Department of Earth Sciences, University of California-Riverside, CA, USA

[3]ICBM, Oldenburg University, Germany

[4]Department of Earth Sciences, University of Oxford, UK

There is an ongoing discussion concerning the global-versus-local origins of trace metal records expressed in sedimentary successions from ancient epicontinental (epeiric) seaways. Properly deciphering these records is of considerable importance because they factor prominently in our understanding of the redox history of the Earth surface environment. Particularly useful and contentious examples of this debate are the black shales deposited in the north European epicontinental seaway (NEES) during the Toarcian Stage of the Early Jurassic. Despite the fact that these marine shales are extremely rich in organic matter and sedimentary sulfides, some show little to no enrichment beyond crustal abundances of many redox-sensitive elements (e.g., Cu, Mo, Ni, V, Zn, U). As these organic-rich rocks have been linked to an interval of widespread marine anoxia/euxinia — the Toarcian Oceanic Anoxic Event (T-OAE) — the muted enrichments have consequently been purported to reflect diminished global seawater inventories of these elements. Conversely, some workers attribute the lack of trace metal enrichment to restriction of the seaway from the open ocean.

In this study, we present a variety of geochemical data from various locations in the northern Europe to explore the character of the Toarcian trace metal record. High-resolution stratigraphic iron and sulfur redox proxy data from within the seaway (Fe/Al, Fe_{HR}/Fe_{total}, Fe_{py}/Fe_{HR}, $\delta^{34}S_{pyrite}$) reveal variable redox conditions and also suggest hydrographic restriction of the seaway, both of which likely played roles in the trace metal depletions. Furthermore, the trace metals records show higher enrichments at locations more proximal to the open ocean, also pointing to restriction within the NEES. However, all the study localities record a temporal pattern of subdued metal enrichment and rates of metal accumulation, which together suggest a global marine depletion during the OAE. Perhaps not surprisingly, therefore, ancient trace metal records of organic-rich rocks contain both global and local features, which can be deciphered through careful integration of parallel geochemical and sedimentological data.

https://doi.org/10.1180/S0026461X00008434 Published online by Cambridge University Press

Variability of ^{13}C-^{14}C in soil CO_2: Impact on ^{14}C groundwater ages

MARINA GILLON[1,2*], FLORENT BARBECOT[2], ELISABETH GIBERT[2], CAROLINE PLAIN[3], JOSÉ ANTONIO CORCHO ALVARADO[4], AND MARC MASSAULT[2]

[1]UMR UAPV-INRA 1114 EMMAH, Avignon, France, marina.gillon@univ-avignon.fr (*presenting author)
[2]UMR CNRS-UPS 8148 IDES, Orsay, France, florent.barbecot@u-psud.fr, elisabeth.gibert@u-psud.fr, marc.massault@u-psud.fr
[3]UMR UL-INRA 1137 EEF, Nancy, France, plain@nancy.inra.fr
[4]Institute of Radiation Physics, University Hospital and University of Lausanne, Lausanne, Switzerland, Jose.Corcho@chuv.ch

The ^{14}C age correction models for groundwater use generally an input function that depends on the carbon isotopic composition (^{13}C and ^{14}C) of the soil CO_2. However, in most cases the activity ($A^{14}C$) of atmospheric CO_2 is directly used as input function without considering processes occurring in soil and leading to significant isotopic changes between the composition of atmospheric CO_2 and of soil CO_2 [1][2]. We present here the role of these processes as well as the associated isotopic changes and their impact on the calculation of the age of groundwater. Our approach is based on the use of experimental data from two sites (Fontainebleau sands and Astian sands, France) and its interpretation by a distributed model [3].

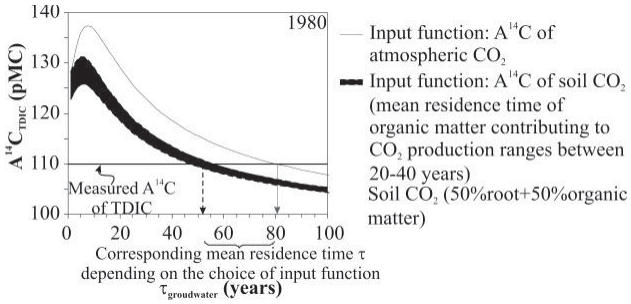

Figure 1: Calculated mean ages of groundwater with respect to different input function; case of a theoretical sampling in 1980.

Since 1950, the evolution of the $A^{14}C$ in soil CO_2 reflects the competition between the fluxes of root derived-CO_2 and organic matter derived-CO_2 due to the residence times of organic matter in the soil. We demonstrate that a mean ^{14}C groundwater age based purely on the ^{14}C atmospheric data may lead to significant biases [2]. For example, a measured $A^{14}C$ of 110 pMC in 1980 corresponds to a mean age of 50±5 or 80±2 y depending on the choice of the input function (Fig. 1). Moreover, the analytical $\delta^{13}C$ of soil CO_2 showed large seasonal variations. Therefore, for dating modern groundwater, a systematic sampling of soil CO_2 has to be integrated into numerical simulations to define ^{13}C-^{14}C content at the water table [4].

[1] Fontes (1992) *Radiocarbon After Four Decades*, 242-261; [2] Gillon et al. (2009), *Geochim. Cosmochim. Acta* **73**, 6488-6501; [3] Gillon et al., *geoderma*, in revision; [4] Gillon (2008), Ph. D. Thesis, Paris Sud XI Univ., France.

What we do and don't know about microbial mercury methylation

CYNTHIA C. GILMOUR[1*], JUDY WALL[2], REMY GUYONEAUD[3] AND DWAYNE ELIAS[4]

[1]Smithsonian Environmental Research Center, gilmourc@si.edu
[2]University of Missouri, Biochemistry Division, wallJ@missouri.edu
[3]UMR IPREM 5254, Universite de Pau, remy.guyoneaud@univ-pau.fr
[4]Oak Ridge National Laboratory Biosciences Division, eliasda@ornl.gov

More than 40 years after the discovery of the Hg methylation process in sediments, we still don't know why some bacteria are capable of methylmercury (MeHg) production and others are not. This paper will present an overview of our understanding of those processes, taken from the recent literature and ongoing research in our groups.

The intimate and complex relationship between mercury and sulfur is a dominant feature of mercury's biogeochemical cycle. However, while sulfate- and iron-reducing bacteria (SRB and FeRB, respectively) are implicated in MeHg production, only a subset of these organisms have the ability to produce MeHg. Other than the observation that most methylators have membership in the *Deltaproteobacteria* , there is no obvious physiological or genetic trait that is common. Recent data suggesting net MeHg production in novel environments, like surface ocean waters, suggest that the diversity of Hg-methylators may be broader than we realize. However, to date, and with modern analytical methods, Hg methylation has only been demonstrated within the *Deltaproteobacteria*.

The earliest work on Hg methylation mechanisms focused on intracellular methylases. Methylcobalamine was identified as the proximate methyl transfer group in one *Desulfovibrio*, but the proposed pathway is also present in many non-methylating SRB and FeRB. The sulfate-reducing apparatus in SRB does not appear to play a direct role in methylation, although the sulfide and other reduced sulfur compounds produced by SRB have dramatic effects on Hg bioavailability to cells

Stable isotope fractionation suggests that some portion of the Hg methylation pathway is enzymatic, but whether that portion is uptake, methylation or even export is unknown. Cell-free protein extracts of methylators exhibit low levels of methylation not seen in extracts of non-methylators. Denaturation of proteins eliminates the activity detected confirming the apparent enzymatic nature of the catalyst. Importantly, Hg-methylators release MeHg from cells very rapidly, and perhaps as a part of a larger organic complex. SRB (and FeRB) also demethylate MeHg, sometimes very rapidly. These organisms do not contain the *mer* operon and the mechanism of demethylation remains a mystery.

More recently, Hg transport has emerged as a potentially distinguishing characteristic of some Hg-methylators. Certain Hg-thiol complexes are highly bioavailable to methylators Nanoparticulate HgS, bound up in organic colloids, is also bioavailable to Hg methylators. However, the uptake mechanism(s) for both remain uncertain. Progress on understanding MeHg production in the environment depends on a fuller understanding of Hg methylation pathways in bacteria. The recent completion of full genome sequences for a number of Hg-methylating SRB may help solve this mystery through phylogenetic comparisons and genetic approaches.

https://doi.org/10.1180/S0026461X00008434 Published online by Cambridge University Press

Geochemical characterization of the initial phase of El Hierro eruption

DOMINGO GIMENO[1*], MERITXELL AULINAS[1] AND GUILLEM GISBERT[1]

[1]Dpt. Geoquímica, Petrologia i Prospecció Geològica, Universitat de Barcelona, Spain domingo.gimeno@ub.edu (* presenting author), meritxellaulinas@ub.edu, ggisbertp@hotmail.com

Ongoing submarine eruption at El Hierro]

A submarine eruption close to the La Restinga village (south of El Hierro island, Canary Archipelago, Spain) started october the 13th 2011 and is still (1st february 2012) ongoing. During some weeks the eruption was manifested by a discoloured plume (green) of dissolved gas (and probably suspended fine-sized particles) marking the site of submarine vents on the sea surface, and by the punctual emission of a rare type of decimetre to metre-sized buoyant pyroclasts, ovoid in shape. At the moment of emerging, pyroclasts crack or explode producing small steam plumes as a consequence of cooling by water. The initial phase of eruption provided mingled massive bombs (the so-called "restingolites") while successively the buoyant pyroclasts became hollow balloons, exclusively basic in composition.

Rhyolite-basanite composite mingled pyroclasts

"Restingolite" pyroclasts are formed by two parts intimately mingled: a white microvesiculated pumice, rhyolitic in composition and a deep green-black glassy basanite with porphyritic (phenocrysts < 3 %) and locally macrovesicular textures. The basanite constitutes the skin of the pyroclasts. while the inner part is formed by planar pumitic discontinuous plastic fragments roll-wrapped with black partings of basanite. Locally, the basanite clearly looks vitreous with concoidal fracture (sideromelane). Under the stereomicroscope, the basanite and rhyolitic glass are sinterized at their contact along planar surfaces, without trace of substantial mixing. The whole pyroclast is very friable, pulling apart as fragments with thin basanitic crust and centimetre thick of pumitic rhyolite; this provides pieces with the appearance of coconut fragments.

Trace element geochemistry and isotopic geochemistry gives evidence of an unequivocal magmatic character for both materials. In fact, the $^{143}Nd/^{144}Nd$ isotope ratios of the pumitic rhyolite and the roll-wrapped basanite are very close (0.512926 ± 0.000005 and 0.512975 ± 0.000007, respectively) and similar to the Nd isotopic data reported in literature for El Hierro magmas. $^{87}Sr/^{86}Sr$ of the basanite component is 0.702947 ± 0.000006 whereas alkaline rhyolite show higher ratios (0.706040 ± 0.000005) the latter indicating an interaction with hydrothermal fluids prior to eruption. Moreover, Nb/Zr ratio of the rhyolite component is close to the ones dispayed by oceanic islands rhyolitic peralkaline rocks [1].

This research has been developed at the Serveis Científicotecnics (SCT) belonging to the Universitat de Barcelona (UB) (Spain), while isotope data were kindly provided by CAI (Centro deGeocronología y Geoquímica Isotópica) from the Universidad Complutenese de Madrid (Spain)

[1] Leat et al. (1986) *J. Geol. Soc. London* **143**, 259-273

New insight into long-term dissolution rates of borosilicate glasses

S. GIN, P. FRUGIER*, F. ANGÉLI, C. JÉGOU, N. GODON, Y. MINET

Commissariat à l'Énergie Atomique (CEA), DEN - Marcoule, 30207 Bagnols-sur-Cèze, France stephane.gin@cea.fr (* presenting author)

Ten borosilicate glass compositions were leached at 90°C for up to 14 years under static conditions in deionised water, and then characterized by SEM, TEM and XRD in order to establish a correlation between the glass composition and the long-term rate. Within a ternary sodium borosilicate glass, some of the key elements present in nuclear glasses (Al, Ca, Zr, Ce) have been progressively incorporated. A qualitative inverse correlation between the forward and residual rates of these glasses has been observed. This unexpected result is related to the effect of gel reorganisation on the diffusive properties of the passivating layer. No simple relations was found between the residual rates and the solution composition. A first-order rate law based on silica fits only the first few weeks, but a large deviation is observed thereafter. In most of the experiments, no real saturation occurs even during the residual rate regime: the silica concentration slowly increases towards saturation with respect to amorphous silica. The role of some glass components is examined. Glasses containing a hardener element (Al or Zr) and Ca have lower residual rates than those containing only one of these two categories of elements. the detrimental effect of precipitation of silicate minerals on the residual rate is also evidenced. Finally, the 6-oxide glass, called CJ4 in this study, as well as the more complicated CJ5 and CJ6 glasses are good analogues of the actual nuclear glass. CJ4 glass has been selected at an international level as a reference glass for a common understanding of glass corrosion mechanisms.,

In conclusion, the residual rate strongly depends on the glass composition. This rate depends on the transport properties of transient amorphous layers formed by glass hydration and in situ reorganization.

https://doi.org/10.1180/S0026461X00008434 Published online by Cambridge University Press

As(III) oxidation by delta-MnO_2: Kinetics, Mechanisms, and Inhibition

MATTHEW GINDER-VOGEL[1,2]*, BRANDON LAFFERTY[2,3], AND DONALD L. SPARKS[2]

[1]Present Address: Environmental Chemistry and Technology, Dept. of Civil and Environmental Engineering, University of Wisconsin – Madison, Madison, WI 53706, mgindervogel@wisc.edu

[2]Dept. of Plant and Soil Sciences, Delaware Institute for the Environment, University of Delaware, Newark, DE 19711

[3]United States Army Corps of Engineers, Engineer Research and Development Center, 3909 Halls Ferry Rd, Vicksburg, MS 39180

Abstract

In the environment, chemical reactions at the mineral/water interface occur over a range of temporal scales, ranging from microseconds to years. Many important mineral surface processes (e.g., adsorption, oxidation-reduction, precipitation) are characterized by a rapid initial reaction on time-scales of milliseconds to minutes, and are often limited by the formation of secondary mineral phases. Knowledge of these initial reaction rates combined with detailed characterization of secondary phases is critical to determining chemical rate constants, and reaction mechanisms.

Here we describe the reactions controlling the oxidation of As(III) by δ-MnO_2 (a poorly crystalline form of hexagonal birnessite) over time-scales rangin from sub-second to hours. Initial As(III) oxidation rates (< 30 s) were measured using batch reactions and quick-scanning X-ray absorption spectroscopy (Q-XAS). Longer-term reaction dynamics were examined using a combination of column and stir-flow reactors combined with molecular-scale characterization of the resultant solid-phases with both Q-XAS and traditional XAS. While the aqueous As(V) and As(III) concentrations were determined using LC-ICPMS analysis.

Q-XAS studies reveal that As(III) oxidation occurs most rapidly during the initial 30 seconds of reaction, followed by slow oxidation over the next several minutes, and that traditional analysis (i.e., ex-situ analysis of $As(III/V)_{aq}$) may underestimate As(III) oxidation rates due to As(V) removal from solution due to sorption on the HMO mineral surface.

In column and stirred-flow experiments, As(III) oxidation by δ-MnO_2 is also initially rapid but slows appreciably after several hours of reaction. Mn(II) is the only reduced product of δ-MnO_2 formed by As(III) oxidation during the initial, most rapid phase of the reaction. However, it appears that observed Mn(III) is a result of conproportionation of Mn(II) sorbed onto Mn(IV) reaction sites rather than from direct reduction of Mn(IV) by As(III). The only evidence of arsenic (As) sorption during As(III) oxidation by δ-MnO_2 is during the first 10 h of reaction, and As sorption is greater when As(V) and Mn(II) occur simultaneously in solution. Our findings indicate that As(III) oxidation by poorly crystalline δ-MnO_2 involves several simultaneous reactions and reinforces the importance of studying reaction mechanisms over multiple time-scales with multiple techniques.

Photodemethylation: a significant actor in the methylmercury budget of Arctic freshwater ecosystems

CATHERINE GIRARD[1*], MARC AMYOT[2]

[1]CEN, Université de Montréal, Département de sciences biologiques, Montréal, Canada, catherine.girard.7@umontreal.ca (* presenting author)

[2]GRIL, Université de Montréal, Département de sciences biologiques, Montréal, Canada, m.amyot@umontreal.ca

Results of field experiments in the Arctic

Photodemethylation of monomethylmercury (MMHg) into inorganic mercury (Hg) has recently been shown to play an important part in the mercury budget of aquatic ecosystems. The objective of our project was to assess photodemethylation potential as well as its chemical drivers in Arctic lakes and thermokarst ponds. In 2008-2011, *in situ* experiments were conducted on Bylot and Cornwallis Islands (Nunavut) to determine which natural compounds drove the process. After week-long incubations of natural water exposed to sunlight, we observed significantly lower levels of MMHg (losses of 34-63%), and the use of light filters showed that short wavelenghts of solar radiation (<410 nm) were most effective at mediating photodemethylation. The process appears to be abiotic, being unnaffected by filtration (0.45 μm). Furthermore, samples amended with sulfur-rich molecules (thiols), chlorides as well as reactive oxygen species producers and scavengers showed that the presence of glutathione, singlet oxygen and chlorides accelerated photodemethylation.

In 2011, another experiment was conducted during which solar radiation was obstructed (98,7% of radiation from 200-750 nm) from a thermokarst pond on Bylot Island to measure the impact of photodemethylation on the pond's total MMHg budget. Monitoring was conducted over a 14-day period, during which time Hg levels remained stable, indicating that the total Hg budget was unaffected. However, MMHg levels fluctuated significantly, with changes in water chemistry occuring concurrently. Hence, the absence of solar radiation induced significant changes in the MMHg budget of the thermokarst pond.

Conclusions

We conclude from both sets of experiments that photodemethylation is a major degradation pathway of MMHg in Arctic thermokarst ponds and lakes, and that it has the potential to significantly affect MMHg budgets in northern aquatic ecosystems. Our results show that the process is most effectively mediated by UV radiation, and that sulfur-rich compounds and singlet oxygen play a significant role in the *in situ* degradation of MMHg via solar radiation.

https://doi.org/10.1180/S0026461X00008434 Published online by Cambridge University Press

HOT-WIRED: THE ROLE OF EXTRACELLULAR ELECTRON TRANSFER IN SUSTAINING PRIMARY PRODUCTION BY HYDROTHERMAL VENT MICROBES

PETER R. GIRGUIS[1*] AND MARK NIELSEN[1]

[1]Harvard University, Cambridge, USA, pgirguis@oeb.harvard.edu*

Introduction

Microbes have evolved a variety of metabolic strategies to flourish in the absence of oxygen (e.g. sulfate reduction, methanogenesis). Recent studies of extracellular electron transfer (or EET) have further expanded the repertoire of metabolic capacities that facilitate life in anaerobic environments. EET is a process whereby microbes shuttle charge to or from solid phase electron acceptors or donors. EET was first described in iron-reducing proteobacteria by Lovley and Philips (*1*), which use iron oxides as terminal electron acceptors for respiration. In recent years is has become apparent that EET is quite widespread, and studies have shown that a diversity of microbes are capable of EET, and that EET is coupled to an equally diverse number of metabolic modes.

Microbial EET at hydrothermal vents

At hydrothermal vents, EET may enable microbes in anaerobic milieus to remotely access dissolved oxidants in the overlying seawater through the semi-conductive metal sulfides cross redox gradients. Here we present laboratory and *in situ* experiments that support this hypothesis, revealing that hydrothermal vent microbes employ and depend upon EET to access spatially remote oxidants via semi-conductive pyrite. To simulate the physical and electrochemical conditions in vent sulfides, we constructed a two-chamber flow-through bioelectrochemical reactor in which a pyrite electrode was enclosed in one chamber and subject to simulated hydrothermal conditions. Substantial electroactive biofilms formed on pyrite in electrical continuity with oxygenated water. Phylogenetic and metagenomic analyses revealed a diversity of autotrophic and heterotrophic archaea and bacteria, markedly different in composition from the control (pyrite without electrical continuity). Stable carbon isotopic tracer experiments further reveal differences in carbon fixation among communities in and out of electrical continuity with oxygen. The data presented here reveal that microbial communities use conductive minerals such as pyrite to enable the reduction of spatially remote oxidants. Thus EET, by enabling sustained access to terminal electron acceptors while maintaining the functioning of strictly anaerobic metabolisms, may alleviate the limitation of oxidants commonly associated with anaerobic environs.

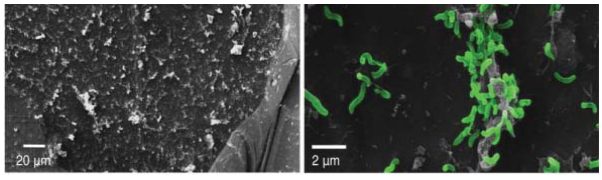

Figure #1: SEM image of electroactive biofilm, and SEM image with false color added to microbial cells to provide contrast.

[1] Lovley, D.R., and Phillips, E.J. (1988). *Appl. Environ. Microbiol.* **54**, 1472.

Subduction-related fluids influence on the Oligo-Miocene transitional magmatism of the Sulcis area (SW Sardinia, Italy)

GUILLEM GISBERT[1]*, DOMINGO GIMENO[1], MERITXELL AULINAS[1]

[1]Universitat de Barcelona, Facultat de Geologia, Barcelona, Spain, ggisbertp@hotmail.com (* presenting author), domingo.gimeno@ub.edu ,meritxellaulinas@ub.edu

The Sardinia-Corsica microplate was involved in Oligo-Miocene times in a SE-ward drift and counterclockwise rotation from the European margin in western Mediterranean to its current position. This movement was caused by the roll-back play of a NW-ward subducting oceanic plate under this margin and produced the detachment of this microplate from the continental margin and the openning of the Liguro-Provençal basin. As a result of the subduction abundant calc-alkaline magmatism of orogenic affinity occurred, mostly in the western sectors of Sardinia. In the final stages of the Miocene subduction and magmatism, coinciding with an increase in extensional tectonics, in the Sulcis area magmatism shifted from typical orogenic andesites to more evolved products of transitional character, ranging from trachydacites to rhyolites, with the relevant presence of peralkaline magmas (comendites), which were emplaced mostly as widespread ignimbrites reaching up to 20 km^3 in volume and forming a pile over 200 m thick.

The present work is focused on the study of the evolved rocks of the Sulcis area. Literature was reviewed for data, and new sampling was done. Major and trace elements whole rock XRF and ICP (-OES and MS) analyses were done on over 200 new samples covering the whole sequence, as well as Sr, Nd and Pb isotopes on a selection of 26 samples. Mineral chemistry (EMP) was done on a selection of representative samples.

Trace elements and isotope ratios reveal that magmas were originated in a mantle wedge metasomatised by fluids released by the subducting slab which were both hydrous fluids from the oceanic crust and overlying sediments, and sediment partial melts. It is also evidenced that the mantle beneath Sardinia had an original EMI signature which was subsequently modifyed by the Central Atlantic Plume event in Cretaceous times (to get a more EAR-like signature) and finally by the subduction fluids. Isotopes show that fluid influence progressively decreased with time and that assimilation processes during magma evolution were scarce. The transitional character of this magmatism was caused by the increased extensional setting, which controlled magma alkalinity and favoured melting of mantle wedge sectors with less slab-released fluids. Magma evolution in the upper crust was dominated by fractional crystallisation of magmas with slightly different initial alkalinity, producing subparallel evolutionary trends. The peralkaline magmas were originated by the evolution of the more alkaline magmas, with participation of the plagioclase effect and the resorption of cumulate amphibole, which further favoured it.

This work was funded by Spanish research projects CGL2007-63727/BTE (MEC) and CGL2011-28022 (MICINN).

https://doi.org/10.1180/S0026461X00008434 Published online by Cambridge University Press

Reactivity of detrital silicates and carbon storage in the ocean margins

S.R. GISLASON[1*], E.H. OELKERS[1,2], M.T. JONES[1], D. WOLFF-BOENISCH[1], H.A. ALFREDSSON[1] AND K.G. MESFIN[1]

[1]Institute of Earth Sciences, University of Iceland, Reykjavík, Iceland (*sigrg@raunvis.hi.is, morgan@hi.is, boenisch@raunvis.hi.is, haa4@hi.is, kgm1@hi.is)

[2]Géosciences Environnement Toulouse , GET/CNRS, Université de Toulouse, Toulouse, France (oelkers@get.obs-mip.fr)

A recent survey of chemical denudation of continental silicates at the global scale suggests that riverine particulate material-seawater interaction may be essential to the feedback between weathering and atmospheric CO_2 content/climate over geological timescales [1]. Moreover substantial evidence indicates that this pariculate material is reactive once it arrives in the coastal oceans, in part due to its high surface area [2,3]. This study explores the possibility of using the detrital silicate material, located at the continental and volcanic island margins for carbon storage via *in-situ* mineral carbonation.

Continental margin silicate sediments offer a number of advantages to potential carbon storage efforts. In addition to the large surface area of reactive solids, they have subtantial porosity available for carbonate mineral precipitation. The carbonation of silicate sediments can be enhanced by injecting CO_2 fully dissolved in water, which in turn limits the risk associated with buoyancy. The CO_2 dissolution requires large water volumes that may not be available on land. Moreover, public acceptance of ocean sediments storage may be easier than for land storage.

Of particular interest is the carbonation of basaltic and ultramafic sediments [4,5], which comprise a significant proportion of the particulate material transported to the oceans. Natural analogues, laboratory experiments, and reactive transport models suggests that such material is readily transformed into carbonates at low temperature and high CO_2 partial pressure [e.g. 6]. Laboratory experiments suggest that seawater/basaltic sediment interaction is particularly well suited for long-term CO_2 storage [7].

[1] Gislason *et al.* (2006) *Geology* **34**, 49–52. [2] Wallmann *et al.* (2008) *Geochim. Cosmochim. Acta* **72**, 2895–2918. [3] Jones *et al.* (2012) *Geochim. Cosmochim. Acta* **77**, 108–120. [4] Oelkers *et al.* (2008) *Elements* **4**, 333–337. [5] Gislason *et al.* (2010) *Intern. Jour. Greenhouse Gas Control* **4**, 537–545. [6] Roger *et al.* (2006) *Lithos* **92**, 55–82. [7] Wolff-Boenisch *et al.* (2011) *Geochim. Cosmochim. Acta* **75**, 5510–5525.

Controls of polysaccharide chemistry on kinetics and thermodynamics of calcium carbonate nucleation

ANTHONY J. GIUFFRE[1*], LAURA M. HAMM[1], AND PATRICIA M. DOVE[1]

[1]Department of Geosciences, Virginia Tech, Blacksburg, USA, giuffre@vt.edu (* presenting author)

Living organisms produce skeletal structures within a complex matrix of organic macromolecules. These compounds are proposed to actively guide the nucleation and growth of crystalline structures into the organic-inorganic composites we know as biominerals. Good examples are seen in calcareous algae and stromatolite-forming cyanobacteria. An extensive effort has investigated the influence of proteins on calcium carbonate ($CaCO_3$) mineralization. The polysaccharides, however, have received little attention despite their near-ubiquitous occurrence in mineralized tissues and intimate associations with proteinaceous compounds of the organic matrix.

The polysaccharides found at sites of microbial mineralization have complex monosaccharide sequences with various carbohydrate stereochemistries and functionalities (carboxylated, acetylaminated, sulfonated, methylated). This study tests the hypothesis that polysaccharides influence the rate of calcite nucleation by systematic and predictible differences in their chemistry. Using high purity polysaccharides with regular monomer sequences as simple model compounds for more complex macromolecules, we quantify the effect of functional group chemistry (chitosan, hyaluronic acid, heparin, alginic acid) and monomer sequencing (two stereoisomers of alginic acid) on the kinetic and thermodynamic barriers to $CaCO_3$ formation. Substrates were prepared by electrodeposition of these polysaccharides as thin gel-like films onto gold-coated silicon wafers. Using a flow-through cell, heterogeneous nucleation rates of calcite were measured for a suite of supersaturation conditions.

The kinetic measurements show rates of calcite nucleation are dependent on polysaccharide functional group chemistry and monomer sequence. Analysis of the data indicate the kinetic and thermodynamic barriers to nucleation are correlated with surface charge as the number of carboxyl groups per monomer of polysaccharide. Nucleation rates are also correlated with independent measurements of surface free energy of the polysaccharide substrates. These findings indicate polysaccharides may have active roles in promoting the formation of calcite and suggest their presumed function as inert framework molecules should be revisited.

https://doi.org/10.1180/S0026461X00008434 Published online by Cambridge University Press

The use of coupled image analysis and laser-ablation ICP-MS in fission track thermochronology

ANDREW GLEADOW*, BARRY KOHN, RAUL LUGO-ZAZUETA AND ABAZ ALIMANOVIC

School of Earth Sciences, University of Melbourne, Victoria 3010, Australia, gleadow@unimelb.edu.au (* presenting author)

Strategies for the interpretation of fission track data from natural minerals, especially apatite, and the quantitative techniques for forward modeling of thermal histories based on data, have advanced enormously over the past two decades. However the actual techniques used to acquire these data have changed little in this time. Moreover the limitations of that data in terms of both quality and quantity are now providing significant constraint on the further development of fission track thermochronology. Two very important technological developments are currently taking place in fission track analysis that are likely to transform the practice of this technique, and are likely to lead to significant improvements in data quality, inter-user consistency and the efficiency of data acquisition.

The first of these is the emergence of autonomous microscopy and automatic image analysis for the recognition and counting of fission tracks in minerals such as apatite [1], along with new tools for the enhanced measurement of fission track lengths. The second is the adoption of Laser-Ablation ICP-Mass Spectrometry for direct determination of ^{238}U abundances in the same mineral grains, in place of the conventional method using neutron induced fission tracks to measure ^{235}U as a proxy.

Switching from the conventional external detector method to using image analysis and LA-ICP-MS means that a new set of analytical and calibration issues must be addressed. These include practical matters such as transfer of grain coordinates from the microscope to the ablation stage, avoiding ejection of etched grains from the mount during laser ablation, and choice of the most appropriate ablation pattern to adequately sample the ^{238}U distribution. In addition a number of analytical strategies such as optimising instrument settings and developing suitable matrix-matched standards must also be resolved. Working solutions to all of these issues have now been developed.

Limitations of the conventional method for fission track analysis include: laborious and demanding procedures, limited counting statistics, and extremely long sample turnaround times due to the required neutron irradiation (typically several months), as well as safety issues due to the handling of irradiated materials. In contrast, the new approach using automated image analysis and LA-ICP-MS can produce better counting statistics, reduced demands on the analyst and dramatically improved sample turn-around times. In addition only one track density need be measured instead of three with the conventional method. Further, the combination of LA-ICP-MS and fission track data opens the potential for routine double-dating using both U-Th-Pb and FT systems, or even triple dating with (U-Th)/He analysis on the same grains . These advances mean that more data can be collected, with greater consistency and much more rapidly, providing higher quality input for thermal history modelling.

[1] Gleadow, Gleadow, Belton, Kohn, and Krochmal (2009) *Geol. Soc. London Spec. Publ.* **324**, 24-36.

Sulfate reduction and methanogenesis in coal microcosms

A.W. GLOSSNER[1*], L. GALLAGHER[2], L. LANDKAMER[2], L. FIGUEROA[2], J. MUNAKATA-MARR[2], K. MANDERNACK[3]

[1]Department of Chemistry and Geochemistry, Colorado School of Mines, Golden, CO 80401, USA. (aglossne@mines.edu)*

[2]Department of Civil and Environmental Engineering, Colorado School of Mines, Golden, CO 80401, USA. (lgallagh@mines.edu, llandkam@mines.edu, lfiguero@mines.edu, junko@mines.edu)

3Department of Earth Sciences, Indiana University~Purdue University, Indianapolis, Indianapolis, IN 46202 USA (kevinman@iupui.edu)

There is considerable interest in stimulating microbial methanogenesis from coal *in situ*, but limited information available on the interactions of the metabolic groups of organisms involved in this process. In most freshwater systems with sufficient sulfate, sulfate reducing bacteria (SRB) will outcompete methanogens for available acetate and H_2 due to their higher substrate affinity and growth yields . However, SRB can function both as fermenters and syntrophically with methanogens in the absence of sulfate , so their role in coal degradation may depend entirely upon reservoir conditions. In this study we examined the role of SRB in methanogenic coal degradation experiments through the use of variable sulfate concentrations (50 μM – 1mM) and metabolic inhibitors (5 mM molybdate for SRB). We hypothesized that with increasing sulfate concentrations SRB would outcompete methanogens for both the acetate and hydrogen resulting from coal fermentation, and that the absence of sulfate, or presence of molybdate, would enhance methanogenesis relative to the uninhibited, sulfate-amended experiments. Results from these experiments suggest that SRB did not outcompete methanogens for available acetate or hydrogen. Roughly 4-6 μmol sulfate was consumed in each experiment amended with sulfate, regardless of its starting concentration. Experiments performed with molybdate and in the absence of sulfate did not produce more methane than experiments amended with up to 1mM sulfate, suggesting that SRB did not compete with methanogens for the same substrate. Changes to the microbial consortium were montitored using qPCR for the mcrA and dsrA genes for methanogens and SRB, respectively, as well as by phospholipid fatty acid (PLFA) and phospholipid ether lipid (PLEL) analysis. Stable carbon isotope analysis of the microbial phospholipids will help to elucidate carbon flow pathways in these experiments as well. Results from this work help elucidate the microbial carbon transformation pathways that might stimulate in situ methanogenesis from coal.

[1] D. R. Lovley and M. J. Klug (1983) *Applied and Environmental Microbiology* **45**, 187-192.

[2] D. R. Lovley and M. J. Klug (1986) *Geochimica et Cosmochimica Acta* **50**, 11-18.

[3] M. R. Winfrey and J. G. Zeikus (1977) *Applied and Environmental Microbiology* **33**, 275-281.

[4] S. J.W.H, et al. (1994) *FEMS Microbiology Reviews* **15**, 119-136.

https://doi.org/10.1180/S0026461X00008434 Published online by Cambridge University Press

Benthic Iron flux in the Arctic Ocean

CHARLES GOBEIL [1*] AND ROBIE W. MACDONALD

[1]IRS-ETE, Université du Québec, Québec, Canada, charles.gobeil@ete.inrs.ca (* presenting author)
[2]Department of Fisheries and Oceans at IOS, Sidney, Canada, robie.macdonald@dfo-mpo.gc.ca

Between 1990 and 2007, sediments box cores were recovered within the Arctic Ocean at locations spanning shallow to deep water (40-4200 m), and analyzed for total Fe and S, operationally-defined fractions of Fe and S, other inorganic components and organic C. Cores from the basins (defined as depth > 1000 m) are characterized by the lowest concentrations of organic C, undetectable levels of pyrite, and high concentrations and inventories of Fe oxihydroxides (Fe soluble in a dithionite solution at pH 4.8). In contrast, cores from the arctic continental shelves and slopes exhibit relatively higher levels of organic C, detectable concentration of pyrite, and significantly lower levels and inventories of Fe oxyhydroxides. Using these data to determine the sediment sink and relying on literature values for physical transport of material in and out of the polar ocean, we have constructed a budget for highly reactive Fe (FeHR), defined as Fe oxihydroxides plus pyrite-Fe, for the whole Arctic Ocean. This budget reveals that most FeHR comes from rivers and coastal erosion and that almost all of it is trapped within the Arctic Ocean. The amounts of FeHR accumulating in shelf, slope and basin sediments represents 36%, 22% and 33% of its total input, respectively, with pyrite-Fe representing less than 20% of total burial of FeHR in shelf and slope sediments. This budget, combined with the fact that the proportion of FeHR relative to total Fe (FeT) is significantly higher in basin sediments (FeHR/FeT = 0.30±0.03) than in shelf sediments (FeHR/FeT = 0.19±0.07), implies that authigenic pyrite is not a substantial sink for Fe in the Arctic Ocean and that a significant fraction of the Fe recycled as a consequence of Fe oxyhydroxides reduction during the anaerobic metabolism of organic matter in shelf sediments is eventually exported towards the Arctic Ocean interior. Considering that the large-scale distribution of FeHR in the arctic marine sediments is strongly dependent of organic matter metabolism in shelves and that the Arctic Ocean presently contains as much as 50% shelf area, but loses most of that when global sea level falls by ~120 m during glacial maxima, we argue that sea-level fluctuation is a major factor influencing the biogeochemical cycle of Fe in the Arctic Ocean.

Climate change: the future of continental weathering

YVES GODDÉRIS[1*], EMILIE BEAULIEU[1], YANNICK DONNADIEU[2], DAVID LABAT[1], CAROLINE ROELANDT[3]

[1]Géosciences Environnement Toulouse GET, CNRS, Observatoire Midi-Pyrénées, Toulouse, France, yves.godderis@get.obs-mip.fr
[2]LSCE, CNRS, Gif sur Yvette, France, yannick.donnadieu@lsce.ipsl.fr
[3]Geophysical Institute, University of Bergen, Bergen, Norway, caroline.roelandt@gfi.uib.no

Continental weathering has been considered for long as a key process in the global carbon cycle at the geological timescale. Conversely, the evolution of the CO_2 sink by weathering is neglected in all studies dealing with the future of our climate, because weathering is considered as a slow process, almost inert at the secular time scale. However, recent data surveys have demonstrated the potential high sensitivity of weathering to the ongoing climate and land use changes[1,2].

According to future anthropogenic emission scenarios, the atmospheric CO_2 concentration may double before the end of 21st century, resulting in a global warming more than 6°C in the worse case. The global temperature increase will promote changes in the hydrologic cycle through redistributions of rainfall patterns and continental vegetation cover[1,2]. All these changes will impact the chemical weathering of the continental rocks. To evaluate these impacts, we use a process-based model of the chemical weathering of the continental surfaces (B-WITCH[3], spatial resolution 1°x1°) forced by models describing the atmospheric general circulation and the dynamic of the vegetation under increased atmospheric CO_2. We focus on the arctic environment where land use changes can be neglected while the climate change is expected to be important (the Mackenzie watershed)[4]. We calculate that the CO_2 consumption flux related to weathering processes (including carbonate and silicate dissolution) may increase by more than 50% for an atmospheric CO_2 doubling for one of the most important arctic watershed: the Mackenzie River basin. 40% of this increase is directly related to the warming (1.4 to 3°C warming over the watershed) and to the rainfall increase (averaged increase of 7%). But the remaining 60% are due to the direct CO_2 impact on the vegetation. Indeed, under higher CO_2 pressure, plants close their stomata, limiting the evapotranspiration and the fertilization effect promotes below ground CO_2 respiration[4]. Our study stresses the potential role that weathering may play in the evolution of the global carbon cycle over the next centuries.

[1] Raymond et al. (2008) *Nature* **451**, 449-452 [2] Gislason et al. (2009) *Earth Planet. Sci. Lett.* **277**, 213-222 [3] Roelandt et al. (2010) Glob. Biogeochem. Cycles 24, doi:10.1029/2008GB003420 [4] Beaulieu et al. (2012) *Nature Climate Change* **in press**.

https://doi.org/10.1180/S0026461X00008434 Published online by Cambridge University Press

The effect of surface chemistry on dissolution rates of CaF_2 suggests a new dissolution mechanism

JOSÉ R. A. GODINHO[1*], SANDRA PIAZOLO[1,2] AND LENA Z. EVINS[3]

[1] Department of Geological Sciences, Stockholm University, Stockholm, Sweden; jose.godinho@geo.su.se (* presenting author)
[2] GEMOC ARC National Key Centre, Department of Earth and Planetary Sciences, Macquarie University, Sidney, Australia; sandra.piazolo@mq.edu.au.
[3] Swedish Nuclear Fuel and Waste Management Co, Stockholm, Sweden. lena.z.evins@skb.se

We investigated how during dissolution differences in surface chemistry affect the evolution of topography of CaF_2 pellets with a microstructure similar to UO_2 spent nuclear fuel [1]. 3D confocal profilometry and atomic force microscopy were used to quantify retreat rates and analyze topography changes on surfaces with different orientations as dissolution proceeds up to 468 hours. A $NaClO_4$ (0.05 M) solution with pH 3.6 which was far from equilibrium relative to CaF_2 was used.

Measured dissolution rates depend directly on the orientation of the dissolving surfaces. The {111} is the most stable plane with a dissolution rate of (1.2 ± 0.8) x10^{-9} mol.m^{-2}.s^{-1}, and {112} the least stable plane with a dissolution rate 33 times faster that {111}. Dissolution rates were found to be correlated to surface orientation which is characterized by a specific surface chemistry and therefore related to surface energy. It was proposed that every surface is characterized by the relative proportions of the three reference planes {111}, {100} and {110}, and by the high energy sites at their interceptions.

Based on the different dissolution rates observed and ab initio simulations we propose a dissolution model to explain changes of topography during dissolution [2]. Surfaces with slower dissolution rate, and inferred lower surface energy, tend to form leading to an increase of roughness and surface area. This adjustment of the surface during dissolution suggests that dissolution rates during early stages of dissolution are different from the later stages. The time-dependency of this dynamic system needs to be taken into consideration in geosciences and the nuclear waste disposal management when predicting long-term dissolution rates.

[1] Godinho et.al. (2011) J. Nucl. Mat. **419**, 46-51.
[2] Godinho et. al. (2012) Geochim. Cosmochim. Acta (in review)

Application of Light Isotopes as a Tool for Watermasses tracing – Results of South Atlantic JC-057 Cruise

JOSÉ MARCUS GODOY[1,2*], MARIA LUIZA GODOY2, EDNO CAMPOS[3]

[1]Pontificia Universidade Catolica do Rio de Janeiro, Rio de Janeiro, Brazil, jmgodoy@puc-rio.br (* presenting author)
[2]Instituto de Radioproteção e Dosimetria, Rio de Janeiro, Brazil, malu@ird.gov.br
[3]Universidade de São Paulo, São Paulo, Brazil, edno@usp.br

Introduction

As part of the JC-057 cruise, filtered seawater samples were collected from 18 stations at 24 different depth. The samples were directly measured using a L-1102i PICARRO water analyzer (cavity ring down spectrometer, CRDS).Each sample result represents the mean value of four different injections, and for a batch of each six samples a standard and a test sample were measured. Typical combined uncertainty is 0.7‰ for δ(D) and 0.2‰ for δ(^{18}O).

The obtained results shown that light isotopes values are valuable tools to identify watermasses. An example of the obtained output is shown in Fig 1, where is possible, for example,to identify different water masses as, for example, South Atlantic Central Water (SCAW) at the surface and the North Atlantic Depth Water (NADW), at intermediary depth, starting at a latitude of about 40°C. Interisting also to note is the inflow of a botton water mass at 45° S. Good correlation to salinity[1] (Fig. 2) and nutrients, as fosfate, was observed, in particular, of δ(D) values.

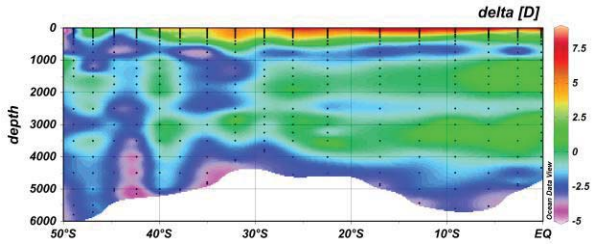

Figure 1: Isoplot of δ(D) values

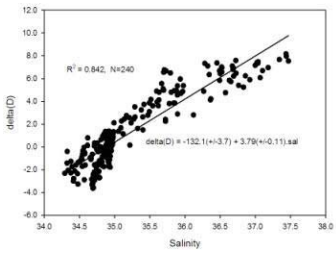

Figure 2: δ(D) and salinity relationship

Conclusions

On a very simple way, applying CRDS, it was possible to trace the different water masses acting at the South Atlantic at long the South American coast.

Povinec, (2011) *Earth and Planetary Letters* **302**, 14-26

https://doi.org/10.1180/S0026461X00008434 Published online by Cambridge University Press

Characterization of S-containing concretions from the North Sea

JOERG GOETTLICHER[1]*, RALPH STEININGER[1]

[1]Karlsruhe Institute of Technology, Institute for Synchrotron Radiation, ANKA, Eggenstein-Leopoldshafen, Germany, joerg.goettlicher@iss.fzk.de (* presenting author)

Sulfur containing concretions can be found from time to time on the German North Sea shore, e.g., on the beach of the island Juist. They show grey to black and yellow to red-brown colors (Fig. 1). Macroscopically they consist of cemented sand intergrown with shell fragments. Because of the red brown colors Fe might be present.

So far, a few of them have been investigated by X-ray powder diffraction and additionally with X-ray absorption spectroscopy (SUL-X beamline, ANKA) at the S K-edge to determine the chemical form of sulfur. The latter technique has been applied because the grey black colored parts may indicate iron sulfides. XANES spectra have been processed with the Athena program [1]. From the X-ray diffractograms quartz (SiO_2), calcite ($CaCO_3$) and calcium sulfate hydrate have been identified. Two sharp reflections (at d values of 3.24 and 3.19 Å) could not yet been assigned. And there are no reflections left that indicate an iron oxyhydroxide or iron sulfide phase because their amounts might be too small or they are not or not well crystalline. Peaks from the S K XANES spectra of the brown parts have been assigned to sulfate (≈ 2481.4 eV, close to the calibration energy of sulfate in scotch tape) and to elemental sulfur (2471.6 eV) by comparison with a spectrum of elemental sulfur (Fig. 2). Brown-black parts show additionally a peak at about 2477.6 eV which is close to S^{4+}. In the grey-black areas mono-sulfide (S^{2-}) has been identified by comparison with a spectrum of pyrrhotite ($Fe_{1-x}S$).

Because of the intergrowth with shells the location of the iron, sulfide, elemental S and sulfate containing concretions may take place on the sea floor. One possibility could be that around a nucleus in the tideland concretions of sand and shells are forming, where Fe and reduced sulfur are delivered from the sediment to form iron mono-sulfides around the quartz grains and shells that partially oxidize to elemental sulfur and sulfate. Fe K XANES spectroscopy is planned to get more information of the Fe mineral phase.

Figure 1: Fe- and S-containing concretion (scale in cm).

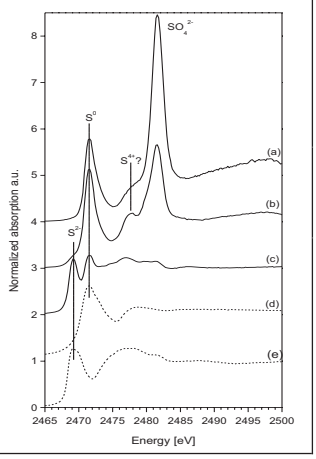

Figure 2: S K XANES spectra of a brown (a), brown-black (b) and grey-black part (c) of the sample compared to reference spectra of elemental S (d) and pyrrhotite (e).

[1] Ravel & Newville (2005). *JSR*, **12**: 537–541

MULTI-ISOTOPE TRACING OF ATMOSPHERIC EMISSONS FROM AN ALUMINUM SMELTER

JULIEN GOGOT[1*], ANDRÉ POIRIER[1], AND AMIEL BOULLEMANT[2]

[1]GEOTOP-UQAM, Science de la terre et de l'atmosphère, poirier.andre@uqam.ca julien.gogot@gmail.com (* presenting author)

[2]Rio Tinto, Australia, QRDC, amiel.boullemant@riotinto.com

Evaluating the net contribution to atmospheric fine particulates of an aluminium smelter is a challenge. For the first time here, we combine osmium (Os) and lead (Pb) isotopes as tracers of the atmospheric emissions from an aluminum smelter in Saguenay (Canada). This smelter reduces alumina (extracted from bauxite) into metallic aluminum using carbonaceous anodes. These anodes are consumed during the electrolytic process and produce atmospheric emissions (mainly CO_2) during reaction with Al_2O_3. Anodes are made of petroleum coke, which is characterized by isotopic compositions of lead and osmium that are significantly differents from other typical anthropogenic sources [1]. These metal's isotopic compositions are transfered into particulate matter emitted along with gases from the smelter process, and can then be traced in the environment. In the immediate surroundings of the aluminum smelter (i.e. on the industrial property) we observed a high Os content in surface deposits, which gradually decrease away from the factory, down to average eroding continental crust at the sampling point closest to the boundary of the industrial property (Fig. 1). For this study, we will compare these findings with Pb isotope results obtained on the same set of samples; Pb stable isotopes systematics being a powerful tool in environmental studies.

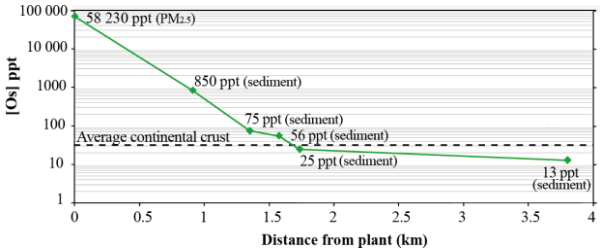

Figure 1. Decrease of osmium content in the near environment of the aluminum smelter.

[1] Boullemant (2011) *Journal of the Air & Waste Management Association*, **61**, 311-318.

https://doi.org/10.1180/S0026461X00008434 Published online by Cambridge University Press

RECONSTRUCTION OF TRACE METAL CONTAMINATION IN COASTAL SEDIMENTS FROM CAPE CORSICA (FRANCE) DURING ANCIENT TIME

JEAN-PHILIPPE GOIRAN[1] NATHALIE FAGEL[2], CLAIRE HALLEUX[2], LUCIE LEFEBVRE[2], PASCAL ARNAUD[3] AND GILLES DE LA BRIERE[4]

[1]UMR 5133 Archéorient, MOM, CNRS, Lyon, France, jean-philippe.goiran@mom.fr (* presenting author)
[2]AGEs, Argiles, Géochimie et Environnement sédimentaires, Université de Liège, Liège, Belgium, nathalie.fagel@ulg.ac.be; Claire.Halleux@student.ulg.ac.be, Lucie.Lefebvre@student.ulg.ac.be
[3]UMR 5189 HISOMA, MOM, Université Lyon 2, Lyon, France Pascal.arnaud@mom.fr
[4]Commission Régionale d'Archéologie Sous-Marine, France gilles.delabriere@wanadoo.fr

The Mediterranean margins were characterised by intense maritime commercial exchanges since Antiquity. We conduct a sedimentological (mineralogy, fossil assemblages, C/N ratio, organic content) and geochemical (trace element concentration, Pb isotope composition) study of lagoon sediments from Cala Francese, a Roman archeological site from Cape Corsica that may have been an ancient harbour. Aims are to reconstruct history of environmental contamination in trace metals over the historical period and, to propose a paleoenvironmental reconstruction. The sedimentary column of core CF10-III is divided in 3 units: an upper clayey unit (0-80cm); a median sandy clayey unit with abundant marine plant (posidonia) remains (80-160 cm) and a lower sandy and gravelly unit (160-220 cm). Radiocarbon ages performed on macroremains in an adjacant core CF10-II suggest that the sedimentary column covers the last 6000 years, with a late Roman age (210-350 AD) obtained at 140-160 cm. In core CF10-III, Pb concentration remains low in the lower unit (10 ppm), it ranges between 30-40 ppm in the intermediate unit and then increase from 60 cm (>115 ppm). A major shift in Pb isotopic composition is observed at 60 cm, with a decrease of $^{206}Pb/^{207}Pb$ ratios from 1.193 to 1.187. Both $^{206}Pb/^{207}Pb$ and $^{208}Pb/^{206}Pb$ ratios are consistent with Pb Roman signatures [1]. A marked Zn-enrichment (from 4 to 80 ppm) is observed at 40-60 cm. Such drastic changes in trace metal content and Pb isotopic signature of sediments is consistent with Human perturbations of the environment during the Roman period. Further investigations are in progress in order to define the sediment deposition conditions and in particular to date the marine-continental transition.

[1] Véron et al., 2006. Geophys. Res. Lett. 33, doi :10.1029/2006GLR02582.

Bioaccessibility of trace metals on mining and smelting impacted dusts: importance of particle size on children exposure

GOIX SYLVAINE[1], OLIVA PRISCIA[1*], CASTET SYLVIE[1], DUPREY JEAN-LOUIS[2], POINT DAVID[1], GARDON JACQUES[3]

[1]Université de Toulouse; IRD; CNRS; GET; F-31400 Toulouse, France (correspondence : sylvainegoix@gmail.com)
[2]IRD, La Paz, Bolivia
[3]IRD, Laboratoire Hydrosciences Montpellier, CNRS-IRD-UM1 34095 Montpellier Cedex 05, France

20d. Metals and human health

Located on the Bolivian Altiplano at 3750 m.a.s.l., Oruro is a mining city with a population of 200 000. The volcanic dome on which lies the city is exploited since centuries for its polymetallic ores (Sn, Ag, Zn, Cu, Pb, Sb, Au) and smelting activities (Sn, Sb) are developed in the direct vicinity of the town, and process half of Bolivia's Sn ore.

An interdisciplinary project (ToxBol) aiming at studying the origins and impacts of trace metal contamination on the environment, human health and society was initiated in 2006 in Oruro. Previous studies have shown differences in polymetallic contents between exposed and non exposed area in children's hair[1] and atmosphere[2]. Correlations were found between air particles and children's exposure except for Pb that show relative low contamination in atmosphere in comparison with children's hair content.

Dusts from football fields were collected in mining and smelting districts. Particles were separated into 5 granulometric fractions: 2000-200 (coarse sand), 200-50 (fine sand), 50-20 (coarse loam), 20-2 (fine loam) and <2 µm (clay). Bulk samples and fractions were analyzed to characterize geochemical and mineralogical dust properties. Bioaccessibility of trace metals was measured on each subsample following the UBM stomach phase procedure[3].

Results and Conclusion

Bulk samples were highly contaminated, especially in the smelting environment with up to 16000 µg/g Pb. Clay fraction was globally the most concentrated in trace metals. Bioaccessibility in bulk sample was different according to the environment: Cd>Pb>Zn>As>Sb=Sn (i.e., 84% to 1%) in smelting district and Cd>Zn>Pb=As>Sn=Sb (i.e., 86% to 1%) in mining district. Highest difference was observed for Pb (62% of bioaccessibility in mining and 13% in smelting bulk dust). Trace metals in smelting environment were globally more bioaccessible in fine sand than in clay. In mining district, fine loam and clay show the highest trace metals bioaccessibility.

Observed differences can be partly explained by mineralogical speciation of trace metals. Exposure doses of particles ingestion for children playing on the field were calculated, and show possible metal absorption higher than those recommanded by WHO.

[1]. Barbieri (2011) *Biol. Trace Elem. Res.* **139** 10-23.
[2]. Goix (2011) *Sci. Total Environ.* **412-413** 170-184.
[3]. Wragg (2011) *Sci. Total Environ.* **409** 4016-4030.

https://doi.org/10.1180/S0026461X00008434 Published online by Cambridge University Press

Controls on Mo isotope fractionations

T. GOLDBERG[1*], S.W. POULTON[2], C. ARCHER[3], D. VANCE[3] AND B. THAMDRUP[4]

[1]Imperial College London, Department of Earth Science and Eng., London, SW7 2AZ, UK, t.goldberg@imperial.ac.uk (* presenting author)
[2]Newcastle University, School of Civil Eng. & Geosciences, Newcastle upon Tyne, UK, simon.poulton@newcastle.ac.uk
[3]University of Bristol, Dept. of Earth Sciences, Bristol, UK, c.archer@bristol.ac.uk, d.vance@bristol.ac.uk
[4]University of South Denmark, Institute of Biology, Odense, Denmark, bot@biology.sdu.dk

Mo isotopes are employed as a palaeoredox indicator, particularly in terms of quantifying the spatial extent of different redox conditions [e.g. 1]. However, the controlling factors on Mo cycling and isotopic fractionations under distinct redox conditions remain poorly understood. Mn and Fe (oxyhydr)oxides, Fe-sulphides, and organic mater have all been proposed to exert an influence on Mo isotope fractionations during diagenesis [2, 3]. To evaluate past ocean redox conditions it is necessary to understand the controls on redox sensitive element and isotope cycling in modern sedimentary environments, as well as the degree of Mo fractionation during Mo uptake by different substrates.

Sediment cores from Danish and Swedish waters were investigated for this purpose. The redox chemistry ranges from Mn- to Fe-rich to sulphidic sediments and pore-waters. An examination of dissolved and particulate Mo isotope measurements with porewater and solid phase Mn, Fe and sulphide characterization, reveals that adsorption and desorption processes heavily influence the porewater δ^{98}Mo values. The highest δ^{98}Mo values, converging towards the global modern seawater (~2.3‰), are recorded in highly sulphidic sediments. Our results suggest that for modern anoxic marine sediments, where deposition occurs beneath an oxic to suboxic water column, sedimentary δ^{98}Mo is dominantly controlled by the relative availability of Mn and Fe (oxyhydr)oxides, and the production of dissolved sulphide [4].

A mechanistic investigation of the isotopic fractionation of Mo during different mineral uptake pathways was also employed. The focus here is on fractionations during redox transformations involving iron-based phases, including those upon Mo interaction with Fe oxides and their sulphide-promoted reductive dissolution. This is a key process affecting Mo cycling in the environment. Preliminary results exhibit species dependant fractionations. The findings add to our understanding of Mo isotope fractionations during syn- to early-diagenesis and their relation to the interpretation of Mo isotope data for ancient sediments.

[1] Kendall et al. (2011) *EPSL* **307**, 450-460. [2] Siebert et al. (2006) *EPSL* **241**, 723-733. [3] Poulson-Brucker et al. (2009) *G*^{3} **10**, 1-25. [4] Goldberg et al. (2012) *Chem.Geol.* **296-297**, 73-82.

On the evolution of Earth's "Geo-bio" atmosphere

COLIN GOLDBLATT[1*]

[1] School of Earth and Ocean Sciences, University of Victoria, PO Box 1700 STN CSC, Victoria, BC Canada V8W 2Y2 czg@uvic.ca (* presenting author)

On of the first predictions of Gaia hypothesis was that the biota exerted dominant control of evolution of the composition of Earth's atmosphere - including for the major atmospheric constituents, oxygen and nitrogen [1]. Here we review this in light of four decades of study. We argue that, other than water vapour (which is controlled by temperature) and the noble gases, all constituents of the atmosphere are controlled by a mix of geological and biological processes. In particular, recent work on nitrogen has shown that there is more nitrogen buried in the mantle than there is in the atmosphere. This is not primordial, but grew from the subduction of biologically fixed NH_4^+ [2]. It is evidence of both the biological contamination of the mantle, and billion-year timescale, non-steady state interaction of life and the atmosphere. By contrast, cycles of other gases range from years (methane) to millions of years (CO_2 via carbonate silicate weathering), and others display strongly non-linear behaviour (oxygen [3]). Can one weave these timescales together to a coherent narrative of coupled geosphere-atmosphere-climate interaction through the history of life on Earth?

[1] Lovelock (1972) *Atmos. Env.* **6**, 679-580. [2] Goldblatt et al. (2009) *N. Geosci.* **2**, 891-896 [3] Goldblatt et al. (2006) *Nature*, **443**, 683-683.

https://doi.org/10.1180/S0026461X00008434 Published online by Cambridge University Press

Scaling of Ecological and Critical Zone Processes in the Prairie Pothole Region, USA and Canada

MARTIN GOLDHABER[1*], CHRISTOPHER MILLS[2], CRAIG STRICKER[3], DAVE MUSHET[4], JEAN MORRISON[5]

[1]USGS, Denver CO, USA, mgold@usgs.gov (*presenting author)
[2]USGS, Denver CO, USA cmills@usgs.gov
[3]USGS, Denver CO USA, cstricker@usgs.gov
[4]USGS, Jamestown ND, USA, dmushet@usgs.gov
[5]USGS, Denver CO, USA, jmorrison@usgs.gov

The Prairie Pothole Region (PPR), occupying 715,000 km^2 of the north central U.S. and S. central Canada, is a vital ecosystem in North America. It contains >10 million wetlands that are habitat for shore and migratory birds. The wetlands are underlain by glacial till and are internally drained within discrete, km-scale basins. We studied the geochemistry of sediments, wetland water, and groundwater in the 92 hectare Cottonwood Lakes area (CWLA) of North Dakota, USA. The CWLA has upland groundwater recharge wetlands with TDS ~150 mg/kg (Ca-HCO_3 dominant), and a discharge wetland at a local topographic low only 200m distant with TDS>3000 mg/kg (Mg-SO_4 dominant). Groundwater and wetland chemistry is controlled by critical zone oxidation of marine shale-derived pyrite in the upper glacial till (mean $\delta^{34}S$ of unoxidzed till=-19.9‰). A sample of the underlying marine shale has $\delta^{34}S$ value of -16.5‰. Oxidation produces an upper iron oxide rich brown zone in the till (mean depth 6.1m) supplying mobile and isotopically light SO_4 ($\delta^{34}S$ from -18.2 to -7.5‰) to the local discharge area. Dissolution of dolomite in the till is the source of Mg. Thus, critical zone oxidation processes dominate wetland water composition, which in turn is a primary control on ecology.

The same combination of upland recharge areas and local discharge areas occurs at a range of scales throughout the PPR. Information from nearly 500 well logs from a 10^3 km^2 area surrounding the study site document oxidation of surface till to an average depth 7.8m. Comparison of CWLA geochemistry with that of literature data from 178 wetlands in this same surrounding area both document the progressive formation of SO_4 with increasing salinity. Thus, geochemical processes identified in the CWLA are likely occurring across a much larger area. Furthermore, based on our analysis of literature data, the same wetland geochemical trends occur in >300 wetlands in southern Canada.

The broad regional impact of critical zone pyrite oxidation on ecology is reflected in two published studies on the S isotope composition of juvenile mallard feathers througout North America. These feathers are isotopically light ($\delta^{34}S$ from -5 to -16‰) in the PPR in contrast to other mallard migration corridors ($\delta^{34}S$ from -2 to +13‰), reflecting the pyrite source for sulfur in PPR breeding ground waters. We conclude that critical zone oxidation of glacial till is a key control on geochemistry and biology in the PPR ecosystem.

Multi-proxy investigation of paleoredox indicators in a permanently euxinic, low sulfate lake

M. GOMES[1*] AND M.T. HURTGEN[1]

[1]Department of Earth and Planetary Sciences, Northwestern University, Evanston, IL, USA (* correspondence: maya@earth.northwestern.edu)

Many paleoclimate investigations require knowledge of the redox state of the ocean-atmosphere system at the time of sediment deposition. This is an essential question because it has implications for what chemical reactions are favored or suppressed in a given system and, importantly, what kinds of organisms could have lived during the time period studied. Yet, it can be very challenging to conclude with certainty whether or not a system was oxic, and could therefore support animal life. Geochemical signatures of sulfur (S) and iron (Fe) preserved in marine sediments have been utilized as paleoredox indicators because they are redox sensitive elements that are transformed as organic matter is degraded in sediment. Many of these proxies have been developed and calibrated using empirical and experimental studies of the modern, high sulfate (~28mM) ocean. However, sulfate concentration in the ocean has varied widely through Earth history from a low of <200μM to the high modern value of 28mM [1].

In this study we examine Fe speciation, S isotopes, and elemental ratios in a modern low sulfate (~275-330μM) system with permanently euxinic (i.e. anoxic and sulfidic) bottom waters. We investigate both a shallow site with oxic overlying water and a deep site with euxinic overlying water. Given the current paradigm of these paleoredox proxies, the S-Fe geochemistry preserved at these disparate sites would lead to interpretations of redox state that are different than what is observed in the modern system. We hypothesize that this is due to the small size of the sulfate reservoir and differences in sedimentation patterns between the two sites. Because sulfate levels are low and organic carbon availability is high, a relatively large fraction of the sulfate reservoir is quickly consumed during early diagenesis resulting in sediment S-Fe geochemistry that would lead to incorrect interpretations of the redox state of the environment. This investigation and future studies in low-sulfate systems are imperative towards improving our understanding of how the redox state of the ocean-atmosphere system varied during long periods of Earth history when marine sulfate levels were much lower than they are in the modern ocean.

[1] Lowenstein, T.K., Hardie, L.A., Timofeeff, M.N., & Demicco, R.V. (2003) *Geology,* **31**, 857-860.

https://doi.org/10.1180/S0026461X00008434 Published online by Cambridge University Press

Anaerobic reduction of adsorbed X-Ferrihydrite (X = 0, AsO_4 and MoO_4) at pH 8 and 10

MARIO A. GOMEZ[1*], AND JIM HENDRY[3]

[1]University of Saskatchewan, Department of Geological Science, Saskatoon, Canada, mag346@mail.usask.ca (* presenting author) and jim.hendry@usask.ca

Introduction

Uranium ore tailings produced in northern Saskatchewan, Canada often contain elevated concentrations of **As, Se, Mo and Ni**, **(elements of concern, EOC).** These EOCs are immobilized within the tailings solid phase through complexation (chemical adsorption) or co-precipitation with ferric oxide (HFO) minerals such as ferrihydrite (FH).[1-2] Although the redox conditions in the tailings are oxic, even after 15 years of storage, concern exists as to impact of the development of anaerobic conditions at depth (E_h~ 500 mV) on the stability of these EOCs. Research suggests HFOs are unstable under moderately reducing conditions (E_h ~ +100 mV). As a result, they may undergo phase transformation and redox active species (such as Fe, As, and Se) may undergo reduction of their oxidation states. To understand the impact of an anoxic environment on the stability of the EOCs, a set of anaerobic reduction test were conducted on pure synthetic adsorbed systems and on more complex tailings samples.[2]

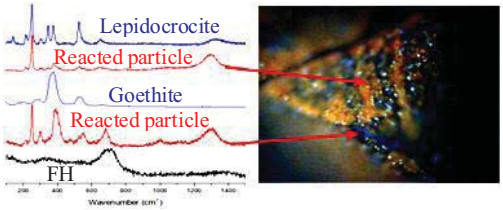

Figure 1: Micro-Raman and optical image of reduced X-FH particle

Results and Conclusion

We investigated solids with X/Fe molar ratios of 0, ~ 4, ~30 (X= 0, As and Mo) which are similar to those found in the DTMF products [1,2] and reacted these under two sets of conditions for all our products: high and low [Fe^{+2}] at pH 8 and 10, using lime as a base (as per the industrial process). In the case of the pure FH @ pH 8 and 10, phase transformation to lepidocrocite-goethite and complete uptake of the Fe^{+2} added were observed (Figure 1). For the AsO_4-FH samples, only samples at higher Fe/As ratios (~4) was phase transformation not observed (via Micro-Raman nor PXRD) at both pH's irrespective of the [Fe^{+2}]. Significant arsenic release (~ 10 ppm) was observed in the case of Fe/As 4 and pH 10. In case of the MoO_4-FH, phase transformation to goethite-lepidocrocite was observed at all Fe/Mo ratio's at pH 8 but not at pH 10. High Mo release (> 20ppm) was observed for the Fe/Mo ~4 solid at pH 8, and pH 10 for both Fe/Mo solid ratios. The difference in chemical properties such as phase transformation and element release of these molecules may be attributed to their X-O bond lengths (As-O= 1.68 Å vs. Mo-O= 1.76 Å), and chelating nature (inner vs. outer sphere) in the adsorbed state to FH.[1,3]

[1] Moldovan *et al.* (2003) *Environ. Sci. Tech* **37**, 873-879.
[2] Shaw *et al.* (2011) *Appl. Geochem.* **26**, 2044-2056. [3] Brinza L. (2010) *PhD Dissertation thesis*, University of Leeds.

Enhanced metal release from acid mine drainage sediments due to the interaction with municipal waste water

MÁRIO A. GONÇALVES[1,2*], JOÃO C. WAERENBORGH[3], FLÁVIA MAIA[4], CLÁUDIA PINTO[1], CÁTIA PRAZERES[5] AND SUSANA SÉRIO[6]

[1]Department of Geology, FCUL, Lisbon, Portugal, mgoncalves@fc.ul.pt (* presenting author)
[2]CREMINER/LARSys, University of Lisbon, Lisbon, Portugal
[3]Instituto Tecnológico e Nuclear/CFMC-UL, Dept. of Chemistry, Lisbon, Portugal, jcarlos@itn.pt
[4]AMPHOS21 Consulting SL, Barcelona, Spain
[5] Laboratório Nacional de Energia e Geologia, Alfragide, Portugal
[6]CEFITEC, Department of Physics, FCT-UNL, Monte da Caparica; Portugal

The mining area of Aljustrel belongs to the well-known Iberian Pyrite Belt in Portugal. In spite of recent reclamation of the land where the old tailings were deposited, there is still a significant production of acid drainage waters that flow to the north in the Ribeira da Água Forte watershed. The stream waters are mixed with municipal waste water at 2 km from the source, for reasons that ultimately reside on the potential attenuation capacity of this high pH, low Eh, and organic-rich water. Although the visual impacts on the landscape seem to be attenuated, this apparently idyllic situation hides an unsuspected increase of metals in the flowing waters all along the stream length. This situation was detected because during large periods of the year in the dry season, the flow along the stream is mostly fed by the waste water with little or no input from the acid drainage waters. However, the stream hydrochemistry reveals that not only all the important trace metals remain equally concentrated in solution, but also that the stream waters are a bit more acidified as compared to the situation when mixing with the acid drainage waters from the old tailings occurs.

A detailed study of the stream sediments mineralogy by XRD and Mössbauer Spectroscopy shows that these sediments have important amounts of jarosite-group minerals and abundant small particle Fe-oxyhydroxides (SPO), mostly ferrihydrite. The sediments down to the mixing zone also have minor quantities of pyrite ± sphalerite. Beyond the mixing zone, sulfides disappear and SPO dominate, while jarosite has a minimum precisely at the mixing zone. Some hundreds of meters downstream schwertmannite was also detected. These findings suggest that the waste water input is actually promoting the reductive dissolution of jarosite and SPO from the stream bed sediments at the mixing area releasing the metals adsorbed onto these phases back into solution. Subsequent Fe hydroxide precipitation and the metastable nature of schwertmannite sustain an acid environment in spite of the feeding waters having a pH above 8. This maintains metals in solution, with the exception of As that is adsorbed on the newly formed Fe-hydroxides along the stream path. All other elements arrive at the discharge point of the stream 10 km away with the same concentration in solution as when they started at the mixing zone.

This work is a contribution from project METALTRAVEL – POCI/CTEGEX/61700/2004, funded by MCTES-FCT, Portugal.

https://doi.org/10.1180/S0026461X00008434 Published online by Cambridge University Press

Organic Matter in Sediments from the North American Arctic Margin

MIGUEL A. GOÑI[1*], ALISON O'CONNOR[2], ZOU ZOU KUZYK[3], CHARLES GOBEIL[4], ROBIE MACDONALD[5]

[1]College of Earth, Ocean & Atmospheric Sciences, Oregon State University, Corvallis, OR 97331, mgoni@coas.oregonstate.edu (* presenting author)

[2]Department of Chemistry and Biochemistry, Oberlin College, Oberlin, OH

[3]Department of Geological Sciences and CEOS,University of Manitoba, umkuzyk@cc.umanitoba.ca

[4]INRS-ETE, Université du Québec, Québec (QC), G1K 9A9, Canada

[5]Department of Fisheries and Oceans, Institute of Ocean Sciences, Sidney BC

Abstract

To better understand the nature and distribution of the sedimentary organic matter in margin sediments off the North American Arctic, we analyzed thirty cores collected from all its major basins, including Baffin Bay/Davis Strait, the Canadian Archipelago, three regions of the Beaufort Sea (Mackenzie River Shelf, East Alaskan and West Alaskan Shelves), as well as the Chukchi and Bering Seas. Measurements included organic and inorganic carbon contents, mineral surface area, stable carbon and radiocarbon compositions of organic matter and a variety of CuO oxidation products derived from both terrigenous vascular plant and non-vascular plant sources. Our analyses showed major differences in the compositions of surface sediments along the North American Arctic margin. For example, while organic carbon contents were relatively uniform in all regions, ranging between 1 and 2 wt%, inorganic carbon contents were extremely elevated in the Canadian Archipelago sites (up to 8 wt%). Based on their depleted ^{14}C signatures, the elevated carbonate contents in these latter sediments reflect inputs from erosion of limestone bedrock in the adjacent terrain. Marked contrasts in the distribution of terrigenous-specific biomarkers indicated significant differences in the inputs of land-derived materials. For example, the highest carbon-normalized yields of lignin phenols were found in sites along the shelf portion of the Beaufort Sea, including off Barrow Canyon and Mackenzie Shelf. In contrast, sediments from Baffin Bay and the Archipelago were relatively devoid of these terrigenous markers. Compositional contrasts among biomarker classes indicated differences in provenance of land-derived organic matter among regions. Inputs from coastal erosion appear to be more important in the western parts of the Beaufort, Chukchi and Bering Seas, whereas export from the Mackenzie River dominate the eastern Beaufort sea.

Is the deuterium isotope composition of amber a reliable inland paleoclimatic indicator?

G. GONZALEZ[1,*] R. TAPPERT[2], A.P WOLFE[1], AND K. MUEHLENBACHS[1]

[1]University of Alberta, Edmonton, Canada, ggonzale@ualberta.ca (*presenting author)

[2]University of Innsbruck, Innsbruck, Austria.

Hydrous deuterium-exchange experiments have shown that a significant fraction of the original D/H composition of bulk kerogens, bitumens and expelled oils may participate in isotopic exchange reactions during burial diagenesis. However, it is unknown to what extent resins and their fossil counterpart amber, exchange hydrogen isotopes following their biosynthesis. This situation hinders the application of resin D/H measurements in paleoenvironmental reconstruction. As compared with other plant-derived compounds resins seem to preserve most of the chemical and isotopic features during their transformation to amber [1,2]. Yet, in fossil resinoids the number of hydrogen-containing functional groups seems to decrease, whereas the number of aromatized groups apparently increases with increasing age [3,5,6]. Accordingly, the possibility of a significant D-isotopic exchange with meteoric waters during burial cannot be ruled out. By using a series of immersion experiments in deuterated (D-enriched) waters over a period of several months at several temperatures, here we investigate whether significant D-isotopic exchange occurs during early thermal maturation and polymerization of conifer and angiosperm resins. At 90 ºC, equivalent to ~3 km of burial, modern conifer and angiosperm resins have an average post-metabolic D exchange of 4.63%, compared to only 1.08% for mature, polymerized ambers. At 55 ºC the degree of exchange is considerably lower: 1.9% for resins and 0.6% for ambers, Our results indicate that most D/H isotopic exchange occurs prior to polymerization reactions of resins, thereby confirming that D/H measurements from amber constitute a potentially sensitive proxy for environmental reconstructions of past climates, ecologies, and hydrological regimes.

[1] Nissenbaum and Yakir (1995) *In* Amber, Resinite and Fossil Resins, 34–42. [2] McKellar et al. (2008) *Can Journ of Earth Sci.* **45**, 1061–1082. [3] Murae et al. (1995) In Amber, resinite and fossil resins (eds. K. B. Anderson & J. C. Crelling) 76–91. [4] Schimmelmann et al. (1999) *Geochim. Cosmochim Acta* **63**, 3751–66. [5] Wolfe et al (2009) *Proceed. Roy. Soc. B: Biol. Sci.* 276, 3403-12. [6] Yamamoto et al. (2006) *Palaeobot. Palynol.* **140**, 27–49.

https://doi.org/10.1180/S0026461X00008434 Published online by Cambridge University Press

Femtosecond laser ablation ICP-MS: high repetition rate diode-pumped ytterbium performance

J.J. GONZALEZ[1,3], H. LONGERICH[2], J.YOO[3] AND R.E. RUSSO[1]

[1]Lawrence Berkeley National Laboratory, Berkeley, USA, jjgonzalez@lbl.gov (* presenting author) rerusso@lbl.gov

[2]Memorial University, Newfoundland, CA henryl@mun.ca

[3]Applied Spectra, Inc, Fremont,CA USA, jyoo@appliedspectra.com

Laser Ablation ICP-MS

Without doubt, the femtosecond laser offers compelling advantages to direct solid sample laser ablation (LA) chemical analysis with detection of elements and isotopes using ICP-MS. The femtosecond laser reduces matrix effects due to a nominal heat-affected zone (no fractionation) and provides a nanometer particle aerosol that is ideal for transport, vaporization and ionization in the ICP. Several groups have shown the benefits of femtosecond LA-ICP-MS, but there remains conflicting reports of the 'optimun' wavelength, energy and pulse duration for geological sample analysis. Fundamental studies have shown in many cases that these parameters are significantly relaxed once the pulse duration is less than approximately 1ps. Most of the previous fs-ablation applications have been demonstrated using Ti:Sapphire lasers. We demonstrated excellent performance for several geological samples using a smaller footprint, lower cost, and more reliable diode-pumped ytterbium femtosecond laser, even using wavelengths at 1um. Precision, sensitivity and accuracy were established and will be reported. In addition, the high repetition rate of this laser was demonstrated for rapid bulk analysis of inhomogeneous granite samples.

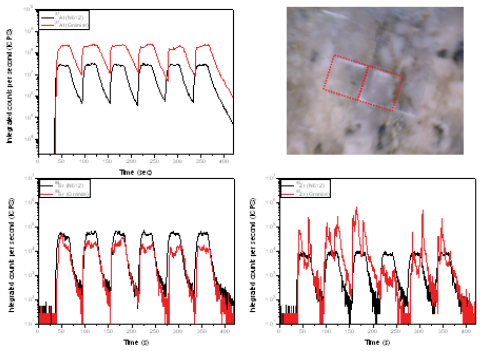

Figure 1: ICP-MS transient signal of selected isotopes produced by high repetition rate femtosecond laser ablation of NIST 612 and granite at 6um spot size, 40mm/sec and 20KHz. Scans show the effect of elemental inhomogeniety.

Conclusion

This talk will describe the current status of femtosecond laser abaltion ICP-MS with emphasis on the benefits of a reliable and stable diode pumped ytterbium solid state laser.

Novel synthesis of iron sulfide for carbon dioxide reduction

JOSIE GOODALL[1]*, HUSN-UBAYDA ISLAM[1], NATHAN HOLLINGSWORTH[1], ANNA ROFFEY[1], KATHERINE B. HOLT[1], GRAEME HOGARTH[1], GOPINATHAN SANKAR[1], JAWWAD A. DARR[1]

[1]University College London, London, UK *j.goodall@ucl.ac.uk

Overview

Despite the high thermodynamic stability of CO_2, biological systems are capable of both activating and converting it into a range of organic molecules, under moderate conditions. Successful conversion of CO_2 into useful chemical intermediates without the need for extreme reaction conditions would be of enormous benefit Iron-nickel sulfide membranes formed in the warm, alkaline springs on the Archaean ocean floor are increasingly considered to be the early catalysts involved the emergence of life. These anaerobic reactions are thought to have been catalyzed by small (Fe,Ni)S clusters similar to the surfaces of present day sulfide minerals.[1]

We have synthesised iron sulfide nanomaterials using a novel synthesis methods based on continuous hydrothermal synthesis, where flows of aqueous solutions of iron and sulfide ions are brought into contact with a flow of superheated water (at 450 ºC). This results in sudden, rapid crystallisation of nanoparticle metal sulfides. A flow reactor such as this offers the potential to affect the particle properties, such as composition, based on modelled predictions of active catalysts. The conditions and processes occurring during synthesis can be compared to those that might occur in hydrothermal vents.[2,3] The electrochemical properties of these materials and their stability and activity towards CO_2 and their selectivity to products can be evaluated.

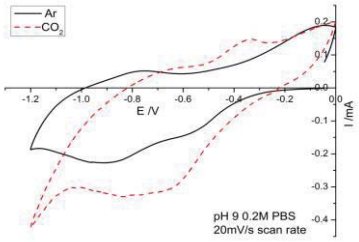

Figure 1: Comparison of the electrochemical behaviour of Ni-doped greigite under argon and CO_2.

Results

Based on comprehensive computational investigations, a number of iron and iron-nickel sulphide nanoparticles have been designed, synthesised, tested, characterised, and evaluated for the activation and chemical modification of CO_2 at low voltages (obtainable from solar energy). Succesful synthesis methods for greigite, mackinawite, pyrrhotite, pyrite and nickel sulfide as well as doped greigite nanostructures have been developed. Structures including nickel-doped greigite (above) show clear differences in electrochemical behaviour in the presence and absence of CO_2.

[1]Russell (2005) *Economic Geology* **100**, 419-438. [2]Crabtree (1997) *Science* **276**, 222-222. [3]Middelkoop (2009) *Chemistry of Materials* **21**, 2430-2435

https://doi.org/10.1180/S0026461X00008434 Published online by Cambridge University Press

Taking control of subsurface behavior with Smart Gels – an oil & gas exploitation perspective

HARVEY GOODMAN[1*]

[1]Chevron Energy Technology Company, Chevron Fellow (hego@chevron.com)

The safe, environmentally friendly and cost efficient exploitation of oil and gas resources is becoming increasingly complex. For example, deepwater subsalt developments require fewer wells that must produce reliably over longer periods of time to justify the large capital expenditures necessary to develop. Enabling technologies being developed focus on a wide range of applications along the entire value chain used to discover, recover and transport high energy density resources to the consumer. This discussion will focus on smart materials, particularly smart gels applications that appear promising for subsurface behaviour illumination or imaging and CO2 sequestration applications. Smart gel actions that can be triggered to respond to specific subsurface conditions is an extremely attractive option for geomechanical model forecasts calibration. Calibration of theoretical models used to predict rock mechanical behaviour during drilling and through production can use smart gel trigger responses to excite the subsurface in an observable manner. This may lead to improved calibration of time-dependent model predictions that consider near-wellbore osmotic effects (pore pressure & swelling) and to ground truth far-field reservoir mechanical response to pressure depletion. With regard to applications in geological storage of CO2, an important risk to containment loss is through leakage pathways associated with injection wells. The well schematic shown in Figure 1 illustrates potential CO2 leakage pathways. Regaining containment by sealing these leakage pathways may be problematic, particularly for extremely small crack apertures. The design and application of smart gels to restore CO2 containment will be discussed.

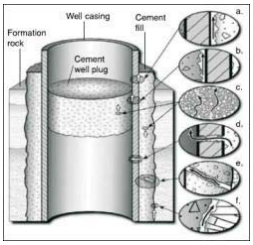

Figure 1: Possible leakage pathways in an abandoned well (modified after Gasda et al., 2004).

[1] Gasda, S. E., S. Bachu, and M. A. Celia (2004), Environ. Geol., 46.

^{54}Cr and $\Delta^{17}O$ in carbonaceous chondrites and an old $^{53}Cr/^{53}Mn$ age of the Paris meteorite

CHRISTA GÖPEL[1]*, JEAN-LOUIS BIRCK[1,2], PIERRE CARTIGNY[1,3], NELLY ASSAYAG[1,4], AND BRIGITTE ZANDA[5]

[1]IPGP, Paris, France, gopel@ipgp.fr (* presenting author)
[2]birck@ipgp.fr, [3]cartigny@ipgp.fr, [4] assayag@ipgp.fr
[5]MNHN, Paris, France, zanda@mnhn.fr

Mn/Cr isotope systematics in meteorites presents an interesting tool because this isotope system holds double information: the ^{53}Cr-^{53}Mn couple allows us to obtain chronological information while the ^{54}Cr isotope systematics yields information on the mixing of nucleosynthetically distinct components. Although the variations of the ^{54}Cr abundances in meteorites are not yet fully understood, they are nevertheless so systematic that they can be used as a classification tool, very similar to the oxygen isotope systematics.
We present Mn/Cr and oxygen isotope data obtained on recently discovered and/or unclassified carbonaceous meteorites. The oxygen isotopic compositions were determined by laser fluorination on small fragments; the Cr isotopic compositions were measured on sequential dissolution steps of bulk rock powders of all meteorites and on separated mineral fractions of two of them. The mineral separates of Paris, forsterite, fayalite, fine-grained material around chondrules (FGR), fall on a line with a slope of $^{53}Mn/^{55}Mn = 6.183 \times 10^{-6}$ and $^{53}Cr_i = -0.165$. This slope can be translated into an age based on the LEW Cliff 86010 anchor [1] and corresponds to $4566.33 \pm 0.63 \times 10^6$ y. This old Mn/Cr age shows that the first chondrules formed rapidly (1-2 $\times 10^6$ y) after CAIs. The mineral isochron obtained on Tafassasset indicates a younger equilibration age: $4563.31 \pm 0.42 \times 10^6$ y.
The ^{54}Cr abundances measured in the bulk rocks of all samples studied as well as the isotopic pattern of the sequential leaching steps allow us to classify Tafassasset as CR, Niger I as CI, Paris as CM and NWA TBC as CV chondrites. Although the existence of a correlation between ^{54}Cr and oxygen in carbonaceous chondrites has recently been questioned [2], our new $\Delta^{17}O$ data for Niger I ($\Delta^{17}O$ = -0.361 ±1.189), NWA TBC (- 4.052 ± 0.550) as well as the ^{54}Cr abundances of Tafassasset (^{54}Cr= 1.42± 0.076), Paris (^{54}Cr= 0.925 ±0.098), Niger I (^{54}Cr= 1.64±0.11) and NWA TBC ^{54}Cr= 1.08±0.19) seem to match such a correlation.

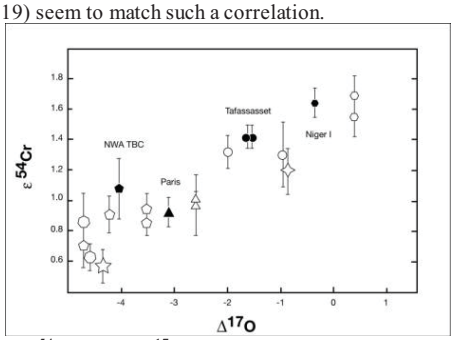

Figure 1: $\varepsilon^{54}Cr$ versus $\Delta^{17}O$ in carbonaceous chondrites, data from new meteorites are shown as solid symbols. Published data of CC from [3-5]

[1] Yuri (2008) *GCA* **72**, 221-232. [2] Qin (2010) *GCA* **74**, 1122-1145. [3] Trinquier (2008) *AJL* **655,** 1779-1185. [4] Clayton (1999) *GCA* **63**, 2089-2134. [5] Petitat (2011) *AJ* **736**, 23-30.

https://doi.org/10.1180/S0026461X00008434 Published online by Cambridge University Press

Isotopic analysis of sulfide captured on photographic film: Laboratory and field experiments

PAUL GORJAN[1*], DAVID A. FIKE[1], AND WILLIAM P. GILHOOLY III[2]

[1]Washington University in St Louis, St Louis MO, USA, pgorjan@levee.wustl.edu (* presenting author), dfike@wustl.edu

[2]Indiana University-Purdue University Indianapolis, Indianapolis, USA, wgilhool@iupui.edu

Sulfide is formed in sediment pore waters or in the water column of stagnant water bodies by the action of anaerobic sulfate-reducing bacteria. Sampling of free sulfide in natural environments has typically been done using syringes (for water column) or cores (for pore water). Yet the resolution of these approaches is often too coarse to capture steep environmental (e.g., redox) or ecological gradients in microbially dominated sediments.

We seek a means to capture a continuous record of ambient sulfide for subsequent stable isotope ($\delta^{34}S$) analysis. Previous work highlighted the potential of sulfide capture on metallic silver disks [e.g., 1-3]. However, this is not suitable for frequent deployments, particularly covering areas greater than a few cm^2. Here we build upon previous work for capturing atmospheric sulfide [e.g., 4,5], via reaction with the silver compound embedded in photographic film to form silver sulfide, which can then be quantified. This technique has the potential to capture a continuous $\delta^{34}S$ record across a wide range of environments and has the advantages of being inexpensive, readily available, rapidly deployable, and can be used *en masse* for sampling [4]. Here we test the reliability of photographic film to accurately capture the $\delta^{34}S$ signature of aqueous sulfide in laboratory experiments as well as in a natural setting.

In laboratory experiments, strips of photographic film were immersed in dissolved sulfide solutions with pH spanning 7–11 in closed systems and in contact with the atmosphere. No isotopic offset was detected for films immersed in high pH solutions. However, at pH ~7 films were consistently depleted by 1–2‰ relative to fluids, which we attribute to fractionation between sulfide species within the solution.

The method was also tested at a field site. Mahoney Lake in British Columbia, Canada, has sulfide present in the water column below ~7 m depth. Photographic film was lowered into the water alongside syringes for sulfide collection and a comparison made between the isotopic composition of sulfide from the film and the syringes. As with the laboratory experiments, the film sulfide was depleted by 1–2‰ compared to the aqueous sulfide under circumneutral pH.

[1] Visscher *et al*. (2000) *Geology* **28**, 919-922. [2] Fike *et al*. (2008) ISME J. **2**, 749 – 759. [3] Fike *et al*. (2009) *GCA* **73**, 6187 – 6204. [4] Horwell *et al*. (2004) *J. Environ. Monit.* **6**, 630 – 635. [5] Horwell *et al*. (2005) *J. Volcanol. Geoth. Res.* **139**, 259 – 269.

Complexation of Neptunium(V) with *Bacillus subtilis* endospores and their exudates

DREW GORMAN-LEWIS[1*], MARK P. JENSEN[2], ZOË R. HARROLD[1] AND MIKAELA R. HERTEL[1]

[1]University of Washington, Seattle, USA, dgormanl@u.washington.edu (* presenting author)

[2]Argonne National Laboratory, USA

Biological media may affect the movement of neptunyl ions, a highly toxic and potentially mobile radionuclide, in the environment. Most previous investigations of neptunyl-microbial interactions have focused on interactions with vegetative bacterial cells. However, endospores are known to comprise up to ca. 50% of the total bacterial populations in some environments and reserachers have identified endospore counts in soils as high as ca. 10^5 CFU/g of soil. Despite endospores being important biological media in the environment, neptunyl-endospore interactions have been ignored. Thus, we investigated neptunyl ion interactions with *Bacillus subtilis* endospore surfaces and their exudates.

B. subtilis endospore exudates are dominated by dipicolinic acid, which is a ligand that strongly binds neptunyl ions. *B. subtilis* endospores contain a large reservoir of dipicolinic acid in their cortex that can be released during germination or changes in permeability of the endospore coat, the latter being the most likely form of release in this work. Spectrophotometric investigations of the chemical form of neptunyl ion in endospore exudate solutions were consistant with the formation of neptunyl-dipicolinate complexes. Due to the strength of the 1:1 neptunyl-dipicolinate complex, neptunyl speciation in these experimental systems was heavily influenced by exudate complexation and controlled the extent surface adsorption. Neptunyl ions weakly adsorbed onto the endospore surface and sorption decreased with increasing pH, which corresponds to increasing aqueous complexation by dipicolinate.

Using spectrophotometric measurements of neptunyl-dipicolinate complexes and neptunyl-endospore adsorption data, we determined thermodynamic stability constants for both species. With stability constants determined in this work, we compared controls on neptunyl partitioning in simulated systems with *B. subtilis* vegetative and sporulated cells, (at dipicolinc acid concentrations corresponding to the extent of sporulation), and generic natural organic matter. Neptunyl complexation by dipicolinic acid exerted the greatest biological control in the simulated systems. This work highlights the importance of considering radionuclide complexation by microbial exudates when trying to understand the fate and transport of radionuclides in the environment.

https://doi.org/10.1180/S0026461X00008434 Published online by Cambridge University Press

Endolithic (bio)weathering and rock varnish in East Antarctica as early-Earth analogs of "protosoils"

SERGEY GORYACHKIN[1*], ALEX CHERKINSKY[2], NIKITA MERGELOV[1] AND ILIA SHORKUNOV[1]

[1]Institute of Geography, Russian Academy of Sciences, Moscow, Russia, goryachkin@igras.ru (* presenting author)

[2]Center for Applied Isotope Studies, University of Georgia-Athens, Athens, USA, acherkin@uga.edu

Introduction

Rock varnish and endolithic organisms being quite informative as early-Earth analogs are very well studied apart however their interaction and possible cogenesis have never been particularly explored, as well as nobody has studied them as soils. Endolithic organisms of Antarctic Dry Valleys inhabit structural cavities in the superficial rock interior [1]. The other common feature of Antarctica is the red-brownish colour of solid rocks (rock varnish).

Results and Conclusion

Our explorations in coastal oases of East Antarctic at field and microscopic scales showed that such system as "endolithic organisms-granitoid rock-weathering products" has all features to be denominated as "protosoil": (1) rock layer exposed to external abiotic factors; (2) this layer is inhabited by living organisms synthesizing and decomposing organic matter (OM); (3) induced by biotic and abiotic factors the initial lithomatrix is transformed *in situ*, the transformation products (e.g. fine earth) are retained and/or taken away, the vertical heterogeneity (microprofile) is formed. Organo-mineral horizons of endolithic soil contain 0,2-3,3% C and 0,02-0,47% N. ^{14}C mean residence time of OM reaches 480±25 y BP, $\delta^{13}C$= -23,7- -21,0 ‰. Major pedogenic products are numerous Fe-C- Si-Al- S-Cl-Ca-Mg-containing bio-coatings which cover cavities in the rock. Main binding material are amorphous Si and Al with incorporated detritus. SEM morphology and composition of coatings correspond to those observed in varnish on rock (Fig. 1).

Thus, certain types of rock varnish could be the products of endolithic (bio)weathering exposed after exfoliation and transformed by external factors. This hypothesis can't explain all rock varnishes (e.g. formed by accretion). However, this "endoliths-varnish" system may be recognized as an early-Earth "protosoil".

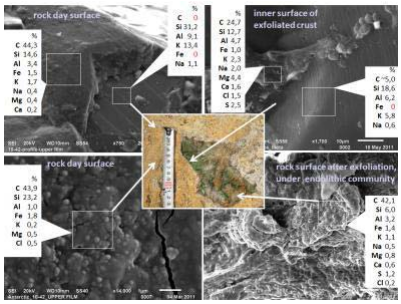

Figure 1: Rock varnish on the surface (left) and endolithic "protosoils" (right) and its elemental composition

[1] Friedmann (1982) *Science* **215**, 1045-1053.

Temporal variation in $^{187}Os/^{188}Os$ of the Arabian Seawater

VINEET GOSWAMI[1*], SUNIL K. SINGH[2]

[1]Physical Research Laboratory, Ahmedabad, India. vineetg@prl.res.in (* presenting author)

[2]Physical Research Laboratory, Ahmedabad, India. sunil@prl.res.in

Residence time of Os is 8-40 ka in the ocean [1], long enough to homogenise its isotopic signature in the global ocean but short enough to track the variations in its supply to ocean on glacial – interglacial time scale. Recent studies have shown variation in Os isotopic composition of seawater over glacial – interglacial time scale [2-5]. These variations have been interpreted in terms of variation in intensity of continental weathering.

To obtain a reliable and high reosolution record of marine $^{187}Os/^{188}Os$ form the Arabian Sea, sediments from a core in the south-eastern Arabian Sea (SS-3101G; 6.0°N, 74.0°E) have been analyzed. Samples have been leached by mild acidic peroxide solution to obtain the seawater Os isotope composition. The results display significant variation in $^{187}Os/^{188}Os$ of marine Os record from the Arabian Sea during last 29 ka. The $^{187}Os/^{188}Os$ of seawater in the most recent sample has a value of 1.04 ± 0.01, close to the Os isotopic composition of present day seawater (1.06 ± 0.01) [6]. The Os isotopic composition of the Arabian seawater vary in phase with that of the global ocean since last lat 29 ka except during the Last Glacial Maxima (LGM). During LGM, $^{187}Os/^{188}Os$ deviates from the trend set by the global ocean and shows an excursion towards higher $^{187}Os/^{188}Os$. Os concentrations of the leachable fraction of sediments from the Arabian Sea are higher during the LGM. Further, the Re contents of the LGM sediments are also higher.

Higher concentrations of Re and Os in the sediments deposited during the LGM indicate more suboxic/anoxic conditions at the sediment water interface during that time. Lower oxygen content in the bottom water of the Arabian Sea could have been caused by the reduced transport of polar waters (North Atlantic Deep water, NADW) into the Arabian Sea. Deviation of Os isotope composition of Arabian Seawater from the global oceanic trend and higher concentration of Re and Os during LGM, thus, indicate the reduced supply of NADW to the Arabian Sea during LGM, resulting in partial isolation of the Arabian Sea from rest of the oceans during the LGM [7-9].

[1] Oxburgh (2001) *G-cubed* 2000GC000104. [2] Oxburgh (1998) *EPSL* **159**, 181–191. [3] Dalai *et al.* (2005) *Chem. Geol.* **220**, 303–314. [4] Williams & Turekian (2004) *EPSL* **228**, 379–389. [5] Oxburgh *et al.* (2007) *EPSL* **263**, 246–258. [6] Levasseur *et al. Science* **282**, 272–274. [7] Pattan & Pearce (2009) *Palaeogeogr. Palaeoclimatol. Palaeoecol.* **280**, 396–405. [8] Sarkar *et al.* (1993) *Geochim. Cosmochim. Acta.* **57**, 1009–1016. [9] Piotrowski *et al.* (2009) *Earth Planet. Sci. Lett.* **285**, 179–189.

https://doi.org/10.1180/S0026461X00008434 Published online by Cambridge University Press

Engineered nanomaterials in rivers – exposure scenarios for Switzerland at high spatial and temporal resolution

F. GOTTSCHALK[1,2*], CHR. ORT[3], R.W. SCHOLZ[2] AND B. NOWACK[1]

[1] Empa – Swiss Federal Laboratories for Materials Science and Technology, Technology and Society Laboratory, fadri.gottschalk@empa.ch (* presenting author), nowack@empa.ch

[2]ETH Zurich, Institute for Environmental Decisions, Natural and Social Science Interface, roland.scholz@env.ethz.ch

[3]Eawag – Swiss Federal Institute of Aquatic Science and Technology, Christoph.Ort@eawag.ch

Introduction and methods

Two models, one based on probabilistic material flow analysis [1] and one based on graph theory [2], were combined to calculate predicted environmental concentrations (PECs) of engineered nanomaterials (ENMs) in rivers at local resolution. PECs for nano-TiO_2, nano-ZnO and nano-Ag were modeled for river sections downstream from 543 sewage treatment plants (STPs) at base flow conditions. Flow measurements over a 20-year period (1988–2007) at 20 selected locations were used to assess temporal variation. Due to the absence or ambiguity of available data on ENM dissolution behavior or agglomeration/sedimentation rates two "extreme" transport scenarios were considered: (i) a reactive scenario *with rapid (complete)* ENM *transformation* or sedimentation in rivers between two STPs and a conservative scenario *without any* ENM removal from the liquid phase.

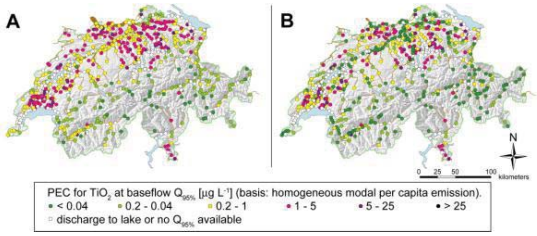

Figure 1: PECs of nano-Ag in Swiss rivers at base flow conditions (A: conservative scenario, B: reactive scenario).

Results

The highest concentrations were found in the midlands or near urban centers. Rural, alpine and pre-alpine values were negligibly small (Fig. 1). Temporal variation of PECs was evaluated by considering a whole range of "typical cases": small to large rivers (highly variable to more attenuated flow rates) and predominantly alpine to urban catchments (low to high ENM input). The alpine Rhine showed the smallest concentrations: the nano-Ag PECs ranged from 0.01 ng L^{-1} to 0.6 ng L^{-1} (conservative scenario). Some of the highest concentrations were observed within a lowland river section: 0.3 ng L^{-1} to 60 ng L^{-1} nano-Ag (conservative scenario).

[1] Gottschalk et al. (2010) Environ. Model. Softw. **25**, 320-332.
[2] Ort et al. (2009) Environ. Sci. Technol. **43**, 3214-3220.

Ultrapotassic lava flows from Colli Albani Volcanic District (Central Italy) give insights into the crystallization of magmatic calcite in effusive rocks

FERNANDO GOZZI[1*], MARIO GAETA[1,2], CARMELA FREDA[2], SILVIO MOLLO[2], TOMMASO DI ROCCO[3], FABRIZIO MARRA[2], LUIGI DALLAI[4], ANDREAS PACK[3]

[1]Sapienza-Università di Roma, Dipartimento di Scienze della Terra, fernando.gozzi@uniroma1.it (*presenting author)
[2]Istituto Nazionale di Geofisica e Vulcanologia, Roma, Italy.
[3]Georg August Universität, Geowissenschaftliches Zentrum, Göttingen, Germany.
[4]CNR-Istituto di Geoscienze e Georisorse, Pisa, Italy.

Calcite crystals are relatively common in alkalic hypoabyssalite and kimberlite rocks, but rarely documented in effusive rocks (e.g. alkaline lava flows). Magmatic calcite in effusive rocks has been usually related to mantle-origine carbonate; only in very few cases, it has been explained throughout magma-sediments interaction.

The ultrapotassic Colli Albani Volcanic District (Central Italy) represents one of the most peculiar volcanic districts on the Earth because of its liquid line of descent characterized by differentiated, low silica (SiO_2≤45wt%), K-foiditic magmas. Field, geochemical, and experimental studies have demonstrated that such a differentiation trend, starting from trachybasaltic parental magma, is mainly due to magma-carbonate sediments interaction. One of the most intriguing question concerning Colli Albani petrology is the occurrence of calcite crystals in the groundmass of some lava flows. In general, Colli Albani lava flows are made up of leucite and clinopyroxene phenocrysts and the groundmass contains leucite, clinopyroxene, and Ti-magnetite. More evolved products may also contain calcite, usually associated with nepheline. A detailed microtextural study of these calcite-bearing lava flows has shown that calcite occurs as follows: i) interstitially, associated with clinopyroxene, nepheline and phlogopite; ii) in ocelli, associated with fluorite and tangentially arranged clinopyroxene; iii) in coronitic reaction zone around K-feldspar xenocrysts. These microtextural features clearly indicate that calcite crystallized under magmatic conditions. Moreover, the high $\delta^{18}O$ (25-29‰ SMOW) and low $\delta^{13}C$ (down to -19‰ PDB) values of calcite crystals prove the sedimentary origin of the carbonate involved in the process. Finally, the occurrence of limestone fragments in the lava flows accounts for a syn-eruptive assimilation of the carbonate sediments. The high activity of fluorine in the Colli Albani magmas, as demonstrated by the occurrence of F-rich mineral phases (i.e, amphibole and mica), associated with fast crystallization due to the low magma viscosity, can have played a central role on the subsistence of sedimentary carbonate melt (then calcite crystals) at atmospheric pressure. This study may help unravelling the formation processes of the so-called "pseudocarbonatites", i.e. carbonated rocks related to the anatexis of crustal limestone.

https://doi.org/10.1180/S0026461X00008434 Published online by Cambridge University Press

Dissolved organic matter concentration and character influence Hg-S bioavailability to Hg-methylating bacteria

ANDREW M. GRAHAM[1*], ALLYSON L. BULLOCK[1], GEORGE R. AIKEN[2], AND CYNTHIA C. GILMOUR[1]

[1]Smithsonian Environmental Research Center, Edgewater MD, USA, grahaman@si.edu (*presenting author)
[2]U.S. Geological Survey, Boulder, CO, USA

Mercury methylation occurs primarily in mildly sulfidic environments where nanoparticulate forms of Hg-S are increasingly recognized to be of significance [1,2]. In this study, we sought to elucidate the role of dissolved organic matter (DOM) in altering the bioavailability of Hg-S to a model Hg-methylating bacterium, *Desulfovibrio desulfuricans* ND132. Methylmercury (MeHg) production by strain ND132 was evaluated in short-term washed cell assays in Hg-S-DOM solutions containing DOM isolates of varied origin, size, and composition, as well as a wide range of [Hg]/[DOM] and [Hg]/[sulfide] concentration ratios.

Under mildly sulfidic conditions (1-10 μM total dissolved sulfide), MeHg production was found to increase linearly with increasing DOM concentration, while relative bioavailability (i.e., fractional Hg methylation) increased logarithmically with increasing [DOM]/[Hg] ratio. Equilibrium speciation calculations indicated that Hg binding to DOM-thiols did not outcompete Hg binding to sulfide, and that solutions were supersaturated with respect to β-HgS(s) (metacinnabar) under most experimental conditions. We hypothesize that DOM enhanced MeHg production by stabilizing small, poorly crystalline HgS particles against growth/aggregation. Supporting this hypothesis, we found no DOM-dependent enhancement in Hg methylation in the presence of a strong Hg-binding ligand (L-cysteine) at concentrations sufficient to outcompete sulfide for inorganic Hg. Further, we found that while all DOM isolates tested (n = 12) enhanced MeHg production to some degree (2- to 25-fold enhancement at 20 mg C/L and 0.5 nM added Hg), the enhancement in Hg methylation correlated with the DOM isolates' specific UV absorbance (SUVA), a measure of DOM size and aromaticity. This finding is significant in that DOM size and aromaticity have been demonstrated to be key characteristics controlling HgS precipitation and dissolution [3], suggesting a link between dynamics of HgS precipitation/dissolution, Hg uptake, and Hg methylation.

Overall, our results point to the limits of existing equilibrium-speciation based models for Hg uptake and methylation. In addition to Hg and sulfide concentrations, DOM concentration and character are potentially important variables for predicting *in-situ* Hg-methylation rates in natural systems.

[1] Deonarine *et al.* (2008) *Environ. Sci. Technol.* ***43***, 2368-2373. [2] Gerbig *et al.* (2011) *Environ. Sci. Technol.* **45**, 9180-9187. [3] Waples *et al. Geochim. Cosmochim. Acta*. **69**, 1575-1588.

Apollo 15 zircons reveal age of young impact

MARION L. GRANGE[1*], ALEXANDER A. NEMCHIN[1], ROBERT T. PIDGEON[1] AND CHARLES MEYER[2]

[1]Curtin University, Perth, Australia, m.grange@curtin.edu.au
[2]Johnson Space Center, Houston, USA.
(* presenting author)

We have investigated microstructures of zircon and apatite grains, their textural context and U-Pb ages, in Apollo 15 sample 15405, aiming to extend the existing database consisting of Apollo 14 and 17 breccia samples. Sample 15405 was chipped from a boulder at Station 6A, south of the landing site and close to the Apennine Front. It is a clast-bearing impact melt breccia, with a crystalline matrix, similar in chemistry to KREEP basalt, and containing KREEP basalt and quart-monzodiorite (QMD) clasts. It contains zircon and apatite grains both within the matrix and in QMD clasts.

Zircon grains in the matrix are abraded or broken fragments. Zircons in both matrix and clasts are anhedral, showing oscillatory and sector zoning in CL. Previous work [1] on zircon included in QMD clasts indicated a disturbed U-Pb system in the grains with an upper concordia intercept at 4294±26 Ma and a lower intercept at 1320 +240/-280 Ma (2σ). New data show comparable patterns, with no age distinction between zircon from the matrix and from clasts: both types show concordant and discordant ages, although oscillatory zoned zircon are systematically concordant. The combination of concordant analyses gives the age of 4335±7 Ma (2σ). When combining these data with discordant ages from zircon and apatite, a lower intercept is obtained at 1570±51 Ma (2σ). In addition, a single spot in one zircon shows a concordant age at 2053±14 Ma (1σ).

These young U-Pb ages have never been found before in lunar zircons that are usually >3.9 Ga. It indicates that the relatively robust U-Pb system in zircon has been severely disturbed at ~1570 Ma (and maybe also at ~2.05 Ga). Such late disturbance is also recorded in Ar-Ar ages at ~1.3 Ga [2] and ~2.1 Ga [3]. These authors [3] interpreted these young ages as disturbance following close-by impacts that they tentatively identified as Aristillus and Autolycus, respectively.

If these young U-Pb ages of zircon can be associated with a particular impact event, this would be the first time a clear link can be established between a specific impact event and a zircon age. This would have major implications for constraining variations in the flux of impactors through the history of the inner Solar System, as so far only relative ages of craters exist. Previous studies [3] showed that even poorly defined ages of specific crater, i.e. much less precise that what can be obtained using zircon, can dramatically increase our understanding of the impact flux of the Moon, and by extension of the Earth. Such opportunities have to be fully explored making breccia 15405 one of the key samples in the lunar collection.

[1] Meyer et al. (1996) *MAPS* **31**, 370-387. [2] Bernatowitz et al. (1978) *Proc. LPSC* **9th**, 905-919. [3] Ryder et al. (1991) *Geology* **19**, 143-146.

https://doi.org/10.1180/S0026461X00008434 Published online by Cambridge University Press

The importance of hickory trees (*Carya*) in biogeochemical cycling of meteoric ^{10}Be

DARRYL E. GRANGER* AND GRACE CONYERS

Department of Earth and Atmospheric Sciences, Purdue University, West Lafayette, IN USA, dgranger@purdue.edu (* presenting author), gconyers@gmail.com

Meteoric ^{10}Be is widely used to monitor weathering and erosion of soils, with little regard to biogeochemical cycling. We found that hickory trees (Carya spp.) strongly bioaccumulate beryllium. Because oak-hickory forests are a dominant biome over much of the eastern United States, hickory trees can play an inordinately large role in the cycling of meteoric ^{10}Be in these areas.

To explore the role of trees in biological cycling of ^{10}Be, we analyzed composite samples of wood and leaves from four dominant tree species (red hickory, Carya ovalis; black oak, Quercus velutina; red maple, Acer rubrum; and tulip poplar, Liriodendron tulipfera) as well as soil at the Martel experimental forest in northern Indiana, USA. We analyzed samples from 1 ha of unmanaged forest growing on loess and loamy till of Late Wisconsinan age.

We found that hickory contains the highest beryllium concentrations by a factor of 50-100, with an average of 0.39 ppm (dry mass) in the wood, subequal to the average exchangeable [Be] in the soil of 0.43 ppm. Abscised hickory leaves have a higher [Be] of 2.0 ppm. The isotopic ratio ^{10}Be/^{9}Be in all four tree species was similar, ranging from 6-8 x 10^{-9}. Using standard allometric equations relating tree biomass to trunk diameter, and assuming that belowground biomass has the same [Be] as aboveground, we calculate that hickory trees at our site contain an average of ~0.5% of the total ^{10}Be under their crown and that 5-15% of this Be is cycled annually by leaf abscission. It is not clear at this point what fraction of Be in litterfall is recycled into the plant, returned to the soil, or carried to groundwater as organic complexes.

Although the fraction of ^{10}Be in standing biomass is small, annual cycling in litterfall can be significant when integrated over thousands of years. Using our values for [^{10}Be] in litterfall, we can estimate the probability that a given atom of ^{10}Be in a forest soil will have passed through a hickory tree. Hickories occupy an average of ~10% of the oak-hickory forest area. Assuming that trees are randomly distributed and that litterfall Be is returned to the soil, and maintaining a constant ^{10}Be budget for generality, we calculate that nearly half of all ^{10}Be in the forest soil will have passed through a hickory tree over the past 10 ky. It is clear that hickories can transport a sizable fraction of the total ^{10}Be in their nutrient cycle, and that they may be responsible for landscape-scale Be mobility.

Biogeochemical cycling of ^{10}Be has not previously been fully appreciated. It is known that many plants and fungi contain Be at the 0.1-0.5 ppm level (ash mass), approximately 10 times lower than in hickory, and that the larch tree (Larix) also accumulates Be. There has been no systematic survey, however, to examine ^{10}Be in the ecosystem. Much more work is needed to understand ^{10}Be mobility in the biosphere, including the influence of ecosystem shifts, land management, harvesting, and burning, both natural and anthropogenic. It is possible that ^{10}Be signals previously attributed to soil erosion may instead be due to biological disturbance.

Weathering at the Mineral-Fungus-Bacteria Interface Analyzed with Scanning Electron Microscopy and Helium Ion Microscopy

K.A. GREENBERG[1]*, Z. BALOGH-BRUNSTAD[1], B.W. AREY[2], S.M. NIEDZIELA[1], A. DOHNALKOVA[2, 3], Z. SHI[3], AND C. K. KELLER[3]

[1] Hartwick College, Oneonta, NY, 13820 USA (*correspondence: balogh_brunz@hartwick.edu)

[2]Environmental Molecular Sciences Laboratory, Pacific Northwest National Laboratory, Richland, WA, USA

[3]School of the Environment, Washington State University, Pullman, WA, USA

Introduction and Methods

Bacteria and fungi are documented agents of chemical weathering and nutrient uptake by higher plants. However, the role of biofilm in these processes is poorly understood. This study examines components of a laboratory column growth experiment to study the mineral-fungus-bacteria interface, morphology of mineral surfaces, and associated microbes and biofilm when calcium and potassium sources are varied. We hypothesized that 1) under limiting Ca and K conditions, thick biofilm cover develops to protect the mineral-fungus-bacteria interface and facilitate direct cation uptake from the minerals; 2) as Ca and K are made increasingly available in the input solutions, biofilm becomes thinner, patchy and less developed.

Red Pine (*Pinus resinosa* Ait.) was grown in leach tubes filled with quartz sand and 0.5 wt% biotite and 1 wt% anorthite. Half of the trees were inoculated with *Suillus tomentosus* and a variety of soil bacteria and the other half were left without inoculation. Columns without biology served as controls. The columns were supplied with Ca and K in irrigation water at 0, 10, 30 and 100% of what a healthy tree would need for growth. A subset of columns were destructively sampled after one month and three months growth. Biotite and anorthite were analyzed from the rhizosphere of each tree and also from the bulk material with helium ion microscopy (HeIM) and scanning electron microscopy (SEM) equiped with energy dispersive x-ray spectroscopy (EDS).

Results and Discussion

Microscopy images show that after one month, bacterial colonization dominated the rhizosphere with few areas of fungal development. By the 3rd month, abundant fungal hyphal cover of rhizospheric minerals developed in the 0 and 10% Ca and K treatments and the 30 and 100% Ca and K treatments remained less colonized. The bulk material of the tree treatments and the controls remained nearly unaffected by microbes. Fungal hyphae appear to "search" for weaknesses of the crystal structure such as particle and step edges, existing fractures and perhaps inpurities or inclusions. Bacteria are associated with fungal hyphae in some places, but do not form large biofilm colonies. Biofilm and polysaccharide cover remained patchy through the 3 month growth period in all treatments, but a slight decrease of cover was detected with increasing concentrations of Ca and K in the irrigation solutions.

In conclusion, our study shows that biofilm is directly affected by Ca and K concentrations in input solutions, but later time points of our experiments (6 and 9 months), most likely with more developed biofilm, will be analyzed to support our first hypothesis.

https://doi.org/10.1180/S0026461X00008434 Published online by Cambridge University Press

Boron isotope based CO_2 record during retreat of the Antarctic ice sheet

ROSANNA GREENOP[1*], GAVIN L. FOSTER[1], PAUL A. WILSON[1]

[1]Ocean and Earth Sciences, National Oceanography Centre Southampton, University of Southampton, Waterfront Campus, Southampton, SO14 3ZH, United Kingdom r.greenop@noc.soton.ac.uk (*presenting author)

Large ice sheets have existed on Antarctica since the Eocene-Oligocene transition (~34 Ma) when atmospheric CO_2 dropped below around 750 ppm. Results of ice sheet modelling experiments suggest that once the land based East Antarctic ice sheets had grown, a powerful hysteresis effect should have acted to make them inherently stable necessitating high CO_2 levels >> 750 ppm to initiate deglaciation [1]. However, the deep sea oxygen isotope record [2] and results of proximal ice drilling [3] suggest that there has been large fluctuation in Antarctic ice sheet volume, while existing CO_2 records appear to have remained relatively low and constant [2].

Here, we explore this hysteresis effect using boron isotopes, measured by MC-ICPMS, to produce high-resolution CO_2 records during the warming into the Mid-Miocene Climatic Optimum, a time interval associated with significant retreat of the Antarctic Ice Sheet [3]. A high-resolution boron isotope record has been produced for the time period between 15.5 and 17 Ma at ODP Site 761 (16°44.23′S, 115°32.10′E 2179 m). Our results show relative changes in atmospheric CO_2 across this time interval. By combining this new record with records of proxy ice volume change we shed new light on our understanding of CO_2 driven retreats of the Antarctic ice sheet.

[1] Pollard & DeConto (2005) *Global and Planetary Change* **45**(1-3), 9-21[2] Zachos *et al.* (2008) *Nature* **451**(7176), 279-283 [3] Passchier *et al.* (2011) *Geol Soc Am Bull,* ***123***(11-12), 2352-2365.

Water in the Moon: D/H and high volatile abundances of lunar apatite

JAMES P. GREENWOOD[1*], SHOICHI ITOH[2], NAOYA SAKAMOTO[3], PAUL H. WARREN[4], LAWRENCE A. TAYLOR[5], HISAYOSHI YURIMOTO[2,3]

[1]Dept. of Earth & Environmental Sciences, Wesleyan University, Middletown, CT 06459 USA

[2]Natural History Sciences, Hokkaido University, Sapporo 060-0810 JAPAN

[3]Creative Research Initiative "Sousei", Hokkaido University, Sapporo 060-0810 JAPAN

[4]Institute of Geophysics & Planetary Physics, University of California, Los Angeles CA 90095 USA

[5]Planetary Geosciences Institute, Dept. of Earth & Planet. Sci., Univ. of Tennessee, Knoxville, TN 37996-1410 USA

In order to study ^{1}H and D distributions in individual apatite grains $\{Ca_5(PO_4)_3(F,Cl,OH)\}$ in a range of lunar rocks collected during the Apollo program, we have been using a new ion microprobe technique that combines quantitative spot analyses with semi-quantitative 2-D ion imaging. We find the Moon has abundant water and a distinct range of D/H compared to known water sources in the solar system [1]. Since our publication, we have measured D/H and OH in lunar apatite in five more samples. New samples include mare basalts 10047 and 12064 that both have high δD, but moderate water contents (<2000 ppmw OH) in comparison to other mare basalts that we have measured. New analyses of mare basalt 12039 have been performed, a rock from which a significant portion of our pubished data was derived. These new analyses of 12039 suggest less variability in D/H than reported for this sample.

We continue to see that the mare basalts have significant hydroxyl in their apatite grains (with the exception of olivine basalt 12040). Estimates for the lunar-mantle water content from apatite grains are fraught with assumptions. However, with some assumptions, we can estimate the H_2O content of the lunar mantle that produced 12039. For 3-5% partial melting, and assuming no assimilation of volatile-bearing material by the magma, a mean partition coefficient of 0.4 for OH between apatite and melt (e.g. [2]), and that apatite is the only OH-mineral crystallizing from the magma, and no degassing of H_2 or H_2O, and, finally, that our highest water content apatite represents 99% crystallization of the magma, we estimate 5-8 ppm H_2O for the 12039 source region.

[1] Greenwood J. P. et al. (2011) *Nature Geosci.,* **4**, 79-82. [2] Boyce J. W. et al. (2010) *Nature* **466**, 466-469.

https://doi.org/10.1180/S0026461X00008434 Published online by Cambridge University Press

Isotopic evidence for the early use of ceramics in cooking meats and processing milk from sheep and goats

MICHAEL W. GREGG[1*], GREG F. SLATER[2]

[1] School of Geography and Earth Sciences, McMaster University greggm@mcmaster.ca (*presenting author)
[2] School of Geography and Earth Sciences, McMaster University gslater@mcmaster.ca

14b. Reciprocal interactions between archaeology and archaeometry focusing on characterization of ancient human settlements and their environmental impacts

This paper presents molecular and isotopic evidence for prehistoric subsistence practices associated with the earliest use of clay and manufacturing of pottery vessels in a narrow geographic corridor linking the Middle East with Central Asia. Through use of our recently-developed protocol for extraction, isolation and transesterification of free fatty acids from archaeological pottery[1], $C_{16:0}$ and $C_{18:0}$ saturated fatty acids with ratios consistent with degraded animal fats[2] were obtained from fired-clay and pottery fragments from Hotu and Belt Caves in northern Iran. These rock shelters, situated on the late Pleistocene shoreline of the Caspian sea in the foothills of the Alborz mountains, were excavated by University of Pennsylvania anthropologist Carleton Coon in the fall of 1949 and the spring of 1951[3,4]. The mid-Mesolithic to late Neolithic period human occupations from which these materials were recovered date between 4850 and 13250 calBC[5,6].

Compound-specific isotopic analyses ($^{13}C/^{12}C$) of $C_{16:0}$ and $C_{18:0}$ fatty acids surviving in 16 of 37 fired-clay and pottery fragments (43%) revealed ratios of $\partial^{13}C$ values consistent with those of modern ruminant milk fats and carcass fats of sheep, goats and pigs[2,1]. These results demonstrate that clay was used in cooking meats during the late Pleistocene and pottery vessels were used in processing milk from sheep and goats at the onset of the Holocene — the earliest direct evidence of these two subsistence practices reported in this region to date. These findings raise many questions concerning core and peripheral areas of independent economic innovation in western Eurasia, and draw attention to the compelling need for additional research into the role of ceramic technologies as a catalyst for a sedentary way of life in Central Asia following the last Ice Age.

[1] Gregg & Slater (2010) *Archaeometry,* **52**:833-854.
[2] Evershed et al. (1997) *Naturwissenschaften,* **84**:402-406.
[3] Coon (1951) *Cave Explorations in Iran 1949.*
[4] Coon (1952) Proc. Amer. Philosophical Soc., **96**/3: 231-249.
[5] Libby (1951) *Radiocarbon Dating,* 72.
[6] Ralph (1955) *Science*, **121**/ 3136: 149-151.

Assessing the effect of macrobenthos diversity on the mineralisation of sediment organic matter

ANTOINE GREMARE[1*], BRUNO DEFLANDRE[1], SABINE SCHMIDT[1], OLIVIER MAIRE[1], ALICIA ROMERO-RAMIREZ[1], EDOUARD METZGER[2], ERIC VIOLLIER[3], FLORIAN CESBRON[2], CELINE LABRUNE[4], JEAN MICHEL AMOUROUX[4], PASCAL LECROART[1], JEAN CLAUDE DUCHENE[1], DAMIEN CABANES[1], AUDE CHARRIER[1], DOMINIQUE POIRIER[1], LAURENCE COSTE AND SABRINA BICHON[1]

[1] University Bordeaux 1 - CNRS, EPOC a.gremare@epoc.u-bordeaux1.fr (* presenting author)
[2]Universirty of Angers, BIAF,
[3]University Denis Diderot, IPGP,
[4]University Paris 6 - CNRS

Through bioturbation, macrobenthos is known to indirectly control the fate of sedimented organic matter including its mineralisation through early diagenetic processes. The diversity of macrobenthos and more specifically coastal macrobenthos is now at threat to the rise of a large variety of human-induced disturbances. The consequences of a decline of macrobenthos diversity on sedimented organic matter mineralization are still largely unknown. Up to now, they have been mostly studied through an experimental approach consisting in the *in vitro* assessment of mineralisation fluxes at the water-sediment interface in the presence of an increasing complexity of macrobenthic assemblages [1]. This approach has most often resulted in the determination of slight unpredictable effects. It suffers from major drawback including the fact: (1) that macrobenthos assemblages are reconstructed at random whereas species extinction does not, and (2) the importance of diversity relative to other potential controlling factors is not assessed.

We will present another possible approach consisting in assessing the effect of diversity by carrying out comparative *in situ* studies. In order to unravel the effects of possible confounding factors, it should be coupled with a hierarchical approach, which consists in considering that the intensity of mineralization results from the superposition of the effects of different types of ranked factors: first abiotic factors, second the quantity of organic matter, third the quality of organic matter, and only fourth macrobenthos diversity. This approach allows for the assessment of the relative importance of all main potential controlling factors given that co-correlation between them is properly handled. It requires studying a large variety of ecological/biogeochemical situations, which is currently achieved within the framework of the French National program BIOMIN.

This on-going project consists in an interdisciplinary study including the assessment of: (1) abiotic parameters, (2) sedimented organic matter quantitative (e.g., C and N) and qualitative (Chl *a* and EHAA) characteristics, (3) bioturbation (bioirrigation and sediment reworking), and (4) mineralization fluxes (oxygen and nutrients). It is carried out in five main ecosystems located along the French Metropolitan coast, namely: (1) the Rhône River prodelta, (2) the extremity of the dilution area of the Rhône River, (3) The Arcachon Bay, (4) the Garonne River prodelta, and (5) the Bay of Biscaye.

We will first report on preliminary results obtained within the Rhône river prodelta. Based on these results, we will then use the hierarchical approach described above to assess whether or not taking into account macrobenthos diversity enhances the description of mineralization fluxes by abiotic parameters and organic matter characteristics.

[1] Norling *et al. Mar.Ecol.Prog. Ser.* (2007) **332**, 11-23

https://doi.org/10.1180/S0026461X00008434 Published online by Cambridge University Press

The sensitivity of *Mytilus* shell microstructure and geochemistry to environmental change

ERIKA GRIESSHABER[1]*; SABINE HAHN[2], ADRIAN IMMENHAUSER[2] AND WOLFGANG SCHMAHL[1]

[1]Department of Earth and Environmental Sciences, LMU Munich, Germany, E.Griesshaber@lrz.uni-muenchen.de

[2]Institut für Geologie, Mineralogie, Geophysik, Ruhr-Universität Bochum, Germany,sabine.hahn@rub.de

Preservation of biological hard tissues offers unique opportunities for reconstructing environments of formation. Prerequisites for a precise reconstruction are the profound understanding of the studied biological material as well as their ability to record environment derived signatures. Even though bivalves are perfect archives for past environmental change they have not yet been used to interpret ocean acidification events. In a multianalytical approach combining microstructure imaging, crystallographic texture analysis and trace element geochemistry we investigated the microstructural and geochemical responses of *Mytilus galloprovincialis* shells to seawater acidification. Live specimens of *M. galloprovincialis* were transplanted from Ischia harbour (Mediterranean Sea) to nearby CO2 vents and exposed to mean seawater pH of 8.07 (harbor) and 7.25 (vent). The shells recorded the shock of transplantation and environmental change in both, their microstructure, texture (Figure 1), trace element (Figure 2) and carbon and oxygen isotope record [1]. We explore in this paper the potential of three different proxies within the same carbonate archive and test the potential of *Mytilus* to preserve in its shells acidified seawater conditions.

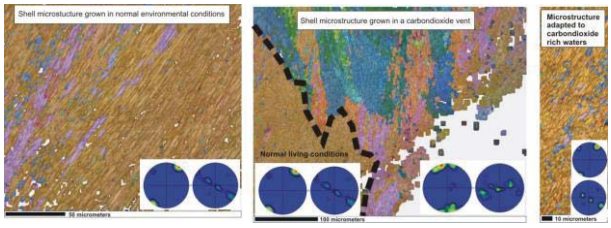

Figures 1. The shock of transplantation from normal to acid environmental conditions recorded in the microstructure and texture of *Mytilus galloprovincialis*.

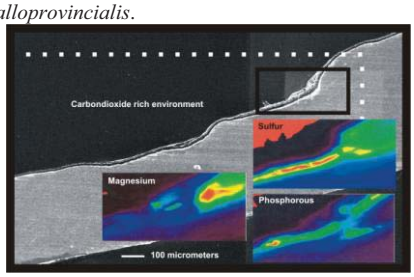

Figures 2. The transplantation from normal to an acid environment is manifested in the shells ultrastructure and in its major and minor element chemical variation.

[1]. S. Hahn, R. Rodolfo-Metalp2, E. Griesshaber, W. W. Schmahl, D. Buh1, J. M. Hall-Spencer, C. Baggin2, K. T. Fehr, and A. Immenhauser (2012) *Biogeosciences Discuss*. **8**, 10351–10388.

Coal-to-gas: Uncertainty in CH_4 emissions and climate impacts

W. MICHAEL GRIFFIN[1*] AND STEFAN SCHWIETZKE[2]

[1]Carnegie Mellon University, Tepper School of Business, Engineering and Public Policy, wmichaelgriffin@cmu.edu (* presenting author)

[2]Carnegie Mellon University, Engineering and Public Policy, sschwiet@andrew.cmu.edu

Section Heading

Increasing the use of natural gas (NG) for power generation and other industrial purposes is perceived as an part of a portfolio to decarbonize the domestic and global economy. While many studies indicate greenhouse gas (GHG) emissions reductions from NG production and use relative to coal [1], the potential climate benefits remain largely uncertain and depend on three main factors. First, CH_4 emissions from NG production, distribution and use are uncertain, and some estimates eliminate the overall GHG reductions [2]. Second, the combined climate response due to direct and indirect radiative forcing from GHG and aerosol emissions remains to be quantified [3]. Third, the rate of a potential coal-to-gas transition can influence future temperature change trajectories [4], and has not been analyzed in detail.

Our analysis addresses these issues by combining data and models from life cycle assessment (LCA), an emissions accounting tool, and climate science. We determine a reduced range of possible life cycle CH_4 emissions through comparison with atmospheric observations and modeling results from the literature. Methods to generate these top-down estimates include a combination of (a) measuring CH_4 concentrations from a global observation network, (b) employing atmospheric emissions transport models, and (c) measuring CH_4 isotope ratios to distinguish emissions sources [5]. We further establish coal-to-gas transition scenarios based on constraints for resource availability and industry development. A probabilistic climate model is used to translate the emissions distributions and scenarios into temperature change trajectories. The model accounts for uncertainty in the magnitude of aerosol forcing and climate feedbacks, which represent low probability and high impact events [6].

Results and Conclusion

Preliminary results show that CH_4 emissions estimates can be significantly constrained. For example, over a 10-year period the upper bound life cycle CH_4 emissions overestimate observed absolute emissions by 75-100%. In terms of climate impacts, the degree to which lower CO_2 and aerosol emissions from reduced coal combustion compensate for higher CH_4 emissions due to higher NG varies depending on the transition scenario. Work in progress investigates the probability of each scenario to cross the policy relevant 2 degree celsius temperature threshold.

[1] Venkatesh et al. (2011) *Env. Sci. Tech.* **45**, 8182-8189. [2] Howarth et al. (2011) *Climatic Change* **106,** 4, 679-690. [3] Wigley (2011) *Climatic Change* **108,** 3, 601-608. [4] Schwietzke, Griffin, Matthews (2011) *Env. Sci. Tech.* **45**, 8197-8203. [5] Bousquet et al. (2006) *Nature* **443**, 439-443. [6] Goes et al. (2011) *Climatic Change* **109,** 3-4, 719-744.

https://doi.org/10.1180/S0026461X00008434 Published online by Cambridge University Press

The end of the Hadean: The world turns over

W.L. GRIFFIN[1*],. V. MALKOVETS[1,2], E.A. BELOUSOVA[1], SUZANNE Y. O'REILLY[1] AND N.J. PEARSON[1]

[1]ARC Centre of Excellence for Core to Crust Fluid Systems, Department of Earth and Planetary Sciences, Macquarie University, Sydney, NSW 2109, Australia

bill.griffin@mq.edu.au (*presenting author);

elena.belousova@mq.edu.au; sue.oreilly@mq.edu.au;

norman.pearson2mq.edu.au

[2] Institute of Geology and Mineralogy, Russian Academy of Sciences, Novosibirsk, Russia, 630090

vladimir.malkovets@gmail.com

Context and Results

A U-Pb/Hf-isotope study of >16,000 zircons from sources worldwide has demonstrated that at least 70% of Earth's continental crust probably formed in Archean time [1], and much probably is >3 Ga old. The model-age (T_{RD} and T_{MA}) distributions of ca 500 low-Re sulfides in mantle-derived peridotite xenoliths, mainly from the Kaapvaal, Siberian and Slave cratons, peak between 2.5-3.0 or 3.0-3.5 Ga, depending on locality. In detail, at each locality the oldest T_{MA} model ages from the mantle sulfides correlate well with the oldest U-Pb ages and Hf model ages from crustal zircons. Younger T_{MA} peaks commonly coincide with later major crustal events.

The sulfides in mantle xenoliths are secondary phases, and Os model ages probably are biased toward young ages. Most of the studied sulfides are from garnet-bearing peridotites, and garnet is generally a secondary phase in these rocks [2]. In Siberian xenoliths, model ages of sulfides included in garnet are younger on average than those of sulfides included in olivine. However, detailed searches of the most depleted peridotites available have thus far revealed very few sulfides with model ages >3.5 Ga, just as the oldest widespread crustal ages are around 3.5 Ga.

Conclusions

These data suggest that the oldest crust and the oldest, highly depleted SCLM are broadly coeval, and are interpreted as forming during massive mantle overturns that produced the residual Archean SCLM, providing buoyant "life rafts" that ever since have supported and preserved the continental crust. The 3.5 Ga overturn event changed Earth's fundamental tectonic behaviour, and truly marks the end of the Hadean period

[1] Belousova *et al*. (2010) *Lithos* **119**, 457-466. [2] Malkovets *et al.* (2007) Geology 35, 339-342.

Investigating controls on calcium isotope ratios in marine carbonates and barite across the Paleocene-Eocene Thermal Maximum

ELIZABETH M. GRIFFITH[1*], MATTHEW S. FANTLE[2], THOMAS D. BULLEN[3], ANTON EISENHAUER[4], AND ADINA PAYTAN[5]

[1]Kent State University, Kent, USA, egriffi9@kent.edu (* presenting author)

[2]Pennsylvania State University, University Park, USA, mfantle@psu.edu

[3]U.S.Geological Survay, Menlo Park, USA, tdbullen@usgs.gov

[4]IFM-GEOMAR, Kiel, Germany, aeisenhauer@geomar.de

[5]University of California, Santa Cruz, USA, apaytan@ucsc.edu

The stable calcium isotopic composition of seawater can be controlled over million-year time scales by the relative fluxes of Ca into and out of the ocean, given knowledge of the isotopic compositions of these fluxes. Ocean acidification, such as occurred at the Paleocene-Eocene Thermal Maximum (PETM), should perturb the riverine input of Ca relative to Ca output as pelagic $CaCO_3$. We therefore expect coincident variability in the Ca (and C) cycles that should be evident in the Ca isotope record. Yet environmental and post-depositional factors can affect the isotopic composition of a recording phase resulting in values inconsistent with changes in seawater Ca isotopic composition. This study measures Ca isotopes in marine barite and bulk carbonates over the PETM in order to evaluate their use as recorders of seawater $\delta^{44}Ca$.

This study reports high temporal resolution (~25 ka) Ca isotopic compositions ($\delta^{44}Ca$, relative to Bulk Earth) of bulk marine carbonates and coeval marine pelagic barite from ODP Leg 199 Site 1221C (Equatorial Pacific) and bulk carbonates from ODP Leg 198, Site 1212B (Shatsky Rise). The study also reports $CaCO_3$ content and bulk carbonate $\delta^{13}C$ and $\delta^{18}O$ for 1221C and 1212B. The marine barite Ca isotope record decreases by 0.3‰ after the benthic extinction event (BEE), increases to a maximum (-0.7‰) as $CaCO_3$ accumulation rates peak, and returns to values near modern day (-1.3‰) <100 ka after the BEE. Interestingly, bulk carbonate $\delta^{44}Ca$ values are distinct from the barite record. At Site 1221C, carbonate $\delta^{44}Ca$ increases just after the barite $\delta^{44}Ca$ drop and stays high (~0.4‰) until the barite record returns to near modern $\delta^{44}Ca$ values. Sediments at 1221C decrease to near zero $CaCO_3$ accumulation at the BEE, strongly suggesting that dissolution occurred. By comparison, the 1212B core has high $CaCO_3$ content (80-98%) over this interval and exhibits trends that are similar to the 1221C marine barite record but vary in absolute magnitude.

One hypothesis to explain the observed differences is that post-depositional diagenetic reactions (dissolution/recrystallilzation) in the sedimentary column influence the measured $\delta^{44}Ca$. Alternately, it is possible that variations in local Ca cycling can explain the differences in the carbonate and barite records. We will explore both hypothesis using numerical models and various data.

https://doi.org/10.1180/S0026461X00008434 Published online by Cambridge University Press

A high-resolution paleoclimate reconstruction using C and N isotopes in a subarctic environment, northern Canada

FRITZ GRIFFITH[1*], IAN CLARK[1], TIM PATTERSON[2], ANDREW MACUMBER[2], JENNIFER GALLOWAY[3], AND HENDRIK FALCK[4]

[1]University of Ottawa, Dept. of Earth Sciences, Ottawa, Ontario, Canada, fgrif103@uottawa.ca (* presenting author)
[2]Carleton University, Dept. of Earth Sciences, Ottawa, Ontario, Canada
[3]Geological Survey of Canada, Calgary, Alberta, Canada
[4]Northwest Territories Geoscience Office, Yellowknife, Northwest Territories

The Tibbitt-to-Contwoyto Winter Road (TCWR) is the sole overland route servicing diamond mines north of the city of Yellowknife, Northwest Territories (NWT), Canada. Because the majority of the TCWR traverses frozen lakes, late freezing or early thawing of these lakes can drastically shorten the transportation season, imparting significant economic consequences on mining operations. Such was the case in 2006, when a warm and stormy winter season associated with an El Niño Southern Oscillation (ENSO) event resulted in a significant and costly reduction of shipments to the mines. As the use of the TCWR is projected to increase in the coming years, planners and policy makers require a sound scientific understanding of past regional climate variability upon which to base their development strategies. Previous research has been valuable in gaining a broad understanding of regional long-term climate change; however, no research has provided a climate record with a resolution high enough to identify medium- to short-term climate phenomena that might be affecting this region (e.g. sub-decadal ENSO cycles and the decadal-scale Pacific Decadal Oscillation [PDO]).

This study is an integral component of a larger-scale study designed to develop a comprehensive database of high-resolution paleoclimate data for the NWT, using a variety of proxies. As part of the larger study, freeze cores were taken in 2010 from 10 lakes along the TCWR and sliced at 1-mm intervals using a custom-designed freeze core microtome. We report here the results of preliminary bulk ^{13}C and ^{15}N isotope analyses, taken at 1-cm intervals throughout the Danny's Lake and Horseshoe Lake cores. Higher-resolution analysis is underway for sections of the Danny's Lake core in order to identify short-term climate cycles. Additionally, C and N isotopic compositions are currently being analysed for surface sediment samples of over 90 lakes scattered along a latitudinal gradient throughout the NWT. These data will be used to create a paleoclimatic transfer function, which will correlate spatial variations in isotope values to climate parameters, and provide a means of using temporal variations in these isotopes down-core to quantitatively reconstruct past climate change.

Preliminary results from the Danny's Lake core show clear trends in isotopic compositions for both C and N isotopes and suggest distinct stages of lake evolution. Previous to 6700 BP, there are large long-term fluctuations in isotope values, which may be related to significant variations in vegetation or lake water levels. At 6700 BP, a sudden change in trends, as well as a sharp colour change in the sediment, suggest a significant and abrupt shift in lake dynamics, the source of which is currently under investigation. A positive correlation between the C/N ratio, %C, and %N from 6700-4000 BP suggests an increase in terrestrial organic matter input to the lake. This increase stops at 4000 BP and is stable to the present. Comparison of these preliminary results to the paleoclimatic transfer function will provide greater insight into the causes of these trends.

Influence of mineral surfaces on Re speciation in sulfidic porewaters

LAURA M. GROSKREUTZ[1*] AND TRENT P. VORLICEK[1]

[1]Minnesota State University, Mankato, Minnesota, USA, laura.groskreutz@mnsu.edu (*presenting author) trenton.vorlicek@mnsu.edu

Introduction

The thioperrhenate anions may be important species in the chemical pathway to Re deposition within sulfidic waters. Thioperrhenate formation reactions may be written:

$$Re^{VII}O_4^-{}_{(aq)} + nH_2S_{(aq)} \rightleftharpoons Re^{VII}O_{4-n}S_n^-{}_{(aq)} + nH_2O_{(l)}\ (n = 1\text{-}4)$$

Because of their immense areas and hydrated properties, oxide surfaces are known to influence various environmentally relevant reactions within porewaters of soils and sediments [1,2]. Mineral catalysts have been shown to greatly enhance the rate of thiomolybdate reactions [1]. To test the conjecture that thioperrhenate reactions are also catalyzed by oxide surfaces, solutions were prepared to contain 0 to 10 g/L δ-Al_2O_3, 10 µM ReO_4^- and10 mM ΣS^{2-} at pH = 7.0. ReO_4^- remaining in the filtered solutions after 0.2 and 22 days was quantified using ion chromatography (IC) with suppressed conductivity detection.

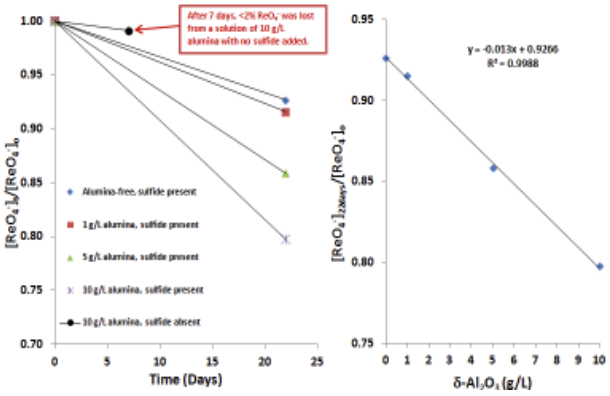

Figure 1: Left: loss of ReO_4^- from test solutions over time. Right: loss of ReO_4^- after 22 days as a function of δ-Al_2O_3 mass loading.

Conclusion

The left panel of the figure shows an increasing rate of ReO_4^- loss as the mass loading of δ-Al_2O_3 increases. Closed circles indicate <2% of initial ReO_4^- is lost from analogous sulfide-free suspensions; observed losses in the sulfidic suspensions cannot be due to adsorption of ReO_4^-. The right panel shows the loss of ReO_4^- after 22 days exhibits linearity with increasing mass loading. These data demonstrate that δ-Al_2O_3 enhances the rate of a sulfidation reaction(s) involving ReO_4^-. Further inquiry is required for definitive identification of reaction product(s). These results may help to explain observations that Re removal only occurs below the sediment-water interface in temporally anoxic basins, even when the overlying water column is also sulfidic [3].

[1] Vorlicek & Helz (2002) *Geochim. Cosmochim. Acta* **66**, 3679-3692.
[2] Lan, Deng, Kim & Thornton (2007) *Geochem. Trans.* **8**:4 doi: 10.1186/1467-4866-8-4.
[3] Chappaz, Gobeil & Tessier (2008) *Geochim. Cosmochim. Acta* **72**, 6027-6036.

https://doi.org/10.1180/S0026461X00008434 Published online by Cambridge University Press

Mechanisms of subglacial groundwater recharge as derived from noble gas, ^{14}C, and stable isotopic data

TIM GRUNDL[1*], NATHAN MAGNUSSON[1], MATTHIAS BRENNWALD[2], ROLF KIPFER[2]

[1*] University of Wisconsin-Milwaukee, Geosciences Department, Milwaukee, USA
[2]EAWAG, Swiss Federal Institute of Aquatic Science and Technology, Duebendorf, Switzerland

Major ion, noble gas, stable isotope and ^{14}C data collected from a transect along groundwater flow path within a confined Paleozoic aquifer in northeastern Wisconsin, USA are used to deduce the effect of the Laurentide Ice Sheet (LIS) on the underlying aquifer. Major ion trends, ^{14}C ages and $\delta^{18}O$ derived temperatures that decrease to -5.6 ºC during the last glacial maximum (~10 kyr. B.P. to ~26 kyr. B.P.) indicate that recharge continued when ice covered the area. A $\delta^{18}O$ derived temperature record that extends well below freezing, a contrasting noble gas temperature record that remains constant at ~3º C (Figure 1), high excess air (ΔNe) values

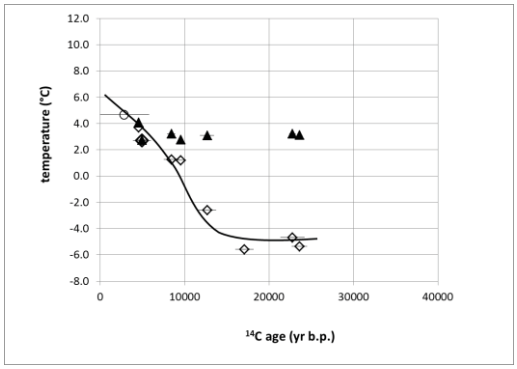

Figure 1: Oxygen isotope temperature (open diamonds) and noble gas temperatures (solid triangles) versus corrected ^{14}C ages.

and strong noble gas fractionation patterns indicate that supraglacial melt was the dominant constituent of aquifer recharge. Recharge occurred within the ice sheet as a part of a very dynamic englacial hydrologic system that experienced recharge heads of as much as 7.8m. Comparisons to a similar transect taken 150 km to the south [1] show different recharge mechanisms occurring near the terminus of the ice sheet. To the author's knowledge this is the first time that noble gas and isotope tracers have been used to deduce the mechanism of aquifer recharge beneath continental ice sheets.

[1] Klump, Grundl, Purtschert, and Kipfer (2008) *Geology* **Volume 36(5)**, 395-398.

Enrichment of Li in fluids exsolved from the Harney Peak leucogranite Black Hills, South Dakota

MARK L. GRZOVIC[1*] AND PETER I. NABELEK[1]

[1]Department of Geological Sciences, University of Missouri-Columbia, Columbia, MO, USA, mlg6wc@mail.missouri.edu (* presenting author)

Fluid inclusions provide a way to directly sample the composition of magmatic fluids and are therefore a key to investigating the role of fluids in differentiation of magmas and element mobility within plutonic systems. Laser ablation (LA) ICP-MS analysis and microthermometry were used to determine quantitatively the chemical compositions of individual fluid inclusions in the Harney Peak granite-pegmatite (HPG) system in South Dakota. HPG has a simple mineralogy, it has had no interaction with meteoric fluids and it has not been metamorphosed [1]. In the HPG system, magmatic fluids were key to development of pegmatitic segregations and a broad field of Li-bearing pegmatites. Moreover, Wilke et al. [2] attributed an enrichment of Li in the metamorphic aureole of the HPG to expulsion of Li-bearing fluids from the HPG. The objective of this study was to determine the composition of the putative magmatic fluids in order to evaluate their potential role in the differentiation of the HPG and development of the pegmatite field and metasomatic aureoles.

All analyzed fluid inclusions were hosted in quartz. Types of inclusions are: type 1 (H_2O-CO_2+salts), type 2 (H_2O+salts), type 3 (CO_2-rich) [3]. Concentrations of Li, B, Na, K, Rb and Cs were measured by LA-ICP-MS. Raw data were reduced using the AMS data reduction software [4].

Results indicate elevated concentrations of alkali elements in the fluid inclusions. The inclusions are primarily composed of Na (up to 25.7 wt.%), K (up to 0.8 wt.%) and Li (up to 0.9 wt.%), but also contain minor concentrations of Rb (≤0.01 wt.%) and Cs (up to 0.05 wt.%). Initial analysis also suggests a significantly higher Li concentrations is secondary type 2 inclusions compared to primary type 1 inclusions. Secondary type 2 inclusions on average have concentrations of 0.3 wt.% Li whereas primary inclusions contain less than 0.1 wt.%. This suggests that these elements were concentrated in the magmatic fluid when it seperated from the HPG magma, and that Li was further concentrated in the aqueous fluid when the magmatic fluid unmixed into carbonic and aqueous fractions.

Li is important in pegmatite formation as at elevated concentrations it can reduce the viscosity of a magma and inhibit crystal nucleation, leading to the crystalization of few large crystals [5]. The results suggest that Li in magmatic fluid was important in the formation of the pegmatite field and the metasomatism of the aureole.

[1] Nabelek & Ternes (1997) *Geochim. Cosmochim. Acta* **61**, 1447-1465. [2] Wilke et al. (2002) *Am. Mineral.* **87**, 491-500. [3] Sirbescu & Nabelek (2003) *Geochim. Cosmochim. Acta* **67**, 2443-2465. [4] Mutchler et al. (2008) *Mineral. Assoc. Can. Short Course* **40**, 318-327. [5] Nabelek et al. (2010) *Contrib. Mineral. Petrol.* **160**, 313-325.

https://doi.org/10.1180/S0026461X00008434 Published online by Cambridge University Press

KAOLINITE PRECIPITATION RATES AT PH 4 AND 25 °C.

S. GUDBRANDSSON [1], V. MAVROMATIS[2], Q. GAUTIER[3], N. BOVET [4], J. SCHOTT[5] AND E.H. OELKERS[6]

[1] GET, CNRS/UMR 5563-Université Paul Sabatier, Toulouse, France, snorgud@hi.is (*),[2] GET, CNRS/UMR 5563-Université Paul Sabatier, Toulouse, France, mavromat@get.obs-mip.fr, [3] GET, CNRS/UMR 5563-Université Paul Sabatier, Toulouse, France, gautier@get.obs-mip.fr, [4] Nano-Science Center, Department of Chemistry, University of Copehagen, Denmark. bovet@nano.ku.dk,[5] GET, CNRS/UMR 5563-Université Paul Sabatier, Toulouse, France,schott@get.obs-mip.fr, [6] GET, CNRS/UMR 5563-Université Paul Sabatier, Toulouse, France, oelkers@get.obs-mip.fr

This study focuses on the precipitation rates of kaolinite ($Al_2Si_2O_5(OH)_4$), a common low temperature secondary clay mineral forming during silicate rocks weathering. To date a number of studies have reported kaolinite dissolution rates (1, 2, 3, 4) but far fewer precipitation rates have been reported (1, 2, and 4). Rates were measured at pH 4 and 25 °C as a function of saturation state using low defect Georgia kaolinite, KGa-1b, as seeds in constant volume mixed flow reactors. Precipitation was induced by injecting into the reactor at similar rates two separate aqueous solutions, one Al-rich and one Si-rich. All fluids were fixed to ionic strength of 10 mM using NaCl. Reactive fluids were sampled daily, keeping the volume in the reactor constant. Sampled fluids were filtered and analyzed for Si and Al concentration. Solids recovered after all experiments exhibit identical X-ray diffraction patterns compared to those of the initial seed. Similar results were observed for the Al/Si surface ratio of these solids as measured by XPS. These observations demonstrate that the only mineral phase precipitating in our experiments was kaolinite. Furthermore, precipitation rates obtained from aqueous Si concentrations are closely consistent with those obtained from aqueous Al concentrations. Measured rates exhibit a systematic variation, increasing linearly with the square root of the kaolinite saturation index (see Fig.). This behaviour, consistent with TST-derived rate laws, indicates that kaolinite growth is controlled by the simple incorporation of Al and SiO_2 at the numerous growth sites (likely crystal edge sites) present at kaolinite surface.

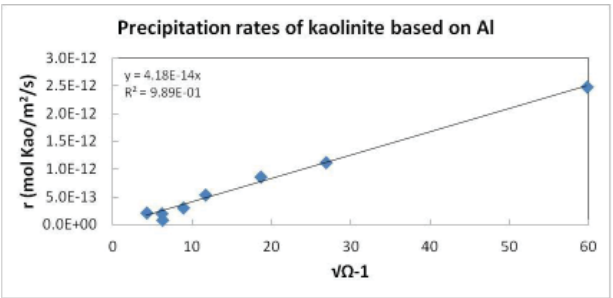

[1] Nagy K. L., Blum A. E. and Lasaga A. C. (1991). *Am. J. Sci.* **291**, 649–686.
[2] Devidal J. L., Schott J. and Dandurand J. L. (1997). *Geochim. Cosmochim. Acta* **61**, 5165–5186.
[3] Cama J., Metz V. and Ganor J. (2002) *Geochim. Cosmochim. Acta* **66**, 3913–3926.
[4] Yang L. And Steefel C. I. (2008). *Geochim. Cosmochim. Acta* **72**, 99–116.

1.1 Billion-years-old biomarkers from a microbial mat

NUR GUENELI[1*], ERIC LEGENDRE[2], AND JOCHEN J. BROCKS[1]

[1]The Australian National University, Research School of Earth Sciences, Canberra, Australia
nur.gueneli@anu.edu.au (* presenting author)
jochen.brocks@anu.edu.au
[2]Fluids and Organic Geochemistry Department, TOTAL, Pau Cedex, France

Biomarkers and the Proterozoic

Molecular fossils, or biomarkers, are altered biogenic compounds that can be preserved in the geological record for hundreds of millions of years and assigned to specific precursor molecules. Therefore, biomarker analysis makes it possible to assess major groups of organisms that contributed organic matter to ancient microbial communities. The mid-Proterozoic interval, ~1.8 Ga to 0.8 Ga ago, comprises major steps in the evolution of life and Earth chemistry. However, in a re-appraisal of published biomarkers from this period, we only found indigenous bitumens in 9 geological basins, and only 3 fall into the age bracket 1.4 Ga to 0.9 Ga; the 1.2 Ga Hongshuizhuang Fm. N China [1], the 1.1 Ga Taoudeni Basin, NW Africa [2] and the 1.0 Ga Nonesuch Fm., NE USA [3]. Here, we present a detailed study of biomarkers from microbial mats in the Taoudeni Basin.

Mat biomarkers of the 1.1 Ga Taoudeni Basin, NW Africa

The shales of the Taoudeni Basin belong to an organic-rich mat facies [2]. We found TOC levels as high as 16%, and Rock Eval parameters reveal low thermal maturity. *n*-Alkanes range from C_{12} to C_{37} with a maximum at C_{17}. Pristane and phytane are present but we did not detect any higher acyclic isoprenoids. Hopanes are abundant, including 3β-methylhopanes, although concentrations of 2α-methylhopanes were very low. Even though the mats contain simple fossils of eukaryotic orgin, diagnostic eukaryotic steranes were not detected. However, we found triaromatic steroids of possible methanotrophic bacterial origin. Most significantly, we detected aryl isoprenoids with distinct substitution patterns. These biomarkers together describe a shallow-water microbial mat community that was presumably inhabited by oxygenic cyanobacteria, anoxygenic phototrophic purple (Chromatiaceae) and green (Chlorobiaceae) sulphur bacteria, as well as methanotrophic bacteria. The biomarker assemblage is very similar to biomarkers from the 1.64 Ga Barney Creek Formation (BCF) in northern Australia [4], which has been described as an euxenic deep water environment. However, this new data suggests that it may instead represent a shallow water habitat harbouring microbial mats.

Our results represent the oldest direct observation of the complexity of Precambrian microbial mat ecosystems.

[1] Li *et al.* (2004), *Organic Geochemistry* **35,** 531-541.
[2] Blumenberg *et al*. (2012) *Precambrian Research* **196-197,** 113-127. [3] Pratt, Summons & Hieshima (1991) *Geochimica et Cosmochimica Acta* **55,** 911-916. [4] Brocks *et al.* (2005) *Nature* **437,** 866-870.

https://doi.org/10.1180/S0026461X00008434 Published online by Cambridge University Press

Chemical-hydrodynamic control of arsenic mobility at a river confluence

PAULA GUERRA[1], CHRISTIAN GONZALEZ[1], CRISTIAN ESCAURIAZA[1], CARLOS BONILLA[1], GONZALO PIZARRO[1], PABLO PASTEN[1*]

[1]Pontificia Universidad Catolica de Chile, Santiago, Chile, ppasten@ing.puc.cl (* presenting author)

River confluences are natural reactors where key process controlling the fate of contaminants at different scales occur. A better understanding of the interactions between biogeochemical reactions and the hydrodynamics of a river confluence may lead to innovative strategies for contaminant risk evaluation and management.

The Lluta river is a precious water resource for Arica y Parinacota in northern Chile, an extremely arid region. Although the construction of a dam is being planned to increase water availability, the likely accumulation of arsenic-rich iron oxyhydroxides in the dam sediments has prompted careful analysis from environmental authorities and the local scientific community. The main source of As-rich fine particles is the confluence between two rivers in the Chilean Altiplano, the Caracarani and the Azufre river, thus making it a perfect natural laboratory to study interactions between biogeochemical reactions and hydrodynamics.

We performed field and laboratory studies to characterize the chemistry and hydrodynamics at this confluence. After mixing of the Caracarani (pH=8; Fe, As<0.1 mg/L, low turbidity, Q~150L/s) and the Azufre river (pH=2, Fe=80 mg/L, As=2 mg/L, low turbidity, Q=50 L/s), a highly variable spatial distribution of pH and turbidity was found within the first 300m downstream of the confluence. Characteristic light-brown fine particulate material was found in stagnant areas with varying As concentrations up to 600 mg As/kg sediment for low flows. We reproduced the mixing of these waters at different velocities using jar-test type of experiments. Although the production of fine oxyhydroxides was also observed, the concentration of arsenic in the flocculated material (particles >0,45 um) was remarkably lower (<50 mgAs/kg of sediment) compared to the natural flocs. Furthermore, we found that the mixing velocity is a critical parameter determining the As sequestration potential by te oxyhydroxides.

Acoustic Doppler velocimetry at the confluence showed spatially variable turbulence intensities at the streamwise and across-stream directions, producing heterogenous distribution of particulate material on the river bed. Fresh flocs are thus exposed to varying chemical environments and hydrodynamic turbulent stresses determining arsenic sorption, floc formation, and floc strength. At larger time and spatial scales, flow characteristics during flood and drought seasons are likely to determine the formation/mobilization of arsenic repositories within the watershed.

Project funded by Conicyt, Fondecyt 1100943.

From peak metamorphism to orogenic collapse: insights into the exhumation history of the Clearwater metamorphic core complex

V.E. GUEVARA[1*], J.A. BALDWIN[1], D.A. FOSTER[2], AND R.S. LEWIS[3]

[1]University of Montana, Missoula, MT, USA victor.guevara@umontana.edu (* presenting author) julie.baldwin@umontana.edu

[2]University of Florida, Gainesville, FL, USA dafoster@ufl.edu

[3]Idaho Geological Survey, Moscow, ID, USA reedl@uidaho.edu

Abstract

Metamorphic core complexes are ubiquitous features in orogenic belts around the world and offer exceptional opportunities to investigate the rheological and thermal characteristics of the middle crust during orogenesis. The Clearwater metamorphic core complex in northern Idaho, U.S.A. exposes some of the deepest rocks in the Cordilleran orogen and records a complicated polymetamorphic history starting in the Paleoproterozoic, with the youngest high-grade metamorphism resulting from late Cretaceous Sevier crustal thickening.[1, 2, 3] Categorization of the Clearwater complex as a core complex has recently been confirmed based on structural data, thermobarometric data, and $^{40}Ar/^{39}Ar$ cooling ages, all of which suggest rapid Eocene exhumation of regionally metamorphosed mid- and lower-crustal rocks within the complex.[1, 3] Despite these data, the structural and thermal evolution of the Clearwater complex during Eocene exhumation remains cryptic.

The Clearwater complex is comprised of two lithologically and structurally distinct zones: an internal zone comprised of basement schist, gneiss, and anorthosite, and an external zone with both Archean to Paleoproterozoic basement and metapelitic rocks of the overlying Mesoproterozoic Belt Supergroup.[1, 4] These zones are bound by conjugate sets of E- and W-verging normal faults. The geological significance of these faults is unclear. This paper integrates new $^{40}Ar/^{39}Ar$ muscovite and biotite cooling ages along an E-W transect across the Clearwater complex with respect to major extensional structures, 1:24,000-scale mapping, microstructural analysis, and metamorphic phase equilibria modelling in order to constrain the structural and thermal evolution of the Clearwater complex from maximum crustal thickness to Eocene gravitational collapse of the Sevier orogenic belt.

[1] Doughty et al. (2007) *GSA Special Paper,* **434**, 211-241. [2] Nesheim et al. (2012) *Lithos*, **134-135**, 91-107. [3] Grover et al. (1992) *American Journal of Science*, **292**, 474-507. [4] Lewis et al. (2011) *Northwest Geology*, **40**, 143-158.

https://doi.org/10.1180/S0026461X00008434 Published online by Cambridge University Press

SCAVENGING OF ^{230}TH AND ^{231}PA AT THE BERMUDA RISE

ABEL GUIHOU[1*], J. KIRK COCHRAN[1], DAVID BLACK[1]

[1] School of Marine and Atmospheric Sciences, Stony Brook University, Stony Brook, NY 11794 USA, abel.guihou@stonybrook.edu (* presenting author)

Abstract

The Bermuda Rise is a site of great paleoceanographic interest due to its high sediment accumulation rates, due in part to intense lateral advection. The particle-reactive U-series nuclides ^{230}Th and ^{231}Pa have been used at the Bermuda Rise and elsewhere as tracers of ocean circulation (e.g. AMOC), but their use is complicated by the influence of particle composition on the scavenging of these radionuclides. The recently initiated Bermuda Rise Flux Project (BaRFlux) offers an opportunity to resolve some of the processes controlling the delivery of ^{230}Th and ^{231}Pa to the seafloor. BaRFlux aims to better constrain the sedimentation process at the Bermuda Rise through sampling filterable particles in the water column as well as sinking particles caught in sediment traps. We have deployed a mooring consisting of 10 sediment traps, with two traps each at water depths of 300, 1000, 1500, 2500 and 4200 meters. Each depth has a trap collecting particles as a function of time and a trap separating particles in situ according to their settling velocity. The sediment trap mooring is turned around ever 3 months. Seawater samples also have been taken to characterize the distributions of ^{230}Th and ^{231}Pa in the water column. This contribution will present preliminary results on the effects of particle flux, particle sinking velocity and lateral advection on the scavenging of ^{230}Th and ^{231}Pa from the water column to the sediment at this site.

Understanding gas dynamics in unsaturated fractured granite using SF_6, CO_2, Rn and other noble gases.

S. GUILLON[1,2*], E. PILI[1,2], J.-C. SABROUX[3], P. AGRINIER[2]

[1]CEA, DAM, DIF, F-91297 Arpajon, France, sophie.guillon@cea.fr (* presenting author)

[2]Institut de Physique du Globe de Paris, 1 rue Jussieu, F-75005 Paris, France

[3]Institut de Radioprotection et de Sûreté Nucléaire, Centre de Saclay, F-91191 Gif-sur-Yvette France

The Roselend Natural Laboratory

In the Roselend Natural Laboratory (French Alps), a tunnel provides access to the heart of unsaturated fractured crystalline rocks at 55 m depth below ground surface (Figure 1). This underground research facility allows studying gas transfer between a 60 m^3 chamber isolated at the dead-end of the tunnel and vertical and horizontal boreholes at the surface. Transport properties were determined at various scales using these boreholes and chamber.

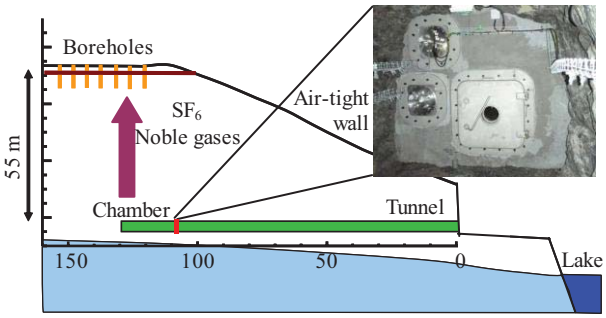

Figure 1: Setting of the Roselend Natural Laboratory, near the artificial Roselend lake, with the isolated chamber and boreholes.

Experimental and numerical results

We carried out a field-scale tracing experiment using SF_6 with the aim to serve for a forthcoming experiment using helium-3 and other noble gases. SF_6 was injected in the isolated chamber at 150 mbar above atmospheric pressure during 2 hours. SF_6 breakthrough was detected after only 10 hours at the ppb level in several surface boreholes, consistent with advective transfer in major fractures. SF_6 concentration in the surface progressively increased up to 30 ppm, and started to decrease 4 months after injection, indicating slow migration in the porous matrix.

^{222}Rn and CO_2 (concentration and $\delta^{13}C$) are monitored on the long term in the tunnel and at the surface. These gases are naturally produced by the rock. Air without tracer repeatedly injected from the chamber is able to flush large amounts of these gases out of the porosity.

These experiments are used to better understand gas dynamics and residence time in this dual porosity medium, in response to natural solicitations (meteorological, biological, geochemical, mechanical) and particularly barometric pressure fluctuations and variable water saturation. Numerical modeling is presented to account for the driving processes deduced from observations.

https://doi.org/10.1180/S0026461X00008434 Published online by Cambridge University Press

TTG Lu-Hf isotope evidence for a deep mantle-continental crust connection

M. GUITREAU[1,2]*, J. BLICHERT-TOFT[1,2], H. MARTIN[3], S.J. MOJZSIS[2,4] AND F. ALBARÈDE[1,2]

[1] Ecole Normale Supérieure de Lyon, 69007 Lyon, France (*presenting author: martin.guitreau@ens-lyon.fr)
[2] Université Claude Bernard Lyon 1, 69622 Villeurbanne, France
[3] Université Blaise Pascal, 63000 Clermont-Ferrand, France
[4] University of Colorado, Boulder, CO 80309, USA

The principle that growth of continents depletes the upper mantle from its most fertile fraction goes back several decades [1,2]. A widely held tenet is that continental crust grows either by melting of oceanic crust [3,4] or by fluxing the mantle wedge above subduction zones [5]. An alternative view holds that continents form through magmatic processing at subduction zones, not of regular oceanic crust, but of oceanic plateaus [6,7]; this would account for the apparent episodic character of crustal growth [8]. The present work reports MC-ICP-MS Lu-Hf isotope data for a large collection of Archean granitoids belonging to typical TTG (Tonalite-Trondhjemite-Granodiorite) suites. Both the whole-rock and zircons were analyzed, and the results are discussed in the broader context of the extensive literature database on Hf isotopes in zircons. Our results demonstrate that the Lu/Hf ratio of the mantle source of TTGs has not significantly changed over the last 4 Gyr. Continents therefore most likely grew from nearly primordial unfractionated material extracted from the deep mantle via rising plumes that left a depleted melt residue in the upper mantle. The deep mantle could retain its primitive relative element abundances over time because sinking plates are stripped barren of their oceanic and continental crustal components at subduction zones; this process results in only small proportions (<15-25%) of present-day continental mass getting recycled to great depths. Zircon populations extracted from the analyzed TTGs have Hf isotopic compositions very consistent with those of their host whole-rocks, whereas the U-Pb system in the same grains is often disturbed. This discrepancy creates spurious positive correlations with age when variable initial ε_{Hf} values are determined. The problem is endemic to the Archean detrital zircon record and consistent with experimental results bearing on the relative retentivity of Hf vs. U and Pb in zircon [9]. We argue that this behavior accounts for the generally negative ε_{Hf} values reported for Archean zircons and which are at odds with the present TTG data set. If Hadean Jack Hills zircons are considered in light of our results, the mantle source of continents appears to have remained unchanged for the last 4.3 Gyr.

[1] Hofmann (1988) *Earth and Planetary Science Letters* **90**, 297-314. [2] Jacobsen and Wasserburg (1979) *Journal of Geophysical Research* **84**, 7411-7427. [3] Drummond and Defant (1990) *Journal of Geophysical Research* **95**, 503-521. [4] Martin (1993) *Lithos***30**, 373-388. [5] Kelemen (1995) *Contributions to mineralogy and Petrology* **120**, 1-19. [6] Boher (1992) *Geophysical Research* **97**, 345-369. [7] Stein and Goldstein (1996) *Nature* **382**, 773-778. [8] Albarède (1998) *Tectonophysics* **296**, 1-14. [9] Cherniak and Watson (2003) *Reviews in mineralogy and geochemistry* **53**, 113-143.

Phase Equilibria constraints on the origin of the Peridot Mesa basanite

Amber Gullikson[1], Gordon Moore[2*], Kurt Roggensack[1]

[1] Arizona State University, School of Earth and Space Exploration, Amber.gullikson@asu.edu, Kurt. Roggensack@asu.edu
[2] University of Michigan, Department of Earth and Environmental Sciences, Gordon.moore@asu.edu*

Peridot Mesa is well-known for its gem quality peridot (Wrucke et al. 2004) and xenoliths of spinel-bearing peridotite (Frey and Prinz, 1978). Little is known of the lava that brought these mantle xenoliths to the surface however. The purpose of this study was to gain a better understanding of the origins of alkali basalts, and in particular the pre-eruptive conditions of the Peridot Mesa basanite. Phase equilibria experiments were performed on the Peridot Mesa basanite, over a range of various pressures, temperatures, and volatile content.

The phenocryst assemblage of the Peridot Mesa basanite is clinopyroxene, olivine, plagioclase, and spinel. An important feature of this lava is the presence of two phenocrystic olivine compositions. The first population is Mg-rich (Fo 73-80), and averages in size from 20-100 microns, and does not appear to have been in equilibrium at the time of eruption. The observation of prominent diffusion rims, re-equilibrating to a higher Fe content around the outer portion of the crystal supports this conclusion. The second olivine group has a lower Mg content, ranging between Fo 65-69. This population of olivine is 4-10 microns in size, with a less common, reversed zoning, making the rim slightly more Mg-rich (Fo 70). The presence of two compositionally different olivine phenocrysts can possibly be explained by a magma mixing event that occurred just before eruption, although these features are not seen in any of the other phenocryst phases.

In order to replicate the natural phase assemblage and determine magma conditions prior to eruption, a series of phase equilibria experiments were performed using a 1-atm Deltech furnace and a non-end loaded piston cylinder. The starting material for all runs was made by melting the natural sample at 1 atm and an oxygen fugacity of NNO, and quenching to a glass to ensure homogeneity. For the high P runs, glass chips were sealed in an AuPd capsule and run under anhydrous, CO_2-rich, or H_2O under-saturated conditions, ranging between 1050°C-1250°C and 0.1 MPa up to 2 GPa of pressure. The majority of H_2O under-saturated experiments contained 2wt% H_2O or less, with a few runs conducted at 5 wt% added H_2O.

Despite numerous experiments performed at a wide range of conditions, the mineral assemblage of this lava has yet to be reproduced experimentally. Plagioclase, a ubiquitous mineral in the Peridot Mesa lava, has failed to crystallize in any experiment. Significant temperature, pressure, and volatile constraints have been placed on the basanite by the presence of hydrous minerals, and the stability of olivine and clinopyroxene. Samples run under pressures greater than 500 MPa, and temperatures cooler than 1150°C crystallized phlogopite and amphibole minerals readily, neither of which are found in the lava. Also, olivine phenocrysts only occurred at temperatures 1100°C or cooler, and the amount of water present in the system is restricted by the appearance of hydrous minerals and/or the lack of olivine and clinopyroxene.

Phase equilibria experiments on the Peridot Mesa basanite have provided insight into the poorly understood history of this alkali basalt. The fact that hydrous minerals are present at 500 MPa or greater in pressure, even in anhydrous runs, leads to the conclusion that the phenocrysts formed under low pressure and low-H_2O content conditions. The stability of olivine also requires crystallization temperatures at or below 1100°C. The observation of two olivine populations in the natural sample, and the fact that plagioclase could not be reproduced in the lab, supports the possibility of magma mixing and a complex origin and eruption history for this lava.

https://doi.org/10.1180/S0026461X00008434 Published online by Cambridge University Press

A new strategy for the production of homogeneous standards for microbeam techniques

DETLEF GÜNTHER[1]*, DANIEL TABERSKY[1], NORMAN A. LUECHINGER[2] AND SAMUEL C. HALIM[2]

[1]ETH Zurich, Department of Chemistry and Applied Biosciences, Laboratory of Inorganic Chemistry
(*correspondence: guenther@inorg.chem.ethz.ch)
[2]Nanograde, Wolfgang-Pauli-Str., P/O 239, 8093 Zurich, Switzerland

The glass series of NIST 61x have been the major standard materials particularly useful for quantification for laser ablation – inductively coupled plasma mass spectrometry (LA-ICP-MS) [1]. However, heterogeneities have been reported in some sample charges [2]. Furthermore, geologically important elements such as Ti, Fe, and Mg are very low in concentration; platinum group elements (PGE) are either absent in these materials or present in very low concentrations. Therefore, alternative methods for the production of standard materials were investigated with the aim to extend quantifiable elements in the NIST glass series, in particular the PGEs, and to provide materials which overcome the reported heterogeneities.
A novel approach now provides standard materials with heterogeneities in the size range of 20-50 nm. This approach further provides PGE concentrations in the range of 500 mg/kg; multiple analyses of these novel standard materials confirm a RSD for PGEs in the order of 1-3 %.

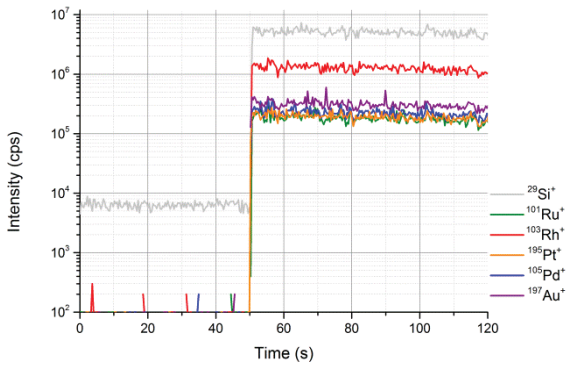

Figure: Transient LA-ICP-MS of the PGE-doped silicate.

The glass series NIST 61x and the newly synthesized materials provide identical ablation characteristics. The setup of production, preliminary results and first figures of merit will be discussed.

.[1] K.P. Jochum et al. (2011), Geostand Geoanal Res, **35**, 397
[2] S.M. Eggins and J.M.G. Shelley (2002), Geostand Geoanal Res, **26** 269

^{13}C-^{18}O bonds in dissovled inorganic carbon: Toward a better understanding of clumped isotope thermometer in biogenic carbonates

WEIFU GUO[1*], SANG-TAE KIM[2], JIE YUAN[3], JAMES FARQUHAR[4], BENJAMIN H. PASSEY[5]

[1]Woods Hole Oceanographic Institution, Woods Hole, MA, USA wfguo@whoi.edu (* presenting author)
[2]McMaster University, Hamilton, Ontario, Canada
[3]Chinese Academy of Science, Guiyang, Guizhou, P. R. China
[4]University of Maryland, College Park, MD, USA
[5]Johns Hopkins University, Baltimore, MD, USA

Application of the 'clumped isotope' thermometer in biogenic carbonates yields invaluable information regarding paleotemperatures [1]. Most biogenic carbonates analyzed so far appear to be free of clumped isotope vital effects [1], except for some surface corals [2,3]. This constrasts against ubiquitous oxygen isotope vital effects in biogenic carbonates, and potentially consitutes another advantage of clumped isotope thermometer. To better understand the incorportation of clumped isotope signals in biogenic carbonates, we present new experimental and theoretical constraints on equilibrium and kinetic clumped isotope fractionations among different dissovled inorganic carbon (DIC) species.

Sodium (bi)carbonte solutions of different pH were prepared and equilibrated at 25°C and 50°C, and the DIC species in each solution were then quantitatively precipitated as barium carbonate (yields >95%). Based on clumped isotope analyses of these precipitates, we determined, relative to statistical distribution, the abundance anomalies of ^{13}C-^{18}O bonds in CO_3^{2-}(aq) are 0.392±0.016‰ and 0.354±0.020‰(2σ) respectively at 25°C and 50°C (assuming the clumped isotope fractionation during phosphoric acid digestion of barium carbonate is 0.015‰ smaller than calcite [4]). These values are 0.041±0.014‰ and 0.009±0.029‰(2σ) lower than those in HCO_3^-(aq) equilibrated at the same temperatures, consistent with our lastest theoretical estimation of the equilibrium clumped isotope fractionations among different DIC species. This could potentially explain the general absence of clumped isotope vital effects in most biogenic carbonates [5,6]. We note, however, the oxygen isotope fractionation between disssolved HCO_3^- and CO_3^{2-} we determnined from our experiments are 0.3-0.4‰ smaller than those reported in previous studies [7,8].

We also estimated the kinetic fractionations of clumped isotope species associated with CO_2 hydration and hydroxylation reactions based on first principles transition state theory, and will discuss their implications for clumped isotope thermometry in biogenic carbonates.

[1] Eiler (2011) *Quarternary. Sci. Rev.* **30**, 3575-3588; [2] Ghosh et al. (2006) *Geochim. Cosmochim. Acta* **70**, 1439-1456; [3] Saenger et al. (2011) *AGU Fall Meeting,* Abstract PP41A-1726; [4] Guo et al. (2009) *Geochim. Cosmochim. Acta* **73**, 7203-7225; [5] Guo et al. (2009) *AGU Fall Meeting,* Abstract PP34B-07; [6] Thiagarajan et al. (2011) *Geochim. Cosmochim. Acta* **75**, 4416-4425; [7] Beck et al. (2005) *Geochim. Cosmochim. Acta* **69**, 3493-3503; [8] Kim et al. (2006) *Geochim. Cosmochim. Acta* **70**, 5790-5801.

https://doi.org/10.1180/S0026461X00008434 Published online by Cambridge University Press

Carbonate chemistry response of the North Atlantic mixed layer and thermocline to the Paleocene-Eocene Thermal Maximum

MARCUS GUTJAHR[1*], PHILIP F. SEXTON[2], RICHARD D. NORRIS[3] AND GAVIN L. FOSTER[1]

[1]National Oceanography Centre, Ocean and Earth Sciences, Southampton, UK, m.gutjahr@soton.ac.uk (* presenting author), Gavin.Foster@noc.soton.ac.uk

[2]Centre for Earth, Planetary, Space & Astronomical Research, The Open University, Milton Keynes, UK P.F.Sexton@open.ac.uk

[3]Scripps Institution of Oceanography, University of California, San Diego, La Jolla, U.S.A. rnorris@ucsd.edu

With between 2,000 and 12,000 Gt of carbon released over ≤10 ka (see [1] and references therein), the Paleocene-Eocene Thermal Maximum (PETM) is regarded as the best analogue for understanding the long-term effects of present-day fossil carbon combustion (e.g. [2]). Deep ocean acidity displayed a strong response to this carbon cycle perturbation, witnessed in the substantial temporary shoaling of the Carbonate Compensation Depth (by >2 km) [3] but, as yet, no constraints exist for the response of surface water *p*H through this event. If the initial injection of carbon occurred sufficiently rapidly (relative to the mixing time of the oceans) it should have resulted in a significant drop in surface water *p*H that subsequently recovered to near pre-event values. Such a perturbation of surface water *p*H is potentially traceable by means of the boron isotopic composition (expressed in $\delta^{11}B$) of marine carbonates.

In this presentation we will investigate the upper ocean's *p*H response through the PETM with new $\delta^{11}B$ records from two species of planktic foraminifera from the North Atlantic (DSDP Site 401). We present complementary boron isotope and B/Ca records for the mixed layer (using *Morozovella subbotinae*) and the thermocline (using *Subbotina patagonica*), both sampled from the same sedimentary depths at high resolution spanning the entire event. Planktic foraminifera at Site 401 are very well preserved, implying minimal diagenetic alteration of their primary $\delta^{11}B$ and B/Ca signatures.

Through calculations assuming various seawater $\delta^{11}B$ and alkalinity configurations, we aim to provide new constraints on the evolution of surface water *p*H and atmospheric pCO_2 across the PETM to better constrain the amount of carbon released and, hence, its likely source.

[1] Dickens (2011) *Climate of the Past* **7**, 831-846. [2] Ridgwell and Schmidt (2010) *Nature Geoscience* **3**, 196-200. [3] Zachos et al. (2005) *Science* **308**, 1611-1615.

The Gulf of Mexico Pb isotope response to elevated deglacial freshwater fluxes

MARCUS GUTJAHR[1*] AND ANNA NELE MECKLER[2]

[1]National Oceanography Centre, Ocean and Earth Sciences, Southampton, UK, m.gutjahr@soton.ac.uk (* presenting author),

[2]Swiss Federal Institute of Technology Zurich (ETHZ), Geological Institute, Zurich, Switzerland nele.meckler@erdw.ethz.ch

The disintegration of the North American Laurentide ice sheet during progressive warming throughout the last deglaciation provides an excellent opportunity to study changes in continental surface conditions and its effect on the dissolved runoff signal. The climate in interior North America shifted from glacial conditions dominated by intense (sub-)glacial physical and significantly reduced chemical weathering rates to wetter and warmer conditions in the transition to the Holocene. Various mineral phases in freshly exposed rock substrate weather relatively quickly, resulting in increased dissolved runoff fluxes for many major and trace elements during deglacial warming (cf. [1]). For tracing ice sheet retreat, elements displaying incongruent chemical weathering behaviour are particularly useful as long as these elements have short residence time in seawater such as dissolved Pb ($\tau \sim 20$-30 years).

At the NW Atlantic Laurentian Fan and deeper Blake Ridge, two Pb isotopic data sets suggest a significant increase in riverine input from proximal North American sources eastward during and after the Younger Dryas [2, 3]. The magnitude of change between these two sites suggests a proximal-distal relationship with the source of this radiogenic Pb signal most likely being located within the Gulf of St Lawrence. Together with Laurentide ice sheet margin retreat patterns presented from interior North America, oxygen isotope records derived from the Gulf of Mexico [4] and one multi-proxy data set from the outer St. Lawrence estuary [5], these Pb isotope records suggest that the signal recorded in the NW Atlantic very likely traced a major runoff reorganisation in interior North America during the mid-Younger Dryas.

Apart from [5], the identification of increased deglacial freshwater input into NW Atlantic sites by means of surface water $\delta^{18}O$ has proven difficult if not impossible [6]. Conversely, the supposedly preceding mid-deglacial Laurentide-derived freshwater runoff into the Gulf of Mexico was clearly recorded in surface-dwelling foraminifera in the open Gulf of Mexico [4, 7]. In order to complement the existing NW Atlantic Pb isotope records, we therefore present a new authigenic Fe-Mn oxyhydroxide derived Pb isotope record from core MD02-2550 within the Orca Basin in the Northern Gulf of Mexico. This core has a well-dated deglacial section and contains oxygen isotopic and organic matter content-based evidence for enhanced freshwater runoff during this key interval [7], allowing direct comparison with the new Pb isotope records.

[1] Vance et al. (2009) *Nature* **458**, 493-496. [2] Gutjahr et al. (2009) *EPSL* **286**, 546-555. [3] Kurzweil et al. (2010) *EPSL* **299**, 458-465. [4] Leventer et al. (1982) *EPSL* **59**, 11-17. [5] Carlson et al. (2007) *PNAS* **308**, 1611-1615. [6] Keigwin and Jones (1995) *Paleoceanography* **10**, 973-985. [7] Meckler et al. (2008) *EPSL* **272**, 251-263.

https://doi.org/10.1180/S0026461X00008434 Published online by Cambridge University Press

Fluid-rock interaction in the Strange Lake peralkaline granitic pluton, Canada: Implications for REE/HFSE mobility

A.P. GYSI* AND A.E. WILLIAMS-JONES

Dept. of Earth and Planetary Sciences, McGill University, Montreal, Quebec H3A 2A7, Canada, alexander.gysi@mail.mcgill.ca (* presenting author)

Alkaline and peralkaline intrusions, such as at Strange Lake [1] and Thor Lake [2] in Canada, are unusually enriched in rare earth elements (REE) and in the high-field strength elements (HFSE) yttrium (Y), zirconium (Zr) and niobium (Nb). Understanding the geochemistry of this type of intrusions is urgently required because of the need to develop resources of the REE/HFSE to meet increasing societal demands for new technologies employing these elements.

Previous studies have demonstrated the importance of hydrothermal remobilization in concentrating the HFSE and REE in alkaline and peralkaline intrusions [1,2,3]. These intrusions are typically enriched in fluorine, which other studies have shown substantially affects the geochemical behavior of HFSE/REE in fluids and melts. In the present study, we focus on the alteration observed in subsolvus granites and pegmatites located in the northwestern part of the Strange Lake pluton. This zone is strongly enriched in HFSE/REE and is characterized by intense fluid-rock interaction due to the infiltration of F-rich fluids. Field relations indicate multiple infiltration events with the formation of veins and breccias, and pervasive alteration of the granites. The infiltration was largely confined to a NE-SW trending zone enriched in pegmatites, which we suspect formed a porous path for focused fluid flow. Mineral textures provide strong evidence for hydrothermal fluid-rock interaction involving the co-precipitation of secondary HFSE/REE minerals with hydrothermal fluorite. Preleminary results indicate that zirconosilicates were the primary source for the rare metals, and suggest that upon dissolution of these minerals, the rare metals complexed with F^- present in the fluid and were remobilized. Previous studies have also shown the importance of other complexes including Cl^- and CO_2^{-3} in mobilizing HFSE/REE [1]. We have investigated the capability of such fluids to leach rare metals from the primary rock and control the remobilization and concentration of the HFSE and REE.

The availability of Ca is one of the major factors controlling fluoride activity (aF^-) and mobility of HFSE/REE in peralkaline granites. Two of the keys to successful exploration for HFSE/REE in F-rich igneous systems, such as Strange Lake, are understanding the mechanisms of fluid-rock interaction from the magmatic-hydrothermal transition to the final stages of fluid-rock interaction, and correctly evaluating the associated alteration assemblages.

[1] Salvi & Williams-Jones (2006) *Lithos* **91**, 19-34. [2] Sheard et al. (2012) *Econ. Geol.* **107**, 81-104. [3] Salvi et al. (2000) *Econ. Geol.* **95**, 559-576.

https://doi.org/10.1180/S0026461X00008434 Published online by Cambridge University Press

Investigating bioalteration products on seafloor basalts, Fe sulfides and Fe oxyhydroxides using scanning transmission X-ray microscopy (STXM) and absorption spectroscopy

AMANDA G. HADDAD[1*], COLLEEN L. HOFFMAN[1], FRIEDER KLEIN[2], SARAH A. BENNETT[1,3] ROMAN A. BARCO[1] AND KATRINA J. EDWARDS[1]

[1]University of Southern California, Los Angeles, USA, agturner@usc.edu (* presenting author)
[2]Woods Hole Oceanographic Institution, Woods Hole, USA, fklein@whoi.edu
[3]NASA Jet Propulsion Laboratory, Pasadena, USA, sarah.a.bennett@jpl.nasa.gov

Section Heading

Seafloor hydrothermal vent chimneys and the basaltic ocean crust are chemically reduced at the time of their formation but quicky undergo alteration following exposure to the oxygenated seawater. Alteration reactions (namely Fe and S oxidation and hydration) begin immediately at the rock-seawater interface yet when occuring abiotically, these reactions are kinetically inhibited, occuring very slowly if at all. It is suggested that microbes influence, if not control, these low-temperature alteration reactions at the rock-seawater interface in order to fix an estimated ~1x10^{19}g C per year [1]. In doing so, they influence global cycling of C, Fe, Mn, S and many other biogeochemically salient elements [2].

Understanding seafloor microbe-mineral interactions requires that we characterize how the minerals are changing as a result of being colonized by microbes. To investigate bioalteration products of seafloor microbe-mineral interactions, polished panels of common seafloor substrates (basalts, Fe sulfides, Fe oxyhydroxides) were allowed to react with in situ bottom water on the flanks of the Lo'ihi Seamount, Hawai'i for up to three years. After reaction, these panels developed thin (micron-scale) veneers of secondary alteration products and have been shown to harbor microbes found on seafloor basalts and hydrothermal sulfides (Haddad, unpub. data). We examined the products for morphology via scanning transmission X-ray microscopy (STXM) and changes in chemistry and mineralogy via C K-, Fe K- and O K-edge near edge X-ray absorbtion fine structure (NEXAFS). The alteration products on the reacted panels are amorphous Fe(III) and short-range Fe(III) mineralloids similar to those found on seafloor basalts. We present the range in chemistry and particle morphologies observed and discuss the variability with mineralogy.

[1] Bach (2003) *Geochim Cosmochim Acta* **67**, 3871-3887.
[2] Orcutt (2011) *Microbio Mol Bio Rev* **75**, 361-422.

Modeling the dioctahedral smectites CEC variation versus structural Iron reduction level

J. HADI[1*], C. TOURNASSAT[1], I. IGNATIADIS[1], L. CHARLET[2]

[1]BRGM, Avenue Claude Guillemin, BP 36009, 45060 Orléans, Cedex 2, France
[2]ISTERRE, BP 53, 38041 Grenoble, Cedex

Abstract

Iron is one of the most common redox species in soils and sedimentary rocks. Amongst iron-bearing phases, phyllosilicates might play key roles in various bio-geochemical processes involving redox reactions, where structural Fe (Festr) acts as a renewable source/trap of electron. A large set of data from kinetics, spectroscopic or electrochemical studies on dioctahedral smectites demonstrate that reduction of Festr impacts many clay properties such as colour, layer charge, swelling pressure, and colloidal properties that are linked to layer structural changes. Experiments also suggest that this mechanism is partly reversible, depending on type and properties of the primary oxidized clay and on extent of iron reduction level. The complexity of the involved mechanisms makes the prediction of Festr redox properties challenging. For instance, only empirical models are currently available to quantify structural changes as a function of reduction level. However, a predictive and mechanistic model of these changes is a prerequisite to develop a thermodynamic model for Festr redox properties. In this contribution, we propose a mechanistic statistical model to explain 2:1 layer excess negative charge changes induced by chemical reduction (dithionite) of structural Fe(III) to Fe(II). This model completes this published by Drits and Manceau [1] and was calibrated on data from our own and from the literature.

[1] Drits, V. A. and Manceau A. (2000) *A model for the mechanism of Fe^{3+} to Fe^{2+} reduction in dioctahedral smectites*. .Clays and Clay Minerals **48#**, 185-195.

https://doi.org/10.1180/S0026461X00008434 Published online by Cambridge University Press

Weathering of marine sediments in a natural high-CO_2 environment: A geochemical investigation of the hydrothermal seeps of Yonaguni Knoll, Okinawa Trough

MATTHIAS HAECKEL[1]*, VOLKER LIEBETRAU[1], DIRK DE BEER[2], STEFFEN KUTTEROLF[1]

[1]GEOMAR Helmholtz Centre for Ocean Research Kiel, Kiel, Germany, mhaeckel@geomar.de (* presenting author), vliebetrau@geomar.de, skutterolf@geomar.de

[2]Max Planck Institute for Marine Microbiology, Bremen, Germany, dbeer@mpi-bremen.de

Carbon dioxide capture and storage (CCS) has been recognized as one practical option for mitigating anthropogenic CO_2 emissions and several demonstration projects aim at storage units below the seafloor. However, the likelihood for potential CO_2 leakage and its impacts on the marine environment are still unclear and have to be assessed.

One approach is the study of natural analogues, i.e. natural CO_2 seeps, mainly of volcanogenic origin. Here, we present geochemical data from the sediment-covered hydrothermal seeps of Yonaguni Knoll in the southern Okinawa Trough, NE off Taiwan.

Two seep sites were investigated in detail: (a) Abyss Vent, where hot, supercritical CO_2 is percolating through the sediment, and (b) Swallow Chimney, where liquid CO_2 and CO_2 hydrate form in the surface sediments. Geochemical and isotopic analyses of the porewater and solid phase indicate intense weathering of the sediments: carbonates are completely dissolved in the surface sediments, but also reactive silicate minerals, such as K-feldspars, plagioclases and pyroxenes, are leached by the low-pH fluids. Consequently, the CO_2-saturated porewaters are relatively enriched in K, Ca, Mg, and also contain high alkalinity values of 30-60 meq/l typically buffering the pH at 4.6-4.8.

While at Abyss Vent CO_2 and fluids are emitted into the water column at high advection velocities, in contrast, at Swallow Chimney the condensed liquid CO_2 and/or gas hydrates seem to have reduced the permeability trapping the CO_2 effectively below the seafloor in a depth of 30-100 cm. Here, intensive reactions with the sediments are observed. Applying a transport-reaction model to both data sets, natural weathering rates for high CO_2 conditions are determined. Strontium isotopic composition of the porewater, bulk sediment, chimney and volcanogenic material helps to constrain the mass balance of the weathered compounds.

Exploring the effects of bedrock nutrient density on life and topography in the Sierra Nevada Batholith, California

W. JESSE HAHM[1*], SAYAKA ARAKI[1], BARBARA S. JESSUP[1], CLAIRE E. LUKENS[1], ANNE E. KELLY[2], AND CLIFFORD S. RIEBE[1]

[1]University of Wyoming, Laramie, USA, whahm@uwyo.edu (*presenting author)

[2]University of California, Irvine, USA

As primary producers, plants form the basis of ecosystems. Plants themselves, however, depend on underlying substrates for mineral nutrients, which are ultimately derived from weathering of local bedrock and influxes of allocthonous dust [1]. Substrates that lack essential nutrients may preclude colonization of plant life. Where plants are absent, soil production and retention are hindered, leading to exposure of bedrock, which in turn inhibits erosion relative to surrounding soil-mantled, vegetated terrain [2]. This raises the possibility of a feedback wherein exposed bedrock hillslopes emerge in relief as stable features due to low intrinsic nutrient density. We explore the potential for such a feedback in the Sierra Nevada Batholith, California, which provides a natural laboratory for studying how gradients in intrinsic nutrient density correspond with gradients in vegetation. We restrict our analysis of controls on vegetation to minimally disturbed, unglaciated terrain, thus eliminating potentially confounding effects of intensive land use and glacial scour. We measured bedrock bulk geochemistry for slopes spanning a wide range in above-ground biomass, thus quantifying variations in intrinsic nutrient density. We leverage these point measurements of geochemistry with existing geochemical databases and geologic maps. Using spatial analysis we compare our geochemical data with measurements of above-ground biomass, net primary productivity, and remotely sensed vegetation density. Across our study area, nutrient density, as revealed by concentrations of phosphorus and magnesium in bedrock, varies by more than an order of magnitude. Biomass likewise varies widely, ranging in extremes from densely vegetated giant sequoia (*Sequoiadendron giganteum*) groves to sparsely distributed stands of stunted conifers within otherwise bare-bedrock landscapes. We find that bedrock with low intrinsic nutrient density is often associated with low biomass per unit area at sites where local climate is similar to that of forests with high biomass and productivity. This implies that bedrock nutrient density may serve as a first-order control on vegetation distributions across some portions of our study area. Our measurements of cosmogenic nuclides from exposed bedrock surfaces indicate that they are eroding slower than surrounding soil-mantled terrain, confirming that linkages between intrinsic nutrient density and vegetation could regulate relief at hillslope to mountain scales.

[1] Chadwick, Derry, Vitousek, Huebert, and Hedin (1999) *Nature* **397**, 491-497.
[2] Portenga and Bierman (2011) *GSA Today* **21**, 4-10.

https://doi.org/10.1180/S0026461X00008434 Published online by Cambridge University Press

Computer simulations of iron-nickel sulphides in water

SAIMA HAIDER*, DEVIS DI TOMMASO, RICARDO GRAU-CRESPO, ALBERTO ROLDAN, NORA H. DE LEEUW

University College London, Department of Chemistry, UK
*saima.haider.09@ucl.ac.uk (presenting author),
n.h.deleeuw@ucl.ac.uk

The structural analogy between FeS/(Fe,Ni)S minerals and the (Fe,Ni)S clusters present in biological enzymes has led to suggestions that these minerals could have acted as catalysts for the origin of life. It has been suggested that life arose from a redox and pH front on the Hadean ocean floor [1], whereby the meeting between the hydrothermal front generated in the oceanic crust with the acidic oceanic fluid led to a spontaneous precipitation of FeS and NiS 'membranes/bubbles' which acted as reaction centres for carbon-carbon bond forming reactions. Here we present a computational study aimed at investigating the structure, dynamics and stability of Fe_xS_y (x, y $\leq$ 4) clusters in water. We shall also discuss violarite ($FeNi_2S_4$) surface structures and stabilities, and their affinity towards water

First, we will present first principles molecular dynamics simulations of the nucleation of iron sulphide clusters from aqueous solution, where our calculations of the Fe and S ions and the primary building unit FeS in water reveal that the effect of sulphur on the hydration structure of iron is to significantly reduce its first coordination shell compared with isolated Fe^{2+} and Fe^{3+} ions in water. However, simulations of Fe_xS_y particles (x, y $\geq$ 2) show that these clusters are unstable in water under the ambient conditions in our simulations, where we discuss any competing reactions such as the formation of iron hydroxides.

Because Ni is an important impurity in iron sulphides and potentally plays a vital role in the catalytic reactions, we will also present our calculations of the uptake and distribution of Ni ions in greigite-structured materials, employing a joint thermodynamical and statistical mechanical approach.

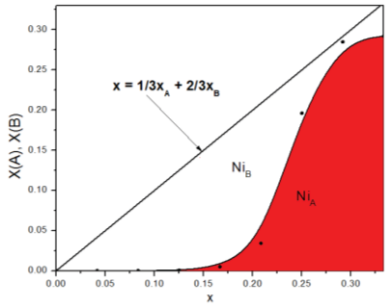

Figure 1: Distribution of Ni over tetrahedral (A) and octahedral (B) greigite sites, as a function of the total Ni concentration (x) at 600 K.

Finally, we have calculated the surface structures and stabilities of violarite - the fully-orded $FeNiS_2$ mineral – and investigated their interaction with the aqueous environment and propensity towards dissolution.

[1] Russell, Martin, (2004) *Trends Biochem. Sci.*, **29**, 358-363.

Molecular dynamics simulations of Y in silicate melts and implications for element partitioning

V. HAIGIS[1*] AND S. JAHN[1]

[1]GFZ German Research Centre for Geosciences, Telegrafenberg, 14473 Potsdam, Germany, haigis@gfz-potsdam.de (* presenting author)

Element partitioning depends strongly on the composition and structure of the involved phases. Whereas the influence of mineral phases is well described by the lattice strain model [1], the dependence of partition coefficients on melt chemistry is still poorly understood. However, there is ample evidence that the distribution of, e.g., rare earth elements between mineral and melt or between two immiscible melts varies considerably with melt polymerization [2]. Hence, if one uses trace element contents of igneous rock samples to constrain *P-T-t* paths of the material, the dependence of geochemical affinities on melt composition has to be understood.

We performed molecular dynamics simulations to investigate the coordination environment of Y (as an exemplary trace element) in silicate melts of different compositions in the model system $CaO-Al_2O_3-SiO_2$ [3]. This structural information was then linked to the partitioning behavior of Y. A wide range of melt polymerization was sampled by varying the relative abundance of network-modifying CaO. The results show that the local atomic structure around Y depends systematically on melt composition: when melt polymerization decreases (i.e. CaO content increases), the coordination of Y by oxygen decreases, as well as the average Y-O bond length. These changes are reflected by an increased oxygen order around Y and were confirmed by extended x-ray absorption fine structure (EXAFS) spectroscopy on glasses of the same composition as in the simulations. Moreover, we found a tendency of Y to form clusters with Ca and conclude that the presence of network modifiers facilitates the incorporation of Y into melts. This observation is in agreement with the observed trend of rare earth elements to partition preferentially into more depolymerized melts.

In a more quantitative approach, we modelled exchange reactions of trace elements and major elements between different phases. The computational method of thermodynamic integration allows the calculation of equilibrium constants and free energies of these reactions, which are directly related to fractionation processes. The thermodynamic results confirm the more qualitative explanation of partitioning behavior in terms of melt structure.

We emphasize that the method, applied here to Y in silicate melts, is very general and can be used, in principle, to predict element partitioning between arbitrary phases quantitatively. It thus complements the lattice strain model (which focuses on the role of mineral phases) by taking into account the influence of melt or fluid structure on element partitioning.

[1] Blundy and Wood (1994) Nature **372**, 452-454.
[2] Schmidt et al. (2006) Science **312**, 1646-1650.
[3] Haigis et al. (2012) (submitted)

https://doi.org/10.1180/S0026461X00008434 Published online by Cambridge University Press

Carbon- isotope stratigraphy; a correlation tool for Cenomanian–Turonian carbonates in Southern Iran

*Elham Hajikazemi[1], Ihsan Al-Aasm[2,4], And Mario Coniglio[3]

[1]Department of Geology, Iranian Offshore Oil Company, Tehran, Iran, ekazemi@iooc.co.ir (*presenting author)
[2]Department of Earth and Environmental Sciences, University of Windsor, Ontario, Canada, alaasm@uwindsor.ca
[3]Department of Earth and Environmental Sciences, University of Waterloo, Ontario, Canada, coniglio@uwaterloo.ca
[4]The Petroleum Institute, Abu Dhabi, UAE

Introduction:

The Cenomanian-Turonian Sarvak Formation forms one of the main hydrocarbon reservoirs in southern Iran and the Persian Gulf. Surface and subsurface sections from this heterogeneous carbonate reservoir were examined to define the chemical conditions of the Mid- Cretaceous basin. The obtained data were compared to previously published data of the Tethyan region for stratigraphic correlation. This was carried out using detailed petrography, stable carbon, and oxygen and strontium isotope analysis.

Results:

The $\delta^{13}C$ values (range from -6.4‰ to 4.1‰, VPDB) for Sarvak carbonate matrix fall well within the Mid-Cretaceous marine values. Superimposing of these data on the Cenomanian-Turonian $\delta^{13}C$ curve shows a good global correlation, including similar $\delta^{13}C$ excursions. These positive excursions in $\delta^{13}C$ values reflect the Cenomanian-Turonian Oceanic Anoxic Event (OAE). The occurrence of thinly laminated Ahmadi shales and Khatiyah bituminous shaly limestone (members of the Sarvak Formation) confirms the anoxic condition and corresponding OAE of Mid-Cretaceous basin in the studied area. These shales could be considered as a potential source for the Upper Sarvak Formation and also the other important reservoirs of the younger ages.

There is a positive shift in $\delta^{13}C$ values within the strata with values of between +3.3 and +4.1 ‰ which corresponds to the well-defined Mid-Cenomanian Event (MCE). This positive excursion is detected both in surface and subsurface sections.

Negative values (e.g. -6.4‰) were obtained from samples collected along the paleoexposure surfaces on top of the Sarvak Formation which reflect the effect of meteoric diagenesis on these carbonates.

The $^{87}Sr/^{86}Sr$ ratios from surface and subsurface samples plotted on the Cenomanian-Turonian portion of the secular seawater curve of Burke et al. (1982) [1] show that the majority of the obtained values fallow the Cenomanian portion of the curve and confirm the validity of present carbon-isotope data.

Conclusions:

Carbon- isotope stratigraphy could be used as a regional and global correlation tool in Cenomanian-Turonian carbonates even in heterogeneous Formations (i.e. Sarvak Formation).

The results of this study added new data to the isotopic composition records and confirmed the occurrence of OAE in the eastern margin of the Neo-Tethys Ocean.

[1]Burke, W.H., Denison, R.E., Hetherington, E.A., Koepnick, R.B., Nelson, H.F. and Otto, J.B. (1982). Variation of seawater $^{87}Sr/^{86}Sr$ throughout Phanerozoic time. Geology, 10, 516-519.

Stratigraphic constraints on critical fluxes in the Phanerozoic sulfur cycle

I. Halevy[1,*], S. E. Peters[2] and W. W. Fischer[3]

[1]Weizmann Institute of Science, Rehovot, Israel, itay.halevy@weizmann.ac.il (*correspondence)
[2]University of Wisconsin–Madison, Madison, WI, USA
[3]California Institute of Technology, Pasadena, CA, USA

Understanding the influence of sulfur cycle processes on the evolving oxidation state of the oceans and atmosphere, on the chemical composition of seawater and on the respiration of sedimentary organic matter requires knowledge about the removal of sulfur from the oceans as pyrite and as sulfate evaporites. Most approaches have attempted to constrain the magnitude and isotopic composition of influxes to the ocean and have used measurements of isotopic ratios in sedimentary pyrite and sulfates to constrain the relative magnitude and isotopic composition of the outfluxes in the context of isotope mass balance models [1-4]. These studies suggest an average Phanerozoic fractional pyrite burial rate (f_{pyr}) of approximately 0.4 [1-4], with the notion that variation in f_{pyr} values reflects changes in the rates of sulfate reduction.

Taking an inverse approach, we attempted to constrain the burial flux of sulfate evaporites and then test various sulfur cycle models for consistency with independent physical understanding of the sulfur cycle. Our data were derived from a comprehensive stratigraphic database [5], with unprecedented spatial and lithological resolution in North America and the Caribbean (NAC). Using constraints on deposit age, we converted evaporite volumes into burial rates. On long timescales, the burial rates correlate with the area of continental shelf at latitudes of net evaporation (±10–50°), whereas short-timescale variability in sulfate deposition corresponds to variability in the rate of sea level change. We used these relationships to scale the NAC data globally and to generate a synthetic record of global Phanerozoic sulfate burial rates. The average Phanerozoic sulfate evaporite burial rate is $\sim 3.3\times10^{11}$ mol yr^{-1}. Sulfur entering the ocean in excess of this amount must exit as pyrite and given estimates of riverine sulfate influxes to the ocean ($1.5–3.5\times10^{12}$ mol yr^{-1} [3,6]), the implication is that f_{pyr} has had a value of ~0.7–0.9 over Phanerozoic time.

The results describe a marine sulfur cycle where the majority of net outputs and inputs are burial and oxidative weathering of sedimentary pyrite, respectively. While perturbations to the pyrite burial rate have likely occurred over short timescales, models of constant or slowly varying pyrite burial yield results that are consistent both internally and with existing observations of seawater sulfate concentration and $\delta^{34}S$. Over the time intervals resolved by the data, the long-term value we estimate for f_{pyr} is generally high, and large downward excursions in its value are associated with high rates of sulfate evaporite burial, rather than times of less pyrite burial. High values of f_{pyr} also imply a larger than previously thought role for the sulfur cycle in stabilizing atmospheric oxygen levels.

[1] Berner (1987) *Am J Sci* **287**, 177. [2] Garrels & Lerman (1984) *Am J Sci* **284**, 989. [3] Canfield (2004) *Am J Sci* **304**, 839. [4] Kampshulte & Strauss (2004) *Chem Geol* **204**, 255. [5] Peters & Heim (2010) *Paleobiology* **36**, 61. [6] Kump & Garrels (1986) *Am J Sci* **286**, 337.

https://doi.org/10.1180/S0026461X00008434 Published online by Cambridge University Press

Nitrogen-Helium-Argon isotope relationships in subglacial glasses from Iceland's Neovolcanic zones

S. A. HALLDÓRSSON[1*], D. R. HILTON[1], P. H. BARRY[1], E. FÜRI[2], T. P. FISCHER[3], K. GRÖNVOLD[4]

[1]Scripps Institution of Oceanography, UCSD, La Jolla, USA,(*presenting author, shalldor@ucsd.edu)

[2]CRPG/CNRS, Vandoeuvre-les-Nancy, France

[3]University of New Mexico, Albuquerque, USA

[4]University of Iceland, Reykjavík, Iceland

Nitrogen isotopes in Ocean Island Basalt (OIB) glasses show positive values, up to +6 ‰, which has led to ideas on ancient nitrogen recycling from the surface to the deep mantle [1]. If indeed the source of the N is the deep mantle then there should be correspondence between the highest primordial noble gas signatures (i.e. highest $^{3}He/^{4}He$ ratios) and the positive $\delta^{15}N$ signatures. However, the current database of $\delta^{15}N$ from high $^{3}He/^{4}He$ OIB is limited. Given the excellent exposure of fresh and glassy material, Iceland remains one of the few hotspot localities where this hypothesis can be tested in detail.

We report new high-precision nitrogen isotope data for 34 geochemically well-characterized subglacial basaltic glasses using newly developed methods at Scripps [2]. The glasses, which cover all the currently- active volcanic zones of Iceland, span a wide range in helium isotope (8-26 R_A) but show rather limited $^{40}Ar/^{36}Ar$ ratios (298-1330) [3]. N-isotopes in samples with sufficient, i.e., detectable, N_2 (> 2 $\mu cm^3STP/g$) range from -2.9 ‰ to +6.2 ‰. To avoid samples potentially affected by degassing-induced isotopic fractionation and/or air interaction, we have filtered the $\delta^{15}N$ dataset using $^{4}He/^{40}Ar^*$ ratios to identify (and remove) highly degassed samples (n= 8). In contrast to He-isotopes, there appears to be no spatial control on the filtered $\delta^{15}N$ dataset; however, we note the dominance of positive values in the Eastern Rift Zone.

We investigate simple binary He-N_2 isotope mixing and show that these data can be explained with K mixing values ($K=(N/He)_{MORB}/(N/He)_{PLUME}$) between 1 and 50 indicating that the high $^{3}He/^{4}He$ signature may in fact be coupled with a high $\delta^{15}N$ endmember [4] that has either i) lost He before mixing with the MORB endmember, similar to the two-step model of He depletion followed by open-system degassing developed by [3], and/or ii) excess N_2. We speculate that the high $\delta^{15}N$ endmember needed to explain these mixing relationships strongly suggest recycled N-components in the Icelandic mantle.

[1] Marty & Dauphas, (2003) *EPSL*, [2] Barry et al., (2012) *G-cubed*, [3] Füri et al., (2010) *GCA*, [4] Prade et al., (2009) AGU.

The accessory mineral record of metamorphism and protracted melt crystallization in a metamorphic core complex

BENJAMIN W. HALLETT[1*] AND FRANK S. SPEAR[1]

[1]Rensselaer Polytechnic Institute, Troy, New York, USA, halleb3@rpi.edu (* presenting author), spearf@rpi.edu

Partial melting during high grade metamorphism is an important mechanism of crustal differentiation. In the northern East Humboldt Range metamorphic core complex of Nevada, USA, Late Cretaceous high grade metamorphsim and leucogranite intrusion was followed by decompression, resulting a steep P–T path segment across fluid absent dehydration melting melting reactions in aluminous pelites.

U/Th-Pb and trace element SHRIMP analyses of zircon and monazite from metapelites indicate a complex metamorphic and partial melting history that includes protracted zircon crystallization and 3–4 chemically distinct phases of monazite growth in each sample. Monazites from within the Winchell Lake nappe (WLN) show moderate Y cores, low Y/higher Th mantles, and high Y rims, giving Th-Pb ages of ~84 Ma, 72–63 Ma, and 30–40 Ma respectively. Monazites from lower structural levels (beneath the WLN) commonly show irregularly-shaped low U cores that give Jurassic–Early Cretaceous Th-Pb ages. These cores may constitute the only evidence for an earlier Mesozoic metamorphic event in the East Humboldt Range. Chemical zoning patterns are generally similar to WLN monazite, but Cretaceous monazite core growth began >10 m.y. earlier. Higher U cores/mantles from these monazites fall in two age groups, near 96 Ma with low Y, and near 84 Ma with more moderate Y. High Y monazite from a sillimanite-bearing leucosome gives a weighted mean age of 83 ± 2 Ma, interpreted to represent leucosome crystallization beneath the WLN. Thin, higher Y monazite rims beneath the WLN give ages near 71 Ma and 35 Ma.

Zircons from migmaties within the WLN give concordant U-Pb ages spanning from 78–61 Ma, interpreted to represent protracted crystallization of in situ anatectic melt. Zircon grown during melt crystallization, in both leucosome and melanosome domains, shows a moderate depletion in heavy rare earth elements (HREE). This is consistent with growth during melt crystallization and resorption of observed HREE-depleted garnet on the decompression and cooling path. Garnet zoning patterns suggest fairly rapid cooling from peak temperature conditions (~750°C, 7 kbar), evidenced by relatively narrow diffusion profiles for resorbed garnet that back-reacted with melt. A lack of significant residual alkali feldspar and muscovite indicates that a large portion of the anatectic melt was lost from the system.

Zircon U-Pb and Ti data from the WLN are consistent with an extended presence of small amounts of melt at near-solidus conditions (~680°C, 5 kbar) for nearly 15 million years, suggesting that cooling nearly ceased at these conditions and melt-enhanced ductile flow did not occur at this time in the East Humboldt Range. As a result, retrograde net transfer reactions involving melt or a residual fluid phase are limited (1) kinetically, by grain boundary and volume diffusion, and (2) by the evolution of the reactive bulk compositon due to segregation and crystallization of anatectic melt.

https://doi.org/10.1180/S0026461X00008434 Published online by Cambridge University Press

The origins of Earth's volatiles

ALEX N. HALLIDAY[1*]

[1]Department of Earth Sciences, University of Oxford, Oxford, U.K., alexh@earth.ox.ac.uk (* presenting author)

The decay of ^{40}K to ^{40}Ar allows calculation of Earth's current ^{36}Ar budget. For example, if K/U_{BSE} =13,800 [1] and average mantle $^{40}Ar/^{36}Ar$ = 10,000-30,000 (based on OIB, MORB and well gas data [2,3]), then only 1 to 3% of Earth's ^{36}Ar is in the mantle ((4-11)×10^{37} atoms). This holds regardless of whether the mantle is residual to degassing or largely unrelated to the present atmosphere. It has been argued that much of the mantle's Ar and other volatiles are recycled by subduction in which case primordial degassing was presumably closer to 99%. However, significant Ar recycling is hard to reconcile with the apparent K-Ar age of the mantle of 4.0 Ga.

The upper mantle ^{3}He concentration [4] and atmosphere-corrected noble gas patterns in MORB and OIB sources [2] facilitate calculation of noble gas concentrations in the seismic lower mantle using the above total mantle ^{36}Ar budget. These are 5 to 10 times higher than in the upper mantle. If much of the Ar, Kr and Xe is recycled the mass balance of primordial Ne should be different. In fact $^{20}Ne/^{36}Ar$ in OIB and MORB sources are similar [2]. This upper / lower mantle mass balance is based on the degree of degassing, which in turn is based on the K/U_{BSE} which assumes chondritic refractory elements (hence U and Th) in the BSE. If instead impact erosion has stripped Earth's incompatible elements [5], depletion of U and Th by ~40% would yield an upper / lower mantle that is roughly balanced in concentrations for K, U, ^{36}Ar and ^{20}Ne.

Earth's atmospheric $^{20}Ne/^{36}Ar$ is close to that of Venus, Mars, and CI and enstatite chondrites, contrasting with 4 orders of magnitude variation in other solar system reservoirs. This and other evidence suggests that the terrestrial planets acquired most of their volatiles from chondrite like materials and not from fractionated solar nebular gases, consistent with the Kr isotopic composition of the mantle [6]. The $^{20}Ne/^{22}Ne$, $^{36}Ar/^{38}Ar$ and $^{20}Ne/^{36}Ar$ ratios of the atmosphere are consistent with a minor solar component, consistent with that in the mantle [2-4]. If carbonaceous or enstatite chondrites are the ultimate starting materials for Earth's volatiles there has been up to 2 orders of magnitude depletion in ^{1}H, ^{12}C, ^{14}N and ^{130}Xe relative to ^{3}He, ^{20}Ne, ^{36}Ar and ^{84}Kr. A similar pattern is shown by the atmospheres of Venus and Mars. Like Xe, but unlike other noble gases, C and N form low temperature species [7] with an EUV first ionization potential less than that of H. Therefore, depletion in these elements could be related to ionization with EUV in the inner solar system and / or core formation. The present C/N of Earth and the atmospheres of Mars and Venus are close to chondritic providing evidence that these budgets were established by later chondritic veneers. However, a major fraction of Earth's water (~70% but dependent on assumptions about the mantle inventory) would appear to predate this late acquisition, as argued by Drake [8].

[1] Arévalo Jr et al. (2009) *EPSL* **278**, 361-369. [2] Trieloff & Kunz (2005) *PEPI* **148**, 13-38. [3] Ballentine& Holland (2008) *Phil Trans R Soc A* **366**, 4183-4203. [4] Porcelli & Ballentine (2002) *Rev Min Geochem* **47**, 411-480. [5] O'Neill & Palme (2008) *Phil Trans R Soc A* **366**, 4205-4238. [6] Holland et al. (2009) *Science* **326**, 1522-1526. [7] Lodders (2003) *Ap J* **591**, 1220-1247. [8] Drake (2005) *MAPS* **40**, 1-9.

Nickel removal mechanisms from neutral contaminated drainage by sulfate-reducing passive biofilters

AÏSSA HAMANI-ZALAGOU[1*], BRUNO BUSSIERE[1], CARMEN MIHAELA NECULITA[1] AND GERALD J ZAGURY[2]

[1]Université du Québec en Abitibi-Témiscamingue, 445 boul. de l'Université, J9X 5E4, Rouyn Noranda, Canada, Aissa-zalagou-M.Hamani@uqat.ca*

[2]Ecole Polytechnique de Montréal, 2900 boulevard Édouard Montpetit, H3T 1J4, Montréal, Canada, gerald.zagury@polymtl.ca

Contaminated neutral drainage (CND) is generally characterized by low sulfate concentrations, but with metals concentrations exceeding the norms. The treatment of CND by sulfate reducing passive biofilter (SRPB) is an attractive option for the mining industry. The main challenge for its long-term effectiveness lies in the choice and the proportion of the components in the reactive mixture. In this study, two reactive mixtures were tested in duplicate for the treatment of synthetic CND (pH of 6.5 and 7.8) contaminated with nickel (2.26 mg/L Ni) by SRPB. The first mixture was composed of leaf compost, poultry manure, sawdust, and wood chips, whereas in the second, the compost was replaced by peat. The results of the batch tests showed Ni removal efficiencies higher than 90% in all mixtures. However, the mechanisms of Ni removal seemed different in the two mixtures and also over time for the same mixture. The higher rate of sulfate removal in the first mixture indicates that it would promote sulfate reduction, while Ni removal in the second mixture would be essentially related to sorption mechanisms. Overall, the SRPB filled with both mixtures can be effective for the treatment of DNC in order to reduce Ni concentrations to values below the regulatory criteria.

Keywords: Contaminated neutral drainage, Nickel removal, Biofilter, Reactive mixture, Sulfate reduction

https://doi.org/10.1180/S0026461X00008434 Published online by Cambridge University Press

Top-down growth of travertine veins revealed from U-Th dating at Little Grand Wash (Utah)

B. HAMELIN[1*], P. DESCHAMPS[1], J-P. GRATIER[2], E. FRERY[2,3], N. ELLOUZ-ZIMMERMAN[3], A. RØYNE[4], F. RENARD[2,4], D. DYSTHE[4]

[1]CEREGE, UMR Aix-Marseille Univ. - CNRS - IRD, Aix-en-Provence, France, hamelin@cerege.fr
[2]ISTerre, University Grenoble 1 & CNRS, BP 53, Grenoble 38041, France
[3]IFP- Energies Nouvelles, Rueil-Malmaison, 92852, France
[4]Physics of Geological Processes, University of Oslo, 0316 Oslo, Norway

Thermogenic travertine mounds may be examined as an outcrop analog for natural CO_2 long-term storage. As they form at the mouth of springs where CO_2 degassing drives carbonate precipitation from waters flowing from depth along active faults, they record the complex history of leakage/sealing of natural deep CO2 reservoirs.

The morphology of these mounds is often characterized by widespread and intriguing decimetric veins of white calcium carbonate, that lay parallel or oblique to the usual stratigraphic travertine. These veins may extend horizontally over several tens of meters, and may represent up to 50% of the total volume of the travertine mound.

We present here U-Th ages obtained from one such vein from the Little Grand Wash area (Utah), near the Crystal Geyser. ^{230}Th/U ages were determined by thermo ionization mass spectrometry. Very high U concentrations (7.2 – 9.2 ppm) combined with high (^{234}U/^{238}U) ratios and low detrital ^{232}Th concentrations result in U-Th age uncertainties of ± 9-14 yr for a mean age of the vein of 6 Kyr. Taking advantage of this high accuracy and resolution, we show that the vein grew unexpectedly from top to bottom over about a thousand years. The chemical composition of the geothermal fluid remained stable during this period, as indicated by very small variations of the $(^{234}U/^{238}U)_0$ activity ratio between 4.19 and 4.26 ± 0.005.

We propose that this counter-intuitive downward growth can be driven by the force of crystallization, implying that this mechanism is able to uplift the rock above the vein. We also show that the growth rate of the vein is fully compatible with the over-saturation state and with the expected percolation rate of the fluids. The inferred mechanism may possibly be generalized to the formation of horizontal veins in other geological settings. This study also shows that one must be very careful when interpreting travertine data, for example geochemical evolution, from samples removed from drill hole since the ages of the successive layers are not necessarily continuous from top to bottom or in stratigraphic order.

Atypical depleted mantle components at Mohns Ridge and along the Mid-Atlantic Ridge near the Azores

CÉDRIC HAMELIN[1*], ANTOINE BEZOS[2], LAURE DOSSO[3], JAVIER ESCARTIN[1], MATHILDE CANNAT[1], CATHERINE MEVEL[1] AND ROLF B. PEDERSEN[4]

[1]IPGP, 1 rue Jussieu, 75252 Paris cedex 05, France, *ced.hamelin@gmail.com, escartin@ipgp.fr; cannat@ipgp.fr; mevel@ipgp.fr.
[2]LPGN, UMR 6112, 2 rue de la Houssiniere, 44322 Nantes, France, antoine.bezos@univ-nantes.fr
[3]CNRS, UMR 6538, Ifremer, 29280 Plouzané, France, laure.dosso@univ-brest.fr
[4]Centre for Geobiology, Postboks 7800, NO-5020 Bergen, Norway, Rolf.Pedersen@geo.uib.no

Lu-Hf and Sm-Nd isotopic systems have proven useful to track ancient mantle depletion signals in basalts. For both isotopic systems, during mantle melting events, parent-daughter ratios are higher in the residue than in the melt. Since these two isotopic systems have similar geochemical behavior during magmatic processes, a time-integrated evolution is expected to produce a strong correlation. However, in the particular case of mid-oceanic ridges samples, it has long been documented that Hf and Nd isotope compositions can be decoupled [1]. We present Hf, Nd, Pb and Sr isotope and trace element data for basalts from the Lucky Strike segment of the Mid-Atlantic Ridge together with published data from Mohns ridge area [2]. In a Hf-Nd isotope diagram, these two data sets define a similar correlation with a slope significantly steeper than the mantle array (Fig. 1). Two different hypotheses are discussed to explain this atypical Hf-Nd correlation: (i) a kinetic process during the current melting event [2] and (ii) an anomalous mantle source created by an ancient melting event with residual garnet [3]. Based on our sampling of the Lucky Strike segment, we show that the unusual Hf isotope signature can be the result of re-melting a refractory component in the mantle rather than the effect of disequilibrium melting. This observation provides new constraints on the structure of the Mid-Atlantic ridge upper mantle around the Azores and along Mohns ridge.

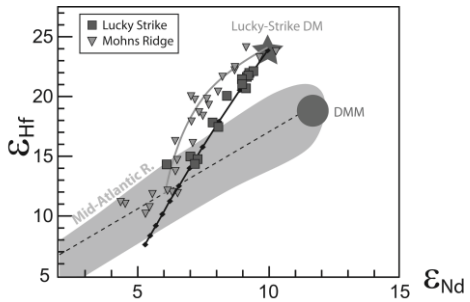

Figure 1: Atypical Hf-Nd isotopes values in Lucky Strike and Mohns ridge depleted mantle.

[1] Salters and Hart (1991) EPSL, 104(2-4), 364-380.
[2] Blichert-Toft (2005) G3, 6(1), Q01E19.
[3] Paulick (2010) EPSL, 296(3-4), 299-310.

https://doi.org/10.1180/S0026461X00008434 Published online by Cambridge University Press

Avanavero Large Igneous Province: a short-lived and widespread Paleoproterozoic mafic event in the Guiana Shield, Amazonian Craton: U-Pb geochronological, geochemical and paleomagnetic evidence

MIKE A. HAMILTON[1*], NELSON J. REIS[2], WILSON TEIXEIRA[3], FRANKLIN BISPO-SANTOS[4], MARCELO ALMEIDA[2], AND MANOEL D'AGRELLA-FILHO[4]

[1]University of Toronto, Geology, Toronto, Canada, mahamilton@geology.utoronto.ca (* presenting author)
[2]Geol. Survey of Brazil, Manaus, Brazil, nelson.reis@cprm.gov.br, marcelo.esteves@cprm.gov.br
[3]Universidade de Sao Paulo, Geociencias, Sao Paulo, Brazil, wteixeir@usp.br
[4]Universidade de Sao Paulo, Geofísica, Sao Paulo, Brazil, frankb@iag.usp.br, dagrella@iag.usp.br

The Avanavero Large Igneous Province (LIP) constitutes the most important Paleoproterozoic mafic magmatic event in the Guiana Shield, northern Amazonian craton. It comprises voluminous tholeiitic dykes and sills, the latter intrusive into regional sedimentary cover sequences such as Roraima Supergroup and Urupi Formation. Geochemical evidence suggests variable influence and modification by continental lithosphere, similar in many respects to chemically equivalent Karoo and Columbia River continental flood basalts of the Phanerozoic.

We present new U-Pb (ID-TIMS) baddeleyite ages of 1795 ± 2 Ma and 1793 ± 1 Ma from the Pedra Preta and Quarenta Ilhas gabbroic sills occurring in the Pakaraima and Urupi Blocks, respectively, at the north and south extremes of the Guiana Shield, north of the Phanerozoic Amazon basin. Combined with a single earlier ID-TIMS U-Pb age of 1794 ± 4 Ma for a mafic dyke [1], these ages confirm a broad suspicion from earlier isotopic studies (Rb-Sr, K-Ar, U-Pb SHRIMP) for the existence of a major ca. 1.78-1.80 Ga Avanavero magmatic event spanning eastern Venezuela-Guyana-Suriname-northern Brazil. The new results, however, potentially collapse the duration of intrusive activity to only a few Myr. Moreover, coeval gabbroic magmatism (Crepori sill) in the Central Brazil Shield suggests the Avanavero LIP originally extended across Brazil, south of the Amazon basin, towards the opposite side of Amazonia.

A synoptic summary is provided regarding the interpreted geometry of this expansive magmatic province, and we explore possible links between the dominant suite of sills and potential feeder dyke swarms. Available reliable paleomagnetic data favour a Laurentia/Baltica/Amazonia link at 1.78 Ga, and this large landmass may have represented the core of a hypothesized Columbia (Nuna) supercontinent during Paleo- and Mesoproterozoic times.

[1] Norcross et al. (2000) *Precamb. Res.* **102**, 69-86.

Kinetics and thermodynamics of calcite nucleation on self-assembled monolayers

LAURA M. HAMM[1*], NIZHOU HAN[1], ANTHONY F. GIUFFRE[1], JAMES J. DE YOREO[2] AND PATRICIA M. DOVE[1]

[1]Virginia Polytechnic Institiute and State University, Blacksburg, Virginia, USA, (correspondence: maehamm6@vt.edu)
[2]Lawrence Berkeley National Laboratory, Berkeley, California, USA

Sites of biogenic calcification are comprised of a complex macromolecular assemblage that is implicated in regulating the onset of mineralization. Previous studies have qualitatively investigated the influence of functional group chemistry on calcium carbonate ($CaCO_3$) formation using self-assembled monolayers (SAMs) as proxies for the macromolecules associated with biominerals. While these efforts have demonstrated that chemical functionality influences calcium carbonate phase, morphology, and nucleating face, they cannot provide insights into the kinetics of nucleation or the energy barrier associated with mineralization.

This study tests the hypothesis that specific chemical functional groups regulate the kinetics and thermodynamics of $CaCO_3$ formation by using SAMs with different termini (-COOH, -PO_4, and -SH) as substrates for calcite nucleation. We measured nucleation rates on each substrate at a variety of chemical driving forces both above and below the reported solubility of amorphous calcium carbonate (ACC), although ACC formation was not observed in these systems. Using classical nucleation theory to interpret the kinetic data, we calculated calcite-substrate interfacial energies and estimated substrate-specific effects on the thermodynamic barrier to nucleation. Calcite – substrate interaction forces were quantified with independent dynamic force microscopy measurements. A second part of the study investigated the effect of magnesium on calcite nucleation rates and barriers for selected substrates.

The kinetic measurements show a strong dependence of calcite nucleation rate on functional group chemistry. Interfacial free energies for 16-C alkanethiols terminated by –COOH and –SH were reduced to 82 and 91 mJ/m^2, respectively, from approximately 110 mJ/m^2 reported for calcite in solution. The kinetic behaviour is accurately described with classical models of nucleation, and calcite-substrate interaction force is positively correlated with the reduction in interfacial free energy. Rate measurements from solutions containing progressive amounts of magnesium demonstrate reductions in calcite nucleation rate without affecting the thermodynamic barrier to nucleation.

https://doi.org/10.1180/S0026461X00008434 Published online by Cambridge University Press

The role of sulfides on high field-strength element budget during enstatite chondrite melting

TAHAR HAMMOUDA[1,2,3], CAMILLE CARTIER[1,2,3], MAUD BOYET[1,2,3], BERTRAND MOINE[2,3,4], JEAN-LUC DEVIDAL[1,2,3]

[1]Clermont Université, Université Blaise Pascal, Laboratoire Magmas et Volcans, BP 10448, F-63000 CLERMONT-FERRAND, France, t.hammouda@opgc.univ-bpclermont.fr
[2] CNRS, UMR 6524, LMV, F-63038 CLERMONT-FERRAND
[3] IRD, R 163, LMV, F-63038 CLERMONT-FERRAND
[4] Université Jean-Monnet, Saint-Etienne FRANCE

Introduction

High field-strength elements (HFSE) are usually considered to be incompatible lithophile elements during planetary magmatic processes. However, troilite analyses in enstatite chondrites and achondrites (aubrites) show high Ti concentrations, which are not found in ordinary chondrites [1]. In order to quantify this behavior and to check whether is applies to the other HFSE, we have conducted melting experiments relevant to enstatite chondrites under controlled (and low, down to IW-5) oxygen fugacity. Experiments were performed at 1 atmosphere using evacuated silica tubes, and 5 GPa, using multianvil apparatus. Starting material was doped and experimental products were analyzed using microbeam techniques (electron probe, laser ablation ICP-MS).

Results

For oxygen fugacity (fO_2) about IW-2, sulfide / silicate melt partition coefficients for all HFSE are below 1. As fO_2 is lowered below IW-4, Ti is preferentially incorporated in Fe-rich sulfide. The same applies to V, Nb, and Ta. V and Nb have about the same D (sulfide / silicate melt), while Ta is about one order of magnitude lower. These observations are similar to previous observations on metal / silicate partitioning [2]. However, in the case where metal is present we find that V and Ta have about the same D (metal / silicate melt), about one order of magnitude lower than that of Nb. This result differs from [2]. For the cited elements, pressure does not seem to affect partitioning in the investigated range. In the case of Zr and Hf we find that low fO_2 favors their incorporation into the sulfide phase, while no notable change is found for the metal. Moreover, our results suggest that Zr may be compatible in the sulfide phase at low fO_2 (D sulfide / silicate melt > 1), while D for Hf approaches unity. Pressure appears to increase Zr and Hf solubility in the sulfide phase.

Discussion

The chalcophile character of Zr (and maybe for Hf at more reduced conditions) is a new feature, which may be related to observed Ti behavior in enstatite chondrites and achondrites [1]. If we consider that the Earth's differentiation started at reducing conditions (close to those of enstatite chondrites), Zr and Hf may have been trapped by sulfide melts and stored in a sulfur dominated reservoir. This reservoir may then have been assimilated into the core or, alternatively, it may have remained a separate reservoir in the silicate mantle.

[1] K Keil (1969) Earth Planet. Sci.Lett. **7**, 243-248.
[2] J Wade, BJ Wood (2001) Nature **409**, 75-78.

CALCIUM ISOTOPE FRACTIONATION IN A TYPICAL KARST FOREST ECOSYSTEM, SOUTHWEST CHINA

GUILIN HAN[1*] AND ANTON EISENHAUER[2],

[1]Institute of Geochemistry, Chinese Academy of Sciences, Guiyang, China, hanguilin@vip.skleg.cn (presenting author)
[2]GEOMAR | Helmholtz Centre for Ocean Research Kiel, Wischhofstraβe 1-3, 24148 Kiel, Germany, aeisenhauer@geomar.de

Recent studies have used Ca isotope fractionation to directly trace Ca transport along different biogeochemical pathway in various terrestrial ecosystems [1-3]. In an extension of these studies we present Ca isotope and Mg/Ca compositions of rain water, groundwater, bedrock (carbonates), soil and plant samples measured by TIMS using a ^{43}Ca-^{48}Ca double spike to gain information about the biogeochemical processes in a typical karst forest (Guizhou province, Southwest China).

The $\delta^{44/40}Ca$ of rainwater and groundwater are very similar, both of them are enriched in the ^{44}Ca when compared to bedrock, indicating that groundwater is supplied mainly by rain and that there is no significant Ca isotopic fractionation during the dissolution of Ca originating from the carbonate bedrock. Our results confirm previous findings that Ca isotopes will be fractionated down the line from bedrock (0.36 ‰) to forest soil (0.04 ‰) and to leaves (-0.26‰). Organic rich soils are enriched in ^{40}Ca relative to organic depleted soils, following the sequence farm land > burnt grass land > forest land > shrub land > grass land. In contrast, Mg/Ca ratios increase from in the same sequence indicating a distinct loss of Ca due metabolisation in plants. The recycling of plant material and soils as well as the variation in $\delta^{44/40}Ca$ and Mg/Ca in plant-soil ecosystem can be well described by an open-system Rayleigh fractionation model, indicating the preferential enrichment of ^{40}Ca and Ca in plants.

This work was supported jointly by the Innovation Program of Chinese Academy of Sciences (No. KZCX2-YW-QN109) and the Chinese National Natural Science Foundation (No. 40973088).

[1] Cobert et al. (2011) GCA **75**, 5467-548. [2] Hindshaw et al. (2011) GCA **75**, 106-118. [3] Farkas et al. (2011) GCA **75**, 7031-7046.

https://doi.org/10.1180/S0026461X00008434 Published online by Cambridge University Press

Seasonal and interannual change in mercury sequestration at Dome Fuji, Antarctica

YEONGCHEOL HAN[1*], YOUNGSOOK HUH[1], SUNGMIN HONG[2], SOON DO HUR[3], HIDEAKI MOTOYAMA[4]

[1]Seoul National University, Korea, hanlove7@snu.ac.kr (* presenting author), yhuh@snu.ac.kr
[2]Inha University, Korea, smhong@inha.ac.kr
[3]Korea Polar Research Institute, Korea, sdhur@kopri.re.kr
[4]National Institute of Polar Research, Japan, motoyama@nipr.ac.jp

The total mercury concentration (Hg_T) was determined with high precision in snow pit samples collected every 2.5 cm down to 2 m, covering ~27 years (1983-2010), at Dome Fuji in East Antarctica. This high-resolution data provide new information on seasonal and interannual change in mercury sequestration rate and factors affecting it.

The Hg_T ranged between 0.20 (±0.02, 2σ) and 5.20 (±0.05) pg g^{-1} with variations at seasonal and interannual time scales. The mean mercury sequestration rate was estimated to be 3.1 ± 0.1 pg cm^{-2} yr^{-1}, slightly higher than the previous estimate at Dome Fuji [1]. By comparison with sulfate concentration, $\delta^{18}O$-δD and deuterium excess profiles, the seasonality was characterized by summertime maxima in Hg_T, even though the peaks were not always exactly in phase. The enhanced mercury sequestration may be related to the active photochemical dynamics of mercury in summer [2]. We ascribe the interannual change to the variation in the atmospheric circulation over Antarctica that regulates the meridional transport of aerosols containing oxidant precursors, continental dust, moisture and heat, each of which is thought to play a role in the mercury dynamics on the Antarctic Plateau [3].

[1] Han et al. (2011) *Mineral. Mag.* **75**, 972. [2] Brooks et al. (1998) *Atmos. Environ.* **42**, 2877-2884. [3] Han et al. (2011) *Bull. Korean Chem. Soc.* **32**, 4258-4264.

The Southeast Indian Ridge: Scale of Source Heterogeneity and Origin of the DUPAL Anomaly

B. HANAN[1]*, J. BLICHERT-TOFT[2], K. SAYIT[1], A. AGRANIER[3], C. HEMOND[3], A. BRIAIS[4], M. MAIA[3], D. GRAHAM[5], F. ALBARÈDE[2]

[1]San Diego State University, San Diego, CA 92182-1020, USA (*correspondence:Barry.Hanan@sdsu.edu)
[2]Ecole Normale Supérieure, 69007 Lyon, France
[3]University of Brest-CNRS, IUEM, 29280 Plouzané, France
[4] CNRS-OMP, BGI, 31400 Toulouse, France
[5] COAS, Oregon State University, Corvallis, OR 97331, USA

Results

Pb and Hf isotope ratios from 139 basalt glasses sampled at < 10 km intervals along 2000 km of the Southeast Indian Ridge (SEIR) between 86°E and 110°E show bimodal distributions. The bimodality in both Pb and Hf isotope ratios confirms the presence of ancient compositional streaks in the Indian Ocean upper mantle [1]. The density of streaks is well described by a Poisson distribution having a characteristic thickness of ~25 km.

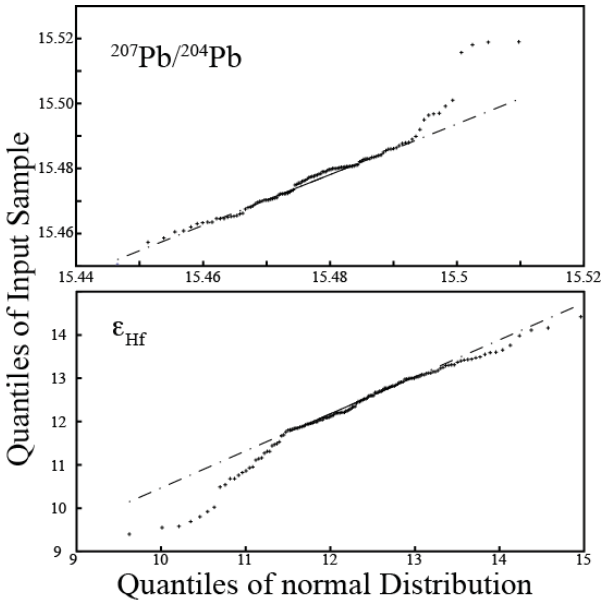

Figure 1: QQ plots for Pb and Hf isotopes for 139 SEIR glasses [this work; 1, 2] show that these MORB melts reflect a mantle source in which the isotope compositions are bimodal rather than a single gaussian population.

Implications

Pb isotopes in SEIR basalts all carry a DUPAL [3] isotope signature. Two possible origins for the bimodality and DUPAL signature are: (1) ancient melting that involved garnet fractionation, with subsequent pollution of the upper mantle by continental material during Gondwana breakup; (2) inherited heterogeneity from the early Earth.

[1] Graham et al. (2006) *Nature* **440**, 199-202.
[2] Mahoney et al. (2002) *J. Petrology* **43**, 1155-1176.
[3] Hart (1984) *Nature* **309**, 753-757.

https://doi.org/10.1180/S0026461X00008434 Published online by Cambridge University Press

Synthesis of Mn minerals at ambient temperature and pressure

MATTHIAS HÄNDEL[1*], THLIO RENNERT[1,2], AND KAI U. TOTSCHE[1]

[1] Friedrich-Schiller-Universität Jena, Institut für Geowissenschaften, Burgweg 11, D-07749 Jena, Germany, matthias.haendel@uni-jena.de (* presenting author), kai.totsche@uni-jena.de

[2] Technische Universität München, Lehrstuhl für Bodenkunde, D-85350 Freising-Weihenstephan, Germany, thilo.rennert@wzw.tum.de

Manganese minerals are widespread in soils, sediments, water and ores. Particularly, Mn oxides play important roles in many soil chemical processes, are effective sorbents for metal ions and can oxidize organic and inorganic contaminants. Manganese oxides mostly occur together with other minerals and are therefore difficult to separate. To study fundamental processes on reactivity and kinetics pure phases are needed.

The objective of this work was to synthesize Mn minerals at ambient conditions and without the use of strong acids and bases. We designed 4 different experimental approaches based on $KMnO_4$ reduction. The reaction time varied between 1 and 550 days and the influence of the organic modificators acetate, citrate and lactate was checked. The reaction products were characterized mineralogically (XRD, FTIR), morphologically (SEM, BET) and chemically (SEM-EDX, ICP-OES, IC).

After a period of 1 day a poorly crystalline precursor birnessite [$K_4Mn_{14}O_{27}$•$9H_2O$] was the sole mineral phase that was formed in all reaction batches. Depending on the educts and on the modificator, several transformations of birnessite were observed over time. In 3 of 4 experiments without modificator, birnessite remained stable but increased in crystallinity and decreased in surface area with time. In one approach birnessite was stable in the first 90 days followed by slow dehydration and transformation to cryptomelane [KMn_8O_{16}].

The modificator acetate showed no effects on both crystallization behavior and mineral transformation. Birnessite that was formed in the presence of either citrate and sulfate, or citrate and chloride partly transformed to rhodochrosite [$MnCO_3$]. Chloride especially promoted this carbonization, which ended after 185 days in an equilibrium state. The final precipitate contained 80% rhodochrosite and 20% birnessite. Citrate had no effects on the reaction in the other 2 approaches and birnessite remained stable. Also lactate promotes the formation of rhodochrosite in the presence of sulfate or chloride. In contrast to citrate, lactate transformed the residual birnessite to manganite [γ-MnOOH]. In the other 2 approaches lactate induced a complete transformation of the precursor birnessite to feitknechtite [β-MnOOH] between 7 and 30 days after starting. The lactate- induced transformation of birnessite to manganite or feitknechtite could be related to the strong reducing property of lactate.

Our pathways to synthesize Mn minerals are feasible on a large scale, can produce crystallites in different sizes and with a well-defined surface area. The products can serve as model minerals in studies on kinetics and reaction behaviors of Mn minerals, and may also have a potential for remediation of contaminated sites.

Magmatic degassing in contrasting volcanic systems of the Vanuatu arc: constraints from uranium-series isotopes

HEATHER HANDLEY[1*], SIMON TURNER[1], MARK REAGAN[2], GUILLAUME GIRARD[2], AND SHANE CRONIN[3]

[1]Department of Earth and Planetary Sciences, Macquarie University, Sydney, Australia, heather.handley@mq.edu.au (* presenting author), simon.turner@mq.edu.au

[2]Department of Geoscience, University of Iowa, Iowa City, IA, United States, mark-reagan@uiowa.edu, guillaume-girard@uiowa.edu

[3]Institute of Natural Resources, Massey University, Palmerston North, New Zealand, s.j.cronin@massey.ac.nz

Recent and present volcanism in the Vanuatu arc (South West Pacific Ocean) occurs at a variety of volcano types that exhibit a wide range of eruptive behaviour: from post-caldera lava-lake activity and lava flows at shield volcanoes (Ambrym), moderately explosive sub-plinian events and associated pyroclastic-flows and lava flows at stratovolcanoes (Lopevi), to persistent strombolian and vulcanian-style eruptions at scoria cones (Yasur). This precludes a generic model of magmatic and eruptive behaviour for the Vantuatu arc volcanoes and necessitates a detailed study of each system.

Uranium-series disequilibria in volcanic rocks offer unique insights into pre-eruptive magmatic systems over process-relevant timescales e.g., ^{238}U-^{230}Th (380 Ka), ^{230}Th-^{226}Ra (8 Ka) and ^{226}Ra-^{210}Pb (100 a). The short half-life of ^{210}Pb ($t_{1/2}$ = 22.6 years) and the volatile nature of the intermediate isotope, ^{222}Rn, (intermediate between the ^{226}Ra parent and ^{210}Pb daughter) provide valuable information on magma transport, evolution and degassing over a timescale more pertinent to the processes leading up to volcanic eruptions.

We present new Uranium-series isotope data (U-Th-Ra-^{210}Pb) for young (< 100 years old) volcanic samples from Ambrym, Lopevi and Yasur volcanoes to investigate the timescales of magmatic evolution and degassing in the contrasting volcanic systems. ^{210}Pb deficits ($(^{210}Pb/^{226}Ra)_0 < 1$) in Ambrym and Yasur volcanic rocks suggest effective open-system magmatic degassing of ^{222}Rn, consistent with the persistent lava-lakes/exposed magma and significant gas emissions observed at both volcanoes. Lopevi, on the other hand, displays excess ^{210}Pb ($(^{210}Pb/^{226}Ra)_0 > 1$) in the most mafic samples suggesting that ^{222}Rn gas accumulation and fluxing preceding and/or during eruption (on a decadal timescale) may be responsible for the more explosive-style of eruption witnessed at this volcano. Significant accumulation of recently crystallised plagioclase phenocrysts can also create ^{210}Pb excesses in volcanic rocks, however, this process is not supported by the petrographic and geochemical data. In summary ^{210}Pb-^{226}Ra disequilibria in Vanuatu volcanic rocks reveal a strong link between pre-eruptive magma degassing systematics and the resultant style of volcanic activity.

https://doi.org/10.1180/S0026461X00008434 Published online by Cambridge University Press

Mechanism of microbial hydroxyapatite manufacture and its application to radionuclide remediation

STEPHANIE HANDLEY-SIDHU[1]*, JOANNA C. RENSHAW[1], BJORN STOLPE[1], JAMIE R. LEAD[1], RICHARD A.D. PATTRICK[2], JOHN M. CHARNOCK[2], STEPHEN J. BAKER[1], MARK O. CUTHBERT[1], LYNNE E. MACASKIE[1]

[1] The University of Birmingham, Edgbaston, B15 2TT, UK (*correspondence: s.handley-sidhu@bham.ac.uk)

[2] The University of Manchester, Oxford Road, M13 9PL, U.K.

Introduction

Hydroxyapatite (HAP) shows potential for the remediation of metal contaminated waters [1, 2]. *Serratia sp.* contains high levels of an atypical phosphatase enzyme located in the bacterial periplasmic space and attached to extracellular polymeric substance; this enzyme cleaves glycerol-2-phosphate, liberating inorganic phosphate and providing the nucleation site for the growth of biological hydroxyapatite (Bio-HAP) crystals [1, 3]. Evidence suggests that the growth of Bio-HAP is controlled within spatial localisation of the biological space on and in close proximity to cells [1, 3]. Crystalline HAP [$Ca_{10}(PO_4)_6(OH_2)$] is described as ten calcium cations aligned in 2 non equivalent sites denoted as Ca(1) and Ca(2). The Ca(1) site contains four cations each surrounded by nine oxygen atoms, whereas, the Ca(2) site contains six cations each surrounded by 7 oxygen atoms [4].

Experimental

Various techniques (Atomic force microscopy, scanning and transmission electron microscopy, BET surface area, X-ray diffraction) were used to characterise the properties and structure of HAP. To investigate how HAP properties influence metal uptake, portions of biomineral were heated at different temperatures ranging from 200-700 °C before the sorption of key radionuclides (Eu^{3+} as an analogue for trivalent actinides, U^{6+}, Sr^{2+} and Co^{2+}). The amount of absorbed species was determined by inductively coupled plasma mass spectroscopy and synchrotron X-ray absorption spectroscopy (XAS) was used to determine the local environment.

Results and Conclusions

Controlled biomineral growth produces amorphous HAP, with a large surface area and more reactive surface. Untreated HAP viewed under TEM and AFM appeared as chain/needle structures of < 50nm length. As the HAP was heated from 200-700 °C the organics content and HAP surface area decreased and the mineral became more crystalline. Heat treating to 700 °C caused the HAP to anneal and larger spheres >100 nm in length formed. The potential of microbial HAP to remediate radionuclides and the stability of bound metals will be presented.

[1] Handley-Sidhu et al., (2011) *Environ. Sci. Technol.* **45**, 6985-6990. [2] Handley-Sidhu et al., (2011) *Biotechnol. Lett.* 2011, **33**, 79-87. [3] Thackray et al., (2004) J. Mater. Sci. Mater. Med. **15**, 403-406. [4] Terra et al., (2009) *Phys. Chem. Chem. Phys.* **11**, 568-577.

Redox Conditions and Metasomatic Activity beneath the Wesselton kimberlite, South Africa

BRENDAN J. HANGER[1*], GREGORY M YAXLEY[1], ANDREW J. BERRY[1,2] AND VADIM S. KAMENETSKY[3]

[1]Research School of Earth Sciences, Australian National University, Canberra, ACT 0200, Australia, brendan.hanger@anu.edu.au (* presenting author)

[2]Department of Earth Science and Engineering, Imperial College London, South Kensington, SW7 2AZ, UK,

[3]ARC Centre of Excellence in Ore Deposits, University of Tasmania, Hobart, TAS 7001. Australia

The redox state in mantle-derived garnet peridotite can be determined using the ratio of $Fe^{3+}/\sum Fe$ in garnet, which can be measured using Fe K-edge X-ray Absorption Near Edge Structure (XANES) [1] spectroscopy. This is a synchrotron based method which allows for *in-situ* measurement with high spatial resoloution. Redox state is expressed as oxygen fugacity (fO_2) and is an important control on carbon speciation in the mantle, particularly defining the boundary between carbonate stability relative to diamond or graphite.

A suite of garnet harzburgite and lherzolite xenoliths from the Wesselton kimberlite pipe, South Africa was analysed using electron probe microanalysis, LA-ICP-MS and Fe K-edge XANES spectroscopy with the aim of investigating the relationship between metasomatic enrichment and changes in redox conditions in the cratonic mantle beneath the Wesselton kimberlite pipes.

The suite shows evidence of multiple metasomatic events, including zonation in some garnet grains in which Ca, Fe and Ti enriched rims have overgrown highly refractory cores. Two distinct garnet REE patterns occur within the suite, 'sinusoidal' patterns typical of harzburgitic garnet in the cores, with 'normal' patterns typical of lherzolitic garnet on the rims. We quantitatively mapped the Fe^{3+} distribution in these grains using XANES and calculated average rim and core fO_2 values using the oxybarometer of Gudmundson and Wood [2]. The results indicate $\Delta \log fO_2$ of -1.37 (relative to FMQ) on the rim and -3.79 in the core at 1060 °C and 50 kbar. These values both fall in the diamond stability field in P-T-fO_2 space, however the rim fO_2 value is close to carbonate stability. Our results are in broad agreement with those of McCammon *et al.* [3] on similar samples.

We interpret this data in terms of quenching of the xenoliths caused by eruption of the kimberlite, during a strongly oxidising metasomatic event.

[1] Berry *et al.* (2010) *Chem. Geol.* **278**, 31-37.
[2] Gudmundsson and Wood (1995) *Contrib. Mineral. Petrol.* **119**, 56-67.
[3] McCammon *et al. (2001) Contrib. Mineral. Petrol.* **141**, 287-296.

https://doi.org/10.1180/S0026461X00008434 Published online by Cambridge University Press

Geochemistry of the Bolkardağı Bauxite Province, Karaman-Turkey

NURULLAH HANİLÇİ

İstanbul University, Department of Geological Engineering
nurullah@istanbul.edu.tr

Abstract

Bolkardağı bauxite province is located in the Tauride Belt, southern Turkey (Fig.1). This province hosts a large number of bauxite deposits (e.g. Karataş, Bolkardede T., Arpaçukuru, Kızıldağ, Öşün Yaylası, Göztaşı, Kavaközü, Baharpınarı, Kemikli T.,) which occurred within the Bolkardağı Unit (BU), Namrun Tectonic Unit (NTU) and Aladağ Unit (AU), and these tectono-stratigraphic units are imbricated [1]. Both the lateritic and karstic-type bauxite deposits developed in the province. While the phyllites-schists are the footwall of the lateritic-type deposits, the recrystallised limestones are the footwall for the karstic-type. The Middle Jurassic recrystallised limestones overlies the bauxite deposits in the province. The deposits consist mainly of diasporite and hematite with minor boehmite, kaolinite and anatas minerals.

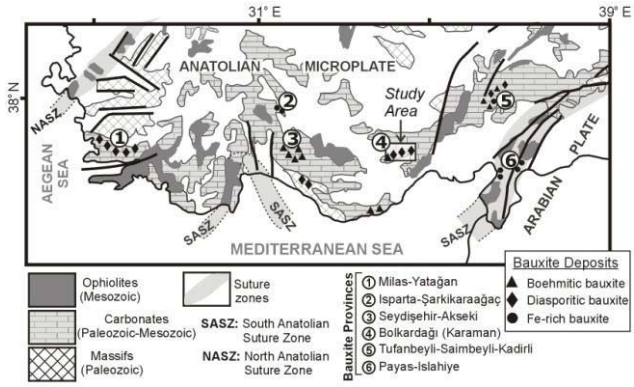

Figure 1: The bauxite provinces of the Turkey

The deposits contains 40.13 to 76.2 wt. % Al_2O_3 (aver. 53.3 %), 0.7 to 29.8 wt. % Fe_2O_3 (aver. 18.8 %), 0.6 to 24.9 wt. % SiO_2 (aver. 12 %), 11 % average LOI, 1.92 to 4.1 wt. %TiO_2 (aver. 2.7 %).

Al, Fe and Ti are mainly enriched elements during the bauxitization processes. The Al_2O_3 content increases from 28.6 % in average parent rock to 53.3% in average bauxite. Similar increases occur from 1.4 % to 2.7 % for TiO_2 content, from 7.6 % to 18.8 % for Fe content. The alkali (Na, K, Rb), alkali earth (Mg, Ca, Sr, Ba) elements, and silica content of the bauxites are lower than the parent rocks and saprolite, indicating extreme leaching during the bauxitization. The Ti, Zr, Hf, Nb, and Ta are the strongly immobile elements during the bauxitization processes, and the Fe, Ti, Sn, V, Pb, Ni and Cr are the gained elements in bauxitic zones in the Bolkardağı province.

From the stratigraphic evidence and geochemical data it is concluded that the Lower and Upper Triassic fillates-schists could have been the precursor rock for the bauxite deposits in Bolkardağı province. The bauxitization processes occurred pre-Middle Jurassic time, and the deposits included boehmite. The boehmitic bauxite was transformed to diasporitic bauxite due to post Cretaceous overtrusting and imbrication.

[1] Hanilci et.al., (2006) *59th Geological Congress of Turkey, Proceedings Book*. 157-159.

Interaction of subsurface pesticides with some metal-organic frameworks

ASSIA BOUCIF[1], ZAKIA HANK[1*], DJAMEL ABDESSEMED[2] AND SULTANA BOUTAMINE[1]

[1]Université des Sciences et de la Technologie Houari Boumediene (USTHB), Faculté de Chimie, Laboratoire d'Electrochimie, Corrosion, Métallurgie et Chimie Minérale, BP 32, El Alia, Bab-Ezzouar,16111, Algiers Algeria. z_hank@yahoo.fr, zhank@usthb.dz
[2]Université des Sciences et de la Technologie Houari Boumediene (USTHB), Faculté de Génie des Procédés, Laboratoire de Sciences, Génie des Procédés et Environnement, BP 32, El Alia, Bab-Ezzouar,16111, Algiers Algeria

Introduction

Particular chemicals like pesticides which use, in agriculture, became inescapable are engendering an environmental pollution and more particularly that of the waters as well of surfaces as ground-water sheets.

It is urgent, for preservation of public health, to reduce at most our exposure to these substances and to operate everything to reduce and control these pollutants.

So, the presence of pesticides in drinkable waters is severely regulated and the producing companies of water, to conform to the established standards, are obliged to include in their networks of water treatment, processes to eliminate them.

The adsorption on the synthetized metal organic complexes may be a technique to disinfect waters polluted by pesticides and other chemicals.

In this context, some coordination compouds of manganese, copper, zinc and cobalt were tested in the adsorption of mitrobuzin present in contaminated water. The retained organis molecules are natural products (flavonoids and purines)

Results and Conclusion

The preliminary results seems encouraging and we report them here. They are compared to those obtained with a classic adsorbing agent, namely powdered activated carbon F400

https://doi.org/10.1180/S0026461X00008434 Published online by Cambridge University Press

The origin of platinum-group element enrichments in alkalic porphyry systems: evidence from melt inclusions

JACOB J. HANLEY[1]

[1]Department of Geology, Saint Mary's University, Halifax, Nova Scotia, Canada, jacob.hanley@smu.ca (* presenting author)

Introduction

To elucidate some uncertainties concerning PGE enrichment in alkalic porphyry systems, we have performed a comprehensive study of the mineralogy, bulk rock geochemistry and melt inclusion chemistry of two porphyry systems in British Columbia, Canada.

Results and Discussion

Discrete PGE minerals in these systems are represented by Hg-rich Pd-Pt-As-Sb species (naldrettite-stibiopalladinite-sperrylite) and Pd-Te-Hg species (kotulskite-temagamite). However, these mineral phases are unambiguously late-stage, having formed during either remobilization of the PGE during a stage of carbonate-chlorite alteration, or during an epithermal stage whereby low salinity vapour transported Pd, along with Au, Sb, As, and S and deposited these in quartz carbonate-pyrite veins that cross-cut the porphyry-stage veining.

An indication of the nature of primary enrichment in PGE is supported by LA-ICPMS analyses of primary silicate melt inclusions within leucite-olivine-clinopyroxene-phyric, high-Mg basalt flows that are coeval with the porphyry rocks. The inclusions preserve Pd/Pt ratios, determined by LA-ICPMS, that are very similar to Pd/Pt ratios in bulk ore samples, suggesting that the basalts and porphyry rocks are genetically related (e.g., mixing of mafic and felsic endmembers to produce a hybrid PGE-rich porphyry magma, or contamination of a mafic magma by crustal material during ascent).

Only limited decoupling of Pd from Pt occurred during melt fractionation or mixing, melt ascent, fluid exsolution, and ore precipitation. PGE precipitation in the porphyry stage occurred in pyrite (as a dissolved trace constituent) and was coincident to Co and Ni enrichment in the pyrite, an association that is observed in found in IOCG deposits and Outukompu-type (mantle-peridotite associated) Cu-Co-Ni deposits.

A global Os isotope signal in a narrow seaway – the Late Jurassic from the Barents Sea to S. England

J.L. HANNAH[1,2,3*], S. GEORGIEV[1,2], G. XU[1,2], H.J. STEIN[1,2,3]

[1] Geological Survey of Norway, 7491 Trondheim, Norway, judith.hannah@colostate.edu (*presenting author)
[2] AIRIE Program, Colorado State University, Fort Collins, CO, USA
[3] Physics of Geological Processes, University of Oslo, Norway

Late Jurassic organic-rich shales are the dominant source rock for expansive hydrocarbon reserves in the corridor extending from the North Atlantic through the North and Norwegian Seas to the Barents Sea. An enormous accumulation of organic matter is contained in shales deposited over ca. 15 m.y. from the Late Jurassic (Oxfordian) through the earliest Cretaceous (Berriasian). At this time, the region was a drowned continental shelf; a narrow seaway cluttered with small landmasses tenuously linked the Arctic and Tethyan marine systems. Re-Os geochronology is now available from four sites along this seaway, from NE to SW: Nordkapp Basin in the Barents Sea, Troms III on the northern Norwegian Shelf, Staffin Bay on the Isle of Skye (western Scotland) [1], and the Kimmeridge sea cliffs at Dorset (southern England) [2]. Shales from the four sites differ significantly in depositional environment and proximity to shoreline, and in related variations in trace metal chemistry. Despite this complexity, seawater $^{187}Os/^{188}Os$ captured in the shales is remarkably consistent for a given depositional age.

At the two northern locales, Nordkapp Basin and Troms III, Hekkingen Formation shales are divided into a basal Alge Member and overlying Krill Member. At Troms III, the distinction is clear: relative to the rich Alge source rock, the Krill has lower total organic carbon (TOC) and lower gamma radiation. At Nordkapp Basin, this distinction is blurred. TOC is high throughout the Hekkingen section and trace metal concentrations are significantly higher than at Troms III, even when normalized to TOC. Also, biostratigraphy indicates that the units are time-transgressive; Krill deposition ended earlier at Nordkapp Basin than at Troms III.

Our new Re-Os data show a consistent increase in the initial $^{187}Os/^{188}Os$ ratio through the Late Jurassic. Alge shales at Troms III and Nordkapp Basin, with isochron ages of ~152 and ~158 Ma, have relatively low initial $^{187}Os/^{188}Os$ ratios of about 0.51 and 0.45, respectively. Upsection, Krill shales with isochron ages <150 Ma, have ratios >0.6. The correspondence continues to the south, where Staffin Bay shales near the Oxfordian-Kimeridgian boundary yield an age of 154.1 ± 2.1 Ma with initial $^{187}Os/^{188}Os = 0.53 \pm 0.02$ [1]. The Kimmeridge Clay shales yield an age of 155 ± 4.3 Ma but with higher initial $^{187}Os/^{188}Os = 0.59 \pm 0.07$ [2]. Although the imprecise Kimmeridge isochron age is similar to that of the Staffin Bay and Alge shales, the biostratigraphy (*wheatleyensis* Subzone) indicates an early Tithonian age, more likely correlative with the Krill shales.

The rising initial $^{187}Os/^{188}Os$ shale ratios through the Late Jurassic closely mimic the $^{87}Sr/^{86}Sr$ seawater curve. Our study shows that seawater Os is well mixed, even in narrow, confined seaways with relatively shallow water and nearby shorelines. Seawater $^{187}Os/^{188}Os$ is faithfully recorded in organic-rich shales.

NRC Petromaks project 180015/S30. [1] Selby (2007) *Nor. J of Geol.* **87**: 291-299. [2] Cohen et al. (1999) *EPSL* **167**: 159-173.

https://doi.org/10.1180/S0026461X00008434 Published online by Cambridge University Press

Microbial and geochemical synergy in manganese oxide formation

COLLEEN M. HANSEL[1*], DERIC R. LEARMAN[2], CAROLYN A. ZEINER[1], CARA M. SANTELLI[3] AND SAM M. WEBB[4]

[1]Harvard University, Cambridge, MA, USA, hansel@seas.harvard.edu (*presenting author)
[2]Central Michigan University, Mount Pleasant, MI, USA, deric.learman@cmich.edu
[3]Smithsonian Institution, Washington, DC, USA, santellic@si.edu
[4]Stanford Synchrotron Radiation Lightsource, Menlo Park, CA, USA, samwebb@slac.stanford.edu

Manganese (Mn) oxides are among the strongest sorbents and oxidants within the environment, controlling the fate and transport of numerous elements and the degradation of recalcitrant carbon. Both bacteria and fungi mediate the oxidation of Mn(II) to Mn(III/IV) oxides but the genetic and biochemical mechanisms responsible remain poorly understood. Furthermore, the physiological basis for microbial Mn(II) oxidation remains an enigma.

We have recently reported that a common marine bacterium (*Roseobacter* sp. AzwK-3b) oxidizes Mn(II) via reaction with extracellular superoxide (O_2^-) produced during exponential growth [1]. Here we expand this superoxide-mediated Mn(II) oxidation pathway to fungi, introducing a surprising homology between prokaryotic and eukaryotic metal redox processes. For instance, *Stilbella aciculosa*, a common soil Ascomycete filamentous fungus, precipitates Mn oxides at the base of asexual reproductive structures. This distribution is a consequence of localized production of superoxide by the well-known NADPH oxidase enzymes, leading to abiotic oxidation of Mn(II) by superoxide. Disruption of NADPH oxidase activity using the common oxidoreductase inhibitor DPI leads to diminished cell differentiation and subsequent Mn(II) oxidation inhibition.

We also show here that similar to fungi extracellular superoxide production is widespread throughout the bacterial domain. Yet, superoxide production does not, in fact, confer the ability to produce Mn oxides. This is a consequence of a backreaction between the products (Mn(III) and hydrogen peroxide) formed upon Mn(II) and superoxide reaction, leading to the regeneration of Mn(II). Indeed, we show that superoxide-mediated Mn oxide formation is reliant upon the removal of the hydrogen peroxide product. Thus, the formation of Mn oxides by the *Roseobacter* and *Stilbella* spp. requires both the production of superoxide and consumption of hydrogen peroxide. We believe that this need for hydrogen peroxide consumption hints to the role of heme peroxidases (recently implicated Mn oxidases) in bacterial Mn oxidation.

Taking into consideration that superoxide is a strong and versatile redox reactant serving as both an oxidant (e.g., Mn) and reductant (e.g., Fe, Cu, Hg) of metals, biological superoxide production may have profound influences on metal biogeochemistry beyond Mn.

[1] Learman et al. (2011) *Nature Geo.* **4**, 95-98.

Structural constraints on Mn(II) oxidation by biogenic Mn oxides

COLLEEN M. HANSEL[1*], DERIC R. LEARMAN[2], ANDY S. MADDEN[3], SCOTT D. WANKEL[1] AND SAM M. WEBB[4]

[1]Harvard University, Cambridge, MA, USA, hansel@seas.harvard.edu (*presenting author)
[2]Central Michigan University, Mount Pleasant, MI, USA, deric.learman@cmich.edu
[3]University of Oklahoma, Norman, OK, USA, amadden@ou.edu
[4]Stanford Synchrotron Radiation Lightsource, Menlo Park, CA, USA, samwebb@slac.stanford.edu

Manganse (Mn) oxides are vital components of environmental systems, controlling the fate and transport of contaminants, bioavailability of nutrients, degradation of recalcitrant carbon, and respiratory capacity of microbial populations. The oxidation of Mn(II) to Mn(III/IV) oxides has been primarily attributed to biological processes, due in part to the faster rates of bacterial Mn(II) oxidation compared to observed mineral-induced and other abiotic rates.

Here we reveal the reactivity of biogenic Mn oxides formed by a common marine bacterium (*Roseobacter* sp. AzwK-3b), which has been previously shown to oxidize Mn(II) via the production of extracllular superoxide [1]. The reactivity of the biogenic Mn oxides was explored by harvesting and characterizing Mn oxides formed within *Roseobacter* AzwK-3b filtrate at various time points followed by reaction with Mn(II) under an array of aqueous conditions [2]. Oxidation of Mn(II) by extracellular superoxide within *Roseobacter* filtrate results in the formation of colloidal (~20-40 nm in diameter) Mn oxides. These oxides are most similar to δ-MnO_2 – a highly disordered birnessite phase with turbostratic stacking and hexagonal symmetry. These colloidal Mn oxides are extremely reactive and induce further Mn(II) oxidation and Mn oxide formation. Interestingly, the oxidation of Mn(II) mediated by the colloidal Mn oxides includes a number of reaction pathways, involving the formation of organic and oxygen radicals at the oxide surface.

The reactivity of these Mn oxide minerals, however, is short-lived due to the rapid evolution of the initial hexagonal birnessite phase to a non-reactive triclinic birnessite phase. Thus, this structural evolution imposes the need for continuous production of new colloidal hexagonal particles for Mn(II) oxidation to be sustained, illustrating an intimate dependency of enzymatic and mineral-based reactions in Mn(II) oxidation. Further, the coupled enzymatic and mineral-induced pathways are linked such that enzymatic formation of Mn oxide is requisite for the mineral-induced pathway to occur. These findings highlight the important (yet frequently overlooked) role that reactive metabolites and biominerals play in metal redox biogeochemistry.

[1] Learman, et al. (2011) *Nature Geo.* **4**, 95-98. [2] Learman, et al. (2011) *Geochim. Cosmochim. Acta* **75**, 6048-6063.

https://doi.org/10.1180/S0026461X00008434 Published online by Cambridge University Press

He-Ne-Ar isotope systematics of the HIMU reservoir; implications to K and U budget in the mantle

T. HANYU[1]*, Y. TATSUMI[1] AND J.-I. KIMURA[1]

[1]Institute for Research on Earth Evolution, Japan Agency for Marine-Earth Science and Technology, Yokosuka, Japan, hanyut@jamstec.go.jp (* presenting author)

Noble gas isotopes could have the potential to provide the evidence for recycled origin of some mantle reservoirs. We present a new set of He-Ne-Ar isotopic compositions of lavas from the Cook-Austral Islands in the south Pacific, which exhibit HIMU and EM characteristics in terms of radiogenic isotopes. $^{3}He/^{4}He$ of the HIMU lavas are lower than MORB values, as previously demonstrated, but a coherent variation in $^{3}He/^{4}He$ with Pb isotopes indicates two-component mixing to form the lavas. Since the HIMU reservoir plots at the radiogenic Pb isotopic end of the mixing trend, $^{3}He/^{4}He$ of this reservoir must be 6 Ra or less. The other mixing component is the local lithosphere, which is commonly involved in EM lavas.

K/U of the HIMU reservoir is constrained by the relative abundances of radiogenic and nucleogenic ^{4}He, $^{21}Ne^*$ and $^{40}Ar^*$. The HIMU lavas show systematic variations in $^{4}He/^{40}Ar^*$-$^{4}He/^{21}Ne^*$ space, in which they define a trend that is parallel to, but offset from the trend previously observed for other OIBs. Using $^{4}He/^{21}Ne^*$ to correct for elemental fractionation of noble gases, $^{4}He/^{40}Ar^*$ of the HIMU reservoir is higher than the $^{4}He/^{40}Ar^*$ production ratio in the mantle. This indicates that the HIMU reservoir had lower time-integrated K/U (approximately 3000) than the canonical mantle value (13000). Low $^{3}He/^{4}He$ and K/U are best explained by a model where the HIMU reservoir originates from ancient subducted oceanic crust that preferentially lost He and K relative to U by dehydration during its subduction.

Since the subducted oceanic crust is enriched in U, but not in K, the preservation of the subducted oceanic crust in the mantle modifies the previous estimates of K/U and K concentration in the bulk silicate Earth (BSE), that did not take this reservoir into consideration. The estimated K/U of BSE may be changed from 13000 down to 8000-10000, if significant amounts of subducted oceanic crust have accumulated to form an isolated reservoir. This fact partially (but not always totally) reconciles $^{40}Ar^*$ paradox. More importantly, subduction and accumulation of the oceanic crust affects the distribution of fluid-mobile and fluid-immobile elements in the mantle.

Mapping of heavy metal sorption to cell-iron-mineral aggregates on the µm-scale

LIKAI HAO[1*], GREGOR SCHMID[1], ANDREAS KAPPLER[1], MARTIN OBST[1]

[1] University of Tuebingen, Germany, Center for Applied Geoscience likai.hao@uni-tuebingen.de (* presenting author) gregor. schmid@ uni-tuebingen.de, andreas.kapple@ uni-tuebingen.de, martin.obst@uni-tuebingen.de

The distribution of heavy metals such as Ni, Cu, Zn, As, Cd, and Hg in environmental biofilm-system is often controlled by the sorption to organic biomacromolecules and by the sorption to and co-precipitation with abiogenic and biogenic iron minerals [1,2]. Changes in pH or redox-potential in micro-environments can result in the release and mobilization of heavy metals in the environment and thus affect ecosystems and/or human health. Therefore, to understand the fate and environmental behaviour of metals in the environment it is essential to acquire information on the partitioning of the respective metals in complex systems such as biofilms which contain a heterogeneous mixture of intact cells, polysaccharides and iron miernals.

Whereas high-resolution imaging such as electron microscopy or scanning transmission X-ray microscopy are suitable to gain detailed insights into binding mechanisms of heavy metals, they usually do not allow for mapping regions at a spatial scale that is relevant for the environment. Thus, we use metal sensitive fluorescent dyes that were developed for cell-biology [3] in combination with confocal laser scanning microscopy (CLSM) [4] to qualitatively and semi-quantitatively map *in-situ* the distribution of heavy metals such as Ni, Cu and Zn within biofilms formed by Fe(II)-oxidizing bacteria at µm to mm-scales. At the same time we localize and map the organochemical composition of the biofilm using various DNA-, protein-, polysaccharide- and lipid-specific fluorescent dyes [3]. Mineral particles were mapped using the reflection signal of the laser. Correlation analysis allowed for identification of binding sites of heavy metals at the µm to mm scale within pristine and metal-contaminated environmental biofilms. Ni and Zn were mainly bound to bacterial cells and polysaccharides, but Cu was found to preferentially be bound to polysaccharides and iron minerals.

Acknowledgements: Funded by DFG Emmy-Noether program to M.O. (OB 362/1-1). We thank E. Struve, K. Stögerer and the Geomicrobiology group at the U. of Tuebingen for support and discussion.

[1] Bakkaloglu (1998), *Water Sci & Tech* **38**, 269-277. [2] Cornell (2003), *The Iron Oxides*, Weinheim: Wiley-VCH. [3] Sabins (2010), *Handbook of Biological Dyes and Stains*. John Wiley & Sons. [4] Pawley (2006), *Handbook of Biological Confocal Microscopy*, **3rd ed**, Springer.

https://doi.org/10.1180/S0026461X00008434 Published online by Cambridge University Press

Fire activity in Northern Eurasia from 2002 to 2010 and its contribution to Arctic black carbon

WEI MIN HAO*[1], ALEX PETKOV[2], BRYCE NORDGREN[3], RACHEL CORLEY[4], AND SHAWN URBANSKI[5]

[1]USDA Forest Service, RMRS Fire Sciences Laboratory, Missoula MT, USA, whao@fs.fed.us (* presenting author)
[2]USDA Forest Service, RMRS Fire Sciences Laboratory, Missoula, MT, USA, apetkov@fs.fed.us
[3]USDA Forest Service, RMRS Fire Sciences Laboratory, Missoula, MT, USA, bnordgren@fs.fed.us
[4]USDA Forest Service, RMRS Fire Sciences Laboratory, Missoula, MT, USA, rcorley@fs.fed.us
[5]USDA Forest Service, RMRS Fire Sciences Laboratory, Missoula, MT, USA, surbanski@fs.fed.us

Introduction

Northern Eurasia covers 20% of the global land mass and contains 70% of boreal forest. Biomass burning in this region may be a significant source of atmospheric black carbon that would deposit on Arctic ice and accelerate ice melting. We examined the daily fire occurrence in different land cover categories at a 1 km x 1 km resolution from 2002 to 2010 over Northern Eurasia. The results are important in assessing the contribution of fire emissions in this region to the black carbon deposition on Arctic ice. This research is also critical in understanding the impact of climate change on the fire dynamics and emissions in Northern Eurasia.

Results and Conclusion

Northern Eurasia is divided into seven geographic areas. The fire locations were based on the MODIS active fire products and MODIS MOD12Q1 product was used for the classification of land cover types. Agricultural fires dominated biomass burning in Northern Eurasia during the nine-year period, accounting for about 52% of the MODIS fire detections, followed by grassland fires (17%), forest fires (16%), and shrubland fires (8%). Approximately 61% of the active fire detections in Northern Eurasia occurred in Russia. The remainder of fire activity largely occurred in Central and Western Asia (21%) and in Eastern Europe (8%). In Russia, about 51% of the fire detections were agricultural fires, 24% were forest fires, and 17% were grassland and shrubland fires. Agricultural residues are often burned after harvest in the autumn or before plowing in the spring. In Central and Western Asia, about 58% of the fire detections were grassland fires, and 37% were agricultural fires. The years 2003 and 2008 had 43% and 47%, respectively, more fire detections than the annual mean (303,856) from 2002 to 2010. The unusually high fire activity in 2003 and 2008 was a result of extensive burning on cropland in Russia and Central and Western Russia, and over forest and grassland and shrubland in Russia. There is no apparent trend of fire occurrence in the entire Northern Eurasia, within each geographic area, or within each of the land cover types between 2002 and 2010. We will present the results of the study and discuss its significance on the spatial and temporal extent of black carbon emissions from forest, agricultural, and grassland and shrubland fires in Northern Eurasia.

Distribution of helium isotope ratio in the central Indian Ocean

T. HARA[1] *, N. TAKAHATA[1], Y. SANO[1], K. SHIRAI[1], K.OHMORI[2] AND T.GAMO[1]

[1]Atmosphere and Ocean Reserch Institute, The University of Tokyo, 5-1-5, Kashiwanoha, Kashiwa-shi, Chiba 277-8564, Japan (*correspondence:hrtaka@aori.u-tokyo.ac.jp)
[2]Department of Natural History Sciences, Graduate School of Science, Hokkaido University, N10W8, Kita-ku, Sapporo, 060-0810, Japan

Introduction

The ocean circulation plays an important role in global biogeochemical cycles. Understanding the dynamics of the deep ocean is essential to study global climate change because the ocean has a great capacity to store and transport heat and material. The $^3He/^4He$ ratio is one of the most sensitive and conservative tracers in chemical oceanography because of the primordial signature, rapid mobility and chemical inertness of the isotopes. We have collected about 80 samples at 10 stations along or near 70°E from 20°N to 60°S at various depths (200m ~ 5000m) in the central Indian Ocean. Sampling was carried out during the KH-09-5 cruise of a Research Vessel, Hakuho Maru. Helium isotopes in this area have not beeen much investigated yet.[1]

Analysis

The $^3He/^4He$ ratios were measured on a conventional noble gas mass spectrometer after extraction, purification and separation using Ti getters and cryogenic charcoal traps.[2] The observed $^3He/^4He$ ratios were calibrated against atmospheric helium. To estimate the influence of air contamination, the $^4He/^{20}Ne$ ratios were measured by an on-line quadrupole mass spectrometer before cryogenic separation of He from Ne.

Results and Discussion

The $^3He/^4He$ ratios increased downward, and maximum excess ^3He of ~17% were observed at mid-depth (2000–3000 m), and then decreased in the bottom water. The distribution revealed a north-south gradient with relatively high anomalies in the northern and equatorial Indian Ocean and low anomaly in the southern Indian Ocean.

The high $^3He/^4He$ ratios at mid-depth possibly derived from the mid ocean ridge in the Indian Ocean. These results are consistent with counterclockwise deep circulation in the north-west Indian ocean. The north-south gradient might be due to the inflow of deep seawater with the lower $^3He/^4He$ ratios in Atlantic Ocean or in Antarctic Ocean.

References

[1] Srinivasan *et al*. (2004) *J. Geophys. Res*. **109**, C06012
[2] Sano *et al*. (2008) *Anal. Sci*. **24,** 521-525

https://doi.org/10.1180/S0026461X00008434 Published online by Cambridge University Press

Modeling a rise of atmospheric oxygen induced by Paleoproterozoic snowball Earth event

MARIKO HARADA[1*], EIICHI TAJIKA[2], AND YASUHITO SEKINE[2]

[1]University of Tokyo, Earth and Planetary Science, Tokyo, Japan, harada@astrobio.k.u-tokyo.ac.jp

[2]University of Tokyo, Complexity Science and Engneering, Chiba, Japan

Recent geological studies suggest that Paleoproterozoic snowball glaciations may have possibly caused a rise in atmospheric oxygen [1,2]. The hypothesis is that a global warming in a glacial aftermath enhances chemical weathering on land and provides nutrients to the ocean, which leads to a cyanobacterial bloom [2]. In order to verify the hypothesized oxidation process quantitatively, we developed a simple atmosphere-ocean biogeochemical cycle model and simulated the atmosphere and ocean perterbation after deglaciation.

We set an initial condition under high atmospheric pCO_2 (~0.7 atm), assuming a situation immediately after the Paleoproterozoic snowball deglaciation. Chemical weathering rate is given as a function of temperature and atmospheric pCO_2, mutipled by weahtering efficiency f (f = 1 at present) which depends on soil biological activity and continental area at the time. Nutrient supply is represented by riverine phosphorous input via chemical weathering, which is assumed to be consumed fully by photosenthesis. For the global oxygen cycle, we adopt a redox system model given by Goldblatt et al. (2006) [3].

Our results indicate that, immidiately after the deglaciatoin, global temterature rises as high as 330 K, resulting in extremely high levels of riverine phosphorous input due to the enhanced chemical weathering (~10–20 times higher than that of today). Assuming all the provided phosphorous are consumed by oxygen-producing photosenthesis via cyanobacteria, total amount of oxygen generated by photosenthesis may reach 10^{23} mol during 10^5 years immediately after the deglaciation. Atmospheric oxygen level rises from less than 10^{-5} PAL (present atmospheric level) to ~1 PAL during the first 5 million years, and then gradually decreases to a stable level of ~0.01 PAL. In this model, oxygen concentration rises up to ~0.1 PAL in the first 100 years, probably because of a large perterbation induced by glaciation and subsequent suppression of methane oxidation, which is a major sink of oxygen, by ozone layer formation. However in reality, such an extremely rapid rise in productivity and O_2 level might have been dampened, considering timescale needed for cycnobacteria to recover after the severe glaciation or phosphous adsorption into iron oxides in the shallow ocean. We will therefore also discuss influences of iron-manganese cycles which couple to the phosporus cycle, as well as variations of marine carbon isotopic composition.

[1] Kirschvink et al. (2000) *Proc. Natl. Acad. Sci. USA*, **97**, 1400-1405. [2] Sekine, Y et al. (2010) *Geochem. Geophys. Geophys* **11**, 1-10. [3] Goldblatt, C (2006) *Nature* **443**, 683-686.

Spectrophotometric analysis for As(V) sorption mechanism in the aluminum hydroxide coprecipitation method

D. HARAGUCHI[1*], C. TOKORO[2] AND S. OWADA[2]

[1]Waseda university, Tokyo, Japan, d.haraguchi@aoni.waseda.jp

[2]Waseda university, Tokyo, Japan, tokoro@waseda.jp

[3]Waseda university, Tokyo, Japan, owadas@waseda.jp

Hydroxide coprecipitation method is widely used in a treatment of wastewater containing dilute toxic anions. But now detail mechanism or quantitative characteristic is not well understood and also demanded. This study discussed a sorption mechanism of dulute arsenic (As(V)) in wastewater using aluminum hydroxide coprecipitation method by analyzing filtrates and precipitates for an artificial wastewater.

Sorption mechanism of As(V) coprecipitation with aluminum hydroxide was investigated using four kinds of experimental methods: (i) sorption instherm formation, (ii) zeta potential mesurement, (iii) XRD analysis, and (iv) FT-IR analysis. We compared between coprecipitation experimental results and simle adsorption ones in which As(V) was just adsorbed on the sysnthized aluminum hydroxide.

In the only coprecipitation experiments, sorption isotherms of As(V) on aluminum hydroxide exhibited a BET type isotherms and sorption densities abruptly increased when the initial As/Al molar ratio was more than 1.5. And zeta potential hardly changed even if sorption densities increased when the initial As/Al molar ratio was more than 1.5. Moreover, the results of XRD and FT-IR analysis represented that patterns and spectra were similar to not the ones of amorphous aluminum hydroxide but amorphous aluminum arsenate when the initial As/Al molar ratio was more than 1.5. On the other hand, these unique tends was not shown in the adsorption experiments [1].

Thus, the inherent phenomena which can sorb more As(V) than single layer adsorption has occurred in the only coprecipitation experiments. The results of XRD and FT-IR analysis suggested that the precipitates have changed depending on the initial As/Al molar ratio and a surface precipitation such as amorphous aluminum arsenate was formed when the initial As/Al molar ratio was more than 1.5, whereas simple tow-dimentional adsorption of As(V) onto the surface of aluminum hydroxide when the initial As/Al molar ratio was less than 1.5. These trends were qualitatively accorded with sorption mechanism of dilute As(V) with ferrihydrite [2].

[1] D., Haraguchi; C., Tokoro; S., Owada. (2011) *Jour. of MMIJ.* **127** 82-87.

[2] C., Tokoro; Y., Yatsugi; H., Koga; S, Owada. (2010) *Environ. Sci. Technol.* **44**, 638-643.

https://doi.org/10.1180/S0026461X00008434 Published online by Cambridge University Press

The weathering forefront for permafrost carbon: priorities for critical zone research

JENNIFER HARDEN[1*], STEPHANIE EWING[2], TORRE JORGENSON[3], CHARLES KOVEN[4], COREY LAWRENCE[1], MARJORIE SCHULZ[1], MARK WALDROP[1]

[1]U.S. Geological Survey, Menlo Park, USA, jharden@usgs.gov
[2] Montana State University, Bozeman, USA, stephanie.ewing@montana.edu
[3]Ecosystems, Fairbanks, USA, ecoscience@alaska.net
[4]Lawrence Berkeley National Lab, Berkeley, USA, CDKoven@lbl.gov

Little is known about mineral weathering in permafrost soils. Yet as permafrost thaws, mineral stabilization of carbon may become exceedingly important owing to the large stores of permafrost carbon that will thaw over the next century. In areas where permafrost is not present, carbon is often stabilized by organo-mineral binding and complexation driven by mineral weathering. Hydrology and biogeochemistry are key to pathways and transit times of carbon fluxes to the atmosphere. Above the permafrost (the active layer), water and ice contents influence thermal conductance and rates of thawing; decomposition of organic matter increases dramatically upon thaw; organic matter structure is linked to soil moisture and vegetation characteristics. In deeper soils with permafrost, the amounts and forms of carbon have been characterized according to processes of C stabilization (Figure 1), but carbon forms have not been related mechanistically to water, mineral surfaces, and biogeochemistry in a way that addresses processes at meaningful scales.

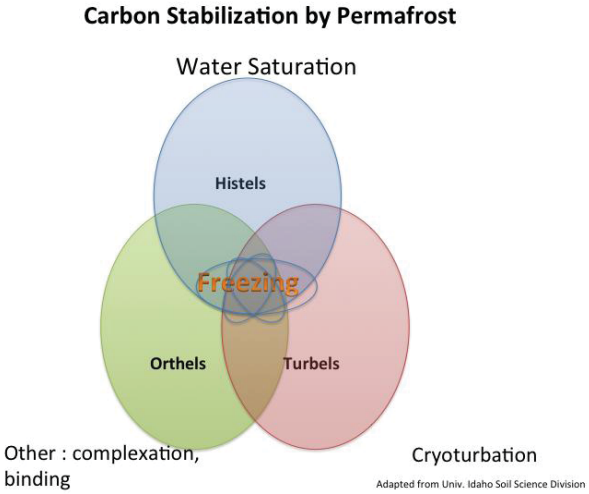

Figure 1. Processes of carbon stabilization by the three suborders of permafrost soils called Gelisols.

Thus the processing and microenvironments of permafrost carbon at the micro and macroscale will be key to understanding how and where permafrost carbon may be stabilized or destabilized upon thaw.

New insights from FOAM: iron and trace metal cycling in highly sulfidic pore waters beneath an oxic water column

DALTON S. HARDISTY*[1], NATASCHA RIEDINGER[1], BEN C. GILL[2], DAVID T. JOHNSTON[3], CHRISTOPHER T. REINHARD[1], NOAH PLANAVSKY[1], DAN ASAEL[4] AND TIMOTHY W. LYONS[1]

[1]University of California, Riverside, Riverside, USA, dhard003@ucr.edu (*presenting author)
[2]Virginia Tech, Blacksburg, USA
[3]Harvard University, Cambridge, USA
[4]University Brest, Brest, France

A 50-cm sediment core was collected from the FOAM site (Friends of Anoxic Mud) with pore waters being extracted immediately on-site. FOAM is a well-described, nearshore study site in Long Island Sound characterized by high TOC and pore water sulfide concentrations of a few mM overlain by an oxic water column. Going well beyond any past work at FOAM, and to complement our Fe analyses, we analyzed a suite of trace metals including Mo, Cr, V, and U. Our data for Fe-speciation show high ratios of pyrite (Fe_{py}) to highly reactive Fe (Fe_{HR}; Fe_{py}/Fe_{HR} >.99), intermediate Fe_{total}/Al (≈.5) and low Fe_{HR}/Fe_{total} (< .3), consistent with near-complete pyritization of the highly reactive Fe delivered with the detrital mineral flux. Importantly, these conditions do not yield high Fe_{HR}/Fe_{total} and Fe_{total}/Al ratios and degrees of pyritization, our standard fingerprints of anoxia/euxinia, despite protracted exposure to high dissolved sulfide concentrations. Data from the FOAM site, in combination with past work in the Black Sea, show the necessity for additional inputs of reactive Fe to generate high Fe_{HR}/Fe_{total}, Fe_{py}/Fe_{HR}, Fe_{total}/Al, and degrees of pyritization, likely via an Fe-shuttle in association with syngenetic pyrite formation under euxinic conditions. Because of the oxic bottom waters, these processes are not significant at FOAM, confirming past work by Canfield et al. [1, 2]. Then, as now, FOAM provides a mechanistic keystone in our understanding of the Fe paleoredox proxies. Trace metal concentrations in FOAM sediments show only intermediate enrichment, despite very high [H_2S] in the shallow pore waters. The muted trace metal enrichments at FOAM confirm that water-column euxinia is uniquely responsible for very high concentrations and further validate the utility of the proxies in our search for euxinia in the ancient oceans. In addition, coupled Fe and Mo isotopes from both the FOAM sediments and pore waters have the potential to improve the paleoproxy potential of Fe and trace metal expressions that distinguish between euxinia and sulfide-rich and sulfide-poor diagenetic environments overlain by oxic bottom waters.

[1]Canfield, DE, Raiswell, R, Bottrell, S (1992). *Am. J. Sci*, **Volume 292**: 659-683
[2]Canfield, DE, Lyons, TW, and Raiswell, R (1996). *Am. J. Sci*, **Volume 296**: 818-834.

.

https://doi.org/10.1180/S0026461X00008434 Published online by Cambridge University Press

Alteration of zircon in alkaline fluids: Nature and experiment

D.E. HARLOV[1*], A. LEWERENTZ[2], A. SCHERSTEN[2]

[1]GeoForschungsZentrum, Telegrafenberg, 14473 Potsdam, Germany, dharlov@gfz-potsdam.de (* presenting author)
[2]Dept Earth Sciences, Lund University, 22362 Lund, Sweden, alexander.lewerentz@gmail.com, anders.schersten@geol.lu.se

Natural alteration of zircon can take place either via partial dissolution coupled with partial overgrowth or via fluid-aided coupled dissolution-reprecipitation or both processes in tandem [1][2]. Coupled dissolution-reprecipitation results in the zircon being partially to totally replaced by compositionally re-equilibrated zircon, a new mineral phase, or both.

In this study, fragments (50 to 200 μm) from an inclusion-free, relatively non-metamict euhedral zircon (nepheline syenite pegmatite, Seiland magmatic province, northern Norway) were experimentally reacted in 20 mg batches with Ca-bearing fluids (1 mg $Ca(OH)_2$ + 5 mg H_2O) plus 5 mg (ThO_2 + $ThSiO_2$ + SiO_2) in sealed Pt capsules at 900 °C and 1000 MPa for 6 to 11 days (piston cylinder press, CaF_2 setup, cylindrical graphite oven). In the experiment, the fluid reacted with the zircon. This took the form of partial replacement of the zircon with compositionally altered zircon via coupled dissolution-reprecipitation. The reacted zircon is characterized by a sharp compositional boundary between the altered and original zircon. The altered zircon generally contains a micro-porosity. Inclusions of baddelyite (ZrO_2) are seen outlining the reaction front between the altered and unaltered zircon. SIMS analysis of the altered zircon indicates that it is strongly enriched in Th + Si, heavily depleted in U, and heavily to moderately depleted in (Y+REE). In all experiments radiogenic ^{206}Pb (3 to 5 ppm in the unaltered zircon) is strongly depleted in the altered zircon. Hf concentrations in the altered zircon retain the same approximate value as in the original zircon. The results from these experiments indicate that zircon can be compositionally altered via Ca-bearing fluids via coupled dissolution-reprecipitation processes under high-grade conditions and that their internal geochronometer can be reset due to the massive loss of U and radiogenic Pb and the additon of Th.

The baddelyite-zircon textures from these experiments replicate similar, highly-localized zircon-baddelyite textures seen in albitised, 2.9 to 2.7 Ga, amphibolite- and granulite-facies granitoid rocks from SW Greenland [3]. Here Ca was released into the fluid during the albitisation of plagioclase. Baddelyite should not be stable in the presence of SiO_2 (present in both the experiments and in the granitoid rocks) but rather react with SiO_2 to form zircon. However, if sufficient Ca is present in the fluid, it appears to complex with the SiO_2 as $CaSiO_3$ thereby lowering the SiO_2 activity such that baddelyite is stable with co-existing zircon and quartz. The experiments also demonstrated that, with sufficiently high enough concentrations of SiO_2 in the fluid, not all of the SiO_2 will complex with Ca allowing for the activity of SiO_2 to remain at 1. In this case baddelyite did not form in or with the altered zircon.

[1] Geisler et al., 2007 **Elements** 3, 43-50 [2] Putnis, 2009 **Rev Mineral Geochem**, vol 70, 87-124. [3] Windley and Garde (2009) Earth Sci Rev 93, 1-30

Multiple sulfur isotope model of temperature dependent isotope fraction in *Archaeoglobus fulgidus*

BRIAN HARMS[1*], KRISTEN MITCHELL[2], KIRSTEN HABICHT[3], JOOST HOEK[1], JAMES FARQUHAR[1]

[1]Department of Geology and ESSIC, University of Maryland, College Park, Maryland, USA (*Correspondence: bharms@umd.edu)
[2]Department of Earth and Environmental Sciences, University of Waterloo, Waterloo, Ontario, Canada
[3]Institute of Biology, Nordic Center for Earth Evolution (NordCEE), University of Southern Denmark, Odense, Denmark

Dissimilatory sulfate reduction (DSR) has a central role in the global sulfur cycle. Understanding how environmental factors and physiological variables influence DSR-mediated sulfur isotope fractionation is therefore crucial for interpting the sedimentary sulfide record. The hyperthermophile *Archaeoglobus fulgidus* grows over a wide range of temperature conditions (54°-92°C [1]), making it an ideal test subject for investigating how aspects of the DSR pathway respond to temperature extremes. A previous study of *A. fulgidus* [1] found that fractionations between sulfate and sulfide were greatest at intermediate temperatures. An inverse correlation between cell specific sulfate reduction rate and fractionation was found in the intermediate temperature range, but this correlation broke down at the extreme hot and cold limits of growth. A potential solution to a flow network model [2] was proposed, one in which sulfate exchange across the cell membrane controlled fractionation at high and low temperatures, and internal sulfur transformations were the dominant influence at intermediate temperatures [1].

Here we present multiple sulfur isotope results from the same culture experiments in [1]. Our calculated flow parameters (f_3 and f_5) give a markedly different trend from that predicted in [1], and our observed $\Delta^{33}S$ values also implicate a DSR flow network in which large fractionations (as in e.g. [3]) are permitted. The mismatch between predictions and results suggests a different physiological response to temperature change than expected. Several possibilities are investigated. Following the framework of [4], we also investigate solutions in which the fractionation factor associated with the reduction of sulfite to sulfide is not a fixed quantity.

[1] Mitchell et al. (2009) *Environ Microbiol* **11**, 2998-3006. [2] Canfield et al. (2006) *Geochim, Cosmochim. Acta* **70** 548-561. [3] Brunner and Bernasconi (2005) *Geochim. Cosmochim. Acta* **69** 4759 – 4771. [4] Bradley et al. (2011) *Geobiology* **9** 446-457.

https://doi.org/10.1180/S0026461X00008434 Published online by Cambridge University Press

Isotopic Variations in the Northern Galápagos Volcanic Province

KAREN S. HARPP[1,2*], WILLIAM SCHLITZER[1], THOMAS MORROW[2], ERIC MITTELSTAEDT[3], AND THE MV1007 SCIENTIFIC PARTY

[1]Colgate University, Hamilton, NY, USA, kharpp@colgate.edu *presenting author
[2]University of Idaho, Moscow, ID, USA
[3]Woods Hole Oceanographic Institution, Woods Hole, MA, USA, emittelstaedt@whoi.edu

The Northern Galápagos Volcanic Province (NGVP), located between the Galápagos Archipelago and the Galápagos Spreading Center (GSC), is ideally located to provide insight into the mechanisms of plume-ridge interaction. The plume is located south of the GSC, close enough to have profound geochemical and geophysical influences on the ridge. During the 2010 MV1007 research cruise, we collected geophysical data and >40 dredges across the NGVP, in a survey bounded by the Wolf-Darwin Lineament (WDL) to the west and Genovesa Island to the east.

Preliminary Sr, Nd, and Pb isotopic data reveal several important observations about the composition of lavas in the NGVP: a) most NGVP lavas are more enriched than those from the northern margin of the Galápagos Platform; b) consistent with previous work in the archipelago [1, 2], geochemical variations of Nazca Plate lavas require 3 distinct isotopic endmembers, a dominant one with elevated $^{207}Pb/^{204}Pb$ and $^{208}Pb/^{204}Pb$ for a given $^{206}Pb/^{204}Pb$ (like WD from [2]), one with moderate Sr, Nd, and Pb ratios (like PLUME from [2]), and a depleted MORB-like composition; c) lavas from Pinta Island eastward are binary mixtures of WD and depleted mantle; d) lavas erupted on the Cocos Plate may be influenced by a 4th endmember with elevated $^{206}Pb/^{204}Pb$ and $^{87}Sr/^{86}Sr$ (i.e., FLO from [2]); and e) there are no systematic spatial variations in isotopic ratios along volcanic lineaments on the Nazca Plate (e.g., the WDL).

Our results have implications for plume-ridge interaction and the composition of the Galápagos plume. The NGVP is dominated by the elevated $^{207}Pb/^{204}Pb$ and $^{208}Pb/^{204}Pb$ component, with only minor influence of the material supplying the western Galápagos shields, the locus of the plume. This suggests that the plume is strongly spatially zoned or that there is an additional source of enriched mantle material limited to the GSC area. The lack of spatial patterns in geochemistry across the Nazca Plate in the NGVP further indicates that enriched material is distributed throughout the mantle between the ridge and the plume and reaches the surface through crustal weaknesses generated by regional stresses [3, 4]. The presence of enriched material in Cocos Plate lavas suggests plume-related material is bypassing the zone of upwelling beneath the GSC as it flows to the north. These results confirm that the Galápagos system may be mirroring Hawaii and other plumes that exhibit strong north/south spatial zonation [5], The Galápagos are distinct from Hawaii, however, in that the more radiogenic Pb component is in the northern arm of the plume instead of the south.

White et al. (1993) *J. Petrol.* **98**, 19533-19563. [2] Harpp & White (2001) *G-Cubed* **2**, 2000GC000137. [3] Harpp and Geist (2002) *G-Cubed* **3**, 2002GC000370. [4] Mittelstaedt & Ito (2005) *G-Cubed* **6**, 2004GC000860. [5] Huang et al. (2011) *Nat. Geosci.,* NGE01263.

Manganese, Fenton Chemistry, and Disease: The proof is in the inflammation.

ANDREA D. HARRINGTON[1]*, STELLA E. TSIRKA[2], AND MARTIN A.A. SCHOONEN[1]

[1] Stony Brook University, Department of Geosciences, Andrea.Harrington@stonybrook.edu (*presenting author) Martin.Schoonen@stonybrook.edu
[2] Stony Brook University, Pharmacological Sciences, stella@pharm.stonybrook.edu

Exposure related diseases can be, for the most part, broken down into two categories, mutagenic and toxic. While a mutagenic disease results from disruption of normal cell replication, an illness based on particle toxicity is derived from the ability of the material to generate an inflammatory stress response (ISR), dysregurate the cell, and possibly lead to cell death. Particle-derived cellular oxidative stress is likely a key contributor to many occupational health diseases, such as silicosis and coal workers' pneumoconiosis.

Reactive oxygen species (ROS), and the hydroxyl radical in particular, are known to cause oxidative stress. Earth materials can generate ROS in two different ways, via surface defects and oxidative dissolution. The oxidative dissolution of minerals allows for metal cations to enter the solution. Once in solution, these cations can partake in Fenton chemistry.

While iron is the most recognized Fenton metal, new research indicates that chromium, copper, vanadium, recently manganese can also generate ROS, although the reaction mechanisms are not well understood [1-3]. Originally only taking iron into account, the Fenton reaction can now be generalized to [4]:

$$H_2O_2 + M^{n+} \rightarrow M^{(n+1)+} + {}^{\cdot}OH + OH^-$$

where M is a metal cation which can donate one electron and be stable at this new oxidation state [4].

Exposure to manganese is thought to be the root for many neurological diseases, such a Parkinson's, Alzheimer's and Huntington's. However, its role in the development of pulmonary diseases through stimulating inflammation is unknown. In the present study, the ability of different species of manganese to generate ROS and an ISR at the cellular level is examined. Furthermore, the confounding effects of having iron and/or quartz in the system are investigated.

Experiments using dissolved manganese and iron species are performed to compare their abilities to generate ROS and an ISR. These tests are performed utilizing an array of geochemical and biochemical techniques [5,6]. More intricate experiments will be performed using iron and/or manganese as co-contaminates and co-precipitates onto synthetic quartz.

Initial experiments have demonstrated the ability of manganese to elicit an ISR. Furthermore, the higher solubility of manganese compared to iron, which precipitates out into a relatively inert ferric phase, allows for a considerably steady ISR over time and a response that continuously increases with loading.

[1] Valko M, Morris H, Cronin MTD (2005) *Curr Med Chem*, **12:**1161-1208. [2] Pierre JL, Fontecave M (1999) *Biometals*, **12:**195-199. [3] Srivastava S & Dubey RS (2011) *Plant Growth Regul*, **64:**1-16. [4] Prousek J (1995) *Chemicke Listy*, **89:**11-21. [5] Harrington AD, Tsirka SE & Schoonen MAA (accepted) *Geochem Trans*. [6] Cohn CA *et al.* (2009) *Geochemical Transactions* 2009, **10:**8-16.

https://doi.org/10.1180/S0026461X00008434 Published online by Cambridge University Press

Documenting magmatic processes at Filicudi Island, Aeolian Arc, Italy: integrating plagioclase textural and in situ compositional data

Michelle Harris[1*], Wendy Bohrson[2]

[1]Central Washington University, Ellensburg, USA harrism@geology.cwu.edu (* presenting author)

[2]Central Washington University, Ellensburg, USA bohrson@geology.cwu.edu

Documenting the physiochemical processes that influence magma composition is critical for forecasting eruption style and managing volcanic hazards. Although studies have documented how compositional diversity develops in magmas on Earth, controversy exists regarding the roles that recharge, assimilation and fractional crystallization (RAFC) play in magma evolution. Studies of Filicudi Island, Italy, document a compositional range from calc-alkaline basalt (51 wt. % SiO_2) to high-K andesite (62 wt. % SiO_2) that cannot be simply related by FC, implying magma recharge and crustal contamination/assimilation played vital roles. Integration of plagioclase textural and in situ compositional data allows documentation of the quantitative roles and chronology of RAFC.

Filicudi Island is one of seven major islands of the Aeolian archipelago in the southern Tyrrhenian Sea, Italy. Stratigraphic studies define four main cycles of activity that range in age from 1.02 to 0.04 Ma (*1*). Cycles are characterized by a succession of plagioclase bearing magmas that show recurrent reversals to more MgO-rich magmas, a lack of systematic correlation between SiO_2 and MgO, and an overall SiO_2 increase with time, implying recharge, assimilation, and fractional crystallization took place. Images obtained from Nomarski Differential Interference Contrast and Back-Scattered Electron methods document five main texture types within seven samples that span the compositional range of Cycle Three, the most widely exposed cycle. Identified textural types include monotonous, complex oscillatory, sieved cores with oscillatory rims, oscillatory cores with sieved rims, and sieved cores and rims.

Detailed core-to-rim traverses of crystals of each textural type using Electron Microprobe analysis document mostly core-to-rim decreases in Anorthite content, although a few significant core-to-rim increases do occur. Similarly, incompatible trace elements generally show increases from core-to-rim with decreasing Anorthite content, or more complex trends, providing evidence that (A)FC processes played a dominant role. Conversely, core-to-rim increases in Anorthite content with associated Fe and Mg increases provide strong evidence that at least one recharge event occurred within the associated magma body. LA-MC-ICPMS analyses will be performed on selected crystals that encompass the range of Anorthite, trace element and textural types to document core-to-rim changes in $^{87}Sr/^{86}Sr$. Isotopic data will further characterize the RAFC history of these magmas as well as will complete a data set that can be quantitatively modeled to provide thermal and mass constraints on this phase of magmatic activity at Filicudi Island.

1. A. P. Santo, Volcanological and geochemical evolution of Filicudi (Aeolian Islands, south Tyrrhenian Sea, Italy). *Journal of Volcanology and Geothermal Research* **96**, 79 (2000).

Reactive transport modeling of CO_2 sequestration in mine tailings

Anna L. Harrison[1*], Ian M. Power[1], Siobhan A. Wilson[2], Gregory M. Dipple[1], K. Ulrich Mayer[1], and Sergio A. Bea[3]

[1]University of British Columbia, Vancouver, Canada, aharriso@eos.ubc.ca ([*] presenting author), ipower@eos.ubc.ca, gdipple@eos.ubc.ca, umayer@eso.ubc.ca

[2]Monash University, Clayton, Australia, sasha.wilson@monash.edu

[3]Lawrence Berkeley National Laboratory, Berkeley, United States of America, sabea@lbl.gov

Mineralization of atmospheric CO_2 within carbonate minerals occurs passively in ultramafic mine tailings via weathering of Mg-silicates and hydroxides [1]. If this process were accelerated, large mines may have the capacity to sequester millions of tonnes of CO_2 annually. Supplying elevated partial pressures of CO_2 (pCO_2) into tailings may accelerate CO_2 sequestration by increasing dissolved inorganic carbon and enhancing mineral dissolution. Passive carbon mineralization has been documented at the Mount Keith Nickel Mine (MKM) in Western Australia [2]. MKM produces tailings consisting primarily of Mg-silicate minerals. Brucite [$Mg(OH)_2$] is present at lower abundance [2], yet is more rapidly carbonated, thus was practical for experiments and modeling.

Gas streams with elevated pCO_2 have been used to enhance brucite carbonation rates in zero-dimensional batch experiments. In tailings, however, multi-dimensional flow means that interactions between transport and chemical reactions will play a role in governing carbonation rates. To investigate carbonation efficiency in tailings under elevated pCO_2 conditions, brucite columns were supplied with 10 vol.% CO_2. Quantitative mineralogical analyses of solids indicate the extent of carbonation declined with distance from the injected CO_2.

Two modeling studies have been undertaken using the reactive transport code, MIN3P [3], to calibrate the model and to elucidate the processes likely to govern the rate and extent of carbonation in tailings. Modeling of column experiments indicated a strong advective gradient in the gas phase was developed due to CO_2 injection, thereby enhancing vertical CO_2 transport. A second modeling study was undertaken in which passive carbonation in an active tailings storage facility at MKM was modeled and calibrated with field data to complement previous work simulating an inactive facility at this mine [4]. The active facility is periodically replenished with slurries of fresh tailings, resulting in lateral flow in addition to the evaporative driven vertical flow occurring in the inactive facility. This more complex flow regime may affect both reactive cation transport and the ingress of atmospheric CO_2, thereby altering the extent of carbonation.

These studies permitted the development of a comprehensive model that describes both passive and accelerated CO_2 sequestration in tailings. Our calibrated model will enable assessment of sequestration potential and help guide implementation of accelerated sequestration strategies at mine sites.

[1] Wilson et al (2009) *Econ. Geol.* **104**, 95-112. [2] Wilson (2009), PhD thesis, UBC. [3] Molins and Mayer (2007) *Water Resour. Res.* **43**, W05435. [4] Bea et al (*in press*) *Vadose Zone J.*

https://doi.org/10.1180/S0026461X00008434 Published online by Cambridge University Press

Li Isotopes of Hawaiian Lavas: Kea vs Loa Source Variation

LAUREN HARRISON[1*], DOMINIQUE WEIS[1], MIKE GARCIA[2], ELSPETH BARNES[1], AND DIANE HANANO[1]

[1]Pacific Center for Isotopic and Geochemical Research, University of British Columbia, Vancouver, BC, Canada, lharriso@eos.ubc.ca
[2]Department of Geology and Geophysics, University of Hawai'i, Honolulu, HI, 96822, USA, mogarcia@hawaii.edu

Hawaiian volcanism delineates into two distinctive geographical series, the Kea and the Loa trends, identified by their unique geochemical and isotopic characteristics. Traditionally, these trends have been attributed to mixing of different components in the source of the Hawaiian mantle plume, mainly an enriched end-member (Ko'olau) characterized by the presence of recycled oceanic crust ± sediment, a more depleted end-member (Kea) with high ε_{Nd}, ε_{Hf}, and $^{206}Pb/^{204}Pb$, and a more primitive component defined by high $^{3}He/^{4}He$ (Lo'ihi). Because of the sizeable fractionation of lithium isotopes in low temperature environments, lithum serves as a powerful tracer for the presence of altered oceanic crust and sediments in the sources of oceanic island basalts. Lithium can thus be used to help distinguish the source components of Hawaiian lavas, most importantly for post-shield and rejuvenated lavas, where depleted/recycled components are thought to play a larger role.

This study analyzed fifty-six samples of Hawaiian shield (13), post-shield (36) and rejuvenated lavas (7) for lithium isotopes. Post-shield volcanics exhibit the lightest δ^7Li values, ranging from 0.75 ± 0.33‰ to 5.20 ± 0.20‰, while rejuvenated lavas from Kaua'i, Ka'ula, and West Ka'ena Ridge are intermediate with an average of 3.72‰. Finally, shield basalts exhibit the highest δ^7Li, ranging from 3.03 ± 0.27‰ to 5.19 ± 1.07‰. For both post-shield and shield lavas, δ^7Li is able to delineate between Kea and Loa trends (e.g., post-shield Kea average: 3.67‰ and post-shield Loa average: 2.48‰). Lithium isotopes correlate positively with Pb and Nd isotopes, indicating that Li isotopic signatures survive residence time in the mantle and are suitable tracers of source components [1], in this case ancient subducted oceanic crust and/or sediments, in Hawaiian volcanism. In $^{206}Pb/^{204}Pb$ and ε_{Nd} vs δ^7Li diagrams, Loa shield lavas plot along the extension of Kea shield lavas with lower δ^7Li, ε_{Nd} and $^{206}Pb/^{204}Pb$. Enriched Loa shield lavas from West Ka'ena Ridge, the Mile High Section of Mauna Loa, and subaerial Ko'olau show higher δ^7Li, but with their lower ε_{Nd} and $^{206}Pb/^{204}Pb$, these lavas define a sub-parallel trend that indicates there are at least two enriched end-members in the Loa source, one in Ko'olau [2] and one in Loa trend lavas [3]. Finally, Hualalai post-shield volcanics show the lowest δ^7Li values, ranging from 0.75 ± 0.33‰ to 3.53 ± 0.53‰, which might reflect the presence of recycled oceanic crust.

In this study, lithium isotopes not only suggest the presence of a recycled component in post-shield, rejuvenated, and Loa shield lavas, they also help distinguish Loa enriched source components. Further characterization of the trends in lithium isotopes may unearth some additional insights into the source of Loa-type volcanism [4].

[1] Vlastélic *et al* (2009) *Earth and Planetary Science Letters* **286**, 456-466. [2] Tanaka *et al*. (2007) *Earth and Planetary Science Letters* **265,** 450-465. [3] Weis *et al.* (2011) *Nature Geosciences* **4**, 831-838. [4] Hanano *et al* (2010) *G3* **11**, doi:10.1029/2009GC002782

Incorporation of Perrhenate into Nitrate Sodalite

JAMES B. HARSH*[1], JOHNBULL O. DICKSON[1], AND ERIC M. PIERCE[2]

[1]Washington State University, Pullman, WA, USA, harsh@wsu.edu (* presenting author)
[2]Oak Ridge National Laboratory, Oak Ridge, TN, USA

Technetium-99 (Tc), a long-lived radionuclide, is one of the most widespread contaminants within the Hanford subsurface with an estimated inventory of 5.31×10^3 curies. For example, Tc contamination has been found in the sediments beneath the C, S, SX, T, and TX Tank Farms as a result of high-level waste (HLW) solutions that have leaked or spilled from Hanford Tanks. The HLW solutions are characterized as highly alkaline (hydroxide ion concentration > 8.5 M) and high ionic strength solutions (up to saturation with respect to $NaNO_3$). Previous research focused on Sr-90 and Cs-137 has demonstrated that these elements are incorporated into feldspathoid minerals, such as nitrate sodalite $[Na_8(Al_6Si_6O_{24})(NO_3)_2]$, that formed as a result of the contact between Hanford sediments and the HLW solutions (Chorover et al., 2008; Deng et al. 2006). The desire to immobilize Tc in aluminosilicate minerals through the application of subsurface amendments for contaminated sediments as well as the production of mineralized wasteforms further emphasizes the need to understand the long-term stability and release of Tc from aluminosilicate minerals, specifically the feldspathoid mineral sodalite.

Nonradioactive perrhenate (ReO_4^-) was used as a surrogate for TcO_4^- due to its similar ionic potential. Sodalite was synthesized over 24 h at 80C from 1.76 M solutions of NO_3 + ReO_4, with ReO_4 concentrations of 0, 0.18, 0.35, 0.71, 0.88, and 1.76 M with NaOH and 4A zeolite added as sources of Na, OH, Al, and Si. Perrhenate concentrations in the sodalite ranged from 0 to 13 mmol kg^{-1} in the 0 – 0.88 M ReO_4 samples. The 1.76 M sample, without NO_3, contained 760 mmol kg^{-1}. Using the 211 x-ray diffraction peak to determine alteration of crystal structure, no significant shifts occurred, except in the NO_3-free sample where the 211 d-spacing increased by 0.01 nm. Increased reaction time from 1 to 7 d narrowed the peak widths, implying more crystallinity, but ReO_4 incorporation did not change in a consistent manner. We conclude that the larger ReO_4 ion (r = 260 pm) does not form as stable a sodalite structure as the NO_3 (r = 190 pm). Further experiments will determine the role of ion size in the formation of sodalite in the presence of more than one species.

[1] Chorover, J., Choi, S., Rotenberg, P., Serne, R.J., Rivera, N., Strepka, C., Thompson, A., Mueller, K.T., O'Day, P.A., 2008, *Geochimica et Cosmochimica Acta* **72**, 2024-2047.
[2] Deng, Y., Harsh, J.B., Flury, M., Young, J.S., and Boyle, J.S. 2006, *Applied Geochemistry*, **21**, 1392-1409.

https://doi.org/10.1180/S0026461X00008434 Published online by Cambridge University Press

Meridional ocean circulation intensity through MIS 11 from Nd isotopes in South Atlantic cores

ALISON E. HARTMAN[1*], STEVEN L. GOLDSTEIN[1], SIDNEY R. HEMMING[1]

[1]Lamont Doherty Earth Observatory; Columbia University, Palisades, NY, USA, ahartman@ldeo.columbia.edu (* presenting author)

Abstract

The waxing and waning of North Atlantic Deep Water (NADW) in the South Atlantic has been used to monitor changes in meridional overturning circulation. Neodymium (Nd) isotopes are a valuable water mass tracer in this region because the ε_{Nd} value of intermediate and deep waters is dependent on the mixing ratio of southern- and northern-sourced water. A spliced record from deep cores RC11-83 (42.07ºS, 9.717ºE, 4718m) and TNO57-21 (40.6ºS, 7.816ºE, 4918 m) showed higher values (>2ε_{Nd} units) during the LGM compared with today, indicative of a weakening or shoaling of NADW in the South Atlantic during glacial periods[1]. Nearby core TNO57-6 (42.92ºS, 8.88ºE, 3750m) is slightly further south and significantly shallower than RC11-83/TNO57-21 and showed a substantially greater Last Glacial Maximum (LGM) to Holocene offset (>4 ε_{Nd} units)[1,2]. However, further studies have indicated that the methods for obtaining the bottom water ε_{Nd} signal at site TNO57-6 were likely compromised by a contaminating phase within the fine sediment during leaching. We modified our previous procedure, in line with the Cambridge group[3], and are extracting the ε_{Nd} values of dissolved Fe-Mn oxide encrusted, mixed-species, planktonic foraminifera. Confirmation of the results as a bottom water signal is indicated by agreement with the ε_{Nd} values of fish debris from the same depth[3]. The resulting record shows a Holocene ε_{Nd} value around -9.7 with a gradual increase of ~3 ε_{Nd} units to an LGM value around -6.5 ε_{Nd} units. This trend is similar to the TNO57-21/RC11-83 record. We have applied the new procedure down-core, and developed a set of glacial-interglacial pairs for each transition since MIS 11. All interglacial stages show ε_{Nd} values similar to Holocene values (-9.5) and each glacial shows an increase of about 2 ε_{Nd} units, with the exception of MIS 8, which appears to show a smaller increase of ~1 ε_{Nd} unit. We interpret these data as recording changes in the presence of NADW in the South Atlantic between glacials and interglacials, and indicating similar intensities in the export during interglacials through MIS 11, and also in glacials except for MIS 8. The record may also be interpreted as indicating stronger shoaling of the northern component waters during MIS 2, 6 and 10 than during MIS 8, and this will be further investigated. Overall the data indicate similar levels of stability were reached during the warm and cold phases of several glacial-interglacial cycles.

[1] Piotrowski, *et al*. (2004) *Earth Planet. Sci. Lett*. **225**, 205. [2] Rutberg, et al. (2000) *Nature*, **405**, 935. [3] Roberts, *et al*. (2010) *Science*. **327**, 75.

Stable isotope and trace element records in Holocene stalagmites from Java: Paleoarchive of climate change and human activity?

A. HARTMANN[1], E. EICHE[1], T. NEUMANN[1*], J. FOHLMEISTER[2], A. SCHRÖDER-RITZRAU[2], A, MANGINI[2]

[1]Karlsruhe Institute of Technology, Institute for Mineralogy and Geochemistry, neumann@kit.edu (*presenting author)

[2]Forschungsstelle Radiometrie, Heidelberger Akademie der Wissenschaften, 69120 Heidelberg, Germany

Speleothems are important archives to trace paleoclimate and paleoenvironmental changes. This has widely been proven in temperate zones, but there is a lack of studies from the tropics. To further close this gap, active stalagmites, formed since the early Holocene, from Bribin cave located in the Gunung Sewu karst, Middle Java, Indonesia have been analysed in high resolution.

The $\delta^{18}O$ values vary between -6 and -8 ‰ with lowest values approximatily 8.5 ka ago indicating a period of high rainfall amount in the early Holocene. This assumption is supported by a continuous concurrent lowering of corresponding Sr/Ca and Mg/Ca ratios with time, displaying a shorter contact time with the limestone in the Karst.

During the early and mid-Holocene, relatively low $\delta^{13}C$ values of 12.2 ± 0.24 ‰ were recorded which is indicative of a predominant contribution of carbon from C3 plants of the overlying tropical rain forest. However, the $\delta^{13}C$ values show a dramatic, but almost continuous increase from -12.0 to -7.8 ‰ over the last ~1.1 ka. This increase may reflect a change in vegetation density (less isotopically light plant material) and/or composition (C4 instead of C3 plants) at the surface.However, during the corresponding period of time, no distinctive trend was detectable for the $\delta^{18}O$ values with oscillations around -6.8 ± 0.25 ‰. Consequently, a possible change in vegetation cannot be explained by considerable climatic changes alone which would have also influenced the $\delta^{18}O$ signal. Mg/Ca and Sr/Ca ratios partially positively correlate with the $\delta^{13}C$ record over the last 1.1 ka indicating that some changes in the water balance still might be of importance resulting in longer or shorter contact time with the karstic limestone. An alternative interpretational approach may relate the marked $\delta^{13}C$ increase of the last millenium to human activities. Pollen and sedimentological studies from the area strongly suggest that extensive and organized forest clearance has been taking place on Java for the last 1.5 or 1.2 ka, respectively [1].

[1] Sémah & Sémah (2012) *Quaternary International* **249**, 120-128.

https://doi.org/10.1180/S0026461X00008434 Published online by Cambridge University Press

Steps towards a global chemical weathering model framework: The role of erosion and supply limitation

J. HARTMANN[1*], N. MOOSDORF[1], R. LAUERWALD[1], A.J. WEST[2], S. COHEN[3], A.J. KETTNER[3]

[1] Institute for Biogeochemistry and Marine Chemistry, KlimaCampus, University of Hamburg, Hamburg, Germany, geo@hattes.de [* presenting author], nils.moosdorf@zmaw.de, ronny.lauerwald@zmaw.de

[2] Department of Earth Sciences, University of Southern California, Los Angeles, USA, joshwest@usc.edu

[3] Community Surface Dynamics Modeling System (CSDMS), Institute of Arctic and Alpine Research (INSTAAR), University of Colorado, Boulder CO, USA, sagy.cohen@colorado.edu, kettner@colorado.edu

Chemical weathering is an integral part of the rock cycle, and its relationship with physical erosion has been a subject of long-standing interest. Empirical correlations between erosion and weathering have been observed for headwater catchments [1] but such correlations have been more difficult to identify at the scale of Earth's largest river basins [2]. This may be the result of the many different factors that influence weathering, including the strong observed dependence on runoff [2, 3].

In this study, we explore the hypothesis that low rates of erosion and associated development of deeply weathered soils, particularly in the humid tropics, reduces chemical weathering over large spatial scales, significantly influencing fluxes from large river basins. As a starting point, we use functional equations for chemical weathering that have been trained empirically based on data from the Japanese Archipelago [3], across a range of different lithologies [4]. These equations were applied to large catchments in tropical areas, and the importance of supply limited weathering was assessed in two ways: (i) using a correction factor based on maps of the distribution of deeply weathered soils and wetlands, and (ii) by comparing weathering fluxes with modeled physical erosion rates [5].

In general, weathering fluxes calculated using the island arc model are significantly over-estimated for the low-lying tropical river basins. An average soil correction factor of 90% was found to account for this supply limited effect. The reduction in chemical weathering rates scales with calculated physical erosion in a comparable pattern to that identified for headwater catchments with felsic lithologies [1].

The results of this study highlight the importance of accounting for the scaling of chemical weathering with erosion at the scale of Earth's largest river basins. Weathering fluxes from island arcs are among the globally highest, because of the young and fresh mineral surfaces, but the weathering equations derived in these settings can be applied to estimate weathering fluxes globally by accounting for supply limitation based on physical erosion rates.

[1] West et al. (2005) *Earth Plan. Sci. Lett.* **235**, 211-218. [2] Gaillardet et al. (1999) *Chem. Geol.* **159**: 3-30. [3] Hartmann & Moosdorf (2011) *Chem. Geol.* **287**, 211-257. [4] Dürr et al. (2005) *Global Biogeochem. Cycles* **19**, GB4S10. [5] Cohen et al. (2012) *Computers & Geosciences*, in press

Ocean-like water in Jupiter-family comet 103P/Hartley 2

PAUL HARTOGH[1*], DARIUSZ C. LIS[2], DOMINIQUE BOCKELÉE-MORVAN[3], MIGUEL DE VAL-BORRO[1], NICOLAS BIVER[3], MICHAEL KÜPPERS[4], MARTIN EMPRECHTINGER[2], EDWIN A. BERGIN[5], JACQUES CROVISIER[3], MIRIAM RENGEL[1], RAPHAEL MORENO[3], SLAWOMIRA SZUTOWICZ[6], GEOFFREY A. BLAKE[2]

[1]Max Planck Institute for Solar System Research, Katlenburg-Lindau, Germany, hartogh@mps.mpg.de (* presenting author)

[2]California Institute of Technology, Pasadena, USA, dcl@caltech.edu

[3]LESIA Observatoire de Paris, CNRS, UPMC, Université Paris-Diderot, France, Dominique.Bockelee@obspm.fr

[4]Rosetta Science Operation Centre, European Space Astronomy Centre, Madrid, Spain, michael.kueppers@sciops.esa.int

[5]Astronomy Department, University of Michigan, Ann Arbor, USA, ebergin@umich.edu

[6]Space Research Centre, Polish Academy of Sciences, Warsaw, Poland, slawka@cbk.waw.pl

Abstract

For decades, the source of Earth volatiles, especially water, has been a subject of debate. Proposed explanations include accretion of material in the vicinity of the Earth orbit or delivery by impacts of asteroids or comets during the late heavy bombardment (LHB). The source of water reservoirs can be accurately traced by measurements of the deuterium-to-hydrogen isotopic ratio (D/H). Previous measurements of this ratio in several Oort cloud comets resulted in a value twice as high as that in the Earth oceans, leading to the generally accepted conclusion that comets are unlikely to be the primary source of ocean water. Together with orbital modeling, these measurements suggested instead that asteroids with composition similar to that of CI meteoroids were the main water source. As part of our solar system observation programme [1], using the HIFI instrument [2] on the Herschel Space Observatory [3], we have obtained the first measurement of the D/H ratio in a Jupiter-Family comet (103P/Hartley 2) [4]. It turned out that 103P's D/H-ratio is consistent with VSMOW. This result substantially expands the reservoir of Earth ocean-like water to include some comets, and is consistent with the emerging picture of a complex dynamical evolution of the early Solar System. We discuss the implications of these observations for the origin of water and the evolution of its distribution in the solar system.

[1] Hartogh *et al.* (2009) *Planet. Space Sci.* **57**, 1596-1606. [2] de Graauw *et al.* (2010) *Astron. Astrophys.* **518**, L4. [3] Pilbratt *et al.* (2010) *Astron. Astrophys.* **518**, L1. [4] Hartogh *et al.* (2011) *Nature* **478**, 218-220.

https://doi.org/10.1180/S0026461X00008434 Published online by Cambridge University Press

High-pressure dehydration of antigorite-serpentinite and its effect on boron isotope fractionation in the shallow mantle wedge.

JASON HARVEY [1*], CARLOS J. GARRIDO[2], SAMUELE AGOSTINI [3], JOSÉ-ALBERTO PADRÓN-NAVARTA [4], VICENTE LÓPEZ SÁNCHEZ-VIZCAÍNO [5], IVAN P. SAVOV [1], CLAUDIO MARCHESI [2]

[1] School of Earth & Environment, University of Leeds, UK feejh@leeds.ac.uk (*presenting author)
[2] IACT, CSIC-UGR, Armilla, Granada, Spain
[3] Istituto di Geoscienze e Georisorse, CNR, Pisa, Italy
[4] Géosciences, Montpellier, CNRS (France)
[5] Departamento de Geología, Universidad de Jaén, Linares, Spain

The ultramafic rocks of Cerro del Almirez Massif in Spain preserve field evidence for the subduction-related, prograde transition from antigorite-serpentinite (ant-serp) to chlorite-harzburgite (chl-harz) [1]. This study investigates the influence of dehydration reactions on B isotope fractionation in the sub-arc region, where fluid loss accompanies prograde metamorphism under well constrained P-T conditions (650 °C, 1.7 GPa [2]).

B isotopes are strongly fractionated during the dehydration of ant-serp, with a sharp decrease of $\delta^{11}B$ across the ant-serp to chl-harz isograd. Ant-serp has a $\delta^{11}B$ of +22.6 ‰ (± 1.6; n=2), similar to the heaviest $\delta^{11}B$ in forearc serpentinites of the active Mariana subduction zone [3, 4]. Transitional ant-chl-ol-opx serpentinite samples preserve a $\delta^{11}B$ of +3.3 ‰ (± 0.3), and the dehydration reaction product, granofels-textured chl-harz, has a $\delta^{11}B$ of -3.5 ‰ (± 0.3). Spinifex-textured chl-harz formed by crystallisation of atg-breakdown products and sampled some distance from the isograd, has a $\delta^{11}B$ of +2.7 ‰ (± 0.4). The anomalously heavy $\delta^{11}B$ of the spinifex-textured chl-harz may be attributable to interaction with a second, boron-bearing fluid associated with the formation of the spinifex textures or to a less efficient fractionation process due to the fast mineral and textural transformations that took place.

The drop in $\delta^{11}B$ approaching the isograd demonstrates that massive B isotope fractionation occurs in the shallow segments of the slab-mantle interface during the dehydration of ant-serp. Moreover, the effects survive to higher P-T conditions. The continuing stability of chlorite beyond the antigorite breakdown reaction limits the release of H_2O, and therefore B, to about 6–7 wt% H_2O, whereas without the "chlorite-in" reaction the dehydration would yield > 12 wt% H_2O loss and thus a larger B flux). This likely results in a chlorite-hosted, B-rich reservoir with a heterogeneous $\delta^{11}B$. This reservoir may contribute B to the fluids necessary to trigger melting under volcanic arcs and in addition to the proposed deeply subducted serpentine [5] may contribute to the heavy and often very heterogeneous $\delta^{11}B$ signatures of island arc volcanoes

[1] Trommsdorff et al. (1998) *Contrib. Min. Petrol.* **132**, 139-148. [2] Padrón-Navarta et al. (2011) *J. Petrol.* **52**, 2047-2078. [3] Savov et al. (2007), *J. Geophys. Res*, doi:10.1029/2006JB004749.[4] Pabst et al. (2012) *Lithos* **133**, 162-179. [5] Ullmer & Trommsdorff (1995) *Science* **268**, 858-861.

Identification and characterization of phase governing Eu(III) uptake in granite by microscopic observations

Y. HASEGAWA[1], K. FUKUSHI[1*], K. MAEDA[1], Y. YAMAMOTO[2], D. AOSAI[2] AND T. MIZUNO[2]

[1]Kanazawa Univeristy, Kanazawa, Japan, fukushi@kenroku.kanazawa-u.ac.jp (presenting author)
[2]Japan Atomic Energy Agency, Mizunami, Japan

Sorption behaviors of trace elements on single mineral surface have been extensively studied. However, there have been very few researches for the trace elements sorption on complex mineral assemblages such as rocks, sediments and soils. In order to make predictions for the trace elements migration on geologic media, it is crucial to understand the molecular-scale interaction of trace elements with complex mineral assemblages, and to construct the thermodynamic sorption models based on the molecular-scale information. In the present study, the sorption of trace level of Eu(III) on complex mineral assemblages, slightly altered granite, as function of pH was studied by microscopic approaches.

The granite sample was collected from a borehole at a depth of 400m from the Mizunami Underground Research Laboratory constructed by Japan Atomic Energy Agency in central Japan. The granite sample was visually fresh. However, the microscope observation as well as the X-ray diffraction patterns of clay fraction shows that the occurrences of smectite, chlorite, vermiculate, calcite and hydrous iron oxides. The thin sections of the granite were prepared for Eu(III) sorption experiments. The thin sections were reacted for 24 hours in solutions of which pH were adjusted to 4, 5 and 6 under 0.01 M NaCl support electrolyte and analyzed by electron probe micro analyzer (EPMA). Then, the same thin sections were reacted for 24 hours in solutions of which 1.5 ppm of Eu(III) was added into solutions mentioned above. The resulting thin sections were served for observation and analyses by EPMA.

EPMA analyses of the thin sections after Eu(III) sorption shows that the Eu contents in quartz, plagioclase, K-feldspar, chrolite, calcite and iron hydroxide were less than detection limit. In contrast, smectite always contains up to 4 wt% of Eu. Part of biotite grains also contains up to 8 wt% of Eu. Because the Eu concentration in solution is 1.5 ppm, the concentrated factors of Eu in smectite and biotite are more than ten thousands. Quantitatively, the amount of smectite in the granite is negligible. We concluded that biotite is most important phase governing Eu(III) uptake on the granite. The texture of Eu enriched parts in the biotite grain were different from the original texture. The Eu enriched parts were distorted and the distinct cleavages appear. There is good negative correlation between K and Eu in the affected biotite grain. The relationship shows the uptake mode of Eu on biotite is ion-exchange of K in biotite and Eu(III) in solution. The number of the Eu affected biotite grain increases with decreasing pH. This indicates that the intercalation of Eu(III) to K in biotite favors at low pH conditions. The macroscopic sortpion behavior of Eu(III) on granite (Maeda et al. this volume) is consistent with the microscopic observations.

Ref.: K. Maeda, K. Fukushi, Y. Hasegawa, Y. Yamamoto, D. Aosai and T. Mizuno: "Modeling Eu(III) sorption on granite, In this volume.

https://doi.org/10.1180/S0026461X00008434 Published online by Cambridge University Press

Organic-poor Neoarchean Banded Iron Formations from the Slave and North China Cratons

BREANA HASHMAN[1], DOMINIC PAPINEAU[2,3], WOUTER BLEEKER[4], AND YUSHENG WAN[5]

[1] Department of Earth Sciences, Dickinson College, United States, hashmanb@dickinson.edu
[2] Department of Earth and Environmental Sciences, Boston College, United States.
[3] Geophysical Laboratory, Carnegie Institution of Washington, United States.
[4] Geological Survey of Canada, Ottawa, Canada.
[5] Beijing SHRIMP Center, China.

Geochemical data suggest that Banded Iron Formations (BIFs) preserve a record of both abiological and biological processes. Rare earth elements, compositional, and mineralogical data of BIFs over the last thirty years have led Klein (2005) to suggest that BIFs are hydrothermally-influenced chemical precipitates. This view complements that of Li et al. (2011) who used the presence of Fe (III) acetate salt, and apatite+magnetite associations to suggest that bacteria played a role in the formation of Paleoproterozoic BIFs from Western Australia. Ferruginous metasedimentary rocks from the Eoarchean Akilia Association in Greenland have apatite+graphite mineral-pairs that might represent biosignatures (Papineau et al., 2010; Mojzsis et al., 1996), but recent work has shown that these mineral associa¬tions can also be fluid-deposited later in the history of BIFs (Papineau et al., 2011). In order to further understand the genesis of these rocks, a study was performed on ca. 2.85 Ga BIFs from the Slave Craton in Canada and on ca. 2.53 Ga BIFs the Anshan province of the North China Craton.

Mineral occurrences of possible biological relevance like apatite, sulfides, and carbonates were mapped in petrographic thin sections from both localities and found to typically occur in bands parallel to bedding. This is consistent with an authigenic origin from the sedimentary or diagenetic environment. No apatite-graphite associations were found in BIFs from either location, although these mineral-pairs were found in Neoarchean turbidites from the Slave Craton. Only BIFs from Anshan province contained minor amounts of carbonates, typically occurring in bands, with isotopically light $\delta^{13}C_{carb}$ values ranging from -9‰ to -27‰. Diagenetic oxidation of organic matter likely accounts for this carbonate as well as for the low amount of organic carbon in the samples. Only one BIF sample from the Slave had detectable levels of organic carbon with only about 0.02wt% TOC and $\delta^{13}C_{org}$ value of -25.7‰. Current work is focused on major and minor element compositions to establish detailed comparisons with other Archean BIFs.

Mid-Miocene volcanism in the Owyhee Mountains (ID) and implications for coeval epithermal precious metal mineralization

ZACHARY HASTEN[1*], MATTHEW BRUESEKE[1], JAMES SAUNDERS[2], AND WILLIS HAMES[2]

[1]Kansas State University, Department of Geology, Manhattan, Kansas, USA, zhasten@k-state.edu (* presenting author) and brueseke@k-state.edu
[2]Auburn University, Department of Geology and Geography, Auburn, Alabama, USA, saundja@auburn.edu and hameswe@auburn.edu

The inception of the Yellowstone hotspot is associated with a period of extensive mid-Miocene volcanism in and adjacent to the northern Great Basin (NGB) and the Oregon Plateau (OP). This volcanism is also associated with spatially and temporally contemporaneous precious metal mineralization throughout the region. This relationship between mid-Miocene volcanism and gold/silver mineralization is present in the Silver City district, Owyhee Mountains ID (OM), USA. This study focuses on the mid-Miocene magmatism in OM and its relationship to coeval volcanism in the region as well as the relationship and controls on the accompanying gold and silver mineralization. The mid-Miocene magmatic suite in OM is compositionally diverse and ranges from locally erupted Steens Basalt through high-Si rhyolite. Field relationships and geochemistry of the silicic units indicates that there were at least two chemically and spatially distinct magmatic reservoirs underlying the OM. The distinct reservoirs produced at least three physically and chemically identifiable effusive silicic units: the previously identified Silver City rhyolite [1], a quartz latite unit [2], and a transitional (between the two) silicic unit. While some major and trace element concentrations overlap between these units, other trace element data, including Zr, Nb, Ba, and Nd, show well defined separations. The OM silicic volcanic suite also chemically physically resembles lava flows found in other coeval, regional eruptive systems. Sr-Nd-Pb isotope data currently being obtained will provide additional constraints that will help constrain the petrogenesis of the silicic units, including whether they were sourced from Cretaceous granitoid upper crust and how the intermediate magmas formed. Previous work in OM has yielded K-Ar and $^{40}Ar/^{39}Ar$ ages of ~16.6 to 14 Ma [3], while recent $^{40}Ar/^{39}Ar$ dating of adularia from epithermal veins has provided mineralization ages ranging from 16.1 to 15.5 Ma, with the majority of mineralization occurring around 15.7 Ma [4]. Already obtained Pb isotope data from OM gold and gangue samples will be compared to Pb isotope compositions of OM volcanic units and local crust to better understand the role that mid-Miocene volcanism plays in the mineralization process and the fundamental relationship between the source of the ores (e.g. mantle or crust) and the source of the magmas.

[1] Lindgren (1900) *USGS Annual Report* **20**, pt 3 65-256. [2] Pansze (1975) *Idaho BMG* **P-161**. [3] Bonnichsen and Godchaux (2006) *Idaho BMG* **DWM-80**. [4] Aseto (2011) *GSA Abstracts with Programs* **43,** 28.

https://doi.org/10.1180/S0026461X00008434 Published online by Cambridge University Press

Stability of Reduced Carbon in the Mantle

PATRICK T. HASTINGS JR.[1*], ANTHONY C. WITHERS [1] AND MARC M. HIRSCHMANN[1]

[1]University of Minnesota, Minneapolis, United States, phasting@umn.edu (* presenting author)

Reduced carbon in the mantle is commonly thought to be chiefly in diamond, but experiments suggest that at >250 km the mantle contains small amounts (0.1-1 %) of FeNi alloy. [**1, 2, 3**]. Thus, alloy may be a significant host of reduced C [**4**], but little is known about C solubility of FeNi alloy under mantle conditions.

To determine the carbon solubility in FeNi alloy and melt, we conducted experiments in the system Fe-Ni-C with bulk compositions having 5 wt. % C and variable Fe/(Fe+Ni) at 3 to 7 GPa and 1000 – 1400°C. Experiments at 3 GPa and 1000-1250 °C were performed in an end loaded piston cylinder apparatus; those at 5 and 7 GPa and 1200-1400°C were performed in a 1000 ton Walker-style octahedral multianvil.

At 3 GPa, Fe-rich melts contain up to 4.5 wt. % C, but Ni-rich (>25 mole% Ni) compositions remain subsolidus at 1250°C. The solubility of carbon in pure Fe and Ni metal are 2 wt. % and 1 wt. % respectively, but in the alloy passes through a minimum of 0.4 wt. % for $Fe_{0.2}Ni_{0.8}$. Assuming that these concentrations apply at higher temperatures and pressures (as will be tested by future experiments) allows a first estimate of the potential storage of C in FeNi alloy in the mantle. If the mantle at 250 km contains 0.1-0.2 wt.% Ni-rich (Fe0.4Ni0.6) alloy, increasing with depth to 1 wt.% Fe-rich (Fe0.88Ni0.12) alloy at 700 km [**1,2**], then maximum storage of C in alloy rises from 5 ppm in the deep upper mantle to 180 ppm in the shallow lower mantle. For mantle similar to the MORB source, with ~10-30 ppm C [**5**], alloy cannot store all C in the deep upper mantle but can in the lower mantle. For OIB sources with 33-500 ppm C [**5**], complete storage in alloy is less likely. Additional phases will be diamond in the upper mantle, as our experiments and previous work **[6]** indicate that carbide is not stable in equilibrium with Ni-rich alloy, and carbide melt in the lower mantle.

[1] Frost et al (2004) *Nature* **428** 409-412 [2] Frost and McCammon (2008) *EPSL* **36** 389-420 [3] Rohrbach et al. (2011) *J.Petrol* **52** #717-731 [4] Dasgupta et al. (2009) *GCA* **73** 6678–6691 [5] Dasgupta and Hirschmann (2010) *EPSL* **298** 1-13 [6] Romig and Goldstein (1978) Metal *Trans. Met. AIME* **9a** 1599-1609

Rare earth elements in Andaman Island surface seawater: Geochemical tracers for the monsoon

ED HATHORNE[1*], MARTIN FRANK[1], P.M. MOHAN[2]

[1]GEOMAR | Helmholtz Centre for Ocean Research Kiel, Wischhofstr. 1-3, Kiel, Germany, ehathorne@geomar.de (* presenting author)

[2]Department of Ocean Studies and Marine Biology, Pondicherry University, Port Blair 744 103, Andaman & Nicobar Islands, India

The Asian summer monsoon affects the lives of billions of people. With the aim of identifying geochemical tracers for the monsoon related freshwater input from the major rivers draining into the Bay of Bengal and Andaman Sea we have taken surface seawater samples from various locations up and down the Andaman Islands during 2011. Importantly, in some locations samples have been taken in March, July and November, covering most of a seasonal cycle and different monsoon phases. Samples were collected from the side of small wooden boats or while swimming and were filtered within a few hours at 0.45 or 0.22 microns using the vacuum produced by a water jet or a hand operated peristaltic pump. Filtered and unfiltered samples were acidified to < pH 2 and analysed for Y and the REEs with an automated online preconcentration ICP-MS technique [1].

The local input of REEs from streams and sediment rich areas such as mangrove environments is clearly identified by middle REE enrichments in the shale normalised patterns of some samples. These middle REE bulges accompany large increases in dissolved REE concentrations at some locations, especially for the July samples obtained during the peak monsoon season with frequent storms. Y/Ho fractionation aslo occurs during the local input of dissolved REEs with affected samples having lower Y/Ho ratios. Conversly, some samples, in particular those taken after heavy rainfall in March, show strong REE scavenging accompanied by the prefferential removal of dissolved light REEs and higher Y/Ho ratios.

The time series at a location away from local input sources shows remarkably similar REE patterns and concentraions in March and July. Then in October-November, following the peak in monsoon river discharge, the dissolved REE concentration increases by almost a factor of 2. The notable exception to this seasonal pattern is the Ce anomally which is around 0.3 in March and November but 0.6 in July, implying less oxidative removal of Ce(IV) during the peak summer monsoon rains. With the exception of elevated dissolved Ce concentrations, the North Pacific Deep Water normalised REE patterns are similar to those reported for offshore samples from the Bay of Bengal and Andaman Sea [2]. These seawater normalised patterns are distinctive having a middle REE enriched arc with similar light and heavy REE values suggesting the input from large rivers in the region is traceable using seawater REE chemistry.

[1] Hathorne et al. (2012), Online preconcentration ICP-MS analysis of rare earth elements in seawater, *Geochem. Geophys. Geosyst.*, 13, Q01020, doi:10.1029/2011GC003907.
[2] Amakawa et al. (2000), *Geochim. Cosmochim. Acta* 64, 1715-1727.

https://doi.org/10.1180/S0026461X00008434 Published online by Cambridge University Press

Ecodynamics of trace metals in assisted phytoextracted contaminated soils

N. Hattab[1*], M. Motelica- Heino[1], X. Bourrat[1]; R. Guégan[1] and M. Mench[2]

[1]ISTO, UMR 6113 CNRS Université d'Orléans, France, nour.hattab@univ-orleans.fr(*). mikael.motelica@univ-orleans.fr Xavier.Bourrat@univ-orleans.fr regis.guegan@univ-orleans.fr

[2]BIOGECO, UMR INRA 1202, Université de Bordeaux 1, av. des Facultés, 33405, Talence, France, mench@bordeaux.inra.fr.

Introduction

Many domestic, industrial and agricultural activities result in soil contamination by trace metals(Adriano,2001).The methodological guide of the French Geological Survey (BRGM) has reported the lack of knowledge on metal(loid)s in soils. Total metal(loid) concentrations in soils establish the hazard source but delivers little information on the risks. Moreover the physico-chemical analysis is not enough to evaluate the toxicity of soils on living organisms . In contrast the simultaneous investigation of the ecodynamic of trace metals and their ecotoxicological effects on an instrumented site shows several advantages. Additionally the characterisation of the ecotoxicological impact(s) by biotests representative of the various organisation levels of the ecosystems is a complementary step in the environmental risk assessment.Several investigations were performed to assess the (im)mobilisation mechanisms of metal(loid)s in CCA contaminated soils and the effects of the mineral and/or organic amendments and phytoextraction strategies.

Material and methods

The studied site is located in South-western France, Gironde County (44°43'N; 0°30'O). This site has been contaminated with high concentrations of CCA (Cu,Co,As). The site is divided into five pieces depending on the increasing of the concentration of Cu contamination in topsoils. One kilo of soil from each sub plot was put in the pots. Grains of dwarf beans (Phaseolus vulgaris L. cv vroege Limburgs) were sown in all pots and cultivated (18 days) under controlled conditions. Then the moisture of soil was raised to 80% at the beginning of germination stage of grains. In the end of the period the plants were harvested and biometrical parameters, i.e. fresh weight (FW) of roots, shoots and primary leaves, and leaf surface area, were determined together with the leave dry weigth. The solution of soil was extracted by Rhizons and DGT (diffusive gardients in thin films) were deplyed for 24h in the soils to assess the remobilsiation of trace metals.

Results and conclusion

Results suggested that plant extractable amounts of Cu are increased by the incorporation of organic and mineral amendments in the soils. Additionaly both the organic compost and addition of dolomite provide a mechanism for metal retention in the soil.

[1] Adriano, D.C., 2001. *Trace elements in terrestrial environments: biogeochemistry, bioavailability and risks of metals. 2nd Springer-Verlag, New York, Berlin, Heidelberg*

North Atlantic's hold on the Earth's asymmetric climate

GERALD H. HAUG[1], GAUDENZ DEPLAZES[1], YVONNE HAMANN[1], ANDREAS LÜCKGE[2], LARRY C. PETERSON[3], DANIEL M. SIGMAN[4]

[1]Geological Institute, ETH Zürich, 8092 Zürich, Switzerland, gerald.haug@erdw.ethz.ch, gaudenz.deplazes@erdw.ethz.ch, yvonne.hamann@erdw.ethz.ch

[2]Bundesanstalt für Geowissenschaften und Rohstoffe, 30655 Hannover, Germany, andreas.lueckge@bgr.de

[3]Rosenstiel School of Marine and Atmospheric Science, University of Miami, Miami, FL 33149, USA, lpeterson@rsams.miami.edu

[4]Department of Geosciences, Guyot Hall, Princeton University, Princeton, NJ 08544, USA, sigman@princeton.edu

Modern climate is characterized by a strong bias in temperature toward the northern hemisphere, a feature that has been described as the result of Atlantic Ocean circulation and/or the concentration of continental area north of the equator. Sediments from the Cariaco Basin off Venezuela and the northeastern Arabian Sea record this asymmetry, which manifests itself in the position and strength of the Intertropical Convergence Zone (ITCZ) over the Cariaco Basin and in summer monsoon strength over the Arabian Sea. New sediment core records of unprecedented temporal resolution indicate an unbroken correspondence between warm climate conditions over Greenland, a northerly position of the Atlantic ITCZ, and a strong Indian summer monsoon over the last 110,000 years. Given that Greenland temperature changes cannot be explained by insolation changes or by the lower latitude forcings, the tight coupling among records can only be explained by a dominant role of the North Atlantic in the hemispheric asymmetry of climate. The abruptness of the Cariaco Basin and Arabian Sea changes requires fast communication from the North Atlantic via the atmosphere.

Over millennia, the maintenance of North Atlantic conditions and their influence on global climate points to an underlying control of the Atlantic Meridional Overturning Circulation (AMOC) associated with Heinrich events. However, it apparently cannot explain some of the climate structure of the Dansgaard-Oeschger cycles: Heinrich events populate only a fraction of the cold stadials, and they occur at the end – not the beginning – of those stadials. Our new sediment records indicate that, during peak stadials, a southward shift in the trade winds caused the boreal summertime ITCZ to remain south of the Cariaco. This ITCZ shift would have reduced summertime equatorial Atlantic upwelling, reducing ocean heat transport to the North Atlantic. This positive feedback between subpolar North Atlantic cooling and ITCZ position represents a mechanism for Dansgaard-Oeschger cycles that complements AMOC changes.

https://doi.org/10.1180/S0026461X00008434 Published online by Cambridge University Press

Pliocene warmth: ocean gateways and polar oceans

GERALD H. HAUG[1], DANIEL M. SIGMAN[2], RALF TIEDEMANN[3]

[1]Geological Institute, ETH Zürich, 8092 Zürich, Switzerland, gerald.haug@erdw.ethz.ch
[2]Department of Geosciences, Guyot Hall, Princeton University, Princeton, NJ 08544, USA, sigman@princeton.edu
[3]Alfred Wegener Institute for Polar and Marine Research, Bremerhaven, Germany, Ralf.Tiedemann@awi.de

Paleoceanographic time series from numerous sediment cores retrieved in the Atlantic and Pacific Oceans and in the Caribbean Sea show that the Panamanian Seaway closure had a major impact on ocean circulation beginning at 4.6 Ma. The Gulf Stream intensified and introduced warm and saline water masses to high northern latitudes, which led to Pliocene warmth at 4.6 Ma. The world during the Pliocene warm interval was globally warmer than the past interglacial maxima and was characterized by a Northern Hemisphere without major ice shields. Since 2.7 Ma, the cycle between ice ages and warm interglacials has dominated the climate on Earth. Our understanding of the Pliocene warm period and the ice age cycles is that subtle variations in Earth's orbit and rotation are amplified by internal feedbacks, yielding dramatic climate change over hundreds to thousands of years. The time interval between 4.5 and 3.1 Myr was dominated by a pronounced long-term minimum in the amplitude of the 41 kyr cycle in the obliquity of Earth's rotation which would have failed to produce particularly cold northern hemisphere summers, the key requirement posited by Milankovitch for the onset of major northern hemisphere glaciations. During this time interval, there may have been several aborted shifts toward glaciation, for example between 4.1 - 3.9 Myr and 3.5 - 3.3 Myr. During late Pliocene and early Pleistocene, a high amplitude in the obliquity cycle resulted in periods of low tilt angle, which, in turn, would have yielded periods with cold summers in the Northern Hemisphere. Thus, it has been suggested that the progressive increase in the amplitude of the obliquity cycle tipped the scale between 3.1 - 2.7 Myr, allowing for long-term expansion of Northern Hemisphere ice. In short, our long-held view of the temperature requirement of glaciation is largely consistent with the timing of the onset of Northern Hemisphere Glaciation.In addition, atmospheric carbon dioxide appears to represent the key internal feedback to explain Pliocene warmth, being more abundant during the Pliocene thermal maximum (≥400ppm) than during warm interglacial periods (280-300ppm) and scarce during ice ages (180-200ppm). However, it is not conclusively explained what caused atmospheric carbon dioxide to change. Carbon dioxide is sequestered in the ocean interior by the photosynthetic production of organic carbon that subsequently sinks out of the low latitude surface ocean before being converted back to carbon dioxide. However, rapid vertical mixing in warmer polar ocean regions such as the Antarctic and the Subarctic North Pacific allows this deeply sequestered carbon dioxide to escape back into the atmosphere through the polar ocean surface. Measurements of the N isotopes and biogeochemical properties in sediment cores indicate that vertical stratification of the polar ocean reduced this polar CO_2 leak during cold times, has provided a satisfyingly simple physical explanation for this cooling-induced stratification. This hypothesis has been recognized as the critical piece in the Plio/Pleistocene CO_2 puzzle.

High-resolution chemostratigraphy of the 2.46 Ga Joffre banded iron formation, Western Australia: implications for the hydrosphere-atmosphere-lithosphere in the early Palaeoproterozoic

RASMUS HAUGAARD*[1]; ERNESTO PECOITS[1]; STEFAN V. LALONDE[2]; NATALIE AUBET[1]; MARTIN J. VAN KRANENDONK[3]; KURT O. KONHAUSER[1]

[1]Earth and Atmospheric Sciences, University of Alberta, Edmonton, Alberta, Canada, T6G 2E3. (*Correspondance: rasmus@ualberta.ca)
[2]Universite´ Europe´ene de Bretagne, Institut Universitaire Europe´en de la Mer, Plouzane´ 29280, France.
[3]University of New South Wales, Kensington NSW 2052, Australia.

Here we present new geochemical data of a 355 m long drill core from the single largest banded iron formation (BIF) known, the 2460 Ma [1] Joffre BIF, Western Australia. By directly preceding the 2.45-2.32 Great Oxygenation Event (GOE), this BIF was deposited prior to one of the most important periods in Earth history. The Joffre BIF consists predominantly of chert-hematite-riebeckite microbands (<1mm) alternating with chert-Fe dolomite-siderite-crocidolite mesobands (>1cm) and denser magnetite-hematite mesobands, respectively. The precursors of these mineral phases were laid down on a large stable and clastic-starved continental shelf [2]. Very fine-grained occasionally oolitic, bands of potassium-rich greenalite and stilpnomelane occur throughout, documenting input of tuffaceous material from evolved volcanic sources, similarly to the Woongarra rhyolite, in the vicinity of the depository. Preliminary geochemical results show that K_2O and Ba are strongly correlated to immobile elements such as Al_2O_3, TiO_2, Zr, La, Nb, Hf and various trace metals such as V, Cr, Ni and Co, suggesting minimum degree of K- and Ba-mobilisation. Relative to the profound Cr enrichment in the overlying Weeli Wolli BIF [3], very low Cr content (3-10 ppm) are found within Joffre BIF which indicate that the atmospheric O_2 and the oxidative weathering of continental pyrite was suppressed at the time. In contrast to the underlying Dales Gorge BIF, elevated values are found of P_2O_5 (up to 2.4 wt.%), B (up to 33 ppm), Li (up to 9 ppm) and Au (up to 8.4 ppm). Since none of these elements are hosted within the tuffaceous material they likely were sourced from elevated submarine hydrothermal activities related to the emplacement of the 2449 +/- 3 Ma large, bimodal igneous province of Weeli Wolly-Woongarra Formations [4].

[1] Trendall et al. (2004) *Australian Journal of Earth Sciences* **51**, 621-644
[2] Morris (1993) Precambrian Research **60**, 243-286
[3] Konhauser et al. (2011) Nature **478**, 369-373
[4] Barley et al. (1997) Nature **385**, 55-58

https://doi.org/10.1180/S0026461X00008434 Published online by Cambridge University Press

Interpreting phosphate mobility on Mars and the implications for habitability

ELISABETH M. HAUSRATH[1*] ; CHRISTOPHER T. ADCOCK[1]; VALERIE TU[1]

[1]University of Nevada, Las Vegas, Las Vegas, NV USA
Elisabeth.Hausrath@unlv.edu

Phosphate is a crucial nutrient on Earth, used by life in ATP, DNA, RNA and phospholipid membranes [1]. Phosphate has also been proposed as essential in the prebiotic formation of RNA on Earth [2]. Interpreting phosphate behaviour on Mars is therefore important in characterizing habitability. Phosphate mobility on Mars, however, differs in important ways from phosphate mobility on Earth. In addition to fluorapatite, common on Earth, chlorapatite and merrillite are important primary phosphate minerals in martian meteorites [3-5]. Amorphous and poorly crystalline secondary phases have been documented on Mars [6, 7], suggesting that amorphous phosphate phases may similarly be important to the phosphate cycle on Mars. Environmental conditions affecting the behaviour of secondary phosphates such as oxidation state, pH, and water: rock ratios also likely differ between Earth and Mars. In order to interpret phosphate mobility on Mars, we are therefore performing dissolution experiments, investigating apatite weathering in the field, and modeling using the reactive transport code CrunchFlow.

Mineral dissolution rates are being measured of the phosphate-rich primary minerals fluorapatite, whitlockite, merrillite and chlorapatite, which are found in Mars meteorites. Due to the likely importance of amorphous phases, dissolution rates are also being measured of amorphous Al- and Fe-phosphate. Thin sections of weathered basalt from the phosphate-rich Mars analog Craters of the Moon, ID [8] are being examined to interpret phosphate mobility during incipient weathering. These data are then being used in reactive transport modeling of phosphate behavior under Mars-like conditions.

Measured dissolution rates suggest that whitlockite dissolves more quickly than fluorapatite at pH values < 4. Preliminary results suggest that amorphous Fe-phosphate dissolves more rapidly than its crystalline counterpart. Phosphate availability on Mars may therefore be greater than on Earth, with important implications for habitability. Reactive transport modeling indicates that secondary phosphate phases may preserve important environmental characteristics of habitability, including pH, water: rock ratio, and oxidation state. Future analyses of phosphate on Mars will likely yield important characteristics of possible habitability.

[1] Madigan et al. (2000) Prentice Hall 991 p.
[2] Powner et al. (2009) *Nature* **459** 239-242.
[3] McSween and Treiman (1998) *Planetary Materials* 6-1-6-53.
[4] Bridges and Grady (2000) *EPSL* **176** 267-279.
[5] Greenwood et al. (2003) *GCA* **67** 2289-2298.
[6] Tosca and Knoll (2009) *EPSL* **286** 379-386.
[7] Rampe (2011) Arizona State University 201p
[8] Usui et al. (2008) *JGR Planets* **113** doi:10.1029/2008JE003225.

The Crystallization of a Layered Mafic Sill from the Neoproterozoic Franklin LIP, Victoria Island, Arctic Canada

HAYES, B.[1*], BÉDARD, J.H.[2], LISSENBERG, C.J.[1]

[1]School of Earth & Ocean Sciences, Cardiff University, UK, hayesb@cardiff.ac.uk (* presenting author)

[2]Geol. Survey of Canada, Québec, Canada

A diabasic sill with an olivine-enriched base from the Neoproterozoic (ca. 723 & 716 Ma) Franklin LIP has been studied in detail through the combined use of whole-rock and in-situ mineral compositions, accompanied with detailed petrology and textural observations. The Franklin LIP has a well-exposed, unmetamorphosed, sill-dominated plumbing system, outcropping within the Shaler Supergroup, in the Minto Inlier of Victoria Island. The Shaler stratigraphy is riddled with sills and is capped by the ≤1 km thick Natkusiak flood basalts. A significant amount of magma has passed through this plumbing system, with a large portion of it remaining as sills in the crust. Whole-rock data from numerous sill chills sampled across the Minto Inlet region indicate two populations of magmas: 1) a younger diabasic event with flatter REE profiles; and 2) older diabasic sills characterized by LREE enrichment, some of which have olivine-enriched zones near their base. Of the latter type, the >40m thick Uhuk massif is thought to be one of several fault-controlled magmatic feeder zones within the Franklin LIP, and has a thick ol-rich layer. The >20m thick 'Lower Pyramid sill' from the Boot Inlet region, occupies the same stratigraphic position as the Uhuk massif, and we propose an explicit correlation of the two, with the Lower Pyramid representing a well-preserved distal (>40 km) injection of the same magma.

The Lower Pyramid sill has been divided into 7 facies zones; 1) a lower chilled margin (LCM); 2) a lower border zone (LBZ); 3) an olivine-cumulate zone (OZ); 4) a pyroxene-cumulate zone (PZ); 5) a diabase zone (DZ); 6) an upper border zone (UBZ); and, 7) an upper chilled margin (UCM). Due to the relatively rapid cooling regime of this sill and the occurrence of an olivine-rich base, the Lower Pyramid sill provides a snapshot into differentiation mechanisms operating within basaltic magma reservoirs. Using detailed petrography, coupled with whole-rock and in-situ mineral chemistry, a model of crystallization is proposed. During the initial emplacement of magma within the sill, melt chilled rapidly against the 'cold' host rock preserving a parental melt composition with 13% MgO. This was followed by crystallization of the LBZ and UBZ. The UBZ is characterized by acicular clinopyroxene with long axes oriented towards the roof, indicative of rapid heat loss in the upper sill margins. After the initial emplacement of the sill, olivine (trapped in the LCM and LBZ), clinopyroxene and plagioclase began to crystallize. As the early melt emplacement event continued to crystallize, the sill was re-intruded by a relatively primitive magma (~22% MgO) charged with olivine crystals, injected along the interface between the LBZ and the DZ. This incoming melt interacted with the rocks of the host intrusion, resetting some of its crystal composition values (An in plagioclase and Mg in clinopyroxene). The distribution of such zoning seems to suggest a complex interaction of melt and crystals in a cooling permeable mush when the olivine-slurry came in. There is also an increase seen in Fo and NiO content within olivine at the boundary of the olivine-zone, which contrasts with the more normal fractionation trends displayed in the LCM and LBZ. Some olivine crystals within the LBZ and the OZ display NiO-Fo decoupling trends, with NiO peaks towards the rim, which may well be caused by the influx of primitive melts sourced from the olivine-slurry, soaking into the LBZ mush below. The upper section of the olivine-zone has a 'harristic'-like texture suggesting that the DZ mush may have been largely crystallized and fairly cold at the time of the olivine replenishment event. As the OZ crystallized, residual melts enriched in SiO_2-Al_2O_3-CaO-Na_2O-K_2O might have percolated up through the OZ mush to pond below the diabasic rocks and affected the PZ, characterized by evolved plagioclase and clinopyroxene rims. Both plagioclase and clinopyroxene core compositions within the PZ fall on the same trends as the corresponding cores in the LBZ and DZ, which may also imply that there was a population of micro-phenocrysts entrained within the original magma. The DZ above the PZ is dominated by typical ophitic gabbros indicating the co-crystallization of plagioclase and clinopyroxene, with both cumulus and interstitial Fe-Ti oxides (as well as biotite and amphibole).

https://doi.org/10.1180/S0026461X00008434 Published online by Cambridge University Press

The nature of boundary scavenging in the North Pacific Ocean

CHRISTOPHER T. HAYES[1*], ROBERT F. ANDERSON[1], MARTIN Q. FLEISHER[1] AND RAINER GERSONDE[2]

[1]Lamont-Doherty Earth Observatory of Columbia University, Palisades, NY, cth@ldeo.columbia.edu (* presenting author)
[2]Alfred Wegener Institute for Polar and Marine Research, Bremerhaven, Germany, Rainer.Gersonde@awi.edu

The radionuclides ^{231}Pa and ^{230}Th are useful tracers in the ocean of chemical scavenging, or the process of removal from the water column by adsorption onto sinking particles. This is because of their well-known and uniform source from the decay of U. The residence time of ^{231}Pa in the water column (50-200 yrs) is roughly five times greater than that of ^{230}Th (10-40 yrs), and thus their combined distributions provide information on scavenging processes occuring over different timescales. The increase of the ^{231}Pa/^{230}Th ratio in surface sediments toward ocean margins has been used as evidence that ^{231}Pa is laterally transported (to a greater degree than ^{230}Th because of its longer residence time) by diffusive fluxes from areas of low scavenging intensity to areas of high scavenging intensity [1]. This process is termed boundary scavenging [2] and potentially affects all scavenged elements whose residence time is long enough to allow basin-wide isopycnal diffusion. Little data exist, however, to support this phenomenon on the basis of ^{231}Pa/^{230}Th in the water column. Along lateral gradients in scavening intensity, the theory predicts inversely corresponding lateral gradients in [^{230}Th] (high scavenging, low [^{230}Th] and vice versa), and smaller lateral gradients for [^{231}Pa], reduced by isopycnal transport.

From the Innovative North Pacific Experiment (INOPEX) cruise of 2009, profiles of dissolved ^{230}Th and ^{231}Pa situated along strong lateral productivity gradients in the subarctic Pacific show virtually no lateral concentration gradients for either radionuclide, at odds with the traditional boundary scavenging explanation. From the subarctic to subtropical and tropical North Pacific, based on published data from this area, much larger lateral gradients in [^{231}Pa] and [^{230}Th] exist, even over lateral productivity gradients of similar magnitude to those within the subarctic. From subtropics to subarctic, in the upper 2.5 km, the lateral gradient is larger for [^{231}Pa] than for [^{230}Th], exactly the opposite of the expectation based on their residence times. We link this behavior to the geographical distirbution of biogenic opal, a strong scavenger of Pa. Below 2.5 km depth, however, ^{231}Pa has a more uniform distribution across the North Pacific, whereas ^{230}Th displays a relatively large contrast primarily between areas north and south the subarctic front. While more water column data are needed to determine the influence of inflow from the South Pacific, it is suggested that in deep waters isopycnal diffusion dominates over the lateral gradient in scavenging intensity for ^{231}Pa. The sensitivity of ^{230}Th and ^{231}Pa to differences in scavenging intensity across gyes but not within them suggests a new biogeographic dimension to boundary scavenging that deserves more attention.

[1] Bacon (1988) *Philos. T. Roy. Soc. A.* **325**, 147-160. [2] Spencer et al. (1981) *J. Mar. Res.* **39**, 119-138.

Global warmth during the Pliocene: a CO_2 paradox?

ALAN HAYWOOD[1*], DANIEL LUNT [2], AISLING DOLAN[3], DANIEL HILL[4]

[1]School of Earth and Environment, University of Leeds, earamh@leeds.ac.uk (* presenting author)
[2]School of Geographical Sciences, University of Bristol, d.j.lunt@bris.ac.uk
[3]School of Earth and Environment, University of Leeds, eeamd@leeds.ac.uk
[4]School of Earth and Environment, University of Leeds, d.j.hill@leeds.ac.uk

Multiple sources of geological proxy data indicate higher than modern surface temperatures, relative to present-day, during intervals of the Pliocene. Recently there has been a suggestion that the increase in global annual mean temperature of the planet for the Pliocene (~2 to 3°C) is inconsistent with CO_2 forcing alone, since it would require a very high climate sensitivity. Other mechanisms that are not currently, or only poorly, represented in climate models have been invoked as a means to provide a significant contribution to Pliocene warmth, in addition to CO_2.

This argument is based upon the premise that we define climate sensitivity during the Pliocene in the same way that we define climate sensitivity in response to a CO_2 doubling during this century. This premise may be invalid because in the deep palaeo proxy records provide evidence for the response of climate to a carbon cycle perturbation over far longer timescales than are used to understand 21st century climate sensitivity. Over such timescales feedback s from slow responding components of the climate system (e.g. vegetation and ice sheets) have the ability to enhance any surface temperature rise caused by CO_2.

Here we demonstrate this concept through the presentation of a suite of climate model simulations using the Hadley Centre Coupled Climate Model Version 3, in which fast and longer term feedbacks to a CO_2 rise to 400 ppmv are considered. The direct climate response in the short-term indicates a climate sensitivity in line with the best estimates of the IPCC for the coming century (~3°C). Feedbacks from vegetation and ice sheets to the CO_2 forcing (probably in response to orbital forcing as well) are able to significantly increase the total change in global mean temperature. Our results are corroborated by initial model outputs produced by the Pliocene Model Intercomparison Project.

Overall we conclude that the Pliocene paradox can easily be resolved when different timescales of environmental response to a given carbon cycle perturbation are considered.

https://doi.org/10.1180/S0026461X00008434 Published online by Cambridge University Press

What minerals were present at life's origins?

ROBERT M. HAZEN[1]
[1]Carnegie Institution of Washington,
Geophysical Laboratory, Washington, D.C. 20015, USA
(*correspondence: rhazen@ciw.edu)

Scenarios for life's origins often invoke varied minerals in such roles as catalysts or reactants for molecular synthesis, templates for selection and concentration of potential biomolecules, and protective environments for protolife [1-4]. However, any such model for biogenesis must consider the relatively limited prebiotic mineral diversity. We estimate that prebiotic Earth held no more than ~500 different mineral species, compared to more than 4500 recognized today [5,6]. Modes of mineral paragenesis at 4.0 Ga were severely limited compared to the last 3.0 billion years. Important mineral-forming mechanisms not established at 4 Ga include atmospheric oxidation, emplacement of complex pegmatites, subduction zone volcanism, and the rise of the terrestrial biosphere, which collectively led to as many as 4000 of the known species.

In spite of these constraints, most minerals previously invoked in origins-of-life research are plausible participants in prebiotic reactions. In particular, clay minerals, so often employed in origins studies for their ability to adsorb and template organic molecules, would have been present, though distributions of clay mineral species were significantly different from the modern world. Serpentinization would have produced abundant serpentine and talc, as well as brucite, while anoxic weathering of volcanic deposits may have yielded montmorillonite and kaolinite. This suite of clay minerals contrasts with the modern production, which is dominated by terrestrial clay minerals through oxic and biological weathering. Most common rock-forming silicates, including Fe-Mg olivine, pyroxene, amphibole, and mica, as well as all major varieties of Na-K-Ca feldspar and feldspathoid would have been present, as well. Though volumetrically much less important, reactive Fe-Ni phases, including metal alloys, sulfides, and the phosphide schreibersite were all available continuously in the near-surface environment in the form of iron meteorites. Similarly, quartz, carbonates, and phosphate minerals, though present, appear to have been volumetrically insignificant, and it is not obvious that any borate minerals were available prior to 3.5 Ga [7].

[1] V.M.Goldschmidt (1952) *New Biology* **12**, 97-105; [2] J.D.Bernal (1951) *The Physical Basis of Life*. London: Routledge and Kegan Paul; [3] N.Lahav (1999) *Biogenesis*. NY: Oxford; [4] R.M.Hazen (2005) *Genesis*. Washington, DC: National Academy Press; [5] R.M.Hazen et al. (2008) *Am.Mineral*. **93**, 1692-1720; [6] D.Papineau (2010) *Elements* 6, 25-30; [7] E.Grew, J.L.Bada, R.M.Hazen (2011) *Orig. Life Evol. Biosph*. **41**, 307-316.

Noble gas isotopes in Cenozoic mantle xenoliths from the North China Craton

HUAIYU HE[1,*], FEI SU[1], YING WANG[1], LIANGLIANG WANG[1], AND RIXIANG ZHU[2]

[1]Key Laboratory of the Earth's Deep Interior, Institute of Geology and Geophysics, Chinese Academy of Sciences, Beijing, China, huaiyuhe@mail.iggcas.ac.cn
[2] State Key Laboratory of Lithospheric Evolution, Institute of Geology and Geophysics, Chinese Academy of Sciences, Beijing, China, rxzhu@mail.iggcas.ac.cn

Section 17k

The North China Craton (NCC) is one of the oldest cratons on Earth (3.8 Ga) and is also one of the major Archean cratons in eastern Eurasia. However, the craton experienced fundamental lithospheric rejuvenation in late Mesozoic and Cenozoic, resulted in replacement of the old, cold, thick (>180 km), and depleted lithospheric mantle by young, hot, thin (70-80 km), and fertile lithospheric mantle. The NCC can be divided into eastern part (ENCC) and western part (WNCC) by the NS trending Daxing'anling - Taihangshan Gravity Lineament (DTGL) that separates two topographically and tectonically different regions.

The ENCC experienced widespread lithospheric thinnin. The preexisting Tan-Lu Fault Zone, main active strike-slip fault zone in eastern China, is believed to have acted as a major channel for the ascending of asthenosphere and played an important role in the Mesozoic-Cenozoic thinning of the North China Craton lithosphere. WNCC, lithospheric removal was possibly relative limited, and the elevation are about 1000m higher than ENCC. The difference of lithospheric thin between ENCC and WNCC is also supported by the contrast of thickness of crust and lithospheric mantle, heat flow and gravity anomaly. Geophysical and geochemical study suggest that the asthenospheric upwelling beneath the ENCC at late Cretaceous and upwelling beneath the WNCC recently.

Noble gas isotopic ratios would provide unique and important constraints for the evolution of the subcontinental mantle and delineate similarities and differences between the MORB reservoir and the subcontinental mantle.We present one-step crushing noble gas isotope data from corundum and co-existed mantle xenoliths and megacrystals from the middle part of the Tan-Lu Fault Zone, ENCC and from Yangyuan, WNCC. The $^{3}He/^{4}He$ ratio is 7.6–8.3 times the atmospheric ratio (Ra) in corundum, indicating contribution of fluid from convective asthenosphere. The olivine and opx in lherzolite show high helium content and homogeneous isotopic helium ratio, 6.9–7.0 Ra for ENCC and 7.6-8.5 Ra for WNCC.

Conclusion

Combined with isotope correlation diagrams, the systematic difference in ^{4}He abundance, the $^{3}He/^{4}He$ and $^{4}He/^{40}Ar^{*}$ ratios of cpx, opx and olivine in pyroxenite and lherzolite suggest refertilization of lithospheric mantle in the ENCC maybe early than WNCC.

https://doi.org/10.1180/S0026461X00008434 Published online by Cambridge University Press

Canadian oil sands; a window on the deep petroleum biosphere

IAN M. HEAD[1] *,

NEIL D. GRAY[1], ANGELA SHERRY[1], MICHAEL J. MAGUIRE[1], RUSSELL J. GRANT, CASEY R.J. HUBERT[1], CAROLYN AITKEN[1], D. MARTIN JONES[1], THOMAS OLDENBURG[2], BARRY BENNETT[2] AND STEVE LARTER[2]

[1]NRG, School of Civil Engineering and Geosciences, U. Newcastle, Newcastle upon Tyne, UK. i.m.head@ncl.ac.uk (* presenting author)

[2]PRG Dept Geosciences, U. Calgary, Calgary, Canada., slarter@ucalgary.ca

Covering an area over 100,000 km^2 the Canadian oil sands deposits are a vast testament to the consequences when the biosphere meets the geosphere. By integrating laboratory and field based studies of the microbiology, geochemistry and geology of the Canadian oil sands we have developed a more complete understanding of the processes that led to their formation and factors that may control in-reservoir petroleum biodegradation. Studies of methanogenic oil degradation in the laboratory suggest that in the initial stages of biodegradation when the bulk of the crude oil hydrocarbons, principally saturated hydrocarbons, are removed, oil degradation is driven by consortia of bacteria from the *Syntrophaceae* and methanogenic archaea. However field studies of the microbial communities currently predominant in the heavily biodegraded oil sands paint a very different picture with apparent predominance of known hydrocarbon degrading taxa conventionally considered to be aerobes. In addition, the communities in produced water samples contrast with communities detected in core samples and are dominated by *Epsilonproteobacteria* which are typically thought to play a role in sulfur cycling. The reasons for the contrasting views obtained using different approaches and sampling strategies will be explored and linked to geochemical patterns characteristic of heavy oil reservoirs.

Based on the occurrence of geochemical gradients in biodegraded petroleun reservoirs it was initially inferred that the petroleum reservoir microbiota should be most abundant and active at the base of the reservoir where oil staurated rock transitions to water saturated rock [1]. This theory appears to hold up to empirical scrutiny and we have shown that bacterial 16S rRNA gene abundance is around 2 orders of magnitude greater in these oil water transition zones. We will discuss our most recent findings integrating geochemical and metagenomic results to gain further insights into the potential role of the microbiota currently dominant in oil sands reservoirs and the implications for the petroleum deep biosphere and other hydrocarbon-impacted anoxic environments.

[1] Head I.M., Jones D.M. and Larter S.R. (2003). Biological activity in the deep subsurface and the origin of heavy oil. *Nature* 426, 344-352.

Orbitrap high resolution mass spectrometry characterization of Athabasca oil sands acids in environmental samples

JOHN V. HEADLEY*[1], KERRY M. PERU[1], BRIAN FAHLMAN[2], JONATHAN BAILEY[1] AND DENA MCMARTIN[3]

[1]Environment Canada, Saskatoon, Canada, John.Headley@ec.gc.ca

[2]Canadian Forest Service - Great Lakes Forestry Centre, Sault Ste. Marie, Canada, brian.fahlman@ec.gc.ca

[3]Environmental Systems Engineering University of Regina, Regina, Canada, DenaMcMartin@uregina.ca

Type The Athabasca oils sands region of Alberta, Canada is one of world's largest bitumen reserves with a proven 170 billion barrels of crude oil. Approximately 3 barrels of river water are used during the alkaline/hot water extraction process of the mined oil sand for every barrel of oil produced. During the extraction process, acidic bitumen components (including naphthenic acids) are solubilized in the water. This oil sands process water (OSPW) is stored in tailings ponds in accordance with a zero discharge policy. There is a growing need for development of analytical methods that can distinguish between compounds found within industrially derived OSPW from those derived from natural weathering of oil sands deposits. This is a difficult challenge as possible leakage beyond tailings ponds containments will likely be in the form of a mixture of water soluble organic acids that are similar to those leaching naturally to aquatic environments. An overview is given on the progress of analytical developments and the current state of mass spectrometry analysis of environmental samples. The potential for Orbitrap high resolution mass spectrometry and accurate mass measurements for chemical fingerprinting of oil sands acids from tailing ponds, interceptor wells, groundwater and reference river surface waters is evaluated. Particular emphasis is given to (i) new developments which recognize that the oil sands acid fraction contains more components than the traditional structures of naphthenic acids; and (ii) the influence of extraction procedures on what is being measured. Significant differences in high resolution mass spectrometry results were observed for the same sample set that are attributed to the extraction procedure and/or extraction solvent of choice.

https://doi.org/10.1180/S0026461X00008434 Published online by Cambridge University Press

C, N, O abundances and isotopic compositions in the Sun

V.S. HEBER[1], D.S. BURNETT[2], Y. GUAN[2], A.J.G. JUREWICZ[3], S. SMITH[4], C. OLINGER[5], K.D. MCKEEGAN[1*]

[1]Dept. Earth and Space Sciences, UCLA, Los Angeles, CA, USA, mckeegan@ess.ucla.edu ; [2] California Institute of Technology, Pasadena, CA, USA; [3]Arizona State University, Tempe, AZ, USA; [4]Evans Analytical Group, Sunnyvale, CA, USA; [5]Neutron Science and Technology, LANL, Los Alamos, NM, USA.

For most elements, their solar (≡cosmic) abundance and primordial isotopic composition have historically been determined via precise laboratory measurements of primitive meteorites. However, this approach is not possible for highly volatile elements which are strongly depleted, relative to the solar photosphere, even in CI chondrites. Similarly, isotopic compositions, especially for N and O, are so variable among planetary bodies and components of meteorites that distinguishing an average starting composition for the solar nebula was impossible prior to the Genesis mission [1]. By analyzing solar wind (SW) captured in high purity targets, the Genesis science team established that the nitrogen [2] and oxygen [3] isotopic compositions of the Sun are grossly different than those of Earth and almost all planetary materials of the inner solar system. The mechanisms to establish isotopic fractionations of ~40% (N) and ~7% (non-mass-dependent for O) from the average solar nebula starting composition are still being investigated and it is interesting to consider the isotopic shifts in the light of elemental depletions in planetary matter. For this and other purposes, it is necessary to know the solar elemental composition of elements heavier than He.

Photospheric determinations of the solar abundances of the most significant volatile elements (C, N, O) have recently undergone serious revision downward by factors of 1.7 (O), 1.7 (N) and 1.3 (C), thus reducing the solar "metallicity" from 0.0201 to 0.0134 [4]. While solving some long-standing astronomical problems related to the Sun's composition and age, the new results are at odds with models of the solar interior based on helioseismology [see 4]. This discrepancy remains unresolved. We analyzed Genesis Si and SiC targets to determine the fluences of C, N, and O in captured SW. These data can be related to absolute abundances in the Sun when considered with H fluence and a model of ion fractionation in formation and acceleration of the SW.

Fluences of C, N, and O were obtained by back-side depth profiling of passive (Si) collectors that had been mechanically thinned [5]. Even with this approach, background corrections were relatively high: ~4 % for ^{12}C, ~20% for ^{16}O and ~6% for ^{14}N. The O fluence can be measured with lower background on the SiC target of the SW Concentrator by utlizing the known concentration factor as a function of radius determined from ^{20}Ne data [6]. Preliminary results for the inter-element ratios C/O and N/O agree within uncertainty with the new photospheric compositions, suggesting that high first ionization potential elements are not fractionated relative to each other and lending confidence to the new photospheric abundances.

References: [1] Burnett et al. (2011) *PNAS* **108**, 19147-19151. [2] Marty et al. (2011) *Science* **332**, 1533-1536. [3] McKeegan et al. (2011) *Science* **332**, 1528-1532. [4] Asplund et al. (2009) *Ann. Rev. Astron. Astrophys.* **47**, 481-522. [5] Heber et al. (2011) *LPSC* 42, #2642. [6] Heber et al. (2011) *MAPS* **46**, 493-512.

Ion specific effects at the calcite(104) – water interface

FRANK HEBERLING [1*], PETER J. ENG [2], JOHANNES LÜTZENKIRCHEN [1], JOANNE E. STUBBS [2], THORSTEN SCHÄFER [1], HORST GECKEIS [1]

[1] Institute for Nuclear waste Disposal, Karlsruhe Institute of Technology, Karlsruhe, Germany, (* presenting author, Frank.Heberling@kit.edu)

[2] GSECARS, The University of Chicago, Chicago, United States of America

In this study the influence of Li^+-, Na^+-, K^+-, Rb^+-, and Cs^+-chloride solutions on the calcite zeta-potential is investigated and surface diffraction data that can be used to relate the observed ion specific effects to the calcite(104) – water interface structure is presented.

Specular and off-specular resonant surface diffraction data are used to locate and quantify Rb^+ ions at the calcite(104) – water interface. In a 0.01 molar RbCl solution equilibrated with atmospheric CO_2 and calcite (pH = 8.2), we observe the main Rb^+ species (~0.17 mono layers (ML)) 3.2 Å above the surface, associated with the second well ordered water layer at the interface, a position that might mark the upper end of a Stern layer at the calcite(104) surface [1]. An unexpected result is that there seems to be inner-sphere adsorbed Rb^+ (< 0.1 ML) closely associated with the surface carbonate groups. Additionally there are outer-sphere Rb^+ species at ~5 and ~11 Å above the surface, likely associated with Rb^+ in the diffuse layer above the calcite surface. In order to test to what extent these results are specific for Rb^+ or whether they can be transferred to the other alkali-metal cations we measured specular surface diffraction data on calcite(104) in contact with equilibrated 0.01 molar alkali chloride solutions across the whole series from Li^+ to Cs^+, and indeed certain trends are observable. The analyses of these data is still ongoing and it is not yet clear if changes are due to the increasing number of electrons in the series Li^+ – Cs^+ or due to actual changes in interface structure.

Streaming potential measurements performed on an Anton Paar SurPASS electrokinetic analyzer show that, if we successively add Ca^{2+} to a solution containing 0.01 mol/L of an alkali metal chloride as background electrolyte at fixed pH (~9), remarkable changes in the behavior of the calcite zetapotential are observed across the series of 0.01 molar alkali chloride solutions: the Ca^{2+} concentration at which zero zetapotential is measured is 0.5 mmol/L in CsCl solution and increases continuously across the series of alkali metals, up to 2.5 mmol/L in LiCl solution. For Ca^{2+} concentrations >5 mmol/L the calcite zetapotential reaches a plateau. The plateau zetapotential value lies at 5 mV in the LiCl system and at 20 mV in the CsCl system. These two effects clearly demonstrate the ion specific effect of the alkali metal cations on the affinity of Ca^{2+} ions to the calcite(104) surface. The calcite zetapotential measured as a function of pH in the absence of added Ca^{2+} is the same in 0.01 molar solutions of all alkali metal chlorides investigated. These results may have important implications e.g. for calcite growth-, adsorption-, or surface complexation models.

[1] Heberling et al. (2011) *Journal of Colloid and Interface Science* **354**, 843-857.

https://doi.org/10.1180/S0026461X00008434 Published online by Cambridge University Press

Structural Development and Petrogenesis along the Southern Central Indian Ridge

K. U. HEESCHEN[1]*, U. SCHWARZ-SCHAMPERA[1], AND H. FRANKE[1],

[1] Federal Institute for Geosciences and Natural Resources (BGR), D 30655 Hannover, Germany, Katja.Heeschen@bgr.de (* presenting author)

The southern Central Indian Ridge (S-CIR) was the target of the cruise INDEX 2011, which was aming to examine the bathymetry, structural geology, magnetic signatures, and crustal development of the area with special emphasis on the petrogenesis and hydrothermal processes.

The S-CIR is characterized by intermediate to slow spreading rates and a highly variable regional to small-scale structural pattern of seafloor spreading [1] with recent volcanic activity focussing on cone-shaped volcanoes and neovolcanic ridges in the central valley or along its flanks. The structural development has triggered complex petrogenetic processes including differentiation and fractionation processes as well as the exhumation of deep oceanic lithosphere. The ridges in the Indian Ocean generally show strong indications for intense plume-ridge interactions, all of which leads to the formation of a wide and variable range of rock compositions [2, 3]. The deep and active fault systems and sustainable heat supply have also triggered a range of fossil and recent hydrothermal activity alongside the rift valley.

For the detailed petrological and geochemical study a large variety of rock samples were collected along the S-CIR using dredge and TV-grab. The rock suite includes basalts, gabbros, and ultramafic rocks from five different ridge sections along the active spreading center. Next to the analysis of major and trace elements in bulk samples of fresh rocks and volcanic glass, microanalytical studies allow for the analysis of specific minerals for petrogenetic purposes.

First results gained from bulk analysis of the mafic rocks indicate small but explicit differences with respect to the differentiation and fractionation processes, especially pronounced in the major and trace element composition. This is true for the rock suites from different ridge sections investigated during INDEX2011 as well as deviations from data published on the CIR [e.g. 2]. More specifically their character appears less differentiated, however, fractionation and the involvement of mantle heterogeneities or variable depths sources are suggested by elevated concentrations of incompatible and volatile elements.

[1] Briais (1995) *Marine Geophysical Researches* **17**, 431-467. [2] Murton (2005) *Geochem. Geophys. Geosyst.* **6**, Q03E20. [3] Rehkämper (1997) *Earth and Planetary Science Letters* **147**, 93-106.

Tracing anthropogenic Hg deposition in peat bogs with Hg stable isotopes

HEIMBÜRGER, LARS-ERIC[1*], ENRICO, MAXIME [1,2,3], LE ROUX, GAEL[2,3], SONKE, JEROEN E.[1]

[1]CNRS; Geosciences Environment Toulouse, 31400, Toulouse, France, heimburger@get.obs-mip.fr (* presenting author)
[2] Université de Toulouse; INP, UPS; EcoLab (Laboratoire Ecologie Fonctionnelle et Environnement); ENSAT, Avenue de l'Agrobiopole, 31326 Castanet Tolosan, France, gael.leroux@ensat.fr
[3] CNRS; EcoLab; 31326 Castanet Tolosan, France

Abstract

Ombrotrophic peatlands integrate atmospheric deposition and are therefore used as archives to interpret variations of natural and anthropogenic mercury (Hg) emission sources. However, the question remains whether peat Hg profiles reflect local, regional or global Hg deposition. On a global scale, coal combustion is today the major anthropogenic Hg source to the atmosphere. The unique range of Hg isotopic compositions observed in coal deposits suggests that Hg isotope signatures may offer a new tool to track coal Hg emissions and deposition. We examined 3 peat cores from the Pinet peat bog (French Pyrenees, 42°51'52N, 1°58'29E, 880m a.s.l.). for variability of Hg accumulation rates and Hg isotopic signatures. Loss on ignition, water content, density and radionuclides were measured in each core. The 3 cores have been dissected in slices of 1cm allowing a temporal resolution of 20 years at the bottom part and less than 2 years in the top part. The Pinet peat bog is relatively sheltered from direct emission sources and integrates therefore mostly Hg transported over long distances. However, local mining and smelting activities in neighboring valleys might have been additional sources during the last 200 years. A combined ^{210}Pb-^{14}C age-depth model was applied to all cores and revealed that the Wardenaar cores of approximately 75cm-length go back in time until 2300BC. Mercury accumulation rates (Hg AR) are around 1.5µg.m^{-2}.y^{-1} before times of significant industrial emissions (2300 to 1900BC), consistent with other European peat records. First signs of anthropogenic impacts are evidenced by an increase of Hg AR to 8µg.m^{-2}.y^{-1} (1650 to 1900AD). Hg AR continue to increase in the 20th century to values of 38µg.m^{-2}.y^{-1}. Major Hg AR peaks of 42, 52, 62 and 100µg.m^{-2}.y^{-1} occur in the periods 1956, 1979, 1994 and 2001 respectively. Only very recently a decrease in Hg AR of 28% is visible. This decrease might be attributed to reduced Hg emssions following the implementation of antipolution policies.

A modified combustion and trapping method was used to isolate and purify Hg from the organic peat matrix before analysis of Hg isotopes using MC-ICPMS. Mercury's isotopic signatures in the Anthropocene (δ^{202}Hg: -0.84 to -1.65‰) are different from the Holocene (δ^{202}Hg = -0.5‰) and correspond to that of average coal (δ^{202}Hg = -1.3‰; [1,2]).

[1] Lefticariu et al. (2011) *Environ. Sci. Technol.* **45(4)**, 1724-1729
[2] Biswas et al. (2008) *Environ. Sci. Technol.* **42(22)**, 8303-8309

https://doi.org/10.1180/S0026461X00008434 Published online by Cambridge University Press

The Art of augering, observing, and connecting processes across threshold landscapes

ARJUN M. HEIMSATH[1*], JEAN L. DIXON[2], ROMAN A. DIBIASE[3], AND KELIN X. WHIPPLE[1]

[1]School of Earth and Space Exploration, ASU, Tempe, USA, Arjun.Heimsath@asu.edu (* presenting author)
[2]Deutsches GeoForschungsZentrum GFZ, Potsdam, Germany, jeannie@gfz-potsdam.de
[3]Geological and Planetary Sciences, CalTech, Pasadena, USA, rdibiase@caltech.edu

Abstract

We focus here on the soil-mantled landscapes found in high-relief, steeply sloped landscapes typically thought to be at a critical threshold of soil cover. Soil found across such landscapes fits the conceptual framework of a physically mobile layer derived from the underlying parent material with some locally-derived organic content. The extent and persistence of such soils depends on the long-term balance between soil production and erosion. We present cosmogenic Be-10-derived soil production and erosion rates that show that soil production increases with catchment-averaged erosion, suggesting a feedback that enhances soil-cover persistence, even in threshold landscapes [1]. Soil production rates do decline systematically with increasing soil thickness, but hint at the potential for separate soil production functions for different erosional regimes. We also show that a process transistion to landslide-dominated erosion results in thinner, patchier soils and rockier topography [2], but find that there is no sudden transition to bedrock landscapes.

These findings focusing on the physical processes of soil production and transport are coupled with extensive measurements of major and trace elements in soils, saprolites and bedrock across different physiographic regimes ranging from low to high gradient in the same field area of the San Gabriel Mountains, California. Connecting the processes shows that average chemical depletion fractions (soil loss relative to parent material) decrease with increasing elevation and decreasing temperature, reflecting a combination of climate influence and potential dust flux. On low-gradient slopes weathering rates increase with increasing erosion rates, reflecting the influence of mineral supply, while on high-gradient slopes both weathering intensity and rates decrease with increasing erosion rate [3].

Finally, we draw an important conclusion connecting the physical processes producing and transporting soil and the chemical processes weathering the parent material by measuring parent material strength. We observe that parent material strength increases with overlying soil thickness and, therefore, the weathered extent of the saprolite. Soil production rates, thus, decrease with increasing parent material competence. These observation highlight the importance of quantifying hillslope hydrologic processes where our multi-facted measurements are made. Art did it!

[1] Heimsath et al. (2012) *Nature Geoscience* **DOI:** 10.1038/NGEO1380. [2] DiBiase et al. (2012) *Earth Surface Processes and Landforms* **DOI:** 10.1002/esp.3205. [3] Dixon et al. (2012) *Earth and Planetary Science Letters* **DOI:** 10.1016/j.epsl.2012.01.010.

Copper partitioning during magmatic-hydrothermal phase separation — revisited: Fluid inclusions in coeval quartz, topaz and garnet

SEO, JUNG HUN[1,2] AND HEINRICH, CHRISTOPH A.[1*]

[1]ETH Zurich, Switzerland, heinrich@erdw.ethz.ch (* presenting author)
[2]Present address: Seoul National University, Korea, seo28@snu.ac.kr

Recent experimental studies have raised concerns that Cu concentrations in natural quartz-hosted magmatic-hydrothermal fluid and melt inclusions can be modified after entrapment. Li, Cu^+, Na^+, Ag^+ and probably H^+ may undergo selective diffusional exchange between inclusions hosted by quartz and the surrounding aqueous fluid [1, 2]. Using LA-ICPMS multi-element analysis including sulfur, we have analysed coexisting brine and vapor inclusions hosted in topaz and garnet, from samples where previous analyses had been obtained from similar and likely coeval inclusions hosted by quartz [3]. We found that the concentration of Cu in the quartz-hosted fluid inclusions deviate from those hosted by garnet or topaz in the same sample. In particular, the selective enrichment of Cu found in quartz-hosted vapor inclusions is not observed in the topaz-hosted counterparts, whereas S and all other metals have overlapping concentrations in each of the samples, irrespective of host mineral.

Our data from natural samples are in line with the experimental study of Lerchbaumer and Audétat [2], indicating selective inward diffusion of copper into the quartz-hosted vapor inclusions after their entrapment and during cooling from ~450°C. Electrolytic diffusion experiments have previously demonstrated that small monovalent cations, such as Li^+ and to lesser degrees Na^+, can selectively diffuse along the channels oriented parallel to the c-axis of the quartz structure [4].

Post-entrapment modification of natural fluid inclusions depends on a chemical driving force. In cooling magmatic-hydrothermal systems, a chemical potential gradient in μ_{Cu^+} can be established by the high original H_2S content of magmatic vapor inclusions, in excess relative to chalcophile metals [3] as confirmed by our new data from garnet and topaz inclusions. Cu^+ may be driven to diffuse from a gradually H_2S-depleted grain-boundary fluid outside the quartz crystals (where Cu^+ activity remains high due to consumption of H_2S by reaction with ferromagnesian silicates to pyrite) towards the vapor inclusions in which Cu^+ activity gradually decreases by precipitation of a daughter crystal of chalcopyrite, $CuFeS_2$. This S-driven exchange mechanism explains why S/Cu ratios in natural fluid inclusions are commonly close to the stoichiometric proportion of Cu:S = 1:2, as in chalcopyrite [3].

[1] Zajacz Z., Hanley J.J., Heinrich C.A., Halter W.E., Guillong M. (2009) *Geochimica et Cosmochimica Acta* **73**, 3013-3027. [2] Lerchbaumer L. and Audétat A. (2011) *European Geophysical Union General Assembly*, Vienna: **EGU2011**, 11906. [3] Seo J.H., Guillong M. and Heinrich C.A. (2009) *Earth and Planetary Science Letters* **282**, 323-328. [4] Harris, P.M. and Waring, C.E. (1937) *Journal of Physical Chemistry* **41**, 1077-1085

https://doi.org/10.1180/S0026461X00008434 Published online by Cambridge University Press

Suitability of IAEA-603 as a replacement of NBS19 for small sample carbonate analysis

JEAN-FRANÇOIS HÉLIE[1*], CLAUDE HILLAIRE-MARCEL[1], MANFRED GROENING[2]

[1] GEOTOP-UQAM, Montréal, Canada,
[1]helie.jean-francois@uqam.ca (* presenting author)
[1]hillaire-marcel.claude@uqam.ca
[2]IAEA Terrestrial Environment Laboratory, Vienna, Austria,
[3]m.groening @iaea.org

The VPDB scale is anchored by NBS19 and LSVEC with absolute values for $\delta^{13}C$ [1]. For $\delta^{18}O$ values, the only carbonate material with an absolute value is NBS19 [2]. It is thus a critical reference material. NBS19-TS is now exhausted and IAEA is proposing IAEA-603 as a replacement, produced from Carrara marble. Most of the carbonate international reference materials are distributed with a grain size of about 200 to 500 µm to minimize water adsorption. Thus, the analysis of 100 µg of these international reference materials is often given by 1 grain resulting in less than desirable reproducibility. IAEA will not distribute smaller grain sizes due to possible isotopic exchange at a large surface area exposed to CO2 and moisture, and grinding by individual laboratories may result in heating and conversion of calcite to aragonite accompanied by a small but measurable fractionation. Here, we evaluate the suitability of IAEA-603 for calcium carbonate isotopic analysis at the 100 µg level. About 15 kg of ground and sieved material was uniformly divided into 31 bottles by IAEA. A subsample of each bottle was ground and sieved resulting in 4 differend fractions: i) the original material (200 to 500 µm), ii) a fraction <90 µm, iii) a fraction between 90 and 125 µm and iv) a fraction >125 µm. All 4 fractions were analyzed for $\delta^{13}C$ and $\delta^{18}O$ of all 31 subsamples on an Isoprime™ triple collector IRMS in dual inlet mode coupled to a MultiCarb™ system. Preliminary results show that average values vary little from one fraction to another (table 1). However, the largest standard deviations are obtained with the original material and the lowest one for the fraction of less than 90 µm. X-ray diffraction analysis of a subsample and all of its fractions shows that only calcite is present in all fractions. Following these preliminary results, IAEA has decided to wash the original material to remove the fine dust fraction, and subsamples of the washed material will be analyzed following the same protocol.

Table 1. Average $\delta^{13}C$ and $\delta^{18}O$ and standard deviations of all subsamples

	$\delta^{13}C$ ‰ vs VPDB	STDev (1σ)	$\delta^{18}O$ ‰ vs VPDB	STDev (1σ)
Grains	2,466	0,024	-2,437	0,038
<90	2,469	0,012	-2,405	0,027
90-125	2,461	0,016	-2,371	0,025
>125	2,455	0,021	-2,408	0,033
all	2,466	0,018	-2,406	0,038

[1] Coplen, T.B. & al. (2006) *Anal. Chem.* **78**, 2439-2441.
[2] Coplen, T.B. (1995) *Nature* **375#**, 285.

Mechanisms of chemical weathering: nanoscale-analytical measurements yield evidence for a weathering continuum

R. HELLMANN[1*], J.P. BARNES, D. DAVAL

[1]ISTerre, University of Grenoble 1 and CNRS, Observatory for Earth, Planetary and Space Sciences (OSUG), F-38041 Grenoble Cedex 9, France; roland.hellmann@obs.ujf-grenoble.fr (* presenting author)
[2]CEA-Leti, Minatec Campus, 17 rue des Martyrs, F-38054 Grenoble Cedex 9, France; barnesjp@cea.fr
[3]LHyGeS, University of Strasbourg/EOST-CNRS, F-67084 Strasbourg, France; ddaval@unistra.fr

Chemical weathering in the field occurs under complex conditions, characterized by variable degrees of aqueous chemical saturation and chemically complex fluids that may contain significant concentrations of ions, metals, ligand complexing agents, inorganic and/or organic acids or bases. In addition, weathering may also occur in very specific environments, such as in µm-sized pore spaces or in contact with mycorrhiza. Becasue of the complexity inherent to natural chemical weathering environments, it is not surprising that many types of alteration have been documented; two of the commonest reveal a) mineral-mineral replacement b) formation of amorphous, silica-rich surface layers. The question addressed in this talk is whether it is possible to define a unique nanoscale mechanism that controls chemical weathering.

Here we present recent measurements of the structure and chemical composition of mineral surface interfaces associated with the natural weathering of granite and serpentinite. The samples investigated were extracted from environments that are characterized by subaerial, shallow soil, and biological/abiological alteration. As detailed in a recent publication (Hellmann et al., 2012), one of the most promising techniques for studying chemical weathering at the nanoscale is based on sample preparation by focused ion beam (FIB), and measurements using high resolution transmission electron microscopy techniques, in particular HRTEM, STEM-HAADF, and EFTEM/EELS. The latter technique is particularly useful for providing nm-scale chemical maps of mineral surface interfaces.

The mineral surface interfaces that were investigated show evidence for spatially coincident and very abrupt structural and chemical changes (nm-scale sharp gradients) at the boundary between the unaltered parent mineral and the silica-rich amorphous surface layer. This type of chemical weathering was observed in all samples. The sharp structural and chemical boundaries that we measured are compatible with an interfacial dissolution-reprecipitation mechanism, and not solid-state volume interdiffusion associated with preferential cation loss and leached layer formation. Based on these results, as well as published studies on mineral-mineral replacement, we propose a chemical weathering continuum based on a dissolution-reprecipitation mechanism that unifies the different types of weathering observed in nature.

[1] Hellmann (2012) *Chemical Geology* **294-295**, 203-216.

https://doi.org/10.1180/S0026461X00008434 Published online by Cambridge University Press

What mechanism controls rhenium deposition from euxinic waters?

GEORGE R. HELZ*[1]

[1] University of Maryland, College Park MD 20742 USA, helz@umd.edu (* presenting author)

Rhenium is often enriched in black shales and euxinic basin sediments by 100 to 1000 times over its crustal abundance. Enrichment previously has been attributed to reduction of ReO_4^-, the principal Re species in natural waters. The product is assumed to be an insoluble Re(IV) oxide or sulfide. So far, the specific biotic or abiotic mechanism of reduction has escaped identification. Pure cultures of sulfate and iron reducing bacterial fail to precipitate Re, but precipitation has been observed in Re-enriched natural sediments under sulfate reducing conditions. In this talk, I explore an alternate, non-reductive mechanism of fixing Re in sediments: sulfidation of ReO_4^- to particle-reactive thioperrhenates ($Re^{VII}O_nS_{4-n}^-$) or to Re^{VII} sulfide precipitates or coprecipitates. Using UV-vis spectroscopy, equilibrium constants for formation of ReO_3S^- and ReS_4^- as well as a solubility constant for a colloidal Re_2S_7 polymer have been measured for the first time. From these constants, I conclude that most euxinic environments contain insufficient sulfide to stabilize thioperrhenates as major species. Similarly, Re_2S_7 polymers are too soluble to form in near-neutral pH waters, although they might form in acidic mine waters or during supergene-hypogene enrichment processes. To explain remarkable similarities between Mo and Re vertical profiles in the Black Sea, I propose that both elements become thiolated and coprecipitate at surfaces of the Fe-Mo-S colloidal phase that has previously been proposed to explain Mo deposition from euxinic basins. Coprecipitation implies that the critical step for Re removal from euxinic basins involves neither reduction nor thiolation of ReO_4^-, but instead saturation of sulfidic waters with the Fe-Mo-S phase. Coprecipitation favors removal of Mo more than Re from the aqueous phase, explaining increasing aqueous phase Re/Mo ratios as these elements are depleted from sulfidic waters. This process is well-described by the Raleigh fractionation law. Similar partition coefficients describe the evolution of Re/Mo ratios quantitatively both in sulfidic Black Sea waters and in sulfidic Hingham Bay pore waters. This implies that Re chemistry in sulfidic pore waters does not differ from that in sulfidic water columns in any fundamental way, contrary to some previous views. This mechanism accounts for the remarkable coherence in the profiles of Re and Mo in the Black Sea and for the failure of Re to be precipitated in pure sulfate reduction cultures that lack Mo.

Inter-laboratory Evaluation of $^{40}Ar/^{39}Ar$ Data for Sanidines from the Fire Clay Tonstein

S.R. HEMMING[1,2], , M.T. HEIZLER[3], B. JICHA[4], M. MACHLUS[2], E.T. RASBURY[5], P. R. RENNE[6], B. S. SINGER[4], C.C. SWISHER III[7], B.D. TURRIN[7]

[1]Columbia University, New York, USA, sidney@ldeo.columbia.edu
[2]Lamont-Doherty Earth Observatory, Palisades, USA
[3]NM Bureau of Geology and Mineral Resources, Socorro, NM, USA
[4]University of Wisconsin, Madison, WI, USA
[5]Stony Brook University, Stony Brook, NY, USA
[6]Berkeley Geochronology Center, Berkeley, CA, USA
[7]Rutgers University, Piscataway, NJ, USA

Because the $^{40}Ar/^{39}Ar$ method requires age standards, an important step towards improving the overall precision and accuracy of the method is to develop standard materials for inter-laboratory comparisons that span a wide array of age. It has been previously demonstrated that sanidines of the Carboniferous Fire Clay tonstein give analytically indistinguishable plateau ages over a 300 km distance in the Appalachian Basin [1]. Here we show that sanidines from the Carboniferous Fire Clay Tonstein of the Appalachian Basin of the southern United States are homogeneous at the single crystal scale, at least as measurable with single collector approaches, and reasonably reproducible among laboratories.

The reproducibility of the Fire Clay populations for the 8 iterations in the LDEO experiment (including 304 individual grains of Fire Clay sanidine and 137 of Fish Canyon) is 0.03% (1σ, analytical only). Encouraged by these results we distributed aliquots to four other labs for inter-laboratory comparisons.

Preliminary results are promising. All labs find a small range of ages, although the reported estimates are not all overlapping with estimated analytical errors. The agreement in terms of *R*-values, defined as the $^{40}Ar^*/^{39}Ar_K$ of the Fire Clay sanidine relative to the Fish Canyon sanidine standard, is quite reasonable with an interlaboratory average of 12.0799 ± 0.0296 (0.24%), and the small variability of ages suggests the potential for probing interlaboratory biases. This *R*-value translates to 315.3 ± 0.7 Ma and 314.6 ± 1.1 Ma using the calibrations of [2] and [3,4], respectively, including full systematic uncertainties. The Fire Clay tonstein is a promising natural sample for inter-laboratory comparisons and is a good candidate for producing a Carboniferous sanidine monitor standard.

[1] Kunk and Rice, 1994

[2] Renne et al., 2011, GCA, 75, 5097-5100.

[3] Kuiper et al., 2008, Science, 320, 500-504.

[4] Min et al., 2000, GCA, 64, 73-98.

https://doi.org/10.1180/S0026461X00008434 Published online by Cambridge University Press

The geochemical signal of the provenance of ice-rafted deposits and ice sheet dynamics

S.R. HEMMING[1,2]

[1]Columbia University, New York, USA, epierce@ldeo.columbia.edu
[2]Lamont-Doherty Earth Observatory, Palisades, USA

Ice sheets are important components of the climate system. Their high albedo leads to a positive cooling feedback, and their presence affects atmospheric and oceanic circulation. Understanding the temporal record of ice sheets in the past and how they correlate to other climate-sensitive processes are important to understanding the vulnerability of ice sheets in a warming world. The distribution of ice-rafted detritus in marine sediments has been used in the polar oceans to provide significant insights into ice sheet behavior and processes that control climate conditions. A key element for understanding ice sheet interactions in the climate system is identifying the major sources of ice-rafted detritus. I will review some examples of the application of radiogenic isotope provenance studies of glaciogenic marine sediments. Because of the fortuitous patchwork distribution of continental terranes with variable geologic age and history, radiogenic isotopes are powerful tracers of sediment provenance that can provide important clues about past ice sheet behavior. In favorable cases application to marine sediments allows developing a precise time line of ice sheet behavior that can be integrated with evidence for paleoclimate and paleoceanography changes. Additionally ocean sediment archives tend to have relatively continuous sediment accumulation, so although they are separated from the more direct continental evidence, they provide an important complement to the study of land-based glacial features.

There is a wide array of fruitful approaches to geochemical provenance of glaciogenic marine sediments. Because sediments produced from glaciers tend to be dominantly from strongly mechanical weathering regimes, the degree of chemical alteration is a good indication of the abundance of recycled sedimentary sources. Approaches that use bulk sediments have the advantage of providing an average of the contributing sources and the disadvantage of providing a mixed signal. Approaches that use measurements of individual grains have the advantage of separating multiple source contributions and the disadvantage of being much more costly and time-consuming. The combination of bulk-sediment and individual grain approaches is preferred. A combination of petrographic and geochemical approaches helps to mitigate the inevitable biases of each individual approach, although most geochemical approaches are biased against detecting mafic contributions.

^{236}U in seawater – contaminant and tracer

GIDEON M. HENDERSON[1*], NICK S. BELSHAW[1], REBECCA NEELY[1], ALEX L. THOMAS[1], PHILIP F. HOLDSHIP[1], KEN O. BUESSELER [2]

[1] University of Oxford, Department of Earth Sciences, South Parks Road, Oxford, OX13AN, UK, gideonh@earth.ox.ac.uk
[2] Woods Hole Oceanographic Institution, USA.

U-236 is generated from ^{235}U by the neutron flux of a nuclear explosion or power plant. Resulting ^{236}U/^{238}U ratios from such processes can be as high as $5x10^{-3}$ [1] and up to 8 orders of magnitude higher than expected theoretically for the natural environment. In contrast, ^{238}U/^{235}U ratios vary by only 4 orders of magnitude between weapons grade and residual depleted uranium. U-236 is therefore a more sensitive tracer of the presence of nuclear contamination. In seawater, the conservative behaviour of uranium means that this tracer may provide information not only about contamination, but about ocean mixing and advection away from point sources of such contamination.

U-236 has not frequently been measured in the natural environment, but most studies to have done so rely on accelerator mass spectrometry (AMS) to achieve the high abundance sensitivity required to accurately assess the ^{236}U/^{238}U ratio. In this study, we demonstrate the use of ICP mass spectrometry (with a large-geometry Nu-Instruments 1700 MC-ICP-MS) to measure ^{236}U/^{238}U ratios as low as 10^{-8}. Although this detection limit is not as low as that of AMS, the ICP approach allows measurement on significantly smaller samples (≈200mL of seawater) and for more routine sampling and analysis.

We present measurements on a suite of 30 seawater samples collected from the upper 50 m of the water column offshore the Fukushima power-plant in the months immediately following the disaster at that plant. The samples were collected from the RV KOK during a cruise (June 4-19 2011) sponsored by the Gordon and Betty Moore Foundation, and are set in the context of Cs isotope results. A wide range of other contaminant radionuclides will also be measured on seawater samples from this cruise, enabling the release of ^{236}U from the Fukushima plant into the marine environment to be well constrained, and the relative impact of atmospheric versus hydrographic routes to the ocean to be assessed. This case study will also provide an assessment of the future use of ^{236}U as a tracer of ocean contamination and transport.

[1] S.F. Boulyga and K.G. Heumann, 2006, *Journal of Environmental Radioactivity* **88** 1-10.

https://doi.org/10.1180/S0026461X00008434 Published online by Cambridge University Press

Uranium series rate meters for ocean processes

GIDEON M. HENDERSON[1*], YU-TE HSIEH[1], MARK D. BOURNE[1], WALTER GEIBERT[2], FEIFEI DENG[1], ALEX L. THOMAS[1]

[1] University of Oxford, Department of Earth Sciences, South Parks Road, Oxford, OX13AN, UK, gideonh@earth.ox.ac.uk
[2] University of Edinburgh, School of Geosciences, Edinburgh, UK

Uranium-series nuclides have a range of solubility in seawater which, coupled to their diverse half-lives, make them excellent timekeepers for a wide variety of ocean processes. Not only do they record the timing of growth of marine precipitates (most notably corals) but they provide information about the rates of ocean processes such as mixing and circulation, and about chemical fluxes into and out of seawater and sediments. Recent analytical advances are reinvigorating the use of U-series approaches to assess ocean processes. This presentation will illustrate the power of these new measurement techniques to assess three critical ocean processes.

Development of new mass-spectrometric approaches to measurement of ^{228}Ra in seawater [1] allow lower detection limits and higher precision. This precision allows use of ^{228}Ra to quantify ocean mixing and chemical inputs more accurately than before, and in settings not previously investigated, as we will demonstrate with results from the Cape Basin (South Atlantic) and Loch Etive (Scotland).

Measurement of Th isotopes in dissolved form and settling particles enables assessment of downward fluxes of material in the oceans. Th-234 has been widely used to assess downward carbon fluxes, for instance. But increasing precision of ^{230}Th and ^{228}Th measurements in seawater now allow these nuclides to be used to provide complementary information about downward fluxes on other timescales. These tools have huge potential for assessment of other ocean fluxes, including those of micronutrients critical for ocean life and, via measurement of a fourth Th isotope – ^{232}Th – of detrital inputs to seawater such as mineral dust [2].

Th-230 is also frequently used as a constant flux proxy to assess variations in sedimentation rate. We will illustrate how this approach can be used to assess the duration of past events [3] with well-constrained uncertainties, and to assess chemical fluxes both into and out of marine sediments.

[1] Hsieh and Henderson (2011) Journal of Analytical Atomic Spectrometry **26(7)**, p1338-1346.
[2] Hsieh et al. (2011) EPSL **312** p280-290
[3] Knudsen et al. (2007) GRL **34(22)** L22302

Silicon isotopes in glassy sponges as a tracer of silicic acid in seawater

KATHARINE R. HENDRY[1,2]
LAURA F. ROBINSON[2,3]

[1]School of Earth and Ocean Sciences, University of Cardiff, Main Building, Park Place, Cardiff, CF10 3AT, UK, HendryKR@cardiff.ac.uk
[2]Department of Marine Chemistry and Geochemistry, Woods Hole Oceanographic Institution, Woods Hole Road, Woods Hole, MA 20543, USA.
[3]Department of Earth Sciences, Bristol University, Wills Memorial Building, Queen's Road, Bristol, BS8 1RJ, UK.

Dissolved silicon, or silicic acid, is an essential nutrient that feeds the growth of opaline diatoms, which are a photosynthetic organism responsible for a significant proportion of carbon export production in the oceans. Deep-sea glassy sponges also produce their skeletal elements, spicules, out of opal and, while they most likely play a less important part in carbon cycling, they can provide valuable information about seawater composition. Recent work has shown that the silicon isotope composition of spicules reflects the concentration of silicic acid in the ambient seawater in which the sponge grew. Here, we present a global dataset of silicon isotopes in modern and core top spicules, which shows that the relationship between silicic acid concentration and silicon isotopes in sponges is universal. A biological mechanism, linking uptake kinetics of silicic acid in sponges and fractionation, can explain this relationship. This theoretical framework, together with the modern and core top calibration work, supports the view that the isotopic composition of sponge spicules is a robust geochemical proxy, and downcore records can be interpreted in terms of past ocean silicic acid concentration.

https://doi.org/10.1180/S0026461X00008434 Published online by Cambridge University Press

Insights on biomineralisation and the nature of 'vital effects' using Boron isotopes

HENEHAN, MICHAEL J.[1*], FOSTER, GAVIN L.[1], RAE, JAMES W. B.[2], RIES, JUSTIN B.[3], EREZ, JONATHAN[4], BOSTOCK, HELEN C.[5], KUCERA, MICHAL[6], CASTILLO, KARL D.[3], MARTÍNEZ-BOTÍ, MIGUEL A.[1]

[1] University of Southampton, National Oceanography Centre, Southampton, UK, M.J.Henehan@soton.ac.uk*
[2] California Institute of Technology, Pasadena, California, USA, james.rae@bristol.ac.uk
[3] University of North Carolina, Chapel Hill, North Carolina, USA, riesjustin@gmail.com
[4] Hebrew University of Jerusalem, Jerusalem, Israel, erez@vms.huji.ac.il
[5] National Institute for Water and Atmosphere Research, Wellington, NZ, Helen.Bostock@niwa.co.nz
[6] Eberhard-Karls-Universität, Tübingen, Germany, Michal.Kucera@uni-tuebingen.de

The boron isotopic compositions of foraminiferal and coral carbonate provide invaluable tools for the reconstruction of past CO_2 levels [e.g.1, 2]. However, calibration studies in both foraminifera and corals have illustrated that many organisms do not conform fully to our theorectical understanding of the proxy and there is often (but not always) a biological imprint upon recorded values. In order to construct reliable palaeo-pH and CO_2 records, it is crucial that we understand, quantify and correct for biological influence or 'vital effects' when applying the proxy to any given organism[3].

Here we present the results of efforts to quantify the biological influence on the boron isotopic signatures of planktic foraminiferal and coral carbonates. Calibration (via MC-ICPMS) of both symbiont-bearing and non-symbiont-bearing foraminifera (from cultures, tows and sediments) provides insight into the influence of symbiont photosynthesis, symbiont-host respiration and host calcification on the microenvironment pH around the foraminifera and thus the recorded boron isotopic signature of calcite. In this way, biological and environmental signals can be disentangled and proxy records extended.

In addition, analyses of coral carbonate (*Siderastrea siderea*) cultured under controlled pH not only constitute a new species-specific $\delta^{11}B$ calibration for palaeo-application, but shed light on the calcifying fluid pH of scleractinian corals when viewed in the context of recent pH micro-electrode measurements[4].

[1] Foster (2008) *EPSL* **271,** 254-266.
[2] Hönisch et al. (2004) *Geochimica et Cosmochimica Acta* **68**, 3675-3685.
[3] Pagani et al. (2005) *Geochimica et Cosmochimica Acta* **69**, 953-961.
[4] Ries (2011) *Geochimica et Cosmochimica Acta* **75**, 4053-4064.

Groundwater evolution under permafrost conditions, South-West Greenland

EMILY HENKEMANS[1*], SHAUN FRAPE[1], TIMO RUSKEENIEMI[2], LILLEMOR CLAESSON LILJEDAHL[3], ANNE LEHTINEN[4] AND JON ENGSTRÖM[2]

[1]University of Waterloo, Earth Science, ehenkema@uwaterloo.ca (*presenting author), shaun@uwaterloo.ca
[2]GTK, Finland, timo.ruskeeniemi@gtk.fi, jon.engstrom@gtk.fi
[3]SKB, Sweden, lillemor.claesson-liljedhal@skb.se
[4]POSIVA, Finland, anne.lehtinen@posiva.fi

The Greenland Analogue Project (GAP) aims to further the understanding of groundwater evolution due to the influence of a continental ice sheet and continuous permafrost. Geochemical and hydrogeological processes are being studied in the area around Kangerlussuaq, Greenland. Geochemical and isotopic (^{18}O, ^{2}H, ^{3}H, ^{37}Cl, ^{87}Sr and ^{34}S and ^{18}O of SO_4) tracers are used to interpret the flow and geochemical evolution of groundwater in this crystalline environment.

Three boreholes have been drilled since 2009. Two boreholes are equipped with groundwater sampling devices: DH-GAP01 intersects a talik beneath a large lake and DH-GAP04 provides 3 sampling sections beneath and adjacent to the ice.

Talik waters from DH-GAP01 and the first groundwaters sampled at DH-GAP04 appear to be geochemically similar in many ways, such as high concentrations of sulphate. High sulphate groundwaters are also found in other permafrost impacted crystalline environments in Northern Canada [1],[2]. GAP borehole waters are depleted in $\delta^{18}O$ and $\delta^{2}H$ compared to modern precipitation when a simple linear mixing model is used to calculate final compositions of DH-GAP04 based on the concentration of tracer in the samples (Fig. 1). Further sampling of DH-GAP04 is planned for 2012.

A spring located directly infront of Leverett Glacier, about 10 km south of DH-GAP01, yields groundwaters that are geochemically distinct from the waters sampled from the boreholes with elevated iron concentrations up to 14.8 mg/L.

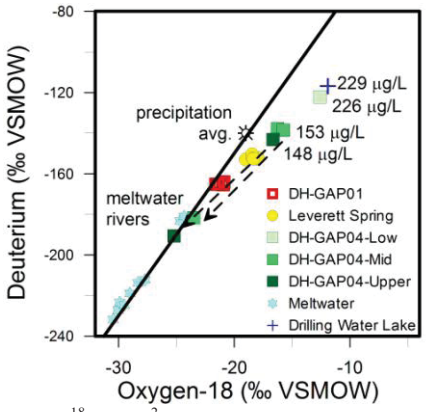

Figure 1: $\delta^{18}O$ vs $\delta^{2}H$ for groundwaters and glacial meltwaters. Concentrations are the sodium fluorescein tracer used in drilling.

[1] Stotler *et al.* (2009) *J. Hydrol* **373**, 80-95. [2] Frape, Fritz & McNutt (1984) *Geochim. Cosmochim. Acta* **48**, 1617-1627.

https://doi.org/10.1180/S0026461X00008434 Published online by Cambridge University Press

Clumped isotope thermometry of Carboniferous brachiopods and the effects of burial heating

GREGORY A. HENKES[1*], ETHAN L. GROSSMAN[2], THOMAS E. YANCEY[2] AND BENJAMIN H. PASSEY[1]

[1]Department of Earth and Planetary Sciences, The Johns Hopkins University, Baltimore, MD, USA 21211 (*ghenkes1@jhu.edu)
[2]Department of Geology and Geophysics, Texas A&M University, College Station, TX, USA 77843

Clumped isotope thermometry of well-preserved carbonate fossils holds great promise for detangling the effects of paleotemperature and seawater oxygen isotope composition on the oxygen isotope composition of fossils. Meaningful application of this paleothermometer requires accurate calibration curves, as well as an understanding of the burial temperatures where solid-state reordering of C-O bonds becomes significant. We describe the results of a clumped isotope calibration for modern brachiopods and mollusks, then use this calibration to determine paleotemperatures from a suite of nominally pristine Carboniferous brachiopod fossils. Apparent paleotemperatures of the brachiopods range from 15 to 197 °C. Thus, while the Δ_{47}-derived temperatures of many of the fossils are consistent with formation at Earth's surface, some shells give paleotemperatures that are clearly inconsistent with biological mineralization. We have conducted laboratory heating experiments on natural calcites to determine Arrhenius parameters for solid-state C-O reordering. These parameters are used in numerical models to predict the Δ_{47} evolution of the Carboniferous brachiopods, where the T-t paths are constrained by independent geological data. We observe a reasonably close correspondence between predicted and observed Δ_{47} values, and the models predict that reordering becomes important at temperatures above ~100-125°C for dwell timescales of 10^8 years.

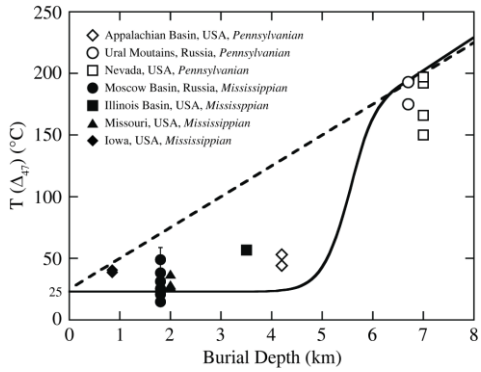

Figure 1: Clumped isotope temperatures and estimated burial depths (based on independent geological information) for pristine Carboniferous brachiopods from several Paleozoic sedimentary basins. The solid line is a modeled solid-state reordering pathway showing the clumped isotope temperature evolution of a shell buried at a rate of 0.25 km/Ma under a geothermal gradient of 25 °C/km (dashed line). Samples undergoing solution-precipitation should plot in the area bounded by the solid and dashed lines.

Monopolar and highly asymmetric nucleation at low temperatures: Insights from tourmaline

D.J. HENRY[1*], B.L. DUTROW[1]

[1]Louisiana State University, Dept. Geology & Geophysics, Baton Rouge, LA, USA, dutrow@lsu.edu

Minerals overcome the nucleation barrier to growth by numerous methods. Epitaxial growth can be found between different minerals that share structural features e.g. kyanite and staurolite. Alternatively, new growth can nucelate on substrates of the same mineral. In low-temperature systems, crystallographically congruent overgrowths are common such as the often observed quartz overgrowths on quartz. Here, composition of the substrate is nearly identical, except for trace element compositions. In contrast, at diagenetic and low grade metamorphic conditions, tourmaline supergroup minerals commonly nucleate on substrates of pre-existing tourmaline, even when their compositions are substantially dissimilar.

In these environments, the substrate, a detrital core, is distinctly different in composition such that it may be classified as a different species that may manifest as a contrasting color (Fig. 1). These interfaces appear sharp with little-to-no diffusion across the interface. In addition, these oriented overgrowths are in optical continuity with the detrital grain and are more pronounced at the $+c$ axis of the crystal providing a crystallographic identifier. Such overgrowths suggest distinct and major differences in surface energy at different poles of the crystal. At diagenetic conditions the tourmaline overgrowth is monopolar – only at the $+c$ axis. At low grades of metamorphism the overgrowths are highly asymmetric along the c axis with significant differences in composition at the opposite poles. With increasing metamorphic grade the asymmetric differences in overgrowth dimensions and compositions diminish and converge at roughly 550°C. Tourmaline is one of the few minerals to exhibit such features at low temperatures and supports the fact that preferred nucleation reduces the nucleation barrier. Because of the temperature dependence of the asymmetric development of tourmaline, it is likely that differential surface energy plays a very significant role in tourmaline nucleation.

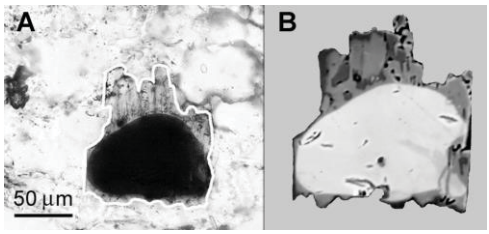

Figure 1: Detrital tourmaline grain with asymmetric overgrowth developed in chlorite zone metawacke. (A) Optical photomicrograph with dark detrital core and lighter overgrowth highlighted by white outline. (B) Backscattered electron image showing some of the textural and chemical variability of the overgrowths. [1]

[1] Henry, D.J., and Dutrow, B.L. (1992) Tourmaline in a low-grade clastic metasedimentary rock - an example of the petrogenetic potential of tourmaline. Contributions to Mineralogy and Petrology, **112,** 203-218.

https://doi.org/10.1180/S0026461X00008434 Published online by Cambridge University Press

Iron Oxides Chemistry from High-grade Iron Ore, Iron Quadrangle

ANA-SOPHIE HENSLER[1*], STEFFEN HAGEMANN[1], CARLOS ALBERTO ROSIERE[2], THOMAS ANGERER[1] AND SARAH GILBERT[3]

[1]Center for Exploration Targeting, University of Western Australia, hensla01@student.uwa.edu.au (*presenting author)
[2]Universidade Federal de Minas Gerais, Brazil, crosiere@gmail.com
[3]University of Tasmania, Australia, sgilbert@utas.edu.au

Abstract

Most of the high-grade iron ore deposits in the Iron Quadrangle (IQ), Brazil are hosted by itabirites of the Caue Formation, a Paleoproterozoic Lake-Superior type Banded Iron Formation. The IQ was affected by two main orogenies, the Transamazonian (2.6 – 2.0 Ga) and the Brasiliano (0.7 – 0.45 Ga) resulting in a western low-strain and an eastern high-strain domain. Iron ore bodies in the western domain are dominated by early-stage martite and granoblastic hematite, whereas ore bodies of the eastern domain contain mainly late-stage microplaty hematite and specularite.

Minor and trace element contents (Mg, Mn, Al, Cr, V, Ti, Ga, Ni, Co, Zn, As, Bi and REE) of selected iron ore deposits in the IQ, such as Aguas Claras, Pau Branco, Casa de Pedra, Bau and Conceicao were analysed using Laser Ablation ICPMS. At a deposit-scale, the minor and trace element patterns of specific iron oxide phases (e.g., martite) are consistent within an ore body, but show significant variations, when compared to another iron oxide phase of the same ore body (e.g., to microplaty hematite). A progressive depletion of elements, (most significantly Mg, Al, Cr, Ti, and Ni) is recorded when comparing paragenetically older (i.e., granoblastic hematite) with younger (i.e., microplaty hematite, specularite) oxides (Figure 1). At a scale of the IQ, chemistry of iron oxides that formed during the early Transamazonian event (i.e., martite after magnetite and granular hematite) shows consistent Mn, Al, Ti, Ga, Co, Zn, As, and Bi contents. This is distinct from late crystallised oxides (i.e., microplaty hematite, specularite), which display also consistent but different chemical patterns (e.g., Mn, Cr, Ti, Ga, and As) when compared to the "early" oxides. Therefore, different tectonometamorphic stages may have a major influence on the mineral chemistry of the iron oxide generations. The actual factors, that may control the mineral chemistry patterns of iron oxides and are currently under investigation, are the host and country rock petrology, fluid source type(s) and/or the mineral-specific preference of cation substitution.

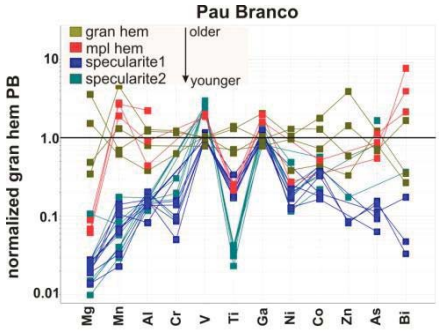

Figure 1: Chemical signature of iron oxide species from Pau Branco (PB) iron ore deposit, normalized to granoblastic hematite. Abbreviations: Gran hem = granoblastic hematite; mpl hem = microplaty hematite

Pilot-scale barrier system for removal of nitrate in mine drainage

ROGER HERBERT[1*] AND HARRY WINBJÖRK[2]

[1] Department of Earth Sciences, Uppsala University, Uppsala, Sweden, roger.herbert@geo.uu.se (* presenting author)
[2] LKAB, Malmberget, Sweden, harry.winbjork@lkab.com

Introduction

Undetonated ammonium nitrate - based explosives are readily soluble in water and quickly enter into the mine water and process water at a mine site. Process water is eventually discharged to a surface water body and, without treatment, can lead to eutrophication in the recipient. In order to investigate the application of nitrate removal by denitrification in the cold climate of northern Sweden, laboratory and field experiments have been conducted. Laboratory column experiments were designed to determine denitrification rates at relevant temperatures for northern Sweden. Based on the column experiments at low temperature, a hydraulic residence time of ca. 24 hours was one of the design criteria used for dimensioning a barrier system in the field. In autumn 2009, a pilot-scale barrier system was constructed of sheet metal at the Malmberget iron ore mine. The barrier (9m x 2m x 1.5m) appears as an open basin with three inner dividing walls, and is filled with a reactive mixture consisting of crushed rock, sawdust, and sewage sludge. A small fraction of the water discharging from the Malmberget clarification pond was fed by pump to the barrier at a rate of ca. 5 m^3 day^{-1}.

Results

In the pilot-scale barrier system, analytical results from 2010 indicated that nitrate (NO_3^-) removal generally lay in the range between 11 and 77% of influent nitrate concentrations. In order to achieve a higher removal rate, the barrier system needed to be supplemented with an additional carbon and energy source for denitrifying bacteria. In 2011, a sodium acetate solution as an external electron donor was continuously added to the barrier system along with the influent water. Analytical results from 2011 indicate that the barrier system in Malmberget removes >95% of the incoming nitrate during summer months (average daily temperature 14°C for 2011) with the addition of acetate. The barrier did exhibit decreases in performance toward the end of the study period in 2011, but this is likely the result of a lower hydraulic residence time in the barrier at this time.

Nitrite (NO_2^-) concentrations in effluent waters were initially in excess of influent values, indicating the production of nitrite in the barrier. However, both nitrite and ammonium (NH_4^+) concentrations decreased to below detection limits after the addition of acetate (CH_3COO^-), suggestion the occurrence of anaerobic ammonium oxidation (anommox) in the barrier substrate. During this period, alkalinity values peaked at 500 mg HCO_3^- L^{-1} in effluent waters, indicative of organic carbon (acetate) oxidation through denitrification:

$$5CH_3COO^- + 8NO_3^- + 3H^+ \rightarrow 4N_2(g) + 10HCO_3^- + 4H_2O$$

Stable isotope analyses of $\delta^{15}N$ and $\delta^{18}O$ in nitrate demonstrate an enrichment in ^{15}N and ^{18}O along the flowpath, supporting the conclusion that denitrification is responsible for nitrate removal.

https://doi.org/10.1180/S0026461X00008434 Published online by Cambridge University Press

Geochemical Proxies Linked to Astronomical Climate Forcing in Dynamic Sedimentary Environments: Western Canada Sedimentary Basin.

BENJAMIN D. HEREDIA[1], JONATHAN R. GAYLOR[2], KLAUS MEZGER[1], FRITS HILGEN[3], KLAUDIA KUIPER[3]

[1]University of Bern, Bern, Switzerland, benjamin.heredia@geo.unibe.ch (* presenting author); klaus.mezger@geo.unibe.ch

[2]University Paris-Sud XI, Paris, France, jonathan.gaylor@u-psud.fr
[3]University of Utrecht, Utrecht, The Netherlands, fhilgen@geo.uu.nl; kkuiper@geo.uu.nl

Abstract

Generally, coal-deposits and associated organic-rich horizons in continental successions in North-America have been interpreted to represent swamp deposits, which accumulated on the floodplain as a consequence of autocyclic or tectonic processes. However, spectral-based analyses of geochemical proxies have shown precession-eccentricity controlled stacking patterns in the Tongue River Member of the Fort Union Formation in the US. Similarly, Upper Cretaceous alternations of sand-silt-organic-rich horizons likely represent precession-controlled cycles in the Horseshoe Canyon Formation in the Western Canada Sedimentary Basin. To support the lithological proxy-data, mainly represented by the color, geochemical data has been generated for each single layer that include some of the soluble, moderately soluble and insoluble elements, and compared them with seawater and upper crustal partition abundances. All different lithologies show the same characteristics: increased abundances of Mg, Ba, Cr, Zn and lower abundances of Ca relative to the very homogeneous Coal 13 or Nevis Coal. Although the chemical index of alteration (CAI) is the most widely accepted weathering index applied to siliciclastic sedimentary rocks and it has been successfully applied to evaluate various climatic conditions in the Precambrian, in the Horsehoe Canyon Formation the CAI does not yield any clear paleoclimatic information, most probably due to mobilisation of Na^{+}, K^{+} and Ca^{2+} during diagenesis or the presence of apatite. In addition a combination of grain-size effects and the possible incorporation of older weathered material may have affected the CAI-values for the deposits. For some of the elemental ratios, the redox sensitive (Cr/V)-proxy, and the Mg#, the data show trends that mirror those observed in the color proxy when normalized to the reference layer coal. Furthermore, when applying wavelet analysis to the records, periodicities appear to be more evident. This, in combination with new paleomagnetic, Ar-Ar and U-Pb (CA-TIMS) data, will enable us to link our records to the Maastrichtian, including the C29R and the K-Pg boundary. This research is funded by the European Community's Seventh Framework Program (FP7/2007-2013) under grant agreement no. 215458.

Micro- to macro-scale investigations of manganese in soil-plant systems

ELIZABETH M. HERNDON[1*], JAMES KUBICKI[2], AND SUSAN L. BRANTLEY[3]

[1]Dept. of Geosciences, Penn State University, University Park, PA, United States, eherndon@psu.edu (* presenting author)
[2]Dept. of Geosciences, Penn State University, University Park, PA, United States, jdk7@psu.edu
[3]Earth and Environmental Systems Institute, Dept. of Geosciences, Penn State University, University Park, PA, United States, sxb7@psu.edu

Industrial processes have emitted large quantities of metals into the atmosphere which have been subsequently redistributed across the Earth's surface. As a result, we can observe enrichment of many metals in air, water, soil, and biota. Vegetation can impact the residence time of these metals in soils and their rate of transfer from soils to river systems. In particular, biotic uptake into vegetation can slow leaching and outflux of manganese contaminants from soils. Mn that is taken up by vegetation can be stored in standing biomass or returned to the soil through litterfall. In order to better predict Mn mobility in the environment, it is necessary to characterize the abundance and chemical forms of Mn-compounds in mineral soil, soil organic matter, and vegetation. Here, we combine spectroscopic techniques with molecular modeling and mass balance models to develop better ecosystem-scale understanding of Mn transport through vegetation and soils.

Spectroscopic techniques (XRF and XANES) reveal the chemical transformations of Mn that occur during its movement through the plant-soil system. Mn(II) is complexed to organic matter in roots, branches, and foliar tissue. Mn is concentrated in the foliage, where Mn(II)-organic complexes dominate, but where we have also observed a distinct chemical form of Mn localized in Mn-rich black spots. Foliar Mn is oxidized and immobilized as mixed-valence Mn-oxides in the soil during decomposition of litterfall.

To complement the spectroscopic data, molecular modeling is being used to calculate ligand-dependent shifts in the Mn K-edge energy and provides insight into the Mn oxidation state and coordination environment. Furthermore, bulk chemistry data is combined with the spectroscopic data to create mass balance models and estimate Mn fluxes between reservoirs in the soil-plant system. While bulk chemistry itself alone yields important information about Mn dynamics, techniques such as μXRF and μXANES can deliver further insight into the spatial distribution, oxidation state, and chemical form of Mn in soils and vegetation. As demonstrated here, integration of microscale techniques with ecosystem analysis can prove valuable to understanding ecosystem metal dynamics.

https://doi.org/10.1180/S0026461X00008434 Published online by Cambridge University Press

Input and transport of ^{129}I in the Canadian Arctic: evidence of a Fukushima pulse

MATT N. HEROD[1]*, IAN D. CLARK[1], W.E. KIESER[2], XIAO-LEI ZHAO[3]

[1]University of Ottawa, Earth Sciences, Ottawa ON, Canada mhero065@uottawa.ca (*presenting author)
[1]University of Ottawa, Earth Sciences, Ottawa ON, Canada idclark@uottawa.ca
[2]University of Ottawa, Physics, Ottawa ON, Canada liam.kieser@utoronto.ca
[3]University of Toronto, Physics, Toronto ON, Canada xiaolei.zhao@utoronto.ca

Since the 1950s, nuclear fuel reprocessing and nuclear accidents have released large amounts of anthropogenic ^{129}I into the atmosphere. This ^{129}I has spread throughout the northern hemisphere, increasing concentrations above natural fallout and geogenic levels in these regions. Because it is very mobile and readily absorbed by living organisms, ^{129}I is considered a contaminant of concern, especially in terms of the long term disposal of radioactive waste.

The Arctic has been identified as a location that may be affected by ^{129}I fallout from nuclear activities in Europe and Asia. A multi-year comparison of ^{129}I concentrations, ratios and fluxes between Arctic watersheds is a valuable tool to assess the origin and extent of contamination, and to understand ^{129}I transport dynamics. Water samples from a number of watersheds were collected in the Yukon Territory, Canada in 2010 and 2011. Sampling was conducted in Whitehorse (60°43′00″N) and continued north along the Dempster Highway as far as Tsiigehtchic, Northwest Territory (67°26′26″N). ^{129}I was extracted from water samples by redox separation, precipitated as AgI, and analyzed using accelerator mass spectrometry (AMS). Total iodine was determined using ICP-MS. Mean concentrations for ^{129}I northwest Canadian rivers were 16.1x10^{6} atoms/L in 2010 and 66.8 x10^{6} atoms/L for 2011. These values significantly exceed previously published values for waters containing only geogenic or cosmogenic ^{129}I. A comparison of ^{129}I flux over the two years for a subsection of the sampling area also shows a 10-fold increase in the fallout of ^{129}I (atoms/m^2/yr) in the watersheds between 2010 and 2011. The source of ^{129}I in the Arctic is mainly from nuclear fuel reprocessing releases which are transported atmospherically through a cycle of deposition and revolatilization to remote regions throughout the northern hemisphere. The substantial increase in ^{129}I fallout in these watersheds from 2010 to 2011 is consistent with elevated levels of ^{131}I measured on the western coast of North America in the days following releases from the Fukushima Daiichi nuclear power plant in March 2011.

U isotopes in marine calcareous algae: a paleo-redox proxy?

ACHIM D. HERRMANN[1*], STEPHEN J. ROMANIELLO[1], R. PAMELA REID[2], ARIEL D. ANBAR[1,3]

[1] School of Earth and Space Exploration, Arizona State University, Tempe, AZ, USA, achim@asu.edu (* presenting author)
[2] Rosenstiel School of Marine and Atmospheric Science, University of Miami, Miami, FL, USA
[3] Department of Chemistry & Biochemistry, Arizona State University, Tempe, AZ, USA

Significant variability in the uranium isotopic composition of natural samples [1] is largely due to isotope fractionation during redox transformations associated with uranium deposition in reducing sediments. This suggests that the uranium isotopic composition of seawater may be determined by the redox state of the global ocean. Limited evidence indicates that scleractinian corals record the uranium isotopic composition of seawater [1]. Thus, changes in the uranium isotopic composition of carbonates through time may reflect changes in the redox conditions of the global oceans. More work is needed, however, to confirm that uranium values of biogenic carbonate sediments in general reflect seawater values, irrespective of the biomineralization pathways that led to the formation of the calcium carbonate. In particular, it will be critical to establish that carbonates faithfully record uranium values of seawater without fractionation. Here, we report uranium isotope values from a range of different marine algae from the Bahamas to further test the potential of calcium carbonates as a paleo redox proxy.

It has long been known that calcareous algae incorporate different amounts of uranium [2] and have different biomineralization pathways that affect the δ^{13}C and δ^{18}O of the precipitated carbonate [3]. These difference might also lead to a fractionation of uranium isotopes during the formation of calcium carbonate in different algae. However, our results indicate that fractionation of uranium during biomineralization of algae does in fact not take place. Despite difference in uranium concentrations (ranging from ~1ppm to ~2.5ppm) and different biomineralization pathways (*Acetabularia* sp., *Rhipocephalus* sp., *Halimeda incrassata*, and *Penicillus capitatus*), the uranium isotopic compositions in these various algae are the same and reflect seawater values (δ^{238}U ~-0.40‰). The δ^{238}U values of the calcareous green algae are indistinguishable from δ^{238}U values of scleractinian corals (*Diploria* sp, *Siderastrea* sp., and *Porites* sp.) collected in the same area. Futhermore, δ^{234}U values of all samples are indistinguishable from seawater values.

Our results show that biominearlization pathways do not lead to fractionation during the uptake of uranium isotopes and calcareous algae are thus excellent candidates to serve as paleo-redox proxies. Since calcareous algae are important producers of fine sediment in carbonate settings, the lack of fractionation within the algal material further implies that bulk sediment analyses of carbonate rocks dominated by algal material as a tracer of paleo-redox are possible.

[1] Weyer el al. (2008) *GCA* **72**, 345–359. [2] Edgington et al. (1970) *Limnol Oceanogr* **15**, 945-955. [3] Lee and Carpenter (2001) *Chem Geol* **172,** 307-329.

https://doi.org/10.1180/S0026461X00008434 Published online by Cambridge University Press

Origin of spherulitic concretions in Cambro-Ordovician black shales, St. Lawrence Estuary, Quebec, Canada

REINHARD HESSE[1*], CHRISTOPHER FONG[2]

[1]Earth & Planetary Sciences (McGill), Montreal, Canada, Reinhard.Hesse@mcgill.ca*
[2] Apt. 102, No.16, Lane 3292, Hongmei Road, Shanghai, 201103 China, Fongchristopher@hotmail.com

Introduction and Results

Spherulitic concretions are very rare among carbonate concretions which are a trademark of organic-matter rich sediments and normally consist of micritic carbonate. The occurrence in Cambro-Ordovician black shales of unknown stratigraphic age on mid-channel islands in the St. Lawrence Estuary in Quebec is among four hitherto known examples [1,2,3] of spherulitic concretions and their origin is still poorly understood. These concretions occur in close association with and show various transitions to cone-in-cone structure. The spherules are 0.5 to 12 mm in diameter. They consist of intergrown fine fibers of ferroan calcite and quartzine, pointing to the formation of the concretions below the sulfate reduction zone. A phenomenological theory of spherulitic crystallization [4] relates the thickness δ of an impurity-rich layer in front of impurity-rejecting growing crystals to the impurity-diffusion coefficient D and the growth velocity G of the crystal by δ=D/G. In spherulite-forming environments, extremely small values of δ (on the order of $<10^{-4}$cm) in conjunction with cellulation lead to spherulitic fibre growth. The intimate association of calcite and quartzine in the concretions seems hard to understand. Most spherules precipitated experimentally in the laboratory crystallized in a gelatinous medium in the presence of impurities. Silica gel is the most common medium used. The occurrence of silica gel has not been reported from clastic or biogenic siliceous pelagic deep-sea sediments, not even in hydrothermally sourced ponds of mid-oceanic ridges. However, experimental spherulite precipitation has also been achieved from alkaline aqueous solutions. Alkaline conditions are established during early diagenesis in the lower sulfate reduction zone so that fibrous calcium carbonate precipitation in the presence of impurities may easily start in the carbonate-reduction (methane-generation) zone. The switch from carbonate precipitation to silica precipitation into the pore spaces of coarse, open-texture fibrous carbonate spherulite may be achieved by the dissolution of sponge spicules or radiolarians which would lead to low supersaturation allowing the direct precipitation of quartzine.

Conclusion

Intergrown spherulitic carbonate/quartzine concretions seem to require special chemical conditions of pore-water composition and burial-diagenetic evolution that may shed important light on unusual early diagenetic chemical environments. Sperulitic concretion growth can be explained in view of a phenomenological crystallization theory [4] and experimental results.

[1] Allen (1936) *Am. Min.* **21**, 369-373, [2] Hodgson (1968) *J. Sed. Petrol.* **38**, 1254-1263, [3] Morse & Donnay (1936) *Am. Min*. **21**, 391-426, [4] Keith & Padden (1963) *J. Appl. Phys*. **34**, 2409-2421

New insights into the origin of the Shatsky Rise from Sr-Nd-Pb-Hf isotopes of volcanic rocks from IODP Exp. 324

KEN HEYDOLPH[1*], JOERG GELDMACHER[1], KAJ HOERNLE[1]

[1]GEOMAR | Helmholtz Centre for Ocean Research, Kiel, Germany, kheydolph@geomar.de (* presenting author)
jgeldmacher@geomar.de
khoernle@geomar.de

Shatsky Rise: a unique large igneous province

The submarine Shatsky Rise plateau, situated in the northwest Pacific Ocean ca. 1500 km east of Japan, is the only large intraoceanic plateau, which formed during the Late Jurassic to Early Cretaceous at a time period with numerous reversals of the Earth's magnetic field. Combined with bathymetric data, the magnetic reversals allow a detailed reconstruction of the original tectonic setting, spatial evolution and approximate seafloor age from the magnetic record [1]. Accordingly, the three main volcanic edifices Tamu, Ori, and Shirshov massifs formed by massive volcanism during a short time span along a southwest - northeast trending, rapidly spreading triple junction. After the initially voluminous stage, which created the large Tamu massif, the volcanism waned to less voluminous phases, creating Ori and eventually the smallest Shirshov massif.

We present here Sr-Nd-Pb and Hf isotope data from relatively fresh basaltic lava flows from Site U1347A drilled during IODP Expedition 324 and Site 1213B (ODP Leg 198) both located on the southernmost (oldest) volcanic edifice of Shatsky Rise. Initial $^{143}Nd/^{144}Nd$: 0.512903 to 0.512981 and $^{176}Hf/^{177}Hf$: 0.283076 to 0.283100 isotopic compositions from Site U1347A samples are quite uniform throughout the entire hole and show neither distinct MORB nor intraplate (Ocean Island Basalt) affinity. Site 1213 samples are slightly less radiogenic in Nd and Hf isotopic compositions. In a Nd vs. Hf isotope plot Site U1347 form a tight cluster at the edge of the Pacific MORB field below the present-day Hf-Nd mantle array. Site 1213 samples have less radiogenic Nd and Hf isotopic compositions. Although initial Pb double spike $^{206}Pb/^{204}Pb$ and $^{208}Pb/^{204}Pb$ isotopic compositions for Site U1347 range from 18.13 to 18.46 and 37.71 to 37.96 respectively and overlap with MORB-like compositions, they trend towards more radiogenic, intraplate-like values.

In general, our isotopic data from Tamu massif show a very homogeneous and relatively depleted isotopic composition. Such composition could reflect a large degree of melting, consistent with an origin of the initial (oldest) phase of Shatsky volcanism from an arriving hot plume head [2].

[1] Nakanishi (1999) *J. Geophys. Res.* **104**, 7539-7556
[2] Farnetani and Hofmann (2011) *Encyclopedia of solid earth physics*

https://doi.org/10.1180/S0026461X00008434 Published online by Cambridge University Press

Large and heterogeneous isotopic anomalies of Sm and Gd in the Norton County meteorite

HIROSHI HIDAKA[1*] AND SHIGEKAZU YONEDA[2]

[1]Hiroshima University, Earth and Planetary Systems Science, Higashi-Hiroshima 739-8526, Japan, hidaka@hiroshima-u.ac.jp
[2]National Museum of Nature and Science, Science and Engineering, Tsukuba 305-0005, Japan, s-yoneda@kahaku.go.jp

Introduction

Cosmic rays in space penetrate a few meters into the surface of planetary materials, and produce cosmogenic nuclides in the materials. The exposure history of meteorites has been characterized by several cosmogenic nuclides. Sm and Gd isotopic shifts by neutron capture reactions also provide useful information for understanding the exposure records of meteorites, because ^{149}Sm and ^{157}Gd have very large thermal neutron capture cross sections and shift to ^{150}Sm and ^{158}Gd, respectively.

Enstatite achondrites (aubrites) are highly reduced achondrite meteorites, and must have formed in a very unique part of the solar nebular. The Norton County aubrite is known as one of the longest cosmic-ray exposure ages (111 Ma [1]), and its recovery of the main mass over 1000 kg is large enough to accumulate many kinds of cosmogenic nuclides. Therefore, Norton County is one of the best examples to study cosmic-ray irradiation effects [2-5]. We found very large and heterogeneous isotopic shifts of Sm and Gd in specific phases of Norton County, and would like to discuss the possible existence of preirradiation materials migrating into the meteorite body.

Experiments

In this study, whole rock, handpicked material of the light-colored phase (consisting mainly of enstatite), and chemical separates obtained by a sequential acid-leaching method (acetic acid-ammonium acetate, 0.1 M HCl, 2 M HCl, aqua regia, and the residue) were prepared from the same single fragment of Norton County. Sm and Gd were separated from the individual samples by a conventional method using cation exchange methods [6]. A thermal ionization mass spectrometer was used for the isotopic measurements of Sm and Gd.

Results and Conclusions

Large and heterogeneous isotopic variations of ^{150}Sm/^{149}Sm and ^{158}Gd/^{157}Gd due to neutron capture reactions caused by cosmic-ray irradiation were found in chemical and mineral separates from the Norton County meteorite. The light-colored separates have a very large neutron fluence of 1.98×10^{17} n cm^{-2}, which is 10 times higher than that of the whole rock. Furthermore, four chemical separates showed a large variation in neutron fluences, ranging from 1.82×10^{16} to 1.87×10^{17} n cm^{-2}. The variable amounts of neutron fluences from a small single fragment of the Norton County meteorite cannot be simply explained by single-stage cosmic-ray irradiation in space.

[1] Lorenzetti et al. (2003) *GCA* **67,** 557-571. [2] Eugster et al. (1970) *JGR* **75,** 2753-2768. [3] Hidaka, Ebihara & Yoneda (1999) *EPSL* **173,** 41- 51.[4] Hidaka, Yoneda & Marti (2006) *GCA* **70,** 3449-3456. [5] Herzog et al. (2011) *MAPS* **46,** 284-310. [6] Hidaka & Yoneda (2007) *GCA* **71,** 1074-1086.

Microscopic Structure of Interfaces of Minerals in Relation to Macroscopic Ion Adsorption Phenomena

TJISSE HIEMSTRA[1] AND WILLEM VAN RIEMSDIJK[1]

[1]Wageningen University, Wageningen, The Netherlands

Mineral-water interfaces are important in regulating the free ion concentration of many minor elements in nature. In the interface, a bulk mineral meets the water network, forming a reactive structure for ion adsorption in which surface groups are a key for understanding reactivity. Surface groups and surface complexes can be characterized with modern spectroscopy (e.g. X-ray techniques, FTIR) and computational approaches (MO/DFT and MD simulations). Microscopic surface complexation is usually conditional, i.e. it will depend on pH, ionic strength, the concentration of the ion involved as well as the presence of cooperative and competitive ions. Surface complexation models (SCM) can be used to generalize experimental microscopic information and to rationalize macroscopic adsorption behavior as a function of environmental conditions. Microscopic data and tools are also highly valuable for parameterization and development of mechanistic adsorption frameworks, such as the CD and MUSIC model. Achievements and challenges will be discussed.

The variable surface speciation of a particular ion is largely regulated by the joint electrostatic interactions of all ions in the interface and there is a feedback from the water network. The structure of interfacial water and location of interfacial charge are essential. Interfacial structure and mechanisms of charging of minerals are very different. This will be illustrated, comparing metal oxides, silver halides, and ice, using experimental information as well as computational data.

https://doi.org/10.1180/S0026461X00008434 Published online by Cambridge University Press

Chlorine-rich fluid in granulite facies continental collision zone

FUMIKO HIGASHINO[1*], TETSUO KAWAKAMI[1], M. SATISH-KUMAR[2], MASAHIRO ISHIKAWA[3], KENSHI MAKI[1], NORIYOSHI TSUCHIYA[4], GEOFF GRANTHAM[5], AND TAKAFUMI HIRATA[1]

[1]Department of Geology and Mineralogy, Kyoto University, Kyoto, Japan, fumitan@kueps.kyoto-u.ac.jp (* presenting author).
[2]Shizuoka University, Shizuoka, Japan
[3]Yokohama National University, Yokohama, Japan
[4]Tohoku University, Sendai, Japan
[5]Council for Geoscience, Pretoria, South Africa

In the granulite facies rocks, CO_2-rich fluid has been considered important and studies on Cl-rich fluid are not sufficiently available, because Cl-rich fluid inclusions are less observed than CO_2-rich ones. However, Cl-bearing brines are increasingly recognized as playing an important role in high-*T* metamorphic rocks [1]. Using Cl concentration of minerals, it is possible to decipher the Cl-rich fluid activity and its role during metamorphism.

We have investigated the field distribution of Cl-rich Bt in the pelitic gneisses of the Sør Rondane Mountains, East Antarctica where Late Proterozoic to Cambrian granulites are widely exposed [2]. Among more than 20 samples studied, a Grt-Bt-Sil gneiss from Balchenfjella was selected as best suited sample to constrain the *P-T-t* condition of Cl-rich fluid activity. This gneiss contains Grt porphyroblasts (5-10 mm) that have P-rich core with oscillatory zoning in P. The Grt core includes Cl-poor Bt and Ap. This core is once resorbed and discontinuously overgrown by the P-poor rim, in which Cl-rich Bt and Ap are included. Coarse-grained (ca. 100 μm), round Zrn grains are exclusively included in the rim of the Grt porphyroblast and present in the matrix. This mode of occurrence suggests that Cl-rich Bt and Ap, and coarse Zrn were formed almost simultaneously. The *P-T* conditions of the Cl-rich Bt entrapment in the Grt rim were estimated to be ca. 800 ºC and 8 kbar, and those of the peak metamorphic condition were ca. 850 ºC and 11 kbar, using Grt-Bt geothermometer and GASP geobarometer [3]. The f_{HCl}/f_{H2O} ratio of the fluid in equilibrium with Cl-rich Bt [4] and Ap [5] in the Grt rim are ten times larger than that in equilibrium with Cl-poor Bt and Ap in the matrix and the Grt core. The LA-ICPMS U-Pb dating of the coarse Zrn gave $^{206}Pb/^{238}U$ age of ca. 600 Ma. Therefore, the Cl-rich fluid infiltration took place at near metamorphic peak condition of ca. 800 ºC and 8 kbar at ca. 600 Ma.

The field distribution of Cl-rich fluid activity is somewhat linear. Some of them are located near the ductile shear zones [6], and suggesting its relation to high-strain zones [e.g. 7]. Regional distribution of near-peak metamorphic Cl-rich fluid activity in the Sør Rondane Mountains implies that it is one of the major phenomenon in the continental collision processes.

[1] Newton & Manning (2010) *Geofluids* **10**, 58-72. [2] Shiraishi *et al*. (2008) *Geol. London Sp. Pub.* **308**, 21-67. [3] Hodges & Spear (1982) *Am. Min.* **67**, 1118-1134. [4] Selby & Nesbitt (2000) *Chem. Geol.* **171**, 77-93. [5] Piccoli & Candela (1994) *Am. J. Sci.* **294**, 92-135. [6] Ishikawa et al. (2011) NIPR symposium abst. [7] Kullerud *et al*. (2001) *J. Pet.* **42**, 1349-1372.

Cenozoic seawater chemistry – insights from Mg isotopes in pelagic carbonate sediments and pore-fluids

JOHN A HIGGINS[1] AND DANIEL P SCHRAG[2]

[1]Princeton University, Princeton, NJ, jahiggin@princeton.edu*
[2]Harvard University, Cambridge, MA

10b. Seawater chemistry changes through time

Large changes in seawater chemistry accompanied a decline in atmospheric CO_2 and cooling of Earth's climate over the Cenozoic. Sources and sinks of magnesium in seawater have distinct isotopic compositions, making the magnesium isotopic composition of seawater a tracer of the processes that control seawater chemistry [1]. Here we present Mg isotope data from both pore-fluids and pelagic carbonate sediments from ODP sites 1265 and 807A in the Atlantic and Pacific ocean basins, resepecitvely. Pore-fluid profiles of Mg and Ca in deep-sea carbonate sediments can be explained to first order by the recrystallization of biogenic carbonate and changes in Cenozoic seawater Mg and Ca. Our results are consistent with a substantial (>10 mmol) increase in seawater Mg over the Neogene, approximately balanced by a similar decline in seawater Ca. Magnesium isotope ratios measured in pelagic carbonates and corrected for re-crystallization vary systematically: peaking in the Paleogene, declining by ~0.4‰ to the Oligocene-Miocene boundary and remaining approximately constant from the Miocene to the present. Using a numerical model of global geochemical cycles (C, Mg, Ca, alkalinity), we explore mechanisms for changing seawater Mg and Ca and discuss implications for carbon cycling during the Neogene.

10b. Seawater chemistry changes through time

[1] Higgins (2010) *Geochimica et Cosmochimica Acta* **74**, 5039-5053.

https://doi.org/10.1180/S0026461X00008434 Published online by Cambridge University Press

Arsenic speciation and stable isotope chemistry in an arsenic contaminant plume at a landfill site

BRENDAN HILDUM[1*], RUDOLPH HON[1], SHAKIB AHMED[1]

[1]Department of Earth and Environmental Sciences, Boston College, Chestnut Hill, MA, USA, Hildum@bc.edu ([*]presenting author)

A groundwater plume beneath a capped landfill in North-Central Massachusetts contains dissolved arsenic concentrations exceeding 15,000 ppb in some locations. Disposal of solid wastes at the landfill spanned nearly a century with little documentation of the material disposed. The source(s), fate, and transport of arsenic in the landfill aquifer have been studied extensively; however site characterization has yet to be fully defined. The primary source of the arsenic is not believed to be directly from the landfill based on several lines of evidence, including naturally derived arsenic mobilization due to reducing conditions created by in-situ bioremediation at a nearby airfield (less than 0.5 miles), the existence of extremely high arsenic concentrations in sediment (8,500 ppm) in the bordering marshland, and prior studies performed at the site including arsenic leachate potential from landfill and aquifer materials [1]. Potential natural sources include a layer of peat located beneath the landfill believed to be a part of a historic marshland, previously insoluble iron hydroxides within the glacial sands, and/or bedrock due to oxidation of sulfides containing arsenic.

Arsenic species, including inorganic As(III) and As(V) as well as organic monomethyl arsenic acid (MMA) and dimethyl arsenic acid (DMA), along with groundwater parameters such as pH and redox conditions may provide information as to where the arsenic is primarily originating from and how it is transported through the aquifer. Furthermore, the analysis of stable isotopic ratios of groundwater from different zones of the landfill with varying arsenic concentrations will aid in the delineation of probable arsenic sources, the mobilization processes, and arsenic transport modes within the aquifer. The role of strong redox gradients and the various redox ladder reactions involving water are likely to create characteristic isotopic signatures which might lead to a better understanding of biogeochemical processes within and beneath the landfill waste pile and also assist with future remidiation of the aquifer.

[1] United States Army Corp of Engineers (USACE) (2010) *Five-Year Review Report for Former Fort Devens Army Installation , Devens, Massachusetts* 1,053p.

FORAMINIFERAL ISOTOPES IN THE SEA-ICE ENVIRONMENT

CLAUDE HILLAIRE-MARCEL[1]* AND ANNE DE VERNAL[2]

[1] GEOTOP-UQAM, Montréal, Canada, chm@uqam.ca

[2]GEOTOP-UQAM, Montréal, Canada, devernal.anne@uqam.ca

The only abundant planktic foraminifer in cold environments, *Neogloboquadrina pachyderma* left coiled (Np), is generally seen as a deep dwelling species forming its shell along the pycnocline. This may be true in the North Atlantic Ocean but can be challenged in the Arctic Ocean and sea-ice environment in general. Np occurs in sea-ice brine bubbles, especially near the base of the ice characterized by higher temperature and food availability [1]. It also occurs in cold and shallow waters where salinity is ≥34 and/or potential density ≥27.25 [2]. In sea-ice environment, Np-$\delta^{18}O$ often shows negative offset vs. isotopic equilibrium for calcite precipitated at mid-pycnocline depth. In the Arctic Ocean, the offset ranges –1 to –3‰ in the Western Arctic and there is a negative size-dependent isotopic gradient between light/small and heavy/large shells, which is opposite to what is observed in subarctic seas [3-5]. In sea ice, freezing of low $\delta^{18}O$ sea-surface waters produces isotopically-light brines that either concentrate in the sea-ice itself or sink deeper in the water column. *In vitro* experiments by Spindler [1] have shown that formation of new Np-shell chambers still occur in salinities of up to 58. A simple Rayleigh distillation equation governs the ^{18}O-content of brines. From a mean Arctic surface water (S ~ 30; $\delta^{18}O_{WATER}$ ~ -1‰ vs. VSMOW), brines with salinity of 34-58 and temperature of -2 to -3.5°C [6] have $\delta^{18}O$ ranging - 0.2 to -1.5‰, which may thus account for large Np isotopic offset. The brines sinking in the water column may partly accumulate along the pycnocline with the underlying saltier and warmer North Atlantic water carrying Np-tests and alive specimens. When dominant, Np is by itself a good indicator of polar water and sea-ice. When isotopic offsets vs. equilibrium increase, a longer seasonal duration of sea-ice cover may be inferred. A proxy calibration is not totally out of reach, but remains difficult because of highly variable conditions within sea-ice environment. In any case, the specific adaptation of Np to sea-ice has to be taken into account for the interpretations of paleo-records. It results in unreliable stratigraphy of $\delta^{18}O_{Np}$ -records from deep-Arctic cores [7] whereas the large amplitude shifts towards exceptionally light $\delta^{18}O_{Np}$-values, which accompanied Np abundance peaks in the glacial North Atlantic, are more likely a response to the spreading of sea-ice rather than the direct impact of glacial ice meltwater on salinity [8].

[1] Spindler (1986) *Proc. NIPR Symp. Polar Biology* **9**, 85–91
[2] Bergami *et al*. (2009) *Marine Micropaleontology* **73**, 37-48
[3] Kohfeld *et al.* (1996) *Paleoceanography* **11**, 679–699
[4] Bauch *et al*. (1997) *Earth and Planetary Science Letters* **146**, 47–58
[5] Hillaire-Marcel *et al*. (2004) *Quaternary Science Reviews* **23,** 245-260
[6] Golden *et al*. (2007) *Geophysical Research Letters* **34**
[7] Not and Hillaire-Marcel (2010) *Quat. Sci. Rev.* **29**, 3665-3675
[8] Hillaire-Marcel and de Vernal (2008) *Earth and Planetary Science Letters* **268**, 143-150

https://doi.org/10.1180/S0026461X00008434 Published online by Cambridge University Press

He-CO_2-N_2 systematics of the Tengchong Geothermal Province, SW China: Degassing along a plate boundary

DAVID R. HILTON[1*], ZHENGFU GUO[2], PETER H. BARRY[1], M. ZHANG[2], Z. CHENG[2]

[1]Scripps Institution of Oceanography, La Jolla, California, USA 92093-0244, drhilton@ucsd.edu (* presenting author).
[2] Key Laboratory of Cenozoic Geology and Environment, Institute of Geology and Geophysics, Chinese Academy of Sciences (CAS), 100029, Beijing, China.

The Tengchong Geothermal Province (TGP) is located on the northeast edge of the Indian-Eurasian plate collision zone, immediately east of the region of low-angle subduction of the Indian plate beneath the Burma microplate. It lies within the Gaoligong fold belt of the Tibetan-Yunnan fold system, between Myitkyina and the Nujiang suture. The TGP is characterized by recent volcanism, geothermal activity, and frequent earthquakes. Seismic evidence suggests that (a) faults in the region extend to the lower crust, with the Tengchong fault penetrating the Moho, and (b) melt in the region is generated in the upper mantle [1]. We aim to determine the volatile systematics of this shear zone by sampling thermal waters and geothermal gases along the Tengchong fault zone and in the nearby Kunming Province. Through analysis of He, C, and N (relative abundances and isotopic compositions) we consider the distribution of magmatic inputs to the volatile inventory, spatial controls on the degassing fluxes, and provenance characteristics of the volatiles.

We report new results from 16 geothermal gas and thermal water locations: 12 along a N-S transect within the Tengchong Block and 4 on the Eurasian plate in the Dali and Kunming areas. In the Tengchong Block, He isotope ($^3He/^4He$) ratios vary between 0.2 and 5 R_A (where R_A is the $^3He/^4He$ value of air), indicating a mixture between mantle (8 ± 1 R_A) and crustal (0.1–0.01 R_A) sources. Carbon isotope ($\delta^{13}C$) values of CO_2 range from -12.2 to -2.8 ‰ (vs. VPDB). $CO_2/^3He$ ratios range from 1.2×10^9 to 5.4×10^{12} with the majority of values falling between 10-100 times greater than the MORB value ($\sim2\times10^9$). Nitrogen isotope ($\delta^{15}N$) values of N_2 range from -2.1 to +5.8 ‰ (vs. air), but the majority are > 0 ‰, consistent with a crustal source. In contrast, Eurasian plate samples are dominated by radiogenic helium and $^3He/^4He$ does not exceed 0.6 R_A. In addition, $\delta^{15}N$ varies from +0.7 to +8.2 ‰, $CO_2/^3He$ ranges from 8×10^8 to 5.4×10^{12}, and $\delta^{13}C$ values range from +0.52 to -14.5 ‰.

The contrast in $^3He/^4He$ ratios between Tengchong and the Eurasian plate indicates that regional mantle degassing is narrowly focused on the Tengchong shear zone. Based on a ternary mixing model, CO_2 provenance is highly variable within the Tengchong Block, with contributions from mantle-derived CO_2, and crustal limestone and organic matter. Most samples have less than 10% mantle contribution, but mantle CO_2 exceeds 60% at two localities. The results are consistent with magma in the crust being derived from the upper mantle - in agreement with seismic evidence - we find no evidence for the presence of a slab-influenced mantle wedge. Thus, deep faulting in the Tibetan-Yunnan fold system must sustain sufficiently high crustal permeability to allow mantle volatiles to degas via the TGP. The results add to a growing body of evidence that strike-slip plate boundaries (e.g., San Andreas Fault and the North Anatolian Fault) represent important pathways for mantle volatile loss although, to date, their relative contributions to the total degassing budget remains unknown.

[1] Wang, C-Y. and Huangfu, G. (2004) *Tectonophysics* **380**, 69-87.

Climatic and geomorphic controls on the erosion of carbon from mountain forest: Implications for Earth's thermostat

ROBERT. G. HILTON[1*], ALBERT GALY[2], NIELS HOVIUS[2], SHUH-JI KAO[3], MING-JAME HORNG[4], HONGEY CHEN[5]

[1]Department of Geography, Durham University, Durham, UK, r.g.hilton@durham.ac.uk (* presenting author)
[2]Department of Earth Sciences, University of Cambridge, Downing Street, Cambridge CB2 3EQ, UK, albert00@esc.cam.ac.uk, nhovius@esc.cam.ac.uk
[3]Research Centre for Environmental Changes, Academia Sinica, Taipei, Taiwan, sjkao@gate.sinica.edu.tw
[4]Water Resources Agency, Ministry of Economic Affairs, Taipei, Taiwan, mjhorng@gmail.com
[5]Department of Geoscience, National Taiwan University, Taipei, Taiwan, hchen@ntu.edu.tw

Erosion of particulate organic carbon (POC) occurs at very high rates in mountain river catchments, yet the proportion derived recently from atmospheric CO_2 in the terrestrial biosphere ($POC_{biomass}$) remains poorly constrained. In these settings, export of $POC_{biomass}$ with large amounts of clastic sediment can drive geological CO_2 sequestration [1]. However, erosion can also mobilise fossil POC from bedrocks (POC_{fossil}) and this needs to be quantified. Here we examine the fluvial transport of $POC_{biomass}$ in suspended sediments of mountain rivers in Taiwan and assess the extent to which climatic and tectonic boundary conditions drive carbon transfer from atmosphere to lithosphere.

In 11 major river catchments in Taiwan, we have previously corrected for POC_{fossil} input using N/C, $\delta^{13}C$ and $\Delta^{14}C$ [2]. Here, $POC_{biomass}$ measurements are combined with water discharge (Q_w, $m^3\ s^{-1}$) and suspended sediment concentration (mg L^{-1}) over 2 years, with samples from flows between 0.1 and 20 times the long-term mean Q_w. In these catchments, $POC_{biomass}$ concentration (mg L^{-1}) was positively correlated with Q_w, with enhanced loads at high flow attributed to rainfall driven supply of $POC_{biomass}$ from forested hillslopes. This climatic control on $POC_{biomass}$ transport was moderated by catchment geomorphology: the gradient of a linear relation of $POC_{biomass}$ concentration and Q_w increased as the proportion of steep hillslopes (> 35°) in the catchment increased. The data suggest enhanced supply of $POC_{biomass}$ by erosion processes which act most efficiently on the steepest sections of forest.

Across Taiwan, $POC_{biomass}$ yield was correlated with suspended sediment yield, and did not limit at high physical erosion rates. Our data demonstrate that, for a constant set of geomorphic conditions, the fluvial transfer of $POC_{biomass}$ from mountain catchments is driven by climate through the activation of erosion and transport processes during heavy rainfall. A move to a wetter, stormier climate should enhance the erosional export of $POC_{biomass}$. In settings with strong coupling between depositional sinks and terrestrial inputs this offers a feedback in the Earth System, whereby climate can modify rates of CO_2 sequestration through erosion and burial of $POC_{biomass}$ [1,3].

[1] Galy *et al.* (2007) *Nature* **450,** 407-410. [2] Hilton *et al.* (2010) *Geochimica et Cosmochimica Acta* **74**, 3164-3181. [3] Hilton *et al.* (2008) *Nature Geoscience* **1**, 759-762.

https://doi.org/10.1180/S0026461X00008434 Published online by Cambridge University Press

Stable calcium isotope fractionation in basaltic catchments (Iceland)

R. S. HINDSHAW[1,2*], B. C. REYNOLDS[1], K. W. BURTON[3] AND B. BOURDON[4]

[1]IGP, ETH Zurich, Zurich, Switzerland, ruth.hindshaw@ngu.no (* presenting author)
[2]NGU, Trondheim, Norway
[3]Durham University, Durham, UK
[4]LGL, ENS Lyon, CNRS and UCBL, Lyon, France

Calcium (Ca) isotope studies of river water have potential to reveal information about biogeochemical processes affecting calcium, one of the most abundant elements in the Earth's crust. In this study, river water samples were taken from twenty-five different rivers draining basaltic lithology in Iceland. Previous studies in this region have shown that 1) calcium containing secondary phases are prevalent in these catchments [1] and 2) there are clear differences in weathering regime between different parts of the island [e.g. 2]. The aim of this study was to investigate whether the aforementioned factors would impact on the calcium isotopic composition of river water, and thus help develop the use of Ca isotopes as a viable tracer of catchment scale biogeochemical processes.

Calcium isotopic compositions were measured by TIMS, after chemical purification, using a ^{43}Ca-^{46}Ca double-spike. The measured water samples span a range of 0.22‰ in $\delta^{44/42}$Ca (0.45‰ – 0.67 ‰), with rivers draining glaciated catchments tending to have higher $\delta^{44/42}$Ca values than rivers unaffected by present-day glaciation. An ice-melt sample, representing precipitation inputs, and a hydrothermal sample were also measured.

The Ca isotopic composition of river water samples draining un-glaciated catchments was consistent with a mixture of the basaltic rock isotopic composition ($\delta^{44/42}$Ca = 0.41‰) and precipitation, which is characterised by a seawater Ca isotopic composition ($\delta^{44/42}$Ca = 0.95‰). Mixing between rock and precipitation sources for divalent cations was corroborated by radiogenic strontium measurements.

Calcium isotopic compositions from rivers draining glaciated catchments could not be explained by mixing of known sources and it is probable that isotope fractionation processes affect the Ca isotopic compositions of these rivers. The water samples from the presently glaciated samples fitted a simple Rayleigh distillation model, consistent with isotope fractionation during the removal of Ca from the dissolved phase by the formation of secondary minerals.

This study demonstrates that in Iceland 1) differences in riverine Ca isotopic values may simply reflect differences in precipitation volume and 2) glaciation significantly affects the weathering regime, resulting in different controls on Ca isotopic compositions, as compared to unglaciated terrain.

[1] Crovisier *et al.* (1992) *Appl. Geochem.,* **Suppl. Issue No. 1**, 55-81. [2] Georg *et al.* (2007) *Earth Planet. Sci. Lett.*, **261**, 476-490.

Interaction of Fe(II) with phosphate and sulfate on iron oxide surfaces: Implications for interfacial electron transfer

MARGARET ANNE G. HINKLE[1*] AND JEFFREY G. CATALANO[1]

[1]Washington University in St. Louis, Earth and Planetary Sciences, St. Louis, USA, (*correspondence: mhinkle@eps.wustl.edu)

Adsorption and coprecipitation reactions on iron oxide surfaces exert considerable controls on trace element and oxoanion concentrations in soil and aquatic environments [1]. Biogeochemical cycling of iron by microorganisms, involving the reductive dissolution and oxidative precipitation of iron oxides, activates interfacial electron transfer and atom exchange (ET-AE) reactions between aqueous Fe(II) and solid Fe(III) oxide minerals, causing mineral recrystallization [2,3]. This dynamic recrystallization of iron oxide minerals causes the incorporation of divalent metal adsorbates into the mineral and the release of preincorporated divalent metal ions to solution [4,5]. However, the effect of ET-AE reactions on the behavior of structurally incompatible oxoanions is not well understood. Recent research has shown that Fe(II) does not signficantly affect arsenate adsorption mechanisms, yet Fe(II) adsorption is suppressed in the presence of arsenate through competative adsorption processes [6]. This indicates that oxoanion adsorption can affect as well as be affected by ET-AE interactions between aqueous Fe(II) and Fe(III) oxides.

Here we consider the effect of aqueous Fe(II) on phosphate and sulfate adsorption onto hematite and goethite, and the effect of phosphate and sulfate on Fe(II) adsorption. We observe that the pH dependent adsorption of Fe(II) onto hematite and goethite slightly increases in the presence of phosphate and sulfate. The effect of phosphate and sulfate on Fe(II) adsorption, probed by metal release from doped iron oxides reacted with Fe(II) and oxoanions, will also be presented. We find that sulfate and phosphate adsorption also increases with the addition of Fe(II). If the observed adsorption behavior is the result of electrostatic effects, ET-AE reactions may be promoted. However, if the behavior is due to ternary complexation then ET-AE reactions may be suppressed because such complexes may stabilize adsorbed Fe(II) or inhibit electron transfer to the surface. The effect of Fe(II) on oxoanion adsorption mechanisms, determined by ATR-FTIR spectroscopy, will also be discussed. This work will further clarify the interactions between iron oxide minerals and common aqueous species in regions with active biogeochemical iron cycling.

[1] Brown & Parks (2001) *Int Geol Rev* **43**, 963-1073. [2] Handler *et al.* (2009) *Environ Sci Technol* **43**, 1102-1107. [3] Yanina & Rosso (2008) *Science* **320**, 218-222. [4] Frierdich & Catalano (2012) *Environ Sci Technol* doi: 10.1021/es203272z. [5] Frierdich, Luo & Catalano (2011) *Geology* **39**, 1083-1086. [6] Catalano, Luo & Otemuyiwa (2011) *Environ Scie Technol* **45**, 8826-8833.

https://doi.org/10.1180/S0026461X00008434 Published online by Cambridge University Press

New results from metamorphic nucleation experiments

DAVID M. HIRSCH[1*], CRAIG E. MANNING[2]

[1]Western Washington University, Bellingham, WA USA, hirschd@geol.wwu.edu (* presenting author)

[2]University of California Los Angeles, Los Angeles, CA USA, manning@ess.ucla.edu

Introduction

The rates and mechanisms of metamorphic crystallization remain poorly understood despite decades of study. In particular, nucleation processes such as the relationship of nucleation rate to driving force have proven difficult to quantify. Nucleation theory predicts that the nucleation rate can be expressed as:

$$\frac{dN}{dt} = C_1 \exp\left(\frac{-C_2}{T\Delta G_{rxn}^2}\right) \quad (1)$$

where N is the number of nuclei per unit volume, T is the absolute temperature, ΔG_{rxn} is the Gibbs free energy of the chemical reaction, and C_1 and C_2 are constants, which can be related to other, less well-constrained properties of the system [1]. However, this theory has not been adquately tested against geological data.

Experimental Method

We have undertaken a experimental pilot project to model nucleation, focusing on the reaction An + Wo = Grs + Qtz from an initial assemblage An+Wo+Qtz. This reaction is simple enough to make the experiments tractable, yet retains key basic features of reactions studied by others working on crystallization kinetics: aluminous garnet is the nucleating phase and the reaction involves multiple reactants and products. In order to remove temperature as a variable, all experiments are performed at constant temperature (1100 °C), and nucleation is initiated by a change in pressure only (1.41-1.90 GPa). Stereological methods were used to determine 3D nucleation counts.

Results

The experiments successfully nucleated grossular in runs within its stability field. Nucleation rates are generally replicable from run to run. Our preliminary results show that there is a systematic relationship between nucleation rate and driving force. By fitting equation (1) to the data, values for the constants are estimated at C_1=8.9 x 10^6 and C_2=2.0 x 10^4 (Fig. 1). The results support the theoretical prediction of a sharp increase in nucleation rate with driving force.

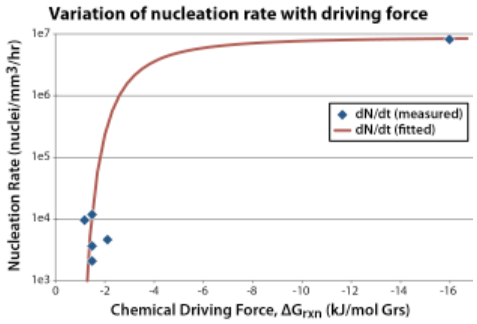

Figure 1: Nucleation rate as a function of thermodynamic driving force.

[1] Kelton, Greer, Thompson (1973) *J Chem. Phys.* **79**, 6261-6276.

Magma ocean influence on early atmosphere composition and mass

MARC M. HIRSCHMANN[1*] , HONGLUO ZHANG[1]

[1]Dept. Earth Sci. U. Minneosta Minneapolis, MN USA mmh@umn.edu (*presenting author)

The composition and mass of the atmosphere overlying early terrestrial magma oceans (MOs) likely had a key influence on Earth's early thermal and dynamical evolution, its geochemical differentiation, its path to an equable climate, and development of prebiotic chemistry. It also set the initial conditions for development of deep Earth volatile cycles. Key questions are how MO processes partitions volatiles between the atmosphere, mantle, and core and how reaction between the the MO and overlying vapor influences the composition of the nascent atmosphere.

The availability of Fe alloy in a MO creates reducing conditions, and the expectation that overlying atmospheres consist chiefly of H_2 and CO, but this may be incorrect if the mean depth of alloy-silicate equilibration is deep, if convection in the MO homogenizes Fe^{3+}/Fe^T throughout the magma column, and if the effect of decreased pressure on the chemical potentials of Fe^{2+} and Fe^{3+} in the magma increases relative f_{O2}. Low pressure data [1,2] suggest the opposite – decreases in Δf_{O2} on isochemical decompression – but Mössbauer spectroscopy of andesite glasses quenched from 1-6 GPa provisionally indicate that this relationship reverses at high pressure. Consequently, it is likely that the overlying atmosphere consisted chiefly of H_2O+CO_2, whilst reducing (~IW-1.5) conditions prevailed deep in the MO.

Owing to low solubility of C-species in reduced magma, virtually all of the available C in the MO and the atmosphere may be partitioned into alloy, leaving a virtually C- free mantle and exosphere. However, it is likely that the MO equilibrates with only a small fraction of metal (<5% **[3]** and possibly <1%). As the alloy cannot absorb ~ 8 wt.% C, excess reduced C may saturate as diamond. This too will greatly limit the partial pressure of CO_2 in the overlying atmosphere. Floatation of diamond in the MO **[4]** and could create the principle initial reservoir of C in the BSE.

Following or coinciding with segregation of metal (but not diamond) to the core, the Moon-forming impact resets the volatile distribution in the BSE: virtually all that did not escape ends up in a superheated atmosphere. On cooling, much of the remaining H_2O and some of the CO_2 redissolves in the MO. Upon MO crystallization, much of the H_2O and possibly nearly all the the C returns atmosphere. However, homogenization of Fe^{3+}/Fe^T in the MO should again produce a vertical f_{O2} gradient in the MO and the solubility of CO_2 diminishes by >10X on cooling from a MO adiabat to the peridotite solidus. Thus, precipitation of a C-rich phase (diamond, carbide, or alloy) during crystallization of this final MO is likely, setting up conditions for a MO carbon pump [5] that draws down much of the CO_2 in the atmosphere and deposits much of the BSE C in the mantle rather than the exosphere. This speculative, but plausible, scenario may produce a mantle with a high H/C ratio compared to the exposphere, as remains true at present [6].

[1] Kress&Carmichael (1991) *Contrib. Mineral. Petrol.* **108**, 82-92. [2] O'Neill et al. (2006) *Am. Mineral* **91**, 404-412.[3] Dahl & Stevenson (2010) *EPSL* **295** 177-186. [4] Suzuki et al. (1995) *Science* **269** 216-281. [5] Hirschmann (2011) ***42nd*** *LPSC Abstracts* #2321. [5] Hirschmann&Dasgupta (2009) *Chem. Geol*. **262** 4-16.

https://doi.org/10.1180/S0026461X00008434 Published online by Cambridge University Press

Diffusion in the deep Earth: Is it all about grain boundaries?

MATT HISCOCK[1]*, GEOFFREY BROMILEY[1] AND EIMF[2]

[1]Grant Institute of GeoSciences, University of Edinburgh, Edinburgh, UK, Matt.Hiscock@ed.ac.uk (* presenting author)
[2]Edinburgh Ion Microprobe Facility, University of Edinburgh, Edinburgh, UK, ionprobe@ed.ac.uk

We can consider two mechanisms by which diffusion can occur in Earth's deep interior: 1) through mineral lattices: lattice diffusion or 2) along the boundaries between grains: grain boundary diffusion. To date very little work has been conducted on grain boundary diffusion of volatiles under mantle conditions. Here we present recently acquired experimental data obtained using a novel method to determine grain boundary diffusion rates under mantle conditions, initially looking at hydrogen. The data is considered in terms of the mobility of hydrogen in the mantle and how an understanding of this can help to constrain the influence it has on bulk mantle properties. Preliminary results suggest that grain boundary diffusion rates may be of similar magnitude to diffusion through crystal structures, suggesting that very small diffusing species are indiscriminate towards their surroundings/host (mineral lattice versus grain boundary).

Further data is presented on a complimentary study of diffusion of titanium in quartz. Single crystal diffusion rates for Ti in quartz are very slow, potentially acting as a limiting factor for Ti abundance in crystallising quartz – with implications for the applicability of Ti in quartz thermometry.

Tuning the interactions of PNIPAM Gel Nanoparticles

REX P. HJELM*[1], LISE ARLETH[2], ZHIBING HU[3], JIANZHONG WU.[4]

[1]Los Alamos Neutron Science Center, Los Alamos National Laboratory, Los Alamos, New Mexico, 87544 USA, hjelm@lanl.gov.
[2]Department of Basic Sciences and Environment, University of Copenhagen, Frederiksberg, Denmark. lia@life.ku.dk
[3]Departments of Physics and Chemistry, University of North Texas, Denton, Texas, 76203, USA. zhibing@unt.edu
[4]Department of Chemical and Envronmental Engineering, University of California, Riverside, California, 92521, USA. Jianzhong.wu@ucr.edu

The presence of a lower critical solution temperature (LCST) at 33C in PNIPAM gels is well known. Above the LCST the gel in water collapses from a solvent swollen state. Previously, we syntesized and studied the properties of 5 nm PNIPAM gel nanoparticles [1]. The size of these particles allowed us to characterizae the ttemperature-dependent changes in the particle interactons using light scattering and small-angle neutron scattering (SANS) with the unanticipated result that the interactions go from highly repulsive to attractive as the temperature is increased above the LCST. The magnitude of the repulsive interaction was larger than that anticipated for hard sphere excluded volume effects.

With the aim of understanding the interaction potential of these PNIPAM gel nanoparticles and the relation to the LCST, we studied the concentration and temperature-dependent phase map, using SANS to probe the structures of the fluid, crystalline and glassy phases. Concentration is used to explore the distance dependency of the interaction potential, while temperature is used to tune this potential through the repulsive to attractive states. The overall goal of this work is to understand the underlying phaysics of these and like materials for the development of environmentally responsive systems.

[1] Arleth, L., Xia, X., Hjelm, R.P. Hu, Z. and Wu, J. (2005) *J. Polym. Sci. B: Polym. Phys.*, **43**, 849-860.

https://doi.org/10.1180/S0026461X00008434 Published online by Cambridge University Press

Stable carbon and nitrogen isotopic variations in latest Pleistocene to Holocene organic matter from Lake Ontario, Canada

RYAN HLADYNIUK[1*] AND FRED J. LONGSTAFFE[1]

[1]The University of Western Ontario, London, Canada, rhladyni@uwo.ca (* presenting author), flongsta@uwo.ca

We have examined the variations in organic carbon (OC) and nitrogen (TN) contents, C/N ratios (7-10) and stable carbon and nitrogen isotopic compositions of bulk organic matter (OM) from Lake Ontario (the easternmost Great Lake) since 12.3 ka BP. Samples were obtained from three piston cores that contain sediments from each of Lake Ontario's major sub-basins. These data indicate low primary productivity during glacial times (12.3-10.8 ka BP), consistent with the cold and dry period proposed for this region by Lewis et al. (2008) [1]. That said, the carbon isotopic compositions of OM in glacial sediments display different upward variations in cores from west to east across the Lake Ontario sub-basins: Niagara sub-basin (west), an increase from -29 to -27 per mil (VPDB); Mississauga sub-basin (central), a decrease from -27 to -28.5 per mil (VPDB); Rochester sub-basin (east), an increase from -28 to -27 per mil (VPDB). These differences likely arise from greater contributions of terrestrial OM both in the west and the east as glacial meltwater entered the lake via the Niagara River (west) and directly from the Laurentide Ice Sheet (east). A short-lived influx of glacial meltwater from 10.8-10.5 ka BP is indicated by increased mass accumulation rates (MARs) during this interval of time. Upon cessation of glacial meltwater supply at 10.5 ka BP, the carbon-isotope composition of Lake Ontario OM decreased to -29.5 per mil across the basin. With hydraulic closure of Lake Ontario during the early Holocene, rising lacustrine productivity is indicated by progressively increasing OC and TN concentrations and OM carbon- and nitrogen-isotope compositions. Return of upper Great Lakes water to Lake Ontario during the region's Nipissing Rise at 5.0 ka BP correlates well with a temporary lowering of primary productivity in Lake Ontario. This decrease is followed shortly thereafter by a return to increasing OC, TN and OM carbon- and nitrogen-isotope compositions as modern Lake Ontario emerged. This history of lacustrine productivity for Lake Ontario is similar to that reported for Lake Superior [2], the deepest and largest of the Laurentian Great Lakes. Such comparisons may facilitate future regional synthesis of primary productivity in the Great Lakes during their changing histories from the latest Pleistocene to the present.

[1] Lewis et al. (2008) *EOS* **89**, 541-542. [2] Hyodo and Longstaffe (2011) *Quaternary Science Reviews* **30**, 2988-3000.

Mineralogical and Geochemical Investigation of Tungsten in natural environments: An Emerging Contaminant

CHAD HOBSON[1*], TAHMINEH JADE MOHAJERIN[2], , KAREN JOHANNESSON[2], KATHERINE TELFEYAN[2], RYAN TAPPERO[3] SAUGATA DATTA[1],

[1]Kansas State University, Manhattan, US, chobson@ksu.edu (* presenting author), sdatta@ksu.edu

[2]Tulane University , New Orleans, US,

[3]NSLS Brookhaven National Lab, New York, US

W is one of the most widely used and poorly understood elements today [1][2]. A lack of knowledge about its biogeochemistry coupled with its unique and advantageous properties have led to an explosion of W based products for domestic, military, and ind ustrial applications [1]. Recently W has come under scrutiny following a CDC investigation of a leukemia cluster in Fallon, Nevada which implicated high levels of W in the drinking water as a probable cause [1][2]. Besides W's potential health hazards, recent studies have shown that the WO_4^{2-} oxyanion is soluble in water, capable of moving through soils. Also, dissolution of W metal leads to decreases in bacterial biomass in soils and increases in fungal biomass, also having adverse effects on plant life [2][3][4].

The hypothesis to be tested is that the physical and chemical changes from chemical weathering, mineral dissolution and precipitation, and/or redox reactions catalyzed by microbial activity control W transport and sequestration. These parameters control W by means of adsorptive/desorptive reactions, reductive/oxidative mineral dissolution or aqueous complexation with sulfide. Three sites have been chosen for geochemical and mineralogical analysis; two sites of high W concentrations (Fallon and Hoisington, KS) and one site of low concentration (Carrizo aquifer, Texas). Surface samples from within the town of Fallon and in-lake sediments from Cheyenne Bottoms Refuge in Hoisington have both shown high levels of W. The first step used in understanding the W-sediment association is x-ray microprobe aided speciation and bulk XANES, utilizing synchrotron radiation. This is done with μXRF mapping accompanied by μXANES and μXRD on mineral/sediment grains and also elucidates the association of W with other elements (Ca, Fe, Mn, Fe, As, Cu, Mo, Ti, Zn). Sediment samples from Fallon were analyzed for bulk W speciation, and the data showed predominately W-VI, though the presence of minor shoulders in the spectra may indicate the presence of other species. The μXRF map revealed that the highest density of W hotspots was in samples nearest the hard-metal facility, and good correlations were found with Fe. Sequential extractions are also being done to understand the partitioning of sediment fractions and preference of W to bind with variuos fractions.

[1] Koutsospyros, Braida, Christodoulatos, Dermatas, Strigul (2006) *J. Hazard. Mat.* **136**, 1-19. [2] Strigul, Koutsospyros, Arienti, Christodoulatos, Dermatas, Braida (2005) *Chemo* **61**, 248-258. [3] Johnson, Inouye, Bednar, Clarke, Winfield, Boyd, Ang, Goss (2009) *Land Cont. & Reclam.* **17**, 141-151. [4] Ringelberg, Reynolds, Winfield, Inouye, Johnson, Bednar (2009) *J. Environ. Qual.* **38**, 103-11

https://doi.org/10.1180/S0026461X00008434 Published online by Cambridge University Press

Weathering phenomena involving mineral nanoparticles, one of the last unexplored geochemical components in soils and sediments: A tribute to Art White

MICHAEL F. HOCHELLA, JR.

Department of Geosciences, Virginia Tech, Blacksburg, VA, USA, hochella@vt.edu.

Art White has made a difference in how we understand Earth. He has been a geochemist in the mold of Victor Goldschmidt in terms of a lifetime of deeply insightful thinking, and in Art's case, he has been a masterful unraveler of the critical zone. Remarkably, some of his experiments have lasted more than a decade. He is one of the best in the world at interpreting soil chronosequences, and is also a world authority on linking field- vs. laboratory-based weathering rates. In my career, he was the first to convince me that seemingly hopelessy complicated Earth systems could be untangled and in fact understood.

Recently, we have realized that the field of nanoscience is important in weathering phenomena. Worldwide, soils blanketing the continents contain an estimated 10^7 to 10^8 terragrams (Tg = one million metric tons) of mineral nanoparticles, with roughly 10^3 to 10^4 Tg being transported to the continental margins annually via rivers. Nanoscience comes into play because experimental and theoretical evidence suggests that dissolution rate is a function of particle size in the nanoscale. Although quite difficult to measure, to date accelerated dissolution rates are associated with smaller nanoparticle sizes for silica, iron oxides/hydroxides, titanium dioxide, zinc oxide, and lead sulfide, and nanothin clay edges dissolve much faster than basel surfaces. However, this is not the case for all minerals. Calcium phosphate minerals, in particular, may experience a dramatic retardation of dissolution rates at the nanoscale relative to larger crystals. This may be because there is a critical particle radius required for the formation of etch pits on these phosphates.

More recently, it has been clearly verified that there are other factors besides size that dramatically affect the dissolution rates of mineral nanoparticles. For example, the exact aggregation state is key: in tightly aggregated clusters, where water is reduced to nanofilms that we can now directly observe, dissolution rates can be reduced by orders of magnitude, essentially quenching the overall reaction per surface area available. In other words, even the fluids in this case are presenting dramatically different properties than in the bulk state, again the hallmark of nanoscience. Examples of mineral nanoparticles where this has been shown include goethtite, lead sulfide, and zinc oxide. In addition, we have recently shown that nanotubular voids that intersect the surface of hematite nanoparticles act as highly reactive sites for reductive dissolution driven by organic acids. So again, acceleation and inhibition of dissolution can be dramatically manifested in different nanofeatures of nanoparticles.

Such minute phenomena can have global consequences. For example, it has recently been realized that phytoplankton (key to CO_2 drawdown from the atmosphere) can acquire one of its vital limiting nutrients, iron, from iron oxide nanoparticles in the oceans that have been shed from the continents. This depends on iron oxide dissolution controlled by some of the factors described above.

Using pore-scale simulations to better quantify mixing and mass transformation in upscaled models

DAVID L. HOCHSTETLER[1*], MASSIMO ROLLE[1,2], PETER K. KITANIDIS[1]

[1]Department of Civil and Environmental Engineering, Stanford University, Stanford, CA , USA

[2]Center for Applied Geosciences, University of Tübingen, Tübingen, Germany

*(presenting author: dhochste@stanford.edu)

We perform pore-scale simulations of different transport scenarios in order to analyze irreversible bimolecular reactive transport with the objectives of: i) finding an empirical relationship that describes the effective kinetic rate constants in upscaled (Darcy scale) models; ii) determining the appropriateness of using intrinsic kinetic rate constants in upscaled models; iii) enhancing understanding of how compound-specific diffusivites affect mass transformation of reactive solutes at the pore-scale; and iv) quantifying the importance of accounting for compound-dependent mixing properties in predicting plume lengths and mass transformation at the Darcy scale. We evaluated transient displacement problems with a range of intrinsic kinetic rates as well as steady-state reactive plumes with a range of flow rates and "fast" and "slow" kinetics.

The results show that an empirical relationship can relate the ratio of the effective rate constant over the intrinsic rate constant to the inverse of the Damköhler; this is similar to what has been found for 1st-order [1] and biofilm [2] reactions. Furthermore, increasing Da does increase the amount of reactant segregation [3] but does not necessarily significantly increase mass overprediction because the reactant transformation may be mostly mixing limited. Thus, using an intrinsic rate constant in an upscaled model resulted in only about 10% overprediction of product mass for our problem set-up [4]. For the steady-state problems, we compare the adequacy of using the traditional linear parameterization for transverse dispersion to using a non-linear compound-specific parameterization [5] to predict reactive transport at the Darcy scale. We quantify the differences for product mass and plume lengths between the pore-scale results and the upscaled predictions using the linear and non-linear transverse dispersion coefficients.

[1] Dykaar and Kitanidis (1996) *Water Resour. Res.* **32**, 307-320.
[2] Wood et al. (2007) *Adv. Water Resourc.* **30**, 1630-1647.
[3] Kapoor et al. (1997) *Water Resourc. Res.* **33**, 527-536.
[4] Hochstetler and Kitanidis. (2012) (submitted).
[5] Rolle et al. (2012) *Transp. Porous Media* (in press).

https://doi.org/10.1180/S0026461X00008434 Published online by Cambridge University Press

When iron and silver nanoparticles meet natural organic matter: Probing NP-NOM interactions with molecular spectroscopy and quartz crystal microgravimetry

W.C. HOCKADAY[1*] AND B.L.T. LAU[2]

[1*] Baylor Univ., Waco TX 76706 (william_hockaday@baylor.edu)
[2] Baylor Univ., Waco TX 76706 (boris_lau@baylor.edu)

As natural organic matter (NOM) is ubiquitous in natural waters and known to complex with nanoparticle (NP) surfaces, it is important to study NP-NOM dynamics to better understand the fate and transport of NPs. This work combines molecular spectroscopy and quartz crystal microgravimetry (QCM) to determine the mechanisms and kinetics of NOM interaction with the surfaces of NP and silica. Hematite NPs (FeNPs) and silver NPs (AgNPs) were used to represent natural and engineered NPs in this study.

The identity and affinity of NOM on NP surfaces can affect the way NPs behave in aquatic systems. ^{1}H NMR and Raman spectroscopy were used to identify the reactive organic functional groups in Suwanee River NOM and probe the mechanism of covalent and non-covalent bonding. FeNPs was observed to expedite the spin-lattice relaxation time (T_1) of aromatic and heteroatom-substituted aliphatic groups, which suggests a decrease in molecular motion (intra- and inter-molecular) upon interaction with the NPs. Raman spectroscopy was used to probe the interatctions of NOM with AgNPs having a polyvinyl pyrrolidone (PVP) capping agent. Raman spectroscopy suggested that O-substituted alkyl groups in the NOM interacts with both the polyvinyl domain of (PVP) and the oxygen atom of the PVP-capped AgNPs. These spectroscopy results have important implications for the fate of NPs in aqueous suspensions, as NOM may change the stability of NPs.

While NP's interactions with "free" NOM in the bulk solution is critical in predicting their mobility, NP's associations with "immobilized" NOM on mineral or other environmental surfaces are equally important in controlling their transport in natural waters. With high sensitivity (ng/cm^2) to quantify mass deposition on substrate surfaces, QCM was used as a tool in determining the extent and kinetics of NP adsorption in real-time. Preliminary QCM experiments revealed observable differences in the adsorption dynamics of FeNPs and AgNPs on silica substrate when NOM is coated on either the particle surface or substrate surface or both. For example, at pH 6, deposition of FeNPs on silica substrate was found to be at least two order of magnitude slower in the presence of NOM. QCM results also suggested that humic and fulvic fractions of the NOM exert differing degrees of influence on the adsorption of AgNPs.

Mobility of antimony in soils under changing redox conditions

KERSTIN HOCKMANN[1*], SUSAN TANDY[1], MARKUS LENZ[2,3] AND RAINER SCHULIN[1]

[1]Institute of Terrestrial Ecosystems, ETH Zurich, Switzerland, kerstin.hockmann@env.ethz.ch (* presenting author)
[2] University of Applied Sciences and Arts Northwestern Switzerland (FHNW), Institute for Ecopreneurship
[3] Wageningen University, Sub-Department of Environmental Technology, The Netherlands

Human activities have led to highly elevated antimony (Sb) concentrations in many soils and, consequently, to increased exposure of biota to this toxic element. Knowledge about the risks of Sb leaching from such soils is, however, very limited.

A key factor regarding the mobility of Sb in soils is the water regime. Many soils are subject to permanent or periodic water-logging. Under aerobic conditions, Sb is stable as the pentavalent $Sb(OH)_6^-$ in soil solution. Under reducing conditions, the trivalent $Sb(OH)_3$ becomes dominant [1]. Both species strongly differ in their affinity to iron (Fe) and manganese (Mn) (hydr)oxides. The interplay of Sb redox transformations, differential sorption and reductive dissolution of Mn and Fe (hydr)oxides during water-logging and its effect on Sb mobility has received little attention though.

Here, we investigated changes in Sb speciation and solubility over a reduction-reoxidation period in Sb-contaminated shooting range soil (pH 7.8). Lactate was used as carbon source to stimulate microbial activity. Antimony(V) concentrations strongly decreased with the development of reducing conditions (Figure 1), while dissolved Sb(III) concentrations remained low. During further reduction, soluble Sb(III) increased together with dissolved Fe(II) concentrations. Reoxidation of the soil batches caused Sb(III) to decrease and soluble Sb(V) to increase again.

The results indicate that water logging conditions at first led to the immobilization of Sb by reduction of Sb(V) to Sb(III), since the latter has a higher binding affinity to metal hydroxides. When reducing conditions continued, the previously bound Sb(III) was released into the solution again due to reductive dissolution of the (hydr)oxides, resulting in increased mobility.

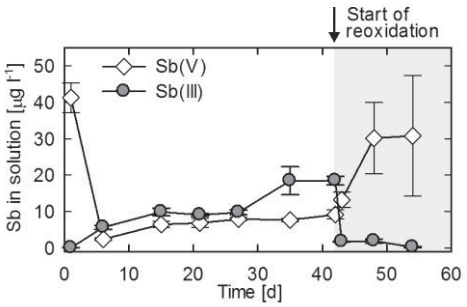

Figure 1: Antimony(III) and Sb(V) concentrations during varying redox conditions. Error bars are the standard deviation of triplicates.

[1] Filella, Belzile & Chen (2002) *Earth-Sci. Rev.* **57**, 125 - 176.

https://doi.org/10.1180/S0026461X00008434 Published online by Cambridge University Press

Direct infusion lipidomics: profiling the oil sands microbiome

P. HODGSON*, B. E. MCCARRY

McMaster University, Chemistry and Chemical Biology
hodgspa@mcmaster.ca, (* presenting author),
mccarry@mcmaster.ca

Introduction

Oil sands processing recycles large quantites of water from settling ponds employed to settle out the fine particulate matter end products of bitumen extraction. Settling pond characterization has indicated vibrant microbial communities and thus there is a strong likelihood that at least some portion of this community is present in process water; where their impacts on extraction efficiency and/or settling pond water quality remain unknown. We are applying a comprehensive bacterial lipid profiling method previously developed [1,2] to characterize the bacterial community associated with process water collected prior to discharge into the settling pond in an effort to identify possible microbially linked strategies for improved management and process efficiencies.

Results

Process water samples were treated with organic solvents to extract the non-polar constituents, using a developed method [1,2] capable of detecting profiles of eight lipid classes using direct infusion electrospray mass spectroscopy in a triple quadrupole mass spectrometer. The profiles of individual lipid classes were obtained by infusion of a $CHCl_3$:MeOH solution of the process water extract in the presence of 4mM LiCl; each lipid class is detected using tandem mass spectrometry with a neutral mass loss specific to each phospholipid class. For example, phosphatidylethanolamines (PE) undergo a neutral loss of 147 mass units while phosphatidylcholines lose 189 mass units. The presence of lithium chloride not only affords more intense neutral losses but also simplifies the mass spectrum by affording a single metal ion (Li^+) adduct. By using phospholipid standards it is possible to quantify the intact lipid components in the extracts. This work is being undertaken in concert with phospholipid fatty acid (PLFA) analyses. Results indicate microbial lipids in the process water sample. Phospholipid profiles of this microbial community will be presented.

References

[1] Basconcillo *et al.* (2009) J. Lipid Res., **50,** 1120-1132
[2] Basconcillo *et al.* (2009) J. Chromatogr. B: Anal. Technol. Biomed. Life Sci., **877,** 2873-2882

^{10}Be Basin averaged erosion rates from the Cordillera Blanca, Peru: a record of interacting climate and tectonics.

KEITH HODSON[1*], SARAH HALL[2], MELANIE MICHALAK[3], DANIEL FARBER[4], AND JEREMY HOURIGAN[5]

[1]McGill University, Montreal, Canada, keith.hodson@mail.mcgill.ca (* presenting author)
[2]McGill University, Montreal, Canada, sarah.hall@mcgill.ca
[3]University of California, Santa Cruz, USA, melanie@ucsc.edu
[4]University of California, Santa Cruz, USA, farber2@mac.com
[5]University of California, Santa Cruz, USA, jhourigan@es.ucsc.edu

Overview

Current numerical and analog models predict discrete interactions and feedbacks between tectonic deformation and climate-driven denudation [1]. To test the applicability of these models, we utilize cosmogenic radionuclides (CRN) to quantify basin-scale erosion rates in the Cordillera Blanca Mountain Range (CB) of Northern Peru [2]. The range is an actively deforming, NNW trending massif running from ~8-10°S. The CB is closely associated with pronounced extension along the Cordillera Blanca Detachment Fault (CBDF) that delineates the western margin of the grano-tonalitic batholith. The ~200 km long, NNW trending CBDF accommodates significant crustal scale extension in the heart of the dominantly contractile Andean Orogen [3]. Previous thermochronologic and CRN based studies have outlined the potential for linkages between patterns of long-term (Ma) exhumation/uplift and short-term (ka) rates of fault slip [4,5]. Exhumation data, while sparsely dispributed, suggest elevated rates of uplift from ~4-6 Ma in the central portion of the range relative to the flanks (~0.5 km Ma^{-1} and ~0.2 km Ma^{-1}, respectively). More recent exhumation rates spanning ~2-4 Ma suggest a unform ~0.5 km Ma^{-1} along the entire range. Spatial trends in CRN-based fault slip rates are reminescent of those from 4-6 Ma exhumation rates, and decrease dramatically by an order of magnitude towards the south. Our new CRN dataset fills a crucial gap in the development history of the range, representing landscape modification on the order of 10^3 to 10^5 years in response to both tectonic and climatic variations within the batholith.

Results and Conclusion

Preliminary calculated erosion rates range from 0.0096 to 4.1 mm yr^{-1}. Highest erosion rates are located near the center of the range, correlating with the highest peak elevations and the highest degrees of glacial cover. Spatial patterns follow those of 4-6 Ma exhumation rates and CRN fault slip rates, suggesting a long-lived, tectonic control on range development. Erosion and uplift are likely encanced in basins with higher degrees of glaciation due to isostatic responses to glacial erosion.

[1] Whipple (2009) *Nat. Geosci.* **2**, DOI:10.1038. [2] von Blanckenburg (2005) *Earth Plan. Sci. Let.* **237**, 462-479. [3] McNulty (2002) *Geology* **30**, 567-570. [4] Giovanni (2007) *Ph.D. Thesis, Univ. CA, Los Angeles.* [5] Farber, *in preparation.*

https://doi.org/10.1180/S0026461X00008434 Published online by Cambridge University Press

Organic matter and Fe oxide coatings reduce the relevance of laboratory rates to mineral dissolution in soil

SAMUEL A. PARRY[1], MARK E. HODSON[1*], SIMON J. KEMP[2], ERIC H. OELKERS[3]

[1]University of Reading, Reading, UK, s.a.parry@pgr.reading.ac.uk, m.e.hodson@reading.ac.uk (* presenting author)
[2]British Geological Survey, Keyworth, UK, sjk@bgs.ac.uk
[3]GET-OMP, Toulouse, France, oelkers@ltmg.obs-mip.fr

The minerals present in a soil and the reactive surface area of those minerals are key factors in determining element release rates from soils due to mineral dissolution. This study examines the contribution and influence of the relatively un-reactive soil organic matter (SOM) and amorphous and free Fe oxide phases to soil surface area and element release from the dissolution of primary silicate minerals within two podzol soil profiles. Soils were sampled systematically with depth (using a coarse-stepped continuous strategy) from granitic podzols directly overlying bedrock in Dartmoor and Glen Dye, UK. The geometric and BET specific surface area and porosity of bulk soil samples were calculated and measured prior to and following the removal of SOM and amorphous and free Fe oxide phases. Batch and flow through dissolution experiments were then performed on the different sample sets.

Bulk soil surface area and porosity decreased overall from the base of the soil profiles to the soil surface, largely due to the loss of relatively reactive primary minerals up the soil profiles and an associated increase in the proportion of residual quartz, the quartz dilution effect [1]. Superimposed over these variations were the contributions and influences of the SOM and amorphous and free Fe oxide phases on soil surface area. SOM aggregated and coated soil mineral grains, increasing the effective diameter of the mineral grains and occluding underlying mineral surfaces and porosity, thus reducing bulk soil surface area. Amorphous and free Fe oxide phases contributed to soil surface area as discrete fine particles and architecturally elaborate and porous surface coatings. They were also present as aggregate binding agents and smooth surface coatings (amorphous only) that occluded mineral surfaces and reduced soil surface area. Podzolisation translocated the SOM, amorphous and free Fe oxide phases down the soil profile and in doing so redistributed un-reactive mineral surface area and porosity between the eluvial and illuvial horizons. This exacerbated the quartz dilution effect between these horizons and resulted in a relative peak in bulk soil surface area in the illuvial horizon.

The presence of SOM, amorphous and free Fe oxide phases typically reduced bulk soil Si release rates through the contribution of unreactive surface area and/or the occlusion of underlying reactive mineral surface area. The exception was the contribution of biogenic silica to reactive soil surface area and Si release rates in the upper soil profile. As a result, pristine mineral laboratory dissolution studies do not account for the influence of SOM, amorphous and free Fe oxide phases reactive surface area in the field environment and thus the derived dissolution rates are not representative of aggregated and coated field grains.

[1] Bern (2009) *Applied Geochemistry* **24**, 1429-1437.

Geochemical Zonation of Mantle Plumes: Lower Mantle Chemical Heterogeneity and Plume Splitting

KAJ HOERNLE [1*], JOANA DEPPE[1], FOLKMAR HAUFF[1], REINHARD WERNER[1], JASON PHIPPS MORGAN[2]

[1] GEOMAR Helmholtz Centre for Ocean Research Kiel, Germany (* presenting author khoernle@geomar.de)
[2] Cornell University, Ithaca, NY, U.S.A.

The geochemistry of basalts from single hotspot tracks contains important clues about the compositional heterogeneity of the Earth's mantle. Increasingly spatial chemical zoning has been recognized as a long-term feature (up to 80 Ma) of hotspot tracks, including the Galapagos [1,2], Hawaii [3,4], Marquesas, Somoa [5] and Tristan-Gough [6] hotspot tracks. It is argued that geochemical zonation of hotspot tracks reflect lateral zonation in the plume stem in the form of stripes or filaments that ultimately reflect tapping of different geochemical reservoirs in the plume source [1,4-9]. An important question is what plume zonation tells us about the plume source in the lower mantle. Seismic tomographic studies show the existence of two large seismic low-velocity anomalies in the lower mantle beneath the southern Pacific and beneath southern and western Africa [e.g.10]. It has been proposed that the zoned plumes are related to the margins of these large-scale low-velocity anomalies and that the orientation of the zoning can provide information about the chemical composition of these lower mantle seismic anomalies [4,5,6]. The talk will discuss problems with this model and how these problems might be resolved. The talk will also explore other implications of zoned plumes, for example, if plume zonation can led to the breakup/splitting of the plume conduit or alternatively if plume-splitting allows us to identify chemical zonation in plumes.

[1] Hoernle et al. (2000) Geology 28: 435-438. [2] Werner et al. (2003) G^3 4(12), 1108. [3] Abouchami et al. Nature 434: 851-856 (2005). [4] Weis et al. (2011) NGS 4(12): 831-838. [5] Huang et al. (2011) NGS 4(12): 874-878. [6] Deppe et al. (in revision) NGS. [7] Farnetani & Samuel (2005) GRL 32, L07311. [8] Lohmann et al. (2009) EPSL 284: 553-563. [9] Farnetani & Hofmann (2009) EPSL 282: 314-322. [10] Ritsema et al. (2011) GJI 184: 1223-1236.

https://doi.org/10.1180/S0026461X00008434 Published online by Cambridge University Press

Building Eoarchean crust: the arc tholeiite – TTG connection

J. Elis Hoffmann[1,2*], Carsten Münker[1], Thorsten J. Nagel[2], Tomas Næraa[3,4], Ali Polat[5] and Minik T. Rosing[4]

[1] Institut für Geologie und Mineralogie, Universität zu Köln, Germany (hoffjoel@uni-bonn.de)
[2] Steinmann-Institut, Abt. Endogene Prozesse, Universität Bonn
[3] Geological Survey of Denmark and Greenland, Copenhagen, DK
[4] Nordic Center for Earth Evolution (NORDCEE), Natural history museum of Denmark , DK
[5] University of Windsor, Ontario, Canada

A pertinent issue in Archean research is the genetic relation between the TTG suite and the associated mafic supercrustals. Here we present a coherent model for the geodynamic evolution of the oldest (3.65 to 3.85 Ga) continental crust in southern West Greenland. Within the Isua Supracrustals, tholeiitic and boninite-like metabasalts dominate the sequence, both displaying trace element patterns consistent with a subduction-related origin. This is well demonstrated by correlated trace element variations in Nb/Th, La/Yb, Gd/Yb, Zr/Nb in Isua tholeiites [1]. Boninite-like rocks in Isua are derived from ultradepleted sources with εHf(3720) of up to ca. +12.9 [2], providing for the first time Hf-isotope evidence from the mafic rock record for the preservation of depleted Hadean mantle domains.

Petrological phase equilibria and trace element modeling suggest a close relationship between Isua arc tholeiites and the TTGs [3,4]. Notably, Hf-Nd isotope signatures between the two lithologies overlap in both showing the characteristic decoupling of initial Hf-Nd isotope compositions. Systematically elevated ^{142}Nd anomalies of tholeiites and TTGs [5] are also in agreement with a related origin. The decoupled Hf-Nd signature is likely an inherited feature from melting of the tholeiites. This is also underlined by new Hf and O in zircon data from Eoarchean TTGs [6] that indicate melting of a thickened mafic crust to form the TTGs. We therefore propose an arc-arc collisional setting, where the TTGs formed by polybaric melting of arc tholeiites at 10-20% of partial melting.

The cause for the decoupling of the Hf and Nd isotope systems is most likely a subduction-related mantle source overprint. Cumulate segregation processes in an early magma ocean or an early metamorphic overprint during intrusion of the TTGs might be alternative scenarios, but they cannot account for all trace element characteristics found in mafic rocks from the Isua region [1].

[1] Hoffmann, J.E. et al. (2011a) *GCA* **75**, 6610-6628. [2] Hoffmann, J.E. et al. (2010) *GCA* **74**, 7236–7260. [3] Nagel et al. (2012) *Geology* doi:10.1130/G32729.1. [4] Hoffmann, J.E. et al. (2011b) *GCA* **75**, 6610-6628. [5] Caro et al. (2006) GCA **70**, 164–191. [6] Næraa, T. et al. (submitted).

Holocene intermediate water circulation at the Carolina Slope from sedimentary ^{231}Pa/^{230}Th

Sharon S. Hoffmann [1*], Jerry F. McManus[1]

[1]Lamont-Doherty Earth Observatory of Columbia University, Palisades, NY, USA, sharonh@ldeo.columbia.edu (* presenting author), jmcmanus@ldeo.columbia.edu

Meridional overturning circulation (MOC) may play a crucial role in global climate change both at Milankovich and abrupt timescales, making it an important target for paleoceanographic study. Measured ratios of ^{231}Pa/^{230}Th in sediment cores are sensitive to deep and intermediate water residence times, and may provide a dynamical tracer of past MOC strength in the waters overlying core sites. We will present a new ^{231}Pa/^{230}Th record from core KN140-2-51GGC on the Carolina continental slope at 1790 m. This core has an expanded Holocene section [1], allowing for detailed examination of circulation during the 8.2 ka event, resumption of Labrador Sea Water Production, mid-Holocene climate optimum, and cooler late Holocene.

Previous records of Holocene ^{231}Pa/^{230}Th at intermediate depths show no net ^{231}Pa transport [2] (sedimentary ratios at the seawater production ratio of 0.093) or a transition from low ratios in the erly Holocene to production-ratio levels in the mid-to-late Holocene [3]. Sedimentary ratios similar to the production ratio may suggest sluggish MOC in intermediate water in the eastern and central Atlantic. Our results indicate that sedimentary ratios at the Carolina slope remained below the ^{231}Pa/^{230}Th production ratio in seawater throughout the Holocene. These ratios, falling between 0.08 and 0.07 in the earliest Holocene and between 0.07 and 0.06 through the remainder of the Holocene, indicate export of ^{231}Pa, possibly through vigorous ventilation at intermediate depths. This discrepancy between our record and published sites may point to influence of Labrador Sea Water, or the influence of the deep western boundary current along the North American continental slope, at our site. Sediment composition analyses, particularly biogenic opal content, will allow for better constraints on the influence of particle type on ^{231}Pa scavenging at this site. ^{231}Pa/^{230}Th results will be compared to predictions from advection/scavenging models to assess the role of MOC vs. water column ingrowth/scavenging in determining sedimentary ratios. This new record will enable improved comparison between intermediate and deep sites, enhanced understanding of existing water mass boundary records through the addition of a dynamical tracer of ventilation strength, and cross-basinal comparison of ventilation at intermediate depths.

[1] Keigwin (2004) *Paleoceanogr.*, **19,** PA4012, doi:10.1029/2004PA001029 [2] Hall *et al.* (2006) *Geophys. Res. Lett.* , **33**, L16616. [3] Gherardi *et al.* (2009) *Paleoceanogr.*, **24**, PA2204.

https://doi.org/10.1180/S0026461X00008434 Published online by Cambridge University Press

Kinetic isotope fractionation of ionic species in D_2O and methanol

AMY E. HOFMANN[1*], IAN C. BOURG[1], JOHN N. CHRISTENSEN[1], & DONALD J. DEPAOLO[1,2]

[1]Lawrence Berkeley National Laboratory, Earth Sciences Division, Berkeley, CA 94720, USA aehofmann@lbl.gov (* presenting author)

[2] University of California–Berkeley, Department of Earth & Planetary Science, Berkeley, CA 94720, USA

Certain kinetic processes, such as the self-diffusion and desolvation of ions in aqueous solution, have been shown via experiments[1,2] and molecular dynamics (MD) simulations[2,3,4] to fractionate Li^+, K^+, and Ca^{2+} isotopes. Both the self-diffusivities and desolvation rates of these isotopes in pure water follow an inverse power-law dependence on isotopic mass. In other words, lighter isotopes diffuse faster and exchange water molecules between their first hydration shell and the bulk liquid more quickly than heavier isotopes of the same species. In order to better elucidate the mechanism(s) responsible for kinetic fractionations associated with these processes, we performed MD simulations of ions in D_2O and diffusion experiments of ions in methanol comparable to previous experiments and simulations of the same ionic species in pure H_2O.

MD simulations involved one cation and 550 D_2O molecules in a periodically replicated cell at 298 K. Heavy water was modeled by altering the mass of SPC/E water but leaving all other model parameters unchanged. Simulation results indicate that both self-diffusion and desolvation of Li^+ and K^+ in D_2O produce larger isotopic fractionations compared to those determined for the same species in pure H_2O. For Ca^{2+}, ion desolvation rates in D_2O had no isotopic mass dependence, whereas data obtained in H_2O showed $^{44/40}Ca$ kinetic fractionations of order 3 ‰[4,5]. Kinetic isotope fractionations associated with self-diffusion of Ca^{2+} isotopes in D_2O are ambiguous at best due to the magnitude of the errors: simulation results predict diffusive fractionations between ^{44}Ca and ^{40}Ca of ca. 0.8 ± 5 ‰; by comparison, $^{44/40}Ca$ kinetic isotope fractionation by diffusion in H_2O is 0.43 ± 0.05 ‰[2]. Experimental corroboration of our D_2O simulation results is forthcoming.

Preliminary experimental results indicate that diffusion of K^+ in methanol produces larger isotopic fractionations than diffusion in pure H_2O. We are currently testing appropriate force field models for MD simulations of Li^+, K^+, and Ca^{2+} in methanol. Together, these observations reveal how properties of the solvent (and, hence, kinetic processes that chemically couple the solute to the solvent) may play a critical role in the isotopic fractionation of cations in solution.

[1] Richter et al. (2006) *GCA* **70**, 277-289. [2] Bourg et al. (2010) *GCA* **74**, 2249-2256. [3] Bourg & Sposito (2007) *GCA* **71**, 5583-5589. [4] Hofmann et al. (2011) *Mineral. Mag.* **75**, 1035. [5] Hofmann et al., in prep.

Influence of nitrate on the Eu(III) uptake by calcite: A TRLFS study

SASCHA HOFMANN[1] , THORSTEN STUMPF[2]

[1] Karlsruhe Institute of Technology, Institute for Nuclear Waste Disposal, Karlsruhe, Germany, sascha.hofmann@kit.edu

[2] Karlsruhe Institute of Technology, Institute for Nuclear Waste Disposal, Karlsruhe, Germany, thorsten.stumpf@kit.edu

Introduction

Calcite is present up to high amounts in clay minerals which are being discussed as a host rock formation and is formed by the degradation of cementitious material as a secondary phase. Furthermore, nitrate is very common in the geological environment and can influence the sorption behaviour of radionuclides. Because of the high impact of trivalent actinides (Pu, Am, Cm) on the radiotoxicity on long time scales, we used Europium as a homologue due to its spectroscopical properties and chemically similar behaviour. Earlier studies[1] have shown that Eu forms solid solutions with calcite under moderate conditions (T=25°C, IS=0.01M, ClO_4^- trace concentration). Three different sites were determined by TRLFS (dotted line, fig.1). By measurement of the fluorescence lifetimes after direct on-site excitation, these have been identified as one sorption (site A) and two incorporation species (sites B and C). For charge compensation, sodium must be present:

$$Eu^{3+} + Na^+ \leftrightarrow 2Ca^{2+}$$

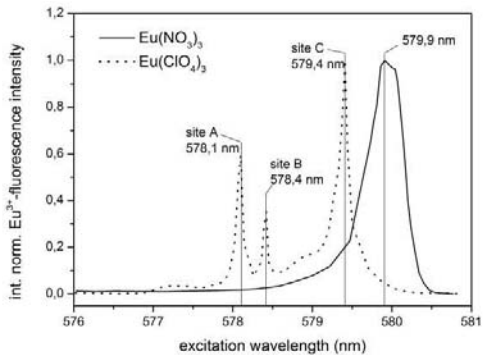

Figure 1: TRLFS excitation spectra of Eu^{3+} doped calcite with nitrate (one site) and perchlorate (three sites) as counterion

Results and Conclusion

By using 2 µM europium nitrate (T=25°C, IS=0.02M) instead of a perchlorate solution, a bathochromic shift of the emission maximum of about 0.5 nm was observed (solid line, fig.1). The long emission lifetime of this species (602 ± 59 µs) indicates that there are no water molecules left in the first coordination sphere of the lanthanaide ion (Horrock's equation[2]). As no other sites could be found, a new mechanism of Eu incorporation in the presence of NO_3^- -ions has to be assumed. Therefore, the uptake of Eu^{3+} by calcite is stongly influenced by the presence of trace amounts of NO_3^-. Considering the ubiquity of nitrate in the geosphere, this will highly affect modelling calculations for long term safety of nuclear waste deposits.

Reference

[1] Schmidt (2008) *Angew. Chem. Int. Ed* 47, 5846–5850

[2] Horrocks (1979) *J. Am. Chem. Soc.* 101, 334

https://doi.org/10.1180/S0026461X00008434 Published online by Cambridge University Press

Trace element abundances in Doushantuo cap dolostones from platform and slope settings, Yangtze Platform, South China

S. V. HOHL [1*], H. BECKER[1], D. HIPPLER[2], W. BÄRO[1]

[1] Freie Universität, Berlin, Germany
[2] Technical University, Berlin, Germany
(*correspondence author: shohl@zedat.fu-berlin.de)

Shallow and deep water facies cap carbontes of the Ediacaran Doushantuo Formation (Yangtze Platform, South China) were studied to evaluate the extent of diagenetic alteration and to asses temporal and spatial variations of Ediacaran seawater chemistry. The mineralogical composition and textures of the samples were prescreened using SEM and XRD, and 20 mg sample aliquots were obtained by drilling into presumably unaltered domains of polished rock chips. For analysis of major and trace element concentrations and Sr isotopic composition, sample powders were leached in 10 % acetic acid.

REE+Y patterns of deep water cap dolostones from a slope section (Huanglian section, Songtao, Guizhou Province) have high Y/Ho_{PAAS} ratios up to 1.9 and Pr/Yb_{PAAS} of 0.45 to 0.8 and may reflect relatively undisturbed seawater signatures. In detail, the base of the section shows a relative enrichment in MREE, no Ce anomaly and a positive Eu anomaly (1.2). The middle part of the section displays weak negative Ce anomalies (Ce/Ce* = 0.8-0.9) whereas the upper part of the section shows no Ce but a small positive Eu anomaly. These results are in contrast with data from nearby Panmen section [Becker et al., this meeting], where no or positive Ce anomalies are obtained from acetic acid leachates of cap dolostones.

REE+Y patterns of cap dolostones of the shallow water facies from Hubei Province (Tianjiayuanzi, Wuhe-Gaoxi, Jijiawan sections) are flat to variably depleted in the LREE and show variable Y/Ho_{PAAS} (1-1.3) or Ce/Ce* (1-1.4). These results are different from the shallow water section at nearby Jiulongwan section (Hubei Province), the latter displaying prominent negative Ce anomalies [1]. The most compelling explanation for the section to section variability in REE+Y systematics in both shallow and deep water sections is the variable influence of secondary processes such as diagenesis and fluid flow. $^{87}Sr/^{86}Sr$ ratios in deep water cap dolostones at Huanglian range from 0.7246 right above the diamictites and drop to values of 0.7175 at the top of the section. The $^{87}Sr/^{86}Sr$ ratios of cap dolostones from the shallow water sections are lower (0.7081 - 0.7113) and similar to recently published data for the Three Gorges Area [2]. Samples from slope sections show a strong overprint by hydrothermal fluids containing very radiogenic Sr, with limited redistribution of REE+Y. Cap dolostones from shallow water sections also reveal variable redistribution of REE+Y abundances. These observations indicate decoupling of REE+Y behavior from fluid mobile elements such as Sr or O. SEM work is helpful in the identification of homogeneous carbonate domains, but it does not guarantee that such domains have retained pristine compositions.

[1] Huang et al. (2009) *Chinese Science Bulletin* **54**, 3295-3302.
[2] Sawaki et al. (2010) *Precambrian Research* **176,**46-64.

C-, O- and Sr-isotopes in marbles from the Eastern Alps

BARBARA PUHR[1], RALF SCHUSTER[2], GEORG HOINKES[1*], SYLVAIN RICHOZ[1], BEATRIX MOSHAMMER[2]

[1]University of Graz, Graz, Austria, barbara.puhr@edu.uni-graz.at, georg.hoinkes@uni-graz.at (* presenting author), sylvain.richoz@uni-graz.at
[2]Geologische Bundesanstalt, Vienna, Austria, ralf.schuster@geologie.ac.at, beatrix.moshammer@geologie.ac.at

Introduction

Marbles of the polymetamorphic, medium-grade, greenschist to eclogite facies Koralpe-Wölz nappe system (Eastern Alps) were investigated regarding their geochemical and isotope compositions. Focus was set on a characterization of different lithostratigraphic units by their distinct compositions and a comparison of revealed chemostratigraphic information with un- to weakly metamorphosed equivalents of the Austroalpine and Southalpine units.

Results and conclusion

Geochemical screening of the marbles using Mn/Sr, Rb/Sr-ratios and C-, O- and Sr-isotope signals, which reflect the diagenetic and metamorphic imprints, allows distinguishing between primary compositions and altered samples, as can be expected from highly metamorphosed metacarbonates. A limiting factor for Mn/Sr is proposed by ≤2 and for Rb/Sr by ≤0.02. The upper limit of primary Sr-values is given by 0.709250 reflecting the highest Sr-seawater value. Feasible samples with regard to C- and O-isotope contents fall within -1 to 4 and -8 to 0, respectively. Mn/Sr-ratios scatter in a range of 0.036 and 2.814, from which just 4 samples exceed values above 2. The Rb/Sr-values vary between 0 and 0.132 (17 samples exceeding the upper limit). Two distinct groups of marbles, based on isotope compositions and different alteration signals, are present. Group I is characterized by relatively low and solely slightly variable Sr-values between 0.707997 and 0.708465. However, these marbles possess strongly scattering $\delta^{18}O$- (-11.08 - 0.10‰) and $\delta^{13}C$-data (-1.58 - 4.78‰). Group II shows Sr-ratios above 0.708556 with a maximum at 0.711090. Δ18O-values of this group are strongly scattering (-12.95 - -4.01‰), whereas $\delta^{13}C$-isotope signatures fluctuate in a narrow span between -0.9 and 2.02. Due to best fitting geochemical and isotope constraints, marbles of at least two lithostratigraphic complexes, namely the Rappold and Millstatt Complexes, reflecting group I and group II respectively, are interpreted to possess most likely primary geochemical signatures.

These best preserved samples were used for further chemostratigraphic interpretation by means of a correlation with isotope seawater curves. For marbles of group I a depositional age in the late Early to Middle Devonian (400-385 Ma) is indicated. For metacarbonates of group II a sedimentation in the latest Silurian to Early Devonian (420- 405 Ma) is concluded.

Based on the depositional age, geochemistry and on its lithological successions, group I occurring in the southeastern part of the Austroalpine unit show similarities with the directly overlying Graz Palaeozoic, whereas units of group II which is present further north and west can be attributed to the other weakly metamorphosed Palaeozoic sequences of the Austroalpine and Southalpine units.

https://doi.org/10.1180/S0026461X00008434 Published online by Cambridge University Press

Migration and evolution of oil sands tailings pond seepage through glacial till sediments: combined field and laboratory investigations

A. HOLDEN[1*], M. KONE[1], K. U. MAYER[2], A. ULRICH[1]

[1] University of Alberta, Civil and Environmental Engineering, Edmonton, Canada, aholden@ualberta.ca (*presenting author), macoura@ualberta.ca, aulrich@ualberta.ca

[2] University of British Columbia, Earth and Ocean Sciences, Vancouver, Canada, umayer@eos.ubc.ca

In Northern Alberta, at least three major oil sands tailings impoundments have been constructed atop aquifers, mantled by a layer of glacial till. Despite these favourable conditions, absolute containment within these enormous, man-made structures is not achievable, and oil sands process water (OSPW) from the ponds is expected to infiltrate through the aquitard, impacting groundwater quality on site and potentially beyond [1]. However, to date, there has been no research investigating the evolution and migration of OSPW in glacial till sediments, and thus the nature of contaminants entering the groundwater-bearing formations remains unclear.

The present study seeks to a) characterize the potential for glacial till sediments to attenuate, or to modify the composition of, ingressing major ions contributing to salinization; and b) to clarify the key geochemical processes governing system behaviour. Of novelty, groundwater was monitored for 6 years, from its pristine state through to first ingress of OSPW, and results are interpreted in conjunction with radial diffusion cell experiments [2] using the same sediments.

Field observations show that OSPW intrusion resulted in high concentrations of Na, Cl and alkalinity (likely HCO_3), at approximately 900, 370 and 1350 (as $CaCO_3$) mg L^{-1} respectively. In agreement with findings from radial diffusion experiments, initial ingress of sodium-rich OSPW exchanged with sediment-bound Ca, while NO_2, NO_3 and high concentrations of SO_4 were mitigated, due to reduction reactions. However, displacement of exchangeable Mg was observed in the laboratory but not on site, though perhaps the change too subtle or localized to be detected by annual sampling.

Field monitoring enables the detailed assessment afforded under the well-controlled conditions of the diffusion cells, to be expanded to include field-scale heterogeneity in mineralogy and hydrology, and variable climate. Together, the unified results are expected to aid future remediation and environmental management strategies.

[1] MacKinnon *et al.* (2004). *IAHS Publ.* **297**, 71-80.
[2] van der Kamp *et al.* (1996) *Water Resour. Res.* **32**, 1815-1822.

Bacterial Diversity in Athabasca Oil Sands Composite Tailings Components

STEVEN P. HOLLAND[1]*, TARA COLENBRANDER NELSON[1], KATE STEPHENSON[1], KATIE KENDRA[1], TARA PENNER[2], LESLEY A. WARREN[1]

[1]School of Geography and Earth Sciences, McMaster Universiy, Hamilton, ON, Canada, hollansp@mcmaster.ca (*presenting author), tnelson@mcmaster.ca, steph2k@mcmaster.ca, kendrake@mcmaster.ca, warrenl@mcmaster.ca

[2]Syncrude Canada Ltd., Edmonton, AB, Canada, Penner.Tara@syncrude.com

Sustainable reclamation of tailings, process water, and disturbed land represents the largest environmental challenge facing the Alberta Oil Sands industry. Bitumen extraction generates immense quantites of composite tailings (CT), a material that remains, to date, uncharacerized with regards to bacterial genetic diversity. Syncrude Canada Ltd. is currently building the first large-scale reclamation freshwater fen overlying sand-capped CT. Unexpected hydrogen sulfide (H_2S) gas emissions coinciding with dewatering of the CT associated with fen construction has highlighted the need to more thoroughly constrain S biogeochemistry in these materials. Recently initiated work is now investigating microbial linkages between S cycling and the generation of H_2S gas in untreated CT as well as CT undergoing reclamation fen development. CT consists of process water, gypsum, sand, and fluid fine tailings (FFT), a process waste that is rich in microbial life as well as Fe-bearing clay content. Understanding the putative microbial links to H_2S generation thus requires a thorough characterization of the microbial players that may be present in the starting materials, as well as those in the composite tailings *in situ*, and their potential impact for S cycling. The objectives of this work are to characterize the bacterial diversity of FFT, CT, and overlying sand cap materials, as well as process water, via molecular, cultivation-independent 16S approaches. Results of this genetic charactierzation, as well as Fe and S metabolic enrichment from these materials, and the potential linkages to H_2S gas generation will be presented.

https://doi.org/10.1180/S0026461X00008434 Published online by Cambridge University Press

Discriminating factors affecting incorporation: Comparison of the fate of Eu^{3+}/Cm^{3+} in the Sr carbonate/sulfate system

KIEL HOLLIDAY[1,2*], AURÉLIE CHAGNEAU[1,3,4], MORITZ SCHMIDT[1], FRANCIS CLARET[3], THORSTEN SCHÄFER[1,4], AND THORSTEN STUMPF[1]

1 Karlsruhe Institute of Technology, Institute for Nuclear Waste Disposal, P.O. Box 3640, 76021 Karlsruhe, Germany; E-mail: holliday7@llnl.gov, mschmidt@anl.gov, thorsten.schaefer@kit.edu, thorsten.stumpf@kit.edu

2 Lawrence Livermore National Lab, 7000 East Ave., Livermore, CA 94551 USA; E-mail: holliday7@llnl.gov

3 Bureau de Recherches Géologiques et Minières, 3 avenue Claude-Guillemin, BP 36009, Orléans Cedex 2, France; E-mail: aurelie.chagneau@kit.edu, f.claret@brgm.fr

4Institute of Geological Sciences, Department of Earth Sciences, Freie Universität Berlin, Berlin, Germany.

The aim of this work is to assess the effect of ligand strength, symmetry, and coordination number on solid solution formation of trivalent actinides and lanthanides in carbonate and sulfate minerals. This is of particular importance in radionuclide migration where trivalent actinides such as Pu, Am, and Cm are responsible for the majority of radiotoxicity after 1,000 years. Time-resolved laser fluorescence spectroscopy was used to study trace concentrations of the dopant ion after interaction with the mineral phase. This study expands on previous work with aragonite and gypsum where it was found that aragonite incorporates Eu^{3+} and Cm^{3+} while only surface sorption is observed in gypsum. This study uses isostructural minerals strontianite ($SrCO_3$) and celestite ($SrSO_4$) to decouple the effect of structure from that due to the anion. It is demonstrated that while distribution coefficients can predict the amount of dopant ion associated with the mineral phase, they do not have any correlation with solid solution formation. This substitution mechanism is most likely dictated by the symmetry of the site being substituted and the electronic structure of the dopant atom.

Table 1: Lifetime and position of fluorescence emission in Eu^{3+} and Cm^{3+} doped aragonite, strontianite, and celestite.

Sample	Wavelength (F_0 or $S_{7/2}$)/nm	Lifetime/ms
Eu-$CaCO_3$[1]	579.4	1.6
Eu-$SrCO_3$	578.5	1.6
Eu-$SrSO_4$	577.7	3.1
Cm-$CaCO_3$[1]	612.7	0.64
Cm-$SrCO_3$	608.5	0.47
Cm-$SrSO_4$	596.3	1.1

[1] Schmidt, M., Stumpf, T., Walther, C., Geckeis, H., Fanghänel, T. (2009) *Dalton Trans.* **33**, 6645.

Dissolved organic matter characterization for a Prairie Potholes ecosystem

JOANN M. HOLLOWAY[1]*, MARTIN B. GOLDHABER[1], CHRISTOPHER T. MILLS[1], GEORGE R. AIKEN[2], AND KENNA D. BUTLER[2]

[1]U.S. Geological Survey, Denver, CO, USA, jholloway@usgs.gov (* presenting author), mgold@usgs.gov, cmills@usgs.gov

[2]U.S. Geological Survey, Boulder, CO, USA, graiken@usgs.gov, kebutler@usgs.gov

The Prairie Potholes region of the northern Great Plains includes an extensive system of small (< 0.5 hectare), discrete wetlands that occur within a hummocky topography formed by the retreat of Pleistocene glaciers. The Cottonwood Lake Study Area, located in the Prairie Potholes region near Jamestown, North Dakota (USA), includes 16 wetlands. These wetlands receive water primarily from snowmelt and are hydrologically connected by groundwater flow within a 92-hectare basin that lacks surface drainage. The objectives of this study were to 1) determine if different wetland vegetation communities affect the quantity and quality of dissolved organic matter (DOM), and 2) determine the extent to which vegetation-DOM is partitioned into groundwater.

Wetland salinity ranged from 150 mg kg^{-1} in recharge wetlands receiving only meteoric input to >3000 mg kg^{-1} in discharge wetlands receiving groundwater flow from topographically higher wetlands. The pH of individual wetlands ranged from 6.7 to 8.8 and has been linked to variable wetland salinity that supports differing plant community structures. Unusually high concentrations of dissolved organic carbon (DOC) accumulate from the decay of vegetation and algae in wetland waters (27 to 56 mg C L^{-1}), an order of magnitude greater than most natural waters. The hydrologic connection between the wetlands and shallow groundwater was reflected by elevated DOC concentrations (20 to 46 mg C L^{-1}) from wells screened within this flow path. Deeper groundwater isolated from direct wetland recharge had lower DOC concentrations (2.5 to 10 mg C L^{-1}). Specific UV absorbance ($SUVA_{254}$) is an index of aromaticity. Wetlands with near neutral pH had a greater $SUVA_{254}$ than alkaline wetlands, although aromatic dissolved organic matter is generally more soluble in alkaline waters. Thus, we interpret this trend to be in part a function of organic matter source. Groundwater had a lower $SUVA_{254}$ than the wetlands, indicating a lower proportion of aromatic compounds. We are also applying fluorescence-based techniques in evaluating the quality of DOM associated with these wetlands. These data give insights on how varying vegetation communities can affect types of DOM associated with these wetlands and the exchange of organic matter between surface and groundwater.

https://doi.org/10.1180/S0026461X00008434 Published online by Cambridge University Press

Subduction eroded continental crust and sediment derived fluids in the genesis of arc magmas in the SVZ, Andes

PAUL MARTIN HOLM[1*], NINA SØAGER[1], CHARLOTTE THORUP DYHR[1]

[1] University of Copenhagen, Copenhagen, Denmark, paulmh@geo.ku.dk (*presenting author)

New Sr, Nd and Pb isotope and trace element data is presented from young volcanic rocks from Maipo and Laguna del Maule Transitional and Northern Southern Volcanic Zone (SVZ) of the Andes, respectively. The trace element enrichment of many of the volcanic rocks from the 34-38°S in the Southern Volcanic Zone, SVZ, display a relative enrichment of Th to Ba indicating that source enrichment by fluids is not the most important process. All rocks have negative Nb and positive Pb anomalies indicating that the magmas have an important component of continental crust or/and had a fluid-enriched source.

To avoid most effects on incompatible trace element ratios from fractional crystallization and from afc processes we used only incompatible element ratios of the most primitive rocks in our modelling (Mg# > 60).

Nb/Th, Ba/Th and La/Th ratios in rocks from the Central-Transitional-Northern SVZ correlate well and suggest that two components dominate their compositions. In this respect the Andes rocks with the relatively highest ratios are comparable to the Marianas and Tonga, which have been argued to be derived from a fluid-enriched source [2,3]. The low Ba/Th component has lower Ba/Th and La/Th than GLOSS, local trench sediments and average continental crust. This end-member most resemble average upper crust, and its relatively low Ba/Rb and La/Rb suggest it to be of evolved magmatic composition. Volcan Maipo rocks approximates this end-member for the Northern SVZ and very little fluid-borne enrichment is required to generate these magmas. This is in accord with the radiogenic Sr ($^{87}Sr/^{86}Sr$ = 0.7049-0.7055) and unradiogenic Nd ($^{143}Nd/^{144}Nd$ = 0.5125-0.5126) of the Maipo rocks, lower than 0.5127-.5128 of Chile Trench sediments. For the Transitional and Central SVZ crust with similar geochemistry but different isotopic composition is indicated. We suggest that the subducting Nazca plate abraded the South American upper crust at the leading edge and transported it below the lithosphere where it partially melted, as also suggested by e.g. [4]. The fluid-borne enrichment is characterized by its Sr and Nd isotope composition of $^{87}Sr/^{86}Sr$ around 0.7040 and $^{143}Nd/^{144}Nd$ 0.5128. This composition is common for several SVZ volcanoes and isotopically overlap with Chile Trench sediments in Sr, Nd and Pb isotopic composition, and is very different from both Pacific MORB and the OIB-type source of the back-arc magmas which probably is an important end-member in the local asthenosphere. The fluid borne enrichment is therefore indicated to be derived from subducted sediments. The well defined trend towards higer Nb/Th for the rocks rich in this end-member show that they were derived from a rather fixed proportions of fluid plus mantle.

[1] Plank(2010) J. Petrol. 46, 921-944, [2] Elliot et al.(1997) J. Geophys. Res. 102, 14991-15019, [3]Turner et al.(1997) Geochim.Cosmochim.Acta 61, 4855-4884, [4] Stern(2011)Gondwana Res. 20, 284-308.

Organic geochemical insights into the formation of the Here's Your Chance lead-zinc-silver deposit

ALEX HOLMAN[1*], KLITI GRICE[1], CAROLINE JARAULA[1], JEFFREY DICK[1], ARNDT SCHIMMELMANN[2] AND KATY EVANS[3]

[1]WA Organic and Isotope Geochemistry Centre, Department of Chemistry, Curtin University, Perth, Australia, A.Holman@curtin.edu.au (* presenting author)

[2]Department of Geological Sciences, Indiana University, Bloomington, United States of America

[3]Department of Applied Geology, Curtin University, Perth, Australia

The Here's Your Chance (HYC) lead-zinc-silver deposit is located in the Barney Creek Formation (BCF), a 1639 ± 2 Ma carbonaceous marine deposit in the Northern Territory of Australia. The HYC deposit has been extensively studied as an example of hydrothermal alteration of well-preserved Proterozoic organic matter [1,2].

Samples were collected from five sites along the flow path of hydrothermal fluid. The freely-extractable hydrocarbons (Bitumen I) from these samples have been analysed by Williford *et al.* [2]. This study has investigated hydrocarbons that were occluded within the kerogen/mineral matrix (Bitumen II), following hydrofluoric acid digestion and extraction as per Nabbefeld *et al.* [3].

Bitumen II *n*-alkanes display a markedly different distribution to those of Bitumen I, characterised by an unusual even-over-odd distribution and the preservation of long-chain alkanes up to *n*-C_{38}, indicating a biological source such as sulfate-reducing bacteria [4]. It is believed that hydrocarbons in Bitumen II have been protected from alteration by the kerogen / mineral matrix; hence it is likely that these bacteria were associated with the depositional environment. Bitumen II *n*-alkanes are 5 ‰ more negative in $\delta^{13}C$ compared to Bitumen I, suggesting that Bitumen I hydrocarbons originate from a different source. Other explanations for the origin of Bitumen II are also under investigation.

The isomer ratios of Polycyclic Aromatic Hydrocarbons (PAHs) in sediments are temperature dependant, and are widely used to estimate thermal maturity [3]. Bitumen I PAH ratios indicate a higher maturity than Bitumen II, supporting the theory that PAHs were generated at higher temperatures below the BCF, then transported up with the mineralising fluid [2]. Preliminary thermodynamic calculations based on PAH distributions in these proceedings [5] have placed an upper limit on mineralising fluid temperature which is in agreement with previous studies [2].

[1] Chen *et al.* (2003) *Earth and Planetary Science Letters* **210**, 467-479.
[2] Williford *et al.* (2011) *Earth and Planetary Science Letters* **301**, 382-392.
[3] Nabbefeld *et al.* (2010) *Organic Geochemistry* **41**, 78-87.
[4] Melendez *et al.* (2012) *Geology*, in review.
[5] Dick *et al.* (2012) *Goldschmidt 2012*, submitted abstract.

https://doi.org/10.1180/S0026461X00008434 Published online by Cambridge University Press

Molecular dynamics simulations of the three-layer hydrate in smectites: A sensitivity analysis

MICHAEL HOLMBOE* AND IAN C. BOURG

Earth Sciences Division, Lawrence Berkeley National Laboratory, Berkeley, USA,
mholmboe@lbl.gov (* presenting author)

Abstract

Bentonite (smectite-rich) clays is under consideration as a buffer material for geological nuclear waste repositories in many countries. Molecular simulation techniques such as Monte Carlo (MC) and molecular dynamics (MD) simulations have played an important role in characterizing these materials by yielding detailed atomistic insights into the structural, dynamical and thermodynamic properties of water in smectite interlayer nanopores. Most of these studies used classical MD simulations of small smectite/water systems (< 10^4 atoms) with fixed smectite clay layers, in order to save computational time, although size dependent effects using more realistic and flexible smectite layers were observed in large-scale MD simulations (> 10^5 atoms) of flexible smectite layers [1]. In this work we compare the results of MD simulations with 6900, 7710 and 8520 atoms, carried out with either fixed or flexible smectite layers of a typical 2:1 sodium exchanged smectite (Wyoming montmorillonite), at different water contents and temperatures. The simulations were performed using the MD code LAMMPS with the SPC/E water model and the ClayFF force field, which are known to correctly reproduce structural and thermodynamical properties of smectite interlayer water and exchangeable cations [2]. We focus in particular on the diffusion coefficents and structural data for the three-layer hydration state, which is expected to be the predominant hydration state in different concepts for geological nuclear waste disposal, such as the Swedish KBS-3 method [3].

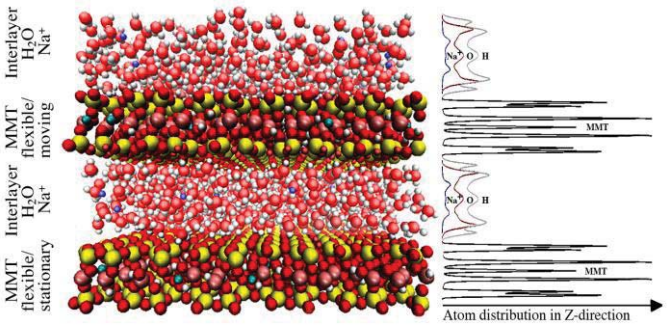

Figure 1: Typical "snapshot" from a MD simulation of two montmorillonite layers in the three-layer hydrate state. Right hand side shows the atom distribution in the vertical direction.

[1] Suter et al. (2007) *J. Phys. Chem. C.* **111**, 8248-8259.
[2] Bourg & Sposito. (2010) *Environ. Sci. Technol.* **44**, 2085-2091.
[3] Holmboe et al. (2012) *J. Contam. Hydrol.* **128**, 1-4, 19-32.

Ca-isotope tracing of submarine groundwater discharge—Florida Bay

C. HOLMDEN[1], D. A. PAPANASTASSIOU[2], P. BLANCHON[3] AND S. EVANS[4]

[1]Saskatchewan Isotope Laboratory, Saskatoon, Canada
[2]Jet Propulsion Laboratory/Caltech, Pasadena, USA
[3]Instituto de Ciencias del Mar y Limnologìa, Natl. Univ. of México
[4]Dept. of Geosciences, Boise State University, USA

Florida Bay is a seasonally hypersaline estuarine lagoon located on the southernmost tip of the submerged Florida shelf. It is roughly triangular in shape with barriers that limit circulation with open marine waters. To the east, the nearly continuous exposure of Pleistocene limestone, composing the Florida Keys, keeps surface Atlantic waters out of Florida Bay (with the exception of a few tidal passes). To the south, a series of shallow mudbanks limits circulation with the Gulf of Mexico. To the north, Florida Bay is bounded by mangrove wetlands of the Florida Everglades. Waters are typically <3 m deep, and it is common to find areas that have been scoured of sediment to reveal the underlying Pleistocene limestone bedrock. Outcrop exposures of Pleistocene limestone occur in the coastal region of northern Florida Bay extending into the wetlands of the southern Everglades.

The coastal region of northeastern Florida Bay has been indentified in hydrogeological models as an area of submarine groundwater discharge (SGD) [1]. Other studies have shown seawater penetration beneath the southern Everglades extending for 25 km inland from the coastline [2], and that brackish groundwaters are not conservative with respect to Ca, showing an 'excess Ca' effect; i.e., more Ca than would be expected on the basis of seawater-freshwater mixing in the subterranean estuary [3]. The excess Ca originates from the dissolution of carbonate-aquifer minerals.

The tracer potential of Ca-isotopes ($\delta^{44/40}$Ca values) in this setting stems from the ~1.1‰ difference between $\delta^{44/40}$Ca values of carbonate bedrock (–1.1‰) and seawater (0‰). Therefore, the excess Ca picked up during the circulation of seawater in the subsurface serves as a fingerprint of SGD inputs into coastal Florida Bay, where water circulation restriction enables the seepage flux of isotopically light Ca to be resolved before it is 'mixed out' by circulation with the ocean. A 0.7‰ gradient in $\delta^{44/40}$Ca values is found in both waters and sediment of northeastern Florida Bay, decreasing towards the Florida Everglades. Results of a quantitative Ca-isotope mixing model indicate that 20% of the water and 30% of the Ca in Joe Bay is from SGD. The estimates are even higher in the southern Mangrove fringe of the Florida Everglades [4].

More work is needed to determine the global-scale SGD Ca-flux to the oceans. Quantitative flux estimates would help to close the Ca isotope budget of the oceans, where the traditional input Ca-fluxes from rivers and hydrothermal fluids are too small to balance the output Ca-flux into carbonate sediments.

[1] Langevin et al. (2004) USGS Open File Report 2004–1097, 30p. [2] Fitterman and Deszcz-Pan (1998) *Explor. Geophys.* 29, 240–243. [3] Price et al., (2006) *Hydrobiology* 569, 23–36. [4] Holmden et al. (2012) *Geochim. Cosmochim. Acta*, IN PRESS.

https://doi.org/10.1180/S0026461X00008434 Published online by Cambridge University Press

Long Term Trend in the Aerosol Black Concentrations in the Arctic Region

LIAQUAT HUSAIN[1,2], VINCENT A. DUTKIEWICZ[2], TANVEER AHMED[2], ANTHONY DEJULIO[1], PHILIP K. HOPKE[3*], JAMES R. LAING[3], AND JUSSI PAATERO[4]

[1]Department of Environmental Health Sciences, School of Public Health, SUNY, Albany, NY. 12201-0509

[2]Wadsworth Center, NYS Department of Health, Albany, NY 12201-0509

[3]Center for Air Resources Engineering and Science, Clarkson University, Potsdam, NY 13699

[4]Finnish Meteorological Institute, Helsinki, Finland

Introduction

Carbon, primarily a byproduct of incomplete combustion of fossil fuel and biomass burning constitute only a few % of the total PM mass, but disproportionately affect the global climate by absorbing the incoming sunlight and directly warm the atmosphere. BC coated with sulfate is even more effective than externally mixed BC and SO4 particles. Recent studies have indicated that substantial radiative forcing in the Arctic is due to the indirect impact of BC on the albedo of snow and ice surfaces. We are determining the concentrations of BC, SO4, selected trace elements in weekly samples collected at Kevo, Finland, from 1964-2010 to assess the impact of aerosols on (1) radiative forcing, (2) source regions that have contributed to the burden of BC and SO4 in the Arctic region, and (3) how the regional emissions impacting Arctic have changed with time.

Methods

Samples were collected over 7 day periods beginning in October 1964 through the present in Kevo [1], Finland in an automated system to measure airborne radioactivity. These samples were analyzed using the approach developed by Husain et al. [2]. The light absorption of each new filter was measured with a Magee OT21 transmissometer.

Results and Conclusions

Figure 1 shows the annual average values for 1965 to 2000. The concentrations of BC aerosols during 1965 were 430 ng m^{-3}. From 1966 thru 1987 it varied from ~250 to 430 ng m^{-3}. Beginning in 1989, concentrations showed a systematic decrease to about 150 ng m^{-3}. From 1989 to 2002, the concentrations have remained between 150 and 230 ng m^{-3}. The data from 2003 to 2010 is not yet available.

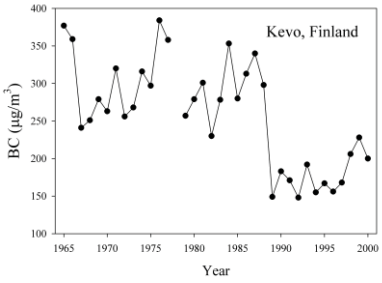

These data show that there was a substantial decrease in BC concentrations around the time of the collapse of the Soviet Union and the change in political systems in eastern Europe. More detailed analyses will be performed in the future.

[1] Yli-Tuomi, T., et al., 2003. *Atmospheric Environ.* **37**, 2355-2364.

[2] Li, J., et al., 2002, *Atmospheric Environ*. **36**, 4699–4704.

Aluminium affecting copper speciation in Swedish freshwaters

SABINA HOPPE[1*], KURIA N´DUNGU[1], HANS BORG[1]

[1]Stockholm University, Dept. of Applied environmental science, Sabina.hoppe@itm.su.se (* presenting author)

Abstract

Swedish fresh waters are often rich in aluminium depending on the underlying bedrock, water chemistry e.g. acidification status and TOC. Aluminium forms, present at circum neutral pH are not toxic to aquatic biota, but may however influence the bioavailability of other metals. This will occur due to competition of Al on organic carbon binding sites which will relese free metal ions affecting metal speciation (Fig.1) as well as toxicity. Measured free/labile Cu levels, using electro chemical detection - Anodic Stripping Voltammetry (ASV), combined with modeling (Visual minteq) showed that this occurs until a threshold level of Al in the water is reached. The concentration of free Cu increased and the organically complexed Cu (Cu-FA) decreased when Al was added (Fig. 1)

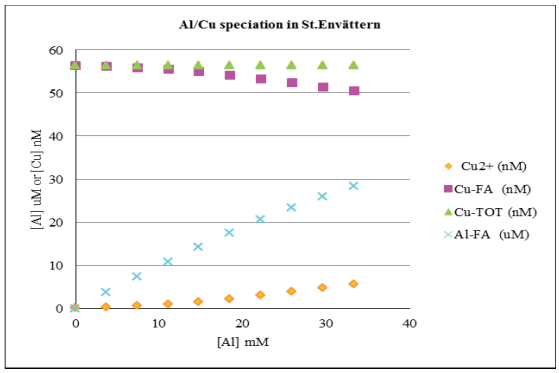

Figure 1: Cu-species at increased amount of Al added to water from Lake St. Envättern, Sweden. Cu-FA, Al-FA: metal complexes with humus.

These findings also have a marked influence on the Cu-toxicity to crustaceans (*Daphnia magna*) as shown by preliminary results from toxicity tests using lake waters in the presence of Al well below the toxic concentration of Al (Fig.2).

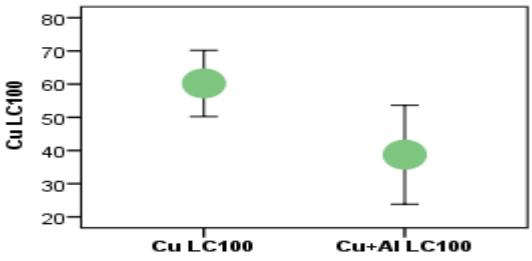

Figure 2: Cu LC_{100} values with and without Al addition (20 µg/L) for *D.magna*.

Conclusion

Aluminium, thou not bioavailable at circum neutral pH-values, can affect Cu speciation, toxicity and bioavailability in freshwaters already at moderately elevated Al-concentration.

https://doi.org/10.1180/S0026461X00008434 Published online by Cambridge University Press

EVOLUTION, ECOLOGY AND BIODIVERSITY IN OLD, INFERTILE LANDSCAPES

STEPHEN D. HOPPER[1]

[1]Royal Botanic Gardens, Kew, Richmond, Surrey, UK, s.hopper@kew.org

OCBIL theory[1] aims to develop an integrated series of hypotheses explaining the evolution and ecology of, and best conservation practices for, biota on very old, climatically buffered, infertile landscapes (OCBILs). Conventional theory for ecology and evolutionary and conservation biology has developed primarily from data on species and communities from young, often disturbed, fertile landscapes (YODFELs), mainly in the Northern Hemisphere. OCBILs are rare, but are prominent in the Southwest Australian Floristic Region, South Africa's Greater Cape, and Venezuela's Pantepui Highlands (Fig 1). They may have been more common globally before Pleistocene glaciations. Based on the premise that natural selection has favoured limited dispersability of sedentary organisms, OCBILs should have elevated persistence of lineages (Gondwanan Heritage Hypothesis) and long-lived individuals (Ultimate Self Hypothesis), high numbers of localised rare endemics and strongly differentiated population systems. To counter such natural fragmentation and inbreeding due to small population size, ecological, cytogenetic and genetic mechanisms selecting for the retention of heterozygosity should feature (the James Effect). The climatic stability of OCBILs should be paralleled by persistence of adjacent semi-arid areas, conducive to speciation (Semiarid Cradle Hypothesis). Special nutritional and other biological traits associated with coping with infertile lands should be evident, accentuated in plants, for example, through waterforaging strategies, symbioses, carnivory, pollination and parasitism. The uniquely flat landscapes of southwestern Australia have had prolonged presence of saline lakes along palaeoriver systems favouring evolution of accentuated tolerance to salinity. Lastly, unusual resiliences and vulnerabilities might be evident among OCBIL organisms, such as enhanced abilities to persist in small fragmented populations but great susceptibility to major soil disturbances. In those places where it is most pertinent, OCBIL theory hopefully lays a foundation for future research and for better informed conservation management.

Figure 1: Old granite landscapes in South Africa (left) and Western Australia (middle), unglaciated since the Permian (photos S.D. Hopper), and the sandstone Neblina massif (right) in the Guiana Highlands (photo B. Stannard).

[1] Hopper S.D. (2009) *Plant and Soil* **322**, 49-86.

Reconstructing deep-ocean nutrients with paired Cd/Ca and Cd isotopes in deep-sea corals

TRISTAN J. HORNER[1]*, GIDEON M. HENDERSON[1], ROSALIND E.M. RICKABY[1], AND JESS F. ADKINS[2]

[1]Dept. Earth Sci., University of Oxford, Oxford OX1 3AN, UK *Tristan.Horner@earth.ox.ac.uk (presenting author)

[2]Div. Geol. Planet. Sci., Caltech, Pasadena, CA 91125, USA

The abyssal ocean is a major sink for nutrients, heat, and carbon, and plays an important role in modulating glacial-interglacial climate. Archives of deep-water chemistry, particularly those which can be precisely dated, are therefore of great use in understanding the temporal interactions between ocean circulation and global climate.

Deep-sea corals, which typically live between 500–2,000 m, are well positioned to record changes in deep-water chemistry in their aragonitic skeletons, which can be absolutely dated with U-series techniques [1]. In particular, they have shown some utility in recording oceanic Cd/Ca [2] which can be used to reconstruct seawater phosphate concentrations (because Cd is pseudo-linearly correlated with P). However, physiological 'overprinting' of the environmental signal is a significant issue in deep-sea corals and requires empirical calibration before such archives can be used to reconstruct seawater compositions (e.g. [3]).

Here, we investigate the controls on the Cd isotope composition of deep-sea coral aragonite using a previously collected series of modern and fossil samples from the New England Seamounts located in the North Atlantic [4]. Inorganically precipitated calcium carbonate has previously been shown to have a constant fractionation from seawater [5], therefore deviations from constant fractionation in coral aragonite would indicate a biological overprint that may enable interpretation of Cd/Ca ratios in terms of biomineralization and past seawater composition. The isotope composition of coral aragonite may also allow reconstruction of the past isotope composition of deep-waters, providing clues to changing nutrient cycling during periods of global change.

[1] Cheng *et al*. (2000) *Geochim. Cosmochim. Acta* **64**, 2401-2416.
[2] Adkins *et al*. (1998) *Science* **280**, 725-728.
[3] Gagnon *et al*. (2007) *Earth Planet. Sci. Lett*. **261**, 280-295.
[4] Robinson *et al*. (2007) *Bull. Mar. Sci.* **81**, 371-391.
[5] Horner *et al*. (2011) *Earth Planet. Sci. Lett.* **312**, 243-253.

https://doi.org/10.1180/S0026461X00008434 Published online by Cambridge University Press

Greenhouse gas footprint of shale gas obtained by hydraulic fracturing

ROBERT W. HOWARTH[1*], RENEE SANTORO[2], ANTHONY INGRAFFEA[3]

[1]Cornell University, Ecology & Evolutionary Biology, howarth@cornell.edu (* presenting author)
[2]Cornell University, Ecology & Evolutionary Biology, rls75@cornell.edu
[3]Cornell University, Civil & Environmental Engineering, ari@cornell.edu

Introduction

Only in the past 10-15 years have high-volume hydraulic fracturing and precision directional drilling been combined to make extraction of natural gas from shale commercially viable. Industry and many governments promote shale gas, often describing shale gas as a bridge fuel that allows continued use of fossil fuels while reducing greenhouse gas emissions (GHG) compared to other fuels. In April 2011, we published the first comprehensive analysis of the GHG footprint of shale gas, concluding that in fact full-lifecycle GHG emissions from shale gas are comparable to or larger than those from oil and coal [1]. Since our paper was published, the US EPA issued new estimates on GHG emissions from natural gas systems, and many other papers and reports have also evaluated aspects of the GHG footprint of shale gas. In Feburary 2012, we published a paper synthesizing and summarizing this new information [2]. In this talk, I will further update the rapidly changing state of knowledge on the GHG footprint of shale gas.

Uncertainties and sensitivity analysis

Methane venting and leakage dominates the GHG footprint of shale gas, particularly when considered using the most recently available information on global warming potential that integrates the effect of methane over a 20-year time period. The influence of methane is diminished at the 100-year time frame. Over a wide range of estimates of methane emission, the GHG footprint of shale gas is worse than other fossil fuels, when viewed at the 20-year scale. The most recent evidence suggests that many studies continue to underestimate the magnitude of methane emisisons.

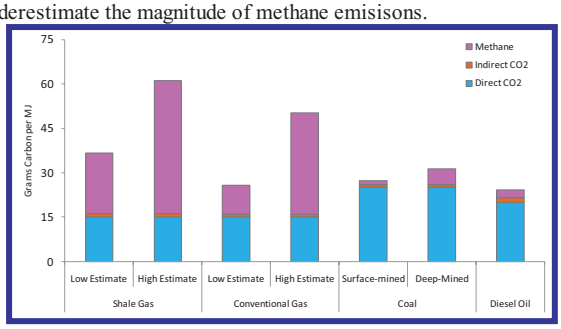

Figure 1: Comparison of the GHG footprint of shale gas with other fuels, using 20-year global warming potentials for methane. From [1].

[1] Howarth et al. (2011) *Climatic Change Letters,* doi: 10.1007/s10584-011-0061-5. [2] Howarth et al. (2012) *Climatic Change*, doi:10.1007/s10584-012-0401-0.

Trace element partitioning in mixed-habit diamonds

D. HOWELL[1]*, W.L. GRIFFIN[1], W. POWELL[1], P. WIELAND[1], N. PEARSON[1], S.Y O'REILLY[1]

[1]CCFS ARC Centre of Excellence, GEMOC, Macquarie University, Sydney, NSW 2109, Australia (*daniel.howell@mq.edu.au)

Mixed-habit diamonds are those that exhibit periods of growth during which they were bound by two surface forms [1], namely smooth faceted octahedral growth in combination with hummocky, non-facetted "cuboid" surfaces whose mean orientation is {100} [2]. This type of diamond is commonly referred to as *star* or *centre-cross*, because the cuboid sectors can sometimes have a much darker appearance compared to the gem-quality octahedral sectors.

Analysis of mixed-habit diamonds has already revealed a preferential partioning of nitrogen between the two sectors [3]. Nickel has also been identified as being present and the cause of the green luminescence in these diamonds [3]; however, exact concentrations or trace element patterns have never been reported.

Laser ablation inductively coupled plasma mass spectrometry (LA-ICPMS) analysis of diamonds has yielded abundant valuable trace-element information and helped to further our understanding of metasomatic fluids in the deep Earth. Traditional *in situ* techniques have had to overcome the issue of using a suitable standard reference material [4-8], but have provided great insights when applied to fluid inclusion-rich diamonds. More recently a closed-system (i.e. off-line) laser ablation technique has been developed [9] that has been applied succesfully to measure the low impurity levels present in gem-quality diamonds. The sacrifice made to obtain these low detection limits is a loss of spatial resolution. This is due to the large ablation areas required (approximately 500 × 500 μm in area, with depths ranging from 200 – 400 μm).

In this study we present a modified off-line LA-ICPMS method for analysing diamonds. Instead of trapping the ablated material in a closed cell, it is collected in a liquid. We apply this larger-scale ablation technique to investigating the partitioning of trace elements between octahedral and cuboid sectors in a collection of large (>6mm) mixed-habit diamonds. This is the first set of trace element data to be collected from mixed-habit diamonds, and integrated with several other types of analysis (infrared mapping, cathodo-luminescence imaging and spectroscopy, in-situ carbon-isotope analysis by secondary ion mass spectrometry), they will provide further insights into the specific geochemical conditions of formation for this interesting subset of diamonds.

[1] Frank (1967) *Proc. Int. Industrial Diamond Conf., 119-135*. [2] Lang (1974) *Proc. R. Soc. Lond.,* **A. 340**, 233-248, [3] Welbourn et al. (1989) *J. Crystal Growth*, **94**, 229-252, [4] Rege et al. (2005) *J. Anal. At. Spectrom.*, **20**, 601-611, [5] Resano et al. (2005) *J. Anal. At. Spectrom.*, **18**, 1238-1242, [6] Tomlinson et al. (2005) *Geochim. Cosmochim. Acta*, 69, 4719-32, [7] Weiss et al. (2008) *Chem. Geol.*, **252**, 158-168, [8] Dalpe et al. (2010) *J. Forensic Sci.,* **55**, 1443-1456, [9] McNeill et al. (2009) *J. Phys.: Condens. Matter*, **21**, 364207.

https://doi.org/10.1180/S0026461X00008434 Published online by Cambridge University Press

Engineering controls on fly ash chemistry: Examples from Kentucky power plants

JAMES C. HOWER[1]

[1] University of Kentucky Center for Applied Energy Research, 2540 Research Park Drive, Lexington, KY 40511, james.hower@uky.edu

The chemistry of fly ash is controlled by a number of factors: 1/ chemistry of the feed coal (and added fuels, such as petroleum coke, tires, biomass, etc.), 2/ size consist of the fuel feed (controlled by pulverized fuel vs. cyclone combustion, maintenance of pulverizers, etc.), 3/ design of the boiler and pollution control system, and 4/ temperature of the flue gas at the collection point. In general, for any electrostatic precipitator (ESP) or baghouse system, the concentrations of volatile trace elements in fly ash will increase with a drop in the flue gas temperature and a decrease in the particle size. Mercury is an exception, requiring carbon to be present in the fly ash for any appreciable amount of Hg to be captured.

Changes in the design of two Kentucky power plants, both originally using central Appalachian coal sources, and the consequent impact on the fly ash chemistry were examined through sampling for a number of studies from 2000 to 2012. One plant, typically burning medium-S eastern Kentucky coals, bypassed two rows of mechanical (cyclone) collectors, consequently sending coarser fly ash to the ESPs. Among the consequences of the design change are a 1st-row ESP C, As, and Hg content than in the ESP fly ash without the coarse ash. The utility is currently installing dry scrubbing to control SO_2 emissions, allowing them to broaden their fuel supply to include high-S coals.

A second plant was burning low-S coal, but installed flue-gas desulfurization (FGD) in anticipation of more stringent regulation of emissions. As with the first plant, this change allows them to pursue a wider range of coals than the central West Virginia sources previously utilized; over 2.5% total S vs. 0.8% prior to the FGD installation. The post-FGD-installation fly ash contains much higher Fe_2S and CaO and lower Al_2O_3 and SiO_2 than the pre-FGD fly ash. The Hg content, while never as high as at some power plants, is below the detection limit in the post-FGD fly ash.

The Coupling of Voltammetric Microelectrodes with Optical Microscopy: A Novel Combination as Applied to the Study of Neutrophilic Iron Oxidizers

PATRICIA L. HREDZAK-SHOWALTER[1*], SEAN T. KREPSKI[2], CLARA S. CHAN[2], DAVID E. EMERSON[3], GEORGE W. LUTHER III[1]

[1]School of Marine Science and Policy, College of Earth, Ocean and Environment, The University of Delaware, Lewes, DE 19958, USA (*hredzak@udel.edu)

[2]Department of Geological Sciences, The University of Delaware, Newark, DE 19716, USA

[3]Bigelow Laboratory for Ocean Sciences, West Boothbay Harbor, ME 04575, USA

Voltammetric solid-state Au/Hg microelectrodes measure multiple analytes, including dissolved oxygen, sulfide, thiosulfate, polysulfides, iodide, Fe^{2+}, Mn^{2+}, and FeS simultaneously at the (sub)millimeter scale. These electrodes are ideal for the *in situ* quantification of the chemical gradients within redox transition zones, ubiquitous in the natural environment or created in the laboratory, and have been used to examine Fe(II) oxidation by neutrophilic iron oxidizers. Use of Au/Hg microelectrodes alone in redox transition zones have inherent limitations as the exact location of the electrode tip where analytes are detected cannot be pinpointed.

To advance chemical and microbial studies we have coupled voltammetric solid-state Au/Hg microelectrodes with optical microscopy using an optical resolution of 0.55 μm in specially designed microslide growth chambers. Higher optical resolutions can be used on the microslides alone. The resulting microslide profiles yield quantifiable chemical gradients including O_2 and Fe(II) associated with both isolated species in artifical media and with samples of naturally occuring flocculent material in freshwater believed to contain iron oxidizers. These profiles are consistent with other profiles obtained from sediments and microbial mats. This novel combination allows for high resolution images to be simutaneously aquired with the electrochemical measurements and the exact location of the electrode tip is known. The coupling of voltammetric microelectrodes with high resolution microscopy is applicable to the study of the chemistry of the microenvironments of other types of microbes as well as microbial biofilms.

https://doi.org/10.1180/S0026461X00008434 Published online by Cambridge University Press

Clumped Isotope Paleothermometry: Interpreting Lacustrine Climate Records

HREN, M.T. [1*], SHELDON, N.D.[2], LOHMANN, K.[2]

[1]University of Tennessee, Knoxville, TN, USA mhren@utk.edu (* presenting author)
[2]University of Michgan, Ann Arbor, MI, USA, ndsheldon@umich.edu
[3]University of Michgan, Ann Arbor, MI, USA, kacey@umich.edu

"Clumped Isotope" measurements of carbonate offer a powerful tool for reconstructing the paleotemperature of past environments. One of the key challenges to interpreting clumped isotope measurements is to understand both the temperature-dependent relationship of the system, and how carbonate formation temperatures relate to broader climatic conditions. We examine timescales of carbonate formation in terrestrial systems to determine how clumped isotope temperature measurements relate to climate. Specifically, we use surface temperature records from lakes spanning a wide range of latitudes and elevation to develop transfer functions that relate seasonal temperature to mean annual air temperature. These functions enable determination of mean annual climate from proxies that record a seasonal signal. Transfer function relationships are applied to an example from the Isle of Wight, UK, to constrain the magnitude of temperature change during the Eocene-Oligocene transition using freshwater biotic carbonate. Δ_{47} measurements of pristine, aragonitic gastropod carbonate produce unreasonably high Eocene and Oligocene paleotemeprature estimates using established temperature-dependent relationships. However, transfer functions that account for timing of carbonate formation produce reasonable measures of mean annual temperature and the overall change in MAT during the Eocene-Oligocene transition. These data show that the Δ_{47} paleotemperature proxy provides a powerful and accurate measure of paleoclimate when appropriate transfer functions that relate timescales of carbonate formation are employed. Such an approach must be considered in the application of this proxy to terrestrial systems for problems ranging from paleoclimate to paleoelevation studies.

Evaporite assimilation 'window' triggers sulfide immiscibility

HRYCIUK, M.[1*], BÉDARD, J.H.[2], MINARIK, W[1]. AND WING, B.[1]

[1]McGill University, Montréal, Canada, matthew.hryciuk@mail.mcgill.ca * (presenting author)
[2]Geological Survey of Canada, Québec, Canada

The assimilation of sulfur from sedimentary evaporites by mafic and ultramafic intrusions may trigger the formation of Noril'sk-Type Ni-Cu-PGE (platinum group element) deposits. The Neoproterozoic Minto Inlier on Victoria Island of the western Canadian Arctic exposes dikes, sills and flood basalts from the Franklin Large Igneous Province and sedimentary rocks of the Shaler Supergroup. The Franklin intrusives have many features in common with those in the Noril'sk region of Russia. Both intrude a sequence of carbonates, shales, evaporites and sandstones and are sill-dominated with fault-controlled conduit systems. The excellent exposure on Victoria Island enables intrusive-host rock interactions to be studied directly.

In order to investigate the process of evaporite assimilation, we collected samples through a 5m thick evaporite-hosted sill and the underlying 5m of sedimentary rocks. The host evaporites are part of the Minto Inlet Formation and consist of interbedded carbonate, gypsum and anhydrite. The host sulfate evaporites have $\delta^{34}S$ values between +15.9 and +16.2‰ and the sill has elevated $\delta^{34}S$ values between +11.4 and +12.9‰ in the core and upper sill that imply contamination from crustal sulfate source. However, the lower chilled margin has a $\delta^{34}S$ value of only +1.9‰, within the range of primary igneous values from other sills in the area.

The sulfur isotope value of the chill margin indicates that sulfur was not directly introduced into the sill from the sedimentary rocks below. Possible explanations for elevated S-isotope values within the sill include stoping and mechanical assimilation along the upper sill contact; or the delivery of sulfate contamination from upstream in a later magma pulse. Using simple mixing calculations, we estimate that the sill has assimilated up to 0.4 to 0.7 wt% anydrite. Based on calibrated relationships between evaporite assimilation, sulfur solubility and oxidation state, this range of evaporite assimilation is within a favourable 'window' for ore deposits. It is enough to generate sulfide immiscibility, while being low enough to avoid oxidation of the magma and resorption of the sulfur.

https://doi.org/10.1180/S0026461X00008434 Published online by Cambridge University Press

Using ^{228}Ra to assess ocean mixing and nutrient fluxes in the Cape Basin

YU-TE HSIEH[1*], WALTER GEIBERT[2,3], E. MALCOLM S. WOODWARD[4], AND GIDEON M. HENDERSON[1]

[1]University of Oxford, Department of Earth Sciences, Oxford, UK, yuteh@earth.ox.ac.uk (* presenting author)
[2]University of Edinburgh, School of Geosciences, Edinburgh, UK
[3]Scottish Association for Marine Sciences, Oban, UK
[4]Plymouth Marine Laboratory, Plymouth, UK

In the South Atlantic Ocean, the Cape Basin holds an important position for dynamic inter-ocean exchange between the Atlantic Ocean and the Indian Ocean (e.g. Agulhas Current Leakage), and for transition from the macronutrient-limited subtropical gyre to the micronutrient-limited Southern Ocean [1]. Nutrients and micronutrients play important roles in marine productivity in the Cape Basin, but their sources and fluxes to this region remain unclear.

Radium-228 has been applied to the study of a variety of oceanographic processes, including tracing of water masses; quantifing mixing processes; and constraining fluxes of dissolved species to the ocean [2]. With a short half-life of 5.75 years, ^{228}Ra is very suitable to assess ocean mixing rates, and the fluxes of nutrients and trace metals into the euphotic zone by vertical and horizontal mixing [3]. In this study, we measure the distribution of seawater ^{228}Ra and ^{226}Ra in the water column of the Cape Basin during the UK-GEOTRACES cruise (GA10E) and use these measurements to calculate horizontal and vertical mixing rates, and resulting nutrient fluxes to the surface ocean of the Cape Basin. A newly developed MC-ICP-MS technique with improved analytical precision has been applied to measure of seawater ^{228}Ra and ^{226}Ra in this study [4]. Vertical and horizontal ^{228}Ra profiles are used to determine the diapycnal and isopycnal mixing rates respectively in the surface ocean of the Cape Basin. The ^{228}Ra-derived vertical mixing rates coupled with the vertical nutrient profiles (nitrate, phosphate and silicate) are then used to estimate the upward nutrient fluxes into the euphotic zone. Assuming steady state, the upward nitrate fluxes are coverted to the organic carbon fluxes in the surface ocean. The observations of the vertical nutrient fluxes suggest that the marine productivity in the Cape Basin is nitrogen-limited in early spring of the southern hemisphere. This study provide important estimates of ocean mixing and nutrient fluxes in the Cape Basin, which enable us to understand the nutrient cycles and biological activities in the macronutrient-limated subropical gyre.

[1] Gordon (1985) *Science* **227**, 1030-1033. [2] Moore et al. (2008) *Nature Geosci.* **1**, 309-311. [3] Ku and Luo (2008) *Radioactivity in the Environment* **13**, 307-344. [4] Hsieh and Henderson (2011) *J. Anal. At. Spectrom.* **26**, 1338-1346.

The Reduction and Surface Complexation of Mercury by *Geobacter sulfurreducens* PCA

HAIYAN HU[1,2], WANG ZHENG[1], JEFFRA SCHAEFER[3], XINBIN FENG[2], LIYUAN LIANG[1], DWAYNE ELIAS[1], AND BAOHUA GU[1*]

[1]Oak Ridge National Laboratory, Environmental Sicences Division, Oak Ridge, TN 37830, USA, gub1@ornl.gov
[2]Institute of Geochemistry, Chinese Academy of Sciences, Guiyang, China
[3]Department of Geosciences, Princeton University, Princeton, NJ 08544, USA

Understanding the biogeochemical processes that control mercury (Hg) redox transformations is necessary to predict Hg availability for microbial methylation, its fate and transport in the environment. Previous studies have shown that a wide variety of microorganisms are capable of reducing the mercuric Hg(II) to elemental Hg(0) under anaerobic conditions, but others have indicated an inverse correlation between microbial biomass and Hg(0) production. In this study, we systematically examined the reduction kinetics and surface interactions between Hg(II) and washed cells of *G. sulfurreducens,* as influenced by the growth stage of cells, cell density, the presence or absence of various complexing ligands, including glutathione and naturally dissolved organic matter (DOM). We found that Hg(II) can be rapidly reduced to Hg(0) upon contact with washed cells, but reduction rates and extent are influenced by the growth stage, cell density and Hg(II)/cell ratio. The initial reduction rates can generally be described by a pseudo-first order kinetics with half-lives on the order of minutes to less than 2 hr. An optimal reduction of Hg(II) at a fixed concentration of 50 nM was observed at a cell density of ~10^{11} L^{-1}; an increase in cell density inhibited the reduction of Hg(II) due to surface adsorption and complexation of Hg(II) on bacterial cells. Similarly, the presence of complexing organic ligands inhibited the Hg(II) reduction at varying degrees, with glutathione among the most effective in inhibiting Hg(II) reduction and surface complexation by *Geobacter* cells. Our findings explain some previously observed inconsistencies with respect to the roles of microorganisms in Hg(II) reduction and may have important implications to the availability and bioaccumulation of Hg in the aquatic food web.

https://doi.org/10.1180/S0026461X00008434 Published online by Cambridge University Press

Mg isotope composition of the bulk silicate earth constrained by first princeples calculation

FANG HUANG[1*], ZHONG-QING WU[2], LI-JUAN CHEN[1]

[1] CAS Key Laboratory of Crust-Mantle Materials and Environments, School of Earth and Space Sciences, USTC, Hefei, Anhui 230026. Email: fhuang@ustc.edu.edu

[2] School of Earth and Space Sciences, University of Science and Technology, Hefei, Anhui 230026, China

Comparisons of stable isotope composition of the bulk silicate earth (BSE) with chondrites have provided a plethora of important insights into the Earth's generation and evolution processes. Many recent studies argue that the Earth may have similar Mg isotope composition with the CI chondrites, suggesting that planetary accretion or mantle melting does not significantly fractionate Mg isotope composition [e.g., 1,2]. Because mantle samples from the depths greater than 150 km are rare, most studies used basalts and spinel-peridotite xenoliths representing the BSE assuming no measurable variation of δ^{26}Mg (<0.1‰) at the mantle's P-T conditions. However, recent studies clearly show that substantial equilibrium Mg isotope fractionation could occur to mantle minerals due to different C.N. and ionic strengths of Mg in the minerals [e.g., 3,4]. Thus it is necessary to examine the assumption before using shallow mantle samples to represent the BSE.

We use first-principles calculation to predict Mg isotope variations in mantle minerals with depths down to the core-mantle boundary. Our results show that increasing temperature dramatically decreases isotope fractionation, while increasing pressure can enhance it. Therefore, significant fractionation of Mg isotopes between mantle minerals at high P-T can still be expected. Along the mantle's geotherm, $\Delta^{26}Mg_{olivine\text{-}garnet}$ varies from ~0.5‰ (2GPa) to 0.2‰ (13.4 GPa, ~410 km), owing to the combined effects of different C.N. (6 in olivine vs. 8 in garnet) and increasing temperature. Wadsleyite is enriched in heavy Mg isotopes relative to olivine and ringwoodite likely due to mineral structure change. At 670 km discontinuity, ringwoodite (C.N.=6) is isotopically heavier than Mg-perovskite (C.N.=8) by 0.28‰ while it is identical with periclase (C.N.=6).

Our preliminary results suggest that Mg isotope compositions of the mantle peridotites could be quite heterogeneous. This brings up some uncertainties when extrapolating δ^{26}Mg of the BSE from basalt and spinel-peridotite data. Specifically, olivine and garnet, the two dominant Mg-bearing minerals in the upper mantle, show varying Δ^{26}Mg by ~ 0.3‰ with increasing the depth, meaning that olivine, garnet, or both have variable δ^{26}Mg. Therefore, it is difficult to predict variations of δ^{26}Mg of olivine and garnet along the temperature-pressure gradient. As δ^{26}Mg of the bulk mantle is a weighted average of the six- and eight- coordinated minerals, Mg isotope composition of the BSE may still be an open question.

[1] Bourdon B. et al. (2010) ***GCA***, 74: 5069-5083. [2] Teng F.-Z. et al. (2010). ***GCA***, 74: 4150-4166. [3] Liu S.-A. et al. (2011) ***EPSL***, 308: 131-140. [4] Schauble E.A. (2011) ***GCA***, 75: 844-869.

Weathering of mafic rocks and early animal evolution in the Ediacaran of South China

JING HUANG[1], XUELEI CHU[2*], TIMOTHY W. LYONS[3], NOAH J. PLANAVSKY[4] AND HANJIE WEN[5]

[1]Institute of Geology and Geophysics, CAS, Beijing 100029, China, jhuang@mail.iggcas.ac.cn

[2]Institute of Geology and Geophysics, CAS, Beijing 100029, China, xlchu@mail.iggcas.ac.cn (* presenting author)

[3]Dept. of Earth Sciences, Univ. of California, Riverside, CA 92521, USA, timothyl@ucr.edu

[4]Dept. of Earth Sciences, Univ. of California, Riverside, CA 92521, USA, planavsky@gmail.com

[5]Institute of Geochemistry, CAS, Guiyang, Guizhou 550002, China, wenhanjie@vip.gyig.ac.cn

Acanthomorphic acritarch fossils, including some interpreted to be early animal embryos and the resting stages of Metazoa offspring, first appear in the Doushantuo Formation of the Yangtze Gorges area (YGA)[1]. Previous investigators have linked the rise of acanthomorphic acritarchs to the termination of the Marinoan glaciation and diversafacation of early eumetazoans, but without specific ties to conditions in the YGA. Recently, however, Bristow *et al*. suggested that non-marine environments might have hosted the acanthomorphic acritarchs preserved in YGA[2]. Their principal argument supporting the non-marine hypothesis is the appearance of the trioctahedral clay mineral saponite in the lower part of Doushantuo Formation, which can form in alkaline conditions (pH > 9) most commonly found in non-marine settings. However, other possibilities exist for its formation. For instance trioctahedral clays can forms during weathering of mafic rocks.

Major and trace elemental compositions of the Doushantuo Formation from the YGA imply that sediments overlying the cap carbonate reflect two distinct sources. Member 2 was derived from surrounding Neoproterozoic mafic-to-ultramafic rocks, and Members 3 and 4 were likely sourced from recycled sediments with an average shale composition. Using a coupled geochemical and sedimentological approach we argue that the trioctahedral clay mineral saponite in the lower Doushantuo of the YGA are better explained as weathering products from the regional mafic-to-ultramafic hinterland delivered by rivers to a shelf lagoon of the Yangtze Gorges Basin. Therefore, the saponite of the YGA and the associated fossils are easily interpreted within a marine depositional context and, thus, the semi-restricted setting may have favored deposition of sediments with a local provenance signature.

Although weathering of mafic volcanics commonly leads to the formation of a mix of trioctahedral and dioctahedral clays, there have been reported cases of the formation of predominantly trioctahedral clays. Further, trioctahedral clays are the dominant products during the early stages of mafic rock weathering, with subsquent formation of dioctahedral clays. Thus, it is reasonable to imagine that rapid weathering rates after the Neoproterozoic Snowball Earth favored trioctahedral clay formation and preservation.

[1] Yin *et al.* (2007) *Nature* **446**, 661-663. [2] Bristow *et al.* (2009) *Proc. Natl. Acad. Sci. USA* **106**, 13190-13195.

https://doi.org/10.1180/S0026461X00008434 Published online by Cambridge University Press

Towards an improved understanding of Paleoceanographic proxies for Antarctic Intermediate Water Circulation: A core-top perspective

KUO-FANG HUANG*, DELIA W. OPPO, WILLIAM B. CURRY AND JERZY S. BLUSZTAJN

Department of Geology and Geophysics, Woods Hole Oceanographic Institution, Woods Hole, MA, USA.

kfhuang05@gmail.com (*presenting author)

Abstract

The Atlantic Meridional Overturning Circulation has been recognized as a major component of the climate system and is important for oceanic heat transport on millennial and glacial-interglacial timescales (Burton et al., 1997; Rutberg et al., 2000; Piotrowski et al., 2005; Roberts et al., 2010). The records for an important component of this circulation - Antarctic Intermediate Water - are ambiguous, giving rise to conflicting interpretations about the long-term history of AAIW flow into the North Atlantic (Came et al., 2008; Pahnke et al., 2008). To further constrain the past AAIW variability, we systematically examine water mass proxies, such as nutrient tracers (Cd/Ca and $\delta^{13}C$) in benthic foraminifera and the Nd isotopes in uncleaned planktonic foraminifera using a set of multicore tops (KNR197-3, spanning depths of 380 to 3300 m) and measured seawater chemistry from the Demerara Rise in the western tropical Atlantic. AAIW and NADW overlie the Demerara Rise sediments at these water depths.

Both seawater Cd and $\delta^{13}C$ at Demerara Rise closely mimic salinity. Cd/Ca of the three benthic foraminifera (*C. pachyderma*, *C. wuellerstorfi* and *Uvi. spp*.) capture the regional seawater Cd profiles and are best explained by a single partition coefficient D_{Cd}= 2.7, similar to values typically found below 2000 m. $\delta^{13}C$ of individual specimens (*C. pachyderma* and *C. wuellerstorfi*) from multicore tops also reflect the different water mass isotopic compositions. Our seawater Nd isotope data follows the distribution of salinity, demonstrating conservative mixing of Nd in the water column at Demerara Rise. Furthermore, ε_{Nd} in uncleaned planktonic foraminfera faithfully record the seawater ε_{Nd}, suggesting that we will be able to reconstruct changes in the shape of bathymetric profile of ε_{Nd} through time and downcore ε_{Nd} changes at a single site in our study area. Preliminary downcore work will be presented.

[1] Burton *et al*. (1997) *Nature* **386**, 382-385. [2] Rutberg *et al*. (2000) *Nature* **405**, 935-938. [3] Piotrowski *et al*. (2005) *Science* **307**, 1933-1938. [4] Roberts *et al*. (2010) *Science* **327**, 75-78. [5] Came *et al*. (2008) *Paleoceanography* **23**, PA1217. [6] Pahnke *et al*. (2008) *Nat. Geosci*. **1**, 870-874.

Relationship between the Isotopic Compositions of Earth and Chondrites: Constraints from Calcium Isotopes

SHICHUN HUANG[1]* AND STEIN B JACOBSEN[1]

[1]Department of Earth and Planetary Science, Harvard University, huang17@fas.harvard.edu; jacobsen@neodymium.harvard.edu

Chondritic meteorites have been used to estimate the elemental and isotopic compositions for refractory lithosphile elements of the bulk Earth. Recent studies reported both mass-dependent and mass-independent isotopic differences between terrestrial rocks and chondrites. Such isotopic differences have been used to argue for (i) a hidden reservoir burried deep at the bottom of the mantle; (ii) certain elements partitioning into the Earth's core; or (iii) that the bulk Earth does not have a chondritic composition for the refractory lithosphile elements.

Here we present Ca isotopic measurements of three groups of chondrites (carbonaceous, ordinary and enstatite chondrites). Our results show that Ca is the only major element in addition to O that show both mass-dependent (δ-values) and mass-independent (ε-values) isotopic variations among chondrite groups. In contrast, all chondrite groups have essentially the same Mg, Si and Fe isotopic compositions. Our results show that $\delta^{44/40}Ca$ decreases in the order of enstatite chondrites > ordinatry chondrites > carbonaceous chondrites, with enstatite chondrites having the same $\delta^{44/40}Ca$ as the estimated bulk Earth value. Carbonaceous chondrites also have up to 3 ε units of ^{48}Ca excess compared to the Earth. In contrast, such ^{48}Ca excess is not observed in ordinary or enstatite chondrites.

Enstatite chondrities and the Earth have the same isotopic compositions for all major and minor elements (O, Ca, Ti, Cr) which exhibit substantial isotopic variations among different chondrite groups, with Si being the only exception. Available data show that enstatite chondrites have lower $\delta^{30}Si$ compared to the Earth's mantle. Since only EH chondrites, which have high metal contents and whose metals have very different Si isotopic composition, have been analyzed for Si isotopes, the measured Si isotopic compositions in EH chondrites may not represent the isotopic composition of their parental nebular reservoir.

The identical isotopic compositions of the Earth and enstatite chondrites and their very different chemical compostions imply that they are derived from the same parental nebular reservoir, but experienced different formation processes.

https://doi.org/10.1180/S0026461X00008434 Published online by Cambridge University Press

Rare earth element geochemistry of marine carbonate reservoir in northeast Sichuan, China

HUANG YI[1,2*], LIU SHUGEN[3], ZHANG WEI[1], CHEN YING[1], HU QIANG[1], WU HAO[1], TANG QING[1],

[1]Department of Geochemistry, Chengdu University of Technology, Sichuan, PRC, huangyi@cdut.cn (* presenting author)
[2]Applied Nuclear technigues in Groscience Key Laboratory of Sichuan Proviance, PRC
[3]State Key Lab of Oil and Gas Reservoir Geology and Exploitation, Chengdu University of Technology, Sichuan, PRC

Abstract

Samples were collected from marine carbonate reservoir of northeast of Sichuan province, China. And REE of those samples were analyzed to statement ΣREE, LREE, HREE, δEu and δCe geochemical characteristics. Using the mechanism of REE migration, enrichment and fractionation, the nature of fluid and diagenesis environment were distinguished. The impact of deep fluid was also analyzed to study the formation of carbonate rock geochemistry and the diagenesis environment.

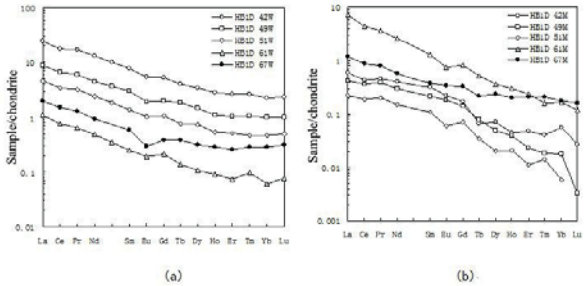

Figure 1. The REE partitioning patterns for (a) wall rock, and (b) veins

Results and Conclusion

The results show that during the diagenesis process of the original marine limestone, REE in protolith has been constantly depleted and manifested similar ΣREE values between wall rock and the veins. The δEu value of samples from wells Heba1 and Ma2 are greater than zero and less than 1, which indicates an open oxidizing environment. The δEu values of other drilling samples are greater than 1, which suggests an effect of high temperature hydrothermal fluids with Eu anomalies and hot water dissolution. Comparing with the veins and the Earth REE patterns, there're similar REE patterns between veins and the original mantle, which could be related to the activities of the mantle fluids.

[1] Huang J. Chu X. L., Chang H. J., Feng L. J. (2009) *Chinese Science Bulletin,* **54(2)**, 3498-3506.

A new pore-scale model of diffusion and advection of reactant in a dissolving porous media

CHRISTIAN HUBER[1*], BABAK SHAFEI[1], AND ANDREA PARMIGIANI[2]

[1]Georgia Institute of Technology, Atlanta, GA 30332, USA, christian.huber@eas.gatech.edu , babakshafei@gatech.edu
[2]University of Geneva, Geneva, Switzerland, andrea.parmigiani@unige.ch

We have developed a new model of pore-scale reactive transport based on the lattice Boltzmann method (LBM). LBM has already been successfully applied to reactive transport by Kang and co-workers [1 & 2]. Our model offers a natural approach to handle porosity changes in the solid matrix during dissolution and precipitation. It also uses an iterative solver for the coupling of the reactant transport with surface reactions which allows us to explore a wide range of reaction rates and non-linear heterogeneous reactions. In a first application, we present the results of calculations aiming at investigating the effect of matrix dissolution during multiphase flow (e.g. CO_2 injection into an aquifer). We find that although dissolution processes and multiphase flows in porous media generally lead to channelization, i.e. wormhole structure and capillary instabilities respectively, dissolution during multiphase flows stabilizes the reactive front leading yielding a homogeneous distribution of CO_2 in the pore space (see Fig. 1) [3]. In a second application, we incorporate subgrid-scale roughness at the solid-fluid interface in a single phase reactive transport model. The presence of surface roughness can significantly increase the reactive surface area at the pore-scale. We propose some simple laws for the development and evolution of a time-dependent local surface roughness as function of reaction rates and local chemical disequilibrium and investigate its effect on the development of flow and reactive patterns at the mesoscale (~100 pores/physical dimension).

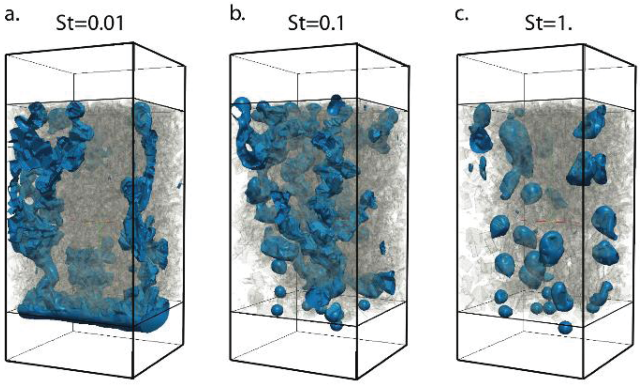

Figure 1: Snapshots of volatile (CO2) transport (blue) in a dissolving porous media with dissolution rates increasing from left to right.

[1] Kang, Zhang and Chen (2003) *PRE* **65**. [2] Kang, Lichtner and Zhang (2006) *JGR* **111**. [3] Parmigiani *et al.* (2011) *JFM* **686**, 40-76.

https://doi.org/10.1180/S0026461X00008434 Published online by Cambridge University Press

Shale Gas: A Panacea for the Energy Woes of America?

J.D. HUGHES[1]

[1]Post Carbon Institute and Global Sustainability Research Inc., davehughes@xplornet.com

The Hype

Shale gas has been heralded as a "game changer" in the struggle to meet America's demand for energy. The "Pickens Plan" of Texas oil and gas pioneer T.Boone Pickens suggests that gas can replace coal for much of U.S. electricity generation, and oil for, at least, truck transportation[1]. Industry lobby groups such as ANGA declare "that the dream of clean, abundant, home grown energy is now reality"[2]. In Canada, politicians in British Columbia are racing to export the virtual bounty of shale gas via LNG to Asia (despite the fact that Canadian gas production is down 16 percent from its 2001 peak). And the EIA has forecast that the U.S. will become a net exporter of gas by 2021[3].

The Reality

Shale gas is expensive gas. In the early days it was declared that "continuous plays" like shale gas were "manufacturing operations", and that geology didn't matter. One could drill a well anywhere, it was suggested, and expect consistent production. Unfortuately, Mother Nature always has the last word, and inevitably the vast expanses of purported potential shale gas resources contracted to "core" areas, where geological conditions were optimal. The cost to produce shale gas ranges from $4.00 per thousand cubic feet (mcf) to $10.00, depending on the play. Natural gas production is a story about declines which now amount to 32% per year in the U.S. So 22 billion cubic feet per day of production now has to be replaced each year to keep overall production flat. At current prices of $2.50/mcf, industry is short about $50 billion per year in cash flow to make this happen[4]. As a result I expect falling production and rising prices in the near to medium term.

The Environmental Costs

The mantra that natural gas is a "transition fuel" to a low carbon future is false. The environmental costs of shale gas extraction have been documented in legions of anecdotal and scientific reports. Methane and fracture fluid contamination of groundwater, induced seismicity from fracture water injection, industrialized landscapes and air emissions, and the fact that near term emissions from shale gas generation of electricity are worse than coal. A sane energy security strategy for America must focus on radically reducing energy consumption through investments in infrastructure that provides alternatives to our current high energy throughput. Shale gas will be an important contributor to future energy requirements, given that other gas sources are declining, but there is no free lunch.

[1] http://www.pickensplan.com/.
[2] http://anga.us/why-natural-gas/abundant/shale-plays .
[3] http://www.eia.gov/forecasts/aeo/er/ .
[4]http://arcfinancial.com/research/energy-charts/who-is-eating-at-the-petroleum-club/.

Spatial and seasonal variations of the δ^{30}Si signatures in the Amazon Basin

H.J. HUGHES[1], F. SONDAG[2], L. ANDRÉ[1]*, D. CARDINAL[3]

[1]Royal Museum for Central Africa, Tervuren, Belgium (* presenting author), harold.hughes@africamuseum.be
[2]LMTG (Université de Toulouse III, CNRS, IRD), Brasilia, Brazil
[3]LOCEAN, Université Pierre et Marie Curie, Paris, France

The Amazon Basin is the world's largest basin and covers an area of 6.1 million km^2 occupied for more than 96% of its surface by silicate rocks [1]. We present here the first large-scale study of riverine silicon isotopes signatures in the Amazon Basin. The Amazon and its main tributaries, which can be considered as representative of the main types of rivers in the basin, were studied at different seasons of the annual hydrological cycle. Concentrations of dissolved silicon (DSi) and of biogenic silica particles were measured as well as isotopic signatures of DSi. An occasional impact of diatoms growth on the silicon cycle and isotopic signatures is observed, but outside these periods of high biologic influence, δ^{30}Si signatures of the different rivers are shown to correlate with DSi concentrations. This is probably a consequence of the more important impact of clay formation during low flow period. The mean δ^{30}Si signature measured in the Amazon River itself is +1.0‰ (n=6), a value similare to that measured in the Congo River (+0.96‰ [2]). Very low isotopic signatures were measured in the upper Río Negro, confirming recent observations in Congolese black rivers. We also tested the homogeneity of the Amazon River regarding DSi concentration and isotopic ratio: A river cross-section shows the homogeneity of the Amazon River when diatoms activity is low. Our data provide evidences that silicon isotopic signatures of rivers result from a complex combination of biological and geological processes which contribution to the silicon biogeochemical cycle varies spatially and seasonally.

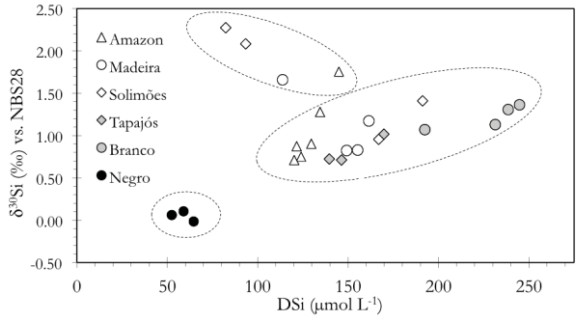

Figure 1:. Three groups of samples can be defined in the Amazon Basin: Samples showing a decreasing DSi concentration for increasing δ^{30}Si ratio, most probably due to diatoms uptake; samples showing a simultaneous increase of DSi concentration and δ^{30}Si ratio; and the Rio Negro samples

Reference

[1] Amiotte-Suchet et al., (2003) *Global Biogeochem. Cycles* **1**, 1038-1051.
[2] Hughes et al. (2011) *Limnol. Oceanogr.* **56**, 551-561.

https://doi.org/10.1180/S0026461X00008434 Published online by Cambridge University Press

Experimental climate warming in a French peatland: impact on the abundance and distribution of branched GDGTs

A. HUGUET[1*], C. FOSSE[2], F. LAGGOUN-DEFARGE[3], AND S. DERENNE[1]

[1] BioEMCo, CNRS/UPMC UMR 7618, Paris, France, arnaud.huguet@upmc.fr (* presenting author)
[2] Chimie ParisTech (ENSCP), Paris, France
[3] ISTO, UMR 7327 CNRS–Univ. d'Orléans, Orléans, France

Branched glycerol dialkyl glycerol tetraethers (GDGTs) are complex lipids of high molecular weight, recently discovered in soils and produced by still unknown bacteria. They are increasingly used as paleoclimate proxies. Their degree of methylation, expressed in the MBT, was shown to depend on mean annual air temperature (MAAT) and to a lesser extent on soil pH, whereas the relative abundance of cyclopentyl rings of branched GDGTs, expressed in the (CBT), was related to soil pH. Northern peatlands contain approximately one third of the world's organic carbon and may play an important role in the responses of the global carbon cycle to climate change. The aim of this work was to study the effects of experimental climate warming on the abundance and distribution of branched GDGTs in a *Sphagnum*-dominated peatland (French Jura Mountains). Air temperature was experimentally increased using a warming system consisting of in situ open mini-greenhouses (Open-Top Chambers – OTCs). The effect of the OTCs was especially apparent in spring and summer, with an increase of mean and maximal air temperatures of ca. 1 and 3°C respectively. Branched GDGTs either present as core lipids (CLs; presumed of fossil origin) or derived from intact polar lipids (IPLs, markers for living cells) were analysed. Results showed that despite the short duration of the climate experiment (26 months), branched GDGT distribution was significantly affected by the temperature rise, supporting the empirical relationship between MBT and MAAT established from a large range of soils. The difference in branched GDGT-derived temperatures between the control and the OTC plots was in the same range as the increase in maximal temperature induced by the OTCs in spring and summer, suggesting that branched GDGT-producing bacteria might be more active during the warmest months of the year. The OTC treatment had no significant effect on the abundance of branched GDGTs, mainly present as "fossil" CLs (70 to 85% of the total extractable branched GDGTs). Furthemore, no significant differences in branched GDGT distribution were observed between CLs and IPLs, which both provided higher MBT and MAAT values for the OTCs. This suggests that the fossil pool of branched GDGTs has a very fast turnover (less than the 2 year duration of the experiment) at peat surface and that branched GDGT distribution may rapidly reflect changes in environmental conditions.

This work was funded as part of the PEATWARM initiative through an ANR (French National Agency for Research) grant (ANR-07-VUL-010).

Dissolved platinum in major rivers of East Asia

YOUNGSOOK HUH[1*], TSEREN-OCHIR SOYOL-ERDENE[2]

[1]Seoul National University, Seoul, Korea, yhuh@snu.ac.kr (* presenting author)
[2]Korea Polar Research Institute, Incheon, Korea, soyoloo@kopri.re.kr

Dissolved platinum concentrations of eleven large pristine river systems in East Asia (~200 samples) were determined to better constrain the oceanic platinum budget. Most samples had concentrations less than 1.4 pM, and relatively high concentrations up to 5.8 pM were measured in only approximately 6% of the samples. Principal component analysis was carried out using Pt, major elements (Na, K, Mg, Ca, HCO_3^-, Cl^-, SO_4^{2-}, Si), Sr, and $^{87}Sr/^{86}Sr$ of the dissolved load to derive the potential sources of Pt. The Pt in the main (<1.4 pM) group was best clustered with Mg, HCO_3^-, Ca, Sr, and SO_4^{2-}, interpreted as weathering of carbonates and associated gypsum. The Pt in the outlier group was best clustered with Si, K, $^{87}Sr/^{86}Sr$, Ca, and HCO_3^-, interpreted as weathering of silicates. The median Pt concentrations of the individual river systems had only a small range, from 0.18 pM (Duman) to 0.63 (Huang He), and the difference in Pt yield mainly resulted from the difference in runoff. The rivers draining the eastern Tibetan Plateau – the Salween, Mekong, Chang Jiang (Yangtze), Hong (Red), and Huang He (Yellow) – had relatively higher Pt yield than the rivers of the Russian Far East – the Amur, Lena, Yana, Indigirka, and Kolyma. The discharge-weighted mean Pt concentration was 0.36 pM for the eleven river systems of East Asia. If this value is extrapolated globally, the estimated riverine flux of dissolved Pt to the ocean is 13×10^3 mol y^{-1}. Based on this riverine flux, the estimated oceanic residence time of Pt is 3×10^4 years.

https://doi.org/10.1180/S0026461X00008434 Published online by Cambridge University Press

Atom exchange between aqueous Fe(II) and Fe oxides: Fate of As(V)

BRITTANY L. HUHMANN*, MICHELLE M. SCHERER, AND ANKE NEUMANN

Department of Civil and Environmental Engineering, The University of Iowa, Iowa City, USA (*correspondence: brittany-huhmann@uiowa.edu)

Human exposure to arsenic in groundwater is a global concern, and arsenic mobility in groundwater is often controlled by iron minerals. Recently, it has been shown that electron transfer and atom exchange between aqueous Fe(II) and iron oxides can enable structural incorporation of trace elements into iron oxides [1]. The structural incorporation of As(V) into magnetite has been observed during magnetite precipitation [2], and during the reductive transformation of lepidocrocite [2] and 2-line ferrihydrite [3] to magnetite. As(V) does not appear, however, to be incorporated into goethite and hematite in the presence of aqueous Fe(II) [4]. To better understand the controls on As(V) incorporation into iron oxides, we investigate whether the presence of As(V) inhibits atom exchange between aqueous Fe(II) and goethite or magnetite, and whether As(V) is incorporated into goethite, magnetite, and ferrihydrite in the presence of Fe(II).

Enriched Fe isotope experiments were used to investigate the extent of Fe atom exchange between aqueous Fe(II) and goethite in the presence of varying concentrations of As(V). Near-complete atom exchange between aqueous Fe(II) and goethite was observed at 1 mg/L As(V), whereas exchange was severely inhibited at the exceedingly high concentration of 20 mg/L As(V). Surface-adsorbed As was determined by phosphate extraction, and the remaining As was recovered by complete dissolution of the solid. As(V) remained adsorbed to the surface of the goethite rather than being incorporated, with 96% of the As(V) recoverable by a phosphate extraction on the time frame of near-complete atom exchange.

Additional experiments are underway to explore the fate of As(V) during Fe atom exchange between aqueous Fe(II) and magnetite and ferrihydrite. We hypothesize that atom exchange between aqueous Fe(II) and magnetite will occur in the presence of As(V) and that that As(V) may be incorporated into the magnetite structure, since As incorporation into magnetite has been observed in other systems [2,3].

[1] Frierdich *et al.* (2011) *Geology* **39**, 1083-1086. [2] Wang *et al.* (2011) *Environ. Sci. Technol.* **45**, 7258-7266. [3] Coker *et al.* (2006) *Environ. Sci. Technol.* **40**, 7745-7750. [4] Catalano *et al.* (2011) *Environ. Sci. Technol.* **45**, 8826-8833.

Tungsten isotopic evolution of the earliest terrestrial mantle

MUNIR HUMAYUN[1*], ALAN D. BRANDON[2], KEVIN RIGHTER[3],

[1]Department of Earth, Ocean & Atmospheric Science & NHMFL, Florida State University, Tallahassee, FL 32310, USA, humayun@magnet.fsu.edu.

[2]Department of Earth & Atmospheric Sciences, University of Houston, Houston, TX 77204, USA, abrandon@uh.edu.

[3]NASA Johnson Space Center, Mail Code KR, Houston, TX 77058, USA, kevin.righter-1@nasa.gov.

Introduction

Recently, two reports of $\varepsilon^{182}W>0$ in Archean samples [1-2] challenge previous conceptions of a homogeneous W isotopic composition of the mantle. The removal of these positive anomalies by late accretion of a chondritic veneer [1] can be quickly refuted by comparison with lunar breccia siderophile element abundances which contain too low an accreted meteoritic component to affect a mantle-wide change in W isotope composition. Here, we present two sets of alternative models to interpret this incredible finding.

Results and Conclusions

Post core-formation mantle: Because D(metal-silicate) for W diminishes with increasing depth [3], the deep mantle has a higher W abundance, and a lower Hf/W ratio and consequently evolves a negative anomaly in $\varepsilon^{182}W$ while the upper mantle evolves a positive $\varepsilon^{182}W$. Subsequent solid-state convection (4.55-2.8 Ga) mixes away the complementary $\varepsilon^{182}W$ anomalies. This set of models predicts that the complementary negative anomalies in $\varepsilon^{182}W$ should eventually be discovered in ancient magmatic rocks.

Hadean melting models: Tungsten is significantly more incompatible (like U, Th and Ba) than Hf, the latter being similar in compatibility to Nd and Sm. Our results show that extraction of low-degree partial melts (<2%) leaving a Hadean depleted mantle that can have Sm/Nd~20% higher than chondrites [4] also creates a $f_{Hf/W}$~2-3, sufficient to generate the anomalies observed [1,2] in the first 100 Ma of Earth history. These models increase Hf/W and Sm/Nd ratios in a correlated fashion explaining the tendency of positive anomalies of $\varepsilon^{182}W$ to occur in rocks with positive $\varepsilon^{142}Nd$. Recycling of the complementary Hadean crust would result in negative anomalies, while partitioning of W into an enriched "hidden reservoir" [5] would not. Evidence from Hadean zircons indicates crust was preserved from 4.4 Ga onwards [6], too late to constrain $\varepsilon^{182}W$ anomalies which are more challenging to create after the first 100 Ma. ^{142}Nd anomalies indicate a melting event around 35-75 Ma after solar system formation [4], the upper end of which is consistent with our models of Hf/W fractionation that also yield a depleted mantle composition consistent with DMM [7]. The presence of $\varepsilon^{182}W$ anomalies in the Hadean mantle complicates the search for W isotopic evidence of core-mantle interaction, now predicted to be $\varepsilon^{182}W$~ -0.1 [8].

[1] Willbold et al. (2011) *Nature* **477**, 195-198. [2] Touboul et al. (2011) *Min. Mag.* **75**, 2026. [3] Righter (2011) *EPSL* **304**, 158-167. [4] Bennett et al. (2007) *Science* **318**, 1907-1910. [5] Boyet and Carlson (2005) *Science* **309**, 576-581. [6] Wilde et al. (2001) *Nature* **409**, 175-178. [7] Salters and Stracke (2004) *G-cubed* **5**, Q05004, doi:10.1029/2003GC000597. [8] Humayun (2011) *G-cubed* **12**, Q03007, doi:10.1029/2010GC003281.

https://doi.org/10.1180/S0026461X00008434 Published online by Cambridge University Press

Multi-isotope monitoring of enhanced weathering of glauconitic sands under controlled high pCO_2 conditions

PAULINE HUMEZ[1*], JULIE LIONS[1], VINCENT LAGNEAU[2], PHILIPPE NEGREL[1].

[1]BRGM, Orléans, France, p.humez@brgm.fr (* presenting author)
[2]MINES PARITECH, Fontainebleau, France

Enhanced water-rock interaction in aquifers overlying CO_2 storage sites in deep saline formation can be expected in the case of CO_2 leakage, leading to a release of geogenic compounds into freshwater resources. Our study investigates the use of trace elements and several isotope systematics (B, Li, C, O, D, Sr) as monitoring tools to detect CO_2-leaks in aquifers. For this, we develop batch experiments under controlled pCO_2 conditions. The glauconitic Albian greensands of the Paris Basin were chosen as interacting solid phase because i) the Paris Basin contains aquifers identified as CCS targets and ii) the Albian aquifer is a deep freshwater resource of strategic national importance. The selected greensand sample consists mainly of quartz with presence of glauconitic minerals and traces of apatite, rutile, ilmenite. The water used for the experiments was pumped from the confined part of the Albian aquifer. PTFE reactors (liquid/solid ratio of 10, pCO_2= 2 bar; room temperature, continuous pH measurements) were run simultaneously, over 1 day, 1 week, 2 weeks and 1 month. A pH drop from 6.6 to 4.9 was noticeable immediately after the injection, due to CO_2 dissolution (ΔHCO_3 = 0.8 mmol/L). Cations and silica increased by a factor of 2 (Ca), 2 (SiO2), 1.5 (K), 1.3 (Mg), 1.5 (Sr), 3.7 (Li), 4.2 (B) for t=1 month. From 1 day to 1 month of contact with CO_2, the $\delta^{13}C_{DIC}$ decreased from -15.7 ‰ to -21 ‰ vs. PDB suggesting a proton-consuming process which entails supplementary CO_2 dissolution. Weathering reactions and surface complexation consume acidity and account for the observed chemical variations. Glauconitic minerals being the main B-bearing phase, the evolution of the aqueous B concentrations indicates their implication in the water-gas-mineral interactions. This is supported by a shift of $\delta^{11}B$ towards more negative values in the presence of CO_2. The $\delta^{11}B$ is different according to the origin of the B (surface or structural), which gives additional information of the actual processes at stake during the evolution.

We focus here on the complex weathering behavior of glauconitic minerals, as poorly defined phases with regards to its mineral structure, under pCO_2 and low-pH conditions, constraining e.g. dissolution rates and surface complexation models through isotope and geochemical data.

A comparative mineral magnetic study of the intrabasaltic palaeosols and modern soils from the Deccan volcanic province, India

Sajid Hundekari[1*], Satish Sangode[2] and Mohammed Rafi Sayyed[3]

[1]Geology Department, Poona College, Pune, India, sajid_hundekar@yahoo.com (presenting author)
[2]Geology Department, University of Pune, India, sangode@unipune.ac.in
[3]Geology Department, Poona College, Pune, India, mrgsayyed@yahoo.com

Total 65 samples representing a variety of red, green and brown bole beds (intrabasaltic palaeosols), the associated underlying and overlying Deccan trap basalts and the modern soils (developed upon the basalts during Holocene) are studied for their mineral magnetic characterization augmented with field examination. The red boles show highest Fe-oxide concentrations amongst the studied intrabasaltic palaeosols but lower than the modern soils formed over these basalts. The qualitative mineral magnetic parameters however indicate a polygenetic control of the mineral species for of these bole beds with a unimodal finer superparamagnetic (SP) fraction that may be of pedogenic origin or product of baking. Comparisons of mineral magnetism of with the unbaked modern soils however suggest that the finer faction is from baking effects. This depicts a complex recycled nature for the red boles with pigmentary hematite imparting the red colouration over a combination of detrital mixtures. The green boles with low ferrimagnetic concentration indicate less oxidative but humid conditions that may possibly occur during the short events of volcanic winters. Although the bole beds largely depict the recycled nature of the magnetic mineral concentrates disproportionate to the concentrations of magnetic minerals in the underlying (/parent) basalts (unlike the modern soils). This suggests in a profile indicate the independent controls like the intensity and duration of baking in the red boles in particular and the palaeoweathering and palaeoenvironments in general (in all the bole beds). The mineral magnetic results further do not support existence of systematic soil profiles amongst any of the studied sections and the genesis of bole beds is largely governed by the surface water interaction with the weathering products. A detailed knowledge on these bole beds can lead to understanding on the post-eruptive paleoweathering and palaeoenvironmental conditions and hence demand a during the formation of these intrabasaltic bole beds employing a multi-proxy approach is therefore warranted in further understanding and characterizing the genesis of large variety of intrabasaltic bole beds which abundantly occur in the Deccan volcanic province of India including mineral magnetism.

https://doi.org/10.1180/S0026461X00008434 Published online by Cambridge University Press

Helium-4 dating of groundwater in the Green River Formation, Piceance Basin, northwestern, Colorado, USA

ANDREW G HUNT[1*], PETER B. MCMAHON[1], JUDITH C. THOMAS[2] AND RICHARD J. MOSCATI[1]

[1]U.S. Geological Survey, Denver, CO, USA
ahunt@usgs.gov (* presenting author)
pmcmahon@usgs.gov, rmoscati@usgs.gov
[2]U.S. Geological Survey, Grand Junction, CO, USA
juthomas@usgs.gov

Renewed oil and gas production/development in Colorado has highlighted a need to evaluate groundwater resources that overlie current and future production reservoirs in order to define the potential impacts of development activities. Our study focuses on the Piceance Basin in northwestern Colorado, where current hydrocarbon production/development could threaten water quality in the Green River Formation. Given the environmental and economic importance of the bedrock aquifers and associated sediments and the complexity of the bedrock hydrogeology, it is important to develop an understanding of basic system characteristics such as dissolved gas composition, groundwater residence time (or age), and sources of recharge. Our approach was to sample pre-existing well clusters in the basin for dissolved gas compositions, chemistry, noble gas isotopes, and tritium to develop conceptual models of groundwater flow in the upper aquifers.

The application of ^{4}He as an indicator of groundwater residence time has been used to interpret groundwater age for time scales of tens of years to hundred of thousands of years, making it a unique tracer that has both strengths and weaknesses over other radiogenic tracers (e.g. ^{3}H, ^{85}Kr, ^{14}C, ^{36}Cl, and ^{81}Kr) currently in use. Considerable debate has arisen over the interpretation of estimated ^{4}He production rates owing to a lack of understanding of the actual *in-situ* helium production and definition of possible flux of ^{4}He from deeper sources. Error can be further exaggerated by the presence of older reservoirs that interact within the younger, active flow-systems at or near flow boundaries, violating assumptions inherent to the dating application. For the Green River Formation, the possibilities of variable recharge altitudes and migration of gas from deeper sources could complicate the simple application of the ^{4}He dating method. Despite these possibilities, most samples show noble gas compositions that reflect normal air saturated water associated with high altitude recharge, allowing for a simple interpretation of excess helium in the samples. Current age calculations combine the measured concentrations of uranium and thorium in the aquifer and confining units to produce an *in-situ* flux model for ^{4}He accumulation in the basin aquifers, showing an age distribution that agrees well with the conceptual model of groundwater flow and indicate increasing biogenic methane concentrations with increasing age.

Non-gem diamonds from the Diavik diamond mine, Canada: Tracers for cratonic mantle metasomatism

LUCY HUNT[1*], THOMAS STACHEL[1], D. GRAHAM PEARSON[2], RICHARD STERN[1], KARLIS MUEHLENBACHS1 VANESSA MARCHEGGIANI-CRODEN[1] AND HAILEY MCLEAN[2].

[1]University of Alberta, Edmonton, Canada, lchunt@ualberta.ca (* presenting author)
[2]Rio Tinto, Diavik Diamond Mines Inc., Yellowknife, Canada, Hayley.McLean@riotinto.com

Non-gem diamonds are valuable tracers of mantle metasomatism, trapping micro-inclusions of the melt/fluids which formed them and allowing direct analysis of the changing chemical environment in which they grew. Approximately 600 non-gem diamonds were selected for this research, including: coated diamonds; fibrous cubes, and polycrystalline boart. We aim to establish the changes in physical and chemical conditions accompanying the transition from gem to non-gem diamond growth and how this affects the sub-cratonic lithospheric mantle (SCLM).

Cathodoluminescence (CL) of five sectioned non-gem diamonds revealed fine scale complexities not observed in visible light, likely related to differences in nitrogen centres. A subset of diamonds change outward from fibrous cubic {100} to more gem-like octahedral habit. This transition may be linked to decreasing supersaturation in the diamond precipitating melt/fluid (e.g. [1]).

Secondary Ion Mass Spectromotry was used to determine N content and δ^{13}C along transects perpendicular to growth of the diamond sections. The coats are generally higher in N content (average 1700ppm) with more negative δ^{13}C (-8 to -5.5‰) than the associated cores (1300ppm and -4.5 to -5‰). The change from gem to non-gem growth appears visually sharp and may represent precipitation from two distinct fluids. However, a subtle shift in N content and δ^{13}C is already observed prior to the visible core-coat transition in two of the three coated stones. This suggests that a more continuous evolution of the diamond preciptating medium, possibly through mixing processes, may have prompted non-gem growth after a critical point of supersaturation was reached. The mantle-like δ^{13}Cvalues suggest a melt/fluid derived from the asthenosphere. Such an interpretation was also made based on Sr–Nd–Pb isotopes and trace elements of fibrous diamonds [2]. The authors suggested fluid mixing from at least two distinct sources — ancient enriched lithosphere and the underlying convecting mantle.

Detailed research on a 54 carat Diavik boart fragment indicates formation from a different type of fluid/melt. The δ^{13}C is typical of eclogitic diamonds (~23.6‰), however, the intergrown minerals are predominantly G9 garnet and peridotitic clinopyroxene. This suggests interaction of a slab derived melt/fluid with a very negative δ^{13}C with mantle peridotite.

Non-gem diamonds thus provide vessels to carry both samples of, and evidence for, melts/fluids operating as metasomatic agents in the SCLM.

[1] Sunagawa (1984). *Material Science of the Earth's Interior*. 303-330. [2] Klein-BenDavid, Pearson, Nowell, Ottley, McNeill and Cartigny (2010). *Earth and Planetary Science Letters*, **289**, 123-133.

https://doi.org/10.1180/S0026461X00008434 Published online by Cambridge University Press

Impact of seasonally variable soil carbonate formation on paleotemperature records from clumped isotopes

KATHARINE W. HUNTINGTON[1*], NATHAN PETERS[2], AND GREGORY D. HOKE[3]

[1]University of Washington, Dept. of Earth and Space Sciences, Seattle, USA, kate1@uw.edu (* presenting author)
[2]University of Washington, Dept. of Earth and Space Sciences, Seattle, USA, petersn@uw.edu
[3]Syracuse University, Dept. of Earth Sciences, Syracuse, USA, gdhoke@syr.edu

Reconstructing environmental temperatures from the continental geologic record is important for investigating the evolution of life, climate, tectonics, and landforms, yet direct temperature estimates are difficult to obtain from conventional isotopic and paleobotanical proxies. Measurement of 'clumped' ^{13}C-^{18}O bonds in calcium carbonate provides independent estimates of the formation temperature, $\delta^{13}C$ value, and $\delta^{18}O$ value of the carbonate and enables calculation of the $\delta^{18}O$ value of the water from which the mineral grew--each of which can provide important paleoenvironmental constraints. When applied to pedogenic carbonates, clumped isotope thermometry can quantify Earth surface paleotemperature and the $\delta^{18}O$ value of ancient surface waters, from which changes in climate or surface elevation might be inferred. However, recent studies suggest a strong seasonal bias in soil carbonate growth, complicating the interpretation of both temperature and $\delta^{18}O$ data from paleosols.

We use clumped isotope thermometry of recent soil carbonates and monitoring of local weather and soil subsurface conditions to investigate how seasonal variations in environmental factors such as soil temperature, precipitation, and vegetation influence rates of soil carbonate formation. Pedogenic carbonate samples formed in Holocene to Recent soils were collected from soil pits along a transect spanning 2 km of relief in the southern Central Andes of Argentina (33°S) with high seasonal variations in precipitation, air temperature, and soil temperature.

Because soil carbonate formation is generally favored in warm, dry conditions, we expected carbonate growth temperatures from clumped isotope thermometry to exceed mean annual soil temperatures at the sample sites. Instead, we find clumped isotope temperatures vary significantly between mean annual and and greater than mean annual soil temperatures. Samples below 2000 m elevation (where winters are dry) record temperatures from 0 to 4.5°C above mean annual soil temperature, while samples above 2000 m (where summers are dry) are >5.5°C above mean annual soil temperature, suggesting the influence of seasonal variations in both temperature and precipitation. For some sites, clumped isotope temperatures for samples at depths >50 cm in the soil profile exceed maximum soil temperatures measured over the period of record, likely reflecting enhanced carbonate formation during warm periods over the last 10^2-10^3 years. Temperatures for these deeper samples also exceed temperatures for samples near the surface, suggesting that sampling paleosols deep in the soil profile, a practice designed to avoid large temperature bias, could actually introduce greater biases in soil temperature estimates used to interpret conventional $\delta^{18}O$ data.

The effect of different metal species on the evolution with pressure of hydration clusters in water vapour

N.C. HURTIG*, A.A. MIGDISOV AND A.E. WILLIAMS-JONES

Earth & Planetary Sciences, McGill University, Montreal, QC, Canada (*presenting author: nicole.hurtig@mail.mcgill.ca)

The hypothesis that transport of metals by vapour is a viable mechanism for ore formation in magmatic-hydrothermal systems is supported by fluid inclusion data and the occurrence of metal-rich incrustations around fumaroles. A feature of this hypothesis is that hydration of metal species in water vapour is an essential factor in making such transport possible [1,2]. Indeed, hydration has been shown to increase concentrations of Ag and Au in the gas phase by several orders of magnitude over those calculated using volatility data. Nevertheless metal concentrations determined experimentally are substantially lower than those reported for vapour inclusions in magmatic hydrothermal systems.

We have shown previously that hydration numbers are not constant but increase exponentially with increasing water pressure. As a result, metal solubility increases by orders of magnitude from its values at low pressure to those at conditions approaching saturation of the vapour with liquid. In the current study, we are building on this earlier work by conducting experiments designed to determine the effect of different metallic vapour species on the nature of the surrounding hydration cluster with changing P_{H_2O}.

The experiments were conducted in batch-type Ti autoclaves at a constant oxygen fugacity, buffered by the assemblage MoO_2-MoO_3. From comparison of the experimental data sets for $AuCl(H_2O)_n$ and $MoO_3(H_2O)_n$, it is apparent that the solubility of these two species is described by different exponential functions. The solubility of the Au-chloride species is, within experimental error, independent of pressure below 87 bars P_{H_2O} and increases with increasing pressure to a value three log units higher at conditions approaching saturation of the vapour with liquid. By contrast, the solubility of the Mo-oxide species is only observed to increase above 150 bars P_{H_2O}, and at conditions approaching saturation, is only 1.5 log units higher than at pressures below 150 bars P_{H_2O}. This likely indicates that the molecular structure or the type of bonding of the metal species has an important control on the nature and size of the hydration clusters.

Experiments performed at conditions of saturation, i.e., with vapour and liquid present, indicate that there is a continuum between metal solubility in the vapour and that in the corresponding liquid. Above the critical point, the form of the hydration curve does not change significantly, indicating the formation of stable hydration clusters under these conditions and a continuous increase in solubility with increasing P_{H_2O} from vapour-like to liquid-like supercritical fluids.

[1] Migdisov et al. (1999) *Geochim. Cosmochim. Acta* **63**, 3817
[2] Archibald et al. (2001) *Geochim. Cosmochim. Acta* **65**, 4413

https://doi.org/10.1180/S0026461X00008434 Published online by Cambridge University Press

Weathering & heterogeneous phase distribution in brachinite NWA 4872

BRENDT C. HYDE[1*], JAMES M. D. DAY[2], KIM T. TAIT[1], RICHARD D. ASH[3] AND DAVID W. HOLDSWORTH[4]

[1]Royal Ontario Museum, Department of Natural History, Toronto, Canada, brendth@rom.on.ca (*presenting author)
[2]Scripps Institution of Oceanography, Geosciences Research Division, La Jolla, CA 92093, U.S.A.
[3]University of Maryland, Department of Geology, College Park, MD 20742, U.S.A.
[4]Robarts Research Institute, Imaging Research Lab, London, Canada

Brachinites are thought to be the residuum of a partially melted asteroid [e.g. 1-3] and offer insights into the initial stages of asteroid differentiation. Multiple splits from single brachinites show differences in highly siderophile element (HSE) abundances, likely reflecting the effects of heterogeneous phase distribution and uneven weathering [3]. Weathering is an important issue as it can obscure primary information on parent-body processes. We report a detailed Raman spectroscopy, micro-computed tomography (micro-CT) and laser-ablation inductively coupled plasma mass spectrometry (LA-ICP-MS) study of weathering and phase distribution for brachinite Northwest Africa (NWA) 4872.

Raman analyses employed for investigating weathering products used a Horiba LabRAM Aramis micro-Raman spectrometer with a 532 nm, 50 mW laser (filtered to 10% power). *In situ* mineral REE and HSE abundance analyses used a New Wave Research UP213 (213 nm) laser-ablation system coupled to a Thermo-Finnigan Element 2 ICP-MS. Micro-CT scans employed for investigating phase distribution were run with a GE eXplore speCZT using a X-ray voltage of 110 kV and a beam current of 32 mA.

Raman analyses showed a redistribution of S from the initial troilite resulting in S-rich areas (mostly marcasite) and S-poor areas (mostly Fe-oxide). Studies of weathering in martian meteorites have found marcasite [e.g. 4] and sulphur removal from troilite has been linked to hot desert weathering [5]. Absolute abundances of HSE were hard to determine by LA-ICP-MS due to variable degrees of alteration, but relative abundances reveal that positive Ru-anomalies that are characteristic of brachinites [3] are common to weathered sulphide grains as well as to fresh troilite. Variability in elements were observed relative to the Ru-anomaly and grain-to-grain variations in Re and Os were seen. This accounts for differences in HSE abundances and Re/Os seen in separate splits of NWA 4872.

The light REE, Ba, Sr, U and Pb did not show elevation related to weathering in whole rock analyses [3]. This is consistent with the observed weathering. Weathered sulphide and metal were widespread; however, silicates showed no obvious weathering, no carbonate was found and sulfate was minimal. The measured splits of NWA 4872 appear to be influenced mostly by uneven weathering. However, micro-CT analysis showed a heterogeneous distribution of high density grains. This is likely true of other brachinites and could affect measured bulk trace element abundances.

[1] Day et al. (2009) *Nature* **457**, 179-182. [2] Goodrich (1998) *MAPS* **33**, A60. [3] Day et al. (2012) *GCA* **81**, 94-128. [4] Floran et al. (1978) *GCA* **42**, 1213-1229. [5] Lee & Bland (2004) *GCA* **68(4)**, 893-916.

https://doi.org/10.1180/S0026461X00008434 Published online by Cambridge University Press

Experimental constraints on the evolution of alkaline magmas from Ross Island, Antarctica: A case for CO_2-dominated volcanism

KAYLA IACOVINO[1*], CLIVE OPPENHEIMER[1], BRUNO SCAILLET[2], PHILIP KYLE[3]

[1] University of Cambridge, Dept. of Geography, Cambridge, UK, ki247@cam.ac.uk (* presenting author) co200@cam.ac.uk

[2] Université d'Orléans, ISTO, Orléans, France bscaille@cnrs-orleans.fr

[3] New Mexico Institute of Mining and Technology, New Mexico, USA kyle@nmt.edu

Background and Experimental

Erebus volcano on Ross Island, Antarctica is home to the only phonolite lava lake in the world and, in combination with the continuous suite of alkaline lavas found in outcrop, provides an excellent natural laboratory for studying the genesis and evolution of alkaline magmas at a rift setting. Two geochemical lineages make up the majority of lavas erupted from Erebus and the surrounding basaltic volcanic centers at Hut Point Peninsula and Mts. Bird and Terror: The Erebus Lineage (EL) lavas and the Dry Valley Drilling Project (DVDP) lavas taken from drill core [1]. The occurence of kaersutite phenocrysts in DVDP lavas, attributed to a higher f_{H2O} and lower temperatures, is the key mineralogical distinction between these two lineages. Modelling suggests that both lineages evolved through fractional crystallization from parental basanite melt [2].

High pressure and temperature experiments (2−4 kbars; 1000−1150 ° C) with added H_2O and CO_2 (X_{H2O} varying between 0−1) were performed with primitive members from both EL and DVDP lavas to investigate the evolution of these magmas.

Results and Conclusions

Preliminary results show that only very CO_2-rich conditions (X_{H2O} approaching 0) reproduce the mineralogy of natural samples, even for kaersutite-bearing assemblages. This is consistent both with measurements of gas emissions and melt inclusion data. Kaersutite, which only occurs in DVDP lavas, is the liquidus phase in experiments carried out with EL samples, even when no water was added to the experimental capsule (some H_2O is present, however, even in “dry” runs from the reduction of Fe_2O_3 in the melt). This indicates that: a) DVDP and EL lavas are likely sourced from the same parent magma – that is, the differences in mineralogy and geochemistry between DVDP and EL lavas is caused by slight variations in differentiation and eruption conditions, and b) assuming that f_{H2O} controls the presence or lack of kaersutite, only a very small amount (<1 wt%) of H_2O is needed to stabilize the phase, making it a very precise threshold indicator of dissolved H_2O contents in Ross Island melts. In contrast, the occurrence of amphibole in calc-alkaline magmas is typically indicative of at least 4 wt% dissolved H_2O.

Previous work has made the case for deep CO_2-fluxing at Erebus to explain CO_2-rich gas emissions and the induction of crystallization in the magmatic system [2]. Further work aims to determine whether CO_2-fluxing is necessary to achieve the gas composition at Erebus and, ultimately, to determine the deep source of the carbon feeding the volcano.

[1] Kyle (1981) *J. Pet.* **22** 451-500 [2] Kyle *et al.* (1992) *J. Pet.* **33** 849-875. [3] Oppenheimer *et al.* (2011) *EPSL* **306** 261-271.

Late Cretaceous migmatites in the southern Mojave Desert and their contribution to gabbro genesis and magmatic diversity

ADAM J. IANNO* AND SCOTT R. PATERSON

Department of Earth Sciences, University of Southern California, Los Angeles, CA, USA, ianno@usc.edu, paterson@usc.edu

Within the tilted crustal section found at Joshua Tree National Park in the southern Mojave Desert of California, we observe a >100 km long "heterogeneous sheeted complex" composed of meter-thick, tabular, intrusive igneous sheets that were intruded into Proterozoic gneisses that were locally partially molten. The sheeted complex contains a wide range of composition and texture, but is primarily composed of tonalites and two-mica garnet granites. We are testing the hypothesis that the genesis of this sheeted complex is likely intricately connected to the partial melting by a mantle-derived heat source of a heterogeneous package of Proterozoic host rocks.

In this study, we focus on the subset of hornblende gabbros present to better trace migmatization and crystal segregation processes. We have analyzed samples for bulk rock and single mineral chemistry, Sr and Nd isotopes, and U-Pb zircon ages to complement geologic mapping and microscopy for these hornblende gabbros. Samples contain hornblende + plagioclase ± clinopyroxene or biotite ± quartz, are medium to coarse-grained, and are equigranular to porphyritic in texture (hornblendes range up to 3 cm in length in hand sample). Samples range in melt fraction and amount of host rock present, and some sheets and pods observed have a cumulate texture and predominance of hornblende suggestive of fractional crystallization. Later greenschist-facies metamorphism overprints many of the gabbros observed. Crystallization ages are 74-78 Ma (U-Pb in zircon), although all samples have inherited zircon cores of ~1700 Ma. Two diatexites have been measured at 0.707 to 0.709 Sr_I, -12.4 to -13.6 εNd.

The hornblende gabbros of Joshua Tree National Park are primarily formed by a combination of partial melting of metamafic rocks and mantle-sourced magmatism. In some cases, this is followed by a period of fractional crystallization to form hornblende cumulates. Leucosomes derived from partial melting of metamafic rocks or melt extracted from these hornblende gabbro magmas are plagioclase-dominated and leucotonalitic to leucodioritic. As leucosomes and neosomes from metamafic protoliths rise and mix with those from metafelsic/quartzofeldspathic protoliths and mantle-sourced magmas, a continuum of melt compositions between tonalite and peraluminous granite is formed. Evidence of mixing exists down to the thin section scale and may explain the formation of biotite in some samples of otherwise K-deficient hornblende gabbro diatexites. These mixing and fractionation processes occur in igneous compositions beyond the gabbros and can also explain the textural diversity of magmas observed in the heterogeneous sheeted complex.

https://doi.org/10.1180/S0026461X00008434 Published online by Cambridge University Press

What Remains? Molecular and spectroscopic analysis of non-hydrolyzable St. Lawrence

MINA IBRAHIM[1*], YVES GÉLINAS[2], ANDRÉ SIMPSON[3]

[1] Concordia University & GEOTOP, Montreal, Canada, mi_ibra@hotmail.com (* presenting author)
[2] Concordia University & GEOTOP, Montreal, Canada, ygelinas@alcor.concordia.ca
[3]University of Toronto, Mississauga, Canada, asimpson@utsc.utoronto.ca

Sediments are the ultimate long-term sink for organic carbon (OC) on Earth, thus playing an important role in the global cycles of O_2 and CO_2. Estuaries and river deltas are major conduits for terrestrial organic matter (OM) into marine systems, where it is mixed with locally produced OM and is eventually deposited and buried in the sediment bed. About 45% of global OC burial occurs along these river deltas and estuaries [1], therefore it is of interest to follow OM deposition and preservation in these terrestrial to marine transition zones. We chemically fractionated bulk OM from a series of sediments from the St. Lawrence Estuary and Gulf into distinct reactivity classes. We define three such OM fractions based on pioneering work by Hedges and Keil (1995) who classified OM based on chemical reactivities: labile (degradable at similar rate under oxic and anoxic conditions), non-hydrolyzable (degraded primarily under oxic conditions), and refractory (preserved on long time scales independently of redox conditions). Here we present data on the spectroscopic (HR-MAS $^{1}H/^{13}C$ NMR) characterization of the non-hydrolyzable fraction because of its importance in the long-term burial of OC below the seafloor. We used mild oxidation methods (RuO_4) followed by chromatographic and compound-specific isotope analysis ($\delta^{13}C$ CSIA) of the oxidation products. Combining results from the bulk and molecular analytical techniques provides insights into the composition and cycling of non-hydrolyzable OM in transitional system, from which OM preservation can be better understood.

[1] Hedges (1995) *Marine Chemistry* **49**,81-115

Diamond growth from organic carbon suggested by coupled $\delta^{18}O$-$\delta^{13}C$ variations in diamonds and garnet inclusions

RYAN B. ICKERT[1*], THOMAS STACHEL[1], RICHARD A. STERN[1], JEFF W. HARRIS[2]

[2]Canadian Centre for Isotopic Microanalysis, Department of Earth and Atmospheric Sciences, University of Alberta, Edmonton, Canada, ryan.ickert@gmail.com
[2]School of Geographical and Earth Sciences, University of Glasgow, Glasgow, Scotland

The sources of carbon in the mantle and the mechanisms of its transport and precipitation as diamond are poorly understood. Diamond itself contains only a limited amount of geochemical information, primarily in the form of carbon isotope ratios and nitrogen abundances, and therefore a substantial effort has focussed on relating syngenetic mineral inclusions to their diamond hosts. For example, it is well known that, on a worldwide scale, diamonds with eclogitic inclusions have a distinct $\delta^{13}C$ distribution when compared to more abundant diamonds with peridotitic inclusions. Eclogitic diamonds have a distribution that extends from mantle-like $\delta^{13}C$ values (ca. -5‰), to very light carbon (<-20‰), whereas peridotitic diamonds have a distribution that clusters close to -5‰, without the long tail. The relatively low $\delta^{13}C$ values have been explained by either the subduction of organic carbon [1], the presence of heterogeneous primordial carbon reservoirs in the mantle [2], or high-temperature fractionation [3].

Here we report high-precision SIMS $\delta^{18}O$ measurements ($2\sigma <$ ±0.4‰) of eclogitic garnet inclusions in diamonds from three distinct deposits, Damtshaa (near the Orapa mine) in Botswana; Argyle in Australia; and ultradeep inclusions from Jagersfontein, South Africa. The measured $\delta^{18}O$ values are highly variable, and the distributions of each locality are clearly distinct. Damtshaa garnet inclusions range from +4.8‰ to +8.8‰ (n=15) and have a broadly similar distribution to $\delta^{18}O$ values of eclogite xenoliths. Argyle garnet-inclusions range from +5.9‰ to +10.8‰ (n=29), and are skewed towards ^{18}O-rich isotopic compositions. Ultradeep, majoritic garnet inclusions from Jagersfontein have a narrow range between +8.6‰ and +10.0‰ (n=11).

All three localities are distinct from each other in their univariate $\delta^{18}O$ and bivariate $\delta^{18}O$-$\delta^{13}C$ distributions. Damtshaa has negatively correlated $\delta^{18}O$-$\delta^{13}C$, Argyle has a distribution that is offset from "mantle-like" ^{18}O-^{13}C distributions, and Jagersfontein has low-variance $\delta^{18}O$-$\delta^{13}C$, but at anomalously high-$\delta^{18}O$ and low-$\delta^{13}C$. Importantly, none have the distribution expected from independent knowledge about $\delta^{18}O$ values of cratonic eclogites and the sampling distribution of $\delta^{13}C$ values in eclogitic diamonds. The association of crustal-like $\delta^{18}O$ values with low $\delta^{13}C$ values suggests that the carbon responsible for the low $\delta^{13}C$ values is subducted organic material.

[1] Sobolev & Sobolev (1980) *Dokl Akad Nauk SSSR* **250**, 683-685.
[2] Deines (1980) *GCA* **44**, 943-961.
[3] Javoy *et al*. (1986) *Chem Geol* **57**, 41-62.

https://doi.org/10.1180/S0026461X00008434 Published online by Cambridge University Press

Nb-Zr systematics of U-Pb dated achondrites

TSUYOSHI IIZUKA[1,2*], WAHEED AKRAM[3], YURI AMELIN[2] AND MARIA SCHÖNBÄCHLER[3]

[1]DEPS, University of Tokyo, iizuka@eps.s.u-tokyo.ac.jp (*presenting author),
[2]RSES, Australian National University
[3]SEAES, University of Manchester,

The short-lived radionuclide ^{92}Nb decays to ^{92}Zr with a half-life of 36 Ma [1]. Nb and Zr are both refractory lithophile elements and can fractionate from each other during partial melting of the mantle. Thus, Nb-Zr isotope systematics can potentially place chronological constraints on early planetary silicate differentiation. This application requires the initial abundabce of ^{92}Nb (or ^{92}Nb/^{93}Nb) and its homogeneity in the solar system to be unambiguosly defined. Yet previously reported initial ^{92}Nb/^{93}Nb values range from ~10^{-5} to >10^{-3} [2-6], and remain to be further constrained. All but one of the previous studies estimated the initial ^{92}Nb/^{93}Nb using Zr isotope data for single phases with fractionated Nb/Zr in meteorites such as zircons and CAIs, under the assumption that their source materials and bulk chondrites had had identical initial ^{92}Nb/^{93}Nb and Zr isotopic compositions [2-5]. To evaluate the homogeneity of the initial ^{92}Nb abundance, however, it is desirable to define internal mineral isochrons for meteorites with known absolute ages. Although Schönbächler et al. [6] defined Nb-Zr internal isochrons for two meteorites (Estacado and Vaca Muerta), their absolute crystallization (or possibly recrystallization) ages are not precisely constrained, leading to uncertainties in the resultant estimate for the initial ^{92}Nb/^{93}Nb of the solar system.

To establish the solar system intial ^{92}Nb/^{93}Nb and its homogeneity, we are studying the Nb-Zr systematics of minerals from achondrites whose absolute crystallization ages were precisely determined with the U-Pb chronometer. Abundances of trace elements including Nb and Zr were determined by LA-ICPMS for pyroxene, plagioclase, pyrite, spinel and/or opaque minerals from 3 eucrites (Agoult, Ibitira and A-881394), 5 angrites (SAH99555, D'Orbigny, NWA2999, NWA4590 and NWA4801) and Acapulco. The results reveal that Agoult, Ibitira and NWA4590 contain phases with reasonably high Zr contents and a good spread in Nb/Zr (<0.01 for pyroxene and ~3 for opaque minerals and spinel) to define precise internal isochrons. These minerals and whole rock samples were further processed for Zr separation and analyzed for Zr isotopes by MC-ICPMS. We found that the spinel and opaque mineral fractions have restricted positive ^{92}Zr anomalies up to 30 ppm relative to the terrestrial standard samples. We are still in the process of determining their Nb/Zr isotopic ratios, but preliminary results of Zr isotope analyses, combined with the approximate Nb/Zr of minerals estimated by LA-ICPMS, suggest that the initial ^{92}Nb/^{93}Nb is in the order of ~10^{-5}, consistent with the results of previous work using the internal isochron approach [6].

[1] Nethaway et al. (1978) *Phys. Rev. C* **17**, 1409–1413. [2] Sanloup et al. (2000) *EPSL* **184**, 75-81. [3] Yin et al. (2000) *ApJ* **536**, L49-L53. [4] Münker et al. (2000) *Science* **289**, 1538-1542. [5] Hirata (2001) *Chem. Geol.* **176**, 323-342. [6] Schönbächler et al. (2002) *Science* **295**, 1705-1708.

The role of extracellular polymeric substances in nanoparticle-biofilm interactions

KAORU IKUMA[1*], ANDREW S. MADDEN[2], AND BORIS L. T. LAU[1]

[1]Department of Geology, Baylor University, Waco, TX, USA, kaoru_ikuma@baylor.edu (* presenting author), boris_lau@baylor.edu
[2]School of Geology and Geophysics, University of Oklahoma, Norman, OK, USA, amadden@ou.edu

Introduction

Environmental surfaces are ubiquitously covered with biofilms that are primarily made of "sticky" bacterial extracellular polymeric substances (EPS). While various nanoparticles (NPs) have previously been shown to interact strongly with biofilms and EPS, the mechanisms of interaction have remained unclear. EPS consist of a range of organic compounds including various polysaccharides, proteins, and lipids that may play different roles in NP-biofilm interactions. Our objective in this work is to determine the different surface interactions between NPs and individual EPS components. A quartz crystal microbalance with dissipation monitoring (QCM-D) was used to quantify the kinetics and extent of the deposition of hematite NPs (FeNPs) and galena NPs (PbNPs) onto surfaces coated with model and natural EPS components.

Results and Discussion

Frequency shifts were observed during the deposition of EPS components and NPs onto QCM-D sensors (e.g., protein and PbNPs in Fig 1A). Such observed shifts were used to calculate changes in NP mass deposited onto various surfaces. For example, FeNP deposition (in 10mM NaCl, pH 6) was 1.6 fold slower but ~10% greater onto surfaces coated with a model polysaccharide (alginate) compared to a model protein (bovine serum albumin; BSA) (Fig 1B). We expect that the observed differences between varying EPS components were due to differences in charge and hydrophobicity. Experiments are currently underway to test this hypothesis.

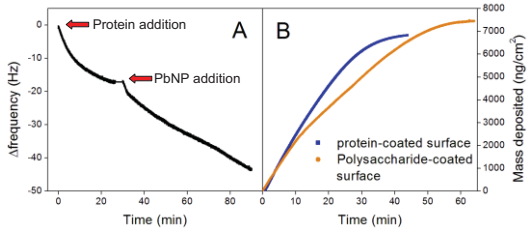

Figure 1: NP deposition onto QCM-D sensor surface coated with EPS components. (A) Frequency shifts measured by QCM-D during protein and PbNP deposition onto the sensor surface. (B) FeNP deposition onto surfaces coated with proteins or polysaccharides.

Environmental Implications

As natural biofilms may act as a major sink for NPs, a detailed mechanistic understanding of the role of EPS and its components in NP-biofilm interactions is crucial for determining the environmental fate and transport of engineered NPs.

https://doi.org/10.1180/S0026461X00008434 Published online by Cambridge University Press

Biogenic methane and bacterial community structure in Ordovician shales, Michigan Basin, Ontario

DIMITRI ILIN*, HOSSEIN MOHAMMADZADEH, ALEXANDRE POULAIN AND IAN CLARK

University of Ottawa, Ottaawa, Canada, dilin083@uottawa.ca,, mohammadzadeh@ferdowsi.um.ac.ir, apoulain @uottawa.ca, idclark@uottawa.ca

As a component of geoscientific investigations for a deep geological repository in Middle Ordovician strata of the Michigan Basin near Tiverton, Ontario, methane from hypersaline pore waters ($Cl^- > 6$ molal) in shale and limestone core samples was analysed for concentration, $\delta^{13}C$ and δD.

CH_4 is highly depleted in ^{13}C and D from the top of the Queenston Formation down through the Cobourg Formation. Based on the location of the isotopes on a discrimination diagram for methane, the isotopes are interpreted to be of biogenic origin. An associated zone of ^{13}C-enriched CO_2 strengthens this interpretation and constrains production to the lower Georgian Bay and upper Blue Mountain formations. The $\delta^{13}C$ and δD signatures of methane from the limestones below the Cobourg Formation increase sharply to values consistent with methane of thermocatalytic origin.

In an attempt to resolve whether methanogenic archaea may still be active in these strata, environmental DNA was extracted from core samples and PCR amplified using 16S rDNA primers. PCR performed with archaeal 16S rDNA and methanogen-specific (*mcrA*) primers yielded no DNA, whereas low, but measurable, yields were obtained for bacterial primers. Gene analysis indicated that bacterial sequences similar to *Proteobacteria*, *Cyanobacteria*, *Firmicutes*, and *Actinobacteria* were present.

The majority of identified bacterial species were uncultured extremophilic heterotrophs. We believe that identified bacteria have survived in the rocks for a prolonged period of time by utilizing available energy sources that were trapped during deposition or by assuming a state of dormancy. In contrast, methanogenic archaea are considered to be halophobic and their absence today is not surprising. We hypothesize that the biogenic methane in the Upper Ordovician shales is of para-diagenetic origin, and has been preserved in-situ for some 400 My.

Sulphur isotopy in a sequence of iron-limited organic rich deposits

P. ILLNER[1], Z. BERNER[1], H. ALSENZ[2], S. ASHCKENAZI-POLIVODA[3], T. NEUMANN[1], W. PÜTTMANN[2], S. ABRAMOVICH[3], A.ALMOGI- LABIN[4], S. FEINSTEIN[3]

[1]Karlsruhe Institute of Technology (KIT), Germany (peter.illner@kit.edu)
[2]J.W. Goethe Universität, Frankfurt am Main, Germany
[3]Ben GurionUniversity of the Negev, Beer Sheva, Israel
[4]Geological Survey of Israel, Jerusalem, Israel

In the Negev, the transition from latest Campanian to early Maastrichtian is marked by organic- and phosphate-rich sediments deposited in a high productivity regime induced by coastal up-welling along the southern margin of the Tethys. The study aims at tracing small scale fluctuations in the depositional conditions in this coastal upwelling system, by exploring the isotopic composition of different forms of sulphur in a ca. 50 m thick sequence, encompassing the top of the Phosphate Unit (PU) of the Mishash Formation and the Oil Shale Member (OSM) of the Ghareb Formation.

Different sulphur compounds, including acid soluble sulphates (ASS), acid volatile sulphides (AVS), chromium reducible sulphur (CRS), organic sulphate (OS) and organic bond reduced sulphur (ORS) were separated according to the protocol suggested by Mayer and Krouse [1] and were characterized for their isotopic composition.

In oil shales most of the sulphur (up to 94%) is bond to the organic fraction, decreasing gradually toward the top of the OSM to 40-60% of the sulphur present in sediment. Pyrite-S (CRS), which is the second most common form of sulphur, is low in the basal, most organic rich part of the OSM (<10%), but it can represent up to 40-50% of sulphur in the central part of the section. In the PU and in the marls that top the oil shales, sulphate-S (gypsum, apatite-bond-S) becomes the dominant S-species (>80% of total).

The $\delta^{34}S$ values of the reduced organic sulphur vary throughout the section in a relatively close range between -6 and +1‰, and are always considerably higher than the much more scattered values recorded for the pyrite-S. Sulphur in pyrite is typically strongly depleted in ^{34}S (-43 to -34‰), except in the PU and in the lowest, most organic-rich part of the OSM where the $\delta^{34}S$-values can be as high as -16‰.

The incorporation of sulphur into sedimentary pools with distinct isotopic composition is interpreted in terms of depositional conditions/ primary environmental signals (e.g., availability of reactive iron and degradable organic matter, sulphate diffusion, bottom water oxygenation, sedimentation rate) which were in part overprinted by late/ post diagenetic effects.

[1] Mayer, B. & Krouse, H.R. (2004) In: Procedures for Sulfur Isotope Abundance Studies (ed. P.A. de Groot.) *Handbook of stable isotope analytical techniques*. pp. 538-596.

https://doi.org/10.1180/S0026461X00008434 Published online by Cambridge University Press

The chemical nature of Titan's organic aerosols; constraints from spectroscopic and mass spectrometric observations.

HIROSHI IMANAKA[1*]

[1]University of Arizona, Lunar and Planetary Laboratory, Tucson, USA, himanaka@lpl.arizona.edu (* presenting author)

Introduction

The Cassini-Huygens observations greately extend our knowledge about Titan's organic aerosols. The Cassini INMS and CAPS observations clearly demonstrate the formation of large organic molecules in the ionosphere. The VIMS and CIRS instruments have revealed spectral features of the haze covering the mid-IR and far-IR wavelengths. This study attempts to speculate the possible chemical nature of Titan's aerosols by comparing the currently availabe observations with our laboratory study.

Results and Conclusion

We have conducted a series of cold plasma experiment to investigate the mass spectrometric and spectroscopic properties of laboratory aerosol analogs [1, 2]. Titan tholins and C_2H_2 plasma polymer are generated with cold plasma irradiations of N_2/CH_4 and C_2H_2, respectively. Laser desorption mass spectrum of the C_2H_2 plasma polymer shows a reasonable match with the CAPS positive ion mass spectrum. Furthermore, spectroscopic features of the the C_2H_2 plasma polymer in mid-IR and far-IR wavelegths qualitatively show reasonable match with the VIMS and CIRS observations. These results support that the C_2H_2 plasma polymer is a good candidate material for Titan's aerosol particles at the altidues sampled by the observations.

[1] Imanaka et al. (2004) *Icarus* **168**, 344-366. [2] Imanaka et al. (2012) *Icarus* **218**, 247-261.

B-Sr-U isotope systematics and ^{14}C dating of groundwaters from southwestern France.

C.INNOCENT[1*], E. MALCUIT[2], C. FLEHOC[1], C. GUERROT[1], W. KLOPPMANN[1], E. PETELET-GIRAUD[1] AND P. NEGREL[1]

[1]BRGM – MMA, Orleans, France, c.innocent@brgm.fr
[2]BRGM – SAR/SGR-AQI, Pessac, France, e.malcuit@brgm.fr

The Eocene sands aquifer has been extensively studied for its hydrology, hydrogeochemistry, and also for stable isotopes and groundwater residence time using ^{14}C [1, 2]. Recently, in the framework of the CARISMEAU project, groundwaters have been in addition characterized for B, Li, Sr and U isotopes (Négrel et al., 2008).

The second step of the CARISMEAU research project is aimed at studying the restricted "Entre-Deux-Mers" area, where Eocene groundwaters displays high sulfate and fluorine contents that exceed the regulation limits for drinking water use. B and Sr isotopes have been measured in 18 water samples. The isotopic signal of these groundwaters emphasize the influence of carbonate and evaporitic sources, and also of clay lithologies in some samples, as indicated by B isotopes.

Uranium activity ratios are also available for 18 waters samples (which do not match those analyzed for B and Sr). U activity ratios are in any case higher than the equilibrium value, ranging from 2.9 to 8.6. Such high values confirm those previously measured in Eocene groundwaters during the first step of the project [4].

Finally, ^{14}C activity has been measured in 2009 on 30 groundwaters. The calculated residence times are compared when possible to ^{14}C dates obtained during the 90's on water samples recovered from the same sites. New dates are surprizingly much younger. In addition, a slight shift in $\delta^{13}C$ is observed between the 90's data and those obtained in 2009. The significance of these new ^{14}C data is discussed in the light of both groundwater sampling procedures and the impacted status of this aquifer due to overpumping.

[1] André (2002) *PhD thesis, University of Bordeaux III,* 320 p.
[2] André et al. (2005) *Journal of Hydrology,* **305**, 40-62.
[3] Négrel et al. (2008) *BRGM Report RP-56291-FR,* 193 p.
[4] Innocent and Négrel, *Applied Geochemistry,* submitted.

https://doi.org/10.1180/S0026461X00008434 Published online by Cambridge University Press

Carbon chemostratigraphy of the Paleoproterozoic Belcher, Nastapoka, and Richmond Gulf Groups

KATHERINE INTERLICHIA[1*], DOMINIC PAPINEAU[1,2], WOUTER BLEEKER[3], CHRISTIAN HALLMANN[4], CHRIS SWARTH[5], ZHENBING SHE[1,6], AND MARILYN FOGEL[2]

[1] Department of Earth and Environmental Sciences, Boston College, Boston, United States, interlik@bc.edu (*), dominic.papineau@bc.edu
[2] Geophysical Laboratory, Carnegie Institution of Washington, United States, m.fogel@gl.ciw.edu
[3] Geological Survey of Canada, Ottawa, Canada, Wouter.Bleeker@nrcan-rncan.gc.ca
[4] Max-Planck Institute for Biogeochemistry and MARUM, University of Bremen, Bremen, Germany, hallmann@mit.edu
[5] Jug Bay Wetlands Sanctuary, Maryland, United States, cswarth10@gmail.com
[6] Department of Mineralogy and Petrology, China University of Geosciences, Wuhan, China, zbsher@gmail.com

The Paleoproterozoic Lomagundi $\delta^{13}C_{carb}$ excursion between 2.22 and 2.06 Ga corresponds to the most significant period of atmospheric oxygenation and is referred to as the "Great Oxidation Event" (GOE). Large $\delta^{13}C_{carb}$ excursions are often followed by periods of accelerated biological evolution, suggesting that rocks deposited immediately after 2.06 Ga might preserve changes in environmental chemistry and microbial communities after the GOE. The poorly studied rocks of the Belcher, Nastapoka, and Richmond Gulf Groups, along the northwestern margin of the Superior Craton, Canada, have been dated between 2.03 and 1.870 Ga (Chandler and Parrish, 1989; Hamilton et al., 2009), and thus represent ideal rocks to investigate the evolution of microbial communities and of the carbon cycle in a higher redox state. These Paleoproterozoic successions contain exceptionally well-preserved carbonates with abundant and diverse stromatolites. The Belcher Group preserves three successive transgressions of a drowning carbonate platform between two major volcanic episodes (Ricketts and Donaldson, 1989). Progressive transitions from green/gray to red argillites/mudstones and the development of beds of carbonate concretions indicate a progressive oxidation of fine-grained marine sedimentary rocks and organic matter near the end of the second and third megacycles (Tukarak and Costello-Laddie Fms.). Data from the McLeary and Kasegalik Fms. in the Belcher Group show uniform $\delta^{13}C_{carb}$ values around +0.1‰ and $\delta^{13}C_{org}$ values between -26.1‰ and -22.1‰. Current work is focused on completing the carbon isotope chemostratigraphies to establish geochemical correlations between the entire Belcher Group and the correlative Richmond Gulf and Nastapoka Groups.

Formation and evolution of cratonic lithospheric mantle in central Siberia

D.A. IONOV[1*], I.N. BINDEMAN[2], L.S. DOUCET[1], I.V. ASHCHEPKOV[3], A.V. GOLOVIN[3] NAME[3]

[1]Université J. Monnet (PRES-Lyon), Saint Etienne, France, dmitri.ionov@univ-st-etienne.fr (* presenting author)
[2]University of Oregon, Eugene OR, USA, bindeman@uoregon.edu
[3]Inst. Geology & Mineralogy, Novosibirsk, Russia, avg@igm.nsc.ru

Degrees, depth, settings and age of partial melting

A major reason why various models for the formation of cratonic mantle continue to be debated [1] is that the modal and chemical composition of initial melting residues, hence melting conditions, remain poorly constrained. Spl harzburgite xenoliths (Mg# 0.92-0.93) from the Udachnaya kimberlite in the central Siberian craton, unlike most published data on cratonic peridotites, form clear trends on major oxide plots and based on experimental results [2] are residues of 35-40% fractional partial melting of upwelling fertile mantle over a broad depth range (7-1 GPa). By contrast, the majority of garnet peridotites from Udachnaya show metasomatic enrichments in Fe, Ti etc. relative to the residual harzburgites. Dunites (melting degrees >40%) are extremely rare.

Unmetasomatized spl harzburgites yield isochron Lu-Hf age of 1.8 Ga and Sm-Nd age of 2.0 Ga [3]. The early Proterozoic formation of the Siberian lithospheric mantle is also indicated by Re-depletion ages for coarse peridotites from this study [4] that range from 1.5 to 2.6 Ga (av. 1.8 Ga). The Re-Os age range may reflect metasomatic overprinting rather than prolonged craton creation. Garnet peridotites yield Hf- and Nd-isotope WR-isochron ages of 0.7 Ga, apparently dating a major metasomatic event [3].

O-isotope data and the origin of opx-rich peridotites

We report laser-fluorination O-isotope data for olivine and opx from 32 Udachnaya peridotites. Average δ18O for the olivines is 5.18 ± 0.26‰ (2σ), i.e. identical to the mantle olivine average of 5.18 ± 0.28‰ [5]; the opx are on average 0.5‰ heavier than coexisting olivine. Calculated bulk compositions are similar for spl and coarse and sheared garnet peridotites (~5.3‰) and show no relation to modal or major oxide abundances. A sub-group of Udachnaya spl harzburgites have too much opx (31-43% vs. 7-22% in 'normal' harzburgites) to be melting residues. The high opx in Siberian and other cratonic peridotites are commonly attributed to hydrous melting or post-melting silica enrichments in subduction zones. Bulk O-isotope compositions of the opx-rich spl harzburgites are similar to those for all other Udachnaya peridotites. There is no evidence that processes producing opx-rich (or metasomatized) cratonic peridotites impart distinctive O-isotope characteristics; their links to subduction settings remain unsupported by chemical or isotope data. The opx-rich rocks could form by mineral segregation in unconsolidated residues, crystallization of pockets of trapped residual melt etc. We find no evidence that intitial melting residues were dunites later refertilized to harzburgites in subduction zones.

[1] Pearson & Wittig (2008) *J Geol Soc* **165**, 895-914. [2] Herzberg (2005) *J Petrol* **45**, 2507-2530. [3] Doucet *et al.* (2012) *This volume.* [4] Doucet *et al.* (2011) *Miner Mag* **75**, 777. [5] Mattey et al. (1994) *EPSL* **128**, 231-241.

https://doi.org/10.1180/S0026461X00008434 Published online by Cambridge University Press

Sr isotopic investigations of calcium-rich matrices by LA-MC-ICPMS

JOHANNA IRRGEHER [1,a*], PATRICK GALLER[2] , ANDREAS ZITEK[1], MARIA TESCHLER-NICOLA[3], AND THOMAS PROHASKA[1]

[1]University of Natural Resources and Life Sciences, Department of Chemistry, Division of Analytical Chemistry, VIRIS Laboratory, A-3430 Tulln, Austria, johanna.irrgeher@boku.ac.at (* presenting author)

[a]Recipient of a DOC-fFORTE-fellowship of the Austrian Academy of Sciences

[2]Elkem Technology - Lab projects, ,NO-4675 Kristiansand S., Norway, patrick.galler@elkem.no

[3]Natural History Museum Vienna, Department of Anthropology, A-1010 Vienna, Austria, maria.teschler@nhm-wien.ac.at

The use of $^{87}Sr/^{86}Sr$ ratios is a powerful tool in the field of analytical ecogeochemistry, above all for the investigation of migration, mobility and movement due to its outstanding properties of regional difference and Sr abundance in nature. Only recently, variation of the $^{86}Sr/^{88}Sr$ ratio due to natural fractionation processes induced by weathering and temperature effects were reported, as well.

Laser ablation coupled to multiple collector inductively coupled plasma mass spectrometry (LA-MC-ICPMS) stands out due to its attributes as a semi-invasive means for the fast and direct investigation of Sr isotope ratios and marginal sample preparation required. However, direct stable Sr isotope ratio measurements in calcium phosphates and carbonates suffer from significant matrix-related interferences such as molecular ions, e.g. $(^{40}Ca\text{-}^{31}P\text{-}^{16}O)^+$, $(^{40}Ar\text{-}^{31}P\text{-}^{16}O)^+$, $(^{43}Ca\text{-}^{44}Ca)^+$ as well as in many cases concomitant atomic ions, e.g. $^{87}Rb^+$, $^{174}Hf^{2+}$. Interferences on Sr isotopes analyzed by LA-MC-ICPMS have been subject to numerous debates and discussions among scientists during the last couple of years. Interpretations of generated data are highly diverse regarding the trustworthiness of LA-MC-ICPMS, as corrections are approached in different ways and diverse sources of interferences are presumed. The major part of observations report trends towards higher $^{87}Sr/^{86}Sr$ ratios for LA-MC-ICPMS compared to solution-nebulisation based MC-ICPMS when analyzing apatite matrices and lower ratios in case of calcium carbonate matrices.

This study is dedicated to the systematic investigation of the effect of interferences and instrumental mass discrimination on Sr isotopic investigations using LA-MC-ICPMS and the assessment and validation of possible correction strategies. This includes evaluating the potential of the implementation of externally added elements (e.g. Zr) for mass bias correction.

The major focus was set on analyzing human tooth samples, fish hard parts and geological carbonates. Laser ablation data and corresponding data established using solution nebulisation based approaches were compared and potential sources of interferences identified by e.g. using high resolution ICPMS. The combined corrections of interferences and adequate mass bias correction procedures lead to accurate data even though increased uncertainties have to be taken into account. The obtained results are discussed along with coexisting approaches for data correction in laser ablation analysis.

Speciation and Localization of Cd in the Hyperaccumulator Plant *Arabidopsis halleri* Grown in the Field and in Controlled Conditions by XAS Techniques

MARIE-PIERRE ISAURE[1*], STEPHANIE HUGUET[1], CLAIRE-LISE MEYER[2], NATHALIE VERBRUGGEN[2], GERALDINE SARRET[3]

[1]LCABIE / IPREM UMR 5254, Université de Pau et des Pays de l'Adour & CNRS, Pau, France, marie-pierre.isaure@univ-pau.fr.

[2] LPGMP, Université Libre de Bruxelles, Brussels, Belgium, nverbru@ulb.ac.be.

[3]ISTerre UMR 5275, Université Joseph Fourier & CNRS, Grenoble, France, geraldine.sarret@ujf-grenoble.fr.

Some higher plants naturally grow on metal contaminated soils due to their ability to cope with metal toxicity. They can be used in phytoremediation to extract (phytoextraction) or stabilize (phytostabilization) metals accumulated in soils. These techniques can be an alternative to invasive physico-chemical remediation techniques. However, to develop phytoremediation, it is necessary to understand the mechanisms involved in metal accumulation, and particularly the way that plants transfer and store metals. These mechanisms have not been elucidated yet [1]. In this context, synchrotron radiation based techniques, and particularly micro-focused X-Ray Fluorescence (μXRF), and X-ray Absorption Spectroscopy (XAS) appear as powerful tools to determine the localization and the chemical forms of metals in plants, and thus the mechanisms involved in the metal accumulation capacity [2, 3]. In this study, we have investigated the Zn, Cd hyperaccumulator *Arabidopsis halleri*, which naturally develops on some contaminated soils in Europe. This work presents the application of μXRF and Cd μXANES to determine the distribution and speciation of Cd in *Arabidopsis halleri*, in combination with bulk Cd EXAFS/XANES spectroscopy. We particularly compared *Arabidopsis halleri* collected on the field and in various controlled conditions. Results show that Cd is mainly located in veins and mesophyll of leaves and that hot spots are found in trichomes (epidermal hairs), although this compartment is not a major compartment of storage for the metal. The speciation of Cd varies with the various conditions of Cd treatments but also differs from the plants originated from the site. This study highlights the difficulty to extrapolate the laboratory experiments to the field in a remediation context.

[1] Verbruggen et al. (2009) *New Phytologist* **181**, 759-776.
[2] Lombi and Susini (2009) *Plant Soil* **320**, 1-35.
[3] Isaure et al. (2006) *Spectrochimica Acta Part B* **61**, 1242-1252.

https://doi.org/10.1180/S0026461X00008434 Published online by Cambridge University Press

Search for Early Archean mantle lacking the late-veneer component

AKIRA ISHIKAWA[1,2*], MASANORI SHIMOJO[1], KATSUHIKO SUZUKI[2], KENNETH D. COLLERSON[3] AND TSUYOSHI KOMIYA[1]

[1] Earth Science and Astronomy, The University of Tokyo, Tokyo 153-8902, Japan, akr@ea.c.u-tokyo.ac.jp (*presenting author)
[2]IFREE, JAMSTEC, Yokosuka 236-0016, Japan
[3]Earth Sciences, Univ. Queensland, Brisbane Qld 4072, Australia

The overabundance of highly siderophile elements (HSEs) in the modern terrestrial mantle, relative to predicted composition is frequently attributed to the late influx of chondritic materials (late veneer) after the efficient stripping of HSEs to the metallic core. Although this model is not universally accepted due to insufficient knowledge of metal-silicate partitioning under high P-T conditions, broadly chondritic ratios of HSEs in fertile peridotites from a variety of tectonic settings provide strong support for the late veneer model.

A recent discovery of ^{182}W enrichments in ~3.8 Ga crustal rocks from Isua, West Greenland suggests that this area of Earth's surface has escaped addition of the late veneer, and remained unaffected by subsequent replenishment [1]. Furthermore, possible secular increase of HSE abundances for the komatiite source has been attributed to the progressive pollution of the HSE-poor deep mantle by the late veneer component between 3.5 and 2.9 Ga [2]. These studies raise the possibility that ~3.8 Ga ultramafic rocks from West Greenland and Labrador, Canada, can be used to establish HSE abundances of the Earth's mantle before the arrival of the late veneer.

We present HSE abundances and Re-Os systematics for a set of ultramafic rocks from Saglek-Hebron area of northern Labrador. Based on field and geochemical data, they were classified into two suites: residual peridotites occurring as tectonically-emplaced slivers of lithospheric mantle, and metakomatiites comprising mostly pyroxenite layers in supracrustal units. The samples analysed here have been investigated previously for Sm-Nd and Pb-Pb systematics, supporting their >3.8 Ga formation [3, 4]. Thus, the primary aim is to test whether the meta-peridotites and komatiites record peculiar HSE signatures of the early Archean shallow and deep mantle, respectively.

The two suites display contrasting HSE patterns that are consistent with their inferred protoliths. The harzburgitic to dunitic metaperidotites are typically marked by depletion of Pt, Pd and Re relative to Os, Ir and Ru, resulting from extensive melt extraction. In contrast, metakomatiites show smooth patterns with gentle positive slopes (except for Re). Overall, in terms of HSE patterns and abundances, both suites do not differ from their late Archean equivalents, such as the harzburgitic to dunitic xenoliths from North Atlantic Craton [5] and the 2.7 Ga Belingwe/Abitibi komatiites [6]. Moreover, a rare lherzolitic sample shows a very similar HSE pattern to that of PUM estimate [7]. These observations suggest that 3.8 Ga mantle has been influenced by the late veneer. We will discuss the possible reasons for the decoupling between W isotope evidence from crustal rocks and HSE signatures in mantle materials.

[1] Willbold *et al.* (2011) *Nature* **477**, 195-198. [2] Maier *et al.* (2009) *Nature* **460**, 620-623. [3] Collerson *et al.* (1991) *Nature* **349**, 209-214. [4] Wendt & Collerson (1999) *Precamb. Res.* **93**, 281-297. [5] Wittig *et al.* (2010) *Chem. Geol.* **276**, 166-187. [6] Puchtel *et al.* (2009) *GCA* **73**, 6367-6389. [7] Becker *et al.* (2006) *GCA* **70**, 4528-4550.

Coupling between separative techniques and inductively coupled plasma mass spectrometry for lanthanides separation and on-line isotope ratio measurements

ISNARD H. [1*]., GOURGIOTIS A.[1]., MIALLE S.[1], BOURGEOIS M.[1], VIO L.[1], NONELL A.[1], CHARTIER F.[2]

[1] Commissariat à l'Energie Atomique, DEN/DPC/SEARS/LANIE, 91191 Gif-sur-Yvette Cedex, France, helene.isnard@cea.fr
[3] Commissariat à l'Energie Atomique, DEN/DPC, 91191 Gif-sur-Yvette Cedex, France

The precise lanthanide (Nd, Sm, Eu) isotope composition is of major interest in geosciences (geochronology, erosion studies, paleo-circulation reconstruction…) as well as in nuclear industry (determination of nuclear fuel burn-up, management of the spent fuel nuclear fuel…). Direct determination of lanthanides by mass spectrometry is hampered by isobaric interferences and so previous chemical separations are then required before mass spectrometric measurements. In most cases isotope ratio are determined off-line after chemical separation processes.

We would like to present here the simultaneous online determination of some lanthanides (Nd, Sm, Eu) isotopic composition in nuclear samples by the hyphenation of two separative techniques with inductively coupled plasma mass spectrometry.

The first one is the coupling between liquid chromatography and ICPMS [1]. The LUNA SCX column which includes benzene sulfonic acid group and 2-hydroxy-2-methylbutyric acid as a complexing agent in eluent solution were used for the separation. The column has been directly coupled to ICPMS. Data acquisition and correction of mass bias by different approaches are discussed.

The second one present the development and conception of a microchip for the lanthanides separation. This microchip is based on the isotachophoresis (ITP) separation of lanthanides and was directly coupled to an MC-ICPMS for the on-line measurements of Nd and Sm isotopic ratio [2]. This is the first time that such a coupling is performed and the feasibility is demonstrated in this study. These on-line methods are a great challenge related to the limited signal duration [3] but a very attractive approach to decrease the sample size and the sample preparation time. Such a coupling and further applications could be envisaged for geochemical applications.

[1] Bourgeois M. et al. (2011) *JAAS* **26**, 1660-1666. [2] Vio et al. (2012) *JASS* accepted, in press. [3] Günther-Leopold et al. (2004) *Anal. Bioanal. Chem.* **378**, 241-249.

https://doi.org/10.1180/S0026461X00008434 Published online by Cambridge University Press

Concentrations and chemical forms of trace metals in coastal seawater in coral reefs and their relationship to coral mucus

AKIHIDE ITOH[1*] AND SHOKO GANAHA[1]

[1]University of the Ryukyus, Science education, Okinawa, Japan, akihide@edu.u-ryukyu.ac.jp (* presenting author)

Coastal seawater in coral reefs near Okinawa Island in Japan, which is in oligotrophic conditions, has a diverse and unique ecosystem. It is possible that nutrient salts and trace metals, classified into nutrient type, are effectively supplied to marine phytoplankton and zooxanthellae from seawater. However, the concentrations and chemical forms of trace metals in coastal seawater in coral reefs have been scarcely reported so far. In addition, it is reported that the coral mucus plays an important role as a nutrient supply to fishes and other animals, and scavengers of suspended particles [1]. In the present study, firstly, the characteristics of the concentrations and chemical forms of trace metals in coastal seawater in coral reefs were investigated according to seasonal variation. Secondly, the relationship between concentrations of trace metals in seawater in coral reefs and in coral mucus were discussed.

A monitoring investigation of the coastal seawater in coral reefs, located near the northern part of Okinawa Island, was carried out once every month from Sep. 2010 to Aug. 2011. After the chemical species in the seawater were separated into dissolved, acid-soluble particulate, and ionic ones, an analytical method using a chelating resin disc and a disposable syringe was employed for desalination and preconcentration of trace metals. After that, trace metals in the concentrated solutions were measured by ICP-MS. On the other hand, coral mucus was sampled from *Acropora nasuta* exposed to sunlight and then analysed by ICP-MS.

As a result, 10 elements in the dissolved form of each sample could be determined. The average concentrations (unit: $\mu g\ L^{-1}$)for all samples were as follows: Mo:10.8, U: 3.2, V:1.6, Mn:0.14, Ni:0.16, Zn:0.13, Cu:0.070, Pb:0.023, Co:0.0022, Cd:0.0019. The concentrations for most trace metals were close to ones at the surface of open seawater in the North Pacific Ocean, but the concentrations of Co, Ni, Cu, Zn, and Cd, classified into nutrient type, were significantly lower than ones in other coastal seawater. These results suggest that the coastal seawater in coral reef ecosystems were in oligotrophic conditions. The most of Mo, V, and U exist in dissolved forms, while most Fe exists in acid-soluble form. 50–70 % of Cu, Zn, Pb, and Co and 21–42 % of Cd, Mn, and Ni existed in acid-soluble particles. These results suggest that some trace metals in the nutrient type exist as biogenic particulate matter. As for their relationship to coral mucus, the concentrations of Mn, Fe, Co, Ni, Zn, Cd, and Pb in coral mucus were 10-150 times larger than those dissolved in coastal seawater in coral reefs, while those of Na, Mg, K, V, and U in coral mucus were almost the same as the dissolved forms. The elements which showed high concentration for acid-soluble particles in June and January were almost the same as those in coral mucus. Therefore, the concentrations of trace metals in acid-soluble particles in June and January may be affected by coral mucus, which combined with sediment and was lifted by tidal flows.

[1] C. Wild et al, (2004), *Nature* **428**, 66-70.

Can Nd tell us about Mediterranean Outflow Water?

RUŽA IVANOVIĆ[1*] MARCUS GUTJAHR[2], RACHEL FLECKER[3], PAUL VALDES[4], TANJA KOUWENHOVEN[5], JÖRG RICKLI[6], ROB ELLAM[7], ANDRIA NICODEMOU[8]

[1]University of Bristol, Bristol, UK, Ruza.Ivanovic@bristol.ac.uk (* presenting author)
[2]NOC, Southampton, UK, M.Gutjahr@soton.ac.uk
[3]University of Bristol, Bristol, UK, r.flecker@bristol.ac.uk
[4]University of Bristol, Bristol, UK, p.j.valdes@bristol.ac.uk
[5]University of Leuven, Belgium, tj.kouwenhoven01@gmail.com
[6] University of Bristol, Bristol, UK, J.Rickli@bristol.ac.uk
[7] SUERC, East Kilbride, UK, r.ellam@suerc.gla.ac.uk
[8] University of Bristol, Bristol, UK

Although εNd is a well established water provenance tracer for deep ocean circulation, there remains some debate over the practicability of Neodymium (Nd) isotopes at intermediate water depth on the continental-margin. Using the method of Vance and Burton (1999), we intend to answer some of the questions on how useful Nd can be for tracking Mediterranean Outflow Water (MOW), and whether or not Nd isotopes (expressed as ε_{Nd}) measured in foraminfera from this setting represent a true water-column signal, or a post-depostional one.

We have measured ε_{Nd} in 90 foraminiferal samples (each containing 400-900 individuals) and fish-remains samples in order to assess whether or not Nd extracted from these palaeo archives can elucidate on the evolution of MOW at high temporal resolution. We examined Late Quaternary samples, to make direct comparisons between our data, other Quaternary MOW reconstructions[e.g.2] (including different phases from the same samples) and modern observations[e.g.3]. We also analysed samples from the Late Miocene, 8-6 Ma, when progressive tectonic restriction of the Betic-Rif region caused Mediterranean-Atlantic water exchange to fluctuate dramatically, making the period a good test-case for MOW extremes. We further interpreted our ε_{Nd} record within the context of more finely resolved Sr and foram assemblage records, including data we obtained from the same samples as the Nd.

From these results, we propose that ε_{Nd} in foraminifera and fish teeth can tell us about MOW evolution. For example, we clearly detect changes in water provenance, indicative of marine shallowing events and corridor 'closure'. Furthermore, our data suggest that foraminfera-hosted Nd is not diagenetic and thus our planktic Nd indeed appears to be a 'true' water-column signal. However, questions remain over whether or not boundary exchange[4] and localised riverine inputs have confused the extracted ε_{Nd} signal, and although our Sr and benthic assemblage data do present some clues to the answers, these are by no means exhaustive tests. In short, there remain significant challenges in fully understanding this continental-margin ε_{Nd} record, and we advise that although Nd can provide valuable information about changes in MOW, a multi-proxy approach is essential for making robust interpretations of the data.

[1] Vance & Burton (1999) *EPSL* **173 (4)**, 365-379. [2] Stumpf *et al.* (2010) *Quaternary Science Reviews* **29 (19-20)**, 2462-2472. [3] Spivack & Wasserburg (1988) *Geochim. Cosmochim. Acta* **52,** 2762–2773. [4] Lacan & Jeandel (2005) *EPSL* **232 (3-4)**, 245-257.

https://doi.org/10.1180/S0026461X00008434 Published online by Cambridge University Press

Rock boring fungi in subseafloor basalts

MAGNUS IVARSSON[1*]

[1]Swedish Museum of Natural History, Department of Palaeozoology, Stockholm, Sweden, magnus.ivarsson@nrm.se (* presenting author)

Fossilized fungal hyphae in subseafloor basalts bear witness of extensive weathering and tunneling in vein and vesicle filling secondary mineralisations (carbonates and zeolites). The minerals have been chemically dissolved and penetarted by the fungal hyphae, which have produced and occur in complex mycelium-like networks within the minerals. The hyphae frequently branch and anastomoses between branches occur, a mechanism that is not fully understood. Rock boring hyphae in subseafloor basalts have been observed from two separate locations: the Emperor Seamounts, Pacific Ocean, and the volcaniclastic apron of Gran Canaria, Atlantic Ocean, thus, it is not an isolated phenomenon [1]. Selection towards Fe-rich carbonates (siderite) over Fe-poor carbonates (calcite) indicates a possible trophic strategy in a few samples. Otherwise, the strategy of tunnelling probably is due to migration through the system or acquiring of habitable space. Subseafloor, hydrothermal settings are dynamic environments characterised by extreme shifts in, for example, temperature or pH, thus, the tunneling can be a response mechanism to environmental stress. Fungi are known as a powerful geobiological agent in terrestrial environments that promotes mineral weatherin and decomposition of organic matter. It is probable to assume that fungi would play a similar role in the ocean crust and mediate weathering and mobilization of elements.

[1] Ivarsson *et al.* (2011) *Astrobiology* **11**, 633-650.

XAFS investigation for sorption mechanism in As(V) coprecipitation with ferrihydrite

SAYAKA IZAWA[1*], CHIHARU TOKORO[2], YUJI ODA[3], DAISUKE HARAGUCHI[4], AND SHUJI OWADA[5]

[1]Waseda University, Tokyo, Japan, izasaya@ruri.waseda.jp
[2]Waseda University, Tokyo, Japan, tokoro@waseda.jp
[3]Waseda University, Tokyo, Japan, my-happy-ending@ruri.waseda.jp
[4]Waseda University, Tokyo, Japan, d.haraguchi@aoni.waseda.jp
[5]Waseda University, Tokyo, Japan, owadas@waseda.jp

Coprecipitation method using ferrihydrite has been commonly applied to remove As(V) from acid mine drainage. However, the mechanism in coprecipitation is unclear. Therefore, it is demanded to clarify how coprecipitation of As(V) with ferrihydrite occures in acid mine drainage.

In the previous paper, we investigated the sorption mechanism of dilute As(V) with ferrihydrite using three kinds of experimental studies for an artificial wastewater in which the ion strength was 0.05 and pH was 5; (i) sorption isotherm formation, (ii) zeta potential mesurment and (iii) XRD analysis. We already confirmed that As(V) was formed a simple two-dimentional adsorption onto the surface of ferrihydrite when the initial As/Fe molar ratio was less than 0.4, whereas a surface precipitation of amorphous ferric arsenate was formed when the initial As/Fe molar ratio was more than 0.4 [1]. In this study, XAFS analysis was conducted to know more detail mechnism of As(V) sorption to ferrihydrite in coprecipitation proess. Additionaly, the effect of ionic strength to As(V) sorption mechanism with ferrihdyrite in coprecipitation process was also discussed.

Both of XANES and EXAFS analysis on K-edge of As showed As(V) coprecipitates with ferrihydrite was mixture of As(V) adsorbed ferrihydrite and amorphous ferric arsenate. When the ion strength was 0.05 in an artificial wastewater containing As(V), estimated weight ratio of amorphous ferric arsenate in As(V) coprecipitates became above 0.5 when the initial molar ratio of As/Fe≥0.5 was used. These results corresponded with results by XRD analysis. EXAFS analysis assuming one surface complex for As-Fe bond showed the coordination number of As to Fe in As(V) coprecipitates increased with increasing the initial molar ratio of As/Fe. Moreover, EXAFS analysis assuming three kinds of surface complexes for As-Fe bond showed the coordination number for 2.85 Å of As-Fe bond increased and it for 3.24 Å of As-Fe bond decreased with increasing the initial As/Fe molar ratio. All experimental data obtained in this study showed As(V) co-precipitation mechanism shifted gradually from As(V) complexation to the surface of ferrihydrite toward amorphous ferric arsenate.

On the other hand, when the ion strength was 0.5, the sorption density of As(V) to ferrihydrite obtained from coprecipitation process was lower than it at ion strength of 0.05. Results of XRD and XAFS analysis revealed that the formation of surface precipitation was prevented when the ion strength was high, whereas simple two-dimentional adsorption of As(V) onto the surface of ferrihydrite was not so prevented by the higher ion strength.

[1] C.Tokoro, Y.Yatsugi, H.Koga and S.Owada (2010) *Environment Science and Technology*, **44**, pp.638-643.

https://doi.org/10.1180/S0026461X00008434 Published online by Cambridge University Press

Silica, Al and Pb in atmospheric PM10 and in human lungs in Upper Silesia,Poland

JABLONSKA MARIOLA [1], JANECZEK JANUSZ[1], LESNIOK MIECZYSLAW [2] LUCYNA LEWIŃSKA-PREIS[1]

[1]University of Silesia, Department of Geochemistry, Mineralogy and Petrology; Sosnowiec, Poland
mariola.jablonska@us.edu.pl;
janusz.janeczek@us.edu.pl
[2]University University of Silesia, Department of Climatology,Sosnowiec, Poland,

Upper Silesia (US) is the most densely populated (>1600 people/km^2) and the most polluted region of Poland. Annual average of PM10 concentration is still higher then national standars set by the regulators at 40 μg/m^3. That situation poses a high risk to human health as evidenced by the medical data. In this study silica, aluminium and lead were determined in atmospheric PM10 and in human lung tissues. Silica occurs as quartz and amorphous phase, whereas aluminium is in clay minerals, feldspars, amorphous alumino-silicates etc. Lead occurs in the form of galena, lead chloride and lead oxide. All of those mineral particles are abundant in respirable fraction of PM10 and in ultrafine particles.

Fifteen samples of PM10 and 34 samples of lung tissues from autopsy donors from US (13 female and 21 male) were analysed. Silica was determinated by colorimetry, and aluminium and lead were determined using inductively coupled plasma-atomic emission spectrometry (ICP-AES).

The concentration of silica in PM10 is the range of 1,00 – 34,98 wt. % (the average is 12,11±5,19 wt. %). In human lung tissues the average concentration of silica is 3,03±0,84 wt. % (the minimum value is 0,37 wt. % and the max. 5,65 wt. %). The concentration of aluminium in PM10 ranges from 0,58 wt.% to 2,78 wt. %. The average concentration of Al of 1,69±0,42 wt. % is distinctly higher than the average of Al in human lungs (0,197±0,08 wt. %). The lead content in PM10 ranges from 45 ppm to 1473 ppm, with the average 296±92 ppm. In human lungs the content of lead is 13±3 ppm, (min. 2 ppm, max. 47 ppm).

The presence of abundant Si, Pb, and Al in ultrafine particles is particularly worrisome as it is known, that particles with a diameter less than 0.5 μm immediately infiltrate into blood circulation system similarly to gases [1]. 100% of Pb hosted by ultraparticles is absorbed by lung tissues [2].

References

[1] Migaszawski Z.,Galuszka A., (2007) *Essentials of Environment Geochemistry, Science –Technical Publisher, Warsow (in Polish)*
[2] Goyer R.A., (1991) *Toxic effects of metals*. In: Amdur M.O., Doull J., Klaassen C.D. (eds.) Casarett and Doull's *Toxicology*, *The Basic Science of Poisons*. *New York, Pergamon Press*

SEQUENTIAL DISSIPATION OF A POORLY-VENTILATED WATER MASS UPON THE LAST GLACIAL TERMINATION

SAMUEL L. JACCARD[1*], ERIC D. GALBRAITH[2], ALFREDO MARTINEZ-GARCIA[1], ROBERT F. ANDERSON[3]

[1]ETHZ, Zurich, Switzerland, samuel.jaccard@erdw.ethz.ch; alfredo.martinez-garcia@erdw.ethz.ch
[2]McGill University, Montreal, Canada, eric.galbraith@mcgill.ca
[3]LDEO, Columbia University, USA, boba@ldeo.columbia.edu

It is believed that no single mechanism can account for the full amplitude of past CO_2 variability. But although multiple synergistic processes may be involved, intensified isolation of deep-water masses from the atmosphere has emerged as a central mechanism for low glacial CO_2. This could have resulted from increased oceanic density stratification, increased sea ice cover, or a decrease wind-driven vertical mixing. Recent evidence is consistent with the existence of a poorly ventilated, carbon-rich water mass in a large portion of the glacial Pacific and Southern Oceans. However, the mechanisms by which this water mass dissipated upon glacial terminations remains a subject of debate.

Here, we present a compilation of sedimentary redox-sensitive trace metal records from the subarctic Pacific and the Southern Ocean to reconstruct changes in deep ocean oxygenation – and, by inference, respired carbon storage - across the last glacial termination.

Our results suggest that the abyssal Pacific and Southern oceans were depleted in oxygen during the last glacial maximum, though they were not anoxic. The large and abrupt increase in sedimentary opal accumulation observed in the Southern Ocean at approx. 18 kyr is accompanied by a decrease in authigenic uranium concentrations suggesting better oxygenation at the depth of the core site. Enhanced mixing within the Southern Ocean, driven by stronger winds and/or changes in the density profile of the water column, would have invigorated circulation at depth, The increase in the rate of nutrient supply to the surface would have enhanced the strength of the Southern Ocean High Nutrient Low Chlorophyll (HNLC) region, and increased the leakage of nutrients into intermediate and mode waters of the southern hemisphere. Simultaneously, the decrease in nutrient-poor NADW to the deep sea, caused by the freshwater forcing associated with Heinrich Event 1, allowed nutrient-rich AABW to dominate the deep ocean. Both of these mechanisms would have increased global preformed nutrient concentrations, previously shown to contribute to higher atmospheric pCO_2, and could have explained the large-scale transfer of carbon from the deep ocean to the atmosphere between 18 and 15 ka. In the subarctic Pacific, the arrival of well-oxygenated abyssal waters appears to have taken place at the onset of the Bolling/Allerod, 14.7 ka, accompanying the reinvigoration of North Atlantic Deep Water, which increased the overall rate of deep ocean ventilation, even as it contributed to an overall decrease in the preformed nutrient load of the global ocean. The fact that atmospheric pCO_2 stopped increasing at this time is consistent with this interpretation. Our results suggest that this stepwise reinvigoration of deep water circulation, resulting from the buffeting of ocean density structure by large inputs of freshwater, was responsible for driving carbon out of the abyssal ocean during the melting of the large continental ice sheets.

https://doi.org/10.1180/S0026461X00008434 Published online by Cambridge University Press

Helium solubility in ring site bearing minerals and implications for noble gas recycling

COLIN R.M. JACKSON[1*], SIMON P. KELLEY[2], STEPHEN W. PARMAN[1]. REID F. COOPER[1]

[1]Brown University, Providence, United States colin_jackson@brown.edu (* presenting author)
[2]The Open University, Milton Keynes, England

Noble gas solubility in minerals is generally assumed to be low, leading to the assumption that noble gases are not recycled back in to the mantle (e.g. 1). However, applicable experimental data remain scarce. To explore possible mechanisms of noble gas recycling, we conducted a series of experiments defining He solubility in a suite of amphiboles and cyclosilicates using an externally heated, gas-pressure-medium apparatus. Analysis was conducted using by laser-ablation mass spectrometry. Helium was the pressure medium in all experiments. Pressures and temperatures ranged from 50 to 170 MPa and 650 to 800°C, respectively. Helium solubility in both cyclosilicates (tourmaline, beryl, cordierite) and amphibole (richterite, paragasite, actinolite) is remarkably high and correlates with the density of vacant (i.e., unoccupied by a cation) ring sites. Helium is >1,000x more soluble in vacant ring rich cordierite, beryl, and actinolite than in olivine.

The concentration of He dissolved into cordierite and beryl is linearly dependent on P_{He}, demonstrating Henrian behaviour, and thus applicable to natural systems. Depth profiles were completed on each phase investigated and showed that He concentrations are homogenous. This indicates a close approach to equilibrium and an absence of inclusions affecting the analysis. The observed solubilities are independent of experimental duration (7-27 hrs) and temperature (650 to 800°C).

The ring site is a lattice structure constituting six $Si/AlO_4^{4-/5-}$ tetrahedra linked in a hexagonal ring. It is large, hosting alkali cations, and has no net charge when vacant. Following lattice strain theory, the ring site is an energetically favorable environment for noble gas dissolution. Excess argon is commonly observed in natural samples of ring-bearing minerals (amphibole, mica, cyclosilicates) (2, 3), corroborating our conclusion that noble gas solubility can be associated with ring sites.

Ring-site-bearing minerals, including mica, serpentine, talc, and amphibole, are common in recycled lithologies (4) and may provide a possible mechanism for widespread recycling of noble gases back into the mantle. Moreover, ring-site bearing minerals are the major minerals responsible for recycling water and halogens. Thus, water and halogen recycling may be mineralogically linked to noble gas recycling.

[1] C. J. Allegre, A. Hofmann, K. Onions, (2006). *GRL*, **23**, 3555 [2] S. Kelley (2002). *Chem. Geo*, **188**, 1 [3] P. E. Damon, J. L. Kulp, (1958). *Am. Min.* **43**, 433 [4] S. Poli, M. W. Schmidt, (2002). *Annual Review of Earth and Planetary Sciences* **30**, 207

Trace element composition of a non-chondritic Earth: Potential solutions and geodynamic implications

MATTHEW G. JACKSON[1*], A. MARK JELLINEK[2]

[1] Boston University, Department of Earth Sciences, Boston, MA, 02115, USA (jacksonm@bu.edu)
[2] Department of Earth and Ocean Sciences, University of British Columbia, Vancouver, British Columbia, V6T 1Z4, Canada (mjallinek@eos.ubc.ca)

The bulk composition of the silicate part of the Earth (BSE) has long been assumed to be tied to chondrites, where refractory, lithophile elements like Sm and Nd are thought to exist in chondritic relative abundances in the Earth. However, recent work exploring the $^{142}Nd/^{144}Nd$ systematics of modern terrestrial samples identifies ratios that are 18±5 ppm higher than the chondrite reservoir that challenges the traditional BSE model [1]. Here we investigate a hypothesis that this terrestrial ^{142}Nd excess is related to a Sm/Nd ratio 6% higher than chondritic. We develop a non-chondritic BSE trace element model in which the elevated Sm/Nd requires a shift of BSE $^{143}Nd/^{144}Nd$ from 0.51263 to 0.51300 that demands, in turn, corresponding changes to $^{87}Sr/^{86}Sr$ and $^{176}Hf/^{177}Hf$, as well as the associated parent-daughter ratios—Rb/Sr, Lu/Hf. These modified parent-daughter ratios define a normalized trace element pattern, or spidergram, that is depleted in highly incompatible elements relative to the chondrite-based BSE. We use the ^{40}Ar abundance of the atmosphere, crust and depleted mantle to constrain the minimum K in the Earth (155 ppm), and anchor the spidergram to this K concentration to determine the concentrations of the other geochemically important incompatible elements, such as U and Th. An upper limit (170 ppm K) is estimated by assuming that abundances of the least incompatible elements (e.g., Lu) do not exceed chondrite-based BSE concentrations. This non-chondritic BSE trace element model requires that >78% of the mantle mass contribute to the formation of continental crust. The reduced concentrations in heat-producing elements U, Th and K in our new BSE compositional model implies a ~30% reduction in the current rate of radiogenic heating and, thus, a proportional increase in the heat flow delivered to Earth's surface by plate tectonics, the implications of which we explore in parameterized thermal history models.

[1] Boyet and Carlson (2005) *Science* **309**, 576-581.

https://doi.org/10.1180/S0026461X00008434 Published online by Cambridge University Press

Shale gas and its environmental footprint

R.B. JACKSON[1*], A. VENGOSH[2], N.R. WARNER[3], AND S.G. OSBORN[4]

[1]Duke University, Nicholas School of the Environment and Center on Global Change, Durham, NC, 27708, USA, jackson@duke.edu (* presenting author)
[2]Duke University, Nicholas School of the Environment, Durham, NC, 27708, USA, vengosh@duke.edu
[3]Duke University, Nicholas School of the Environment, Durham, NC, 27708, USA, nathaniel.warner@duke.edu
[4]Cal Poly Pomona, Department of Geological Sciences, Pomona, CA, 91768, USA, sgosborn@csupomona.edu

The Marcellus shale is one of the largest natural gas reservoirs in the United States and, like other shale gas reserves, has been developed through advances in drilling technologies and production strategies. Concerns over potential environmental impacts have accompanied natural gas extraction around the country. We have sampled shallow groundwater systems of >200 homeowners in NE Pennsylvania and New York for brines, dissolved gases, and other attributes of water quality for the last two years. In particular, we have exampled possible relationships between water quality and distance to natural gas wells.

In our first study publishd in May of 2011 [1], we found no evidence of increase salt concentrations or fracturing fluids with distance to gas wells, but dissolved methane concentrations were 17 times higher on average for water wells found within 1km of them. Higher chain hydrocarbons (ethane, propane, and butane) were detected more often in active areas (21, 8, and 3, respectively) compared to non-active areas (3, 0, and 0, respectively), indicating a more thermogenic methane character. The carbon isotope values of methane (δ^{13}C-CH4), in active extraction areas were on average less negative (-37±7 ‰) than non-active extraction areas (-54±11‰). We conclude from these, and newer follow-up results, that there are important differences in methane concentration, natural gas composition, and δ^{13}C-CH_4 values in some shallow groundwater wells near natural gas extraction areas. Furthermore, the dissolved gas geochemistry nearer gas wells appears to be consistent with a more thermally mature source of organic matter. New results from additional sampling in 2011 will be presented.

[1] Osborn, Vengosh, Warner, Jackson (2011) *Proceedings of the National Academy of Sciences, U.S.A,* **108**, 8172-8176.

Mapping element concentrations and Ce^{4+}/Ce^{3+} ratios in zircon by LA-ICP-MS

SIMON E. JACKSON[1*] AND JOHN B. CHAPMAN[1]

[1]Geological Survey of Canada, Ottawa, Ontario, Canada, simon.jackson@nrcan-rncan.gc.ca (* presenting author); john.chapman@nrcan-rncan.gc.ca

A LA-ICP-MS procedure has been developed for simultaneously generating element, element ratio and isotope ratio maps of individual zircon grains. The instrumentation used was a Photon Machines Analyte.193 laser ablation system and Agilent 7700 quadrupole ICP-MS with addition of a second rotary interface pump that doubles instrument sensitivity. The procedure involves performing lines of individual spot ablations, resulting in true spot size-limited spatial resolution. Each spot ablation is preceded by several laser cleaning pulses and a short period of flushing to remove surface contamination (from condensation and other sources). For each element, signals for each individual spot are integrated into single readings, then calibrated using an external standard (NIST 612) and an internal standard (SiO_2) for element concentration measurements, and against a zircon (GJ-1) for Pb-U isotope ratio measurement. The concentration or ratio data are then presented as colour pixel maps by assigning colours according to concentration (or ratio) using a choice of different colour assignment schemes (linear, logarithmic, percentile)

Zircon ($ZrSiO_4$) is an abundant accessory mineral in granitoid igneous intrusive rocks that are associated with porphyry and other magmatic-hydrothermal mineral deposits. Using spot sizes as small as 7 microns in diameter, Ce and the REE from Nd-Lu, Pb, Hf, Th and U can be detected routinely in zircons. Measurement of this suite of REE allows, by extrapolation, calculation of Ce^{4+}/Ce^{3+} ratios, which are a proxy for oxidation state of the source magma which has been linked to its fertility for generation of porphyry-style Cu (±Au±Mo) mineralization [1]. Distribution maps for key trace elements and Ce^{4+}/Ce^{3+} ratios in single zircons thus allow the geochemical evolution of the magmatic system, including oxidation state, to be visually documented.

The procedure is been applied to zircons from a suite of Jurassic and Cretaceous granitoid intrusions from the Canadian Cordillera, including samples from igneous host rocks to porphyry-style deposits, to determine whether systematic differences exist in the geochemical trends between mineralised and non-mineralised intrusions. Pb/U ratio and age maps for the zircons are also being generated, allowing identification of inherited cores and, potentially, multiple crystallisation ages for zircons that have had a protracted crystallisation history. Also being evaluated is whether zones with anomalous ages can be identified and whether these correlate with the chemistry of the REE, or other elements, as has been proposed [2].

[1] Ballard et al. (2002) *Contrib. Mineral. Petrol.* **144**, 347-364.
[2] Black et al. (2004*) Chem. Geol.* **205**, 115–140.

https://doi.org/10.1180/S0026461X00008434 Published online by Cambridge University Press

Distribution and stable isotopic composition of ClO_4^- in the Atacama Desert.

W.ANDREW. JACKSON[1], BALAJI RAO[5], J.K. BÖHLKE[2], PAUL B. HATZINGER[3], NEIL STURCHIO[4], BAOHUA GU[5], ALFONSO DAVILIA[6], MARK CLAIR[7]

[1]Texas Tech University, TX; andrew.jackson@ttu.edu
[2]U.S. Geological Survey, Reston, VA; jkbohlke@usgs.gov
[3]Shaw Environmental, NJ; paul.hatzinger@shawgrp.com
[4]University of Illinois at Chicago, IL; sturchio@uic.edu
[5]Oak Ridge National Laboratory, TN; gub1@ornl.gov
[6]NASA Ames, Moffett Field, CA; adavila@seti.org
[7]U. of Washington, Seatle, WA; mclaire@astro.washington.edu

High concentrations of atmospheric ClO_4^-, ClO_3^-, and NO_3^- occur in the Atacama Desert where dry and oxic conditions allow oxyanions to accumulate near the surface over long periods. We collected sediment samples from vertical profiles (~1-3 m depth) over a 1000 km longitudinal transect along the central depression in the Atacama. ClO_4^-/NO_3^- molar ratios (350-3,500) and NO_3^- stable isotopes were relatively consistent both with depth and along the longitudinal transect except for locations receiving >2 cm of annual precipitation. ClO_4^-/ClO_3^- molar ratios were similar for most sites (~1). In contrast, ClO_4^- exhibited substantial variation in its stable isotopic composition ($\delta^{18}O$ and $\Delta^{17}O$) with respect to location along the longitudinal transect. In addition, the $\delta^{18}O$ and $\Delta^{17}O$ of O in ClO_4^- were strongly correlated (r^2=0.89). Elevated $\Delta^{17}O$ values indicate ClO_4^- formed largely by O_3 mediated oxidation of Cl, possibly in the stratosphere. However, substantial variation in $\delta^{18}O$ (-25 to -3 per mil) and $\Delta^{17}O$ (+4 to +10 per mil) of ClO_4^- is intriguing given the long salt accumulation times (~10^6 years). This isotopic variation may indicate some unknown process is controlling deposition over a large area for long time periods, atmospheric ClO_4^- isotopic composition has varied in geologic time, or some surface process (generation or alteration) that varies spatially is affecting the ClO_4^-isotope composition by transformation, exchange, or dilution. Insights from our work are relevant to models of oxyanion production and accumulation in areas with little biologic activity.

Enstatite Chondrites and the Composition of the Earth

STEIN B JACOBSEN[1*], MICHAIL PETAEV[1] AND SHICHUN HUANG[1]

[1]Department of Earth and Planetary Science, Harvard University, jacobsen@neodymium.harvard.edu (*)

The nearly identical O isotopic compositions of the enstatite chondrites (EC), Earth's mantle, and Moon were used [1] to argue that the EC provide the best Solar System material for estimating the chemical composition of the Earth. A possible link between the EC and Earth is further supported by recent observations that EC and Earth have the same isotopic compositions for both major and minor elements (O, Ca, Ti, Cr) which exhibit substantial variations among different chondrite groups [e.g., 2-4], with Si being the only exception.

However, there is a huge mismatch in chemical compositions between the EC and Earth. For example, the EC have much too high Rb/Sr and K/U ratios and are depleted in FeO and refractory lithophile elements compared to the composition of Earth's mantle deduced from terrestrial rocks. This discrepancy could be resolved by assuming that the Earth and EC had a common nebular precursor but they have experienced different chemical evolution. Such an assumption is supported by the mineralogy and O isotopic data for the most primitive EH3 chondrites.

The abundant FeO-bearing silicates, compositionally similar to those in other classes of chondrites, are well documented in ECs [5-8], with most silicates having O isotopic compositions of the bulk EC values [7-8]. Recent studies [9-11] showed that the chalcophile behaviour of Ca, Mg, Na, and other elements in EC is due to secondary processing of FeO-bearing silicates in an H-poor environment with high f_{S2} (Fe-FeS buffer) and f_{O2} close to the CO-CO_2 buffer.

We propose that the nebular reservoir that produced the precursor material for EC has also produced the building blocks for the Earth, chemically similar to the widely accepted Earth's composition of [12]. Interestingly, the Nd isotope variations in the Earth and EC are consistent with a bulk mantle-crust system that followed the CHUR evolution curve [13].

[1] Javoy M. (1995) *GRL* **22**, 2219-2222.
[2] Clayton (2003) *SSR* **106**, 19-32.
[3] Huang et al. (2012) *LPS* **42**, #1334.
[4] Trinquier et al. (2009) *Science* **324**, 374-376.
[5] Lusby D. et al. (1987) *JGR* **92**, E679-695.
[6] Weisberg M. K. et al. (1994) *Meteoritics* **29**, 362-373.
[7] Kimura M. et al. (2003) *MAPS* **38**, 389-398.
[8] Weisberg M. K. et al. (2011) *GCA* **75**, 6556-6569.
[9] Lehner S. W. et al. (2011) *LPS* **42**, #1863.
[10] Petaev M. I. et al. (2011) *LPS* **42**, #2323.
[11] Petaev M. I. et al. (2012) *LPS* **43**, #2229.
[12] McDonough W.F. & Sun S.-s (1995) *Chem. Geol.* **120**, 223-254.
[13] Jacobsen S. B. and Wasserburg G. J. (1984). *EPSL* **67**, 137-150.

https://doi.org/10.1180/S0026461X00008434 Published online by Cambridge University Press

Investigating cloud absorption effects I and II: Global and Arctic absorption properties of black carbon and tar balls in clouds and aerosols

MARK Z. JACOBSON[1*]

[1]Stanford University, Stanford, U.S.A., jacobson@stanford.edu (* presenting author)

This is a study to understand better Cloud Absorption Effects I and II, which are the effects on cloud heating of absorbing inclusions in hydrometeor particles and of absorbing aerosol particles interstitially between hydrometeor particles at their actual relative humidity (RH), respectively [1]. The GATOR-GCMOM model was used to study these effects as well as optical properties and the mixing states of black carbon (BC) and tar balls (TB) in clouds and aerosols. The globally- and annually-averaged modeled 550-nm aerosol mass absorption coefficient (AMAC) of externally-mixed BC was found to be 6.72 (6.3-7.3) m^2/g, within the laboratory range (6.3-8.7 m^2/g). The global AMAC of externally- plus internally-mixed (IM) BC was 16.2 (13.9-18.2) m^2/g, less than the measured maximum at 100% RH (23 m^2/g). The resulting AMAC amplification factor due to internal mixing was 2.41 (2-2.9), with highest values in high RH regions. The global 650-nm hydrometeor mass absorption coefficient (HMAC) due to BC inclusions within hydrometeor particles was 17.7 (10.6-19) m^2/g, ~9.3% higher than that of the IM-AMAC. The 650-nm HMACs of TBs and SD were half and $1/190^{th}$, respectively, that of BC. Modeled aerosol absorption optical depths were consistent with AERONET and OMI data. In column tests, BC inclusions in low and mid clouds (CAE I) gave column-integrated BC heating rates ~200% and 235%, respectively, those of interstitial BC at the actual cloud RH (CAE II), which itself gave heating rates ~120% and ~130%, respectively, those of interstitial BC at the clear-sky RH. Globally, cloud optical depth increased then decreased with increasing aerosol optical depth, consistent with boomerang curves from satellite studies. Thus, CAEs, which are largely ignored, heat clouds significantly.

[1] Jacobson (2012) *J. Geophys. Res.* **doi:10.1029/2011JD017218**.

Electron Donor Utilization During the Bioreduction of Uranium

PETER R. JAFFE[1*], MELISSA BARLETT[2], LEE KERKHOFF[3], PHILIP E. LONG[4], DEREK LOVLEY[5], LORA MCGUINNESS[6], HEE SUN MOON[7], AARON A. PEACOCK[8], HUI TAN[9], KENNETH H. WILLIAMS[10]

[1]Princeton University, Princeton, USA, jaffe@princeton.edu (* presenting author)
[2]University of Massachusetts, Amherst, USA, mbarlett@mvcc.edu
[3]Rutgers Univ., New Brunswick, USA, kerkhof@marine.rutgers.edu
[4]LBNL, Berkeley, USA, PELong@lbl.gov
[5] Univ. Massachusetts, Amherst, USA, dlovley@microbio.umass.edu
[6] Rutgers U., New Brunswick, USA, mcguinne@marine.rutgers.edu
[7] Princeton University, Princeton, USA, hmoon@snu.ac.kr
[8]Microb. Insights, Rockford, USA, Aaron.peacock@peakenvbio.com
[9] Princeton University, Princeton, USA, huitan@princeton.edu
[10]LBNL, Berkeley, USA, KHWilliams@lbl.gov

Stimulating microbial reduction of soluble U(VI) to less soluble U(IV) is a promising strategy for remediating uranium contaminated groundwater. Little is known about optimizing the electron donor for promoting this process, nor what fraction of the electron donor is utilized by the target microbial population. Results presented here focus first on the effect of several electron donors on the microbial community and the overall uranium removal efficiency, and then on the specific utilization of acetate by target microorganisms.

Acetate and lactate, as well as more complex and commercially used donors such as a hydrogen-releasing compound (HRC) and vegetable oil were examined in terms of their effect on uranium removal and the microbial community, using flow-through column experiments. The composition of the microbial communities was evaluated with quantitative PCR probing specific 16S rRNA genes and functional genes, phospholipid fatty acid analysis, and clone libraries. For equivalent amounts of donor in terms of total organic carbon, acetate was least effective in U(VI) removal, while vegetable oil and HRC were most effective.

Utilization of acetate was examined closer by utilizing C-13 labeled acetate to determine which microorganisms take up acetate during biostimulation, and how the uptake of acetate by specific organisms, especially *Geobacter sp.*, changes over time during a long-term (~ several months) biostimulation experiment. A biostimulation experiment was performed, operating eight columns in parallel under continuous flow conditions, amended with 3 mM C-12 acetate. At regular time intervals, C-12 acetate flow into a column was switched to C-13 acetate for 36 hours before that column was sacrificed for detailed geochemical and microbiological analyses. Phospholipid fatty acid analysis (PLFA) and stable isotope probing (SIP) were used for the microbial characterization and to differentiate between the biomass that incorporated C-12 vs. C-13. Results showed that the *Geobacter* population remained fairly constant throughout the duration of the experiment (pre and post sulfate reduction), and that of the total amount of acetate incorporated into the overall biomass, about 40% was incorporated into the *Geobacter* biomass throughout the duration of the experiment.

The final experiment to be discussed shows that a very large fraction of acetate supplied for the biostimulation is utilized by methanogens, and that for very long biostimulation times and sufficiently high acetate levels to reduce all available sulfate, methane bubbles will form in the porous medium, which has implications for the system's permeability.

The differentiation of continental crust in arcs

OLIVER JAGOUTZ[1]*, MAX W SCHMIDT[2], ANDREAS ENGGIST[2]

[1]Dep. Earth Atmos. Planet. Sciences, MIT, Cambrige, USA, jagoutz@mit.edu (* presenting author)
[2]Dep. Earth Sciences, ETH Zurich, Switzerland

Processes resulting in the chemical stratification of the continental crust have since long been studied but, limited information is available on the extend and origin of stratification of the initial juvenile continental crust formed in arcs. This lack of knowledge renders the quantification of secondary reworking processes in the continental crust difficult. Here we present an extended dataset documenting the magnitude and nature of chemical stratification of the juvenile Kohistan arc crust. The Kohistan arc (NE Pakistan) is the only complete exposed arc section preserved in the geological record, ranging from upper mantle peridotites and ultramafic cumulates at the bottom to unmetamorphosed sediments at its top. The bulk composition of the Kohistan arc, formed during intra oceanic subduction, is andesitic and similar to the bulk continental crust [1]. As postcollisional secondary reworking processes in Kohistan are negligible, the chemical stratification observed of the Kohistan arc represents the best available initial stratification state of the juvenile continental crust formed in arcs.

We used in total ~60 own and published geobarometric results (Al-in-hbl and various net-transfer reactions) to constrain the (re)crystallisation depth of the different plutonic rocks of the entire Kohistan arc. The calculated (re)crystallisation pressures coincide well with inferred intrusion depths of the different units based on magmatic phase relationships and form a regionally consitent pattern of increasing pressures from the unmetamorphosed sediments in the north to the upper mantle peridotites in the south. We thus interpret the geobarometric results to generally reflect magmatic emplacement pressures. Based on these results, we used standard krigging methods to approximate the intrusion depth of > 200 sample for which geochemical whole rock compositions exist. The result is a profound chemical stratification between the lower and upper crust. Whereas the upper part of the crust is internally only weakly stratified and compositional rather homogenous the lower arc crust section is compositionally strongly stratified and complementary to the upper crust. This indicates that the juvenile continental crust formed in arcs inherits a strong primary compositional stratification before secondary (e.g. remelting) processes may set in.

[1] Jagoutz O. Schmidt M.W. (2012) *Chem.Geol.* doi:10.1016/j.chemgeo.2011.10.022

Multi-tool dating for polymetallic deposits (Antimony Line, RSA)

JUSTINE JAGUIN[1*], MARC POUJOL[1], PHILLIPE BOULVAIS[1], GILLES RUFFET[1], LAURENCE ROBB[2], VALERIE BOSSE[3] AND JEAN-LOUIS PAQUETTE[3]

[1]Laboratoire Géosciences Rennes,UMR CNRS 6118, France justine.jaguin@univ-rennes1.fr
[2]Department of Earth Sciences, University of Oxford, UK
[3]Laboratoire Magmas et Volcans, UMR CNRS 6524, France

The 3.09-2.97 Ga Murchison Greenstone Belt is one of several Archean volcano-sedimentary belts within the Kaapvaal Craton in southern Africa [1]. It hosts a variety of ore deposit types: VMS style Cu-Zn mineralization [2], pegmatite related emerald and orogenic-style Sb-Au deposits along the Antimony Line (AL), the latter an unusual Precambrian Sb-dominant set of deposits located in a major quartz-carbonate altered ductile structure. Various models (magmatic, volcanogenic-derived, orogenic-gold…) have been proposed for the AL, which emphasize its overall complexity.

The Malati Pump mine, at the eastern end of the AL, hosts Au-Sb mineralization in the cupola of one of a number of granodiorite plugs intrusive into the belt. Its U-Pb (Zircon) dating and Pb-Pb dating of the Au-Sb-related sulphides yield an age of 2.97 Ga, identical to the age of the VMS Cu-Zn and the emerald deposits. Thus the granodiorites emplacement was probably the main trigger for this polymetallic metallogenic system at different crustal levels (Fig).

The AL is also clearly related to hydrothermal fluid circulation. Albitites run along the AL and were developed at the expense of a granodioritic protolith. Their systematic enrichment in Sb highlights a genetic link between the Sb mineralization and the albitization process. U-Pb data on hydrothermal monazites spread along the Concordia from 2.8 down to ca 2.0 Ga. Chemical analyses on the dated monazite allow us to interpret the data as a Discordia (combination of a major fluid circulation at 2.8 Ga followed by a thermal/fluid event at ca 2.0 Ga) rather than as a multi-events system.

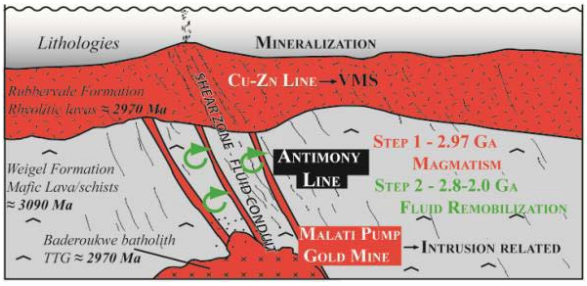

Figure: Model for the AL deposit formation and evolution.

Fluid dating is rather complex as is the AL system as a whole. This study illustrates that a combination of conventional U-Pb zircon dating to accurately identify the emplacement ages of the major meta-igneous host rocks, with Pb-Pb dating of sulphide minerals and U-Pb dating of monazites to date stages of mineralization, plus mineral chemistry studies of the various dated phases combined with $^{40}Ar/^{39}Ar$ geochronology represents a useful methodology for uncovering the history of metallogenically complex regions.

[1] Poujol et al (1996) *Econ Geol* **91**, 14551461. [2] Schwarz-Schampera et al (2010) *Miner Depos* **45,** 113-145.

https://doi.org/10.1180/S0026461X00008434 Published online by Cambridge University Press

Shear deformation of olivine at high pressures and temperatures: An atomic scale perspective

SANDRO JAHN

GFZ German Research Centre for Geosciences, Telegrafenberg, 14473 Potsdam, Germany, jahn@gfz-potsdam.de

Olivine, $(Mg,Fe)_2SiO_4$, is assumed to be the most abundant mineral of the Earth's upper mantle. The knowledge of its physical properties in the relevant range of pressures and temperatures therefore provides important constraints on the dynamic behavior of the upper mantle. Plastic deformation of olivine has been investigated for a long time but recent experimental [1] and computational [2] studies suggest a pressure and strain rate dependence of the dominant olivine dislocation slip system from [100] slip at low pressures and low strain rates to [001] at high pressure and high strain rates.

Here, an atomic scale modeling approach is used to investigate the pressure and temperature dependence of the shear deformation mechanism of the magnesium end member, Mg_2SiO_4 forsterite. The simulations combine classical molecular dynamics with metadynamics using the scaled simulation cell box matrix as dynamic variables [3]. The particle interactions are described by an advanced polarizable ion potential [4]. Pressure was varied between atmospheric and 20 GPa, temperature between 1000 K and 2000 K. At high pressures (> 5 GPa), the dominant shear is observed in [001], which is consistent with the experimental studies. The dominant shear plane changes from (100) to (010) with increasing pressure and temperature. At lower pressures (< 5 GPa), both shear in [100] and combined shear in [001] and [100] are observed.

Besides identification of shear plane and direction, insight into the atomic scale mechanism of shear is obtained. The most interesting observation is a change of shear mechanism in [001](010) from a two-step process at lower pressure, in which SiO_4 tetrahedra remain intact and the stacking order of oxygens unchanged, to a three-step process, which involves breakage of Si-O bonds and changes in the stacking order of the oxygen sublattice. The latter mechanism is observed at the highest pressure, where the free volume needed for the other shear mechanism becomes energetically too expensive. Finally, possible relations between shear deformation and high pressure phase transitions of single crystal forsterite will be discussed.

The shear deformation observed in these simulations does not describe the process of dislocation creep but it provides useful guidelines and insights that are not available otherwise. The method used in this study may therefore complement other efforts to understand the rheological behavior of mantle minerals, including the very promising multiscale simulation method presented very recently [5].

[1] e.g. Mainprice et al. (2005) *Science* **433**, 731-733; Raterron et al. (2007) *Am. Mineral.* **92**, 1436-1445; Demouchy et al. (2009) G*eophys. Res. Lett.* **36**, L04304; Hilairet et al. (2012) *J. Geophys. Res.* **117**, B01203. [2] Durinck et al. (2005) *Phys. Chem. Minerals* **32**, 646-654; Durinck et al. (2007) *Eur. J. Mineral.* **19**, 631-639. [3] Martonak et al. (2003) *Phys. Rev. Lett.* **90**, 075503. [4] Jahn and Madden (2007) *Phys. Earth Planet. Int.* **162**, 129-139. [5] Cordier et al. (2012) *Nature* **481**, 177-180.

Mineralogical controls on arsenic bioaccessibility in mine waste and body fluids

HEATHER JAMIESON[1*], MACKENZIE BROMSTAD[1], SUZETTE MORMAN[2], AND GEOFFREY PLUMLEE[2]

[1]Queen's University, Geological Sciences and Geological Engineering, jamieson@geol.queensu.ca (*presenting author)
[2]U.S. Geological Survey, gplumlee@usgs.gov, smorman@usgs.gov

Arsenic associated with ores is typically hosted in arsenopyrite and/or arsenical pyrite. In mine waste, arsenic mineralogy is much more complicated as a result of weathering, ore processing and the ability of As to be incorporated as As(V), As(III) or reduced As in a wide range of secondary minerals. Gastric to intestinal extraction tests indicate decreasing As bioaccessibility from Ca Fe arsenate > lead arsenate > arsenic trioxide > amorphous iron arsenate > As-bearing Fe oxyhydroxide > arsenical pyrite > As sulfide (realgar) > arsenopyrite.. There are likely to be additional factors affecting As uptake in the gastro-intestinal system including changes in pH, redox conditions and availability of Fe and S to combine with dissolved As.

Field and laboratory observations of the stability of As secondary minerals in mine waste may provide insight into the anticipated complexities and As phase transformations in the gastro-intestinal system. Arsenopyrite (FeAsS) is typically coarse-grained relative to secondary minerals, explaining why it does not react during bioaccessibility tests which involve exposure to gastric fluids for only an hour or so. Scorodite ($FeAsO_4 \cdot 2H_2O$) forms as a oxidation product of arsenopyrite (Fe/As = 1 for both minerals) and is stable in low pH environments which explains why it releases little As to acid gastric fluids, even when the starting solid is nanocrystalline [1]. As pH increases, scorodite is transformed to hydrous ferric arsenate (Fe/As>1), which may explain why more As is released to circum-neutral pH intestinal fluids. Tooeleite ($Fe_6(AsO_3)_4(SO_4)(OH)_4 \bullet 4H_2O$) has been recognized only rarely in mine waste but precipitates readily when As(III) is combined with Fe(III) under acid conditions (pH<4) [2] suggesting that if sufficient Fe is available (Fe/As=.66), this phase may form under gastric conditions and limit As bioaccessibility. Arsenic trioxide (As_2O_3) is a product of ore processing which is stable over a wide range of pH and, in some contaminated soils, persists for many decades. In other situations, arsenic trioxide combines with Fe(III) to form scorodite in acid drainage [3] or with reduced S to form secondary As sulfides [4]. It is possible that similar transformations may occur in the body, both of which would reduce As bioaccessibility. Finally, Ca-Fe arsenate minerals (e.g. yukonite $Ca_7Fe_{12}(AsO_4)_{10}(OH)_20 \bullet 15H_2O$) have Fe/As>1 form under pH-neutral conditions where carbonate minerals are stable. These minerals are soluble in acid fluids and exhibit high As bioaccessibility in gastric solutions.

Laboratory results indicate that As bioaccessibility can actually be higher per mass in simulated lung fluids than gastric, but the overall dose is smaller due to the lower amounts that reach the lung.

[1]Meunier *et al*. (2010) *Environ. Sci. Tech.* **44**, 2667-2674. [2]Opio *et al.* (2011) *Proc.2nd Environmine Sem.*[3]Haffert & Craw (2007) *App. Geochem.* **23,** 1467-1483.[4]Fawcett & Jamieson (2011) *Chem. Geol.* **283,** 109-118.

https://doi.org/10.1180/S0026461X00008434 Published online by Cambridge University Press

Chromium isotope fractionation during reduction of Cr(VI) under saturated flow conditions

JULIA H. JAMIESON-HANES[1*], BLAIR D. GIBSON[1], MATTHEW B.J. LINDSAY[1,2], YEONGKYOO KIM[3], CAROL J. PTACEK[1], AND DAVID W. BLOWES[1]

[1]Dept. of Earth and Environmental Sciences, University of Waterloo, jhjamies@uwaterloo.ca (* presenting author), bgibson@uwaterloo.ca, ptacek@uwaterloo.ca, blowes@uwaterloo.ca

[2]Dept. of Earth and Ocean Sciences, University of British Columbia, mlindsay@eos.ubc.ca (current address)

[3]Dept. of Geology, Kyungpook National University, Korea, ygkim@knu.ac.kr

Chromium (VI) is a pervasive groundwater contaminant that poses a considerable threat to human health. Remediation techniques have focused on the reduction of the highly mobile Cr(VI) to the sparingly soluble Cr(III) species. Reduction has been shown to produce significant Cr isotope fractionation, characterized by an enrichment in the $^{53}Cr/^{52}Cr$ ratio in the remaining Cr(VI) pool [1]. Chromium isotopes are promising indicators of Cr(VI) reduction in groundwater; however, the influence of transport on fractionation has not been fully examined.

A laboratory column experiment was conducted to evaluate isotopic fractionation of Cr during Cr(VI) reduction under controlled flow conditions. Simulated groundwater containing 20 mg L^{-1} Cr(VI) was pumped through a saturated column containing quartz sand with 10% (v/v) organic carbon. Isotope measurements were performed on both effluent and profile samples. Dissolved Cr(VI) concentrations decreased while $\delta^{53}Cr$ increased, indicating that reduction of Cr(VI) occurred. Solid-phase analysis by scanning electron microscopy (SEM) and X-ray absorption near edge structure (XANES) spectroscopy confirmed the presence of Cr(III) on the surface of the organic carbon. The $\delta^{53}Cr$ data followed a linear regression equation yielding a fractionation factor (α) of 0.9979, whereas previous studies of batch experiments under similar geochemical conditions demonstrated Rayleigh-type isotope fractionation. Both the results of the solid-phase Cr and isotope analyses suggest a combination of Cr(VI) reduction mechanisms, including reduction in solution, and sorption prior to reduction [2]. The linear characteristic of the current $\delta^{53}Cr$ data may reflect the contribution of transport on Cr isotope fractionation.

[1] Ellis *et al.* (2002) *Science,* **295**, 2060-2062; [2] Park *et al.* (2005) *Water Res.,* **39**, 533-540.

Mechanisms of reaction driven porosity and permeability generation

BJØRN JAMTVEIT[*], OLIVER PLÜMPER, ANJA RØYNE AND ANDERS MALTHE-SØRENSSEN

Physics of Geological Processes, University of Oslo, P.O. Box 1048, Blindern, N-0136, Oslo, Norway (bjorn.jamtveit@geo.uio.no)

The evolution of the Earth's lithosphere is, to a major extent, affected by reactions in which magmatic or metamorphic rocks consume fluid components such as H_2O and CO_2. Examples include serpentinization of the oceanic lithosphere and weathering of continental rocks. The progress of such reactions, as well as many other replacement processes that depend on the presence of a fluid phase, requires that porosity is maintained to keep fluid in contact with reactive solid surfaces.

As most volatilization reactions lead to a reduction in rock density, and thus an increase in the volume of solid, the initial pore volume will tend to become filled with new mineral phases during such processes, in the absence of porosity-generating processes. However, observations at scales ranging from nanometer to outcrop scales, indicate that a variety of porosity generating processes are operating. For example, replacement reactions mediated by dissolution-reprecipitation mechanisms have been observed to produce micro-porous products in a variety of systems [1], while reactions associated with a significant volume increase often lead to fracturing [2]. However, the detailed mechanisms of these porosity- producing processes have been poorly understood.

In this contribution, we review examples of reaction driven fracturing, and propose a new model for how stress is generated at reacting olivine surfaces during serpentinization. This model emphasizes the role of interface coupled dissolution-reprecipitation processes in producing the surface roughness required to generate stress concentration and associated fracturing at the reactive surface. This process results in the hierarchical fracture network [3] represented by the characteristic mesh-structure of partly serpentinized olivine grains. Similar patterns are also observed in a variety of other systems.

[1] Putnis, A. (2009) *Reviews in Mineralogy*, **70,** 87-124. [2] Jamtveit, B., Putnis, C., Malthe-Sørenssen, A., (2009) *Contributions to Mineralogy and Petrology,* **157**, 127-133. [3] Iyer, K**.,** Jamtveit, B., Mathiesen, J., Malthe-Sørenssen, A., and Feder, J., (2008) *Earth and Planetary Science Letters***, 267**, 503-516.

https://doi.org/10.1180/S0026461X00008434 Published online by Cambridge University Press

The relationship between PM10 and meteorological conditions in Sosnowiec (Poland) in view of potential health hazard

JANECZEK JANUSZ[1*], JABLONSKA MARIOLA[1],
LESNIOK MIECZYSLAW[2],

[1]University of Silesia, Department of Geochemistry, Mineralogy and Petrology; Sosnowiec, Poland
janusz.janeczek@us.edu.pl; mariola.jablonska@us.edu.pl
[2]University University of Silesia, Department of Climatology,Sosnowiec, Poland,
mlesniok@op.pl

The aim of this study was to determine concentrations and chemistry of PM10 in one of the major cities in densely populated and industrial region of Upper Silesia, SW Poland, in relation to meteorological conditions. Meteorological conditions and atmospheric circulations play an important role in dispersion of air pollutants [1].

Both concentrations of PM10 and meteorological parameters were monitored from June to December 2011. In addition, the collected PM10 was investigated by analytical scanning and transmission electron microscopies (SEM, TEM). The identification of phases in PM10, their morfology, chemical compositions, structure and particle size enabled the precise pinpointing of the emission sources.

The abundant ultraparticles occur in the PM10 fraction. Those ultraparticles are carriers of heavy metals inluding Pb, Zn, Cd, U and others. The most common constituent of PM10 is soot. A large number of nano-sized particles containing toxic elements adhered to the soot surface and together with respirable soot particles can be inhaled by the humans.

Quartz, iron oxides, amorphous and crystalline alumino-silicates are also abundant in PM10 and in ultraparticles. Regardless of their size they may have a negative impact on human health as suggested by medical data for this part of Poland. All of the observed mineral phases in PM10 are typical of fossil fuels combustion and of car exhausts.

As expected, the highest concentrations of PM10 was observed during the prevalence of anticyclonic conditions, at low speed winds, and the lack of precipitation. The extremaly high concentrations of PM10 were associated with the thermal inversion. The presence of some mineral phases in PM10 (e.g. Zn, Pb, Cd-sulfides, Sn alloys) combined with back-tracing of air flow allowed precise location of particular sources of dust emissions.

[1] Niedzwiedz T.(2005) *The role of cities in climate modification – selected issues. Global Change* **12**, 23-33

Authigenic neodymium isotopes recording change in Arctic Ocean circulation

KWANGCHUL JANG[1*], YEONGCHEOL HAN[1], YOUNGSOOK HUH[1], SEUNG-IL NAM[2]

[1]Seoul National University, Seoul, Korea, wkdrhkd3@snu.ac.kr (* presenting author), hanlove7@snu.ac.kr, yhuh@snu.ac.kr
[2]Korea Polar Research Institute, Incheon, Korea, sinam@kopri.re.kr

We analyzed neodymium isotope ratios of Fe-Mn oxide coatings in sediments from the Mendeleev Ridge collected during RV Polarstern Expedition ARK-XXIII/3. According to our age model constructed using AMS ^{14}C ages (n=4) and by correlating $\delta^{18}O$ and $\delta^{13}C$ with neighbouring cores 94B16 [1] and 0503-8JPC [2], the record extends to MIS 5a. The average ε_{Nd} value (n = 39) was -10.2, which is quite similar to the present-day water column values of the Canada and Makarov basins [3]. Two significant deviations from the average ε_{Nd} were observed. Middle MIS 3 displayed unradiogenic ε_{Nd} accompanied by decreases in $\delta^{18}O$ and $\delta^{13}C$ of planktonic foraminifera (*N. pachyderma* sin.) and an increase in $\%CaCO_3$. The unradiogenic dissolved Nd of the Mackenzie River [4] and carbonate-rich lithology of the Canadian Archipelago suggest that the melting of the Laurentide Ice Sheet (LIS) was mainly responsible. Additionally, the pinkish carbonate layer observed at this depth interval is reported to be derived from Banks and Victoria islands of the Canadian Archipelago [5]. The radiogenic ε_{Nd} peak during Late MIS 4–Early MIS 3 period coincided with decreases in $\delta^{18}O$ and $\delta^{13}C$ values and low $\%CaCO_3$. The radiogenic dissolved Nd of the Ob and Yenisei rivers [6] and the carbonate-poor lithology of western Siberia suggest that outburst of ice-dammed lakes from this region could have affected the western Arctic Ocean [7].

The two contrasting sources mentioned above imply that the water circulation pathway has changed. During the Mid-MIS3, transport via the Beaufort Gyre may have expanded and water from the Canadian Archipelago bathed the southern Mendeleev Ridge. On the other hand, during the Late MIS 4–Early MIS 3 period, the Beaufort Gyre may have weaked and water from western Siberia dominated on the southern Mendeleev Ridge. According to Morison et al. [8], the strength of the Beaufort Gyre is modulated by the Arctic Oscillation (AO). Consequently, our results suggest that the negative mode of AO is associated with the warmer Mid-MIS3 and the positive mode with the colder Late MIS 4-Early MIS 3.

[1] Poore et al. (1999) *Geology* **27**, 759-762. [2] Adler et al. (2009) *Glob. Planet. Change* **68**, 18-29. [3] Porcelli et al. (2009) *Geochim. Cosmochim. Acta* **73**, 2645-2659. [4] Woo and Thorne (2003) *Arctic* **56**, 328-340. [5] Polyak et al. (2004) *Palaeogeogr. Palaeoclimatol. Palaeoecol.* **203**, 73-93. [6] Zimmermann et al. (2009) *Geochim. Cosmochim. Acta* **73**, 3218-3233. [7] Spielhagen et al. (2004) *Quat Sci Rev* **23**, 1455-1483. [8] Morison et al. (2012) *Nature* **481**, 66-70.

https://doi.org/10.1180/S0026461X00008434 Published online by Cambridge University Press

A Physiochemical Analysis of the Transport and Retention of Technetium in Unsaturated Hanford Formation Sediments

DANIELLE P. JANSIK[1,2*], DAWN M. WELLMAN[1], JONATHAN ISTOK[2], JIM SZECSODY[1], KENT PARKER[1], ELSA CORDOVA[1]

[1]Pacific Northwest National Laboratory, Richland, United States, Danielle.Jansik@pnnl.gov

[2]Oregon State Univeristy, Corvallis, United States

The transport of Tc, like many other radionuclides, is of interest due to the potential for human exposure and impact on ecosystems. Specifically, Tc is a contaminant of concern at several DOE facilities including the Hanford, Oak Ridge, Paducah, Portsmouth, and Savannah River Sites.

Current conceptual models do not fully explain the distribution and persistence of technetium in vadose zone environments such as the Hanford site, Eastern Washington. In an oxic environment with low organic content the residence time of technetium in the soil would be expected to be low, due to its low sorption and high mobility. While $Tc^{VII}O_4$ can be reduced, it is also readily oxidized, so temporary reducing environments are not expected to alter the general rapid Tc migration in the subsurface. Inexplicably, nearly 50 years following the release of contamination into the site, a significant fraction of Tc has persisted in the subsurface in the 200 Area.

In these experiments we examined the unsaturated transport of pertechnetate at very low water content using an Unsaturated Flow Apparatus (UFA) to evaluate breakthrough curve behavior and the potential impact of immobile domains, anion exclusion and sorption on the transport and retention of technetium. The analysis confirmed that Tc was transported at pore water velocity and that transport was not altered by the presence of immobile domains, anion exclusion, or sorption. The experimental dispersivity increased with decreasing saturation.

Using borehole sediments from the Hanford site 200 Area where Tc was co-disposed with a variety of chemicals and has been in contact with the sediment for decades, a series of sequential extractions was conducted to evaluate the mineral associations of technetium in natural Hanford sediments. The sequential extractions targeted the Tc associated with the ion exchange layer, carbonate minerals, aluminosilicate minerals and iron oxides. The analyses indicated that while most Tc was associated with an aqueous extractable phase, some Tc was associated with oxalic acid and nitric acid extractable phases. The preliminary results indicate a portion of the Tc may be less mobile than originally indicated. EXAFS and XANES will be used to identify Tc surface phases, as the surface Tc may be incorporated in minerals or coated by non-Tc precipitates. Results from extractions and additional geochemical analysis will be presented.

Saline groundwater discharges in the Athabasca oil sands region: a chemical mass balance

S. JASECHKO[1*], J.J. GIBSON[2,3], S.J. BIRKS[2,4], Y. YI[2,3], A. MARANDI[5]

[1]Department of Earth and Planetary Sciences, University of New Mexico, Albuquerque, New Mexico (jasechko@unm.edu)

[2]Alberta Innovates, Victoria, British Columbia, Canada

[3]Department of Geography, University of Victoria, Victoria, British Columbia, Canada

[4]Department of Earth and Environmental Sciences, University of Waterloo, Waterloo, Ontario, Canada

[5]Institute of Geology, Tallinn Technical University, Tallin, Estonia

Quantifying water quality impacts of oil sands developments in western Canada will require decoupling natural contributions of organic and inorganic contaminants from potential releases from tailings ponds, oil sands mining, and in-situ bitumen production. Here, we quantify natural saline groundwater contributions to the Athabasca River by applying a chemical mass balance (Cl^-) to monthly chemical and discharge data collected between 1987 and 2009, using data available from the Long Term River Network.

The results of the chemical mass balance indicate that saline springs are an important control on the chemistry of the Athabasca River, despite comprising <3% of the river's discharge. The impact of these discharges on the chemistry of the Athabasca River is greatest during periods of low river flow. The shift in chloride concentrations measured between Fort McMurray and the Peace Athabasca Delta can only be explained if saline groundwater along this stretch are in the range of 500 to 3400 L/s. This finding is supported by the subcrop exposure and known seepage of Devonian- and Cretaceous-aged aquifers bearing saline fluids along this reach of the Athabasca River. While this study does not exclude the possibility that tailings discharge to the Athabasca River could be occurring, the observed increase in chloride measured between Fort McMurray and the Peace-Athabasca Delta cannot be accounted for using tailings pond seepages alone. The range of chloride concentrations reported for a wide range of tailings ponds are very low in comparison with the groundwater seeps entering the river and the total increase in chloride along this stretch cannot be reconciled using just mixing with tailings pond water.

Given the important role discharges of saline groundwater from Cretaceous and Devonian formations appears to play in the geochemical evolution of the Athabasca River, a more comprehensive evaluation of regional groundwater flowpaths and groundwater surface water interactions is warranted. These results suggest that any future water quality monitoring efforts for the Athabasca River should try to better quantify the contribution of groundwater inflow to changes in river water quality.

https://doi.org/10.1180/S0026461X00008434 Published online by Cambridge University Press

Historical atmospheric deposition of PAHs in lakes east of the Athabasca oil sands operations

JOSUÉ JAUTZY[1*], JASON M. E. AHAD[2], CHARLES GOBEIL[1], AND MARTINE M. SAVARD[2]

[1]INRS Eau Terre Environnement, Québec City, Canada, Josue.Jautzy@ete.inrs.ca (* presenting author), Charles.Gobeil@ete.inrs.ca

[2]Geological Survey of Canada, Natural Resources Canada, Québec City, Canada, Jason.Ahad@nrcan.gc.ca, MartineM.Savard@nrcan.gc.ca

The growth of bitumen mining activities in northeastern Alberta poses significant environmental challenges. One of the main concerns is a potential increase in emissions of harmful organic contaminants such as polycyclic aromatic hydrocarbons (PAHs). PAHs are widespread in the environment and result from incomplete organic matter combustion (kinetic process) or maturation (thermodynamic process), which makes them good markers of pyrogenic or petroleum input.

In order to understand the impact of oil sands-related mining activities to the environment it is essential to examine PAH emissions in the context of variability in natural background levels. Here we report geochronological records of PAH atmospheric deposition fluxes over the last century in two headwater lakes located approximately 50 km downwind from the main area of oil sands operations. Assessing PAH levels over the last 100 years allowed us to differentiate the deposition fluxes prior to the modern period of bitumen mining activities (i.e., pre-1970). Concentrations of the 16 EPA priority PAHs in addition to coronene, retene, perylene and 6 alkylated groups were measured in dated cores from both lakes. PAH molecular diagnostics ratios were used in order to discriminate preliminary sources and their variation over time.

Results and conclusion:

Our results showed an increase of parent and alkylated PAHs (2-fold for alkylated PAHs and 0.5-fold for 16 EPA priority PAHs) in both lakes over the past decade. Alkylated PAHs are generally related to petroleum sources. A possible explanation for this increase may be the expansion of open mine pit area resulting in greater sensitivity to wind erosion and transport. PAH molecular diagnostics ratios revealed two distinct groupings using two different sets of ratios: a pre-1980s combustion dominated type, and a post-1980s petroleum dominated one. These results point to an increasing contribution from recent oil sands mining activities, though it should be noted that overall PAH levels in these lakes are relatively low. In light of these results, and taking into consideration the future expansion plans of bitumen mining activities, it is possible that PAH fluxes in this region may continue to rise. Further insight into PAH source apportionment is expected from ongoing work involving compound-specific isotope analysis.

Meridional distribution of the atmospheric $^3He/^4He$ isotopic ratio

P. JEAN-BAPTISTE[1*], E. FOURRE[1]

[1]LSCE, CEA-CNRS-UVSQ, Gif/Yvette, France, pjb@lsce.ipsl.fr

Due to the release of crustal helium by natural gas and oil production and by coal mining with a low $^3He/^4He$ ratio, the atmospheric $^3He/^4He$ ratio may be decreasing with time. The direct detection of this change is problematic due to the difficulty in finding well preserved ancient air samples and has led to conflicting results. Most of the He release occur in the northern hemisphere, therefore it may create an interhemispheric gradient in the atmospheric $^3He/^4He$ ratio, as already observed for other anthropogenic gases such as CH_4, CFC or ^{85}Kr. We performed precise helium isotope measurements on air samples collected at various latitudes going from 82°30'N (Alert Station) to 78°38'S (Vostok Station). The mean helium isotope ratio (relative to our Saclay air standard) are identical for both hemisphere : 1.0004 ± 0.0005 for the northern hemisphere and 1.0004 ± 0.0009 for the southern hemisphere respectively, thus showing no detectable meridional gradient. However, as shown in Fig. 1, $^3He/^4He$ values are very homogeneous from the northermost latitudes to 20°S but the two southernmost data points show diverging trends. Therefore, additional data are needed south of 20°S.

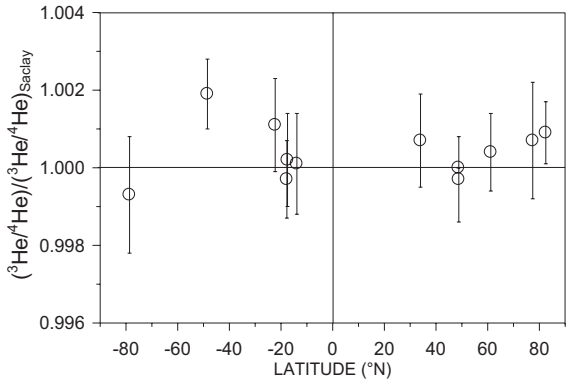

Figure 1: Meridional distribution of the helium isotopic ratio of air

The lower value for Vostok could be due either to the high elevation (3500 m) or to the relative isolation of the air masses over the Antarctic interior. If we consider this latter data point as an outlier, the mean $^3He/^4He$ value for the southern hemisphere becomes 1.0006 ± 0.0009. The two mean values, $^3He/^4He = 1.0004$ for the northern hemisphere and $^3He/^4He \leq 1.0006$ for the southern hemisphere, can be used to estimate the value of the anthropogenic helium flux using a simple two-box model of the atmosphere with an interhemispheric mixing time of about 1 year [1-2] and a anthropogenic helium input function proportional to the world release of fossil carbon since 1850. Model results indicate that the He/C molar ratio may be $\leq 2\times10^{-4}$, with a decrease of the atmospheric $^3He/^4He$ ratio $\leq 0.7\%$ over the industrial period.

[1] Ehhalt D.H. (1978) *Tellus* **30**, 169-176.
[2] Prather M. et al. (1987) *J. Geophys. Res.* **92**, 6579-6613.

https://doi.org/10.1180/S0026461X00008434 Published online by Cambridge University Press

Ferric oxyhydroxide microbial mat community metabolic model based on metagenome sequence analysis

RYAN DEM. JENNINGS[1*], ROSS P. CARLSON[2], KRISTOPHER A. HUNT[2], ZACKARY J. JAY[1], JACOB P. BEAM[1], MARK A. KOZUBAL[1], MARGARET F. ROMINE[3] AND WILLIAM P. INSKEEP[1]

[1]Montana State University, Land Resources and Environmental Science, Bozeman, Montana, United States of America, rdemjennings@gmail.com (* presenting author)

[2]Montana State University, Chemical and Biological Engineering, Bozeman, Montana, United States of America.

[3]Pacific Northwest National Laboratory, Richland, Washington, United States of America.

Introduction and Approach

Ferric oxyhydroxide microbial mats in acidic high-temperature springs of Norris Geyser Basin, Yellowstone National Park (Wyoming, USA) are inhabited by an environmentally constrained consortia of archaea. These extreme environments are ideal sites to study microbial interactions in natural communities where gradients in temperature and oxygen occur over spatially resolvable distances. The goal of this study was to generate a stoichiometric metabolic model as an incremental step in describing the microbial ecology within these chemotrophic systems. We obtained a metagenome of a ferric oxyhydroxide mat community in One Hundred Springs Plain via Sanger sequencing (DOE-Joint Genome Institute). *De novo* assemblies were obtained using the Celera (J. Craig Venter Institute) assembler and evaluated using nucleotide word frequency-principal components analysis. These communities are comprised of several dominant populations including chemolithoautotrophic *Metallosphaera yellowstonensis*, as well as heterotrophic Thermoproteales, Desulfurococcales, and a novel, deeply rooted archaeon (NAG1). *De novo* assemblies corresponding to these populations were annotated and *in silico* stoichiometric metabolic models were created for each organism focusing on mass and energy fluxes within and between community members.

Results and Conclusion

Multiscale metabolic systems analysis was used to predict possible modes of microbial interaction where autotrophic metabolism of *M. yellowstonensis* supports Thermoproteales, Desulfurococcales, and NAG1 growth via metabolic exchange of co-factors as well as different types of reduced carbon. These metabolite exchanges suggest autotroph-heterotroph relationships constrained by fluxes of major electron donors/acceptors and sources of carbon. This work provides a rational, *in silico* framework for understanding the microbial ecology within a thermophilic ferric oxyhydroxide mat community.

Enhanced soil remediation by microwave irradiation with sodium hydroxide and iron powder

SANGJO JEONG[1,*] AND HANG-DEUK KIM[1]

[1]Korea Military Academy, Department of Civil Engineering and Environmental Sciences, sangjo.jeong@gmail.com

Abstract

Thermal treatment is one of the fast and effective methods to remediate highly contaminated soils with organic contaminants such as gasoline, diesel fuel, and organic solvents, etc. However, the energy efficiency of thermal treatment is relatively low, compared to other soil remediation techniques. In this study, microwave irradiation was applied for contaminated soils to efficiently desorb and degrade organic contaminants. The effects of additives such as iron powder and sodium hydroxide (NaOH), activated carbon on desorption and degradation of organic contaminants in soils were investigated.

The modified microwave oven (2,450 MHz, 800W) was used as a reactor. Tetrachloroethylene (PCE) and hexachlorobenzene (HCB) were selected as representative organic contaminants. Sandy soil, clay soil, *and* zeolite were used as adsorbents. Each soil sample was intentionally contaminated with organic contaminant which was dissolved in methanol, respectively, and dried in the fume hood. The contaminated soils were located in the microwave reactor and irradiated with microwave for 9 minutes in nitrogen condition. About 10% of additives and 20% of water were also mixed with the contaminated soils and treated with the same method for contaminated soils. During microwave irradiation, effluent gas was collected with methanol. After microwave irradiation, residual organic contaminants were extracted from soils with by methanol. Desorbed and residual organic contaminants were analyzed with both gas chromatography (GC, Shimadzu GC 2014) with electron capture detector (ECD) for mass balance and GC with mass spectrometry (Agilent 5795C VL MSD) for degradation products. The chloride ions were extracted from soils after microwave irradiation and analyzed with ion chromatography (Dionex ICS-2000) to investigate the degradation of chlorinated organic contaminants.

The results of chloride ion analysis showed that chlorinated organic contaminants in soils were degraded by microwave irradiation with iron powder and NaOH. Desorption of organic contaminants from soils was enhanced by the addition of water. Microwave irradiation for 9 minutes with additives (e.g., 10% Fe / 5% NaOH, 10% activated carbon) removed most of the contaminant from PCE contaminated sandy soils. However, it was not sufficient for HCB contaminated sandy soils. Later on, the properties of pyrolyzed organic contaminants will be investigated using zeolite and the differences of soil remediation properties between sandy and clay soils will also be examined. These results will contribute to develop more energy efficient soil remediation techniques, which is applicable to highly contaminated soils with organic contaminants.

https://doi.org/10.1180/S0026461X00008434 Published online by Cambridge University Press

Geochemical characteristics of suspended matters and sediments in a small watershed of the central Guizhou province and its weathering implications

JI HONGBING[1, 2*], JIANG YONBIN[1, 2], ZHAO XINGYUAN[1]

[1] The College of Resource Enviroment and Tourism, Capital Normal University, Beijing 100048, China
[2] School of Civil and Environmental Engineering, University of Science and Technology Beijing, Beijing 100083, China (*correspondence: hongbing.ji@yahoo.com)

Southwest China is one of the three biggest karst areas in the world. Over the past few decades, land use changes in this area have resulted in a series of severe ecological and environmental problems. This paper presents data on trace elements and C, N isotopes of suspended matters and sediments collected from the Qianzhong watershed in the central Guizhou province, Southwest China. Results showed that the contents of trace elements are different between rivers and lakes, also between suspended and sedimentary phases; the spatial and temporal distribution of OC contents, $C_{organic}/N_{total}$ and $\delta^{13}C$ in total suspended matter (TSM) and sedimentary matter showed different variation, indicating the transfer and arrival of allochthonous organic matter and the ecosystem changes during past sedimentary period. $\delta^{15}N$ ratios reflected the combined results of information of sources and a series of biogeochemical processes. Although $\delta^{15}N$ ratios could provide limited information of sources, it can be used to trace some special biogeochemical processes. The conclusion was testified the element characteristics and material conveying status in chemical weathering and physical erosion processes in the small watershed, And by the analysis of end members. C_3 plant debris and soil organic matter from decomposition of a mixture of C_3 and C_4 plant debris are the dominant sources for SED-OC, and aquatic plants for POC. The fractionation of $\delta^{13}C$ caused by decomposition of organic matter or diagenesis was minor. There are two models for the relationship between physical erosion and chemical weathering there: the co-promotion model for regions which have serious anthropogenic effects, and the increase and decrease model for regions where anthropogenic input is less significant. Both models would likely to be occurring in global scale.

From schwertmannite to natrojarosite: aging processes involving precipitation and dissolution reactions

AMALIA JIMÉNEZ[1*], ANGELES FERNÁNDEZ-GONZÁLEZ[1], ANA HERNÁNDEZ[1] AND MANUEL PRIETO[1]

[1]University of Oviedo, Spain, amjimenez@uniovi.es*

Introduction

Minerals of the jarosite group ($MFe_3(SO_4)_2(OH)_6$) are involved in different mineralogical and geochemical processes ocurring in the environment (acid mine water drainage, chemical weathering). Here, the objective is studying the genesis of natrojarosite during aging processes at ambient temperature. For this purpose, a set of experiments was carried out by mixing $Fe_3(SO_4)_2$ (0.5N) and NaOH (0.5N) parent solutions which were kept at constant agitation for specific reaction periods (1 hour to 50 days). Similar experiments were performed using 1N concentration of parent solutions. Composition and crystallinity were determined by X-ray powder diffraction (XRD) using the computer program X'Pert Plus (Panalytical). The aqueous solution composition was analysed by ICP-OES, and the pH was monitored at the beginning and end of the experiments. Speciation and aqueous solution modeling was carried out using PHREEQC code [1].

Results and Conclusion

XRD results reveal that schwertmannite ($Fe_8O_8(SO_4)(OH)_6$) precipitate in the early stages of the experiments, regardless of the initial concentration. In the case of the experiments carried out with 0.5 N parent solutions, schwertmannite remains during the entire aging process. In contrast, using 1N parent solutions, schwertmannite evolved to form natrojarosite ($NaFe_3(SO_4)_2(OH)_6$). The main XRD reflections (012, 021 and 113) of natrojarosite become more apparent and undergo a progressive decrease of widthness (FWHM) and an increase of intensity which indicate an increasing degree of crystallinity at the end of the aging process. The analysis of the aqueous solution shows that there is a virtually complete removal of Fe due to the precipitation of schwertmannite. In the experiments performed with 1N parent solution, the evolution of the aqueous composition is consistent with the initial precipitation of schwertmannite and subsequently, the precipitation of natrojarosite with increasing of crystallinity. The reactions takes place in acidic conditions (pH~2.2) in all experiments. Although PHREEQC considers many other phases susceptible to precipitate, any of these were identified in the diffractograms.

A set of reactions, including precipitation of schwertmannite and its transformation into natrojarosite takes place simultaneous in a highly supersaturated aqueous medium for both phases.

[1] Parkhurst and Appelo (2000), US Geological Survey Water-Resources Investigations Report 99-4259, 312 p.

https://doi.org/10.1180/S0026461X00008434 Published online by Cambridge University Press

Towards a unifying theory of geomicrobial kinetics

QUSHENG JIN[1*]

[1]Department of Geological Sciences, University of Oregon, Eugene, OR, USA, qjin@uoregon.edu (* presenting author)

Geomicrobial kinetics studies how fast microbial metabolism proceeds in natural environments – a key question of low-temperature geochemistry [1]. It differs from microbial kinetics by considering wide spectra of tempertaures, pHs, availibilities of energy sources and growth nutrients, and other environmental factors. Geomicrobial kinetics also differs from geochemical kinetics in that it accounts for life's essential functions, including energy conservation, growth, and maitenance, and considers how thermodynamics impacts reaction rates.

Geomicrobial rates can be predicted on the basis of rate laws that applicable to natural environments [2]. These rate laws carry relatively large numbers of kinetic and thermodynamic parameters in order to account for various environmental and microbial factors. But application of the rate laws present a special challenge – how to assign values for the parameters.

Jin and Roden propose a best-choice approach to assign parameter values [1]. In theory, microbial parameters can be seperated into two groups, extant and intrinsic [3]. Extant parameters describes how rates are influenced by microbial adaptation to the environments, and include half-saturation constants for electron donor oxidation, acceptor reduction, and nutrient consumption, and specific maitnenance rate. These parameters vary with the availability of energy and nutrient sources, and should be determined directly using samples from the environment.

Intrinsic parameters describe the dependence of microbial rates on cellular enzymes and pathways, and include rate constant, growth yield, ATP yield, phosphorylation energy, and average stoichiometric number. These parameters bear the relationships determined by microbial physiology. Taking anaerobic respiration as an example, ATP yield and average stoichiometric number vary with electron donors and acceptors, and can be determined on the basis of respiratory pathways. Also, because microbial growth depends on ATP synthesis, growth yield increases linearly with ATP yields. As a result, we can taken intrinsic parameters as constants of microorganisms, and extraploate the values determined for pure cultures directly to the environment.

Taking the simulation of microbial sulfate reduction and methanogenesis as examples, I demonstrate how to select parameter values that are consistent with our current knowledge of microbial physiology and relavant to the environment of interest. I then apply the parameter sets and simulate microbial metabolism in batch reactors of mixed culture, flow-through sediment columns, and lake sediments. The results demonstrat that the best-choice approach reduces the task of parameter fitting and ensures the quality of simulation.

[1] Jin and Roden (2012) *Geomicrobial Journal*, in press. [2] Jin and Bethke (2007) *American Journal of Science* **307**, 643-677. [3] Grady, Smets, and Barbeau (1996) Water Research **30**, 742-748.

Experimental study on carbonation of Portland cement in sodium chloride solutions

HWANJU JO[1*], HO YOUNG JO[1], AND YOUNG-NAM JANG[2]

[1]Korea University, Earth and Environmental Sciences, Seoul, Republic of Korea, chohwanju@korea.ac.kr (*presenting author)

[2]Korea Institute of Geoscience and Mineral Resources, CO_2 sequestration Research Department, Daejeon, Republic of Korea

Carbonation behavior of cement has been extensively studied because cement carbonation affects the conrete stength and corrosion resistance of the steel reinforcement. Various factors can affect the carbonation of cement. This study presents the influence of salinity on the carbonation behaviors of cement material.

The leaching and carbonation tests were conducted on ordinary Porland cement(OPC) using a Teflon reacter at various NaCl concentrations (0 ~ 2.0 M) under ambient temperature and pressure conditions. For the carbonation tests, CO_2 gas (99.9%) was injected in the slurry, which was obtained by mixing the soluiton and OPC.

For the leaching tests, the slurry pHs increased to 12.0 ~ 12.9, regardless of the NaCl concentration, after 24-hours leaching due to dissolution of $Ca(OH)_2$. The electrical conductivities (ECs) of the slurries increased steadily during the leaching test at low NaCl concentrations (< 1.0 M), whereas decreased at high NaCl concentrations (> 1.0 M). The Ca concentration in the slurry increased with increasing the NaCl concentration. After the leaching tests, dissolution of C_3S and $Ca(OH)_2$ and formation of C-S-H and Friedel's salt were indentified by XRD, SEM-EDX, and TGA analysis. The NaCl concentration affected the extent of the C-S-H formation during the leaching tests. The C-S-H content in the reacted OPC was the highet at the 1.0 M NaCl solution. During CO_2 injection, the pH decreased due to the dissolution of CO_2 and the carbonation reaction. Precipitation of well-crystallized calcite ($CaCO_3$) and halite (NaCl) in the reacted OPC obtained after the carbonation tests were identified by XRD, SEM-EDX, and TGA analysis. The C-S-H content decreased but the $CaCO_3$ content increased with incresing the NaCl concentration after the carbonation tests. Theses results sugesst that the presence of NaCl enhances the dissolution of $Ca(OH)_2$ in the OPC during hydration and the precipitation of $CaCO_3$ by the elevated dissolution of C-S-H during CO_2 injection.

https://doi.org/10.1180/S0026461X00008434 Published online by Cambridge University Press

Combined silicon, oxygen isotope and trace element microanalysis of giant spicules of the deep-sea sponge *Monorhaphis chuni* for paleoclimate research

KLAUS PETER JOCHUM[1*], XIAOHONG WANG[2], JAN A. SCHUESSLER[3], BÄRBEL SINHA[1], BRIGITTE STOLL[1], ULRIKE WEIS[1], MEINRAT O. ANDREAE[1], AND WERNER E.G. MÜLLER[4]

[1]Max Planck Institute for Chemistry, Mainz, Germany, k.jochum@mpic.de (* presenting author)
[2]National Research Center for Geoanalysis, Beijing, China
[3]German Research Centre for Geosciences GFZ, Potsdam, Germany
[4]Universitätsmedizin Mainz, Germany

The deep-sea sponge *Monorhaphis chuni* forms giant spicules, which can reach lengths of 3 m and diameters of 10 mm [1]. Because of the long lifespan of this sponge (several thousands years), the spicules offer a unique opportunity to record environmental change of past oceanic and climatic conditions [2]. To get a detailed time-resolved record over the lifetime of the sponge, analyses at a high resolution in the nm to µm range were performed. We investigated several giant spicules from the East and South China Sea along center-to-surface segments by determining Si isotopes with UV fs-LA-MC-ICP-MS at GFZ, and O isotopes with NanoSIMS and trace elements with LA-ICP-MS at MPI. No clear trend in Si isotope variability outside external analytical reproducibility (±0.2 ‰, 2SD) could be identified in the spicule MC from the East China Sea; average δ^{29}Si and δ^{30}Si values relative to NBS 28 were -0.67±0.21 and -1.30±0.35 (2SD), respectively. According to [3], the Si isotope fractionation is influenced by seawater Si concentration with lower isotope ratios being associated with sponges collected from waters high in Si. This implies that no significant change in Si concentration in the ambient seawater occurred during the lifetime of the sponge. Average δ^{29}Si values for the specimen SCS-3 and Q-E from the South and the East China Sea, respectively, are different: -0.43±0.22 (SCS-3) and -1.28±0.23 (Q-E) indicating different Si contents of the seawater. In contrast to these measurements, oxygen isotope data and Mg/Ca ratios of the spicule MC show a small trend in $\delta^{18}O_{VSMOW}$ from about 36±1 (rim) to 38.5±0.5 (core) and Mg/Ca from 0.062 (rim) to 0.055 (core), which can be interpreted as an increase in seawater temperature of about 3 °C during the lifespan of this specimen, similar to the results of the giant spicule QB [2].

[1] Wang et al. (2009) *Int. Rev. Cell Biol.*, 273, 69-115. [2] Jochum et al. (2012) *Chem. Geol.*, in press. [3] Wille et al. (2010) *Earth Planet. Sci. Lett.*, 292, 281-289.

Gold, Gilding and gilded marble sculpture in Antiquity: new methods, new results.

PHILIPPE JOCKEY[1*]

[1]Aix-Marseille Université, Centre Camille Jullian, Aix-en-Provence, France, philippe.jockey@univ-amu.fr

Gilding marble statues in Antiquity was rather a common practice, as testified both by ancient literary and epigraphical sources. However, for a long time, scholars showed some reluctance to admit it, due to the lack of archaeological evidence. Today, on the contrary, new scientific methods of surveying, evidencing and analysing marble surface treatments, by combining for instance videomicroscopy and X-ray fluorescence spectroscopy, confirm without any doubt the success of gilded marble statues in ancient Greece as in Rome[1]. They also give informations about gilding an regilding processes, documenting gold leaf thickness as well as the techniques of applying it on the marble layer by layer. By crossing archeological and archeometrical evidence, it becomes then possible to reconsider both ancient taste and gilded statues functions. For instance, a bright white marble hellenistic copy of the Famous classical Greek sculptor Polycletes, found in Delos [Figure 1] at the beginning of the 20th century was originally wholly gilded [Figure 2], leading to new conclusions as regards the status and functions of such a work[2]. But at the present time, some decisive information remain unknown, as for instance the provenance of the gold itself, a central historical and economic topic for Historians and Archaeologists. We need to find the missing link between antique gold mines and gilded or gold artefacts. The present talk aims also at arousing new collaborations focused on this topic.

Figure 1: The so-called Polycletes's Diadoumenos at the very time of its discovery (©efa).
Figure 2: 3D digital Reconstruction of its original look (©Fauquet, Bourgeois, Jockey).

[1] Bourgeois, Jockey (2005), "La dorure des marbres grecs. Nouvelle enquête sur la sculpture hellénistique de Délos", *JdS*, juil.-déc., 253-316.
[2] Bourgeois, Jockey, Karydas (2009), "New Researches on Polychrome Hellenistic Sculptures in Delos, III: the Gilding Processes. Observations and Meanings" in Jockey (2009), *Leukos lithos. Interdisciplinary Studies on Mediterranean Ancient Marble and Stones*, 645-661.

https://doi.org/10.1180/S0026461X00008434 Published online by Cambridge University Press

Sources of organic matter fueling As mobilization in groundwaters of West Bengal, India: Evidence from reactive transport modeling

KAREN H. JOHANNESSON[1*], SAUGATA DATTA[2], T. JADE MOHAJERIN[1], KATHERINE TELFEYAN[1], NINGFANG YANG[1], CHRISTOPHER D. WHITE[3] AND BRAD E. ROSENHEIM[1]

[1]Department of Earth and Environmental Sciences, Tulane University, New Orleans, LA, USA, kjohanne@tulane.edu (* presenting author)

[2]Department of Geology, Kansas State University, Manhattan, KS, USA, sdatta@k-state.edu

[3]Department of Petroleum Engineering, Louisiana State University, Baton Rouge, LA, USA, cdwhite@lsu.edu

It is generally agreed that microbial reduction of Fe(III) oxides/oxyhydroxides coupled to organic matter (OM) oxidation is an important mechanism by which arsenic (As) is mobilized to groundwaters within the Bengal Basin of Bangladesh and West Bengal, India. Nonetheless, the source of the OM driving the respiratory processes remains contentious [1]. Some researchers argue that recently constructed perennial ponds are a major source of recharge waters, and hence dissolved organic matter (DOM) to the As affected groundwaters, whereas others maintain that the sediments contain sufficient OM to fuel microbial respiration [2, 3]. Here we employ reactive transport modeling to simulate transport of DOM in aquifers from the Murshidabad district of West Bengal, India. The goal was to assess the possibility that OM originating in surface ponds could be transported to depth in the local sediments where As is chiefly being mobilized (i.e., ~ 30 m below ground surface). A one-dimensional advective-dispersive transport code was linked to the generalized, two-layer surface complexation model (SCM) for Fe(III) oxides/oxyhydroxides to evaluate DOM transport within local sediments. We present the results of different scenarios that include variable aquifer heterogeneity, DOM lability, and different potential surface water sources (i.e., river Bhagirathi and constructed perennial ponds). The model runs indicate that transport of pond-derived and river-derived DOM to depths in the underlying aquifer where As mobilization is greatest is unlikely to be significant over time scales consistent with the estimated ages of groundwater at these depths (e.g., ~ 50 years). Instead, DOM from surface waters would require at least 1000 years to reach the top of the As affected aquifers in Murshidabad. Results of the modelling support an *in situ*, sediment source for the DOM.

[1] Reich (2011) *Nature* **478**, 437-438. [2] Harvey et al. (2002), *Science* **298**,1602-1606. [3] McArthur et al. (2004) *Appl. Geochem.* **19**, 1255-1293.

A triple-proxy approach to reconstrucing seawater $\delta^{18}O$

CÉDRIC M. JOHN[1*], ANNA JOY DRURY[1], ANNE-LISE JOURDAN[1]

[1]Department of Earth Science and Engineering, Imperial College London, London SW7 2AZ, United Kingdom. cedric.john@imperial.ac.uk (* presenting author), a.j.drury10@imperial.ac.uk, a.jourdan@imperial.ac.uk

Reconstructing changes in the oxygen isotopic composition of seawater ($\delta^{18}O_{seawater}$) through geologic times is a high-value target as this proxy informs us on the evolution of Earth's crysophere (waxing and wanning of ice sheets), changes in ocean currents (with subtle differences in $\delta^{18}O_{seawater}$) and salinity effects related to the amount of evaporation of surface waters (the lighter ^{16}O isotope being preferentially fractionated in the water-vapor phase during evaporation). Unfortunately, geologic samples of biogenic marine calcite ($\delta^{18}O_{calcite}$) record the combined effects of changes in $\delta^{18}O_{seawater}$ and changing water temperature. For instance, a phase of expended high-latitude ice sheets during a glaciation will result in heavier $\delta^{18}O_{seawater}$ (due to ^{16}O preferrentially stored in the continental ice) but would also be associated with a global cooling of the ocean, thus further increasing the $\delta^{18}O_{calcite}$ values. This makes assessing the relative impact of each mechanism on $\delta^{18}O_{calcite}$ difficult, and hinders quantitative assessments of changes in $\delta^{18}O_{seawater}$.

The paleoceanography community has tried to come around this limitation by pairing $\delta^{18}O_{calcite}$ with other temperature proxies independent of $\delta^{18}O_{seawater}$. One of the most succesful proxies to date is the Mg/Ca ratio of benthic foraminifers. Foramiferal Mg/Ca ratio has been shown to be temperature dependent for many species, and the Mg/Ca ratio of seawater is thought to be conservative on the timescale of 1 million years. However, on timescales greater than a million year the Mg/Ca ratio of seawater is likely to change, implying that this proxy is a good proxy for relative temperature changes, but that it cannot unambiguously resolve absolute seawater termperatures for periods older than the Pleistocene. Furthermore, the concentration of carbonate ions seem to impact Mg/Ca intake in benthic foraminifers, and thus changes in carbonate ion concentrations in the ocean could impact on the temperature estimates from foraminiferal Mg/Ca.

This review talk will highlight how adding a third, novel proxy (clumped isotopes) could resolve some of the issues at hand. The "Clumped isotope paleothermometer" is based on thermodynamics, and thus is independent of $\delta^{18}O_{seawater}$. Calibrations have shown that clumped isotopes are independent of nearly all changes in ocean chemistry, though some exceptions occur (for instance, in hypersaline conditions). Clumped isotopes suffer from their own set of limitations, notably because the measurements require a significant amount of time and sample material (up to 25 mg if three replicates are made). However, we will show through some preliminary data what strategies can be put in place to overcome this limitation, and how a "triple-proxy" approach based on high-resolution $\delta^{18}O_{calcite}$ measurments, medium resolution foraminiferal Mg/Ca measurements and low-resolution clumped isotope mesurements could help resolve some of the issues currently faced by the paleoclimate community.

https://doi.org/10.1180/S0026461X00008434 Published online by Cambridge University Press

The role of nano-components in contaminated mine water outflow crossing a redox boundary

CAROL A. JOHNSON[1*], GINA FREYER[2], KIRSTEN KÜSEL[2], MICHAEL F. HOCHELLA JR[1]

[1]Department of Geosciences, Virginia Tech, Blacksburg, VA, USA, cjohns49@vt.edu (* presenting author), hochella@vt.edu

[2] Institute of Ecology, Friedrich-Schiller University, Jena, Germany, gina.freyer@uni-jena.de, kirsten.kuesel@uni-jena.de

Especially in the last 15 years, Earth scientists have been exploring the role of nano-sized materials in a number of environment-related processes, including the transport and transformation of organic and inorganic contaminants. In this study, with both the geochemistry and microbiology in mind, we chose to study a highly dynamic environmental system (Ronneburg Mining District, Germany) where groundwater outflow from a former uranium mine is negatively impacting the downstream environment. The outflow contains high amounts of Fe(II) and, upon exposure to air at pH 5.8-6.0, iron oxyhydroxide particles form. Our principal goal was to determine the role that nanoparticulate formation has on the (bio)geochemistry of this complex and dynamic system. From June to October of 2011, water and sediment was carefully collected at four sites along portions of the flow path of greatest interest: at the groundwater outflow point, at rust-colored terraces where the outflow water flowed over a creek bank, from the creek adjacent to the terrace, and from the creek about 1 km downstream. A multi-scale approach was used to analyze the samples including XRD, ICP-MS, SEM and analytical TEM (HR-TEM, EDS, and SAED).

The first indication of nanocrystalline particles comes from the broad XRD peaks of the sediment samples, many of which match goethite and akaganeite. XRD of suspended particles shows even broader diffraction maxima that cannot readily be indentified, but do indicate the predominance of nano- and/or very poorly crystalline or amorphous particles. TEM corroborates this to a point, but also reveals very important details. For example, suspended particles (40-300 nm) in terrace and creek sites tend to be roughly spherical, and found in aggregates of amorphous iron oxyhydroxides intimately mixed with and sometimes coated by amorphous silica. Various types of nanocrystalline phases were found in the sediment samples as well, including nanoneedles of goethite growing from 100-300 nm spherical particles, and even smaller and smoother spherical particles that are clearly mixtures of amorphous silica and the very earliest stages of iron oxyhydroxide crystallization manifested by uniform lattice fringes that can be traced over only 2 to 5 nanometers. Interestingly, in the groundwater outflow, suspended nanometer-thin ferrous sulfate pseudo-hexagonal platelets (containing small amounts of Zn) were discovered. We have tentatively identified these as the mineral rozenite using electron diffraction analysis.

As these rozenite particles in the outflow become unstable, they are an important source of Zn, which is the metal with the fourth-highest concentration downstream. Zn and Ni were not primarily associated with larger suspended particles (> 0.1 μm), unlike the metals at trace concentrations (U, Cu, Cr, and Pb). Interestingly, Sn oxide oval-shaped nanoparticles (5-20 nm) were found multiple times in terrace site water samples, and their significance is presently being investigated.

In this ongoing study, we have shown again why knowledge of the formation, transformation, reactivity, and dissolution of the nano-components are important in understanding the behavior and evolution of the entire system.

From mineral interfaces to 200 million tons per year: A geologic perspective of the surface-catalyzed iron redox cycle

CLARK M. JOHNSON[1,*]

[1]Department of Geoscience, University of Wisconsin, Madison, USA, clarkj@geology.wisc.edu

Evidence for redox-driven reactions at the mineral-fluid interface of iron oxides may be found in the largest iron deposits on Earth, banded iron formations (BIFs), which were largely deposited in the Neoarchean and Paleoproterozoic. The insights gained by detailed, mechanistic studies of mineral-fluid reactions demonstrate that the major volume of BIF deposits was not formed by "passive" accumulation of iron oxide minerals on the seafloor but instead record an extensive redox history during formation and early diagenesis prior to lithification. Redox-driven reactions are the fundamental process that inhibits iron oxides from behaving as "inert" particles, and, in fact determine not only the isotopic compositions of redox-sensitive elements such as Fe, but also the O isotope compositions through breakage of Fe-O bonds. In addition, the structural changes that occur in iron oxides upon subsitution of Si, an important component in marine environments in the Precambrian, produce signficant changes in stable isotope compositions. Redox-driven reactions between aqueous Fe(II) and Fe(III) oxides that are catalyzed by biology may produce signficiantly different end products and elemental mass balance than abiologic Fe(II)-Fe(III) oxide interactions, and this contrast may be expressed as distinct isotopic compositions. In the case of BIFs, the isotopic fingerprints of microbially-catalyzed redox cycling is expressed in fine-scale isotopic heterogeneity that produces compositions out of equilibrium with ambient seawater. Importantly, the end product of extensive biological reduction of Fe(III) oxides are not mixed Fe(II)-Fe(III) minerals such as magnetite, which are produced at moderate extensts of reduction, but Fe(II)-bearing carbonates (siderite, ankerite). Although perhaps not imemdiately obvious, iron carbonates actually contain the best evidence for the magnitude of microbially-catalyzed redox cycling of iron oxides in BIFs, and C, O, and Fe isotope compositions clearly indicate biological Fe(III) reduction. The C, O, and Fe isotope compositions of the largest BIFs, the 2.5 Ga Brockman (Pilbara craton, Australia) and Kuruman (Kaapvaal craton, South Africa) iron formations, indicate that virtually all of the Fe in these deposits has been cycled by microbes. These BIFs provide the majority of the world's iron, in economic deposits that reflect later hydrothermal mobilization, oxidation, and deposition. These BIFs are mined at a rate of ~200 million tons per year in the Pilbara craton alone, an impressive testament to the importance of surface-catalyzed redox cycling.

https://doi.org/10.1180/S0026461X00008434 Published online by Cambridge University Press

Rapid early- to mid-Holocene thinning of Pine Island Glacier detected using cosmogenic exposure dating

JOANNE S JOHNSON[1*], JOERG M SCHAEFER[2], MICHAEL J BENTLEY[3], CHRIS J FOGWILL[4], JAMES A SMITH[1], IRENE SCHIMMELPFENNIG[2] AND KARSTEN GOHL[5]

[1]British Antarctic Survey, Cambridge, UK, jsj@bas.ac.uk (*presenting author)
[2]Lamont-Doherty Earth Observatory, Columbia University, New York, USA
[3]Durham University, Durham, UK
[4]University of New South Wales, Sydney, Australia
[5]Alfred-Wegener Institut, Bremerhaven, Germany

The West Antarctic Ice Sheet is thought to be inherently unstable and has the potential to contribute up to 3.3 metres to sea level rise. Recent years have seen dramatic rates of thinning of major ice streams flowing into the Amundsen Sea, and in particular Pine Island Glacier. Onshore measurements of these changes are restricted to decadal timescales and in particular the satellite era, which makes it difficult to judge their significance and whether such changes are unprecedented. One way to place these events in a longer-term context is to study the geological record of past ice sheet change. This approach also provides data that are critical for building reliable ice sheet models that will predict the magnitude and timing of sea level change.

Recent advances in exposure dating afford new approaches for dating Holocene ice sheet thinning: we present the first study combining precise ^{10}Be and in-situ ^{14}C surface exposure ages from Antarctica. We used glacially-transported erratic cobbles as a vertical 'dipstick' for tracing past fluctuations in thickness of the West Antarctic Ice Sheet, focusing on the lower elevations of three nunataks in the Hudson Mountains (immediately north of Pine Island Glacier and close to its present-day grounding line). Exposure ages from the lowermost 100 m of two nunataks (Mt Moses and Maish Nunatak) suggest that rapid thinning was sustained there over a few hundred years in the early- to mid-Holocene, and brought the ice sheet surface close to its present elevation by ~6 ka. We also report exposure ages from within 40 m of the modern ice surface at Meyers Nunatak.

Formation of the Si-rich layer on olivine surfaces during carbonation under *in-situ* conditions

NATALIE C. JOHNSON[1,*], BURT THOMAS[2], KATHERINE MAHER[3], DENNIS K BIRD[3], ROBERT J.ROSENBAUER[2], GORDON E. BROWN, JR.[1,3,4]

[1]Department of Chemical Engineering, 381 North-South Mall, Stauffer III, Stanford University, Stanford CA 94305
[2]United States Geological Survey, 345 Middlefield Rd, Menlo Park CA 94025
[3]Department of Geological and Environmental Sciences, 450 Serra Mall, Braun Hall Builidng 320, Stanford University, Stanford CA 94305
[4]Stanford Syncrotron Radiation Lightsource, 2575 Sand Hill Rd, Menlo Park CA 94025
[*]nataliej@stanford.edu

Olivine dissolution releases divalent cations (Mg^{2+}, Fe^{2+}) into solution and in the presence of dissolved CO_2 will result in the precipitation of carbonate minerals. This process, known as mineral carbonation, has the potential to safely store CO_2 in the subsurface over geologic time. Although the reaction is thermodynamically favored and occurs naturally, the kinetics are typically slow at temperatures < 100°C and thus limit industrial applications of the process. Previous results from this group and others have shown that the dissolution rate of olivine drops over two orders of magnitude as the reaction solution approaches saturation with respect to amorphous silica (a by-product of metal silicate carbonation). This study aims to understand why and how the rate drop occurs, using a series of batch reactions in a three-phase system (water, solid, and supercritical CO_2) at conditions relevant to in-situ carbonation (60°C, 100 bar P_{CO2}). Analysis of the mineral reaction products indicates the formation of a Si-rich, Mg-depleted layer on the olivine surface as soon as 2 days after reaction is started and before the bulk solution reaches silica saturation. Ion probe analysis of olivine grain surfaces produced by reaction with a ^{29}Si-spiked, CO_2-containing aqueous solution suggests that a Si-rich layer up to 1.5 μm deep forms on the grain surfaces, and that after 2 weeks of reaction this layer is primarily due to preferential removal of cations (leaching) rather than re-precipitation of silica. At t<20 days and pH<5, the Si-rich layer appears to control the rate of olivine dissolution. After 20 days, the layer no longer controls the dissolution rate, the rate increases, and carbonation occurs. Although Mg-carbonate precipitation requires significant oversaturation with respect to magnesite, the overall rate-limiting step for olivine carbonation as measured in our experiments involves the formation and subsequent break-down of the Si-rich layer. Current work is aimed at preventing the formation of the leached layer.

https://doi.org/10.1180/S0026461X00008434 Published online by Cambridge University Press

Interrogating the mechanisms controlling sulfur isotope fractionation during sulfate reduction

DAVID T. JOHNSTON*, WILLIAM D. LEAVITT, MARIAN SCHMIDT, SCOTT D. WANKEL, ALEX S. BRADLEY AND PETER R. GIRGUIS

Harvard University, Dept. of Earth and Planetary Sciences, Cambridge, MA, USA, johnston@eps.harvard.edu (*presenting author)

The sedimentary sulfur isotope record represents a unique opportunity to learn about Earth's environmental history. This great interpretability is related to the fact that the sulfur cycle captures the interplay of numerous redox sensitive biological processes and preserves an extraordinary geological signal, both of which are accessible with a multiple isotope system. The precision with which we can tell these stories, however, rests with the quality of our calibrations. To date, isotopic calibrations have targeted microbial sulfate reduction; an anaerobic metabolism that is both the dominant contributor to the preserved sulfur isotope variability and provides the tight, quantitative links between the sulfur, oxygen and carbon cycles. Decades of classic batch experiments with whole cells of sulfate reducers underpin our understanding of the fractionation capacity of this metabolism, coarsely linking cellular and volumetric rates of reduction to the inverse of the magnitude of $^{34}S/^{32}S$ fractionation (*1*). Although informative, it is possible to both place tighter quantitative constraints on this relationship, as well as to develop a more fundamental understanding of the physiological mechanisms driving the observed fractionation patterns. With this level of calibration, and through the inclusion of minor isotope fractionation patterns, a more refined picture of Earth surface evolution is possible.

In what follows we present data from a suite of continuous culture experiments with two pure *Desulfovibrio* strains of sulfate reducer: *D. vulgaris* Hildenborough and *D. alaskensis* G20. Through these experiments we varied sulfate concentrations from 1-100% of modern values and modulated the electron delivery rate over an order of magnitude in order to induce varying degrees of limitation in electron availability. These experiments thus target the two primary controls on sulfate reduction – electron donation rate (lactate flux) and reception (sulfate availability) – and map onto distinct geological questions. For example, in the case of sulfate availability, the difference in isotopic composition between Proterozoic sulfates and sulfides is often inferred as related to $[SO_4^{2-}]$; our experiments directly address this assumption as they span the presumed $[SO_4^{2-}]$ for that time interval (0.5-5 mM). Our entire data set presents fractionation that in $^{34}S/^{32}S$ range from the ordinary (< 25‰) to the extraordinary (> 50‰), and can be contoured by electron consumption rates. When paired with the minor isotope data, the flux of sulfur through a bacterium can be more specifically solved for. This is in part because of the steady-state character of the experiments and through additional insight gained from oxygen isotope geochemistry. In the case of the oxygen isotope work, we lean on new experimental calibrations of the sulfite-water isotope equilibrium conducted over a range of temperatures and pH (data presented herein). Together with an updated metabolic model (*2*), this study allows for the internal operation of the metabolism to be solved.

Through the tight constraints allowed by our experimental design, and with the direct measurement of all sulfur bearing phases present in the reactor at each time point (satisfying elemental and isotopic mass-balance), we link electron utilization to isotopic fractionation (*3*) in a manner that allows for geological records to be more fully interpreted. This work also helps to open the 'black box' of large fractionations produced by sulfate reduction through solid physiological and geochemical constraints. The sum of the information gained through this work will allow Proterozoic and Phanerozoic oxidant budgets to become more accessible.

(*1*) D. E. Canfield, in *Stable Isotope Geochemistry*. (2001) 607-636. (*2*) A. S. Bradley et al., *Geobiology* **9**, 446 (2011). (*3*) L. A. Chambers et al., *Canadian Journal of Microbiology* **21**, 1602 (1975).

Neutron scattering reveals conformations of the transcriptional regulator MerR in complex with its operator DNA

ALEXANDER JOHS[1*], STEPHEN J. TOMANICEK[1], HAO-BO GUO[1], ANNE O. SUMMERS[2], AND LIYUAN LIANG[1]

[1]Oak Ridge National Laboratory, Oak Ridge, TN, U.S.A., johsa@ornl.gov (* presenting author)

[2]University of Georgia, Athens, GA, U.S.A.

Bacterial resistance to heavy metals is controlled by metal-responsive transcriptional regulators. For example, bacterial resistance to inorganic and organic mercury compounds is conferred by the *mer* operon, which is typically located on transposons or plasmids [1,2]. These proteins are involved in Hg(II) import, proteolysis of organomercurials and Hg(II) reduction to Hg(0). Expression of the *mer* operon genes is controlled by the transcriptional repressor-activator MerR.

How Hg(II) binding affects the changes in the conformation of MerR, which in turn propagate through DNA contacts to its operator DNA (MerOP) is unknown. In this study we investigate Hg(II)–induced conformational changes of MerOP in complex with its regulator MerR to reveal the transcription control mechanism conferred by MerR. Experimentally, we purified MerR and prepared a complex with a 23bp MerOP dsDNA construct. In vivo, MerR tightly binds to MerOP in a region of dyad symmetry between the -10 and -35 RNA polymerase recognition sites. In the absence of Hg(II), RNA polymerase binds to its promoter and forms a stable pre-initiation complex with dimeric MerR acting as a repressor preventing RNA polymerase from accessing the -10 recognition site. In the experiments, we examined the MerR-MerOP complex in the presence and absence of Hg(II) using small-angle neutron scattering (SANS) (Fig. 1). A contrast variation series allowed us to detect changes in the conformation of MerR and MerOP, respectively. Homology modeling and molecular dynamics simulations were used to generate atomic resolution models to interpret the data. The results provide insights on the allosteric change in MerR triggered by Hg(II), which causes a reorientation of the -10 recognition site and ultimately initiation of transcription by RNA polymerase [3].

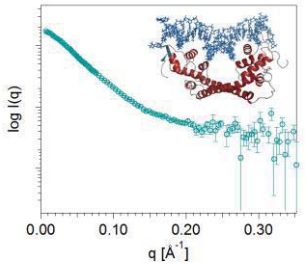

Figure 1: Small angle neutron scattering intensities I(q) vs momentum transfer (q) in 100% D_2O buffer and a model of the MerR-MerOP complex.

[1] Barkay et al. (2003) *FEMS Microbiol Rev* **27**, 385-384.
[2] Summers et al. (1986) *Annu Rev Microbiol* **40**, 607-634.
[3] Ansari et al. (1995) *Nature* **374**, 371-375.

https://doi.org/10.1180/S0026461X00008434 Published online by Cambridge University Press

Are River Basins affected by Climatic Variations?: A study from a major river in Central Mexico, Mexico.

M.P. JONATHAN[1*], P.D. ROY[2], P.F. RODRÍGUEZ-ESPINOSA[1] AND N.P. MUÑOZ-SEVILLA[1]

[1]Centro Interdisciplinario de Investigaciones y Estudios sobre Medio Ambiente y Desarrollo (CIIEMAD), Instituto Politécnico Nacional (IPN), Calle 30 de Junio de 1520, Barrio la Laguna Ticomán, C.P. 07340, Del. Gustavo A. Madero, México, D.F., México.
mpjonathan7@yahoo.com (*presenting author)
pedrof44@hotmail.com, npmsevilla@gmail.com
[2]Instituto de Geología, Universidad Nacional Autónoma de México (UNAM), Ciudad Universitaria C.P. 04510, Coyoacan, México DF., México.
p_debajyotiroy@yahoo.com

Variations in climatic cycle during different periods often affect various aspects in the earth, especially it shows more diversity in the aquatic region. Our study focuses mainly on the geochemical aspects of river sediments from River Amajac, Panuco and its lagoons which are located in the north eastern part of the Mexico. The whole system runs through the Sierra Madre Oriental in Central part of Mexico and finally drains into the Gulf of Mexico. The difference in the weathering pattern in the sediments of the river basin could be related to the changes in the climatic cycle in the region [1-2]. The results also clearly indicate that the decrease in rainfall events during the last three decades have affected the farming land and has resulted in deforestation and subsequently it has resulted in erosion of finer particles into the aquatic system. The analysis of major, trace elements and the calculated weathering pattern results suggest that the region is frequently vulnerable to erosion. The concentration and distribution pattern of the geochemical elements also indicate that the higher concentration of toxic elements is mainly anthropogenic, which can be related to the industrialization of the region.

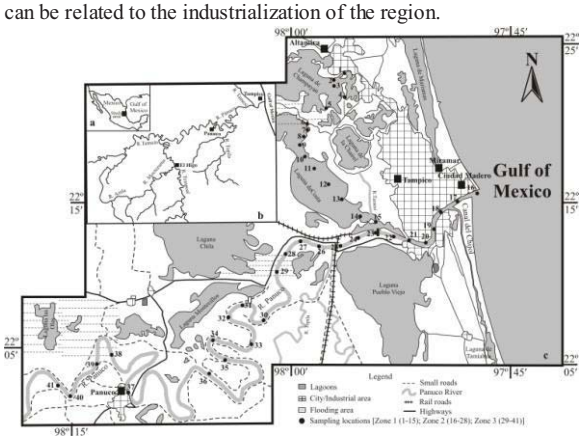

Figure 1. A part of the study area in north eastern part of Mexico.

[1] Hudson (2003) J of Latin Amer Geog **1**, 58-68. [2] Fiechter *et al*. (2006) Estu Coast & Shelf Sci **70**, 297-306.

Evidence for a manganous surface sea at 2.5 Ga

C. JONES[1*], S. W. POULTON[2], S. A. CROWE[1], AND D.E. CANFIELD[1]

[1]Nordic Center for Earth Evolution, Institute of Biology, University of Southern Denmark, Odense, Denmark
carriayne@biology.sdu.dk (* presenting author), sacrowe@biology.sdu.dk, dec@biology.sdu.dk
[2]School of Civil Engineering and Geosciences, Newcastle University, Newcastle upon Tyne, United Kingdom
simon.poulton@newcastle.ac.uk

The Transvaal Supergroup in South Africa hosts one of the most pristine Archean sedimentary successions known, with largely flat lying strata and sub-greenschist metamorphism [1]. The relevant section of this unit records an intertidal carbonate platform deepening upward to a basinal iron formation. The carbonates from the platform, especially the Lower Nauga formation, have relatively high Mn concentrations, but more limited Fe. We propose that this resulted from surface sea waters containing substantial Mn and a paucity of Fe, based on the ideal partitioning coefficients of Mn and Fe into calcite and dolomite lattices [2].

Fe speciation data from deep basin sediments indicate deposition under anoxic, ferruginous conditions, implying that the water column was stratified with manganous surface waters overlying ferruginous bottom waters. Surface sea waters could be devoid of Fe^{2+} for a number of reasons, including photic zone oxygen production, anoxygenic phototrophic Fe^{2+} oxidation, or sulfide scavenging of Fe^{2+}. Dissolved Mn^{2+} can persist through all of these scenarios; however, pervasive oxygenation could be expected to oxidize Mn as well. Had Mn been deposited as oxide, the $\partial^{13}C$-CO_3 should move to more negative values, reflecting the $\partial^{13}C$ composition from the organic matter used during dissimilatory reduction. Platform carbonates of the Campbellrand Subgroup from the intertidal to the lagoonal to the shelf margin have previously been shown to have $\partial^{13}C$-CO_3 compositions around -0.5 ‰ [3], a signal indicative of water column carbonate precipitation. The speciation of Fe present on the carbonate platform also indicates anoxic surface water. The vertical extent of the depositional environments of these Mn rich carbonates from the intertidal zone to the shelf margin together with the roughly 600 m of elevated Mn:Fe ratios in the carbonates suggest a substantially thick manganous surface layer above the more reducing (mostly ferruginous) deep basin.

[1] Beukes (1983) in *Iron Formation: Facts and Problems*, 131-209.
[2] Mucci and Morse (1990) *Aquatic Sciences* **3,** 217-254.
[3] Fischer, Schroeder, Lacassie, Beukes, Goldberg, Strauss, Horstmann, Schrag, and Knoll (2009) *Precambrian Research* **169**, 15-27.

https://doi.org/10.1180/S0026461X00008434 Published online by Cambridge University Press

Field evidence of Sr exchange between particulate material and seawater in estuaries

M.T. JONES[1*], S.R. GISLASON[1], K. BURTON[2], C.R. PEARCE[3], V. MAVROMATIS[4] & E.H. OELKERS[1,4]

[1]Institute of Earth Sciences, University of Iceland, Sturlugata 7, Reykjavik, Iceland, morgan@hi.is *presenting author, sigrg@raunvis.hi.is

[2] Department of Earth Sciences, Durham University, Durham, UK, kevin.burton@durham.ac.uk

[3] Department of Environment, Earth and Ecosystems, CEPSAR, The Open University, Milton Keynes, UK, c.pearce@open.ac.uk

[4] GET-Université de Toulouse-CNRS-IRD-OMP, Toulouse, France, mavromat@get.obs-mip.fr, oelkers@lmtg.obs-mip.fr

The reactivity of riverine particulate material upon arrival in the oceans is an important consideration for global element cycles, as this flux dominates for the majority of elements [1]. A small amount of particulate dissolution in saline water would have a noticeable impact on land-to-ocean fluxes of key elements such as Ca, Mg and Sr. A recent study showed significant dissolution and/or exchange of strontium between riverine particulate material and seawater in laboratory conditions [2]. If replicated in the natural environment, the calculated Sr release upon arrival in estuarine waters would be of a similar order of magnitude to hydrothermal exchange at mid-ocean ridges. To date, no study has found evidence of Sr exchange in field studies, potentially because the concentrations of Sr in seawater are high and there is experimental evidence for contemporaneous precipitation of Sr-bearing phases [2].

This study focuses on the Borgarfjörður estuary in western Iceland. The basaltic lithology of the catchment and the shallow depth of the fjord make this site ideal for detecting any interaction between solid and liquid phases, as this should equate the most easily weathered material and the highest sediment to water ratio in the natural environment. Two independent field trips collected water, suspended material and bedload samples in transects along the fjord, and subsequently analyzed for major element concentrations and $^{87}Sr/^{86}Sr$ values. While dissolved Sr concentrations are controlled by the extent of mixing with saline water, the $^{87}Sr/^{86}Sr$ values of both the dissolved and suspended load display evidence that unradiogenic Sr is liberated from solid particles upon first contact with saline water. Bedload samples show a systematic increase in $^{87}Sr/^{86}Sr$ values along the length of the estuary. These analyses represent the first *in situ* evidence of considerable Sr exchange between riverine particulate material and seawater, and demostrate that particulate material can play an important role in defining the chemistry of coastal waters. These findings have important consequences for global Sr budget calculations and the general use of isotopes as tracers of biogeochemical processes.

[1] Oelkers et al. (2011) *Appl. Geochem.* **26**, S365-S369.

[2] Jones et al. (2012) *Geochim. Cosmochim. Acta* **77**, 108-120.

Subduction erosion, magmatism and continental crust formation in the southern Central Andes

ROSIE JONES[1*] LINDA KIRSTEIN [1], RICHARD HINTON[1], SIMONE KASEMANN[2], BRUNO DHUIME[3] AND TIM ELLIOTT[3]

[1]School of GeoSciences, University of Edinburgh, UK r.e.jones-3@sms.ed.ac.uk (* presenting author)

[2]Department of Geosciences, University of Bremen, Germany

[3]Department of Earth Sciences, University of Bristol, UK

Subduction zones, such as the Andean convergent margin, form large recycling systems and are the main producers of new continental crust. The subduction of continental material through either tectonic subduction erosion or sediment cycling is an important component when estimating the mass flux through an active margin over time. Suduction erosion in particular has been highlighted as an important process along certain parts of the Andean continental margin, especially to the west of the Central Andes [1, 2].

It has been suggested that the rate of subduction erosion along the north-central Andean margin has varied over time with constant, fast rates between 150 and 20 Ma and slower rates during the Neogene [3]. A near constant rate of subduction erosion between 150 and 20 Ma suggests a continuous supply of continental material into the subduction zone, during this time.

We have combined high resolution, U-Pb dating, isotope geochemistry, and major and trace element analyses, from a suite of magmatic rocks sampled from the southern Central Andes (28º to 32ºS), in order to investigate source contamination by subducted continental material between the late Cretaceous and the late Miocene.

The results of new, in-situ U-Pb dating of magmatic zircons by SIMS place further constraints on the presence of a widespread period of reduced arc magmatism in the southern Central Andes during the late Eocene to late Oligocene (35 - 26 Ma). Oxygen and hafnium isotopic analysis, of the same magmatic zircons (by SIMS and LA-ICPMS respectively), reveal variations in $\delta^{18}O_{(VSMOW)}$ of between 9.78 ± 0.21‰ and 3.59 ± 0.21‰ and in εHf of between 10.4 ± 1.3 and -4.4 ± 0.8. This new data, when combined with the results of whole rock, major and trace element analysis, provides increased constraint on the amount of continental material being subducted to depth and recycled to the continental crust via arc magmatism during this key time in the evolution of the Andes.

[1] Stern (1991) *Geology,* **19**, 78-81.

[2] Stern (2004) *Rev. geol. Chile,* **31**, 161-206.

[3] Clift and Hartley (2007) *Geology,* **35**, 503-506.

https://doi.org/10.1180/S0026461X00008434 Published online by Cambridge University Press

Size-dependent surface charging of TiO_2 nanoparticles

CAROLINE M JONSSON*, JENNY PEREZ HOLMBERG, ELISABET AHLBERG, MARTIN HASSELLÖV, JOHAN BERGENHOLTZ, AND ZAREEN ABBAS

University of Gothenburg, Department of Chemistry and Molecular Biology, Gothenburg, Sweden
caroline.jonsson@chem.gu.se (* presenting author), perezj@chem.gu.se, ela@chem.gu.se, martin.hassellov@chem.gu.se, jbergen@chem.gu.se, zareen@chem.gu.se

Metal oxide nanoparticles show variations in their structure relative to corresponding larger microparticles of the same material, often with new unexpected features occurring in the nanoscale size range. Generally, nanoparticles have increased roughness and curvature of the surface, large specific surface area and high abundance of active binding sites; thus are very reactive. The surface charge is highly affected by the surrounding media, which in turn affects the colloidal stability of nanoparticles.

This study focuses on the size-dependent surface charging of TiO_2 (anatase) nanoparticles. TiO_2 nanoparticles with well-defined particle sizes (<30 nm) and without any coatings or surfactants were synthesized using low-temperature hydrolysis of $TiCl_4$. Temperature during synthesis reaction, dialysis and storage was found to strongly influence the particle size and crystal structure, according to [1]. The nanoparticles were extensively characterized using several techniques and were found to have a sphere-like shape. In order to study the size-dependence on the pH_{PZC} (point of zero charge), potentiometric titrations were used to determine the surface charge of the TiO_2 nanoparticles at 25 °C, and at varying ionic strengths obtained with NaCl as background electrolyte. Further, zeta potential measurements were performed under similar conditions.

The experimentally determined size-dependent surface charging behavior of TiO_2 nanoparticles are compared with the corresponding surface charge densities calculated by classical surface complexation models, as well as by the Corrected Debye-Hückel (CDH) theory [2].

[1] Abbas *et al.* (2011) *Colloids Surf. A: Physicochem. Eng. Aspects* **384**, 254-261. [2] Abbas *et al.* (2008) *J. Phys. Chem. C*, **112**, 5715-5723.

Biomineralization and fate of the Fe^{II}-Fe^{III} hydroxy salt green rust *vs.* magnetite

JORAND FRÉDÉRIC*, ZEGEYE ASFAW, SERGENT ANNE-SOPHIE, REMY PAUL-PHILIPPE, LARTIGES BRUNO AND HANNA KHALIL

University of Lorraine LCPME UMR 7564 CNRS –, Jean Barriol Institute, 405 rue de Vandoeuvre, 54600 Villers-lès-Nancy, France (*correspondence: frederic.jorand@univ-lorraine.fr)

It is well known that iron oxide reduction by *Shewanella* spp. bacteria promotes the formation of Fe^{II} bearing minerals, such as the mixed Fe^{II}-Fe^{III} hydroxysalt green rusts (GRs), in anaerobic conditions. Although the microbial-promoted generation of GRs is widely demonstrated, the mechanisms and factors governing the GR formation as the main secondary iron mineral at the expense of other products in lab-scale investigations or environmental systems are largely unknown. As GR is an effective reductant for several contaminants the mechanism controlling the formation routes of GR merit investigation, from both the environmental and engineering points of view.

Some factors such as cellular material (i.e. autoclaved cells and/or bacterial polymers), synthetic anionic polymers or oxyanions have been identified to control the route of the GR mineralization as secondary mineral at the expense of other products such as magnetite.

The arrangement mode of the heterogeneous aggregates resulting from the interactions between bacterial cells, iron oxide particles and polymers was suggested to influence the routes of formation of secondary iron minerals by limiting the diffusion of reactive species and thus creating favorable microenvironment for GR formation. In these aggregates, the electron transfer from cells to iron oxides is supported by organic electron shuttles.

On the other hand, anionic polymers, colloidal and aqueous silicates were found to also influence the nature of the secondary iron minerals through the stabilization of the GR crystals.

These results indicate clearly that the bacterial cells drive indirectly the nature of the secondary Fe^{II}-bearing mineral. Moreover, they give new insights into the understanding of the mechanisms of « biogenic » mineral formation based on the electron transfers from bacteria towards iron oxides. Finally, this work contributes to our understanding of the processes leading to green rust formation in environmental systems, such as soils or aquatic systems biofilms, in which a very high cell density can be found at a micro-scale level, associated to exo-cellular polymers and natural silica mineral composites.

https://doi.org/10.1180/S0026461X00008434 Published online by Cambridge University Press

Soil vapour characterization and intrusion to indoor air: a reactive transport modelling approach

P. JOURABCHI[1*], I. HERS[2], S. MOLINS[3], AND M. LAHVIS[4]

[1]Golder Associates Ltd., Burnaby, Canada, pjourabchi@golder.com (* presenting author)
[2]Golder Associates Ltd., Burnaby, Canada, ihers@golder.com
[3]Lawrence Berkeley National Lab, Berkeley, USA, SMolins@lbl.gov
[4]Shell Global Solutions, Houston, USA, Matthew.Lahvis@shell.com

Introduction

Vapour intrusion to indoor air often represents a significant exposure pathway for risk assessment at sites contaminated by volatile petroleum hydrocarbons. While the importance of biodegradation processes on the fate and transport of petroleum hydrocarbon vapours is well established [1; and references therein], fewer studies have investigated site specific factors such as source concentration and location with respect to the building, pressure conditions, and soil properties, all of which have been shown to impact the potential for vapour intrusion [e.g., 2-4]. In this numerical modelling study, site specific factors are evaluated using the multi-component reactive transport code MIN3P-DUSTY [5-6]. The model includes the key processes of hydrocarbon volatilization, gas- and aqueous-phase diffusion, gas-phase advection, aerobic biodegradation (using dual-Monod kinetics formulation) and sorption in a domain comprising the subsurface and the building foundation. Benzene and iso-octane are used as surrogates of the aromatic and aliphatic compounds of the gasoline vapours. Initially, a sub-model for transport through concrete and within foundations cracks was developed and benchmarked against an analytical solution. The model was calibrated based on a high quality data set for an unoccupied research house located above a petroleum hydrocarbon plume (located in North Battleford, Saskatchewan, Canada), and then used to predict the hydrocarbon vapour distribution for a range of observed and hypothetical conditions.

Results & Conclusion

For the observed site conditions, the calibrated model indicates soil vapour transport is dominated by diffusion and aerobic biodegradation, and that building pressures and soil gas advection have little influence on soil vapour concentrations. Comparison of wetter (spring) and drier (winter) conditions indicate that the vadose zone oxygen concentrations above the contamination source area are lower for wetter spring conditions because of the reduced diffusion through relatively wet surface soils. For most scenarios simulated, there is rapid attenuation of benzene within approximately 1 m of the source; however, less attenuation of iso-octane is predicted, consistent with site data. For a shallow NAPL scenario, a concrete foundation slab resulted in an oxygen shadow and increase in benzene and iso-octance concentrations below the building.

[1] Verginelli & Baciocchi (2011) *J. Contam. Hydrol.* **126**, 167-180. [2] Abreu &Johnson (2005) *Environ. Sci. Technol.* **39**, 4550-4561. [3] Pennell et al. (2009) *J. Air &Waste Manage. Assoc.* **59**, 447-460. [4] Yu et al. (2009) *J. Contam. Hydrol.* **107**, 140-161. [5] Mayer et al. (2002) *Water Resour. Res.* **38**, doi:10.1029/2001WR000862. [6] Molins & Mayer (2007) *Water Resour. Res.* **43**, doi:10.1029/2006WR005206.

Clumped isotope Vs. fluid inclusion thermometry in crystals from Oman.

A.-L. JOURDAN[1*], CÉDRIC M. JOHN[1], SIMON DAVIS[1] AND VEERLE VANDEGINSTE[1]

[1]Department of Earth Science and Engineering, Imperial College London, London SW7 2AZ, United Kingdom. a.jourdan@imperial.ac.uk (* presenting author), cedric.john@imperial.ac.uk, s.davis@imperial.ac.uk, v.vandeginste@imperial.ac.uk

Clumped isotopes are a new exciting tool in the domain of paleothermometry. The "clumped isotopes carbonate paleothermometer" has been tested and used as a new temperature proxy for paleoclimate studies during the last few years. Indeed, clumped isotopes (Δ47) appear to be a great proxy since they are based on the degree of association of ^{13}C and ^{18}O into the carbonate ions, a function of thermodynamics. Therefore, measuring Δ47 allows the determination of the formation temperature of the carbonate material independent of the isotopic composition of the precipitating fluid. Furthermore, unlike other proxies, Δ47 seems insensitive to potential 'vital effects'.

However, there is still a lot to unravel in this field of geochemistry, and some improvement and development are necessary. Some processes, such as kinetic fractionation, need to be identified and better understood in order to apply this proxy in the most precise way possible. Studies need to include comparisons between clumped isotopes and other temperature proxies.

Here we intend to compare data from both fluid inclusions microthermometry and clumped isotopes measurements carried out on the same material. Our focus has been placed on calcite crystals sampled in the carbonate carapace of a salt dome at Jebel Madar, Oman, where preliminary data suggest a low temperature precipitation.

As carbonates are very reactive minerals, diagenesis and metamorphism could re-order the isotope clumping configuration in the carbonate and the measurements would reflect the equilibrium temperature of recrystallisation. Hence, careful consideration needs to be given to sampling strategies. Calcite crystals were sampled in fractures showing multiple pulses of opening, and the crystals themselves show evidence for growth zoning and fracture healing. We focus our study on deciphering and understanding the processes and effects of diagenesis on the reliability of the carbonate clumped isotope paleothermometer.

The project is part of the Qatar Carbonate and Carbon Storage Research Centre (QCCSRC), funded jointly by Qatar Petroleum, Shell and the Qatar Science and Technology Park.

https://doi.org/10.1180/S0026461X00008434 Published online by Cambridge University Press

Sources and processes identification for Zn cycling in the Seine river, France

DELPHINE JOUVIN[1*], ALEXANDRE GÉLABERT[2], PASCALE LOUVAT[2], GUILLAUME MORIN[3], FARID JUILLOT[3], AND MARC F. BENEDETTI[2]

[1]IDES UMR 8148, Université Paris Sud - CNRS, Orsay, France (*delphine.jouvin@u-psud.fr)
[2]Univ. Paris Diderot – Sorbonne Paris Cité - IPGP, Paris, France (gelabert@ipgp.fr, louvat@ipgp.fr, benedetti@ipgp.fr)
[3]IMPMC CNRS UMR7590, UMPC, Paris, France (guillaume.morin@impmc.upmc.fr, farid.juillot@impmc.upmc.fr)

An accurate determination of the ecological status of the Seine River (flowing through greater Paris, France) is required as it is one of the most severely damaged European rivers. However, important evaluation limitation still exists, partly because the metal cycling in this system is not fully understood, with for instance half the Seine river Zn not having clearly identified sources[1]. Along with Zn isotopic measurements, this study proposes to use XAS (X-ray Absorption Spectroscopy) to determine precisely the speciation of Zn complexes, and thus to define the proportion of water mixing vs. processes for Zn transfer in the watershed. A geographical sampling transect has been performed downstream Paris, where the contamination is maximum – 5 samples from the Seine River and 3 tributaries.

Significant isotopic signature variations are observed, varying from $\delta^{66}Zn$ = 0.04 to 0.14 ± 0.05‰ in the particulate phase, and from $\delta^{66}Zn$ = -0.23 to 0.10 ± 0.06‰ for the dissolved phase. These results are in line with previous work by Chen et al.[2] on the Seine River, but as we focus on the most polluted downstream part of the river, the $\delta^{66}Zn$ variation range in both dissolved and suspended loads is much narrower. The XAS analysis performed on the suspended load samples at the Zn K-edge confirmed however a real heterogeneity by showing different speciations with a major contribution of sulfides, iron oxides, amorphous silica and organic ligands.

The dissolved phase displays systematically lower isotopic signatures than the particulate phase, resulting from adsorption processes [3, 4]. A significant discrepancy was observed between summer and winter for the dissolved phase, with higher values in winter high-water stages, reflecting a bigger contribution of natural sources ($\delta^{66}Zn$ is 0.88‰ for chalk [2]) than during summer low-water stages dominated by anthropogenic sources.

The regional major wastewater treatment plant (WWTP) in Achères (shortly after Paris) brings significantly heavier Zn to the Seine River particulate material. This change in $\delta^{66}Zn$ follows a change in Zn speciation, with a strong decrease in sulfides contribution after Achères. This WWTP impacts both dissolved and particulate phases on concentration, speciation and isotopic signatures. Comparison with Chen et al.[2] indicates a significant variability of the WWTP Zn signal that needs further investigation.

[1] Thevenot et al. (2007) *Science Total Environ.* **375**, 180-203. [2] Chen et al. (2008) *Environ. Science Tech.* **42**, 6494-6501. [3] Juillot et al. (2008) *Geochim. Cosmochim. Act*. **72**, 4886-4900. [4] Jouvin et al. (2009) *Environ. Science Tech.* **43**, 5747-5754.

Geochemical Assessment of the Metallogenic Potential of Proterozoic LIPs of Canada

S. M. JOWITT[1], AND R. E. ERNST[2*]

[1]School of Geosciences, Monash University, Melbourne, VIC3800, Australia, simon.jowitt@monash.edu
[2]Dept. of Geology, Carleton University and Ernst Geosciences, 43 Margrave Avenue, Ottawa, Ontario, Canada K1T 3Y2, richard.ernst@ernstgeosciences.com (* presenting author)

The lithogeochemistry of eight Proterozoic Large Igneous Provinces (LIPs) within Canada has been studied to determine the Ni-Cu-PGE prospectivity of these major magmatic events. Three of the LIPs discussed here, the 1.87 Ga Chukotat, 1.27 Ga Mackenzie and the 2.49-2.45 Ga Matachewan LIPs, host known magmatic Ni-Cu-PGE sulphide mineralisation; in addition, the 0.72 Ga Franklin LIP may be associated with the coeval and mineralised Dovyren intrusion in Siberia and several Franklin-related Ni-Cu-PGE prospects are known within northern Canada. The other four LIPs, the 1.14 Ga Abitibi, 0.59 Ga Grenville, ~1.25 Ga Seal Lake and 1.24 Ga Sudbury (distinct from the Sudbury impact event) LIPs, have no known Ni-Cu-PGE mineralisation.

The mineralised Chukotat, Mackenzie and Matachewan LIPs are characterised by basalts with Ti/V ratios below 50, Gd/Yb ratios close to primitive mantle values and variable La/Sm ratios. The magmas that formed these LIPs assimilated significant amounts of crustal material and samples representing both chalcophile depleted and undepleted magmas are present within these LIPs. This suggests that the magmas that formed these LIPs were fertile and S-undersaturated when they left the mantle and subsequently underwent a S-saturation event, forming immiscible magmatic sulphides. The close relationship between chalcophile element depletion and crustal contamination evident in the geochemistry of these LIPs suggests that S-saturation was caused by assimilation of crustal material, most likely by assimilation of crustal sulphides. The magmatic sulphides produced during this event were presumably segregated from silicate magmas and were deposited in cogenetic mafic-ultramafic sills and intrusives associated with these LIPs.

The Grenville and part of the Franklin LIPs have similar magma source characteristics to LIPs with known Ni-Cu-PGE mineralisation. However, although magmas from both LIPs were fertile and assimilated crustal material, the Grenville LIP did not undergo a S-saturation event prior to emplacement, whereas the Franklin LIP may have; the timing and location of this S-saturation event may be a useful guide during exploration for Ni-Cu-PGE mineralisation. The Abitibi, Sudbury and Seal Lake LIPs are alkaline, dominated by alkali basalts and are characterised by high Gd/Yb ratios, a wide range in La/Sm ratios and Ti/V ratios higher than 50. All samples from the Abitibi, Seal Lake and Sudbury LIPs are chalcophile element depleted, suggesting that these magmas left residual sulphide within the mantle during partial melting, and indicating that these LIPs are probably unprospective for Ni-Cu-PGE sulphide mineralisation.

https://doi.org/10.1180/S0026461X00008434 Published online by Cambridge University Press

Sulfate adsorption at buried mineral/solution interfaces probed via vibrational surface spectroscopy

AARON M. JUBB[1] AND HEATHER C. ALLEN[2*]

[1]The Ohio State University, Columbus, USA, ajubb@chemistry.ohio-state.edu

[2]The Ohio State University, Columbus, USA, allen@chemistry.ohio-state.edu (* presenting author)

Introduction

Understanding the structure and energetics of adsorbed ions at the buried mineral/solution interface has great importance to the geochemical and atmospheric chemistry communities. Vibrational spectroscopy is a powerful tool for the study of mineral/solution interfaces as these techniques can be applied *in situ*, are sensitive to surface structures, and are generally non-destructive. Sulfate (SO_4^{2-}) adsorption at buried mineral (fluorite, silica, hematite)/sulfate-solution interfaces was studied using either vibrational sum frequency generation spectroscopy (VSFG), which is inherently interface specific, or total internal reflection (TIR) Raman spectroscopy. Sulfate is a simple, inorganic anion whose behavior is important to understand as it is ubiquitous in the environment being the third most prevalent ionic species in seawater by weight [1].

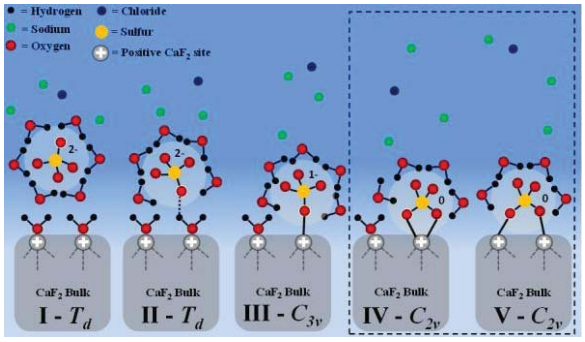

Figure 1: Idealized possible sulfate adsorption complexes at fluorite surface.

Results and Conclusions

The use of VSFG and TIR-Raman allows for the spectral resolution of anion adsorption complex structure, i.e. inner-sphere versus outer-sphere adsorption, Figure 1, at the mineral surface. Utilizing VSFG the sulfate anion is observed to adsorb with a bidentate inner-sphere structure at the fluorite surface with a surface free energy of adsorption of -33 ± 2 kJ/mole for pH 7 solutions at 298 K. The use of TIR-Raman spectroscopy to examine sulfate behavior at silica and hematite surfaces, which feature differing surface charges at pH 7, allows for the direct observation of anion adsorption behavior as a function of the model oxide mineral surface charge.

[1] Kester *et al.* (1967) *Limnol Oceanogr.* **12(1),** 176-180.

Use of in vivo and in vitro assays for refining human health exposure assessment for As-contaminated soil

ALBERT JUHASZ[1,2*], EUAN SMITH[1,2], JOHN WEBER[1,2] AND RAVI NAIDU[1,2]

[1]Centre for Environmental Risk Assessment and Remediation, University of South Australia, Adelaide, Australia, Albert.Juhasz@unisa.edu.au

[2]Cooperative Research Centre for Contamination Assessment and Remediation of the Environment, Adelaide, Australia

Introduction

When quantifying exposure to arsenic (As) for human health risk assessment calculations, As bioavailability is assumed to be 100% which presumes that all of the As has been solubilised in the gastrointestinal tract and absorption into systemic circulation has occurred. In reality, a fraction of the soil-borne As may only be bioavailable and as such this assumption may overestimate the chemical daily intake thereby influencing risk assessment [1]. In order to refine risk calculations by adjusting the default bioavailability value, reliable assays are required that can quantitatively measure site specific bioavailability.

In this study, As bioaccessibility and As relative bioavailability was assessed in contaminated soils using a variety of *in vitro* and *in vivo* assays. In vitro results were compared to in vivo relative As bioavailability data (swine assay) to determined which methodologies have the potential to act as surrogates for in vivo assays.

Materials and Methods

Contaminated soils used in this study were collected from regional areas where the soil type, source of As and As-soil residence time varied. Arsenic bioaccessibility was determined using SBRC [2], IVG [3], PBET [1], DIN [4] and UBM [5] assays while in vivo As relative bioavailability was determined using a swine model according to Rees et al. [6].

Results and Conclusions

Comparison of in vitro and in vivo results demonstrated that the in vitro assay encompassing the SBRC gastric phase provided the best prediction of in vivo relative As bioavailability (r^2 = 0.75, Pearson correlation = 0.87). However, As relative bioavailability could also be predicted using gastric or intestinal phases of IVG, PBET, DIN and UBM assays but with varying degrees of confidence (r^2 = 0.53-0.67, Pearson correlation = 0.73-0.82).

[1] Ruby *et al*. (1996) *Environ. Sci. Technol*. **30**, 422-430. [2] Kelley *et al.* (2002) Assessing Oral Bioavailability of Metals in Soil. Battelle Press, Ohio. [3] Rodriguez *et al.* (1999) *Environ. Sci. Technol*. **33**, 642-649. [4] DIN (2000) Soil Quality - Absorption availability of organic and inorganic pollutants from contaminated soil material. DIN E 19738. [5] Wragg *et al.* (2011) *Sci. Total Environ*. **409**, 4016-4030. [6] Rees *et al*. (2009) *Environ. Geochem. Health* **31**, 167-177.

https://doi.org/10.1180/S0026461X00008434 Published online by Cambridge University Press

Light is an active contributor to vital effect in coral skeleton proxies

ANNE JUILLET-LECLERC[1*], STEPHANIE REYNAUD[2], DELPHINE DISSARD[1,3], GUILLAUME TISSERANT[2] AND CHRISTINE FERRIER-PAGES[2]

[1]LSCE, Gif sur Yvette, France
Anne.Juillet@lsce.ipsl.fr (*presenting author)
[2]CSM, Monaco, Principality of Monaco
sreynaud@centrescientifique.mc
[3]School of Earth and Environment, Crawley, Australia

Biologists emphasize the Light Enhanced Calcification (LEC) for a long time, although the interaction between light and calcification in coral skeleton formation remains not understood. $d^{18}O$, Sr/Ca and Mg/Ca are regarded as temperature tracers. However, we have no information concerning potential light influence on proxies.

Symbiotic colonies of the coral *Acropora* sp. were cultured, under constant conditions, in a factorial design of three temperatures (21, 25 and 28°C) and two light intensities (200 and 400 □mol photon m^{-2} s^{-1}). Metabolic, growth and geochemical measurements ($d^{18}O$, $d^{13}C$, Sr/Ca and Mg/Ca) were conducted on 6 colony sets representing each environmental (light temperature) condition. The experiment intended firstly to identify the separated influences of temperature and light on metabolism and calcification rates and secondly to compare them with corresponding skeletal $d^{18}O$, $d^{13}C$, Sr/Ca and Mg/Ca variations.

Metabolic parameters responded as biologists could expect: photosynthesis increased with temperature, being always higher at high light. When colony was maintained at low light zooxanthellae (coral symbionts) density was higher at 25 and 28°C than under high light, illustrating the coral capability of shadow-adaptation. Calcification rate was also positively correlated to temperature, the quantity of deposited aragonite being always higher under high light. In opposite, surface expansion (equivalent to linear extension) did not show straightforward behavior. In addition, mean (for each data set) photosynthetic activity was related to mean calcification rate following logarithmic relationship.

Proxy responses showed huge scattering especially under high light and high temperature, exceeding by several °C the value calculated by using conventional calibrations, thus compromising the robustness of commonly admitted temperature tracers. The average assessed by the 6 values of $d^{13}C$, Sr/Ca and Mg/Ca measured on the 6 nubbins of each set were correlated to averaged calcification rates, following logarithmic relationship. Furthermore, they seemed to obey to the temperature-light synergy. In □opposite, correlation between $d^{18}O$ and calcification rate strongly depended on the light intensity, although $d^{18}O$ seemed the most relevant temperature tracer. Examination of isotopic micro-measurements confirmed that isotopic fractionation could differ following light intensity. By considering individual values measured on each colony developed under high light, we underlined that photosynthetic activity, covering the total measured amplitude, was strongly related to symbiotic algae density, regardless temperature value, such as individual proxy values showed strong correlation with calcification rate according to light intensity, regardless temperature value. We deduced that in these conditions the high scattering that we observed could be due to the light effect, at least under high light.

No coral proxy is dependent on the sole temperature and no temperature calibration could be regarded as a universal law.

Distribution of vanadium in a basaltic aquifer of Jeju Island, Korea: effects of geochemical reactions and hydrological mixing

HEE-WON JUNG[1*], SEONG-TAEK YUN[1], BERNHARD MAYER[2], KYOUNG-HO KIM[1], YOUNG-HWA GO[1], SANG-SIL OH[3], AND KYUNG-GOO KANG[4]

[1]Korea University, Green School and the Department of Earth and Environmental Sciences, South Korea, indra832@korea.ac.kr (* presenting author)
[2]University of Calgary, Geoscience, Canada
[3]Jeju Special Self-Governing Province Institute of Environment Research, Jeju, South Korea
[4]Jeju Special Self-Governing Province Development Corporation, Jeju, South Korea

Hydrochemistry data (i.e., major cations and anions, and trace metals such as Fe, Mn, V, As, Mo and U) of 25 groundwater samples from the Gosan area at the southwestern part of Jeju volcanic island, South Korea, were examined to investigate physico-chemical factors controlling the spatio-temporal distribution of vanadium in a basaltic aquifer. The study area is comprised of a wide coastal agricultural land with hills with moderate slopes in the northeast. Groundwater sampling was conducted in May 2009 and October 2010. Groundwater in the study area usually contains high concentrations of V with an average of 12.2 μg/L (max. 28.8 μg/L). Except for two samples that were influenced by seawater intrusion, as indicated by higher concentrations of Cl, Mg and SO_4 and elevated $\delta^{34}S$ values (14.5~18.9 ‰), groundwater in the study area is clustered into two major hydrochemical types: 1) a Mg-Cl-NO_3 type and 2) a Na-HCO_3 type. The latter type is characterized by higher pH values (8.2~8.9, avg 8.6), compared to water type 1 (pH: 6.9~8.3, avg 7.3). The concentrations of V are strongly correlated with pH (γ^2 = 0.89) and are higher in the Na-HCO_3 type water. In addition, positive correlations were observed between pH and Cl-normalized concentrations of Na (γ^2 = 0.79), K (γ^2 = 0.49), and HCO_3 (γ^2 = 0.64). These observations indicate that water-rock interactions during southwestward regional groundwater flow in the basaltic aquifer largely control the observed hydrochemical changes and increasing V concentrations. However, V concentrations also tend to decrease in samples with higher concentrations of NO_3 characteristic for Mg-Cl-NO_3 type waters. Examination of relationships between concentrations and $\delta^{15}N$ and $\delta^{18}O$ values of nitrate in the study area revealed that nitrate is mainly derived from synthetic fertilizers (~3 to 4 ‰ $\delta^{15}N_{NO3}$) applied to agricultural fields. During infiltration of rainwater into the aquifer, agricultural nitrate is locally attenuated by partial denitrification to low nitrate levels (~8 ‰ $\delta^{15}N_{NO3}$). These observations suggest that there are two major paths of groundwater recharge in the study area: 1) regional flow accompanying water-rock interactions with V leaching from basalts, and 2) local flow dominated by direct infiltration of rainwater through agricultural land, accompanyed by nitrate loading. We suggest that V concentrations of groundwater will decrease with increasing nitrate concentrations at times of increased local recharge.

https://doi.org/10.1180/S0026461X00008434 Published online by Cambridge University Press

Fate of Metallic Silver Nanoparticles in a Sewer System

RALF KAEGI[1*], ANDREAS VOEGELIN[1], BRIAN SINNET[1], HARALD HAGENDORFER[2] AND CHRISTOPH ORT[1]

[1]Eawag: Swiss Federal Institute of Aquatic Science and Technology, Dübendorf, Switzerland, ralf.kaegi@eawag.ch (* presenting author)

[2]Empa: Swiss Federal Institute of Materials Science and Technology, Dübendorf, Switzerland, harald.hagendorfer@empa.ch

The biocidal properties of Ag^+ ions have led to the incorporation of metallic Ag nanoparticles (Ag-NP) in a wide range of industrial and commercial products. Therefore, the emission of Ag-NP to the aquatic environment seems inevitable, most likely occuring via urban water systems. However, the understanding of the transport behavior of Ag-NP in urban water systems is still incomplete. It has been shown that Ag-NP are readily transformed to Ag_2S during wastewater treatment [1] and based on laboartory studies, Liu et al. [2] speculated that the transformation might already occur in the sewer system. To assess whether Ag-NP sorb to and are retained by the sewer biofilm and to investigate the physical-chemical changes during the transport in a sewer line, we conducted experiments in a 5-km sewer stretch (no exfiltration, no confluents).

The wastewater flow rate for our experiment was adjusted to 30 l/sec. Over 30 seconds, we spiked 1g of Ag-NP (15 nm diamter) to the wastewater. Subsequntly, wastewater samples were collected at three locations 500 m, 2.4 km, and 5 km downstream. The transit times for unretarded Ag-NP at the respective locations were derived from tracer experiments and equalled 10 min, 60 min, and 120 min, respectively. Around these times, forty wastewater samples were collected at each location and immediately acidified for analysis of total Ag contents. Additional samples were prepared for transmission electron microscopy (TEM) and X-ray absorption spectroscopy (XAS) to assess changes in Ag-NP aggregation state and speciation along the sewer stretch.

Between 95 and 105% of the spiked Ag were recovered at all sampling stations, indicating that Ag retention by the sewer biofilm was negligible, which was also confirmed by Ag contents in the biofilm before and after the experiment. TEM revealed that the Ag-NP did not aggregate amongst themselves but were dominately attached to other colloids. Energy dispersive X-ray analysis indicated that the Ag-NP were partially transformed into Ag_2S already after 500 m (10 min), consistent with high acid-volatile sulfide levels of 0.15mM in the raw wastewater. The quantitative Ag speciation will be determined in XAS measurements scheduled for March 2012.

[1] Kaegi, R. *et al.* (2011) *Environ. Sci. & Tech.,* **45(9)**, 3902–3908.
[2] Liu, J. *et al.* (2011) *Environ. Sci. & Tech.,* **45(17)**, 7345–7353.

Zinc isotope fractionation during metabolic uptake by bacteria

FOTIOS-CHRISTOS KAFANTARIS[1*] AND DAVID M. BORROK[1]

[1]University of Texas at El Paso, El Paso, Texas, USA., fkafantaris@miners.utep.edu (* presenting author), dborrok@utep.edu

Zinc is a trace metal responsible for the normal operation of living organisms but can be toxic at elevated concentrations. The biogeochemical processing of Zn in microorganisms may be reflected in changes in the ratios of stable Zn isotopes. If so, the isotopic signatures of Zn might be used as a tool to learn more about cellular metal processing and toxicity. Despite pioneering work on how Zn isotopes are fractionated during interaction with diatoms and plants, Zn isotopes in bacterial systems remain largely unexplored.

In this study, we conducted a series of metabolic uptake experiments with bacteria using different concentrations of Zn-citrate. Experiments were conducted using the Gram-negative bacteria, *Pseudomonas mendocina* and *Escherichia Coli*, as well as with a natural consortium of desert soil bacteria. Each experimental system was sampled as a function of time/cell growth and the elemental and isotopic compositions of Zn were determined for both the bacterial cells and the solution.

When exposed to 2 ppm of Zn, the growth curves for both *E. coli* and the natural consortium were similar in that the stationary phase occurred 8 days after inoculation. The stationary phase for *P. mendocina* occurred at 6 days after inoculation. However, when *P. mendocina* cells were exposed to 20 ppm of Zn, there was a time lag and the populations reached stationary phase 9 days after inoculation. Cell counts also suggested that fewer bacteria grew under the elevated Zn concentrations. In the 2 ppm experiments, *E. coli, P. mendocina* and the natural consortium incorporated a maximum of 17, 16 and 29 ppm of Zn, respectively. In contrast, when exposed to 20 ppm of Zn in the growth solution, *P. mendocina* incorporated 509 ppm of Zn. Zn isotopes, reported as $\Delta^{66}Zn_{bacteria\text{-}solution}$, for the 2 ppm Zn experiments varied as a function of the growth phase. A separation factor of +0.22‰ was measured for the log phase of *E. coli*, but this decreased to slightly negative values during the death phase. In contrast, *P. mendocina* showed the most negative $\Delta^{66}Zn_{bacteria\text{-}solution}$ during the log phase of its growth (-0.4‰). When *P. mendocina* cells were exposed to 20 ppm of Zn, the $\Delta^{66}Zn_{bacteria\text{-}solution}$ was positive, ranging from +1.02 to +1.5‰. The largest values were again found in the log phase of growth. The natural bacterial consortium did not substantially fractionate Zn isotopes ($\Delta^{66}Zn_{bacteria\text{-}solution}$ = -0.04 to +0.05‰) when exposed to 2 ppm of Zn.

Despite some broad similarities, our experiments demonstrate that the bacterial species, growth phase, and the dosage of Zn all impact the Zn isotopic composition of bacteria. This may suggest that Zn isotopes could be used as a chemical tool for understanding Zn homeostasis within cells. The observation of a dose-dependent fractionation further suggests that Zn isotopes might serve as a tool for understanding toxicological impacts on these microorganisms. However, because of these same complexities, the use of Zn isotopes as a possible biological marker in natural systems deserves further scrutiny.

https://doi.org/10.1180/S0026461X00008434 Published online by Cambridge University Press

Estimation of S, F, Br and Cl Fluxes at Mid Ocean Ridges

T. KAGOSHIMA[1*], Y. SANO[1], N. TAKAHATA[1], J. JUNG[1], H. AMAKAWA[2], AND H. KUMAGAI[3]

[1]Atmosphere and Ocean Research Institute, the University of Tokyo, Chiba, Japan (*correspondence: kagoshima@aori.u-tokyo.ac.jp)
[2]National Taiwan University, Department of Geoscience, Taipei, Taiwan
[3]JAMSTEC, Kanagawa, Japan

Introduction

It is known that superficial volatile elements of the Earth have been accumulated mainly by degassing from the solid Earth. Studies that used noble gases as tracers have been conducted to investigate the degassing history of the Earth, which suggests that the significant degassing occurred in the early Earth [1, 2]. Carbon and nitrogen fluxes were well documented in literatures, and they provided other constraints on the hypothesis of degassing history [3, 4]. It is important to study the degassing history of the Earth from the mantle based on the other volatile elements, thus we measured sulfur (S), fluorine (F), bromine (Br) and chlorine (Cl) concentrations trapped in vesicles in mid-ocean ridge basalts (MORBs) and back-arc basin basalts (BABBs) and compared them with helium-3 (^{3}He) concentrations to estimate their fluxes from the mantle.

Analysis

Approximately 1 g of fresh glassy aliquots were picked up from MORB and BABB glasses and were put in a stainless-steel crusher with 1-2 cm^3 of distilled aqueous sodium hydroxide (1-4 mol/L) and a stainless-steel ball. The alkali solution was frozen at the temperature of liquid nitrogen (77K). When the crusher was shaken up and down, the glassy aliquots were crushed together with the frozen solution by the stainless-steel ball. Highly reactive elements including S, F, Br and Cl were extracted from vesicles of glasses by mechanical fracturing and immediately dissolved into a small portion of melted alkali solution. While helium (He), not dissolved into the solution, was introduced into a vacuum line and purified, then helium-4 (^{4}He) intensity and ^{3}He/^{4}He ratio were measured by a VG5400 mass spectrometer. S, F, Br and Cl concentrations in the alkali solution were measured by ion chromatography (Dionex-320).

Results and Discussion

Concentrations of volatile elements trapped in vesicles were (4 – 31) × 10^{-15} mol/g for ^{3}He, (20 – 430) × 10^{-9} mol/g for S, (60 – 5000) × 10^{-9} mol/g for F, (5 – 1300) × 10^{-9} mol/g for Br and (160 – 450) × 10^{-9} mol/g for Cl. Under an assumption that the samples in this study represent typical MORBs, global fluxes of S, F, Br and Cl were estimated using mole ratios X/^{3}He of the samples and the ^{3}He flux of 1060 mol/yr from the mantle [5]. These estimated fluxes from mid ocean ridges will be discussed in comparison with those from volcanic arcs.

References

[1] Ozima (1975) *GCA* **39**, 1127-1134. [2] Graham (2002) *Rev. Min. Geochem.* **47**, 247–317. [3] Marty and Jambon (1987) *EPSL* **83**, 16-26. [4] Sano et al., (2001) *Chem. Geol.* **171**, 263–271. [5] Lupton and Craig (1975) *EPSL* **26**, 133-139

Magnetism of Individual Magnetosomes in Magnetotactic Bacteria

SAMANBIR S. KALIRAI[1*], KAREN P. LAM[1], DENNIS A. BAZYLINSKI[2], ULYSSES LINS[3], ADAM P. HITCHCOCK[1]

[1]McMaster University, Chemistry and Chemical Biology, kaliras@mcmaster.ca (* presenting author)
[2]University of Nevada, Las Vegas, Life Sciences
[3]Universidade Federal do Rio de Janeiro, Microbiologia Geral

Magnetotactic bacteria (MTB) synthesize chains of intracellular, membrane-bound, single crystals of magnetite or greigite in the 30-80 nm size range, an exquisite example of biomineralization. We used Scanning Transmission X-ray Microscopy as a chemically and magnetically sensitive probe to investigate the magnetism of individual magnetosomes and thereby study the mechanism of magnetosome biomineralization. The Fe $L_{2,3}$ X-ray magnetic circular dichroism (XMCD) of cultured cells of *Candidatus* Magnetovibrio blakemorei (MV-1) has the same shape and intensity as abiotic magnetite indicating that the magnetic moment of the magnetosomes is nearly saturated (Fig. 1) [1,2].

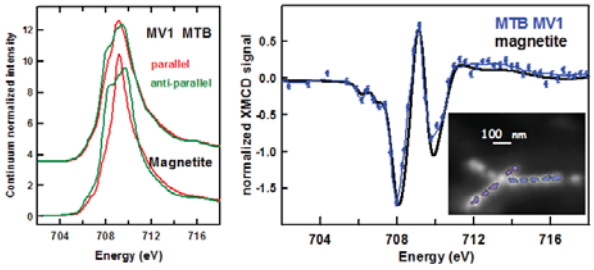

Figure 1: (Left) Fe L_3 and **(Right)** Average XMCD spectrum of magnetosome chains (dots) from two magnetosome chains (see inset) compared to the XMCD of magnetically saturated abiotic magnetic (black). The average magnetosome magnetic moment is 3.6(2) μB [2], 0.93(6) of that of magnetite [3].

Many cells of MV-1 show characteristic gaps between magnetosome chains that occasionally yield intracellular chain orientation reversals. In these gaps there is a reasonably strong Fe L_3 signal very similar to that of magnetite, but without XMCD. These are possibly the result of incomplete or defective magnetite biomineralization and thus may provide insights into the mechanism of chain formation and alignment as well as biogeochemical factors affecting magnetosome chain growth. We will report our recent XMCD-STXM findings of this phenomena and the implications with respect to the mechanism of chain formation.

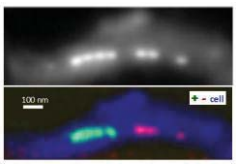

Figure 2 (Upper) Average of all Fe L_3 images of a single MV-1 cell. **(Lower)** Composite of parallel (green) and antiparallel (red) XMCD and the pre-Fe L_3 signal outlining the cell (blue)

[1] Lam et al. (2010) *Chem. Geol.* **270** 110-116. [2] Kalirai et al. (2012) *Chem. Geol.* in press. [3] Goering et al. (2007) *J. Magn. Magn. Mater.* **310**, e249–e251. [4] Research supported by NSERC, Canada Research Chair, CFI. Work performed at the Canadian Light Source, supported by CFI, NSERC, CIHR and U. Saskatchewan.

https://doi.org/10.1180/S0026461X00008434 Published online by Cambridge University Press

The Meso- and early Neoproterozoic deep ocean REE issue

BALZ S. KAMBER[1*], ELIZABETH C. TURNER[2], SEAN P. O'HARE[2], GEOFFREY J. BALDWIN[2] AND KATHERINE HAHN[2]

[1]Trinity College Dublin, Department of Geology, Dublin, Ireland, kamberbs@tcd.ie (* presenting author)

[2]Laurentian University, Department of Earth Sciences, Sudbury, ON, Canada, eturner@laurentian.ca, sp_ohare@ laurentian.ca, gj_baldwin@laurentian.ca, kx_hahn@laurentian.ca

The sulphidic deep ocean model for the post-1.85 Ga Proterozoic elegantly combines several lines of evidence and reasoning, including: release of sulphate from land into the ocean; the increase in extent of S-isotope fractionation; the lack of significant Mo enrichment in black shales; and the absence of BIF. However, sediment redox proxies for the latest Neoproterozoic have more recently suggested that the deep ocean might have reverted from a sulphidic to a ferruginous state many 10 Ma before the Sturtian BIF deposition. In addition, little direct sedimentological or other geological evidence exists for the proposed sulphidic nature of Proterozoic deep ocean sedimentary rocks.

The present work aims to add to this debate from a rare earth element (REE) perspective. Archaean and Palaeoproterozoic hydrogenous sediments show very pronounced positive Eu anomalies. This well-established aspect of the seawater REE chemistry reflects the fact that the REE from high temperature hydrothermal fluids were not scavenged onto Fe-oxyhydroxides. In other words, hydrothermal vents were a significant source of dissolved REE to the ocean. By contrast, Phanerozoic seawater proxies consistently have either no or a slight negative Eu anomaly. The expectation from these observations for a sulphidic deep ocean, in which hydrothermal Fe combined with S (from sulphate) to form pyrite, is that the positive Eu anomly would persist. Pyrite cannot accommodate Eu in its lattice and the post-1.85 Ga deep ocean could thus be expected to still carry a strong Eu excess.

New data from the ≤711 Ma Rapitan Gp., the 845 Ma Little Dal Gp. and the 1040 Ma Arctic Bay Fm. (all Canada) will be presented. The deeper waters sampled by the Rapitan BIF show neither a negative Ce anomaly nor a positive Eu anomaly and are therefore consistent with a ventilated deep ocean. The carbonate facies of the Little Dal Gp. and the ca. 1040 Ma Arctic Bay Fm. sampled surface waters that were sufficiently oxygenated to generate a negative Ce anomaly. Corresponding black shales and deep water laminites, respectively, were deposited below a chemocline where Ce was re-released from particles. However, none of the deep water samples shows have a significant positive Eu anomaly. This observation is confimed by reactive Fe speciation in the Little Dal black shale, which rarely record sulphidic conditions. While supportive of a reduced deep ocean, these data cannot be explained if all hydrothermal Fe was sequestered as sulphide.

In summary, the redox evolution during the Neoproterozoic was likley very complex and may have involved a ventilated stage as well as ferruginous and sulphidic episodes. The lack of a strong positive Eu anomaly in Mesosproterozoic and early Neoproterozoic deep waters requires a more complex deep ocean redox in general, likley to have been influenced by the relative supply of Fe, S and C.

Application of PTR-MS to an incubation experiment of the marine diatom *Thalassiosira pseudonana*

SOHIKO KAMEYAMA[1*], HIROSHI TANIMOTO[2], SATOSHI INOMATA[3], KOJI SUZUKI[4], DAISUKE D. KOMATSU[5], AKINARI HIROTA[6], UTA KONNNO[7] AND URUMU TSUNOGAI[8]

[1]National Institute for Environmental Studies, Tsukuba, Japan, now at Hokkaido University, Sapporo, Japan, skameyama@ees.hokudai.ac.jp

[2]National Institute for Environmental Studies, Tsukuba, Japan, tanimoto@nies.go.jp

[3]National Institute for Environmental Studies, Tsukuba, Japan, ino@nies.go.jp

[4]Hokkaido University, Sapporo, Japan, kojis@ees.hokudai.ac.jp

[5]Hokkaido University, Sapporo, Japan, now at Nagoya University, Nagoya, Japan, damboo@mail.sci.hokudai.ac.jp

[6]Hokkaido University, Sapporo, Japan, now at National Institute of Advanced Industrial Science and Technology, Tsukuba, Japan, aki-hirota@aist.go.jp

[7]Hokkaido University, Sapporo, Japan, not at National Institute of Advanced Industrial Science and Technology, Tsukuba, Japan, yu-konno@aist.go.jp

[8]Hokkaido University, Sapporo, Japan, now at Nagoya University, Nagoya, Japan, urumu@mail.sci.hokudai.ac.jp

Emission of trace gases from the marine diatom *Thalassiosira pseudonana* (CCMP1335) was continuously monitored with a proton transfer reaction-mass spectrometry (PTR-MS) in an axenic batch culture system under a 13:11-h light:dark cycle. Substantial increases in the signals at *m*/*z* 49, 63, and 69, attributable to methanethiol, dimethyl sulfide (DMS), and isoprene, respectively, were observed in response to increases in cell density. Signals at *m*/*z* 69 showed diurnal variations throughout the experiment whereas those at *m*/*z* 49 were more pronounced at the beginning of the incubation. Interestingly, the signals at *m*/*z* 49 and 69 changed immediately following the light-dark and dark-light transitions, suggesting that light plays a crucial role in the production of methanethiol and isoprene. However, in the latter half of the experiment, methanethiol showed negligible diurnal variations regardless of light conditions, suggesting the production of methanethiol from enzymatic cleavage of DMS. The trend in signals at *m*/*z* 63 was similar to that of the abundance of senescent cells plus cell debris rather than vegetative cells. The results suggest that aging or death of phytoplankton cells could also substantially control DMS production in natural waters along with the other microbial processes related to bacteria and zooplankton.

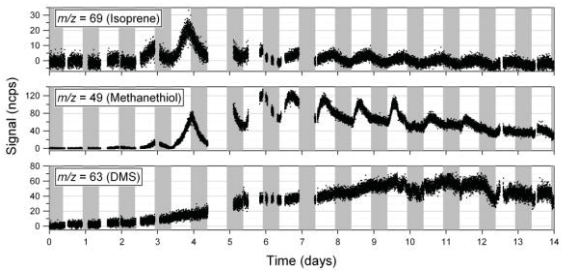

Figure: Time series of PTR-MS signals at *m*/*z* 69, 49, and 63

https://doi.org/10.1180/S0026461X00008434 Published online by Cambridge University Press

Sulfur isotope systematics of sulfide oxidation intermediates: implications for organic geochemistry

A. KAMYSHNY, JR.[1]

[1]Geological and Environmental Sciences, Ben-Gurion University of the Negev, Beer Sheva, Israel, alexey93@gmail.com

Bacterial sulfate reduction in natural anoxic aqautic systems produces hydrogen sulfide. Chemical and biological oxidation of sulfide results in formation of sulfate as well as variety of intermediate species, such as polysulfides (S_n^{2-}), elemental sulfur (S_8), thiosulfate ($S_2O_3^{2-}$), sulfite (SO_3^{2-}) and polythionates ($S_nO_6^{2-}$). Many of sulfide oxidation intremediates are highly reactive toward other inorganic and organic species. Such reactions result in formation of secondary products including dimethylpolysulfanes, carbonyl sulfide, and sulfur cross-linked oganic macromolecules [1-3]. Sulfurization of organic matter during early diagenesis occurs due to reactions of organic molecules with polysulfides and possibly with other sulfide oxidation intremediates (e.g. thiosulfate, sulfite) [4,5].

Bacterial sulfate reduction and bacterial sulfur disproportionation are known to result in relatively high sulfur isotope fractionation. On the other hand, processes involved in reoxidative part of sulfur cycle produce only small sulfur isotope fractionations. For example, $\delta^{34}S$ values of fractionation between H_2S and HS^- were reported to be up to 2.7‰ [6], between sulfur and hydrogen sulfide (by anaerobic bicterial sulfide oxidation) – 2‰ [7], between HS^- and inorganic polyuslfides (S_n^{2-}) – up to 4‰ [8], and between thiosulfate and sulfide during bacterial reduction of thiosulafte – 10‰ [9].

A new powerful tool, sumultaneous mesurement of abundances of all four stable isotopes of sulfur, was recently applied for studying reoxidative part of biogeochemical sulfur cycle [10-12]. First miultiple sulfur isotope fractionation fingerprints look promising for future decoupling of various pathways of sulfide reoxidation in natural aquatic systems.

Future application of multiple sulfur isotope approach to formation of sulfide oxidation intermediates as well as to reacions between sulfide oxidation intermedates and organic molecules have a potential to shed a light on mechanisms of diagenetic sulfurization of organic matter as well as on oil formation scenarios.

[1] Ginzburg *et al.* (1999) *Environmental Science & Technology* **33**, 571-579. [2] Kamyshny *et al.* (2003) *Environmental Science & Technology* **37**, 1865-1872. [3] Amrani *et al.* (2007) *Geochimica et Cosmochimica Acta* **71**, 4141-4160. [4] Amrani and Aizenshtat (2004) *Organic Geochemistry* **35**, 1319-1336. [5] Werne *et al.* (2003) *Chemical Geology* **195**, 159-179. [6] Fry *et al.* (1986) *Chemical Geology* **58**, 253-258. [7] Fry *et al.* (1986) *Journal of Bacteriology* **165**, 328-330. [8] Amrani *et al.* (2006) *Inorganic Chemistry* **45**, 1427-1429. [9] Smock *et al.* (1998) *Archives of Microbiology* **169**, 460-463. [10] Zerkle *et al.* (2009) *Geochimica et Cosmochimica Acta* **73**, 291-306. [11] Zerkle *et al.* (2010) *Geochimica et Cosmochimica Acta* **74**, 4953-4970. [12] Kamyshny *et al.* (2011) *Marine Chemistry* **127**, 144-154.

Biomineralization of Mg-rich calcite by aerobic microorganism enriched from rhodoliths

SERKU KANG[1, *], SUNGJUN YOON[2], AND YUL ROH[3]

Chonnam National University, Gwangju, Korea, rohy@jnu.ac.kr

Introduction

The formation of carbonate minerals by biological processes may play an important role in carbon and metal geochemistry in natural environments. The objectives of this study were to investigate biomineralization of the carbonate minerals using microorganisms enriched from rhodoliths and to identify environmental factors that control the formation of calcite by the microorganisms.

Materials and Methods

Carbonate forming microorganisms were enriched from rhodoliths, which were sampled at Seogwang-ri coast in the western part of Wu Island, Jeju-do, Korea. Microorganisms enriched from rhodoliths were aerobically cultured at 25℃ in D-1 media containing various concentrations (0, 30, 100 mM) of Ca and Mg-acetate, and the microorganisms were analyzed by 16S rRNA gene DGGE analysis to confirm microbial diversity. Mineralogical characteristics of the rhodoliths and carbonate minerals preciptated by the enriched microrganisms were determined by XRF, XRD, and SEM-EDS analyses.

Results and Conclusion

XRF and XRD analyses showed the rhodoliths mainly consisted of CaO (46%) and and MgO (5%) and major mineral is Mg-rich calcite. A 16S rRNA sequence analysis showed the enriched microorganisms contained carbonate forming microorganisms such as *proteus micrailis* and *marinobacterium coralli* [1, 2]. The enriched microorganisms precipitated carbonate minerals using D-1 media containing Ca and Mg-acetate (30, 100 mM) and mineralogy of the precipitated carbonate mineral was Mg-rich calcite. Whereas, the microorganisms did not form carbonate minerals without Ca and Mg-acetate in D-1 media. SEM-EDS analyses showed that the Mg-rich calcite formed by the microorganisms had a rhombohedron shape and consisted of Ca, Si and Mg with extracelluar polymeric subtance (EPS). These results indicate that the microorganisms induce precipitation of Mg-rich calcite on the cell walls and EPS via the accumulation of Ca and/or Mg ions on the cells. Therefore, microbial precipitation of carbonate minerals may play one of important roles in metal and carbon biogeochemistry as well as carbon sequestration in natural environments.

[1] Xi *et al.* (2002) *Infect. Immun.***70(1),** 389-394.
[2] Chimetto *et al.* (2011) *Int J. Syst. Evol. Microbiol.* **60(1)**, 60-64.

https://doi.org/10.1180/S0026461X00008434 Published online by Cambridge University Press

Effect of Oxalic Acid on Geological Storage of CO_2 Using Serpentinite

SEUNG-HEE KANG[1*], NATALIE C. JOHNSON[2], BURT THOMAS[3], KATE MAHER[1], DENNIS K. BIRD[1], ROBERT J. ROSENBAUER[3], AND GORDON E. BROWN, JR.[1]

[1]Stanford University, Geological & Environmental Sciences, envlover@stanford.edu (*presenting author)
[2]Stanford University, Chemical Engineering, nataliej@stanford.edu
[3]United States Geological Survey, burt.thomas@gmail.com

Mineral carbonation of Mg-silicates ensures stable CO_2 storage over geologic time periods. This reaction takes place in natural systems but is kinetically slow [1]. In order to make mineral carbonation an efficient means of sequestering CO_2, we have investigated the effect of oxalic acid in enhancing the kinetics of the serpentinite-CO_2-H_2O reaction.

Serpentinite used in this study was obtained from the New Idria, California serpentinite massif and consists primarily of antigorite. For faster reaction, the rock was ground and sieved, and the 60 to150 μm size range was separated. After washing with methanol five times, the serpentinite was characterized by XRD, XPS, SEM-EDX, and XRF.

Our experiments were conducted under 100 bars CO_2 at 60˚C in 0.5M NaCl solution for one month with a water-to-rock mass ratio of 20:1. A Dickson-type rocker bomb reactor used for these experiments is able to maintain constant pressure and temperature while samples are withdrawn at regular intervals. Thorough mixing was achieved by rocking the reactor.

Magnesite and siderite were generated within 25 days, as revealed by XRD and SEM/EDX analyses. SEM and EDX analysis showed widely dispersed magnesite on the edges of serpentinite grains. Siderite, although less abundant than magnesite, showed more euhedral shapes. The overall carbonation reaction was enhanced in the presence of oxalic acid.

Solution pH was calculated from alkalinity and was found to increase from 3.0 to 5.3 within two days as H^+ was consumed during Mg^{2+} dissolution from serpentine. The serpentinite surface was positively charged under all experimental pH conditions as revealed by zeta potential measurements, suggesting that oxalate anions are likely to be electrostatically attracted to the particle surfaces. Therefore oxalate is predicted to form Mg- and Fe-complexes, which should enhance dissolution. The amounts of Mg, Ca, Fe, and Si released during dissolution were quantified using ICP-OES and indicate initial incongruent dissolution (excess concentrations of Mg, Ca, and Fe, relative to Si). The Mg and Fe concentrations along with pH changes in this experiment indicated favorable conditions for magnesite and siderite formation.Although Krevor and Lackner discussed enhanced serpentine dissolution in the presence of oxalate for CO_2-H_2O-serpentine reaction [2], the present study presents new data on both Mg dissolution and magnesite formation, which will be presented.

[1] P. B. Kelemen and J. M. Matter, *In situ* carbonation of peridotite for CO_2 storage. *PNAS* **105** (2008) 17295-17300.
[2] S. C. Krevor and K. S. Lackner, Enhancing process kinetics for mineral carbon sequestration. *Energy Procedia* **1** (2009) 4867-4871.

The Volcanic Rocks of Bima Formation, Sangri Group in Gangdese Belt: Products of Intra-Oceanic Subduction

ZHI-QIANG KANG[1]*, JI-FENG XU[2], DI-CHENG ZHU[3], JIN-LIN CHEN[3], ZUO-HAI FENG[1], XI-JUN LIU[1], BING-KUI MIAO[1], BAO-CHENG PANG[1], WEI FU[1], QING-WEI ZHANG[1]

[1]College of Earth Sciences/Guangxi Key Laboratory of Hidden Metallic Ore Deposits Exploration,Guilin University of Technology,Guilin 541004, China, zk99201@163.com (* presenting author)
[2] State Key Laboratory of Isotope Geochemistry, GIG, CAS, China
[3] School of Earth Sciences and Resources, CUGB, Beijing, China

The Sangri group volcanic rocks lie in Middle-Eastern part of south edge of Gangdese belt, thought to be the production of Neo-Tethys' northward subduction. However, its geochronology, feature and tectonic setting remains a debate. The previous researches mainly focus on the underlying Mamuxia formation, which originated from the melting of subducted oceanic crust[1,2]. But so far, there is not any study about the overlying Bima formation, so in this study, we focus on the Bima formation and acid intrusions in Sangri group, in order to understand its petrogenesis, tectonic setting and constrain the age and evolution of the whole Sangri arc. The two conclusions as following:

1.We selected zircons from the acid intrusion to do LA-ICPMS U-Pb dating, obtaining an age of 93.4±1.1Ma, which can constrain the upper limit of Sangri group's age. Combining our new data with previously zircon SHRIMP U-Pb age of andesite from the underlying Mamuxia formation by Zhu[2], we firstly obtain the activity time of Sangri group, from 136.5Ma to 93.4Ma.

2. Bima formation mainly consists of basalt, basalt-andesite and andesite. We chose the most mafic rocks to discuss magmatic origin and tectonic setting.These rocks are tholeiite basalt, with high Al_2O_3 (average 17.72wt%), MgO (average 7.82wt%), $Mg^{\#}$ (average 65.52), Cr (215ppm) and Ni (140ppm), hinting that the magma did not undergo significant differentiation. In the spider diagram its geochemical characteristics are similar with those of island arc volcanic rocks, e.g., the enrichment of LILE and depletion of HFSE. However, the basalts have very low K_2O（average: 0.13wt%）、Th（average: 0.8ppm）and flat REE pattern（La_N/Sm_N=1.37; La_N/Yb_N=2.12), the initial Sr^{87}/Sr^{86} ratios vary in range of 0.703965~0.704316, while Nd^{143}/Nd^{144} ratios are from 0.512895 to 0.512944 with high εNd (5.78~6.30), all these characteristics indicate that the basalts were likely generated from partial melting of the depleted mantle wedge without remarkable crustal and sediment influence. So we suggest that Bima formation volcanic rocks are not from the northward subduction of Neo-Tethy along the southern margin of Gangdese belt but products of an intra-oceanic subduction system.

[1] Yao P et al., 2006, *Acta Petrologica Sinica,* 22(3): 612-620
[2] Zhu DC et al., 2009,*Journal of Asian Earth Sciences,* 34: 298-309

This study was supported by the Chinese National Natural Science Foundation Grant(No.41003018)

https://doi.org/10.1180/S0026461X00008434 Published online by Cambridge University Press

The Phanerozoic minimum in seawater $^{87}Sr/^{86}Sr$: Middle Permian mid-Panthalassan seamount record

TOMOMI KANI[1*], CHIHIRO HISANABE[1], AND YUKIO ISOZAKI[2]

[1]Kumamoto University, Kumamoto, Japan
kani@sci.kumamoto-u.ac.jp (* presenting author)
[2]The Univerisity of Tokyo, Meguro, Japan
isozaki@ea.c.u-tokyo.ac.jp

We report a detail secular change of the Late Guadalupian (Permian) seawater $^{87}Sr/^{86}Sr$ ratio with the unique "Permian minimum" interval detected in mid-Panthalassa (superocean) paleo-atoll carbonates. The analyzed two sections at Akasaka and Kamura (Japan) occur as exotic blocks within the Jurassic accretionary complex. The two sections are separated from each other for 500 km at present, thus were likely derived from different paleo-seamounts formed in mid-Panthalassa. The detected intervals of the minimum and the following increase in $^{87}Sr/^{86}Sr$ are common between the two sections. The new data of the lowest ratio (0.706808) in the Capitanian *Yabeina* (fusuline) Zone at Akasaka give the minimum $^{87}Sr/^{86}Sr$ ratio not only of the Paleozoic but also of the entire Phanerozoic. The extremely low values lower than 0.70690 were detected from 18 samples in the *Yabeina* Zone and the barren interval. In particular, the extremely low values continued up to the topmost barren interval immediately below the Guadalupian-Lopingian (G-L) boundary.

The newly detected Sr record likely represents the general trend of the Guadalupian seawater in mid-Panthalassa. The rapid increase during the Late Permian-Early Triassic interval suggests that a large amount of radiogenic terrigenous clastics have been shed into Panthalassa through rift-related new drainage systems in Pangea [1]. The initial breakup of Pangea may have started around the G-L boundary, clearly before the final opening of the Atlantic in the Jurassic [2].

[1] Kani *et al.* (2008) *J. Asian Earth Sci.* **32**, 22-33.
[2] Isozaki (2009) *J. Asian Earth Sci.* **36**, 459-480.

Effect of fluid flow rate on Fe^{3+}/Fe^{2+} ratios of Paleoproterozoic paleosols and its implication for atmospheric oxygen levels

YOSHIKI KANZAKI* AND TAKASHI MURAKAMI

Department of Earth and Planetary Science, the University of Tokyo, Tokyo 113-0033, Japan
(*Correspondence: kanzaki@eps.s.u-tokyo.ac.jp)

The Great Oxidation Event (2.5 – 2.0 Ga) is one of the most important events in the Earth's history because of its coevolution with organisms and redox surface-environments. Compiled geological records constrain the timing of the oxygen rise and the threshold levels of oxygen concentration, but few investigations have not shown quantitative estimation of oxygen variation as a function of age during the Paleoproterozoic. As demonstrated by Murakami et al. (2011) [1], paleosols allow us to challange such estimation. The recorded behavior of Fe(II) and Fe(III) in paleosols can lead us to understand redox conditions of the Earth's surface at the time of ancient weathering. To properly interpret the behavior of Fe, one must consider: (1) dissolution from primary minerals, (2) oxidation of Fe(II) into Fe(III) (which immediately precipitates as (oxyhydr)oxides), and (3) transport of dissolved Fe(II) outside the weathering profile by fluid (groundwater). The weathering model that considers these factors can calculate Fe(III)/Fe(II) ratios for a given oxygen level, and therefore, predict inversely the P_{O_2} levels from the recorded Fe(III)/Fe(II) ratios in paleosols [2].

The sensitivity analysis of the weathering model revealed that the relationships between Fe(III)/Fe(II) ratios and oxygen levels vary with fluid flow rate. This causes large uncertainty in the predicted levels of P_{O_2}. To properly predict the P_{O_2} levels, the fluid flow rates must be constrained.

The estimation of fluid flow rates for five Paleoproterozoic paleosols has been made based on Si behavior during weathering; loss of Si in each paleosol (mol km^{-2}) against Si in corresponding parent rock was used for the estimation. Using the calculated amounts of Si loss from the paleosols and assuming 50 kyr – 5 myr of weathering duration, the relationships between silica flux (mol km^{-2} yr^{-1}) and runoff (cm yr^{-1}) for basalt and granite [3] gave estimated values of fluid flow rate ranging from 8×10^{-3} to 46 m yr^{-1}. These estimates match well with those calculated based on the mass balance principal of Si between water and rock assuming steady state concentrations of dissolved silica as 10^{-4} – 10^{-3} mol L^{-1}, average porosity of a whole weathering profile as 0.2 and weathering duration as 50 kyr – 5 myr.

The weathering model adopting an average value of the estimated fluid flow rates, that is ~ 0.1 m yr^{-1}, have calculated P_{O_2} levels from the Fe(III)/Fe(II) ratios of the five Paleoproterozoic paleosols. Although there remains an uncertainty about the fluid flow rate, the most likely results suggest a gradual rise of atmospheric oxygen, from < ~ 10^{-6} to > ~ 10^{-3} atm between 2.5 and 2.0 Ga.

[1] Murakami et al. (2011) *Geochim. Cosmochim. Acta* **75**, 3982-4004. [2] Murakami and Yokota (2008) *Geochim. Cosmochim. Acta* **72**, Suppl. 1, A665. [3] Bluth and Kump (1994) *Geochim. Cosmochim. Acta* **58**, 2341-2359.

https://doi.org/10.1180/S0026461X00008434 Published online by Cambridge University Press

Microbial Fe, Mn & As redox transformations and their contributions to As removal from drinking water in household sand filters in Vietnam

ANDREAS KAPPLER[1]*, KATJA NITZSCHE[1], ANKITA BHANSALI[1], MICHAEL BERG[2], PHAM THI KIM TRANG[3], PHAM HUNG VIET[3], SEBASTIAN BEHRENS[1]

[1]Geomicrobiology Group, University of Tuebingen, Germany, andreas.kappler@uni-tuebingen.de (*presenting author)

[2]Eawag, Swiss Federal Institute of Aquatic Science and Technology, Dübendorf, Switzerland

[3]Center for Environmental Technology and Sustainable Development (CETASD), Hanoi University of Science

Worldwide more than 100 million people ingest detrimental concentrations of arsenic by consuming groundwater contaminated from natural geogenic sources. Many Asian countries, in particular Vietnam, Bangladesh, India, and Cambodia are known to be affected by high groundwater arsenic concentrations as a result of reducing aquifer conditions [1]. Household sand filters are simple to operate and remove most of the arsenic from the groundwater containing arsenic and ferrous iron with an iron/arsenic ratio of at least 50 leading to As values of <50 or even <10 µg/L [2]. The installation and operation costs of household sand filters are low and the construction materials are locally available. The filters can treat a reasonable amount of groundwater within a short time and they are easily installed by the affected communities. Oxidation of dissolved iron present in the groundwater leads to the formation of sparsely soluble iron (oxyhydr)oxide particles in the sand filters, which bind negatively charged and neutral arsenic species and reduce arsenic concentrations in the water [2, 3].

Although household sand filters are an effective technical solution for mitigating arsenic exposure, not much is known about microbial iron, manganese, and arsenic redox transformations occurring in the filters and their effect on filter efficiency. Therefore, one of the goals of this study was to isolate, identify, and quantify Fe, Mn, and As-oxidizing and -reducing microorganisms from a arsenic removal sand filter and to study their specific Fe, Mn, and As redox activities. Water samples and filter solids were collected from a local sand filter close to the city of Hanoi, Vietnam. The samples were geochemically and mineralogically characterized. Total iron, arsenic, manganese, and phosphate concentrations, pH, TOC, TIC measurements, as well as total cell counts were performed on samples from various depths of the sand filter. Most probable number counts confirmed the presence and activity of various iron, manganese, arsenic redox-processes and their distribution within the water filter. This research aims to better understand the microbial redox transformation processes that drive arsenic/manganese/iron mineral interactions in household sand filters and to give recommendations for improved filter use and filter material disposal.

[1] Winkel *et al.* (2008) *Nature Geosci.* **1**, 536-542. [2] Berg *et al.* (2006) *Eviron. Sci. Technol.* **40**, 5567-5573. [3] Kleinert *et al.* (2011) *Eviron. Sci. Technol.* **45**, 7533-7541.

First principles study of the structure and compressibility of $MgSiO_3$ glass

DIPTA GHOSH[1], BIJAYA KARKI[1*] AND LARS STIXRUDE [2]

[1]Louisiana State University, Baton Rouge, USA, dghosh2@lsu.edu, karki@csc.lsu.edu (* presenting author)

[2]University College London, London, UK, l.stixrude@ucl.ac.uk

Silicate glasses have been widely studied because they are considered as analog of geologically relevant silicate melts. Experimental studies have suggested that silicate glasses undergo significant structural changes including irreversibility under compression. Here, we report first-principles molecular dynamics study of the equation of state and structure of $MgSiO_3$ glass at 300 K as a function of pressure. Our simulations show that the glass at ambient condition is composed of primarily Si-O tetrahedra (with ~95% abundance, the mean coordination number being ≥ 4), which are partially linked with each other via bridging oxygens (present in 35%, the remaining being non-bridging oxygens). As pressure increases, the mean Si-O coordination gradually increases to 6 occurring through the increased appearance of five-fold (pentahedral) states at low pressure and then six-fold (octahedral) states at high pressure. On the other hand, Mg-O coordination, which is a mixture of four-, five- and six-fold species at zero pressure, picks up more high-coordination (seven- to nine-fold) species on compression and its mean value increases from 4.5 to 8 over the pressure range studied. Consistently, the anion-cation coordination increases under pressure with the appearance of oxygen triclusters (O atoms coordinated with 3 Si or 3 Mg atoms) and the mean O-Si (O-Mg) coordination eventually reaching (exceeding) 2. We find that glass densification is rather rapid initially and becomes more gradual at pressures above 20 GPa. This behavior can be associated with the way the glass structure changes in terms of bond distances, bond angles and coordination environments as pressure increases. On decompression, the system fails to revert back to its initial structural state, consistent with the experimental observations, and this irreversibility can be attributed to the memory effects, i.e., to continuing existence of high coordination species (pentahedra and octahedra) to larger volumes.

https://doi.org/10.1180/S0026461X00008434 Published online by Cambridge University Press

Mechanisms of isotopic fractionation of Mo on ferromanganese oxides based on the systematics of its surface complex structures

TERUHIKO KASHIWABARA[1]* AND YOSHIO TAKAHASHI[2]

[1]Japan Agency for Marine-Earth Science and Technology (JAMSTEC), teruhiko-kashiwa@jamstec.go.jp*

[2]Hiroshima University, ytakaha@hiroshima-u.ac.jp

Molybdenum (Mo) shows a large mass-dependent isotopic fractionation during adsorption on ferromanganese oxides, which is responsible for isotopic composition of Mo in modern oxic seawater [1]. This fractionation process is the basis of the utility of Mo isotope system as a paleocean redox proxy. The aim of this study is to reveal the fractionation mechanisms of Mo isotopes during adsorption on natural ferromanganese oxides. We investigated surface complex structures of Mo on various Fe/Mn (oxyhydr)oxides, key factors for the isotopic fractionation, and discussed the relationship among the degree of isotopic fractionation, surface complex structures, and characteristics of various oxides.

Our XAFS analyses revealed that Mo forms a *Td* outer-sphere complex on ferrihydrite and distorted *Oh* inner-sphere complexes on δ-MnO_2 [2]. In addition, Mo forms inner-sphere complexes as *Td* edge-sharing (46%) and *Oh* double corner-sharing (54%) for goethite, and as *Td* double corner-sharing (14%) and *Oh* edge-sharing (86%) for hematite [3]. This structural information showed the excellent correlation with the degree of isotopic fractionation of Mo reported in previous studies: the proportion of *Oh* species in surface Mo species becomes larger in the order of ferrihydrite < goethite < hematite < δ-MnO_2, a trend identical to the degree of isotopic fractionation [4]. Based on the comparison with previous reports for surface Mo species on various oxides such as MgO, Al_2O_3, and TiO_2, the symmetry change from *Td* to *Oh* is suggested to be driven by the formation of inner-sphere complexes on specific sites of the oxide surfaces. In addition, the mode of attachment (inner- or outer-sphere) of surface Mo species is well correlated with the hydrolysis constant of the cation (e.g. Mg^{2+}, Al^{3+}, Fe^{3+}, Ti^{4+}, and Mn^{4+}) in oxides. These facts imply that large isotopic fractionation as the case of Mo between seawter and marine ferromanganese oxides could occur as a general phenomena for other unknown elements and/or adsorbents[5], which would considerably influence their isotope systems in the environment.

[1] Barling et al., (2001) *Earth Planet. Sci. Lett.*, **193**, 447-453.
[2] Kashiwabara et al., (2009) *Geochem. J.* **43**, e31-e36.
[3] Kashiwabara et al., (2011) *Geochim. Cosmochim. Acta.* **75**, 5762-5784.
[4] Goldberg et al., (2009) *Geochim. Cosmochim. Acta*, **73**, 6502-6516.
[5] Kashiwabara et al., (2010) *Chem. Lett.* **39**, 870-871.

Sr and Nd isotopes from Diorites and Granites (Damara Orogen, Namibia): Partial melting of juvenile mafic crust?

NICO KASTEK[1], STEFAN JUNG[1], JASPER BERNDT[2] AND ANDREAS STRACKE[2]

[1]Mineralogisch-Petrographisches Institut, Universität Hamburg Germany, nico_kk@web.de

[2]Institut für Mineralogie, Westfälische Wilhems-Universität, Münster, Germany

The high-grade central zone of the Pan-African Damara Orogen in Namibia hosts abundant granitoidswith ages from c. 540 to c. 480 Ma. New LA-ICP-MS zircon ages of 541±3 Ma obtained on qtz diorites show that these rocks intruded close to the first peak of regional metamorphism, whereas granodiorites and granites intruded close to the main peak of metamorphism (506±6 Ma). Qtz diorites are meta-aluminous with A.S.I (A.S.I.: Al/(Ca+Na+K)(molar)) up to 0.8. The granites are slightly peraluminous high-K calc-alkaline I-type granites. All rocks are enriched in light rare earth elements relative to heavy rare earth elements with La_N/Yb_N ranging from 13 to 18 in the qtz diorites and from 9 to 26 in the granodiorites and granites. The qtz diorites have Eu/Eu* (Eu/Eu*: Eu/√(Sm*Gd)) from 0.8 to 0.9 whereas the granites have Eu/Eu* = 0.1-0.4. The qtz diorites have the most radiogenic Nd isotope composition among the qtz diorites of the Damara orogen (εNd_i: -1.50 to -1.78) together with unradiogenic Sr isotope compositions ($^{87}Sr/^{86}Sr_i$: 0.7049-0.7058). The granodiorites and granites have less radiogenic Nd isotopic compositions (εNd_i: -2.74 to -5.31) and more radiogenic initial Sr isotope ratios ($^{87}Sr/^{86}Sr_i$: 0.7071-0.7082). Although fractional crystallization processes were operative, the lack of correlation between isotope ratios and elemental concentrations indicate that both rock types represent partial melts of juvenile crustal sources. Compared to experimental studies, a medium-K/high-Al-metabasaltic rock is the most plausible source for the qtz-diorites. For the granites, high-K andesitic to tonalitic rocks are plausible sources. Although both rock types were formed during the main phases of regional metamorphism, internal crustal heat production rates are probably not sufficient to generate qtz diorites and I-type granites from pre-existing crustal sources. One plausible model involves underplating of mantle derived magmas followed by sill-like intrusions in the lower crust close to the peak of high-grade metamorphism producing excess temperatures that promote partial melting of fertile crustal sources.

https://doi.org/10.1180/S0026461X00008434 Published online by Cambridge University Press

Don't Neglect Serpentinization

JAMES F. KASTING

Department of Geosciences, Penn State University, University Park, PA, USA, jfk4@psu.edu

Why did atmospheric O_2 only increase at 2.45 Ga when various indirect indicators suggest that oxygenic photosynthesis had already evolved by 2.7 Ga or earlier? This question has perplexed geologists for the past decade or more. Suggested hypotheses include: 1) Oxygenic photosynthesis was not actually invented until 2.45 Ga; 2) O_2 could not rise until the dissolved ferrous iron in the ocean was titrated out; 3) The mantle became more oxidized with time so that volcanic gases also became more oxidized; 4) The continents became more oxidized with time so that metamorphic gases became more oxidized; 5) The ratio of C and S relative to H in volcanic gases increased with time because of more active recycling of carbon and sulfur; and 6) A gradual switch from submarine to subaerial volcanic outgassing caused volcanic gases to become more oxidized with time. This last hypothesis has at least two variants, presented, respectively, by Kump and coauthors [1,2] and Gaillard et al. [3]. These variants differ with respect to the temperature at which submarine volcanic gases last equilibrate with basalts before being vented into the ocean. Here, I suggest that hypothesis (6) is indeed correct, but that the interaction of hydrothermal fluids with seafloor rocks is not well accounted for by any of the existing models [1-3]. Warm (~350°C) water can react with ultramafic rocks, generating hydrogen, by the process of serpentinization. This process happens only in restricted environments today, e.g., in deep fracture zones around the Mid-Atlantic ridge. However, on the early Earth, a hotter mantle may have generated thicker, more ultramafic oceanic crust, along with widespread hydrothermal activity. Gradual cooling of the mantle led to a change in tectonic styles, reflected by the Archean-Proterozoic geologic boundary, and also to a reduction in production of hydrogen from serpentinization. Thus, this hypothesis is closely related to the Kump and Gaillard models, but it includes additional types of water-rock interactions.

References: [1] Kump LR, Seyfried WE. 2005. *Earth Planet. Sci. Lett.* 235: 654-662. [2] Kump LR, Barley ME. 2007. *Nature* 448: 1033-1036. [3] Gaillard F, Scaillet B, Arndt NT. 2011. *Nature* 478: 229-232.

Experimental and field studies of Li cycling in subduction zones

Miriam Kastner[1]*, Evan A. Solomon[2]

[1]Scripps Institution of Oceanography, La Jolla, CA 92093, USA, mkastner@ucsd.edu
[2] School of Oceanography, University of Washington, Seattle, WA 98195, USA, esolomn@u.washington.edu

Li is one of the most prominent tracers that provides insights on fluid-rock diagenetic or metamorphic reactions, hence, on the subsurface hydrology in subduction zones. Like the other alkali elements it strongly partitions into the fluid-phase, in particular at moderate to elevated temperatures; the magnitude of the partition is strongly temperature dependent. Li and its isotopes have been used for tracing fluid reactions and cycling at plate boundaries. In subduction zones the nature of the subducted material has a strong influence on the observed variations in Li isotopes. Data from two subduction zones, Costa Rica, and Nankai Trough, will be presented.

Recent hydrothermal experiments by Wei Wei on MORB-seawater and smectite-seawater, 35-350 °C at 25 °C steps, and 600 bars, greatly expanded the data-base and insights on the behavior of Li. The results indicate that Li is released into the fluid-phase throughout the temperature range of the experiments, with a strong threshold of significant release at ~250 °C; indeed, Li concentrations increase in fluids with depth in subdution zones. Accordingly, because clay-rich sediments and altered oceanic crust are enriched in Li and the Li isotope values are lower than seawater value; the fluids that migrate up-dip from a deeper source into the ocean should have a lower isotope signature, eventually approaching the source material, as observed in the pore fluids of the décollement zones at the Costa Rica and Nankai Trough subduction zones. The experiments show a linear trend starting at seawater and decreasing with temperature (δ^7Li versus T), and can facilitate estimation of the fluid source temperature if the mineralogy of the subducting material is known.

The formation fluids recently recovered at two sites at the Costa Rica subduction zone provide, for the first time, two-year records on temporal variations (1) on the chemistry of the incoming plate upper basement formation fluid, (2) on the décollement fluid at 0.6 km arcward of the deformation front, and (3) on the relations of chemistry, tectonic events, and flow rates. The formation fluid Li concentrations and isotope data at the ODP reference Site 1253 support mixing between seawater and a deep-sourced fluid in the forearc of the Costa Rica subduction zone, implying that the uppermost permeable basement serves as pathway of fluid expulsion from the forearc. At the Nankai Trough décollement the Li concentrations are significantly higher and the δ^7Li value is lower than at Costa Rica, reflecting the different sediment inputs and geothermal gradients at these two subduction zones.

https://doi.org/10.1180/S0026461X00008434 Published online by Cambridge University Press

Redox oscillations in a freshwater analogue of marine pelagic sediments: Lake Superior

S. KATSEV[1*], J. LI[1], S.A. CROWE[2], D. MIKLESH[1], M. KISTNER[1] AND D.E. CANFIELD[2]

[1]Large Lakes Observatory, University of Minnesota Duluth, Duluth, MN, USA, skatsev@d.umn.edu (* presenting author)
[2]NordCEE, University of Southern Denmark, Odense, Denmark

Much attention has been given recently to the dynamics of redox boundaries in environments ranging from coastal sediments to flood planes to abyssal Arctic sediments [1]. We report on a multi-year investigation of transient diagenetic phenomena in a freshwater system. Deep (160-318 m) sediments in Lake Superior have sedimentation rates (0.01-0.04 cm y^{-1}) similar to those in marine hemipelagic and pelagic sediments and are similar to such sediments in terms of oxygen uptake, carbon degradation rates, carbon mineralization efficiency, and surface bioturbation rates. The reactivity of deposited organic carbon decreases with age according to a power law similar to the one established for marine environments. In Lake Superior, oxygen penetration into sediments ranges from 3.5 to >12 cm. Seasonal variations of only ~20% in bottom water oxygen concentrations cause it to vary by several cm, more than previously acknowledged. Using measurements and diagenetic modeling, we analyze the causes of these variations and their effects on sediment diagenesis and fluxes. On decadal time scales, our results show that multiple Mn- and Fe-rich (up to 10 wt %) layers in Lake Superior sediments are diagenetically mobile even where organic carbon is only weakly reactive (k≈0.005 y^{-1}). We draw parallels with the metal-rich layers that are found in deep Arctic sediments where they are often used as indicators of paleo-redox conditions [2] and discuss the diagenetic mobility of such layers on time scales up to 100 ky.

[1] Katsev et al. (2006) *Limnol. Oceanogr*. **51**, 1581-1593.
[2] März et al. (2011) *Geochim. Cosmochim. Acta* **75**, 7668-7687.

Impact of Ternary Surface Complexes on Metal Ion Adsorption

LYNN E. KATZ[1]*

[1]University of Texas, Austin, USA,
lynnkatz@mail.utexas.edu (* presenting author)

Introduction

The fate and transport of metal ions released into the environment rely heavily upon their interactions with the mineral–water interface. Surface complexation models (SCMs) such as the Charge Distribution Multi-Site Complexation (CD-MUSIC) model are capable of describing and predicting adsorption processes over a range of environmental conditions in well-controlled systems with few competing or co-adsorbing species. In recent years, research objectives have focused on applying these models to more complex systems containing multiple adsorbing species and mixed mineral assemblages.

Results

In this research, surface charge, isotherm, and pH adsorption edge data taken from several published studies were modeled using CD-MUSIC to examine how different adsorbents (goethite and gibbsite) and complexing ligands (e.g. carbonate, chloride, selenite, and sulfate) influence metal ion adsorption and surface speciation (e.g. Figure 1). Mineral's surface site density was estimated, when possible, using a new approach that incorporates the proton reactive site density [1], along with maximum oxyanion adsorption data and pertinent crystallographic information regarding the adsorbent of interest. The impact of ternary complexes was ligand and adsorbent dependent.

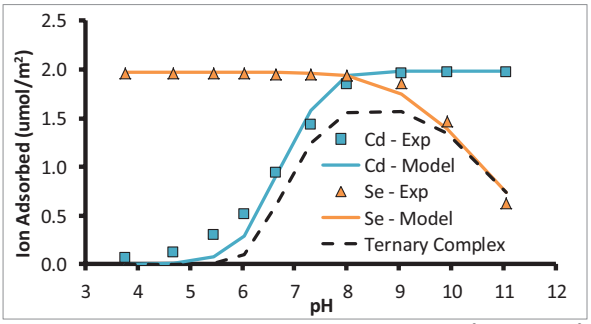

Figure 1: Adsorption and CD-MUSIC model for Cd^{2+} and SeO_3^{2-} bi-solute adsorption to goethtite. Model predictions of the $CdSeO_3$ ternary complex are represented by the dashed line.

Conclusion

This investigation reveals the pivotal role that ternary surface complexes can play in adsorption processes, and further illustrates the necessity of accurately depicting surface and aqueous complexes in SCM predictions.

[1] Salazar-Camacho and Villalobos (2010) *Geochim. Cosmochim. Acta* **74**, 2257-2280.

https://doi.org/10.1180/S0026461X00008434 Published online by Cambridge University Press

Solubilization of trace elements from coal fly ash in relation to chemical speciation

NAVDEEP KAUR[1], DEAN L. HESTERBERG[1]*, OWEN W. DUCKWORTH[1], DAVID B. BUCHWALTER[1] & COLIN R. WARD[2]

[1]NC State University, Raleigh, United States, dean_hesterberg@ncsu.edu (* presenting author)
[2] University of New South Wales, Sydney, NSW, Australia, C.Ward@unsw.edu.au

Abstract

In December 2008, approximately 4.2 million cubic meters of coal fly ash were discharged into the Emory and Clinch Rivers from a holding pond in Kingston, TN. A fundamental understanding of the chemistry of the ash is required to develop long-term management strategies for the site. The objective of this study was to relate the pH-dependent kinetics of trace-element dissolution to chemical speciation in the ash. A fly ash sample from TVA's Kingston power plant contained 60% aluminosilicate glass in addition to mullite, quartz, and other minerals. Synchrotron x-ray absorption spectroscopy (XAS) indicated that trace elements (As, Cr, Cu, Se, Sr, and Zn) were associated with both the glass and mineral phases.

Initial experiments on dissolution kinetics were conducted on suspensions of ash in 0.05 M KCl (10 g kg^{-1}) in a continuously stirred batch reactor at 25 °C under oxic conditions, both at pH 5 and at ambient pH (buffered at pH 10) over a period of 10 days. Similar trends in increasing dissolved Sr and Ca concentrations with time at both pH levels were observed, and both elements were found predominantly in the glassy phase. General trends of increasing dissolution with time of As, Cr, Se, and S at pH 10, and of Zn, Mn, and Fe at pH 5 were observed. Speciation analyses of unweathered ash samples indicated the presence of mainly As(V), Se(IV) and Cr(III), along with ferrihydrite-like Fe and discrete Zn phases. A decline in dissolved concentrations of some elements with time was attributable to precipitation of secondary solids. Results from a stirred-flow reactor system will also be presented.

Conclusions

Over time, alkaline fly ash residues in circumneutral or acidic river sediments are expected to become acidified. Elemental speciation in fly ash provides insights on solubilization of potentially toxic trace elements under varying pH conditions. However, transformations of initial solid-phase species into other, possibly more insoluble species, must also be considered. Continuing experiments across a range of geochemical conditions to which fly ash residues might be exposed will assess potential, long-term environmental impacts of ash-contaminated sediments.

This research was funded by Tennessee Valley Authority (TVA) through a grant administered by Oak Ridge Associated University (ORAU). We appreciate Dr. Neil Carriker's assistance in obtaining fly-ash samples for this research. Synchrotron XAS analyses were done at Beamline X11A at the DOE's National Synchrotron Light Source, Brookhaven National Laboratory and at Beamline 4-3 at the Stanford Synchrotron Radiation Lightsource.

Modeling the impact of soil aggregate size on selenium immobilization

MATTEO KAUSCH[1]* AND CÉLINE PALLUD[1]

[1]ESPM, University of California, Berkeley, USA, mkausch@berkeley.edu (* presenting author)

Soil mineral and organic particles are commonly bound together into mm to cm sized microporous structures (aggregates) separated by macropores. While fast advective transport prevails in macropores, the transport inside aggregates is mostly diffusive (slow) which leads to the formation of aggregate-scale concentration gradients impacting biogeochemical reactions. Selenium (Se) is an essential micronutrient that has recently emerged as an environmental contaminant. The bioavailable oxyanions selenate, Se(VI), and selenite, Se(IV), can be microbially reduced to solid, elemental Se, Se(0), and anoxic microzones within aggregates are thought to promote this process in soils. A mechanistic understanding of Se reduction and retention in soil aggregates can lead to better predictions of Se transport and attenuation in seleniferous soils which may help improve the management of such ecosystems.

Using a dynamic 3D reactive transport model of a single idealized aggregate, we model the coupling between physical transport and biogeochemical reactions controlling Se reduction at the aggregate scale. The model was developed and validated based on a series of flow-through reactor experiments involving artificial soil aggregates. Each experiment/model scenario consisted of a spherical aggregate (experimental diameter: 2.5 cm) surrounded by a constant flow providing Se(VI) (0.4 or 0.8 mM) and pyruvate (0.3 or 1.2 mM) for 8 days under oxic or anoxic conditions. Aggregates contained a Se-reducing bacterial strain (*Enterobacter cloacae* SLD1a-1) that oxidizes pyruvate while reducing Se(VI) to Se(IV) and Se(IV) to Se(0). These two reactions were implemented in the model as double-Monod rate equations with literature based kinetic parameters. Reactions were coupled to transport of pyruvate, O_2, and Se species modelled *via* advection-diffusion equations with static flow fields calculated using Navier-Stokes/Brinkman equations (macropore/aggregate). Concentrations of Se(VI) and reduced Se (Se(IV)+Se(0)) were measured in the outflow solution (temporally resolved) and in concentric solid phase sections of aggregates (spatially resolved). This data was used to validate the dynamics of the reactive transport model and all subsequent simulations where performed within experimentally validated dimensions ($\leq$ 2.5 cm, 8 days).

Simulations predict that larger aggregate size leads to increased Se retention. For example aggregates, surrounded by oxic conditions and a flow of 0.3 mM pyruvate/0.4 mM Se(VI) solution, are predicted to retain 0.4 and 0.1 nmol/g/day of Se(IV) and Se(0) respectively if they are 2.5 cm in diameter, but this decreases continuously over the simulated size spectrum to 0.07 and 0.01 nmol/g/day for 1 cm diameter aggregates. While the absolute amount of reduction depends on aeration, as well as Se(VI) and carbon concentrations, this trend persists across all chemical conditions investigated. Promoting soil aggregation on seleniferous agricultural soils, through addition of organic matter and decreased use of tillage may thus be an effective management practice to decrease impacts of Se contaminated drainage water on downstream ecosystems.

https://doi.org/10.1180/S0026461X00008434 Published online by Cambridge University Press

Rainfall induced isotope effects in rice (*Oryza sativa* L.) grain organics: A palaeo perspective

RITIKA KAUSHAL[1*], PROSENJIT GHOSH[1], WILLI A. BRAND[2], AND HEIKE GEILMANN[2]

[1] Centre for Earth Sciences, Indian Institute of Science, Bangalore, India, rithikakaushal@ceas.iisc.ernet.in (* presenting author), pghosh@ceas.iisc.ernet.in

[2] Max Planck Institute for Biogeochemistry, Jena, Germany wbrand@bgc-jena.mpg.de , geilmann@bgc-jena.mpg.de

The relationship between $\delta^{18}O$ of environmental water and organic-starch present in rice (*Oryza sativa* L.) and its usefulness to reconstruct precipitation patterns from archaeological samples is being explored in this paper. Rice grows in an environment saturated with water which is derived primarily from rainfall. Being a crop which grows across latitude from tropical to temperate regions, it offers the possibility to explore the relationship that it exhibits with the oxygen isotopic composition of rainfall. Rainfed water is the primary source of water in agricultural fields and is responsible for controlling the growth and productivity of the rice crop. A strong and significant relationship was found to exist between the all-India rice production and Indian summer monsoon rainfall [1]. Here we used $\delta^{18}O$ signature of rice grain samples originating from different latitudes, and compared it with the zonal temperature and respective precipitation isotopic ratios. Oxygen isotope ratios in rice grains were obtained from the literature [2, 3] and were also generated upon analysis of samples originating from different locations over India. The isotopic composition of precipitation and temperature were retrieved from International Atomic Energy Agency–Global Network of Isotopes in Precipitation (IAEA – GNIP) dataset [4]. A careful inspection of precipitation isotope ratios and rice isotopic composition, allowed the determination of $\delta^{18}O$ fractionation factor between rice organics and precipitation water. The fractionation factor observed in here varies between ~23‰ to ~35‰ and is mainly controlled by temperature. The latitudinal effect on rice isotopic composition and rainfall is observed in majority of the locations. However, the regions affected by dual monsoon show tendency of large scatter owing to contribution of moisture from different ocean basins [5]. The oxygen isotope ratios in rice samples will provide an opportunity to understand the rainfall pattern from isotopic composition of rice samples belonging to archaeological sites of older civilizations.

[1] Kumar *et al.* (2004) *Int. J. Climatol.* **24,** 1375–1393.
[2] Korenga *et al.* (2010) *Analytical Sciences* **26,** 873-878.
[3] Kelly *et al.* (2002) *Eur Food Res Techno.* **214,** 72–78.
[4] GNIP/ISOHIS, Isotope Hydrology Information System of International Atomic Energy Agency, (IAEA), Vienna, Austria. The ISOHIS Database. 2001, Available at: http://isohis.iaea.org
[5] Breitenbach, *et al.* (2010) *Earth Planet. Sci. Lett.* **292,** 212-220.

Stable-isotope insights into mineral-fluid redox reactions

ABBY KAVNER[1,*], JAY R. BLACK[1,2]

[1]University of California. Los Angeles, Earth and Space Sciences Department akavner@ucla.edu (* presenting author)
[2]Geoscience Australia, Canberra ACT 2601 jay.black@ga.gov.au

We present a synthesis of a series of experiments which use metal stable isotope behavior as a probe of the kinetics of redox reactions at an aqueous/solid interface. Measurements of isotope fractionation during potentiostat-controlled electroplating has led to observations of large isotope fractionation factors in a large variety of metal systems including Fe [1-3], Zn [2-5], Li [6], and Cu[7]. Our observed isotope fractionations vary strongly as a function of electrochemical driving force and temperature. We interpret our observations in terms of a competition between two rate-limiting steps at a redox-sensitive interface: mass transport to the interface, which results in small isotope signatures, and the steps associated with the electron transfer reaction, which results in much larger isotope signatures. Our experimental data which measures both overall reaction rates and rate-dependent isotope separation cannot be explained simultaneously using rate laws involving simple single-step activated processes governing mass transport and redox reaction steps. Instead, to explain all of our observations, we require rate-dependent isotope fractionation factors. Our results are consistent with a theory predicting isotope-dependent electrochemical reaction rates that is based on theory for electron transfer reactions[1,4]. The results imply that stable isotope behavior at a redox-active interface provides an exquisitely sensitive probe of the details of the activated processes governing the reactions, eslucidating small variations in rate that cannot be observed by measuring reaction rates alone. This is especially true in regimes where redox processes are not rate-limited by mass transport of material to the reaction zone.

[1] Kavner *et al.* (2005), GCA **69**, 2971. [2] Black *et al.* (2010), **74**, 809-817. [3] Black *et al.* (2010), GCA **74**, 5187-5201. [4] Kavner *et al.* (2008), GCA **72**, 1731-1741. [5] Black, *et al.* (2012), ms in prep. [6] Black *et al.* (2009), JACS **131** 9904-9905 [7] Black *et al.* (2011), ACS Symposium Series **1071** 345–359.

https://doi.org/10.1180/S0026461X00008434 Published online by Cambridge University Press

High-precision temperature change at the western Japan during the past 10,000 years and its effect on the human activity

HODAKA KAWAHATA [1]*, MEGUMI MATSUOKA[1], AMI TOGAMI[1], AND NAOMI HARADA[2]

[1] Atmosphere and Ocean Research Insttitute, The University of Tokyo, Kashiwanoha 5-1-5, Kashiwa, Chiba 277-8564, Japan, kawahata@aori.u-tokyo.ac.jp (* presenting author),
[2] JAMSTEC, Natsushima 2-15, Yokosuka, 237-0061, Japan

A continuous record of terrestrial environments is difficult to reconstruct because terrestrial sediments are often eroded and transported away by wind or water. In contrast, marine sediments often provide a continuous record of both marine and terrestrial environments in their sedimentary sequence. Therefore, we collected a shallow-marine sediment cores near Hiroshima-city, located near Inland Sea of Japan in the western Japanese Islands, and conducted the reconstruction of Holocene environmental change with ultra-high resolution of environmental change during 700-1700 AD. SST (sea surface temperature) declined (26.2-23.7oC) from 10,300 to 3,900 cal. Yr. BP), which is quite different from those recorded in surrounding areas including Yellow Sea, Japan Sea, and the western Pacific, which show increase in SST or a maximum around mid-Holocene. We attributed the decrease in SST to the large heat capacity of Inland Sea of Japan and general decrease in insolation. SST fluctuated between 22.3 and 24.3 during 1900BC-1800AD). With respect to historical record, Asuka (592-610AD) and Nara (710-794AD) eras showed reduced and enhanced SSTs, respectively. The former half of Heian era (794-1000AD) showed very mild and optimal climate, which enabled aristocracy by noblemen. In contrast, SST drastically declined from the latter half of Heian era to majority of Kamakura eras (1000-1230AD), which could promote the change to Samurai government by power politics. After that a relative mild climate prevailed about 200 years (1230-1500AD) and then cold weather was observed during 1500-1800AD, corresponding to Little Ice Age.

Melt inclusions in zircon from the migmatite zone, Ryoke belt, Japan

TETSUO KAWAKAMI[1*], ISAO YAMAGUCHI[1,2], AKIRA MIYAKE[1], KENSHI MAKI[1], TOMOYUKI SHIBATA[1], TAKAOMI D. YOKOYAMA[1], AND TAKAFUMI HIRATA[1]

[1]Department of Geology and Mineralogy, Kyoto University, Japan. t-kawakami@kueps.kyoto-u.ac.jp (* presenting author).
[2]DOWA Holdings Co. Ltd., Tokyo, Japan

Melt inclusions in Zrn is a clear evidence of the presence of melt during Zrn formation and therefore, places an important constraint on the timing of Zrn growth. In the Ryoke belt at the Aoyama area, Japan, pelitic and psammitic schists dominate in the north, and migmatites dominate in the south [1]. Zrn in pelitic and psammitic schists from the low-*T* part of the Grt-Crd zone is coarse-grained and shows almost no syn-metamorphic overgrowth. On the other hand, Zrn in migmatites from the mid-*T* and high-*T* parts of the Grt-Crd zone has thin, bright annulus under BSE image along which tiny inclusions of several microns are aligned [cf. 2]. TEM observation of the inclusions gave halo patterns, revealing that they are glass rich in Si, Al and K. This inclusion alignment divides the Zrn into the core with various detrital ages and the rim with 92.6±2.0Ma $^{206}Pb/^{238}U$ concordant age. Presence of the melt inclusions at the core/rim boundary shows that the melt was present when the Zrn rim grew. Low Th/U ratio (<0.02) of the Zrn rim implies that Mnz also coexisted then. A reaction Bt+Sil+Qtz = Grt+Crd±Kfs±Ilm+melt is considered responsible for partial melting in this area [1]. However, Bt is not an important sink of Zr [3], and Bt breakdown cannot supply sufficient Zr to form Zrn rim. Therefore, dissolution of pre-existing Zrn is required to grow new Zrn rim. It would be difficult to saturate melt in Zrn component by dissolving Zrn when the amount of melt is increasing. Therefore, 92.6±2.0Ma Zrn rim probably crystallized during the solidification of the melt in migmatites, possibly near the wet-solidus. Thin, similar-aged rim is developed in Zrn from the mid-*T* part as well. These data suggest that presence of the melt controls dissolution and recrystallization of Zrn [e.g. 4].

Although the whole-rock Zr content is not especially high in the pelitic-psammitic schists from the low-*T* part, modal amount of Zrn (>20μm) is higher in them. Zrn (<20μm) is confirmed to become common in mid-*T* and high-*T* parts, and young, ca. 30μm Zrn without detrital core are rarely found in the high-*T* part. These Zrn are probably newly nucleated grains during the Ryoke metamorphism.

On the other hand, Mnz grows at amphibolite facies grade and the presence of the melt does not largely affect its recrystallization [4]. In the Aoyama area, Mnz from the migmatites records the prograde growth age of 96.5±1.9Ma during the regional metamorphism [5]. Using the difference of growth timing of Mnz (prograde) and Zrn (retrograde), the duration of metamorphism higher than the amphibolite facies grade can be constrained to be ca. 4Ma for the Ryoke metamorphism at the Aoyama area.

[1] Kawakami (2001) *JMG* **19**, 61-75. [2] Cesare et al. (2003) *CMP* **146**, 28-43. [3] Bea et al. (2006) *Can Min* **44**, 693-714. [4] Rubatto et al. (2001) *CMP* **140**, 458-468. [5] Kawakami & Suzuki (2011) *Island Arc*, **20**, 439-453.

https://doi.org/10.1180/S0026461X00008434 Published online by Cambridge University Press

Crustal Destruction: Delamination Processes and Rates

ROBERT W. KAY[1*] AND SUZANNE M. KAY[1]

[1]Cornell University, Earth and Atmospheric Science and INSTOC, Ithaca, NY, USA rwk6@cornell.edu

Narratives of Earth's continental crust formation need to devote time to both crustal creation and destruction. For creation, mantle melting yields magmas that add new mass; destruction involves sediment subduction, subduction erosion, and lower crustal delamination (foundering, dripping) and slab breakoff. Processes like relamination only involve recycling. Issues include rate and relative importance of basaltic versus andesitic magmas, criteria for identification of destruction processes and rates. Here, we examine criteria for identifying delamination and focus particularly on the role of delamination in ultimately producing an andesitic crust. In general, delamination occurs in contractional regimes, is episodic, and recycles mafic/ultramafic lower crust. On-going delamination is being observed in seismic images of the mantle and crust under areas like the high Central Andean plateau and the Sierras and Colorado Plateau of the western US. Abrupt changes in magma composition and xenolith populations along with structural changes and uplift complement and provide a temporal context to geophysical observations. Adakitic rocks that form in equilibrium with dense eclogitic residues are distinctive, as is the presence of magmatic "flare-ups". In older contractional orogens, similar thermal-compositional-structural observations, constrained by high precision chronology permit identification of delamination episodes as in the Tertiary Tibetan Plateau and in the Proterozoic Grenville. In accretionary orogens like the Palaeozoic Altaids (central Asia) identification of delamination is aided by present-day analogues. In collages of sutured arc terranes, mafic lower crust and forearcs often appear under-represented and were presumably destroyed. In contrast, regions like the Ural arc-continent collision zone appear to have remained largely intact. Integrated over a long time scale, the rate of lower crustal destruction by delamination at subduction zones and during continental collision is on the order of 2 AU (Armstrong units at km^3/year globally).

EM-like sources in Patagonian plateau basalts: Auca Mahuida case

SUZANNE M. KAY[1]* AND HELEN JONES[1]

[1]Cornell University, Earth and Atmospheric Science and INSTOC, Ithaca, NY, USA smk16@cornell.edu

Plateau basalts in the northern Patagonian ~1.8 to 0.8 Ma Auca Mahuida volcanic field, which is centered at 37.8°S and 68.7°W and is ~225 km from the Andean Southern Volcanic Zone arc front, have trace element and Sr, Nd and Pb isotopic similarities to nearby early Miocene basalt flows as well as oceanic OIB basalts that are primarily mixtures of EM1 and depleted mantle. The isotopic ratios and the presence of positive Sr, K, Ba and Rb spikes on primitive mantle normalized plots of both the Auca Mahuida basalts and the early Miocene basalts indicate a mantle source containing old slab modified continental lithosphere. As similar positive spikes are absent on trace element patterns of north-central Patagonian ~48-32 Ma backarc basalts with more depleted isotopic signatures, major additions of slab-modified lithosphere and crust into the mantle source are conjectured to have occurred in the late Oligocene to early Miocene as the Andean margin adjusted to major changes in plate convergence parameters. Relatively higher Ba, Rb, Th, U and K concentrations and subtly lower La/Ta ratios in the Auca Mahuida basalts than in the early Miocene basalts are attributed to interaction of the local mantle source with slab-derived fluids or melts during the episode of late Miocene shallow subduction of the Nazca plate recorded in the near-by arc-like Chachahuén volcanic complex.

On the scale of the Auca Mahuida volcanic field, the relatively homogeneous trace element and isotopic chemistry of the basaltic lavas are consistent with their formation as melt batches of a similar mantle source. Calculated temperatures and pressures for the most primitive basalts are 1350° to 1380°C at 1.8 to 2.0 GPA, which correspond to depths of 65-74 km. These depths are consistent with independent estimates for the depth to the base of the lithosphere from xenolith and seismic studies in the same region by others. Calculated melting percentages from a moderately enriched mantle source for the most mafic basalts range from about 6% to 3%. The associated mugearitic, trachyandesitic and trachytic volcanic rocks can be modelled as being derived from fractionation of the basaltic magmas along with some mixing with evolved magmas, and possibly with partial melts of recently underplated magmas. The small range of Sr, Nd and Pb isotopic variation in the Auca Mahuida volcanic suite fits with little old crustal contamination of the magmas in the refractory crust left over from the major melting event that produced the Permo-Triassic Choiyoi granite-rhyolite province.

https://doi.org/10.1180/S0026461X00008434 Published online by Cambridge University Press

Examining the root exudate-induced cycling of reactive manganese species in the rhizosphere

MARCO KEILUWEIT[1,2]*, PETER NICO[3], JEREMY BOUGOURE[2], JENNIFER PETT-RIDGE[2], AND MARKUS KLEBER[1]

[1] Department of Crop and Soil Science, Oregon State Universtity, Corvallis, USA, marco.keiluweit@oregonstate.edu (* presenting author)
[2] Lawrence Livermore National Laboratory, Physical and Life Sciences Directorate, Livermore, USA
[3] Lawrence Berkeley National Laboratory, Earth Sciences Division, Berkeley, USA

Dynamics of reactive metals and soil organic matter (SOM) operating in the rhizosphere can be dramatically different from those occurring in the surrounding bulk soil due to the many interactions between roots, microorganisms, soil particles, and SOM. One of the main driving forces in changing the chemical, biological, and physical properties of the rhizosphere is the exudation of low molecular weight (LMW) organic compounds by the root. LMW exudates represent a significant C flux into soil ecosystems; compounds such as simple sugars, organic acids, and phenols have also been shown to facilitate cycling of redox active metals (e.g., Fe and Mn). This phenomenon is not only observed in aquic and poorly drained soils, but seems to be common in any upland soil with moisture regimes other than aridic or xeric.

In the research presented here we assumed that LMW exudates and microbial activity in the rhizosphere act together to create redox active microsites in soil. We further hypothesize that redox active microsites are short-lived and continuously recreated, thereby generating a steady supply of reactive manganese (Mn) species. This rhizosphere redox cycling may control the availability of reactive forms of Mn that have been mechanistically linked to the oxidative breakdown of complex organic substrates such as lignin.

We tested our hypothesis by examining the effect of different LMW exudates (oxalate, glucose, acetate, and vanillin) on the Mn dynamics of two different soil types in rhizosphere microcosms. Artificial roots allowed for the release of LMW exudates into structurally intact soil at realistic rates. Results from O_2 microsensor measurements as well as bulk and spectroscopic analyses show how root exudates vary in their ability to (i) induce reducing conditions, (ii) influence the activity of lignolytic enzymes, and (iii) affect the abundance and speciation of reactive Mn species in the rhizosphere.

Our results indicate that Mn redox cycling in the rhizosphere may be plant-driven. If confirmed for natural soil environments, the exudates-induced formation of reactive Mn species may have important implications for the turnover of complex biopolymers such as lignin in the rhizosphere.

Ongoing Formation of Continental Crust: Batholiths Are Forever

PETER B. KELEMEN[1*], BRADLEY R. HACKER[2], MARK D. BEHN[3] AND OLIVER E. JAGOUTZ[4]

[1]LDEO, Palisades NY, USA, peterk@LDEO.columbia.edu (*presenting author)
[2]UCSB, Santa Barbara CA, USA, hacker@geol.ucsb.edu
[3]WHOI, Woods Hole MA, USA, mbehn@whoi.edu
[4]MIT, Cambridge MA, USA, jagoutz@mit.edu

We propose that formation of continental crust is a uniformitarian process dominated by arc magmatism and gravitational instabilities that remove dense lithologies and/or add buoyant ones. Rates have varied, lithologies other than arc rocks are present in continental crust (CC), and weathering has modified the composition, but all of these factors are relatively unimportant.

Some arc lavas are geochemically identical to bulk CC. These include andesites and dacites with molar Mg# > 0.5 in the western Aleutian arc, that are the most isotopically depleted arc magmas worldwide. They contain little or no material recycled from older CC. Throughout the Aleutians, sparse data show that intermediate to felsic plutons also have compositions similar to CC. Thus, modern arc processes form voluminous juvenile igneous rocks identical to CC.

The Talkeetna and Kohistan arc crustal sections may have andesitic rather than basaltic bulk compositions. For Talkeetna, there is a gap in exposure from ~ 7 to 20 km paleodepth, so the bulk crustal composition is uncertain. When the missing section is assigned the composition of upper crustal, felsic plutonic rocks, bulk crust is andesitic and calculated seismic sections are similar to the modern IBM arc (Behn & Kelemen JGR 2006; Hacker et al. JGR 2008). For Kohistan, combined barometry and geochemistry yield a more certain, andesitic bulk crust (Jagoutz et al. EPSL 2011, Jagoutz & Schmidt Science 2012). Foundering of dense ultramafic rocks and garnet granulites may help convert basaltic to andesitic arc crust.

Talkeetna and Kohistan (and the central Aleutians, based on geologic and seismic data) have chemically stratified sections, with felsic rocks in the upper crust, mafic rocks in the lower crust, and ultramafic plutonic rocks directly overlying residual mantle peridotite. When such sections undergo subduction, during arc-arc or arc-continent collision, felsic upper crustal rocks with layer thickness more than ~ 100 m will rise as buoyant diapirs, either back up a subduction channel or through the mantle wedge, returning substantial masses of felsic material to overlying arc or continental crust (Behn et al., Nature Geoscience 2011; Hacker et al. EPSL 2011). Similar instabilities likely return andesitic trench sediments (greywacke) to the base of arc crust following subduction erosion.

Based on isotope data, felsic arc batholiths > 50% juvenile material (< 50% older, recycled CC). If such batholiths have been forming at the same average rate since the early Archean, and most of these remain in the crust via buoyancy instabilities as described above, the mass of juvenile felsic material formed in this way could be greater than or equal to the present mass of CC. So far, we have only calculated this approximately for North America. By the 2012 Goldschmidt, we will formalize and evaluate this hypothesis using data on batholiths from all of the continents.

https://doi.org/10.1180/S0026461X00008434 Published online by Cambridge University Press

Secular geochemical evolution linked to atmospheric oxidation

C. BRENHIN KELLER* AND BLAIR SCHOENE

Department of Geosciences, Princeton University, Princeton NJ, USA (*cbkeller@princeton.edu, bschoene@princeton.edu)

Secular geochemical evolution of the Earth's crust has typically been obscured by the geochemical heterogeneity of the rock record along with imperfect sampling[1]. In order to ameliorate this problem, we have taken a new approach: weighted bootstrap resampling Monte Carlo analysis of a ~70,000 sample igneous rock database. In addition to gradual trends in compatible and incompatible elements expected from secular cooling, the results reveal a period of dramatic geochemical change near the Archean/Proterozoic boundary. Temporal correlation of this event with stepwise atmospheric oxidation circa 2.4 Ga[2] may suggest a link between deep earth geochemical processes and the rise of atmospheric oxygen on Earth.

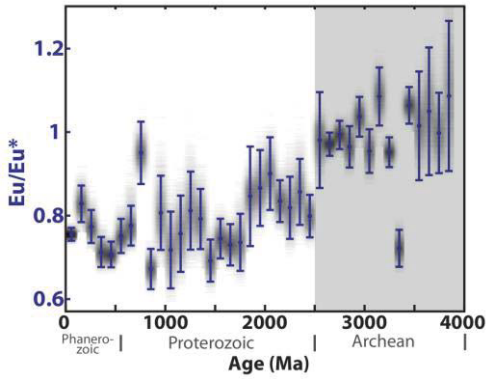

Figure 1: Monte Carlo analysis of mean europium anomaly in felsic (62-73% SiO_2) samples through time. Error bars: 2σ standard error.

Notable changes across the boundary include decreases in deep meltitng/fractionation indicators such as La/Yb and Eu/Eu* of felsic rocks (Figure 1), as well as decreases in mantle melt fraction in basalts. In the context of observed increases in preserved crustal thickness across the Archean-Proterozoic boundary[3,4], these data suggest a model where high degree Archean mantle melting produced a thick, mafic lower crust, leading to deep crustal delamination; delamination and associated lower crustal anatexis in turn resulted in abundant tonalite-tronhjemite-granodiorite (TTG) magmatism and a thin preserved Archean crust.

Since higher pressure restitic assemblages may contain substantial Fe^{3+}, we speculate that deep melting or deep fractionation in the Archean may have resulted in magmas with lower Fe^{3+}/Fe^{2+}, and consequently larger budgets of reduced volcanic volatiles. Cessation of abundant deep crustal melting at the end of the Archean may therefore have resulted in decreased reducing flux to the atmosphere, contributing to the atmospheric Great Oxidation event.

[1] Hawkesworth & Kemp (2006). *Nature* **433**, 811–817. [2] Kump (2008). *Nature* **451**, 277–278. [3] Artemieva (2006). *Tectonophysics* **416**, 245–277. [4] Durrheim & Mooney (1991). *Geology* **19**, 606–609.

The role of pre-nucleation clusters in the crystallization of $CaCO_3$

MATTHIAS KELLERMEIER* & DENIS GEBAUER

Physical Chemistry, University of Konstanz, D-78457 Konstanz, Germany, matthias.kellermeier@uni-konstanz.de (* presenting author), denis.gebauer@uni-konstanz.de

Introduction

Recent studies have revealed that stable pre-nucleation clusters exist in both super- and undersaturated solutions of calcium carbonate prior to the formation of a solid phase [1]. Computer simulation data indicate that the thermodynamic stability of these species is based on strong hydration in combination with a distinct entropic contribution, resulting from the high degree of disorder inherent to their dynamic chain-like structure [2]. Nucleation of solid particles from this solute form appears to occur through aggregation of the clusters, rather than by the stochastic assembly of ions into metastable nuclei envisaged in classical theories [3,4]. However, direct insight into these processes has not yet been gained.

The phase initially precipitated from these pre-nucleation clusters was found to be amorphous calcium carbonate (ACC) exhibiting distinct short-range structural features, which resemble the long-range order in calcite or vaterite [5] and moreover seem to be already encoded in the clusters [1]. Transformation of ACC into more stable crystalline polymorphs usually takes place within minutes unless kinetic stabilization is provided, as for instance achieved by coating the nanoparticles with silica [6].

Results and Conclusions

In the present contribution, we outline the concept of non-classical nucleation via stable ion clusters and highlight experimental evidence supporting this scenario for the case of calcium carbonate as well as other important minerals. It is furthermore demonstrated that silica can be used as an additive slowing down or impeding the nucleation process due to colloidal shielding of the clusters [7]. In this manner, details of the transformation of ion clusters into ACC nanoparticles could be resolved experimentally. Results corroborate that nucleation of ACC relies on aggregation and coalescence of the clusters, yielding primary particles that exceed a certain critical size. In addition, our methodology facilitates preparation of solutions rich in pre-nucleation clusters, which – despite high supersaturation – do not nucleate even after periods of more than a year, as the classical ion-by-ion pathway is obviously not accessible under the given conditions. Colloidal stabilization with silica even allows for a direct isolation of these elusive species, which may be a key step for the analysis of their structure. Our findings are likely to be relevant for crystallization phenomena in various geological settings.

[1] Gebauer, Völkel & Cölfen (2008), *Science* **322**, 1819-1822. [2] Demichelis, Raiteri, Gale, Quigley & Gebauer (2011), *Nat. Commun.* **2**, 590. [3] Gebauer & Cölfen (2011), *Nano Today* **6**, 564-584. [4] Pouget *et al.* (2009), *Science* **323**, 1455-1458. [5] Gebauer *et al.* (2010), *Angew. Chem. Int. Ed.* **49**, 8889-8891. [6] Kellermeier *et al.* (2010), *J. Am. Chem. Soc.* **132**, 17859-17866. [7] Kellermeier *et al.* (2012), *Adv. Funct. Mater.* submitted.

https://doi.org/10.1180/S0026461X00008434 Published online by Cambridge University Press

Modeling mantle mixing and the persistence of geochemical reservoirs

LOUISE H. KELLOGG[1*]

[1]Department of Geology, University of California, Davis, CA USA kellogg@ucdavis.edu (* presenting author)

Understanding the dynamics of mixing in the mantle is fundamental to understanding the origins of the isotopic heterogeneity observed in oceanic islands and at mid-ocean ridges. Heterogeneity is introduced into the mantle thoughout geologic time by processes associated with melting, alteration, and subduction. Heterogeneity is continously destroyed by convection, as the stretching and folding common to all kinematic mixing processes stirs the mantle. Thus it has long been a goal of computational geodynamics to understand the factors controlling the rate and efficacy of mantle mixing. The time and spatial scales of mixing are influenced by the kinematics of flow, plate motion, viscosity variations, compositional heterogeneity, and phase transitions. Chaotic mixing is observed in time-varying 2-D flows; by contrast, the factors controlling mixing in 3-D remain somewhat poorly understood. We investigate a series of methods for computing and evaluating mixing in 3-D, and compare their utility for assessing mantle mixing and the interpretation of mantle heterogeneity. We explore a suite of models of convection in a layer and in a spherical shell. Passive tracer particles are introduced into time-varying and steady-state models of mantle flow; the particles are tracked over time as they disperse and deform, allowing the use of quantitative measures of mixing. Mixing can be assessed by calculating a Lyapunov exponent (which characterizes the separation of tracers that are initially close to each other), or by treating the tracers as ellipsoidal strain markers and computing their deformation, or by determining the configurational entropy of the sytem of tracers. Stirring may be rapid on a regional scale, while heterogeneities at the global scale are retained because of isolation across long-wavelength cells. Essentially, the regions that exhibit high rates of stretching and thinning have the most important influence on mixing, and packets of material that are stirred rapidly in regions of high strain rate are carried wholesale into regions of more sluggish convection.

Geochemical perspectives on local versus global ocean redox at 1.64 Ga

AMY E. KELLY[1,2,3*], TIMOTHY W. LYONS[2], ERIC B. ALSOP[3], GORDON D. LOVE[2], NOAH J. PLANAVSKY[2], BRIAN KENDALL[3], AND ARIEL D. ANBAR[3]

[1]Shell Oil Company, Houston, U.S.A., Amy.A.Kelly@shell.com (* presenting author)

[2]University of California, Riverside, U.S.A., timothy.lyons@ucr.edu, gordon.love@ucr.edu, noah.planavsky@email.ucr.edu

[3]Arizona State University, Tempe, U.S.A, eric.alsop@asu.edu, brian.kendall@asu.edu, anbar@asu.edu

The chemistry and redox structure of the ancient ocean played a key role in influencing the evolution of life throughout Earth's history. Surface waters in the mid-Proterozoic ocean (~1.8-1.0 billion years old [Ga]) were oxygenated, but a number of lines of evidence point toward anoxic, iron-rich (ferruginous) and sulfide-rich (euxinic) deeper waters. Geochemical data indicate that euxinia was confined to ocean margins and restricted basins. Nevertheless, these euxinic waters may have impeded diversification of eukaryotic life.

We studied a suite of thermally well-preserved black shales from drill core of the 1.64 Ga Barney Creek Formation using detailed biomarker, sulfur isotope, iron speciation, and trace metal redox proxies. High abundances of Type 1 microaerophilic methanotrophic bacteria, as evidenced by elevated 3β-methylhopane indices suggest low marine sulfate concentrations, an inference corroborated by highly variable, heavy pyrite sulfur isotopic values, and likely reflects globally low values exacerbated by local restriction of the Glyde Sub-basin. Iron speciation and organic biomarker data provide evidence for extensive and persistent euxinic waters within the sub-basin.

Despite the presence of oxic surface waters and euxinic deep waters in the sub-basin, the predicted light iron isotope signature of an iron shuttle, like that in the Black Sea, is not observed. Typically, with the shuttle, isotopically light iron from oxic sediments on the shelf is transported to and trapped in sediments of the deep euxinic basin via pyrite formation in the water column. In contrast, our iron isotope values are positive, so the source had to have been isotopically heavy. There are several possible interpretations for this observation. We are intrigued by the possibility that the source of heavy iron was precipitated iron oxide from the redoxcline in a ferruginous ocean, which converted to Fe^{2+} and then to pyrite in a sulfidic local environment, which suggests a relatively high iron ocean with strong redox stratification. It is also possible that the positive values are linked to both removal of isotopically light sulfides in a moderately Fe-rich system and transport of heavy dissolved iron, since sulfide formation may have a positive kinetic isotope fractionation. Both hypotheses necessitate a fundamentally different iron cycle compared to that found in Phanerozoic/modern restricted basins.

Our integrated results point to a sub-basin with oxic surface waters and euxinic deep-waters. This restricted basin was likely connected to an ocean with oxic surface waters, ferruginous deep-waters, and limited expanses of euxinic conditions along productive margins, as well as within other restricted basins. Nevertheless, euxinia in the mid-Proterozoic ocean was likely orders of magnitude more widespread than it is today, and the deleterious impacts on nutrient availability could have been enough to throttle the early evolution and expansion of eukaryotic organisms.

https://doi.org/10.1180/S0026461X00008434 Published online by Cambridge University Press

Detrital zircon: a foggy window into early Earth evolution

JEFFREY VERVOORT[1], ANTHONY KEMP[2*] AND MARTIN WHITEHOUSE[3]

[1]Washington State University, Pullman, USA, vervoort@wsu.edu
[2]The University of Western Australia, Perth, Australia, tony.kemp@uwa.edu.au (* presenting author)
[3]Swedish Museum of Natural History, Stockholm, Sweden, martin.whitehouse@nrm.se

A basic tenet of terrestrial geochemistry is that the continental crust has been extracted from the mantle leaving the latter depleted in incompatible elements. Nd and Hf isotopes have long shown that this process has been an essential feature of the Earth throughout its history, yet the details of the isotopic record—and the implications for the timing and rates of mantle depletion and continental crust extraction—remain debated. Recently, much attention has been given to detrital zircons in both modern and ancient sediments. Integration of the crystallization history of the zircon from the U-Pb chronometer with its Hf isotopic composition can reveal whether the zircon derived from juvenile or reworked crust. This approach critically requires that the crystallization age of the zircons can be unambiguously determined. We suggest that this represents an important—but generally overlooked—limitation in the Hf isotope record from detrital zircons.

The quality filter most often used to assess the integrity of zircon U-Pb systematics is concordance; if a zircon is concordant, it is assumed that the U-Pb age is accurate. A concordance filter is less effective in old zircons because ancient Pb loss, viewed today, parallels concordia. Ancient Pb loss in zircons produces an apparent age less than the true magmatic age, and so the initial Hf isotopic composition will be anomalously low (by ~2.2 epsilon Hf units per 0.1 Ga). Hf model ages, calculated from these parameters, will be artificially old and spurious. The combination of unradiogenic Hf and Hf model ages > U-Pb ages in the zircon record are often given as prima facie evidence of crustal reworking and recycling during Earth's early history, and underpin models for large volumes of ancient continental crust. For many old zircons these features may simply reflect unrecognized ancient Pb loss.

A more robust picture of the isotopic evolution of the Earth can be gained from an integrated approach of Hf and Nd isotopes in well age-constrained magmatic samples: careful U-Pb zircon geochronology; Hf isotopic composition of the zircons; and Hf and Nd isotopic measurements of the whole-rocks. We also highlight strategies for minimising complexities from ancient Pb loss, with respect to Hadean detrital zircons from the Jack Hills and zircons from multiply metamorphosed Archean TTG gneisses of Greenland and Scotland. In these cases, oxygen isotopes, time-resolved Pb/U isotope profiles, trace elements and microstructures provide additional quality filters. An important part of this approach is the realization that not all rock samples (or zircons!) yield useful, unambiguous results. Inclusion of all Hf isotope data from large zircon databases, unscrutinized for quality and lacking in context, will do more to obscure the isotopic evolution of the first billion years of Earth history than to clarify it.

The Hf-Nd isotope barcode of crust formation in the Archean Earth

ANTHONY KEMP[1*], JEFFREY VERVOORT[2], MARTIN WHITEHOUSE[3], ARTHUR HICKMAN[4], MARTIN VAN KRANENDONK[5] AND TOMAS NAERAA[6]

[1]The University of Western Australia, Crawley, Australia, tony.kemp@uwa.edu.au (* presenting author)
[2]Washington State University, Pullman, USA, vervoort@wsu.edu
[3]Swedish Museum of Natural History, Stockholm, Sweden, martin.whitehouse@nrm.se
[4]The Geological Survey of Western Australia, Perth, Australia, Arthur.Hickman@dmp.wa.gov.au
[5]The University of New South Wales, Sydney, Australia, m.vankranendonk@unsw.edu.au
[6]GEUS, Copenhagen, Denmark, tomn@geus.dk

Information from long-lived radiogenic isotope tracers has long been used to argue for the extraction of at least 50% of the Earth's continental crust before the end of the Archean [1]. This implies high, but largely cryptic rates of ancient silicate Earth differentiation not matched by preserved crustal materials of these ages. The geodynamic environment for the generation of these putative early continents remains enigmatic, and this affects models for mantle and atmospheric evolution. Plume-driven crustal growth accords with a hotter early Earth and with inferred episodicity in crust formation, but is difficult to test in the absence of diagnostic chemical signatures. Other studies invoke convergent plate margin processes by 3.8 Ga or earlier – yet, given evidence that crust generation and crust destruction rates are balanced at modern subduction zones, rapid crustal growth at ancient arcs would require a fundamentally different subduction regime to that of the present day. Impediments to understanding early Earth geodynamics include the fragmentary Archean geological record, preservation and sampling bias and overprinting by younger thermal events. It is also increasingly recognised that the isotope testimony of a key mineralogical witness to early Earth processes, zircon, is not always robust.

We examine the constraints on the timing and composition of crust formation from the Hadean to the end of the Archean Eon, focussing on the Hf-Nd isotope record. This information is compared to isotope-time patterns produced by igneous rocks of subduction-related Phanerozoic orogens. The simple Hf isotope-time array defined by the Hadean Jack Hills zircons is not consistent with arc magmatism in its modern guise, but suggests repeated remelting of a basaltic protocrust extracted from primitive mantle at ~4.5 Ga, perhaps during magma ocean solidification [2]. Felsic rocks of the oldest continental nuclei in Greenland (3.85-3.82 Ga) and the Pilbara Craton (3.65-3.42 Ga) appear to have tapped an undifferentiated, near-chondritic mantle source, possibly of deep-seated origin. Both cratons record distinct switches in Hf-Nd isotope signatures after 3.1 Ga that reflect changes in magma sources and enhanced recycling of crust into the mantle. The resulting temporal Hf-Nd isotope trends resemble those produced by plate tectonic processes involving arc accretion and ocean closure, and suggest a transition from a deep to a shallow mantle source of new continental crust after 3.1 Ga.

[1] McCulloch, M. and Bennett, V. (1993) *GCA* **58**, 4717-4738.
[2] Kemp, A.I.S. et al (2010) *EPSL* **296**, 45-56.

https://doi.org/10.1180/S0026461X00008434 Published online by Cambridge University Press

Rhenium data from shales confirms ferruginous Proterozoic deep oceans

B. KENDALL[1*], A.D. ANBAR[1,2], R.A. CREASER[3], T.W. LYONS[4], A. BEKKER[5] AND S.W. POULTON[6]

[1]School of Earth and Space Exploration, Arizona State University, Tempe, AZ, USA, brian.kendall@asu.edu (* presenting author)
[2]Department of Chemistry and Biochemistry, Arizona State University, Tempe, AZ, USA, anbar@asu.edu
[3]Department of Earth and Atmospheric Sciences, University of Alberta, Edmonton, AB, Canada, robert.creaser@ualberta.ca
[4]Department of Earth Sciences, University of California, Riverside, CA, USA, timothy.lyons@ucr.edu
[5]Department of Geological Sciences, University of Manitoba, Winnipeg, MB, Canada, bekker@cc.umanitoba.ca
[6]School of Civil Engineering and Geosciences, Newcastle University, Newcastle upon Tyne, UK, simon.poulton@ncl.ac.uk

A new view of Proterozoic ocean chemistry is emerging from sedimentary Fe speciation and Mo abundance and isotope data from black shales. Fe speciation has revealed examples of anoxic/sulfidic (euxinic) mid-depth waters that were underlain by anoxic/ferruginous (Fe^{2+}-rich) deep waters. Mo data indicate a moderate-sized oceanic Mo inventory, consistent with pervasive oxidative weathering but a pronounced Mo sink into euxinic sediments. However, Fe speciation is strictly a local redox proxy. Furthermore, the high efficiency of Mo burial in sulfidic environments relative to oxygenated and ferruginous settings renders the oceanic Mo inventory sensitive to small changes in the extent of water column euxinia.

To test the hypothesis of ferruginous Proterozoic deep oceans we turned to Re abundances in black shales. Like Mo, Re is oxidatively mobilized from the upper crust and accumulates in oxygenated seawater. Re and Mo have long oceanic residence times (~10^5 years today) that enable their use as global redox proxies. Both metals are removed in sulfidic marine settings. In contrast, Re burial rates in O_2-deficient sediments beneath low-O_2/ferruginous and mildly oxygenated bottom waters are high and low, respectively, whereas Mo burial rates in these settings are low and negligible, respectively.

We found that Re abundances in most Paleoproterozoic and Mesoproterozoic shales are similar to those in Late Archean shales. Re (up to 50 ppb) is enriched relative to upper crust (~1 ppb), indicating that dissolved Re was supplied to the oceans via oxidative weathering. However, the low Re abundances in Proterozoic shales point to widespread low-O_2/ferruginous conditions that maintained a low oceanic Re inventory. Higher Mo (but not Re) abundances in Proterozoic relative to Late Archean shales is consistent with increased oxidative weathering, limited extent of sulfidic conditions, and low Mo burial rates beneath ferruginous deep waters. Re is a global redox proxy, so our data confirm the widespread ferruginous Proterozoic deep oceans inferred from local Fe speciation data.

Exceptions to the Late Archean-to-Mesoproterozoic baseline are found in black shales deposited during the Paleoproterozoic Lomagundi positive carbon isotope excursion (the later stage of the Great Oxidation Event) and the late Mesoproterozoic. Re abundances in these shales reach 200 ppb, similar to the lower end of the range observed in Ediacaran and Phanerozoic shales, and hence suggests a greater extent of ocean oxygenation at these times.

Microbial hydrogen sulfide generation within Syncrude composite tailings

KATHRYN KENDRA[1*], KATE STEPHENSON[1], TARA COLENBRANDER NELSON[1], RODERICK AMORES[1], STEVEN HOLLAND[1], TARA PENNER[2] AND LESLEY WARREN[1]

[1]School of Geography and Earth Sciences, McMaster University, Hamilton, Canada, kendrake@mcmaster.ca (*corresponding author)
[2]Syncrude Environmental Research, Edmonton, Canada, penner.tara@syncrude.com

Surface mining of Alberta's Oil Sands has led to significant land disturbance, making reclamation one of the largest challenges facing the industry today. With increased production from Alberta's Oil Sands, sustainable development of this resource has emerged as a substantial environmental issue facing Canadians. Syncrude Canada Ltd. has developed an innovative technique to reclaim composite tailings (CT) through constructed wetland landscapes and is currently investigating the viability of a pilot-scale freshwater fen built over sandcapped CT. Episodes of hydrogen sulfide (H_2S) gas release have been encountered during the initial stages of fen construction; these occurrences were not predicted by abiotic geochemical models, thus highlighting the likely importance of microbial metabolic activity in controlling H_2S generation. Previous research in our group has demonstrated the occurrence of H_2S within CT and sandcap porewaters. The interfacial surficial sandcap between the CT and fen has revealed a widespread presence of diverse microbial communities capable of Fe and S metabolisms, suggesting that microbial Fe and S activity within the deeper CT itself is likely. However, to date, no systematic study of CT Fe and S biogeochemistry has occurred. The objectives of this study are to: (1) characterize the mineralogy, microbial Fe and S metabolisms and biologically accessible Fe and S pools with depth in the CT (over 40m) and; (2) constrain microbial and geochemical variables affecting H_2S generation throughout laboratory experimentation. Microcosm experiments are being conducted in an effort to monitor H_2S generation in CT collected from 2 different depths under varying microbial Fe and S metabolic influence. Preliminary results of these experiments will be presented in conjunction with the field based mineralogical, geochemical and microbial CT characterization to identify the constraining variables of the system.

https://doi.org/10.1180/S0026461X00008434 Published online by Cambridge University Press

Frictional Melting in Volcanoes.

JACKIE E. KENDRICK[1*], YAN LAVALLÉE[1], LINDA PETRAKOVA[1], GIULIO DI TORO[2] AND DONALD B. DINGWELL[1]

[1] Department of Earth and Environmental Sciences, Ludwig Maximillians University, Munich, Germany
Kendrick@min.uni-muenchen.de *
Lavallee@min.uni-muenchen.de
Linda.Petrakova@min.uni-muenchen.de
Dingwell@min.uni-muenchen.de
[2] Department of Geosciences, Padova University, Padova, Italy
giulio.ditoro@unipd.it

Introduction

Seismogenic faulting and rapid slip (>0.1 m/s) of rock may result in non-equilibrium frictional melting [1] at temperatures >1000 °C after few centimetres of slip [2]. Upon cooling (and recrystallization) this melt forms a pseudotachylyte [3].

In active volcanoes, the transition from endogenous to exogenous growth is generally attributed to a shift in magma rheology into the brittle regime. The ascent of this high-viscosity magma can form discrete shear zones via strain localisation along conduit margins [4]. Although comparable to tectonic faults, little information regarding the slip processes and generation of fault products in such shear zones are known. Pseudotachylytes have, until now, rarely been noted in volcanic materials [5, 6], and seldom in active volcanic environments [4, 7] despite laboratory experiments which support magma's propensity for frictional melting [8].

Here, we combine field evidence and experimental data to demonstrate that pseudotachylyte ought to be a common product of volcanic activity due to simultaneously high ambient temperatures and differential stresses, and propose a hypothesis for this conspicuous absence of pseudotachylytes in the volcanic record.

Results and Conclusion

Experimental results demonstrate that higher slip rate and/or axial load increases the rate of heat production by friction. At volcanoes, repeated slip events at a high ambient temperature during the ascent of a magma may thus promote melting (as well as subsequent cooling) in (near-)equilibrium, hence eradicating some of the key pseudotachylyte characteristics, including heterogeneous melt filaments formed by selective melting of crystals [9]. Our studies suggest that the indentification of volcanic pseudotachylytes relies upon combined investigations of structural characteristics, magnetic properties (Curie temperature, remanence, susceptibility and domain state) and calorimetric glass transition, which can identify different P-T equilibrium conditions between the wallrock and pseudotachylyte.

[1] Shimamoto & Lin (1994) *Struct. Geol. (Journal of the Tectonic Research Group of Japan)* **39**, 79-84. [2] Di Toro et al. (2006) *Science* **311**, 647-649. [3] Sibson (1975) *Geophys. J. Roy. Astr. S.* **43**, 775-794. [4] Tuffen & Dingwell (2005) *Bull. Volc.* **67**, 370-387. [5] Schwarzkopf *et al.* (2001) *International Journal of Earth Sciences* **90**, 769-775. [6] P. Kokelaar (2007) *J. Geol. Soc.* **164**, 751-754. [7] Kendrick *et al.* (2012) *J. Struct. Geol.* **In press**. [8] Lavallée *et al.* (2012) *J. Struct. Geol.* **In press.** [9] Lin & Shimamoto (1998) *J. Asian Earth Sci.* **16**, 533-545.

Extremely high iodine and noble gas abundances in forearc serpentinites

MARK A KENDRICK[1*], MASAHIKO HONDA[2], THOMAS PETTKE[3], DAVID PHILLIPS[1]

[1]School of Earth Sciences, University of Melbourne, Victoria, Australia. (*mark.kendrick@unimelb.edu.au)
[2]Research School Earth Sciences, Australian National University, Canberra, Australia.
[3]Institute of Geological Sciences, University of Bern, CH-3012 Bern, Switzerland.

Combined Cl, Br, I and noble gas analyses have been undertaken on 16 'seafloor serpentites' obtianed from IODP drill cores (Atlantic and Hess Deep MOR; Marianas and Guatemala forearcs; Iberian and Newfoundland passive margins; see [1]). The serpentinite halogen data overlap those of sedimentary marine pore fluids, with forearc serpentinites being most enriched in iodine (Fig 1). The maximum iodine concentration of ~50 ppm, is similar to the iodine content of organic-rich marine sediment.

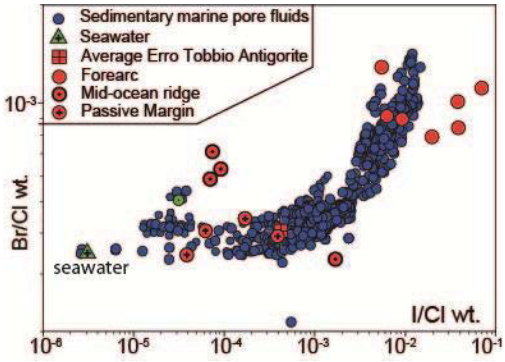

Figure 1: Br/Cl versus I/Cl three element plot showing the compositional range of sedimentary marine pore fluids (refs in ref [3]) and seafloor serpentinites.

The chrysotile-lizardite serpentinites all have atmospheric He, Ne, Ar, Kr and Xe isotope signatures. The maximum noble gas abundances of ~2×10^{-11} mol ^{36}Ar g^{-1} exceed those of antigorite serpentinites, by an order of magnitude[2]. Noble gas abundances are not simply correlated with serpentinites halogen signatures. However, the serpentinites preserving Br/Cl and I/Cl closest to the pore fluid trend have the highest ^{36}Ar concentrations. The data suggest that serpentinisation takes place at variable water-rock ratios. Serpentinites formed at low W/R, with pore fluids 'consumed' during serpentinisation, preserve halogen signatures close to the marine pore fluid trend, and the highest noble gas abundances. Serpentinites formed at higher W/R, do not preserve the halogen signature of the marine pore fluid, and trap an order of magnitude less noble gas.

The combined halogen and noble gas data show that the conditions of serpentinisation, as well as the involvement of sedimentary marine pore fluids in near subduction zone settings, exert critical controls on subduction zone volatile budgets.

[1] Kodolanyi et al., (2012) *Journal of Petrology* **53**, 235-270.
[2] Kendrick et al., (2011) *Nature Geoscience* **4**, 807-812.
[3] Kendrick et al., (2011) *Applied Geochemistry* **26**, 2089-2100.

https://doi.org/10.1180/S0026461X00008434 Published online by Cambridge University Press

Soil gas exploration at Rotokawa geothermal field, New Zealand

SIMON BLOOMBERG[1], CLINTON RISSMANN[2], TRAVIS HORTON[1], AGNES MAZOT[3], DARREN GRAVLEY[1], CHRISTOPHER OZE[1], AND BEN KENNEDY[1*]

[1]University of Canterbury, Geological Sciences, NZ
simon.bloomberg@pg.canterbury.ac.nz
Ben.kennedy@canterbury.ac.nz*
[2]Environment Southland, Invercargill, NZ
[3]GNS Science, Wairakei, NZ

Soil CO_2 as a proxy for heat and mass flow

A significant challenge to geothermal exploration is accurate quantification of the heat and mass flow between deep reservoir(s) and the surface. Here, we use high resolution measurement (10's of m's) of carbon dioxide (CO_2) flux and heat flow at the land surface to characterise the mass (CO_2 and steam) and heat released from the geothermal reservoir. Statistical and isotopic characterisation of atmospheric, biogenic and hydrothermally sourced CO_2 reduces the level of uncertainty when deriving mass (emissions) and heat flow estimates from high temperature reservoirs. Our results include soil CO_2 flux, soil $\delta^{13}C$, and soil temperature (0.1m depth) measurements at the surface of Rotokawa geothermal field (2.5km^2), in the Taupo Volcanic Zone, New Zealand. Data is modelled and interpolated to predict total CO_2 emissions which are used in conjunction with historic fumarolic discharges to calculate reservoir mass and heat flow. Soil temperature measurements are converted to heat flow units and summed to produce a surface heat flow value.

Initial results indicate a total CO_2 emission rate of 633 ± 16td^{-1} which includes 22td^{-1} from biogenic and atmospheric sources. The $\delta^{13}C$ range (-16 and -8‰) is plotted as an isoscape (i.e. isotope value contours) and illustrates spatial variance in magmatic, biogenic and atmospheric CO_2 contribution. The reservoir's steam mass flow of 10,150td^{-1} is calculated from the total hydrothermal CO_2 emission (611 ± 16td^{-1}) multiplied by the H_2O:CO_2 molar weight ratio (16.6) characterised for major fumaroles. The equivalent thermal energy of the mass flow of the reservoir is 317 ± 8MW, while the observed surface heat flow through soil is equivalent to 73 ± 5MW. The discrepancy in these two heat flow values is attributed to water vapour condensing (scrubbed) within cool (<160ºC) meteoric groundwaters that overly the high temperature reservoir prior to reaching the surface. In contrast, CO_2 is more conservative and therefore less susceptible to scrubbing by meteoric groundwaters making it a better proxy for heat and mass release from the deep reservoir.

By spatially mapping and comparing the soil flux, temperatures, and $\delta^{13}C$, there is more control over the soil permeability/soil gas flux (magnitude) relationship. The connectivity from the deep source through to the shallow subsurface through structural (fault/fracture) control of fluid flow pathways can be constrained with more certainty by identifying the CO_2 source.

This study concludes that the combination of CO_2 flux and $\delta^{13}C$ can successfully quantify heat flow and predict connectivity to deeper heat sources as well as illustrate shallow spatial variation in permeability.

The effect of extracellular polysaccharides on the mobility of phosphates bound to iron oxides

JANICE P.L. KENNEY [1*] AND PER PERSSON[1]

[1]Department of Chemistry, Umeå University, Umeå, Sweden,
(* presenting author: janice.kenney@chem.umu.se)

Introduction

The biogeochemical cycle of P is unique due to its strong tendency to adsorb to environmental particles, such as iron oxides, resulting in the formation of sparingly soluble solid phases. Furthermore, phosphorus does not form volatile compounds in the environment; hence the biogeochemical cycle of phosphorus occurs exclusively in the biosphere. Thus, due to the high stability of phosphates, key processes for biomass production are the transfer of phosphorus from adsorbed, solid, or organically bonded states into bioavailable forms, and these processes occur primarily at primarily at solution interfaces with minerals, microbes, or organic ligands.

The types of environmental perturbations that may result in the release of phosphates from iron oxide surfaces are not well understood. For example, many microorganisms and plants can release extracellular polysaccharides (EPS) into their local environments. EPS is known to adsorb to environmental particles, including iron oxides, and therefore the adsorption of EPS may out-compete the adsorbed phosphate, or even preferentially bind the oxyanion. It was previously thought that organics that form inner sphere complexes with the iron oxides would be able to out-compete the phosphates and remobilize them into solution. However, Lindegren et al. [1] found that strong, multiple H-bond donors and acceptors, in lieu of inner sphere species, out-compete phosphate. Therefore, EPS may be expected to have an effect on phosphate mobility in the subsurface. Currently, there is little information available regarding the ability of EPS to remobilize essential nutrients, such as phosphate, into the environment.

Experimental

In this study we investigated the remobilization of both inorganic and organophosphate following their adsorption to iron oxides. The inorganic phosphate used was orthophosphate and the organophosphate was the phosphate monoester, glucose phosphate. We examined qualitatively and quantitatively the effect of alginate, which was used as a model for EPS, on the remobilization mechanisms and competition reactions of pre-adsorbed phosphates. This was accomplished by a combination of in-situ infrared spectroscopy and wet-chemical experiments. Data were collected as a function of phosphate and alginate concentrations, pH, and time, and the collective results from these experiments will be presented and the co-adsorption and competitive mechanisms will be discussed. These results are important as they provide constraints on the mobility and, thereby, bioavailability of phosphate in the environment.

[1] Lindegren (2009) *European Journal of Soil Science* **60**, 982-993.

https://doi.org/10.1180/S0026461X00008434 Published online by Cambridge University Press

Modeling the impact of variable pH and dissolved salt concentrations on metal ion transport observed in field experiments

DOUGLAS B. KENT[1*], MATTHIAS KOHLER[2], GARY P. CURTIS[3], GILLIAN M. FAIRCHILD[4], AND DENIS R. LEBLANC[5]

[1]U. S. Geological Survey, Menlo Park CA, USA, dkbent@usgs.gov (*presenting author)
[2] U. S. Geological Survey, Menlo Park CA, mkohler@usgs.gov
[3] U. S. Geological Survey, Menlo Park CA, gpcurtis@usgs.gov
[4] U. S. Geological Survey, Northborough MA, gfairchi@usgs.gov
[5] U. S. Geological Survey, Northborough MA, dleblanc@usgs.gov

Field experiments show that the mobility of the divalent metal ions Ni, Zn, and Pb in a mildly acidic aquifer varies with both pH and dissolved salt concentrations. Field experiments were conducted by injecting groundwater with added Ni, Zn, and Pb at 2 or 20 μM into a shallow aquifer on Cape Cod, Massachusetts, USA. The mineralogy of the sediments is dominated by quartz but the sorption properties are controlled by well-ordered, nanometer-size Al-substituted goethite and micrometer-size clay minerals like chlorite and illite in mineral-grain coatings [1]. Uncontaminated groundwater had approximately 90 μM Na, 8 μM K, 20 μM Mg, and 9 μM Ca. Concentrations in a wastewater-contaminated zone of the aquifer were 10-20 times higher. Much more extensive retardation of Ni and Zn were observed in the uncontaminated zone at pH 6 over a one-meter transport distance than in the wastewater-contaminated zone. Much less extensive retardation of Zn and minimal retardation of Ni was observed in the uncontaminated zone at pH 5 than at pH 6. Concentrations of Pb remained above background in the injection ports for several months under all sets of conditions. Lead still had not been detected one meter downgradient one year after the injection but was readily mobilized by EDTA.

Models for metal ion sorption were calibrated by using laboratory experiments conducted with site-specific aquifer sediments over the relevant range of chemical conditions. Sorption of all three metal ions increased with increasing pH (4.8-6.3). Sorption decreased with increasing dissolved salt concentrations, but the impact on Pb sorption was much less extensive than for Ni and Zn. Sorption of Na, K, Mg, and Ca also increased with increasing pH. Sorption could be described quantitatively by using a set of cation exchange and surface complexation reactions: M^{n+} + $nHY = MY_n + nH^+$ and $Me^{2+} + >SOH = >SOMe^+ + H^+$, where M = Na, K, Mg, Ca, Ni, Zn, or Pb; Me = Ni, Zn, or Pb; and HY and >SOH represent generic surface sites.

Reactive transport simulations incorporating the laboratory-calibrated sorption models capture the principal trends in the field experimental data. Mobility of Ni is controlled by ion-exchange-type reactions, mobility of Pb by surface-complexation-type reactions, and mobility of Zn by both types of reactions. Results show that simple model structures like this can account for the impact of pH and dissolved salt concentrations on metal ion mobility.

[1] Zhang et al. (2011) *J. Contam. Hydrol.* **124**, 57-67.

Changes in North Atlantic deepwater circulation during the past 4 Myr

NABIL KHÉLIFI[1*], MARTIN FRANK[1], AND DIRK NÜRNBERG[1]

[1]Helmholtz Centre for Ocean Research (GEOMAR), Kiel, Germany, nkhelifi@geomar.de (* presenting author)

Abstract

Changes in northern North Atlantic deep water circulation during the past 4 million years (Ma) were studied at a suite of five IODP/ODP sites at water depths from 2400 to about 5000 m. Benthic $\delta^{13}C$ records at these sites oscillate in parallel around values lower than today by ~0.2 ‰ during interglacials and by ~0.7 ‰ during pronounced glacials of the late Pliocene warm period. However, Pliocene Mg/Ca-based deep-water temperatures were 2 to 3 °C higher than today during interglacials and near modern levels during glacial periods. The coeval changes in ventilation at a lower level than today may indicate a weaker difference between these warm water masses than today, which is probably caused by water mixing in the northern North Atlantic. This is corroborated by ε_{Nd} bottom seawater values near -9 to -10 at all sites, which differs markedly from the modern situation characterized by clear differences in ε_{Nd} signatures between the water masses at these sites. Accordingly, the lesser ventilated, warm, and mixed water masses are most likely the result of the weaker overturning in the northern North Atlantic during that time of global warmth [1].

After 1.6 Ma, benthic $\delta^{13}C$ records show a gradually improving ventilation, with pronounced glacial/interglacial oscillations, which came close to the modern-to-late-Pleistocene levels. This ventilation change in deep water masses was coeval with a clear divergence in ε_{Nd} of bottom water masses between the different sites towards modern signatures. This is apparently linked to a significant change in the sources of circulating deep waters in northern North Atlantic. Accordingly, the first reorganization of the deep circulation in northern North Atlantic towards the modern situation appears to have started only after ~1.6 Ma, most likely as a response to increases in the amplitude of the Earth's obliquity cycle during that time [2].

[1] Haywood & Valdes (2004) *Earth and Planetary Science Letters* **218**, 363-377. [2] Laskar *et al.* (1993) *Astronomy and Astrophysics* **270**, 522-533.

https://doi.org/10.1180/S0026461X00008434 Published online by Cambridge University Press

$U_K^{37'}$ in eastern tropical Pacific surface sediments: Implications for alkenone paleothermometry at the 'warm end'

M. KIENAST[1*], G. MACINTYRE[1], N. DUBOIS[1,2], S. HIGGINSON[1], S.S. KIENAST[1], AND T.D. HERBERT[3]

[1]Dalhousie University, Dept. Oceanography, Halifax, Nova Scotia, Canada, markus.kienast@dal.ca (* presenting author)
[2]now at: School of Earth, Atmospheric and Environmental Sciences, The University of Manchester, Manchester, UK
[3]Brown University, Dept. of Geological Sciences, Providence, Rhode Island, USA

Introduction

The eastern equatorial Pacific (EEP) is arguably the oceanic region where reconstructions of past sea surface temperature (SST) variability based on different proxies disagree most significantly. For instance, foraminiferal Mg/Ca and alkenone paleothermometry-based SST estimates disagree on the timing and pattern of the glacial-interglacial warming, and the inferred amplitude of the glacial cooling, in particular in the cold tongue off Peru, ranges from 2 to 8 °C depending on the proxy used.

Results and Conclusion

Here we present the first regional calibration of alkenone unsaturation in surface sediments versus World Ocean Atlas (WOA) 09 mean annual sea surface temperatures (maSST). Based on 81 new and 48 previously published data points, it is shown that open ocean samples conform to established global regressions of $U_K^{37'}$ versus maSST and that there is no systematic bias from seasonality in the production or export of alkenones, or from surface ocean nutrient concentrations or salinity. The flattening of the regression at the highest maSSTs is found to be statistically insignificant. For the near-coastal Peru upwelling zone between 11-15 °S and 76-79 °W, however, we corroborate earlier observations that $U_K^{37'}$ SST estimates significantly over-estimate maSSTs at many sites. We posit that this is caused either by uncertainties in the determination of maSSTs in this highly dynamic environment, i.e. by substantial small-scale SST variability not captured by WOA, or by biasing of the alkenone paleothermometer toward El Niño events as postulated by Rein et al. [1].

[1] Rein, B., et al. (2005), El Niño variability off Peru during the last 20,000 years, *Paleoceanography*, 20(4), doi:10.1029/2004PA001099

Ancient water and isolated ecosystems in crystalline bedrock

RIIKKA KIETÄVÄINEN[1*], LASSE AHONEN[1], ILMO T. KUKKONEN[1], NINA KORTELAINEN[1], MARI NYYSSÖNEN[2,3], AND MERJA ITÄVAARA[3]

[1]Geological Survey of Finland, Espoo, Finland, riikka.kietavainen@gtk.fi (* presenting author), lasse.ahonen@gtk.fi, ilmo.kukkonen@gtk.fi, nina.kortelainen@gtk.fi
[2]Lawrence Berkeley National Laboratory, Berkeley, CA, USA, mjnyyssonen@lbl.gov
[3]Technical Research Centre of Finland, Espoo, Finland, Merja.Itavaara@vtt.fi

Introduction

Saline groundwaters with distinct water stable isotope composition above the Global Meteoric Water Line (GMWL) are common in continental shields all over the world [1]. Microbial life thrives in these extreme environments. The 2516 m deep Outokumpu Deep Drill Hole, located in eastern Finland, is an uncased hole hosted by Palaeoproterozoic turbiditic metasediments, ophiolite-derived altered ultramafic rocks and pegmatitic granitoids, and provides a direct access to gas rich formation waters, where diverse microbial communities have been found [2]. Isotopic composition of water and dissolved strontium as well as geochemistry has been used to characterise the drill hole water profile in order to trace water origin and evolutionary time scales [3]. Along with microbiological studies this helps to reveal the extent of isolation of sub-surface ecosystems.

Results and conclusions

Water stable isotope composition of the Outokumpu Deep Drill Hole water is typical for shield brines, and clearly different from shallow fresh groundwater in the area. High salinity up to 70 g l^{-1} of total dissolved solids and high $^{87}Sr/^{86}Sr$ ratio also indicate strong water-rock interaction. Five isotopically and geochemically distinct water types occur along the 2.5 km drill hole section. Two-component mixing between the ^{18}O and ^{2}H enriched saline water and lighter meteoric water can not explain the isotopic composition and trends observed. Instead, ancient meteoric waters recharged at different, warmer than present climatic conditions and subsequent evolution of groundwater by hydration of silicates is the most likely cause for the observed variation. In the plate tectonic and palaeoclimatic framework, residence times in the order of tens of millions of years are suggested. However, the time which these waters have been isolated from surficial waters and from each other may differ substantially between the water types. Changes in bacterial communities with depth correlate with the different water types indicating the occurrence of separate ecosystems at different depths.

[1] Kloppmann et al. (2002) *Chem. Geol.* **184**, 49-70. [2] Kukkonen (2011) *Geol. Surv. Finl. Spec. Pap.* **51**. [3] Kietäväinen et al. (subm.) *Appl. Geochem.*

https://doi.org/10.1180/S0026461X00008434 Published online by Cambridge University Press

Reassessment of the dispersion of uranium originating from nuclear test explosions across East Asia through the atmosphere

YOSHIKAZU KIKAWADA[1*], YUSUKE MATSUMOTO[1], TAKAO OI[1], MASAO NOMURA[2] AND KATSUMI HIROSE[1]

[1]Sophia University, Materials and Life Sciences, Tokyo, Japan, y-kikawa@sophia.ac.jp (* presenting author), t-ooi@sophia.ac.jp, hirose45037@mail2.accsnet.ne.jp

[2]Tokyo Institute of Technology, Research Laboratory for Nuclear Reactors, Tokyo, Japan, mnomura@nr.titech.ac.jp

Background and Methodology

We have already reported that some Japanese atmospheric deposits have been contaminated with the uranium whose isotope ratio ($^{235}U/^{238}U$) had been fractionated from the natural ratio [1, 2]. For example, the uranium with a high $^{235}U/^{238}U$ ratio relative to the natural ratio (enriched uranium) has continuously been transported to the western side of the Japanese Islands since the 1960s until today. This suggests that the debris of nuclear test explosions conducted in Asia before the 1980s have continuously drifted east through the atmosphere. These debris must have been transported to the east end of Asia not only directly but also through several resuspension processes from their hypocenter region. However, the actual source region and transportation processes of such nuclear debris have never been identified clearly. In this context, we preliminarily measured the uranium isotope ratios of the dry deposits from Asian mineral dust events at Nagasaki, Japan and of surface soils across East Asia to clarify the mechanisms for the transportation of nuclear debris. The dry deposits from dust events had been collected at Nagasaki, which is located at western Japan near the Korean Peninsula, in March 2001, just at the time of a huge Asian mineral dust (Kosa, yellow-sand) event.

Results and Remarks

The $^{235}U/^{238}U$ ratios in the dry deposits samples from Nagasaki are obviously higher than the natural ratio (maximally *ca.* +20‰). Contrastively, no obvious fractionation in the uranium isotope ratio is found for the surface soils in the East Asian region served to this study, although they tend to have slightly higher $^{235}U/^{238}U$ ratio than the natural one. Our results undoubtedly reveal that Asian mineral dust has been transported with nuclear debris which contains enriched uranium. The contribution of secondary processes like repeated resuspension of contaminated surface soils, which had been overlaid with nuclear debris through fallout processes, to the anomalous uranium isotope ratios found in Japanese atmospheric deposits may not be so substantial.

[1] Kikawada *et al.* (2009) *J. Nucl. Sci. Technol.* **46**, 1094-1098.
[2] Kikawada *et al.* (2011) *Mineral. Mag.* **75**, 1182.

Decrease of Arsenate Adsorption onto Bacteriogenic Iron Oxies by the Presence of Organic Materials

S. KIKUCHI [1*] AND Y. TAKAHASHI[1]

[1]Graduate School of Science, Hiroshima University, Hiroshima 739-8526
([*]correspondence: m103384@hiroshima-u.ac.jp)

The adsorption behaviour of trace elements onto iron (Fe) oxides has been well demonstrated for their importance in water chemistry. Especially, bacterial-induced iron oxides (Bacteriogenic iron oxides: BIOS) are of common interest because of their ubiquity and characteristics of adsorption of various ions. In this study, arsenate adsorption behaviour onto (A) synthetic ferrihydrite, (B) natural BIOS collected from Okinawa hydrothermal vent, (C) synthetic BIOS obtained by incubation of iron-oxidizing bacterium (*Mariprofundus ferroxydans*) were compared. BIOS synthesis was performed using a set of diffusion cells by which can obtain pure BIOS free from other inorganic and organic materials which are abundant in natural BIOS (e.g., silica, clay mineral, and other ions adsorbed onto BIOS). Adsorption experiments were performed under sea water condition (I: 0.7 M; initial arsenate concentration: 70 mg/L; adsorbent: approx. 0.5 mg) as a function of pH 4-10. Iron mineral species of iron oxides were specified by Fe K-edge X-ray adsorption fine structure (XAFS) [1] and adsorption structure of arsenate was examined by As K-edge XAFS analysis.

Iron K-edge XAFS analysis revealed that both natural and synthetic BIOS consisted mainly of ferrihydrite with 45-55 % of highly amorphous Fe hydroxides that is characterized by the primitive Fe hydrothesis stages. The crystal size was nano-scale which was smaller than the synthetic ferrihydrite. Thus, It was expected that BIOS sholud have more arsenate adsorption capacity than synthetic ferrihydrite. However, the amount of arsenate adsorbed onto each iron oxides decreased in the order of synthetic ferrihydrite > natural BIOS = synthetic BIOS with a same adsorption trend as a function of pH. XAFS and μ-XRF analysis indicated that arsenate was mainly adsorbed onto Fe phase within natural and synthetic BIOS forming inner-sphere complexatation to the Fe oxides. These results were consistent with previous results on arsenate adsorbed onto synthetic ferrihydrite. Contrary to their reduced crystal particle size, specific surface areas of synthetic BIOS was decreased by 25% from synthetic ferrihydrite, which is possibly caused by the coprecipitation of Fe oxides with organic materials [2]. Thus, it is suggested that strong aggregation of Fe particles by the presence of orgainic material reduces (i) the surface area and/or (ii) the active adsorption site within BIOS, which ultimately result in the decrease of the arsenate adsotion onto BIOS. These results also suggests that direct and indirect effects of organic material sholuld be taken into account to evaluate the anion adsorption onto BIOS.

[1] Kikuchi et al. (2011) *Chem. Lett.* **40**, 680-681
[2] Mikkuta et al. (2008) *Geochim. Cosmochimi. Acta.***72**, 1111-1127.

https://doi.org/10.1180/S0026461X00008434 Published online by Cambridge University Press

Magmatic processes at Mt. Ruapehu, New Zealand: melt-mush interactions determined from melt inclusions

GEOFF KILGOUR[1,2*], JON BLUNDY[2], KATHY CASHMAN[2,3], HEIDY MADER[2]

[1]Wairakei Research Centre, GNS Science, Taupo, New Zealand g.kilgour@bristol.ac.uk (* presenting author)
[2]School of Earth Sciences, University of Bristol, Bristol, UK
[3]Dept. of Geological Sciences, University of Oregon, USA

Mt. Ruapehu is an andesitic cone volcano situated at the southern end of the Taupo Volcanic Zone. Historical activity has consisted of frequent small phreatic and phreatomagmatic eruptions through Crater Lake - a warm, acidic lake. Eruptions are difficult to predict due to the very short seismic precursors and typically provide only minutes of warning. Three popular ski fields are located on the mountain and therefore it is important that the processes responsible for the generation of eruptions are better constrained.

Ruapehu scoria exhibit phenocrysts of plagioclase, clinopyroxene, and orthopyroxene with rare microphenocrysts of ilmenite and magnetite. We present geochemical data and volatile contents of phenocryst-hosted melt inclusions and groundmass glass from scoria erupted in 1969, 1971, 1977, 1995, and 1996. The groundmass glass composition spans a similar range to the melt inclusions (58-74 wt % SiO_2). The volatile content of melt inclusions is very low in H_2O (~ 1.5 wt %), high in F (up to ~ 2000 ppm), and high in CO_2 (up to ~ 1000 ppm). These magmas record some of the lowest H_2O contents of an andesite in an arc setting.

Many phenocryst-hosted melt inclusions plot on a separate mixing line from the groundmass glass, which suggests that the phenocrysts are exotic to the melt. We show that the small volume magmas that are erupted at Ruapehu leave a remnant crystal mush that is re-entrained by the following eruption. This is seen in eruptions where the time interval between eruptions is short (e.g. 1969/1971 and 1995/1996). Consequently, most Ruapehu magmas interact with a resident crystal mush prior to eruption. The interation of magmas with a crystal mush is probably a common process at other volcanoes, and the small volume of magmas at Ruapehu allows for more common preservation of these magmatic interactions at depth.

Mineral Dissolution Kinetics Under Conditions Relevant to Geological Storage

ANDREW D. KILPATRICK*, JÖRGEN ROSENQVIST AND BRUCE W. D. YARDLEY

School of Earth and Environment, University of Leeds, Leeds, LS2 9JT, United Kingdom
ee07adk@leeds.ac.uk (* presenting author)
j.rosenqvist@leeds.ac.uk, b.w.d.yardley@leeds.ac.uk

In the field of geological storage of carbon dioxide, a detailed understanding of the geochemical behaviour of the host reservoir is important in terms of both storage potential and security. Currently, most predicitions of geochemical behaviour rely on sparse data from single mineral experiments conducted under a wide variety of pressures, temperatures and salinities not all of which will be relevant to specific storage sites.

Our experiments aim to bridge some of these knowledge gaps: CO_2 solubility and the kinetics of mineral dissolution in CO_2-mineral-brine systems have been examined in a number of batch experiments at sub-critical (3 bar – 30 bar, 20°C – 70°C) conditions. Common reservoir mineral and rock samples have been utilised in these experiments, including dolomite, quartz, feldspar and UK sandstone. Figure 1 shows the results from an experiment following cation release from c.150µm sized dolomite in a CO_2 saturated brine at 21°C and 3 bar CO_2 pressure. Concentrations plateau at between 400 and 500 hours, a fairly long time relative to dissolution rates expected for calcite. The dissolution is highly incongruent, with calcium concentrations five to six times higher than those of magnesium. The exact reaction mechanism is still under investigation. These rates appear to be closer to those expected for silicate minerals and suggest that reaction rate imbalance between carbonate rocks and silicate rocks must be evaluated for specific lithologies and mineralogies.

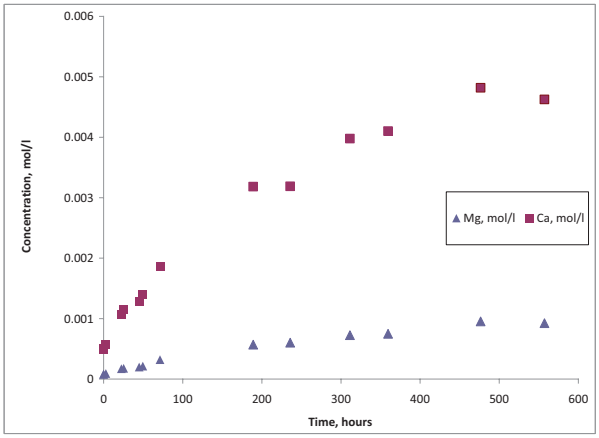

Figure 1: Ca and Mg release during a CO_2-brine-dolomite batch experiment. Temperature: 21°C, Pressure: 3 Bar, Brine: 1.36M NaCl.

https://doi.org/10.1180/S0026461X00008434 Published online by Cambridge University Press

Fluvial and windborne transport of arsenic-bearing mine tailings in semi-arid environments

CHRISTOPHER S. KIM[1*], DAVID H. STACK[1], JAMES J. RYTUBA[3]

[1]Chapman University, School of Earth and Environmental Sciences, Orange, USA, [*]cskim@chapman.edu

[3]U.S. Geological Survey, Menlo Park, USA, jrytuba@usgs.gov

Gold and silver mining throughout the state of California has left an environmental legacy of exposed mine wastes (tailings) containing elevated levels of arsenic (As) and other potentially toxic trace elements. The uncontrolled movement of mine tailings by erosion and natural transport processes poses challenges to the long-term containment and remediation of these contaminated materials.

The typically fine-grained size distribution of mine tailings combined with decades of exposure and weathering of large tailings piles has resulted in the mobilization of As-bearing mine wastes by both fluvial means (rainwater runoff and streams) and by transport of windblown mine waste particles. While airborne mobilization of mine tailings is diffuse and covers large areas, in semi-arid mining areas with relatively low rainfall rates fluvial transport is both sporadic and much more localized down narrow semi-linear streambeds (washes), facilitating the movement of tailings across significant distances and into ephemeral lakes/playas.

We have conducted extensive geochemical, mineralogic, and spatial characterization of tailings throughout the Mojave Desert, CA to assess the degree of surface arsenic enrichment in soils surrounding tailings piles, identify arsenic concentration trends with distance in sediments located within different washes, and measure arsenic in surface water runoff from a tailings pile during a rare storm event. EXAFS spectroscopy was also applied to selected samples to determine arsenic speciation at various locations.

Intense precipitation events were determined to mobilize mine wastes as a series of discrete pulses down a wash, which could be effectively modeled as a series of overlapping pulses with power-law exponential decay characters. Similar exponential decay behavior was observed by windblown tailings and maximized in the direction of prevailing winds. In the majority of samples, arsenic was found to exist as As(V), either in the form of secondarily-mineralized iron arsenate phases or in a sorbed phase onto iron (hydr)oxide phases.

By examining fluvial and windborne transport of As-enriched tailings at various mines throughout the western Mojave Desert, we have developed a conceptual model for the transport of mine wastes within alluvial systems that provides a sound basis for formulating strategies for the effective remediation and monitoring of historic mine areas in semi-arid environments.

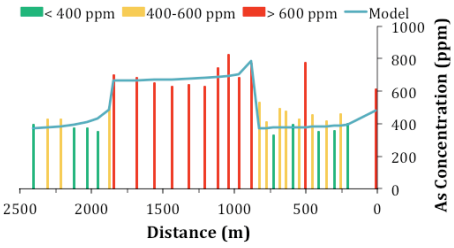

Figure 1: Arsenic concentration as a function of distance from mine point source, with exponential decay model overlying data.

Evaluation of Rice Wine Waste as Substrate for Use in Acid Mine Drainage Treatment

GYOUNGMAN KIM, SANGSOO KANG[*], JUNGSEOCK KANG, HWANJO BAEK

[1]Kangwon National University, Dept. of Energy resources Engineering, Chuncheon, Korea, yaong011@kangwon.ac.kr

[2] Korea Institute of Geoscience and Mineral Resources, Daejeon, Korea, kss@kigam.re.kr (* presenting author)

[3] Korea Institute of Geoscience and Mineral Resources, Daejeon, Korea, kangjs@kigam.re.kr

[4]Kangwon National University, Dept. of Energy resources Engineering, Chuncheon, Korea, hwanjo@kangwon.ac.kr

Introduction

The spent mushroom compost(SMC) has been generally used as substrate for passive treatment systems, especially for SAPS in Korea. More effective substitutes to replace the SMC have always been a key concern. In this study, rice wine waste(RWW) was tested as substrates for use in acid mine drainage treatment.

Materials and methods

Batch tests were conducted to evaluate the material's efficacy in reducing sulfates and removing heavy metals within the artificial AMD. AMD was made from the standard solution for some heavy metals, mixed with distilled water and strong acid. During the test, limestone aggregates were added for increasing the pH of AMD. Batch test was continued for 27 days, and samples were taken every 3 days. The ORP, pH, and the sulfate concentration of each sample were recorded, and the concentration of heavy metals was measured with ICP.

Results and Conclusion

Test results showed that both SMC(#1) and RWW(#2) have similar efficiency in total sulfate reduction capacity(Fig. 1). However, the RWW has a little higher reducing rate, and the mixture of SMC and RWW(#3) showed the highest reducing rate. In terms of the heavy metal removal, including Fe, Al, and Cu, both materials showed similar results. Overall, the batch test results indicated that RWW has a good potential as a substrate for SAPS.

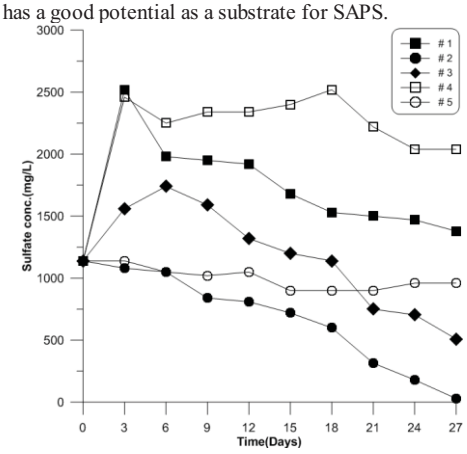

Fig. 1. Changes in sulfate

https://doi.org/10.1180/S0026461X00008434 Published online by Cambridge University Press

Bayesian statistical interpretation of hydrochemistry data to delineate the groundwater vulnerability to nitrate contamination

HO-RIM KIM[1*], KYOUNG-HO KIM[1], SEONG-TAEK YUN[1], KYUNG-GOO KANG[2], HYANG MI KIM[3], YOUNG-HWA GO[1], AND SOO-HYUNG MOON[2]

[1]Korea University, Green School and the Department of Earth and Environmental Sciences, South Korea, honeius@korea.ac.kr (* presenting author)

[2]Jeju Special Self-Governing Province Development Corporation, South Korea

[3]University of Calgary, Mathmatics and Statistics

Nitrate contamination of groundwater is a serious environmental problem in South Korea and elsewhere. Better understanding of the source(s) and spatial land use control of groundwater nitrate pollution is required to manage nitrate contamination. In this context, we used a GIS technique integrated with a Bayesian statistical approach to interpret hydrochemistry data of groundwater, in order to produce a spatial map reliably showing groundwater vulnerability to nitrate contamination. For this purpose, we used the hydrochemistry data of 45 groundwater samples from the Pyosun Watershed located on Jeju volcanic island, Korea. The studied groundwater system is considered to be highly susceptible to non-point contamination sources such as agricultural pollutants because of the short residence time in the permeable basaltic aquifer.

The vulnerability (i.e., pollution probability) was initially predicted using a logistic model on the relationship between observed nitrate concentrations and the distribution of agricultural fields within a land use map. However, the initial results on vulnerability prediction were not satisfactory yielding a few unreliable results. This is likely due to inherent uncertainties of the adopted statistical model (i.e., model error) and the land use classification obtained from the GIS technique (i.e., data error). To assess such uncertainties, we re-evaluated the spatial information with the membership probability in relation to the extent of agricultural lands, using a fuzzy algorithm on a remote sensed image. In the next step, the results estimating data error were compared with the improved spatial map showing the probability of the nitrate concentrations to exceed a natural background (2.5 mg/L in the studied area). Finally, we compared the results of two probability maps for each GIS grid cell using the Bayesian regression, in order to assess the model uncertainty. As a result of these steps, the obtained results on groundwater vulnerability were significantly improved to yield a significant correlation between predicted nitrate concentrations and observed nitrate concentrations. Therefore, our technique developed in this study can be successfully used for evaluating groundwater vulnerability to nitrate contamination based on the hydrochemistry and land use data in agricultural areas.

Interaction of supercritical CO_2 with bentonite

JIN-SEOK KIM[1]*, HO-YOUNG JO[1], AND SEONG-TAEK YUN[1]

[1]Korea university, Earth and Environmental science, Seoul, Republic of Korea, darkach@korea.ac.kr (*presenting author)

Physical properties (e.g., porosity and permeability) of caprocks may be altered by interaction between Supercritical (SC) CO_2 and caprock. Caprocks in potential geological carbon sequestration sites can have clay minerals, which is mainly affected by SC CO_2. In this study, interaction between SC CO_2 and clay minerals was evaluated at various conditions. Bentonite was used in this study because bentonite mainly consists of montmorillonite, which is the expandable clay mineral.

SC CO_2/bentonite/water interaction kinetic tests were conducted in a stainless steel autoclave reactor at various conditions for a week to investigate how bentonite is altered in saline water when contacted with SC CO_2. The tests were conducted at 50℃ and 12 MPa. Two reaction systems (SC CO_2/bentonite and SC CO_2/water/bentonite) were used to mimic the geologic CO_2 sequestration environment. The water/bentonite system without addition of SC CO_2 was also used as a reference system. 1N NaCl, $MgCl_2$, and $CaCl_2$ solutions and sea water were used to investigate the effect of salts on the bentonite alteration in the presence of SC CO_2.

In the SC CO_2/bentonite system without water, the mass and volume of bentonite sample decreased probably due to pore water in bentonite gradually dissolved in SC CO_2. In the SC CO_2/water/bentonite system, blue and greenish mineral precipitation was observed on surface of bentonite samples. In addition, the bentonite samples swelled during the interaction. The bentonite samples swelled in the presence of salts, even though the degree of swelling was less than that without salts. These results implies that salinity and water content can affect the extent of bentonite alteration in the presence of SC CO_2. Further evaluation of the effect of precipitation and dissolution of minerals on the physical properties of bentonite when contacted SC CO_2 is needed.

https://doi.org/10.1180/S0026461X00008434 Published online by Cambridge University Press

Effect of Dissolved Ions on $\delta^{18}O$ Measurement of Saline Aqueous Solutions: Experimental Results

SANG-TAE KIM[1*], SEONG-SOOK PARK[2], AND SEONG-TAEK YUN[3]

[1]McMaster University, School of Geography and Earth Sciences, Hamilton, Canada, sangtae@mcmaster.ca (* presenting author)
[2]Hanyang University, Department of Natural Resources and Environmental Engineering, Seoul, Republic of Korea, pss2907@hanyang.ac.kr
[3]Korea University, Department of Earth & Environmental Sciences, Seoul, Republic of Korea, styun@korea.ac.kr

The oxygen isotope ratios of aqueous solutions have been typically determined by either "the classic CO_2–H_2O equilibration method" or a quantitative conversion of H_2O to a gas (e.g., CO, CO_2, or O_2), followed by an isotopic analysis of the gas on an isotope ratio mass spectrometer (IRMS). However, many stable isotope laboratories use the classic CO_2–H_2O equilibration technique for their routine $\delta^{18}O$ analysis of aqueous solution samples due to its analytical simplicity. In recent years, the classic CO_2–H_2O equilibration method has gained more popularity because of the introduction of an automated on-line CO_2–H_2O equilibration system coupled to a continuous-flow isotope-ratio mass spectrometer (CF-IRMS). This relatively new but innovative CF-IRMS technique requires a considerably smaller amount of aqueous solutions, compared to the conventional off-line or on-line CO_2–H_2O equilibration technique for a dual-inlet isotope ratio mass spectrometer (DI-IRMS).

Whatever the type of preparation technique or the stable isotope ratio mass spectrometry, the kinetics of oxygen isotope exchange for a given CO_2–H_2O system have to be carefully evaluated in order to accurately determine the oxygen isotope ratio of the corresponding aqueous solution when the classic CO_2–H_2O equilibration method is employed. This is because oxygen isotope exchange kinetics in the CO_2–H_2O system for a high ionic strength solution (e.g., hydrothermal brines) are not the same as that for a low ionic strength solution (e.g., freshwater) [1, 2]. Guidelines for the $\delta^{18}O$ analysis of high ionic strength solutions of geological importance will be presented at the meeting based on the experimentally determined results of oxygen isotope exchange kinetics and equilibrium isotope effects in various CO_2–high ionic strength solution systems, such as CO_2–a 1.0 molal solution of Na_2SO_4.

[1] Fortier (1994) *Chem. Geol.* **116**, 115-162.
[2] Lécuyer *et al.* (2009) *Chem. Geol.* **264**, 122-126.

Lithium isotopic signature Oman ophiolite during hydrothermal alteration of the ancient oceanic crust

TAEHOON KIM[1*], SHUN'ICHI NAKAI[2], HODAKA KAWAHATA[3], KYOKO YAMAOKA[4] AND YOSHIRO NISHIO[5]

[1]Korea Polar Research Institute, Inchon, Korea, tkim@kopri.re.kr (* presenting author)
[2]Earthquake Research Institute, The Universty of Tokyo, Tokyo, Japan
[3]Atmosphere and Ocean Research Institute, The University of Tokyo, Kashiwa, Japan
[4]Geological Survey of Japan, National institute of Advanced Industrial Science and Technology, Tsukuba, Japan
[5]Kochi Institute for Core Sample Research, JAMSTEC, Kochi, Japan

Oman ophiolites are regarded as a fossil oceanic crust which was hydrothermally altered by seawater-derived fluid [1]. Li isotopes can be utilized for tracing hydrothermal alteration because of their large isotopic fractionation at low-to-medium temperature between rock and fluid phase [2]. Here, we determined the Li abundances and isotopic compositions of the ophiolites from the Wadi Fizh section in Oman with multi-collector ICP-MS, IsoProbe in the University of Tokyo and Neptune in JAMSTEC. The precisions of δ^7Li measured by IsoProbe and Neptune are ± 0.7 and 0.3 ‰ (2σ), respectively.

The Li abundances vary from 0.1 to 8.0 ppm, and decrease with depth. The δ^7Li values of the Wadi Fizh section represent a variation ranging from +2.9 to +23.5‰, which is heavier than those of normal MORB. The samples deeper than 2 km also show heavy Li-isotopic signatures, different from drill hole samples of the ODP sites 504B and 896A in the present oceanic crust [3]. There is no distinct correlation between the δ^7Li values and depth. The sheeted dike and dolerite dike samples near the boundary between the sheeted dike and gabbro layer have heavy δ^7Li values up to ca. +23‰. These large variations in the δ^7Li values are likely to result not only from temperature variation, but from changes in the Li composition of hydrothermal fluid and water/rock ratios.

The Li compositions of initial hydrothermal fluid which altered the samples of ophiolites were calculated with changing water/rock ratios, and show deviation from the reaction array between seawater and fresh MORB. This suggests that the initial fluid of the Wadi Fizh section has evolved via other pathway than the simple interaction array between seawater and fresh MORB. The range of inferred initial fluid is similar in the Li compositions with pore fluids in high-temperature diagentic environment and marine brines [4, 5]. It is suggestive that the Li composition of initial hydrothermal fluid in the Wadi Fizh section is modified by another process by the interaction between original seawater-derived fluid and sediment or secondary mineral at the surface level of the oceanic crust.

[1] Kawahata et al. (2001) *Jour. Geophy. Res.* **106**, 11083-11099. [2] Seyfried et al. (1998) *GCA* **62**, 949-960. [3] Chan et al. (2002) *EPSL* **202**, 187-201. [3] Chan and Kastner (2000) *EPSL* **183**, 275-290. [4] Chan et al. (2002) *GCA* **66**, 615-623.

https://doi.org/10.1180/S0026461X00008434 Published online by Cambridge University Press

Mercury Sorption on Apatite: Effects of pH and Ionic Strength

YOUNG JAE KIM[1], SOO-OH PARK[1], YOUNG JAE LEE[1*]

[1]Department of Earth and Environmental Sciences, Korea University, Seoul 136-701, Korea (*Correspondence: youngjlee@korea.ac.kr, jjbsnlove@korea.ac.kr, orange261@korea.ac.kr)

Mercury (Hg) has been the subject of interest due to its substantial toxicity on humans and living organisms. Apatite such as hydroxylapatite (HAP, $[Ca_5(PO_4)_3OH]$) is one of abundant minerals in nature but also the essential constituent for bone of vertebrates. In spite of such importance, Hg sorption on hydroxylapatite (HAP) has been barely adressed yet. In this study, sorption of mercury on HAP is investigated through batch experiments over a wide range of physicochemical conditions such as different pHs and concentrations of background electrolyte in solution.

Upon [Hg] < 20 μM, Hg sorption on HAP shows that mercury uptake by HAP increases with increasing the mecury concentration in solution over a wide range of pH between 5.0 and 9.0. Total amount of mercury sorbed on HAP decreases with increasing pH; the total amount of Hg sorption on HAP at pH 5.0 is twice greater than that of pH 8.5, suggesting that the sorption of Hg could be critically controlled by pH at the HAP-water interface. Compared to that of pH 8.5, we found that an ionic strength dramatically influences Hg uptake by HAP at pH 5.0, showing that Hg sorption increases with increasing the concentration of background electrolyte at pH 5.0. Although this study is an on-going research, it is likely that these observations would be relevant to Hg species as a function of pH. With PHREEQC modeling for Hg speciation, our results show that $Hg(OH)_2^0$ is dominant at pH 8.5, whereas at pH 5.0 $HgCl_2^0$ plays as a major species under the experiment conditions in this study, indicating that changes in Hg species as a function of pH play an important role in the sorption of Hg on HAP. In kinetic experiments at pH 8.5, the initial uptake of Hg by HAP is rapid and ~85% of Hg is rapidly sorbed on the HAP within 1 hr, suggesting that adsorption plays a key role in the initial uptake of mercury at the HAP-water interface. With our results, it is found that the mercury uptake by HAP is greatly influenced by different physicochemical conditions such as pH and ionic strength of the solution.

Silver reduction and synthesis of elemental silver nanoparticles by metal-reducing bacteria

YUMI KIM* AND YUL ROH

Chonnam National University, Gwangju, Korea, rohy@jnu.ac.kr

Introduction

In the recent years, a new dimension of the microbe-metal interactions has been explored for synthesis of metal nanoparticles such as gold and silver[1]. Although Ag(0) is known to be an antibacterial agent, metal-reducing bacteria such as *Geobacter* sp. and *Shewanella* sp. have shown the surprising ability of actively growing and precipitating Ag(0) nanoparticles within and around the cell surface via reduction of Ag(I) [2-3]. The objectives of this study were to synthesize Ag(0) nanoparticles via microbial Ag(I) reduction as well as to determine the effects of various experimental conditions such as silver nitrate concentrations, pHs, temperatures, and reaction time controlling for the optimal biosynthesis of Ag(0) nanoparticles.

Materials and Methods

The Ag(0) nanoparticles were synthesized by metal-reducing bacteria (Suncheon-1) enriched from inter-tidal flat sediments from southwestern part of South Korea. The 16S rRNA gene DGGE analysis showed the metal-reducing bacteria consisted of *Shewanella* sp., *Clostridium* sp., and *Vibrio* sp. Microbial synthesis of Ag(0) nanoparticles was examined under different concentrations of silver nitrate (1 − 10 mM), medium pHs (6.5 − 8.5), incubation temperatures (5 − 35℃) and reaction time (for 7 days) for crystal growth. The precipitates resulted from silver reduction by the bacteria were analyzed with XRD and TEM-EDS for mineralogical characterization.

Results and Conclusion

The metal-reducing bacteria (Suncheon-1) enzymatically transformed silver nitrate to Ag(0) nanoparticles with their metabolism. The Ag(0) nanoparticles were rapidly synthesized when silver nitrate ($AgNO_3$) was injected into the medium enriched the bacteria compared with initial injection at once. Microbial reactions with silver ion led formation of homogeneous sized Ag(0) nanoparticles (5 − 15 nm) by reduction of silver nitrate (0.5 − 1 mM) under the conditions around 15 − 25℃ and medium pH 8.5 within 3 days of incubation time. These results show that metal-reducing bacteria enzymatically reduced Ag(I) to Ag(0) and formed homogeneous size and shape of Ag(0) nanoparticles. Moreover, the capability of silver precipitation by microbial Ag(I) reduction suggests expanded application of recovering silver nanoparticles from silver-containing water and/or silver enriched natural environments.

[1] Fayaz *et al.* (2011) *Appl. Process Biochem.***46**, 1958-1962.
[2] Law *et al.* (2008) *Appl. Environ. Microbial.***74**, 7090-7093.
[3] Wang *et al.* (2010) *J. Bacteriol*. **192**, 1143-1150.

https://doi.org/10.1180/S0026461X00008434 Published online by Cambridge University Press

Copper speciation in variably toxic sediments: Ely Copper Mine Superfund Site, Vermont

BRYN E. KIMBALL[1*], ANDREA L. FOSTER[2], ROBERT R. SEAL II[1], NADINE M. PIATAK[1] AND JANE M. HAMMARSTROM[1]

[1]US Geological Survey, Reston, VA, USA, bekimball@usgs.gov (* presenting author), rseal@usgs.gov, npiatak@usgs.gov, jhammars@usgs.gov

[2]US Geological Survey, Menlo Park, CA, USA, afoster@usgs.gov

Near the Ely Copper Mine, a Superfund site in Vermont, both surface water and sediment quality are impacted by acid rock drainage and elevated metal concentrations, with Cu being the dominant metal and contaminant of concern [1]. Chronic water-quality criteria for Cu are exceeded in the section of Ely Brook that drains mine waste. In this same section, however, stream bed sediment toxicity, as measured by detritus-feeding invertebrates called amphipods, varies. At an upstream sample location where surface and *in situ* pore water pHs are near 7, stream bed sediments display high toxicity (6% survival), but at a downstream sample location where surface and *in situ* pore water pHs are near 3, stream bed sediments have lower toxicity (91% survival) [1]. Because Cu concentrations in Ely Brook stream bed sediments are high throughout the study area (0.33 – 0.93 wt.%), the toxicity results suggest that Cu in upstream sediments is more bioavailable than Cu in downstream sediments. In sediment samples examined using bulk X-ray diffraction, no Cu minerals were detected above detection limits, so we hypothesize that the variable Cu toxicity is due to differences in the identity, relative abundance, and/or distribution of solid-phase Cu species, where Cu is a trace to minor component.

In an effort to characterize Cu speciation in these distinct toxicity environments, we collected six stream bed sediment samples along the toxicity gradient and conducted meso-scale (50-100 µm beam size) X-ray fluorescence microscopy (XRF) on sediment thin sections, and X-ray absorbance spectroscopy (XAS) on bulk dried sediment powders and representative model compounds. Both datasets were collected under ambient conditions.

Preliminary XRF results indicate that Cu in the relatively toxic upstream sample correlates with Mn, and generally coats mineral grain surfaces. In less toxic downstream samples, Cu correlates strongly with S and Zn, and weakly with Fe. Preliminary analysis of calibrated and normalized X-ray absorption near edge spectra (XANES) shows clear evidence of the presence of a Cu-sulfide phase in downstream, low-toxicity sediments. The upstream, high-toxicity sample displays an overall XANES spectrum similar to spectra for Cu-sorbed Fe- and Mn-(hydr)oxides. The relative abundance of dominant Cu species is being determined by linear-combination, least-squares fitting. Preliminary results indicate that downstream sediment spectra are fit 80-90% by chalcopyrite and 10-20% by Cu-jarosite. The upstream sediment spectrum is fit nearly 100% by Cu-sorbed MnO_2. The spectroscopic findings are consistent with the toxicity results given the lower solubility of Cu sulfides relative to Cu sorbed phases under relevant environmental conditions.

[1] Seal, R.R. II *et al.* (2010) *US Geological Survey Scientific Investigations Report* 2010-5084.

Sulphate inhibition of magnesite dissolution: An in-situ AFM study

HELEN E. KING[1*] AND CHRISTINE V. PUTNIS[1]

[1]Institut für Mineralogie, University of Münster, Münster, Germany, hking_01@uni-muenster.de (* presenting author), putnisc@uni-muenster.de

Magnesite is the expected product phase of CO_2 sequestration in strategies involving Mg-silicates. Its formation and stability in these environments will be controlled by the ions present in rock pore fluids, e.g. NaCl and sulphates, as well as temperature and pH. The effect of different ligands on magnesite stability has been studied at aquifer conditions, i.e. low concentrations, in *ex-situ* flow-through experiments where sulphate was shown to enhance the dissolution [1]. To test whether this effect is also prominent at higher sulphate concentrations we have conducted *in-situ* dissolution experiments of the $\{10\bar{1}4\}$ magnesite surface using atomic force microscopy (AFM) at room temperature with Na_2SO_4 concentrations between 0.01 and 0.1 M. Solutions were acidified to pH 2 because magnesite dissolution under ambient conditions is slow. However, rather than observing an increase in dissolution under our experimental conditions, sulphate dramatically reduced the magnesite dissolution rate. To determine whether this effect was a consequence of the mixed electrolytes used in the experiments of Pokrovsky et al. [1] magnesite dissolution in solutions of 0.1 M NaCl and 0, 0.01, 0.03 or 0.1 M Na_2SO_4 was tested. Experiments at approximately 40 °C were also conducted to study the role of temperature on the sulphate effect.

Increased dissolution was observed with 0.1 M NaCl without sulphate in comparison to dissolution in 0.1 M Na_2SO_4. The effect of sulphate was not diminished by the concomitant presence of chloride even when the concentration of the different anions was equal. Increasing the solution temperature also did not change the effect of sulphate on magnesite dissolution. Formation of Mg-sulphate interactions are expected to be facilitated by the presence of NaCl in solution due to its effect on ion hydration [2]. Similarly, higher temperatures have been shown to increase the number of contact ion pairs between Mg and sulphate in solution [3]. Both of these effects are possibly a consequence of changes in the ion hydration. Therefore, it would be expected that the presence of sulphate in higher ionic strength solutions or higher temperatures would also retard magnesite dissolution. A precipitate was observed on the surface during the experiments despite the undersaturation of the input solution with respect to Mg-carbonate phases and the inhibition of magnesite dissolution in the presence of sulphate. This indicates that in our experiments the fluid boundary layer present at the mineral surface plays a crucial role in the reaction. Thus, sulphate in this boundary layer, which could be present in nature but was minimized in previous *ex-situ* flow-through experiments, plays a critical role in magnesite reactivity.

[1] Pokrovsky et al. (2009) *Chemical Geology* **265**, 33-43.
[2] Ruiz-Agudo et al. (2011) *Chemical Geology* **281** 364-371.
[3] Rudolph et al. (2003) *Physical Chemistry Chemical Physics* **5**, 5253-5261.

https://doi.org/10.1180/S0026461X00008434 Published online by Cambridge University Press

Petrogenesis of CAMP dolerites from Suriname and West Africa

NICOLE KIOE-A-SEN[1*] AND MANFRED VAN BERGEN[2]

[1]Anton de Kom University of Suriname, Paramaribo, Suriname, nicole.kioe-a-sen@uvs.edu (* presenting author)
[2] Department of Earth Sciences, Utrecht University, The Netherlands, m.j.vanbergen@uu.nl

We performed a petrological and geochemical investigation on dolerites from Suriname and West Africa to explore the extent to which CAMP products from areas on opposite sides of the present-day Atlantic have a common petrogenetic heritage. Dykes in Suriname and the Ivory Coast (IC) are mainly tholeiitic basalts, while sills in Burkina Faso (BF) are mostly basaltic-andesites with tholeiitic as well as calc-alkaline affinities. The Surinamese rocks are slightly more evolved (Mg#=34-46) than the IC dolerites (Mg#=43-51), whereas the BF dolerites include the least evolved compositions (Mg#=45-66).

A geographic subdivision into high-Ti (1.9-3.7 wt.% TiO_2) and low-Ti (0.9-1.2 wt.%) dolerites is consistent with findings in other CAMP regions. Nevertheless, overall geochemical characteristics of the studied rocks tend to be distinct. The Surinamese and IC dolerites fall in a narrow zone of high-Ti magmatism along the margins of the present-day Atlantic Ocean, where preferential upwelling shortly before initial rifting has been proposed. Trace-element signatures and inferences from partial melting models suggest that mantle sources of the Surinamese and IC dolerites were different from those of the BF rocks. Modestly contrasting geochemical signatures point to source inhomogeneity and variations in melting conditions on regional as well as local scales. Relatively deep melting of a garnet-rich source with primitive-mantle like composition may have produced the Suriname and IC magmas, whereas the BF magmas possibly originated by shallower melting of a more spinel-rich source that might have been affected by subduction-type enrichment. Our findings indicate that chemostratigraphic criteria, used in correlations of northern CAMP basalts, are not directly applicable to southern counterparts on both sides of the Atlantic.

Plutonium redox chemistry under anoxic conditions in the presence of iron(II) bearing minerals

REGINA KIRSCH[1,2*], DAVID FELLHAUER[3,4], MARCUS ALTMAIER[4], LAURENT CHARLET[2], THOMAS FANGHÄNEL[3], ANDREAS C. SCHEINOST[1]

[1]Institute of Resource Ecology, HZDR, Dresden, Germany, kirsch@esrf.fr (*presenting author), scheinost@esrf.fr
[2]ISTerre, UdG/CNRS, Grenoble, France, charlet38@gmail.com
[3]EC-JRC-ITU, Karlsruhe, Germany, thomas.fanghaenel@ec.europa.eu
[4]Institute for nuclear waste disposal, KIT, Karlsruhe, Germany, marcus.altmaier@kit.edu, david.fellhauer@kit.edu

The environmental fate of plutonium, the major transuranium actinide in nuclear waste, is largely impacted by its sorption onto and redox reactions with iron oxide, carbonate or sulfide minerals that form as corrosion products of steel in the "near field" and occur widely in sediments. To obtain information on oxidation state and local structure of Pu in the presence of Fe(II) bearing minerals, electrolytically prepared Pu(V) or Pu(III) (^{242}Pu, 1-3·10^{-5} M) were, under anoxic conditions, reacted with magnetite ($Fe^{II}Fe^{III}_2O_4$) (pH 6-8.5), chukanovite ($Fe_2(CO_3)(OH)_2$) (pH 8.5) and mackinawite (FeS) (pH 6-8.5). Pu-L_{III}-edge X-ray absorption spectra (XAS) were collected after 40 d and 8 months of reaction.

In all 14 samples, more than 98 % of Pu was associated with the solid phase and its redox speciation thus accessible by XAS. With magnetite, only the sample prepared at the highest pH and highest Pu loading contained $Pu(IV)O_2$ while in all others Pu was solely present as a tridentate Pu(III) surface complex [1]. The three chukanovite samples all contained both Pu(III) (15 to 40 %) and PuO_2. With mackinawite at pH 6 only Pu(III) was present, while all samples prepared at pH 7 and higher contained mostly PuO_2 and up to approx. 10 % Pu(III).

Through comparison of the different types of minerals (oxide, carbonate, sulfide), reaction pH and Pu/mineral ratios, it becomes apparent that the type of surface complexation (e.g. inner-sphere on magnetite vs. outer-sphere on mackinawite) and total mineral surface area are key parameters in controlling concentrations of dissolved Pu and in determining whether a PuO_2 solid phase precipitates. While PuO_2 provides an upper limit for concentrations of dissolved Pu, the available mineral surface area and sorption complex stability control what percentage of Pu is present in surface complexes. Under reducing conditions as established through the Fe(II) bearing minerals used here, this mineral surface associated Pu was found to be trivalent. Surface complexed Pu(III) and PuO_2 can be thought of being in equilibrium with each other via two processes: a sorption reaction between dissolved and surface complexed Pu(III) and a heterogeneous redox reaction between dissolved Pu(III) and solid phase $Pu(IV)O_2$. It remains to be investigated if and through what mechanisms the Pu solid phase speciation (sorbed Pu(III) vs. solid phase PuO_2) might impact the migration behavior of Pu and how, for risk assessment purposes, Pu(III) surface complexes with iron minerals can be implemented into geochemical models.

[1] Kirsch et al. (2011) *Environ. Sci. Technol.* **45**, 7267-7274.

https://doi.org/10.1180/S0026461X00008434 Published online by Cambridge University Press

Archean "whiffs of oxygen" go Poof!

JOSEPH L. KIRSCHVINK[1,*], TIMOTHY D. RAUB[2], & WOODWARD FISCHER[1]

[1] Division of Geological and Planetary Sciences, California Institute of Technology, Pasadena, California, USA.

[2] Department of Earth Sciences, University of St. Andrews, St. Andrews, United Kingdom.

NASA's scientific drillcore ABDP-9 penetrated ~90 m of strata from the Archean-Paleoproterozoic boundary interval in the mid-Hamersley Basin of the Pilbara craton, Western Australia beneath ~100 m of regolith. A series of geochemical studies of the core in the past 5 years starting with [1, 2] have reported Mo and Re concentration enrichments, mass-independent sulfur isotope fractionations, ^{15}N-enrichments, and iron speciation that were argued to represent "whiffs" of atmospheric oxygen. These datasets have lent support to controversial traces of biomarkers in both this unit and strata elsewhere in the Hamersley Basin that have been interpreted to contain evidence for cyanobacteria and eukaryotes inhabiting widespread late Archean niches. Similar, though less conspicuous Mo, Re, S, N, Fe, and lipid biomarker anomalies in ~2.7-2.5 Ga marine strata of South Africa's Kaapvaal cratonic margin have been interpreted in context of ABDP-9 "whiffs" of oxygen to suggest even "pervasive" Late Archean oxygenation. These interpretations are surprising because they appear to conflict with other longstanding geological proxies (e.g. red beds, redox-sensitive detrital grains, mass independent S fractionation) that suggest the rise of oxygen occurred several hundred million years later. If correct, these data solicit a complete reevaluation of our knowledge of how solid Earth and surface Earth processes operate to keep oxygen in balance over geological time. It is reasonable to ask whether the inferences made from elemental and isotopic relationships captured in these rocks are sufficiently strong to warrant such reevaluation.

We present new observations from ABDP-9 that reveal significant open-system, post-depositional alteration of the sedimentary rocks in this region of the Hammersley Basin: these include observations of widespread highly-crystalline, high-temperature, late-stage chlorite veins, preferentially developed within shale lithologies and concentrated in the "whiff" interval, locally associated with iron and sulfur metasomatism; and regionally set in ~300-450 °C burial metamorphic, multiply-deformed terrane. Preliminary micro-scale work to measure isotopic and elemental abundances show clear texture-specific differences that may allow untangling of several episodes of diagenesis and metasomatism to provide a framework for better interpreting the bulk data.

These post-depositional features in ABDP-9 argue that the 'whiffs' are metasomatic artifacts. We suspect similar problems in other Archean cores, which are sulfide-remagnetized during orogenic episodes associated with Pb-Zn-mineralizing crustal fluids in the foreland. We note that a late origin of oxygenic photosynthesis can explain the Lomagundi-Jutali event, the Makganyene snowball, the Kalahari Mn field, the Sishen iron deposit, and Shungite deposition [3]. The timing is consistent with recent molecular clock estimates for the radiation of the Eukaryotes, which post-date 2 Ga. [4].

[1] Kaufman et al., Science **317**(2007): 1900-1903. [2] Anbar et al., Science **317**(2007): 1903-1906. [3] Kirschvink et al., GCA **73,** A662-A662. [4] Parfrey et al., PNAS **108** (2011): 13624-13629.

Nitrate transformation and immobilization: effects of biotic-abiotic and oxic-anoxic conditions

FIONA KIZEWSKI[1*], JASON KAYE[1], AND CARMEN ENID MARTÍNEZ[1]

[1]The Pennsylvania State University, Department of Crop and Soil Sciences, frk2@psu.edu (*), jpk12@psu.edu, cem17@psu.edu

Biogeochemistry under redox-dynamic conditions: processes, speciation, and fluxes

It has been hypothesized that incorporation of dissolved inorganic nitrogen into organic matter (OM) via abiotic (chemical) prossesses is one of the mechanisms that account for the high N retention observed in temperate forest soils [1]. Soil incubations under sterile conditions have shown that N from nitrate (N-NO_3^-) is rapidly transformed to organic nitrogen [2, 3]. Transformation of N-NO_3^- to organic nitrogen involves a decrease in N oxidation state. Hence, NO_3^- reduction to nitrite (NO_2^-) or other more reduced species may be a required step prior to N immobilization. In this study, solid OM was spiked with $^{15}NO_3^-$ and incubated in suspensions in four combinations of biotic-abiotic and oxic-anoxic conditions at pH 6.5 for five days. Our objectives are to elucidate how biotic-abiotic and redox conditions affect NO_3^- transformations and to determine whether N-NO_3^- will be incorporated into solid OM under abiotic conditions.

Within the first hour, the experimental (NO_3^- spiked) system incubated under biotic and oxic (Bio-Ox) conditions showed a drastic decrese (22%) in NO_3^- concentration, which increased again towards the end of incubation. Increases in the concentrations of NH_4^+ and dissolved organic nitrogen (DON) in the experimental system were of the same magnitude as in the blank (no NO_3^- spiked) systems. However, significant increases did not occur until after ~3 days in the blank. These results suggest that NO_3^- addition accelerates microbial activity, which facilitates N mineralization to NH_4^+. Incubations of experimental and blank systems under abiotic oxic (Abio-Ox) conditions showed no significant change in NH_4^+ with time; but a steady increase, of the same magnitude, was observed for DON. The experimental system showed a steady decrease in NO_3^- of 8% with time under Abio-Ox conditions. Comparison of Bio-Ox and Abio-Ox systems thus suggests that microbial activity is not required for the production of DON, but seem to be needed for DON mineralization to NH_4^+.

We also performed incubations under anoxic conditions to test whether the same mechanisms are operative in reduced environments, e.g., in the interior of soil aggregates or wetlands. Under anoxic conditions, the spiked NO_3^- disappeared within the first 24 h in both the biotic and abiotic experimental systems. In these systems, NO_2^- was detected; its concentration first increased then droped to zero. Biotic anoxic (Bio-Anox) systems showed an increase in the concentration of NH_4^+ with time. However, the increase of NH_4^+ in the experimental system was twice that of the blank. Another striking result is that DON in the blank increased with time whereas it remained constant in the experimental system. Under abiotic anoxic (Abio-Anox) conditions, the experimental and blank systems showed the same trend and magnitude in DON decrease and NH_4^- increase.

Disappearance of NO_3^- and NO_2^- detection under anoxic conditions suggest that NO_3^- is reduced to NO_2^- which is either volatized or incorporated into the solid OM. Under biotic conditions, immobilization (microbial and chemical) seems to be the primary pathway for NO_3^- disappearance. Our interpreation of the fate of NO_3^- under various conditions will be further verified by ^{15}N measurements.

[1] Aber *et al.* (1998) *Bioscience* **48**, (11), 921-934. [2] Dail *et al.* (2001) *Biogeochemistry* **54**, (2), 131-146. [3] Fitzhugh *et al.* (2003) *Global Change Biology* **9**, (11), 1591-1601.

https://doi.org/10.1180/S0026461X00008434 Published online by Cambridge University Press

Zn-rich chromite in Ni-ore of the Thompson Nickel Belt, Canada

INGRID M. KJARSGAARD[1*], M. BETH MCCLENAGHAN[2], STUART A. AVERILL[3], AND GAYWOOD MATILE[4]

[1] Consulting Mineralogist, Ottawa, CANADA, ikjarsgaard@sympatico.ca (*presenting author)
[2]Geological Survey of Canada, Ottawa, CANADA, bmcclena@NRCan.gc.ca
[3]Overburden Drilling Management Ltd., Ottawa, CANADA, odm@storm.ca
[4]Manitoba Geological Survey, Winnipeg, CANADA, gaywood.matile@gov.mb.ca

Abstract

A comparative till and bedrock study in the Thompson Nickel Belt (TNB), Manitoba, Canada, was carried out by the Geological Survey of Canada (GSC) and Manitoba Geological Survey in collaboration with a Canadian Mining Industry Research Organization (CAMIRO) project with the aim of identifying potential resistate indicator minerals for Ni-Cu-mineralization. The TNB is a 10 to 35 km wide belt consisting of variably reworked Archean gneisses and Early Proterozoic cover rocks along the northwestern margin of the Superior Craton in central Canada. It hosts several world-class magmatic Ni-Cu deposits that have been strongly metamorphosed under upper amphibolite to granulite conditions. Nickel sulphide mineralization is associated with komatiitic ultra-mafic bodies (meta-pyroxenite, meta-peridotite) within the lower part of the Proterozoic Ospwagan Group. Of all the potential resistate minerals picked from till and representative bedrock samples of the main lithological units within the TNB, chromite is the most useful indicator mineral because it is more resistate than the sulphides, occurs both in ore and barren ultramafic rocks and has distinctly different compositions in mineralized samples compared to un-mineralized. Chromite in barren TNB peridotite contains moderate MgO (1.5 - 5 wt.%) and 40 to 52 wt.% Cr_2O_3 while chromite in massive sulphide ore varies from chromian magnetite to extremely Mg-poor, Zn-rich chromite in contact with pyrrhotite. The chromite analyzed in the massive Ni-ore contained > 2 wt.% to 8 wt.% ZnO. Chromite in till samples immediately down ice of the Thompson and Pipe deposits, are MgO-poor chromite - gahnite solid solutions spanning the entire range from 2 to 18% ZnO. In contrast, chromite in barren ultramafics and in till samples from non-mineralized areas of the TNB consistently contain <2 wt.% ZnO.

While Zn-rich chromite has been observed in other areas of the world hosting magmatic NiCu-deposits (e.g. Vammala belt, Finland and Kambalda, Australia), the compositions found in the TNB are extreme and are attributed to the high metamorphic grades reached during peak metamorphism.

Magma chamber heterogeneities recorded by melt inclusions from Mt. Somma-Vesuvius, Italy

RITA KLÉBESZ[1,2*], ROBERT J. BODNAR[1], BENEDETTO DE VIVO[2], ROSARIO ESPOSITO[1], ANNAMARIA LIMA[2], PAOLA PETROSINO[2], KALMAN TÖRÖK[3]

[1]Virginia Tech, Blacksburg, VA, USA, krita@vt.edu (* presenting author), rjb@vt.edu, rosario@vt.edu
[2]University of Naples "Federico II", Naples Italy, bdevivo@unina.it, anlima@unina.it, petrosin@unina.it
[3]Eötvös Loránd Geophysical Institute of Hungary, Hungary, torokklm@elgi.hu

Nodules (coarse-grain "plutonic" rocks) from the ~20 ka Pomici di Base (PB)-Sarno eruption of Mt. Somma-Vesuvius, Italy show petrographic features, such as porphyrogranular texture, slight zonation and irregular edges of phenocrysts, and crystallized melt pockets, which are all consistent with the interpretation that these nodules represent the crystal-rich part of the mush-zone of the active plumbing system beneath Mt. Somma-Vesuvius.

Melt inclusions (MI) are abundant in clinopyroxenes in the nodules. All MI observed in this study are partially to completely crystallized, suggesting they cooled relatively slowly after trapping. Two types of MI can be distinguished based on petrography. Type I consists of mica, Fe-Ti-oxide minerals and/or dark green spinel, clinopyroxene, feldspar and a vapor bubble. No volatiles (CO_2, H_2O) were detected in the bubbles during Raman analysis. Type II inclusions are generally lighter in color and they contain subhedral feldspar and/or glass and oxides. Both types of MI are randomly distributed in the crystals or they occur along a growth zone and are interpreted to be primary. MI were homogenized and analyzed to determine their major and trace element, and volatile compositions. MI homogenized between 1227°C and 1267°C, with most homogenizing at 1230-1235°C. In addition to petrographic differences, the two types of MI can also be distinguished based on their chemical compositions. Type I MI can be classified as phono-tephrite – tephri-phonolite – basaltic trachy-andesite, while Type II MI have a mainly basaltic composition. The two different types of MI also show different trace element patterns. Type I MI are more enriched in incompatible elements compared to Type II MI. SIMS analysis of homogenized MI show variations in the volatile composition of the melt, both within and between MI types.

The presence of spatially associated MI with different compositions in individual phenocrysts is interpreted to represent small scale heterogeneities within the magma chamber due to reaction of crystals and/or wall rock in the mush zone at the margin of the magma chamber with the newly intruded magma [1].

[1] Danyushevsky et al. (2004) *J. Petrol*. **45**, 2531-2553

https://doi.org/10.1180/S0026461X00008434 Published online by Cambridge University Press

Compositional controls on hydrogen generation during serpentinization

FRIEDER KLEIN*[1], WOLFGANG BACH[2], THOMAS M. MCCOLLOM[3]

[1] Woods Hole Oceanographic Institution, Woods Hole, MA 02543, USA, fklein@whoi.edu

[2] Geoscience Department, University of Bremen, Klagenfurter Str., 28359 Bremen, Germany, wbach@uni-bremen.de

[3] CU Center for Astrobiology and Laboratory for Atmospheric and Space Physics, University of Colorado, Boulder, CO 80309-0392, USA, mccollom@lasp.colorado.edu

At the Earth's surface peridotites and pyroxenites are inevitably unstable in the presence water causing the formation of serpentine, brucite or talc, magnetite and, most notably hydrogen. We compute equilibrium mineral assemblages, mineral compositions and the fluid/gas chemistry during serpentinization of an array of olivine- and/or pyroxene-rich rocks under near surface conditions from 25-400 °C and 50 MPa at a water-to-rock mass ratio of one. Our results indicate that the optimal temperature for hydrogen generation during serpentinization of olivine (Ol, Fo90)-rich peridotite and dunite is at about 300-330°C. At this temperature we predict that rocks having an Ol -orthopyroxene (Opx) mass ratio > 1 generate more hydrogen during serpentinization than rocks having an Ol – Opx mass ratio < 1. There is a direct link between the fayalite content of olivine, its stability relative to water, temperature, and redox conditions. Fayalite-rich olivine is stable to significantly lower temperatures in the presence of water than fayalite-poor olivine. Accordingly, the most reducing conditions during serpentinization of fayalite-rich olivine develop at temperatures lower than 330 °C. Notwithstanding the lower temperatures, rocks having abundant fayalite-rich olivine are predicted to generate significantly more H_2,aq during serpentinization than typical forsterite-rich (Fo90) mantle rocks.

Our modeling results indicate that serpentinization of Fe-rich ultramafic rocks might represent one of the most reducing environments at or close to the Earth's surface. The results also suggest that serpentinization on Mars, where Fe contents of olivine in peridotites are higher than in terrestrial counterparts, will generate higher levels of H_2.

Partitioning of F between nominally fluorine-free minerals and basaltic melts: Implications for the global cycle of halogens

S. KLEMME [1*], C. BEYER[1], C. VOLLMER[1], M. WIEDENBECK[2] AND A. STRACKE [1]

[1]Institut für Mineralogie, University of Münster, Germany stephan.klemme@uni-muenster.de (*presenting author) christian.vollmer@uni-muenster.de, stracke.andreas@uni-muenster.de, christopher.beyer@uni-bayreuth.de

[2]GFZ, Potsdam, Germany, michawi@gfz-potsdam.de

We present preliminary experimentally determined partition coefficients for fluorine (F) between nominally fluorine-free minerals and corresponding basaltic melts in the systems CaO-MgO-Al_2O_3-SiO_2+F, Na_2O-CaO-MgO-Al_2O_3-SiO_2+F, and in natural compositions at pressures up to 2.5 GPa and temperatures between 1285°C and 1445°C. F is incompatible in olivine, whereas the F in orthopyroxene is slightly more compatible. Our preliminary partition coefficients agree well with our analyses of F in natural olivines and orthopyroxenes from spinel peridodites and oceanic basalts, both indicating that F is much more compatible in olivine and orthopyroxene than hydrogen. Based on high-resolution TEM images of one of the samples, we argue that the F incorporation into the olivine structure is mass balanced via oxygen defects.

Hence, fluorine, and to a lesser extend chlorine, may be effectively stored in nominally fluorine-free mantle minerals such as olivine and orthopyroxene. By considering their high modal proportions in the upper mantle, both phases are the major hosts for F in the Earth's mantle, and must be taken into account when calculating the Earth's budget of halogens or global cycles of halogens in the deeper Earth. It, therefore, seems that other F-bearing minerals such as amphibole or phosphates are not required in order to balance the F concentrations between crust and mantle.

Applying our new partition coefficients to primitive olivine hosted melt inclusion data from mid-ocean ridge basalt (MORB) and from primary melt inclusions from ocean island basalts (OIB), we suggest slightly higher fluorine contents in OIB than in MORB.

https://doi.org/10.1180/S0026461X00008434 Published online by Cambridge University Press

Recrystallization of Barite in the presence of Ra at elevated temperatures up to 90 °C

MARTINA KLINKENBERG[1*], FELIX BRANDT[1], KONSTANTIN ROZOV[1], GIUSEPPE MODOLO[1], DIRK BOSBACH[1]

[1] IEK-6 Nuclear Waste Management and Reactor Safety, Forschungszentrum Jülich, Germany m.klinkenberg@fz-juelich.de(*presenting author), f.brandt@fz-juelich.de, k.rozov@fz-juelich.de, g.modolo@fz-juelich.de, d.bosbach@fz-juelich.de

The uptake of Radium by Barite via solid solution formation is an important process controlling the solubility of Ra in aqueous systems. Recent studies have focused on ambient conditions (Bosbach et al., 2010; Curti et al., 2010). Here, we have focused on the understanding of kinetics and uptake mechanisms at elevated temperatures.

New experimental data of batch recrystallization experiments at room temperature (RT) and 90 °C are presented. A pure barite solid was put into contact with an aqueous solution (0.1 n NaCl) with an initial Ra/Ba ratio of 0.3 ($5 \cdot 10^{-6}$ mol/L Ra) and neutral pH. The solid/liquid ratio was 5 g/L. A barite which consists of blocky crystals with a particle size of > 10 µm and a specific surface area of 0.17 m²/g was used for the recrystallization experiments at close to equilibrium conditions. The evolution of the Ra and Ba concentration in solution with time was monitored via Gamma spectrometry and ICP-MS. Furthermore, the morphological evoution of the barite crystals was investigated by SEM.

A faster decrease of the Ra concentration in solution is observed at 90 °C compared to room temperature. A steady state of the Ra concentration is reached at $3 \cdot 10^{-8}$ mol/L for experiments at 90 °C after 30 days and after 70 days at $3.5 \cdot 10^{-9}$ mol/l for experiments at room temperature.

Our results agree with the thermodynamic data of the $RaSO_4$ and $BaSO_4$ endmembers. At room temperature, $RaSO_4$ is less soluble than $BaSO_4$ whereas estimated solubilities indicate that $RaSO_4$ is more soluble than $BaSO_4$ at 90 °C. As a consequence, a lower retention capacity for Ra can be expected for 90 °C.

Electron microscopy results of the crystal morphology show a distinct influence of the presence of Ra on recrystalization at close to equilibrium conditions and 90 °C. In the presence of Ra, the crystals show plain crystal faces. In the absence of Ra rough surfaces and deep holes in the crystals are observed. These differences clearly indicate different recrystallization mechanisms.

TEM studies will be carried out to achieve a nanoscopic system understanding of micro structural evolution and Ra incorporation into the barite crystal as well as its spatial distribution in the crystal.

Bosbach, D.; Böttle, M. & Metz, V. (2010) *Waste Management, Svensk Kärnbränslehantering AB*
Curti, E.; Fujiwara, K.; Iijima, K.; Tits, J.; Cuesta, C.; Kitamura, A.; Glaus, M. & Müller, W. (2010) *Geochimica et Cosmochimica Acta*, **74**, 3553-3570

Prebiotic selection of D-ribose on mineral surfaces

K. KLOCHKO[1*], R.M. HAZEN[1,2], D.A. SVERJENSKY[1], AND G.D. CODY[1]

[1]Geophysical Laboratory, Carnegie Institution of Washington, Washington DC, USA, kklochko@ciw.edu (* presenting author)
[2]Department of Earth and Planetary Sciences, Johns Hopkins University, Baltimore, USA

Pentose sugars are major biochemical building blocks. Prebiotic syntheses have been proposed leading to complex mixtures including 4-, 5-, and 6-carbon sugars [1,2]. However, the pentose sugar D-ribose has the greatest biological importance because it is the sugar found within modern nucleic acids. We are investigating whether this is due to some exceptional characteristic of ribose associated with its interaction with mineral surfaces.

Some studies have shown that D-ribose can be stabilized in the presence of borate [3] or silicate [4] minerals. Recent study of the adsorption of nucleosides and nucleotides on rutile [5] indicates that adjacent OH-groups on the ribose part of these molecules play a critical role in the attachment to mineral surfaces. The four pentose sugars ribose, xylose, lyxose and arabinose differ only in the arrangement of the OH-groups and their stereochemistry in solution. This suggests that the different structures of these sugars might lead to selective adsorption on mineral surfaces.

The present study is focused on interactions of pentose sugars on rutile (α-TiO_2, pH_{PPZC} = 5.4, BET = 18.1 m^2/g) in the presence of light: in pure water; and in the dark: in pure water, 10 and 100 mM NaCl solutions over a wide range of pH conditions (5-11).

In the presence of light, the results of our batch adsoption experiments indicate an occurance of a photocatalytic reaction between rutile surface and four pentoses. Xylose and lyxose form threose via loss of an aldehyde group. The reaction product of ribose or arabinose and rutile has not yet been identified.

In dark conditions, batch adsorption experiments of the four sugars individually and in mixtures indicate that adsorption increases with increasing pH and salt concentration of the solution. The salt effect and pH dependancy of adsorption is more pronounced for ribose. Ribose adsorption is the strongest among the pentose sugars, suggesting that ribose's cis diol OH-groups play a critical role in the attachment to mineral surfaces. Overall, our results are consistent with the hypothesis that mineral surfaces could potentially have played a role in selecting ribose relative to the other pentose sugars.

[1] Springsteen and Joyce (2004) *J. Am. Chem. Soc.* **126**, 9578-9583. [2] Shapiro (1988) *Origin Life Evol. Biosphere* **18**, 71-85. [5] Ricardo *et al.* (2004) *Science* **303**, 196. [4] Vazquez-Mayagoitia *et al.* (2011) *Astrobiology* **11**, 115-121. [5] Cleaves *et al.* (2010) *Astrobiology* **10**, 311-323.

https://doi.org/10.1180/S0026461X00008434 Published online by Cambridge University Press

Man made water cycles: Isotope tracing of desalinated seawater through water supply, sewage and groundwater

WOLFRAM KLOPPMANN[1*], IDO NEGEV[2], JOSEPH GUTTMAN[2], CATHERINE GUERROT[1], CHRISTINE FLEHOC[1], MARIE PETTENATI[1], ORLY GOREN[3], AVIHU BURG[3].

[1]BRGM, Orléans, France, w.kloppmann@brgm.fr (* presenting author)
[2]Mekorot National Water Company, Tel Aviv, Israel
[3]Geological Survey of Israel, Jerusalem, Israel

Non-conventional water resources like desalinated water and treated sewage play today a key role in the water balance of many developed countries in arid and semi-arid regions. The worldwide capacity of desalination is expected to double within ten years to reach 62 Mm^3/d in 2015 [1]. This massive arrival of "man-made" fresh water in the water cycle is expected to change geochemical and isotope characteristics of surface and groundwater. A pilot study in 2008 [2] has shown the highly specific isotope signatures of reverse osmosis (RO) desalinated seawater. Our current study presents isotope data (B, $H+O_{H2O}$, $S+O_{SO4}$) on the largest system of soil-aquifer treatment (SAT) in the Middle East - the Shafdan site, Israel - where 130 Mm^3/Y of treated wastewater from the greater Tel Aviv region are infiltrated through ponds into the sandy Mediterranean Coastal Aquifer, recovered and then transported 70 km further to the South for unrestricted irrigation in the Negev desert. In Sept. 2010 and Feb. 2011, we analysed treated wastewater before infiltration, together with groundwaters at different distances from the infiltration ponds, as well as samples from the Tel Aviv drinking water supply and the product waters from two RO desalination plants. B isotopes of sewage show a siginficant shift from 1994 with a $\delta^{11}B$ of +9.7 ±2.8‰ *vs.* NBS951 [3] to 2010-11 with + 40.4 ±0.7‰ (n=5). This shift is explained with (1) a change in legislation lowering considerably the perborate contents in washing powders (1999-2008) and (2) the massive arrival of desalinated seawater in the drinking water supply ($\delta^{11}B$ of 53±3‰, [2]) since 2007. The breakthrough of this new boron signature has not yet been observed in the aquifer, not even for the wells closest to the infiltration ponds and no significant shift was observed between the two campaigns. This can be due to temporary sorption on clays leading to an important delay of B with respect to water [4] inducing a highly non-conservative behaviour. δ^2H and $\delta^{18}O_{H2O}$ in wastewater and groundwater can be quantitatively explained by the different components of regional water supply, including the new desalination permeate. $\delta^{34}S$ and $\delta^{18}O$ of sulphates in wastewater, observed in the vicinity of the infiltration pond, are very different from desalinated seawater, the latter very depleted in SO_4^{2-}, as sewage sulphate is dominated by other sources. This study reveals the usefulness of multi-isotope tracing for elucidating the mixing components and pathways of water and solutes in a nearly completely artificial regional water cycle.

[1] Fritzmann *et al.* (2007) *Desalination* **216**, 1-76. [2] Kloppmann *et al.* (2008) *Environ. Sci. Technol.* **42**, 4723-4731. [3] Venghosh *et al.* (1994) *Environ. Sci. Technol.* **28**, 1968-1974.

NO_2^--induced abiotic redox processes during microbial NO_3^--dependent Fe(II) oxidation

NICOLE KLUEGLEIN*, AND ANDREAS KAPPLER

University Tuebingen, Geomicrobiology, Germany
nicole.klueglein@uni-tuebingen.de (* presenting author)
andreas.kappler@uni-tuebingen.de

Anaerobic, neutrophilic nitrate-reducing Fe(II)-oxidizing bacteria are found in many anoxic environments and were suggested to play an important role in nitrogen and iron cycling. In this study we conducted batch experiments with the mixotrophic, nitrate-reducing, iron(II)-oxidizing *Acidovorax* sp. strain BoFeN1 isolated from anoxic littoral sediments [1]. This strain produces nitrite in the low mM range as an intermediate during denitrification. Nitrite has long been identified as a strong oxidant for Fe(II) particularly under acidic pH conditions [2] but also at neutral pH in the presence of minerals and heavy metal ions that function as catalysts [3,4]. This raises the question whether the oxidation of ferrous iron is indeed enzymatically catalyzed or whether to a large extent it is just a chemical reaction as a consequence of microbial nitrite formation during acetate oxidation. A key problem occurring during investigation of these processes is the quantification of Fe(II) oxidation over time in the presence of nitrite that forms during denitrification. The acidification of the samples with HCl during dissolution of the iron mineral phases followed by the widely used spectrophotometric ferrozine assay leads to a rapid, abiotic oxidation of Fe(II) by even small amounts of nitrite. This abiotic Fe(II) oxidation in turn leads to underestimated and thus incorrect values and therefore to an overestimation of oxidation rates. To obtain correct Fe(II) data we used a revised Fe extraction protocol and added 40 mM sulfamic acid to our samples. Sulfamic acid reacts with the nitrite and prevents abiotic Fe(II) oxidation by nitrite. With this revised analytical procedure we observed a much slower Fe(II) oxidation rate with BoFeN1 (3.4 mM/day) than previously published (6 mM/day) [5]. We also quantified abiogenic oxidation of ferrous iron by mM concentrations of nitrite added to sterile culture medium at neutral pH and found rapid Fe(II) oxidation suggesting that the abiotic oxidation of Fe(II) by nitrite produced during heterotrophic denitrification contributes significantly to overall Fe(II) oxidation rates observed. Additionally, we grew strain BoFeN1 at different temperatures and found that at lower temperatures nitrite accumulated to a higher extent than in cultures growing at room temperature. This suggests that abiotic nitrite-dependent Fe(II) oxidation is even more important in low-temperature environments such as lake sediments. In summary, our experiments demonstrate the importance of nitrite formation during heterotrophic nitrate reduction in mixotrophic nitrate-reducing, Fe(II)-oxidizing cultures. The ability of nitrite to oxidize ferrous iron in the presence of biogenic Fe(III) minerals also at neutral pH raises the question if the importance of the biological process was overestimated until now. Accurate measurements of Fe(II) concentrations over time with the described revised Fe extraction method are necessary to reevaluate the Fe(II) oxidation rates of known Fe(II)-oxidizing strains. This may allow to better understand the role of abiotic Fe(II) oxidation by nitrite in these systems.

[1] Kappler, Schink & Newman (2005) *Geobiology* **3**, 235-245.
[2] Van Cleemput & Baert (1983) *Soil Biol. Biochem.***15**, 137-140.
[3] Hansen, Borggaard & Sørensen (1994) *Geochim. Cosmochim. Ac.* **58**, 2599-2608.
[4] Moraghan & Buresh (1977) *Soil Sci. Soc. Am. J.* **41**, 47-50.
[5] Muehe et al. (2009) *FEMS Microbiol. Ecol.* **70**, 335-343.

https://doi.org/10.1180/S0026461X00008434 Published online by Cambridge University Press

Noble gases in geothermal waters as tracers for deep fluid circulation

STEPHAN KLUMP[1*], MATTHIAS S. BRENNWALD[2], DAVID MORRISON[3] AND ROLF KIPFER[2,4]

[1]EBA, A Tetra Tech Company, Whitehorse, Canada, sklump@eba.ca (* presenting author)
[2]Eawag: Swiss Federal Institute of Aquatic Science and Technology, Duebendorf, Switzerland, matthias.brennwald@eawag.ch
[3]Yukon Energy Corp., Whitehorse, Canada, david.morrison@yec.yk.ca
[4]Swiss Federal Institute of Technology, ETH Zurich, Zurich, Switzerland, rolf.kipfer@eawag.ch

Introduction

Dissolved noble gases make excellent environmental tracers to study physical processes in groundwater and other aquatic environments. Especially helium isotopes have been widely used to trace residence time and deep circulation in groundwater systems.

Elevated $^{3}He/^{4}He$ isotope ratios were found in areas with increased geothermal resource potential in the Basin and Range Province, western United States [1]. The authors suggest that high $^{3}He/^{4}He$ anomalies, i.e., areas with admixture of mantle-derived helium in groundwater, indicate enhanced crustal permeability coupled with local zones of deep fluid production and/or hidden magmatic activity.

As part of a geothermal exploration project, samples were collected from five warm and hot springs in southern and central Yukon, Canada. All samples were analyzed for noble gas abundances of He, Ne, Ar, Kr, Xe and the isotope ratios $^{3}He/^{4}He$, $^{20}Ne/^{22}Ne$, and $^{36}Ar/^{40}Ar$, as well as stable isotopes (^{2}H, ^{18}O), tritium (^{3}H), and routine inorganic chemistry.

Results and Conclusions

All samples contained a significant component of mantle-derived helium which is characterized by a higher $^{3}He/^{4}He$ isotope ratio compared to crustal helium. The presence of a mantle-derived helium component typically suggests the existence of a deep fluid pathway, usually a steeply inclined fault or fault zone. This is in agreement with the conceptual models for the warm and hot springs which include a deep circulation system for meteoric water to reach a sub-surface heat source and a suitable, fast conduit back to surface.

However, it remains unknown whether the noble gas signatures from the warm and hot springs represent local anomalies being characteristic for areas with geothermal resource potential. If this is the case, noble gas data, especially helium isotope ratios, could be used as an exploration tool for geothermal resource assessments once background values have been established. More noble gas data from both thermal waters and cold groundwater in the wider areas of known warm and hot springs would be required to answer this question.

[1] Kennedy and van Soest (2007) *Science*. **318**, 1433-1436.

Molecular Dynamics study of Aqueous Solution: solubility calculation with kinetic and thermodynamic approaches

KAZUYA KOBAYASHI*, YUNFENG LIANG, AND TOSHIFUMI MATSUOKA

Kyoto university, Kyoto 615-8540, Japan
* Presenting author: k_kobayashi@earth.kumst.kyoto-u.ac.jp

Aqueous solutions are fundamental to chemistry, biology, geology and technology. Predicting the shape of growing crystals is of essential importance for industrious crystallization process. In geology, crystalization is also one of the most siginifcant phenomenon to be better understood.

The rock-salt crystal structure is the stable solid phase in contact with a saturated solution of NaCl at atomspheric pressure and at room or higher temperature, while the dihydrate is stable solid phase in contact with a saturated solution of NaCl below 0.1°C. The question is that how this different stable solid phase in contact will be reflected from the hydration structure of the solutions(namely, how the hydration structure varies with temperature), how the different hydration structure will influence the salt-solution interfacial structure and eventually affect the crystal growth. Solubility is one of the significant and measurable properties, which is directly related to these three particular aspects: 1)crystal growth; 2) salt-solution interfacial structure and 3) the ionic hydration structure.

Here, we have investigated the salt-solution interface system and the salt solution single-phase system at different temperatures by using molecular dynamics. The solubilities were calculated by using the direct calculation and the free energy calculation, which are kinetic approach and thermodynamic approach, respectively. The direct calculation employs a salt-solution combined system. When the system is equilibrated, the concentration in the solution area is the solubility. In the free energy calculation, we calculate separately the chemical potential of two systems: solid and solution. And the two chemical potential values are compared. When the chemical potential of the solution phase is equal to the chemical potential of the solid phase, the concentration of the solution system is the solubility.

Very interestingly, it was found that the crystal shapes obtained from the direct calculations are significantly different between high and low temperatures: while the clusters were observed at the crystal surface at low temperatures, the layered rock salt structure is formed at high temperatures. We found that the clustering behavior is tightly conncted with the adsorbed water.

The calculated solubilties from two different approaches have a general good agreement, where the values at low temperatures exhibit slightly lager deviation than those at high temperatures. We remarked that the solubility value from the direct calculation might be affected by the kinetic reasons: the newly formed crystal structure and the adsorbed water molecules.

https://doi.org/10.1180/S0026461X00008434 Published online by Cambridge University Press

Strategies of aerobic microbial Fe acquisition from montmorillonite: siderophores and Fe(III) reduction

K. KOEHN[1]*, J. DUBOIS[2], P. MAURICE[1]

[1]University of Notre Dame, 156 Fitzpatrick Hall, Notre Dame, IN 46556, USA, kkoehn@nd.edu, pmaurice@nd.edu (* presenting author)

[2]University of Notre Dame, 251 Nieuwland Hall, Notre Dame, IN 46556, USA (jdubois@nd.edu)

Abstract

Iron bioavailability in aerobic, circumneutral environments is limited by low solubilities and slow dissolution kinetics of Fe-bearing minerals. Aerobic microorganisms have developed a number of strategies to obtain Fe, including release of siderophores, which are low molecular-weight Fe(III)-specific chelators. This research investigated the role of siderophores and other Fe acquisition strategies in Fe acquisition from the Fe(III)-bearing clay mineral montmorillonite (MMT) by an aerobic *Pseudomonas mendocina* bacterium. Fe-limited batch experiments were conducted using a wild-type (WT) *P. mendocina* strain that produces siderophore and an engineered mutant with a siderophore(-) phenotype. Based on measurements of population densities coupled with a molecular biosensor assay that monitors the promoter activity of the siderophore biosynthesis gene, and measurements of cells' reducing ability, it appears that both siderophore -related and -independent Fe acquisition strategies may play a role in Fe acquisition.

WT siderophore-producing cells actively grow and metabolize when MMT is the sole Fe source, but sideorphore sorption to clay particles may limit the concentration of dissolved siderophore (and Fe-siderophore complex) accessible to cells at any given time. Cells may also obtain Fe from MMT by reducing clay-associated Fe(III), but because *P. mendocina* does not produce an exogenous reductant, such reductive Fe acquisition only occurs when direct physical contact is established between cells (or organic biofilm components) and MMT. Siderphore(-) mutant cells were able to increase intercellular Fe concentrations at earlier growth stages and to attain higher maximum population densities than the WT. This suggests that cell-associated reduction of MMT Fe(III) may potentially provide cells with a more rapid and energy-efficient Fe acquisition strategy from clays as compared with siderophore-dependent mechanism(s). Moreover, the reducing mechanism may be assisted by biofilm production that ensures direct contact with the clay and has the potential to physically limit diffusion of siderophores away from cells in batch cultures.

Changes in Southern Hemisphere atmospheric circulation over the past 2400 years inferred from the WAIS Divide ice core dust record

BESS G. KOFFMAN[1*], KARL J. KREUTZ[1], NATALIE M. MAHOWALD[2]

[1]University of Maine, Orono, USA, bess.koffman@maine.edu; karl.kreutz@maine.edu (* presenting author)

[2]Cornell University, Ithaca, USA, mahowald@cornell.edu

Abstract

The strength of the atmospheric circulation around Antarctica is intimately coupled to the rate of deepwater ventilation in the Southern Ocean, hypothesized to be the dominant control on atmospheric CO_2 concentrations on glacial-interglacial timescales [1, 2]. During the past ~2000 years, preindustrial atmospheric CO_2 concentrations changed significantly and, at times, rapidly [3]. There are several possible explanations for these observed changes, including changes in terrestrial biomass linked to human activities. However, the role of Southern Hemisphere westerly wind intensity on inter-annual to centennial timescales has not been evaluated fully, and may be important. High-resolution ice core microparticle records hold promise for reconstructing the strength of the atmospheric circulation because, as we have observed, the background dust particle size distribution (PSD) is primarily a function of wind strength. Moreover, PSD varies independently of total particle flux, implying different meteorological and climatic drivers. We present results from continuous analysis of mineral dust in the upper 577 m of the West Antarctic Ice Sheet (WAIS) Divide deep ice core (79.468° S, 112.086° W) and discuss the dominant controls on dust flux and PSD, as determined using reanalysis data and climate model output. In addition, we evaluate the periodicity of the dust flux and PSD records using wavelet analysis. We find that changes in the periodicity of the PSD (notably at ~1300 and 1600 C.E.) appear to be coincident with shifts in the strength of the Southern Annular Mode (SAM) climate oscillation, as inferred using the Law Dome sea salt proxy record [4]. We extend our interpretations of the dust record to the past 2400 years, offering new insights into how the atmospheric circulation around Antarctica changed, with possible impacts on ocean ventilation and atmospheric CO_2.

[1] Toggweiler, J.R., *et al.* (2006) *Paleoceanography* **21**. [2] Anderson, R.F., *et al.* (2009) *Science* **323**, 1443-1448. [3] Macfarling Meure, C., *et al.* (2006) *Geophysical Research Letters* **33.** [4] Goodwin, I.D., *et al.* (2004) *Climate Dynamics* **22,** 783-794.

https://doi.org/10.1180/S0026461X00008434 Published online by Cambridge University Press

Riparian soils control metal loading of natural organic carrier phases

STEPHAN J. KÖHLER[1*], THOMAS GRABS[2], JOSE L. J. LEDESMA[1], KEVIN BISHOP[2], FREDRIK LIDMAN[3] AND HJALMAR LAUDON[4]

[1]Department of Aquatic Sciences and Assessment, Uppsala, Sweden, stephan.kohler@slu.se, (*presenting author).
[2]Dept. of Geosciences, Uppsala University, Uppsala, Sweden.
[3]Dept. of Ecology and Environmental Science, Umeå University, Umeå, Sweden.
[4]Dept. Forest Ecology and Management, Swedish Agricultural University, Umeå, Sweden.

Dissolved organic carbon (DOC) originating from wetland and riparian soils is known to effectively bind rare earth elements, uranium, aluminum and iron and play an important role for the mobilization and transport of these elements from soils to the surface waters [1]. In this study we present long-term data from 15 nested streams and several riparian soils draining granitic till covered soils ranging over almost three pH units. We analyze for which metals dissolved organic matter can function as carrier across scales and during varying hydrochemical conditions.

Metal loading (mM Metal per mM Carbon) in the various subcatchment changes over scales in a very characteristic manner that is dominated by the relative distribution of the three prevailing landscape types: forest, wetland and sediment area. The almost constant relationship between La and U loading of organic matter throughout the whole 68km^2 large catchment is controlled by homogeneous mineralogy in the source areas, flow pathways and metal release in the riparian soils.

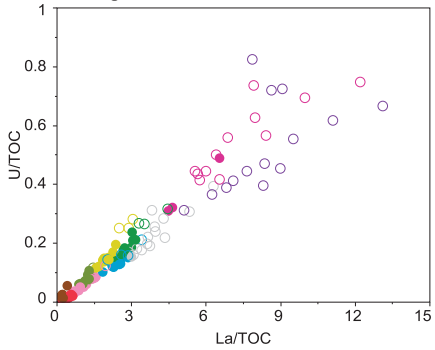

Fig. 1 Organic matter loading of U and La at all sites.

Soil solution data from one detailed soil catena along a hypothetical flowline indicate that organic matter leaches increasing amounts of trace metals during the riparian soil passage. The very similar Al and Fe loadings from 10 other riparian soils from different subcatchments are in accordance with the gradual change observed in the above transect for Al [2]. Our experimental data for metal speciation are in general accordance with those modelled using Visual Minteq [3] and confirm the importance of organic matter for metal mobility across scales from riparian soils.

[1] Andersson, K. et al. (2006) GCA, **70** (13), 3261-3274. [2] Cory, N. et al. JGR-Biogeosciences 2007, **112** (G3). [3] Gustafsson, J. P. et al. (2003) *Environ. Sci. Technol.*, **37** (12), 2767-2774.

Multiple growth events in diamonds from Murowa; evidence from FTIR mapping of N and H defects.

S.C.KOHN*, G.P. BULANOVA, C.B. SMITH, M.J. WALTER, A. MARKS AND A.P. MCKAY

School of Earth Sciences, University of Bristol, BS8 1RJ, UK
simon.kohn@bristol.ac.uk

The Murowa kimberlites [1] are located near the southern edge of the Zimbabwe craton. The few available measured ages suggest that the xenoliths and diamonds in the kimberlites date to 3.2 Ga and the kimberlite exhumation dates to 0.5 Ga, giving a residence time in the mantle for the diamonds of 2.7 Ga [2].

Here, we present FTIR maps of Murowa diamonds that show a range of growth histories. Whereas most diamonds show uninturrupted octahedral growth, or transitions from cubic to octahedral growth, a few show very clear evidence for at least two growth events. For example, one diamond (Mur-82) contains 130 ppm N in the core which is 82% aggregated to B centres, and a rim zone with 630 ppm N and only 16% aggregation. If both core and rim are assumed to be close in age, with a mantle residence time of 2.7 Ga, the core gives a temperature of 1205°C and the rim a temperature of 1087°C. A drop in lithospheric temperature of 120°C over a short time scale seems unlikely, so alternative scenarios with various combinations of temperature evolution through the period of growth have been modelled. Consideration of both the nitrogen aggregation zoning in individual diamonds, and the residence temperatures obtained for the collection of diamonds as a whole suggests that more than one period of diamond growth may be sampled. The implications of the results to models of the evolution of the craton (e.g. [3]) will be discussed. Detailed maps of hydrogen incorporated in diamond can also be obtained, and in some cases (e.g. Fig. 1) there is a hydrogen-rich zone or overgrowth at the rim. This implies a late stage growth event, possibly from a hydrogen-rich fluid.

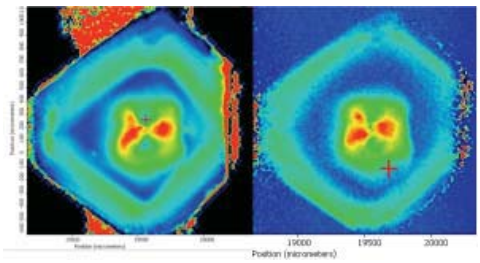

Figure 1: Contoured map of nitrogen concentration (left) and hydrogen concentration (right) in diamond Mur-79 . The diamond shows a transition from N and H rich cubic-growth core to octahedral-growth rim. Note also that the N-rich zone in the rim does not coincide with the H-rich zone at the very outer edge.

[1] Smith C.B. et al. (2004) *Lithos* **76** 219-232. [2] Smith C.B. et al. (2009) *Lithos* **112S**, 1120-1132. [3] Shirey (2004) *Lithos* **77**, 923-944.

https://doi.org/10.1180/S0026461X00008434 Published online by Cambridge University Press

Atmospheric particulate matter in proximity to mountaintop coal mines

ALLAN KOLKER[1*], MARK A. ENGLE [1,2], WILLIAM H. OREM[1], CALIN A. TATU[1], MICHAEL HENDRYX[3], MICHAEL MCCAWLEY[3], LAURA ESCH[3], NICHOLAS J. GEBOY[1], LYNN M. CROSBY[1], AND MATTHEW S. VARONKA[1]

[1]U.S. Geological Survey, Reston, VA, USA, akolker@usgs.gov (* presenting author)
[2]University of Texas at El Paso, El Paso, TX, USA engle@usgs.gov
[3]West Virginia University, Morgantown, WV, USA mhendryx@hsc.wvu.edu

Introduction and Approach

In collaboration with West Virginia University, the U.S. Geological Survey is conducting a study of potential human health impacts associated with coal extraction by mountaintop mining (MTM). This practice, common in portions of Appalachia, exposes coal for production by explosion and removal of non-coal-bearing siliceous overburden. Past studies have primarily considered the geochemical impact of overburden disposal in valleys on aquatic life. Recent epidemiological work suggests disparities in the rates of some diseases between comparable MTM and non-MTM areas [1]. In the present study, we are evaluating potential human exposure to air- and water-sourced contaminants from MTM activity. Preliminary results reported here focus on air quality impacts. For this portion of the study, sized atmospheric particulate matter (PM) and geochemical window wipes were collected in two MTM areas and a control site over several days in June, 2011 (Table 1).

	V	As	Cd	Al	Ga	Rb	Ce
E/M fine	2.4	1.8	2.0	15.8	20.1	9.3	10.6
T/M fine	1.7	1.6	1.7	8.4	12.1	5.2	6.5
E/M	ND	ND	2.4	9.5	6.8	7.6	10.1
T/M coarse	ND	ND	3.4	7.5	5.5	5.6	5.9

Table 1: Results for selected trace elements in sized PM samples expressed as concentration ratios for MTM communities E and T vs. control area M. ND = Not detected.

Results and Conclusions

Results for PM and window wipes show anthropogenic contaminants (SO_4, V, Ni, Cu, As, and Cd) are comparable in concentration for MTM and non-MTM sites suggesting little additional local contribution in the MTM areas. However, "crustal" elements (Al, Ti, Fe, Ga, Rb, and rare earths) were much higher in concentration in the MTM areas. A preliminary analysis shows that local sources contributed 80 to 96% of these elements at sites E and T during the sampling period. Based on this analysis, residents of MTM communities are exposed to much higher levels of locally derived siliceous lithogenic material compared to the control. These results will be combined with drinking water quality data, expanded epidemiological mapping, and toxicologic studies to assess the impact of environmental factors in MTM areas on health outcomes.

[1] Hendryx et al. (2011) *J Community Heath* DOI: 10.1007/s10900-011-9448-5.

Geology of the Nain Complex, Labrador, Canada: Occurrence of the Early Archean Supracrustals

T. KOMIYA[1*], M. SHIMOJO[1], S. YAMAMOTO[1], Y. SAWAKI[2], A. ISHIKAWA[1], K. KAZUMASA[1], K. D. COLLERSON[3]

[1]Dept Earth Science & Astronomy, Komaba, University of Tokyo, Tokyo, Japan, komiya@ea.c.u-tokyo.ac.jp
[2]JAMSTEC, Yokosuka, Kanagawa, Japan
[3]The University of Queensland, Brisbane, Australia

The Hadean is the most mysterious period because no rocks and geologic bodies are preserved except for only the zircons in Western Australia, Canada, China and Greenland [1]. But, it is the most important period because the early evolution possibly clinched the earth's history. We try to find the earliest supracrustal rocks in the world to investigate the Hadean tectonics. As far, the oldest supracrustal rocks are found in Akilia association in West Greenland, Nuvvuagittuq in Quebec, and Nain Complex in Labrador [2,3].

We made geological survey in the Nain Complex, and reinvestigated the occurrence of the supracrustal rocks and their relationship with the ambient orthogneisses. Previous works focused on distribution of the supracrustal belts within the orthogneisses [e.g. 4], but the detailed field occurrence of the supracrustal rocks within the belts is still ambiguous. Therefore, we focus on their internal structures.

The supracrustal belts are repeatedly intruded by granitic intrusions with some ages and their original structures are obscured, but their lithostratigraphies are relatively well preserved in Nulliak, Big and Shuldham islands and St Jones Harbor. The supracrustal belts in Nulliak and Big islands comprise ultramafic rocks, mafic rocks and mafic sediments intercalated with feldspathic sediments and banded iron formations in ascending order. In the St Jones Harbor, it is composed of ultramafic rocks, mafic rocks, banded iron formation, and clastic sediments, intercalated with chert in the middle and with bedded carbonate rocks in the upper part, respectively, in ascending order. In the Shuldham Island, it consists of ultramafic rocks, layered gabbro with precursors of plagioclase and pyroxene accumulation layers, mafic rocks and terrigenous sediments in ascending order. The lithostratigraphies are very similar to oceanic plate stratigraphy. The fact that some supracrustal belts are intruded by Uivak I orthogneisses and presence of >3.86 Ga zircons in the supracrustal rocks [e.g. 3] suggest that the supracrustal belts have early Archean ages. In addition, despite of the still ambiguous relationship between Nanok Gneiss and supracrustal rocks, presence of Nanok Gneiss (3.85 to 3.91 Ga) in this area [5] implies that the supracrustal belts date back to the earliest Archean.

[1] Froude *et al.* (1983) *Nature* **304**, 616-618; Nelson *et al.* (2000) *EPSL* **181**, 89-102; Mojzsis & Harrison (2002) *EPSL* **202**, 563-576; Iizuka *et al.* (2006) *Geology* **34**, 245-248; Wang *et al.* (2007) *CSB* **52**, 3002-3010. [2] Bowring & Williams (1999) *CMP* **134**, 3-16; Nutman *et al.* (1996) *Precamb. Res.* **78**, 1-39; O'Neil *et al.* (2008) *Science* **321**, 1828-1831. [3] Schiøtte *et al.* (1989) *Can Jour Earth Sci.* **26**, 2636-2644. [4] Bridgwater *et al.* (1974) *Geol Surv Canada, Paper* **75-1 Part A**, 282-296. [5] Collerson (1983) in *Abstracts for Early Crustal Genesis Field Workshop, LPI,*

https://doi.org/10.1180/S0026461X00008434 Published online by Cambridge University Press

Banded Iron Formation as Seawater Proxies

KURT O. KONHAUSER[1*], LESLIE J. ROBBINS[1], MERLE EICKHOFF[2], ELIZABETH D. SWANNER[2] AND ANDREAS KAPPLER[2]

[1]University of Alberta, Edmonton, Canada (*kurtk@ualberta.ca)
[2]University of Tuebingen, Tuebingen, Germany

Banded iron formations (BIF) are iron rich (~20-40% Fe) and siliceous (~40-50% SiO_2) marine sedimentary deposits that precipitated throughout much of the Precambrian. Recently, their trace element compositions have been used to determine paleo-seawater chemistry, with the ultimate goal being to better understanding nutrient availability (e.g., P, Ni, Zn) for the ancient marine biosphere [1-3]. Using BIF as ancient seawater proxies requires an understanding of the initial mineral precipitates, the adsorption/co-precipitation reactions that took place in the ocean water column, and the potential for post-depositional changes in sediment nutrient content. It has generally been accepted that ferric hydroxide, $Fe(OH)_3$, particles were the precursor sediment, and that mineral precipitation was intimately linked to the metabolism of planktonic bacteria. The nutrients that later became incorporated into BIF were either supplied as sorbates of the iron hydroxide particles or were components of the cellular biomass [4]. Subsequent deposition and burial of the mineral-cell aggregates then provided an abundant supply of electron donors and acceptors to the seafloor, which fueled sediment diagenesis and metamorphism. Preliminary work on the experimental transformations of ferric hydroxide-biomass composites at elevated temperatures and pressures has demonstrated that all of the ferrous iron minerals in BIF can be formed during late-stage diagenesis. Current experiments are being directed at understanding whether post-depositional alteration may have affected nutrient mobility, and thus, whether BIF composition can indeed be used as an ancient seawater proxy.

[1] Bjerrum, C.J. & Canfield, D.E. (2002) *Nature* **417**, 159-162.
[2] Konhauser, K.O. et al. (2009) *Nature* **458**, 750-753.
[3] Planavsky, N.J. et al. (2010) *Nature,* **467**, 1088-1090.
[4] Yi-Liang, L. et al. (2011) *Geology*, **39**, 707-710.

Mineralogical control of Se and Te signatures in peridotites: implications for the primitive mantle

STEPHAN KÖNIG[*1,2], JEAN-PIERRE-LORAND[3], FRANK WOMBACHER[2], AMBRE LUGUET[2] AND D. GRAHAM PEARSON[4]

[1] Universität Bonn, Steinmann Institut für Mineralogie, Germany, stephan.koenig@uni-bonn.de (* presenting author) [2] Universität zu Köln, Institut für Geologie und Mineralogie, Germany [3] Laboratoire de Planétologie et Géodynamique de Nantes, University of Nantes, France [4] University of Alberta, Department of Earth and Atmospheric Sciences, Edmonton, Canada

Selenium and tellurium belong to the group of highly siderophile elements (HSE) that are believed to constitute key tracers for planetary processes such as formation of the Earth's core and the Late Veneer composition. Constraints on HSE systematics on the planetary scale require, however, a previous understanding regarding the behaviour of these elements during petrogenetic processes and their abundances in the primitive upper mantle (PUM). Recent studies have shown systematic differences in Se/Te between fertile lherzolites and depleted harzburgites. In contrast to fertile lherzolites which remain at broadly chondritic values [1], depleted peridotites are highly fractionated with up to suprachondritic Se/Te (up to 35), where high Se/Te correlates with decreasing Te concentrations [2]. Fractionation is also observed at the scale of a single sample and results from the heterogeneous distribution of micrometer sized Te-bearing host phases in residual peridotites. On the whole rock scale this effect results in a more incompatible behaviour of Te compared to Se, once base metal sulfides are highly depleted and in some cases entirely consumed by partial melting. The marked differences in Se-Te systematics observed between fertile lherzolites and depleted harzburgites can be explained by the combined effect of i) different abundances and proportions of residual and metasomatic base metal sulfides and ii) discrete micrometric to nanometric platinum-group minerals. Hence, it is critical to fully understand Se-Te systematics in harzburgites if we are to provide new insights into the behaviour of Se and Te during mantle depletion. This knowledge is a prerequisite to further constrain the Se and Te abundances of the primitive upper mantle.

[1] Lorand and Alard (2010) *Chem Geol* **278**, 120-130. [2] König et al. (2012) *GCA* **in press**.

https://doi.org/10.1180/S0026461X00008434 Published online by Cambridge University Press

Complex burrow system of the mud shrimp *Laomedia astacina* and nutrient fluxes through its burrow

Bon Joo Koo [1*] and Chul-Hwan Koh[2]

[1]Korea Ocean Research and Development Institute, Ansan PO Box 29, Seoul 425-600, Korea, bjkoo@kordi.re.kr
[2]School of Earth and Environmetal Science, Seoul National University, Seoul 151-742, Korea, chkoh@snu.ac.kr

Abstract

Laomedia astacina had large and unique burrow systems (Fig. 1), and its extensive burrows increased the total area of the sediment-water interface by roughly 1,044%, the highest value among reported data on marine invertebrates. Oxygen concentrations in a *Laomedia* burrow showed large fluctuations with respect to tidal variation, and the burrow was flushed by active irrigation, which caused a more than 100 times increase in oxygen supply to the burrow when compared to passive irrigation. The range of oxygen concentrations was different depending on the location of the burrow. It seemed to be determined by the activity of the shrimp and by the burrow structure. Burrow water mainly out-flowed through the mound lumen (about 90% of total water flow) and in-flowed only through the funnel lumen. The average burrow irrigation rate during flooding of about four hours duration was 24.7ℓh^{-1} in the mound and 2.9ℓh^{-1} in the funnel. At this irrigation rate, the inhabitants would flush their burrow water a maximum of 9.4 times during a flooding event. Nutrient flux through *Laomedia* burrows ranged from 23~224% of that on tidal flats, which included the flux through both macrofaunal burrows and the sediment surface, indicating that large and actively-irrigated burrows are important in material exchange between sediments and overlying water. These results suggested that nutrient flux may not be correctly determined unless tidal variation, daily variation, and deep burrows are taken into consideration.

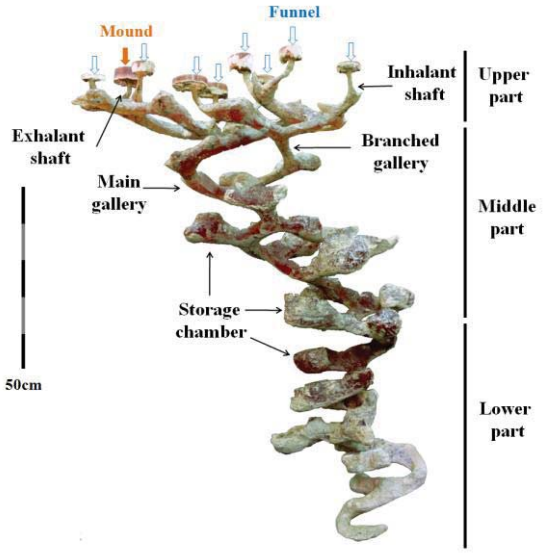

Figure 1: The complex burrow system of the mud shrimp *Laomedia astacina* recovered from Korean tidal flat.

This study was funded by KORDI (pe98781)

Use of 10^{12} and 10^{13} Ohm resistors in TIMS analysis of Sr and Nd isotopes in sub-nanogram geological and environmental samples

J.M. KOORNNEEF[1*], CLAUDIA BOUMAN[2], AND G.R. DAVIES [1]

[1]Department of Petrology, Vrije Universiteit Amsterdam, the Netherlands, janne.koornneef@falw.vu.nl (* presenting author)
[2] Thermo Fisher Scientific, Bremen, Germany.

Analysis of isotope ratios in small geological and environmental samples such as inclusions in diamonds or individual human hairs is ultimately limited by the detection system of the mass spectrometer. Here we report a technique using a TRITON Thermal Ionisation Mass-Spectrometer (TIMS) equipped with nine Faraday cups to measure sample sizes up to 10 times smaller than currently feasible. Use of current amplifiers with 10^{12} Ohm and 10^{13} Ohm resistors instead of the standard 10^{11} Ohm resistors promises a 3-fold and 4-5 fold improvement in signal to noise ratios, respectively. This improvement results in higher precision on analyses of small ion beams.

The precision of measurements of 100 pg Nd and Sr standards is found to be a factor of ~2 better for the 10^{12} ohm resistors compared 10^{11} Ohm resistors (i.e., 2RSE of 64 ppm instead of 110 ppm for a Nd analysis). The reproducibility of the $^{143}Nd/^{144}Nd$ and $^{87}Sr/^{86}Sr$ ratios for 100 pg standards using 10^{12} Ohm resisitors is 235 ppm for Nd (2RSD, n=20) and 133 ppm for Sr (2RSD, n=10). Thus, variability in Nd and Sr isotope ratios in the 4th decimal place, e.g. $^{143}Nd/^{144}Nd$ 0.5110 – 0.5119 or $^{87}Sr/^{86}Sr$ 0.7100-0.7109, can be resolved in such small samples, provided that the procedural blanks and chemical separation are optimal.

Preliminary data using current amplifiers with 10^{13} Ohm resistors indicate that the precision (2SE) on Nd isotope ratios for beam sizes of 40 μV (~2500 cps) is 1%. The high gain amplifiers can thus be used instead of multi ion counting and/or in the range between ion counting and Faraday cups, equipped with the standard 10^{11} Ohm resistors. Use of the 10^{13} Ohm resistors is prefered over multiple ion counting systems as potential problems with non-linearity, instability, or the limited dynamic range of the ion counters are avoided. This new methodology thus potentially opens up new applications in a range of studies on small sample sizes.

https://doi.org/10.1180/S0026461X00008434 Published online by Cambridge University Press

Adsorption of Metals and Oxyanions on Mineral Assemblages

CARLA M. KORETSKY *[1]

[1]Western Michigan University, Department of Geosciences, Kalamazoo, MI, USA, carla.koretsky@wmich.edu (* presenting author)

Trace metal contamination of near surface aquatic systems has created a need for accurate predictive models of inorganic contaminant speciation and transport in the natural environment. Thermodynamically-based surface complexation models (SCMs) can successfully describe adsorption of single metals and oxyanions on a diverse suite of pure substrates, including bacteria, amorphous and crystalline solids. Application of SCMs to better understand metal fate and mobility in natural systems requires models that can correctly predict adsorption in mixed mineral assemblages and over broad ranges of pH, ionic strength, pCO_2 and metal loading.

Adsorption edges for Cd, Co, Pb, and Cu have been measured as a function of pH (~3-10), ionic strength (0.001-0.1 M $NaNO_3$) and solid loading (~2-5 g/L solid; 10^{-6} to 10^{-4} M metal) on pure kaolinite (KGa-1b), silica, and hydrous ferric oxide (HFO). Adsorption of the metals on synthetic mixtures of kaolinite, quartz and HFO are well predicted using diffuse layer models (DLMs) developed from data for the pure endmember systems under similar conditions. However, for systems of pure solids and for synthetic mineral assemblages, the DLM approach often fails to correctly capture adsorption trends over broad ranges of ionic strength and solid loading. This is a significant problem which should be recognized and explicitly addressed if SCMs developed for single solids are to be applied to natural systems.

Redox-sensitive sorbates, such as (Cr(VI), pose another challenge in developing SCMs that can correctly predict speciation in complex natural systems. Cr(VI) sorption on γ-alumina, a substrate which does not promote Cr(VI) reduction, is rapid and reversible. Single adsorption edges (pH ~4-10) measured at constant ionic strength (0.001 to 0.1 M $NaNO_3$), pCO_2 (0-2.5%) and loading (10^{-4} to 10^{-5} M Cr(VI) on 5 g/L solid) are well described using constant capacitance, double layer or triple layer models. However, none of the SCMs correctly describes Cr(VI) sorption over broad ranges in pH, ionic strength and pCO_2. Likewise, Cr(VI) sorbs quickly and reversibly on hydrous managanese oxide, and single edges are well described using the SCM approach. On clay minerals, however, development of SCMs is much more problematic due to slow and irreversible sorption, which likely reflects reduction of Cr(VI) to Cr(III) by organic matter or Fe(II) in the clay mineral lattices. On untreated kaolinite, Cr(VI) sorption at pH 3 is extremely slow, failing to reach a steady state even after 2 weeks of reaction time. Although sorption is rapid on untreated montmorillonite (Swy-2), on both kaolinite and montmorillonite, Cr(VI) fails to desorb at pH 10, even after several days. On kaolinite treated with HCl, hydroxylamine HCl or hydrogen peroxide, Cr(VI) sorption reaches steady state much more quickly, and more sorption occurs at pH 3-7 compared to the untreated kaolinite. These data point to the need for spectroscopic data to constrain SCMs describing Cr(VI) sorption on clay minerals.

Secondary Mineral Phases in a Uranium Mill Pilot Study

JOCELYN KOSHINSKY[1*], JOSEPH ESSILFIE-DUGHAN[2], M. JIM HENDRY[3]

[1]University of Saskatchewan, Saskatoon, Canada, jocelyn.koshinsky@usask.ca (* presenting author)
[2]University of Saskatchewan, Saskatoon, Canada, joe377@mail.usask.ca
[3]University of Saskatchewan, Saskatoon, Canada, jim.hendry@usask.ca

Introduction

The uranium milling process at Cameco's Key Lake operation in nothern Saskatchewan, Canada leaches untargeted elements of concern (EOC; e.g., arsenic, molybdenum, selenium, iron, radium-226) that have the potential to adversely impact local groundwaters and surface waters. [1] Studies at similar uranium milling operations indicate As concentrations are controlled by Fe oxide mineral phases such as ferrihydrite. [2-5] The environmental impact of EOCs in the Key Lake mill waste solution (raffinate) is mitigated by neutralizing the pre-discharge mine tailings with slaked lime, resulting in the formation of secondary As-, Mo-, Se-, and Fe-bearing mineral phases as well as co-precipitation of ^{226}Ra phases. This serves to control EOC concentrations at very low levels in the tailings porewater.

As part of an ongoing investigation into the long-term stability of EOCs in the Deilmann Tailings Management Facility (DTMF) at Key Lake, secondary mineral phases formed during the neutralization process must be characterized and the controls on the aqueous phase concentrations of EOCs defined for a variety of ore blends. A pilot-scale model of the Key Lake mill neutralization circuit was thus developed (Figure 1) to assist in quantifying the redistributon of EOCs during the milling process. Secondary precipitates and supernatants in the physical model are separated and analyzed using ICP-MS, XRD, and Raman spectroscopy. The results are compared to geochemical modeling of the mill neutralization process.

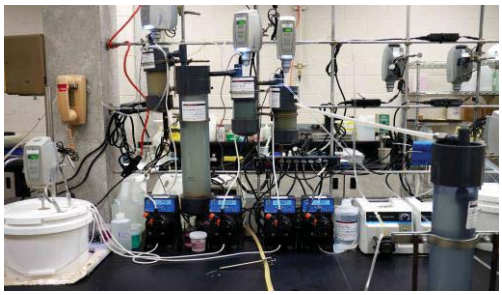

Figure 1: EOCs are removed from the raffinate by precipitation with slaked lime and thickener settling at pH set points.

Conclusions

A comparison of EOC percent removal efficiences from the pilot-scale model and the Key Lake milling process indicates that the model successfully reproduces conditions in the mill.

[1] Liu & Hendry (2011) *Appl. Geochem.* **26**, 2113-2120. [2] Jia *et al.* (2006) *Environ. Sci. Technol.* **40**, 3248-3253. [3] Mahoney *et al.* (2007) *Appl. Geochem.* **22**, 2758-2776. [4] Moldovan, Jiang & Hendry (2003) *Environ. Sci. Technol.* **37**, 873-879. [5] Moldovan, Hendry & Harrington (2005) *Appl. Geochem.* **39**, 4913-4920.

https://doi.org/10.1180/S0026461X00008434 Published online by Cambridge University Press

Prediction of B, Li and Si equilibrium isotope fractionation between minerals, aqueous solutions, melts and metals at high P and T

PIOTR M. KOWALSKI*, BERND WUNDER AND SANDRO JAHN

GFZ German Research Centre for Geosciences, Telegrafenberg, 14473 Potsdam, Germany; email: kowalski@gfz-potsdam.de

"Non-traditional" stable isotopes of light elements such as B, Li and Si are important geochemical tracers widely used in petrology. B and Li isotopes strongly fractionate between minerals and fluids during fluid-rock interaction. The fractionation of Si isotopes between silicate melt and iron-rich metal during Earth's core formation is assumed to produce the observed difference in isotopic signatures between the Bulk Silicate Earth and Chondrite meteorites. In order to understand the origin of these isotopic signatures we need to know the equilibrium isotope fractionation factors between the different materials of interest. They can be determined in high P/T experiments, which due to extreme conditions is often a difficult task, or computed. In order to deliver the required information we have developed an efficient *ab initio* based computational method for prediction of the equilibrium isotope fractionation factors between different phases at high P and T, including fluids and melts. We have tested our method by computing the B and Li isotope fractionation factors between complex B/Li-bearing crystalline solids (tourmaline, staurolite, spodumene and micas) and aqueous solution, and by comparison of the results with the existing experimental data. We show that we are able to reproduce correctly the experimental isotope fractionation sequences: fluid-tourmaline-mica for B and staurolite-fluid-mica-spodumene for Li and compute the fractionation factors with an uncertainty comparable to the experimental error [1]. In addition, we are able to get a valuable atomic-scale insight into the processes driving the fractionation of isotopes, such as coordination environment of cations, or speciation in fluids [1,2]. The computations also provide a better understanding of the experimental results such as "contradicting" measurements of B isotopes fractionation between mica and tourmaline [2]. With our method well tested on B/Li systems we attempt to derive the fractionation factors of Si isotopes between silicate melt and iron-rich metal fluid at the condition of Earth's core formation. We believe that the results of such theoretical investigation will help to better constrain the Si fractionation factors and address the question on the silicon content of the Earth's core.

[1] Kowalski, P. M. and Jahn, S. (2011) *Geochim. Cosmochim. Acta* **75**, 6112-6123.
[2] Kowalski, P. M. Wunder, B. and Jahn, S. (2012) *Geochim. Cosmochim. Acta* submitted.

Cd mobilization from Fe(III)-hydroxides by an isolated Fe(III)-reducing *Geobacter* strain and its impact on enhanced phytoremedation

UTE KRÄMER[1*], E. MARIE MUEHE[2], MARTIN OBST[3], ADAM HITCHCOCK[4], ANDREAS KAPPLER[2]

[1]Plant Physiology, University of Bochum, Germany Ute.Kraemer@ruhr-uni-bochum.de (* presenting author)
[2]Geomicrobiology, University of Tuebingen, Germany eva-marie.muehe@uni-tuebingen.de
[3]Environ. Analy. Microscopy, University of Tuebingen, Germany
[4]Canada Research Chair in Materials Research, McMaster University Hamilton, Canada

Habitats worldwide have strongly been contaminated with industrial waste metals, such as Cd, which may potentially enter the food chain through plants. These contaminant metals have drastic effects on human and environmental health. Hence, there is a demand for the development and application of new techniques to efficiently remediate contaminated soils.

In the present study, we present a new Fe(III)-reducing *Geobacter* strain, isolated from a highly Cd-contaminated soil in Germany. This *Geobacter* strain reduces Cd-loaded Fe(III) hydroxide fast and to a large extent and thus mobilizes the Fe-mineral-bound Cd. Using X-ray diffraction we identified and characterized the Fe(III) minerals present during and after Fe(III) reduction. Synchrotron-based STXM-XRF analysis was used to locate Cd in the cell-mineral aggregates. Taking into account the data presented in this study, Fe(III)-reducing bacteria could potentially mobilize Cd in Cd-contaminated soils and make it more bioavailable. We are currently investigating whether the mobilized Cd is taken up and accumulated by the Cd hyperaccumulator plant Arabidopsis halleri, leading to the net removal of Cd from the contaminated site. Hence, combining enhanced natural attenuation and phytoremedation could potentially be a technique to remove metals from contaminated sites more time- and cost-efficiently. First studies in plant-microbe-soil microcosms showed that the presence of the naturally occurring microbial community compared to sterile conditions leads to a higher uptake of Cd into the plant A. halleri, potentially due to the presence and higher activity of Fe(III)-reducing bacteria.

https://doi.org/10.1180/S0026461X00008434 Published online by Cambridge University Press

Past changes in riverine input and ocean circulation in the Gulf of Guinea

STEFFANIE KRAFT[1*], SYEE WELDEAB[2], ED HATHORNE[1], MARTIN FRANK[1]

[1]GEOMAR | Helmholtz Centre for Ocean Research Kiel, Wischhofstr. 1-3, Kiel, Germany, skraft@geomar.de (* presenting author)
[2]University of California, Santa Barbara, USA

Large river systems draining the West African Monsoon area deliver sediments and dissolved trace elements into the Gulf of Guinea (GoG) in the easternmost equatorial Atlantic. The different catchment areas of these river systems are characterized by different geological ages and rock types releasing distinct radiogenic neodymium isotope compositions during weathering which are supplied to the GoG. The main rivers discharging into the GoG are the Niger, the Sanaga, the Nyong and the Ntem with present day εNd signatures of -10.5 [1], -12.3, -12.5 and -28.1 [2], respectively. These riverine inputs mix with the tropical Atlantic surface waters. At intermediate water depths Antarctic Intermediate Water (AAIW) prevails whereas the deep basin at this location is mainly filled with NADW.

We focus on a marine sediment core that was recovered off the Sanaga and Ntem Rivers and we reconstruct changes in riverine inputs and in mixing of surface and deep water masses over the past 140,000 years.

Changes in riverine inputs most likely reflecting latitudinal shifts of the rainfall zones across the different catchment areas were obtained from the Nd isotope signatures of the residual detrital fraction of the sediment. Sediment leachates of several GoG core top samples reflect the riverine input from nearby rivers indicating transport of particles coated in the rivers. Both the sediment leachates and the residual detrital fraction show similar patterns, with shifts towards radiogenic values during the interglacials and least radiogenic values during glacial periods. This shift in εNd values may be attributed to the migration of the rainfall zones towards the north during interglacial times and thus implies the increased influence of the northern rivers, the Sanaga and Nyong.

The oxidatively-reductively cleaned planktonic foraminiferal calcite of the core top samples in the GoG reflects surface seawater signatures. Non-reductively cleaned planktonic foraminiferal tests and cleaned shallow endo-benthic and epi-benthic foraminiferal tests were used to acquire information about past bottom waters. Difficulties in cleaning down core foraminiferal samples were experienced and these samples appear to be contaminated by secondary manganese and iron bearing phases, even after cleaning. Those phases may have overprinted the original surface water Nd isotope composition in the planktonic foraminiferal tests. As the planktonic and benthic foraminiferal values are overall similar to the sediment leachates, the foraminiferal isotope signatures are most likely overprinted by isotopic signals originating from the rivers due to remobilization processes in the sediments and formation of secondary phases such as Mn-carbonates, which are attached to the foraminiferal calcites.

References:

[1] Goldstein et al. (1984) *Earth and Planetary Science Letter* **70**, 221-236.
[2] Weldeab et al. (2011) *Geophysical Research Letter* **38**, pp. 5.

Mg-dolomite nucleation in biofilm of sulfate-reducing bacteria at modern seawater salinity

STEFAN KRAUSE[1*], VOLKER LIEBETRAU[1], STANISLAV GORB[2], MÓNICA SÁNCHEZ-ROMÁN[3], JUDITH A. MCKENZIE[4] AND TINA TREUDE[1]

[1]GEOMAR, Department of Marine Biogeochemistry, Kiel, Germany
skrause@geomar.de (* presenting author)
vliebetrau@geomar.de
ttreude@geomar.de
[2]CAU, Zoological Institute, Kiel, Germany
sgorb@zoologie.uni-kiel.de
[3]Centro de Astrobiología, Madrid, Spain
msanz78@gmail.com
[4]ETH, Geological Institute, Zürich, Swizerland
judy.mckenzie@erdw.ethz.ch

Sulfate-reducing bacteria (SRB) have been identified to facilitate present-day dolomite formation under hypersaline conditions. Our laboratory study demonstrates for the first time, to our knowledge, primary Mg-rich dolomite formation in biofilms of the marine sulfate-reducing strain *Desulfobulbus mediterraneus,* under modern seawater salinity and Mg/Ca ratio. Spatial distribution of crystals within the biofilm was investigated using confocal laser scanning microscopy. Crystal morphology and mineralogy were examined with scanning electron microscopy, X-ray diffraction, and electron microprobe. Values of $\delta^{44/40}$Ca of crystals, biofilm, and bulk fluid were analyzed by double spike thermal ionization mass spectrometry. Mg-dolomite crystals precipitated in association with extracellular polymeric substances (EPS) in the biofilm. Three days after inoculation, nucleation of single nano-spherulites (~50 nm) was observed, subsequently aggregating to spherulites of ~2–3 μm in diameter after 14 days. Differences in Mg/Ca molar ratios and $\delta^{44/40}$Ca (‰) values between the biofilm material (including cells and EPS; 0.87 ± 0.01 [2 SD] and 0.48‰ ± 0.11 [2 SE], respectively), the crystals (1.02 ± 0.11 [2 SD] and <0.08‰ ± 0.24 [2 SE], respectively), and the liquid bulk medium were observed after mineral precipitation (4.53 ± 0.04 [2 SD] and 1.10‰ ± 0.24 [2 SE], respectively). These data indicate that the EPS bind relatively more Ca^{2+} than Mg^{2+}. We also propose a two-step fractionation process for Ca, shown by successive relative enrichment of ^{40}Ca in the biofilm and the crystals, compared to the bulk medium. Our results demonstrate the capability of EPS to overcome kinetic inhibition for dolomite, also suggesting contribution of SRB to dolomite deposition during periods of low oxygen concentration in the Phanerozoic.

https://doi.org/10.1180/S0026461X00008434 Published online by Cambridge University Press

Biogenicity of iron microfossils based on the morphology, physiology, and behavior of modern iron-depositing microbes

SEAN T. KREPSKI[1]*, PATRICIA L. HREDZAK-SHOWALTER[2], DAVID EMERSON[3], GEORGE W. LUTHER III[2] AND CLARA S. CHAN[1]

[1]Dept. of Geological Sciences, University of Delaware, Newark, DE 19716, USA (*krepskis@udel.edu)
[2]School of Marine Science and Policy, College of Earth, Ocean and Environment, University of Delaware, Lewes, DE 19958, USA
[3]Bigelow Laboratory for Ocean Sciences, West Boothbay Harbor, ME 04575, USA

Many iron-depositing microorganisms make distinctive iron mineralized filaments, which form iron mats in oxic-anoxic transition zones. These organisms and their mineral byproducts are found in environments ranging from wetlands to deep-sea hydrothermal vents. Iron-depositing microbes have likely been significant biogeochemical agents throughout much of Earth's history (e.g. deposition of iron formations). Iron filaments, similar to those of modern iron-depositing microbes, are found in the rock record. If we can confidently determine biogenicity and interpret physiology, these structures could be powerful tools to understand the microbiological and redox history of Earth. In our research, we are developing quantitative biogenicity criteria, based on multiple extant organisms and environments, and linked to physiology.

We investigated growth and biomineralization by the marine *Mariprofundus ferrooxydans* PV-1, as well as *Leptothrix*-like organisms enriched from a freshwater iron seep. Microbes were grown in opposing O_2/Fe(II) concentration gradients in flat glass growth chambers, which allowed for direct microscopic observation of growth. We documented microbial biomineralization by time-lapse light microscopy, and measured filament widths and directionality (as circular variance) over space and time. Microscopy was also coupled with solid-state electrode voltammetry to pair imaging with *in situ* measurements of chemical microenvironments. Our results show that microbial iron filaments display a narrow range of widths, and strong directional formation (showing small circular variance values) parallel to redox gradients. Biomineralization occurred under low oxygen levels, indicating the oxygen microenvironment of iron-depositing microbes. Filament widths and directionality varied over space and time, reflecting microbial growth and chemotaxis. We also made similar measurements on putative iron microfossils and found that they showed quantitatively similar patterns with regard to filament width and directionality. This work shows that iron filaments with a narrow range of widths, and directional formation can form the basis for strong morphological biosignatures. These signatures can be indicative of microaerophilic iron-depositing microbial activity and physiology in ancient environments. Strong biogenicity criteria will aid in the interpretation of iron microfossils, and will help us to piece together the redox history of Earth.

New water column profiles of dissolved thorium and protactinium in the western North-Atlantic

SVEN KRETSCHMER[1]*, PERE MASQUE[2], WALTER GEIBERT[3], MICHIEL RUTGERS VAN DER LOEFF[1]

[1]Alfred Wegener Institute for Polar and Marine Research, Bremerhaven, Germany, sven.kretschmer@awi.de (* presenting author), Michiel.Rutgers.v.d.Loeff@awi.de
[2]Universitat Autònoma de Barcelona, Departament de Fisica, Institut de Ciència i Tecnologia Ambientals, Bacelona, Spain, Pere.Masque@uab.cat
[3]University of Edinburgh, School of GeoSciences, Edinburgh, UK, walter.geibert@ed.ac.uk

The strength of the Atlantic Meridional Overturning Circulation (AMOC) is a major factor in the global thermohaline circulation system. Because of this central role of AMOC in the global climate system, it is important to have reliable tools to reconstruct the strength of deep water ventilation in general and of AMOC in particular during major phases of past climate variability. The basin-wide Atlantic $^{231}Pa/^{230}Th$ signature in sediment archives has been identified as a powerful tracer for the intensity of the AMOC in the past. The information on ocean circulation arises from an overall higher export rate of ^{231}Pa over ^{230}Th within NADW from the entire Atlantic basin to the Southern Ocean due to the somewhat lower particle reactivity of ^{231}Pa.

A fundamental complication for reliable applicability of this tool arises from the fact that there is a severe lack of data of these isotopes in the critical areas of the modern AMOC. Only very few ^{230}Th and ^{231}Pa profiles in the Labrador Sea, in the NE Atlantic, and in the tropical and South Atlantic have been published [1, 2, 3, 4].

To remove this gap, 14 water column profiles were sampled under trace metal clean conditions during the expedition of RV Pelagia (GEOTRACES Cruise GA02) on a transect following the North Atlantic deep water (NADW). At all stations the deepest sample was collected within the bottom nepheloid layer, providing information on the latest stage of signal development in the water column. Here we will present the first results on 5 profiles of dissolved ^{230}Th and ^{231}Pa along NADW between 15 and 55°N including also the crossover station Bermuda Atlantic Time-Series (BATS). With this study we aim to provide missing information of the factors controlling signal generation in order to answer the questions: What is the $^{231}Pa/^{230}Th$ isotope composition of the main water masses of the AMOC and how do the ^{230}Th and ^{231}Pa activities in NADW evolve on its way south and east? Can they be explained by ventilation or are there other controlling factors to identify such as the composition of suspended particles?

[1] Moran et al. (2002) *Earth Planet. Sci. Lett.* **203**, 999-1014.
[2] Moran et al. (1997) *Earth Planet. Sci. Lett.* **150**, 151-160.
[3] Moran et al. (1995) *Geophys. Res. Lett.* **22**, 2589-2592.
[4] Vogler et al. (1998) *Earth Planet. Sci. Lett.* **156**, 61-74.

https://doi.org/10.1180/S0026461X00008434 Published online by Cambridge University Press

Neutron diffraction, excess sorption and infrared study of CO_2 interaction with Na-rich montmorillonite at CCS P-T conditions

ELIZABETH KRUKOWSKI [1*], ANGELA GOODMAN[2], GERNOT ROTHER[3], EUGENE ILTON[4], GEORGE GUTHRIE[2], ROBERT BODNAR[1]

[1*] Virginia Tech, Blacksburg, VA, USA, egk@vt.edu*, rjb@vt.edu
[2] National Energy Technology Laboratory, U.S. Department of Energy, Pittsburgh, PA, USA, angela.goodman@netl.doe.gov, george.guthrie@netl.doe.gov
[3] Oak Ridge National Laboratory, Oak Ridge, TN, USA, rotherg@ornl.gov
[4] Pacific Northwest National Laboratory, Richland, WA, USA, eugene.ilton@pnnl.gov

The interaction of CO_2 with Na-rich montmorillonite clay (Na-mont) as an analog for a clay-rich caprock was studied to better understand how CO_2 might interact with caprock at P-T conditions relevant to carbon capture and storage (CCS). Neutron diffraction, excess sorption and Attenuated Total Reflectance – Fourier Transform Infrared Spectroscopy (ATR -FTIR) analyses of Na-mont at 35°C and 50°C, and pressures relevant to CCS, were conducted.

Neutron diffraction and excess sorption measurements were conducted on Na-mont at CO_2 pressures from 0-200 bars. Neutron diffraction measurements show a shift in the d(001) spacing from 12.10 Å to 12.55 Å and a decrease in the intensity of the d(001) peak, both of which are consistent with CO_2 entering the interlayer region of the clay. Excess sorption isotherms were determined gravimetrically to provide a better understanding of changes in the density of CO_2 near clay surfaces. Maxima in the excess sorption isotherms were observed at a bulk density ≈0.15 g/cm^3 and pressures of 58 bars (35°C) and 64 bars (50°C). As the bulk density of the CO_2 increases, the amount of CO_2 sorbed to the clay decreases.

To better understand the specific structural locations of CO_2 interaction with the Na-mont, the same clay sample examined by neutron diffraction and excess sorption was studied using ATR-FTIR. Measurements were conducted on both dried and hydrated Na-mont from 1-82 bars at 35° and 50°C. ATR-FTIR data show that the asymmetric stretch and bending mode of sorbed CO_2 is impacted by the presence of interlayer water, but the absorption bands due to adsorbed water between 3564 and 2975 cm^{-1} are not affected by the presence of CO_2. Specifically, the frequency of the asymmetric sorbed CO_2 band is at 2339 cm^{-1} in dehydrated clay, but at 2344 cm^{-1} in hydrated clay. The sorbed CO_2 bands increase in intensity with increasing CO_2 pressure. The stretching mode for the isolated inner hydroxyl groups at 3623 cm^{-1} is present in both the hydrated and dehydrated clay and is not affected by the presence of CO_2.

Analysis of the data indicates that sorbed CO_2 enters the interlayer space and potentially sorbs onto the edges of octahedral sheets in the Na-mont structure. If CO_2 does enter the Na-mont interlayer it could affect the rheological properties of the caprock, but further work is needed to determine if this might lead to a degradation or enhancement of seal quality.

Origin of Q-gases in pristine meteorites: an experimental study

M. KUGA[1*], B. MARTY[1], Y. MARROCCHI[1], L. TISSANDIER[1] AND L. ZIMMERMAN[1]

[1]Centre de Recherche Pétrographique et Géochimique - CNRS, Nancy, France (* correspondence : mkuga@crpg.cnrs-nancy.fr)

Most of heavy noble gases (Ar, Kr and Xe) trapped in primitive meteorites are hosted in the so-called phase Q which is commonly thought to be part of the Insoluble Organic Matter (IOM) of primitive meteorites [1]. This enigmatic phase is found in many classes of meteorites, implying that it was widespread in the early solar system [2]. Q-gases are characterized by an important fractionation relative to solar composition in favor of the heavy elements and isotopes (up to 1.3%/amu for xenon isotopes, the least-prone to isotopic fractionation) [2]. Despite many effort, the origin of Q-gases and the nature of their carriers are still poorly understood. Several experiments performed in the past decades showed that Q-gas characteristics could be reproduced to some extent by trapping ionized noble gases in various solids [3-7]. It has been interpreted by [6-7] as evidence for anomalous adsorption of xenon on growing or crumbled surfaces. This process takes place at low ion energy (<10 eV) and involves chemical bonds between ionized xenon and reactive sites onto the surface. Such a process could have occurred in the outer part of the protoplanetary disk or in the parent cloud, where gases and organics are subjected to intense UV light from the young Sun or near-by stars [8]. However, it remains unclear whether this process controls the xenon isotopic fractionation and if it can account for the light noble gas fractionation reported in phase Q [2].

The goal of this study is to better constrain the trapping and the isotopic fractionation of noble gases under ionizing conditions. Thus, we investigated the synthesis of carbonaceous particles in presence of noble gas ions by dissociating CO in a microwave plasma, at low pressure and ambient temperature. Solid particles were characterized by SEM, TEM, Raman Microscopy and Infrared Spectroscopy. The abundances and the isotopic ratios of noble gases were analyzed by static Mass Spectrometry.

Xenon trapped in carbonaceous particles is enriched in heavy isotopes by a factor of 0.2 to 1.7%/amu, depending mostly on the duration of the experiment. Assuming Henry's law for xenon trapping in carbonaceous particles, the trapping yield of xenon ions is 12000 mbar.(cm^3.g^{-1})$^{-1}$ in average, which can largely account for the amount of xenon trapped in phase Q [2,7]. Preliminary element ratios Ar/Xe and Kr/Xe are in the range of those measured in meteorites [2]. Future investigations will focus on the role of plasma parameters on the trapping efficiency and isotopic fractionation of Ar, Kr and Xe.

[1] Lewis et al. (1979) *Science* **190**, 1251-1262. [2] Busemann et al. (2000) *Met. Planet. Sci.* **35**, 949-973. [3] Frick et al. (1979) *LPSC 10th*, 1961-1972. [4] Dziczkaniec et al. (1981) *LPSC 12th*, 246-248. [5] Bernatowitcz et al. (1986) *GCA* **50**, 445-452. [6] Hohenberg et al. (2002) *Met. Planet. Sci.* **37**, 257-267. [7] Marrocchi et al. (2011) *GCA* **75**, 6255-6266. [8] Ribas et al. 2010, *Astr. Phys. J.* **714**, 384-395.

https://doi.org/10.1180/S0026461X00008434 Published online by Cambridge University Press

Partial-equilibrium concepts to model trace element uptake

DMITRII A. KULIK[1*], BRUNO THIEN[1], ENZO CURTI[1]

[1]Paul Scherrer Institut, Villigen PSI, Switzerland, dmitrii.kulik@psi.ch (* presenting author)

Uptake of trace elements into host minerals involves various mechanisms - from ion exchange and inner-sphere adsorption via surface entrapment or in-diffusion to structural incorporation upon precipitation or recrystallization. Even at long reaction time, their interplay may result in a metastable distribution of minor elements that deviates from complete aqueous- solid solution thermodynamic equilibrium. Uptake processes may proceed at widely different rates, e.g. fast (minutes to hours) for ion exchange and slow for re-crystallization (days to years), with important consequences for the reactive transport of contaminants. In this work, we explored how the rate-dependent uptake and metastability can be implemented in geochemical models using the partial equilibrium principle.

Thermodynamic models cannot be directly related to particular molecular mechanisms or their locations. Yet, some information can be retained in the model by introducing (i) multiple metastability constraints; (ii) mineral surface areas and site densities; and (iii) a set of 'layered', intrinsically metastable solid phases. In particular, the additional time-step-dependent metastability constraints [1] can be imposed on the amounts of solid solution end members. Because the specific free energy of the solid-aqueous interface is usually positive, solids with large specific surface area are metastable relative to coarse-crystalline counterparts. The surface free energy decreases due to adsorption, the extent of which is limited by the site density and the solid surface area. The limited adsorption can be modeled using the activity coefficient terms [2] or, more commonly, by adding the mass balances for surface- or permanent charge sites [3,4].

In usual aqueous - solid solution (AqSS) models, metastability constraints can only be set on bulk amounts of host and trace end members. In the new aqueous – layered solid (AqLS) model, 'seed' grains with defined specific surface, representing metastable cores of the solid, are enveloped by layers of the overgrown (or re-crystallized) solid solution phase. This 'overgrowth' part has its own metastability constraints linked to the surface area of 'seed' phase. The 'adsorption solution' phase can be linked to the surface area of either the 'layer' (in AqALS) or the 'seed' phase (AqAS).

These partial equilibrium concepts, combined with different models of uptake kinetics [5], have been implemented in the GEM-Selektor code (http://gems.web.psi.ch) and tested in simulations of uptake into carbonates, sulfates, and goethite. Major trends in the experimental data were reproduced well in all cases. A more detailed time-dependent distribution of trace elements in AqLS and AqALS models could be reconciled with the inferred uptake mechanisms.

The research leading to these results has received funding from the European Atomic Energy Community's Seventh Framework Programme (FP7/2007-2011) under grant agreement n° 269688.

[1] Karpov et al. (2001) *Geochem. Internat.* **39**, 1108-1119. [2] Kulik (2006) *Interf. Sci. Technol.* **11**, 171-250. [3] Bradbury & Baeyens (2006) *Interf. Sci. Technol.* **11,** 518-538. [4] Kulik (2009) *RiMG* **70**, 125-180. [5] Thien et al. (2012), this conference.

Application of iron nanoparticles for subsurface remediation: geochemical interaction and transfer

NARESH KUMAR[1,2], DELPHINE KAIFAS[3], JEROME ROSE[1,2], JEROME LABILLE[1,2], ARMAND MASION[1,2], PIERRE DOUMENQ[3], PETR KVAPIL[4], JEAN-YVES BOTTERO[1,2*]

[1]CEREGE UMR 6635 AMU-CNRS, Aix-en-provence, France
[2]GDRI-iCEINT, Aix-en-provence, France
[3]ISM2 UMR 6263, Université Paul Cézanne,Aix-en-provence, France
[4]AquaTest a.s., Praha, Czech Republic
(bottero@cerege.fr)

Use of metallic nanoparticles in the groundwater treatment is a relatively new concept. Due to their small size nanoparticles exhibit both the critical necessities, a large surface area to volume ratio and ability to transport through finest porosity. Zero valent iron nano particles (nFe°) are perhaps the most used and kinetically efficient reactive material for in-situ groundwater treatment. Effective treatment ability of any reactive material does not depend only on maintaining reactive surface area and oxidation but also on the mobility through the finest pores within the sediment to be able to reach the targeted contaminants. Although there have been several studies recently, discussing the transport of nanoparticles in model porous media but the behaviour and interaction in real sediment is poorly understood. Geochemical interactions, non-uniform porosity and aggregation and oxidation of particles make it difficult to predict the effectiveness of treatment systems. We setup several bench scale flow through columns in laboratory to investigate the behaviour of the nFe° in subsurface transport. Several organic coatings were tested for surface modification to improve dispersion in aqueous media and mobility in sediment. Different porous media i.e. model sand, contaminated sediment and interaction with iron oxides were also tested for possible impact on mobility of nanoparticles. Oxidation kinetics of nanoparticles in aqueous medium was followed using different analytical tools like XAS, TEM and XRD analysis.

Our results show that the transfer of nanoparticles was largely affected by the geochemical interactions within the transfer medium. Transport of iron nanoparticles in model sand media was found to be largely different from the real sediment given the similar physico chemical parameters. We observed upto 95% transfer of nano particles in sandy porous media and upto 64 % in real sediment. The oxidation kinetics of nanoparticles after suitable surface coating in aqueous media was found to be relatively slow (~14 days), which allowed a relatively complete decontamination when tested against TCE contaminated groundwater in our experiments. Latest results will be presented.

Acknowledgement: This work is a contribution of project NanoFrezes funded under ANR program ECOTECH (ANR-09-ECOT-012).

https://doi.org/10.1180/S0026461X00008434 Published online by Cambridge University Press

Killed by geochemistry: Mass extinction in toxic oceans

LEE R. KUMP[1*]

[1]Dept. of Geosciences, Penn State University, University Park, USA, lkump@psu.edu (* presenting author)

The boundaries between geological periods often mark major losses of biodiversity, i.e., mass extinctions. Geochemistry is used to investigate these events, both to determine the trigger for the event (asteroid/comet impact, volcanism) and the event's cause (abrupt warming, anoxia, trace metal poisoning, loss of habitat by sea-level fall, global wildfires, etc.). For the Cretaceous-Paleogene event, although the trigger is well established to be asteroid impact, the kill mechanism is less clear, and trace metal poisoning may have played a role. For the end-Permian, evidence for oceanic anoxia and the spread of sulfidic waters into the photic zone is widely associated with the extinction horizon in marine sedimentary rocks. Detailed studies of the spatio-temporal distribution of geochemical and isotopic proxies together with numerical simulations of these events is leading to a clearer picture of the cause and consequence of mass extinction in Earth history.

Super-high atmospheric oxygen levels during the Great Oxidation Event

LEE R. KUMP[1*]

[1]Dept. of Geosciences, Penn State University, University Park, USA, lkump@psu.edu (* presenting author)

A combination of geological and isotopic evidence demonstrates that the atmosphere became oxygenated for the first time in Earth history roughly 2.5 billion years ago. The proxies for atmospheric oxygen in the rock record are quite sensitive, though; an atmosphere sufficiently oxygenated to support animal life may not have been established for hundreds of millions of years after this initial rise.

A new repository of geological information has recently become available, the result of scientific continental drilling in Fennoscandia (FAR-DEEP). Kilometers of drill core potentially record a detailed history of the path atmospheric oxygenation took through the critical interval from 2.5 to 2.0 billion years ago. Preliminary analysis of these cores has revealed an excursion in the carbon isotope composition of the ocean/atmosphere system that is best explained by a massive oxidation of the continental crust. The event terminates a well-known, equally anomalous but oppositely signed carbon isotope excursion that likely reflects a large accumulation of oxygen in the atmosphere from about 2.2 to 2.0 billion years ago. The hypothesis that arises from these observations is that atmospheric oxygen levels built up to levels that may have exceeded modern during the earlier interval, leading to pervasive oxidative weathering of the continental crust, the first in Earth history, and a large consumption of atmospheric oxygen during the termination event. The suggestion that oxygen levels may have exceeded modern levels during the early stages of planetary oxygenation is provocative, but is consistent with singular geologic events that happened at this time, including the generation of natural nuclear reactors resulting from concentration of uranium by oxygenated groundwaters, and the enrichment in the iron content of banded iron formations by oxidative weathering into ore-grade deposits.

https://doi.org/10.1180/S0026461X00008434 Published online by Cambridge University Press

Determination of line tension via pressure profile: a molecular dynamics study

MAKOTO KUNIEDA[1], YUNFENG LIANG[1,*], SATORU TAKAHASHI[2] AND TOSHIFUMI MATSUOKA[1]

[1]Kyoto university, Kyoto 615-8540, Japan
[2]Japan Oil, Gas and Metals National Corporation (JOGMEC), Chiba 261-0025, Japan
* Presenting author: y_liang@earth.kumst.kyoto-u.ac.jp

The oil-water-vapor three-phase systems are investigated by molecular dynamics methods. The line tension has been calculated directly from local pressure profile. In this work, the line tension of decane-water-vapor system is estimated to be around -8.2×10^{-12} N, while the line tension of decane/heptane/toluene multicomponent-oil-water-vapor system has been obtained to 9.1×10^{-12} N. We suggested that the precursor thin film of toluene, which spreads preferentially over the water ahead of the bulk oil, is responsible for the fact that the line tension of decane-water-vapor system have increased from negative to positive values by adding heptane and toluene.

Zn isotope composition of Paleoproterozoic carbonates, banded iron formation and manganese formation

MARCUS KUNZMANN[1*], PAOLO A. SOSSI[2], GALEN P. HALVERSON[1], AND JENS GUTZMER[3]

[1]Department of Earth & Planetary Sciences/GEOTOP, McGill University, Montréal, Canada, marcus.kunzmann@mail.mcgill.ca (* presenting author), galen.halverson@mcgill.ca
[2]Research School of Earth Sciences, Australian National University, Canberra, Australia, paolo.sossi@anu.edu.au
[3]Helmholtz-Institute Freiberg for Resource Technology, Freiberg, Germany, j.gutzmer@hzdr.de

Previous studies of Zn isotopes in the modern open marine realm demonstrate a consistent biological control of the Zn isotopic composition of the surface ocean. The micronutrient Zn is assimilated in the surface ocean by primary producers and exported to the deep ocean, where it is released by remineralization. Preferential uptake of the light isotopes enriches the surface ocean compared to the source (river-derived Zn in surface ocean, hydrothermal mantle Zn in deep ocean), resulting in a surface-to-deep isotope gradient akin to that of $\delta^{13}C$ of dissolved inorganic carbon. Since Zn is incorporated in carbonates without significant isotopic fractionation, Zn isotope ratios of carbonates precipitated in the surface ocean should track fluctuations in primary productivity.

We analyzed the Zn isotopic composition of ~2.2 Ga old shallow and deep marine carbonates, banded iron formation (BIF) and manganese formation (MnF) from the Kalahari Manganese Field in South Africa, which formed in a small rift basin. The $\delta^{66}Zn$ ($^{66}Zn/^{64}Zn$) composition of the carbonate fraction of dolostones mainly ranges from 0.20–0.63‰ (vs JMC-Lyon) and systematically varies with inferred paleo-waterdepth. $\delta^{66}Zn$ of BIF samples range from -0.25–0.49‰ and MnF samples from -0.36–0.68‰.

The observed range in $\delta^{66}Zn$ cannot be easily explained by analytical artefacts, such as spectral interferences or diagenetic re-equilibration. Hence, we argue that these data represent the composition of the stratified seawater in a Paleoproterozoic rift. Whereas microbial carbonates deposited above the chemocline are enriched (up to 0.63‰) due to the biological pump, deep marine rhythmites are closer to the mantle value (0.2-0.3‰). Upward deepening of the succession, from intertidal microbialaminites to subtidal thrombolites, is accompanied by a gradual decrease in $\delta^{66}Zn$ values. The highest Zn isotope values are significantly lower than those reported from Neogene carbonates, which could be due to lack of eukaryotes in the 2.2 Ga old ocean. Eukaryotes have higher Zn requirements than cyanobacteria and, therefore, more efficiently deplete ^{64}Zn in the surface ocean. MnF and BIF likely owe their large variability to formation close to the chemocline, resulting in enriched $\delta^{66}Zn$ values if deposited above the chemocline and mantle values if formed below the chemocline. Values depleted with respect to the mantle signature might be due to preferential adsorption of light isotopes by Fe and Mn hydroxides as observed during previous reported experiments.

https://doi.org/10.1180/S0026461X00008434 Published online by Cambridge University Press

Combined Lu-Hf and Sm-Nd isotope systematics of Martian meteorites

E. KURAHASHI[1,2*], E. E. SCHERER[2], T. KLEINE[1] AND K. MEZGER[3]

[1]Institut für Planetologie, Westfälische Wilhelms-Universität Münster, Wilhelm-Klemm-Str. 10, 48149 Münster, Germany (*e.kurahashi@uni-muenster.de, thorsten.kleine@uni-muenster.de)
[2]Institut für Mineralogie, Westfälische Wilhelms-Universität Münster, Corrensstrasse 24, 48149 Münster, Germany (escherer@uni-muenster.de)
[3]Institute of Geological Sciences, University of Bern, Baltzerstrasse 1, 3012 Bern, Switzerland (klaus.mezger@geo.unibe.ch)

The radioisotope systems of ^{176}Lu-^{176}Hf ($t_{1/2}$ = 3.71×10^{10} yr) and ^{147}Sm-^{143}Nd ($t_{1/2}$ = 1.06×10^{11} yr) are well suited to investigating Martian mantle evolution. All four of these elements are refractory and lithophile, so they should not have been fractionated during planetary accretion or metal-silicate separation during core formation. In contrast, silicate differentiation, e.g., melt extraction from the mantle, produces melts and residual mantle whose Sm/Nd and Lu/Hf differ from those of the parental reservoir. Over time, these secondary reservoirs diverge isotopically from the parental reservoir. To gain a better understanding of Martian mantle evolution, we are conducting a systematic investigation on Martian meteorites and their minerals, measuring both isotope systems on the same sample aliquot. Eleven bulk Martian meteorites (5 shergottites, 4 nakhlites, and 2 chassignites) have been examined so far. For each, 70 to 240 mg of powder were spiked with ^{176}Lu-^{180}Hf and ^{149}Sm-^{150}Nd, then digested in a closed Teflon vial with HF + HNO_3 (2:1) overnight on a hot plate, and again in steel-jacketed Teflon bombs for 5 days at 180 C°. After ion exchange chemistry, Lu and Hf isotopic compositions were measured by MC-ICP-MS (Isoprobe, Münster), and Sm and Nd were analyzed by TIMS (Triton, Münster). Initial ε^{176}Hf and ε^{143}Nd values range from +49.0 to +51.3 and +34.7 to +47.8, respectively, for depleted shergottites, -13.3 to -17.4 and -6.3 to -6.5 for enriched shergottites, +1.8 to +14.5 and +13.4 to +15.6 for nakhlites, and +16.3 to +24.9 and +15.3 to +15.4 for chassignites. These values from unleached samples agree well with those of previous studies [e.g., 1-7]. The initial ε^{143}Nd values of nakhlites and chassignites exhibit low variation relative to ε^{176}Hf. The time-integrated ^{176}Lu/^{177}Hf and ^{147}Sm/^{144}Nd of all investigated source reservoirs define a narrow trend within the terrestrial MORB + OIB field, with the sources of nakhlites and chassignites falling between those of depleted and enriched shergottites. Shergottites themselves display a large range of ^{147}Sm/^{144}Nd, with higher values at a given ^{176}Lu/^{177}Hf relative to MORB + OIB. The constraints placed by these data on the differentiation history, mineralogy, and dynamics of the Martian mantle critically depend on the accuracy of the samples' crystallization ages. In particular, the ages of shergottites have been debated (e.g., [2,3,7]). Evidence for young (474-150 Ma) and old ages, and the implications for models of silicate differentiation on Mars will be evaluated.

[1] Blichert-Toft J. et al. (1999) *EPSL*, **173**, 25-39. [2] Bouvier A. et al. (2005) *EPSL*, **240**, 221-233. [3] Bouvier A. et al. (2008) *EPSL*, **266**, 105-124. [4] Debaille V. et al. (2008) *EPSL*, **269**, 186-199. [5] Debaille V. et al. (2009) *Nature Geoscience*, **2**, 548-552. [6] Shafer J. T. et al. (2010) *GCA*, **74**, 7307-7328. [7] Lapen T. J. et al. (2010) *Science*, **328**, 347-351.

Noble gas distribution and migration in the oceanic crust: new results from ODP Hole 1256D

MARK D. KURZ [1]*, JOSHUA CURTICE [1], DEMPSEY E. LOTT III[1] AND THE IODP EXPEDITION 335 SCIENCE PARTY

[1]Department of Marine Chemistry and Geochemistry, Woods Hole Oceanographic Institution, Woods Hole, Massachusetts, 02543, USA, mkurz@whoi.edu

In an effort to understand the relative contributions of mantle, radiogenic, and atmospheric/hydrothermal noble gas components in the ocean crust, we have performed helium, neon and argon measurements on a suite of gabbros, granoblastic dikes, and diorite veins in Pacific oceanic crust. The samples were collected during IODP Expeditions 312 and 335 to Hole 1256D, a deep crustal borehole drilled into 15 Ma ocean crust formed at the East Pacific Rise during an episode of superfast spreading (>200 mm/yr). The measurements were carried out by coupled vacuum crushing and melting in order to determine the fraction of gases held by fluid inclusions. Total helium abundances in the whole rock gabbros range from 0.46 to 1.22 micro cc STP/gram, which is 2 to 5 times higher than literature data, all of which are from the slow spreading Southwest Indian Ridge (Kumagai et al., 2003; Moreira et al., 2003). These strikingly higher helium concentrations place constraints on the thermal crustal history (due to relatively rapid helium diffusivity) and are assumed to reflect fundamentally different emplacement/degassing processes within crust formed at a super-fast spreading rate. Contact metamorphosed granoblastic dikes have total helium contents lower than the gabbros (typically ~ 0.15 micro cc STP/gram), but significantly higher than the assumed degassed basaltic protolith, suggesting that metamorphism adds helium to the crust. The helium isotopes obtained by crushing of the gabbros and granoblastic dikes are dominated by mantle helium, with average ^{3}He/^{4}He = 6.5 ± .2 times atmosphere (Ra). This value is at the low end of the range for normal Pacific MORB helium data and is interpreted to represent the mantle source. Crushing in vacuum releases a larger fraction of total neon and argon (28 to 64 %), suggesting that atmospheric/hydrothermal/alteration neon and argon are loosely bound, most likely in secondary alteration minerals. Small mantle argon isotopic components are only found in a few samples, mainly during the heating experiments. These data suggest that the atmospheric noble gas components are most likely to be expelled during subduction of the ocean crust.

A transect across an amphibole diorite vein within granoblastic basalt reveals remarkable heterogeneity with respect to noble gases, on a centimeter scale. The amphibole and plagioclase at the vein center have 5-10 times higher abundances of He, Ne, and Ar, and slightly elevated ^{3}He/^{4}He and ^{40}Ar/^{36}Ar. The length scale of the variability, the age of the crust, and the present temperature of the hole, place an upper limit on the bulk helium crustal diffusion coefficient of ~2 x 10^{-14} cm^{2}/sec at 70 C. The abundances and isotopic compositions are consistent with hydrous melting models of ocean crust for production of diorite veins. The small He and Ar isotopic variations might be due to post emplacement radiogenic components, and distribution of K, Th, and U, suggesting possible applications to geochronology.

https://doi.org/10.1180/S0026461X00008434 Published online by Cambridge University Press

Comparing felsic and mafic volcanics along Central America with implications for interaction with continental crust

STEFFEN KUTTEROLF[1] (*), KEN HEYDOLPH[1], ARMIN FREUNDT[1], KAJ HOERNLE[1], FOLKMAR HAUFF[1], WENDY PERÉZ[1], HEIDI WEHRMANN[1], DIETER GARBE-SCHÖNBERG[2], HANS-ULRICH SCHMINCKE[1]

[1] GEOMAR, Kiel, Germany, skutterolf@geomar.de(*)
[2] IfG at university of Kiel, Germany

The subduction of the Cocos plate beneath the Caribbean plate has formed the Central American Volcanic Arc (CAVA) extending from Guatemala through central Costa Rica. We have analyzed all Pliocene through Holocene felsic tephras along the volcanic front, which we compare with mafic tephras and lavas in terms of major and trace element as well as Sr-Nd-Pb-Hf isotope compositions. Thus we extend previous geochemical studies that have largely focused on mafic rocks while attempting to constrain mantle-source conditions. In contrast, our mafic-felsic comparison aims to identify crustal influences on evolving magmas along the CAVA.

Along the southern CAVA, incompatible-element and isotope ratios of mafic and felsic rocks co-vary in a fashion expected from simple fractional crystallization of mantle-derived melts. However, felsic compositions along the northern CAVA, from central El Salvador through Guatemala, deviate from the associated mafic compositions particularly for radiogenic and some HFS elements in a way that suggests interaction with Mesozoic continental crust. Our observations have two implications:

(1) The onset of the geochemical deviation places the transition from mafic to continental crust between San Vincente volcano and Ilopango caldera in central El Salvador.

(2) The reason that crustal contamination has affected the cooler felsic rather than the hotter mafic magmas argues against partial melting of crustal rocks but rather favors hydrothermal interaction of magma reservoirs with host rocks such that contamination of felsic magmas benefits from their longer residence times allowing for longer-lasting interaction of hot fluids with both the resident magma and the host rocks.

210Pb and 137Cs in margin sediments of the Arctic Ocean: controls on boundary scavenging

ZOU ZOU KUZYK[1*], CHARLES GOBEIL[2], AND ROBIE MACDONALD[3]

[1]Department of Geological Sciences and CEOS, University of Manitoba, Winnipeg MB, Canada, umkuzyk@cc.umanitoba.ca (* presenting author)
[2]INRS-ETE, Université du Québec, Québec QC, Canada, Charles_Gobeil@inrs-ete.uquebec.ca
[3]Department of Fisheries and Oceans, Institute of Ocean Sciences, Sidney BC, Canada, Robie.Macdonald@dfo-mpo.gc.ca

Abstract

Scavenging and burial of particle-reactive elements along continental margins play important roles in the oceanic biogeochemical cycling of many elements and may be particularly important in the Arctic Ocean, where the shelves are disproportionally large and there are extreme contrasts in productivity, particle supply and sedimentation between the margins and interior ocean. Water-column distributions of radioisotopes have provided insight into scavenging processes in the interior Arctic Ocean but the importance of, and controls on, scavenging in margin areas, which are not dominated by vertical processes, remain poorly understood. In this study, we report new measurements of the naturally-occurring radioisotope 210Pb and the artificial radioisotope 137Cs in 25 sediment cores that were collected broadly along the North American Arctic margin, from the North Bering Sea eastward to Baffin Bay/Davis Strait. We apply sediment profiles and inventories of 210Pb and 137Cs to the dual objectives of (1) determining and validating the sediment accumulation rates in the cores; and (2) assessing the intensity of scavenging and burial of particle-reactive elements along the North American Arctic margin. Outside the North Bering and Chukchi Sea shelves, most sediments contain an actively mixed surface layer and a subsurface layer in which sediment mixing appears to be negligible relative to sediment accumulation. Variation in sediment accumulation rates among the cores explains much of the variation in sediment inventories of 137Cs but little of the variation in the sediment inventories of 210Pb, which everywhere meet or exceed the total supply of 210Pb to the ocean by atmospheric deposition and 226Ra decay. Although the data imply enhanced scavenging all along the North American arctic margin, relative to the interior Arctic Ocean, there are also pronounced regional differences in the accumulation of 210Pb. Geographic disparities in the distributions of 210Pb and 137Cs in margin sediments are examined with regard to regional variations in sea ice cover, degree of terrestrial influence, productivity and strength of lateral exchanges with the interior ocean.

https://doi.org/10.1180/S0026461X00008434 Published online by Cambridge University Press

Adding value to exploration and the mining environment with isotopes

KURT KYSER[1]

[1]Queen's University, Dept Geol Sci & Geol Engin, Canada
kyser@geol.queensu.ca

Isotopes in exploration

Elemental geochemistry has proven invaluable in exploring for undercover ore deposits using a multitude of surface media. The anomalous concentrations of metals and compounds in ore deposits will disperse with geologic time and may result in slight aberrations in the normal background levels in the environs of the deposit. The challenge in exploration geochemistry is in finding those particular elements that reflect this process when the ore deposits reside at some depth below the surface. Most elements of interest have more than one isotope whose ratios can provide the most sensitive and precise way to fingerprint the source of an element, even though the concentration may not differ from backgroud.

The use of isotopes as definitive tracers of the origin of an element is exemplified by radiogenic Pb that has migrated from uranium deposits and non-radiogenic Pb that has migrated from VHMS deposits. The $^{207}Pb/^{206}Pb$ ratios in permeable sandstones, along unconformities or in fractures of cemented lithologies several kms from known sandstone-hosted uranium mineralization are aberrantly low and unsupported by co-existing U. This indicates that radiogenic Pb was introduced from the deposits post-mineralization. Similar results are evident using H, Li, C, N and U isotopes from U deposits. Similarly, low $^{206}Pb/^{204}Pb$ ratios in soils and vegetation above VHMS deposits at depth discriminate mineralized bodies buried ca. 100m below cover from background signals. S, Cu and Zn isotopes have the same response, despite surface media over the deposits and the background having similar elemental concentrations.

Carbon, N, O and S isotopic compositions in conjunction with elemental concentrations differentiate the least-altered from moderately-altered rocks as well as the specific geochemical alteration associated with the ore stage. Isotopic compositions and trace elements of these fluids are recorded in the ores and concomitant alteration and can be used to guide exploration at both regional and local scales.

Use of isotopes in the mining environment

As in exploration, isotopes can be used in the mining environment to fingerprint the origin of elements. For example, explosives used in mining and residual sulfides are potential sources of nitrate and sulfate pollution in the environs mines in S. Africa and Chile. However, isotopes of B, C, N and S indicate that the mine sites contribute only minor amounts of these compounds to the environment, but anthropogenic and agricultural sources of nitrate and sulfates are substantial. Similarly, the isotopic compositions of Cu, Zn and Pb are distinct from mining and anthropogenic activities on local, regional and even global scales.

Conclusion

Isotopes can add value to exploration for all types of ore deposits and provide new avenues to move up learning curves for both effective exploration and targeting of remediation strategies for mining.

https://doi.org/10.1180/S0026461X00008434 Published online by Cambridge University Press

Access to the largest geosphere laboratory in the world – the Äspö Hard Rock Laboratory

MARCUS LAAKSOHARJU[1], IOANA GURBAN[2*]

[1]Nova, Oskarshamn, Sweden, marcus.laaksoharju@gmail.com
[2] 3D Terra, Montreal, Qc, Canada, gurban@videotron.ca (* presenting author)

Nova FoU (Nova R&D) www.novaoskarshamn.se is a joint research and development platform at Nova Centre for University Studies Research and Development in Oskarshamn, Sweden. The platform is a cooperation between the Swedish Nuclear Fuel and Waste Management Co (SKB) and the municipality of Oskarshamn. SKB has a general policy to broaden the use within society concerning research results, knowledge and data gathered within the SKB research program. Nova FoU is the organisation which implements this policy by facilitating access for external research and development projects to SKB's facilities in Oskarshamn, Sweden (Fig. 1 and 2). The facilities are: Äspö Hard Rock Laboratory Äspö HRL) (located 450 meters underground), the Bentonite Laboratory, the Canister Laboratory and Site Investigations Oskarshamn.

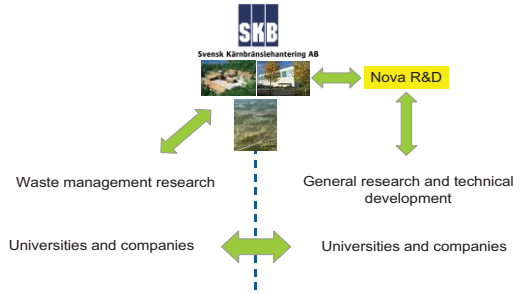

Figure 1: Nova FoU gives free access to the SKB facilities in Oskarshamn for general resarch and technical development within various geospehere projects and for technical development.

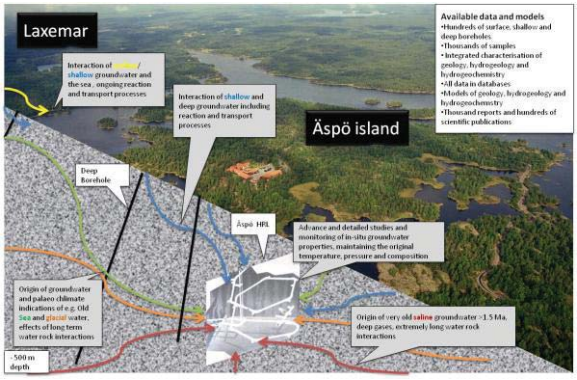

Figure 2: Research possibilities at Äspö HRL through Nova FoU

The unique Äspö Hard Tock laboratory is now open for new research outside the field of spent nuclear fuel. The present Nova status is that more than 20 projects are ongoing and engage 80 researchers. The total project value is 5 million USD. Major domestic universities and international universities are involved.

A new way to look at mantle heterogeneities : Multiple sulfur-isotope on Pacific Antarctic ridge

JABRANE LABIDI[1*], PIERRE CARTIGNY[1], CEDRIC HAMELIN[2], MANUEL MOREIRA[3], LAURE DOSSO[4] AND NELLY ASSAYAG[1]

[1]Stable isotope Laboratory, IPGP, Paris, France. (*labidi@ipgp.fr)
[2]Marine Geosciences laboratory, IPGP.
[3]Geochemistry and Cosmochemistry Laboratory, IPGP.
[4]CNRS, Domaines Océaniques, IFREMER, 29280 Plouzané, France.

On- and off-axis basalts have been collected along the Pacific-Antarctic Ridge (PAR) during the PACANTARCTIC cruises, between 65 and 40°S. The distance between this area and any of the numerous pacific hotspots (d>1000 km) allows determination of the average local upper mantle composition, undisturbed by any mantle plume [1]. Previous study [2] has revealed a subtle but significant Sr-Nd-Hf-Pb-He isotope variability for on-axis samples, mostly seen as the consequence of a large-scale melting process of a marble-cake assemblage. The off-axis samples, collected between 50 and 40°S, show more radiogenic $^{87}Sr/^{86}Sr$, $^{206}Pb/^{204}Pb$, and $^{4}He/^{3}He$ ratios, varying between the local mean MORB value and 0.703065, 20.2 and 180 000 respectively. Such values reflect an increased contribution of the marble-cake enriched component.

In order to better assess the nature of the local components and their distribution in the Pacific Antarctic mantle, we conducted a Sulfur multi-isotopes study on 29 on-axis and 8 off-axis samples from the PAR. Using an improved method allowing quantitative recovery of sulfur from basaltic glasses, we report data with external precision to be ± 0.005‰, 0.10‰ and 0.10‰ in 1σ for $\Delta^{33}S$, $\delta^{34}S$, and $\Delta^{36}S$ respectively.

All our samples are homogeneously ^{33}S and ^{36}S slightly depleted compared to the theoretical mass-dependent prediction, with a mean $\Delta^{33}S$ of -0.015 ± 0.004 (1σ) and a mean $\Delta^{36}S$ of -0.186 ± 0.046 (1σ). Besides, almost all the basalts are ^{34}S depleted when compared to the Canyon Diablo Troilite (CDT) standard. Their mean $\delta^{34}S$ is -0.68 ± 0.42 ‰ (1σ), varying between -1.2 and +0.6‰. $\delta^{34}S$ of our samples appears constant over lengthscales of several hundred kilometers with localized spikes of ^{34}S-enriched values, recorded mainly in on-axis samples. The $\delta^{34}S$ background of on-axis samples is constant at -0.8‰ from 65 to 46°S and reaches -1.2 ‰ northward. The off-axis basalts are equally ^{34}S depleted and also record the $\delta^{34}S$ background transition at 46°S.

We interpret the spike-like ^{34}S enrichments as the result of oceanic crust assimilation, in agreement with their high Cl/K ratios (>0.2) typical of fast-spreading ridge context. Taken together, the negative $\delta^{34}S$ recorded in the on- and off-axis basalts show that the local depleted mantle is statistically distinct of the chondrite reservoir ($\delta^{34}S$ = 0.0 ± 0.4 ‰), from the sulfur isotopes point of view. Finally, along ridge variation in the $\delta^{34}S$ background at the northern end of the area is concomitant with a Pb isotopic evolution toward less radiogenic values. This illustrates the isotope variability of the local enriched component, revealing that the marble-cake assemblage may contain more than one recycled constituent.

[1] Moreira et al. (2008) G.*R.L.* **35**, 49-54. [2] Hamelin et al. (2011) *Earth Planet. Sci. Lett.* **302**, 154-162.

https://doi.org/10.1180/S0026461X00008434 Published online by Cambridge University Press

Infiltration-driven metamorphism of dolomite rock

T. Labotka[1*], M. DeAngelis[2], and D. Cole[3]

[1]University of Tennessee, Knoxville TN, USA, tlabotka@utk.edu (* presenting author)

[2]University of Arkansas, Little Rock AR, USA

[3]Ohio State University, Columbus OH, USA

Marble with brucite and calcite is commonly the result of metamor-phism of dolomite rock in the presence of an H_2O-rich fluid through the reaction dolomite = periclase + calcite + CO_2 with subsequent replacement of periclase by brucite. We have conducted laboratory experiments to determine the rate and mechanism of the breakdown of dolomite and have found that dolomite converts to the product assemblage by the shrinking-core process, in which H_2O and CO_2 diffuse through a reaction rim of calcite and periclase. The reaction rate is diffusion controlled with an average rate given by $\langle d\xi/dt \rangle = 0.01\ t^{-0.75}$ (μmol/mm^2·s). The rate is a function of the composition of the fluid and approaches zero at the equilibrium value of x_{CO_2}, which is about 0.23 at the conditions of the experiments, 700 °C, 100 MPa. With these data, we can construct a kinetic model for metamorphism of dolomite rock in an infiltration system, as might occur in contact-metamorphic aureoles. The goal of the model is to compare the extent of reaction accounting for the finite reaction rate with the extent expected simply by assuming local equilibrium only. The model is isothermal and isobaric, to use the kinetic parameters determined by our experiments, and one-dimensional. Adjustable parameters include the flux at the inlet, the composition of the infiltrate, and the initial hydraulic conductivity of the dolomite. The model accounts for the production of porosity during reaction and the fluid pressure resulting from the change in composition during reaction. As an example, Figure 1 shows the composition of the fluid after infiltration of 1 mol H_2O/m^2·y for three times. For a dolomite rock with 1.52×10^4 mol dolomite/m^3, two orders of magnitude more time are required for the downstream fluid composition to change, and reaction is confined to the first meter. Even though the rate of dolomite breakdown is fast, its finite value can result in reaction over a zone a few meters wide.

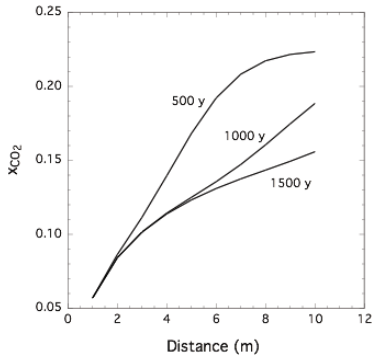

Figure 1: Fluid composition during infiltration with a flux at the inlet of 1 mol/m^2·y

Experimental study for determination of trace element sequestration in chrysotile

ROMAIN LAFAY [1*], GERMAN MONTES-HERNANDEZ [1], EMILIE JANOTS[1], DAMIEN LEMARCHAND[2]

[1] Institut des Sciences de la Terre (ISTerre), UJF-CNRS, F-38041 Grenoble, Cedex 9, France (*romain.lafay@ujf-grenoble.fr).

[2] Laboratoire d'Hydrologie et de GEochimie de Strasbourg (LHyGeS), UMR7517 CNRS, Strasbourg, Cedex, France

Introduction

Olivine alteration by serpentine is crucial to understand the fluid-mobile-elements cycle in geological systems. However, few hydrothermal experiments have quantified the partitioning of trace elements during serpentine precipitation is still poorly known and new experimental data are required.

Experimental protocols

In this study we characterized the trace elements (B, Li, As, Sb, Cs) partitioning between serpentine and alkaline fluids using two distinct experimental protocols. Alkaline conditions were choosen for the fast kinetic of reaction and the formation of few secondary phases. First, chrysotile nanofibers were synthetized from H_2SiO_3-$MgCl_2$-NaOH "silicagel system" at 300°C, Mg/Si=1.5, P_{sat}, (pH=13.5 at 25°C) in presence of a single trace element (5 to 200mg/L in solution in the starting fluid) to model equilibrium isotherms (Fig.1b). The second protocol, "alteration system", consists in serpentinisation of olivine grains at 200°C, fluid/rock=15, (pH=13.5 at 25°C), 3h<t<6 months with three olivine starting grain size. Serpentinisation reaction was characterized using XRD, FESEM (Fig.1a,c) and FTIR. Thermogravimetric analyses (TGA) was used as an inovative method to determinate kinetic of serpentinization.

Results

Fast serpentinization is observed in this "alteration system" leading to full olivine replacement by a porous assemblage of chrysotile nanotubes and Fe-rich hexagonal brucite in less than 30 days (for <30µm grain size). Chrysotile fibrous growing from "silicagel system" are very homogeneous and the presence of trace elements influence the size and morphology of partiles.

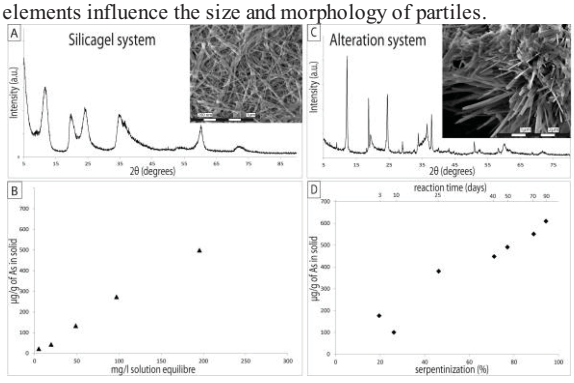

Figure 1: Exemple of results obtained in the two protocols

Results indicate that trace elements are significantly sequestreted by chrysotile in the both systems (e.g. up to 2000 ppm for Sb). Surprisingly, boron is the element with the lowest partitioning in serpentine in alkaline condition. In alteration systems, As (Fig.1d) and Cs incorporation follow rationally serpentinization advancement, Li and B seems not only controlled by chrysotile growth.

https://doi.org/10.1180/S0026461X00008434 Published online by Cambridge University Press

Timing constraints on the deep crustal residence and uplift of the Repulse Bay block, Nunavut

C.LAFLAMME[1*], C.MCFARLANE[2], D. CORRIGAN[2].

[1]University of New Brunswick, Fredericton, Canada, d6g44@unb.ca*

[2]University of New Brunswick, Fredericton, Canada, crmm@unb.ca

[3]GSC, Ottawa, Canada, dcorrigan@nrcan.ca

5f. Characterizing mid- to lower-crustal flow related to orogenic processes

The Repulse Bay block of Melville Peninsula, Nunavut, is hypothesized to be a crustal block that accreted to the Rae craton prior to terminal collision of the Superior craton during the Trans Hudson orogeny. The block consists primarily of Archean granitoid lithologies with interleaved sedimentary sequences that were deformed and metamorphosed at amphibolite to granulite facies. Within what is known as a central granulite facies domain, two different units were chosen for this study: a 2670 Ma enderbitic intrusion and a younger migmatitic metapelitic gneiss. The timing of 1) prograde and peak metamorphism, 2) deep crustal residence and 3) subsequent uplift of the Repulse Bay block are constrained using *in situ* LA-(MC)-ICPMS studies of Sm-Nd in apatite, and U-Pb in apatite and monazite from the study units. Within the migmatitic metapelitic gneiss, the timing of muscovite dehydration is well constrained by ca. 1847 Ma monazite and zircon in leucosomes, and the timing of biotite dehydration, interpreted to represent peak metamorphism having reached 800˚C and 9.5 kbar, is constrained by **ca.** 1811 Ma large monazite grains partially enclosed by peritectic garnet. The duration of deep crustal residence is documented by *in situ* Sm-Nd analyses on 50-200 μm magmatic apatite grains in the enderbite that reveal complete resetting of the Sm-Nd system during peak Trans-Hudson metamorphism. Based on the experimental diffusion data for Nd in apatite of Cherniak (2000), complete loss of radiogenic ^{143}Nd is expected to occur over a crustal residence time >2 myr for temperatures of 800˚C; quantitative accumulation of radiogenic ^{143}Nd is not expected until cooling below 725˚C for the apatite diameters we encountered. The decompression path is also recorded in the metapelitic gneiss by cordierite + spinel coronas surrounding garnet, indicative of near-isothermal decompression. Abundant small (< 10 μm) monazite inclusions within these coronas have a ^{207}Pb/^{206}Pb age of ca. 1770 Ma, interpreted to represent the timing of near- isothermal uplift to 4.5 kbar. Finally, preliminary U-Pb apatite geochronology demonstrates that the granulite facies domain then cooled to 450˚C by ca. 1700 Ma.

Results and Conclusions

These results suggest that the Repulse Bay block encountered a classic Himalayan-style orogenic cycle that was marked by relatively rapid burial followed by slow cooling during subsequent uplift. The sub-horizontal ductile fabrics preserved in the block are interpreted to have formed during granulite-facies mid-crustal flow between 1840-1810 Ma. The block was then uplifted to upper-crustal levels by 1700 Ma before final exhumation along major terrain-bounding shear zones.

Re-suspension of lead-contaminated soils a major health burden in cities

M.A.S. LAIDLAW[1], S. ZAHRAN[2], H.W. MIELKE[3], M.P. TAYLOR[1], D. MORRISON[4], AND G.M. FILIPPELLI[4*]

[1] Environmental Science, Macquarie University, North Ryde, Sydney NSW 2109, Australia

[2] Department of Economics and Center for Disaster and Risk Analysis, Colorado State University, Fort Collins, CO 80523-1784, USA

[3] Department of Chemistry and Center for Bioenvironmental Research, Tulane University, New Orleans, LA 70118, USA

[4] Department of Earth Sciences and Center for Urban Health, Indiana University - Purdue University Indianapolis (IUPUI), Indianapolis, IN 46202, USA, gfilippe@iupui.edu

Introduction

Soils in older areas of cities are highly contaminated by lead, due largely to past use of lead additives in gasoline, the use of lead in exterior paints, and industrial lead sources. Soils are not passive repositories and periodic re-suspension of fine lead contaminated soil dust particulates (or aerosols) may create seasonal variations of lead exposure for urban dwellers.

Results and Discussion

Atmospheric soil and lead aerosol data from the Interagency Monitoring of Protected Visual Environments (IMPROVE) database were obtained for Pittsburgh, Detroit, Chicago, and Birmingham (Alabama), USA [1]. The temporal variations of atmospheric soil and lead aerosols in these four US cities were examined to determine whether re-suspended lead contaminated urban soil was the dominant source of atmospheric lead. Soil and lead-in-air concentrations were examined to ascertain whether lead aerosols follow seasonal patterns with highest concentrations during the summer and/or autumn. Atmospheric soil and lead aerosol concentrations on weekends and Federal holidays were compared to weekdays to evaluate the possibility that automotive turbulence results in re-suspension of lead contaminated urban soil. The results show that the natural logs of atmospheric soil and lead aerosols were associated in Pittsburgh from April 2004 to July 2005 (R^2=0.31, $p < 0.01$), Detroit from November 2003 to July 2005 (R^2=0.49, $p < 0.01$), Chicago from November 2003 to August 2005 (R^2=0.32, $p < 0.01$), and Birmingham from May 2004 to December 2006 (R^2=0.47, $p < 0.01$). Atmospheric soil and lead aerosols followed seasonal patterns with highest concentrations during the summer and/or autumn. Atmospheric soil and lead aerosols are 3.15 and 3.12 times higher, respectively, during weekdays than weekends and Federal Government holidays, suggesting that automotive traffic turbulence plays a significant role in re-suspension of contaminated roadside soils and dusts.

Conclusions and Recommendations

To decrease urban atmospheric Pb concentrations, subsequent Pb-rich dust deposition and penetration into homes, and its consequent deleterious effect in childhood Pb levels, it is necessary to remediate and or isolate urban soils contaminated with Pb. While the US Federal Government has enacted legislation covering clean air and clean water, there is no universal clean soil act, although there are several standards pertaining to acceptable values. These guidelines are inconsistent across the US and in light of the evidence, they need to be harmonized and re-evaluated so as to develop a unified strategy to mitigate an unnecessary and preventable exposure pathway.

[1] Laidlaw, Zahran, Mielke, Taylor & Filippelli, 2012. *Atmospheric Environment* **49**, 302-310.

https://doi.org/10.1180/S0026461X00008434 Published online by Cambridge University Press

The mechanism for inhibition of calcite recrystallisation by organic molecules

LAKSHTANOV L.Z. [1,2,*], BELOVA D.A.[1], AND STIPP S.L.S.[1]

[1]NanoGeoScience, Dept of Chemistry, Copenhagen Univ, Denmark, leonid@iem.ac.ru (* presenting author), bd@gmail.com, stipp@nano.ku.dk

[2]Institute of Experimental Mineralogy, Chernogolovka, Russia.

The inhibitory effect of biopolymers, particularly by polysaccharides, could explain the extremely slow recrystallization rates of biominerals such as the calcite coverings on some species of algae that make chalk. Recrystallization can be considered as a series of simultaneous and consequent elementary events of dissolution and precipitation that leads to the diagenetic phenomenon known as grain coarsening. A driving force of recrystallization in geological environments is usually either the difference between lithostatic and hydrostatic pressures or the dependence of the chemical potential of the interface on the grain size. This coarsening process, where larger particles grow at the expense of smaller ones, is called Ostwald ripening.

It is well known [1] that the presence of aqueous organic anions (such as alginate) negligibly affects calcite dissolution rate. On the other hand, there is evidences that alginate significantly inhibits calcite precipitation [2]. Thus, it can be supposed that precipitation is the rate-limiting stage of the overall process of recrystallization, which, in turn should be affected by the presence of alginate. This conclusion is supported by our experimental study of ^{14}C isotope uptake during calcite recrystallization in a pure system and in the presence of alginate. Isotope concentration was monitored during the experiment, yielding the total amount of isotope uptake into the solid phase. An assumption about the mechanism of isotope uptake (i.e. burial into calcite layers newly formed during recrystallization) allows us to quantify the amount of newly formed material. Extent of inhibition of the calcite recrystallization rate because of alginate adsorption is comparable with that of calcite precipitation. This inhibition would take place as long as alginate is present in the solution. If there is no effective alginate supply, inhibition would sooner or later be decreased by exhausting the solution and burying the alginate molecules under the newly formed calcite layers, the more so, because adsorbed alginate could function as a substrate for calcite growth, initiated by the interaction of Ca with the negative end of the –C=O bond of the alginate functional group.

[1] Oelkers et al. (2011) *Geochim. Cosmochim. Acta*, **75**, 1799-1813. [2] Lakshtanov et al. (2011) *Geochim. Cosmochim. Acta*, **75**, 3945-3955.

Photochemical alteration of $\delta^{13}C$ of dissolved organic matter in big rivers

KARINE LALONDE[1]*, ANSSI VAHATALO[2], YVES GÉLINAS[3]

[1]Concordia University, Chemistry and Biochemistry, k_lalonde@hotmail.com

[2]University of Helsinki, Bio- and Environmental Sciences, anssi.vahatalo@helsinki.fi

[3]Concordia University, Chemistry and Biochemistry, ygelinas@alcor.concordia.ca

Organic matter (OM) depleted in $\delta^{13}C$, is considered an excellent tracer for terrestrial OM in aquatic systems. As a bulk measurement, it was also thought that $\delta^{13}C$ is less susceptible than molecular biomarker proxies toward bacterial reworking and degradation. It has been shown however, that $\delta^{13}C$ in total dissolved organic matter (DOM) can change as a result of photochemical reactions, with coloured, aromatic-rich terrestrial OM most susceptible to these reactions [1,2]. Here we further assess the viability of $\delta^{13}C$-DOM as a tracer for terrestrial OM in coastal systems by assessing the susceptibility of this proxy to UV radiation, which causes the photochemical destruction of chromophoric DOM. Our data set comprises 10 large rivers, which cumulatively account for approximately 1/3 of the world's freshwater discharge to the global ocean. We show that irradiation causes a 1.5‰ enrichment in $\delta^{13}C$ in almost all riverine DOM samples, demonstrating that riverine DOM, almost entirely terrestrial in nature, can artificially be branded as a mixture of terrestrial and marine DOM due to photochemical reactions. Photochemical alterations in $\delta^{13}C$ therefore bias mass balance calculations of terrestrial OM discharge and degradation in coastal oceans towards the marine end-member.

[1] Vahatalo et al. (1998) *Limnology and Oceanography* **53**, 1387-1392.

2] Osburn et al. (2022) *Marine Chemistry* **126**, 182-294.

https://doi.org/10.1180/S0026461X00008434 Published online by Cambridge University Press

Germanium and silicon isotopic evolution of seawater inferred from Precambrian Iron Formations

STEFAN V. LALONDE[1*], KURT O. KONHAUSER[2], AND OLIVIER J. ROUXEL[3]

[1]European Institute for Marine Studies, UMR 6538 Domaines Océaniques, Plouzané, France, stefan.lalonde@univ-brest.fr (* presenting author)
[2]University of Alberta, Edmonton, Canada, kurtk@ualberta.ca
[3]IFREMER, Dept. Géosciences Marines, Plouzané, France, olivier.rouxel@ifremer.fr

The metalloid germanium behaves as silicon's geochemical twin as the result of their near-identical ionic radii and coordination environments, and the behaviour of Ge and Si in modern seawater are tightly correlated. However, two important exceptions exist: (1) in hydrothermal systems where Ge/Si is elevated due to Si uptake during quartz precipitation, and (2) in continental runoff, where Ge/Si is depressed due to Ge retention during clay formation. Contrasting Ge/Si of these two major marine Ge and Si inputs has led to the suggestion that Ge/Si ratios of siliceous sediments may be used as a paleo-proxy for evolving marine Si sources and sinks. Germanium has five stable isotopes (^{70}Ge, ^{72}Ge, ^{73}Ge, ^{74}Ge, ^{76}Ge), and natural Ge stable isotope variations stand poised to provide additional constraints on marine Ge and Si cycling past and present [1]. In this work, we examine secular changes in Ge/Si and the Ge and Si isotopic compositions of Si-rich metalliferous deposits to better understand their inter-relationship and implications for the evolution of marine silicon cycling. We focus on Precambrian iron formations as they predate the modern biological silicon pump and represent >3 Gyr of inorganic marine Si cycling that remains largely unexplored. Both $\delta^{74/70}$Ge and $\delta^{30/28}$Si data demonstrate a nearly 3‰ variation over geological time and Archean IF that are isotopically light relative to later deposits. A heavy excursion in Ge isotopes alone appears to coincide with atmospheric oxygenation ca. 2.5-2.3 Ga. This new dataset will be discussed in light of the proposal that silicon isotopes in Precambrian cherts record waning hydrothermal input and cooling seawater over geological time [2].

[1] Rouxel et al. (2006) *Geochim. Cosmochim. Acta* **70**, 3387-3400.
[2] Robert & Chaussidon (2006) *Nature* **443**, 969-972.

Size-fractionated particle mass and composition during the U.S. GEOTRACES North Atlantic Zonal Transect

PHOEBE J. LAM[1*], MAUREEN E. AURO[1], DANIEL C. OHNEMUS[1,2]

[1]Department of Marine Chemistry and Geochemistry, Woods Hole Oceanographic Institution, Woods Hole, USA, pjlam@whoi.edu
[2]MIT-WHOI Joint Program in Oceanography, Woods Hole, USA

Particles are a key parameter for the international GEOTRACES program because of their role in mediating the cycles of so many trace elements and isotopes (TEIs). For example, the atmospheric or margin input of lithogenic particles is a source of many TEIs to the ocean; primary producers and consumers (biogenic particles) mediate the internal cycling of TEIs; and particles of all compositions are the vector for the scavenging removal of particle-reactive TEIs to the sediments. One of the key recommendations to emerge from the 3rd GEOTRACES Data-Model Synergy Workshop was the importance of measuring total suspended mass and major particle composition for GEOTRACES. These parameters are crucial for understanding the scavenging behaviour of many TEIs.

Here we present the major particle composition and the chemically-derived particle mass of the suspended (<51μm) and sinking (>51μm) size fractions for particles collected by in-situ filtration on the U.S. GEOTRACES North Atlantic Zonal Transect in occuppied in 2010 and 2011 (NAZT'10 and NAZT'11). Results from NAZT'10 Stn 10 in the eastern tropical Atlantic, 500 km away from the Mauritanian coast, show that particulate organic matter accounts for over 80% of suspended particle mass in the euphotic zone, declining to 25% near the seafloor at 3300m. The opal and $CaCO_3$ contributions at this station were less than 8% and 27%, respectively, of the suspended particle mass. The lithogenic fraction increased with depth until it accounted for 41% of suspended particle mass by 3300m. We will contrast this station with profiles from a selection of stations that represent a wide range of particle compositions, including the oligotrophic gyres, the TAG hydrothermal site, and the western and eastern margin stations.

https://doi.org/10.1180/S0026461X00008434 Published online by Cambridge University Press

Identification of trace amounts of H_2O in CO_2-rich fluid inclusions in granulite facies rocks

HECTOR LAMADRID[1*], ROBERT J. BODNAR[1], WILLIAM LAMB [2] AND M. SANTOSH [3]

[1] Department of Geosciences, Virginia Tech, Blacksburg, VA, USA, (lamadrid@vt.edu*)

[2] Department of Geology and Geophysics, Texas A&M University, College Station, TX, USA, (lamb@geo.tamu.edu)

[3] Department of Interdisciplinary Science, Faculty of Science, Kochi University, Kochi, Japan, (santosh@cc.kochi-u.ac.jp)

Granulite facies metamorphism is characterized by mostly anhydrous mineral assemblages that include orthopyroxene, plagioclase, garnet and quartz. It has been proposed that granulites are generated during dry melting of the deep crust at ultra high P-T conditions. The role of the fluids during granulite formation has been the subject of debate for decades. The debate is centered on whether or not low a_{H2O} fluids were present during metamorphism [1]. Numerous workers have reported high density "pure" CO_2 fluid inclusions as evidence that granulite facies fluids are carbonic and do not contain H_2O. However, silicate minerals show low solubilities in CO_2 and the poor wetting ability at grain boundaries inhibits infiltration, making it more difficult to dissolve silicate minerals and transport elements such as U and Rb out of the lower crust [1].

We show that H_2O is a common but minor fluid component in "pure" CO_2 fluid inclusions from various previously well-studied granulites. The inclusions were analyzed at 150°C using a recently developed technique that involves a Raman microprobe coupled with a Linkam THSG 600 heating/cooling stage [2]. Over a wide range of temperatures, CO_2 and H_2O are largely immiscible. Because of this, and because H_2O is the "wetting" phase, at room temperature small amounts of H_2O in CO_2-rich fluid inclusions will be present as a thin film wetting the walls and will be optically unresolvable [3]. In this study, fluid inclusions were heated from room temperature (~25°C) to a temperature above the one-phase / two phase boundary (≈150°C), and the liquid H_2O phase that occurs as a thin film at room temperature evaporated into the CO_2 phase. Raman analysis of this homogeneous phase at elevated temperature revealed the presence of H_2O, as evidenced by a small but sharp peak at ~3641 cm^{-1}. H_2O was detected in all primary-appearing fluid inclusions in quartz that formed at peak metamorphic conditions. In secondary fluid inclusions in garnet from Southern India, H_2O was not detected. Rather, hydrogarnet was found covering the walls of inclusions in this phase, as evidenced by a peak at ~3661 cm^{-1}. The hydrogarnet is interpreted to be a "step-daughter" phase that was formed by reaction of the H_2O in the fluid with the garnet host during retrogression. These observations suggest that granulites may not be as dehydrated as previously thought, and provide evidence for an H_2O-bearing fluid that could transport LILE out of the lower crust.

[1] Newton et al., (1998) *Precambrian Research* **91**, 41-63.
[2] Berkesi et al. (2006) *J of Raman Spectroscopy* **40**, 1461-1463.
[3] Roedder (1972) *USGS Professional Paper* **440**, 164 pp

CHARACTERISTICS OF LATE MESOZOIC GRANITIC ROCKS IN SW CORNER OF SOUTHERN VIETNAM

Ching-Ying Lan*[1], Tadashi Usuki[1], Tuan A Nguyen[2], Phu Hung Tran[2], Tran Thien Quy Ngo[2], Sun-Lin Chung[3], Stanley A. Mertzman[4]

[1]Institute of Earth Sciences, Academia Sinica, Taipei, *kyanite@earth.sinica.edu.tw, usu@earth.sinica.edu.tw

[2]University of Science, Ho Chi Minh City, tnguyen@geosun.sjsu.edu, tphung@hcmus.edu.vn, nttquy@hcmus.edu.vn,

[3]Department of Geosciences, National Taiwan University, Taipei, sunlin@ntu.edu.tw

[4]Department of Earth and Environment, Franklin and Marshall College, Lancaster, Penn., stan.mertzman@fandm.edu

Late Mesozoic magmatic belt stretches north- south in the central Vietnam to the northern part of southern Vietnam. In the central Vietnam, at the eastern part of the Dalat zone, the Late Mesozoic plutonic and contemporaneous volcanic rocks are widespread, and are interpreted as subduction-related products (Nguyen Thi Bich Thuy et al., 2004a, b). The Late Mesozoic granitic rocks are divided into three suites: the Dinhquan, the Deoca and the Ankroet suites. The Dinhquan and Deoca suites are widely developed as a northeast-southwest trending belt south of the Kontum Massif and along the coast. The Dinhquan and Deoca granitic rocks are crosscut by Ankroet granitic rocks. The Ankroet suite is more quartz-rich with predominantly leucocratic sub-alkaline granites. Beside the main granitoid suites of Dalat zone, there are few scattered igneous bodies, especially the southwest corner of southern Vietnam, such as That Son and Ba Den batholiths. The Dinhquan, the Deoca and the Ankroet suites are also given for these batholiths although they are separated over 400 to 500 km from the Dalat zone. Our previous studies indicate the late Mesozoic granitic rocks of Dalat zone can be divided into two suites: the Dinhquan-Deoca I-type granite and the Ankroet A-type granite suites. In the field, mafic microgranular enclaves are rather common in late Mesozoic granitic rocks of Dalat zone. However, enclaves are less common in late Mesozoic granitic rocks in SW corner of southern Vietnam. We will present in-situ U-Pb zircon dating and Lu-Hf isotopic analyses, and whole rock geochemical and Nd-Sr isotopic analysis of Dinhquan, Deoca and Ankroet suites in SW corner of southern Vietnam in order to compare the characteristics of these granites suites with those from the Dalat zone.

https://doi.org/10.1180/S0026461X00008434 Published online by Cambridge University Press

Deciphering sedimentary recycling via multiproxy *in situ* analyses

PENELOPE J. LANCASTER*, SHANE TYRRELL AND J. STEPHEN DALY

University College Dublin, School of Geological Sciences, penelope.lancaster@ucd.ie (* presenting author); shane.tyrrell@ucd.ie; stephen.daly@ucd.ie

Sedimentary rocks and modern sediments sample large volumes of the Earth's crust, and preserve units that vary greatly in age and composition. Determining the provenance of component minerals is complicated by the ability of some minerals to be recycled through multiple sedimentary cycles, so minerals from completely unrelated sources may end up in the same sedimentary basin. To untangle these multi-stage signals, two or more chemical signatures measured in minerals with different stability are required. For instance, labile minerals, such as feldspar, can break down rapidly during sedimentary transport, while refractory minerals, such as zircon, can be much more resilient and survive repeated recycling.

One sedimentary succession suitable for testing this hypothesis is the Upper Carboniferous Millstone Grit Group, a fluvio-deltaic, upward-coarsening sequence of mudstones, sandstones and conglomerates deposited in the Pennine Basin of northern England. New data from throughout this sequence clearly indicate two main feldspar populations, consistent with previous work [1], but also a minor third group which may represent an additional source. Since rocks of similar ages typically describe overlapping domains on a $^{207}Pb/^{204}Pb$ vs. $^{206}Pb/^{204}Pb$ plot, the addition of zircon U–Pb and Hf measurements from the same sediments may help to discriminate between possible source areas.

Previous zircon U–Pb analyses in parts of the sequence have identified three main zircon populations at c. 500, 1000–1800 and 2700 Ma, with the proportion of young to old ages increasing up section [2]. This data set has now been extended to the rest of the sequence to create a statistically significant database covering c. 14 Ma of deposition in the Pennine Basin. With the addition of new Hf isotope data from the same zircons, the combination of all three isotope systems from the same units should fingerprint discrete source terrains within potential source areas, such as Greenland, north-west Scotland and the Southern Uplands of Scotland. As such, these data have significant implications for transport distances of both labile and refractory minerals.

[1] Tyrrell *et al.* (2006) *J. Sed. Res.* **76**, 324-345.
[2] Hallsworth *et al.* (2000) *Sed. Geol.* **137**, 147-185.

Combination of water isotopes to improve temperature reconstruction.

AMAELLE LANDAIS[1*], RENATO WINKLER[1], EUGENI BARKAN[2], ARNAUD DAPOIGNY[1], ALEKSEY EYKAKIN[3], SONIA FALOURD[1], ELISE FOURRÉ[1], PHILIPPE JEAN-BAPTISTE[1], BOAZ LUZ[2], BÉNÉDICTE MINSTER[1], JEAN-ROBERT PETIT[4], FRÉDÉRIC PRIÉ[1] AND CAMILLE RISI[5]

[1]Laboratoire des Sciences du Climat et de l'Environnement (IPSL/CEA/CNRS/UVSQ), Gif sur Yvette, France amaelle.landais@lsce.ipsl.fr (* presenting author) Renato.winkler@lsce.ipsl.fr, ,Elise.fourre@lsce.ipsl.fr Philippe.Jean-Baptiste@lsce.ipsl.fr,
[2] The Institute of Earth Sciences, The Hebrew University of Jerusalem, Jerusalem, Israel eugenib@cc.huji.ac.il, boaz.luz@huji.ac.il
[3] Arctic and Antarctic Research Institute, St Petersburg, Russia ekaykin@mail.ru
[4] Laboratoire de Glaciologie et Géophysique de l'Environnement, CNRS-UJF, St Martin d'Hères, France. Jean-robert.Petit@lgge.obs.ujf-grenoble.fr
[4] Laboratoire de Météorologie Dynamique, Paris, France Camille.Risi@lmd.jussieu.fr

Introduction

Reconstruction of past temperature from water isotopic records in deep ice cores in remote East-Antarctica is limited by several artefacts such as precipitation seasonality, limited knowledge of water isotopic fractionation at low temperature, temporal changes in hydrological cycle , post-deposition effects and possible input of stratospheric water. In order to address these issues, we present new combined measurements of all water stable isotopes ($\delta^{18}O$, δD and $\delta^{17}O$) at the remote East Antarctica site of Vostok (78°27 S, 106° 50 E) at three timescales: seasonal, interannual and over the last 150 kyears Before Present. Indeed, the combination of water isotopes such as d-excess ($\delta D - 8\times\delta^{18}O$) and ^{17}O-excess ($\ln(\delta^{17}O+1) - 0.528\times\ln(\delta^{18}O+1)$) are especially sensitive to organisation of the hydrological cycle, changes in kinetic vs. equilibrium fractionations and post-deposition effects.

Results and Conclusion

The relationships between $\delta^{18}O$, d-excess and ^{17}O-excess display very different patterns on the three different timescales. The results on the seasonal cycle suggest a much more important influence of temperature on d-excess and ^{17}O-excess than previously assumed which is helpful to constraint fractionation conditions at very low temperature. It also shows that seasonality should be taken into account when interpreting deep ice cores isotopic records.On the opposite to seasonal cycle variations, we show that the strong variations of $\delta^{18}O$, d-excess and ^{17}O-excess observed at interannual timescale can not be explained only by temperature effects but that processes such as post-depositionnal effects or hydrological cycle reorganizations should be invoked. Finally, we compare these different results with general circulation model outputs including water isotopes to test the capacity of such models to represent water isotopic composition in remote regions of East Antarctica.

https://doi.org/10.1180/S0026461X00008434 Published online by Cambridge University Press

Measurement of the reactive surface area relevant to CO_2 mineralization in a reservoir sandstone

GAUTIER LANDROT*, JONATHAN B. AJO-FRANKLIN, STEPHANO CABRINI, CARL I. STEEFEL

Lawrence Berkeley National Laboratory, Berkeley, USA, gjlandrot@lbl.gov (* presenting author)

Introduction

The accessible surface area of reactive minerals considered in reactive transport models are needed to multiply rate constants associated with the reactive minerals, since the latter are typically normalized to a unit surface area. An experimental approach is developed and applied in this study that enables the measurement of the surface area of each reactive mineral located within the connected pore network of a sandstone from a carbon sequestration pilot site in Cranfield, Mississippi [1]. Several analytical techniques are used that probe the sample at different scales and dimensions, including X-ray based micro-tomography (u-CT), Energy Dispersive X-ray Spectroscopy-Scanning Electron Microscopy (SEM-EDX), Backscattered Electron Microscopy (BSE-SEM), and Focus Ion Beam-Scanning Electron Microscopy (FIB-SEM). In contrast to the methods commonly employed to measure mineral surface areas, our approach accounts for the fraction of the mineral surface that is accessible to transport. Our method thus may help minimize the discrepancy often observed in the literature between the rates predicted by models and those measured in the field, and could be used in reactive transport models that would accurately predict the fate of CO_2 in the deep subsurface.

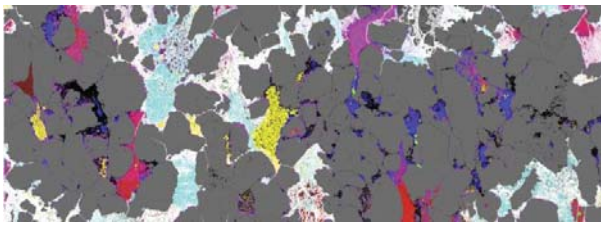

Figure 1: Mineral accessibility mapping

Results and Conclusion

The accessible surface area of each reactive mineral present in the sandstone is inferred, in m^2/g, by multiplying the fraction of each reactive mineral next to the connected pore network, measured in 2D (Figure 1), with the surface area of the connected pore network in the rock, which is measured in 3D from u-CT tomography images.

The characterization approach employed in this study is suitable for mapping the mineral distribution and pore structure found in a reservoir sandstone currently being considered as a sequestration site. Our approach could be also employed to characterize the physical and chemical properties of the rock after CO_2 injection. This would be useful in determining where precisely carbon dioxide is trapped in the rock and in identifying the CO_2 sequestration mechanisms.

[1] Landrot et al. (2012) *Chem. Geol.* in review

The density, thermal expansion and compressibility of FeO in model basalts (An-Di-Hd) and a lunar basalt: Fe^{2+} in 6-fold coordination

REBECCA A. LANGE[1*], XUAN GUO[1], QIONG LIU[1], YUHUI AI[1]

[1]University of Michigan, Ann Arbor, USA, becky@umich.edu (* presenting author)

FeO is an important component in both terrestrial and lunar basalts and yet its partial molar volume at one bar is not well known because of the difficulty of performing double-bob density measurements under reducing conditions. Moreover, there is growing evidence from spectroscopic studies that Fe^{2+} occurs in 4, 5, and 6-fold coordination in silicate melts, and it is expected that its partial molar properties will vary accordingly. We have conducted both density and relaxed sound speed measurements under reducing conditions on four liquids in the An-Di-Hd ($CaAl_2Si_2O_8$-$CaMgSi_2O_6$-$CaFeSi_2O_6$) system: (1) Di-Hd (50:50), (2) An-Hd (50:50), (3) An-Di-Hd (33:33:33) and (4) Hd (100), as well as a lunar basalt. All the multi-component (model basalts and lunar basalt) liquid density data were combined with published density data on SiO_2-Al_2O_3-CaO-MgO-K_2O-Na_2O liquids (Lange, 1997), and CaO-Al_2O_3-TiO_2-SiO_2 liquids (Lange and Carmichael, 1987) in a fit to a linear volume equation; the results lead to a partial molar volume for FeO = 12.2 (± 0.1) and TiO_2 = 23.9 (± 0.1) cm^3/mol at 1723 K, and dV/dT for FeO = 3.45 (± 0.62) 10^{-3} and TiO_2 = 3.88 (± 1.43) 10^{-3} cm^3/mol-K. The partial molar volume for FeO is similar to that for crystalline FeO at 298 K (halite structure; 12.06 cm^3/mol), which suggests an average Fe^{2+} coordination of ~6 in these model basalt and lunar basalt compositions. In contrast, the fitted partial molar volume of FeO in pure hedenbergite liquid is 14.6 ± 0.3 at 1723 K, which is consistent with an average Fe^{2+} coordination of 4.3 derived from EXAFS spectroscopy (Rossano, 2000). Similarly, the compressibility data for the three model basalt and lunar basalt liquids were combined with compressibility data on SiO_2-Al_2O_3-CaO-MgO liquids (Ai and Lange, 2008) and new sound speed data on CaO-MgO-TiO_2-SiO_2 liquids in a fit to an ideal mixing model for melt compressibility; the results lead to a partial molar compressibility (± 1 σ) for FeO = 3.25 (± 0.15) 10^{-2} and TiO_2 = 8.67 (± 0.06) 10^{-2} GPa^{-1} at 1723 K. In contrast, the compressibility of FeO in pure hedenbergite liquid is significantly larger than that in the basalts: 6.3 (± 0.2) 10^{-2} GPa^{-1}. When these results are combined with density and sound speed data on CaO-FeO-SiO_2 liquids at one bar (Guo et al., 2009), a systematic and linear variation between the partial molar volume and compressibility of the FeO component is obtained, which appears to track changes in the average Fe^{2+} coordination in these liquids. Therefore, the three most important conclusions of this study are: (1) ideal mixing of volume and compressibility does not occur for all FeO-bearing liquids, owing to changes in Fe^{2+} coordination, (2) the partial molar volume and compressibility of FeO varies linearly and systematically with Fe^{2+} coordination, and (3) ideal mixing of volume and compressibility does occur among the three multicomponent An-Di-Hd liquids and extends to lunar basalt compositions, presumably because of a common, average Fe^{2+} coordination of ~6.

https://doi.org/10.1180/S0026461X00008434 Published online by Cambridge University Press

A multi-proxy study of the Mackenzie Shelf waters

BRUNO LANSARD[1*], ALFONSO MUCCI[2], KRISTINA BROWN[3], AND MARCEL BABIN[4]

[1]LEGOS, Université Paul Sabatier, CNRS, Toulouse, France, bruno.lansard@legos.obs-mip.fr
[2]GEOTOP and Earth and Planetary Sciences, McGill University, Montréal, Canada, alfonso.mucci@mcgill.ca
[3]Earth and Ocean Sciences, University of British Columbia, Vancouver, Canada, kbrown@eos.ubc.ca
[4]Takuvik, Université Laval, Québec, Canada, marcel.babin@takuvik.ulaval.ca

The Arctic Ocean is one of the most intense CO_2 sinks of the oceanic realm due to the low temperature and relatively high primary productivity of its waters [1]. Nevertheless, the Arctic Ocean is prone to rapid transformations in response to climate change, such as changes in sea-ice melt and freezing rates, increased freshwater, nutrient, and particulate input due to higher riverine discharge, as well as changing carbon and sediment fluxes caused by coastal erosion and permafrost thawing. Given the complex interplay between these factors, predicting how the strength of the Arctic Ocean atmospheric CO_2 sink will vary in the future is still a matter of debate [2]. In this context, we address how CO_2 in the surface mixed layer (SML) of the Arctic Ocean may change in response to increased sea-ice melt and riverine inputs.

During the summer of 2009, we conducted high resolution water column sampling on the Mackenzie and Beaufort Shelves (Canadian Arctic) to examine the impact of sea-ice melt and river runoff on surface ocean CO_2 chemistry. We used a combination of natural tracers (salinity, total alkalinity (TA) and stable oxygen isotopic composition ($\delta^{18}O$-H_2O)) to distinguish between sea-ice melt (SIM) and meteoric water (MW) [3]. SIM is characterised by a low TA (415 ± 35 μmol kg^{-1}), a relatively high $\delta^{18}O$-H_2O (-2.0 ± 0.5‰) and relatively low CO_2 partial pressure (pCO_2≈300 μatm). MW is characterised by a high TA (1618 ± 55 μmol kg^{-1}), low $\delta^{18}O$-H_2O (-18.9 ± 0.1‰), and relatively high pCO_2 (>450 μatm). In addition, we analysed the stable carbon isotopic composition ($\delta^{13}C$) of dissolved inorganic carbon (DIC) to determine the origin of the CO_2, i.e. metabolic or atmospheric.

During the study period, significant contributions of MW (>50%) to the SML were only observed on the inner Mackenzie Shelf. In contrast, SIM contribution to the SML reached 30% close to the ice pack, located beyond the shelf break. The admixture of SIM to the SML may therefore allow for the absorption of atmospheric CO_2. A preliminary analysis of the $\delta^{13}C$-DIC data reveals two distinct patterns indicating that CO_2 was either taken up from the atmosphere or produced *in situ* by microbial respiration.

[1] Takahashi et *al.* (2009) Deep-Sea Research II **56**, 554–577. [2] Cai et *al.* (2010) Science **329**, 556-559. [3] Lansard et *al.* (in press) Journal of Geophysical Research

Trace element interactions with altered surfaces in smelter affected acidic soils; Sudbury, Canada

SONIA LANTEIGNE[1*], MICHAEL SCHINDLER[1], ANDREW MCDONALD[1]

[1]Laurentian University, Sudbury, Canada, sx_lanteigne@laurentian.ca (* presenting author)
[1]Laurentian University, Sudbury, Canada, mschindler@laurentian.ca
[1]Laurentian University, Sudbury, Canada, amcdonald@laurentian.ca

Elevated concentrations of metal(loids) in silica rich alteration layers has recently been described for altered surfaces at the solid-water and solid-atmospheric interfaces in tailings, and in the vicinity of smelters, respectively. To determine if similar coatings occur in acidic soils, samples were taken from unlimed areas around three major smelting centers in Sudbury, Ontario, Canada. Coated grains were extracted from these samples and individually mounted to be analysed with SEM, Micro-raman spectroscopy, Laser Ablation ICP-MS and XPS. Preliminary results indicate that coatings are mainly composed of Fe and Si, and that trace elements seem to be associated primarily with coatings having Si : Fe ratios greater than 1, whereas coatings with Si : Fe ratios less than 1 have lower concentrations of associated trace elements. The silica-rich coatings were most likely formed through the precipitation of amorphous silica in iron hydroxide. Their higher metal concentrations with respect to Fe-rich coatings can be explained either by the promoted growth and encapsulation of jarosite group minerals by a silica matrix, or by higher sorption of metal(loids) by iron hydroxide minerals with high silica content which have a lower positive surface charge, lower crystallinity and number of polymerized polyhedra, as well as a higher reactivity than Si-depleted Fe-hydroxides. In conclusion, micro-coatings are capable of taking up and in some cases preserving metal(loid)s such as As,Pb,Se,Cu and Zn among others, and therefore play an important role in the interaction of trace elements with soils, and may affect their behaviour within the soil environment.

Soil grain with multiple coatings

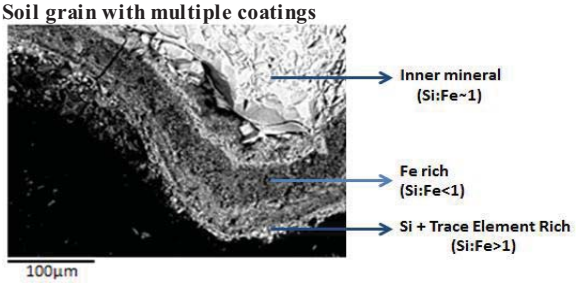

Figure 1. SEM backscatter image of a grain with multiple coatings; a bright Si-rich coating with associated trace elements and a darker Fe-rich coating.

[1] Durocher et al. (2011) *Applied Geochemistry*, pp.1-16
[2] Mantha et al. (2012) *Geochimica Cosmogeochimica Acta* (in press)
[3]Dyer et al. (2010) *J. Colloid Interface Science*, 348, pp.65-70

https://doi.org/10.1180/S0026461X00008434 Published online by Cambridge University Press

A record of Northern Hemisphere climate variability during the Penultimate Glacial from high resolution speleothem data

ZACHARY LAPOINTE[1*], YEMANE ASMEROM[1], VICTOR POLYAK[1], MATTHEW LACHNIET[2]

[1]Department of Earth and Planetary Sciences, Albuquerque, USA, zoneldc@unm.edu

[2]Department of Geoscience, University of Nevada, Las Vegas, USA, matthew.Lachniet@unlv.edu

Numerous paleoclimate records have contributed to our understanding climate change during the Last Glacial. Data for previous glacial cycles are rare however, due to the lack of absolutely dated continuous records. Here we present stable isotope and elemental data of an absolutely dated stalagmite (FS-TR3) from Fort Stanton Cave, New Mexico, that reveal the character and timing of Northern Hemisphere (NH) climate variability during the Penultimate Glacial (MIS 6). These data show links to summer insolation, rapid North Atlantic cold/warm anomalies or lack thereof, and climatic oscillations resembling the 1500-year cycle.

Previous results from the study area showed that δ18O values from stalagmite FS2 mimic the δ18O record of the Greenland Ice Core in both general trends and higher frequency variations such as the Dansgaard–Oeschger (DO) and Heinrich events (HEs) (Asmerom et al., 2010 ref 1) . The new FS-TR3 stalagmite extends our record to the Penultimate Glaciation. Stalagmite FS-TR3, based on high-resolution U-series chronology, grew continuously from 165 to 130 ka. At the orbital scale, the trend is dominated by insolation, upon which are superimposed millennial scale variations. The millennial scale variations are more muted than HE and DO events during the Last Glacial. In contrast to the millennial scale variability, the transition to peak cooling during MIS 6 was abrupt and pronounced, and followed by a very rapid Termination II. Time series analyses of the stable isotope and elemental data show climatic oscillations similar to those exhibited by NH Last Glacial records, such as the 1500-yr cycle. A growth hiatus at 130.3 ka is coincident with the termination of NH Glacial-II from other records. Our record is comparable to that of stalagmite SB11 from Sanbao Cave, China (Wang et al. 2008 ref 2), and this comparison shows that the atmospheric teleconnections between Greenland, the SW USA, and China are likely hemispherical in scale through the Penultimate NH Glacial.

[1] Asmerom (2010) *Nature* **3**, 113-117.
[2] Wang (2008) *Nature* **451**, 1090-1093.

Stable isotope tracing of ZnO nanoparticles in complex systems

F. LARNER[1*], S. DOGRA[2], J. FABREGA[2], A. DYBOWSKA[3], A. AMER[2], A. FILBY[2], L. J. BRIDGESTOCK[1], M. REHKÄMPER[1,3], E. VALSAMI-JONES[3,4], C.R. TYLER[2]AND T.S. GALLOWAY[2]

[1]Imperial College, Earth Science & Engineering, London, UK, fiona.larner04@imperial.ac.uk (* presenting author)

[2]University of Exeter, Biosciences, Exeter, UK

[3]Natural History Museum, Mineralogy, London, UK

[4]University of Birmingham, Geography, Earth & Environmental Sciences, Birmingham, UK

Whilst nanomaterials are employed in an increasing range of commercial and industrial products, analytical difficulties obstruct the scientific understanding of their toxicological properties and environmental fate. ZnO nanomaterials (NMs) are of particular interest as these are used in sunscreens and cosmetics as a UV filter, and reach the biosphere through a variety of routes. Due to the high natural background levels of Zn, the detection of ZnO NMs in ecotoxicologically relevant exposures cannot be attained through concentration data alone. However, highly sensitive detection can be achieved using purpose-made ZnO nanoparticles (NPs) labelled with a stable Zn isotope [1]. This approach also negates handling difficulties and time restrictions associated with radioactive tracing. Even with relatively inexpensive ^{68}Zn as the isotope label, ZnO nanoparticle concentrations as low as 5 ng/g can be precisely quantified against a background of 100 μg/g Zn when measured using MC-ICP-MS.

ZnO NPs (30 nm, TEM) labelled with ^{68}Zn were synthesized by hydrolysis from an acetate precursor [2]. Parallel 10-day exposures of *Corophium volutator* to labelled ^{68}ZnO NPs, bulk ^{68}ZnO and soluble $^{68}ZnCl_2$ were performed in artificial seawater in the presence of sediment [3]. Dialysis experiments were used to determine the rate and extent of dissolution for both bulk and nanoparticulate ^{68}ZnO in the test medium. The subsequent analyses of organisms, sediment and water samples for Zn isotope compositions and concentrations were carried out by MC-ICP-MS following preconcentration of Zn by anion exchange chromatography [4].

For all exposures, including those utilizing dissolved $^{68}ZnCl_2$, the sediments accumulated the largest pool of the ^{68}Zn label. This finding and the low final ^{68}Zn contents of the aqueous media are indicative of significant Zn transfer from the water column to sediments, presumably as a result of Zn sorption [5]. The observations that (i) the ^{68}Zn levels determined for the organisms were approximately scaled in proportion to the dissolved ^{68}Zn concentrations that are expected based on the dialysis experiments and (ii) the organisms featured $^{68}Zn/^{66}Zn$ isotope ratios lower than those measured for the corresponding water samples, suggest that the uptake of ^{68}Zn by the organisms from ^{68}ZnO NPs occurred through the dissolved state.

[1] Croteau *et al*., (2011) *Nanotoxicology*, **5**, 79-90 [2] Dybowska *et al.,* (2011) *Environ. Poll.,* **159**, 266-273 [3] Scarlett *et al*., (2007) *Mar. Environ. Res.,* **63**, 457-470 [4] Arnold *et al*., (2010) *Anal. Bioanal. Chem.,* **398**, 3115-3125 [5] Jain *et al*., (2004) *J. Haz. Mat.*, **B114**, 231-239

https://doi.org/10.1180/S0026461X00008434 Published online by Cambridge University Press

Fingerprinting Himalayan convergence accommodation processes

KYLE LARSON [1*], LAURENT GODIN[2], AND JOHN COTTLE[3]

[1]University of Saskatchewan, Department of Geological Sciences, Currently at University of British Columbia Okanagan, Department of Earth and Environmental Science kyle.larson@ubc.ca (* presenting author)
[2]Queen's University, Department of Geological Sciences and Geological Engineering, godin@geol.queensu.ca
[3]University of California, Santa Barbara, Department of Earth Science, cottle@geol.ucsb.edu

Conceptual models of convergence accommodation processses that operated during the Tertiary evolution of the Himalayan orogen have commonly been examined from an 'end member' point of view. Many previous studies have used geologic data to attempt to characterize these processes in terms of either channel flow or wedge taper models. These models, however, are not mutually exclusive [1] as supported by recent field-based research that demonstrates they are intrinscially related both spatially and temporally [2,3]. Key to undertanding the relationship between channel-type mid-crustal flow and wedge taper processes is appreciating the spatial variation in displacement and distortion throughout a large, hot orogen. Moreover, it is also critical to recognize how initially spatially and deformationally distinct domains may be later juxtaposed.

The exhumed metamorphic core of the Himalaya is well exposed in the Manaslu-Himal Chuli region of central Nepal. This transect has been subject to much geologic research including spatially expansive P-T determinations and new geochronologic controls. These data, coupled with detailed mapping that covers most of the exhumed metamorphic core, provide the constraints necessary to characterize the convergence accommodation processes that imparted those characteristics. The lower portion of the exhumed mid-crust is characterized by structurally-downward decreasing P-T conditions and monazite ages interpreted to reflect subcretion of material to the base of the mid-crust as it was exhuming, consistent with wedge taper processes in the shallow foreland [2]. The upper portion of the exhumed mid-crust, however, preserves a condensed right-way up pressure gradient, an invariant temperature gradient, and monazite ages that are consistent with ductile mid-crustal flow in the deep hinterland [3]. The present-day juxtaposition of these two contrasting domains and the characteristics they record is compatible with the crustal scale channel flow models of Jamieson et al. [4]. Channel flow and wedge taper processes are, therefore, not mutually exclusive.

[1] Beaumont and Jamieson (2010) *USGS Open-File Report* **2010-1099**, 2p. [2] Larson et al. (2010) *GSA Bulletin* **122**, 1116-1134. [3] Larson et al. (2011) *Lithosphere* **3**, 379-392. [4] Jamieson et al. (2004) *Journal of Geophysical Research* **109**, B06407.

Mercury exposure in a sub-arctic population 80 years ago

THORJØRN LARSSEN[1*], MARTHE T.S. JENSSEN[1], HANS FREDRIK BRAATEN[1], AND INGER NJØLSTAD[2]

[1]Norwegian Institute for Water Research, thorjorn.larssen@niva.no (* presenting author)
[2]Department of Community Medicine, University of Tromsø

Mercury exposure to humans from consumption of fish and sea food is a global concern. Mercury releases to the environment from human activities have increased over the past several hundred years. Along with the historical increase in releases, concentrations of mercury in the environment has also increased. As mercury undergo long range transport, elevated concentrations can be found in the environment far from the sources, including in the Arctic. Samples from museum collections, such as, teeth from humans and marine mammals, hair from polar bears and feathers from birds, have shown that mercury concentrations increased rapidly from around 1900 [1].

Historical samples of biological material are scarce and usually only available from a very limited number of individuals . We have come across a set of several hundred human hair samples from a remote population in sub-arctic Norway (a coastal village in Finnmark County) collected as part of a tuberculosis study in the period 1928-1932. A sub set of 218 samples covering all age groups and both sexes was analysed for methyl mercury.

Mean hair methyl mercury concentration was 1.5 mg kg^{-1} (median 1.3 mg kg^{-1}; range 0.3-6.1 mg kg^{-1}). A compareable modern day population (sampled in Tromsø in 2007-2009) had mean hair mercury concentration 1.3 mg kg^{-1} (median 1.0 mg kg^{-1}; range 0.02-11.9 mg kg^{-1}; n=4973) [2]. The relatively similar mean concentrations in the data from around 1930 and from 2007-2009, despite that concentrations of mercury in fish around 1930 were considerably lower than today, are probably due to higher fish intake and hence similar total mercury exposure 80 years ago.

Contrary to the modern day population, the data set from around 1930 shows no differences between age groups or sexes. Modern day data typically show increasing concentrations with age and higher concentrations in men than women. The differences between age groups and sexes in the modern day population can be explained by food consumption habits. The lack of differences between sub groups in the old data probably shows that there were minor differences in food consumption habits, related to high dependency on local fish and limited choice of food due to poverty and relative geographical isolation at the time.

[1] Dietz, R. *et al.*, (2009) *Sci. Total Environ*. **407,** 6120-6131.
[2] Jenssen, M.T.S. *et al.* Mercury exposure and links to human health in Tromsø, Arctic Norway. *Manuscript in preparation.*

https://doi.org/10.1180/S0026461X00008434 Published online by Cambridge University Press

Vanadate complexation to ferrihydrite: X-ray absorption spectroscopy and CD-MUSIC modeling

MAJA A. LARSSON[1], JON PETTER GUSTAFSSON[2]*, CARIN SJÖSTEDT[2] AND INGMAR PERSSON[3]

[1]Department of Soil and Environment, Swedish University of Agricultural Sciences, Box 7014, 750 07 Uppsala, Sweden
[2]Department of Land and Water Resources Engineering, KTH (Royal Institute of Technology), Teknikringen 76, 100 44 Stockholm, Sweden, gustafjp@kth.se (* presenting author)
[3]Department of Chemistry, Swedish University of Agricultural Sciences, Box 7001, 750 07 Uppsala, Sweden,

Sorption of vanadate(V) to iron (hydr)oxides is one of the most important processes affecting vanadium bioavailability and transport in soils. We characterised vanadate(V) adsorption to 2-line ferrihydrite by means of batch experiments, EXAFS spectroscopy, and surface complexation modeling using the CD-MUSIC model for ferrihydrite [1, 2].

Vanadate(V) sorption was strongest at low pH, and it decreased in the presence of *o*-phosphate, as expected. Results from EXAFS spectroscopy showed that vanadate(V) is sorbed primarily as an edge-sharing bidentate complex with a single V···Fe distance of ~2.87 Å. Our conclusion differs from earlier work on vanadate(V)-sorbed goethite, for which a corner-sharing bidentate complex with V···Fe distances of ~3.25 Å was identified [3].

The CD-MUSIC model could describe vanadate(V) sorption well when two surface complexes were considered. One of them was a bidentate $\equiv FeO_2VO_2^{1.5-}$ complex (in line with the EXAFS results), which dominated vanadate(V) sorption under most conditions. The best modeling results were obtained when one of the surface oxygens of this complex was assumed to be singly coordinated to iron, whereas the second one was doubly coordinated. At low pH and at low Fe:V ratios the modeling exercise suggested the additional presence of another complex, which may be an outer-sphere surface complex involving $H_2VO_4^-$ and a diprotonated $\equiv FeOH_2^{½+}$ surface group. The implications of these results are that vanadate(V) may be strongly sorbed to iron (hydr)oxides in acid to neutral environments; however, the sorption affinity is related strongly to, e.g., competition with *o*-phosphate.

[1] Hiemstra & Riemsidjk (1996) *J. Colloid Interface Sci.* **179**, 488-508. [2] Gustafsson *et al.* (2009) *Appl. Geochem.* **24,** 454-462. [3] Peacock and Sherman (2004) *Geochim. Cosmochim. Acta* **68,** 1723-1733.

The location of microrganisms in petroleum reservoirs

STEVE LARTER[1]*, BARRY BENNETT[1], THOMAS OLDENBURG[1], JENNIFER ADAMS[1,2] AND IAN HEAD[3]

[1]PRG, Dept Geosciences, U. Calgary, Calgary, Canada., slarter@ucalgary.ca * presenting author)
[2]Current address: ConocoPhillips, Houston, USA.,
[3]NRG, Civil Engineering and Geosciences, U. Newcastle, Newcastle, UK. i.m.head@ncl.ac.uk

Summary

Geochemical and geological inferences have suggested, based on analysis of chemical gradients in biodegraded oil reservoirs that the site of microbial activity must be largely focussed at the oil-water-transition zone (OWTZ) at the base of the oil column[1]. Using a combined geochemical, geological and microbiological analysis of an actively biodegrading Canadian heavy oil reservoir shows that petroleum degrading microorganisms are indeed focussed in a zone of high water saturation at the base of the oil column in the OWTZ but that surprisingly, it is much thicker than expected, occupying a zone of active biological activity exceeding 10 meters. Through the oil column, gradients in biodegradation related oil physical and chemical properties are driven from this OWTZ with chemical gradients in, for example, concentrations of alkylaromatic hydrocarbons and aromatic heterocompounds significantly steepening in this "biological burn out zone". 16S rRNA gene qPCR data suggest on the order of 10^6 to 10^7 cells/gm of sediment are present in the burn out zone, numbers that are consistent with an active biological system and around 10^4 to 10^5 cells/gm outside the burnout zone. The bacterial abundances in the OWTZ are in line with the trend of bacterial abundance with depth that has emerged from extensive analysis of microbial cells in deep subsurface sediments [2], implying that in terms of the deep biosphere, oil reservoirs are nothing special! The bacterial abundance is about 2 orders of magnitude higher within the burnout zone than within the oil leg, consistent with the notion that microbial activity and abundance in the deep subsurface is elevated at geochemical interfaces[3]. This broad result appears to support the original hypothesis that microbial activity must be largely focussed at the oil-water-transition zone (OWTZ) at the base of the oil column. We discuss the impact of these results on both the uniformity of processes in the deep biosphere and the substantial challenges this imposes on engineering accelerated microbial conversion of liquid petroleum to methane or hydrogen on production timescales.

[1] Larter S.R., Wilhelms A., Head I., Koopmans M., Aplin A., Di Primio R., Zwach C., Erdmann M. and Telnaes N. (2003). The controls on the composition of biodegraded oils in the deep subsurface: (Part 1) Biodegradation rates in petroleum reservoirs. Organic Geochemistry, 34, 601-613.
[2] Parkes R.J., Cragg B.A., Bale S.J., Getlifff J.M., Goodman K., Rochelle P.A., Fry J.C., Weightman A.J. and Harvey, S.M. (1994). Deep bacterial biosphere in Pacific- Ocean sediments. Nature 371, 410-413. (1994).
[3] Parkes R.J., Cragg B.A., Weightman A.J., Webster G., Newberry C.J., Ferdelman T.G., Kallmeyer J., Jørgensen B.B., Aiello I.W. and Fry J.C. (2005). Deep sub-seafloor bacteria stimulated at interfaces over geological time. Nature 436, 390-394.

https://doi.org/10.1180/S0026461X00008434 Published online by Cambridge University Press

Foliar transfer of TiO_2 and Ag nanoparticles in lettuce

CAMILLE LARUE[1*], LAURIC CECILLON[1], HIRAM CASTILLO-MICHEL[2], VERONIQUE BARTHES[3], VALERIE MAGNIN[1], NATHANIEL FINDLING[1], SARAH BUREAU[1], GERALDINE SARRET[1]

[1]ISTerre, UMR 5275, (ex UJF-LGIT), CNRS and University J. Fourier, BP 53, 38041 Grenoble cedex 9, France. camille.larue@ujf-grenoble.fr (*presenting author), lauric.cecillon@irstea.fr, valerie.magnin@ujf-grenoble.fr, nathaniel.findling@ujf-grenoble.fr, sarah.bureau@ujf-grenoble.fr, geraldine.sarret@ujf-grenoble.fr

[2]European Synchrotron Radiation Facility, beamline ID21, Grenoble, France. hiram.castillo_michel@esrf.fr

[3]LCSN, LITEN/L2T, CEA Grenoble, France. veronique.barthes@cea.fr

Introduction: The possible transfer of engineered nanoparticles (ENPs) into plants should be evaluated in the perspective of human exposure through ingestion of crops. The mechanisms of ENPs transfer and on their fate inside plants are poorly understood, particularly for the foliar pathway [1]. The fate of TiO_2 and Ag^0 ENPs in lettuce leaves was studied after foliar exposure by wet deposition. The localization of ENPs and the speciation of Ti and Ag were studied by SEM- and TEM-EDX, micro X-ray fluorescence (μXRF) and micro X-ray absorption spectroscopy (μXAS) based on synchrotron radiation.

Results and Conclusion: TiO_2 exposure did not induce any visible toxicity symptoms, whereas Ag (both ionic and nano) induced some necroses on leaves. Imaging techniques show the presence of large agglomerates of Ti or Ag both on the surface of the epidermis and inside leaves (Figure 1). No sign of TiO_2 dissolution was observed by μXAS whereas Ag ENPs are partially dissolved with the formation of secondary Ag species (Ag^+ bound to organic ligands). These results suggest that crops exposed to atmospheric deposition of ENPs may undergo contamination due to foliar transfer of ENPs.

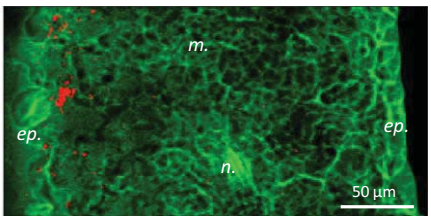

Figure 1: Ti (red) and K (green) distribution in lettuce leaves after foliar exposure. *ep. epidermis, m. mesophyll, n. nerve.*

[1] Fernandez & Eichert (2009) *Crit. Rev Plant Sci.* **28**, 36-68.

Chemistry of H-Li-Na-K-Cl-H_2O brines up to high concentrations (< 40 molal) and temperatures (0 - 250°C)

A. LASSIN[1]*, C. CHRISTOV[2], L. ANDRÉ[1], M. AZAROUAL[1]

[1]BRGM, Orléans, France, a.lassin@brgm.fr (* presenting author), l.andre@brgm.fr, m.azaroual@brgm.fr

[2]GeoEco Consulting 2010, San Marcos, CA, USA, hristovi@sbcglobal.net

Introduction

Lithium interest for industrial production has been increasing during the last few years. This alkali metal is of primary importance in the battery production for electricity storage, in vehicles and electronic devices. Because of very high solubility of lithium in water, the chemical behaviour of lithium minerals – brines systems is highly non-ideal and very complex. Its characterization requires specific approaches. The ion-specific interactions model developed by Pitzer [1] is particularly well suited for dealing with ionic strengths ranging from low up to very high salinities, i.e. above several tens of moles per kg of water [2].

Description of the work

In this work, we studied the H-Li-Na-K-Cl-H_2O chemical system, and determined new relevant Pitzer interaction parameters using the recent procedure developed by André et al. [3]. In the binary LiCl-H_2O system, this set of parameters, together with the aqueous complexation constant of the $LiCl^0$ aqueous species, allows the description of the phase diagram for temperatures ranging from 0 to 250°C and for salinities up to saturation, i.e. up to 40 mol/kgw. The presence of the $LiCl^0$ aqueous species has been investigated by NMR (Nuclear Magnetic Resonance) as described in a companion communication [4]. Using this parametrization (which includes the $LiCl^0$ aqueous species) in the ternary LiCl-KCl-H_2O, LiCl-NaCl-H_2O, and LiCl-HCl-H_2O systems, phase diagrams can be satisfactorily described up to 30 mol/kgw, and 150°C.

The set of new interaction parameters determined in this study should allow the description of the chemical behaviour of the quinary LiCl-KCl-NaCl-HCl-H_2O system over a wide range of salinities (0.001 to 40 molal) and temperatures (0 to 250°C). The model presented here is a continuation of the previously established model for lithium hydroxide systems [5], and is consistent with the related set of specific interaction parameters. This extension is of great importance to better characterize the chemical behaviour of complex systems like natural Li-bearing brines found in hydrothermal systems (e.g., Soultz-Sous-Forêt, Salton Sea, etc.).

[1] Pitzer (1991) *Activity coefficients in electrolyte solutions*, 2nd ed., CRC Press
[2] Lassin et al. (2009) *19th Goldschmidt Conf.*
[3] André et al. (2009) *19th Goldschmidt Conf.*
[4] Montouillout et al. (2012) *22nd Goldschmidt Conf.*
[5] Lassin et al. (2011) *21st Goldschmidt Conf.*

https://doi.org/10.1180/S0026461X00008434 Published online by Cambridge University Press

Evaluation of sources of error in $^{186}Os/^{188}Os$ measurements via NTIMS

JOHN C LASSITER[1]*, RUDRA CHATTERJEE[1], SHUANGQUAN ZHANG[1], STACI LOEWY[1]

[1]University of Texas, Jackson School of Geosciences lassiter1@mail.utexas.edu (* presenting author)

The ^{190}Pt-^{186}Os decay system may be useful for monitoring signals of core/mantle interaction in plume-derived lavas [c.f., 1]. However, the total natural variation in $^{186}Os/^{188}Os$ is small (~150 ppm), requiring the highest levels of accuracy and precision in $^{186}Os/^{188}Os$ measurements to discern natural variations that may reflect such interaction. Previous studies have examined several potential sources of systematic and non-systematic error in $^{186}Os/^{188}Os$ measurements deriving from uncertainties in the O-isotope composition of OsO_3^-, potential interferences from PtO_2^-, PtO_3^-, and WO_3^-, and departures from exponential mass fractionation [2]. We have undertaken a $^{186}Os/^{188}Os$ study of both laboratory Os standards and natural samples to better quantify the primary sources of analytical error in $^{186}Os/^{188}Os$ measurements and refine analytical procedures to minimize these errors.

Inter- and intra-run variations in oxygen isotope composition of measured OsO_3 peaks produce correlated errors in $^{186}Os/^{188}Os$, $^{189}Os/^{188}Os$, and $^{190}Os/^{188}Os$ ratios. Although significant O-isotope variation is observed between analyses, intra-run variation is sufficiently small that O-isotope composition determination through pre- and post-run measurement of $^{192}Os^{16}O_2{}^{18}O$ and other high-mass oxide peaks is suffiicent. Uncertainties derived from oxide corrections can be further reduced by utilizing the $^{189}Os/^{188}Os$ ratio for mass fractionation corrections rather than $^{192}Os/^{188}Os$, but the reduced error from oxygen isotope uncertainties is offset by increased error in the fractionation factor. However, the excellent reproducibility of $^{189}Os/^{188}Os$ measurements (<10ppm 2σ) using $^{192}Os/^{188}Os$ for mass fractionation indicates that these uncertainties are not the primary sources of error in $^{186}Os/^{188}Os$ measurements.

For the quantities of Os and beam intensities utilized in previous $^{186}Os/^{188}Os$ studies (several 10s of ng Os, ~80-120 mV ^{186}Os with a 10^{11} ohm resistor), the largest source of analytical error is shown to be Johnson Noise on interblock baseline measurements, which significantly exceeds error derived from counting statistics. Because ^{186}Os is a relatively minor isotope of Os (~1.6%), it is affected by Johnson Noise error propagation to a much greater extent than higher abundance isotopes. Analytical precision on the smaller Os-isotope peaks can be significantly improved without increasing sample size simply by increasing the duration of baseline measurements in proportion to signal measurement time [3]. Further improvement is obtained by utilizing a 10^{12} ohm resistor for measurement of $^{184}OsO_3$ and $^{186}OsO_3$ peaks. Finally, several $^{186}Os/^{188}Os$ analyses previously reported in the literature appear to be compromised by an as-yet unidentified, possibly organic interference that impacts both the $^{186}Os/^{188}Os$ and $^{184}Os/^{184}Os$ ratios. We present an improved method for monitoring potential interferences in future $^{186}Os/^{188}Os$ studies.

[1] Brandon, et al. (1999) *Earth Planet. Sci. Lett.* **174**, 25-42. [2]Luguet et al. (2008) *Chem. Geol* **248**, 342-362. [3] Ludwig (1997) *Chem. Geol.* **135**, 325-334.

Reactivity of U^{VI} with pure, oxidized, and Ti-substituted magnetites

DREW E. LATTA[1*], CAROLYN I. PEARCE[2], CHRISTOPHER A. GORSKI,[3] KEVIN M. ROSSO[2], EDWARD J. O'LOUGHLIN[1], KENNETH K. KEMNER[1], MICHELLE M. SCHERER[4], MAXIM I. BOYANOV[1]

[1]Argonne National Laboratory, Argonne, IL, USA, dlatta@anl.gov (* presenting author)

[2]Pacific Northwest National Laboratory, Richland, WA, USA.

[3]Swiss Federal Institue of Aquatic Science and Technology, Eawag, Duebendorf, Switzerland.

[4]The University of Iowa, Iowa City, IA, USA

Reduction of U^{VI} to U^{IV} through coupled biotic-abiotic processes can significantly decrease uranium mobility in subsurface environments. To understand the abiotic factors contributing to this process, we investigated the reduction of U^{VI} to U^{IV} by magnetite, a common rock forming mineral and product of microbial Fe^{III} respiration. U^{VI} reactivity with pure, stoichiometric magnetite ($Fe^{II}Fe^{III}{}_2O_4$, $Fe^{2+}/Fe^{3+} = 0.5$) is compared to that with a series of oxidized ($Fe^{2+}/Fe^{3+} < 0.5$) and Ti-substituted magnetites. Ti^{4+}-for-Fe^{3+} substitution is common in natural magnetite [1, 2] and results in a solid solution ($Fe_{3-x}Ti_xO_4$, $0 < x < 1$) where Ti^{4+} incorporation is charge balanced by proportional increases in Fe^{2+}.

Using x-ray absorption spectroscopy (XANES and EXAFS) at the U L_{III}-edge we observe that the Fe^{2+}/Fe^{3+} ratio in magnetite is a major control on its ability to reduce U^{VI}. Stoichiometric and partially oxidized magnetites ($Fe^{2+}/Fe^{3+} \geq 0.38$) reduce U^{VI} to uraninite ($U^{IV}O_2$) nanoparticles, whereas more oxidized magnetites ($Fe^{2+}/Fe^{3+} < 0.38$) adsorb U^{VI} as an inner-sphere complex without transferring electrons. The observed redox reactivity between magnetite and U^{VI} can be correlated with measured reduction potentials for magnetite and with published thermodynamic parameters for U^{IV}/U^{VI} redox couples [3].

Titanomagnetite nanoparticles with Ti formula contents up to $x = 0.5$ and Fe^{2+}/Fe^{3+} ratios between 0.5 and 1.2 can also reduce U^{VI} to U^{IV}. EXAFS spectra indicate that the reduced U^{IV} atoms are *not* incorporated in uraninite. The speciation of U^{IV} appears to be controlled by Ti-content and not by the Fe^{2+}/Fe^{3+} ratio, as the reduction of U^{VI} by partially oxidized $x = 0.5$ titanomagnetite results in the same non-uraninite U^{IV} species.

This work highlights previously unexplored thermodynamic and geochemical factors that may influence the speciation and solubility of uranium in the subsurface. The observation of non-uraninite U^{IV} species in this study, as well as in carbonate and phosphate bearing systems in previous studies [4-6] suggests the need for a better understanding of the stability of reduced U^{IV}.

[1] Pearce, et al. Am. Mineral., 2010. **95**: p. 425-439.

[2] Baer, et al. Phys. Chem. Earth Pt. A/B/C, 2010. **35**: p. 233-241.

[3] Latta, et al. Environ. Sci. Technol., 2011. **46**: p. 778-786.

[4] Cologgi, et al. Proceedings of the National Academy of Sciences, 2011. **108**: p. 15248-15252.

[5] Veeramani, et al. Geochim. Cosmochim. Acta, 2011. **75**: p. 2512-2528.

[6] Boyanov, et al. Environ. Sci. Technol., 2011. **45**: p. 8336-8344.

https://doi.org/10.1180/S0026461X00008434 Published online by Cambridge University Press

Mobility of nanoscale zero-valent iron in quartz and carbonate sands

SUSANNE LAUMANN[1], VESNA MICIĆ[1], THILO HOFMANN[1,*]

[1]Department of Environmental Geosciences, University of Vienna, Vienna, Austria, susanne.laumann@univie.ac.at, vesna.micic@univie.ac.at, thilo.hofmann@univie.ac.at (*presenting author)

Abiotic dechlorination of chlorinated solvents by nanoscale zero-valent iron (nZVI) is an alternative remediation technology for deep aquifers or those underneath infrastructures. Its effectiveness depends on the nZVI properties and concentration, as well as concentration and distribution of contaminats. One prerequisite for a succesfull application of this technology is the delivery of nZVI particles to the contaminats [1]. Delivery is limited by nZVI mobility due to aggregation and deposition, all depending on water chemistry, nZVI properties, and aquifer surface properties.

Adsorbed anionic polyelectrolyte coatings provide electrostatic double layer repulsions between negatively charged nZVI particles [2], hindering their aggregation and also deposition on the negatively charged quartz surfaces (prevailing in aquifers). However, it is shown that the presence of surface charge heterogeneities in the aquifer, such as carbonates, effects the particle mobility [3].

Hereby we evaluated the mobility of commercially available nZVI particles in porous media that have different surface charges, namely quartz and carbonate sands.

Column experiments showed that the mobility of nZVI was reduced by ~45% in pure carbonate sand, compared to that in pure quartz sand. These results revealed substantially different attachment efficiencies of nZVI to these aquifer solids with different surface charges. The zeta potential varied from -40.6 mV in pure quartz sand to -13.6 mV in pure carbonate sands at pH value of 9.1 and 9.6, respectively. The results demonstrated the influence of surface chemistry of the two often encountered aquifer matrices on the mobility of nZVI particles. Further experminets are carried out aiming to evaluate the influence of other surface charge heterogeneities (such as presence of NOM and iron oxides) as well as of different groundwater chemistry on nZVI mobility.

[1] Tratnyek, P.G., Johnson, R.L. (2006), ***Nano Today*** **1**, 44-48. [2] Saleh, N. et al., (2007), ***Environmental Engineering Science*** **24**, 45-57. [3] Johnson, P. R. et al., (1996), ***ES&T*** **30**, 3284-3293.

The diversity of granitoids in the northern Kaapvaal craton records late-Archæan geodynamic changes

OSCAR LAURENT[1*], HERVE MARTIN[1], REGIS DOUCELANCE[1], JEAN-FRANÇOIS MOYEN[2] AND JEAN-LOUIS PAQUETTE[1]

[1]Clermont Université, Université B. Pascal, Laboratoire Magmas et Volcans (CNRS-UMR6524), BP10448, F-63000 Clermont-Ferrand, France. O.Laurent@opgc.univ-bpclermont.fr (* presenting author)

[2]Université Jean Monnet, Département de Géologie (CNRS-UMR6524), 23 rue Dr. Paul Michelon, F-42043 Saint-Étienne, France.

We studied the emplacement ages (LA-ICP-MS dating on zircons) and petrogenesis (major- and trace-elements, Nd isotopes) of granitoid rocks along a cross-section in South Africa, from the Murchison greenstone belt in the Kaapvaal craton to the Central Zone of the Limpopo mobile belt.

The 'basement' of the northernmost Kaapvaal craton is made up of deformed and variously migmatized granitoid gneisses of TTG affinity that emplaced as discrete events, in the time range of 3.20 to 2.85 Ga. The peraluminous biotite granites from the Turfloop batholith and Duiwelskloof area, located between the Murchison and Pietersburg belts, emplaced at ~2.78 Ga and have a crustal origin (TTGs, possibly metasediments). At the suture between the Kaapvaal craton and the Limpopo Belt, several metaluminous, high-K calc-alkaline granitoids intruded at ~2.69 Ga (Mashashane, Matlala, Matok, Moletsi). Their geochemical features indicate that they are composite complexes, whose genesis involved melts derived from both the reworked TTGs and mantle-derived intermediate to mafic material. Finally, the Bulai pluton (~2.59 Ga) emplaced in the Central Zone of the Limpopo belt further north. It shares unequivocal affinities with sanukitoids. It was generated by differentiation of primary monzodiorites [1], themselves deriving from a mantle source previously enriched by a sediment-derived felsic melt [2].

Therefore, while 'classical' Archæan petrogenetic mechanisms prevailed until ~2.85 Ga (protracted generation and recycling of TTG), the late-Archæan evolution is marked by a diversification of granitoid sources and crustal growth processes. In addition, whereas TTGs of all ages are randomly distributed throughout the whole area, younger magmatism shows a strict structural control: from south to north, emplacement ages decrease while mantle contribution increases.

This spatial and temporal evolution of granitoid magmatism in the northern Kaapvaal records fundamental geodynamic changes. In particular, while typical Archæan TTGs are only derived from meta-basalts at various depths [3], the magmas emplaced at the Archæan-Proterozoic transition involved a greater range of sources (from recycling of various crustal lithologies up to inputs of juvenile, mantle-derived material), thus resulting in a wide range of medium- to high-K granitoids. As the distribution, geochemistry and temporal evolution of granitoids in the northern Kaavaal recall those of post-Archæan late-orogenic settings, we propose that these rocks witness the progressive initiation of modern-style geodynamic processes.

[1] Laurent *et al*., *Precambrian Research*, submitted. [2] Laurent *et al*. (2011) *Lithos* **123,** 73-91. [3] Moyen (2011) *Lithos* **123**, 21-36.

https://doi.org/10.1180/S0026461X00008434 Published online by Cambridge University Press

The influence of temperature on carbon chemistry of organomineral complexes

JOCELYN M. LAVALLEE [1]*, RICH T. CONANT[1], MARTIN OBST[2], THOMAS BORCH[3], AND TOM REGIER[4]

[1]Natural Resource Ecology Laboratory, Colorado State Univervity, Fort Collins, USA, jocelyn.lavallee@colostate.edu (* presenting author) , rich.conant@colostate.edu

[2]Center for Applied Geoscience Eberhard Karls University Tuebingen, Tuebingen, Germany, martin.obst@uni-tuebingen.de

[3]Department of Soil and Crop Sciences, Colorado State University, Fort Collins, USA, thomas.borch@colostate.edu

[4]Canadian Light Source, Saskatoon, Canada, Tom.Regier@lightsource.ca

Soil organic matter can interact with soil mineral surfaces to form stable organomineral complexes. These organomineral complexes effectively protect carbon compounds against microbial decomposition and play a large role in regulating global carbon cycling rates. Because the interactions between the organic matter and mineral surfaces are chemical reactions, there is reason to believe that they are regulated by temperature, but this remains unknown. As part of an ongoing study, we are investigating the impact of temperature on the rates of formation of organomineral complexes and the chemical properties of the carbon within those complexes. We are employing scanning transmission X-ray microscopy (STXM) and carbon near edge X-ray absorption fine structure (CNEXAFS) to map the spatial distribution of carbon forms in organomineral complexes at different temperatures. We are also using CNEXAFS with a spot size of 1000µm x 100µm to gather comprehensive chemical data on the effect of temperature on organic matter fractionation. We will present data from ongoing experiments utilizing two types of samples: synthesized iron oxide-organic matter complexes and soils gathered from field climate manipulation experiments. The climate manipulation experiments are part of the Old-field Community Climate and Atmospheric Manipulation Experiment carried out in Oak Ridge, Tennessee from 2003 to 2005. We fractionated the climate manipulation soils by density prior to measurement. The laboratory experiments provide the benefit of control over the materials used, while the climate manipulation soils are more representative of the effects of temperature that we would see in the field. Thus far, results suggest that temperature can impact organic matter fractionation at mineral surfaces. Of particular interest, we see an influence of temperature on the absorption peak at 290.2 eV, which under our experimental conditions may be caused by Fe-O-C bonds rather than carbonates. We also present methodological considerations for CNEXAFS measurements, as well as plans for future experiments.

Multiple glass transitions in natural volcanics: a demonstration of shallow magma mixing during Strombolian eruptions at Yasur Volcano, Vanuatu

YAN LAVALLÉE[1*], SIMON KREMERS[1], JONATHAN HANSON[1,2], KAI-UWE HESS[1], MAGDALENA ORYAËLLE CHEVREL[1], JOACHIM WASSERMANN[1], DONALD B. DINGWELL[1]

[1] Ludwig-Maximilians-University Munich, Earth and Environmental Sciences, lavallee@min.uni-muenchen.de (*presenting author)

[2] University of Bristol, Department of Earth Sciences

Introduction

Strombolian activity is often regarded as a product of the rapid ascent of gas slugs entraining a deep magma [1], which mingle with a batch of shallow magma upon eruption [2]. The presence of a range in crystallinities as well as bimodal bubble-size distributions, in the eruptive products, generally support this view. The regular intervals of strombolian activity suggest a continuum in an open system [3], where the surface activity is inferred to reflect the ascent of magma batches at various rates, driven by the relative buoyancy of bubbles with contrasting sizes [4,5]. Mt. Yasur volcano (Vanuatu) has been increasingly recognized for its high-frequency Strombolian eruptions, where three active vents display eruptions of different intensities at contrasting intervals of minutes to tens of minutes. Here, we constrain this range of behaviour using information locked in at the glass transition.

Result and conclusion

A rheological investigation of the eruptive products indicates that basaltic-andesitic eruptive products containing an apparently homogeneous glass phase exhibit evidence of a distinct range of glass transition temperatures with multiple peaks occurring in individual samples. Such anomalous behavior, is proposed to result from the mingling of magmas with contrasting oxidation state. We resolved this hypothesis through complementary calorimetric analyses on remelted rocks prepared under different oxigen fugacities, which attest of the range in glass transitions with oxidation states as well as reveal the instability of such basaltic-andesitic melts in the reduced state. The anomalous nature of the measured glass transition behavior of eruptive products leads us to the inference that mingling is located in the shallow parts of the eruptive conduits, in parts due to rejuvenation of material slumped from the crater walls into an open conduit system. The dynamics of this process may reflect the periodicity of the eruptions themselves.

[1] Walker (1973) *Geologische Rundschau* 62, 431-446. [2] Lautze & Houghton (2005) *Geology* 33, 425-428. [3] Metrich *et al.* (2010) *J. Petrology* 51, 603-626. [4] Vergniolle (1996) *Earth Planet Sci Letter* 140, 269-279. [5] James *et al.* (2008) *Geol. Soc. London Special Publication* 307, 147-167.

https://doi.org/10.1180/S0026461X00008434 Published online by Cambridge University Press

Neptunium biogeochemistry and the manganese cycle

GARETH T. W. LAW[1], CLARE L. THORPE[1*], SAM SHAW[2], AMY ATKINS[2], FRANCIS R. LIVENS[3], CAROLINE L. PEACOCK[2], JONATHAN R. LLOYD[1], MELISSA A. DENECKE[4], KATHY DARDENNE[4] AND KATHERINE MORRIS[1]

[1]Centre for Radwaste and Decommissioning, The University of Manchester, UK, clare.thorpe-2@postgrad.manchester.ac.uk (* presenting author)

[2]Earth Surface Science Institute, School of Earth and Environment, Leeds, UK, S.S.Shaw@leeds.ac.uk

[3]Centre for Radiochemistry Research, The University of Manchester, UK, francis.livens@manchester.ac.uk

[4]Karlsruhe Institute of Technology, Institut fur Nukleare Entsorgung, Karlsruhe, Germany

Neptunium is a key risk-driving radionuclide in geological disposal and is predicted to be the most mobile transuranic in the subsurface at nuclear contaminated sites. However there is a lack of information concerning Np environmental behavior; notably in relation to manganese, a ubiquitous element in any geological setting that has been implicated in actinide beogeochemical cycling [1]. To explore this relationship further, we have characterised Np biogeochemical behaviour in: (i) a ^{237}Np(V) amended δMnO_2-rich sediment treatment where we have poised the system at Mn-reducing conditions; and (ii) a range of ^{237}Np(V) amended synthetic Mn mineral systems (pure-phase δMnO_2, tri-clinic and acid birnessite, todokrokite, hausmennite and rhodochrosite).

In the sediment system, acetate addition stimulated microbially-mediated bioreduction and the rate of Np sorption to sediment increased during both Mn-reduction and Fe(III) reduction. By the onset of sulfate reduction, all (>99 %) of the added Np(V) (~0.3 μM) had been removed from solution. Parallel XAS experiments (Np(V) ~ 0.3 mM) underwent a similar biogeochemical evolution and data collection is ongoing. In the pure-mineral systems, Np(V) (0.3 μM – 0.3 mM) rapidly (minutes – hours) sorbed to each mineral phase except rhodochrosite, which showed more limited Np sorptive potential. XAS analysis of each mineral phase is ongoing and we expect a range of Np speciation and co-ordination environments related to the Mn-mineral structure and average oxidation state.

[1] Law et al. (2010) *Environmental Science and Technology* **44**, 8924-8929.

Modeling the influence of organic acids on soil weathering

COREY R LAWRENCE[1*], KATE MAHER[2], MARJORIE SCHULZ[1], AND JENNIFER HARDEN[1]

[1]USGS, Menlo Park, USA, clawrence@usgs.gov (* presenting author)

[2]Stanford University, Stanford, USA, kmaher@stanford.edu

The potential infuences of low molecular weight organic acids (LMWOA) on the dissolution of soil minerals and, conversly, the stabilization of organic compounds by complexation with minerals or weathering products are well characterized. Mineral weathering is enhanced through several processes including: ligand promoted dissolution; the influence of organic-metal comlexation on dissolution reaction affinity; and/or the changes in soil pH resulting from organic acid dissociation and the production of CO_2 through the decomposition of organics [1]. Protection of organic matter occurs through adsorption of organics on mineral surfaces, complexation of organics with metals in solution, the formation of soil aggregates and/or other processes that limit the microbes access to organic compounds or increase the energy required to initiate decomposition [2]. Although these processes are well documented, the net influence of these interactions in a natural soil weathering system has yet to be quantified.

Reactive transport modeling of soils provides a viable framework for examining the organic-mineral interactions at the field scale. The inclusion of LMWOA in simulations of soil development at the Santa Cruz Marine Terrace Chronosequence yields supprising results with regard to mineral weathering. Our work suggests that inclusion of reactions describing the complexation of organic acids and aqueous Al species does not dramatically alter the spatial extent of primary mineral dissolution (and hence the overall weathering rate), but has a comparativly greater influence on seondary mineral precipiation (e.g. kaolinite). In our model system, complexation of organic acids with trace metals competes with kaolinite precipitation as a sink of Al^{3+}; effectively reducing precipiation in the top 0.5 m of the study soils but not leading to large enough changes in the saturation state of albite or K-feldspar to increase the dissolution rate of those minerals. Furthermore, our results show how the spatial extent of weathering fronts may control the distribution of organic substrates. Several other processes linking organic acids to mineral weathering still need to be encorporated into this model framework, but these results demonstrate that our understanding of organic-mineral interactions in soils may be advanced through consideration of these processes in natural systems.

[1] Ganor (2009) *Reviews in Mineralogy & Geochemistry* **Volume 70**, 259-369. [2] v. Lützow (2006) *European Journal of Soil Science* **Volume 57**, 426-445.

https://doi.org/10.1180/S0026461X00008434 Published online by Cambridge University Press

Oxygen Isotope Proxies of Tropical Cyclones: Suitable Species

JAMES LAWRENCE[1], ROSALIE MADDOCKS[1], NIALL SLOWEY[2], AND BRENDAN ROARK[2]

[1]University of Houston, Earth and Atmospheric Sciences, Houston, Texas, USA, jimrslawrence@gmail.com*
[2]Texas A&M University, Geosciences, College Station, Texas, USA

Results

The human experience of climate change is not one of gradual changes in seasonal or yearly changes in temperature or rainfall. Despite that, most paleoclimatic reconstructions attempt to provide just such information. Humans experience climate change on much shorter time scales. We remember hurricanes, weeks of drought or overwhelming rainy periods

Tropical cyclones produce very low isotope ratios in rainfall. Thus, climate proxies that potentially record these low isotope ratios offer one of the most concrete records of climate change to which humans can relate.

The oxygen isotopic composition of tropical cyclone rainfall has the potential to be recorded in fresh water carbonate fossil material, cave deposits and corals. The waters in ephemeral ponds in Texas have been shown to contain anomalously low isotope ratios following the passage of tropical cyclones. The Class of carbonate organisms known as Ostracoda (Arthropods) form their carapaces very rapidly and have been shown to provide an isotopic record of the storm passage [1]. The Class of organisms known as Charophyceae (specialized algae) form desiccation resistant ooganis ("carbonate fruits") on their stems in response to the sudden appearance of water in dry ponds. Thus fresh water ephemeral ponds in the subtropics are ideal locations for isotopic studies.

A region that shows considerable promise is South Texas /Northeast Mexico. In 2010 rains from Hurricane Alex, Tropical Depression 2 and Tropical Storm Hermine flooded ephemeral ponds in south Texas. Isotopic analysis of water and fossil Ostracoda and Charophyceae from ephemeral ponds in south Texas are planned. A core (50 cm in length) was taken in one of these ponds where living Ostracoda and Charophyceae were found and collected.

[1] Lawrence (2008) *Quat. Res.* **Volume 70 pp 339-342**.

Biogeochemical Dynamics of Aqueous Fe and Mn in Soil Pore-Waters and Stream with Respect to Dissolved Organic Matter (DOM) Quantity and Quality

O. LAZAREVA[1*], D.L. SPARKS[1], W. PAN[1], J. KAN[2], A. AUFDENKAMPE[2]

[1]University of Delaware Environmental Institute, Newark, USA, olazarev@udel.edu*, dlsparks@udel.edu, wpan@udel.edu
[2]Stroud Water Research Center, Avondale, USA, jkan@stroudcenter.org, aufdenkampe@stroudcenter.org

Iron (Fe) and manganese (Mn) oxides, hydroxides and oxyhydroxides are well known redox-sensitive and reactive mineral components of environmental systems. Soil horizons with abundant Fe and Mn oxides/hydroxides have high mineral surface area and thus a high capacity to complex carbon (C), reducing susceptibility of C to microbial degradation. At the same time, Mn and Fe oxides are strong oxidizing agents under anaerobic conditions and could facilitate the microbial degradation of organics and formation of humic compounds.

The National Science Foundation (NSF) Critical Zone Observatory program is a system of six environmental observatories in the USA within a growing network throughout the world. The Christina River Basin-Critical Zone Observatory (CRB-CZO), located in the Piedmont region of Southeastern Pennsylvania and northern Delaware, is a partnership between the University of Delaware and the Stroud Water Research Center. At the White Clay Creek Watershed (WCCW) of the CRB-CZO we study how biogeochemical dynamics of Fe- and Mn- along redox gradients affect the C cycle within a floodplain forest.

We investigated the composition of soil pore-waters and stream over a 9 month-period with respect to the concentration of dissolved organic carbon (DOC) and the quality of dissolved organic matter (DOM) coupled with aqueous Fe and Mn, pH, temperature, alkalinity, conductivity, major anions, major cations, δD, and δ18O. DOM quality was characterized using UV-visible absorbance and fluorescence metrics such as absorption coefficient at 254nm (a_{254}), specific-UV absorbance ($SUVA_{254}$), slope ratio (S_r) humification index (HIX), fluorescence index (FI), protein-like and other indices obtained from PARAFAC modeling of fluorescence excitation-emission matrices (EEMs). The biogeochemical approach above was combined with an advanced in-situ monitoring of biogeochemical parameters including redox, soil moisture and temperature. The sensors are being used to characterize geochemical gradients and how they change over time, and to enable targeted sampling at hot spots and during hot movements.

Our preliminary results demonstrated a significant redox gradient across the interface between anoxic wetland soils and valley-bottom gravel layers within a floodplain forest. Variations in redox gradients near the streambed may drive changes in Fe- and Mn-oxide precipitation and dissolution affecting C complexation or destabilization. DOM quality fluctuated in time and space indicating the existence of humic, microbial, or protein regions depending on the redox envirоinment.

https://doi.org/10.1180/S0026461X00008434 Published online by Cambridge University Press

Iron redox and viscosity of Erebus volcano phonolite lava (Antarctica): implications for lava lake convection and degassing processes

CHARLES LE LOSQ[1*], DANIEL R. NEUVILLE[1], ROBERTO MORETTI[2,3], DOMINIQUE DE LIGNY[4], YVES MOUSSALAM[5], FRANÇOIS BAUDELET[6], CLIVE OPPENHEIMER[5]

[1]Géochimie&Cosmochimie, IPGP, Paris, France, lelosq@ipgp.fr (* presenting author)

[2]Centro Interdipartimentale di Ricerca in Ingegneria Ambientale (CIRIAM) & Dipartimento di Ingegneria Civile, Napoli, Italia, moretti@ov.ingv.it

[3]Istituto Nazionale di Geofisica e Vulcanologia, Napoli, Italia, moretti@ov.ingv.it

[4]Laboratoire de Physico-Chimie des Matériaux Luminescents, Université Lyon 1, Villeurbanne, France, dominique.de-ligny@univ-lyon1.fr

[5]Geography Dept, Cambridge, UK, co200@cam.ac.uk

[6]SOLEIL, St Aubin, France, francois.baudelet@synchrotron-soleil.fr

Erebus is an intraplate volcano associated with extensional tectonics, mantle upwelling and high heat flow. It is famous for its long-lived lava lake, a rare phenomenon seen at just a few other volcanoes. Such lava lakes imply steady-state magma input, convection and degassing. They represent particularly convenient "windows" into the behaviour of magma plumbing systems. The Erebus lava lake is further distinguished by its phonolitic composition, with abundant megacrysts of anorthocolase feldspar. The eruptive activity is characterised by two kinds of behaviour: (i) passively degassing lava lake, and (ii) intermittent Strombolian eruptions. An important question to address is what physico-chemical mechanisms drive these contrasting styles of eruption. One hypothesis is that the lava lake activity is associated with open-system degassing, while the Strombolian phases are related to closed-system degassing.

Observations of the emissions of passive and explosive degassing and analysis of the sulfur contents of melt inclusions from the Erebus magmatic lineage are both consistent with a reducing-upwards redox trend in the magma system. Oxygen fugacity changes, occuring between the magma chamber and the lava lake surface, will control the redox state of sulfur and iron, impacting both the melt's thermodynamic and rheologic properties.

The next key step is to make direct measurements of redox conditions in Erebus samples to test model results. Moreover, no rheological data exist on Erebus lava. Therefore, we performed X-ray absorption spectroscopy (XAS) at the iron K-edge experiments under controlled atmosphere at high temperature, and viscosity experiments on the lava. The obtained data bring informations about the oxygen fugacity evolution of the lava between the magma chamber and the surface, and its rheology in the superficial lava lake. These data will constrain the existing eruptive models, and allows to better understand the Erebus dynamic and behavior.

Holocene deposition of atmospheric REE in Europe

GAËL LE ROUX[1,2],*, NATHALIE FAGEL[3], FRANCOIS DE VLEESCHOUWER[1,2], NADINE MATIELLI[4] AND WILLIAM SHOTYK[5]

[1]Université de Toulouse; INP, UPS; EcoLab (Laboratoire Ecologie Fonctionnelle et Environnement); ENSAT, Avenue de l'Agrobiopole, 31326 Castanet Tolosan, France, gael.leroux@ensat.fr

[2] CNRS; EcoLab; 31326 Castanet Tolosan, France

* presenting author

[3] AGEs, Department of Geology, Liège University, Belgium,

[4] IPE, Sciences de la Terre et Environnement, Université Libre Bruxelles, Belgium

[5] Department of Renewable Resources, University of Alberta, Edmonton, Alberta T6G 2H1 Canada

Abstract

Three peat bogs from Eastern French Pyrenees, German Black Forest and Swiss Jura provide three parallel records of REE deposition in Europe. The Swiss site shows considerable variation in dust deposition during the past 15,000 years with abrupt changes in fluxes at 12 k.y. cal. BP, 9.2 k.y. cal. B.P., 8.4 k.y. cal. B.P., 7.2 k.y. cal. B.P. and 6 k.y. cal. B.P [1]. Using Nd isotopes and Rare Earth Elements, it is possible to clearly distinguish between volcanic inputs and those driven by climate change such as the long-term aridification of the Sahara and regional erosion due to forest clearance and soil cultivation. Our results indicate that a major dust event in Central Europe precedes the 8.2 k.y. cold event by 200 years. The French and German sites show also considerable variation in dust deposition but represent only respectively 10,000 and 8,000 years of peat accumulation. Unlike the French and Swiss sites located on a limestone plateau, the German peat bog is located on a granite massif, which strongly influences the chemical composition of aerosols falling into the peat. These findings show that the inorganic fraction of high-resolution peat records can provide remarkably sensitive indicators of dust load and its local and remote sources. Our study supports the priority to better identify the impact of dust cycles during the Holocene in terms of direct and indirect impacts on environmental and climate changes.

[1] Le Roux G. et al. Volcano- and climate-driven changes in atmospheric dust sources and fluxes since the Late Glacial in Central Europe. Geology, in press

https://doi.org/10.1180/S0026461X00008434 Published online by Cambridge University Press

Scaling and nature of melting processes in the mantle wedge: a record from the Josephine Peridotite (Klamath Mountains, USA)

VERONIQUE LE ROUX[1*], HENRY DICK[1], NOBUMICHI SHIMIZU[1]

[1]Woods Hole Oceanographic Institution, Woods Hole, USA, vleroux@whoi.edu (* presenting author)

The selected peridotite samples come from the Josephine ophiolite, emplaced 157 My ago and now part of the western Jurassic belt of the Klamath Mountains in Northern California and Southwest Oregon [1]. The ophiolite is partly dismembered but presents a complete ophiolitic section from mantle peridotites in the lower part (our samples) to pillow lavas at the top. The Josephine peridotite extends over >800km^2 and has most likely originated in a fore-arc or back-arc setting [1]. It is mostly composed of massive harzburgites, believed to be the residue of partial melting processes, crosscut by several generations of dykes and veins of variable lithologies [2]. Previous studies have mainly focused on the dunite bodies because of their importance as melt extraction channels in the upper mantle. They are believed to have formed through melt-rock reactions between depleted melts and the mantle wedge [3-6].

However, large areas of the Josephine peridotite have yet to be investigated. Here we propose to focus on the compositional variability of harzburgites and lherzolites, which likely represent the protolith of mantle wedge before the diking and veining events that later affected the massif. Our goal is to constrain the scale of melting processes in the upper mantle in subduction environments and better assess the role and distribution of subduction-derived fluids in the melting process. In order to achieve this, our study is based on the observation of geochemical gradients (major, minor and trace elements in minerals and whole-rocks) throughout the selected harzburgites and lherzolites. Based on major elements and most minor and trace element trends (e.g. HREE, Ti, Ni versus MgO wt%) we find that harzburgites and lherzolites are genetically related by a partial melting event, as suggested in previous studies [2]. However the concentrations of the most incompatible elements (e.g. LREE) and fluid-mobile elements (Ba, Rb, Sr) cannot result from a partial melting process but require the later addition of fluids and/or melts superimposed to the partial melting features recorded by the Josephine peridotites.

Mapping out the melting and melt percolation processes that took place in the Josephine Peridotite should shed a new light on the extent and nature (dry or hydrous) of melting in the upper mantle from subduction environments.

[1] Harper, G.D. (1984), *Geological Society of America Bulletin*. **95**, 1009-1026.
[2] Dick, H.J.B. (1977), *American Journal of Science*. **277**, 801-832.
[3] Kelemen, P.B. and H.J.B. Dick (1995), *Journal of Geophysical Research*. **100**, 423-438.
[4] Warren, J.M., G. Hirth, and P.B. Kelemen (2008), *Earth and Planetary Science Letters*. **272**, 501-512.
[5] Morgan, Z., Y. Liang, and P. Kelemen (2008), *Geochemistry Geophysics Geosystems*. **9**.
[6] Kelemen, P.B. (1990), *Journal of Petrology*. **31**, 51-98.

The nanoSIMS as a tool to study zonation around/in melt inclusions

MARION LE VOYER[1, 2*], MEGAN NEWCOMBE[1], EDWARD M. STOLPER[1], AND JOHN M. EILER[1]

[1]California Institution of Technology, Pasadena, CA, USA, mlevoyer@caltech.edu (* presenting author).
[2]Presently at Carnegie Institution, Washington DC, USA.

Melt inclusions preserve geochemical records of magmatic processes and can provide windows into melt composition prior to near-surface fractionation processes such as degassing, crystal fractionation, and mixing that can influence the compositions of erupted magmas. The compositions of melt inclusions are usually measured near their centers using in-situ analytical techniques such as electron microprobe, ion probe, or LA-ICPMS. However, melt inclusions can experience post-entrapment modifications through crystallization or exchange with the host mineral or the outside melt via diffusion through the host mineral. For example, water loss (or gain) can occur by diffusion of H-bearing species through the host mineral toward (or from) the enclosing melt. Zonation in melt inclusions and their host minerals provide information on such post-entrapment modifications. We present a new approach to the study of such zonation using the nanoSIMS Cameca 50L high-resolution ion microprobe. Our data document mechanisms of chemical evolution of melt inclusion after entrapment and can constrain the nature and timescales of syn-eruptive processes.

The distinctive capabilities of the nanoSIMS are (1) small spot sizes – typically as small as ~0.2 μm for major elements, 1 μm for minor elements, and several microns for trace elements (including H in nominally anhydrous minerals); and (2) multicollection with large mass range, permitting simultaneous analysis of low- and high-mass elements.

We characterized H and F gradients in olivine around volatile-rich melt inclusions from two arc basalts. The H gradients are anisotropic and can be modeled by diffusion by the proton-polaron mechanism (D_a=100D_b). The length scales of these gradients (from < 20 μm to > 125 μm) indicate that diffusion from the melt inclusion to the olivine produced these gradients on timescales of a few hours,.

We also discovered concentric major and volatile element concentration gradients inside melt inclusions (i.e., zonation within the glass) from various geological settings. Given the high rates of chemical diffusion in silicate melts, the preservation of these gradients implies that these gradients formed during or just prior to eruption on timescales on the order of 0,1-1 hour. For example, gradients in MgO and Al_2O_3 in inclusions from the Siqueiros fracture zone can be modeled as due to coupled olivine growth on inclusion walls and diffusion in the melt inclusion on timescales of ~10 min, presumably in the last stages of eruption. Gradients in H and F inside melt inclusions are more complex, likely reflecting the coupling of olivine crystallization with loss of H and F from the melt inclusion into the host olivine.

https://doi.org/10.1180/S0026461X00008434 Published online by Cambridge University Press

POTENTIAL ENVIRONMENTAL FATE AND BEHAVIOUR OF INORGANIC MANUFACTURED NANOPARTICLES IN THE AQUATIC ENVIRONMENT

J.R. LEAD*[1],

[1] School of Geography, Earth & Environmental Sciences, University of Birmingham, Birmingham, UK, j.r.lead@bham.ac.uk (presenting author)

Introduction

Manufactured nanoparticles are usually defined as materials between 1 and 100 nm. They are widely used industrially and in consumer products because of their novel properties and ease of use; metals (e.g. Ag, Au, Fe) and their oxides (e.g. Ti, Zn and Fe) are of particular ubiquity and are produced in high volumes. It is certain that these nanoparticles are entering the aquatic environment in large volumes and are present in low but increasing concentrations. Once in the environment, these nanoparticles are subject to transformations due to alterations in the physical and chemical environment. Potentially the nanoparticles are subject to interactions with salts, natural organic macromolecules (NOM) such as humic substances and polysaccharides and are potentially altered by pH variation. Changes include surface alterations such as oxidation followed by dissolution and possibly regrowth and sulfidation followed by reduced dissolution especially for Ag, shape changes and coating or corona formation often leading to reduced aggregation or even diaggregation. Microbiological effects are also observed.

This paper will discuss these changes in relation to NP properties such as core material type, capping agent and size with particular examples drawn form ceria and silver. Both natural aquatic and toxicological media will be considered.

The sulfur isotope fractionation of dissimilatory sulfite reductase (Dsr)

WILLIAM D. LEAVITT*[1], ALEXANDER S. BRADLEY[1], INÊS C. PEREIRA[2], RENATA CUMMINS[1], AND DAVID T. JOHNSTON[1]

[1]Harvard University, Cambridge, MA, USA, wleavitt@fas.harvard.edu (*presenting author), johnston@eps.harvard.edu

[2]Instituto De Technologia Quimica E Biologica, Oeiras, Portugal

The sedimentary sulfur isotope record is an integrator of biochemical processes, among the most quantitatively important of which is microbial sulfate reduction (MSR). Interpretations of the sedimentary sulfur isotope record rely largely on our understanding of the fractionation associated with MSR. This has been empirically determined by numerous cellular-scale studies [1, 2]. Still, a mechanistic understanding of the controls on this fractionation has proven elusive. Here, through whole-cell (*in vivo*) and pure-enzyme (*in vitro*) experiments, we provide the next generation of quantitative constraints on the fractionation capacity of a key reductive step in the MSR metabolic network. We present data from experimental work with purified dissimilatory sulfite reductase (Dsr) protein, from which we can extract enzyme-specific isotope fractionation factors. These data represent the first enzyme level constraints on isotope fractionation during MSR, and serve as a template for evaluating the other prominent enzymatic reduction steps within this metabolic process. Akin to the early carbon isotope work on RuBisCO and its importance to the carbon cycle [3], the work presented herein will help to unlock the secrets of the sulfur cycle and ultimately allow for the full isotopic interpretation of Earth's sulfur isotope records.

Metabolic isotope models of MSR are at the heart of interpreting modern and ancient sulfur isotope records [2], but models require a quantitative understanding of the magnitude of fractionation at each node within the metabolic network. To provide fundamental boundary conditions for the metabolic fractionation models of MSR [2, 4], we measured the enzyme-specific (*in vitro*) isotope fractionation factors for the key enzyme Dsr ($^{34}\alpha_{Dsr}$) which catalyzes sulfite reduction. Our pure Dsr enzyme fractions are from the model bacterial sulfate reducer *Desulfovibrio vulgaris* Hildenborough (DvH). In replicate closed-bottle experiments, Dsr catalyzed sulfite reduction at the expense of molecular hydrogen. After freeze-quenching the reaction, products and residual reactant were collected and quantified. In all cases, elemental and isotopic mass balance was satisfied. Individual sulfur pools were isolated from the bulk solution by sequential precipitation. To support the novel *in vitro* experiments, we also performed a set of continuous culture controls and classical *in vivo* closed bottle growth experiments. During closed bottle experiments, MSRs were grown first utilizing sulfate, then sulfite or thiosulfate. These later experiments represent an attempt to get whole-cell quantification of the same reductive process that the pure enzyme experiments facilitated.

Taking an enzyme-level approach to understanding isotopic fractionation in MSR provide the most fundamental constraints on the biogeochemical sulfur cycle. It is through coupled biochemical and physiological observations that we are able to better quantify the key fractionations during MSR. As a result, we gain insight into the physicochemical controls on the directionality of sulfur flow through a bacterium and resulting net sulfur isotope fractionation signatures.

[1] Kaplan & Rittenberg (1964) *J. Gen. Micrbio.* 34, 195-212. [2] Johnston *et al.* (2007) *GCA* **71**, 3929–47. [3] Park & Epstein (1960) *GCA* **21**, 110–26. [1141-62. [4] Bradley *et al*. (2011) *Geobio.* 9, 446-57.

https://doi.org/10.1180/S0026461X00008434 Published online by Cambridge University Press

Carbon and nitrogen isotopes cycling recorded in sediments from anoxic and ferruginous Lake Pavin

OANEZ LEBEAU[1]*, VINCENT BUSIGNY[1], DIDIER JEZEQUEL[1] AND MAGALI ADER[1]

[1]Univ. Paris Diderot-IPGP, Sorbonne Paris Cité, UMR7154 CNRS, Paris, France, olebeau@ipgp.fr

Over geological timescale, the Earth's oceans were affected by several periods of total or partial anoxia. Timing, causes and consequences of the ocean oxygenation can potentially be better understood from past C and N cycles. Studies on modern analogues are essential for interpreting the biogeochemical signal recorded in ancient sediments. Lake Pavin (French Massif Central) is permanently stratified with anoxic Fe-rich deep waters (from 60 to 92m depth) overlain by oxic shallow waters (from 0 to 60m depth) and can be regarded as an analogue for the ocean during periods of redox stratification with ferruginous deep water column.

In order to determine if the primary C and N isotope signatures are preserved or modified in this type of environment, we analyzed bulk C and N isotope compositions in 3 sediment cores from different depths in Lake Pavin: in the oxic zone (31.5m depth), at the oxic-anoxic boundary (60m depth), and the last one at the peak of H_2S production from SO_4^{2-} reduction (65m depth). For the cores of the anoxic layer the C and N isotopic compositions show little variability: $\delta^{13}C_{org}$ = -26.8±0.4‰ (1σ) and $\delta^{15}N_{tot}$ = -1.1±0.2‰ (1σ). Such $\delta^{15}N$ values suggest a dominance of N_2-fixers in the water column, which is expected in stratified system where nitrates are strongly denitrified at the redox boundary. For the core of the oxic layer, both $\delta^{13}C_{org}$ and $\delta^{15}N_{tot}$ increase with depth, from -28.6 to -25.3‰ and -3.4 to -1.7‰, respectively. This variation indicates either a modification of the primary signal by oxic early diagenesis or a change of the biomass contributing to the isotopic signal. Further investigations are still needed to explain this variability.

Preliminary analytical approaches to investigate the biogeochemical role of selenomethionine in aquatic ecosystems

KELLY LEBLANC[1]*, AND DIRK WALLSCHLÄGER[1]

[1]Trent University, Peterborough, ON, Canada,
* kellyleblanc@trentu.ca, dwallsch@trentu.ca

Recent changes to legislation relating to acceptable environmental selenium (Se) concentrations in North America have provided an increased need to better understand the element's natural biogeochemical cycle. Although toxicity tests modeling parts of this cycle generally expose organisms to the organic Se species selenomethionine (SeMet), to our knowledge it has not been shown that this form of Se is present in the abiotic compartments of the natural environment for uptake in real ecosystems.

It is well established that algae, the lowest trophic level in most aquatic systems, have the ability to uptake inorganic Se and metabolize it into SeMet – as both free and proteinaceous forms.[1] For this reason, as a preliminary investigation into the ability of SeMet to be released from organisms (upon their death) back into their surrounding environment, we have grown algal cultures (3 species of *Chlorophyta* and 1 *Cyanobacterium*) in the presence of selenate and examined the resulting metabolites that are present both within the cells and released into the growth media.

For the analysis of SeMet and other metabolites we have optimized existing anion-exchange chromatography inductively-coupled plasma mass spectrometric (AEC-ICP-MS) methods to allow for baseline resolution between various organic Se species of similar retention, while still allowing for quantitative analysis of inorganic metabolites such as selenite and selenocyanate. Using this method it has been observed that free SeMet is one of the main Se species within algal cells though only trace amounts are found in the growth media; potentially due to efficient re-uptake after this metabolite is released. To further confirm the identity of SeMet in algal growth media, electrospray tandem mass spectrometry (ES-MS/MS) was used and characteristic fragmentation patterns of the molecular ion were observed for various isotopes of Se.

The overall goal of this work involves determining whether SeMet is present in the abiotic compartments of the natural environment, which would make it available for uptake into the lowest tropic level of aquatic food webs and likely play a vital role in the initial stages of Se toxicity in these ecosystems. Preliminary evidence of discrete organic Se species in an impacted river system, as well as the potential implications of this will be discussed.

[1] Fan *et al.* (2002) *Aquat. Toxicol.* **57**, 65-84

https://doi.org/10.1180/S0026461X00008434 Published online by Cambridge University Press

Carbon isotope clues on the origin of Frere granular iron formation from the Paleoproterozoic Earaheedy Basin

JACQUES L. ERFFMEYER[1*], DOMINIC PAPINEAU[1,2], AND FRANCO PIRAJNO[3]

[1] Department of Earth and Environmental Sciences, Boston College, United States.
[2] Geophysical Laboratory, Carnegie Institution of Washington, United States.
[3] Geological Survey of Western Australia, Perth, Australia.

The rocks of the late Paleoproterozoic Earaheedy Basin in Western Australia were deposited on a continental passive margin between the Pilbara and Yilgarn Craton and preserve a prominent horizon of granular iron formation (GIF). A drill core through the 1.83 to 1.79 Ga Frere Formation intersects the iron-rich horizon and was investigated for possible biological activity using carbon isotopes, which may provide clues on the origin of GIFs. Microbial involvement in the formation of granules is a possibility that remains to be demonstrated. The lowermost part of the studied section of the core consists of stromatolitic dolomite of the Yelma Formation, with mm- to cm-thick layers and veins of pyrite and galena. The lack of weathering and low metamorphic grades experienced by these rocks yield a particularly interesting suite of rock samples to investigate the local carbon cycle.

Granules with sizes between ~100 to ~500 microns were observed to be composed of chert associated with variable assemblages of microplaty hematite, magnetite, greenalite, sulfides, and organic matter. In a few samples, granules are exclusively composed of chert and organic matter, which forms rounded sub-structures, of possible diagenetic origin, a few tens of microns in size inside the granules. Initial results indicate large ranges of $\delta^{13}C_{org}$ values ranging from -14.0 to -33.1‰ for generally low total organic carbon contents between 0.01 to 0.50%wt. However, organic carbon could not be detected in all samples and many also contain carbonate carbon. Current work is focused on expanding the carbon isotope dataset of both organic and carbonate carbon, which will allow for a better characterization of the original depositional environment and of diagenetic and possibly metamorphic alteration.

The tracer-dependence of biodiffusion coefficients

PASCAL LECROART[1*], OLIVIER MAIRE[1], SABINE SCHMIDT[1], ANTOINE GREMARE[1], PIERRE ANSCHUTZ[1], FILIP J.R. MEYSMAN[2]

[1] Universite de Bordeaux, laboratoire EPOC, Talence, France p.lecroart@epoc.u-bordeaux1.fr (* presenting author)
[2] Netherlands Institute of Ecology (NIOO-KNAW), Department of Ecosystem Studies, Yerseke, The Netherlands

Bioturbation refers to the mixing of sediment particles resulting from benthic faunal activity. It is the dominant particle mixing process in most marine sediments and exerts an important control on biogeochemical processes. In models, bioturbation is usually treated as a diffusive process where the biodiffusion coefficient (Db) characterizes the biological mixing intensity. Biodiffusion coefficients are classically computed by fitting a diffusive model to vertical profiles of particle-bound radioisotopes.

One peculiar observation is tracer-dependence: Db values from short-lived tracers tend to be larger than those obtained from long-lived tracers from the same site. Recent theoretical work, based on random walk theory and Lattice Automaton Bioturbation Simulations (LABS), has suggested that this tracer-dependence is simply a model artifact and has concluded that the biodiffusion model is not applicable to the short observational time scales associated with short-lived radioisotopes.

Here we have compiled a global dataset of Db values obtained from different radiotracers to assess tracer-dependence from a data perspective. Tracer-dependence is significant in low-mixing environments like slope and deep-sea sediments, but is not present in intensely mixed coastal areas. Tracer-dependence is absent when the number of mixing events is larger than 20, or the potential length scale is greater than 0.5 cm. Roughly this comes down to tracer-derived Db values greater than 2 $cm^2\ yr^{-1}$. This condition is met for 68%, 50%, and 8% of published Db values obtained from coastal, continental slope, and abyssal environments, respectively.

These results show that short-lived radioisotopes are suitable to quantify biodiffusion mixing in sedimentary environments featuring intense bioturbation.

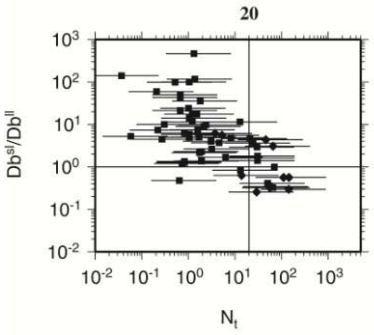

Fig. Evolution of the ratio between Db derived from short-lived tracers (Db^{sl}) and Db derived from long-lived tracers (Db^{ll}) as a function of the number of mixing events (Nt).

https://doi.org/10.1180/S0026461X00008434 Published online by Cambridge University Press

Characterization of fluids in the transition from deep porphyry Cu to shallow high-sulfidation epithermal mineralization at Red Mountain, AZ

PILAR LECUMBERRI-SANCHEZ[1*], ROBERT J. KAMILLI[2], ROBERT J. BODNAR[1]

[1]Virginia Tech, Blacksburg, USA, pilar@vt.edu*
[2]U.S. Geological Survey, Tucson, USA, bkamilli@usgs.gov

In recent years, significant efforts have been made to better understand the genetic relationship between deeper porphyry and shallower epithermal ore-forming systems [1,2,3]. Advanced argillic alteration is frequently associated with high-sulfidation epithermal systems and is typically absent in porphyry copper systems from the southwestern US. However, Red Mountain (AZ) has experienced relatively little erosion, leading to the occurrence of a well-preserved transition between a deep porphyry and a shallow high-sulfidation epithermal system. Hypogene mineralization at Red Mountain occurs as chalcopyrite-bornite ore at depth and transitions gradually to shallow chalcocite-enargite mineralization.

Early fluids in the deep part of the system are represented by chalcopyrite-bearing fluid inclusions that typically homogenize to liquid at 350-380 °C and have salinities of 2-5 equivalent wt% NaCl. For this range of salinity and Th the slope of the isochore is about 6 bar/°C so that the trapping temperature may be significantly greater than Th depending on the pressure of entrapment.

Later fluids in the deep part of the system are represented by halite+chalcopyrite-bearing fluid inclusions with consistent Th but variable halite dissolution temperatures of 350-420 °C within fluid inclusion assamblages. The consistent Th and variable Tm indicates that, unless necking down occurred after halite precipitation and before bubble nucleation, the fluid entrapped by this inclusions was halite saturated and therefore provides a constraint on the pressure and temperature of entrapment. The halite-bearing fluid inclusions are in secondary trails with chalcopyrite blebs. Therefore, these inclusions represent the mineralizing fluid and the trapping conditions represent the mineralization conditions.

Towards the surface and the high sulfidation epithermal system, the fluid inclusions are generally less saline and evidence of boiling is more frequent. Fluid inclusions spatially related to enargite-chalcocite mineralization have homogenization temperatures above 480 °C.

[1] Hedenquist, Arribas & Reynolds (1998) *Economic Geology* **93**, 373-404 [2] Pudack et al. (2009) *Economic geology* **104**, 449-477 [3] Muntean & Einaudi (2001) *Economic geology* **96**, 743-772

How to recognize and use primary cherts for studying Archean seawater?

MORGANE LEDEVIN[1*], NICHOLAS ARNDT[2] AND ALEXANDRE SIMIONOVICI[3]

[1*]ISTerre, OSUG, Grenoble, France, morgane.ledevin@ujf-grenoble.fr (* presenting author)
[2] ISTerre, OSUG, Grenoble, France, nicholas.arndt@ujf-grenoble.fr
[3] ISTerre, OSUG, Grenoble, France, Alexandre.Simionovici@ujf-grenoble.fr

Archean cherts are a powerful tool for studying physico-chemical conditions at the seafloor during the early history of the Earth. Numerous studies use geochemistry to infer the characteristics of Archean seawater (e.g. temperature, salinity, composition), but surprisingly few use rigorous petrological and field observations which are critical to understand the origin of analyzed cherts, their environmental context of emplacement, and their diagenetic history.

We sampled four sites in the Archean (3.5 – 3.2 Ga) Barberton Greenstone Belt in South Africa and identified three types of chert. Primary cherts are directly precipitated on the seafloor, secondary cherts come from the silicification of any kind of protolith, and fracture-filling cherts are precipitated from fluids circulating through the crust. Using field and petrological observations, we define reliable criteria to identify primary cherts, which are most likely to represent Archean seawater geochemistry.

Our field observations focus on the depositional environment and particularly on evidence of direct deposition on the seafloor. Several criteria are defined: (1) First, primary cherts are homogeneous and translucent, concordant with surrounding sedimentary rocks and they lack well-developed internal sedimentary structures (i.e. layering). (2) They contain recurrent undulating surfaces with troughs filled by the overlying sediment (i.e. load casts). (3) The presence of microbial mats on bedding surfaces indicates shallow-water deposition. (4) Slab conglomerates are interpreted as tempestites composed of angular fragments of reworked chert representing material that was precipitated and indurated on the sea floor.

When those criteria are absent, we use petrological observations to distinguish primary and secondary cherts. We show that primary cherts are exclusively made of microcrystalline quartz (<200µm in size), with little porosity (<1%) and without any internal sedimentary-like structures (i.e. layering). This homogeneity is inherited from early chert deposition as a colloidal silica phase. Cathodoluminescence and X-ray microfluorescence mapping confirm the homogeneity of primary chert which are composed also entirely of silica and contain extremely low concentrations of other elements. The very good preservation of Barberton samples is shown by an absence of major recrystallization and lack of metamorphic and/or alteration minerals.

Finally, we tested the validity of geochemical criteria to identify the primary oceanic signature in cherts. We show that such proxies are extremely dependent on the environmental context of deposition, and that no conclusions can be made without careful field and petrologic studies.

https://doi.org/10.1180/S0026461X00008434 Published online by Cambridge University Press

Metal stable isotopes for sediment core GC-99 from Lake Baikal

DER-CHUEN LEE[1,*], HSIN-TING LIU[2], SHUN-CHUN YANG[3]

[1]Institute of Earth Sciences, Academia Sinica, Taipei, Taiwan, ROC, dclee@earth.sinica.edu.tw (* presenting author)
[2]Dept. of Earth Sciences, Nat. Normal Univ., Taipei, Taiwan, ROC, 49444039@ntnu.edu.tw
[3]Dept. of Geological Sciences, Nat. Taiwan Univ., Taipei, Taiwan, ROC, d98224001@ntu.edu.tw

Metal stable isotopes, e.g., Fe, Zn, Mo, and Cd, have been analyzed for the authigenic portion of a sediment core, GC-99, of Lake Baikal, Russia, in order to study the sources and sinks for these trace metals in the Lake Baikal, the largest fresh water lake in the world, as well as potential proxy for the past climate changes in this region. Lake Baikal is located in the southern region of the Siberia of Russia, and was formed through rifting. It has very thick sediments, and is relatively undisturbed due to its high latitude and isolation, and hence may provide a complete record of the local geological history [1]. In this study, a ~ 3 meters gravity core (GC-99; 52°05'23"N, 105°15'24"E) sampled near the bore hole of BDP-99 in Lake Baikal is used. Samples are taken continuously every cm interval for the entire core. For the initial test, one sample is selected for every 10 cm interval continuously throughtout the entire core. In order to extract the authigenic portions, a series of leaching procedures were used to remove the carbonates, and to collect the authigenic fractions, while leaving the lithogenic sediments unaffected. Double spike technique is used for all four metal stable isotopic measurements in this study.

Initial results showed that there are significant isotopic variations for all four isotope systems, and in general, the data are plotted away from the bulk silicate Earth (BSE). For Fe isotope, the $\delta^{56}Fe/^{54}Fe$ varies from the BSE at 0 to -2, while most of the sample centering around -1. For Zn isotope, the $\delta^{66}Zn/^{64}Zn$ is noticeably lighter than the BES, varying from -0.6 to 0 in the top 50 cm. In contrast, the $\varepsilon^{114}Cd/^{110}Cd$ varies from the BSE at +2 to +6 in the top 50 cm, and the observed +6 $\varepsilon^{114}Cd/^{110}Cd$ is most likely the results of bio-activity, e.g., diatom. For the top 50 cm, if the top surface sample is discarded, there seems to be a general positive correlation among the Fe, Zn, and Cd data, and if these correlations are real, they probably reflect a mixing relationship between the dissolved portions from the sources and the isotopic signature that had experienced the uptake of bio-activity. More data, for the extire sediment core and other biological indicators and mineralogical compositions, are needed in order to test if this is correct. Unlike the other metals, Mo data are more of an indicator for the sediment source and/or redox condition of the lake. Preliminary data for the top 50 cm also show observable variations. Although preliminary, the results seem to indicate evidence of source variations and biological activities in the sediment core of Lake Baikal. More data and, in particular, the chronology of the sediment core are needed in order to better constrain the relationship between the Lake Baikal and regional climate changes in the past.

[1] Kuzmin M.I. and Yarmolyuk V.V. (2006) *Geol. Geophy.* **47**, 5-23.

Distribution of lead and lead isotopes in the Indian Ocean: data from the Japanese Indian Ocean GEOTRACES transect

JONG-MI LEE[1*], YOLANDA ECHEGOYEN-SANZ[2], EDWARD A. BOYLE[1], TOSHITAKA GAMO[3], HAJIME OBATA[3] AND KAZUHIRO NORISUYE[4]

[1]Massachusetts Institute of Technology, Cambridge MA, USA, jm_lee@mit.edu (*presenting author)
[2]University of Zaragoza, Zaragoza, Spain
[3]University of Tokyo, Tokyo, Japan
[4]Kyoto University, Kyoto, Japan

Anthropogenic Pb inputs have altered distributions of Pb and Pb isotopes in the modern ocean, but the impact of anthropogenic Pb inputs to the Indian Ocean has been unknown due to the lack of data. Here we discuss the distribution of Pb from 11 deep stations from the Japanese Indian Ocean GEOTRACES cruise (2009 Nov-Dec), from the Bay of Bengal and Arabian Sea to the Antarctic (18degN to 65degS). We will also show the Pb isotopic composition ($^{206}Pb/^{207}Pb$ and $^{208}Pb/^{207}Pb$) of these waters for the first time.

Because of the later industrialization and a delayed phase out of the leaded gasoline in the African and South Asian countries (and limited convection in the north), Pb concentrations in the surface waters of the Indian Ocean are higher (40-80 pmol/kg) than in the present-day North Atlantic and North Pacific (20-30 pmol/kg). The anthropogenic Pb has not penetrated deeply in the Indian Ocean yet; high Pb is confined to the upper 2000m and deep waters have low Pb (<10 pmol/kg, and as low as ~3 pmol/kg at some stations). Pb at the surface has low isotopic ratios ($^{206}Pb/^{207}Pb$ ranging 1.141-1.151 and $^{208}Pb/^{207}Pb$ ranging 2.417-2.429), and the ratios generally increase with depth due to the mixing with Pb of higher isotopic ratios in deep waters. The low isotopic ratios of the surface Pb reflect the anthropogenic origin of the Pb in the Indian Ocean: they fall onto the range of Pb isotopic ratios found in the aerosols collected from the major cities around the Indian Ocean [1]. The Pb isotopic ratios are lower in the northern stations (>20degS) than in the southern stations due to their proximity to anthropogenic Pb sources. The southernmost station (65degS) appears to be least affected by anthropogenic Pb inputs given the low Pb concentrations (4-9 pmol/kg) and distinctively high Pb isotopic ratios ($^{206}Pb/^{207}Pb$ =1.17-1.19; $^{208}Pb/^{207}Pb$ =2.44-2.46).

[1] Bollhöfer and Rosman (2000) *GCA* **64**, 3251-3262.

https://doi.org/10.1180/S0026461X00008434 Published online by Cambridge University Press

Analysis of Carbon Cycling Within a Malaysian Watershed

KERN LEE[1*], JAN VEIZER[1] AND IAN CLARK[1]

[1]University of Ottawa, Dept. of Earth Sciences, Ottawa, Canada klee029@uottawa.ca (* presenting author), jveizer@uottawa.ca, idclark@uottawa.ca

Introduction and Objectives

Carbon cycling in Southeast Asian watersheds remains poorly understood, and has been addressed by only a handful of studies. With regards to the stable carbon isotope systematics of these areas, the paucity of information is even greater. Such studies can help clarify the nature of carbon inputs into these fluvial systems, in addition to constraining sources and sinks of carbon in the associated watershed [1]. This information can then shed light on the importance and role of tropical rivers within the global carbon cycle.

Results and Conclusion

Initial results indicate that the dissolved organic carbon (DOC) within Langat River is sourced predominantly from C3 type vegetation, with an average $\delta^{13}C$ value of -27.4 ± 3.1 ‰. DIC $\delta^{13}C$ averages about -12.7 ± 2.4 ‰, which suggests that weathering of mineral substrates by soil-derived carbonic acid plays a central role in riverine DIC. Further ^{13}C enrichment may occur *in situ*, due to CO_2 outgassing from the river surface. Measured concentrations of DIC and DOC showed greater variance, averaging 3.5 ± 2.1 ppm and 5.3 ± 3.5 ppm, respectively. These concentration data plot negatively and positively with $\delta^{13}C$, respectively. The negative correlation is consistent with the proposition that biologic activity plays an important role in DIC generation. The factors behind the DOC $\delta^{13}C$ relationships are less certain, but could be indicative of external inputs of more ^{13}C enriched carbon relative to C3 plants sources.

Using the pH and DIC data, averaged values of -18.5 +/- 2.8 ‰ and 2958 +/- 2475 ppm were calculated for $\delta^{13}C_{CO2(g)}$ and [pCO_2], respectively. Throughout the year, the Langat River is supersaturated with respect to CO_2 in the overlying air. Atmospheric CO_2 has therefore a minimal impact on the riverine carbon budget. Instead there is a net efflux of carbon from the river surface, in accord with the proposition based on carbon isotope data implying that the fluvial CO_2 is predominantly sourced from biologically-respired carbon [2].

A rough, low-end estimate of evasion flux of carbon from the river to the atmosphere is about 3.8 kg C m^{-2} yr^{-1}, comparable to the world-average value of 2.7 kg C m^{-2} yr^{-1} for tropical streams [3]. This suggest that a minimum of 8.5 kt C yr^{-1} is being outgassed, approaching the magnitude of the total carbon export of 20 kt C yr^{-1} to the sea, as estimated based on river flow and DIC/DOC concentration data. These results confirm previous studies that highlight the active role of rivers in global carbon cycling, beyond that of simple conduits of carbon transport from land to sea.

[1] Schulte *et al*. (2011) *Earth Sci. Rev.* **109**, 20-31. [2] Dubois *et al*. (2009) *Appl. Geochem.* **24,** 988-998. [3] Aufdenkampe *et al.* (2011) *Front. Ecol. Environ.* **9**, 53-60.

Experimental evidence that redox state influences amino acid stability under hydrothermal conditions

NAMHEY LEE[1,2], DIONYSIS I. FOUSTOUKOS[2], DIMITRI A. SVERJENSKY[1,2], GEORGE D. CODY[2], ROBERT M. HAZEN[2]

[1]Department of Earth and Planetary Sciences, Johns Hopkins University, Baltimore, MD, Email: namheyl@jhu.edu
[2]Geophysical Laboratory, Carnegie Institution of Washington 5251 Broad Branch Rd., NW, Washington D.C.

The stability of amino acids under hydrothermal conditions is of great interest to geochemists and biochemists in understanding the metabolic cycles of the biosphere near deep-sea hydrothermal vents and potential mechanisms for the origin of life in such environments. Thermodynamic calculations suggest that amino acid stability is sensitive to both temperature and the redox state of the environment [1]. Previous experimental studies have shown that parameters such as temperature and catalytic reactor surfaces strongly affect the stability of amino acids under hydrothermal conditions [2]. However, despite the potential relevance, the redox state of amino acid systems has never been controlled experimentally. Here experiments were conducted to investigate the influence of redox conditions on the stability of glutamic acid under hydrothermal conditions in a flow-through cell with temperatures from 150 ^{o}C to 250^{o}C at 136 bars. The redox state was controlled by equilibrating ~14 mmolal $H_{2(aq)}$ in solutions containing glutamic acid with varying pHs. Results indicate that under hydrothermal conditions glutamic acid is converted to the cyclic pyroglutamate, a redox neutral reaction, following first-order kinetics. Other reaction products including $CO_{2(aq)}$, NH_4^+, formate, and succinate are formed through redox controlled reactions. The concentrations of the reaction products are observed to be strongly dependent on the redox state of the system. This finding indicates that redox state defined by aqueous H_2 is an essential variable in determining the stability of biomolecules under hydrothermal conditions.

[1] Shock & Canovas (2010) *Geofluids* **Volume 10**, 161-192.
[2] Cox & Sewald (2007) *Geochim. Cosmochim. Acta.* **Volume71**, 797-820.

https://doi.org/10.1180/S0026461X00008434 Published online by Cambridge University Press

Laboratory TIR Emission Spectroscopy of Silicic Melts

R. J. LEE[1*], M. S. RAMSEY[1], AND P. L. KING[2]

[1]University of Pittsburgh, Pittsburgh, PA USA, rjl20@pitt.edu (* presenting author)
[2]University of Pittsburgh, Pittsburgh, PA USA, mramsey@pitt.edu
[3]Australian National University, Research School of Earth Sciences, Acton ACT 0200, AUS, penny.king@anu.edu.au

Introduction

Silicic glass is ubiquitous in volcanic environments, and is known to affect TIR remote sensing data. Glasses display similar TIR spectral features regardless of composition, making them difficult to distinguish spectrally [3,4], and their features vary with physical state [1,2]. To quantify these spectral changes, and provide calibrated laboratory melt data, a custom-built micro-furnace has been developed for use with a Nexus 670 FTIR spectrometer. It has been used to collect the very first *in-situ* laboratory TIR emissivity spectra of actively melting/cooling rhyolitic to dacitic compositions.

Methods

Absolute emissivity spectra were acquired using an empty Pt-lined furnace cavity as the blackbody calibration source. Crushed synthesized glass (1 to 2g) was placed into Pt crucibles in the micro-furnace. Emissivity spectra were acquired in 100°C intervals to the melting point temperature (MPT). To mimic the cooling behavior of lava, data were also acquired at 100°C intervals as the melt cooled. Spectra of seven glasses were taken at 20°C intervals from MPT to ~1100°C, to determine the approximate glass transition (Tg).

Results and Conclusions

Changes in the position, depth and spectral morphology of the absorption band with physical state have been quantified. Significant findings include a reduction in average melt emissivity, and identification of ~ Tg. Preliminary results show this approach is applicable to melt petrology and could be used with remote sensing data to better characterize and map glassy volcanic environments.

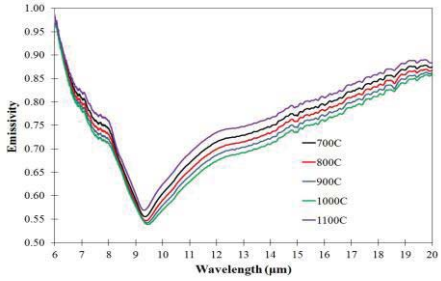

Figure 1: Glass emissivity spectra from 700C to 1100C, showing changes in spectral morphology with physical state.

[1] Dalby and King (2006) *Am. Mineral*., **91**, 1783-1793. [2] Lee et al. (2010) *J. Geophys. Res*., **115**, B06202. [3] Minitti et al. (2007) *J. Geophys. Res*., **112**, E05015. [4] Wyatt et al. (2001) *J. Geophys. Res*., **106**, 14711-14732.

In-situ observations of the formation of a single-layer gibbsite-like phase on the muscovite (001) surface

SANG SOO LEE[1*], MORITZ SCHMIDT[1], KATHRYN L. NAGY[2], AND PAUL FENTER[1]

[1]Argonne National Laboratory, Chemical Sciences & Engineering, Argonne, IL, USA. sslee@anl.gov
[2]University of Illinois at Chicago, Earth and Environmental Sciences, Chicago, IL, USA

Hydrolysis of a multivalent cation in aqueous solutions often precedes secondary reactions such as oligomerization. It is known that such reactions can be controlled by the presence of solid surfaces [1]. Previous work showed that crystalline Al-hydroxide phases formed on the surface of muscovite mica with an apparent epitaxial relationship to the underlying surface [2], but the molecular-scale interfacial processes that initiate the reactions are not well understood. We investigated the formation of an Al-hydroxide phase on the basal surface of single crystal muscovite by monitoring changes in muscovite-solution interfacial structure using in-situ high resolution x-ray reflectivity. Experimental solutions were prepared with a fixed total Al content (1 mM) as a function of pH. At pH 4, we observed sorbed Al^{3+} species formed an approximately 2Å thick film. The thickness and the vertical structure of the film matches those of a single Al dioctahedral sheet, i.e., gibbsite, $Al(OH)_3$, phase. The films formed at lower pH (2 and 3) are structurally more disordered and are less dense (i.e., covered a smaller fraction of the surface) than that formed at pH 4. These observations can be attributed to decrease in the concentration of hydrolyzed Al species with decreasing pH, both in the solution and at the surface. No film formation was observed at alkaline conditions (pH 9-12) where Al^{3+} occurs primarily as an anionic species, $Al(OH)_4^-$. The difference implies that the formation of the film is initiated by adsorption of positively-charged Al species at the negatively charged surface.

The results demonstrate that the growth of secondary minerals and the structural control of underlying substrates can be investigated in situ, in real time, and with a molecular-scale resolution. The results also suggest a new capability to characterize the reactivity of nanomineral films [3] with a high resolution.

[1] Scheidegger et al. (1998) Geochim Cosmochim Acta **62** 2233-2245.
[2] Nagy et al. (1999) Geochim Cosmochim Acta **63** 2337-2351.
[3] Hochella et al. (2008) Science **319** 1631-1635.

https://doi.org/10.1180/S0026461X00008434 Published online by Cambridge University Press

Biogenic and abiogenic nucleation of uranium in anaerobic environments

SEUNG YEOP LEE[1*], JONG MIN OH[1], MIN HOON BAIK[1], AND JONG WON CHOI[1]

[1]Korea Atomic Energy Research Institute, Daejeon, Korea, seungylee@kaeri.re.kr

Biogenic uranium transformation

Biogenic UO_2 (uraninite) nanocrystals may be formed as a product of a microbial reduction process in urnaium-enriched environments near the Earth's surface [1]. We investigated the size, nanometer-scale structure, and aggregation state of UO_2 formed by iron-reducing bacterium, *Shewanella putrefaciens*, from a uranium-rich solution. The UO_2 nanoparticles were highly aggregated by extracellular polymeric substances (EPS) (Figure 1), which limited a dispersal of the nanoparticulate uranium phase. Nearly all of the nanocrystals were networked in more or less 100 nm diameter spherical aggregates that displayed some concentric UO_2 accumulation with heterogeneity.

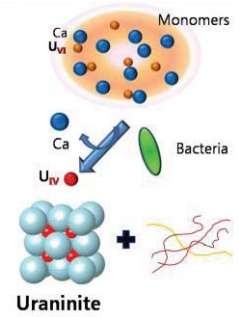

Figure 1: The microbial UO_2 formation and aggregation by EPS

Abiogenic U(IV) phase catalyzed by a biogenic sulphide mineral

Sulphate-reducing bacteria (SRB) and their by-products, such as iron sulfides, are widely distributed in subsurface environments, and can affect subsurface chemisty. There was a catalytic reduction and nucleation of uranium by fast-growing biogenic mackinawite (FeS), which is a common iron monosulphide observed in the anaerobic subsurface. The formed uranium phase was a nanoparticulate U(IV) phase. However, the U(IV) nanoparticles were easily released and dispersed without aggregation. It shows that a mobility of the reduced uranium phase might exist and be influenced by the ways that it was reduced in a heterogeneous microbial system.

[1] Suzuki *et al*. (2002) *Nature* **419**, 134.

Strontium, Carbon, Hydrogen and Oxygen Isotope Geochemistry from two hot spring waters in Busan area, Korea

SEUNG-GU LEE[1*], TOSHIO NAKAMURA[2], TONG-KWON KIM[1], YOON YEOL YOON[1], TOMOKO OHTA[2], TAEJONG LEE[1] AND HYUNG CHAN KIM[1]

[1]Korea Institute of Geosciences and Mineral Resources, Daejeon, Korea, sgl@kigam.re.kr; tkkim@kigam.re.kr; yyyoonl@kigam.re.kr; khc@kigam.re.kr

[2]Nagoya University, Center for Chronological Research, Nagoya, Japan, nakamura@nendai.nagoya-u.ac.jp

Introduction

Dongrae and Haeundae hot springs are one of the representative hot springs with water temperatures more than 58°C in South Korea. Both hot springs occur in Mesozoic granite area which is located in the Busan city at the margin of southeastern coastal side of the Korean peninsula, and have been used for spa for the past 1,000 years. Here we report ^{14}C, ^{3}H, $\delta^{18}O$, $\delta^{2}H$ and $^{87}Sr/^{86}Sr$ isotopic data for the Haeundae and Dongrae hot spring waters, which were collected for 2004-2011. Based on the geochemical data mentioned above, the groundwater cycle between hot spring waters and shallow graoundwaters, and heat source of the hot springs in Busan area will be discussed.

Results and Discussion

Geochemically, both of the hot spring waters are of Na-Cl type. The result of stable isotope compositions of O and H suggested that both of the hot spring waters should be derived from meteoric water. Furthermore, the chemical components of the hot spring waters indicate that they all were derived from hot spring water-rock interaction rather than through anthropogenic input. The $^{87}Sr/^{86}Sr$ ratio in Dongrae hot spring waters during the past 8 years ranges from 0.705632 ± 0.000012 to 0.705694 ± 0.000010. And the $^{87}Sr/^{86}Sr$ ratio in Haeundae hot spring waters ranges from 0.706023 ± 0.000011 to 0.706082 ± 0.000011. The ^{14}C ages in Dongrae hot spring waters ranged from 1,271 to 2852 years(BP) whereas those from the Haeundae from 2037 to 6687 years(BP). Such age difference corresponds well with aquifer depth of hot spring waters.

Conclusion

In this study, we could observe that there was no variation in the $^{87}Sr/^{86}Sr$ ratio from both hot spring waters during last 8 years. The chemical component also does not show significant variaton in their compostion. These all indicate that the hot spring waters in Busan area might be a product of long-term water-rock interaction rather than short-term water-rock interaction due to the input of recent meteoric water. In this research, we could confirm that $^{87}Sr/^{86}Sr$ ratio in the groundwater can be used as a tracer for monitoring the groundwater mixing history among several different aquifers such as shallow and deep groundwaters.

https://doi.org/10.1180/S0026461X00008434 Published online by Cambridge University Press

Effects of common groundwater constituents on coupled Mn(II)/U(IV) oxidation by *Bacillus* sp. SG-1

SUNG-WOO LEE[1*], KELLY L. PLATHE[2], ZIMENG WANG[3], JUAN S. LEZAMA-PACHECO[4], JOHN R. BARGAR[4], DANIEL E. GIAMMAR[3], RIZLAN BERNIER-LATMANI[2], AND BRADLEY M. TEBO[1]

[1]Oregon Health & Science University, Beaverton, OR, USA lees@ebs.ogi.edu (* presenting author), tebo@ebs.ogi.edu

[2]Ecole Polytechnique Federale de Lausanne, Lausanne, Switzerland kelly.plathe@epfl.ch, rizlan.bernier-latmani@epfl.ch

[3]Washington University in St.Louis, St.Louis, MO, USA zimengwang@wustl.edu, giammar@wustl.edu

[4]SLAC National Accelerator Laboratory, Menlo Park, CA, USA jlezama@slac.stanford.edu, bargar@slac.stanford.edu

Abstract

Bioreduction of U(VI) to U(IV) is considered a promising strategy for immobilizing U in the subsurface. Until recently, the product of U(VI) reduction was considered to be crystalline uraninite (UO_2). Recent studies have shown that other non-UO_2 phases may also exist including monomeric U(IV) which is presumed to be more labile relative to UO_2 [1]. Manganese oxides (MnO_2) which can be formed microbially even under low oxygen concentrations, can oxidize U(IV) to U(VI), and thereby jeopardize the stability of U(IV) [2]. Once oxidized by biogenic MnO_2, the resulting U(VI) can sorb to the MnO_2 surface. As the presence of MnO_2 can greatly impact the fate and transport of U in the subsurface, it is imperative to understand the effect a variety of common groundwater constituents may have on microbial Mn(II)-oxidation rates and the structure of the biogenic manganese oxides which in turn potentially affect the stability of U(IV).

In this study, the effects of common groundwater constituents, O_2 (0-5 %), Ca^{2+} (5 mM), Mg^{2+} (5 mM), and HCO_3^- (1 mM), on the coupled Mn/U processes were investigated. A model Mn(II)-oxidizing microorganism, *Bacillus* sp. SG-1 spores, was incubated with Mn(II) in the presence and absence of the above solutes and U(IV) as either biogenic UO_2 or monomeric U(IV). It is hypothesized that conditions that stimulate microbial Mn(II)-oxidation or lead to the formation of U(VI) complexes will lead to faster Mn(II) and U(IV) oxidation rates. In contrast, constituents that provide more stability for U(IV) species or sorb strongly to the MnO_2 surface and reduce its ability to oxidize U(IV) will decrease or have little impact on the rate of U(IV) oxidation. As expected, increasing O_2 concentration led to increased Mn(II)-oxidation rates. Addition of Ca^{2+} stimulated Mn(II)-oxidation while Mg^{2+} inhibited Mn(II)-oxidation in the presence of U(IV). Specific experiments probed the biological and chemical basis for the stimulatory and inhibitory effects of individual groundwater constituents on Mn(II)-oxidation in the presence of U(IV).

[1] Alessi et al (2011) *Mineral. Mag.* **75**, 422.
[2] Chinni et al (2008) *Environ. Sci. & Technol.* **42**, 8709.

Cyanide Sorption on Granular Activated Carbon and Its Attenuation by UV-Light

SOO-OH PARK[1], HYO EUN LEE[1], YOUNG JAE KIM[1], GIEHYEON LEE[2], YOO HYUN SUNG[3], CHAN OH PARK[3], YOUNG JAE LEE[1*]

[1]Department of Earth and Environmental Sciences, Korea University, Seoul 136-701, Korea (*Correspondence: youngjlee@korea.ac.kr, orange261@korea.ac.kr , hyonim@korea.ac.kr, jjbsnlove@korea.ac.kr)

[2]Department of Earth System Sciences, Yonsei University, Seoul 120-749, Korea (ghlee@yonsei.ac.kr)

[3]Development and Environment Team, Korea Resources Corporation, Seoul 156-406, Korea (sungyh77@gmail.com, pckores@lycos.co.kr)

Cyanide (CN) has been the subject of interest due to its heavy toxicity on humans and ecosystems. Carbons such as charcoal and granular activated carbon (GAC) are commonly used to remove contaminants in environments. Despite the popular usage of carbon, cyanide uptake by GAC has not been systematically adressed yet. In addition, effects of UV-light on cyanide attenuation are barely studied over a wide range of physicochemical conditions. Thus, in this study, we investigate cyanide sorption on GAC and its attenuation by UV-light over a wide range of conditions such as different pHs and concentrations through batch experiments.

Cyanide uptake by GAC is effective at $[CN]_{initial} < 2$ mg/L. At pH 7.0, the sorption of cyanide on GAC is greater than that of pH 9.0. It is also found that the ratio of CN uptake by GAC increases at pH 9.0 whereas the ratio decreases at pH 7.0, suggesting that reactivity of GAC would increase as a function of pH. The cyanide uptake by GAC rapidly increases during the first 30 min, followed by sharp desorption until 3 hr, and then the sorption increases and reaches the maximum sorption during the duration of experiments, implying that the sorption mode could be changed. Total amount of cyanide desorbed from the GAC during the duration of the desorption is less than 1.5% of total sorbed cyanide, indicative of strong and stable sorption of cyanide on the GAC. It is noted that UV-light is much effective on the attenuation of cyanide but also the attenuation is achieved until $[CN]_{total}$ is up to 10 mg/L. Our findings demonstrate that both GAC and UV-light are very effective on the attenuation of cyanide over a wide range of environmental conditions.

https://doi.org/10.1180/S0026461X00008434 Published online by Cambridge University Press

Review of environmental multi-tracer sensitivity to groundwater discharge in river

KARINE LEFEBVRE[1]*, FLORENT BARBECOT[1], MARIE LAROCQUE[2], BASSAM GHALEB[3], JEAN-FRANÇOIS HELIE[3], AURELIE NORET[1], SYLVAIN GAGNE[2]

[1]Université Paris-Sud, Sciences de la Terre et de l'Univers
karine.lefebvre@u-psud.fr (*presenting author)
florent.barbecot@u-psud.fr; aurelie.noret@u-psud.fr
[2]UQAM, Sciences de la Terre et de l'atmosphère
larocque.marie@uqam.ca; gagne.sylvain@uqam.ca
[3]GEOTOP-UQAM, Sciences de la Terre et de l'atmosphère
ghaleb.bassam@uqam.ca; helie.jean-francois@uqam.ca

Abstract

Assessing the distribution of groundwater inflow to small watersheds is of utmost interest to appreciate the sensitivity of humid zones to environmental changes. However, this distribution is poorly constrained because the resolution on river flow measurements is generally low. Different environmental tracer experiments have been proposed during the last decade [1]. In this work, we investigate the significance of $\delta^{18}O_{water}$, $\delta^{2}H_{water}$, $\delta^{13}C_{TDIC,}$ $A^{222}Rn$ coupled with *in situ* measurements (Q, T°, EC, pH, alcalinity) to better understand groundwater inflow to rivers. These tracers have been chosen as they may depict signals significantly different from groundwater to surface water. Here, we focus on processes and kinetics that sustain tracer evolution in surface waters.

The experimental site is a small watershed (219 km²) located in northern France. The Hallue River is 15 km long and flows over the Chalk aquifer. Stream flow was measured manually using a velocimeter and reflects variations in groundwater discharge along the river length. T, EC, pH and alkalinity were measured *in situ* at 11 locations along the Hallue River. Sampling for $\delta^{18}O_{water}$, $\delta^{2}H_{water}$, $\delta^{13}C_{TDIC}$ and $A^{222}Rn$ was performed in different glass bottles on the 11 locations with a peristaltic pump. Analyses of $\delta^{18}O_{water}$ and $\delta^{2}H_{water}$ were done in the IDReau laboratory (University Paris Sud, France) whereas the others were made at the "Département des sciences de la Terre et de l'atmosphère de l'UQAM" and at the GEOTOP (laboratory). The results of $\delta^{18}O_{water}$ and $\delta^{2}H_{water}$ show that there is no evaporation of the river water. The correlations between ^{222}Rn, CE and $\delta^{18}O_{water}$ and between $\delta^{13}C_{TDIC}$ and pH are high. ^{222}Rn and $\delta^{13}C_{TDIC}$ are anti-correlated and respond rapidly to groundwater inflow to the river. As a result, ^{222}Rn and $\delta^{13}C_{TDIC}$ processes are modeled using a diffusion exchange approach discretized along the river, as suggested by Cook et al. (2006) for ^{222}Rn [2]. The model fits very well the evolution of ^{222}Rn. Yet, the sensitivity of the model is too low for $\delta^{13}C_{TDIC}$.

[1] Gleason and al. (2009), Water Resour. Res. [2] Cook and al. (2006), Water Resour. Res., 42.

The Lower St. Lawrence Estuary: A suitable analogue for OMZs?

STELLY LEFORT[1*], YVES GRATTON[2], ALFONSO MUCCI[1], DENIS GILBERT[3] AND ISABELLE DADOU[4]

[1]McGill University, Montreal, Quebec, stelly.lefort@gmail.com (* presenting author)
[2]INRS-Ete, Quebec City, Canada
[3]Maurice-Lamontagne Institute, Fisheries and Oceans Canada, Mont-Joli, Canada
[4]LEGOS, Paul Sabatier University, Toulouse, France

When the rate of oxygen consumption in water exceeds the rate of supply, the oxygen concentration decreases and may reach levels that threaten the survival of many aquatic organisms. Waters with such low oxygen levels are termed severely hypoxic ($[O_2] < 62.5$ μmol L^{-1}).

The dissolved oxygen concentration in the deep water of the Lower St. Lawrence Estuary (Eastern Canada) has progressively decreased during the last century, concomitent with an increase in temperature. The severely hypoxic threshold was reached in the early 1980s where it has hovered ever since [1].

Using a 2D diffusion-advection model for oxygen, we examined the causes of large-scale hypoxia in the bottom waters (> 150 m depth) of the Lower St. Lawrence Estuary [2] and estimated the volumetric evolution of these hypoxic waters in response to further changes in the boundary conditons (biogeochemical properties of the waters that enter the estuary from the North Atlantic Ocean). The physics of the system and the source water properties were identified as the main cause of oxygen depletion and shown to control the oxygen distribution pattern in the deep water column [2]. Preliminary results on the evolution of hypoxia reveal that a ~2°C increase of the bottom water temperature would cause widespread anoxia throughout the Lower St. Lawrence Estuary and into the western Gulf.

[1] Gilbert et al. (2005) *Limnology & Oceanography* **50**, 1654-1666.
[2] Lefort et al. (submitted) *JGR-Oceans*.

https://doi.org/10.1180/S0026461X00008434 Published online by Cambridge University Press

Remediation of Coal-Mine Drainage by Sulfate-Reducing Bioreactor

LILIANA LEFTICARIU[1,2,*], PAUL T. BEHUM, JR[2], CHARLES W. PUGH[3] AND KELLY S. BENDER[3]

[1]Southern Illinois University, Department of Geology, lefticar@siu.edu (*presenting author)
[2]Southern Illinois University, Environmental Resources and Policy, pbehum@siu.edu
[3]Southern Illinois University, Department of Microbiology, bender@micro.siu.edu

Acid mine drainage (AMD) associated with abandoned coal mines is produced by biochemical weathering of organic (e.g., macerals) and inorganic (e.g., pyrite and other sulphides, clays, carbonates) components found in coal, overburden, and mine waste piles [1, 2]. Hydrologic conditions allow most coal mines in the Illinois Basin to be reclaimed without deleterious drainage problems. However, localized AMD from historic surface and underground mining within the basin have required remediation.

A passive-treatment system constructed in 2006 at one of these sites, the Tab-Simco mine near Carbondale, Illinois, remediates AMD characterized by low-pH (~2.9) and high-metal concentrations. Over the past five years the treatment system has increased the median pH of the AMD to ~6.0 and decreased the median acidity to 22.7 mg/L CCE, SO_4^{2-} from 2,981 to 1,750 mg/L, Fe from 450.6 to 3.76 mg/L, Al from 113 to 3.42 mg/L, and Mn from 36.4 to 23.3 mg/L. Continuous monitoring over the past five years has revealed significant temporal trends, including (1) seasonal variations in acidity, dissolved SO_4^{2-} and metals, (2) a general decline in the amount of alkalinity produced, and (3) an overall decline in the efficiency of the of treatment system in removing sulphate and metals. Bacterial community analyses targeting 16S rRNA and dsrAB genes indicated that the pre-treated samples were dominated by bacteria related to iron-oxidizing Betaproteobacteria, while the post-treated water directly from the reactor outflow was dominated by sequences related to sulfur-oxidizing Epsilonproteobacteria and complex carbon degrading Bacteroidetes and Firmicutes phylums. While initial microbiological results indicated that the passive treatment system was successful in stimulating sulfate-reducing bacteria to a certain extent, the algae and bacteria related to sulfur and iron oxidizers dominated the system. Cultures capable of sulfate-reduction have been enriched from the bioreactor and isolates are being used to determine optimal growth substrates. Molecular analysis targeting the 18S rRNA gene is also being used to characterize the algal and microscopic eukaryotic communities present in order to determine their metabolic contribution to the site chemistry. The geochemical and biological trends suggest that the AMD treatment system has to be modified in order to both stimulate sulfate-reducing bacteria and inhibit sulfur-oxidizing bacteria.

Our study demonstrates that passive treatment is an important technology for remediation of streams impacted by coal mining. This result is significant because it provide evidence that reclamation of abandoned coal mines can reduce significantly the environmental impact to water quality degradation.

[1] Behum *et al.* (2011) *Appl. Geochem.,* **26**, S162–S166. [2] Burns *et al.* (2011) *Biodegradation* doi:10.1007/s10532-011-9520-y

Street sediment and lichen as proxies to constrain source of urban lead pollution using lead isotopes

ERIN LEGALLEY[1*], ELISABETH WIDOM[1], MARK P.S. KREKELER[1], AND DAVID C. KUENTZ[1]

[1]Department of Geology and Environmental Earth Science, Miami University, Oxford, Ohio 45056, U.S.A., legallem@muohio.edu (* presenting author)

Introduction and methodology

Street sediment and lichen samples were used as proxies to investigate the source of urban lead (Pb) pollution in Hamilton, Ohio. Pb is a well-known environmental pollutant that poses a significant risk to human health and the greater environment. The study area includes a coal-fired power plant, the Great Miami River, athletic fields, industry, residential neighborhoods, and roadways.

Previously studied street sediment samples exhibit high concentrations of heavy metals (Pb, Zn, Cr, Cu, and Ni) and contain evidence of coal-derived pollution such as fly ash spherules.[1] Lichens are extensively used as bioindicators of atmospheric pollution[2,3] and have not been previously investigated in this study area. Heavy metal concentrations and Pb isotopic compositions of street sediment and lichen samples are combined to develop a more complete picture of local pollution. Major potential sources of Pb pollution in the study area include road paint containing $PbCrO_4$ as a yellow pigment and emissions from the coal-fired power plant.

Samples of local coal, fly ash from an anonymous coal-fired power plant in Kentucky, local road paint, lichen, and sieved (<38 μm) street sediment were analyzed. Two soil samples and one glacial till sample representing regional background were also analyzed. Elemental concentrations were determined by ICP-MS and Pb isotope ratios were determined by either TIMS or MC-ICP-MS.

Results and discussion

Street sediment samples exhibit highly variable Pb concentrations ranging from 130 to 1398 ppm. Pb concentrations in lichen range from 11 to 54 ppm. Pb concentrations range from 17 to 94 ppm in coal and fly ash samples and from 14 to 18 ppm in regional background samples. Road paint samples contain up to 0.63 wt% Pb. Pb isotope ratios in sample materials also exhibit substantial variability and potential pollution sources are isotopically distinct.

Street sediment and lichen samples exhibit strong positive correlations of $^{206}Pb/^{204}Pb$ vs. $^{208}Pb/^{204}Pb$ and $^{208}Pb/^{206}Pb$ vs. $^{207}Pb/^{206}Pb$, consistent with two-component mixing between regional background and road paint samples. In $^{206}Pb/^{204}Pb$ vs. $^{207}Pb/^{204}Pb$, coal and fly ash samples fall distinctly off this mixing trend, confirming the dominant contribution of Pb from road paint. Electron microscopy investigations of street sediment and the utilization of lichens as bioindicators of atmospheric pollution demonstrate the fine particulate nature of Pb pollution, and efforts to reduce health and environmental risks are encouraged.

[1] LeGalley, Krekeler, Widom, and Kuentz. (2011) *GSA Abstracts with Programs* **43**, 409. [2] Conti and Cecchetti (2001) *Environ. Pollut.* **114**, 471-492. [3] Cloquet, Carignan, and Libourel (2006) *Atmos. Environ.* **40**, 574-587.

https://doi.org/10.1180/S0026461X00008434 Published online by Cambridge University Press

Metals in black shales

BERND LEHMANN[1*]

[1*]Technical University of Clausthal, Mineral Resources, bernd.lehmann@tu-clausthal.de

Post-Archean marine black shales with organic carbon content of several wt% have long been known to be enriched in a broad metal spectrum. These metals reflect accumulation of biogenic matter with a composition relatively close to that of planktonic organisms. A suite of redox- and particle-sensitive metals also accumulates through precipitation/adsorption from seawater and reflects the environmental conditions of the ocean bottom water as a function of bacterial respiration/organic matter degradation. Oxic conditions are characterized by enrichment of Mn and locally Ba, whereas suboxic (also denitrifying) conditions typically have high P, and in places high V or Cr concentrations; anoxic and euxinic conditions (both sulfate reducing) may display V, U, Mo, and Ni enrichments..

Advanced organic matter decay under reducing conditions will release Ni, Cu, Zn from biogenic matter which may be incorporated in pyrite or in other sulfides. Consequently, Ni, Cu, Zn may indicate the original presence of organic matter even if partially or totally lost after deposition. Lateral facies variation with distinct metal zoning between these different depositional environments corroborates the general model, which, at very advanced reaction progress, is best preserved in restricted and stratified Early Cambrian basins on the Yangtze Platform of South China. Hydrodynamically induced winnowing of hardground with oolithic Mo-S-C and Ni sulfide compounds has here produced spectacular metal tenors in the % range in euxinic portions, grading into suboxic V-rich black shale (V in illite), with huge stratigraphically equivalent phosphorite deposits in oxic/suboxic settings, as well as 10s of meter thick "stone coal" (sapropelite).

Anoxic/euxinic marine environments may also provide the reducing milieu for focussed seafloor metal precipitation from hydrothermal fluids related to sediment-hosted massive sulfide systems (Cu-Pb-Zn-Ag-Ba), as documented by the presence of host basal black shale units in many SEDEX massive sulfide ore deposits (such as Rammelsberg, Germany; HYC, Australia; Howards Pass and Sullivan, Canada; Red Dog, USA). Basal black shale is also found related to Late Archean/Early Proterozoic banded iron formation (Minas Gerais and Carajás, Brazil).

Black shales preserve their reducing lithology with geological time and may then act as epigenetic traps for redox-sensitive metals in a broad hydrothermal ore deposit spectrum. Examples are orogenic gold and Carlin-type gold deposits where gold deposition is controlled by carbonaceous host rocks, or unconformity-related uranium deposits which are controlled by graphite-rich basement rocks. Roll-front/sandstone-hosted uranium deposits are also controlled by reducing host rocks within a much wider oxidizing depositional environment. The same applies to the European Kupferschiefer and Central African copper shale deposits where basinal brines leach postorogenic red bed/molasse basins and Cu (Co) + other minor redox-sensitive elements are deposited at thin carbonaceous rock units.

Links between sediment reactivity, sediment oxygen demand, and the N isotope effect of benthic N loss: Model and field observations

MORITZ F. LEHMANN[1]* AND MOHAMMAD ALKHATIB[2]

[1] Universität Basel, Department for Environmental Science, Basel, Switzerland, moritz.lehmann@unibas.ch (* presenting author)

[2] GEOTOP, UQAM-GRIL, Département des Sciences Biologiques Montreal, Canada, alkhatib.mohammad@courrier.uqam.ca

Abstract

We report $^{15}N/^{14}N$ ratios of pore water nitrate and reduced dissolved nitrogen (RDN=DON+NH_4^+) in sediments from various marine environments, where microbial nitrate reduction has previously been identified as a significant sink for fixed nitrogen (N). In order to address the combined isotope effects of benthic N-cycle processes (ε_{sed}) on the water column nitrate pool and to assess the dependence of ε_{sed} on various environmental factors, we calculated the net fluxes of dissolved N across the sediment-water interface from simulated pore water profiles corresponding to denitrification under varying sedimentation regimes. The model simulations suggest that differences in sediment reactivity and sediment oxygen demand have a significant effect on the geometry of the oxic layer and the denitrification zone, and thus on the expression of the biological N-isotope effect of denitrification in the water column. Model predictions were confirmed by observational benthic isotope flux data from an estuarine environment characterized by gradients in organic matter (OM) reactivity, bottom water oxygen concentrations, as well as benthic respiration rates. In agreement with the model, observed values for ε_{sed} ranged between 1 and 6 ‰ and diffusion-limitation of nitrate to the depth of denitrification was identified as the main cause of the general under-expression of the biological fractionation (>20‰) at the sediment water interface. The pore water RDN pool in the sediments was enriched in ^{15}N relative to the water column so that the (OM reactivity-controlled) efflux of RDN to the water column acts to enhance ε_{sed} . ε_{sed} reflects the $\delta^{15}N$ of the N_2 lost from marine sediments and thus best describes the isotopic impact of N elimination on the oceanic fixed N pool. Our mean value for ε_{sed} (4.6‰) is larger than assumed by earlier work, questioning current ideas with regards to the state of balance of the modern N budget.

https://doi.org/10.1180/S0026461X00008434 Published online by Cambridge University Press

A multiproxy approach ($^{87}Sr/^{86}Sr$, $\delta^{44}Ca$, $\delta^{13}C_{DIC}$) for tracking seasonal changes in permafrost dynamics

GREGORY O. LEHN[1*], ANDREW D. JACOBSON[1] THOMAS A. DOUGLAS[2], JAMES W. MCCLELLAND[3], AMANDA J. BARKER[2], MATT S. KHOSH[3], CHRIS HOLMDEN[4]

[1]Northwestern University, Earth and Planetary Sciences, Evanston, IL, United States, greg@earth.northwestern.edu (*presenting)
[2]U.S. Army Cold Regions Research and Engineering Laboratory-Alaska, Ft. Wainwright, AK, United States.
[3]Marine Science Institute, The University of Texas at Austin, Austin, TX, United States
[4] University of Saskatchewan, Dept. of Geological Sciences, Saskatoon, SK, Canada

Global change predictions indicate the warming will be greatest in the high latitudes, where permafrost soils have historically been a large carbon sink. As temperatures increase, the seasonally thawed active layer will extend downward into previously frozen soils, potentially releasing large quantities of greenhouse gases to the atmosphere, thus accelearting the pace of warming. In addition, dramatic changes in the hydrology and biogeochemistry of Arctic landscapes will result. A better understanding of the dynamics of permafrost thaw is needed to gauge the importance of feedbacks between Arctic warming and global climate change. Conventional methods for probing the depth of the active layer are labor intensive and may not address the spatial heterogeneity of Arctic soils. Alternatively, geochemical gradients in permafrost may be harnessed as spatially integrative, natural tracers of the downward movement of the active layer. This study evaluates $^{87}Sr/^{86}Sr$, $\delta^{44}Ca$, and $\delta^{13}C_{DIC}$ in stream water as potential tracers of seasonal variations in permafrost thaw.

Surface waters were collected from six watersheds on the North Slope of Alaska between May and October of 2009 and 2010, focusing on early spring thaw through late season freeze-up. All rivers drain continuous permafrost: three drain tussock tundra-dominated watersheds, and three drain bare bedrock catchments with minor tundra influences.

Large interstream variations in $^{87}Sr/^{86}Sr$ ratios imply heterogeneity in soil composition across watersheds. However, within individual watersheds, $^{87}Sr/^{86}Sr$ ratios vary with changes in discharge, including early season melt, base flow, and large rain events. During periods of high discharge, slightly elevated $^{87}Sr/^{86}Sr$ ratios indicate flushing of the shallow soil pool, which has a relatively low carbonate mineral content. $\delta^{44}Ca$ values in tundra streams decrease during the melt season while $\delta^{44}Ca$ values in bedrock streams increase. In tundra streams, low $\delta^{13}C_{DIC}$ values in the early season indicate silicate weathering. Higher mid- to late-season $\delta^{13}C_{DIC}$ values indicate carbonate weathering. Bedrock streams have nearly constant $\delta^{13}C_{DIC}$ values and high dissolved sulfate concentrations throughout the year, indicating the signficance of sulfuric acid carbonate weathering. In late fall of 2010, $\delta^{13}C_{DIC}$ values suggest a shift from sulfuric acid- to carbonic acid-dominated weathering, possibly due oxygen limitation during active layer freezing. Our initial findings illustrate how seasonal changes in mineral weathering have potential for tracking active layer dynamics.

Model of isotope distribution during water-rock interactions

LEMARCHAND D.[1*], DI CHIARA ROUPERT R.[1]

[1]LHyGeS-EOST, University of Strasbourg, Strasbourg, France, lemarcha@unistra.fr (* presenting author)

Soil particles evolve by contact with weathering agents supplied by meteoritic waters (mainly protons) or produced by the near activity of living organisms (protons, organic acids and ligands). The chemical budget of soil-forming reactions depends primary on the nature of the parent bedrock but also on the extent and rates of the weathering reactions. The mechanisms and controls of soil particles (trans)formation depend on multi-parametrized and non-linear reactions that are therefore difficult to characterize and even more to model on the basis of chemical composition alone.

In the present study, we developed a general model of isotopic evolution of bulk soil samples in response to progressing weathering reactions. It is based on mass and isotopic budgets and treats the bulk soil evolution as a simple gain-and-loss problem in which soil-forming reactions consist in mineral dissolution (loss) and secondary mineral precipitation (gain) including exchange of matter with the surrounding soil solution. Since dissolution and precipitation reactions have distinct effects on stable isotopic systems (like B, Ca, Li, Mg, Si, and many other metals of intermediate mass), then analyses of bulk soil samples give insights on the degree of soil evolution by comparison with a reference material that can be either the parent bedrock or a deeper soil layer. Adding analyses of the soil solution with knowledge of the water velocity provides additional information on the reaction rates as well as helps distinguishing reactions currently active from those active the past.

Because the water-rock interaction system may rapidly be under-determined, we developed a population-based stochastic search technique based on a modified Particle Swarm Optimization approach (PSO) to solve our system of differential equations. This has the advantage to provide sets of solutions without requiring the precise knowledge of model parameters like isotopic fractionation factors or the relative mass of parent material lost.

The model has been tested with B chemical and isotopic compositions in two soil profiles developed on granitic bedrock from the Strengbach watershed (Vosges Mountains, France) and showing different dissolution/precipitation dynamics. First numerical solutions are consistent with our hydrological and mineralogical knowledge of the two soils. They also clearly show varying intensity of soil-forming reactions with depth in line with the tree roots density or the soil horizons. These results encourage further work coupling isotopes with advanced numerical approaches for investigating water-rock interactions in multi-parametrized systems.

https://doi.org/10.1180/S0026461X00008434 Published online by Cambridge University Press

The role of Fe(III) (hydr)oxide structure in controlling the kinetics and products of biogenic sulfide oxidation in low sulfate media with *Desulfovibrio* sp.

CHRISTOPHER J. LENTINI[1*], SCOTT D. WANKEL[2], COLLEEN M. HANSEL[1,2]

[1]School of Engineering and Applied Sciences, Harvard University, Cambridge, MA, U.S.A.,

[2] Earth and Planatery Sciences, Harvard University, Cambridge, MA, U.S.A.,

(* presenting author; lentini@fas.harvard.edu)

Iron (hydr)oxides are a diverse groups of minerals which exist in a spectrum of crystallinities and subsequent bioavailabilities; ranging from ferrihydrite (poorly crystalline) to hematite (well crystalline). While the organisms responsible for the reduction of the poorly crystalline phase ferrihydrite have been well documented (*Geobacter* and *Shewanella*), these model dissimilatory iron-reducing microorganisms (DIRMs) show diminished abilities to reduce the more crystalline Fe(III) (hydr)oxide phases, goethite and hematite. In agreement with this, we have previously shown through enrichment experiments that these model DIRMs are enriched on goethite and hematite yet their presence does not correlate with reduction of these more crystalline phases. Instead, within Fe(III)-reducing enrichments supplemented with lactate, the reduction of goethite and hematite was detected in significant amounts (30–60%) and appeared to be a function of organisms associated with sulfate reduction, *Desulfovibrio putealis* and *Desulfovibrio vulgaris*. Media specific thermodynamic calculations along with enrichment data suggest that sulfate reduction may dominate and control Fe(III) reduction when more recalcitrant Fe(III) phases are provided as the terminal electron acceptor.

Interestingly, sulfate concentrations (200 μM) and subsequent sulfide oxidation alone could not account for the amount of Fe(III) reduction observed, without the cycling of sulfur. Consequently, the data suggest that either *Desulfovibrio* directly participates in the reduction of goethite and hematite or catalytic amounts of sulfur are being cycled multiple times.

In order to further elucidate the mechanisms of Fe(III) reduction by sulfate-reducing bacteria, pure culture Fe(III)-reducing experiments with *Desulfovibrio* species were conducted using three Fe(III) (hydr)oxides (ferrihydrite, goethite, hematite) and varying freshwater sulfate concentrations (0-800 μM). In order to track how intermediate Fe and S species varied as a function of Fe(III) (hydr)oxide type and S:Fe ratio, a variety of spectroscopic techniques were coupled with voltammetric microelectrodes. This aqueous data was combined with S and Fe EXAFS to further elucidate the products of sulfide oxidation and Fe(III) reduction. These findings will further illuminate how sulfate reduction kinetics in low-sulfate waters controls Fe(III) reduction of structurally diverse Fe(III) (hydr)oxides. In addition, the role that Fe(III) (hydr)oxide mineralogy and S:Fe ratios play in controlling the stoichiometry of different oxidized S species will be highlighted.

Did life turn the global weathering thermostat back up after turning it down?

TIMOTHY M. LENTON[1*]

[1]University of Exeter, Exeter, UK, t.m.lenton@exeter.ac.uk (*presenting author)

It is now widely accepted that plants (and their associated soil communities) amplify the weathering of silicate rocks, thus accelerating the drawdown of atmospheric CO_2 and ultimately leading to a lower stable state for CO_2 and global temperature. In metaphorical terms, land life has turned down the dial on the global weathering thermostat. Indeed it may have done so several times.

This is a neat way of explaining episodes of global cooling. Most notably, the rise of rooted vascular plants has been linked to the Late Devonian and Permo-Carboniferous glaciations. Recently, we suggested that the earlier rise of the first non-vascular plants could have been responsible for the Late Ordovician glaciations [1]. More speculatively, we have argued that lichen-like land colonisers could explain the episode of extreme glaciations in the Neoproterozoic [2]. Others extend the argument even further back in time [3].

But why were these cold episodes in Earth history transient ones? If the effects of life on weathering persisted each time, one would expect it to have remained cold. One can appeal to a steadily brightening Sun to warm things up again, but that is far too slow a process to explain the rather striking returns to warmer conditions. Often geological mechanisms are invoked to explain recovery from the cold. But it would be rather surprising if every time a biological innovation cooled the planet, some tens of millions of years later a change in geological forcing acted to warm it up again.

Here I suggest that biotic increases in weathering are naturally followed by biotic decreases in weathering. The key mechanism is a transition from weathering-fuelled phases of land colonisation to recycling-based ecosystems. Initially, new colonisers of the land must weather their rocky substrate to extract essential elements for growth, but as that substrate becomes exhausted and soils become established, ecosystems switch to internal recycling of essential elements. Also, by stabilising landscapes and suppressing erosion, vegetation and soils further suppress chemical weathering.

This could provide an intrinsic mechanism by which biotically-driven cooling of the planet would be followed by a relaxation back towards warmer conditions. In other words; perhaps after turning down the weathering thermostat, life turns it back up again.

[1] Lenton *et al.* (2012) *Nature Geoscience* **5**, 86-89.
[2] Lenton & Watson (2004) *GRL* **31**, L05202.
[3] Schwartzman & Volk (1989) *Nature* **340**, 457-460.

https://doi.org/10.1180/S0026461X00008434 Published online by Cambridge University Press

Natural organobromine in terrestrial and marine environments

ALESSANDRA C. LERI[1*] AND SATISH C. B. MYNENI[2]

[1]Marymount Manhattan College, New York, NY, USA, aleri@mmm.edu (* presenting author)
[2]Princeton University, Princeton, NJ, USA, smyneni@princeton.edu

In natural systems, bromine (Br) is generally believed to exist in the form of inorganic bromide. The perception of bromide as unreactive in soils justifies its frequent use as a hydrological tracer. Similarly, the oceanographic classification of Br as a conservative element in the water column has persisted for decades. We have recently shown that stable organobromine of natural origin is ubiquitous in terrestrial [1] and marine [2] environments. Using a novel quantitative technique based on XRF and X-ray absorption spectroscopy, we quantified organobromine concentrations in estuarine and marine sediments. Organobromine occurs in correlation with organic carbon and varies with sediment depth (Fig. 1) due to biogeochemical cycling of Br.

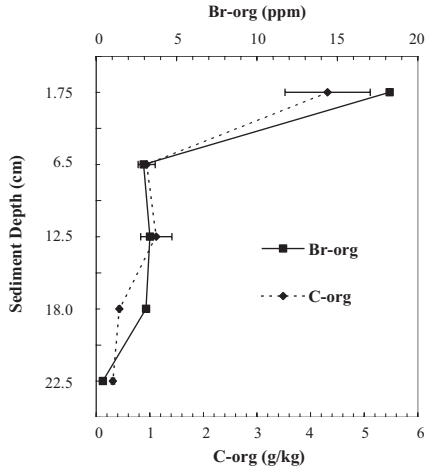

Figure 1: Organobromine and organic carbon concentrations with depth in estuarine sediments from Cape Cod, MA, USA.

X-ray spectromicroscopic images of sediment sections reveal a heterogeneous Br distribution, with associations between organobromine and metals such as iron and calcium. Organobromine also appears in particulate material from sediment traps deployed in the water column, suggesting that some fraction of sedimentary organobromine originates in overlying waters.

In the terrestrial environment, the Br in plant litter, organic-rich surface soils, and isolated humic substances is exclusively bonded to carbon. Terrestrial organobromine production is linked with plant litter decay and may be catalyzed by haloperoxidase-like enzymes in the soil environment.

These findings overturn the paradigmatic classification of Br as unreactive in the environment, shedding light on a biogeochemical cycle that may ultimately contribute to our understanding of the environmental fate of anthropogenic organobromine pollutants.

[1] Leri & Myneni (2012) *Geochim. Cosmochim. Ac.* **77**, 1-10.
[2] Leri *et al*. (2010) *Global Biogeochem. Cycles* **24**, GB4017.

Redox and Ca/Mg/Fe ratios in clay formations

C. LEROUGE[1*], C. TOURNASSAT[1] AND E.C. GAUCHER[1]

[1]BRGM, Orléans, France, c.lerouge@brgm.fr (* presenting author)

Redox control and Ca/Fe/Mg ratios remain among sensitive factors to improve modelling of porewaters chemistry in geological clay barriers. The existing models consider pure phases at equilibrium with porewater [1, 2], however accurate observations show more complexe mineralogy. In that way two marine clay formations (Callovian-Oxfordian (COx) clay at Bure, France and Opalinus (OPA) clay at Mont Terri and Benken, Switzerland) were investigated to describe diagenetic minerals, the processes involved in their deposition and the effects of these processes on redox conditions and phase stabilities.

Mineralogical constraints in COx clay [3] and OPA clay

Diagenetic sequence defined in the three clay formations consists of: 1) dominant micritic calcite with minor dolomite, and pyrite resulting from bacterial reduction of dissolved marine sulphate; calcite and dolomite are characterized at this stage of low Fe/(Fe+Mg) ratios (<0.4);

2) calcite, Fe-rich dolomite/ankerite, siderite ($Ca_{0.1\text{-}0.3}$ $Fe_{0.5\text{-}0.7}$ $Mg_{0.2\text{-}0.4}$ CO_3) and glauconite. Calcite and siderite have Fe/(Fe+Mg) ratios higher than 0.5-0.6 in the both clay formations. At contrary Fe-rich dolomite shows heterogenous Fe/(Fe+Mg) ratios depending of the clay formation: ~ 0.1 in COx clay, ~ 0.35 in OPA Clay of Mont Terri and up to 0.7-0.8 in OPA clay of Benken;

3) galena, sphalerite, celestite, calcite veinlets.

Redox control

Redox is controlled by pyrite in the models [1, 2, 4]. When Sphalerite and galena are taking account in the COx porewater model, the three sulfides are not at equilibrium with porewater. Further investigations on the distribution of sphalerite and galena in the clay formation are needed to affine the chemical system (introduction of Zn and Pb or not) to control the redox.

Ca/Fe/Mg ratios in porewaters

The cation exchanger of clay rocks reflects the relative amounts of exchanged cations in porewater through exchange equilibrium reactions [3]. Porewater is also at equilibrium with some diagenetic minerals. In Pearson [1] (OPA Clay model) and Gaucher [2] (COx Clay model), porewaters are likely at equilibrium with calcite (for Ca), dolomite (for Mg), siderite (for Fe) and celestite (for Sr). The large chemical variations of carbonates and their distribution (present at the scale of the formation or only at some levels) must be taken account to improve the models. Further work is to precise the carbonate compositions at equilibrium with present-day porewaters, specifically of dolomite in COx, ankerite and siderite in OPA, and to calculate the solubility constants of the carbonate solid solutions for Ca/Mg/Fe ratio control. The Fe control by siderite in the COx model will be discussed, siderite being present at a level of the COx Clay.

This research has been financially supported by the ANDRA BRGM–scientific partnership, the University of Bern and by the Mont Terri Consortium.

[1] Pearson (2011) *Applied Geochemistry* **Volume26**, 990-1008,
[2] Gaucher (2009) *GCA* **Volume73**, 6470-6487,
[3] Lerouge (2011) *GCA* **Volume75**, 2633-2663,

https://doi.org/10.1180/S0026461X00008434 Published online by Cambridge University Press

Experimental constraints on Fe-isotope fractionation at the core-mantle boundary

CHARLES E. LESHER[1*], JAMES BRENAN[2], GRY H. BARFOD[1], AND JUSTIN GLESSNER[1]

[1]Dept Geology, University of California, Davis, USA, celesher@ucdavis.edu (* presenting author), ghbarfod@ucdavid.edu, jjglessner@ucdavid.edu

[2]Dept Geology, University of Toronto, Canada, j.brenan@utoronto.ca

Background

The core-mantle boundary (CMB) is the largest thermal boundary layer within the Earth with temperature differences estimated between 1000-1500 K over length scales of 10-100's km. This complex boundary layer, including reaction products between the outer core (molten Fe ± light elements) and the lowermost mantle (silicates), may be partially molten and bounded below by a stagnant layer (10-100's km thick) of buoyant molten iron alloy. The conductive geothermal across the CMB and uppermost portion of the outer core thus creates a setting wherein diffusive transport of components along a temperature gradient can occur. This process of thermal (Soret) diffusion can be an agent of isotopic fractionation. The sense, magnitude and rates of isotopic fractionation by Soret diffusion of core-forming melts are largely unknown.

Results and Conclusion

We report experimental results of Soret diffusion of pure Fe and Fe (Ni-S-C) alloy melts conducted at 2 GPa within a temperature gradient from 1750 and 2000°C. We show that the sense of fractionation is consistent with Chapman-Enskog theory based on classical mechanics predicting that lighter isotopes are preferentially enriched at the hot end, while heavy isotopes are enriched at the cold end of the temperature gradient [1]. At steady-state, $\Delta\delta^{56}Fe/^{54}Fe$ between the hot and cold ends of the temperature gradient are 6-8 ‰ - similar in magnitude to those reported for silicate melts [2-4]. Steady-state profiles are also linear in temperature at high temperatures – as also observed for silicate melts. Time studies show that the approach to the steady state occurs rapidly and governed by Fe self diffusion. Simple scaling suggests that significant fractionation of Fe isotopes can occur across a stagnant boundary layer at the top of the outer core transporting heavy Fe into the overlying mantle. Soret effects should not be dismissed as an agent of iron isotope fractionation in the vicinity of the CMB.

[1] Lacks (2012) *PRL,* **108**, 065901. [2] Kyser (1998) *CMP*, **133**, 373-381. [3] Richter (2008) *GCA* **72**, 206-220. [4] Huang (2010) *Nature* **464**, 396-400.

Clay minerals and geochemical indicators of past environments on Earth and Mars

RICHARD J. LÉVEILLÉ[1*], JENNIFER BENTZ[1,2]

[1] Canadian Space Agency, St-Hubert, QC, Canada, richard.leveille@asc-csa.gc.ca ([*] presenting author)

[2] University of Saskatchewan, Saskatoon, SK, Canada, S7N 5A8

Introduction and Background

Identifying and characterizing specific minerals present on Mars is critical to reconstructing past environmental conditions and geological processes, and is essential for accurately assessing past habitability. Various clay minerals have been identified in ancient rocks on Mars, including rocks at Gale Crater, and their presence suggests an early, active hydrologic system. The formation of these minerals would have required the presence of persistent liquid water over extended periods of time. However, the timing, duration, and extent of hydrologic activity and nature of mineral formation processes are poorly constrained. While Al- and Fe-Mg-phyllosilicates seem to be most common on Mars, Mg-rich phyllosilicates (e.g., serpentine, talc, saponite, Mg-smectite) have also been identified. Due to the greater solubility and mobility of Mg, compared to Fe and Al, Mg-clay minerals generally indicate sustained aqueous conditions (either long-term presence of liquid water or high water-to-rock ratios). On Earth, Mg-clay minerals form most commonly in circumneutral to alkaline conditions, either by direct precipitation (neoformation) or via transformation of precursor phases. In fact, pH is a major control on clay mineral precipitation and Mg-phyllosilicates will form mostly at a pH >8.0, with specific minerals often being indicative of narrow pH ranges. Hence, the presence of Mg-phyllosilicates on Mars may indicate areas of increased or extended liquid water activity, and/ (or) aqueous environments where circumneutral pH may have favored habitable conditions or the preservation of organics. However, Mg-clay minerals can also form at high temperatures in hydrothermal systems, such as deep-sea hydrothermal vents, or during low-grade metamorphism. Therefore, developing criteria to distinguish between low and high temperature Mg-clay formation is needed to assess past environmental conditions and habitability of Mars.

Results and Conclusion

We present the results of our characterization of analog natural and synthetic clay minerals using a Terra XRD instrument, a laboratory laser-induced breakdown spectroscopy (LIBS) instrument, a prototype multi-spectral microscope, and regular laboratory analytical facilities. We critically assess the likelihood of distinguishing clay minerals formed at low and high temperatures on Mars by combining mineralogical, elemental and isotopic information. In particular, we target elemental indicators of hydrothermal activity, such as Ti, Mn, and Ba within clay minerals, that can be readily detected by LIBS. This information will be invaluable for the Mars Science Laboratory mission, where an integrated mineralogical and geochemical approach using a suite of instruments will enable accurate mineral identification, geochemical analyses, and paleoenvironmental reconstructions on Mars.

https://doi.org/10.1180/S0026461X00008434 Published online by Cambridge University Press

Baseline characterization of surface water at the Coles Hill uranium deposit, Virginia

DENISE M. LEVITAN[1*], MADELINE E. SCHREIBER[1], ROBERT R. SEAL II[2], ROBERT J. BODNAR[1], AND JOSEPH G. AYLOR JR.[3]

[1]Department of Geosciences, Virginia Tech, Blacksburg, VA, USA, dlevitan@vt.edu (* presenting author)
[2]U.S. Geological Survey, Reston, VA, USA
[3]Virginia Uranium, Inc., Chatham, VA, USA

Increasing interest in uranium deposits in temperate locales such as Virginia requires a reassessment of existing characterization methods. The goal of a pre-operational baseline characterization is to provide data which will enable both the identification of potential environmental impacts during mining and the establishment of post-mining closure targets.

A baseline surface water characterization study has been conducted at the undeveloped Coles Hill uranium deposit in agricultural Pittsylvania County, southern Virginia, USA. The study area included locations in stream reaches and ponds both upgradient and downgradient of potential mining, milling, and storage sites within the footprint of the deposit, as well as sampling locations in surrounding watersheds outside the area of potential operations.

Twenty-two stream sites were sampled twice, in early spring during high flow and late summer during low flow. Water samples were analyzed for major and trace elements, dissolved organic carbon (DOC), O and H isotopes, and field parameters. Major and trace elements abundances and mineralogy of sediment samples were also determined. Water at a subset of nine sites was sampled monthly for the above constituents and for radioisotopes. Discharge was measured to calculate loading. Fourteen ponds were sampled quarterly for the same analytes.

Statistical tests were used to compare analyte concentrations in stream reaches upstream and downstream of the deposit to evaluate the effect of the undeveloped deposit on surface water quality. Geochemical data collected at the site will also be compared to publicly available data from elsewhere in the Appalachian Piedmont and other uranium deposits to test for anomalies at Coles Hill.

Surface waters in the vicinity of the deposit are circumneutral (pH 3.9–7.6) with low total dissolved solids (specific conductance 3–93 µS/cm). Radionuclides, including U, ^{226}Ra and ^{228}Ra, and Th species, gross alpha and beta radiation, and trace metals, including As, Ba, and Pb, are below EPA regulatory limits for drinking water.

Statistically significant differences in composition were observed among streams, in particular in small drainages flowing near the ore bodies relative to other streams studied. Compositions at individual sites vary over time but indicate no regular trend. Positive correlations between DOC and dissolved trace metals such as Fe, Al, U, Ba, and Pb suggest complexation of metals by organic ligands. Higher concentrations of total metals relative to dissolved reflect metal transport via suspended sediment.

Sedimentary evolution in the northern South China Sea since Oligocene and its responses to tectonics

LI ANCHUN[1*], HUANG JIE[1,2], JIANG HENGYI[1,2], WAN SHIMING[1]

[1]Key Laboratory of Marine Geology and Environment, Institute of Oceanology, Chinese Academy of Sciences, Qingdao 266071, China, acli@qdio.ac.cn (* presenting author)
[2]Graduate University of Chinese Academy of Sciences, Beijing 100049, China, huang.211@163.com

Introduction

The South China Sea (SCS), one of the largest marginal sea of the West Pacific, has complex geological structure, unique development mode and has been controled by the Eurasian plate, Pacific plate and Australia - the Indian plate interaction since the late Mesozoic. Its formation underwent continental rifting, separation and seafloor spreading[1]. The tectonic evolution has a close relationship with peripheral geological units and can be recorded by sedimentary strata. This work is try to reconstruct sedimentary evolution of the SCS and its response to tectonics since Oligocene based on a multi-proxies including a monomineralic quartz oxygen isotope (δ^{18}O), grain-size of isolated terrigenous materials, terrigenous mineral accumulation rate of sediment samples from Ocean Drilling Program (ODP) Site 1148 in the northern SCS.

Results and Conclusion

The results show that the sedimentary evolution of the northern SCS Basin could be divided into five stages: period of initial expansion (34～28.5), period of intense tectonic activity (28.5～23), period of reduced tectonic activity (23～16.5), period of thermal subsidence (16.5～3.5) and period of Taiwan uplift (3.5 Ma to present). Terrigenous mineral composition and oxygen isotope values of quartz altered significantly between 28.5 Ma and 23 Ma during which provenance transition took place, corresponding to the most active period of the SCS since Oligocene. Sediments of the study area were mainly from southern source (presumptively from Palawan) during the early spreading period of the SCS. With the extensive spreading of the SCS, especially when the spreading axis of the SCS jumped to south during 25～23 Ma, Palawan continental block moved away from the study site, while northern sources did not set up as Tibetan Plateau uplift had not spread to Yunnan-Guizhou Plateau, so that, terrigenous mass accumu-lation rate was very low. Later owing to the rapid uplift of Qinghai-Tibet Plateau, rivers such as Pearl River developed gradually, so did the headward erosion, as a result, South Mainland of China turned to be the main source of ODP Site 1148, and in the meantime the northern SCS converted to distal deposition. While the hiatus of ODP Site 1148 in the late Oligocene resulted from the lack of terrigenous materials supply, sea level rise and relatively stronger currents during the source transformation. With uplift and development of Taiwan island, it turned to be the major sediment provenance of the study area since 3.5 Ma.

[1] Li (2008) Evolution of China's marginal seas and its effect of natural resources. Beijing: Ocean Press (in Chinese), 228-240.

https://doi.org/10.1180/S0026461X00008434 Published online by Cambridge University Press

A highly stratified Cryogenian marine basin recorded in the Datangpo Formation, South China

CHAO LI[1,2*], GORDON D. LOVE[2], TIMOTHY W. LYONS[2], CLINT SCOTT[2], LIANJUN FENG[3], JING HUANG[3], HUAJIN CHANG[3], QIRUI ZHANG[3], XUELEI CHU[3]

[1] State Key Laboratory of Biogeology and Environmental Geology, China University of Geosciences, Wuhan 430074, China, chaoli@cug.edu.cn (* presenting author)

[2] Department of Earth Sciences, University of California, Riverside, CA 92521, USA, glove@ucr.edu, timothyl@ucr.edu, clintscott001@gmail.com

[3] Institute of Geology and Geophysics, Chinese Academy of Sciences, Beijing 100029, China, ljfeng@mail.iggcas.ac.cn, jhuang@mail.iggcas.ac.cn, changhj@163.com, qrzhang@mail.iggcas.ac.cn, xlchu@mail.igcas.ac.cn.

Changes in ocean redox chemistry during the Cryogenian are likely to have had a strong influence on the emergence of animals[1]. A detailed, multi-element (Fe-C-S-Mo) biogeochemical study was conducted for two outcrop sections reflecting different water depths for the ca. 663-654 Ma Datangpo Fm. The Datangpo was deposited between the two major Neoproterozoic glacial episodes (Sturtian and Marinoan) in the restricted Nanhua Basin, South China. Basinal restriction may have been a common feature throughout the world in association with widespread rifted margins during global sea-level lowstands, particularly during build-up of the Marinoan ice sheet. Our findings are consistent with a highly stratified basin in which water column chemistry was strongly controlled by Fe and other nutrient fluxes, low dissolved marine sulfate concentrations, varying inputs of marine organic carbon delivered via primary production, and changing sea-level. Sea level was the overarching control on much of the observed variation. A compilation of new and published S isotope data for the Datangpo Fm. suggests a ^{34}S-enriched deep marine sulfate pool generated, in part, during the Sturtian glaciation by bacterial sulfate reduction in combination with suppressed riverine sulfate inputs and restriction of the basin during a dramatic drop in sea level. This study highlights the importance of both global and local controls in determining the chemical conditions in Neoproterozoic basins.

[1] Love et al. (2009) *Nature* **457**, 718-721.

Fluid cell TEM shows direction-specific interactions control crystal growth by oriented attachment

DONGSHENG LI[1]*, MICHAEL H. NIELSEN[2], JONATHAN R. LEE[3], CATHRINE FRANDSEN[4], JILLIAN BANFIELD[5] AND JAMES J. DE YOREO[1]

[1]Materials Science Division, Lawrence Berkeley National Laboratory, Berkeley, CA, USA, (*presenting author), dongshengli@lbl.gov, jjdeyoreo@lbl.gov

[2]Department of Materials Science and Engineering, University of California, Berkeley, CA, USA, mhnielsen@lbl.gov

[3]Physical Sciences Directorate, Lawrence Livermore National Laboratory, Livermore, CA, USA, lee204@llnl.gov

[4]Department of Physics, Technical University of Denmark, 2800 Kongens Lyngby, Denmark, fraca@fysik.dtu.dk

[5]Department of Earth and Planetary Science, University of California, Berkeley, CA, USA, jbanfield@berkeley.edu

Introduction

Oriented attachment (OA) of molecular clusters and nanoparticles in solution is now recognized as an important mechanism of crystal growth in many materials, yet the alignment process and attachment mechanism have not been established. Here we performed high-resolution TEM using a fluid cell to directly observe attachment of iron oxyhydroxide nanoparticles. Images were recorded with lattice fringe-resolution, enabling us to track particle orientations throughout the experiments.

Results and Conclusion

We find that the primary particles undergo continuous rotation and interaction until they find a perfect lattice match. A sudden "jump to contact" then occurs over < 1nm, followed by lateral atom-by-atom addition initiated at the contact point. Interface elimination proceeds at a rate consistent with the curvature-dependence of the Gibbs free energy. From the measured translational and rotational accelerations we calculate the magnitude of the inter-particle forces. The results show that highly-direction-specific interactions drive crystal growth via OA, and are likely the result of electrostatic forces.

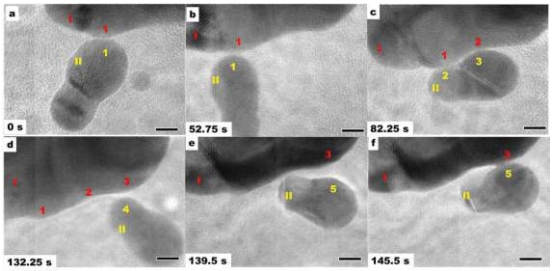

Figure 1: Typical dynamics of attachment process. Scale bar: 5 nm.

The findings of this study provide a dynamic view of the process of OA and answer the essential question of whether co-alignment occurs prior to attachment or comes about afterwards. In the case of freely diffusing nanoparticles, either near-perfect crystallographic orientation or a specific twin orientation that ensures interfacial coherence is required for attachment to occur. The results also shed light on the magnitude and nature of the forces that drive OA.

https://doi.org/10.1180/S0026461X00008434 Published online by Cambridge University Press

Strains of *Clostridium* sp. induce formation of carbonate minerals

FUCHUN LI, WENWEN GUO and JINPING WANG

College of Resources and Environmental Sciences, Nanjing Agricultural University, Nanjing 210095, China. fchli@njau.edu.cn

Large amounts of natural sediments and bacterial experiments have evidenced that microorganism in nature might be very important in formation of carbonate minerals. In order to study the mechanism of bacterially induced formation of carbonate minerals, a series of culture experiments using Lagoa Vermelha medium with 6:1 molar Mg/Ca ratio within 55 days at 28℃ and starting pH=7.5 was made under the mediation of two stains of *Clostridium* sp., which were isolated from the Nanjing suburb soil (named MH18 strain) and from the Qinghai Lake sediment in NW China (named SN-1 strain), respectively. At the same time, the aseptic experiments were carried out as control.

In the mediation experiments with strains, the morphologies of formed carbonate minerals were various, including club-shaped, dumbbell-like, spherical, rhombohedral and irregular. However, in the sterile experiments, only the rhombohedral minerals appeared. We propose that this morphological variation might be related with different nucleation sites and with different growth stages. At the initial stage, the microbe-generated organic acid with low molecular weight and extracellular polymer substance (EPS) could only affect the microenvironment surrounding the bacteria bodies. The carbonate crystals might be nucleated and grew on the cell surfaces of the bacteria, and the rod-like minerals with a morphology closely analogous to bacterial shape were formed. Afterwards, these “clubs” gradually developed to dumbbells, as well as spheres. However, in the EPS, the carbonate could be nucleated and grew with an irregular shape. Along with the longer reaction times, deamination of bacteria resulted in rising pH values of the whole medium. Consequently, carbonate super-saturation and homogeneous nucleation took place locally. Finally, the carbonate crystals were formed with a rhombohedral shape.

It is usually considered that the high-magnesium environment is favourable for formation of aragonite, but not for calcite. At the same time, the monohydrocalcite is a thermodynamically unstable mineral. Nevertheless, our study results showed that high-magnesian calcite and monohydrocalcite were dominant minerals in our experiments by using MH18 and SN-1 strains.

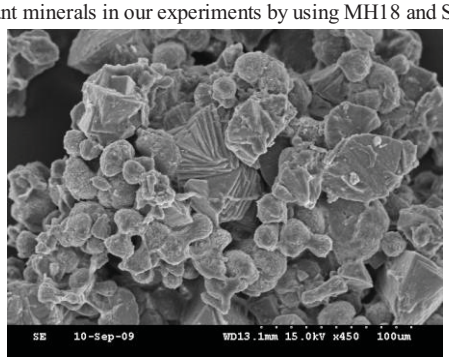

Figure 1 SEM images of carbonate minerals with different morphologies at the 55-th day by using SN-1 strain

Geochemical signatures of Tibetan dust

GAOJUN LI[1*]

[1]Department of Earth Sciences, Nanjing University, Nanjing 210093, China, ligaojun@nju.edu.cn (* presenting author)

Asian dust is one of the major components of global dust inventory. Provenance identification of Asian dust is helpful for understanding the paleo-environmental implications of the eolian deposits such as the loess on Chinese Loess Plateau, the pelagic sediments in North Pacific, and the dust in Greenland ice cores. Geochemical methods are effective ways to trace the provenance of eolian dust. Previous source tracing of Asian dust using geochemical methods mainly focus on the arid lands in North China and the neighboring Mongolia as the major potential source regions. However, recent studies indicate that Tibetan Plateau is probably an important source region of Asian dust. Tibetan dust, which only needs to be uplifted by 1-2 Km, could be carried into westerly jet and thus enable a long-distance transportation. The northern Tibetan Plateau, especially the arid lands in Qaidam Basin, is also probably an important source region of the loess on Chinese Loess Plateau. This study will systematically investigate the geochemical compositions of the surface materials on Tibetan Plateau, hoping to find out the geochemical signatures of Tibetan dust. Through comparing the geochemical compositions, this study will also confirm the possible contribution of Tibetan dust to the loess on Chinese loess, the pelagic sediments in North Pacific, and the dust in Greenland ice cores.

https://doi.org/10.1180/S0026461X00008434 Published online by Cambridge University Press

Brines and saline fracture waters in the terrestrial subsurface: A niche for the deep biosphere and unique analog for Mars

L. LI[1*], B. SHERWOOD LOLLAR[1], G. HOLLAND[2, 3], G.F. SLATER[4], C.J. BALLENTINE[3], G. LACRAMPE-COULOUME[1]

[1] University of Toronto, Toronto, Canada, longli@geology.utoronto.ca (* presenting author)
[2] Lancaster University, Lancaster, UK, g.holland@lancaster.ac.uk
[3] University of Manchester, UK, chris.ballentine@manchester.ac.uk
[4] McMaster University, Hamilton, Canada, gslater@mcmaster.ca

Saline waters and brines have been widely observed in deep fractures in the Precambrian igneous rocks of the Canadian Shield and South Africa. Recent molecular studies indicate that these deep brine waters contain low-abundance, low-diversity microbial ecosystems [1, 2] distinct from those found in the shallower, less saline fracture waters. This discovery has significantly expanded our understanding of life in the deep anaeorobic terrestrial environment and provided an important analog for studies of early life on Earth and for the search for life on Mars.

To understand the dependence of microbial ecosystems on water chemistry, we studied the brine waters from Timmins (Ontario), and Thompson (Manitoba) in the Canadian Shield. The fracture brine waters are dominant by Ca, Na, Cl with salinities of 150-290 g.TDS/L. Na-Cl-Br relationships exclude the possiblilty of brine sourced by freezing seawater during the Pleistocene glaciation as had been recently suggested [3]. The geochemistry of Na-Cl-Br favors a source related to evaporated seawater which may originate from the mid-Devonian or even earlier [4]. Oxygen and hydrogen isotope compositions of these brine waters lie well above the global meteoric water line, indicating significant oxygen and hydrogen isotope modification by fluid-rock interaction. Noble gas studies indicate 100s Ma to possibly Ga gas components in the fractures, suggesting little or no disturbance of these fractures over geological time scales and bulk water residence times on the order of millions of years – again supporting an a geologically ancient origin for these fluids.

Based on above observations, we propose that the fracture saline waters and brines in the deep terrestrial subsurface provide the best opportunity to host microbial ecosystems that have been separated from those on the surface for millions of years and sustained on the limited energy and nutrient sources produced by fluid-rock interaction. They demonstrate the potential for life to sustain its activity over geologic time in ancient low temperature tectonically quiescent rock fractures that serve as an important analog for the Martian subsurface.

[1] Lin *et al.* (2006) *Science* **314**, 479-482. [2] Chivian *et al.* (2008) *Science* **322**, 275-278. [3] Katz & Starinsky (2003) *Geology* **31**, 93-94. [4] Bottomley *et al.* (2002) *Geology* **30**, 587-590.

Research on the Basin Formation and the Eruption of volcano During Carboniferous period in front of the Kelamli Mountain in Junger Basin

L LI[1], X LUO[2*], LH HOU[3], YZ WEI [4], XF QI[5], X ZHAO[6]

[1]China University of Petroleum, Beijing, China; Xinjiang Oil Company, Petrochina, Uramuqi, China; llin@petrochina.com.cn
[2,3,4,5,6] Research Insitute of Petroleum Exploration and Development, Petrochina,Beijing, China, [2] luoxia69@petrochina.com.cn, [3] houlh@petrochina.com.cn , [4] weiyanzhao@petrochina.com.cn , [5]qxuefeng@petrochina.com.cn , [6] zhaox601@petrochina.com.cn
(* presenting author)

Experiments and results

Junger Basin was located among the intersection of Kazakhstan, Tarim and Siberia plates during Palaeozoic. The research on the basin formation and the volcanos during this period were never stopped because of the complicated structural settings and great breakthough of gas exploration has gained in Carboniferous volcanos.

12 Volcanic rocks samples dating by SHRIMP and LA-ICPMS and elemental analysis, palynologic analysis were conducted in this essay. The results were follows. There were different eruption structural settings of volcano during carboniferous period in front of Kelamli Mountain. The duration of early stage was about from 354Ma to 330Ma. The range of dating detection is 350Ma~335Ma.Volcanos were arc. The samples points are in the arc areas in the figure of logτ-logσ. Elements Nb, Ta, Ti are parrent deficit and element Sr is abnormal in the figure of the distribution of elements cobweb. All of above were interrelation with the lagoon or tide of sedementary environment in this period. The duration of late stage was about from 320Ma to 295Ma. Volcanos were intraplate. The sample points are in the intraplate areas in the figure of logτ-logσ such as typical sample DX17. Elements Nb, Ta, Ti are little deficit and element Pb is abnormal in the figure of the distribution of elements cobweb. All of the above were interrelation with the occurrence of considerable granite aging from 314 Ma to 295Ma in the mountain around the basin in the same period. This indicates that geological setting was extended. During the period between 330Ma and 320Ma, volcanic activity stopped and a set of sedmentary rock deposited.

The evolution of the carboneferous system as follows. The early volcanic eruption stage indicated that Junger basin and its near areas were in a concourse geological setting. Kelamli Ocean began to dive and a lage scale of volcanos erupted during this period. During the 330Ma to 320Ma, Kelamli Ocean had dived into the plate of Yemaquan and had been died out since then. Accompany with this, a depression was formed in front of the mountain. During the late of the carboneferous, with the gelogical setting changing from concourse to extend, another large-scale of volcanic activity occurred again.

Conclusions

There were 3 evolution stages during carbonferous. From early to late stage, there were coexisting volcanos and sedments, maily sedments and volcanos respctively. In a all, there formed two sets of source rocks and two sets of reservoirs during carboniferous period.

https://doi.org/10.1180/S0026461X00008434 Published online by Cambridge University Press

A mixing model for crustal growth in Northeastern China as revealed by U-Pb age and Hf isotopes of detrital zircons from modern rivers

MING LI[1*], SHAN GAO[1], GINGLIANG GUO[1], KANG CHEN[1] AND XIANLEI GENG[1]

[1]State Key Laboratory of Geological Processes and Mineral Resources, China University of Geosciences, Wuhan 430074, China, liming19820426@163.com (* presenting author)

Northeastern (NE) China consists of the eastern part of the Central Asian Orogenic Belt (CAOB), which is the most important site of juvenile crustal formation in the Phanerozoic. Detrital zircons from young sediments, or in modern river sediments, may record crustal material that has not been preserved or is no longer exposed. Here, we report U-Pb ages and Hf isotopes of 1381 detrital zircons in 13 sand samples from 5 modern rivers, which drain the most part of NE China, in order to characterize the crustal growth and evolution. These zircons give three magmatic age groups of 100-600 Ma, 1600-2000 Ma and 2300-2700 Ma. The third group from the Songhua river characterizes the North China craton. The first and second group zircons were derived from rivers that drain within CAOB, and display a large spread in Hf isotope two-stage model ages (T_{DM2}) between 400 and 3000 Ma but with a significant peak at 600-1600 Ma. They suggest that 98% of the crust for much of NE China formed 500 Ma ago. However, NE China has significant production of juvenile crust in the Paleozoic [1]. Clearly, the obtained Hf model ages are a mixing product. To estimate the true crust formation age, we simply assume the mixing source consists of the depleted mantle (juvenile crustal addition) and the regionally known oldest crust components, whose proportions can thus be calculated for each zircon from its U-Pb age and Hf isotope. The mixing model shows that proportions of the juvenile crustal component are about 50-90% in the 100-400 Ma age group, 40-70% in the ~500 Ma age group and below 50% in the 1600-2000 Ma age group. The corresponding crustal growth rates suggest that 20%, 47% and 98% of the present crustal volume were formed by 2700 Ma, 200 Ma and 100 Ma ago, respectively (Figure 1).

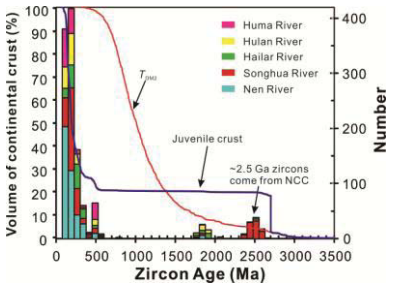

Figure 1: Histogram of concordant U-Pb ages and crust growth curves based on two-stage Hf crust formation ages and our mixing model for detrital zircons from rivers in NE China.

[1] Wu *et al.* (2000) *Tectonophysics* **328**, 89-113.

Geochronology and geochemistry of the Mesozoic volcanic rocks from the Hailar basin, NE China

SHUANG-QING LI, FUKUN CHEN, JIA-DE WU, YUE QI, QUN LONG

CAS Key Laboratory of Crust-Mantle Materials and Environments, School of Earth and Space Sciences, University of Science and Technology of China, Hefei, 230026, China

Mesozoic volcanic rocks and granitoids are widespread in northeastern China, which are interpreted as a large igneous province in eastern Asia and are distinguished by extensive Phanerozoic crustal growth as a part of the Central Asian Orogenic Belt. These Mesozoic volcanic and pyroclastic rocks are important reservoir rocks of petroleum in the basins distributed in NE China, e.g. the Songliao basin that has been a major oil and gas field in China. This study focuses on a successive volcanic rock series that are exposed along the northwestern bank of the Hulun Lake of the Hailar basin.

Two rock formations, the Shangkuli Formation and the Tamulangou Formation, contain volcanic rocks in the Hailar basin. Zircon U-Pb dating of six rhyolitic samples successively collected from the Shangkuli Formation in a profile along the western bank of the Hulun Lake yields ages of 137 Ma to 147 Ma, possibly implicating a long term of volcanic activities in this area. This magmatism is likely related to the closure of the Mongolia-Okhotsk Oceans in late Mesozoic. The volcanic rocks are characterized by low contents of MgO and compatible elements in spite of the variations in major element contents. Both the basic and acid volcanic rocks of the Tamulangou and the Shangkuli Formations are characterized by slightly depleted Nd isotopic composition with initial ε_{Nd} values of 0.63 to 2.67 and relatively low initial $^{87}Sr/^{86}Sr$ values of 0.7033 to 0.70548. Homogeneous Sr-Nd isotopic composition of different volcanic rocks in context of the spatial and temporal relationship indicate that they were derived from a similar mantle source and formed through different degrees of fractional crystallization of the primary melt(s). This study is supported by the Ministry of Science and Technology of China (grant No. 2009CB219305).

https://doi.org/10.1180/S0026461X00008434 Published online by Cambridge University Press

Ice nucleation in supercooled nano water droplets

TIANSHU LI[1*], DAVIDE DONADIO[2], AND GIULIA GALLI[3]

[1]George Washington University, Civil and Environmental Engineering, Washington DC, USA, tsli@gwu.edu (* presenting author)
[2]Max Planck Institute for Polymer Research, Mains, Germany, donadio@mpip-mainz.mpg.de
[3]University of California, Department of Chemistry & Department of Physics, Davis, USA, gagalli@ucdavis.edu

Abstract

The prediction of contribution to global radiative budget and future climate change by cirrus clouds requires computation of the formation rates, growth rates, shape evolution and size distribution of small ice particles. The formation of ice particles under various thermodynamic, dynamic, and chemical environments still remains very poorly understood. Here we report a large-scale numerical study of spontaneous ice nucleation from supercooled nano water droplets, with the size of droplets ranging from 6 nm to 12 nm at 230K. In this study, we combined forward flux sampling method [1] with molecular dynamics simulations, and employed a recently developed coarse-grained water model [2]. The large number of nucleation trajectories (500) sampled in this study allowed obtaining nucleation rates directly from molecular simulations and identifying ensembles of various crystal structures and morphology of the fully crystallized ice clusters. The calculated nucleation rates show strong size dependence below 10 nm: it increases from $1.97\pm0.92\times10^{8}$ $m^{-3}s^{-1}$ to $1.08\pm0.47\times10^{14}$ $m^{-3}s^{-1}$ as the size of water droplets increase from 6 nm to 9.5 nm. When the size of water droplets is beyond 10 nm, the calculated ice nucleation rates become indistinguishable from the calculated ice homogenous nucleation rates in bulk supercooled water at the same temperature [3]. The preferential location of the formation of ice embryos also shows variation with the size of water droplets, with a strong preference for the location identified within the subsurface (1~1.5 nm below the immediate surface) for larger water droplets (>7.6 nm). The fully crystallized ice clusters are found to be mixtures of both hexagonal ice (I_h) and cubic ice (I_c), and display a variety of structures and shapes. In consistent with previous study in bulk water [3], we also identified the five-fold twin boundary (FFTB) structure in ice cluster. A single FFTB per ice cluster yields a nearly decahedral shape of crystallized ice cluster. In addition, we have also identified a more complex and highly symmetrical defect structure that is composed of 12 FFTB merging and forming a 512 water cage at the center of the defect. Such defect structure results in a nearly icosahedral shape, which also displays nearly 5 fold rotational symmetry.

[1] Allen, Frenkel, and Wolde (2006) *J. Chem. Phys.* **124**, 024102.
[2] Molinero and Moore (2009) *J. Phys. Chem. B* **113**, 4008.
[3] Li, Donadio, Russo and Galli (2011) *Phys. Chem. Chem. Phys.* **13**, 19807-19813.

Fe isotope and U-Th-Pb evidence for a reduced 3.4 Ga Archean ocean

WEIQIANG LI[1,2*], CLARK M. JOHNSON[1,2], BRIAN L. BEARD[1,2], AND MARTIN VAN KRANENDONK[3]

[1]Univ. Wisconsin, Dept. of Geoscicence, Madison WI, USA, wli@geology.wisc.edu (* presenting author)
[2]NASA Astrobiology Institute, Madison WI, USA
[3]School of Biological, Earth and Environmental Sciences, University of New South Wales, Sydney, Australia

Evolution of Earth's early atmosphere is critical to understanding the geologic history of the Earth, yet the levels of oxygen in Earth's atmosphere in the Archean continue to be debated. The hematite-bearing 3.4 Ga Marble Bar Chert (MBC) at Marble Bar area of the Pilbara Craton, NW Australia, has been used to argue that Earth's early atmosphere contained significant amounts of oxygen [1]. We measured Fe and U-Th-Pb isotope composition of the MBC samples. Our results indicate that the Marble Bar Chert was deposited from a Fe-rich, but U-poor ocean. The δ^{56}Fe values of hematite in MBC range between 1.71‰ and 2.63‰, which are the most positive δ^{56}Fe dataset that has ever been reported from natural rocks (Figure 1). Given that hydrothermal sources of aqueous Fe^{2+} should have had a δ^{56}Fe value of around 0‰ [2], and that Fe isotope fractionation between hydrous ferric oxides and aqueous Fe^{2+} is ~3-4‰ [3][4], the high δ^{56}Fe values of hematite in MBC requires partial oxidation of aqueous Fe^{2+}. This suggests that the oxidant was extremely limited and the main body of ocean water was reduced and rich in Fe^{2+}. In addition, U concentrations of the MBC samples are over one order of magnitude lower than those of Phanerozoic cherts, indicating lower U content of Archean ocean water than modern ocean water. Moreover, U-Th-Pb isotope analysis shows that the MBC samples has actually undergone U addition during the Phanerozoic, which further attests to low U contents during deposition at 3.4 Ga. This indicates low O_2 levels in Archean atmosphere.

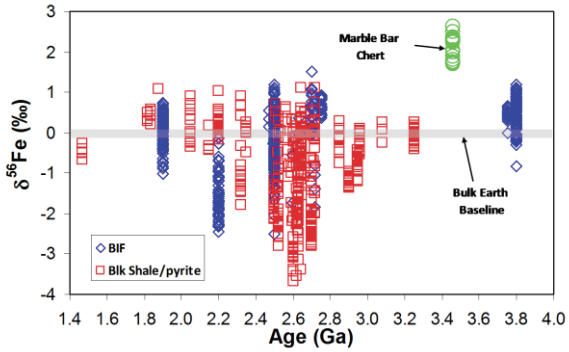

Figure 1. Compilation of δ^{56}Fe values for minerals and rocks from the Archean and Proterozoic sedimentary rocks

[1] Hoashi et al. (2009) *Nature Geoscience* **2**, 301-306. [2] Johnson et al. (2008). *Annual Review of Earth and Planetary Sciences* **36**, 457-493. [3] Johnson et al. (2002) *Earth and Planetary Science Letters* **195**, 141-153. [4] Wu, et al. (2012) *Geochimica et Cosmochimica Acta* **in press**.

https://doi.org/10.1180/S0026461X00008434 Published online by Cambridge University Press

Trace metals in atmospheric particular matters over the northern South China Sea (SCS): regional sources and long-range atmospheric transport

WEIHAI XU[1], XIANGDONG LI [2*], WEN YAN [1], GAN ZHANG [3], JUN LI [3], LI MIAO[1], WEIXIA HUANG [1]

[1]CAS Key Laboratory of Marginal Sea Geology, South China Sea Institute of Oceanology, Chinese Academy of Sciences, Guangzhou 510301, China

[2]Department of Civil and Structural Engineering, The Hong Kong Polytechnic University, Hung Hom, Kowloon, Hong Kong, cexdli@polyu.edu.hk (* presenting author)

[3]State Key Laboratory of Organic Geochemistry, Guangzhou Institute of Geochemistry, Chinese Academy of Sciences, Guangzhou 510640, China

Abstract

A total of 65 daily aerosol samples were collected in two open cruises covering the whole northern SCS in September 2005 and August 2007, respectively. The concentrations of Cr, Cu, Ni, Zn and Pb in particular matters (PM) of the northern SCS were comparable to the values measured in suburban and background sites of south China. Cu showed relatively high concentrations during the two sampling periods, suggesting the regional sources of Cu pollution in the Pearl River Delta (PRD) area, south China. The calculated enrichment factor (EF) values of Cu, Zn and Pb were generally greater than 10, indicating the strong influences of anthropogenic inputs. As shown by the backward air trajectory analysis, the high concentrations of trace metals in the air during the sampling periods were mainly related to the air mass passing over the neighboring cities or countries around the SCS. Elevated concentrations of Pb and Zn in the daytime of the 2007 summer criuse may indicate the effects of traffic emissions from the nearby cities around the SCS. The relatively high concentrations of trace metals during the northeastern monsoons in 2005 were probably attributed to local emissions and long range atmospheric transport of pollutants by the Asian monsoon.

Fluorescent nanoparticle tracers

YAN VIVIAN LI[1*], LAWRENCE M. CATHLES[2]

[1]The KAUST-CU Center of Energy and Sustainability, Cornell University, Ithaca, NY, USA, yl398@cornell.edu (* presenting author),

[2]Department of Earth and Atmospheric Science, Cornell University, Ithaca, NY, USA, lmc19@cornell.edu

Introduction

Tracers are perhaps the most direct and efficient way of determining subsurface fluid flow pathways. Particle tracers could arrive faster at a detection site because they would not diffuse, as would chemical tracers, from the fractures where flow occurs. Indeed their early arrival could measure the fraction of flow that occurs through the fractures. A requirement is that the particles not aggregate or stick to mineral surfaces. Here we describe our method for screening paticles for stickiness and present results for 8 nanoparticles that suggests small size and neutral charge keep particles from sticking.

We inject a slug of artifical brine that contains nanoparticles into a column filled with crushed calcium carbonate, and follow this slug with particle-free brine. The particle concentration in the effluent is measured by the fluorerscence of the nanoparticles, and the fraction recovered is determined by intgration over time. Results are shown in Figure 1 for 8 nanoparticles: small ethanolamine carbon dot (light blue, CNP-2), large ethanolamine carbon dot (CNP-3), small Jeffamine carbon dot (CNP-1), commercial silica (SiNP-1), silica coated with polyethylene glycol (SiNP-2), polystyrene commerical (PSNP), polyacrylonitril (PANNP), and a

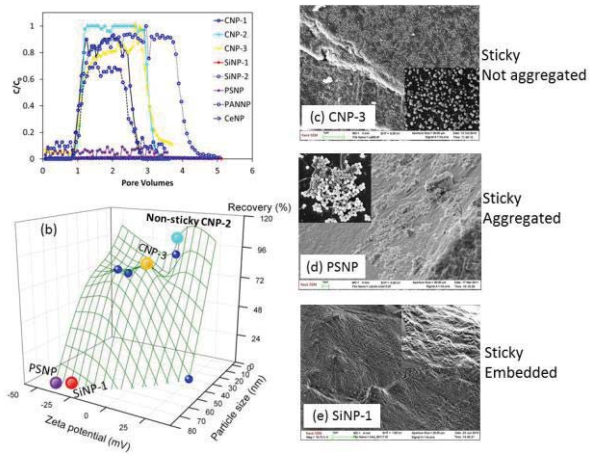

Ce-fluoride (CeNP).

Figure 1. (a) NP concentration (in brine) as a function of injection pore volumes. (b) 3D-countour plot showing particle recovery as a function of particle size and zeta potential. (c-e) SEM images of the CNP-3, PSNP and SiNP-1 particles.

Results and Conclusion

The nanoparticles that showed the least stickiness is the small 3 ± 2 nm ethanolamine carbon dot (CNP-2 light blue on plots) which has zeta potential near zero.

https://doi.org/10.1180/S0026461X00008434 Published online by Cambridge University Press

Relationship between Leaf Phosphorus and Soil Phosphorus：A Case Study of Degraded Grassland in western Jilin Province, NE China

Y.F.LI[1*], S.WAN[1], D.Y.WANG[1], Q.FU[1], D.Y. GUO [1]AND Y. Y.YANG[1]

[1] College of Earth Sciences, Jilin University, Changchun 130061, China, yfli@jlu.edu.cn(* presenting author), Lasoukhan_09@yahoo.com, wang_dy@jlu.edu.cn, fly19881118@yahoo.com.cn, jluguodongyan@163.com, yyyang10@mails.jlu.edu.cn

Introduction

Plant growth should be expected to be limited by phosphorus (P) availability in most terrestrial ecosystems. The previous studies indicate that the leaf P concentrations of Chinese terrestrial plants should be considerably lower than the global average, resulting in a higher leaf N/P ratio. However, how does the content of soil total P and available P influence leaf P and N/P ratio? It has been one of the hotly-discussed issues in the ecological stoichiometry. However, the P stoichiometry in the leaves of Leymus chinensis and soil conditions from the Jiangjiadian grassland in Da'an city in western Jilin Province, NE China, provides insights for the above issue. Our objective is to determine how and to what extent soil total P and available P influence leaf P and N/P ratio in the study region.

Material, Method, Results and discussion

This paper reports the total P and available P contents of 25 surface soil samples and the leaf P contents of 25 Leymus chinensis samples.The results indicate that the content of leaf P ($1.3mg \cdot g^{-1}$) is lower than the global average content ($2.0mg \cdot g^{-1}$), however, the N/P ratio in Leymus chinensis leaf (15.26) is higher than the global average value (13.8). These findings are consistent with previous findings[1]. Moreover, the contents of soil total P and available P are $0.34mg \cdot g^{-1}$ and $5.25mg \cdot kg^{-1}$, respectively. The available P content of degraded grassland in western Jilin province is higher than Chinese soils ($3.83mg \cdot kg^{-1}$), United States soils ($3.41mg \cdot kg^{-1}$) and Australian soils ($2.17mg \cdot kg^{-1}$). But, available P is lower than the global soils ($7.65mg \cdot kg^{-1}$). In addition, Pearson correlations analyses done by SPSS software indicate that soil total P(r=0.345) and available P(r=0.25) do not exhibit evidently positive correlations with leaf P concentrations. The soil total P concentrations has no significant correlation with N/P ratio(r=-0.3). While the soil available P has significantly negative correlation with N/P ratio($r_{0.05}$=-0.416*). Taken together, it is suggested that the soil total P and available P can influence leaf P concentrations, but be not necessarily leading factor, because contents of soil total P and available P are not accurately reflect leaf P concentrations. Compared with leaf P concentrations, leaf N/P ratio is more related to soil P concentrations, especially to soil available P concentrations.

Conclusion

Therefore, we conclude that low leaf P and high N/P of Leymus chinensis are caused by low soil P content on one hand, on the other hand they are likely caused by other factors such as plant characteristics, climate, and external environment and so on.

The fate of mercury at a contaminated site

DAVID WATSON, CARRIE MILLER, JANE HOWE, FENG HE, ERIC PIERCE, LIYUAN LIANG*

Oak Ridge National Laboratory, PO Box 2008 Oak Ridge, TN, 37831-6038, U.S.A., liangl@ornl.gov (*presenting author)

Soils contaminated with mercury present unique challenges for remediation due to the variety of chemical forms in which mercury occurs. Mercury, like many other heavy metals, cannot be degraded in the environment and its remediation must therefore involve either removal or immobilization. The characteristics of the mercury in sediment, i.e., Hg(0) beads with or without coatings of HgO and $Hg(OH)_2$, or oxidized Hg(II) that is attached to sediment minerals, or precipitated Hg as mercury sulfide (HgS), underpins the technologies that can be effective for clean up. When selecting mercury remediation technologies at a given contaminated site it is essential that the form of mercury—especially speciation—is well understood.

During the mercury use era at the Y-12 National Security Complex, Oak Ridge, Tennessee, large quantities of mercury were lost to the subsurface environment[1]. Spilled elemental mercury has undergone complex biogeochemical transformations under both saturated and unsaturated conditions. High-levels of mercury have recently been found in soil collected from a Hg use area (which housed a mercury retort furnace from 1957 until 1962[2]). Hg concentrations, determined by atomic absorption following core collection, sampling and soil digestion, ranged from 0.2 to 19000 ppm. Hg(0) was the dominant form in sediment samples where mercury beads were visually present[3]. Additionally micron-sized Hg(0) beads were also observed. Although the formation process is under investigation, the observed micron-sized beads may have formed in situ due to high vapor pressure and/or disintegrated from the original Hg(0) beads over the last 50 years in the subsurface. New SEM and XRD evidence shows that the coatings of the mercury beads are predominantly HgO, but that native clay minerals are also

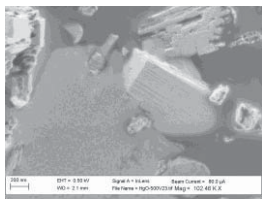

present. These results are being incorporated into further laboratory tests focused on evaluating the fate and transport of mercury as well as the development of new remediation strategies.

1. Brooks, S. C., Southworth, G. R., 2011. Environmental Pollution 159, 219-228.

2. King, D. A., 2010. Characterization report for the 8110 area in the Upper East Fork Poplar Creek area at the Oak Ridge Y-12 national security complex, Oak Ridge, Tennessee, DOE/OR/01-2485&D1, Oak Ridge Institute for Science and Education

3. Miller, C., Watson, D., Phillips, D., Lowe, K., Lester, B., Liang, L., 2011. Field and laboratory characterization of mercury contaminated soils: Implication on mercury transformation and remediation, Halifax, Nova Scotia, Canada.

https://doi.org/10.1180/S0026461X00008434 Published online by Cambridge University Press

A two-lithology model for melting and melt migration in an upwelling and chemically heteogeneous mantle

YAN LIANG[1]

[1]Department of Geological Sciences, Brown University, Providence, RI 02912, USA (yan_liang@brown.edu)

Several lines of evidence suggest that the melt generation and segreatation regions of the mantle are heterogeneous consisting of chemically and lithologically distinct domains of variable size and dimension. Partial melting of such heterogeneous mantle source regions give rise to a divers range of basaltic magmas erupted on the sea floor. Although the diversity and importance of mantle source heterogeneity have long been recognized, simple models for trace element fractionation during concurrent melting and melt migration in a lithologically heterogeneous mantle have not been fully developed. In this study we develop a two-lithology model for trace element fractionation during concurrent melting and melt migration in a vertically upwelling, chemically and lithologically heterogeneous mantle column. As a first model, we consider a special case in which strings of enriched lithology are regularly distributed in a depleted background or ambiment mantle. The enriched and depleted lithologies, referred to as channel and matrix, respectively, are treated as two overlapping continua each with a prescribed melting rate and starting composition. Part of the melt generated in the matrix is segregated into the channel along the upwelling column. Part of the channel melt is extracted into a melt-filled open network within the channel continuum at a prescribed depth. Analytical solutions for the abundances of a trace element in the matrix melt, channel melt, and open channel melt have been obtained. Essential features of the two-lithology model have been investigated through simple analysis and case studies. Using the two-lithology model as a module, we have also developed a "bundle of columns" model for melting and melt migration in a heterogeneous mantle over a broad upwelling region.

Applications of the two-lithology model to REE abundances in olivine-hosted melt inclusions in one hand sample from Mid-Atlantic Ridge and $^{87}Sr/^{86}Sr$, $^{143}Nd/^{144}Nd$, La/Sm ratios and REE abundances in basalts in near-ridge seamounts and axial valleys from East Pacific Rise demonstrate the importance of melting and melt migration-induced mixing in a two-component mantle and magma mixing at the top of the melting column in producing compositional diversities and variations observed in basalts erupted on the surface. Such mixing poses considerable challenges to deciphering the original mantle source composition and lithology based on compositions of basalts erupted on the surface.

Mineralogy and oxygen-isotope geochemistry of clays from the Te Mihi area, Wairakei Geothermal Field, New Zealand

RYAN B. LIBBEY[1*], FRED J. LONGSTAFFE[2], ROBERTA L. FLEMMING[2]

[1]McGill University, Montreal, Canada, ryan.libbey@mail.mcgill.ca (*presenting author)
[2]The University of Western Ontario, London, Canada

Abstract

Drill cuttings recovered from the Te Mihi area of the Wairakei Geothermal Field, New Zealand, have been analyzed to determine the mineralogical, morphological, and isotopic systematics of hydrothermal clays present in these samples. These data provide a tool for assessment of the paleo-hydrological conditions and temperature variations that have operated in the subsurface. Mixed-layer illite-dioctahedral smectite (I-S) and R0 chlorite-trioctahedral smectite phases are the principal clay minerals present. Mixed-layer I-S clays in well WK244 display a well-defined prograding sequence exhibiting R1 to R3 ordering and illite proportions grading from 50 to >90% over a 160 m depth interval. The interlayer proportion of illite in I-S correlates positively to measured downhole temperatures with a correlation coefficient (r) of 0.98. SEM photomicrographs demonstrate a change in clay morphology from micron-scale laths and hairy fibers to pseudo-hexagonal plates alongside this illitization sequence. Methylene blue estimates of swelling clay percentages show a strong inverse relation to %I of mixed-layer I-S with a correlation coefficient of -0.91, which further validates this method as a tool for delineating illitization sequences in active geothermal environments. The oxygen isotope compositions of I-S exhibit a continuous downhole depletion of ^{18}O, which tracks the corresponding gradation of subsurface temperatures prevailing at the time of clay formation. The oxygen isotopic compositions are used to calculate fluid compositions, under isotopic equilibrium assumptions, and assess thermal changes in the subsurface. Estimates of water/rock mass ratios calculated using the I-S oxygen isotope compositions display an inter-stratigraphic variability that correlates with known unit permeabilities. The isotopic methods applied in this study have proven useful for delineating reservoir evolution and detailed permeability characteristics in an active geothermal system.

https://doi.org/10.1180/S0026461X00008434 Published online by Cambridge University Press

A complex ecological role for submarine groundwater discharge in the formation of toxic *Pseudo-nitzschia* spp. blooms

JUSTIN D. LIEFER*, WILLIAM C. BURNETT[2], HUGH L. MACINTYRE[3]

[1] Dauphin Island Sea Lab, Dauphin Island, AL 36528 USA, jliefer@disl.org (* presenting author)
[2]Department of Earth, Ocean and Atmospheric Sciences, Florida State University, Tallahassee, FL 32306, USA, wburnett@fsu.edu
[3]Dalhousie University, Halifax, NS B3H 4J1 Canada, hugh.macintyre@dal.

Abstract

The potentially-toxic diatom *Pseudo-nitzschia* is common in th northern Gulf of Mexico (NGOM), including the coastal waters of Alabam The NGOM shoreline near Little Lagoon, AL, is a hot spot for blooms of *Pseudo-nitzschia* spp. and their population density is correlated with proxi for groundwater discharge[1]. Little Lagoon, AL (USA) is a shallow coasta lagoon that lacks riverine inputs but has persistent salinity gradients betwee the ends and the narrow pass connecting it to the Gulf of Mexico. Covarian between salinity and the groundwater tracer ^{222}Rn in Little Lagoon indicate that submarine groundwater discharge (SGD) is responsible for the salinity gradients and is likely the primary source of freshwater to the lagoon. Clus analysis based on temperature, salinity and two proxies of SGD revealed tw regimes with different drivers for nutrient concentrations and chlorophyll a samples characterized by high discharge, total nitrogen (TN) was negatively correlated with salinity and total phosphorus (TP) was correlated with temperature. In samples characterized by low discharge and higher temperatures, both TN and TP were highly correlated with temperature and inferred to originate from benthic efflux.

Monitoring within Little Lagoon from 2007 to 2010 showed tha phytoplankton community structure during periods of high aquifer discharg was distinct from other periods and tended to be dominated by diatoms and chlorophytes. *Pseudo-nitzschia* spp. abundances were also greatest during these periods and were correlated with increases in groundwater elevation. *Pseudo-nitzschia* spp. abundance had a negative relationship with measures nutrient availability and nutrients were relatively low during periods of high *Pseudo-nitzschia* spp. and high aquifer discharge. Other blooms of *Pseudo nitzschia* spp. in coastal Alabama were also associated with periods of high aquifer discharge and low nutrient availability. Dilution grazing experiment also indicated that the effects of SGD are likely to favor *Pseudo-nitzschia* spp. due to their high growth rates and susceptibility to grazing. We hypothesize that the link between SGD and *Pseudo-nitzschia* spp. blooms i not due simply to nutrient inputs, but rather that SGD is part of a disturbanc regime that favors fast-growing, heavily grazed diatoms like *Pseudo-nitzsc* spp.

[1] Liefer et al. (2009) *Harmful Algae* **8**: 706-714.

Relating microbial community structure and geochemistry in the Bisley watershed, Puerto Rico

LAURA LIERMANN[1*], SUSAN BRANTLEY[1], ISTVAN ALBERT[2], HEATHER BUSS[3], MORGAN MINYARD[4]

[1]The Pennsylvania State University, Earth and Environment Systems Institute, University Pare, PA, USA, ljl8@psu.edu (* presenting author), sxb7@psu.edu
[2]The Pennsylvania State University, Biochemistry and Molecular Biology, University Park, PA, USA, iua1@psu.edu
[3]University of Bristol, School of Earth Sciences, Bristol, UK, h.buss@bristol.ac.uk
[4]U.S. Defense Threat Reduction Agency, Edgewood, MD, USA

Abstract

Using next generation sequencing and metagenomics analysis tools, bacteria community composition and structure were assessed in the context of chemical and mineralogical characteristics of a 9.2 m depth regolith profile developed on volcaniclastic material of the Fajardo formation in the Bisley watershed in Puerto Rico. We have hypothesized that Fe oxidation is important in weathering of intact bedrock to disaggregated regolith, and that chemolithoautotrophic microorganisms play a role in Fe cycling at depth.

The regolith forms along a gradient between conditions of low oxygen and higher pH at depth, to higher oxygen and lower pH at the surface. Secondary clay minerals and Fe oxides are present from the surface down to 8.3 m, while the weathered primary minerals chlorite and feldspar were detected from 8.3 m to the bedrock at 9.2 m. Both total cell counts and heterotrophic cell counts generally decreased from the surface to ~9 m, with variations in bacterial numbers correlating with variations in clay content. Cell numbers in iron-oxidizing media decreased with depth, but increased near the weathering front at 8.3 m depth. Increased concentrations of organic-bound iron at 8.3 m were observed as well.

Rarefaction curves generated at a 97% similarity value indicated that the regolith was representatively sampled for determining community richness. At all depths analyzed, 4 phyla were dominant – Proteobacteria, Acidobacteria, Planctomycetes, and Actinobacteria. Sub-phylum groups containing known iron-oxidizing microorganisms (e.g. subclass Acidimicrobidae) were found in the deepest samples, near the regolith-bedrock interface, consistent with the hypothesis that chemolithoautotrophic bacteria play an important role in weathering and element cycling in the deep regolith. Iron-reducing groups (e.g. *Geobacter* and *Anaeromyxobacter*) were detected as well. The data obtained from this study are consistent with the hypothesis of an iron-cycling community that in turn supports heterotrophs at depth. It is furthermore possible that this Fe-related ecosystem at depth contributes to disaggregation of bedrock to form noncohesive regolith.

https://doi.org/10.1180/S0026461X00008434 Published online by Cambridge University Press

Active filtration of phosphorus with hydrated oil-shale ash in constructed wetlands: geochemical modelling and phosphorus removal efficiency

MARTIN LIIRA[1]*, MARGIT KÕIV[2], RIHO MÕTLEP[1], CHRISTINA VOHLA[2], ÜLO MANDER[2], KALLE KIRSIMÄE[1]

[1] University of Tartu, Department of Geology, martin.liira@ut.ee (*presenting author)
[2]University of Tartu, Department of Geography, margit.koiv@ut.ee

Kerogenous Oil-shale used at Estonian thermal power plants is a solid fuel of low energetic value. More than 95% of power production in Estonia relies on the use of oil-shale and about 45-50% of oil-shale remains after combustion as calcareous ash. The ash is rich in free lime (CaO) and anhydrite (CaSO4), with an Al-Si glass-like phase and secondary Ca(Mg)-silicate minerals [1]. The ash is hydraulically transported to large open plateaus, and due to hydration reactions forms a variety of secondary Ca-minerals ettringite, portlandite, Ca-aluminates and calcite. More than 280 million tons of ash is deposited and these dumps are considered as point source of contamination which almost completely lacks any further use.

Recent studies [2] [3] have shown a large potential of Estonian oil-shale fly ash and the hydrated ash sediment as an alternative media for phosphorous (P) removal in constructed wetland systems via active filtration through the alkaline media. The active filtration technique uses the direct immobilization of phosphates into low soluble forms and extensive super-saturation of pore-water is required for the precipitation of stable Ca-phosphate phases.

We studied the phosphorus binding capacity of hydrated oil shale ash in onsite pilot-scale experiment (with subsurface flow filters) in Estonia, using pre-treated landfill leachate (median P 3.4 $mg \cdot L^{-1}$) for a total of 12 months. The results show efficient P removal (median removal of phosphates 99%) in filters. The P removal efficiency of the hydrated ash increases with increasing P loading, suggesting direct precipitation of Ca-phosphate phases.

A computer programme Geochemist's Workbench was employed to calculate the saturation-index (SI), according to the data obtained from the experiment, with respect to hydroxyapatite (HAP) and Ca-minerals in ash (e.g. ettringite, portlandite). The SI values for the different Ca- minerals were between -2 to -12, indicating dissolution of these minerals. and thus providing Ca^{2+} ions to the pore-water.Especially ettringite (with average SI= -6.5) is most important mineral providing Ca^{2+} ions for the precipitation of HAP. The SI values for HAP were more than 8 during all the experiment.

[1] Kuusik *et al.* (2005) Characte rization of oil shale ashes formed at industrial-scale CFBC boilers. *Oil Shale* **22**, 407e 421. [2] Vohla *et a.* (2005) Alternative filter media for phosphorous removal in a horizontal subsurface flow constructed wetland. *J. Environ. Sci. Health*, **A40**, 1251 –1264. [3] Kaasik *et al.* (2008) Hydrated calcareous oil-shale ash as potential filter media for phosphorus removal in constructed wetlands. Water Res. **42**, 1315-1323.

Precambrian palaeosol from Baltica – reconstructing the Neoproterozoic climate

SIRLE LIIVAMÄGI[1*], KALLE KIRSIMÄE[1], PEETER SOMELAR[1], JUHO KIRS[1]

[1]University of Tartu, Department of Geology
sirle.liivamagi@ut.ee (*presenting author)

Precambrian palaeosol profiles provide important and direct evidence for early weathering conditions reflecting the past climate (temperature, precipitation), atmospheric composition (pCO_2, pO_2) and (microbial)biota. In this contribution we study a well-preserved Neoproterozoic weathering crust that is widespread under the Ediacaran-Phanerozoic sedimentary cover at the southern margin of the Baltic Shield, Baltic Basin.

The palaeosol marks an unconformable contact of peneplained Palaeoproterozoic – Mesoproterozoic metamorphic-plutonic rocks and overlaying unmetamorphosed Ediacaran sandstones –claystones. Palaeosol profiles were developed on rapakivi granites, sillimanite-cordierite and biotite-amphibole gneisses, amphibolites in the northern part and pyroxene and amphibole gneisses in the southern part of the area. The maximum age of the palaeosol is estimated at 1.3-0.8 Ga by the age of major denudation in Fennoscandia and the minimum age is defined by the age of overlying Ediacaran terrigenous sediments estimated at 600 Ma, which suggest that the age of weathering falls into the period of final stage of atmosphere oxygenation during Cryogenian.

Palaeosol is accessed in more than 100 drillcores where the thickness of the alteration profiles varies from few meters to exceptional 152 m on fractured-faulted sections of alumo-gneiss parent rocks. Palaeosol is preserved unmetamorphosed, but probably slightly modified by diagenetic illitization.

Palaeosol profiles are characterized by well-developed alteration zones grading gradually from (lateritic?) kaolinitic zone (kaolinite content 30-40wt%) to smectite-illite/smectite and chlorite(illite)-smectite zones and into saprolite and fresh basement rocks. Chemical Index of Alteration (CIA, [1]) reaches values >90(95) in the uppermost parts of the alteration profiles. The Ti/Al ratios from parent rock into uppermost kaolinitized laterite are in most profiles constant at ~0.04-0.06 or 0.15-0.17 depending on host rock composition, suggesting *in situ* formation of profiles. Several profiles are characterized by Fe accumulation (Fe_2O_{3tot} are as high as 20%.) in the zone below strongly kaolinitized upper part of the palaeosol.

The quantitative weathering indicators suggest intense weathering in well drained landscapes under humid and warm conditions, with mean annual precipitation estimated at 1500-1800 mm/yr. This interpretation well agrees with palaeoposition of the Baltica continent at equator at the transition from Mesoproterozoic to Neoproterozoic [2], but there is no indication of global Snow Ball Earth glaciations that are believed to have occurred in the same period at about 710 and 635 Ma [3].

[1] Nesbitt and Young (1982) Nature 299, 715-717 [2] Cocks and Torsvik (2005) Earth Science Reviews 72, 39-66. [3] Hoffman et al. (1998) Science 281, 1342-1346.

https://doi.org/10.1180/S0026461X00008434 Published online by Cambridge University Press

Electro-osmostic removal of PAHs: A journey from the lab to the field

ANA T. LIMA[1,2*], PHILIPPE VAN CAPPELLEN[1], J.P. GUSTAV LOCH[2]

[1] University of Waterloo, Waterloo, Canada, atlima@uwaterloo.ca
[2] Utrecht University, Utrecht, the Netherlands

Polycyclic aromatic hydrocarbons (PAH) are persistent and toxic contaminants of difficult removal from fine porous materials using conventional remediation techniques. Electro-osmosis is a potential remediation technique for the mobilization and cleanup of hydrocarbon contaminants [1-3]; it may be a promising and cost-effective technology for the removal of PAHs from clay-rich soil. By applying an electrical potential gradient, a flow of water, generally from the anode to cathode, is induced. Together with the movement of water, PAHs may be entrained towards the cathode as well. In order to demonstrate this process, we carried out studies with a custom made electro-osmosis cell (Figure 1), described elsewhere [4]. Clayey soil from Olst, the Netherlands, was used as it presents a unique study matrix: the site has been contaminated by asphalt industry for over 100 years. Using the experimental cell, up to 30% of PAHs were removed by electro-osmosis with the aid of Tween 80 [5].

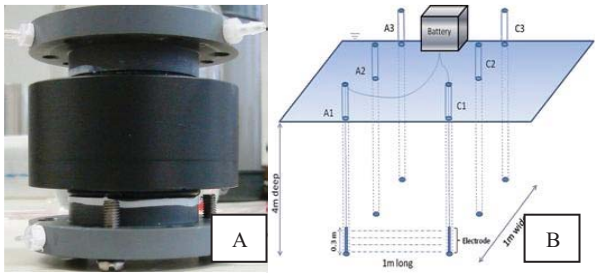

Figure 1: Picture of the electro-osmostic cell used for lab experiments (a) and design of the field experiment (b)

The Tween 80-assisted electro-osmotic clean-up was subsequently scaled up to the Olst field site (Figure 1). A release of PAHs from the soil was observed, with significant concentrations accumulating at the cathode after 90 days of continuous application of an electrical field [6]. However, most of the PAHs could not be remobilized. The percentages of PAHs that could be removed from the Olst soil, both in the laboratory and in the field, fall well below those reported for experiments with artificially spiked soils. This is likely due to the presence of PAHs in pure solid phase tar particles, from which release by dissolution is very slow. Aging effects with respect to sorption must also be taken into account when extrapolating laboratory tests to field conditions.

[1] Saichek (2005) *Critical Reviews of Environmental Science and Technology* **35**,115-192.
[2] Pamukcu (1992) *Environmental Progress* **11**, 241-250.
[3] McNab Jr. (1998) *Chemosphere* **37**, 925–636.
[4] Loch (2010) *Journal of Applied Electrochemistry* **40**, 1249-1254.
[5] Lima (2011) *Separation and Purification Technology* **79**, 221-229.
[6] Lima (2012) *Electrochimica Acta* doi:10.1016/j.electacta.2011.12.060

Synchrotron XAS and single-crystal EPR study of arsenic speciation in struvite

JINRU LIN[1], NING CHEN[1, 2], YUANMING PAN[3]

[1] University of Saskatchewan, Department of Geological Sciences, Canada, email: jil368@mail.usask.ca
[2] University of Saskatchewan, Canadian Light Source, Canada, email: Ning.Chen@lightsource.ca
[3] University of Saskatchewan, Department of Geological Sciences, Canada, email: yuanming.pan@usask.ca

Abstract

Arsenic contamination in groundwater, natural or man-made, has become a major environmental concern worldwide, with adverse effects to human health[1]. The mobility, toxicity and bioavailability of arsenic in groundwater are known to strongly depend on its nature and speciation in source rocks. Also, when incorporated in the bulk rather than simply adsorbed on the surfaces, arsenic is less susceptible to secondary contamination. In this context, enormous efforts have been devoted to investigate arsenic uptake and speciation in minerals and synthetic materials[2]. Struvite, a common biomineral and increasingly important fertilizer recovered widely from sewage and waste water treatment plants, is known to accommodate a wide range of toxic metalloids, including arsenic. Experiments have been conducted to investigate the pH dependence of arsenic uptake in struvite. Microbeam synchrotron X-ray flurorescence (μ-SXRF) imaging shows heterogeneous distribution of arsenic in synthetic struvite. Arsenic K edge X-ray absorption near edge spectra (XANES) reveal that As in struvite occurs predominantly in the pentavalent oxidation state. Similarly, single-crystal electron paramagnetic resonance (EPR) spectra identified at least four varieties of paramagentic $(AsO_3)^{2-}$ centers derived from diamagentic $[^{V}AsO_4]^{3-}$ precursors at the $[PO_4]^{3-}$ positions, further supporting the presence of lattice-bound As^{5+} in struvite.

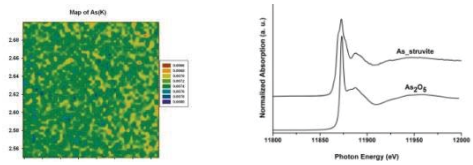

Figure 1: μ-SXRF map of As(K) and As K-edge XANES spectra

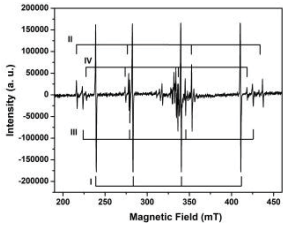

Figure 2: Single-crystal EPR spectrum of gamma-ray-irradiated struvite measured at the magnetic field B approximately parallel to the crystallographic axis **b**, showing four $[AsO_3]^{2-}$ centers with characteristic ^{75}As hyperfine structures (labeled I, II, III and IV).

[1] Smith *et al.* (2000). Bulletin of the World Health Organization, **78**(9), 1093-1103. [2] O'Day P.A. (2006) Chemistry and mineralogy of arsenic. Elements, **2**, 77-83.

https://doi.org/10.1180/S0026461X00008434 Published online by Cambridge University Press

Time series of elemental carbon concentrations at Alert, Canada

COURTNEY BELDEN,[1] PHILIP K. HOPKE,[1] LIN LIN,[1*] SHELDON LANDSBERGER[2]

1. Institute for a Sustainable Environment, Clarkson University, Potsdam, NY, llin@clarkson.edu
2. Department of Mechanical Engineering, University of Texas at Austin

Introduction

There is significant interest in the concentration of elemental carbon in the Arctic ambient aerosol because of its potential climatic effect in reducing the albedo of the snow cap. Ambient particulate matter samples have been collected at Alert, Nanuvut, Canada (latitude 82.3" N, longitude 62.5" W) since 1980 by Environment Canada. In 1989, they began making hourly black carbon mearusrements using an aethalometer [1] and the time series of these data are presented in Figure 1.

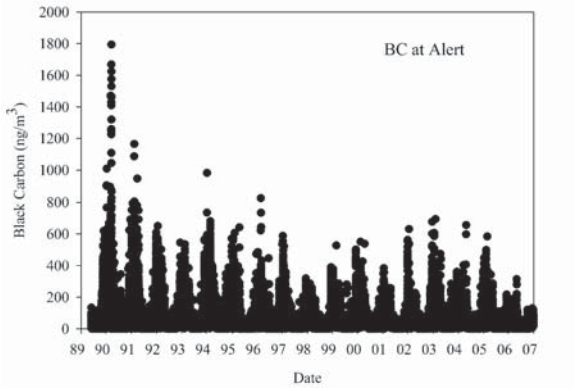

Figure 1. Environment Canada data for light absorbing carbon measured at Alert with an Aethalometer.

Methods

High volume samples have been collected on 20 x 25 cm Whatman 41 filters for 7 day periods. These filters were then cut into strips and we are analyzing one of these strips. The analysis follows the procedures developed by Husain et al.[2]. The filter material is dissolved in a concentrated $ZnCl_2$ solution. The elemental carbon particles are then collected on a baked quartz filter and the carbon determined using a Sunset carbon analyzer implementing the NIOSH protocol for organic and elemental carbon [3]).

Results and Conclusions

We will report the EC concentrations in almost 400 samples begiing with 1980 that we have analyzed. Thus, we will present the results in terms of the trends observed over the full 30 years spanned by these samples as well as fill in some of the gaps when the aethalometer was not functioning.

[1] Data from http://www.ec.gc.ca/donneesnatchem-natchemdata/default.asp?lang=En&n=22F5B2D4-1

[2] Husain, L., Khan, A.J., Ahmed, T., Swami, K., Bari, A. and Li, J, (2008) J. Geophysical Research., **113**, D13102, doi:10.1029/2007JD009398

[3] Birch, M.E., Cary, R.A., 1996. Aerosol Science and Technology, **25**, 221–241

Archaeal and bacterial tetraether lipids in carbonate chimneys of the Lost City Hydrothermal Field

SARA A. LINCOLN[1*], ALEXANDER S. BRADLEY[2], SHARON A. NEWMAN[1] AND ROGER E. SUMMONS[1]

[1]Massachusetts Institute of Technology, Earth, Atmospheric and Planetary Sciences, Cambridge, MA 02139 USA slincoln@mit.edu ([*]presenting author)

[2]Washington University in St. Louis, Earth & Planetary Sciences, St. Louis, MO 63130 USA

The Lost City Hydrothermal Field is a peridotite-hosted hydrothermal system near the mid-Atlantic ridge [1] with a rich microbial ecosystem. Microbes inhabiting carbonate chimneys are sustained by reducing fluids that contan methane and H_2 derived from serpentinization reactions. Extensive tag sequencing of archaeal communities in Lost City revealed diversity to be low: biofilms composed almost exclusively of *Methanosarcinales* are common in active chimneys, inactive chimneys contain ANME-1, and a phylotype similar to Marine Group I *Crenarchaeota* was detected in the active chimneys with the hightest fluid temperatures. Less abundant phylotypes include groups similar to the order *Thermoplasmatales* and Marine Benthic Groups 1-2 [2].

Organic geochemical investigations provide a time-integrated record, offering insight complementary to nucleic acid-based studies. Previous work focusing on diether membrane lipids common to *Methanosarcinales* found evidence for methanogenesis and carbon limitation at Lost City [3]. Here, we present data on membrane-spanning glycerol dialkyl glycerol tetraether (GDGT) lipids from six active and five inactive chimneys. Although the distribution of individual GDGTs is similar across sites, concentrations are higher in inactive chimneys where biomarkers record the cumulative history of microbial history over years of active venting and dormancy.

We detected three GDGTs not commonly reported in marine systems: an H-shaped isoprenoidal GDGT found in thermophilic archaea isolated from hydrothermal systems and two branched, non-isoprenoidal GDGTs. Branched GDGTs, attributed to bacteria and abundant in many soils, have been used as a proxy for the input of terrestrial organic matter to marine sediments (BIT index, [4]). Their presence at Lost City, together with that of other GDGTs, suggests that input of hydrothermal sediments may complicate paleoproxies based on tetraether lipid distributions. Large, non-systematic variations in both the BIT index and the sea surface temperature proxy TEX_{86} [5] were observed in Lost City samples.

Finally, we discuss the likely archaeal and bacterial source organisms of GDGTs at Lost City.

[1] Kelley *et al.* (2005) *Science* **307**, 1428–1434. [2] Brazelton *et al.* (2010) *P Natl Acad Sci USA* **107,** 1612-1617. [3] Bradley *et al.* (2009) *Geochim Cosmochim Ac* **73,** 102-118. [4] Hopmans *et al.* (2004) *Earth Planet Sc Lett* **224,** 107-116. [5] Schouten *et al.* (2002) *Earth Planet Sc Lett* **204,** 265-274.

https://doi.org/10.1180/S0026461X00008434 Published online by Cambridge University Press

Biogeochemistry of permeable reactive barriers for arsenic and selenium remediation

MATTHEW B.J. LINDSAY[1,2*], DAVID W. BLOWES[1], AND CAROL J. PTACEK[1]

[1]Earth and Environmental Sciences, University of Waterloo, Waterloo, ON, Canada, blowes@uwaterloo.ca, ptacek@uwaterloo.ca

[2]Present Address: Earth and Ocean Sciences, University of British Columbia, Vancouver, BC, Canada, mlindsay@eos.ubc.ca (*presenting author)

Introduction

Contamination of groundwater by arsenic (As) and selenium (Se) arises from the natural weathering of geologic materials, but can be exacerbated by mining activities. Column experiments were conducted to evaluate treatment of oxic groundwater containing As and Se using permeable reactive barriers (PRBs). Three columns were packed with varied mixtures of granular iron filings (GIF) from two separate suppliers (a and b), organic carbon (OC) and silica sand. An input solution containing 2 mg L^{-1} As(V) and 0.8 mg L^{-1} Se(VI) was passed through the 0.3 m long columns for 325 days.

ID	GIF-a	GIF-b	OC	Sand
C1	50			50
C2		50		50
C3	25		25	50

Table 1: Composition of columns given as volume percentages.

Water chemistry was monitored over time, and solid-phase samples were collected at the conclusion of the experiment. Reaction products were examined by field emission-scanning electron microscopy-energy dispersive spectroscopy (FE-SEM-EDS). Solid-phase As and Se speciation was investigated by X-ray absorption near edge structure (XANES) spectroscopy. Microbial ecology was assessed by tag encoded FLX amplicon pyrosequencing (TEFAP) of the bacterial 16S rRNA gene.

Results and Conclusions

Effective removal of As and Se was observed for all columns. Effluent concentrations of As and Se concentrations were generally < 2 μg L^{-1} for C1 and C2. Treatment improved over time for C3, with effluent As concentrations decreasing to < 2 μg L^{-1} after 120 days and Se concentrations remaining < 30 μg L^{-1} after this time. Examination by FE-SEM-EDS revealed the common presence of discrete As-bearing phases in C1 and C2. Results of XANES analysis indicate that As(V) and As(III) occurred in differing proportions within C1 and C2, whereas As predominantly exhibited a reduced oxidation state in C3. Solid-phase Se was consistently present in a reduced oxidation state in all columns. The microbial community within C3 exhibited the greatest phylogenetic and metabolic diversity. However, sulfate reducers were common to all columns, even in the absence of OC in C1 and C2. Results of this study demonstrate that As and Se removal by PRBs may result from various biogeochemical processes. Understanding these processes is critical for assessing long-term treatment performance and the potential stability of reaction products.

Crystal chemical constraints on element distribution in oxides

DONALD H. LINDSLEY,

Geosciences, Stony Brook University, Stony Brook, NY, USA

donald.lindsley@stonybrook.edu

Spinels

The oxide spinel structure, one of the first to be determined by x-ray diffraction, is based on a unit cell of 32 oxygens, which are (nearly) cubic-close-packed when viewed along the cube diagonals {1,2]. For stoichiometric spinels in the space group Fd3m, half the possible octahedral interstices (B) and one-quarter of the possible tetrahedral interstices (A) are occupied by cations, yielding the nominal formula AB_2O_4. Spinels may be normal or inverse, depending on whether the B cations are restricted to the octahedral sites or are split between the sites. The spinel structure is extraordinarily flexible; this stems from the fact that (1) the entire oxygen framework can expand *and* (2) the position of oxygens shared by tetrahedral and octahedral sites can shift along (111); the latter causes a puckering of the oxygen planes. This shift is measured by the **u** parameter, which ideally is 0.25, but can be either larger or smaller depending on the relative sizes of the tetrahedral and octahedral cations. The ideal spinel would contain cations having ionic radii of 0.0315 nm (tetrahedral) and 0.0575 nm (octahedral), but in fact at least 30 different caions, with valences ranging from +1 to +6 and ionic radii ranging from 0.026 to 0.103 nm, can form **major** components of spinels. As a great many trace elements have properties falling within these limits, the ability of spinels to host such elements is quite large.

Rhombohedral Oxides

The rhombohedral oxides, exemplified by hematite or corundum (A_2O_3) and ilmenite ABO_3, crystallize in space groups $R\bar{3}c$ and $R\bar{3}$ respectively. Oxygen forms planes parallel to (111) of the rhombohedral cell [(0001) of the equivalent hexagonal cell]; these planes are stacked in (nearly) hexagonal-close-packing, with 18 potential octahedral cation sites per 18 oxygens. Typically 2/3 of those sites are occupied by cations, most often as the couples 3^+-3^+ or 2^+-4^+ (as in hematite and ilmenite respectively). In hematite, oxygen layers alternate with cation layers, while in ilmenite the sequence of layers is O-Fe-O-Ti, thus leading to the lower symmetry. Again, however, at least 30 different cations with valences from +1 to +5, and ionic radii ranging from 0.039 to 0.095 nm (although the majority are 0.06-0.075) can form **major** components in the rhombohedral oxides. If the flexibility of the rhombohedral phases is not quite so great as that of spinels, their capacity to host many trace elements is still large.

Conclusions

In view of the great flexibility of the spinel and rhombohedral oxide structures, a more appropriate title for this abstract might well be "*Lack of* crystal chemical constraints..."

[1] Waychunas (1991) *Reviews in Mineralogy.* **Volume 25**, 11-68.
[2] Lindsley (1969) *Reviews in Mineralogy.* **Volume 3**, L1-L60.)

https://doi.org/10.1180/S0026461X00008434 Published online by Cambridge University Press

Constraints on the origins of adakites by using magnesium isotopes

MING-XING LING[1, 2*], FANG-ZHEN TENG[2], WEIDONG SUN[3]

[1]State Key Laboratory of Isotope Geochemistry, Guangzhou Institute of Geochemistry, CAS, Guangzhou 510640, P.R. China, mxling@gig.ac.cn (* presenting author)

[2]Isotope Laboratory, Department of Geosciences, University of Arkansas, Fayetteville, AR 72701, USA, fteng@uark.edu

[3]Key Laboratory of Mineralogy and Metallogeny, Guangzhou Institute of Geochemistry, CAS, Guangzhou 510640, P.R. China, weidongsun@gig.ac.cn

Adakite is a certain series of andesitic, dacitic and sodic rhyolitic rocks or their intrusive equivalents, with unique geochemical characteristics, e.g., $SiO_2 \geq 56$ wt%, $Al_2O_3 \geq 15$ wt%, Y≤18 ppm, Yb≤1.9 ppm and Sr≥400 ppm. It has attracted intensive attention because of its similar geochemical characteristics to Archaean tonalite-trodhjemite-granodiorite series (TTG) and its close association with many large porphyry copper-gold deposits. The genesis of adakites has been controversial, particularly on whether formed by partial melting of thickened/delaminated lower continental crust (LCC) or partial melting of subducting oceanic crust. A combination of major elements, trace elements and traditional isotopic systems was used to discrimate adakites formed by partial melting of subducting oceanic crust or LCC. However, traditional Sr-Nd-Pb isotopic composition can be easily altered by upper crust during magma ascent. By contrast, such processes cannot affect Mg isotopes significantly because the mantle has much higher Mg content than the crust. Magnesium isotopes may therefore shed light on the different origins of adakites.

In this study, Mg isotopic composition of a suite of adakites from three districts of central eastern China, the Lower Yangtze River belt (LYRB), the Dabie orogen and the Dexing porphyry deposits, were investigated to constrain their origins, e.g., slab melting or partial melting of thickened/delaminated LCC. The results indicate that adakites from the LYRB have relatively homogeneous mantle-like Mg isotopic composition, with δ^{26}Mg ranging from -0.366 ± 0.066 to -0.213 ± 0.078 (2SD). The adakites from the Dexing porphyry deposits have slightly scattered δ^{26}Mg from -0.340 ± 0.067 to -0.146 ± 0.068 (2SD), but with mantle-like average. By contrast, those from the Dabie orogen have heterogeneous Mg isotopic composition (δ^{26}Mg = -0.161 ± 0.065 to -0.059 ± 0.065, 2SD), slightly heavier than that of mantle (δ^{26}Mg = -0.25 ± 0.07). These distinct Mg isotopic compositions indicate different origins of these adakites, i.e., adakites form the LYRB and Dexing formed from slab melting whereas the adakites from the Dabie orogen presumably have contributions of the LCC components, consistent with previous studies [1,2]. Our studies suggest Mg isotopes may be a powerful tool for constraing the origins of adakites.

[1] Ling, M. X. *et al.* (2009) *Econ. Geol.* **104#**, 303-321.

[2] Ling, M. X. *et al.* (2011) *International Geology Review* **53#**, 727-740.

Radiotracer studies on the kinetics and equilibrium characteristics of adsorption of humic matter

HOLGER LIPPOLD[1*], JOHANNA LIPPMANN-PIPKE[1]

[1]Helmholtz-Zentrum Dresden-Rossendorf (HZDR), Institute of Resource Ecology, Germany, h.lippold@hzdr.de

Introduction

Humic substances are ubiquitous in near-surface natural waters, and they are known to act as carriers for organic and inorganic contaminants [1, 2]. In order to assess the impact of such humic-bound mobilization, transport models are developed (see [3] for a review). As a prerequisite, reaction rates for adsorption and desorption are commonly assumed to be high enough to ensure a steady local equilibrium under flow conditions. For humic matter as a polydisperse system of highly charged colloids, however, it is unclear whether a dynamic adsorption equilibrium (i.e., a permanent run of adsorption and desorption at equal rates) actually exists. Low recoveries in column experiments with geological materials suggest a limited reversibility.

Experimental

Using kaolinite as an adsorbent, the kinetics of adsorption and desorption were studied for a humic acid (Aldrich) and a fulvic acid (isolated from bog water). Their radiolabeling with ^{14}C (accomplished by azo coupling with [^{14}C]aniline) allowed sensitive detection and enabled tracer exchange experiments at surface saturation, providing direct insight into the dynamics of the adsorption equilibria for the first time. In these studies, a negligible amount of radiolabeled humic or fulvic acid was contacted with equilibrated systems of kaolinite and non-labeled humic material at different durations ranging from 6 hours to 4 weeks.

Results

The equilibrium state of adsorption was attained within few hours for the fulvic acid, whereas the process took considerably longer for the humic acid (~ 2 days), possibly as a consequence of competition effects within the polydisperse system [4]. In desorption experiments, initiated by diluting the supernatant, not any release was observed within a time frame of 4 weeks, neither for the humic acid nor for the fulvic acid. In view of transport modeling, this finding is rather disturbing since the basic assumptions do not hold if adsorption is irreversible. Our tracer exchange experiments, however, revealed that labeled humic material is adsorbed even though it is confronted with a saturated surface. Consequently, an exchange must take place, indicating a reversible process, albeit an exchange time of ~ 4 weeks was required for both materials until the adsorption equilibrium was quantitatively represented by the tracer. Apparently, the competitive situation in its presence is a stronger driving force for desorption than is a concentration gradient. Models for humic-bound transport are thus applicable under comparable conditions.

[1] MacKay & Gschwend (2001) *ES&T* **35**, 1320-1328. [2] Dearlove *et al.* (1991) *Radiochim. Acta* **52/53**, 83-89. [3] Lippold & Lippmann-Pipke (2009) *J. Contam. Hydrol.* **109**, 40-48. [4] Van de Weerd *et al.* (1999) *ES&T* **33**, 1675-1681.

https://doi.org/10.1180/S0026461X00008434 Published online by Cambridge University Press

Glacial Atlantic Circulation - Insights from combined sedimentary ε_{Nd} and $^{231}Pa/^{230}Th$ records

JOERG LIPPOLD[1*], MARCUS GUTJAHR[2], FRANK WOMBACHER[3], EMANUEL CHRISTNER[1], MARCUS CHRISTL[4]

[1]University of Heidelberg, Institute of Environmental Physics, joerg.lippold@iup.uni-heidelberg.de (* presenting author)
[2]National Oceanography Centre, Earth and Ocean Sciences, Southampton, UK, m.gutjahr@soton.ac.uk
[3]University of Cologne, Institute of Geosciences
[4]ETH Zurich, Institute of Particle Physics

In contrast to the modern situation, several proxies point to a very different structure of water mass distribution in the Atlantic Ocean during the Last Glacial. However, there is still no consensus about variations of the circulation strength and timing or causation of such changes.

Seawater-derived ^{231}Pa, ^{230}Th, and neodymium isotopes, extracted from marine sediments, are promising inorganic proxies to reconstruct the past deep Ocean hydrography and water mass export. $^{231}Pa/^{230}Th$ yield information about the rate of overturning circulation, whereas ε_{Nd} derived from ferromanganese coatings carries a water mass provenance signal.

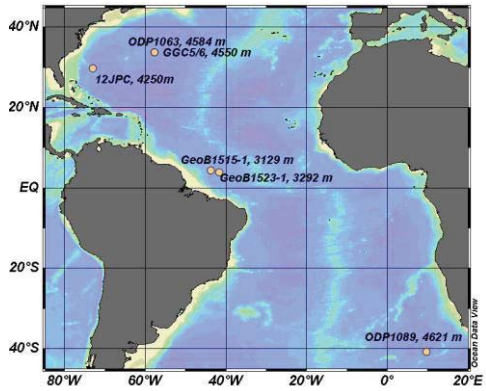

Fig.1: Locations of combined $^{231}Pa/^{230}Th$ and ε_{Nd} measurements.

First combined records of these tracers on the same sediment samples from the NW Atlantic (Bermuda Rise, ODP1063 and GGC5/6) vitally improved our knowledge about the timing of changes in past Ocean Circulation particularly with respect to centennial- to millennial-scale water column reorganisations [1,2]. We compare these earlier records to new North and South Atlantic core sites to better resolve basin-wide water column variations back to 30,000 years.

Our results show a general high level of concordance of both proxies. This is in agreement to former studies applying different circulation proxies [3,4,5], implying that both tracers indeed recorded invasion of Southern Source Water (high ε_{Nd}) during times of a weakened influence of North Atlantic Deep Water formation (high $^{231}Pa/^{230}Th$) in the Deep Atlantic Ocean.

[1] Roberts et al. (2010) Science **327**, 75. [2] Gutjahr and Lippold (2011) Paleoceanography **26,** Pa2101. [3] Curry and Oppo (2005) Paleoceanography **20,** Pa1017. [4] Lynch-Stieglitz et al. (2007) Science **316**, 66. [5] Praetorius et al. (2008) Nature Geoscience **1**, 449 – 452.

Highly Siderophile and Chalcophile element systematics in Mid-Ocean Ridge Basalts

MORITZ LISSNER[1*], AMBRE LUGUET[1] AND STEPHAN KÖNIG [1,2]

[1] Steinmann Institut für Mineralogie, Universität Bonn, Germany moritz.lissner@uni-bonn.de, ambre.luguet@uni-bonn.de, stephan.koenig@uni-bonn.de (* presenting author)
[2] Institut für Geologie und Mineralogie, Universität zu Köln, Germany

Highly Siderophile Elements (HSE: Os, Ir, Ru, Pt, Pd, Re) as well as chalcophile elements (S, Se, Te) are potential key tracers of large-scale planetary processes such as core formation and late veneer addition. Therefore their signatures and concentrations in the primitive upper mantle (PUM) should be estimated based on our understanding of their behaviour and signatures in the mantle rocks and in partial melts at both the whole-rock and host-minerals' scales.

While a relatively large database is available for HSE, data for S, Se and Te are scarce for MORBs and peridotites. Recent preliminary investigations in depleted peridotites [1] support an incompatible behaviour of both Se and Te during mantle melting, with Te being more incompatible. This is in agreement with experimental data on sulfides [2] but is not supported by the few MORB data available, which show similar Te concentration range than peridotites [3, 4]. Additionally, an increase of Se/Te ratios for decreasing Te concentrations is observed for a suite of peridotites as well as within replicate analyses on a single sample [1], revealing the strong control of heterogeneously-distributed micrometric Te-rich phases on the Se-Te systematics in mantle residues. Strikingly, similar Se/Te fractionations are also observed in available MORB data [3].

We will present a comprehensive HSE and S-Se-Te dataset for a large suite of MORB samples, in order to provide, in the light of S and HSE, further constrains on the behaviour of Se and Te during partial mantle melting. This dataset will contribute to the characterisation of the coupled chalcophile-highly siderophile elements signatures in the terrestrial silicate reservoirs.

[1] König et al. (2012) *GCA* **in press**. [2] Helmy et al. (2011) *GCA* **74**, 6174-6179. [3] Hertogen et al. (1980) *GCA* **44**, 2125-2143. [4] Yi et al. (2000) *JGR* **105 (B08)**, 18927-18948.

https://doi.org/10.1180/S0026461X00008434 Published online by Cambridge University Press

The isotopic mass balance of zinc in the oceans

S. H. LITTLE[1*], D. VANCE[1], D. M. SHERMAN[1], T. W. LYONS[2]

[1]Bristol Isotope Group, School of Earth Sciences, University of Bristol, Bristol, UK, s.little@bristol.ac.uk (*presenting author)
[2]Department of Earth Sciences, University of California, Riverside, USA, timothy.lyons@ucr.edu

Zinc isotopes represent a new tool that could track biological usage of trace metals in the ocean through time. Such an endeavour, however, must rest on a sound understanding of the biogeochemical cycling of zinc isotopes. Here we summarise this current understanding through analysis of the inputs and outputs of Zn to and from the modern ocean. The present Zn isotopic composition of the deep ocean is uniform, at ca. 0.5‰ for $\delta^{66/64}$Zn. This value is also an upper limit on the composition of the average whole ocean. Unlike some other transition metal isotopic systems studied so far, including Mo and Cu, this average value of δ^{66}Zn is similar to typical rock and detrital values (0.3‰) and to the principal sources of Zn to the oceans (including average global rivers = 0.33‰ [1], hydrothermal input = 0.24‰ [2], and dust ~0.2-0.4‰ [1,3]).

Both Mo and Cu isotopes are fractionated in seawater by preferential sorption of the light isotope onto Mn oxides in oxic settings. Ferromanganese crusts are isotopically light, and the imprint of their formation is stamped on the resulting heavy dissolved pool in seawater. Laboratory sorption experiments of Zn on δ-MnO_2 indicate that δ-MnO_2 also sorbs the light isotope of Zn, and an EXAFS study of three ferromanganese crusts indicates that Zn is associated with birnessite (δ-MnO_2) in these samples. This association with birnessite in nature, and the preferential uptake of the light isotope onto birnessite in experiments, are features that Zn shares with Cu and Mo. However, Zn isotope values from natural Fe-Mn crusts are uniformly heavier (at 0.7-1.2‰) than the deep ocean value. Either Zn is in a different crystal chemical environment on the oxide in experiment versus nature, or biology is, by an unknown mechanism, superimposed on Zn isotopes in crusts. In either case, the oxic sink for Zn, as sampled by Fe-Mn crusts, does not appear to significantly impact the average ocean isotopic composition. If anything, the isotope data for the inputs and for dissolved Zn in the deep ocean imply a total output that preferentially removes the light isotope. It is possible that the uptake of light isotopes into organic material [4] at least balances removal of the heavy isotope to Fe-Mn oxides.

The other key sink of redox sensitive elements is in anoxic settings, where, like Mo, Zn seems to undergo no isotopic fractionation on removal from seawater in to sediments. Data from the most Zn-enriched euxinic sediments of the Black Sea and Cariaco Basin give almost identical values to the deep ocean, of 0.5-0.6‰, whilst non-euxinic sediments from the margin of the Black Sea record the expected detrital value of 0.3‰. Hence the observed, small, difference between the input of Zn to the oceans and the average ocean isotopic composition is neatly replicated in these local anoxic-oxic settings.

[1] Brown, C. (2009) *MSci thesis, UoB*. [2] John, S.G. *et al*. (2008) *EPSL* **269** 17-28. [3] Maréchal, C.N. *et al*. (2000) G^3 **1** 1-15. [4] John, S.G. *et al*. (2007) *Limnol. Oceanogr*. **52**(6), 2710–2714.

Orbitally-paced oscillations in benthic $\delta^{18}O$ in the early Paleogene: Implications for variations in deep sea temperature and ice-volume

KATE LITTLER[1]; JAMES C. ZACHOS[1]; ALEXIS KERSEY[1]; URSULA RÖHL[2]; THOMAS WESTERHOLD[2]

[1]University of California, Santa Cruz, USA.
klittler@ucsc.edu (* presenting author); jzachos@ucsc.edu; akersey@ucsc.edu.
[2]MARUM, University of Bremen, Germany.
uroehl@marum.de; twesterhold@marum.de

Introduction

The early Paleogene is generally accepted to have been a warm greenhouse world, with relatively high pCO_2 levels and little evidence for large-scale ice-sheets. However, ample geochemical and palaeontological evidence exists for both sustained and transient fluctuations in global climate during this time, which are often coupled to significant changes in the carbon-cycle [1, 2, 3, 4, 5, 6]. Controversially, some oxygen-isotope and sequence-stratigraphic evidence has been put forward to suggest that continental ice-volumes were large enough to drive significant changes in global eustatic sea-level during the early Paleogene [7, 8]. If ice-sheets capable of affecting global sea-level did exist, presumably on Antarctica, one would expect two things to be observed in early Paleogene marine geochemical records; 1. The presence of significant variance in eccentricity and obliquity periods in high-resolution benthic oxygen-isotope records, as is commonly observed in the icehouse world of the Oligocene–Neogene; and 2. A distinct residual seawater oxygen-isotope signal (i.e., $\Delta\delta^{18}O_{SW}$) once the temperature contribution to the benthic foraminifer $\delta^{18}O$ signal is extracted by applying the Mg/Ca or some other paleothermometer.

Results and conclusions

Here we present benthic foraminiferal $\delta^{18}O$ data from the South Atlantic (Site 1262, Walvis Ridge), which show orbitally-paced cyclic variations during the Late Paleocene and Early Eocene. Spectral analysis of these records reveals a strong eccentricity pacing throughout the entire ~6 Myr record, but no significant power in the obliquity band, suggesting global ice volumes were too low to influence $\delta^{18}O_{SW}$ beyond the background noise. Additionally, ongoing Mg/Ca analysis of benthic species at Site 1262 demonstrates that there were changes in deep-water temperature associated with eccentricity-paced carbon cycle fluctuations in the Late Paleocene, concurrent with changes in the oxygen-isotope record. Furthermore, these Mg/Ca records allow absolute temperatures to be estimated for the deep water of the South Atlantic during the Late Paleocene, which may help to establish a baseline for pre-PETM climate.

[1]Kennett & Stott (1991) *Nature* **353**, 225–229. [2]Zachos *et al*., (2001) *Science* **292**, 686–693. [3]Cramer *et al*., (2003) *Paleoceanography* **18(4)**, 1097. [4]Tripati & Elderfield (2005) *Science*, **308**, 1894–1898. [5]Zachos *et al,* (2010) *EPSL* **299**, 242–249. [6] McInerney & Wing (2011) *Annu. Rev. Earth Planet. Sci.* **39**, 489–516. [7]Miller *et al*., (2005) *Marine Geology* **217**, 215–231. [8]Boulila *et al*., (2011) *Ear. Sci. Rev* **109**, 94–112.

https://doi.org/10.1180/S0026461X00008434 Published online by Cambridge University Press

Zircon U-Pb ages and O-Nd isotopic composition of the Qinling Group in North Qinling, central China

BING-XIANG LIU, FUKUN CHEN, WEI WANG, YUE QI, QUN LONG, JIA-DE WU

CAS Key Laboratory of Crust-Mantle Materials and Environments, School of Earth and Space Sciences, University of Science and Technology of China, Hefei, 230026, China

The Qinling Group exposed in the North Qinling orogenic belt, central China, has been interpreted as the oldest basement rocks of Precambrian in age and it records crustal formation and evolution of the North Qinling orogenic belt. However, previous studies have demonstrated different formation ages such as Paleoproterozoic, Mesoproterozoic, and Neoproterozoic for the Qinling Group. In this study, we present U-Pb ages and O isotopic data of zircons obtained on the same analytical spot by the SIMS technique and Nd isotopic composition of whole-rocks from two different types of metamorphic rocks collected from the Qinling Group in the eastern part of the North Qinling orogenic belt. They are felsic gneiss and amphibolite in composition and both are major components of the Qinling Group.

Zircons of a biotite plagioclase gneiss show clear oscillatory zoning of magmatic origin but with complex core-rim structures shown in cathodoluminescence (CL) images. The cores of zircons mostly yield U-Pb ages of ca. 930 Ma, suggesting a Neoproterozoic formation age of the Qinling Group. The rims give U-Pb ages of about 500 Ma, recording an Early Paleozoic metamorphic event. Zircon grains have $\delta^{18}O$ values of 6.5 to 9.3‰ and whole-rocks yield low initial ε_{Nd} values of about -20, suggesting an origin of crustal material for magma(s) of the precursors. Zircons of amphibolite samples do not have clear oscillatory zoning and the residual cores are irregular shown in CL images. The SIMS dating yields U-Pb ages clustering in two peaks of 850 Ma and 510 Ma, also recording the Neoproterozoic formation age and the Early Paleozoic metamorphism. Zircons $\delta^{18}O$ values cluster around the mantle value with an average of 5.3 ±0.1‰, implying that the parental magma was derived from a mantle source. Initial ε_{Nd} values of whole-rocks range from -13.9 to -10.0, showing significant contribution of crustal material.

In combination with previous geochronological data and the results reported here, it is proposed that the Qinling Group formed in early Neoproterozoic. This rock group is obviously composed of variable rocks of different formation ages. The North Qinling block underwent metamorphism in Early Paleozoic related to the North Qingling orogenic event along the southern margin the North China Craton. This study is supported by the Ministry of Science and Technology of China (grant No. 2012CB416606).

Sr isotope study of Marinoan Cap carbonates from southwestern Mongolia

CHAO LIU[1], FRANCIS MACDONALD[2], ZHENGRONG WANG[1]

[1]Yale University, New Haven, CT, USA, chao.liu@yale.edu, zhengrong.wang@yale.edu

[2] Harvard University, Boston, MA, USA, fmacdon@fas.harvard.edu

The basal Ediacaran (Marinoan) Ol cap carbonate rests above the second of two glacigenic horizons in the Tsagaan Oloom Formation of southerwestern Mongolia [1]. This cap-carbonates is composed of a basal buff-colored micro-peloidal dolostone with tubestone cements, and an upper lime-mudstone with peudomorphosed aragonite crystal fans in between. In this work, we studied the Sr isotope compositions of the cap-carbonate to understand the origin of Sr isotope variability in basal Ediacaran cap carbonates globally.

Forty cap carbonate samples from Ol member, Tsagaan Oloom formation in Mongolia, were analyzed for $^{87}Sr/^{86}Sr$. An incremental leaching technique using 1N ammonium acetate and various concerntrations of acetic acid and hydrocloric acid was applied to extract Sr from different phases in the cap-carbonates (including surface adsorbed Sr, calcite, dolomite and clay minerals). The leacheates were then passed through chromatographic columns and pure Sr was analyzed using MC-ICP-MS (Neptune) at Yale university.

Our results show that the lowest $^{87}Sr/^{86}Sr$ values among all leacheates from each sample span 0.7089-0.7092, which is higher than both the overlying carbonate crystal fans and limestones (0.7082-0.7087), the least-altered samples from the Tayshir member below Khongoryn diamictite [1,2], and the lowest $^{87}Sr/^{86}Sr$ values previously reported in global basal Ediacaran carbonates (~0.7075) [3]. Very small $^{87}Sr/^{86}Sr$ variation has been observed throughout the 6-meter cap-dolomite section and leachates from the carbonate portion of each sample, suggesting these dolostones are quite uniform in chemical compositions, consistant with sub-per mil variation in $\delta^{18}O$ (-7.2 ± 0.8 ‰) and $\delta^{13}C$ (-1.2± 0.7‰) of these samples. The relatively high, but uniform $^{87}Sr/^{86}Sr$ ratios in the Ol cap dolostones could be explained by high-degree alteration or dolomitization process involving local waterbody with more radiogenic $^{87}Sr/^{86}Sr$, implying Sr isotope compositions in these dolostones might not be suitable for chemostratigraphic correlation.

[1] Macdonald et al., (2009) *Geology* **37**, 123-126.
[2] Brasier et al., (1996), *Geological Magazine*, **133**, 445-485.
[3] Halverson et al., (2007) *PAELEO* **256**, 103-129.

https://doi.org/10.1180/S0026461X00008434 Published online by Cambridge University Press

Pore-scale Process Coupling and Apparent Surface Reaction Rates

CHONGXUAN LIU[1]*, CHANGYONG ZHANG[1], ZHI SHI[1], JIANYING SHANG[1], SEBASTIEN KERISIT[1], AND JOHN ZACHARA[1]

[1]Pacific Northwest National Laboratory, Fundamental and Computational Directorate, Chemistry and Material Sciences Division, Richland, WA 99354, USA. chongxuan.liu@pnnl.gov

Introduction

Surface reactions such as metal oxide dissolution, reduction, and surface complexation occur in coupling with transport processes at the pore scale in subsurface sediments. The transport processes provide reactants and remove reaction products for continuous reactions, while reactions change concentration gradients and porous media properties that affect subsequent transport processes. This presentation discusses how the pore-scale process coupling affects the manifestation of surface reaction rates at the grain and Darcy scales. Uranium silicate dissolution, uranyl surface complexation, and hematite reductive dissolution by quinone-type reductants will be used as examples to demonstrate the coupled effects of reactions with transport processes on the apparent reaction rates.

Results and Discussion

Microscopic characterization revealed that geochemical reactions of interest often occur in intragranular domains in subsurface sediments such as in intragranular fractures, pores, or grain coating porous regions where reaction rates are affected by intragranular diffusion and intergranular diffusion and advection. Uranium silicate dissolution and uranyl surface complexation are two examples of such reactions that have been found to control contaminant release and transport in US Department of Energy (DOE) Hanford site [1, 2]. Experimental and modelling results at various scales consistently showed that the apparent rates of both uranium silicate dissolution and uranyl surface complexation reactions decreased with increasing scale from a single phase, to the grain scale, and to the Darcy scale. Pore-scale simulations in intragranular and flow domains revealed that the scale-dependence of the apparent reaction rates can be explained from the pore-scale coupling of the reactions with transport processes. A micromodel with complex pore-networks with pore surfaces coated with hematite are used to rigorously investigate the pore-scale coupling of reactions, diffusion, and advection and its effects on the apparent reaction rates. The surface-coated hematite in the micromodel was reduced by quinone-type reductants to mimic microbial reduction of iron oxides in the intragranular domains through a biogenic electron shuttling process. Local scale measurements within the micromodel and effluent monitoring, as well as pore-scale simulations, are collectively used to explore the coupling effect of reactions with the transport processes. The presentation will also discuss challenges to scale reaction rates at different scales and discuss effective approaches to the scale the reaction rates that can be used in reactive transport modelling at the continuum scale.

[1] Liu et al. (2004), *Geochim. Cosmochim. Acta*, 68, 4519-4537.
[2] MicKinley et al. (2007), Geochim. Cosmochim. Acta, 71, 305-325.

Age structure of lithospheric mantle beneath southeastern (SE) China

CHUAN-ZHOU LIU[1,*], FU-YUAN WU[1], JING SUN[1]

[1]Institute of Geology and Geophysics, Chinese Academy of Sciences, chzliu@mail.iggcas.ac.cn (* Presenting author)

Cenozoic basalts are widespread in southeastern China and commonly contain abundant deep-seated mantle xenoliths. In this study, we report the Re-Os isotope compositions of Cenozoic mantle xenoliths from two localities (Xinchang and Mingxi) to reveal the age structure of the lithospehric mantle beneath SE China. Twelve Xinchang mantle xenoliths have been analyzed, including two spinel lherzolites, seven spinel harzburgites and three garnet lherzolites. The relatively refractory spinel harzburgites contain 0.95-1.73% Al_2O_3, and 0.65-1.49% CaO. They have $^{187}Re/^{188}Os$ ratios ranging from 0.01 to 0.06 and $^{187}Os/^{188}Os$ ratios varying from 0.11999 to 0.12258, giving rehenium depletion ages (T_{RD}), relative to the primitive upper mantle, of 0.99-1.35 Ga and model ages (T_{MA}) of 1.09-1.48 Ga. In contrast, the fertile spinel- and garnet-lherzolites have higher Al_2O_3 contents (2.4-5.43%) and more radiogenic $^{187}Os/^{188}Os$ (0.12424-0.12801), which yield T_{RD} of 0.22-0.75 Ga.

The studied twenty-six Mingxi mantle xenoliths include eight spinel lherzolites, eight spinel harzburgites, nine garnet lherzolites and one garnet harzburgite. The spinel lherzolites have Al_2O_3 contents of 1.89-4.46%, whereas spinel harzburgites have lower Al_2O_3 contents (0.83-1.41%). The garnet lherzolites have Al_2O_3 contents of 1.41-3.59%, whereas the only garnet harzburgite contains 0.83% Al_2O_3. The spinel harzburgites display $^{187}Os/^{188}Os$ ratios ranging from 0.11685 to 0.12197, giving T_{RD} ages of 1.08-1.97 Ga. The $^{187}Os/^{188}Os$ ratios of the spinel lherzolites (0.11889-.13037) are more radiogenic than the spinel harzburgites, which yield T_{RD} ages ranging from 1.51 Ga to modern age. The garnet lherzolites have $^{187}Os/^{188}Os$ ratios of 0.12313-0.12733 and T_{RD} ages of 0.33-0.96 Ga. In contrast, the garnet harzburgite has a depleted $^{187}Os/^{188}Os$ ratio of 0.11737 and an old T_{RD} age of 1.72 Ga.

Our results show that spinel harzburgites from both localities have Proterozoic T_{RD} ages, which supports the existence of the Proterozoic mantle relics in the shallow depths beneath SE China. The garnet harzburgites and some garnet lherzolites from Mingxi also have unradiogenic $^{187}Os/^{188}Os$ ratios and ancient T_{RD} ages. This suggests that the ancient lithospheric mantle relic beenath Mingxi is thicker than that beneath Xinchang. In contrast, most spinel- and garnet-lherzolites from both localities have Os isotope compositions indistinguishable from the modern convecting upper mantle [1], representing the juvenile accretion of asthenospheric mantle in SE China. The juvenile mantle accretion in SE China could be accompanied with the lithospehric extension in this region since the Mesozoic [2].

[1] Liu *et al.* (2008) *Nature* **452**, 311-316; [2] Liu *et al.* (2012) *Chem. Geol.* **291**, 186-198.

https://doi.org/10.1180/S0026461X00008434 Published online by Cambridge University Press

Molecular Dynamics Calculation of the Calcite Zeta Potential in Brine

HONGYI LIU[1,2*] AND LAWRENCE M. CATHLES[2]

[1]The KAUST-Cornell Center for Energy and Sustainability, Cornell Unviersity, Ithaca, NY, U.S.A., hl373@cornell.edu (* presenting author) ,

[2]The Department of Earth and Atmospheric Science, Cornell Unviersity, Ithaca, NY, U.S.A., lmc19@cornell.edu

Introduction

The surface charge on minerals in an aqueous enironment can affect rock strength, oil-particle adhesion, and other properties. The surface charge originates from defects in the minerals, but the charge that often counts is the electrostatic potential (zeta potential) at the distance from the mineral surface at the which the aqueous fluid becomes mobile. Here we use molecular dynamic (MD) methods to calculate the zeta potental adjacent to a calcite surface emersed in water of diffirent salinities.

Our forcefield for calcite is from a 2010 publication where MD methods successfully simulated the growth of calcium carbonate [1]. The brine solution is placed between a pair of planar numerical (1 0 4) calcite surfaces. We set the surface charge by removing Ca^{2+} or CO_3^{2-} ions from the top layer of the calcite crystal, and then calculate the electrostatic potential from the outer edge (symmetry boundary) of the calcite. The slipping plane is determined by inducing fluid flow with a gravity force and noting where the fluid movement starts. The electrostatic potential is shown as a function of distance from the calcite surface in Figure 1.

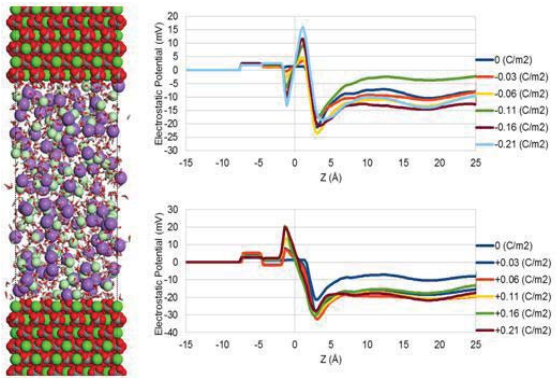

Figure 1: (a) The molecular calcite-brine sandwich (Ca: green, O: red, C: gray, Na: violet, Cl: aqua, and H_2O: red sticks). (b) The electrostatic potential of negatively charged surfaces and (c) postively charged surfaces. Z=0 marks the average VDW surface of the lower calcite layer.

Results and Conclusion

The vacancies where Ca^{2+} ions were removed are mostly ocuppied by sodium ions, while those where carbonate CO_3^{2-} ions were removed are occupied by Cl^- and Na^+ ions. The slipping plane lies about 5Å from the calcite surface (z=0 on plot). The plot shows that the sign of the zeta potential is negative whether the surface charge is positive or negative and ranges from -10 to -25 mV. If this holds true for other minerals it could help explain why the zeta potential of minerals tends to be negative.

[1] Raiteri, *et al.* (2010) *J.A.C.S* **132**, 17623-17634.

Characterization of various biochars used for mercury treatment and assessment of their potential to release soluble components

PENG LIU[1*], CAROL J. PTACEK[1], DAVID W. BLOWES[1], WILLIAM R. BERTI[2], AND RICHARD C. LANDIS[2]

[1] University of Waterloo, Department of Earth and Environmental Sciences, p26liu@uwaterloo.ca (* presenting author)

[2] E. I. du Pont de Nemours and Company, Wilmington, DE, USA,

21b. Soil and sediment remediation

Biochars (BCs), waste organic matter pyrolyzed under low temperature and oxygen conditions, have attracted great interest in environmental remediation processes [1]. However, few studies have focused on the characterization of BC prepared from a range of sources and their potential to release soluble components. In this study, eight groups of BCs produced from different materials at 300 °C and 600 °C, one group of charcoals (CL), and one group of activated carbon (AC) as a control were characterized for physical and chemical properties. Batch tests were conducted by adding BCs at a 1:75 mass ratio to river water (10 μg L^{-1} Hg). The experiments were sampled after two days to evaluate both the reduction of Hg and increase of soluble constituents in the river water. In the batch systems containing AC, CL and BCs pyrolyzed at 600 °C, concentrations of Hg were observed to decrease by >90%. In the systems containing the other BCs, concentrations of Hg decreased by 40-90%. The BCs with the highest Hg removals had relatively high specific surface areas, C and S contents, which likely contributed to Hg removal. Results obtained from FT-IR showed all BCs had hydroxyl, carboxylic and quinone functional groups, which also likely contributed to the Hg removal; the spectra of BCs prepared at 600 °C had fewer peaks compared to BCs pyrolyzed at 300 °C. Batch test results indicated that river water equilibrated with BCs prepared at 600 °C had higher pH and alkalinity and released more PO_4-P and NH_4-P than those prepared at 300 °C; however, BCs prepared at 300 °C released higher concentrations of dissolved organic carbon (DOC), short chain organic acids, NO_3^-, NO_2^-, and SO_4^{2-}, which were consistent with the FT-IR results. Biochars are promising reactive media to treat Hg contaminated waters and sediments; however, some BCs released DOC, sulfate, and organic acids, which could be utilized by methylating microbes to stimulate Hg methylation. Therefore further research needs to be performed to evaluate long term effect of the leached constituents from BCs amendments.

Results and Conclusion

Mercury concentration decreased by 40-99% in river water after two days of biochar amendment. Biochars pyrolyzed at different temperatures showed different chemical and physical properties.

Biochars are promising reactive media to treat Hg contaminated waters and sediments; however, further research still needs to be performed to evaluate long term effect of the leached constituents from BCs amendments.

[1] Lehmann (2009). *Biochar for Environmental Management: Science and Technology*. Earthscan, London & Sterling, VA.

https://doi.org/10.1180/S0026461X00008434 Published online by Cambridge University Press

Trace element of titanomagnetite in layered mafic-ultramafic intrusions: implications for oxide ore genesis

PINGPING LIU[1*], MEI-FU ZHOU[2] JIANFENG GAO[3], AND CHRISTINA YAN WANG[4]

[1] The University of Hong Kong, Earth Seicences, Hong Kong, China, liupp@hku.hk (* presenting author)
[2] The University of Hong Kong, Earth Seicences, Hong Kong, China, mfzhou@hkucc.hku.hk
[3] The University of Hong Kong, Earth Seicences, Hong Kong, China, gao_jianfeng@yahoo.com
[4] Guangzhou Institute of Geochemistry, Chinese Academy of Sciences, Guangzhou, China,wang_yan@gig.ac.cn

Titanomagnetite has always been considered as a late crystallizing phase from basaltic magma. Precipitation of titanomagmetite is usually initiated after a lengthy period of fractionation of olivine and plagioclase, which has been proved to increase both the Fe content and the oxygen fugacity of the evolving magma [1]. However, early saturation of Fe-Ti oxides was proposed because of the occurrence of abundant Fe-Ti oxide inclusions in olivine and plagioclase [2]. In this study, we carefully examine the distribution, microtexture and chemical composition of Fe-Ti oxide minerals of Baima Fe-Ti oxide deposit in Emeishan Large Igneous Province, Southwest China. Titanomagnetite occurs as interstitial phase coexisting with a minimum amount of sulfides (Fig. 1a), or as droplet enclosed in olivine with/without other mineral assemblage (Fig. 1b, c). The major element compositions of titanomagnetite determined by electonic microprobe are highly variable, partially due to the extensive exsolution of ilmenite and spinel. Trace elements, including Ti, Zn, Cr, V, Mg, and Ni, are dertermined using in situ LA-ICP-MS. These datsets are compared with those of bulk compositions of oxide separates. From this study, the evolution stage of differentiation of titanomagnetite is revealed [3]. Combining with petrography of the oxide ores, the new dataset indicates that titanomagnetite formed from immiscible Fe-Ti-(P) melts in silicate magmas. From these immiscible melts, sulphur was saturated, resulting in the formation of sulfide blebs in oxide ores.

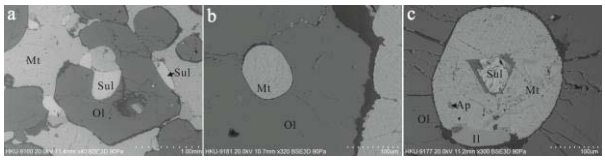

Figure 1: Titanomagnetite occurring as net-textured mass (a) or inclusions in olivine (b, c). Sul-sulfide, Mt-titanomagnetite, Ol-olivine, Ap-apatite, Il-ilmenite.

[1] Reynolds (1985) *Econ. Geol.* **80**, 1089-1108. [2] Pang (2008) *CMP* **156**, 307-321. [3] Duchesne (1999) Miner Depos 34, 182-198.

Theoretical calculations of equilibrium clumped isotope signatures beyond harmonic approximations

QI LIU, XINYA YIN AND YUN LIU*

State Key Laboratory of Ore Deposit Geochemistry, Institute of Geochemistry, Chinese Academy of Sciences, Guiyang, China, liuyun@vip.gyig.ac.cn (* corresponding author)

Clumped isotope geochemistry studies isotope distribution of isotopologues containing more than one rare isotope which could provide unique information such as formation temperatures of geological events. The measurement of clumped isotope signatures in laboratory needs calibration between observed isotopic data and formation temperatures in order to take account isotope fractionations in experimental procedures. One method of calibration is to measure the clumped isotope signatures of temperature-known materials to scale the temperature curve made of experimental data. Theoretical calculation using quantum chemistry methods could also become a powerful tool to study clumped isotope signatures. However, the precision required for clumped isotope calculation is very high. Theoretical treatments beyond harmonic approximations are therefore highly recommended.

In this study, theoretical treatments beyond the harmonic level by including several higher-order corrections to the Bigeleisen-Mayer equation are used to predict accurate Δ_i and Δ_{mass} results for ^{13}C-^{18}O and ^{13}C-^{2}H (or ^{13}C-D) clumps in carbonates and organic compounds. The details of these higher-order corrections can be found in [1]. Our preliminary results suggest significant improvement on the calculation of ^{13}C-D clumped isotope fractionations.

[1] Liu et al. (2010) *Geochim. Cosmochim. Acta* **74**, 6965-6983.

https://doi.org/10.1180/S0026461X00008434 Published online by Cambridge University Press

Study on the Effects between Soil Trace Elements and Apple-Pear Quality

Q.LIU[1*], D.Y.WANG[1], Y. Y.YANG[1], Y. SHANG[2] AND Q.FU[1]

[1] Jilin University, College of Earth Sciences, Changchun, China, 26246117@qq.com*, wang_dy@jlu.edu.cn, yangyuan52415241@163.com, fly19881118@yahoo.com.cn

[2] Land Surveying and Mapping Institute of Shandong Province, Jinan, China, rulyshang@yahoo.com.cn

Introduction

With a wide range of fertilizer applications in agriculture, soil trace elements are paid more and more attention in improving crop yields, especially in terms of the quality of agricultural products.

Material, Method, Results and Discussion

This study, for the first time, systematically analyzes and tests the 40 surface soil sample in the apple-pear growing areas of the total elements of Cu, Zn, B, Mo, Mn , the available elements and the corresponding quality indicators in the apple-pear samples of total sugars, total acid , soluble solids , water content and hardness in Yanbian area, Jilin (NE China). Correlation analyses are done by SPSS, calculated the correlation coefficient among the total elements of soil trace elements, the available elements and the quality indicators of the apple-pear respectively. The results show that the total sugar content of apple-pear and the total elements of soil trace elements Mn, Mo have extremely remarkable positive correlations, with the total elements of Cu, Zn exhibiting significant positive correlations, with the available Mn, Mo showing significant positive correlations. Total acid only have significantly negative correlations with the available Zn. Soluble solids, the total elements of Zn, Mn, Mo and the available Mo show extremely remarkable positive correlations, with the total elements of Cu, B having significant positive correlations. Water content and the total elements of Zn exhibit extremely remarkable negative correlations; the total elements of Cu, Mn and the available Mo show significant negative correlations. Hardness, the total elements of Mo and the available Mn, Mo indicate extremely significant negative correlations, with the total elements of Cu, Zn, Mn and the available Zn having significant negative correlations.

Conclusion

Taken together, the above analysis shows that the soil trace elements have the negative and the positive effects on the apple-pear and effects are remarkable. Therefore, it will make an important sense to combine the characteristics of the soil trace elements and fruit quality. The improving of the quality of agricultural products, reasonable landing using and scientific products program planning are of great significance.

Microscopic structures and acid chemistry of interfaces between phyllosilicates edges and water

XIANDONG LIU[1*], XIANCAI LU[1], EVERT JAN MEIJER[2], RUCHENG WANG[1], HUIQUN ZHOU[1]

[1]State Key Laboratory for Mineral Deposits Research (Nanjing University), School of Earth Sciences and Engineering, Nanjing University, Nanjing 210093, P. R. China

[2]Van't Hoff Institute for Molecular Sciences and Amsterdam Center for Multiscale Modeling University of Amsterdam, Nieuwe Achtergracht 166, 1018 WV Amsterdam, The Netherlands

xiandongliu@nju.edu.cn (* presenting author)

Theme 18 Frontiers in Computational Geochemistry

Knowledge on phyllosilicates (2:1- and 1:1-type)–water interfaces is critical for both understanding natural processes and guiding development of advanced hybrid materials. Due to the layered structures, their surfaces can be grouped into basal surfaces and edge surfaces (i.e. broken surfaces). Compared to basal surfaces whose properties have been well realized, chemical properties of edge surfaces are much more subtle and therefore are impossible to reveal by experimenting or force field based simulations.

With FPMD (first principles molecular dynamics) and free-energy calculation techniques [1~3], we investigated the structures and acid chemistry of these complicated interfaces [4, 5]. According to systematic simulations, the following has been achieved. (1) Through investigating the leaving processes of coordinated waters of edge cations, interfacial hydration states are revealed and thus the topologies are pictured (see Fig. 1 for 2:1-type) (2) Interfacial acidic sites have been figured out with detailed analyses of H-bonding networks. (3) Acidity constants of those acidic sites are derived by free-energy calculations for proton transfer reactions.

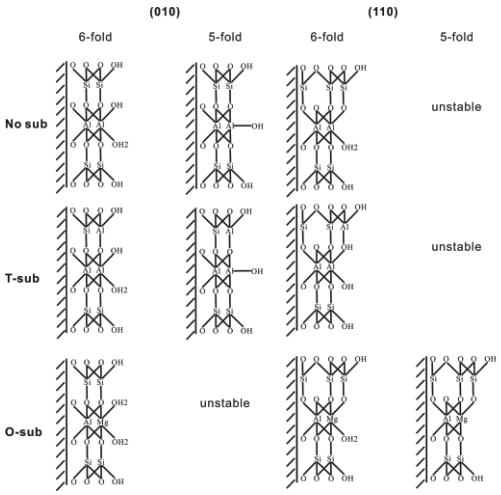

Figure 1: Topologies of edge surfaces of 2:1-type phyllosilicates.

[1] Car &Parrinello (1985) *PRL* **55**, 2471-2474. [2] Sprik (1998) *Far. Dis.* **110**, 437-445. [3] Sulpizi & Sprik (2008) *PCCP* **10**, 5238-5249. [4] Liu et al. (2011) *GCA* **75**, 4978-4986. [5] Liu et al. (2012) *GCA* **81**, 56-68.

https://doi.org/10.1180/S0026461X00008434 Published online by Cambridge University Press

FLUID ACTIVITY AND PARTIAL MELTING IN THE EVOLUTION OF UHP ROCK: EVDIENCES FROM ZIRCON U-PB AGE AND HF-O ISOTOPES

XIAOCHI LIU[1], YUANBAO WU[1*], AND JOHN M. HANCHAR[2]
[1]Faculty of Earth Sciences, China University of Geosciences, Wuhan, China, liuchicug@163.com; yuanbaowu@cug.edu.cn (* presenting author)
[2]Department of Earth Sciences, Memorial University of Newfoundland, St. Johns, Canada, jhanchar@mun.ca

In subduction- or collision-related metamorphism, fluid activity and partial melting occur at different stages and play key roles in many geological processes including metasomatism, crustal rheology, anatexis, resetting of isotopic clocks, transformation of mineral assemblages, and the creation and preservation of high-pressure (HP) and ultrahigh-pressure (UHP) rocks. The timing and features of fluid activity and partial melting, however, are quite difficult to constrain. In this study, in situ U–Pb geochronology, O and Hf isotopes in zircon have been done on a retrograde eclogite, a quartz vein and a leucosome vein enclosed in the eclogite and a country rock gneiss from the Xitieshan UHP terrane in the North Qaidam metamorphic belt, northwest China. Zircon from the quartz vein was dated at 438.0 ± 11 Ma and is consistent with the timing of peak UHP metamorphism in this region. This demonstrates that there was fluid activity during the peak UHP metamorphism. The homogeneous, bright in cathodoluminescence, zircon cores in the quartz vein contain O and Hf isotope compositions similar to the zircon in the eclogite, indicating that the zircon cores of quartz vein may be related to, or possibly derived from, the eclogite. In contrast, the oscillatory-zoned rims in the zircon crystals in the quartz vein have O and Hf isotope compositions consistent with the country rock gneiss sample. Most zircons from the leucosome vein have oscillatory zoning or wholly caliginous homogeneous in cathodoluminescence. The zircon U–Pb age of the leucosome vein is 419.6 ± 3.9 Ma, which can be regarded as the timing of extensive partial melting of the Xitieshan UHP rocks. The O and Hf isotope composition of the leucosome vein zircon is also consistent with the country rock gneiss. Therefore, the O and Hf isotopes in both the zircon rims of quartz vein and the zircons in leucosome vein are compatible with their origins from the surrounding felsic gneiss. The metamorphic zircon cores grew in the presence of fluids during the peak UHP metamorphism, whereas the younger zircon grew during partial melting of the surrounding gneiss during exhumation following granulite-facies metamorphism. This suggests that the fluid flow at the peak conditions might induce a low-degree of partial melting of the subducted slab and promote the initiation exhumation of the continental crust.

Tracing continental weathering using Li and Mg isotopes:

Insights from rivers draining the Columbia River Basalts

XIAO-MING LIU[1*], ROBERTA L. RUDNICK[1], WILLIAM F. MCDONOUGH[1], AND FANG-ZHEN TENG[2]
[1]University of Maryland, College Park, MD, USA, xliu1235@umd.edu (* presenting author), rudnick@umd.edu, & mcdonoug@umd.edu
[2]University of Askansas, Fayetteville, AR, USA, fzteng@uark.edu

Chemical weathering may have an important influence on continental crust evolution, as weathering of basalt removes Mg and can shift the crust composition towards more andesitic compositions, thus helping to solve the crustal composition paradox [e.g., 1]. We are exploring the use of soluble elements like lithium and magnesium, and their isotopes, to monitor chemical weathering of the continents. These elements are preferentially transfered to the rivers during weathering, coupled with large isotopic fractionations [e.g., 2], and therefore could be useful tracers of weathering processes. Here, we report chemical and isotopic analyses of small rivers and streams whose catchments lie entirely within the Columbia River Basalts in order to understand the processes associated with basalt weathering.

Soluble elements, such as Na, Mg and Ca are positively correlated with TDS (Total Dissolved Solids) in the rivers. The river water chemistry (e.g., Mg/Na vs. Ca/Na) reveals that more than 95% of the dissolved load comes from silicate weathering, consistent with the lithology of the catchments (basalt). There are large variations in the lithium isotopic composition of the river waters (δ^7Li varies from +9 to +30) and a negative correlation between δ^7Li and normalized Li concentration in the dissolved load, which likely marks the influence of two weathering regimes on river chemistry: incipient weathering (generating large isotopic fractionation, δ^7Li up to +30) vs. advanced weathering (with less significant isotopic fractionation, δ^7Li is around +10). This trend is opposite to that found in a previous study from rivers draining a multi-lithology basin [3]. Nonetheless, combined δ^7Li and normalized Li concentration may be a good tracer of weathering intensity. By contrast, the magnesium isotopic signature in river waters does not display an obvious difference between these two weathering regimes, which may due to the influence of additional factors, such as different isotopic fractionation associated with various secondary mineral formation, as well as biological activity on the Mg isotope signatures. Nonetheless, river waters have isotopically light δ^{26}Mg (varying from -0.8 to -0.2) relative to the basalts (-0.2 ± 0.1), consistent with equilibrium isotopic fractionation between water and regolith.

[1] Liu and Rudnick (2011) *Proceedings of National Academy of Sciences* **108**, 20873-20880. [2] Teng et al. (2010) *Earth and Planetary Science Letters* **300**, 63-71. [3] Millot et al. (2010) *Geochimica et Cosmochimica Acta* **74**, 3897-3912.

https://doi.org/10.1180/S0026461X00008434 Published online by Cambridge University Press

Characterization of EPS fractions before and after adsorption to goethite

X. LIU[1], K. EUSTERHUES*[1], J. THIEME[2], C. HÖSCHEN[3], CARSTEN W. MÜLLER[3], I. KÖGEL-KNABNER[3], K.U. TOTSCHE[1]

[1]Institut für Geowissenschaften, Friedrich-Schiller-Universität Jena, Germany (*correspondence: karin.eusterhues@uni-jena.de)
[2]NSLS-II, Brookhaven National Laboratory, Upton, NY, USA
[3]Lehrstuhl für Bodenkunde, Technische Universität München, Germany

Extracellular polymeric substances (EPS) are produced by many different microorganisms and are crucial for their initial attachment to solid surfaces. They consist of a mixture of polysaccharides, proteins, lipids and nucleic acids, i.e. of compounds, which are known to be easy degradable. In soils however, microbial-derived polysaccharides seem to be effectively stabilized against degradation when adsorbed to minerals. We therefore assume that EPS may be a long-term stable and significant component of organic coatings on soil minerals. This is of environmental concern as the coverage of mineral surfaces by EPS will completely change interface properties such as solubility, charge, and hydrophobicity.

We performed batch adsorption experiments using EPS extracted from liquid cultures of *Bacillus subtilis* and goethite. The pure EPS and the EPS covered goethites were characterized by atomic force microscopy (AFM), Fourier-transform infrared spectroscopy (FTIR), scanning transmission X-ray microscopy (STXM) and high-lateral-resolution secondary ion mass spectrometry (NanoSIMS). The original EPS was found to be spatially separated into three fractions which differ in their content of polysaccharides, proteins and aromatic groups. During reaction with goethite, we observed the formation of an additional fraction, rich in lipids and proteins, which is preferentially adsorbed. Polysaccharides, in contrast, remained in solution. NanoSIMS allowed to map the spatial distribution of C, P, N, and S. Phosporous was homogenously distributed throughout the whole EPS, whereas N was only found where EPS was in close association with goethite. Sulfur was enriched in some patches (~ 500 nm in diameter) of the goethite associated EPS.

We conclude, that mainly proteins and lipids, i.e., the EPS components which preferentially adsorb to goethite will be stabilized against biodegradation. Likewise, mainly these components, will change the surface properties and hence the reactivity of goethite.

Acidophilic Population Succession in Pilot Uranium Bioleaching Process

LIU YAJIE[1,2], LI JIANG[2], XU WEIYUN[2], D.B.JOHNSON[3], KEVIN HALLBERG[3], WANG XUEGANG[2], SUN ZHANSUE[2], LIU JINHUI[2], XU LINGLING[2], LIU JIANGSHE[1*]

[1] School of Envrionmental Science and Engineering, Donghua University, Shanghai, China. 201620 (*Correspondence: liujianshe@dhu.edu.cn)
[2] Department of Water Resources and Environmental Engineering, East China Institute of Technology, Fuzhou, Jiangxi Province, China. 344000 (yjliu@ecit.cn, lij@ecit.cn, wyxu@ecit.cn, xgwang@ecit.cn, zhxsun@ecit.cn, liujh@ecit.cn, llxu@ecit.cn)(*presenting author)
[3] *College of Natural SciencesBangor University, LL57 2UW, Wales, U.K.(d.b.johnson@bangor.ac.uk)*

Microorganisms community changes and develops with its environment. In uranium bioleaching, acidophilies especially some chemolithotrophic play an important role as well as some heterotrophic and mixtrophic acidophiles[1]. This paper investigated the acidophilic community successions by double layer solid plate and molecular methods such as t-RFLP, RFLP and Gene Clone Library methods.

Two different type minerals for bioleaching were set up as a 5000-ton heap and a 3-ton column, respectively. The main uranium mineral was pitchblende and the average uranium content was 0.021% and 0.290%, respectively. 9 mineral samples were taken from the bioleaching heap or column sites during the process of bioleaching, meanwhile, the chemical parameters such as pH value, Eh value, Ferric ion, total iron and uranium IV concentration of PLS before and after the samples were analysis. After 120 days and 116 days, the uranium extraction rate were reached to 55.92% and 90.20%, respectively. Results showed that the predominant bacteria of the 5000-ton heap were *At. thiooxidans, L. ferriphilum, Sulfobacillus thermotolerans*, *L. Ferrodiazotrophum*, *At. caldus* and *Acidocella sp.* and of the 3-ton column were *At. thiooxidans, L. ferriphilum, L. Ferrodiazotrophum*. It confirmed that *L. ferriphilum* always an active and predominant species in our laboratory and so did in the column, but not in the waste rock heap. It concluded that the bacterial population of the column bio-leaching was less influenced by the natural acidophilic bacteria, while in the 5000-ton heap, the bacteral population was highly influenced by the natural ones. More over, the population succession was evident with the temperature and bioprocessing.

ACKNOWLEDGEMENT

Thanks for the supports of Jiangxi Provincial Department of Education Project (GJJ08309) , National Natrual Science Foudation (50974043) and Ministry of Science and Technology Project (2012CB723101) .

REFRENCES

[1]D.BarrieJohnson(1998) *FEMS MicrobiologyEcology*, 27, 307-317.

https://doi.org/10.1180/S0026461X00008434 Published online by Cambridge University Press

MSS-sulfide melt partitioning of PGE and semi metal at controlled f_{o2}-f_{s2} conditions

YANAN LIU[1] AND JAMES BRENAN[1]

[1]University of Toronto, Geology
liu@geology.utoronto.ca (* presenting author)
j.brenan@utoronto.ca

Field evidence indicates that phases rich in the semi metals (As, Se, Sb, Te and Bi) may sequester significant amounts of Platinum Group Elements (PGE) relative to base metal sulfide at the magmatic stage [1,2]. To better understand the role of the semi metals on affecting PGE distribution within magmatic sulfides, a series of partitioning experiments have been conducted between Monosulfide Solid Solution (MSS) and sulfide melt at f_{o2}-f_{s2} close to natural conditions.

All the partitioning experiments were carried out in evacuated silica tubes, with Fe-Ni-Cu-S mixtures pre-melted and doped with approximately 80 ppm each of PGEs and semi metals. The oxygen fugacity was buffered by Fayalite-Magnetite-Quartz (FMQ), and the sulfur fugacity was calculated from the composition of the coexisting pyrrhotite. The correlation between sulfur fugacity and pyrrhotite composition [3] was independently calibrated at different sulfur buffers (Ru-RuS_2, Pt-PtS and Ir_2S_3-IrS_2), using a freshly synthesized FeS microprobe standard. The PGE partitioning experiments were conducted at 900 °C, 915 °C and 930 °C, while the semi metal doped runs at 915 °C, 900 °C and 885 °C. A comparison experiment was also conducted with all the PGE and semi meal dopants at 900 °C to test the effect of semi metals on PGE partitioning. The duration of experiments was 3-7 days.

Results indicate that the MSS/melt partition coefficient (D) of these semi metals are all less than one, with the relative order of compatibility: Se>As>Te>Sb≥Bi. There is a linear decrease in logD for the semi metals with their increasing covalent radius. These partition coefficients are not sensitive to variations in temperature, oxygen fugacity, or sulfur fugacity within the range of experimental conditions. Yet for any given semi metal element (except Se), the partition coefficient exhibits a weak dependence on the cation / anion ratio of the residual sulfide melt. D values for the PGEs remained unchanged by the addition of semi metals. These data imply that the crystallization of MSS can potentially lead to semi metal enriched residual liquid, resulting in the formation of immiscible semi metal rich melt or discrete semi metal rich Platinum Group Minerals (PGM). Thus the semi metal PGMs at Sudbury Ontario (tellurides and bismuthides being the most common ones, associated with late-stage low sulfur and haloes-bearing liquid around massive sulfide bodies [4]) could as well be produced by extreme fractionation of sulfide melt.

[1] Gervilla et al. (1996) *Can. Mineral* **34**: 485-502. [2] Dare et al. (2010) DOI 10.1007/s00126-010-0295-6. [3] Toulmin and Barton (1964) *Geochim. Cosmochim Acta* **28**, 641-671. [4]Farrow and Watkinson (1997) *Can. Mineral* **35**: 817-839.

Water, water, everywhere on the Moon

YANG LIU[1*] AND LARRY A. TAYLOR[1]

[1]Planetary Geosciences Institute, Department of Earth & Planetary Sciences, University of Tennessee, Knoxville, TN 37996, USA. (yangl@utk.edu)

Different forms of "water" have been reported from surface of the Moon to igneous samples, as shown by many recent discoveries [1-10]. Reflectance IR identified OH (and possible HOH) on the upper-most lunar soil (top few mm) of 10-5000 ppmw H_2O [1-3]. An impact experiment on a permanently shadowed crater in lunar south pole observed 5.9 ±2.9 wt% H_2O ice in the impact site [4]. Using Secondary ion mass spectrometry, we have seen high amounts of H, regarded as OH, in volcanic glasses (<46 ppmw H_2O, [5]), apatite (<7000 ppmw H_2O, [6-8]), and melt inclusions (370-1410 ppmw H_2O, [10]). These studies of magmatic apatite and glasses suggest that the lunar mantle may contain OH comparable to that of Earth [5, 10]. These discoveries highlighted new questions about the formation and evolution of the Moon from surface to interior, and the total "water" budget on the Moon.

We are actively involved in the research of "water" on the Moon. Our most recent studies have focussed on a search of host phases of lunar "water" [11, 12]. We have discovered significant amounts of OH in lunar soils. The D/H isotope values suggest a depleted source (solar-wind) and an enriched source (likely meteorites or comets). These results provide direct evidence for meteorite inputs to lunar surface OH/H_2O. The observation of abundant solar-wind-like OH also supports models that suggest its migration as OH to ice in the permanently shadowed craters in lunar poles [13, 14]. Here, we will summarize our recent studies and its implications on the formation mechanisms of surface OH/H_2O on airless terrestrial bodies, and we will also attempt to quantify the total budget of the OH/H_2O, particularly on the surface of the Moon.

[1] Pieters et al. (2009) *Science,* **326,** 568-572. [2] Clark (2009) *Science,* **326,** 562-564. [3] Sunshine et al. (2009) *Science,* **326,** 565-568. [4] Colaprete *et al.* (2010) *Science* **330**, 463-468. [5] Saal, *et al.* (2008) *Nature* **454**, 192-196. [6] Liu et al. (2010) LPSC 41st, #2649. [7] Boyce, J. W. *et al.* (2010) *Nature* **466**, 466-469. [8] McCubbin *et al.* (2010) *Proceedings of the National Academy of Sciences* **107**, 11223-11228. [9] Greenwood *et al.* (2011) *Nature Geosci* **4**, 79-82. [10] Hauri et al. (2011) *Science* **333**, 213-215. [11] Liu et al. (2012) LPSC 43rd #1864. [12] Liu et al. (2012) LPSC 43rd #1866. [13] Crider and Vondrak (2000). *J. Geophys. Res.* **105**, 26773-26782. [14] Crider and Vondrak (2002). *Advances in Space Research* **30**, 1869-1874.

https://doi.org/10.1180/S0026461X00008434 Published online by Cambridge University Press

Passive treatment of perchlorate, nitrate, and sulfate in contaminated groundwater using zero valent iron and wood chips

YINGYING LIU *, CAROL J. PTACEK, DAVID W. BLOWES

University of Waterloo, Waterloo, Canada, yy4liu@uwaterloo.ca

21i. Groundwater Remediation

Perchlorate is widespread in the environment due to its use in rocket propellants, explosives, fireworks, and other applications. Its high mobility and ecotoxicity make treatment of perchlorate-contaminated water urgent [1]. Reactive media can be used to remove perchlorate in water in permeable reactive barriers and a variety of bioreactors [2]. In this study, a series of four column experiments was used to evaluate the effectiveness of reactive media for use in passive treatment systems for removal of perchlorate, nitrate, and sulfate from contaminated water associated with mining and blasting sites.

One column was packed with silica sand as a control, the other three columns were packed with granular zero valent iron (ZVI), wood chips (WC), a mixture of granular zero valent iron and wood chips, adjusted with 50 vol.% of silica sand. The experiments were operated in two stages; the flow rate was maintained at 0.5 pore volume (PV) day^{-1} in the first stage and at 0.1 PV day^{-1} in the second stage (after approximately 100 PV of flow in each column).

Results and Conclusion

Nitrate, sulfate, and perchlorate were effectively removed during the second stage of the experiment: nitrate (~10.8 mg L^{-1} NO_3-N) was almost completely removed to concentrations <0.02 mg L^{-1} NO_3-N in all columns; sulfate was removed with a variable removal of up to 70% of input sulfate (~24.5 mg L^{-1}) in Column WC; perchlorate (~857 µg L^{-1}) was effectively removed to concentrations <28 µg L^{-1} in Column WC and to concentrations <2 µg L^{-1} in Column ZVI+WC during the last 30 pore volumes in the second stage of the experiment.

The removal of nitrate and perchlorate followed first-order and zero-order kinetic equations, respectively. Nitrate and perchlorate were removed simultaneously within Columns WC and ZVI+WC, however, nitrate was removed much more rapidly than perchlorate. Nitrate inhibition of perchlorate removal was observed in Column WC at nitrate concentrations >2 mg L^{-1} NO_3-N. However, adding ZVI into WC effectively eliminated the inhibition of perchlorate removal by nitrate in Column ZVI+WC. Sulfate did not inhibit perchlorate removal in any of the columns in this study.

[1] Ward (2008) *Springer* [2] Giblin et al. (2000) J. *Environ. Qual.* **Volume29**, 578-583.

Triassic high-Mg adakitic andesites from Linxi, Inner Mongolia: Insights into the fate of the Paleo-Asian ocean crust and fossil slab-derived melt-peridotite interaction

YONGSHENG LIU*, XIAOHONG WANG, DONGBIN WANG, DETAO HE, KEQING ZONG, CHANGGUI GAO, ZHAOCHU HU

[1] State Key Laboratory of GPMR, China University of Geosciences, Wuhan 430074, China, yshliu@hotmail.com (* presenting author)

As the eastern Chinese extension of the central Asian orogenic belt, the Inner Mongolia-Daxinganling orogenic belt (IMDOB) has been regarded as a complex collage of island arcs, microcontinental blocks and fragments of oceanic crust that were amalgamated together during the Paleozoic closure of the eastern Chinese segment of the Paleo-Asian Ocean between the North China Craton and south Mongolia Block. The IMDOB is celebrated for its subduction-accretion tectonics and as being the world's most important juvenile crust production in Phanerozoic times.

Bulk element and isotopic compositions, single zircon U-Pb ages and trace element compositions of the Triassic high-Mg adakitic andesites (HMAs) from the Linxi area in the IMDOB were studied in this work to understand its petrogenesis and implications for Phanerozoic crustal growth. The Linxi HMAs are characterized by typical features of high-SiO_2 adakite with high Mg# and high Cr and Ni contents. Coarse clinopyroxene (cpx) phenocrysts with reverse zoning were found. These cpx phenocrysts have cores with lower Mg# and Ni contents, and higher incompatible element contents (e.g., Zr and La) compared to their mantles and rims. Bulk rock Sr-Nd isotopic compositions ($^{87}Sr/^{86}Sr_I$ = 0.70382 - 0.70396 and $\varepsilon_{Nd(t)}$ = 3.2 - 4.5) fall in the range of mid-ocean ridge basalt (MORB) and modern subduction-related adakites. Single zircon U-Pb dating by LA-ICP-MS suggests an eruption at ca. 238 Ma. Combined with the tectonic setting and Precambrian zircon age spectrum, these features suggest that the Linxin HMAs were derived from the subducted Paleo-Asian oceanic slab with sediments shed from the north China Craton and hybridized by peridotite in the mantle.

Trace element-age variations of zircons indicate that the oceanic crust was formed during Carboniferous-early Permian times, and then subducted during ca. 270 – 260 Ma. Melting of the subducted oceanic slab and hybridization by peridotite could have been initiated at ca. 250 Ma. It is suggested that the southern accretionary zone between the North China Craton and the Solonker suture in the IMDOB, where the Linxi HMAs are located, could have been consolidated by Carboniferous-Permian times. This implies that the Linxi HMAs could have been derived from partial melting of a fossil oceanic slab after the subduction, and subduction-related melting may have been delayed if the slab was subducted under an old, cold craton. Although we are unsure of the true extent of the fossil oceanic slab, the genesis of the Linxi HMAs is essentially a snapshot of the melting of a subducted slab lagging behind subduction, and melting of fossil oceanic slab could have played an important role in the Phanerozoic crustal growth in the IMDOB.

https://doi.org/10.1180/S0026461X00008434 Published online by Cambridge University Press

Equilibrium Mg and O isotope fractionations between silicates at high T and P: the test of a new calculation method

YUN LIU*, XIAOBIN CAO, XUEFANG LI, JIE YUAN

State Key Laboratory of Ore Deposit Geochemistry, Institute of Geochemistry, Chinese Academy of Sciences, Guiyang, China, liuyun@vip.gyig.ac.cn (* presenting author)

For the test of a cluster-model-based method which we developed for estimating isotopic fractionations of solids, Mg and O isotope fractionations between spinel, diopside, pyrope, omphacite and forsterite at different temperatures and pressures are investigated. There is a tremendous interest in developing a cluster-model-based method of isotope fractionation calculation for solids because most of the new techniques developed in modern quantum chemistry are for molecules which usually are represented by cluster models. Many local properties of solids (e.g., isotopic effect) can be calculated using much higher theoretical treatments if using cluster models. Another reason we developed this method is to remedy problems raised from a similar method used by Rustad and co-workers (e.g.,[1]), especially to enhance its implementation on isotope fractionation calculations between solids and aqueous species.

Recent studies (e.g., [2],[3],[4]) suggested the possibility of using equilibrium inter-mineral Mg isotope fractionations as a thermometer at mantle conditions. Here, we calculate equilibrium Mg and O isotope fractionation factors of geologically important silicate minerals by using our new method. Although our results of silicate minerals are generally close to those of Schauble (2011), our result of magnesite vs. Mg^{2+}(aq) ion is significantly different from his result. Our results are very close to existing Mg and O isotope experimental data, suggesting broad applications of this method in future.

Because an good isotope thermometer is required to exclude pressure effects, we checked the pressure effects of Mg and O isotopes of those silicate minerals mentioned up to 13GPa (i.e., roughly the upper mantle condition). Very small pressure effects are found within the lower pressure range (e.g. less than 4 GPa). However, slowly increasing pressure effects are found with the increase of pressure to 13GPa. We suggest to correct the pressure effects if the samples are from the lower part of the upper mantle.

[1] Rustad et al. (2010) *GCA*, **74**, 6301-6323. [2]Young et al. (2009) *EPSL*, **288**, 524-533. [3] Li et al. (2011), *EPSL*, **304**, 224-230. [4] Huang et al. (2010) *GCA*, **75**, 3318-3334. [5]Schauble (2011) *GCA*,**75**, 844-869.

Nanoscale Measurement of Manganese Valence in Mn-oxides

KENNETH J.T. LIVI[1*], BRANDON LAFFERTY[2,3], MENGQIANG ZHU[2, 4], SHOULIANG ZHANG[5], ANNE-CLAIRE GAILLOT[6], DONALD L. SPARKS[2]

[1]HRAEM, Depts. of Earth and Planetary Sciences and Biology, Johns Hopkins University, Baltimore, MD 21218 klivi@jhu.edu (* presenting author)

[2]Plant and Soil Sciences, University of Delaware, Newark, DE 19717-1303

[3]U.S. Army Engineer Research & Development Center, 3909 Halls Ferry Rd, Vicksburg, MS 39180

[4]Earth Sciences Division, Lawrence Berkeley National Laboratory, Berkeley, CA 94720

[5]Texas Material Institute, University of Texas at Austin Austin, TX 78712

[6]Institut des Matériaux Jean Rouxel, Université de Nantes, CNRS, 2 rue de la Houssinière, BP 32229, 44322 Nantes Cedex 3, France

Manganese (Mn) oxides are among the strongest mineral oxidants in the environment and impose significant influence on mobility and bioavailability of redox-active substances, such as arsenic, chromium, and pharmaceutical products, through oxidation processes. Oxidizing potentials of Mn oxides are determined by Mn valence states (II, III, IV). In this study, the effects of beam damage during Electron Energy-Loss Spectroscopy (EELS) measurement in the Transmission Electron Microscope have been investigated to determine the "safe dose" of electrons [1]. Time series analyses demonstrate that some Mn-oxide minerals experience a reduction of Mn valence during intense or prolonged electron beam exposure. We have determined the safe dose fluence (electrons/nm^2) for todorokite (10^6 e/nm^2), acid birnessite (10^5), triclinic birnessite (10^4), randomly-stacked birnessite (10^3) and δ-MnO_2 ($<10^3$) at 200 kV. The results show that precise measurements of the mean Mn valence can be acquired by EELS if proper care is taken. EELS anayses are shown to be as precise as chemical titration analyses, but with twelve orders of magnitude less volume (~5 attoliters, 10^{-18}).

The value of EELS analysis is demonstrated by two applications: 1) Analysis of run products from experiments reacting 1 mM dissolved Mn^{2+} with δ-MnO_2 in the presence of other cations (Na^+, Ca^{2+} Zn^{2+} and Ni^{2+},). These experiments, designed to determine reaction rates of the reduction of Mn(IV) in poorly-crystalline Mn-oxides by Mn^{2+}, produce mixtures of phases with variable mean valence. Unlike bulk chemical tiration or X-ray absorption spectroscopy, EELS, in concert with energy-dispersive X-ray analysis (EDS), can determine the individual phase valences and their mineral formulae (including other divalent cations). 2) Analysis of todorikite in a Mn-oxide crust from the Pacific ocean floor. This natural todorokite includes Fe(II,III) and other minor elements. EELS is capable of measuring the mean valence for both Mn and Fe, while simulaneously acquiring quantitative EDS analyses.

[1] Livi et al. (2012) *Environmental Science & Technology* **46,** 970-976.

https://doi.org/10.1180/S0026461X00008434 Published online by Cambridge University Press

A modeling study of ecosystem carbon and nutrient cycling following oil sands mining

EMILY LLORET[1*], SYLVIE A. QUIDEAU[1], AND ROBERT GRANT[1]

[1]Department of Renewable Resources, University of Alberta, Edmonton, Canada, lloret@ualberta.ca (* presenting author)

Oil sands in northern Alberta provide a valuable resource for the national and international production of gas and petroleum. However after this resource is extracted, industries must restore disturbed landscapes to a productivity equivalent to that of natural landscapes. Carbon and nitrogen cycling play important roles in the restoration of this productivity. To examine these roles, we compared modelled vs. measured effects of three different depths of mixed peat-mineral soil covers on ecosystem productivity, soil quality and salinity in a disturbed landscape at the South Hills site of the Syncrude mine in northern Alberta. We then compared the productivities of these landscapes with that of a natural landscape to determine the depth of soil cover required to restore the productivity of a reclaimed landscape to that of a natural one. These results are preliminary pending more detailed measurements of site and soil properties.

Single cell genomics of uncultured subsurface archaea

KAREN G. LLOYD[1*], LARS SCHREIBER[2], DORTHE G. PETERSEN[2], MICHAEL RICHTER[3], KASPER KJELDSEN[2], MARK LEVER[2], SABINE LENK[3], SARA KLEINDIENST[3], ANDREAS SCHRAMM[2], AND BO B. JORGENSEN[2]

[1]University of Tennessee, Knoxville, TN, USA, klloyd@utk.edu (* presenting author)
[2]Center for Geomicrobiology, Aarhus University, Aarhus, Denmark
[3]Max Plank Institute for Marine Microbiology, Bremen, Germany

Abstract

Microorganisms are dominant players in global biogeochemical cycling, and the marine subsurface contains many deeply-branching groups of archaea that have no cultured relatives.[1,2] Much of these archaea come from the Miscellaneous Crenarchaeotal Group (MCG) and the Marine Benthic Group D (MBG-D), which are globally distributed in anoxic environments. The phylogenetic identity of these archaea has only been established through genetic information in the 16S rRNA gene. Metabolic capacity, on the other hand, can be inferred by presence of functional genes that represent specific metabolic pathways. In order to link phylogenetic identity to metabolic capacity of these uncultured archaea, we sorted a single cell of each and sequenced the entire genome of each using a hybrid approach with 454 FLX and Illumina methods. We then compared this to abundance data in Aarhus Bay sediments to determine potential roles for these groups in marine non-seep sediments.

Out of the 56 single copy genes conserved in all cultured archaea, we found 14 and 29, MCG and MBG-D, respectively. A concatanation of these conserved genes provide support for an evolutionary grouping of the MCG within the mesophilic Crenarchaeota (or Thaumarchaeota) and the MBG-D within the Order Thermoplasmatales within the Euryarchaeota. MCG and MBG-D were found to comprise the bulk of the archaeal population, using qPCR as well as 454 FLX sequencing of archaeal 16S genes. The genomes of MCG and MBG-D contain nearly complete pathways for the tricarboxylic acid cycle, as well as transporters for externally-derived organic molecules. They both contain variations on pathways for amino acid degradation. These data support a heterotrophic lifestyle for uncultured archaea in the marine subsurface, as was predicted by bulk biomass isotopic ratios.[1] No evidence was found for commonly used inorganic terminal electron acceptors such as oxygen, sulfate, iron, or CO_2 (for methanogenesis). Therefore the physiology of MCG and MBG-D most likely diverges from those of their aerobic closest relatives.

[1] Biddle, J. F., et al. (2006) *PNAS* **103**, 3846-3851.
[2] Whitman, W.B., et al. (1998) *PNAS* **95**, 6578-6593.

https://doi.org/10.1180/S0026461X00008434 Published online by Cambridge University Press

High sensitivity laser ablation MC-ICP-MS

NICHOLAS S. LLOYD[1*], STEVE SHUTTLEWORTH[2], CLAUDIA BOUMAN[1], ANNE TRINQUIER[1], JOHN ROY[2] AND JOHANNES B. SCHWIETERS[1]

[1]Thermo Fisher Scientific, Bremen, Germany, nicholas.lloyd@thermofisher.com (* presenting author)
[2]Photon Machines, Redmond, USA, shutts@photon-machines.com

The Thermo Scientific NEPTUNE *Plus* MC-ICP-MS with Jet Interface option has previously been demonstrated to offer the highest ICP-MS analyte sensitivities for desolvated solutions [1] and for laser ablation [2]. A combination of nitrogen addition, special cones and a high capacity interface pump improved laser ablation Hf sensitivity by a factor of more than seven. The resulting sensitivity enabled highly precise and accurate $^{176}Hf/^{177}Hf$ isotope ratios to be measured from zircon 91500 using 25 µm diameter laser ablation spots, whereas typically 100 ppm 2σ external precision is only achieved using 50 µm diameter spots (with four times the ablated volume). It was noted that with increased sensitivity the Yb and Hf fractionation factors diverge further, highlighting the importance of independent measurement of the Yb fractionation factor used for the ^{176}Yb correction.

For these experiments a Photon Machines Analyte.G2 193 nm laser ablation system was operated with moderate fluence and repetition rate (6.22 J/cm^2 at 7 Hz). The short pulse width and short wavelength of this excimer laser ablation system is ideal for ablation of zircon mineral grains. The Analyte.G2 is equipped with a two-volume HELEX 2 cell for the fastest washout time. The combination of improved ICP-MS sensitivity and fast response laser ablation cell is critical for the emerging field of 'geochron, imaging' by LA-ICP-MS.

In this study we investigate the factors that influence external precision of $^{176}Hf/^{177}Hf$ isotope ratios from zircons, including the effects of nitrogen addition on analyte sensitivity and mass bias stability. We also describe a new multi-ion counting collector configuration that has been designed for the Thermo Scientific NEPTUNE *Plus*. This allows for increased flexibility of analysis, using combinations of ion counters and Faraday cups to accommodate the range of U-Pb isotope beam intensities expected from both young and old zircons.

[1] Bouman et al (2009) *Geochim. Cosmochim. Acta* **73**(13, Supplement 1), A147. [2] Lloyd et al. (2011) *Min. Mag.* **75**(3), 1351.

Setting and Styles of Hydrothermal Mudstones near the Lemarchant volcanogenic massive sulfide deposit, Newfoundland Appalachians.

S. LODE ([1]*), S.J. PIERCEY[1], D. COPELAND[2], C. DEVIVE[2], B. SPARROW[2]

[1]Department of Earth Sciences, Memorial Univ., St. John's, Canada (*correspondence: slode@mun.ca)
[2]Paragon Minerals Corporation, 140 Water Street, Suite 605, St. John's, Canada

In some volcanogenic massive sulfide (VMS) deposits there is a close association of black shales and hydrothermal mudstones and massive sulfide mineralization, yet our understanding of the relationship of these muds to VMS deposit genesis and exploration is incomplete. The Lemarchant VMS deposit, Central Mobile Belt, Newfoundland Appalachians, Canada, is an excellent location to study the relationship of black shales/hydrothermal muds to VMS mineralization because there is an intimate relationship between precious-metal bearing Zn-Pb-Cu sulfides and hydrothermal sedimentary rocks. The Lemarchant VMS deposit is hosted by the late Cambrian Tally Pond volcanic belt and represents a bimodal felsic VMS deposit with a typical stratigraphic sequence consisting of rhyolite domes and/or breccias with a stockwork stringer zone, overlain by the massive sulfides, one or more barite bed(s), and capped by hydrothermal sediments/mudstones. Mafic volcanic flows, predominantly pillowed basalts, are deposited on top of this sequence and represent a new cycle of volcanic activity. Metalliferous mudstones represent a hiatus in this volcanic activity, where the deposition of hydrothermal matter dominates over the abiogenic pelagic background sedimentation. These hydrothermal sediments comprise brown to black graphite-rich mudstones and fine laminated shales, which can be intercalated by siliclastic and/or kidney-shaped chert layers as well as by fine layers of organic matter. The main sulfide phases are pyrite and pyrrhotite plus minor amounts of chalcopyrite, sphalerite, arsenopyrite and galena. Pyrite mostly occurs as diagenetic euhedral grains or as framboids, whereas pyrrhotite forms fine granulates or irregular shaped grains to massive grains that infill veins.

Preliminary lithogeochemical results illustrate that relative to upper crust normal shales, the hydrothermal sedimentary rocks have anomalous base and precious metals, volatile metals (e.g., Tl, Sb), high Fe/Al ratios, variable Ce/Ce*, Y/Ho ~27, and have Eu/Eu*≧1, indicative of deposition from reduced, hot hydrothermal fluids with only a minor detrital input. Ongoing research includes detailed mineralogical-petrographical studies of the sulfides, additional whole-rock lithogeochemical analyses, and sulfur isotope geochemistry. The research is aimed at understanding both the role that basin redox conditions has on the genesis of the Lemarchant deposit, discriminating the relative contributions of hydrothermal, detrital or hydrogenous (seawater-derived) materials in the genesis of the shales, distinguishing between hydrothermal, diagenetic and biological sulfur sources in the sediments, and utilizing the latter to create potential exploration vectors at Lemarchant and for other shale-associated VMS systems.

https://doi.org/10.1180/S0026461X00008434 Published online by Cambridge University Press

Trace element geochemistry of VMS-deprived and VMS-endowed 2720 Ma greenstone belts in the Wawa Subprovince, Superior Craton

R.W.D. LODGE[1*], H.L. GIBSON[2], AND G.M. STOTTT[3]

[1]Mineral Exploration Research Centre, Laurentian University, Sudbury, Ontario, Canada, rx_lodge@laurentian.ca (*presenting author), HGibson@laurentian.ca

[2]Ontario Geological Survey (ret.), Stott Geoconsulting Ltd., Sudbury, Ontario, Canada, stottgeoconsult@gmail.com

The northern margin of the Wawa subprovince of the Superior craton is marked by four relatively well studied greenstone belts that have vastly different endowments of economic volcanogenic massive sulphide (VMS) mineralization. These coeval greenstone belts (2720 Ma) are inferred to have formed within similar tectonic environments and to have experienced similar styles of volcanism, and therefore would be expected to have the same VMS-potential. Yet, significant exploration over the past century has yet to yield an economic VMS deposit in the Shebandowan and Vermilion greenstone belts (SGB, VGB, respectively). The smaller Winston Lake and Manitouwadge greenstone belts (WGB, MGB respectively) host the Geco (~50 Mt), Willroy (~4.5 Mt) and Winston Lake (~3.1 Mt) VMS deposits. This study aims to determine if the VMS metallogeny of barren versus endowed greenstone belts is related to different geodynamic settings or differences in the petrogenesis of their host volcanic successions.

VMS deposits are products of synvolcanic, high-temperature hydrothermal systems in extensional submarine geodynamic settings. Primitive mantle-normalized trace element contents of basalts have distinctive geochemical signatures depending on the geodynamic setting. Arc basalts have negative Nb, Ta, and Ti anomalies and LREE enrichment, whereas MORB have depleted to flat LREE patterns. Felsic-intermediate rocks commonly associated with VMS mineralization have flat REE patterns or slight LREE enrichment (FII–FIV rhyolites). Regional- and property-scale sampling and mapping in each greenstone belt have been completed to clarify the spatial distribution of these geochemical signatures in order to determine if there are differences in the geodynamic evolution and/or petrogenesis of VMS endowed versus barren 2720 Ma greenstone belts. Initial results suggest the dominance of FI felsic volcanics (Figure 1), arc-like mafic volcanics, and plume-fed ultramafic sequences hindered VMS-development in the SGB.

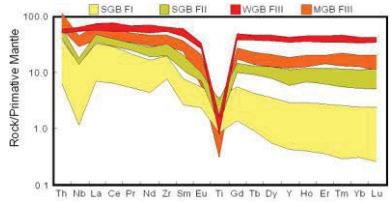

Figure 1: Trace element geochemistry of the Shebandowan (SGB), Winston Lake (WGB), and Manitouwadge greenstone belts (MGB).

[1] Corfu & Stott (1998) *GSA Bulletin* **110**, 1467-1484.

Fluoride complexation of hafnium under hydrothermal conditions

A. LOGES[1]*, A.A. MIGDISOV[2], T. WAGNER[3], A.E. WILLIAMS-JONES[2], G. MARKL[1]

[1] Department of Geosciences, University of Tuebingen, D-72070 Tübingen, Germany, anselm.loges@uni-tuebingen.de (* presenting author)

[2] Department of Earth and Planetary Sciences, McGill University, Montreal, Quebec, Canada H3A 2A7, artas65@gmail.com

[3] Institute of Geochemistry and Petrology, ETH Zurich CH-8902 Zurich, Switzerland, thomas.wagner@erdw.ethz.ch

Hydrothermal transport and deposition of high field strength elements (HFSE) attracts increasing attention as demand for these strategic metals rises. Data on the stability of aqueous complexes of geochemical twins, such as zirconium (ionic radius 590 pm) and hafnium (580 pm), can provide us with insights into the processes that concentrate these elements in HFSE deposits. Fluoride is an important ligand in such systems, greatly enhancing the solubility of HFSE. Fluorine-rich hydrothermal processes are also known to fractionate geochemical twins (including Zr/Hf) much more strongly than other geological processes.

Here we report experimentally determined Hf fluoride formation constants for 150, 200, and 250°C and saturated water pressure. The data were obtained using the method applied by Migdisov et al. [1] to determine Zr speciation in fluoride-bearing aqueous fluids. The pH and fluoride concentration range considered was 1.3 to 2.5 and 7e-4 to 2e-1, respectively.

Our experiments show that Hf is complexed exclusively as di-fluorohydroxy species under the conditions of our experiments. Zirconium forms either mono- or di-fluorohydroxy complexes under the same conditions, depending on fluoride activity [1]. This shows that Hf has a higher affinity for F than Zr. The di-fluorohydroxy complexes of Hf are more stable than those of Zr.

We conclude that the differential behavior of Zr and Hf in fluoride-bearing aqueous fluids is the reason for the high temperature fractionation of of these metals in hydrothermal HFSE deposits. In combination with other geochemical information, the data presented here allows us to better quantify the behaviour of Zr and Hf during HFSE ore-formation.

[1] Migdisov et al. (2011) *Geochim. Cosmochim. Acta* **75**, 7426-7434.

https://doi.org/10.1180/S0026461X00008434 Published online by Cambridge University Press

Temporal and Spacial Variation of Microbial Community Structures in Oil Sand Tailing Ponds

NADINE LOICK[1]*, ERNEST CHI FRU[2], CHRISTOPHER WEISENER[1]

[1]Great Lakes Environmental Institute for Research, University of Windsor, Windsor, Canada, nloick@uwindsor.ca*
[2]Swedish Museum of Natural History, Department of Palaeozoology, Stockholm, Sweden

Introduction

The process of extracting bitumen from oil sands produces large volumes of tailings that are deposited in large settling basins to become denser mature fine tailings; ultimately aiming at reclamation of the land by establishing viable envionmental systems such as wetlands or lakes.

Microorganisms enhance particulate matter sedimentation rates and the dewatering of tailings materials, releasing water for bitumen extraction. They are critical to biogeochemical elemental cycles and the degradation of toxic hydrocarbon contaminants coupled to greenhouse gas production in oil sands fine fluid tailings and influence remediation and land-reclamation efforts.

Results

Microbial community patterns were analysed using population ecology tools. A bioreactor study showed that after 300 days no significant differences existed between the microbial communities of the bioreactors and the fiel samples. This studdy suggests that bioreactor studies reflect field conditions. It also proposes a whole community succession pattern from bacterial dominance to a new assemblage predominated by archaea [1].

To reinforce these findings, a comparison between different sampling locations within the same tailings ponds was carried out and shows the degree of heterogeneity of the material; comparisons between ponds of different ages give an insight into the temporal changes in the microbial community composition during the settling of the material under field conditions.

Conclusions

These results will have implications for the stepwise development of microbial model systems for predictive management of field scale tailings basins. They will aid in the determination of times and locations within the pond where greenhouse gas (CH_4 and CO_2) production is likely to happen. This will assist in managing the ponds, as well as help remediation and land reclamation efforts.

Reference

[1] Chi Fru (2012) *Environmental Science &Technology,* in review

Manipulating uranium redox status in an alluvial aquifer: insights from electron donor amendment experiments

P. E. LONG[1*] K. H. WILLIAMS[1], J. BANFIELD[2], J. BARGAR[3], J. A. DAVIS[1], P. FOX[1], K. HANDLEY[2], K. HATFIELD[4], D. LOVLEY[5], N. VERBERKMOES[6], M. WILKINS[7], K. WRIGHTON[2], S. YABUSAKI[7], AND THE RIFLE IFRC SCIENCE TEAM

[1]LBNL, Berkeley, CA, USA, PELong@lbl.gov (* presenting author)
[2]University of California, Berkeley, CA, USA
[3]Synchrotron Radiation Light Source, Stanford, CA, USA
[4]University of Florida, Gainsville, FL, USA
[5]University of Massachusetts, Amherst, MA, USA
[6]Oak Ridge National Laboratory, Oak Ridge, TN, USA
[7]Pacific Northwest National Lab, Richland, WA, USA

Introduction

Starting in 2002, field-scale biostimulation experiments have been conducted in a uranium-contaminated, shallow alluvial aquifer located along the Colorado River in western Colorado. In parallel the naturally reduced zones in the aquifer have been examined. These experiments and observations have provided insight into the coupling of microbiological, biogeochemical, and hydrogeological processes controlling mobility of uranium in subsurface environments. Research at the U.S. Department of Energy's Integrated Field Research Challenge site (IFRC) at Rifle, Colorado, USA, initially focused on testing the concept that Fe-reducing bacteria such as *Geobacter sp.* could reduce soluble U(VI) to insoluble U(IV) during electron donor amendment (acetate) and that this could be used as a bioremediation strategy for uranium-contaminated aquifers.

Summary of Results

Initial experiments demonstrated a stimulation of microbial Fe(III) reduction *in situ* that correlated with an increase in Geobacter sp. within the subsurface microbial community and a decrease in soluble U(VI) concentration in the groundwater consistent with laboratory studies and the known physiological trait of *Geobacter sp.* to enzymatically reduce U(VI). After approximately 20-30 days, the dominant microbial process shifted from Fe(III) reduction to sulfate reduction and U(VI) concentrations increased. Subsequent experiments directly linked gene expression for metal reduction pathways in *Geobacter sp.* to decreases in U(VI) concentration. More recently it has been possible to sample and analyze both *in situ* proteomes and metagenomes during biostimulation, leading to a comprehensive understanding of both the metabolic potential of the biostimulated microbial community and its actively expressed metabolism.

Future Directions

Future research at the Rifle IFRC will focus on understanding the plume-scale behavior of uranium the context of the metabolic potential of the subsurface microbial community enabled by metagenomic sequencing. Initial results show assembly of nearly complete genomes for microbes present at ≥0.5% abundance is achievable. Coupled with proteomics, transcriptomics, and selected physiological studies, prediction of microbially-mediated uranium fate and transport should be possible for aquifers under conditions that include natural microbially-mediated reduction of uranium.

https://doi.org/10.1180/S0026461X00008434 Published online by Cambridge University Press

Magma chamber processes leading to the January 1835 eruption of Cosigüina volcano, Nicaragua

MARC-ANTOINE LONGPRÉ[1*], JOHN STIX[1], ANGÉLICA MUÑOZ[2], AND EVELING ESPINOZA[2]

[1]McGill University, Montréal, Canada
m-a.longpre@mcgill.ca (* presenting author)
[2]INETER, Managua, Nicaragua

Cosigüina volcano, in northwest Nicaragua, erupted violently in January 1835, producing pumice, scoria, and ash fall deposits, as well as pyroclastic flows for a total volume of ~6 km^3 [1]. Here, we present new geochemical data on bulk-rocks, matrix glasses, melt inclusions and minerals from the 1835 deposits, with the aim of shedding light on the magmatic processes that led to the eruption.

The deposits of the 1835 eruption are chemically zoned; a small volume of dacite pumice was erupted first, followed by silicic andesite scoria and andesite scoria, the latter representing by far the largest magmatic component. The dacite pumice is composed of microlite-free glass (65.6 wt.% SiO_2, 0.9 ± 1.6 (1σ) wt.% H_2O (by difference)), and scarce crystals of plagioclase (An_{50-65}, some with a An_{80} core), clinopyroxene (Mg#=64-68), orthopyroxene (Mg#=57-62), magnetite (14.6 wt.% TiO_2) and apatite that commonly occur as glomerocrysts. Rare melt inclusions are of dacitic composition and contain 4.0 ± 1.7 wt.% H_2O. In comparison, the andesite scoria comprises microlite-rich glass (62.1 wt.% SiO_2, 1.0 ± 0.8 wt.% H_2O), abundant crystals of plagioclase (An_{75-95}) and sparse clinopyroxene (Mg#=64-75), orthopyroxene (Mg#=59-72) and magnetite (8.4 wt.% TiO_2) generally occuring as individual crystals. Abundant melt inclusions trapped in An_{80} plagioclase are of andesitic composition and contain 3.3 ± 1.7 wt.% H_2O. Mineral-melt thermometry and hygrometry [2] suggest magmatic temperatures of 930°C and 1030°C and dissolved water contents of 4.5 wt. % and 3.3 wt. %, in agreement with H_2O-by-difference results, in the dacite and andesite magmas, respectively. Assuming water saturation, this translates into magma storage pressures of ~100-150 MPa. Parallel REE patterns for dacite and andesite show a negative Eu anomaly, particularly pronounced for the former. Yet, andesite bulk-rock Al_2O_3 contents depart from the glass and melt inclusion trend, implying that early extensive fractionation was followed by 15-30 % plagioclase addition in the andesite.

Together these observations suggest that the 1835 eruption was fed by a chemically and thermally zoned magma chamber and that the dacite and andesite magmas are closely related through crystal fractionation. However, the lack of plagioclase of intermediate compositions in the 1835 magmas requires efficient and 'sudden' separation (through e.g., gas-driven filter pressing [3]) of a dacitic melt, from which An_{50-65} plagioclase began crystallising. Accumulation of free gas at the top of the magma chamber may have led to the abrupt collapse of a foam layer, triggering the eruption and rapidly ejecting the dacite. Decompression associated with the eruption onset may have caused microlite growth in the andesite melt prior to its expulsion in the later stages of the eruption.

[1] Scott et al. (2006) *GSA Bull. Special Paper* **412**, 167-187. [2] Putirka (2008) *Rev. Mineral. Geochem.* **69**, 61-120. [3] Sisson and Bacon (1999) *Geology* **27**, 613-616.

Bacterial Interactions with radionuclides in Bentonite Samples from Spanish Clays

MARGARITA LOPEZ FERNANDEZ[1*], ALBERTO MORENO GARCIA[1], JAIME LAZUEN ALCON[2], ANDREA GEISSLER[3], MOHAMED L. MERROUN[1]

[1]Department of Microbiology, University of Granada, Spain, margaritalopez@ugr.es (* presenting author), merroun@ugr.es
[2]CIC, University of Granada, Spain, jlazuen@ugr.es
[3]Institute of Ressource Ecology, HZDR, Dresden, Germany, a.geissler@hzdr.de

A reliable performance assessment of radioactive waste repository depends on a better knowledge on the interactions of radionuclides and natural microorganisms of geological formations (salts, granitic rocks and clays) used as host rock candidate for these disposal systems. Microbes are able to interact efficiently with actinides affecting their transport and mobility in the environment [1] .The main goals of the current work are: a) to characterize the bacterial diversity of two bentonite samples (BI and BII), recovered from Spanish clay deposits considered in this study as host rock candidate for geological disposal of radioactive wastes, and b) to investigate how these bacterial community will respond to uranium toxicity.

Results and conclusions

16S rRNA gene sequence analysis was used to explore the bacterial community structure of the two bentonite samples which indicated that the sample BI showed a higher diversity than the sample BII. Bacteroidetes (*Flavisolibacter* spp.), Alfaproteobacteria (*Rhodobacter* spp.), Cyanobacteria (*Phormidium* spp.) for example were identified in the sample BI. In contrast, the sample BII was dominated by Betaproteobacteria (*Ralstonia* spp.). Bacteria belonging to Actinobacteria (*Arthobacter* spp.), Gammaproteobacteria (*Stenotrophomonas* spp.), Firmicutes (*Bacillus* spp.), etc. were isolated by culture dependent methods from both samples and assayed for their tolerance to uranium. *Stenotrophomonas* spp. (strain BII-R6r) presented the highest level of U tolerance, being able to grow up to 8 mM of this radionuclide.

Flow cytometry studies (live/dead staining) indicated that the cellular viability of the U-exposed cells of the strain BII-R6r was not affected by this radionuclide (85% viable cells at 3 mM U) compared to that of *Bacillus simplex* (strain BII-S2) wich was U-sensitive showing 60% viable cells at only 1 mM U. In addition, results on the behaviour of the cells of *Stenotrophomonas* spp. BII-R6r in response to the oxidative stress, in term of membrane potential activation alterations and ROS production, caused by uranium will be discussed. Microscopic analysis indicated that uranium precipitation as uranium phosphate mineral phases (e.g. meta-autunite) was involved in the mechanisms of bacterial tolerance to this radionuclide.

This work was supported by the Grant CGL2009-09760 from the Spanish Ministry of Science and Innovation.

[1] Merroun (2011) *Journal of Hazardous Materials*. **197**: 1-10.

https://doi.org/10.1180/S0026461X00008434 Published online by Cambridge University Press

Platinum-group minerals in upper mantle peridotites : Implications for our understanding of whole-rock signatures of HSE.

LORAND, J.P.[1](*), LUGUET, A[2] AND ALARD, O.[3]

[1] LPGN, UMR-CNRS 6112, University of Nantes, Nantes, France,(jean-pierre.lorand@univ-nantes.fr)

[2] Steinmann Institute für Endogene process, Universität Bonn, Germany

[3] Geosciences Montpellier, UMR-CNRS, 5243, University of Montpellier II, Montpellier, France

Platinum-group elements (PGEs) have now been recognized to be highly sensitive geochemical tracers of Earth's mantle. However, compared to lithophile trace elements, PGEs occur as ultra-trace elements which may occasionally be present as major elements in discrete platinum-group minerals (PGMs) in addition to the base-metal sulfides (BMS). PGMs are not expected to be stable in the upper mantle because PGEs are highly soluble (at wt. % levels) in base metal sulfides (BMS), which control the largest part of the PGE budget in the uppermost mantle. However, micrometric PGMs (0.1 μm-3μm) have now been identified in a large panel of mantle-derived rocks (abyssal peridotites, orogenic peridotites, basalt-borne spinel peridotite xenoliths, cratonic peridotites) within both lherzolitic and harzburgitic compositions. These minerals may impact analytical precision (e.g. Os-Ir) and reproducibility of whole-rock analyses by generating nugget effects on some elements (e.g. Pt) and incomplete dissolution of some acid-resistant minerals (Os-Ir).

The PGMs so far recovered from the study of peridotites are invariably associated with BMS phases or derived from a BMS precursor indicating the key role of the BMS in the PGMs genesis. Decreasing temperature, decreasing activity of S or increasing semi-metal concentrations (Te, Bi, As, Sb…) are major factors triggering crystallization of PGMs. Adiabatic partial melting processes generate refractory PGMs (Pt-Ir-(Os) alloys Os-Ir-Ru alloys/ sulfides) by consuming all of the available BMS in the mantle residues. Refractory PGMs are long-lived minerals that may survive recycling and rejuvenation of residual peridotites while preserving Os isotopic signatures of Archean partial melting events. Reactions at decreasing melt–rock ratios (« mantle metasomatism ») as well as magmatic « refertilization » concentrate volatile semi-metals (Te, As, Bi…) which precipitate as high-temperature Pt-Pd-Te-Bi or Pt-As-S microphases intimately associated with Cu-Ni-rich sulfides. Transient fluid - rock interactions, subsolidus cooling, crustal contamination and serpentinization are also PGM-maker (PdSb, PdCuNi, Pt-Bi-Sb phases ; Pt-Fe-Ru alloys; Pd sulfides, native gold….). These non cogenetic HSE-rich minerals have thus important implications for our interpretation of the mantle HSE signatures and their use to constrain planetary processes.

Experimental insights into fluid-rock interactions in granite-hosted and CO_2-saturated geothermal systems

CAROLINE LO RÉ[1], JOHN P. KASZUBA[1, 2*], JOSEPH MOORE[3], AND BRIAN MCPHERSON[3]

[1]University of Wyoming, Department of Geology & Geophysics, Laramie, WY, USA, flore@uwyo.edu

[2]University of Wyoming, School of Energy Resources, Laramie, WY, USA, John.Kaszuba@uwyo.edu (* presenting author)

[3]University of Utah, Energy & Geoscience Institute, Salt Lake City, UT, USA, jmoore@egi.utah.edu, b.j.mcpherson@utah.edu

Hydrothermal experiments and geochemical modeling were conducted at 250°C and 25 to 45 MPa to evaluate geochemical and mineralogical relationships in a granite-hosted geothermal system. Experiments and geochemical models emulate geothermal conditions of typical granitic reservoirs and are based on the Roosevelt Hot Springs thermal area, Utah, USA. Additional experiments and modeling were also conducted to determine how these geothermal systems may respond to CO_2.

Hydrothermal experiments were conducted in rocker bombs and Au-Ti reaction cells (Dickson cells) using established methods. The granite consists of 75% ground (<45 um) and 25% chipped (0.1-0.7 cm) mineral separates, including sub-equal portions of quartz, perthitic K-feldspar (~25% wt% albite and 75% wt% K-feldspar), oligoclase (An_{23}), and 4 wt% Fe-rich biotite. The use of mineral chips allows post-experimental examination of textures, while use of powder enhances reactivity and kinetic rates. The synthetic brine ($I \cong 0.1$) contains ~ 0.1 molal Na and Cl and millimolal quantities of SiO_2, Al, Ca, Mg, K, SO_4, and HCO_3.

Five water+granite+/-epidote experiments reacted for ~28 days (water:rock ≅ 20:1). Two water+granite experiments and one water+granite+epidote experiment were subsequently injected with supercritical CO_2 and reacted for an additional 42 days. Excess CO_2 is injected to produce a separate supercritical fluid phase, ensuring aqueous CO_2 saturation for the duration of each experiment.

Prior to injection of CO_2 into water-granite experiments, relatively constant concentrations of aqueous Cl, Na, SO_4, and ΣCO_2, increasing aqueous SiO_2, K, and Al, and decreasing aqueous Mg are observed. Aqueous Ca concentrations initially increase and then decrease over time. Relatively constant concentrations of aqueous Cl, Na, and K are observed post-injection. Concentrations of aqueous Ca, SO_4, and Al decrease during the first 5 days after injection while concentrations of aqueous Mg and ΣCO_2 increase over the same period of time. Post-injection concentrations of aqueous SiO_2 gradually decrease over time.

Mg-Fe-rich illite and kaolinite precipitated in water+granite experiments whereas illite, kaolinite, and Fe-rich smectite precipitated in water+granite+CO_2 experiments. Decreasing aqueous Mg concentrations during the first 5 days of each experiment are consistent with illite formation. Increasing aqueous Mg concentrations during the first 2 days after injecting CO_2 may signal a shift in stability from illite to smectite. No carbonate minerals were observed as reaction products. These results are relevant to understanding processes in natural and enhanced geothermal systems.

https://doi.org/10.1180/S0026461X00008434 Published online by Cambridge University Press

Mass anomalous fractionations of sulfur isotopes in the Talvivaara Ni deposit, Finland - evidence for hydrothermal input

KIRSTI LOUKOLA-RUSKEENIEMI [1]*, SETH A.YOUNG[2], LISA M.PRATT[2], BO JOHANSON[1]

[1]Geological Survey of Finland, Espoo, Finland, kirsti.loukola-ruskeeniemi@gtk.fi (* presenting author)

[2]Indiana University, Department of Geological Sciences, Bloomington, Indiana, USA, seayoung@indiana.edu

Talvivaara black shale-hosted Ni deposit

The Talvivaara deposit contains 1 550 Mt of Ni-Cu-Co-Zn-Mn-U ore and was deposited in a stratified marine basin ca. 2 Ga ago. The deposit is characterized by high C_{org} and S concentrations with median values of 7.6% and 9.0%, respectively, and the occurrence of layers with Mn ≥ 0.8%. Pyrite, pyrrhotite, chalcopyrite, sphalerite, alabandite and pentlandite occur both as fine-grained disseminations and as coarser grains in quartz-sulfide veins.

The median $\delta^{34}S$ values of both pyrite and pyrrhotite are -3‰ in the Ni-rich black shales. In the black shales with Ni < 0.1% the $\delta^{34}S$ values are -4‰ in pyrite and -5‰ in pyrrhotite [1, 2]. Both thermochemical and biogenic sulfate reduction were important for the generation of reduced S as has been reported from the Sullivan Pb-Zn-Ag deposit in Canada [3] where $\delta^{34}S$ patterns resemble those at Talvivaara.

The black shales have undergone medium grade regional metamorphism but spheroidal pyrite with grain size < 0.01 mm and containing up to 0.7% Ni is still preserved in places.

Results

Sequentially extracted S fractions analyzed for 27 Talvivaara samples show mass anomalous $\Delta^{33}S$ values for spheroidal pyrite. For example, in one drill core sample (map sheet 3433, drill core 305, depth 150.89 m in the drill core), the values for spheroidal pyrite range between -2.27‰ to -7.73‰ for $\delta^{34}S$, -0.60 to -4.38‰ for $\delta^{33}S$ and 0.57 to -0.40‰ for $\Delta^{33}S$.

Values for recrystallized pyrite and pyrrhotite in the same sample range from -3.09 to -6.25‰ for $\delta^{34}S$, -1.57 to -3.20‰ for $\delta^{33}S$ and 0.01 to 0.05‰ for $\Delta^{33}S$.

Conclusions

Previous MIF sulfur anomalies have been reported for rocks older than 2.4 Ga. However, anomalous S isotope signatures may also result from reactions between organic matter and S-bearing aqueous solutions under hydrothermal conditions [4] which is the most likely case at Talvivaara. The uniform distribution of Ni in the extensive black shale unit indicates mixing between seawater and Ni-rich fluids.

[1] Loukola-Ruskeeniemi & Heino (1996) *Econ. Geol.* **91**, 80-110. [2] Loukola-Ruskeeniemi (1995) *Geological Survey of Finland, Special Paper* **20**, 31-46. [3] Taylor (2004) *Chem. Geol.* **204**, 215-236. [4] Lasaga et al. (2008) *Earth and Planetary Science Letters* **268**, 225-238.

Dating old groundwater by multiple tracers including Krypton 81

A.J. LOVE[1*], R. PURTSCHERT[2], Z-T LU[3], S. FULTON[4], P. SHAND[5], W. JIANG[3], P. MUELLER[3], G-M. YANG[3], D. WOHLING[6], W. AESCHBACH-HERTIG[7], L. BRODER[7], R. KIPFER[8], S. PRIESTLEY[1], P. GEUETIN[1], M. KEPPEL[1], Y.TOSAKI[9]

[1]Flinders University and the NCGRT, Adelaide Australia, andy.love@flinders.edu.a

[2]University of Bern Switzerland, purtschert@climate.unibe.ch

[3]Argonne National Laboratory, USA, lu@anl.gov

[4]NRETAS, Darwin, Australia, Simon.Fulton@nt.gov.au

[5]CSIRO, Land and Water, Adelaide, Australia, Paul.Shand@csiro.au

[6]Department for Water, Adelaide, Australia, Daniel.Wohling@sa.gov.au

[7]University of Heidelberg, Germany, aeschbach@iup.uni-heidelberg.de

[8]EAWAG, Switzerland, rolf.kipfer@eawag.ch

[9]GSJ, Japan, yuki.tosaki@aist.go.jp

22f

The Great Artesian Basin (GAB) of Australia is one of the largest groundwater basins in the world and contains the largest storage of potable groundwater in the Australian continent. Because of its vast size and the potential for large regional flow systems to occur, the GAB has been considered an ideal basin to test emerging groundwater dating techniques such as Cl-36 and He-4. However both of these techniques are subjected to large degrees of uncertainty, as they require a detailed understanding of different sources and sinks of these two isotopes. Contrasting this Kr-81 is considered to be an ideal tracer as it contains only one source, the atmosphere with no or at most minimal sub surface production. Our study area is focused on the western margin of the GAB between the Finke River system in the Northern Territory and the iconic Dalhousie springs in South Australia. This represents the direction of groundwater flow from recharge to discharge through the Dalhousie spring complex. For the first time we have provided a comprehensive suite of analyse not only of Cl-36, He-4, C-14, Ar-39, stable isotopes of the water molecule and noble gases but also, Kr-85 and Kr-81. Our preliminary results indicate a spectrum of "tracer groundwater ages" ranging from modern as indicated by C-14 and Ar-39 up to hundreds of thousands of years as indicated by Kr-81, Cl-36 and He-4. We suggest that this groundwater flow transect may represent an ideal type section for understanding different isotope systematic in order to obtain a greater knowledge of regional groundwater flow.

https://doi.org/10.1180/S0026461X00008434 Published online by Cambridge University Press

Tracking Proterozoic Biospheric Evolution and Marine Redox Structure using Lipid Biomarkers

GORDON D. LOVE[1*], AMY E. KELLY[1], CHAO LI[1,2], MEGAN ROHRSSEN [1]

[1] Department of Earth Sciences, University of California, Riverside, CA 92521, USA, glove@ucr.edu (*presenting author), Amy.A.Kelly@shell.com, mrohr001@ucr.edu

[2] State Key Laboratory of Biogeology and Environmental Geology, China University of Geosciences, Wuhan 430074, China, chaoli@cug.edu.cn

Molecular geochemical analyses of Proterozoic rocks and oils that have experienced a reasonably mild thermal history generally reveal a wide diversity of hydrocarbon compounds. Robust biomarker information can be recovered from many Proterozoic rocks given due attention to potential contamination and thermal preservation issues, and novel evolutionary insights include the earliest record of ecologically significant Cryogenian-age animal biomass from distinctive C_{30} steranes from demosponges [1].

Despite speculation to the contrary [2], evidence for abundant anoxygenic photosynthetic bacterial primary production in mid-Proterozoic pelagic marine settings is not supported by fossil carotenoid biomarker evidence in most thermally immature sedimentary rocks and oils from China and Australia. Only in certain organic sedimentary facies of the 1.64 Ga Barney Creek Formation deposited in the northern depocenter of the Glyde Sub-basin [3], particularly for intervals influenced by dolomotic turbidite flows [4] bringing photosynthetic benthic mats from the shelf, are aromatic carotenoid markers for Chlorobiaceae and Chromatiaceae (green and purple S bacteria) detected in abundance. The biomarker assemblages associated with unusual organofacies reported from the Barney Creek Fm. in the Glyde Sub-basin has seemingly given a misleading picture of mid-Proterozoic ocean redox structure and the general mode of pelagic bacterial production, although poorly constrained groups of bacteria appear to be the dominant source organisms.

[1] Love et al. (2009) *Nature* **457**, 718-721. [2] Johnston et al. (2009) *PNAS* **106**, 16925-16929. [3] Brocks et al. (2005) *Nature* **3**, 653-659. [4] Davidson and Dashlooty (1993) *Australian Journal of Earth Sciences* **40**, 527-543.

Nature Abhors a Vacuum: Geothermal gases at Yellowstone

LOWENSTERN J.B.[1*], EVANS, W.C.[1], BERGFELD, D.B.[1]

[1]U.S. Geological Survey, Menlo Park, CA, USA, jlwnstrn@usgs.gov (* presenting author)

Though off limits to geothermal development, Yellowstone remains the world's most prominent single source of geothermal heat, with many high-temperature aquifers underlying thousands of square km of alpine terrain. Our studies of gas and water compositions provide many lessons for the assessment of geothermal resources and the source of heat, solutes, and gases in long-lived hydrothermal systems in the shallow continental crust. We highlight three below.

Don't mix apples, oranges, and helium: Components in geothermal fluids originate from separate sources. Based on stable isotopes of H_2O, researchers recognized early on that >90% of the thermal water in Yellowstone comes from meteoric recharge. Yet most thermal waters have $^3He/^4He \geq 7R_A$, implying ~50% mantle He. Methane, a trace gas in meteoric waters and most magmatic gases is produced by thermogenesis of crustal sediments, and emerges in greatest abundance in the east side of the park. Additional CH_4 is generated through in situ equilibration of C-H-O gases. Each gas or isotope provides a different perspective on the source of heat, gas and water to a geothermal fluid.

All good things come to those who wait: An important insight from recent studies of gas composition and CO_2 flux at Yellowstone is that radiogenic He is emitted in quantities far too great to be accounted for by steady state ingrowth through radioactive decay. At the Heart Lake Geyser Basin, we measured thermal water discharge and the diffuse and fumarolic CO_2 flux. He isotopic ratios demand that 90-95% of the He is generated in the crust, yet discharge of 21 mmol L^{-1} of dissolved CO_2, and the CO_2/He ratio of the gases requires that 4.6 x 10^{-4} mol s^{-1} of He are released from this small thermal area (~1% of the thermal water discharge at Yellowstone). A He flux of this magnitude would require steady-state ingrowth of U-rich crust (7 ppm U and Th/U = 3.5) equivalent to the entire area of Yellowstone National Park down to 8 km depth. This astonishing calculation implies: i) igneous heat liberates ^4He produced by millions (and in some cases billions) of years of radioactive decay and He storage, and ii) the fluid flow and crustal degassing is ultimately short-lived on a geologic timescale, generating remarkable bursts of crustal gas.

A leopard cannot change its spots: The $CO_2/^3He$ ratio of Yellowstone gases is consistent throughout the park, with values between 10^9 and 10^{10} and shows no correlation with either gas chemistry or isotopes. The constant ratio of these gases and the similarity to mantle values demonstrates that the crustal component of CO_2 is < 50% of total CO_2 and that crustal and mantle CO_2 are well-mixed at depth. Moreover, thermodynamic models for CO_2 fugacities in calcite-bearing geothermal systems predict 2-3 orders of magnitude variation in CO_2 pressure over the 100-300°C range of geothermal temperatures. Clearly, deep magmatic and metamorphic degassing flood the geothermal system with CO_2. Low temperature solution-mineral equilibria provide little control on the $CO_2/^3He$ ratio of emitted gases.

https://doi.org/10.1180/S0026461X00008434 Published online by Cambridge University Press

Formation mechanisms of carbonate concretions of the Monterey Formation: Analyses of clumped isotopes, iron, sulfur and carbon

SEAN J. LOYD[1]*, WILLIAM M. BERELSON[2], TIMOTHY W. LYONS[3], DOUGLAS E. HAMMOND[2], ARADHNA K. TRIPATI[1], JOHN M. EILER[4], AND FRANK A. CORSETTI[2]

[1]Univ. Calif., Los Angeles, Los Angeles, USA, seanloyd@ess.ucla.edu (* presenting author)
[2]Univ. So. Calif., Los Angeles, USA
[3]Univ. Calif., Riverside, Riverside, USA
[4]Calif. Inst. Tech., Pasadena, USA

Carbonate concretions can form as a result of organic matter degradation within sediments. However, the ability to determine specific processes and formation temperatures of particular concretions has remained elusive. Here, we employ concentrations of carbonate-associated sulfate (CAS), $\delta^{34}S_{CAS}$ and clumped isotopes (along with more traditional approaches) to characterize the nature of concretion authigenesis within the Miocene Monterey Formation.

Integrated analyses reveal that at least three specific diagenetic reaction pathways can be tied to concretion formation. One calcitic concretion from the Phosphatic Shale Member at Naples Beach yields $\delta^{34}S_{CAS}$ values near Miocene seawater sulfate (~ +22‰ VCDT), abundant CAS (ca. 1000 ppm), depleted $\delta^{13}C_{carb}$ (~ –11‰ VPDB), very low concentrations of Fe (ca. 700 ppm) and Mn (ca. 15 ppm) and clumped isotope temperatures of ~18°C—characteristics most consistent with shallow formation in association with microbially mediated, organic matter degradation by nitrate, iron-oxides and/or minor sulfate reduction. Cemented concretionary layers of the Phosphatic Shale Member at Shell Beach display elevated $\delta^{34}S_{CAS}$ (up to ~ +37‰), CAS concentrations of ~600 ppm, mildly depleted $\delta^{13}C_{carb}$ (~ –6‰), moderate amounts of Mn (ca. 250 ppm), relatively low Fe (ca. 1,700 ppm) and clumped isotope temperatures of ~27-35°C, indicative of somewhat deeper formation in sediments dominated by sulfate reduction. Finally, concretions within a siliceous host at Montaña de Oro and Naples Beach show minimal CAS concentrations, positive $\delta^{13}C$ values (up to +16‰), the highest concentrations of Fe (ca. 11,300 ppm) and Mn (ca. 440 ppm) and clumped isotope temperatures of ~28-35°C, consistent with formation in sediments experiencing methanogenesis in a highly reducing environment. This study highlights the promise in combining CAS and clumped isotope analyses with more traditional techniques to more precisely characterize subsurface biospheric processes and particularly how they relate to Fe-S-C cycling in ancient sediments.

Two contrasting Sn- and W-bearing granites in the Nanling Range, South China: evidence from Hf isotopes

JIANJUN LU, RUCHENG WANG, DONGSHENG MA, WEIFENG CHEN, LEI XIE AND RONGQING ZHANG

State Key Laboratory for Mineral Deposits Research, School of Earth Sciences and Engineering, Nanjing University, Nanjing, 210093, China (lujj@nju.edu.cn)

The Nanling Range where many granite-related lager-superlarge rare-element deposits occur, is the most important area in terms of W-Sn deposits in the world. The Middle-Late Jurassic period (170-140Ma) is the most important metallogenic time for W and Sn in this area. The most granites associated with W-Sn deposits formed during this time can be divided into two groups: the W- and Sn-bearing granites. These two kinds of granites have different petrochemical and trace element geochemical features [1]. The W-bearing granites comprising biotite granites, two-mica granites and muscovite granites are peraluminous and belong to S-type, whereas the Sn-bearing granites consisting of hornblende-bearing biotite granites and biotite granites and containing little muscovite are metaluminous and belong to A-type [2].

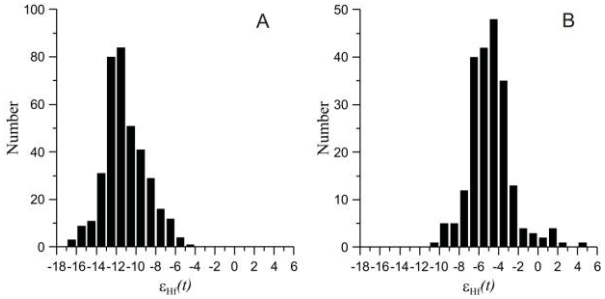

Figure 1: Histograms of zircon Hf isotopic compositions for the W-bearing (A) and Sn-bearing (B) granites

We have investigated the Hf isotope compositions of zircons in both the W- and Sn-bearing granites. The εHf(t) values of the zircons in the W-bearing granites vary from -8 to -14, with a peak value of -12; whereas the εHf(t) values of the zircons in the Sn-bearing granites range from -2 to -8, with a peak value of -5. The hafnium isotope compositions for these two kinds of ore-bearing granites in the Nanling Range indicate that the W-bearing granites were dominantly derived from the continental crustal materials; whereas the Sn-bearing granites were mainly generated by the crust-mantle mixed sources.

This work was financially supported by the NSFC (40873029) and China Geological Survey (1212010632100).

[1] Chen, Lu, Chen, et al. (2008) *Geological Journal of China Universities,* **14**, 459-473. [2] Lu, Zhang & Wang (2011) *Mineralogical Magazine* **75**, 1359.

https://doi.org/10.1180/S0026461X00008434 Published online by Cambridge University Press

^{81}Kr-dating is now available

Z.-T. LU,[1,2*] W. JIANG,[1] A. SHARMA,[1,2] K. BAILEY,[1] P. MUELLER,[1] T.P. O'CONNOR,[1] S.-M. HU,[3] R. PURTSCHERT,[4] N.C. STURCHIO[5]

[1]Argonne National Laboratory, Argonne, USA (* LU@ANL.GOV)
[2]The University of Chicago, Chicago, USA
[3]University of Science and Technology of China, Hefei, China
[4]University of Bern, Bern, Switzerland
[5]University of Illinois at Chicago, Chicago, USA

Due to its simple production and transport processes in the terrestrial environment, the long-lived noble-gas isotope ^{81}Kr is the ideal tracer for old water and ice in the age range of 10^5-10^6 years, a range beyond the reach of ^{14}C. ^{81}Kr-dating, a concept pursued over the past four decades by numerous laboratories employing a variety of techniques, is now available for the first time to the earth science community at large. This is made possible by the development of ATTA-3, an efficient and selective atom counter based on the Atom Trap Trace Analysis method and capable of measuring both ^{81}Kr/Kr and ^{85}Kr/Kr ratios of environmental samples in the range of 10^{-14}-10^{-10}. The instrument was calibrated with 12 samples whose ^{85}Kr/Kr ratios were independently measured using Low Level Decay Counting, including six samples that were measured in a blind arrangement. Compared to the previously reported ATTA-2 instrument, the counting rates of ATTA-3 are higher by two orders of magnitude and the required sample size lower by one order of magnitude. For ^{81}Kr-dating in the age range of 200 – 1,500 kyr, the required sample size is 5 – 10 micro-L STP of krypton gas, which can be extracted from approximately 100 – 200 kg of water or 40 – 80 kg of ice. Moreover, a laser-induced quenching scheme was developed to enable measurements of both the rare ^{81,85}Kr and the abundant ^{83}Kr, whose isotopic abundances differ by 11 orders of magnitude. This scheme allows ATTA-3 to directly determine ^{81}Kr/Kr and ^{85}Kr/Kr ratios without other supplemental measurements. Combining the significant reduction in sample size with several advances in the measurement procedure, ATTA-3 represents the state-of-the-art instrument for routine analysis of these rare noble gas tracers for a wide range of earth science applications.

More information regarding ATTA-3 is posted at http://www.phy.anl.gov/mep/atta/. This work is supported by the U.S. DOE, Office of Nuclear Physics, under contract DE-AC02-06CH11357; and by NSF, Division of Earth Sciences, under Award No. EAR-0651161.

Climate controls the fluctuations of fish mercury levels in Québec lakes

MARC LUCOTTE[1]*, SERGE PAQUET[1], AND MATTHIEU MOINGT[1]

[1]GEOTOP, UQAM, Montréal, Canada
lucotte.marc_michel@uqam.ca
paquet.serge@uqam.ca, matthieumoingt@yahoo.fr

Data mining

The compilation of data bases of Québec Ministry of Environment, Hydro-Québec, COMERN strategic network as well as Environment Canada's CARA research program allowed us to reconstruct the history of total mercury levels (Hg) over the 1979-2011 period in two predatory fish species most consumed in mid-northern Québec (Canada): northern pike (*Esox lucius*) and walleye (*Sander vitreus*). We present results for a series of 82 large lakes frequently fished by sport fishers. In order to compare different years and lakes among each other, we calculated fish flesh Hg levels at standardized lengths using von Bertalanffy growth models. We also used fish growth rates data whenever available. We run our statistical analysis considering 20 GIS variables (lake order, watershed slopes, drainage density, mining sites, vegetation cover, geological substratum) and 15 climatic variables (monthly precipitations, temperatures, and sulfate deposition).

Trends in mercury levels in walleye and pike over the last three decades

Climatic factors such as annual mean temperatures and winter precipitations could explain 60% of the variations of walleye Hg levels. In turn, these climatic variables appeared to strongly control walleye growth rates. In addition, logging activities equivalent to at least 20% of the watershed surface every 10 years could explain 15% of the variations of waleye Hg levels. The influence of mining activities in lakes watershed appeared to be masked by the dominant climatic conditions and eventual logging activities. In fact, walleyes caught in lakes heavily impacted by mining activities such as Chibougamau and Matagami lakes presented some of the lowest Hg levels at standardized length. 35% of the variations of pike Hg levels could be explained by the nature of the watershed, rather steep slopes having a positive influence on the bioaccumulation of the heavy metal in that fish species. Mining activities in the watershed also explained 15% of the variations of pike Hg levels. Watershed characteristics (10 to 20% slopes and higher fraction of the watershed covered by mixed forest) was in turn linked to fish growth rates, which by itself explained 45% of the variations of pike Hg levels.

Climate conditions control fish mercury levels

Hg levels in walleyes and to some extent in pikes in large lakes of mid-northern Québec have been significantly increasing from the 1980's to the 1990's due to colder and dryer conditions prevailing at that time and sharply decreasing since then mainly because of average temperatures rises, in turn stimulating fish growth rates. The effect of measured decreased acid rain deposition could not be detected with our data set. In the absence of monitoring stations of wet and dry atmospheric Hg deposition in the region, the effects of decreased Hg atmospheric emissions at the continental scale could not be evidenced either.

https://doi.org/10.1180/S0026461X00008434 Published online by Cambridge University Press

The geochemistry of aqueous fluids and hydrous melts in subduction zones

STEFANIE LUGINBUEHL[1*], PETER ULMER[1] AND THOMAS PETTKE[2]

[1]Dept. Earth Sciences, ETHZ, 8092 Zurich, Switzerland, (*correspondence: stefanie.luginbuehl@erdw.ethz.ch)
[2]University of Bern, Institute of Geological Sciences, 3012 Bern, Switzerland

Aqueous fluids and silicate melts released from dehydrating slabs play a crucial role in mass transfer in subduction zones. Therefore, it is important to quantify the nature and composition of these mobile phases in order to understand elemental transport from the slab to the mantle wedge and the consequences for arc magmatism. We performed experiments at 2-3 GPa and temperatures between 700 and 1100°C on a K-free, H_2O-saturated and trace element-doped basaltic composition representing altered, oceanic lithosphere. This pressure-temperature range corresponds to a depth in subduction zones where hydrous phases, most prominently epidote group minerals and amphibole, are stable and constitute hosts for a number of trace elements like REE, HFSE, some LILE as well as U and Th.

Due to experimental and analytical difficulties in measuring the composition of fluids and melts directly and quantitatively, a "freezing stage" [1] is employed to determine compositions of frozen liquids and fluids by Laser ablation-ICP-MS. By applying this method, the loss of any potential precipitates and unquenchable solutes upon preparation for subsequent analyses is prevented. The employment of diamond traps in the experiments allows mobile phases to be collected in the trap and being analysed by this procedure. Coexisting eclogitic residual mineral assemblages are likewise measured by EMPA and LA-ICP-MS in order to obtain partition coefficients between fluids/melts and solid residual phases.

Preliminary results show hydrous phase assemblages with amphibole and epidote stable at lower temperatures (700 and 800°C), that are replaced by dominantly anhydrous phase assemblages with clinopyroxene and garnet coexisting with trondhjemitic melt at higher temperatures. Rutile is present as accessory mineral at all temperatures. H_2O contents of the liquid phase indicate an aqueous fluid being stable at 700°C and hydrous melts coexisting with eclogite above 800°C. Partition coefficients between hydrous mobile phases and the solid residue indicate garnet controlling Heavy REE at higher temperatures while Light REE, as well as Th and Sr, show strong compatibilities and suggest epidote group minerals controlling these elements below 800°C.

[1] Aerts M. *et al.* (2010) *American Mineralogist,* **95**, 1523-1526.

Recycled material in MORB sources: Os isotopes and HSE in the fossil Galapagos Rise lavas

AMBRE LUGUET[1*], KARSTEN HAASE[2] AND MARCEL REGELOUS[2]

[1]Steinmann Institut, Universität Bonn, Germany (* presenting author), (ambre.luguet@uni-bonn.de)
[2]Geozentrum Nord-Bayern, Universität Erlangen-Nürnberg, Germany (karsten.haase@geol.uni-erlangen.de, regelous@geol.uni-erlangen.de)

There is now growing evidence from trace elements and lithophile-element based isotopes (e.g. Sr, Nd, Pb) that enriched lithologies (e.g. pyroxenites) are significant contributors to the heterogeneous signatures of the Earth's mantle and a major source component in enriched basaltic melts such as the E-MORBs or OIB [1, 2].

Owing to the opposite geochemical behaviour of Re and Os during partial melting, the Re-Os isotopic system may be most sensitive to trace recycling and thus provide further insights into the mantle heterogeneity and its origin. We have analysed N-MORBs and E-MORBs from the fossil Galapagos Rise for $^{187}Os/^{188}Os$ ratios and highly siderophile elements (HSE). The distinct signatures in trace elements and Sr-Nd-Pb isotopic systems between these N- and E-MORBs have been attributed to variable contributions of a pyroxenitic source component due to variable mantle melting degrees and the ceasing of the spreading [3].

Both E- and N-MORBs show the overall positive-sloped HSE patterns, typical of partial melts. However, the E-MORBs are generally richer in Os, Ir, Ru Pt and Pd but contain less Re than the N-MORBs. E-MORBS contain 3.5 to 38 ppt Os and 117-230 ppt Re (Re/Os=6-33) while the N-MORBs have <1-4.5 ppt Os and 230-1190 ppt Re (Re/Os=115-690). N-MORBs have slightly radiogenic to radiogenic initial $^{187}Os/^{188}Os$ ratios (0.19-0.74) while the E-MORBs have extremely radiogenic initial $^{187}Os/^{188}Os$ ratios (0.90-0.99). Strikingly, the Galapagos Rise MORBs define a positive trend between Os concentrations and initial $^{187}Os/^{188}Os$ ratios, opposite to what is usually observed in OIB [4]. This trend suggests that the extremely radiogenic signatures of the E-MORBs may be a primary feature revealing a MORB source reservoir with a long-term Re-enrichment (i.e. high Re/Os).

Whole-rock pyroxenites and eclogites as well as their sulfides and platinum group minerals are likely candidates as source materials since they can develop similarly radiogenic signatures especially if residing in the mantle for a few billion years [5].

[1] Stracke and Bourdon (2009), *GCA* **73**, 218-238. [2] Sobolev et al., (2007) *Science* **316**, 412-417.[3] Haase et al., (2011) *G3*, **12**, Q0AC11. [4] Widom (1997), *Physica A* **244**, 484-49. [5] Luguet et al., (2008), *Science* **319**, 453-456.

https://doi.org/10.1180/S0026461X00008434 Published online by Cambridge University Press

Permeability change from CO_2 injection: Experimental considerations

ANDREW J. LUHMANN[1*], BENJAMIN M. TUTOLO[1], XIANG-ZHAO KONG[1], KANG DING[1], MARTIN O. SAAR[1], WILLIAM E. SEYFRIED, JR.[1]

[1]University of Minnesota, Department of Earth Sciences, Minneapolis, USA, luhm0031@umn.edu (*presenting author)

Abstract

Geologic carbon sequestration experiments were conducted using a hydrothermal flow system. The flow system design enables a continuous record of permeability and periodic fluid chemistry sampling during experiments at elevated temperatures and pressures. Initial experiments were conducted with deionized water saturated with CO_2 at room temperature and arkose sediment from the Eau Claire Formation. Outlet pore pressure was 11MPa and confinement pressure was 20MPa throughout the experiments, and temperature of the core was incrementally increased from room temperature to 150ºC. Some temperature step increases were followed by relatively quick changes in permeability, such that measured permeability decreased by 3-4 orders of magnitude during a given experiment. Scanning electron microscopy (SEM) revealed clay mineral formation on potassium feldspar grains (Fig. 1). While some geochemical changes did occur, the relative role of different potential permeability-reducing mechanisms is not constrained by these initial experiments. Potential mechanisms include geochemical changes as well as physical redistribution of grains and CO_2 exsolution. Ongoing experiments are being conducted to isolate the roles of these different mechanisms. Experiments with pure St. Peter quartz sand and fluid supersaturated with CO_2 isolate the effect of CO_2 exsolution, and experiments with solid arkose cores and fluid undersaturated with CO_2 constrain geochemical controls on permeability changes.

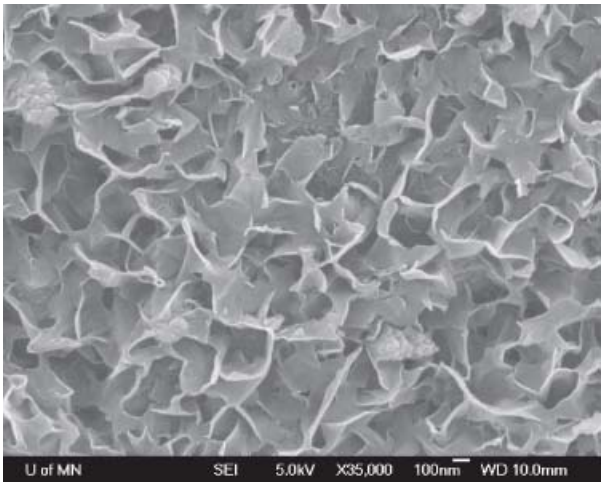

Figure 1: Clay precipitation on K-feldspar grain surface post-experiment.

Chemical speciation of sediment phosphorus and iron suggesting burial of iron-bound phosphorus in the northern Baltic Sea

KAARINA LUKKARI[1*], SANNA KUJANSUU[2], AND HANNA KAASALAINEN[3]

[1]Marine Research Centre/Finnish Environment Institute, Helsinki, Finland, kaarina.lukkari@ymparisto.fi *

[2]University of Helsinki, Finland, sanna.kujansuu@helsinki.fi

[3]University of Iceland, Reykjavik, Iceland, hannakaa@hi.is

Introduction

Biogeochemistry of phosphorus (P) is of special interest in the eutrophied Baltic Sea. Large areas of the sea-floor, especially in the central basin and in the Gulf of Finland, suffer from hypoxia, which affects P cycling and its burial [1]. Formation of authigenic carbonate fluorapatite, which is an important sink for reactive P in many marine sediments [2], is not significant in the Baltic. Instead, P is buried mostly as organic P [3]. However, in some estuary sediments, P is buried also in iron (Fe) bound form [4].

The Gulf of Bothnia is separated from the main basin by a sill and it has better oxygen conditions than the Baltic Proper. The Gulf receives high riverine input of organic and inorganic material. In order to assess whether part of P may become buried in the Fe-bound form in this Fe-rich basin, we collected samples at two oxic sites in the Gulf of Bothnia and, for comparison, from one anoxic site in the northern Baltic Proper. We made sequential extractions to assess the different forms of sediment P and Fe [5,6] and analysed nutrients and metals from the pore waters and the solid phases.

Results and Conclusions

P and Fe species in the two oxic sediments in the Gulf of Bothnia differed from those in the anoxic sediment in the Baltic Proper. At the anoxic site, sediment P was dominated by organic and detrital apatite-P and it was poor in P bound to hydrated oxides of Fe. This suggests that this redox-dependent form of P was lost during anoxia. Accordingly, reducible Fe oxides were relatively low, and Fe-speciation suggested that Fe was associated with sulphide, carbonate, and silicate phases. This was in agreement with the low dissolved Fe concentrations and the presence of hydrogen sulphide in the pore water. At certain sediment depths in the oxic Gulf of Bothnia, Fe-bound P formed more than 50% of total P concentration. Fe-speciation showed high concentrations of easily reducible and reducible Fe oxides at these same sample depths. Pore water data indicated reduction of Fe oxides and consequent release of dissolved Fe to the pore water below the 5 cm depth at both sites. However, relatively high concentrations of Fe-bound P was found down to 15-20 cm depth suggesting that part of it can be buried. Presence of benthic fauna may partly explain this finding.

[1] Conley et al. (2009) *Environ. Sci. Technol.* **43**, 3412-3420. [2] Ruttenberg (2003) *Treat. Geochem.* **8**, 585-643. [3] Mort et al. (2010) *Geochim. Cosmochim. Acta* **74**, 1350-1362. [4] Hyacinthe & Van Cappellen (2004) *Mar. Chem.* 91, 227-251. [5] Jensen & Thamdrup (1993) *Hydrobiologia* **253**, 47-59. [6] Poulton & Canfield (2005) *Chem. Geol.* **214**, 209-221.

https://doi.org/10.1180/S0026461X00008434 Published online by Cambridge University Press

Deep Pacific ventilation ages during the last deglaciation: Evaluating the influence of diffusive mixing and source region reservoir age

DAVID C. LUND[1*]

[1]University of Michigan, Earth and Environmental Sciences, Ann Arbor, MI, USA, dclund@umich.edu (*presenting author)

The rise in atmospheric carbon dioxide during the last deglaciation may have been driven by the release of carbon sequestered in the deep ocean. If this was the case, it would imply that deep Pacific ventilation ages should have A) been greater than today during the LGM and B) decreased during the deglaciation. Yet recent results based on the projection age method suggest Pacific ventilation ages during the LGM were similar to today and increased during the deglaciation, opposite the expected pattern [1]. Because the projection age method does not account for tracer diffusion [2] it can potentially yield spurious results and therefore requires validation with alternative techniques.

Here we determine ventilation ages using the transit-time distribution (TTD) method that explicitly accounts for diffusive mixing in the ocean interior [3]. To estimate TTD ages, we assumed an initial TTD width of 600 years, an equilibration-time distribution (ETD) mean of 900 years, and an ETD width of 1600 years. The ETD mean is equivalent to the average surface water reservoir age for the deep water formation region in the Southern Ocean [3]. We used five separate Monte Carlo chains with prior mean TTD values of 1000, 1500, 2000, 2500, and 3000 years. In each case, the chains were run 2000 times to ensure they had converged on a common ventilation age.

Both the TTD and projection age methods imply the ventilation age of the deep Pacific increased by ~1000 years during Heinrich Stadial 1 (H1) and ~500 years during the Younger Dryas (YD). Thus, explicitly accounting for mixing has little impact on the key features of the deep Pacific ventilation history. The similar results are due in part to the projection age error analysis in [1] that fully accounts for the uncertainty in calendar ages and benthic $\Delta^{14}C$ estimates. The resulting projection age distributions are similar to the transit time distributions produced by diffusive mixing in the TTD method.

Our ventilation age results imply that either: 1) the ventilation rate of the deep Pacific decreased during the deglaciation, 2) the surface water reservoir age in the Southern Ocean increased, or 3) there was an influx of ^{14}C-depleted carbon from another source into the deep Pacific. The first scenario would likely increase the residence time of deep water in the Pacific basin and promote oceanic sequestration of respired carbon. Although we cannot rule out this possibility, it seems unlikely given that atmospheric CO_2 increased during both H1 and the YD [4]. Alternatively, an increase in surface water reservoir age in the deep water formation region may have driven the ventilation age signal, but the timing of the required increase is inconsistent with upwelling proxies from the Southern Ocean [5]. Results from a simple geochemical box also show that a 2x increase in Southern Ocean mixing yields negligible changes in deep Pacific $\Delta^{14}C$. Turning off North Atlantic Deep Water formation reduces the quantity of ^{14}C-enriched carbon entering the deep Atlantic but increases the flux of atmospheric ^{14}C into the surface ocean in general, resulting in little net change in Pacific $\Delta^{14}C$. The lack of an obvious oceanographic mechanism implies that input of old carbon from another reservoir may have responsible for the deglacial ventilation age anomalies in the deep Pacific.

[1] Lund, Mix & Southon (2011) *Nature Geoscience* **4**, 771-774. [2] Adkins and Boyle (1997) *Paleoceanography* **12**, 337-344. [3] DeVries and Primeau (2010) *Earth and Planetary Science Letters* **295**, 367-378. [4] Monnin et al. (2001) *Science* **291**, 112-114. [5] Anderson et al. (2009) *Science* **323**, 1443-1448.

Non-traditional isotope ratios in the Sonju Lake layered mafic intrusion: insight into magma differentiation

CRAIG C. LUNDSTROM

[1]Dept. of Geology, University of Illinois at Urbana–Champaign, Urbana, IL USA (lundstro@uiuc.edu)

The Sonju Lake Intrusion (SLI) is a 1200 m thick layered mafic intrusion that directly underlies the equal volume Finland Granite (FG). These intrusions, part of the Proterozoic Keweenaw rift, provide a puzzle to standard models of igneous petrogenesis: examination of mineral modes, mineral compositions and even incompatible trace element ratios grade systematically between the two bodies as if the two intrusions were genetically related while U-Pb ages overlap. Yet, simple volume relationships argue against any fractional crystallization-like process linking the intrusions.

Despite expectations of minimal fractionation in igneous rocks, non-traditional isotope ratios show signficant variations with differentiation index in many igneous suites. Thus, examination of non-traditional systems may provide insight into the differentiation process and the SLI-FG genetic relationship. The sample set analyzed here provides a complete top to bottom transect; 10 samples come from the bottom of the SLI (the SNA drill core reaches the bottom contact); 8 come from the AC-1 drill core through the Finland Granite (these show the granite to be heterogeneous, possibly reflecting sill accumulation); another 20 field-collected samples span the SLI and SLI-FG contact zone. Results of MC-ICPMS analysis show clear distinction in $^{87}Sr/^{86}Sr$ testifying to the FG and SLI coming from different sources. $\delta^{56}Fe$ changes with stratigraphic height. The basal SNA drill core samples average -0.01 but have values as low as -0.2. The middle SLI samples average around the mean mafic earth but show systematic oscillations. The FG samples vary in $\delta^{56}Fe$ with heaviest values (0.35) in the most silicic samples.

The correlation of non-traditional isotope ratios with differentiation could reflect: 1) effects of fractional crystallization; 2) effects of fluid loss; 3) crustal contamination processes; 4) a temperature gradient effect. With regard to #1, the peak in Fe-Ti oxides in the SLI shows no relationship to the variations in $\delta^{56}Fe$; as magnetite tends to enrich in heavy Fe isotopes, the lack of correlation does not support control by FC. Although heavy $\delta^{56}Fe$ occurs in silicic FG samples (which have more radiogenic $^{87}Sr/^{86}Sr$), the relationship between Sr and Fe isotopes within each intrusion argues against crustal contamination (#2). Loss of a fluid (#3) is more difficult to assess but appears inconsistent because FG samples which are most fluid rich have the highest $\delta^{56}Fe$. A model of thermal migration zone refining shows that SLI modes and compositional trends are reproduced by a top down sill injection process; differentiation of a uniform composition basalt occurs by temperature gradient based diffusion-reaction above the sill [2]. The $\delta^{56}Fe$ pattern observed is generally consistent with the "S" shaped pattern with depth predicted by #4. If so, the FG could reflect a ripening effect of a basaltic sill system (the SLI) cooking an already existing rhyolite flow or dome into the Finland Granophyre.

[1] Shahar et al. (2008) *EPSL* **268**, 330-338.
[2] Lundstrom et al. (2011) *Intl Geol. Rev.* **53** 377-405.

https://doi.org/10.1180/S0026461X00008434 Published online by Cambridge University Press

The origin of Earth's water: Local or remote source?

JONATHAN I. LUNINE*

[1]Department of Astronomy, Cornell University, Ithaca NY, USA. jlunine@astro.cornell.edu (*)

Two Planets are Better than One

The classical idea that comets supplied the Earth's oceans [1] ran into trouble when dynamical models showed that no more than 10% of Earth's crustal water could have come from comets [2]. Since the final stage of the assembly of the Earth almost certainly involved collisions among lunar- to Mars-sized embryos, it is reasonable to imagine [2] that embryos from what is now the asteroid belt provided most of Earth's water. Our scenario works from a dynamical point of view, but probably adds too much carbonaceous chondritic material to Earth to satisfy geochemical constraints [3]. An alternative is that water was adsorbed or chemisorbed into grains locally where the Earth formed, a view championed by Mike Drake [4].

A potential test of local versus remote sources of Earth's water comes from examining Mars. Because of its small size Mars could not have gained water through the addition of large embryos—it is one of them—and so under the remote source hypothesis, a much larger fraction of Martian water must be cometary than is the case for the Earth [5]. *If* the cometary D/H is significantly higher than Earth's (SMOW) and that of Martian water, the local-source hypothesis is supported. Meteoritic evidence [6] suggests a slightly elevated D/H for early Martian water relative to SMOW, but D/H in comets varies from 1-2 times SMOW [7], so the jury is still out.

The Grand Tack Maneuver Outflanks the Geochemists

Walsh et al [8] showed that if Jupiter formed before Saturn, its interaction with the disk moved it inward to as close as 1.5 AU; the subsequent formation and entry into resonance of Saturn cause both planets to then move outward. This "Grand Tack" introduced outer solar system planetesimals into the inner solar system with a high collision probability, from which the Earth could have acquired much of its water [9] without excessive accretion of carbonaceous chondritic material. Of course, the composition of these colder bodies is not known, but being plausibly more water-rich than any known chondrite, their geochemical signature on the Earth may have been muted relative to those in our "classic" scenario.

At Odds with my Boss on Science, but Collegially So

It is said that one should never lend money to a close friend nor get into a scientific disagreement with one's Department Head. I've only done the latter. Mike Drake was my senior colleague at Arizona for 27 years and my Department Head for 18 of those. Although we disagreed on how the Earth acquired its water, it never affected our personal or professional relationship. No Department Head could have been more supportive of my professional development than Mike was. He was truly a statesman of science.

[1] Delsemme (1992) *Adv. Space Res.* **12,** 5-12. [2] Morbidelli *et al.* (2000) *Met. Plan. Sci.* **35**, 1309-1320. [3] Drake&Righter (2002) *Nature* **416,** 39-44. [4] King *et al.* (2010) *Earth Plan. Sci. Lt.* **300**, 11-18. [5] Lunine *et al.* (2003) *Icarus* **165**, 1-8. [6] Leshin (2000) *GRL.* **27**, 2017-2020. [7] Hartogh *et al.* (2011) *Nature* **478**, 218-220. [8] Walsh *et al.* (2011) *Nature* **475,** 206-209. [9] Morbidelli *et al.* (2012) *AREPS* **40**, 251-275.

Sr-Nd isotope fractionation against water depth: a case study of Datong gauge station of Yangtze River

CHAO LUO [1*], HONGBO ZHENG [1] WEIHUA WU [1] AND PING WANG [1]

[1] Institute of Surficial Geochemistry, School of Earth Sciences and Engineering, Nanjing University, Nanjing 210093, China. chaoluo.niki@gmail.com (* presenting author)

This study reports Sr-Nd isotopic compositions as well as grain size distribution of suspended sediment collected from different water depths at Datong gauge station of Yangtze River during the raining season of year 2010, in order to investigate the influence of hydrological sorting during transportation on Sr-Nd. Samples were collected biweekly from surface, middle and bottome of river depth during June 12th, 2010 to Augest 29th , 2010.

Our results show that, $^{87}Sr/^{86}Sr$ decreases from surface to bottom, ranging from 0.730332 to 0.720857. $\varepsilon_{Nd}(0)$ ranges from -14.75 to -10.09, with surface sediments having the most negative values. In Yangtze River, $\varepsilon_{Nd}(0)$ decrease from the upper reaches to the lower reaches while $^{87}Sr/^{86}Sr$ increased. [1]

Hence, Sr-Nd isotopic compositions of suspended sediments in large rivers are heterogeneous from surface to bottom. In our findings, the isotope composition of suspended sediment collected from the middle of river channel can best represent the mean isotopic composition of suspended sediment transported by river. Stratification of Sr-Nd isotope may be caused by varied contributions of sources to different depths. At least in the Yangtze River, contribution from the upper reaches is larger in the bottom sediment than in the surface sediment.

Although Sr-Nd isotope is a well acknowledged tool in provenance study, our current results indicate that it is necessary to take the grain size and sampling location into consideration.

[1] Yang et al. (2007) *Science in China* **37**, 682-690.

https://doi.org/10.1180/S0026461X00008434 Published online by Cambridge University Press

EVALUATION OF UNCERTAINTY BUDGETS OF Pb AND U DETERMINATIONS IN GLASSES AND ZIRCON AT HIGH SPATIAL RESOLUTION

Yan Luo Chris McFarlane

Department of Earth Sciences, The University of New Brunswick, Box 4400, 2 Bailey Drive, Fredericton, NB, Canada, E3B 5A3
yanluo@unb.ca*; crmm@unb.ca

Laser ablation inductively coupled plasma-mass spectrometry (LA-ICP-MS) has been widely used for element and isotope analyses in geological study. Recent research has highlighted that matrix induced laser fractionations between commonly used external reference materials (NIST61x SRMs), natural silicate reference materials (USGS glasses) and zircon are significant at high spatial resolution.[1] Question raised here is if such fractionation effect is the significant uncertainty source to combined uncertainty for the whole trace element analytical procedure. Luo et al (2007)[2] has addressed the uncertainty budget of Co, La and Th trace analysis using LA-ICP-MS. The results indicated that Poisson counting statistics prevailed for the uncertainty budget when the signal was relatively low. However, elements which have significant fractionation effect - such as Pb and U - at higher spatial resolution have not been addressed. Therefore, the objective of this study is to evaluate the uncertainty budget of Pb and U determination and assess the effect of elemental fractionation to their combined uncertainties. Experiment was conducted at 193nm excimer LA-ICP-MS lab at Department of Earth Science, University of New Brunswick. Spot sizes from 45 to 13 micron were chosen for evaluation. Calibration was performed using NIST610 with internal standardization using Ca or Si. NIST 612, NIST 614, USGS glasses and Zircon 91500 were treated as unknowns. Elemental fractionation and the matrix effect arising from 193 nm excimer laser ablation ICP-MS were evaluated in detail in this uncertainty budget study.

References

[1] Hu et al. (2011). Journal of Analytical Atomic Spectrometry **26**, p425-p430.

[2] Luo et al. (2007). Journal of Analytical Atomic Spectrometry **22**, p122-p130.

The influence of deep water circulation on the distribution of ^{231}Pa and ^{230}Th in the water column and sediments of the Pacific Ocean.

YIMING LUO*, ROGER FRANCOIS AND SUSAN E. ALLEN

Department of Earth and Ocean Sciences, University of British Columbia, 6339 Stores Road, Vancouver, BC, Canada V6T1Z4
(correspondence: yluo@eos.ubc.ca)

SESSION 12b:
"Pa and Th distributions in the ocean: controlling mechanisms"

The Atlantic Meridional Overturning Circulation (AMOC) is increasingly recognized as paramount to controlling the broad distribution pattern of sediment ^{231}Pa/^{230}Th in the Atlantic Ocean [1,2]. In contrast, for the Pacific, "boundary scavenging", i.e. the enhanced removal of ^{231}Pa in high particle flux, opal dominated regions, is generally considered as the dominant factor [3,4,5].

We have revisited this apparent dichotomy by developing a two-dimentional Pacific scavenging model to investigate the possible influence of the Pacific Meridional Overturning Circulation (PMOC) on the distribution of sediment ^{231}Pa/^{230}Th. The circulation strength and geometry in the model are based on published field observations [6] and the scavenging parameters are chosen to reproduce the broad features of dissolved ^{231}Pa and ^{230}Th profiles measured in the Pacific Ocean. Boundary scavenging is taken into account by adding a removal term derived from a two-box model following [7]. The sediment ^{231}Pa/^{230}Th generated in the model between 30°N and 30°S is then compared to the existing database.

The results show that both boundary scavenging and overturning circulation play an equally important role in determining the distribution of ^{231}Pa/^{230}Th in Pacific sediments. The former by increasing ^{231}Pa/^{230}Th in zones of enhanced scavenging and the latter by producing distinct vertical and horizontal ^{231}Pa/^{230}Th gradients. As anticipated, the boundary scavenging effect is more prominent in the eastern equatorial Pacific but the influence of circulation in this region can still be recognized in the data. In areas of lower scavenging intensity, measured sediment ^{231}Pa/^{230}Th varies with water depth in accordance with model predictions, suggesting that PMOC strength and geometry are the main controlling factors. This finding suggests that past changes in the strength and geometry of the PMOC could be derived from the distribution of ^{231}Pa/^{230}Th in the low productivity regions of the Pacific.

[1] Luo et al., (2010) Ocean Science, **6**, 381-400.
[2] Lippold et al., (2011) Geophys. Res. Lett., **38**
[3] Yang et al., (1986) Geochim Cosmochim Ac, **50**, 81-89.
[4] Anderson et al., (1990) Earth Planet Sci. Lett., **96**, 287-304.
[5] Yu et al., (2001) Earth Planet Sci. Lett., **191**, 219-230.
[6] Sloyan and Rintoul (2001) J Phys Oceanogr., **31**, 143-173.
[7] Roy-Barman (2009) Biogeosciences, **6**, 3091-3107.

https://doi.org/10.1180/S0026461X00008434 Published online by Cambridge University Press

MGMTP Software to obtain tritium concentration in precipitation

YUE LUO[1*], YANHONG ZHANG[1], SHUJUN YE [1] AND JICHUN WU[1]

[1] Department of Hydrosciences, Nanjing University, Nanjing, China kuaikuaikaikai@126.com

Tritium, as one of various environmental tracers, has been broadly applied in hydrogeology. However, observations of tritium concentration in precipitation are generally scarce. The utilization of tritium concentration is strongly limited by our knowledge of the natural distribution of tritium in precipitation over both space and time. The modified global model of tritium in precipitation (MGMTP) was developed by Zhang et al. (2011) [1]. For the purpose of making MGMTP model easy to use, the MGMTP software, a MATLAB Software Package, was developed to obtain the annual mean tritium concentration in precipitation in the area from 80°S to 80°N over the period from year 1960 to 2005. The MGMTP model was developed by improvement of Doney model [2] based on the method of factor analysis. The annual mean tritium concentration in precipitation $c_p(t)$ at any place in the MGMTP model is established by the equation:

$$c_p(t) = b + f_1\hat{c}_p(t,1) + f_2\hat{c}_p(t,2) + \varepsilon_a(t) \quad (1)$$

Where $\varepsilon_a(t)$ is the error term; $\hat{c}_p(t,1)$ and $\hat{c}_p(t,2)$ are the two reference curves (factor scores), which is determined by factor analysis using tritium data from International Atomic Energy Agency(IAEA) covering all the stations from 50°S to 70°N over period from 1960 to 2005. The coefficients f_1 and f_2 are unique for each station and are similar to the factor loadings; b represents the mean of the vector. Parameters of b, f_1 and f_2 are calculated from the least-squares solution for each selected station. The global maps of model factor coefficients f1, f2 and b are generated using a kriging interpolation method. The Software Package includes a MAT-file and a M-file. It was originally inspired by a MATLAB toolbox. The values of five parameters in MGMTP model have been stored in the MAT-file. User could easily update MAT-file if new observation data is available, because MATLAB offers functions of factor analysis and regression analysis. The role of the M-file is to solve equation (1). User can get tritium concentration with the input of specific latitude, longitude and time. The Software Package's Syntax is c = feval (Latitude, longitude, time).

Acknowledgements

Funding for this research from 973 Program No. 2010CB428803, from NSFC No. 40872155, 40725010 and 41030746, and also from Fundamental Research Funds for the Central Universities No.020614300003 is gratefully acknowledged.

[1] Zhang, Ye & Wu(2011) *Hydrological processes*, **25**, 2379–2392. [2] Doney, Glover & Jenkins (1992) *Journal of Geophysical Research-Oceans,* **97**(C4), 5481-5492.

Understanding sediment interfaces with voltammetric microelectrodes: Two decades of science and fun with Bjørn Sundby

GEORGE W. LUTHER, III[1,*], ANDREW S. MADISON[1], ALFONSO MUCCI[2], BRADLEY M. TEBO[3], BJØRN SUNDBY[2]

[1] School of Marine Science and Policy, College of Earth, Ocean and Environment, University of Delaware, Lewes, DE 19958, USA ([*]correspondence: luther@udel.edu; amadison@udel.edu)

[2] Department of Earth and Planetary Sciences, McGill University, Montreal, QC., Canada H3A 2A7 (alfonso.mucci@mcgill.ca; bjorn_sundby@uqar.ca)

[3] Division of Environmental and Biomolecular Systems, Oregon Health & Science University, Beaverton, OR 97006, USA (tebo@ebs.ogi.edu)

Abstract

GWL had the pleasure to meet Bjørn Sundby at a Black Sea conference in Gotebørg, Sweden in 1986 hosted by David Dyrssen. After that George and Bjørn communicated on a regular basis and when our Delaware group developed solid state (micro)electrodes that could measure O_2, H_2S, Fe(II) and Mn(II), it was obvious that we should join forces on studying sediment biogeochemisry. In this talk, I will show our collaborative work in the St. Lawrence estuary and Portuguese salt marshes. This includes detailed work on Mn chemistry with the O, Fe and N cycles leading to new insights on soluble Mn(III) chemistry, and interesting Pb chemistry as the redox state of the sediment changes. The collaboration has been frutiful beyond our wildest imagination, and has led to much fun and the development of a great friendship for us as well as our students and colleagues.

[1] Luther, G. W., III, B. Sundby, B. L. Lewis, P. J. Brendel and N. Silverberg (1997) Interactions of manganese with the nitrogen cycle: alternative pathways to dinitrogen. *Geochimica Cosmochimica Acta* **Volume61**, 4043-4052.
[2] Sundby, B, M. Caetano, C. Vale, C. Gobeil, G. W. Luther III and D. B. Nuzzio (2005) Root induced cycling of lead in salt marsh sediments. *Environmental Science & Technology* **Volume39**, 2080-2086.

https://doi.org/10.1180/S0026461X00008434 Published online by Cambridge University Press

THE ORIGIN OF SULFUR ISOTOPE MASS-INDEPENDENT FRACTIONATION IN ARCHEAN ROCKS

JAMES LYONS[1*], DOUGLAS BLACKIE[2], GLENN STARK[3], JULIET PICKERING[4]

[1]Dept. Earth & Space Sciences, UCLA, Los Angeles, USA, jimlyons@ucla.edu (* presenting author)
[2]Physics Dept., Imperial College, London, UK, douglas.blackie01@imperial.ac.uk
[3]Physics Dept., Wellesley College, Wellesley, USA, gstark@wellesley.edu
[4]Physics Dept., Imperial College, London, UK, j.pickering@imperial.ac.uk

Introduction

The discovery of unusual sulfur isotope fractionation in Archean and Paleoproterozoic rocks has promised to yield insights into the rise of O_2 and the nature of the sulfur cycle on ancient Earth [1], but interpretation has been hampered by the lack of a clear mechanism for the sulfur isotope signature. Proposed mechanisms include SO_2 photolysis [1-4], mass-independent fractionation (MIF) during atmospheric S_3 (thiozone) formation, and thermal sulfate reduction in sediments [5]. Studies focusing only on SO_2 photolysis, including measurements of isotopic cross sections [6], have yielded results differing greatly from theory [4], and have resulted in improbable interpretations [7].

Results

Here we report high-resolution ultraviolet cross section measurements of the sulfur isotopologues of SO_2 made with the UV FTS at Imperial College. This instrument has a dual-beam configuraton, allowing the D_2 lamp intensity to be monitored simultaneously with the gas absorption, effectively removing the lamp as a noise source. We measured cross sections at 1 cm^{-1} spectral resolution for $^{32}SO_2$, $^{33}SO_2$ and $^{34}SO_2$. Incorporating these cross sections into a simple atmospheric photochemical model, with a solar UV flux, yields sulfur MIF signatures for optically thin abundances of SO_2 due to small differences in the integrated cross sections. The $\Delta^{33}S$ values for SO and S produced by photolysis of SO_2 and SO, respectively, are positive in the 190-220 range, in contrast to the results of lower resolution cross section measurements of [6]. We therefore do not need to invoke an additional absorber to modify the sign of the MIF signature, as was done using OCS in [7]. We find that additional MIF by self-shielding by $^{32}SO_2$ places an upper limit on SO_2 of about 1 ppb. Our results imply that SO_2 photolysis alone is responsible for most of the Archean sulfur MIF record, and that sulfur MIF is a good proxy for the rise of O_2 in the earliest Paleoproterozoic. Work on $^{36}SO_2$ is in progress.

[1] Farquhar (2000) *Science* **289**, 756-758. [2] Farquhar (2001) *JGR* **106**, 32829-32840. [3] Pavlov & Kasting (2002) *Astrobiology* **2**, 27-41. [4] Lyons (2007) *GRL* **34**, L22811. [5] Watanabe et al. *Science* **324**, 370-372. [6] Danielache et al. (2008) *JGR* **113**, D17314. [7] Ueno et al. (2009) *PNAS* **106**, 14784-17789.

https://doi.org/10.1180/S0026461X00008434 Published online by Cambridge University Press

Tracing crustal contamination along the Java segment of Sunda Arc, Indonesia

JOLIS, E. M.[1*], TROLL, V. R.[1, 4], DEEGAN, F. M.[2], BLYTHE, L. S.[1], HARRIS, C.[3], FREDA, C.[4], HILTON, D.[5], CHADWICK, J.[6], VAN HELDEN, M.[6]

[1]Dept. Earth Sciences, CEMPEG, Uppsala, Sweden (*ester.jolis@geo.uu.se)
[2] Lab. for Isotope Geology, SMNH, Stockhom, Sweden
[3] Dept. of Geological Science, UCT, South Africa
[4] Istituto Nazionale di Geofisica e Vulcanologia, Rome, Italy
[5] Scripps Oceanographic Institute, San Diego, USA
[6] Dept. Petrology, Vrije, Universiteit Amsterdam, Netherlands

Arc magmas typically display chemical and petrographic characteristics indicative of crustal input. Crustal contamination can take place either in the mantle source region or as magma traverses the crust (e.g. [1]). While source contamination is generally considered the dominant process (e.g. [2, 3, 4]), crustal contamination in high level magma chambers has also been recognised at volcanic arcs (e.g. [5, 6]). In light of this, we aim to test the extent of upper crustal versus source contamination along the Java segment of the Sunda arc, which, because of its variable upper crustal structure, is ideal for the task.

We present a detailed geochemical study of 7 volcanoes along a traverse from Anak-Krakatau in the Sunda strait through Java (Gede, Slamet, Merapi, Kelut, Kawah-Ijen) and Bali (Batur). Using rock and mineral elemental geochemistry and radiogenic (Sr, Nd and Pb) and, stable (O) isotopes, we show a correspondence between changes in composition of the upper crust and the apparent degree of upper crustal contamination. There is an increase in $^{87}Sr/^{86}Sr$ and $\delta^{18}O$, and a decrease in $^{143}Nd/^{144}Nd$ from Krakatau towards Merapi, indicating substantial input from the thick quasi-continental basement beneath East and Central Java. Volcanoes to the east of Merapi, and the Progo-Muria fault zone, where the upper crust is thinner and increasingly oceanic in nature have lower $^{87}Sr/^{86}Sr$ and $\delta^{18}O$, and higher $^{143}Nd/^{144}Nd$ indicating a stronger influence of the mantle source [7]. Our new data represent a systematic and high-resolution arc-wide sampling effort that allows us to distinguish the effects of the upper crust on the compositional spectrum of individual volcanic systems along the Sunda arc.

[1] Davidson, J.P, Hora, J.M, Garrison, J.M & Dungan, M.A (2005), *J. Geotherm. Res.,* **140**, 157-170.
[2] Hilton, D.R., Fischer, T.P. & Marty, B. (2002), *Rev. Mineral. Geochem.,* **47**, 319-370.
[3] Gertisser, R. & Keller, J. (2003). *J. Petrol.*, **44**, 457-489
[4] Debaille, V., Doucelance, R., Weis, D., & Schiano, P. (2005), *Geochim. Cosmochim. Acta,* **70**,723-741.
[5] Gasparon, M., Hilton, D.R., & Varne, R. (1994), *Earth Planet. Sci. Lett.,* **126**, 15-22.
[6] Chadwick, J.P., Troll, V.R., Ginibre, C., Morgan, D., Gertisser, R., Waight, T.E. & Davidson, J.P. (2007), *J. Petrol.,* **48**, 1793-1812.
[7] Whitford, D.J. (1975), *Geochim. Cosmochim. Acta,* **39**, 1287-1302.

Multi-scale modeling of transverse reactive mixing in a coastal aquifer

H. M. NICK[1,3*], A. RAOOF[1], M. THULLNER[1,2], P.A.G. REGNIER[3]

[1]Faculty of Geosciences, Utrecht University, Utrecht, The Netherlands (*correspondence: h.m.nick@uu.nl, a.raoof@uu.nl)
[2]Department of Environmental Microbiology, UFZ – Helmholtz Centre for Environmental Research, Leipzig, Germany (martin.thullner@ufz.de)
[3]Department of Earth and Environmental Sciences, Université Libre de Bruxelles, Brussels, Belgium (pregnier@ulb.ac.be)

The transverse mixing between freshwater and seawater in coastal aquifers is a key process controlling the chemistry of submarine groundwater discharge (SGD). The quantification of such mixing and its effects on the fate of reactive chemical compounds in coastal waters are still the subject of debate. We developed reactive transport model approaches to study the mechanisms responsible for controlling reactive mixing processes in coastal aquifers. These models employ hybrid numerical methods for solving flow and transport [1,2], and benefit from utilizing the biogeochemical reaction network simulator (BRNS) [3].

Critical to advancing our understanding is the study of the interplay between reaction and flow. We particularly investigated the impact of dispersion, heterogeneity induced velocity variations and biogeochemical reactivities on reactive transport for density driven flow scenarios representing seawater-groundwater-interface in coastal aquifers. Our numerical observation showed e.g., that for highly reactive dissolved organic carbon (DOC) degradation processes are limited by the porous media properties controlling dispersion, whereas for relatively less reactive DOC degradation is controlled by reaction kinetics.

In general, we found three reactive flow regimes: reaction controlled, reaction-dispersion controlled and dispersion controlled transport. This is supported by further simulations utilizing pore-scale models to investigate these regimes at the smaller scale. Our results suggest that the chemical reactivity as well as dispersivity are important parameters governing the biogeochemical dynamics of SGD. Hence, an adequate representenation of these processes in the macro-scale models is essential.

[1] S.K. Matthai, et al. (2009) *Transport in Porous Media* **83**, 289-318.
[2] A. Raoof, et al. (2010) *Vadose Zone Journal* **9**, 624-636.
[3] P. Regnier, et al. (2002) *Applied Mathematical Modeling* **26**, 913-927.

https://doi.org/10.1180/S0026461X00008434 Published online by Cambridge University Press

Mantle Evolution from Plate Subduction to Post-orogenic Extension: Evidence from Permo-Triassic Mafic Dike Swarms in Northern Tibet Plateau

CHANGQIAN MA[1,2*], JINYANG ZHANG[2], FUHAO XIONG[2], BIN LIU[2], JIAN HUANG[2] AND BAIHUA WANG[2]

[1] State Key Lab. of Geological Processes and Mineral Resources, Wuhan, China, cqma@cug.edu.cn (* presenting author)

[2] China University of Geosciences,Wuhan,China

Five large mafic dike swarms have been discovered within the ~270 km-long Xiangride-Golmud segment of the East Kunlun belt, Northern Tibet Plateau, which are named, from east to west, the Balong, Binggou, Xiaomiao, Bairiqili and Nanshankou dyke swarms. The number of dikes in a given swarm can vary from 10 to 42, and the width of individual dikes ranges from 0.1 to 5 m. Most of the dikes trend N-S. The widest dikes are clearly banded with coarser textures and more phenocrysts in the middle portions than in the margins. Most of the dikes are porphyritic diabase with the coarser-grained varieties grading into diorites. All of the mafic dikes are composed chiefly of clinopyroxene, plagioclase and amphibole.

Based on the field relationships, hornblende Ar-Ar and zircon U-Pb dating we consider that the dike swams were formed in three episodes; Early Permian, late Permian and Triassic to Late Triassic. The Xiaomiao (277 Ma) and Binggou (225 Ma) mafic dikes are calc-alkaline in composition with low ∑REE (＜100 ppm) and relatively flat, chondrite-normalized REE patterns with no Eu anomalies. These rocks also have low Ni, Cr and V but are enriched in Rb, K, Pb and P, and depleted in Nb and Ta. In contrast, the Balong dike swarms (253 Ma) have high ∑REE (~100 to >150 ppm） and are enriched in HREE, with higher trace element contents than the other dikes. The Xiaomiao and Binggou dike swarms have similar Sr-Nd isotopic characteristics with ISr = 0.707-0.711 and εNd(t) ranges from -3.4 to 3.9, whereas the Bairiqili (251 Ma) and Balong dikes have somewhat more enriched and variable compositions, with ISr = 0.709-0.719 and εNd(t) ranging from -7.8 to -3.6. The geochemical similarities of the Permin –Triassic East Kunlun, South Qiangtang and north Himalaya dike swarms and basalts indicate that the north boundary of Gondwana reached the East Kunlun block at that time.

Further study of these dike swarms should lead to a better understanding of the influence of subducted slabs on the mantle source and subduction mechanics during the evolutionary stage between the Paleo-Tethyan oceanic plate subduction and post-orogenic extension.

Heterogeneous mantle sources of the alkaline-tholeiitic intraplate basalts from the Aleppo Plateau, NW Syria

GEORGE S.-K. MA[1,2*], JOHN MALPAS[2], KATSUHIKO SUZUKI[3], CHING-HUA LO[4], KUO-LUNG WANG[1], YOSHIYUKI IIZUKA[1] AND COSTAS XENOPHONTOS[2]

[1]IES, Academia Sinica, Taipei 11529, Taiwan, georgema@earth.sinica.edu.tw

[2]Department of Earth Sciences, The University of Hong Kong, Hong Kong

[3]IFREE, JAMSTEC, Japan

[4]Department of Geosciences, National Taiwan University, Taiwan

Mantle-derived magmas are characterised by considerable chemical and isotopic variability that is difficult to reconcile with partial melting of a peridotite mantle alone. This reflects the presence of heterogeneities in the mantle, originated from, for instance, recycled oceanic crust or metasomatised lithosphere [1, 2, 3]. Identification of such heterogeneities and thus the mineralogy of the mantle source becomes more ambiguous because both crustal contamination and crystal fractionation may mask important source characteristics.

We present age, chemical and isotopic data to constrain the source and the chemical evolution of the continental alkaline-tholeiitic intraplate magmas from the Aleppo Plateau and vicinity, NW Syria. With the aid of new $^{40}Ar/^{39}Ar$ ages, two phases of volcanism have been recognised in the Miocene, ~19-18 Ma (Phase 1) and ~13.5-12 Ma (Phase 2), in the studied area. The chemical and isotopic compositions [$^{87}Sr/^{86}Sr$ = 0.7036-0.7051, $^{143}Nd/^{144}Nd$ = 0.51269-0.51287 and $(^{187}Os/^{188}Os)_t$ = 0.151-0.453] of the lavas reflect the unequivocal influence of crustal assimilation and fractional crystallisation. However, it is interpreted that the two phases of volcanism likely sampled a mineralogically heterogeneous source, as reflected by their compositional variations seen in the most-primitive, least contaminated magmas. Such variations are: (1) relatively high Si, low Ti and trace-element contents in the Phase 1 lavas, consistent with partial melting of a largely peridotitic mantle source; (2) relatively low Si, high Ti, Fe, Ca, P, alkalis, and L-MREE/HREE, plus sub-chondritic Th-(U)/Nb, Pb/Ce and Zr/Sm in the Phase 2 lavas, approaching compositions of experimental melts of amphibole-rich metasomatic veins [3]. Thus, it is inferred that the Syrian lithosphere had been pervasively metasomatised and contained veins of amphibole-rich cumulates shortly before volcanism, and that the changing compositions of the Phase 1 to Phase 2 lavas (increasing Si-undersaturation) reflected an increasing contribution from the metasomatic vein-derived melts.

[1] Hofmann (1997) *Nature* **385**, 219-229. [2] Jackson & Dasgupta (2008) *EPSL* **276**, 175-186. [3] Pilet *et al*. (2008) *Science* **320**, 916-919.

https://doi.org/10.1180/S0026461X00008434 Published online by Cambridge University Press

Using Uranium Isotopes to Determine Salinity Sources in Rio Grande Waters

LIN MA[1*], ANNA SZYNKIEWICZ[1], DAVID BORROK[1], AND JENNIFER C. MCINTOSH[2]

[1]Department of Geological Sciences, University of Texas at El Paso, El Paso, TX 79968, USA, lma@utep.edu (* presenting author), aaszynkiewicz@utep.edu, dborrok@utep.edu

[2]Department of Hydrology and Water Resources, University of Arizona, Tucson, AZ 85721, USA, mcintosh@hwr.arizona.edu

Abstract

The Rio Grande flows from Southern Colorado through New Mexico and West Texas down to the Gulf of Mexico. It serves as an important water supply for agricutural and municipal needs. In Rio Grande waters, total dissolved solids (TDS) increase from ~40 mg/L at the headwaters to 500-1500 mg/L at El Paso, Texas. The elevated TDS values in downstream water cause various problems such as reduction in crop productivity and deterioration of soil quality due to salt loading. A number of natural and anthropogenic factors may lead to increased salinity, so the exact sources and their relative contributions to the salt load remain unclear. U isotopes (e.g., ^{234}U and ^{238}U) fractionate naturally when released from rocks to waters during chemical weathering processes at Earth's surface. It has been suggested that the degree of U isotope fractionation depends largely on local lithology and climate conditions, which affect chemical weathering and U release rates. U isotopes in natural waters thus have great potential to serve as natural tracers for chemical weathering processes, which in turn can help to determine the origins of dissolved solids (i.e., salts) and their history.

Here, we measured the U concentrations and isotope ratios for water samples collected along a ~ 1000 km stretch of Rio Grande (from the headwaters in Colorado to El Paso, Texas), as well as from streams and springs in the Jemez Mountains, a small drainage basin that recharges to Rio Grande in northern New Mexico. The comparison of these two case studies reveals different evolution histories for U in surface waters. In the Jemez Mountain region where human impacts are minimal, U isotope ratios in surface waters are largely controlled by rhyolite weathering, and both U concentrations (0.01-0.19 ppb) and ($^{234}U/^{238}U$) activity ratios (1.5-3.0) vary systematically with elevation (2600-2900 m). Here, solutes in streams largely represent mixing of two sources: young surface water (e.g., several months old) with low U concentrations and high ($^{234}U/^{238}U$) ratios and relatively old shallow groundwater that has higher U concentrations and lower ($^{234}U/^{238}U$) ratios. Similar ranges of U concentrations and ($^{234}U/^{238}U$) ratios are observed for the headwater regions of the Rio Grande. U concentrations in the Rio Grande increase significantly downstream (0.12 to 5.97 ppb) and correlate well with Ca^{2+}, Mg^{2+}, and HCO_3^- ions, revealing a control of carbonate dissolution/precipitation on river water chemistry. This is probaly due to a change of lithology. In addition, both ($^{234}U/^{238}U$) ratios (1.6-2.1) and U concentrations in the Rio Grande waters show strong seasonal patterns, reflecting the human impacts on river chemistry, such as the regulation of river flows by reservoirs and dams, agricultural irrigation return flows, and pumping of cold/geothermal aquifer waters.

Petrogenesis of the Aolunhua igneous complex, eastern Central Asian Orogenic Belt: Geochemical, and Sr–Nd–Hf isotopic constraints

XINGHUA MA[1*], BIN CHEN[1,2], AND ZHIQIANG WANG[1]

[1]Key Laboratory of Orogenic Belts and Crustal Evolution, Peking University, Beijing 100871, China, maxh@pku.edu.cn (* presenting author)

[2]Institute of Geology and Exploration Engineering, Xinjiang University, Urumchi 830046, China, binchen@pku.edu.cn

A large-scale Early Cretaceous magmatic-metallogenic belt (known as the Xar moron belt) has recently been recognized in the eastern Central Asian Orogenic Belt (CAOB), but the process and mechanism for the formation of this belt are controversial. Here we report geochemical and Sr–Nd–Hf isotopic data for the Aolunhua igneous complex (genetically related to a porphyry-type Mo deposit), to reveal its petrogenesis, source nature, and implications for the Mesozoic tectonic evolution of eastern CAOB.

The complex consists of a batholith (monzogranite-porphyry) and late-stage bimodal dyke swarms (quartz-porphyry and diorite dykes). Geochemically, the monzogranite-porphyry exhibits features of arc rocks such as conspicuous Nb, Ta negative anomalies and LILE enrichment (e.g., Sr and Ba). It has low I_{sr}, positive $\varepsilon_{Nd}(t)$ values of +0.5 to +1.4 and $\varepsilon_{Hf}(t)$ values of +3.5 to +9.8. These features, together with young inherited zircons (< 360 Ma) from the source region, suggest a juvenile basement dominated by the late Paleozoic island-arc series. The mafic enclaves hosted in the monzogranite-porphyry are characterized by containing H_2O-bearing minerals (e.g., Hb and Bi) and more calcic plagioclases, variable elements compositions, high $Mg^{\#}$, enrichment of Sr and LREE, and radiogenic Nd-Hf isotopic compositions ($\varepsilon_{Nd}(t)$ = +0.7 to +1.6 and $\varepsilon_{Hf}(t)$ = +3.3 to +10.9), indicating that they originated from a subduction-modified mantle, followed by a significant fractionation of ferromagnesian phases such as pyroxene and hornblende. Petrological and geochemical evidences including hornblende-rimmed quartz ocelli, pervasive acicular apatites in mafic enclaves, compositional disequilibrium in plagioclases and high $Mg^{\#}$ features of the host rocks, demonstrate that mixing between mantle magma and crustal melts have played an important role in the formation of monzogranite-porphyry. The quartz-porphyry dykes show high SiO_2 concentrations, low $Mg^{\#}$, conspicuous negative Eu anomalies and relatively flat REE patterns. The contemporaneous diorite dykes, however, show geochemical and isotopic characteristics similar to the mafic enclaves. The two kinds of dykes probably have been originated from melting of lower crust and mantle source, respectively, in a late stage when the monzogranite-porphyry batholiths was solidified.

In summary, the Aolunhua igneous complex formed due to the reactivation of the juvenile CAOB in the Early Cretaceous when the Paleo-Pacific oceanic slab subducted beneath eastern China, and triggered the upwelling of asthenosphere, which resulted in lithospheric thinning and extensive magmatism in the eastern CAOB.

https://doi.org/10.1180/S0026461X00008434 Published online by Cambridge University Press

Investigations into temporal and spatial variations in atmospheric helium isotopes

J.C. MABRY[1*], B. MARTY[1], P. BURNARD[1]

[1]CRPG-CNRS, 54501 Nancy, France (*correspondence: jmabry@crpg.cnrs-nancy.fr)

This work describes the development of a method to measure atmospheric helium isotopes at a very high precision (0.2% or better). The primary motivation is to look for potential temporal or spatial variations in the helium isotopic composition of the atmosphere. Since crustal helium has a large excess of ^{4}He relative to atmospheric helium, recent anthropogenic activities such as fossil fuel exploitation may give rise to a change in the atmospheric composition [1, 2]. However, previous measurements have put an upper limit on this near current measurement abilities [3, 4]. There are significant analytical challenges to improving the precision of atmospheric helium measurments as helium is only present in trace quantities in the air (5.24 ppm) and there are are many of orders of magnitude difference in the abundance of the two isotopes ($^3He/^4He_{air} = 1.38 \times 10^{-6}$).

To improve our ability to measure helium isotopes precisely, we have constructed an automated extraction line which can rapidly switch between measuring aliquots of sample with standards. For each measurement we purify a relatively large amount of gas (~20 cm^3) so that we can make many repeat analyses of the same sample gas. A major component of our method features an adjustable bellows on the sample aliquot volume that enables us to adjust the size of a sample aliquot to precisely match the standard, eliminating biases arising from nonlinear pressure effects in the mass spectrometer.

Prior to analysis we remove the neon (and any other gases remaining after purification) with a cryo trap. This lowers the pressure in the mass spectrometer and makes it easier to be sure that the standard and sample aliquots are the same size. There is an additional cryo trap on the mass spectrometer volume to maintain low background levels. Adding the cryo trap reduced the statistical errors of repeated standard analysis within one day from 0.5% to 0.3% (2σ). Meanwhile the absolute scatter of measurements over several days fell from ~5% before the addition of the cryo trap to better than 0.5%. We believe much of this remaining scatter can be attributed to an instability discovered in the high voltage power supply of the source.

All of the previous measurements were made on a GV Instruments Helix split flight tube multi-collector mass spectrometer, which was specifically designed for helium isotope measurements. Future measurements will be made on a new version of the same machine built by Thermo Scientific and recently installed in our lab (January 2012). The new machine has already demonstrated approximately three times higher sensitivity as well as better electronic stability. First results with the new machine will be presented at the conference.

[1] Oliver *et al.* (1984) *GCA* **48**, 1759-1767. [2] Pierson-Wickman *et al.* (2001) *EPSL* **194**, 165-175. [3] Sano *et al.* (2010) *GCA* **74**, 4893-4901. [4] Lupton and Evans (2004) *GRL* **31,** L13101.

Metagenome-enabled investigation of microbial sulfur precipitation in a carbonate aquifer

JENNIFER L. MACALADY[1*], DANIEL S. JONES[1], IRENE SCHAPERDOTH[1], CLARA CHAN[2] AND KEVIN CABANISS[2]

[1]Penn State University, Geosciences Dept., University Park, PA, USA (*presenting author, jlm80@psu.edu)

[2]Univ of Delaware, Earth, Ocean & Environment, Newark, DE, USA

Microbial coupling between carbon and sulfur elemental cycles in iron-poor, carbonate-rich environments results in the dissolution of carbonate minerals, precipitation of gypsum, and/or the precipiation and dissolution of elemental S. In particular, the incomplete oxidation of sulfide to elemental S strongly affects the availability of H2S and H2SO4, acids which contribute to limestone dissolution. The sulfidic Frasassi caves provide a superb model environment for understanding biotic and abiotic controls on the balance of these processes, which affect porosity development and fluid flow in sedimentary aquifers and the diagenesis of marine carbonates.

In the Frasassi system, four types of sulfide-oxidizing biofilm communities develop in separate niches defined by dissolved sulfide:oxygen ratios and hydrodynamic shear [1]. Elemental analyses suggest that S precipitates most rapidly in locations where turbulent mixing brings sulfidic water in contact with cave air, resulting in biofilms that are 40-80% sulfur by mass. Major populations in the biofilms include members of widely-dispersed and uncultivated sulfur-oxidizing clades, including Gammaproteobacteria related to "Thiobacillus baregensis" (Tbar) and Sulfurovumales-group Epsilonproteobacteria. Based on FISH population counts with genus and group-specific probes, Sulfurovumales are successful only when the sulfide:oxygen ratio exceeds 150. In contrast, Tbar populations are not correlated with concentrations of sulfide, oxygen, or the dissolved sulfide:oxygen ratio.

To further investigate the geochemical and ecological factors that favor the growth of Tbar and Sulfurovumales populations, and implications for sulfur precipitation and limestone dissolution, we investigated the metabolic capabilities of the sulfur-precipitating biofilms using enrichment culturing and metagenomics. Initial enrichment culturing efforts suggest that Tbar and Sulfurovumales populations are autotrophic or mixotrophic, and that batch (rather than flow-through) culturing methods favor the growth of Tbar over Sulfurovumales. Four metagenomes derived from biofilms naturally enriched in Tbar and Sulfurovumales populations are currently in production, and will provide genetic clues necessary to enhance enrichment culturing efforts and constrain the metabolic potential of these ecologically successful groups, including pathways for partial or complete S oxidation, S reduction, C and N fixation, heterotrophy, and biofilm formation.

[1] Macalady (2008) *ISME Journal* **2**, 590-601.

https://doi.org/10.1180/S0026461X00008434 Published online by Cambridge University Press

Isotopic and mineralogical properties of surface sediment from the circum Arctic

JENNY MACCALI[1*], CLAUDE HILLAIRE-MARCEL[1]

[1]GEOTOP-UQAM, Montréal, Canada, jenny.maccali@gmail.com (* presenting author)

Radiogenic isotopes (RI) have been used to trace sediment origin in various ocean basins [1, 2, 3, 4, 5, 6]. This method is particularly useful in sites where ire-rafting deposition (IRD) represents an important sediment transport mechanism, as illustrated recently by RI-analyses in cored sediments from Fram Strait [7], the main sea-ice exit pathway from the Arctic Ocean towards the North Atlantic. Mineral-lattice bound Pb-, Sr- and Nd- isotopes (i.e., linked to detrital sediment supplies) from this sedimentary sequence displayed two distinct temporal trends since the Last glacial Maximum [7]. In this study, three main detrital supply areas were defined, based on literature data, respectively, the Canadian and Russian margins, and northern Greenland. Broad sea-ice paleocirculation patterns were then proposed based on the Fram Strait RI-record. In order to refine sea-ice paleo-circulation reconstructions, we have undertaken a more detailed survey of potential circum-Arctic sediment sources, using surface-sediment samples from the Canadian Arctic Archipelago, the Beaufort Shelf, Bering Strait, the Chukchi Sea, the East Siberian, Laptev, Kara and Barents seas. Nd- and Sr- isotope data now define more detailed isotopic domains with, for instance, low epsilon Nd values corresponding to North American cratons, and high epsilon Nd values linked to Pacific inputs through Bering Strait. These domains are compared with relevent mineralogical information (e.g. iron-oxides) from Darby [8]. This 'RI-mapping' data set should improve quantitative estimates of IRD sources and mixing in sedimentary records from the Arctic, thus of the dynamics of surrounding continental ice-margins during the Quaternary.

[1] Fagel et al. (2004) *Paleoceanography* **19**, 1-16. [2] Frank et al. (2002) *Reviews of Geophysics* **40**, 1-38. [3] Haley et al. (2008) *Paleoceanography* **23**. [4] Tütken et al. (2002) *Marine Geology* **182**, 351-372. [5] Winter et al. (1997) *Geochimica and Cosmochimica Acta* **19**, 4181-4200. [6] O'Nions et al. (1978) *Nature* **273**, 435-438. [7] Maccali et al. (2012) *Paleoceanography* **27**. [8] Darby (2003) *Journal of Geophysical Research: Oceans* **108**, 13-1.

In Situ Determination of Sulfide Oxidation Rates in the Green Sulfur Bacterium *Chlorobaculum tepidum*

Daniel J. MacDonald[1*], Alyssa Findlay[1], Kevin Shuman[1], Daniel Hess[1], Thomas E. Hanson[1], and George W. Luther[1]

[1]College of Earth, Ocean, and Environment, University of Delaware, Lewes, DE 19958
*uri@udel.edu

Sulfur cycling in many environments is regulated by microbial activity. As the most reduced form of sulfur, H_2S, is toxic to many aerobic organisms; however, *Chlorobaculum tepidum* uses sulfide as an electron donor during photosynthesis. Microbial sulfide oxidation is a major sulfide removal mechanism, yet the relevant microbial oxidation rates are relatively unknown. In a recent study biological sulfide oxidation rates were determined to exceed abiotic oxidation rates by several orders of magnitude[1]. Voltammetric data will be presented that examines the rate of sulfide loss due to microbial uptake and oxidation over a variety of physical and biochemical parameters, such as the effects of light intensity, biomass concentration and total sulfide concentration. Speciation of sulfide oxidation products, such as elemental sulfur and polysulfides, and the rates at which these products form, will be presented. Initial data show that these organisms follow Michaelis-Menten kinetics with an approximate apparent saturation rate of 100 μM sulfide.

[1] Luther et. al. (2011) *"Thermodynamics and Kinetics of sulfide oxidation by oxygen: a look at inorganically controlled reactions and biologically mediated processes in the environment"* Frontiers in Microbiology**. 2.**

https://doi.org/10.1180/S0026461X00008434 Published online by Cambridge University Press

Natural-abundance stable carbon isotopes of small-subunit ribosomal RNA (SSU rRNA): first results from Guaymas Basin (Mexico)

BARBARA J. MACGREGOR*, HOWARD MENDLOVITZ, DANIEL ALBERT, AND ANDREAS P. TESKE

University of North Carolina, Dept. of Marine Sciences
*bmacgreg@unc.edu, mendlovitz@unc.edu, dan_albert@unc.edu, teske@email.unc.edu

Introduction

Small-subunit ribosomal RNA (SSU rRNA) is a phylogenetically informative molecule found in all cells. Being poorly preserved in most environments, it is a useful marker for active microbial populations. At Guaymas Basin, hydrothermal fluids interact with abundant sedimentary organic carbon to produce natural gas and petroleum. Where this reaches the sediment surface, it can support dense patches of seafloor life, including *Beggiatoa* mats. We report here on the stable carbon isotopic composition of SSU rRNA from a *Beggiatoa* mat transect, a cold background site, and a warm site with high oil concentration. Our initial hypotheses were that rRNA isotopic composition would be strongly influenced by methane supply, and that archaeal rRNA might be lighter than bacterial due to contributions from methanogens and anaerobic methane oxidizers.

Results and Conclusion

The central part of the mat overlay the steepest temperature gradient, and was visually dominated by orange *Beggiatoa*. This was fringed by white *Beggiatoa* mat and bare, but still warm, sediment. Methane concentrations were saturating beneath the mat and at the oily site, lower beneath bare sediment, and below detection at the background site.

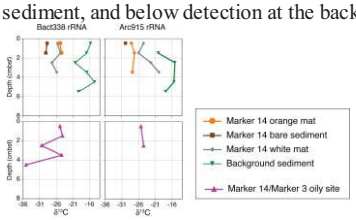

Figure 1. Stable carbon isotope composition of rRNA captured by magnetic bead capture hybridization [1].

We used biotin-labeled oligonucleotides to capture Bacterial and Archaeal SSU rRNA for isotopic determination (Fig. 1). Background-site rRNA was isotopically heaviest, and bacterial RNA from below 2 cm at the oily site was lightest, consistent with control by methane. Within the mat, however, rRNA from the bare periphery was lightest. There was no consistent isotopic difference between the probes, although RNA recoveries were too low for capture at depths where methanogens and methane oxidizers are expected.

Our prediction that rRNA isotopes would correlate directly with methane supply was clearly oversimplified. Future work will include the isotopic characterization of other potential carbon substrates. We are also investigating Gulf of Mexico sediments, where methane is significantly more ^{13}C-depleted than at Guaymas Basin.

[1] Miyatake et al. (2009) *Appl. Environ. Microbiol.* **75**, 4927-4935.

Surface complexation modeling of Na^+ and Rb^+ adsorption by rutile to 250°C

MICHAEL L. MACHESKY[1]*, MILAN PŘEDOTA[2], MOIRA K. RIDLEY[3], AND DAVID J. WESOLOWSKI[4]

[1]Univ. of Illinois, Illinois State Water Survey, Champaign IL, USA, machesky@illinois.edu (* presenting author)
[2]Univ. South Bohemia, České Budějovice, Czech Republic, predota@prf.jcu.cz
[3]Texas Tech Univ., Dept. of Geosciences, Lubbock, TX, USA, moira.ridley@ttu.edu
[4]Oak Ridge National Laboratory, Oak Ridge, TN, USA, dqw@ornl.gov

Surface complexation models (SCMs) provide the means to rationalize and extend (to uncharacterized conditions) cation adsorption data, and increasing use is being made of molecular level experimental and/or modeling results to constrain SCM parameter space. One rather surprising finding of this molecular-level information is that monovalent alkali metal cations can bind in inner-sphere fashion to oxides such as rutile. Given the very common use of alkali metal salts as background electrolyte media for adsorption experiments, it therefore becomes necessary to incorporate inner-sphere adsorption of alkali metal cations into SCMs to best represent molecular-level reality.

Ridley et al [1] demonstrated that the CD-MUSIC model of Hiemstra, van Riemsdijk and co-workers can successfully accommodate inner-sphere binding of Na^+, K^+, and Rb^+, as gleaned from ab initio constrained classical molecular dynamics (CMD) simulations (for Na^+, Rb^+) and X-ray reflectivity measurements (for Rb^+) in fitting 25°C rutile surface titration data. We have extended this CD-MUSIC approach to rutile surface titration data collected to 250°C in NaCl, NaTr(Tr=triflate) and RbCl electrolyte solutions. CMD results that track Na^+ and Rb^+ adsorption by the 110 surface of rutile at 25, 150, and 250°C and several charge states are used to constrain the allowable CD-MUSIC model parameters and it is shown that the resulting SCM can adequately mirror most of the CMD results over the broad ambient to hydrothermal temperature range.

[1] Ridley et al. (2009) *Geochim. Cosmochim. Acta* **73**, 1841-1856.

https://doi.org/10.1180/S0026461X00008434 Published online by Cambridge University Press

Discharge-driven harmful algal blooms in the NE Gulf of Mexico

H.L. MACINTYRE[1*], J.D. LIEFER[2], L. NOVOVESKA[2], W.C. BURNETT[3], N. SU[3], K.T. ELLER[3], W.L. SMITH[4], C.P. DORSEY[4], R.H. PETERSON[5] AND R.F. VISO[5]

[1]Dalhousie University, Halifax, Canada, hugh.macintyre@dal.ca (* presenting author)
[2]Dauphin Island Sea Lab, Dauphin Island, USA, jdl602@jaguar1.usouthal.edu, lucie.novoveska@gmail.com
[3]Florida State University, Tallahassee, USA, wburnett@fsu.edu, nisu1111@gmail.com, eller@ocean.fsu.edu
[4]Alabama Department of Public Health, Mobile, USA, billandelinor72@yahoo.com, Carol.Dorsey@adph.state.al.us
[5]Coastal Carolina University, Conway, USA, rpeters2@coastal.edu, rviso@coastal.edu

The state of Alabama (USA) has only 100 km of coastline but has had recurring harmful algal blooms (HABs) at two shallow-water hot-spots. Both are in the same hydrological unit on the eastern margin of Mobile Bay. The first, Weeks Bay, is a sub-estuary on the eastern margin of Mobile Bay and is the site of diverse dinoflagellate blooms that cause hypoxia and fish-kills. The second, the Gulf of Mexico shoreline adjacent to Little Lagoon, a shallow and saline lagoon, is the site of toxic blooms of the diatom *Pseudo-nitzschia* spp. Initiation of both dinoflagellate and diatom blooms is correlated with discharge from the aquifer.

Microalgal community composition appears to be driven by the interaction of temperature and submarine groundwater discharge. Dinoflagellates bloom in Weeks Bay during periods of low discharge in both winter (*Prorocentrum minimum*) and summer (*Karlodinium veneficum*). *Pseudo-nitzschia* spp. bloom predominantly in the spring after periods of high discharge [1], as part of a cohort of diatoms that includes other bloom-forming taxa [2]. Comparison of community composition with physico-chemical characteristics of Little Lagoon showed a very high correlation between the degree of dominance by diatoms and water age (inferred from the excess ^{224}Ra:^{223}Ra ratio) when subsurface resistivity showed that the water table was high. There was no correlation between community indices and water age when the water table was low.

The surficial aquifer is contaminated with very high N (up to c. 5 mM DIN plus DON) and the sediments in Weeks Bay and Little Lagoon have even higher concentrations of both N and P. Although the supply of nutrients by groundwater is important in supporting very dense blooms, the magnitude of discharge is likely as important in structuring the community. The conditions under which both dinoflagellate and diatom blooms occur are consistent with ordination of their niches in terms of habitat productivity and stability [3]. Because global climate change is predicted to alter seasonal patterns of precipitation, hence aquifer discharge, it is likely that the niches for these HAB taxa will expand.

[1] Liefer et al. (2009) *Harmful Algae* **8**: 706-714. [2] MacIntyre et al. (2011) *J. Plankt. Res.* **33**: 273–295. [3] Grime (1977) *Amer. Natur*. **111:** 1169-1194.

Nanodiamonds and carbonaceous grains in Bull Creek Valley, Oklahoma

ANDREW S. MADDEN[1*], ANDREW L. SWINDLE[1], LELAND C. BEMENT[2], BRIAN J. CARTER[3], ALEX R. SIMMS[4], AND MOURAD BENAMARA[5]

[1]University of Oklahoma, Norman OK, USA, amadden@ou.edu (* presenting author), aswindle@ou.edu
[2]Oklahoma Archaeological Survey, Norman OK, USA, lbement@ou.edu
[3]Oklahoma State University, Stillwater OK, USA, brian.j.cater@okstate.edu
[4]University of California Santa Barbara, Santa Barbara CA, USA, asimms@geol.ucsb.edu
[5]University of Arkansas, Fayetteville AR, USA, mourad@uark.edu

Sediments in the Bull Creek Valley document the Pliestocene-Holocene transition, including the period corresponding to the Younger Dryas climate anomaly. Conflicting reports of nanodiamond presence/ absence, spatial/ temporal distribution, and polymorphic phase identification [e.g., 1,2] are perhaps not surprising given the challenges of recovering and identifying such materials within bulk sediments. Nanodiamonds form extraterrestrially; their distribution in Earth sediments may relate to the intensity of extraterrestrial bombardment. It has been suggested that a nanodiamond spike in Younger Dryas strata records an impact event, contributing to cooling on a global to regional scale [1].

For this study, sediments corresponding to alluvial, paleosol, and loess horizons were collected from multiple profiles across the Bull Creek Valley at approximately 10 cm intervals. Carbon dates ranged from ~33,000 years before present to recent. The clay fraction was separated from the bulk soil and then digested by a series of strong acid treatments. Residues were resuspended in ammonium hydroxide and prepared for transmission electron microscopy (TEM) by centrifugation onto grids with carbon support films. Grids were analyzed with TEM, high-resolution TEM (HRTEM), energy-dispersive x-ray analysis (EDS), and electron energy loss spectroscopy (EELS).

Nanodiamonds were identified in multiple horizons, including sediment dated to the Younger Dryas. Individual grains ranged from approximately 3-50 nm, although most grains were 5-10 nm. Most or all grains correspond to the n-diamond polymorph, as suggested by lattice fringe spacings. Lesser amounts of cubic nanodiamonds qwere also tentatively identified. EELS of these particles was consistent with sp^3-bonded carbon. Other micron-scale particles morphologically similar with those previously identified as hexagonal diamond [3] were graphene/graphane mixtures based on electron diffraction and EELS.

[1] Kennett et al. (2009) *Science* **323**, 94. [2] Daulton et al. (2010) *PNAS* **107**, 16043-16047. [2] Kennett et al. (2009) *PNAS* **106**, 12623-12628.

https://doi.org/10.1180/S0026461X00008434 Published online by Cambridge University Press

Reactive transport in compacted bentonite: porosity concepts, experiments and applications

URS MÄDER[1]*, ANDREAS JENNI[1], RAÚL FERNÁNDEZ[2], AND ISABEL DE SOTO GARCÍA[2]

[1]University of Bern, Geological Sciences, Bern, Switzerland
* urs.maeder@geo.unibe.ch, andreas.jenni@geo.unibe.ch
[2]Universidad Autonóma de Madrid, Departamento de Geología y Geoquímica, Madrid, Spain, raul.fernandez@uam.es,isabel.desoto@uam.es

Porosity concepts and scales

Chemical and transport processes in compacted bentonite are operating at the nanometer scale of smectite interlayers but cannot be resolved at this scale by analytical or imaging techniques. Porosity concepts are treated as macroscopic averaged properties but are based on the microscopic scale using electrostatics and explicit or averaged Poisson-Boltzman theory for the distribution of electrolyte species adjacent to mineral surfaces bearing permanent charge. Implementation into reactive transport numerical models is debated, ranging from an averaged single-phase solid-liquid electrolyte [1] to complex multi-porous models assigning transport parameters specific to each type of porosity [2]. Here, we examine the relative merits and limitations of different multi-porous models as applied to experimental data of various complexity.

Reactive transport modelling of experimental data

A long-term multi-component advective-diffusive reactive transport experiment with compacted bentonite can be modelled satisfactorily with either a dual porous concept (small proportion of charge-balanced "free" eletrolyte, large proportion of interlayer-type electrolyte with Donnan approximation), or more complex model assigning separate porosities to the interlayers and a pore space close to external surfaces of smectite particles. Transport of the solvent was additionally constrained by a D_2O tracer.

Modelling of short-term simple major-component through-diffusion experiments is not discriminating between models of various complexity and leads to a strong dependency of transport coefficients on the porosity concept.

PHREEQC and Crunchflow were used as numerical models, both capable of treating multiple porosities, electrostatics in the form of diffuse-layer theory, and species-specific and porosity-specific transport properties.

References [1] Birgersson M. & Karnland O. (2009) *Geochim. Cosmochim. Acta,* **73**, 1908-1923. [2] Tournassat C. & Appelo C.A.J. (2011) *Geochim. Cosmochim. Acta*, **75**, 3698-3710.

Modeling Eu(III) sorption on granite

K. MAEDA[1*], K. FUKUSHI[1], Y. HASEGAWA[1], Y. YAMAMOTO[2], D. AOSAI[2] AND T. MIZUNO[2]

[1]Kanazawa Univeristy, Kanazawa, Japan, koushi@stu.kanazawa-u.ac.jp (presenting author)
[2]Japan Atomic Energy Agency, Mizunami, Japan

There have been very few researches for the trace elements sorption on complex mineral assemblages such as rocks, sediments and soils. In order to make predictions for the trace elements migration on geologic media, it is crucial to understand the nano-scale interaction of trace elements with complex mineral assemblages, and to construct the thermodynamic sorption models based on the molecular-scale information. In the present study, the batch sorption experiments of Eu(III) on granite were conducted as function of pH and ionic strength. The sorption behavior was modeled based on our microscopic observation (Hasegawa et al. this volume).

The granite sample was collected from a borehole at a depth of 400 m from the Mizunami Underground Research Laboratory constructed by Japan Atomic Energy Agency in central Japan. The granite was visually fresh. However, the microscope observation and the X-ray diffraction analysis of clay fraction show the occurrences of smectite, chlorite, vermiculate, calcite and hydrous iron oxides. Eu(III) sorption experiments on granite in the Teflon vessels were conducted as function of pH (2 to 8), ionic strength (I=0.01 and 0.1) and Eu concentration (1 and 10 uM) under ultra-pure N_2 atmosphere in room temperature.

The experiments and modeling results are shown in the Figure. Sorption ratio of Eu(III) was almost zero at pH 2. They abruptly increase with pH up to 3.5. Above pH 3.5, the sorption ratio indicates almost constant. The sorption strongly depends on ionic strength at the pH more than 3.5. Our microscopic observations show that Eu(III) is selectively scavenged by biotite and that sorption mode of Eu(III) is identified to be exchange reaction with inter-layer K in biotite and Eu(III). The sorption behaviors at pH more than 3.5 are consistent with the cation exchange reaction. At low pH conditions, less than pH 3.5, the release of the Al and/or Fe must occur with dissolution of minerals. The Al and/or Fe should be competed with Eu(III) on the exchange site of biotite. The sorption modeling is simply considering ion exchange reaction and solubility of hydrous iron oxide. The model reasonably reproduces the overall sorption behavior.

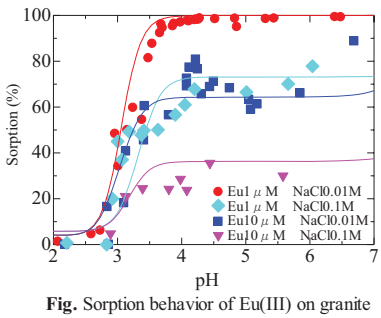

Fig. Sorption behavior of Eu(III) on granite

Ref.: Y. Hasegawa, K. Fukushi, K. Maeda, Y. Yamamoto, D. Aosai and T. Mizuno: "Identification and characterization of phase governing Eu(III) uptake in granite by microscopic observations", In this volume

https://doi.org/10.1180/S0026461X00008434 Published online by Cambridge University Press

More than just "brown layers": Manganese in Quaternary Arctic Ocean sediments

C. MÄRZ[1,2,*], A. STRATMANN[2], J. MATTHIESSEN[3], S.W. POULTON[1], A.-K. MEINHARDT[2], S. ECKERT[2], B. SCHNETGER[2], C. VOGT[4], R STEIN[3] AND H.-J. BRUMSACK[2]

[1]School of Civil Engineering and Geosciences, Newcastle University, UK, christian.maerz@ncl.ac.uk (* presenting author)
[2]Institut für Chemie und Biologie des Meeres, Carl-von-Ossietzky-Universität Oldenburg, Germany
[3]Alfred-Wegener-Institut für Polar- und Meeresforschung, Bremerhaven, Germany
[4]ZEKAM, Fachbereich Geowissenschaften/MARUM, Universität Bremen, Germany

In Quaternary deposits of the Arctic Ocean, brown Mn-rich layers are well-known, widespread, but also debated features. Both glacial-interglacial climatic variations (in river runoff, bottom water ventilation etc.) and early diagenetic processes might explain the sedimentary Mn distributions. We applied inorganic geochemical analyses to pore waters and sediments of two sediment cores from the western Arctic Mendeleev Ridge (RV Polarstern Expedition ARK-XXIII/3) [1]. Our results show that most brown layers are associated with detrital (ice-rafted) and biogenic carbonate enrichments. In addition, all Mn-rich layers are enriched in Fe (oxyhydr)oxides, and in Co, Cu, Mo and Ni that were most probably scavenged by Mn/Fe (oxyhydr)oxides. Distinct bioturbation patterns (i.e., brown burrows into the underlying sediments) suggest these metal enrichments formed close to the sediment–water interface.

We infer that the metal-rich layers formed under warmer (interglacial/interstadial) conditions with an intensified continental hydrological cycle and only seasonal sea ice cover. Metals were delivered to the ocean by rivers/sea ice/coastal erosion [2], while seasonal productivity increased the reactive organic matter export to the sea floor. The coeval deposition of organic matter and Mn/Fe (oxyhydr)oxides triggered an intense diagenetic Mn and Fe cycling at the sediment-water interface. These climate-induced primary and secondary processes resulted in the enrichments of Mn/Fe (oxyhydr)oxides, scavenging of trace metals, and the degradation of labile organic matter. With the onset of glacial/stadial conditions, the riverine/erosive delivery of metals strongly decreased, a solid sea ice cover terminated the production and export of fresh organic matter, and gray-yellowish sediments with lower metal contents were deposited. Our data do not support glacial/stadial bottom water oxygen depletion that might have affected the Mn distribution.

Despite the climatic control on the composition of the brown layers, pore water data show that diagenetic redistribution of Mn and Mo is still affecting the deeper sediments. The degree of Mn remobilisation (potentially causing complete dissolution of existing, and formation of new Mn layers) largely depends on the availability and reactivity of Mn (oxyhydr)oxides and organic matter.

[1] C. März, A. Stratmann, J. Matthiessen, A.-K. Meinhardt, S. Eckert, B. Schnetger, C. Vogt, R. Stein, H.-J. Brumsack (2011) *Geochim. Cosmochim. Acta* **75**, 7668-7687.
[2] R.W. Macdonald and C. Gobeil (in press) *Aquat. Geochem.*

SIMS sputter pit volume estimation in SHRIMP zircon analysis using an $^{18}O_2^-$ primary beam

CHARLES W. MAGEE JR.[1*], JIM FERRIS[2], CHARLES W. MAGEE[2]

[1]Australian Scientific Instruments, Canberra, Australia, cwmagee@gmail.com (* presenting author)
[2]Evans Analytical Group, East Windsor NJ, USA

Abstract

A novel method of estimating the volume of sputtered material was discovered while performing SHRIMP (Sensitive High-Resolution Ion MicroProbe) zircon U/Pb geochronology using an $^{18}O_2^-$ primary beam. During analysis, the ratio of Th and U oxide isotopologues was found to be equal for each individual spot. Assuming that the $U^{16}O/U^{18}O$ (or $Th^{16}O/Th^{18}O$) ratio was equal to the $^{16}O/^{18}O$ ratio of the sputtered material, multiplying this by the total ^{18}O primary beam fluence (true beam current times analytical time) yields total sputtered oxygen. Dividing by the density of oxygen in the zircon crystal lattice (about 63 atoms per nm^3) yields an analytical volume.

Comparison with pit volumes from AFM (Atomic Force Microscopy) shows that this isotopic volume estimation agrees with AFM pit measurements to within 10%. This relationship holds for primary beam impact energies from 5 to 15 kV.

This agreement in volume between isotopic and AFM measurements suggests that oxygen migration in the sputtering process is limited. As oxygen activity is crucial to governing the Pb/U vs UO/U calibration that makes accurate SIMS U/Pb geochronology possible, further investigations are planned into minerals such as baddeleyite, which calibrate poorly.

As the SHRIMP duoplasmatron consumes only \$50-\$100 of $^{18}O_2$ per day, this method appears to be cost-competitive with paying for analytical time on a second instrument for analytical volume determination. However, it requires that the sample and the primary beam are the only sources of oxygen in the sputtering process.

https://doi.org/10.1180/S0026461X00008434 Published online by Cambridge University Press

Measurement of nitrous oxide isotopologues and isotopomers by the MAT 253 Ultra

PAUL MAGYAR[1*], SEBASTIAN KOPF[1], VICTORIA ORPHAN[1] AND JOHN EILER[1]

[1]California Institute of Technology, Pasadena, CA, USA, pmagyar@caltech.edu (* presenting author)

The global budget of nitrous oxide is dominated by terrestrial and marine biological sources and atmospheric sinks. Details of the budget remain unclear, including the cause of increasing atmospheric N_2O concentrations. Marine sources of N_2O include denitrification and nitrification. Our understanding of the major microbial players in the nitrogen cycle has changed in recent years (for example, the nitrifying Archaea), and the overall contributions of these organisms to N_2O production and their isotopic signatures are poorly constrained [1].

Here we examine the suitability of the MAT 253 Ultra, a new high resolution gas source mass spectrometer [2], for measurements of rare, previously unanalyzed isotopologues and isotopomers of N_2O, including 'clumped' species and high-precision direct analysis of ^{17}O-substituted species. Such measurements could provide additional constraints to the global cycle of N_2O, and in particular offer a fresh opportunity for distinguishing among biosynthetic N_2O sources. Preliminary experiments include examining N_2O produced by pure cultures of denitrifying bacteria.

In the instrument's 'medium resolution' setting (16 μm entrance slit; resolving power ~16-18,000, M/ΔM), [$^{14}N^{15}N^{18}O$ + $^{15}N^{14}N^{18}O$] is well resolved from $^{13}C^{18}O^{16}O$ and the $^{15}N^{18}O$ fragment from $^{17}O^{18}O$. In zero-enrichment measurements, precision of 0.2‰ was achieved for mass 47 species and 0.4‰ for $^{15}N^{18}O$; both equaled counting statistics limits for the integration times used (11 and 17 minutes, respectively) and should be improved by increasing the source pressure, reducing resolution (e.g., using a 20 μm entrance slit) or increasing counting time. At mass 45, $^{14}N_2{}^{17}O$ is well resolved from [$^{14}N^{15}N^{16}O$ + $^{15}N^{14}N^{16}O$], with external precision of 0.03‰ achieved after 11 minutes of integration (again, counting statistics limited and potentially improvable).

By measuring both these species (as well as unsubstituted and singly substituted isotopologues), the position-specific clumping (i.e., clumping of ^{15}N with ^{18}O, and its dependence on site preference of ^{15}N) can be examined. Such measurements will complement the information already available from N_2O site preference measurements alone. Calculations suggest that site preference of ^{15}N in thermodynamically equilibrated N_2O will differ by ~1‰ between ^{16}O and ^{18}O isotopologues [3]. A larger range of signals could arise from photochemical and biological fractionations. Precise measurement of ^{17}O will enable detection of even subtle contributions of atmospheric mass-independent fractionation, or study of variations in mass laws of biological and other fractionations.

[1] Santoro *et al.* (2011) *Science* **333**, 1282-1285. [2] Eiler *et al.* The MAT 253 Ultra — a novel high-resolution, multi-collector gas source mass spectrometer. Goldschmidt 2012. [3] Wang *et al.* (2004) *Geochim. Cosmochim. Acta* **68,** 4779-4797.

Oxygen isotopes from Chinese caves: records not of monsoon rainfall but circulation regime

BARBARA A MAHER [1] * , ROY THOMPSON [2]

[1]University of Lancaster, Lancaster, UK, b.maher@lancaster.ac.uk (* presenting author)

[2]University of Edinburgh, roy@ed.ac.uk

Current interpretation of cave $\delta^{18}O$ records

Oxygen isotope variations in Chinese stalagmites have been widely interpreted as a record of the amount of East Asian summer monsoonal rainfall. This interpretation infers decreasing monsoonal rainfall from the mid-Holocene and large, dipolar rainfall oscillations within glaciations. However, the cave $\delta^{18}O$ variations conflict with independent palaeoclimate proxies (cave $\delta^{13}C$, loess/palaeosol magnetic properties, n-alkanes), which indicate no systematic decline in rainfall from the mid-Holocene, and no glacial rainfall maxima.

Mass balance calculations show moisture source is key control

Using mass balance calculations, we demonstrate that the cave $\delta^{18}O$ variations cannot be accounted for by summer rainfall changes, nor rainfall seasonality nor winter cooling, but instead reflect changes in moisture source. A possible driver of the $\delta^{18}O$ variations in Chinese stalagmites is precessional forcing of inter-hemispheric temperature gradients, in a mechanism similar to that of the modern day Indian Ocean dipole. Through such forcing, Indian monsoon-sourced $\delta^{18}O$ may have dominated at times of high boreal summer insolation, local Pacific-sourced moisture at low insolation. Suppression of summer monsoonal rainfall during glacial stages may reflect diminished sea and land surface temperatures and the radiative impacts of increased regional dust fluxes.

https://doi.org/10.1180/S0026461X00008434 Published online by Cambridge University Press

Defining the chemical and physical length and time scales that control chemical fluxes from landscapes

KATE MAHER[1*], CLAIRE KOUBA[1], ALEX K. HEANEY[1] AND VALERIE B. ROSEN[1]

[1]Dept. of Geological and Environmental Sciences, Stanford University, Stanford, CA, USA, kmaher@stanford.edu (* presenting author)

As fluids move through the subsurface they acquire solutes at a rate that is controlled primarily by the available surface area, the reaction kinetics of the individual minerals and the thermodynamic departure from chemical equilibrium [1]. As a result, both the physical length scale (or cumulative mineral surface area) and the time available for the fluid to react (or the fluid residence time) should exert a coupled influence on the solute fluxes from a given landscape. For example, if actual fluid residence times exceed the theoretical time required to reach chemical equilibrium, then the solute fluxes are optimized. However, because rivers and streams average over spatial domains that include an array of length scales and fluid residence times, determining the length and time scales that control solute generation has proven difficult. Defining and linking these length and time scales presents a key challenge to fields of geochemistry, geomorphology, biology and hydrology. Yet, if the length and time scales that control solute fluxes could be defined, this knowledge may provide a mechanistic approach for interpreting catchment to global-scale solute fluxes.

A comparison between soil profile solute evolution from stable and eroding landscapes, and concentration-discharge relationships (C-Q) both for small rivers from the U.S. Geological Survey's Hydrologic Benchmark Network (HBN) and large rivers from the Global Environmental Monitoring System (GEMS) database suggests that even with increasing discharge and catchment area, the ratio between the physical and chemical length scales may remain relatively constant. Catchments that show little variability in concentration with discharge (or "chemostatic behavior") are characterized by average fluid residence times that exceed the time required to reach chemical equilibrium. Chemostatic rivers may also represent rivers that are at their optimal solute flux. Conversely, decreases in concentration with increasing discharge are explained by average residence times shorter than required to approach chemical equilibrium, resulting in dilution. In these systems, if fluid residence times increase or chemical equilibration lengths decrease, solute fluxes are expected to increase to the optimum level. The fluid residence time model could provide an alternative framework for assessing both the relationship between discharge and concentration for individual catchments and controls on the solute fluxes of larger rivers. However, more detailed studies of the chemical and physical length and time scales and the development of scaling approaches are necessary to refine the simple model presented here. In particular, the time required to reach chemical equilibrium is perhaps the most poorly constrained variable in the fluid residence time model.

[1] White, A.F., et al. (2008) *Geochim. Cosmochim. Acta*, **73**, 2769-2803.

Assessing limitations for PAH biodegradation in long-term contaminated soils using bioavailability assays

NAGISSA MAHMOUDI[1*], GREG SLATER[1] AND ALBERT JUHASZ[2]

[1]School of Geography and Earth Sciences, McMaster University, 1280 Main St. W., Hamilton, ON, Canada (*mahmoun@mcmaster.ca) (gslater@mcmaster.ca)

[2]Centre for Environmental Risk Assessment and Remediation (CERAR), University of South Australia, Adelaide, SA, Australia (Albert.Juhasz@unisa.edu.au)

Polycyclic aromatic hydrocarbons (PAHs) are a class of organic contaminants that are ubiquitous in the environment through the incomplete combustion of organic matter such as diesel, coal and wood as well as being present at industrial sites due to use in a range of industrial processes. Once PAHs enter the environment, the predominant mechanisms for removal are biological via microbial activity, although physiochemical processes such volatilization can reduce the concentration of some PAHs. However, due to their hydrophobic structure, PAHs have the potential to partition onto soil organic matter thereby decreasing their bioavailability to microorganisms and limiting their degradation in the environment. This explanation was felt to be the reason for a lack of evidence of PAH biodegradation in a study of long-term contaminated soils. Instead, natural organic matter was being utilised as a carbon source resulting in the persistence of PAHs at this site [1].

Although biodegradation may be limited by a variety of environmental factors, bioavailability is considered to be a major limitation in contaminated soils. To test the hypothesis that bioavailability was the limiting factor for biodegradation in theses soils, PAH bioavailability was determined using non-exhaustive extraction (propanol, butanol, hydrooxypropyl-β-cyclodextrin) and oxidation (persulfate) methodologies designed to determine the fraction of contaminants within soil which are available for biological uptake [2, 3]. By comparing the initial PAH concentrations to the residual PAH concentrations following each assay, it was determined that the majority of PAHs in the soils were inaccessible to microorganisms which suggested that bioavailability limitations were the primary cause for the lack of observed biodegradation at this site.

These results highlight the importance of bioavailability to PAH degradation as well as the effectiveness of these assays as a rapid, and inexpensive method for determining the endpoints of PAH bioremediation. Such assays have the potential to provide a decision making tool on the suitability of bioremediation for soil treatment with minimal cost and time impacts and high accountability.

[1] Mahmoudi et al. (2011), submitted to *Env Sci & Technol*
[2] Juhasz et al. (2005) *Biorem J* **9**, 99-114.
[3] Dandie et al. (2010) *Chemosphere* **81**, 1061-1068.

https://doi.org/10.1180/S0026461X00008434 Published online by Cambridge University Press

Aerosol impacts on climate and biogeochemical cycles

NATALIE MAHOWALD[1], DANIEL WARD[1*], SILVIA KLOSTER[2], MARK FLANNER[3], COLETTE HEALD[4], NICHOLAS HEAVENS[1], PETER HESS[5], JEAN-FRANCOIS LAMARQUE[6], PATRICK CHUANG[7]

[1]Earth and Atmospheric Science, Cornell University, Ithaca, United States, dsw25@cornell.edu (* presenting author)
[2]Land in the Earth System, Max Planck Institute for Meteorology, Hamburg, Germany
[3]Atmospheric, Ocean, and Space Sciences, University of Michigan, Ann Arbor, United States
[4]Atmospheric Science, Colorado State University, Fort Collins, United States
[5]Biological and Environmental Engineering, Cornell University, Ithaca, United States
[6]Atmospheric Chemistry Division, National Center for Atmospheric Research, Boulder, United States
[7]Earth and Planetary Sciences, University of California, Santa Cruz, United States

Aerosols play an important role in our understanding of the Earth's climate through direct interactions with atmospheric radiation and indirect interactions by modifying cloud properties. These impacts take place on timescales in the troposphere of days to weeks. Longer timescale impacts of aerosols on climate through biogeochemical feedbacks are less well understood. Aerosols transport mass which may include nutrients or toxins across long distances and have been shown to effect the production of ecosystems that are distant to the aerosol source. The purveyors of these important nutrients are often naturally emitted aerosols such as mineral dust, volcanic ash, or biomass burning aerosols. Natural aerosols have generally received less study than anthropogenic aerosols, but here we use model simulations of preindustrial and present day aerosols to isolate the relative importance of different aerosol types for various climate impacts. Radiative forcings for the different aerosol types are estimated from the literature. We also give estimates for the contributions of various aerosol sources and types to nutrient transport in the atmosphere.

The impacts of aerosols on ecosystem production feedback onto the climate by changing the amount of carbon emitted or sequestered by the affected ecosystem. In addition, aerosols modify the carbon uptake capacity of the land surface and the ocean by altering climate through these biogeochemical effects and the more commonly referenced direct and indirect cloud effects.

Here we present the first quantitative assessment of the total indirect effects of aerosols onto climate through their effects on biogeochemical cycles. The aerosol indirect biogeochemistry effect is found to be similar in magnitude to the aerosol direct effect, with higher uncertainties, and yet the impacts on climate could be even greater because the biogeochemical impacts take place over longer time scales. The cooling influence of the indirect biogeochemical effects suggests that abatement costs for projected CO_2 concentrations could be underestimated. Due to the potential importance for our understanding of the land-atmosphere-ocean coupled climate and for policy, aerosol indirect effects on biogeochemistry warrant greater consideration in studies of aerosol and climate interactions.

Characterization of Corn Rhizosphere (*Zea mays*) Grown in Metal-contaminated Soil

NAHED MAHROUS[1]*, SHEILA MACFIE[1] AND GORDON SOUTHAM[1,2]

[1]Department of Biology, The University of Western Ontario, London, Canada, N6G 5H4, nmahrous@uwo.ca (*presenting author)
[2]Department of Earth Sciences, The University of Western Ontario, London, Canada, N6G 5H4

As industrialization encroaches on agricultural settings, it has become increasingly more important to investigate the microbe-mineral interactions within the rhizosphere. Currently, there is an incomplete understanding of metal contaminants and distribution (i.e., the bioavailability of different forms of metals) in soils that result in the uptake and accumulation in plants [1]. A more focused study on metal concentrations in edible plants is important to avoid possible risks to human health [2]. In this study, the examination of the rhizosphere was made possible by developing a new embedding procedure resulting in successful preservation of the inorganic and organic materials, i.e., structure and chemistry, within the rhizosphere (Figure 1).

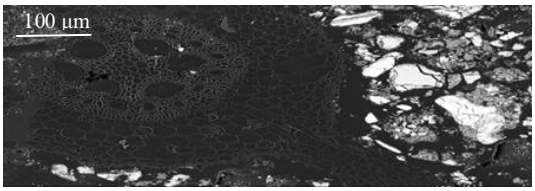

Figure 1: A BSE-SEM micrograph of a soil core containing roots and soil, i.e., rhizosphere.

ICP-AES analysis demonstrated that concentrations of bioavailable metals (Cd, Cu, Pb and Zn) were higher within the rhizosphere than the bulk soil. While the bacterial communities within the bulk soil and rhizosphere were capable of using similar types of carbon for growth, i.e., biodiversity was not affected by the growth of corn, the activity of the bacterial community inhabiting the rhizosphere (measured by using the Biolog Ecoplate™ system) was greater than the soil control. This increase in activity, which was reflected by a decrease in pH in the rhizosphere, can presumably be expected to influence heavy metals uptake by plants. The use of scanning electron microscopy combined with energy dispersive spectroscopy (SEM-EDS) and wavelength dispersive x-ray spectroscopy (SEM-WDS) revealed the presence of particles containing lead (Pb). Under these conditions, the use of micro-synchrotron x-ray fluorescence (micro- XRF), x-ray absorption fine structure (XAFS) and x-ray absorption near edge structure (XANES) are required to probe the spatial and chemical relationships of plant roots and the soils in which they grow.

[1] Chen & Cutright (2001). *Chemosphere*. **45**, 21-28. [2] Kamnev & Lelie (2000). *Bioscience Reports*. **20**, 239-258.

https://doi.org/10.1180/S0026461X00008434 Published online by Cambridge University Press

U(VI) sorption on montmorillonite in the presence of phosphate.

F. MAILLOT[1]*, J.G. CATALANO[1], D.E. GIAMMAR[2]

[1]Earth & Planetary Sciences, Washington Univ., St. Louis, MO 63130, USA, fabien.maillot@wustl.edu (*presenting author), catalano@wustl.edu

[2]Energy, Environmental and Chemical Engineering, Washington Univ., St. Louis, MO 63130, USA, giammar@wustl.edu

Uranium (U) contamination of soils and groundwater is a serious environmental concern due to past mining, processing, and waste disposal activities. In oxidizing environments, U(VI) is the most stable valence state for uranium, occurring in the linear uranyl ion, UO_2^{2+}. Among the in-situ remediation strategies for oxic subsurface environments, phosphate-based treatments have generated significant interest. U(VI) has a strong affinity for phosphate, which can lead to the nucleation of low-solubility U(VI)-phosphate minerals or enhance U(VI) sorption to subsurface minerals via the formation of ternary surface complexes. In addition, U(VI)-phosphate associations are common forms of U(VI) in contaminated soils and sediments at U.S Department of Energy (DOE) facilities, and have been observed in the Hanford 300 Area, the Oak Ridge Reservation, and the Fernald Site. However, the molecular mechanisms controlling U(VI) speciation in heterogeneous phosphate-bearing systems are currently poorly constrained, which hinders the design of efficient remediation strategies and the prediction of uranium transport in treated systems.

Previous work by coworkers in the U(VI)-PO_4^{3-}-goethite (α-FeOOH) system [1] has pointed towards the existence of ternary surface complexes at the goethite surface. The characterization of these species was possible thanks to the use of extended X-ray absorption fine structure (EXAFS) spectroscopy at the uranium L_{III}-edge. Following a similar approach in the present work, we investigated the effect of phosphate on U(VI) sorption on montmorillonite, a dioctahedral 2:1 clay mineral. Montmorillonite was chosen because phyllosilicate clays are a common component of the fine fraction of soils and sediments at many DOE sites. Previous work has also shown that montmorillonite is a strong sorbent for U(VI) [2,3].

In order to identify chemical divides that separate regimes where specific mechanisms (e.g. ternary surface complexation or precipitation of U(VI) phosphates) dominate, we determined U(VI) adsorption isotherms as a function of [PO_4^{3-}], pH, P_{CO2}, and electrolyte cation. To further characterize the nature of U(VI) speciation in these separate regimes, relevant samples were analyzed in more detail using EXAFS and XRD. Besides providing new knowledge of the U(VI)-PO_4^{3-}-montmorillonite system, comparison with the previously studied goethite system will allow determinations of how sorbent structure influences uranium-phosphate reactions in heterogeneous systems, which is fundamental for potential remediation applications involving real soils and sediments.

This work is supported by the U.S Department of Energy, Office of Biological and Environmental Research, Subsurface Biogeochemistry Research Program through grant DE-SC0006857.

[1] Singh *et al.* (2010) *Geochim. Cosmochim. Acta* **74**, 6324-6343.
[2] McKinley *et al.* (1995) *Clays and Clay Minerals*, **43**, 586-598.
[3] Turner *et al.* (1996) *Geochim. Cosmochim. Acta* **60**, 3399-3414.

Radiocarbon Analysis of Microbial DNA and PLFA from Arsenic Impacted Aquifers in Bangladesh.

BRIAN J. MAILLOUX[1*], ELIZABETH TREMBATH-REICHERT[1], JENNIFER CHEUNG[1], MARLENA WATSON[1], AUDRA DOCHENETZ[1], MARTIN STUTE[1], GREG A. FREYER[2], ANDREW FERGUSON[3], KAZI MATIN AHMED[4], MD, J. ALAM[4], BRUCE A. BUCHHOLZ[5], GREG F. SLATER[6], LORI A. ZIOLKOWSKI[6], JAMES THOMAS[7], ALICE LAYTON[8], YAN ZHENG[9], ALEXANDER VAN GEEN[9]

[1]Environmental Science Department, Barnard College, NY, NY 10027, USA. bmaillou@barnard.edu

[2]Environmental Health Science, Columbia University, NY, NY 10032, USA

[3]Department of Civil Engineering and Engineering Mechanics, Columbia University, NY, NY 10027, USA

[4]Department of Geology, University of Dhaka, Dhaka 1000, Bangladesh

[5]Center for Accelerator Mass Spectrometry, Lawrence Livermore National Lab, Livermore, CA 94551-9900, USA

[6]Geography & Earth Science, McMaster University, Hamilton, ON L8S 2S4, Canada

[7]Hydrologic Sciences, Desert Research Institute, Reno, NV, 89512, USA

[8]Dept of Microbiology and Center for Environmental Biotechnology, University of Tennessee, Knoxville, Tennessee, USA

[9]Lamont-Doherty Earth Observatory, Columbia University, Palisades, NY 10964, USA

Abstract

It is generally agreed that microbial respiration drives the release of arsenic from the sediment to water in drinking water aquifers throughout Southeast Asia. This microbial respiration requires organic carbon, and it is this source of organic carbon that is poorly constrained. It has been hypothesized that the carbon could be derived from: 1) young anthropogenic sources, 2) carbon deposited with the sediments, 3) carbon from organic rich peat lenses, or 4) older petroleum byproducts. However, no method is currently available to directly determine the source of organic carbon. In order to better constrain the source of organic carbon we developed a method to determine the radiocarbon signature of microbial DNA and phospholipids fatty acids (PLFAs) from groundwater samples. The radiocarbon signatures of the DNA and PLFA will reflect the source of organic carbon utilized by heterotrophic microbes. For DNA, the method includes filtering over 2,000 liters of groundwater onto a 0.2 µm filter followed by DNA extraction and purification. For PLFAs the method includes filtering over 1,000 liters of groundwater onto a newly developed carbon free filter. The DNA method enables us to collect, extract, and purify over 150 µg of DNA with an absorbance at 260/280>1.8 and an A260/230>2; indicating pure DNA. The new method was utilized at Site F in the Lashkardi Village, Araihazar, Bangladesh. The site represents an area where rapid recharge of anthropogenic carbon might occur. Results indicate that in the Holocene Aquifer the DNA is significantly older than groundwater ages and does not contain modern carbon but is younger than estimated sediment ages. We hypothesize that the carbon in the aquifer is recharged at the water table and is significantly retarded as it is tranported to depth. Further utilization of this novel method should help to better constrain the carbon sources driving arsenic release in the shallow aquifers of Southeast Asia.

https://doi.org/10.1180/S0026461X00008434 Published online by Cambridge University Press

Constraining E- and N-type components in Baffin Island picrites

MELISSA MAISONNEUVE[1*], DON FRANCIS[2], AND JOHN STIX[3]

[1]McGill University, Earth and Planetary Sciences, melissa.maisonneuve@mail.mcgill.ca (* presenting author)
[2]McGill University, Earth and Planetary Sciences, donald.francis@mcgill.ca
[3]McGill University, Earth and Planetary Sciences, john.stix@mcgill.ca

The Baffin Island picrites are interpreted to represent primitive magmas (up to ~22 wt% MgO) that are minimally changed since leaving their mantle source. Lead and neodymium-samarium isotopes indicate that these lavas may be melts of a primordial mantle reservoir (~4.45-4.55 Ga). Silicate melt inclusions (MIs) trapped within olivine crystals during their crystallization are considered to be aliquots of their parental melts and thus their compositions provide a unique insight into the geochemical nature of the oldest known terrestrial mantle reservoir.

In this study, the ratio of potassium to titanium (K/Ti) is used as an analog for trace element enrichment as both these elements are incompatible in the olivine and plagioclase phenocrysts present in these lavas. We define depleted glass compositions (N-type) as those with K/Ti < 0.2 and enriched glass compositions (E-type) as those with K/Ti > 0.2, based on an apparent population minimum at ~ 0.2. The N-type MIs are characterized by low K/Ti, La/Lu, Zr/Y and chlorine contents (Cl ≤ 50 ppm) while the E-type MIs appear to be mixtures of two distinct liquids, one a depleted end-member similar in composition to the N-type MIs and the other an enriched end-member characterized by high K/Ti, La/Lu, Zr/Y and chlorine contents (50 ≤ Cl ≤ 200 ppm). The chlorine concentration increases with trace element enrichment in E-type MIs which may indicate a relatively high Cl content in the E-type component. Whereas N-type MIs are hosted in olivines with a narrow range of forsterite contents, from Fo_{89} to Fo_{87}, the E-type MIs are found mostly in olivines with lower Fo contents (Fo_{87}-Fo_{83}), suggesting either the incorporation of the E-type component occurred later in the crystallization history of the N-type magmas or that the E-type component was less magnesian.

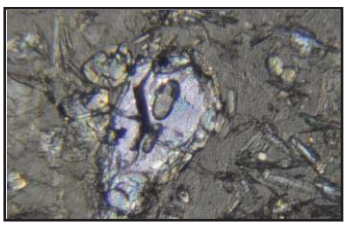

Figure 1: Melt inclusions in olivine crystal. Field of view is approximately 1 mm.

The large variation in K/Ti (0.05 to 0.6) in multiple melt inclusions within single olivine crystals suggests either that the growth of olivine phenocrysts during the magmatic differentiation of the N-type magma records the incorporation of the E-type component, or that the E- and N-type components were intermixed on a fine scale. The presence of two finely intermingled magmatic components in the mantle source of the Baffin picrites implies that Earth's primordial mantle was as heterogeneous as the asthenospheric source of modern-day mid-ocean ridge basalts.

Identity of oxidation products on surface of metallic antimony

FRANTISEK MAJS[1*], ANASTASIA G. ILGEN[1], AMANDA J. BARKER[1,2], THOMAS A. DOUGLAS[2], AND THOMAS P. TRAINOR[1]

[1]University of Alaska Fairbanks, Chemistry and Biochemistry, fmajs@alaska.edu*, anastasia.ilgen@alaska.edu, ajbarker@alaska.edu, tptrainor@alaska.edu
[2]US Army Corps of Engineers, Cold Regions Research and Engineering Laboratory, Fort Wainwright, AK, Thomas.A.Douglas@usace.army.mil

Introduction

Small arms bullets are predominantly made of lead (Pb) but antimony (Sb) is commonly used to harden bullets and can comprise up to 10% of the total mass. The fate of Pb in firing range soils has been investigated in a number of studies while the fundamental geochemical processes controlling the fate of Sb in soils and surface water are largely unknown. Anthropogenic deposition of Sb to soils on military and recreational shooting ranges represents an environmental risk due to Sb toxicity. Oxidation of bullet fragments containing metallic antimony under surface soil conditions ultimately leads to the release of Sb(V) to the soil solution and an accumulation of Sb(V) in soil. While Sb(III) is usually absent from soil solution or contaminated soil, its oxide (Sb_2O_3) precipitates readily during oxidation of Sb(0) under model conditions with deionized water and simulated groundwater. Mechanisms controlling speciation of precipitated Sb_2O_3 as well as relationship between solid and aqueous Sb speciation are not clearly understood.

Methods

The experimental study focused on understanding the effect of common cations (Na^+, Ca^{2+}) on the formation of precipitates on an Sb(0) surface during oxidation in simulated groundwater. Solutions were prepared at fixed ionic stregth (I = 0.01 mol L^{-1}) and a range of environmentally relevant pH values. We compared these results to the same processes in background solutions containing either deionized water or 30% hydrogen peroxide (H_2O_2). We determined the speciation and preferred orientation of the precipitates with grazing incidence x-ray diffraction and texture measurements, respectively. Results of the laboratory experiments were compared to Sb(0) weathered under field conditions in soils of varied texture and pH.

Results and Conclusion

The surface of Sb(0) oxidizes rapidly and within 24 hours we observed the formation of cubic and orthorhombic polymorphs of Sb_2O_3 (senarmontite and valentinite) of which valentinite exhibited strong preferential orientation with the *a* axis normal to the Sb(0) surfaces. An oxidation end member, hydrated Sb_2O_5, precipitated on Sb(0) surfaces only under the extremely oxidizing conditions of the H_2O_2 solution. The valentinite fraction in the precipitate increases with increasing solution pH but no measurable difference in speciation was found between Na^+ and Ca^{2+} background solutions. Drawing a connection between environmental conditions like soil pH and Sb(0) oxidation mechanisms helps to predict the fate of spent bullets and assists land managers in identifying appropriate soils to use in constructing new shooting ranges.

https://doi.org/10.1180/S0026461X00008434 Published online by Cambridge University Press

Thermodynamic prediction of aqueous As concentration in scorodite-rich tailings

JURAJ MAJZLAN

Institute of Geosciences, Burgweg 11, Friedrich-Schiller University, D-07749 Jena, Germany, Juraj.Majzlan@uni-jena.de

Hydrometallurgical processing of As-rich ores for the extraction of gold or other metals produce voluminous fine-grained, As-rich waste which is disposed of in the tailing ponds and stored in these facilities over a long time. Under predominantly acidic conditions, the principal As carrier in these tailings is the mineral scorodite, $FeAsO_4 \cdot 2H_2O$. Field and laboratory studies revealed a wide variation of the aqueous As concentrations in such tailings or in aqueous solutions with scorodite. This study explains these concentrations and their large scatter by thermodynamic modelling of scorodite-rich waste.

For the calculations, we have used recently measured or estimated thermodynamic properties from our work of As-rich hydrous ferric oxide (As-HFO) [1], scorodite [2], crystalline iron oxides goethite and lepidocrocite [3], and ferrihydrite [4].

At pH < 2.5, scorodite dissolves congruently and controls and aqueous As concentrations in the tailings. In this region, most of the experimental studies agree with respect to the measured and predicted As concentrations.

Above pH of ~2.5, Fe^{3+} phases (As-HFO, goethite, lepidocrocite, ferrihydrite) will start precipitating. These reactions drive the aqueous Fe^{3+} concentration down, force further dissolution of scorodite, and hence elevate the aqueous As^{5+} concentration. As each of these phases has a different stability in the environment of the tailings, the influence of each phase on the Fe^{3+} and As concentration is different. Yet, we show that the majority of the scattered experimental measurements fall into the field defined by the models where scorodite dissolves and Fe oxides precipitate. This field is bound for the curves which represent the scorodite-goethite (scorodite dissolves, goethite precipitates) and scorodite-ferrihydrite model. These two phases are expected to constitute the boundaries of the field because goethite is the most stable and ferrihydrite the least stable phase in the system.

Hence, using our data and models, we can reconcile all published experimental and field data with the thermodynamic values for the participating phases. We can also show that the As concentrations is likely to change in time as the Fe oxides age and transform to more stable phases or phase assemblages.

[1] Majzlan, J. (2011) *Environmental Science & Technology* **45**, 4726-4732. [2] Majzlan, J., Drahota, P., Filippi, M., Grevel, K.-D., Kahl, W.A., Plášil, J., Boerio-Goates, J., Woodfield, B.F. (2012) *Hydrometallurgy* (in press) [3] Majzlan, J., Grevel, K.-D., Navrotsky, A. (2003) *American Mineralogist* **88**, 855-859. [4] Majzlan, J., Navrotsky, A., Schwertmann, U. (2004) *Geochimica et Cosmochimica Acta* **68**, 1049-1059.

Fracture Mineral Investigation in Crystalline Rock, SW Greenland

W.R.M. MAKAHNOUK[1*], S.K. FRAPE[1], A.R. BLYTH[2], T. RUSKEENIEMI[3], M. CONIGLIO[1], AND R.J. DRIMMIE[4]

[1]University of Waterloo, Earth & Environmental Sciences
mak@uwaterloo.ca shaun@uwaterloo.ca coniglio@uwaterloo.ca
[2]Nuclear Waste Management Organisation (NWMO)
ablyth@nwmo.ca
[3]Geological Survey of Finland (GTK)
timo.ruskeeniemi@gtk.fi
[4]Isotope Trace Technologies Inc. (IT^2)
bob@it2isotopes.com

Abstract

This current study is associated with the Greenland Analogue Project (GAP), an international collaboration between the Nuclear Waste Management Organization (Canada), Posiva (Finland), and SKB (Sweden). The objective of this project is to further understand groundwater evolution in bedrock as influenced by the presence of a continental ice-sheet. Physical and chemical characteristics of secondary minerals within fracture networks in the bedrock were examined to provide insights into paleo-hydrological processes (e.g. hydrothermal, metamorphic, or glacial events).

Two boreholes were drilled into granitic gneiss near the margin of the Greenland ice-sheet. The first was drilled beneath a talik lake and instrumented to sample groundwater (GAP01). The second borehole was drilled to ~350 m to determine the depth of the permafrost (GAP03). Preliminary results, specifically, carbon ($\delta^{13}C$) and oxygen ($\delta^{18}O$) isotope geochemistry of carbonate fracture fillings, are now available (Fig. 1). Calcite analyses reveal a vertical $\delta^{18}O$ trend in the GAP01 borehole, indicative of hydrothermal carbonates. This is further corroborated by the ^{18}O depleted dolomite in that borehole. Dolomite in the GAP03 borehole corresponds to a fracture filling that is coated with a thin layer of calcite (arrow identifies isotopic signature in Fig.1), indicative of two different crystallization events based on the large difference in $\delta^{18}O$ values.

Ongoing fluid inclusion studies are anticipated to elucidate minimum carbonate mineral crystallization (trapping) temperatures and fluid salinities. Formation temperatures are used to calculate the isotopic composition of the parent fluids from which these carbonates precipitated. Estimates for $\delta^{13}C$ of DIC and $\delta^{18}O$ of paleo-fluids are powerful tools to distinguish meteoric or glacial water from fluids that have been subjected to water-rock interaction.

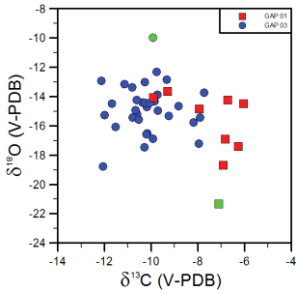

Figure 1: $\delta^{13}C$ and $\delta^{18}O$ isotope signatures of carbonates sampled from Greenland core - calcite (red and blue) and dolomite (green).

https://doi.org/10.1180/S0026461X00008434 Published online by Cambridge University Press

Detrital zircons from the Higo and Abukuma metamorphic terranes, Japan: implication for the sediment provenance

KENSHI MAKI[1*], MAYUKO FUKUYAMA[2], KAZUHIRO MIYAZAKI[3], TZEN-FU YUI[4], KUO-LUNG WANG[4], TADASHI USUKI[4], TAKAFUMI HIRATA[1], AND MARTY GROVE[5]

[1]Kyoto University, Kyoto, Japan, k-maki@kueps.kyoto-u.ac.jp (* presenting author)
[2]Akita University, Akita, Japan
[3]Geological Survey of Japan, AIST, Tsukuba, Japan
[4]Academia Sinica, Taipei, Taiwan
[5]Stanford University, Stanford, California, USA

In the Cretaceous low-pressure and high-temperature metamorphic terranes of Japan, the Higo (south-west Japan) and Abukuma (north-east Japan) metamorphic terranes are characterized by the occurrences of peraluminous metapelitic rocks and impure marbles, and absence of chert, and zircon U-Pb age of ca. 260Ma, suggesting that these terranes might be the eastern extension of the North China-South China collision zone [1,2,3,4]. However, new results of our zircon SHRIMP and LA-ICP-MS U-Pb dating do not necessary support the possibility of eastern extension of the North China-South China collision zone. Lu-Hf isotopic data for the detrital zircon may imply that the possible provenance for the Higo and Abukuma metamorphic terranes is the South China Craton.

The metamoprhic age of ca. 260 Ma could not be replicated from the Higo and Abukuma metamoprhic terranes in this study. Detrital zircons from the Higo and Abukuma metamorphic terranes show an age peak around the Carboniferous to early Jurassic, wchich is agree with previous works [5,6; i.e. 330 to 184Ma and 280 to 200Ma, respectively]. These lines of evidence may imply that the age of ca. 260 Ma shows a protoligh age for the metamoprhic terranes. Moreover, the Permian-Triassic detrital zircons from the Higo metamorphic terrane are characterized by positive $\varepsilon Hf_{(T)}$ values ($+7 < \varepsilon Hf_{(T)} < +10$) with high Th/U ratio ($0.2 < Th/U < 0.5$). Many Permian-Triassic granites are present within the Yangtze and Cathaysia Blocks of the South China craton [7], and zircons with positive $\varepsilon Hf_{(T)}$ values were found in the Permian-Triassic felsic rocks of the Emeishan large igneous province [8]. We concluded that the provenance for the Higo and Abukuma metamorphic terranes may be indicative of the South China Block implying that they may not be the eastern extension of the North China-South China collision zone.

[1] Isozaki and Maruyama (1991) *Jour. Geog.* **100**, 697-761. [2] Osanai *et al*. (2006) *GR* **9**, 152-166. [3] Isozaki *et al*. (2010) *Jour. Geog.* **119**, 999-1053. [4] Omori and Isozaki (2011) *Jour. Geog.* **120**, 40-51. [5] Hiroi *et al*. (1998) *Jour. Metamor. Geol.* **16**. 67-81. [6] Sakashima *et al*. (2003) *Jour. Asian Earth Sci.* **21** 1019-1039. [7] Wang *et al*. (2005) *Earth Planet. Sci Lett.* **230**, 339-354. [8] Xu *et al*. (2008) *Geoch. Cosmoch. Acta* **72**, 3084-3104.

Chemistry and petrography of detrital magnetite applied to mineral exploration in glaciated terrains

S.MAKVANDI[1*], G.BEAUDOIN[2], B.MCCLENAGHAN[3]

[1]Université Laval, Département de géologie et de génie géologique, 1100, avenue de la Medecine, Québec, Québec, Canada, G1V 0A6, sheida.makvandi.1@ulaval.ca
[2]Université Laval, Département de géologie et de génie géologique, 1100, avenue de la Medecine, Québec, Québec, Canada, G1V 0A6, Georges.Beaudoin@ggl.ulaval.ca
[3]Geological Survey of Canada, 601 Booth St., Ottawa, Canada, K1A 0E8, bmcclena@NRCan.gc.ca

The spinel structure of magnetite has potential to carry unique chemical and petrographic signatures imposed by compositional and physico-chemical conditions during crystallization and subsequently during metamorphism or weathering. The chemical composition of detrital magnetite is applicable in provenance studies, in particular for mineral exploration. Its ubiquity in mineral deposits, its resistance to weathering and abrasion, and ease of magnetic separation have led magnetite to be considered an indicator mineral. This study aims to determine the usefulness of chemistry and petrographic features of detrital magnetite in mineral exploration in glaciated terrain. A total of 186 grains from the 0.18-2.0 mm ferromagnetic fraction of till deposited down-ice of the Halfmile Lake VMS deposit (Bathurst Camp) were investigated. To find out the effect of erosion of surrounding lithologies on the formation of till, 176 grains from hostrocks and magnetite alteration zones in the area were examined. Mineral grains were liberated from rocks using a small plate crusher. Minor and trace elements of the grains in till and bedrock (K, Ca, Al, Si, Ti, Mg, Mn, Cr, V, Cu, Zn, Ni) were measured using the Electron Probe Micro-Analysis. Various plots of these elements show that till samples generally form a cluster of very similar compositions that are different from magnetite in the Halfmile deposit country rocks especially because of their lower Si and higher Ti and V content. Electron microscopy and Mineral Liberation Analysis (MLA) are also applied to study these till and bedrock grains to evaluate relationships between mineralogy, abundances and associations of minerals. Results indicate that up to 90 percent of magnetite in both till and country rocks are polymineralic, and that detrital magnetite is Ti-bearing and is most often accompanied with titanomagnetite, ilmenite and hematite. In the Halfmile deposit bedrock samples, in contrast, magnetite is mostly in association with sulfide and/or silicate minerals. These heterogeneities in composition and mineral associations of till and most of rock samples suggest that magnetite in till is largely derived from distant sources. Detrital magnetite shows the greatest chemical similarities with magnetite from nearby granitic rocks.

https://doi.org/10.1180/S0026461X00008434 Published online by Cambridge University Press

Geochemical characterization of mineralized groundwaters in the Aquitaine Basin (SW France): lateral and vertical variability of the Eocene formations, hydrodynamic and geochemical processes of acquisition of the mineralization.

ELINE MALCUIT[1,3*], PHILIPPE NEGREL[2], EMMANUELLE PETELET-GIRAUD[2], OLIVIER ATTEIA[3], MICHEL FRANCESCHI[3], ALAIN DUPUY[3]

[1]BRGM, Regional Geological Survey Service Bordeaux, France, e.malcuit@brgm.fr (* presenting author)
[2]BRGM, Metrology Monitoring Analysis Department, Orleans, France, p.negrel@brgm.fr; e.petelet@brgm.fr
[3]EA 4592, ENSEGID - IPB, Pessac, France, Olivier.Atteia@ipb.fr; Michel.Franceschi@ipb.fr; Alain.Dupuy@ipb.fr

Section Heading: 22a. Tracing groundwater variability

In the sedimentary Nord Aquitaine Basin (SW France), the large Eocene aquifer, mostly confined, is one of the main resources for drinking water. In this aquifer, a large saline area has been identified, where the groundwaters show high values of mineralization and anomalous levels of critical elements, such as sulfates and fluoride, leading to difficulties of resource exploitation for drinking water supply. Geochemical and isotopic characterization of withdrawn groundwaters shows a common origin of the mineralization.

The Eocene aquifer formations include several geological layers, which have different lithological, mineralogical and hydrodynamic properties. Since the beginning of the century, many boreholes in the area for drinking water supply have locally modified the natural water flows of the system. Our investigation shows the need for a precise and detailed knowledge of the vertical distribution of the hydrodynamic and geochemical properties of each layer. Indeed, the average concentration in the borehole water depends on the centimetre scale variation of water fluxes and concentrations. Geochemical models fully explain the composition of groundwaters across the study area and improve the understanding of geochemical processes taking place at the borehole scale.

To understand the acquisition of the groundwaters' geochemistry, it is necessary to consider the lateral and vertical variations in facies and mineralogy, geochemical processes (mineral dissolution and/or precipitation, phenomenon of diffusion in contact with low permeability and mineralized layers) and local fluid mixing processes within the borehole and its immediate surroundings.

Cu-isotope systematic of magmatic PGE-Cu-Ni sulfide ores from the Talnakh and Kharaelakh intrusions, Noril'sk Province (Russia)

KRESHIMIR N. MALITCH[1*] AND RAIS M. LATYPOV[2]

[1]Institute of Geology and Geochemistry of the Uralian Branch of Russian Academy of Sciences, Ekaterinburg, Russia, dunite@yandex.ru (* presenting author)
[2]Department of Geosciences, University of Oulu, P.O. Box 3000, Oulu, Finland, rais.latypov@oulu.fi

We have undertaken for the first time the examination of the Cu isotope composition of primary high temperature Cu-Ni sulfde ores from world-class PGE-Cu-Ni sulfide deposits associated with the economic Talnakh and Kharaelakh intrusions and native copper ores from the Noril'sk Province (Russia). Copper isotope ratios are reported as $\delta^{65}Cu‰=((^{65}Cu/^{63}Cu_{sample}/^{65}Cu/^{63}Cu_{NIST\ 976\ standard})-1) \times 10^3$. The isotope measurements were carried out with an MC ICP-MS (ThermoFinnigan Neptune) using sample-standard bracketing as outlined by Larson et al. [1].

Main set of samples of this study form three major $\delta^{65}Cu$ clusters that well match $\delta^{65}Cu$ signatures of two distinct reservoirs as defined for iron meteorites and carbonaceous chondrites, respectively [2-4]. The mean $\delta^{65}Cu$ value of massive sulfide ores at Talnakh forms the first cluster around zero ‰ (-0.1 ± 0.15 ‰, respectively), close to the $\delta^{65}Cu$ signatures of the Bulk Earth and iron meteorites. Similarly, the mean $\delta^{65}Cu$ value of disseminated sulfide ores at Talnakh forms the second cluster around –0.7 ‰ (–0.7 ± 0.4 ‰), matching that of the carbonaceous chondrites. The third cluster with the mean $\delta^{65}Cu$ values, represented by massive and disseminated ores of the Kharaelakh intrusion (-1.52 ± 0.24 ‰ and -1.6 ± 0.4 ‰, respectively) lie very close to the light-isotope end of the $\delta^{65}Cu$ range expressed by the carbonaceous chondrites. A $\delta^{65}Cu$ value measured in a sample and a replicate represented by native copper from the Arylakh deposit of the Noril'sk Province gave indistinguishable result of -1.9±0.15 ‰.

The determined $\delta^{65}Cu$ variability is interpreted to represent a primary signature of the ores, though a magmatic fractionation of copper isotopes and/or assimilation of the ore material from external source (in case of the Kharaelakh ores) can not be ruled out.

The study was supported by the Academy of Finland (grant No. 131619) and the Uralian Division of Russian Academy of Sciences (12-U-5-1038).

[1] Larson *et al*. (2003) *Chemical Geology* **201**, 337-350.
[2] Luck *et al*. (2003) *GCA* **67**, 143-151.
[3] Luck *et al*. (2005) *GCA* **69**, 5351-5363.
[4] Wasson & Choi (2003) *GCA* **67,** 3079-3096.

https://doi.org/10.1180/S0026461X00008434 Published online by Cambridge University Press

Hafnium isotopic compositions of Abyssal Peridotites from the Southwest Indian Ridge

SOUMEN MALLICK[1], MICHAEL BIZIMIS[1,2*]

[1]University of South Carolina, EOS, smallick@geol.sc.edu, [2]mbizimis@geol.sc.edu (* presenting author)

We report Hf isotopic compositions of clinopyroxene mineral separates from abyssal peridotites from the 9-25° E segment of the Southwest Indian Ridge (SWIR). Peridotites from 15.4° E are plagioclase-free with low Na-Ti abundances and depleted chondrite normalized REE patterns in clinopyroxene (cpx) suggesting residual characteristics, The cpx show a limited variability and plot at the radiogenic end of the MORB field in Nd-Hf isotope space (ε_{Nd} ~ 13.1, ε_{Hf} ~ 18.5), consistent with the estimates for the DMM reservoir. However these peridotites are more radiogenic than spatially associated SWIR basalts, suggesting the presence of an enriched component in the source of these basalts. A regression line through these peridotites and co-located basalts in ε_{Nd}-ε_{Hf} space has a slope of 1.21 (R^2 = 0.94), similar to the slope of mantle array, suggesting that the enriched component must lie within the mantle array. The un-radiogenic extension of the regression line in ε_{Nd}-ε_{Hf} space passes close to the proposed local enriched endmember, similar to the Bouvet hotspot lavas. Assuming a Bouvet-like enriched composition in the source of the SWIR mantle, maximum 40% of the Hf budget in the basalts is contributed from the depleted peridotites (15.4° E), which translates to a maximum of 10% enriched component in the basalt source. In contrast, peridotites from 9.98° E and 16.64° E have relatively high Na-Ti contents, high LREE/HREE ratios and are often plagioclase bearing, suggesting re-fertilization. The cpx from both locations plot towards the un-radiogenic end of MORB field (ε_{Nd} = 4.8-7.9 ε_{Hf} = 9.9-14.2). They are however distinct in Nd-Hf space and overlap with their co-located basalts. The above data is consistent with variable degree of equilibration between these peridotites and local basalts. Model calculations show that 4% addition of local basalts-like melt to the most depleted (15.4° E) local peridotites can explain the Nd and Hf isotopic compositions of re-fertilized 9.98° E and 16.64° E peridotites, however, this estimate does not match the REE patterns of the re-fertilized peridotites. This could indicate that local melts have reacted with a protolith, which is a residue of variable degree of melting but has an Nd-Hf isotope ratio similar to 15.4° E peridotites.

The high Sm-Nd and Lu-Hf ratios of the depleted peridotites (15.4° E) combined with their DMM-like Nd and Hf isotopes suggest recent depletion of a DMM – type mantle, likely related to recent melting underneath the SWIR. This observation is in contrast to the recently reported highly radiogenic Hf isotopic compositions (ε_{Hf} up to 291) of abyssal peridotites from the Gakkel Ridge, which have been interpreted to reflect an ancient (> 1Ga) depletion and melt-rock interaction processes. Our observation, together with Gakkel Ridge peridotites indicates that earth's mantle is more heterogeneous than basalts suggest and investigation of Nd-Hf isotopic compositions of abyssal peridotites from other areas will help us to better constrain the upper mantle composition.

Genesis of alkaline magmas by reaction of MORB-eclogite derived carbonated melt with lherzolite

ANANYA MALLIK*[1], RAJDEEP DASGUPTA[1] AND VAIBHAV MISHRA[1]

[1]Rice University, Houston, TX, USA (*am33@rice.edu)

Ocean island lavas such as HIMU basalts are silica-undersaturated [1] and present evidence of recycled oceanic crust in their mantle source. Partial melts of neither volatile-free peridotite nor subducted oceanic crust (MORB-eclogite) can explain the degree of silica-undersaturation and high TiO_2 and high MgO, respectively of HIMU lavas. While reaction of MORB-eclogite derived, volatile-free melts with peridotite produce alkalic basalts at low melt-rock ratios [2], the reacted-melts are not low enough in SiO_2 and Al_2O_3 and high enough in FeO* and CaO to explain most of the HIMU lavas. Here we explore whether MORB-eclogite derived CO_2-bearing partial melts and volatile-free peridotite reaction can generate the required chemical attributes for primary HIMU-type magmas.

Reaction experiments were performed between lherzolite KLB-1 and two different MORB-eclogite-derived partial melts – (1) an alkalic melt with 8.5 wt.% CO_2 (G2CPM1; [3]) and (2) a basaltic andesite with 2 wt.% CO_2 (G2CPM2) – at 1375 °C, 3 GPa, a condition which is above the respective liquidii of both the melts but below the solidus of peridotite. The amount of melt, mixed homogenously with peridotite, was varied from 8 to 50 wt.%. In all the experiments, the original melt underwent partial reactive crystallization, leading to CO_2-enrichment in the reacted melt in equilibrium with a residue of garnet lherzolite to garnet-bearing olivine websterite. Reaction of G2CPM1-KLB-1 produced reacted melts which, on a volatile-free basis, show a decrease in SiO_2 from ~37 wt.% to ~35 wt.%, Al_2O_3 from ~7 wt.% to ~6 wt.%, FeO* from ~17 wt.% to ~12 wt.%, Na_2O from ~6 wt.% to ~3 wt.% and increase in TiO_2 from ~6 wt.% to ~8 wt.%, MgO from ~15 wt.% to ~21 wt.%, and Mg# from ~62 to ~75 with decreasing melt-rock ratio. The reacted melts produced from 25-33 wt.% G2CPM2 have ~39 wt.% SiO_2, 8.5-9.5 wt.% Al_2O_3, >10.5 wt.% FeO*, 15.4-16.5 wt.% MgO, 9-10 wt.% CaO, and Mg# of 72-73.

We demonstrate that carbonated MORB-eclogite derived mildly alkalic melt evolves to more primitive, strongly alkalic compositions with variable melt:peridotite ratio. More importantly, an andesitic melt with only 2 wt.% CO_2 evolves to melts similar to melilititic, nephelinitic, and HIMU lavas. At a given MgO content, the reacted melts evolved from G2CPM2 are a better match for alkaline ocean island lavas in terms of SiO_2, Al_2O_3, FeO*, CaO, and MgO as compared to partial melts of carbonated peridotites and eclogites. We suggest that percolative flow of siliceous or mildly alkalic carbonated melts in a subsolidus peridotitic mantle is a widely occurring process, causing partial reactive crystallization of the original melts and leading to formation of primary alkalic magmas. The reacted melts have the potential to erupt as alkalic OIBs or to act as metasomatic flux to shallower source regions.

[1] Jackson and Dasgupta (2008) *EPSL* **276**, 175-186. [2] Mallik and Dasgupta (in press) *EPSL*. [3] Gerbode and Dasgupta (2010) *JPetrol* **51**, 2067-2088.

https://doi.org/10.1180/S0026461X00008434 Published online by Cambridge University Press

Field scale investigation of geochemical parameters controlling high and low As occurrence in Murshidabad District, West Bengal: India

SANKAR M.S*[1], KATHERINE TELFEYAN[2], SOPHIA FORD[1], ANDREW NEAL[3], TAHMINEH JADE HAUG[2], KAREN JOHANNESSON[2] AND SAUGATA DATTA[1]

[1]Kansas State University, Manhattan, KS, USA, mssankar@ksu.edu (* presenting author)

[2]Tulane University, New Orleans, LA, USA

[3]Virginia Water Resources Research Center, Virginia Tech, Blackburg, VA, USA

The assessment of incidence of arsenic (As) and the other major ions is evaluated in the groundwaters of Murshidabad, West Bengal. This work is executed over an area of about ~497 km^2. Water samples were collected from 39 hand pumped tube wells (~90-110ft), 9 ponds and 6 irrigation wells (~60-80ft) along with 4 sediment cores (~150ft) from these sites. Field sites are located east and west of the river Bhagirathi, a tributary of the river Ganges, flowing N-S through Murshidabad. The western part of Bhagirathi river is mainly occupied by Suja formation, older alluvium of Pleistocene age (oxidized ferruginous sand, silt and clay with caliche), whereas the eastern part of the river is occupied by Bhagirathi Ganga formation, newer alluvium of Holocene age (sand, silt and clay).

Comparative study of major water quality parameters reveal high As (10->500ppb) and low Mn (0.1-1.6ppm) in the areas like Beldanga, Hariharpara (east bank of the river) while low As (0-30ppb) and higher Mn (0.2-8ppm) is found in Nabagram, Kandi (west bank of the river). DO, NO_3^- and NH_3 do not show appreciable variation among the high and low As areas and they range from 1.5-5ppm, 0-2.7ppm and 0-0.06ppm respectively. TDS and conductivity do not show considerable variation among the high and low As areas and range from 0.001-6.2g/l and 2.6-988 µS/cm respectively. High As areas show a pH of 4.5-7.8 while pH in the low As areas is 5.1-8.2. Alkalinity values range from 10-18 mg/l at high and 10-180mg/l at low As areas. PO_4^{3-} values of high As areas range 0.2-11ppm and at low As areas the range is 0.3-1.3ppm. Cl^- values are higher at low As areas (40-148ppm) and lower at high As areas (10-60ppm). Fe^{2+} values at high and low As areas are 0.05-6ppm and 0.1-1.4ppm respectively. Analyses show positive correlation of arsenic with Fe^{2+}, PO_4^{3-} and TDS content in most of the high As areas, whereas the Mn and Cl^- ions are negatively correlated with high As in most areas. During field work it is observed that there is good correlation between tube well platform color and high As concentration areas which agrees with a recent study near Chakdaha, south of Murshidabad [2]. Stable isotope data from our sites show that groundwaters of this region are directly recharged by local precipitation without significant evaporation [3]. Organic matter within aquifer sediments drive dissimilatory iron reduction reaction and thus release As to the ground water [3].

[1] McArthur *et al*. (2012) *ES&T* **46**, 669-676. [2] Biswas *et al.* (2012) *ES&T* **46**, 434-440. [3] Datta *et al.* (2011) *Geophys. Res. Lett*., 38, L20404, doi: 10.1029/2011GL049301.

The effect of Li on pegmatitic textures – experimental results

VICTORIA MANETA[1*] AND DON R. BAKER[1]

[1]McGill University, Earth and Planetary Sciences, Montreal, Canada, viktoria.maneta@mail.mcgill.ca (* presenting author), don.baker@mcgill.ca

Introduction

According to the most prevalent models that explain the genesis of pegmatites, crystallization takes place after appreciable liquidus undercooling in a medium rich in fluxing components, such as H_2O, B, F and P [1, 2, 3]. The present study examines the potential of Li as another fluxing agent and its effect on the formation of pegmatites.

Pegmatitic textures are developed in experimental samples that contain a starting material of common granitic composition, but enriched in Li_2O, 3% seed crystals of K-feldspar, albite and quartz, and varying amounts of H_2O. The experimental procedure involves initially heating the samples in a piston-cylinder apparatus to 1000˚C and 550 MPa for 1 hr, followed by cooling at 50˚C/min to temperatures from 600 to 900˚C and 500 MPa and keeping those conditions constant for 100 hrs.

The results show the formation of graphic intergrowths between quartz and K-feldspar that closely resemble the ones encountered in pegmatites. Additionally, numerous K-feldspar crystals exhibiting spherulitic and skeletal morphologies are formed in the experimental samples, suggesting rapid growth rates for the crystals that grow in the Li-enriched medium. The growth rates measured for the K-feldspar in the samples range from approximately 5 x 10^{-11} m s^{-1} to 2 x 10^{-9} m s^{-1}. Experiments conducted under the same conditions but with Li-free starting material do not exhibit the same tendency.

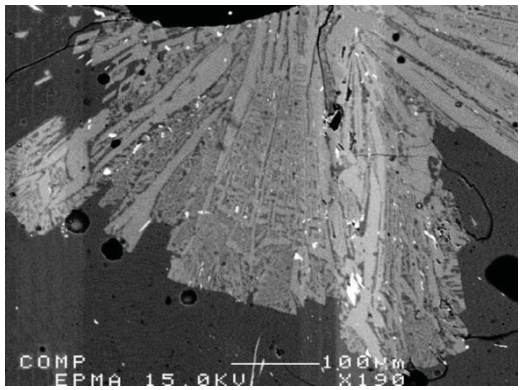

Figure 1: Graphic intergrowth between K-feldspar and quartz developed experimentally (2% added Li_2O, 12% added H_2O, P=500 MPa, T= 600˚C, t=100 hrs)

Conclusion

The experimental results indicate that the presence of Li in the system promotes the fast growth of crystals as well as the development of graphic quartz-feldspar intergrowths, both typical characteristics of pegmatites.

[1] Fenn (1986) *American Mineralogist* **71**, 325-33. [2] Jahns & Burnham (1969) *Economic Geology* **64**, 843-864. [3] London (2008) Pegmatites, 347p.

https://doi.org/10.1180/S0026461X00008434 Published online by Cambridge University Press

Response of methanogenic communities to glacial-interglacial climate changes in the Siberian Arctic

K. MANGELSDORF[1*], J. GRIESS[1,2], A. GATTINGER[3] AND D. WAGNER[1]

[1]GFZ Potsdam, Telegrafenberg, D-14473 Potsdam, Germany, K.Mangelsdorf@gfz-potsdam.de (* presenting author)

[2]AWI Potsdam, Telegrafenberg, D-14473 Potsdam, Germany

[3]Helmholtz Centre Munich, Ingoldstädter Landstr. 1, D-85758 Oberschleissheim, Germany

Introduction

The Arctic has gained specific attention within the current debate on climate change. With the thawing of permafrost large amounts of stored carbon become accessible again for microbial degradation and will form a potential source for the release of CO_2 and methane to the atmosphere having a positive feedback on the global warming. Therefore, it is of specific interest to understand the microbial driven greenhouse gas dynamics of the Siberian Arctic and their response to glacial-interglacial changes in the past.

Sample material was drilled on Kurungnahk Island (Russian-German expedition LENA 2002) located in the southern part of the Lena Delta and in lake El'gyggytgyn (ICDP-project) in Northeast Siberia. The Kurungnahk samples comprise Late Pleistocene to Holocene deposits, whereas the lake El'gyggytgyn samples cover Middle to Late Pleistocene sediments. Samples were investigated applying a combine biogeochemical and microbiological approach.

Results and Conclusion

The methane profile of the Kurungnahk core reveals highest methane contents in the warm and wet Holocene and Late Pleistocene (LP) deposits and correlates largly to the organic carbon (TOC) contents. Archaeol concentrations, being a biomarker for past methanogenic archaea, are also high during the warm and wet Holocene and LP intervals and low during the cold and dry LP periods. This indicates that part of the methane might be produced and trapped in the past. However, biomarkers for living microorganisms (bacteria and archaea) and microbial activity measurements of methanogens point, especially, for the Holocene to a viable archaeal community, indicating a possible *in-situ* methane production. Furthermore, warm/wet-cold/dry climate cycles are recorded in the archaeal diversity as revealed by genetic fingerprint analysis.

In contrast to the results from the Kurungnakh core, in general the bacterial and archaeal biomarker profiles from the lake El'gygytgyn deposits reveal no distinct glacial-interglacial variability. This might be due to the fact that the overlying lake water buffers the temperature effect on the lake sediments which never became permafrost. The microbial abundance rather correlates to the TOC contents in the sediments forming the accessible carbon and energy source for the indigenous microbial communities. Also the diversity of methanogenic archaea, being still active in 400 ka old sediments, appears to vary with the organic carbon content. TOC-rich lake intervals seem to sustain a divers microbial ecosystem independent from glacial-interglacial climate cycles.

Oxygen and di-nitrogen (N_2) dynamics in the hypoxic zone of the St-Lawrence Estuary

ROXANEMARANGER[1*], MARK ALTABET[2], DENIS GILBERT[3], ALFONSO MUCCI[4], LAURA BRISTOWE[5], BJORN SUNDBY[4]

[1]Université de Montréal, Montréal, Canada, r.maranger@umontreal.ca (* presenting author)

[2]University of Massachusetts at Dartmouth, Dartmouth, US

[3]Intitut Maurice Lamontagne, Mont Jolie, Canada

[4]McGill University, Montréal, Canada

[5]University Southern Denmark, Odese, Denmark

Di-nitrogen (N_2) is the terminal end product of denitrification and annamox, microbial processes that eliminates fixed-Nitrogen (N) from ecosystems. N loss is critical given the key role of N in coastal eutrophication. The Lower St-Lawrence Estuary (LSLE) is a heavily stratified ecosystem, where persistent hypoxic conditions have established and steadily increased over the last 80 years. In order to estimate fixed-N loss, we tracked the change in N_2 concentrations along an isopycnal that progressively loses oxygen as it moves landward from the Laurentian Channel into the LSLE. We found a very strong relationship between N_2 excess and the O_2 deficit in the LSLE, where excess N_2 could be predicted linearly from AOU with an r^2=0.84. We estimate fixed-N losses from the change in N_2 excess along the isopycnal of around 685-1370 μmol N m^{-2} d^{-1}. Compared with other methods estimating fixed-N loss, we found that our lower estimate corresponds with the higher estimates determined in core incubations, whereas our higher estimate, corresponds to the lower estimate as predicted using N*. Using excess N_2 represents however the most integrative approach at the basin scale.

https://doi.org/10.1180/S0026461X00008434 Published online by Cambridge University Press

Geochemical, mineralogical and geomechanical effects of impure CO_2 on reservoir sandstones during the injection and geological storage: an experimental approach

HERWIG MARBLER[1], MICHAEL SCHMIDT[1], KIRSTEN P. ERICKSON[1], CHRISTOF LEMPP[1], AND HERBERT PÖLLMANN[1]

[1]Martin-Luther-University Halle-Wittenberg, Institute for Geosciences, Von-Seckendorff-Platz 3, 06120 Halle, Germany herwig.marbler@geo.uni-halle.de

Within the German national project COORAL* the behaviour of reservoir rocks from deep saline aquifers during the injection and geological storage of CO_2 with inherent impurities such as SO_X and NO_X is studied in laboratory experiments. Samples are taken from sandstone outcrops of possible reservoir formations of Rotliegend and Bunter Sandstones from the North German Basin. A combination of geochemical/mineralogical alteration experiments and geomechanical tests was carried out on these rocks to study the potential effects of the impurities within the CO_2 pore fluid. Mineralogical alterations were observed within the sandstones after the exposure to supercritical (sc)CO_2 with SO_X/NO_X and brine, mainly of the carbonatic, but also of the silicatic cements, as well as of single minerals. Besides the partial solution effects, secondary mineral precipitations of carbonates and subsidiary silicates were observed within the pore space of the treated sandstones. The evaluation of the chemical composition of the reaction fluid during the course of the autoclave experiments also indicate that dissolution and precipitation processes occur in the system fluid/rock/gas. The alterations affect the porosity and permeability of the treated sandstones and also weaken their grain structure. Results of geomechanical experiments on untreated samples indicate that the rock strength as well as the amount of injected $scCO_2$ is influenced by the chemical composition of the pore pressure fluid ($scCO_2$ + SO_X/NO_X). After long-term autoclave treatment with impure $scCO_2$, sandstone samples exhibit reduced strength parameters and modified deformation behaviour compared to untreated samples.

* The project "COORAL" ("CO2 Purity for Capture and Storage"; acronym derived from German project title) is supported by the German Federal Ministry of Economics and Technology on the basis of a decision by the German Bundestag. Third-party funding: Alstom, EnBW, E.ON, Vattenfall Europe, VNG.

Systematics of biodegradation of sulfur compounds in heavy oil reservoirs

MARCANO N.[1], OLDENBURG, T.B., MAYER, B[1].

AND LARTER S[1].

[1]University of Calgary, Department of Geoscience, Calgary, Canada

The growing trend of producing and refining large volumes of high-sulfur content petroleum leads to a need for exploring new ways of meeting environmental regulations regarding the allowable sulfur emissions and sulfur content of petroleum derivatives. Biodesulfurization is one of the new technologies currently being considered [1,2]. In this study, we use a natural biodegradation site to examine the systematics of biodegradation of sulfur compounds in oil at reservoir conditions. The biodegradation of alkylbenzothiophenes (alkylBT) and alkyldibenzothiophenes (alkylDBT) were investigated in oil columns with progressively biodegraded oil from top to bottom, using gas chromatography mass spectrometry and sulfur isotopic compositions of bulk oil and oil fractions. The concentrations of alkylBT and alyklDBT decrease from hundreds of ppm to almost complete removal in biodegraded oil columns with different ranges of biodegradation levels. The order of sensitivity to biodegradation was found to be generally dibenzothiophene (DBT), dimethylBT (DMBT) > trimethylBT (TMBT) > methylDBT (MDBT) > dimethylDBT (DMDBT). The preferential removal or preservation of some of the isomers gives insights into reaction mechanisms. Changes are also seen in alkylated high molecular weight S and mixed SNO species observed using Fourier Transform Mass Spectrometry (FTICRMS), providing evidence for dealkylation of even very high molecular weight S bearing species. Despite multiple changes at the molecular level in the thioaromatic and NSO fractions, the bulk sulfur content of the oil did not change significantly in the studied oil columns. The $\delta^{34}S$ values of bulk oil also did not change systematically with increasing biodegradation of sulfur compounds, while slight variations in the oil thioaromatic and asphaltene fractions may be related to the microbial alteration process. We propose a route forward for studying the natural and industrial scale sulfur systematics of biologically altered crude oils.

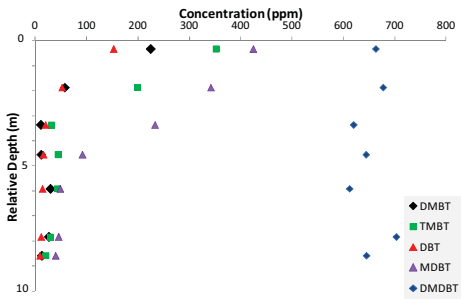

Figure 1: Progressive biodegradation of sulfur compounds in progressively biodegraded oil towards the reservoir base.

[1] Marcelis et al. (2003) *Biodegradation* **14 (3)**, 173-182.
[2] Mohebali and Ball (2008) *Microbiology* **154**, 2169-2183.

https://doi.org/10.1180/S0026461X00008434 Published online by Cambridge University Press

Making sense of large sets of XANES spectra

MATTHEW A. MARCUS[1*], THOMAS LENOIR[2], PHOEBE J. LAM[3], ALAIN MANCEAU[2]

[1]Advanced Light Source, Lawrence Berkeley Laboratory, Berkeley CA USA mamarcus@lbl.gov

[2]University of Grenoble 1 and CNRS Grenoble, France, thomas.lenoir@ifsttar.fr; manceau@ujf-grenoble.fe

[3]Department of Marine Chemistry and Geochemistry, Woods Hole Oceanographic Institution, Woods Hole, USA, pjlam@whoi.edu

Natural materials are often heterogeneous, and must be sampled at many points to be understood. We demonstrate new PCA-based statistical techniques for estimating the number of end-member components required to describe a dataset. Also, we have developed a visualization tool which allows us to examine projections of the multidimensional dataset in such a way as to gain clues to the underlying statistical structure of the data. We show the example of the XANES analysis of Fe-bearing suspended marine particles from two regions, 214 spectra from particles collected in the Northwest Pacific, and 126 from the Southern Ocean. The data from the NW Pacific require more components to describe than those from the Southern Ocean. As shown in Figure 1, a well-chosen projection can let one identify distinct clusters of spectra having distinct features.

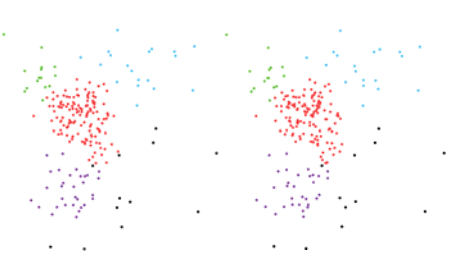

Figure1: Stereogram of 3D projection of the first 6 PCA components of the NW Pacific dataset, with groups of spectra colored in. Each dot represents one XANES spectrum, and nearby dots correspond to similar spectra.

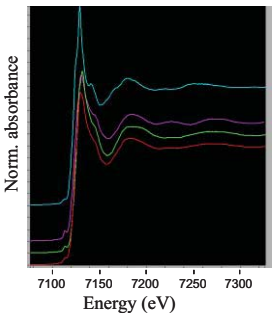

Figure 2: Averaged XANES spectra for the clusters shown above. The colors correspond to those in Figure 1.

Least-squares fits to the spectra shown in Figure 2 indicate clays+poorly-crystalline Fe oxyhdroxide (red), oxidized phyllosilicates (green), biotite+chlorite+clay (cyan) and magnetite+Fe^{2+} silicate+ Fe oxyhdroxide (purple).

Conclusion

Statistical tools can allow one to see patterns in data which would otherwise be invisible when examining spectra individually. We demonstrate how a complex XANES dataset can be simplified so that important characteristics such as dominant minerals and their distribution may be identified.

In situ Fe and multiple S isotope analyses of an Archean pyrite nodule

JOHANNA MARIN-CARBONNE[1,2*], CLAIRE ROLLION-BARD[3], AXEL HOFMANN[4], EMILIE THOMASSOT[3], KEVIN MCKEEGAN[1], ANDREY BEKKER[5] AND OLIVIER ROUXEL[6]

[1] UCLA, Los Angeles, USA, jmarin@ess.ucla.edu, mckeegan@ess.ucla.edu

[2]Institut de Physique du Globe, Paris, France

[3] CRPG, Nancy, France, rollion@crpg.cnrs-nancy.fr, emilie@crpg.cnrs-nancy.fr

[4]University of Johannesburg, South Africa, ahofmann@uj.ac.za

[5]University of Manitoba, Winnipeg, Manitoba, R3G 2K4 Canada, bekker@cc.umanitoba.ca

[6]Universite de Bretagne Occidentale, Ifremer, Brest, France, olivier.rouxel@univ-brest.fr

Studies of Fe and multiple S isotope composition of sedimentary pyrites have placed important constraints on the chemistry and the redox evolution of the ocean and the atmosphere over the geological time [1,2,3]. Additionally, Fe isotopes have been explored as a proxy for microbial metabolism [2]. Pyrite in black shales is predominantly formed either in the water column or during early diagenesis close to the sediment-water interface and so potentially records chemical evolution of the ocean. Previous studies mostly used bulk samples, although individual pyrite nodules often show complex internal textures such as concentric lamination. Large isotopic variability within individual nodules has been shown for S isotopes [4] but not yet for iron isotopes.

We have performed coupled situ Fe and multiple S isotope analyses of a pyrite nodule hosted by c. 2.7 Ga black shale from Zimbabwe. This mm-size nodule is composed of pure pyrite. Fe isotopes were measured with ims 1270 ion probes at both UCLA and CRPG [5]. We also performed multiple S isotope measurements with the ion probe ims 1280 HR2 at CRPG. The measurements performed at CRPG and UCLA are in agreement with a reproducibility better than 0.2 ‰ (2σ) in δ^{56}Fe. Reproducibility for δ^{34}S is ~ 0.2 ‰ (2 σ) and ~ 0.1 ‰ (2 σ) for Δ^{33}S.

The mean δ^{34}S and δ^{56}Fe values of this nodule are +2.9 ± 0.5 ‰ and -1.08 ± 0.7 ‰, close to the bulk values of +3.2 ‰ and -1.46 ‰, respectively. Two profiles have been performed in one nodule and show large variations in both δ^{56}Fe (~ 2.5 ‰) and δ^{34}S (~5 ‰). The δ^{56}Fe profile shows ^{56}Fe enrichment in the rim relative to the core. The δ^{34}S profile shows large isotopic variation that have no systematic relationship with the location. Δ^{33}S values are negative in the core and positive in the rim. The pyrite nodule was likely formed in a closed system during diagenesis, under reducing conditions but also record some iron oxidation in the water column. S isotopes reflect mixing and different reactivity of two sulfides pools (sulfate and elemental sulfur photochemically produced in the atmosphere) in sediments. Coupled S and Fe isotope composition at µm-scale provides new insights into Archaean ocean chemistry.

[1] Rouxel et al. (2005) *Science*, **307**, 1088-1091, [2] Johnson et al. (2008) *Annu. Rev. Earth Planet. Sci.* **36,** 457-493, [3] Farquhar et al. (2000), *Science*, **298**, 756-758, [4] Kamber and Whitehouse (2007), *Geobiology*, **5,** 5-17, [5] Marin-Carbonne et al. (2011) *Chemical Geology*, **285**, 50-61

https://doi.org/10.1180/S0026461X00008434 Published online by Cambridge University Press

FREZCHEM: A geochemical model for cold aqueous solutions

GILES M. MARION[1*]

[1]Desert Research Institute, Reno, Nevada, USA, giles.marion@dri.edu (*presenting author)

FREZCHEM Model

FREZCHEM is an equilibrium chemical thermodynamic model parameterized for concentrated electrolyte solutions (to ionic strengths = 20 molal) using the Pitzer approach [1] for the temperature range from –100 to 25°C (CHEMCHAU version has temperature range from 0 to 100°C) and the pressure range from 1 to 1000 bars [2]. The current version of the model is parameterized for the Na-K-NH_4-Mg-Ca-Fe(II)-Fe(III)-Al-H-Cl-ClO_4-Br-SO_4-NO_3-OH-HCO_3-CO_3-HSO_3-SO_3-HS-S-CO_2-O_2-CH_4-NH_3-SO_2-H_2S-Si-H_2O system and includes 115 solid phases including ice, 16 chloride minerals, 36 sulfate minerals, 16 carbonate minerals, six sulfite minerals, five solid-phase acids, four nitrate minerals, seven perchlorates, six acid-salts, five iron oxide/hydroxides, four aluminum hydroxides, two silica minerals, two ammonia minerals, two gas hydrates, two bromide sinks, and one sulfide mineral (pyrite). Fortran codes and an Internet working model are available at http://frezchem.dri.edu.

Applications for FREZCHEM can be very diverse because of its extensive physical ranges. For example, if ammonia/ammonium and methane are prevalent on Titan, that can lead to interesting chemistries over the temperature range of 173-273 K (Fig. 1). Notice that SO_4 largely precipitates, but CH_4 (aq) increases, which may be why methane is a major component on the surface of Titan where the temperature is 94 K.

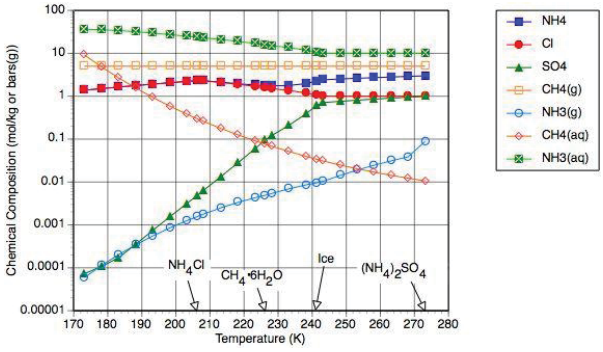

Figure 1. The chemical compositions as temperature decreases from 273 to 173 K beneath Titan surface. Arrows on the X-axis indicate when solid phases start to precipitate.

[1] Pitzer (1991) *Activity Coefficients in Electrolyte Solutions* CRC Press. [2] Marion & Kargel (2008) *Cold Aqueous Planetary Geochemistry with FREZCHEM* Springer.

Post OIS6 climate-change records in the Lower Mississippi Valley and mid-Atlantic Coastal Plain

HELAINE W. MARKEWICH[1*], MILAN J. PAVICH[2], DOUGLAS A. WYSOCKI[3], RONALD J. LITWIN2

[1]U.S. Geological Survey, Atlanta, GA, helainem@usgs.gov (* presenting author)

[2] U.S. Geological Survey, Reston, VA, mpavich@usgs.gov , rlitwin@usgs.gov

[3] U.S. Department of Agriculture, National Soil Survey Center, Lincoln, NE, doug.wysocki@lin.usda.gov

Published and on-going investigations allow comparison of post OIS6 chrono- and pedo-stratigraphic and palynologic records in the Lower Mississippi Valley (LMV) and mid-Atlantic Coastal Plain (MACP) of the unglaciated USA. Data indicate that in both regions W-NW winds were responsible for loess and eolian-sand deposition and that in both regions depositional periods were coeval with Northern Hemisphere glaciations and characterized by boreal environments.

The LMV was the major meltwater conduit associated with the Laurentide Ice Sheet (LIS). Loess dominates the OIS6, 3, and 2 LMV stratigraphic record. Sand dunes are a minor component. The Susquehanna and Delaware rivers were conduits for glacial meltwater that had an impact on the Chesapeake Bay area of the MACP. Eolian deposits are more spatially and temporally restricted in this area than in the LMV and are most prevalent within 300 km of the glacial border. Eolian sand dominates the OIS 3 and 2 MACP stratigraphic record.

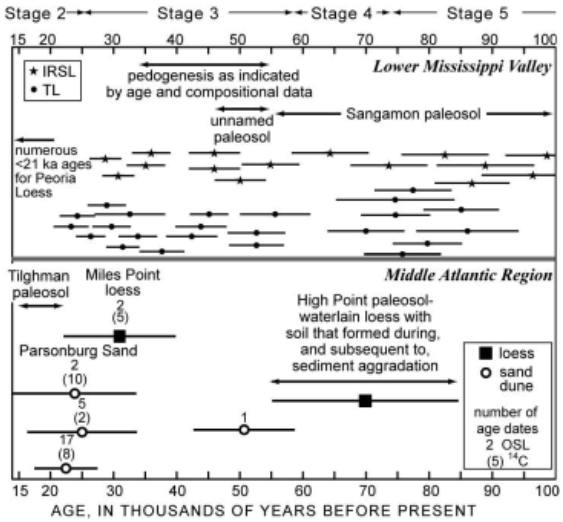

Figure 1: Age data for loess, eolian sand, and paleosols from the LMV[1] and the mid- Atlantic region[2][3][4].

Palynologic and paleowind data, along with the chrono- and pedo-stratigraphic records, are adequate to allow preliminary comparisons of late Pleistocene climates in the two regions.

[1] Markewich *et al.* (2011) *Geo. Soc. Am. Bull.* **123**, 21-39. [2] Lowery *et al.* (2010) *Quaternary Sci. Rev.* **29,** 1472-1480. [3] Pavich *et al.* (2010) *Geo. Soc. Am. Abs. with Prog.***42**, 231. [4] Wysocki *et al.* (2010) *Soil Sci. Soc. Am.* http://a-c-s.confex.com/crops/2010am/webprogram/Paper60303.html.

https://doi.org/10.1180/S0026461X00008434 Published online by Cambridge University Press

Analysis of 33 Uranium Ore Concentrate Samples: A Case Study in Nuclear Forensics

NAOMI MARKS[1]*, IAN D. HUTCHEON[1], MARTIN ROBEL[1], LARS E. BORG[1]

[1]Lawrence Livermore National Lab, USA, marks23@llnl.gov (* presenting author)

Nuclear forensics is a scientific discipline interfacing law enforcement, nuclear science and non-proliferation. Information on the history and on the potential origin of intercepted nuclear material can be obtained through nuclear forensic analysis. Using commonly available techniques of mass spectrometry, microscopy and x-ray diffraction, we have gained insight into the processing and origin of a suite of uranium ore concentrate (UOC) samples.

The 33 UOC samples are in the form of ammonum di-uranate (ADU). The sample suite is thought to represent a time series collected at the same location over a number of years. The rare earth element (REE) patterns match the REE patterns for phosphorites reported in [1], implying that the samples are derived from a phosphorite deposit (Figure 1). The REE patterns are fairly consistent throughout the series, although absolute concentrations of REEs decrease through the time sequence (Figure 1) suggesting improvments in metallurgy with time.

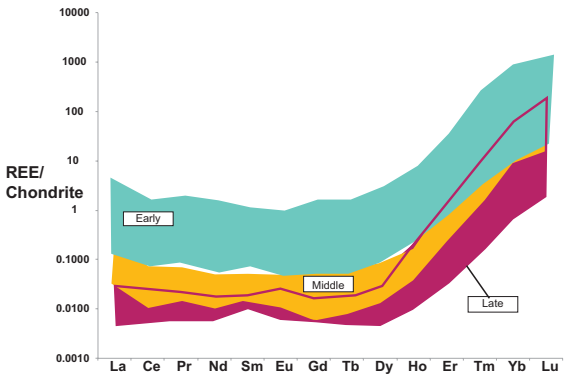

Figure 1: Chondrite normalized REE patterns for the suite of UOC samples.

The U purification process appears to be OPPA solvent extraction based on the form of the UOC (as ADU). The first few samples in the time series have higher concentrations of almost all impurity elements, and lower concentrations of U, than subsequent samples. Some of the later samples have on up to 40% higher concentrations of alkali earths and alkali metals, indicating slight variations in feedstock. The consistency in trace element patterns, however, suggests the samples are derived from geologically related ore bodies. This study illustrates one way in which nuclear forensic analysis can provide insight into the ore geology and production and purification methods used to produce UOC.

[1] Varga (2010) *Talanta* **80**, 1744-1749. This work performed under the auspices of the U.S. DOE by Lawrence Livermore National Laboratory under Contract DE-AC52-07NA27344.

The Terceira Rift, Azores: a melt inclusion study of submarine lavas

A.F.A. MARQUES[1*], S.D. SCOTT[2], P. MADUREIRA[3,4], P. CONCEIÇÃO[4], N. LOURENÇO[4], AND C.J.P. ROSA[5]

[1]CREMINER (LARSyS) Faculdade de Ciências da Universidade de Lisboa, Lisbon, Portugal, afamarques@fc.ul.pt (* presenting author)

[2]University of Toronto, Dept. of Geology, Toronto, Canada

[3]Centro de Geofísica de Évora / Dept. Geociências da Universidade de Évora, Évora, Portugal

[4]EMEPC – Estutura de Missão para a Extensão da Plataforma Continental, Lisbon, Portugal

[5]LNEG – Laboratório Nacional de Energia e Geologia, Lisbon, Portugal

The Azores plateau, a bathymetric high seated on an anomalous mantle domain is located in the Azores Triple Junction where the American, EUR and AFR lithospheric plates meet. The cause for these anomalies is controversial but many authors consider the presence of an anomalously hot/wet enriched mantle probably supplied by a plume [1]. The origin, size and present location of the plume is under debate but an area near Terceira is the favoured plume centre [2]. The Terceira Rift (TR) defines the EUR/AFR plate boundary of the Azores triple junction. The TR is a 550 km long, generally ESE trending line of volcanic massifs (e.g. São Miguel, D. João de Castro, Terceira and Graciosa) alternating with deep basins (e.g. Hirondelle basin). The latter are interpreted to be volcanically unfilled rift valley segments [3]. Vesicular, porphyritic basalts were sampled along the Terceira Rift during Portuguese scientific cruises (EMEPC 2007-2009). Initial studies focused on the adjacent areas Don João de Castro - DJC (submarine volcano) and Hirondelle - Hir (basin). Major and trace element data of phenocrysts (olivine, clinopyroxene, plagioclase), groundmass and exposed melt inclusions in these vesicular lavas depict only slight differences between the two sites although DJC samples have somewhat higher Fo and Mg# in olivine and clinopyroxene, respectively. Chondrite-normalized REE data indicate that groundmass material is LREE-enriched in both Hir and DJC lavas. Exposed melt inclusions (MI) show similar REE patterns compared to their hosts. Clinopyroxene in both sites displays L-MREE enriched, HREE depleted sinusoidal patterns. MI were found in olivine, clinopyroxene and plagioclase phenocrysts. MI are glassy to completely opaque and devitrified, with one or more bubbles, and sulfide globules (SG). SG are spherical, depict two-phase lamellar intergrowths of Fe-Ni and Cu-Fe phases, and are ubiquitous in DJC and Hir lava samples. Some lavas display SG within clinopyroxene-hosted MI and dispersed in the groundmass. Preliminary data suggest that lavas found in these areas of the Terceira Rift were sulfur-saturated in different stages of their evolution; during early fractionation and prior to eruption. The geochemistry of melt inclusion will contribute to the understanding of mantle source, melting and mixing processes in the Terceira Rift, Azores.

[1] Asimow et al. (2004) *Geochem. Geophys. Geosyst.* **5**, Q01E16,
[2] Jean-Baptiste et al. (2009) *EPSL* **281**, 70-80.
[3] Vogt (2004) *EPSL* **218**, 77-90.

https://doi.org/10.1180/S0026461X00008434 Published online by Cambridge University Press

Sorption of Lanthanides and trivalent actinides on montmorillonite in the presence and absence of carbonate

M. Marques Fernandes[1*], B. Baeyens[1], R. Dähn[1], T. Stumpf[2] and M. H. Bradbury[1]

[1]Paul Scherrer Institut, Villigen, Switzerland, *maria.marques@psi.ch

[2]Karlsruher Institut für Technologie, Eggenstein-Leopoldshafen, Germany

The fate of released RNs in a deep geological radioactive waste repository is primarily controlled by sorption/desorption processes onto mineral surfaces. Clay minerals are major constituents in both the man-made engineered barriers and in the argillaceous host rock formations currently being considered for a deep high level radioactive waste (HLW) repository in Switzerland. In the near-field of HLW repositories, reducing conditions are expected to prevail and the RNs are present in their lowest oxidation states. Trivalent actinides such as Am(III), Cm(III) and Pu(III) make a significant contribution to the radiotoxicity of HLW. In natural environments, the predominant aqueous phase reactions of lanthanides and trivalent actinides (Ln/An(III)) are hydrolysis and complexation with dissolved inorganic ligands, such as carbonates. Such complexation reactions could potentially decrease the metal ion sorption and thus increase the migration rates of these RNs.

The sorption of Ln/An(III) on montmorillonite in the absence and presence of dissolved carbonate was investigated by a combination of different approaches. Batch sorption experiments, surface complexation modelling, Time-Resolved Laser Fluorescence Spectroscopy (TRLFS) and Extended X-ray Absorption Fine Structure (EXAFS) spectroscopy were applied to investigate the uptake of Ln/An(III) on montmorillonite at low surface loadings ($\leq$ 3 mmol·kg^{-1}). The macroscopic sorption experiments showed that the presence of carbonate leads to a pronounced decrease of Ln/An(III) uptake on montmorillonite. Modelling the experimental data with the 2SPNE SC/CE sorption model under the assumption that carbonate complexes do not sorb, clearly under predicted the experimental data, suggesting the formation of ternary Ln/An(III)–carbonate surface complexes. In order to verify this assumption, EXAFS and TRLFS were applied. The differences in the TRLFS spectra obtained for samples in the presence and absence of carbonate *i.e.* red-shift of excitation and emission spectra, as well as the increase of fluorescence lifetimes, unambiguously showed the influence of carbonate, and were fully consistent with the formation of Ln/An(III)(III) surface species involving carbonate complexes. The EXAFS parameters derived by fitting the spectra of the carbonate free sample were consistent with bond lengths from Am-O and Am-Si/Al backscattering pairs, and clearly indicated that An(III) forms inner sphere complexes at the montmorillonite surface. The EXAFS parameters obtained by fitting the spectra of the sample prepared in the presence of carbonate was consistent with the formation of an An(III) complex at the montmorillonite surface with 1 to 2 carbonate groups. The application of EXAFS and TRLFS clearly supported the macroscopic sorption experiments and modeling results and confirmed the formation of ternary Ln/An(III)-CO_3 complexes at the montmorillonite surface.

Comparison of grain size and BET surface area trends in modern glacial and non-glacial fluvial sediments as a proxy for deep-time climate

Kristen R. Marra[1*], Megan E. Elwood Madden[1], Gerilyn S.Soreghan[1], and Allison R. Stumpf[1]

[1]ConocoPhillips School of Geology and Geophysics, University of Oklahoma, kmarra@ou.edu (* presenting author)

Chemical and physical weathering in sediments is highly contingent upon erosion rates and climatic variables (temperature and precipitation). Sediment grain size and surface area also impose critical controls on mineral-water reaction rates, where finer grain sizes are correlated to higher surface areas and thus increased chemical weathering, even in glacial environments [1]. However, sediment surface area is generally not evaluated or reported for natural systems. Here we document grain size and BET surface area trends within the mud fraction (< 63 μm) of proximal fluvial sediments in a cold-arid, glacial (Clark Glacier Stream, Wright Valley, Antarctica) and a warm semi-arid, non-glacial (Blue Beaver Creek, Wichita Mountains, Oklahoma) environment. Both systems are of similar basin drainage size (40 km^2), relief (360-465 m), and bedrock lithology (granitoid).

In the polar glacial transect, the mud fraction coarsens with distance along transect, with a corresponding decrease in BET surface area, indicating rapid dissolution of fines. In the non-glacial transects, grain size decreases downstream while surface area increases, reflecting precipitation of clay-sized weathering products. Aqueous chemistry of stream water samples collected simultaneously with stream sediments supports the conclusion that silicate dissolution dominates in the glacial environment, whereas incongruent chemical weathering of silicate phases is predominant the non-glacial environment. The occurrence of opposing trends within climatically distinct settings indicates that the production and fate of fine-grained sediments may be diagnostic of glacial and non-glacial regimes and potentially evident in the rock record. Additionally, systematic quantification of sediment surface areas provides critical constraints on evaluating the effect of chemical weathering on modern and deep-time global carbon cycles.

[1] Anderson (2005) *Geomorphology* **67**, 147-157.

https://doi.org/10.1180/S0026461X00008434 Published online by Cambridge University Press

Sulfur isotopes in high-pressure rocks

HORST R. MARSCHALL[1*], NOBUMICHI SHIMIZU[1]

[1]WHOI, Woods Hole, MA, USA, hmarschall@whoi.edu (* presenting author), nshimizu@whoi.edu

Models of the global sulfur cycle are afflicted with a lack of knowledge on the efficiency and isotopic effects of subduction processes. Primitive undegassed basalts, as well as sulfide inclusions in mantle xenoliths and in eclogite-type diamonds display a relatively large variation in $\delta^{34}S$ (Seal, 2006) providing evidence for significant mantle heterogeneities in S isotopes. It has been speculated that recycling of sulfur in subduction zones is in part responsible for these variations. However, models of the deep mantle sulfur cycle ignore any processes operating during subduction. Estimates on the subduction input into the mantle are reduced to using the compositions of un-metamorphosed oceanic rocks, because little is known on the behavior of sulfur and sulfur isotopes during high-*P* metamorphism and subduction zone devolatilization. This study aims to close this gap, and investigates the S isotope composition of sulfides in natural high-*P* rocks.

Sulfur isotope analyses were conducted by SIMS on pyrite and chalcopyrite. Based on petrographic evidence, the sulfides were attributed to formation during two contrasting stages of the subduction-exhumation cycle: (1) sulfides formed prior to or during subduction, and (2) sulfides in revolatilization zones formed during exhumation, probably by fluids released from the subducting slab. The first type bears on the isotopic composition of sulfur in different lithologies subducted to various depths, while the second type complements these data by reflecting the composition of fluids released from the slab.

Preliminary data from various samples investigated so far include both types of sulfide from various localities (Cycladic blueschist belt, Greece; Zermatt-Saas Fee, Italian Alps; Western Gneiss Region, Norway; New England Fold belt, Australia; Franciscan fm., California) and present the following picture:

(i) $\delta^{34}S$ values of prograde pyrite and chalcopyrite in eclogites are mainly positive: ~0 to +14 ‰, although some individual pyrite grains show negative values down to –3.4 ‰. The grains are typically unzoned in S isotopes.

(ii) prograde pyrite and chalcopyrite from a high-*P* metasediment shows grains unzoned in $\delta^{34}S$ with values as low as –31 ‰.

(iii) $\delta^{34}S$ values of retrograde pyrite show a heterogeneous picture with unzoned grains having negative (as low as –21 ‰) or positive values, as well as mm-sized grains with ~8 permil $\delta^{34}S$ core-to-rim zonation.

The results obtained to date suggest that altered igneous crust carries a positive $\delta^{34}S$ signal down to the UHP eclogite stage, while sediments are probably depleted in ^{34}S. Evidence for high-$\delta^{34}S$ fore-arc fluids is found in retrograde pyrite. However, some retrograde pyrite shows very low $\delta^{34}S$ values, which may be related to metasedimentary sources in the slab. High-*P* serpentinites and harzburgites will be one of the future foci of this ongoing study into the subduction zone sulfur cycle.

[1] Seal RR (2006) Sulfur isotope geochemistry of sulfide minerals. MSA Reviews in Mineralogy and Geochemistry, 61: 633–677.

Warm Arctic Peatlands – Future Methane Factories?

CHRIS MARSHALL*[1], DAVID J LARGE[1], WILL MEREDITH[1], COLIN E SNAPE[1], BARUCH F SPIRO[2] AND MALTE JOCHMANN[3*]

[1] Chemical &Environmental Engineering, University of Nottingham, enxcm3@nottingham.ac.uk

[2]Natural History Museum, London baruch.spiro@gmail.com

[3]Store Norske Grubekompani AS Longyearbyen Malte.Jochmann@snsk.no (* presenting author)

Palaeocene Arctic coal represents a unique terrestrial record of peatland processes and carbon storage during the last period of Arctic warmth. Modern high latitude warming is accelerated when compared to global averages [1] indicating future Arctic peatlands may bear closer resemblance to Palaeocene peatlands than those seen at the present time.The Svalbard coals formed around 60Ma at latitude 68°N. Previous studies of mid-latitude Paleocene coals, [2] provide evidence of significant methanogenic communities within peatlands before and during the PETM event. Modern high latitude methane fluxes have been linked to polar stratospheric cloud formation [3] and accelerated Arctic warming This study aims to use organic petrology and geochemistry to find evidence of such methane fluxes in Palaeocene, Svalbard and study the implications for modern peatlands

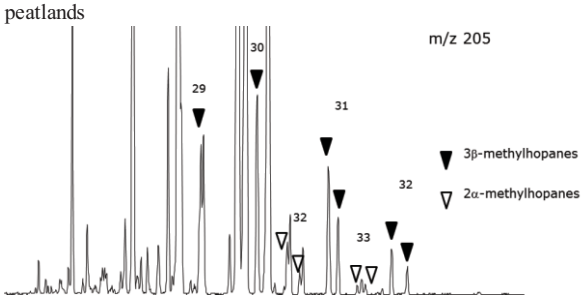

Figure 1: M/z 205 gas chromatograms showing 2 & 3 Methyl-hopanes in Svalbard coal extracts.

Total hopane concentrations (bacterial biomarkers) in Svalbard coals are 45- 125mg/g extract indicating the coals are massively enriched in microbial lipids compared to other source rocks (<2mg/g extract [4]). High detrovitrinite contents in the Svalbard coals also indicate high levels of biodegradation for the latitude. This is probably a feature of high peatland seasonality with winter productivity lowered but temperatures sufficient, to allow continued biodegradation.

Methanotrophic biomarkers, 3-methyl hopanes (figure 1) are enriched (1.26mg/g extract) significantly compared to other source rocks (<300µg/g extract, [4]). This increase is thought associated with the general increases in biodegradation shown by the hopanes. This is reflected by 3Me/Total Hopane ratios of 2-3%, which are consistent with other source rocks [4]. Consequently, if future Arctic peatlands evolve similarly, biodegradation would be expected to increase rapidly, increasing the Arctic terrestrial carbon flux and accelerating subsequent high latitude warming.

[1] Holland & Bitz (2003) *Climate Dynamics* **2**, *221-232* [2] Pancost *et al.* (2007) *Nature* **449,** 332-335. [4]Sloan & Pollard (1998) *Geophysical Research Letters* **25,** *3517-3520* [4] Farrimond *et al.* (2004) *Geochimica et Cosmochimica Acta* **68**, 3873-3882.

https://doi.org/10.1180/S0026461X00008434 Published online by Cambridge University Press

Uranium incorporation during iron (oxyhydr)oxide crystallisation at hyperalkaline pH

T. A. MARSHALL[1*], G.T.W. LAW[2], K. MORRIS[2], J.F.W. MOSSELMANS[3] AND S. SHAW[1].

[1]ESSI, School of Earth and Environment, University of Leeds, UK. eetam@leeds.ac.uk (*presenting author)
[2]RCRD and CRR, Schools of Earth, Atmopsheric and Environmental Sciences and Chemistry, The University of Manchester, UK.
[3]Diamond Light Source, UK.

Geological disposal of the legacy of radioactive wastes stored at Earth's surface is now the accepted management pathway for these materials and is a task of importance for nuclear power generating countries. In many radioactive waste disposal scenarios, intermediate level wastes are grouted and the geological disposal facility (GDF) will have cement present as a ubiquitous engineering material. Further, cementitious grouts have been considered as backfill for the GDF. Therefore, post-closure leaching of cementitious materials in a GDF is expected to create hyperalkaline conditions in and around the repository. These high pH fluids will react with the repository components and host rock, resulting in mineral alteration and crystallisation. Iron within the host rock derived from the alkaline breakdown of Fe-bearing silicate minerals (e.g. biotite, chlorite) or corrosion products formed within the repository will form iron (oxyhydr)oxide minerals. The formation and re-crystallisation of these reactive minerals, which may sequester radionuclides through reduction to less soluble forms and/or incorporation to more stable secondary iron oxide phases [1], may prove key to the fate of radionuclides in such environments.

To evaluate the signficance of these processes, ferrihydrite was crystallised under CO_2-free oxic and anoxic conditions, in two U(VI) amended synthetic cement leachates, representing early (pH 13.1) and late (pH 10.5) stage cement evolution for a cementitious ILW GDF. Under oxic conditions ferrihydrite crystallised to hematite (pH 10.5) and goethite (pH 13.1). Under anoxic contitions in both leachates, and in the presence of Fe(II), ferrihydrite crystallised to magnetite. X-ray Absorption Spectroscopy was used to characterise uranium association with each of the iron (oxyhydr)oxide phases during the crystallisation reactions. Under oxic conditons at pH 10.5, U(VI) rapidly (hours) sorbed to the ferrihydrite. Thereafter, during crytallisation, analysis indicates that U(VI) became structually incorporated in the hematite lattice. At pH 13.1, U(VI) remained 0.22 μm soluble and did not sorb to either ferrihydrite or goethite. Under anoxic conditions, in both leachates, uranium was rapidly (minutes) removed from solution as the ferrihydrite crystallised to magnetite (catalysed by Fe(II) in solution). Here, U(VI) was reduced to U(IV) and XAS analysis suggests it was directly substituted into octhedral sites of the magnetite structure.

These data have significant implications for the safety case for uranium behaviour in alkaline conditions in a GDF and in contaminated land scenarios. Details of uptake and bonding mechanisms of uranium in the iron oxide phases will be presented.

[1] Boland et al. (2011) *Environ. Sci. Technol.* **45**, 1327-1333.

Advanced Geological Applications Using XRF Elemental Mapping and Small Spot Analysis

Al Martin [1*], Didier Bonvin [2], Chris Shaffer [3], Kurt Juchli[4]

[1]Thermo Scientific, The Woodlands, TX, USA, al.martin@thermofisher.com (* presenting author)
[2]Thermo Fisher Scientific, Ecublens, Switzerland, Didier.bonvin@thermofisher.com
[3]Thermo Fisher Scientific, Ecublens, Switzerland, Christopher.shaffer@thermofisher.com
[4]Thermo Fisher Scientific, Ecublens, Switzerland, kurt.juchli@thermofisher.com

23d. General geochemistry

Geochemical and R&D applications offer interesting analytical challenges in the sense that these materials can represent a wide elemental coverage, wide concentration ranges and varied sample matrices and sizes. Analytical performance of wavelength dispersive X-ray fluorescence (WDXRF) instruments is being constantly advanced in order to cope with such challenges.

While traditionally WDXRF technique has always demanded homogeneous samples, the latest developments permit analysis of small spots down to 0.5mm as well as mapping of a selected area of a sample. These new possibilities open up the WDXRF technique to heterogeneous samples where segregations, defects or inclusions can now be determined. Coupling these capabilities with standardless analysis permits quantification of up to 79 elements of the periodic table on selected points of the sample.

In this presentation, several examples will be presented and finally tied into one thorough application in which the power and flexibility of new WDXRF instruments are fully exploited.

https://doi.org/10.1180/S0026461X00008434 Published online by Cambridge University Press

Chemical weathering fluxes through a coastal aquifer, the Pingtung Plain, southwest Taiwan

CAROLINE MARTIN[1]*, ALBERT GALY[1], NIELS HOVIUS[1], MIKE BICKLE[1], IN-TIAN LIN[2], MING-JAME HORNG[3], DAMIEN CALMELS[4], HAZEL CHAPMAN[1] AND HONGEY CHEN[5]

[1]Dept. Earth Sciences, University of Cambridge, UK, ceam4@cam.ac.uk (* presenting author)
[2]Institute of Earth Sciences, Academia Sinica, Taipei, Taiwan, itlin@earth.sinica.edu.tw
[3]Water Resources Agency, Ministry of Economic Affairs, Hsin-Yi Road, Taipei, Taiwan
[4]Institute de Physique du Globe, Paris, France, calmels@ipgp.fr
[5]Dept. of Geosciences, National Taiwan University, Taipei, hchen@ntu.edu.tw

Tracing groundwater offshore has resulted in a wide range of submarine groundwater discharge (SGD) estimates for specific marine locations, but complementary, similarly-focused studies measuring potential throughput on land are few. We analysed the waters from 43 wells at varying depths through a 264 m window in the Pingtung Plain for major dissolved cations, anions, dissolved SiO_2, and stable isotopic composition of oxygen and hydrogen of water, and used Darcy's Law to compute their subsurface fluxes. Compared to chemical flux estimates from the adjacent Kaoping River, results show that 1.1 to 12.3 % of combined surface runoff and potential subsurface discharge to the ocean can be attributed to groundwater-derived weathering fluxes. Estimated propagated errors at 2σ on subsurface fluxes are ± 30 % assuming the hydraulic conductivity is known by ±10 %. Multi-year daily hydraulic head data gives the direction of groundwater flow through the plain, and indicates that pumping has led to episodic reversals of flow, facilitating seawater intrusion in the near-coast aquifer. Hydrological connectivity exists throughout the drilled depth of the basin, whereas chemical gradients suggest that stratified flow is in operation, with up to a two-fold increase in silicate-derived Na^+ seen in deeper horizons as compared to the near surface. For all ions except Ca^{2+} and SO_4^{2-}, the average concentrations of dissolved species in the distal groundwaters exceed those of the river, ranging from a factor of 1.2 in the case of Li^+, K^+ and Mg^{2+} to 5.4 in the case of Ba^{2+}. At 12.3 %, the relative groundwater flux of Ba^{2+} exceeds that of all other elements by at least a factor of two. Furthermore, Ba^{2+} concentrations in the near surface coastal aquifer exceed those in deeper horizons by up to a factor of 7.9. The observation of increasing Ba^{2+} in the shallow subsurface could be accounted for by a desorption mechanism. However, the correlation of Ba^{2+} and ionic strength is poor, requiring an additional mechanism that could affect Ba, (additional dissolution of Ba-bearing phases), and/or the ionic strength (~Na^+), such as reverse weathering. Results suggest that, with the exception of Ba^{2+}, submarine groundwater chemical fluxes into the Taiwan Strait are modest in comparison to those related to surface runoff. If reverse weathering is promoted in seawater-intruded aquifers, the silicate weathering fluxes in the Pingtung Plain would still be underestimated after the incorporation of SGD.

Isotopic insight into volcanic sulfate formation in the troposphere.

ERWAN MARTIN[1(*)], SLIMANE BEKKI[2], CHARLOTTE NININ[1], AND IYA BINDEMAN[3].

[1]ISTEP-UPMC, Paris, France. erwan.martin@upmc.fr, charlotte.ninin@etu.upmc.fr
[2]LATMOS-IPSL, Paris, France. slimane@latmos.ipsl.fr
[3]Dprt of Geological Sciences, Univ. of Oergon, Eugene, USA. bindeman@uoregon.edu

We present analyses of oxygen and sulfur isotopic composition of sulfate extracted from volcanic ash collected near volcanoes few hours or days after eruptions. This study is based 10 volcanic eruptions that occurred from the equator to 65°N.

Very significant variability is observed in the dataset with SO_4 concentration ranging from 350 to 7500ppm, $\delta^{18}O$ from 0.2 to 13.2‰, $\Delta^{17}O$ from -0.14 to 0.35‰ and $\delta^{34}S$ from 3.9 to 10.5‰.

While $\delta^{34}S$ of volcanic sulfate is expected to reflect processes that mainly occurred in the volcanic plume, the O-isotopes clearly trace the oxidation pathways of volcanic SO_2 in the atmosphere and more specifically in the troposphere for our samples.

Assuming that $\Delta^{17}O$ = 0‰ and $\delta^{18}O$ = 5-7‰ in SO_2 coming out from the volcanoes, the resulting sulfate $\Delta^{17}O$ would be significantly different from 0‰ only if a substantial fraction of SO_2 was oxidized via mass-independent fractionating oxidation pathways (reaction with O_3 or H_2O_2). On the other hand, the $\delta^{34}S$ of sulfate was expected to fall within the initial volcanic SO_2 range, which is $\delta^{34}S$ = 6-8‰. The fluctuations of about 2‰ outside this range in the measured sulfate may reflect some Rayleigh distillation processes in the volcanic plume.

The different volcanic events analysed here correspond to different environmental conditions (latitude, season…) for the oxidation of volcanic SO_2. We analyse, via 3-D chemistry-transport model calculations, the expected levels of SO_2 oxidants in the atmospheric column above the studied volcanoes. For each eruption, we are able to compare the measured $\Delta^{17}O$ with the $\Delta^{17}O$ estimated in sulfate produced by SO_2 oxidised in model-calculated background conditions.

Our results indicate that, for the vast majority of the cases, the main oxidant for volcanic SO_2 in the troposphere is OH radicals or, at least, that SO_2 is not significantly oxidised via a mass-independent fractionating channel. OH in the very dry stratosphere carries a substantial mass-independent isotopic anomaly while in the humid troposphere this anomaly is thought to be lost through isotopic exchanges with H_2O. It is likely that the low pH of volcanic aerosol clouds could reduce very significantly the heterogeneous oxidation via the mass-independent O_3 and H_2O_2 in the troposphere.

https://doi.org/10.1180/S0026461X00008434 Published online by Cambridge University Press

Fluid evolution along a cross section through the Central Alps, Switzerland

K. MARTINEK[1*], T. WAGNER[1], M. WÄLLE[1], AND C.A. HEINRICH [1]

[1]Geochemistry and Petrology, ETH Zurich, Clausiusstrasse 25, CH-8092 Zürich, Switzerland, klara.martinek@erdw.ethz.ch

The classical Alpine fissure veins, large cavities lined by occasionally giant quartz crystals, occur in regionally metamorphosed rocks in the Central Alps. They record important information about the composition and evolution of metamorphic fluids, and fluid sources and mass transfer during fluid-rock interaction. The fluid composition shows a distinct evolution with increasing metamorphic grade, where consecutive zones are dominated by (1) heavier hydrocarbons, (2) methane, (3) aqueous fluids, and (4) aqueous-carbonic fluids [1]. This study addresses the chemical evolution of fluids in Alpine fissure veins in the Central Swiss Alps by integrating field work, fluid inclusion studies (microthermometry and LA-ICPMS microanalysis of individual fluid inclusions), and geochemical modeling.

The field locations were selected along a cross section through the Central Alps that covers different lithologies and metamorphic conditions. This includes vein systems in the Aar massif (Gauli glacier, Gerstenegg vein, Tiefen glacier), the Bedretto valley, and the Cavagnoli and Faido region. The fluid inclusions from the Aar massif are low-salinity aqueous two-phase, whereas the Cavagnoli and Faido samples dominantly contain aqueous-carbonic fluid inclusions. The salinity increases from the Gauli samples with 4.5-5.0 wt% equivalent (eqv.) NaCl to those from the Gerstenegg and Tiefen glacier with salinities of around 10-11 wt% eqv. NaCl. The aqueous-carbonic fluids of the Faido and Cavagnoli region have very low salinities of around 3.4 and 0.4 wt% NaCl, respectively. This differences in salinity are also reflected in their major and trace element concentrations, as determined with LA-ICPMS. Higher salinities do systematically correlate with higher concentrations of elements that are largely complexed by chlorine such as the alkali and earth alkaline metals, and divalent transition metals [2]. The concentrations of base metals such as Pb, Zn and Ag are consistently higher in the fluid inclusions from the Gerstenegg and Tiefen glacier than in the Gauli samples. The Cavagnoli and Faido samples contain even higher concentrations of ore metals (up to several tens of ppm) and sulfur, reflecting their higher metamorphic grade. The measured fluid compositions will be compared with results from multicomponent-multiphase fluid-mineral equilibria modeling to evaluate the status of fluid-rock equilibrium along the metamorphic gradient.

[1] Mullis, J., Dubessy, J., Poty, B., O'Neil, J. (1994) *Geochim. Cosmochim. Acta* **58**, 2239-2267. [2] Yardley, B.W.D. (2005) *Econ. Geol.* **100**, 613-632.

Evidence for the accumulation of heterocyclic N compounds in temperate forest soils as a function of depth

CARMEN ENID MARTÍNEZ[1*], JOSEPH DVORAK[2]

[1]The Pennsylvania State University, Department of Crop and Soil Sciences, University Park, PA, USA, cem17@psu.edu (* presenting author)

[2] Brookhaven National Laboratory, National Synchrotron Light Source, Upton, USA, jdvorak@bnl.gov

Leaching of dissolved organic nitrogen (DON) from forest (organic–rich) surface soils is likely the primary vehicle for the observed movement of N into underlying mineral soils. Our goal is to understand the accumulation and storage of nitrogen in soils. The overarching hypothesis that drives this research is that heterocyclic N compounds derived from the decomposition of litter are transported and accumulate in the soil column. The analytical approaches typically used to study N-containing compounds are not sensitive to the presence of heterocyclic N. This has resulted in the general belief that amide-N (as in proteins/peptides) is the only N form important in N accumulation and storage in soils. Still, biomolecules such as DNA are composed of heterocyclic N containing subunits and these molecules, although in lower concentrations than amide-N in proteins/peptides, are chemically recalcitrant, sorb onto soil solids, and are thus expected to accumulate and persist in natural soil environments. In this investigation, we used an innovative technique, nitrogen X-ray absorption near edge structure (N-XANES) spectroscopy, to determine the N chemical forms in temperate forest soils as a function of depth and varying mineralogy.

Soil columns (down to approx. 1 meter) were collected from two forest locations in Pennsylvania. These include an Inceptisol soil with mineralogy dominated by illite and chlorite, and a Spodosol soil with mineralogy dominated by Fe oxides, illite and kaolinite, but that also contains organic matter accumulations at depths of about 25-50 cm. The N K-edge (409.9 eV) XANES spectra was collected at the National Synchrotron Light Source, BNL.

The N-XANES spectra of these forest soils can be divided into two regions: π* resonances at 398-404 eV and σ* resonances at 404-420 eV. Furthermore, the spectra reveal two well-resolved π* resonances, one (lower energy π*) corresponding to spectral features present in biomolecules such as DNA/RNA and their contituent nucleic acids, and a second resonance (higher energy π*) which is present in proteins and their contituent amino acids and polypeptides. We observed an increase in the lower energy π* resonace with soil depth that was mirrored by a decrease in the higher energy π* resonace. This trend is consistent for all soil columns, except when an accumulation of organic matter occurs in deep soil layers. The lower energy π* resonance originates from molecular structures with extended π-electron systems and indicate the presence of heterocyclic N compunds. Thus, our results indicate N long-term leaching processes result in the selective accumulation of heterocyclic N compounds at soil depths. The accumulation of heterocyclic N at soil depths might be a consequence of its presumed recalcitrance and/or bonding to mineral surfaces.

https://doi.org/10.1180/S0026461X00008434 Published online by Cambridge University Press

Trace element mobility and root iron plaque effects on rice growth in a coal mining area of North Vietnam

RAUL E. MARTINEZ, J. EDUARDO MARQUEZ*, THI BICH HOÀNG-HÒA , AND RETO GIERÉ

Universität Freiburg, Geowissenschaften, 79104 Freiburg, Germany raul.martinez@minpet.uni-freiburg.de, jorge.eduardo.marquez@gmail.com (* presenting author), hoahtb@gmail.com, reto.giere@minpet.uni-freiburg.de

The Cam Pha area in Northen Vietnam is known for its coal mining activities. The Coc Sau open pit coal mine has been operative in this area for at least the past 50 years. Rice paddies located ~2 km away from the Coc Sau mine are irrigated with water contaminated by acid mine drainage. Bulk chemical analysis of rice paddy soil from the Cam Pha area shows relatively high concentrations of several toxic metals attributable for the most part to the coal mining activities, including Cr, Cu, Zn, As, Cd, and Pb (60, 27, 48, 14, 0.2, and 35 ppm, respectively).

Preliminary experiments with model *Oryza sativa* cv. (Asia) rice species exposed to contaminated paddy soil from the Coc Sau mining area showed a hindered growth as a function of increasing soil concentrations added to rice growth media under controlled laboratory conditions. Figure 1 shows a clearly a detrimental effect of this soil on the growth of model *Oryza sativa* cv. (Asia) rice species.

In the next step, we will perform sequential extraction analyses of the soil to determine the most mobile metals. Moreover, we are currently studying the effects of root iron plaques and the presence iron oxide mineral phases in regards to toxic metal immobilization.

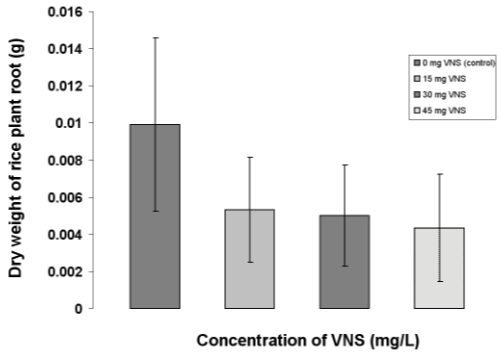

Figure 1: Plot of dry rice plant root weight as a function of concentration of Vietnamese rice paddy soil (VNS) from Cam Pha area.

δ^{11}B-based atmospheric CO_2 records during the Pliocene at orbital resolution

MIGUEL A. MARTÍNEZ-BOTÍ[1*], GAVIN L. FOSTER[1], MARCUS P.S. BADGER[2], RICHARD D. PANCOST[2], DANIELA N. SCHMIDT[3], DANIEL J. LUNT[4]

[1]Ocean and Earth Science, National Oceanography Centre Southampton, University of Southampton Waterfront Campus, European Way, Southampton SO14 3ZH, UK, M.A.Martinez-Botí@noc.soton.ac.uk (*presenting author), Gavin.Foster@noc.soton.ac.uk.

[2]Organic Geochemistry Unit, School of Chemistry, University of Bristol, Cantock's Close, BS9 1TS, U.K., Marcus.Badger@bristol.ac.uk, R.D.Pancost@bristol.ac.uk.

[3]Department of Earth Sciences, University of Bristol, Wills Memorial Building, Queen's Road, BS8 1RJ, U.K, D.Schmidt@bristol.ac.uk.

[4]School of Geographical Sciences, University of Bristol, University Road, Bristol BS8 1SS, U.K., D.J.Lunt@bristol.ac.uk.

The Mid-Pliocene is the most recent time in Earth's history when mean global temperatures were substantially warmer and sea levels higher than they are today [1]. The subsequent intensification of the Northern Hemisphere Glaciation (iNHG) represents the key final step in the climatic transition from the warm Pliocene to the current "icehouse" climate. Recent modeling and proxy-based results [2-4] suggest that this climate shift was forced by a reduction in atmospheric CO_2 concentrations (pCO_2), which highlights the relationship between climate and this important greenhouse gas. Hence, there is significant potential in the use of the Pliocene as an analogue for future global warming in modeling studies and as a key period to study the role of CO_2 in driving major climatic shifts. Despite recent advances in the reconstruction of pCO_2 change during this important period [3-4], detail at the orbital scale is currently lacking.

Boron isotopes in planktic foraminifera are a proven proxy for surface oceanic pH [5], which has been shown to provide valuable insights into past changes in the ocean carbonate system and ultimately into past atmospheric pCO_2. Here we will provide foraminiferal δ^{11}B-based records to determine the temporal evolution of pCO_2 for an interval spanning the Pliocene Warm Period and the iNGH at orbital scale temporal resolution. Our record provides valuable insights into the causes and consequences of the changes in the atmospheric concentration of this important greenhouse gas.

[1] Haywood *et al.* (2000) *Geology* **23**, 1063-1066. [2] Lunt *et al.* (2008) *Nature* **454**, 1102-1105. [3] Pagani *et al.* (2010) *Nature Geoscience* **3**, 27-30, [4] Seki *et al.* (2012) *Earth and Planetary Science Letters* **292**, 201-211. [5] Sanyal *et al.* (2001) *Paleoceanography* **16**, 515-519.

https://doi.org/10.1180/S0026461X00008434 Published online by Cambridge University Press

Mercury methylation, pore water geochemistry and legacy mercury contamination along the floodplain of the Connecticut River

ANNA MARTINI[1*], JON WOODRUFF[2], DANIEL KEKACS[1], HANNA BOUBERHAN[1], AND CARYL ANN BERCERRA[1]

[1]Amherst College, Geology, Amherst, U.S., ammartini@amherst.edu (* presenting author)

[2]University of Massachusetts, Geosciences, Amherst, U.S., woodruff@geo.umass.edu

Mercury has long been stored in the fine-grained sediment along the various tributaries, ponds, lakes, and coves connected to the Connecticut River. Concentrations rose above background (<80 ppb) by the dawn of the Industrial Revolution and have, for the most part, mirrored the rise and fall of atmospheric mercury concentrations[1]. Total mercury concentrations in the sediment peak upstream in the Oxbow at approximately 500 ppb and near the mouth of the river, in Hamburg Cove, increase to nearly 3000 ppb. This sixfold rise is further exacerbated by the changing sedimentation rate from a low at the Oxbow (~1.5 cm/yr) to extremely high values for Hamburg Cove (~4.1 cm/yr)[1]. The rise in sedimentation rates towards the Long Island Sound are due to the influence of tidal pumping, allowing significant quantities of sediment fines to accumulate in these depocenters. In comparing mass accumulation rates (as $\mu g/m^2/yr$), Hamburg Cove accumulates mercury at nearly an order of magnitude greater than at the upriver Oxbow. In both locations, organic content ranges from 4 to 14%, but does not correlate well with mercury concentrations (R^2 = 0.2664). Although mercury readily adsorbs onto organic matter, the peaks in mercury concentration are more correlative with atmospheric loading and local mercury inputs than simply TOC. Methylmercury concentrations are also quite distinct in each location, with Hamburg containing over 1.5 ppb in its uppermost sediments while Oxbow concentrations never rise above 0.5 ppb. Variations in MeHg concentrations do not, however, correspond to those of total inorganic mercury, but instead suggest that SO_4 in pore water and the actions of SRB are needed to methylate the stored inorganic mercury. qPCR results also indicate the presence of sulfate reducers in these environments, just below the sediment interface. For Hamburg Cove this suggests that significant introduction of the bioavailable form of mercury is controlled by the occasional influx of salt water (with its high SO_4 concentration). With sealevel rise, it is likely that the magnitude of re-introduction of legacy mercury will increase and will eventually effect other floodplain waterbodies further up the Connecticut River Channel.

[1] Varekamp (2003) *Environmental Geology* **Volume43**, 268-282.

Computational study of the most stable pyrophyllite edge surfaces for metal adsorption

DAVID M. S. MARTINS[1,*], MÁRIO A. GONÇALVES[1], JOSÉ MIRÃO[2], STEPHEN C. PARKER[3]

[1]Department of Geology and CREMINER/LARSyS, Faculty of Sciences of the University of Lisbon, Lisbon, Portugal (*dmmartins@fc.ul.pt, mgoncalves@fc.ul.pt)

[2]Department of Geosciences and Center of Geophysics, University of Évora, Portugal (jmirao@uevora.pt)

[3]Department of Chemistry, University of Bath, Bath BA2 7AY, United Kingdom (s.c.parker@bath.ac.uk)

Abstract

Metal adsorption on mineral surfaces is a topic extensively pursued by researchers to improve the understanding of the environmental fate of metals, and provide natural low-cost adsorbents for remediation as this is an active mechanism in controlling the fate of metal ions in natural waters. Despite the wealth of available information focused mostly with basal surfaces, because edge surfaces are difficult to model, few studies were devoted to edge surfaces of clays.[1-3]

Pyrophyllite was chosen as a model because it is a non expanding phyllosilicate with neutral layers that do not require encapsulation of couter-ions, making it the best candidate for calculations that intend to discern such an important and complex problem.

The work presented herein follows on from experimental work done in our group,[4] and aims at interplaying with such results *via* the investigation of the metal adsorption mechanisms at the edge surface sites of pyrophyllite. Having been started with a non biased and systematic approach using atomistic simulation techniques, initially, the static simulation code METADISE[5] was used to cleave and hydroxylate low Miller index surfaces, and explore their structure and stability. Subsequent to ranking the cuts, classical modeling of the hydrated clay-edge surfaces showed that from the large set of Miller index planes cut, the (110), (-110), (010), and (100) surfaces are the most stable leading to a pseudo-hexagonal crystal shape generated with the first three surface planes, as documented for phyllosilicates. These edge surfaces were further optimised using DFT within the VASP code,[6] to calculate the energy of the diferent hydroxylated ensembles in oder to ascertain the most stable and hence the most likely for metal surface complex formation.

[1] Bickmore B. R., Rosso K. M., Nagy K. L., Cygan R. T., and Tadanier C. J. (2003) *Clays and Clay Miner.* **51(4)**, 359-371. [2] Churakov S.V. (2006) *J. Phys. Chem. B* **110(9)**, 4135-4146. [3] Rotenberg, B., Marry, V., Malikova, N. and Turq, P. (2010) *J. Phys.: Condens. Matter*, **22**, 284114. [4] Gonçalves, M. A. and Rodrigues, A. S., *Submitted to Chem. Geol*. [5] Watson G. W., Kelsey E. T., deLeeuw N. H., Harris D. J., and Parker S. C. (1996) *J. Chem. Soc., Faraday Trans.* **92(3)**, 433-438. [6] Kresse G. and Furthmuller J. (1996) *Phys. Rev. B* **54(16)**, 11169-11186.

https://doi.org/10.1180/S0026461X00008434 Published online by Cambridge University Press

Nitrogen composition of the ancient atmosphere from fluid inclusion analysis of Archean quartz

B. MARTY[1*], L. ZIMMERMANN[1], M. PUJOL[1,2], R. BURGESS[3] AND P. PHILLIPOT[4]

[1]CRPG-CNRS, Université de Lorraine, Vandoeuvre les Nancy, France, bmarty@crpg.cnrs-nancy.fr
[2]ETH, Zürich, Switzerland, pujol@erdw.ethz.ch
[3]University if Manchester, UK, ray.burgess@manchester.ac.uk
[4]IPGP, Paris, France, philippot@ipgp.fr

Introduction

Knowning the composition of the Archean atmosphere is extremely important for a number of reasons. First, the Sun was ~25 % fainter than Today and, because there is no evidence of glaciation in the Archean, rhe lower solar energy delivery was presumably compensated by a stronger greenhouse effect. Such an effect is not recorded in geological proxies of the paleo partial pressure of CO_2, and it has been proposed that doubling the pN_2 in the Archean atmosphere could have broadened by Rayleigh scattering the adsorption line of radiatively active gases, strengthening the greenhouse effect [1]. Because nitrogen isotopes are fractionated by bacteria, the isotopic siganture of this element in old sedimentary rocks is used to investigate the early development of the biosphere. Thus the isotopic value of the atmosphere at different time periods is equally important to document. Previous works have proposed that it remained constant through time within a few permil [2].

Nitrogen and argon isotopes in irradiated Archean quartz

We have analyzed nitrogen and argon isotopes in 3.5 Ga old hydrothermal quartz from the North Pole area, Pilbara, NW Australia. In the same sample we have previoulsy determined a Ar-Ar plateau age of 3.0±0.2 Ga indicating that the age of trapped fluids is within 3.0-3.5 Ga. The Xe isotope signature intermediate between Chondritic and Atmospheric was interpreted as representing atmospheric Xe trapped ≥ 3.0 Ga ago [3]. Gases were extracted by vacuum crushing and heating of the remaining powder, nitrogen and noble gases were purified independently, and nitrogen and argon isotopes and abundances were sequentially analyzed by static mass spectrometry (overall $\delta^{15}N$ error : 1-2 ‰). In a first step we analyzed non-irradiated samples, and data are consistent with mixing between an hydrothermal end-member and a paleo-atmospheric component having a $\delta^{15}N$ value close to the modern one. We then irradiated a second batch of samples in order to quantify the chlorine and potassium contents of the extraction steps from ^{37}Ar, ^{38}Ar and ^{39}Ar and to correct data for mixing (and ageing for Ar). The $\delta^{15}N$ values are very similar to the ones obtained from the non-irradiated sample runs, showing neglible production of nitrogen isotopes during neutron irradiation. Premiminary results confirm $\delta^{15}N$ values between 0 ‰ and 5 ‰, and suggest a partial pressure of atmospheric nitrogen comparable to the present-day one.

[1] Goldblatt, C., et al., (2009) *Nature Geosci.* **2**, 891-896.
[2] Sano, Y. & Pillinger, C.T. (1990) *Geochem. J.* **24**, 315-325.
[3] Pujol, M., et al. (2011) *EPSL* **308**, 298-306.

The volatile element record of Earth's accretion

B. MARTY[1]

[1]CRPG-CNRS, Université de Lorraine, Vandoeuvre les Nancy, France, bmarty@crpg.cnrs-nancy.fr

Isotope signatures of volatile elements

The stable isotopes signatures of terrestrial nitrogen and hydrogen suggest strongly that most volatile elements on Earth originated from a cosmochemical reservoir that also sourced asteroidal bodies. However, in the Earth's mantle, a minor solar-like volatile component is present and best seen in the Ne (and possibly N and H) isotope composition(s) of mantle-derived rocks. Ne isotopes in minerals from mantle plume provinces discriminate against contribution of dust implanted with solar ions, and instead support trapping of volatile elements directly from the nebular gas. Atmospheric escape to space has been long advocated to account for the atmospheric $^{20}Ne/^{22}He$ isotope ratio lower than the Solar value. I shall argue instead that mixing between solar and chondritic components accounts well for Ne isotope variations in the Earth-atmosphere system. In a $^{20}Ne/^{22}Ne$ versus $^{36}Ar/^{22}Ne$ diagram, both the atmosphere and the MORB mantle plot on a mixing line joining the solar and the chondritic (A-type component) end-members [1].

Earth's accretion seen from volatile elements

The above geochemical compositions on one hand, and dynamical modelling of planetary formation [2] on another hand, are consistent with the following scenario. Planetary embryos of the size of Mars accreted and differentiated in a few Ma [3], while the nebular gas was still present. Solar-like atmospheres were gravitationnally bound and solar gases were dissolved in molten silicates, imposing reducing conditions that participated to metal segregation. Such conditions might have also permitted the trapping of minor amounts of solar, isotopically light, N and H. Such contribution is larger than the late veener advocated in the case of PGEs. Giant shocks that characterized the accretion of Earth, but not of Mars, did not completely dry up the proto-Earth : volatile elements were gravitationnaly bound as were less volatile, or non volatile, elements also vaporized during the Moon-forming impact. Delayed accretion of asteroidal bodies or of volatile-rich dust orginating from close to the snowline added chondritic-like volatiles : a contribution of 2±1% carbonaceous chondrite-type material is indeed sufficient to supply water, carbon, nitrogen, halogens, and most noble gases to the Earth (including the surface reservoirs) [1]. In the light of existing data, the contribution of comets might not have exceeded a few percents of that of asteroidal material. The isotopic fractionation of atmospheric xenon (and, to a lesser extent, of atmospheric krypton) is probably related to non-thermal escape processes involving selective ionization, possibly on embryos, or during the Hadean-Archean eons [4] when the young Sun was more energetic than Today in the far UV range [5].

[1] Marty, B., (2012) *EPSL* **313-314**, 56-66.
[2] Walsh, K.J., et al., (2009) *Nature* **475**, 206-209.
[3] Dauphas N. & Pourmand, A., (1990) *Nature* **473**, 489-493.
[4] Pujol, M., et al., (2011) *EPSL* **308**, 298-306.
[5] Ribas, I., et al., (2011) *Astrophys. J.* **714**, 384–395.

https://doi.org/10.1180/S0026461X00008434 Published online by Cambridge University Press

Mercury stable isotope time trends in cryogenically archived ringed seal livers from the Alaskan Arctic

J. MASBOU[1*], D.POINT[1], J.E. SONKE[1], P.R. BECKER[2]

1 Observatoire Midi-Pyrénées, Geosciences Environnement Toulouse, CNRS-IRD-Université de Toulouse 3, France. jeremy.masbou@get.obs-mip.fr (* presenting author)

2 National Institute of Standards and Technology, Hollings Marine Laboratory, Charleston, South Carolina, USA

Because of its long residence time in the atmosphere, gaseous mercury (Hg) emitted from distant anthropogenic sources reaches high latitude regions carried by air flow [1]. Springtime atmospheric Hg depletion events (AMDEs) were early on recognized as a potential key control on Hg entering the Arctic ecosystem. Even if a large amount of AMDE Hg deposited is immediately re-emitted to the atmosphere, the remainder is mobilized by meltwater [2] and transformed by bacteria into methyl-Hg. This neurotoxic form is able to bio-accumulate along the trophic chain and high concentrations are observed in top predators. Global emission Hg trends and AMDEs alone are however unable to explain observed temporal trends in biota Hg in Western and Eastern Arctic sectors [4]. Marine mammal's exposure to MeHg therefore needs additional consideration of physiological, ecological and climate change factors such as feeding behavior, habitat utilization, and sea-ice dissappearance. Recent work on arctic seabird eggs [5] has shown a possible link between sea-ice cover and biota Hg isotope signatures. It was inferred that by blocking UV radiation the sea-ice diminishes photochemical breakdown of bioavailable surface ocean MeHg.

Here we further explore the potential influence of climate change on Arctic Hg biogeochemistry. We focus on ringed seals, a sea-ice dependent species considered as apropriate Hg biomonitors in the Arctic region. Indeed, their high degree of site fidelity allows spatio-temporal analysis of biomarkers. Hg speciation (inorganic Hg, MMHg) and stable isotopic composition (C, N, Hg) measurements were made on 53 ringed seal liver samples archived at the US Marine Environmental Specimen Bank. Sampling covers a period of 14 years (1988-2002), allowing an accurate time trend analysis. The isotopic signature Δ^{199}Hg, which is a tracer for inorganic or methyl Hg photochemistry in surface waters, varied from 0.05 to 1.04 ‰.This variation was not related to in-vivo metabolic effects or ecological effects such as feeding habitat (δ^{13}C) and trophic level (δ^{15}N). Δ^{199}Hg shift from +0.37±0.08‰ (SE, n=5) in 1988 to +0.59±0.07‰ (SE, n=7) in 2002, and show a significant increase of 4.8% yearly (R^2=0.70, p*<0.05) in this period. We suggest that this reflect the progressive decrease in sea-ice cover between 1988 and 2002. This is coherent with our previous study [5].

[1] Macdonald et al. (2005) *Sci Total Environ*, **342**, 5-86
[2] Steffen et al. (2002) *Atmos Environ,* **36**, 2653-2661.
[3] Loseto et al. (2004) *ES&T,* **38**, 3004-3010.
[4] Gaden et al. (2009) *ES&T*, **43**, 3646-3651
[5] Point et al. (2011) *NGS,* **4**, 188-194.

Characterization of combustion products from biomass pellets

CHRISTOPH MASCHOWSKI[1*], RETO GIERÉ[1], AND GWENAËLLE TROUVÉ[2]

[1] Universität Freiburg, Geowissenschaften, 79104 Freiburg, Germany, christoph@maschowski.de (* presenting author), giere@uni-freiburg.de

[2] Université de Haute-Alsace, Laboratoire de Gestion des Risques et Environnement, Mulhouse, France, gwenaelle.trouve@uha.fr

Two different types of biomass pellets (a DIN+ wood pellet and a new pellet made of the *Miscanthus* grass) and their combustion products (bottom ash and fly ash) were investigated by Atomic Absorption Spectroscopy (AAS), Scanning Electron Microscopy (SEM), Electron Microprobe Analysis (EMPA), and X-ray diffraction (XRD). Also, an attempt was made to characterize combustion-derived particles in the exhaust gas by using SEM images and EDX spectra.

The fuels were combusted in a glass tube reactor using a heating ramp (20-820°C @ 20°C/min). The particles were collected by an Electrical Low Pressure Impactor (ELPI) on twelve stages depending on their aerodynamic diameter. The main focus was put on the alkali, alkaline earth and silicon contents as these compounds commonly lead to the formation of corrosive deposits in biomass power plants and may also contribute to hazardous primary and secondary particulate matter in the atmosphere.

The results reveal relatively higher potassium and calcium contents in the Miscanthus fuel and its combustion products. On the other hand, the silicon contents of the fuel and the combustion products are almost identical for the two pellet types. The unexpected high silicon content in the wood pellet is inferred to result from contamination during harvesting and pellet production, a hypothesis supported by the presence of extraneous quartz grains observed by SEM. In the Miscanthus pellet potassium and silicon were also found inside the cells, and thus represent inherent inorganic material. In the bottom ash of the Miscanthus pellet, a multitude of mineral phases, predominantly lime, have been identified by XRD, and evidence for ash melting was obtained from SEM observations. In the bottom ash of the DIN+ wood pellet, only quartz and calcite were detected, with no indication for ash melting.

The inorganic particles collected from the flue gas were classified on the basis of their chemical composition and shape in order to assign them to a probable mineral phase. In the Miscanthus particulate matter samples, twelve different inorganic particle types with mean diameters from 1-20µm were identified. In the DIN+ particulate matter sample, a total of seven different particle types were found, but the main fraction (~80%) is represented by quartz grains with mean diameters > 10µm.

The major part of the inorganic (ash-forming) fraction of the DIN+ pellet is represented by extraeneous material, whereas significant amounts of the inorganic constituents of the Miscanthus pellet are located inside the biostructures. This may lead to higher reactivity during combustion and the formation of secondary phases such as lime and melilite, and the formation of a wide variety of particle types.

https://doi.org/10.1180/S0026461X00008434 Published online by Cambridge University Press

Speciation of commercial CeO2 nanocomposites during aging.

A. MASION[1,2*], L. SCIFO[3], P. CHAURAND1,[2], M.A. DIOT[1,2], J. LABILLE[1,2], M. AUFFAN[1,2], J.Y. BOTTERO[1,2] AND J. ROSE[1,2]

[1]CEREGE, CNRS-Aix Marseille Univ., France. masion@cerege.fr
[2]iCEINT, Aix en Provence, France
[3]TECNALIA, Montpellier, France

In many commercial nanoproducts, nanoparticles are surface modified to obtain new properties and/or to facilitate their dispersion in a matrix. Regular use, aging, and improper handling may cause the release of residues into the environment. As a consequence, assessing the risks associated with a given nanoproduct needs to take into account these residues throughout the entire life cycle of the product.

For example, outdoor wood paint contains CeO_2 nanoparticles as long-term UV-absorber to stabilize paints against degradation. The nanoparticles are citrate coated for better dispersion in the aqueous paint. This work aimed at investigating the transformation occurring at the nanoparticle surface during simulated aging in the lab.

Two sets of experiments were conducted: aging of the Ce based nanocomposite in aqueous suspensions, and aging of a paint containing CeO_2 nanocomposites.

In both cases, the experiments were carried out over several months, with UV/Vis illumination to simulate sunlight, and, in the case the paint samples, included rain cycles at fixed intervals. During the aging, the samples were analyzed in terms of leached Ce content (paint), and physical-chemical properties (size, charge...) and chemical nature of the residues using mainly microscopy and spectroscopy techniques.

Towards a new clinopyroxene geothermometer for alkaline, differentiated magmas

MATTEO MASOTTA[1*], SILVIO MOLLO[2], CARMELA FREDA[2], MARIO GAETA[1,2] AND GORDON MOORE[3]

[1]Sapienza Università di Roma, Rome, Italy
matteo.masotta@uniroma1.it (* presenting author)
[2]Istituto Nazionale di Geofisica e Vulcanologia, Rome, Italy
[3]Department of Chemistry and Biochemistry, Arizona State University, USA

In the last decades several clinopyroxene geothermometers have been proposed with the aim to constrain pre-eruptive conditions of volcanic systems [1]. However, the compositional bounds of the calibration dataset represent a serious limitation in their use. In fact, the more the composition of the investigated natural rocks deviates from the compositions in the calibration dataset, the larger the uncertainty in the estimate of temperature will be.

At the present, clinopyroxene geothermometers are mainly calibrated on magma compositions ranging from basalt to rhyolite, leaving poorly constrained or even unconstrained, alkaline differentiated composition. Moreover, the effect of melt-water content on phase compositions is usually neglected. Given the magnitude of the alkaline, explosive volcanism, these two factors cannot be ignored in future calibrations of geothermometers.

In this study, we present a new clinopyroxene geothermometer specifically calibrated for hydrous, alkaline compositions ranging from phonolite to trachyte. This model is based on a broad dataset consisting of 35 phase equilibria experiments, carried out at 200 MPa, in the temperature range 850-1000°C and at variable X_{H2O}-X_{CO2} (H_2O ranging from 0 to 6 wt.% and CO_2 ranging from from 0 to 0.5 wt.%). The equations have been obtained by means of least squares regression analysis of the experimental dataset, yielding a better accuracy of temperature estimate than previous models. Notably, the accuracy of the model largely increases by including the water-melt content parameter in the equations, whereas the presence of CO_2, which actually does not affect the composition of clinopyroxene and melt, scarcely influences the temperature estimate.

[1] Putirka (2008) *Rev. Mineral. Geochem.* **69**, 61-120.

https://doi.org/10.1180/S0026461X00008434 Published online by Cambridge University Press

Classification of Groundwater from a Coastal Granitoidic Fracture Network

FRÉDÉRIC MATHURIN[1*], BIRGITTA KALINOWSKI[2], MATS ÅSTRÖM[3] AND MARCUS LAAKSOHARJU[4]

[1]Linnaeus University at Kalmar, Sweden, frederic.mathurin@lnu.se (*presenting author)
[2]Swedish Nuclear Fuel and Waste Management Co, Sweden birgitta.kalinowski@skb.se
[3]Linnaeus University, Sweden, mats.astrom@lnu.se
[4]Nova FoU, Sweden, marcus@geopoint.se

Introduction

A groundwater classification system, using the distribution of the two groundwater conservative parameters Cl and $\delta^{18}O$ was developed at Äspö Hard Rock Laboratory (Äspö HRL).

Groundwater from boreholes was sampled during the years 1987-2009 from a total of 284 packed-off sections representing depths of 8 m to 984 m below the sea level. The groundwater classification system was based on the conceptual hydrological understanding of the region, including five end-members which, in ascending order with respect to their age, are: deep saline water of old age [1] but unknown origin (referred to as "old-saline water"), glacial melt water formed during the last Pleistocene glaciation, Littorina Sea water (mid-Holocene), current meteoric water and Baltic Sea water.

Results and Conclusions

Most of the samples in Fig 1 plot in the Mixed class indicating influences from several end-members. The Meteoric, Marine and Saline classes are also well represented by the samples. Few samples plot close to the Littorina and Glacial end-member indicating less influence in the sampled water."

The groundwater classification and results presented here are relevant for recognition of conditions of importance in terms of bedrock disposal of toxic waste materials as technical barriers may be influenced by hydrogeological and hydrochemical changes over time.

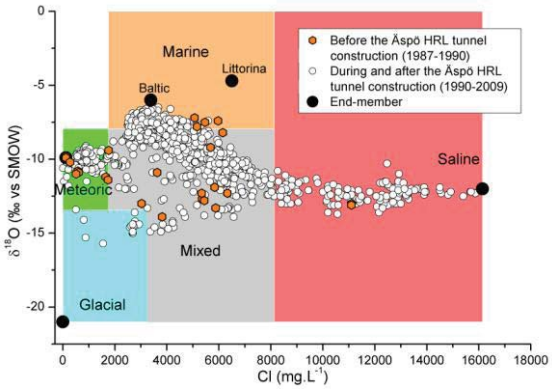

Fig. 1. Sampled groundwater plotted according to the established classes: Saline, Glacial, Marine, Meteoric and Mixed.

[1] Laaksoharju et al (2008) *Applied Geochemistry* **23**, 1921-1940.

Petolorogical diversity of chromian spinel bearing Matsue Basalt in Shimane Prefecture, Japan.

ICHIRO MATSUMOTO[1*], TOMOYUKI TSUBOTA[2], ATSUSHI KAMEI[3] AND DAISUKE SATO[4]

[1] Department of Education, Shimane University, Matsue, Japan, chromim@edu.shimane-u.ac.jp (* presenting author)
[2] Saidaiji Junir High School, Okayama, Japan
[3] Department of Geoscience, Interdisciplinary, Shimane University, Matsue, Japan
[4] Institute of Geology and Geoinfomation, AIST, Tsukuba, Japan

Matsue Alkaline Basalt

Matsue city located in Japan Sea coast side of southwest Japan arc. There are many alkaline basic-intermediate lavas that we called "Matsue Basalts" in Matsue city area. The activity of the Matsue Basalt is about 10 Ma ago. Matsue basalt basically consist of 6 basic lavas and some it's pyroclastic deposite (sandstone and tuff) [1, 2]. The purpose of this study is clarifying geochemical characteristics of Matsue basalt. We here report the Bulk rock chemical composition, and mineral assemblage and chemistry of Matsue Basalt. And we classified Matsue basalt into five groups. And we found chromian spinels from two groups. This study adds a new data and idea to the Tsubota and Matsumoto (2008) [2].

Results and discussion

Bulk rock chemical compositions of Matsue Basalt are divided into 6 groups, which are 3 basalt groups (Chausuyama, Hanamagari and Agenogi groupes), 2 basaltic andesite groups (Tsuda and Rakuzan groups) and 1 andesite group (Toukodai groupe) based on their volcanic Stratigraphy. However, Tsuda and Rakuzan groups are show same chemical feature. That is Matsue Basalt is chemically consists of 5 groups. Chausuyama and Agenogi basalts show particularly with respect to their low FeO*/MgO ratios and high Cr content. And these two basalts have chromian spinels in and around olivine grains. Chromian spinels from Chausuyama and Agenogi basalts have Cr# (Cr/(Cr+Al) atomic ratio) of 0.16-0.40, and olivines from these basalts have Fo of 88-76. Arai (1987, 1994) proposed that Fo-Cr# relations depend on the tectonic setting, due to differing melting conditions (pressure, temperature and water vapour conditions) [3, 4]. That is Chausuyama and Agenogi basalts of Matsue Basalt derived from the relatively depleted lerzolitic mantle. Furthermore, above two basalts may be the different magma origins by Cr and Ni bulk rock chemical composition.

After 5 Ma of activity of Matsue basalt, eruption of adakite magam enters active time at the almost same location as Matsue basalt [5]. That is, it may be able to explain the chemical diversity of Matsu basalt in which it is related also with motion of a Philippine Sea Plate and activity of adakite magma in Japan sea coast side south west Japan arc.

[1] Miyajima et al. (1972) *Mem. Fac. Lit. & Sci., shimane Univ., Nat. sci.* **5**, 131-138. [2] Tsubota & Matsumoto (2008) *GCA,* Abstract Vol. **72**, A960. [3] Arai (1987) *N. Jb. Miner. Mh.* 347-354. [4] Arai (1994) *J. Volcanol. Geotherm. Res.* **59**, 279-294. [5] Sato *et al.* (2011) *Jour. Geol. Soc. Japan.* **117**, 439-450.

https://doi.org/10.1180/S0026461X00008434 Published online by Cambridge University Press

Zn isotope fractionation in Archean komatiites and associated lava-flows

N. MATTIELLI[1,*], P. HAENECOUR[1,2] AND V. DEBAILLE[1]

[1]Laboratoire G-Time, Université Libre de Bruxelles, Brussels, Belgium (*correspondence : nmattiel@ulb.ac.be)
[2]Laboratory for Space Sciences, Washington University in St. Louis, St. Louis, USA.

Komatiites are volcanic ultramafic rocks with high MgO content (>18Wt.%), which make up the first few blocks of the Archean crust and are indicative of the earliest stages of the Earth mantle dynamics.

The present study reports high-precision MC-ICP-MS measurements of Zn isotopic compositions in whole rocks and mineral separates from Fred's Flow and Theo's Flow, two thick Archean differenciated flows (2.7 Ga) located in the Abitibi greenstone belt (Munro Township, Canada). Fred's Flow has a komatiitic affinity, and is classified as Al-undepleted type, whereas Theo's Flow has an Fe-rich tholeiitic affinity and is classified as Al-depleted type. Their geographical relationship as well as their complementary geochemical compositions suggest that they are genetically related. Characterizing fractionation processes of their Zn isotope compositions would provide constraints on diffusion transport, crystallisation processes, and melting conditions involved in the komatiites petrogenesis.

Small but significant shift in δ^{66}Zn values for whole rocks is systematically observed between Fred's flow (mean δ^{66}Zn = +0.30±0.04‰ (2SD)) and Theo's flow profiles (mean δ^{66}Zn = +0.39±0.03‰). For each flow, the Zn isotopic profile is relatively monotonous, except for the gabbroic units with slightly lower δ^{66}Zn (down to +0.28±0.04‰) and the basal ultrabasic units where enrichments in heavy Zn isotopes are clearly obvious (δ^{66}Zn up to +0.55±0.05‰).

Zn isotopic compositions in mineral separates vary on a large range of 1.6 δ-unit, and their relative modal contributions can explain the whole rock isotopic trends. As a whole, mineral separates reproduce the same isotopic shift between the two flows, as previously shown by the bulk rocks, suggesting a fractionation control by the crystallisation/melting conditions. Individually, chromites show especially strong enrichments in light Zn isotopes, relative to the silicates. Olivine, clinopyroxene and plagioclase exhibit generally smaller isotopic fractionation with respect to each other, but are characterized by contrasted δ^{66}Zn values suggesting correlation with the polymerization degree. No relationship has been observed between the Zn isotope fractionation and (light) alteration degree of the lava flow or mineral.

Further analyses are needed to discriminate secondary Zn mobilization, crystallisation or cooling rate effects, and establish interesting comparison with Mg and Fe isotopic results reported by Dauphas et al. (2010) on Alexo komatiites.

[1] Dauphas et al. (2010) *Geochimica et Cosmochimica Acta* **74**, 3274-3291.

Ni partitioning between olivine and high-MgO silicate melts: Implications for Ni contents of forsteritic phenocrysts in basalts

A.K. MATZEN, M.B. BAKER, J.R. BECKETT, E.M. STOLPER*

California Institute of Technology, Pasadena, CA, USA
ems@caltech.edu (* presenting author)

There has been considerable interest in the presence in basalts of forsteritic olivine (*ol*) phenocrysts with elevated NiO contents (i.e., up to 0.5-0.6 wt. % NiO, substantially higher than in normal peridotitic *ol*, [typically 0.35-0.40 wt. % NiO]). It is difficult to produce such high NiO contents in peridotitic *ol* via simple melting processes; so assuming that *ol* phenocrysts that crystallize at low P mimic the compositions of *ol* in deeper residual magmatic sources, the existence of phenocrysts with such elevated NiO contents would require that *ol* in these sources contain comparably elevated NiO contents. This has led to several hypotheses to explain NiO-rich *ol* in mantle sources of basalts (e.g., contamination of the lower mantle by the core; metasomatism of normal mantle by silica-rich melts of eclogite). If, however, the partition coefficient of NiO between *ol* and melt (D_{Ni}) depends strongly on T and/or P, *ol* phenocrysts that crystallize at lower P's and T's than those at which their host magmas last equilibrated with mantle need not mimic the compositions of *ol* in their residual sources. This would provide an explanation for NiO-rich *ol* phenocrysts that does not require NiO-enriched mantle *ol*.

We measured D_{Ni} between *ol* and picritic liquid at 0.001-30 kbar; by adjusting the T at each P, we kept liquid MgO contents similar (~17-18 wt. %) for all experiments. This experimental feature was critical because D_{Ni} is a strong function of liquid MgO content; so by keeping the MgO content essentially constant, we isolated the dependence of D_{Ni} on P and T from its dependence on MgO. D_{Ni} in our experiments decreases from 5.0 to 3.8 (by wt.) as T increases from 1400 to 1550°C. Our results are well described by a simple Ni-Mg exchange equilibrium assuming (1) ideal models for the liquid and *ol* and (2) the standard state ΔV and ΔC_P of the reaction are zero. Previous measurements of D_{Ni} are scattered, but the same model can describe simultaneously our isochemical results and the literature data in which T and MgO (and P) vary considerably.

Using our model, we calculated the NiO contents of Hawaiian *ol* phenocrysts that would crystallize at 1 kbar from primary magma separated from its residue at ~35 kbar. If the T difference between the residue and the conditions of phenocryst crystallization is ~150°C and the NiO content of residual *ol* is 0.37±0.02 wt. %, the calculated NiO content of *ol* phenocrysts is 0.47±0.025 wt. %. This is not as high as the highest NiO contents of Fo-rich Hawaiian phenocrysts, but it matches most of the data (0.44±0.07 wt. % NiO; 2σ). This simple calculation demonstrates that the effect of T on D_{Ni} can explain much of the range in NiO contents of Hawaiian *ol* phenocrysts without invoking processes that enrich mantle *ol* in Ni. Although such Ni-enrichment processes may operate, their contributions to basalt genesis need not be as large as suggested by models that do not consider the effects of T differences between source regions and the environments of phenocryst formation. A similar calculation reproduces the moderate enrichment in NiO in komatiitic *ol* assuming komatiitic magmas are dry, deep, and hot melts of the upper mantle.

https://doi.org/10.1180/S0026461X00008434 Published online by Cambridge University Press

Geochemical signature and evolution of granitic rocks in Sulawesi Island, Indonesia: evidence for Gondwana involvement

ADI MAULANA[1,4], KOICHIRO WATANABE[1], AKIRA IMAI[2], KOTARO YONEZU[1], TAKANORI NAKANO[3]

[1]Kyushu University, Fukuoka, Japan, adi-m@mine.kyushu-u.ac.jp (* presenting author)
[2]Akita University, Akita, Japan, akira@gipc.akita-u.ac.jp.net
[3]Research Institute of Human and Nature, Kyoto, Japan,nakanot@chikyu.ac.jp
[4]Hasanuddin University, Makassar, Indonesia, adi-maulana@unhas.ac.id

Tertiary granitic rocks from Sulawesi record series of complex history where subduction and collision occur and are still active. One of the products of these events is granitic magmatisms which are widely dispersed from southern part to northern part of the island. The granitic rocks were exposed to form a NS trending belt along the west to north plutono-volcanic arc province. The granitic rocks are of particular interest since they provide an insight into the geological processes that were operating at the eastern margin of Eurasian Plate.

In this study, major- and trace- element chemistry of granitic pluton from nine areas which represent the whole granitic distribution in Sulawesi Island were studied in order to elucidate the geodynamic evolution. In addition, the geochemical signatures coupled with isotopic results are used to determine the corresponding constraint on Gondwana involvement in the evolution of the island.

The results indicate that the granitic rocks ranges from acid to intermediate (granitic to tonalitic in composition) and are dominated by granodiorite with enclave of microdiorite and gabbro. They are identified as medium- to high-K, calc-alkaline, metaluminous and I-type granitoid emplaced as volcanic arc granites. With the exception of tonalitic rocks in Gorontalo area in the northern part of the island, all granitic samples resemble the upper continental crust pattern in their trace and rare earth element normalized pattern. Enrichment of large ion lithophile elements (Rb and Sr) and depletion of high field strength element (especially Nb and Ta) suggests an arc magma affinity. Negative Eu anomaly in most of the samples shows the occurrence of plagioclase fractionation in magma chamber. Most of the samples show high $^{87}Sr/^{86}Sr$ value but low $^{143}Nd/^{144}Nd$ suggesting strong upper crustal component source. In addition, they have high ^{206}Pb, ^{207}Pb and ^{208}Pb isotope ratios. However, microdioritic enclave and tonalitic rocks from Gorontalo shows lower $^{87}Sr/^{86}Sr$ value but higher $^{143}Nd/^{144}Nd$ and relatively higher ^{206}Pb, ^{207}Pb and ^{208}Pb value, significantly different from other samples.

The magma sources of these granitic rocks were interpreted derived from the upper continental crust. The most plausible nature of such affinity was Gondwana fragment which were dispersed during Cenozoic. They were then emplaced above subduction zone during the syn- to late collision stages with eastern part of Sundaland.

The overall geochemical signature of the Sulawesi granitic rocks suggests the evidence of Gondwana fragment involvement in geodynamic evolution of the island, particularly in the western and central Sulawesi.

Experimental investigations of the structural environment of metal (Nb, Ta) ions in silicate glass-water systems to high P-T conditions

ROBERT A. MAYANOVIC[1*], ALAN J. ANDERSON[2], MANELICH LUNA[1], GIULIO SOLFERINO[2] AND HAO YAN[1]

[1]Missouri State University, Springfield, MO, U.S.A., robertmayanovic@missouristate.edu (* presenting author)
[2]St. Francis Xavier University, Antigonish, NS, Canada, aanderso@stfx.ca

The study of silicate and aluminosilicate glasses and water systems at high P-T conditions has importance for understanding natural systems and for technological applications. The interrogation of the interaction of water in silicate melts and glasses on the structural level is critical for establishing a better understanding of the effect of dissolved water on the thermodynamic and physical properties of water-saturated magmas and of industrial glasses that are in contact with high P-T aqueous fluids. In this work, we discuss our *in situ* Ta L_3 and Nb K-edge x-ray absorption spectroscopic (XAS) investigations of the structural environment of metal (Nb, Ta) ions in haplogranitic glasses, water-saturated melts, and silicate-rich aqueous fluids at high temperatures and pressures. The starting materials, which consisted of water and a Ta (~1400 ppm)- or Nb (~5000 ppm)-bearing haplogranitic glass of peraluminous composition, were loaded into an hydrothermal diamond anvil cell and subjected to temperatures between 25 and 960 °C, and pressures up to 600 MPa. Pre-edge peak analysis of the Nb K-edge x-ray absorption near edge structure (XANES) measured from the Nb-bearing glass+water system to 760 °C shows a transition (in the 300 to 400 °C range) from a double to a single peak in the vicinity of the glass transition. In addition, the overall intensity of the pre-edge peak feature of the Nb-bearing glass+water system increases monotonically with increasing temperature. A doublet occuring in the white line feature of the Ta L_3-edge XANES is present in the spectra measured from the hydrous glass/melt to 700 °C and from the silicate-rich aqueous fluid at 960 °C. The white line feature results from dipole allowed transitions of the Ta $2p_{3/2}$ core electron to empty quasi-bound states in the continuum having Ta 5d atomic character. The Ta L_3-edge XANES spectra measured from a peraluminous silicate glass and water system have been analyzed using multi-peak fitting techniques. The normalized XANES spectra were fit in the vicinity of the white line using pseudo-Voigt peak functions. The relative intensities of the individual peaks in the Ta L_3-edge XANES white-line doublet vary with increasing temperature of the glass+water system, suggesting a shift in occupation of the electronic density of states in the vicinity of Ta 5d states probed by the $2p_{3/2}$ core photoelectron. *In situ* XANES is shown to be a sensitive probe of the modifications in the structural environment surrounding the metal (Nb, Ta) ion in the hydrated peraluminous glass/melt and in the silicate enriched aqueous fluid with increasing P-T conditions. We discuss the results of modeling of the XANES spectra and calculations of the projected angular momentum density of states (*l*-DOS) for the glass+water systems using FEFF code.

https://doi.org/10.1180/S0026461X00008434 Published online by Cambridge University Press

Pb and Hf isotope composition of hornblende-bearing lavas (Central European Volcanic Province): a lithospheric mantle source?

BERNHARD MAYER[1*], STEFAN JUNG[1], ROLF L. ROMER[2], CARSTEN MÜNKER[3]

[1] Universität Hamburg, Mineralogisch-Petrographisches Institut, Hamburg, Germany, Bernhard.Mayer@uni-hamburg.de (* presenting author)
[2] Deutsches GeoForschungsZentrum, Potsdam, Germany
[3] Universität zu Köln, Institut für Geologie und Mineralogie, Köln, Germany

Primitive alkaline mafic volcanic rocks – like the hornblende-bearing basanites from the Rhön area (Central European volcanic Province; CEVP) – provide important information about the chemical composition in the Earth's mantle. The presence of amphibole requires wet melting conditions; hence the source for the hornblende-bearing lavas is thought to be located in the lithospheric mantle. Strontium and Nd isotope compositions are well within the range commonly observed in CEVP magmas (εNd: +3.4 to +4.4; $^{87}Sr/^{86}Sr$: 0.7034-0.7041) and, although moderately evolved, are not indicative of crustal contamination.

Beside some differences in major and trace element geochemistry and Sr and Nd isotopes relative to other primitive volcanic rocks in CEVP, the Pb isotope composition is broadly similar to lavas from other volcanic centers located in the eastern part of the CEVP (i.e., Vogelsberg, Hessian Depression) in having $^{206}Pb/^{204}Pb$ ratios < 19.5, which contrasts to the Pb isotope composition of volcanic centers in the west (Eifel, Siebengebirge, Westerwald) with $^{206}Pb/^{204}Pb$ ratios > 19.5. The Rhön lavas have Pb isotope compositions ($^{206}Pb/^{204}Pb$: 19.1-19.4, $^{207}Pb/^{204}Pb$: 15.61-15.64, $^{208}Pb/^{204}Pb$: 38.9-39.2) that plot slightly above the NHRL (Northern Hemisphere Reference Line) in the $^{206}Pb/^{204}Pb$-$^{207}Pb/^{204}Pb$ and $^{206}Pb/^{204}Pb$-$^{208}Pb/^{204}Pb$ diagram, indicating that the source of the western CEVP must have a slightly higher U/Pb and Th/Pb ratio than the source of the eastern CEVP. In general, the Pb isotope compositions of the lavas plot at the unradiogenic end of Pb isotope range obtained on mantle xenoliths from the CEVP.

The hornblende-bearing lavas have initial εHf values ranging from +4.6 to +6.6, which is at least one εHf unit lower than in other lavas from the CEVP having similar εNd values and Pb isotope compostions. Since the Lu/Hf ratios of the hornblende-bearing lavas are similar to other lavas from the CEVP, the Hf isotope composition must be a source feature which is related to distinct Lu/Hf ratios in the mantle. The less radiogenic Hf isotope composition requires a source with a time-integrated lower Lu/Hf ratio relative to the mantle that produced other CEVP lavas with more radiogenic Hf isotope compositions. This inferred lower Lu/Hf ratio is compatible with a mantle with less or even no garnet, i.e. the spinel-bearing lithospheric mantle. Alternatively, participation of metasomatism-related minerals with low Lu/Hf ratios can explain the inferred slightly lower Lu/Hf ratios of the mantle source.

Sources and Seasonal Transformations of Nitrate in Lake Winnipeg (Manitoba, Canada)

BERNHARD MAYER[1]* AND LEONARD I. WASSENAAR[2]

[1]University of Calgary, Calgary, Alberta, Canada, bmayer@ucalgary.ca (* presenting author)
[2]Environment Canada, Saskatoon, Saskatchewan, Canada, current e-mail: L.Wassenaar@iaea.org

Lake Winnipeg (Manitoba, Canada) is in an eutrophic state from a century of increased riverine loadings from agricultural and urban nitrogen (N) and phosphorus (P) sources. This study investigated seasonal patterns of the isotopic composition of nitrate (NO_3^-) in Lake Winnipeg and its contributing rivers to gain insight into current N nutrient sources and in-lake N dynamics. Elevated NO_3^- concentrations in Lake Winnipeg tributaries between 0.36 and 2.44 mg/L NO_3^--N were associated with high $\delta^{15}N$ values between +5.0 and +13.9 ‰, while $\delta^{18}O_{NO3}$ values were <+15.0 ‰. The three major riverine inputs had distinctive mean $\delta^{15}N_{NO3}$ values of +8.1 ‰ for the Red River, -0.6 ‰ for the Winnipeg River, and +5.0 ‰ for the Saskatchewan River. The isotopic composition of NO_3^- in Lake Winnipeg was partly controlled by the isotopic composition of the riverine nitrate for instance via the predominant nitrate input to the South basin from the Red River. Nitrate assimilation and late season mineralization of phytoplankton and N_2 fixing cyanobacteria were identified as important additional processes affecting the isotopic composition of lake NO_3^- resulting in low $\delta^{15}N_{NO3}$ values, especially in the North basin. In the South basin, elevated $\delta^{15}N_{NO3}$ values in spring that changed to lower values by summer indicated a dynamic N cycle within the lake. This study demonstrates the need for sesoanlly resolved concentration and isotope analyses on samples from a large number of sampling sites to assess the highly dynamic in-lake fate of nitrogen inputs to Lake Winnipeg.

https://doi.org/10.1180/S0026461X00008434 Published online by Cambridge University Press

Delivery and release of organic carbon associated with iron oxyhydroxides in the Mississippi River-Delta

LAWRENCE M. MAYER[1]*, LINDA L. SCHICK[1], MARGARET L. ESTAPA[2], ROTA WAGAI[3], MATTHEW STEVENSON[1]

[1]University of Maine, Walpole ME USA Lmayer@maine.edu (* presenting author)
[2]Woods Hole Oceanographic Institution, Woods Hole MA USA mestapa@whoi.edu
[3]National Institute for Agro-Environmental Sciences, Tsukuba, Japan, rota@affrc.go.jp

Iron oxyhydroxides commonly associate with organic matter in terrestrial environments, but can become reductively dissolved in coastal environments. We examined the organic carbon content of these reducible phases using two carbon-free extraction approaches in Mississippi River suspended particulates and in its adjoining deltaic sediments. Contents of reductively dissolved iron decreased from river to depocenter and with distance from river outfall, and accompanied by similar losses of reductively soluble organic carbon. Both also decreased with depth in coastal cores. The ratios of organic carbon to iron released were less than the 0.22 g-OC g-Fe^{-1} that represents the approximate sorption limit of iron oxyhydroxides for dissolved organic matter, suggesting that the released organic matter was adsorbed. At these ratios, the solid phase iron and organic carbon are in approximate redox balance, so that import of either oxidant or reductant may not be necessary for metabolism. The reductively soluble organic carbon generally made up <5% of total organic carbon and its loss thus accounted for small fractions of total organic carbon losses during sediment transport and diagenesis. Extrapolation to global scale suggests a greater impact of perhaps 10% of global river delivery of particulate organic carbon in this form.

Hydrogen production from low temperature (55-100ºC) water-rock reactions

L. MAYHEW[1*], E. ELLISON[1], T. MCCOLLOM[2], AND A. TEMPLETON[1]

[1]University of Colorado-Boulder, Geological Sciences lmayhew@colorado.edu (* presenting author)
[2] University of Colorado-Boulder, Laboratory for Atmospheric and Space Physics

Hydrogen (H_2) produced from water-rock reactions at ~150-300ºC is known to support thriving microbial communities on Earth (e.g. Lost City hydrothermal vents [1,2]) and similar geochemical process have been suggested to occur on Mars and Europa [3,4]. However, the potential for mafic rocks and minerals to produce enough H_2 to support microbial life at temperatures below 100ºC remains a matter of debate (e.g. [4,5]) and is relatively unexplored in the laboratory.

We are conducting laboratory experiments to assess the potential of 12 rock and mineral substrates to produce H_2 when reacted with seawater under anoxic conditions at 55 and 100ºC. Time series measurements were obtained for key gaseous and aqueous constituents. Magnetite, hypersthene, fayalite, San Carlos olivine and San Carlos peridotite produce 20-180 nmol H_2/gram mineral at 55ºC. The same 5 substrates as well as chromite produce 50-210 nmol H_2/gram mineral at 100ºC. In contrast, hortonolite, hedenbergite, augite, enstatite, diopside, and basalt do not produce significant H_2. Our H_2 measurements agree with previously reported results from mineral-water reactions at 30, 50, and 70ºC [4,6]. However, previous studies did not conduct an analysis of the mineral products thus the reactions responsible for H_2 gas production are unknown. To address this issue and define the reaction pathways, we are using synchrotron-based μXRF and μXANES investigations to identify Fe-bearing secondary phases and to constrain the partitioning of Fe and the mechanisms of H_2 generation as a function of mineral composition and temperature. Investigations into the effect of the starting materials (e.g. surface area of the substrates and substrate and fluid composition) on H_2 production are also being undertaken. This work will allow us to constrain the reactions that produce H_2 under low temperature conditions and will provide insight into the potential for water-rock reactions to support microbial life in the deep subsurface and on other planetary bodies.

[1] Kelly (2001) *Nature* **412**, 145-149. [2] Boston (1992) *Icarus* **95**:300-308. [3] McCollom (1999) *J. Geophys. Res.* **104**, 30729-30742. [4] Stevens & McKinley (2000) *Env. Sci. Tech* **34**, 826-831. [5] Anderson (2001) *Env. Sci. Tech* **35**, 1556-1557. [6] Neubeck (2011) *Geochem. Trans.* **12**:6.

https://doi.org/10.1180/S0026461X00008434 Published online by Cambridge University Press

Carbon dioxide degassing and estimation of thermal energy release from White Island volcano , New Zealand

AGNES MAZOT[1],SIMON BLOOMBERG[2*], TRAVIS HORTON[2], CLINTON RISSMANN[3], CHRISTOPHER OZE[2], DARREN GRAVLEY[2] AND BEN KENNEDY[2]

[1]GNS Science, Wairakei, NZ
a.mazot@gns.cri.nz
[2]University of Canterbury, Geological Sciences, NZ
Simon.bloomberg@pg.canterbury.ac.nz*
[3]Environment Southland, Invercargill, NZ

Accurate quantification and mapping of the total carbon dioxide (CO_2) emitted from a variably permeable volcano still remains a challenge. We used high resolution measurements of CO_2 flux and heat flow within the crater floor of White Island to characterise the mass (CO_2 and steam) and heat released. White Island is an andesite stratocone and New Zealand's most active volcano. Frequent phreatic, phreatomagmatic and magmatic eruptions have occurred throughout the 19th and 20th century. White Island's most recent magmatic explosive eruption occurred in 2000. Currently, the hydrothermal system is manifested by localised vigorous fumarolic activity, mud pools and mounds, and an acidic (pH ≈–0.4) 200 m diameter crater lake, and diffuse degassing through the crater floor.

CO_2 flux degassing and thermal budget

In 2011, we performed 691 measurements of CO_2 flux using the accumulation chamber method. CO_2 flux values measured were ranged between of 0.1 – 29,896 g m^{-2} d^{-1}. Total CO_2 emission rate estimated by stochastic simulation was 116 ± 2 td^{-1} within the crater floor (0.31 km^2). The $\delta^{13}C$ range (-10 and -2‰) reflects the spatial variance in magmatic CO_2 contribution. Based on CO_2 flux data and a mean H_2O/CO_2 wt ratio of 15.3, the flux of thermal energy released from the crater floor totals 54 ± 1MW. The associated rate of steam condensation is 1760 ± 25td^{-1}. The spatial distribution of surface heat flow, soil gas $\delta^{13}C$, surface hydrothermal features and CO_2 flux indicates high gas and thermal permeability at old crater margins, and breaks in slope (crater floor/wall, crater floor/mound). We suggest that areas of high degassing are associated with advective gas transport adjacent to persistent fumarole pathways. Areas of low permeability are associated with sulphur/anhydrite and iron oxide-silica precipitation crusts which limit gas diffusion to the surface. In addition, we explore the influence of sea water and meteoric water influx into the hydrothermal system.

Evidence of paleo sulfate methane transition zone in marine sediments

A.PEKETI[1], A. MAZUMDAR[1*] , R. K. JOSHI[1], H. JOAO, D. J. PATIL[2], L.S. SRINIVAS[2], A. M DAYAL[2]

[1] Gas Hydrate Research Group, Geological Oceanography, National Institute of Oceanography, Donapaula, Goa-403004, India maninda@nio.org (* presenting author)
[2]National Geophysical Research Institute, Uppal Road, Hyderabad-500606, India

The sulfate methane transition zone (SMTZ) denotes a redox interface within the anoxic sediment column where pore water sulfate and methane concentration profiles intersect and are depleted to non detectable concentrations. This depletion in sulfate and methane concentrations are attributed to the anaerobic oxidation of methane (AOM) performed by a syntrophic consortium of CH_4-oxidizing archaea and sulfate-reducing bacteria [1]. AOM causes marked enrichment in H_2S and HCO_3^- ion concentrations in the porewaters within the SMTZ, resulting in precipitation of Fe-sulfides, Ca-Mg-carbonates. Sulfate concentration profile, depth to SMTZ and thickness of SMTZ depend on the methane flux. High methane flux results in linear sulfate concentration gradient and shallow SMTZ and vice versa. In the Krishna-Godavari (K-G) basin, Bay of Bengal, seismic data [2] show regional presence of gas hydrates manifested in the form of a bottom simulating reflector (BSR). Sediment cores for the study were collected on-board Marion Dufresne and JOIDES Resolution as part of the gas hydrate exploration program in the K-G basin offshoe. Our results show multiple carbonate bearing zones in the sediment with pronounced carbon isotopic depletion typical of AOM. Biogenic methane with $\delta^{13}C$ ranging from -80 to -100‰ (VPDB) have earlier been reported [3] from K-G basin. In contrast, we have not recorded any appreciable barium front in any of the cores. The barium front possibly diappeared whenever the SMTZ moved up across an existing Ba front. However carbonate layers are not subject to such dissolution. The zones with deplted carbon isotope ratios are enriched in pyrite with heavy sulfur isotope ratios suggesting Rayleigh fractionation in a closed system. The sharp rise in $^{34}S_{CRS}$ indicate focussed sulfate reduction in SMTZ. In the long core NGHP-01-10D several such zones with heavy sulfur isotope ratios have been noted indicating paleo SMTZ transition zones We propose that content and stable isotope ratios of authigenic carbonate and pyrite in marine sediments may serves as an ideal tool to detect fossil sulfate methane transition zone in the absence of barium front.

[1] Boetius et al. (2000) *Nature,* **407,** 623– 626.
[2] Ramana et al. (2004) *International Jour. Enviormental Studies* **64,** 675-693.
[3] Mazumdar et al. (2009) *Geophy.Geochem.Geosys*., **10,** 1-15.

https://doi.org/10.1180/S0026461X00008434 Published online by Cambridge University Press

Pore-water chemistry in clays and shales: Methods and applications

MARTIN MAZUREK[1*], H. NIKLAUS WABER[1] AND TAKAHIRO OYAMA[2]

[1]Institute of Geological Sciences, University of Bern, Switzerland, mazurek@geo.unibe.ch (*presenting author), waber@geo.unibe.ch
[2]CRIEPI, Abiko-shi, Chiba, Japan, ooyama@criepi.denken.or.jp

A suite of techniques to extract pore waters from clays and shales and to analyse them for major ions and isotope ratios have been developed over the last decade. Sophisticated techniques are needed to obtain the full pore-water composition, while simple crush/leach tests and other laboratory protocols provide information on conservative chemical constituents, such as Cl^-, Br^-, $\delta^{18}O$, δ^2H and dissolved noble gases. Concentration profiles of these constituents across shale formations are typically curved, indicating a transient state of diffusive exchange with the embedding aquifers. Transport modelling is used to quantify the time scales related to this process, using initial and boundary conditions based on palaeo-hydrogeological evidence [1]. This procedure provides insights on transport processes and on the upscaling of laboratory-derived transport parameters to the formation scale.

A comprehensive set of pore-water data has been obtained from drillcores of the Schlattingen borehole, penetrating a Mesozoic, clay-mineral rich, low-permeability sequence in NE Switzerland. Squeezing tests at 200-500 MPa yielded sufficient water for chemical and isotopic analysis (Fig. 1), in spite of low water contents (3-5 wt.-%). Salinity decreases with squeezing pressure, which is an artefact related to the membrane properties of the rocks. The decline of salinity in the lower part of the profile indicates the presence of a low-salinity boundary below 1000 m depth, leading to out-diffusion of Cl^- from the low-permeability sequence. The time scales related to this process are evaluated by transport modelling.

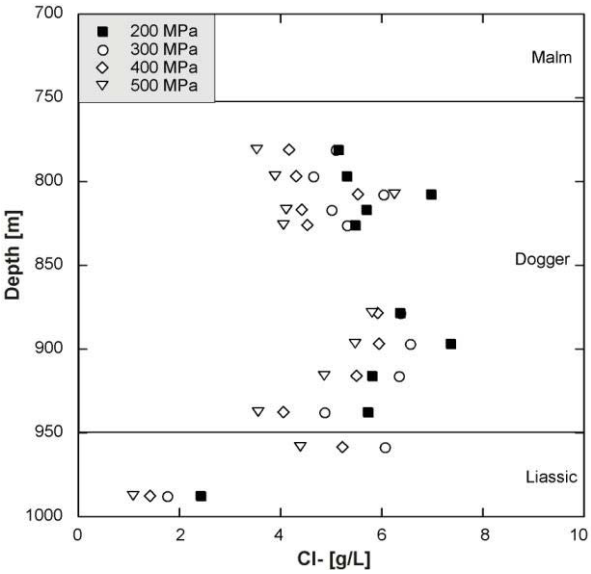

Figure 1: Cl^- concentrations in pore waters from the Schlattingen borehole obtained by squeezing experiments

[1] Mazurek *et al.* (2011) Appl. Geochem. **26**, 1035-1064.

Investigating marine corrosion communities using tagged pyrosequencing and single cell genomics

JOYCE M. MCBETH[1*] AND DAVID EMERSON[1]

[1]Bigelow Laboratory for Ocean Sciences, East Boothbay, ME, USA jmcbeth@bigelow.org (* presenting author) demerson@bigelow.org

It was recently discovered that members of the Fe(II)-oxidizing *Zetaproteobacteria* (*Zetas*) rapidly colonize mild steel surfaces that represent a ready source of Fe(II) [1], and that a robust microbiologically influenced corrosion (MIC) community develops on steel that includes *Zetas* and *Epsilonproteobacteria* [2]. Here we summarize our efforts to expand our understanding of marine steel MIC bacterial and archaeal communities. We present results from two time series incubations, the first conducted in Great Salt Bay salt marsh in summer 2010, and the second conducted below the marine intertidal zone in Boothbay Harbor, ME in summer 2011.

We used tagged pyrosequencing (V4 region, SSU rRNA gene) to examine bacterial and archaeal communities on mild steel surfaces from the salt marsh time series (2010). *Zetas* were identified in both sediment and steel sample pyrosequencing libraries, and unique *Zeta* OTUs on the steel reflected the numbers observed in the sedimentary *Zeta* communities we analyzed. *Epsilonproteobacteria* (in particular *Sulfurimonas* and *Arcobacter* relatives) were enriched on the steel in comparison with sediments. Unique *Deltaproteobacterial* OTUs present increased with incubation time to near sediment levels, likely reflecting colonization of the steel by Fe(III)-reducing and sulfate-reducing bacteria (SRB). Archaeal results were dominated by a potentially novel order of *Euryarchaeota*, most closely related to the *Thermoplasmatales*. Quantiative PCR of these samples and associated sediments with 16S rRNA gene primers for *Zetas* and functional gene primers for SRB showed that, on average, *Zeta* gene copies in sediments were an order of magnitude less abundant than SRB. *Zeta* gene copies on the steel increased rapidly over the first 10 days, exceeding copies quantified in the sediment by an order of magnitude. The SRB numbers on the steel were 10 fold lower than in sediments during the first days of incubation, but increased to near the sediment levels by 40 days.

A 9 day sample from the 2011 time series was subjected to whole genome amplification. Screening of single amplified genomes (SAGs) for bacteria identified 148 bacterial SAGs; 18 (12%) *Zetas*, 61 (42%) *Epsilonproteobacteria* (near relatives of *Sulfurimonas* sp.), and 46 (32%) *Gammaproteobacteria* (notably 15 relatives of *Hydrogenovibrio* sp., an autotrophic H_2-oxidizing bacterium).

When compared to previous work [2], this study provides evidence for rapid development of a core corrosion community on mild steel. Use of tagged pyrosequencing and single cell genomics enhances our understanding of MIC community richness and provides the possibility of exploring the genomes of individual community members.

[1] McBeth *et al* (2011) *Appl Env Microbiol* **77**, 1405-12.
[2] Dang *et al* (2011) *Env Micro* **13**, 3059-74.

https://doi.org/10.1180/S0026461X00008434 Published online by Cambridge University Press

The origin and composition of polyphase inclusions in tourmaline from the Greenbushes pegmatite

TRAVIS J. MCCARRON[1*] and ALAN J. ANDERSON[2]

[1]Carleton University, Ottawa, Canada, tmccarro@connect.carleton.ca (* presenting author)
[2]St. Francis Xavier University, Antigonish, Canada, aanderso@stfx.ca

The (2.527 Ga) Greenbushes rare-element pegmatite in Western Australia is an important source of lithium and tantalum. The pegmatite, which was emplaced syngenetically into the Donnybrook-Bridgetown shear zone within the Western Gneiss terrain of the Yilgarn Craton, consists of five distinct petrologic zones. Zoned tourmaline crystals in the Ta-rich albite zone of the pegmatite contain numerous solid-liquid-vapor inclusions. The inclusions occur within an inner brown-green pleochroic growth zone and are distributed as planar arrays in healed microcracks, oriented subnormal to the c-axis, and as isolated groups. The inclusion-bearing tourmaline is overgrown by an inclusion-free blue-green growth zone. Solid phases in the inclusions were identified using Raman spectroscopy and one representative polyphase inclusion was analysed using a dual beam focused ion beam-scanning electron microscope (FIB-SEM) for three-dimensional textural and chemical characterization. Fluid inclusion assemblages (FIA) show highly variable liquid-vapor-solid phase proportions. Measurements of phase ratios using a petrographic microscope and image analysis system show a direct relationship between inclusion size, percent volume solids and mineralogy. Large inclusions (>300μm^2) containing >50% volume solids are dominated by a silicate assemblage, which may contain quartz, pollucite, lepidolite, zabuyelite and an arsenic-antimony rich phase (predominantly native arsenic, senarmontite, paakonenite and/or arsenolite) and aqueous carbonic fluid. Intermediate sized inclusions ranging from 5-50% volume solids may contain zabuyelite, an arsenic- bearing phase and aqueous carbonic fluid. The smallest inclusions (<100μm^2) have less than 5% volume solids and contain aqueous carbonic fluid and an arsenic-bearing solid phase. Rare nahcolite and lithiophosphate were also identified in some inclusions. The variability in inclusion size and phase proportions within a FIA is attributed to mineral precipitation prior to trapping and inclusion necking. The inclusions are interpreted to represent the products of a silicate-rich aqueous carbonic fluid that was entrapped during the growth and recrystallization of the early brown-green tourmaline.

Extreme Fractionation of Rare Earth Elements in Volcanogenic Massive Sulfides of the Bathurst Mining Camp: Evidence from Europium Anomalies in Hydrothermal Apatite

SEAN MCCLENAGHAN[1*], DAVID LENTZ[2], AND PAUL SYLVESTER[3]

[1]New Brunswick Geological Surveys Branch, Bathurst, Sean.mcclenaghan@gnb.ca (* presenting author)
[2]University of New Brunswick, Department of Earth Sciences, Fredericton, Dlentz@unb.ca
[3]Memorial University of Newfoundland, Department of Earth Sciences, Psylvester@mun.ca

Rare earth element (REE) mobility in hydrothermal systems has been the focus of numerous studies [1,2], with the most direct evidence coming from active hydrothermal vents [3], which display prominent enrichments in Eu and LREE. Exhalative sedimentary rocks generally contain small quantities of REE when compared to volcanic and clastic sedimentary lithotypes; *e.g.*, massive sulfides of the Bathurst Mining Camp (BMC) have ∑REE contents that average 36.8 ppm, and range from 0.93 to 249 ppm. Nevertheless, REE in massive sulfides of these exhalative horizons can exhibit considerable fractionation, with chondrite-normalized REE profiles [4] displaying prominent Eu anomalies. Values of Eu_N/Eu^* calculated for massive sulfides are consistently positive with values as high as 36.7 (ave., 6.26). A positive Eu_N/Eu^* correlation (n=286) with Sn (r'=0.55) and In (r'=0.40) suggests enrichment in primary hydrothermal fluids associated with base-metal sulfide precipitation.

Petrography and micro-analytical data for massive sulfides have shown that exhalative gangue and accessory minerals, in particular phosphates control REE contents; this is supported by a strong correlation (bulk) between ∑REE and P_2O_5 (r'=0.53). Fluorapatite is the most abundant phosphate in exhalites of the BMC, occurring as nodular to colloform masses and intimate mixtures with carbonate and sulfide minerals. Imaging of fluorapatite reveals a distinct cathodoluminescence consistent with the substitution of Mn^{2+} and Eu^{2+} in the fluorapatite mineral structure and suggests formation under reducing hydrothermal conditions.

In situ laser-ablation ICP–MS analyses (n=169) reveal elevated ∑REE contents in fluorapatite, averaging 1,548 ppm, and ranging from 250 to 24,038 ppm. Europium accounts for approximately ¼ of all REE substitution in apatite, with Eu contents as high as 1,554 ppm (ave., 295 ppm). Chondrite-normalized REE profiles display prominent enrichment in Eu, with Eu_N/Eu^* values as high as 222 (ave., 19.0). To date, these anomalies represent the largest reported fractionation of Eu in the solar system, exceeding values for mesosiderites, and both terrestrial and lunar anorthosites [5]. This extreme fractionation of Eu suggests protracted growth of apatite or some precursor phase (i.e., francolite) under reducing (low fO_2) and high temperature hydrothermal (>250ºC) conditions, further corroborated by the prevailing pyrrhotite-pyrite-chalcopyrite stockwork assemblage. Apatite associated with lower temperature assemblages exhibits diminished Eu signatures, reflecting a more-distal hydrothermal environment and defining a vector for mineralization.

[1] Graf (1977) *Econ Geol* **72**, 527-548. [2] Campbell *et al*. (1984) *Chem Geol* **72**, 181-202. [3] Michard (1989) *Geochim Cosmochim Acta* **53**, 745-750. [4] McDonough and Sun (1995) Chem Geol 120, 223-253. [5] Mittlefehldt *et al*. (1992) Science **257**, 1096-1099.

https://doi.org/10.1180/S0026461X00008434 Published online by Cambridge University Press

Serpentinization and the flux of reduced volatiles to the seafloor

THOMAS M. MCCOLLOM[1*], FRIEDER KLEIN[2], WOLFGANG BACH[3], BRUCE MOSKOWITZ[4], THELMA BERQUÓ[5], AND ALEXIS TEMPLETON[1]

[1]University of Colorado, Boulder, CO, USA, mccollom@lasp.colorado.edu (* presenting author)
[2]Woods Hole Oceanographic Institution, Woods Hole, MA, USA
[3]University of Bremen, Bremen, Germany
[4]Institute for Rock Magnetism, University of Minnesota, Minneapolis, MN, USA
[5]Concordia College, Moorhead, MN, USA

Serpentinization of ultramafic rocks has long been recognized to be a source of reduced volatile compounds, particularly hydrogen (H_2) and methane (CH_4). Over the last couple of decades, there has been increasing scientific interest in the capacity of these reduced compounds to support chemolithoautotrophic biological communities, both now and on the early Earth. In the deep sea, serpentinization of ultramafic rocks can serve as a source of H_2 and CH_4 to biological communities living within the ocean crust, at the seafloor where fluids are discharged from serpentinites, and in the overlying water column. The abundance and spatial distribution of serpentinite-supported autotrophic communities depends on when, where, and how much reduced volatiles are generated.

The production of reduced volatiles during serpentinization depends strongly on the fate of Fe as the reaction proceeds, since the generation of reduced compounds is directly linked to the oxidation of Fe(II) to Fe(III). Serpentinization is often portrayed as a fairly straightforward process whereby ultramafic rocks are converted to a limited set of minerals dominated by serpentine polymorphs, brucite, and magnetite. Within this rather simple framework, however, there is a lot of room for complexity. In particular, it is increasingly clear from petrologic studies, laboratory experiments, and numerical modeling that the distribution of Fe among reaction product minerals, and the oxidation state of Fe in those products, is highly variable, and is dependent on a complex mixture of factors including temperature, kinetics of dissolution, precipitation and diffusion, bulk rock and mineral compositions, extent of reaction, and thermodynamic constraints. A recent bevy of laboratory experiments by both ourselves and others [e.g., 1-3] focusing on the fate of Fe during serpentinization is providing new insights into pathways leading to generation of H_2 and other reduced compounds, and will provide the basis for improved models of the flux of reduced volatiles from serpentinization environments within the ocean crust. We will present results from a series of experiments that examine production of H_2 and concurrent mineral alteration during serpentinization of olivine and peridotite at temperatures from 230 to 320 ºC.

[1] Seyfried et al. (2007) *Geochim. Cosmochim. Acta* **71**, 3872-3886. [2] Marcaillou et al. (2011) *Earth Planet. Sci. Lett.* **303**, 281-290. [3] Malvoisin et al. (2012) *J. Geophys. Res.* **117**, doi:10.1029/2011JB008612.

Investigating biomineralized structures and morphology associated with laminated freshwater stream terraces: Stromatolites?

C. MCCORT[1]*, E. CHI FRU[2], S. GOUDEY[3], AND C.G WEISENER[1]

[1]Great lakes Institute for Environmental Research, University of Windsor, Windsor, Canada, candace.mccort@gmail.com; weisener@uwindsor.ca
[2] Department of Paleozoology, Swedish Museum of Natural History, Stockholm, Sweden, ernest.chifru@nrm.se
[3]Limnos Ltd., Calgary, Canada, sg.limnos@gmail.com

Introduction

Biogeochemical cycles are considered the driving force behind how elements are transported and buried in sediments. A principle mechanism in the addition and removal of elements in biogeochemical cycles involves biomineralization. In the strict context we can classify biomineralization as extracellular, intracellular or as catalytically induced depending on the organisms in question. Investigation of the Erickson Creek watershed BC Canada, has led to the discovery of interesting phenomena involving cementation of the streambeds possibly affecting aquatic habitats adjacent to coal mine impacted riparian zones.

These mineralized mats are calcareous in nature and have managed to form densely layered sequences associated with proliferation of freshwater mosses/biofilms. The streams support localized assemblages charaterized by benthic, alkaliphilous diatoms with relatively low species richness. To investigate the process attributing to the biomineralized event, samples were collected to determine the casual relationships been the mosses, bacteria and the *in situ* mineralization that is taking place (Figure 1). SEM and Raman microscopy provide structural, morphological, and chemical information about the biomineralized structure within aged layers. In addition, DNA extraction, species richness and identification, was used to determine biological composition.

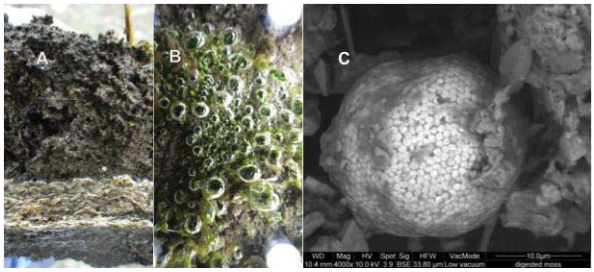

Figure 1: (A) laminated structure of biomineralized mat, (B) top down surface showing freshwater moss, (C) SEM micrograph suggesting the existence of localized chemically reduced microhabitats with S/Fe precipitation.

Conclusion

This data will provide insight and address questions pertaining to the cementation process at this location and its affects on aquatic habitats influenceing the biogeochemistry and microorganisms that live in this environmental system.

https://doi.org/10.1180/S0026461X00008434 Published online by Cambridge University Press

Microbially-accelerated carbon sequestration

JENINE MCCUTCHEON[1*], IAN M. POWER[2], ANNA L. HARRISON[2], GREGORY M. DIPPLE[2] AND GORDON SOUTHAM[1]

[1]Department of Earth Sciences, The University of Western Ontario, London, ON CANADA, jmccutc3@uwo.ca (*presenting author)
[2]Department of Earth and Ocean Sciences, The University of British Columbia, Vancouver, BC CANADA

This investigation modelled microbially-accelerated carbon sequestration through the precipitation of carbonate minerals. A microbial consortium, collected from a natural hydromagnesite playa near Atlin, British Columbia, Canada, was used to inoculate a 10 m long flow-through bioreactor. The consortium contained cyanobacteria, which are able to mediate magnesium carbonate precipitation by changing the water chemistry, particularly by increasing pH. A bicarbonate-rich nutrient solution containing 1 g/L Mg was added to the bioreactor at a rate of 5 L/day for 7 weeks. Major ion concentrations, pH, dissolved oxygen, and conductivity were monitored weekly along the length of the bioreactor. The concentration of Mg^{2+} and other major cations was determined using inductively coupled plasma atomic emission spectroscopy, while ion chromatography was used for major anions. An alkalinity titration was used to quantify the bicarbonate concentration. The precipitation of carbonate minerals was inferred by the measured decrease in [Mg^{2+}] and alkalinity along the length of the bioreactor. Carbonate precipitation occurred, primarily as dypingite, which was confirmed using light microscopy, scanning electron microscopy, and x-ray diffraction. The first 3 m of the bioreactor, dubbed the active zone, was responsible for removing over 37% of the Mg added to the bioreactor from solution, versus 61% Mg removed from the entire system. A mass of 0.362 kg of Mg carbonate precipitated in the active zone via microbially-mediated mineralization. This amount of mineral precipitation over the course of the experiment translates to a carbon sequestration rate of 5.88 kg of CO_2/m^2 of microbial mat/year.

This investigation demonstrated the process of microbe-induced carbonate precipitation on a larger scale than previous studies [1,2]. This biogeochemical process may have industrial applications if it can be implemented on the scale of mine tailing storage facilities such as those at the Mount Keith Nickel Mine in Western Australia. Magnesium weathered from ultramafic waste rock would react with CO_2 in the presence of the microbes and aqueous chemistry conditions studied in this investigation. The Mount Keith Mine produces tailings at a rate of 11 Mt/year, with tailings covering an area of ~19 km^2 [2,3]. Application of the biogeochemical process studied in this investigation to the Mount Keith Mine could result in a CO_2 sequestration rate of over 111 700 t/year. Globally, there are many mine sites with microbially-accelerated carbon sequestration potential, making the results of this study relevant to the current efforts to reduce net greenhouse gas emissions.

[1] Power *et al.* (2007) *Geochem. Trans.* **8**:13 [2] Power *et al.* (2011) *Env. Sci. and Technol.* **45**, 9061-9068. [3] Grguric (2003) *Aust. J. Mineral.* **9**, 55-71.

Compositional models of the Earth and early planetary evolution

WILLIAM F. MCDONOUGH

Geology, Univ Maryland, College Park, USA mcdonoug@umd.edu

New chemical data along with a broad range of other chemical, isotopic and physica data that have come to light over the last decade will be integrated into a coherent planetary model. Present day compositional models for the planet are non-unique and strongly influenced by the method used in its construct: cosmochemical, geochemical/petrological, and geophysical. Cosmochemical models examine candidate accretion materials (i.e., chondrites) from which the Earth was built and compares these compositional input against physical data that describes the planet to minimize the misfit. Geochemical models deconvolve compositional data from samples of the mantle and crust to estimate the concentration of elements in the primitive mantle and then compares these input against chondrite data to describe the core composition with a minimum misfit. Geophysical models use the present day boundary condition for the Earth to find consistent solutions to the thermal evolution of the planet and the mineralogy of the mantle.

Recently reported geoneutrino data are consistent with most existing Earth models, and now exclude, at the 67% confidence level, models that invoke a homogeneous, fully radiogenic Earth model. Stable (O, Ca, Ti, Cr, Ni, Mo) and radiogenic (142Nd, Sr, Hf) isotope data for chondrites provide a perspective and perhaps a constraint on which group of chondrites best fit the bulk Earth composition. Increasingly, these data find the greatest misfit between the composition of the Earth and that of carbonaeous chondrites, whereas better fits are observed for the Earth and enstatite and ordinary chondrites. Models that describe the planetary proportion of Fe, O, Si, Mg (>90% of the Earth's mass) define the mass of core and mineralogy of the mantle, with the latter potential describing a compositionally layered state. No chondritic material, present in our collections, are consistent with data for the Earth and demonstrate that adhoc adjustments are needed to describe the nature of the building blocks of the Earth. Matching compositional models of the primitive mantle with that for the continental crust constrains the family of permissible compositional and mineralogical models for the present day mantle and any potential stratification. Data and uncertainties will be presented for quantitative models that describe the concentration and distribution of elements, particularly the heat producing elements, in the present day mantle. Models invoking deep mantle reservoirs (BMOL, 142Nd-layer, primitive mantle regions, upper/lower boundaries) will be assessed quantitatively. All model predictions from the three approaches described above are presently permissible given uncertainties, however ever accumulating geoneutrino data sets will provide tighter bounds by which one can critically assess the viability of Earth model compositions.

https://doi.org/10.1180/S0026461X00008434 Published online by Cambridge University Press

Episodic, post-supereruption resurrection of the Peach Spring magmatic system (western Arizona, USA) over ~2 Ma

SUSANNE M. MCDOWELL[1*], CALVIN F. MILLER[1], CHARLES A. FERGUSON[2], AND JOE WOODEN[3]

[1]Vanderbilt University, Earth & Environmental Sciences, susanne.m.mcdowell@gmail.com (* presenting author)
[2]Arizona Geological Survey, caf@email.arizona.edu
[3]Stanford University, jwooden@standford.edu

The Silver Creek caldera (southern Black Mountains, western Arizona) is the source of the 18.8 Ma supereruption that produced the Peach Spring Tuff (PST), a ≥700 km^3 ignimbrite that crops out in northwestern Arizona, southern Nevada, and southeastern California [1, 2, 3]. Intruding the caldera's eastern margin is a ~30 km^2 epizonal, intermediate to felsic plutonic complex. The complex reveals a ~2 Ma history of episodic, post-PST magmatic recharge, suggesting that this magmatic system was periodically revitalized long after its colossal eruption.

Indications of magmatic rejuvenation are evident throughout the intrusive complex, which consists of two primary, texturally-diverse units: the coarse-grained Moss porphyry (~62-68 wt. % SiO_2) in the north, and the fine- to coarse-grained, commonly granophyric Times porphyry (>70 wt. % SiO_2) in the south. The Moss displays locally abundant, 2-10 cm rounded enclaves (59 wt. % SiO_2). Near the Moss/Times contact along Silver Creek, a crystal-rich Times matrix consisting of rounded feldspars set in a fine-grained groundmass hosts 0.5-2 m enclaves with intermediate compositions. Rapakivi feldspars appear in both units, and mafic, intermediate, and felsic porphyry dikes crosscut the entire complex.

U-Pb SHRIMP zircon ages and mineral geochemistry support field evidence for magmatic recharge. The Times, the Moss, and a distinctive porphyry similar to the Moss yield zircon age spectra of ~16.8-19 Ma (coeval with nearby volcanics), though PST-age zircons are notably scarce. Probability density analysis indicates two main age peaks at ~17.4 and ~18.2 Ma, with the Moss containing a larger population of older grains than the Times. Moss zircon and sphene record increasing concentrations of Ti and Zr, respectively, from core to rim, consistent with reheating.

A preliminary interpretation of the data is that the Moss was emplaced in the shallow crust at ~18 Ma and substantially reheated and reactivated at ~17.4 Ma, roughly coincident with emplacement of the Times. The wide zircon age spread may reflect other recharging events that are irresolvable via SHRIMP dating. Regardless, the shallow subvolcanic system appears to have been sporadically resurrected over one to two million years following the PST supereruption.

[1] Ferguson et al. (in review) *Geology*. [2] Buesch et al. (1992) *GSA Bulletin* **104**, 1193-1207. [3] Glazner et al. (1986) *Geology* **14,** 840-843.

Lacustrine cave carbonates: novel, absolute-dated paleohydrologic archives in the Bonneville Basin (Utah, USA)

DAVID MCGEE[1,*], JAY QUADE[2], R. LAWRENCE EDWARDS[3], WALLACE S. BROECKER[4], HAI CHENG[3,5], AND ELENA STEPONAITIS[1]

[1]Massachusetts Institute of Technology, Cambridge, USA, davidmcg@mit.edu (* presenting author), estep@mit.edu
[2]Univ. of Arizona, Tucson, USA, quadej@email.arizona.edu
[3]Univ. of Minnesota, Minneapolis, USA, edwar001@umn.edu
[4]Columbia Univ., New York, USA, broecker@ldeo.columbia.edu
[5]Xi'an Jiaotong Univ., Xian, China, cheng021@umn.edu

Records of past changes in closed basin lake levels and lake water isotopic composition provide key insights into past variations in the hydrological cycle; however, these records are often limited by dating precision and temporal resolution. Here we present data from lacustrine cave carbonates, a novel class of carbonates that comprise a promising new archive of past hydrologic changes in the Bonneville Basin of the northeastern Great Basin (U.S.A.). These dense carbonates precipitated within caves, crevices and other protected spaces flooded by Lake Bonneville during its highstand in the last glacial period. We focus on deposits in Cathedral and Craners caves, located ~50 km apart at a similar elevations approximately 100 m above the modern Great Salt Lake and almost 200 m below Lake Bonneville's highstand shoreline. Carbonates from the two caves show similar chronologies, mineralogical transitions, isotopic compositions and trace element concentrations. These findings suggest that lacustrine cave carbonates record changes in lake level and in the isotopic composition and chemistry of lake water. Importantly, the deposits can be precisely dated by U-Th methods, providing the first high-precision, absolute-dated records of Lake Bonneville's water balance changes.

We use dates for the onset and cessation of lacustrine cave carbonate deposition to offer new constraints on past changes in lake level and the carbonate saturation state of lake water. We also present precisely dated, high-resolution oxygen and uranium isotope records from the deposits. Within a first phase of deposition reflecting the lake's transgression between 26 and 18 ka, our isotopic data suggest a large influx of freshwater during Heinrich Stadial 2. A hiatus in deposition beginning 18.2 ± 0.3 ka may be the result of freshening related to the lake's overflow. Calcite deposition resumes at Cathedral Cave at 16.4 ± 0.2 ka, suggesting that basin overflow had ceased by this time and that the lake re-entered calcite saturation; this interpretation implies that the lake's deglacial regression began well before the Bølling warming. Cessation of this second phase of deposition at 14.7 ± 0.2 ka may reflect the lake's drop below Cathedral Cave's elevation.

We have located similar deposits at over forty locations in the basin spanning almost the entire ~270 m elevation range between the modern Great Salt Lake and the highstand shoreline. We present data from several elevations that offer additional constraints on changes in lake level and lake chemistry during the last glacial period and deglaciation.

https://doi.org/10.1180/S0026461X00008434 Published online by Cambridge University Press

Life at the fringe: redox conditions around a 1.6 Ga submarine vent

PETER MCGOLDRICK[1*], JOSHUA GUILLIAMSE[2], TOBY DAWBORN[3], AND DONNA SATTERTHWAIT[4]

[1]CODES ARC Centre of Excellence in Ore Depoits, University of Tasmania, Hobart, Australia, p.mcgoldrick@utas.edu.au (*presenting author)
[2]Geological Survey of Western Australia, Perth, Australia, Joshua.Guilliamse@dmp.wa.gov.au
[3]Teal Exploration & Mining, Chingola, Zambia, toby@tealming.com
[4]School of Earth Sciences, University of Tasmania, donna.satterthwait@utas.edu.au

The supergiant Century sediment-hosted Zn-Pb-Ag deposit formed in an outer shelf setting [1] from a submarine hydrothermal vent system developed on, or very near, the seafloor[2]. The mine sequence comprises variably sulfidic (mainly sphalerite) and sideritic siltstones and carbonaceous shales [1,3]. It is somewhat (~1.5x) thicker than equivalent strata observed in a drill-core (MMG788) 5km to the west, suggesting sub-basin development at the site of ore deposition [3]. Unlike other northern Australia Proterozoic sedex Zn deposits, Century is relatively low in pyrite.

Sideritic siltstones in the mine sequence are characterised by crinkly and whispy carbonaceous, bedding-parallel seams, previously interpreted as stylolites. We have re-interpretted these features as microbialites. Their diversity and abundance in the mine sequence, compared to drill-core MMG788, is consistent with locally abundant biological activity at the site of ore formation.

Major element geochemical data and iron speciation measurements from samples from the mine and MMG788 indicate anoxic (ferruginous, *not* sulfidic) conditions mostly prevailed [3]. This is despite several hundred million tons of biogenically reduced S having been sequestered into the Century deposit.

We will present new Mo, P and organic C data from the mine sequence that speak to locally high primary organic productivity. Organic matter thus produced may have been fuel for biogenic sulfate reduction sufficient to form the Century Zn sulfide orebody.

[1] Andrews *et al*. (1998) *Economic Geology* **93**, 1132-1152.
[2] Feltrin *et al*. (2009) *Computers & Geoscence* **35**, 108-133.
[3] Guilliamse (2010) *Unpub. BSc(Hons) thesis, University of Tasmania* 86pp.

Geologic Storage Mavericks: Insights and Promise from Laboratory and Field Pilot Studies in Flood Basalts

B. PETER MCGRAIL

Pacific Northwest National Laboratory, Richland, Washington, USA, pete.mcgrail@pnnl.gov

Abstract

"Maverick" according to the Merriam-Webster dictionary is defined as "One that refuses to abide by the dictates of or resists adherence to a group." Hence, "maverick" is apropos for anyone seriously studying flood basalts for sequestration of carbon dioxide. Continental flood basalts represent one of the largest geologic structures on earth but have received comparatively little attention for geologic storage of CO_2. In fact, flood basalts have flow tops that are porous, permeable, and have enormous capacity for storage of CO_2 or other gases of interest. In appropriate geologic settings, interbedded sediment layers and dense low-permeability basalt rock flow interior sections may act as effective containment for injected gases. For CO_2 sequestration purposes, containment is critical so that sufficient residence time is established for mineralization reactions to occur. Initial laboratory experiments conducted nearly a decade ago with $scCO_2$ showed rapid chemical reaction of CO_2-saturated pore water with basalts to form stable carbonate minerals. However, recent discoveries in laboratory tests with water-saturated supercritical CO_2 show that mineralization reactions occur directly in this phase as well, providing a second and potentially more important mineralization pathway than was previously understood. In fact, in deep geologic settings, mineralization by water-wet $scCO_2$ is the dominant mineralization pathway. But, despite many years of laboratory investigation, the remarkable 10 fold variability in reactivity of different basalts remains an unresolved scientific question, defying easy correlation to mineral makeup or chemical compositional differences in the basalts.

In this paper, we will also discuss an important leveraging application of the work on CO_2 sequestration in basalts for compressed air energy storage to help manage electric grid stability in the Pacific Northwest. Here, mineralization reactions need to be avoided to prevent reservoir permeability decline over the course of many air injection and extraction cycles. Oxygen depletion through reaction with Fe(II) in the basalts also might need mitigation if the extracted air is to be used directly in a combustion turbine.

Field testing of CO_2 storage in basalts is proceeding with drilling of the world's first supercritical CO_2 injection well in flood basalt being completed in May 2009 near the township of Wallula in Washington State and corresponding CO_2 injection permit granted by the State of Washington in March 2011. Injection is in the final planning stage. In Iceland, the CARBFIX project has drilled an injection well and several monitoring wells and plans to test injection of groundwater saturated with a CO_2-H_2S gas mixture obtained from a geothermal power plant. If proven viable by these field tests and others that are in progress or being planned, major flood basalts in the U.S., India, and perhaps Australia would provide additional CO_2 storage capacity and regional sequestration options in these countries where conventional storage is limited, and also provide tangible benefits for future applications in energy transmission and storage.

https://doi.org/10.1180/S0026461X00008434 Published online by Cambridge University Press

The role of surface charge and exchange cation speciation on the structure of interfacial water in nontronite suspensions

JUSTIN V.T. ROTH,[1] CHRISTOPHER A. HEIST,[1] AND MOLLY M. MCGUIRE[1*]

[1]Bucknell University, Department of Chemistry, Lewisburg, PA, U.S.A., mmcguire@bucknell.edu (* presenting author)

Attenuated total reflection infrared spectroscopy (ATR-FTIR) was used to investigate the structure of water at the surface of suspensions of the nontronites, NAu-1 and NAu-2. Raw ATR spectra were converted to absorption index (k) spectra via the Kramers-Kronig transform to allow direct comparison of samples with different indices of refraction. Difference spectra produced from these k spectra allowed subtle shifts in the O-H stretching region to be discerned, thereby providing information about differences in the degree of hydrogen bonding. Suspensions of both NAu-1 and NAu-2 exchanged with either Na+ or K+ exhibit increased hydrogen-bonding at the mineral/water interface as compared to bulk water. NAu-1, which has greater total and tetrahedral charge than NAu-2, shows no change in water structure upon reduction of structural Fe or the addition of a small excess of electrolyte. These observations suggest that the ordering of interfacial water in NAu-1 suspensions is dominated by the highly charged mineral surface. Reduction of structural Fe in NAu-2 results in changes to the interfacial water structure that are dependent on the exchange cation species. In this case, reduction produces a significant increase in tetrahedral charge, which alters the interactions of the exchange cations with the surface.

A Tertiary record of Australian plate motion from ages of diamondiferous alkalic intrusions

BRENT MCINNES[1*], NOREEN EVANS[1,2], FRED JOURDAN[1], BRAD MCDONALD[1,2], JOHN GORTER[3], CELIA MAYERS[1] AND SIMON WILDE[1]

[1] John De Laeter Centre for Isotope Research, Curtin University, Perth Australia, b.mcinnes@curtin.edu.au ([*] presenting author), f.jourdan@curtin.edu.au, Celia.Mayers@curtin.edu.au, s.wilde@curtin.edu.au

[2] CSIRO Earth Science and Resource Engineering, Perth, Australia, noreen.evans@csiro.au, brad.mcdonald@csiro.au

[3] Eni Australia Ltd, Perth, Australia, John.Gorter@eni.com

Multiple geo/thermochronometry datasets (zircon (U-Th)/He[1], phlogopite $^{40}Ar/^{39}Ar$ and wadeite $^{40}Ar/^{39}Ar$) have been acquired from four Western Australian kimberlite and lamproite localities distributed over 850 km. The linear orientation of the eruption centres (~015°), southwardly younging emplacement ages, and apparent co-linearity with modern geodetic measurements has implications for Australian plate geodynamics (Fig. 1).

The Fohn diatreme field consists of ~30 lamproite pipes discovered during oil exploration in the Timor Sea[2]. Phlogopite recovered from lamproite cuttings in an offshore exploration well (Fohn-1) returned a robust plateau $^{40}Ar/^{39}Ar$ age of 29.4 ± 0.7 Ma (P=0.99). A diamond pipe from the North Kimberley kimberlite field (Seppelt) yielded four zircon grains with thermally reset (U-Th)/He ages averaging 25 Ma. Diamondiferous pipes at Ellendale contain xenocrystic zircon grains with (U-Th)/He ages of 20.6 ± 2.8 Ma that were thermally reset by lamproitic intrusions. Other researchers[3] report K-Ar ages for the Noonkanbah lamproite field of ~19 Ma, whereas $^{40}Ar/^{39}Ar$ dating of wadeite from the Walgidee Hills lamproite yielded plateau ages of 17.46 ± 0.17 Ma (P=0.44).

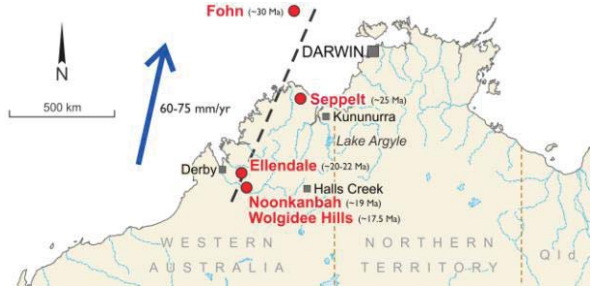

Figure 1: *Age-distance relationships of WA lamproites (red) and Australian plate motion as determined by GPS (blue arrow).*

Geodetic measurements indicate that the Australian plate is currently moving NNE at a rate of 60-75 mm/year relative to the Eurasian plate, whereas long period geospeedometry estimates range from 50-78 mm/year[4]. The age-distance relationship between the Fohn and Wolgidee Hills sites in this study are consistent with a plate motion of 70 mm/yr during the Tertiary.

[1] McInnes et al (2009) *Lithos* **112S**, 592-599. [2] Gorter and Glikson (2002) *AJES* **49**, 847-868. [3] Jaques et al (1986) *GSWA Bull.* **132,** pp. 267. [4] Wellman and McDougall (1974) *Tectonophys.* **23** 49–65.

https://doi.org/10.1180/S0026461X00008434 Published online by Cambridge University Press

Effects of polydispersity on natural organic matter fate and transport

DANIEL MCINNIS, LINDSAY SEDERS DIETRICH, DIOGO BOLSTER, AND PATRICIA MAURICE*

University of Notre Dame, Civil Engineering & Geological Sciences, 156 Fitzpatrick Hall, Notre Dame, IN 46556, USA dmcinnis@nd.edu, lseders@gmail.com, bolster@nd.edu, pmaurice@nd.edu (* presenting author)

Natural Organic Matter (NOM) is a polydisperse material whose components display a range of adsorption rates and affinities as determined largely by molecular weight (MW). In this study, the mobility of NOM was examined in sand columns at pH 5-8, in 0.001 to 0.1 M $NaClO_4$. Effluent data were modelled using the advection-dispersion equation (ADE). Greater overall mobility of NOM was observed at higher pH and lower ionic strength. High-pressure size exclusion chromatography (HPSEC) was used to monitor the MW distribution of column effluent; results were consistent with fractionation by preferential adsorption of intermediate to high MW components, as previously observed in many batch systems. Transport rates of different components were quantified by dividing the MW distribution into separate 'bins' and examining breakthrough curves for each bin. Heterogeneity in the retardation factor (*R)* led to heavy tailing of breakthrough curves as the experiments progressed. This non-Fickian transport behaviour was described using a continuous time random walk (CTRW) model designed to address variability in geochemical properties controlling sorption-desorption kinetics. Results of this study demonstrate that the effects of NOM compositional heterogeneity on transport can be addressed through a systematic coupling of geochemical and hydrologic approaches.

Origin, distribution and hydrogeochemical controls on methane occurences in shallow aquifers in southwestern Ontario

JENNIFER MCINTOSH[1*], STEPHEN OSBORN[2], STEPHEN GRASBY[3], AND STEWART HAMILTON[4]

[1]Department of Hydrology and Water Resources, University of Arizona, Tuscon, AZ 85721, USA, mcintosh@hwr.arizona.edu

[2]Geological Sciences Department, California State Polytechnic University Pomona, Pomona, CA 91768, sgosborn@csupomona.edu

[3]Geological Survey of Canada, Calgary, Alberta, AB T2L 2A7 Steve.Grasby@NRCan-RNCan.gc.ca

[4]Ontario Geological Survey, Sudbury, Ontario P3E 6B5, stew.hamilton@ontario.ca

Abstract

Fractured organic-rich shales, such as the Marcellus, Antrim, and Utica are major targets for thermogenic and biogenic production in Michigan, New York, Pennsylvania, and Quebec. Age-equivalent shales extend into southwestern Ontario (Findlay Arch region), where there has been no shale gas production to date and little information exists on the origin and distribution of natural gas, despite historical accounts of gas in water supply wells screened in shales. To determine the origin and extent of natural gas, and investigate water quality associated with natural gas occurrences, 912 water supply wells were sampled for gas composition, isotopes, and water chemistry in Paleozoic bedrock and overburden formations throughout southwestern Ontario.

Methane concentrations, measured at the well head, ranged from <5 to 415% in-situ saturation (0 to ~251 ppm) with the highest concentrations in wells screened in the Georgian Bay, Dundee, Marcellus, Hamilton Group, and Kettle Point formations, and overlying glacial drift deposits. Carbon isotopes values of CH_4 (-89.9 to –52.3‰), the correlation of hydrogen isotopes of CH_4 and water, and the lack of higher chain hydrocarbons (C_2+<0.8 mole%), indicates the gas is biogenic in origin. Isotopic signatures of methane in overburden deposits were similar to gas accumulations in underlying bedrock formations, suggesting the gas migrated vertically into shallow aquifers, rather than being generated in-situ. Groundwater associated with methane accumulations are dominantly Na-HCO_3 type, with no dissolved oxygen, low Fe (<0.06 mM), low SO_4 (<0.44 mM), and low H_2S (<0.5 mM). Alkalinity concentrations ranged from 0.2 to 15.0 mM, and there was no correlation with CH_4 concentrations. High CH_4 concentrations were observed in groundwater with variable $\delta^{18}O$ values (-18.6 to –8.3‰), representing microbial methanogenesis associated with both modern and Late Pleistocene recharge. Results from this study provide important baseline data on dissolved gases and water quality in shallow aquifers overlying shales, in the case of future shale gas production, hydraulic fracturing and/or geologic sequestration of carbon dioxide to evaluate potential environmental impacts.

https://doi.org/10.1180/S0026461X00008434 Published online by Cambridge University Press

Anatexis and uranium protore in the Wollaston Domain, Saskatchewan

CHRISTINE L. MCKECHNIE [1,2*], IRVINE R. ANNESLEY [2,3], AND KEVIN M. ANSDELL[2]

[1] CanAlaska Uranium Ltd., Saskatoon, caustman@canalaska.com (* presenting author)

[2] Department of Geological Sciences, University of Saskatchewan, Saskatoon, Canada, kevin.ansdell@usask.ca

[3] JNR Resources Inc.., Saskatoon, Canada, jnrirvine@sasktel.net

The Fraser Lakes Zone B U-Th-REE-bearing granitic pegmatites are located within the Wollaston Domain of northern Saskatchewan, Canada. The mineralized zone lies circa 25 km from the southeastern edge of the highly prolific Athabasca Basin; home to some of the world's highest grade uranium deposits.

The granitic pegmatites intruded into a NNE-plunging regional fold structure at/near the highly deformed contact between Archean orthogneisses and overlying Paleoproterozoic metasedimentary rocks of the Wollaston Group.[1,2,3] Their intrusive contacts suggest the pegmatites formed during the later stages of the ca. 1.8 Ga Trans-Hudson Orogeny.[1,2,3] This agrees with CHIME dating of uraninite in the uranium-rich pegmatites (a cluster of ages between 1.85 and 1.80 Ga). A primary magmatic age has yet to be determined for the Th-LREE-rich pegmatites, which have contact relationships similar to the strongly U-rich pegmatites. High-grade metamorphism and migmatization occurred concurrently with pegmatite intrusion, at peak temperatures of up to T ca. 850°C at P ca. 9 kbar (i.e. lower granulite facies) followed by retrograde amphibolite-facies metamorphism.

A combination of partial melting of a metasedimentary-dominated source at depth, accessory mineral entrainment, and assimilation-fractional crystallization processes during ascent and emplacement is thought to be responsible for U, Th, and REE enrichment of the granitic pegmatites.

These pegmatites show similarities to the alaskite-hosted uranium deposits at Rossing (Namibia) and to uraniferous pegmatites in the Grenville Province (Canada).[1] Similar pegmatites have also been found in the proximity of some of the Athabasca Basin basement-hosted unconformity-type uranium deposits, including Moore Lakes, Eagle Point, and Millennium. Hence, it has been proposed [4,5,6,7] that such pegmatites are protore for the formation of these uranium deposits in the Athabasca Basin. Hydrothermal alteration (i.e. chlorite, hematite, and clay minerals) similar to that in the alteration halos around some of the Athabasca deposits is also found at Fraser Lakes Zone B [1,2,3,7], indicating that fluids of similar composition may have passed through the pegmatites.[7] The presence of younger, secondary, hydrothermal U mineralization within fractures cutting the pegmatites also supports this hypothesis.

[1] Austman *et. al.* (2010) *SEG 2010 Conference Abstr.* **Ext. Abstr. F-1**. [2] Annesley *et. al.* (2010) *GeoCanada 2010 Abstr. No.* **815**. [3] Annesley *et. al.* (2010) *SGS Open House Abstr. Vol.* **2010**, 8. [4] Annesley *et al.* (2000) *Sask. Geol. Survey Sum. of Invest.2000 Vol.* **2**, 201-211. [5] Hecht & Cuney (2000) *Miner. Deposita* **35**, 791-795. [6] Mercadier *et. al.* (2010) *Lithos* **115**, 121-136. [7] Mercadier *et.al.* (submit.) *Econ. Geol.*

Mineral and element vectoring in the Pilley's Island VMS district, Newfoundland Appalachians, Canada

C.P. MCKINLEY [1*], S.J. PIERCEY[1], L. WINTER[2], AND J.G. THURLOW[3]

[1]Department of Earth Sciences, Memorial University of Newfoundland, St. John's, Canada, cmckinley@mun.ca (*presenting author), spiercey@mun.ca

[2]Altius Minerals Corporation, St. John's, Canada, lawrence@altiusminerals.com

[3]Corner Brook, Canada, geoffthurlow@gmail.com

A major challenge in ancient volcanogenic massive sulfide (VMS) districts is that many have been strongly affected by metamorphism and deformation, resulting in mineralization being hosted within imbricated, thrust-faulted terranes, with abundant stratigraphic offset and juxtaposition. In such environments, barren volcanic units are often juxtaposed next to those that may be VMS-bearing, causing difficulty in stratigraphic reconstruction and in the discrimination of prospective from less prospective stratigraphy. These stratigraphic and structural uncertainties result in the requirement for the integration of lithogeochemistry and detailed mineralogy with traditional mapping, to vector towards mineralization at the prospect and regional scale. Pilley's Island, Newfoundland is an ideal location to demonstrate this vectoring because it hosts several VMS deposits in a small area (10 km^2), it is heavily faulted with barren mafic volcanics thrust between VMS-bearing felsic volcanic panels, and has excellent surface exposure and archived drill core for detailed geological and geochemical visualization.

Results from mapping, lithogeochemistry, and shortwave infrared-near infrared (SWIR-NIR) spectroscopy have identified alteration haloes around the VMS deposits of Pilley's Island. The distribution of AlOH, FeOH, and MgOH hull absorption values from SWIR-NIR spectra defines, from proximal to distal to mineralization, haloes of illitic phengite, phengite, illitic muscovite, muscovite, and Fe- to Fe-Mg- to Mg-chlorite. Surface and 3D gridding of lithogeochemical data have also identified prospective zones for mineralization. In particular, useful vectors include Na, K, and alteration indices. For example, zones with highest Na depletion, with K addition and associated with illitic phengite alteration are most prospective for sulfide mineralization.

Despite this VMS district being intensely imbricated, the integration of mapping, drill core reconstructions, lithogeochemistry, and SWIR-NIR spectroscopy readily distinguishes the mineralization-related thrust faulted panels from those that are barren of mineralization. The integration of both geochemical and mineralogical vectoring methods exemplified at Pilley's Island, can be useful in the exploration and delineation of VMS and other hydrothermal deposits elsewhere in the Appalachians and in other heavily faulted collision zones worldwide.

https://doi.org/10.1180/S0026461X00008434 Published online by Cambridge University Press

Carbon Dioxide Groundwater Mixing and Mineralization Reactions with Reservoir Rocks at a Natural Analogue Site, Soda Springs, Idaho, USA

TRAVIS L. MCLING[1]*, ROBERT W. SMITH[2], AND WILLIAM SMITH[3],

[1] Idaho National Laboratory-Center For Advanced Energy Studies, Idaho Falls, ID, USA, travis.mcling@inl.gov*.

[2] University of Idaho-Center for Advanced Energy Studies, Idaho Falls, ID, USA, smithbob@uidaho.edu

[3]Idaho State University, Pocatello, Idaho, USA, smitwill@isu.edu

Analogue sites are particularly relevant and useful to the study geologic carbon dioxide sequestration for a number of reasons, particularly because they offer the opportunity to examine a system that has operated on a time scale (centuries to eons) that laboratory and field experimentation (days to decades) cannot compare. One such example of a mafic rock CO2 analogue is the Soda Springs site located in Caribou County of Southeastern Idaho, USA. At this site, CO2 and formation fluids generated by the dissolution of Paleozoic carbonates at depth are migrating and reacting with a series of shallower thoelitic basalt flows that host a fresh water aquifer. We believe that the layered basalt flows are acting as a reactive barrier to the vertical migration of the deep CO2 charged fluids. However, in several cases the CO2 charged reservoir fluids make it to the surface and are expressed as either carbonated springs, or as cold-water geysers caused by wells that encounter the system at depth. Analysis of these sources of water shows a steady evolution of groundwater from unaffected by the basalt (deep wells) to more fully reacted (springs).

Data from this system makes a compelling argument for the ability of basalt flows to maintain containment for CCS applications. Our study has shown that CO2 charged fluids migrating upwards are being neutralized by mineral dissolution and precipitation within the basalt flows. These neutralization reactions have resulted in a specific chemical signature being imparted to the formation fluid that can be used to determine which minerals are dissolving and precipitating. Through and integrated study of this natural analogue site including field and laboratory experiments, the relative roles of mineral dissolution and precipitation and phase assemblage are being characterized for this basalt-hosted system.

The benefit of studying this natural analogue is that it has been active for many 1000's of years and depending on sample location and depth, the resulting fluid chemistry carries the chemical signature (tracer) indicative of the degree of reaction within the basalt formation. Additionally, the study of this system is helping define the appropriate laboratory scale experiments that will be needed to accomplish the larger objective of the project, understanding changes in aqueous geochemistry associated with progressing CO2-water-interactions.

Reconstructing the large-scale deep and intermediate ocean circulation in the North Atlantic during the LGM and last deglaciation

JERRY F. MCMANUS[1*], SHARON S. HOFFMANN[1], NATALIE ROBERTS[2], GENE HENRY[1], LOUISA BRADTMILLER[3], KAIS MOHAMED[4], SAM JACARD[5], JIMIN YU[6], ALEX PIOTROWSKI[2], DELIA W. OPPO[7], WILLIAM B. CURRY[7], SUMMER K. PRAETORIUS[8], AND LAURA F. ROBINSON[9]

[2]Lamont-Doherty Earth Observatory of Columbia University, NY, USA jmcmanus@ldeo.columbia.edu (* presenting author)

[2]University of Cambridge, Cambridge, UK, nr297@cam.ac.uk

[3]Macalester College, St. Paul, MN, USA, lbradtmi@macalester.edu

[4]University of Vigo, Vigo, ES, kmohamed@uvigo.es

[5]ETHZ, Zurich, CH, samuel.jaccard@erdw.ethz.ch

[6]Lawrence Livermore National Laboratory, CA, USA, yu26@llnl.gov

[7]Woods Hole Oceanographic Institution, USA, doppo@whoi.edu

[8]Oregon State University, Corvallis, spraetor@coas.oregonstate.edu

[9]University of Bristol, Bristol, UK, Laura.Robinson@bristol.ac.uk

The large-scale subsurface circulation of the ocean is an important component of the Earth's climate system, and contributes to the global and regional transport of heat and mass. More than two decades ago, geochemical analyses of deep-sea sediments in the Atlantic Ocean revealed that the distribution of water masses and their characteristics were significantly different at the LGM and other times in the past when compared to modern observations. Although some of the paleodata have been reproduced and shown to be robust, there has been continued debate about the implications of these results for the dynamics of the large-scale circulation and the consequences for the storage and transport of heat, freshwater, nutrients and carbon in the past. There is also no consensus on the variations in water mass and dynamics that occurred between the LGM and the establishment of the modern Atlantic circulation despite the development of time series and maps of more than a half dozen paleo proxies for various aspects of the circulation.

Here we present a discussion of new and previously published Pa/Th, $\delta^{13}C$, SS, εNd, $\Delta^{14}C$, Cd/Ca, B/Ca, Zn/Ca and other data. We consider which aspects of past circulation during the LGM and deglaciation are robustly established and which remain open to competing interpretations. These results combine to confirm that the Atlantic circulation was different both in terms of water masses and their fluxes. The LGM Atlantic was characterized by rapidly overturning intermediate waters, consisting of more than one water mass, most likely of northern origin, and southern-sourced deeper waters with a longer residence time in the basin. Early in the deglaciation, during the H1 iceberg discharge and ensuing stadial, the boundary between intermediate and deep water masses shoaled, although a shallower overturning cell persisted throughout. We seek to reconcile apparently conflicting new and existing proxy evidence regarding any substantial change in the rate of deep water production and residence time during H1. Shortly after 15 ka, nearly all proxies indicate a rejuvenation of deep overturning, followed by a reduction during the Younger Dryas event (12.7 – 11.5 ka), and the subsequent development of the modern Atlantic circulation in the Holocene.

https://doi.org/10.1180/S0026461X00008434 Published online by Cambridge University Press

From Rhizosphere To Ecosystem: Heavy Metals and Plant Defense

David H. McNear Jr. [1*]

[1]Unvieristy of Kentucky, Lexington, U.S.A., dave.mcnear@uky.edu

Human use and manipulation of our natural resources, especially since the industrial revolution, has accelerated the introduction of HM's into soils resulting in a dramatic increase in their concentration in many soils of the United States (and beyond). Many of these HM's even at very low concentrations are toxic and reside in sites that are close to large and often socially downtrodden populations, and hence, pose a significant threat to both human health and the environment. Few remediation technologies have been effective at treating HM enriched soils *in-situ*. Phytoextraction, the use of specialized metal hyperaccumulating plants to remove metals from soils has been growing in popularity because it overcomes many of the limitations of conventional remediation methods. address the ecological implications that could arise from planting non-native plants capable of transferring metals from the soil to the shoots of the plant where they can then be introduced into the food chain, and/or have undesirable effects on ecosystem structure and function.

Elucidating how metals in specialized metal hyperaccumulating plant tissues influence plant physiology and insect feeding behavior is fundamental to understanding the evolution of this unique trait and the influence these plants may have on ecosystem structure and function. The elemental defense hypothesis (EDH) states that metals taken up and stored are effective at protecting plants from insect herbivores because of the inherent toxicity or unpalatability of the metals. A concomitant hypothesis, known as the trade-off hypothesis, states that plants will trade more physiologically costly chemical defenses (e.g. glucosinolates (GL's)) for less costly metal defenses. The objectives of this study were to investigate these hypotheses by examining the spatial and temporal relationship between Zn and GL concentration and speciation in leaves of the model Zn hyperaccumulator *Noccaea caerulescens* (formerly *Thlaspi caerulescense*) and assess how these patterns influence insect feeding behavior. A six week greenhouse study was conducted with *N. caerulescens* grown in soil receiving 250, 500 and 1000 uM Zn treatments. At the end of the experiment whole plant metal concentrations were determined in addition to the analysis of young, medium and old leaves for total metal content (ICP-MS), total GL's (as glucose) and GL species (HPLC). Metal distribution was also determined in young, medium and old leaves using synchrotron based x-ray fluorescence (SXRF) mapping and scanning electron microscopy (SEM-EDX), and the spatial distribution of specific GL's determined using matrix assisted laser desorption time of flight mass spectrometry (MALDI TOF/TOF MS) chemical mapping. The influence of these patterns on insect feeding behavior was assessed using the generalist herbivore *Trichoplusia ni* (Cabbage looper) in choice and no-choice feeding experiments. Preliminary results show that the concentration and distribution of Zn in young, medium and old leaves is inversely proportional to that of GL's with the younger leaves having a higher GL content than older leaves. Feeding patterns are alterned in response ot Zn concentrationa and distribution in the leaves providing evidence for the trade-off hypothesis.

Siqueiros Transform MORB; characteristics of a S-saturated suite

Andrew McNeill[1], Leonid Danyushevsky[1*], Kevin Klimm[2], Alexei Ariskin[3], Mike Perfit[4]

[1]CODES, University of Tasmania, Hobart, Australia, Leonid.danyushevsky@utas.edu.au (* presenting author)

[2]Johann Wolfgang Goethe University, Frankfurt, Germany, klimm@em.uni-frankfurt.de

[3]Vernadsky Intstitute, Moscow, Russia, ariskin@geokhi.ru

[4]University of Florida, Gainesville, USA, perfit@geology.ufl.edu

Geochemically diverse mid-ocean ridge basalts, with a significant range of major and trace element contents in pillow-rim glasses, were recovered from the Siqueiros Transform Fault, in the East Pacific Ocean. All these glasses were S-saturated at eruption, on the basis of the presence of immiscible sulfide globules (Fig. 1A). Based on the compositions of silicate melt inclusions in early-crystallised olivine phenocrysts, previous workers [1] have interpreted the early Siqueiros liquids, which were less fractionated than the pillow-rim glasses, to be S-undersaturated. However, since we have observed numerous inclusions of immiscible sulfides in the same early olivine phenocrysts, we interpret that most of Siqueiros parental liquids were S-saturated early in their fractionation history. The compositions of these immiscible sulfide liquid inclusions in olivine are consistent with those from other MORB suites [2] and estimates of sulfide liquid compositions from mantle rocks (e.g., [3]). In the Siqueiros samples S-Saturation appears to be largely independent of liquid composition over a wide compositional range, and is only controlled by total Fe content (Fig. 1B).

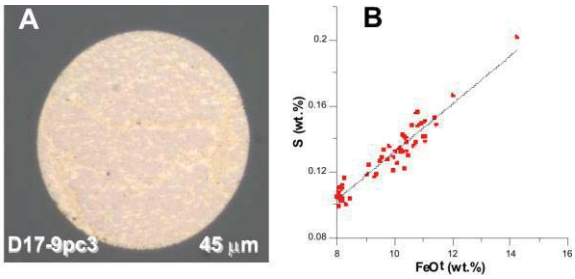

Figure 1: A; reflected light image of a 'quenched' immiscible sulfide globule in pillow-rim glass. B; relationship between FeO^t (all Fe as FeO) and S for Siqueiros Transform Fault pillow-rim glasses. The strong correlation indicates S-saturation (see [4]).

Laser Raman analyses, using the method of [5], of primitive and evolved pillow-rim glasses indicate that all S is present at S^{2-} and that the maximum fO_2 is therefore close to QFM. Mössbauer analyses are being completed to confirm the fO_2 of the pillow rim glasses.

Our data from the erupted basalts and inclusions provides a well constrained natural dataset that has been combined with experimental data to produce a new sulfur saturation model [6] and can be used to test the results of this and other models.

[1] Saal *et al.* (2002) *Nature* **419**, 451-455. [2] McNeill *et al.* (2009) *Proc. Xi'an Int. Ni-Cu Deposit Symposium.*, 4-5. [3] Luguet *et al.* (2003) *Geochim et Cosmochim acta* **67**, 1553-1570. [4] Wallace and Carmichael (1992) *Geochim et Cosmochim acta* **56**, 1863-1874. [5] Klimm *et al.* (submitted). [6] Bychkov *et al.* (2010) *13th IAGOD Symposium*, 304-305.

https://doi.org/10.1180/S0026461X00008434 Published online by Cambridge University Press

A Microbial Fuel Cell enhances Bioremediation of Gasworks Contaminated Groundwater

B. MC POLIN[1*], R. DOHERTY[1], M.J. LARKIN[2]

[1] Environmental Engineering Research Centre, SPACE, Queen's University Belfast (*correspondence: bmcpolin03@qub.ac.uk), (r.doherty@qub.ac.uk)
[2] School of Biological Sciences, Medical Biology Centre, Queen's University Belfast (M.Larkin@qub.ac.uk)

Microbial Fuel Cell (MFC) technology has been applied to many different remedial technologies, including bioremediation of contaminated groundwater. As of yet full scale implementation of the technology in relation to remediation projects has not been proven. In regards to groundwater bioremediation a MFC consists of bacteria oxidising contaminants such as organic pollutants within an anaerobic area of a plume (the anode) and the transfer of electrons through a circuit to a cathode where terminal electron acceptors are reduced. This results in the generation of a low current and the depletion of contaminants.

From geophysical analysis a large MFC (50+mV) was observed to be functioning at a gasworks site containing high levels of organic and ammonium contamination in groundwater. The aim of this research is to investigate what parameters play a role or drive the MFC and can it be utilised as a sustainable remediation tool.

Experiments involve constructing a MFC with graphite electrodes connected by wire that provides a direct circuit from high contamination (the anode) to an area of bioelectric activity (the cathode). A variable resistor and datalogger are used to monitor current production. Comparison of water samples using chemical analysis (monitoring levels of TOC, Ammonium, Nitrate & Nitrite) and molecular microbiology techniques (characterising the microbial population at the anode and cathode using PCR, DGGE, and metagenomics approaches) before and after electrode operation would indicate whether the MFC has enhanced bioremediation. Initial results indicate considerable microbial diversity between the anode and cathode on site and a large Self-Potential (electrical) difference. There is also evidence of microbial utilisation of ammonium.

Genetic analysis of the shift in microbial population before and after MFC installation would highlight the involvement of microbes in the bioremedial process. Characterising the microbial biofilm formed at the anode and cathode would give a better understanding of the role the active microbial communities play in electrical conductivity and ultimately a better understanding of the potential bioremedial/ bioelectric potential of the native microbial consortia which can be exploited for bioremediation.

Comparing the soil solution chemistry of soils amended with nano-sized copper oxide, micron-sized copper oxide, and with a copper salt.

HEATHER MCSHANE[1,*], JOANN K WHALEN[1], GEOFFREY SUNAHARA[2], WILLIAM HENDERSHOT[1]

[1]University of McGill Dept. of Natural Resource Sciences, Ste Anne de Bellevue, Quebec, Canada, Heather.Mcshane@mail.mcgill.ca (* presenting author)
2: National Research Council Canada - Biotechnology Research Institute, Montreal, Quebec, Canada, geoffrey.sunahara@cnrc-nrc.gc.ca

Engineered copper oxide nanoparticles (nano-CuO) are likely to be used in agriculture in the future but little is known about their effects on soil biota. As nano-CuO particles dissolve, they release Cu^{2+}, which can be measured as Cu activity, and which is thought to be the main form of bioavailable Cu in soils. Copper bioavailability may change over time as the Cu redistributes between soil solid and solution phases. Soluble Cu salts have been used to evaluate Cu^{2+} transformations but they can reduce soil pH and increase the concentration of dissolved cations in the soil solution, and they may overestimate bioavailable Cu. In this study, we amended two natural soils with 500 mg Cu / kg soil as nano-sized or micron-sized CuO, or as Cu nitrate, and measured the change in Cu activity, pH, and concentrations of dissolved Ca, Mg, and Zn in the amended soils over a period of 56 d. The initially low Cu activity in the oxide-amended soils increased over the course of the experiment, whereas the initially high Cu activity in the salt-amended soil declined. Soil pH was lower and dissolved cation concentrations were higher in the salt-amended soils than in the oxide-amended soils for the duration of the experiment. We conclude that amending soils with Cu nitrate does not accurately reflect Cu^{2+} transformations in soils amended with nano- and micron-sized CuO.

https://doi.org/10.1180/S0026461X00008434 Published online by Cambridge University Press

In-situ geochemical characterization of experimental partial melts

FIONA C. MEADE[1,2*], MATTEO MASOTTA[3], VALENTIN R. TROLL[2], CARMELA FREDA[4], BÖRJE DAHRÉN[2], JON P. DAVIDSON[5] AND ROBERT M. ELLAM[6]

[1]University of Glasgow, Glasgow, UK, fiona.meade@glasgow.ac.uk (* presenting author)
[2]Uppsala University, Uppsala, Sweden, valentin.troll@geo.uu.se
[3]Sapienza Università di Roma, Rome, Italy, matteo.masotta@uniroma1.it
[4]INGV, Rome, Italy, carmela.freda@ingv.it
[5]Durham University, Durham, UK, j.p.davidson@durham.ac.uk
[6]SUERC, East Kilbride, UK, r.ellam@suerc.gla.ac.uk

Understanding partial melting of ancient gneiss terranes is crucial when considering crustal contamination in volcanic systems, for example, as these rocks are unlikely to melt completely at magmatic temperatures (900-1200 °C) and crustal pressures (<500 MPa). Variations in the bulk composition of the protolith, magma temperature, pressure (depth), the composition and abundance of any fluids present will produce a variety of melt compositions. This may range from partial melts enriched in incompatible elements to more complete melts, nearing the bulk chemistry of the parent gneiss.

We have used piston cylinder experiments to simulate partial melting in a suite of 10 gneisses from NW Scotland and Eastern Greenland at magma chamber temperatures and pressures (P = 200 MPa, T = 975 °C). These gneisses form the basement to much of the North Atlantic Igneous Province, where crustal contamination is frequently identified. However, the actual compositions of the crustal partial melts are poorly constrained. Partial melts were produced in all 10 experiments. The experimental charges were quenched so that partial melts were preserved as glass, making them suitable for in-situ microanalysis. Electron microprobe spot analyses of the glasses indicate they are compositionally heterogeneous and are significantly different to the bulk chemistry of the parent gneisses. The samples were mapped using energy-dispersive x-ray spectroscopy (EDX), which deciphered the spatial variation in melt chemistry and revealed evidence of intense mixing and mingling processes. Individual melt domains were microdrilled for Sr and Pb isotope ratios.

This novel petrological, experimental and in-situ geochemical approach allows quantification of partial melting in a volcanic context, providing accurate geochemical end-members for modelling crustal contamination processes.

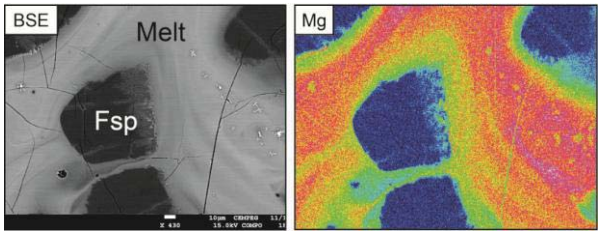

Figure 1: BSE image and EDX map of a partial melting experiment showing heterogeneous composition and mixing/mingling textures. Images and analyses were collected using the FE-EPMA facility at Uppsala University (http://www.geo.uu.se/mpt).

Pumping away: Impact of benthic macrofauna on flow, redox dynamics and sediment N cycling

C. MEILE[1,*], T. DORNHOFFER[1], S. KAZA[2], N. VOLKENBORN[3] AND G.G. WALDBUSSER[4]

[1]Dept. of Marine Sciences, The University of Georgia, Athens, GA 30602, USA, *cmeile@uga.edu, dorntd@uga.edu
[2]Institute for Artificial Intelligence, The University of Georgia, Athens, GA 30602, USA, priyak@uga.edu
[3]Dept. of Biological Sciences, University of South Carolina, Columbia, SC 29208, USA, nils@biol.sc.edu
[4]College of Oceanic and Atmospheric Science, Oregon State University, Corvallis, OR 97331, USA, waldbuss@coas.oregonstate.edu

Burrowing organisms have long been recognized to play a major role in biogeochemical cycling in aquatic sediments. However, only recently have advances in sensor developments and computational capabilities provided the opportunity to detail the flow dynamics and oscillatory redox conditions driven by the pumping activity of benthic infauna. Here we present a coupled flow-reaction model analysis linked to observations in experimental microcosms.

While volumetric pumping rates are fairly well known and experimentally accessible, flow patterns in the subsurface are not. However, they are important to quantify location and extent of oxic-anoxic interfaces which are critical in determining the biogeochemical cycling of redox sensitive elements. We present the determination of such velocity fields using optical flow anlysis of fluorescent dye tracers in antfarm experiments.

Our work then focuses on the role of burrowing organisms on O_2 dynamics and nitrogen cycling in coastal sediment. We will present model analyses of the impacts of burrowing depth, irrigation intensity and activity patterns. Our results show a distinct role for all these factors on denitrification. Model simulations show a significant impact of volumetric water exchange on areal denitrifaction; notably, they also predict a different trajectory of total denitrification with increasing burrow depth for continuous vs. episodic biologically induced flow.

Our findings have significant implications for removal of N from shallow water environments, and the controls thereof. Initial results suggest that nitrate removal is controlled not only by spatial structuring of the sediment (e.g. concentration gradients), but also by temporal dynamics (duration and frequency) of anoxic conditions forming in the sediment domain. Our findings also suggest that bioirrigation models which depict organism activity as an averaged continuous, unidirectional process miss the temporally dynamic character of biologically active sediments that may profoundly affect sediment nitrogen cycling.

https://doi.org/10.1180/S0026461X00008434 Published online by Cambridge University Press

Behavior of uranium isotopes in shallow aquifers of southern Québec, Canada

PAULINE MÉJEAN[1], GENÈVIEVE VAUTOUR[3], DANIELE L. PINTI[4], BASSAM GHALEB[2], MARIE LAROCQUE[5]

[1,2,3,4]GEOTOP-UQAM, Montréal, QC, Canada
[1] mejeanpauline@gmail.com (* presenting author)
[2] ghaleb.bassam@uqam.ca
[3] vautour.genevieve@courrier.uqam.ca
[4] pinti.daniele@uqam.ca
[5]Département des Sciences de la Terre et de l'Atmosphère, UQAM, Montréal, QC, Canada
[5] larocque.marie@uqam.ca

A multi-isotopic study was initiated in order to quantify the groundwater resources available in a shallow aquifer of southern Québec. Uranium content and its isotopes ^{234}U and ^{238}U, which are partially dependent of redox conditions and physical/lithological characteristics of the aquifers and their recharge were measured. In specific cases, $^{234}U/^{238}U$ activity ratios can give information on the residence time of groundwater, a fundamental piece of information for a correct estimation of groundwater sustainability.

The target area is the lower portion of the Bécancour River watershed located between Montréal and Québec. Groundwater flows in shallow sands intercalated with clays of the Champlain Sea (Holocene age) and deeper fractured carbonates of Ordovician age of the St. Lawrence Lowlands. Water chemistry is dominantly bicarbonate.

Two transects (15 wells) were preliminary selected. The first follows the main flow path from the Appalachian Mts. (the main recharge area) downstream to the St. Lawrence River. The second transect is perpendicular to the first one and contains more mineralized waters. Along the flow path, there is a clear decreasing trend of the $^{234}U/^{238}U$ activity ratio, from a maximum of 3.12 measured close to the recharge to a value of 1.14, on the plain next to the St. Lawrence River.

During decay of ^{238}U to ^{234}Th, an α particle is emitted. The recoil energy is sufficiently important for the mineral to eject ^{234}Th to groundwater or to weak mineral sites were ^{234}U will be produced, making it easily leachable. Consequently, recharging groundwater would be enriched in ^{234}U when compared to ^{238}U and this mechanism might explain the high $^{234}U/^{238}U$ activity ratios observed close to the recharge areas.

The observed decrease of the $^{234}U/^{238}U$ ratio along the flow path could be interpreted by the radioactive decay of the excess of ^{234}U compared to that of ^{238}U at the ^{234}U time scale (10^6 yrs). However, a recent noble gas survey shows clearly that groundwater in the recharge area contains tritiogenic ^3He with ages younger than 20 years. A different process should be evoked to explain the isotopic fractionation of $^{234}U/^{238}U$. There is a clear relation between the alkalinity of waters (and the HCO_3^- content) and the $^{234}U/^{238}U$ activity ratio. This relation suggests that the mobility of uranium might be related to HCO_3^- and CO_3^{2-} ions complex. It is known that carbonates and hydroxyls could be efficient agents of complexation inducing higher mobility of ^{234}U after the "recoil". Thus the high activity ratios observed could be related to the enhanced mobility of ^{234}U in bicarbonate waters.

Low energy absorption edges of NS3 glass, albite and silicon investigated using x-ray Raman scattering

KOLJA MENDE[1*], ALEXANDER NYROW[1], CHRISTIAN STERNEMANN[1], CHRISTIAN SCHMIDT[2], MAX WILKE[2], LAURA SIMONELLI[3], MARCO MORETTI SALA[3], CHRISTOPH SAHLE[1], THORSTEN BRENNER[1], JOHN TSE[4] AND METIN TOLAN[1]

[1]Fakultät Physik, TU Dortmund, Dortmund, Germany
*kolja.mende@tu-dortmund.de
[2]Geoforschungszentrum Potsdam, Potsdam, Germany
[3]European Synchrotron Radiation Facility, Grenoble, France
[4]Department of Physics and Engineering Physics, University of Saskatchewan, Saskatoon, Canada

X-ray Raman Scattering (XRS)

The investigation of processes of geological relevance is directly connected to environments of extreme conditions, e.g., high pressure and high temperature. For in situ studies of materials under such conditions one needs to use special sample chambers with highly absorbing sample environments such as diamond anvil cells, which prevent the use of electron or soft x-ray techniques like EELS or XANES, combined with laser or resistive heating.

XRS is a non resonant inelastic photon-in-photon-out scattering process. The incoming high energy photons are scattered by core-hole electrons, exciting them to unoccupied states by transferring a relatively small amount of energy [1]. The application of hard x-rays makes x-ray Raman scattering a unique tool to investigate low energy absorption edges for binding energies between 10 eV and 2 keV of low Z elements like silicon, sodium, iron or oxygen under geologically relevant conditions.

XRS is very sensitive to changes of the electronic and local atomic structure, e.g., the oxidation or spin state of the studied atom. It provides the similar information as soft x-ray absorption and electron energy loss spectroscopy.

NS3 glass, albite and silicon

Silicon is the subject of many current studies. These include silicate melts and glasses due to their geological relevance, as well as pure silicon [2,3]. We present first results of an XRS study of the sodium K-edge of dry and water bearing NS3 glass ($Na_2Si_3O_7$) and albite ($NaAlSi_3O_8$) as well as results on the aluminum L-edge of albite. Furthermore we show recent in situ measurements of pure silicon at the Si L-edge at pressures up to 20 GPa.

[1] Schülke (2007) *Electron Dynamics by Inelastic X-ray Scattering* (Oxford University Press)
[2] Weigel *et al.* (2008), *J. Phys.: Condens. Matter* **20**, 135219
[3] Farges *et al.* (2006), *AIP Conf. Proc.* **882**, 214-216

https://doi.org/10.1180/S0026461X00008434 Published online by Cambridge University Press

Greener and leaner soil and sediment remediation: an overview of *in-situ*

CHARLES MENZIE [1]

[1]Exponent Inc., Alexandria VA, USA, camenzie@exponent.com

Abstract

Over the past decade there has been heightened interest in using in-situ remediation for contaminated sediments and in-situ technologies for soils have been underway for the past few decades. Such technologies include methods for degrading the contaminants in place or arresting or blocking exposures through the use of various barriers and amendments. These approaches appeal to common sense as they can be less costly to implement, can be less disturbing to the environment, and may pose lower risks to humans. But often the arguments regarding pros and cons of in-situ vs. removal technologies focus on specific aspects of the remedial process. What can be lost in narrow arguments is the fuller understanding of the life cycle of the various technologies with respect to overall economic, environmental, and human health benfits.

The economic benefits aspects are often the easiest to grasp and to compare among removal and in-situ remedial technologies. Less obvious are overall ecological benefits. Understanding relative ecological benefits typically requires a broad understanding of the ecological risks/impacts that contaminants are having within the system, the degree to which these risks will be reduced in the short and long-term by the remedial technologies, and the short and long-term impacts of the remediation.

A variety of methodologies have arisen to capture the relative environmental risks and benefits of alternative technologies. These include Net Environmental Benefits Analysis (NEBA), Integrated Environmental Benefits Analysis (IEBA), and Relative Risk Methods (RRM). Implementation of these methods requires knowledge of the various ecological systems and associated ecological srvices.

Relative human health risks and benefits involve a comparison of technologies in the short and long-term for the full range of remedial elements. Particular attention has been given to the life-cycle aspects that influence site-related risk reduction, potential risks associated with remediation, and even risks to remedial workers. While the last has gotten much discussion, it is important to note that “risk acceptability” is itself a variable that is not constant over all populations.

This talk will weave together the above aspects into a consideration of the “greener” and “leaner” nature of in-situ remediation and the efforts that are needed to make that case.

Origin of uranium deposits revealed by their rare earth element signature

JULIEN MERCADIER*, MICHEL CUNEY, PHILIPPE LACH, MARIE-CHRISTINE BOIRON, JESSICA BONHOURE, ANTONIN RICHARD

G2R, Université de Lorraine, CNRS, CREGU, 54506 Vandoeuvre-lès-Nancy, France (*julien.mercadier@g2r.uhp-nancy.fr)

Uranium deposits have formed in a wide range of geological settings including deep metamorphic/magmatic to surficial conditions and range in age from Archean to recent time. These temporal and spatial variations have given rise to an extreme diversity of deposits [1]. However, understanding their genesis and exploring for uranium deposits have remained challenging. In particular, very limited link between trace element or isotopic composition of uranium oxide and the conditions for their accumulation to economic grades have been clearly established.

Here we report REE abundances in uranium oxides, measured by microbeam methods (SIMS and LA-ICP-MS), for a series of 20 worldwide uranium occurrences from six of the major uranium deposit types. This study demonstrates that the REE contents of uranium oxides are very specific to each deposit type, regardless of the age or variations in local geological settings. Thus, REE abundances reflect directly the mineralising processes specific to each deposit type. We propose an evaluation of the first order parameters (T, REE sources and fluid composition) controlling the REE behaviour in each mineralized system. When applied to giant unconformity-related deposits, REE abundances enable to better understand their formation. Our results demonstrate that the REE patterns of uranium oxides are powerful tools for refining metallogenic models, and a key for the definition of the genetic model of new uranium discoveries [2].

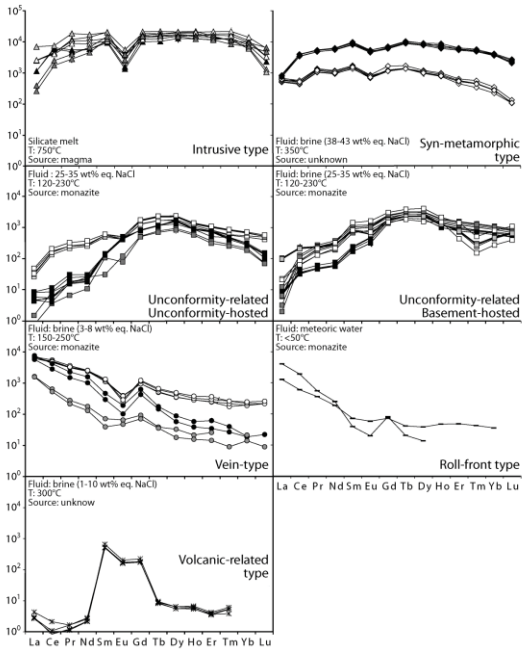

Figure 1:chondrite-normalized REE patterns of uranium oxides for six different types of worldwide U deposits. Source : source of REE

[1] Cuney (2009) *Mineralium Deposita* **44**, 3-9. [2] Mercadier et al. (2011) *Terra Nova* **23**, 264-269.

https://doi.org/10.1180/S0026461X00008434 Published online by Cambridge University Press

Pre-eruptive conditions of ore-forming magma that produced the Henderson molybdenite deposit, CO: Insights from melt inclusions and mineral thermobarometry

CELESTINE N. MERCER[1*], ALBERT H. HOFSTRA[1], TODOR I. TODOROV[1], AND ERIN E. MARSH[1]

[1]USGS, Denver, USA, cmercer@usgs.gov (* presenting author)

The Henderson ore body is a Climax-type porphyry molybdenum deposit related to Oligocene high-silica rhyolite intrusions of the Red Mountain Complex near Empire, Colorado [1, 2]. The Hideaway Park rhyolite ashflow tuff outcrops 17 km NE of the Henderson deposit, and is thought to be a co-genetic extrusive expression of the intrusive complex that formed the Henderson deposit [3, 4]. We use quartz-hosted melt inclusions and phenocryst mineral chemistry to place constraints on the pre-eruptive magmatic conditions (P, T, f_{O2}, f_{S2}), volatile contents (H_2O, CO_2, F, Cl, S), and metal concentrations to better understand the process of metal segregation within Climax-type ore-forming stocks.

Melt inclusions in the Hideaway Park rhyolite are comprised of glass, devitrified glass, crystals, and vapor. Crystals typically include quartz, alkali feldspar, magnetite, fluorite, zircon, and monazite. No molybdenite crystals have yet been identified within the crystallized inclusions, however some inclusions likely contain them because preliminary trace element analysis by LA-ICP-MS reveals several inclusions with anomalously high Mo concentrations (15-115 ppm) compared to the modal Mo concentration (10 ppm).

Accessory minerals in the Hideaway Park rhyolite include magnetite, ilmenite, biotite, zircon, and monazite. Preliminary magnetite-ilmenite pairs indicate crystallization at an f_{O2} of NNO+1.7 and an a_{TiO2} of 0.4 [6].

SEM-CL images of quartz phenocrysts show alternating bright-to-dark euhedral growth rims and resorbed zones. Ti concentrations in quartz measured by electron microprobe range from 39 to 66 ppm corresponding to crystallization temperatures [7] between 720-790°C (assuming a_{TiO2} = 0.4 and a preliminary pressure estimate of 2 kbar, equivalent to a shallow crustal magma reservoir at ~6 km depth). Quartz phenocrysts contain zircon inclusions, but pyrrhotite and molybdenite inclusions have not yet been found in any phenocrysts. Given that the Henderson deposit was formed in an extensional tectonic regime, carries a deep crustal/upper mantle signature (Mo/Rb = 0.013-0.040), and is only moderately oxidized, the magma is likely to be saturated with both molybdenite and pyrrhotite [5]. Assuming pyrrhotite and magnetite saturation at 750°C and an f_{O2} of NNO+1.7, the Hideaway Park rhyolite should saturate with molybdenite with 8 ppm Mo in the melt [5]. The modal Mo value of 10 ppm may be indicative of a slightly higher average crystallization temperature (+10-20°C) or a slightly higher prevailing f_{O2} of NNO+2.

[1] Wallace (1978) *B Soc Econ Geol* **73**, 325-368. [2] Seedorff (2004) *Econ Geol* **99**, 3-37. [3] Adams (2009) *GSA Annual Meeting* **93-7**. [4] Geissman (1992) *GSA B* **104**, 1031-1047. [5] Audétat (2011) *J Petrol* **52**, 891-904. [6] Ghiorso (2008) *Am J Sci* **308**, 957-1039. [7] Huang (in press) *Geochim Cosmochim Ac.*

Experimental solubility of silica in nano-pores

LIONEL MERCURY[1,*], MAJDA BOUZID[2,3], JEAN-MICHEL MATRAY[3]

[1] Institut des Sciences de la Terre d'Orléans, UMR 7327 Université d'Orléans/CNRS/BRGM, 1A rue de la Férollerie, 45071 Orléans Cedex, France. (* presenting author)

[2] IDES, UMR 8148 CNRS/Université Paris-Sud, bâtiment 504, 91405 Orsay cedex, France

[3] IRSN, DEI/SARG/LETS, BP 17, 92262 Fontenay-aux-Roses cedex, France

We used a pressure membrane extractor (Model 1020, Soil Moisture Equipment Corp.) to study the silica content at equilibrium with the decreasing pore sizes of amorphous silica. The principle is to extract the aqueous solution through a sequential process from the larger (micrometric) pores to the thinner (some nm) pores. Each extraction step is followed by an equilibration period.

The measurements confirmed earlier observations [1,2] that the concentration in dissolved silica decreases when the extraction pressure increases. The direct conclusion is that the silica solubility is pore-size dependent. These results are interpreted with the Young-Laplace relationship, at constant silica-solution surface tension, which means to attribute an elasto-capillary pressure to the solid.

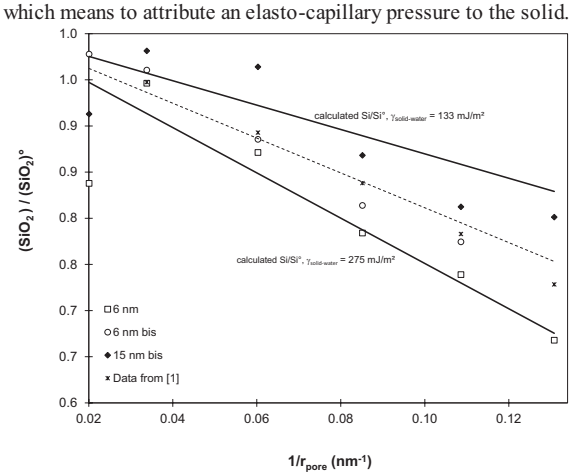

Figure 1: Decreasing silica solubility extracted from pores having decreasing radii.

The geological implication can be illustrated using a simple scheme (e.g. [3]), wherein aquifer compartments with changing pore sizes are successively put along a flowing line (in series). Depending on the modeling assumption (pore sizes, succession type, equilibrium state of the solution), this process can result in a preferential cementation of the thin or the large pores.

Our experiments demonstrate that the negative curvature of the solids has a geochemical feed-back on the solid-solution interactions, with a threshold size at around 0.1 µm.

[1] Dandurand J.-L., Mizele J., Schott J., Bourgeat F., Valles V., and Tardy Y. (1982) *Sci. Géol. Bull.* **35**, 71−79. [2] Emmanuel S. and Berkowitz B. (2007) *Geophys. Research Letters* **34**, L06404. [3] Mizele J., Dandurand J.-L., and Schott J. (1985) *Surf. Sci.* **162**, 830-837.

https://doi.org/10.1180/S0026461X00008434 Published online by Cambridge University Press

Carbon isotope diffusion in quartz & apatite and its relationship to biosignatures

SEBASTIAN T. MERGELSBERG[1,2]*, DANIELE J. CHERNIAK[1] AND E. BRUCE WATSON[1,2]

[1]Department of Earth & Environmental Sciences, Rensselaer Polytechnic Institute, Troy, NY 12180, USA (*correspondence: merges@rpi.edu)
[2]New York Center for Astrobiology, Rensselaer Polytechnic Institute, Troy, NY 12180, USA

While organisms live, their enzymatic reactions tend to accumulate certain isotopes of particular elements more than others. The most abundant element in any organism – carbon – is no exception and its lighter isotope is preferentially accumulated and incorporated, leading to a general $\delta^{13}C$ of around -40.00‰ to -10.00‰. When an organism dies, its remains may be taken up by a growing host mineral, such as quartz or apatite. This inclusion would "freeze" the ratio, creating a biosignature that is thought to be stable over time. Most of the evidence for the earliest life forms on Earth is found in the form of isotopic biosignatures. Durable and inert minerals such as apatite and quartz are potential hosts for these isotopic anomalies, but their ability to accommodate carbon is uncertain, especially in the case of quartz. Recently, the origin and validity of biosignatures have been questioned, suggesting abiotic origins of lower $\delta^{13}C$ isotope ratios [1] rather than being strictly derived from enzymatic action.

To investigate the potential of apatite and quartz to record and retain biosignatures, the solubility and diffusion of different carbon species in these minerals were investigated. Carbon is detectable in both apatite and quartz treated at high temperature and pressure in the presence of graphite, CO, CO_2, and CO_3^{2-}. Regardless of primary carbon species, however, the diffusion rates remained more or less constant. In addition, the values seemed to line up quite well with oxygen isotope diffusion data in quartz, when the diffusing species was CO_2 [2]. Based on these findings, it seems possible that the primary diffusion of carbon in these minerals depends greatly on the production of CO/CO_2 and thus the oxygen fugacity in the system.

Recent studies of isotope fractionation in the production of these gases from carbon indicate that CO production may lead to great distortion of the isotope ratio in the parent material. Evidence of such mechanisms would be suggesting a certain fallibility in interpretating isotopic ratios as biosignatures and recognizing proof of early life on earth.

[1] Horita, J (2005) *Chemical Geology* **218**(1-2), 171-186.
[2] Sharp, ZD, Giletti, BJ and Yoder, HS (1991) *Earth and Planetary Science Letters* **107**, 339-348.

The use of trace elements in Fe-oxides in deducing the fractionation history of a silicate magma: A LA-ICP-MS study

J. MERIC[1*], S.A.S.DARE[1], S.-J. BARNES[1] AND G. BEAUDOIN[2]

[1]Université du Québec à Chicoutimi, Québec, Canada, G7H 2B1
[2]Université Laval, Québec City, Québec, Canada, G1V 0A6

Knowledge of the trace element compositions of Fe-oxides will help to develop indicator minerals for exploration in addition to improving our understanding of the petrogenesis of the deposit. This study has characterized Fe-oxides, using laser ablation ICP-MS, from the upper part of Sept-Îles layered intrusion (Québec, Canada), which hosts an Fe-Ti-P deposit, rich in magnetite, ilmenite and apatite. The Fe-oxides record a sequence of fractional crystallization that evolves from the bottom to the top of the deposit. Trace elements in both magnetite and ilmenite vary as a function of their stratigraphic position (Fig. 1). Aluminium, Co, Cr, Mg and V decrease in the Fe-oxides up sequence whereas Ga, Ge, Hf, Mn, Mo, Nb, W, Sc, Sn, Ta, Zr and Zn increase. These geochemical variations appear to be controlled by the partition coefficients of compatible (e.g., V) and incompatible (e.g., Mo) elements into the co-crystallizing phases (olivine, plagioclase, magnetite, ilmenite and apatite) and in the magma during fractional crystallization of the silicate magma. Although magnetite and ilmenite show similar variations (Fig. 1), elements partition differently between the two. For example, Hf, Mg, Nb, Sc, Ta, Ti, W, and Zr are more abundant in ilmenite whereas Al, Co, Cr, Ga, Ge, Mo, Ni, Pb, Sn and V are more abundant in magnetite.

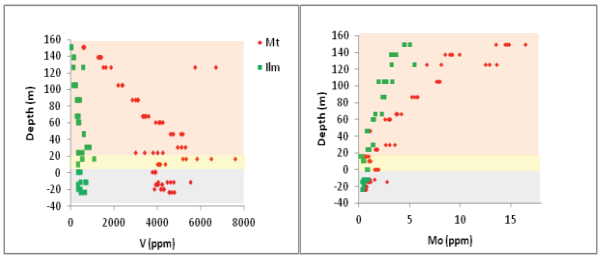

Figure 1: Variation of V and Mo in magnetite (Mt) and ilmenite (Ilm) as a function of depth in the Fe-Ti-P deposit of Sept-Îles. The layered sequence comprises, from bottom to top: magnetitite (grey), nelsonite (yellow) and nelsonitic-gabbro (orange).

This study shows that the chemical composition of Fe-oxides varies over a wide range within a single Fe-Ti-P deposit as a result of fractional crystallization. Thus it is necessary to understand the processes that control the chemical variability of the Fe-oxides in any given deposit in order to develop an effective exploration tool for the mining industry.

https://doi.org/10.1180/S0026461X00008434 Published online by Cambridge University Press

Improved representation of dust-nutrient deposition to the ocean for the Earth System Models

MESKHIDZE*, N. AND M. S. JOHNSON

North Carolina State University, Raleigh, USA,
*nmeskhidze@ncsu.edu, msjohns2@ncsu.edu

With the development of comprehensive Earth System Models (coupled climate-carbon models with land and ocean biogeochemistry) there is an increased need for improved representation of atmospheric fluxes of essential nutrients, i.e. iron (Fe), phosphorus (P), and nitrogen (N) to the surface oceans. These micronutrients have a controlling effect on marine ecosystem productivity and therefore can influence the global carbon cycle and climate. Today it is well established that models that consider interactive representation of aerosol-climate-carbon cycle do better job in predicting future climate. Since Fe at the dust source regions is thought to be primarily in an insoluble form with increasing bioavailability through the interaction of mineral particles with acidic trace gases, it is believed that anthropogenic activities may exert sizable influence on micronutrient fluxes to the ocean.

In this study the state-of-the-art dust-nutrient dissolution scheme has been implemented in the global 3-D chemistry transport model GEOS-Chem. The Fe-dissolution module of Meskhidze et al. (2005) [1] was updated to consider dust-mineralogy in different desert regions, Fe-organic acid (oxalate) interaction, the photoreductive dissolution of Fe containing minerals (hematite, goethite and aluminosilicates), and the redox cycling between relatively more soluble ferrous, Fe(II) and highly insoluble ferric, Fe(III) forms of iron. Dissolution of P containing minerals is carried out using acid-based chemistry [2], while nitrate production occurs through the deposition of gas phase nitric acid on mineral dust. Our calculations using dust-nutrient dissolution scheme show high temporal and spatial variability in nutrient deposition fluxes over the ocean. Preliminary results indicate (see Fig. 1) that simplified Fe dissolution schemes, with the prescribed amounts of soluble iron, are unable to capture the complex nature of micronutrient deposition to the surface ocean. Our study reveals that in order to properly account for the effects of anthropogenic activities on ocean biogeochemical cycles, next generation Earth System Models should consider implementation of more comprehensive modules for nutrient mobilization from mineral dust.

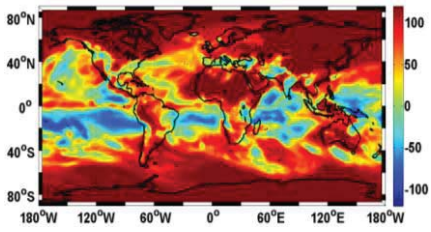

Figure 1: Percent difference (1% - model)/model in soluble Fe deposition during January 2009.

[1] Meskhidze *et al.* (2005) *J. Geophys. Res.* **110**, 1-23.
[2] Nenes *et al.* (2011) *Atmos. Chem. Phys*. **11**, 6265–6272.

Influence of zostera meadows on geochemistry and meiofauna of the sediment of a tidal lagoon (Arcachon Basin): new technical approaches

EDOUARD METZGER[1*], DIDIER JEZEQUEL[2], EMMANUELLE GESLIN[1], FLORIAN CESBRON[1], LAURIE CHARRIEAU[1], MARIE-LISE DELGARD[3], BRUNO DEFLANDRE[3], FRANS JORISSEN[1], AND PIERRE ANSCHUTZ[3]

[1]Univ. Angers, LPGN-BIAF, OSUNA, Angers, France,
edouard.metzger@univ-angers.fr (* presenting author)
[2]Univ. Paris Diderot, Sorbonne Paris Cité, IPGP, France
[3] Univ. Bordeaux, EPOC, UMR 5805, Talence, France

Tidal lagoons are by definition very dynamic environments. Sediments from such environments are very heterogeneous especially because of direct action of living organisms (i.e. bioturbation). The intertidal flats of Arcachon basin are highly covered by seagrass meadows of *Zostera noltii*. The seasonnal dynamics of these meadows enhance the lateral heterogeneity of the sediment by influencing sedimentation and organic matter accumulation. The present study shows preliminary results from very new techniques which were applied to understand the relationship between the root system of seagrass and meiofauna such as foraminifera. Those are able to respire oxygen and nitrate as well as bacteria. Our hypothesis is that roots bring oxygen to the anoxic sediment maybe generating nitrate-rich microenvironments. Since foraminifera are able to denitrify, we suppose that some specialized taxa can gather in such environments.

Methodologically, our goals are: i) to document at a submillimetric scale and in 2 dimensions relevant redox species (e.g. H_2S, Fe(II), PO_4, NO_3) in the pore waters using combined DGT-DET gels and in the solid phase by X microflurescence; ii) to describe foraminiferal species related to documented microenvironments using a highly discriminant staining technique for living specimen (i.e. CTG fluorogenic probe). The metabolism of anoxia tolerant taxa is quantified using microchambers equiped with microsensors.

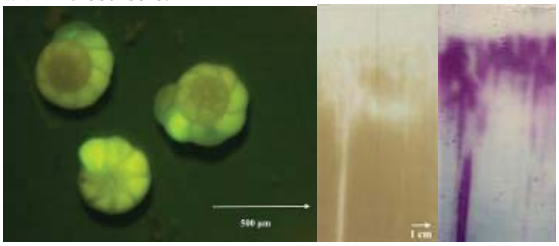

Figure 1: CTG Fluorescent foraminifera observed using an epifluorescence binocular (left) and 2D DET images (right): H_2S in brown, Fe(II) in pink and PO_4 in blue

2D DET gels show very heterogeneous redox layers which are very influenced by burrowing organisms and seagrass root webs. The first results seem to show that foraminferal densities are also influenced by the root web related to sedimentary redox interfaces. Anoxic sediment is dominated by *Eggerella* sp. which ability to denitrify is presently being assessed in the laboratory.

https://doi.org/10.1180/S0026461X00008434 Published online by Cambridge University Press

The source of Si in terrestrial plants: amorphous silica vs clay minerals

JEAN-DOMINIQUE MEUNIER*, MUHAMMAD RISWAN, JING SHA AND CATHERINE KELLER

Aix-Marseille Université, CNRS, CEREGE, Europôle Méditerranéen de l'Arbois, 13540 Aix-en-Provence, France, meunier@cerege.fr

Although Si is generally not considered as a nutrient for terrestrial plant, there are increasing evidences showing a beneficial effect of Si particularly under environmental stresses. Recent studies have suggested that land use and particularly agriculture can modify the Si cycle through a depletion of soil available Si. The extent of the perturbation, its impact on the plant cycle and food production is challenging and requires a better assessment of the biogeochemical acquisition of Si by plant. Si accumulated in plants originates from the dissolution of soil silicates. In soil solutions, Si is mostly present as the neutral molecule $Si(OH)_4$ (silicic acid). $Si(OH)_4$ is absorbed by the roots by a mechanism that is not fully understood. Both active and passive uptakes have been evidenced. In shoots, $Si(OH)_4$ is polymerized through the elimination of water by evaporation and, eventually, phytoliths (amorphous opaline silica particles) form. Steady state models show that plants absorb a significant fraction of dissolved Si that originates from litterfall decomposition i.e phytolith dissolution. Laboratory experiments show that phytoliths are a source of silica amongst the most soluble of the soil minerals at slightly acid to neutral pH. However, because the concentration of phytoliths in soil is generally low (below 10 mg/g), the contribution of clay minerals as a source of bioavailable silica is poorly documented but could be crucial in nutrient-limited soils where highly soluble primary silicates have been exhausted. A pot experiment using Durum wheat was conducted to assess the capacity of different silicate sources to release bioavailable silicon. For this purpose we used three types of sources: quartz (Q), clay (C, vermiculite) and amorphous silica (D, diatomite, as an analogue for phytoliths). Mixtures (Q + C and Q + D) were prepared in different proportions. Wheat plants were grown for 60 days in these mixtures. We found that the plants grown in the Q + D mixtures accumulated in their shoots about twice more silica (16-22 g kg^{-1}) than those grown in the Q + C mixtures (7-13 g kg^{-1}). These results show that, although soil amorphous silica (phytoliths) constitutes the most bioavailable Si pool for plants, the contribution of clay minerals should be more fully evaluated.

Nucleosynthesis and Isotopic Anomalies in FUN CAIs

BRADLEY S. MEYER[1*]

[1]Department of Physics and Astronomy, Clemson University, Clemson, SC, 29634-0978, USA, mbradle@clemson.edu (* presenting author)

Introduction

Millions of stars working over Galactic history generated the mix of isotopes present in the interstellar medium 4.6 billion years ago. Importantly, each of the roughly 280 different naturally-occurring isotopes in the Solar System had a different production route during this history, and present Solar System objects may contain a chemical memory of these varying histories [1]. Isotopes of Ca, Ti, Cr, Mo, and Ba in particular show anomalies in primitive Solar System samples, which thus give evidence of such chemical memory (e.g., [2]-[4]), and a key goal of isotope cosmochemistry in the coming years will be to understand what these anomalies are telling us about nucleosynthesis, Galactic chemical evolution, and Solar System formation.

Neutron-Rich Iron-Group Isotopes and FUN CAIs

The anomalies in the neutron-rich iron-group isotopes found in FUN (fractionation and unknown nuclear effects) CAIs (calcium-aluminum-rich inclusions) present a long-standing example of a likely cosmic-chemical memory effect [2]. FUN CAIs show correlated excesses and deficits in the isotopes ^{48}Ca, ^{50}Ti, and ^{54}Cr. All three of these isotopes have substantial production in a low-entropy environment [5], most likely the thermonuclear disruption of a dense white dwarf star [6]. At the same time, ^{50}Ti and ^{54}Cr, but not ^{48}Ca, have substantial production in massive stars (e.g., [7]). It is likely that the dust in the interstellar medium is highly anomalous. When this dust is incorporated into the Solar cloud, the Solar System will inherit these anomalies, and processing within the protoplanetary disk incorporates those anomalies in the FUN CAIs. In order to understand all of this history, we are making estimates of the siting of these isotopes in the interstellar dust along with their expected isotopic anomalies.

Tools for Understanding Nucleosynthesis and Galactic Chemical Evolution

Nucleosynthesis and chemical evolution are complex subjects that researchers best understand by running their own calculations. All of the computational tools we are developing to understand chemical memory in Solar System samples are open source and available for download (e.g., [8]), and we hope these tools will help others gain a better appreciation for nucleosynthesis and Solar System isotopic anomalies.

[1] Clayton (1978) *Moon and Planets* **19,** 109-137. [2] Lee, Papanastassiou, & Wasserburg (1978) *Astrophys. J. Lett.* **220,** L21-L25. [3] Niederer, Papanastassiou, & Wasserburg (1980) *Astrophys. J. Lett.* **240,** L73-L77. [4] Qin, Carlson, & Alexander (2011) *Geochim. Cosmochim. Acta* ***75,*** 7806-7828. [5] Meyer, Krishnan, & Clayton (1996) *Astrophys. J.* **462,** 825-838. [6] Woosley (1997) *Astrophys. J.* ***476,*** 801-810. [7] Meyer , The, & El Eid (1996) *Lunar and Planet. Sci.* **27,** 875. [8] http://sourceforge.net/projects/nucnet-tools/.

https://doi.org/10.1180/S0026461X00008434 Published online by Cambridge University Press

Fractionation of highly siderophile elements in the lower oceanic crust at ODP Site 735b, SW Indian Ridge

C. MEYER[1]*, H. BECKER[1]

[1]Freie Universität Berlin, Institut für Geologische Wissenschaften, chmeyer@zedat.fu-berlin.de

Compared to the mantle, abundances of some HSE in gabbroic oceanic crust and ocean ridge basalts are lower by a factor of 1000 or more, with Re, Au and Pd being more abundant than Os, Ir, Ru, or Rh. It has been suggested that the highly variable abundances may reflect sulfide fractionation processes in the deeper oceanic crust [1]. Samples from ODP site 735b, legs 118 and 176, a 1500 section of tectonically exhumed middle to lower oceanic crust were analyzed for abundances of HSE and Os isotopic composition. For reconnaissance study, 30 samples characterized by little alteration were selected to cover a range of lithologies, including olivine gabbro, gabbro, troctolitic gabbro, troctolite and disseminated oxide gabbro and oxide gabbro. 2.5 g of powder was digested in inverse aqua regia in a high pressure asher at 320°C. HSE separation and analyses methods follow those established in our lab. In a Re-Os isochron diagram, the most radiogenic samples (with large errors) plot along a 11 Ma reference line, in good agreement to the crustal age of site 735b [2]. Two troctolitic gabbros and 3 olivine gabbros with $^{187}Os/^{188}Os$ of 0.14 - 0.24 display a different linear trend that yields an apparent age of 244 ± 77 Ma with an initial $^{187}Os/^{188}Os$ of 0.126 ± 0.022. CI-chondrite normalized abundances of HSE in the lower crustal rocks cover a wide range (at the most extreme 10^{-3} to 10^{-7} x CI chondrite for Os), with relatively high abundances of all HSE in some troctolitic gabbros to more fractionated HSE patterns and much lower abundances of Os, Ir, Ru, Rh and Pt in other lithologies. Re is the least variable, with typical abundances in gabbros of 0.2 – 0.5 ppb, considerably lower than in most MORB. Au concentrations in most analyzed samples are typically <0.1 ppb. Au is more strongly depleted than Re compared to MORB [3] and most mantle rocks. This would imply that Au is more incompatible than Re during fractional crystallization, at least in this section of oceanic crust. From HSE abundance and ratio data, it appears that olivine gabbros behave as a coherent group, whereas troctolitic gabbros may reflect other processes. HSE abundances, Au/Ir, Pd/Ir and Os/Ir in "primitive" olivine gabbros reach values >100 and decrease substantially with decreasing Mg#, Cr, Ni and MgO. The progressive depletion of HSE in olivine gabbros may be related to fractional crystallization from progressively evolved basic melts. This process appears to result in a strong increase in Re/Os from olivine gabbro via gabbro to leuco gabbro and in a decrease of Au/Ir, Pd/Ir and Os/Ir. Consequently, while Re/Os in melts increase during fractional crystallization, Au/Ir, Pd/Ir and Os/Ir decrease. The evolution of troctolitic gabbros, increasing Au/Ir and Pd/Ir with decreasing Mg# and Cr, follows different trajectories and implies more complicated processes, presumably, hybridization of ultramafic cumulates or mantle tectonites by basic melts..

[1] Hertogen et al. (1980) *GCA* **44**, 2125 – 2143.
[2] Dick et al. (1991) *Proceedings of the ODP, Scientific Results* **118**, 439 – 538.
[3] Keays and Scott (1976) *Economic Geology* **71**, 705 – 718.

Control of copper enrichment in Lau Basin magmas by sulfide segregation and sulfur degassing

P.J. MICHAEL[1*], A. BÉZOS[2], C. LANGMUIR[3], S. ESCRIG[4]

[1]Dept. Geosciences, University of Tulsa, Tulsa, OK USA 74104 pjm@utulsa.edu (* presenting author)
[2]Lab. Planet et Geodynamique, Univ. de Nantes, Nantes, France, Antoine.Bezos@univ-nantes.fr
[3]Dept. Earth & Planet Sci, Harvard Univ, Cambridge, MA, USA 02138 langmuir@eps.harvard.edu
[4]École Polytech. Féd. Lausanne, Lausanne, CH-1015, Switzerland stephane.escrig@epfl.ch

Lau Basin magmas show how magma ascent, crystallization and degassing can lead to either enrichment or depletion of Cu (and other chalcophile elements) in differentiated magmas. In these magmas, S degassing is correlated with H_2O degassing. Dissolved S occurs almost entirely as sulfide (S^{2-}) in analyzed glasses.

Glasses from the northern part of Eastern Lau Spreading Center (ELSC), located in the backarc, far from the active Tofua arc, are similar to MORB. They have not degassed H_2O, and their dissolved S contents are high and correlated with Fe. They have not degassed much S but have segregated immiscible sulfide liquids which leads to a MORB-like trend of decreasing Cu with decreasing MgO. Further south, ELSC (and its continuation, Valu Fa Ridge:VFR) is shallower and only 35-60 km from Tofua arc. Its magmas include a greater subduction component, especially H_2O which has degassed. Low S contents show that they have also degassed variable amounts of S. Cu contents are slightly elevated compared to northern ELSC and MORB, and Cu decreases with decreasing MgO.

In contrast, the small seamounts located a few km from the ELSC-VFR axis have Cu contents that *increase* with decreasing MgO, and reach much higher values than ELSC-VFR. They have degassed large amounts of H_2O and almost all of their Sulfur. Most seamounts are more primitive than the nearby spreading axis. A few analyzed glasses from the nearby Tofua volcanic arc are similar to the seamounts in their behavior of S and Cu.

We propose that Cu contents in differentiated magmas are controlled by immiscible sulfide liquid segregation and S degassing. Like MORB, glasses from northern ELSC undergo sulfide segregation that depletes Cu from residual liquids, while very little S is lost by degassing. Magmas from southern ELSC and VFR start crystallizing at moderate depths (6-8 km) where they segregate some sulfide liquid, and lose Cu. They also undergo degassing of H_2O and S as they crystallize and ascend to shallower levels, limiting the amount of formation of sulfide liquids and its consequent Cu depletion. In contrast, seamount (and arc) magmas ascend rapidly to shallow levels and degas H_2O and S before they have a chance to segregate immiscible sulfide liquid. Cu remains in the silicate liquid and its concentration increases in differentiated magmas.

An alternative mechanism to account for high Cu in some magmas is that during larger extents of partial melting beneath the arc and seamounts (caused by high H_2O in the source), sulfide in the mantle source is exhausted, releasing all Cu into the melt. However, low Cu in primitive seamounts suggests elevated Cu results from differentiation, not melting.

https://doi.org/10.1180/S0026461X00008434 Published online by Cambridge University Press

Potentially hazardous trace elements in biomass burned in power plants

MAREK MICHALIK[1], RENATA GASEK[2], WANDA WILCZYŃSKA-MICHALIK[2]

[1]Institute of Geological Sciences, Jagiellonian University, Kraków, Poland, marek.michalik@uj.edu.pl (* presenting author)

[2] Institute of Geography, Pedagogical University, Kraków, Poland, rgasek@ap.krakow.pl, wmichali@up.krakow.pl

The study is based on eight samples of biomass (OTR- corn bran; SLON-1 and SLON-2 – sunflower; TRO – sawdust; OLI – olive residue; SLOM - straw; BUK – beech bark; PAL – palm kernels) used in power plants in southern Poland and ashes obtained in relatively low temperature (475°C). Results are compared with average trace element contents in coal and coal ash [1].

Fourteen elements were selected as components of major environmental concern (As, Cd, Co, Cr, Cu, Hg, Mn, Mo, Ni, Pb, Sb, Se, V, Zn). Average values for hard coal are exceeded in biomass only for four elements (Table 1). The concentration of trace elements in biomass ash can be very high and for eight elements significantly exceed average values determined for coal ash (Table 2). The results indicate that concentration of several trace elements in biomass used as fuel and in biomass ash could be dangerous for environment.

Element	Average for hard coal	Highest values for studied biomass samples
Cd	0.2	0.31(TRO)
Cu	16	25 (OLI); 23 (PAL)
Mn	71	333 (PAL); 126 (OTR); 88 (BUK)
Zn	28	79 (OTR); 46 (PAL)

Table 1. Highest values of trace elements in biomass samples exceeding average value for hard coal (in ppm)

Element	Average for coal ash	Highest values for studied biomass ash samples
Ag	590	5319 (TRO)
Cd	1.2	71 (TRO); 2.1 (OTR); 1.66 (SLON-2)
Cu	110	587 (TRO); 509 (PAL); 266 (SLON-2); 255 (SLON-1); 178 (OTR); 169 (OLI)
Mn	430	>10 000 (TRO); 7373 (PAL); 2148 (OTR); 1507 (BUK); 444 (SLOM)
Mo	14	14.7 (OTR)
Ni	37	49 (PAL); 38 (OLI)
Pb	55	69 (TRO)
Zn	170	1923 (TRO); 1485 (OTR); 1051 (PAL); 428 (BUK); 399 (SLON-2); 321(SLON-1)

Table 2. Highest values of trace elements in biomass ash samples exceeding average value for hard coal ash (in ppm)

[1] Ketris & Yudovich (2009) *International Journal of Coal Geology* **78**, 135-148.

Study was supported by NCN grant No. 0579/B/P01/2011/40.

Synchysite: Implications for Titanite Destabilisation and Differential REE, Y and Th Mobility in the Soultz Monzogranite

A. W. MIDDLETON[1*], H.-J. FÖRSTER[2], I. T. UYSAL[1] AND S. D. GOLDING[1]

[1]University of Queensland, Queensland 4072, Australia (*correspondence: alexander.middleton@uqconnect.edu.au)

[2]GeoForschungsZentrum, Potsdam, Germany

High heat-producing granitic rocks (HHPGs) are characterised by abnormally enriched values of radiogenic U, Th and K above upper continental crustal averages. In recent years, HHPGs have received considerable attention as they can be targeted for enhanced geothermal systems (EGS). The Soultz-sous-Forêts monzogranite is a notable example. With the exception of K, U and Th commonly occur with rare earth elements and yttrium (REE and Y, REY) in primary accessory phases [1]. Upon interaction with hydrothermal fluids, accessory phases such as titanite, may destabilise and form polymineralic metasomatic assemblages. Analysis of these metasomatic minerals is integral for understanding not only the chemistry of the hydrothermal fluid, but also the mobility of elements previously held in primary accessory phases. As such, this study focuses on the comparative EPMA of primary and metasomatic accessory phases to further the understanding of REE, Y and Th mobility in the Soultz monzogranite.

Petrographic studies show primary REY and Th-bearing titanites have been altered to anatase + calcite + quartz + synchysite-(Ce) [(Ce,Ca,Th)$(CO_3)_2$F] ± bastnaesite-(Ce) [(Ce,Th)(CO_3)F] or monazite-(Ce) [(Ce,Th)PO_4] + xenotime-(Y) [(Y)PO_4] ± thorite [$ThSiO_4$]. These observations represent the first documented citing of synchysite-(Ce) formation through titanite destabilisation. The purely fluorocarbonate-bearing assemblage is restricted to samples exhibiting minor selective alteration. Phosphate-bearing assemblages are, however, found in pervasively altered samples where primary apatite was significantly affected. Comparative mass balance studies of titanite, synchysite-(Ce) and monazite-(Ce) found $HREE_2O_3$, Y_2O_3 and ThO_2 levels to be relatively depleted in fluorocarbonate-bearing samples. Although ThO_2 levels were maintained in monazite-(Ce) relative to parent titanite, $HREE_2O_3$ and Y_2O_3 appeared lower due to the presence of xenotime.

Following the experimental work of Hunt and Kerrick [2], the ingress of CO_2-rich fluid was integral for titanite destabilisation. On the other hand, fluorine in synchysite was most likely sourced from proximal chloritised biotite. Following synchysite formation, excess FCO_3^- or HCO_3^- anions may have remained in solution and led to the significant mobilisation of HREE, Y and Th through complexation. Our study provides evidence for not only differential REE and Y mobility in the Soultz monzogranite, but also that Th, conventionally considered an immobile element, is mobilised under certain hydrothermal conditions.

[1] Bea (1996) *J Petrol* **37**, 521-552. [2] Hunt & Kerrick (1977) *Geochim Cosmochim Ac* **41**, 279-288

https://doi.org/10.1180/S0026461X00008434 Published online by Cambridge University Press

Modelling the vapour transport of Au, Ag, and Cu chlorides at high temperature based on new experimental data

ART. A. MIGDISOV[1*], N. HURTIG[1], AND A.E. WILLIAMS-JONES[1]

[1]McGill University, Earth & Planet. Sci., Montreal, QC, Canada (*correspondence: artas65@gmail.com)

The fact that water can significantly increase the gaseous transport of weakly volatile compounds has been long-known and is attributed to hydration, namely the formation of gaseous clusters involving H_2O molecules. However, laboratory experiments performed in simple H_2O-bearing systems have yielded concentrations of metals, e.g., Cu and Au, considerably lower than reported for vapour inclusions in many natural samples. Furthermore, calculations of the stability of known Cu- and Au-bearing gaseous clusters have shown that these clusters cannot explain the very high concentrations Cu and Au predicted for some vapour-dominated hydrothermal systems. Assuming that the source of this disagreement lies in the models that have been developed for the hydration process, we have re-visited the Au-HCl-H_2O, AgCl-HCl-H_2O, CuCl-HCl-H_2O, and $CuCl_2$-HCl-H_2O systems, and conducted additional experiments that allow us to more accurately determine the hydration numbers of metal-bearing gas clusters.

Our experiments involved determining the solubility of metal chlorides (or metals) in HCl-bearing water vapour at a variety of water vapour pressures and temperatures ranging from 300 to 450 °C. The experimental technique employed in this study is identical to that reported in our previous publications [1]. The data obtained from these experiments demonstrate that, in contrast to conclusions in our earlier publications, hydration numbers of metal-bearing clusters are not constant, but increase with increasing fugacity of water. This results in an exponential increase in the saturation concentrations of metals in water wapour at elevated pressures and temperatures.

We fitted our experimental data to a simplified model similar to that developed by Pitzer and Pabalan [2] for the solubility of NaCl in low-density fluids. The model accounts for a set of hydrated species of the common stoichiometry $MeCl(H_2O)_n$, where n ranges from 1 to 14. After independent treatment of each of the experimental isotherms, it was found that the Gibbs free energy of each of the modelled clusters varies linearly with the reciprocal absolute temperature (1/TK). This allows extrapolation of the data collected at 300 to 450 °C to much higher temperatures. The new model has been tested against the measurements of Simon et al. [3] for the solubility of Au and Ag at 1000 to 1400 bar and 800° and yield reasonable results. .In addition, the concentrations of Ag and Au (the experiments on Cu are still in progress) calculated for 500 °C show much closer approximation to those determined in natural fluid inclusions than in any previous models

[1] Archibald et al. (2001) *Geochim. Cosmochim. Acta*, 65, 4413
[2] Pitzer and Pabalan (1986) *Geochim. Cosmochim. Acta*, 50, 1445
[3] Simon et al. (2005) *Geochim. Cosmochim. Acta*, 69, 3321

The role of changing abstraction patterns in the contamination of a low-arsenic aquifer in Bangladesh

I. MIHAJLOV[1*], M. STUTE[1,2], B.C. BOSTICK[1], I. CHOUDHURY[3], K.M. AHMED[3] AND A. VAN GEEN[1]

[1]Lamont-Doherty Earth Observatory of Columbia University, Palisades, NY, USA, mihajlov@ldeo.columbia.edu (* presenting author)
[2]Barnard College, New York, USA
[3]Dhaka University, Dhaka, Bangladesh

The installation of deeper aquifer community wells has been one of the primary arsenic mitigation strategies in Bangladesh, a country where a large portion of shallow tubewell groundwaters exceed the WHO limit of 10 µg/L As. Shifting groundwater abstraction patterns, in particular the increased pumping from deeper aquifers, could potentially threaten this resource by vertical transport of As and organics between aquifers and across leaky confining units. While this scenario has been addressed by Bengal basin-wide models [1], hydrogeologic conditions across the basin are variable.

Our study focused on a site 25 km east of Dhaka where a community well was installed twice in a low-As aquifer separated from the shallow aquifer by >10m of silty clay, but As levels in both wells rose within <18 months. An increasing downward hydraulic gradient across clay units in the vicinity, as well as a lack of evidence of mechanical failures at the site, led us to suspect vertical leakage across the clay. Thus, a network of pumping and monitoring wells was established on the site to conduct pumping tests and continuously monitor hydraulic heads. Lithologs, sediment X-ray fluorescence (XRF) and chemical extraction profiles were collected during well installation, and groundwater was sampled for water chemistry, DIC ^{13}C and ^{14}C, ^{2}H, ^{18}O, ^{3}H, and noble gas analysis.

Lithologs and XRF profiles established that stratigraphy and sediment composition were laterally uniform. Pumping from long-screen wells in either aquifer did not induce measurable drawdown in the other, but the time plot of drawdown in the confined aquifer was characteristic of a leaky aquifer. Given the present downward hydraulic gradient of ~1m between the aquifers, continuous slow downward transport of As and/or organics across the clay may exist.

High-As groundwater is absent at the depth of the community well failures, but the upper ~10m of the aquifer (below the clay) is ^{3}H-dead and displayed high dissolved conc. of Fe, As, and NH_3. The well-advanced reduction in this stratum was accompanied by elevated Na, DOC, and DIC levels, and a lower pH. Depressed ^{14}C and heavy ^{13}C signature of the DIC there, along with low diss. [Ca], was characteristic of microbial consumption of old organic C (potentially leached from the clay with Na) and methanogenesis. Water level and ^{3}H data, however, also implied that a flow of recently recharged water exists below this upper portion of the aquifer, presumably due to pumping from a nearby factory. While the community wells probably failed due to vertical transport of As within the aquifer itself, it is presently unclear if the source of As and DOC in the upper part of the aquifer is from clay leakage or if that layer is a zone of low flow where resident organic C is currently consumed.

[1] Radloff et al. (2011) *Nature Geoscience* **4**, 793-798.

https://doi.org/10.1180/S0026461X00008434 Published online by Cambridge University Press

Late Miocene Central Anatolian surface uplift and orographic rainout from stable hydrogen and oxygen isotope records

TAMÁS MIKES[1,2]*, ANDREAS MULCH[1,2], FABIAN SCHEMMEL[2], DOMENICO COSENTINO[3], BORA ROJAY[4] AND ERKAN AYDAR[5]

[1] Goethe University, Institute of Geosciences, Frankfurt am Main, Germany, mikes@em.uni-frankfurt.de (* presenting author)
[2] Biodiversity and Climate Research Centre (BiK-F), Frankfurt am Main, Germany, andreas.mulch@senckenberg.de; fabian.schemmel@senckenberg.de
[3] Department of Geosciences, University Roma Tre, Rome, Italy, cosentin@uniroma3.it
[4] Middle East Technical University, Institute of Geological Engineering, Ankara, Turkey, brojay@metu.edu.tr
[5] Hacettepe University, Department of Geological Engineering, eaydar@hacettepe.edu.tr

A stable isotopic aproach to surface uplift history of the S margin of the Central Anatolian Plateau (CAP), the second largest orogenic plateau in the Alpine-Himalayan belt, is the focus of this work. Extending at average elevations of 1 km and bordered by the 2-3 km-high Tauride Mts to the S, Mediterranean mantle dynamics have been instrumental in governing regional surface uplift [1], yet with detailed temporal and spatial patterns of surface uplift remaining conjectural. For the first time, we apply a paleoaltimetric approach to the CAP by (1) looking at stable hydrogen and oxygen isotope ratios of continental deposits (such as paleosol and lacustrine carbonates and hydrated volcanic glasses), taking advantage of their recent, precise age calibration based on chrono- and biostratigraphy, and (2) providing a robust template of stable hydrogen and oxygen isotopes from modern surface waters on the CAP and across the Tauride Mts, against which the continental proxy data can be validated. We show that integrity of the modern meteoric water data nicely images the present-day topographic structure of the CAP and the Tauride Mts. with ca. -24 ‰/km and -3 ‰/km isotopic lapse rates for δD and $\delta^{18}O$, respectively. We then compare two sets of $\delta^{18}O$ data of fossil meteoric waters as recorded in proxy minerals from Upper Miocene to Quaternary deposits in front of the growing Tauride Mts and in its N rainshadow. The data reveal fairly uniform isoscapes at the S plateau margin until 6.3 Ma, with a major isotopic shift occurring between 8.2 and 5.5 Ma, with a $\Delta(\delta^{18}O_{windward\text{-}leeward})$ of 3.4 to 5.6 ‰. This difference corresponds to ca. 50 to 75% of that of the present-day altitude effect on isotope fractionation across the Taurides. Combined with stratigraphic evidence from margin-capping shallow-marine deposits of 8.4 to 8.1 Ma age [1], and with basin subsidence history at the Tauride front revealing a major clastic influx at 5.5 Ma [2], we conclude that 1000 to 1500 m of surface uplift occurred in less than 2.7 Ma, pointing to notably high uplift rates of 0.4 to 0.6 mm/yr for the Taurides in the Tortonian to Messinian. Our data compare well to short-term Quaternary uplift rates on incised river terraces [3].

[1] Cosentino et al. (2012) *GSA Bull.* **124**, 133-145.
[2] Cipollari et al. (accepted) *GSL, Spec Publ.*
[3] Schildgen et al. (2012) *EPSL* **317-318**, 85-95.

Evidence for distinct stages of magma evolution recorded in the composition of accessory phases and whole-rocks in silicic magmas

ANDREW MILES[1*], COLIN GRAHAM[1], MARTIN GILLESPIE[2], CHRIS HAWKESWORTH[3], RICHARD HINTON[1] AND EIMF[4]

[1]Grant Institute of GeoSciecnes, University of Edinburgh, Edinburgh, UK, Andrew.Miles@ed.ac.uk (* presenting author)
[2]British Geological Survey, Edinburgh, UK, mrg@bgs.ac.uk
[3]School of Geography and Geoscicences, University of St Andrews, St Andrews, UK, chris.hawkesworth@st-andrews.ac.uk
[4]Edinburgh Ion Microprobe Facility, University of Edinburgh, Edinburgh, UK, ionprobe@ed.ac.uk

Accessory minerals may contain a detailed record of the evolution of silicic magmas. Different stages of magma evolution are preserved in the trace element compositions of apatite inclusions and their host rocks in the normally zoned Criffell pluton, southern Scotland. Apatites in metaluminous outer zones define a trend of variable La (277 to 2677 ppm) and less variable Y (0 to 662 ppm) (trend 1), and lie on the same trend as that defined by the whole-rocks (WR) throughout the pluton. By contrast, apatites from peraluminous inner zones show variable Y (276 to 2677 ppm) and low La (<1079 ppm) (trend 2). WR isotopic and elemental trends have previously been modelled by assimilation and fractional crystallization (AFC) [1]. Zircon $\delta^{18}O$ varies by more than 3‰ between zones, but zircons within individual zones (within which apatite is included) are mostly within analytical error (0.4‰ 2σ) and thus show limited evidence for assimilation during crystallization of apatite and zircon. Crucially, in each metaluminous zone only the most primitive (La-rich) apatites crystallized from melts that closely match its WR composition. Both the WR and the most primitive apatites in each metaluminous zone therefore preserve liquidus compositions, and little open system fractionation occurred throughout the crystallization of accessory phases in these zones. Trend 2 reflects the effects of monazite crystallization in peraluminous zones that led to depletion of La in accessory phases that crystallized after monazite saturation. However, no WR compositions lie on trend 2, indicating that they were not influenced by monazite fractionation. Variations in apatite trace element concentrations within each zone therefore reflect the effects of *in situ* crystallization of allanite in metaluminous zones and monazite in peraluminous zones. The independently determined compositions of WR and apatites support numerical models for the existence of crustal hot zones in the formation of silicic magmas [2]. WR compositions are determined at depth while textural maturity and the compositions of accessory minerals such as apatite and zircon are largely determined at shallower depths by the presence or absence of other accessory phases during *in situ* crystallization of small melt batches.

[1] Stephens et al (1985) Contributions to Mineralogy and Petrology **89**, 226-238.
[2] Annen et al (2006) Journal of Petrology **47**, 505-539.

https://doi.org/10.1180/S0026461X00008434 Published online by Cambridge University Press

Picrite-driven cratonization: a perspective from the NeoArchean Ungava craton

DEJAN MILIDRAGOVIC[1]*, DON FRANCIS[1], AND DOMINIQUE WEIS[2]

[1]McGill University, Earth and Planetary Sciences, Montreal QC
dejan.milidragovic@mail.mcgill.ca (*presenting author)
don.francis@mcgill.ca

[2]Univ. British Columbia, EOS, PCIGR, Vancouver BC
dweis@eos.ubc.ca

Zoned ultramafic/mafic plutonic rocks emplaced at mid-crustal depths occur scattered across the disparate terranes of the Ungava craton of the Archean Superior Province. These Qullinaaraaluk (Q-suite) intrusions are coeval with the ca. 2.74-2.72 Ga pyroxene-bearing granitoids and high-K granitoids that dominate the Ungava craton [1], and their wide spread distribution suggests that mantle-derived magma may have played a key role in cratonization of the northern Superior province at the end of Archean. The Q-suite intrusions are small, irregularly-zoned cumulate bodies that include a spectrum of lithologies, ranging from olivine-dominated adcumulate-mesocumulate cores to more evolved gabbro(norites). Their parental magmas appear to have been H_2O-rich as indicated by the abundance of oikocrystic amphibole in the mesocumulate rocks. Electron microprobe analyses of olivine (Fo_{max} = 85) from peridotitic cores across the peninsula, suggest that the parental magmas were enriched in Fe relative to present day picritic magmas. Although the Q-suite intrusions intrude a number of isotopically distinct terranes (Boily et al. 2009), their trace element signatures are strikingly similar across the entire 300$^+$ km width of the Ungava Craton. Despite the Fe-rich composition of their parental magmas, Q-suite rocks are characterized by "calc-alkaline" trace element signatures, with relatively flat $(MREE/HREE)_{PM}$, elevated $(LREE/MREE)_{PM}$, and strong depletions in the HFSE, in particular Nb and Ta (Fig. 1). Furthermore, the pyroxene-bearing granitoids have compositions that span the gap between the coeval Q-suite and high-K grantoids, indicating intimate interaction between mantle-derived magmas and crustal melts. Geochemical, mineralogical and field data thus suggest that the craton-wide emplacement of Fe-rich picritic magma with "calc-alkaline" trace element affinities may have been responsible for the crustal melting episode that stabilized the Ungava craton at the end of the Archean.

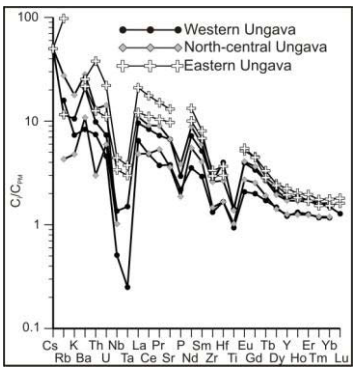

Figure 1: Primitive mantle-normalized trace element abundances in representative Q-suite websterites and wehrlites

[1] Maurice et al. (2009) Prec Res 168, 45-65. [2] Boily et al. (2009) Prec Res 168, 23-44.

Li and B isotopic composition of basement rocks, Dawn Lake area, Athabasca Basin, Saskatchewan

ROBERT MILLAR[1,3*], IRVINE R. ANNESLEY[2,3], ROBERTA L. RUDNICK[4], XIAOMING LIU[4], AND KEVIN ANSDELL[3]

[1]Saskatchewan Research Council, Saskatoon, Canada,
millar@src.sk.ca (* presenting author)

[2]JNR Resources, Saskatoon, Canada, jnrirvine@sasktel.net

[3]University of Saskatchewan, Saskatoon, Canada,
kevin.ansdell@usask.ca

[4]University of Maryland, College Park, United States of America,
rudnick@umd.edu, xliu1235@umd.edu

Recent literature suggests Li isotopic fractionation can occur during weathering, hydrothermal alteration, igneous and metamorphic processes [1], while the B isotopic signature preserved in refractory minerals, such as tourmaline, can aid in determining the source of fluids and P-T conditions during crystallization [2]. The objectives of this research are to determine the δ^7Li and δ^{11}B of relatively fresh to strongly altered basement lithologies in the vicinity of uranium mineralization in the Athabasca Basin (SK, Canada) and to evaluate if bulk isotopic analysis of Li and B can provide insight into the fluids that precipitated this mineralization with implications as a possible vectoring tool.

The largest high grade uranium deposits in the world are found within the Athabasca Basin of northern Saskatchewan, although the source of the uranium and the ultimate depositional mechanism are still highly debated. A suite of samples from the Dawn Lake area (12.9 M lbs @ 1.69% U_3O_8) include fresh to strongly altered graphitic pelitic gneiss and granitic pegmatites. Li concentrations from bulk chemical analysis range between 76 and 369 ppm, whereas B concentrations vary between 62 and 915 ppm. The elevated concentrations of Li and B are related to the presence of hydrothermal clay minerals and tourmaline, while the latter is also present as earlier formed magmatic and/or metamorphic minerals. The significant concentrations of Li and B were more then adequate for isotopic analysis, δ^7Li measured by MC-ICP-MS relative to L-SVEC display values between +4‰ and +13‰ for pelitic and graphitic pelitic gneiss and +6.2 to +18.6‰ for granitic pegmatites. The δ^{11}B measured by HR-ICP-MS relative to NBS951 was determined for granitic pegmatites to be in the range from -5.3 to 1.6 ‰, whereas the δ^{11}B for metasediments range from -0.8 to 3.5 ‰. There is no correlation between the elemental concentration of Li and B and the isotopic composition, but large variations in δ^7Li and δ^{11}B may be due to mixing of magmatic/metamorphic and hydrothermal components (eg., [3]) in these bulk samples. Further work will aim to unravel the cause of the isotopic variability and determine whether δ^7Li and δ^{11}B of bulk samples can aid in vectoring towards U mineralization.

[1] Teng et al. (2006) *American Mineralogist* 91, 1488-1498.[2] van Hinsberg, Henry and Marschall (2011) *The Canadian Mineralogist* **49,** 1-16. [3] Mercadier, Richard and Cathelineau, (2012) *Geology*, doi: 10.1130/G32509.1

https://doi.org/10.1180/S0026461X00008434 Published online by Cambridge University Press

Iodide and iodate interactions with clay minerals

ANDREW MILLER[1*], JESSICA KRUICHAK[1], HERNESTO TELLEZ[1], YIFENG WANG[1]

[1]Sandia National Laboratories, Albuquerque, USA, andmill@sandia.gov (* presenting author)

Abstract

Clay minerals are likely candidates to aid in waste isolation due to their low permeability, favorable swelling properties, and high cation sorption capacities. Iodine-129 is often the major driver of exposure risk from nuclear waste repositories at timescales >10,000 years. Therefore, understanding the geochemical cycling of iodine in clays is critical in developing defensible quantitative descriptions of nuclear waste disposal.

Anions are not typically considered to interact with most clays as it is assumed that the fixed negative charge of clays actively repels the dissoloved anion. This is corroborated by many batch studies, but diffusion experiments in compacted clays have shown iodide retardation relative to chloride. The reasons for this are unknown; however, several possible hypotheses include: redox transformation controls on sorption behavior, complex surface charge environments due to overlapping charge domains, and sorption to ancillary minerals or weathering products.

A series of clay minerals have been examined using several techniques to chracterize the surface charge environment of the clays, as well as to discern the potential for redox transformation and variable sorption behavior of different iodine oxidation states. Surface charge environments were examined through surface titrations and cation exchange capacity determination with methylene blue. Batch sorption experiments were completed with illite and palygorskite samples with both iodide and iodate. The batch experiments were completed at a range of pH values from 4-10, and at a constant ionic strength of 0.1M NaCl. Sorption experiments were performed at 20g/L solid:solution ratios to exacerbate sorption properties. The results show a range of sorption behaviors based on the clay mineral involved, as well as chemical conditions such as pH. Palygorskite has a higher sorption affinity for iodide compared to illite. There is evidence for some anion exhchange capacity on palygorskite; iodide sorption led to fluoride release. While not typically considered as a disposal medium, this result points to the use of alternative clay minerals to further isolate anionic components in nuclear waste.

Sandia National Laboratories is a multi-program laboratory managed and operated by Sandia Corporation, a wholly owned subsidiary of Lockheed Martin Corperation, for the U.S. Department of Energy's Nation Nuclear Security Administration under contract DE-AC04-94AL85000.

Peach Spring Tuff, Arizona-California-Nevada, USA: Generating an isolated supereruption

C.F. MILLER[1*], A.S. PAMUKCU[1], C.A. FERGUSON,[2] , T.L. CARLEY[1], G.A.R. GUALDA[1], J.L. WOODEN[3], W.C. MCINTOSH[4], M. LIDZBARSKI[5], J.S. MILLER[5], AND S.M. MCDOWELL[1]

[1]Vanderbilt Univ, Earth & Env Sciences, Nashville USA, calvin.miller@vanderbilt.edu (* presenting author)
[2]Arizona Geological Survey, Tucson USA, caf@email.arizona.edu
[3]Stanford U, Geol & Env Sci, Stanford USA, jwooden@stanford.edu
[4]NM Tech, Earth & Env Sci, Socorro USA mcintosh@nmt.edu
[5]San Jose State Univ, Geology, marshalidz@aol.com

The >700 km^3 Peach Spring Tuff (PST) is exposed through much of the western Colorado Plateau and the extended terrane of southern Nevada, SE California, and NW Arizona. Voluminous early volcanism and plutonism characterized the early Miocene history of this region, but large ignimbrites were rare and PST was almost an order of magnitude larger than any other erupted deposit.

Discovery of the source of PST (Silver Creek caldera, southern Black Mtns, AZ [Ferguson 2008]), a refined $^{40}Ar/^{39}Ar$ sanidine age (18.78±0.02 Ma, intracaldera & outflow [Ferguson et al in rev]), and detailed studies of pumice [Pamukcu et al in revision] shed light on the eruption and magma chamber evolution that preceded it. Phenocryst assemblages are consistently san>plag+bio+ hbl>qtz+px, +prominent sphene+zrc+all/chev. However, intracaldera pumice is distinct from distal outflow: richer in phenocrysts (~30-40%, showing strong resorption textures, vs ≤10%, mostly euhedral), trachyte rather than rhyolite (66-69 wt% SiO_2 vs 74-76 wt%). Thick proximal sections have common high-Si pumice, but in their upper parts crystal-rich, low-Si rhyolite-trachyte pumice is present. Core-rim zoning in zrc and sph in lower-Si pumice have compositions suggesting late growth from hotter less evolved melt (e.g. zrc rims to 50 ppm Ti: T >~900 C), in contrast to normally-zoned counterparts in high-Si pumice. Crystal size distributions and resorption textures also point to late heating in low-Si but not high-Si pumice.

We propose that trachyte in the caldera and proximal outflow represents basal cumulate mush within a zoned magma body, and that Si-rich outflow pumice was derived from higher levels. Only the lower portion was affected intensely by a pre-eruption heating event. Rhyolite-MELTS simulations suggest that the trachyte was melt-poor and ineruptible prior to reheating. The most plausible mechanism for heating and destabilizing of the mush, and perhaps for triggering eruption as well, is basal injection of hot, more mafic magma. Mafic injection is consistent with presence of sparse andesite magmatic enclaves within the ignimbrite and of a near-caldera basaltic andesite lava that was was emplaced just prior to the PST supereruption.

Regional uniqueness of the PST poses a conundrum: either super-quantities of eruptible magma or triggers to destabilize them must have been generally lacking, yet regional magma flux was high and interaction between felsic and mafic magma was ubiquitous.

https://doi.org/10.1180/S0026461X00008434 Published online by Cambridge University Press

Identification of the geographical origin of exotic wood species using $^{87}Sr/^{86}Sr$ isotope amount ratios

KERRI MILLER[1*], TYLER COPLEN[2], AND MICHAEL WIESER[1]

[1]Department of Physics and Astronomy, University of Calgary, 2500 University Drive NW, Calgary, AB, T2N 1N4, Canada, kamiller@ucalgary.ca (*presenting author)

[2]US Geological Survey, 12201 Sunrise Valley Drive, Reston, VA, 20192, USA

Rosewood species constitute only a small amount of the Dalbergia genus, however this wood is highly sought after for use in expensive cabinetry, flooring, musical instruments, and decorative objects. As a result, rosewood is an over-exploited resource and three species of the Dalbergia genus are currently controlled by the Convention on International Trade in Endangered Species of Wild Flora and Fauna (CITES). Because some rosewood species are threatened with extinction, trade for commercial purpose is illegal. Despite the efforts of international trade officials to prevent illegal export of this wood species, it is still common to hear about new investigations taking place. The goal of this study is to use strontium isotopic composition to aid in the determination of the geographical origin of wood samples in an effort to prevent the illegal trade of exotic timber.

The $^{87}Sr/^{86}Sr$ isotope amount ratios in 120 wood samples were analyzed by thermal ionization mass spectrometery. Samples were identified by species and country of origin. Isotope amount ratios varied from 0.704174 to 0.790101 with external repeatabilities typically on the order of 20 ppm (2s). Many regions exhibited a distinct isotopic fingerprint.

Magma dynamics beneath the ancient Mt. Etna: Clinopyroxene isotopic and thermobarometric constraints

S.A. MILLER[1*], M. MYERS[1], J.G. BRYCE[1], J. BLICHERT-TOFT[2]

[1]University of New Hampshire Earth Sciences, Durham, NH USA (*smiller@alumni.caltech.edu, correspondance)

[2]Ecole Normale Supérieure de Lyon, Lyon, France

Early stages of volcanism associated with Mount Etna, Europe's largest and most active volcano, began at ~0.5 Ma [1] and are now preserved around the perimeter of the modern-day edifice [2]. Magmatic products of these early centers, including those of ancient alkali centers active between ~200 and ~100 ka, generally have mantle-derived isotopic signatures consistent with contributions from both enriched and depleted source components. More recent Etna volcanics exhibit tell-tale signs of assimilation, but the degree to which this affected the early products is debated. Here we use an approach combining clinopyroxene (cpx) thermobarometry with an investigation of Pb, Hf and Nd mineral-whole rock isotopic (dis)equilibrium to constrain the depths at which magmas crystallized beneath these alkali centers and to gain insight into the nature of the source of ancient Etna lava isotopic signatures. The advantage of using these three isotopic systems together lies in coupling two slowly diffusing elements (Hf and Nd) with a more rapidly diffusing one (Pb), thereby providing the potential to infer any links between the timing of magma mixing (or assimilation) and eruption [cf. 3].

We have applied detailed single-cpx and cpx-liquid thermobarometric modeling based on back-calculated liquids from whole rock compositions [4] and the models of Putirka [5]. Crystals from two mafic flows from ancient alkali centers yield temperatures of 1140-1180 °C and 1090-1130 °C. Calculated initial crystallization depths lie at or below the Moho [6], consistent with polybaric fractionation and shoaling crystallization depths over time. Hf-Pb-Nd isotopic data from cpx phenocryst separates of ancient alkali lavas indicate no difference between whole rock and cpx values. Accordingly, we infer that the isotopic signatures of these magmas were locked in at pressures, at minimum, corresponding to early cpx crystallization. The lack of isotopic disequilibrium also suggests that the magmas were relatively well-mixed by the time they ascended to the depths at which cpx crystallization began.

Taken together, our results support the interpretation that observed isotopic systematicatics in ancient Etna lavas result from mixing between MORB-like and enriched mantle sources, with volatile-bearing peridotite and pyroxenite components preferentially melting to generate ancient alkaline volcanism. Shallower crystallization depths recorded in some phenocrysts correspond to the current location of a high-velocity body in the upper crystalline basement [7], indicating that this may be a long-lived feature.

[1] Gillot et al. (1994) *Acta Volcanol.* **5**, 81-87 [2] Tanguy et al. (1997) *JVGR*, **75**, 221-250 [3] Bryce and DePaolo (2004), *GCA* **68**, 4453-4468 [4] Armienti et al. (2007) *GSA Sp. Paper,* **418**, 265-276 [5] Putirka, (2008) *Rev. Mineral.,* **69**, 61-120 [6] Nicolich et al. (2000) *Tectonophys.*, **329**, 121-139 [7] Patanè et al. (2003) *Science*, **299**, 2061-2063.

https://doi.org/10.1180/S0026461X00008434 Published online by Cambridge University Press

Solubility of fish-produced high magnesium calcite

FRANK J. MILLERO[1]* AND RYAN WOOSLEY[1]

[1]Rosenstiel School of Marine and Atmospheric Science,University of Miami, Miami, FL 33149, USA, fmillero@rsmas.miami.edu (* presenting author)
rwoosley@rsmas.miami.edu

It has been suggested that the fish produced high 10 to 48% magnesium calcite can contribute to the input of calcite to the oceans. Fish produce this material as part of the physiological mechanisms for maintaining salt and water balance. In this paper, we report on the first measurements of the solubility of this high magnesium calcite in seawater. The solubility ($pK^*_{sp} = 5.89 \pm 0.09$) of this material is approximately two times higher than aragonite ($pK^*_{sp} = pK^*_{sp} = 6.18$) and similar to the high magnesium calcite generated on the Bahamas Banks ($pK^*_{sp} = 5.90$). The dissolution of this fish-produced $CaCO_3$ input to the oceans will be discussed. The higher solubility of this fish-produced carbonate to surface ocean waters may partially explain the increase in total alkalinity above the aragonite saturation horizon in the oceans. More recent work has shown that the production of this high-magnesium calcite may affect the total alkalinity of coral reefs.

Ultra-high precision Fe isotope analysis of eucrites and diogenites - Fe stable isotope fractionation during planetary differentiation?

M.-A. MILLET[1,*], J.A. BAKER[1], M. SCHILLER[2], J. CREECH[1], J. DALLAS[1], M. BIZZARRO[2]

[1]Victoria University of Wellington, Wellington, New Zealand, *marc-alban.millet@vuw.ac.nz

[2]Center for Star and Planet Formation, Natural History Museum of Denmark, University of Copenhagen, Denmark

The redox state of mantle sources, fractional crystallization of minerals with varying Fe^{3+}/Fe^{2+} ratios, diffusion processes and high pressure silicate-metal segregation have been identified as the main causes of Fe stable isotope variations in terrestrial magmatic rocks [1-4]. However, samples from smaller reduced planetary bodies show limited Fe stable isotope variations similar to chondritic values, which may indicate that Fe isotopes are not fractionated by any other processes during planetary formation and differentiation [1,5]. However, the limited number of samples measured and the precision of the available data preclude this as a definitive interpretation.

Diogenites and eucrites originate from the HED parent body, thought to be the asteroid 4-Vesta, and may have been generated during the crystallization of a nearly complete magma ocean within a few millions years of Solar System formation [6]. As such, they offer a unique opportunity to investigate the fractionation of Fe stable isotopes during planetary formation and differentiation, provided suitable analytical precision can be attained.

Here we present ultra-high precision Fe stable isotope measurements on a suite of diogenites and eucrites obtained by high-resolution MC-ICP-MS using a ^{57}Fe-^{58}Fe double spike to correct for instrumental mass bias (2 sd = 0.02‰, [7]) along with major and trace element concentrations and $\mu^{26}Mg^*$ values (for diogenites only, [6]). This dataset will allow us to investigate in detail the processes occuring during the development of planetary embryos and if Fe stable isotope fractionation occurred during differentiation of the HED parent body.

[1] Dauphas et al. (2009) *EPSL* **288**, 255-267. [2] Liu et al. (2010) *GCA* **74**, 6249-6262. [3] Teng et al. (2011) *EPSL* **308**, 317-324. [4] Polyakov (2009) *Nature* **323**, 912-914. [5] Weyer et al. (20050 *EPSL* **240**, 251-264. [6] Schiller et al. (2011) *ApJ lett* **740**, L22. [7] Millet et al. (2012) *Chem. Geol.* in press.

https://doi.org/10.1180/S0026461X00008434 Published online by Cambridge University Press

U-Th-Pb geochronology of meta-carbonatites and meta-alkaline rocks

LEO J. MILLONIG[1*], AXEL GERDES[2], LEE A. GROAT[1]

[1]Department of Earth and Ocean Sciences, University of British Columbia, Vancouver, Canada, lmillonig@eos.ubc.ca (*presenting author), lgroat@eos.ubc.ca
[2]Institut fuer Geowissenschaften, Goethe University Frankfurt, Germany, gerdes@em.uni-frankfurt.de

U-Pb and Th-Pb ages of zircons from eight meta-carbonatite and four meta-alkaline rock samples provide evidence for three distinct episodes of carbonatite and alkaline magmatism in the southern Canadian Cordillera spanning a period of ~460 Ma. The earliest (Neoproterozoic) event occurred at ~800-700 Ma and coincides with the postulated initial break-up of Rodinia. The second, previously undocumented, event of carbonatitic magmatism is constrained to the Late Cambrian to Early Ordovician at ~500-490 Ma and corresponds to a period of extensional tectonics that affected the western continental margin of North America from the Canadian Cordillera to the southwestern United States. The youngest and most prevalent period of alkaline igneous activity occurred in Late Devonian to Early Carboniferous times at ~360-340 Ma and also resulted from extensional tectonics. In addition, different episodes of amphibolites facies metamorphism subsequently affected the igneous rocks between ~170-50 Ma.

The magmatic emplacement ages, as well as the time of subsequent metamorphism, were further confirmed and constrained by U-Th-Pb dating of the accessory minerals baddeleyite, titanite, monazite, allanite, pyrochlore, and apatite (Figure 1).

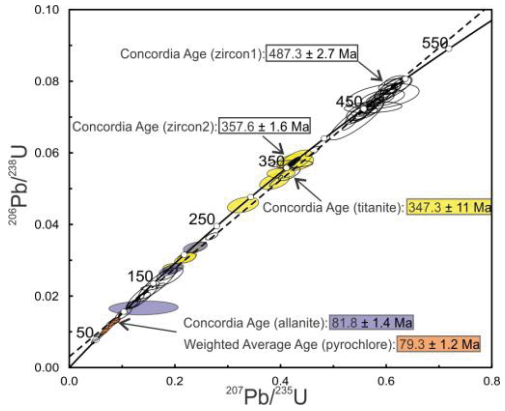

Figure 1: Concordia diagram of zircon, titanite, allanite and pyrochlore analyses from a meta-carbonatite sample (HwCr-001) defining a linear array with upper and lower intercepts of 436 and 71 Ma. However, this 'simple' linear array obscures the complex behavior of different isotope systems in the accessory phases and the complex geological history that led to the above pattern.

In combination, these datasets put new constraints on the timing of carbonatite and alkaline igneous activity and the evolution of (ancestral) North America's western continental margin from Neoproterozoic to Carboniferous times, and elucidate the applicability of different geochronometers and their sensitivity to amphibolites facies metamorphism in this set of unusual high-alkaline rocks.

Lithium isotopes systematics in Geothermal systems

ROMAIN MILLOT[1*], PHILIPPE NÉGREL[2], AND BERNARD SANJUAN[3]

[1]BRGM, Metrology Monitoring Analysis Department, Orléans, France, r.millot@brgm.fr (* presenting author)
[2] BRGM, Metrology Monitoring Analysis Department, Orléans, France, p.negrel@brgm.fr
[3] BRGM, Department of Geothermal Energy, Orléans, France, b.sanjuan@brgm.fr

Assessing the origin and behaviour of lithium and the distribution of Li isotopes in geothermal systems is of major importance in order to increase our knowledge of the lithium cycling in the Earth's crust. Lithium is a fluid-mobile element and due to the large relative mass difference between its two stable isotopes, it is subject to significant low and high temperature mass fractionation which provides key information on the nature of water/rock interaction processes. The main objective of the present work is to constrain the behaviour of Li and its isotopes in geothermal systems both for geothermal water samples representing deep circulation in the crust and by using an experimental approach.

The behaviour of Li and its isotopes (δ^7Li) have been characterized in geothermal systems located in volcanic island arc areas: Guadeloupe, Martinique islands [1] and in New Zealand [2]. Moreover, one particularly important aspect of this work was to establish the nature, extent and mechanism of Li isotope fractionation as a function of temperature during water/rock interaction.
And, we also report results of Li isotope exchange experiments during seawater/basalt interaction (from 25 to 250°C). These results confirm that Li isotopic exchange is strongly temperature dependent, and demonstrate the importance of Li isotopic fractionation during the formation of Li-bearing secondary minerals and allow us to determine the following empirical relationship between isotopic fractionation and temperature: $\Delta_{solution - solid} = 7847 / T - 8.093$.

This work shows that the fractionation of Li isotopes is dependent upon the extent of water/rock interaction in terms of intensity (i.e. temperature that control primary mineral dissolution and secondary mineral formation in geothermal systems). Altogether, this study highlights that the use of Li isotopic systematics is a powerful tool for characterizing the origin of geothermal waters as well as the nature of their reservoir rocks.

[1] Millot *et al.* (2010) *Geochim. Cosmochim. Acta* **74**, 1852-1871.
[2] Millot *et al.* (2012) *Applied Geochem.* doi:10.1016/j.apgeochem.2011.12.015

https://doi.org/10.1180/S0026461X00008434 Published online by Cambridge University Press

Modelling long term carbon and sulphur cycling over the Proterozoic

BENJAMIN MILLS[1*], ANDREW J. WATSON[1], COLIN GOLDBLATT[2] AND TIMOTHY M. LENTON[3]

[1]University of East Anglia, Norwich, UK.
b.mills@uea.ac.uk (* presenting author)
a.watson@uea.ac.uk
[2]University of Victoria, Victoria, British Columbia, Canada.
czg@uvic.ca
[3]University of Exeter, Exeter, UK.
t.m.lenton@exeter.ac.uk

Current zero-dimensional carbon and sulphur cycle models provide estimates of O_2 and CO_2 concentration over the Phanerozoic eon, and show a reasonable correlation with available proxys [1][2].

In this work we attempt to further extend these techniques to address conditions throughout the Proterozoic. As well as the controlling processes in the Phanerozoic, this model must include the interaction of the surface system with the mantle, the steady accumilation of carbon in the crust and the change in removal pathways as the continental area expands – processes which have been addressed individually in previous work [3][4][5].

Initial results show that the accumilation of crustal carbon in the combined model agrees well with previous modelling, and the predicted surface temperature and isotopic fractionation fall within reasonable limits. However, the baseline model does not predict the expected low oxygen concentration throughout the Proterozoic, instead predicting a stable concentration of around 0.2-0.5 PAL (present atmospheric level). The conclusion is that important processes may be missing.

Thankfully there are many candidates for the missing process (e.g. reduced organic burial due to limited nutrient delievey [6]), and we therefore use our model framework as an assesment tool: for each possibility, model predictions for O_2, CO_2, temperature and the isotopic fractionation of carbon and sulphur are compared to all available geochamical proxies, allowing the evaluation of these mechanisms, and hopefully the beginnings of a combined model for Earth evolution.

[1] Bergman *et al*. (2004) *Am. J. Sci.* **304,** 397-437. [2] Berner (2006) *Geochim. Cosmochim.* **70,** 5653-5664. [3] Hayes and Waldbauer (2006) *Phil. Trans. R. Soc. B* **361,** 931-950. [4] Bjerrum and Canfield (2004) *Geochem. Geophys. Geosyst.* **5,** Q08001. [5] Sleep and Zahnle (2001) *J. Geophys. Res.* **106,** 1373-1399. [6] Lenton and Watson (2004) *Geophys. Res. Lett.* **31,** L05202.

Concentration and transport of solutes drive by transpiration at the edge of a Prairie Pothole wetland

CHRISTOPHER T. MILLS*, MARTIN B. GOLDHABER, CRAIG A. STRICKER

United States Geological Survey, Denver, CO, 80225, USA
*presenting author (cmills@usgs.gov)

The Prairie Potholes region (~715,000 km^2) extends from Alberta, Canada to Iowa, USA. Retreat of Pleistocene glaciers left millions of pothole-like depressions that are internally drained. Topographically low, groundwater discharge wetlands tend to be saline (often Ca-Mg-SO_4-HCO_3) due to reaction of groundwater with glacial till rich in pyrite, gypsum, and calcite. However, several other processes influence discharge wetland chemistry, including plant transpiration at the wetland edge. This process can concentrate solutes and change hydrologic gradients at the wetland margin causing it to alternate between a source and sink of water and solutes to the wetland. We used $\delta^{18}O_{H2O}$, $\delta^{2}H_{H2O}$, and $\delta^{34}S_{SO4}$ values of groundwater and wetland water to investigate this process at the edge of wetland P1 in the Cottonwood Lake study area near Jamestown, North Dakota (USA).

Solutes (including SO_4) were least concentrated in wetland P1 water and deep (several meters below ground surface) groundwater upgradient of P1. Solutes were more concentrated in mid-depth (150 cm) to shallow (60 to 90 cm) groundwater at the edge of the wetland due to plant transpiration. Transpiration did not affect $\delta^{18}O_{H2O}$/ $\delta^{2}H_{H2O}$ values of mid-depth groundwater samples which were similar to deep, upgradient groundwater and fell on the meteoric water line ($\delta^{18}O_{H2O}$ from -14.6 to -12.0‰). Deep and mid-depth groundwater samples also shared similar $\delta^{34}S_{SO4}$ values (-18.2 to -15.1‰). Water from P1 fell below the meteoric water line ($\delta^{18}O_{H2O}$=-4.6‰) and had more positive $\delta^{34}S_{SO4}$ values (-4.2‰).

Shallow groundwater from the wetland edge had $\delta^{18}O_{H2O}$/ $\delta^{2}H_{H2O}$ and $\delta^{34}S_{SO4}$ values that were intermediate between deeper groundwater and wetland water. A plot of $\delta^{34}S_{SO4}$ versus the deuterium offset showed shallow groundwater to be a mixture of deeper groundwater and wetland water. Samples taken at different times of day located differently along the mixing line indicating dynamic mixing. Samples collected earlier in the day showed a smaller contribution of wetland water than samples collected later in the day. This may be a result of a diurnal cycle of the hydrological gradient at the wetland edge due to plant transpiration. This study clearly demonstrated the use of natural abundance isotope systems for investigating this hydrochemical process and the potential impact of plant physiology on wetland geochemistry.

https://doi.org/10.1180/S0026461X00008434 Published online by Cambridge University Press

Current Status of Phosphate (U-Th)/He Thermochronology of Meteorites

KYOUNGWON MIN[1*], SEUNG RYEOL LEE[2]

[1]University of Florida, Department of Geological Sciences, Gainesville, USA, kmin@ufl.edu (* presenting author)
[2]Korea Institute of Geoscience & Mineral Resources, Daejeon, Korea, leesr@kigam.re.kr

Traditional whole-rock (U-Th)/He methods applied to meteorites commonly yield apparently younger ages than expected from other thermochronologic tools, suggesting that (U-Th)/He systems are disturbed by thermal event(s) after the primary cooling. However, recent investigations applied to phosphates at a grain scale have revealed that some of the phosphate (merrillite, apatite) grains retain their pristine (U-Th)/He ages, allowing for determination of the temporal and temperature conditions that their parent bodies experienced during the primary cooling or shock events. In this contribution, we aim to explain the current status of the (U-Th)/He methods applied to extraterrestrial phosphates.

For unshocked meteorites, the single-grain (U-Th)/He methods provide a unique way to determine absolute ages when the meteorites have passed through temperatures below ~200 °C. Recent stepped heating experiments indicate that the closure temperatures of merrillite and chlorapatite are generally in the range of 85-145 °C and 7-108 °C, respectively, for a wide range of cooling rates (0.1– 100 °C/Ma) and at a diffusion domain radius of 50 μm. Two examples of the single-grain (U-Th)/He thermochronometry used to constrain low T thermal histories are for the Acapulco and St. Séverin meteorites whose pristine ages are well consistent with the medium-to-high T cooling curves. For shocked meteorites, the phosphate (U-Th)/He ages can provide crucial information regarding shock temperature conditions. Due to the high He diffusivity in phosphates, the transient shock event causes significant fractional loss of He (f_{He}), which can be utilized for thermal modeling and peak T estimation. Because most of the phosphate crystals are severely fractured, most likely during the shock event, diffusion domains are smaller than crystals; therefore, requiring detailed petrographic examination and image analysis of phosphate grains for modeling. This approach has been applied to the Los Angeles, ALHA84001, Zagami and EETA79001 Martian meteorites. Some of the results from this approach indicate bias from the peak T estimated from traditional shock recovery experiments. (U-Th)/He study of Zagami indicates relatively high peak T (> 400 °C); whereas, shock recovery experiments yield minor shock conditions (post-shock T ~ 60 °C). It is unclear what causes such a large discrepancy. In order to improve phosphate (U-Th)/He methods, the following issues need to be thoroughly addressed. First, because the morphology-based α recoil correction is essentially impossible for meteoritic samples, an alternative way of avoiding this correction has been suggested. Although there is a tendency that large grains with other phases attached yield more pristine ages without α recoil correction, there are some exceptional cases that are not fully understood. Second, the He diffusion properties in meteoritic apatite seem to show relatively large sample-to-sample variations, rendering additional efforts to constrain the diffusion properties for various meteoritic phosphates.

The evolution of clay minerals and rift structure in Zhanhua Depression, China

Zhao Ming[1*], Ji Junfeng[2], Chen Xiaoming[3], Wu Changzhi[4], Wu Bing[5] and Pan Yuguan[6]

[1]Nanjing University, China, Earth Sciences and Engineering, zming412@nju.edu.cn
[2]Nanjing University, China, Earth Sciences and Engineering, jijunfeng@nju.edu.cn
[3]Nanjing University, China, Earth Sciences and Engineering, xmchen@nju.edu.cn
[4]Nanjing University, China, Earth Sciences and Engineering, jcwu@nju.edu.cn
[5]Nanjing University, China, Earth Sciences and Engineering, guojichun2006@yahoo.com.cn
[6]Nanjing University, China, Earth Sciences and Engineering, yuguan.pan@gmail.com

Introduction, Results and Conclusion

Zhanhua Depression is located in Bohai Bay Basin, China. The depression has an area of about 3800km^2. It is a major oil and gas exploring district in the basin.

The study on diagenesis of clay minerals in Zhanhua Depression shows that the disordered mixed-illite/smectite (R_0I/S) and kaolinite in the Neogene were formed at the burial depths <2000m during the post-rift in Zhanhua Depression, while the appearance of the ordered mixed-illite/smectite ($R_{\geq 1}$I/S) in the Paleogene at the burial depths >2000m and the disappearance of kaolinite at the same depths were symbolized as the syn-rift in the depression. This regularity is referred to the burial depths, which are controlled by the paleotemperatures in the evolution of the clay minerals.

By using the chlorite geothermometer [1, 2, 3], the forming temperature of chlorites during the rift period in the Paleogene is calculated as 135-180℃ in Zhanhua Depression. The relationship between the chlorite diagenetic temperature and its burial depth indicates that the paleogeothermal gradient is about 38℃/km in the Paleogene in Zhanhua Depression. It is higher than the present geotemperature (34.5-32℃/km [4]). This phenomenon was attributed to the evolution of the structural dynamics in the rifted basin [5, 6].

Acknowledgements: This work is supported by the National Natural Science Foundation of China (Project number 40772027, 41172040). The authors would like to thank the help from the session convenors of the Goldschmidt 2012 Conference.

[1] Battaglia (1999) *Clay and Clay Minerals,* **47**, 54-63. [2] Nieto (1997) *Europe Journal of Mineral,* **9**, 829-841. [3] Rausell-Colom, Wiewiora (1991) *American Mineralogist,* **76**, 1373-1379. [4] Gong, Wang, Liu, et al (2003) *Sci China Ser D-Earth Sci*, **33**, 384-391.[5] Xie, Jiao, Tang, et al (2003) *AAPG Bull,* **87**, 99-119. [6] Zhao, Chen, Ji, et al (2006) *Acta Petrol Sin (in Chinese),* **22**, 2195-2204

https://doi.org/10.1180/S0026461X00008434 Published online by Cambridge University Press

Hydrocarbon adsorption on Carbonate and Silica surfaces: a First Principles study with van der Waals interactions

VAGNER A. RIGO[1] AND CAETANO R. MIRANDA[1*],

[1]Universidade Federal do ABC (UFABC), Santo Andre-SP, Brazil, caetano.miranda@ufabc.edu.br (* presenting author)

We study the adsorption of hydrocarbon molecules on carbonate minerals and silica surfaces by means of first-principles calculations based on Density Functional Theory (DFT) with and without van der Waals (vdW) corrections. The inclusion of vdW corrections in ab-initio methods can improve the description of these systems particularly, the long range weak dipole-dipole interaction as well as provide a fully electronic description for the interface of hydrocarbon molecules and mineral surfaces. To take into account the vdW dispersion forces, we used the DFT with the Dispersion-Corrected Atom-Centered Potentials model (DCACP) [1] Energetic, electronic, structural and kinetic properties have been determined for the adsorption of the representative hydrocarbons (benzene, anthracene, naphthalene, toluene, heptane and hexane) on calcite ($CaCO_3$) and dolomite [$CaMg(CO_3)_2$] (10-14) and quartz (SiO_2) surfaces. Our results suggest that Ca sites are the most energetically favorable for hydrocarbon adsorption on both carbonate systems. The calculations also indicate a weak interaction between the hydrocarbon with the bare silica surface for all hydrocarbons studied. The vdW corrections strengthen the hydrocarbon-surface bond with a corresponding reduction in the bond distance between the benzene and the surfaces. The inclusion of London dispersion forces to benzene results in an increase of 70% in the surface-molecule energy interaction. The energy barrier, for the displacement of the hydrocarbons along the calcite and quartz SiO_2 surfaces were determined using the Nudged Elastic Band method, and adsorption energies for the most stable sites show the same order of magnitude. The highest energy barriers associated with the hydrocarbon displacements on the surfaces are of the same order of the adsorption energies for the most stable sites. By taking into account the vdW interactions within the energy barriers in complement to adsorption energies in a model for hydrocarbons/mineral-rocks interaction can give us a more realistic description to the hydrocarbon carbonate/silicate interactions.

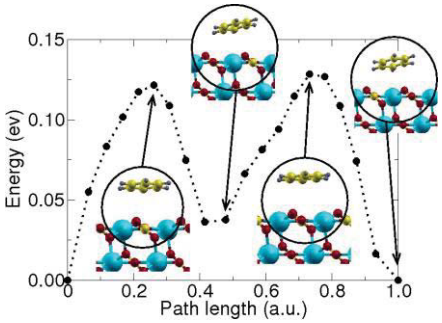

Figure1 - Energy barriers for benzene displacement along [48-1] direction for calcite (10-14) surface

[1] Lin et al. (2007) *Phys. Rev. B* **75**, 205131

Litho-, chrono- and S-MIF-chemo-stratigraphy of late Archean Dharwar Supergroup, south India

KAORU MISHIMA[1]*, RIE YAMAZAKI[2], M. SATISH-KUMAR[2], TOMOKAZU HOKADA[3], YUICHIRO UENO[1]

[1]Department of Earth & Planetary Sciences, Tokyo Institute of Technology, Tokyo, Japan. mishima.k.ab@m.titech.ac.jp
[2]Institute of Geosciences, Shizuoka University, Shizuoka, Japan
[3]National Institute of Polar Research, Tachikawa, Tokyo, Japan

Earth's tectonic and climatic systems may have fundamentaly changed through the late Archean period, which is characterized by major deposition of banded iron formation (BIF) and appearance of stromatolite reef along continental margins. Also, mass-independent fractionation of sulfur isotopes (S-MIF) demonstrated that Earth's atmosphere and ocean were virtually oxygen-free before 2.3 Ga [1]. In the late Archean, the S-MIF signature changed dramatically: minimam $\Delta^{33}S$ at around 2.9 Ga, subsequent large $\Delta^{33}S$ variation culminated at 2.5 Ga and its sudden drop at the end of Archean. These changes may reflect perturbation of atmospheric chemistry. However, almost the S-MIF record so far came from Pilbara and Kaapvaal cratons, that may have been a single continent (Vaalbara) at that time [2], and thus the observed S-MIF may possibly reflect local environment. It is important to test the "globalism" of the S-MIF signature for tracing the atmospheric evolution.

We studied late Archean volcano-sedimentary sequence of the Dharwar Supergroup, distributed in the Chitradurga schist belt, western Dharwar craton. Our new field mapping and zircon U-Pb dating allows us to reconstruct detailed lithostratigraphy. The lower unit (post-3.0 Ga) consists of basal conglomerate, stromatolitic carbonate, silici-clastics with diamictite, chert/BIF and pillowed basalt in assending order, all of which are older than 2676 Ma magmatic zircon ages from dacite dyke intruded into the topmost pillowed basalt. The upper unit unconformably overlies the pillow lava, and consists of conglomerate/sandstone with ~ 2600 Ma detrital zircons, komatiite lava, BIF and silici-clastic sequence with mafic volcanics. Sulfur isotope analysis of extracted sulfide of these sedimentary rocks show a clear $\Delta^{33}S$-$\Delta^{36}S$ correlation with a $\Delta^{36}S/\Delta^{33}S$ slope of -0.98. This trend is similar to those reported from Pilbara-Kaapvaal equivalents, thus could be a global signature, whereas $\delta^{34}S$-$\Delta^{33}S$ relation from each stratigraphic level shows somewhat different trend, possibly reflecting local environment and/or postdepositional overprint.

[1] Farquhar (2000) *Science,* **289,**756-758. [2] de Kock et al. (2009) *Precambrian Res.* **174**, 145-154.

https://doi.org/10.1180/S0026461X00008434 Published online by Cambridge University Press

Global oxygen isotope survey of lithospheric mantle: Implications for the evolution of cratonic roots

A. MIŠKOVIĆ[1]*, R.B. ICKERT[2], D.G. PEARSON[2], R. A. STERN[2], M. KOPYLOVA[3] AND B. KJARSGAARD[4]

[1]Northwest Territories Geoscience Office, Yellowknife, Canada, amiskovic@eos.ubc.ca (* presenting author)
[2]CCIM - Earth & Atmospheric Sciences, University of Alberta, Edmonton, Canada
[3]Earth & Ocean Sciences, University of British Columbia, Vancouver, Canada
[4]Geological Survey of Canada, Ottawa, Canada

The sub-continental lithospheric mantle (SCLM) forms the roots to the earliest crust and represents the most ancient mantle domain on Earth. Hundreds of oxygen isotope data have been reported for various mantle domains in the past three decades, yet the full geodynamic significance of these data is largely unappreciated. When coupled to the major element systematics, oxygen isotopes have the potential to illuminate the longstanding conundrum of the origin of highly depleted lithospheric roots beneath the Archean crust given that the current debate on their genesis is centred on quantifying the relative contributions of mantle plumes (asthenospheric source) and subduction zone processes (lithospheric source).

We present isotope analyses for 61 grains of olivines extracted from peridotite xenoliths entrained by kimberlites and pericratonic basalts worldwide; the most extensive high-precision *in situ* $\delta^{18}O$ database to date. Olivines analysed by multi-collector SIMS in this study were collected at: Paleogene to Jurassic Diavik and Jericho kimberlites (Slave Province), Cretaceous Somerset Island kimberlites (Rae Craton), Late Neoproterozoic kimberlites of Western Greenland (North American Craton), Middle Cretaceous to Late Mesoproterozoic Kimberly, Finsch, Letseng-la-Terae and Premier kimberlites (Kaapvaal Craton), Early Carboniferous Udachnaya pipe (Siberian Platform), and Miocene Vitim alkaline basalts.

The SCLM $\delta^{18}O$ data are normally distributed about the mean value of 5.30 ‰ (±0.22; 2σ) and largely corroborate previous upper mantle compilations [1]. There is no correlation between $\delta^{18}O$ and major or trace element chemistry, rhenium-depletion ages or equilibrium pressure-temperature conditions from which the mantle xenoliths were derived. Based on the new data we find no statistical difference between the oxygen isotope composition of cratonic peridotites and modern MORB-source mantle. These observations rule out an origin for SCLM via subcretion of serpentinised oceanic lithosphere [2]. However, we cannot discriminate between the subduction of relatively unaltered oceanic lithospheric mantle versus a plume origin. Furthermore, the overlap of the SCLM data with the mean global δ18O value of MORBs of 5.17‰ (±0.21; 2σ) has important implications for the long-term relationship between the convecting asthenospheric mantle and refractory cratonic roots.

[1] Mattey, D., Lowry, D, and Macpherson, C. (1994) *Oxygen isotope composition of mantle peridotite*. **EPSL 128**, 231-241.
[2] Schulze, D. (1986) *Calcium anomalies in the mantle and a subducted metaserpentinite origin for diamonds*. **Nature 319**, 483-485.
[3] Canil, D. and Lee, C.-T. A. (2009) *Were deep cratonic mantle roots hydrated in Archean oceans?* **Geology 37**, 667-670.

Improved Analytical Method for Determination of B Isotopes by Magnetic Sector ICP-MS

SAMBUDDHA MISRA[1*], JOANNA KERR[1], MERVYN GREAVES[1], HENRY ELDERFIELD[1]

[1]University of Cambridge; Dept. of Earth Sciences; Cambridge, UK (*presenting author: sm929@cam.ac.uk)

The boron isotopic composition of seawater, as recorded by foraminifera, can be used as a tracer of past variations in atmospheric pCO_2 [1, 2]. However, widespread application of B isotopes in geochemical studies is limited by the large relative mass requirement for high precision measurements, large memory effect, high procedural blanks, artificial fractionation induced by matrix purification methods, and low matrix tolerance [3]. We present an improved method for B istope ratio ($\delta^{11}B$) determination with low mass consumption (5 to 10 ng-B per quintuplicate analyses), high precision (± 0.5‰, 2σ), low blanks (< 9 pg-B/ml), and high matrix tolerance using Element XR® Single Collector ICP-MS (***figure)***. The present ICP-MS method is optimised for analysis of < 0.5 mg foraminifera samples.

Preliminary analyses of B standards following standard – sample bracketing technique gave external precision (quintuplicate) of ± 0.50‰ independent of analyte concentration (4 ppb – 10 ppb). Moreover, this new ICP-MS method has relatively large tolerance for Na, Mg, and Ca – the dominant matrix elements in foraminiferal calcite and provides an improved methodology to investigate B isotopic variations of planktonic and benthic foraminifera samples over geologic timescales.

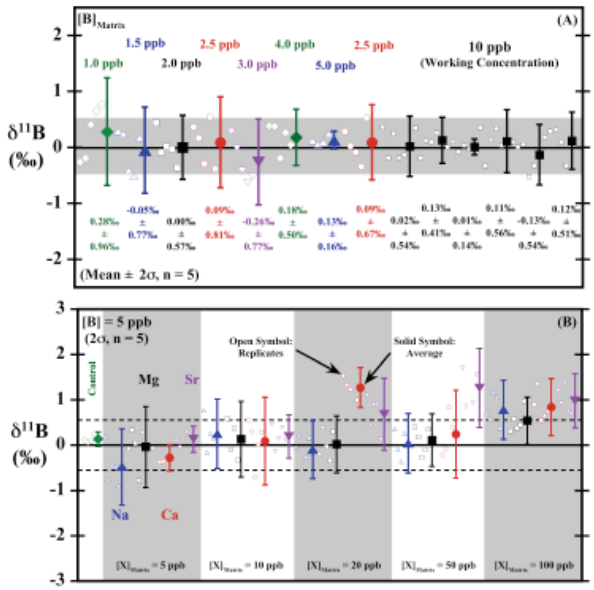

Figure: Results of **(A)** Boron concentration experiment, and **(B)** matrix experiment. All samples analysed following standard – sample bracketing technique. Analyses of sample in quintuplicates.

[1] Pearson and Palmer (2000) *Nature.* **406**, 695-699.
[2] Hemming & Honisch (2007) *Proxies in late Cenozoic paleoceanography*, **1 (17)**. 717-734
[3] Aggarwal et al., (2003) *Chemical Geology* **199,** 331-342

https://doi.org/10.1180/S0026461X00008434 Published online by Cambridge University Press

Potential of Microbiologically Induced Mineralisation to Increase Geologic CO_2 Storage Security

ANDREW C. MITCHELL[1]*, ADRIENNE J. PHILLIPS[2], ELLEN LAUCHNOR[2], JAMES CONNOLLY[2], LOGAN SCHULTZ[2], ROBIN GERLACH[2] AND ALFRED B CUNNINGHAM[2].

[1]Institute of Geography and Earth Sciences, Aberystwyth University, Aberystwyth, UK, nem@aber.ac.uk (* presenting author)

[2]Center for Biofilm Engineering, Montana State University, Bozeman, USA,

During the operation of Geologic Carbon Capture and Storage (CCS) and the injection of supercritical CO_2 into underground formations, microbe-rock-fluid interactions occur. These interactions may be important for controlling the ultimate fate of the injected CO_2, and may also be manipulated to enhance the storage of the CO_2, via mineral-trapping, solubility trapping, formation trapping, and leakage reduction.

We have demonstrated that engineered microbial biofilms are capable of enhancing formation, mineral, and solubility trapping in carbon sequestration-relevant formation materials. Batch and flow experiments at atmospheric and high pressures (> 74 bar) have shown the ability of microbial biofilms to decrease the permeability of natural and artificial porous media [1], survive the exposure to $scCO_2$ [2], and facilitate the conversion of gaseous and supercritical CO_2 into long-term stable carbonate phases as well as increase the solubility of CO_2 in brines [3].

Ongoing microscopy and modelling studies aim to understand these processes at both the pore- and core-scale in order to facilitate larger scale understanding and potential manipulation for biologically based CCS engineering [4,5]. Successful development of these biologically-based mineralisation concepts could result in microbially enhanced carbon sequestration strategies as well as CO_2 leakage mitigation technologies, which can be applied either before CO_2 injection or as a remedial measure around injection wells.

[1] Mitchell *et al.* (2009) *International Journal of Greenhouse Gas Control* **3**, 90-99.
[2] Mitchell *et al.*(2008) *Journal of Supercritical Fluids* **47**, 318-325.
[3] Mitchell *et al.* (2010) *ES&T* **44**, 5270-5276.
[4] Schultz *et al.* (2011) *Microscopy Today* **19**, 12-15.
[5] Cunningham *et al.*(2011) *Energy Procedia* **4**, 5178-5185.

Isotope fractionation of selenium during sorption to iron oxide and iron sulfide minerals

K MITCHELL[1*], R-M COUTURE[1], T M JOHNSON[2], PRD MASON[3] AND P VAN CAPPELLEN[1]

[1]University of Waterloo, Waterloo, Canada (*presenting author: kristen.mitchell@uwaterloo.ca)

[2]University of Illinois, Urbana, USA

[3]Utrecht University, Utrecht, The Netherlands

Sorption and abiotic reduction are important processes influencing the mobility and cycling of Se in natural environments. Although these processes have received increasing attention in recent years, the associated isotopic fractionations are poorly known [1, 2]. In this study we determined the rates of reaction and isotopic fractionations of Se(IV) and Se(VI) during sorption to iron oxides (2-line ferrihydrite, hematite and goethite) and iron sulfides (FeS and FeS_2) in batch reactor experiments. No change in Se oxidation state was observed when Se(IV) and Se(VI) sorbed to iron oxides. In contrast, XANES spectra showed evidence of reduction on the iron sulfides. Reaction rates were obtained using inverse modeling of dissolved Se concentration time series, following the mixed-reaction modeling approach of [3]. Sorption rates were highest in the Se(IV)-goethite system, while Se(VI) sorbed slowly on 2-line ferrihydrite and not at all on hematite and goethite. Reduction was fastest in the Se(IV)-FeS system and slowest for Se(VI)-FeS_2. Changes in the isotopic composition of aqueous Se were monitored as a function of time. The results revealed the absence of measurable equilibrium isotope fractionation for all systems studied. Kinetic fractionation was observed in the case of Se(IV) sorbing to 2-line ferrihydrite and Se(IV) being reduced by FeS_2. Figure 1 illustrates the $\delta^{82/76}$Se trends of aqueous and solid-bound Se(IV) sorbing to 2-line ferrihydrite. The data follow the standard Rayleigh fractionation model, except for the last two time points, as the system approaches equilibrium.

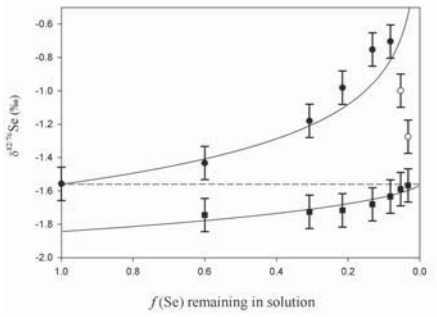

Figure 1: Se(IV) sorption to 2-line ferrihydrite. Circles show measured $\delta^{82/76}$Se of the remaining Se(IV) in solution, squares the calculated $\delta^{82/76}$Se of Se(IV) sorbed to 2-line ferrihydrite. The open symbols correspond to the two last samples collected, whose data were excluded when fitting the data with the Rayleigh fractionation model. Error bars indicate the precision of $\delta^{82/76}$Se measurements.

[1] Johnson (2003) *Geochim. Cosmochim. Acta* **67**, 413-419.
[2] Johnson (1999) *Geochim. Cosmochim. Acta* **63**, 2775-2783.
[3] Zhang (2005) *Environ. Sci. Technol.* **39**, 6101-6108.

https://doi.org/10.1180/S0026461X00008434 Published online by Cambridge University Press

Dislocation microstructures of ferropericlase at high pressures.

NOBUYOSHI MIYAJIMA[1*] AND TETSUO IRIFUNE[2]

[1]Bayerisches Geoinstitute, Bayreuth Universität, Bayreuth, Germany, nobuyoshi.miyajima@uni-bayreuth.de
[2]Geodynamics Research Center, Ehime University, Matsuyama, Japan, irifune@dpc.ehime-u.ac.jp

Introduction

The rheological behavior of magnesium silicate perovskite (MgPv) and ferropericlase (Fp) at high pressure and temperature is indispensable for discussing dynamics of the Earth's lower mantle. Deformation of plastically weaker Fp than coexisting MgPv is likely to be responsible for bulk strain of the rock, if it develops a sufficient grain connectivity in a fabric development at high temperature. Particularly, lattice preferred orientations (LPO) of the polycrystalline Fp can be important to explain observed seismic anisotropies in the bottom of Earth's lower mantle, so called "D'' layer". For understanding deformation mechanisms to create a LPO pattern, dislocation microstructures of Fp under lower mantle conditions are very important, because dislocation creep mechanisms could become one of dominant mechanisms in the D'' layer. To discuss the influence of pressure on the active slip system in Fp, we report dislocation microstructures of Fp in a pyrolite mineral assemblages synthesized at 44 GPa and 2073 K [1], in comparion to those of lower pressure samples, by using TEM.

Results and Conclusion

In the pyrolite mineral assemblage, MgPv contained a few dislocations and Fp displayed a high density of dislocations (Figure 1). In a Fp grain, straight long screw dislocations with $\boldsymbol{b}$ = 1/2[1-10] were nucleated on the (110) and/or (11-1) planes (Figure 1a) and the other dislocations with $\boldsymbol{b}$ = 1/2[01-1] was also along the (011) plane (Figure 1b) in the same grain.

Dislocation microstructures of Fp synthesized at high temperatures and different pressures from 0 to 44 GPa were compared in the TEM images. The highest pressure sample indicate that an active slip system of 1/2<110>{110} in Fp, consistent with previous experimental studies at lower pressures. The characteristic textures of straight screw dislocations along a specific crystal orientation strongly imply that the Peierls friction for movement of 1/2<110> dislocations in Fp increases with increasing pressure. The dislocation microtextures are compared with a current theoritical study of dislocation mobilities in MgO [2].

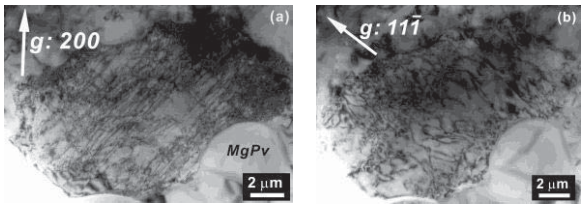

Figure 1: Bright field TEM micrographs of Fp in a pyrolite mineral assemblage at 44 GPa and 2073 K.

[1] Irifune, Shinmei, McCammon, Miyajima, Rubie & Frost (2010) *Science* **327**, 193-195. [2] Cordier, Amodeo & Carrez (2012) *Nature* **481**, 177-180.

Local structure of Al in Al-Zn hydroxide coprecipitates

AKANE MIYAZAKI[1*], KAORI ETOU[1], MAYUMI ETOU[2], KOTARO YONEZU[3], IOAN BALINT[4], AND TAKUSHI YOKOYAMA[5]

[1]Japan Women's University, Tokyo, Japan, miyazakia@fc.jwu.ac.jp (* presenting author)
[2]Faculty of Science, Kyusyu University, Fukuoka, Japan
[3]Faculty of Engineering, Kyusyu University, Fukuoka, Japan
[4]Institute of Physical Chemisty, Bucharest, Romania

Al-Zn hydroxide coprecipitate

Zn^{2+} adsorption onto alumina, which represents the behavior of heavy metal ions in soil systems, can be devided into three processes; adsorption due to formation of inner-sphere complex, desorption of Zn^{2+} accompanied with dissolution of Al^{3+}, and then re-adsorption of Zn^{2+} [1]. Recently, the final product of the above three processes was found to have AlO_4 species in its structure [2]. The formation of AlO_4 was induced by Zn^{2+} adsorption and it relats deeply to the dissolution and re-adsorption of Al^{3+}. There are two possible assignement for the AlO_4 species; one is Keggin-like structure, and the other is substitution of Zn^{2+} by Al^{3+} in the structure of zinc aluminate, $ZnAl_2O_4$. Because the adsorption experiments were performed at constant pH of 6.5, where Keggin is not stable, the formation of Keggin-like structure seems to be unlikely. On the other hand, $ZnAl_2O_4$ is a member of the spinel family and Al^{3+} can substitute four coordinated Zn^{2+} in its structure. Zinc aluminate is known to be prepared by calcining Al-Zn hydroxide coprecipitates [3]. In the process of Zn^{2+} adsorption onto alumina, it is possible that the desorbed Zn^{2+} and dissolved Al^{3+} coprecipitate to form zinc aluminate-like structure as the final products of adsorption. In order to examine this possibility, Zn-Al hydroxide coprecipitates having various Zn/Al ratios were prepared and chemical states of Al was compared to the final product of adsorption using ^{27}Al MAS NMR.

^{27}Al MAS NMR spectra of the coprecipitates

Figure 1 shows the ^{27}Al MAS NMR spectra of coprecipitates prepared by hydrolysis of mixed solution of zinc and aluminum nitrates. Peaks at around 60 ppm, which correspond to AlO_4 species, increased by decrease of Zn/Al ratios. Fig. 1 shows that the AlO_4 species can be formed by coprecipitation of Al and Zn, without calcination. AlO_4 species increased by lowering Zn/Al ratios. Therefore, less Zn^{2+} seems to cause more isomorphic subsbitution by Al^{3+}. The shape of ^{27}Al MAS NMR spectra of the coprecipitate with low Zn/Al ratio is almost identical to that of the final product of Zn^{2+} adsorption onto alumina. Therefore, it is highly possible that Zn^{2+} adsorption onto alumina induced the formation of Zn-Al hydroxide coprecipitate having zinc aluminate-like structure.

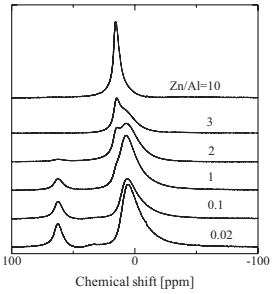

Figure 1: ^{27}Al MAS NMR spectra of the Zn-Al hydroxide coprecipitates

[1] Miyazaki *et al*, (2003) *Geochem. Cosmoshim. Acta* **67**, 3833-3844.
[2] Miyazaki *et al*, (2011) *Goldschmidt*, 08/3045.
[3] van de Laag *et a*l, (2004) *J. Eur. Ceram. Soc.* **24**, 2417-2424.

https://doi.org/10.1180/S0026461X00008434 Published online by Cambridge University Press

High-pressure and high-temperature experimental study of carbon isotope fractionation in the Mg-Si-C-O system

SHOGO MIZUTANI[1*], M. SATISH-KUMAR[1], TAKASHI YOSHINO[2], AND MUTSUMI KATO[3]

[1]Department of Geosciences, Shizuoka University, Shizuoka, Japan,
[2]ISEI, Okayama University, Misasa, Japan
[3]Graduate School of Science, Chiba University, Chiba, Japan

Carbon is the fourth most cosmic abundant element in the solar system. It has a key role in the melting phase relations of mantle rocks and can move within mantle as carbonate rich melts [1]. Additionally, carbon is deposited in the ocean floor as carbonate minerals and organic matter, and is recycled into the mantle during subduction. Carbon isotopic composition serves as an efficient tool to understand the carbon cycle, both in the shallow and deep Earth environments. Recently, the presence of low $\delta^{13}C$ diamonds was considered to provide evidence for deep cycling of surface carbon of the organic matter origin [2], however recent experimental results in the Fe-C system suggests an alternate possibility of light carbon in the core [3]. Therefore, it is essential to understand the carbon isotope fractionation at mantle *P-T* conditions. Here, we present results on experimental determination of partitioning of carbon isotopes at high-pressure and high-temperature conditions, analogous to melting of carbonated mantle in the presence of graphite/diamond, and discuss the carbon movement in the mantle.

High-pressure experiments were performed in the Mg-Si-C-O system using a Kawai type multi-anvil high-pressure apparatus at the Institute for Study of the Earth's Interior, Okayama University, Misasa, Japan. Starting materials comprise of natural enstatite, synthetic magnesite ($\delta^{13}C$ = -32.8‰), San Carlos olivine and pure graphite ($\delta^{13}C$ = -16‰), that were mixed in the molar ratio 3:2:1:1 or 3:2:1:3. This mixture is assumed as simplified carbonated harzburgite in a upper mantle. Experiments were carried out at pressures of 5 and 10 GPa at varying temperature conditions between 1100 ºC and 1800 ºC. Retrieved samples from HPHT experimental runs were mounted in epoxy and cut into two halves and polished. One half was used for petrographic observations and chemical analysis using an electron microprobe and the other half for carbon isotope measurements. Run products were mechanically and/or chemically separated and carbon isotope measurements were carried out using a conventional gas source isotope ratio mass spectrometer (IRMS).

Preliminary results indicate that runs at 5 GPa and above 1500 ºC have melted and the chemical composition of the melt varied widely, such as C-rich melt or Si-rich melt. Carbon isotope results show considerable partitioning between graphite/diamond and carbonate melt at temperatures and pressures corresponding to upper mantle conditions. We discuss the carbon isotope systematics during melting of carbonated mantle and implications for deep carbon cycle based on our experimental results.

[1] Dasgupta & Hirschmann (2006) *Nature*, **440**, 659-662 [2] Walter et al., (2011) *Science*, **334**, 54-57 [3] Satish-Kumar et al., (2011) *Earth Planet. Sci. Lett.* **310**, 340-348

Influence of DOM quality on arsenic mobilization in a Bangladesh Aquifer

NATALIE MLADENOV[1,2*], DIANE M. MCKNIGHT[1], BAILEY SIMONE[1], TERESA LEGG[1], DIANA NEMERGUT[1], JESSICA EBERT[1], KATHLEEN A. RADLOFF[3,4], AND YAN ZHENG[3,4]

[1]University of Colorado, Boulder, CO, USA, diane.mcknight@colorado.edu, bailey.simone@colorado.edu, leggeteresa@gmail.com, diana.nemergut@colorado.edu, jlebert@gmail.com
[2]Kansas State University, Manhattan, KS, USA, mladenov@ksu.edu (* presenting author)
[3]Queens College, City University of New York, Flushing, NY, USA
[4]LDEO, Columbia University, Palisades, NY, USA, yzheng@ldeo.columbia.edu, kradloff@gradientcorp.com

There is broad consensus that the main mechanism for the mobilization of arsenic (As) in reducing groundwater is the microbial reductive dissolution of iron (Fe) oxyhydroxides driven by the oxidation of labile organic matter (Figure 1). There is increasing evidence that the chemical quality of dissolved organic matter (DOM) may have an additional influence on arsenic (As) mobilization in reducing groundwater. [1] For example, humic substances, a major part of the DOM pool, are known electron shuttles that may also be involved in metal complexation (Figure 1). We used UV-vis absorbance and novel fluorescence techniques to characterize DOM in groundwater with dissolved As concentrations ranging from 2 to >400 µg/L and spanning a wide spatial extent in Araihazar, Bangladesh. For a subset of wells, we also determined % fulvic acid and performed elemental and ^{13}C-NMR analyses on fulvic acid isolates.

Our results consistently showed that terrestrially-derived aromatic organic compounds with low protein-like character were found where dissolved As concentrations are elevated. Moreover, the lowest As concentrations were found in village wells that had sewage pollution-derived DOM signatures. Together with highly significant relationships between arsenic and aromaticity and fluorescence of the fulvic acid isolates, our results provide strong evidence that humic substances have an important role in arsenic mobilization and potentially its maintenance in solution (Figure 1).

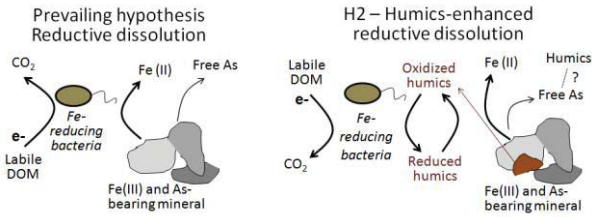

Figure 1: Conceptual diagram showing the "reductive dissolution" hypothesis (left) and an expanded "humics-enhanced reductive dissolution" hypothesis (H2; right) in which labile DOM and reactive DOM (including humic quinones) serve to donate and shuttle electrons, and are involved in complexation reactions. Sedimentary organic matter sources of labile and reactive DOM shown in brown.

[1] Mladenov, N. et al. (2010) *Env. Sci. Tech.* **52**, 47-59.

https://doi.org/10.1180/S0026461X00008434 Published online by Cambridge University Press

Petrography and composition of iron formation from the ca. 3.8 Ga Nulliak Supracrustal Association (northern Labrador, Canada)

ALEKSANDRA M. MLOSZEWSKA[*1]; RASMUS HAUGAARD[1]; KURT O. KONHAUSER[1]

[1]Earth and Atmospheric Sciences, University of Alberta, Edmonton, Canada, mloszews@ualberta.ca (*corresponding author)

Banded iron formations (BIFs) are important sources of information on the composition of ancient seawater [1,2]. Eoarchean BIFs in particular may disclose information on the nutrient levels bracketing the evolution of early microbial metallo-enzymes. Only a limited amount of pre-3.6 Ga year old BIFs are know, and chemical sediments from the ca. 3.8 Ga year old Nulliak Supracrustal Association of northern Labrador (Canada) [3] offer an exciting opportunity to expand our data base.

We present new petrographic and geochemical data on these Fe- and Si-facies iron formations, by integrating geochemical relationships observed between minerals in thin section and whole rock chemistry. This approach provides an important framework for studying the chemical variations in these sediments, on several scales. Preliminary results show that the Nulliak sediments are relatively aluminous (Al_2O_3>1 wt%), with correspondingly high abundances of Zr (up to 20 ppm) and other high-field strenght elements (e.g., Nb, Hf), suggesting a non-trivial detrital component. These chemical sediments contain noteworthy abundances of Cr, Ni, Zn, Sr, and Ba, while other elements tend to be <25 ppm. The high Ni and Zn abundances correlate well with previous studies on Eoarchean-aged iron formations, suggesting that these metals were found globally in high concentrations during the Eoarchean [3,4]. Rare earth element and yttrium profiles tend to show seawater-like anomalies (LREE<MREE<HREE; positive La and Eu anomalies, and superchondritic Y/Ho ratios) despite granulite-facies metamorphic overprinting. Collectively, these findings indicate that at least some of the original seawater signature has been preserved. Neverthless, these sediments may not be an accurate seawater proxy, as detrital material tends to obscure seawater signals. Instead, they may provide a measure of balanace between hydrothermal- and terrestrial inputs affecting the composition of Eoarchean seawater composition as reflected in BIFs.

[1] Bjerrum and Canfield (2002) *Nature* 417, 159-162
[2] Konhauser et al. (2009) *Nature* **458**, 750-753
[3] Nutman et al. (1989) *Canadian Journal of Earth Sciences* **26**, 2159-2168
[4] Mloszewska et al. (2012) *Earth and Planetary Science Letters* 317-318, 341-342.

GOLIATH: A systems biology, geochemical and physiological approach to discern microbial transformations of Mercury and Methylmercury.

JAMES G. MOBERLY[1], CARRIE L. MILLER[1], RICHARD A. HURT, JR, STEVEN D. BROWN[1], SCOTT C. BROOKS[1], CRAIG C. BRANDT[1], MIRCEA PODAR[1], ANTHONY V. PALUMBO[1], DWAYNE A. ELIAS[1*]

[1]Oak Ridge National Laboratory, Oak Ridge, USA, eliasda@ornl.gov (* presenting author)

BACKGROUND: Mercury (Hg) contamination is a global concern. Hg methylation is an important biogeochemical process, which generates the potent neurotoxin monomethylmercury (MeHg). Net MeHg production in aquatic ecosystems is linked to environmental and geochemical parameters along with electron donor and acceptor availability. Recently we found that methylating communities contained high populations of Desulfobulbus and Geobacter spp. To gain a deeper understanding of the microbial community populations invlolved in, and geochemical influences on, Hg methylation, physiological and meta-omic analyses were performed. **METHODS**: Intact sediment cores from two methylating sites (NOAA, upstream; New Horizon, downstream) and a background site were collected and used to construct sediment microcosms from different depths with 6 different carbon/electron sources. All microcosms were spiked with Hg stable isotope tracers to enable quantification of both Hg methylation and MeHg demethylation and incubated under anaerobic conditions in the dark for 48 hours at room temperature. DNA from the original core material and incubations were hybridized to functional gene arrays and sequenced via 454 16S rRNA gene pyrosequencing. **RESULTS**: Functional gene array results revealed a greater relative abundance of Hg(II)-reduction genes at NOAA while actual methylation was higher downstream at New Horizon. Each of the latter two sites displayed ~15X more methylation than the background site. Upstream at NOAA, methylation was moderately stimulated by methanol and ethanol but not by acetate, lactate, propionate or cellobiose, while downstream at New Horizon cellobiose stimulated methylation relative to unamended controls. Meta -genomic, -transcriptomic, and -proteomic analyses as well as 454 pyrosequencing are currently underway. **CONCLUSIONS**: The multidisciplinary combination of the above approaches are being employed together for the first time in order to more comprehensively ascertain the influence of geochemistry on the microorganisms, genes, and gene products that are differentially present, abundant and expressed in active MeHg generating ecosystems.

https://doi.org/10.1180/S0026461X00008434 Published online by Cambridge University Press

The magmatic and metasomatic formation of zircon in the Nechalacho deposit at Thor Lake, Northwest Territories, Canada

VOLKER MÖLLER[1*], ANTHONY E. WILLIAMS-JONES[1]

[1]McGill University, Earth and Planetary Sciences, Montreal, Canada, volker.moeller@mail.mcgill.ca (* presenting author)

The Nechalacho Rare Metal Deposit represents a world-class resource of REE, Y, Nb, Ta, Zr and Ga. Two densely mineralized horizons are hosted in intensely altered rocks of the upper part of the Nechalacho Layered Syenite Suite. These evolved, fluorine-rich peralkaline rocks are dominated by acmite, annite, sodalite, nepheline and feldspars. Primary REE- and HFSE-minerals include eudialyte, zircon, pyrochlore, britholite and Na-zircono-silicates. During alteration, eudialyte syenites were converted to an assemblage of zircon, quartz, magnetite and phlogopite. Secondary REE- and HFSE-bearing phases in the two REE-mineralized horizons comprise zircon, fergusonite, allanite-(Ce), bastnäsite-(Ce), synchisite-(Ce), parisite-(Ce), monazite and columbite[1].

The average whole rock content of ZrO_2 ranges from 2 to 3 wt. % and locally exceeds 10 wt. % in the deposit, making zircon an important rock-forming mineral. Three textural types of this mineral have been recognized: 1. rare magmatic phenocrysts in fresh or partially altered syenite; 2. quartz-hosted euhedral zoned crystals in the upper mineralized zone; 3. unzoned subhedral crystals intergrown with quartz in pseudomorphs after eudialyte in the lower mineralized zone.

Based on new Laser ICP-MS and electron microprobe data, magmatic zircon has a low trace element content (e.g., 80 to 6500 ppm REE) and displays heavy REE-enriched, near-linear chondrite-normalized profiles with strong positive Ce and negative Eu anomalies (avg. Ce/Ce*=3.4, avg. Eu/Eu*=0.44). Secondary type 2 and 3 zircon varies widely in composition, is strongly enriched in REE, Y, Nb and F, has elevated P and displays non-linear chondrite-normalized REE profiles with weak or absent Ce anomalies and strong Eu anomalies. Type 2 zircon has an average content of 2.3 wt. % REE, 1.1 wt. % Y and 1.3 wt. % Nb, has light and heavy REE enriched rims and cores respectively and contains significant fluorine. Relict magmatic cores and rims in the upper zone are distinguished by their low REE-contents and positive Ce anomalies which are comparable to type 1 zircon. Secondary zircon in the lower zone (Type 3) is strongly enriched in heavy REE and contains 2.8 wt. % REE, 1.7 wt. % Y and 1.6 wt. % Nb on average.

The HFSE mineralogy suggests that miaskitic and agpaitic rocks occurred in close spatial association. Metasomatic-hydrothermal replacement of both magmatic zircon and zircono-silicates was important for the formation of REE-enriched varieties of zircon. A possible mechanisms for the incorporation of such high levels of the REE is the formation of hydrated varieties at the alteration stage.

[1] Sheard, E.R, Williams-Jones, A.E., Heiligmann, M., Pederson, C and Trueman, D.L. (2012) *Controls on the concentration of zirconium, niobium, and the rare earth elements in the Thor Lake Rare Metal Deposit, Northwest Territories, Canada* **Economic Geology 107**, 81-104.

Deglacial forcing of rapid deoxygenation and seafloor ecological change, Santa Barbara Basin, CA

SARAH E. MOFFITT[1*], TESSA M. HILL[2]

[1]University of California at Davis, Bodega Marine Laboratory, Bodega, smyhre@ucdavis.edu (* presenting author)

[2]University of California at Davis, Bodega Marine Laboratory, Bodega, tmhill@ucdavis.edu

Background

Deglacial sediment from Santa Barbara Basin (SBB) are high-resolution records of regional climate, intermediate and surface water processes, and benthic ecology. Patterns of bottom water oxygenation in sediment records, and thus the presence of Oxygen Minimum Zones (OMZs), can be reconstructed by proxy using the oxygenation and environmental tolerances of modern taxa. We construct a record of deglacial community ecology, intermediate water oxygenation and coastal oceanography for SBB (34° 15'N, 119° 45'W) using a core from the northwestern basin slope at 418 m water depth (MV0811-15JC).

Results

The 9.2m core, which spans 4-16ky, is completely bioturbated. Significant faunal community deoxygenation horizons are evident at deglacial Termination 1A (~14.5 ky) and 1B (~10.9 ky), demarcated by the loss of ostracod, mollusc and brittle star fossils. The faunal record has high-resolution structure across taxa groups, indicating that stressful hypoxic events occur very rapidly at this depth. Results indicate the capacity for both rapid and sustained expansion of OMZs, the gradation of biological responses, and the spatial oceanographic processes that impact oxygenation across the coastal basin feature through the deglaciation.

Figure 1: Spetangoid heart urchin fossills in deglacial marine sediment, Santa Barbara Basin, CA. Note the biological orientation of the respiratory structures, indicating preservation at the time of death.

https://doi.org/10.1180/S0026461X00008434 Published online by Cambridge University Press

Assessing the role of Holocene sapropels on the Black Sea methane cycle

JOSÉ M. MOGOLLÓN [1*], SABINE KASTEN[1]

[1]Alfred Wegener Institute for Polar and Marine Research, Jose.Mogollon@awi.de (* presenting author) Sabine.Kasten@awi.de

Sapropels, sedimentary intervals rich in organic matter, represent a substantial carbon source which directly affects the sedimentary redox conditions in marine sediments. While recently-deposited sapropels produce a shoaling of the redox zonation, the long term effect of sapropelic sediments once these become buried over several millennia and lose their most labile carbon fraction requires further addressing. In the northern Black Sea, the changing limnic to marine conditions due to the flooding of the Bosphorous straight and subsequent connection with the Mediterranean Sea circa 9.5 kyr before present (BP), led to local geochemical conditions which favored ocean stratification and an increase in the amount of organic matter reaching the sediment between 8.0 and 3.5 kyr BP. Through reactive transport models which focus on the methane cycle, we track the geochemical effects of the sapropel since its initial deposition up to present time. Our results reveal that, from the onset of their deposition, sapropels heavily influence the methane cycle by controlling the position of the sulfate-methane transition (SMT) through organoclastic sulfate reduction. Nevertheless, the influence of the sapropels on methanogenesis will ultimately depend on the time required for the sapropel to be buried below the SMT. Consequently, methane formation will be favored in locations with high sedimentation rates, or locations receiving turbidites and slumps, such that the sapropel can be quickly buried into the methanogenic zone.

Determining thiotungstate stability constants for low temperature, low ionic strength aqueous solutions

T. J. Mohajerin[1*] & K. H. Johannesson[2]

[1] Tulane University, New Orleans, USA, thaug@tulane.edu (* presenting author)

[2] Tulane University, New Orleans, USA, kjohanne@tulane.edu

Abstract

Due to recent findings that suggest childhood leukemia may be linked to exposure to tungsten in drinking water, a need has arisen to better understand geochemical reactions affecting W concentrations and speciation in groundwater flow systems. Preliminary data show that W has a strong and statistically significant positive correlation ($p \leq 0.001$) with dissolved sulfide [i.e., S (-II)] concentration ($r = 0.95$) in the Carrizo Sand aquifer where groundwaters become anoxic. We hypothesize that like Mo [1], W may form thiotungstate complexes in sulfidic groundwaters. In sulfidic waters the general form of the thiotungstate forming reaction is:

$$WO_xS_{4-x}^{2-} + H_2S \leftrightarrow WO_{x-1}S_{5-x}^{2-} + H_2O$$

where x is 0 – 4, and the concentration product, Q, which is used to obtain the conditional equilibrium constants, is given as:

$$Q = [WO_{x-1}S_{5-x}^{2-}]/\{[WO_xS_{4-x}^{2-}][H_2S]\}.$$

To better understand the geochemical behavior of thiotungstates, we are measuring the stability constants for these species in dilute, aqueous solutions. As the thiotungstate forming reaction occurs, sulfur replaces oxygen in the tungstate oxyanion. Changes in solution composition are measured by periodic scanning of the absorption spectrum (200 nm $\leq \lambda \leq$ 450 nm) by UV/Vis spectrophotometry. As shown in Figure 1, the wavelegth pattern changes with time as different thiotungstate species are produced. Using the absorbsion coefficients and absorption at the maximum spectra for each thiotungstate species, Beer's Law is employed to calculate the concentration of each thiotungstate species, from which Q for each reaction can be determined. The stability constants are then calculated from Q using a modified Debye-Hükel equation. Determination of the stability constants of each of thiotungstate species is then used in a geochemical model to predict their importance in groundwater systems. Preliminary data are presented for the stability constants of the thiotungstate complexes in dilute aqueous solutions.

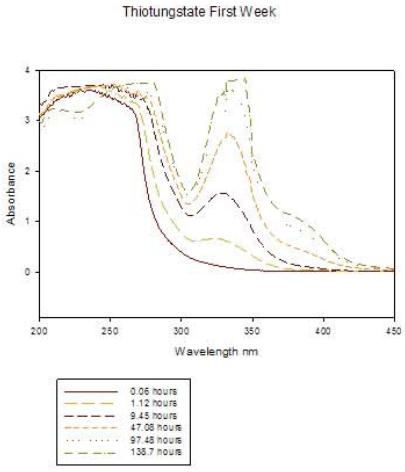

Figure 1: Spectral changes occurring during the time interval when WO_4^{2-} changes to WO_3S^{2-}, and is beginning to form $WO_2S_2^{2-}$

[1] Erickson & Helz (2000) Geochemica et Cosmochimica Acta **64**, 1149-1158

https://doi.org/10.1180/S0026461X00008434 Published online by Cambridge University Press

Investigating geochemistry and the stable isotope ($\delta^{18}O$ & $\delta^{2}H$) composition of Karde Carbonate lake water (NE Iran)

MOHAMMADZADEH HOSSEIN [1], MOJTABA HEYDARIZAD[2]

[1] Groundwater Research Center (GRC), Ferdowsi University of Mashhad, Mashhad, Iran, mohammadzadeh@um.ac.ir (* presenting author)

[2] Ferdowsi University of Mashhad, Department of geology, amour_elle_86@yahoo.com

Introduction

Karde dam's lake is a carbonate-precipitating and diamictic lake, which supplies irrigation and potable water for more than 4 million inhabitant of Mashhad city (NE Iran). In the following survey, Vertical (five depths 1, 5, 10, 15, 20) and temporal distribution of major cations and anions (especially nitrogen) in lakes water are investigated during 15 months (Jan 2010 to June 2011).

Results

The Calcite, Dolomite and Aragonite saturation index of lakes water and evaluation of Na, Mg, Ca concentration in lake, local ground water and rock samples in ternary diagram indicate that Na, Ca and Mg concentrations are mainly governed by incongruent dissolution of local carbonate (Mozdooran formation) and silicate (Neogen red formation).

Identification of dissolved minerals with ion activity (a) and $Log(aCa^{2+}/a(H^{+})^{2})$ versus $Log(aMg^{2+}/a(H^{+})^{2})$ graph for Carbonate minerals and $Log(aMg^{2+}/a(H^{+})^{2})$ and $Log(aCa^{2+}/a(H^{+})^{2})$ versus $Log(aNa^{+}/a(H^{+})^{2})$ for silicate minerals show that carbonate minerals "Calcite and Dolomite" and silicate minerals "Kaolinite, Laumontite and Clinochlore" are the dominate dissolved minerals within dam lake water. Vertical distribution of N in lake water shows significant increasing in NH_4^+ and NO_2^- concentrations with depth when the NO_3^- concentration decreases. Principal Component Analysis (PCA) of hydrochemical analyses revealed 3 components which explain 67% of the variance observed. In the first component, strong relationship between EC, TDS, Mg^{2+}, HCO_3^- and hardness reflect carbonate weathering. The variables in the second component are NH_3, NH_4^+, dissolved oxygen and depth. All the variables are directly related except dissolved oxygen which has inverse relationship with this component. This factor represents high Organic production in Karde dams' lake water. The third component shows relationships in the concentrations of Na^+, Ca^{2+}, SO_4^{2-} indicating the weathering of evaporative minerals especially gypsum ($CaSO_4$) and Glabuer's salt (Na_2SO_4) in the upper hand basin.

In the classical plot of $\delta^{18}O$ vs $\delta^{2}H$, the isotopic signature of lake water samples (-6.82‰, -48.3‰) plot further to (LMWL) comparing to the local ground water (-8.21‰, -57.5‰) and upstream river (-8.7‰,-61.8‰) which appear to be controlled by evaporation loss of the lake water.

References

[1] Cioni et al. (2002) *Volcanology and geothermal research* **120**, 179-195.

[2] Marini et al. (2000) *Geochemica et Cosmochimica Acta,* **64**, 2617-2635.

[3] Hong-jun et al. (2006) *Enviromental science,* **19**, 689-695.

Estimation of He diffusion coefficients in low permeability sedimentary rocks

RATAN MOHAPATRA[1*], TOM AL[2], AND IAN CLARK[1]

[1]Earth Sciences, University of Ottawa, Ottawa, Ontario, Canada, Ratan.Mohapatra@uOttawa.ca (*presenting author)

[2]Earth Sciences, University of New Brunswick, Fredericton, New Brunswick, Canada

With a view toward establishing a deep geological repository for low- and intermediate-level radioactive waste, a geoscientific site characterization program has been conducted on the eastern margin of the Michigan Basin at the Bruce nuclear site. Drilling and collection of cores within an ~ 860 m near-horizontally layered Paleozoic sedimentary sequence, resting atop the Precambrian basement, has provided an opportunity for porewater and groundwater sampling and analysis with an unprecedented level of detail. This abstract presents a methodology for estimating diffusion coefficients for He in low permeability sedimentary rocks obtained from the drilling.

Drill core samples (76 mm diameter) of Ordovician shale and limestone were preserved in the field inside N_2-purged and vacuum-sealed bags; first polyethylene and then aluminized polyethylene. The samples were transported to the University of Ottawa where a sub core (6 mm diameter and ~ 20 mm long) was removed from the centre of the larger core and encapsulated in a stainless steel container at 1×10^{-2} Torr. Gas accumulating in the head space by room temperature (20 °C) diffusion was periodically sampled for He and Ne isotopic measurements using a MAP L 215-50 Noble Gas Mass Spectrometer. A typical experiment involved 5 gas measurements over a period of 24 hr. The measured He was corrected for air contamination using accompanying ^{20}Ne data. The time-series of He concentrations in the head space are treated as an out-diffusion experiment and numerical simulations were conducted to estimate the He diffusion coefficients by matching simulated out-diffusion profiles to the measured data. Simulations were conducted by running the reactive transport model MIN3P under the control of the parameter estimation code, PEST.

In general, there is a good match between the measured He data and the simulations (Fig. 1); D_p values ranging from 1 to 4 × 10^{-11} m^2/s. However, samples from a 70 m interval that straddles the Blue Mountain Formation shale and the underlying Cobourg Formation limestone are an exception. This is a zone with high organic carbon content and the He release profiles suggest a delayed release of He – perhaps due to out gassing from an organic or petroleum phase.

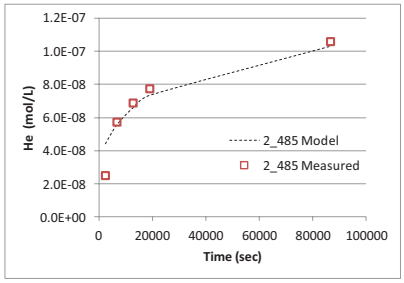

Figure 1. Example of He out diffusion showing measured He concentrations in the stainless steel container head space (open squares) and simulated out-diffusion profile indicating $D_p = 3.2 \times 10^{-11}$ m^2/s.

https://doi.org/10.1180/S0026461X00008434 Published online by Cambridge University Press

Paleo-environmental reconstruction of mercury and terrigenous organic matter dynamics in large Northern Quebec boreal lakes: an assessment of anthropogenic activities occuring in their watersheds

MATTHIEU MOINGT[1]*, MARC LUCOTTE[1], SERGE PAQUET[1], AND BASSAM GHALEB[1]

[1]GEOTOP-UQAM, Montréal, H3C 3P8, Canada
matthieumoingt@yahoo.fr (* presenting author)
lucotte.marc_michel@uqam.ca
paquet.serge@uqam.ca
ghaleb.bassam@uqam.ca

Mercury dynamics in boreal lakes is of special concern as human populations may be exposed to the contaminant through fish consumption.To evaluate the impact of watershed pertubations on the mercury dynamics in boreal aquatic systems, we studied sediment cores retrieved in six large boreal lakes of Québec (Canada) with watersheds disturbed by anthropogenic activities such as logging or mining activities, and in two undisturbed lakes chosen as reference lakes. Sediment rates were estimated by ^{210}Pb dating and range from 0.03 to 0.33 cm/yr. Total mercury (THg) contents and lignin biomarkers (refering to both quantity and quality of terrestrial organic matter (TOM)) were measured in all eight cores whereas watershed modifications over a 30 year period were determined by analysis of remotely sensed images using GIS. In all cores, THg concentrations significantly increased over recent years with maximum values comprised between 70 and 370 ng/g, the lowest THg contents being observed in reference lake cores. Anthropogenic Sedimentary Enrichment Factor (ASEF) is comprised between 2 and 15 and surprisingly, not all the lakes with disturbed watersheds present an ASEF superior to the value of 3.5 usually reported in the literature [1]. Our results allowed us to emphasize the importance of mean slope inclination, repartition of slopes in classes and vegetation cover in the drainage area on Hg fluxes reaching lake sediments. Results from this study suggest that in large boreal lakes ecosystems, the size and the characteristics (e.g. nature of the vegetation cover, mean slope) can promote the uptake of atmospheric Hg leading to enahanced presence of THg in sediments. Then, supplementary Hg transfers from the watershed to the aquatic systems due to anthropogenic activities (e.g. logging and mining activities) can be masked in sedimentary profiles. This study also underlines the importance of TOM as vector of Hg since sedimentary Hg enrichment appears proportional to the amount of TOM coming from the watershed.

[1] Lucotte *et al.* (1995) Water, Air, and Soil Pollution **80**, 467-476.

Cave sediments as repositories of very old fossil invertebrates

OANA T. MOLDOVAN[1*], SILVIU CONSTANTIN[1], IOANA N. MELEG[1], LADISLAV MIKO[2], LAURA EPURE[1], CRISTIAN PANAIOTU[3], RELU ROBAN[3], AND ANDREJ MIHEVC[4]

[1]* "E. Racovitza" Institute of Speleology, Cluj, Romania, oanamol@hasdeu.ubbcluj.ro
[2]European Commission, Bruxelles, Belgium, Ladislav.MIKO@ec.europa.eu
[3]University of Bucharest, Bucuresti, Romania, cristian.panaiotu@gmail.com
[4]Karst Research Institute, Postojna, Slovenia, mihevc@zrc-sazu.si

Introduction

Cave sediments preserve the geological and paleoenvironmental past as well as biological and anthropological information, important for the terrestrial continental history, where correlative sediments are mostly missing [1]. Our studies are first attempts to use fossil invertebrates from cave sediments as proxy in paleoclimate studies. Microbiological studies have been added to explain the processes of preservation.

Results

Six caves (S-E Europe) provided fossil invertebrates, mostly mites, springtails and ostracods, originating from the surface environments. All these groups are excellent as paleoecological bioindicators and were identified in Pliocene-Pleistocene sediments (Fig. 1). Their presence has been correlated with other proxies and provided reliable information about the type of vegetation on the surface and the deposition condition inside caves. Microorganisms isolated from the sediments were extremely scarce, with differences in the amount of bacteria or fungi.

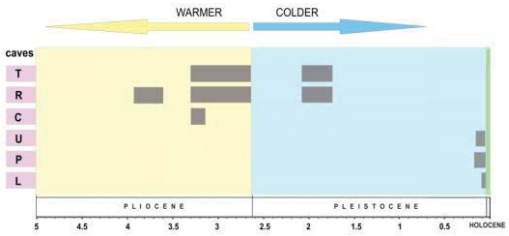

Figure 1: Invertebrate fossils found in the studied caves.

Conclusion

The depositional mechanisms and the low intensity of biochemical processes can explain the relatively good state of preservation of old invertebrate remains both in the cave sediments and Arctic lake sediments [2]. Considering the age of sediments, the state of preservation is relatively good. This may suggests a combination of: (1) a relatively short and slow transport to the site of deposition, (2) a rapid burial, i.e. a high sedimentation rate, and (3) subdued microbial and biochemical processes that could have altered the entire organisms. The difference we found in the concentration of bacteria or fungi, at different sediment levels, can also be correlated with dry/wet periods [3] and the work is still in progress.

[1] Sasowsky & Mylroie (2004) *Studies of Cave Sediments*. Kluwer Academic. [2] Moldovan *et al.* (2011) *Biogeosciences* **8**, 1825-1837 [3] de Vries *et al.* (2012) *Nature Climate Change*, DOI: 10.1038/NCLIMATE1368

https://doi.org/10.1180/S0026461X00008434 Published online by Cambridge University Press

Investigation of coupled flow and geochemical reactions at the pore scale by direct numerical simulation

S. MOLINS [1*], C. SHEN[2], D. SILIN[1], C.I. STEEFEL[1] AND D. TREBOTICH[2]

[1]Lawrence Berkeley National Laboratory, Earth Sciences Division, Berkeley, USA, SMolins@lbl.gov (* presenting author)
[2]Lawrence Berkeley National Laboratory, Computational Research Division, Berkeley, USA

Prediction of chemical fate and transport in subsurface environments often relies on reaction rate constants applicable to each grid block of continuum-scale numerical models. Typically, laboratory-determined reaction rates are applicable to a scale smaller than that resolved by the continuum-scale models. Upscaling of these rates to a grid block is possible under certain conditions; otherwise, microscopic and macroscopic scales need be considered simultaneously (e.g. [1], [2]). This is often the case in carbon sequestration or remediation applications where the subsurface geochemical system is driven to far-from-equilibrium conditions in relatively short time scales, which result in short characteristic length scales. In addition, induced geochemical reactions such as mineral precipitation and dissolution can modify the geometry and structure of porous media, which further affects the macroscopic reactions rates.

Direct numerical simulation techniques in which the Navier-Stokes or Stokes equations are solved using conventional methods (e.g. finite volume, differences) allow for incorporation of complex multicomponent reaction networks into pore scale models. We employ pore scale modeling based on direct numerical simulation of flow and multicomponent reactive transport to investigate the two-way coupling between precipitation-dissolution reactions and flow. We focus on calcite dissolution-precipitation as system of environmental relevance. We observe that non-uniformity in the flow field at the pore scale decreases the overall reactivity of the system in equivalent continuum-scale systems. The effect becomes more pronounced as the heterogeneity of the reactive grain packing increases, particularly where the flow slows sufficiently such that the solution approaches equilibrium locally and the average rate becomes transport-limited.

Simulations show that dissolution and precipitation reactions affect the pore space non-uniformly. As a result, a simple porosity-permeability correlation may be insufficient to describe the complexity of the reaction-induced pore space evolution. The relative magnitude of the reaction rate constants affects the evolution of the permeability-porosity relationship. In dissolution simulations, fast reactions result in localized effects and further evolution of permeability is relatively unaffected by subsequent porosity increase. In contrast, slow reactions cause a less localized dissolution, with the result that the permeability increase is consistent with the porosity increment.

[1] Battiato, Tartakovsky (2011), *J. Contam. Hydrol.*, 120-121,18-26
[2] Wood (2009) *Adv. Water Resour.*, 32, 723–736.

Comparison of three organic geochemical proxies for sea-surface temperatures in a four year sediment trap record

GESINE MOLLENHAUER[1,2*], ELEONORA ULIANA[2], ANDREAS BASSE[1,2], JUNG-HYUN KIM[3], OSCAR ROMERO[4], ENNO SCHEFUß[2], JENS HEFTER[1] AND GERHARD FISCHER[2]

[1]Alfred-Wegener Institute, Bremerhaven, Germany, gesine.mollenhauer@awi.de (* presenting author)
[2]Marum Center for Marine Environmental Research, Bremen, Germany
[3]Royal Netherlands Institute for Sea Research, Texel, the Netherlands
[4]University of Granada, Granada, Spain

The most well-established organic-geochemical SST proxy index $U^{K'}_{37}$ based on haptophyte produced long-chain ketones (alkenones) has been shown to yield robust estimates of annual mean SSTs but may be more problematic in high productivity eastern boundary upwelling areas. In the last decade, two types of new organic geochemical SST proxies, i.e., the TEX_{86} index based on archaeal glycerol dialcyl glycerol tetraether (GDGTs) and two indices based on long-chain diols derived from diatoms (DCI) and eustigmatophytes (LDI) have been proposed. Those proxies have been suggested to be applicable in settings where the alkenones are less reliable or absent. On the other hand, each of the new indices has its own caveats. These include, but are not limited to: 1) the fact that GDGT producing archaea thrive throughout the water column and perhaps also in the sediment; 2) limited understanding of the physiological role of the respective lipids in their precursor organisms; 3) incomplete understanding of the export mechanismns responsible for the transport of lipids from the depth of production to the sediments; 4) concerns regarding differential degradation of individual lipids.

Here we address several of these questions using sediment trap samples collected at 1-2 week intervals between June 2003 and March 2007. The trap was moored off Cape Blanc in an area strongly influenced by seasonal coastal upwelling. We measured $U^{K'}_{37}$, TEX_{86}, and the diol indices as well as concentrations and fluxes of the respective lipids. The results are compared with total, carbonate, opal and organic matter fluxes as well as diatom abundances. For all indices, we observe pronounced seasonal cycles, while flux-weighted averages agree well with values measured in underlying surface sediments. Reconstructed SSTs based on $U^{K'}_{37}$ and TEX_{86} correspond generally well with satellite measured SSTs but reveal that $U^{K'}_{37}$ is more uncertain during periods of highest productivity. The DCI shows a well pronounced but reverse relationship with SST than originally proposed. Fluxes of all lipids are closely tied to total fluxes, implying that ballasting is an important mechanism. Delays between observed and reconstructed SST maxima are within the expected range for alkenones and larger but similar for GDGTs and diols, implying that these lipids are predominantly exported as diatom-rich aggregates known to sink at lower velocities than carbonate containing aggregates. We find no evidence for substantial sub-surface export of GDGTs.

https://doi.org/10.1180/S0026461X00008434 Published online by Cambridge University Press

Investigating Silver Nanoparticle Transport in Soil via Synchrotron X-Ray Microtomography

IAN L. MOLNAR[1*], DENIS M. O'CARROLL[1], JASON I. GERHARD[1] AND CLINTON S. WILLSON[2]

[1]University of Western Ontario, London, Canada, imolnar@uwo.ca (*presenting author)

[2] Louisiana State University, Baton Rouge, U.S.A., cwillson@lsu.edu

The rapidly increasing production and use of nanoparticles carries with it a risk of their release into the subsurface environment, contaminating aquifers that are either used for municipal drinking water or discharge into surface water bodies. To consider their risk, it is necessary to understand nanoparticles' fate in the subsurface. However, nanoparticle transport in the subsurface environment remains poorly understood and developed relationships are specific to the imposed experimental conditions and particle type. This research aims to improve our ability to non-destructively measure pore-level concentrations and distribution of nanoparticles in an effort to better understand the soil - nanoparticle interactions and role of pore geometry.

Synchrotron x-ray computed microtomography (SXCMT) is widely used for imaging soil and rock cores and fluids occupying their pore space. The high resolution, three-dimensional, quasi-real time datasets output by SXCMT are capable of accurately quantifying silver nanoparticle concentrations within a porous media. These datasets can provide valuable information about silver nanoparticle distribution throughout the pore-network and even within each individual pore. This presentation will: outline an SXCMT method for imaging and quantifying aqueous silver nanoparticle solutions in porous media, present and analyze and number of time-lapse images of silver nanoparticles invading and evacuating a variety of water saturated soil types and examine the role of intra and inter-pore geometry on nanoparticle transport and deposition.

Targeting sites for exploration for precious metal mineralization in the Guanajuato district, Mexico using petrography and fluid inclusions

D. MONCADA* AND R.J. BODNAR

Department of Geosciences, Virginia Tech, Blacksburg, VA 24061 USA, moncada@vt.edu (*presenting author)

The search for mineral deposits is a time consuming, risky and very expensive process. Any technique that can help the explorationist to quickly and inexpensively discriminate between areas with high potential for economic mineralization and those with lower potential provides a competitive advantage to those applying the technology. In this study, we describe a technique based on petrography of gangue minerals and fluid inclusion characteristics that may be applied in exploration for precious metal deposits to identify targets from surface, drill holes and underground workings.

The Guanajuato mining district in Mexico was discovered 1548. This initial discovery was in the la Luz area with major northwest trending vein systems. The mining in the area has been continuous and recent exploration programs to search for new targets have been successful. Mineralization in veins show variability, from gold-rich to silver-rich, in going from west to east. Ore textures also vary and include void space that formed during multiple fissuring events, banded quartz veins, vuggy quartz, lattice bladed calcite, lattice bladed calcite replaced by quartz, massive quartz veins and stockworks with adularia and sericite/illite. More than 200 samples from nine veins representing all different styles of mineralization were collected from the La Luz system, and the mineral textures and fluid inclusion characteristics of each sample have been defined. In addition, each sample was assayed for Au, Ag, Cu, Pb, Zn, As and Sb. Some drill holes were assayed for 34 elements.

Samples from the La Luz system show a wide range in silica textures. The veins that have been studied show a range in textures, including colloform, plumose and jigsaw texture, quartz that are all indicative of rapid precipitation, such as occurs when fluids boil. Other mineral phases, including illite, adularia and bladed calcite are also indicative of rapid growth in a hydrothermal system and are characteristic of boiling systems. Because boiling is an effective mechanism for precipitating gold and silver from hydrothermal fluids, the presence of mineral textures indicative of boiling is a desirable feature in exploration. In many samples, textural evidence for boiling is supported by coexisting liquid-rich and vapor-rich fluid inclusions, or Fluid Inclusion Assemblages consisting of only vapor-rich inclusions, suggesting "flashing" of the hydrothermal fluids. Several traverses along outcrop on the surface and perpendicular to the veins show that samples collected from within 25 m of the main veins show increasing precious metal abundances that correlate with an increase in features that indicate boiling. Drill core samples show the same behavior, with evidence of boiling increasing within 0 to 5 m of where precious metal abundances increase. This approach helps to establish new targets for detail exploration. Importantly, textural and fluid inclusion evidence for boiling has been observed in the deepest levels of the La Luz system, suggesting that additional precious metal resources may occur beneath these levels.

https://doi.org/10.1180/S0026461X00008434 Published online by Cambridge University Press

Mineralogical and geochemical processes occurring in sulfide-rich tailings after 60 years of subaqueous storage

MICHAEL C. MONCUR[1,2*], CAROL J. PTACEK[1], DAVID W. BLOWES[1], MATHEW B.J. LINDSAY[1,3], AND JOHN L. JAMBOR[1]

[1]Earth and Environmental Sciences, University of Waterloo, Waterloo, ON, Canada mmoncur@uwaterloo.ca (* presenting author) ptacek@uwaterloo.ca , blowes@uwaterloo.ca

[2]Alberta Innovates-Technology Futures, Calgary, AB, Canada,

[3]Present Address: Earth and Ocean Sciences, University of British Columbia, Vancouver, BC, Canada mlindsay@eos.ubc.ca

The oxidation of sulfide minerals in subaerial tailings deposits generates acid and releases sulfate and metals to pore water. Subaqueous disposal of tailings is a common method for limiting sulfide-mineral oxidation. Numerous short-term studies have demonstrated that shallow water covers are effective at limiting oxygen diffusion to submerged tailings; however, long-term studies are lacking. The former Sherritt-Gordon Zn-Cu mine, located in Sherridon, Manitoba, Canada, deposited sulfide-rich tailings into Fox Lake during 1951. The tailings formed a number of small exposed islands with the majority of material submerged underwater, extending outward into the Lake. Exposed tailings were visually oxidized and submerged tailings commonly were overlain by naturally-established vegetation. Surface water, porewater and core samples were collected in 2001 and 2009 to examine long-term biogeochemistry of land-deposited tailings and the submerged tailings under approximately 1 m of water.

Mineralogical examination of the land-deposited tailings showed a well-defined, ochreous oxidation zone that extended from surface to about 40 cm depth. The interval from 40 to 60 cm was a transitional or intermediate zone of much weaker oxidation, and at depths >60 cm sulfide minerals in the tailings were not altered. In contrast to the thickness of the oxidation zone in the land-based tailings, the equivalent zone in the submerged tailings extended <6 cm below the water-solids interface. Porewater collected from the land-based tailings was characterized by low pH, depleted alkalinity and elevated concentrations of dissolved sulfate and metals. Microbial communities within these tailings were dominated by neutrophilic sulfur oxidizing bacteria. Conversely, the natural colonization of vegetation over the subaqueous tailings resulted in the development of strong reducing conditions evident from circumneutral pH conditions, low concentrations of dissolved sulfate and metals, H_2S production and strong $\delta^{34}S_{SO4}$ and $\delta^{13}S_{DIC}$ fractionation indicating microbially-mediated (dissimilatory) sulfate reduction. Within the submerged tailings, secondary marcasite was observed in the relic ochreous zone occurring as coatings on primary minerals. This observation indicates that, following a period of oxidation, metals were subsequently sequestered from solution in this zone. This finding further emphasizes the influence of reducing conditions and microbial activity on metal mobility within mine tailings. Results from this study provide insight for the submergence of sulfide-rich tailings under a shallow water cover as a viable method for long-term storage.

Isotopic fractionation of U(VI) during reduction by sulphide

NIKHIL MONGA[1*], STEPHEN J. ROMANIELLO[1], AND ARIEL D. ANBAR[1,2]

[1]School of Earth and Space Exploration, Arizona State University, Tempe, AZ, USA, nikhil.monga@asu.edu (* presenting author)

[2] Department of Chemistry & Biochemistry, Arizona State University, Tempe, AZ, USA, anbar@asu.edu

Understanding isotopic fractionation of $^{238}U/^{235}U$ between soluble U(VI) and insoluble U(IV) is useful in various ways, from undersanding the geochemistry of U to its use as a paleoredox proxy [1]. In the environment, deposits of uranium formed by low temperature redox processes (e.g. black shales, roll front deposits) are observed to be isotopically heavy compared to the fluid from which they precipitated by 0.4-1.0‰ (e.g. the $^{238}U/^{235}U$ of the Black Sea sediments is consistantly heavier than the overlying water column) [1,2,3]. This idea is consistent with theoretical calculations which predict that U^{4+} should be heavier than UO_2^{2+} by 1.3‰, primarily due to nuclear volume effects [4,5]. Despite the prevelance of this effect in nature, it has been suprisingly difficult to produce isotopically-heavy reduced U phases experimentally. Two independent studies have shown that the reduction of U(VI) using zero-valent Zn and Fe produces no isotopic fractionation [2,6]. In experiments with two different cultures of U-reducing bacteria, researchers found that the reduced phase was isotopically light by 0.31-0.34‰, opposite of observations in the environment.

Motivated by this discrepancy and reasoning that sulfide is a common and abundant reductant in environmental settings, we set up experiments to measure isotopic fractionation during abiotic U reduction by sulfide. We reduced a 4 ppm U(VI)-CO_3 solution in the presence of 2.1 mM sulfide and 4.11 mM bicarbonate, maintained at a pH of 6.8 using a TRIS/HCO_3 buffer under a UHP He atmosphere [7]. At regular time intervals, the solution containing the soluble U(VI) and a suspended insoluble precipitate, presumably U(IV) in the form of uraninite [7], was sampled using a syringe and rapidly separated using syringe filtration.

Our initial results are well-described by a Rayleigh model and indicate that the reduced uranium phase is lighter than the solution by 0.189±0.097‰ (α = 0.999811±0.000097, 2σ). This effect is opposite that observed in nature but similar to results observed for U-reducing bacterial cultures. Since all laboratory experiments so far produce moderately light or unfractionated reduced U, it is possible that isotopic equilibration of U(VI)⇌U(IV) is not achieved on laboratory timescales. Alternatively, the chemical details of the lab experiments may differ from natural systems and theoretical models in some key respect. For example, U speciation may have a large effect, or other reactions, such as U adsorption, could occur.

[1] Weyer *et al.* (2008*) Geochim. Cosmochim. Acta* 7**2**, 345-359**5**,1370–1375 [2] Stirling *et al.* (2007) *Earth Planet. Sci. Lett.* **264,** 208-225. [3] Romaniello *et al* (2009) *AGU Fall meeting 2009*, abstract # V54C-06. [4] Bigeleisen (1996) *J. Am. Chem. Soc.* **118,** 3676-3680. [5] Abe et al (2008) *J. Chem. Phys*. **129,** 164309. [6] Rademacher *et al* (2007) Environ. Sci. Technol. 2010, 44, 5927–5933 [7] Hua *et al.(2006) Environ. Sci. Technol 40 , 4666-4671*

https://doi.org/10.1180/S0026461X00008434 Published online by Cambridge University Press

Growth of nanostructured calcite under hydrothermal conditions in presence of organic and inorganic selenium

G. MONTES-HERNANDEZ[1*], G. SARRET[1], R. HELLMANN[1], L. CHARLET[1], F. RENARD[1]

[1]Institut des Sciences de la Terre (ISTerre), OSUG/CNRS, UJF, BP 53X, 38041 Grenoble, France

Abstract

Selenium is an important trace metalloid, whose global cycle is controlled by fluid-rock interactions in the Earth's upper crust, interactions with bio-molecules in soils and living systems, and atmospheric transport in ashes. The cycling of selenium is often intimately associated with carbonate phases, with Se being generally incorporated as an impurity in calcite crystals or adsorbed on carbonate nanoparticles. In order to better understand the interaction of aqueous selenium species with carbonates, we studied the precipitation of calcite under hydrothermal conditions (30-90°C, 25-90 bar) in a CO_2-H_2O-$Ca(OH)_2$ medium in the presence of aqueous inorganic and organic selenium compounds. Aqueous carbonation reactions in the presence of selenium at elevated temperatures and pressures, relevant for long-term CO_2 sequestration in reservoirs and other natural geological systems, have until now not been investigated to the best of our knowledge. Macroscopic measurements, Electron microscopy (FESEM and TEM) and synchrotron X-ray absorption spectroscopy (XAS) were used in a complementary manner to investigate kinetic effect of Se, crystal size, structural order (crystallinity), morphology of crystal faces, crystal organization, and selenium speciation in the calcite samples. XAS data analysis showed clear evidence for the incorporation of selenite oxyanion (SeO_3^{2-}) into the calcite crystal structure. At low Se content (1.3 mg/g calcite), a single site was observed with Se surrounded by six Ca atoms, whereas additional sites, probably corresponding to surface sorption sites, were found with increasing Se content. XAS also showed that seleno-L-cystine (Secys) was chemically fragmented during carbonation, and the solid phase contained elemental and oxidized Se, in hexagonal or amorphous form depending on the experimental conditions, with a minor proportion of Se(IV). Moreover, FESEM and TEM measurements revealed a very complex effect of Secys on the particle size and aggregation/agglomeration process, leading to the following calcite morphologies: rhombohedra, elongated rhombohedra (*c*-axis elongation), scalenohedra, star-like and shell-like crystal aggregates, and irregular calcite polycrystals. The aggregates and irregular polycrystals, which we designate as nanostructured calcite material, were constituted of nanometer-sized calcite crystallites (<100nm). The star and shell-like crystal aggregates, which were observed only in the presence of Secys, may be due to crystal growth in the presence of associated secondary organic compounds due to a simultaneous chemical fragmentation of Secys. Overall, the results from this study show that selenium (of biotic or abiotic origin) can be integrated into the crystallographic structure of calcite under hydrothermal conditions. This has relevance for geological processes in diverse environments, such as hydrothermal systems along mid-ocean ridges, or underground reservoirs associated with massive injection of CO_2 for long-term geological sequestration. For more details refer to Montes-Hernandez et al. [1-3].

[1] Montes-Hernandez et al. (2011) *Chem. Geol.* **290**, 109-120. [2] Montes-Hernandez et al. (2009) *J. Hazardous Mater.* **166**, 788-795. [3] Montes-Hernandez et al. (2008) *Crystal Growth & Design.* **8**, 2497-2504.

Compositional data analysis to constrain the geochemical footprint of iron oxide copper-gold deposits

JEAN-FRANÇOIS MONTREUIL[1*], LOUISE CORRIVEAU[2], AND ERIC GRUNSKY[3]

[1]Institut de la Recherche Scientifique –Eau-Terre-Environnement, jean-francois.montreuil@ete.inrs.ca (* presenting author)

[2]Geological survey of Canada, Québec, louise.corriveau@nrcan.gc.ca

[3]Geological Survey of Canada, Ottawa, eric.grunsky@nrcan.gc.ca

Introduction

Lithogeochemical analysis of alteration haloes is an important exploration vector towards hydrothermal ore deposits. Iron oxide copper-gold (IOCG) systems display a systemic development of hydrothermal alteration types from sodic, to calcic-iron, and high to low temperature potassic-iron and potassic alteration paragenesis that indiscriminately replace host rocks at local and regional scales. Where intense and pervasive, alteration leads to complete and systemic mineralogical, chemical and textural transformation of precursor rocks, resulting geochemical composition for each alteration type is reproducible irrespective of the nature of the original host. However the zoning in the alteration haloes and the types of deposits formed vary as a function of unidirectional, cyclical or non unidirectional evolution of the hydrothermal system [1]. To further the development of geochemical vectors to IOCG and affiliated deposits and orient exploration campaign in under-explored settings, we document the geochemical signature of hydrothermal alteration from the Great Bear magmatic zone (GBmz) IOCG systems through the application of compositional data analysis based on the log-ratio approach and principal component analysis (PCA).

Results and Conclusions

PCA has enabled the characterisation of the geochemical signature of the diagnostic alteration types. When compared to the other IOCG alteration types defined in the preceding section, potassic and potassic-iron alteration show relative enrichment in K, Al, Ba, Si, Rb, Zr, Ta, Nb, Th and U. In contrast, when compared with the other alteration types, calcic-iron alteration exhibit relative enrichment in Ca, Fe, Mn, Mg, Zn, Ni and Co. Sodic alteration is relatively enriched in in Na, Sr and Zr compared to the other alteration signatures.

The observed compositional variations established for each alteration type were thereafter portrayed in IOCG alteration indexes. Combined with the IOCG alteration vector to mineralization model, the resulting IOCG alteration indexes led to the development of an IOCG alteration discrimination diagram that provides a useful tool to quickly evaluate if a geochemical composition is related to IOCG –associated hydrothermal alteration. Plotting the alteration indexes on the GBmz regional geology map further demonstrates that the IOCG alteration indexes can provide a framework for field evaluation of the potential fertility and maturity of the GBmz IOCG systems and ultimately vector to ore during exploration.

[1] Corriveau, Williams & Mumin (2010) GAC, Short Course Notes, **20**, 89-110

https://doi.org/10.1180/S0026461X00008434 Published online by Cambridge University Press

Electrical conductivity of serpentine fluids at subduction zone conditions

MAINAK MOOKHERJEE[1,2*], M. A. GEETH MANTHILAKE[2A] AND NOBUYOSHI MIYAJIMA[2B]

[1]Earth and Atmospheric Sciences, Cornell University, Ithaca, USA, mainak.mookherjee@gmail.com (* presenting author)
[2]Bayerisches Geoinstitut, Bayreuth, Germany,
[A]Geeth.Manthilake@uni-bayeruth.de,
[B]Nobuyoshi.Miyajima@uni-bayeruth.de

Owing to pervasive faults, sea water interacts with oceanic crusts and stabilizes a suite of layered hydrous silicate phases. As the oceanic crusts subducts, the hydrous phases are also dragged along with the subduing slab. These hydrous phases have limited thermal stabilities and they eventually dehydrate, releasing fluids. These fluids are less buoyant and hence migrates upwards. The fluids interact with the overlying mantle wedge. These released fluids rehydrates the mantle wedge i.e., rehydrates peridotitic mantle and stabilizes serpentinite. From geophysical observations, the mantle wedges of subduction zone are characterized by low seismic velocities and electrical resistivities. In order to asses the role of fluids and serpentine, we have measured the electrical conductivity of natural serpentinites at pressure (2 GPa) and temperatures (up to 1000 K) relevant to mantle wedge conditions. Among the two natural serpentinite sample investigated, one contained antigorite and traces of carbonate and the other contained chrysotile and carbonate. We distinguish the various polytypes of serpentine by careful analysis of the crystal structure using transmission electron microscopy (TEM). The measured contuctivity of serpentinite (10^{-4} Sm^{-1}) is higher than anhydrous olivine (10^{-6} Sm^{-1}) by two orders of magnidute at 1000 K. Upon dehydration, serpentine releases fluids which were also measured in our expreiment and showed a very high conductivity of the order of 10^{-2}-10^{0} Sm^{-1} range. This can easlily explain the high conductivities observed in many subduction zones.

Epitaxial garnet-muscovite interfaces: Molecular modelling

STEPHANIE J. MOORE[1*], KATE WRIGHT[2], JULIAN D. GALE[3], WILLIAM D. CARLSON[4]

[1]The University of Texas at Austin, Austin, U.S.A., sjmoore@utexas.edu (* presenting author)
[2]Curtin University, Perth, Australia, kate@ivec.org
[3]Curtin Univeristy, Perth, Australia, julian@ivec.org
[4]The University of Texas at Austin, Austin, U.S.A., wcarlson@mail.utexas.edu

Introduction

Computer simulations of garnet-muscovite interfaces provide a means of assessing the importance of interfacial energetics to epitaxial nucleation. Experiments and natural samples provide information about specific grain boundary orientations and their prevalence and invite speculation on the importance of particular orientations, but the determination of grain boundary energies from these data is difficult. Currently, there are few constraints on the interfacial energies of naturally occurring minerals and no studies have focused on garnet, a mineral that is of great significance to the metamorphic community. Combining data on grain boundary orientations from natural and experimental samples with molecular modelling that uses energy minimization allows for the determination of relative energies for naturally-occurring grain boundaries between garnet and muscovite.

Methods

Force-field simulations are particularly well-suited to the task of calculating grain-boundary energies for a specific set of conditions; here the General Utility Lattice Program (GULP) simulation code is employed for this purpose [1]. A 2-D periodic slab model is used to investigate muscovite-garnet interfaces. Here each phase is represented by two regions: an interfacial region in which the atoms are fully relaxed, in contact with a second rigid region that represents the underlying bulk material. The two unconstrained regions of garnet and muscovite are then placed in contact to create the interface, while the bulk regions are allowed to rigidly translate relative to each other in order to minimize the total energy. The total potential energy of this final configuration is compared to that of the two bulk structures and by dividing the difference between the two by the area of the interface, an interfacial energy is calculated. The parameters used to describe the energetics of the muscovite and garnet structures include Buckingham potentials, an oxygen core-shell spring constant, a three-body term to describe the O-Si-O bonding angle, and a Morse bond to describe the H-O bond [2,3].

Results

Initial simulations indicate that a garnet slab six unit cells thick and a muscovite slab five unit cells thick are sufficient for simulating the $(110)_{grt} \parallel (001)_{ms}$ with $[100]_{grt} \parallel [100]_{ms}$ interface. Additional simulations reveal that certain surface terminations of the muscovite and garnet slabs create more stable surfaces to be used in the garnet-muscovite interface simulations. The stability of these surfaces may be a guide to determining the precise interfaces between garnet and muscovite in natural samples.

[1] Gale & Rohl (2003) *Molecular Simulation* **29**, 291-341. [2] Steele *et al.* (2000) *Geochimica et Cosmochimica Acta* **64**, 257-262. [3] van Westrenen *et al.* (2000) *Geochimica et Cosmochimica Acta* **64**, 1629-1639.

https://doi.org/10.1180/S0026461X00008434 Published online by Cambridge University Press

Characterization of dissolved organic matter (DOM) from diverse oceanic environments by reverse osmosis and electrodialysis

KENNETH MOPPER[1*], JOHN R. HELMS[1], HONGMEI CHEN[1], NELSON GREEN[2], ARON STUBBINS[3], E. MICHAEL PERDUE[2], PATRICK G. HATCHER[1], AND JINGDONG MAO[1]

[1] Old Dominion University, Department of Chemistry and Biochemistry, 4402 Elkhorn Avenue, Norfolk, VA ,USA, kmopper@odu.edu* (presenting author)

[2] Georgia Institute of Technology, School of Earth and Atmospheric Science, 311 Ferst Drive, Atlanta, GA, USA, mperdue@eas.gatech.edu

[3] Skidaway Institute of Oceanography, 10 Ocean Science Circle, Savannah, Georgia, USA, aron_stubbins@gmail.com

The oceans contain approximately 685 x 10^{15} g of dissolved organic carbon (DOC), a pool similar to current atmospheric CO_2 of ~861 x 10^{15} g C, and is thus a major component of the global carbon cycle. However, only a small fraction of marine DOM is readily identifiable. Determining the chemical nature of the remaining fraction of oceanic DOM has been impeded by the lack of efficient and non-fractionating methods of isolation/desalting. Here, reverse osmosis- electrodialysis (RO/ED) [1] was used for isolating a representative DOM fraction (~75%) for analysis by advanced solid-state 13C- NMR, UV-vis spectroscopy and wet chemical techniques. Samples were obtained from biogeochemically diverse environments; i.e., photobleached surface gyre, productive coastal upwelled, oxygen minimum, deep Atlantic, and old deep Pacific waters. NMR spectral editing revealed new insights into carbohydrate biodegradation, and preservation of carboxyl groups and condensed aromatic structures (deep sea samples). Quaternary anomeric carbons were identified as an important component of bio-refractory carbohydrates. However, despite some differences, these diverse samples yielded remarkably similar DOM compositions. Our results support the 3-pool DOM model (labile, semi-labile, and refractory) [2]. Evidence of 'background' refractory carbon was seen throughout the ocean DOM samples, and the high carboxyl signal in the deep Pacific sample supports the hypothesis that a major fraction of the refractory pool consists of carboxylic-rich alicyclic molecules (CRAM) [3].

RO/ED appears to be the most promising method to date for DOM isolation from seawater; as it can isolate up to 95% of marine DOM (average 75%; compared to 15-40% for other methods) and the extracted DOM has properties closely resembling the unextracted DOM [1,4]. As the method is capable of processing large volumes of seawater, it can potentially be used to collect marine DOM reference material from different oceanic environments, which currently do not exist and would be useful for comparison to terrestrial DOM reference materials.

[1] Koprivnjak et al. (2009). *Geochim. Cosmochim. Acta* **73,** 4215-4231. [2] Hansell& Carlson (2001) *Oceanogr.* **14,** 41-49. [3] Hertkorn et al. (2006) *Geochim. Cosmochim. Acta* **70**, 2990-3010. [4] Mopper et al. (2007) *Chem. Review* **107,** 419-442.

Groundwater vulnerability to climate change in high elevation catchments of the Sierra Nevada

JEAN E. MORAN[1*], MICHAEL J. SINGLETON[2], DARREN HILLEGONDS[2], GLENN SHAW[3], MARTHA CONKLIN[4], BRADLEY K. ESSER[2] AND ATE VISSER[2]

[1]California State University East Bay, Hayward, CA, USA, jean.moran@csueastbay.edu (* presenting author)

[2] Lawrence Livermore National Laboratory, Livermore, USA, singleton20@llnl.gov; hillegonds1@llnl.gov; esser1@llnl.gov visser3@llnl.gov

[3]Montana Bureau of Mines and Geology, Butte, USA, gshaw@mtech.edu

4University of California Merced, Merced, USA, mconklin@ucmerced.edu

Study Design

Snowmelt is an important component of groundwater recharge in high elevation watersheds of the western United States. In these watersheds, the predicted climate change impacts on snowmelt will likely alter the amount and timing of groundwater recharge, which may lead to reduced groundwater production, declining water tables, and reduced baseflow to streams.

We apply dissolved noble gas tracers to answer questions about recharge location and aquifer residence times in two catchments of differing size in the northern Sierra Nevada. The Olympic Valley near Lake Tahoe is a 22 km^2 alpine catchment while the Upper Merced catchment has an area of 465 km^2 and drains through Yosemite Valley. In both valleys, deep, high capacity production wells located in the upper portion of the valley draw groundwater from over much of the sediment thickness. These wells were sampled for tritium and dissolved noble gases in order to determine recharge temperatures (used to esimate to recharge elevation), and tritium-helium groundwater ages.

Results

Noble gas recharge temperatures point to the lower slopes of the mountains, just above the valley floor, as important recharge areas for both catchments. Tritium-helium aquifer residence times are somewhat greater in Yosemite Valley wells (10-28 years) than in Olympic Valley wells (<1-23 years), but in both areas the results indicate relatively rapid turnover of groundwater in the coarse alluvium of the upper valley reaches. The much larger Upper Merced catchment thus supplies only somewhat greater buffering to perturbations in recharge and runoff that would be expected due to warmer temperatures. Using the information gathered from these tracers, differing scenarios characterized by earlier snowpack melting and a higher proportion of precipitation as rain are evaluated with regard to potential impacts to recharge.

https://doi.org/10.1180/S0026461X00008434 Published online by Cambridge University Press

Dynamical and chemical modeling of terrestrial planet accretion

ALESSANDRO MORBIDELLI[1*], DAVID C. RUBIE[2]

[1]Observatoire de la Cote d'Azur, Nice, France, morby@oca.eu (*presenting author)

[2]Bayerisches Geoinstitut, Bayreuth, Germany, dave.rubie@uni-bayreuth.de

The "Grand Tack" dynamical model

The classic dynamical models of terrestrial planet formation, starting from a disk of planetesimals extended from the Sun to the current orbit of Jupiter, typically produce in ~ 100 Ma a few planets in the terrestrial zone on orbits comparable to the real ones [1], but the synthetic planets located near 1.5 AU are systematically more massive than Mars. The large Earth/Mars mass ratio seems to require a strong depletion of solid mass beyond ~1 AU [2]. The "Grand Tack" model [3] explains such a depletion by coupling the early orbital migration of the giant planets with the terrestrial planets accretion process. More precisely, the model assumes that, when the giant planets formed in a proto-planetary disk still dominated by gas, Jupiter first migrated towards the Sun and then, as a consequence of the formation of Saturn, reversed its migration and spiralled outwards. This possibility is supported by hydro-dynamical simulations [4]. If the reversal (or tack) of Jupiter's migration occurred when the planet was at ~ 1.5 AU, the region beyond 1 AU would have been strongly depleted by the passage of Jupiter. The simulations in [3] show that this model is consistent with the existence and the structure of the asteroid belt between 2 and 4 AU, it produces in 30-50 Ma terrestrial planets on orbits consistent with the real ones and, in particular, it explains why Mars is 10 times smaller than the Earth and formed 10 times faster [5]. Thus, the Grand Tack model is so far the most successful model of terrestrial planet formation from the dynamical point of view.

Chemical modelling

To test the Grand Tack model further, we are now applying geochemical constraints. The model is consistent with the delivery of 2000 ppm of water to the Earth from planetesimals of chondritic composition, which agrees with recent estimates of the Earth's water budget and its isotopic composition [6]. Moreover, we are modeling core-mantle differentiation [7] using the accretion history of the planets obtained in the Grand Tack simulations. Assuming that the material originally inside ~1.5 AU had a reduced composition and that beyond this threshold was oxidized, our chemical models result in a FeO content of 8 wt% for the Earth's mantle and ~18 wt% for the Martian mantle, results that are consistent with observed concentrations [8,9]. In the future we will extend our analysis to include more elements (e.g. sulphur, volatile elements, HSEs and water) and we will use more than two initial bulk compositions for accreting material.

[1] Raymond *et al.* (2009) *Icarus* **203**, 644-662. [2] Hansen (2009) ApJ **703**, 1131-1140. [3] Walsh *et al.* (2011) *Nature* **475**, 206-209. [4] Pierens & Raymond (2011) *A&A* **533**, A131. [5] Dauphas & Pourmand (2011) *Nature* **473**, 489-492. [6] Marty (2012) *EPSL* **313**, 56-66. [7] Rubie *et al.* (2011) *EPSL* **301**, 31-42. [8] Palme & O'Neill (2003) In: *Treatise on Geochemistry* **v 2**, 1-38. [9] Dreibus & Wanke (1985) *Meteoritics* **20**, 367-381.

Interaction between Eu(III), phenolic acids and Al_2O_3 nanoparticles.

PAULINE MOREAU[1*], SONIA COLETTE-MAATOUK[1], PASCAL E. REILLER[1], ELISABETH GIBERT-BRUNET[2] AND PIERRE GAREIL[3]

[1] Commissariat à l'Energie Atomique et aux Energies Alternatives, DEN/DANS/DPC/SEARS/LANIE, Gif-sur-Yvette , France, pauline.moreau@cea.fr

[2] Direction Générale de l'Armement, Bagneux, France, elisabeth.gibert-brunet@dga.defense.gouv.fr

[3] Chimie ParisTech, Laboratory of Physicochemistry of Electrolytes, Colloids and Analytical Sciences Paris, France, pierre-gareil@chimie-paristech.fr

Introduction

Natural colloid-borne transport of metal ions in ground water is known to occur. The implications of this kind of transport are especially important in the context of radionuclide migration in subsurface water to evaluate risks of pollutants migration in contaminated soils [1,2]. Furthermore, dissolved organic matter plays a crucial role on metal ions transport. In particular, phenolic acids, resulting from lignin degradation, may be involved in the process of metal ion adsorption onto mineral nanoparticles, as it is the case for aliphatic acids [3]. Our aim is to investigate the sorption of Eu(III) (rare earth and analogue of trivalent actinides) onto Al_2O_3 nanoparticles in the presence of a hydroxybenzoic acid series (4-hydroxybenzoic, 3,4-dihydroxybenzoic, and 3,4,5-trihydroxybenzoic acids).

Results

First, the binary systems were characterized. Eu(III) was shown to have a high sorption capacity on our Al_2O_3 sample, as already described elsewhere [4,5]. Combining sorption data analysis with time-resolved luminescence spectroscopy (TRLS) for Eu(III), at least 2 sorption sites of different energies were evidenced, as in *Rabung et al*. [5]. Complexation constants between Eu(III) and acids were determined using TRLS. It appears that the complexation constant increases from $\log_{10}K° = 2.1$ to 5.3 with the number of phenoxy groups on the benzoic ring. As expected, the sorption isotherms of the Al_2O_3-phenolic acid binary systems show different sorption capacities that cannot be explained by the hydrophobicity of the acids Indeed 4-hydroxybenzoic acid, which is the most hydrophobic compound of the series, has the lowest sorption capacity on Al_2O_3. These results are consistent with published data, demonstrating that increasing the number of phenoxy groups on the benzoic ring of analogue compounds increases sorption on alumina [6]. Besides, the sorption isotherm of 3,4,5-trihydroxybenzoic acid at pH 5 can only be fitted using sequential Langmuir isotherms, which evidences different sorption sites for this acid on Al_2O_3.

The same strategy was applied to study the ternary systems. Sorption isotherms were obtained as well as the TRLS spectra which permit to discuss the pertinency of mixed-surface complexes that involves Eu(III), hydroxybenzoic acids and aluminol sites.

References

1 Kersting et al. (1999) *Nature* **397**, 56-59.
2 Utsunomiya et al. (2009) *Environ. Sci. Technol.* **43**, 1293-1298.
3 Alliot et al. (2006) *J. Colloid Interface Sci*., **298**, 573-581
4 Janot et al. (2011) *Environ. Sci. Technol.* **45**, 3224-3230.
5 Rabung et al. (2000) *Radiochim. Acta*. **88**, 711-716
6 Hidber et al. (1996) *J. Eur. Ceram. Soc.*, **17**, 239-249

https://doi.org/10.1180/S0026461X00008434 Published online by Cambridge University Press

Role of weak complexing agents in metal uptake by phytoplankton

FRANÇOIS M.M. MOREL*, LUDMILLA ARISTILDE, AND YAN XU*

Princeton University, Department of Geosciences, morel@princeton.edu (* presenting author)

The presence of weak ligands enhances the bioavailability of metals bound to strong chelating agents. For example, addition of cysteine (Cys) to EDTA-buffered media increases the rate of uptake of zinc (Zn) by model phytoplankton. Such enhancement of uptake may result from 1) specific uptake of the Zn-Cys complexes, 2) alleviation of diffusion limitation by dissociation of the complexes in the boundary layer of the cells, or 3) exchange of Zn with uptake ligands, X, via formation of a ternary complex X-Zn-Cys. Mechanism 1 is ruled out by the facts that L- and D- isomers of Cys are equally effective at enhancing the Zn uptake rate and that weak ligand addition increases rather than decreases uptake in the absence of EDTA. Mechanism 2 does not explain the effect of weak ligands, for this effect is seen when diffusion does not limit uptake of the free metal. The enhancement of Zn uptake kinetics by weak ligands under various conditions is consistent with mechanism 3: i) enhancement of uptake is particularly effective in Zn-deplete cells whose high affinity transport molecules should be most able to exchange Zn with external ligands; ii) a variety of weak ligands have similar effects on uptake, showing that the mechanism is relatively non-specific; and iii) ligands that bind Zn in complexes that make the formation of a ternary complex difficult do not increase Zn uptake. When essential metals are bound to strong chelating agents in natural waters, binding to weak complexing agents may increase their bioavailability to ambient microorganisms.

The amphoteric behaviour of water in silicate melts: Raman observations and physico-chemical description

ROBERTO MORETTI[1,2,*], CHARLES LE LOSQ[3], DANIEL R. NEUVILLE[3]

[1] Dipartimento di Ingegneria Civile, Seconda Università di Napoli, Italia, roberto.moretti@unina2.it (*presenting author)
[2] Istituto Nazionale di Geofisica e Vulcanologia, Napoli, Italia, roberto.moretti@ov.ingv.it
[3] Géochimie&Cosmochimie, IPGP, Paris, France, lelosq@ipgp.fr neuville@ipgp.fr

Water plays a fundamental role in the dynamics and evolution of magmas in the deep interior and during volcano eruption. However, water speciation in silicate melts is not fully understood, despite Infrared, Raman and NMR spectroscopy had provided some valuable information about the H_2O/OH speciation and its variations as a function of temperature, pressure, and water contents of melts. Some issues still remain unsolved about OH and H_2O linkages to the silicate network and we lack a general physico-chemical description of acid-base exchanges of water in melts. This includes the amphoteric behavior displayed by the water component into depolymerized glasses and melts.

By adopting a Raman-spectroscopy calibration of water dissolved in aluminosilicate melts [1], we studied the Raman OH-stretching bands of hydrous glasses. OH-stretching Raman band records the vibrations of OH groups in molecular water or differently linked to the glass structure or metal cations. To constrain more in detail the evolution of such bands, we performed a set of in situ experiments on rhyolite, basalt and albite glasses using a micro-furnace at ambient atmosphere. We observed new high-temperature Raman features near 3650-3700 cm^{-1}, and also changes of water speciation that occurred below glass transition while quenching to room temperature. Our results will be used to constrain the acid-base exchanges occurring in melts and give insights into the relations between water and silicate network in melts.

[1] Le Losq, C., Neuville, D. R., Moretti, R., Roux, J., 2012. Determination of Water Content in Silicate Glasses using Raman Spectrometry: implications for the study of explosive volcanism. American Mineralogist, in press.

https://doi.org/10.1180/S0026461X00008434 Published online by Cambridge University Press

The cataclysmic Campanian Ignimbrite eruption (Campi Flegrei, Southern Italy): Volatile melt-fining processes and the effects of physico-chemical heterogeneities

R. Moretti[1,2], I. Arienzo[2], F. Brun[3], L. Civetta[4,2], M. D'Antonio[5,2], C. Le Losq[6], L. Mancini[2], D.R. Neuville[6], G. Orsi[2],

[1]Dip. Ing. Civile, Seconda Univ. Napoli, Italy (*presenting author)
[2]Istituto Nazionale di Geofisica e Vulcanologia, Napoli, Italy.
[3]Dip. Scienze Fisiche, Univ.Napoli "Federico II", Italy.
[4]Dip. Scienze della Terra, Univ.Napoli "Federico II", Italy.
[5]Géochimie&Cosmochimie, IPGP, Paris, France
[6]Sincrotrone Trieste S.C.p.A., Basovizza (TS), Italy.

The late Pleistocene trachytic Campanian Ignimbrite (CI; 300 km^3 DRE) covers the Campanian Plain near Naples, and is found behind ridges more than 1,000 m high at 80 km from source, the Campi Flegrei caldera (CFc). Very dilute pyroclastic density currents suggest a magma reservoir highly enriched in volatiles. Volatile concentration, H_2O particularly, exceeds significantly that of other explosive CFc eruptions. To understand such an enrichment and come out with a significant budget of discharged volatiles, particularly H_2O, we analyzed products from the different eruptive phases. Together with FTIR analyses on melt inclusions (MIs), we also characterized pumice glasses for their water content by adopting Raman spectroscopy. CI pumices display high values of porosity (> 60%, but typically > 70%), usually determined by density measurements on bulk samples. However, microscale analyses (2D and 3D) of natural pumices show a significant variability of porosity and permeability within samples. Such a variability may encompass up to 50% of porosity and contrasts with the typical values inherited by pumices at magma fragmentation. This variability is too often overlooked in the pertinent literature and ascribed to local effects within the large-scale dynamics occurring at the moment of the volcanic explosion and leading to generation of Plinian columns. Therefore, we also characterized, at the same micrometric scale of Raman investigations, pumice structure by means of conventional X-ray μCT tomography at the Elettra synchrotron facility in Trieste (Italy). Data substantiate a model in which water accumulation in the CI magma chamber is made possible by a melt fining process, similar to chromatographic separation, that occurs over a time scale comparable to that of magma residence time. This process produced extensive gas fluxing within the magma chamber, leading to an overpressurized CO_2-dominated gas cap (about 150 km^3), uniformly distributed at the top of the magma chamber. The main features of the magmatic "chromatographic" column can be retrieved by our joint Raman and synchrotron X-Ray μCT approach, that allowed investigating the effects of water exsolution and the structural changes in the polymeric network of the pre-fragmentation melt (quenched in the pumice glass).

Geochemical signature of an injection complex in the deep middle crust

Samuel Morfin[1*], Edward Sawyer[1] and Daniel Bandyayera[2]

[1]Université du Québec À Chicoutimi, Sciences Appliquées
[2]Bureau de l'Exploration géologique du Québec
samuel.morfin@uqac.ca (* presenting author)
ewsawyer@uqac.ca
Daniel.Bandyayera@mrnf.gouv.qc.ca

Introduction

Upward transfer of anatectic magma from its lower crustal source is the mechanism of crustal differentiation [1][2]. Recently, it has become evident that a large proportion of anatectic magma does not reach the brittle/ductile transition depth. Field studies show that in the granulitic crust, anatectic magma is mostly transported in a pervasive network of narrow veins. Consequently, the upward migration of magma is arrested at, or close to, the level of the granite solidus and much leucogranite is accumulated at the granulite/amphibolite transition in the form of an injection complex [3]. This changes our perspective on the overall process of chemical differentiation of the crust

Method

Since the formation of an injection complex is mostly controlled by the depth of the solidus, which changes over the time span of a regional metamorphic event, it is expected that at a single crustal depth leucogranites should show a wide degree of chemical evolution.

Results

Both major and trace elements indicate that the Opinaca Injection Complex (Québec) contains a continuum of leucogranite compositions ranging from cumulate to highly fractionated (Fig. 1).

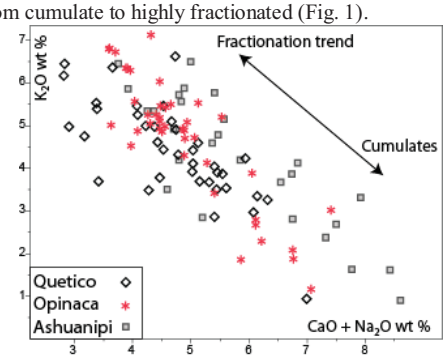

Figure 1: Na_2O+CaO vs K_2O plot showing that (1) the variety of fractionation degree in the Opinaca is similar to deeper crustal levels (Ashuanipi Subprovince) with (2) a greater proportion of evolved compositions although less evolved than higher crustal levels leucogranites (Quetico Subprovince).

Conclusion

Development of injection complex in the deep middle crust result in the accumulation of large volumes of leucogranites of various degrees of evolution close to the granite solidus depth. Evolved granites are thus not only concentrated in the upper crust, many remain in the deep middle crust. Crustal differentiation is thus not as efficient as presently thought both in terms of volume and chemical distribution. Consequences of these changes should be considered into future crustal scale models (e.g. presence of water, heat distribution).

[1] Sawyer et al. (2011) Elements **7**, 229-234. [2] Brown et al. (2011) Elements **7**, 261-266. [3] Morfin et al. (submitted) Lithos.

https://doi.org/10.1180/S0026461X00008434 Published online by Cambridge University Press

Evidence for Mo, organic molecule, and mineral interactions

CAITLIN M. CARNEY[1], JOHN P. LISHER[1], KELLY A. MURPHY[1], PHILLIP R. SLOGOFF-SEVILLA[1], ANTHONY D. WISHARD[1], AND JENNIFER L. MORFORD[1*]

[1]Franklin & Marshall College, Department of Chemistry, jennifer.morford@fandm.edu (*presenting author)

Introduction

Molybdenum (Mo) is relatively conservative in oxic seawater but is removed to the solid phase under sulfidic conditions. Investigators have been encouraged to use Mo solid phase concentrations or accumulation rates to infer past changes in reducing conditions in sediments and/or overlying waters. However, difficulties in fully using Mo as a proxy derive from a lack of information regarding the controlling factors for the removal of Mo from the aqueous phase to the solid phase. A commonly accepted hypothesis involves the thiolation of molybdate to a form that is more easily scavenged by particles[1,2]. A subsequent hypothesis instead suggests that the precipitation of a nanoscale Fe(II)-Mo(VI) sulfide mineral dictates Mo removal from the aqueous phase[3]. However, persuasive correlations between Mo concentrations and sulfurized organic matter hint at a role for organic molecules in Mo fixation and preservation in sediments[4].

We seek to clarify the influence of organic matter on Mo sequestration by determining the role of organic molecules, either aqueous or bound to solid surfaces, in the transition of Mo between the aqueous and solid phases. Simple organic molecules and single minerals are used as analogs for more complex humic material and heterogenous sediments, respectively, present in the environment.

Results

Initial results suggest that the nature of the organic molecule and the type of functional groups are important for aqueous molybdate-organic interactions. Molybdate preferentially complexes with organic molecules that have two phenolic functional groups on adjacent carbons as seen using ^{1}H and ^{13}C NMR. Analysis of molybdate with either 1,2-dihydroxybenzene or 2-mercaptopropionic acid using UV/Vis and ESMS supports the formation of a 1:2 Mo:organic complex.

Molybdate adsorption to aluminum oxide or pyrite is pH dependent with greater adsorption under acidic conditions. All adsorption experiments are consistent with a one-site adsorption surface as modelled with a Langmuir isotherm. The addition of 2-mercaptopropionic acid possibly inhibits the adsorption of molybdate to pyrite, although it is still uncertain whether the thiol competitively occupies pyrite adsorption sites or complexes molybdate, thereby making it incapable of adsorbing to the solid surface. Ultimately, the results of this research should clarify the influence of organic matter on Mo sequestration in modern sediments.

[1] Helz et al. (1996) *Geochim. Cosmochim. Acta* **60**, 3631-3642. [2] Bostick et al. (2003) *Environ. Sci. Technol.* **37**, 285-291. [3] Helz et al. (2011) *Chem. Geol.* **284**, 323-332. [4] Tribovillard et al. (2004) *Chem. Geol.* **213**, 385-401.

Redox reactions affecting arsenic at iron-(oxyhydr)oxide mineral surfaces

GUILLAUME MORIN[1*], GEORGES ONA-NGUEMA[1], KARIM BENZERARA[1], FARID JUILLOT[1], YUHENG WANG[1], CLAUDIA HOHMANN[2], MARTIN OBST[2], ANDREAS KAPPLER[2], GORDON E. BROWN JR[3].

[1]Environmental Mineralogy, IMPMC, CNRS-UPMC, Paris, France. (guillaume.morin@impmc.upmc.fr; * presenting author)
[2]Geomicrobiology, University of Tübingen, Germany.
[3]Surface & Aqueous Geochemistry Group, Department of Geological and Environmental Sciences, Stanford University, Stanford, CA, USA.

For the last few decades, a great deal of attention has been focused on better understanding and predicting the fate of arsenic in the environment. Indeed, due to natural as well as anthropogenic inputs, this element has been recognized as a pollutant in several countries, with major impacts on human health. One of the main conclusions drawn from the numerous studies conducted on natural and laboratory systems is that nanometer-sized iron-(oxyhydr)oxide minerals play a key role in the scavenging of arsenic in water, soils and sediments via sorption reactions. In addition, redox transformations of arsenic have been shown to greatly influence its mobility and toxicity, with As(III) species generally more mobile and toxic than As(V) species. Despite this extensive knowledge base, important questions remain about the detailed mechanisms of particular As oxidation and reduction reactions in complex heterogeneous media, and about the ultimate fate of this element in the presence of various electron donors and acceptors [1-4].

In the present communication, we will review important pathways for arsenic redox transformations that can be driven by either abiotic or abiotic processes. Examples will be chosen from recent studies using synchrotron-based X-ray absorption specoscopy (XANES, EXAFS) to monitor the redox state of arsenic in natural and laboratory systems. Focus will first be given to redox transformations that are usually slow at room temperature, but which can be catalyzed by chemical and physical factors. Particular attention will be paid to the complex interplay between Fe(II)/Fe(III) and As(III)/As(V) redox couples in the presence or absence of oxygen, and the role of photocatalysis in redox reactions [1-4]. Regarding these processes, classical artifacts involving catalysis of redox reactions during exposure to synchrotron radiation will be discussed as possible indicators of light-induced reactions.

In addition, examples of biotic redox transformations able to contribute to As sequestration by oxidized [5-7] or reduced iron-containing minerals [8] will be discussed in relation to the differing affinities of As(III) and As(V) species for specific mineral surfaces [9].

[1] Charlet et al. (2011) ***CRGeosci.*** 343, 123-139. [2] Bandari et al. (2011) ***ES&T*** 45, 2783–2789. [3] Ona-Nguema G. et al. (2010) ***ES&T*** 44, 5416–5422. [4] Amstaetter et al. (2010) ***ES&T*** 44, 102-108. [5] Benzerara et al. (2008) ***GCA*** 72, 3949-3963. [6] Hohmann *et al.* (2010) ***ES&T*** 44, 94-101. [7] Hohmann et al. (2011) ***GCA*** 75, 4699-4712. [8] Ona-Nguema et al. (2009), ***GCA*** *73*, 1359-1381. [9] Wang et al. (2010) ***ES&T*** 44, 109-115.

https://doi.org/10.1180/S0026461X00008434 Published online by Cambridge University Press

Geochemical composition of erosion products in Central Nepal : contraints on landslide and soil erosion processes.

GUILLAUME P. MORIN[1*], CHRISTIAN FRANCE-LANORD[1], MAARTEN LUPKER[1], FLORIAN GALLO[1], JÉRÔME LAVÉ[1], ANANTA PRASSAD GAJUREL[2]

[1] CRPG-CNRS, 15 rue Notre-Dame-des-Pauvres, 54501, Vandoeuvre-les-Nancy, France gmorin@crpg.cnrs-nancy.fr (* presenting author)
[2]Department of Geology, Tribhuvan University, Kathmandu, Nepal

In order to interpret continental sedimentary archives in terms of erosion processes in the past, we made an effort to characterise actual landslides and soils geochemical signatures, in order to trace these processes in the river suspended load (SL) throughout a monsoon season.

To assess this question, daily monitoring of SL chemistry have been conducted during 2010 monsoon in two watersheds : the Narayani river that drains whole central Nepal and the Khudi khola, one of its minor High Himalayan tributaries. In addition, systematic sampling was conducted on hillslopes material from soils and landslides in Khudi. This catchment was chosen because it represents typical South flank Himalayan basin exposed to severe precipitations (3.5 m/yr), and undergoes intense erosion rates as high as 2-3 mm/yr [1]. Characteristics of this watershed are : 800 to 4500 m elevation, 152 km^2, dense forest cover up to 3500 m, and active landslide erosion for at least one decade.

Source rocks, soil and landslide samples are compared to river suspended sediment using mobile to immobile element ratios. Data clearly show that soil material has undergone weathering with loss of Na, K and Ca relative to average source rocks. In contrast, landslide products and suspended sediments have close chemical signature and are only slightly depleted relative to source rocks. Geochemical composition of the Narayani SL have similar characteristics suggesting that even at large scale the erosion is dominated by physical erosion processes rather than by progressive soil development.

The results of this study show that chemical composition of SL are close to those of pristine source rocks, and contrasted with those of soil products. Therefore, active and steep reliefs are mostly eroded through landsliding rather than through soil erosion. The later is difficult to quantify using SL composition in spite of enhanced soil erosion by agricultural activity [2-3] that is significant in the Narayani Basin.

[1] Gabet *et al.* (2008) *Earth and Planetary Science Letters* **267**, 482–494. [2] Gautam *et al.* (2003) *Agriculture, Ecosystems & Environment* **99**, 83–96. [3] Merz (2004) ICIMOD *Institute of Geography, University of Berne, Switzerland*.

Electron microprobe and LA-ICP-MS analyses of ilmenite from lunar samples

CAROLINE-EMMANUELLE MORISSET[1*], SIMON JACKSON[2], MARIE-CLAUDE WILLIAMSON[2], VICTORIA HIPKIN[1] AND KIMBERLY TAIT[3]

[1]Canadian Space Agency, Saint-Hubert, Canada, (* presenting author: caroline-emmanuelle.morisset@asc-csa.gc.ca), victoria.hipkin@asc-csa.gc.ca
[2]Geological Survey of Canada, Ottawa, Canada, simon.jackson@NRCan.gc.ca, marie-claude.williamson@NRCan.g.ca
[3]Royal Ontario Museum, Toronto, Canada, ktait@rom.on.ca

Oxygen can be liberated from ilmenite at lower temperature than from silicates present in the lunar regolith, making ilmenite a key resource for human settlement on the Moon. Major and trace element concentrations of ilmenite contained in twelve samples selected from the six Apollo landing sites (10 basalts, one impact melt, and one impact breccia) and in one lunar meteorite (NEA 001) have been determined using electron microprobe and LA-ICP-MS. These analyses help us to understand the role of ilmenite in the crystallization of magma on the Moon and to determine if the ilmenite from different rock types has a specific chemical signature. Ilmenite can reach a modal proportion of up to 20% in basaltic rocks. Some ilmenite grains contain rutile, Cr-spinel and baddeleyite needles. The TiO_2 in the analyzed ilmenite from the Apollo samples varies from 52.4 to 55.9 wt% while it is noticeably lower in the meteorite sample (i.e. 51.7 to 52.8 wt%). In all samples, FeO varies from 37.4 to 46.7 wt% and MgO from 0.1 to 5.1 wt% except in the impact melt where it is higher (5.3-5.7 wt%). The largest variation observed in MgO within an ilmenite grain is of 0.3 wt% (e.g. 4.7-5.0 MgO wt%), implying that the observed variation between grains cannot be attributed to mineral zoning. So far, three basaltic samples have been analyzed by LA-ICP-MS. Cr varies from 1080 to 7580 ppm, V varies from 80 to 453 ppm and both elements are positively correlated with MgO. Zr (123-2330ppm) and Hf (5.95-85 ppm) concentrations are highest in the baddeleyite-bearing ilmenite grains. Nb (20-107 ppm) and Ta (1.85-8.52 ppm) are positively correlated but are not well correlated with Zr or Hf. REE patterns show enrichment in HREE (Ce_N/Lu_N: 0.0001-0.005) with a strong negative Eu anomaly (Eu/Eu* from 0.003 to 0.413). The ratio of MgO vs TiO_2 of the ilmenite permit discrimination of what type of sample the ilmenite is from. Ilmenite from the basaltic samples form a trend (n=355; slope=1.89; r^2=0.86) that is richer in TiO_2 for the same MgO than the impact breccias (n=11; slope=1.5; r^2=0.91) and the meteorite (n=10; slope=4.38; r^2=0.42) samples. LA-ICP-MS analysis of the remaining samples will permit evaluation of whether the observed geochemical distinctions between the three sample groups are identifiable using trace elements.

https://doi.org/10.1180/S0026461X00008434 Published online by Cambridge University Press

Recovery and reproducibility of the conventional and accelerated solvent extraction methods for lipid biomarkers

ANJA MORITZ[1]*, KARINE LALONDE[2], YVES GÉLINAS[3]

[1]Concordia University, Montreal QC, Canada, anjamoritz@hotmail.com (*presenting author)
[2]Concordia University, Montreal QC, Canada, k_lalonde@hotmail.com
[3]Concordia University, Montreal QC, Canada, ygelinas@alcor.concordia.ca

Abstract

Biomarkers are widely used as tracers of the processes affecting organic matter cycling in the environment. Lipids, or more specifically hydrocarbons, sterols and fatty acids, are used extensively as indicators of the sources of organic matter as well as its alteration by photochemical or microbial degradation. The extraction of these lipids from sediments consists in a liquid-solid extraction using a mixture of non-polar solvents (most often dichloromethane and methanol). Conventional extraction of lipids from solid matrices traditionally involves ultrasonic extraction combined with shaking, or Soxhlet-based solvent refluxing. These two techniques are long and tedious and use low temperature and low pressure conditions to extract lipids. We recently found out that iron oxides associate very intimately with sedimentary organic matter, leading to the preservation of labile organic material, likely through covalent bonding [1]. Our results show that a fraction of the extractable lipids are not quantitatively recovered when using low temperature and low pressure methods for iron oxide-containing sediments. An extraction at high pressure and high temperature using an accelerated solvent extractor (ASE) disrupts these iron-organic matter structures, releasing the lipids into solution. The reproducibility and lipid recovery of the ultrasonication and ASE methods will be presented and discussed.

[1] Lalonde et al. (in press) *Nature*.

Sourcing hydrocarbons at two continental sites of present-day serpentinization: The Tablelands, NL, CAN and The Cedars, CA, USA

PENNY MORRILL[1], AMANDA RIETZE[1], NATALIE SZPONAR[1], J.GIJS KUENEN[2],SHINO SUZUKI-ISHII[3], AND KENNETH H. NEALSON[3].

[1] Dept. Earth Sciences, Memorial University of Newfoundland, NL, CAN, pmorrill@mun.ca (* presenting author)
[2] Delft University of Technology, Delft, Netherlands
[3] J. Craig Venter Institute, San Diego, CA, USA

The hydration of ultramafic rocks, via the serpentinization reaction, is a suspected source of putative hydrocarbons (methane and possibility higher molecular weight gases hydrocarbons) on Mars. On Earth, serpentinization produces hydrogen gas and the reducing conditions necessary for abiogenic hydrocarbon synthesis, while also producing conditions amenable for chemolithotrophic life. Additionally, on Earth, continental sites of serpentinization are often assoicated with buried sedimentary organic matter (SOM) that can possibly contribute thermogenic hydrocarbons to the ultra-basic reducing springs associated with the serpentinization. This study sources hydrocarbons from two continental sites (the Tablelands, NL, CAN and The Cedars, CA, USA) of present-day serpentinization where methane and higher molecular weight hydrocarbons are present in the ultra-basic reducing springs discharging from altered ultramafic rocks.

The Cedars was the first site to be described where ultramafic rocks are undergoing present-day serpentinization at shallow depth and low temperature. The Cedars is part of California's Coast Ranges and is a section of a peridotite body that was obducted as part of the Franciscan Subduction Complex (Late Cretaceous). Conversely, the much older Tablelands Ophiolite, NL is part of the Bay of Island Ophiolite. The Tablelands Ophiolite is composed of ultramafic rocks that were obducted onto the eastern edge of ancient North America (Ordovician). Elevated concentrations of H_2, CH_4 and higher molecular weight hydrocarbons have been detected in the ultra-basic reducing springs discharging from The Cedars and the Tablelands. Our geochemical investigations show that the methane at The Cedars is primarily microbial in origin (for example C_1/C_{2+} = 6000, $\delta^{13}C$ = -68.0 ‰), while the methane sampled from the Tablelands is not (for example C_1/C_{2+} = 5, $\delta^{13}C$ = -26.3 ‰). However, the source of the higher molecular weight hydrocarbons may differ from the source of methane (The Cedars average $\delta^{13}C_{C2-C6}$ ~-23.6 ‰ and the Tablelands $\delta^{13}C_{C2-C6}$ ~-30.7‰). Both The Cedars and the Tablelands could have thermogenic and/or abiogenic hydrocarbons contributing to the hydrocarbons detected in the springs. The purpose of this study is to source the higher molecular weight hydrocarbons through the analyses of the hydrocarbons in the ultra-basic reducing springs and the SOM associated with the Ophiolite.

https://doi.org/10.1180/S0026461X00008434 Published online by Cambridge University Press

Microbial transformation of radionuclides - the radionuclide biomineral interface.

K. MORRIS[1*], D. BROOKSHAW[1], V. EVANS[1], C. THORPE[1], A. WILLIAMSON[1], G. T. LAW[1,2], A. RIZOULIS[1], F.R. LIVENS[1,2] AND J.R. LLOYD[1]

[1]Research Centre for Radwaste and Decommissioning and Williamson Research Centre, and [2]Centre for Radiochemistry Research, The University of Manchester, Manchester, M13 9PL. (*correspondence: katherine.morris@ manchester.ac.uk)

Microbial processes can have a profound effect on the solubility of radionuclides in natural and engineered environments. The scope of these processes is significant with clear evidence that radionuclide solubility may be altered enzymatically via mediated redox reactions, by indirect redox reactions with, for example, Fe(II)-bearing biominerals andfor non-redox active species, even by incorporation reactions into neo-formed biominerals formed as physicochemical conditions change. Understanding these reactions is important across radionuclide impacted environments from contaminated land environments where bioreduction and biomineralisation processes may be harnessed to control radionuclide mobility, through nuclear facilities where biological processes are often poorly constrained yet may be critical in long term management and control of radionuclides, and finally to radioactive waste disposal scenarios where there is a paucity of information on the influence of microbial processes on bio-mineralisation and radionuclide behaviour under geological disposal facility conditions.

Recent work exploring the behaviour of Sr, U and Np will be discussed with a focus on (bio)mineralisation, reduction and reoxidation reactions and their impact on radionuclide behaviour. The products of biomineralisation in terms of bulk element cycles and (bio)geochemistry will be discussed in the context of radionuclide solubility. Studies relevant to a range of environments including radioactively contaminated land, nuclear legacy ponds, and high pH environments relevant to environments expected in geological disposal of cementitious waste forms will be discussed. The biogeochemical fate of radionuclides across these systems and in the sometimes "extreme" environments that these systems pose will be highlighted.

Critical zone weathering of glacial till in the Prairie Potholes Region: A major control on wetland ecology

JEAN M. MORRISON[1]*, MARTIN B. GOLDHABER[2], CHRISTOPHER T. MILLS[2], KARL J. ELLEFSEN[2]

[1]U.S. Geological Survey, Denver, United States, jmorrison@usgs.gov (* presenting author)
[2]U.S. Geological Survey, Denver, United States

The Prairie Potholes Region (PPR), a vital ecosystem in North America comprising a 715,000 km^2 region in the north-central U.S. and south-central Canada, is characterized by millions of closed-basin wetlands. Sulfate is the dominant anion in these wetlands. A thick oxidized brown (iron oxide-bearing) zone which transitions to unoxidzed, gray till has been widely reported in the PPR.

The objective of this study is to characterize till alteration in the 92 hectare Cottonwood Lake Area (CWLA) near Jamestown, ND, where Pleistocene-age glacial till overlies pyrite-rich marine shale. We studied the geochemistry and mineralogy of three cores drilled along a topographic gradient from an upland position (ground surface at 569 m) to the edge of a low lying discharge wetland (ground surface at 560 m) referred to as P1, whose anion content is dominated by SO_4^{2-}. A brown-gray transition was recognized whose depth systematically decreased from 13.3 m in the upland core to 7.3 m at the wetland edge. We also analyzed archived cutting samples from a groundwater well drilled in 1978 near the margin of wetland P1. This well penetrated to bedrock at 136 m and the brown-gray transition was observed at 12.3 m.

Semi-quantitative X-ray diffraction (XRD) analysis of material from the cores and cuttings detected gypsum in the brown zone that ranged from trace amounts to 8 wt % with the highest concentrations at or below the water table. Gypsum was below detection (<1 wt%) in the samples from the gray zone. These results were confirmed by water leaches for soluble sulfates. Using a terrain conductivity meter, the electrical conductivities of subsurface were measured along a transect parallel to the core samples. The brown zone was more conductive than the gray zone (120-150 mS/m vs. <120 mS/m) likely due to the presence of gypsym. Both XRD and quantative reductive dissolution assays showed that gray zone samples, including those from the deep well, contain pyrite in the range 0.3 to 1.1 wt %.

We conclude that shale-derived pyrite in the till has been slowly oxidized to SO_4^{2-}, which is leached to groundwater and responsible for the consistently high content of S in the CWLA wetlands. These weathering processes drive groundwater and wetland geochemistry, resulting in dramatic variations in salinity over short distances depending upon where individual wetlands reside in local groundwater systems. Variations in wetland chemistry influence the flora and fauna that inhabit the wetlands. Therefore, understanding the long-term alteration processes in the till has a close link to wetland ecology in this region that is known as the duck factory of North America.

https://doi.org/10.1180/S0026461X00008434 Published online by Cambridge University Press

Structure and Energetics of Smectite Interlayer Hydration: Molecular Dynamics Investigations of Na- and Ca-Hectorite

CHRISTIN P. MORROW[1]*, A. ÖZGÜR YAZAYDIN[2], GEOFFREY M. BOWERS[3], ANDREY G. KALINICHEV[4], AND R. JAMES KIRKPATRICK[5]

[1]Department of Chemistry, Michigan State University, East Lansing, MI, USA, morrowc9@msu.edu (*presenting author)

[2]Department of Chemistry, Michigan State University, East Lansing, MI, USA and Department of Chemical Engineering, University of Surrey, Guildford, UK, yazaydin@msu.edu

[3]Division of Chemistry and Department of Materials Engineering, Alfred University, Alfred, NY, USA, bowers@alfred.edu

[4]Department of Chemistry, Michigan State University, East Lansing, MI, USA and Laboratoire SUBATECH, Ecole des Mines de Nantes, Nantes Cedex 3, France, kalinich@subatech.in2p3.fr

[5]College of Natural Sciences, Michigan State University, East Lansing, MI, USA, rjkirk@cns.msu.edu

Molecular-scale interactions present at mineral-water interfaces and in clay interlayer galleries control numerous environmental processes, including chemical interactions in soils and transport of nutrients and pollutants through them.[1-4] Understanding these processes requires accurate knowledge of the structure, energetics, and dynamics of the interaction among the mineral substrate, ions, and water molecules.[5, 6] Challenges to this objective include experimental difficulties in probing these interfaces and interlayers at the molecular scale; fully characterizing the mineral substrate; and identifying how the mineral surface, ions, and water molecules each contribute to the overall structure, energetics, and dynamics of these systems.[6] Linked computational molecular dynamics (MD) simulations and experimental nuclear magnetic resonance (NMR) studies are particularly effective in addressing these issues.[7-9]

Here we focus on MD studies of Na- and Ca-smectite (hectorite) interlayer galleries to provide a molecular-scale picture of the structure and dynamics of their hydration[9, 10] and to complement our earlier NMR investigations of these systems.[7-9] Classical MD simulations were undertaken in the *NPT* and *NVT* ensembles to determine the structural and energetic changes with increasing hydration with focus on the single- and double-layer hydrates. The results show substantial changes in the hydration of the interlayer cations, the orientations of the water molecules, the hydrogen bond network involving the water molecules and basal oxygen atoms, and the resulting potential energies as the interlayer gallery expands.

[1] Scheidegger *et al.* (1996) *Soil Science* **161** 813-831. [2] Stumm (1997) *Colloids and Surfaces A-Physicochemical and Engineering Aspects* **120** 143-166. [3] O'Day (1999) *Reviews of Geophysics* **37** 249-274. [4] Koretsky (2000) *Journal of Hydrology* **230** 127-171. [5] Wang *et al.* (2001) *Chemistry of Materials* **13** 145-150. [6] Wang *et al.* (2006) *Geochimica et Cosmochimica Acta* **70** 562-582. [7] Bowers *et al.* (2008) *Journal of Physical Chemistry C* **112** 6430-6438. [8] Bowers *et al.* (2011) *Journal of Physical Chemistry C* **115** 23395–23407. [9] Bowers *et al.* (2012), unpublished. [10] Morrow *et al.* (2012) *Journal of Physical Chemistry C*, submitted.

Reconstructing a young martian history with igneous microbaddeleyite rimmed by metamorphic zircon

D. E. MOSER[1*], K.R. CHAMBERLAIN[2], K.T. TAIT[3], A.K. SCHMITT[4], I. R. BARKER[1], B.C. HYDE[3], J. DARLING[1]

[1]Western University, London, Canada, desmond.moser@uwo.ca

[2]University of Wyoming, Laramie, U.S.A.

[3]Royal Ontario Museum, Toronto, Canada

[4]UCLA, Los Angeles CA, U.S.A.

A current paradox in martian geochronology is that basaltic shergottites yield whole rock and unradiogenic mineral isotopic Pb-Pb compositions consistent with a primary Noachian (>4 Ga) age for crystallization whereas mineral isotopic analyses consistently return 'young' post-Amazonian (<0.6 Ga) dates. To assess the significance of the mineral dates, we have combined single-grain isotopic SIMS U-Pb microbaddeleyite dating with chemical and deformation microstructure data obtained with electron nanobeam techniques (e.g. CL, EBSD) to resolve baddeleyite paragenesis and potential for isotopic disturbance by shock processes. We have focused on microbaddeleyites from shergottite NWA 5298, an enriched basaltic shergottite exhibiting a primary phaneritic igneous texture which has similarities to other basaltic shergottites. The baddeleyites are generally subhedral to euhedral blocky to bladed grains, 2 to 20 μm long, at the boundaries of larger main phase minerals. SE and BSE imaging of grain interiors showed that grains are often composed of equant microdomains that give the appearance of a granular texture. Grains are often surrounded by discontinuous rims of zircon a few microns wide identified by EDS and EBSD. CL zoning types in baddeleyite include simple bright, narrow rims of variable thickness surrounding dark cores, and patchy to diffuse and mottled CL domains at the margins of grains or in areas of crystal disruption and apparent granular texture. A subset of grains exhibits oscillatory planar growth banding similar to that which we have observed in terrestrial igneous baddeleyite. Our EBSD mapping indicates clearly that the baddeleyite is now quasi-amorphous and is hosted by amorphous maskelyinite, whereas zircon is crystalline and apparently unshocked, although an investigation at higher resolution for the high pressure polymorph, reidite, is ongoing. SIMS analysis of 12 grains yielded $^{206}Pb/^{238}U$ dates ranging from 209 ± 22 Ma (2σ) to 26 ± 2 Ma. An unforced discordia line has an upper intercept with concordia at 0.9 +1.2/-0.7 Ga and a zero age lower intercept. Our SIMS data together with microtextural data for the baddeleyites are consistent with U-Pb disturbance of primary, post-Noachian igneous crystals during shock, recent shock heating, and zircon growth. A scenario is favoured wherein bulk melting of ancient 4 Ga parent material produced the NWA 5298 source magma through volcanic or impact melting. This would reconcile 'young' mineral dates and isochrons with the unradiogenic and whole rock Pb-Pb age data from basaltic shergottites.

https://doi.org/10.1180/S0026461X00008434 Published online by Cambridge University Press

Remobilisation of uranium from contaminated sediments: effect of the bioturbation

MIKAEL MOTELICA-HEINO [1]*, F.LE MOING[2], SANDRA LAGAUZERE [2], JEAN-MARC BONZOM[2], LAURENINE FEVRIER[2] AND VIRGINIE CHAPON[3]

[1]ISTO, University of Orléans, Orléans, France, mikael.motelica@univ-orleans.fr
[2]IRSN, Cadarache, France, jean-marc.bonzom@irsn.fr
[3]CEA,Cadarache, France, virginie.chapon@cea.fr

Introduction

The main thrust of this work is to bring some answers to the following question: what either distinct or combined role do the different physico-chemical and biological (benthic macro-organisms) play on the reactivity, the transfer and the biotic impact of metallic contaminants in sediments? To achieve this goal, experimentations wre carried out in microcosmes with different forcing parameters (oxia, anoxia, with and without macro-benthic organisms).

Material and methods

15 sediment cores were samples in the Pontabrier lake within the village of Compreignac north of Limoges (Haute-Vienne, France). These sediments are heavily contaminated in uranium (34 317 Bq/Kg m.s.). Cores were untouched and were used as the characterisation cores (cores « C »). 6 other cores were then depleted in benthic macro-organisms by addition of niyrogen gas for 24 h. Half of the cores depleted in macro-organisms were populated with 1060 Tubifex tubifex by core with a mean density of 60 000 individualss /m² close to what observed in some environments (cores « T »). The three remaining cores were submitted to gamma irradiation (delivered dose: 40 Kgy) during 6 days t sterilise them (cores « S »). At day 0 and after a month, peepers-gels DET probes (diffusive equilibrium in thin-films) were inserted for 24 h in all probes to determine the concentration profiles of the dissolved species.

Results and conclusion

Results suggested the enhanced release of uranium from the sediment by bioturbation (figure 1). The present study provides further evidence of the enhanced release of uranium from the sediment by bioturbation, possibly from the dissolutive reduction of iron oxyhydroxydes coated with uranium. The bioturbation is in fact likely to shift the redox processes with the further addition of dissolved oxygen by the Tubifex activity.

Figure 1: U pore-water profiles by DET

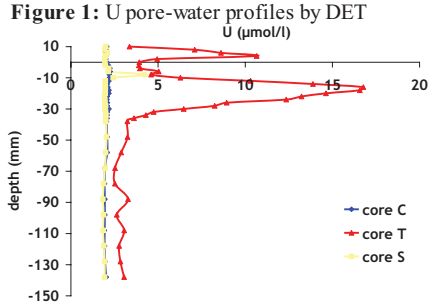

In situ high pressure changes to the O *K*-edge electronic structure of $CaMgSi_2O_6$: An x-ray Raman approach

B.J.A. MOULTON[1*], M. KANZAKI[2], H. FUKUI[3], N. HIRAOKA[4] AND G.S. HENDERSON[1]

[1]University of Toronto, Toronto, Canada, bja.moulton@utoronto.ca*; henders@geology.utoronto.ca
[2]Institute for Study of the Earth's Interior, Okayama University, Misasa, Japan, mkanzaki@misasa.okayama-u.ac.jp
[3]University of Hyogo, Hyogo, Japan, fukuih@sci.u-hyogo.ac.jp
[4] National Synchrotron Radiation Research Center, SPring-8, Hyogo, Japan, hiraoka@spring8.or.jp

Abstract

X-ray Raman spectroscopy (XRS) is a rapidly developing technique for in situ observation of the near edge structures in the soft x-ray regime. This region includes the K- and L-edges of most common silicate melt forming elements including Si, Al, Mg and O. This is the only technique that provides direct in-situ observation of the near edge features of these elements at high pressure. This study uses a panoramic diamond anvil cell and beryllium (Be) gasket in the through gasket geometry to investigate the oxygen (O) K-edge within $CaMgSi_2O_6$ glass, an important high pressure phase. Experiments were performed on the Taiwanese inelastic x-ray scattering beamline BL12XU at SPring 8, Japan.

Preliminary results show a prominent edge feature at 533 eV. With increasing pressure the edge first shifts to slightly lower values (~0.1 eV/GPa) until 17.5 GPa whereupon the edge shift becomes positive. At 8 GPa, the O K-edge changes from being a single asymmetric peak (537 eV) at ambient pressure to a distinct double peak (537 and 541 eV). Above 8 GPa, the main peak retains these features though the resolution becomes degraded. The changes in the O K-edge are related to the changes in Si-O-Si glass network.

In comparison to XRS studies on the O K-edge of SiO_2[1], and its polymorphs, the edge features for $CaMgSi_2O_6$ glass are substantially more broad, indicating more complex bonding interactions of local structures. Additionally, the development of an intense peak at 544 eV in SiO_2 glass, thought to represent the presence of $Si^{[6]}$ found in stishovite, is lacking. Although the absense of the 544 eV feature does not preclude the presence of higher coordinated Si species within the glass structure, it does suggest that a more in-depth understanding of the O K-edge under pressure is essential to directly observing, interpreting and understanding the structural role of O within silicate melts at high pressure.

[1] Lin, Fukui, Prendergast, Okuchi, Cai, Hiraoka, Yoo, Trave, Eng, Hu and Chow (2007) *Physical Reviews B* **75**, 012201:1-4.

https://doi.org/10.1180/S0026461X00008434 Published online by Cambridge University Press

Volatile budget of the 2011 Cordon Caulle eruption (Chile) from various and integrated approaches.

S. MOUNE[1*], S. CARN[2], N. CLUZEL[1], F. AGUILERA[3], A. AMIGO[4]

[1]. Laboratoire Magmas et Volcans, OPGC-UBP-CNRS, Clermont-Ferrand, France, S.Moune@opgc.univ-bpclermont.fr
[2]. Department of Geological and Mining Engineering and Sciences, MTU, Houghton, USA, scarn@mtu.edu
[3]. Departamento de Geología, Universidad de Atacama, Copiapó, Chile, felipe.aguilera@uda.cl
[4]. SERNAGEONIM, Santiago, Chile, aamigo@sernageomin.cl

Estimates of volatile budgets for volcanic eruptions are often based on volatile concentrations measured in melt inclusions (MIs) versus groundmass glass and on measurements made by direct sampling and remote sensing techniques. Here, we present new measurements and estimates of volatile budget of the 2011 Cordon Caulle eruption in Chile. The eruption from the Cordón Caulle rift zone, part of the basaltic-to-rhyolitic Puyehue-Cordón Caulle volcanic complex, began on 4 June 2011. The first phase of the eruption was characterized by an explosion from Cordón Caulle that produced a 5-km-wide ash-and-gas plume that rose to an altitude of 12.2 km a.s.l. We used three different approaches to assess the volatile budget and how the volatile content of the magma controls the explosivity of such an eruption.

1- Pumice samples were collected on June 18th, a few hours after their eruption. Volatile (S, Cl, F) and major element concentrations were measured in MIs trapped in plagioclase (An54-56) and pyroxene (Mg#39-44) phenocrysts and also in groundmass. Homogeneous dacitic to rhyolitic compositions were observed in the MIs with maximum concentrations up to 160ppm S, 2600ppm Cl and 800ppm F. The difference between the maximum volatile concentrations in the MIs and those measured in the groundmass indicates that ~0.2Mt SO_2, 0.5Mt HCl and 0.3Mt HF were released into the atmosphere during the Cordon Caulle eruption.

2- Satellite remote sensing data from instruments in NASA's A-Train spacecraft constellation, including the Ozone Monitoring Instrument (OMI) on Aura and the Atmospheric Infrared Sounder (AIRS) on Aqua, indicate a total SO_2 emission of ~0.2 Mt from the initial explosive phase of the 2011 Cordon Caulle eruption. The Microwave Limb Sounder (MLS) also detected HCl in the volcanic plume, providing some constraints on the SO_2/HCl ratio.

3- These two previous preliminary results will be discussed and compared with ash-leachate analyses. Leachates from pristine ash collected on June 21st will also provide a plume-gas proxy.

Experimental simulation of brine re-injection under subcritical and supercritical conditions

BRUCE W. MOUNTAIN[1]* AND ROMAIN SONNEY[2]

[1]GNS Science, Wairakei Research Centre, Taupo, New Zealand, b.mountain@gns.cri.nz (*presenting author)
[2]University of Neuchâtel, Centre for Hydrogeology and Geothermics (CHYN), Neuchâtel, Switzerland, romain.sonney@unine.ch

The re-injection of flashed brine at geothermal power plants is used to avoid adverse impacts of surface disposal. These fluids contain solutes that can precipitate and thus are detrimental to re-injection aquifer permeability. The deposition of silica is a particular issue that must be managed through brine aging and/or acid/base dosing. These treatments modify brine properties such that it is highly out of equilibrium with the aquifer mineralogy. The re-injection of fluids into deep (>4 km) drillholes, that may encounter supercritical conditions, also poses interesting questions in terms of fluid-rock interactions influencing reservoir permeability. Existing thermodynamic data used in modelling programmes are insufficient to provide adequate information on the effects of fluid-rock interactions in these situations. A viable alternative is direct simulation using experimental apparati.

Re-injection scenarios have been simulated using a continuous flow apparatus. The experiments replicate the interaction between waste brine with fractured greywacke, a typical re-injection aquifer lithology at power plants in the Taupo Volcanic Zone. Deoxygenated brine from Kawerau power station (SiO_2 950 mg/kg, Na 799 mg/kg, K 131 mg/kg, Cl 1027 mg/kg, SO_4 423 mg/kg) was reacted with crushed, sieved and cleaned greywacke at T/P conditions of 157^{o}C/27 bar, 204^{o}C/35 bar and 400^{o}C/279 bar. At the lowest temperature both polymerized and depolymerized brine were used to assess the effect of fluid aging. SEM/EDS examination showed that polymerized brine produced a continuous coating of amorphous silica composed of variable size silica spherules (<500 nm) cemented by dissolved monomeric silica. Using depolymerized brine, amorphous silica was also produced, the spherule size was uniform (80 nm) and the coating was more discontinuous. At 204^{o}C, precipitated minerals include chlorite, potassium feldspar, a clay mineral phase and a Ca-Na aluminosilicate, most likely a zeolite, based on its morphology. SiO_2 concentration dropped below amorphous silica saturation but no SiO_2 polymorph was identified indicating that the decrease in SiO_2 concentration was the result of precipitation of the minerals listed above. At 400^{o}C, the surfaces of the greywacke fragments were covered with continous coating of acicular secondary minerals. These include a fibrous Na-Ca-Fe-Mg aluminosilicate (pargasite?), a Na-Fe silicate with a distinct amphibole morpholgy (riebeckite?) and an unidentified Ca-aluminosilicate. Titanite was also present, likely derived from the sample chamber. These experiments show that laboratory simulations can be successfully used to reproduce fluid-mineral interactions that correlate with temperature conditions found in re-injection aquifers. They also provide information on changes in surface roughness and permeability of fractures during re-injection of geothermal brines.

https://doi.org/10.1180/S0026461X00008434 Published online by Cambridge University Press

Compositional trends in tourmalines from granites and quartz-tourmaline rocks from the Penamacor-Monsanto pluton (Eastern Central Portugal)

I. Ribeiro da Costa[1,2], I.M. Antunes[3], F. Guimarães[4], J.M. F. Ramos[2], C. Recio[5], F.J.A.S. Barriga[1,2], C. Mourão[2*]

[1] Departamento de Geologia, Faculdade de Ciências da Universidade de Lisboa, Portugal, isabelrc@fc.ul.pt, fbarriga@fc.ul.pt
[2] CREMINER/LARSyS (Lab.Assoc.), Portugal, Farinha.Ramos@ineti.pt, ccmourao@fc.ul.pt (*presenting author)
[3] Escola Superior Agrária, Instituto Politécnico de Castelo Branco, Portugal, imantunes@ipcb.pt
[4] LNEG: Laboratório Nacional de Energia e Geologia (S. Mamede de Infesta), Portugal, fernanda.guimaraes@lneg.pt
[5] Servicio General de Isótopos Estables, Facultad de Ciéncias de la Universidad de Salamanca, Spain, crecio@usal.es

Abstract

Peraluminous two-mica granites are predominant in the late-Hercynian Penamacor-Monsanto pluton [1], intrusive into a massive schist-greywacke sequence, and most marginal granites contain tourmaline, hinting at late-magmatic boron-metasomatism. This is further supported by occurrences of quartz (± mica) -tourmaline rocks along the narrow contact aureole. Tourmaline colour and colour zoning patterns are related to Ti abundance and Fe/Mg ratios, according to X-ray mapping. Notwithstanding ubiquitous late crystallization of euhedral to subhedral tourmaline in the marginal granites, textural and X-ray compositional evidence suggest that some tourmaline may nucleate on biotite and eventually replace it. Given their high proportion of *X*-site vacancies (58 to 78%), tourmalines from marginal granites are classified as foitites and those in the quartz-tourmaline rocks as foitites and Mg-foitites. Schorl-type substitution predominates over elbaite-type substitution, especially in granite tourmalines, which tend to be richer in Fe^{2+} and Al (± Mn) and poorer in Mg and Na (± Ca, Cr, V, Ti) than tourmalines from quartz-tourmaline rocks. In spite of their chemical differences, both tourmaline populations seem to bear a close genetic relationship, as evidenced in the (Fe+Mn)/(Fe+Mn+Mg) *vs.* Al/(Al+Mg+Li) linear trend, strongly suggesting that the same late-magmatic, B-enriched aqueous fluid was involved in their genesis.

Analytical and isotopic work currently in progress will soon add to these preliminary results on the Penamacor-Monsanto tourmalines.

We acknowledge financial support of PTDC/CTE-GIX/116204/2009.

[1] Neiva, A.M.R & Costa Campos, T.F. (1993) *Mem. Not. Publ. Mus. Lab. Mineral. Geol. Univ. Coimbra* **116**, 21-47.

An integrated study with benthocosms on the impact of different functional groups of macrofauna on benthic N-processes in coastal sediments of the St. Lawrence Estuary

Aurélia Mouret[1*], Gwénaëlle Chaillou[2], Philippe Archambault[3], Roxane Maranger[4], Bjorn Sundby[5] and Alfonso Mucci[6]

[1]Institut des Sciences de la MER-UQAR, Rimouski, Canada, aurelia.mouret@uqar.qc.ca (* presenting author)
[2]Institut des Sciences de la MER-UQAR, Rimouski, Canada, philippe_archambault@uqar.qc.ca
[3]Université du Québec à Rimouski, Rimouski, Canada, gwenaelle_chaillou@uqar.qc.ca
[4]Université de Montréal, Montreal, Canada, r.maranger@umontreal.ca
[6]McGill University, Earth and Planetary Sciences, Montreal, Canada, bjorn.sundby@mcgill.ca
[6]McGill University, Earth and Planetary Sciences, Montreal, Canada, alfonso.mucci@mcgill.ca

Previous studies in the Laurentian Channel revealed that 2/3 of the dissolved oxygen depletion of bottom water is caused by changes in ocean circulation patterns in the northwestern Atlantic [1]. Nevertheless, elevated organic matter fluxes to the seafloor, from eutrophication due to enhanced fertilizer use in the watershed, could also increase locally the bottom water and sedimentary oxygen demand. The aim of this study was to improve the knowledge of the N budget in the coastal environments of the St Lawrence Estuary in order to better evaluate system's capacity to buffer anthropogenic N loading. Some studies showed that macrofauna of these coastal environments have an impact on benthic biogeochemical fluxes. Develop the understanding on complex interactions between sediment and benthos requires the use of innovative approaches because fauna activity and patchy distribution of organic matter introduce another level of complexity and initiate a heterogenic pattern of microzones. In this perspective, a closed-circulation, water jacket-insulated laboratory basins, called benthocosms, were used to preserve sediment mesocosms of 0.16 m^2 surface area, with controlled conditions of salinity and temperature. 5 different treatments were set up to specify the impact of different functional groups of macrofauna on nitrification, denitrification, anammox. A treatment without fauna was compared to a treatement with biodiffusers (*Mya arenaria* and *Macoma balthica*) and to a treatment with biodiffusers + gallery-diffusers (*Nereis virens*). Additional treatments were amended with NH_4^+ to mimic NH_4^+ excretion by organisms or with allylthiourea to inhibit nitrification by sediment bacteria. Fluxes of O_2, NO_3^-, NO_2^-, NH_4^+ have been determined by incubations. O_2 profiles were realised with microelectrodes and the vertical distributions of NO_3^-, NO_2^-, NH_4^+ were measured on porewater extracted by centrifugation. Isotope Pairing Technique was used to determine denitrification, anammox rates.

[1] Gilbert et al. (2005) *Limnology and Oceanography* **50(50)**, 1654-1666. [2] Michaud et al. (2005) *Journal of Experimental Marine Biology and Ecology* **326**, 77-88. [3] Michaud et al. (2009) *Journal of Marine Research* **67**, 43-70.

https://doi.org/10.1180/S0026461X00008434 Published online by Cambridge University Press

Mineral reactions at high pH relevant to radwaste disposal: a 15 year experimental study

E.B.A. MOYCE[1]*, K. MORRIS[2], A.E. MILODOWSKI[3], C. ROCHELLE[3], S. SHAW[1]

[1]Earth Surface Scienec Institute, University of Leeds, Leeds, UK (*correspondence: eeem@leeds.ac.uk)
[2]Research Centre for Radwaste and Decommissioining, SEAES, The University of Manchester, Manchester, UK
[3]British Geological Survey, Keyworth, UK

The use of cement within waste forms, engineering and potentially as backfill in the geological disposal of radioactive waste will produce a high pH (~pH 13-10) leachate plume as the geological disposal facility (GDF) evolves over hundreds to millions of years. This plume will create a chemically disturbed zone (CDZ) within the host rock causing alteration, dissolution and secondary precipitation of minerals. This has clear potential to change the rock's physical and chemical properties and affect radionuclide transport in the geosphere through alteration of flow paths or change in the host rock sorption capacity for radionuclides.

Here we describe analysis of a unique series of batch experiments which contain Borrowdale Volcanic Group (BVG) rock (quartz, orthoclase and dolomite with clay coatings) reacted in CDZ leachates at 70 ºC for 15 years. Two leachates were used: young cement leachate (pH 13.00, KOH and NaOH dominated); and evolved leachate equilibrated with a model deep groundwater (pH 12.2, $Ca(OH)_2$ and NaCl dominated)[1]. Experiments were characterised at 15 months and in this most recent work, at 15 years.

At 15 months mineral dissolution and formation of Ca-bearing silicate phases, e.g. apophyllite and Ca-K-Al silicate clays, was observed. However, recent work shows that by 15 years, extensive de-dolomitisation had occurred; here the dissolution of $CaMg(CO_3)_2$ resulted in extensive $CaCO_3$ re-precipitation and release of Mg^{2+}. By 15 years, it is apparent that this Mg^{2+} had reacted with silica in solution and clay particles on the primary mineral surfaces to produce Mg(K)(Al)-silicates of varying composition, structure and morphology as the major alteration products. The Ca-bearing silicates observed after 15 months of reaction were not present at 15 years. At all points, the alteration level was greatest in the young leachate, but the processes described occurred in both fluids.

Overall, these results demonstrate that the stability of secondary phases formed within the CDZ may change significantly over time and may affect both flow and radionuclide speciation. Clearly, this has implications for GDF safety case development.

[1] Rochelle *et al.* (1997) BGS technical report WE/97/16

Planetary scale Sr isotopic heterogeneity

FREDERIC MOYNIER[1*], JAMES M.D. DAY[2,3], WATARU OKUI[4], TETSUYA YOKOYAMA[4], AUDREY BOUVIER[5], RICHARD J. WALKER[3], FRANK A. PODOSEK[1]

[1]Department of Earth and Planetery Science and McDonnell Center for Space Sciences, Washington University, St Louis, MO 63130, USA (moynier@levee.wustl.edu) (*presenting author)
[2]Geosciences Research Division, Scripps Institution of Oceanography, La Jolla, CA 92093-0244, USA
[3]Department of Geology, University of Maryland, College Park, MD 20742, USA
[4]Department of Earth and Planetary Sciences, Tokyo Institute of Technology, Tokyo 152–8551, Japan
[5]Department of Earth Sciences, University of Minnesota, Minneapolis, MN 55455-0231 USA

Isotopic anomalies in planetary materials may reflect both early solar nebular heterogeneity inherited from presolar stellar sources [1], and processes that generated non-mass dependent isotopic fractionations [2,3]. The characterization of isotopic variations in heavy elements among early Solar System materials brings important insight into the stellar environment and formation of the solar system, and may also provide critical information about initial isotopic ratios relevant to long-term chronological applications [4]. One such heavy element, strontium, is a central element in the geosciences due to the widespread application of the long-lived ^{87}Rb-^{87}Sr radioactive system ($\lambda=1.393x10^{-11}y^{-1}$ [5]) as a chronological tool.

Through high-precision Sr isotopic measurements we show that the stable isotopes of Sr were heterogeneously distributed at both the mineral- and the planetary-scale in the early Solar System, and also that the Sr isotopic heterogeneities correlate with mass independent oxygen isotope variations. This correlation implies that most Solar System material was formed by mixing of at least two isotopically distinct components: a refractory inclusion-like component (rich in *p*-process ^{84}Sr or *s*-process ^{88}Sr, and ^{16}O), and an H-chondrite-like component (poor in ^{84}Sr or ^{88}Sr, and ^{16}O).

The heterogeneous distribution of Sr isotopes, most notably with respect to ^{84}Sr, may indicate that variations in initial $^{87}Sr/^{86}Sr$ of early Solar System materials reflect isotopic heterogeneity instead of having a chronological significance, as interpreted previously. For example, the corrected age difference between the formation of refractory inclusions and eucrites, as determined from Sr isotopic differences, is much shorter than previously suggested, placing the Sr chronology in agreement with other long and short-lived systems, such as U-Pb and Mn-Cr [6].

[1] Birck, J. L.. *Rev Mineral Geochem* **55**, 26-63 (2004). [2] Fujii, T., Moynier, F. & Albarède, F. *Earth Planet. Sci. Lett.* **247**, 1-9 (2006).[3] Thiemens, M. H.. *Science* **283**, 341-345 (1999). [4] Brennecka, G. A. *et al. Science* **327**, 449-451, (2010). [5] Nebel, O., Scherer, E. E. & Mezger, K. *Earth Planet. Sci. Lett.* **301**, 1-8, (2011). [6] Lugmair, G. W. & Shukolyukov, A. *Geochim. Cosmochim. Acta* **62**, 2863-2886 (1998).

https://doi.org/10.1180/S0026461X00008434 Published online by Cambridge University Press

Exploring the relative influence of fluid and particle residence times on chemical weathering using a coupled geomorphic and geochemical model

SIMON M. MUDD[1*], KYUNGSOO YOO[2], KATE MAHER[3]

[1]School of GeoSciences, University of Edinburgh, Edinburgh, UK, simon.m.mudd@ed.ac.uk (* presenting author)
[2]Department of Soil, Water and Climate, University of Minnesota, St. Paul, MN, USA, kyoo@umn.edu
[3]School of Earth Sciences, Stanford University, Stanford, CA, USA, kmaher@stanford.edu

Minerals enter the weathering zone as landscapes erode and weathering fronts propagate downward through the near surface. In many, if not most landscapes, this process involves minerals first being chemically weathered and subsequently being subject to both chemical weathering and mechanical disturbance. The timescale of mineral transformation is on the order of thousands to millions of years [1]; this timescale is similar to the residence time of minerals within the physically disturbed, mobile regolith of eroding landscapes [2]. The chemistry of mobile weathered material on eroding hillslopes will reflect the integrated effects of different weathering environments along the hillslope profile. Thus it is crucial to account for sediment transport if one is to use the solid state chemistry of hillslope materials to infer weathering rates over long (10^3-10^6 yr) timescales [3, 4]. It has been postulated that the rate that minerals weather is partly a function of the time they spend in the weathering zone [5] and this time is closely related to the erosion rate. It has also been suggested that fluid, rather than mineral residence time plays a dominant role in determining the rate of chemical weathering in near-surface materials [6]. To examine the relative importance of mineral vs. fluid residence time or to examine if these two factors co-evolve we have developed a numerical model that traces minerals through the weathering zone, including their transit through a mobile, mixed regolith. The model is designed to assimilate field data so that hypotheses concerning the controls of chemical weathering rates can be tested with solid state chemistry and mineralogy from soil pits or cores. Chemical weathering in the model can be simulated using either the time the mineral has spent in the weathering zone or using a geochemical model that accounts for fluid flow and chemistry. Here we use the model to examine the sensitivity of weathering zone evolution to erosion rate. We also compare model predictions to geochemical data from a transect in Tennessee Valley, California in order to explore if variations in either fluid or mineral residence times can explain the observed geochemical patterns.

[1] Lasaga et al. (1994) *Geochima et Cosmochimica Acta* **58,** 2361-2386.
[2] Mudd and Yoo (2010) *Journal of Geophysical Research-Earth Surface* **115**, doi:10.1029/2009JF001591.
[3] Mudd and Furbish (2006) *Journal of Geophysical Research-Earth Surface* **111,** doi:10.1029/2005JF000343.
[4] Yoo et al. (2007) *Journal of Geophysical Research-Earth Surface,* **112,** doi:10.1029/2005JF000402.
[5] White and Brantley (2003) *Chemical Geology* **202**, 479-506.
[6] Maher (2010) *Earth and Planetary Sci. Letters* **294,** 101-110.

Binding environment of As(V) during microbial reduction of As-bearing biogenic Fe(III) minerals

E. M. MUEHE[1]*, L. SCHEER[1], G.MORIN[2], A. KAPPLER[1]

[1] Geomicrobiology, University of Tuebingen, Germany eva-marie.muehe@uni-tuebingen.de (* presenting author)
[2] Environmental Mineralogy, IMPMC, CNRS-UPMC, France guillaume.morin@impmc.upmc.fr

Aqueous As in As-contaminated groundwater and soil enters the human food chain (in)directly via drinking water, plants and animals, potentially having a devastating impact on the health of people. Correspondingly, research has put its focus on (bio)geochemical processes leading to the mobilization (release) and immobilization (removal) of As from aquifers and soil. Previous studies by Hohmann *et al.* [1] revealed that Fe(II)-oxidizing bacteria efficiently immobilize the two most common inorganic As species, As(V) and As(III), in aqueous systems by the formation of biogenic Fe(III) oxyhydroxides (ferrihydrite and goethite). Detailed analyses of these biogenic precipitates formed in the presence of dissolved As indicated As is efficiently removed from the aqueous phase via sorption to the mineral surfaces [2].

Environments that contain Fe(III) minerals and organic matter are usually also inhabited by Fe(III)-reducing microorganisms, suggesting that potentially microbial reduction of the biogenic Fe(III) (oxyhydr)oxides occurs. The microbially-mediated dissolution of these biogenic Fe(III) minerals could cause a release of the bound As or result in further immobilization of As due to the formation of secondary Fe(II/III) mineral phases. Additionally, the redox state of As might change during microbial Fe cycling and thus affect the mobility of As, since As(III) is generally more mobile than As(V).

In the study presented here, we followed the reduction of biogenic As-bearing Fe(III) minerals by the Fe(III)-reducer *Shewanella oneidensis* MR-1. Arsenic concentration and oxidation state were monitored in the liquid and solid phases. Mineralogy of the incubated solid phases was determined by X-ray diffraction and electron microscopy, whereas the As redox species and bonding environment in the mineral precipitates were analyzed by X-ray adsorption spectroscopy. We found that As(V) is immobilized during microbial reduction of biogenic As-bearing Fe(III) (oxyhydr)oxides while As(III) is mobilized to a significant extent. The immobilized As(V) is bound either to the remaining goethite or to the newly formed Fe(II) minerals and no mobilization occurred even though As(V) was transformed to As(III).

[1] Hohmann *et al.* (2010) *ES&T* **44**, 94-101. [2] Hohmann et al. (2011) *GCA* **75**, 4699-4712.

https://doi.org/10.1180/S0026461X00008434 Published online by Cambridge University Press

Early planetary differentiation and volatile accretion recorded in deep mantle Xenon isotopes

SUJOY MUKHOPADHYAY [1*], MARIA PETO[1], RITA PARAI[1], AND JONATHAN TUCKER[1]

[1]Harvard University, Cambridge, MA, USA, sujoy@eps.harvard.edu

^{129}Xe, produced from the radioactive decay of extinct ^{129}I, and ^{136}Xe, produced from extinct ^{244}Pu and extant ^{238}U, have provided important constraints on early mantle outgassing and volatile loss from Earth[1,2]. The low ratios of radiogenic to non-radiogenic xenon (^{129}Xe/^{130}Xe) in ocean island basalts (OIBs) compared to mid-ocean ridge basalts (MORBs) have been used as evidence for the existence of a relatively undegassed primitive deep mantle reservoir[1]. However, the low ^{129}Xe/^{130}Xe ratios in OIBs have also been attributed to mixing between subducted atmospheric Xe with MORB Xe, obviating the need for a less degassed mantle reservoir[3,4].

We present new noble gas data from OIBs and MORBs that demonstrate for the first time that the lower ^{129}Xe/^{130}Xe ratios in OIBs are derived from a lower I/Xe ratio in the OIB mantle source and cannot be explained solely through mixing between atmospheric Xe and MORB-type Xe. As ^{129}I became extinct prior to 100 Myrs after the start of the Solar System, OIB and MORB mantle sources must have differentiated by 4.45 Ga and subsequent mixing must have been limited. Thus, if the Moon-forming giant impact led to large scale planetary equilibration, it must have happened within 100 Myrs of the start of the Solar System.

The new precise xenon measurements also allow us to compute the proportion of Pu to U-derived fission Xe. Our measurements indicate that the plume source has a higher proportion of Pu- to U-derived fission Xe, requiring the plume source to be less degassed than the MORB source and supporting the long-term separation of MORB and OIB mantle sources. These conclusion are independent of noble gas concentrations and the partitioning behavior of the noble gases with respect to their radiogenic parents.

Calculated I/Pu ratios for the plume source is lower than the MORB source. This suggests that early accretion was volatile-poor compared to later accreting material, supporting the hypothesis of heterogeneous accretion[5]. Overall, the noble gases suggest at least two separate sources of volatiles for Earth and require that 4.45 Gyrs of mantle convection have not erased the signature of Earth's early differentiation. Finally, if noble gases in OIBs are derived from the Large Low Shear Wave Velocity Provinces (LLSVPs), then our study requires LLSVPs to be stable features that have existed since the formation of the Earth and are not exclusively composed of subducted slabs.

[1] Allegre, et al. (1987) EPSL 81, 127-150. [2] Marty (1987) EPSL 94, 45-56. [3] Holland & Ballentine (2006) Nature 441, 186-191. [4] Trieloff & Kunz (2005) PEPI 148, 13-38. [5] Schonbachler et al (2010) Science 328, 884-887.

Sr-Nd-Hf-Pb isotopic constraints on the origin of alkalic basalts in the northern Cascade Arc

E. K. MULLEN*, M. CARPENTIER AND D. WEIS

PCIGR, University of British Columbia, Vancouver, BC Canada V6T 1Z4, emullen@eos.ubc.ca (*presenting author)

Calc-alkaline basalts are the predominant primitive magmas in the Cascade Arc. However, the northernmost segment of the arc, the Garibaldi Volcanic Belt (GVB), shows a progressive northerly shift from calc-alkaline to alkalic basalts. At the northern end of the arc, hawaiite and basanite occur at Salal Glacier, Bridge River, and Mt. Meager volcanic complexes. The gradient in alkalinity is accompanied by a northerly reduction in the "arc signature" and increases in P and T of basalt generation. These trends may be related to the age of the subducting plate, which decreases by ~4 Myr, potentially leading to reduced slab inputs and consequently smaller melt fractions formed at greater depths [1]. We have obtained new high-precision whole-rock Sr-Nd-Pb-Hf isotope and trace element data on GVB basalts to geochemically characterize the mantle beneath each volcanic center and determine whether the geochemical gradients displayed by the basalts can be explained solely by changes in slab input or require multiple mantle components.

Relative to other primitive Cascade arc basalts, GVB basalts have lower ^{208}Pb/^{204}Pb at a given ^{206}Pb/^{204}Pb (18.67-18.92) and higher ε_{Nd} (3.8-8.5) at a given ^{87}Sr/^{86}Sr (0.70310-0.70396). The alkalic GVB basalts have the most depleted Pb isotopic ratios yet identified in the Cascade Arc. In Pb isotopic space, the GVB defines a linear array extending from Juan de Fuca MORB to subducting sediment in the northern Cascadia basin, which we interpret as a mixing line indicating variable sediment input to the mantle. A northerly La/Nb decrease from ~4.25 at Glacier Peak to ~0.78 at Bridge River confirms the reduction in arc signature, but an inverse correlation between ε_{Nd} and ε_{Hf} (8.7-13.3) indicates arc-parallel mixing between two isotopically distinct mantle sources, one dominating in the south and the other in the north.

Trace element modeling, phase equilibria and thermobarometry indicate that the alkalic GVB basalts segregated from the mantle at high pressures and MORB-like temperatures (up to ~2.7 GPa, 1475°C) and have garnet lherzolite residues. The mantle source is not modified by a subduction component and is isotopically depleted, yet it is enriched in incompatible elements. These correlations indicate either long-term mantle source depletion coupled with a recent metasomatic enrichment event, or extremely low melt fractions. In contrast, calc-alkaline basalts of the southern GVB (Mt. Baker, Glacier Peak) were generated near the base of the crust from depleted lherzolite or harzburgite metasomatized by sediment melt or fluid.

Because the alkalic basalts lack an arc signature, have a hot, recently-enriched mantle source, and are located at the termination of the currently subducting slab, we propose that they are generated by a "slab edge effect". Decompression melting is triggered by upwelling of asthenospheric mantle through a window between the active Juan de Fuca plate and near-stagnant Explorer plate [2,3].

[1] Green (2006) *Lithos* **87**, 23-49. [2] Audet et al. (2008) *Geology* **36**, 895-898. [3] Riddihough (1984) *J. Geoph. Res.* **89**, 6980-6994.

https://doi.org/10.1180/S0026461X00008434 Published online by Cambridge University Press

Accuracy of in-situ Sr isotope analysis of biogenic phosphates by LA-MC-ICPMS – a problem reassessed

WOLFGANG MÜLLER[1, *)], ROBERT ANCZKIEWICZ[2]

[1]Dept. of Earth Sciences, Royal Holloway University of London, Egham, UK, w.muller@es.rhul.ac.uk

[2]Inst. of Geological Sciences, Polish Academy of Sciences, Krakow, Poland, ndanczki@cyf-kr.edu.pl

In-situ Sr isotope analysis by LA-MC-ICPMS has been available for more than fifteen years [1]. While precise and accurate data can be obtained in this way for (high-Sr) carbonates and other materials, for phosphates accuracy (and precision) of in-situ analyzed Sr isotope data have proven difficult to obtain [2, 3]. Specific to Ca-phosphates, CaPO, a molecular interference on mass 87 ($^{40}Ca^{31}P^{16}O$), as well as doubly-charged Yb & Er in case of REE-rich inorganic apatite have been invoked as analytical obstacles, besides $^{84,86}Kr$, ^{87}Rb, Ca-Argides. Moreover, all is exacerbated by the relatively low Sr concentrations of biogenic phosphates (<100 to few 100 ppm Sr).

In view of the importance of Sr-isotopes in biogenic phosphate as mobility proxy in vertebrates - in teeth potentially providing sub-seasonal resolution when analyzed in-situ by LA-MC-ICPMS - we have evaluated in-situ Sr-isotope analysis for a range of biogenic phosphates. Using a RESOlution M-50 193 nm excimer laser-ablation system, featuring a Laurin two-volume cell, coupled to a Neptune MC-ICPMS, we evaluate spectral interferences on ^{87}Sr by focussing on: 1) Routine 'robust' plasma conditions ($ThO^+/Th^+ < 0.1$ %), which because of the highest oxide bond strength for ThO [4] imply that all other oxides will be present in lower abundances. 2) Accurate naturally invariant $^{84}Sr/^{86}Sr$ ratio (0.0565 after mass bias correction) as monitor of appropriate interference corrections (Kr, CaAr, REE^{2+}). 3) Careful mass scans at medium mass resolution ($M/\Delta M = 4000$) because CaPO and ^{87}Sr are resolvable above $M/\Delta M = 3900$. 4) Focus on the accuracy of the ^{87}Rb-correction on mass 87 since mammalian bioapatite can have relatively high $^{85}Rb/^{86}Sr$ of up to ~0.01 and sometimes even higher.

For the analytical (plasma) conditions utilized, we find no evidence for any molecular interference (CaPO) at mass 87 using medium resolution mass scans. Furthermore we obtain accurate $^{84}Sr/^{86}Sr$ ratios (0.0565) for both shark teeth (high-Sr) as well as mammalian enamel (few 100 ppm Sr maximum). $^{87}Sr/^{86}Sr$ ratios for modern shark teeth of 0.70917 ± 3 (2 SD) are indistinguishable from modern seawater (0.70917). Comparing TIMS and LA-MC-ICPMS Sr isotope data of the same tooth enamel characterized by variable Sr-isotope ratios inevitably highlights the problem of scale because mg-sized fragments are utilized for TIMS vs. ~100 μm spot sizes for LA-ICPMS. Nevertheless we find very good agreement in $^{87}Sr/^{86}Sr$ for corresponding enamel sections using both methodologies, but the ultimate accuracy depends on the magnitude of the necessary ^{87}Rb correction; corresponding results will be presented.

[1] Christensen *et al* (1995) *Earth Planet. Sci. Lett.* **136**, 79-85. [2] Simonetti *et al* (2008) *Archaeometry* **50,** 371-385. [3] Horstwood *et al* (2008) *Geochim. Cosmochim. Acta* **72,** 5659-5674. [4] Kent & Ungerer (2005) *J. Anal. Atom. Spectrom.* **20,** 1256-1262.

Evaluation of contaminated sediment remediation techniques

CATHERINE N. MULLIGAN [1*]

[1*]Concordia University, Montreal, Canada, mulligan@civil.concordia.ca

Introduction

An evaluation of the management options must be made for contaminated sites. In particular, the various techniques must be considered for the remediation of sediments when the sediment leads to the accumulation of contaminants in aquatic life or when the release of hazardous materials from sediments becomes a serious problem. The options can include capping, dredging, or physical, biological, and/or chemical treatments. Sustainable management options for contaminated sediments are required and will be evaluated. In situ remediation could be beneficial over dredging due to a reduction in costs and lack of solid disposal requirements.

Approach

Selection of the most appropriate remediation technology must coincide with the environmental characteristics of the site and the ongoing sediment fate and transport processes. To be sustainable, the risk at the site must be reduced, and the risk should not be transferred to another site. The treatment must reduce the risk to human health and the environment. Cost-effectiveness and permanent solutions are significant factors in determining the treatment. Sites vary substantially, and there can be substantial uncertainty involved in the evaluation process. However, decisions must be made based on the information available.

Both in situ and ex situ treatment approaches are examined. For example, environmental dredging requires evaluation of the risk of dredging, determination of disposal methods and/or potential beneficial use. Innovative integrated decontamination technologies must be utilized.

Results and Conclusions

To work towards sustainability, indicators must be identified and quantified, including waste must be minimized, natural resources must be conserved, landfill deposition should be minimized and benthic habitats and wetlands must not be lost and must be protected. Innovative integrated decontamination technologies must be utilized. The fate and transport of contaminants must be understood more thoroughly to develop appropriate strategies. A long term vision is needed. Otherwise, natural resources will continue to be depleted, landfills will continue to be filled with contaminated sediments, and biodiversity in the aquatic geoenvironment will be diminished. Integrated innovative management practices need to be developed and applied such as in situ techniques that reduce waste management requirements.

https://doi.org/10.1180/S0026461X00008434 Published online by Cambridge University Press

Arsenic Mobility is Mediated by Bacterial Reduction in New Jersey Shallow Groundwater

A. C. MUMFORD[1*], J. L. BARRINGER[2], P. A. REILLY[2] AND L. Y. YOUNG[1]

[1]Rutgers University, New Brunswick, NJ, USA amumford@eden.rutgers.edu, (*presenting author) lyoung@aesop.rutgers.edu

[2]US Geological Survey, NJ Water Science Center , West Trenton, NJ, USA. jbarring@usgs.gov, jankowsk@usgs.gov

Introduction

The mobilization of arsenic bound to aquifer sediments is a source of contamination in groundwater in New Jersey. Deep Coastal Plain sediments have average As concentrations of 15-23 mg/kg [1,2], and As concentrations of 26 mg/kg have been recorded in shallow glauconitic sediments[3]. In a prior study [3] we demonstrated that As reducing bacteria promote As release and mobility in groundwater at a New Jersey Coastal Plain site. We have expanded this study to investigate the potential for microbial As mobilization beneath the streambeds at two other sites, Six Mile Run and Pike Run, in the New Jersey Piedmont. Groundwater at the Six Mile Run site has an As concentration of 27 µg/L, which is in excess of the 5µg/L limit set by the NJDEP, while the As concentration at the Pike Run site is 2.1 ug/L.

Methods:

Groundwater was sampled on gaining reaches of Pike Run and Six Mile Run in the New Jersey Piedmont Physiographic Province, and inoculated into anaerobic microcosms with acetate as a carbon source and As(V) as an electron acceptor. Arsenic reduction was monitored by HPLC. Groundwater was filtered on site, and DNA was extracted from the filters for amplification and cloning of the16S rRNA gene and the arsenate respiratory reductase gene, *arrA*, a biomarker for As(V) respiration [4]. 16S rRNA gene sequence data was analyzed using ARB [5] and the SILVA 108 NR 16S rRNA gene database [6]. *arrA* gene sequence analysis was performed using ARB [6]. Operational Taxonomic Unit (OTU) analysis was performed with mothur [7].

Results and Conclusions

Microcosms developed from Six Mile Run groundwater reduced 1 mM of As(V) to As(III) in 30 days, while microcosms from Pike Run did not reduce As. Based on a 97% similarity cutoff, 10 OTUs unique to Six Mile Run were identified, and 11 OTUs unique to Pike Run were identified. The sites shared 4 OTUS out of the 25 sequenced, suggesting that distinct bacterial communities were present at each site. Based on the *arrA* gene, distinct arsenic respiring communities were identified at each site, with 8 unique OTUs found at Six Mile Run, and 11 unique OTUs shared at Pike Run. Globally, the *arrA* sequences recovered from both Pike Run and Six Mile Run are most similar to those recovered from the Meuse River in France, and distinct from those recovered from marine environments. Our findings demonstrate that while the *arrA* gene may indicate the presence of As reducing organisms, microcosm studies are necessary to predict microbial As reduction and mobilization from sediments.

[1] Dooley (1998) *The New Jersey Geological Survey Technical Memorandum 98-1*. [2] Dooley (2001) *N. J. Geological Survey Investigation Report* [3] Mumford *et al.* (2012) *Water Res. In Review* [4] Malasarn *et al.* (2004) *Science* **306**, 455. [5] Ludwig *et al.* (2004) Nucleic Acids Res **32,** 1363-1371, [6] Pruesse *et al.* (2007) Nucleic Acids Res **35,** 7188-7196 [7] Schloss *et al.* (2009) Appl Env Microb **75,** 7537-7541

Combining macroscopic invasion percolation with mass transfer to model bubble-facilitated transport of VOCs in groundwater

KEVIN G. MUMFORD[1*], PAUL R. HEGELE[1], MAGDALENA M. KROL[2,3] AND BRENT E. SLEEP[3]

[1]Queen's University, Dept. of Civil Engineering, Kingston, Ontario, Canada, kevin.mumford@civil.queensu.ca (*presenting author)

[2]Western University, Dept. of Civil and Environmental Engineering, London, Ontario, Canada, mkrol4@uwo.ca

[3]University of Toronto, Dept. of Civil Engineering, Toronto, Ontario, Canada, sleep@ecf.utoronto.ca

Gas bubbles present in otherwise water-saturated porous media can affect the transport of volatile organic compounds (VOCs) in groundwater. The partitioning of VOCs to gas bubbles, with the bubbles acting as a variable-volume sink, can retard VOC transport, and can also affect the transport of other volatile species (e.g., dissolved atmospheric or biogenic gases). If sufficient gas volumes exist for bubbles to be vertically mobilized, the transport is also affected by the creation of an additional mass transport pathway – the buoyant advection of the bubbles – which can carry mass away from regions with higher aqueous concentration to those with lower aqueous concentration, resulting in mass partitioning from the bubble back to the aqueous phase. This type of transport has been observed in a variety of systems, including: the natural attenuation of hydrocarbon plumes, the expansion of trapped gases above non-aqueous phase liquid (NAPL) sources, and remediation by in situ thermal treatment.

In these types of systems, where the expansion and mobilization of the gas bubbles is controlled by the mass transfer between the aqueous phase and the trapped gas phase, it is important to model both the partitioning of multipe volatile species and the subsequent discontinuous bubble flow as mass transfer and immicible displacement occur over similar time scales. One promising approach is the use of macroscopic invasion percolation (MIP) to model gas movement, combined with continuum-scale simulation of aqueous-phase transport and mass transfer between phases. The MIP routine can be modified to include gravity for biased vertical growth, as well as fragmentation and mobilization to reproduce bubble behaviour, provided that gridblock sizes are less than a critical length scale required for mobilization. Here, simulations of VOC transport in the presence of mobilized gas bubbles were compared to an intermediate-scale laboratory flow cell experiment, where non-monotonic changes in concentrations were observed at higher-than-expected elevations above a dense non-aqueous phase liquid (DNAPL) pool. Additional simulations that investigated the potential role of bubbles during in situ thermal remediation showed greater mass removal from a targetted heating area due to bubble formation and mobilization. Finally, a third set of simulations investigated bubble-facilitated transport of VOCs in heated and unheated, heterogeneous systems.

https://doi.org/10.1180/S0026461X00008434 Published online by Cambridge University Press

Blatchford Lake intrusive suite, new geochronology and barometric estimates: implications for mineralization

THOMAS MUMFORD[1*], BRIAN COUSENS[1]

[1]Carleton University, Ottawa, Canada, tmumford@connect.carleton.ca (* presenting author)
[2]Carleton University, Ottawa, Canada, bcousens@earthsci.carleton.ca

Introduction

The Paleoproterozoic Blatchford Lake intrusive suite, can be subdivided into two cogenetic separate lobes: a metaluminous western lobe and a peralkaline eastern lobe which is host to the world class Nechalacho rare metal deposit. The western lobe consists of a multi-phase layered gabbroic sequence, cross-cut by a series of sills varying from syenite to granite. The eastern lobe comprises a large sub-circular granite that grades to a syenite core. Underlying the syenite core is a layered suite of silica-undersaturated rocks collectively known as the Nechalacho layered syenite series (NLSS). Rare metal mineralization occurs in the upper units of the NLSS, which have been overprinted by intense hydrothermal alteration. Approximately two kilometers east of the Nechalacho mineralized zone, two small plutonic stocks, believed to be related to the regional Compton Intrusive suite [2], cross-cut the peralkaline granite.

In situ U-Pb zircon laser ablation ion-coupled plasma mass spectrometry (LA-ICP-MS) was used to date the Compton Intrusives stocks (1895±5 Ma) and to provide the first reliable age estimate for the NLSS (2187±8 Ma). These new dates help define relationships between phases in the eastern lobe, and resolve discrepencies in the chronology of the Blatchford Lake intrusive suite.

Using the Al-in-hornblende barometer [1], pressure estimates were made on hornblende and edenite crystals from granitic and syenitic phases of the western lobe. These result indicate a mid-crustal emplacement (~3.5 kbar) for the late cross-cutting granite and syenite sills. Given that the ages between the eastern and western lobes are within analytical error, these pressure estimates can be used to infer the pressure conditions during crystallization of phases within the eastern lobe.

This new geohronological and barometric information helps to constrain the overall evolution of the Blatchford Lake intrusive suite, and therby aids in developing models to explain the exceptional enrichment in rare-metals in select phases.

[1] Schmidt (1992) *Contributions to Mineralogy and Petrology* **110**, 304-310. [2] Davidson (1978) *GSC current research* **71-8A**, 119-127.

PGE systematics of refractory mantle: role of Pt alloy

JAMES E MUNGALL[1*] FRANCES JENNER[2], RICHARD ARCULUS[2], JOHN MAVROGENES[2]

[1]University of Toronto, Canada [2]Australian National University, Canberra, Australia * mungall@geology.utoronto.ca

Pt/Pd variability in the mantle and picrites

The primitive mantle has slightly sub-chondritic Pt/Pd values close to 1.1 [1]. Extreme degrees of melt depletion, as recorded by decreases in CaO, Al_2O_3, and increases in Mg/(Mg + Fe) in whole rock or olivine, confer a distinctively high Pt/Pd ratio to the mantle restite, ranging from 5 to 10 in some massif peridotites to as high as > 100 in ultradepleted mantle xenoliths from the Kaapvaal craton [2,3]. A complementary reduction in Pt/Pd to values similar to unity is observed in a global compilation of data for picrites, which evolve to still lower Pt/Pd approaching 0.1 by fractional crystallization in the absence of sulfides [4]. We present data for primitive boninites from Chichi Jima and the northern Tonga arc, which equilibrated with $Fo_{>90}$ olivine and show extremely low Pt/Pd with values ranging from 0.1 to 0.5, while also showing strong depletions in Ir and Ru compared to Rh that we have previously attributed to the existence of Ir-Ru alloy or laurite in the restite [5].

Partition coefficients and models

Bulk partition coefficients D^*_{Pt} and D^*_{Pd} estimated from studies of fractionated lava lakes are approximately 0.2 - 0.6 and 0.1 - 0.2 [6]. Experimental determinations of D_{Pt} and D_{Pd} for olivine are < 0.01 and 0.006 at the FMQ oxygen buffer [7]; values for pyroxenes are similar and, even in chromite they are <0.03 [8].

The existence of Pt/Pd fractionations spanning two to three orders of magnitude between parental picritic magmas and their mantle residues positively requires the existence of a restite phase with dramatically higher D_{Pt} than D_{Pd}. Alloys of Os-Ru-Pt have been observed in mantle peridotite [9,10], and consideration of Os solubility in sulfide liquid and bulk Os concentration in the mantle requires the existence of Os alloy even in the presence of sulfide melt in the mantle [11]. Our models show that the range of Pt/Pd observed in peridotite massifs, mantle xenoliths, boninites, and tholeiitic picrites is consistent with the ubiquitous occurrence of alloy-hosted Pt in amounts ranging from 2 to 7 ppb, whereas Pd appears to be hosted only by sulfide phases, becoming extremely incompatible once sulfide has been consumed during partial melting.

The Bushveld complex of SA, with Pt/Pd between 1.5 and 5, is a unique exception [12]. An unusual process may have destabilized Pt alloy in the highly refractory SCLM of the Kaapvaal craton during emplacement of the Bushveld.

References

[1] Becker (2006) *Geochim Cosmochim Acta* **70**, 4528-4550. [2] Lorand et al. (1999) *J Petrol* **40,** 957-981. [3] Pearson *et al.* (2004) *Chem Geol* **208**, 29-59. [4] references available from corresponding author. [5] Mungall *et al.* (2011) AGU Fall meeting. [6] Puchtel *et al.* (2004) *Geochim Cosmochim Acta* **68**, 1361-1383. [7] Brenan *et al.* (2003) *Earth Planet Sci Lett* **212**, 135-150. [8] Brenan *et al.* (2011) *Chem Geol* in press. [9] Luguet *et al* (2003) *Geochim Cosmochim Acta* **67**, 1553-1570. [10] Kogiso *et al* (2008) *Geochem Geophys Geosys* doi:10.1029/2007GC001888. [11] Brenan (2002) *Earth Planet Sci Lett* **199**, 257-268. [12] Barnes *et al*. (2010) *Econ Geol* **105**, 1491-1511.

https://doi.org/10.1180/S0026461X00008434 Published online by Cambridge University Press

Is the bulk Earth Nb/Ta chondritic?

CARSTEN MÜNKER[1*], ANDREAS STRACKE[2], VERENA BENDEL[3], HERBERT PALME[4], ANDREAS PACK[3]

[1]Institut für Geologie und Mineralogie, Universität zu Köln, Germany, c.muenker@uni-koeln.de (* presenting author)
[2]Institut für Mineralogie, Universität Münster, Germany,
[3]GZG, Universität Göttingen, Germany
[4]Forschungsinstitut Senckenberg, Frankfurt, Germany

The accessible silicate Earth is characterized by a Nb deficit of ca. 30% relative to most groups of chondrites [1]. This Nb deficit has been attributed to a slightly siderophile affinity of Nb during high-pressure formation of the Earth's core [1,2]. The finding of low Nb/Ta ratios in CV chondrites (ca. 17 [1]), however has challenged this model, as CV chondrites closely resemble the Earth's composition in their relative abundances of volatile and refractory elements. If the bulk Earth indeed had a CV-chondritic or even lower Nb/Ta ratio, the Nb deficit in the silicate Earth would be much less pronounced, and models using Nb/Ta ratios to assess conditions during core formation [e.g., 3,4] would neeed some revision.

In order to investigate the cause for the low Nb/Ta in CV chondrites, we analyzed small ca. 0.6 g slices taken from a single piece of Allende [5], together with an aliquot of the Smithsonian powder that is representative for bulk Allende. Ratios of HFSE were determined at high precision using isotope dilution and the Neptune MC-ICPMS at Cologne-Bonn [6] and are compared to high precision data for REE previously determined at ETH Zürich and RSES Canberra [5, unpulished]. The Smithsonian Allende powder yielded a Nb/Ta of 19.1±0.8 (2σ), within error of values for other chondrite groups (19.9±0.6, [1]). Conversely, the Nb/Ta measured for the small Allende slices span a wide range from 14.2 to 22.0. Ratios of Zr/Nb are correlated with Nb contents and range towards values as low as 10, much lower than the chondritic value (13.5, [3]).

The Nb/Ta systematics found for Allende indicate that in contrast to Zr-Hf, Nb and Ta are not distributed homogenously in CV chondrites. However, the data for the large Smithsonian powder aliquot suggest that the bulk Allende parent body had a Nb/Ta indistinguishable from other types of chondrites. Notably, the Nb/Ta in the small Allende slices are negatively correlated with Tm/Er ratios (0.16 to 0.26). At near-chondritic Tm/Er (ca. 0.16 [7]), the mesured Nb/Ta in the Allende splits scatter around a value of 20, typical of the chondrite average. It has previously been argued that the elevated Tm/Er in many CV chondrites can be attributed to the presence of type II CAIs [5]. Low Nb/Ta ratios occasionally found in CV chondrites may reflect selective enrichment group II CAI.

The co-variation between Nb/Ta and Tm/Er could imply that the bulk Earth exhibits a superchondritic Tm/Er, if it had a low Nb/Ta. This is clearly not the case, as the silicate Earth displays a Tm/Er that is not resolvable from that of CI-chondrites [7]. The Nb/Ta of the bulk Earth should therefore overlap the chondritic value and the Nb deficit in the Earth's mantle reflects its siderophile behaviour.

[1] Münker *et al.* (2003) *Science* **301**, 84-87. [2] Wade & Wood (2001) *Nature* **409**, 75-78.[3] Palme & O'Neill (2003) *Treatise on Geochemistry* **2**, 1-38, Elsevier, Oxford. [4] Corgne *et al.* (2008) *GCA* **72**, 574-589. [5] Stracke *et al.* (2012) *GCA*, in press.[6] Münker (2010) *GCA* 74, 7340-7361. [7] Pourmand et al. (2012) *Chem Geol* **291**, 38-54.

Microchemistry of amphiboles near the roof of a mafic magma chamber

J. BRENDAN MURPHY[1*], STEPHANIE BLAIS[1], MICHAEL TUBRETT[2], DANIEL MCNEIL[1] AND MATTHEW MIDDLETON[1]

[1] St. Francis Xavier University, Earth Sciences, bmurphy@stfx.ca
[2] Memorial University of Newfoundland, MicroAnalysis Facility - Inco Innovation Centre (MAF-IIC),

The Late Neoproterozoic Greendale Complex is a suite of arc-related appinitic rocks ranging from ultramafic to felsic in composition that crystallized at shallow crustal levels under conditions of high pH_2O. Amphibole is the dominant mafic mineral in ultramafic to mafic rocks and displays the extraordinary variability in texture and modal abundance that is characteristic of appinite suites. These features allow sensitivity of amphibole composition (major, trace and REE) to the evolution of water-rich magma to be investigated.

All amphiboles in mafic and ultramafic rocks are calcic, with $(Ca+Na)_B \geq 1.34$ and $Na_B < 0.67$ apfu, with Si^{IV} between 6.1 and 7.3. They predominantly range in composition from tschermakite, to tschermakitic hornblende, to magnesio-hornblende and display a dominance of edenite ($Na,K_A + Al^{IV} = Si^{IV}$) substitution. Although each sample exhibits remarkably uniform $Mg/(Mg+Fe^{2+})$ over a wide range in Si of up to one formula unit, the mafic rock amphiboles are characterized by lower (0.5 to 0.7) $Mg/(Mg+Fe^{2+})$, compared to the ultramafic rocks (0.7 and 0.9). REE and trace element profiles of amphiboles from mafic rocks are remarkably consistent. REE profiles are bow-shaped, and are characterized by depletion in LREE (La/Sm ≈ 0.61), a slight depletion in HREE (Gd/Yb ≈ 1.55) as well as a negative Eu anomaly, which is attributed to co-precipitation of plagioclase. REE and trace element profiles of ultramafic amphiboles are divided into two groups that correspond to different textural settings: Group A amphiboles occur in all specimens analyzed and are very similar to the profiles of the mafic rocks. In contrast, Group B amphiboles display relative enrichment in light REEs (La/Sm ≈ 2.05), have lower ΣREE, and lack a negative Eu anomaly relative to Sm and Gd. Group B amphiboles are more enriched in Th and U and show a more pronounced depletion in Ta, Nb, Ti and Y. Group B amphiboles grew in a reaction relationship with olivine and pyroxene. Groups A and B are virtually indistinguishable with respect to the major elements used for amphibole classification, suggesting that REE and selected trace element data when combined with textural observations may provide important additional insights into phase equilibria and conditions of crystallization.

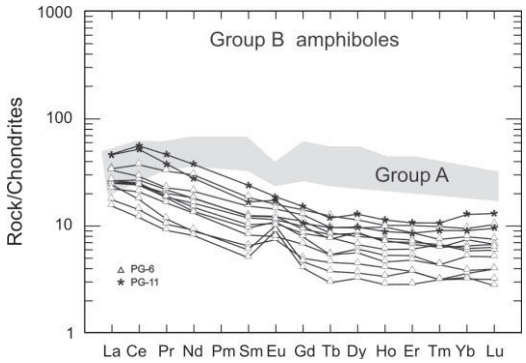

Figure 1. Contrasting REE profiles of amphiboles in ultramafic rocks

https://doi.org/10.1180/S0026461X00008434 Published online by Cambridge University Press

The fate of volcanic ash in marine sediments

RICHARD W. MURRAY[1](*), JULIE C. SCHINDLBECK[2], RACHEL P. SCUDDER[1], STEFFEN KUTTEROLF[2]

[1]Department of Earth Sciences, Boston University, Boston, MA, USA, rickm@bu.edu; rscudder@bu.edu.

[2]GEOMAR, Kiel, Germany, jschindlbeck@geomar.de; skutterolf@geomar.de

Volcanic ash transported to the oceans is one of the main mechanisms by which terrigenous material and nutrients are delivered to the deep sea. Alteration of volcanic glass in the ocean is an important component of marine biogeochemical cycling, with the ash acting as a source and/or sink of many major and trace species.

Ash in marine sediment also provides an important record of explosive subduction zone volcanism. Discrete, visible ash layers are common in the vicinity of subduction zones and have originated from larger explosive eruptions at the volcanic arc. The chemistry and provenance of these visible ash layers are mostly well known and the layers themselves facilitate direct or indirect dating and can therefore be used as marker horizons in marine sedimentology and stratigraphy. Ash layers may also help estimate eruptive volumes, and contribute to the chemistry of sediments and fluids in these regimes. Normal grading and mineral enrichment at the base, glass shard morphology, as well as changes in ash color that are mostly correlated to variations in the chemistry of the primary glass, are features that are relatively easily recognized within the marine sediment column.

The qualitative and quantitative fate of discrete ash layers in sedimentary sequences is only partly known. In theory, bioturbation should destroy layers less than ~10 cm thick, yet well preserved layers of a few cm's thickness are found even in bio-irrigated deposits. By detailed geochemical and sedimentologic study, we here quantify how the incorporation of the primary volcanic ash in marine sediments proceeds above ash layers and with distance from the source. We further discuss how ash is captured within the sediment column and recycled in subduction zones, and quantitatively address how ash layers compositionally affect the hosting sediment column.

Stratigraphic sampling of sequential 1-3 cm slices above primary ash layers from offshore Central America show that densities decrease due to lesser amounts of volcanic glass in the silty clay marine sediments. The bulk rock chemistry reflects this gradation as well and can be quantified for single elements like U, Cr, Zr, V, and Pb, depending on the composition of the volcanic glass (mafic versus felsic). The most important component for those changes is the <32 µm fraction, since ~14 wt% of this is still composed of volcanic glass. Additionally, we see a decreasing frequency of ash layers with increased distance from the source (e.g., 200 vs. 350 km). Quantification of this decrease will help establish a volcanic matter correction factor for chemical and sedimentological parameters with distance from source in subduction zone settings.

Analog studies of brine cryoenvironments in the Canadian high Arctic

NADIA MYKYTCZUK[1*], SUSAN TWINE[2], BOSWELL WING[3], SIMON FOOTE[2], KELLY FULTON[2], CHARLES GREER[4], LYLE WHYTE[1]

[1]McGill University, Natural Resource Sciences, Montreal, Canada, nadia.mykytczuk@mcgill.ca (*presenting author); lyle.whyte@mcgill.ca

[2]National Research Council Canada, Institute for Biological Sciences, Ottawa, Canada, susan.twine@nrc-cnrc.gc.ca; simon.foote@nrc-cnrc.gc.ca; kelly.fulton@nrc-cnrc.gc.ca

[3]McGill University, Earth and Planetary Sciences, Montreal, Canada, boswell.wing@mcgill.ca

[4]National Research Council Canada, Biotechnology Research Institute, Montreal, Canada, charles.greer@nrc-cnrc.gc.ca

The Canadian high Arctic offers several unique cryoenvironments including cold saline springs and extensive permafrost that are working analogs to the conditions that are known, or are suspected, to exist on Mars, and potentially on other astrobiological targets. In particular, fluvial features linked to past and current processes on the surface of Mars suggest that liquid brines near the surface exist and could have been a potential abode for past or extant microbial life. Our recent research focused on detecting and examining microbial life in the unique cold saline/brine springs on Axel Heiberg Island. The microbiology and geochemistry of a habitat found within the Gypsum Hill (GH) spring site will be presented, describing a constant circum-zero saline (7.5 % salinity) habitat that is host to chemolithotrophic sulfur-oxidizing bacterial filaments that flourish in the Arctic winter. The GH spring site is a sulfide (25-100 ppm) and sulfate (2300-3700 mg/L) abundant system serving as an analogue for the abundant sulfate deposits and potential sulfate-rich brines on Mars. The GH springs support viable, active (down to -10°C), and low diversity microbial communities dominated by *Thiomicrospira* spp.. Environmental meta-omic analyses (genomic, proteomic, transcriptomic) were aimed at uncovering insights into: a) the sulfur metabolizing community; b) the diversity of core metabolic genes required to utilize essential nutrients (C, N) within this extreme environment; c) the pathways of energy utilization i.e. CH_4, H_2, sulfur; d) the evolutionary and physiological traits required for microbial life in this subzero, hypersaline cryoenvironment. The meta-analyses provided greater insight into the predominant *Thiomicrospira* metabolic enzymes expressed as part of the active microbial growth, activity and adaptive traits during the late Arctic spring. *In situ* geochemical and isotopic analyses of the fractionation of multiple-sulfur isotopes resulting from bacterial sulfur-metabolism vs. abiotic isotope exchange illustrated the route of biogeochemical sulfur cycling and traced the formation and preservation of potential sulfur-based biosignatures ($\delta^{33}S$, $\delta^{34}S$ and $\delta^{36}S$ stable isotopes). These studies demonstrate how complimentary molecular tools provide a functional link between microbial life and the geochemistry of their environments, how we can predict potential biosignatures of microbial activity and illustrate unique traits linked to microbial survival within these brine cryoenvironments analogous to past or perhaps present conditions on Mars.

https://doi.org/10.1180/S0026461X00008434 Published online by Cambridge University Press

Speciation of colloidal Fe in terrestrial and marine environments using synchrotron X-ray spectroscopy and microscopy

SATISH C.B MYNENI[1*], BJORN P. VON DER HEYDEN[2], ALAKENDRA N. ROYCHOUDHURY[2], GUSTAVO A. MARTINEZ[3], TOLEK TYLISZCZAK[4]

[1]Department of Geosciences, Princeton University,
[2]Department of Earth Sciences, Stellenbosch University,
[3]Department of Crops and Agroenvironmental Science, University of Puerto Rico,
[4]Advanced Light Source, Lawrence Berkeley National Laboratory,
*Corresponding author: smyneni@princeton.edu

Iron is an essential element for all organisms, and it is a limiting nutrient in many parts of the oceans, including the unproductive regions of the Southern Ocean. Although Fe is not a common limiting nutrient in terrestrial aquatic systems, Fe-minerals control the solubility and bioavailability of several nutrients and contaminants. While the dominant fraction of Fe occurs in the form of particulates in aquatic systems, its speciation and mineralogy are less well understood. Here we show how Fe *L*-edge spectroscopy can be used to study the speciation of iron in Fe-rich colloids.

Previous studies have shown that Fe *L*-edge XANES spectra can be used to identify the distribution of ferrous and ferric species accurately. Our study shows that the spectral features in the L_3-edge XANES spectra are sensitive not only to the oxidation state of Fe, but also to small changes in the structural environment of Fe. We use the differences in energy and the spectral intensities of different Fe *p-d* transitions to identify different iron oxides and oxyhydroxide phases. However, saturation and self-absorption problems, associated with transmission and fluorescence spectra of Fe-rich compounds respectively, make positive identification of some of the Fe-phases difficult.

Using the *L*-edge XANES spectroscopy studies on crystalline and amorphous Fe-oxides and oxyhydroxides, we conducted speciation of Fe in the colloidal fraction of Southern Ocean water, and in several South African streams flowing into the Atlantic Ocean. We find that the Fe in the riverine environments is present in the ferric form, which is associated primarily with amorphous Fe-oxides. These Fe-oxides also often exhibit Al substitution. The colloidal Fe-speciation also changed dramatically with distance away from South Africa, and with different Fe-species in different frontal zones in the Southern Ocean. Characterization of colloidal Fe in freshwater lakes also indicates the abundance of amorphous Fe-oxide phases. Although crystalline iron oxides are found in several samples, amorphous Fe-oxides appear to be much more abundant than the crystalline phases, at least in the colloidal pool. A detailed discussion of the method, and its application to the identification of different Fe-phases will be discussed.

^{26}Al-^{26}Mg and ^{10}Be-^{10}B systematics in CAIs from CO and CV chondrites

KUNIHIRO MYOJO[1*], TETSUYA YOKOYAMA[1], YUJI SANO[2], NAOTO TAKAHATA[2], AND NAOJI SUGIURA[3]

[1]Department of Earth and Planetary Sciences, Tokyo Tech, myojo.k.aa@m.titech.ac.jp (* presenting author)
[2]Atmosphere and Ocean Research Institute, The Univ. of Tokyo
[3]Department of Earth and Planetary Science, The Univ. of Tokyo

Fine-scale chronology is very important to discuss the dynamic evolution of the early solar system. Most of the critical events such as the formation of Ca, Al-rich inclusions (CAIs) and chondrules as well as the accretion and early differentiation of planetary bodies have occurred within several Myr from the collapse of the molecular cloud [1]. Short-lived chronometers are extremely useful to obtain highly-precise ages for a variety of extraterrestrial materials. In contrast to the most commonly used ^{26}Al-^{26}Mg system, the ^{10}Be-^{10}B chronometer has been rarely used because of the uncertainty if the parent nuclide (^{10}Be, $T_{1/2}$=1.5 Myr) was homogeneously widespread in the solar nebula. In order to attest the usefulness of the ^{10}Be-^{10}B system, we have measured the ^{10}Be-^{10}B ages in CAIs from two CO chondrites (Moss and Felix) and one CV chondrite (NWA 2364) coupled with their ^{26}Al-^{26}Mg ages. CO chondrites are known to have chemical and mineral compositions similar to those in CV chondrites. However, *in-situ* analysis of CAIs in CO chondrites has been hindered by their relatively small mineral sizes compared to CV CAIs. In this study, fine-grained CAIs were measured by NanoSIMS installed at the AORI, Univ. of Tokyo.

The meteorite fragment containing CAIs was mounted in a resin, and thoroughly polished. Because boron contamination is one of the major problems in SIMS analysis for B-poor samples, we cleaned the polished sample surface with diluted HF prior to analysis. The mineral compositions of CAIs were observed by the SEM-EDX at the Univ. of Tokyo. We found some melilite grains (~50 μm) in CAIs from Moss and Felix, which were subject to the ^{10}Be-^{10}B and ^{26}Al-^{26}Mg analyses using NanoSIMS. We found no melilite in CAIs from NWA 2364, and only the ^{26}Al-^{26}Mg system was analyzed by using hibonite grains.

We observed excess ^{10}B/^{11}B ratios in Moss CAIs, which yielded an initial ^{10}Be/^{9}Be = $(1.05\pm0.56)\times10^{-3}$. This is consistent with the canonical value of Allende CAI, $(1.04\pm0.09)\times10^{-3}$, within analytical uncertainty [2]. In contrast, we were unable to obtained the initial ^{10}Be/^{9}Be ratio for Felix CAI, because of the limited Be/B ratios in the melilite grains analyzed. We speculate that this is caused by B contamination, because we cleaned the mounted Felix by relatively mild HF (0.01M), while Moss was cleaned by 0.1M HF. This implies that the removal of B contamination is critical for the measurement of ^{10}Be-^{10}B system in CAIs. For the ^{26}Al-^{26}Mg system, all CAIs yielded initial ^{26}Al/^{27}Al ratios identical to the canonical value (5.11×10^{-5}, [3]) within analytical uncertainties. This reinforces the usefullness of the ^{10}Be-^{10}B system as for a chronometer in the early solar system.

[1] Kleine, T. et al. (2009) *GCA* **73**, 5150-5188. [2] McKeegan, K.D. and Davis, A.M. (2007) *Treatise on Geochemistry* **1**, 1.16. [3] Jacobsen, B. et al. (2008) *EPSL* **272** 353-364.

https://doi.org/10.1180/S0026461X00008434 Published online by Cambridge University Press

North American ice sheet dynamics controlled by obliquity (41 ka) during the early Pleistocene

B.D.A. NAAFS[1,2*], J. HEFTER[1], G. ACTON[3], G.H. HAUG[2,4], A. MARTÍNEZ-GARCIA[2,4], R. PANCOST[5], AND R. STEIN[1]

[1]Alfred Wegener Institute for Polar and Marine Research, Department of Marine Geology and Paleontology, D-27568 Bremerhaven, Germany, david.naafs@awi.de (* Presenting author)

[2]Leibniz Center for Earth Surface and Climate Studies, Institute for Geosciences, Potsdam University, D-14476 Potsdam, Germany

[3]Department of Geology, University of California, CA 95616 Davis, USA

[4]Geological Institute, ETH Zürich, 8092 Zürich, Switzerland

[5]Organic Geochemistry Unit, Bristol Biogeochemistry Research Centre, School of Chemistry, University of Bristol, BS8 1TS Bristol, United Kingdom

During the Pleistocene, large continental ice sheets episodically appeared in the Northern Hemisphere, covering large parts of Europe and North America. Besides the results based on benthic oxygen isotope records, which predominantly represent variations in global ice volume, little is know about the timing of and astronomical control on the advances and retreats of the continental ice sheets in the Northern Hemisphere during the late Pliocene and early Pleistocene (3-2 million years (Ma) ago).

Here we therefore present the first orbitally-resolved records of terrestrial higher plant leaf wax input to the North Atlantic covering the last 3.5 Ma, based on the accumulation of long-chain *n*-alkanes and *n*-alkanl-1-ols at IODP Site U1313 [1]. These lipids are a major component of dust, even in remote ocean areas, and have a predominantly aeolian origin in distal marine sediments. Our results demonstrate that around 2.7 Ma, coinciding with the intensification of the Northern Hemisphere glaciation (NHG), the aeolian input of terrestrial material to the North Atlantic increased drastically. Since then, during every glacial the aeolian input of higher plant material was up to 30 times higher than during interglacials. We argue that the increased aeolian input at Site U1313 during glacials is predominantly related to the episodic appearance of continental ice sheets in North America and the associated strengthening of glaciogenic dust sources. The records thus reflect the timing of the advances and retreats of the North American ice sheets. Evolutional spectral analyses of the *n*-alkane records were therefore used to determine the dominant astronomical forcing in North American ice sheet advances over the last 3.5 Ma. These results demonstrate that during the early Pleistocene North American ice sheet dynamics responded predominantly to variations in obliquity (41 ka), which argues against previous suggestions of precession-related variations in Northern Hemisphere ice sheets during the early Pleistocene [2].

[1] Naafs *et al.* (2012) *Earth Plan. Sci. Lett.* **317-318**, 8-9. [2] Raymo *et al.* (2006) *Science* **313**, 492-495

A strain-heating model for the seismic low-velocity zone along the Main Himalaya Thrust

PETER I. NABELEK[1*] AND JOHN L. NABELEK[2]

[1]Dept. of Geological Sciences, University of Missouri, Columbia, MO 65211, USA, nabelekp@missouri.edu (* presenting author)

[2] College of Oceanic and Atmospheric Sciences, Oregon State University, Corvallis, OR 97331, USA, nabelek@oce.orst.edu

Seismic low-velocity zone along the MHT

Recent Hi-CLIMB seismic experiment, using an 800 km long, densely spaced seismic array across Nepal and southern Tibet, has revealed a narrow low-velocity zone along the Main Himalaya Thrust [1]. The zone extends approximately from the 28.5°N latitude, dipping to ~40 km depth at the latitude of the Yarlung Tsangpo Suture (YTS), and then continues horizontally beneath the Lhasa Block to approximately 32°N latitude. Nabelek et al. [1] interpreted this deep low-velocity zone to be the result of increased ductility and partial melting. The narrowness of the low-velocity zone along most of the length of the MHT requires a mechanism by which the partial melting is localized. Strain heating along the ductile portion of the MHT provides such a mechanism.

Parameters of numerical model

Development of the partially molten zone was modeled numericaly following [2]. The model domain is 600x140, 1 km grid. The initial conditions are steady-state with subduction of the Indian lithosphere beneath the Himalayas and Tibet at 3 cm/y. Temperature is 25°C at the surface and 1300°C at the bottom of the lithosphere. Radiogenic heat production (Ah) in the Indian crust was constrained by the average 70 mW/m^2 surface heat flux of the stable northern Indian crust. Ah in the upper plate was assumed to be 2 $\mu W/m^3$ throughout and in the mantle 0.01 $\mu W/m^3$. Subduction of the Indian lithosphere at 3 cm/y keeps the crust above the MHT refrigerated. The model accounts for temperature-dependent thermal diffusivity [2, 3] and power-law temperature dependence of the shear strength (τ) of quartz [4]. Strain heating in the ductile regime is given by $\tau \cdot \varepsilon$, where ε is the strain rate. Strain rate in a 3 km wide shear zone is $3 \cdot 10^{-13}$ s^{-1}. Heat production at this strain rate is ~100 $\mu W/m^3$ at 550°C and ~10 $\mu W/m^3$ at 750°C [2].

Model results

Strain heating was assumed to occur along the length of the MHT, but only within the ductile regime. With subduction only, shearing produces a narrow, partially molten zone that extends from below the Himalayas to the northern end of the model domain. The partially molten zone is underlain by an inverted temperature gradient. The ductile regime extends further to the south along the MHT, in accord with observations [1]. Thus, the calculations demonstrate the feasibility of producing the observed low-velocity, partially-molten zone along the MHT in the deep crust.

[1] Nabelek, J.L. et al. (2009) *Science* **325**, 1371-1374.
[2] Nabelek, P.I. et al. (2010) *J Geophys Res* **115**, B12417.
[3] Whittington et al. (2009) Nature **458**, 319–321.
[4] Rutter, E.H. & Brodie, K.H. (2004) *J Struct Geol.* **26**, 2011–2023.

https://doi.org/10.1180/S0026461X00008434 Published online by Cambridge University Press

Depleted Mantle as the Source of Gold in Archean Alkaline Magmatic-Hydrothermal Systems

OLIVIER NADEAU[1*], ROSS STEVENSON[1], MICHEL JÉBRAK[1]

[1] UQAM-Géotop, Département des Sciences de la Terre et de l'Atmosphère , nadeau.olivier@uqam.ca (* presenting author)

Field relations, trace element and isotopic compositions and isotope dating suggest that 2.6 to 2.7 Ga. old gold-bearing syenites, lamprophyres (sensu stricto) and carbonatites of the Abitibi greenstone belt are genetically related. Their chondrite-normalized REE signatures are very similar and a survey of isotope data in the literature reveals ε_{Nd} and $^{87}Sr/^{86}Sr$ values that are consistent with a depleted mantle source. Preliminary results from syenites and lamprophyres of the Duquesne gold mine indicate that they have similar REE patterns in addition to both mantle and crustal isotopic compositions.

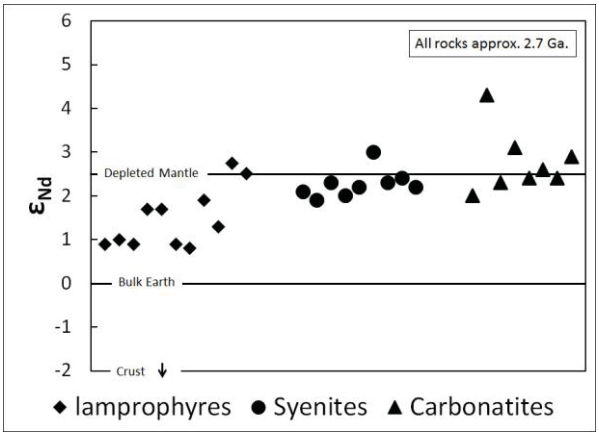

Figure 1: ε_{Nd} values for 2.6 to 2.7 Ga. lamprophyres, syenites and carbonatites of the Abitibi greenstone belt. The three lithologies display similar, mantle values, although the lamprophyres show some crustal alteration.

These results allow us to shed light on the petrogenesis of these rocks and their relationship to the gold deposits. Lamprophyres are quenched, volatile-rich, mafic porphyric rocks that interact very little with the crust as they rise from the mantle. Syenites also appear to be derived from a depleted mantle source that has interacted very little with the crust during their evolution. We propose that the syenites were produced by fractional crystallization of lamprophyre magmas in the crust. In this model, gold could have been carried from the mantle to its site of deposition in shallow level syenitic porphyries via a mantle-derived, carbothermal fluid. This model also finds support in the coexistence of carbonic-fluid-saturated, hybrid silicocarbonatites of Abitibi and most late-Archean gold deposits.

SO_2 emissions and their role in eruptive activity at Fuego Volcano, Guatemala

PATRICIA A. NADEAU[1, 2*], GREGORY P.WAITE[1], AND JOSÉ L. PALMA[1, 3]

[1]Michigan Technological University, Department of Geological and Mining Engineering and Sciences, Houghton, MI, USA, panadeau@mtu.edu (*presenting author)

[2]Now at: American Museum of Natural History, Department of Earth and Planetary Science, New York, NY, USA

[3]Now at: Center for Geohazards Studies, University at Buffalo, Buffalo, NY, USA

Magmatic volatiles have an important role in many aspects of volcanism, from magma generation to initiation of seismic phenomena to influence on eruption style. It follows that many models of volcanism and volcanogenic phenomena rely on behavior of such volatiles. UV cameras offer enhanced temporal resolution over previous SO_2 emission rate measurement techniques and also offer a synoptic view of plumes and degassing behavior. Integrated UV camera and seismic measurements recorded in January 2008 and January 2009 at Fuego volcano, Guatemala, provide new insight into the system's shallow conduit processes.

In 2008, an inter-explosion period was marked by pseudo-cyclic patterns of SO_2 emission rate. Comparison of the data with band-pass-filtered seismic data indicates that the onsets of increases in SO_2 emission rate are accompanied by very long period (VLP) seismic events. Larger amplitude VLPs are associated with larger pulses of SO_2 and shorter preceding inter-event times. Other VLPs associated with explosions at Fuego have been linked to pressurization at the intersection of two cracks [1], but the non-explosive nature of these VLPs may indicate a different source process.

UV camera data in 2009 reveal patterns of SO_2 emission rate relative to explosions and low-frequency seismic tremor that indicate tremor and degassing share a common source process. Progressive decreases in emission rate appear to represent inhibition of gas loss from magma as a result of rheological stiffening in the upper conduit. Measurements of emission rate from two closely-spaced vents, made possible by 2-dimension nature of camera data, help constrain this model.

Eruptive activity at Fuego appeared superficially similar in January 2008 and 2009, with a passive gas plume and sporadic, ash-rich explosions. Gas emission data obtained via UV camera, in combination with seismic data, enabled elucidation of different eruptive processes driven by the movement and escape of volatiles.

[1] Lyons and Waite (2011) *Journal of Geophysical Research* **116**, B09303.

https://doi.org/10.1180/S0026461X00008434 Published online by Cambridge University Press

Alteration and isotopic vectoring at the syenite-hosted Young-Davidson gold deposit, Matachewan, Ontario

N. NADERI[1*], R. MARTIN[2], R. LINNEN[1], J. ZHANG[3], S. LIN[2] AND N.R. BANERJEE[1]

[1]University of Western Ontario, Department of Earth Sciences, London, Ontario, Canada, nnaderi@uwo.ca (*presenting author)
[2]University of Waterloo, Earth and Environmental Sciences, Waterloo, Canada
[3]University of Hong Kong, Earth Sciences, Hong Kong, China

The Young Davidson mine is a syenite-hosted orogenic gold deposit at the western end of the Cadillac-Larder-Lake deformation zone in the southern Abitibi greenstone belt, Canada. The earliest stage of veining (V_1) consists of folded and boudinaged quartz-ankerite veins. V_2 is comprised of folded quartz-pyrite veinlets and disseminated sulphides and V_3 consists of en echelon or planar quartz-carbonate veins with sulphide minerals. The major phase of Au mineralization is associated with V_2 veins. Gold occurs as inclusions in V_2 pyrite, along quartz-carbonate grain boundaries in V_3 veins and as inclusions in disseminated pyrite in zones of intense potassic-hematite alteration.

Contouring of whole rock drillcore data indicate that Au is correlated with K_2O, S and Ba, consistent with the result of core logging, which established an association of Au with intense potassic-hematite alteration, quartz veining, pyritization and decreased magnetic susceptibility. Increases of K_2O (2 to 9 wt%) and Ba (600 to 3800 ppm) and a decrease of whole rock $\delta^{18}O$ values (11.4 to 9.2 ‰) is observed for some of the mineralized zones. Thus potassic alteration and whole rock $\delta^{18}O$ contours show promise as vectors to Au mineralization likely associated with high temperature magmatic fluids.

Bulk rock XRD analysis supports the idea of different alteration zones extending from shallower to deeper parts of the deposit. In shallower parts, ankerite abundance increases and that of calcite decreases towards the zone of mineralization. In deeper parts, this distribution pattern is reversed. In terms of oxide minerals, shallow mineralization is dominated by hematite (the concentrations of rutile and barite are also high enough to be identified in XRD patterns). In the deeper zones of mineralization hematite abundance decreases and magnetite abundance increases towards the mineralized zones.

Temperatures calculated from mineral pair oxygen isotope thermometry indicate the fluids ranged from approximately 330° to 460°C.Calculated V3 vein fluid compositions range from 6.4 to 11.9 ‰ and V1 from 6.6 to 7.4 ‰. In the deeper zones Au mineralization is correlated to high K_2O alteration, high sulphur concentrations and low $\delta^{18}O$ values, which indicate magmatic fluid involvement. However, in shallower zones gold mineralization is consistent with high $\delta^{18}O$ values, which is interpreted that the fluids were at lower temperatures and/or dominated by metamorphic fluids reflecting a separate and possibly later mineralizing event. We conclude that there are multiple stages of Au mineralization at Young-Davidson and that $\delta^{18}O$ whole rock values, potassic alteration and sulphur concentrations can be used as vectors for mineralization within different alteration zones.

Magnetite - An indicator mineral for hydrothermal ore deposits

PATRICK NADOLL[1]*, JEFFREY L. MAUK[2], RICHARD LEVEILLE[3], LOUISE FISHER[1], ROBERT HOUGH[1]

[1]CSIRO, 26 Dick Perry Ave, Kensington, 6151 Perth, WA, Australia
[2]University of Auckland, New Zealand
[3]Freeport McMoRan, Phoenix, United States

Magnetite and other Fe-Ti –oxides have been recognized as potential indicator minerals for exploration purposes since the 1980s. However, only recent studies have presented data that illustrate characteristic variations among magnetites of hydrothermal origin and describe distinct compositional signatures that can discriminate specific geologic settings such as hydrothermal ore deposits. The major controls for the geochemistry of hydrothermal magnetite are lithology/fluid composition, T, fO_2/fS_2 and re-equilibration processes. Exploratory data analysis has established the following upper threshold concentrations for hydrothermal magnetite from Ag-Pb-Zn veins, porphyry Cu-Mo, and skarn deposits (Table 1). The most important overall discriminators for the minor and trace element geochemistry of hydrothermal magnetite are Mg, Al, Ti, V, Co, Mn, Zn, and Ga. Nickel and Cr, which can have significant concentrations in igneous magnetite, are not commonly present at levels above their respective detection limits. Hydrothermal magnetite is typically depleted in Ti compared to igneous magnetite. Aluminum and V display a similar trend although the overlap between hydrothermal and igneous magnetite is more pronounced for these elements. Depleted Ti and V concentrations in combination with enriched Mg contents up to wt% values are in particular characteristic for hydrothermal magnetite from magnesian skarn. Manganese concentrations vary significantly among hydrothermal and igneous magnetites but concentrations are commonly lesser in hydrothermal magnetite with values up to several 1000 ppm. Cobalt, Zn, and Ga are enriched in hydrothermal magnetite from skarn compared to other hydrothermal magnetite. In addition to minor and trace element concentrations, the occurrence, abundance and composition of inclusions in magnetite is a potential tool to discriminate magnetite sample populations and fingerprint mineral deposits. Minor and trace elements that are commonly associated with micro- or nano-inclusions in magnetite include Ca + REEs (apatite and carbonates), Si (silicates), Cu (Cu-sulfides), Nb (rutile). Copper can be particularly indicative for mineralized zones where magnetite is closely associated with Cu-sulfides such as chalcopyrite or chalcocite.

Table 1: Upper threshold concentrations in ppm for n-number of hydrothermal magnetites from a range of geological settings.

	Ag-Pb-Zn	Porphyry	Mg-skarn	Skarn
n	30	126	17	57
Mg	740	490	25810	8780
Al	900	3180	2730	11330
Ti	4160	10500	20	8820
V	170	1460	20	14190
Co	10	40	5	320
Mn	1220	1880	1600	2900
Zn	110	280	260	5470
Ga	10	60	30	600

https://doi.org/10.1180/S0026461X00008434 Published online by Cambridge University Press

Hf isotope evidence for a transition in the geodynamics of continental growth after 3.2 Ga

T. NÆRAA[1,2], A. SCHERSTÉN[3], M.T. ROSING[2], A.I.S. KEMP[4], J.E. HOFFMANN[5,6], T.F. KOKFELT[1], M. WHITEHOUSE[7].

[1]Geological Survey of Denmark and Greenland (GEUS), Øster Voldgade 10, 1350 København K, Denmark
2) Nordic Center for Early Earth Evolution, Copenhagen University, Øster Voldgade 3-5, 1350 København K., Denmark
3) Department of Geology, Lund University, Sölvegatan 12, 223 62 Lund, Sweden
4) School of Earth and Environmental Sciences, James Cook University, Townsville 4811 Australia
5) Steinmann Institut für Geologie, Mineralogie, Paläontologie. Rheinische Wilhelms-Universität, Poppelsdorfer Schloss, 53115 Bonn, Germany
6) Geologisch-Mineralogisches Institut, Universität zu Köln, Zülpicher Str. 49a, Köln, Germany
7) Swedish Museum of Natural History, Box 50007, SE-104 05 Stockholm, Sweden

Earth's lithosphere likely experienced an evolution toward the modern plate tectonic regime, due to secular changes in mantle temperature. Gradually declining growth rates of the continental crust through time has been suggested, and recent estimates suggest that ≥70% of the present continental crustal reservoir was extracted by the end of the Archaean [1]. Patterns of crustal growth and reworking in rocks younger than 3.0 billion years (Ga) are thought to reflect the assembly and breakup of supercontinents by Wilson Cycle processes and mark an important change in lithosphere dynamics. It has been argued that subduction settings and crustal growth by arc accretion go back to 3.8 Ga in southern West Greenland [2-4]. We present in-situ zircon U/Pb, Hf and O isotope data from basement rocks in southern West Greenland across the time-period where modern style tectonic regimes might have started. Our data show that pronounced differences in the εHf-time patterns occurred, implying changing source rock characteristics. The observations suggest that 3.9-3.5 Ga rocks differentiated from a ≥3.9 Ga initially chondritic to slightly depleted mafic proto-crust. In contrast, rocks formed after 3.2 Ga register the first additions of juvenile depleted material since 3.9 Ga. Crustal growth after 3.2 Ga is characterised by upward εHf shifts and correlate in age with regional meta-volcanic supracrustal belts, stabilised felsic crust are characterised by downward εHf excursions, a pattern that compare with Phanerozoic accretionary orogens [5,6]. The isotope data reveal a transition from a crustal evolutionary signature unlike that of modern subduction-related orogens that didn't seem to generate or stabilise juvenile zircon-bearing crust, to an isotope-time pattern after 3.2 Ga that is compatible with arc accretionary processes and plate tectonics.

[1] Belousova et al., (2010) *Lithos,* **119**, 457–466. [2] Komiya et al., *J. Geol*. **107,** 515-554 [3] Nutman et al., (2009) *Precam. Res.* **172,** 212–233 [4] Furnes et al. (2007) *Science* **315,** 1704-1707. [5] Kemp et al., (2009) *Earth Planet. Sci. Let.* **284,** 455–466 [6] DeCelles et al., (2009) *Nature Geoscience* **2,** 251-257

Oxygen isotopic exchange reaction between silicate melt and ambient gas

HIROKO NAGAHARA[1]* AND KAZUHITO OZAWA[2]

[1]The University of Tokyo, Department of Earth and Planetary Science, Tokyo, Japan, hiroko@eps.s.u-tokyo.ac.jp (* presenting author)
[2] The University of Tokyo, Department of Earth and Planetary Science, Tokyo, Japan, ozawa@eps.s.u-tokyo.ac.jp

Oxygen Isotopic Variation of Planetary Materials

Chondrite, nonchondritic meteorites, and planets show wide variations of oxygen isotopic compositions, which incude mass-dependent and mass-independent fractionations. Mass-independent oxygen isotopic fractionation has been one of the most extensively studied subjects of meteorite study, whereas mass-dependent isotopic fractionation has not been paid attentions. It is, however, contorlled by physics, and is potentially an excellent indicator for environments. Here, we quantitatively study the role of isotopic exchange reaction between silicate melt and gas, and evaluate mixing lines on the oxygen three isotope plot.

Method

We have developed a kinetic condensation model that assumes totally molten silicate melt sphere cooling from an above liquidus temperature in a closed or open system, which has a composition of the solar abundance except for hydrogen. The model includes three free parameters; cooling rate of the system, initial oxygen abundance in gas relative to metallic elements, and oxygen isotpopic exchange efficiency. The model consists of the Hertz-Knudsen equation that describes condensation/evaporation flux and isotopic exchange reactions.

Results

We found that isotopic exchange reactions play a critical role in evolution of condensing silicate melt: silicate melt gets highly mass-fractionated composition if isotopic exchange does not work, which results in deviation of a straight mixing line but in formation of a fractionation trend with a slope of 1/2 on a oxygen three isotope plot. An isotopic exchange reaction greatly suppresses mass-dependent isotopic fractionation, which is tends to form a straight mixing line. The effect of fractionation is more conspicuous when the relative abundance of oxygen in the ambient gas against silicate melt is small. The degree also depends on isotopic exchange efficiency, but it is not dependent on cooling rate of the system. If the oxygen isotopic exchange efficiency does not change largely, the degree of deviation from a straight mixing line corresponds to the melt/gas ratio in a planetary environment or dust/gas ratio in a protoplanetary disk environment.

Discussions

The calculation results show that the straight mixing lines observed in various chondritic components such as CAIs and chondrules are explained by condensation in the presence of oxygen in the ambient gas by more than two orders of magnitude than the metallic elements. Otherwise, the mixing lines should be curved toward □^{18}O-rich side. The average O/M ratio (M: metallic elements) of the solar abundance is ~100, which suggests that CAIs and chondrules that show straight mixing lines were formed in an oxygen enriched environment than the average solar abundance. The model is further applied to the Earth-moon system, where homogenization of oxygen isotopic composition is easy at the stage of magma ocean.

https://doi.org/10.1180/S0026461X00008434 Published online by Cambridge University Press

Separation of Mo, W and HFSEs from rock samples for the study of isotope anomalies in meteorites

YUICHIRO NAGAI[1*], TETSUYA YOKOYAMA[1] AND RICHARD J. WALKER[2]

[1] Dept. of Earth and Planetary Sciences, Tokyo Institute of Technology, Tokyo, Japan. (* nagai.y.ab@m.titech.ac.jp)
[2]Dept. of Geology, Univ. of Maryland, College Park, MD, USA

Recent innovations in mass spectrometry have enabled detection of small isotope anomalies in some heavy elements present in a variety of meteorites. To make highly-precise and "accurate" isotope analysis, chemical separation of the target element from various types of meteorites must be developed from the following standpoints: 1) Achieve of nearly 100% recovery to avoid mass fractionation during chemical separation. 2) Complete removal of unwanted elements that can interfere with isotope analysis. 3) Maintain high sample/blank ratios. 4) Simultaneously separate as many elements as possible from a single sample. The last point is important not only to preserve precious meteorites, but also for performing multi-elemental isotope analysis on heterogeneous samples. In this study, we have developed a chemical separation method for Mo, W and HFSEs (High Field Strength Elements; e.g., Zr, Hf) from meteorite samples, all of which are intriguing elements for the study of isotope anomalies in the early solar system. We also show our prelimiary analysis of Mo isotope compositions in bulk chondrites and their acid leachates.

The separation method consists of a two-stage column chemistry using anion exchange resin (BioRad AG1X8). We have evaluated the performance of our technique by using a synthesized multi-element solution and some terrestrial rock samples decomposed by HF. A quadrupole-type ICP-MS (*ThermoFisher X SERIES II* at Tokyo Tech.) was used to determine the elution profile, as well as the recovery yield of Mo during the column chemistry. Molybdenum isotopes were analyzed by N-TIMS (TRITON-*plus* at Tokyo Tech).

In the first column, HFSE, W and Mo were successively eluted by 9M HCl-0.05M HF, 9M HCl-1M HF, and 6M HNO_3-3M HF, respectively. Unwanted elements in the Mo fraction (Zn, Nb and trace Ru) were further separated in the second column. The column size and total amount of acids were dramatically reduced compared to previous techniques. The Mo recovery was 94.5 ± 2.9 % in the first column and 101.3 ± 5.0 % in the second column. By applying this technique, we have determined Mo isotope compositions in bulk samples of Murchison (CM2) and Allende (CV3), as well as their acid leachates. The Mo isotope anomalies in bulk Murchison and a leachate indicate deficits of *s*-process Mo isotopes, consistent with previous studies [1, 2]. In contrast, anomalies observed in bulk Allende and its leachates are enigmatic, which may require a reassessment of the isotopic compositions of end-member components calculated by current nucleosynthetic theories.

[1] Burkhardt et al. (2011a) *EPSL* **312**, 390-400. [2] Burkhardt et al. (2011b) *LPSC* **42**, #2592.

Characterizing the cessation of arc-normal mid-crust extrusion, NW Nepal Himalaya

CARL NAGY [1*], LAURENT GODIN [1], JOHN COTTLE [2] AND BORJA ANTOLÍN [1]

[1] Queen's University, Department of Geological Sciences and Geological Engineering, Kingston, Canada, carl.nagy@queensu.com (* presenting author)
[2] University of California, Department of Earth Sciences, Santa Barbara, USA

The metamorphic and anatectic core of the Himalaya, the Greater Himalayan Sequence (GHS), has been hypothesized to represent exhumed mid-crustal material via a channel flow model [1 and references therein]. Characterizing the cessation of this lateral mid-crustal extrusion is integral in providing a comprehensive understanding of mid-crustal flow during orogenesis.

Field mapping, structural and microstructural analysis, geochronology, and thermochronology confirm the existence of the Gurla-Mandhata-Humla fault, an orogen-oblique strike-slip dominated fault in the High Himalaya of northwestern Nepal. Detailed across-strike transects reveal shallow-dipping mylonitic foliations and strongly-developed shallow plunging mineral stretching lineations interpreted to represent the terminal stages of arc-normal directed extrusion of mid-crustal material, and onset of orogenic extension [2]. Furthermore, late-stage deformation along this fault system overprints the GHS and its upper bounding fault, thus confirming a cessation of and transition from extruding GHS to subsequent arc-parallel deformation. A study of this fault system therefore provides documentation of the final stages of arc-normal directed extrusion of mid-crustal material.

The shear zone is characterized at upper structural levels by well-developed type-1 cross-girdle quartz c-axis fabrics and symmetric a-axis fabrics, indicating plane strain conditions. C-axis fabrics transition to type-2 cross girdles at ~ 1.2 km below the fault, suggesting an ostensible contribution of constrictional strain at depth. This deviation towards constriction is consistent with measured quartz a-axes, which show a progression towards upright cleft girdle patterns at similar depths. Quartz c-axis opening angles and quartz and feldspar recrystallization mechanisms show a progressive increase in deformation temperatures from ~ 350°C along the zone of maximum strain, to upwards of ~ 630°C at depths greater than ~ 5.5 km below the fault. Abundant asymmetrical fabric elements and conjugate shear bands in conjunction with a calculated mean kinematic vorticity number of 0.60 (c. 58% pure shear) attest to an important contribution of pure shear. U-Th-Pb in situ monazite geochronology, U-Pb zircon geochronology, and $^{40}Ar/^{39}Ar$ muscovite thermochronology reveal crystallization, decompression melting, and cooling within ≤ 7 Myr.

These data indicate that the final stages of the extruding mid-crust are characterized by a particularly high vertical gradient in deformation temperatures, deviations from plane strain at depths, and a significant contribution of pure shear. Furthermore, chronological data suggest that cooling and cessation of arc-normal extrusion of the mid-crust occurred within a geologically confined period.

[1] Godin et al. (2006) *Geol. Soc. Spec. Publ.* **268**, 1-23. [2] Murphy & Copeland (2005) *Tectonics*. **24**. TC4012, doi:10.1029/2004TC001659.

https://doi.org/10.1180/S0026461X00008434 Published online by Cambridge University Press

Phase relations in meta-komatiites during dehydration melting

NAIR,R.[1*] CHACKO, T.[2] VERWIMP, J.[1]

[1]Department of Geoscience, University of Calgary, Canada T2K 1N4(*rnair@ucalgary.ca)

[2]Department of Earth and Atmospheric Sciences, University of Alberta, Canada T6G 2E3

Komatiitic-basalts and komatiites are relatively abundant in the volcanic record of Archean cratons compared to Phanerozoic terranes. It has been suggested that these rocks may have constituted the Archean oceanic crust. It is important to understand the role these rocks would have played in the transformation of oceanic crust during purported processes like slab melting, eclogite formation etc. Whereas metamorphic phase relations of mid-ocean ridge (MORB) type basalts have been widely studied in the past, there is a paucity of knowledge on the phase relations of komatiitic basalts and komatiites.

We report results of preliminary dehydration melting experiments (1000°C, 7-20 kbar) on a natural amphibolite of komatiitic composition with starting composition in wt.% oxides : SiO_2 48.26, TiO_2 0.50, Al_2O_3 7.19, Fe_2O_3 13.31, MnO 0.23, MgO 18.66, CaO 8.49, Na_2O 0.51, K_2O 0.05 (1). The experiments were conducted on a piston cylinder apparatus for a duration of 2-7 days using procedures outlined in (2).

Experiment	P (kbar)	T (°C)	Phases Present
7IG006	7	1000	Ol,Cpx, (Opx), Melt
7IG005	10	1000	Ol,Cpx, Opx, Melt
7IG004	12.5	1000	Ol,Cpx, Opx, Melt
7IG001	15	1000	Grt, Cpx, Opx, Melt,(Amph)
7IG003	15	1000	Grt, Cpx, Opx, Melt,[Amph]
7IG002	17.5	1000	Grt, Cpx, Opx, Melt
7IG007	20	1000	Grt, Cpx, Opx, Melt

Table 1: Experimental conditions and phase relations. Abbreviations after (3). (), [] indicate minor and trace proportions, respectively.

Phase relations (Table 1) indicate a melt residue dominated by ol, opx and cpx at P <15 kbar and grt, opx and cpx at P ≥ 15 kbar. The incoming of garnet is at a significantly higher pressure than in MORB compositions (~10 kbar). Our results present interesting comparisons with recent crystallization experiments on a komatiite bulk composition at similar P-T conditions (4). This earlier study reported Ol coexisting with grt at P >14 kbar and no olivine at P<14 kbar. A melt phase was not reported at 1000°C and 10-18 kbar in these earlier experiments, but is ubiquitous in our experiments. A first order implication of the new results is that if Archean oceanic crust were komatiitic, crustal thickness >45 km is required to stabilize garnet in the melt residue. This is important to consider in Archean geodynamic models like crustal delamination that invoke density inversions resulting from stabilization of garnet bearing assemblages in the mafic lower-crust.

[1] Furnes et al. (2007) *Science.***315,** 1704-1707.[2] Nair and Chacko (2002) *J. of Petrol.***43,** 2121-2142. [3] Kretz (1983) *Am. Mineral.* **68**, 277-279.[4] Foley et al. (2003) *Nature* **421**, 249-252.

Transport of uranyl and arsenate in the presence of SiO_2, Al_2O_3, TiO_2 and FeOOH

SREEJESH NAIR[1*], BRODER J MERKEL[1]

[1] Department of Hydrogeology, Technische Universität Bergakademie Freiberg, Gustav-Zeuner Str.12, 09599 Freiberg, Germany

sreejeshmc@gmail.com (* presenting author)

merkel@geo.tu-freiberg.de

Uranium is a naturally occurring radioactive and chemically toxic metal, which is widespread in nature. Reactive transport of U(VI) with various ligands and different minerals has been studied extensively. Arsenic is analogous to phosphate and is a well-known contaminant to the environment. Uranyl-arsenate complex formation at near-neutral to alkaline pH conditions was proved by XAS and XANES [1]. They reported the formation of $UO_2AsO_4^-$, analogous to $UO_2PO_4^-$. However, little information is available about the migration of U(VI) and As(V) in systems containing both elements. The changes in sorption behaviour of U(VI) and As(V) in columns containing bentonite [2] and iron-coated sand [3] were reported. Since As(V) co-exists with U(VI) in several mining areas, it is important to understand the species behaviour to implement proper remediation procedures. Less or no information is available about the transportation of U(VI) and As(V) in the presence of SiO_2, Al_2O_3, TiO_2 and FeOOH, which are very common in natural environments. Hence column experiments were carried out for uranium (0.5 µM/L), arsenate (0.5 µM/L) and both uranium and arsenic containing solutions (0.5:0.5 µM/L) with SiO_2 (10 g), Al_2O_3 (10 g), TiO_2 (0.5 g) and FeOOH (0.1 g) at pH 6.5. Transport behaviour of U(VI) and As(V) through SiO_2 packed columns are identical for solutions containing either U(VI) or As(V) separately, or both together. Almost identical transport behaviour was observed for TiO_2 column also. In the presence of equimolar U(VI) and As(V) a substantial increase in As(V) mobility and slight decrease in U(VI) migration through Al_2O_3 was observed. When Al_2O_3 is replaced by FeOOH, a significant change in the pattern of mobility was shown for As(V) and minor changes for U(VI). The changes in transport behaviour of both elements can be attributed to the competitive sorption between uranyl and arsenate species or due to the formation of the above mentioned uranyl-arsenate species. Further investigations are recommended in order to understand the migration of contaminants in the environment and to implement proper measures in the remediation process.

[1] Gezahegne *et al.*(2009) *Geochimica Et Cosmochimica Acta 73*, A430-A430.

[2] Bachmaf *et al.*(2009) *Geochimica Et Cosmochimica Acta 73*, A 67-A67.

[3] Schulze & Merkel (2011) *The New Uranium Mining Boom: Challenge and Lessons Learned*, 573-578

https://doi.org/10.1180/S0026461X00008434 Published online by Cambridge University Press

An experimental study on stable isotope fractionation of rare earth elements during the adsorption on iron and manganese oxides

RYOICHI NAKADA[1*], YOSHIO TAKAHASHI[1, 2], AND MASAHARU TANIMIZU[1, 2]

[1] Hiroshima University, Higashi-Hiroshima, Hiroshima, ryo-nakada@hiroshima-u.ac.jp

[2] Japan Agency for Marine-Earth Science and Technology (JAMSTEC), Nankoku, Kochi

Recent development of analytical instruments, especially multiple collector (MC) ICP-MS, has enabled us to discuss the mass-dependent isotopic fractionation of heavy elements. Although several rules controlling the isotopic fractionation has have been suggested, it is still insufficient to discuss which chemical properties are the most important factor to evaluate bond stiffness in the equilibrium isotopic fractionation. This study, therefore, exhibits the results of stable isotopic fractionation of rare earth element (REE) during the adsorption experiment to discuss the cause of the isotopic fractionation among REE.

Lanthanum, Ce, Nd, and Sm chloride solutions with various concentrations were respectively added to both synthesized ferrihydrite and δ-MnO_2 suspensions. In all the systems, pH was adjusted to 5.00 (±0.05) and shaken for 6 hours before the filtration. Stable isotope ratios in both liquid and solid phases were determined using MC-ICP-MS. REE-Cl_3 solutions used in the adsorption experiment were employed as standard solutions and the isotope ratio of each element was expressed in epsilon notation relative to the average standards, which is shown in the equation as follows: $\varepsilon = (R_{sample}/R_{STD} - 1) \times 10^4$, where R was defined as $^{139}La/^{138}La$, $^{142}Ce/^{140}Ce$, $^{145}Nd/^{143}Nd$, or $^{149}Sm/^{147}Sm$, respectively. For the solid phase, K-edge EXAFS of filtered samples was measured at BL01B1 in SPring-8 to obtain the information of the coordination environment.

Though accurate determination of La isotope ratio was difficult due to the large difference in the isotopic abundance between ^{138}La and ^{139}La, a broad trend obtained in this study suggested that the lighter La isotope was selectively partitioned into the solid phase. In Ce system, it is clearly shown that the lighter isotope was partitioned into solid phase, whereas in Nd and Sm systems, lighter isotopes remained in the liquid phase, suggesting that physicochemical factors have been changed between Ce and Nd. According to the EXAFS analysis, split first shell (La-O bond) was observed for La-adsorption system, suggesting that the first coordination sphere is distorted in the system. Such distortion was also expected for Ce-adsorption system from their EXAFS results. On the other hand, split first shell was not observed for Nd and Sm systems. Thus, it is expected that the slight change in coordination environment, which can also cause the difference in their hydration numbers, affects the direction and degrees of mass-dependent isotope fractionations among REE.

Mechanism and conditions for strain softening in gabbro

PRITAM NASIPURI[1*], HOLGER STUNITZ[1], LUCA MENEGON[1], AND ALFONS BERGER [2]

[1] Departmnent of Geology, University of Tromsø, Norway, pritam.nasipuri@uit.no (* presenting author), holger.stunitz@uit.no, luca.menegon@uit.no

[2] University of Copenhagen, Denmark, ab@geo.ku.dk

Introduction

Weakening of lower crustal rocks due to fluid infiltration and metamorphism is responsible for the development of ductile shear zones. In this contribution, we describe the mechanism of formation of ductile shear zones in a granulite facies gabbro, followed by fabric formation during retrogression after eclogite facies metamorphism in rocks from Flakstadøy, Lofoten, Norway [1].

Results

Several mm to cm wide ductile shear zones are observed within the leuco-gabbro. Pl_0, Ol_0 and Opx_0 form the cumulus igneous texture. Opx_1 and Grt_1 corona around Pl_0 and Ol_0 indicate granulite facies metamorphism (M_1). Alternate bands of mafic (Opx_0+ Omp + $Grt_{I/II}$) and felsic (Pl + Amp + Spl) layers characterize the shear zone. The Opx_0 porphyroclasts are mantled by recrystallized Opx_{II} grains (20-30 mm) and show asymmetrical σ-porphyroclast indicative of sinistral sense of shear (D_1). Static overgrowth of Omp ± Grt_{II} around $Opx_{0/II}$ is the peak pressure metamorphic stage (M_{2A}). Subsequently, Cpx - Pl symplectite (M_{2B}) form at the outer rim the Omp. Breakdown of Grt $_{I/II}$ to Amph ± Pl (An rich) ± Spl with opposite shear sense in the $Opx_{0/II}$ defined fabric characterize M_3 metamorphism.

Alternate bands of mafic (Cpx + Pl + Qtz + Grt_{II} – Ol_0 - Opx_0 - Omp) layer (≈M_{2B})and felsic (Pl+ Amp + Cz – Spl) layer characterize the fabric in the retrograde eclogite. Amp and Cz overgrows at the contact between the mafic and felsic layers (≈ M_3).

In the ductile shear zone, chemical similarity and CPO data of Opx_0 and Opx_{II} indicate that Opx_0 deformed by cracking (D_1) at the onset of M_1-metamorphism. The fine-grained Pl shows a strong CPO indicative of inheritance of the CPO from D_1 deformation. The CPO of amphibole suggests that amphibole re-orients by rigid body rotation forming aligned (100) planes during post D_1 deformation.

In the retrograde variety, the CPO data of Cpx from the mixed phase mafic layers is consistent with the (010) [001] dominant slip system but is interpreted as oriented-growth-fabric during diffusion creep, because the mixed-phase-fabric does not indicate dislocation creep microstructures. CPO data of recrystallized plagioclase in the mono-mineralic felsic layers indicate (010) [100] as dominant slip system during dislocation creep.

Conclusions

This study indicates that deformation of Opx via cracking (D_1) requires very high differential stress at lower crustal conditions [3] during M_1 stage. However, in the retrograde eclogite, Omp breakdown will produce fine-grained Cpx+Pl mixtures [4] and promotes diffusion creep accommodated fabric formation.

[1] Markl & Bucher (1997) *Lithos* **42**, 15-35. [2] Kretz (1983) *Am. Min.* **68**, 277-279. [3] Steltolphel et al. (2006) *Geosphere* **2**, 61-72. [4] Anderson & Mocher (2007) *Contrib. Min. Pet.* **154**, 253-277.

https://doi.org/10.1180/S0026461X00008434 Published online by Cambridge University Press

Origin of Magnetite "Lava Flows" at El Laco Volcano, Chile

H.R. NASLUND[1*], F.J. HENRIQUEZ[2], J.O. NYSTRÖM[3], J.A. NARANJO[4] AND R.D. MATHUR[5]

[1]SUNY-Binghamton, Geological Sciences, Naslund@Binghamton.edu (*presenting author)
[2]Universidad de Santiago de Chile, fhenriqu@gmail.com
[3]Swedish Museum of Natural History, jan.nystrom@nrm.se
[4]SERNAGEOMIN, Santiago, Chile, cotonaranjo@gmail.com
[5]Juniata College, Huntingdon, PA, MATHUR@juniata.edu

Introduction:

Iron ore bodies at El Laco volcano have the appearance of dikes, lava flows, scoria, ash, and other pyroclastics and are composed of almost pure magnetite. Although an origin as Fe-oxide magmas has been proposed by many investigators [1], others have suggested an origin as hydrothermal or metasomatic replacement deposits [2, 3].

Magnetite Composition:

Excluding samples with obvious minor pyroxene or apatite, magnetite ore samples are 95 to 97% iron oxide with: 0.6-1.5% SiO_2; 0.01-0.03% TiO_2; 0.15-0.69% Al_2O_3; 0.002-0.039% MnO; 0.09-1.20% MgO; 0.18-1.18% CaO; 0.03-0.38% Na_2O; 0.05-0.21% K_2O; and 0.8-2.5% P_2O_5. Trace element abundances in the ore average: 90 ppm Ba; 96 ppm Co; 26 ppm Cr; 212 ppm Ni; 9 ppm Sc; 147 ppm Sr; 793 ppm V; 105 ppm Zn; 5 ppm Zr; and 24 ppm Y. Relative to associated unaltered andesites, the ores are enriched (ores/andesites) in Ni (7.7), P (7.3), V (5.3), Cu (2.6), and Zn (1.6), and depleted in Cr (0.7), Sc (0.6), Sr (0.3), Ba (0.2), Mn (0.1), Zr (0.03), and Ti (0.02). The ores are enriched in REEs (La 150X and Yb 14X chondritic) with steep LREE slopes (La_N/Sm_N = 8.1), relatively flat HREE slopes (Sm_N/Yb_N = 1.7), middle REE depletions (Sm/Sm* = 0.23), and negative Eu anomalies (Eu/Eu* = 0.5). In contrast, associated unaltered andesites have similar abundances (La 145X and Yb 12X chondritic) but less steep LREE (La_N/Sm_N = 4.6), steeper HREE (Sm_N/Yb_N = 2.7), less middle REE depletion (Sm/Sm* = 0.39), and less Eu depletion (Eu/Eu* = 0.65). Fe isotopes in the ores (δ56 = 0.52-0.90‰) are elevated relative to fumarolic and vein deposits (δ56 = 0.23-0.29‰) or andesites (δ56 = 0.49‰) at El Laco. In a single ore sample measured, Re = 460 ppt, Os = 23 ppt, $^{187}Os/^{188}Os_{measured}$ = 0.52, $^{187}Re/^{188}Os_{measured}$ = 2, and $^{187}Os/^{188}Os_{initial}$ = 0.51 indicates that there is a large contribution of Os from the continental crust.

Conclusions:

The high abundance of some relatively immobile elements (V, Ni, Y, and REEs) and the low abundance of other immobile elements (Zr, Ti, Cr, and Sc) is inconsistent with a hydrothermal or replacement origin for the ores. δ56 Fe in the ores is systematically higher than δ56 Fe in hydrothermal magnetite. Immiscibility between silicate magma and volatile-rich Fe-P-S-O magma, possibly initiated by crustal contamination, is compatible with all of the data.

[1] Naslund et al. (2002) *Hydrothermal iron-oxide copper-gold & related deposits* **Volume 2**, 207-226. [2] Rhodes et al. (1999) *Soc. of Econ. Geol. Spec. Pub.* **Volume 7**, 299-351. [3] Sillitoe & Burrows (2002) *Economic Geology* **Volume 97**, 1101-1109.

Mudstone pore networks: characterization and flow modeling

ALEXIS NAVARRE-SITCHLER[1*], KATHERINE MOUZAKIS[1], GERNOT ROTHER[2], JASON HEATH[3], TOM DEWERS[3], JOHN MCCRAY[1]

[1]Department of Civil and Environmental Engineering, Colorado School of Mines, Golden CO, USA, asitchle@mines.edu (*presenting author)
[2] Oak Ridge National Laboratory, Oak Ridge TN, USA
[3] Sandia National Laboratories, Albuquerque NM, USA

In geochemically active systems the pore network is arguably the most important physical characteristic of a rock because it provides pathways for reactive fluid flow and solute transport. The pore network is defined by an interface that advances and retreats with mineral precipitation and dissolution. These geochemical reactions can change important physical rock properties, such as interfacial roughness and area, and pore volume and connectivity, that in turn influence rates and mechanisms of future geochemical reactions and fluid flow. Despite their importance on geochemical behaviour of rocks, pore networks and their evolution with geochemical reaction are poorly understood. However, characterizing pore networks is not straightforward due to their dynamic nature and features at different length scales (nm to mm).

Problems associated with the characterization of pore networks are compounded in fine-grained rocks such as shales and mudstones that have a high percentage of nm scale pores. However, these rock types are increasingly important due to the role they play in unconventional natural gas production and geologic CO_2 storage. Small angle neutron scattering (SANS) is an ideal tool to study structural heterogeneties in porous materials on nanometer to micron length scales and compliments other traditional techniques such as sorption, mercury intrusion porosimetry (MIP), or microscopy.

In this study we characterized the nm to mm scale pore network in samples from three different mudstone formations using SANS, MIP, BET gas adsorption techniques and focused ion beam scanning electron microscopy imaging. These formations all serve as seals for containment of CO_2 in prospective geologic storage sites. Porosity and surface area in pores < 700 nm diameter was measured with small angle neutron scattering. According to this data pores < 10 nm radius contribute 20-50% of the total porosity and > 80% of the total surface area of these mudstones. The total pore volume determined from small angle neutron scattering is higher than porosity determined from mercury instrusion porosity for most of the samples. The discrepancy between these measured porosities may be related to low pore connectivity or the inability of MIP to fully access the pore network due to pressure limitations of the method. A comparison of cumulative pore fractions determined from SANS and MIP suggests that < 30% of the total porosity is accessible through pore throats < 1 nm radius. At these length scales Fickian diffusion of solutes and Knudsen diffusion of gas become the dominant transport mechanisms.

These data demonstrate the importance of very small pores to the overall pore structure of the mudstones. To really understand pore scale processes we need to not only develop a fully realized view of what the pore network looks like at multiple length scales but also understand how different techniques provide windows into that view. Results from flow simulation using pore networks created from FIB-SEM data will be presented. These simulations will help determine the contribution of different types of flow mechanisms and will form the basis for reactive transport models of geochemial processes.

Sandia is a multiprogram laboratory operated by Sandia Corporation, a Lockheed Martin Company, for the U.S. DOE under contract DE-ACOC4-94AL85000.

https://doi.org/10.1180/S0026461X00008434 Published online by Cambridge University Press

Analysis of sea ice and phytoplankton biomarkers in marine sediments from the Nordic Seas - a calibration study

ALBA NAVARRO RODRIGUEZ[1*], PATRICIA CABEDO SANZ[1], SIMON BELT[1], THOMAS BROWN[1], JOCHEN KNIES[2], KATRINE HUSUM[3], AND JACQUES GIRAUDEAU[4]

[1]Plymouth University, Plymouth, UK, alba.navarrorodriguez@plymouth.ac.uk (* presenting author)
[2]Geological Survey of Norway, Trondheim, Norway, Jochen.Knies@NGO.NO
[3]University of Tromsø, Tromsø, Norway, katrine.husum@uit.no
[4]Université Bordeaux, Bordeaux, France, J.Giraudeau@epoc.u-bordeaux.fr

Abstract

The work presented here is part of the Changing Arctic and Sub-Arctic Environment (CASE) program which is an Initial Training Network (ITN) that focuses on biological proxies and their use in reconstructing climate change and, in particular, the marine environment. One of these proxies is the sea ice diatom biomarker IP_{25} which is a highly branched isoprenoid (HBI) alkene synthesised by some Arctic sea-ice diatoms and has been shown previously to be a specific, stable and sensitive proxy measure of Arctic sea ice when detected in underlying sediments [1].

The current study focuses on three key elements: (1) An analytical calibration of IP_{25} isolated from marine sediments and purified using a range of chromatographic methods was conducted in order to improve the quantification of this biomarker in sediment extracts [2]. (2) Analysis of >30 near-surface sediments from the Nordic Seas was carried out to quantify biomarkers previously suggested as indicators of open-water phytoplankton (brassicasterol) [3] and sea-ice (IP_{25}) conditions [4]. The outcomes of the biomarker analyses were used to make comparisons between proxy data and known sea ice conditions in the study area derived from satellite record over the last 20 years. (3) A consideration of possible processes occurring within surface sediments and the implications of these on downcore analysis of biomarkers for palaeo-climate reconstructions.

[1] Belt et al. (2007) *Org. Geochem.* **38**, 16-27. [2] Belt et al. (2012) *Environ Chem Lett* DOI 10.1007/s10311-011-0344-0. [3] Müller et al. (2011) *EPSL* **306,** 137-148. [4] Belt et al. (2010) *Quaternary Science Reviews*, **29** 3489-3504.

Energetic Studies of Nanophase and Amorphous Carbonate Minerals

ALEXANDRA NAVROTSKY[1]*

[1]Peter A. Rock Thermochemistry Lab, University of California Davis, Davis, CA 95616 USA, anavrotsky@ucdavis.edu

13f. Physicochemical constraints of the marine carbonate system: recent insights into the reactivity of carbonate minerals in aqueous solutions

Solution calorimetric methodology has been applied to measuring the energetics of formation and transformation of amorphous and nanophase carbonates in the CaCO3 - MgCO3 - FeCO3 system. The data point to several general conclusions, summarized here. (1) Amorphous calcium carbonate (ACC) exists in two forms: a heavily hydrated material initially precipitated from strongly oversaturated aqueous solution and a less hydrated form, which is energetically similar whether formed by biomineralization or by thermal dehydration of the initially precipitated phase. Transformation in the sequence hydrated ACC – relatively anhydrous ACC – vaterite – aragonite – calcite is energetically downhill and thus ACC can be a precursor to any of these crystalline phases. (2) Amorphous magnesium carbonate (AMC), despite being energetically more metastable than ACC, is more persistent (can be kept for a year rather than a few days before crystallizing under ambient conditions). This is attributed to the kinetic difficulty of removing water of hydration from the environment of Mg2+. (3) Amorphous iron carbonate (AFC) is energetically similar to AMC but is very susceptible to crystallization and oxidation. The energetics of the amorphous versus crystalline carbonate phases may be controlled by the ionic radius of the cation. (4) The ACC – AMC system shows a striking change in energetic behavior near Ca/Mg = 1. More Mg-rich compositions, though amorphous, appear to be heterogeneous and consist of nanoscopic regions of dolomitic and magnesitic composition. The amorphous material with Ca/Mg = 1 may be a precursor to dolomite. (5) Measurement of the surface energies of calcite, aragonite, and vaterite is currently in progress. These general trends are discussed in the context of carbonate formation in biological, carbon sequestration, diagenetic, and fresh water and oceanic environments.

https://doi.org/10.1180/S0026461X00008434 Published online by Cambridge University Press

Nanoscale Effects on the Thermodynamics of Oxidation-Reduction Equilibria in Transition Metal Oxide Systems

ALEXANDRA NAVROTSKY[1]*

[1]Peter A. Rock Thermochemistry Lab, University of California Davis, Davis, CA 95616 USA, anavrotsky@ucdavis.edu

Keynote Speaker

Many low temperature aqueous geochemical processes involve the precipitation, dissolution, and redox reactions of fine - grained (nanophase) transition metal oxide minerals. Because phases with different oxidation states have different structures and, often, different surface energies, their redox phase boundaries can be significantly shited in oxygen fugacity - temperature space at the nanoscale. We have shown, for example, that FeO (wustite) has no stability field at the nanoscale, and that the stability field of magnetite is expanded relative to both reduction (to iron) and oxidation (to hematite) for small particles. A current calorimetric study suggests that fayalite has a higher surface energy than the assemblage magnetite plus quartz, thus shifting the QFM buffer to more reducing conditions for nanoparticles. In the manganese oxides, the phase field of Mn3O4 (hausmannite) is expanded relative to reduction to MnO and oxidation to Mn2O3, and the Mn2O3-MnO2 equilibrium is also affected. Furthermore, there appears to be complex involvement of water in these redox reactions, with possible reversible formation of hydrated amorphous layers at the nanoscale. The thermodynamic effects of particle size on reactions at bulk and nanoscale in the system magnetite - maghemite - ulvospinel are also under investigation. Thus significant nanoscale thermodynamic effects are a general phenomenon and must be considered, in addition to kinetic factors, in redox reactions in mineral and mineral - water systems at low temperature.

Amphiboles from the subcontinental lithospheric mantle of the Northern Victoria Land (Antartica): implications for the water activity and metasomatism

S. NAZZARENI[1*], C. BONADIMAN[2], P. COMODI[1], B. FACCINI[2] , P.F. ZANAZZI[1], M. COLTORTI[2], AND G. GIULI[3]

[1] Department Earth Sciences, University of Perugia, Italy sabrina.nazzareni@unipg.it

[2]Department Earth Sciences, University of Ferrara. Italy

[3] Scuola di Scienze e Tecnologia, University of Camerino

Spinel-bearing lherzolites and wehrlites from Baker Rocks (Northern Victoria Land, Antartica) have pargasitic amphiboles as metasomatic phase [1]. We investigated the amphiboles in order to estimate the physico-chemical conditions of their formation and, combined with the H2O content in coexistent pyroxenes, to estimate the total water budget of this mantle domain. The samples were analysed by Single-Crystal XRD, EMPA, SIMS and XANES to have an accurate crystalchemical formula and to calculate the fH2 and ultimately the fO2 and aH2O. The crystalchemical data showed that these amphiboles have similar composition, irrespective of the textural position and lithotype. The high equivalent thermal factor and cation off-centering suggest partition of Ti at M1 site. The high M3 site distortion and low <M3-O> distances suggest the presence of Fe3+ at M3 site. Starting from the crystallographic data we calculated dehydrogenation using the Oberti et al.'s method [2], whereas Fe3+/Fetot was measured by Fe K-edge XANES spectroscopy at GILDA beamline. Dehydrogenation varies from 0.80 to 1.07 a.f.u., with the lowest values for samples with lowest Ti and Fe. The measured Fe3+/Fetot and the crystallographic data suggest that dehydrogenation occurred by Ti-oxy substitution with only a minor Fe-oxy component. These data were used to estimated the aH2O and the fO2 of the mineral assemblage, following Lamb & Popp [3] and Ballhaus et al. [4] methods. Pressure estimates indicate a relatively shallow lithospheric mantle (P: 0.5-1.6 GPa) and T in the range of 800-1000 °C, implying an aH2O for the amphibole formation in the range of 0.01- 0.02. The calculated aH2O values are quite low if compared with those reported for the stability field of the reaction in the T-aH2O diagrams [3]. Δlog fO2 values relative to FMQ buffer range from -1.4 to -0.4. This range perfectly overlaps that of anhydrous samples from a locality nearby, as well as those obtained from peridotite xenoliths from continental setting [Δlog (FMQ) = -1.5 - +1.5; T=900-1100; P= 1.0-1.5 GPa. The low water content of amphibole is in agreement with that of the coexisting pyroxenes, which are about two times lower than those from other intraplate off-craton mantle xenolith [5], discharging the hypothesis that their low H2O contents may have resulted from the OH being preferentially partitioned in amphibole. This fact confirms the anomalously low whole-rock water content shown by the Antarctic sublithospheric mantle domain in a rifting setting.

[1] Coltorti et al.(2004) *Lithos*, **75**, 115-139. [2] Oberti et al. (2007) *Rev. Mineral MSAGS*, **67**, 125-164171; [3] Lamb & Popp (2009) *Am. Mineral*, **94**, 41-59; [4] Ballhaus et al. (1991) *Contrib. Mineral. Petrol,***78**, 27-40 [5] Bonadiman et. Al. (2009) *Eur. J. Min*., **21**, 637-647

https://doi.org/10.1180/S0026461X00008434 Published online by Cambridge University Press

Biogeochemical weathering of serpentinite in field and laboratory studies

K. NEGRICH[1*], J.L. BAUMEISTER[2], E. YARDLEY[1], J. MACRAE[1], E.M. HAUSRATH[2], AND A.A. OLSEN[1]

[1]University of Maine, Orono, USA, kimberly.negrich@maine.edu (*presenting author); eileen.yardley@maine.edu; jean.macrae@umit.maine.edu; amanda.a.olsen@maine.edu

[2]University of Nevada, Las Vegas, USA, baumeis5@unlv.nevada.edu; elisabeth.hausrath@unlv.edu

Biological processes, specifically mediated by microbial communities, are closely tied to mineral weathering. Serpentinites, for example, exert strong controls on the biota that develop on them. The bulk chemistry of serpentinite rocks is high in Mg and trace elements and low in nutrients such as Ca, K, P, and N. This causes an extreme and stressful environment for plants and microbes, that has been extensively studied by ecologists [1]. However, the role that serpentine biota play in development of serpentine soils has not been examined. In order to address this question, we have observed biogeochemical weathering of serpentinite in the field, and we are conducting laboratory studies to examine how iron-oxidizing bacteria and oxalic acid influence weathering rates of serpentine minerals.

Field samples from the Trinity Ultramafic Complex in the Klamath Mountains, California were analyzed by biological activity reaction tests (BART™) to test for the presence of iron-related bacteria. The BART™ indicators tested positive for iron-related bacteria in both rock and soil cores, [2] suggesting that biological impacts on Fe cycling may be important. However, future work is needed to compare lizardite dissoltuion in the presence and absence of Fe-oxidizing bacteria.

Lab experiments were performed to test the effect of oxalic acid on lizardite dissolution. Oxalic acid is an exudate from many soil fungi, and is an important ligand that binds to metals in the surrounding soil. We found that oxalate in concentrations of 50 mMol enhanced lizardite weathering by a factor of six [3].

We also plan to complete similar lab experiments with iron-oxidizing bacteria. We hypothesize that iron-oxidizing bacteria enhance lizardite dissolution, contributing to early serpentinite weathering in deep profiles. Crushed lizardite grains will be reacted in batch solutions with *Acidithiobacillus ferrooxidans*; a species common in acid mine drainage [4], *Ferritrophicum radicicola*; a neutrophilic species isolated from a wetland rhizosphere, and in abiotic solutions [5]. Experiments will be conducted at a range of pH values, but constrained by the survival needs of each species. Aliquots of solution will be extracted and analyzed for Mg, Si, Fe, Al, Ni, Cr, Cu, Co, and Ti using ICP-MS. Magnesium and silicon release rates will be used to calculate dissolution rates of lizardite in both biotic and abiotic experiments. Iron-oxide precipitates will be analyzed with SEM-EDS. Measured dissolution rates in the presence of microorganisms will be compared to abiotic dissolution rates, and used in reactive transport modeling of the field area.

[1] Kazakou et al. (2008) *Biological Reviews* **83**, 495-508. [2] Baumeister et al., in prep. [3] Yardley, E. (2012) M.S. Thesis. [4] Santelli et al. (2001) *Chemical Geology* **180**, 99-115. [5] Weiss et al. (2007) *Geomicrobiology Journal* **24**, 559-570.

Chemical zoning of eclogite lenses in subduction complexes: an example from the Leaota Massif, South Carpathians

ELENA NEGULESCU[1*] AND GAVRIL SĂBĂU[1]

[1]Geological Institute Of Romania, Bucharest, Romania elinegu@yahoo.com (*presenting author), g_sabau@yahoo.co.uk

The Leaota Massif basement comprises several concordant units characterized by internal lithologic and metamorphic contrasts. Eclogite and metagabbronorite lenses, hosted in a semipelitic matrix, appear sandwiched between two units of pelitic/meta-igneous composition.

The eclogite lenses are chemically zoned, as best exemplified by the Bughiţa Albeştilor (BA) occurrence, displaying several well-defined concentric zones, from fine-grained massive phengite-free domains that grade outwards into phengite-rich zones. The mineral assemblage of the phengite-free domain is garnet + omphacite + amphibole + zoisite + quartz + rutile. The phengite-rich zone preserved a low-variance mineral assemblage of garnet - omphacite - phengite - paragonite - amphibole - kyanite - clinozoisite - quartz – rutile. Mg-rich staurolite (X_{Mg} = 0.29 – 0.40) was rarely identified in kyanite porphyroblasts. Whole-rock compositions approach N-MORB to E-MORB, the latter ones also displaying HFSE-depletion.

The macro- and the microscopic features of these zones, together with their trace elements patterns that resemble N-MORB except the LILE (Rb, Ba, K, U) enrichment in the rind (fig. 1, 2), support the interpretation of the phengite-rich domains as a metasomatic rind of the phengite-free inner part, ensuing interaction with subduction-zone fluids.

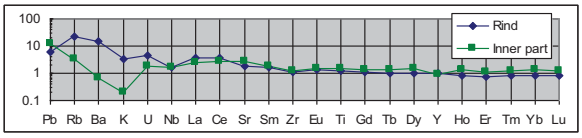

Figure 1: N-MORB-normalized [1] trace elements abundance of the inner part and its metasomatised rind of the BA-eclogites

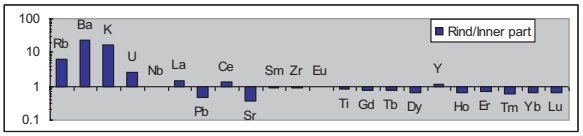

Figure 2: Chemical variation between the inner part and its metasomatised rind of the BA-eclogites

The geochemical features of the eclogite and metagabbronorite knockers, especially the distinctive LILE enrichment, document subduction-zone metamorphism of normal and SSZ ocean floor remnants enclosed in a subduction mélange. The LILE-metasomatism of the semipelitic matrix rocks themselves, demonstrated by high Ba contents of K-white micas [2], also support this interpretation.

[1] Sun, McDonough (1989) *Geol.Soc.Special Publications* **42**, 313-345. [2] Negulescu, Săbău (1999) *An. Univ. Bucureşti* ***XLVIII****,55-58.*

https://doi.org/10.1180/S0026461X00008434 Published online by Cambridge University Press

Micas and columbite-tantalite from some Portuguese granitic aplite-pegmatites

A.M.R. NEIVA[1*], P.B. SILVA[2], AND J.M.F. RAMOS[2]

[1]University of Coimbra, Geosciences Centre Earth Sciences, Portugal, neiva@dct.uc.pt (* presenting author)

[2]National Laboratory of Energy and Geology, S. Mamede de Infesta, Portugal, paulo.bravo@lneg.pt; farinha.ramos@lneg.pt

Different micas occur in granitic beryl-columbite-phosphate subtype aplite-pegmatite veins and sills from the Sabugal area. Subhedral lithian muscovite surrounds relics and penetrates along cleavages of primary muscovite, showing sharp contacts. The lithian muscovite containing higher Fe^{2+}, Li and F contents replaces primary muscovite. Radial lithian muscovite from aplite presents lighter areas (richer in Fe^{2+}, Li and F) surrounding and penetrating darker areas (richer in Al^{VI}, $Al^{IV} + Al^{VI}$ and OH) in BSE images and showing sharp contacts, suggesting that the former areas replace the latter areas. Primary muscovite and lithian muscovite from aplite and aplite-pegmatite have higher Fe^{2+}, Li, Rb and F contents and lower Mg content than primary muscovite from the parent granite and define a trend in the Li-Mg diagram. Very rare lepidolite from aplite-pegmatite surrounds lithian muscovite. In aplite-pegmatite, zinnwaldite penetrates along cleavages and partially surrounds lithian muscovite, suggesting that the former replaces the latter. Locally zinnwaldite and lithian muscovite seem to show different orientations. All contacts are sharp. Rare polylithionite partially surrounds lithian muscovite from aplite. The rim has higher Si, Li, Rb and F contents and lower $Al^{IV} + Al^{VI}$ and OH contents than the core. The compositions of the micas studied are well distinguished in Li-R^{3+} + Ti-R^{2+} and $Al^{IV} + Al^{VI}$ versus Fe + Mg diagrams. The lithium micas resulted from the accumulation of F and Li in derivative silicate liquids. Primary muscovite is texturally and chemically identified. Lithium micas have higher Li, F contents and lower Al^{VI}, $Al^{IV} + Al^{VI}$ and OH contents than primary muscovite.

Columbite-tantalite from granitic aplite-pegmatites veins and sills from the Sabugal area occurs associated with K-feldspar, albite, quartz, muscovite and beryl. Columbite-(Fe) is more abundant than columbite-(Mn) and tantalite-(Fe) is rare. Individual crystals of columbite-(Fe) are complexely zoned, showing alternating light BSE contrast zones high in W, Ta, Sn and F and dark BSE contrast zones high in Nb and Ti. Other complexely zoned crystals have col-(Mn) containing higher Nb, Mn contents, and lower Ta, Fe contents and Ta/(Ta+Nb) value than col-(Fe). A zoned columbite-(Fe) crystal shows the lighter zones containing higher Ta, Fe contents and Ta/(Ta+Nb) value and lower Nb content than the darker zones. In this crystal, a partial thin rim of tantalite-(Fe) is the richest in Ta, Sn, Ti, Sc, Fe and Mg contents and Ta/(Ta+Nb) value and the poorest in W, Nb and Mn contents. Columbite-tantalite is a primary phase. Crystals are complexely zoned, showing sharp contacts between zones, with exchange of Nb↔Ta and Fe↔Mn, suggesting that magmatic fluxes may have played a role, but diffusive reequilibration was not very important. The increasing content of fluxing elements like Li, F. B and P increase the solubility of columbite-(Mn). This type of zoning may be due to disequilibrium conditions.

Using a surface precipitation approach to model the continuum between Hg adsorption and precipitation onto *Bacillus subtilis*

RYAN M. NELL*, JENNIFER E.S. SZYMANOWSKI, JEREMY B. FEIN

University of Notre Dame, Civil Engineering and Geological Sciences, Notre Dame, IN 46556 (*presenting author, rnell@nd.edu)

The effect of bacterial cell wall adsorption on the precipitation of mineral phases in supersaturated systems is not well constrained experimentally, although there is circumstantial evidence for enhanced precipitation in these systems with the presence of bacteria. Surface complexation modeling has been applied successfully to model the adsorption of a wide range of aqueous metal cations onto bacterial cell walls. Surface precipitation theory represents an extension of surface complexation modeling that can bridge the continuum between adsorption and precipitation. However, only a small number of studies have examined the effect of bacteria on mineral precipitation reactions in well-controlled experiments, so testing and calibration of the surface precipitation modeling approach is limited for bacterial systems. In this study, we measured the extent of Hg(II) removal from solution, in the presence and absence of non-metabolizing cells of *Bacillus subtilis* in both sulfide-free and sulfide-bearing systems under a range of concentrations from undersaturation to supersaturation with respect to solid phase HgO and HgS, respectively. Initial Hg molalities ranged from 10^{-5} to 10^{-2} m at pH 4.5; ionic strength was buffered by conducting the experiments in 0.01 M $NaClO_4$, and the wet mass of bacteria used in each biotic experiment was held constant at 5 g/L. Sulfide-free experiments were conducted aerobically with a two-hour equilibration period. Sulfide experiments were conducted with varying concentrations of Na-sulfide under anaerobic conditions. Samples from both types of experiments were filtered and analyzed for aqueous Hg by a Hydra II AF Mercury Analyzer following the ASTM International standard test method for mercury in water.

The biotic systems exhibited enhanced Hg(II) removal relative to the abiotic controls in undersaturated conditions, likely due to Hg(II) adsorption onto cell wall functional groups. However, under the highest Hg concentrations studied in the sulfide-free system, the bacteria inhibit precipitation, maintaining high concentrations of Hg in solution. We use surface precipitation modeling to account for the range of Hg removal that we observed in the sulfide-bearing system, yielding equilibrium constants that can quantitatively account for Hg adsorption and precipitation with a single set of parameters. This approach offers promise for modeling the fate and distribution of aqueous metals in geologic systems with a wide range of saturation state conditions.

https://doi.org/10.1180/S0026461X00008434 Published online by Cambridge University Press

Microstructures in lunar zircon: key to interpretation of U-Pb ages

ALEXANDER A. NEMCHIN[1*], MARION L. GRANGE[1], NICHOLAS E. TIMMS[1] AND ROBERT T. PIDGEON[1]

[1]Curtin University, Perth, Australia, nemchina@kalg.curtin.edu.au

The interpretation of internal microstructures has become an integral part of geochronological studies using the U-Pb system in zircon from terrestrial samples. However, U-Pb analysis of lunar zircon was abandoned in late 80s and only recently resumed and combined with imaging utilising different methods available to reveal internal microstructures in these grains. Extensive study of lunar zircons during the last few years resulted in accumulation of data sufficient to build a preliminary classification of their internal structures. This classification is essential for the correct interpretation of U-Pb ages. It is particularly important because majority of lunar zircons occur as abraded, broken fragments in the matrix of the breccias, with no evidence of their origin or history. Also, increasingly, we are finding zircon grains with complex U-Pb age patterns, which makes interpretation difficult. The only way of addressing these issues is studying the textures and structures in lunar zircons and cross correlating this information with the observed pattern of U-Pb ages determined by ion microprobe analyses.

Lunar zircons are classified according to: (i) textural relationships between zircon and surrounding minerals in the breccias, (ii) the internal microstructures of the zircon grains and (iii) in-situ analyses of Th-U-Pb isotopic systems with ion microprobe. Both igneous (primary) and impact (secondary) features can be identified in lunar zircon.

Primary zircons occur as part of a cogenetic mineral assemblage (lithic clast) or as individual mineral clasts and are unzoned, or have sector zoning or rarely oscillatory zoning. U-Pb ages of zircons exhibiting these microstructures determine the timing of magmatic crystallisation.

Secondary microstructures include locally recrystallised domains, localised amorphization, crystal-plastic deformation, planar deformation features and fractures, and are associated with impact metamorphism. The first two types often yield internally consistent, concordant U-Pb ages that date impact events. The absolute ages of other secondary microstructures cannot be determined. Nevertheless, it is possible to define their relative timing from the relationships with other microstructures. In addition, regular occurence of these features (e.g. planar deformation features are found in lunar zircon along {001}, {110}, and {112}, typically with 0.1-25 μm spacing and {112} commonly contain micro-twin lamellae with 65° / <110> misorientation relationships, while dislocation creep commonly forms deformation bands parallel to {100} planes) can be explained in terms of elastic anisotropy of zircon and used to predict conditions experienced by different zircon grains during the impacts.

Planar deformation features, crystal-plastic deformation and micro-fractures can provide channels for Pb diffusion and their identification can explain some instances of partial resetting of the U-Pb isotopic system. Consequently their identification in a zircon grain should prompt a careful examination of the U-Pb ages obtained in this grain and their significance.

Metal speciation and dynamics of carrier phases in a boreal forested catchment under transient chemical conditions

ELISABETH NEUBAUER [1*], STEPHAN KÖHLER [2], FRANK V.D. KAMMER [1], HJALMAR LAUDON [3] AND THILO HOFMANN [1]

[1]University of Vienna, Department of Environmental Geosciences, Vienna, Austria, elisabeth.neubauer@univie.ac.at, thilo.hofmann@univie.ac.at (*presenting author)

[2]SLU, Department of Aquatic Sciences and Assessment, Uppsala, Sweden

[3]SLU, Department of Forest Ecology and Management, Umeå, Sweden

The formation and fate of natural aquatic colloids was investigated in a boreal catchment (68 km^2) with transient pH conditions (pH 3.8-6.4) and diverse landcover types (wetland, forest and sediment dominated). We examined the influence of colloids on metal speciation, i.e. iron, aluminum, arsenic, manganese, and rare earth elements (REE).

Flow-Field Flow Fractionation [1], membrane filtration (0.2 μm), cation exchange column separation [2], ultrafiltration (1 kDa) and scanning electron microscopy were used to characterize colloids and to quantify colloid-metal associations.

In the small headwater catchments, complexation with natural organic matter (NOM) was dominating the speciation of iron, aluminum, manganese and REEs. 50-70% of the total arsenic was associated with NOM, and substantial concentrations were present as dissolved species. Along the natural pH gradient we observed a gradual increase of iron in form of iron-oxy(hydr)oxide particles (50 nm up to several hundred nm). Despite this increase, REEs were still associated to colloidal NOM, while up to 30% of arsenic and manganese adsorbed or co-precipitated with the iron particles.

Chemical equilibrium modelling confirmed that complexation of REEs to NOM was stronger than the sorption of REEs to iron-oxy(hydr)oxides. The concentration of iron minerals can only be explained by a stronger than expected Fe-NOM complexation. The complexation constant would then be higher than in the data base of Minteq [3].

We quantified fluxes from all sub-catchments and used landscape type analysis for the estimation of metal export. Mass balances indicate that there is no loss of iron and trace elements during the transport through the catchment, despite the formation of relatively large iron-oxy(hydr)oxides particles. An additional source of iron, manganese, and sulphate through groundwater influx accounts for the observed total export from the catchment. Our study implies that the trace metals mobilized from the different upstream sites behave mainly conservative despite shifts in speciation. Mass balance calculation does allow for the quantification of the relative contribution of the different landscape elements for total metal flux.

[1] Neubauer et al. (2011) *J. Chromatogr., A.* **1218**, 6763-6773. [2] Hruska et al. (1996) *Water Resour. Res.* **32**, 2841-2851. [3] Sjöstedt et al. (2010) *Environ. Sci. Technol.* **44**, 8587-8593.

https://doi.org/10.1180/S0026461X00008434 Published online by Cambridge University Press

Interfacial Fe(II)-Fe(III) electron transfer and atom exchange in smectites: effect of smectite properties

ANKE NEUMANN[1*] AND MICHELLE M. SCHERER[1]

[1]Department of Civil and Environmental Engineering, The University of Iowa, Iowa City, USA, anke-neumann@uiowa.edu (* presenting author)

Heterogeneous reactions between aqueous Fe(II) and Fe(III) oxides have extensively been studied, leading to a new conceptual framework which includes electron transfer between aqueous Fe(II) and structural Fe(III), bulk electron conduction, and Fe(II)-Fe(III) atom exchange [1]. A recent study showed that interfacial electron transfer between aqueous Fe(II) and structural Fe(III) also occurred in one clay mineral [2]. Whether this observation can be generalized for all clay minerals and whether similar processes as observed for the heterogeneous redox reaction in Fe(III) oxides are also crucial for clay mineral redox reactions is unclear.

Studies on chemical reduction of structural Fe in smectites showed that the type of reductant as well as smectite structural properties determined the extent of Fe reduction and the resulting structural Fe(II) entities. Thus, we investigated well-characterized smectites differing in structural Fe content, location of structural Fe (octahedral vs. tetrahedral), and location of excess charge (octahedral vs. tetrahedral) for their reaction with aqueous Fe(II), a reductant abundant in natural anaerobic environments.

Stable isotope specific Mössbauer spectroscopy was used to determine the extent of reduction of structural Fe in smectites after exposure to aqueous ^{56}Fe(II), which is invisible in Mössbauer spectra. Experiments with aqueous Fe(II) enriched in ^{57}Fe were carried out to determine the exchange of stable Fe isotopes between aqueous Fe(II) and structural Fe(III) in smectites. Different pools of Fe(II) and Fe(III) were investigated by sequential extraction procedures and solid reaction products were characterized with X-ray diffraction and electron-based microscopic methods.

[1] Gorski & Scherer (2011) *Aquatic Redox Chemistry*, **1071**, 315-343, [2] Schaefer, Gorski & Scherer (2011) *Environ. Sci. Technol.* **45**, 540-545.

Paired ^{87}Sr/^{86}Sr - $\delta^{88/86}$Sr values in Paleozoic conodonts

LEONID NEYMARK*, WAYNE PREMO, AND POUL EMSBO

US Geological Survey, Denver, Colorado, USA lneymark@usgs.gov (* presenting author), wpremo@usgs.gov, pemsbo@usgs.gov.

The isotopic composition of Sr (^{87}Sr/^{86}Sr) is widely used as a tracer in paleooceanographic, paleoclimatologic, paleotectonic, and stratigraphic investigations. Until recently, the stable Sr-isotopic ratio (^{88}Sr/^{86}Sr) was assumed to be constant and was used for internal normalization to correct for instrumental mass fractionation, thus masking any natural mass-dependent Sr-isotopic fractionation. Newly developed MC-ICPMS and Double Spike (DS) TIMS methods, however, document measurable Sr isotope fractionation in natural systems.

We present the first DS TIMS $\delta^{88/86}$Sr (‰) data ($\delta^{88/86}$Sr = (^{88}Sr/^{86}Sr$_{sample}$/^{88}Sr/^{86}Sr$_{NBS\text{-}987}$-1)×1000) for fossil biogenic marine phosphates (conodonts). The ^{84}Sr-^{87}Sr DS preparation and data reduction followed recommendations in [1]. Our DS was calibrated against NIST SRM-987 assuming ^{88}Sr/^{86}Sr = 8.375209 to give $\delta^{88/86}$Sr = 0.002 ± 0.024 ‰ (2SD). External reproducibility was evaluated using USGS Sr isotope standard EN-1 (a carbonate shell of a giant clam Tridacna collected live from the floor of the Enewetak lagoon, Marshall Islands), which yielded $\delta^{88/86}$Sr = +0.262 ± 0.032 ‰ (2SD) and NRC Canada sea-water trace element reference material NASS-6, which yielded $\delta^{88/86}$Sr = +0.371 ± 0.026 ‰ (2SD).

Paired ^{87}Sr/^{86}Sr - $\delta^{88/86}$Sr values were measured in 30 Paleozoic conodont samples from different stratigraphic horizons (Middle Ordovician to Middle Mississippian). The samples were screened for diagenetic alteration so that only conodonts with Color Alteration Index CAI≤ 3.0 were analyzed. The $\delta^{88/86}$Sr values in these samples vary from slightly positive to significantly negative (up to –1.05 ‰). This range is significantly broader than the variability observed in Paleozoic marine brachiopods [2] but is similar to the range in human tooth enamel and bone [3]. The reasons for this variability in conodonts are not well understood, but likely reflect changes in seawater composition and/or biogenic fractionation of Sr isotopes. The range in $\delta^{88/86}$Sr also causes ^{87}Sr/^{86}Sr values based on DS measurements to deviate appreciably from ^{87}Sr/^{86}Sr values determined using conventional mass-fractionation corrections.

Our results indicate that the study of conodont $\delta^{88/86}$Sr values has the potential for better constraining the marine Sr cycle and its relation to secular changes in marine chemical and biologic systems.

[1] Rudge et al. (2009) *Chemical Geology* **265**, 420-431.
[2] Vollstaedt et al. (2011) *Geophysical Research Abstracts* **13**, EGU2011-7257
[3] Knudson et al. (2010) *J. Archaeol. Sci.* **9**, 2352-2364.

https://doi.org/10.1180/S0026461X00008434 Published online by Cambridge University Press

Using PLFA to constrain microbial distribution related to S-cycling in oil-sands composite tailings during reclamation

NGONADI, N.*[1], ZIOLKOWSKI, L.A.[1], PENNER, T.[2], SLATER, G.F.[1]

[1]McMaster University, Hamilton, Canada gslater@mcmaster.ca
[2] Syncrude Environmental Research, Edmonton, Canada

Understanding the extent and nature of biogeochemical cycling by microbial communities is a critical component of predicting and managing their impact within systems. This study is applying phospholipid fatty acid (PLFA) analysis to investigate the microbial communities associated with reclamation of composite tailings recently initiated at Syncrude's Mildred Lake site. PLFA concentrations and distributions were determined within the sand cap that separates the fen reclamation from the CT below, as well as in the CT itself. The goal was to determine how cell densities and microbial community parameters varied between the CT and the sand cap, and to determine the relatively importance of these communities to biogeochemical cycling of sulphur, particularly H_2S generation.

Results from sand cap samples show cell densities in the 10^7 range based on generic conversion factors, not unexpected for oligotrophic conditions. The presence of branched PLFA, particularly iso and anteiso C15:0 are indicative of the presence of sulphate reducing organisms in the sand cap. Such organisms have also been enriched from these samples. Analysis of CT samples in on-going and will be compared to these surface samples to determine whether microbial cycling rates are expected to be lower or higher within the CT which has a highly distinct geochemistry to the sand cap, including the presence of abundant sulphate, used in flocculation of tailings.

The results of these studies will yield insight into the cycling that may be carried out by these communities. They also provide the foundational understanding for on-going isotopic studies of microbial carbon sources and cycling.

Identifying the arsenic source in glacial aquifer sediments, west-central Minnesota, USA

SARAH L. NICHOLAS[1]*, BRANDY M. TONER[2], MELINDA L. ERICKSON[3], ALAN R. KNAEBLE[4]

[1]Land and Atmospheric Sciences Graduate Program, Department of Soil, Water, and Climate, University of Minnesota, Saint Paul, MN, USA (*presenting author) nich0160@umn.edu
[2]Department of Soil, Water, and Climate, University of Minnesota, Saint Paul, MN, USA toner@umn.edu
[3]United States Geological Survey Minnesota Water Science Center, Mounds View, Minnesota USA merickso@usgs.gov
[4]Minnesota Geological Survey, Minneapolis, Minnesota USA knaeb001@umn.edu

X-ray absorption spectroscopy (XAS) and sequential extractions were used to identify and quantify different arsenic (As) species present in glacial aquifer materials from west-central Minnesota, USA. Sample locations were chosen based on proximity to domestic drinking water wells with As concentrations exceeding the $10 \mu g L^{-1}$ maximum contaminant level for drinking water in the United States. Glacial sediments were collected from rotary-sonic drill cores (25-100m depth).

Sequential extractions were used to quantify arsenic species concentrations. Total (all species) arsenic concentrations of the glacial aquifer sediments are not unusually high, however the concentration of labile species of arsenic are unusually high. Here the labile species are defined operationally as those liberated by anion exchange with Cl^- and PO_4^{-3}. Labile As concentrations in many samples are near or above the crustal average of about 1-1.8mg kg^{-1} for all forms of solid-phase arsenic.

X-ray absorption spectroscopy of the samples shows that arsenic is present in three oxidation states: As^{5+}, As^{3+}, and $As^{1-\text{ to }2-}$. Non-uniform distribution of oxidized arsenic may explain the spatial heterogeneity of high As wells in the area.

Arsenic-bearing sulfide minerals in the Cretaceous shale fragments found in these glacial sediments are frequently hypothesized to be the source of arsenic in drinking water in west-central Minnesota. Our data suggest that the solid-phase arsenic sources in water are likely to be the more labile, oxidized species found in unusual abundance in these samples. Most As-bearing sulfide minerals would be expected to be chemically refractory in the reduced groundwater of the area.

https://doi.org/10.1180/S0026461X00008434 Published online by Cambridge University Press

Geomicrobiological and Geochemical Study on Pockmarks in the SW Barents Sea

JULIA NICKEL[1*], KAI MANGELSDORF[1], JENS KALLMEYER[2], ROLANDO DI PRIMIO[1], AND DANIEL STODDART[3]

[1] Helmholtz Centre Potsdam GFZ German Research Centre for Geosciences, Telegrafenberg D-14473 Potsdam, Germany, nickel@gfz-potsdam.de (* presenting author)

[2] University of Potsdam, Karl-Liebknecht-Strasse 24, Haus 27, D-14476 Potsdam, Germany

[3] Lundin Petroleum Norway, Strandveien 50D, 1366 Lysaker, Norway

Introduction

Widespread areas of the seabed in the southwestern Barents Sea are dominated by pockmarks, being manifestations of hydrocarbon venting and are, therefore, of considerable interest as possible indicators for deeper hydrocarbon reservoirs. Concomitantly, they form specific habitats for microbial communities. These pockmarks and the associated microbial ecosystems are in the focus of the current study using biogeochemical and microbiological approaches.

During two research cruises in 2009 and 2011, funded by the Swedish oil company Lundin, about 42 surface sediment cores of up to 2.5 m length were selected. For comparison cores were taken inside and outside of the pockmark structures.

Results and Conclusion

The analysis of methane within the pockmarks reveals only marginal amounts of gas, indicating that nowadays the pockmarks system is more or less inactive. Also microbial activity is astonishingly low in the entire sampling area as indicated by low sulfate reduction rates. Processes like anaerobic oxidation of methane (AOM) can be excluded for this depth interval since methane concentration and net sulfate consumption are very low.

Different biomarkers have been analyzed being indicators for fossil hydrocarbons (e.g. *n*-alkanes, hopanoids and steranes), or past microbial populations (glycerol dialkyl glycerol tetraethers (GDGTs)). Biomarker profiles do not show significant differences between pockmark and reference sites, inferring that fluid flow through the present pockmarks is currently not taking place. However, in the deeper core section an increase for hydrocarbons and microbial markers is detectable which might indicate the transition to the interval of paleo-seepage.

The results show that the observed pockmarks are rather relicts of paleo-seepage than indicators for active fluid flow. Their formation is most likely related to paleo-events of decaying gas hydrates induced by the pressure release from the melting ice shield during last deglaciation (approx. 13ka B.P.). [1]

Microorganisms, which are involved in the methane cycle, show a characteristic light carbon isotopic composition ($\delta^{13}C$). [2] Currently, the $\delta^{13}C$ values of GDGTs from top and bottom part of the sample cores are investigated to unravel a possible correlation of the biomarker increase to paleo-seepage.

Furthermore, a piece of a carbonate crust, sampled from an active seep in the Norwegian Sea is being analyzed to compare its biomarker composition to our previously investigated samples.

[1] Nickel et al. (2012) *Marine Geology,* in press.
[2] Aloisi et al. (2002) *Earth and Planetary Science Letters,* **203**(1), 195-203.

Bulk redox status or redox microenvironments: Which is more important for controlling trace element transport?

PETER S. NICO[1*], CHARULEKA VARADHARAJAN[1], HARRY R. BELLER[1], RUYANG HAN[1], LI YANG[1], EOIN L. BRODIE, MARK CONRAD, MARKUS BILL, AARON J. SLOWEY[1], WILLIAM MOSES[1]

[1]Lawrence Berkeley National Laboratory, Berkeley, CA, USA
psnico@lbl.gov (* presenting author)
cvaradharajan@lbl.gov
hrbeller@lbl.gov
rhan@lbl.gov
lyang@lbl.gov
elbrodie@lbl.gov
msconrad@lbl.gov
mbill@lbl.gov
ajslowey@lbl.gov
wwmoses@lbl.gov

The redox form of trace elements is frequently the major control on the tansport of those elements within soil and sediment systems. However, what controls the transformation from one redox form to another is much more debatable. Clearly the dominant or bulk redox condition of a sytem has an important impact on the chemical form of the trace metals therein. However, rarely can trace metal behavior be simply predicted by bulk redox measurements. The current presentation will focus on recent work studying the bioreduction of Cr(VI) to Cr(III) under differing dominant terminal electron acceptor (TEA) conditions (i.e. NO_3^-, native Fe(III)-containing minerals, and SO_4^{2-}) and the subsequent remobilization of that Cr via reoxidation.

For the bioreduction phase of the experiment, advective flow laboratory columns packed with Hanford 100H aquifer sediments were subject to oxygen-free, synthetic groundwater containing Cr(VI) and lactate in the presence of different electron acceptors (NO_3^-, native Fe(III)-containing minerals, and SO_4^{2-}). Chromate removal was observed under all conditions to varying degrees. The nitrate-treated columns, all of which exhibited denitrifying conditions, as well as in some of the sulfate-amended columns in which fermentative conditions were dominant, showed the most rapid removal of Cr(VI). After approximately one year, selected replicates of the nitrate-amended and sulfate-amended (one fermenting, one not) conditions were removed from the glovebox and presented with oxygen and nitrate containing, lactate- and chromate-free synthetic ground water in order to promote oxidative remobilization of Cr.

Interestingly, the solid-state form of Cr at the end of the bioreduction phase of the experiment appeared to be relatively independent of the dominant TEA present. However, in the reoxidation phase of the experiment, the rate and degree of Cr remobilization was strongly influenced by the bulk redox condition history of the system. These results present an interesting contrast between those behaviors controlled by local conditions and those controlled by bulk conditions.

https://doi.org/10.1180/S0026461X00008434 Published online by Cambridge University Press

Contrasting on- and off-axis melt delivery: a Sr and Nd isotopic study of the Moho transition zone of the Oman ophiolite

MARIE NICOLLE[1]*, DELPHINE BOSCH[2], LAURIE REISBERG[1], DAVID JOUSSELIN[1] AND AURORE STEPHANT[1]

[1]Université de Lorraine, CRPG-CNRS, Vandoeuvre les Nancy, France, mnicolle@crpg.cnrs-nancy.fr (* presenting author)
[2]Université Montpellier 2, Géosciences Montpellier, Montpellier, France

Recent tomographic images from the East Pacific Rise [1] indicate that nearly 50% of the melt is delivered off-axis instead of beneath the ridge axis. The consequences of this process can be studied on land in the Oman ophiolite, where structural mapping has shown the existence of both on- and off-axis melt delivery systems [2]. Off-axis diapirs impinge directly on hydrothermally-altered lithosphere and may be contaminated by this material. Petrologically, off-axis melt delivery results in the development of an unusually thick Moho Transition Zone (MTZ) composed largely of clinopyroxenite, whereas on-axis MTZ contains troctolite and gabbro lenses. We are analyzing the Sr and Nd isotopic compositions of pyroxenites, gabbros, diorites, and dunites, from an on-axis (Maqsad) and an off-axis (Mansah) diapir in the Semail massif of the Oman ophiolite to explore the geochemical consequences of these contrasting settings. Leached and unleached whole rocks, as well as clinopyroxene (cpx) separates are being studied, to allow us to investigate both magmatic and later hydrothermal processes. Initial Nd isotopic compositions from unleached whole rock powders are comparable for the two diapirs (ε_{Nd} = 8.5-9.2 on-axis; ε_{Nd} = 5.6-10.3 off-axis), although off-axis rocks display a larger range of variation. In contrast, whole rock Sr isotopic ratios differ markedly, with on-axis samples displaying a limited range of enriched MORB-like compositions ($^{87}Sr/^{86}Sr$ = 0.703010 - 0.703438) whereas off-axis samples have more radiogenic and highly heterogeneous compositions ($^{87}Sr/^{86}Sr$ = 0.703277 - 0.706192). We attribute this difference to the presence of a magma chamber above the on-axis diapir, which protects the MTZ from the effects of hydrothermal circulation. Separated cpx and leached whole rocks from off-axis pyroxenites have less radiogenic compositions ($^{87}Sr/^{86}Sr$ = 0.703218 - 0.703576) than the corresponding unleached whole rocks. Nevertheless, several of these samples have $^{87}Sr/^{86}Sr$ ratios that approach the upper limit of the Indian MORB field. In outcrop, a mixing zone is observed between pyroxenites and crustal gabbros in the MTZ overlying the off-axis diapir. Samples from this mixing zone have more radiogenic cpx compositions than samples collected further from the Moho, suggesting magmatic contamination of the pyroxenites by incorporation of hydrated material rich in seawater-derived Sr.

[1] Toomey et al. (2007) *Nature* **446**, 409-414. [2] Jousselin and Nicolas (2000) *Marine Geophysical Researches* **21,** 243-257

Weathering in the Rhizosphere Analyzed with Transmission Electron Microscopy

S.M. NIEDZIELA[1]*, A. DOHNALKOVA[2,3], K.A. GREENBERG[1], B.W. AREY[2], Z. BALOGH-BRUNSTAD[1], Z. SHI[3], AND C. K. KELLER[3]

[1] Hartwick College, Oneonta, NY, 13820 USA (*correspondence: balogh_brunz@hartwick.edu)
[2]Environmental Molecular Sciences Laboratory, Pacific Northwest National Laboratory, Richland, WA, USA
[3]School of the Environment, Washington State University, Pullman, WA, USA

Introduction and Methods

It is generally accepted that bacteria and mycorrhizal fungi enhance mineral weathering and nutrient translocation to their host plants. The role of biofilm in rhizosphere (root zone), on the other hand, is not well known and poorly characterized. The goal of our study was to examine the mineral-fungus-biofilm interface under conditions of calcium and potassium limitation, using transmission electron microscopy. We hypothesized that tree-fungus-bacteria association increases biofilm formation under calcium and potassium limitation, and enhances mineral weathering that will be indicated by distinct depletion profiles of elements under fungal and biofilm cover [1].

Red pine (*Pinus resinosa* Ait.) trees were grown in leach tubes filled with quartz sand amended with 0.5 wt% biotite and 1 wt% anorthite. Half of the trees were inoculated with *Suillus tomentosus* and a group of forest soil bacteria, and the other half were left without microbial inoculation. Additional columns without any biology served as controls. Calcium and potassium were supplied in irrigation water at 0, 10, 30 and 100% of rates for healthy tree growth. A subset of the columns were destructively sampled after three months. Whole mount transmission electron microscopy (TEM) grids were prepared from root-system wash solutions used to collect the rhizospheric microbial community. Anorthite and biotite grains were also collected from the rhizosphere to prepare thin sections using focused ion beam – scanning electron microscopy (FIB-SEM). Thin sections of the 0% treatment and a control were analyzed with high resolution TEM coupled with energy dispersive x-ray spectoscopy to test our hypothesis. Multiple chemical profiles were analyzed on the FIB sections under the fungal cover of anorthite and biofilm cover of biotite.

Results and Discussion

Whole mount TEM shows that the 0% treatment has the greatest species diversity, but all treatments have one or two types of bacteria. The overall bacterial population by number is the largest in the 100% treatment. Fungal hyphae are only oberserved with SEM. On the anorthite FIB sections, a slight decrease of Ca is seen under the fungus compared to the control. The same slight depletion is seen for K, Mg and Fe in biotite under biofilm cover, compared to the control. However, these chemical profile differences between treatments and controls are not significant after 3 months reaction time. Further work after 6, 9 and 12 months is planned to further explore our hypothesis.

[1] Bonneville et al. (2011) *Geochim. Cosmochim. Acta* **75**, 6988-7005.

https://doi.org/10.1180/S0026461X00008434 Published online by Cambridge University Press

Thermodynamic feedbacks in kinetic trace metal-calcite solid solution formation

LAURA C. NIELSEN[1*], DONALD DEPAOLO[1,2], JAMES J. DEYOREO[3]

[1]University of California-Berkeley, Berkeley, CA, USA, lnielsen@berkeley.edu (* presenting author)
[2]Center for Isotope Geochiemistry, Lawrence Berkeley National Laboratory, Berkeley, CA, USA
[3]The Molecular Foundry, Lawrence Berkeley National Laboratory, Berkeley, CA, USA

Calcite precipitated from natural terrestrial fluids typically incorporates trace to mole percent amounts of impurities. The resulting solid solutions have solubilities different from the pure phase. To understand the relationships between trace element concentration and the environment of calcite precipitation, it is necessary to know how thermodynamic controls on solid solution composition also affect mineral precipitation kinetics. These two factors together determine the solid solution composition. To evaluate the feedbacks between thermodynamics and kinetics we developed a microscopic model of ion-kink attachment-detachment rates which predicts the inhibition and incorporation behaviour of impurities, and its relationship to solution composition.

For solution supersaturations typical of biomineralizing fluids in seawater and of most natural surface waters, ion attachment and detachment occur primarily at kink sites along step edges on the calcite surface. The net ion attachment rate is controlled by the density of compatible kink sites (i.e. a carbonate site for a calcium ion) and by the kinetic barrier for ion attachment, which is thought to reflect ion and kink desolvation kinetics. Ion detachment from kink sites occurs when the solid-solid bonds between the ion and the adjacent lattice sites are broken. Lattice strain induced by incorporation of poorly fitting trace elements will speed ion detachment kinetics. Ion attachment kinetics are primarily governed by solution properties, whereas ion detachment is controlled by bond energetics of calcite. At equilibrium, ion attachment and detachment rates are equal, so the detachment frequency can be calculated from the equilibrium ion activities, which in turn are dependent on the composition of the calcite. Ultimately, with some assumptions about the form of the kinetic rate laws, we can derive a model that simultaneously accounts for the trace element incorporation and its effects on calcite growth rates.

Our results indicate that step velocities of strontian calcites vary non-linearly with aqueous Sr concentration due to the effect of lattice strain on Ca detachment kinetics. The growth rate of Mg-bearing calcite with increasing aqueous Mg, on the other hand, is inhibited primarily by kink blocking, and Mg incorporation is typically controlled by the relative rates of Ca and Mg desolvation. This suggests that the Mg isotopic composition may similarly be controlled by dehydration kinetics. This model can be used to constrain the composition of fluid from which a given calcite precipitated.

The geochemical behavior of thallium in mantle-derived basalts

NIELSEN, S.G.[1*], LEE, C.T.A.[2], SHIMIZU, N.[1]

[1]WHOI, Dept. of Geology and Geophysics, 266 Woods Hole Rd, 02543 Woods Hole, MA, USA, snielsen@whoi.edu
[2]Department of Earth Science, MS-126, Rice University, 6100 Main St., Houston, TX 77005, USA

Thallium (Tl) isotopes are a new stable isotope system that shows great potential as a tracer in igneous systems [1, 2]. One of the main difficulties when doing any geochemical study of Tl is the scarcity of knowledge about the general behavior of this element in various environments. This problem stems from the fact that historically Earth scientists have rarely analyzed Tl. The physical and chemical properties of Tl allows for the possibility that it can act in four different ways, depending on the geodynamic setting: 1) Chalcophile, 2) Lithophile, 3) Fluid mobile, 4) Volatile.

The few studies that have investigated Tl behavior in igneous systems present somewhat conflicting evidence. McGoldrick et al. [3] concluded that sulfur imparts a strong control on Tl concentrations in mid ocean ridge basalts (MORB), which contrasts the general behavior of Tl in more evolved igneous systems, where Tl appears to follow the alkali metals [2]. The more recent studies present more reliable data produced with inductively coupled mass spectrometers (ICP-MS), but the number of data points is either limited or lack some key complimentary geochemical data that might help reveal the processes that control the transport of Tl from the mantle to the Earth's surface [1, 2, 4, 5].

To obtain a more complete understanding of Tl in primitive igneous systems we will present Tl concentration data for a number of MORB glasses, back arc lavas and melt inclusions. These data are complemented by concentrations of alkali metals, water, Cl and S, which will enable us to identify if Tl changes its geochemical affinity in different geologic settings.

[1] Nielsen, S.G., et al., Earth Planet. Sci. Lett., 2007. 264: p. 332-345.
[2] Nielsen, S.G., et al., Nature, 2006. 439: p. 314-317.
[3] McGoldrick, P.J., R.R. Keays, and B.B. Scott, Geochim. Cosmochim. Acta., 1979. 43: p. 1303-1311.
[4] Jochum, K.P. and S.P. Verma, Chem. Geol., 1996. 130: p. 289-299.
[5] Noll, P.D., et al., Geochim. Cosmochim. Acta., 1996. 60: p. 587-611.

https://doi.org/10.1180/S0026461X00008434 Published online by Cambridge University Press

U–Pb isotopic systematics on shock-metamorphosed baddeleyite

TAKAFUMI NIIHARA[1,2,3]*

[1]Center for Lunar Science and Exploration, Lunar and Planetary Institute, Houston, Texas 77058, USA. niihara@lpi.usra.edu (* presenting author)
[2]Antarctic Meteorite Research Center, National Institute of Polar Research, Japan
[3]Dept. of Polar Science, SOKENDAI, Japan

The issue of the duration of Martian magmatic activity is one the controversial debates recently [e.g. 1]. The young radiometric ages of ~180 Ma for shergottites, a class of Martian meteorites, reflect the timing of crystallization from a magma or rather later events related to shock metamorphism or fluid infiltration. Baddeleyite (ZrO_2) occurs as an accessory mineral in Martian meteorite and is useful for U–Pb isotopic analyses as well as zircon ($ZrSiO_4$) [e.g. 2-4]. Martian meteorites contain varied shock effects; however, there are no available data on the effect of high-pressure/temperateure lead or uranium diffusivities in baddeleyite. To examine whether the U–Pb isotopic systems of baddeleyite are easily reset by shock metamorphism, our group have undertaken shock-recovery and annealing experiments using a propellant gun at NIMS and a vertical gas-mixing furnace and at Univ. of Tokyo, respectively [5].

High-shock pressure slightly caused damages on baddeleyite crystal structures. The brightness of Cathode Luminescence emission increased with the shock pressure of up to 57 GPa. Annealed sample did not show any detectable change from pre-annealing sample (shocked at 47 GPa sample). In addition, Raman peak shifts of 2-4 cm^{-1} from unshocked baddeleyite were observed associate with shock pressures. Those peak shifts were reported on high pressure static experiments [6]. However, there is no evidence on phase transformation from baddeleyite to high-pressure and temperature phases [5].

Lead loss from baddeleyite was not observed for the experimentally shocked samples. In addition, the U–Pb and ^{206}Pb–^{207}Pb ages of shocked and heated baddeleyites are indistinguishable from those of unshocked baddeleyite within errors except minor lead loss from the baddeleyite shocked at 57 GPa and heated 1 h at 1300 ^{o}C. Although duration of peak shock-pressure and grain size of baddeleyite are different from the nature of shock events, our experimental results suggest that it is hard to completely reset U–Pb isotopic systematics of baddeleyite by shock metamorphism.

In some terrestrial crater, occurrences of some baddeleyite grains are explained as breakdown products from zircon to baddeleyite and silica ($ZrSiO_4 \rightarrow ZrO_2+SiO_2$) by shock effects. The baddeleyite grains in RBT 04261, shergottites, do not associate with zircon or silica materials and no signature of Raman peak shift; it imply that grains are not breakdown products from zircon and not affected by shock pressure so much. Three large grains (~10 μm) are found for isotopic analyses, two grains occurred with ilmenite and one grain found in melt pocket. U–Pb age of ~200 Ma was obtained from these grains although the grain sizes are still slightly smaller than primary ion beam of SHRIMP, and may imply the magmatic activity on Mars [4].

[1] Bouvier et al. (2005) *Earth. Planet. Sci. Lett. 240*, 221–233.
[2] Herd et al. (2007) *Lunar Planet. Sci.38*, Abstract 1664.
[3] Misawa and Yamaguchi (2007) *Meteorit. Planet. Sci. 42,* A108.
[4] Niihara (2011) *Jour. Geophis. Res. 116,* E12008
[5] Niihara et al. (2012) *submitted for EPSL.*
[6] Bouvier et al. (2002) *Jour. Nucl. Material. 300*, 118–126.

Rapid reductions in North Atlantic Deep Water during the last interglacial period and their relationship to Greenland ice sheet variability

ULYSSES NINNEMANN[1*], EIRIK GALAASEN[2], NIL IRVALI[3], HELGA KLEIVEN[4], YAIR ROSENTHAL[5], CATHERINE KISSEL[6]

[1]University of Bergen and Uni Bjerknes Centre, Norway, ulysses@uib.no (* presenting author)
[2]University of Bergen, Norway, eirik.galaasen@bjerknes.uib.no
[3]Uni Bjerknes Centre and University of Bergen, Norway, Nil.Irvali@uni.no
[4] University of Bergen and Uni Bjerknes Centre, Norway, kikki@uib.no
[5]Rutgers University, USA, rosentha@marine.rutgers.edu
[6] Laboratoire des Sciences du Climat et de l'Environnement/IPSL, France, catherine.kissel@lsce.ipsl.fr

One uncertainty in future climate and CO_2 projections involves changes in the Atlantic meridional overturning circulation (AMOC) and its response to climate change. Models and proxy data suggest that AMOC is vigorous under interglacial climate conditions with minor changes on millennial timescales. Yet, with the exception of the notable changes associated with the 8.4 kyr BP flood outburst, little is known about the stability or thresholds of deep ocean circulation on shorter timescales. Here we use deep-sea sediment cores to assess the response of North Atlantic Deep Water (NADW), the main constituent of the deep limb of AMOC, to source region warming, Greenland ice sheet (GIS) melting, and ocean freshening.

We present new high-resolution (~20 yr/sample) foraminiferal $\delta^{13}C$ and $\delta^{18}O$ records of near surface and bottom water properties spanning MIS 5e from a core site on the Eirik Drift south of Greenland (MD03-2664). The site lies at 3440m, just below the main axis of the sediment-laden Western Boundary Undercurrent and is optimally situated for recording changes in newly formed NADW. In addition, we use ice rafted detritus (IRD) and foraminifera-based surface property proxies ($\delta^{18}O$, MAT-SST's, Mg/Ca) to assess changes in the GIS and Arctic to North Atlantic freshwater transport.

Bottom water $\delta^{13}C$ values gradually increase through MIS 5e. Superimposed on this trend are large-amplitude (>1‰) reductions in bottom water $\delta^{13}C$, similar in scale to those observed during the 8.4 kyr BP event. These $\delta^{13}C$ decreases last a few centuries before recovering to background values. Using an array of records spanning the abyssal Atlantic we show that the magnitude and spatial geometry of the deep water anomalies is consistent with an expansion of southern source deep water as the influence of NADW waned—a geometry analogous to deep ocean changes during the 8.4 kyr BP event and to millennial scale events of the last glaciation. Surface water proxies and IRD content suggest that these NADW changes occur during a period of rapid GIS retreat and surface water freshening. Taken together, our results demonstrate that "8.4kyr-style" deep ocean property changes occurred at a time when North Atlantic climate was similar to that projected for our future.

https://doi.org/10.1180/S0026461X00008434 Published online by Cambridge University Press

Deformation experiments of mantle materials at the conditions of deep Earth interior

YU NISHIHARA[1*]

[1]Ehime Universtiy, Senior Research Fellow Center and Geodynamics Research Center, yunishi@sci.ehime-u.ac.jp

Introduction

Knowledge on rheology of mantle materials is indispensable in understanding thermal evolution and material transport in the Earth. Since rheological properties strongly depend on temperature and pressure, it is critacally important to conduct deformation experiments at *P-T* conditions corresponding to the deep mantle for accurate understanding of Earth's interior. Recently, quantitative rheological measurements at relatively high pressures (up to 10–20 GPa) and high temperatures (up to 1000–2000 K) are possible by using large-volume presses in conjunction with synchrotron radiation. In this presentation, our recent results on rhelogy under Earth's deep mantle conditions determined by deformation experiments using deformation-DIA appratus are discussed.

Mechanical property of fine-grained forsterite

In order to understand mechanical behavior in grain-size-seisitive creep in the deep upper mantle condition, deformation experiments on dry fine-grained (grain size of ~1 μm) forsterite were performed at P = 3–5 GPa, T = 1473–1573 K and strain rate of 9×10^{-6}–2×10^{-4} s^{-1} [1]. The stress-strain rate data together with data at 0.1–300 MPa by Tasaka et al. (unpublished data) were analyzed using a flow law equation for diffusion creep (n = 1, p = 2) and dislocation creep accommodated grain-boundary sliding (GBS, n = 3.5, p = 2). Based on the analysis, the activation volume both for diffusion creep (V^*_{dif}) and GBS (V^*_{GBS}) of olivine was determined to be ~8 cm^3/mol. Calculation based on the present results implies that typical mantle deformation conditions are close to the mechanism boundary between the diffusion creep and the GBS.

Mechanical property of wadsleyite

Uniaxial deformation experiments on wadsleyite were carried out at P = 14–16 GPa and T = 1500–1700 K with strain rates of 3.4–15 × 10^{-5} s^{-1} [2]. Results suggest that flow strength of wadsleyite is more sensitive to water content than that of olivine.

Lattice preferred orientation (LPO) of olivine

The effects of hydrogen and pressure on LPO of olivine were investigated through simple-shear deformation experiments under asthenospheric upper mantle conditions (P = 2.1−5.2 GPa, T = 1490−1830 K) [3,4]. Formation of the A-type olivine fabric developed by the (010)[100] slip system was observed under water-depleted (C_{OH} < 650 H/10^6Si in olivine), while B-type fabrics by the (010)[001] slip system (or B-typre like fabric) were predominantly formed under water-rich conditions (>1000 H/10^6Si). The water-induced olivine LPO transition from A-type to B-type (-like) fabric results in flow-parallel and flow-perpendicular shear wave splitting under water-depleted and water-rich conditions, respectively.

[1] Nishihara *et al*. (2011) Abstract MR11A-2170 presented at 2011 Fall Meeting, AGU. [2] Kawazoe *et al*. (2011) *A. Mineral.***96**, 1665-1672. [3] Ohuchi *et al*. (2011) *Earth Planet. Sci. Lett.* **304**, 55-63. [4] Ohuchi *et al*. (2011) *Earth Planet. Sci. Lett.* **317-318**, 111-119.

Formation condition of mono-hydrocalcite from Ca-Mg-CO_3 solutions

RISA NISHIYAMA[1*], TAKASHI MUNEMOTO[2], AND KEISUKE FUKUSHI[1]

[1] Kanazawa University, Ishikawa, Japan, rinrin@stu.kanazawa-u.ac.jp (* presenting author)

[2] The University of Tokyo, Tokyo, Japan,

Monohydrocalcite ($CaCO_3$·H_2O: MHC) is rare mineral in geological settings. MHC has been most frequently found in the recent sediment in saline lakes [1]. It also was found from the calcareous sinter of cold spring of Shiowakka, Hokkaido, Japan [2]. A lot of kinds of calcium carbonate minerals, including calcite, vaterite, ikaite and MHC, were also occurred in Shiowakka. MHC occurred in only summer season and frequently associated with green algae. In order to understand the preferential formation of MHC with green algae, we conducted synthesis experiments of carbonate minerals from various concentrations of Ca, Mg and CO_3 to clarify the formation condition of MHC.

The mixing solutions containing $CaCl_2$ and $MgCl_2$ was prepared in the reaction vessels, and Na_2CO_3 solution was added to 50mL of the mixing solutions. The initial concentrations of Ca, Mg and CO_3 in the solutions were 0.025~0.1M, 0~0.05M and 0.03~0.1M, respectively. Immediately after Na_2CO_3 solutions were added to the solution, the whitish suspensions were formed in the reaction vessels. The syntheses experiments were conducted in closed polycarbonate vessels at 25 °C, and the resulting suspension was constantly stirred and aged with mix-rotor for 24 h. After the aging time, the suspensions were filtered. The solids were analyzed by X-ray diffraction and examined by scanning electron microscope. The filtrates were analyzed for the concentration of CO_3 by alkalinity titration. The Ca, Mg and Na concentrations of filtrates were measured by high-performance liquid chromatography.

Four mineral assemblages were obtained from all of the experimental conditions from the XRD results. They are mixture of vaterite and calcite, mixture of aragonite and calcite, MHC and amorphous material. Based on the observations, the formation conditions of MHC can be summarized that the initial Mg concentration is more than 0.01 M and the CO_3/Ca ratio of the initial solutions are more than 1. The IAP of the reacted solutions with MHC formations were greatly higher than anhydrus calcium carbonates. The activity of Ca^{2+} is lower than that of CO_3^{2-} when MHC was formed. Furthermore, the activities of Mg^{2+} and CO_3^{2-} in the solution after MHC and amorphous material formation were almost equilibrium with respect to nesquehonite. By integrating the formation conditions of MHC from both initial solution and reacted solution, we considered that MHC formation requires simultaneous formation of magnesium carbonate (nesquehonite), i.e., the concentration of CO_3^{2-} in the solution must be high enough to produce both MHC and magnesium carbonate.

In Shiowakka, the pH increase by photosynthesis of green algae. The local concentration of CO_3^{2-} near the green algae must increase drastically. Inclease of the cintribution of CO_3^{2-} to HCO_3^- enables to the formation magnesium carbonate even spontaneously with MHC formation. Thus, the MHC is selectively formed in summer season associated with green algae.

[1] Fukushi *et al.* (2011) *Sci. Technol. Adv. Mater*, **12**, 064702.
[2] Ito (1993) *Ganko*, **88**, 485-491.

https://doi.org/10.1180/S0026461X00008434 Published online by Cambridge University Press

Preliminary Pb and Pb isotopes from the US GEOTRACES North Atlantic Transect

ABIGAIL E. NOBLE[1*], YOLANDA ECHEGOYEN-SANZ[2], AND ED BOYLE[3]

[1]Massachusetts Institute of Technology, Cambridge, USA anoble@mit.edu (* presenting author)
[2]Universidad de Zaragoza, Zaragoza, Spain, yolandaechegoyen@gmail.com
[3] Massachusetts Institute of Technology, Cambridge, USA, eaboyle@mit.edu

This study presents preliminary Pb and Pb isotope data from the US GEOTRACES North Atlantic Transect which was sampled during two cruises that took place during the Fall of 2011 and 2012. Almost all of the Pb found in the modern ocean is derived from anthropogenic sources, and the North Atlantic has received significant Pb inputs from the United States and Europe due to emissions from leaded gasoline and high temperature industrial processes. During the past three decades, Pb fluxes to the North Atlantic have decreased following the phasing out of leaded gasoline in the United States and Europe. Following the concentrations and isotope ratios of Pb in this basin over time reveals the temporal evolution of Pb in this highly- affected basin. This cruise included a re-occupation of the Bermuda Atlantic Time Series station (BATS) that was one of 8 occupations since 1979 for Pb and one of 6 for Pb isotopes at approximately 5-year intervals,. Two stations in the Eastern North Atlantic were previously occupied in 1989, 1999, and the data from this expedition provide some comparison of the temporal evolution of Pb in this region. The Pb isotope signatures reflect the relative importance of inputs from the United States and Europe as leaded gasoline was phased out faster in the United States relative to Europe. This is observed in a surface trend towards slightly lower ^{206}Pb / ^{207}Pb ratios in the last decade. Pb concentrations decrease with time in the upper water column (<2000m) with higher concentrations observed in mid-latitude northern stations decreasing southward at the eastern end of the basin. Concentrations and isotopes converge in deep waters with longer residence times. Further results from the section will be presented as data become available.

Isotopic Variability of the Ninetyeast Ridge – Implications for its Mantle Sources

INÊS G. NOBRE SILVA[1]*, DOMINIQUE WEIS[1], JAMES S. SCOATES[1], MALCOLM S. PRINGLE[2] AND FRED A. FREY[2]

[1]Pacific Centre for Isotopic and Geochemical Research, Earth & Ocean Sciences, Univ. of British Columbia, Vancouver, BC V6T 1Z4, Canada, inobre@eos.ubc.ca (* presenting author)
[2]EAPS, MIT, Cambridge MA 02139 USA.

The ~5000 km long north-south oriented Ninetyeast Ridge in the eastern Indian Ocean Basin represents the age progressive, ~80 to ~40 Ma products of the 120 Ma old Kerguelen mantle plume. Basaltic basement samples recovered during DSDP and ODP drilling campaigns are however scarce and debate concerning the nature and number of components in the mantle source of the Ninetyeast Ridge persists. Dredging during a National Science Foundation-funded 2007 cruise recovered basaltic basement from 21 locations along ~3200 km of the ridge. New high-precision isotopic compositions by MC-ICP-MS (Pb, Hf, and Nd) and TIMS (Sr) were obtained on 59 basaltic samples from 21 dredges. Sample choice was based on the lowest degree of alteration (lowest LOI), high Mg#, and variable trace element ratios (e.g., Zr/Nb, Y/Nb, La/Sm). Altogether these samples cover a greater range of Pb-Sr-Nd-Hf isotopic compositions and wider within-site isotopic variability than that covered by the drilled samples recovered during ODP Leg 121, and are generally intermediate between those of the volcanic products of the Kerguelen and Amsterdam-St. Paul mantle plumes. This attests to a compositionally heterogeneous mantle source, and at least three, possibly four, distinct source components with relatively enriched and depleted signatures are required to explain the observed isotopic variability along the Ninetyeast Ridge. Mixing with shallow level Indian MORB does not account for the lower $^{87}Sr/^{86}Sr$ and higher Nd and Hf isotopic ratios of basalts from some of the dredges (i.e., $^{87}Sr/^{86}Sr$ 0.70369-0.70428, $^{143}Nd/^{144}Nd$ > 0.51300 and $^{176}Hf/^{177}Hf$ > 0.28322 for 5 samples from 2 dredges). These depleted signatures are instead consistent with the presence of a previously depleted, garnet-enriched component intrinsic to their deep mantle source that had been identified based on incompatible trace element abundances alone. Together with other Indian Ocean island basalts of typical EM-1-like compositions, the Pb-Hf-Sr-Nd isotopic compositions of the Ninetyeast Ridge basalts are consistent with provenance from a deep mantle source that has incorporated a mixture of recycled sediments and lower continental crust together with altered oceanic crust. This supports a deep origin for the EM-1-like Dupal signatures encountered in ocean island basalts.

https://doi.org/10.1180/S0026461X00008434 Published online by Cambridge University Press

Boron incorporation in synthetic calcite and aragonite revealed by B isotopes and ^{11}B MAS NMR

JOHANNA NOIREAUX[1*], VASSILEIOS MAVROMATIS[2], JEROME GAILLARDET[1], JACQUES SCHOTT[2], PASCALE LOUVAT[1] AND VALERIE MONTOUILLOUT[3]

[1]Laboratoire de Géochimie et Cosmochimie, Institut de Physique du Globe de Paris, Paris, France, noireaux@ipgp.fr (* presenting author)

[2]Geosciences Environnement Toulouse, Université Paul Sabatier, Toulouse, France, schott@lmtg.obs-mip.fr

[3]CNRS-CEMHTI, Orléans, France, valerie.montouillout@cnrs-orleans.fr

Boron isotopes measurements in marine carbonates are used as a proxy of the paleo-pH of the oceans. The reliability of these pH reconstructions lies in our understanding of the mechanisms of boron incorporation in carbonates. The paleo-pH calculations are based on the assumption that one of the two boron species in solution (borate $B(OH)_4^-$) is preferentially incorporated in calcium carbonates [1],[2]. Experiments show that there is a shift between expected and measured boron isotopic ratios ($\delta^{11}B$) at a given pH, which is attributed to the specifics of boron incorporation in biological organisms ("vital effect").

In order to better understand the mechanisms of boron incorporation in carbonates and by comparison, the modifications induced by vital effects, we carried out inorganic precipitation experiments of calcite and aragonite in NaCl solutions of wide-ranging pH values and at temperatures of 25°C and 5°C. Boron isotopic compositions of the carbonates were then measured by MC-ICP-MS and the proportions of trigonal and tetragonal B by ^{11}B MAS NMR.

Our results confirm that the boron isotopic ratio of the carbonates is dependent upon the growth solution pH, but also upon crystal type and temperature. In calcite, both NMR and boron isotopic composition show that boron incorporation is not consistent with the single incorporation of the aqueous borate species $B(OH)_4^-$. Moreover, the NMR measurements show that the proportion of trigonal boron (BO_3) in calcite is higher than what is inferred from the isotopic signal by assuming that both boron aqueous species are incorporated in the carbonate. In aragonite, BO_3 is present in smaller proportions depending on pH and both NMR measurements and $\delta^{11}B$ are in good agreement with the hypothesis of the preferential incorporation of the borate species in calcium carbonates .

[1] Hemming and Hanson (1992) *Geochim et Cosmochim Acta* **56,** 537-543. [2] Vengosh et al. (1991) *Geochim et Cosmochim Acta* **55**, 2901-2910.

As, Sb, Mo, V, W, and Se oxyanions in Yellowstone's thermal waters

D. KIRK NORDSTROM[1*] AND R. BLAINE MCCLESKEY[2]

[1]US Geological Survey, Boulder, USA, dkn@usgs.gov (* presenting author)

[2]US Geological Survey, Boulder, USA

Concentrations of As, Sb, Mo, V, W, and Se have been determined in hundreds of water samples from thermal features in Yellowstone National Park and from the Firehole and Gibbon River systems. Analytical methods include ICP-AES, ICP-MS, HGAAS, and GFAAS. Selenium is consistently less than 1 µg/L everywhere, V is often below detection up to 130 µg/L, Mo occurs up to 360 µg/L, Sb up to 370 µg/L, and As up to 14,600 µg/L. Concentrations of W are limited but generally similar to or a bit higher than those of Sb and Mo.

Arsenic concentrations are typically 0.5 to 3 mg/L but they are highest in Norris Geyser Basin waters, especially in the western part of the basin. This area seems to have accumulated arsenic through precipitation of considerable orpiment and realgar at low pH at or just below the ground surface. One pair of springs demonstrate remarkable mixing between two end-member compositions, a near neutral pH high-As and high-Cl water and a low-As, low-Cl acid water. This range of composition can explain the variable water compositions for many waters occurring in Norris Basin. Most waters exhibit a linear relation of As concentrations relative to Cl concentrations suggesting that arsenic is largely conservative and tends to stay with the aqueous fluid during boiling and dilution. More surprising, arsenic concentrations are not attenuated during 20-30 miles of river drainage. The Gibbon River maintains more than 100 µg/L dissolved As and the Firehole River increases to more than 400 µg/L in the lower reaches. The most likely hypothesis is that the high silica concentrations in the thermal waters precipitate in the river and coat the river bed sediments, decreasing its sorption capacity. There is also very little Fe in the overflows.

A complicating factor for speciation of As, Sb, Mo, and W is the formation of thio-complexes which have been explored for As and Sb but not for Mo and W. Such complexes may help to explain their mobility under reducing conditions.

Concentrations of Sb and Mo tend to track with As, with the highest concentrations occurring with the highest Cl concentrations but there is much more scatter in the data. For the Gibbon and Firehole Rivers, Sb and Mo concentration profiles are strikingly similar showing no attenuation. One anomaly occurs in the Gibbon River profile. A substantial inflow of Mo enters from Terrace Spring just before the convergence of the Gibbon with the Firehole. These trace elements are indicative of the deep geothermal reservoir composition and not greatly affected during transport to the surface.

Concentrations of V behave very differently from the other oxyanions; they are below 10 µg/L for nearly all Cl concentrations above 200 mg/L. Higher concentrations are only found in acid waters of low Cl concentration, regardless of temperature. These results suggest that V is dominantly derived from acid weathering of near surface rocks. Furthermore, V is the element in this group that forms a cation under reduced conditions which also helps to explain its higher concentration in acidic waters.

Both similar and dissimilar trends in these trace elements can be demonstrated. The biggest dissimilarity is the lack of any correlation for V with the other elements. The other elements generally behave similarly with the exception of some local anomalies. When thermal overflows enter river systems there is little to no attenuation likely because of continual silica precipitation and the lack of hydrated iron oxides.

https://doi.org/10.1180/S0026461X00008434 Published online by Cambridge University Press

Natural pyrite weathering rate in a small catchment compared with mined catchments and lab rates

D. Kirk Nordstrom[1*]

[1]US Geological Survey, Boulder, USA, dkn@usgs.gov (* presenting author)

As part of the USGS background study of the Questa mine in northern New Mexico, a small catchment (Straight Creek) of about 2.67 km^2, was studied to determine the hydrogeochemical processes that naturally generate acidic, metal-rich surface waters and groundwaters. The predominant reaction is pyrite oxidation because there is excess pyrite (2-10 wt.%) in quartz-sericite alteration. A mass–balance calculation was performed reacting pure water to the median composition of 14 water analyses from 2000-2003 with median pH of 2.98 and median sulfate concentration of 2,030 mg/L. The most likely mass–balance model consistent with mineralogical analyses, assuming that rates are unaffected by solid/solution ratio or by evaporation, indicates oxidative dissolution of 8.66 mmol pyrite/kg_{H_2O}. When combined with a median discharge of 37.85 L/min measured simultaneously, the weathering rate was 5.46 mmol pyrite/h. This value is larger than batch abiotic laboratory rates, about 0.01 mmol/h for Fe(III) oxidation with pH close to 2, or microbial laboratory rates, about 0.22 mmol/h based on an interlab comparison. Evaporation effects or a "pooling effect" might be the main sources of discrepancy between apparent field rates based on mass balances and laboratory rates. Similar calculations for effluent water at the Leviathan Mine, CA (pH = 1.8) result in an apparent pyrite weathering rate of 40 mmol/h, 200 times higher than expected from laboratory rates; this result could be explained by the extremely fine-grained pyrite that occurs there as well as evaporation effects.

Calculations for Iron Mountain, CA a massive sulphide copper deposit that has been extensively mined and exposed to air and water, result in an apparent pyrite weathering rate of 17,100 mol/h, five orders of magnitude higher than laboratory rates. At Iron Mountain pyrite weathering has produced enormous amounts of efflorescent salts that periodically dissolve and reprecipitate in the underground workings. When the mass–balance is modified in terms of dissolving soluble salts, removal of some iron as goethite is required and the weathering rate becomes 24,800 moles soluble sulfates/h.

Regardless of how mass–balances are calculated, the field rate for pyrite oxidation is much faster than the laboratory rate suggesting that evaporation, pooling, or possibly surface areas, strongly influence these calculations for most mined sites. The pyrite weathering rate might be a guide to whether the mechanism is dominated by pyrite weathering or by precipitation/dissolution of soluble salts. Another conclusion dictated by the mass balance is that large amounts of iron and silica must precipitate. This conclusion is also supported by the saturation indices having reached saturation for silica in many of these waters.

Geochemical signatures of IOCG mineralization and alteration in till

Philippe X. Normandeau[1*], Isabelle McMartin[2], Jeanne Paquette[1], Louise Corriveau[2] and Jean-François Montreauil[3]

[1]Dept. of Earth and Planetary Sciences, McGill University, Montreal, Quebec, Canada philippe.normandeau@mail.mcgill.ca (*presenting author), jeanne.paquette@mcgill.ca

[2]Geological Survey of Canada, Natural Resources Canada, Ottawa, Ontario, Canada, isabelle.mcmartin@nrcan-rncan.gc.ca, louise.corriveau@nrcan-rncan.gc.ca

[3]INRS-ETE, Québec, Canada, jmontreu@nrcan.gc.ca

Introduction

As part of Canada's Geomapping for Energy and Minerals (GEM) Program, an applied Quaternary research activity under the IOCG-Great Bear Project was undertaken in the Great Bear magmatic zone (Northwest Territories, Canada) to provide a practical guide for geochemical and indicator mineral exploration targeting iron oxide copper-gold (IOCG) and affiliated deposits in glaciated terrain. Detailed till sampling (n=111) was completed in the vicinity of the NICO Au- Co-Bi-Cu magnetite-group IOCG deposit as well as the Sue-Dianne Cu-Ag-Au magnetite- to hematite-group IOCG deposit, and near showings hosted within other IOCG-type alteration systems in the GBmz. Samples were collected up-ice, proximal to, and down-ice from mineralization, hydrothermally-altered host rocks and least-altered bedrock. Extensive lihogeochemical data set (n=1243) was available within the IOCG-Great Bear Project.

Results and conclusion

Lithogeochemical signatures of mineralization and/or alteration are reflected in the till matrix (K, Na, Ca, Mg, Ti, Cu, Ba, Cr, Co, Th, Bi, Mo, U, As) despite variable degrees of post-glacial weathering and textural differences. Possible IOCG deposit pathfinder elements in till (<2 and/or <63 µm fraction) include Cu, Mo, Bi and Co (enrichments), as well as Ti (depletion). However, given the high variability of IOCG and affiliated mineralization, a multivariate statistical approach was also applied to see if their associated, and more characteristic, alteration types left a clear signal. A principal component analysis (PCA) was performed on combined data sets of till geochemistry and lithogeochemistry. This innovative approach helps to isolate the role of hydrothermal processes from surface processes such as glacial communition and post glacial weathering in the internal variability of the till geochemistry. Results so far show: 1) grouping of till samples by the first 3 principal components, based on their related IOCG showings; 2) discrimination between anomalous till samples based on multi-enrichments of alteration related elements (K, Ca, Na), and 3) potential to identify the type of bedrock IOCG alteration in overlying till samples.

https://doi.org/10.1180/S0026461X00008434 Published online by Cambridge University Press

Understanding biogeochemical mechanisms for heavy metal removal in SuDS

M. J. Norris[1*], H. L. Haynes[2], C. C. Dorea[3], I.D. Pulford[1], and V.R. Phoenix[1]

[1]University of Glasgow College of Science and Engineering, Glasgow, Scotland G12 8QQ (* m.norris.1@research.gla.ac.uk)
[2]Heriot-Watt University Institute for Infrastructure & Environment, Edinburgh, Scotland EH14 4AS
[3]Université Laval Département de génie civil et génie des eaux, Québec, QC, Canada G1V 0A6

With urbanization on the rise, there has become a growing need for sustainable approaches to cope with increased pollutant load and reduced land available for stormwater infiltration. A type of Sustainable urban Drainage System (SuDS) of particular interest is a filter drain, which utilizes gravel media to filter and treat road runoff laden with pollutants. While the simple concept is known to remove suspended solids and heavy metals typical in road runoff, the design of such systems is based on limited scientific input. This study aims to characterize the biogeochemical mechanisms responsible for pollutant removal, specifically heavy metals, to help improve design and efficiency in SuDS systems.

While metal immobilization in filter drains may be biologically mediated and a subject of future research, initial experimentation explored removal processes by the gravel itself and with the addition of a mineral amendment. Enhancing heavy metal removal with an iron oxide coating has been explored due to the the vast literature evidence of iron oxide minerals sequestering metals [1]. Kinetic batch and flow-through column experiments demonstrated that an iron oxide coated gravel removed similar concentrations of zinc to a locally sourced uncoated microgabbro gravel. Since coated gravel also buffered solution pH away from neutral, it was concluded that the difficult, costly coating process would not be suitable for use in an environmental setting.

Specifically, kinetic batch experiments showed typical adsorption curves and removal rates of zinc by uncoated microgabbro at 80% removal up to 8 hours and nearly 100% after 48 hours. Whereas other types of gravel such as dolomite, sandstone and granite removed between 10-50% less zinc overall than microgabbro. Scanning electron microscope (SEM) images of microgabbro show a rough, high surface area and mineral components of microgabbro have the ability to weather to clay minerals, which also have a high affinity for heavy metals. Further experimentation has proven the weathered surface in fact accelerates zinc immobilization by about 20% compared to an unweathered surface.

The SuDS Manual, which is used in construction and design of new SuDS systems, indicates that filter drain material should be a locally sourced graded stone/rock [2]. While this implies that the geology of the type of rock utilized in such systems does not affect pollutant removal mechanisms, kinetic batch experiments of different rock types indicates otherwise.

[1] Benjamin *et al.* (1996) *Wat. Res* **30**, 2609-2620. [2] Woods-Ballard *et al.* (2007) *The SuDS Manual* 241-249.

Conservative behavior of Uranium vs. salinity in sea ice and brine

Christelle Not[1*], Kristina Brown[2], Bassam Ghaleb[3] and Claude Hillaire-Marcel[4]

[1]GEOTOP-UQAM, Montréal, Canada and AORI-Tokyo University, Kashiwa, Japan, christelle.not@aori.u-tokyo.ac.jp (* presenting author)
[2]University of British Columbia, Department of Earth and Ocean Sciences, Vancouver, Canada, kbrown@eos.ubc.ca
[3]GEOTOP-UQAM, Montréal, Canada, ghaleb.bassam@uqam.ca
[4]GEOTOP-UQAM, Montréal, Canada, hillaire-marcel.claude@uqam.ca

Since studies by Ku et al [1] and Chen et al [2], it is widely accepted that uranium (U) behaves conservatively with respect to salinity (S) in seawater over the salinty range of 30 to 36. However, in low salinity environments, such as estuaries, its behavior seems more variable. Freezing in the Arctic Ocean provides a natural mechanism to concentrate dissovled seawater constituants into high salinitity brine through the formation of sea ice, and reintroduce low salinity water to the surface through melt.

Here we compare U concentration and isotopic composition from samples of low-salinity sea ice, underlying surface seawater, and high salinity brine, covering a salinity range of 0 to 135. Based on these samples, we found that U behaves conservatively across a wide salinity range, producing a U-S relationship slightly different than the one described in previous studies [1] (Figure 1). The isotopic ratio $^{234}U/^{238}U$ from melted sea ice, under-ice seawater, and sea ice brine samples were not statisically different from mean ocean values, within our statistical uncertainties.

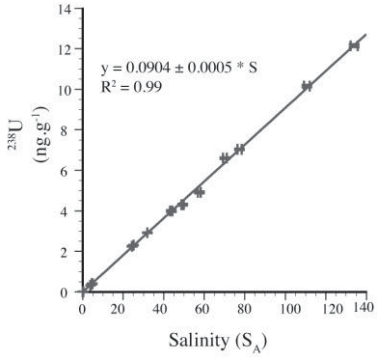

Figure 1: U-Salinity relationship in sea ice, surface sea water, and brine samples [3].

[1] Ku et al (1977) *Deep-sea Res.* **24**, 1005-1017. [2] Chen et al (1986) *Earth Planet. Sci. Lett.* **80,** 241-251. [3] Not et al (2012) *Marine Chem.* **130-131,** 33-39.

https://doi.org/10.1180/S0026461X00008434 Published online by Cambridge University Press

Nitrogen mobility in freshwater peat

MARTIN NOVAK[1*], IVANA JACKOVA[1], FRANTISEK BUZEK[1], LUCIE ERBANOVA[1] AND MARKETA STEPANOVA[1]

[1] Czech Geological Survey, Prague, Czech Republic, martin.novak@geology.cz (* presenting author), ivana.jackova@geology.cz, frantisek.buzek@geology.cz, lucie.erbanova@geology.cz, marketa.stepanova@geology.cz

Peatlands cover less than 5 % of the Earth's land surface, yet they store as much as 15 % of the world's soil N, and 30 % of the world's soil C. Vile et al. [1] have recently reported that ^{210}Pb dated peat in pristine high-latitude bogs contains 20 times more N than could be explained by inputs of atmospheric N. Vile et al. [1] have suggested that the "excess" N in peat is a result of *in-situ* N_2 fixation from cyanobacteria, a process that has been largely overlooked. It is unclear whether in N-polluted areas, where N is not a limiting nutrient, the symbiosis between *Sphagnum* and N-fixing microorganisms is lost. Still, it appears that a major gap in the global biogeochemical cycling of N has been identified.

Here we report a field experiment that might provide an insight into the retention of atmogenic N in peat. We hypothesized that vertical N profiles in peat do not directly reflect historical trends in N deposition and that N is mobile after its burial in peat. We selected two Central European peat bogs, differing in present-day atmospheric N inputs by a factor of 2, and collected 10 peat cores per site. Trends in N deposition since the beginning of the Industrial Revolution have been extremely well documented in the area [2]. The more polluted site VJ exhibited a clear-cut N concentration peak in layers dating from 1950. The less polluted site CB showed a N concentration minimum in layers dating from 1940. In actual fact, the atmospheric N input increased smoothly until 1980, and dropped thereafter [2]. We suggest that N in peat profiles does not record past N deposition levels. We conducted an 18-month reciprocal peat transplant experiment between VJ and CB, using 5 cores as transplants and 5 cores as controls per site. At the end of the experiment, at both sites, bulk N to a depth of 10 cm changed its δ^{15}N value by 3 per mil, converging to that of the host site. Again, the bulk N isotope change indicated a measurable degree of N mobility in peat.

[1] Vile et al. (2011) *Proceedings of AGU Annual Meeting*, San Francisco, December 2011.
[2] Kopacek et al. (2011) *Global Biogeochem. Cycles* 25, GB2017.

Development of a process-based chemical weathering model with consideration of the effective surface area

TAICHI NOZU[1*] AND EIICHI TAJIKA[1,2]

[1]The University of Tokyo, Earth and Planetary Science, tnozu@eps.s.u-tokyo.ac.jp (* presenting author)
[2]The University of Tokyo, Complexity Science and Engineering, tajika@k.u-tokyo.ac.jp

Feedback mechanism between climate and chemical weathering is one of the most important aspects of the Earth system. Despite a significant number of studies for understanding the rate of chemical weathering quantitatively by observational, experimental, and numerical methods, the global chemical weathering rate has not been estimated straightforwardly owing to a significant discrepancy between field and laboratory studies. The discrepancy may be explained as a sum effect of several phenomena such as increase in surface roughness with time and difference in reaction affinities between natural and experimental conditions [1].

We are developing a process-based chemical weathering model to study behaviours of the geochemical cycle system in response to changes in modern- and palaeo-environment. This model is similar to "WITCH" model [2], but the originality of our approach lies on integration of simple soil physics (i.e. heat and moisture transport) and consideration of soil biological activity in the weathering model. The model has been applied to different small (< 10 km^2) watersheds such as Strengbach in France and Lac Clair in Canada to verify the model to reproduce major ion concentrations of modern streams. We introduced a free parameter which represents a ratio of field-scale weathering rate to mineralogical dissolution rate to fit the results to the observational data. Sensitivity analyses show that riverine ionic concentrations of base cations are well reproduced from the model only by tuning this parameter alone. We interpret that this parameter may represent the erosional effect which, in turn, controls the age of the weathering environment. That is, the time dependency of silicate weathering [1] can explain the difference in this parameter. The obtained parameter is also comparable with the ratio of the effective surface area to the BET surface area estimated in previous studies.

Our results imply that the chemical weathering process can be modelled by considering the difference in the effective surface area controlled by lithology and erosion.

[1] White & Brantley (2003) *Chem. Geol*. **202**, 479-506. [2] Goddéris *et al*. (2006) *Geochim. Cosmochim. Acta* **70**, 1128-1147.

https://doi.org/10.1180/S0026461X00008434 Published online by Cambridge University Press

The unique biogeochemical signature of the marine diazotroph *Trichodesmium*

JOCHEN NUESTER[1*], STEFAN VOGT[2], MATT NEWILLE[3], ADAM KUSTKA[4], BENJAMIN S. TWINING[5]

[1]Bigelow Laboratory for Ocean Sciences, W. Boothbay Harbor, ME, USA, jnuester@bigelow.org (*presenting author)
[2]X-ray Science Division, Advanced Photon Source, Argonne National Laboratory, Argonne, IL, USA, f.stefan.vogt@gmail.com
[3]Center for Advanced Radiation Sources, The University of Chicago, Argonne, IL, USA, newville@cars.uchicago.edu
[4]Rutgers University – Newark, Earth and Environmental Sciences, Newark, NJ, USA, kustka@andromeda.rutgers.edu
[5]Bigelow Laboratory for Ocean Sciences, W. Boothbay Harbor, ME, USA, btwining@bigelow.org

Trichodesmium is a globally important nitrogen-fixing, filamentous cyanobacterium. In the present study, we collected *Trichodesmium* colonies from the Sargasso Sea and investigated their elemental signature. Element concentrations and spatial distributions in colonies were compared using inductively coupled plasma mass spectrometry (ICPMS), CHN analysis, and synchrotron x-ray fluorescence (SXRF) mapping. *Trichodesmium*'s cellular stoichiometry of 647C:111N:1P deviated significantly from the canonical Redfield ratio and illustrates the P-limiting condition at the time of sampling. Additionally, ICPMS and SXRF analysis confirmed that the metallome of *Trichodesmium* is enriched in V, Fe and Ni in comparison to other phytoplankton. Surprisingly, V was the most abundant metal in *Trichodesmium*, and the V quota was up to 4-fold higher than the corresponding Fe quota. Furthermore, SXRF mapping revealed the presence of V and Fe hotspots. These hotspots typically spanned over several contiguous cells. The spatial distribution of Ni differed from V and Fe and was enriched in transverse walls between attached cells. As hotspots of V, Fe, or Ni were spatially decoupled from each other, we conclude that external adsorption of aerosol particles on *Trichodesmium* trichomes did not contribute to the elevated element quotas. Fe hotspots were found in only ca. 10% of analysed trichome sections, and Fe enrichment in contiguous cells may be linked to diazocytes as zones of nitrogen fixation in *Trichodesmium*. In contrast, genomic analyses indicated that V is not directly associated with nitrogenase in *Trichodesmium*. V maybe used in V-dependent haloperoxidases to protect the oxygen susceptible nitrogen fixing enzyme nitrogenase from reactive oxygen species (ROS) such as hydrogen peroxide, but genomic evidence for such an enzymatic role of V is also currently lacking. The presence of Ni in transverse walls is in agreement with genomic evidence for the presence of Ni-superoxide dismutase and/or NiFe hydrogenase. Both Ni-containing enzymes are beneficial for nitrogen fixation by either inactivation of the ROS species superoxide or the catalyzation of hydrogen, respectively. We conclude that the enrichment of these metals is directly or indirectly linked to nitrogen fixation in *Trichodesmium*.

Zooming on Heinrich layers H2 to H0 through geochemical and sedimentological analysis of a core raised off Hudson Strait

LAURENCE NUTTIN[1] AND CLAUDE HILLAIRE-MARCEL[1]

1GEOTOP-UQAM, Montréal, Canada, lanuttin@gmail.com

The ~ 9 m-long core (HU08-029-004; 2674 m water-depth; 61°27'N, 58°2'W) was raised from the lower slope of the Labrador Sea, approximately 100 nm off the Hudson Strait shelf edge. It provides a high resolution record of recent detrital carbonate sedimentary pulses through Hudson Strait assigned to "Heinrich events" H2, H1, H0, thus the means to constrain the age and depositional mechanism of the corresponding "Heinrich layers" at near proximity of sediment source. Some special attention is given to depositional mechanisms of fine glacial flour reworked by meltwater vs ice-rafted debris (IRD). Analysis includes, at ~ 10 cm-intervals, uranium and thorium series measurements (^{238}U, ^{234}U, ^{230}Th and ^{232}Th), at 4 cm intervals, semi-quantitative analyses of mineralogical assemblages (XRD), inorganic and organic carbon ($C_{inorg.}$, $C_{org.}$) contents and $C_{org.}$/N data, coarse fraction abundance (>106 μm), which we associate with IRD, CAT-scan images; nine layers provided enough Neogloboquadrina pachyderma (l) shells for ^{14}C measurements. Calibrated ^{14}C ages indicate a mean sedimentation rate of ~ 27 cm/ka, Heinrich-layers included, and of ~ 25 cm/ka when they are assigned a duration from literature data then excluded from the sediment inventory (i.e., "background" sedimentation rate). ^{230}Th-excesses ($^{230}Th_{xs}$) over supported fraction are estimated following Veiga-Pires & Hillaire-Marcel (1999). Preliminary results show that the Heinrich layers contain up to 60% fine detrital carbonates (mostly calcite) and are highlighted by low $^{230}Th_{xs}$ (nearly 0 dpm/g) indicating an extremely fast depositional mechanism of the fine fraction. Coarse fraction peaks highlight intense IRD on both sides of the fine detrital carbonate layer, i.e., from the very beginning until a "late" H-event phase. They likely correlate with the H-layers as observed in more distal North Atlantic sites. $^{230}Th_{xs}$ inventories and background sedimentation rate calculated as above, suggest much higher Holocene $^{230}Th_{xs}$ fluxes at the study site, in comparision to late glacial fluxes, resulting from $^{230}Th_{xs}$-advection by an enhanced Western Boundary Undercurrent.

[1] Hesse et al. (2004), *Geology*, **32**, 449-452.
[2] Rashid et al. (2003a), *Earth and Planetary Science Letters*, **208**, 319-336.
[3] Veiga-Pires *et al.* (1999), *Paleoceanography*, **14**(2), 187-199.

https://doi.org/10.1180/S0026461X00008434 Published online by Cambridge University Press

Potential dissolution of sandstone in the presence of supercritical CO_2-H_2S-H_2O: An experimental and geochemical modelling approach

CHIJIOKE NWANKWOR[1*], MERCEDES MAROTO-VALER[1], DAVID LARGE[1], KEITH BATEMAN[2] AND CHRIS ROCHELLE[2]

[1]University of Nottingham, Nottingham, NG7 2RD United Kingdom, enxcn7@nottingham.ac.uk (*presenting author)

[2]British Geological Survey, Nicker Hill, Keyworth Nottinghamshire, NG12 5GG United Kingdom

Introduction

The high monetary and energy costs associated with the production of pure CO_2, for storage has necessitated the need for consideration of waste stream with some impurities (e.g. H_2S, SO_x, NO_x). However, little knowledge exists on the geochemical impact of these gas mixtures when injected into geological formations for the long term geological storage of CO_2. We report results from initial experiments that have been conducted with pure CO_2 as base cases with which to compare subsequent experiments involving impurities. The experiments investigated the reaction of Permo-Triassic sandstones (the on-shore equivalent of a North Sea reservoir rock) with brine in the presence of supercritical CO_2. Experiments were conducted over 3-6 months using 0.5 M NaCl solution at 70°C and 200 bar pressure, conditions typical of many potential CO_2 geologic storage sites. Modelling of the experimental systems was also carried out using PHREEQC. Figure 1 below shows the schematic content of pressure vessel used for laboratory batch experiments.

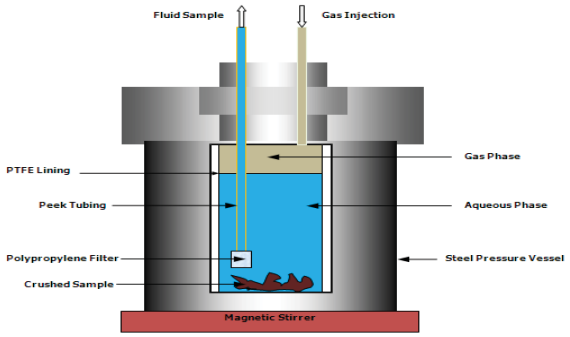

Figure 1: Schematic of pressure vessel

Results and Conclusions

Increasing concentrations of Mg, Ca and K were observed in the experiments over time. Mineralogical analyses and mass balance calculations for reacted and un-reacted rock samples, indicate that increases of Mg and Ca may be explained by dissolution of carbonate minerals such as calcite and dolomite, possibly followed by slight dissolution or ion-exchange with clay minerals. K concentrations are possibly governed by dissolution of trace halide minerals. In non-reactive 'control' experiments representing only the fluid-rock system equilibration using N_2 gas as the pressurising fluid, concentrations of the same elements were much lower.

PHREEQC modelling utilised rates of mineral dissolution and precipitation from the literature. Longer-term trends in observed solution chemistry could be modelled, if some assumptions about reactive surface areas were made. However, the model could not account for observed decreases in concentration of dissolved elements such as Al and Fe. Work is in progress to account for these changes and will be presented at the conference. Preliminary results from on-going experiments involving fluid-rock-CO_2 reaction in the presence of impurities (particularly H_2S) will also be presented.

Use of vegetation, soil, and radiometric survey to locate areas of concealed uranium mineralization at the Jacques Lake area, Labrador.

Praise Nyade[1*], Derek Wilton[1], Henry Longerich[1], Gary Thompson[2], Paul McNeill[3]

[1]Department of Earth Sciences, Memorial University, St John's, NL, A1B3X5, Canada, nyade@mun.ca (* presenting author)

[2]College of North Atlantic, Burin Campus, Burin Bay Arm A0E1G0, Canada, Gary.Thomposon@cna.nl.ca

[3]Auroral Energy Limited, St John's, NL, A1C6H6, Canada, PMcNeill@aurora-energy.ca

Abstract

We applied biogeochemical analysis of black spruce twigs, bark, and Labrador tea shoots with soil geochemistry, and an air-borne magnetic and radiometric survey to delineate areas of uranium enrichment at the Jacques Lake prospect of the Central Mineral Belt, Labrador, Canada. This area is overlain by thick layers of glacial till and peat which effectively obscure the direct observation of mineralized outcrops and accompanying alteration haloes. The topography is rugged with dense coniferous forest cover, lacks access roads, and is characterized by long and extreme winter weather conditions with very high precipitation. Biogeochemical signatures from black spruce twigs show elevated concentrations of U and pathfinder elements Be, Ag, Pb, and Sb over mineralized areas. A PCA plot of the data discriminated the bedrock mineralization with good anomaly contrast for uranium and related pathfinder elements (Be, Ag, Sb, V and Pb). Bark samples of black spruce generally showed weak to moderate anomaly contrasts. Labrador Tea leaves and stems defined very low anomalies or none at all; and possibly attributable to the shallow root system of the shrub. There is metal enrichment and an expression of the bedrock mineralization in the B-horizon soil. The distribution of U, Sb, Cu, Pb and to a less extent V in the soil exhibit anomalous signatures that may reflect a primary mineralized halo associated with the Jacque's Lake U prospect. Uranium concentrations (mixed acid digest) in soil ranged from 0.01 – 867 ppm. Areas of anomalous U concentration in B-horizon soils coincide with the airborne magnetic and radiometric and black spruce twig uranium anomalies that defined the Jacque's Lake deposit.

https://doi.org/10.1180/S0026461X00008434 Published online by Cambridge University Press

Iron L- and M- edges of iron containing minerals measured by x-ray Raman scattering

ALEXANDER NYROW[1*], CHRISTIAN STERNEMANN[1], MAX WILKE[2], KOLJA MENDE[1], CHRISTOPH SAHLE[1], LAURA SIMONELLI[3], ROBERT GORDON[4], NOZOMU HIRAOKA[5], FLORIAN WIELAND[1], METIN TOLAN[1] AND JOHN TSE[6]

[1]Technische Universitaet Dortmund, Germany, alexander.nyrow@tu-dortmund.de
[2]Deutsches GeoForschungsZentrum, Potsdam, Germany
[3]European Synchrotron Radiation Facility, Grenoble Cedex, France
[4]PNC-SRF, Department of Physics, Simon Fraser University, Burnaby, Canada
[5]National Synchrotron Radiation Research Center, Taiwan
[6]University of Saskatchewan, Saskatoon, Canada

Concerning the composition of the Earth's core and mantle, iron is one of the most interesting elements for applications in geosciences. Investigation of its electronic structure is essential to understand the origin of physical properties of different iron containing minerals existing in the Earth's interior. E.g. Fe^{2+}/Fe^{3+} ratios, the spin state as well as the oxygen fugacity can vary significantly at relevant conditions, i.e. pressures up to 1 Mbar and temperatures up to 3000°C [1-2]. Thus, experimental determination of such parameters in situ is crucial to understand the thermodynamic properties of these minerals [3].

X-ray Raman scattering (XRS) provides a possibility to measure electronic excitations by inelastic x-ray scattering which yields similar information like measurement of x-ray absorption edges by x-ray absorption spectroscopy (XAFS) or electron energy loss spectroscopy (EELS) [4]. Because XRS is an energy loss technique and the energy of the incident radiation does not depend on the binding energy of an atom, in contrast to XAFS and EELS, measurments of absorption edges of low Z elements in soft x-ray regime are possible using hard x-rays which allows measurements even in highly absorbing sample environments like diamond anvil cells with resistive or laser heating.

In this study, Fe $L_{2/3}$ and $M_{2/3}$-edges of different iron oxides and iron containing minerals measured by x-ray Raman scattering are presented in comparison with XAFS and EELS results. Furthermore, the momentum transfer dependency of the Fe $M_{2/3}$-edge is discussed. Possible applications in geosciences are pressure induced electronic transitions in iron containing minerals.

[1] Narygina, Kantor, McCammon (2010) *Physics and Chemistry of Minerals* **37**, 407.
[2] Speziale, Milner, Lee, Clark et al. (2005) *Proced. Nat. Acad. Sci.* **102** 17918.
[3] Wilke, Farges, Petit, Brown and Martin (2001) *Amer. Mineral Soc.***86**, 714
[4] Schülke (2007) *Electron Dynamics by Inelastic X-ray Scattering* (Oxford University Press).

https://doi.org/10.1180/S0026461X00008434 Published online by Cambridge University Press

Unravelling Plio-Pleistocene sea surface temperature signals: a multi-proxy latitudinal approach from the South China Sea

CHARLOTTE L. O'BRIEN[1]*, RICHARD D. PANCOST[1] AND GAVIN L. FOSTER[2]

[1]Organic Geochemistry Unit, School of Chemistry, University of Bristol, UK, c.l.obrien@bristol.ac.uk (* presenting author)

[2]School of Ocean and Earth Science, National Oceanography Centre, University of Southampton, UK

The tropical oceans are thought to have played a major role in the evolution of the Earth's climate since the Pliocene, such that accurately reconstructing tropical sea surface temperatures (SSTs) is an essential part of investigating how the global climate system has evolved over the past 5 Ma. Marine sediments from the tropical South China Sea (SCS) have yielded numerous paleotemperature records, however disagreement among different proxies and the potential causes of these differences may be hindering our understanding of the climate system. Using sediments from ODP Sites 1148 and 1143 located in the northern and southern SCS, respectively, we have applied three independent paleo-proxies to examine variations in SST for the past 5 Ma. Specifically, we have generated comparable SST records using the alkenone $U^{K'}_{37}$ index, TEX_{86} and Mg/Ca ratios in planktic foraminifer, *G. sacculifer*.

Our Pliocene TEX_{86}-derived temperatures for both sites indicate SSTs continuously higher than 27°C, exceeding modern mean annual SSTs. The southern SCS is generally warmer (28.0-32.5°C) than the northern SCS (27.0-31.0°C), with ODP Site 1143 displaying both greater variability (4.5°C) and a long-term decrease from 4 to 2 Ma. In contrast, the northern ODP Site 1148 exhibits lower variability (3.5°C) and no apparent trend such that the two records converge to similar values in the Pleistocene. Our Mg/Ca-SSTs show a similar trend to Mg/Ca SSTs at ODP Site 806 in the western equatorial Pacific [1], remaining generally stable (25.5-31.5°C) throughout the last 5 Ma with no indication of any global cooling. Alkenones are abundant in our samples. However, during the Pliocene, concentrations of tri-unsaturated alkenones are below detection limits indicating that SSTs in the SCS were above the limits of the $U^{K'}_{37}$ proxy (27.0-29.0°C) during this time.

The high $U^{K'}_{37}$ indices are consistent with the high SSTs in our TEX_{86} records, implying that SCS SSTs in the Pliocene and early Pleistocene exceeded modern mean annual SSTs. In contrast, our Mg/Ca SSTs (25.5-30.5°C) during this same period are offset from our TEX_{86}-SSTs (27.0-32.5°C) by, on average, >2°C at both SCS sites. Furthermore, our alkenone SSTs for ODP Site 1148 show that the northern SCS has cooled over the last 2 Ma, but this cooling is not seen in our Mg/Ca records. Higher TEX_{86}-derived temperatures may be in part due to TEX_{86}-SST estimates corresponding to warm season SSTs, as reported for a SCS core top sample [2], but it is unclear if such a bias can explain the high $U^{K'}_{37}$-derived SSTs. With these data we shall discuss reconstructing past tropical warmth and the application of various SST proxies in the Pliocene.

[1] Wara *et al.*, (2005) *Science* **309**, 758-761. [2] Shintani *et al.*, (2008) *J. Asian Earth Sci.* **40**, 1221-1229.

Trace element composition of gahnite in Broken Hill-type mineralization in and near the Broken Hill Pb-Zn-Ag deposit, Australia: implications for exploration

Joshua J. O'Brien[1*], Paul G. Spry[1], Graham S. Teale[2], Simon Jackson[3], and Dean Rogers[4]

[1] Iowa State University, Ames, Iowa, jjobrien@iastate.edu (* presenting author), pgspry@iastate.edu

[2] Teale and Associates, Adelaide, Australia, geologists@tealeassociates.com.au

[3]Geological Survey of Canada, Ottawa, Canada, Simon.Jackson@NRCan-RNCan.gc.ca

[4] Perilya Limited, Broken Hill, Australia, dean.rogers@perilya.com.au

Gahnite-bearing rocks ($ZnAl_2O_4$) are volumetrically abundant throughout the Proterozoic Broken Hill Domain, New South Wales, Australia, where they are associated with Broken Hill-type (BHT) Pb-Zn-Ag mineralization (including the supergiant, 200 Mt, Broken Hill deposit). Historically, the presence of gahnite has been utilized as an exploration guide for ores of this type, but has led to relatively limited sulfide discoveries. Major element chemistry has been used successfully to define a compositional range of gahnite associated with metamorphosed massive sulphides deposits, but it fails to distinguish sulfide-rich from sulfide-poor occurrences.

Major and trace element data from LA-ICP-MS and electron microprobe analyses provide valuable insight both into the origin of gahnite at Broken Hill, and its use as an exploration guide. Samples from 12 BHT deposits were analysed to determine whether or not prospective BHT deposits can be compositionally distinguished from non-prospective occurrences based on trace element content. Data were discriminated using a Principal Component Analysis to distinguish gahnite associated with the main ore lode from that associated with unmineralized lode pegmatites and sillimanite gneiss. Gahnite from the main ore bodies at Broken Hill have a relatively restricted compositional range that, based on a series of bivariate plot with density ellipses, overlap with the compositions of gahnite from several minor BHT occurrences. Based on contour maps of ore grade (wt. % Pb + Zn) associated with each gahnite locality, gahnite associated with the highest grades from the minor BHT deposits, have compositions that plot within the field for gahnite from the main ore bodies suggesting that trace element chemistry (e.g., Co: 60-80 ppm, and Cr+V+Mn+Ga: 1,100-2,200 ppm) may be used as an exploration guide for high-grade ore.

https://doi.org/10.1180/S0026461X00008434 Published online by Cambridge University Press

Spatial distribution of As(V) in cell-mineral aggregates formed by NO_3^--reducing Fe(II)-oxidizing bacteria

MARTIN OBST [1*], TINA LÖSEKANN-BEHRENS[2], SEBASTIAN BEHRENS[2], ANDREAS KAPPLER[2], CLAUDIA PANTKE[2], TOLEK TYLISZCZAK[3], ADAM P. HITCHCOCK[4]

[1]Environmental Analytical Microscopy, ZAG, University of Tuebingen, Germany, martin.obst@uni-tuebingen.de

[2]Geomicrobiology, ZAG, University of Tuebingen, Germany, tina-loesekann-behrens@uni-tuebingen.de, sebastian.behrens@uni-tuebingen.de, andreas.kappler@uni-tuebingen.de

[3]Molecular Environmental Science, Advanced Light Source, LBNL, Berkeley, USA, tolek@lbl.gov

[4]Canada Research Chair in Materials Research, CLS-CCRS, B.I.M.R, McMaster University, Hamilton, Canada, aph@mcmaster.ca

Ground water contamination with As is an environmental problem affecting human health [1]. Sorption of As to Fe(III)-(oxyhydr)oxides, is one of the most efficient mechanisms for immobilizing As in the environment. Fe(II)-oxidizing bacteria have recently been identified as possible contributors to As immobilization [2]. The objective of this study was to map the partitioning of As at various stages of precipitation [3] and to clarify the detoxification mechanisms.

The nitrate-reducing, Fe(II)-oxidizing *Acidovorax* strain BoFeN1 was cultured in presence of 0.2-1 mM arsenate. Samples were prepared anoxically for spectromicroscopic identification and mapping of the of cell-mineral aggregates formed during biogenic Fe(II) oxidation. Chemical speciation of As was measured at sub-100 nm spatial resolution by scanning transmission (soft) X-ray microscopy (STXM) using X-ray fluorescence (XRF) detection at beamline 11.0.2, Advanced Light Source (ALS), Berkeley USA.

Biogenic Fe-precipitates formed at different stages of microbial Fe(II) oxidation were found to vary significantly in their affinity for arsenate sorption/coprecipitation. The cytoplasm and the periplasm of cells cultured in the absence of Fe as well as periplasmatic Fe(III) precipitates formed when cultivated with Fe(II)) were highly depleted in As(V). No reduction of arsenate to arsenite was detected, which would be an essential step in the conventional As-detoxification systems. These results together indicate a yet unknown, efficient mechanism of either hindering As(V) from entering the cytoplasm through the phosphate transport mechanisms, or an arsenate-specific efflux pump. Although present in the genome of BoFeN1, the arsC, arsA and the ARR3 genes which are involved in the conventional detoxification, seemed not to play a role in the As depletion of the cells. In contrast, cell-associated extracellular precipitates of mineral-filled cell-residues of late stages of Fe(II) oxidation were enriched in their As(V)-content.

Acknowledgements: Funded by DFG Emmy-Noether program to M.O. (OB 362/1-1), The ALS is supported by the Director, Office of Science, Office of Basic Energy Sciences, of the U.S. DoE, Contract No. DE-AC02-05CH11231.

[1] Smedley (2002) *Appl. Geochem.* **17**, 517-568. [2] Hohmann (2010) *Environ. Sci. Tech* **44**, 94-101. [3] Hitchcock (2012) *Environ. Sci. Tech,* DOI: 10.1021/es202238k.

Origin of Anomalous Isotope Effects in Photo- and Thermo-chemical Reactions of Organosulfur Compounds

HARRY ODURO[1,2]*, ANDREW WHITEHILL[1], JAMES FARQUHAR[2], ROGER E. SUMMONS[1], AND SHUHEI ONO[1]

[1]Department of Earth, Atmospheric, and Planetary Sciences, Massachusetts Institute of Technology, 77 Massachusetts Avenue,Cambridge, MA 02139-4307, USA, mit.edu.

[2]Department of Geology and Earth System Science Interdisciplinary Center (ESSIC), University of Maryland, College Park, Maryland 20742, USA, umd.edu.

(*Author Presenting : Hoduro@mit.edu)

15f. Organic sulfur in the Earth System

There is overwhelming hypothesis about the importance of sulfur mass-independent isotopic (MIF) signatures $\Delta^{33}S$, $\delta^{34}S$, and $\Delta^{36}S$ observed in the early Earth's history[1]. The accumulation of MIF signals in ancient rocks has been linked to UV photolysis of SO_2 that penetrated deep in the Earth's atmosphere during the Archean[2]. Recently, it has been argued that thermochemical sulfate reduction (TSR) produce anomalous sulfur-33 compositions[3], but the source of this anomalous isotope signature have been suggested to result from a magnetic isotope effects (MIE) and the anomaly is limited to the magnetic isotope ^{33}S and not on ^{36}S[4].

In order to elucidate the mechanisms and differentiate between the sulfur isotope anomalies produced by photochemical and thermochemical reactions. We carried out a series of UV photolysis experiments of SO_2 with methane (CH_4), acetylene (C_2H_2), and ethylene (C_2H_4). The photolysis produced a number of methylated sulfoxide aerosol species (such as dimethylsulfone - DSO and methanesulfonic acids -MSA). The different isotope patterns are observed for the radiation under 190 to 220 and 250 to 330 nm UV absorption bands. But all shows anomaly in both S-33 and S-36. New thermochemical experiments of model organosulfur compounds demonstrate that thermolysis of terminal thiyl (such as glutathionine) and aromatic thiane (1,3,5-trithiane) compounds can also produce significant $\Delta^{33}S$ anomalies. These ^{33}S enrichments are attributed to a magnetic isotope effect (MIE) that affects only odd isotopes via the formation of thiyl-disulfide ion-radical pairs.

The findings in this thermal experiment are not consistent with multiple sulfur isotope trends of extracted methylated sulfoxide compounds observed in SO_2-CH_4-C_2H_2-C_2H_4 photochemical experiments, which exhibit significant ^{36}S anomalies and further the assertion that the early Archean record does not reflect this thermally induced radical sulfur chemistry. Detailed reaction mechanisms and processes leading to photochemical and thermochemical S-MIF signals will be presented.

References:
[1] Kaufman A.J. et al., 2007: *Science* **317**, 1900-1903.
[2] Farquhar J., et al., 2001: *J. Geophys. Res.* **106**, 32829 – 32839.
[3] Watanabe Y., et al., 2009: *Science* **324**, 370-373.
[4] Oduro et al., 2011:*PNAS* **108**, 17635-17638.

https://doi.org/10.1180/S0026461X00008434 Published online by Cambridge University Press

Direct evidence for isotopic fractionation during congruent dissolution, precipitation and at equilibrium

ERIC H. OELKERS[1*], CHRISTOPHER R. PEARCE[2], GIUSEPPE D. SALDI[3], AND JACQUES SCHOTT[1]

[1]Géosciences Environnement Toulouse, (GET/ CNRS UMR 5563, 14 Avenue Edourd Belin, 31400 Toulouse, France, oelkers@get.obs-mip.fr (* presenting author)
[2] Department of Environment, Earth and Ecosystems, The Open University, Walton Hall, Milton Keynes, MK7 6AA, UK.
[3] Earth Sciences Division, Lawrence Berkeley Laboratory, 1 Cyclotron Road, Berkeley, CA 94720, USA

This study provides direct experimental evidence of magnesium (Mg) isotope fractionation between an aqueous fluid and magnesite during its congruent dissolution, precipitation, and at equilibrium. Closed-system batch reactor experiments were performed at temperatures from 120 to 200 ºC and at 15 to 30 bars CO_2 pressure. During congruent magnesite dissolution the fluid became enriched in isotopically heavy Mg, with a steady state $\delta^{26}Mg_{fluid}$ composition 0.4 ‰ higher than the dissolving magnesite at 15 bars of CO_2 pressure, and 0.15 ‰ higher at 30 bars of CO_2 pressure. Equilibrium $^{26}Mg/^{24}Mg$ fractionation factors (α_{eqm}) for the were found to be 0.99881 at 150 °C and 0.99912 at 200 °C, close to those predicted by density-functional electronic structure models Magnesite precipitation was provoked by increasing the reactor temperature after equilibrium had been attained via dissolution. Kinetic isotope fractionation effects consistent with Rayleigh fractionation were observed immediately after the reactor temperature was increased and rapid magnesite precipitation occurred. However, isotopic exchange continued as the system equilibrated, eradicating the kinetic signal in the precipitated solid. As most natural systems fail to sustain rapid precipitation rates long-term, this observation suggests that kinetic fractionation effects in precipitated minerals will not be preserved in most geological systems.

The results of this study confirm the concept of dynamic equilibrium during water-mineral processes. Dynamic equilibrium also means that minerals and fluids will continue to equilibrate isotopically long after equilibrium is attained. This conclusion likely has significant consequences for the use of mineral isotopic compositions to illuminate chemical weathering processes, water-rock interaction in the crust, and past environmental conditions.

.

On the competition between kinetic and equilibrium isotope fractionation during low-T silica precipitation

M. OELZE[1*], F. VON BLANCKENBURG[1], D. HÖLLEN[2], M. DIETZEL[2], J. BOUCHEZ[1]

[1] GFZ German Centre for Geosciences, Potsdam, Germany, Oelze@gfz-potsdam.de(* presenting author)
[2]Institute of Applied Geosciences, Graz University of Technology, Austria

Formation of Si-bearing phases due to precipitation or adsorption always favors incorporation of light isotopes (apparent fractionation factor $\Delta_{solid\text{-}fluid} < 0$‰), which is usually explained by kinetic isotope fractionation. We challenge this assumption by conducting two sets of laboratory experiments.

First, Si-adsorption experiments (exp. #1) onto suspended gibbsite were performed at different initial monosilicic acid concentrations ($[Si]_{aq}$= 10, 20 and 40 ppm) at pH 7. Adsorption of silicic acid results in an increase of $\delta^{30}Si_{aq}$ values and a chemical steady state is reached after ~ 300 h of experimental runtime. These experiments confirm that $\Delta_{solid\text{-}fluid} < 0$‰, but also show that the magnitude of $\Delta_{solid\text{-}fluid}$ depends on the initial Si concentration. We show that Si concentrations affect the precipitation rate, but there is no obvious reason why isotope fractionation should depend on precipitation rate in a well-mixed system where no isotope fractionation due to diffusion in the solution should occur.

However, according to DePaolo[1], the fractionation of isotopes between solution and forming solids depends on the ratio of net precipitation rate R_p to the backward reaction rate R_b. When $R_p \approx R_b$, a competition between equilibrium and kinetic fractionation is expected. To test this hypothesis, a second set of experiments (exp. #2) were conducted, where solutions were frozen and thawed within 24 hours up to 130 days and sampled at regular intervals, during which amorphous silica was repeatedly precipitated/adsorbed and redissolved. In this special setup, $R_p << R_b$ might be achieved, a condition for isotope fractionation to reflect equilibrium[1]. Several sets of these experiments were performed at pH 4.5 and 7, with solutions initially containing $[Si]_{aq}$ = 45 ppm and $[Al]_{aq}$ = 2.7 or 27 ppm. We suggest precipitation of an Al-O-OH phase and subsequent adsorption of Si and/or coprecipitation of Si and Al. Experiments with high initial Al concentration show changing $\delta^{30}Si_{aq}$ values with experimental runtime. The $\delta^{30}Si_{aq}$ values increased during the first 20 days to up to 2.4‰ and then shows a decline to almost starting values of 0‰ after 130 days. This setup allows that R_p shifts from values $>> R_b$ to values $R_p << R_b$, which results in a change from kinetically- to equilibrium-dominated isotope fractionation.

In the first set of adsorption experiments (exp. #1), where $R_p > R_b$, kinetic isotope fractionation is assumed as Si rarely exchanges with the solution.

To conclude, the withdrawal of Si in natural systems due to precipitation or adsorption is not necessarily dominated by kinetic isotope fractionation. Instead, isotope fractionation might approach $\Delta_{solid\text{-}fluid} \geq 0$ if $R_p << R_b$, which can then be interpreted as equilibrium isotope fractionation.

[1] DePaolo (2011) *GCA* **75**, 1039-1056

https://doi.org/10.1180/S0026461X00008434 Published online by Cambridge University Press

Mercury speciation in deep-sea waters of the Mediterranean Sea

NIVES OGRINC[1,*], MITJA VAHČIČ[1], ARNE BRATKIČ[1], JOŽE KOTNIK[1], FRANCESCA SPROVIERI[2], NICOLA PIRRONE[2], MILENA HORVAT[1]

[1]Jožef Stefan Institute, Ljubljana, Slovenia, nives.ogrinc@ijs.si (* presenting author)
[2]CNR IIa, Institute for Atmospheric Pollution, Rende, Italy, pirrone@iia.cnr.it

This communication presents results of the investigation of the distribution and speciation of mercury (Hg) in deep-sea waters of the Mediterranean Sea during oceanographic cruise on board the Italian research vessel URANIA as a part of GMOS project. The study includes deep water profiles of dissolved gaseous Hg (DGM), reactive Hg (RHg), total (THg), monomethyl Hg (MeHg) and dimethyl Hg (DMeHg) in open ocean waters. A special attention is paid on the distribution of DGM, which plays the major role in the exchange of Hg between water and atmosphere. Average concentrations of measured Hg species were characterized by seasonal and spatial variations. Overall average THg concentrations ranged between 0.41 to 2.65 pM (1.32 ± 0.48 pM) and were comparable to those obtained in previous studies for the Mediterranean Sea [1,2]. Generally, average THg concentration was higher in W and E Mediteranean Deep Waters (WMDW and EMDW) and Leavantine Intermediate Water (LIW) than overlaying Modified Atlantic Water (MAW). High concentrations and portions of DGM and MeHg indicate high reactivity of Hg in open ocean waters. DGM was present in surface waters mainly as Hg^0 as no DMHg was detected at the surface, while towards the bottom a noticeable, but relatively small portion of DMeHg is present. DGM represents a considerable proportion of total Hg (average 20%, 0.23 ± 0.11 pM). The portion of DGM typically increased towards the bottom, especially in areas with strong tectonic activity (Alboran Sea, Strait of Sicily, Tyrrhenian Sea), indicating its bacterial and/or geotectonic origin. This is also confirmed by the fact that average DGM concentration was the highest in deep water masses (WMDW and EMDW). The percentage of MeHg (0.22 ± 0.12 pM) was on average approximately the same as for DGM. The observed increase of MeHg towards the bottom could be the consequence of photochemical degradation and/or microbial actions in surface and microbiologically mediated methylation in deeper waters [3,4].

Results will be also compared to the results obtained in the last GEOTRACES Atlantic Ocean cruise.

[1] Horvat *et al.* (2003) Atmosph. Environ **37/S1**, 93-108. [2] Kotnik *et al.* (2007) *Mar. Chem.* **107**, 13-30. [3] Monperrus *et al.* (2007) *Mar. Chem.* **107**, 49-63. [4] Heimbürger *et al.* (2010) Geochim. Cosmochim. Acta **74**, 5549-5559.

Hydrochemistry of shallow groundwater in areas affected by livestock burial

JUN-SEOP OH[1*], SEONG-TAEK YUN[1], JEONG-HO LEE[1], KYOUNG-HO KIM[1], KWANG-JUN CHOI[2], DONG-HO KIM[3], TAE-SEUNG KIM[3], JIN-SEOK HAN[3], AND BERNHARD MAYER[4]

[1]Korea University, Earth and Environmental Sciences, South Korea, ohseop@korea.ac.kr (* presenting author)
[2]Rural Research Institute, South Korea
[3]National Institute of Environmental Research, South Korea
[4]University of Calgary, Geoscience, Canada

As a result of an outbreak of foot and mouth disease (FMD) between late 2010 and early 2011 in South Korea, a large number of livestock carcasses (> 3.4 million) were buried in ~4,400 pits (usually 5 m deep) throughout the country. As a result, there is concern about the potential impacts of leachates from livestock burial sites on shallow groundwater. In addition, there are debates about the origin of groundwater contamination around livestock burial sites, as groundwater in agricultural areas is also usually contaminated by nitrogen-bearing compounds and chlorine from preexisting non-point and point sources. Therefore, we conducted hydrochemical surveys of groundwater in a few areas potentially affected by livestock burial, with the main purpose of assessing the potential impacts on groundwater quality. An additional objective was to identify geochemical indicators which can be used for differentiating contamination from agricultural areas and livestock burial sites. We collected hydrochemical (i.e., major cations and anions and trace metals) and isotopic data for nitrate ($\delta^{15}N$ and $\delta^{18}O$) for groundwater from domestic and agricultural wells (< 300 m away from burial sites) as well as leachate samples from burial sites. The obtained data were interpreted using factor analysis to reveal the relationships between variables and to cluster the samples based on hydrochemical processes.

The results show that only a few monitoring wells at distances of < 5 m from the burial sites were impacted by leachate from burial sites yielding groundwater that was strongly anoxic and high in ammonium and other solutes such as HCO_3, Ca, Cl, Mg, Na, K, SO_4, Br, Fe, Mn and B. The leachates and groundwaters affected by burial sites were hydrochemically a Ca-HCO_3 type, while unaffected groundwater was mostly Ca-Cl(NO_3) type due to pervasive impacts from agrochemicals. The isotopic composition of traces of nitrate in leachate and groundwater affected by burial sites were variable and inconsistent with values known for diverse nitrate sources such as fertilizers, manure and sewage, possibly due to nitrification under isotopic disequilibrium or due to other nitrogen transformation processes. We propose the use of following geochemical parameters for differentiating groundwater contamination from leachate of livestock burial sites and from agricultural areas: 1) redox-sensitive parameters such as ammonium, Fe and DO (especially, the occurrence of ammonium ion) and 2) hydrochemical water types in conjunction with (Na+K)/∑cations versus (SO_4+Cl) relationship.

https://doi.org/10.1180/S0026461X00008434 Published online by Cambridge University Press

Evidence for the O_2 and CO_2 rich Archean atmosphere

H. OHMOTO[1*], Y. WATANABE[1], K.E. YAMAGUCHI[2], H. HAMASAKI, J. BRAINARD[1], AND A.P. CHORNEY[1]

[1]NASA Astrobiology Institute and Department of Geosciences, Penn State University, University Park, USA, hqo@psu.edu; yxw129@psu.edu; hzh114@psu.edu; jlb5156@psu.edu; apc5060@psu.edu

[2]Toho University, Chiba, Japan, kosei@chem.sci.toho-u.ac.jp

In the oxygenated world, the CO_2 and O_2 contents of the atmosphere and oceans are regulated at steady-state levels by the balance between the forward and backward reactions of: $CO_2 + H_2O = CH_2O + O_2$. Today, ~100% of the CH_2O formed on land and ~99.7% of the CH_2O formed in the oceans by oxygenic photosynthesis are recycled back to CO_2 in <10 yrs by aerobic oxidation. Burial of the ~0.3% of marine organic matter as kerogen in sediments has been responsible for the long-term (>1,000 yrs) production of O_2 in the atmosphere and oceans. Oxidation of the kerogen during soil formation has been the main pathway for the long-term consumption of O_2.

In the anaerobic world, such as the one postulated by many for the Archean, organic synthesis is carried out by anoxygenic photosynthesis (e.g., $CO_2 + 2H_2 \rightarrow CH_2O + H_2O$). Fresh organic matter decomposes by fermentation (e.g., $CH_2O \rightarrow CO + H_2$ and $3CH_2O \rightarrow 2CO + CH_4 + H_2O$, c.f., Hoeler et al., 2001), but kerogen is not decomposed. In such a world, the atmospheric CO_2 is continuously converted to reduced C compounds (CH_2O, CO, CH_4 and C) and not completely recycled back to CO_2. Thus, the atmospheric CO_2 continuously decreases, even with continuous supplies of CO_2 by volcanic gas and weathering of carbonates, and disappears in <~100 Ma since the emergence of photoautotrophs, creating an icy, dead planet (Ohmoto and Lasaga, 2001). However, the abundances of carbonates and organic C-rich shales, and their $\delta^{13}C$ values, in Archean sedimentary rocks are essentially the same as those in younger ones (Ohmoto, 2004), suggesting that since ~3.8 Ga, the atmosphere and oceans have remained O_2- and CO_2 rich and the modern-styled redox cycle of C has operated.

Black shales with high pyrite contents, which positively correlate with organic C contents, and sulfate-rich sediments are not uncommon in Archean rocks (Ohmoto, 2004). $\delta^{34}S$ values of the pyrites and sulfates show large variations, from -20 to +35‰ and from +2 to +27‰, respectively (Ohmoto, 1992, 2004; Kiyokawa et al., in prep.). The common $\delta^{15}N$ values for kerogen in Archean shales (0 to +15‰) are essentially the same as those in Phanerozoic ones (Yamaguchi, 2004; Kerrich et al., 2006). These data suggest that since >3.5 Ga, the oceans have been rich in SO_4^{2-} and NO_3^-. Researchers have interpreted the isotopic records of S, Fe, Mo and Cr in sedimentary rocks based on anoxic Archean atmosphere models. However, we can better explain these isotopic data, as well as the Pb isotope data and the variations in the Fe^{III}-, Mo-, Ce, and U contents, of Archean rocks with the model of a fully-oxygenated Archean world. The isotopic variations in the 2.7-2.5 Ga Hamersley sediments can be explained by combinations of biological-, diagenetic- and hydrothermal processes in a nearly-closed euxinic basin, which episodically hosted matalliferous brine pools and/or opened to the O_2-, S-, Mo- and U rich oceans.

Many researchers have cited the presence of AIF-S (or MIF-S) and detrital grains of uraninite and pyrite in some Archean-aged sedimentary rocks as strong evidence for an anoxic Archean atmosphere. But such arguments are invalid, as AIF-S and these detrital minerals have also been found in much younger-aged materials (Ohmoto, 2004; Watanabe et al., Goldschmidt 2012).

Trace element composition of size-fractionated particulates in the North Atlantic U.S. GEOTRACES section

DANIEL C. OHNEMUS[1,2*], PHOEBE J. LAM[2]

[1]MIT/WHOI Joint Program in Oceanography, Woods Hole, USA (*dan@whoi.edu)

[2]Department of Marine Chemistry and Geochemistry, Woods Hole Oceanographic Inst., Woods Hole, USA, pjlam@whoi.edu

Sinking (>51μm) and suspended (<51μm) marine particulates were collected via *in situ* filtration during the US GEOTRACES North Atlantic Zonal Transect cruises on the *R/V Knorr* in 2010 and 2011. Total and acetic acid-leachable compositional profiles for key trace elements and isotopes (TEIs—Fe, Al, Zn, Mn, Cd, Cu) and other TEIs of interest (Co, Ti, Ba, V, Ni, Mo) are presented, allowing a first look at particulate composition for a full ocean transect, in sixteen-point depth resolution.

This transect explores a diverse array of sites—the Saharan African and North American continental margins, a mid-ocean ridge hydrothermal plume, several benthic boundary layers, as well as open-ocean sites—which significantly expands our knowledge of the highly-variable and dynamic marine particulate world. Common behaviors are observed for several groups of elements, highlighting differences between lithogenic and biogenic particulate pools, and the dynamics that exchange material between different size-fractions. Acetic acid-leachable particulate data furthermore provides constraints on exchangeable and/or bioavailable elemental pools, and also explores the behaviors of redox-sensitive metals in oxygen minimum zones, benthic boundary layers, and in surface waters. Combination of this dataset with other, forthcoming GEOTRACES results (e.g. ^{234}Th export, dissolved TEI parameters) will be an exciting product of the worldwide GEOTRACES program.

https://doi.org/10.1180/S0026461X00008434 Published online by Cambridge University Press

Bio-mineralization of rare earth elements

T. OHNUKI[1*], M. JIANG[1,2], S. UTSUNOMIYA[2], K. TANAKA[1,3]

[1] Advanced Science Research Center, Japan Atomic Energy Agency, Tokai, Ibaraki, 319-1195 Japan
(*correspondence: ohnuki.toshihiko@jaea.go.jp)
[2] Department of Chemistry, Kyushu University, Fukuoka-shi, Fukuoka-ken, 812-8581 Japan
[3] Department of Earth and Planetary Systems Science, Hiroshima University, Higashi-Hiroshima, Hiroshima, 739-8526Japan

Geochemical behaviors of rare earth elements (REEs) are important to understand the migration of trivalent actinides and fission genic REEs from nuclear power plants and high level radioactive waste. When REEs migrates in environemnts, their chemical states may change by the interaction with inorganic and organic materials. Many researchers have studied the interaction of REEs with inorganic materials. However, the biotransformation of REEs have not fully understood. We have conducted the research on the effects of microorganisms on chemical states change of REEs.

We found that Sm(III) phosphate minerals were formed on the cells surface of gram negative bacterium *Pseudomonas fluorescens* after exposure of Sm(III) solution with the resting cells, even though no phosphate is added. TEM-SAED analysis showed that Sm-monazite was developed directly from the surface of cells. Sm(III) ions were first adsorbed by the functional groups of cells surface, followed by the chemical states change by the reaction with phosphate ions released from inside the yeast cells.

When phosphate is provided in the solution as glycerol phosphate-Ca, Yb concentration decreased abruptly with time after *P. fluorescens* exposed to the solution containing Yb(III) and lactic acid. TEM and XAFS analyses showed the nanoprecipitates containing Yb and P were formed directly from the cells surface. Interestingly, precipitates containing Ca and P, but no Yb were observed on the cells. On the contary, without glycerol phosphate, Yb concentration in the solution slightly decreased with time by the formation of Yb-lactate complex in the solution.

These findings strongly indicate that Yb phosphate mineralization was occurred on the cells surface, even when P was provided from inside and outside cells. Thus, cell surface of microorganisms functions as specific reaction environment for biotransportation of REEs.

Speciation study of copper in stream sediments and soils

ATSUYUKI OHTA[1*], HIROYUKI KAGI2

[1]Geological Suervey of Japan, Tsukuba, Japan, aohta@aist.go.jp
[2] The University of Tokyo, Tokyo, Japan, kagi@eqchem.s.u-tokyo.ac.jp

A sequential extraction method has been used widely to elucidate its chemical binding forms in sediments including soil. However, the method might give misleading results due to alteration of the samples during the individual steps of the extraction [1]. We applied a X-ray absorption fine structure (XAFS) spectroscopy to identify the Cu species in the residues after each step of the sequential extraction. The Cu in 7 geo-standard materials (JSd-1~5: stream sediments, JSO-1 and 3: soils) was extracted using a modified three-step extraction developed by the Community Bureau of Reference (BCR) [2]. The steps and extractants are as follows;

(1) Step1: CH_3COOH (0.11 mol/L).
(2) Step 2: $NH_2OH{\cdot}HCl$ (0.5 mol/L).
(3) Step 3: H_2O_2 (8.8 mol/L) and CH_3COONH_4 (1 mol/L).

The residues after each step of extraction were filtrated by a membrane filter. The $Cu^{3+}_{(aq)}$, $Cu(NO_3)_2$, Cu doped FeOOH (or MnO_2), Cu doped humic materials, and JCu-1 (a geochemical reference material of CuS ores) were prepared As a reference compounds. The Cu K-edge XANES spectra were recorded in a fluoresce mode at the BL-12C of KEK-PF. The fluorescence X-ray was measured by a 19 element pure-Ge SSD.

Figure 1 shows the Cu K-edge XANES spectra of JSd-2 and reference materials and its fitting results. The JSd-2 is a stream sediment reference material collected from the drainage basin having Cu mine. The speciation of Cu in JSd-2 is expected to be a mixture of Cu weakly adsorbed on materials (step 1), Cu bound to Fe-Mn hydroxides (step 2), chalcopyrite (step 3) and silicate materials (residue). The linear fitting result was roughly comparable to the results from the BCR scheme, although the relative amount of Cu extracted at step 3 is underestimated. Thus, the method using XAFS spectroscopy combined with BCR scheme is effective to accurately identify and quantify Cu species in sediment samples.

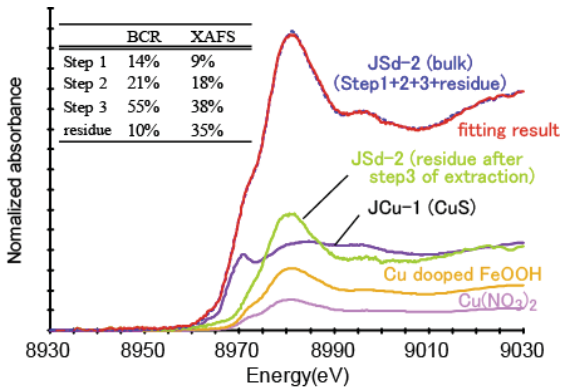

Figure 1. The Cu K-edge XANES spectra of JSd-2 and the residue of JSd-2 after third step in the BCR scheme, and reference materials.

[1] Calmano *et al*. (2001) *Anal. Chem.* **371**, 823-830.
[2] Rauret *et al*. (1999), *J. Environ. Monit*. **1**, 57-61.

https://doi.org/10.1180/S0026461X00008434 Published online by Cambridge University Press

Iron isotopic signature of Fe-Ni metals in ordinary chondrites using LAL-MC-ICPMS technique

SATOKI OKABAYASHI[1*], TETSUYA YOKOYAMA[2], AND TAKAFUMI HIRATA[1]

[1]Laboratory for Planetary Sciences, Kyoto University, Kyoto, Japan, okabayashi-s-aa@kueps.kyoto-u.ac.jp (* presenting author)
[2]Department of Earth and Planetary Sciences, Tokyo Institute of Technology, Tokyo, Japan

Introduction

The ordinary chondrite is the most abundant and primitive meteorite in the solar system. It is widely believed that the formation sequence of the ordinary chondrites tell us details of the early solar system history. Among the various minerals or components found in the ordinary chondrites, the Fe-Ni metal is one of the characteristic materials of ordinary chondrite. Despite the major components, the formation processes of Fe-Ni metals have still been veiled. The Fe isotopic signature is one of the key information to derive the formation processes of Fe-Ni metals in the ordinary chondrites, because (a) Fe is ubiquitously distributed in various minerals or phases in the meteorites, and (b) Fe isotope composition can vary through the formation processes. In this study, the Fe isotopic ratios of Fe-Ni grains in ordinary chondrites were measured. In order to derive inherent and reliable Fe isotopic data from complex Fe-Ni phases, we have developed a new sampling technique described below.

Experimental

In this study, Fe-Ni metals in ordinary chondrites were collected using laser ablation in liquid (LAL) technique [1, 2]. The sample surface was polished and the metal phase was ablated in the deionized water using the femtosecond laser (λ=780 nm). Unlike with the conventional micro-drilling technique, the LAL technique can provide minimum risk of contamination of Fe from equipments. After the LAL sampling procedure, the resulting sample suspension was collected using micropipette and was then subsidized to acid digestion using conc. HCl and conc. H_2O_2. The sample solution was heated until dryness and the resulting sample cake was re-dissolved in 0.1% HCl, and then used for the isotopic analysis of Fe using MC-ICPMS connected to the desolvating nebulizer system.

Results and Conclusion

Total 15 ordinary chondrite metals were analyzed in this study. The δ^{56}Fe data for L chondrites did not vary with the δ^{56}Fe data for LL chondrites. In contrast, Fe in the H chondrites was isotopically lighter than those for L or LL chondrites. These Fe isotopic variations between H, L and LL chondrites are consistent with the data obtained by Theis et al. (2008) [3]. However, these Fe isotopic ratios within the metallic phase in the H, L and LL chondrites cannot be explained by the simple redox reaction suggested by Theis et al. (2008). Possible cause of the present variation of Fe isotopic ratios will be discussed in this presentation.

[1] Okabayashi *et al.* (2011) *J. Anal. At. Spectrom.* **26**, 1393-1400. [2] Douglas *et al.* (2011) *J. Anal. At. Spectrom.* **26**, 1294-11301. [3] Theis *et al.* (2008) *Geochim. Cosmochim. Acta* **72**, 4440-4456.

Vertical distributions of ^{230}Th in the Pacific Ocean and their relation to advection and diffusion

AYAKO OKUBO[1*], HAJIME OBATA[2], TOSHITAKA GAMO[3], MASATOSHI YAMADA[4]

[1]Research Group for Radiochemistry, Japan Atomic Energy Agency, Ibaraki, Japan, okubo.ayako@jaea.go.jp (* presenting author)
[2]Atmosphere and Ocean Research Institute, the University of Tokyo, Chiba, Japan obata@aori.u-tokyo.ac.jp
[3]Atmosphere and Ocean Research Institute, the University of Tokyo, Chiba, Japan gamo@aori.u-tokyo.ac.jp
[4]Institute of Radiation Emergency Medicine, Hirosaki University, Aomori, Japan, myamada@cc.hirosaki-u.ac.jp

In the central Pacific Ocean, which is remote from all the continents, the distributions of trace elements expectedly show the typical vertical profiles of open oceans.

Vertical distributions of ^{230}Th in the Pacific Ocean have been well-described by the reversible scavenging model [1]-[5]. On the basis of the assumption of no lateral ^{230}Th transport in this model, in-situ produced ^{230}Th is scavenged within the basin. In contrast, the effect of lateral advection on Th distribution have been shown in the Southern Ocean and Atlantic Ocean[6]-[8] and using a model caluculation the effect of isopynal diffusion have been discussed [9].

We investigated the vertical distribution of total ^{230}Th in mid-latitudes of the Pacific Ocean. Because of low biogenic particle flux, high ^{230}Th activity in deep water is exhibited in the central gyre. The west–east section (20°N) of ^{230}Th shows a strong gradient in the deep waters around 170°E and 110°W. At depths of 2000–4000 m and 4000 m–bottom, within the time-scale of scavenging residence time of ^{230}Th, the horizontal eddy diffusion could reach 1100–1400 km and 400–700 km, respectively. The horizontal eddy diffusion transport is too weak to affect Th distribution in the deep layers between each station in this study area. We observed the depletion of total ^{230}Th compared with a reversible scavenging model prediction for the deep layers in the mid-latitudes of the North Pacific Ocean. The observed depletion is partly explained by lateral advection, adopting the scavenging-mixing model. Additionally, a bottom scavenging process above the seafloor and a diffusion process are considered to explain the ^{230}Th deficit.

In the Eastern Subtropical Pacific, advection and diffusion of low-^{230}Th water in the high particle flux region could affect the distributions of ^{230}Th. At the station on the East Pacific Rise, we observed exceptionaly depleted ^{230}Th in deep layers. The ^{230}Th depletion would be attributed to the active hydro-thermal activity in this area.

[1]Nozaki et al. (1981), *EPSL*,54, 203-216 , [2]Bacon and Anderson (1982), *JGR* 87, 2045-2056. [3]Nozaki and Nakanishi (1985) *DSR*, 32, 1209-1220. [4]Nozaki et al. (1987), *JGR*, 92, 772-778. [5]Roy-Barman et al. (1996) *EPSL*, 139, 351-363. [6]Rutgers van der Loeff and Berger (1933) *DSR-I*, 40, 339-357. [7]Vogler et al (1998) *EPSL*, 156, 61-74. [8]Moran et al.(2002) *EPSL*, 203, 999-1014. ,[9]Roy-Barman (2009) *Biogeosci.* 6, 3091-3107.

https://doi.org/10.1180/S0026461X00008434 Published online by Cambridge University Press

Characterization of microbial activity by petroleum compositional changes using ultra-high resolution mass spectrometry techniques (FT-ICR-MS)

THOMAS B.P. OLDENBURG[1*], KEN CHANTHAMONTRI[1], ANDREW P. STOPFORD[1], HAIPING HUANG[1], MAN-LING WONG[2], GERRIT VOORDOUW[2], STEVE R. LARTER[1]

[1]Petroleum Reservoir Group, Department of Geoscience, University of Calgary, Calgary, Alberta, Canada, toldenbu@ucalgary.ca (* presenting author), ckchanth@ucalgary.ca, andrew.stopford@ucalgary.ca, huah@ucalgary.ca, slarter@ucalgary.ca

[2]Petroleum Microbiology Research Group, Department of Biological Science, University of Calgary, Alberta, Canada, mlwong@ucalgary.ca, voordouw@ucalgary.ca

Introduction & Methods

Most of the world petroleum reserves are biodegraded with the largest oil reserves being found on the flanks of foreland basins in Canada and Venezuela. Coal as another essential energy source is also known to being partially biodegraded yielding to biogenic gas.

In this study, the compositional changes of fossil fuels during biodegradation in lab experiments and in natural reservoir profiles under aerobic and anaerobic conditions will be shown as well as indicators of microbiological activity.

The fossil fuel compositions were analyzed using an ultra-high resolution Fourier Transform-Ion Cyclotron Resonance-Mass Spectrometry (Bruker12T FT-ICR-MS) and GC-MS techniques. For FT-ICR-MS the ionization methods used include Electrospray (ESI) in positive and negative ion mode as well as Atmospheric Pressure Photoionization (APPI) in positive ion mode.

Results & Discussion

One example of compositional changes during biodegradation of bitumen and assessment of microbial activity is shown in Fig. 1.

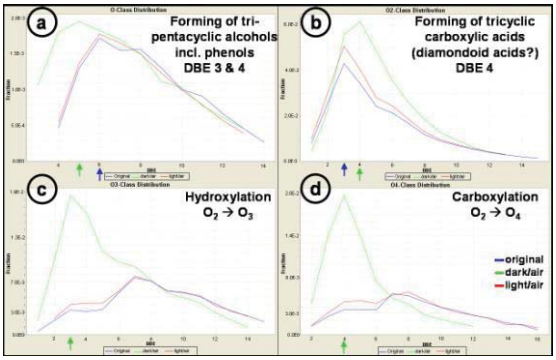

Figure 1: Changes in oxygen compound systematics of aerobic biodegradation lab experiments of oil sands bitumen: a. alcohols, b. carboxylic acids, c. hydroxy-carboxylic acids, d. dicarboxylic acids. All oxygen compound classes (O1-4) are becoming strongly enriched in the absence of light whereas under light no or only minor changes are observed.

Thermodynamic properties of carbonate liquids: required for models of carbonate stability in the mantle

MARY CATHERINE O'LEARY[1*] AND REBECCA A. LANGE[1], AND YUHUI AI[1]

[1] Department of Earth and Environmental Sciences, University of Michigan, Ann Arbor, mcolear@umich.edu (*presenting author)

Not only is mantle carbonate an important reservoir in the global carbon cycle, it also plays a key role in mantle melting processes. Mantle carbonate, of which $MgCO_3$ and $CaCO_3$ are the most important components, has been shown to have a major effect on both the depth of melting and the resultant magma composition (e.g., Dasgupta et al., 2006). In order to fully explore under what T-P conditions mantle carbonate can be subducted into the lower mantle, as well as to examine all possible temperature, pressure, and composition conditions where mantle carbonate influences melting, the number of phase equilibrium experiments needed is prohibitive. Therefore, thermodynamic models of mantle melting that incorporate carbonate are of considerable interest. In order to achieve this, thermodynamic data on $CaCO_3$ and $MgCO_3$ liquids are needed, including their heat capacity, enthalpy, volume, and compressibility. By mixing the alkaline earth carbonates with the alkali carbonates, liquidus temperatures are lowered to those below decomposition (< 1300K), permitting measurement of various thermodynamic properties to be made. This method also tests whether the molar volume, compressibility, and heat capacity of carbonate liquids mix ideally with respect to composition, allowing the partial molar liquid properties for $CaCO_3$ and $MgCO_3$ to be derived. Previous work in the system Li_2CO_3-Na_2CO_3-K_2CO_3-$CaCO_3$ by Liu and Lange (2003) has shown that the volume and thermal expansion mix ideally. In this study, we show that the compressibility and heat capacity of Li_2CO3-Na_2CO_3-K_2CO_3-$CaCO_3$ liquids also mix ideally with respect to composition at one bar. Compressibility measurements were made on eleven liquids (four containing ≤ 50 mol% $CaCO_3$) using frequency-sweep acoustic interferometery at one bar between 800 and 1300 K. When the ideal mixing model for compressibility is applied,

$$\beta_T(X) = \sum X_i \frac{\overline{V}_{i,T}}{\overline{V}_T}\left(\overline{\beta}_{i,T_{1100K}} + \frac{\partial \overline{B}_i}{\partial T}(T - 1100\,K)\right)$$

fitted partial molar compressibilities are acquired (Table 1).

Carbonate Component	$\beta_{T,1100K} \pm 1\sigma$ (10^{-2} GPa^{-1})	$\partial\beta_T/\partial T \pm 1\sigma$ (10^{-2} GPa^{-1})
$CaCO_3$	5.36 ± 0.13	0.0061 ± 0.0010
Li_2CO_3	8.09 ± 0.06	0.0044 ± 0.0008
Na_2CO_3	10.62 ± 0.07	0.0103 ± 0.0006
K_2CO_3	14.09 ± 0.06	0.0135 ± 0.0004

Table 1. Partial molar compressibilities for the carbonates.

A Perkin-Elmer Diamond differential scanning calorimeter is being used to measure liquid heat capacities. We have applied our results to a thermodynamic analysis of the fusion curve of $CaCO_3$ in order to constrain its one-bar enthalpy and entropy of fusion in addition to the pressure dependence of the compressibility (bulk modulus) of $CaCO_3$ liquid (K_0'), using a 3rd-order Birch-Murnaghan equation of state. Currently, our best estimate for the K_0' of $CaCO_3$ liquid is 4.5 ± 0.5. Though DSC measurements are ongoing, our preliminary estimate for the enthalpy of fusion for $CaCO_3$ at one bar is 67.5 ± 0.5 kJ/mol for a one-bar metastable melting temperature of 1295°C.

https://doi.org/10.1180/S0026461X00008434 Published online by Cambridge University Press

Fossil Corals as an archive of Phanerozoic seawater chemistry

ANNE M. O'LEARY[1*], MICHAEL L. BENDER[1], JAROSŁAW STOLARSKI[2], JESS. F. ADKINS[3], KATE J. DENNIS[1], DANIEL P. SCHRAG[4]

[1]Princeton University, Geosciences, Princeton, NJ, aoleary@princeton.edu (*presenting author)
[2]Instytut Paleobiologii, Polska Akademia Nauk, Warszawa, Poland, stolacy@twarda.pan.pl
[3]California Institute of Technology, Geological and Planetary Sciences, Pasadena, CA, jess@gps.caltech.edu
[4]Harvard University, Earth and Planetary Sciences, Cambridge, MA, schrag@eps.harvard.edu

Numerous observations indicate that the composition of seawater has not remained constant through time. It has been hypothesized that such variability is linked to changes in geologic processes such as continental weathering, sea-floor spreading, and continental onlap. Fossil corals may be suitable candidates for studying seawater chemistry. Although there is evidence that incorporation of some elements into the coral skeleton is biologically mediated[1], other elements seem to accurately record certain chemical properties of the seawater from which the corals grow.

We studied a suite of ~12 well-preserved fossil corals dating back to the Triassic. The primary objective of this work was to assemble a collection of fossil corals that have been meticulously tested and shown to be diagenetically unaltered with respect to their original structure and mineralogy. X-ray diffraction, micro-Raman spectroscopy, and cathodoluminescence analyses suggest that these specimens contain little to no secondary calcite. Electron and optical microscopy studies reveal crystal structures consistent with modern coral aragonite. Clumped isotope data for 6 specimens give temperatures that seem either appropriate for what we understand about the time and location at which each coral grew or they appear too low, similar to some modern corals.[2] However, secondary ion mass spectrometry (SIMS) analyses suggest there is some micron-scale alteration indicated by high Mn/Ca, high Mg/Ca, and low Sr/Ca ratios. In fossils with low Mn/Ca, we observe a positive correlation between Na/Ca and S/Ca, as in modern corals.[3] We sometimes observe a negative relation between Sr/Ca and Mg/Ca, also similar to some modern corals.[4]

The second objective of this study is to analyze properties such as Sr/Ca and Mg/Ca in corals to supplement existing records of global seawater chemistry since the Triassic. Initial results from SIMS measurements of Sr/Ca ratios are consistent with some existing records of Sr/Ca in seawater through time; Sr/Ca is relatively constant from the modern to the Triassic. These results are supportive of using corals as archives of paleo-seawater chemistry. Additionally, we find that Mg/Ca ratios in fossil corals decrease with age, but because of possible vital effects, the implications for seawater chemistry are uncertain.

[1] Meibom, A. *et al.* (2007) *Geophys. Res. Lett.* **34,** L02601. [2] Saenger C.P. (2011) *AGU Fall Meeting* PP41A-1726. [3] Mitsuguchi T. *et al.* (2010) *Geochemical Journal* **44,** 261-273. [4] Gagnon A.C. *et al.* (2007) *Earth Planet. Sci. Lett.* **261,** 280-295.

Transport and deposition of engineered nanoparticles (NPs) in saturated porous media (schist): role of interactions between NPs and the rock matrix

PATRICK OLLIVIER*, HÉLÈNE PAUWELS, GUILLAUME WILLE, GILLES BRAIBANT AND GÉRALDINE PICOT-COLBEAUX

BRGM, Water Division, p.ollivier@brgm.fr (* presenting author)

The increasing use of engineered nanoparticles for industrial and household purposes (cosmetics, clothing, electronic, automotive, medical products…) will inevitably lead to their introduction into different environmental compartments, including groundwater. Assessing the risk of groundwater contamination by nanoparticles is worth studying but requires the knowledge of their mobility and environmental reactivity. How far these nanoparticles will travel in waters? A number of studies addressed the processes driving mobility of nanoparticles in simple waters and conditions (clean Quartz sand, bare silica surfaces, uniform and spherical glass beads…). They highlight nanoparticles dispersion in water is highly dependent on physical and chemical key parameters of nanoparticles (solubility, pH_{zpc}, which may vary with chemical composition, crystallinity, size and eventual coating…), and on the overall groundwater composition (pH, ionic strength, major element concentration, e.g. Ca or Na, organic matter contents…). The present study conducted in the frame of the AquaNano project aims at characterising metal oxide nanoparticles (TiO_2 and CeO_2) behaviour and reactivity during transport in schist (heterogeneous medium). Transport (flushing) experiments of nanoparticles suspension through 10 cm long rock column under pressure (up to 5 bars) have been conducted in laboratory. After the experiments, NPs retained in column have been mapped using scanning electron microscopy (SEM). Chemical and physical interactions between NPs and the rock matrix have been constrained using Raman spectroscopy associated with SEM. Results show that NPs deposition and aggregation occurred during their transfer while favorable (repulsive and low ionic strength) transfer conditions were applied in column. Also, it appears a more rapid transfer of NPs concomitant with an increase of NPs retention (by a factor 40) by rock matrix after successives NPs inputs in the column separated by NPs-free water circulation. Experiments conclusively demonstrate that physical and chemical properties of NPs and rock matrix (biotite, quartz…) govern the mobility of NPs. We suggest a rearrangement of NPs (adsorption/desorption processes) in column during NPs-free water circulation and modifications to preferential pathways for NPs circulation while aggregation enhanced NPs deposition.

https://doi.org/10.1180/S0026461X00008434 Published online by Cambridge University Press

Dissimilatory iron reduction and the redox cycling of green rust

EDWARD J. O'LOUGHLIN[1]*, MAXIM I. BOYANOV[1], CHRISTOPHER A. GORSKI[2], MICHAEL L. MCCORMICK[3], MICHELLE M. SCHERER[4], AND KENNETH M.. KEMNER[1]

[1]Argonne National Laboratory, Argonne, IL, USA, oloughlin@anl.gov (* presenting author)
[2]EAWAG, Duebendorf, Switzerland.
[3]Hamilton College, Clinton, NY, USA
[4]The University of Iowa, Iowa City, IA, USA

Introduction

Green rusts (mixed Fe^{II}/Fe^{III} layered double hydroxides) have been identified in Fe^{III}/Fe^{II} transition zones in a variety of natural and engineered subsurface environments including groundwater, soils, and sediments, and among corrosion products in zero valent iron permeable reactive barriers. Many of these environments are characterized by periodic or seasonal cycling of redox conditions (e.g., redoximorphic soils in areas with seasonal flooding) that create the opportunity for cycling of Fe between oxidized and reduced forms. In recent years evidence has been building that suggests that the green rust mineral fougerite plays a central role in Fe redox cycling in these environments.

Experimental Methodology

Carbonate green rust was produced in anoxic defined mineral medium containing 75 mM formate and 80 mM Fe^{III}, in the form of phosphate doped (0.7 mass % P) lepidocrocite, inoculated with *Shewanella putrefaciens* CN32. The green rust was then oxidized by introducing sterile air into the headspace. After 24 h the suspensions were sparged with sterile Ar and re-inoculated with *S. putrefaciens* CN32. Samples were collected for measurement of Fe^{II} and characterization of the secondary mineralization products by powder X-ray diffraction, scanning electron microscopy, and ^{57}Fe Mössbauer spectroscopy.

Discussion of Results

Results of the analysis of the product of green rust oxidation were consistent with ferric green rust. In our experiment, the oxidation of green rust by O_2 to ferric green rust occurred over a period of 24 h without the formation of other Fe^{III} oxide phases. However, the initial green rust was formed in the presence of phosphate and sorption of phosphate or silicate by green rust has been shown to promote oxidation of green rust to ferric green rust by suppressing the dissolution of green rust, a prerequisite for the formation of other ferric phases such as lepidocrocite or goethite. After re-inoculation, total Fe^{II} concentrations rebounded to pre-oxidation concentrations and green rust was observed as the dominant secondary mineralization product. Since phosphate and silicate are typically available in soils and sediments, similar conditions may be encountered in-situ. Thus, our results indicate the potential for cycling of green rust between reduced and oxidized forms under redox dynamics similar to those encountered in environments that alternate between iron-reducing and oxic conditions and are consistent with the identification of green rust in soils/sediments with seasonal redox cycling.

Using laboratory-derived mineral dissolution rates to test biogeochemical weathering in the field

AMANDA ALBRIGHT OLSEN[1*], ELISABETH M. HAUSRATH[2], EILEEN YARDLEY[1], MICHAEL BODKIN[1], JULIE L. BAUMEISTER[2], AND KIMBERLY NEGRICH[1]

[1]University of Maine, Department of Earth Science, Orono, Maine, amanda.a.olsen@maine.edu (* presenting author), eileen.spinney@maine.edu, michael.bodkin@maine.edu, kimberly_negrich@umit.maine.edu.
[2]Department of Geoscience, University of Nevada, Las Vegas, Las Vegas, Nevada. elisabeth.hausrath@unlv.edu, baumeis5@unlv.nevada.edu.

Chemical weathering controls the long-term carbon cycle over million year timescales. Accurate modeling of atmospheric CO_2 requires an understanding of the feedbacks between weathering and CO_2 in natural waters and the atmosphere. However, field-based chemical weathering rates are notoriously hard to measure. Conversely, laboratory-derived mineral dissolution rates are generally two to five orders of magnitude faster than those measured in the field (see [1] and cited references). Additionally, biology plays a critical role in weathering that is very difficult to simulate in the lab or measure in natural environments.

We measured serpentinite dissolution in both laboratory dissolution experiments and in field weathering experiments and modeled our results using the reactive transport code CrunchFlow to try to quantitatively interpret field weathering of serpentinite at two recently glaciated sites in Maine and California. Serpentinites exert a strong control on the ecosystyems that form on them due to the bulk chemistry of serpentinite rocks, high in Mg and trace elements, and low in nutrients such as Ca, K, P, and N, which causes an extreme and stressful environment for biota. Laboratory dissolution studies showed that lizardite dissolves six times times faster in the presence of oxalate, a biological exudate, than in inorganic acids at pH 5. Field samples of a deep profile of the Pine Hill Serpentinite on Little Deer Isle, Maine, show that Ca and other major elements are depleted from the bedrock at depths of up to 1 m, most likely due to the weathering of Ca-rich pyroxenes. Conversely, some trace metals including Cu and Zn show enrichment in the upper meter of the profile. Ongoing reactive transport modeling will allow us to quantitatively interpret the processes contributing to these observed profiles.

[1] Maher et al. (2006) *Geochimica et Cosmochimica Acta 70*, 337-363.

https://doi.org/10.1180/S0026461X00008434 Published online by Cambridge University Press

Experimental study of stibnite solubility and antimony complexation in aqueous sulfide solutions from 20 to 95˚C

NELLIE J. OLSEN[1, 2*], BRUCE W. MOUNTAIN[1], AND TERRY M. SEWARD[2]

[1]GNS Science, Wairakei Research Centre, Taupo, New Zealand, n.olsen@gns.cri.nz (*presenting author), b.mountain@gns.cri.nz
[2]Victoria University, Wellington, New Zealand, terry.seward@vuw.ac.nz

Modeling antimony transport and mobility in natural hydrothermal systems and mitigation of stibnite (Sb_2S_3) scaling in geothermal power stations require precise data on changes in stibnite solubility in response to small changes in pH, sulfide concentration, pressure and temperatures between 20˚C and 350˚C. There is some uncertainty in stability and stoichiometry of antimony(III) sulfide and hydrosulfide species (i.e. thioantimonites and oxythoantimonites) at 25˚C and at higher temperatures, the nature of the thioantimony(III) stoichiometry is poorly constrained.

We have conducted flow-through solubility experiments with natural stibnite to detemine the solubility of stibnite in aqueous sulfide solutions from pH 6.1 to 12.7 and sulfide contents from 0.01 to 0.06 molal S_{total} at 22˚C. Higher temperature experiments up to 60˚C have been completed at pH 11.1 and 0.006 molal S_{total} and experiments up to 95˚C and at variable pH are on-going. Our experimental results are similar to the solubilities found at 25˚C by [1]. Krupp(1988) concluded that $H_xSb_2S_4^{2-x}$ species are dominant between pH 3 to 12. We note that for arsenic(III)-sulfide/hydrosulfide interactions, the dominant thioarsenite stoichiometry is apparently as the $As(HS)_3$ moiety [2], [3], [4]. At 60˚C, our solubilities are also similar to solubilities extrapolated to higher pH and temperature from [1] but predict lower solubilities at 90˚C. Our measurements will provide a complete set of stibnite solubility data from 22˚ to 95˚C in reduced, sulfide-containing fluids and permit a new evaluation of the stoichiometry and stability of thioantimonite species over this temperature range.

References

[1] Krupp R. (1988) *Geochim. et Cosmochim. Acta* **52**, 3005-3015. [2] Bostick B.C., Fendorf S. and Brown Jr.G.E. (2005) *Mineral. Mag.* **69**, 781-795. [3] Beak D.G., Wilkin R.T., Ford R.G. and Kelly S.D. (2008) *Environ. Sci. Technol.* **42**, 1643-1650. [4] Zakaznova-Herzog V.P. and Seward T.M. (2012) *Geochim. Cosmochim. Acta* **76**, doi:10.1016/j.gca.2011.12.022.

Regional Erosion Surfaces and Climatic Readjustments, Midwest USA: Clues from late Pleistocene loess and paleosols (OIS 5e-2)

CAROLYN OLSON*

U.S. Department of Agriculture, Washington, DC, USDA carolyn.olson@wdc.usda.gov

Background

In the Midwestern, USA, early Wisconsinan time was marked by a series of events that until recently were not clearly linked to post-glacial climatic readjustment on a regional scale. Areas outside the Wisconsinan glacial border and adjacent to major river divides in several Midwestern states were examined in an attempt to locate similar adjacent regions on a scale comparable to continental glaciations.

Studies in the early 20th Century in northeastern Iowa identified an extensive erosion surface [1]. Buried by late Wisconsin loess, this surface cut the entire stratigraphic section from the Wisconsin till to the pre-Illinoian till and thus established its relative age as younger than Wisconsin till and older than late Wisconsin loess deposition. Radiocarbon dates for basal Wisconsinan soils, the uppermost unit truncated by the erosion surface, indicated an age of generally greater than 18000 BP. That age indicates its development was a direct response to shifts in climate associated with glacial retreat.

Wisconsin glaciation extended through much of the upper Midwest but at that time, there was no evidence that the surface in Iowa had parallels in adjacent regions. In the 1980's, we began studies of the Ohio/Wabash stream divides in southeastern Indiana traditionally known as "Illinoian till plain' stratigraphically, late Wisconsin loess overlying Illinoian till. From the investigations, it was determined that although the loess was present in a uniformly continuous blanket across these areas, there was little or no Illinoian till beneath. The late Wisconsin loess lay directly on bedrock, pedisediment, or older tills. Borings on subdued highs revealed that these erosional outliers contained complete stratigraphic sections that had been sequentially truncated by an erosions surface [2, 3]. Hidden beneath loess, this erosion surface had cut the slopes that descend in all directions from the remnant outliers to form the floor of the 'till' plain.

Recent Regional Evidence

The Mississippi/Ohio divide in southern Illinois within the Illinoian drift border and well south of the Wisconsinan drift border were examined most recently. Multiple coring sites and soil pits were located near the divides of tributaries to the Big Muddy River drainage. Here, as in Indiana and Iowa, undisturbed thicknesses of late Wisconsin loess directly overlie bedrock, pedisediment or older drift revealing erosional surfaces. Illinoian till is present only in protected coves of the subsurface landscape.

Conclusions

During the waning phases of the last glaciation in North America, a period of significant subaerial erosion occurred that remained largely unknown and undocumented, in part because of a lack of exposures and the difficulty in developing subsurface stratigraphic landscapes. The relative synchroneity, extent, and number of erosion surfaces outside the Wisconsinan drift border suggest a subaerial response to shifts in climatic events occurring during and immediately following the withdrawal of the last glacial ice sheet.

[1] Ruhe, R.V. (1969) *Quaternary landscapes in Iowa,* Iowa State University Press. [2] Gamble, E.E. et al. (1991) *Soil Survey Inv. Rept.* **41**, USDA. [3] Olson, C.G. (1989) *Catena Supplement* **16**, 129-142.

https://doi.org/10.1180/S0026461X00008434 Published online by Cambridge University Press

Nacre as a proxy for water-temperature and hydrostatic-pressure

IAN C. OLSON[1], AND PUPA U. P. A. GILBERT[1*]
[1]Department of Physics, University of Wisconsin, Madison, WI 53706, USA. pupa@physics.wisc.edu (* presenting author)

Many proxies of chemistry, temperature, salinity and pH are based on chemical measurement of mollusk shells, including elemental ratios, and isotopic ratios. These are chemical proxies. Here we present the first evidence of a structural proxy: mollusk shell nacre, or mother-of-pearl, and specifically the angle spread and thickness of aragonite ($CaCO_3$) tablets in modern nacre.

With 20-nm resolution, Polarization-dependent Imaging Contrast (PIC)-mapping [1-4] displays in grayscale the orientation of the aragonite crystal axes in mollusk shell nacre, and it also shows the tablet layer thickness (Fig. 1). Both parameters are species-specific [5]. Furthermore, we found a strong correlation between nacre crystal mis-orientations and environmental temperature, and between nacre tablet thickness and hydrostatic pressure [5]. These observations have far-reaching implications: Nacre tablet thickness may provide insight into the depth at which extinct mollusk species lived, whereas crystal orientations may be used as a paleothermometer of ancient climate, spanning 450 Myr of Earth history.

Thus far we only tested the "nacre as a proxy" hypothesis on modern nacre. Once validated on fossil nacre, e.g. from ammonites, this hypothesis will be put to a test.

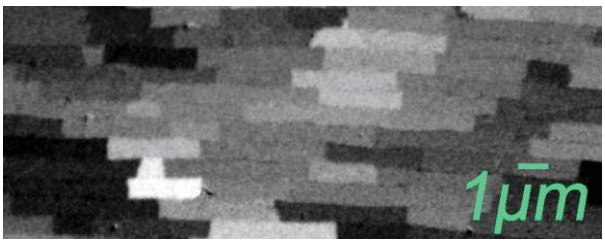

Figure 1: Polarization-dependent Imaging Contrast (PIC) maps of nacre from the fresh-water mussel shell of *Lasmigona complanata*. Different aragonite tablet crystal orientations are shown as different gray levels.

[1] Metzler (2007) *Phys. Rev. Lett.* **98**, 268102.
[2] Metzler (2008) *Phys. Rev. B.* **77**, 064110.
[3] Gilbert (2008) *J. Am. Chem. Soc.* **130**, 17519-17527.
[4] Gilbert (2011) *Procs. Natl. Acad. Sci. USA* **108**, 11350-11355.
[5] Olson (2012) *J. Am. Chem. Soc.* accepted for publication.

Dissolved elements released by the Grímsvötn volcanic ash, 2011

J. OLSSON[1,2*], S.L.S.STIPP[1], AND S.R.GISLASON[2]
[1]Nano-Science Center, Chemistry Department, University of Copenhagen, Denmark, jolsson@nano.ku.dk, stipp@nano.ku.dk
[2]Nordic Volcanological Centre, Institute of Earth Sciences, University of Iceland, Iceland, sigrg@raunvis.hi.is

During the evening of the 21st of May, 2011, the Grímsvötn volcano, located in southeast Iceland, began its strongest eruption in more than 100 years. The ash plume rose to 20 km and spread over Europe and the North Atlantic. The total amount of ash released was estimated by the Icelandic Meteorological Office to be more than 120 million tons and over 90% of it was released during the first 24 hours [1]. The purpose of this study was to measure the release rate of various elements during ash-water interaction and to assess the environmental impacts of the Grímsvötn ash.

Magmatic gases condense onto the surface of ash particles during a volcanic eruption. As the particles react with air and water vapour, the condensed gases form sulphuric and halogen acids and the ash surfaces dissolve [2]. The acid leaches cations from the bulk ash and secondary minerals can precipitate as a thin coating [3]. This material can be highly soluble in water, leading to rapid dispersal of possible harmful elements and/or nutrients into the enviroment when the ash comes into contact with rain or surface waters [e.g. 4].

In the present study, nanopure water (pH 5.9) was pumped through Teflon columns filled with ash of known surface area to monitor change in pH and the release of 70 elements, as a function of time. Initially, release rates were dominated by dissolution of surface salts, then after hours or days, by dissolution of the bulk volcanic ash. Within the first 10 minutes, the concentrations of most measured elements decreased by more than an order of magnitude, including some rare earth elements. Initially, S, Na, Ca, Mg and Cl dominated in the leachate, but after 12 hours, the most abundant element released was Si. The first water exiting the ash filled column had a pH of 7.3 and the pH gradually increased until it reached 9.7 at about 160 minutes. Over the next 4 weeks, pH slowly decreased to 6.5. The total release (mol/g ash) was determined for all harmful elements and compared with the World Health Organization (WHO) guidelines for safe drinking water [5]. The amount of Grímsvötn ash needed per litre of water, to exceed the WHO threshold values for As, Cd, Cr, F, Hg, and Pb, is 3.9, 35, 2.1, 0.10, 720, and 3.0 kg ash/l, respectively. Measured nutrients were P, Fe, V, Mo, and NO_3.

Our study provides valuable information for assessing the environmental impact of ash from volcanic eruptions on vegetation, livestock, and people.

[1] Arason *et al.* (2012) *30th NGW Meeting*, UV4-04 (abstr.), 150.
[2] Rose (1977) *Geology* **5**, 621-624.
[3] Delmelle *et al.* (2007) *Earth Planet. Sci. Lett.* **259**, 159-170.
[4] Gislason *et al.* (2011) *PNAS* **108**, 7307-7312.
[5] Guidelines for Drinking Water Quality (2008) *WHO Press*, Geneva.

https://doi.org/10.1180/S0026461X00008434 Published online by Cambridge University Press

High Arctic perennial spring activity and associated minerals: their value to Mars analogue studies

CHRISTOPHER R. OMELON[1]*, WAYNE H. POLLARD[2], DALE T. ANDERSEN[3], MARCOS ZENTILLI[4]

[1]Department of Geological Sciences, The University of Texas at Austin, Austin, Texas, USA, omelon@jsg.utexas.edu (*presenting author)

[2]Department of Geography, McGill University, Montréal, Québec, Canada, wayne.pollard@mcgill.ca

[3]The Carl Sagan Center for the Study of Life in the Universe, Mountain View, California, USA, dandersen@seti.org

[4]Department of Earth Sciences, Dalhousie University, Halifax, Nova Scotia, Canada, marcos.zentilli@dal.ca

Saline spring discharge in cold environments is of specific relevance to ongoing interest in the search for the presence of water on other planets such as Mars [1]. Inherent to this search is the goal of finding morphological or geochemical evidence that life once existed on these planets. To better understand what these biosignatures may look like, current work aims to understand both how life survives in analogous environments on Earth and how such life interacts with their surroundings to produce biosignatures that may be preserved over geologic timescales.

Saline perennial springs in the Canadian high Arctic are a unique target for such studies. The brines emerge from the subsurface at constant temperatures and flow rates despite extremes in seasonal climate conditions. Mineral precipitates associated with spring discharge include carbonates, sulfates, and chlorides, however the majority of mineral growth occurs during winter months when cold temperatures drive freezing fractionation of salts within the waters to produce large amounts of ice and ice-rich minerals including ikaite ($CaCO_3 \cdot 6H_2O$), mirabilite ($Na_2SO_4 \cdot 10H_2O$), and hydrohalite ($NaCl \cdot 2H_2O$). Halotolerant bacteria inhabit springs at several sites including Gypsum Hill Diapir, Colour Peak Diapir, and Wolf Diapir, but they are restricted to spring outlets where chemical energy such as sulfide and methane are present and temperatures remain near 0˚C. In contrast, it is hypothesized that a lack of energy source coupled with extremely high meaured salinities in waters emanating from Stolz Diapir limits microbial colonization of this habitat.

Examination of mineral precipitates from these sites by microscopy and synchrotron radiation show variations in mineralogies due to differences in source water geochemistry. There is scant evidence of microbial colonization of mineral surfaces or creation of biosignatures at Gypsum Hill and Wolf Diapirs due to low accumulations of mineral precipitates or the souble nature of minerals at near-freezing temperatures. At Colour Peak, however, bacterial sulfate reduction in the deep subsurface is recorded in carbonate precipitates as interbedded FeS_2 laminations, which may be distantly comparable to mineral precipitation associated with a nearby inactive fossil spring adjacent to the White Glacier that formed ancient deposits. Independent data suggests the fossil spring may have been active for several million years and involved warm brines originating at depth, a habitat that could have provided restricted ecological niches for microbial evolution.

[1] McEwen (2001) *Science* **333**, 740-743.

Lead Incorporation within Biological Apatite May Occur through a Polyphosphte Precursor

SIDNEY OMELON*[1]

[1]University of Ottawa, Toronto, Canada, somelon@uottawa.ca (* presenting author)

Introduction

Elevated levels of lead in seawater close to a lead and zinc mine in Greenland has been positivly correlated to lead levels in seaweed, mussels, prawns, and in the liver and bone of wolf-fish and sculpin [1]. Although environmental lead is known to report to bone, the pathway between lead injection and transport to bone mineral has not been elucidated. A new bone mineral nucleation theory suggests that a precursor to biological apatite is calcium polyphosphate. Polyphosphate chelates strongly to calcium, and other divalent cations such as lead [2]. It is possible that polyphosphate chelation to lead could be one of many biological strategies to immobilize lead and prevent it from reacting with other species. A lead-calcium-polyphosphate complex could also be a precursor to biological apatite.

Alkaline phosphatase has been associated with apatite biomineralization [3]; tissue-nonspecific alkaline phosphatase was shown to break down polyphosphate ions into orthophosphate ions [4]. It is proposed that breaking down a calcium polyphosphate complex into orthophosphates increases the apatite saturation and allows for apatite nucleation.

To determine if a lead-calcium-polyphospahte complex could be transformed into biological apatite containing lead, calcium-lead complexes were formed in neutral pH solutions, and exposed to alkaline phosphatase under basic pH conditions.

Figure 1 shows the powder x-ray diffraction of the reaction products.

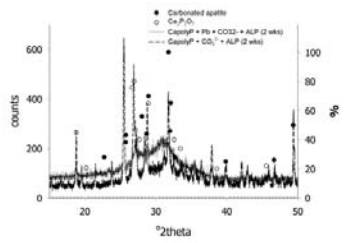

Figure 1: Powder x-ray diffraction of the products of exposing calcium- or lead-calcium polyphosphate to alkaline phosphatase for 2 weeks at 37 °C.

Results and Conclusion

Crystalline materials that have not yet been identified are the product of these in vitro experiments, however, this demonstrates that lead-calcium polyphosphate is a substrate for alkaline phosphatase. With further work on the experimental conditions, lead might be incorporated into biological apatite formed from the degradation products of lead, calcium, and polyphosphate.

[1] Johansen (1991) *Chemistry and Ecology* **5**, 35-55.
[2] Van Wazer (1950) *Journal of the American Chemical Society* **72**, 655-663.
[3] Robison (1923) *Biochemical Journal* **17**, 286-293.
[4] Omelon (2009) *PLoS ONE* **4**, e5634-49.

https://doi.org/10.1180/S0026461X00008434 Published online by Cambridge University Press

ARSENIC BIOREMEDIATION BY BIOGENIC IRON OXIDES AND SULFIDES

[1,2,3*]ENOMA O. OMOREGIE, [4,5]RAOUL-MARIE COUTURE, [4,5]PHILIPPE VAN CAPPELLEN, [1]CLAIRE L. CORKHILL, [1]JOHN CHARNOCK, [1]DAVID A. POLYA, [1]DAVID J.VAUGHAN, [3]KAROLIEN VANBROEKHOVEN, AND [1]JONATHAN R. LLOYD

[1]SEAES, The University of Manchester, Manchester, UK
[2]Department of Earth Sciences, Utrecht University, Utrecht, Netherlands
[3]Flemish Institute for Technological Research, Mol, Belgium
[4]School of Earth and Atmospheric Sciences, Georgia Institute of Technology, Atlanta, Georgia, USA
[5] Earth and Environmental Sciences, University of Waterloo, Waterloo, Canada
*Current location: Centro de Astrobiología, Madrid, Spain (omoregie@cab.inta-csic.es)

Millions of people globally are exposed to groundwaters that exceed the World Health Organization (WHO) safe guideline value of 10 ppb (or 0.13 μM) for arsenic in groundwater [1-3]. In this study we used microcosms containing sediment from an aquifer in Cambodia with naturally elevated levels of arsenic (As) in the associated groundwater to evaluate the effectiveness of microbially-mediated production of iron minerals for *in situ* As remediation. The microcosms were initially incubated without amendments to allow the microbial release of As, and other geogenic chemicals from the sediments into the aqueous phase. Following this period, either nitrate, or a mixture of sulfate and lactate were then added to stimulate biological Fe(II) oxidation and sulfate reduction, respectively.

Without treatment, soluble As concentrations in the microcosms reached 3.9 (±0.9) μM at the end of the 143 day experiment. However, As levels had decreased to 0.01 and 0.41(±0.13) μM in the nitrate, and in the sulfate with lactate treated microcosms, respectively by the end of the experiment. Analyses using a range of biogeochemical and mineralogical tools, indicated that sorption onto freshly formed hydrous ferric oxide (HFO) and ferrous iron monosulfide (FeS) are the likely mechanisms for As removal in the respective treatments. Incorporation of the experimental results into a one-dimensional transport-reaction model suggests that, under conditions representative of the Cambodian aquifer, the *in situ* precipitation of HFO would be effective in bringing groundwaters into compliance with the World Health Organization (WHO) safe water limit for As, although soluble Mn release accompanying biogenic HFO generation presents a potential health concern. In contrast, production of biogenic iron sulfide minerals would not remediate the groundwater As concentration below the recommended WHO limit.

[1] Smedley & Kinniburgh (2002) *Applied Geochemistry, **17**, 517-568*. [2] Ravenscroft P, Brammer H, Richards K (2009) *Arsenic Pollution: A Global Synthesis*. [3] Polya et al. (2005) *Mineralogical Magazine*, **69**, 807-823.

Geochemical and isotopic characteristics of Earth's early mafic crust: a comparison between Nuvvuagittuq and Isua greenstone belt metavolcanic rocks

J. O'NEIL[1*], H. RIZO[1], M. BOYET[1], R.W. CARLSON[2] AND M. ROSING[3]

[1] Laboratoire Magmas et Volcans, Clermont-Ferrand, France (*J.Oneil@opgc.univ-bpclermont.fr)
[2] Carnegie Institution of Washington, Washington DC, USA
[3] University of Copenhagen, Copenhagen, Denmark

Investigation of Earth's primitive crust largely has focused on felsic rocks because they are the most likely host rocks of zircons, providing robust geochronological constraints. However, these felsic rocks cannot be directly produced from melting of the mantle but instead originate by melting of an older mafic precursor. Despite the scarcity of preserved early mafic crusts, the Isua and Nuvvuagittuq greenstone belts are dominated by basaltic metavolcanic rocks. The Isua greenstone belt includes geochemically distinct subterranes dominated by tholeiites and boninite-like rocks (Garbenschiefer) interpreted to have been produced in an arc setting. Similarly, the Nuvvuagittuq belt is mainly composed of a succession of tholeiitic, boninitic and calc-alkaline rocks (Ujaraaluk unit) also sharing geochemical characteristics with suprasubduction related rocks. Both greenstone belts comprise rocks with ^{142}Nd anomalies compared to modern terrestrial Nd. Because ^{142}Nd anomalies can only be produced while ^{146}Sm decay was active, i.e. before 4 Ga, both suites of rocks acquired their ^{142}Nd isotopic composition in the Hadean. The Isua metavolcanic rocks were formed between 3.7-3.8 Ga. Therefore, their elevated ^{142}Nd isotopic composition is consistent with their Eoarchean derivation from an incompatible-element depleted Hadean mantle source. Consequently, they show no correlation between their ^{142}Nd/^{144}Nd and Sm/Nd ratios. However, the Nuvvuagittuq mafic rocks display a positive correlation between their ^{142}Nd/^{144}Nd and Sm/Nd ratios consistent with them being formed in the Hadean, between 4.3 and 4.4 Ga, from a "normal" depleted mantle. The Nuvvuagittuq rocks with the strongest arc-like signature have larger ^{142}Nd anomalies compared to the tholeiitic rocks. However, most Isua mafic rocks analyzed so far for their ^{142}Nd isotopic composition are tholeiites. Here we present a ^{146,147}Sm-^{142,143}Nd isotopic study of the Garbenschiefer which has the strongest arc-like signature in the Isua greenstone belt, allowing comparisons between the different groups of Isua mafic rocks. The studied set of Garbenschiefer rocks covers a relatively wide range of ^{147}Sm/^{144}Nd ratios (0.1650–0.2610) and preliminary analyses suggest that they also yield ^{142}Nd anomalies. The Isua and Nuvvuagittuq greenstone belts represent the oldest preserved mantle-derived suites of rocks and despite the fact that they were most likely formed ~500 million years apart, they share striking geochemical similarities. A geochemical and isotopic comparison between these greenstone belts will allow us to better understand the evolution of Earth's early crust through time and the geological processes responsible for its formation.

https://doi.org/10.1180/S0026461X00008434 Published online by Cambridge University Press

Pressure effects on sulfur mass-independent fractionation during SO_2 photolysis and its implication to the Archean atmospheric chemistry

SHUHEI ONO[1*] AND ANDREW WHITEHILL[2]

[1]Massachusetts Institute of Technology, Cambridge MA, USA, sono@mit.edu (*presenting author)

[2]Massachusetts Institute of Technology, Cambridge MA, USA, arwhite@mit.edu

Large $\Delta^{33}S$ values are measured in pyrite sulfur in rocks deposited before 3.2 Ga and between 2.7 Ga and 2.4 Ga, whereas those between 3.2 and 2.7 Ga yield relatively small $\Delta^{33}S$ values [1,2]. This apparent structure in the Archean $\Delta^{33}S$ signal may reflect changes in the atmospheric chemistry such as an incipient, transient rise of oxygen before the great oxidation event (i.e., *whiff of oxygen*) [1,3], the formation of organic haze aerosols [4], or a change in the redox state of volcanic gases [5].

In order to test various hypotheses, we performed laboratory SO_2 photolysis experiments using a flow through photochemical reactor with a Xe arc lamp as the light source. We will report the results of experiments to test the effect of pSO_2 and pN_2 on the pattern of multiple sulfur isotope fractionation. A new experimental system allows us to experiment at lower pSO_2 (i.e., low SO_2 column density) than using static photochemical cells. The results show that the $\delta^{34}S$, $\Delta^{33}S$ and $\Delta^{36}S$ signatures of the elemetnal sulfur product are a strong function of the SO_2 pressure under the tested range of pSO_2 (0.1 mbar and above), decreasing with decreasing pSO_2. The effect of bath gas pressure was also tested between 250 and 1000 mbar. The results of these experiments suggest that the change in the S-MIF pattern can be linked to the volcanic SO_2 loading in the atmosphere. The implications of this model will be discussed in the context of the early evolution of oxygenic photosynthesis and the resulting effect on the chemistry of the early atmosphere.

References

[1] Ono S. et al. (2006) *South African Journal of Geology*, **109**, 97-108. [2] Farquhar, J., et al. (2007) *Nature* **449**, 706-709. [3] Anbar, A.D. et al. (2007) *Science* **317**, 1903-1906. [4] Domagal-Goldman S. et al. (2008) *Earth and Planetary Science Letters*, **269**, 29–40 [5] Halevy, I., et al. (2010) *Science,* 329, 204-07.

Trace-element control on near IR transmittance of pyrite

M. ORTELLI [1*], K. KOUZMANOV[1], N. UBRIG[2]

[1] Earth and Environmental Sciences, University of Geneva, Switzerland (*correspondence: melissa.ortelli@unige.ch)

[2] Département de Physique de la Matière Condensée (DPMC), University of Geneva, Switzerland

Pyrite, which commonly occurs intergrown with economic ore minerals in a variety of hydrothermal deposits, can be transparent to near-infrared (NIR) light and has been therefore studied by NIR microscopy to observe internal features, such as growth zoning or fluid inclusions. The main limitation of the NIR petrography and microthermometric studies on pyrite is the transmittance of the mineral, which depends on its trace element content, the thickness and the crystallographic orientation of the section used [1].

In this study, we investigate growth zoning in pyrites from two different localities: i) the Toromocho porphyry Cu-Mo deposit, Peru, and ii) the Butte district, USA, by NIR microscopy, electron microprobe (EMP) analysis and FTIR spectroscopy to quantify the effect of minor and trace element substitutions on the NIR light transmittance of the mineral.

Pyrite samples from Toromocho exhibit growth zoning pattern controlled by trace amounts of Co and As. Both elements were often below the detection limit of the EMP, 75 and 470 ppm, respectively. However, As reaches 0.49 wt.% in IR-opaque growth bands (no transmittance detected by FTIR spectroscopy from 0.7 to 5 μm), while the presence of Co was revealed by FTIR transmitted spectrum with its characteristic IR absorption peak at 2 μm [2]. In pyrite samples from the Leonard Mine at Butte, oscillatory growth and sector zoning, observed in NIR light, is controlled by a high Cu content, reaching up to 2500 ppm in some growth bands (Figure 1).

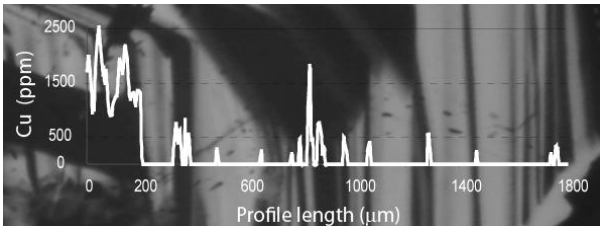

Figure 1 : IR transmitted-light photomicrograph of pyrite (Butte district) superposed to the electron microprobe line scan for Cu. The profile is 1800 μm long and is located along the X-axis.

Trace concentrations of As, Co and Cu decrease significantly the infrared transmittance in pyrite, which is the main limitation for a successful fluid inclusion study. Often trace element content is at the ppm level, thus requiring the use of more sensitive analytical technique, such as LA-ICP-MS, to correctly quantify trace amounts of these elements in the pyrite structure. Correlation between trace element content and quantitative FTIR transmittance spectroscopy allows preselection of samples potentially suitable for fluid inclusion studies.

[1] Lüders & Ziemann (1999) *Chem. Geol.* ***154****, 169-178***.**
[2] Kulis & Campbell (1999) *Geol. Soc. Am. Abstr. Prog.* **31(7)**, 170.

https://doi.org/10.1180/S0026461X00008434 Published online by Cambridge University Press

Interfacial water:properties explored with an Atomic Force Microscope

DEBROAH ORTIZ-YOUNG[1*], HSIANG-CHIH CHIU[2], SUENNE KIM[3] AND ELISA RIEDO[4]

[1]Georgia Institute of Technology, Chemistry Atlanta, Ga USA, dortiz3@gatech.edu
[2]Georgia Institute of Technology, Physics, Atlanta, Ga USA chc@gatech.edu
[3]Georgia Institute of Technology, Physics, Atlanta, Ga USA, suenne.kim@physics.gatech.edu
[4]Georgia Institute of Technology, Physics, Atlanta, Ga USA elisa.riedo@physics.gatech.edu

Structure and dynamics of ions and water at mineral-water interfaces: Insights from experimental and computational studies

The dynamic behaviour of water within nanometres of the solid interface and or under confinement has particularly interesting properties. One among many interests lies in the various geochemical applications [1]. Here, we present Atomic Force Microscope (AFM) force spectroscopy experiments which simultaneously capture the normal (structural) forces and lateral (viscous) forces as a function of tip-sample distance. To link the lateral force and interfacial viscosity, we modify the definition of Newtonian viscosity. When two plates are separated by d, the shear force required to slide one plate parallel to is proportional to the gradient of the fluid velocity, v_x, in the direction perpendicular to the plates.

$$F_L/A = \eta\,(\mathrm{d}v_x/\mathrm{d}z) \qquad (1)$$

The proportionality factor, η, is the viscosity of the liquid and A is the area of the shear. With substitution, we can relate the viscosity on a wetting surface Fig. 1(a), to that of a non-wetting surface, Fig. 1(b) to solve for the slip length, b [2]

$$\eta_{eff} = \eta^{b=0}\, v_{shear}/(d + b) \qquad (2)$$

Where $\eta^{b=0}$ is the interfacial viscosity of water, measured on a surface with zero slippage, and η_{eff} is the interfacial viscosity of water on a surface with slippage. This suggests the boundary viscosity of water strongly depends on the wetting properties of the surface.

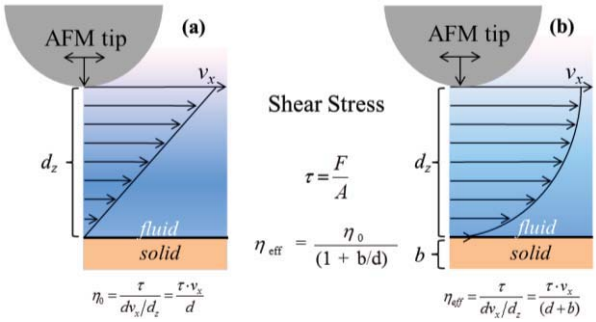

Figure 1. **Schematic of slip length from a shearing an AFM tip.** The wetting case is conveyed in (a) and non-wetting in (b).

We investigated the boundary viscosity and slip length as a function of gap size for mineral, crystalline and other carbon and carbon like surfaces. The slip length values will be discussed relative to surface properties, as well as surface wettability (contact angle), and viscosity.

[1] Stumm (1992) *Chemistry of the Solid-water Interface* **Wiley**.

The Pliocene closure of the Central American Seaway: reconstructing surface-, intermediate- and deep-water connections.

A. H. OSBORNE[1*], M. FRANK[1], R. TIEDEMANN[2]

[1]GEOMAR | Helmholtz-Zentrum für Ozeanforschung Kiel, Germany, aosborne@geomar.de (* presenting author)
[2]AWI, Alfred Wegener Institute for Polar and Marine Research, Bremerhaven, Germany.

Timing of Gateway Closure

The shoaling of the Isthmus of Panama and the associated reorganisation of deep-ocean circulation have been controversially reported as contributing to both a warming and a cooling of global climate. A resulting increase in moisture supply to the northern hemisphere, through the initiation or strengthening of the Gulf Stream, may have been an important precondition for Northern Hemisphere Glaciation. A robust timeframe for the closure of this major ocean gateway is essential for understanding its direct and indirect effects on global climate.

Method

We use radiogenic isotopes of Nd and Pb to reconstruct the history of shallow, intermediate and deep water connections between the Caribbean Sea and the eastern Equatorial Pacific Ocean from 5.0 to 2.0 million years ago. Surface water exchange is characterised using the Nd isotope composition of planktonic foraminiferal calcite. The Nd and Pb isotope compositions of early diagenetic ferromanganese coatings of the same sediment samples are employed to reconstruct intermediate and deep water exchange.

Results and Conclusion

Our results indicate that Caribbean Intermediate Water continued to diverge from a relatively constant Pacific deepwater Nd composition from 5.0 to 2.0 Ma. Comparison with published stable isotope and Mg/Ca records from the same ODP Sites 999, 1000 and 1241 suggest that Caribbean Intermediate Water composition continued to change even after a decrease in surface water exchange with the Pacific (4.5 Ma onwards [1]). A more rapid restriction of mixing between the Pacific and Caribbean at intermediate depths from 4 to 3.5 Ma clearly preceeded the major increase in ice-rafted-debris north of Iceland [2].

[1] Groeneveld *et al*. (2008) G^3 **9**, Q01P23. [2] Jansen *et al*. (2000) *Paleoceanography* **15**, 709-721.

https://doi.org/10.1180/S0026461X00008434 Published online by Cambridge University Press

Reduction of jarosite by *Shewanella oneidensis* MR-1 and its geochemical implication

BINGJIE OUYANG[1]*, XIANCAI LU[1], HUAN LIU[1], JIANJUN LU[1], JUAN LI[1], RUCHENG WANG[1]

[1] Nanjing University, School of Earth Sciences and Engineering, jessicaoy89@gmail.com (* presenting author)

Jarosite is a common mineral in acidic, sulfate-rich environments formed by the oxidation of sulfide in mining area. Decomposition of jarosite by dissimilatory iron reducing bacteria (DIRB) under acidic conditions has been well proved previously [1], and this process influences the mobility of many heavy metals accommodated in jarosite. However, the effects of DIRB on the stability of jarosite under neutral pH conditions have been seldom studied. This study aims to evaluate these effects, and provide a more comprehensive understanding of the geochemical mechanism.

Jarosite was synthesized by microbial oxidation of ferrous ion at 30 °C. The used bacteria strain was Shewanella oneidensis MR-1. We designed a series of batch experiments to study the microbial reduction process of jarosite under anaerobic, aerobic, and no inoculation conditions for 20 days. Lactate was added to the solution as electron donor for MR-1. Temporal evolution of Fe(II) and total dissolved Fe in solution was monitored everyday by using o-phenanthroline method. The concentrations of sulfate, lactate and acetate were determined by ion chromatography (IC). The content of K+ was examined by inductively coupled plasma optical emission spectrometer (ICP-OES). The compositions of the secondary minerals were analyzed by X-ray diffraction and scanning electron microscopy coupled with energy dispersive spectrometer. Diffuse reflection spectroscopy was employed to investigate the component of Fe-bearing minerals. Transformations of jarosite in 40 days and 80 days were also investigated to confirm the reduction process.

Results and conclusions

Our results indicate that jarosite can be reduced by MR-1 under anaerobic condition, and secondary mineralization accompanies the reduction process. Increases in Fe(II), K+, sulfate and acetate concentrations, and a decrease in lactate were observed for the biotic experiment. The release rate of Fe(II) was constant in the beginning period. Microscopic results demonstrated bacterial attachment to the surface of jarosite, which can be regarded as evidence of bacterial absorption. The formation of new minerals as goethite and some green rust was identified. Compared to anaerobic treatment, the concentrations of Fe(II), K+, and sulfate in aerobic treatment and no inoculation treatment were undetectable at first, and tremendously lower than anaerobic treatment after 40 days of reaction. However, reduction of jarosite in aerobic treatment and no inoculation treatment was severely limited, and secondary minerals were either not produced or undetectable.

Acknowledgement

We appreciate the support from the National Natural Science Foundation of China (Grant No. 40930742, 10979018).

[1] Bridge & Johnson (2000) *Geomicrobiol. J.* **17**, 193-206.

Dating zircons from volcanic ash beds in sedimentary successions: magmatic crystallization vs. ash deposition

M. OVTCHAROVA[1*], U. SCHALTEGGER[1], N. GOUDEMAND[2], AND H. BUCHER[2]

[1]Earth and Environmental Sciences, University of Geneva, Switzerland, maria.ovtcharova@unige.ch (*presenting author)
[2]Institute and Museum of Paleontology, Zurich, Switzerland

Detailed calibration of the Late-Middle Triassic time-scale requires precise and accurate age determinations from volcanic ash beds within biostratigraphically well dated marine sedimentary sections. High precision CA-ID-TIMS U-Pb zircon dates of volcanic ash beds have been used to quantify and calibrate the stratigraphic column across the Early-Middle Triassic boundary in South China. Despite an optimal control on the continuity of the stratigraphic record and on the accuracy of analytical procedures, some single ash-beds from the Monggan Wantuo section (Luolou Fm., NW Guangxi, S. China) yield ages that are too old and contradict the stratigraphic succession. How can we improve the confidence in the interpretation of zircon dates as proxies for the age of deposition of these ash beds?

We dated 15 samples of ash beds (four thereof with signs of sedimentary reworking) within the 15m Wantuo Mongan section, applying CA-ID-TIMS techniques on a number of single grains for each sample. In 13 out of 15 ash beds zircon dates are following the stratigraphic succession within analytical uncertainty (from the late Early Triassic Luolou Formation – 248.08 ± 0.12 Ma to the Middle Anisian Transition Beds – 246.43 ± 0.17 Ma). The zircons from two intermediate volcanic ash beds within the Transition Beds at the Early/Middle Anisian boundary yield well clustering $^{206}Pb/^{238}U$ dates at 247.10 ± 0.15 and 247.35 ± 0.11 Ma, clearly indicating that the zircons in this magma batch were crystallizing over a long period of time or remobilized from deeper levels within the same magmatic system. The problem of recurrent zircon dates in a sedimentary succession is common and can only be discovered by sufficiently dense sampling and a sufficient number of data for each ash bed.

We have to keep in mind that for the correct interpretation of dates in stratigraphic sections interlayered with fossil-bearing rocks we need: i) at least one single well preserved stratigraphic section with sufficient absolute or relative chronological control (biochronology, chemostratigraphy, astrochronology) to guarantee that the stratigraphic succession is accurately known; ii) volcanic ash beds that are as much undisturbed as possible (no volcaniclastic material, no sedimentary reworking); iii) sufficient sample and data density to be able to distinguish between magmatic and sedimentary signals coded in the crystallization ages of zircon.

https://doi.org/10.1180/S0026461X00008434 Published online by Cambridge University Press

Enhanced delivery of bioavailable Fe through glacial processes in Kongsfjorden, Svalbard

JEREMY D. OWENS[1*], LAURA M. WEHRMANN[1], ROBERT RAISWELL[2] AND TIMOTHY W. LYONS[1]

[1]University of California- Riverside, Riverside, CA, USA, jowens@student.ucr.edu, laura.wehrmann@ucr.edu, timothyl@ucr.edu (* presenting author)

[2]Leeds University, Leeds, UK, r.raiswell@earth.leeds.ac.uk

Primary production in large portions of the world's ocean is iron-limited, and the supply of bioavailable iron is not well understood. Only recently have glacially derived iron sources been considered a potential major contributor, particularly to high latitude regions. Past workers considered glacial iron to be non-bioavailable or non-reactive more generally. However, we now know that increased delivery of reactive iron to the ocean, as driven by enhanced glacial runoff, has the capacity to increase primary production and concomitant CO_2 uptake. Understanding the role of glaciers in the delivery of bioavailable iron to the ocean has become a priority, and the concentration and reactivity of glacial iron is likely controlled by chemical weathering processes tied to pyrite oxidation and bedrock type within the subglacial environment.

To better understand the factors controlling the delivery of bioavailable iron to glacial fjord environments, we sampled three proglacial streams in the Kongsfjorden region of Svalbard. The streams differed dramatically in the characters of their adjacent glaciers, in their suspended loads and the local bedrock. We quantified the amount of dissolved iron in the glacial meltwaters, determined the reactivity of the iron associated with the fine glacial flour of the streams, and constrained the iron properties of the source bedrock. Here, we present iron data (Fe_{Total}/Al and $Fe_{Highly\ Reactive}/Fe_{Total}$) from each sample type, along with riverine sulfate and bedrock sulfide isotope data ($\delta^{34}S$). The average dissolved iron concentrations varied from glacier to glacier between 4 ppb and 13 ppb, which is only 2 to 3 times higher than in seawater. However, highly reactive iron was enriched in the glacial flour samples at highly variable levels. The overarching suggestion is that the Kongsfjorden glacial systems could deposit large amounts of reactive iron into the fjords via the discharge of glacial flour. The three sampled meltwater streams have comparable and relatively stable pH (~8) coupled with $\delta^{34}S$ values of dissolved sulfate near +10‰, suggesting that the iron is from a source other than just pyrite oxidation. These initial data and specifically the observed variability indicate that bedrock type and other still unknown variables affecting diverse glacial processes control the delivery of bioavailable iron to the ocean in high latitude regions.

Modeling ocean acidification and de-oxygenation: Testing the linkage between large igneous province and Ocean Anoxic Event.

KAZUMI OZAKI [1*], EIICHI TAJIKA[2]

[1]University of Tokyo, Earth and Planetary Science, Tokyo, Japan, ozaki@eps.s.u-tokyo.ac.jp (* presenting author)

[2]University of Tokyo, Complexity Science and Engineering, Chiba-ken, Japan, tajika@k.u-tokyo.ac.jp

Recent geochemical data and chronology enable us to explore biogeochemical dynamics in geological past. The causal linkage between ocean anoxic events and activity of large igeneous provinces has been discussed based on the geochemical imformation, such as the rapid disturbances of osmium isotopic records or metal abundance anomalies before and during ocean anoxic events. It has been discussed that the abundance of nannoconid is rapidly decreased at the initiation of OAE1a, implying the oceanic acidification in sea surface environment. Considering the compensation mechanism of oceanic carbonate system, this must indicate drastic disturbances of Earth's surface environment.

We developed a new atmosphere-ocean biogeochemical cycle model in order to explore the biogeochemical consequences of the activity of large igneous province, and a systematic model sensitivity study is performed with respect to an injection scenario of CO_2 into the terrestrial environment. Examined characteristic timescale of the CO_2 injecation scenarios ranges from 100 year to several hundreds of thoushands of years and the total amount of injection ranges in three orders of magnitudes (0.01-10 EmolC).

Systematic examination shows that (1) the required CO_2 amount for the maximum carbon isotopic anomaly of +1 to 4 permil is approximately from 0.4 to 1.0 Emol (10^{18} mol), providing the theoretical requirements for the carbon isotopic anomaly accompanied with OAE2, and (2) such scenarios result in the global ocean de-oxygenation of approximately 40-80 % (depending on the degassing flux). Our simulation results also indicate that the rapid (less than 10 kyr) and drastic (greater than 100 TmolC/yr) CO_2 injection would be required to explain the strong acidification of sea surface waters and widespread carbonate gap. We conclude that the many characteristic features of OAEs can be explained by the short, rapid and frequent activity of large igneous province.

https://doi.org/10.1180/S0026461X00008434 Published online by Cambridge University Press

In-situ U-Pb dating of baddeleyite in Shergotty and a chassignite: Implications for Martian chronology

SHIN OZAWA[1*], TREVOR R. IRELAND[2], AHMED EL GORESY[3], EIJI OHTANI[1], MASAAKI MIYAHARA[1], AND YOSHINORI ITO[1].

[1] TohokuUniversity, Department of Earth Science, Sendai, Japan, shin.ozawa@s.tohoku.ac.jp (* presenting author)

[2] Australian National University, Research School of Earth Sciences, Canberra, Australia, trevor.ireland@anu.edu.au

[3] Universität Bayreuth, Bayerisches Geoinstitut, Bayreuth, Germany, ahmed.elgoresy@uni-bayreuth.de

Introduction

There is a long-standing debate on the crystallization ages of SNC meteorites, which are considered to be of Martian origin. As to shergottites, young ages of 165–475 Ma have been reported using various radiometric methods [1]. However, Bouvier et al. (2005, 2008) [2, 3] reported old Pb-Pb ages (~4.1 Ga) for basaltic shergottites Shergotty and Zagami, as well as young Rb-Sr, Sm-Nd and Lu-Hf ages (150–180 Ma) for the same meteorites. They concluded that the old ages are their crystallization ages, and the young ages correspond to the timing of shock metamorphism or aqueous alteration. Two different ages were reported for the chassignite NWA 2737. Misawa et al. (2005) [4] reported a whole rock Sm-Nd age of NWA 2737 chassignite as ~1.4 Ga, while Bogard et al. (2008) [5] obtained an ^{40}Ar-^{39}Ar age of 160–190 Ma for the same meteorite. We conducted *in-situ* U-Pb dating of baddeleyite (ZrO_2) in these meteorites using SHRIMP-II and -RG in order to clarify the crystallization ages of Shergotty and NWA 2737 chassignite.

Results and Discussions

We found seven baddeleyite in Shergotty and one baddeleyite in NWA 2737, which can be used for SHRIMP analyses. Before SHRIMP analyses, each baddeleyite was carefully characterized by using FE-SEM, micro-Raman spectrometry and EPMA. The size of the baddeleyite grains range from 3×5 μm to 11×24μm. Baddeleyite usually occurs with ilmenite, titanomagnetite and pyrrhotite.

SHRIMP U-Pb measurements of the seven baddeleyite in Shergotty revealed three clusters of data points on the Concordia diagram, corresponding to ages of ~230, ~400 and older than 3000 Ma, respectively. This result could indicate an old crystallization age of this rock (in excess of 3000 Ma) and recent partial age resetting due to shock-induced melting.

Three U-Pb measurements on the one baddeleyite in NWA 2737 chassignite revealed a U-Pb age of 1640 ± 70 Ma. This is consistent with, but slightly older, than the Sm-Nd age of 1420 ± 70 Ma reported by [4]. It suggests that NWA 2737 chassignite crystallized at 1.4–1.6 Ga and experienced a thermal event, probably by impact, at 160–190 Ma.

For a better understanding of the origin and history of these baddeleyite, FIB-TEM studies are in progress.

[1] Nyquist *et al*. (2001) *Chronology and Evolution of Mars* 96, 105-164. [2] Bouvier *et al*. (2005) *EPSL* 240, 221-233. [3] Bouvier *et al*. (2008) *EPSL* 266, 105-124. [4] Misawa *et al*. *MAPS* 40, A104. [5] Bogard and Garrison (2008) *EPSL* 273, 386-392.

https://doi.org/10.1180/S0026461X00008434 Published online by Cambridge University Press

Combining U and Sr isotope tracers to evaluate water sources and mixing relations in freshwater and estuarine wetlands

J.B. PACES[1*], J.Z. DREXLER[2], F. WURSTER[3], L.A. NEYMARK[1]

[1]U.S. Geological Survey, Denver, CO, USA, jbpaces@usgs.gov (*presenting author), lneymark@usgs.gov
[2] U.S. Geological Survey, Sacramento, CA, USA, jdrexler@usgs.gov
[3]U.S. Fish & Wildlife Service, Suffolk, VA, fred_wurster@fws.gov

Understanding wetland water supplies is important for managing these resources and determining habitat impacts due to climate change or other anthropogenic activities. However, identifying multiple sources and contributions is often difficult due to complex hydrologic, biologic, and chemical processes. Combined $\delta^{87}Sr$ and $^{234}U/^{238}U$ data from wetlands in NV and CA identified 3-component mixing patterns that were not easily recognized by other chemical approaches. Isotopes of Sr and U are particularly useful because they are relatively abundant, can be analyzed with high precision, may have large differences between sources, and remain unchanged by geochemical processes such as evaporation and mineral precipitation or biological fractionation. Mixing models form distorted triangular nets that bound the data and allow contributions from each source to be estimated.

Sources of water in wetlands on the Pahranagat National Wildlife Refuge (PNWR), NV consist of surface flow from high-volume springs from the regional carbonate aquifer and groundwater from local volcanic aquifers. Major ions and H-O-S isotopes are affected by evapotranspiration, mineral precipitation, and sulfate reduction. However, $\delta^{87}Sr$ and $^{234}U/^{238}U$ are unaffected and indicate a 70:20:10 mixture for the irrigation source and a range of mixtures depending on location and water management practices (fig. 1A).

Variations in river water and tidal influence in the Sacramento-San Joaquin Delta, CA, over the last 6,000 years were recorded by $\delta^{87}Sr$ and $^{234}U/^{238}U$ in peat cores. Plants take up substantial dissolved Sr during growth, whereas redox reactions at the peat-water interface causes immobilization of U dissolved in the water column. Analyses of peat cores show coherent changes in space and time, reflecting evolving mixtures of fluvial and seawater sources (fig. 1B). Contributions from hydraulic mine sediment with $\delta^{87}Sr$ >0.0 and $^{234}U/^{238}U$ activities ~1.0 are also apparent in peat-poor samples deposited between 1850 and 1963.

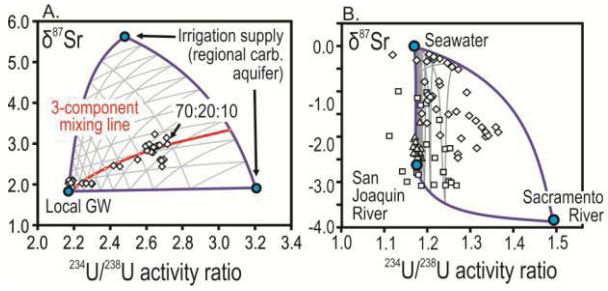

Figure 1: Three-component mixing models showing 10% intervals for water in the PNWR (A) and peat in the Sacramento-San Joaquin Delta (B).

Elucidating the complex thermal and fluid history of Austurhorn Intrusive Complex: zircon elemental and isotopic geochemistry

A.J. PADILLA[1*], C.F. MILLER[1], T.L. CARLEY[1], J.L. WOODEN[2], R.C. ECONOMOS[3], A.K. SCHMITT[3], C.M. FISHER[4] AND J.M. HANCHAR[4]

[1]Vanderbilt U., Earth & Environmental Sciences, Nashville, USA, abraham.j.padilla@vanderbilt.edu (*presenting author), calvin.miller@vanderbilt.edu, tamara.l.carley@vanderbilt.edu
[2]Stanford U.-USGS MAC, SHRIMP-RG Lab, Stanford, USA, jwooden@stanford.edu
[3]U. of California–Los Angeles, Earth & Space Sciences, Los Angeles, USA, economos@ucla.edu, axel@oro.ess.ucla.edu
[4]Memorial U. of Newfoundland, Earth Sciences, St. John's, Canada, c.fisher@mun.ca, jhanchar@mun.ca

The Austurhorn Intrusive Complex (AIC), comprising large bodies of granophyre, gabbro, and a mafic-felsic composite zone, is Iceland's best-studied intrusion (Blake 1966; Furman et al 1992a,b; Thorarinsson & Tegner 2009). However, despite widespread recognition of the value of zircon as a tracer of history and evolution of its parental magma(s), zircon studies are notably lacking for the AIC and other Icelandic plutons. Here, we present the first detailed chronologic, elemental, and isotopic Icelandic plutonic zircon study.

The elemental compositions of AIC zircons generally form a broad but coherent array which, for the most part, overlaps with that of zircons from Icelandic silicic volcanic rocks (Carley et al 2011). With some exceptions (see below), Ti concentrations range from 6-25 ppm (Ti_{zirc} temperatures ~ 730-870°C), and Hf concentrations are low (<10,000 ppm, typical of Icelandic zircon). Epsilon-Hf values are constrained to +13±1, falling between ε_{Hf} for Icelandic basalts from rift and off-rift settings. Similarly, $\delta^{18}O$ values are generally well-constrained at +3 to +4‰, consistent with Icelandic magmatic zircon (Bindeman et al 2012) and suggesting contributions from hydrothermally-altered crust to the petrogenesis of the parental silicic magmas. Zircons from a high-silica granophyre are notable exceptions to the trends described above: a large portion fall well outside of the AIC elemental array, distinguished primarily by extreme Hf concentrations ranging upward to 24,000 ppm (far higher than other analyzed Icelandic zircon), along with generally higher U and Th and lower Ti (down to 2 ppm [~630°C], lowest for Iceland). Their $\delta^{18}O$ values range from "normal" (+4) to extremely low (-6‰). Most of the elementally and isotopically unusual analyses are from CL-dark zones that display convolute and/or irregular zoning. We interpret these zones to reflect hydrothermal crystallization or recrystallization.

Zircon U-Pb geochronology reveals that the AIC was constructed by two distinct major intrusive events, the first at 6.45±0.04 Ma (MSWD=1.3) and a second at 5.99±0.06 Ma (MSWD=1.17). Most ages in the older population are from silicic rocks, while most ages in the younger populations are from a dominantly mafic zone. We interpret the younger age to represent the intrusion of voluminous basalt, which partially reactivated and remobilized the host silicic material ~500k.y. after initial emplacement of the AIC.

https://doi.org/10.1180/S0026461X00008434 Published online by Cambridge University Press

Tracking the Parental Melt of Chromite Using Trace Elements from LA-ICP-MS: an Effective Tool for Chromite Provenance

PAGÉ, PHILIPPE[1]*, BARNES SARAH-JANE[1]

[1] Canada Research Chair in Magmatic Metallogeny, Université du Québec à Chicoutimi, Québec, Canada, G7H 2B1; (Philippe_Page@uqac.ca); (Sarah-Jane_Barnes@uqac.ca)

Chromite is one of the first phases to crystallize in ultramafic - mafic silicate melts, and can thus be used to study early magmatic processes in volcanic and plutonic environments. A better understanding of chromite crystallization is also of economic interest, since it constitutes the only source of primary Cr, and massive chromitites can host important Platinum-Group Element (PGE) concentrations (e.g. UG2, Bushveld Complex).

In our ongoing work, we are studying the composition of chromites, obtained by EMPA and LA-ICP-MS, to i) constrain it's role in the fractionation of certain elements (e.g. Os, Ir, Ru, Sc, Ga, Ni, Co, …) during early magmatic processes (i.e. fractionation of Ru by komatiitic chromite [2, 3]) and ii) investigate the nature of the parental melt involved in the formation of chromitite in both oceanic and continental settings. Using this approach, we have shown a clear similarity between the geochemical signature of chromite from ophiolitic podiform chromitites and chromite from the primitive boninites [1]. This study aims to constrain the nature of the primitive melt involved in the formation of the Stillwater Complex chromitites which have a distinctive geochemical signature compared to chromites from various primitive ultramafic - mafic melts (Fig. 1) suggesting that none of these primitive magmas are involved in their formation. Also, these dissimilarities between the geochemical signature of chromite from the various lavas and from the Stillwater Complex chromitites can be used to discriminate them from one another and thus be used as a provenance mineral.

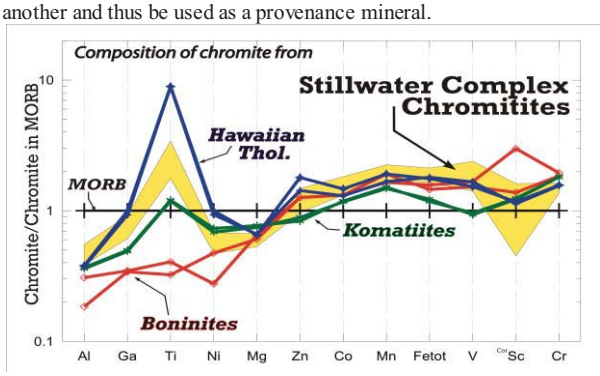

Figure 1: Composition of chromites from the Stillwater Complex chromitites compared to chromite from ultramafic-mafic volcanic rocks, including komatiite, boninite, and Hawaiian tholeiite, all of which have been normalised to the composition of the chromite from the MORB [1].

[1] Pagé & Barnes (2009) *Economic Geology* **104**, 997-1018.
[2] Pagé, Barnes, Bédard & Zientek (in press) *Chemical Geology,* 10.1016/j.chemgeo.2011.06.006.
[3] Locmelis, Pearson, Barnes & Fiorentini (2011) *Geochimica et Cosmochimica Acta* **75**, 3645-3661.

Neodymium isotopic composition of South Pacific bottom water

KATHARINA PAHNKE[1]*, CHANDRANATH BASAK[1] AND RAINER GERSONDE[2]

[1]Max Planck Research Group for Marine Isotope Geochemistry, Oldenburg, Germany (kpahnke@mpi-bremen.de)
[2]Alfred Wegener Institute, Bremerhaven, Germany

Neodymium isotope ratios in seawater are a useful tracer of water masses and marine biogeochemical processes, but our current knowledge of the distribution of Nd isotopes in the ocean is limited by the number of available data. Large areas, particularly in the Southern Ocean, remain unstudied. The international effort of the GEOTRACES program to map the global distributions of trace elements and isotopes in the ocean [1] is improving the basis for the use of Nd isotopes as tracers of present and past processes and changes.

Here we present water column and surface sediment Nd isotope ratios ($^{143}Nd/^{144}Nd$, expressed in ε_{Nd} notation) from the Pacific sector of the Southern Ocean collected during *R/V Polarstern* expedition ANTXXVI-2. Deep and bottom waters in the southwest Pacific within the Antarctic Circumpolar Current (ACC) have an isotopic composition of ε_{Nd} = -9, the characteristic isotope signature of the ACC in the South Pacific and Atlantic [2, 3]. At a station south of the ACC and just north of the Ross Sea (69°S), bottom waters with the temperature-salinity properties of Antarctic Bottom Water formed in the Ross Sea (RSBW), are more radiogenic (ε_{Nd} = -7). These values are consistent with the Nd isotopic composition of sediments and tills in the Ross Sea [4-6]), suggesting an imprint of the Ross Sea signal on RSBW.

We find similar ε_{Nd} values in the authigenic ferromanganese oxide fraction of surface sediments in the southeast Pacific at depths bathed by RSBW, suggesting the northward transport of the Ross Sea ε_{Nd} signal into the southeast Pacific. Our results show a clear contribution of Antarctic Nd sources on the isotopic composition of South Pacific bottom water and suggest that ε_{Nd} can be used to trace the northward flow of RSBW into the southeast Pacific.

[1] GEOTRACES Science Plan (2006) *SCOR*. [2] Stichel et al. (2012) *Earth Planet. Sci. Lett.* **317-318**, 282-294. [3] Carter *et al.* (2012) *Geochim. Cosmochim. Acta* **79**, 41-59. [4] Farmer *et al.* (2006) *Earth Planet. Sci. Lett.* **249**, 90-107. [5] van de Flierdt *et al.* (2007) *Earth Planet. Sci. Lett.* **259**, 432-441. [6] Roy *et al.* (2007) *Chem. Geol*. **244**, 507-519.

https://doi.org/10.1180/S0026461X00008434 Published online by Cambridge University Press

Controls on the formation and crystallization of Mg^{2+}-Fe^{3+}-SO_4^{2-} type layered double hydroxides

SUSANTA PAIKARAY* AND M. JIM HENDRY

Department of Geological Sciences, University of Saskatchewan, Saskatoon, SK, S7N5E2 Canada
Email-sup394@mail.usask.ca

Introduction

Layered double hydroxides (LDH) can play an important role in remediation of hazardous contaminants. Hydrotalcite-like (HTlc) LDH, also known as anionic clays, can be precipitated from numerous divalent (M^{2+}) and trivalent (M^{3+}) cations along with interlayer anions (A^{n-}) where the nature, M^{2+}/M^{3+} ratio and concentation of ions, hydrothermal conditions, aqueous pH can strongly control their formation and crystallization and, as such, their applicability to act as sorbents, catalysts, pharmaceuticals, etc. This study address such aspects using geochemical, spectroscopic, microscopic and diffractogram techniques.

Materials and Methods

HTlc formation was monitored using the coprecipitation synthesis method [1] at ambient temperature and pressure conditions and by varying the pH (7-13), M^{2+}/M^{3+} ratio (0.5-2.5), cation addition rate (2-100 ml h^{-1}), and cation concentrations (0.1-1.0 M) at a constant M^{2+}/M^{3+} ratio (1.0), while assessing the degree of crystallinity over 30 days at three temperatures (22, 65 and 95 °C) and two drying temperatures (100 and 200 °C). The resultant solid phases were studied using X-ray diffraction, Raman and ATR-Infrared spectroscopy, and SEM and thermogravimetric analysis.

Results and Discussion

Formation of HTlc was favored at pH ≥ 9 and $M^{2+}/M^{3+} \geq 0.75$ with both CO_3^{2-} and SO_4^{2-} as interlayer anions. The latttice parameters c and a determined at pH 13 and M^{2+}/M^{3+}=2.5 was ~23.5 Å and ~3.1 Å, respectively. Although HTlc formation was not greatly influenced by the reagent addition rate and M^{2+}-M^{3+} concentrations, slow addition appeared to inhibit development of $d_{(110)}$ plane representing poor 'a' crystallographic development, while slow addition and lower M^{2+}-M^{3+} concentrations facilitated slightly better crystallization. This may be explained by better nucleation and the lack of availability of elevated concentrations of cations [2].

The degree of crystallinity was observed to increase after ageing for 30 days at room temperature (RT, 22±2 °C), increasing the hydrothermal temperature to 95 °C within 1 day and increasing the drying temperature to 200 °C. The crystallization started lowering after 5 days and 1 day at 65 and 95 °C hydrothermal treatment, respectively.

Conclusions

Preliminary observations suggest increasing pH, M^{2+}/M^{3+} ratio, low M^{2+}-M^{3+} concentrations, and a slow mixing rate facilitate HTlc formation and enhance its crystallinity. Although HTlc is likely to develop crystallinity at RT upon prolonged exposure, elevated hydrothermal temperatures may adversely impact its structure.

[1] Cavani et al. (1991) *Catal Today* **11**, 173-301.
[2] Hickey et al. (2000) *J Mater Sci* **35**, 4347-4355.

Boron contamination at the McIntyre tailings, Timmins, Ontario

CORY PALIEWICZ[1]*, MONA-LIZA C. SIRBESCU[1], EDMOND H. VAN HEES[2], AND THOMAS SULATYCKY[3]

[1]Central Michigan University, Earth and Atmospheric Sciences, Mt. Pleasant, MI, USA palie1cc@cmich.edu (* presenting author)
[2]Wayne State University, Dept. of Geology, Detroit, MI, USA
[3]Goldcorp Inc., Timmins, Ontario, Canada

Anomalous concentrations of soluble boron of uncertain origin occur in >40 year old mine tailings of the McIntyre-Hollinger mesothermal gold deposit. We seek to understand 1) the distribution and movement of B in the tailings and 2) sources of soluble B including: the wall-rock of the mineralization, the gangue minerals, and anthropogenic borax that might have been used to smelt the gold ore.

To explore the distribution of boron within an area of about 100,000 m^2, eight boreholes (e.g. H1) were drilled manually to a depth of ~9 m and sampled at ~0.15 or ~1 m intervals. The samples were leached with deionized water at a sediment:water ratio of 1:3 and the filtered leachate was analyzed by ion chromatography. Boron is distributed heterogeneously with depth and distance from the edge of the tailings dam (Fig. 1). Boron contents correlate positively with the ≤38 µm grain size fraction, indicating that absorbtion onto silt-clay particles and/or low permeability result in B build-up. Tailings near surface and at the margin of the dams are coarser and depleted in B. Ephemeral, efflorescent hydrous Mg-borate found along the dam edge is consistent with an outflow of B along paths of high permeability.

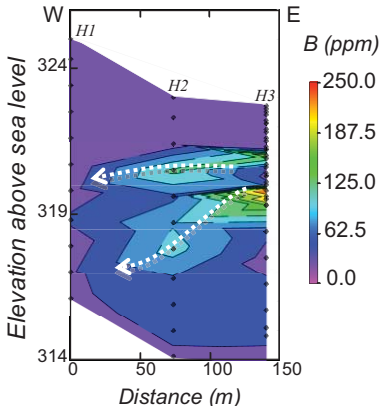

Figure 1: W-E cross-section of B (ppm) distribution and proposed discharge paths to edge of the dam ~20 m west of H1.

The unusual B contents in the McIntyre tailings might originate from altered basaltic wall-rock with B contents <3000 ppm. However, the erratic character of the anomaly suggests that the release of B from the disposal of crushed, borax-fluxed slag into the tailings is also possible. Fresh tourmaline in the tailings sediment and relatively soluble gangue minerals (anhydrite, calcite, siderite, etc.) with <6 ppm B (via laser ablation ICP-MS) cannot account for the amount of soluble B encountered.

https://doi.org/10.1180/S0026461X00008434 Published online by Cambridge University Press

Nature of fluids in the deep mantle (>300km) inferred from a carbon and nitrogen micro-analytical study of a single ultra-deep diamond from Kankan, Guinea

M. PALOT[1*], D.G PEARSON[1], R. STERN[1], T. STACHEL[1]

[1]Department of Earth and Atmospheric Sciences, University of Alberta, Edmonton, Canada, palot@ualberta.ca (* presenting author).

The nature of the deep mantle, especially the transition-zone, is a topic of very broad interest to solid Earth geochemists and geophysicists. Data on actual samples from this region are extremely scarce. Diamonds are derived from the base of the lithosphere down to the lower mantle (>660km) and provide a unique opportunity to sample this region of critical rheological and chemical changes in the Earth. In order to evaluate the nature of fluids percolating through the transition zone, we present the first carbon and nitrogen isotope micro-analytical study of a deep-diamond (Kankan, Guinea) by Secondary Ion Mass Spectrometry (SIMS). This diamond contains a single $CaSiO_3$-walstromite inclusion, presumed to represent retrogressed former $CaSiO_3$-perovskite and hence indicative of an ultra-deep (lowermost transition zone to lower mantle) paragenesis. The large size of the diamond allows to investigate variability in the diamond growth medium along detailed traverses. Combined C-N isotope and N abundance measurements allow us, for the first time, to place strong constraints on the nature of the parental fluid for an ultra-deep diamond.

Carbon isotopic compositions show a small but systematic decrease of $\delta^{13}C$ values from the core to the rim of the diamond. $\delta^{15}N$ is negatively correlated with $\delta^{13}C$, whereas nitrogen abundances show a positive correlation. These co-variations in $\delta^{13}C$-$\delta^{15}N$-[N] are consistent with open system isotopic fractionation where the isotopic and elemental evolution of the fluid is related to diamond crystallisation. The speciation of carbon and nitrogen of the fluid precursor of this deep diamond may be constrained through modelling of these co-variations. Such modelling indicates diamond growth from a reduced, CH_4-bearing fluid, with nitrogen behaving compatibly. Due to uncertainities in $\delta^{15}N$, we cannot constrain whether nitrogen was present in the fluid phase as N_2 or the NH_4^+. Although the origin of the diamond forming fluid (subducted or mantle material) is still a matter of debate, these results have fundamental implications for the fO_2 in the deep mantle and the deep volatile cycle of the Earth.

A critical evaluation of TEX_{86} derived sea surface temperatures in the Paleogene

RICHARD D. PANCOST[1*], KYLE TAYLOR[1] AND CHRIS HOLLIS[2]

[1]Organic Geochemistry Unit, School of Chemistry, The Cabot Institute, University of Bristol, UK, r.d.pancost@bristol.ac.uk (* presenting author)

[2] GNS Science, Lower Hutt, New Zealand

The application of glycerol dialkyl glycerol tetraether (GDGT) based sea surface temperature proxies (e.g. TEX_{86}) has brought about major advances in our understanding of Cenozoic climate. However, TEX_{86} approaches yield very high temperatures at high latitudes during Paleogene hyperthermals, and the resulting low latitudinal temperature gradients challenge our understanding of the physical climate system. Here, we examine existing TEX_{86} data and revisit the modern calibration dataset. A comparison of TEX_{86} SST estimates to those derived from oxygen isotopes or Mg/Ca ratios of well preserved 'glassy' planktonic foraminifera reveals a strong correlation between foraminiferal and GDGT-based approaches, but the latter are 4-6°C warmer. We have also compared TEX_{86} SST estimates from shelf sea settings to associated continental mean air temperatures (MAT) derived from soil bacterial GDGTs (the MBT/CBT index). Again, the two approaches exhibit a strong correlation but with the former yielding 4-6°C warmer temperatures. Intriguingly, SSTs derived from the recently proposed TEX_{86}^L approach are lower and consistent with foraminifera-based approaches and MBT/CBT derived MATs.

We also developed SST records from multiple sites in the SW Pacific, in order to place hyperthermal SST estimates into a longer-term Paleogene context. Our estimates indicate that sea floor and sea surface temperatures increased by 10°C or more from late Paleocene (18 to 23°C) to early Eocene times (30-32°C). MBT/CBT-derived MATs broadly parallel the SST trends, but with 4-6°C lower values throughout the entire sequence. These records suggest that elevated high southern latitude SSTs are reproducible at multiple sites and do document the relative long-term Paleogene climate evolution recorded by benthic foraminifera and inferred from faunal and floral assemblages.

Combined, these two lines of evidence indicate that high latitude EECO temperatures were indeed significantly higher than those of today, but they also suggest that the specific estimates could be as much as 4-6°C too warm. There are multiple explanations for this, but one possibility is an oceanographic and/or ecological control on the GDGT assemblages exported to sediments, an explanation that could also explain the unexpected offset between SSTs derived from TEX_{86}^L compared to other calibrations. Specifically, the offset in both ancient and modern settings is associated with low GDGT-2 to GDGT-3 ratios. In contrast to previous inferences, those low ratios are not limited to cold regions and in fact are associated with shallow water settings and upwelling zones. We propose that this reflects depth-dependant differences in GDGT distributions that are manifested differently in the various TEX_{86} calibrations, with some reflecting primarily shallow water signatures and others reflecting integration over a greater depth range.

https://doi.org/10.1180/S0026461X00008434 Published online by Cambridge University Press

Zinc isotopic variations among ordinary chondrites

RANDAL C. PANIELLO[1,*], FREDERIC MOYNIER[1], JEAN-GABRIEL FRABOULET[1]

[1]Dept of Earth and Planetary Sciences, Washington University, St. Louis, MO, USA, paniellor@wustl.edu (* presenting author)

Zinc is a moderately volatile element that may be capable of movement among minerals or even volatization during thermal metamorphism, despite the absence of partial melts. We obtained high-precision isotopic measurements of zinc by MC-ICP-MS 1,2] from a suite of 70 ordinary chondrites (OCs), in order to study their variation across the metamorphic range. The samples included 23 LL-, 26 L-, and 21 H-chondrites; 26 of the 70 were non-Antarctic falls, 3 were non-Antarctic finds, and 41 were Antarctic finds. Serial leachates were obtained from the LL3.0 Semarkona, and magnetic (metal), silicate and sulfide fractions were separated in three samples in order to determine the contributions of each phase to the total zinc budget. Three whole rock samples were broken into several smaller pieces and each was measured in order to determine the small scale homogeneity of the zinc isotopes.

The $\delta^{66/64}$Zn (reported against the JMC-Lyon standard) for the entire suite, combined with previous data [3,4] generally fell within a narrow range, with a mean of -0.04±0.13 (2se). There was no significant difference measured between Antarctic and Non-Antarctic samples. Isotopic fractionation showed a slight trend across OC subtypes LL<L<H, and unequilibrated OCs were lighter than equilibrated OCs in each subgroup, but these effects were modest. There was also a general trend across petrologicic grade, with the highest subtypes (5-7) heavier than the less metamorphosed subtypes (3-4), by 0.35‰ for LL to 0.68‰ for H. However, zinc concentration did not vary with metamorphic grade, but instead averaged 43-52ppm for all petrologic grades. Leachates and separates show that a large portion of the zinc in OCs is found in sulfide phases. On a small scall, these OCs exhibited a high degree of homogeneity.

The similar zinc content of all OCs rules out significant volatization with increasing metamorphism. Variations in zinc isotopic ratios may reflect pre-accretion nebular processes, or may represent closed-system metamorphic changes in which the zinc moves between phases in a mass-dependent process.

[1] Moynier et al. (2006) GCA **70** 6103-6117, [2] Moynier et al. (2011) **5**, 297-307, [3] Luck et al. (2005) GCA **69** 5351-5363, [4] Moynier et al. (2007) **71** 4365-4379.

Carbonaceous material associated with apatite in the Chassigny meteorite from Mars

DOMINIC PAPINEAU[1,2*]

[1] Department of Earth and Environmental Sciences, Boston College, Chestnut Hill, United States, dominic.papineau@bc.edu

[2] Geophysical Laboratory, Carnegie Institution of Washington, Washington DC, United States.

Following the biologically important elements is key for the search for life beyond Earth. Carbon and Phosphorous are two fundamental biological elements for all life on Earth, and are found throughout Earth's geological record in minerals like graphite and apatite. Associations between disordered carbonaceous material and apatite are reported here for the first time in an extraterrestrial sample. These mineral-pairs were found in the Chassigny meteorite which is an olivine cumulate rock from the Martian mantle. Raman spectra and microspectroscopic images show the presence of disordered carbonaceous material associated with hydroxylapatite-maskelynite inclusions in olivine grains. Optical and electron microscopy suggest that there is a petrogenetic connection between carbonaceous material, hydroxylapatite, maskelynite, Ni-rich pyrrhotite, Cr-rich spinel, orthopyroxene, and olivine. Carbonaceous material is often associated with hydroxylapatite in fields of dozens of 2-30 micron-sized maskelynite inclusions in olivine, which is interpreted here, on the basis of the Raman D- and G-bands, to represent precipitation from low-temperature hydrothermal fluids.

Focused Ion Beam (FIB) was performed to micro-fabricate targets of these mineral associations. Analyses by TEM-EDS show that hydroxylated apatite grains a few microns in size are embedded as inclusions in maskelynite, which was also observed by Raman spectroscopic imaging. In addition, we also found numerous Ni-rich pyrrhotite grains (with up to 4%wt Ni). Cr-rich spinels also occur throughout the olivine cumulates. Such a petrographic context is important because Fischer-Tropsch synthesis produces short-chain alkanes from the reduction of carbon monoxide by dihydrogen and catalyzed by metals such as Ni and Cr.

It is here proposed that apatite acted as a template for aromatic and aliphatic carbonaceous material to condense because apatite and graphite both have an hexagonal structure and there is a near-integer factor of 3.85 difference between their unit cell sizes. The discovery reported here is thus also relevant to the possibility of life on Mars, to the production of organic molecules on Mars (including traces of atmospheric methane), and also to yield a natural example of an early stage of non-biological organic synthesis for the transition from a prebiotic to a biological world.

https://doi.org/10.1180/S0026461X00008434 Published online by Cambridge University Press

Calcrete on Everglades tree islands: human occupation or tree growth?

JEANNE PAQUETTE[1*], MARIE GRAF[2], GAIL L. CHMURA[3], CAMERON BUTLER[4]

[1]Earth & Planetary Sciences, McGill University, Montreal, Canada, jeanne.paquette@mcgill.ca (* presenting author)
[2]Montreal, Canada, graf_marie@hotmail.com
[3]McGill University and Global Environmental and Climate Change Centre, Montreal, Canada, gail.chmura@mcgill.ca
[4]Bioresources Engineering, McGill University, Ste-Anne-de-Bellevue, Canada, cameron.butler@mail.mcgill.ca

New geochemical and petrographic analyses shed light on the origin of the "enigmatic" carbonate layer perched within the soil of some Everglades tree islands. For some time, archaeologists [1, 2] have noticed the presence a 45-70 cm thick calcareous layer in the islands of terrestrial vegetation perched just a meter above the flooded wetlands of the Everglades. This layer, impenetrable without heavy equipment, had been interpreted as a topographic high in the underlying karst platform. Schwadron's archeological excavations of selected islands revealed soil and artifacts below the carbonate layer and a midden just above the karst platform [3]. As Schwadron had not observed artifacts in the layer, she interpreted it as a hiatus in midden/peat deposition. The cultural age of artifacts above and below the layer suggested that it formed ~3800-2700 cal yr BP, a period corresponding to a broad scale climate change recognized in the southeast U.S. and associated with cultural changes from the Late Archaic (Archaic = 9k to 3.5k BP) to Early Woodland culture [4].

Another model [5] proposed for the development of the calcrete layer required no major climate perturbation, only the occurrence of distinct wet and dry seasons where evapotranspiration from vegetation might result in the reprecipitation of calcium carbonate around roots within the soil profile.

Our most recent investigations indicate that a major component of the hardened layer is detrital rather than pedogenic. Most calcareous fragments show textures of an oolitic limestone with isopachous meteoric cements. Their oomoldic porosity is typical of the local underlying Pleistocene bedrock (Miami Limestone). Pedogenic features (needle-fiber calcite, root casts) in the surrounding soil indicate that the limestone fragments have been dissolving in the peaty soil profile. Phreatic acicular calcite cements fill pores in phosphatic bone fragments throughout the layer, enhancing their preservation and fixing phosphorus within the tree island soil.

This provides evidence for layer development that requires neither abandonment nor climate change. The question remains as to whether these limestone fragments were pulled up from a karstic, rubble-covered bedrock by fallen trees or if they were left by human occupants. If vegetation simply enhanced the pedogenic cementation into cohesive calcrete layers of limestone fragments left by early human occupants, these layers might have value as stratigraphic markers.

[1] Mowers (1972) *Fla. Anthropol.* **25**, 129-131.
[2] Carr (2002) *Tree Islands of the Everglades*, 187–206.
[3] Schwadron (2006) *Antiquity* **80**.
[4] Kidder (2010). *Anthropol. Papers AMNH*, **93**, 23-32.
[5] Graf, Schwadron, Stone, Ross, Chmura (2008) *Eos Trans. AGU* **89**, 117-124.

How large is the subducted water flux? New constraints on mantle regassing rates

RITA PARAI[1*] AND SUJOY MUKHOPADHYAY[1]

[1]Harvard University, Cambridge, MA, USA, *parai@fas.harvard.edu

Constraints on the long-term cycling of water between the mantle and exosphere (i.e., the atmosphere, oceans and crust) are critical to our understanding of mantle rheology, the structure and style of mantle convection [1], and the volatile budget of our planet. Volcanic water output from the mantle is offset by input at subduction zones in the form of chemically-bound water in subducting slabs. Water released from subducting slabs at high pressures and temperatures is outgassed to the exosphere by arc and back-arc volcanism. Any water entrained in the mantle wedge or retained in the slab beyond depths of magma generation constitutes a return flux of water to the interior, often referred to as the post-arc subducted water flux. Estimates of the magnitude of the total input flux of water at subduction zones and the magnitude of the return flux beyond arcs into the deep mantle have been used to discuss long-term regassing of the mantle [2-5]. However, these estimates vary widely, and some are large enough to have reduced the volume of water in the global ocean by a factor of two over the Phanerozoic.

In light of uncertainties in the initial hydration state of subducting slabs, magma production rates and mantle source water contents, we use a Monte Carlo simulation of the deep Earth water cycle to set limits on long-term mantle regassing. The simulation is constrained by reconstructions of Phanerozoic sea level change, which suggest that ocean volume is near steady-state, though a sea level decrease of up to 360 m may be supported [6-8]. We find that previous estimates of both the input flux of water into subduction zones and the return flux beyond depths of magma generation are frequently too large to reflect long-term water cycling. Our results [9] suggest a limited extent of serpentinization in subducting lithospheric mantle. For a near steady-state exosphere (0-100 m sea level decrease), we find an average return flux of 1.4–2.0 x 10^{13} moles/yr, corresponding to 2-3% serpentinization in 10 km of lithospheric mantle. For a maximum sea level decrease of 360 m, the average return flux is 3.5 x 10^{13} moles/yr, corresponding to 5% serpentinization in 10 km of lithospheric mantle. Our estimates of the return flux of water past arcs are up to 7 times lower than previously suggested [2-5; 9]. The net imbalance between our estimates of the return flux and the mantle-derived output flux gives an upper limit bulk mantle regassing rate of 24 ppm/Ga. Furthermore, our results indicate that while water in the mid-ocean ridge basalt source may be accounted for by recycling of water carried in subducted slabs, recycled slab water contents may not be high enough to account for the water contents of the ocean island basalt (OIB) source, such that some fraction of OIB source water appears to be juvenile.

[1] Crowley et al. (2011) *EPSL* **310**, 380-388. [2] Schmidt and Poli (1998) *EPSL* **163**, 361-379. [3] Hacker (2008) *Geochem. Geophys. Geosyst.* **9**, 24. [4] Rüpke et al. (2004) *EPSL* **223**, 17-34. [5] van Keken et al. (2011) *JGR Solid Earth* **116**, B01401. [6] Vail et al. (1977) *AAPG Memoir* **26**, 63-97. [7] Haq et al. (1987) *Science* **235**, 1156-1167. [8] Hallam (1992) *Phanerozoic Sea Level Change*. [9] Parai and Mukhopadhyay (2012) *EPSL* **317-318**, 396-406.

https://doi.org/10.1180/S0026461X00008434 Published online by Cambridge University Press

Role of Syntrophy in the Microbial Reduction of Crystalline Iron Oxides

MADHAVI PARIKH[1,*], TAMAR BARKAY[1], NATHAN YEE[1]

[1]School of Environmental and Biological Sciences, Rutgers University, New Brunswick, NJ, USA
(*correspondence: madhavi@eden.rutgers.edu)

Background

Syntrophic microbial consortia composed of anaerobic bacteria are able to catalyze electron transfer reactions that a single organism cannot [1]. Syntrophy is a community-level process that involves interspecies exchange of metabolites between organisms. Cooperative exchange of electrons and hydrogen in microbial communities is known to play an important role in the fermenation of complex natural organic matter to CO_2 and CH_4. Currently, the role of syntrophy in the the reduction of crystalline iron oxides is poorly understood. Here we examined the reduction of crystalline iron oxides by an anaerobic microbial consortium during fermentative growth. We present evidence that the rapid iron reduction rates are enabled by syntrophic interactions between the bacteria that form this consortium.

Materials and Methods

A consortium composed of two microorganisms was cultivated from a sediment core collected from the United States Department of Energy Field Research Center (FRC) in Oak Ridge Tennessee. The consortium consists of a fermenting *Clostridium* species and a hydrogen-oxidizing bacterium belonging to the family *Vellionellaceae*. Iron reduction experiments were conducted to evaluate the ability of this consortium and pure culture to reduce goethite, hematite and ferrihydrite during fermentation of peptone. At periodic time points, samples were collected and analysed for Fe(II) and hydrogen production by ferrozine assay and gas chromatography, respectively. PCR amplification of the 16S rRNA genes and denaturing gradient gel electrophoresis (DGGE) analysis were performed to determine the dominant member of the microbial community.

Results and Discussion

When grown on fermentable substrates, the microbial consortium reduced goethite (α-FeOOH) and hematite (Fe_2O_3) with specific log reduction rates of -3.1 and -3.3 pmol m^{-2} h^{-1} $cell^{-1}$, respectively. DGGE analyses indicated that the *Clostridium* species was the dominant member in the consortium during the reductive dissolution of crystalline iron oxides. In pure culture, the *Clostridium* species was able to reduce ferrihydrite, but it reduced goethite and hematite at 4 to 5 times lower rates than the intact consortium. Finally, we show that the *Clostridium* species produces hydrogen during fermentation, and that the growth of the *Vellionellaceae* partner is stimulated by the presence of H_2 gas. These results suggest that interspecies hydrogen transfer may play a key role in controlling the rates of crystalline iron oxide reduction by fermentative microbial communities.

[1] Summers *et al.*, (2010) *Science*, **330**, 1413-1415.

Profile of sulfate isotopic composition of Lake Matano, Indonesia

G. PARIS[1*], J.F. ADKINS[1], A.L. SESSIONS[1], S.A. CROWE[2], C. JONES[2], D.A. FOWLE[3], D.E. CANFIELD[2]

[1] Division of Geological and Planetary Science, California Institue of Technology, Pasadena CA, USA
[2]Institute of Biology, Nordic Center for Earth Evolution, University of Southern Denmark, Odense, Denmark
[3]Departement of Geology, University of Kansas, Lawrence KS, USA
*corresponding author: gparis@caltech.edu

Lake Matano, Indonesia, is one of the ten deepest lakes in the world and the largest modern ferruginous basin [1,2]. Despite a low thermal gradient, a persistent chemocline at 100 m isolates surface waters with low sulfate concentrations (<25 µmol.l^{-1}) and sulfate-free deep waters [1]. The chemical properties of Lake Matano make it a prospective analogue for the ferruginous Archean ocean and it has been used to study the potential role of anoxygenic phototrophic Fe(II)-oxidizing bacteria in the synthesis of Banded Iron Formations [1] as well as carbon cycling in ferruginous settings [2]. Dissolved sulfate is completely removed between 100 and 150 m by sulfate reduction. However, very low concentrations of sulfide are observed in the Fe(II)-rich chemocline because of efficient removal by precipitation of FeS [2].

To explore the biogeochemical cycling of sulfur in Lake Matano, we investigate the isotopic composition of sulfur in sulfate ($\delta^{34}S_{SO_4}$) from a water profile spanning the surface and chemocline of the lake. Because of the low concentrations of sulfate make the analysis of the sulfur isotopic composition of SO_4 with conventional $BaSO_4$ precipitation is nearly impossible because it would require a huge amount of sample. Here, we use a recently developed method for $\delta^{34}S_{SO_4}$ analysis using the ThermoScientific 'Neptune' multicollector inductively-coupled plasma mass spectrometer (MC-ICPMS). This method allows us to measure the isotopic composition of sulfur from trace sulfates in natural samples. Sulfate was extracted from lake waters using a cation-exchange resin (Dionex AG50X8) and analyzed on the Neptune as Na_2SO_4. Furthermore, using a Cetac 'Aridus' as an introduction system decreases isobaric interference due to O_2 isotopologues on the isotopes ^{32}S, ^{33}S and ^{34}S and ^{32}S-H on ^{33}S. We will also explore the triple isotope variability of this unique system using our new MC-ICPMS method.

Reproducibility of $\delta^{34}S$ better than 0.2 ‰ (1σ) is achieved by running 5 to 20 nmol of sulfate (1 to 10 ml of waters from Lake Matano). Results will provide new constraints on the fractionation of sulfur isotopes in sulfate-poor water, thus helping to constrain our understanding of sulfur cycling during Archean times in a ferruginous ocean.

[1] Crowe, Jones, Kastev, Magen, O'Neill, Sturm, Canfield, Haffner, Mucci, Sundby and Fowle (2008), *Proceedings of the National Academy of Science* **105,** 15938-15934
[2] Crowe, Kastev, Leslie, Sturm, Magen, Nomosatryo, Pack, Kessler, Reesburgh, Roberts, Gonzalez, Douglas, Haffner, Mucci, Sundby and Fowle (2011), G*eobiology* **9**, 61–78

https://doi.org/10.1180/S0026461X00008434 Published online by Cambridge University Press

A biogeochemical orientation study in Mo skarn deposits, Jecheon distict, Korea

JI-YOUNG PARK[1*], JONG-NAM KIM[1, 2], AND HYO-TAEK CHON[1]

[1]Seoul National University, Department of Energy Resources Engineering, Seoul, Republic of Korea, jypakr05@snu.ac.kr (*presenting author), chon@snu.ac.kr

[2]Korea Resources Coportation, Seoul, Republic of Korea, kimjn@kores.or.kr

A biogeochemical orientation survey was conducted in the vicinity of Mo skarn deposits in Jecheon district in Korea. A skarn zone of over 600 m length is hosted in Ordovician carbonate sediments and is adjacent to both Jurrassic and Cretaceous felsic intrusives. Molybedenum occurs in fracture zones within the skarn and in disseminated form. The skarn ore minerals consist mainly of scheelite, molybdenite, galena, and chalcopyrite. The total samples of rocks, soils, and plants – daimyo oak leaves/branches (*Q. dentata*) and sargent cherry leaves (*P. sargentii*) – were collected from the target area and barren control area, and analyzed by ICP-MS. Each of three sampling lines was designed to cross the orebody at 30 m spacing intervals. The soil samples (n=36/10, target/control) collected from the target area show higher values of Mo (<0.1~38.7 ppm) compared with those from the control area (<0.1~3.2 ppm Mo). In all of the plant samples (n=108/30, target/control), Mo concentration from the target area (2.7~95 ppm in *Q. dentata* leaves, 0.2~99.1 ppm in *Q. dentata* branches, and 1.7~69 ppm in *P. sargentii* leaves) is 3~7 times higher than that from the control area (1.9~10.3 ppm in *Q. dentata* leaves, 0.9~6.3 ppm in *Q. dentata* branches, and 2~5 ppm in *P. sargentii* leaves). The variation patterns of Mo in plants are similar to those in soils, suggesting a corresponding Mo anomaly and contrast between soils and plants. The values of Mo in soils and plants are strongly correlated. The biological absorption coefficient (BAC) of Mo in the plants is generally high (*Q. dentata leaves* = 15 and *Q. dentata* branches/*P. sargentii* leaves = 9.1). The three plant organs have high possibilities to be used as indicators for the biogeochemical prospecting of Mo.

Delamination of subcontinental lithosphere beneath the Korean Peninsula: evidence from ultramafic xenoliths in Cenozoic basalts

KYE-HUN PARK[1*], YONG-SUN SONG[2]

[1]Pukyong National University, Earth Environmental Sciences, Busan, Korea, khpark@pknu.ac.kr (* presenting author)

[2]Pukyong National University, Earth Environmental Sciences, Busan, Korea, yssong@pknu.ac.kr

The Cenozoic alkali basalts are widely scattered over Korea and often carry spinel lherzolite xenoliths, indicating that the lithospheric thickness beneath Korea does not reach deep enough to the garnet lherzolite stability field. Interestingly enough, the spinel peridotite xenoliths from Korean peninsula can be divided into two groups based on their geochemical and Sr, Nd, Hf and Pb radiogenic isotopic compositions, i.e. enriched group and depleted group. The former xenoliths have enriched isotopic compositions very similar to their host basalts but show refractory nature of major element compositions with quite low CaO and Al_2O_3 contents indicating their derivation from the old Paleoproterozoic subcontinental lithospheric mantle beneath the Korean peninsula. In contrast, the latter have depleted isotopic compositions similar to mid-oceanic ridge basalts with apparently fertile major element compositions of relatively high CaO and Al_2O_3 contents similar to present day asthenospheric mantle indicating that such asthenosphere-derived materials may have replaced the lithosphere quite recently. In general, the host basalts show isotopic compositions similar to the enriched xenoliths, indicating genetic link between them.

Simple geobarometric calculations indicate that the depths of origination of the xenoliths are in average of ca. 75 km, suggesting that the maximum thickness of the subcontinental lithosphere would not exceed such depth quite much. On the contrary, the crustal evolution of the Korean peninsula seemingly started since the Archean, at least some part of it, suggesting normal lithospheric thickness of 150 km or greater. Such lithospheric thickness of the Korean peninsula significantly thinner than expected is quite similar to the case of North China Craton having lithospheric thickness of ca. 80 km in average, suggesting significant delamination of the lithospheric mantle in a depth scale of a few tens of kilometers during the past geologic time. Such delaminations may have occurred after the continental collisional events of Paleoproterozoic and early Mesozoic, suggested by wide occurrences of igneous and metamorphic events during the 1.9-2.0 Ga and also during the early Mesozoic throughout the Korean peninsula.

https://doi.org/10.1180/S0026461X00008434 Published online by Cambridge University Press

Adsorption of organics and nanoparticles at mineral-water interfaces.

STEPHEN C. PARKER[1*], THOMAS V. SHAPLEY[1], RUNLIANG ZHU[1,2], AND MARCO MOLINARI[1]

[1]Department of Chemistry, University of Bath, Bath BA2 7AY, United Kingdom, s.c.parker@bath.ac.uk (* presenting author)
[2]Key Laboratory of Mineralogy and Metallogeny, Guangzhou Institute of Geochemistry, Chinese Academy of Science, Guangzhou, 510640, China

We present our recent work, developing and applying complementary computational methods to gain atomistic insights into systems comprising mineral-organic-water interfaces. The research scheme involves the use of *ab initio* including van der Waals interactions and experimental data to validate rigid-ion or polarizable potential models which are then applied within energy minimization (EM) and classical molecular dynamics (MD) techniques. This robust approach covers the evolution of systems of different sizes and for different lengths of time allowing the evaluation of structures and dynamic properties.

The focus of our attention is on layered minerals including metal hydroxides, clay minerals and organo-clays interacting in the aqueous environment. The presence of organo-compounds (OCs) and nanoparticles (NPs) which can impact on the environment by entering the food chain, can also disrupt the mineral/water interfaces affecting the physico-chemistry of aqueous systems.

Several examples are discussed including adsorption and transport of OCs on montmorillonite and pyrophyllite and of fullerene on brucite in the presence of water capturing their atomistic features and helping to interpret experiments. The CLAYFF [1] and GAFF [2] or CVFF [3] force fields are applied to the clay surfaces and OCs and NPs respectively. Flexible TIP3P [4] and shell models of water are used in solvated systems. Interatomic potentials are tested against DFT calculations using VASP [5]. EM and MD employ the METADISE [6] and DL_POLY [7] codes.

Our results indicate that the interplay between the adsorption, which is surface-site as well as counter-ion-site dependent, and the transport of OCs and NPs on soil clay significantly disrupts the structure of the mineral-water interface [8,9] which has previously been shown to extend well above both mineral and nanoparticle surfaces [10]. Finally we find that the energy of adsorption is strongly affected by the inclusion of the van der Waals interactions within the DFT simulations and of the polarizability terms in the potential models within classical techniques.

[1] Cygan *et al.* (2004) *J. Phys. Chem. B* **108**, 1255-1266. [2] Wang *et al.* (2004) *J. Comp. Chem.* **25**, 1157-1174. [3] Dauber-Osguthorpe *et al.* (1988) *Proteins: Structure, Function, and Genetics* **4**, 31-47. [4] Cornell *et al.* (2006) *J. Am. Chem. Soc.* **117**, 5179-5197. [5] Kresse & Furthmuller (1996) *Phys. Rev. B* **54**, 11169-11186. [6] Watson *et al.* (1996) *J. Chem. Soc., Faraday Trans.* **92**, 433-438. [7] Smith & Forester (1996) *J. Mol. Graph.* **14**, 136-141. [8] Zhu *et al.* (2011) *Adv. Mater. Res.* **233-235**, 1872-1877. [9] Zhu *et al.* (2011) *Environ. Sci. Technol.* **27**, 6504-6510. [10] Spagnoli *et al.* (2011) *Langmuir* **27**, 1821-1829.

Magnesium isotope fractionation during bacterial mediated carbonate precipitation

I. J. PARKINSON[1*], C.R. PEARCE[1], T.K. POLACSEK[2], C.S. COCKELL[3], M.M. GRADY[2]

[1]Department of Environment, Earth and Ecosystem, The Open University, Walton Hall, Milton Keynes, MK7 6AA, UK
[2]Department of Physical Sciences, The Open University, Walton Hall, Milton Keynes, MK7 6AA, UK
[3]School of Physics and Astronomy, University of Edinburgh, James Clerk Maxwell Building, Edinburgh, EH9 3JZ, UK
[*]i.j.parkinson@open.ac.uk

Magnesium is the eight most abundant element in the Earths crust, and the fourth most abundant species in seawater. As such it is an essential component of life, with pivotal roles in the generation of cellular energy as well as in plant chlorophyll[1]. The bio-geochemical cycling of Mg is associated with mass dependant fractionation (MDF) of the three stable Mg isotopes, ^{24}Mg, ^{25}Mg and ^{26}Mg[1]. The largest MDF of Mg isotopes has been recorded in carbonates, with foraminiferal tests displaying the lowest $\delta^{25}Mg$ and $\delta^{26}Mg$ compositions[2].

Bacterial carbonate precipitation is known to have occurred in modern and ancient Earth surface environments[3,4], with cyanobacteria having a dominat role in carbonate formation during the Archean. In this study, we aim to better constrain the extent to which Mg isotope fractionation occurs during cellular processes, and to identify when, and how, this signal is transferred to carbonates. To quantify these effects we have performed biologically-induced carbonate precipitation experiments using several bacteria strains. The organisms are grown under defined organic and Ca/Mg ratios in artificial seawater, and under temperature controlled conditions that promote carbonate formation. Carbonate spheres of ~100 microns diameter are produced, which are amenable to SEM, EMP and Mg isotopic analysis by MC-ICP-MS. In order to compare our experimental data to natural samples we will present Mg isotope data for modern and ancient stromatolites, which are laminated carbonates produced by micro-organisms. Our new data will shed light on tracing bacterial signals in the geological record.

[1] Young & Galy (2004). Rev. Min. Geochem. 55, p197-230. [2] Pogge von Strandmann (2008). Geochem. Geophys. Geosys. 9 DOI:10.1029/2008GC002209. [3] Castanier, et al. (1999). Sed. Geol. 126, 9-23. [4] Cacchio, et al. (2003). Geomicrobiol. J. 20, 85-98.

https://doi.org/10.1180/S0026461X00008434 Published online by Cambridge University Press

Molecular dynamics simulation of materials

MICHELE PARRINELLO[1*]

[1]ETH Zurich and Università della Svizzera Italiana, Lugano, Switzerland, parrinello@phys.chem.ethz.ch (*presenting author)

Frontiers in Computational Geochemistry

The experimental study of systems under condition of high temperature and pressure provide a considerable challenge. Accurate and reliable computer simulations could be of great help in this area of science. However to reach this goal considerable technical difficulties need to be overcome. We present a number of methods developed in our laboratory that greatly help towards reaching this goal. We apply these techniquese to study the phase diagram of materials, structural phase transition and the nucleation of crystals from solution.

Fluctuations in Precambrian atmospheric and oceanic oxygen levels: a new Precambrian paradigm emerging?

C.A. PARTIN[1*], A. BEKKER[1], N.J. PLANAVSKY[2], B.C. GILL[3], C. LI[4], V. PODKOVYROV[5], A. MASLOV[6], K.O. KONHAUSER[7], G.D. LOVE[2], T.W. LYONS[2]

[1]University of Manitoba, Geological Sciences, Winnipeg, Canada, umpartin@cc.umanitoba.ca (* presenting author), bekker@cc.umanitoba.ca

[2]University of California, Riverside, Earth Sciences, U.S.A., planavsky@gmail.com, glove@ucr.edu, timothyl@ucr.edu

[3]Virginia Tech, Geosciences, Blacksburg, U.S.A., bcgill@vt.edu

[4]China University of Geosciences, Key Laboratory of Biogeology and Environmental Geology, Wuhan, China, chaoli@cug.edu.cn

[5]Russian Academy of Sciences, Institute of Precambrian Geology and Geochronology, St. Petersburg, Russia, vpodk@mail.ru

[6]Russian Academy of Sciences, Zavaritskii Institute of Geology and Geochemistry, Ekaterinburg, Russia, Maslov@igg.uran.ru

[7]University of Alberta, Earth and Atmospheric Sciences, Edmonton, Canada, kurtk@ualberta.ca

The Precambrian atmosphere and oceans are traditionally thought to have undergone a progressive, gradual increase in oxygen content after ~2.4 Ga [1]. This gradual transition from anoxic to oxidizing conditions is assumed to have occurred in two incremental steps, one at the beginning, and one at the end of the Proterozoic Eon. Emerging data require a change to this paradigm. Enrichments of the redox-sensitive element uranium in organic matter-rich shales through time shows that the Earth's surface oxidation had a more dynamic and unexpected history. Archean shales show very low [U] (<10 ppm, average of 3.8 ppm), consistent with a large U sink in anoxic oceans. The Great Oxidation Event (GOE) is accompanied by a rapid increase in maximum [U], up to 60 ppm, which likely reflects the onset of strong oxidative continental weathering releasing soluble U and expansion of oxygenated environments in the oceans. The initial rise of atmospheric oxygen ~2.4-2.32 billion years ago was followed by a dramatic decline to less oxidizing conditions during the Middle Proterozoic, beginning after the cessation of the Lomagundi carbon isotope excursion at ~2.05 Ga, when [U] in shales returned to near-to-crustal levels (average of 3.2 ppm). The subsequently established, steady-state low-oxygen mode persisted for nearly one billion years, terminating with a second oxygenation event in the latest Neoproterozoic, when [U] in shales demonstrate a dramatic increase, up to 94 ppm, by 551 Ma. Utilizing the ubiquitous geological shale record, U concentrations reveal Earth's dynamic path to its presently well-oxygenated atmosphere-ocean system, with unprecedented temporal resolution. We will present evidence for a precipitous rise and (previously unrecognized) fall in atmospheric oxygen early in the Proterozoic, which is in direct contrast to conventional models predicting a unidirectional oxygen rise. With this new paradigm in mind, future models will need to reexamine the links between the co-evolution of life and the chemical composition of the Precambrian oceans.

[1] Kump, L. (2008) *Nature* **45**, 277-278.

https://doi.org/10.1180/S0026461X00008434 Published online by Cambridge University Press

Does Fe electron transfer and atom exchange occur between Fe(II) minerals and aqueous Fe(III)?

TIMOTHY S. PASAKARNIS*, GENE F. PARKIN, AND MICHELLE M. SCHERER

Department of Civil and Environmental Engineering, The University of Iowa, Iowa City, USA, timothy-pasakarnis@uiowa.edu (* presenting author)

Fe oxides are transported as suspended sediment in rivers towards the oceans and act as a major source of iron for primary producers [1]. During this journey, the redox environment changes drastically, from dark, reducing environments in the subsurface, to light, oxidizing environments in fresh and marine surface waters and sediments. Here, we are interested in exploring whether our and others' recent findings of Fe(II)-Fe(III) electron transfer and atom exchange occur under more marine-like redox conditions, where Fe(II) can be structurally bound in a solid phase, and dissolved Fe(III) may be present as a sparingly soluble aqueous species complexed with ligands of various types [2].

In reducing environments, the reaction of Fe(II) and Fe(III) minerals is becoming widely recognized to be more complex than simply surface sorption of Fe(II). Rather, a complex process involving sorption, Fe(II)-Fe(III) electron transfer, and often extensive recrystallization both with and without secondary mineral transformation is beginning to emerge [3]. Whereas there is compelling evidence for oxidation of sorbed Fe(II) by structural Fe(III) in Fe minerals, such as goethite, magnetite, hematite, and ferrihydrite, it is unknown whether electron transfer will occur between sorbed Fe(III) and structural Fe(II) in Fe(II) minerals. It is also unclear whether significant Fe exchange will occur between aqueous Fe(III) and Fe(II) minerals.

We synthesized several Fe(II) containing minerals, such as magnetite, mackinawite, and siderite from ^{56}Fe and reacted it with aqueous ^{57}Fe(III) complexed with various Fe ligands. Mössbauer spectroscopy is specific to ^{57}Fe, and thus by synthesizing the underlying oxide from ^{56}Fe, we can turn off the signal from the solid, and isolate whether the aqueous ^{57}Fe(III) is reduced. In addition, we are using an enriched Fe isotope tracer approach, similar to our previous work [4] to determine whether significant Fe atom exchange occurs between the bulk solids and aqueous phase.

[1] Jickells et al. (2005) *Science* ***308***, 67-71
[2] Rickard and Luther (2007) *Chemical Reviews* **107**, 514-562.
[3] Gorski and Scherer (2011) Aquatic Redox Chemistry, **1071,** 315-343
[4] Handler et al. (2009) *Env Sci Tech* **43**, 1102-1107

Graphite-bearing and graphite-depleted basement rocks in the Dufferin Lake Zone, south-central Athabasca Basin, Saskatchewan: Initial observations and future work.

MARJOLAINE PASCAL[1*], KEVIN ANSDELL[1], IRVINE R. ANNESLEY[1,2], DAN JIRICKA[3], GARY WITT[3] AND AARON BROWN[3]

[1]University of Saskatchewan, Saskatoon, Canada, mjp313@mail.usask.ca, (* presenting author) , kevin.ansdell@usask.ca
[2]JNR Resources, Saskatoon, Canada, jnrirvine@sasktel.net,
[3]Cameco Corporation, Saskatoon, Canada, dan_jiricka@cameco.com, gary_witt@cameco.com, aaron_brown@cameco.com

Unconformity-associated uranium deposits from the Paleo- to Mesoproterozoic Athabasca Basin in Saskatchewan, Canada, include the largest high-grade U ore deposits in the world. Most of the deposits are located at the unconformity between the sedimentary basin and the Archean to Paleoproterozoic basement. Graphite and/or carbonaceous matter (CM) are found in the basement, often concentrated along structures which can be identified as electromagnetic (EM) conductors, and potentially could act as a reductant that could trigger deposition of uranium.

The focus of this study is the Dufferin Lake Zone, an extensive "conductive" block along the trend of the Virgin River Shear Zone in the south-central Athabasca Basin. The Centennial uranium deposit occurs along this trend, although it appears to be located away from the interpreted EM conductor at depth. The significance of this observation is that typical exploration strategies of trying to identify mineralized traps along EM conductors may not always be relevant. In order to address this issue, this study aims to examine, in detail, a drill hole fence of metamorphosed basement rocks that at depth contain variable proportions of graphite, either in structures or in pelitic gneisses, but appear to have lost some or all of their graphite as the unconformity is approached.

A combination of analytical techniques will be used to characterize the textural relationships, crystallinity, and type of CM/graphite in the pelitic gneisses and shear/fault zones at various depths below the unconformity. Lithogeochemistry, fluid inclusion and stable isotope analysis, and synchrotron techniques will be utilized to provide constraints on the chemical variability between graphite-bearing and graphite-depleted rocks, and the likely composition of fluids that may have removed graphite. For example, was the graphite removed by fluids moving along the unconformity or the underlying weathered rocks soon after the basin formed, or was it removed by fluids more directly involved in space and time with uranium mineralization, such as a highly corrosive basinal brine. Initial petrographic observations show much hetereogeneity and complexity in the textural relationships and type of CM/graphite in the pelitic gneisses and shear/fault zones at depth. Further work will first analyze these rocks, and then the rocks within the graphite-depleted zone, prior to establishing the link between the two zones. Did the graphite or its breakdown products act as the reductant for uranium deposition?

https://doi.org/10.1180/S0026461X00008434 Published online by Cambridge University Press

Carbonate clumped isotope closure temperatures

BENJAMIN H. PASSEY* AND GREGORY A. HENKES

Department of Earth and Planetary Sciences, Johns Hopkins University, Baltimore, MD 21218 (*bhpassey@jhu.edu)

Carbonate clumped isotope thermometry can potentially reveal information about the passage of inorganic carbon through the shallow- and mid-crust on its journey to and from the Earth's deep interior. The ordering of rare isotopes of C and O into the same carbonate groups creates 'multiply-substituted' isotopologues such as $Ca^{13}C^{18}O^{16}O_2$ (~67 ppm natural abundance). These isotopologues are surrounded in the mineral lattice by isotopically normal isotopologues such as $Ca^{12}C^{16}O_3$ (~982,000 ppm), and solid-state diffusion of C and O over unit cell distances will act to create and remove multiple substitutions. This short length scale of diffusion leads to the possibility of cooling rate-dependent carbonate clumped isotope closure temperatures in the ~100-300 °C range, much lower than traditional mineral oxygen isotope closure temperatures, and a range useful for studying shallow- and mid-crustal processes. We determined Arrhenius parameters for solid-state reordering of C-O bonds in calcite through a series of laboratory heating experiments. We present a closure temperature equation for carbonate clumped isotope thermometry analogous to Dodson's solution first order loss [1], where the closure temperature is a function of cooling rate and the Arrhenius parameters for solid-state C-O bond reordering. The sensitivity of closure temperature to cooling rate is sufficient for order of magnitude inference of cooling rate, provided the Arrhenius parameters of the studied minerals are well known. The inferred cooling rate of Carrara marble is ~ 3 °C per 10 ka, which is within error of independent estimates of the cooling history of the Alpi Apuane metamorphic core complex.

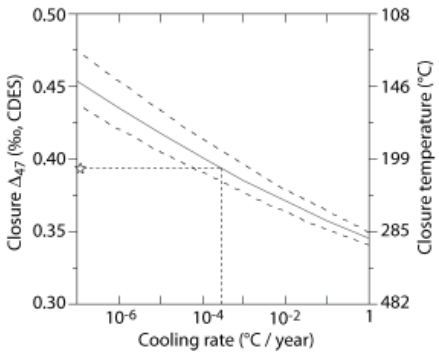

Figure 1: Carbonate clumped isotope closure Δ_{47} and closure temperatures as a function of cooling rate. Solid curved line is the best-estimate closure temperature relationship based on kinetics observed in the laboratory for an optical calcite. The curved dashed lines reflect uncertainty in Arrhenius parameters propagated through the closure temperature model. Star and horizontal dashed line show the mean Δ_{47} value of Carrara marble analyzed in four different laboratories [2]. CDES: 'Carbon dioxide equilibrium scale' [2].

[1] Dodson (1973) *Contrib. Mineral. Petrol.* **40**, 259-274.
[2] Dennis et al. (2011) *GCA* **75**, 7117-7131.

Metamorphic 'cascade effects' due to nucleation-related overstepping

DAVID R.M. PATTISON

Department of Geoscience, University of Calgary, Calgary, Alberta, Canada, pattison@ucalgary.ca

Nucleation difficulty can lead to overstepping of metamorphic reactions. Overstepping can result in multiple reactions being energetically possible, both stable and metastable. The only criterion that has to be satisfied is that each possible reaction lowers the free energy of the system. Overstepping can therefore lead to a 'cascade effect', in which several reactions involving the same reactant phases proceed simultaneously in a small temperature interval. Two different types of cascade effect are recognized. The first, termed the 'Bushveld-type' in respect of its documentation in the Bushveld aureole (Waters & Lovegrove, J Met Geol, 2002), arises from delayed nucleation of a product phase and subsequent production of that product phase from several different reactants. In the Bushveld example, the low-entropy chloritoid to staurolite/andalusite reactions were overstepped to the point that they were overtaken in terms of reaction affinity by high-entropy muscovite+chlorite-consuming reactions. Nucleation of staurolite and andalusite by the latter reactions eliminated the principal kinetic barrier to the progress of the overstepped chloritoid-consuming reactions, such that several staurolite- and andalusite-producing reactions ran in parallel in a small temperature interval, creating a reaction cascade. Fluid release accompanying initial reaction may also have contributed to the cascade effect by facilitating dissolution of chloritoid. The second type of cascade effect, termed the 'Nelson-type' in respect of its documentation in the Nelson aureole (Pattison et al., J Met Geol, 2009; 2011) involves a catalytic trigger related to the sudden build-up or influx of fluid in rocks that have overstepped two or more stable reactions. The result is simultaneous production of different product phases from the same reactant minerals. In the Nelson aureole, the clustering of the garnet, staurolite and andalusite isograds, contrary to their predicted wider spacing according to equilibrium thermodynamics, and the textural evidence that each of these porphyroblasts formed from reaction of the matrix with no evidence of the predicted consumption of the earlier-formed porphyroblasts, suggests the simultaneous operation of several chlorite-consuming reactions. Once the nucleation-related barriers to initial garnet formation were overcome, fluid was released into the grain boundary network, enhancing rates of intergranular transport and possibly further nucleation. This created a positive feedback and a vigorous reaction interval involving production of several porphyroblast phases from the same matrix reactants.

https://doi.org/10.1180/S0026461X00008434 Published online by Cambridge University Press

Paleoceanographic interpretation of the light rare earth elements

GENNA M. PATTON[1], PAMELA A. MARTIN[2], EMILIA SALGUIERO[3], AND ANTJE H.L. VOELKER[3]

[1]University of British Columbia, Vancouver, Canada, gpatton@eos.ubc.ca (* presenting author)
[2]Earth and Environmental Sciences, IUPUI, Indianapolis, IN, United States (martinpa@iupui.edu)
[3] Unidade Geologia Marinha, Laboratorio Nacional de Energia e Geologia, Amadora, Portugal (emilia.salgueiro@lneg.pt, avoelker@softhome.net)

The rare earth elements (REE) in sea water have been used as indicators of the modern oceanic and paleoceanic environments. The Nd-isotopic composition (εNd) of ferromanganese crusts and nodules successfully record water mass changes integrated over 10^4 and 10^5 years; fossil fish teeth and debris pinpoint water mass changes through the Cenozoic, though also with low temporal resolution due to the scarcity of fish remains [*2; 3*]. Records of much higher temporal resolution have been produced from the εNd of bulk sediment leach, and over glacial-interglacial timescales [*4*]. Isolating the εNd of seawater from lithogenic contamination, however, is problematic. Detrital contaminants are much more easily removed from planktonic foraminifera and therefore may be more representative of a seawater signal [*1*]. The phase in which the εNd is associated with foraminiferal calcite is of critical importance for the paleoceanographic interpretation. In addition to Nd, the full sequence of rare earth elements can speak to diagenetic indicators and bottom-water conditions in which the authigenic signal is acquired. Studies of coupled planktonic benthic REE comparison allow for clear indications of diagenetic overprinting. Here, we present data from the Iberian Margin that demonstrate coherent, diagenetic signals indicative of environmental conditions associated with climate signals. Also, we present data generated using X-ray absorption near edge structure analysis that help to identify fine-scale spatial distribution of high concentrations of REE and also the oxidation state of redox sensitive cerium. With a combination of paleorecords and different analytical approaches, we can begin to identify the distinct phases of the REE and as a result, the paleoceanographic interpretation of these elements.

[1] Elmore, A., A. Piotrowski, and J. Wright (2011), Testing the extraction of past seawater Nd isotopic composition from North Atlantic deep sea sediments and foraminifera. [2] Frank, M. (2002), Radiogenic isotopes: tracers of past ocean circulation and erosional input, *40*(1), 1001. [3] Martin, E., S. Blair, G. Kamenov, and H. Scher (2010), Extraction of Nd isotopes from bulk deep sea sediments for paleoceanographic studies on Cenozoic time scales. [4] Piotrowski, A., S. Goldstein, S. Hemming, and R. Fairbanks (2004), Intensification and variability of ocean thermohaline circulation through the last deglaciation, *225*(1-2), 205-220.

Petrology of syn-orogenic S-type leucogranites (Damara orogen; Namibia) – Constraints from Sr, Nd and Pb isotopes

ANDRE PAUL[1*], STEFAN JUNG[1], ROLF L. ROMER[2] AND ANDREAS STRACKE[3]

[1] Mineralogisch-Petrographisches Institut, Universität Hamburg, Germany, andre-paul@hotmail.de ([*]presenting author) stefan.jung@mineralogie.uni-hamburg.de
[2] GeoForschungsZentrum, Potsdam, Germany
[3] Institut für Mineralogie, Westfälische Wilhelms Universität, Münster, Germany

The northern central zone of the Damara Orogen (Namibia) consists of metasedimentary rocks, Pan-African syn- to late-tectonic granites, and rare basement gneisses. Leucogranites of S-Type character with ages of ca. 510-515 Ma appear to be little fractionated although the two suites have high K_2O (5.7-7.3 wt%), Th (30-74 ppm), and U (3-13 ppm) abundances and moderately high but relatively constant Rb/Sr ratios (2.7-4.4). High light rare earth elements but variable heavy rare earth elements concentrations result in high and variable La_n/Yb_n ratios ranging from 16 to 98, suggesting involvement of garnet during crustal melting. The granites have, relative to other syn-tectonic S-type suites from the Damara orogen, more unradiogenic $^{87}Sr/^{86}Sr_{init.}$ ratios (0.7095-0.7140 vs. 0.7150-0.7340). ε–Nd values range from -4.5 to -6.5; the majority of values being similar to those from syn-tectonic S-type granites (ε–Nd -3.0 to -5.5) and match those found in metasedimentary xenoliths (ε–Nd -5.0 to -7.0) from these syn-tectonic S-type granites. The Pb isotopic composition of acid-leached feldspar is broadly similar to the one of metapelitic xenoliths in Damaran syn-tectonic S-type granites suggesting that the leucogranites are derived from isotopically similar metapelitic rocks. Zircon saturation temperatures are high for crustally derived granites, but well within the range commonly accepted for S-type granites (800-840°C). U-Pb monazite ages and Rb-Sr whole rock ages indicate that the leucogranites intruded simultaneously with the main peak of metamorphism. The heating event that promoted melting of fertile rocks at depth might have been subsidized by high heat productivity, which is also reflected in the elevated K, Th, and U abundances of apparently unfractionated granites, and crustal thickening during the Pan African orogeny.

https://doi.org/10.1180/S0026461X00008434 Published online by Cambridge University Press

Lead isotopes in South Atlantic seawater: insights on anthropogenic inputs and ocean circulation

M. PAUL[1*], T. VAN DE FLIERDT[1], D. WEISS[1], M. REHKÄMPER[1]

[1]Imperial College, London, UK (*m.paul@imperial.ac.uk)

Trace elements and their isotopes play an essential role in biological processes in the marine environment. Like many micronutrient elements, lead (Pb) is mainly supplied to the remote parts of the ocean by atmospheric deposition. Unlike nutrients, however, its behaviour in seawater is dominated by passive scavenging onto particles. As Pb is one of the elements which is heavily influenced by anthropogenic contamination, its isotope composition in seawater can give us key information on (i) anthropogenic vs. natural sources affecting the modern oceans, and (ii) the movement of water masses within the global oceans [1,2]

To better exploit the potential of Pb isotopes for research in marine geochemistry, we have developed a new method for accurate high precision analyses of Pb isotopes in seawater. The methodology involves pre-concentration of Pb using $Mg(OH)_2$ co-precipitation [3] and further purification by ion exchange chromatography on two successive columns of AG1X8 100-200 resin. Samples are then loaded on single Re filaments with a mixture of silica gel and phosphoric acid. The isotopic analyses are carried out on a TRITON TIMS instrument at Imperial College London, using a $^{204}Pb/^{207}Pb$ double spike for the correction of instrumental mass fractionation [4].

Using our newly installed and tested technique, we analyzed several depth profiles of seawater from the South Atlantic Ocean collected in the framework of the UK-GEOTRACES program. More precisely, the samples are derived from a transect along 40°S between Cap Town (South Africa) and Montevideo (Uruguay). The key feature of this remote and little studied part of the Atlantic Ocean is a high productivity band in an otherwise nutrient-poor region, which may be due to a number of potential sources of nutrients. Our lead isotope data will help to constrain anthropogenic and natural dust inputs from both South Africa and South America and their migration within the vertical water column. In addition, intermediate and deep water analyses will reveal the presence of Southern Ocean and North Atlantic waters.

[1] Reuer, M.K and D.J. Weiss (2002) *Phil. Trans. of the Royal Society of London Series A: Math., Phys. and Engineering Sciences* **306** (1801), 2889-2904
[2] Von Blanckenburg, F. and H. Igel (1999) *EPSL* **169** (1-2), 113-128.
[3] Wu, J. and E.A. Boyle (1997) *Anal. Chem.* **69**, 2464-2470
[4] Hamelin B., Mahnes G. et al. (1985) *GCA 49,* 173-182

Characterization of Hg leaching from the riverbank sediments of the South River, VA

KRISTA PAULSON[1*], KRISTA DESROCHERS[1], CAROL PTACEK[1], DAVID BLOWES[1], BLAIR GIBSON[1], RICHARD LANDIS[2], JAMES DYER[2], NANCY GROSSO[2]

[1]Earth and Environmental Sciences, University of Waterloo, Waterloo, ON, Canada
kmapauls@uwaterloo.ca (presenting author)
[2]E.I. du Pont de Nemours and Company, Wilmington, DE, USA

A large portion of Hg found in the natural environment originates from sediment and soils that are transported and dispersed by runoff and erosion. The associated particle-facilitated transport depends on the mineralogy and pore-water chemistry of the sediment and can impact the bioavailability and toxicity of Hg [1]. In this study, freshwater river sediments and bank soils that contained elevated concentrations of Hg were collected along two vertical transects perpendicular to the South River, Virginia, USA. The South River system accumulated Hg from industrial processes along the river during the early part of the 20th century. The sediment samples were analysed using a variety of techniques, including sequential chemical extractions and synchrotron-based X-ray absorption spectroscopy (XAS). Column transport experiments were conducted to evaluate Hg leaching from the sediment and bank soils. Specific issues addressed are the extent that Hg leaches from the sediment under varying geochemical conditions, which develop in the frequently inundated riverbanks, and the role of particle-facilitated and colloidal transport of Hg from the bank sediments.

Sediment samples from both transects contained both soluble (up to 32%) and less soluble forms of Hg (up to 94%), as determined by sequential chemical extractions [2]. Micro-XAS analysis produced spectra that were consistent with the mineral phase metacinnabar [HgS]. Column transport experiments conducted with the two sediment samples that contained the elevated concentrations of Hg indicated nearly identical leaching of Hg. These sediments contained similar concentrations of total Hg (280 μg g^{-1} total Hg for a sample collected from the unsaturated zone near the top of the river bank and 187 μg g^{-1} for a sample collected from an elevation just above the base flow level of the river), but contained markedly different fractions of extractable Hg. The effluent concentrations of Hg initially ranged from 1.5 to 3 μg L^{-1} for the 0.45 μm filter fraction for both columns and the unfiltered samples ranging from 2 to 5.3 μg L^{-1}. After 80 pore volumes, the concentrations decreased. Calculated cumulative masses of Hg leached from the sediments reached a plateau at < 2% of the water soluble fraction of Hg, suggesting a diminishing availability of Hg for leaching under saturated flow conditions. These results suggest that there is potential for leaching of elevated concentrations of Hg in both dissolved and particulate forms, that the mass available for leaching under saturated conditions appears to much less than predicted using standardized sequential extraction analyses, and that a portion of the Hg had remained in a relatively stable sulfide phase even after many decades of atmospheric exposure.

[1] Lowry *et al.* (2004) *Environ. Sci. Technol.* **38**, 5101-5111.
[2] Bloom *et al.* (2003) *Anal. Chim. Acta*. **479**, 233-248.

https://doi.org/10.1180/S0026461X00008434 Published online by Cambridge University Press

Sorption models for complex materials – modeling approaches and data requirements

TIMOTHY E. PAYNE

Australian Nuclear Science and Technology Organisation, Lucas Heights, Sydney, Australia, tep@ansto.gov.au

Surface complexation models (SCMs) can be applied to complex geologic materials such as sediments and soils using various approaches, which are generally variants on either the component additivity (CA) or generalised composite (GC) models [1]. The CA approach involves modeling the sorption of a trace metal (or radionuclide) by additively combining sorption models for the individual mineral components of a soil. The GC approach is more generic, but is often parameterised using bulk properties such as the specific surface area (SSA) or ion exchange capacity.

These approaches are demonstated using data for cobalt adsorption on complex materials from Australian field sites. The GC modeling estimated the number of sorbing sites from the measured BET surface area (assuming a site density of 2.31 sites/nm^2 [2,3]). A simplified CA model that conceptualised the surface sites as having equivalent sorption properties to amorphous Fe oxide was also moderately successful in explaining the pH dependence of the Co sorption data sets. This example demonstrates the basic utilility and predictive capability of these modeling approaches. However, as with literature examples of SCMs for complex materials, it does not fully test the underlying assumptions. These outcomes raise questions about the uniqueness and general applicability of these modeling approaches [3].

A principal requirement to further develop the CA modeling approach is adequate models for trace metal sorption on component mineral phases of complex environmental sorbents and conclusive demonstration of their role in each sample. Similarly, the GC approach requires experimental measurement of sorption data on a range of complex samples of differing mineralogy and SSA under various conditions. Given that it is relatively straightforward to experimentally study sorption and measure SSA, it might be expected that numerous sets of trace-metal sorption data for complex samples having a range of properties would be available. However, while individual studies typically report sorption data across a range of chemical conditions (pH, ionic strength, etc), the experiments often involve only a single solid sample (or limited number of samples). Consequently, a significant constraint on obtaining the required data for establishing relationships between sorption and SSA (or other soil properties) is that few literature data sets report sorption as a function of SSA (or mineralogy) for a number of different solid phases. Thus, there is an urgent need for more experimental sorption work with a range of sorbent samples.

[1] Davis *et al.* (1998) *Environ. Sci Technol.* **32**, 2820-2828
[2] Dzombak and Morel (1990) *Surface complexation modeling – hydrous ferric oxide*. John Wiley and Sons, New York, 393pp.
[3] Payne *et al.* (2009). *Applied Radiation and Isotopes*. **67**, 1269-1276.

Deciphering the Cenozoic Tl isotope record of marine ferromanganese crusts – new evidence from adsorption experiments

CAROLINE L. PEACOCK[1*], SUNE G. NIELSEN[2], LAURA E. WASYLENKI[3], ELLEN M. MOON[4] AND MARK REHKÄMPER[5]

[1]School of Earth & Environment, University of Leeds, Leeds, UK, C.L.Peacock@leeds.ac.uk (* presenting author)
[2]Dept. of Geology and Geophysics, Woods Hole Oceanographic Institution, Woods Hole, MA, USA, snielsen@whoi.edu
[3]Dept. of Geological Sciences, Indiana University, Bloomington, IN, USA, lauraw@imap.iu.edu
[4]ANSTO Minerals, Autralian Nuclear Science and Technology Organisation, NSW, Australia, ellenm@ansto.gov.au
[5]Dept. of Earth Science & Engineering, Imperial College London, London, UK, markrehk@imperial.ac.uk

Thallium stable isotopes, recorded in authigenic marine ferromanganese crusts, may provide new constraints on past changes in environmental conditions, the Earth's carbon cycle, and their impact on global climate.[1-3] Specifically, the Cenozoic Tl isotope curve shows a pronounced evolution of Tl isotope composition around the Palaeocene-Eocene boundary, from ~ 6 ε^{205}Tl at 55 Myr to ~ 12 ε^{205}Tl at 45 Myr (where ε^{205}Tl is the deviation of the ^{205}Tl/^{203}Tl ratio of a sample from the NIST SRM 997 Tl isotope standard in parts per 10000).[2] After this pronounced shift, the Tl isotope composition of crusts appears to have changed little over the last 40 Myr, with a globally uniform, modern signature of ~ 13 ε^{205}Tl. Despite the compelling appearance, the record provided by Tl isotopes (and other heavy-metal stable isotope systems) is not straightforward because the temporal shift in isotope composition may reflect either variability in the ε^{205}Tl value of seawater, or changes in the conditions that govern incorporation of the element into the structure of the ferromanganese minerals. Furthermore, modern crusts are ~ 19 ε^{205}Tl (or ~ 2 ‰) heavier than the contemporaneous seawater, and combined with their globally uniform signature this implies there is an equilibrium stable isotope fractionation between Tl in seawater and the Tl incorporated into crust minerals.

To improve our understanding of the Tl isotope record preserved in crusts it is important to develop a detailed characterisation of how Tl is sequestered by ferromanganese minerals, and a quantitative and mechanistic understanding of any stable isotope fractionation that occurs during this process. Here we present the results of novel experimental work that combines molecular-level, X-ray absorption spectroscopy with stable isotope analyses of Tl sorbed to ferromanganese minerals, as a function of time, temperature, pH and ferromanganese mineralogy. Based on the experiments, we have constrained the mechanistic basis for Tl enrichment and stable isotope fraction in ferromanganese crusts, and we will discuss the effect of the experimental parameters on the fractionation factor between simulated seawater and solid minerals.

[1] Rehkämper et al. (2004) *Earth Planet. Sci. Let.* **219**, 77-91. [2] Nielsen et al. (2009) *Earth Planet. Sci. Let.* **278**, 297-307. [3] Baker et al. (2009) *Geochim. Cosmochim. Acta* **73**, 6340-6359.

https://doi.org/10.1180/S0026461X00008434 Published online by Cambridge University Press

Mechanisms of tetrahedral iron formation in ferrihydrite observed via soft x-ray spectroscopy

DEREK PEAK[1*], JAMES J. DYNES[2], ROBERT GREEN[1], AND TOM Z. REGIER[2]

[1]University of Saskatchewan, Saskatoon Canada, derek.peak@usask.ca (*presenting author) robert.green@usask.ca
[2] Canadian Light Source, Saskatoon, Canada, james.dynes@lightsource.ca tom.regier@lightsource.ca

Introduction

Ferrihydrite is a poorly crystalline ferric hydroxide nanomineral. It rapidly transforms to more stable crystalline minerals such as goethite (FeOOH) in the lab, but it is metastable in natural systems and found as persistant coatings as well as discrete particles. Its high reactivity and widespread occurrence make its structure important for geochemists, life scientists (as ferritin), and environmental engineers. However, disagreement among researchers remains as the structure of this enigmatic material. The central question in the structural debate is whether iron in ferrihydrite is purely octahedral, or if tetrahedral ferric iron is present. Recent studies proposing tetrahedral iron in this phase have proposed that it may form via condensation of keggin-type aqueous polymers similar to aluminum, but these have never been directly observed for iron.

Accordingly, the objective of our study was to monitor the precipitation of ferrihydrite from forced hydrolysis of ferric chloride *in situ* using high resolution Fe L-edge XANES spectroscopy of solutions in a flow through liquid cell. Spectra were collected using both Fe partial yield and the newly developed IPFY approach for self absorption-free bulk XAS measurements. The precipitation process was followed from pH 1 to 7.5, and results from these aqueous measurements were compared to air dried samples prepared at the same pH. STXM measurements of wet and dried ferrihydrite were also collected for comparison.

Our results demonstrate clearly that L-edge XANES are extremely sensitive to shifts in ligand field that accompany hydrolysis of metals and coordination changes. There is clear evidence that tetrahedral iron is present in air-dried samples, but that the *in situ* measurements are consistent with only octahedral iron. This suggests that the dominant mechanism for tetrahedral iron in ferrihydrite may be physical dehydration rather than a chemical reaction. This has enormous implications for natural systems, where wetting and drying cycles are expected to strongly influence mineralogy

Novel insights on a traditional proxy: Combining the stable and radiogenic Sr isotope systems to characterise continental weathering

CHRISTOPHER R. PEARCE[1*], IAN J. PARKINSON[1], KEVIN W. BURTON[2], EMILY I. STEVENSON[3], JÉRÔME GAILLARDET[4], ROBERTA L. RUDNICK[5], JOSH WEST[6] AND DOUG E. HAMMOND[6]

[1]Department of Environment, Earth and Ecosystems, CEPSAR, The Open Universtiy, Walton Hall, Milton Keynes, MK7 6AA, UK
[2]Durham University, Durham, UK
[3]Oxford University, Oxford, UK
[4]Institut de Physique du Globe de Paris, Paris, France
[5]University of Maryland, College Park, USA
[6]University of Southern California, Los Angeles, USA
*Presenting and corresponding author: c.pearce@open.ac.uk

The radiogenic strontium isotope system ($^{87}Sr/^{86}Sr$) is one of the most established methods for tracing continental weathering, as subtle, but resolvable, differences in $^{87}Sr/^{86}Sr$ ratios enable the Sr content of water, vegetation and humans to be linked to specific locations and lithologies[1]. On a global scale, shifts in weathering processes control the composition of the oceans, with differences in the relative flux of silicate and carbonate material over geological timescales reflected in the $^{87}Sr/^{86}Sr$ ratio of marine carbonates[2]. Unlike the radiogenic system, variations in stable Sr isotopes ($\delta^{88/86}Sr$) are controlled by mass dependent processes, with the main driver of fractionation thought to be incorporation into carbonates[3]. The combined application of the $^{87}Sr/^{86}Sr$ and $\delta^{88/86}Sr$ systems therefore has the potential to differentiate source variations from other weathering processes, providing a valuable method for assessing strontium transport through the critical zone.

This study presents isotopic data from both Sr systems at various points in the hydrological cycle; $^{87}Sr/^{86}Sr$ and $\delta^{88/86}Sr$ values from glacial ice, precipitation, river water, dust and bedrock are used to constrain the sources and cycling of Sr on the continents. Samples dominated by atmospheric Sr transport typically display lower $\delta^{88/86}Sr$ compositions than equivalent surface waters, and are thought to be influenced by anthropogenic contamination effects. River water samples dominated by surface run-off have $^{87}Sr/^{86}Sr$ and $\delta^{88/86}Sr$ values that depend on the underlying lithology: Continental silicate terrains typically have $\delta^{88/86}Sr$ values within 0.10 ‰ of the global riverine mean (0.34 ‰), whereas rivers draining carbonate and basaltic terrains (i.e. those with $^{87}Sr/^{86}Sr$ ratios <0.7100) show considerably greater $\delta^{88/86}Sr$ variation, ranging from 0.10 ‰ to 0.86 ‰. Differences are also observed within individual drainage basins and between wet and dry flow regimes, confirming the sensitivity of the stable Sr system to fractionation processes during weathering and transport. The findings of this study are compared to other isotopic weathering proxies, and the implications for the future application of the Sr weathering proxy are discussed.

[1] Bentley (2006) *J. Arch. Meth. Theory* **13**, 135-187.
[2] McArthur *et al.* (2001) *J. Geol* **109**, 155-170.
[3] Krabbenhöft *et al.* (2010) *GCA* **74**, 4097-4109.

https://doi.org/10.1180/S0026461X00008434 Published online by Cambridge University Press

Mineral, fluid and gas interactions under CO_2 storage conditions – the role of SO_2, NO_X, and O_2

J. PEARCE[1,2*], D. BIDDLE[2], S. GOLDING[1,2], V. RUDOLPH[2] AND D. KIRSTE[1,3]

[1]Cooperative Research Center for Greenhouse Gas Technologies
[2]University of Queensland, Brisbane, Australia, j.pearce2@uq.edu.au (* presenting author), s.golding1@uq.edu.au, deanb@cheque.uq.edu.au, v.rudolph@uq.edu.au
[3]Simon Fraser University, Vancouver, Canada, d.kirste@sfu.ca

Co-contaminant gases such as SO_2, NO_X, and O_2 are present in gas streams from power stations and oxy fuel power plants. Storage of CO_2 streams containing co-contaminants significantly reduces capture costs however they may have significant physical and chemical impacts on well materials, reservoir and cap rocks when in contact with formation water. Geochemical modelling of SO_2 co-injection indicates formation of sulphuric acid and lowered formation water pH compared to pure CO_2 injection resulting in increased mineral dissolution in the near well bore, and possible precipitation of minerals such as ankerite and dawsonite downstream with a decrease in porosity and injectivity.[1] However modelling is hampered by a lack of experimental data at carbon storage conditions for reactions involving co-contaminants SO_2, O_2 or NO_X.

In this context a new experimental apparatus has been constructed to reproduce in situ carbon storage temperature and pressure conditions for mineral – fluid –scCO_2 – co-contaminant gas reactions, with periodic sampling of fluids and gases for analysis.

Experimental results and geochemical modelling of the dissolution of pure mineral phases siderite, labradorite and illite in CO_2 saturated brines of high (150 g/l NaCl) and low salinity at representative reservoir conditions (80 °C, 200 bar) will be presented. Recent work on far from equilibrium siderite dissolution at up to 100°C and ~50 bar CO_2 shows increased dissolved iron at pH below 5 owing to proton promoted dissolution (PPD).[2] Labradorite dissolution is expected to be incongruent with enhanced release of sodium, calcium and aluminium over silica at our temperature conditions.[3] Labradorite dissolution may be expected to decrease under saline conditions by comparison to feldspar dissolution experiments in the absence of CO_2.[4] The effect on siderite at our conditions is less clear cut, however recently Testemale *et al*. observed an order of magnitude decrease in the rate constant for siderite dissolution at 100°C and 300 bar with the addition of 1 mol kg^{-1} NaCl resulting from competition of Na^+ with H^+ affecting PPD.[4] Further experiments will include the co-contaminants O_2 (5%) and SO_2 (1%). Renard *et al*. observed increased reactivity of carbonate and clay by up to a factor of 10 on addition of SO_2 and O_2.[6] With SO_2 co-injection the lowered pH conditions are expected to increase mineral dissolution rates.

[1] Xu *et al* (2007) *Chem. Geol. 24***2**, 319. [2] Golubev *et al*. (2009) *Chem.Geol.* ***265,*** 13. [3] Carroll *et al.* (2005) *Chem.Geol.**217, 213.* [4] Blake *et al*. (1999) *Geochemica et Cosmochima Acta* **63**, 2043. [5] Testemale *et al.* (2009) *Chem.Geol.* ***259***,8. [6] Renard *et al.(2011) Energy Procedia **1**, 3283.*

Tetraether lipids of Archaea in paleoceanography: Unresolved questions and new directions

ANN PEARSON[1*]

[1]Harvard University, Department of Earth and Planetary Scienes, Cambridge, MA, USA, pearson@eps.harvard.edu (* presenting author)

Abstract

Thaumarchaeota [1, 2], formerly known as Marine Group I Crenarchaeota, are believed to be the primary source of the ubiquitous glycerol dialkyl glycerol tetraether lipids (GDGTs) found in the environment. GDGTs, including the unique compound crenarchaeol, are abundant in marine and terrestrial aquatic environments, in sediments and soils, and over at least an 85°C temperature range from the polar ocean to hydrothermal springs. Experiments on pure cultures, enrichment mesocosms, and empirical correlations for marine sediments (TEX_{86}; [3]) all show a positive relationship between environmental temperature and the number of cyclopentyl or cyclohexyl rings contained within the GDGT structure. The TEX_{86} paleotemperature proxy has been applied across a large temporal range of geologic events and to sediments of widely varying depositional and diagenetic history. Evaluating whether such broad applicability is widely robust requires answers to a number of lingering questions about: (*1*) the physiological mechanism governing the number and distribution of these types of rings; (*2*) the degree to which microbial community structure influences the TEX_{86} relationship, including the extent to which environmental Euryarchaeota also produce GDGTs; (*3*) the mechanism that transfers the TEX_{86} signal to marine sediments; (*4*) the extent to which this signal is modified via diagenesis, *in-situ* production, or sediment redistribution; (*5*) the taxonomic, ecophysiological, and evolutionary significance of the cyclohexyl ring-containing compounds, crenarchaeol and its regioisomer; and (*6*) the fidelity of empirical temperature correlations based on core-top sediments. I will review these questions with a focus on the promise and prospects offered by isotopic approaches, which to date have remained underutilized.

References

[1] Brochier-Armanet, C., Boussau, B., Gribaldo, S., and Forterre, P. (2008) Mesophilic crenarchaeota: proposal for a third archaeal phylum, the Thaumarchaeota. *Nature Reviews Microbiology* **6**, 245-252.
[2] Spang, A., Hatzenpichler, R., Brochier-Armanet, C., Rattei, T., Tischler, P., Spieck, E. *et al.* (2010) Distinct gene set in two different lineages of ammonia-oxidizing archaea supports the phylum Thaumarchaeota. *Trends in Microbiology* **18**, 331-340.
[3] Schouten, S., Hopmans, E.C., Schefuss, E., and Damsté, J.S.S. (2002) Distributional variations in marine crenarchaeotal membrane lipids: a new tool for reconstructing ancient sea water temperatures? *Earth and Planetary Science Letters* **204**, 265-274.

https://doi.org/10.1180/S0026461X00008434 Published online by Cambridge University Press

Development and application of LA-ICP-MS in the geosciences: past, present and future

N.J. Pearson[1] *, W.L. Griffin[1] and Suzanne Y. O'Reilly[1]

[1]ARC Centre of Excellence for Core to Crust Fluid Systems, Department of Earth and Planetary Sciences, Macquarie University, Sydney, NSW 2109, Australia norman.pearson@mq.edu.au (*presenting author); william.griffin@mq.edu.au; sue.oreilly@mq.edu.au

The rapid advances in *in situ* laser ablation (LA) inductively coupled plasma-mass spectrometry (ICP-MS) and multicollector (MC)-ICPMS have provided datasets in geochronology and geochemistry that have revolutionised our understanding of the geodynamic Earth at all scales. The development and application of LA-ICP-MS continues to grow at a dramatic rate and *in situ* analyses for elements and isotopic ratios are now performed routinely in numerous laboratories worldwide. Like other microbeam techniques LA-ICP-MS provides the benefit of high spatial resolution and produces data that can be interpreted in a microstructural context.

The development of new LA-ICP-MS methodologies has been enabled by advances in instrumentation in conjunction with studies of the fundamental processes involved in ablation and in the ICP (e.g. laser-induced elemental and isotopic fractionation, plasma loading, mass bias). The emergence of the multi-collector ICP-MS for high-precision *in situ* measurement of radiogenic (e.g. Hf in zircon [1]) and 'non-traditional' stable isotopes (e.g. Cu and Fe in sulfides) has revolutionised analytical geochemistry. On the laser front, Nd:YAG (266, 213 or 193 nm) or ArF excimer (193 nm) remain the most commonly used laser sources. In comparison with these nanosecond pulse-width systems, ablation using femtosecond lasers has been shown to approach stoichiometric sampling and reduce laser-induced fractionation effects. However the high cost of the commercial femtosecond systems has restricted their uptake.

Despite the significant advances of the last decade, the continued rapid spread and acceptance of the technology may be jeopardized while any significant analytical issues remain unsolved. The accuracy and precision of *in situ* isotope ratio measurements are inherently lower than solution measurements because of the complexity of matrix effects and corrections for mass bias and isobaric interferences. Optimising precision of elemental and isotope ratio measurements while maintaining spatial resolution brings challenges, and emphasises the need for improved understanding of measurement uncertainties and error budgets. Well characterized and readily available reference materials combined with more inter-laboratory comparison exercises are essential.

Future goals for LA-ICP-MS include a quantum increase in sensitivity, fine-scale compositional mapping of geological samples, and overcoming effects of elemental and isotopic fractionation. Elimination of elemental fractionation will accelerate development of procedures to measure major, minor and trace-element abundances without depending on matrix-matched calibration materials and independently determined internal standard concentrations.

[1] Griffin et al. (2000) *Geoch. Cosm Acta* **64**, 133-147.

First record of Ediacaran iron formations: Origin and paleoenvironmental significance

E. Pecoits[1]*, N. R. Aubet[1], M. K. Gingras[1], S. W. Poulton[2], A. Bekker[3], G. Veroslavsky[4] and K. O. Konhauser[1]

[1]University of Alberta, Edmonton, Canada, epecoits@ualberta.ca (* presenting author)

[2]Newcastle University, Newcastle upon Tyne, United Kingdom, simon.poulton@necastle.ac.uk

[3]University of Manitoba, Winnipeg, Canada, bekker@cc.umanitoba.ca

[4]Universidad de la República, Montevideo, Uruguay, gerardo@fcien.edu.uy

It is widely believed that the Earth's oceans became increasingly oxygenated during the late Neoproterozoic, most notably after the end of the Marinoan glaciation approximately ~635 million years ago. However, recent geochemical data for Ediacaran sediments suggest that some deep ocean basins were instead anoxic and ferruginous [Fe(II)-enriched] throughout the Ediacaran and possibly into the Cambrian, suggesting a more complex global redox structure than previously envisioned. An apparent absence of Ediacaran iron formations (IF) presented a challenge to this emerging paradygm; these chemical sediments were common under Fe-rich conditions in the Archean and Paleoproterozoic oceans.

Here, we report detailed sedimentological, stratigraphic, petrographic and geochemical data from an Ediacaran IF and associated rocks, including 'iron-rich' black shales, siltstones and cherts of the Arroyo del Soldado Group in Uruguay [1]. The IF and cherts occur at the top of two siliciclastic units characterized by retrogradational stacking patterns with fining-upward cycles deposited during transgressive system tracts and represent two major episodes of basin flooding and sediment starvation. Geochemically, the IF and cherts have coherent rare earth element and yttrium (REY) patterns and display the essential shale-normalized characteristics of marine precipitates. REY signatures and mixing calculations show that they differ from Archean and Paleoproterozoic IF as far as high-temperature hydrothermal input did not influence their chemistry. Instead, we suggest that low-temperature hydrothermal input may account for the geochemical signatures displayed. By analyzing the REY signature of chemical precipitates (cherts and IF) and evaluating the redox chemistry of the marine water column within a sedimentological and sequence stratigraphic framework, our results confirm that ferruginous conditions dominated the pre-Gaskiers but also the post-glaciation deep-water chemistry. Therefore, global ocean oxygenation may not have occurred unitl well into the upper Ediacaran or even during the Cambrian as was recently proposed [2].

[1] Pecoits et al. (2011) *Precambrian Research* **in press**. [2] Canfield et al. (2008) S*cience* **321**, 92-95.

https://doi.org/10.1180/S0026461X00008434 Published online by Cambridge University Press

Revisited multicomponent chemical geothermometry: application to the Dixie Valley geothermal area

L. PEIFFER*, C. WANNER, N. SPYCHER, E. SONNENTHAL, B.M. KENNEDY

Lawrence Berkeley National Laboratory, Berkeley, USA, lpeiffer@lbl.gov (* presenting author)

The multicomponent chemical geothermometry method [1,2] involves computing the saturation indices of potential reservoir minerals over a range of temperatures, given a known geothermal fluid composition, then inferring reservoir temperature from the clustering of mineral saturation indices near zero. This method was automated as a stand-alone computer program (geoT), easing its application and allowing optimization of model input parameters using parameter-estimation software [3]. The code can process simultaneously multiple water compositions, and correct for dilution and mixing effects as well as gas loss. The temperature of the reservoir is estimated from statistical analysis of computed mineral saturation indices. One difficulty of the method is that it is sensitive to potentially erroneous Al chemical analyses, an issue which can be partly resolved by resorting to computed Al concentrations assuming equilibration with selected Al-bearing minerals [2].

The geothermometry method and new code are being tested on geothermal fluids from Dixie Valley (Nevada, USA) using an extensive set of water and gas analyses [4]. These data include total and dissolved ("ionized") Al analyses in filtered (0.45 and 0.2 μm) and unfiltered water samples, allowing testing the effect of these various reported Al concentrations on predicted temperatures. A set of minerals prevailing in the geothermal reservoir was assumed based on XRD data from well cuttings [5]. Gas analyses were added back to the well waters, and increased salinity effects caused by the reinjection of flashed brines into the reservoir were also considered. Using "ionized" Al concentrations in unfiltered samples, reservoir temperatures of ~250°C were obtained. These temperatures were similar to values obtained by computing Al concentrations assuming equilibrium with Al minerals (albite, microcline, muscovite). These temperatures seem reliable because they are consistent with measured downhole water temperatures. In contrast, the 0.2-μ filtered Al analyses led to lower computed temperatures close to sampling temperatures (160°–180°C) and corresponding to different equilibrated minerals. In this case, the 0.2-μ filtered Al concentrations appear too low, apparently reflecting the filtering-out of colloidal Al formed by cooling. Hot spring waters from the wider Dixie Valley area were also investigated. The lack of consistency between their reconstructed equilibrium temperatures, as well as significant differences in their chemical composition may indicate that Dixie Valley hosts several distinct reservoirs. Batch geochemical modelling and reactive transport simulations are being conducted to understand processes affecting the deep geothermal fluids on their way to the surface and to characterize the hydrologic relations between the deep reservoir and the superficial hot springs.

References

[1] Reed, M.H., Spycher, N.F. (1984), *Geochim. Cosmochim. Acta* **48** 1479-1492. [2] Pang, Z.H., Reed, M.H. (1998), *Geochim. Cosmochim. Acta* **62** 1083-1091. [3] Spycher, N. et al. (2011), *Geoth. Resource Council Transactions* **35** 663-666. [4] Goff, F. et al. (2002), *Los Alamos National Laboratory Report LA-13972-MS, Los Alamos, NM* 71pp. [5] Lutz, S.J. et al. (1998), *Proceedings, Twenty-Third Workshop on Geothermal Reservoir Engineering, Stanford University* 315-321.

Evolutionary Response of S Isotope Fractionation by Sulfate Reducing Microorganisms

ANDRÉ PELLERIN[1]*, NADIA MYKYTCZUK[2], REBECCA AUSTIN[1], GRANT M. ZANE[3], LYLE WHYTE[2], JUDY D. WALL[3], AND BOSWELL WING[1]

[1]Department of Earth and Planetary Sciences, McGill University, Montréal, Canada, andre.pellerin@mail.mcgill.ca (* presenting author), boswell.wing@mcgill.ca, rebecca.austin@mail.mcgill.ca

[2]Department of Natural Resource Science, McGill University, St-Anne de Bellevue, Canada, nadia.mykytczuk@mail.mcgill.ca, lyle.whyte@mcgill.ca

[3]University of Missouri, Biochemistry Division, Columbia, USA, WallJ@missouri.edu, zaneg@missouri.edu

Microbial sulfur isotope fractionation is controlled by the energy metabolism of sulfate reducing microorganisms. It represents a well-defined and precisely measurable characteristic of the phenotype of the microorganism. As such, it is dependent both on the underlying genotype and on the response of that genotype to variability in the local environment. Since genotype and environment have both changed throughout Earth's history, the geological record of biogenic S isotopes must reflect the influence of both environmental change and molecular evolution. However, the basic interplay between microbial evolution and S isotope fractionation has not been examined.

We investigated the evolutionary response of S isotope fractionation in the sulfate-reducing bacterium *Desulfovibrio vulgaris* Hildenborough (DvH). Two bacteria – the wild type DvH as well as a mutant derived from that strain in which one copy of a gene putatively encoding lactate dehydrogenase was deleted and replaced with an antibiotic resistance cassette were used as model organisms. In defined media (sulfate and lactate limited) at 33°C, ancestral wild type and mutant DvH exhibit fractionation factors that reproducibly differ by 0.5‰. We serially transferred six replicate lines of the wild type and six replicate lines of the mutant for 600 generations in batch cultures. Over the course of the experiments, we assayed fitness through direct competition experiments between the ancestral mutant and descendant wild-type strains (or vice versa). In these competition experiments, we used qPCR to monitor the relative abundance of the mutant through a unique genetic barcode associated with the antibiotic resistant cassette. After 300 generations, the descendant strains were markedly more fit than their ancestors, with relative growth rate increases of nearly 30%. This means that the descendant strains have a clear selective advantage in the defined media, illustrating that DvH can undergo evolutionary adaptation on laboratory timescales.

Despite the clear evidence for evolutionary changes over the course of our experiment, isotopic assays of the descendant wild-type and mutant strains reveal that the 0.5‰ difference in their fractionation factors is conserved. Preservation of such a small isotope effect implies that the sulfate reducing energy metabolism is remarkably robust to the selective pressures of our experimental setup.

https://doi.org/10.1180/S0026461X00008434 Published online by Cambridge University Press

Discovery of metals-rich hydrothermal manganese deposits in the South-West Pacific

E. PELLETER[1]*, Y. FOUQUET[1], J. ETOUBLEAU[1], S. CHERON[1], S. LABANIEH[1] AND THE SCIENTIFIC PARTIES

[1]Ifremer c/Brest, Laboratoire de Géochimie et Métallogénie, BP70, 29280, Plouzané, France (*correspondance: ewan.pelleter@ifremer.fr)

Manganese oxides in the deep marine environment can be separated in three genetic groups: (i) hydrothermal, (ii) hydrogenetic, and (iii) diagenetic. The hydrothermal Mn deposits are characterized by low to very low contents of Cu, Ni, Co, Zn whereas the hydrogenetic Mn deposits can be enriched in a characteristic suite of trace elements (e.g. Co, Ni, Zn, REE, HFSE, Pt). As a consequence, only hydrogenetic manganese crusts and polymetallic nodules have been considered as a potential resource for some commercially important metals. Here we report on occurrence of metals-rich hydrothermal manganese deposits discovered in the south-west Pacific during a French cruise (fall 2010). These deposits occur at depth between 800m and 1800m and are controlled by volcanic structures. Volcanism is dominated by pyroclastic rocks (e.g. hyaloclastite, tuffite, pumice) at depth shallower than 1000 m and by pillow-lavas at greater depth. Mineralization occurs as crusts, meter-scale mounds and impregnations composed of well-crystallized birnessite and todorokite with variable amount of iron oxy-hydroxide and nontronite. The manganese oxides exhibit bluish-black to grey-black color with a submetallic luster typical of many hydrothermal Mn mineralizations [1]. Mn oxides are abnormally enriched in Ni (up to 4.6%), Co (up to 2.2%) and Cu (1.5%) but exhibit low REE and HFSE concentrations. Post-Archean Australian Shale-normalized REE patterns exhibit typical seawater signature with prominent negative Ce anomalies. Therefore, trace elements data point to a contribution of hydrothermal fluids for Ni, Co and Cu and a seawater contribution for REE and HFSE. Further, different genetic models to explain the mechanism for metal enrichment will be discussed.

[1] Eckhardt et al. (1997) *Mar. Georesour. Geotechnol.* **15**, 175-208.

Organic geochemisty of the Late Paleozoic black mudstone in Hailaer basin, NE China: Implications for hydrocarbon-forming potential

X.L. PENG*, N. LIU, L. LIU

College of Earth Sciences, Jilin University, Changchun, 130061,China (*correspondence: Pengxl@jlu.edu.cn)

It is being dissussed hotly that whether the Late Paleozoic strata in NE China have hydrocarbon forming potential or not. However, organic geochemical data of the black mudstones from the Late Paleozoic in Hailaer basin provides insights for that. It has been known that the Mesozoic strata in Hailaer Basin NE China, was a famous hydrocarbon accumulation zone. In addition, the outcrop rocks of the Carboniferous and Permian around the basin was in the late stage of diagenetic and low-lever metamorphic belt [1].

Amount to 39 wells of Beier and Wuerxun depression from Hailaer basin were drilled into the Paleozoic black mudstone, and the thickness of the mudstone is about 393m. In this research, organic geochemical analysis has been taken on 40 black mudstone samples from 11 selected wells. It is indicated that the TOC values ranged between 0.09% and 4.407%, with the mean value of 0.73%, and 40% samples are over threshold of the organic matter abundance (0.5).

Organic geochemical analytical data for the Late Paleozoic black mudstones in the well of Wu 9 and Bei 2 of Hailaer basin was collected from Daqing oil field. TOC values from Wu 9 (7 samples) show a mean value of 0.9%, and the maximum value is 1.66%, thus about 43% samples are moderate source rocks. The potential of pyrolysis hydrocarbon generation values are 4.4mg/g ~ 0.01mg/g (average 1.5mg/g), suggesting that 33.3% samples can be regarded as moderate source rocks. For the black mudstones from Bei 2 (29 samples), the average values for TOC and S1+S2 are 0.733% and 0.35 mg/g. The average value for IH is 26mg/g (maximum 123mg/g), showing a typical kerogen type of III. The mean values for Tmax and Ro are 433°C and 0.81, respectivety, suggested that the source rock are high maturity. Combined with the Paleozoic strata in Hailaer Basin is well-protected, we consider that this strata could have a good hydrocarbon-forming potential, and the source rocks from the Late Palezoic strata in Hailaer basin could be an ideal target for a new round of hydrocarbon exploration in NE China.

[1] Hu and Yu. (2009) Acta Petrologica Sinica. 25(8), 2017-2022

This research was financially supported by the Natural Science Foundation of China (40972075) and the Strategic Research Center of Oil & Gas Resources (14B09XQ1201).

https://doi.org/10.1180/S0026461X00008434 Published online by Cambridge University Press

Geogas Nano Material Elements Analysis For Detecting Concealed Structures in Dashui Gold Deposit in Gansu Province, China

XIUHONG PENG[1,2], HUI DENG[3*], BO XU[1],CHENGSHI QING[1],JIANGSU ZHANG[1,4]

[1]Geochemistry Dep., Chengdu University of Technology , China
[2] Key Laboratory of Nuclear Techniques in Geosciences, China
[3] State Key Laboratory of Geohazard Prevention and Geoenvironment Protection, Chengdu University of Technology (*correspondence:dh@cdut.edu.cn)
[4] Third Geology and Mineral Resources Exploration Academy of Gansu Province, Lanzhou, China

The nanoparticles in ore bodies can adsorb on gas and migrate in the updraft. It has strong penetrability which can rise vertically from the deep Earth to the surface, and creates a distribution anomaly (geogas anomaly) of nano material above the projection of ore bodies. Many scholars[1]-[2] have confirmed the prospecting effect of geogas method. From 1988 to 1999, Chunhan Tong et al. [3]-[4] had experimented on the geogas measure method in Laojie Gold Deposit in Yunnan Province and so on successively. They had successfully indicated the locations of ore bodies hundreds of meters deep underground, and observed the nanoparticles in geogas.

The dynamic geogas analysis adopted in this research is to use the pump to exact the geogas in the cover; then the nano materials will be captured by the liquid capture agent; and finally the various kinds of elements in geogas can be analyzed by ICP-MS to obtain the geogas information. Combining the geochemical exploration and the actual situation of the mine, five exploration lines and 40 elements of 139 samples were set in the survey area, including two experiment measuring lines on the known ore bodies.

Results and Conclusion

On the basis of the analysis of the trace elements and rare earth elements characteristics in ores and wall rocks, and the comparison of the geogas experimental profile, the geogas indicating elements were selected. The geogas indicating elements characteristics of the three exploration lines demonstrate that there are two concealed faults: one concealed structure and one ore-controlling structure in the survey area. The first concealed structure goes through No.7-13 measure point of Line a, No.15-19 measure point of Line b and No.7-14 measure point of Line c. The width of the structure (or the combination width of multiple microcracks) is 90-200m. The second ore-controlling structure goes through No.25 measure point of Line a, No.23-27 measure point of Line b and No.23-28 measure point of Line c. The width of the structure is about 80-100m. Because the results of radon survey is as the same as the geogas's, the prospecting exploration efforts should be greatly strengthened in the western periphery of Dashui Gold Deposit.

The authors acknowledge the support of the National Nature Science Foundation of China (No.41103025) and Cultivating Programme of Middle-aged Backbone Teachers of Chengdu University of Technology

[1] Kristanssonk et al. (1990) *Endeavour (New Series)* **14**, 28-33.[2] Wang et al. (2005) *GEOLOGY IN CHINA* **32**, 135-140.[3] Tong et al. (1997) *J MINERAL PETROL* **17**, 83-88.[4] Tong et al. (1999) *CHINESE JOURNAL OF GEOPHYSICS* **42**, 135-142.

The study on the solubility of the vanadium system focused on Panzhihua, China

Y. PENG[1,2], Y. ZENG*[1,2]

[1]College of Materials and Chemistry & Chemical Engineering, Chengdu University of Technology, Chengdu, Sichuan, 610059, P. R. China
[2]Mineral Resources Chemistry Key Laboratory of Sichuan Higher Education Institutions, 610059, P. R. China
(* correspondence: zengyster@gmail.com)

In recent years, the interest of the relationship between microelement and human health increased. Vanadium absence may have negative effects, and it also can be toxic if exposure occurs at high enough levels. It has strong transfer ability in environment. This ability related to the solubility of vanadium in soil solution.

Panzhihua, Sichuan is an important production base of vanadium and titanium magnetite. The vanadium storage is 64% of the total vanadium in China. The vanadium mining and smelting accelerated the vanadium diffusion in soil and water. It causes special environmental problems of vanadium in Panzhihua. Different surface soil in the region, the average mass fraction of vanadium is over 100 $\times$ 10^{-6},[1] far exceeding the background values of Chinese soil vanadium 86 $\times$ 10^{-6}.[2] The amount of vanadium in the soil surrounding smelter is 16.5 times of contrast values. The amount of vanadium in the plant samples is 6.6 times of contrast values.[3]

The solubility of vanadium in soil solution is effected by coexisting ions in soil，such as potassium, sodium, phosphorus and so on. In order to investigate the relationship of solubility between vanadium and the other co-existing ion in soil, the phase equilibria of the quinary system $NaVO_3$ + KVO_3 + NaH_2PO_4 + KH_2PO_4 + $(NH_2)_2CO$ + H_2O and its five quaternary sub-systems were studied at 298 K with isothermal dissoluble method. According to the experimental results, the crystallization form of metavanadate is polyoxovanadate in the weakly acid system. The dissolution and migration of vanadium in aqueous solution has negative correlation with $H_2PO_4^-$ and $(NH_2)_2CO$. The exisiting of K^+ has little effect on the solubility of vanadium. This suggest that in similar soil environment, the solubility of vanadium was restrained by the increase of $H_2PO_4^-$ and $(NH_2)_2CO$, which can affect the transfer ability of vanadium.

The authors acknowledge the support of the National Natural Science Foundation of China(40673050, 41173071), and the Research Fund for the Doctoral Program of Higher Education from the Ministry of Education of China (20115122110001).

[1] Teng, Tuo, Ni. (2003) *Chinese Journal of Geochemistry*, **22**, 253-262. [2] Wei, Chen, Zheng. (1991) *Environmental Science*, **12**, 12-19. [3] Wang, Wei. (1995) *Element Chemistry of Soil Environment*, 231-241.

https://doi.org/10.1180/S0026461X00008434 Published online by Cambridge University Press

Do Critical Zone carbon and water fluxes control chemical denudation?

JULIA N. PERDRIAL[1*], PAUL BROOKS[2], JON CHOROVER[1], KATE CONDON[2], ADRIAN HARPOLD[2], MOLLY HOLLERAN[1], DAVID HUCKLE[2], REBECCA LYBRAND[1], PETER TROCH[2], JEN MCINTOSH[2], TOM MEIXNER[2], REBECCA MINOR[3], BHASKAR MITRA[3], MICHAEL POHLMANN[1], CRAIG RASMUSSEN[1], TYSON SWETNAM[3], ANGELICA VASQUEZ-ORTEGA[1], XAVIER ZAPATA-RIOS[2]

[1]University of Arizona, Department of Soil, Water and Environmental Sciences, Tucson, AZ, USA, jnperdri@email.arizona.edu (*)

[2]University of Arizona, Department of Hydrology and Water Resources, Tucson, AZ, USA

[3]University of Arizona, School of Natural Resources, Tucson, AZ, USA

What controls the magnitude of weathering fluxes in the Critical Zone (CZ) and how vulnerable are those fluxes towards changes in climatic forcing? We believe that these fundamental questions can be uniquely addressed through an integrative approach that includes multiyear CZ water, carbon and lithogenic element flux records using a scaling approach that bridges multiple CZ sub disciplines. Based on the theoretical framework of the Santa Catalina Mountains - Jemez River Basin (SCM-JRB) CZO, we postulate that effective energy and mass transfer (EEMT, MJ m^{-2} y^{-1},[1]) is a predictive variable for chemical denudation. This parameter can be estimated from meteorological variables, as we have done previously for our CZO [2], or it can be measured directly, as we report in this presentation. Within the CZO framework, we are now testing the hypothesis that direct hydrologic and organic geochemical quantifications of EEMT in CZ fluids are correlated with fluxes of major and trace lithogenic elements for several montane forest catchments. Rare earth elements (REE) are investigated as tracers for chemical denudation mechanisms and preliminary data on REE-organic carbon interaction indicate the importance of labile organic carbon (the biomass energy flux component of EEMT) as a key controller of chemical denudation patterns. Climatic impacts on inter-annual variations in EEMT seem to exert an overarching constraint on chemical denudation.

[1] Rasmussen et al. (2010). *An open system framework for integrating critical zone structure and function.* Biogeochemistry. **102**, 15-29.

[2] Chorover et al. (2011). *Probing how water, carbon, and energy drive landscape evolution and surface water dynamics: The Jemez River Basin – Santa Catalina Mountains Critical Zone Observatory*. Vadose Zone Journal. **10**, 884-899.

Modeling the hydrothermal circulation and the hydrogen production at the Rainbow site with Cast3M

FLORIAN PEREZ[1*], CLAUDE MÜGLER[1], PHLIPPE JEAN-BAPTISTE[1] AND JEAN LUC CHARLOU[2].

[1]LSCE, CEA-CNRS-UVSQ, Gif-Sur-Yvette, France florian.perez@lsce.ipsl.fr (* presenting author)

[2] Géosciences Marines, IFREMER, Brest, France Jean.Luc.Charlou@ifremer.fr

Background and Aims

On the Mid-Atlantic Ridge, the Rainbow venting site is described as an ultramafic-hosted active hydrothermal site and releases high fluxes of methane and hydrogen [1, 2]. This behavior has first been interpreted as the result of serpentinization processes. But geochemical reactions involving olivine and plagioclase assemblages, and leading to chlorite, tremolite, talc and magnetite assemblages, could contribute to the observed characteristics of the exiting fluid [2].

Objectives and methods

The predominance of one of these geochemical reactions or their coexistence strongly depend on the hydrothermal fluid circulation. We developed and validated a 2D/3D numerical model using a Finite Volume method to simulate heat driven fluid flows in the framework of the Cast3M code [3, 4]. We also developed a numerical model for hydrogen production and transport that is based on experimental studies of the serpentinization processes [5]. This geochemical model takes into account the exothermic and water-consuming behavior of the serpentinization reaction and it can be coupled to our thermo-hydrogeological model.

Results and conclusion

Our simulations provide temperatures, mass fluxes and venting surface areas very close to those estimated in-situ [6]. We showed that a single-path model [7] was necessary to simulate high values such as the in-situ measured temperatures and estimated water mass fluxes of the Rainbow site [6].

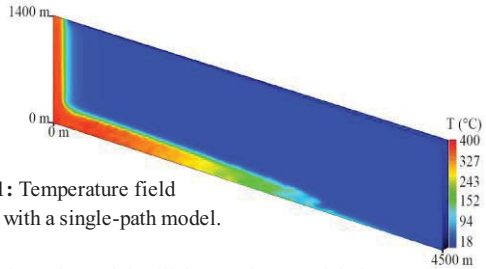

Figure 1: Temperature field obtained with a single-path model.

This single-path model will be used to model the production and transport of hydrogen at the Rainbow hydrothermal site.

[1]Charlou et al. (2010) *AGU Monograph series*. [2]Seyfried et al. (2011) *Geochim. Cosmochim. Acta 75*, 1574-1593. [3]http://www-cast3m.cea.fr. [4]Martin & Fyfe (1970) *Chem. Geol. 6*, 185-202. [5] Marcaillou et al. (2011) *Earth and Planet. Sci. Lett. 303*, 281-290. [6]Perez et al. (2012) submited to Computational Geosciences. [7]Lowell & Germanovich (2004) AGU, Washington DC, USA.

https://doi.org/10.1180/S0026461X00008434 Published online by Cambridge University Press

El Niño impact on mollusk shell biomineralization

ALBERTO PÉREZ-HUERTA[1*], MIGUEL F. ETAYO-CADAVID[1,2], C. FRED T. ANDRUS[1], AND TERESA E. JEFFRIES[3]

[1] Department of Geological Sciences, The University of Alabama, Tuscaloosa, AL 35487, USA, aphuerta@as.ua.edu (* presenting author)
[2] BP America Inc., Houston, TX 77079, USA, metacad@gmail.com
[3] Mineralogy Department, Natural History Museum, London SW7 5BD, UK, t.jeffries@nhm.ac.uk

Marine macroinvertebrates are ideal sentinel organisms to monitor rapid environmental changes associated with climate change. Chemical proxies from mollusk shells are widely used for detecting variations in seawater parameters (e.g., temperature and productivity) related to such changes. However, the influence of known, and recurrent, climatic events on biological processes during active mineralization, and thus on shell chemistry, is still insufficiently understood.

Analysis of Peruvian cockles from the 1982-83 large magnitude El Niño event show significant alterations in shell biomineralization, linked to microstructural changes and the loss of organic matrix components. These alterations are associated to modifications in magnesium and barium content of aragonite cross lamellar shell layers, while strontium content is nearly constant throughout the event. An increase in magnesium is a possible response of the mollusk specimens to the loss of proteins and the need for the stabilization of amorphous calcium carbonate. Additionally, the increase of barium after the El Niño onset is related to upwelling. Overall, these findings contribute to a better understanding the effects of abrupt climate change on mollusk shell structures, while also offering a new view for proxy application to the reconstruction of El Niño events.

Mobility of trace elements from the Sunbury Shale, eastern Kentucky

ROBERT PERKINS[1*], CHARLES MASON[2], AND DAVID PIPER[3]

[1]Portland State University, Department of Geology, Portland, OR, USA, rperkins@pdx.edu (*presenting author)
[2]Morehead State Univeristy, Earth and Space Sciences, Morehead, KY, 40351, USA
[3]U.S. Geological Survey, Mineral Resources Group, Menlo Park, CA, USA

Black shales contain high concentrations of trace elements and may serve as important sources of strategic metals, U and REEs as conventional ore deposits become scarcer. However, the increased use of hydrofracturing for shale gas development as well as possible future mining and processing of black shales for extraction of shale oil could potentially facilitate release of toxic trace elements to hydraulic fracturing or retort process waters, surface water and ground water. Quantifying the concentrations and relative mobility of trace elements from black shales is thus important from both economic and environmental perspectives. A better understanding of trace element mobility from natural weathering of these deposits may also be of use for researchers using outrcop samples to determine paleodepositional conditions.

The Sunbury Shale (lower Mississippian) is one of the youngest units making up the thick Devonian and Mississippian black shale sequence in the Appalachian Basin. This study compares the trace element geochemistry of samples collected from two exposures of Sunbury Shale located < 8 km apart along the eastern margin of the Cincinnati Arch (western flank of the Appalachian Basin). At one site, fresh to minimally weathered samples were collected from a roadcut excavated only a month prior; the second site was a roadcut exposed for ~40 years, wherein the shale was visibly weathered. The Sunbury Shale has, on average, higher levels of trace elements than the much thicker Devonian Ohio Shale that outcrops in the study area (Perkins et al., 2008) and its 5-m thickness readily allowed for comparative sampling of the entire unit from each of the sites. The results indicate that the 40 year period of surface weathering resulted in significant ($\alpha = 0.05$) loss of some trace elements, particularly those associated with sulfides (e.g., Cd, Cu, Ni, Zn). No significant differences were found with respect to the concentrations of Cr, Mo, V that are associated with refractory phases. No significant differences were found with regards to As or Se concentrations, although these elements are also associated with sulfides. This may be due to preferential sorption of these oxyanions under the locally acidic conditions resulting from sulfide oxidation.

[1] Perkins, Piper, and Mason (2008), *Palaeogeography, Palaeoclimatology, Palaeoecology* **265**, 14-29.

https://doi.org/10.1180/S0026461X00008434 Published online by Cambridge University Press

Atmospheric iron from crustal sources: prognostic aerosol composition in GISS/ModelE

JAN P. PERLWITZ[1], CARLOS PÉREZ[1*], RON L. MILLER[1] AND SERGIO RODRIGUEZ[2]

[1]NASA Goddard Institute For Space Studies and Dept of Applied Physics and Applied Math, Columbia University, New York, USA, jan.p.perlwitz@nasa.gov, carlos.perezga@nasa.gov, ronald.l.miller-1@nasa.gov (* presenting author)

[2]Izaña Atmospheric Research Centre, Agencia Estatal de Meteorología, Tenerife, Spain, srodriguezg@aemet.es

Introduction

The emission of aerosol iron from crustal sources is subject to significant uncertainty. Many atmospheric model studies assume spatially homogeneous total iron content at dust sources, typically 3.5% by mass. Moreover, as iron oxides and hydroxides are comprised of more than 50% iron by mass, models usually consider them as the main suppliers of dissolved iron resulting from dust deposition. A recent experiment [1] has shown a large contribution by clays - their low iron content offset by their large solubility - to the total dissolved iron from dust samples. This and other studies suggest the need for explicit representation of individual minerals in dust-climate models in order to improve our understanding of the atmospheric iron cycle and iron deposition as an input to ocean biological productivity.

Methodology

We have implemented prognostic budgets of separate mineral types into an Earth System Model: GISS/ModelE. Each mineral type (composed of iron and/or other elements) is separately transported and modified within the atmosphere. Spatially-dependent concentrations of illite, kaolinite, smectite, calcite, quartz, feldspar, iron (hydr)oxide, and gypsum are predicted by the model based on an updating of the source mineralogy proposed in the seminal work of [2]. We use downwind observations to constrain the mineral content of aerosols leaving the source.

Discussion

We evaluate model results against global observations of mineral aerosols with emphasis on multiyear measurements of size-segregated dust elemental composition at the Izaña Observatory (Tenerife, Canary Islands), situated downwind of important North African dust sources. We highlight the strengths and limitations of the source prescription of [2] and propose new strategies to represent mineral tracers in dust models.

[1] Journet *at al.* (2008) *Geophys. Res. Let* **35,** L07805. [2] Claquin et al. (1999) *J. Geophys. Res* **104, D18,** 22,243-22,256.

Hg stables isotopes assessing methylmercury bioaccumulation, sources, and metabolization in the pelagic food web of Lake Baikal (Russia)

VINCENT PERROT[1]*, MIKHAIL PASTUKHOV[2], VLADIMIR N. EPOV[1], DAVID AMOUROUX[1] AND OLIVIER F.X. DONARD[1]

[1] Laboratoire de Chimie Analytique Bio-Inorganique et Environnement, IPREM, CNRS-UPPA-UMR-5254, Pau, France (*v.perrrot@etud.univ-pau.fr)

[2] Laboratory of geochemical mapping and monitoring, Institute of Geochemistry SB RAS, 1A Favorskogo Street, PB-304, Irkutsk, 664033, Russia

Monomethylmercury (MMHg) is the main chemical form of mercury that threatens human populations via food consumption after its bioaccumulation and biomagnification in food webs [1]. Nowadays, Hg stable isotopes mass dependent and mass independent fractionation (MDF and MIF) is a powerful tool to identify Hg sources and transformations within the environment [2]. In aquatic ecosystems, several Hg transformations may affect Hg molecular speciation and thus Hg isotopes fractionation, inferring toughness to unravel accurately Hg isotopic signature observed in samples. The aim of this study was to investigate Hg bioaccumulation, trophic transfer and its metabolization in top predator organs, through the measurement of total Hg isotopic composition and Hg compounds (i.e. MMHg and inorganic Hg(II)) specific isotopic composition (CSIC) in the pelagic food web of the oligotrophic and remote freshwater Lake Baikal (Russia).

Carnivorous pelagic sculpins fish (Comephoridae and Cottocomephoridae families) and their predator seals (*Phoca sibirica*) were especially investigated. Significant MIF was observed in both samples with no significant differences (Δ^{199}Hg of 4.59±0.55‰ (n=27) and 4.62±0.60‰ (n=7), respectively. This high MIF was related to efficient MMHg demethylation before bioaccumulation in organism's muscles. On the other hand, Hg trophic transfer (from sculpins to seals) does not produce Hg MIF whereas MDF is likely during this process since seals muscles have δ^{202}Hg about 1‰ higher than sculpins muscles. Seals organs (liver, kidney, muscle, hair, intestine …) displayed significantly different Hg speciation, with liver and kidney mostly composed of Hg(II) whereas hair and muscle have more than 80% MMHg (figure 1).

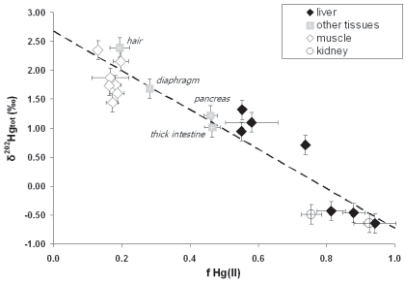

Figure 1. $\delta^{202}Hg_{tot}$ as a function of the fraction of inorganic Hg in seals tissues

Hg CSIC in seals tissues showed MMHg and Hg(II) enriched in heavier and lighter isotopes, respectively, with a δ^{202}Hg difference of about 3.2‰. MMHg demethylation in these top predator mammals was thus identified as a major process leading to MDF, but no MIF, of Hg isotopes before storage and/or elimination within the different organs, such as residual MMHg in muscle and Hg(II) in liver.

[1] Morel et al. (1998). *Annual Review of Ecology and Systematics*, **Volume 29**, pp543-566
[2] Bergquist and Blum (2009). *Elements*, **Volume 5**, pp353-357

https://doi.org/10.1180/S0026461X00008434 Published online by Cambridge University Press

New insights on crystal growth and dissolution by investigating micro-scale entities.

MASSIMO PERUFFO[*1], MICHAEL M. MBOGORO[1] AND PATRICK R. UNWIN[1]

[1]Electrochemistry and Interfaces Group, Department of Chemistry, The University of Warwick, Coventry, CV4 7AL, UK.

M.peruffo@warwick.ac.uk (* presenting author)

Abstract

A new approach to the study of crystal growth/dissolution kinetics is reported, that involves measuring the time-evolution of entire isolated micro-crystals or micro-etch pits in macro crystals via a variety of microscopic techniques (2D and 3D). [1,2] By coupling such measurements to finite element diffusion models, the importance of mass transport to the overall rates can be elucidated readily. Furthermore the approach reveals directly plane-specific intrinsic kinetics free from diffusional effects. Investigations on gypsum ($CaSO_4.2H_2O$) highlight notable sensitivity to solution stoichiometry (Ca^{2+} and SO_4^{2-} ratio) which results in different crystal and pit morphology[3]. In summary, the method is powerful in linking microscopic observations to macroscopic rates and is expected to be of general applicability.

[1] Fan, C.; Teng, H. H. (2007) *Chem. Geol.* **245**, 242-253.

[2] Luttge, A.; Arvidson, R. S. (2010) *J. Am. Ceram. Soc.* **93**, 3519-530.

[3] Zhang, J.; Nancollas, G. H. (1992) *J. Cryst. Growth* **118**, 287-294.

Metasomatic control of water in garnet and pyroxene from Kaapvaal craton mantle xenoliths

ANNE H. PESLIER[1,2*], ALAN B. WOODLAND[3], DAVID R. BELL[4], MARINA LAZAROV[5] AND THOMAS J. LAPEN[6]

[1]Jacobs Technology - ESCG, Houston TX, USA, anne.h.peslier@nasa.gov (* presenting author)

[2]NASA - JSC, Houston TX, USA

[3]Universität Frankfurt, Germany, woodland@em.uni-frankfurt.de

[4]Arizona State University, Tempe AR, USA, David.R.Bell@asu.edu

[5]Universität Hannover, Germany, m.lazarov@mineralogie.uni-hannover.de

[6]University of Houston, TX, USA, tjlapen@uh.edu

Fourier transform infrared spectrometry (FTIR) and laser ablation inductively coupled plasma mass spectrometry (LA-ICPMS) were used to determine water, rare earth (REE), lithophile (LILE), and high field strength (HFSE) element contents in garnet and pyroxene from mantle xenoliths, Kaapvaal craton, southern Africa. Water enters these nominally anhydrous minerals as protons bonded to structural oxygen in lattice defects [1,2]. Pyroxene water contents (150-400 ppm in clinopyroxene; 40-250 ppm in orthopyroxene) correlate with their Al, Fe, Ca and Na and are homogeneous within a mineral grains and a xenolith. Garnets from Jagersfontein are chemically zoned for Cr, Ca, Ti and water contents. Garnets contain 0 to 20 ppm H_2O.

Despite the fast diffusion rate of H in mantle minerals [3], the observations above indicate that the water contents of mantle xenolith minerals were not disturbed during kimberlite entrainment and that the measured water data represent mantle values. Trace elements in all minerals show various degrees of light REE and LILE enrichments indicative of minimal to strong metasomatism. Water contents of peridotite minerals from the Kaapvaal lithosphere are not related to the degree of depletion of the peridotites. Instead, metasomatism exerts a clear control on the amount of water of mantle minerals. Xenoliths from each location record specific types of metasomatism with different outcomes for the water contents of mantle minerals. At pressures $\leq$ 5.5 GPa, highly alkaline melts metasomatized Liqhobong and Kimberley peridotites, and increased the water contents of their olivine, pyroxenes and garnet. At higher pressures, the circulation of ultramafic melts reacting with peridotite resulted in co-variation of Ca, Ti and water at the edge of garnets at Jagersfontein, overall decreasing their water content, and lowered the water content of olivines at Finsch Mine. The calculated water content of these melts varies depending on whether the water content of the peridotite (2 wt% H_2O) or individual minerals (<0.5-13 wt% H_2O) are used, and also depend on the mineral-melt water partition coefficients. These metasomatic events are thought to have occurred during the Archean and Proterozoic, meaning that the water contents measured here have been preserved since that time and can be used to investigate viscocity and longevity of cratonic mantle roots [4].

[1] Bell & Rossman (1992) *Science* **255**, 1391-1397. [2] Peslier (2010) *JVGR* **197**, 239-258. [3] Ingrin & Blanchard (2006) *MSA-RMG* **62**, 291-320. [4] Peslier *et al.* (2010) *Nature* **467**, 78-81.

https://doi.org/10.1180/S0026461X00008434 Published online by Cambridge University Press

Experimental vapor-liquid partitioning of transition metals in NaCl dominated fluids

NICHOLAS J. PESTER[1*], KANG DING[1], AND WILLIAM E. SEYFRIED, JR.[1]

[1]Dept. of Earth Sciences, University of Minnesota, Minneapolis, MN, U.S.A. (* presenting author: peste005@umn.edu)

Multi-phase fluid flow is a common occurrence in magmatic hydrothermal systems, and extensive modeling efforts using empirically derived PVTx properties of the NaCl-H_2O system are frequently conducted. We have performed hydrothermal flow experiments in the near-critical and two-phase region (410-465 °C, 250-400 bars) to derive sufficiently resolute partition coefficients for some important accessory metals. NaCl solutions (3-6 wt%) containing variable amounts (1-20 mmolal) of alkaline earth and transition metal chlorides were pumped through a Ti alloy reactor with an outlet control valve capable of maintaining set pressure within ± 0.5 bars. Flow rates were optimized to obtain the equilibrium vapor phase and the coexisting liquid was then simultaneously sampled. The included figure shows Zn data as a representative example of the metals studied (shown normalized to starting composition of the single phase fluid). Na dominates phase behavior in the system, where all metal cations must be charge balanced

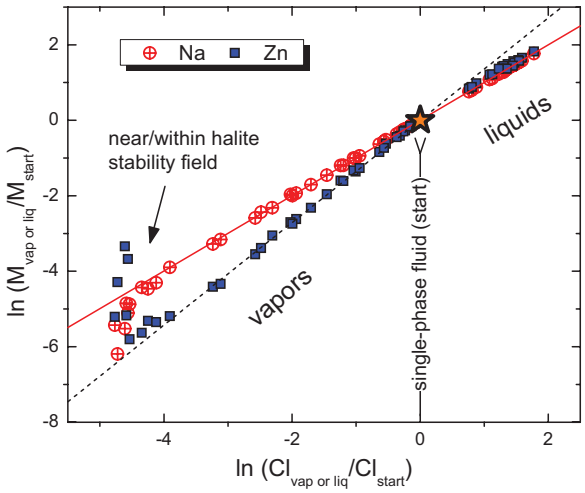

by Cl. The Zn/Na ratio decreases with chlorinity in the vapor phase until conditions approach halite saturation where the trend abruptly reverses with a concommitant decrease in pH (possibly due to hydrolysis). Such volatility may play an important role in concentrating transition metals in magmatic hydrothermal systems. Uniform slopes for each metal in the vapor phase equate to relative partition coefficients (Na = 1) of the order: Cu(I) ≤ Na < Fe(II) < Zn < Mg ≤ Ni(II) ≤ Mn(II) ≤ Co(II) < Ca < Sr < Ba. While the absolute concentration of such elements in natural fluids is controlled to a first order by temperature dependant mineral solubility, phase separation can be decoupled from fluid-mineral equilibria depending on flow rate/residence time. Thus, such partition coefficients can be used to aid in both geochemical modeling and reconstruction of P-T history for multiple hydrothermal fluid samples or inclusions.

Nucleation: concentration fluctuations and polymorph selection

BARON PETERS[1]

[1]University of California at Santa Barbara, Chemical Engineering, baronp@engineering.ucsb.edu

Nucleation is the stochastic process that creates the first stable embryo of a new phase to initiate a phase transition. The mechanism is poorly understood because rare events processes like nucleation present special challenges to both experiments and simulations. The difficulties are particularly acute for multi-component condensed phase nucleation processes where most applications lie. I outline recent advances toward understanding nucleation mechanisms. First, I show how the free energy landscape and dynamics for development of competing polymorphs can be understood using simulations.[1,2] Then I present a new droplet theory of nucleation that couples local concentration fluctuations to nucleus size evolution.[3] The new theory may explain why recent simulations with very different solutes show similar two-step nucleation mechanisms.

[1] Peters (2009) *J. Chem. Phys.* **131**, 224103. [2] Duff, Peters (2011) *J. Chem. Phys.* **135**, 134101. [3] Peters (2011) *J. Chem. Phys.* **135**, 044107 (2011).

https://doi.org/10.1180/S0026461X00008434 Published online by Cambridge University Press

Combining spectroscopic, isotope and modeling techniques to reveal the fate of sulphur in petroleum system studies

HENNING PETERS[1*], OLAF PODLAHA[1], CHAD GLEMSER[2], LAVERN STASIUK[2] AND ERDEM IDIZ[1]

[1]Shell Global Solutions International B.V., Rijswijk, The Netherlands,
Henning.Peters@shell.com (* presenting author)
Olaf.Podlaha@shell.com
Erdem.Idiz@shell.com
[2]Shell Canada Energy LTD, Calgary, Canada
Chad.Glemser@shell.com
Lavern.Stasiuk@shell.com

Introduction

The subsurface geochemical distribution of non-hydrocarbon "sour" gases (H2S, CO2) in oil/gas reservoirs is controlled mainly by thermochemical sulphate reduction (TSR) and organic matter cracking of organic sulfur compounds (OSC) in high temperature reservoirs versus bacterial sulfate reduction (BSR) in low-temperature reservoirs [1]. Their subsequent interactions with the hydrocarbon phase yield organic sulfur compounds in reservoirs and can result in sulfur rich bitumen formation via natural vulcanization processes [2]-[4].

To elucidate such mechanisms as sulfur incorporation and bitumen formation, we developed an integrated experimental approach of organic/inorganic geochemical and spectroscopy methods combined with in-house modeling capabilities. With presenting the main elements of the analytical workflow involving bulk geochemical data, X-ray absorption and photoelexctron spectroscopy techniques, isotope geochemistry, fluid inclusion studies and modeling approaches, we aim for a profound understanding of gas/fluid-rock interactions involving sulfur geochemistry in the suburface realm.

The workflow was developed on stacked Upper Devonian to Mississippian sour gas reservoirs situated in the Rocky Mountains Foothills of Alberta, Western Canadian Sedimentary Basin (WCSB), Canada. Production from these reservoir units is mainly dry gas and condensates with different forms of sulfur. H_2S contents range from 5% to almost 90%.

Results and Conclusions

Preliminary data on studied bitumens from WCSB assets revealed a sequence of solid bitumens with increasing amounts of sulfur incorporated. The distribution of sulfur compounds in the bitumen matrix comprises various oxidation states from -2 to +6. Major sulfur compound classes quantified are sulfide bridged compound classes, thiols, thiophenes and sulfates.

[1] Machel (2001) Sed. Geol. **140**, 143-175.
[2] Kelemen et al. (2010) GCA **74**, 5305-5332.
[3] Kelemen et al. (2008) GCA **72**, 1137-1143.
[4] Walters et al. (2011) Organic Geochem. **42**, 999-1006

Uniform distribution of p-process ^{174}Hf in extraterrestrial materials

STEFAN T.M. PETERS[1,2,*], CARSTEN MÜNKER[1,2]

[1]Institut für Geologie und Mineralogie, Universität zu Köln, Germany; stefan.peters@uni-koeln.de (* presenting author)
[2]Steinmann-Institut für Geologie, Mineralogie und Paläontologie, Rheinische Friedrich-Wilhelms-Universität Bonn, Germany

Nucleosynthetic heterogeneity in extraterrestrial materials is found for several (but not all) p-process isotopes, and reflects the injection of material synthesized by at least one supernova event shortly before the first solar system objects formed. Further information on the distribution of p-process isotopes is relevant to characterise the source of this "late injection" and to unravel the different nucleosynthetic processes producing p-process isotopes. Here we present high precision MC-ICPMS measurements of p-process isotope ^{174}Hf in silicate materials that have originated at different ages and from different regions within the inner solar system. ^{174}Hf is of particular interest because of its similar mass range to p-process ^{180}W, which displays large excesses in iron meteorites [1].

For Hf purification, we optimised the existing protocol by [2]. This was necessary to (1) successfully correct for the interference by isobaric ^{174}Yb; and (2) avoid matrix effects. Furthermore, we extensively tested sample cones with a large aperture ("Jet cones") in combination with an OnTool™ Booster interface pump. This setup enhances instrument sensitivity by a factor of more than 5 (ca. 3000 V/ppm Hf), but we also observed anomalous mass bias behavior in the presence of only minute amounts of matrix. All samples were therefore measured in setup with standard sample and X-skimmer cone, typically consuming ~60 ng Hf at precisions of ±70 ppm (2σ).

^{174}Hf/^{177}Hf ratios in analysed EL, H, L and CV chondrites, eucrites, and one lodranite sample are indistinguishable from the terrestrial value. In contrast, a silicate inclusion of the El Taco IAB iron meteorite and one EL6 chondrite (Pillistfer) exhibit higher ^{174}Hf/^{177}Hf ratios than the terrestrial standard, namely 190 ±72 ppm and 210 ±75 ppm respectively. These are correlated with higher ^{178}Hf/^{177}Hf ratios (18±5 and 21±5 ppm, respectively). The latter most likely result from secondary neutron capture reactions at epithermal energies due to the high Fe content of the samples [3]. The high ^{174}Hf/^{177}Hf ratios therefore most likely reflect a deficit in ^{177}Hf. ^{174}Hf itself has a low neutron capture cross-section (RI ~345 barn [4]) and is expected to be unaffected by cosmic ray interactions.

The absence of nucleosynthetic heterogeneity in ^{174}Hf indicates that either the protosolar nebula was homogenous in ^{174}Hf, or, alternatively, that existing ^{174}Hf heterogeneities had been efficiently homogenized by the time of parent body formation. The second scenario would be consistent with a single source for p-process ^{180}W and ^{174}Hf, and is therefore more plausible.

[1] Schulz & Münker (2011) *Mineral Mag* **75**, 1827. [2] Münker et al. (2001) *G*^{3} **2**, GC000183. [3] Sprung et al. (2011) *EPSL* **295**, 1-11. [4] Trbovich et al. (2009) *Nucl Sc Eng* **161**, 303-320.

https://doi.org/10.1180/S0026461X00008434 Published online by Cambridge University Press

Multi tracer study (^{36}Cl, ^{234}U/^{238}U, ^{14}C) of the Tunisian Continental Intercalaire: inferring recharge areas and groundwater ages.

J. O. PETERSEN[1,*], P. DESCHAMPS[1], B. HAMELIN[1], J. GONCALVES[1], M. MASSAULT[2], J.-L. MICHELOT[2] AND K. ZOUARI[3].

[1] CEREGE, UMR Aix-Marseille Univ.-CNRS-IRD, Aix-en-Provence cedex 4, France (* correspondence: petersen@cerege.fr)

[2] IDES, Université Paris-Sud, Orsay, France

[3] LRAE (ENIS), Sfax Univerty, Sfax,Tunisia

Assessment of groundwater recharge and ages is critical to study the sustainability of groundwater resources. However, determining "active" recharge areas within large aquifer systems, such as the North-Western Sahara Aquifer System (NWSAS) remains challenging. Here, we combine three geochemical tracers (^{14}C, ^{36}Cl and U isotopes) to infer past or recent recharge and evaluate groundwater ages in the Tunisian Continental Intercalaire (CI) Aquifer, the confined aquifer unit of the NWSAS.

Thirty-two boreholes were sampled, covering the whole Tunisian part of the CI aquifer. We paid a special attention on the Dahar Mountains where CI formations outcrop (11 samples). Only two samples located in the Northern Dahar are significantly above background in ^{14}C activity (1 pmc and 1.1 pmc). Uranium content varies from 2.8 to 5×□□$^{-4}$ ppb and ^{234}U/^{238}U activity ratio from 1 to 14. The stepwise decrease in U concentration goes with a high increase of the ^{234}U/^{238}U ratio followed by a decrease, clearly indicating the occurrence of a redox front. ^{36}Cl/Cl ratio varies from 5 to □□□×□□$^{-15}$. Four samples in the upper range (35-40 ×□□$^{-15}$) are again located in the northern oxidizing region of the Dahar as revealed by U concentration. Therefore, these data all converge to indicate that mixing with recent recharge waters occur to some extent in the northern Dahar region, while the southern part of this region shows no evidence of recent recharge.

This constitutes valuable information for hydrodynamic model and comparison with direct simulation of groundwater age (e.g. age-mass approach). We will assess at the meeting the consistency of these data with flow lines of water circulation inferred from piezometric data and hydrological modelling. Crude time constraints and mixing ratios will be also estimated from the comparison between these samples and those collected from the shallower Continental Terminal (CT) aquifer closer to present-day recharge waters.

A structure refinement for monoclinic hydrohematite

KRISTINA M. PETERSON[1]*, PETER J. HEANEY[2] AND JEFFREY E. POST[3]

[1]Pennsylvania State University, Department of Geosciences, University Park, USA, kmp286@psu.edu (* presenting author)

[2]Pennsylvania State University, Department of Geosciences, University Park, USA, pjh14@psu.edu

[3]Department of Mineral Sciences, Smithsonian Institution, USA, postj@si.edu

Introduction

In ferruginous soils, nano- to micro-scale hematite (α-Fe_2O_3) plays a central role in redox processes and contaminant cycling. Hematite is known to incorporate structural OH^- and water, and the requisite charge balance is achieved by iron vacancies. Prior researchers have suggested that the defective hematite structures form unique phases called "protohematite" (PH) and "hydrohematite" (HH) [1-3]. These phases are distinguished from stoichiometric hematite (SH) by their degree of hydration and iron deficiency. Furthermore, past infrared and Raman spectroscopic studies have assigned a lower-symmetry space group to PH/HH (*R*3*c*) relative to that of SH (*R*-3*c*) [4]. However, the existence and structure of these phases has been contentious, largely due to the lack of *in situ* X-ray diffraction data [5].

Here we present a new structure refinement for HH in a monoclinic space group (*I*2/*a*) using time-resolved X-ray diffraction (TR-XRD) data collected at the Advanced Photon Source (APS). Starting with ferric chloride solutions, we collected TR-XRD data during the *in situ* hydrothermal precipitation of akaganéite and its transformation to HH. Sealed quartz capillaries (1.0 mm diameter) were heated at 200 °C while XRD data were collected every 25 – 30 seconds. Rietveld refinements suggested a new monoclinic HH structure.

Results and Conclusions

In our experiments, distinct peak splitting was observed in the hematite diffraction patterns, indicating a violation of the 3-fold rotational symmetry. The observed peak splitting in our data was outside the range calculated for sample displacement, and furthermore video footage obtained during the reaction showed particles uniformly convecting throughout the volume of the capillary. We therefore refined the structure in the various subgroups of *R*-3*c*. As the fit using *I*2/*a* was statistically no worse than that in lower symmetry groups, we selected this space group for our refinement. A monoclinic unit cell with parameters of a = 13.7493(15) Å, b = 5.0121(4) Å, c = 5.4418(6) Å, β = 147.6250(17)° provided a good fit and significant reduction in χ^2 and R_{wp} relative to S.G. *R*-3*c*. Our results demonstrate that the *in situ* formation of the defective hematite phase, HH, was successfully captured. Moreover, HH is structurally distinct from SH and may form as a lower-symmetry monoclinic phase in soils.

[1] Dang *et al.* (1998) *Hyperfine Interact.* **117**, 271-319. [2] Wolska (1981) *Z Kristallogr.* **154**, 69-75. [3] Gualtieri and Venturelli (1999) *Am. Mineral.* **84**, 895-904. [4] Burgina *et al.* (2000) *J. Struct. Chem.* **41**, 396-402. [5] Cornell and Schwertmann *The Iron Oxides, 2nd ed.* Wiley-VCH, Weinheim (2003).

https://doi.org/10.1180/S0026461X00008434 Published online by Cambridge University Press

The microbial role in diagenetic dolomite formation

DANIEL A. PETRASH[1*] AND KURT O. KONHAUSER[1]

[1]University of Alberta, Edmonton, Canada, petrash@ualberta.ca (* presenting author)

In the Neogene, the presence of extensive dolomite intervals exhibiting multigenetic crystal morphologies, distinctive $\delta^{13}C$ signatures and variable concentrations of Fe and Mn, strongly suggest the involvement of various microbial heterotrophic pathways in both dolomite nucleation and ageing [1,2]. However, the relevance of enhanced organic burial, and the catalytic role of microbes in post-depositional dolomite formation, and as an overall control of the Cenozoic abundance of dolomite, remains to be demonstrated.

Most recently, the anaerobic oxidation of methane (AOM), typically by a consortium involving archaea and sulfate reducer bacteria, has been found to be a significant geochemical process in marine sediments [3,4,5]. The activity of microbial communities capable of AOM is usually recorded by a distinctively depleted ^{13}C signal in their carbonate by-products [3]. However, in diffusion-dominated sediments more positive $\delta^{13}C$ could be the result of an admixture of methanogenic $^{13}CO_2$, or alternatively from extensive AOM, which may also increase the residual carbon pool in ^{13}C [5]. In Neogene sequences, the occurrence of multigenic dolomite-rich intervals with $\delta^{13}C$ varying from markedly negative to positive values points to AOM as a likely mechanism of ageing, and potentially extends the microbial dolomite induction zone a few hundred meters below the sediment water interface [e.g., ref. 4].

To fully understand the burial diagenetic history of such intervals, and by extrapolation, their ancient analogues, a comprehensive analytical approach is required. For instance, in addition to the possible presence of ^{13}C-depleted lipid biomarkers [3], when compared with their near-surface precursors dolomite cements formed under the influence of syntrophic AOM should exhibit relatively higher Fe, Mn, and probably bioactive Ni, Zn and Cu concentrations [6]. Unravelling the role of AOM in dolomite formation during burial into the methanogenic zone may provide new insights into the long-standing dolomite problem.

[1] Budd (1997) *Earth Science Reviews* **42**,1-47. [2] Mazzullo (2000) *Journal of Sedimentary Research* **70**, 10-23. [3] Thiel et al. (2001) *Marine Chemistry* **73**, 97-112. [4] Roussel et al. (2008) *Science* **320**, 1046. [5] Alperin and Hoehler (2010) *American Journal of Science* **309**, 958-984. [6] Valentine and Lippard (1997) *Journal of the Chemical Society, Dalton Transactions* **21**, 3925-3932.

Simulating fluoride evolution in groundwater using a reactive multicomponent transient transport model

PETTENATI MARIE[1*], PERRIN JEROME[1,2], PAUWELS HÉLÈNE[1], AND SHAKEEL AHMED[2,3]

[1]BRGM, Avenue Claude Guillemin, BP 36009, 45060 Orléans Cedex 02, France, m.pettenati@brgm.fr (* presenting author)
[2]IFCGR, Indo-French Center for Ground Water Research, NGRI, Uppal Road, 500 007 Hyderabad, India
[3]NGRI, Uppal Road, 500 007 Hyderabad, India

Overexploitation of crystalline aquifers in a semi-arid climate leads to a degradation of water quality. The Maheshwaram watershed is a typical Southern India rural watershed, with intensive groundwater abstraction (more than 700 productive irrigation wells), and a predominant paddy field cropping pattern [1-2]. We outline the process of F accumulation in this small endorheic watershed [3] where the groundwater has a high fluoride concentration of up to 4 mg l^{-1} (WHO guideline value <1.5 mg l^{-1}). The main processes responsible for the observed salt loads are probably being due mainly to irrigation return flow (IRF) and a high evaporation rate [4].

A solute recycling model that includes water/rock interactions and climatic parameters was used to assess the processes controlling fluoride contamination in a crystalline aquifer intensively exploited for paddy field irrigation. we used a 1D PHREEQC reactive-transport column [5] to conceptualize the infiltration of paddy field IRF under watershed-scale evaporation conditions.

Increase of F^- in IRF caused by evaporation and mineral dissolution (no fertilizer input) leads to the accumulation of F- in the aquifer. Crystalline aquifer overexploitation in semi-arid areas enhances geogenic pollution derived from the dissolution of fluoride-bearing minerals (fluorapatite, allanite, biotite) through a combination of complex hydrochemical processes [6]. The present model aims to provide a robust method for the development of prediction tools dedicated to aquifer management in this specific context.

[1] Kumar and Ahmed (2003,) *Curr. Sci.* **84**, 188-196.
[2] Maréchal et al., (2006) *J. Hydrol.* **329**, 281-293.
[3] Négrel et al., (2011) *J. Hydr*. **397**, 55-70.
[4] Perrin et al., (2011) *J. Hydrol*. **398**, 144–154.
[5] Parkhurst and Appelo (1999) *J. Hydrol.* **398**, 144–154.
[6] Pettenati et al., (2012) *Appl. Geochem.,* submitted.

https://doi.org/10.1180/S0026461X00008434 Published online by Cambridge University Press

Metals and microbes: imaging organic matter-mineral relationships at high resolution with STXM/NanoSIMS

JENNIFER PETT-RIDGE[1*], MARCO KEILUWEIT[1,2], JEREMY BOUGOURE[1], PETER S. NICO[3], PETER K. WEBER[1], LYDIA ZEGLIN[2], DAVID D. MYROLD[2], MARKUS KLEBER[2]

[1]Lawrence Livermore National Laboratory, Physical and Life Sciences Directorate, Livermore, CA (*pettridge2@llnl.gov)
[2] Department of Crop and Soil Science, Soils Division, Oregon State University, Corvallis, OR
[3] Lawrence Berkeley National Laboratory, Earth Sciences Division, Berkeley, CA

Advancing understanding of soil organic-mineral interactions requires disentangling the complex interactions between soil mineral surfaces, decomposed organic compounds, and soil microbes in structurally intact soil. To avoid method-related artifacts that are associated with the common physical soil fractionation techniques, non-invasive high-resolution imaging techniques have been recently developed to simultaneously determine the molecular composition, source and fate of added OM, and location of OM within soil micro-aggregates. Simultaneous high-resolution chemical characterization and isotope tracing can be achieved by combining nano-scale imaging mass spectrometry (NanoSIMS) and spatially resolved spectroscopy (STXM/NEXAFS). These techniques allow precise, high-resolution, quantitative measurement of molecular and isotopic patterns in an undisturbed sample.

In a series of recent experiments, we combined these techniques to map organic carbon distribution, and image associations of organics with specific metal-oxide minerals in soil. In these experiments, we used ^{15}N- and ^{13}C-organic matter incubations and NanoSIMS imaging to track the fate of specific microbial and plant polymers. This has allowed us to measure preferential OM associations with Fe and Mn oxides and clay particles. Using synchrotron-based scanning transmission X-ray microscopy (STXM) analysis of the same microstructures, we can then measure the molecular class of these particles, for example, thin amine N coatings covering Fe (hydr)oxides, and microbial lipids coating montmorillonite particles.

These high-resolution imaging approaches are complementary to more traditional bulk analyses (^{14}C dating, NMR, density fractionation) and can yield mechanistic explanations for proceses which influence organic matter decomposition in soil.

This work was performed under the auspices of the U.S. Department of Energy by Lawrence Livermore National Laboratory under Contract DE-AC52-07NA27344.

Investigating controls on chemical weathering in the Cascade Mountains, Oregon

JULIE C. PETT-RIDGE[1*] WILL KRETT[1], NICK CURCIO[1], AND MARKUS KLEBER[1]

[1]Oregon State University Faculty of Soil Science, Corvallis OR, USA, julie.pett-ridge@oregonstate.edu

The steep volcanic terrain of the wet western side of the Cascade Range is likely to support relatively fast weathering rates. In this study we present data from a weathering study at H.J. Andrews Experimental Forest in the western Oregon Cascades. Our goal is to better understand controls on weathering processes, namely the controls on secondary mineral formation and on the magnitude of streamwater dissolved silica fluxes.

Controls on both temporal and spatial variability of streamwater silcia fluxes are investigated using 40+ year streamwater chemistry records from 7 small gauged watersheds within the site, and using synoptic sampling data from 40 locations across the site sampled in 1 day under baseflow conditions. Three sets of paired watersheds with contrasting land-use treatments (control, clear-cut, partial timber harvest, road building) but similar topography, aspect, bedrock and vegetation do not reveal significant land-use effects on streamwater silica fluxes. Over two orders of magnitude variation in instantaneous streamwater silica fluxes across the site is observed in the synoptic sampling. Stream temperature and landscape position correlate with silica flux, suggesting that deeper hydrologic flowpaths are the source of high silica fluxes.

10 soil pits were excavated, sampled, and characterized for physical and chemical properties including clay mineral XRD analyses and selective chemical dissolutions. Paired pits were sited to compare effects of slope aspect, bedrock type, and elevation. We found that higher elevation soils that experience more permanent winter snowpack contained smaller fractions of crystalline Fe-(hydr)oxides and larger fractions of organo-metal complexes relative to lower elavation soils. Among lower elevation soils, neither slope aspect (which corresponds to 30% difference in soil water flux), nor bedrock type (basalt versus andesitic breccia and tuff) varied consistently with soil properties. In this steep mountainous terrain (average slope 60-70%), geomorphic factors such as creep and treethrow appear to play a dominant role in controlling the degree of soil profile development.

Using this and previous data from the well-characterized H.J. Andrews study site, we evaluate weathering processes observed at both soil pit and small watershed scale in the larger context of controls on weathering. Specifically, we evaluate the role of climate variables (runoff, temperature, and snowpack persistence), topography, erosion rate, and hydrologic variables (soil water flux and distributions of fluid residence time) in controlling weathering fluxes as proposed in recent studies.

https://doi.org/10.1180/S0026461X00008434 Published online by Cambridge University Press

The osmium isotope record of seawater: 20 years of research

BERNHARD PEUCKER-EHRENBRINK[1*] AND GREG RAVIZZA[2]

[1]Department of Marine Chemistry and Geochemistry, Woods Hole Oceanographic Institution, Woods Hole, MA, USA behrenbrink@whoi.edu (*presenting author)

[2]Department of Geology and Geophysics, SOEST, University of Hawaii at Manoa, Hawaii, HI, USA ravizza@hawaii.edu

Secular variations in the $^{187}Os/^{188}Os$ of seawater were discovered twenty years ago [1]. Since then, significant progress has been made towards reconstructing $^{187}Os/^{188}Os$ variations throughout the Cenozoic, and select time intervals in the Mesozoic and Palaeozoic.

Osmium is an ultra-trace element in seawater with a residence time of less than 50,000 years, and possibly as short as a few thousand years. While initially thought to be well mixed throughout the oceans, high-precision data – including in the modern ocean - have indicated spatial variations of the order of a few percent. The residence time of osmium makes the isotope system not only ideally suited for tracing processes on time scales of glacial-interglacial variations, but also for investigating longer, tectonically driven changes on the Earth's surface.

Osmium is enriched in marine sediments that have been deposited under reducing, and - to a lesser extent – oxic, conditions. In such sediments, variations in its isotope composition - recorded as $^{187}Os/^{188}Os$ - have left a rich archive that reflects changes on the Earth's surface. The affiliation of osmium with sedimentary organic matter makes the marine $^{187}Os/^{188}Os$ record a sensitive indicator of cycling of old sedimentary organic matter. The lack of a buffering mechanism similar to the formation and weathering of marine carbonates in the $^{87}Sr/^{86}Sr$ record of seawater leads to variations that span most of the range in isotope variations between geochemical endmembers.

Here we focus on the most highly resolved events in the Cenozoic and Mesozoic that are reviewed in detail in the soon to be published chapter 8 in the *Geologic Time Scale 2012* [2]. These events fall into two categories: transient excursions to more radiogenic values that are thought to be caused primarily by hyperthermal events (e.g. PETM), and transient excursions to less radiogenic values that are caused by extraterrestrial impacts (e.g. KTB, late Eocene impacts), large volcanic eruptions (e.g., CAMP, Deccan, and Yemeni-Ethiopian flood basalts), or erosion of osmium-rich, unradiogenic lithologies at convergent plate margins (e.g. erosion of the Papuan ophiolite in the late Eocene).

Widespread anoxia may lead to rapid removal of osmium from the water column, thereby generating conditions for the predominance of local fluxes to seawater in an isotopically non-homogenous water column (e.g. Ocean Anoxic Events in the Mesozoic). In addition, the isolation and reconnection of ocean basins to the global circulation may leave an isotope fingerprint if inputs to such basins deviate from the globally averaged input of osmium to seawater (e.g. Arctic Ocean).

[1] Pegram et al. (1992) *EPSL* **113**, 569-576.
[2] Peucker-Ehrenbrink and Ravizza (2012) *Geologic Time Scale 2012, Chapter 8: Osmium isotope stratigraphy* (Gradstein et al., Eds.), doi: 10.1016/B978-0-444-59425-9.00008-1.

Does the naturally elevated sulfur content of *Ulva lactuca* play a role in the uptake and speciation of arsenic?

CATHERINE PHAM[1,2*], LAURENT CHARLET[2], AND GARRISON SPOSITO[1]

[1]University of California, Department of Environmental Science, Policy & Management, Berkeley, United States, pham@cal.berkeley.edu (* presenting author), gsposito@berkeley.edu

[2]Université de Grenoble, Institut des Sciences de la Terre, Grenoble, France, charlet38@gmail.com

Algae are ubiquitous in surface waters and are known to influence the chemodynamics of the priority toxic metalloid, arsenic (As), in polluted marine environments. Marine algae initially transform As(V) to As(III), after which As(III) is methylated and then converted to a diverse set of organoarsenic compounds by mechanisms that remain unclear.[1] Recently it has become evident that the common marine green alga *Ulva lactuca* contains elevated levels of sulfur (S) and has the capacity to generate toxic concentrations of H_2S in the presence of excess nitrates. In light of the fact that As is chalcophilic, it is important to understand the interaction between As, S, and nitrates in *Ulva lactuca* because the algae may serve as an As reservoir and pose an emerging threat to coastal environments where nitrate inputs are increasing.

In the present study, using synchrotron-based X-ray absorption spectroscopy and X-ray microfluorescence mapping, we investigated the bioavailability and chemical speciation of As in *Ulva lactuca* sampled from contaminated coastal waters in order to understand As cycling in the marine environment. We also conducted batch culture experiments with *Ulva lactuca* to explore the role of thiolation in As biotransformation and toxicity.

Using X-ray microfluorescence mapping, we observed trends in the distribution of S along the thallus of *Ulva lactuca*. We are investigating whether the As distribution and concentration may be correlated with areas of elevated S content along the thallus. Using synchrotron-based X-ray absorption spectroscopy, we characterized the complexation of As with S moities in environmental samples collected from industrially-polluted sites.

Our research aims to determine the potential risks As may pose to both aquatic ecosystem and human health as it is transformed into various chemical forms and moves from algae up trophic levels, potentially to fish and humans.

[1] Edmonds, JS and Francesconi, KA (1977) *Nature* **265**, 436.

https://doi.org/10.1180/S0026461X00008434 Published online by Cambridge University Press

Natural gas leaks in Boston

NATHAN G. PHILLIPS[1*], ROBERT ACKLEY[2], ERIC CROSSON[3], ADRIAN DOWN[4], JON KARR[4], AND ROBERT B. JACKSON[4]

[1]Boston University, Boston, USA, nathan@bu.edu (* presenting author)
[2]Gas Safety, Inc., Southborough, USA, bobackley@gassafetyusa.com
[3]Picarro, Inc, Santa Clara, USA, eric@picarro.com
[4]Duke University, Durham, USA, adrian.down@duke.edu, jkarr@duke.edu, jackson@duke.edu

Introduction and Methods

There are large uncertainties in the fate of lost and unaccounted gas from the natural gas process chain, including in distribution pipeline systems [1,2]. To assess the spatial pattern and typical leak rate of natural gas leaks in an urban distribution system, we drove and mapped leaks on the 785 centerline road miles in the City of Boston. We used a GPS-equipped cavity ringdown methane analyzer, sampling the air above road surfaces. Additionally, to assess leak rates, we deployed gas accumulation chamber on 25 representative gas leaks. Finally, we identified sources of methane leaks using carbon isotope analysis and human olfactory detection of the odorant mercaptan, which is added to pipeline gas.

Figure 1: Methane leaks from natural gas pipelines in the Beacon Hill neighborhood of Boston. Yellow bars represent methane concentrations in parts per million; the highest values recorded exceed 15 times background levels.

Results and Conclusions

We detected ca. 3,900 distinct elevated methane sources within the City of Boston. Isotopic and olfactory methods indicate that a majority of these methane sources are associated with the natural gas pipeline distrib ution system. Individual leak rates ranged from 28 cubic feet per day (CFD) to 315 CFD, averaging 110 CFD, more than half daily US household natural gas use. We conclude that the magnitude of gas lost by typical leaks and their frequency in urban areas like Boston have potential to amount to substantial total lost natural gas. The magnitude of lost and unaccounted gas [1] can represent several percent and more of typical total state greenhouse gas inventories, and total more than $1B nationally. Our discovery of widespread urban gas leaks provides impetus for concerted efforts to determine the total leak rate and corresponding greenhouse warming potential from natural gas distribution systems.

[1] Energy Information Administration, form EIA-176 (2010).
[2] Howarth *et al*. (2011) *Climatic Change* **106**, 679-690.

Isotopic constraints on the genesis of basanitic lavas beneath Haleakala

ERIN H. PHILLIPS WRITER[1*], KENNETH W.W. SIMS[1], VINCENT J.M. SALTERS[2]

[1]University of Wyoming, Department of Geology and Geophysics, Laramie, WY, USA, ephilli8@uwyo.edu (* presenting author), ksims7@uwyo.edu
[2]Florida State University, Department of Geological Sciences, Tallahassee, FL, USA, salters@magnet.fsu.edu

Although tholeiitic volcanism is predominant in Hawaii, the study of smaller volume, late-stage alkaline volcanism is imperative to understanding the magmatic history of the Hawaiian Islands and the dynamics of mantle plumes. Recent basanitic lavas from Haleakala represent an end-member in the compositional range of Hawaiian lavas and are hypothesized to tap magma from the fringe of the Hawaiian plume [1]. Indeed solid mantle upwelling rates inferred from U-series data from a limited number of samples from Haleakala [1] are consistent with both iso-viscous and thermo-viscous fluid mechanical models of plume upwelling [2,3].

However, these conclusions were based on a very small data set (5 samples) and additional isotopic data on alkaline lavas are essential for a more complete understanding of the genesis of late stage and rejuvenated stage volcanism. We present Hf, Nd, Sr, and Pb isotopic data, ^{238}U-^{230}Th and ^{235}U-^{231}Pa-^{227}Ac and major and trace-element data for a suite of 13 samples from Haleakala crater. These samples are relatively young, with ^{14}C ages ranging from 870 ± 40 to 4070 ± 50 years [4]. They are nepheline normative and LREE enriched, indicating that they represent small degree melts. Relative to main-stage tholeiites (Kilauea and Mauna Loa) and late-stage alkali basalts (Mauna Kea and Hualalai), the Haleakala crater samples come from a relatively depleted source (ε_{Nd} = 7.37-8.60; ^{87}Sr/^{86}Sr = 0.70314-0.70333; ε_{Hf} = 12.66-14.68). All samples have ^{230}Th/^{238}U >1 indicating that they originate from a source containing residual garnet. Consistent with earlier studies, the ^{230}Th/^{238}U (1.19-1.32) and ^{231}Pa/^{235}U (1.65-1.79) of these samples are much higher than other young Hawaiian lavas suggesting that basanitic lavas from Haleakala are the manifestation of a small degree of partial melting and relatively slow mantle upwelling rates.

[1] Sims et al. (1999) *Geochim. Cosmochim. Acta*, **63**, 4119-4138. [2] Hauri et al. (1994) *Jour. Geophys. Res.*, **99**, 24,275-24,300. [3] Watson and McKenzie (1991) *J. Pet.*, 32, 501-537 [4] Sherrod and McGeehin (1999) *USGS Open-File Report 99-143*, 14pp.

https://doi.org/10.1180/S0026461X00008434 Published online by Cambridge University Press

Opening the black box: Imaging nanoparticle transport through rock with MRI

VERNON PHOENIX[1*], SUSITHRA LAKSHMANAN[1], WILLIAM SLOAN[2], WILLIAM HOLMES[3].

[1]University of Glasgow, Geographical and Earth Sciences, Glasgow, UK, vernon.phoenix@glasgow.ac.uk (* presenting author)
[2]University of Glasgow, Infrastructure and Environment, Glasgow, UK, william.sloan@glasgow.ac.uk
[3]University of Glasgow, Wellcome Surgical Institute, Glasgow, UK, william.holmes@glasgow.ac.uk

Introduction

Magnetic Resonance Imaging (MRI) is perhaps best known for its use in medicine. However, its ability to non-invasivly image inside materials that are opaque to other imaging methods is of benefit to the geological and environmental sciences. Here we report on the application of MRI to image transport of nanoparticles through sandstone. This approach is beneficial as it enables 2D and 3D 'videos' of nanoparticle transport inside rock to be collected, providing spatially resolved data from which we can enhance our understanding of nanoparticle transport in groundwater systems.

Methods

Commercially available nano-magnetite nanoparticles with an organic polymer cap were used. The superparamagnetic nature of these nanoparticles ensured they were visible to MRI. These were pumped through bentheimer sandstone rock core and MR images were collected every 5 minutes. Images were calibrated to maps of actual nanoparticle concentration using the MRI parameter T_2 (the spin-spin relaxation of ^{1}H nuclei), as $1/T_2$ is proportional to nanoparticle concentration.

Results and conclusion

Transport of positive and negativly charged nanoparticles were succesfully imaged, with transport of positivly charged nanoparticles retarded significantly due to electrostatic attraction to quartz surfaces. Images collected after flushing with nanoparticle free water showed negative nanoparticles were sucesfully removed from the sandstone, while significant quantities of positive nanoparticles remained. Concentration profiles were evaluated with CXTFIT and colloid filtration theory at regular distances along the length of the sandstone core to test for variations in dispersivity, dispersion coefficient, recovery, deposition rate constant, collision efficiency and transport –attachment efficiency. MRI's ability to collect spatially resolved data ensures it can act as a useful tool to unpick nanoparticle transport heterogeneity and test and develop transport models.

Direct Mass Spectrometric Analysis of Position Specific $\delta^{13}C$ in Organics

ALISON PIASECKI [1*], JOHN EILER[1]

[1] California Institute of Technology, Pasadena CA, USA, apiaseck@caltech.edu (*presenting author)

It is recognized that natural organic molecules can exhibit position-specific isotopic fractionations (i.e., differences in isotopic composition for a single element between non-equivalent molecular sites). For example, lipids can exhibit up to ~30 ‰ difference in $^{13}C/^{12}C$ between adjacent carbons as a result of fractionations arising during decarboxylation of pyruvate in lipid biosynthesis [1]. Little in detail is known about such isotope effects in natural products, but it seems possible that observations of isotopic ordering of carbon could distinguishing among the mechanisms and conditions of biosynthetic reactions. And, such position specific isotope effects may be inherited by alkanes produced from thermal degredation fatty acid chains, perhaps modified as functions of the conditions and mechanisms of thermal maturation.

Here we examine the potential of the MAT 253 Ultra, a new kind of high resolution gas source isotope ratio mass spectrometer [2], to make measurements that will permit reconstruction of position specific carbon isotope compositions in organic molecules, as preserved in alkanes. We focus on propane, the smallest alkane that could exhibit position specific carbon isotope differences. Electron impact ionization of propane yields three families of product ions: C1Hn, C2Hn and C3Hn; fragments made by H loss are abundant, including bare carbon ions and clusters. H adducts are present but rare. An analysis of the $^{13}C/^{12}C$ ratio of any two of these familes of product ions constrains the position specific C isotope fractionation in propane, provided such fragment species can be analyzed stably and reproducibly and one has accounted for exchange through recombination. We have demonstrated that $13CH3/^{12}CH_3$, $^{13}C^{12}CH_4/^{12}C_2H_4$, and $^{13}C^{12}C_2H_8/^{12}C_3H_8$ ratios can be analyzed with sub-per mil precision (as good as 0.1 ‰ for the most abundant species), and zero-enrichments yeild accurate results. It remains to be seen whether this approach accurately reproduces independently known position-specific isotopic differences, though the low abundance of adducts suggests recombination will not be a significant artifact; i.e., accuracies similar to the precisions reported here are expected.

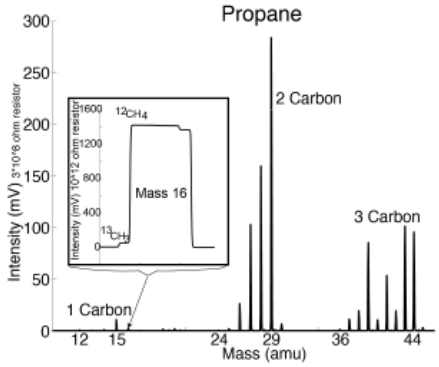

Figure 1: Full spectra of propane as measured on MAT253-Ultra [1] DeNiro, Epstein (1977) *Science* **Volume 197,** 261-263. [2] Eiler et. al (2012) **this volume**.

https://doi.org/10.1180/S0026461X00008434 Published online by Cambridge University Press

Petrogenesis of alkaline mafic rocks from Sivas, Central Anatolia: New insight into ancient continental assembly and break-up

MEGAN PICKARD[1*], TANYA FURMAN[1], BILTAN KÜRKCÜOGLU[2], BARRY HANAN[3], KAAN SAYIT[3]

[1]Department of Geosciences, Pennsylvania State University, University Park, PA, USA, mup163@psu.edu (* presenting author), tfl3@psu.edu

[2]Department of Geological Engineering, Hacettepe University, Ankara, Turkey, biltan@hacettepe.edu.tr

[3]Department of Geological Sciences, San Diego State University, San Diego, CA, USA, bhanan@mail.sdsu.edu, kaansayit@hotmail.com

Alkaline mafic lavas are a common feature of intraplate extensional volcanic settings. We examine mafic lavas from Sivas, Central Anatolia, in order to understand controls on their genesis in a setting with a complex tectonic history extending over the past 1.3 billion years. Continental assembly and break-up, both associated with geochemical modifications to the associated lithosphere, has long played a significant role in Anatolia. The present tectonic regime consists of a complex juxtaposition of rift, strike-slip, and transtensional faulting and an overall WSW movement of the continental microplate.

We identify two groups of alkaline lavas that record different petrogenetic histories. Select incompatible trace element variations (e.g., Ti, Zr) indicate that abundant basalts and basaltic andesites (BBA) evolved by fractional crystallization of a frequently-erupted parental magma with ~9 wt.% MgO. The BBA lavas have overall smooth primitive mantle normalized incompatible trace element patterns that suggest derivation from a source region geochemically similar to that of ocean island basalts. In contrast, basanites erupted over a small geographic area show little fractionation but rather represent individual magma batches with different degrees of partial melting. These lavas exhibit enrichments in Ba, Th, and U and depletions in Rb, Hf and Ti that are characteristic of melts derived from metasomatized lithosphere. Pb abundances in both groups are anomalously high, though this feature is more pronounced in the basanites, suggesting interaction with a Pb-rich continental component.

In general, Sr-Nd-Hf radiogenic isotopic signatures of the BBA lavas are less radiogenic than those measured in the basanites. The BBA and basanite groups overlap in eNd-eHf isotope space, plotting on and above the mantle array between data fields for oceanic basalt-like and continental lithosphere-like compositions. The least radiogenic BBA lavas ($^{87}Sr/^{86}Sr$ 0.7040-0.7044; $^{143}Nd/^{144}Nd$ 0.51278-0.51280) approach compositions of asthenospheric melts. Radiogenic Pb isotope compositions of both groups plot within the range of Indian MORB. Nd model ages of Sivas lavas are consistent with a DUPAL-like source region with Rodinia (~1.2 Ga) continental lithosphere affinity. The observation that basanitic lavas are found only to the southeast of a major strike-slip fault suggests that post-Miocene faulting either controls or reflects significant subsurface chemical heterogeneity related to topography across the lithosphere-asthenosphere boundary.

Reduction of biogenic and abiogenic Fe(III) minerals by humic substances

ANNETTE PIEPENBROCK[1*], IRIS BAUER[2], AND ANDREAS KAPPLER[2]

[1]University of Tuebingen, Center for Applied Geosciences, Tuebingen, Germany, annette.piepenbrock@student.uni-tuebingen.de (* presenting author)

[2]University of Tuebingen, Center for Applied Geosciences, Tuebingen, Germany, andreas.kappler@uni-tuebingen.de

Humic substances (HS) have been shown to shuttle electrons between microorganisms and poorly soluble electron acceptors such as Fe(III) minerals. HS can be reduced by a wide variety of microorganisms including Fe(III)-reducing, sulfate-reducing and dechlorinating bacteria, but also chemically for example by sulfide. In contrast to the reduction of the HS, the second electron transfer step from reduced HS to the Fe(III) minerals proceeds abiotically and is controlled mainly by the properties of the Fe(III) minerals, such as their redox potential. The electron transfer from HS to the Fe(III) minerals is rate limiting for the whole electron shuttling process, but only little is known about the dynamics and limitations of this second electron transfer step itself. This is in particular the case since most laboratry studies were carried out under geochemical conditions differing significantly from those typically encountered in the environment. Thus, the importance of humic substances as electron shuttles under environmental conditions is currently unknown.

To elucidate some of the remaining questions, we aimed to quantify the rate and extent of electron transfer between reduced and non-reduced HS and various Fe(III) minerals. We focused, in particular, on the difference between reduction of biogenic vs. abiogenic Fe(III) minerals by HS. Our studies showed that more electrons were transferred from chemically reduced HS to biogenic than compared to abiogenic Fe(III) minerals. Since biogenic and abiogenic Fe(III) mineral suspensions were normalized to the same BET surface area, it could be ruled out that this outcome resulted from a difference in specific surface area between the mineral suspensions. Furthermore, our results indicate that laboratory experiments with abiogenic Fe(III) minerals might significantly underestimate the amount of electrons transferred between HS and Fe(III) minerals and, as a result, they might also underestimate the importance of HS electron shuttling in environmental systems wherein minerals might be of mainly biogenic origin. This is of great importance, since electron transfer via humic substances has the potential to contribute significantly to the electron fluxes in the environment and thus might affect the fate of organic and inorganic pollutants.

https://doi.org/10.1180/S0026461X00008434 Published online by Cambridge University Press

Evolution of the East Antarctic ice sheet across the mid-Miocene climate transition based on ice-rafted detritus provenance studies

E.L. PIERCE[1*], T. VAN DE FLIERDT[2], S.R. HEMMING[1,3], T. WILLIAMS[3] AND C. COOK[2]

[1]Columbia University, New York, USA, epierce@ldeo.columbia.edu (* presenting author)
[2]Imperial College, London, UK
[3]Lamont-Doherty Earth Observatory, Palisades, USA

The Mid-Miocene Climate Transition (MMCT, ~14 Ma) is an interval of major climate reorganization, accompanied by significant decreases in global temperatures and sea-level. During this interval the East Antarctic Ice Sheet (EAIS) expanded to at least 85% of its present volume, and may have transitioned from a wet- to frozen-bed regime. The geology of East Antarctica exhibits a distinct variation from the Ross Sea to Prydz Bay that allows for the application of geochemical tracers to determine the provenance of ice rafted detritus (IRD) and identify EAIS sectors that supply IRD [1,2]. Prior work from ODP Site 1165 (Prydz Bay) indicates major ice-rafting events sourced from the Adélie and Wilkes margins from late Miocene through early Pliocene, but not during the early Miocene (19-14 Ma) [3], indicating a change in EAIS dynamics and IRD production from these margins through the MMCT.

IODP Site U1356A, located off the coast of Adélie Land, is well positioned to capture the signal of iceberg discharges from this sector. Six peaks in the number of clasts >2mm between ~14.1-13.2 Ma were identified from U1356A; samples were selected across each of these to represent peak, intermediate and low clast counts. Samples were sieved at 150μm, the weight% >150μm was determined, and every hornblende grain >150μm was dated by $^{40}Ar/^{39}Ar$. $^{40}Ar/^{39}Ar$ hornblende ages from each sample show a dominant population of 1400-1600 Ma, consistent with the Mertz shear zone, but slightly younger than the coastal geology of Adélie Land (>1700 Ma), and indicating no significant sourcing of IRD from George V Land or the Ross Sea sector. Ongoing provenance work with 6 additional IRD peaks surrounding the original peaks is underway to further evaluate EAIS evolution over the MMCT.

[1] Roy et al., (2007) *Chemical Geology* **244**, 507-519
[2] Pierce et al., (2011) *Paleoceanography* **26** PA4217
[3] Williams (2010) *EPSL* **290**, 351-361.

Solid-Solution Interfacial Reactions: Effect of Solution Saturation State

ERIC M PIERCE[1*] AND SEBASTIEN N KERISIT[2]

[1]Oak Ridge National Laboratory, Oak Ridge, TN, USA, pierceem@ornl.gov (* presenting author)
[2]Pacific Northwest National Laboratory, Richland, WA, USA, sebastien.kerisit@pnnl.gov

Solid-solution interfacial reactions—specifically silica-rich inorganic surface coatings—play a critical role in the evolution of natural and engineered systems and the transport of radionuclides in the environment. For example, Nugent et al.[1] has shown that development of silica-rich inorganic surface coatings form quickly on albite samples in the field and suggests the formation of these coatings are the reason for the discrepancy between laboratory and field measured weathering rates. Similar surface-layers have been observed in weathering studies conducted with mineral-based glasses, French and Roman glass samples, and surrogate nuclear waste glasses[2,3,4]. Knowledge gaps in the fundamental understanding of alteration layer formation impede the ability to link macroscopic reaction kinetics to nanometer scale interfacial processes that occur at the surface of mineral and glasses, especially under near-saturated conditions.

Therefore to address the scientific challenge of deciphering the complex reactions controlling the formation and evolution of silica-rich surface layers; a series of flow-through experiments were conducted as a function of $a[SiO_2(aq)]$, from dilute to near-saturated conditions with respect $SiO_2(am)$, at pH(23°C) = 9.0 and T = 90°C. Results illustrate that as the saturation state of the solution increases the dissolution rate decreases by approximately two to three orders of magnitude. Furthermore, analysis of reacted grains illustrate significant changes in the elemental composition and structure of the hydrated-surface.

In addition to the afore-mentioned experimental measurements, Monte Carlo simulations are being used to gain additional insight into the evolution of the elemental profiles. Recent advances to the code developed by Kerisit and Pierce [5] enable visualization of the history of the Si sites in a reacted glass sample to determine the origin of elements that comprise the hydrated-surface layer.

Although the data collected to-date provide key information on the processes occuring at the glass-water interface, additional experimentation and modeling will be required to develop a more robust understanding of these reactions.

[1] Nugent et al. (1998), *Nature*, **395**, 588-591.
[2] Hamilton et al. (2001), *GCA*, **65**, 3683-3702.
[3] Pierce et al. (2007), *Appl. Geo.*, **22**, 1841-1859.
[4] Verney-Carron et al. (2008), *GCA*, **72**, 5372-5385.
[5] Kerisit and Pierce (2011), *GCA*, **75**, 5296-5309.

https://doi.org/10.1180/S0026461X00008434 Published online by Cambridge University Press

Voluminous magmas in intra-continental setting: Hf and O isotopes in zircons from Late Paleozoic volcanic rocks in NE Germany

PIETRANIK ANNA[1*], CRAIG STOREY[2], BREITKREUZ CHRISTOPH[3], ELŻBIETA DEJA[1]

[1]University of Wrocław, Geological Sciences, Poland; anna.pietranik@ing.uni.wroc.pl (* presenting author)
[2]University of Portsmouth, Earth and Environmental Sciences, UK craig.storey@port.ac.uk
[3]TU Bergakademie Freiberg, Geology and Paleontology, Germany, Christoph.Breitkreuz@geo.tu-freiberg.de

Voluminous rhyolitic rocks (ca. 34 000 km^3) were formed in the NE German Basin in an intra-continental setting ca. 300 Ma ago. εHf and $\delta^{18}O$ have been measured in dated magmatic and inherited rhyolitic zircons from three drill cores across the NE German Basin. Inherited zircons have crystallisation ages from ca. 1.7 to 0.5 Ga, εHf values of -20 to 7 ε units and $\delta^{18}O$ values of 5.8 to 9.3 ‰. The inherited zircons have Hf model ages of 1.9 - 2.2 Ga, indicating that much of the basement was initially derived from the mantle at that time. High $\delta^{18}O$ magmatic zircons have similar model ages highlighting that the 300 Ma magmatic event involved the melting of sediments derived from basement generated at ca. 2.1 Ga. The εHf values in magmatic zircons vary from -7 to +1 ε units and $\delta^{18}O$ = 6.0 to 9.4 ‰. The range of εHf and $\delta^{18}O$ values in magmatic zircons in the three sites investigated have been modelled by simple assimilation - fractional crystallization processes of mantle derived magma contaminated by sediments with model ages of ca. 2.1 Ga. Zircons record crystallization from magmas with 10-80 % mantle contribution, with an average of 45%. This implies that these silicic magmas contain on average 15000 km^3 of mantle derived material and that they represent a significant contribution to the net growth of the continents. Zircons from the NE German Basin have more inter-grain variability, but they record less complex magma evolution processes than zircon and whole rock data from other large silicic volcanic provinces, e.g. in North America. This is consistent with zircon crystallizing in small magma batches, which are amalgamated in larger, but short - lived upper crustal magma chambers.

The origin of chemical heterogeneity in the Hawaiian mantle plume

AARON J. PIETRUSZKA[1*], MARC D. NORMAN[2], MICHAEL O. GARCIA[3], JARED P. MARSKE[1] AND DALE H. BURNS[1]

[1]San Diego State University, San Diego, CA, USA, apietrus@geology.sdsu.edu (* presenting author)
[2]Australian National University, Canberra, Australia
[3]University of Hawaii, Honolulu, HI, USA

Inter-shield differences in the composition of lavas from Hawaiian volcanoes are generally thought to result from the melting of a heterogeneous mantle source containing variable amounts or types of oceanic crust (sediment, basalt, and/or gabbro) that was recycled into the mantle at ancient subduction zones (e.g., [1-3]). Here we investigate the origin of chemical heterogeneity in the Hawaiian mantle plume by comparing the incompatible trace element abundances of tholeiitic basalts from (1) Kilauea, Mauna Loa, and Loihi Seamount (the three active Hawaiian volcanoes) and (2) the extinct Koolau shield (a compositional end member for Hawaiian volcanoes). Model calculations suggest that the mantle sources of Hawaiian volcanoes contain variable amounts of recycled oceanic crust (ROC) from ~8-16% at Kilauea and Loihi to ~15-21% at Mauna Loa and Koolau. We propose that the Hawaiian plume contains a package of ROC (basalt and gabbro, but little or no marine sediment) that was altered by interaction with seawater or hydrothermal fluids prior to being variably dehydrated in an ancient subduction zone. The ROC in the mantle source of Kilauea and Loihi lavas is dominated by the uppermost portion of the residual slab (gabbro-free and strongly dehydrated), whereas the ROC in the mantle source of Mauna Loa and Koolau lavas is dominated by the lowermost portion of the residual slab (gabbro-rich and weakly dehydrated). The model results suggest that the large-scale distribution of compositional heterogeneities in the Hawaiian plume (at the present time) cannot be described by either a radial zonation [1] or a bilateral asymmetry [4,5]. Instead, the Hawaiian plume is heterogeneous on a small scale with a NW-SE oriented spatial gradient in the amount, type (i.e., basalt vs. gabbro) and extent of dehydration of the ancient ROC.

[1] Hauri (1996) Nature **382**, 415-419. [2] Hofmann & Jochum (1996) J. Geophys. Res. **101**, 11831-11839. [3] Huang & Frey (2005) Contrib. Mineral. Petrol. **149**, 556-575. [4] Abouchami et al. (2005) Nature **434**, 851–856. [5] Weis et al. (2011) Nature Geoscience **4**, 831-838.

https://doi.org/10.1180/S0026461X00008434 Published online by Cambridge University Press

Origin, mobility, and temporal evolution of arsenic from a low-contaminated catchment in Alpine crystalline rocks

ERIC PILI[1,2], DELPHINE TISSERAND[3]*, CORINNE CASIOT[4], AND SARAH BUREAU[3]

[1]CEA, DAM, DIF, Arpajon, France, Eric.Pili@cea.fr
[2]Institut de Physique du Globe de Paris, UMR 7451, Sorbonne Paris Cité, Paris, France, pili@ipgp.fr
[3]Institut des Sciences de la Terre (ISTerre), Grenoble, France, Delphine.Tisserand@ujf-grenoble.fr (*presenting author), Sarah.Bureau@ujf-grenoble.fr
[4]Laboratoire Hydrosciences, Montpellier, France, corinne.casiot@msem.univ-montp2.fr

Introduction

The reduction of the limit for As concentration in drinking water from 50 to 10 µg/l led many resource manager to deal with expensive treatments. In the case of arsenic levels around the limit, knowing its origin and temporal evolution is of great importance. Here, a study case from an alpine basin is presented.

Results

Arsenic speciation, isotopic compositions of pyrites, sulfate and water, and major and trace element concentrations indicate a geogenic source of arsenic due to the dissolution of pyrite. New tools are provided to study As in water: $\delta^{34}S_{SO4}$ and [As] are negatively correlated, $\delta^{18}O_{SO4}$ and $[As^V]/[As^{III}]$ are correlated. A monthly monitoring of [As] in some springs started in 2005 and shows an increase of [As] compared with scattered data from 1998-2002. A 3-year monitoring at high resolution demonstrated that drought conditions enhance pyrite dissolution. The 2003 summer heat wawe had a major effect. The increase in [As] between years 1998-2002 and 2005-2011 may result from the effects of droughts.

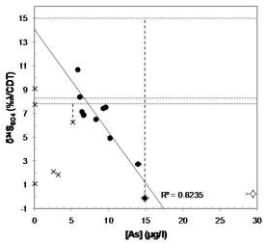

Figure 1 : Arsenic concentrations correlate negatively with $\delta^{34}S$ of dissolved sulfates. Larger As mobilization is linked with larger S-isotope fractionation resulting from larger pyrite dissolution.

Conclusions

As^V is the major arsenic species in the form $HAsO_4^{2-}$ but As originates in a more reducing environment than measured. The increase of fractionation factors leads to a negative correlation between $\delta^{34}S_{SO4}$ versus [As] and oxygen isotopes show that pyrite dissolution appears in anaerobic conditions.Temporal evolution shows that pyrite dissolution is enhanced by droughts.

The Itaju do Colônia Sodalite Litchfieldite Stock, NE Brazil

ADJANINE CARVALHO S. PIMENTA[1*], HERBET CONCEIÇÃO[1], MARIA LOURDES SILVA ROSA[1], ROBERT F. MARTIN [2], DÉBORA CORREIA RIOS[3]

[1]Sergipe Federal University, Núcleo de Geologia, Aracaju, Brazil, adjanine.pimenta@gmail.com
[2]MacGill University, Eath and Planetary Sciences, Montreal, Canada, robert.martin@mcgill.ca
[3]Bahia Federal University, Instituto de Geociências, Salvador, Brazil, dcrios@ufba.br

General Aspects

The Itaju do Colônia sodalite litchfieldite stock is located in the South Bahia Alkaline Province (SBAP) in the São Francisco Craton, NE Brazil. It is an approximatelly 3 km^2 ellipsoidal intrusive body that cuts the Archean–Paleoproterozoic granulitic basement of the Itabuna Belt. SBAP is the unique Brazilian source of the blue sodalitites, and Itaju do Colônia is the most important of them.

Lithogeochemical and Isotopic Data

The crystallization age for these rocks is 732 ± 8 Ma (U–Pb titanite). Diverse types of syenites with variable amounts of blue sodalite constitute this massif. The contacts between syenites and granulitic rocks are sharp, and dykes and pegmatites of syenitic composition are common in those areas. In the Eastern area, a layer of massive blue sodalite (sodalitite) 6-8 m wide occurs. Nearby, the transition between sodalite–nepheline syenites and granulites show interrelated metric apophises of calcite, phlogopitite and carbonatite, in which xenoliths of blue sodalite are common. Flux structures and contact relationship suggest the coexistence of three (3) distinct magmas, that seem to be coeval in this stock: (i) Cl-rich phonolitic, (ii) thomsonite-bearing carbonatitic, and (iii) ultrafemic-ultrapotassic (calcite phlogopititic). The blue syenites show a wide range of textures and sodalite contents. They consist of sodalite, perthitic alkali feldspar, aegirine, nepheline, albite, cancrinite, annite and paragonite; the accessory minerals include calcite, zircon, titanite, apatite, and magnetite. Late fractures are filled with white minerals identified by X-ray diffractometry as natrolite, ferrihydrite, manganosite, halite, gonnardite, halloysite and "chloromagnesite". Lithogeochemical data show that these syenites are strongly fractionated ($53 < SiO_2 < 61$), have high contents of alkalis ($14 < Na_2O+K_2O < 20$); $1.5 < Na_2O/K_2O < 4.2$; and $19 < Al_2O_3 < 25$. These are peralkaline rocks with elevated amounts of chloride (Cl up to 3%), Zr (up to 20,000 ppm), Nb (up to 160 ppm), Y (up to 70 ppm), Th (up to 50 ppm) and Pb (up to 18 ppm). The REE patterns are flat, 10 to 100 times richer than chondrites, and show a strong negative anomaly in Eu.

Concluding Remarks

The new data show that the crystallization of the Itaju do Colônia syenites resulted from a magmatic system in which Cl-rich phonolitic, carbonatitic and ultrafemic-ultrapotassic magmas have developed late and bear complex relationships. *Acknowledgments: This work was supported by CNPq, CBPM and FAPITEC.*

https://doi.org/10.1180/S0026461X00008434 Published online by Cambridge University Press

Epitaxy of calcite on dolomite and kutnahorite (104) surfaces

CARLOS M. PINA[1*], CARLOS PIMENTEL[1], AND ENRICO GNECCO[2],

[1] Departamento de Cristalografía y Mineralogía, Universidad Complutense de Madrid, Spain, cmpina@geo.ucm.es; cpimentelguerra@gmail.com. (* presenting author)
[2] IMDEA Nanociencia, Madrid, Spain, enrico.gnecco@imdea.org.

Carbonate minerals with dolomite-type structure show an anomalous reactivity in aqueous environments. Two examples of this are the complex dissolution paths of kutnahorite, $Mn,Ca(CO_3)_2$, in pure water [1] and the growth inhibition of dolomite, $Mg,Ca(CO_3)_2$, from supersaturated aqueous solutions at ambient conditions, i.e."the dolomite problem" [2]. Key to resolving the problems linked to the reactivity of these minerals is the systematic investigation of the interaction between their surfaces and aqueous solutions with various compositions and saturation states [3,4].

Here we present Atomic Force Microscopy (AFM) observations of the epitaxial growth of calcite on dolomite and kutnahorite (104) faces at room temperature. Growth was promoted by immersing freshly cleaved dolomite and kutnahorite crystals into highly supersaturated aqueous with respect to calcite ($20 < \beta_{calcite} = [a(Ca^{2+})\cdot a(CO_3^{2-})/K_{sp,calcite}] < 100$). Epitaxial growth of calcite occurs by both the spreading of thin layers and the nucleation and growth of oriented three-dimensional islands on (104) substrates. While the growth of calcite thin films is highly anisotropic, the nucleation of 3D-islands occurs preferentially on step edges. This indicates relatively large substrate-overgrowth interfacial energies. Moreover, sequences of AFM images of 3D-islands show that spiral growth on simple or multiple screw dislocations is frequent. The presence of such dislocations can be related to the accommodation of lattice-misfit strains as epitaxial growth proceeds. Additional information provided by recording lateral (friction) forces during the scan with increasing loading forces indicates low adhesion forces between 3D-islands and (104) substrates.

Our AFM observations show that the epitaxial growth of calcite on dolomite and kutnahorite (104) surfaces is a complex phenomenon that leads to the formation of surface patterns at the nanometric scale. The development of such patterns is discussed considering the factors that control the epitaxial growth modes, i.e. Frank-Van der Merwe, Volmer-Weber and Stranski-Krastanov [5].

[1] Mucci (2004) *Aquatic Geochemistry* **10**, 139-169. [2] Lippmann (1973) *Sedimentary carbonate minerals, Springer-Verlag,* 228 pp [3] Hu, Grossie & Higgins (2005) *American Mineralogist*, **90**, 963-968. [4] Higgins & Hu (2005) *Geochimica et Cosmochimica Acta*, **69**, 2085-2094. [5] Chernov (1984) *Modern Crystallography III, Springer-Verlag*, 517 pp.

Next generation of *in situ* chemical analysis of Titan aerosols via laser desorption mass spectrometry

VERONICA PINNICK[1,2*], JOSHUA SEBREE[1], XIANG LI[1,2], MELISSA TRAINER[1], WILLIAM BRINCKERHOFF[1], PAUL MAHAFFY[1]

[1]NASA Goddard Space Flight Center, Greenbelt, MD, USA, veronica.T.Pinnick@nasa.gov*
[2]University of Maryland, Baltimore County, Baltimore, MD, USA

Laser desorption mass spectrometry is an attractive analytical tool for the search for organics in space flight missions. Laser desorption provides complementary information to that obtained via the more ubiquitous methods like pyrolysis GC-MS and EGA because it provides molecular information without the need for sample heating. It is also well suited to space flight missions due to the relative ease (or complete lack) of sample preparation. Many mass analyzers have been used in previous missions, such as time-of-flight and quadrupole mass spectrometers, but ion traps in particular have the potential to operate at higher pressures with lower power requirements. One such space flight mission in the development phase is the Mars Organic Molecule Analyzer (MOMA), aboard the joint NASA/ESA rover ExoMars set to launch in 2018. There, Martian soil core samples from a depth of ~2 meters will be interrogated by either pyrolysis gas chromatography or laser desorption mass spectrometry in ambient atmospheric conditions. The mass analyzer is a linear ion trap, capable of providing chemical structural analysis via tandem mass spectrometry (MS/MS). A similar mass spectrometer can also be used for analysis of atmospheric particulates, if collected or concentrated properly. Potential applications could include the analysis of Titan's atmospheric components or deposited organic material on the surface.

To better understand the instrumental response to Titan-like aerosols, a series of aerosol analogs have been generated via far-UV irradiation of relevant Titan precursors. Aerosols are collected and deposited onto a sample plate interfaced to a commercial version of the MOMA instrument (Thermo MALDI LTQXL). By exploring different aerosol precursors, we are able to test sensitivity of the instrument to different chemical characteristics of the aerosol, including pure hydrocarbons, nitrogen-containing compounds, and large aromatic structures. We will present mass spectrometric results for the range of synthesized analog aerosols; for example, we will compare the spectra of benzene-sourced aerosol to those sourced from the nitrogen-heteroatom equivalent pyridine. These results will highlight the compatibilty of the laser desorption method to give abundant molecular and fragment ions for these classes of compounds. Further, the results from the commercial instrument will be compared to analyses utilizing the prototype MOMA instrument, currently in development.

https://doi.org/10.1180/S0026461X00008434 Published online by Cambridge University Press

Discriminating magmatic sources from fractionation processes using N, Ar and Pb: the Monteregian Hills alkaline province

DANIELE L. PINTI[1*], EMILIE ROULLEAU[2], ROSS K. STEVENSON[3], NAOTO TAKAHATA[4], YUJI SANO[5]

[1] GEOTOP, Montréal, QC, Canada
pinti.daniele@uqam.ca (* presenting author)
[2] The University of Tokyo, AORI, Kashiwa, Japan
eroulleau@aori.u-tokyo.ac.jp
[3] GEOTOP, Montréal, QC, Canada
stevenson.ross@uqam.ca
[4] The University of Tokyo, AORI, Kashiwa, Japan
ysano@aori.u-tokyo.ac.jp
[5] The University of Tokyo, AORI, Kashiwa, Japan
ntaka@aori.u-tokyo.ac.jp

N, He, Ar and Pb isotopic compositions were measured in pyroxenes and amphiboles from Monteregian Hills (Québec, Canada) rocks in order to constrain the mantle sources that originated this alkaline igneous province, a controversial issue lasted for more than 30 years. Most common hypothesis is that Monteregian Hills formed by the passage of the North-American craton over the Great Meteor hotspot [1]. However, melting of subcontinental mantle and magma rising through faulting related to the Cretaceous North-Atlantic opening has been also advocated [2].

Noble gases and N were extracted by crushing. Measured He, Ar and N isotopic and elemental compositions are partially fractioned by magma degassing and fluid-rock interactions during magma ascent. In contrast, $^{40}Ar/^{36}Ar$ ratios are not fractionated, but diluted by an atmospheric/crustal source. An observed correlation between the $^{40}Ar/^{36}Ar$ and $^{208}Pb/^{206}Pb$ ratios suggests two-component mixing. The first component may be related to a plume source with high $^{208}Pb/^{206}Pb$ ratios (≤ 2.06) and moderate $^{40}Ar/^{36}Ar$ ratios (~ 1,200) that are less than the values of depleted mantle ($^{40}Ar/^{36}Ar$ =35,000). The second component shows lower $^{208}Pb/^{206}Pb$ ratios (≤ 1.95) and near-atmospheric $^{40}Ar/^{36}Ar$ ratios (~ 300) and could be related to a recycled source such as HIMU.

Although measured $N_2/^{36}Ar$ ratios are diluted by an atmospheric-like source, they show an inverse correlation with $^{206}Pb/^{204}Pb$. This correlation is interpreted as the mixing between a recycled component (HIMU) and an ambiguous mantle source that could be either a plume source or the depleted mantle. Indeed, the non-fractionated $\delta^{15}N$ values for this mantle source are close to -8‰, which favors a depleted mantle source similar to that feeding N-MORBs ($\delta^{15}N$ = -5±2‰). Consequently, a part of the volatile budget might have a depleted mantle isotopic signature. This study shows the great potential of coupling radiogenic isotopes together with Ar and N isotopes. Nitrogen and argon are efficiently recycled in the mantle and thus can be helpful in discriminating the crustal and mantle sources in oceanic and continental volcanism.

[1] Sleep N. (1990). *J. Geophys. Res* **95**, 21983-21990. [2] McHone, G.J. (1996) *Canadian Mineralogist* **34**, 325-334.

The nearly-primary magmas at the Phlegraean Volcanic District (Italy): new insights by the isotope and trace element whole-rock and in-situ melt inclusion geochemistry

PIOCHI MONICA[1]*, DE ASTIS GIANFILIPPO[2], MORMONE ANGELA[1], MORETTI ROBERTO[3], ZANETTI ALBERTO[4]

[1]Istituto Nazionale di Geofisica e Vulcanologia, sezione Osservatorio Vesuviano, Napoli, Italy , monica.piochi@ov.ingv.it
[2]Istituto Nazionale di Geofisica e Vulcanologia, Roma, Italy , gianfilippo.deastis@ingv.it
[3]Dipartimento di Ingegneria Civile, Seconda Università degli Studi di Napoli, Aversa, Italy, roberto.morettii@ov.ingv.it
[4]Isituto di Geoscienze e Georisorse, Consiglio Nazionale delle Ricerche, Pavia, Italy, zanetti@crystal.unipv.it

The Phlegraean Volcanic District in Italy, including Procida and Ischia islands and the Campi Flegrei caldera, homes to recent volcanism, impressive geothermal system and high volcanic risk. Here, as well along the eastern Tyrrhenian Sea edge, the role of genesis and evolution on magma compositions is continuously debated because of the lack of mantle-derived xenoliths, the paucity of primary rock compositions and the large variability of isotope rock geochemistry. The debate also extends to the significance of high-temperature fumaroles, the origin of which is directly attributed to a deep source, as to the mystery of its geochemical features beneath the Campania. We focus on the least evolved shoshonite that belongs to the sole Procida and defines a roughly common whole-rock chemical trend with the Campi Flegrei products. The new data concerns with: 1) O isotopes for whole-rocks and mineral phases; 2) mineral and glass in-situ major oxide geochemistry by Electron Microprobe; 3) in-situ trace element geochemistry on olivine-hosted melt inclusions and glassy matrix by Laser Ablation Inductively Coupled Plasma Mass Spectrometry and 4) in-situ halogen and B isotope in the olivine-hosted melt inclusions by Secondary Ion Mass Spectometry. These new data on glass and mineral have incremented the diagnostic power of the available information on the geochemistry and isotope Sr, Nd, Pb, B, O and He-systematics of the Phlegraean whole-rocks, supporting the idea that the Procida magmas are the primitive end-member for the Campi Flegrei caldera volcanism. The $\delta^{18}O$ values are <5.88‰ for the Procida samples, wherea the highest values (>7.79‰) characterize the Campi Flegrei samples. The lowest $\delta^{18}O$ is associated with low $^{87}Sr/^{86}Sr$ ($\geq$0.70561), high Mg#, Cr, Ni and $^{3}He/^{4}He$ ($\leq$4.76-5.47Ra) values and Fo-richer olivines; instead, the heavy Sr and He isotopes always increase in the Campi Flegrei rocks. Procida also shows $^{143}Nd/^{144}Nd \leq 0.512553$ and $\delta^{11}B$=-3÷-8‰, higher with respect to the Campi Flegrei. REE produce fractionated patterns with Eu negative anomalies that are absent in the Procida melt inclusions and variously developed in the most evolved Phlegrean glassy matrix and whole-rock. Trace elements are typically enriched with respect to the Enriched MORB composition, with positive spikes for Pb. Interestedly, analyzed Procida melt inclusions mime the OIB composition, although showing very high Cs and Pb and moderate Rb, Ba, Th and U enrichments, as well as Nb and Ti depletions. The detected variation appears correlated to crystallization depth of mineral phases suggesting the main role of evolutionary processes within the crust at the Campi Flegrei caldera.

https://doi.org/10.1180/S0026461X00008434 Published online by Cambridge University Press

From many thousand tons to the laboratory balance pan

Francis F. Pitard [1]

1. Francis Pitard Sampling Consultants, LLC, Broomfield, Colorado, USA. fpsc@aol.com

ABSTRACT

We could define an unshakable optimist as someone who sincerely believes that the analysis of a few milligrams by micro-XRF, ICP-MS, or other sophisticated techniques may be representative of a several-thousand-ton ore block in a mountain or of a full shipment of any commodity traveling around the world. The many steps involved between the many orders of magnitude in weight changes are often dismissed as the steps that will totally ruin the analyst efforts. The assumption that the final analytical subsample is representative of the bulk from which it originated is an audacious one and extreme precautions involving theory and practice must be taken. Unfortunately, many important steps are too often casually addressed at best and the ultimate fault is too often attributed to the incompetence of the analyst, disregarding causes arising out of improper sampling and subsampling. Furthermore, at the laboratory, the most probable assay result is not independent of the weight of the selected subsample analyzed. Case histories are summarized. Solutions borrowed from the well-established Theory of Sampling are suggested. Appropriate sampling and subsampling diagrams providing good visual indicators are recommended. Precautions for the development of Standard Reference Materials are also listed.

The Upper Pennsylvanian Hushpuckney Black Shale Member from the Swope Formation in Kansas: Rhenium – Osmium Isotope Systematics, and the Highly Siderophile Elements.

LYNNETTE L. PITCHER[1*], E. TROY RASBURY[1], RICHARD J. WALKER[2], W. LYNN WATNEY[3]

[1]Stony Brook University, Stony Brook, USA (*presenting author: llpitcher@live.com, erasbury@notes.cc.sunysb.edu)
[2]University of Maryland, College Park, USA rjwalker@umd.edu
[3]Kansas Geological Survey, Lawrence, USA lwatney@kgs.ku.edu

The Pennsylvanian Hushpuckney "core" black shale of the Midcontinent USA has been well studied geochemically and stratigraphically, but lacks Re, Os, and other HSE (Ir, Ru, Pt, and Pd) data. We studied eleven samples from interpreted anoxic and euxinic intervals of four cores and found highly uniform chondrite-normalized HSE patterns. The concentrations are as follows: Os (0.27-9.8), Ir (0.02-0.07), Ru (0.04-0.31), Pt (3.0-11.3), Pd (0.32-13.3), and Re (34.6–1,827), in parts per billion. The Re-Os data show significant scatter on a $^{187}Re/^{188}Os$ versus $^{187}Os/^{188}Os$ isochron plot but give the expected early Kasimovian (Missourian) age of 306 Ma. The HSEs and Mo were used to consider geological processes that might have influenced the Re-Os systematics, and caused the extraordinary spread in $^{187}Re/^{188}Os$ (713-9122). Chondrite-normalized HSE patterns are similar to that of seawater, but with slightly higher relative Re and slightly lower relative Os, consistent with the interpretation that the Midcontinent Seaway had a fairly unrestricted opening to the global ocean. Rhenium and Mo show a positive correlation that suggests sulfidic conditions were, in part, responsible for Re enrichment.

It has been suggested that high Re concentrations from late Permian black shales reflect the unusual conditions during that interval, including warming deep water temperatures and increasing ocean acidity, which were linked to the deterioration of environmental conditions at the end of the Permian[1]. The Re concentrations and $^{187}Re/^{188}Os$ from the Hushpuckney black shale are higher than any reported from the late Permian, suggesting environmental deterioration is not the only reason for late Permian Re enrichment (Fig.1). More data from across the interval that represents the time of unification of Pangea (Early Carboniferous to Late Permian) may offer further insight into processes that control availability of HSE in black shales.

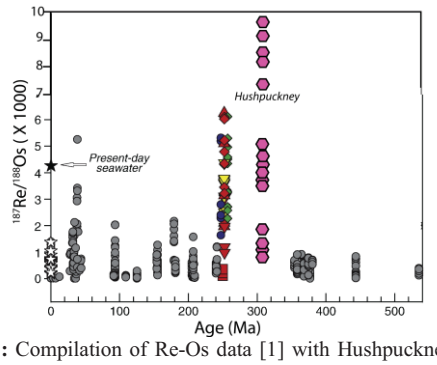

Figure 1: Compilation of Re-Os data [1] with Hushpuckney data shown for comparison.

[1] S. Georgiev *et al.* (2011) *EPSL* **310**, 389-400.

https://doi.org/10.1180/S0026461X00008434 Published online by Cambridge University Press

Natural organic matter roles in floc/sediment Pb dynamics

JANINA PLACH[1*] AND LESLEY WARREN[1]

[1]McMaster University, School of Geography and Earth Sciences, plachj@mcmaster.ca (* presenting author) warenl@mcmaster.ca

Introduction

Natural organic matter (NOM) is a fundamental component of freshwater ecosystems and a geochemically significant substrate for lead (Pb) transport, retention and fate in watersheds. Although Pb release into the environment by atmospheric deposition has declined in recent decades, concern remains whether Pb remobilization from sediments (e.g. pH driven Pb solid-solution partitioning) and subsequent transport by soluble organic-Pb complexes and floc-aggregates may continue to pose risk to freshwater ecosystems. As such, the objectives of this study were to: (1) investigate Pb and NOM distributions among suspended floc, surficial bed sediment and water-column compartments; (2) identify the important solid phases for Pb sequestration in floc and surfical bed sediments; and (3) establish the role of pH (pH 5-8) impacting dissolved organic carbon (DOC) and Pb solid-solution partitioning from natural limnetic floc, as well as lake, stream and wetland sediments both *in situ* and under controlled laboratory settings.

Results and Conclusions

Water, floc and sediments were collected for aqueous Pb and NOM analysis across nine highly variable freshwater (wetland, stream, lake) ecosystems of Ontario, Canada. Results indicate soluble organic-Pb complexes dominated Pb aqueous species in NOM-rich environments. Surficial sediments and floc showed distinct Pb sequestration and solid-solution partitioning patterns across sites driven by differential roles of living versus refractory NOM within each compartment. Stable organo-Pb complexes dominated sediment Pb solid-solution partitioning, as mobilization of DOC and Pb occurred with increasing pH from NOM-rich sediments, while Pb release was inhibited from NOM-poor sediment. In contrast, amorphous Fe oxyhydroxides, collected by microbes and extracellular polymeric substances, were the best predictor of floc Pb solid-solution partitioning and the key floc Pb sequestration phase across sites. These results and their implications for Pb mobility in freshwater catchments from upstream NOM-rich wetlands through to downstream NOM-poor littoral lake environments will be presented.

Significance of sulfidic organic-rich Archean shales

NOAH J. PLANAVSKY[1], CLINTON T. SCOTT[2], CHRIS REINHARD[1], BOSWELL WING[2], TIMOTHY W. LYONS[1]

[1]Univerrsity of California, Riverside, U.S.A., noah.planavsky@email.ucr.edu, timothy.lyons@ucr.edu, christopher.reinhard@email.ucr.edu

[2]McGill University, Montreal, Canada, clinton.scott@mcgill.ca, wing@eps.mcgill.ca

In the past few years multi-proxy studies of black shales have transformed our view of the evolution of Precambrian Earth system processes[1-4]. Part of the utility of black shale studies lies with our ability to tie them to well-understood modern and Phanerozoic analogs. Geochemical signatures in black shales have the potential to hold information about concentrations of key trace nutrients, the emergence of an oxidative biosphere, and the onset of significant oxidative weathering. However, there have been relatively few truly comprehensive, multi-proxy studies of Precambrian units, which has made it difficult to delineate temporal trends from the black shale record and to evaluate the significance of emerging geochemical results. This problem is particularly acute for the Archean. To fill this gap, we have conducted a multielement (C-S-Fe-trace metal) biogeochemical study in black shales from several (ca. 2.7 Ga) drill cores within the Abitibi Greenstone belt in Ontario. We are particularly interested in the Abitibi since it was a strongly hydrothermally influenced basin.

The shales are marked by variable but in some cases extremely high organic carbon concentrations (up to 32% TOC). C-S-Fe systematics and simple sediment dilution calculations suggest that oxygenic photosynthesis was the primary source of organic carbon in the basin. Further, our data reveal a sustained and spatially widespread episode of Fe-limited pyrite formation under an anoxic water column. The Abitibi work, therefore, supports the emerging view that euxinic conditions where a common feature in productive Archean settings. Trace metal systematics allow us to tease apart the influence of hydrothermal systems on abundances of bio-essential metals in Archean anoxic oceans. We will foucus on Mo, Zn, Cu, and U systematics and co-variation.

[1] Anbar *et al.* (2007) *Science,* **317,** 1903-1906
[2] Scott *et al.* (2008) *Nature*, **452**, 456-459
[3] Reinhard *et al*. (2009) *Science,* **326**, 713-716
[4] Scott *et al*. (2011) *Geology,* **39**, 119-122.

https://doi.org/10.1180/S0026461X00008434 Published online by Cambridge University Press

Water loss from melt inclusions in pyroclasts of differing sizes

TERRY PLANK[1*], ALEX LLOYD[1], PHILIPP RUPRECHT[1], ERIK HAURI[2], WILLIAM ROSE[3]

[1]Lamont Doherty Earth Observatory, Columbia Univ., Palisades, NY, USA, tplank@ldeo.columbia.edu (* presenting author)
[2] Carnegie Instit. of Washington, DC, USA, ehauri@ciw.edu
[3]Michigan Tech Univ, Houghton, MI, USA, raman@mtu.edu

Our understanding of the pre-eruptive H_2O contents of parental magmas has come to rely on the measurement of olivine-hosted melt inclusions, and yet there is increasing recognition of the potential short-comings of olivine as a perfect container of undegassed melt. Several laboratory experiments have now demonstrated how melt inclusions can lose or gain H_2O through host olivine on short timescales (hours to days), relevant to eruptive processes. Here we have designed an experiment using natural tephra samples that cooled at different rates: ash (≤ 1 mm diam.), lapilli (2 cm), and bomb (6-7 cm) samples that were deposited on the same day (10/17/74) of the sub-plinian eruption of Volcán de Fuego in Guatemala. Ionprobe, laser ablation-ICPMS and electron probe analyses of olivine-hosted melt inclusions yield a similar range in major element (50-59% SiO_2), trace element (Ba/Zr = 4-6) and olivine compositions (Fo#72-79) in the different clast populations, that also match the range in the host bulk tephra and groundmass. Melt inclusions from the ash and lapilli samples record the highest H_2O contents, up to 4.4 wt%. On the other hand, melt inclusions in the bomb samples indicate up to 30% lower H_2O contents (loss of ~ 1 wt% H_2O), despite similar S, CO_2 and K_2O concentrations, consistent with the longer time available for re-equilibration with degassing magma through the olivine. Inclusions from bombs also record up to 10% post-entrapment crystallization of olivine, while those from the ash samples record none. Thus, taken at face value, melt inclusions from small bombs may lose H_2O and crystallize olivine within the 10 minutes maximum that it takes for a 3-4 cm radius bomb core to cool conductively. This could only occur if the fast redox exchange mechanism for H diffusion in olivine were operating (D ~ 10^{-9} to 10^{-10} m^2/s). On the other hand, several lines of evidence point to some of this water loss also occurring pre-eruptively, during magma ascent and degassing in the conduit. Some of the smallest melt inclusions (< 50 micron diameter) within ash and lapilli appear to have lost up to 10% water, and yet sufficient time is not available during post-eruptive cooling to allow this even given the fastest known H diffusivities. Moreover, inclusions selectively sampled from the outer cm of bomb clasts record greater water loss than those in 1 cm radius lapilli, consistent with a longer timescale for H_2O loss for all the bomb magma, and not just the slowly cooled bomb interiors. Thus, our results point to both slower post-eruptive cooling and slower magma ascent affecting bomb melt inclusions, leading to H_2O loss over the timescale of 10 minutes to hours. The important implication of this study is that a significant portion of the published data on H_2O concentrations in olivine-hosted melt inclusions may record some H_2O loss and not primary water, particularly for samples taken from lavas or bombs, or small inclusions (< 40 microns diameter) in general. Future sampling and analysis should bear these considerations in mind.

Characterisation of the Cr isotopic signature of marine sediments deposited in the S1 Mediterranean sapropel

HELENE PLANQUETTE [1*], RACHAEL H. JAMES [1], IAN J. PARKINSON[2]

[1]National Oceanography Centre, European Way, Southampton, SO14 3ZH, United Kingdom
[2]Department of Environment, Earth and Ecosystems, CEPSAR, The Open University, Walton Hall, Milton Keynes, MK7 6AA, United Kingdom
*Presenting and corresponding author; h.planquette@noc.ac.uk

The record of past changes in the dissolved oxygen concentration of seawater is crucial for understanding past climate changes, and for predicting future climate scenarios. Initial measurements of chromium (Cr) stable-isotope fractionation showed the potential of Cr as a tracer of dissolved oxygen concentrations in groundwaters (Ellis et al., 2002). More recently, analyses of ancient marine carbonates and banded iron formations have revealed large variations in $\delta^{53}Cr$ values, from -0.28 to 5.00‰, (Bonnand et al., 2011; Frei et al., 2009, 2011), which are distinct from the continental crust and terrestrial mantle (~-0.12 ‰; Schoenberg et al., 2008) and are interpreted to reflect past variations in seawater oxygenation.

In order to fully assess the validity of this new proxy, the effects of post-depositional diagenesis on Cr and Cr isotopes need to be quantified. To this end, we will present the results of analyses of Cr isotopes in sediment cores that record the deposition of the most recent eastern Mediterranean sapropel (S1) between 7 and 10 ^{14}C kyrs BP. The sapropel has experienced heavy diagenetic alteration which is revealed by the presence of maxima in the concentration of many redox-sensitive elements outside of the sapropel layer (Thomson et al., 1995). The Cr data will be compared with these other redox-sensitive elements, and measurements of the Cr isotopic composition of seawater samples that have different levels of dissolved oxygen. These new data will allow us to assess the mobility of Cr during diagenesis and the robustness of Cr isotopes as a redox-proxy.

[1] Bonnand, P., et al. (2011) *J. Anal. Atom. Spectrom.*, **26**, 528-535
[2] Ellis, A.S., et al., (2002). *Science*, **295,** 2060–2062
[3] Frei R., C. et al., (2011). *Earth Planet. Sci. Letters*, **312,** 114-125.
[4] Schoenberg, S., et al., (2008). *Chem. Geol*., **249**, 294-306
[5] Thomson J., N.C. et al., (1995). *Geochim. Cosmochim. Acta*, **59**, 3487-3501

https://doi.org/10.1180/S0026461X00008434 Published online by Cambridge University Press

New approaches for the prediction of contaminated neutral drainage

BENOÎT PLANTE[1*], BRUNO BUSSIÈRE[2], AND MOSTAFA BENZAAZOUA[3]

[1]Université du Québec en Abitibi-Témiscamingue (UQAT), Institut de Recherche en Mines et Environnement (IRME), benoit.plante@uqat.ca (* presenting author)
[2]UQAT, IRME, bruno.bussiere@uqat.ca
[3]INSA-Lyon, mostafa.benzaazoua@insa-lyon.fr

Context and objectives

Contaminated neutral drainage (CND) is the presence of metal concentrations above regulatory requirements at circumneutral pH in mine drainage [1]. The generation of CND by tailings and waste rocks is a growing concern for the mining industry due to increasingly restrictive regulatory requirements. Difficulties in CND prediction arise from the low oxidation rates of sulfide minerals and from the metal retention potential within the wastes. The latter induces an important delay in the formation of CND conditions [2]. For now, it is not possible to account for this delay using prediction techniques developed for acid-mine drainage (AMD) prediction, such as humidity cells, columns and lysimeters. This presentation aims to present (1) the main differences in AMD and CND predictions, and (2) new approaches currently under study for CND prediction.

Overcoming the metal retention prediction challenge

The main challenge of CND prediction is to quantify the metal retention potential of mine wastes, especially when sorption phenomena are involved in metal retention [1]. Three approaches are currently used to overcome this difficulty. Firstly, the sorption potential is estimated using batch sorption studies [2, 3]. The second approah consists of artificially saturating the sorption potential of the mine waste [4]. This can be done by contact with a contaminated leachate in sorption-enabling conditions until saturation of the retention potential. These approaches both require that the possible metals involved in CND are known prior to the tests, which require an exhaustive material characterization. Although they enable the qualitative estimation of the retention potentials of mine wastes, their results are virtually impossible to scale up from the lab to the field. A third approah currently under study is to inhibit metal sorption at the source using complexing agents. The ideal complexing agent for this matter would inhibit sorption phenomena by chelating the metals generated by sulfide oxidation, therefore disabling it from any other geochemical reaction, while it would not interfere with any other geochemical processes involved.

Conclusion

New approaches are currently developped to define the sorption potential and its impact in the mobilization of metals for CND prediction. These approaches will help in the development of a CND-specific protocol for the prediction of mine drainage quality.

[1] Nicholson (2004). *MEND Workshop, Sudbury*. [2] Plante, Benzaazoua & Bussière. (2011) *Mine Water Envir* **30**, 2-21. [3] Plante et al. (2010). Appl Geochem 25, 1200-1233. [4] Plante, Benzaazoua & Bussière (2011). *Mine Water Envir* **30**, 22-37

Impact of biological Mn(II) oxidation on the fate of subsurface U(IV)

K.L. PLATHE[1*], S-W. LEE[2], Z. WANG[3], D.E. GIAMMAR[3], B.M. TEBO[2], J.R. BARGAR[4]; R. BERNIER-LATMANI[1]

[1*]École Polytechnique Fédérale de Lausanne, Lausanne, Switzerland, kelly.plathe@epfl.ch (* presenting author)
[2]Orgeon Health & Science University, Portland, OR, USA
[3]Washington University in St. Louis, St. Louis, MO, USA
[4]Stanford Synchrotron Radiation Lightsource, Menlo Park, CA, USA

Uranium contamination of the subsurface, resulting from mining and processing of the radionuclide, is a concern in numerous locales. The oxidized form of U, hexavalent uranium (U(VI)), is soluble and mobile. Therefore, understanding its fate and transport is critical for the management of contaminated environments. U(VI) can be biologically reduced to U(IV) species that are less soluble, such as the mineral uraninite (UO_2) or monomeric U(IV). Stimulating biological activity in the subsurface has emerged as a possible remediation strategy for uranium contamination and would result in the formation of an *in situ* waste form consisting of U(IV). However, the long-term stability of U(IV) in the subsurface is still poorly understood. In particular, the formation of biogenic manganese oxides, known to rapidly oxidize UO_2 [1], may significantly impact the persistence of U(IV). This study focuses on probing the occurrence of Mn oxidation in the subsurface at a U contaminated site (Rifle, CO USA) and the ultimate fate of U in the system. Agarose gel pucks, containing Mn oxidizing spores and reduced U, were prepared as initial probes of the U/Mn redox system to determine if U(VI) was released from the gel after oxidation of U(IV) by Mn oxides. Initial results indicate extensive Mn oxidation within gels and almost no release of U from the gels after a month. U was present as U(VI) in the gels and X-ray absorption results indicate it may be a sorbed species. To investigate such reactions at the field scale, columns containing sediment previously enriched with reduced U *in situ* were prepared for deployment in the same aquifer's sub-oxic zone under Mn oxidizing conditions. Initial results from these experiments indicate U oxidation and release over a two month period. In order to more accurately pinpoint cause and effect in this system, laboratory columns were prepared with the same sediment and artificial groundwater. These experiments will determine the relative contribution of O_2 and Mn(IV) to U(IV) oxidation. Furthermore, TEM and XAS analysis of both field and lab sediments will determine spatial location of U in relation to Mn. These combined methods will give a more detailed view of the interactions between Mn and U in the subsurface. Because bioremedation technology is contingent on the product being stable, this is valuable information which can help evaluate the viability of future remediation approaches.

[1] Chini (2008) *Environ. Sci. Technol.* **42**, 8709-8714.

https://doi.org/10.1180/S0026461X00008434 Published online by Cambridge University Press

Caveats for assessing crystallinity in biogenic minerals

BEN XU, MICHAEL GRUDICH, AND KRISTIN M. PODUSKA*

Memorial University, Department of Physics and Physical Oceanography, St. John's (NL), Canada, kris@mun.ca (presenting author)

Assessing local and long-range order in biogenic minerals

The degree of structural order within biogenic minerals is key for understanding the temporal evolution of mineralization in biological systems.[1] Standard material characterization techniques, including Fourier transform infrared spectroscopy (FTIR) and X-ray diffraction (XRD), are widely used to assess structural differences in biogenic magnesium calcites and carbonated hydroxyapatites.[2,3] However, no single measurement tool can adequately assess both local order (as can be done with FTIR) as well as long-range periodicity (as can be done with XRD). In this work, we identify serious pitfalls that can occur when trying to extract details about the structural order in a mineral from broadened spectroscopic or diffraction peaks. We also show that these challenges can be addressed by using relatively simple analyses to track FTIR spectral changes in amorphous and poorly crystalline materials with biogenic, geogenic, or anthropogenic origins.

Results of diffraction-limited infrared spectroscopic studies

Comparisons between FTIR transmission spectra from conventional bench-top instruments and data collected under spatially resolved, diffraction-limited conditions at the Canadian Light Source (Mid-IR beamline) highlight that there are both structural (material-specific) and measurement geometry contributions to spectral line widths. These conclusions are based on auto-correlation analyses[4] applied to spectra from a series of calcite samples with different particle size distributions. Using similar auto-correlation analyses with carbonated hydroxyapatites and other biominerals is straightforward, but the interpretation and implications of the results present new and interesting questions related to structural order at intermediate length scales. In this context, we compare our approach with other common metrics for tracking crystallinity, including the infrared splitting factor that is routinely reported for apatitic phosphate biominerals.

Conclusions

We demonstrate that the co-existence of material-specific and measurement-specific contributions to infrared peak broadening can be beneficial for extracting information about the differences in structural order that can occur in biogenic, geogenic, and anthropogenic minerals. These effects can be decoupled in FTIR transmission measurements, obtained with standard bench-top instruments, by using a robust auto-correlation analysis of peak widths. An important implication of this result is that infrared spectroscopy has enormous potential as a quantitative tool for tracking changes in the structural order during biomineralization and biomimetic mineralization processes.

[1] Meldrum, Cölfen (2008) *Chemical Reviews* **108**, 4332-4432. [2] Poduska, Regev, Boaretto, Addadi, Weiner, Kronik, Curtarolo (2011) *Advanced Materials* **23**, 550-554. [3] Gueta, Natan, Addadi, Weiner, Refson, Kronik (2007) *Angewandte Chemie International Edition* **46**, 291-294. [4] Balan, Delattre, Roche, Segalen, Morin, Guillaumet, Blanchard, Lazzeri, Brouder, Salje (2011) *Physics and Chemistry of Minerals* **38**, 111-122.

εNd signatures of NW North Atlantic water masses and their recording in deep corals from Orphan Knoll

ANDRÉ POIRIER*[1], SOPHIE RETAILLEAU[1], AURÉLIEN BLENET[1,2], BASSAM GHALEB[1], CLAUDE HILLAIRE-MARCEL[1], AND EVAN EDINGER[2]

[1]GEOTOP-UQAM, Montréal, Canada,
poirier.andre@uqam.ca (*presenting author)
sophie.retailleau@gmail.com
blenet.aurelien@hotmail.fr
ghaleb.bassam@uqam.ca
chm@uqam.ca
[2]Memorial University, St. John's, Canada,
eedinger@mun.ca

Baffin Bay seawater espilon Nd signature was measured more than 25 years ago (Stordal and Wasserburg, 1986) at a very low value when compared to the average North Atlantic Ocean. This unradiogenic value is introduced into the North Atlantic Ocean through the Labrador current that flows on the East coast of Canada.

Seawater from all water masses from Baffin Bay and the Labrador Sea (near Orphan Knoll) were sampled during cruises of CCGS Hudson in 2008 and 2010. Using McLane™ pumping systems equipped with Mn-oxide coated cartridges, dissolved neodymium (Nd) was recovered from ~200 liters of seawater for many casts. The geographical area covered allows us to monitor the present day εNd signatures of Baffin Bay overflow water, as well as that of all other water masses involved in the Atlantic Meridional Overturning Circulation (AMOC).

During the 2010 cruise, the Canadian remotely operated vehicule (ROPOS) was used to sample specimens of deep-water cup corals (alive and fossils) from Orphan Knoll, at a depth of approximately 1700-1800 m below surface, i.e., near the depth-limit of the Present Labrador Sea Water mass. U-Th data in modern (live-collected) specimens of *Desmophyllum dianthus* yield critical information on the efficiency of the cleaning procedure used, with respect to the removal of oxide coatings ("clean" samples must yield zero ^{230}Th-ages), and thus on the representativity of the Nd isotope data obtained. The same approach combined with ^{14}C-ages is used in fossil coral studies, as a means to document, back in time, water mass changes at Orphan Knoll, in relation with the AMOC/climate variability.

[1] Stordal and Wasserburg (1986) Earth and Planetary Science Letters, vol.77, 259–272.

https://doi.org/10.1180/S0026461X00008434 Published online by Cambridge University Press

The geochemical features of the garnets from peridotites of Udachnaya pipe (Yakutia)

LYUDMILA N. POKHILENKO[1]*, VLADIMIR G. MALKOVETS[1], ALEXEY M. AGASHEV[1], AND WILLIAM L. GRIFFIN[2]

[1] V.S.Sobolev Institute of geology and mineralogy SB RAS, Novosibirsk, Russia, lu@igm.nsc.ru (*presenting author)

[2] GEMOC National Key Centre, Macquarie University, Sydney, Australia

Iintroduction

Study of mantle xenoliths from the kimberlite pipes allows to get an important information about the origin and transformations of the lithosphere substance. The most deep-seated rocks of the lithospheric mantle are deformed peridotites, having the features of recrystallization and structures of the flow. These rocks undergo significant transformations and enrichment with different components under the effect of asthenospheric melts penetrating by the cracks and faults [1]. The most depleted rocks which are not affected by the enrichment processes are supposed to be the megacrystalline dunites [2].

Methods and samples

The garnets from 5 deformed lherzolites (mineral composition: olivine, orthopyroxene, clinopyroxene, garnet), and 20 megacrystalline harzburgite-dunites (mineral composition: olivine, garnet, sometimes chromite, orthopyroxene) from the kimberlite pipe Udachnaya (Yakutia) were analyzed by the LAM-ICPMS.

Results and Conclusion

The chondrite normalized [3] REE patterns of garnets from deformed lherzolites are mostly characterized by smooth increasing of LREE values with gradation in the field of HREE. The distribution curves of REE in garnets of megacrystalline dunites have highly sinusoidal character. The very big difference in REE values is seen in the width of dunite field. It shows the different degree and time of their enrichment.

The most of distribution curves for garnets of megacrystalline dunites have the peaks at the LREE and MREE showing increased Ce (7 samples), Pr (4 samples), Nd (7 samples), Sm (2 samples) concentrations proving early enrichment. The sharp sinusoidality of REE distribution curves, early enrichment with the LREE prove that some garnets of studied dunites were not in the equilibrium with the melt. In general these garnets could be formed as a result of transformation of earlier chromites [4], which is confirmed by the increased Cr-concentration in them (for example, garnet UV167/09 contains 11.84 wt.% Cr_2O_3), either as a result of exsolution of primary Al, Cr-containing orthopyroxene, presenting in garzburgites.

[1] Agashev et al.(2010) *Dokl. RAN.* **432**, 510-513. [2] Pokhilenko et al.(1993) *Geol. and Geoph.* **34/1**, 71-84. [3] McDonough & Sun (1995) *Chem.Geol.* **120**, 223-253. [4] Malkovets *et al.* (2007) *Geology* **35**, 339-342.

Composition evolution of peridotites of Siberian craton lithosphere roots: harzdurgite→lherzolite→wehrlite

NIKOLAY P. POKHILENKO*, ALEXEY M. AGASHEV, AND LYUDMILA N. POKHILENKO

VS Sobolev Institute of Geology and Mineralogy SB RAS, blingoreluiy@ya.ru (*presenting author)

Peculiarities of chemical composition and geochemical features of extremely fresh xenolith of unique mantle peridotites from Udacnaya kimberlite pipe were studied. The studied xenoliths were formed at the P-T conditions corresponding to the diamond stability field. A studied collection includes some varieties of megacrystalline Cr-pyrope harzburgites [1,2], metasomatized depleted peridotites [3]; c) fresh sheared Cr-pyrope lherzolites [4].

Obtained results show that ultra depleted peridotites: Cr-pyrope dunites and harzburgites including their diamondiferous varieties were secondary enriched in different scale by two different types of metasomatic agents. The first of them had a geochemical features close to those of carbonatitic melts. Increase of Ca in system caused a transformation of initial paragenesis ol+en+low-Ca knorringite-rich Cr-pyrope to ol+Cr-cpx+high-Ca uvarivite-rich pyrope (up to 76% Ca-comp.). This process caused enrichment of initially depleted peridotites in LREE and Ca.

The second type of metasomatic agent had definitely basanitic composition, and it caused secondary enrichment of initial ultra depleted peridotites by Si, Ti, Al, Fe, Ca, Na, K, incjmpatible and HREE, and obviously this process was synchronous to the kimberlite melt generation. CPX and magnesian ilmenite were a prohibited phases in initial ultra depleted peridotites, and in some the most enriched peridotites their amounts are up to 20 and 5 vol.%, correspondingly.

Sheared pyrope peridotites have a multistage character of a composition evolution including: a) initial depletion as a result of extraction from them melts of high degree of partial melting; b) enrichment by agent with high content of incompatible elements that caused significant increase of La/Yb ratio; c) enrichment by basanitic components synchronous to process of kimberlite formation [5].

[1] Boyd *et al.* (1997) *Contrib. Mineral. Petrol.* **128**, 228-246. [2] Pokhilenko *et al.* (1993) *Russian J. Geol. Geophys.* **34**, 56-67. [3] Pokhilenko *et al.* (1999) *Proc. 7th IKC*, **2**, 689-698. [4] Agashev *et al.*(2006) *Doklady Earth Sciences*, **407A**, 3, 491-494. [5] Pokhilenko (2009) *Lithos*, **112S,** 934-941.

https://doi.org/10.1180/S0026461X00008434 Published online by Cambridge University Press

Mesoarchean hydrous upper mantle: Evidence from the Fiskenæsset Complex, SW Greenland

ALI POLAT

Department of Earth and Environmental Sciences, University of Windsor, Windsor, ON, CANADA, polat@uwindsor.ca

The Fiskenæsset Complex, SW Greenland, contains the world's best preserved Archean (~2970 Ma) layered anorthosite, leucogabbro, gabbro, and ultramafic rock association. The ultramafic rocks consist mainly of olivine-pyroxene hornblendites, peridotites, dunites, and pyroxenites. The complex appears to have been emplaced into Archean oceanic crust (now amphibolite) and later intruded by tonalites, trondhjemites and granodiorites (TTGs). The complex and bordering TTG intrusions and mafic volcanic rocks were variably affected by granulite facies metamorphism and retrogressed under amphibolite facies conditions. Despite poly-phase deformation and amphibolite to granulite facies metamorphism, primary igneous structures and intrusive relationships are well preserved in many outcrops in the complex [1-3]. The Fiskenæsset ultramafic rocks share many petrographic characteristics of unmetamorphosed mafic to ultramafic layered intrusions and Alaskan-type ultramafic complexes. In ultramafic rocks, many orthopyroxene grains occur between amphibole and olivine grains and contain an intergrowth of symplectitic (vermicular) magnetite. These orthopyroxene-magnetite intergrowths appear to have grown at the expense of olivine. The origin of the orthopyroxene-magnetite symplectitic intergrowths is attributed to chemical reactions between residual, hydrous, hornblende-forming melts and olivine. In several locations, the Fiskenæsset ultramafic sills were intruded by a network of 5 to 40-cm-thick hornblendite veins. Given that horblendites and hornblende-bearing gabbros and peridotites are mainly restricted to Phanerozoic supra-subduction zone ophiolites and magmatic arcs, it is suggested that the Fiskenæsset Complex represents a relic fragment of a Mesoarchean oceanic island arc. The trace element systematics of the Fiskenæsset layered rocks and spatially and temporarily associated basaltic amphibolites and TTGs also indicate that these rock suites originated in an oceanic island arc setting. Petrographic observations and geochemical data provide strong evidence for a hydrous sub-arc mantle source for the igneous Fiskenæsset layered intrusion. Amphibole (mostly hornblende) occurs as an interstitial mineral to olivine, pyroxene, plagioclase, chromite and chrome-spinel and as inclusions in these minerals in the cumulates, consistent with an igneous origin. It is suggested that water was recycled to the source of the Fiskenæsset rocks through subduction of altered oceanic crust. Recycling of water to the upper mantle not only resulted in the generation of igneous amphibole in the complex, but it may also have contributed to the generation of neighbouring TTG-dominant continental crust by Archean subduction processes.

[1] Polat *et al.* (2009) *Precambrian Research* **175**, 87-115. [2] Polat *et al.* (2010) *Chemical Geology* **277**, 1-20. [3] Polat *et al.* (2011) *Lithos* **123**, 50-72.

Sorption and incorporation of radio-nuclides at mineral surfaces studied with quantum chemical methods

R. POLLY*, B. SCHIMMELPFENNIG, M. FLÖRSHEIMER, F. HEBERLING, T. STUMPF, R. KLENZE, H. GECKEIS

Karlsruher Institut für Technologie (KIT), Campus Nord, Institut für nukleare Entsorgung (INE), Postfach 3640, 76021 Karlsruhe, Germany (email: polly@kit.edu)

The reliable long-term prediction of actinide migration in geological formations requires understanding of the adsorption/desorption and incorporation mechanism at the molecular level. The sorption and incorporation of metal ions at mineral surfaces is a very important process which leads to the retention/retardation of radionuclides such as actinide ions and fission products.

We present three different investigations in this talk: (1) the interaction of trivalent lanthanides and actinides with the solvated corundum (110) surface, (2) interaction of selenite with the hydrated calcite surface and (3) the incorporation of trivalent lanthanides and actinides in calcite. Study (1) is carried out with orbital based ab inito and DFT methods using TURBOMOLE, whereas (2) and (3) with plane-wave DFT, as implemented in the Vienna Ab initio Simulation Package (VASP).

The corundum (110) surface is a challenging task for a theoretical investigation because singly, doubly and triply coordinated aluminol groups are present simultanously. We used the $Al_{27}O_{75}H_{67}$ cluster in this study as a model system for the corundum (110) surface. In a first step, we determined the structure and deprotonation properties of this cluster and calculated the vibrational frequencies of the surface aluminol groups. These results are compared with experimental data to validate our cluster model. In a second step we determined the structure of the inner-sphere complexes of the trivalent lanthanides and actinides at the surface. Various multidentate surface bound inner-sphere complexes are found to predominate. They are characterized and compared with experimental results.

Se-79 is a fission product of U-235 with a long radioactive half life of $1.1x10^6$ years. Selenite (SeO_3^{2-}) and selenate (SeO_4^{2-}) interact only weakly with common mineral surfaces. Therefore they have been identified as crucial radio nuclides for long term safety assessments of nuclear waste disposal. We determined the structure of the water/calcit interface and identified surface sorbed and incorporated selenite species at the calcite/solution interface.

The last point tackles the incorporation of trivalent lanthanides and actinides into calcite. Earlier spectroscopic investigations suggest incorporation of lanthanide/actinide ions occupying Ca-sites in the calcite lattice. Charge compensation is achieved by the substiution of two Ca atoms by one trivalent lanthanide/actinide and one Na ion. Here, we studied modifications of the calcite structure induced by the substitution.

https://doi.org/10.1180/S0026461X00008434 Published online by Cambridge University Press

Benthic O_2 fluxes measured by Eddy Covariance in a large flume facility

PIERRE POLSENAERE[1,2,3*], CECILE CATHALOT[1], TOM COX[1], FILIP MEYSMAN[1,2], OLIVIER MAIRE[3] AND BRUNO DEFLANDRE[3]

[1]NIOZ Yerseke, Ecosystem Studies
pierre.polsenaere@nioz.nl ([*]presenting author)
cecile.cathalot@nioz.nl
tom.cox@nioz.nl
filip.meysman@nioz.nl
[2]Vrije Universiteit Brussel, Analytical and Environmental Chemistry
[3]University Bordeaux 1, Environnements et Paléoenvironnements Océaniques et Continentaux
o.maire@epoc.u-bordeaux1.fr
b.deflandre@epoc.u-bordeaux1.fr

The Eddy Covariance: a new technique to assess sediment-water O_2 exchanges over various environments

The Eddy Covariance (EC) is a novel technique used to quantify the sedimentary O_2 consumption of marine ecosystems [1]. It measures O_2 exchanges at the sediment-water interface over large spatial scales (> 100 m^2) without being intrusive or disturbance of the flow field. This new technique has recently been used in various natural environments as tropical lagoon [2], tidal flat [3], river [4] and deep ocean [5] systems.

In autumn 2011, EC deployments were carried out in a 18 m long flume tank (NIOZ Yerseke, The Netherlands) filled with muddy sediment (Figure 1). Based on simultaneous measurements of near-sediment velocities (ADV Vector, *Nortek*) and O_2 concentrations (*Unisense* Clark-type microelectrode) at high frequency (64 Hz), O_2 exchanges at the sediment-water interface were calculated by EC. These EC fluxes were then compared with values based on microsensor profiling and chamber incubation.

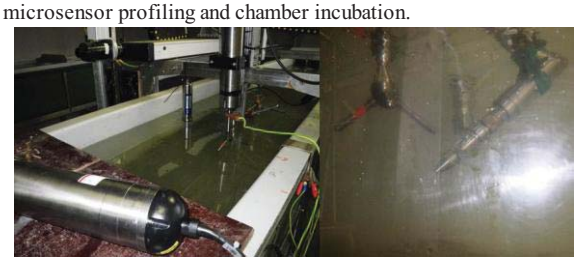

Figure 1: The flume Eddy Covariance deployment (Sept. 2011) showing sensor set-up (velocimeter, left and microelectrode, right).

First results and conclusions

EC O_2 fluxes were similar or greater than those obtained by incubation and microsensor profiling, i.e -23.8˜-62.9, -42.2˜-56.0 and -15.8˜-19.5 mmol m^{-2} d^{-1} respectively. EC fluxes varied with flow velocity, sensor depth and upstream location. The deployment of the EC technique in the flume facility allows to investigate various aspects of boundary layer hydrodynamics under controlled conditions.

[1] Berg et al. (2003) *Mar. Ecol. Pro. Ser.* **261**, 75-83. [2] Hume et al. (2011) *Limnol. Oceanogr.* **56**, 86-96. [3] Kuwae et al. (2006) *Mar. Ecol. Pro. Ser.* **307**, 59-68. [4] McGinnis et al. (2008) *Geophys. Res. Lett.* **35**, doi:10.1029/2007GL032747. [5] Berg et al. (2009) *Limnol. Oceanogr. Meth.* **7**, 576-584.

Theoretical carbon isotope fractionation under deep-earth conditions

VENIAMIN B. POLYAKOV [1*] AND JUSKE HORITA[2]

[1]Institute of Experimental Mineralogy, Russian Academy of Science, Russia, polyakov@iem.ac.ru (* presenting author)
[2]Department of Geosciences, Texas Tech University, Lubbock, TX, juske.horita@ttu.edu

Introduction

In addition to the major component of mantle carbon, which has $\delta^{13}C$ values of about -5±3‰, some reduced (carbide, hydrocarbons) and neutral (diamond, graphite, dissolved C) carbon compounds from mantle xenoliths and other sources have $\delta^{13}C$ values in the range of -20 to -35‰. Contamination of organic carbons near the Earth surface and the recycling of sedimentary organic matter via subduction zones have often been invoked to explain the depleted ^{13}C signatures of these mantle rocks. However an increasing number of studies do not support this scenario. Two other possibilities exist. First, mantle carbon could have been isotopically heterogeneous since the accretion from the solar nebula and the core–mantle segregation in the first 100 My of Earth history. Chondrites, carbonaceous chondrites particularly, which are widely considered to represent primitive undifferentiated materials from which the Earth accreted, have $\delta^{13}C$ values ranging widely from -28 to 0‰. Another possibility is that there exist some mechanisms and processes for large carbon isotope fractionation at high temperatures and pressures. For example, Craig [1] and Deines and Wickman [2] reported *ca*. 12 ‰ differences between graphite and cohenite, $(Fe, Ni, Co)_3C$, from iron meteorites. A recent experimental study by Satish-Kumar *et al*. [3] reported 2.7 - 4.5 ‰ differences between graphite/diamond and FeC melt at 1350 - 2100°C and 5 - 10 GPa.

Theoretical study

Here, we report our updated reuslts of theoreitcal calcualtions on $^{13}C/^{12}C$ fractionation among major C-bearing materials (CO_2, calcite, diamond, graphite, and SiC). Our results show that SiC is depleted in ^{13}C realtive to diamond/graphite and calcite even at very high temperautes: 2.5 - 9 ‰ at 1000 - 2000°C. Our results for SiC is consistent with the experimental results for FeC melt [3]. High preussures (>10's of GPa) under deep-Earth conditions may also affect measurably equilibrium isotope fractionation of C-bearing species [4]. Thus, the recent experimental study and our theoretical calculaitions clealry demonstate that carbides (Fe_3C and SiC) are significatnly depleted in ^{13}C at high tmeperatues and pressures. We need to revise and improve our understanding of carbon cycles and associatted isotope fractionation in the deep-Earth.

[1] Craig (1953) *GCA* **3**, 53-92.
[2] Deines and Wickman (1975) *GCA* **39**, 547-557
[3] Satish-Kumar *et al*. (2011) *EPSL* **310**, 340-348.
[4] Polyakov & Kharlashina (1994) *GCA* **58**, 4739-4750.

https://doi.org/10.1180/S0026461X00008434 Published online by Cambridge University Press

Association with poorly crystalline metal oxides: Effect on soil organic matter storage and stability in four eastern deciduous forest soils

R. Porras[1*], M.Torn[2], K. McFarlane[3]

[1]Lawrence Berkeley National Laboratory, Berkeley, CA, USA, RCPorras@lbl.gov (*presenting author)

[2]Lawrence Berkeley National Laboratory, Berkeley, CA, USA, MSTorn@lbl.gov

[3]Center for Accelerator Mass Spectrometry, Lawrence Livermore National Laboratory, Livermore, CA., USA mcfarlane3@llnl.gov

Redox-active metals and the global carbon cycle

Strong association with mineral surfaces has been suggested as one mechanism underlying the long-term stabilization of organic matter in soils. Several recent studies have demonstrated a positive correlation between the content of poorly ordered crystalline metal oxide and hydroxide mineral phases and soil organic matter (SOM) or ^{14}C-based residence time. This positive correlation suggests that mineral-associated SOM persists over long time scales.

We utilized selective chemical dissolution (acid ammonium oxalate in the dark and sodium pyrophosphate) coupled with radiocarbon measurements to investigate the relationship between poorly crystalline Fe, Al, and Mn oxyhydroxide phases on organic matter storage and turnover time across four deciduous forest sites in the eastern U.S.comprising three different soil orders (inceptisol, spodosol alfisol).

Our results demonstrate that association with poorly-crystalline Fe and Al oxides (via adsorption to mineral surfaces and/or formation of soluble metal-OM complexes) do slow the turnover of SOM, with a significant positive linear relationship between radiocarbon turnover time and the content of oxalate extractable Al and Fe overall (R^2= 0.60,P=0.0001,CL=95%). Piecewise regression analysis on turnover time vs. oxalate extractable metal oxide content for all four sites shows an apparent metal oxide threshold value at 5g kg^{-1}. Sites with oxalate extractable Fe and Al content below this value showed no statistically significant influence on SOM stability, presumably because the metal oxides are present in insufficient quantity to exert a measureable influence on the decomposability of SOM.

Soluble Fe and Al oxyhydroxide-OM complexes extracted via treatment with Na-pyrophosphate had a statistically significant influence on carbon storage at only one site (Bartlett Experimental Forest, spodosol) (R^2=0.92, P<0.0001, 95%CL). However a significant linear relationship between ^{14}C-based turnover time and Na-pyrophosphate extractable Fe and Al could not be demonstrated for any individual site. Thus, complexation of organic matter via reaction with Fe and Al oxide phases does not appear to be the dominant control on turnover time in the 0-15cm depth at the sites under study.

Harvard Forest (inceptisol) had the highest poorly crystalline Fe concentrations estimated as (oxalate extractable Fe) – (Na-pyrophosphate extractable Fe) and exhibited the strongest influence on ^{14}C based turnover times (R^2=0.82, P=0.0003,CL=95%); in this soil, poorly-crystalline Fe oxides and hydroxides are quantitatively important in stabilizing organic inputs against decomposition. Poorly crystalline Mn was found to exert a significant influence on SOM stability at a single site: Missouri Ozark Forest (alfisol) (R^2=0.65,P=0.0051,CL=95%). No significant effect for Mn on SOM storage could be demonstrated for any of the four sites under study.

Analysis of oil inclusions by fs-laser ablation and ToF-SIMS

ROBERT POTTORF[1*], SEBASTIEN DREYFUS[1], SANDRA SILJESTRÖM[2], CHRISTOPHE PECHEYRAN[3], BENOIT CATALAYUD[3], NGAMI PHAN[1], AND MARLENE MADINCEA[1]

[1]ExxonMobil Upstream Research, Houston, USA robert.j.pottorf@exxonmobil.com (* presenting author)

[2]SP Technical Research Institute of Sweden, Borås, Sweden sandra.siljestrom@sp.se

[3]IPREM, LCABIE, UMR 5254, Pau, France christophe.pecheyran@univ-pau.fr

Femtosecond (fs) Laser Ablation

Recent advances in laser technology have led to ultrashort laser pulses capable of selectively opening and liberating oil within single inclusions. Coupling of an on-line femtosecond laser to a gas chromatograph-mass spectrometer successfully analysed hydrocarbon compounds from individual inclusions [1], but C_{19+} compounds were undetected and potentially remained in the ablation chamber. To test this hypothesis, well characterized oils were ablated with an infrared (1030 nm) high repetition rate femtosecond laser and directly collected on filters placed at the exit of the ablation chamber. Analyses of filter extracts by GCxGC-ToF-MS showed the presence of unaltered C_{12+} compounds including biomarkers. The success of the femtosecond laser as a sampling tool for biomarker analysis of oils was extended to the analysis of individual inclusions.

Time of Flight Secondary Ion Mass Spectrometry (ToF-SIMS)

ToF-SIMS technology has been used to detect hopanes and steranes in single oil-bearing fluid inclusions [2]. Standard oil suites were used to calibrate the ToF-SIMS instrument for various hydrocarbon source rock facies allowing the determination of the origin of oils trapped in inclusions within the Elk Basin Field, Big Horn Basin, WY. The oils appear to be derived from a distal carbonate source (Phosphoria Formation) supporting long distance, lateral migration into the Big Horn Basin Fields from a mature Phosphoria source rock ~65-120Ma.

[1] Volk *et al*. (2010) *Organic Geochemistry* **41**, 74–77.
[2] Siljeström *et al.* (2010) *Geobiology* **8**, 37–44.

https://doi.org/10.1180/S0026461X00008434 Published online by Cambridge University Press

Contrasted response of U-Th bearing minerals to albitization:

A case study from 3 albitite occurences in the Pyrenees

MARC POUJOL[1*], PHILIPPE BOULVAIS[1]

1Université de Rennes 1, UMR CNRS 6118 Géosciences Rennes, 35042 Rennes cedex, France. Marc.poujol@univ-rennes1.fr (* presenting author))

Albitization is a common metasomatic process active in various geodynamic environments. In the northern Pyrenees, several occurrences of albitites are described.

Like many other orogenic belts, the Pyrenees recorded numerous fluid-rock interaction events. Fluids led to talc mineralization in dolostones,ophicalcite development at the expense of peridotite massifs and albitization of granitoids and metamorphic rocks.. Because the Pyrenees have undergone the effects of both the Hercynian and Alpine orogenies, precise dating of the different fluid flow events is not straightforward.

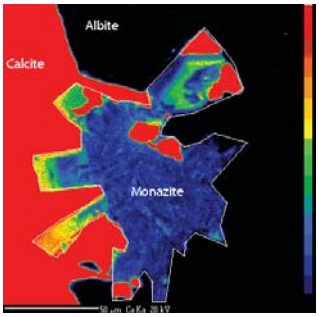

Fig 1: Ca chemical mapping of monazite

In this study, we focused on zircon, monazite and titanite, found either in metasedimenatry or meta-igneous protoliths that undergone pervasive albitization. Zircon grains were present in all the studied samples. Monazites were found only in an albitite occurrence developped from an igneous protolith while titanites were found in a albitized metasedimentary sample. These three types of mineral where selected in well characterized hydrothermal assemblages: zircons in metasomatically Zr-enriched rocks or in hydrothermal structures (millimetric veins cross-cutting granitoids); monazites when associated with calcite and/or albite in centimetric veins (Fig 1) and titanite with albite.

In-situ LA-ICP-MS ages obtained directly in thin sections from euhedral titanite and monazite grains from distinct albitites are 110 ± 8 and 98 ± 2 Ma, respectively [1]. The zircon U-Th-Pb isotopic system did not record this Cretaceous metasomatic event in any of the selected sample. This demonstrates that none of the zircons were affected (or grew anew) during fluid circulations. This confirms the robustness of zircon with respect to interaction with fluids.

We argue that the total time span of 20 Ma recorded by albitites corresponds to a long-lived hydrothermal system that was active during the rotation of Iberia around Europe. Because albitization and talc mineralization share a common spatial and temporal distribution in the Pyrenees, we argue that these two metasomatic phenomena are two independent records of this single, regional-scale, long-lived hydrothermal system.

The bulk composition of Rare Earth Elements (REE), Sc and Y in 36 chondrites: insight into elemental fractionation in the solar nebula

ALI POURMAND[1,2*], NICOLAS DAUPHAS[1], THOMAS J. IRELAND[1]

[1] Origins Lab, Department of Geophysical Sciences, University of Chicago, Chicago, IL 60637, USA

[2*] Neptune Isotope Lab, University of Miami - RSMAS, Miami, FL 33149, USA, apourmand@rsmas.miami.edu (presenting author)

Enrichment or depletion of the REE, Sc and Y in chondritic meteorites, relative to solar abundances preserved in the least equilibrated chondrites, has provided valuable insight into the condensation/evaporation history of refractory lithophile elements in the solar nebula during the early formation of the solar system [1-3]. A large portion of the existing data from bulk meteorite samples and their refractory inclusions, however, suffer from low precisions, or do not include mono-isotopic elements (Pr, Tb, Ho and Tm). Recently, we presented novel analytical techniques, utilizing low-blank fusion with $LiBO_2$ flux, TODGA extraction chromatography, and MC-ICP-MS for measuring the isotopic composition of actinides, REE, Sc and Y in extra-terrestrial materials [4], and revised the accretion age of Mars [5] and the mean of CI-chondrites for these elements [6]. Here, we present bulk concentrations of REE, Sc and Y in 36 (28 falls and 8 finds) carbonaceous (5), ordinary (15) and enstatite (16) chondrites using this new analytical methodology. All meteorite groups show varying degrees of enrichment or depletion in REE, Sc and Y relative to the mean of CI-chondrites. In general, three types of fractionation are dominant among other irregular patterns: 1) more refractory heavy REE (Gd, Tb, Dy, Ho, Er and Lu) are enriched relative to light REE (La, Ce, Pr, Nd, Sm and Tm), 2) more volatile elements (Eu and Yb) show positive or negative anomalies accompanied by minimal fractionation in other REE, 3) all elements show relatively similar enrichment or depletion without significant anomalies. More dispersion is also observed in the anomalies of more volatile elements (*e.g.,* Eu/Eu*) with increasing degrees of equilibration. While some fractionation patterns can be attributed to the presence of (ultra) refractory inclusions [3] or minerals (*e.g.,* phosphate) that concentrate REE in chondrites, other mechanisms may be needed for patterns that cannot be explained by dominance of a particular group of inclusions.

[1] Boynton (1975) *Geochim. Cosmochim. Acta* **39**, 569-584. [2] Evensen et al. (1978) *Geochim. Cosmochim. Acta* **42**, 1199-1212. [3] McPherson et al. (1988) in *Meteorites and the Early Solar System* pp. 746-807. [4] Pourmand & Dauphas (2010) *Talanta* **81**, 741-753. [5] Dauphas & Pourmand (2011) *Nature* **473**, 489–492. [6] Pourmand et al. (2012) *Chem. Geol.* **291**, 38-54.

https://doi.org/10.1180/S0026461X00008434 Published online by Cambridge University Press

Reassesment of the rare earth elements external cycle in french watersheds - a high potential resource for the future

O. POURRET[1*], J. TUDURI[2], R. ARMAND[1], G. BAYON[3] AND M. STEINMANN[4]

[1] HydrISE, LaSalle-Beauvais, Beauvais, France olivier.pourret@lasalle-beauvais.fr (* presenting author)
[2] BRGM, ENAG (BRGM School), Orléans, France
[3] Département Géosciences Marines, IFREMER, Plouzané, France
[4] UMR 6249 Chrono-Environnement, Univ. Franche-Comté, Besançon, France

The distribution of rare earth elements (REE) was studied in streams of the Armorican Massif and the Massif Central (France). The water chemistry of both watersheds was dominated by silicate weathering. The REE distribution patterns of stream water showed, from the source to the catchment outlet, a fractionation of the upper continental crust normalized REE distribution patterns from heavy REE (HREE) enriched to more flat and middle REE (MREE) enriched patterns, together with a progressive disappearance of a negative Ce anomaly. Ultrafiltration data (at 3 or 5 kDa) showed that the ultrafiltrates had HREE-enriched patterns with negative Ce anomalies, whereas the organic colloids showed relatively flat patterns. These data thus suggest that the observed general evolution from HREE-enriched to MREE-enriched patterns with distance is related to a growing importance of organic colloids as REE carriers from upstream to downstream.

The REE patterns of the ultrafiltrates are very similar to seawater patterns. The REE pattern of seawater could thus be inherited from river water. Commonly, the REE patterns of ocean water are usually considered to reflect (i) the respective REE inputs from rivers, aeolian transport, hydrothermal vents and dissolution of marine carbonates and (ii) interactions with the biogeochemical cycle, involving REE-removal from surface waters by adsorption onto settling Fe-Mn particles. The strong Ce depletion and the HREE-enrichment of ocean waters are commonly attributed to the redox chemistry of Ce and to the high stability constants of HREE carbonate complexes. Nevertheless, different processes may lead to REE and/or Ce removal from solution. The most often discussed hypothesis is fractionation during estuarine mixing, enhanced by extremely high particle reactivity of the REE (e.g. with MnO_2).

Results from this study thus allow to reassess the REE external cycle. Indeed, the river input to the oceans has relatively flat REE patterns without Ce anomalies, whereas oceanic REE patterns exhibit strong negative Ce anomalies and HREE enrichment. Indeed, the processes at the origin of seawater REE patterns are commonly thought to occur within the ocean masses themselves. However, the results from the present study illustrate that seawater-like REE patterns already occur in the truly dissolved pool of river input. This leads us to favor a partial or complete removal of the colloidal REE pool during estuarine mixing by coagulation, as previously shown for dissolved humic acids and iron. In this latter case, REE fractionation occurs because colloidal and truly dissolved pools have different REE patterns. Thus, the REE patterns of seawater could be the combination of both intra-oceanic and riverine processes. Eventually, the Atlantic continental shelf could be considered as a potential REE trap and shelf sediments would, similar to metalliferous deep sea sediments, represent a REE potential resource and guide for exploration. This latter hypothesis will be further tested by analysing various fractions (detrital, Fe-Mn oxides, organic compounds) of sediments deposited in river estuaries at the Western Atlantic margin.

On calculating phase equilibria for metamorphic systems

POWELL R[1*]

[1] School of Earth Sciences, University of Melbourne, Vic. 3010, Australia, powell@unimelb.edu.au (* presenting author)

Mike Brown has overseen a revolution in metamorphic geology, as an organiser of meetings, journal creator and editor, supporter of people and contributor to the science itself. I would like to give a personal view of an important part of that revolution—the calculation of metamorphic phase equilibria: where we are, what the challenges are, and what might be the way forward. This will be done via consideration of methodological aspects of what is needed for such calculations: 1) An extensive internally-consistent thermodynamic dataset for the end-members of minerals, fluids and melts; 2) Activity-composition relationships for these phases, extending into parts of composition space where there is little or no experimental control; 3) Methods, for example for calculating phase diagrams, that take into account the "natural" variables that are likely to be critical in metamorphic systems; 4) Software that implements these methods, using the current best thermodynamic descriptions of phases; and 5) An appropriately nuanced appreciation of reaction in metamorphic rocks, for example regarding length-scales, and the likely boundaries of application of equilibrium thermodynamics in the study of metamorphism.

https://doi.org/10.1180/S0026461X00008434 Published online by Cambridge University Press

Hydromagnesite-magnesite playas: A model for carbon storage

IAN M. POWER[1*], SIOBHAN A. WILSON[2], GREG M. DIPPLE[1], AND ANNA L. HARRISON[1]

[1]The University of British Columbia, Vancouver, Canada, ipower@eos.ubc.ca (* presenting author), gdipple@eos.ubc.ca, aharriso@eos.ubc.ca

[2]Monash University, Clayton, Australia, sasha.wilson@monash.edu

Hydromagnesite-magnesite playas (hectare-scale) are found near the town of Atlin, British Columbia, Canada. The playas were first described in 1916 by Young [1] and, most recently, characterized in the context of a biogeochemical model for CO_2 sequestration by Power et al. [2,3]. The weathering of ultramafic bedrock results in Mg-rich groundwaters that discharge into topographic lows where microbial, geochemical and physical processes mediate carbonate precipitation. The playas may be thought of as a natural repository of CO_2. Although magnesite [$MgCO_3$] is the most stable Mg-carbonate mineral, its precipitation is kinetically inhibited as a consequence of the strong hydration of Mg^{2+} ions [4]. As a result, the playas consist of a complex assemblage of hydrated Mg-carbonate mineral phases.

Aragonite [$CaCO_3$], dypingite [$Mg_5(CO_3)_4(OH)_2{\cdot}5H_2O$], and nesquehonite [$MgCO_3{\cdot}3H_2O$] may precipitate directly from surface and ground waters, which undergo diagenesis post-deposition. Playa sediments at depth (up to ~3 m) were collected along a transect (90 m) at 5 and 10 m intervals. The sediments are mainly composed of hydromagnesite [$Mg_5(CO_3)_4(OH)_2{\cdot}4H_2O$], but also contain magnesite. The abundance of magnesite at the surface ranges from 7 to 40 wt.% across the playa. The water table (~1 m depth) coincides with a hard crust containing up to 10 wt.% lansfordite [$MgCO_3{\cdot}5H_2O$]. Below ~1 m, the abundance of magnesite typically increases and may be up to 87 wt.% with hydromagnesite being the remainder. The Mg-carbonate sediments overlay Ca-carbonate sediments containing aragonite and dolomite [$CaMg(CO_3)_2$], which overlay glaciolacustrine sediments. Electron microscopy shows that magnesite forms as a distinct mineral phase and does not show intergrowth with hydromagnesite (Figure 1); meaning that it likely does not form from dehydration of hydromagnesite. The current focus is on understanding the geochemical conditions of low-temperature magnesite formation, which has implications for the long-term storage of anthropogenic CO_2 as Mg-carbonate minerals.

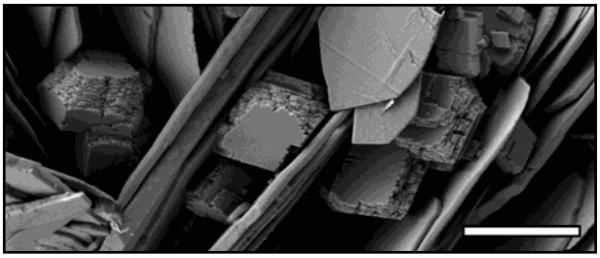

Figure 1: Low-temperature magnesite (rhombohedral crystals) forming between hydromagnesite plates (1 µm scale bar).

[1] Young (1916) *GSA Report*, 50-61. [2] Power *et al.* (2009) *Chem. Geol.* **206**, 302-316. [3] Power *et al.* (2007) *Geochem. Trans.* **8**:13 [4] Hänchen *et al.* (2008) *Chem. Eng. Sci.* **63**, 1012-1028.

Records of atmospheric Pb deposition along the St. Lawrence Valley, Quebec

S. PRATTE[1*], A. MUCCI[1], M. GARNEAU[2]

[1] GEOTOP & Dept. of Earth and Planetary Sciences, McGill University, Montreal, Qc, Canada H3A 2A7 (*correspondence: steve.pratte@mail.mcgill.ca)

[2] GEOTOP & Département de Géographie, Université du Québec à Montréal, Montreal, Qc, Canada

Ombrotrophic peat bogs provide reliable historical records of atmospheric metal deposition, in particular lead [1]. To date, most studies were carried out in Europe and served to document various periods of anthropogenic activities. In contrast, records of atmospheric metal deposition in North America are still scarce. The objective of this study was to reconstruct the recent history of atmospheric metal deposition (Pb, As, Cd, Ni and Zn) along the St. Lawrence Valley (SLV).

Cores (50 to 100-cm long) were collected in four peat bogs along the SLV. They were sub-sampled at 1 to 5-cm intervals and analyzed for their trace metal contents (Pb, As, Cd, Ni and Zn). Here, we present the vertical distributions of Pb and its stable isotopes (204, 205, 206, 207) in the four cores. Core chronologies were established using ^{210}Pb for the surface horizons and ^{14}C for the deeper sections. Regional, natural background metal concentrations and isotopic signatures were established from the analysis of samples taken from the bottom of the bogs. When the latter were not available, values from the upper continental crust (UCC) values were used [2]. Variations from these values within the cores were compared to the isotopic composition of North American major lead-bearing ores (used for the synthesis of gasoline additive) and modern aerosol for U.S. and Canada (1994-1999).

Preliminary results show that anthropogenic Pb concentrations increased sharply from the start of the 19th through the 20th century to reach a maximum between 1940-1970. The age and amplitude of this peak vary spatially along the SLV and, in some cases, can be associated with specific anthropogenic activities (e.g. smelting) or the convergence of different air masses. Since the 60's, lead concentrations have decreased rapidly, following the ban on leaded gasoline, but they have not reached pre-anthropogenic levels. Results show that the southwestern SLV has been more impacted by anthropogenic Pb.

Stable lead isotopes analyses are ongoing and will help discriminate between different anthropogenic and natural sources of atmospheric Pb at the study sites.

[1] Shotyk *et al.* (1996) *Earth Planet Sci Lett.* **145**, 1-7.
[2] Wedephol (1995). *Geochim. et Cosmochim. Acta* **59**(7), 1217-1232.

https://doi.org/10.1180/S0026461X00008434 Published online by Cambridge University Press

CONTAMINATION, MELTING AND SULPHIDE MINERALISATION IN THE BASAL RIVER VALLEY COMPLEX, CANADA

PREVEC[1*], STEPHEN A. AND VILJOEN[1], GREG

[1]Dept of Geology, Rhodes University, P.O. Box 94, Grahamstown, South Africa, 6140, s.prevec@ru.ac.za*

The River Valley Complex (RVC) is a Palaeoproterozoic mafic intrusion lying astride the ca. 1.0 Ga Grenville Front Tectonic Zone (GFTZ). The Complex is the easternmost member of a regionally extensive pod of mafic intrusions, with contemporaneous volcanics and dykes which comprise the Huronian magmatic suite. The RVC is the first member of this suite to show ore-grade prospects for PGE-sulphide mineralisation, as well as the sole instance of ultramafic cumulus rocks. The ores are associated with the Marginal Zone, which is transected by a cross-cutting near-basal unit (the awkwardly named "Inclusion/Autolith-bearing zone") which hosts both autolithic and (more rarely) exotic xenolithic blocks, and has been interpreted [1], on the basis of PGE and HFSE geochemistry, as the product of a late, chemically-boninitic melt, distinct from any other yet reported in this magmatic suite. A xenolithic fragment found in the South Zone of the Dana Lake showing, displaying apparent cumulus layering (only otherwise found higher in the lithostratigraphic sequence), a partial mantle of leucocratic selvage, and sulphide mineralisation, was sampled.

The xenolith is characterised by major and trace element geochemistry comparable to that of a granitoid (e.g., SiO_2 ranging from around 56 wt.% up to nearly 80 wt.%), and features quartz and alkali feldspar prominently. Conversely, the host rock is olivine normative, shows relict cumulus textures, and has REE and other HFSE abundances about an order of magnitude lower than those in the xenolith. Sm-Nd isotopic compositions show a range between $\varepsilon_{Nd}^{2.45}$ of around -1 to -2.3, typical of relatively uncontaminated Palaeoproterozoic mafic rocks regionally. However, the matrix values range between +3.2 and 0, representing the first direct evidence for depleted mantle in the Canadian Palaeoproterozoic. The sulphide mineralogy (po-cpy-py-pn ± sp) varies in mode across the traverse, with fracture-hosted cp-pn dominant in the xenolith, and po-pn-cp in the host rock. Normalised PGE profiles show a PPGE-enriched pattern typical of magmatic sulphide-controlled PGE in both the host rock- and xenolith-hosted sulphides, with the added feature of a negative Ru anomaly. A model involving infiltration metasomatism of fluid-rich crustal (footwall) melt is tentatively proposed to facilitate sulphide liquid precipitation and incorporation.

[1] Jobin-Bevans, L.S. (2004) Platinum-group element mineralisation in Nipissing Gabbro intrusions and the River Valley Intrusion; unpublished Ph.D. thesis, University of Western Ontario, London, Ontario, Canada. 457 pp.

Geochemical Mapping of Mantle Flow between Samoa and the Lau Basin

ALLISON A. PRICE[1*], MATTHEW G. JACKSON[1], PAUL S. HALL[1], JOHN M. SINTON[2], MARK D. KURZ[3]

[1] Boston University, Dept. of Earth Sciences, Boston, MA, 02115 (Price@bu.edu)

[2] University of Hawai'i at Manoa, Dept. of Geology and Geophysics, Honalulu, HI, 96822

[3]Woods Hole Oceanographic Institution, Dept. of Marine Chemistry, Woods Hole, MA, 02543

The juxtaposition of the Samoan plume and the Tonga Trench provides a unique setting for the study of upper mantle flow. The Samoan plume is located only 200 km east of the northern terminus of the Tonga trench. North of the terminus, the Pacific plate "tears," and the resulting tear creates a slab "window" allowing Samoan mantle to flow southward beneath the Vitiaz lineament--which separates the Pacific from the Lau Basin--and into the shallow mantle of the Northern Lau Basin. The presence of high $^3He/^4He$ (up to 28 times atmospheric (R_A)) and latitudinal gradients in trace element and isotopic (Sr-Nd-Pb) enrichment in the N. Lau Basin have been attributed to the southward flow of mantle material from the nearby Samoan hotspot through the slab window. High $^3He/^4He$ ratios (up to 28.1 R_A) have been reported in a swath within the northern Lau Basin but drop rapidly to both the South (~400km south of Peggy ridge) and East (Lupton, 2009.) However, $^3He/^4He$ ratios have not been reported in the region to the West or North of the region of the infiltrating plume, so the geochemical "map" of Samoan plume material in the Lau Basin is incomplete.

We present He, Pb, Sr, and Nd isotopic analyses as well as trace element analyses for glasses in the region just to the west of the location where the highest $^3He/^4He$ ratios were reported. The samples, which span the North Lau and North Fiji Basins, as well as submarine samples from Wallis Island, located just north of the Lau Basin, have $^3He/^4He$ ratios that vary between 6 and 15 R_A. The highest of the new $^3He/^4He$ occur in submarine lavas from Wallis Island, located between the northernmost portion of the Rochambeau Ridge (28.1 R_A) and the Samoan hotspot (up to 35 R_A.) The new data indicate that the Samoan-plume high $^3He/^4He$ mantle does not spread to the west in the Lau Basin, but is confined to a narrow corridor in the Northern Lau Basin that extends from Samoa, through Wallis and into a narrow region of the N. Lau Basin. However, Sr, Nd and Pb isotopic evidence are consistent with low 3He/4He Samoan plume material "leaking" into the N. Fiji basin as far west as Pandora Ridge. This observation places important constraints on changing mantle flow due to the evolving geometry of plume-trench juxtaposition.

https://doi.org/10.1180/S0026461X00008434 Published online by Cambridge University Press

The α-particle dose of the solubility threshold for detrital epidote-group grains from the Yangze River delta

JASON R. PRICE[1*], MICHEAL TUBRETT[2], AND DEREK WILTON[3]

[1]Department of Earth Sciences, P.O. Box 1002, Millersville University, Millersville, PA 17551-0302, USA, Jason.Price@millersville.edu (* presenting author)
[2]CREAIT Network, Memorial University of Newfoundland, St. John's, NL, A1B 3X5 Canada, mtubrett@mun.ca
[3]Department of Earth Sciences, Memorial University of Newfoundland, St. John's, NL, A1B 3X5 Canada, dwilton@mun.ca

The epidote-group minerals are common accessory phases in silicate rocks. These calc-silicate minerals may contain substantial quantities of Th, and concomitantly U. The radioactive decay of ^{232}Th, ^{238}U, ^{235}U to their daughter nuclides results in the radiation-induced transformation from a periodic to an aperiodic structure termed metamictization [1]. Metamictization of epidote-group minerals can increase their solubility and thus these minerals can be important sources of Ca in pore and stream waters that drain silicate terranes [2]. On geologic timescales, dissolved Ca and bicarbonate ions from silicate mineral dissolution are carried by streams to the oceans where they are sequestered in Ca-carbonate minerals [3]. Therefore, the weathering of metamict epidote-group minerals is capable of consuming atmospheric CO_2 and potentially influencing the long-term global climate.

The extent of epidote-group mineral metamictization is a function of age, and Th and U content, which together yield the α-particle dose of the grain [4]. To determine the solubility threshold of epidote-group minerals, the α-particle dose of grains from the Yangtze River delta in China have been calculated. These detrital grains are resistant to chemical weathering and persist into fluvial sediments. Delta sediments from such a large river system provide a suite of epidote-group minerals that approximate the compositional range and radiation damage commonly observed in nature for grains resistant to dissolution. The grain(s) with the highest α-particle dose thus reflect the solubility threshold for the epidote-group minerals.

The Th, U, and Pb isotopic compositions of each grain were measured by laser ablation-inductively coupled plasma-mass spectrometry. ^{232}Th-^{208}Pb ages were corrected for common Pb using an iterative technique [5]. End-member epidote grains contain sufficiently low Th and U concentrations to prevent quantification of an α-particle dose, explaining, at least in part, why they are so resistant to chemical weathering. End-member allanite grains are relatively radioactive, reflect at least four sources of allanite to the delta, and yielded a maximum α-particle dose of ~3.6 x 10^{15} α-decays mg^{-1}. This dose compares very favorably with that of ~3.5 x 10^{15} α-decays mg^{-1} reported for Amazon detrital zircons [6].

[1] Deer et al. (2001) *Rock-Forming Minerals (2nd Edition), Disilicates and Ring Silicates* **1B**. [2] Price et al. (2005) *American Mineralogist* **90**, 101-114. [3] Berner et al. (1983) *American Journal of Science* **283**, 641-683. [4] Holland & Gottfried (1955) *Acta Crystallographica* **8**, 291-300. [5] Chew et al. (2011) *Chemical Geology* **280**, 200-216. [6] Balan et al. (2001) *American Mineralogist* **86**, 1025-1033.

Light activation of steady state copper uptake in marine diatoms

NEIL M. PRICE[1*] AND JUN-WOO KIM[2]

[1]McGill University, Department of Biology, Montreal, Canada, neil.price@mcgill.ca
[2]McGill University, Department of Biology, Montreal, Canada, jun-woo.kim@mail.mcgill.ca (* presenting author)

Marine diatoms of the Thalassiosirales use either a Cu-containing plastocyanin (PC) or an Fe-containing cytochrome (cyt) c_6 to transfer electrons from cyt b_6f to photosystem I in the light reactions of photosynthesis. Growth assays confirm that the PC-containing strains require higher concentrations of Cu for cell division and contain roughly 2-3 times more cellular Cu (30.8 fmol Cu' L^{-1}) than strains with cyt c_6. Under steady state conditions, Cu uptake rates are a linear inverse function of Cu-limited growth rates and not significantly different among PC and cyt c_6-containing strains. Thus, despite having greater cellular demand for Cu, diatoms that use PC are unable to acquire extra Cu. In the presence of high light, however, Cu uptake rates of PC-containing species are increased by 2-10 fold, suggesting that Cu acquisition is somehow light-activated. Steady state Cu uptake rate is proportional to irradiance at both high and low Cu concentrations (Fig. 1). We are currently examining how light affects extracellular Cu(II) reduction in a number of PC and cyt c_6-containing *Thalassiosira* species.

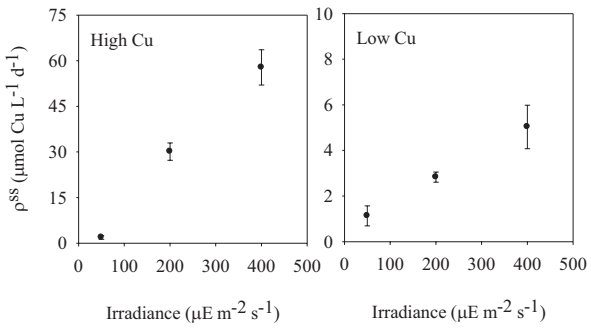

Figure 1: Steady state Cu uptake rate of *Thalassiosira oceanica* normalized to cellular volume as a function of growth irradiance. Values are means of 3-5 replicates and error bars ± 1 std.

https://doi.org/10.1180/S0026461X00008434 Published online by Cambridge University Press

Interfacial tension and nucleation behaviour of minerals (revisited)

MANUEL PRIETO[1*], DIONISIS KATSIKOPOULOS[1], AND ANGELES FERNÁNDEZ-GONZÁLEZ[1]

[1]Department of Geology, University of Oviedo, Oviedo, Spain, mprieto@geol.uniovi.es (* presenting author)

According to the classical nucleation theory (CNT), the nucleation rate depends strongly on the interfacial tension (σ), which in aqueous systems is related to the solubility by the rule that the higher the solubility, the lower σ. Indirect estimations of σ from nucleation experiments [1] are typically used to account for crystallization in natural aqueous systems [2] and to model the precipitation in sequential order of lesser and lesser soluble isochemical mineral phases according to the Ostwald step rule. In a related way, when solid solutions crystallize from supersaturated aqueous solutions the distribution of the substituting ions between the solid and the fluid phase usually differs from the equilibrium values [3]. "More soluble" solid solution compositions are kinetically favoured and tend to nucleate even though the aqueous solution is less supersaturated for these compositions than for less soluble members. This effect has been modelled by considering a linear variation of σ with composition [4]. However, to the authors knowledge, there is no empirical study on the compositional evolution of σ in solid solution systems.

In this work we revisit the concept of interfacial tension in the light of recent findings that challenge the tradictional picture of crystal nucleation, at least in the case of the $CaCO_3$-H_2O system [5]. Our point is that, in the CNT framework, the interfacial tension must be considered more an "artificial" fitting parameter than a measurable magnitude with a precise physical meaning. We show the dependence of CNT-derived σ values on the speciation model, the expression chosen for the driving force, and the shape chosen for the nuclei. Special attention is paid to the polymorphic precipitation of $CaCO_3$ phases. Finally, we determine the CNT-σ parameters for intermediate members of a number of binary (virtually ideal and non-ideal) solid solutions. Our results show a good correlation between the deviations from the ideal mixing behaviour, the solubility, and the obatined CNT-σ values. Positive deviations from ideality (positive enthalpy of mixing) correlate with negative deviations of σ from a linear trend, whereas negative deviations (tendency to ordering) correlate with positive deviations of σ. In each case, the obtained σ values are used to model non-equilibrium distribution coefficients, the results being in good agreement with experimental measurements reported in the literature.

[1] Söhnel (1982) *J. Cryst. Growth* **57**, 101-108. [2] Fritz & Noguera (2009) *Rev. Min. Geochem.* **70**, 371-410. [3] Prieto (2009) *Rev. Min. Geochem.* **70**, 47-85. [4] Pina & Putnis (2002) *Geochim. Cosmochim. Acta* **66**, 185-192. [5] Gebauer, Völkel & Cölfen (2008) *Science* **322**, 1819-1822.

Precipitation of $MgCO_3$ at elevated temperature and CO_2 pressure

VALENTINA PRIGIOBBE[1*]

[1] ETH Zurich, Institute of Process Engineering, Zurich, Switzerland. *Current address:* Dept. of Petroleum and Geosystems Engineering, University of Texas at Austin, Texas, U.S.A. valentina.prigiobbe@mail.utexas.edu (* presenting author)

Introduction and methods

Mineral carbonation is a Carbon Capture and Storage (CSS) technology that consists in fixing CO_2 into stable carbonates, e.g., magnesite ($MgCO_3$) which can be either disposed of or reused [1]. Hydrated phases can initially form which then transform into the stable carbonate [2]. If carbonates are designed to be reused, the precipitation process must be carried out under well-constrained conditions which are still unknown or not fully defined [3,4,5]. Here, we present the results from a $MgCO_3$ precipitation study at 90ºC, 120ºC, and 150ºC and at 100 bar of CO_2 [6]. Batch experiments were performed using a $MgCl_2$-CO_2-Na_2CO_3 aqueous system and monitored with online Raman spectroscopy. Precipitation was modeled using a population balance equation (PBE) [7] coupled with a geochemical model. Nucleation and growth rates were described by empirical equations based on classical nucleation theory and the birth-andspread growth mechanism and the kinetic parameters were estimated by fitting Raman spectroscopy measurements using multivariate kinetics modeling [8].

Results and conclusions

Two types of mechanisms were verified. At all investigated temperatures and at low magnesium concentration (C_{Mg}) $MgCO_3$ precipitated directly (Fig. 1.a). At 120 and 150ºC and at high C_{Mg}, $MgCO_3$ formed simultaneously with hydromagnesite which then transformed into $MgCO_3$ (Fig. 1.b). The kinetics showed no sensitivity to C_{Mg}, small sensitivity to temperature, and a significant sensitivity to supersaturation with respect to $MgCO_3$ (S_M). This allowed the formulation of general rate equations for nucleation and growth given by, respectively,

$$J = 4\times10^{8} e^{(-19/\ln^2 S_M)}, \quad (1)$$

$$G = 29\times10^{-9}(S_M - 1)^{2/3} \ln^{1/6} S_M e^{(-19/\ln^2 S_M)}, \quad (2)$$

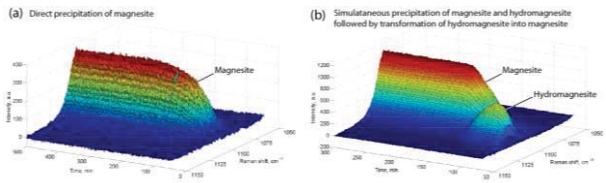

Figure 1: Online Raman spectroscopy measurements.

[1] IPCC (2005). IPCC Special Report on Carbon Dioxide Capture and Storage. Cambridge University Press, 442 pp. [2] Hänchen, Prigiobbe, Baciocchi, Mazzotti (2008). *Chem. Eng. Sci.* **63**, 1012-1028. [3] Sayles, Fyfe (1973) *Geochim. Cosmochim. Acta* **37**, 87-99. [4] Zhang *et al.* (2000) Sandia Nat. Lab. **NM 87185-0750**. [5] Saldi *et al.* (2009) *Geochim. Cosmochim. Acta* **73**, 5646-5657. [6] Prigiobbe, Mazzotti (2012) i*n preparation*. [7] Randolph, Larson (1988) *Theory of particulate processes* Academic Press. [8] Cornel, Mazzotti (2008) *Anal. Chem.* **80**, 9240-9249.

https://doi.org/10.1180/S0026461X00008434 Published online by Cambridge University Press

An early Neoproterozoic dynamic sulphur cycle: evidence from the Shaler Supergroup

JOHN K. G. PRINCE*[1], BOSWELL A. WING[2], ROBERT H. RAINBIRD[3], GALEN P. HALVERSON[4]

[1]Carleton University, Ottawa, Canada, jprince2@connect.carleton.ca (* presenting author)
[2]McGill University, Montreal, Canada, boswell.wing@mcgill.ca
[3]Geological Survey of Canada, Ottawa, Canada, Rob.Rainbird@nrcan-rncan.gc.ca
[4] McGill University, Montreal, Canada, galen.halverson@mcgill.ca

Abstract:

The Neoproterozoic (1000-542Ma) is a dynamic era of Earth history, punctuated by super continental break-up, global glaciations, and the evolution of metazoan life [1,2,3]. During the early to mid-Neoproterozoic, Earth's redox budget was in a state of flux, the evidence for which is preserved in the isotopic records of sulphur and carbon [4]. In order to constrain the initiation of this dynamic behaviour, we described and sampled 3 outcrop stratigraphic sections and a drill core at ~3m intervals through the Minto Inlet Formation of the Shaler Supergroup, which is exposed in the Minto Inlier of NW Victoria Island, NWT.

The Minto Inlet Formation is >250m thick and hosts well-preserved Neoproterozoic sulphate-rich evaporites deposited in a periodically restricted intra-continental marine basin. The Minto Inlet Formation was deposited between ~900Ma and ~800Ma based on detrital zircon geochronology and stratigraphic correlation with well-calibrated sections in the northern Cordillera [4]. We measured multiple sulphur isotopes ($\delta^{34}S$, $\Delta^{33}S$) of the sulphate fraction in all of the stratigraphically controlled dataset of 67 samples.

Current understanding of the sulphur isotope record suggests that the fraction of S buried as pyrite relative to sulphate evaporites was high, approaching 1 for most of the Proterozoic, through the Ediacaran, and into the early Phanerozoic [5]. We used multiple sulphur isotope measurements of Minto Inlet Formation evaporites to constrain models of S fluxes into and out of the ocean prior to the onset of the Cryogenian (720-635Ma). This approach suggests that the relative burial fraction of S as pyrite was extremely low (≈0.2) during the earliest stages of the deposition of the Minto Inlet Formation. Previously, pyrite burial fractions this low had been recorded only at Permian-Triassic time, more than ≈600 Ma after the deposition of the Minto Inlet Formation [5]. Our results indicate large scale variations in ocean redox conditions and a dynamic sulphur-cycle were initiated during the early-Neoproterozoic.

[1] Powell et al. (1993) *Geology,* **21**, 889-892.
[2] Hoffman et al. (1998) *Science,* **281**, 1342-1346.
[3] Halverson and Hurtgen (2007) *Earth and Planetary Science Letters,* **263**, 32-44.
[4] Macdonald et al. (2010) *Science,* **327**, 1241-1243.
[5] Canfield and Farquhar (2009) *PNAS,* **106**, 8123-8127.

Earths Icy Biosphere as a Model for the Microbiology of Other Icy Worlds

JOHN C. PRISCU[1*], KEVIN P. HAND[2]

[1]Montana State University, Land Resources and Environmental Sciences, jpriscu@montana.edu
[2]Jet Propulsion Laboratory, Pasadena, California, kevin.p.hand@jpl.nasa.gov

Antarctic terrestrial environments were initially thought to be devoid of life. However, discoveries of microbial life in Antarctic lake ice, and within and under Antarctic glacial ice have all provided information on the diversity and biogeochemical importance of biology to icy environments. We now know that polar microbiology plays a major role in biogeochemical processes on Earth and offers new insights into the evolution and biodiversity of life on our planet. The discovery of viable microorganisms in icy environments has extended what we know about the limits of life on Earth and provides strong evidence to show that life has successfully radiated into virtually all habitats on our planet containing "free" liquid water. Icy worlds beyond Earth may harbor the greatest volume of habitable space in the Solar System. For at least five of these worlds, considerable evidence exists to support the conclusion that oceans or seas may lie beneath the icy surfaces. The total liquid water reservoir within these worlds may be some 30 to 40 times the volume of liquid water on Earth. For example, data obtained from orbiters have revealed a deep ocean of liquid water beneath a thick chaotic ice cover on Europa where organic matter derived from comets and oxidants provided by radiation from Jupiter's magnetosphere may yield a habitat for life and a reservoir of endogenous and exogenous substances. This vast quantity of liquid water begs the question: Can life emerge and thrive within ice and the cold, lightless oceans beneath many kilometers of ice? To address this broad question, information on water activity, metabolic energy sources, nutrient availability, the ability of the physical environment to support growth and reproduction, and the origin of the biological seed must be known. Studies of Earth's subzero environments will continue to play a crucial role in informing our understanding of habitability on other frozen worlds in our Solar System and guide our development of the robotic tools needed to investigate those distant environments. We will present combined laboratory, numerical, analytical, and field investigations from Earth's polar regions to define the potential habitability of icy worlds beyond Earth.

https://doi.org/10.1180/S0026461X00008434 Published online by Cambridge University Press

Tracing industrial emissions in the Athabasca oil sands region (Alberta, Canada) using stable isotope techniques

BERNADETTE PROEMSE[1*], BERNHARD MAYER[1], AND MICHAEL WIESER[2]

[1]Department of Geoscience, University of Calgary, 2500 University Drive NW, Calgary, AB, T2N 1N4, Canada bcpromse@ucalgary.ca (*presenting author)

[21]Department of Physics and Astronomy, University of Calgary, 2500 University Drive NW, Calgary, AB, T2N 1N4, Canada

The Athabasca oil sands region (AOSR) in northeastern Alberta, Canada, is one of the world's largest oil reservoirs. Its heavy oil will become increasingly important as conventional energy resoures decline. Due to the rapid industrial development in the AOSR, there have been increasing concerns about the impact of the emissions from the oil sands operations on the surrounding terrestrial and aquatic ecosystems. Stable isotope techniques may help to assess such impact in the case where industrial emissions are isotopically distinct from background components. In order to trace nitrogen (N) and sulfur (S) emissions released by the oil sands industry, we have determined chemical and isotopic compositions of various N and S compounds in emissions and several environmental receptors.

Potential source materials such as untreated oil sand, bitumen, elemental sulfur from the sulfur storage block, coke and the by-product ammonium sulfate were analyzed for either $\delta^{34}S$, $\delta^{15}N$ values or both. We also determined stable isotope ratios of sulfate ($\delta^{34}S$, $\delta^{18}O$), nitrate ($\delta^{15}N$, $\delta^{18}O$, and $\Delta^{17}O$) and ammonium ($\delta^{15}N$) of stack emitted $PM_{2.5}$ [1]. The nitrogen and triple oxygen isotopic composition ($\delta^{15}N$, $\delta^{18}O$, and $\Delta^{17}O$) of atmospheric nitrate in bulk deposition and throughfall as well as $\delta^{15}N$ of atmospheric ammonium, and $\delta^{18}O$ and $\delta^{34}S$ of atmospheric sulfate in throughfall and bulk deposition were also measured. Bio-indicators such as lichens and pine needles were collected and analyzed for total N content, $\delta^{15}N$, total S content and $\delta^{34}S$. Industrial N and SO_4 emissions were found to be isotopically distinct. $\delta^{18}O$ and $\Delta^{17}O$ of atmospheric nitrate deposition and $\delta^{18}O$ values of atmospheric sulfate deposition showed trends towards lower values with increasing nitrate and sulfate deposition rates allowing for the quantification of industrial contributions to atmospheric nitrate [2] and sulfate deposition in the AOSR. Lichens responded to elevated N and S deposition in close proximity to the oil sands operations, whereas chemical and isotopic compositions of N and S in pine needles showed no significant industrial impact.

In addition to "traditional" stable isotope techniques, we have investigated the suitability of $\delta^{98/95}Mo$ as an environmental tracer in the AOSR and determined its value in Athabasca bitumen and air filters. Preliminary results reveal that industrial activities are associated with Mo isotope fractionation, providing a potential new tracer for industrial activities in the AOSR.

[1] Proemse, B., Mayer, B., Chow, J., and J. Watson (in review). [2] Proemse, B., Mayer, B., and M. Fenn (in review).

Chemical imaging of isotopic spikes in hard tussues using LA-ICPMS

THOMAS PROHASKA[1*], MONIKA HORSKY[1], JOHANNA IRRGEHER[1,a], ANDREAS ZITEK[1], MARIA TESCHLER-NICOLA[2], TIM SCHULZE-KÖNIG[3] AND THOMAS WALCZYK[4]

[1]University of Natural Resources and Life Sciences Vienna, Department of Chemistry, Division of Analytical Chemistry, VIRIS Laboratory, A-3430 Tulln, Austria, thomas.prohaska@boku.ac.at (* presenting author)

[2]Natural History Museum Vienna, Department of Anthropology, A-1010 Vienna, Austria, maria.teschler@nhm-wien.ac.at

[3]ETH Zürich, Laboratory of Ion Beam Physics, 8093 Zürich, Switzerland, schulze@ohy.ethz.ch

[4]National University of Singapore, Faculty of Science, Food Sciecne and Technology Programme, Singapore 117543, walczyk@nus.edu.sg

[a]Recipient of a DOC-fFORTE-fellowship of the Austrian Academy of Sciences

Laser ablation ICPMS is a widely established method to directly monitor and image the elemetal distribution on solid surfaces with small lateral resolution. The minimal sample preparation and the fact that any solid surface can be analzed irrespective of its nature and composition, has made the method a versatile tool in many areas of science. In addition, the ability of detecting isotope specific information has increased the variety of applications sigificantly. E.g. human and animal teeth as well as otoliths are often used for migration studies.

Beside monitoring the natural isotopic variation, isotopically enriched spikes can be used in natural systems to monitor uptake and distribution of isotopic spikes by hard tissues after administration.

Here, we present the use of Sr isotope spikes for comparing calcium and strontium metabolism in the living organism and tracer distribution within hard tissues (i.e. bones, teeth, otoliths). Our results give new insights into Sr metabolism and turnover. The investigations bear an analytical challenge as spectral interferences have to be accounted for when analysing Sr and Ca isotope ratios with high spatial resolution using LA- ICPMS.

https://doi.org/10.1180/S0026461X00008434 Published online by Cambridge University Press

Nucleation and growth of acicular rutile in garnet: a case of open system precipitation

ALEXANDER PROYER[1*], GERLINDE HABLER[2], RAINER ABART[2], RICHARD WIRTH[3], KURT KRENN[1], AND GEORG HOINKES[1]

[1]University of Graz, Institute of Earth Sciences, Graz, Austria, alexander.proyer@uni-graz.at (* presenting author)
[2]University of Vienna, Department of Lithospheric Research, Vienna, Austria,
[3]GFZ Potsdam, Potsdam, Germany, wirth@gfz-potsdam.de

Crystallographically oriented precipitates of rutile grew within garnet in metapelites from the Greek Rhodope during exhumation and cooling from eclogite and granulite facies conditions. Homgeneous nucleation produced a three-dimensional array of mostly acicular rutile precipitates with aspect rations between 10 and 100. Rutile c-axes are inclined at an average angle of 27° to the needle long axes (oblique extinction), and EBSD analysis reveals a clear but complex crystallographic orientation relationship with the garnet host. TEM-imaging shows semi-coherent to incoherent phase boundaries and a small but significant lattice mismatch even along those phase boundaries with the best relative match. The "idiomorphic" rutile needles are terminated by low-index planes of garnet, the most common ones being (110), (100) and (112).

Another set of micrometer-sized rutile inclusions in the same garnets is more isometric and granular and is interpreted as resulting from heterogeneous nucleation at dislocations; TEM-data show very poor lattice match (complete incoherence along all interfaces). Garnet from another metapelite sample shows arrays of oriented rutile needles embedded in a very fine grained (nanometer-sized) "dust" – most likely a later generation of rutile precipitates – with clear zones free of "dust" around the needles and larger precipitate-free zones (also free of needles) along the garnet rims.

The mechanism of rutile precipitation from garnet is not trivial and in fact impossible stoichiometrically unless one assumes significant amounts of Ti^{4+} on the tetrahedral site in garnet [1, 2]; Yang et al, 2005). Hence, a mechanism called open system precipitation (OSP; Proyer et al. 2008, 2011) is invoked, defined as precipitation made possible by exchange of chemical components with external reservoirs such as the rock matrix and/or fluid inclusions). Several open system reaction equations can be devised, the most effective one being a redox reaction by which Fe^{2+} from the dodecahedral site is oxidized to Fe^{3+} and moves onto the octahedral site in order to replace exsolving Ti^{4+}, accompanied by diffusion of electrons and divalent cations. Part of Ti^{4+} may also be reduced to Ti^{3+} because many of the large primary rutile inclusions found in the same garnets display a colour change from brown to grayish-purple, which is typical for reduced rutile. In that case, Ti^{3+}-bearing overgrowths on primary rutile inclusions would be another type of heterogeneously nucleated precipitate.

Garnets with oriented acicular rutile precipitates are not uncommon from high-grade amphibolite, granulite and also eclogite facies rocks, but the typical garnets from such rocks are precipitate-free, and the actual geological significance – particularly the T-t information recorded by the various precipitate types, their size, spatial distribution and morphology – is yet unclear.

[1] Van Roermund *et al.* (2000) *Geological Journal* **35**, 209-229.
[2] Vang & Liu (2004) *Chinese Science Bulletin* **49/1**, 70-76
[3] Proyer *et al.* (2009) *Journal of metamorphic Geology* **27**, 639-654.

Stable Vanadium Isotope Fractionation During Differentiation

PRYTULAK, J[1,2*], SAVAGE, P.S[1,3], HALLIDAY, A.N[1]

[1]University of Oxford, Oxford, UK (Alex.Halliday@earth.ox.ac.uk)
[2]Imperial College, London, UK (*j.prytulak@imperial.ac.uk)
[3]Washington University, St. Louis, USA (savage@levee.wustl.edu)

Understanding and quantifying fractionation processes is key to the application and interpretation of both traditional and non-traditional stable isotopes. In this study we examine the effects of magmatic fractionation on the nascent stable vanadium (V) isotope system [1, 2]. Vanadium exists in multiple valence states and $\delta^{51}V$ should be strongly influenced by changing oxidation state. We present $\delta^{51}V$ of lavas from Hekla, Iceland [3]. Hekla is a fissure volcano with eruptive products ranging from basalt to rhyolite with remarkably coherent liquid lines of descent. The evolution from basalt to basaltic andesite can be clearly related to crystal fractionation [e.g., 4]. In addition to Sr, Nd, Pb, U-series, and O isotopes, Hekla lavas also boast studies of stable Si [3] Li and Fe [5] isotopes, making them arguably the best-characterized differentiation suite in terms of non-traditional stable isotopes. Hekla is therefore ideal to examine $\delta^{51}V$ against a wide backdrop of geochemical data.

We concentrate on basalt to basaltic andesite lavas where V concentrations decrease sharply from ~300 ppm to ~10 ppm. We find a large range in $\delta^{51}V$ of ~2 ‰, which co-varies with major and trace elements. The crystallising mineral phases are olivine, plagioclase, clinopyroxene and magnetite; with magnetite as the dominant V host.

Co-variation of $\delta^{51}V$ with indices of differentiation could implicate Rayleigh fractionation similar to that proposed for $\delta^{56}Fe$ variations at Hekla [5]. No mineral-melt isotope fractionation factors are available, and a bulk *f* must be assumed. However, unlike Fe, V is dominantly controlled by one phase. If Rayleigh fractionation is occurring, then magnetite must be extremely light in order to drive the lava to the observed heavy $\delta^{51}V$ compositions.

The incorporation of V into magnetite will depend partly on the oxygen fugacity of the system. Determining mineral-melt fractionation factors by measurement of $\delta^{51}V$ in both natural and experimental materials could pave the way for the use of magnetite as a unique single mineral tracer of oxygen fugacity.

[1] Nielsen et al. (2011) *Geostand. Geoanal. Res*. **35**, 293-306.
[2] Prytulak et al. (2011) *Geostand. Geoanal. Res*. **35**, 307-318.
[3] Savage et al. (2011) *Geochim. Cosmochim. Acta* **75**, 6124-6139.
[4] Sigmarsson et al. (1992) *Contrib. Min. Pet*. **112**, 20-34.
[5] Schuessler et al. (2009) *Chem. Geol*. **258**, 78-91.

https://doi.org/10.1180/S0026461X00008434 Published online by Cambridge University Press

Analysis of emerging contaminants in environmental systems

C.J. PTACEK[1,*], D.W. BLOWES[1], S.J. BROWN[2], L.G. GROZA[1], M.C. MONCUR[1,3], W.D. ROBERTSON[1], T. SCHEYTT[4], W.W. WOESSNER[5]

[1]University of Waterloo, Waterloo, Canada, ptacek@uwaterloo.ca (* presenting author), blowes@uwaterloo.ca
[2]Environment Canada, Burlington, Canada, Susan.Brown@ec.gc.ca
[3]Alberta Innovates-Technology Futures, Calgary, Canada, Michael.Moncur@albertainnovates.ca
[4]Technische Universität Berlin, Berlin, Germany, traugott.scheytt@tu-berlin.de
[5]University of Montana, Missoula, USA, william.woessner@mso.umt.edu

22c. Applications of emerging geochemical and isotopic analytical techniques for integrated water resource management and environmental monitoring

Innovative mass spectrometry techniques make it possible to detect emerging contaminants, including pharmaceutical compounds and explosives, at concentrations that are environmentally relevant. Applications of these techniques are challenging because of the very low concentrations of these compounds and because of the complex matrices often encountered in the environment. Sample collection methods and analytical procedures must be refined to provide representative samples and analyses that can be used to assess the potential impacts of emerging contaminants.

Two case studies are used to illustrate steps required for the application of tandem mass spectrometry techniques. These studies involved refinement of sample collection techniques, analyte separation methods, analyte quantification, and modifications of instrument configurations.

A large nation-wide survey of explosives was conducted which initially involved the application of HPLC-MS/MS methods. The HPLC-MS/MS technique required inclusion of several isotope-labelled internal standards at multiple concentrations. Modification of the analytical procedure to an IC-MS/MS procedure resulted in decreased matrix suppression effects and improved analyte quantification. These modifications were particularly important for the analysis of groundwater and saline waters.

On-site wastewater disposal systems represent one of the largest volumes of contaminated water discharged to the subsurface. This wastewater contains elevated concentrations of dissolved organic matter, and nitrogen and phosphorus species. Interaction of this water with natural aquifer materials also can result in the presence of elevated concentrations of dissolved metals. The quantification of trace pharmaceutical compounds within this setting requires consideration of sample acquisition methods, sampling equipment materials, the interaction of these materials with the target compounds, and sample matrix effects. Analyses of a suite of pharmaceutical compounds in the low ng L^{-1} were made for samples collected from wastewater dicharge areas, groundwater and DOC-rich surface water. These studies required diligent use of isotope-labelled internal standards to optimize analytical results. Based on these results, mechanisms controlling transport of these compounds can be better delineated.

Early Earth: an insight from the combined Os-Nd-Hf isotope systematics of Barberton komatiites

IGOR S. PUCHTEL[1*], MATHIEU TOUBOUL[1], JANNE BLICHERT-TOFT[2], AND RICHARD J. WALKER[1]

[1]University of Maryland, College Park, MD 20742, USA, ipuchtel@umd.edu (*presenting author), mtouboul@umd.edu, rjwalker@umd.edu
[2]Ecole Normale Supérieure de Lyon, 69007 Lyon, France, jblicher@ens-lyon.fr

We report ^{190}Pt-^{186}Os, ^{187}Re-^{187}Os, ^{146,147}Sm-^{142,143}Nd, and ^{176}Lu-^{176}Hf isotopic, trace lithophile, and highly siderophile element (HSE) abundance data for remarkably well preserved komatiites from the Komati and Weltevreden Formations of the Barberton Greenstone Belt (BGB). These data provide new insights into the chemical evolution of the early Earth. The 3.48 Ga Komati lavas are mildly depleted in LREE and Th and show strong depletions in HREE, whereas the 3.26 Ga Weltevreden lavas are strongly depleted in LREE and Th and are enriched in HREE; both systems show positive Nb and Ta anomalies. The two komatiite systems are characterized by initial γ^{187}Os of +0.34±0.10 and -0.14±0.03 and ε^{143}Nd of +0.30±0.13 and +0.41±0.11, respectively ($2\sigma_{mean}$), indicating evolution of their sources with time-integrated near-chondritic Re/Os and slightly suprachondritic ^{147}Sm/^{144}Nd. The initial ε^{142}Nd in both systems are not resolvable from that in the terrestrial standard. At the same time, these systems have radiogenic initial ε^{176}Hf of +1.9±0.3 and +4.7±0.8, respectively, implying long-term evolution to the times of melting with suprachondritic ^{176}Lu/^{177}Hf. The Weltevreden system is also characterized by an initial ^{186}Os/^{188}Os of +0.22±0.03, indicating evolution of its source with a time-integrated suprachondritic Pt/Os (3.3±0.2 *vs.* 1.8 in chondrites). Finally, the sources of the two komatiite systems are calculated to have had distinct absolute HSE abundances, containing ~50% (Komati) and ~80% (Weltevreden) of the total HSE estimated for the modern Primitive Mantle. The combined data require early formation and long-term isolation of deep mantle domains enriched in majorite and/or perovskite; these domains served as the melting source regions for the BGB lavas. The isolation must have occurred after ^{146}Sm was no longer extant, but before the mantle accumulated the full complement of the HSE as a result of the late accretion. Our combined data also require deep-sourced formation for the BGB komatiites, most probably *via* dry melting in starting mantle plumes. The potential mantle temperatures calculated from the emplaced lava compositions are in excess of 1800ºC, thus providing evidence for extremely hot conditions that existed in the early Archean mantle.

https://doi.org/10.1180/S0026461X00008434 Published online by Cambridge University Press

Exploring the Geomicrobiology of the Río Tinto subsurface Mars analog by using a life detector biochip

FERNANDO PUENTE-SÁNCHEZ[1*], MERCEDES MORENO-PAZ[1], PATRICIA CRUZ-GIL[1], LUIS RIVAS[1], MARINA POSTIGO[1], MANUEL J. GÓMEZ[1], MIRIAM GARCÍA-VILLADANGOS[1] AND VICTOR PARRO[1]

[1]Centro de Astrobiología (INTA-CSIC), Madrid, Spain, puentesf@cab.inta-csic.es (*presenting author)

Introduction:

The Iberian Pyritic Belt (IPB) is one of the largest massive pyrite deposits in the world, and is considered as a Martian analog. Several studies [1][2] of the acidic, heavy metal rich-Tinto river in the IPB have revealed a surprisingly rich extreme ecosystem, yet little is known about the geomicrobiology of its subsurface. In a previous work [3] we described an antibody microarray which contains more than 200 antibodies against bacterial strains, different fractions of natural extracts, proteins, etc. and reported its usefulness for immunoprofiling of environmental samples and for the detection of biomarkers with different range of universality.

Results and conclusions:

Here we show the results obtained by using LDChip200 (Life Dectector Chip) for immunoprofiling the whole depth of a drill in the IPB at the Tinto river origin. From 0,5 to 1 g of samples from cores up to 160 m depth were processed for a quick analysis with the LDChip200. The results showed the presence of Gram-positive bacteria and peptides or proteins from the ferritin superfamily which might be involved in tolerance to the high iron concentrations present in the IPB subsurface. Biodiversity was also assessed by DNA extraction and analysis with a phylogenetic oligonucleotide microarray for prokaryotes [4], and by cloning and sequencing of the PCR-amplified bacterial 16s rRNA gene. Members of the Gram-positive Firmicutes group of bacteria were detected by the oligonucleotide microarray and sequencing. Sequencing also revealed sequences similar to those of nitrate and sulphate reducing bacteria. Those results allowed us to build a preliminary model of the ecosystem and provided an initial insight into the biology of the deep subsurface of the Iberian Pyritic Belt.

[1] González-Toril (2003) Appl Environ Microbiol 69(8), 4853-65.[2] Amaral-Zettler (2002) Nature 417, 137. [3] Rivas (2008) Anal Chem, 80, 7970-9. [4] Garrido (2008) Environ Microbiol 10, 836-50.

Ar-39 dating of groundwater: How limiting is underground production?

ROLAND PURTSCHERT[1]

[1]Climate and Environmental Physics, University of Bern, Switzerland, purtschert@climate.unibe.ch

With a half-life of 269 years is ^{39}Ar an ideal tracer for groundwater dating in the age range 50-1000 years [1]. Ground water resources beyond the dating range of transient tracers such as ^{3}H/^{3}He, Sf_6, CFC's and ^{85}Kr become increasingly important due to contamination and overexploitation of shallow and young groundwater's. A potential limitation of ^{39}Ar dating of groundwater, besides the difficult sampling protocol, is the possibility of underground production due to neutron activation of potassium [2]. Over modern ^{39}Ar concentrations have for example been observed in U- and Th- rich crystalline rocks [3]. Another important factor is the escape path and probability of ^{39}Ar from the rock matrix into the water permeable pore space. In this review paper the importance of underground production of ^{39}Ar is assessed. Data collected over the last decade in numerous porous and fractured aquifers woldwide are discussed.

[1] Corcho, J.A., et al., (2007). Water Resources Research,. **43,**
[2] Lehmann, B.E. and R. Purtschert, (1997). Appl. Geochem.,. **12(6)**: pp. 727-738.
[3] Andrews, J.N., et al., (1989), Geochim. Cosmochim. Acta,. **53**: pp. 1803-1815.

https://doi.org/10.1180/S0026461X00008434 Published online by Cambridge University Press

The Last Glacial Termination in the Southern Alps, New Zealand

A.E. PUTNAM[1,2*], J.M. SCHAEFER[1], G.H. DENTON[2], M.R. KAPLAN[1], D.J.A. BARRELL[3], B.G. ANDERSEN[4], S.D. BIRKEL[2], A.M. DOUGHTY[2,5], S.E. KELLEY[2,6], T.N.B. KOFFMAN[2], R.C. FINKEL[7], AND R. SCHWARTZ[1]

[1]Lamont-Doherty Earth Observatory, Palisades, NY, USA, aputnam@ldeo.columbia.edu (* presenting author)
[2]Department of Earth Sciences and Climate Change Institute, University of Maine, Orono, ME, USA.
[3]GNS Science, Dunedin, New Zealand.
[4]University of Oslo, Oslo, Norway
[5]Victoria University of Wellington, Wellington, New Zealand.
[6]University of New York at Buffalo, Buffalo, NY, USA.
[7]University of California Berkeley, Berkeley, CA, USA

Abstract

Resolving the timing of the last deglaciation in the Southern Hemisphere can aid discrimination among proposed mechanisms for the last glacial termination. Here, we present records of glacier behavior from three former glacier catchments of the Southern Alps, New Zealand, during the last glacial termination. We used ^{10}Be surface-exposure dating and detailed glacial geomorphologic mapping to produce chronologies of well-preserved glacial landforms tracking the last deglaciation in the Southern Alps. We implemented a glaciological model to derive magnitudes and rates of paleo-snowline changes from our ^{10}Be-dated geomorphological record of glacier behavior. Our glacier/palaeo-snowline reconstruction indicates that Southern Alps ice recession and warming took place in two rapid pulses, separated by an interval of cooling and glacier resurgence during late-glacial time. The timing of these warming pulses coincided with the initiation of stadial conditions in the North Atlantic Ocean. In this regard, we discuss the possible role of a bipolar seesaw mechanism for initiating and sustaining the last glacial termination in the southwest Pacific sector of the Southern Hemisphere.

Transient porosity as an integral aspect of microstructural development during fluid-mineral reaction.

A. PUTNIS[1*], C.V. PUTNIS[1] AND H. AUSTRHEIM[2]

[1]Institut für Mineralogie, University of Münster, Münster, Germany , putnis@uni-muenster.de (* presenting author), putnisc@uni-muenster.de
[2] PGP, University of Oslo, Norway, h.o.austrheim@geo.uio.no

Whenever an aqueous solution interacts with a mineral with which it is out of equilibrium the resultant dissolution process is likely to result in an interfacial solution composition that is supersaturated with respect to different mineral or mineral solid solution phases. At this stage the transport properties of the solution and the probability of nucleation within this interfacial aqueous solution will determine the subsequent behaviour of the system. If the rate-determining step in the dissolution-transport-nucleation process is the dissolution rate, the nucleation of the new mineral phase will take place at the dissolving interface. The microstructural evolution of this solid-fluid two-phase product of the interface reaction depends on the possibility that it can continue to grow at the expense of the parent phase i.e. that the fluid can maintain contact with the parent phase at the migrating reaction interface. This will be the case if the volume of the product solid formed is less than the volume of the parent phase dissolved, allowing the fluid phase to occupy the difference. The solid volume deficit depends on both the molar volumes of parent and product phases and their relative solubility in the interfacial fluid [1]. The volume occupied by the fluid in this two-phase reaction product can be described as a porosity in the product solid. The product solid, together with the porosity which may be on a nanoscale, forms a microstructure characteristic of the reaction mechanism. As with all microstructures this is may be a transient phenomenon and subsequent textural equilibration (recrystallisation) in the presence of fluid may eventually eliminate the porosity. In contrast to microstructures formed in solid-solid reactions, the closure temperature at which no further reaction takes place may be as low as room temperature.

Examples of the microstructural development in natural and experimental fluid-mineral reactions will be given to illustrate these general principles [2].

The most important consequence of this mechanism is that it allows pervasive fluid flow through an initially low permeability rock and the transformation of one mineral assemblage to another [3]. A further aspect of this mechanism is the fact that within micropores a fluid can maintain a higher supersaturation than in a free fluid, and furthermore, the rate of dissolution of the parent phase will define a rate of change of supersaturation in the pores at the migrating interface. These two factors define the threshold supersaturation at which nucleation of the product phase takes place [4]. Taken together with the fact that the fluid composition within the porous parent phase will evolve in time depending on the mass transport though the interconnected porosity, modelling such an interface-coupled dissolution-precipitation process has proven to be a challenge.

[1] Pollok *et al*. (2011) *Am.J.Sci.* **311**, 211-236. [2] Putnis (2009) *Rev.Min.Geochem.* **70**, 47-85 [3] Putnis & Austrheim (2010) *Geofluids*, **10,** 254-269 [4] Prieto *et al.* (1994) *Journ.Cryst.Growth* 142, 225-235.

https://doi.org/10.1180/S0026461X00008434 Published online by Cambridge University Press

The mechanism of leached layer formation during mineral dissolution

CHRISTINE V. PUTNIS[1*], ENCARNACION RUIZ-AGUDO[2], CARLOS RODRIGUEZ-NAVARRO[2], AND ANDREW PUTNIS[1]

[1]Institut für Mineralogy, University of Münster, Münster, Germany, *putnisc@uni-muenster.de, putnis@uni-muenster.de (*presenting author)

[2]Department of Mineralogy and Petrology, University of Granada, Granada, Spain, encaruiz@ugr.es, carlosrn@ugr.es

Many minerals and glasses dissolve non-stoichiometrically, i.e. the elemental ratios measured in the fluid during dissolution experiments are different to those in the solid. This phenomenon results frequently in the formation of the so-called leached layers, which are chemically and structurally altered zones at the fluid–solid interface depleted in some elements relative to the bulk mineral composition [1,2]. The mechanism of non-stoichiometric dissolution and leached layer formation has been a subject of significant research over the past decades, due to its relevance to a wide range of natural and technological weathering processes, as well as being critical to define kinetic laws for mineral reactions. In this study, *in-situ* nanoscale Atomic Force Microscopy (AFM) observations have been made of reacting surfaces during the dissolution of two minerals: 1) a carbonate (dolomite, $CaMg(CO_3)_2$) and; 2) a silicate (wollastonite, $CaSiO_3$), both of which are known to dissolve non-stoichiometrically under acidic conditions and/or to develop leached layers upon dissolution. Combined with chemical analyses of both the output solutions and the reacting surfaces, AFM observations lead to a clearer understanding of the reaction mechanism.

Our study gives clear evidence that a leached layer is formed via an interface-coupled dissolution-precipitation mechanism [3] in a two step process: stoichiometric dissolution of the pristine mineral surfaces and subsequent precipitation of a secondary phase (a Si-rich and Mg-rich surface precipitate, respectively) from a supersaturated boundary layer of fluid in contact with the mineral surface, and not by preferential leaching of cations as postulated by most currently accepted dissolution models. Furthermore, this study demonstrates that *in situ*, direct observations of the reacting mineral surfaces are important to unambiguously ascertain the kinetics and mechanism of mineral dissolution. The kinetics of the process can be quantified from the measurement of etch pit spreading rates, which are unaffected by the formation of a secondary precipitate, whose existence has been neglected or simply not observed in the past.

References

[1] Casey et al. (1993) *Nature*, **366**, 253-256. [2] Hellmann et al. (2012) *Chemical Geology*, **294-295**, 203-216. [3] Putnis (2009) *Reviews in Mineralogy and Geochemistry*, **70**, 87-124.

An *ab initio* and Raman study of Co(II) complexes in water

C. C. PYE[1*], D. C. M. WHYNOT[1], L. APPLEGARTH[2], AND P. R. TREMAINE[2]

[1]Department of Chemistry, Saint Mary's University, Halifax, NS, Canada, cory.pye@smu.ca (* presenting author)

[2]Department of Chemistry, University of Guelph, Guelph, ON, Canada, tremaine@uoguelph.ca

Abstract

The transport of metal ions under hydrothermal conditions such as formation of ore bodies and as corrosion products in nuclear reactors are strongly influenced by temperature, pressure, and the type of complexing ligands. It is difficult to make speciation measurements under extreme conditions, and the interpretation of the measurements is not always unambiguous. *Ab initio* calculations have been shown to be very useful in the interpretation of the spectra of aqueous solutions of metal ions in the presence of complexing ligands, for example Sc^{3+}-Cl^- [1], Zn^{2+}-Cl^- [2] and Zn^{2+}-Br^-[3]. We present here our studies of cobalt(II) in the presence of water, chloride, hydroxide, and ammonia ligands, including predictions of the Raman spectra [4], and compare with recent experimental Raman measurements carried out at the University of Guelph. We will also discuss the stability of mixed OH^-/Cl^- complexes.

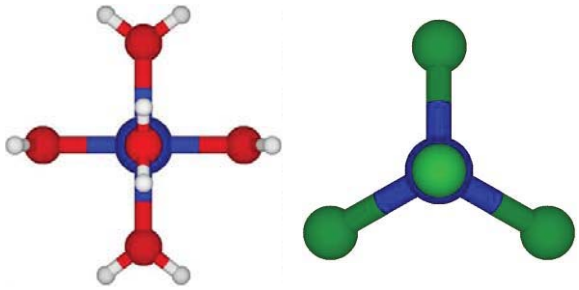

Figure 1: The hexaaquacobalt(II) and tetrachlorocobaltate(II) ions

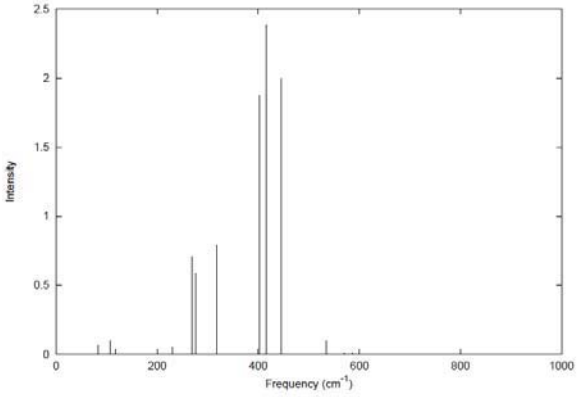

Figure 2: Simulated Raman spectrum of hexaaquacobalt(II) based on a HF/6-31+G* calculation.

[1] Pye et al. (2002) *Can. J. Chem.* **80**, 1331-1342. [2] Pye et al. (2006) *Phys. Chem. Chem. Phys.* **8**, 5428-5436. [3] Pye et al. (2011) *J. Sol. Chem.* **40**, 1932-1954. [4] D. C. M. Whynot (2012), *M. Sc. Thesis*

https://doi.org/10.1180/S0026461X00008434 Published online by Cambridge University Press

Petrogenesis of Quaternary volcanic rocks in the Halaha River and Chaoer River area in Daxing'an Mountain range,North China

QICHENG FAN*, YONGWEI ZHAO, JIANLI SUI

Institute of Geology, China Earthquake Administration, Beijing 100029, email: fqc@ies.ac.cn

The Halaha River and Chaoer River area (HC for short), middle of the Daxing'an Mountain range, is in the north of the North-South Gravity Lineament. 28 Quaternary volcanoes, which scattered along a Quaternary NE strike fault, are found in this area. Based on studies of the volcanic field characteristics, in conjunction with geological dating by K-Ar, it is identified that the volcanism occurred in four periods: Early Pleistocene, Middle Pleistocene, Late Pleistocene and Holocene. Quaternary volcanic rocks in this area, mainly alkaline basalt, cover an area of ca. 1000 km^2. Based on studying of the geochemistry with the Quaternary volcanic rocks in HC, this paper attempts to bring mantle sources and magma genesis in this area to light. The volcanic rocks in HC is of alkali one in sodium series, dominated by alkali olivine basalts. They resemble alkali basalts in Datong, as shown by trace elements distribution patterns, and generally exhibit OIB-like characteristics. They show nearly homogeneous Sr-Nd-Pb isotopic compostition similar to the prevalent mantle. All data show that bsalts of HC have a garnet lherzolite mantle source, low degree partial melting in which at different depth result in the primitive magma. Regional extension triggered asthenospherie upwelling, which may lead to the genesis of magma and subsequent volcanism.

Surpported by NSFC(40972047、41172305).

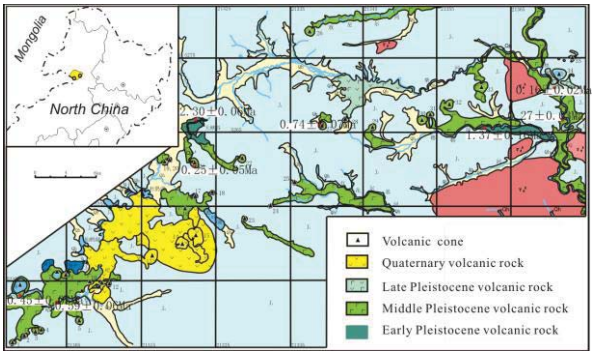

Fig.1 Quaternary volcanic rocks in Halaha River and Chaoer River area in the Great Xing'an Range, North China

^{40}Ar/^{39}Ar geochronology of fluid inclusions

H.N. QIU[1]*, H.Y. WU[2], Z.H. FENG[2], J.B. YUN[2], M. WANG[1], R.G. HU[1], Y.D. JIANG[1], X.J. BAI[3], J.R. WIJBRANS[4]

[1]State Key Laboratory of Isotope Geochemistry, GIGCAS, Guangzhou, China, qiuhn@gig.ac.cn

[2]PetroChina Daqing Oilfield Company Ltd., Daqing, China, wuheyong@petrochina.com.cn

[3]Key Laboratory of Tectonics and Petroleum Resources (China University of Geosciences), Ministry of Education, Wuhan, China, xiuj.bai@gmail.com

[4]Department of Petrology, VU University Amsterdam, The Netherlands, Jan.Wijbrans@falw.vu.nl

Theme 23: General Geochemistry Sessions
Geochronology: the role of fluids

Our primary purpose to date fluid inclusions by ^{40}Ar/^{39}Ar *in vacuo* crushing was to develop a new approach to obtain ore-forming ages of hydrothermal deposits. We suceeded in dating the mineralization ages of W-Sn, Au, Cu and Pb-Zn deposits using this novel technique on quartz, siliceous breccia and sphalerite [1-4]. Our results indicate that the ^{40}Ar/^{39}Ar stepwise crushing technique is very useful to determine the ore-forming ages, however, some samples probably contain too low K-concentrations to be analysed.

Since 2000, we've been investigating the fluid evolution of the Dabieshan eclogites during UHP metamorphism and retrograde metamorphism by the ^{40}Ar/^{39}Ar progressive crushing on garnet, amphibole and quartz [5-7]. The fluid inclusions of garnet revealed the age messages of the Paleozoic UHP metamorphism, and the amphibole and quartz recorded that the retrograde metamorphism of the Dabieshan eclogites occurred from Permian to early Jurassic.

Due to the lack of suitable minerals for dating, the timing of hydrocarbone charging of reservoirs is one of the most difficult problems in geochronology. We recently applied the ^{40}Ar/^{39}Ar progressive crushing into dating the natural gas emplacement in the Songliao Basin, NE China. The igneous quartz from the Cretaceous volcanic rocks that host the gas reservoir contains abundant secondary fluid inclusions with high K contents and high methane pressures, providing an excellent closed system for ^{40}Ar/^{39}Ar dating. The dating results of the igneous quartz by crushing precisely constrained the gas emplacement at 42.4±0.5 Ma [8].

The crushers were improved again and again to make the crushing tubes and dropping pestles shorter and smaller in diameters. It is very important to crush the mineral grains as homogeneously as possible to obtain a good dating result. ^{40}Ar/^{39}Ar geochronology of fluid inclusions is very useful for us to understand various geological processes with fluids.

References:

[1] Qiu *et al.* (1989) *Chin. Sci. Bull.* **34**, 1887-1890.
[2] Qiu (1996) *Chem. Geol.* **127**, 211-222.
[3] Qiu *et al.* (2002) *Geochem. J.* **36**, 475-491.
[4] Qiu *et al.* (2007) *Earth Planet. Sci. Lett.* **256**, 224-232.
[5] Qiu *et al.* (2006) *Geochim. Cosmochim. Acta* **70**, 2354-2370.
[6] Qiu *et al.* (2008) *Earth Planet. Sci. Lett.* **268**, 501-514.
[7] Qiu *et al.* (2010) *J. Metamorph. Geol.* **28**, 477-487.
[8] Qiu *et al.* (2011) *Geology* **39**, 451-454.

https://doi.org/10.1180/S0026461X00008434 Published online by Cambridge University Press

Experimental study of the kinetics of CO_2-sequestration by olivines and Hawaiian picrites

LIN QIU[1]*, ZHENGRONG WANG[1], SHUN-ICHIRO KARATO[1], JAY J. AGUE[1], MICHAEL ORISTAGLIO[1], EDWARD BOLTON[1], AND DAVID BERCOVICI[1]

[1]Department of Geology and Geophysics, Yale University, New Haven, CT, USA

*presenting author: lin.qiu@yale.edu

Mafic/ultramafic rocks have been suggested as promising candidates to store anthropogenic CO_2 permanently. In this study, we employed an experimental approach to quantitatively evaluate the carbonation reaction kinetics as CO_2-rich fluids react with olivine (Fo_{90}) and high-Mg basalts (Hawaiian picrites).

Gem-quality olivine grains, olivine powders (10-20μm) and basalt powders (10-40μm) reacted with CO_2-containing solutions (e.g., 1M and 3M $NaHCO_3$ solution) in gold capsules placed in a hydrothermal autoclave over durations of 1-7 days at 200 ^oC and 150 bar. Dissolution experiments for these samples have also been carried out at three pH values (4.1, 6.9 and 9.3) to understand dissolution kinetics. After completion of experiments, gold capsules were checked for leaks, experimental run products were examined using SEM and electron microprobe, and the solution was analysed for alkalinity and major and trace element compositions at Yale University.

Our preliminary results show that carbonation rates of olivines and basalts are a function of the chemistry of the solution (e.g., concentration of $NaHCO_3$), the grain size, the mineralogy of the solid, and the duration of the experiments. We find that carbonation rates increase with increasing concentration of $NaHCO_3$ and decreasing grain size, but decease with time. For example, an increase of $NaHCO_3$ concentration from 1M to 3M raises the carbonation rate for olivine grain by a factor of 6, and the carbonation rate for 10- 40μm olivine powders with 1M $NaHCO_3$ solution is an order of magnitude greater than that for single olivine grains. Carbonation rates of olivine and basalts in the first day are significantly higher than that of the subsequent days and slow down after 3-days of reaction. A dissolution and precipitation model is formulated to quantitatively simulate this process.

The clumped isotope geothermometer in soil and paleosol carbonate

JAY QUADE[1*], JOHN EILER[2], MATHEIU DAERON[3], AND DAN BREECKER[4]

[1]University of Arizona, Geosciences, quadej@email.ariozna.edu (* presenting author)

[2]California Institute of Technology, Geological and Planetary Sciences, eiler@gps.caltech.edu

[3]CNRS, Science du Climat et de l'Environment, mathieu.daron@gmail.com

[4]Univerisity of Texas at Austin, Geological Sciences, breecker@jsg.utexas.edu

We studied both modern soils and buried paleosols in order to understand the relationship of temperature estimated from clumped isotopes in carbonates ($T°C_{clumped}$) to actual surface and burial temperatures. Carbonates from modern soils in a broad range of climates were sampled from Arizona, Nevada, Tibet, and India. $T°C_{clumped}$ obtained from these soils shows that soil carbonate only forms in the very warmest months of the year, largely in the afternoon, and probably in response to intense soil dewatering. The highest $T°C_{clumped}$ obtained from modern soil carbonate are <40°C On average, $T°C_{clumped}$ significantly exceeds mean annual temperature by 10-15°C due to (1) summertime bias in soil carbonate formation, and (2) sensible heating of soil. Secondary controls on $T°C_{clumped}$ are site aspect, but especially soil depth and shading.

Site mean annual temperature (MAT) across 0-30°C is highly correlated with $T°C_{clumped}$ from soils, following the equation:

$$MAT(°C) = 1.20*T°C_{effective\ air\ T\ from\ clumped} - 21.72 \qquad (r^2=0.92) \qquad (1)$$

where $T°C_{effective\ air\ T\ from\ clumped}$ is the effective air temperature at the site estimated from $T°C_{clumped}$. The effective air temperature represents the air temperature required to account for the $T°C_{clumped}$ at each modern soil site. The highly correlated relationship in equation (1) permits mean annual temperature in the past to be reconstructed from $T°C_{clumped}$ in paleosol carbonate, though it should be noted that soil carbonates appear to principally reflect warm season temperatures and so the proxy might be more precisely used as a measure of warm season climate or, in combination with other mean annual temperature proxies, of seasonality.

We also measured $T°C_{clumped}$ from long sequences of deeply buried (≤5 km) paleosol carbonate in the Himalayan foreland in order to evaluate potential diagenetic resetting. We found that paleosol carbonate faithfully records soil $T°C_{clumped}$ down to 3-4 km burial depth, or ~100°C. Deeper than this and above this

https://doi.org/10.1180/S0026461X00008434 Published online by Cambridge University Press

COMBINING μSXRF, EXAFS AND ISOTOPIC SIGNATURE TO UNDERSTAND THE NI CYCLE IN IMPACTED ULTRAMAFIC SOILS

CÉCILE QUANTIN[1], DELPHINE JOUVIN[1], ALEXANDRE GÉLABERT[2], EMMANUELLE MONTARGES-PELLETIER[3], YANN SIVRY[2], , ISABELLA ZELANO[2] , RÉMY PICHON[1], JÉRÉMIE GARNIER[4*], AND MARC F. BENEDETTI[2]

[1]UMR 8148 IDES, UPS-CNRS, Orsay, France (cecile.quantin@u-psud.fr, delphine.jouvin@u-psud.fr, remy.pichon@u-psud.fr)

[2]UMR 7154, Université Paris Diderot - Sorbonne Paris Cité - IPGP , Paris , France (gelabert@ipgp.fr, sivry@ipgp.fr, zelano@ipgp.fr, benedetti@ipgp.fr)

[3]UMR 7569 LEM, CNRS-Nancy I, Nancy, France (emmanuelle.montarges@univ-lorraine.fr)

[4]Instituto de Geociências, Universidade de Brasilia, Brasilia DF, Brazil (*garnier@unb.br)

Biogeochemical cycles of metals have been deeply modified by anthropogenic activities since the industrial revolution [1]. Since the end of the 90's, the development of metal isotopic ratios analysis provides crucial information about their biogeochemical behaviour. In the case of mining or smelter activities, extracted metals can be clearly followed through their isotopic signatures [2; 3]. Only few publications [4; 5] report the use of Ni isotopes for environmental studies, in spite of its high potential for tracing anthropogenic Ni. The combination of isotopic tools with microspectroscopic techniques (μSRXF and XAS), to unravel metal local distribution and speciation, should improve our understanding of Ni behavior and predict its mobility and bioavailability.

Samples from the ultramafic massives of Barro Alto and Niquelândia (Goiás State, Brazil), constitued in ores, fly ash, slags and natural and waste impacted soils were characterized for their Ni speciation and isotopic signatures. Ni concentrations range from 0.5 to 22.9 $g.kg^{-1}$

Ni K-edge XAS data were collected in bulk and microbeam modes for Ni ore, pristine pyrometallurgical wastes (fly ash and slags) before and after leaching (TCLP and DTPA procedures), to evaluate Ni extractability. TCLP or DTPA leaching leads to the extraction of 0.3 to 8.1% of Ni depending on samples. XANES spectra show that Ni is octahedrally coordinated. Linear Combination Fitting of EXAFS oscillations suggests that Ni in the ore is mainly involved in Ni-phyllosilicates and less than 20% in Ni bearing goethite. The Ni speciation in wastes is dominated by olivine and ferronickel, and leaching procedures only slightly impact Ni speciation.

The relatively high temperature processes occurring during pyrometallurgy processes may be responsible of strong isotopic fractionation [2]. Hence, Ni species from slags and fly ash should be easily distinguished from natural Ni species by their different isotopic signatures. Thus, all anthropogenic materials (ores, fly ash and slags) and soils will be carefully studied for isotopic signatures, in order to trace anthropogenic Ni in this ecosystem.

[1] Rauch & Pacyna (2009) *Glob. Biogeochem. Cycles*, **23**, 1-16. [2] Sivry et al. (2008), *Chem. Geol.*, **255**, 295-304. [3] Juillot et al. (2011), *Geochim. Cosmochim. Act.*, **75**, 2295-2308., [4] Sergeev et al. (2006), *Geochim. Cosmochim. Act.*, **70**, supp., A570., [5] Sergeev et al. (2007), *Geochim. Cosmochim. Act.*, **71**, supp., A918.

Insights into biomineral growth from atomistic simulations of clusters and nanocrystals

DAVID QUIGLEY[1*], MATT BANO[2] AND P. MARK. RODGER[2]

[1]Department of Physics, University of Warwick, Coventry. United Kingdom, d.quigley@warwick.ac.uk (* presenting author)

[2]Department of Chemistry, University of Warwick, Coventry, United Kingdom.

Introduction

The common biomineral calcium carbonate ($CaCO_3$) appears in nature as a variety of crystalline polymorphs and morphologies, exhibiting structure on a hierarchy of length scales which cannot be reproduced synthetically. Molecular simulation has a key role to play in elucidating the earliest stages of biomineral growth where length scales prohibit direct observation by experiment.

Nanoparticle simulations

Our previous free energy calculations based on metadynamics [1,2] have established that amorphous structure is energetically competitive with crystalline calcite for particles smaller than 2nm, with calcite structure increasingly preferred at sizes of 5nm and larger. This confirms experimental evidence that $CaCO_3$ growth can proceed via amorphous precursor phases.

Substantial improvements in the quality of force-fields for $CaCO_3$ [3] are enabling new questions to be addressed. Specifically water content and dehydration of the amorphous phase, and the stability of nanocrystals with aragonite or vaterite structure. The latter of these questions is a necessary step in elucidating the mechanisms of polymorph selection during nucleation and growth.

The traditional method of generating atomic representations of crystalline nanoparticles is the Wulff construction, in which a bulk crystal is cleaved such that the total surface energy is minimised. Our most recent work has demonstrated that such an approach fails for models which correctly capture the $CaCO_3$-water interfacial energetics. Surface *enthalpies* are found to be negative, with the entropic penalty of tightly-bound surface water being sufficient to generate a net interfacial free energy penalty.

We have developed an alternative Monte-Carlo method for generating nanocrystal configurations and applied this to the three $CaCO_3$ polymorphs. A discussion of magic-number effects will be presented, along with simulations comparing the energetics of these particles over a range of sizes in explicit water. Some progress toward simulating transitions between nano-crystalline polymorphs will be presented, along with challenges to calculation of transition kinetics.

Pre-nucleation clusters

Improved atomistic models have also allowed larger scale simulations to probe the earliest stages of ion aggregation, suggesting an explanation for the formation of stable pre-nucleation clusters [4]. This talk will present recent attempts to capture this phenomenon in simple lattice models of nucleation and growth.

[1] Quigley & Rodger (2008) *J. Chem. Phys.* **128**, 221101. [2] Quigley *et al* (2011) *J. Chem. Phys.* **134**, 044703. [3] Raiteri *et al* (2010) *J. Phys. Chem. C.* **114**, 5997-6010. [4] Demichelis *et al* (2011) Nature Comms. **2**, 590.

https://doi.org/10.1180/S0026461X00008434 Published online by Cambridge University Press

Nucleosynthetic anomalies of Ni and other transition metals in chondrites and possible carrier phases

QUITTÉ G.[1*] AND POITRASSON F.[2]

[1]CNRS UMR 5276, ENS de Lyon, Université Lyon 1, Lyon, France, Ghylaine.Quitte@ens-lyon.fr (* presenting author)
[2]GET, CNRS - UPS – IRD, Toulouse, France.

Introduction

The numerous nucleosynthetic anomalies found in refractory inclusions, presolar grains and particular phases carried by chondrites suggest that the matter constituting the solar system results from a mixing between different sources. Over the last few years, Ni isotope heterogeneities – among other elements – have been reported in various meteorites. Many samples including ureilite silicates, CAIs, CB metal nodules fall on a mixing line between an s-process and a e-process components [e.g. 1-2] ; altogether it is clear that meteorites come from at least 3 isotopically distinct Ni reservoirs [2-3]. However, the carrier phases of these nucleosynthetic anomalies have not been fully identified yet.

Leachates of carbonaceous chondrites

Focused studies of specific components or stepwise dissolution of carbonaceous chondrites are powerful tools to characterize the fine-scale isotope heterogeneities of the solar system, even if leaching procedures may induce some mixing between the various nucleosynthetic components. Acid leachates of carbonaceous chondrites already display anomalies for a variety of elements [e.g. 4-5]. A stepwise dissolution procedure similar to those previously used in other studies has been applied to facilitate the comparison of the isotopic results. Nickel is a suitable element to resolve the different nucleosynthetic components as ^{61}Ni is overproduced by s-process (AGB stars) when excesses of ^{62}Ni and ^{64}Ni witness nucleosynthesis in a neutron-rich environment (e.g. supernova explosion). Powdered whole rock samples of Allende, Murchison, and Orgueil were sequentially digested with reagents of increasing acid strength. Nickel is not isotopically uniform among the various host phases. Murchison and Orgueil show similar patterns, with widespread deficits in neutron-rich Ni isotopes. Allende is quite different: most leachates are slightly enriched in those isotopes. In Orgueil, the ^{62}Ni-deficit increases with increasing acid strength, which is consistent with the s-process component being carried by acid-resistant SiC presolar grains. Besides, most of the Ni is dissolved by concentrated acetic acid and nitric acid confirming that metal is a major carrier phase. As ^{58}Fe is the most neutron-rich Fe isotope, a correlation is expected with the neutron-rich Ni isotopes: hint towards negative $\varepsilon(^{58}Fe/^{54}Fe)$ values indeed exists in Orgueil fractions [6]. Isotope measurements of Cu and Zn in the same leachates are in progress with the aim of combining data for several elements from the "iron peak group". Correlations, if any, will potentially bring stronger and more precise constraints on the astrophysical setting where the nuclides have been produced, and help better identify the carrier phases of the isotope anomalies.

[1] Quitté G. et al. (2007) *ApJ* **655**, 678-684. [2] Quitté G. et al. (2010) *ApJ* **720**, 1215-1224. [3] Regelous M. et al. (2008) *EPSL* **272**, 330-338. [4] Rotaru M. et al. (1992) *Nature* **358**, 465-470. [5] Schönbächler M. et al. (2005) *GCA* **69**, 5113-5122. [6] Poitrasson F. and Freydier R. (2006) *MAPS* **41**, A141.

https://doi.org/10.1180/S0026461X00008434 Published online by Cambridge University Press

Boron isotope constraints on deglacial deepwater formation and CO_2 release from the North Pacific

JAMES W.B. RAE[1,2*], ANDY RIDGWELL[1], GAVIN L. FOSTER[3], MICHAEL SARNTHEIN[4], PIETER M. GROOTES[4], TIM ELLIOTT[1].

[1]University of Bristol, Bristol, UK
james.rae@bristol.ac.uk (* presenting author)
[2]now at Geological and Planetary Sciences, Caltech, Pasadena, USA
[3]School of Ocean and Earth Science, National Oceanography Centre, University of Southampton, Southampton, UK
[4]University of Kiel, Kiel, Germany

Deep convective mixing is thought to play a key role in glacial-interglacial cycles in atmospheric CO_2 by providing a pathway for carbon between the deep ocean and the atmosphere. Such mixing is inhibited in the subpolar North Pacific by very low surface water salinity [1], and as a result the North Pacific is not typically thought to play a direct role in glacial-interglacial CO_2 change [2]. Here we challenge this assumption with new boron isotope and radiocarbon data, that track the behaviour of carbon in the deep North Pacific over the last deglaciation. We show that over the last deglaciation deep water formed to 3600 m in the North Pacific. This is supported by experiments with an earth system model, which show that deep mixing in the North Pacific can account for a significant proportion of atmospheric CO_2 rise during deglaciations.

[1] Warren (1983) *Journal of Marine Research* **41**, 327-347. [2] Sigman et al. (2010) *Nature* **407**, 47-55.

Early diagenesis of As and P in tropical deltaic systems

SHAILY RAHMAN[1*] AND ROBERT C. ALLER[1]

[1]School of Marine and Atmospheric Sciences, Stony Brook University, Stony Brook, New York, USA,
sharahma@ic.sunysb.edu (*presenting author)
raller@notes.cc.sunysb.edu

In a comparative study of the diagenetic cycling of As in tropical shelf systems, vertical profiles of dissolved and solid phase arsenic were measured in the Guianas mudbelt, a coastal extension of Amazon delta deposits, and in the clinoform delta of the Gulf of Papua, Papua New Guinea. Both tropical systems are highly energetic, sedimentary depocenters with little anthropogenic contaminant input. Some of the highest concentrations of dissolved arsenic in the world are found in the French Guiana porewater samples, with maxima ranging from 5μM (375ppb) up to 13μM (975ppb). Mudbank As concentrations are typically higher than those found in the upstream Amazon delta (~2 – 4 μM). In contrast, porewater samples from the Gulf of Papua overall exhibited lower As maxima than Amazon-Guianas deposits, most often below 1μM, though in Bamu estuary sediments, concentrations exceeded 5μM. At most sites in the upper 10 – 15cm, dissolved arsenic and SRP appears to correlate with dissolved iron, suggesting concomitant release via dissolution of a solid Fe carrier phase, most likely Fe – oxyhydroxide.

In both the Amazon delta and French Guiana mudbank sediments, high As concentrations extend several decimeters downcore, in some cases showing little sign of attenuation (i.e. KS00-17 LC). In the Gulf of Papua, however, after reaching a subsurface maximum, there is little dissolved As remaining in solution with depth in most cores analyzed to date. Sequential solid phase extractions of French Guiana deposits indicate high amounts of As, reaching 300 nmol/g dry sediment. Solid phase As in the Gulf of Papua is ~10x lower than in the Amazon – Guianas mudbelt. Dissolved and solid phase phosphate were measured in several cores from Kourou – Sinnamary mudbank. Total solid phase phosphate (boiling aqua regia leach) measured between 10 - 19 μmol/g, and showed a marked correlation (r2 ranging from 0.7 – 0.95) with total solid phase iron downcore. Maximum dissolved P, SRP, ranged up to 150 μM. Total P at several Gulf of Papua sites were ~20 – 30 μmol/g.

https://doi.org/10.1180/S0026461X00008434 Published online by Cambridge University Press

Derivation of an accurate force-field for the simulation of carbonates

PAOLO RAITERI[1,*], RAFFAELLA DEMICHELIS[1] AND JULIAN D. GALE[1]

[1]Curtin University, Department of Chemistry, PO Box 1987, Perth WA 6845, Australia, p.raiteri@curtin.edu.au (* presenting author)

In recent years computational methods have become increasingly important in the study of geochemical processes due to the atomistic insight they are able to provide. In particular, force-field simulations are arguably the natural candidates to study processes that occur at the nano-scale due to their ability to approach the experimental conditions. However, the predictive power of force-field simulation strictly depends on the empirical parameters used in the simple formulae that mimic the atomistic interactions, which need to be derived with considerable care.

This work presents the approach followed in our group to derive force-field parameters based on a combination of static and free energy calculations, which are able to reproduce the thermodynamics of minerals in water [1]. Advantages and limitations of this approach will be illustrated, also in view of possible errors in the experimental thermodynamc quantities that are used to train the force field. The application of this approach to the study of carbonates in an aqueous environment will also be presented.

Although force field simulations do not naturally allow for chemical reactions, different approaches to simulate proton reactivity have been proposed in the past years. In this work an overview of two methods, ReaxFF[2,3] and MSEVB[4,5], is also presented.

[1] P. Raiteri *et al.* (2010) *J. Phys. Chem. C*, **114**, 5997–6010.
[2] A. C. T. van Duin, S. Dasgupta, F. Lorant and W. A. Goddard III. (2001), *J. Phys. Chem. A*, **105**, 9396–9409
[3] J. D. Gale, P. Raiteri A. C. T. van Duin (2011) *Phys. Chem. Chem. Phys.*, **13**, 16666–16679
[4] U. W. Schmitt and G. A. Voth (1999), *J. Chem. Phys* **111,** 9361.
[5] P. Raiteri, J. D. Gale and G. Bussi (2011), *J. Phys.: Condens. Matter* **23**, 334213

Cenozoic boron isotope variations in benthic foraminifers

M. RAITZSCH[1*] AND B. HÖNISCH[2]

[1]Alfred Wegener Institute for Polar and Marine Research, Bremerhaven, Germany, raitzsch@awi.de (* presenting author)
[2]Lamont-Doherty Earth Observatory of Columbia University, Palisades, USA, hoenisch@ldeo.columbia.edu

Background

One of the proxies at the forefront of estimating past CO_2 from marine archives is the boron isotopic composition recorded in shells ($\delta^{11}B_c$) of surface-dwelling foraminifers [e.g. 1], which reflects surface seawater pH and relates to atmospheric CO_2. A prerequisite for translating $\delta^{11}B_c$ into pH is the knowledge of the $\delta^{11}B$ of seawater ($\delta^{11}B_{sw}$), which is essentially unknown prior to the Pleistocene. Whereas boron in seawater has a long residence time of 10-20 My, modeling results suggest that $\delta^{11}B_{sw}$ may have changed considerably over millions of years [2,3], thus restricting paleo-pCO_2 reconstructions beyond the Pleistocene to interpretation of relative shifts rather than quantitative estimates.

Estimating $\delta^{11}B_{sw}$ from $\delta^{11}B_c$

Our benthic foraminiferal $\delta^{11}B_c$ approach is based on (i) the observation that deep-sea pH is quasi-constant below 1000 m water depth and (ii) the assumption that past variations in deep-sea pH were muted compared to surface seawater, similar to the dominant control of ice volume on the oxygen isotopic composition of benthic foraminifer shells. Because the distribution of dissolved boron and its isotopes in seawater is conservative, ocean-wide changes in benthic $\delta^{11}B_c$ should thus primarily reflect changes in $\delta^{11}B_{sw}$. The synthesis of multiple individual estimates from spatially distant core locations thus avoids bias due to regional variations in carbonate chemistry, which likely differed between ocean basins. However, modeling studies based on independent evidence from the CCD history of the ocean and atmospheric CO_2 estimates suggest that deep-sea pH has not remained constant over the Cenozoic. To scale our averaged benthic $\delta^{11}B_c$ record to $\delta^{11}B_{sw}$, we therefore account for a linear 0.45 units pH-increase [4] from 50 Ma until today.

Results & Conclusions

Our 50 My benthic foraminiferal $\delta^{11}B_c$ stack, composed of seven core sites from all ocean basins and various water depths, yields a remarkably consistent record. Although a general influence of whole ocean pH-variation has to be accounted for, the history of CCD-variations is not uniform in all ocean basins [5] and would have caused non-uniform changes in pH and thus in benthic $\delta^{11}B_c$. We do not observe such inter-basin differences in $\delta^{11}B_c$ and hence conclude that our record primarily reflects secular variations in $\delta^{11}B_{sw}$. Accordingly, our estimates suggest that $\delta^{11}B_{sw}$ increased by ~2.5‰ since the late Eocene, superimposed on oscillating variations with amplitudes of up to 2‰ over the entire record.

[1] Hönisch et al. (2009) *Science* **12**, 1551-1554. [2] Lemarchand et al. (2000) *Nature* **408**, 951-954. [3] Simon et al. (2006) *Chemical Geology* **225**, 61-76. [4] Tyrrell and Zeebe (2004) *Geochimica et Cosmochimica Acta* **68**, 3521-3530. [5] Van Andel (1975) *Earth and Planetary Science Letters* **26**, 187-194.

https://doi.org/10.1180/S0026461X00008434 Published online by Cambridge University Press

The Influence of Geology and Substrate on Plant Life in Northeastern North America

NISHANTA RAJAKARUNA

[1]College of the Atlantic, Bar Harbor, ME 04609, USA
nrajakaruna@coa.edu

7f. Critical zone processes: their role in ecology and evolution

Within a given climate, geology plays a central role in the distribution and ecology of plant species and their associated biota. The most significant causes of localized or unusual plant distributions are discontinuities in geology. Abrupt changes in geologic conditions can also set the stage for processes generating plant diversity. The study of plants growing on unusual geologies and substrates has contributed much to ecological and evolutionary theory. While much attention has been paid to the influences of geology and substrate on plant life worldwide, such literature for eastern North America is scant. The work we are currently pursuing on the flora of serpentine and granite outcrops, seabird guano deposits, and metal-enriched mine tailings in Maine suggests a unique substrate effect on the regional flora at taxonomic, physiological, and community levels. Our research highlights the need to better document the floras of other under-explored substrates of the region, including limestone, dolomite, and gypsum, and soils overlying metal-enriched geologies, including mine tailings and waste rock piles. These island-like habitats with unusual chemical and physical soil features can provide unique settings for the assembly of distinct plant communities, consisting of rare and endemic species and physiologically distinct ecotypes of more regionally common species. Such edaphically-restricted plants and their associated biota can provide ample opportunities for descriptive and experimental studies in ecology and evolution, ranging from cellular and organismal to population, community, and ecosystem levels.

Bioremediation of Heavy Metals using Transgenic Microalgae

Sathish Rajamani[1*], Surasak Siripornadulsil[2], Vanessa Falcao[3], Moacir Torres[4], Pio Colepicolo[5], and Richard Sayre[6]

[1]New Mexico Consortium, Los Alamos, New Mexico, USA, srajamani@newmexicoconsortium.org
[2]Department of Microbiology, Khon Kaen University, Thailand, surasak@kku.ac.th
[3]Donald Danforth Plant Science Center, St. Louis, Missouri, USA, Vanessa.falcao@gmail.com
[4]Department of Biochemistry, University of Sao Paulo, Sao Paulo, Brazil, wotorres@iq.usp.br
[5]Department of Biochemistry, University of Sao Paulo, Sao Paulo, Brazil, pio.colepicolo@iq.usp.br
[6]New Mexico Consortium, Los Alamos, New Mexico, USA, rsayre@newmexicoconsortium.org

Microalgae account for most of the biologically sequestered trace metals in aquatic environments. Their high metal binding affinities coupled with efficient metal uptake and storage systems make them efficient metal chelators. These factors combined with their large surface: volume ratios aid them bind up to 10% of their biomass as metals. In addition to essential trace metals required for metabolism, microalgae can efficiently sequester toxic heavy metals which often compete with essential trace metals for binding and uptake into cells. We have developed transgenic approaches to further enhance the heavy metal specificity and binding capacity of microalgae with the objective of using these microalgae for the treatment of heavy metal contaminated wastewaters and sediments. These transgenic strategies have included the over expression of enzymes whose metabolic products ameliorate the effects of heavy metal-induced stress and expression of heavy metal chelating protein such as Metallothionein (MT) to sequester heavy metals. The most effective strategies have substantially reduced the toxicity of heavy metals allowing transgenic cells to grow at wild-type rates in the presence of lethal concentrations of heavy metals. In addition, the metal binding capacity of transgenic algae has been increased five-fold relative to wild-type cells. Recently, fluorescent heavy metal biosensors have been developed for expression in transgenic *Chlamydomonas reinhardtii*. These fluorescent biosensor strains can be used for the detection and quantification of bioavailable heavy metals in aquatic environments. Furthermore, we discuss strategies for utilizing these transgenic algae for applications including sequestration of heavy metals in aquatic sediments.

Figure 1: Unicellular green alga *Chlamydomonas reinhardtii*

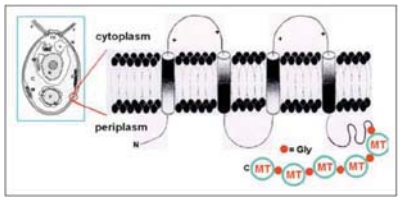

Figure 2: Cartoon depicting algal cell membrane engineered to express surface exposed Metallothionein (MT) units

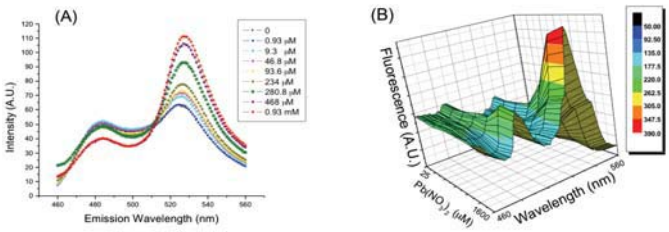

Figure 3: (A) *In vitro* metallothionein fluorescent biosensor showing increased heavy metal lead (Pb) concentration specific response (527nm/485nm).
(B) Intracellular expression of fluorescent biosensor in transgenic algae showing dose dependent response to added Pb.

https://doi.org/10.1180/S0026461X00008434 Published online by Cambridge University Press

Carbonaceous aerosols from biomass burning emissions in Northern India: Chemical characterization and temporal trends

PRASHANT RAJPUT[1]*, M. M. SARIN[2], DARSHAN SINGH[3] AND DEEPTI SHARMA[4]

[1]Physical Research Laboratory, Ahmedabad, India, prashant@prl.res.in (*presenting author)
[2]Physical Research Laboratory, Ahmedabad, India, sarin@prl.res.in
[3]Punjabi University, Patiala, India, dsjphy@yahoo.com
[4]Punjabi University, Patiala, India, deeptisharma271286@gmail.com

Introduction

The impact of biomass burning emissions on atmospheric chemistry and climate has been well recognized in the present–day scenario of rapid increase in the concentration of carbonaceous aerosols. Furthermore, mixing state of carbonaceous aerosols with other chemical species in the atmosphere leads to degradation of regional air–quality. Recent studies from south and south–east Asia have led to diverging views on the sources of carbonaceous aerosols, suggesting dominance of biomass burning emissions vis-à-vis fossil–fuel combustion [1–3]. It is, thus, important to document spatial and temporal variability in the chemical characteristics of carbonaceous aerosols through ground–based measurements from source regions in the Indo–Gangetic Plain (IGP). A large stretch of the IGP in Northern India is influenced by emissions from biomass burning during the wintertime.

Materials and Methods

$PM_{2.5}$ samples were collected (twice a week from October 2008 to May 2009 and from October 2010 to May 2011) from a sampling site (Patiala: 30.2° N, 76.3° E, 250 m asl) using a high–volume sampler. The sampler was operated at a flow rate of ~1.2 m^3/min for ~12 hours to filter about 1200 m^3 of air through tissuquartz filters (20 x 25 cm^2). EC and OC were determined on EC–OC analyzer, using a thermal–optical transmittance protocol [3, 4]. PAHs were extracted by accelerated solvent extraction (ASE), followed by matrix purification on a silica cartridge and quantification on GC–MS [4].

Results and Conclusion

Our comprehensive study on the atmospheric abundances of $PM_{2.5}$, EC, OC, WSOC and PAHs from two distinct post–harvest biomass burning emissions (paddy–residue burning during October–November and wheat–residue burning in April–May) show large temporal and inter–annual variability. This is attributable to the source strength and combustion efficiency of the two biomass burning events in the IGP. Relatively, high mass fraction of OC (Av: 0.33) and low contribution of EC (0.03) in $PM_{2.5}$ are associated with the paddy–residue burning (with high moisture content) compared to wheat–residue burning ($OC/PM_{2.5}$: 0.26; $EC/PM_{2.5}$: 0.07). The OC/EC ratio (Av: 10) for paddy–residue burning is about three times higher than that associated with wheat–residue burning emissions. However, the WSOC/OC ratio (range: 0.41–0.91) exhibits similar characteristic for paddy– and wheat–residue burning emissions.

The ΣPAHs/EC ratio of 4.2 mg g^{-1} is significantly higher from paddy–residue burning than that from wheat–residue (1.2 mg g^{-1}). The particulate concentrations of 5– and 6–ring isomers (normalized to EC) from paddy–residue burning are also about 3–6 times higher. The cross plot of PAHs isomer ratios show distinct dominance of agricultural–waste burning emissions in Northern India [4]. This study brings to focus temporal trends in the dominance of carbonaceous aerosols from biomass burning emissions during the two post–harvest seasons and have implications to atmospheric radiative forcing on a regional scale.

[1] Bracero *et al.* (2002) *J. Geophys. Res.* **107,** D198030.
[2] Gustafsson *et al.* (2009) *Science* **323,** 495–498.
[3] Ram *et al.* (2010) *J. Geophys. Res.* **115,** D24313.
[4] Rajput *et al.* (2011) *Atmos.Environ.* **45,** 6732–6740.

Substrates for anaerobic microbial activity in oil sands tailings ponds

ESTHER RAMOS-PADRON[1]*, LINDSAY N. CLOTHIER[1], SANDRA L. WILSON[1], GERRIT VOORDOUW[1], AND LISA M. GIEG[1].

[1]University of Calgary, Biological Sciences, eramospa@ucalgary.ca (*presenting author)

Alberta, Canada, is home to vast fossil energy reserves in the form of heavy oil or bitumen. Surface mining of the oil sands to recover bitumen using a caustic hot water extraction process generates a large volume of solid and liquid waste that is deposited in large storage areas or tailings ponds. The ponds are managed to promote solids densification so that surface water can be recycled. Surface water contains aerobic microbial communities, while the remaining tailings material at depth harbors anaerobic microorganisms. Such microbial communities can potentially affect gas emissions (H_2S and CH_4), solids densification, and the biodegradation of oil-associated compounds in the tailings such as bitumen, naphtha (a low molecular weight mixed hydrocarbon diluent), and naphthenic acids (NA). We previously measured sulfate reduction and methanogenesis rates with depth in tailings ponds and found that these activities are ongoing at discrete intervals [1]. Microbial community analysis showed that sulfate reducers and methanogens were abundant along with other anaerobes like nitrate and iron reducers [1]. However, the carbon sources driving such indigenous tailings pond communities remained unknown.

Thus, to determine the key substrates driving anaerobic microbial processes in tailings ponds, we established enrichments under a variety of anaerobic conditions using anaerobic tailings as inoculum. The incubations were amended with either bitumen, naphtha, or NA as potential carbon sources. Concentrations of nitrate, sulfate, Fe(II) and methane were determined over time in the substrate-amended incubations relative to substrate-free controls as indicators of anaerobic microbial activity. In some cases, substrate concentrations were also determined by liquid or gas chromatography.

In laboratory incubations, bitumen did not serve as a carbon source for anaerobic communities. However, naphtha and NA did drive several anaerobic activities. Incubations established under methanogenic conditions with naphtha showed enhanced levels of methane relative to substrate-free controls, and that this acitivity was ongoing after transfers of the enrichment. Several naphtha components disappeared over time in the naphtha-amended cultures relative to controls. Naphtha components such as low molecular weight alkanes have been shown to drive methanogenesis in samples collected from other tailings ponds [2], thus naphtha is an important carbon source in diverse tailings ponds. Incubations amended with commercially available model NA showed enhanced levels of nitrate reduction, Fe(III) reduction, and methanogenesis relative to substrate-free controls. Natural NA (extracted from tailings pond water) also stimulated Fe(III) reduction and methanogenesis in laboratory incubations. Little is known about the anaerobic transformation of NA in tailings ponds, but our data suggests that in addition to naphtha, NA may also be an important carbon source for the indigenous anaerobic communities.

[1] Ramos-Padron *et al*. (2011) *Environ. Sci. Technol*. **45**, 439-446.
[2] Siddique *et al*. (2006) *Environ. Sci. Technol*. **40**, 5459-5464.

https://doi.org/10.1180/S0026461X00008434 Published online by Cambridge University Press

Reconstruction of the Indian Summer Monsoon at weekly to sub-weekly resolution using terrestrial Giant African Snail *Lissachatina fulica* from northern India.

RAVI RANGARAJAN[1*], PROSENJIT GHOSH[1]

[1]Centre for Earth Sciences, Indian Institute of Science, Bangalore, India. *ravi@ceas.iisc.ernet.in., pghosh@ceas.iisc.ernet.in. (*presenting author),

Reconstruction of the ISM (Indian Summer Monsoon) at weekly to sub-weekly scales using terrestrial land snails is attempted here. Terrestrial mollusc *Lissachatina fulica* belonging to the Giant African Land Snails (GAL's) are endemic to the African sub-continent and have become an invasive species in most parts of the world. In this study, the stable isotopes of oxygen from the carbonate shells of *L.fulica* are used as a proxy to infer the variation in the ISM during the time period at the beginning of the last century. To establish and validate the suitability of the proxy for monsoon reconstruction, *in vitro* growth rate monitoring and present day comparison of precipitation and shell oxygen isotope has been carried out. The in vitro growth rate experiments showed a high growth rate (2.5 mm/week). Further, the dormancy/aestivation periods associated with non-monsoon time were also defined to explore the possibility for weekly reconstruction of ISM precipitation. The $\delta^{18}O$ of present day shells collected from Kolkata were compared with the already available precipitation isotopic data [1]. The $\delta^{18}O$ values ranged from -2 to -6‰ across the growth period of 3 years with marked cyclicity (Figure 1). The approach was then tested with museum specimens that were collected in the year 1918 from the same region. The $\delta^{18}O$ profile of the archived shells showed a higher depletion of ~1 to 2 ‰ than the present day shells, confirming the variation in the amount of precipitation.

Figure 1: Comparative $\delta^{18}O$ plot of the snail shell carbonates of two individual shell specimens along with the cumulative rainfall data of the region.

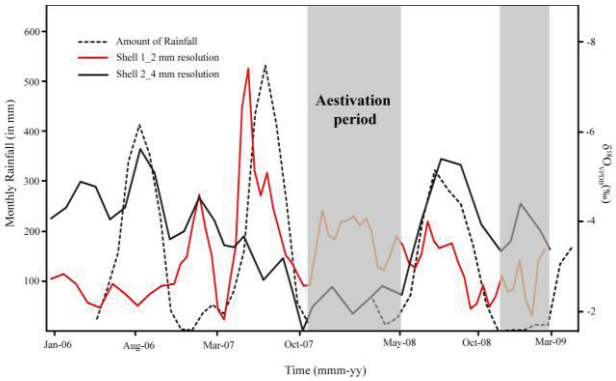

Reference

[1] Sengupta S. and Sarkar A., (2006) *Earth and Planetary Science Letters*. 250, 511-521.

Fractional crystallization of the Lunar Magma Ocean

JENNIFER F. RAPP[1,2*], DAVID S. DRAPER[2]

[1]Lunar and Planetary Institute, Houston, TX, USA, jennifer.f.rapp@nasa.gov (* presenting author)
[2]Astromaterials Research Office, ARES Directorate, NASA Johnson Space Center, Houston, TX, USA, david.draper@nasa.gov

The current paradigm for lunar evolution is that of the crystallization and differentiation of a Lunar Magma Ocean (LMO) [1]. In this model, the crystallization of the LMO gave rise to the plagioclase-rich ferroan anorthosite highlands crust, due to flotation of less dense plagioclase in the mafic magma ocean; and to mafic cumulates rich in olivine and pyroxene, which were later re-melted to produce basaltic magmas such as mare basalts and picritic pyroclastic glasses. LMO crystallization also produced KREEP, which represents the very late-stage incompatible element enriched liquid resulting from magma ocean crystallization, and is thought to have later hybridized with the ascending basaltic magmas (or their source rocks) resulting in specific minor and trace element enrichments seen in lunar basalts.

Numerical simulations have been used to predict the crystallization sequence of the LMO, the extent of fractional crystallization versus bulk crystallization [2], and the density profile of the resultant cumulate pile [3]. However these models, on which a large portion of lunar petrological research is predicated, remain largely untested experimentally. The Snyder model [2] features crystal suspension in the magma ocean due to vigorous convection, and equilibrium crystallization for the majority of LMO crystallization followed by fractional crystallization of the residual magma ocean. This model has been tested experimentally [4], and found to produce a different cumulate assemblage from that predicted by Snyder. We are experimentally simulating fractional crystallization from the outset of LMO solidification, as an alternative end-member model of lunar differentiation. We find that fractional crystallization of the lower portion of the LMO produces a divergence of residual liquid compositions from that of the equilibrium crystallization process, with liquids being somewhat more orthopyroxene-normative, and trending strongly towards plagioclase after approx. 50 volume % of the magma ocean has crystallized. We also find that spinel crystallizes, in small but significant quantities, in our cumulate pile deeper than predicted by previous models [2-4]. These differences are likely to be more pronounced as fractional crystallization proceeds, leading to concomitant differences in crystallizing assemblages including a lack of garnet in the lunar interior, which has implications for the potential thickness of the anorthosite crust. It remains to be seen whether this melt composition will evolve to produce sufficient plagioclase to account for the lunar crust, with a residuum representing KREEP. The outcome of this experimental investigation will enable us to put further constraints on the mechanisms by which the Moon evolved, in particular the extent, if any, to which equilibrium crystallization played an active role in LMO crystallization.

[1] Jolliff et al., (2006). *Reviews in Mineralogy and Geochemistry* 60.
[2] Snyder et al., (1992) *Geochim. Cosmochim. Acta* **56**, 3809-3823.
[3] Elkins-Tanton et al., (2002). *Earth Planet. Sci. Lett.* **196**, 239-249
[4] Elardo et al., (2011) *Geochimica et Cosmochimica Acta* **75**:3024-304

https://doi.org/10.1180/S0026461X00008434 Published online by Cambridge University Press

Flying through time: New microXRF techniques create opportunities to view the past.

AARON FRODSHAM[1], E. TROY RASBURY[1*], ANTONIO LANZIROTTI[2], J.A.D. DICKSON[3]

[1]Stony Brook University, Department of Geosciences
troy.rasbury@sunysb.edu (*presenting author)
afrodsham@stonybrook.edu
[2]University of Chicago
lanzirotti@uchicago.edu
[3]University of Cambridge
jadd1@cam.ac.uk

Abstract

New advances in microprobe technology at beamline X26A, at the National Synchrotron Light Source at Brookhaven National Laboratory, are allowing rapid and high resolution imaging of the distribution and concentration of elements in a sample. With this technique, called a fly-scan, we collect high resolution images in few hours that with conventional XRF scans would take a day. Currently the beam size is approximately 6 x 9 microns, giving a practical limit for the sampling interval of 4 -6 microns. The output of the fly-scan contains the full energy spectra for every detector at each point. To create an image, at each point, a window around the desired spectral peak is summed from each detector. This stacking helps eliminate noise, and provides an additive effect to the sampling time. Thus images of the distribution and concentration of any element whose florescence spectra is within the detection range of the sensors can be created after the data has been collected (Fig. 1).

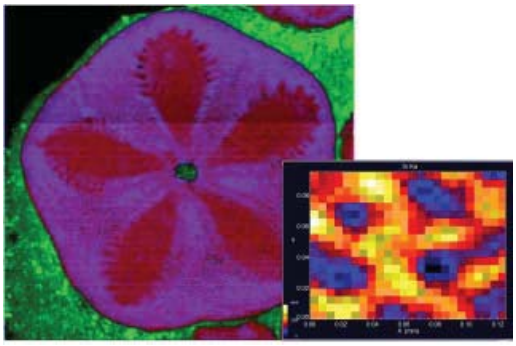

Figure 1: Flyscan image of echinoderm fossil showing distribution of Ca (red) Fe (green) and Sr (blue). Inset of high resolution Sr map from conventional XRF scan showing the typical ossicle structure where the shell is high Sr and the ferroan calcite cement is low Sr.

Carbonate fossils, such as echinoderms, can be used as proxies for the Sr/Ca and Mg/Ca ratios in paleoseawater. However diagenesis and other factors can change the composition of the carbonates. Echinoderm ossicles have a complex porous structure that can rapidly fill with encapsulating cement. This encapsulating cement protects the original carbonate material and creates a microscopic time capsule of the original chemistry [1]. We use fly scan imaging to identify extremely well preserved samples of fossil echinoderms, and measure the composition of the fossil stereom. We then calculate the Sr/Ca ratio of seawater then the fossil was formed. Our results confirm the observations that Sr changes inversely with Mg, and the total strontium concentrations is seawater have fluctuated by a factor of 5, throughout the Phanerozoic [2].

[1] Dickson JAD (2002) *Science*, **298** 1222-1224. [2] Steuber T & Veizer J, (2002) *Geology* **30** no. 12, 1123-1126.

The petrogenesis of monogenetic volcanoes inferred from Lunar Crater Volcanic Field, Central Nevada

C. RASOAZANAMPARANY[1]*, E. WIDOM[1], G.A. VALENTINE[2], E.I. SMITH[3], J.A. CORTES[2], D. KUENTZ[1], R. JOHNSEN[3]

[1]Department of Geology, Miami University, Oxford, USA, rasoazc@muohio.edu (*presenting author)
[2]Department of Geology, State University of New York, Buffalo, USA, gav4@buffalo.edu
[3]Department of Geoscience, University of Nevada, Las Vegas, USA, gene.smith@unlv.edu

The origin of chemical and isotopic variability observed over small spatial scales in basaltic monogenetic volcanic fields is highly controversial, and may be attributed to mantle heterogeneity [1] or to shallow lithospheric assimilation [2, 3], or both. The Lunar Crater volcanic field provides an opportunity to address the importance of shallow versus deep processes in the petrogenesis of basaltic monogenetic volcanoes and the nature of their mantle sources. We have performed Sr, Nd, Pb, Hf and Os isotopes measurement on 19 basaltic lavas from four closely spaced volcanic centers in the northern LCVF. Three eruptive centers (named YMB, OPB and PB [4]) are located within ~500 m of each other; the Marcath volcano, which represents the youngest eruptive center in the field, is located ~6 km SW of these cones. Detailed isotopic studies of the volcanic rocks show a limited range in Nd and Hf isotope ratios, but significant heterogeneity in Sr and Pb isotopes, and superchondritic Os isotope ratios. The lavas are characterized by $^{87}Sr/^{86}Sr$ ranging from 0.7030-0.7037, $^{143}Nd/^{144}Nd$ 0.51286-0.51291, $^{176}Hf/^{177}Hf$ 0.28293-0.28298, $^{206}Pb/^{204}Pb$ 19.16-19.49, $^{207}Pb/^{204}Pb$ 15.55-15.61 and $^{208}Pb/^{204}Pb$ 38.44-38.82. Os concentrations vary from 2 to 241 ppt and $^{187}Os/^{188}Os$ ranges from 0.1336 to 0.61. The lavas produce a well-defined negative correlation between Sr and Pb isotopes that could be attributed to lower crust assimilation. However, the lack of correlation of Sr, Nd or Os isotopes with indices of fractionation (e.g. MgO) suggests a limited role for crustal assimilation. In addition, high (OIB-like) Nb/U ratios and a positive correlation of $^{187}Os/^{188}Os$ with Nb/U argue against an important role for either upper or lower crustal assimilation. These data suggest instead that the basalts are generated by tapping a heterogeneous, enriched mantle source, consistent with trace element chemistry [5]. The HIMU-like trace element patterns and Sr and Pb isotope signatures of the OPB and PB lavas are consistent with derivation from an enriched mantle source with a component of recycled oceanic crust. In contrast, the relatively high Ba, Rb and Cs coupled with lower $^{206}Pb/^{204}Pb$ and higher $^{87}Sr/^{86}Sr$ of the Marcath and YMB lavas are consistent with derivation from an EMI-like mantle source that may be produced by a component of recycled oceanic crust plus sediment. These data indicate that the mantle in this region is characterized by chemical and isotopic heterogeneity over very small spatial scales.

[1] Reiner (2002) *Geochemistry Geophysics Geosystems* **3**, 1011. [2] Chesley et al. (2002) *Earth and Planetary Science Letters* **154**, 1-11. [3] Lassiter and Luhr. (2001) *Geochemistry Geophysics Geosystems* **2**, 1525-2027. [4] Valentine et al. (2011) *Abstract AGU Fall Meet. V33C-2657 [5] Cortes et al., (2011) Abstract AGU Fall Meet. V33C-2663.*

https://doi.org/10.1180/S0026461X00008434 Published online by Cambridge University Press

Archean laboratory models possessing photosynthetic microbial mats

MAIJA RAUDSEPP[1+*], NEIL R. BANERJEE[1] AND GORDON SOUTHAM[1]

[1]Department of Earth Sciences, The University of Western Ontario, London, Canada mraudsep@uwo.ca (*presenting author)

Introduction

Geochemical signatures of oxygen oases are preserved in late Archean shallow marine environments several hundred million years before the globally recorded great oxygenation event at 2.45 Ga [1]. We have created two possible Archean environments to observe geochemical changes in an oxygen oasis over several months. In both experiments a consortium of cyanobacteria, aerobic heterotrophs, iron reducing bacteria, sulphate reducing bacteria, and methanogens were grown on an olivine substrate. In the first experiment no additions were made to the system; in the second experiment ferrous iron equivalent to 0.01mM, a low estimate for an Archean ocean concentration, was added daily.

Results

Microbial growth in both experiments was dominated by oxygenic photosynthesis until the system became limited by inorganic carbon (Fig.1). $H_{2(g)}$ from low temperature serpentinization may have supported small amounts microbial growth.

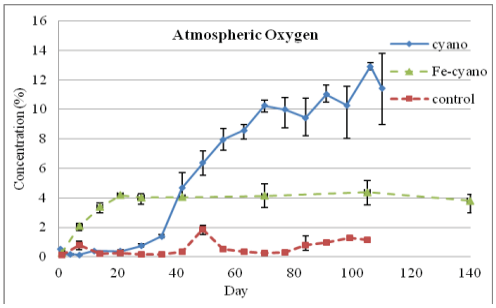

Figure 1: Oxygen accumulation from cyanobacteria mat (cyano), established cyanobacteria mat with iron additions (Fe-cyano) and un-innoculated system with no iron addtions (control).

In the low iron system, scanning electron microscopy showed some sections of mat were mineral free, whereas, other sections had dense accumulations of 0.5-20µm Mg-rich phyllosilicates. Different microbial communities were established on Fe-rich olivine versus Mg-rich olivine. In the high iron system lower oxygen resulted from the oxidation of $Fe^{2+}_{(aq)}$ producing <1µm ferric hydroxides particles. Ferric hydroxides densely covered the cyanobacteria and attached to heterotrophs. Mat growth was not hindered by the addition of iron but greater amounts of exocellular polymeric substances were produced.

Conclusion

This study demonstrates that bacteria in an Archean oxygen oasis had the potential to be fossilized by iron hydroxide minerals. Phyllosilicates, produced in part by biogenic alteration most, likely did not preserve bacteria morphology.

[1] Kendall (2010) *Nature Geoscience* **3**, 647-652.

Anthropogenic alteration of dissolved inorganic carbon fluxes from watersheds

PETER RAYMOND[1]

[1]Yale School of Forestry and Environmental Studies, New Haven, United States, peter.raymond@yale.edu

Section Heading

Introduction. Stream and River dissolved inorganic carbon fluxes represent a key linkage between major reservoirs in the global carbon budget. Over geologic time scales changes in inorganic carbon fluxes from land to sea can cause changes in atmospheric CO2. On shorter time scales alterations in these fluxes can be important to terrestrial carbon budgets, soil chemistry, and the buffering capacity of receiving waters. Here I will discuss what is known about the influence of human's on DIC fluxes from watershed.

https://doi.org/10.1180/S0026461X00008434 Published online by Cambridge University Press

Speckled zircon from mafic granulite: mechanism and meaning

N.M. RAYNER[1*], D. E. MOSER[2], M. SANBORN-BARRIE[1]

[1]Natural Resources Canada, Ottawa, Canada, nrayner@nrcan.gc.ca (* presenting author)

[2]Western University, London, Canada, desmond.moser@uwo.ca

Located in northern Hudson Bay, Southampton Island, Nunavut, is uniquely situated to provide critical insight into the assembly and evolution of northeast Laurentia. Archean and Paleoproterozoic plutonic rocks with 3.0-3.6 Ga Nd model ages dominate the eastern half of the island and include a layered ultramafic complex of which gabbroic anorthosite makes up a minor component. Mineral assemblages and thermobarometry record evidence of granulite-facies metamorphism with peak conditions of 900°C and 10kbar [1]. Zircons recovered from the gabbroic anorthosite are characterized by a distinct speckled zoning pattern in cathodoluminesence (CL) images (Figure 1).

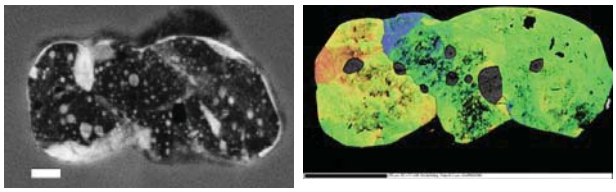

Figure 1: (Left) CL image showing speckled texture in zircon from mafic granulite. Scale bar 20µm. **(Right)** EBSD texture map (after re-polishing) showing relative crystallinity and low angle (up to 4°) misorientation of zircon lattice. Plagioclase inclusions show in grey.

Detailed geochronology, imaging, microstructural analysis and trace element geochemistry are applied to characterize the mechanism(s) responsible for this texture. SHRIMP U-Pb results define a discordia with an upper intercept of ca. 3.0 Ga and a lower intercept of ca. 1.87 Ga. Two interpretations of these results are feasible; the upper intercept may represent the crystallization age of the anorthosite or an inherited component. Accordingly, the lower intercept may record the timing of granulite-facies metamorphism or its crystallization age. EBSD mapping reveals that bright CL 'speckles' are subhedral domains of highly crystalline, unstrained zircon within a zircon matrix exhibiting finer-scale microstructure. Subgrains have rotated by several degrees across transverse, low -angle boundaries, possibly annealed fractures. The latter are sites of zircon recrystallization, suggesting a dynamic deformation and thermal annealing process. This combined isotopic, geochemical and microstructural study allows us to evaluate the two end-member tectonic scenarios; whether the mafic intrusive complex was emplaced and cooled within the deep crust (ca. 30km) during the Paleoproterozoic or whether Paleoproterozoic deep-crustal burial of a Mesoarchean layered complex produced the 'speckled' zircon microstructure and host granulite-facies mineralogy.

[1] Yakymchuk et al (2008) *Atlantic Geoscience Society, 34th Colloquium & Annual Meeting, Program with Abstracts*

Contribution of natural tracers (Cl, He) to development of 3D basin model. Paris Basin, France

ROMAIN REBEIX[1, 2*], HAKIM BENABDERRHAMANE[1], CORINNE LE GAL LA SALLE[3] , BERNARD LAVIELLE[2], VERONIQUE LAVASTRE[4], PHILIPPE JEAN BAPTISTE[5], ELISE FOURRE[5], AGNES VINSOT[1], PHILIPPE LANDREIN[1], JEAN-MICHEL MATRAY[6], MAURICE PAGEL[7] AND JEAN-LUC MICHELOT[7]

[1] CENBG, University of Bordeaux, France (rebeix@cenbg.in2p3.fr)

[2] ANDRA, Chatenay-Malabry, France

[3] GIS-CEREGE, University of Nîmes, France

[4] LMV-LTL, University of Lyon, France

[5] LSCE, CEA, Saclay, France

[6] IRSN, Fontenay-aux-Roses, France

[7] IDES, University of Paris XI, France

The French Radioactive Waste Management National Agency (Andra) is preparing submission of a license to build application for a high level and long lived radioactive waste repository in the Callovo-Oxfordian geological formation in the eastern Paris basin. In this context, flow and solute transport modelling is carried out at the Paris Basin scale in order to understand past and predict future hydrogeological behaviour. The past to present transport characteristics of the basin must be understood to constrain this model. Cl, He and their stable isotopes are considered as good natural tracers to be used for investigating the transport processes and behaviour within a multi-layered aquifer system at regional and local scales. Synthesis of data resulting from over 20 years of study and covering the entire Paris basin provides valuable information which was used to constrain and consolidate a conceptual model of basin evolution.

Chloride transport is dominated by vertical diffusion from the halite level of the Keuper formation in the east of the basin. The mix between primary and secondary brines associated with this level moved laterally into the rest of the basin since the early cretaceous due to uplift of the east border of the basin, generalizing the upward diffusion of chloride from Triassic levels to the entire system. Paleo circulation occurred two times in Dogger and Rhetian at -149±6My and -99±2Ma [1] before general uplift of the basin at the beginning of the Paleogene. Chloride spatial distribution indicates local activities of faults which induced hydraulically conductive links between Triassic, Liassic and Dogger formations.

Helium transport also appears to be dominated by global vertical diffusion from crust to the top of the sedimentary pile in the central and western parts of the basin. This system is separated into two independent domains in the east of the basin by the Keuper halite levels which act as a barrier to diffusion. In the vicinity of present Triassic outcrops in the east of the basin, $^{3}He/^{4}He$ ratios are characteristic of a mantel-derived ^{3}He contribution, quickly changing to a crustal-type $^{3}He/^{4}He$ ratio further along the flow path. The $^{3}He/^{4}He$ ratio in the centre of the basin corresponds to a binary mixing of a southern mantel-derived component and an eastern crustal component.

Simplified 1D modelling of He, Cl, Br and δ37Cl for last 70 My suggests that current lateral advection in the Oxfordian and Dogger formations over and underlying the Callovo-Oxfordian are active since 20 My and 5 My respectively, in the sector considered for the radioactive waste repository.

[1] Pisapia et al., (2011) *; Goldschmidt conf abstract 2011*

https://doi.org/10.1180/S0026461X00008434 Published online by Cambridge University Press

Mineral Precipitation Between Solutions Flowing in Parallel

GEORGE REDDEN*, DON FOX, JAMES HENRIKSON, LUANJING GUO, HAI HUANG, YOSHIKO FUJITA

Idaho National Laboratory, Idaho Falls, ID,USA (George.Redden@inl.gov, Don.Fox@inl.gov, Luanjing.Guo@inl.gov, James.Henriksen@inl.gov, and Hai.Huang@inl.gov (* presenting author)

Engineering mineral precipitation in the subsurface requires generating supersaturated conditions in order for desired minerals to nucleate or grow. For multi-component precipitation reactions, reactants must become mixed at the molecular scale. Different strategies can be used to mix reactants, either prior to introduction into the subsurface or *in situ*. Due to the strong coupling between reactant transport, mixing, and nucleation/growth processes, different mixing strategies will produce different spatial and temporal distributions of precipitates in the subsurface, with distinctly different outcomes with respect to the location of precipitates, changes in media properties and volume averaged rates of reactions. We have been studying the formation of precipitation reaction fronts that are generated by transverse mixing across the interface between solutions flowing in parallel.

Using a flow cell with a homogeneous sand packing, separate solutions containing calcium and carbonate were injected upward in a parallel flow configuration (Figure 1). The solutions, if mixed directly, would create strongly supersaturated conditions for calcite. The objectives were to quantify: 1) the dimensions of the precipitation zone, 2) changes in transverse permeability with distance along the zone, and 3) transient changes in the chemical properties (e.g., pH) on either side of the zone. In addition, we investigated the influence of differences in density of the two solutions on the position of the precipitation zone. The precipitation zone was found to be on the order of 1-2mm across. (This is in contrast to related experiments that involved mixing by double diffusion without advection, where the width of the precipitation zone was >1cm.) A low pH wedge formed on the side containing unbuffered calcium. Formation of asymmetric chemical conditions was consistent with expectations based on the $CaCO_3$ precipitation reaction stoichiometry and the properties of the solutions; however an anticipated disappearance of the pH wedge due to reduced permeability in the precipitation zone was not observed. A two-dimensional numerical model has been developed to simulate the nonlinearly coupled processes of flow, transport, and reaction in the system. Different scenarios with varying flow rate and solution concentrations (engineering controls) have been tested.

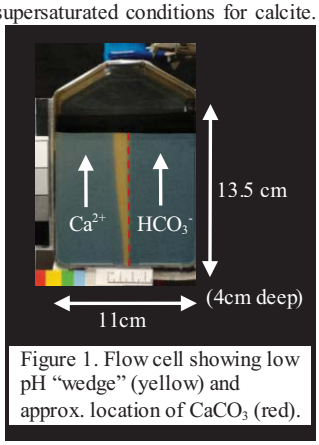

Figure 1. Flow cell showing low pH "wedge" (yellow) and approx. location of $CaCO_3$ (red).

Bioaccessibility of arsenic in soil: method evaluation, comparison to *in vivo* primate data, and influence of soil chemistry

JIM REDWINE[1]*, NICK BASTA[2], RONA DONAHOE[3], MARY MCLEARN[4], AND JAMIE RICHEY[5]

[1]Parsons Environment and Infrastructure, Birmingham AL, USA, James.Redwine@Parsons.com (*presenting author)
[2]School of Environment and Natural Resources, Ohio State University, Columbus OH, USA, basta.4@osu.edu
[3]Department of Geological Sciences, University of Alabama, Tuscaloosa AL, USA, rdonahoe@geo.ua.edu
[4]Electric Power Research Institute, Palo Alto CA, USA, MMCLEARN@epri.com
[5]School of Environment and Natural Resources, Ohio State University, Columbus OH, USA, richey.114@osu.edu

Several studies have shown relatively limited human and animal absorption of arsenic from contaminated soils. Extensive efforts are presently underway to develop less expensive laboratory (*in vitro*) tests that simulate *in vivo* results, and validate them against live animal data. In this study, *in vitro* tests using three common methods were performed on soils for which *in vivo* primate data were available. *In vitro* and *in vivo* test results were then compared. The same soils were treated with iron amendments, to determine if iron treatment reduced arsenic bioaccessibility. Prior to testing, soils were extensively characterized to enable better interpretation of the results of the *in vitro* tests. *In vitro* data by all three methods correlates poorly with primate data. Specifically, with the exception of one iron-rich soil, *in vitro* tests over-estimate bioavailability by factors ranging from 1.3 to 16.7. The presence of calcium carbonate or iron in soil affects the results of the *in vitro* tests. The largest *in vitro* over-estimate occurred for calcium carbonate soils, and iron binds arsenic such that it is less extractable in the *in vitro* tests. As expected, iron treatment significantly reduced arsenic bioaccessibility in the soils studied. A large data base of physical and chemical information was generated for these soils, and with more detailed analysis, could be used to help determine other geochemical influences on arsenic bioavailability and bioaccessibility.

https://doi.org/10.1180/S0026461X00008434 Published online by Cambridge University Press

X-ray pair distribution function and NMR studies of biogenic amorphous calcium carbonate

RICHARD J. REEDER[1*], MILLICENT P. SCHMIDT[1], LAURA M. KUBISTA[1], YUANZHI TANG[2], BRIAN L. PHILLIPS[1]

[1]Stony Brook University, Geosciences, Stony Brook, NY, USA rjreeder@stonybrook.edu (* presenting author), millicentpschmidt@gmail.com, lkubista@gmail.com, brian.phillips@sunysb.edu

[2]Harvard University, Engineering and Applied Sciences, Cambridge, MA, USA tang.yuanzhi@gmail.com

Introduction and Approach

Amorphous calcium carbonate (ACC) is known to serve multiple functions during biomineralization processes: as a transient precursor to crystalline $CaCO_3$, as structural components of functional hard parts, and as temporary storage of calcium. Minor additives play important roles in stabilization of ACC as well as in transformation to crystalline forms. Yet, the specific interactions of the additives with the ACC remain largely unknown. One of the main limitations in understanding ACC stabilization and transformation mechanisms is a lack of knowledge of short- and medium-range structure in the amorphous phase. Recent application of synchrotron total X-ray scattering and pair distribution function analysis has allowed characterization of short- and medium-range structure extending up to length scales of 15 Å in synthetic hydrated ACC [1]. NMR studies provide insight to the role of hydrogen bonding in the local structure. We have applied these same experimental approaches to examine structure in hydrated biogenic ACC to provide a comparison with synthetic ACC. American lobsters produce gastroliths that are composed almost entirely of hydrated ACC.

Results and Conclusions

X-ray PDFs for gastrolith ACC exhibit a weak, sharp peak at 1.3 Å and a strong, sharp peak at 2.4 Å, resulting from first-shell C-O and Ca-O bonds. A weak peak is also evident at ~2.9 Å, appearing as a small shoulder to the 2.4 Å peak. In addition, there are two broad peaks of lower amplitude centered at ~4 and ~6 Å, with even weaker oscillations extending up to ~12 Å. Comparison with the PDF for synthetic hydrated ACC shows essentially identical features, in both position and amplitude. Reverse Monte Carlo refinement has shown that the broad features at 4 and 6 Å represent dominantly Ca-Ca and Ca-O pair correlations [2]. NMR data likewise closely resemble those for synthetic ACC, showing a broad ^{13}C peak near +169 ppm, 3.6 ppm FWHM. Phosphorus present at minor concentrations in the gastrolith yields a ^{31}P NMR peak at 2.8 ppm, similar in position to phosphate in crystalline $CaCO_3$ but much broader (5.5 ppm FWHM), indicating a wide range of local environments. ^{31}P-detected ^{1}H NMR spectra contain a broad sideband envelope characteristic of rigid structural water, similar to ^{1}H spectra of synthetic ACC, suggesting intimate association of phosphate in the gastrolith ACC.

[1] Michel (2008) *Chem. Mater*. **20**, 4720-4728. [2] Goodwin (2010) *Chem. Mater*. **22**, 3197-3205.

The role of lead (Pb) in highly saline fluids of a deep geothermal system: complexation and precipitation

SIMONA REGENSPURG [1]*, RUDOLF NAUMANN [2], ELVIRA FELDBUSCH[1], FIORENZA DEON[1]

[1]GFZ German Research Centre for Geosciences, International Centre for Geothermal Research, Potsdam, Germany, regens@gfz-potsdam.de (* presenting author)

[2]GFZ German Research Centre for Geosciences, Section 4.2 Inorganic and Isotope Geochemistry, Potsdam, Germany rudolf@gfz-potsdam.de

At the geothermal in situ laboratory in Groß Schönebeck (North German Basin) fluid of a Permian sandstone reservoir is produced from about 4.4 km depths, where the temperature is about 150°C at 45 MPa pressure. The brine is characterized by a very high salt content of 265 g/L total dissolved solids, which is mainly composed of NaCl and $CaCl_2$ [1]. During the initial testing phase of the geothermal fluid loop between April and October 2011, fluid was produced from one well at temperatures below 100 °C. After passing a gas seperator and two filter units (< 20 µm), the fluid was re-injected into a second well. During that phase, fluid samples were collected with a special sampling device, allowing to take fluid at in-situ pressure and temperature from the above ground installations after the production well. Fluid samples were collected at various temperatures between 20 and 100 °C. Addionally, filter residues as well as mineral scalings, which precipitated within the well bore have been collected and analyzed. One of the compounds of interest both in fluid and in solid phase is lead (Pb), which was found to be highly enriched (up to 1 mM) in the fluid solution as well as in most of the solid samples.

Solid samples were analyzed by X-ray diffraction (XRD), Scanning Electron Microscopy (SEM) and, after acid extraction by ICP-MS or OES for total elemental composition. Although a large quantity of the material was weakly crystalline or amorphous, some crystalline phases were identified in the samples. Lead occured in different minerals such as laurionite (PbOHCl), galena (PbS), native Pb and PbO, indicating that redox processes play an important role in the borehole.

Fourier Transform Infrared Spectroscopy (FTIR) spectra were collected both on samples of the geothermal brine and on synthetic Pb containing solutions of various composition to identify Pb complexation in the solution.

The aim of these investigations was to understand Pb mobility and the factors affecting Pb solution and precipitation at geothermal conditions.

[1] Regenspurg et al. (2010) *Chemie der Erde* **70(S3)**, 3-12.

https://doi.org/10.1180/S0026461X00008434 Published online by Cambridge University Press

Extracellular reduction of uranium via *Geobacter* conductive pili as a protective cellular mechanism

GEMMA REGUERA*

Michigan State University, Department of Microbiology and Molecular Genetics, East Lansing, USA, reguera@msu.edu

Abstract

The in situ stimulation of Fe(III) oxide reduction by *Geobacter* bacteria leads to the concomitant precipitation of U(VI) from groundwater. Despite its promise for the bioremediation of uranium contaminants, the biological mechanism behind this reaction has remained elusive for almost two decades. Because Fe(III) oxide reduction by *Geobacter* requires the expression of their conductive pili, the contribution of the pili to uranium reduction was investigated in strains of *Geobacter sulfurreducens* with various levels of piliation and in pili-defective strains [1]. Pili expression significantly enhanced the rate and extent of uranium reduction per cell and resulted in the immobilization of the soluble, hexavalent uranium, U(VI), along the pili as a mononuclear tetravalent uranium, U(IV), complexed by carbon containing ligands and with coordinations consistent with a biological mechanism. There was also a direct correspondence between the levels of piliation, the cell envelope respiratory activities, and the cell viability. In contrast, the pili-defective strains preferentially reduced the uranium in the periplasm and had reduced respiratory activities and viability. Furthermore, the degree of periplasmic mineralization in the pili-deficient strains correlated well with their outer membrane *c*-cytochrome content.

It is unlikely that cytochromes released from the outer membrane could have associated with the pili and contributed to the reductive precipitation of uranium, because direct probing of the pilus filaments by scanning tunneling microscopy did not reveal any electronic features resulting from the contribution of cytochrome heme groups [2]. Rather, they show topographic and electronic features intrinsic to the pilus shaft [2]. Furthermore, there was no correlation between the amount of uranium reduction and the cytochrome content of any of the strains tested [1].

Conclusion

The polymerization of the micrometer-long conductive pili on the cell envelope increases the redox-active surface area available for binding and reducing uranium outside the cell. Not only do the pili enhance the reductive precipitation of the soluble U(VI), but also prevent it from penetrating inside the cell, thus preserving the vital respiratory activities of the cell envelope and the cell's viability. Hence, the results support a model in which the conductive pili function as the primary mechanism for the reduction of uranium and cellular protection.

[1] Cologgi et al. (2011) *PNAS* **108**, 15248-52. [2] Veazey et al. (2011) *Phys. Rev. E* **84**, 060901(R).

Carbonate alteration of dolerite intruding coal seams: a natural example of carbon sequestration during fossil fuel combustion and relevance to industrial solutions involving mineral carbonation

DAVID REID[1*], MOTSHIDISI NGWAGWE[1], TENDAI MATHIVHA[1], NICOLE MEYER[1], JACQUES VOGELI[1]

[1]Department of Geological Sciences, University of Cape Town, South Africa, david.reid@uct.ac.za (* presenting author)

Coal seams within the Karoo sequence of South Africa are variably intruded by numerous dolerite dykes and sills that have not only produced a thermal metamorphic effect in the surrounding coal but have themselves been altered by fluids sourced from the original magma and surrounding country rock sediments. While the most significant effect in the adjacent coal is widespread devolatilisation and occasional burning, probably brought about by the heat migrating from the cooling magma, there appears to be a protracted period of hydro- and carbo-thermal fluid activity.

Carbonate alteration of the dolerite is restricted to where the intrusions cut the coal measures and is characterised by pseudomorphic replacement of the primary igneous mineralogy. Olivine and pyroxenes are the first to be replaced, followed by Fe-Ti oxides and finally plagioclase. The degree of replacement varies from essentially complete at the contacts but reduces inwards, with dykes wider than about 3m retaining unaltered interiors. Sills tend to track up and down the stratigraphic sequence along strike so their alteration can vary considerably, depending on proximity to the individual coal seams.

Carbonate replacing the igneous minerals have ternary Ca-Mg-Fe compositions that reflect their hosts, although the correlation is by no means close. There appear to be three broadly defined compositional groups: calcites, dolomites and siderites, that have developed in textural patches dominated by plagioclase, pyroxene and Fe-oxides respectively. These compositional patterns do however confirm the in situ replacement origin by fluids migrating into the solidified dolerite.

Carbon and Oxygen isotope ratios in the carbonates are indicative of a mixture between magmatic and coal sources but require a significant component of the latter, thereby confirming an internal closed system consistent with built in sequestration. Judging from the distribution of dykes through the mine lease area and the proportion of which is carbonated, we estimate that the order of 100s of tonnes of CO2 were taken up by these intrusions. Extending this estimate to incorporate the effect of the sills and to project across the entire coal field is fraught with uncertainty but may involve a factor of 100x. Consequently the natural process probably involved only modest quantities of CO2 and associated C-H-O fluid components.

It is clear that for dolerite to absorb CO2 produced by coal metamorphism, the process was enhanced by near magmatic temperatures, abundant fluid and prolonged geologic time. Low cost energy proxies have to be found for any industrial process that is to be based on the natural phenomenon. However, there are abundant mineral reservoirs with similar bulk composition that are available in South Africa and even worldwide that could be utilised for mineral carbonation.

https://doi.org/10.1180/S0026461X00008434 Published online by Cambridge University Press

Size-associated distribution of ferrous and ferric iron in two Algonquin Park lakes

MICHELLE L. REID[1*], AMY V. C. ELLIOTT[2], AND LESLEY A.WARREN[3]

[1]McMaster University, Hamilton, Canada, reidml@mcmaster.ca (* presenting author)
[2] McMaster University, Hamilton, Canada, elliotav@mcmaster.ca
[3]McMaster University, Hamilton, Canada, warrenl@mcmaster.ca

Iron is integral to global biogeochemical cycling, and is increasingly studied in marine systems based on both speciation as well as size distribution. However, to date, the size-associated distribution of iron species in freshwater lakes has not been investigated. The physico-chemical properties of a lake, as well as interaction with suspended particles, bed sediments, and floc, affect the stability and bioavailability of iron compounds. Iron compounds and trace metals may be present within several operationally defined size fractions, each representing a pool that can differ in bioavailability, sorption reactivity, and mobility. In addition to trace metal concentrations, iron species and abundances are likely to change with depth as well as along creek-lake transects, indicating finer depth scale assessment will provide a more accurate picture of iron-metal dynamics in freshwater systems. Here, the objective is to gain a more thorough understanding of iron distribution within (1) a stratified, anoxic water column as well as (2) along a wetland-lake transect, (Algonquin Park, ON), by determining the relative proportion of iron species in four operationally defined size fractions: particulate (>0.45 um), large colloidal (0.45>0.2 um), small colloidal (0.2>0.02 um), and dissolved (< 0.02 um). Samples from ten depths within the Coldspring Lake water column (July 20-21, 2011) and twelve sites along the Costello Creek - Lake Opeongo transect (August 25-28, 2011) were sequentially filtered into four size fractions, and preserved for trace metal analysis by ICP-MS, and $Fe^{2+/}Fe^{3+}$ quantification by the Ferrozine method. Results assessing Fe^{2+}/Fe^{3+} speciation and abundances, with linkages to trace metal concentrations, in each of these systems will be presented..

OXIDATIVE WEATHERING ON THE EARLY EARTH

CHRISTOPHER T. REINHARD[1*], STEFAN LALONDE[2], TIMOTHY W. LYONS[1]

[1]Dept. of Earth Sciences, Univ. of California, Riverside, CA 92521 USA (*correspondence: christopher.reinhard@ucr.edu)
[2]Institut Universitaire Européen de la Mer (IUEM), Université Européene de Bretagne (UEB), Plouzané 29280, France

Recently accumulating evidence suggests that the biological production of oxygen in Earth's surface oceans preceded the initial accumulation of large amounts of oxygen in the atmosphere by 100 million years or more. However, the potential effects of oxygen production on surface ocean chemistry have remained little explored, and questions persist regarding both the potential role of oxidants other than molecular oxygen and the locus of oxidation of crustal material (i.e., subaerial and/or submarine settings). Here, we revisit the notion of transient and/or spatially restricted 'oxygen oases' in the Archean surface ocean by employing a simple steady-state box model of the surface ocean in a coastal upwelling system, and explore the plausibility that such a system could support the widespread oxidation of reduced crustal minerals. We find that although it is possible to establish strong air-sea gas exchange disequilibrium with respect to O_2, there is an apparent timescale mismatch between the kinetics of oxidative dissolution and the rate at which reduced minerals delivered physically to shallow marine sediments will be buried below the zone of oxidant penetration. In addition, the circum-neutral pH of marine environments places stringent constraints on the efficacy of Fe^{3+} as an oxidant for crustal sulfides, rendering the most important sulfide oxidant in modern weathering systems ineffective. Estimated dissolution timescales compare more favorably with typical timescales of soil development, despite the much lower dissolved oxygen concentrations inferred for a subaerial environment at gas exchange equilibrium with atmospheric pO_2. We suggest that, although the production and accumulation of dissolved O_2 in the Archean surface ocean is probable under certain conditions and should be explored as a biogeochemical agent, it is unlikely that extensive oxidative weathering of chalcophile elements such as Mo, Re, and S occurred within the marine realm.

https://doi.org/10.1180/S0026461X00008434 Published online by Cambridge University Press

Sorption of uranium(VI) and radium(II) at trace level onto kaolinite and montmorillonite

ESTELA REINOSO-MASET*, DELPHINE HAINOS, JACQUES LY

CEA Saclay, DEN/DANS/DPC/SECR/Laboratoire de Mesures et de Modélisation de la Migration des Radionucléides, 91191 Gif-sur-Yvette, France (*estela.reinoso-maset@cea.fr)

Clays are one of the main components of soils and sediments, and are known to have the distinctive property of retaining ions, generally with a high affinity for cationic species. Since retention processes confer a retardation effect on the migration rate of contaminants, the clay content and the intrinsic properties of clays will determine the prevailing process during the transport of contaminants through subsurface environments.

Uranium and the long-lived decay product radium-226 are abundantly present in the vast mine waste produced during uranium extraction activities. However, in the case of release to the surrounding environment, these radionuclides would be found at trace level compared to major cations present in interstitial waters; and hence, the extent of radionuclide sorption will be conditioned by the predominant occupancy of surface sites by the latter solutes. Therefore, the aim of this work was to study the sorption of trace level uranium(VI) and radium(II) on two common phyllosilicate minerals, kaolinite and montmorillonite, alongside with the sorption of sodium, potassium, calcium and magnesium at higher concentration.

Batch type experiments using chemical and radiochemical analytical techniques were carried out to obtain the intrinsic ion-exchange properties of both clay minerals and the ion-exchange equilibria occurring at the mineral-solution interface with the associated selectivity coefficients for Na/H, K/H, Cs/H, Ca/H and Mg/H ion couples. Sodium, K, Cs, Ca and Mg were introduced in sufficiently high amount in separated batches containing the respective homo-ionic clay forms and the adsorbed cation concentration was measured as a function of pH. The results enabled to determine the clay surface sites characteristics (i.e. the number and concentration of sorption site types) and to confirm the multi-site ion-exchanger properties of these clay minerals, as previously observed for montmorillonite [1]. The sorption of U(VI) and Ra(II) at trace level was determined through distribution coefficient (K_d) measurements at different pHs.

Finally, the sorption data for both clays was processed according to a general multi-site sorbent / multi-species sorbate model which has already been applied to successfully describe the sorption reactions on mineral surfaces [2, 3]. The modeling results will provide with fundamental sorption equilibria stoichiometries and constants crucially needed for the calculation of the interfacial chemistry to be coupled to transport in predictions of radionuclide migration rates.

[1] Ly et al. (2002) *1st International Meeting on "Clays in natural and engineered barriers for radioactive waste confinement"*, Reims, France.
[2] Motellier et al. (2003) *Applied Geochemistry* **18**, 1517-1530.
[3] Jacquier et al. (2004) *Applied Clay Science* **26**, 163-170.

Reevaluating osmium isotopes as tracers of glacial-interglacial cycling

LAURIE REISBERG[1*], DOMINIQUE BLAMART[2], AND CATHERINE ZIMMERMANN[1]

[1]CRPG-CNRS, Université de Lorraine, reisberg@crpg.cnrs-nancy.fr (* presenting author); Vandoeuvre-lès-Nancy, France
[2] LSCE (CEA-CNRS-UVSQ), Dominique.Blamart@lsce.ipsl.fr, Gif-sur-Yvette, France

Over the past 15 years, several studies [1-5] have demonstrated correlations between the Os isotopic compositions of hydrogenous marine sediments and glacial-interglacial variations. These are often attributed to decreased continental erosion during glacial episodes. However, the short Os marine residence time (< 5ka) inferred from these rapid variations is inconsistent with that derived from mass balance considerations (~25 to 40 ka, [6-8]). This observation has prompted the proposal that rapid weathering during deglaciations produces transient spikes in the concentration and/or isotopic composition of Os delivered to the ocean, thus arguing that the riverine flux and the oceans are far from steady state equilibrium [9].

Nevertheless, these interpretations rest on the assumption that the available Os isotopic records faithfully reflect the past Os compositions of global seawater. However, many records may be biased by basin isolation, detrital input, and low sedimentation rate. To obtain a reliable, high resolution record of Quaternary marine Os isotopic variations, we are analyzing sediments from ODP Leg 175, Site 1084, drilled beneath the Benguela Upwelling System (BUS) off Namibia. As an open ocean site with rapidly deposited (~ 18 cm/kyr) organic rich sediments, it should be unaffected by the problems noted above. Results from 24 samples analyzed to date, spanning the past ~130 ka, show much less variability ($^{187}Os/^{188}Os$ =1.037 ±.026; 2σ) than that found in previous studies (~10%), and no correlation with glacial-interglacial variations. Instead, the uniformity of the BUS Os record ressembles that of an early Pleistocene record from the equatorial Pacific Ocean [9]. One explanation for the discrepancy between the BUS results and other late Quarternary records may be that the latter reflect local, rather than global, processes. However, while this explanation seems logical for sediments deposited in semi-isolated near-shore basins [2-4], local effects are unlikely to modify the Os compositions of open ocean sites [1,5]. Instead, we consider the fact that dissolved Os may be present in several oxidation states, and experimental studies suggest that it is difficult to pass from one to another [11]. Os incorporated into metalliferous sediments [1] or planktic foraminifera [5] under oxidizing conditions may not be in the same form as that incorporated under the reducing conditions prevailing in the BUS. Thus it may be too simplistic to consider that all of the Os present in the oceans is contained within a single uniform reservoir with a well-defined residence time.

[1] Oxburgh (1998) *EPSL* **159**, 181-191 [2] Dalai et al. (2005) *Chem. Geol.* **220**, 303-314 [3] Williams & Turekian (2004) *EPSL* **228**, 379-389 [4] Oxburgh et al. (2007) *EPSL* **263**, 246-258 [5] Burton et al. (2010) *EPSL* **295**, 58-68 [6] Oxburgh (2001) *G-cubed* 2000GC000104 [7] Levasseur et al. (1998) *EPSL* **174**, 7-23 [8] Paul et al. (2010) *GCA* **74**, 3432-3448 [9] Vance et al. (2009) *Nature* **458** 493-496 [10] Dalai & Ravizza (2010) *GCA* **74**, 4332-4345 [11] Paul et al. (2009) *Chem. Geol.* **258**, 136-144.

https://doi.org/10.1180/S0026461X00008434 Published online by Cambridge University Press

The vapour-liquid fractionation of Cu stable isotopes: a new tool for porphyry research

KIRSTEN U. REMPEL[1,2*], ROLF L. ROMER[1,3], AXEL LIEBSCHER[1,4]

[1] GFZ German Research Centre for Geosciences, Potsdam, Germany
[2] rempel@gfz-potsdam.de (* presenting author)
[3] romer@gfz-potsdam.de , [4] alieb@gfz-potsdam.de

Copper is an essential element for green technologies such as long-life Cu batteries, thin films and other highly conductive materials, while porphyry Cu-Mo deposits are a major source of other metals crucial to green industry (Mo and Re). The formation of these deposits typically involves a two-phase magmatic fluid comprised of aqueous vapour and liquid, and significant quantities of Cu may be transported in both of these phases. The stable isotope signature of Cu in each fluid phase could be of use in tracking the evolution of the fluid system, or in identifying zones of a porphyry deposit formed from the vapour- and liquid-dominated fluid regimes. In order to investigate these possibilities, we have conducted an experimental study of the vapour-liquid (V-L) fractionation of Cu and its stable isotopes ($^{65}Cu/^{63}Cu$).

Closed-system V-L fractionation was measured experimentally at P-T conditions applicable to porphyry formation (up to 450°C and 400 bar) by the removal of V and L sample pairs from a batch of bulk fluid contained within an autoclave, with each pair taken at successively lower total pressure. For most sample pairs, the isotopic compositions of the vapour and liquid were equal within uncertainty.

However, from the intial compositions of the bulk start solutions to those of the final, lowest-pressure V and L sample pairs extracted from the autoclave, a shift to heavier values of $\delta^{65}Cu$ was seen. Specifically, between the starting compositions and those of the lowest-pressure vapour samples, the increases in $\delta^{65}Cu$ values were 0.16, 0.69 and 0.10‰ (all ±0.07‰) at 350, 400 and 450°C, respectively. This compositional shift is roughly proportional to the volume of vapour extracted between sample pairs in order to decrease total pressure (6-35% of the total bulk fluid removed as vapour), indicating that $^{65}Cu/^{63}Cu$ fractionation may be described by a Rayleigh distillation process.

These results suggest that in a closed, boiling hydrothermal ore-forming environment, Cu isotopes exhibit conservative fractionation, and coexisting V and L will preserve the isotopic signature of the fluid source. However, in a structurally open system in which periodic vapour removal occurs, the movement of the escaped vapour outward from the magmatic source will result in cooling and condensation of liquid droplets with heavier $\delta^{65}Cu$ values. This process will give the evolving vapour a progressively lighter $\delta^{65}Cu$ than the residual fluid near the source, although individual liquid droplets will be only marginally heavier in composition than the vapour from which they condensed. It follows that V and L fluid inclusions trapped at shallower depths (e.g., epithermal vein systems), or primary Cu(I) minerals deposited from those fluids, will have lighter $\delta^{65}Cu$ values than their deeper magmatic counterparts and the ore fluid source.

Glacial-interglacial simulations of ε_{Nd}

JOHANNES REMPFER[1,2,*], THOMAS F. STOCKER[1,2], FORTUNAT JOOS[1,2], JEAN-CLAUDE DUTAY[3]

[1]Climate and Environmental Physics, University of Bern, 3012 Bern, Switzerland, rempfer@climate.unibe.ch (* presenting author), stocker@climate.unibe.ch, joos@climate.unibe.ch
[2]Oeschger Center for Climate Change Research, University of Bern, Bern, Switzerland
[3]Laboratoire des Sciences du Climat et de l'Environnement (LSCE), IPSL, CEA/UVSQ/CNRS, Orme des merisiers, 91191 Gif sur Yvette, France, jean-claude.dutay@lsce.ipsl.fr

The Atlantic Meridional Overturning Circulation (AMOC) is an important component of the climate system. Reconstructions of past changes in AMOC are possible via records of paleocirculation proxies that reflect the distribution of water masses or the rate of ocean circulation and that can be measured in sediment cores. However, their interpretation is not unequivocal in some cases.

Covariation of Nd isotopic composition (ε_{Nd}) with salinity and potential temperature, indicates the potential of ε_{Nd} as a complementary water mass tracer [1]. Variations of ε_{Nd} can be reconstructed from sediment cores and are interpreted as past water mass changes [2].

Numerical simulations may contribute to the quantitative interpretation of such reconstructions. However, to date only few simulations of past ε_{Nd} are available [3]. Systematic studies of its paleoceanographic potential were limited by computational costs. We have included Nd isotopes (^{143}Nd and ^{144}Nd) into a cost-efficient climate model of intermediate complexity [4] with which we run 125,000-year simulations of ε_{Nd}.

In this study we present results of the first glacial-interglacial simulations of ε_{Nd}. Simulated ε_{Nd} is in good qualitative agreement with the few available reconstructions from the Atlantic Ocean. Inferences on changes in the AMOC during the entire last glacial cycle are therefore possible. However, our results indicate that relationships between variations in ε_{Nd} and overturning strength in the North Atlantic, or in the deep South Atlantic, are not straightforward during the entire last glacial cycle.

Besides allowing to further constrain changes in pattern and strength of the AMOC during the last glacial cycle, our results therefore provide important new insight into the paleoceanographic potential of ε_{Nd}.

[1] Goldstein and Hemming (2003) *Treatise on Geochemistry, Elsevier, Oxford*, 453-489. [2] Piotrowski *et al.* (2008) *Earth and Planetary Science Letters* **272**, 394 – 405. [3] *Arsouze et al.* (2008) *Climate of the Past* **4**, 191-203. [4] Rempfer *et al.* (2011) *Geochimica et Cosmochimica Acta* **75**, 5927-5950.

https://doi.org/10.1180/S0026461X00008434 Published online by Cambridge University Press

Reactivity of chemically synthesized *versus* biomineralized Fe^{II}-Fe^{III} green rusts with both organic and inorganic pollutants

REMY PAUL-PHILIPPE, HAZOTTE ALICE, SERGENT ANNE-SOPHIE, HANNA KHALIL, JORAND FREDERIC *

*LCPME UMR 7564 CNRS-University of Lorraine, Jean Barriol Institute, 405 rue de Vandoeuvre, 54600 Villers-lès-Nancy, France (*correspondence: frederic.jorand@univ-lorraine.fr)

Green rusts (GR) are mixed ferrous–ferric hydroxides that have layered structures consisting of alternating positively charged hydroxide layers and hydrated anion layers. These compounds can be obtained by chemical co-precipitation of Fe^{II} and Fe^{III} species or from bioreduction of ferric oxides by iron reducing bacteria. Due to the spatial configuration of structural Fe^{II}, green rusts show high reactivity against both organic and inorganic pollutants. While numerous works were mainly focused on the reactivity of a chemically synthesized GR, no report has appeared on the reactivity of biogenic GR with environmental pollutants. In the case of biogenic GR, the presence of exo-polymeric substances, bacterial cells, etc. could contribute to enhance GR stability. This work is devoted to compare the reactivity of chemically synthesized and biogenic GRs towards two pollutants: Methyl Red (MR) and cationic mercury, Reductive transformation of MR was monitored by spectrophotometric method and cationic mercury by ICP-AES. Results show that both abiotic and biotic carbonated GR can reduce Hg^{II} and MR. The effect of stabilizing agents such as phosphate and silicate on the GR reactivity was also tested.

Studies of surface ocean nitrate utilization in the Subarctic North Pacific using multiple nitrogen isotope recorders in the surface sediment

H. Ren[1*], R. F. Anderson[1], A. S. Studer[2], S. Serno[1], D. M. Sigman[3], G. Winckler[1], R. Gersonde[4] and G. H. Haug[2]

[1]Lamont-Doherty Earth Observatory, Columbia University, Palisades, NY, USA, hren@ldeo.columbia.edu (* presenting author)
[2]Geological Institute, ETH Zurich, Zurich, Switzerland
[3]Department of Geosciences, Princeton University, Princeton, NJ, USA
[4]Alfred Wegener Institute for Polar and Marine Research, Bremerhaven, Germany

In this study, we map and compare spatial patterns of three nitrogen isotope recorders: bulk sedimentary $\delta^{15}N$, diatom frustule-bound $\delta^{15}N$ (DB-$\delta^{15}N$), as well as planktonic foraminifera test-bound $\delta^{15}N$ (FB-$\delta^{15}N$) from 37 multicore core-top sediments across the open Subarctic North Pacific (SNP) and the Bering Sea between 60°N and 35°N, which were obtained during the INOPEX cruise in 2009. Both the bulk sedimentary $\delta^{15}N$ and the DB-$\delta^{15}N$ vary between 4 and 8‰, with increasing values towards the more nitrate-deplete lower latitudes, generally consistent with changes in the surface ocean nitrate consumption in the SNP. Bulk sedimentary $\delta^{15}N$ is more variable, which could be due to sedimentary processes altering or contaminating the isotopic signal. Consistent with previous studies [1], the $\delta^{15}N$ of both recorders are 2~4‰ higher than the expected $\delta^{15}N$ of the sinking flux, calculated using the World Ocean Atlas 09 summer surface ocean nitrate concentration in a Rayleigh model, assuming the same nitrate source (with the mean deep ocean nitrate concentration and $\delta^{15}N$), and the fractionation factor during nitrate assimilation as a function of the summer mixed layer depth [2]. The diatom-to-sinking flux offset is constant around 2‰ in the Bering Sea and the southwestern zonal transect, but is greater (around 4‰) in the northwestern and eastern regions. While basin-wide measurements of the $\delta^{15}N$ of the surface nitrate and the sinking flux will be needed to evaluate the offset, we suspect that the changes in the offset may be due to variations in the nitrate source $\delta^{15}N$: higher subsurface nitrate $\delta^{15}N$, originating from the eastern Pacific, has been observed in the northward coastal current off of British Columbia, and may penetrate westward as in the polar half of the North Pacific gyre, while lower nitrate $\delta^{15}N$ from N fixation in the North Pacific subtropical gyre may influence stations along the southern margin of the gyre. The lack of spatial patterns in the $\delta^{15}N$ differences between opal size fractions argues against large effects from variations in diatom assemblage; however, the assemblage effect will be directly analyzed once diatom species counts are completed. While we have limited FB-$\delta^{15}N$ data, the $\delta^{15}N$ of *N. pachyderma* (mostly sinistral) appears most similar to the DB-$\delta^{15}N$, within 1‰.

[1] Robinson et al. (2008) *Quaternary Sci. Rev.* **27**, 1076-1090. [2] DiFiore et al. (2010) *Geophys. Res. Lett.* **37**, L17601, doi:10.1029/2010GL044090.

https://doi.org/10.1180/S0026461X00008434 Published online by Cambridge University Press

Saturation state of $CaCO_3$ precipitation from seawater at raised alkalinity

PHIL RENFORTH[1*], GIDEON M. HENDERSON[1], TIM KRUGER[2], RICHARD C. DARTON[3]

[1]Department of Earth Sciences, South Parks Road, University of Oxford, Oxford, OX1 3AN, United Kingdom (* presenting author) Phil.Renforth@earth.ox.ac.uk,gideonh@earth.ox.ac.uk

[2]Oxford Geoengineering Programme, Oxford Martin School, University of Oxford, Oxford, OX1 3BD, United Kingdom Tim.Kruger@oxfordmartin.ox.ac.uk

[3]Department of Engineering Science, University of Oxford, Parks Road, Oxford, OX1 3PJ, United Kingdom, Richard.Darton@eng.ox.ac.uk

Spontaneous abiotic carbonate precipitation in the oceans is substantially inhibited by the presence of dissolved magnesium and sulphate [1] so that seawater is ≈supersaturated with respect to calcite and aragonite without precipitation occuring. Concern over ocean acidification has let to considerable efforts to understand the impact of lower seawater saturation on (particularly biogenic) carbonate precipitation. But there has been less effort to constrain the impact of increased saturation levels on carbonate precipitation since the early 1990s [e.g. 2]. This issue remains important, however. Recent ideas have suggested a role for changing ocean alkalinity (and therefore saturation state) as a mechanism to drive past glacial-interglacial atmosphereic CO_2 changes. And a range of geoengineering schemes rely on increased ocean alkalinity through carbonate, hydroxide or silicate mineral addition to the surface ocean to induce uptake of atmospheric CO_2 into seawater [3]. The efficiacy of these geoengineering approaches is dependent on a comprehensive understanding of abiotic carbonate precipitation.

Here we present results from laboratory experiments which are specifically designed to investigate the spontaneous precipitation of $CaCO_3$ as saturation state increases in seawater under controlled P_{CO2} and alkalinity. Solutions of seawater were continuously dosed with $Ca(OH)_2$ and $Mg(OH)_2$ over an extended period in a closed system in which the CO_2 concentration in the gas phase was continuously monitored. CO_2 was drawn into solution and pH was measured at discrete intervals. Through analysis of trace-metal incorporation into carbonate phases, we determine the saturation state and rate at which carbonate precipitation occurs, complimenting existing techniques that analyse changes in major element composition.

[1] Berner, R.A. (1975) The role of magnesium in the crystal growth of calcite and aragonite from sea water, *Geochimica et Cosmochimica Acta*, **39**, 4, 489-494
[2] Morse, J.W., Shiliang, H.(1993), Influences of T, S and P_{CO2} on the pseudo-homogeneous precipitation of $CaCO_3$ from seawater: implications for whiting formation, *Marine Chemistry*, 41, 4, 291-297
[3] Kheshgi, H.S. (1995) Sequestering atmospheric carbon dioxide by increasing ocean alkalinity, *Energy*, 20, 9, 915-922,

Mesoarchean TTG melt formation and migration in the Skjoldungen region of South-East Greenland

BARRY L. RENO*[1,2], TOMAS NÆRAA[1] AND LEON BAGAS[3]

[1] Geological Survey of Denmark and Greenland, Copenhagen, Denmark, blr@geus.dk (*presenting author)

[2] Institute for Geography and Geology, University of Copenhagen, Denmark

[3] Centre for Exploration Targeting, University of Western Australia Perth, Australia

The Skjoldungen region of South-East Greenland exposes a well-preserved section of Mesoarchean mid- to lower-continental crust that provides a unique window into crustal evolution and differentiation processes during the Archean. The central portion of the region comprises a sequence of mafic granulite rocks exhibiting clear textural evidence for having been subjected to in-situ partial melting, and subsequent generation of TTG melt. These rocks exhibit an aerially extensive network of former melt-bearing veins that preserve evidence of TTG melt generation in the lower crust and transport from mm-scale leucosomes within the mafic granulite to m-scale dikes that are structurally discordant to the mafic granulites and appear to be feeding larger-scale mid-crustal TTG bodies.

The Px–Pl-bearing mafic granulites have a LREE-enriched calc-alkaline basaltic protolith. Metamorphism and TTG-melt formation and migration occurred either during a crustal differentiation event at ca. 2.86 Ga or during collisional orogenesis at 2.8 – 2.7 Ga [1]. Leucocratic layers within the mafic granulite are characterized by cm-scale peritectic Opx, and form a large-scale network of former melt-bearing veins, in which smaller mm-scale foliation-parallel leucosomes are petrographically continuous with larger cm-scale structurally-discordant former melt-bearing channels which are texturally consistent with having fed large TTG sheets. The cm–m scale TTG layers exhibit enrichment in the most incompatible elements, HREE depletion, and are characterized by strong Pb enrichment, a subchondritic Nb/Ta ratio and higher Mg-number (~50). Trace element systematics are broadly consistent with these TTGs falling in the medium-(to high-) pressure sodic TTG groups of Moyen [2], suggesting partial melting of the mafic granulites occurred at pressures around ~1.5 GPa. Some of the larger-scale TTG dikes in exposures of structurally higher crustal levels exhibit similar geochemical characteristics, suggesting that partial melting of Px-Pl mafic granulites is one source of TTGs in South-East Greenland.

[1] Kolb, J., Thrane, K., Bagas, L., (in press) *Gondwana Research*
[2] Moyen, J.F. (2011) *Lithos* **123**, 21-36.

https://doi.org/10.1180/S0026461X00008434 Published online by Cambridge University Press

The energetic and kinetics of uranyl reduction on pyrite, hematite, and magnetite surfaces: a powder microelectrode study

D. RENOCK[1]*, M. MUELLER[2], R.C. EWING[2], AND U. BECKER[2]

[1]Dept. of Earth Sciences, Dartmouth College, Hanover, NH., USA, Devon.J.Renock@Dartmouth.edu (* presenting author)

[2] Dept. of Earth and Environmental Sciences, University of Michigan, Ann Arbor, MI., USA, ubecker@umich.edu

There are many studies describing the influence of parameters such as pH, pCO_2, and complexing ligands on the sorption of aqueous uranyl ions on mineral surfaces. However, few of these studies describe the reduction reaction mechanisms and the factors that influence the rate of reduction, despite the fact that the oxidation state of uranium is the most important factor controlling the mobility of uranium. In this study, the energetics and kinetics of the U(VI) reduction half-reaction on pyrite, hematite, and magnetite were investigated by electrochemical methods using a powder microelectrode (PME) as the working electrode. Anodic and cathodic peaks corresponding to the 1 e^- reaction redox couple, U(VI)/U(V), were identified in cyclic voltammograms of pyrite, hematite, and magnetite at pH 4.5. A second oxidation peak, corresponding to the oxidation of U(IV), was identified and provides evidence for the formation of reduced uranium phases on the mineral surfaces. In addition, uranium-containing precipitates were identified on pyrite surfaces after polarization in a PME. High Tafel slopes (> 220 mV/dec on all minerals evaluated) suggest that uranyl reduction is mediated by insulating oxide layers that are present on the semiconducting mineral surfaces. The onset potential for uranyl reduction was determined for pyrite (>0.1 V *vs*. Ag/AgCl), and hematite and magnetite (between -0.02 and -0.1 V *vs*. Ag/AgCl). The onset potential values establish a baseline kinetic parameter that can be used to evaluate how solution conditions (*e.g.*, dissolved reductants, complexing ligands, and polarizing ions) affect the kinetics of uranyl reduction.

In addition, this is the first study that uses a PME, instead of a conventional mineral electrode, to evaluate redox processes on mineral surfaces. Stable and reproducible voltammograms obtained for pyrite, hematite, and magnetite were obtained with minimal electrode preparation. The results of this study demonstrate the feasibility of using PME's to evaluate redox energetics, kinetics, and mechanisms for other environmentally-relevant, mineral-analyte systems.

^{238}U-^{230}Th equilibrium in arc magmas: Implications for the time scales of fluid transfer in subduction zones.

Reubi O[1*], Sims KWW [2], Bourdon B[3]

[1] IGP, ETH Zurich, Switzerland (olivier.reubi@erdw.ethz.ch)

[2] University of Wyoming, USA; [3] LGL, Ecole Normale Supérieure de Lyon UCBL and CNRS, France

The transfer of fluids in subduction zone can be fingerprinted in the chemistry of erupted magmas. However, there remain uncertainties regarding the processes and location of material transport from the subducting plate to the mantle wedge. Constraints on the timing of transfer relative to mantle melting are essential to understand the processes at play and the volatile cycles. Large excesses in ^{238}U and ^{226}Ra measured in some arc magmas are taken as indicating short time scales (hundreds to thousands of years) and, therefore, direct causality between slab fluid fluxes and mantle melting. A large proportion of arc magmas are, however, in or close to ^{238}U-^{230}Th equilibrium. This is generally interpreted as resulting from "buffering" of the young slab-fluid U-series signal by an older sediment component in secular equilibrium (i.e. >400 kyr).

Samples from Volcan de Colima, Mexico demonstrate that magmas in ^{238}U-^{230}Th equilibrium can have significant ^{231}Pa and ^{226}Ra excesses. Chemical modelling indicates that, in this case, the U-Th contribution from the sediments is not sufficient to offset the ^{238}U excesses produced by slab fluids. Melting of a mantle source that returned to secular equilibrium after addition of the slab components (time interval >400 kyr) and production of ^{231}Pa and ^{226}Ra excesses during melting is the most likely scenario at Colima. Compilation of U-series data suggests that this scenario is common in arc settings, implying that the time span and consequently the causal relationship between slab-fluid addition and mantle melting are variable at regional and global scales.

https://doi.org/10.1180/S0026461X00008434 Published online by Cambridge University Press

Solubility of scorodite and 6-line ferrihydrite with sorbed arsenic in the presence of *Shewanella* sp. CN32 and *Shewanella* sp. ANA-3 in a chemically defined growth medium containing various phosphate concentrations

E. REVESZ[1*], D. PAKTUNC[2], AND D. FORTIN[3]

1. Dept. Earth Sciences, University of Ottawa, Ottawa, Canada ereve067@uottawa.ca (* presenting author)
2. CANMET Mining and Mineral Sciences Laboratories and Dept. Earth Sciences, University of Ottawa, Ottawa, Canada Dogan.Paktunc@NRCan-RNCan.gc.ca
3. Dept. Earth Sciences, University of Ottawa, Ottawa, Canada, dfortin@uottawa.ca

Scorodite ($FeAsO_4 \cdot 2H_2O$) is a common As-rich mineral found in mining environments. In addition to its low solubility, it is relatively stable under oxidizing conditions, but its stability in the presence of known iron- and arsenic-reducing bacteria is poorly understood, especially under environmentally relevant conditions such as mine tailings. We investigated the reduction of synthetic scorodite in the presence of *Shewanella* sp. CN32, an iron and arsenic reducer, and *Shewanella* sp. ANA-3, a well-known arsenic reducer in a chemically defined medium containing various phosphate concentrations (15μM to 400 μM). The average initial rates of reaction found for arsenic reduction are 10.1 fmol/(cell·day) for ANA-3 and 5.4 fmol/(cell·day) for CN32 indicating that ANA-3 is a more efficient arsenate reducer than CN32. The concentration of dissolved Fe(II) is significantly lower than the concentration of dissolved As(III), and these concentrations are inversely related to the phosphate concentration. The solid phase post-reduction by-products were characterized by XRD, SEM, HRTEM and XAFS. Results so far for bacterial reduction of scorodite indicate that the residue is largely amorphous with domains that are rich in either iron or arsenic.

Preliminary results of reductive, bacterial assisted dissolution of 6-line ferrihydrite containing sorbed As in a chemically defined growth medium will also be discussed.

Sr-Nd-Pb isotope composition of Greenland river sediment constrains provenance of silt on the Eirik Drift

ALBERTO REYES[1*], ANDERS CARLSON[1], BRIAN BEARD[1], DAVID ULLMAN[1], ROBERT HATFIELD[2], AND JOSEPH STONER[2]

[1]University of Wisconsin-Madison, Geoscience, avreyes2@wisc.edu (* presenting author), acarlson@geology.wisc.edu, beardb@geology.wisc.edu, ullman@geology.wisc.edu

[2]Oregon State University, Earth Ocean and Atmospheric Sciences, rhatfield@coas.oregonstate.edu, jstoner@coas.oregonstate.edu

The Sr-Nd-Pb isotope composition of silt in the Eirik Drift off south Greenland can be used as a proxy for the presence/absence of ice on southern Greenland bedrock terranes. This approach requires characterization of different bedrock sources that can be compared with marine sediment core records. We present an updated dataset of Sr-Nd-Pb isotope composition for over 50 silt samples from rivers draining large subglacial basins under the Greenland Ice Sheet.

Distinct differences in the age and crustal evolution of major southern Greenland bedrock terranes are largely mirrored in the isotope composition of sediment in meltwater streams draining the ice sheet. Silt from rivers draining the Archean Block, the oldest south Greenland terrane, have the lowest $^{207}Pb/^{206}Pb$ and ε_{Nd}, and the highest $^{87}Sr/^{86}Sr$; in contrast, the young Paleogene volcanics of southeast Greenland and Iceland yield silt with the highest ε_{Nd} and lowest $^{87}Sr/^{86}Sr$. Silt from the Proterozoic Ketilidian Mobile Belt, in southernmost Greenland, is distinguished by very high $^{206}Pb/^{204}Pb$. Rivers draining the Nagsuggtoqidian Mobile Belt, comprising largely Archean rocks affected by Proterozoic metamorphism, have silt loads with relatively low ε_{Nd} and low $^{87}Sr/^{86}Sr$.

Suspended sediment discharged from the southern Greenland Ice Sheet during deglacial and interglacial intervals is transported via the Western Boundary Undercurrent to the Eirik Drift, where several long (>400 ka), well-dated marine sediment cores have been collected. The stream sediment isotope data presented here are used as end-members in a four-component mixing model, which allows us to determine the fractional contribution of silt from south Greenland bedrock terranes in the marine sedimentary record and, ultimately, to estimate the extent of the southern Greenland Ice Sheet during Pleistocene interglaciations.

https://doi.org/10.1180/S0026461X00008434 Published online by Cambridge University Press

Transformation of lead into pyromorphite by fungi

YOUNG JOON RHEE[1]*, STEPHEN HILLIER[2], AND GEOFFREY M. GADD[1]

[1]Division of Molecular Microbiology, College of Life Sciences, University of Dundee, Dundee DD1 5EH, Scotland, UK, y.j.rhee@dundee.ac.uk (*presenting author), g.m.gadd@dundee.ac.uk

[2]The James Hutton Institute, Craigiebuckler, Aberdeen AB15 8QH, Scotland, UK, Stephen.Hillier@hutton.ac.uk

Introduction

Lead is a serious environmental pollutant in all its chemical forms. Attempts have been made to immobilize lead in soil as the mineral pyromorphite using phosphate amendments (e.g., rock phosphate, phosphoric acid and apatite [1-2]). Lead metal, an important structural and industrial material, is subject to weathering, and soil contamination also occurs through hunting and shooting. Although fungi are increasingly appreciated as geologic agents [3-5], there is a distinct lack of knowledge about their involvement in lead geochemistry. We examined the influence of fungal activity on lead metal and discovered that metallic lead can be transformed into chloropyromorphite, the most stable lead mineral that exists. This is of geochemical significance, not only regarding lead fate and cycling in the environment but also in relation to the phosphate cycle and linked with microbial transformation of inorganic and organic phosphorus. In this contribution, we provide the first report of mycogenic chloropyromorphite formation from metallic lead and highlight the significance of this phenomenon as a biotic component of lead biogeochemistry, with additional consequences for survival in lead-contaminated environments and bioremedial treatments for lead-contaminated land.

Conclusion

The results from present study clearly demonstrate a previously unknown biogenic step in the biocorrosion of lead metal and transformation into pyromorphite through fungal action. This discovery represents an addition to our understanding of the biogeochemical cycling of lead, as well as phosphorus, and the importance of fungi as agents of geochemical changes (Rhee, Y.J., Hillier, S., and Gadd, G. M. (2012). Lead transformation to pyromorphite by fungi. Current Biology, doi:10.1016/ j.cub.2011.12.017).

[1] Ma *et al*., (1993). Environ. Sci. Technol. **27**, 1803–1810.
[2] Basta *et al*., (2004). Environ. Pollut. **127**, 73–82
[3] Gadd (2007). Mycol. Res. **111**, 3–49.
[4] Gadd (2010). Microbiology **156**, 609-643.
[5] Gadd et al., (2011). Environ. Microbiol. Report. DOI: 10.1111/j.1758-2229.2011.00283.x

Chemical zoning in calc-silicate rocks: stratigraphic control versus metasomatism (Northern Portugal)

MARIA AREIAS[1], MARIA A. RIBEIRO[1*], ARMANDA DÓRIA13

[1]Centro Geologia Universidade Porto, DGAOT-FCUP, R. Campo Alegre, 4169-007 Porto, Portugal (* presenting author: maribeir@fc.up.pt

Introduction

In a sheared gneiss-migmatite massif, in the border of a sin-tectonic variscan granite (coastal area of NW Portugal), metatexites and diatexites occur associated with metapelitic and calc-silicate rocks. Calc-silicate resisters (decimetric to metric bodies) are abundant mostly in the metatexitic zones, with ovoid or ellipsoidal geometry resulting from stretching and boudinage, associated with the shear foliation. The calc-silicate bodies are sub-parallel to the migmatitic foliation, striking N20° to N160°, with sheet folds [1].

Results and conclusion

The calc-silicate nodules present an internal structure with three zones: (i) core zone (CZ) with Wo+Cpx+Cal+An+ Qtz+Sph+/-Ep+/-Clzo; (ii) intermediate zone (IZ) where amphibole occurs and clinopyroxene disappears, and (iii) an external zone (EZ) with Bt+Qtz+Plg_{An50}+/ ilm. Taking into account field, petrographic and geochemical data, the IZ may be the result of mass transfer processes between different protoliths, coeval with de metamorphism, migmatization and deformation: the CZ represents a metagreywacke, with some carbonate concretions; the EZ a metapsamite and the IZ represents the metasomatic edges of the CZ. The chemical composition of the three zones is consistent to this explanation. In relation to the CZ, the IZ is richer in Na, K, Fe, Mg, P, LILE, Sc, Nb and Ta. In relation to the IZ, the EZ is enriched in Na and LILE and has less concentration at HSFE and transition metals. With support in these data it is considered that the IZ has input from the EZ (Mg, Fe, Na, K, P, LILE, Sc, Nb and Ta) and from CZ (HSFE). The geometry, internal structure, petrographic and geochemical composition of the calc–silicate boudins points to a model of diffusional metasomatism promoted by chemical potential between the CZ and the EZ - boundary metasomatism [2].

This work has been supported by POCI 2010 (FCT-Portugal, COMPETE/FEDER).

[1] Ribeiro *et al.* (2011) *Mineralogical Magazine* **75 (3)**, 1717.
[2] Zharikov *et al.* (2007) *IUGC-SCMR* **9** Metasomatism and metasomatic rocks (Cambridge Univ.Press).

https://doi.org/10.1180/S0026461X00008434 Published online by Cambridge University Press

Mixture of phases "phlogopite-talc" in the emerald deposit of Santa Terezinha de Goiás, Brazil.

ANA MARIA RIBEIRO-ALTHOFF*

Laboratório de Geologia Isotópica, Universidade Federal do Rio Grande do Sul, Porto Alegre, Brazil
ana.althoff@yahoo.com.br

Introduction – General Geology

The emerald deposits in Brazil represent a particular type of mineralization hosted mainly Proterozoic volcano-sedimentary sequences. The K-Ar and Ar/Ar geochronology of emerald mineralization from Santa Teresinha of Goias resulted in very disturbed spectra with significant variations in age values. This work deals with the different factors that may have caused the observed perturbations.

The emerald deposit of Santa Teresinha is the result of two processes (Giuliani et al., 1990): the first is the regional metamorphism responsible for the formation of carbonated talc-schists; the second is the infiltration of hydrothermal fluids that originated the phlogopite-schists hosting the emeralds (650-600 Ma, Brasiliano Orogeny).

Characterization of the phlogopite-talc mixture

The petrographic and X-ray diffraction examination of samples of phlogopite-talc-schists showed a great heterogeneity in the distribution of the association phlogopite + talc (+ chlorite). This heterogeneity was also observed in $^{40}Ar/^{39}Ar$ analysis: the age spectra of the three grains of phlogopite presented very different results.

Two single grains Sta11g provided upward-convex spectra with ages ranging from 530-635Ma (Sta11g-a) and 530-545Ma (Sta11g-b) while Sta11a provided a plateau age of 520 + 2Ma with 97% of ^{39}Ar released.

Excess argon in the talc

The presence of talc could explain the observed perturbations in the age spectra. As theoretically potassium is not part of talc composition, it is believed that the residual ^{40}Ar found in talc is a consequence of diffusion from neighboring minerals during a Proterozoic thermal event.

^{40}Ar degasing in talc was studied in a quadrupole spectrometer by continuous heating and temperature steps: maximum degasing occurs close to 1000°C (with H_2O and CO_2).

To evaluate the effects of the mixing on the K-Ar age, a mixing-model from degasing curves with the integrated K-Ar age was established. In this way it was possible to determine the age range based on the mixture (Ribeiro-Althoff, 1997).

Conclusion

The irregular shape of the age spectra obtained for the phlogopite could be explained by the mixing of varying proportions of two ^{40}Ar components: a radiogenic component (phlogopite) and an inherited component (talc), with different degasing curves. The apparent-age difference between the single grains indicates that the excess Ar varies from one grain to another.

[1] Giuliani et al. (1990) *Miner. Depos.*, **25**, 57-64.
[2] Ribeiro-Althoff (1997) *Thesis INPL/CNRS*, 214 pp.

The origin of mineralising brines in unconformity-related U deposits: Insights from noble gases and halogens in fluid inclusions

ANTONIN RICHARD[1*], MARK A. KENDRICK[2] AND MICHEL CATHELINEAU[1]

[1]G2R, Université de Lorraine, Vandoeuvre-lès-Nancy, France
antonin.richard@univ-lorraine.fr (* presenting author)
michel.cathelineau@univ-lorraine.fr

[2]The School of Earth Sciences, The University of Melbourne, Aus.
mark.kendrick@unimelb.edu.au

In the Proterozoic Athabasca Basin (Canada) unconformity-related UO_2-ores are associated with U-rich fluid inclusions (FIs) that are either NaCl-rich or $CaCl_2$-rich, and are hosted by quartz and dolomite [1, 2]. In order to constrain the origin of these brines we analysed the naturally occurring isotopes of Ar, Kr and Xe, together with halogens (Cl, Br and I), K, Ca and U in samples containing representative FIs. This was achieved by in vacuo crushing of irradiated samples using extended ^{40}Ar-^{39}Ar methodology [3].

The FIs have molar Br/Cl ratios from 7×10^{-3} to 13×10^{-3}, and I/Cl ratios from 2×10^{-6} to 12×10^{-6}. These compositions are consistent with the fluids deriving the bulk of their salinity by sub-aerial evaporation of seawater, beyond the point of halite saturation. The low I/Cl ratios do not favour fluid interaction with organic matter, or hydrocarbons, as a reductant for localizing U mineralisation.

One sample collected adjacent to high-grade U ore (~40 wt % U) has a less than atmospheric $^{40}Ar/^{36}Ar$ ratio of 180-220. This is ascribed to nucleogenic production of ^{36}Ar from ^{35}Cl in the FIs, due to an exceptionally high neutron fluence in the immediate (<1m) vicinity of the high-grade ores.

The majority of samples contain FIs with age-corrected $^{40}Ar/^{36}Ar$ of between the modern atmospheric value of ~300 and 450. These values are considered representative of the fluids initial composition and are typical of upper crustal sedimentary formation waters. The $^{40}Ar/^{36}Ar$ ratio is correlated with $Cl/^{36}Ar$ in several of the samples and defines $^{40}Ar_E/Cl$ values of between 6×10^{-5} and 10^{-7}. Combined with the salinities (25-35 wt.% salts), the $^{40}Ar_E/Cl$ values, indicate fluid $^{40}Ar_E$ concentrations of 7×10^{-10} to 200×10^{-10} mol.g^{-1} ($^{40}Ar_E$ denotes crustally-derived excess ^{40}Ar).

The FIs non-radiogenic $^{84}Kr/^{36}Ar$ and $^{129}Xe/^{36}Ar$ ratios are intermediate of air and air-saturated brines. The fluids have elevated ^{36}Ar concentrations of up to twenty times air-saturated seawater. The data are interpreted to reflect preferential acquisition of $^{36}Ar>^{84}Kr>^{129}Xe$ from sedimentary rocks. The lack of a strong enrichment in radiogenic ^{40}Ar and preservation of low $^{40}Ar/^{36}Ar$ ratios, suggests interaction of the brines with basement rocks occurred at high water-rock ratios or low temperatures (<200 ºC).

[1] Richard (2010) *Terra Nova* **22**, 303-308.
[2] Richard (2011) *Geochim. Cosmochim Ac.* **75**, 2792-2810.
[3] Kendrick (2012) *Chem. Geol*. **292-293**, 116-126.

https://doi.org/10.1180/S0026461X00008434 Published online by Cambridge University Press

THEREDA – A thermodynamic database for increasing confidence in waste disposal

ANKE RICHTER[1*], FRANK BOK[1], AND VINZENZ BRENDLER[1]

[1]Helmholtz-Zentrum Dresden-Rossendorf e.V., Institute of Resource Ecology, Dresden, Germany, Anke.Richter@hzdr.de (* presenting author)

Motivation and Implementation

For geochemical modeling of scenarios for the disposal of radioactive and (chemo)toxic waste, comprehensive and internally consistent thermodynamic data are required as well as sorption data for the surrounding host rocks. The use of different databases renders it difficult to compare results of geochemical modeling, due to incompleteness, inconsistencies, resticted ranges of variation (temperature, density, pressure), limitations in solution composition (ionic strength) and last but not least missing sorption data.

Features of the Thermodynamic Database THEREDA

THEREDA (THErmodynamic REference DAtabase, www.thereda.de) – a cooperative project of leading research institutes in Germany – adresses these issues, providing full documentation, transparency of all data and a detailed quality assurance scheme [1,2]. THEREDA contains data for the three ion-ion interaction models extendend Debye-Hückel, Specific Ion Interaction Theory, and Pitzer model. At present, two datasets has been released: the oceanic salt system (Na^+, K^+, Mg^{2+}, Ca^{2+}, Cl^-, SO_4^{2-}, H^+, and H_2O(l) within a temperature range of 273.15–523.15 K) and Am/Nd/Cm (Am(III), Nd(III), Cm(III), Na^+, Mg^{2+}, Ca^{2+}, Cl^-, H^+, H_2O(l) at 273.15 K). Tailored parameter files for various geochemical modeling codes are provided (PhreeqC, ChemApp, EQ3/6, Geochemist's Workbench). Documented benchmark calculations allow comparisons with other databases as well as between the different geochemical codes. All data, documentation and references are freely accessible via the projects homepage. Additionally, a user forum allows direct contact with the THEREDA members.

Integration of Sorption Data of RES³T

A holistic view of geochemical processes in the context of a safety analysis requires the inclusion of sorption calculations. A thermodynamically consistent treatment of these processes is only possible with surface complexation modeling (SCM). Respective data are already compiled in the RES³T database [3] (www.hzdr.de/res3t), providing competing entries for many systems. An integration into THEREDA thus not only requires a synchronization of data structures but also a rigorous review process, leading to uniform recommended data sets for each sorbent-sorptive system. This data review process is already in progress.

[1] Altmaier *et al.* (2011) *Report GRS-265*, 63 p. [2] Altmaier *et al.* (2008) *ATW* **53**, 249-253. [3] Brendler *et al.* (2003) *J. Contam. Hydrol*. **61**, 281–291.

Applications of Synthetic Uranium Reference Materials for Geochemistry Research

STEPHAN RICHTER[1*], HEINZ KŰHN[1], ROGER EYKENS[1]AND YETUNDE AREGBE[1]

[1]Institute for Reference Materials and Measurements (IRMM), Geel, Belgium, stephan.richter@ec.europa.eu (* presenting author)

Introduction

For many applications in geochemistry research isotope ratio measurements play a significant role. For instance, in geochronology isotope abundances of uranium and its daughter products thorium and lead are being used to determine the age and history of various samples of geological interest. For measuring the isotopic compositions of these elements by mass spectrometry, suitable isotope reference materials are needed in order to validate measurement procedures and to calibrate Faraday cup multi-collector and ion counting detector systems. IRMM is a well recognized provider for nuclear isotope reference materials to the nuclear industry and nuclear safeguards authorities, which are also being applied widely for geochemical applications.

Synthetic Uranium Reference Materials and their Applications

The preparation of several new synthetic uranium reference materials at IRMM during the recent five years has provided significant impacts on geochemical research. These synthetic isotope reference materials are prepared based on proven methods of purifying and gravimetrically mixing oxides or solutions from isotopically highly enriched uranium materials.

Firstly, the double spike IRMM-3636 [1] with a $^{233}U/^{236}U$ ratio of about 1:1 was prepared which allows an internal mass fractionation correction for high precision $^{235}U/^{238}U$ ratio measurements. The ^{234}U abundance of this double spike material is low enough to allow an accurate and precise correction of $^{234}U/^{238}U$ ratios, even for measurements of close to equilibrium uranium samples. This double spike has been used successfully for characterizing uranium isotopic ratios in various materials of geochemical interest [2] as well as natural consensus standards [3], i.e. NBL CRM 112A [4], and was found very valuable for U-Pb and U-Th geochronology.

Secondly, the application of the IRMM-074/1-10 series of isotopic of isotope reference materials [5] for linearity investigations of secondary electron multiplier (SEM) detectors will be discussed and new procedures introduced. This is of high relevance for U-Pb and U-Th geochronology by isotope mass spectrometric methods.

A general and historical overview about the preparation and certification of uranium isotope reference materials at IRMM will be given, including plans for future certification projects.

[1] Richter (2008), Int. Journal of Mass Spectrometry, **269**, 145–148

[2] Brennecka (2010), Earth and Plan. Science Letters, **291**, 228–233

[3] Condon (2010), Geoch. et Cosmoch. Acta, **74**, 7127–7143

[4] Richter (2010), Int. Journal of Mass Spectrometry, **295**, 94–97

[5] Richter (2009), Int. Journal of Mass Spectrometry, **281**, 115-125.

https://doi.org/10.1180/S0026461X00008434 Published online by Cambridge University Press

Tight coupling of life and metals throughout evolution

ROSALIND E. M. RICKABY*, TRISTAN J. HORNER, RENEE B. Y. LEE, GIDEON M. HENDERSON AND R. J. P. WILLIAMS

University of Oxford, South Parks Road, Oxford, OX1 3AN, UK, rosr@earth.ox.ac.uk (* presenting author)

The chemistry of the environment is intimately tied to the chemistry of life in a feedback system. The original reductive chemistry of life inexorably drove oxidation of Earth's surface. The contrast in solubility products between hydroxides and sulfides lead to a predictable sequence of altered environmental concentrations of metals. Some metals increased in availability: notably the latecomers, Cu and Zn, but others decreased e.g. Fe. Such changes are charted in the chemistry of ancient sediments.

Signals of the changing metal environment can also be found in the genomes of extant life. A rise in the number of Cu and Zn metal domains in proteins, fundamental to the advancement of life towards complexity and multicellularity, parallels the increasing Cu and Zn in the environment. This implies that the initial rise of oxidative products, and newly available metals, at first toxic to life, could be turned to advantage by leading to the emergence *de novo* of catalysts allowing increased complexity to evolve [1].

By contrast, a decrease in environmental availability of metals already exploited by enzymes, can drive substitution by new metals to perform old functions, at least in labile enzymes. An example is the change in metallocentre found in "cytochrome-c oxidase". The original protein was likely based on Fe only but later it became the copper-dependent, O_2-reducing enzyme cytochrome oxidase, seen today.

The recent identification of an unusual Cd/Zn carbonic anhydrase from the marine diatom *Thalassiosira weissflogii* [2] has revealed a biochemical function for Cd, substituting for Zn. This discovery holds the potential to explain the long-standing mystery as to why Cd, regarded as toxic to life, displays a nutrient-like profile in the modern ocean and isotopic ($^{114}Cd/^{110}Cd$) compositions which indicate removal into phytoplankton. We investigate whether this single known biological role for Cd can account for its apparent nutrient like behaviour by analysing the isotopic fractionation of Cd in the model bacteria, *Escherichia coli,* which have been transformed to express the CDCA1 gene. Our results demonstrate that whole cells accumulate and fractionate Cd regardless of CDCA1 expression. Our analysis of different cellular components suggest that, rather than direct use of Cd, it is detoxification in response to inadvertent Cd acquisition which is responsible for the fractionation of Cd isotopes. Such detoxification mechanisms are highly conserved across the diversity of life, and we conclude that detoxification acts as the driving force of the observed seawater Cd concentration and isotopic variations. In order to explain the negligible response of Cd uptake to expression of CDCA1, we shall explore if this unusual enzyme is a labile form of the conventional, non-exchanging carbonic anhydrases.

[1] Williams and Rickaby, *Evolution's Destiny,* in press, [2] Xu, *et al.,* (2008) *Nature* **452,** 56-61.

Interrogating >1Myr Time-Scale Controls On Ocean Chemistry In A 3D Model?!

ANDY RIDGWELL[1]*

[1]University of Bristol, Bristol, UK, andy@seao2.org (* presenting author)

Marine archives of paleo environments, particularly when encoded in deep-sea sediments, can be highly spatially hetrogeneous. Whilst box models have had success in interpreting environmental hetrogeniety on a basin-scale, fully 3D ocean-based models are required to resolve the geological record at any finer spatial resolution than this. However, the extreme scale contrast between the typical time-step required by dynamical ocean models – order days (or considerably shorter), and the 100 kyr time-scale of weathering feedback to >1 Myr residence time of many trace metal and isotope systems of interest, presents a seemingly insurountable barrier (unless one is prepared to wait the best part of a year for a model experiment to finish).

I will present a new methodology applied to a 3D Earth system model ('cGENIE') that involves alternating its behavior between fully 3D climate+carbon cycle and mass balance 'box' model modes. In so doing, solving the silicate weathering feedback can, for example, be accelerated by a factor of 10-100 compared to a fully dynamical calculation but with a virtually identical end result. To avoid boring you stupid with a discourse of pure technical model details, I will illustrate how the δ^7Li compostion of the ocean responds to massive CO_2 release and warming and how the encoding of this emerging weathering proxy in marine carbonates relates to more established proxies (e.g. wt% $CaCO_3$, $\delta^{13}C$) for tracking changes in global carbon cycling.

https://doi.org/10.1180/S0026461X00008434 Published online by Cambridge University Press

Ion adsorption on nanocrystalline anatase surfaces: Integrating experimental and theoretical studies through surface complexation modeling

MOIRA K. RIDLEY[1]*, JAMES D. KUBICKI[2], AND MICHAEL L. MACHESKY[3]

[1]Texas Tech University, Dept. of Geosciences, Lubbock, TX, USA, moira.ridley@ttu.edu (* presenting author)
[2]The Pennsylvania State University, University Park, PA, USA jdk7@psu.edu
[3]University of Illinois, Illinois State Water Survey, Champaign, IL, USA, machesky@illinois.edu

Detailed experimental studies have been undertaken to quantitatively examine particle-size effects on proton-induced surface charge and accompanying ion adsorption phenomena on a suite of nanocrystalline anatase (TiO_2) phases. Commercially available, crystalline, monodispersed anatase particles ranging in diameter from 3 to 40 nm were used in the study. Extensive characterization of these particles revealed that the [101] face predominates. Bulk surface titrations were completed in LiCl, NaCl, KCl, RbCl and $NaCF_3SO_3$ (NaTr) electrolyte solutions, over a wide range of ionic strengths (0.0005 to 0.3 *m*). Additionally, the specific adsorption of divalent ions (e.g., Sr^{2+}) has been investigated as a function of pH and loading in NaCl media.

Molecular simulation, DFT-MD, calculations were completed to complement the surface adsorption studies. Specifically, bonding geometries on the anatase [101] surface were predicted for the adsorption of cations and anions used in the experimental studies. The DFT-MD simulations show inner-sphere binding for all cations, with bidentate geometries predominating. Conversely, monovalent anions form outer-sphere complexes.

To integrate the experimental results with molecular-level insights gained from the simulation studies, surface complexation modelling (SCM) was performed. The CD-MUSIC model, coupled with a Basic Stern layer description of the electric double layer, was used to successfully provide a surface structural description of the ion adsorption data. All fitting parameters within the SCMs were constrained by the DFT simulation results. The resulting SCMs rationalize successfully the subtle differences observed in the surface reactivity of the anatase particles as a function of particle size. For example, the small decrease in pH_{znpc} values with increasing particle diameter are accounted for by slight differences in protonation constants, K_H. Similarly, binding constants for adsorbed ions and capacitance values for the EDL vary with particle size.

Anaerobic oxidation of methane coupled to iron reduction in deep marine sediments

N. RIEDINGER[1*], M.J. FORMOLO[2], T.W. LYONS[1], S. HENKEL[3], A. VOßMEYER[4], B.K. REESE[5], H.J. MILLS[6], AND S. KASTEN[7]

[1]Dept. of Earth Sciences, Univ. of California, Riverside, CA 92521 USA (*correspond.: natascha.riedinger@ucr.edu)
[2]Dept. of Geosciences, The Univ. of Tulsa, OK 74104 USA
[3]Instit. Geology and Mineralogy, Univ. of Cologne, 50674 Cologne, Germany
[4]Center for Geomicrobiology, Aarhus Univ., 8000 Aarhus C, Denmark
[5]Dept. Biological Sciences, Univ. of Southern California, Los Angeles, CA 90089, USA
[6]Dept. of Oceanography, Texas A&M Univ., College Station TX 77843 USA
[7]Alfred Wegener Instit. for Polar and Marine Research, 27570 Bremerhaven, Germany

Anaerobic oxidation of methane (AOM) is an important process in the global methane cycle and contributes to the regulation of methane release to the atmosphere. In sulfate depleted environments, methane can be oxidized anaerobically via microbial consortia tied to other electron acceptors.

Emphasizing the inorganic geochemistry, we explored the process of iron reduction coupled to AOM (Fe-AOM) in marine sediment samples from the Argentine Basin taken during RV Meteor expedition M78/3 (May – July 2009). The essential geochemical requirement for Fe-AOM is the juxtaposition of elevated methane concentrations and abundant reactive Fe(III) in anoxic sediments lacking reactive organic matter. These conditions are met in the Argentine Basin, where dynamic depositional conditions lead to the rapid burial of highly reactive metal phases. Additionally, reworked organic matter is delivered to deeper marine sediments resulting in the dilution by, and subsequent burial of, refractory organic carbon.

Our results show elevated dissolved iron concentrations in the pore water below the sulfidic zone accompanied by high amounts of highly reactive Fe (III) phases. This evidence indicates active iron reduction. In the same sediment, methane concentrations are high, while sulfate and sulfide are depleted. Low TOC contents (<0.8 wt%) throughout the sediment column and sulfate reduction rates close to or at the detection limit argue against the availability of highly reactive organic matter. This suggests that the refractory organic pool does not provide a sufficient energy source for dissimilatory iron reducing microorganisms in these deeper sediments. Thus, we propose that contributions from organo-clastic Fe reduction in these methane-rich sediments are minor. Instead, the concomitant occurrence of abundant methane and reactive ferric iron in the absence of sulfide argues for reduction of biologically available Fe(III) coupled to anaerobic oxidation of methane. The presence and release of dissolved iron and associated alteration of iron minerals in deep sulfate-depleted sediments has been observed in various marine environments, suggesting that Fe-AOM is important in the modern ocean, and, perhaps particularly so, in the sulfate-poor but highly methanic ancient ocean.

https://doi.org/10.1180/S0026461X00008434 Published online by Cambridge University Press

Tracing particulate scavenging fluxes using ^{210}Po and ^{210}Pb during North Atlantic GEOTRACES

S. RIGAUD[1*], T. CHURCH[1], M. BASKARAN[2], G. STEWART[3], Y. CHOI[3], V. PUIGCORBE[4], AND P. MASQUE[4]

[1]School of Marine Science and Policy, University of Delaware, Newark, USA, rigaud@udel.edu(*presenting author), tchurch@udel.edu

[2]Department of Geology, Wayne State University, Detroit, USA, baskaran@wayne.edu

[3]Earth and Environmental Sciences, Queens College, City University of New York, Flushing, USA, Gillian.Stewart@qc.cuny.edu

[4]Institut de Ciencia I Tecnologia Ambientals, Universitat Autonoma de Barcelona, Barcelona, Spain, viena.puigcorbe@uab.cat, pere.masque@uab.cat

Session 13d. Geotraces, the international science program

Quantifying the flux of oceanic particles is central to understanding the coupling of carbon and nutrient cycles that control the functioning of the ocean ecosystems and ultimately the global climate. The natural ^{210}Po and ^{210}Pb nuclide pair affords a radiometric means to model scavenging particle fluxes in the ocean on seasonal to annual time periods.

Data on the dissolved (<0.2 μm), particulate (>0.2 μm, >53μm) and/or the total phases of ^{210}Po and ^{210}Pb has been gathered during two GEOTRACES cruises at the western (GA02, spring 2010) and eastern (GA03, fall 2010) basins of North Atlantic, that include entire (GA03) and upper (GA02) water profiles.

Excess of ^{210}Pb relative to its parent nuclide ^{226}Ra is observed in surface water indicating atmospheric inputs. These inputs are more significant in the subtropics, in association with Saharian dust deposition. In the sub-surface, ^{210}Pb activities decrease and generally attain either equilibrium or deficit with respect to ^{226}Ra, indicating ^{210}Pb removal by scavenging. The surface ^{210}Pb maximum generally corresponds to a minimum in ^{210}Po. Such surface ^{210}Po depletion reflects beside atmospheric input, large particle formation and export to deeper water, where ^{210}Po is regenerated in excess with respect to ^{210}Pb. The highest surface ^{210}Po depletion and deeper regeneration is encountered at the eastern boundary of North Atlantic. Evident here is the expression of enhanced surface production induced from nearby continental sources and upwelling off Africa, and benthic boundary processes.

Based on the ^{210}Po-^{210}Pb and ^{210}Pb-^{226}Ra disequilibria, the upper water profiles of ^{210}Po and ^{210}Pb will be modeled using a steady-state box model for the assessment of particle scavenging fluxes. These can then be compared to the shorter term rates using ^{234}Th nuclide from the same cruises over weeks to months. Thus scavenging rates of several important components such as particulate organic carbon can be assessed over different time scales. Based on the different biogeochemical properties of these nuclides, a distinction can be made between biogenic and lithogenic scavening associated with particle fluxes in both basins of North Atlantic. As important, these scavening rates can be compared to the legacy of modeling these nuclides over the past decades to assess transient changes in basin biodynamics.

Estimation of the mineral reactive surface area during CO_2 mineralization in natural hydrothermal fields.

JEAN RILLARD [1, 2]*, PIERPAOLO ZUDDAS [3]

[1]Earth Sciences Department of University of Lyon 1, Lyon, France, jean.rillard@etu.univ-lyon1.fr (* presenting author)

[2]National Institute for Industrial Environnement and RISk, Paris, France

[3]University Pierre and Marie Currie Paris-Sorbonne ISTEP, Paris, France, pierpaolo.zuddas@upmc.fr

19b Linking experimental and field observations of mineral carbonatation for in-situ long-term carbon storage

The quantitative description of fluid-rock reactivity in natural geothermal field is a useful tool in predicting become and fate of CO_2 artificially injected in natural geological reservoirs. The complex process of CO_2 mineralization involving a set of mineral dissolution and precipitation reactions is probably the best way to permanently storage CO_2. However the overall process strongly depends on the real amount of mineral able to react in the CO_2 mineralization process. In this work we report results of an original methodology able to estimate the Reactive Surface Area (RSA) of the minerals in the high CO_2 fluid geothermal system of Galicia (Spain). This field is characterized by fluids having pH ranging from 6 to 10 with corresponding pCO2 partial pressure varying from 10^5 to 1 Pa and CO_2 content linearly correlated to the variation of the major dissolved cations.

The methodology to estimate the variation of RSA during the CO_2 neutralization is based on an inverse model approach using the composition of springs and borehole fluids as input data. Assuming the continuum equilibrium condition, the irreversible mass transfer process has been described by the overall degree of reaction advancement using a set of polynomial equations solved independently of time scale. The apparent rate of mineral dissolution was estimated by the observed pH and equilibrium conditions. Calculations were carried out for albite, K-feldspar, biotite and calcite, assuming dissolved aluminum and silica activities controlled by quartz and kaolinite equilibriums.

We found that RSA of calcite, albite and K-feldspar increases by 2 orders of magnitude over the entire CO_2-fluid-rock interaction process, while RSA of biotite increases by 4 orders of magnitude. This shows that reactive surface area of minerals is not constant and changes by several orders of magnitude along the entire CO_2-water-rock process. Our work quantifying the evolution of this key kinetic parameter allows new constrains in modelling reactive transport of fluid-rock interaction processes and the safe mineralization of artificially injected CO_2 in natural reservoirs.

https://doi.org/10.1180/S0026461X00008434 Published online by Cambridge University Press

Bendego IC-Iron: HSE and Re-Os

DEBORA RIOS[1,2*], WILTON CARVALHO[2], RICHARD WALKER[3], DONALD DAVIS[1], AND ELIZABETH ZUCOLOTTO[4]

[1]Dept. Of Geology, University of Toronto, Toronto-ON, Canada, debora.rios@utoronto.ca (* presenting author)
[2]UFBA/FAPESB, Salvador-BA, Brazil, wilton@atarde.com.br
[3]University of Maryland, Maryland, USA.
[4]Museu Nacional/UFRJ, Rio de Janeiro-RJ, Brazil.

The Bendego Meteorite is a >5 ton iron found in Northeastern Brazil in 1784. Presently the main mass is hosted at the Brazilian National Museum, being the 16th largest specimen in the world. Bendego is a coarse octahedrite displaying kamacite bands (1.8 mm) of irregular Widmanstatten pattern and abundant Neumann lines. It belongs to the rare IC-group of (11) irons and contains abundant troilite, which occurs as macroscopic nodules as well as microscopic bands, both elongated and aligned. Macroscopic inclusions of cohenite exhibit internal nodules of troilite. Inclusions of plessite, schreibersite, rabdite, $[(Fe,Ni)_3P]$ polymorphs, and chromite were also recognized. It has 6.1-6.9% Ni, 0.40-0.51% Co, 600ppm Cr; 0.05% S; 54-56ppm Ga; 0.17-0.22ppm Ir; and smaller values of As (5.3-6.0ppm) and Au (0.69-0.80ppm), which are slightly different from values reported for other IC-group meteorites.

Re-Os and Highly Siderophile Element (HSE) analyses

This work reports the first Re/Os isotope results from the IC-group. Seven samples collected in different areas of Bendego were analysed at the University of Maryland. Iron meteorites are much richer in siderophiles (1284 < Re < 3249 ppt; 15 < Os < 48 ppb) than terrestrial crust and mantle rocks (Re ~390 ppt; Os ~50 ppt). Bendego has 99-114 ppb Os and 10-12 ppb Re. Ir, Ru, Pt and Pd concentrations were also measured. Normalized to the Orgueil meteorite (CI) these data result in a unique pattern (Figure) that differs from that of other magmatic iron meteorites and pallasites.

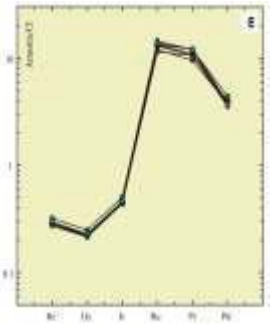

Figure: Bendego Meteorite HSE' multi-elementar diagram.

Concluding Remarks

IC-group meteorites are believed to have formed by magmatic processes similar to those of meteorites in groups IIAB, IIIAB and IVA, even they are thought to have formed on a separate parental body. Our data show: (i) negligible fractionation of highly siderophile elements over the volume of material sampled and (ii) a very distinct highly siderophile element pattern compared to the more voluminous iron groups. It is difficult to make any conclusions about crystal-liquid fractionation processes or the composition of the starting metal but the observed pattern clearly indicates a unique set of conditions compared to the other groups. The Re-Os isotopes of this sample are consistent with a primordial isochron, but given the essentially invariable Re/Os of all pieces analyzed, this cannot yet be confirmed. More samples from the same group will have to be analyzed for a better understanding of Bendego's HSE distribution and its relationship to a chondritic precursor.

The Nordic Seas in the Pliocene: A hot spot or not?

BJØRG RISEBROBAKKEN[1*], CARIN ANDERSSON[1,2], ERIN MCCLYMONT[3], AND LISBETH JENSEN[2]

[1]Bjerknes Centre for Climate Research, Bergen, Norway, bjorg.risebrobakken@uni.no (* presenting author), carin.andersson@uni.no
[2]Department of Earth Sciences, University of Bergen, Norway, lisbeth.jensen@student-uib
[3]Department of Geography, Durham University, England, erin.mcclymont@durham.ac.uk

Pliocene climatic and oceanographic conditions of the Nordic Seasneeds to be better constrained. Therefore, the Pliocenen section of ODP Site 642B (Eastern Nordic Seas, 1286 meter water depth) is studied with the aim to determine the role of the Nordic Seas as a gateway linking the North Atlantic and the Arctic Oceans. Site 642B is located underneath today's pathway of the Norwegian Atlantic Current, and will detect changes in polar heat transport within a current regime comparabla to the present. A multi-proxy approach is used to characterize surface, subsurface and bottom water conditions at the site throughout the Pliocene. The presented results is based on planktic and benthic oxygen and carbon isotopes, planktic foraminiferal counts and SST estimates, and alkenones.

The predominant conditions of the Nordic Seas changed at several occation through the Pliocene, e.g. with the surface water temperatures swiching between longer periods with 1-2°C warmer than present conditions to colder than present by 1°C. Occationally there is indications of strong fresh water influence at the surface, corresponding with reduced ocean-atmosphere gas exchange. However, strong ocean-atmosphere gas exchange or high productivity was the more normal Pliocene situation. Throughout the Pliocene large variability is seen within the mixed layer, however, independent of this variability colder and/or saltier than today's water is seen most of the time. The bottom water conditions at the site swiched between being comparable to and significantly saltier than at present. Reduced stratification between subsurface and bottom water characterize most of the Pliocene. The bottom water was less ventilated than presently through much of the Pliocene, however, conditions more similar to the present occurred towards the early to mid Piacenzian.

The oceanographic conditions of the Nordic Seas was distinctly different from the present day through much of the Pliocene. However, at no point through the Pliocene does our records show extreme polar amplification or strong deep convection and ventilation in the Nordic Seas.

https://doi.org/10.1180/S0026461X00008434 Published online by Cambridge University Press

Early mantle dynamics inferred from ^{142}Nd variations in Archean rocks from southwest Greenland

H. RIZO[1]*, M. BOYET[1], J. BLICHERT-TOFT[2], M. ROSING[3] AND J.-L. PAQUETTE[1]

[1] Université Blaise Pascal, 63038 Clermont-Ferrand, France (*H.Rizo@opgc.univ-bpclermont.fr)
[2]Ecole Normale Supérieure de Lyon, 69007 Lyon, France
[3]University of Copenhagen, Øster Voldgade 5-7, DK-1350 København K, Denmark

Because of the limited geological record, the composition and evolution of the silicate Earth during the Hadean/Eoarchean is widely debated and largely unknown. The short-lived ^{146}Sm-^{142}Nd chronometer applied to 3.7-3.8 Ga old rocks from Greenland has revealed excesses of ^{142}Nd (10-20 ppm) compared to modern samples and terrestrial Nd standards [1-7]. Since the parent isotope, ^{146}Sm, was extant only during the first few hundred million years of the Solar System, this implies that the Greenland samples were derived from a source formed in the Hadean. Combining ^{146,147}Sm-^{143,142}Nd systematics, we have estimated the differentiation age of the reservoir of Greenland rocks (amphibolites from the Isua region) to be between 4.53 and 4.42 Ga [1]. Here we present our ^{146}Sm-^{142}Nd data for a suite of mantle-derived samples with ages of 3.8, 3.7, 3.4 and 3.3 Ga, also collected in the Isua region. Covering over 500 million years of the early history of the Earth, they offer a unique opportunity to constrain the compositional evolution and dynamics of the early Earth mantle. The different groups of rocks were dated with the Sm-Nd and Lu-Hf isotope systems on whole-rocks, and by U-Pb analysis of rare zircons found in some of the samples. Preliminary results reveal ^{142}Nd anomalies in 3.4 Ga rocks, while the ^{142}Nd record of primordial heterogeneities in the Isua mantle source seems to have been completely erased after 3.3 Ga. Therefore, the chemical heterogeneities detected in the southwest Greenland mantle and inferred to have formed during the 4.53-4.42 Ga period appear to have resisted mixing by mantle convection until at least 3.4 Ga. These results add strong constraints on mantle dynamics during Earth's early history and the survival/mixing timescale of mantle heterogeneities.

Rizo et al., (2011) *Earth Planet. Sci. Lett.* **312**, 267-279. [2] Bennett et al., (2007b) *Lunar Planet. Sci.* **37**, 2139. [3] Boyet et al., (2003) *Earth Planet. Sci. Lett* **214**, 427-442. [4] Boyet and Carlson (2006) *Earth Planet. Sci. Lett* **250**, 254-268. [5] Caro et al., (2003) *Nature* **423**, 428- 432. [6] Caro et al., (2006) *Geochim. Cosmochim. Acta* **70**, 164-191. [7] Harper and Jacobsen (1992) *Nature* **360**, 728-732.

Paleo-marine trace element partitioning relationships recorded in Precambrian Iron Formations

LESLIE J. ROBBINS[1*], STEFAN V. LALONDE[2], AND KURT O. KONHAUSER[1]

[1]University of Alberta, Edmonton, Canada, lrobbins@ualberta.ca (* presenting author), kurtk@ualberta.ca
[2]European Institute for Marine Studies, Technopôle Brest-Iroise, Plouzané, France, stefan.lalonde@univ-brest.fr

Ancient metalliferous sediments such as Precambrian Iron Formations (IF) retain geochemical signatures of the composition of the seawater from which they precipitated. Recent efforts to back-calculate paleo-marine trace element abundances from these signatures [1,2,3] have utilized the distribution coefficient (K_D), a special case of the Freundlich isotherm where the Freundlich exponent equals one and sediment concentrations (c_s) are linearly related to aqueous concentrations (c) by the factor $K_D = c_s / c$. However, only a few IF-applicable K_D values have been proposed to date, all were adopted from modern seawater [1] or experimentally estimated [2,3], and their applicability to Precambrian oceans has been assumed. The growing IF trace element record itself has not been thoroughly evaluated for geochemical relationships that should exist after trace element adsorption to Fe oxides, for example scaling with Fe. Here we describe the analysis of a large IF geochemical dataset for evidence of partitioning relationships preserved by the rock record itself. As might be expected, insoluble elements such as Al, Ti, Hf, and Sc show inverse Fe scaling behaviour that follows crustal mixing lines, reaffirming their detrital origin. Many trace elements in IF of presumed seawater origin do indeed scale with Fe in a manner consistent with simple partitioning onto iron oxides. Fe scaling relationships are often best represented in the data at maximal c_s, where K_D-respecting trace element partitioning and open system conditions appeared to prevail. Apparent deviations below these maxima may signify that drawdown of trace elements occurred at times as the result of prolonged iron oxide precipitation. From our data it is possible to estimate the lumped factor K_D*c that directly characterizes paleo-marine elemental partitioning; we briefly evaluate the implication of these apparent factors for select trace elements. This work represents a first step towards a more vigorous exploration of metalliferous proxies for paleo-marine trace element evolution.

[1] Bjerrum & Canfield (2002) *Nature* **417** 159-162. [2] Konhauser et al. (2007) *Science* **315** 1234. [3] Konhauser et al. (2009) *Nature* **458** 750-753.

https://doi.org/10.1180/S0026461X00008434 Published online by Cambridge University Press

Magmatic Processes in the Bishop Tuff Rhyolitic Magma Based on Trace Elements in Melt Inclusions and Pumice Matrix Glass

J. ROBERGE[1]*, P.J. WALLACE[2], A.J.R. KENT[3]

[1]Instituto de Geofisica, UNAM, Mexico D.F., Mexico, robergejulie@gmail.com*
[2] University of Oregon, Eugene, USA, pwallace@uoregon.edu
[3] Oregon State University, Corvallis, USA, adam.kent@science.oregonstate.edu

Abstract

To investigate the origin of compositional zonation in the Bishop Tuff magma body, we have analyzed trace elements in the matrix glass of pumice clasts and in quartz-hosted melt inclusions. Our results show contrasting patterns for quartz in different parts of the Bishop Tuff. In all samples from the early part of the eruption, trace element compositions of matrix glasses are similar to but slightly more evolved than quartz-hosted melt inclusions. This indicates a cogenetic relationship between quartz crystals and their surrounding matrix glass, consistent with in situ crystallization. The range of incompatible element concentrations in melt inclusions and matrix glass from single pumice clasts requires 16-20 wt.% in situ crystallization. This is greater than the actual crystal content of the pumices (<15% crystals). In contrast to the pattern for the early pumices, pyroclastic flow samples from the middle part of the eruption show contrasting trends: in some clasts the matrix is more evolved than the inclusions whereas in other clasts the matrix is less evolved. In the late Bishop Tuff all crystal-rich samples have matrix glasses that are less evolved than the melt inclusions. Trace element abundances indicate that the cores of quartz in the late Bishop Tuff crystallized from more differentiated rhyolitic magma that was similar in many ways, yet distinct from, the early erupted Bishop Tuff. Our results are compatible with a model of secular incremental zoning (Hildreth and Wilson, 2007), in which melt batches from underlying crystal mush rise to various levels in a growing magma body according to their buoyancy. Early and middle erupted quartz crystallized from highly evolved rhyolitic melt, but then some parts of the middle erupted magma were invaded by less differentiated rhyolite such that the matrix melt at the time of eruption was less evolved than the melt inclusions. A similar process occurred but to a greater extent in magma that erupted to form the late Bishop Tuff. In addition, there was a final, major magma mixing event in the late magma that formed Ti-rich rims on quartz and Ba-rich rims on sanidine, trapped less evolved rhyolitic melt inclusions, and resulted in dark and swirly crystal-poor pumice that is a rare type throughout much of the Bishop Tuff.

$(^{231}Pa_{ex}/^{230}Th_{ex})_0$ records from a depth transect in the NE Atlantic 0-20 ka

N. L. ROBERTS[1]*, J. F. MCMANUS[2], A. M. PIOTROWSKI[1]

[1]University of Cambridge, Cambridge, UK, nr297@cam.ac.uk (* presenting author)
[2]Lamont-Doherty Earth Obervatory, Palisades, NY, USA

Paleoclimate proxy records of $(^{231}Pa_{ex}/^{230}Th_{ex})_0$ have been used to infer past changes in deep water-mass advection rates in the North Atlantic [1, 2]. However, data from several studies suggest changing particle flux and composition may cause complications to the use of the sedimentary $(^{231}Pa_{ex}/^{230}Th_{ex})_0$ solely as an advection rate proxy [3, 4, 5]. Modelling studies have also shown that values of $(^{231}Pa_{ex}/^{230}Th_{ex})_0$ recorded in shallow cores differ from deep cores [6, 7], and may also be a function of distance of a core from the deep-water formation region [6], as well as possible effects from sea-ice [8]. It is therefore essential to monitor changes in the local environment and sedimentary parameters as closely as possible in order to accurately interpret $(^{231}Pa_{ex}/^{230}Th_{ex})_0$ measured in marine sediment cores.

Here I will present $(^{231}Pa_{ex}/^{230}Th_{ex})_0$ records from four cores, spanning between 1 and 4 km water depth, in close proximity to each other in the eastern North Atlantic and thus approximating a true depth transect. All four cores have therefore experienced similar changes in productivity and particle composition through time. This allows us to easily account for shared changes in sediment production above the sites and to interpret these records in terms of depth-dependent water column processes. I will present sediment data, including opal and $CaCO_3$ fluxes, along with measured $(^{231}Pa_{ex}/^{230}Th_{ex})_0$ from the last glacial maximum (20 ka) to the present. I will interpret the $(^{231}Pa_{ex}/^{230}Th_{ex})_0$ results, some of which are above the production ratio, in the context of changing sedimentary parameters, changing environmental influences, and ocean advection rates, giving further insight into the controls on $(^{231}Pa_{ex}/^{230}Th_{ex})_0$ and its use as a geochemical proxy.

[1] McManus et al (2004) *Nature* **428**, 834-837. [2] Gherardi et al (2005) *EPSL* **240**, 710-723. [3] Bacon et al (1988) *Trans. R. Soc. Ser* **325** 147-160. [4] Walter et al (1997) *EPSL* **149** 85-100. [5] Chase et al (2002) *EPSL* **204** 215-229. [6] Luo et al (2010) *Ocean Sci.* **6** 381-400. [7] Gherardi et al (2010) *Paleoceanography* **25** PA2207. [8] Henderson et al (1999) *Deep-Sea Res.* **46** 1861-1893.

https://doi.org/10.1180/S0026461X00008434 Published online by Cambridge University Press

CONSTRAINING THE SIZE OF HEINRICH EVENTS USING AN ICEBERG/SEDIMENT MODEL AND A 3D ICE SHEET MODEL

W.H.G. ROBERTS[1*], P.J.VALDES[1], A.J.PAYNE[2]

[1]BRIDGE, School of Geographical Sciences, University of Bristol, U.K. (*william.roberts@bristol.ac.uk)

[2]Bristol Glaciology Centre, School of Geographical Sciences, University of Bristol, U.K.

Heinrich Layers, anomalously thick layers of ice borne sediment in the north Atlantic ocean, and the events that caused them have long been associated with abrupt climate changes during glacial times. However, there is still no consensus about either how much ice is needed to transport this sediment or how such a large volume of ice could be produced. Estimates for this ice volume do exist and may be broadly separated into two categories: estimates derived from ice sheet models, and estimates derived from isotope records. There is a wide discrepancy between these two sets of estimates with the isotope derived estimates being at least one, and sometimes two, orders of magnitude larger than those from ice sheet models.

We shall describe here two different methods to further constrain these events. First, we use an iceberg model that includes sediment to simulate the delivery of sediment to the north Atlantic during a Heinrich Event. Second we use a three dimensional ice sheet model (Glimmer) with realistic topography to determine the volume of ice that leaves Hudson Strait during the thermo-mechanical surging events that the model simulates.

We show that the iceberg model can simulate the pattern of ice raft debris from a Heinrich Event and that we can simulate the sediment layer thickness that would result from the volume of ice released by the different estimates. We show that to best fit the observed Heinrich layer sediment thickness, 60×10^4 km^3 of ice needs to be released during the event. This matches the icesheet derived estimates better than the isotope derived estimates and suggests that Heinrich Events released relatively small volumes of ice. The surges from the 3-D ice sheet produce a larger volume of ice for each Heinrich Event than the iceberg model suggest is needed to form the Heinrich Layers, but the volume is consistent with other ice sheet models and significantly smaller than the volume that the isotopes suggest.

Variation in volatile content: Chichinautzin volcanic field, Mexico.

PHILIPPE ROBIDOUX[1*], JULIE ROBERGE[2], PAOLINA CAROLINA REYES LUNA[3], ARMANDO VÁZQUEZ CAMARGO[3], MARIE-NOËLLE GUILBAUD[1], LUIS ROBERTO JUSTO ESPINOSA[3], ÁNGEL BRISEÑO ARELLANO[3]

[1] Instituto de Geofisica, Universidad Nacional Autonoma de Mexico (UNAM), Av Universidad 3000, Ciudad Universitaria rphil85@hotmail.com (*presenting autor)

[2] Instituto Politécnico Nacional, Av. Ticomán No. 600, Col. San José Ticomán

[3]Facultad de Ingeniería, (UNAM), Av Universidad 3000, Ciudad Universitaria

Project

The Chichinautzin volcanic field (CVF) includes more than 220 volcanoes (cinder cones, shield volcanoes, maars) as well as larger stratovolcanoes (Popocatepetl) which erupted important quantity of volatiles since the Quaternary. It is located in the central portion of the Trans Mexican Volcanic Belt which is largely affected by the subduction of the Cocos plate and by effect of intra-continental rifting in Central Mexico [1]. This work focus on the volatiles content of three cones from the CVF selected based on their location, different range of documented ages and compositions [2]; Xitle (1665 yr B.P.), Pelagatos (< 14 000 yr B.P.), La Cima (<10 410 yr B.P.). Analyses of major gasses (H2O, CO2, Cl, S) trapped inside olivine-hosted melt inclusions were used to establish degassing mechanism. Crystals were selected from the main tephra deposits of these three cinder cones. Preliminary results show an overall dissolved sulphur concentrations varying between below detection limit (~ 50 ppm) and 1450 ppm and chlorine content varying from 56 to1601 ppm. FTIR analysis of doubly intersected olivine-hosted melt inclusions show that the dissolved H2O and CO2 contents vary from 0.1 to 4.31 Wt% and from 51 to 976 ppm respectively. The maximum H2O and CO2 content obtained for each volcano is presented in the table below:

	Xitle	Pelagatos	La Cima
H2O (%)	2.47	4.31	2.66
CO2 (ppm)	630	976	780

Table 1: Maximum H2O and CO2 content for each of the studied volcano.

Conclusion

For Xitle volcano, most melt inclusions have relatively low H2O and. This was previously found by [1] and may indicate that degassing at Xitle started at great depth as it is the case for the neighbour stratovolcano Popocatepetl [3]. Pelagatos volcano has the highest values, La Cima also have significant CO2 contents, but overall lower H2O compare to Pelagatos. The variations in volatile content suggest distinctive degassing mechanisms for each volcano.

[1] Wallace and Carmichael (1999), Cont. to Mineralogy and Petrology 135, 291-314. [2] Siebe et al. (2004), Bull. of Volcanology 66, p.203-225. [3] Roberge et al. (2009), Geology 37, 107-110.

https://doi.org/10.1180/S0026461X00008434 Published online by Cambridge University Press

Sources, sinks and cycling of seawater ^{232}Th in the north and south Atlantic basins.

LAURA F. ROBINSON[1, 2, *], KUO-FANG HUANG[1], MAUREEN E. AURO[1], ROBERT F. ANDERSON[3], CHRISTOPHER T. HAYES[3], MARTIN Q. FLEISHER[3], HAI CHENG[4,5], R. LAWERENCE EDWARDS[5], S. BRADLEY MORAN[6] AND MAK SAITO[1]

[1]Woods Hole Oceanographic Institution, Woods Hole, MA
[2]University of Bristol, Bristol, United Kingdom, lrobinson@whoi.edu
[3] Lamont-Doherty Earth Observatory of Columbia University, Palisades, NY, cth@ldeo.columbia.edu
[4]Institute of Global Environmental Change, Xi'an Jiaotong University, Xi'an, China cheng021@umn.edu
[5]University of Minnesota, Minneapolis, MN, edwar001@umn.edu
[6]University of Rhode Island, Narragansett, RI moran@gso.uri.edu
(* presenting author)

This study examines the distribution of the long-lived thorium isotopes ^{232}Th and ^{230}Th in the Atlantic Ocean. ^{232}Th in the ocean is derived from the partial dissolution of lithogenic minerals. ^{230}Th is produced at a predictable rate by the decay of uranium, and its subsequent removal by efficient reversible scavenging onto settling particles provides a method to quantify ^{232}Th fluxes to the ocean, and eventually to the seafloor. As such, combining analysis of these two isotopes in seawater has the potential to improve our ability to calculate present and past detrital fluxes to the ocean. Challenges to using this approach are both analytical, for example ^{232}Th contamination issues encountered by many labs during the international GEOTRACES intercalibration, and the lack of systematically collected sample sets. The GEOTRACES program is helping to overcome these issues, giving deeper insights into the processes controlling the sources, sinks and cycling of thorium isotopes in the ocean.

In this study we analyze ^{232}Th and ^{230}Th in two zonal Atlantic transects, crossing a range of oceanographic settings. The first is the U. S. GEOTRACES North Atlantic Zonal Transect, between 17N and 40N, for which six stations have been analysed thus far. The second consists of three stations from the CoFeMUG cruise across the South Atlantic at about 30S. All profiles are full depth and were analyzed together with GEOTRACES intercalibration standards. The CoFeMUG sites have ^{232}Th concentrations that range from 15 to 60 pg/kg, are similar across the basin, particularly in the upper 1000m and show no surface enrichment. Station 13 in the east has the highest ^{232}Th values at depth, but this small difference between sites is overwhelmed by the difference from the concentrations in the North Atlantic. The GEOTRACES samples in the eastern basin (stations 1 to 12) range from 25 to 191 pg/kg. The highest values both at the surface and at depth are from stations 9 and 10 which are the closest to the African coast. These high values likely reflect the input of Saharan dust. We discuss the controls on the ^{232}Th distributions in the context of local and basin scale processes.

Widespread expansion of intermediate water suboxia at 2 Ma

REBECCA S. ROBINSON [1*], PHILIPPE M. MARTINEZ[2], JOHAN ETOURNEAU[3], RALPH SCHNIEDER [4]

[1]University of Rhode Island, Narragansett, RI, USA, rebeccar@gos.uri.edu (* presenting author)
[2]Université Bordeaux I, Talence cedex, France, philippe.martinez@u-bordeaux1.fr
[3]Université Pierre et Marie Curie, Paris, France, jelod@locean-ipsl.upmc.fr
[4]Christian-Albrechts-Universitaet Kiel, Kiel, Germany schneider@gpi.uni-kiel.de

ABSTRACT

The transition from the warm Pliocene to the cool Pleistocene appears to accompany a decrease in intermediate water oxygenation. The Plio-Pleistocene cooling begins with the onset of major Northern Hemisphere glaciation, around 3.0-2.7 million years ago (Ma). High latitude cooling and extension of the polar ice caps led to cooling of the deep ocean and shoaling of the thermocline. Cooling of the whole surface ocean and establishment of strong zonal and meridional atmospheric circulation occurred around 2.0 Ma. A compilation of high-resolution nitrogen isotope records from the eastern tropical Pacific, North Pacific, and the Arabian Sea and a global multi-site survey, indicates that regional intensification of oxygen minimum zones (OMZs) and expansion of water column denitrification accompanied the surface cooling and circulation changes at ~2.0 Ma. Large-scale open ocean suboxia intensified with the inception of a modern polar frontal system, despite lower temperatures and thus higher initial oxygen contents of the mode waters themselves. This likely reflects the increased importance of aged mode waters as the principle conduit of nutrients and oxygen to the OMZs and stresses the importance of ocean circulation in regulating oxygenation.

https://doi.org/10.1180/S0026461X00008434 Published online by Cambridge University Press

Morphologies of fungal Mn oxide biomineralization in southern Appalachian caves

LEIGH ANNE ROBLE[1], SARAH K. CARMICHAEL[1], CARA M. SANTELLI[2], BRYAN ZORN[3], AND SUZANNA BRÄUER[3]

[1]Department of Geology, Appalachian State University, Boone, NC 28608, USA. roblela@email.appstate.edu (*presenting author)
[2]Mineral Sciences, Smithsonian Institution, National Museum of Natural History, Washington, DC, 20560 USA
[3]Department of Biology, Appalachian State University, Boone, NC 28608, USA

A common characteristic of southern Appalachian caves are thin, brown-black manganese (Mn) oxide coatings on the walls, on flowstone associated with springs and seeps, and on pebbles and cobbles in streams and pools. These mineral coatings are often associated with bacterial communities, suggesting that microbial activity plays a role in the precipitation of Mn(III/IV) oxides (through catalyzing the oxidation of Mn(II) compounds). Until recently, a fungal contribution to this Mn biomineralization process in caves has been largely overlooked.

In this study, we sought to examine the role of fungi in Mn biomineralization in Daniel Boone Caverns in southwest Virginia and Carter Salt Peter Cave in east Tennessee, all located in the Ordovician Knox Dolomite. Sample locations were chosen based on the presence of black or brownish-black mineral coatings or biofilms on the cave walls and floors, or growing on materials left in the cave by human and animal visitors (tape, socks, feces). X-ray diffraction analyses indicate that the primary cave substrates supporting the Mn oxide coatings was either nontronite clay, dolomite, or anthropogenic materials. Mn oxidation was confirmed in the field using the leucoberbelin blue (LBB) assay, a colorless chemical compound that turns bright blue in the presence of Mn(III) or Mn(IV) compounds. Oxidation was observed in both pristine and agriculturally-contaminated cave systems.

We isolated several different species of Mn(II)-oxidizing fungi from the variety of cave samples. Fungal isolates were analyzed by scanning and transmission electron microscopy (SEM and TEM). TEM imaging with STEM analysis revealed that in several samples, Mn oxidation occurred along the fungal hyphae cells, particularly where new hyphal branches were forming. In other cultures, Mn oxides formed crumpled sheets surrounding the entire exterior of fungal hyphae. In addition to the hyphae-associated oxidation, Mn oxides were produced at the base of fruiting bodies. Interestingly in one culture, fungal spores appearred to be sequestering Mn^{2+} within the spore, but no Mn oxides were present on the cell exteriors.

The Mn oxides produced by fungal cultures were poorly crystalline and amorphous to laboratory-based X-ray sources. Tentative crystallographic identification of Mn oxides by single crystal micro-X-ray diffraction indicate that buserite and todorokite (layer and tunnel structures, respectively) were the dominant Mn oxides present in samples isolated from biofilms in Carter Salt Peter Cave. In the cave environment, the presence of cations, such as Ca^{2+}, may result in the transformation of poorly-crystalline oxide phases to more crystalline and stable forms, such as birnessite and todorokite.

Dynamics of Uranium Release from the Capillary Fringe of Contaminated Hanford Sediments

KENTON A. ROD[1*], DAWN M. WELLMAN[2], MARKUS FLURY[3], ERIC PIERCE[4], JAMES B. HARSH[5], ZHEMING WANG[6]

[1]Washington State University, Pullman, WA, USA, kenton.rod@pnnl.gov (* presenting author)
[2]Pacific Northwest National Laboratory, Richland, WA, USA, Dawn.Wellman@pnnl.gov
[3]Washington State University, Puyallup, WA, USA, flury@wsu.edu
[4]Oak Ridge National Laboratory, Oak Ridge, TN, USA, pierceem@ornl.gov
[5]Washington State University, Pullman, WA, USA, harsh@wsu.edu
[6]Pacific Northwest National Laboratory, Richland, WA, USA, zheming.wang@pnnl.gov

Introduction

The fate and transport of radionuclides from contaminated sediments represents a major long-term risk at department of energy (DOE) sites. Waste disposal units at DOE sites have undergone source zone removal, however, a number of persistent subsurface plumes remain. Sediment analysis from these sites suggests the residual contamination has migrated into sediment fractures, pores and pore-throats and is influenced by coupled nanometer scale reactions. These pore scale reactions affect pore-scale contaminant concentrations and control the presence of persistent subsurface plumes. Our objective was to quantify the dynamics of U concentrations in the pore water of micropores compared to large pores.

Methods

We investigated the dynamics of U release to pore water during river stage changes from two contaminated capillary fringe sediments, sampled from 7.0 m and 7.6 m below ground surface (bgs) in the Hanford 300 area. Sediments were packed into columns and saturated with Hanford groundwater for three to 84 days. After specified times, sediment pores > 48 μm radius were drained, followed by draining pores to 15 μm radius.

Results

U release in the first two weeks was similar between sediments and pore sizes with a range of 4.4 to 5.6 μM U in the two-week sample. The 7.0 m bgs sediment U declined steadily in the larger pores to 0.22 μM at day 84, whereas the smaller pores released U to 9.4 μM at day 28 then to 6.7 μM at day 84. The 7.6 m bgs sediment released 6.2 μM U on day 28 and 1.4 μM on day 84, in the large pores. MINTEQ simulations where pH was increased from 8.1 to 8.35 can be used to model the U release and reincorporation into a solid phase. A mineral phase in the sediments was identified as a U-carbonate species, similar to rutherfordine.

https://doi.org/10.1180/S0026461X00008434 Published online by Cambridge University Press

Geographic and lithologic test of the Mesoarchaean S-MIF minimum

KRISTYN RODZINYAK[1*], LÉA BRASCHI[1], CHRISTIE ROWE[1], ANDREY BEKKER[2], PHILLIPS THURSTON[3], BOSWELL WING[1]

[1]McGill University, Earth and Planetary Sciences, Montreal, Canada, kristyn.rodzinyak@mail.mcgill.ca (* presenting author)
[2] University of Manitoba, Geological Sciences, Winnipeg, Canada
[3] Laurentian University, Department of Earth Sciences, Sudbury

The disappearance of mass independent fractionation in sulfur isotopes (S-MIF) around 2.45 billion years ago is associated with an increase in atmospheric oxygen content. However, the large S-MIF that characterizes the Archaean has not yet been identified in Mesoarchaean (3.2 to 2.8 Ga) rocks. This diminished variability has been attributed to atmospheric compositional changes including fluctuations in atmospheric oxygen, variations in volcanic SO_2- H_2S ratios, and high-altitude methane hazes. In order to constrain the geographic and lithologic distribution of the diminished Mesoarchaean S-MIF signal, we obtained S isotope data from a variety of lithologies from previously uninvestigated Mesoarchaean terrains.

Samples were collected from four greenstone belts within the Superior Province in Northwestern Ontario (Finlayson Lake, Lumby Lake, Red Lake, and Woman Lake) that span an age range of 2.99 to 2.87 Ga. Metamorphic grade within the sampled portions of each belt is no higher than greenschist facies. We studied multiple lithologies, including shales, cherts, carbonates, banded iron formation (BIF), volcanic massive sulfide (VMS) showings, pillow basalts as well as greywackes and phyllites of volcanoclastic and siliciclastic origin. Whole rock samples and individual macroscopic sulfide grains were analyzed for their multiple S isotope compositions.

Sulfide $\delta^{34}S$ values range from -4.6‰ to 8.9‰ V-CDT, while the associated $\Delta^{33}S$ values range from -0.93‰ to 2.32‰ V-CDT. Samples with significant $\Delta^{33}S$ values also have $\Delta^{36}S$ values that fall on a slope of approximately -1, which is typical for Archaean S-MIF. The clastic rocks in our sample suite exhibit near-zero $\Delta^{33}S$ values, while the non-clastic rocks preserve significant S-MIF.

Macroscopic pyrites within some samples show resolvable differences in their multiple S isotope compositions. For example, the silica-rich layers in BIF seem to have more positive $\delta^{34}S$ and $\Delta^{33}S$ values compared to the silica-poor layers. Other samples contain different types of sulfides with similar isotopic compositions. Chalcopyrite and pyrite grains within a single VMS sample, for example, show negligible difference in their multiple S isotope compositions.

Compared to literature data for the Mesoarchaean, we observe a slightly larger spread in both $\delta^{34}S$ and $\Delta^{33}S$ values. The overall S-MIF range is still much reduced relative to the rest of the Archaean. The identification of diminished S-MIF range in multiple localities and lithologies (including shales, carbonates, cherts, and BIFs) suggests that this is a primary feature of the Mesoarchaean atmosphere rather than the effect of sampling bias. This interpretation is supported by the lithologic controls on S-MIF preservation that we have identified here.

Despite the reduced S-MIF magnitude, the full Mesoarchaean sulfur isotope distribution shows similar systematics to other parts of the Archaean. For example, the observed $\Delta^{33}S$ and $\delta^{34}S$ variability can be explained by covariation along the Archean reference array and a horizontal spread of $\delta^{34}S$ values all with similar $-\Delta^{33}S$ values. These features suggest that the diminished Mesoarchaen S-MIF record may be best explained through dilution by a S source without S-MIF, either in the atmosphere or in the marine reservoir, rather than by changing the photochemical regime producing S-MIF.

Searching for traces of early life in Earth's oldest sulfate deposit: the ca. 3520 Ma Londozi barite, Swaziland

DESIREE ROERDINK[1*], PAUL MASON[1], FRAUKJE BROUWER[2], MARTIN WHITEHOUSE[3], NOAH NHLEKO[4]

[1]Department of Earth Sciences, Utrecht University, Utrecht, The Netherlands, d.l.roerdink@uu.nl (*presenting author), p.mason@uu.nl
[2]Department of Petrology, VU University, Amsterdam, The Netherlands, fraukje.brouwer@vu.nl
[3]Swedish Museum of Natural History, Stockholm, Sweden, martin.whitehouse@nrm.se
[4]Geological Survey and Mines Department, Mbabane, Swaziland, nhlekon@swazi.net

Microbial sulfate reduction may have been one of the earliest metabolisms to emerge on Earth. Paleoarchean pyrite and barite deposits potentially record such metabolic activity through stable sulfur isotope fractionation, but this requires proof that microbial signatures were not obscured by metamorphic processes. Here, we discuss the origin of isotopically depleted pyrite in the oldest known sulfate deposit on Earth: the Londozi barite in western Swaziland, for which we obtained a minimum age of 3521±13 Ma by U-Pb zircon dating of felsic volcanics overlying the barite.

Field evidence indicates that the barite was formed in a low-energy marine environment with dominant mafic volcanism and intense hydrothermal activity. It was subsequently affected by amphibolite facies metamorphism and extensive metasomatism. Dominant mineral assemblages include Ca-rich phases actinolite, diopside and epidote with secondary Ba-rich feldspar (celsian and hyalophane) and witherite.

SIMS multiple sulfur isotope analyses of pyrite in the Londozi deposit identified three distinct populations of sulfide: (1) barite-hosted grains with average $\delta^{34}S$ = -5.2‰ and $\Delta^{33}S$ = -1.0‰ (n = 18), (2) massive chert-hosted grains with average $\delta^{34}S$ = -1.1‰ and $\Delta^{33}S$ = 0.2‰ (n = 7) and (3) grains in a silicified silicate matrix with average $\delta^{34}S$ = -0.2‰ and $\Delta^{33}S$ = -0.6‰ (n = 71). We hypothesize that silicate-hosted pyrite was derived from a sulfide pool generated by microbial reduction of sulfate, showing a shift in $\delta^{34}S$ of 5-8‰ relative to the barite. In contrast, association of the most ^{34}S-depleted pyrite with barite might not reflect microbial processes, but could represent sulfide produced during metasomatic remobilization of the barite by reductive dissolution. This process is in agreement with an average sulfur isotope temperature of 524°C calculated for barite-pyrite mineral pairs, and explains the presence of secondary barium-rich feldspar with increasing Ba content towards the barite.

Our work, therefore, demonstrates that the geological context of isotopically depleted sulfides must be carefully interpreted before arguing for the presence of sulfate reducing prokaryotes in the Paleoarchean.

https://doi.org/10.1180/S0026461X00008434 Published online by Cambridge University Press

Si isotope fractionation during silica precipitation in batch-reactor experiments

DESIREE ROERDINK[1], SANDER VAN DEN BOORN[1,3], MANFRED VAN BERGEN[1]*, PIETER VROON[2]

[1]Department of Earth Sciences, Utrecht University, Utrecht, The Netherlands, d.l.roerdink@uu.nl, m.j.vanbergen@uu.nl (*presenting author)

[2]Department of Petrology, VU University, Amsterdam, The Netherlands, p.z.vroon@vu.nl

[3]Shell Projects and Technologies, Kessler Park 1, 2288 GS, Rijswijk, The Netherlands, sander.van-den-boorn@shell.com

Recent research has demonstrated the versatility of silicon isotopes in reconstructing pathways and processes in (bio)geochemical systems. Interpretations of data from siliceous chemical sediments in the rock record rely on quantitative insight into isotopic fractionation during precipitation from silica-carrying solutions. We performed batch-reactor experiments to explore the isotopic fractionation behavior of precipitating silica in low-temperature environments.

Supersaturated silica solutions were obtained by cooling a 90°C saturated solution to temperatures of 10-35°C in silica-seeded batch reactors. Decreased silica solubility induced by the temperature drop resulted in deposition of monomeric silica on the seeds. Solution samples, taken at regular time intervals, were analyzed for silicon isotopic composition by MC-ICP-MS with a typical precision of 0.12‰ (2σ) [1]. The isotope fractionation followed Rayleigh distillation trends and proceeded in two consecutive stages. Initially (stage I), at high degrees of oversaturation, fractionation factors ($\varepsilon_{ppt\text{-}dis}$) were negative and ranged between -1.1 and -2.0‰. Subsequently (stage II), when saturation levels had decreased, fractionation factors were positive and ranged from +0.4 to +0.7‰. The magnitude of the fractionation factor appeared to increase with decreasing temperature in both stages.

We propose that silicon isotope fractionation is controlled by the degree of oversaturation in the reactor, resulting in dominant precipitation in stage I and partial re-dissolution of precipitated silica in stage II. We hypothesize that fractionation during precipitation occurs due to energetically preferred breaking of ^{28}Si-O bonds in the dissolved silica ($\varepsilon < 0$), before formation of new Si-O-Si bonds at the surface of silica grains. In stage II, the system approaches equilibrium, and decreased oversaturation allows partial re-dissolution of Si from the surface with a relatively high rate for ^{28}Si. Consequently, more ^{28}Si goes back into the solution than precipitates, with the net effect that ^{30}Si is preferentially retained in the solid ($\varepsilon > 0$).

Our results suggest that the ultimate isotopic composition of cherts and non-biogenic silica deposits is a function of the degree of oversaturation, for example in cases where rising hydrothermal fluids with different loads of dissolved silica cool down to the same ambient temperature when venting at the seafloor.

[1] Van den Boorn, S.H.J.M. *et al*. (2006) *J. Anal. At. Spectrom.* **21**, 734-742

Discordant polymetamorphic zircons: the rule in crystalline nappes of the SW Norwegian Caledonides

C. ROFFEIS[1*], F. CORFU[1]

[1]Department of Geosciences, University of Oslo, Norway

* cornelia.roffeis@geo.uio.no (presenting author)

5a. What zircons tell us about crustal evolution

Resetting of zircons is commonly due to Pb loss related to metamictisation and subsequent alteration, or to other processes such as strain and recrystallization disturbing the crystal lattice. In general it is possible to identify domains of zircons that have escaped partial resetting. Such domains can then be isolated and analyzed separately. In the crystalline nappes of the SW Norwegian Caledonides, however, zircon populations typically yield data that are variously discordant, defining either discordia lines or, in more complex cases, scattered arrays. The most common pattern is exemplified by zircons in orthogneisses from a klippe on Hardangerjøkulen near Finse, that defines a line with an upper intercept age of 1658 ± 9 Ma, indicating magmatic formation, and a lower intercept age of 968 ± 26 Ma, reflecting the Sveconorwegian metamorphic overprint. The discordia line is defined by seven precise ID-TIMS measurements on clear, inclusion free, optically undisturbed zircon fractions on mainly short prismatic grains subjected to either air or chemical abrasion. The fact that even chemical abrasion did not remove the discordance indicates that the discordance is frozen in by recrystallization. The grains themselves show little indication of metamorphic new growth. Coexisting titanite, however, formed during Sveconorwegian metamorphism. Although the nappe was emplaced during the Caledonian orogeny, the U-Pb data were left nearly completely unaffected by these secondary events. This type of behavior is very common in the gneisses of comparable nappes in the Hardanger-Ryfylke Complex to the south and the Jotun Complex to the north of Hardangerjøkulen, although a Caledonian influence is more evident in some cases and creates more scatter. A very different U-Pb discordant pattern is observed instead in anorthositic-jotunitic gneisses of the northern Lindås Nappe, where the Caledonian amphibolite facies overprint and local deformation strongly affected the zircon populations, causing strong Caledonian resetting and local new growth. In zircons of one of the anorthosite localities the resetting can be linked to strain and plastic deformation, but the other key factors seem to be metamorphic reactions and the release of chemicals that allow to form new zircons.

https://doi.org/10.1180/S0026461X00008434 Published online by Cambridge University Press

The stability of iron–nickel carbides in the Earth's mantle

ARNO ROHRBACH[1,2*], MAX W. SCHMIDT[2], SUJOY GHOSH[2], CLAZINA H. WIJBRANS[1] AND STEPHAN KLEMME[1]

[1]Institute for Mineralogy, WWU Münster, 48149 Münster, Germany arno.rohrbach@uni-muenster.de (* presenting author), stephan.klemme@uni-muenster.de, ineke.wijbrans@uni-muenster.de

[2]Institute of Geochemistry and Petrology, ETH, 8092 Zürich, Switzerland, max.schmidt@erdw.ethz.ch, sujoy.ghosh@erdw.ethz.ch

A substantial amount of carbonate entrained in partially altered lithosphere likely survives shallow devolatilisation during subduction [1] and will thus be carried by the downgoing plate deep into Earth's mantle. Such carbonates are liberated as carbonatitic liquids whenever the subducting plate is heated to ambient mantle temperatures [2], e.g. when the lithosphere deflects into the transition zone above the 660 km discontinuity. When such carbonatites infiltrate the mantle they have to face an environment where oxygen fugacity is potentially lower than defined by the iron–wustite equilibrium, i.e. where (Fe,Ni)-metal is likely to be an accessory phase (at depths greater than ~250 km) [3–5]. When carbonatites become reduced by such (Fe,Ni)-metal, graphite or diamond would not form as long as excess metal is present, but instead (Fe,Ni)-carbides should be stable. Such carbides may form along the boundaries of carbonatite infiltration zones, where the mass of pervasively infiltrating carbonatites is insufficient to oxidize all metal. We thus performed experiments in the Fe–Ni–C ternary, to define the stability of the various carbides in this system. The subsolidus ternary was determined at 1050 °C, 10 GPa. Diamond coexists with (Fe,Ni)-metal to an X_{Fe} (molar, =Fe/(Fe+Ni) of ~0.48, and no carbide is stable on the Ni-rich side of the ternary. $(Fe,Ni)_3C$ is only stable in the range of X_{Fe} = 1.00 to ~0.75, opening a 3-phase field (Fe,Ni)-metal – $(Fe,Ni)_3C$ – diamond. The phase $(Fe,Ni)_7C_3$ is stable up to X_{Fe} ~0.89 and defines together with $(Fe,Ni)_3C$ (X_{Fe} ~0.82) and diamond a second 3-phase field. A second series of experiments indicates that Fe–Ni–C melting temperatures appear to be lower than expected; at 10 GPa, melting is observed down to 1150 °C, which is at least 200 °C lower than both an average mantle geotherm and the previously determined eutectic temperature in the Fe–C binary [6]. If confirmed by further experiments, such low eutectic temperatures would imply that any adiabatic mantle containing metallic iron and iron carbide, i.e. any mantle at depths >300 km with an average mantle C-content, must contain a small (0.1–1 wt%) fraction of (Fe,Ni)-C melt. The infiltration of carbonatite melts should then also lead – in an intermittent stage – to such (Fe,Ni)-carbide melts.

[1] Connolly (2005) *EPSL* **236**, 524–541. [2] Rohrbach & Schmidt (2011) *Nature* **472**, 209–212. [3] Frost et al. (2004) *Nature* **428**,409–412. [4] Rohrbach et al. (2007) *Nature* **449**, 456–458. [5] Rohrbach et al. (2011) *J.Pet.* **52**, 717–731. [6] Lord et al. (2009) *EPSL* **284**, 157–167.

Bio-inspired Fe_3S_4 catalyst for CO_2 reduction: DFT study

ALBERTO ROLDAN,* NORA H. DE LEEUW

University College London, Department of Chemistry, United Kingdom.
alberto.martinez@ucl.ac.uk (* presenting author)
n.h.deleeuw@ucl.ac.uk

Introduction

Carbon dioxide capture and utilisation is gaining attention, driven not only by enviromental factors but by the posibility to use it as chemical feedstock. The main challenge in CO_2 reduction is increasing the energy efficiency of the process, which is hindered primarily by its high reduction over-potentials. However, this process takes place under mild conditions in chemoautotrophic bacteria catalysed by FeS cubane clusters [1]. Similar structures are found in the iron thiospinel mineral (Fe_3S_4) which is present in deep sea vents and marine anoxic sediments. We present a theoretical (DFT+U) [2] investigation using Fe_3S_4 as a catalyst to transform CO_2.

Results and Conclusions

In agreement with previous benchmarks, we find that the CO_2 adsorption/activation process is the determinant step. This step consists of an electron transfer form the metallic atom in the surface to the empty antibonding orbital on the molecule leading to $CO_2^{\bullet-}$. The presence of other transition metals, such as Ni, can enhance the electronic rearrangement making the CO_2 activation energetically possible. A thermodynamically more favorable process is the H_2 dissociative adsorption either on pure or doped greigite. Thus, H_2 becomes a source of (H^++e^-) which can be added to the co-adsorbed $CO_2^{\bullet-}$ molecule by a common Langmuir-Hinshelwood mechanism. We also find a downhill pathway for that addition leading to products of interest, such as formic acid (Fig. 1).

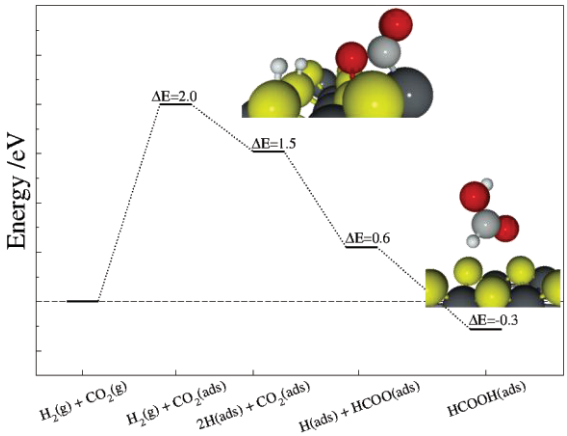

Figure 1: Potential energy diagram for CO_2 transformation to formic acid catalysed be pure greigite.

[1] Huber, C.; Wachtershauser, G. (1997) *Science*, ***276***, 245-247. [2] Devey, A. J.; Grau-Crespo, R.; de Leeuw, N. H. (2009) *Phys. Rev. B*, ***79,*** 195126-195133.

https://doi.org/10.1180/S0026461X00008434 Published online by Cambridge University Press

Experimental and modeling investigation of conservative and reactive transverse mixing in porous media

MASSIMO ROLLE[1,2]*

[1]Center for Applied Geosciences, University of Tübingen, Sigwartstrasse 10, 72706 Tübingen, Germany
[2]Department of Civil and Environmental Engineering, Stanford University, 473 Via Ortega, CA 94305, Stanford, USA (correspondance: mrolle@stanford.edu)

Transverse mixing is of primary importance in many relevant groundwater quality scenarios. For instance, the transport and natural attenuation of organic contaminants is often controlled by the extent of mixing of soluble reactants at the plume's fringe. Conservative and (bio)reactive flow-through experiments have been performed for a detailed investigation of transverse mixing and its coupling with reactive processes. The experiments were carried out at the laboratory bench-scale in quasi two-dimensional flow-through systems, including both homogeneous and heterogeneous saturated porous media. Since the extent of mixing in groundwater systems is typically small, the characteristics of the flow field that result in enhanced mixing are of particular significance. The experiments showed that flow focusing in high-permeability inclusions significantly enhances dilution of conservative tracers as well as transverse mixing of reactants.

Numerical simulations have been performed to extend the experimental results to field-scale scenarios where conservative and reactive transport were evaluated in complex heterogeneous hydraulic conductivity fields. In such systems, measures such as the flux-related dilution index and the flux-related spatial moments have been proposed to quantify mixing [1]. These measures are useful since they allow one to define a mixing-relevant upscaled transverse dispersion coefficient. This parameter accounts not only for the variability of flow in the heterogeneous formation (e.g., flow-focusing in high-permeability inclusions and defocusing in low-conductivity zones) but also for small scale, compound-specific effects. The latter include incomplete dilution in the pore channels, which was investigated in pore-scale simulations and multi-tracer laboratory experiments, and was shown to lead to a non-linear compound-specific parameterization of local transverse dispersion [2]. For reactive transport, the effects of a correct quantification of transverse mixing on the length of reactive solute plumes are illustrated.

[1] Chiogna et al. (2011) *Water Resour. Res.,* 47, W02505, doi:10.1029/2010WR009608.
[2] Rolle et al. (2012) *Transp. Porous Media* (in press).

Incorporation and early diagenesis of Mo and U isotope records in Bahamian carbonate sediments

STEPHEN J. ROMANIELLO[1*], ACHIM D. HERRMANN[1,2], ARIEL D. ANBAR[1,3]

[1]School of Earth and Space Exploration, Arizona State University, Tempe, AZ, USA, sromanie@asu.edu (* presenting author)
[2] Barrett Honors College, Arizona State University, Tempe, AZ, USA
[3] Department of Chemistry & Biochemistry, Arizona State University, Tempe, AZ, USA

Transition metal concentrations and isotopes are widely used to understand past changes in ocean redox. Most of these proxies were developed for use in black shales. However, black shales are not ubiquitous in the geologic record and so our conception of ocean redox evolution may be biased by the conditions of resistricted marginal basins in which such shales are often deposited. Along with other groups, we are exploring the use of complementary lithologies, such as carbonates, which are abundant in the geologic record and often deposited along open ocean margins [1-3].

Here, we examine the incorporation and early diagenetic evolution of Mo and U isotopes in shallow Bahamian carbonate sediments. The Bahamas is one of the largest and best studied Holocene carbonate platforms, and its location far from continental land masses results in sediments which contain very little siliclastic detritus. Our sample set consists of a wide variety of modern coral, algae, ooids, and mollusk samples ("primary precipitates") as well as 4 short push cores taken from tidal flats, sea grass meadows, and an organic-rich, tidal pond.

We find that Mo and U concentrations are much higher in shallow carbonate sediments than in primary precipitates, increasing from <0.1 ppm Mo to an average of 5.6 ppm Mo, and from an average of 1.5 ppm U to 4.1 ppm U, respectively. In almost all cases, the lowest sediment Mo and U concentrations were as high or higher than the highest concentrations found in primary precipitates, consistent with authigenic accumulation of Mo and U from reducing porewaters. $\delta^{234/238}U$ and $\delta^{238/235}U$ were very close to seawater values in all of the primary precipitates, but $\delta^{238/235}U$ in sediments was 0.2-0.4‰ heavier than in seawater. $\delta^{98/95}Mo$ ranged from ~1.0‰ lighter than seawater in a tidal flat core with low organic matter and low porewater sulfide, to values similar to or even slightly exceeding that of seawater in the most organic- and sulfide-rich cores, a pattern also consistent with control by porewater H_2S concentrations.

These results indicate that authigenic accumulation of Mo and U under sulfidic porewater conditions strongly affects Mo and U concentrations and isotopes in carbonate sediments. The extent of this process appears sensitive to porewater H_2S, and thus indirectly to sediment organic content. In the Bahamas, these parameters can vary over 100s of meters, with potential implications for Mo and U isotopic records in the geologic record. For example, in one case $\delta^{98/95}Mo$ of sediments varied by ~1‰ between a tidal flat region and core in a sea grass meadow ~100m away. To cope with such effects, proxies for porewater redox conditions may be required (e.g. organic content, iron speciation, or trace metal distributions).

[1] Voegelin et al. (2009) *Chemical Geology* **265**(3-4), 488-498 [2] Voegelin et al. (2010) *Precambrian Research* **182**(1-2), 70-82 [3] Brennecka et al. (2011) *PNAS* **108**(43): 17631-17634.

https://doi.org/10.1180/S0026461X00008434 Published online by Cambridge University Press

Kinetics of Pyrrhotite Oxidation in Seawater: Implications for Mining Seafloor Hotsprings

GINA Y. ROMANO[1], MICHAEL A. MCKIBBEN[1]

[1]University of California, Riverside, USA, groma002@ucr.edu, michael.mckibben@ucr.edu

A rapid increase in the price of transition metals in recent years has piqued interest in deep sea in situ mining of seafloor massive sulfide (SMS) deposits. There are unique incentives to seafloor mining that make it more attractive than traditional land mining of sulfides, but these are accompanied by important unanswered questions about the potential environmental effects, including localized sulfuric acid generation. Currently there is a paucity of data on the oxidation kinetics of sulfide minerals in seawater. Pyrrhotite specifically is of interest because it is a major non-economic component of SMS deposits that will be disposed of on or above the seafloor during mining. Pyrrhotite oxidizes rapidly via an irreversible, acid-producing reaction. Knowledge of sulfide mineral oxidation rates will also provide constraints on metal and sulfur cycling in oceans by quantifying the natural, abiotic weathering rates of SMS deposits.

Laboratory experiments have been performed to evaluate the effects of pH, temperature, oxidant concentration, and mineral surface area on the rate of oxidation of pyrrhotite in seawater. Temperature controlled circulation baths, Teflon reaction vessels, synthetic seawater, and pure, hand sorted natural pyrrhotite crystals are used in experiments. Both batch and flow-though reactor methods are employed. Reaction products are analyzed using ICP-MS. The rate law is expressed as follows:

$$R = -k\,(M_{O2,aq})^{a}(M_{H+})^{b}$$

where R is the specific oxidation rate of pyrrhotite, k is the rate constant (a function of temperature and surface area), and a and b are reaction orders for reactant concentrations (M) that need to be determined experimentally. The initial rate method is used to isolate the reaction order of each reactant.

Current data from batch experiments indicate positive influences of oxidant concentration, surface area, temperature, and $[H^{+}]$ on the initial rate. Pyrrhotite oxidizes significantly faster than chalcopyrite, providing an upper limit to the anthropogenic and natural weathering rates of SMS deposits, but acid production rates do not appear to exceed the buffering capacity of seawater. There will be potential for microbial studies in the future to quantify the effects of bacterial oxidation of pyrrhotite using this study as a baseline.

Evaluation of non-conventional geothermal potential in a Volcanic Island

CARLOS ROSA[1,2*], RITA CALDEIRA[1,3], DIOGO ROSA[1,4] AND LUISA RIBEIRO[1,5]

[1] LNEG – UGCG, National Laboratory of Energy and Geology, Dept. Geology and Geol. Mapping, Portugal, carlos.rosa@lneg.
[2]CREMINER/LA-ISR, Dept. Geology, Faculty of Science, Lisbon, Portugal
[3]CeGUL – Geology Center, Faculty of Science,Lisbon University, Portugal, rita.caldeira@lneg.pt
[4]GEUS – Geological Survey of Denmark an Greenland, Dept. Petrology and Economic Geology, Copenhagen, Denmarke
[5]Geosciences Center, Coimbra University, Portugal, luisa.duarte@lneg.pt

Madeira, is an intraplate volcanic island, located at the eastern North Atlantic Ocean, with an emerged area of 737 km^2 and maximum altitude of 1861 m. Although there are no historical eruptions, the existence of recent volcanism (6 my) with well preserved volcanic cones and thermal evidences, such as the occurrence of hot water rich in CO2, suggest a heat source at subsurface and the existence of rocks/water with significant temperatures at depths likely to be exploitable for economic generation of electricity.

In a volcanic geothermal system the heat source comes from magma emplacement at relatively shallow levels, thus knowledge of magma chamber(s) depth is one of the keys to geothermal reservoir assessment. In the evaluation of Madeira island geothermal potential, geophysical methods are being applied but, these are most useful for locating chambers beneath active volcanoes. Petrological and geochemical methods supported on whole rock analysis and mineral chemistry can be a helpful tool to constraint the crystallization temperatures and pressures/depths of magmas and to unveil the physical-chemical crystallization history of selected phenocrystals, hence the depth of magma chambers. Volcanic rocks (effusive and explosive) in Madeira are predominantly alkaline basalts. Generally they are holocrystaline presenting porphyritic texture with phenocrystals of olivine and clinopyroxene and, sometimes, calcic plagioclase in a groundmass composed by plagioclase microlites, clinopyroxene, oxides and occasionally interstitial glass. Petrographic and chemical criteria show that phenocrystals had a polibaric crystallization, suggesting that they paused in crustal magma chambers prior to eruption, and that the first minerals to crystallize were olivines and clinopyroxenes. One of the methods to determine the pressure of crystallization is the Ol-Cpx-Plag cotetic method that requires glass composition, or an assumption of it. We applied selected geothemobarometers, based on olivine-liquid and clinopyroxene-liquid equilibrium, to core-mantle analysis of olivine and clinopyroxene phenocrysts to estimate P, which is related to the depth at which magma resides in a chamber, and T of equilibrium crystallization. When required, oxygen fugacity (fO_2) was calculated from oxides and whole rock composition. The first results seem to point out a concentration of core crystallization occurring between 2 to 4 kb/6 to 12 km, which is a good indication of a single and wide magma chamber beneath the island.

https://doi.org/10.1180/S0026461X00008434 Published online by Cambridge University Press

Interaction between lamprophiric and riolitic magmas in the Neoproterozoic Sergipano Belt, NE Brazil

MARIA LOURDES SILVA ROSA[1*], VINÍCIUS A. CARVALHO LISBOA[1], HERBET CONCEIÇÃO[1], JOANE ALMEIDA CONCEIÇÃO[1], ANA CAROLINE SOARES OLIVEIRA[1], CLEVERTON CORREIA SILVA[1], DÉBORA CORREIA RIOS[2]

[1]Sergipe Federal University, Núcleo de Geologia, Aracaju, Brazil, lrosa@ufs.br

[2]Bahia Federal University, Instituto de Geociências, Salvador, Brazil, dcrios@ufba.br

The Neoproterozoic Sergipano Belt occurs on the northeastern margin of São Francisco Craton and in south of and Pernambuco-Alagoas Domains. At the north area of Sergipe State a voluminous granitic rocks intrude a turbiditic Neoproterozoic sequence (Macururé Domain), which due to the action of a low to medium grade regional metamorphism, result in garnet-schists, meta-pelitic e meta-graywacke. In the core, these granitic plutons show magmatic foliation and, at some places, also a tectonic foliation, however in the border with metamorphic country rocks the contacts are abrupt, frequently showing dykes and an increasing of the metamorphic regional grade. The plutons are constituted by muscovite-granite on borders which gradually or suddenly become biotite-granites, hornblende-granites, hornblende-granodiorite, and sometimes, to monzonites, suggesting a magmatic zoning. These granites are medium to coarse rocks, with allotriomorphic, and occasionally porfiritic textures. The magmatic flux foliation is give by the hornblende, biotite or feldspar mineral alignment. Mafic-ultramafic rocks occur as micro-granular enclaves, with a variety of sizes, with or without a border of biotite or amphibole, and as well sin-plutonic dykes. The main enclaves mineralogy is composed by hornblende, biotite, opaque minerals, diopside, alkali-feldspar and plagioclase. The accessory minerals comprise apatite, allanite, carbonate and occasionally zircon. These rocks are correlated to lamprophyres and mafic-monzonites. The presence of these enclaves are indicative of felsic-mafic magmas co-existence and mixing. The geochemical data show that the granites have a shoshonitic to high-K calc-alkaline signature, and the enclaves are ultrapotassic. In the Harker's diagrams the alignment from mafic-ultramafic enclaves to granites from different massifs area straight. Yb and Ta contents suggest a volcanic arc signature. The field and geochemical data point out that some of the granitic rocks from Sergipano Belt are products of the interaction between mafic-ultramafic lamprophiric magmas and riolitic magmas of crustal nature. *Acknowledgements: We thanks the financial funds from FAPITEC and CNPq to the development of this project.*

Simulating iron(III) oxyhydroxide precipitation kinetics using a polymer-based modelling approach

ANDREW L. ROSE[1*]

[1]Southern Cross GeoScience, Southern Cross University, Lismore, Australia, andrew.rose@scu.edu.au (* presenting author)

Conceptual Framework

The precipitation/dissolution behaviour of iron(III) oxyhydroxides (FeOx) is relatively well understood empirically at a macromolecular scale, but poorly described at the mechanistic level. Previously we have used a polymer-based kinetic modelling approach to describe these processes at the molecular scale (i.e. via mechanistic steps), and shown through a steady-state analysis of the resulting differential equations that this approach is consistent with the thermodynamic notion of a solubility limit.[1] Here I extend this approach to numerically simulate temporal evolution of FeOx precipitation and ageing, and compare simulation results with experimentally observed trends.

Modelling Approach

FeOx precipitation is described by sequential addition of monomeric Fe species (denoted by Fe') to other Fe' molecules and existing FeOx polymers, with kinetics controlled by the rate of water loss from Fe' molecules. FeOx dissolution is described by the sequential loss of Fe' from FeOx polymers, and FeOx ageing is described by internal reorganisation of the bonding structure in polymers. Model simulations with several thousand reactions of this type were run using Kintecus.[2]

Results and Conclusion

The polymer-based approach enabled simulation of key aspects of FeOx precipitation and ageing behaviour, including decreasing apparent reactivity and increasing particle size over time (Figure 1).

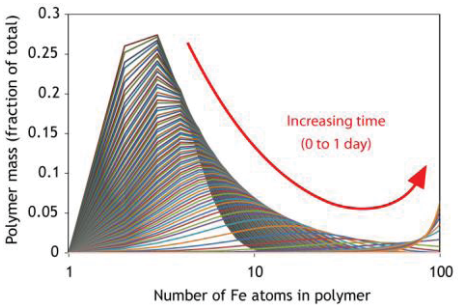

Figure 1: Evolution of FeOx particle size distribution over time at pH 8, as predicted by the polymer-based kinetic modelling approach.

The model was able to simulate the effect of pH on FeOx formation and dissolution kinetics, and successfully reproduced several other experimentally observed phenomena. The polymer-based kinetic modelling approach therefore appears useful to interpret and explain diverse experimental observations in the context of fundamental aquatic chemical reactions.

[1] Rose & Waite (2007) *Geochim. Cosmochim. Acta* **71**, 5605-5619
[2] Ianni (2012) *Kintecus v4.50*, www.kintecus.com

https://doi.org/10.1180/S0026461X00008434 Published online by Cambridge University Press

Trace metals and soil solids: effects of soil heterogeneity on Zn mobility

C.E. ROSENFELD[1*], R.L. CHANEY[2], A. LANZIROTTI[3], C.E. MARTÍNEZ[1]

[1]Pennsylvania State University, Department of Crop and Soil Sciences, University Park, PA, USA, cer196@psu.edu(* presenting author), cem17@psu.edu

[2] USDA ARS Environmental Chemistry Laboratory, Beltsville, MD, USA Rufus.Chaney@ars.usda.gov

[3]Consortium for Advanced Radiation Sources, University of Chicago, Chicago, IL, USA lanzirotti@uchicago.edu

Abstract

Trace metal contamination in soils is a global problem, often causing plant and microbial toxicity and leading to diminished crop production or decreased land cover and subsequent land degradation. In soils, the majority of trace metal contaminants such as Zn are associated with solid phase materials. This can be through cation exchange sites, surface adsorption and/or mineral (co-) precipitation. The specific forms or speciation of metals in soils determines both their bioavailability to plants and microorganisms and their mobility within and out of soils.

In this experiment, we used five contaminated field soils with a variety of sources and Zn:Cd ratios. Bulk soil Zn concentrations ranged from 112 mg/kg up to 26,237 mg/kg with Cd:Zn ratios between 0.05 and 0.003. Each soil was separated using sodium polytungstate, a variable density liquid, into fractions with density less than 1.6 g/mL (light fraction), between 1.6 g/mL and 2.8 g/mL (medium fraction), and greater than 2.8 g/mL (heavy fraction). It is expected that the light fraction contains organic matter, the medium fraction contains aluminosilicate primary and secondary minerals, and the heavy fraction contains high density minerals such as Fe and Mn oxides and their coprecipitates. Each fraction was analysed using μ-XRF, μ-XRD, and μ-XANES to determine the Zn solid phase forms in the natural soils.

The majority of the Zn in four of the five soils resided in the light fraction, though the smelting contaminated soil contained roughly equal light and heavy fraction Zn. A substantial portion of Zn was also present in the medium and heavy fractions of all soils, indicating the transfer of large quantities of Zn between different fractions, regardless of the initial Zn form applied. Based on XANES analysis, the light and heavy fractions from the different soils contain Zn in different chemical environments. Elemental distributions indicated Zn co-location with Fe and/or Mn in heavy fractions, while light fractions often contained Zn co-located with Ca and K as well as Fe and occasionally Mn. μ-XRD data for all soils will also be analysed to confirm differences in mineralogy between fractions and to link with Zn chemical forms.

Soil solids retain substantial portions of toxic trace metals, maintaining the metals within the soil profile and potentially limiting leaching losses to ground and surface waters. Regardless of the initial form, large amounts of the metals are able to transfer between density fractions (e.g. organic matter associated to aluminosilicate associated), indicating that the metals can still be quite mobile among fractions, perhaps impacting their bioavailability as well as their potential for loss via leaching.

Kinetics of Ca-Na ion exchange, induced by CO_2-driven acid dissolution of carbonate minerals

JÖRGEN ROSENQVIST* AND BRUCE W. D. YARDLEY

School of Earth and Environment, University of Leeds, Leeds LS2 9JT, United Kingdom

j.rosenqvist@leeds.ac.uk (* presenting author)

b.w.d.yardley@leeds.ac.uk

During carbon dioxide sequestration in deep geological formations, injected CO_2 will dissolve into the formation water, thus lowering the pH and promoting dissolution of carbonate minerals, e.g. calcite and dolomite. The Ca^{2+} and Mg^{2+} ions from these minerals may stay in solution until eventually reprecipitated as carbonates, but the increased concentrations might also trigger ion-exchange reactions if any clays capable of ion-exchange (e.g. smectites) are present (c.f. [1]). Our knowledge of the kinetics of such ion-exchange reactions is limited, and it is unclear how protons are involved, if at all.

To study the kinetics of the Ca-Na ion-exchange, and the role of protons in the exchange, we have constructed a vessel that allows us to react carbonate minerals and clays in a CO_2-environment at elevated temperature and pressure. pH is continuously monitored, while the concentrations of dissolved ions are determined from fluid samples withdrawn periodically.

The results from two calcite-montmorillonite experiments in different ionic media are presented in Figure 1. In both experiments, calcite dissolution occurred in days, causing rapid increase of calcium in solution. A slow decrease of calcium over the next 2 weeks is attributed to ion exchange, and analysis of the clay fraction at the end of the experiment confirmed a significant increase in Ca. The role of protons is however not clear.

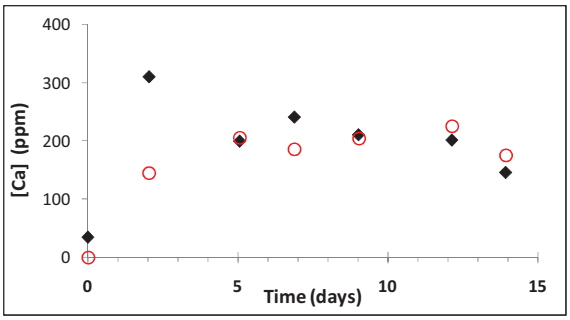

Figure 1: Measured Ca-concentration vs time, in experiments where calcite and Na-montmorillonite were reacted at 70°C and 80 bar CO_2. Filled diamonds: 0.01 M NaCl medium, open circles: 1.0 M NaCl medium.

Our results confirm that the first effect of increased acidity due to CO_2 injection will be dissolution of carbonates in host sediments, but clay minerals are likely to further modify pore water chemistry by ion exchange on the time scale of an injection cycle. This has implications for subsequent precipitation and modification of permeability.

[1] Assyag et al. (2009) *Chemical Geology* **265**, 227-235.

https://doi.org/10.1180/S0026461X00008434 Published online by Cambridge University Press

Revisiting the ^{142}Nd deficits in the 1.48 Ga Khariar alkaline rocks, India

ANTOINE ROTH[1*], ERIK SCHERER[2], COLIN MADEN[3], THORSTEN KLEINE[4], AND BERNARD BOURDON[5]

[1*]ETH Zurich, Institute of Geochemistry and Petrology, Switzerland, antoine.roth@erdw.ethz.ch (* presenting author)
[2]Universität Münster, Institut für Mineralogie, Germany, escherer@uni-muenster.de
[3]ETH Zurich, Institute of Geochemistry and Petrology, Switzerland, maden@erdw.ethz.ch
[4]Universität Münster, Institut für Planetologie, Germany, thorsten.kleine@uni-muenster.de
[5]ENS Lyon, CNRS, and UCBL UMR 5276, France, bernard.bourdon@ens-lyon.fr

The short-lived ^{146}Sm-^{142}Nd chronometer is a sensitive tracer of early silicate Earth differentiation. Expected variations in the abundance of ^{142}Nd are small (max 10-30 ppm) and their detection requires very clean separation of Nd to lower isobaric interferences to negligible levels and multidynamic acquisition scheme during TIMS measurements to account for drifts in detector and amplifier efficiency. The detection of ^{142}Nd deficits may also be hampered by inappropriate mass bias correction if Nd evaporates from multiple domains that are fractionated to different degrees [1].

Whereas early mantle depletion is well documented by <15 ppm ^{142}Nd excesses in Archean rocks [2], evidence for complementary early-enriched reservoirs remains sparse, e.g., [3]. Deficits in ^{142}Nd of up to about 20 ppm were reported for the 1.48 Ga alkaline rocks from the Khariar nepheline syenite complex in southeastern India [4]. These rocks crystallized long after ^{146}Sm was effectively extinct. It was therefore concluded that the Khariar rocks had inherited the Nd signature of an early-formed, low-Sm/Nd reservoir that was preserved (i.e., escaped mixing back into the convecting mantle) for at least 2.7 billion years.

Here we report the results of replicate analyses (double-blind experiment) performed at ETH Zurich for the four Khariar rocks DU-36, DU-1/2, DU-1/4, and DU-9/2. Each sample was digested once. Nd was isolated by classical ion exchange chromatography and Ce was removed using liquid-liquid extraction. Each Nd cut was then split onto two filaments and measured as Nd^+ with a Thermo Triton (TIMS) in multidynamic mode. Repeated measurements of the JNdi-1 standard yielded an external precision of ±5 ppm 2 SD (n=7). Our replicate analyses for the four Khariar rocks show no resolvable ^{142}Nd anomalies and no evidence of mixing among differently fractionated domains on the filament, e.g., [1]. This is in contradiction with previously reported anomalies for the samples DU-1/4 (-13.6 ppm) and DU-36 (-14.4 ppm) [4].

We are currently investigating the reason for the discrepancy between the two data sets, such as mass fractionation, detector linearity, and duration of measurements.

[1] Upadhyay et al. (2008) *JAAS,* **23**, 561-568.
[2] Caro et al. (2006) *GCA*, **70**, 164-191.
[3] O'Neil et al. (2008) *Science* **321**, 1828-1831.
[4] Upadhyay et al. (2009) *Nature* **459**, 1118-1121.

Helium isotopes and gas compositions in Aira caldera: Comparative study of hydrothermal activity at Sakurajima volcano and Wakamiko submarine crater, Japan

EMILIE ROULLEAU[1*], YUJI SANO[2], NAOTO TAKAHATA[3] AND SHINSUKE KAWAGUCCI[4]

[1] The University of Tokyo, AORI, Kashiwa, Japan eroulleau@aori.u-tokyo.ac.jp (* presenting author)
[2] The University of Tokyo, AORI, Kashiwa, Japan ysano@aori.u-tokyo.ac.jp
[3] The University of Tokyo, AORI, Kashiwa, Japan ntaka@aori.u-tokyo.ac.jp
[4] JAMSTEC, Yokosuka, Japan kawagucci@jamstec.go.jp

Aira caldera, located in Kagoshima bay, southern Kyushu, Japan, is a typical example of submerged caldera; it is composed of an active subaerial volcano, Sakurajima, and an active submarine crater, Wakamiko. Sakurajima is a stratovolcano which had its eruptive activity reinforced in the Showa crater since October 2009. Hydrothermal activity such as hot springs is widely observed in the foot of Sakurajima volcano. Wakamiko crater is a submarine depression where lies a hydrothermal activity such as fumarolic gas emissions on the seafloor. Wakamiko hydrothermal activity is considered to be related to the magmatic activity of Sakurajima volcano, but there have been no comparative studies yet to prove it.

In this study, we report He isotopes and gas compositions of hydrothermal waters for both Sakurajima volcano (hot springs) and Wakamiko crater (seawater) to constrain this relationship. First results of helium isotopes for Sakurajima and Wakamiko indicate very consistent values between the two edifices. The ^{3}He/^{4}He ratios for Sakurajima and Wakamiko range from 0.99 to 5.74Ra and 1.09 to 2.81Ra, respectively. Sakurajima ^{3}He/^{4}He ratios are explained by mixing of mantle-derived (MORB) and atmospheric helium dissolved in water (air-saturated water, ASW). Helium ratios in Wakamiko seawater samples increase with depth below the sea surface. Higher δ^3He in samples from 150 to 200m depth indicate a mixing between a mantle-derived component and ASW, as deduced for Sakurajima volcano. The ^{3}He/^{4}He ratio of injected mantle-derived helium component is 6.0±0.3Ra for Sakurajima volcano and 5.9±0.2Ra for Wakamiko crater. This similarity of He signatures for the magmatic source of Wakamiko seawater and Sakurajima hot springs suggests that (1) Wakamiko and Sakurajima share the same magmatic system and (2) the injected mantle-derived helium into the Wakamiko system comes from Sakurajima volcano itself. First results of $CO_2/^3$He ratios (207 to 611×10^9) in Sakurajima hot springs are higher than the average $CO_2/^3$He ratios observed in gas samples in Japan (10×10^9) [1]. High $CO_2/^3$He ratios in hot springs are commonly explained by physical fractionation processes, related to the difference of solubility between He and CO_2 in ground water [2]. However, the ^{3}He/^{4}He and $CO_2/^3$He ratios for Sakurajima decrease with increasing distance from the vent (Showa crater), suggesting that the source of CO_2 (as it is for He) is related to the volcanic activity. These correlations suggest that high $CO_2/^3$He ratios are also the result of addition of CO_2 by decomposition of carbonates from sediment rocks [3].

[1] Hilton et al. (2002). *Rev. Mineral. Geochem.* **47**, 319-370. [2] Sano et al. (1998) *J. Geophys. Res.* **103**, 22,863-22,873. [3] Urabe et al. (1985) *Geoch. J.* **19**, 11-25.

https://doi.org/10.1180/S0026461X00008434 Published online by Cambridge University Press

High ^{36}Cl/Cl ratios and non reactive transport in Chernobyl groundwaters

C. ROUX[1,2*], C. LE GAL LA SALLE[1*], C. SIMONUCCI[2], S. BASSOT[2], D.BOURLES[1], K. FIFIELD[3], N. VAN MEIR[2], L. DE WINDT[4], D.BUGAI[6], J. LANCELOT[1]

[1] UMR 7330, CNRS/Nîmes University/Aix-Marseille University, F-30035, Nîmes cedex 1, France (*correspondences : celine.roux.1@etu.univ-cezanne.fr, corinne.legallasalle@unimes.fr)

[2] IRSN, POB 17, F-92262 Fontenay-aux-Roses, France (caroline.simonucci@irsn.fr)

[3] Department of Nuclear Physics, Australian National University, Canberra ACT 0200, Australia

[4] Mines ParisTech, F-77300 Fontainebleau, France

[5] IGS, National Ukrainian Sciences Academia, U-01054 Kiev, Ukraine.

Introduction

To reduce radiation exposure rates at the site and prevent atmospheric resuspension of radionuclides (RN) released by the Chernobyl reactor 4 explosion (april 1986), about 800 trenches were dug on site to dispose contaminated material: debris, organic matter and topsoil containing reactor fuel particles. Since 1999, the CPS (Chernobyl Pilot Site) project was set up to study the migration of radionuclides from one of these trenches, the trench T22, through the unsaturated and saturated zone. A plume of ^{90}Sr was identified downstream from the trench [1]. The fate of buried RN and migration processes hence needs to be characterised. The aim of this study is to investigate processes governing non-reactive transport from the trench to the groundwater by studying the behaviour of a conservative tracer: ^{36}Cl.

Results and discussion

Significant ^{36}Cl contamination of the groundwater was demonstrated [2] with ^{36}Cl/Cl ratios approximately 10^2 to 10^4 higher than the theoretical natural ratio. New measurements have been performed to complete the dataset. The main source of ^{36}Cl in groundwater is most likely ^{36}Cl from the trench however other ^{36}Cl sources are probable which origins may be: (i) residual contamination after site clean-up and (ii) contamination from upstream trenches. Mixing processes are shown between these two sources. These observations lead to a conceptual non-reactive transport model in the groundwater, which includes the results of previous studies on recharge and groundwater flow system [3][4].

This conceptual non-reactive transport model will be quantitavely tested using the chemistry-transport Hytec code [5]. In a second stage, this model will be considered as a basis to investigate reactive transport for major elements, U and Sr.

[1] Dewiere (2004) *Journal of Environmental Radioactivity* **74**, 139-150.
[2] Roux (2011) *Mineralogical magazine* **75 (3)**, 1760.
[3] Bugai (2011) *Applied Geochemistry*, in press.
[4] Le Gal La Salle (2011) *Applied Geochemistry*, in press.
[5] van der Lee (2003) *Computers and Geosciences* **29**, 265-275.

Coupled Fe and S-isotope composition of sedimentary pyrite: Implications for Precambrian ocean chemistry and isotope biosignatures

OLIVIER J. ROUXEL[1] AND ANDREY BEKKER[2]

[1] IFREMER, Centre de Brest, and UEB-IUEM, 29280 Plouzané, France, (orouxel@ifremer.fr)

[2] University of Manitoba, Winnipeg, Canada, (bekker@cc.umanitoba.ca)

The rise of atmospheric oxygen level at ca. 2.3 Ga have led to dramatic shifts in the Fe-C-S oceanic cycles. Past studies of the Fe and S isotope record in sedimentary sulfides over geological time have placed important constraints on the evolution of the Precambrian ocean chemistry. Since the biogeochemical cycles of Fe and S are closely coupled in marine systems, Fe-limitation and S-limitation for pyrite formation in black shales should leave a coupled imprint on the isotopic record of both elements.

Here, we investigated the fine scale variations of Fe and S isotopic compositions of diagenetic pyrite nodules in several Devonian, Paleo-proterozoic and Archean black shales in order to (1) explore potential biosignatures using co-variations of Fe- and S-isotopes at the grain-size scale; (2) assess potential diagenetic effects on Fe-isotope fractionation during sulfide formation; and (3) assess potential mixing between isotopically distinct pools of Fe and S using multiple S isotope data. Results show that Devonian pyrite display a range of 50‰ in δ^{34}S values whereas δ^{56}Fe values vary between –1.0 and +0.1‰ consistent with Fe isotope variations in modern marine sediments. Similarly, pyrite in the 1.88 Ga Gunflint Formation has δ^{34}S values ranging from –32‰ to +10‰ and displays a range of δ^{56}Fe values between 0 to –0.4‰. In contrast, Archean black shales display a smaller range of δ^{34}S values between –5 and +18‰ but a larger range of δ^{56}Fe values from –3.5 to +0.2‰. A transitional period between 2.3 and 1.8 Ga is marked by a larger spread of δ^{34}S values from –34 to +28‰ and a larger range of δ^{56}Fe values from –1.7 to +1.1‰. These results confirm that after the rise of atmospheric oxygen, the Paleoproterozoic ocean became stratified and gradually affected by an increase of sulfate concentration in an Fe-limited system whereas pre-2.3 Ga ocean was S-limited and characterized by extensive Fe-oxide precipitation and redox cycling. This transition was also linked to profound changes of microbial processes, diagenetic conditions, and Fe redox cycling, that are all ultimately linked to the evolution of the global ocean chemistry.

We also investigated the chemolithostratigraphic variations of Fe-isotopes and Fe speciation in order to establish an Fe isotopic mass balance in black shales and its relation to environmental conditions. All together, our results confirm the existence of an isotopically negative, anoxic, Fe-rich seawater pool before 2.3 Ga, which may be in part fueled by dissimilatory Fe reduction as well as hydrothermal input. Regardless of potential Fe sources, light Fe isotope signatures in Archean and Paleo-proterozoic oceans are consistent with partial Fe oxidation in the photic zone, leading to the precipitation of isotopically enriched Fe-oxides and fueling extensive microbial Fe cycling.

https://doi.org/10.1180/S0026461X00008434 Published online by Cambridge University Press

Deep Sea Metalliferous Deposits as Modern Analogues for Ancient Marine Environments

OLIVIER J. ROUXEL[1,2*], YOHANN RESNAIS[2], NOLWENN CALLAC[1], AND PIERRE ANSCHUTZ[3]

[1] IFREMER, Centre de Brest, Dept. Ressources physiques et Ecosystèmes de fond de Mer , 29280 Plouzané, France, (orouxel@ifremer.fr)
[2] Université Européene de Bretagne, IUEM, 29280 Plouzané, France
[3] Université de Bordeaux 1, UMR CNRS 5805 EPOC, 33405 Talence, France

Modern seafloor metalliferous deposits provide unique analogues of ancient deposits currently mined on land. Their study is crucial for the establishment of genesis models and their relationships to oceanic and crustal evolution through time. Trace metal concentrations and isotopic compositions of laminated, organic matter-rich sediments (i.e. black shales) and iron formations are now widely used to draw inferences concerning paleoredox conditions as well as metal inventories in ancient oceans. Transition metal isotope geochemistry (e.g. Fe and Mo isotopes) is of special interest due to its potential to provide information about the biogeochemical cycling of bio-reactive metals, which allows both quantitative and qualitative estimates of their sources and sinks in the oceans. However, despite the increasing number of investigations, it is still unclear whether ancient metalliferous deposits and organic matter-rich rocks faithfully record ocean-scale processes, considering the importance of diagenetic and hydrothermal overprinting.

Here, we will focus on "calibrating" and "proving" a range of proxies - in particular Fe-isotopes - by undertaking a comparison between ancient metal deposits and modern seafloor metalliferous deposits. We will present geochemical and Fe-isotope signatures of (1) exhalative metalliferous sulfide and oxide deposits from the Atlantis II Deep, Red Sea which offers a unique modern analogue of laterally extensive metalliferous deposits such as ancient SEDEX deposits and possibly banded iron formation; (2) organic matter-rich sediments from the Guaymas Basin seafloor hydrothermal field as modern analogue of Precambrian black shales that are considered to be affected by hydrothermal metal input and reworking; (3) hydrothermal Fe-oxide deposits and microbial mats from the Loihi Seamount hydrothermal field which provides an ideal system in which to test hypotheses on biotic vs. abiotic origin of iron formation and Fe-isotope biosignatures.

This comparative approach should provide better constraints on the effects and signatures of hydrothermal overprinting on the ancient ocean rock record, ultimately leading to a better understanding of mechanisms of metal redox-cycling and microbiological interactions in ancient oceans.

Individual organic compounds in oil sands process-affected waters: identification and toxicity

STEVEN ROWLAND*, CHARLES WEST, ALAN SCARLETT AND DAVID JONES

Plymouth University, Biogeochemistry Research Centre, srowland@plymouth.ac.uk (* presenting author)

Introduction

The toxicity of oil sands process-affected water (OSPW) has often been at least partially attributed to compounds given the uninformative term 'naphthenic acids' (NA). Until our studies in 2011, no-one knew what any of these NA in OSPWwere, or how toxic they were [1-4]. Even now, many compounds remain to be identified and the concentrations remain to be accurately measured with isotopically-labelled analogues.

The present study therefore describes use of gas chromatography x gas chromatography-mass spectrometry (so-called' 2D GCMS'or GCxGC-MS) with both nominal and accurate mass resolution, 'normal' and 'reversed' phase GC column couplings and synthesised isotopically labelled authentic standard compounds, to identify and measure the individual NA components of OSPW. The distributions of the acids can be used to profile and distinguish different sources of NA in the environment.

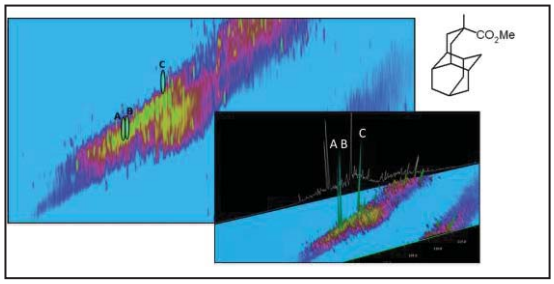

Figure 1: GCxGC-MS mass chromatogram of some of the individual isomers of tetracyclic acids (methyl esters) in OSPW.

Results and Conclusion

Use of trideuterated analogues of diamondoid acids (e.g. esters of adamantane carboxylic acids) and measurement of electron ionisation response factors for the analytes and for the deuterated internal standards, allowed the cocntrations of individual NA in OSPW from different industrial processors of oil sands ore, to be measured for the first time. GCxGC-MS with high accuracy mass resolution and reversed phase GCxGC columns allowed novel acids to be identified with greater certainty. Synthesis of novel acids allowed the toxicity to a number of biological endpoints to be determined. Such studies remove some of the need for speculation about the actual toxicants in OSPW.

[1] Rowland *et al*. (2011)*Environ. Sci. Technol.* **45,** 3154-3159. [2] Rowland *et al*. (2011) *Rapid Commun. Mass Spec.* **25,** 1198-1204. [3 Rowland *et al*. (2011) *Environ. Sci. Technol.* **45,** 9806-9815. [4] Jones *et al*. (2011) *Environ. Sci. Technol.* **45,** 9776-9782.

https://doi.org/10.1180/S0026461X00008434 Published online by Cambridge University Press

A short oceanic residence time for Hf: element/isotope comparison

M. ROY-BARMAN[1*], S. MARCHANDISE[2]

[1]Laboratoire des Sciences du Climat et de l'Environnement, France, Matthieu.Roy-Barman@lsce.ipsl.fr (* presenting author)
[2]Laboratoire des Sciences du Climat et de l'Environnement, France, Sandra.Marchandise@lsce.ipsl.fr)

The oceanic residence time of isotopic tracers is a key parameter for their use in paleo-oceanography. Despite the recent direct determination of the Hf isotopic composition (ε_{Hf}) of seawater and of high resolution GEOTRACES sections, the Hf oceanic residence time remains poorly relatively constrained. River input budget suggest a residence time of 400-1500 y [1,2]. The variability of ε_{Hf} are difficult to use to estimate Hf residence time because the ε_{Hf} of continental inputs to dissolved Hf are not well constrained due to the storage of the Hf of crustal rocks in unsoluble and unradiogenic zircons. It is generaly admitted that the Hf residence time is grossly in the same range as the Nd residence time.

Here litterature data available are reviewed and used to constrain the isotopic residence time of Hf as well as the isotopic variability of the continental inputs:

- Hydrothermal plumes do not seem to affect Hf vertical profiles demonstrating that Hf is primarily of continental origin [2].
- As Hf and Nd inputs are dominated by lithogenic sources, it is likely that Hf inputs to the ocean are dominated by "boundary exchange" like Nd rather than by river inputs.
- A first order estimate of the Hf residence time can be obtained from the fraction of Hf in seawater present in the labile/seawater-derived fraction of particulate matter [3]. Comparison between Hf, Nd and Th suggests a Hf ocean residence time of 100 (compared to 380 y for Nd).
- Simple modeling implies that there is an inverse relationship between the ocean residence time of a radiogenic tracer such as (ε_{Hf}) and the variability of its isotopic composition in the ocean compared to its souce. A residence time as short as short 100 y implies that the variability of ε_{Hf} in the ocean is smaller but close to the variability of ε_{Hf} in continental sources of dissolved Hf. It implies that in a ε_{Hf} - ε_{Nd} diagram, the slope of seawater array matches the slope of the continental inputs and is only 1/3 of the slope of the terrestrial array.
- Inventory of Lu-Hf rich minerals in marine sediments confirms that Hf is mainly contained in zircons even in fine sediments allowing a preferential release of radiogenic Hf. Preferential storage of Lu in xenotime and zircon limits this preferential release [4].

The short residence time of Hf compared to Nd explains the decoupling observed between ε_{Hf} and ε_{Nd} in the present and past ocean.

[1] Zimmerman (2009) *Geochim. Cosmochim. Acta* **73**, 91–101.
[2] Firdaus et al. (2011) *Nat. Geosci.* **4**, 227-230.
[3] Firdaus et al. (2008) *J. Oceanogr.* **64**, 247-257.
[4] Marchandise et al. (2012) *Earth Planet. Sci. Lett.* **Submitted.**

Synthesis, characterization and stabilities of Mg-Zr(IV)-Al-Cl containing layered double hydroxides (LDHs)

KONSTANTIN ROZOV[1*], HILDE CURTIUS[1], AND DIRK BOSBACH[1]

[1]Forschungszentrum Jülich, Institut für Energie- und Klimaforschung, IEK-6, Jülich, Germany, k.rozov@fz-juelich.de (* presenting author)

Layered double hydroxides (LDHs) are of interest as potential sorbents for anionic radionuclides. In the present study the investigation of Zr-containing LDHs was performed because such substances were identified as specific secondary phases in corrosion products under repository relevant conditions of disposed research reactor fuel elements [1].

LDHs $Mg_3Al_{1-x}Zr_x(OH)_8Cl_{1+x}\cdot nH_2O$ with variable Zr(IV) content and fixed cationic ratio $Mg^{2+}/(Zr^{4+}+Al^{3+}) \approx 3$ were synthesized by co-precipitation method at 25 °C and pH = 10.00±0.05. PXRD measurements confirm the presence of a LDH single LDH phase. Cell parameters as a function of zirconium content (x_{Zr}) follow Vegard's law and corroborate the existence of a continuous solid solution series.

Results of infrared (IR) spectroscopic measurements clearly show strong OH^- (3482 cm^{-1}) and H_2O (1636 cm^{-1}) stretching and bending bands. The presence of small quantities of CO_3^{2-}-groups in the interlayer was detected by observation of the very weak band at 1376 cm^{-1}.

TGA measurements demonstrated the temperatures at which interlayer H_2O, Cl^--anions and OH-groups are lost. Moreover, we established that the increase of Zr(IV)-content in LDH solids does not result in a visible changes of the temperatures of removal of the interlayer H_2O, dehydroxylation of brucite-like layers and lost of Cl^-- anions.

Using the Gibbs free energy minimization software GEMS [2] and based on chemical analyses of the LDH solids and corresponding liquids after syntheses we provided the first estimates of $G°_{298}$ of Zr-containing hydrotalcites.

For the further investigations with Zr(IV)-containing hydrotalcites additional careful designed synthesis and dissolution studies at elevated temperatures will be performed. These studies will provide more data about thermodynamic properties (i.e. standard molar Gibbs free energies, entropies and heat capacities) of such phases in order predict their behaviour and retention properties at conditions of nuclear waste disposal environments.

[1] *Curtius et al (2009) Preparation and characterization of Zr-IV containing Mg-Al-Cl layered double hydroxide* ***Volume 97****, 423- 428.*
[2] *Kulik GEM-Selektor. Research package for thermodynamic modeling of aquatic (geo)chemical systems by Gibbs Energy Minimization. http://gems.web.psi.ch.*

https://doi.org/10.1180/S0026461X00008434 Published online by Cambridge University Press

Generation of moderately to very alkalic young Honolulu Series lavas from Th-U-Os-Pb-Nd-Sr isotopes

K.H. RUBIN[1*], D.G. PYLE[1], C.R. RUSSO[1], D. VONDERHAAR[1], G. RAVIZZA[1], D.A. CLAGUE[2]

[1]Dept. of Geology & Geophysics, Univ. of Hawaii, Honolulu, HI 96822 USA (*correspondence: krubin@hawaii.edu)
[2]MBARI, 7700 Sandholdt Road, Moss Landing, CA 95039 USA

The Honolulu Series volcanics on the Hawaiian Island of Oahu, are a type locality of alkalic ocean island rejuvenation stage magmatism. They have been studied by multiple researchers over the past several decades. Rejuvenation volcanism episodically spanned nearly 1 Myr. Our study focuses on the last two groups of eruptions (at ca 80 Kyr, Rubin et al., unpub.), which are known to represent the compositional extremes of the series. Lavas and pyroclasts of the Koko (subaerial/submarine) and Tantalus (subaerial) rift zones are mildly to highly silica undersaturated and alkalic (45-47 and 37-41wt% SiO2; 3.5-5 and 5.5-7 wt% tot. alkalis, respectively), and thought to be derived by small degrees of melting of one or two oceanic mantle source(s), perhaps containing exotic residual mineralogy (multiple authors, too numerous to cite).

We find highly correlated variations in Th/U and age-corrected ($^{230}Th/^{238}U$) in both lava groups, ranging to extreme disequilibria of >50%. Very small degree melts are likely involved. Both groups span the same U-series range, with no correlation to alkali content or other major element indicators of rock composition (e.g., SiO_2, MgO, TiO_2). Disequilibria are not correlated with trace element indicators of residual garnet (e.g., La/Yb). Relationships to tracers that would be sensitive to a Cretaceous lithosphere influence (e.g., $^{187}Os/^{186}Os$) are weak to non-existent. Sr-Nd-Pb isotopic variations are smaller in our sample set than the extant literature. Ratios are nearly constant in the Tantalus samples; Koko lavas display small but significant Pb and more subtle Nd isotopic variations, indicating variable or mixed source chemistry. Pb and Nd isotopes are correlated with U-series signatures on the Koko rift zone. We use these data to discuss the petrogenenis of these magmas and to evaluate both previously proposed and new models for their generation in the asthenosphere, lithosphere or both. The U-series disequilibria appear to require a magmatic phase that can strongly enrich Th relative to U without a strong effect on most LIL or REE.

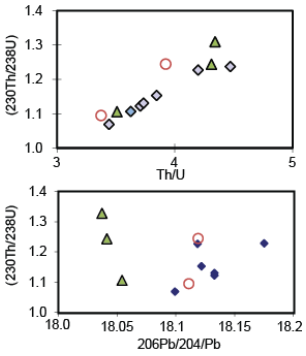

Figure #1: $(^{230}Th/^{238}U)_{meas.}$ verus Th/U and $^{206}Pb/^{204}Pb$ in Koko (diamonds), submarine Koko (circles) and Tantalus (triangles) lavas.

Craton formation

ROBERTA L. RUDNICK*[1]

[1]Geochemistry Laboratory, Department of Geology, University of Maryland, College Park, MD 20742 USA

Archean cratons throughout the world share key features indicating a commonality of processes in their formation and modification. These features include: a) a thick (110 to 220 km) keel of refractory peridotite (typical Fo of 92-93), b) generally increasing fertility of peridotites in the lowermost sections of keels, c) rhenium-depletion model ages of cratonic peridotites that are similar to the age of the overlying crust, d) presence of lithospheric diamonds, as well as diamonds with lower mantle mineral inclusions, now described from most cratons, e) low surface heat flow, averaging 40 mWm^{-2}, f) a ~40 km thick crust composed of granites and greenstone belts at the surface, with increasing seismic velocities with depth, but average intermediate to felsic bulk crustal compositions.

The two classes of competing hypotheses for formation of Archean cratons: plume subcretion vs. stacking and accretion of subducted oceanic lithosphere, do not account for all of the above features, particularly the presence of evolved continental crust overlying refractory mantle peridotite (whose complementary melt must be high Mg-Fe basalt, picrite, or komatiite, -- rare lithologies in cratons). If cratonic peridotite forms via melt extraction at Archean oceanic spreading centers [e.g., 1], and assuming that the density of the Fe-rich basaltic crust is sufficient to cause the lithosphere to founder (subduct?), then cratonic mantle may form from buoyant diapirs of harzburgite mechanically segregated from downgoing lithosphere in the transition zone or deep mantle (where some diamonds grow?) that underplate nacsent cratonic crust formed during partial melting of the downgoing basaltic/picritic crust. Rare eclogites found within cratonic mantle lithosphere may be fragments of the (residual?) oceanic crust that were entrained in the buoyant harzburgite diapirs. Assuming the buyoant tonalitic melts that formed by partial melting of foundering oceanic crust intrude and rise to the top of pre-existing picritic crust, there is still a need to remove picritic material from the deep crust. This could be accomplished by delamination [2] or overturn of lithospheric mantle [3], followed by recycling of eclogitic material. The latter hypothesis has the added attraction of explaining the late granite blooms that occur in most cratons well after their original formation and stabilization. The common occurrence of more fertile peridotite near the base of cratonic keels likely reflects refertilization associated with intrusion of basaltic magmas over the long history of the cratons as they move about the surface of the Earth.

[1] Herzberg et al., (2010) *Earth and Planetary Science Letters* **292**, 79-88. [2] Bedard, J.H. (2006) *Geochimica et Cosmochimica Acta* **70**, 1188-1214. [3] Percival, J.A. and Pysklywec, R.N. (2007) *Earth and Planetary Science Letters* **254**, 393-403.

https://doi.org/10.1180/S0026461X00008434 Published online by Cambridge University Press

Kinetic and step-specific effects on boron incorporation into calcite during growth

ENCARNACION RUIZ-AGUDO[1,2], CHRISTINE V. PUTNIS[2], MAGDALENA KOWACZ[3], AND ANDREW PUTNIS[2*]

[1]Dept. Mineralogy and Petrology, University of Granada, Granada, Spain, encaruiz@ugr.es

[2]Institut für Mineralogie, Universität Münster, Münster, Germany, putnisc@uni-muenster.de (*presenting author)

[3]Instituto de Tecnologia Química e Biológica, Universidade Nova de Lisboa, Oeiras, Portugal, magda@itqb.unl.pt

Reconstructions of ancient ocean pH are critical for evaluating past changes in the atmospheric CO_2 concentration and thus to obtain insights into the evolution of Earth's climate. These reconstructions are currently based on analysis of the boron composition of marine carbonates such as foraminifera or corals, e.g. [1,2]. The correlations observed between B concentrations and $\delta^{11}B$ in carbonates and the pH of the precipitating fluid in inorganic experiments [3,4] suggest that $\delta^{11}B$ and, possibly, the boron composition of carbonates, reflect changes in the pH of the solution from which they precipitated.

Nevertheless, there are still several aspects on the use of boron isotopes for the reconstruction of past seawater pH that require further investigation. In particular, questions related to the mechanism of boron coprecipitation with carbonates remain essentially unexplored. Although the increase in B incorporation with increasing pH can be explained largely by the change in boron speciation, it cannot be ruled out that other factors, such as kinetic effects associated with changes in growth rate [3], may also play a role.

As has been shown for many other elements, boron incorporation mechanisms cannot be simply studied by means of macroscopic measurements; molecular-scale studies are essential to obtain truly representative information of the surface processes taking place during B coprecipitation with calcite. In this study, boron incorporation during calcite growth was investigated using Atomic Force Microscopy (AFM), as a function of pH, supersaturation and boron concentration. Our results indicate that, together with pH, changes in the saturation degree of the precipitating solution and, as a consequence, in the calcification rate are a key factor to consider when using boron in marine carbonates as a paleo-pH proxy, as these factors could influence the extent of boron incorporation and, maybe, its isotopic signature. As well, this study shows that the calcite crystallographic form in which boron is incorporated may be also a critical factor controlling the amount of boron incorporated and that a change in the site preference of boron for its incorporation into calcite could occur depending on the species which is incorporated and, consequently, on the pH of the precipitating solution. Finally, our nanoscale observations give indirect evidence of the incorporation of boron in non-lattice sites.

[1] Rollion-Bard, C. and Erez, J. (2010) *Geochimica et Cosmochimica Acta* **74**, 1530-1536. [2] Rollion-Bard, C. et al. (2010) *Geochimica et Cosmochimica Acta* **75**, 1003-1012. [3] Hobbs, M.Y, and Reardon, E.J. (1999) *Geochimica et Cosmochimica Acta* **75**, 1003-1012. [4] Sanyal et al. (2000) *Geochimica et Cosmochimica Acta* **64**, 1551-1555.

Nucleation and crystal growth in confined nanopores

ANNE RUMINSKI[1] AND JEFFREY URBAN[1]

[1]Lawrence Berkeley National Laboratory, Molecular Foundry, Materials Sciences Division

Storage of carbon dioxide in deep geological formations has emerged as an important option in managing anthropogenic CO_2 [1]. One concern of this storage method is the unknown long-term stability of injected CO_2. Moreover, it will be necessary to seal injection reservoirs to prevent release of gases and fluids. The precipitation of metal carbonate bearing minerals in pore spaces is one possible path for both sealing off reservoirs and securely binding injected CO_2. In general, crystallization from solution occurs at solid-liquid interfaces. The detailed structure of the solid surface plays a critical role in liquid-solid phase transformations [2]. Nucleation and crystallization of these metal carbonates are greatly influenced by the surface shape, roughness, chemical species present, and nanoscopic confinement of the native metal oxides. Current understanding of the thermodynamics and kinetics of nucleation and growth is primilarly based upon analyses of homogenous systems near equilibrium; distinctly different from the supersaturated systems with complex interface structures that would be found at real reservoir sites.

Our aim is to bridge this gap, gaining a better understanding of how the subsurface environment influences the earliest stages of mineralization of sequestered CO_2 at nanoscale dimensions. We will examine the rates of metal carbonate nucleation and growth as a function of material surface structure and chemistry. Thin films of silica containing nanometer sized pores of different shapes and dimensions will be screened for preferential crystal nucleation and growth. In-situ transmission electron microscopy utilizing a fluid cell designed with temperature and electrochemical control will be employed to monitor and drive surface-directed crystal growth in real time.

[1] Metz *et. al.* (2005) *Special Report on Carbon Dioxide Capture and Storage, Intergovernmental Panel on Climate Change.* [2] Diao, *et al*., (2011) *Langmuir*, **27**, 5324-5334.

https://doi.org/10.1180/S0026461X00008434 Published online by Cambridge University Press

Glacier sensitivity to climate change: observations and modeling

SUMMER RUPPER[1*], JOERG M. SCHAEFER[2], LANDON BURGENER[1], RYAN SMITH[1]

[1]Geological Sceinces Brigham, Young University, Utah, USA, summer_rupper@byu.edu (*presenting author) landonburgener@gmail.com ryan.glen.smith@gmail.com

[2]Lamont-Doherty Earth Observatory, Columbia University, New York, USA, schaefer@ldeo.columbia.edu

Glacier Sensitivity to Climate

A suite of general circulation model simulations and a glacier equilibrium line altitude model are used to test the sensitivity of Asian glaciers to climate changes at the Last Glacial Maximum (21 ka) and mid-Holocene (6 ka) [1,2]. The model simulations provide a test of glacier sensitivity to changes in climate boundary conditions. The results show that glacier sensitivity is strongly dependent upon the accumulation setting. In particular, the high accumulation regions of the southeastern Himalaya are most sensitive to changes in temperature and least sensitive to changes in precipitation. The reverse is true in the dry, interior plateau.

The intermodal differences for both 21 ka and 6 ka highlight regions where climate model uncertainty is greatest [3]. In particular, the southeastern Himalaya is a region where intermodel variability in temperature is extremely high, yet few paleoclimate proxies and glacier studies are available to help constrain the models. This is a region where paleoclimate and glacier reconstructions can provide crucial information for global and regional climate modelling efforts.

Southeastern Himalaya: Bhutan

Glacier retreat in the Himalayas impacts societies in the most densely populated area on earth by affecting river-discharge, hydro-energy and agricultural production, and glacial lake outburst flood potential. Bhutan sits in the bulls-eye of highest accumulation, where glacier sensitivity to temperature is greatest, and where there is a severe modern and paleo-climate data gap. Bhutan is therefore a region of potential scientific importance. In addition, Bhutan is representative of the potential societal impacts of glacier changes. Here we present quantitative predictions for glacier area and meltwater flux changes in Bhutan. Based on gridded climate data and a simple glacier melt model, our results show that Bhutan's glaciers lag behind the climate forcing considerably. Under the conservative scenario of an additional 1°C warming, about half of Bhutan's glaciers would disappear and the meltwater flux would drop to 20% of today's value. Even with no additional warming, almost 20% of the glaciated area would vanish and the meltwater flux would drop by 50%.

The results of the Bhutan study highlight the need to decrease uncertainty in glacier sensitivity to climate change. Given the transient nature of current climate and glacier systems, quantifying glacier sensitivity will rely heavily on well-documented glacier and climate histories. These longer term records are critical to quantifying the non-stationarity of glacier sensitivity, placing recent glacier and climate changes into context of longer term patterns, and validating both glacier and climate models.

[1] Rupper and Roe (2008) *J. of Climate* **21**, 5384-5401. [2] Rupper *et al.* (2009) *Quaternary Res.* **72**, 337-346. [3] Rupper and Koppes (2010) *IOP Earth and Environmental Science*. doi:10.1088/1755-1315/9/1/012009.

Mantle signals in olivine phenocrysts in arc volcanics

PHILIPP RUPRECHT[1*], TERRY PLANK[1]

[1] Lamont Doherty Earth Observatory of Columbia University, Palisades, NY, USA, ruprecht@ldeo.columbia.edu (* presenting author)

Volcanism is fed by crustal storage reservoirs recharged ultimately with mantle-derived primitive melts. In particular withinin arc magmatic systems the nearly ubiquitous processes of mixing, hybridization, and crystallization combine to obscure the diversity of melts from the mantle. Isotope and trace element ratios of volcanic rocks and melt inclusions may help to reveal mantle inputs, but we explore here an alternative approach that uses trace element zonation in primitive olivines. Such zonation patterns both record the diversity of primary melts and provide a mechanism to constrain the timescales of mantle recharge and magma ascent through the entire crustal column.

Laser ablation-ICPMS and electron microprobe traverses provide extensive datasets of major and trace element zonation profiles in large populations of olivine (n>100). We focus here on Irazú volcano, in Costa Rica, as a typical strato-volcano from a continental arc, but we have extended our approach to other arc volcanic systems (Volcano A and West Mata in Tonga and Los Hornitos in Chile). The hybrid basaltic andesites that erupted from Irazú in 1963-65 bear abundant, primitive olivine crystals (up to 70 % of olivines include zones of >Fo88). Ni zonation varies within individual crystals by more than 500 ppm at nearly constant, high Fo content (>Fo88), recording the mixing of different mantle melts. The overall range of Ni in these magnesian olivines (2000-4000 ppm) is consistent with pyroxenitic and peridotitic mantle sources. Zonation profiles can be modeled by diffusive re-equilibration of Ni following a mixing event that sometimes creates a reversal (increase) in Ni. We calculate mixing time scales for these near-primary olivine phenocrysts that range from seven months to five years, accounting for anisotropic elemental diffusion in olivine (lattice orientation with respect to diffusion direction determined by electron backscattered diffraction). These short timescales are on the order of the duration of the eruption itself, providing new evidence for recharge of melts directly from the mantle, feeding on-going andesite eruptions at large stratovolcanoes. As the mixing of these distinct mantle melts occurs at least below the Moho (~ 35 km beneath Irazú), we can calculate average ascent rates of 10-100 m per day for magma to traverse the entire crustal column. Given that syn-eruptive ascent is likely very fast in the uppermost part of the magmatic column (typically from 5-10 km depth of the shallow magma chamber to the surface) we can infer that even in the lower and middle crust average ascent rates are >10 m per day. These rates are relevant to real-time geophysical observations of volcanic plumbing systems from the mantle to the surface.

https://doi.org/10.1180/S0026461X00008434 Published online by Cambridge University Press

Planetary oxidation and the biogeochemistry of exoplanets

ANDREW J. RUSHBY[1*], ANDREW J. WATSON[1], MARK W. CLAIRE[1]

[1]School of Environmental Sciences, University of East Anglia, Norwich, U.K.
*andrew.rushby@uea.ac.uk

Atmospheric oxygen is considered a fundamental prerequisite for the evolution of complex organisms with high metabolic demands. On Earth, this requirement can only be met by aerobic respiration. The main source of oxygen on Earth is biological, originating as a by-product of oxygenic photosynthesis. However, geological and planetary factors are important in controlling the relative abundance of oxygen in the atmosphere.

Over geological timescales, planetary oxidation is controlled by two mechanisms: the burial of organic carbon [1] and hydrogen escape from the upper atmosphere [2]. The relative importance of these processes varies significantly over time; hydrogen escape was an important oxidising mechanism during the early evolution of the planetary atmosphere, but represents only a limited source of oxidising power today when compared to the burial of organic carbon.

However, it seems that the 'default' state of the planetary atmosphere is reducing [3], and the oxidising atmosphere of the Earth is unusual. The homeostasis of atmospheric oxygen is perhaps the most obvious example of biogeochemical coupling on the Earth. Is the co-evolution of oxygen and biosphere likely to be a fundamental characteristic of habitable, life-bearing planets?

Planetary characteristics undoubtedly exhibit a fundamental control over these oxidising processes, but our understanding of these factors remains limited. Planet mass may play a particularly important role in controlling hydrogen escape for example, and an upper and lower mass limit must exist beyond which this mechanism fails or operates too slowly or too rapidly to contribute any lasting geochemical signal. Biology is the primary controlling factor in regards to carbon burial, representing the main pathway for organic carbon fixation. However, geological recycling processes enable the burial of organic carbon, and the rate and duration of these mechanisms are sensitively dependent on a number of planetary variables.

Modern biogeochemical models (eg: COPSE [4]) can resolve the rise of oxygen in acceptable agreement with geochemical proxies, but are difficult to apply to planets other than the Earth. Preliminary results from a simplified version of this model return estimates for 'oxygenation time' that vary over several orders of magnitude when forced by either hydrogen escape or carbon burial alone. It is hoped that this model can begin to reconcile these two fundamental processes over time, but also resolve potential oxygen fluxes operating on extrasolar planets, with extensive application to the search for habitable extrasolar planets as well as the emerging field of astrobiology.

[1]Hayes and Waldbauer (2006) *Phil. Trans. R. Soc. B* **361** 931-950 [2] Catling et al. (2001) *Science* **293** 839-843 [3] Kasting et al. (1993) *Journal of Geology* **101** 245-257 [4] Bergman et al. (2004) *American Journal of Science* **304** 397-437

Origin of silicic magmas in the primitive, intra-oceanic Tongan arc

T. RUSHMER[1*], S.TURNER[1], J. CAUFILED[1], M. TURNER[1], S. CRONIN[2] AND I. E. SMITH[3]

[1]Department of Earth and Planetary Sciences, Macquarie University, Sydney 2109, Tracy.Rushmer@mq.edu.au*
[2]Insitute of Natural Resources, Massey University, Palmerston North, New Zealand, S.J.Cronin@massey.ac.nz
[3]Department of Geology, Auckland University, Auckland, PB92019, New Zealand, ie.smith@auckland.ac.nz

The origin of felsic magmas (> 60% SiO_2) in intra-oceanic arc settings is a matter of much current debate. In essence, two very different processes are currently invoked: fractional crystallization of basaltic magma and partial melting of lower crustal amphibolites. Importantly, the physical conditions, such as pressure, melt reactions, rates of melting and fluid dynamics of melt extraction differ markedly between the two mechanisms. Concurrently, a number of sophisticated numerical models of lower crustal amphibolite melting have been developed over the past decade. Such models are becoming widely invoked so there is a need for their applicability to be tested. Fonualei is unusual amongst subaerial volcanos in the Tonga arc because it has erupted dacitic vesicular lavas, tuffs and phreomagmatic deposits for the last 165 years and makes for an excellent natural laboratory. All of the products are crystal-poor and formed from relatively low viscosity magmas inferred to have had temperatures of 1100-1000 ºC, 2-4 wt. % H_2O and oxygen fugacities 1-2 log units above the QFM buffer.

Major and trace element data, along with Sr-Nd-Pb and U-Th-Ra isotope data, are used to assess competing models for the origin of the dacites. Positive correlations between Sc and Zr and Sr rule out evolution by closed-system crystal fractionation and an origin by direct partial melting of amphibolite cannot reproduce the data either. Instead, we develop a model in which the dacites reflect mixing between two dacitic magmas, both products of fractional crystallization of basaltic-andesite magma. Mixing was efficient because the two magmas had similar temperatures around 1000 ºC. This is inferred to have occurred around 6 km depth beneath the volcano and the relative proportion of the fractionation-derived dacite has increased over the 165 year eruption period implying crystal fractionation and mixing may all have occurred on a similar timescale. U-Th-Ra disequilibria in the basaltic-andesite and andesite indicate that the magmas parental to the fractionation produced dacite had fluids added to their mantle source regions less than 8 kyr ago.

https://doi.org/10.1180/S0026461X00008434 Published online by Cambridge University Press

Real-time elemental and isotopic analysis at atmospheric pressure in a laser ablation plasma

R.E. Russo[1*], X.L. Mao[1], A.A. Bol'shakov[2], and J.Yoo[2]

[1]**Lawrence Berkeley National Laboratory, Berkeley, USA,**
rerusso@lbl.gov (* presenting author)
xlmao@lbl.gov
[2]Applied Spectra, Inc, Fremont,CA USA,
alexandb@appliedspectra.com
jyoo@appliedspectra.com

Laser Ablation Molecular Isotopic Spectroscopy (LAMIS)

Would the ability to immediately analyze any sample in the field for elemental and isotope content be of value to the geological community? It is possible and this talk will describe a new technology that offers just that capability. The technology has been named LAMIS for Laser Ablation Molecular Isotopic Spectroscopy. By expanding the capabilities of a classical laser plasma technology known as LIBS (Laser Induced Breakdown Spectroscopy) to emphasize the measurement of molecular emission spectra in addition to elemental, LAMIS provide geologist with a tool for measuring all elements and their isotopes, including light elements like Li, Be, C which are impossible with XRF. The basis of LAMIS is to analyze a tiny amount of the sample using the laser beam. No sample preparation or consumables are needed. We have developed LAMIS to date by establishing its ability to measure B, C, H, D, Sr and other isotopes. We have demonstrated down to percent levels for sensitivity and have experimental plans to meet ppm levels. This talk will describe the previous isotope work that has been reported in LIBS plasmas and show how LAMIS expands those capabilities.

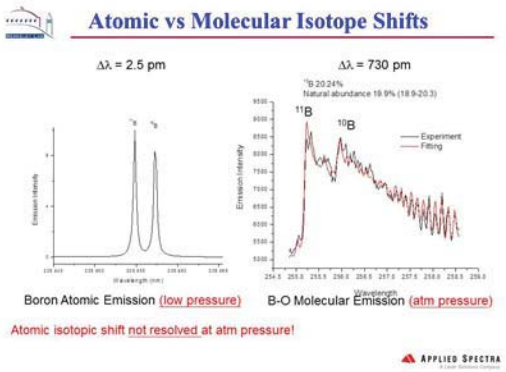

Figure 1: Demonstration of atomic versus molecular isotope emission spectra in laser plasmas

Conclusion

This talk will describe previous isotope work that has been reported in LIBS plasmas and show how LAMIS expands those capabilities.

1. Mao, X.L., Bol'shakov, A.A., Perry, D.L., Sorkhabi, O., and Russo R.E., *Spectrochimica Acta B66, 767-775 (2011).*
2. Mao, X.L., Bol'shakov, A.A., Perry, D.L., Sorkhabi, O., and Russo, R.E., *Spectrochimica Acta, Part B, 66, 604-609 (2011).*
3. Russo, R.E., A.A. Bol'shakov, X.L. Mao, C.P. McKay, D.L. Perry, and O. Sorkhabi, *Spectrochimica Acta, Part B, Vol. 66, Issue 2, pp. 99-104, (2011).*

Changes in $^{231}Pa/^{230}Th$ signatures in the bottom water of the ocean

Michiel Rutgers van der Loeff[1*], Sven Kretschmer[1], Celia Venchiarutti[1]

[1]Alfred-Wegener-Institute for polar and marine research, Bremerhaven, Germany, mloeff@awi.de (* presenting author)

There has recently been much development in the description and modeling of the particulate $^{231}Pa_{xs}/^{230}Th_{xs}$ ratio in the ocean as proxy for the meridional ocean circulation, especially to study the situation in the glacial Atlantic Ocean. Many studies have investigated the effects of ventilation, mass flux and particle composition on $^{231}Pa_{xs}/^{230}Th_{xs}$ ratios. The interpretations as paleoproxy rely usually on the assumption that the isotopic signal stored in the sediment is determined by the composition of suspended or sinking particles when these arrive at the respective water depth. This composition is controlled by exchange with the deep water column [1]. At depths >2500m, Scholten et al. [2] found agreement between $^{231}Pa_{xs}/^{230}Th_{xs}$ ratios in suspended material and surface sediments. Chase et al. [3] observed no difference in activity ratio between surface sediment and a fluff layer present on top of their cores. However, there are several processes that may cause the ratio in surface sediments to differ from the ratio in sinking particles. Bottom currents transport and redistribute the sediment and fractionate grain size [4] and isotopes [5,6]. As a result of this transport and of early diagenetic reactions in the sediment, surface sediments may have a chemical composition and reactivity that is different from sinking particles. We will discuss the possible bias that these processes can give to the signals measured in bottom waters and stored in the sediment.

Whereas Pa/Th ratios have mostly been studied in relation to deep water formation in the North Atlantic, the formation of deep water in the Weddell Sea (Weddell Sea Bottom Water, WSBW) also effects the distribution of ^{230}Th and ^{231}Pa. We will present some new water column data confirming the strong effect of ventilation on the distribution of ^{231}Pa and ^{230}Th in the Atlantic sector of the Southern Ocean. Both nuclides accumulate at intermediate depth in the Weddell Sea while concentrations are appreciably lower in the newly formed Weddell Sea Bottom Water.

[1] Thomas et al. (2006) *Earth Planet. Sci. Lett.* **241**, 493-504.
[2] Scholten et al. (2008) *Earth Planet. Sci. Lett.* **271**, 159-169.
[3] Chase et al. (2003) *Deep-Sea Res. II* **50**, 739-768.
[4] McCave, I. N. and Hall, I. R. (2006) *Geochem. Geophys. Geosyst.* **7**, Q10N05.
[5] Kretschmer et al. (2010) *Earth Planet. Sci. Lett.* **294**, 131-142.
[6] Kretschmer et al. (2011) *Geochim. Cosmochim. Acta* **75**, 6971-6987.

.

https://doi.org/10.1180/S0026461X00008434 Published online by Cambridge University Press

Copper isotope fractionation during uptake and translocation in strategy I and strategy II plants

RYAN, B.M.[1*], KIRBY, J.K.[2], MCLAUGHLIN, M.J.[1,2],
DEGRYSE, F.[1], SCHEIDERICH, K.[2], HARRIS, H.[3]

1Soil Sciences, University of Adelaide, Australia,
(* correspondence: brooke.ryan@adelaide.edu.au)
[2]Land and Water, CSIRO,Adelaide, Australia
[3]Chemistry and Physics, University of Adelaide, Australia

Copper is an essential micronutrient for plant growth, yet is a toxin at above optimal concentrations. It currently remains unclear how plants mobilise, absorb and translocate Cu in soil-plant systems. It has been reported that strategy I plants (dicotyledons or non-graminaceous monocotyledons) can reduce Cu(II) by the secretion of Fe(III) reductases, and that strategy II plants (graminaceous monocotyledons) can complex and absorb Cu(II) using Fe(III) complexing phytosiderophore root exudates [1, 2]. Stable isotopes have the potential to provide in situ information on these mechanisms [3]. This knowledge can assist in developing better agricultural management strategies to enhance uptake in Cu deficient conditions, to limit Cu uptake to allow faster revegetation on contaminated lands, and to trace contamination sources.

A controlled hydroponics experiment that examined the fractionation of Cu isotopes was conducted to assess Cu uptake and translocation mechanisms in higher plants. *Lycopersicum esculentum* (Roma Tomatoes, strategy I), and *Avena sativa* (Oats, strategy II), were grown under nutrient conditions that controlled Cu speciation for 30 days, with an iron deficiency induced on half the plants for the last 6 days of growth.The plants were harvested and separated into roots, stems and leaves for isotopic analysis.

It was expected that if Cu were taken up through Fe acquisition mechanisms, Fe deficiency would increase Cu uptake. Indeed, Cu concentrations were significantly higher in the Fe-deficient plant roots of both species. Furthermore, preliminary Cu isotope data ($\delta^{65/63}$Cu) show Fe-deficient tomato roots being *ca.* 0.5‰ lighter than Fe-sufficient plants, with an average $\Delta^{65}Cu_{(root\text{-}solution)}$ of -2.3‰ in the Fe-deficient tomato plants. The strong negative fractionation suggests reduction of Cu(II) is occuring prior to uptake, possibly at the root surface. Oat roots also showed a light isotopic composition, with a $\Delta^{65}Cu_{(root\text{-}solution)}$ of ca. -1.0‰. However, no significant difference was observed between the control and Fe-deficient oat roots.

Copper isotope data from plant tissues, together with solid-phase Cu speciation from synchotron-based bulk X-ray absorbance spectroscopy, will be used to infer Cu uptake and translocation mechanisms in higher plants.

[1] Welch, R.M. et al., (1993) *Planta,* **190(4)**, 555-561.
[2] Chaignon, V. et al., (2002) *New Phytologist*, **154(1)**, 121-130.
[3] Jouvin, D., et al., (2012) *Environmental Science and Technology*

https://doi.org/10.1180/S0026461X00008434 Published online by Cambridge University Press

Black Shales and massive sulfide deposist in the Iberian Pyrite Belt

REINALDO SÁEZ[1](*); CARMEN MORENO[1]; FELIPE GONZÁLEZ[1]; GABRIEL R. ALMODÓVAR[1]

[1]University of Huelva, Huelva, Spain, (*) saez@uhu.es

Introduction

Many massive sulfide deposits at the Iberian Pyrite Belt (IPB) are hosted by black shales. This relationship is well constrained in some of the major deposits at the province, including Neves-Corvo [1], Tharsis[2], Sotiel [3], and Aznalcóllar [4]. Geochemical environment during ore deposition has been atempted only at the Filon Norte deposit, within the Tharsis District [5][6]. New geochemical data from the black shales hosting the MS at Aznalcóllar and Sotiel show significant differences in terms of environmental conditions for ore generation. Considering the differences in metal content of each deposit, this could be noteworthy for exploration.

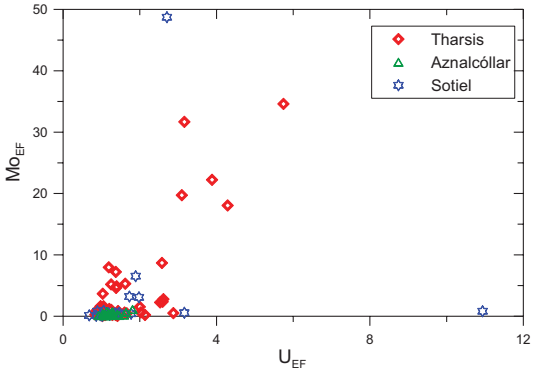

Figure 1: U_{EF} *vs* Mo_{EF} diagram for black shales hosting some IPB ore deposits. Cluster close to x-axis includes the Aznalcóllar and most of the Sotiel samples.

Inorganic geochemical proxies such V/Cr and V/V+Ni suggest general dixosic condition for Tharsis, Aznalcóllar and Sotiel. Recent studies enhance the role of U and Mo as proxies for paleo-environmental reconstructions [7]. Black shales data of these three dstricts on the U_{EF} - Mo_{EF} diagram (Fig. 1) point to disparate environmental conditions. The low absolute values as well as the absence of covariation for the Aznalcollar and Sotiel samples sugest general oxic botom water environents. At Tharsis, the positive correlation together with the dispersion of values sugest changing conditions fron oxic to strongly anoxic, and even euxinic conditions, for the depositional environment.

[1] Oliveira et al (2004) Mineralium Deposita, **39**, 422-436
[2] González et al (2002) Jour. Geol. Soc. London, **159**, 229-232
[3] González et al (2006) Geological Magazine, **143**, 821-827
[4] Almodóvar et al (1998) Mineralium Deposita, **33**, 111-136
[5] Tornos et al (2008) Economic Geology, **103**, 185-214
[6] Sáez et al (2011) Mineralium Deposita, **46**, 585-614
[7] Algeo & Tribovillard (2009) Chemical Geology, **268**, 211-225

This study is a contribution to research project P-S ANOXIA (CGL2011-30011)

Chemical U-Th-total Pb ages in recycled metamorphic terranes: the case of the South Carpathian basement units

GAVRIL SĂBĂU[1*] AND ELENA NEGULESCU[1]

[1]Geological Institute of Romania, Bucharest, Romania, g_sabau@yahoo.co.uk ([*] presenting author), elinegu@yahoo.com

Monazite chemical geochronology

Monazite geochronology has emerged as a reliable dating method for metamorphic ages, as monazite, at variance with other widely employed minerals of geochronological relevance, grows coevally with metamorphic assemblages and displays subsequent chemical and isotopic stability; even dating by chemical methods assuming isotopical equilibrium proved to be accurate enough. Yet, few data refer to metamorphic formations with complex history and thorough succesive overprints, for which the basement units of the South Carpathians represent a typical example.

Previous geochronological data and interpretation

The basement units of the South Carpathians are involved in intricate Variscan and Cretaceous thrust and wrench tectonics. Consisting mainly of medium-grade metamorphic rocks, all types of basement were traditionally considered Precambrian in age [1]. Extensive U-Pb zircon dating revealed Gondwanan provenance and protholith ages ranging from Early Proterozoic to Early Paleozoic [2]. Ar-Ar dating aimed to decipher the metamorphic history overwhelmingly indicated Variscan ages [3], sometimes at odds with cover-basement and intrusion – host-rock relationships. Therefore electron microprobe U-Th-Pb chemical chronology was attempted on rock units of the main basement complexes in order to elucidate the building blocks and temporal details of Variscan tectonometamorphic events.

Results and Conclusions

The age values derived from microprobe U-Th-Pb analyses revealed variable responses of monazite to polymetamorphic events, as well as frequent post-climactic records, resulting in age plateaus often joined by quasi-continuous spectra in case of reworked pre-Variscan complexes. Purely Variscan age patterns in rock units, also displaying microstructures and chemical zonation patterns consistent with a monometamorphic history, sandwiched between pre-Variscan terms, indicate frequent imbrication of reworked and juvenile metamorphic units during the Variscan thermotectonic events in the South Carpathian basement. The recorded evolution is consistent with complex interactions of migrating slivers that originate from the northern Gondwanan margin, up to the time of the Variscan collision. Accidental Alpine age values, mostly unrelated to pervasive metamorphic overprints, indicate low-temperature recrystallization domains in monazite, which call for caution in interpreting monazite age data.

[1] Kräutner *et al*. (1988) *in Zoubek (ed.) Precambrian in younger fold belts*, Wiley & Sons, 639-660. [2] Dallmeyer *et al.* (1998) *Tectonophysics* **290**, 111-135. [3] Balintoni *et al.* (2009) *Gondwana Research* **16**, 119-133.

https://doi.org/10.1180/S0026461X00008434 Published online by Cambridge University Press

Clumped and magnesium isotopes in corals: a comparison with traditional paleothermometers

SAENGER C[1*], THIAGARAJAN N[2], FELIS T[3], LOUGH J[4], HOLCOMB M[5], GAETANI G[6], COHEN AL[6], AFFEK HP[1] AND WANG Z[1]

[1]Yale University, New Haven, CT, USA, casey.saenger@yale.edu (* presenting author)
[2]California Institue of Technology, Pasadena, CA, USA.
[3]MARUM, University of Bremen, Bremen, Germany.
[4]Australia Institute of Marine Science, Townsville, Australia.
[5]University of Western Australia, Perth, Australia.
[6]Woods Hole Oceanographic Institution, Woods Hole, MA, USA.

Corals represent valuable paleoclimatic archieves that may record sub-annual sea surface temperature (SST) over many centuries. Despite strong correlations with SST, the interpretation of traditional proxies (i.e. $\delta^{18}O$, Sr/Ca) is not straightforward because variations in seawater composition and biological vital effects can overprint climatic signals. Evidence for vital effects include 1) proxy-SST calibrations that differ significantly from abiogenic relationships and 2) inter/intra-coral differences in proxy-SST calibrations. Carbonate clumped isotopes (Δ_{47}) and magnesium isotopes ($\delta^{26}Mg$) have emerged as new paleotemperature proxies that may be less prone to seawater variability and vital effects.

Based on the temperature dependent "clumping" of ^{13}C and ^{18}O into a single bond, Δ_{47} temperatures, at equilibrium, do not depend on the composition of the solution from which a carbonate forms. Furthermore, similar Δ_{47}-SST relationships in biogenic carbonates and inorganic precipitates argue against vital effects. However, early sub-annual coral Δ_{47} data deviates from the cannoical Δ_{47}-SST relationship and may reflect a vital effect [1]. We present a survey of Δ_{47} shallow water corals from the Atlantic, Pacific and Red Sea. Sub-annual Δ_{47} in two *Porites* corals shows a temperature sensitivity similar to abiogenic calibrations, but offset toward higher Δ_{47} values that underestimate SST by ~9ºC. This effect cannot be attributed to laboratory artifacts or environmental variables such as salinity, but may result from fast coral calcification. Possible mechanisms for this apparent link to calcification will be discussed.

Like Δ_{47}, temperature dependent magnesium isotope fractionation [2] is unlikely to be affected by solution composition, suggesting it may also be a valuable paleo-thermometer. Sub-annual $\delta^{26}Mg$ variability in two *Porites* corals shows obvious annual cycles that are in phase with $\delta^{18}O$ and Sr/Ca, suggesting a temperature dependence not seen in previous bulk sampling [3]. However, the temperature sensitivity of coral $\delta^{26}Mg$ appears to be larger than abiogenic experiments raising the possibility of a vital effect. Potential sources for this discrepancy will be discussed.

[1] Ghosh et al. (2006) *Geochim. Cosmichim. Acta* **70**, 1439-1456.
[2] Wang et al. (2011) *AGU Fall Meeting* **PP51E-07**.
[3] Wombacher et al. (2011) *Geochim. Cosmichim. Acta* **75**, 5797-5818.

Was Mineral Surface Toxicty an Impetus for Evolution of Bacterial Extra-cellular Polymeric Substances (EPS)?

NITA SAHAI[1*], JIE XU[2], CHUNXIAO ZHU[3], NIANLI ZHANG[4], AND WILLIAM J. HICKEY[3]

[1]University of Akron, Akron, U.S.A., *sahai@uakron.edu
[2]George Washington University, Washington D.C., U.S.A., gail_xu_1982@hotmail.com
[3]University of Wisconsin, Madison, U.S.A., czhu3@wisc.edu, wjhickey@wisc.edu
[4]University of Michigan, Ann Arbor, U.S.A., nianliz@umich.edu

Bacterial community-living at the mineral-water interface is enabled by an extracellular, polymeric, biofilm matrix. Despite the energetic penalties of EPS production, biofilm formation capability likely evolved on early Earth because of several proposed crucial cell survival functions. The potential toxicity of mineral surfaces towards cells in promoting biofilm formation, however, has not been fully appreciated.

We examined here the effects of nanoparticulate oxides (amorphous SiO_2, anatase β-TiO_2, and γ-Al_2O_3) on EPS- and biofilm-producing wild-type strains and their isogenic knock-out mutants which are defective in EPS-producing ability. In particular, we used the Gram-negative wild-type *Pseudomonas aeruginosa* PAO1 and its EPS knock-out mutant *Δpsl*, and the Gram-positive wild-type *Bacillus subtilis* NCIB3610 and its EPS-knock-out mutant *yhxB*Δ. Results showed that (a) cell viability was lower in the presence of each oxide relative to its oxide-free control, (b) toxicity was mineral-specific, and could be related to surface charge and particle size, (c) toxic minerals could induce EPS production, (d) the amount of EPS generated in the presence of oxides was related to relative toxicity of the minerals, and (e) Gram-positive cells were less susceptible to mineral toxicity than Gram-negative cells. Taken together, these results indicated a previously unrecognized role for microbial extracellular polymeric substances (EPS) in shielding bacterial cells against the toxic effects of mineral surfaces.

The function of EPS proposed here is distinct from the previously proposed roles. It is likely that EPS played multiple functions, including our hypothesized role of protecting against mineral toxicity. Furthermore, not all minerals are toxic or benign, and toxicity depends on surface chemistry and particle size. Our results provide insight to the potential impact of nanoparticulate mineral surfaces in promoting increased complexity of cell surfaces, including EPS and biofilm formation, on early Earth.

https://doi.org/10.1180/S0026461X00008434 Published online by Cambridge University Press

The Role of Water Molecules in Stabilizing Amorphous Calcium Carbonate: A Computer Simulation Study

M. SAHARAY[1*], A. OZGUR YAZAYDIN[2], AND R. JAMES KIRKPATRICK[3]

[1]Department of Chemistry, Michigan State University, East Lansing, Michigan 48824, USA, saharaym@chemistry.msu.edu (* presenting author)

[2]Department of Chemical Engineering, University of Surrey, Guildford, GU2 7XH, United Kingdom, a.yazaydin@surrey.ac.uk

[3]College of Natural Science, Michigan State University, East Lansing, Michigan 48824, USA, rjkirk@cns.msu.edu

Session 18b. Nucleation, Growth, and Dissolution in Aqueous Environments: Elementary Processes and Atomistic Models

Amorphous calcium carbonate (ACC) is a critical transient phase in the inorganic precipitation of $CaCO_3$ and in bio- and biomimetic mineralization. Proteins known to be responsible for the biomineralization of, for instance, bird egg shells, bind to ACC nanoparticles and lower or remove the energy barrier to crystallization. The mechanisms of these processes are related to the structures of hydrous and anhydrous ACCs, but the details are poorly known. To advance fundamental molecular-level understanding of the bulk hydrous and anhydrous ACC, we studied these systems using both classical and quantum mechanical simulation methods. Car-Parrinello molecular dynamics (CPMD) simulations of calcium carbonate solvated in a bath of water molecules have been performed at a temperature of 300K to elucidate the microscopic structure, dynamics, and electronic properties of water molecules in the first two solvation shells of calcium carbonate. The reorientational dynamics of near-neighbor water molecules around Ca^{2+} and CO_3^{2-} ions are investigated through first- and second-order time correlation functions, and are in good agreement with nuclear magnetic resonance experiments. The intramolecular vibrations of CO_3^{2-} ion have also been examined through an analysis of the velocity autocorrelation function of the atoms and are compared with that of isolated $CaCO_3$ and existing vibrational spectra of calcium carbonate. In addition, classical molecular dynamics simulations of pre-nucleated ACC are carried out to understand the role of water molecules in stabilizing these clusters. Starting from a hydrous ACC model with a $CaCO_3/H_2O$ ratio of 1/1, we gradually reduced the water concentration of the system to completely dehydrated ACC. Simulation results using the DL_POLY software on the structure and dynamics of the constituent molecules due to drying will be presented.

Acknowledgements

We thank Prof. Richard J. Reeder and Prof. Brian Phillips for providing the atomic positions from the reverse Monte Carlo model of ACC [1].

[1] Goodwin, A. L.; Michel, F. M.; Phillips, B. L.; Keen, D. A.; Dove, M. T.; Reeder, R. J.(2010) *Chemistry of Materials* **22**, 3197.

New U-Pb ages for gabbro sills within the Ramah Group, northern Labrador: implications for Paleoproterozoic extension in Nain craton, and metallogeny

T. SAHIN[1*], M.A. HAMILTON[1], P.J. SYLVESTER[2], AND D.H.C. WILTON[2]

[1]University of Toronto, Geology, Toronto, Canada, tsahin@geology.utoronto.ca (* presenting author); mahamilton@geology.utoronto.ca

[2]Memorial University, Earth Sciences, St John's, Canada, psylvester@mun.ca; dwilton@mun.ca

Archean gneisses of the North Atlantic craton (NAC) in northern Labrador are unconformably overlain by three principal Paleoproterozoic supracrustal remnants – the mostly clastic Snyder/Falls Brook Group, the dominantly volcanic Mugford Group, and, furthest north, the chiefly sedimentary Ramah Group.

Ramah Group is an ~1700m thick cover sequence of lowermost siliciclastic quartz sandstone capped by a distinct supratidal dolomite horizon, together defining a west-facing shallow shelf sequence, overlain by euxinic, pyritic shales and mudstones and pyrite-chert associations (Nullataktok Formation). Upwards, this unit passes through a mixture of carbonate debris flow breccias, and then into voluminous turbiditic sandstones. Sills of diabase or gabbro extensively intrude the upper sedimentary units. The sills typically exhibit chilled margins, and are clearly transgressive to their host sediments. Sills reach up to ~100 m in thickness, though many are only a few meters thick, in many places with preserved primary layering. The entire sequence of sedimentary rocks and sills was deformed and (locally) metamorphosed to amphibolite facies, as part of an east-verging fold-and thrust belt on the east margin of the 1.78 Ga Torngat Orogen. The depositional age of the Ramah Group has only been bracketed only between its late Archean (ca. 2.5 Ga), Nain craton-derived detrital zircons, and Torngat deformation.

We have dated both gabbroic and ultramafic compositional variants of Ramah sills, from samples collected from thick sheets intruding the Nullataktok Formation. ID-TIMS U-Pb baddeleyite analyses yield identical ages of emplacement at 1888 ± 5 and 1887 ± 4 Ma. These represent the first precise U-Pb dates for extension-related mafic magmatism of this age in the NAC in Labrador, and provide a new minimum age for the host Ramah Group sediments. Mafic magmatism of this age is unknown in the Greenland portion of the craton, but is well represented in the Circum-Superior belt, including the ca. 1883 Ma Molson dyke swarm and Fox River sill of Manitoba (Molson Igneous Events), the 1890-1870 Ma Raglan-Expo-Katiniq sills of the Cape Smith belt, Ungava, and the 1884-1874 Ma mafic-ultramafic magmatism of the Labrador Trough.

By analogy with contemporaneous Circum-Superior sediment-sill complexes (Thompson, Birchtree, Raglan-Expo), Ramah Group may have potential for magmatic Ni-Cu-PGE sulfide deposits.

https://doi.org/10.1180/S0026461X00008434 Published online by Cambridge University Press

Ocean redox changes in the wake of the Marinoan glaciation

S. K. SAHOO[1]*, N. J. PLANAVSKY[2], B. KENDALL[3], X. WANG[4], X. SHI[4], A. D. ANBAR[3,5], T. W. LYONS[2] AND G. JIANG[1]

[1]Dept. Geoscience, Univ. Nevada, Las Vegas, NV, USA (*presenting author: sahoos@unlv.nevada.edu), and ganqing.jiang@unlv.edu
[2]Dept. Earth Science, Univ. California, Riverside, CA, USA noah.planavsky@email.ucr.edu and timothy.lyons@ucr.edu
[3]SESE, Arizona State Univ. Tempe, AZ, USA brian.kendall@asu.edu and anbar@asu.edu
[4]Sch. Earth Sc. & Res., Univ. Geosciences, Beijing, China wxqiang307@yahoo.com.cn and shixyb@cugb.edu.cn
[5]Dept. Chem/Biochem, Arizona State Univ. Tempe, AZ, USA

Metazoans first appeared in the fossil record shortly after the termination of the late Cryogenian (Marinoan) glaciation about 635 Myr ago [1]. It has been long hypothesized that an oxygenation event was the driving factor behind the rise and early diversification of metazoans [2], but there is little evidence for a direct link between animal and redox evolution. Here we report new geochemical data from early Ediacaran organic-rich black shales of the basal Doushantuo Formation in South China. These shales were deposited with a strong connection to the open ocean [3] and span the interval of the earliest metazoan fossil [1]. The temporal record of trace metal enrichments (particularly molybdenum) in euxinic shales currently provides one of the clearest signals for a significant redox shift in the Neoproterozoic [4,5]. However, prior to our study the oldest known occurrences of Phanerozoic-like trace metal enrichments are found near the end the Ediacaran (ca. 551 Ma) [4,5], long after the radiation of complex metazoans [1].

In contrast, we found very high, Phanerozoic-like, redox sensitive trace element (molybdenum, vanadium and uranium) abundances in euxinic shales (as identified by sedimentary Fe speciation) that were deposited between 635 and 630 Ma, within five million years of the Marinoan glaciation and coincident with the appearance of the earliest metazoan fossils. Moreover, highly negative pyrite sulphur isotope ($\delta^{34}S_{pyrite}$) values down to –35‰ from basinal samples also point toward an oxidizing ocean-atmosphere system. The isotope fractionation between pyrite and coeval sulphate in the deep basin section is >65‰—equivalent to the maximum fractionations observed in the Phanerozoic rock record [6]. As increase in the fractionation in the Neoproterozoic has been commonly linked to growth of the marine sulphate reservoir and surface oxidation [5], the large sulphur isotope fractionation, therefore, point toward a well oxidized ocean-atmosphere system. Our data provide the first direct evidence for a significant early Ediacaran postglacial oxygenation event. Our results support a casual link between one of the most severe glaciations in Earth's history, the oxygenation of the Earth's surface, and the earliest diversification of complex animals.

[1] Yin (2007) *Nature* **446,** 661-663. [2] Knoll (1999) *Science 284,* 2129-2137. [3] Jiang (2011) *Gondwana Research* **19**, 831-849. [4] Scott (2008) *Nature* **452**, 456-459. [5] Och (2011) *Earth-Science Reviews* **110**, 26-57. [6] Sim (2011) *Science* **333**, 74-77.

Radium interactions with iron (oxy)hydroxide minerals.

M. SAJIH[1*], N.D.BRYAN[1], D.J. VAUGHAN[2], M. DESCOSTES[3], V. PHROMMAVANH[3], KATHERINE MORRIS[1,2]

[1] Centre for Radiochemistry Research and Research Centre for Radwaste and Decommissioning and [2]Williamson Research Centre for Molecular Environmental Science, The University of Manchester, Manchester, M13 9PL. [3]AREVA NC - Business Group Mines, Direction R&D, BAL 3720C, Tour AREVA, 1, Place Jean Millier, 92084 Paris La Défense Cedex, France. (*correspondence: mustafa.sajih@ manchester.ac.uk)

Typically, radium is the most significant contributor to dose in mining effluents from legacy uranium mining operations. However, little is known regarding the uptake of Ra^{2+} by iron (oxy)hydroxide minerals under environmental conditions representative of the mining wastes. Here, we assess the behaviour of Ra^{2+} (and Ba^{2+} as a chemical analogue of Ra^{2+}) to provide surface complexation constants that will be used in the prediction of Ra^{2+} speciation, mobility and fate across a range of environmental conditions.

Radium and barium uptake onto ferrihydrite and goethite was studied in the concentration range nM to mM and from pH 5 - 10, conditions commonly found in legacy U-mine wastes. For ferrihydrite, uptake of Ra^{2+} at nM concentrations was strong at pH > 7. At higher concentrations (μM - mM) Ba^{2+} sorption to ferrihydrite was slightly weaker than that of Ra^{2+}. Experiments with goethite showed weaker binding for both metal ions in all systems studied. Ongoing experiments are exploring the reversibility of these systems. In addition, we are exploring the behaviour of Ra^{2+} during transformation of ferrihydrite to goethite, a process of potential importance in the impacted environments.
Surface complexation modelling has successfully simulated Ra^{2+} and Ba^{2+} sorption across the pH and concentration ranges studied. These data will be used in underpinning the safety case for legacy mining sites.

https://doi.org/10.1180/S0026461X00008434 Published online by Cambridge University Press

Ectomycorrhizal sclerotia formation and status of organo-mineral complex aluminum in low pH *Fagus* forest

NOBUO SAKAGAMI[1*] AND MAKIKO WATANABE[2]

[1]Ibaraki University, College of Agriculture, sakagami@ams.kuramae.ne.jp (* presenting author)
[2]Tokyo Metropolitan University, Department of Geography, m.wata@tmu.ac.jp

Sclerotia of ectomycorrhizal fungus *Cenococcum geophilum* are preserved in soils with *Cenococcum* mycorrhizae.[1] Ferricrocin is known as an ectomycorrhizal siderophore of *Cenococcum geophilum*.[2, 3] In our previous studies, we reported a characteristic concentration of aluminum in sclerotium and the relationship between aluminum (plus iron) content in sclerotia and active aluminum and iron in soils.[4, 5] Absorption of aluminum and iron may be an evidence of activity of *C. geophilum* associated with its siderophore. This fact harmonizes with microbial dissolution of aluminum and iron from minerals studied on ectomycorrhizal fungus.[6] In this study, we established 10 × 10-m quadrat beneath the *Fagus* forest in northeastern Japan, and then subdivided the plot using a 2 × 2-m grid. Thirty six surface soil samples were collected at each grid node.

The SEM-EDX observation (JSM-6610LV, JEOL) on distribution of elements in a cross section of soil aggregate including a sclerotium showed a slight accumulation of aluminum on soil surrounding sclerotium (Fig.1).

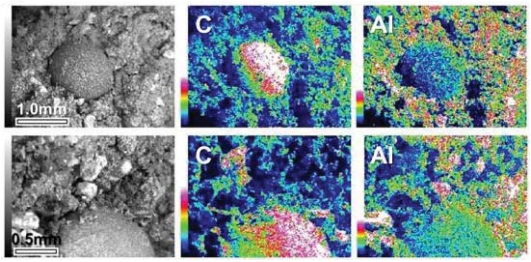

Figure 1: Distribution of C and Al in a cross section of soil aggregate including a sclerotium by SEM-EDX analysis.

According to the analytical results of the sclerotia content, and the status of aluminum in soil (dithionite-citerate, oxalate, pyrophosphate, ammonium acetate, and water extractable aluminum), we discuss the interaction between sclerotia formation and the status of soil aluminum. Furthermore, the interaction between soil and ectmycorrhizal activities in the investigated forest soils are noted regarding with micro topography, *Fagus* stands and floor vegetation.

[1] Trappe (1964) *Lloydia* **27**, 100-106. [2] Haselwandter & Winkelmann (2002) *BioMetals* **15**, 73-77. [3] Hoffland et al. (2004) *Front. Ecol. Env.* **2,** 258-264. [4] Watanabe *et al*. (2001) *Soil Sci. Plant Nutr*. **47**, 411-488. [5] Sakagami et al. (2007) *Proc. OMD 2007*, 402-403 [6] Watteau & Berthelin (1994) *Euro. J. Soil Biol.* **30**, 1-9.

Spectroscopic studies on sedimentary organic material

FANI SAKELLARIADOU

University of Piraeus, Maritime Studies Dept, Piraeus, Greece, fsakelar@unipi.gr

Introduction

Sediment samples from the Saronicos gulf, belonging to the Aegean Sea, were studied for the characterization of humic substances (HS) and dissolved organic matter (DOM). HS are significant sediment constituents performing in metal and toxic material scavenging and transport. Infrared and fluorescence spectroscopy were applied. DOM corresponds to the most active and mobile form of soil organic matter and the major soluble component of natural aquatic systems, with significant functions in the ecological and environmental system. DOM was studied by fluorescence spectroscopy.

Results and discussion

Spectroscopic methods on HS: The application of IR spectroscopy gives spectra with the characteristic peaks for hydroxyl, methyl, methylene, aromatic bond, carbonyl, carboxyl, phenol, alcohol, polysaccharide and silicate impurities. Conventional fluorescence spectroscopy [1] provides with emission spectra with maximum emission intensity at 415-427nm, excitation spectra with a major excitation peak at 355 to 330nm, and synchronous-scan excitation spectra with a very structured form; suggesting the presence of humic-like material with a marine origin.

Spectroscopic methods on DOM: Mono-dimensional emission spectra reveal one typical broad peak with a maximum between 442 and 439 nm. Excitation spectra show three peaks or shoulders at 330 nm, 351 nm, 377-381 nm, and a shoulder at 440 nm. Synchronous scan excitation spectra show one strongest peak at 340-345nm and another much lower or lower intensity peak or shoulder at 385-387nm. Therefore, it seems that fulvic acids, aquatic humic acids and natural organic matter are present. Higher humification index [2, 3], related to a more condensed nature, corresponds to areas with weaker seawater circulation [4]. Excitation/emission matrix spectra (EEMS) exhibit the peak M [5] corresponding to the marine humic fluorophore, strongly correlated with biological activity

[1] Senesi *et al.* (1991) *Soil Science* **152**(4), 259-271. [2] Ohno (2002) *Environ. Sci. and Technol.* **36**, 742-746. [3] Zsolnay *et al* (1999) *Chemosphere* **38**, 45-50. [4] Luciani e*t al*. (2008) *Mar. Environ. Res.* **65**, 148-157. [5] Sakellariadou (2012) *IJOO* **6**, 27-43.

https://doi.org/10.1180/S0026461X00008434 Published online by Cambridge University Press

A coupled biomarker-genetic approach to understanding the $U^{k'}_{37}$ SST proxy in estuaries

JEFF SALACUP[1*], TIMOTHY HERBERT[1], WARREN PRELL[1]

[1]Brown University, Providence, RI, USA,
Jeffrey_Salacup@brown.edu (* presenting author)

Towards a mechanistic understanding of $U^{k'}_{37}$

The $U^{k'}_{37}$ SST proxy has been widely and successfully applied in the reconstruction of open ocean temperatures on centennial to orbital timescales and has proved an indispensable tool in our investigations of past climates. However, the utility of the $U^{k'}_{37}$ SST proxy is thought to break down in near shore settings experiencing more dynamic nutrient and salinity fluctuations. Given the importance of coastal systems, , knowledge of past local to regional SST variability is critical to habitat adaptation and restoration strategies. Furthermore, the rapid deposition of both marine and terrestrial organic and inorganic material in estuarine and coastal systems makes them valuable archives of high-resolution paleo-environmental information.

Here, we present the results of a 3-year-long monthly to sub-weekly resolved record of water column $U^{k'}_{37}$ and alkenone concentration (C_{37}total) and associated instrumental SST suggesting that while important and informative seasonal inconsistencies exist, especially during alkenone blooms, the integrated $U^{k'}_{37}$ signal preserved in Narragansett Bay sediments reflects mean annual instrumental SST. A subset of samples were analyzed for haptophyte-specific 18S ribosomal RNA (rRNA) to understand the composition of the alkenone-producing community during times of instrumental-$U^{k'}_{37}$ coherency and incoherency, alike. So far, the only alkenone-producing species detected in Narragansett Bay, *E.huxleyi* and *G.oceanica* - which dominate open-ocean production and form the foundation of the $U^{k'}_{37}$-SST calibration – were detected in the high salinity lower-Bay during the spring bloom of 2010. A second 'brackish' alkenone-producing population is suspected on the basis of high contributions of the $C_{37:4}$ alkenone in the low-salinity upper Bay.

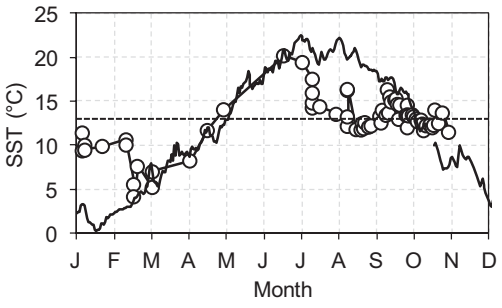

Figure 1. An example of the discrepancy between instrumental SST (solid line) and $U^{k'}_{37}$-inferred SST (open circles) from 2010. C_{37}total-inferred haptophyte blooms peaked in Feb and Aug during periods of maximum instrumental-$U^{k'}_{37}$ SST divergence. Black dashed line is the mean annual instrumental SST for Narragansett Bay for 2009-2011 (~13.4°C).

Fingerprinting uranium-bearing material: development and validation of methods

A. SALAÜN[1*], A. HUBERT[1], J. AUPIAIS[1], E. PILI[1], F. POINTURIER[1], S. DIALLO[1], A.-L. FAURE[1] AND P. RICHON[1].

[1]CEA, DAM, DIF, F-91297 Arpajon, France,
anne.salaun@cea.fr (*presenting author)

The nuclear forensics project

Many parameters such as trace elemental impurity patterns [1], uranium or oxygen isotopic compositions [2, 3] and anionic impurities [4] are known to be tracers of geographical origin of uranium-bearing materials. These parameters can allow to go back to a part of the history (industrial treatment or origin) of a seized nuclear material when they are used individually (Figure 1).

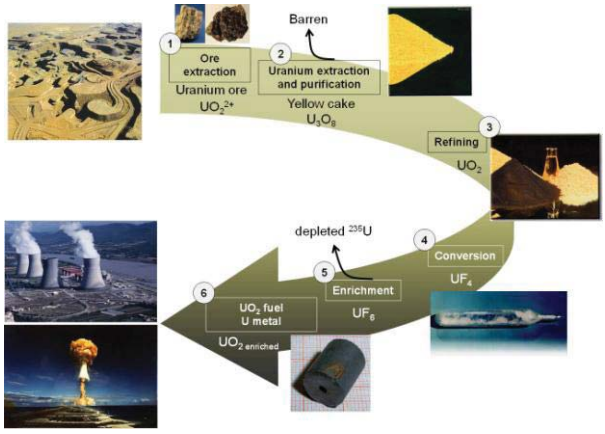

Figure 1: From ore to fuel: a variety of steps for uranium fingerprinting

But in some cases, they are not enough discriminating. We herein document a complete characterization of reference and unknown uranium ore concentrates for which REE, ($^{234}U/^{238}U$) and oxygen isotopic compositions were determined. This original approach which combined all three determinations covers a more global overview of such material.

Methods

A complete analytical procedure has been developed on a single sampling for trace-level determination of lanthanides and U isotopic composition in yellow cakes using ICP-MS, TIMS and PERALS (Photon Electron Rejecting Alpha Liquid Scintillation). The method was validated by the measurement of a reference material and will be applied for the analysis of unknown yellow cakes from various origins. Similarly, oxygen isotopic compositions of reference yellow cakes are currently under measurement by SIMS (Secondary Ion Mass Spectrometry) on particles and by fluorination on bulk samples.

[1] Varga (2010) *Radiochimica Acta* **98**, 771-778.
[2] Keegan (2008) *Applied Geochemistry* **23**, 765-777.
[3] Tamborini (2002) *Analytical Chemistry* **74**, 6098-6101.
[4] Badaut (2009) *J. Radioanal. Nucl. Chem.* **280**, 57-61.

https://doi.org/10.1180/S0026461X00008434 Published online by Cambridge University Press

Kinetic modeling of olivine carbonation reaction: study of the rate dependence on temperature and pCO_2 in open and closed systems

GIUSEPPE D. SALDI[1*], DAMIEN DAVAL[1,2] AND KEVIN G. KNAUSS[1],

[1]Lawrence Berkeley National Laboratory, Berkeley, CA, gdsaldi@lbl.gov (* presenting author); ddaval@lbl.gov; kgknauss@lbl.gov

[2] LHyGeS, CNRS UMR 7517, Strasbourg, France

Although both olivine dissolution and magnesite precipitation rates have been studied and modeled over a significant range of temperatures and aqueous chemical compositions, the mechanisms of the process that combines these two reactions have not been adequately described from a kinetic standpoint.

It was shown that the formation of a silica passivating layer at the interface between pristine olivine and aqueous solution can significantly slow down or even stop the dissolution of this mineral, thus hindering the attainment of the conditions necessary to initiate the carbonation reaction [1, 2]. Recent experimental measurements also indicate that magnesite precipitation can be the rate limiting step to forsterite carbonation in some other conditions [3].

To improve the understanding of mineral carbonation processes and provide new data that can contribute to its kinetic description we conducted a series of experiments in pure water from 90 to 180 °C, at a pCO_2 of 100 and 200 bar, using both the well characterized San Carlos olivine and a pure synthetic forsterite sample. Batch experiments were performed in flexible Au bags whereas steady-state carbonation rates were investigated at 150 °C by means of a mixed-flow Ti-reactor. The study of the chemistry of aqueous solution and the analysis of reacted olivine samples by XRD, SEM-EDX and Rockeval 6 allowed us to describe quantitatively the carbonation reaction as a function of pCO_2 and temperature. All experiments were characterized by the ubiquitous presence of a silica-rich layer at the olivine-aqueous solution interface. The nature of this layer changes as a function of temperature, and can lead to increasing rates of carbonation as magnesite precipitation rates increase with increasing temperature.

Comparison between the results obtained from two one-month-long batch and mixed-flow reactor experiments at 150 °C show that the extent of carbonation is limited by the saturation with respect to a silica polymorph, and possibly by the formation of secondary Mg-silicates. In the closed system, olivine to magnesite conversion rates are <1 %, whereas the extent of carbonation are significantly higher in the open system (8-9 % at least) and magnesite precipitation was found to be the rate limiting step of the reaction in this latter case.

The role of Fe in the passivating properties of the silica layer and its incorporation into the carbonate phase under reducing conditions is also being studied and some experimental results will be presented.

[1] Bearat et al. (2006) *Environ. Sci. Technol.***40**, 4802-4808. [2] Daval et al. (2011) *Chem. Geol.***284**, 193-209. [3] Saldi et al. (2012) *Geochim. Cosmochim. Acta*, doi:10.1016/j.gca.2011.12.005.

High precision 4-isotope Sulfur measurements using the CAMECA IMS 1280-HR

P. PERES, F. FERNANDES, M. SCHUHMACHER, P. SALIOT*

CAMECA, 29 quai des Grésillons, 92622 Gennevilliers Cedex, France, peres@cameca.com

Secondary Ion Mass Spectrometry (SIMS) technique provides direct in situ measurement of elemental and isotopic composition in selected µm-size areas of the sample. The CAMECA IMS 1280-HR is an ultra high sensitivity ion microprobe that delivers unequalled analytical performance for a wide range of SIMS applications: isotope ratio measurements, geochronology applications (U-Pb dating in Zircon), trace element analyses, particle screening measurements,...

Conventional Sulfur isotope studies focus on the two most abundant isotopes ^{32}S and ^{34}S. However, there has been an increasing interest in the minor ^{33}S (~0.7%) and ^{36}S (~0.02%) isotopes since mass independent fractionation effects have been discovered [1-3].

This paper presents 4-isotope Sulfur data obtained on standard and unknown pyrite samples. Measurements have been performed using a small 10µm Cs^+ beam spot, and high mass resolution conditions (~4,500) to resolve the hydride mass interferences. The four S isotopes have been collected simultaneously: ^{32}S, ^{33}S and ^{34}S on Faraday Cup detectors, and the low abundance ^{36}S (intensity ca. $2x10^5$ c/s) on an Electron Multiplier. The EM yield drift has been automatically monitored and corrected using a propriatery algorithm. More than 100 spot analyses have been performed in fully automated mode, with an analysis time of 4 minute/spot.

Data on the standard sample show that a precision < 0.2 permil (1SD) can be achieved for $\delta^{34}S$, $\delta^{33}S$ (and $\Delta^{33}S$). An excellent precision, < 0.3 permil (1SD), is also obtained for $\delta^{36}S$ (**Figure 1**) and $\Delta^{36}S$.

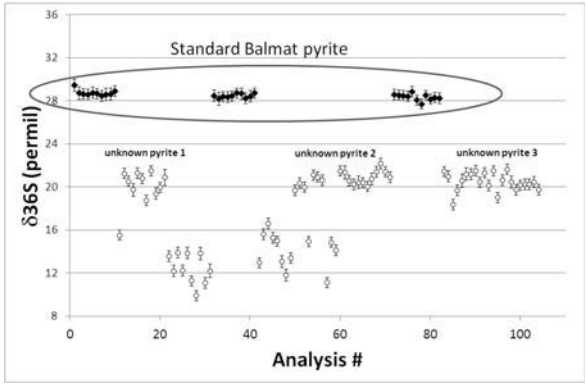

Figure 1: $\delta^{36}S$ data on standard and unknown pyrite samples.

This measurement protocol with multicollection configuration FC-FC-FC-EM allows to work with good spatial resolution (spot size ~10µm) and yields excellent precision for all Sulfur isotopes, including for the lowest abundance ^{36}S.

[1] Kamber and Whitehouse (2007) *Geobiology* 5, 5-17.
[2] Williford et al. (2011) *GCA* 75, 5686-5705.
[3] Whitehouse (2011) *Goldschmidt 2011 abstract*, 2155.

https://doi.org/10.1180/S0026461X00008434 Published online by Cambridge University Press

Ultra depleted mantle at the Gakkel Ridge

VINCENT SALTERS[1*], AFI SACHI KOCHER1, HENRY J.B.DICK[2]

[1]NHMFL and EOAS, Florida State University, Tallahassee, Florida, USA, salters@magnet.fsu.edu (* presenting author) [8pt font size]

[2]MG&G, Woods Hole Oceanographic Institution, Woods Hole, Massachusetts, USA, hdick@whoi.edu

The Gakkel Ridge is one of the slowest spreading ridge segments in the global ridge system and with some of the thinnest oceanic crust. In some locations there is little or no evidence for volcanic activity and oceanic mantle is directly exposed on the ocean floor. This provides an excellent opportunity to investigate the heterogeneity of the oceanic mantle in situ.

We have analyzed a number of peridotites from the western end of the Sparsely Magmatic Zone (3° to 28°E as well as samples further west up to 65°E) and found highly radiogenic Hf and Nd isotopic composition. All but five samples are more radiogenic in either Nd or Hf than MORB. Six samples lie in the extension of the OIB MORB array with ε_{Nd} up to 23.7 and ε_{Hf} up to 54.6. The remainder of the data (14 samples) lie above the OIB-MORB array and its extension with ε_{Nd} values up to 27.4 and ε_{Hf} values up to 291! These values are the most extreme values measured for oceanic mantle. This data confirms the ultra depleted nature of the Gakkel Ridge mantle [1] and its highly heterogeneous nature [2].

Since the Hf and Nd system is expected to behave similar during melting, melt can be added back in the peridotite until the Hf and Nd model age coincide. These calculations show that depleted Gakkel Ridge peridotites have very little melt extracted from them (<1%) and have model ages that ranges from 2.4Ga to future ages with most between 600Ma and 1.2 Ga. The MORB Hf-Nd isotope systematics indicate this depleted component (ReLish) is ubiquitous [3] but under-sampled in basalts due to its depleted character. The presence of ReLish decrease the amount of melt a heterogeneous parcel of mantle can yield during ascent and average melt rate can be much lower requiring depth of melting to start deeper.

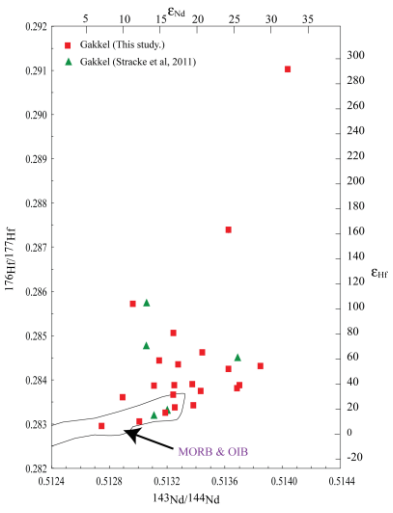

[1] Stracke, A, *et al*., *Earth Plan. Sci. Lett*, **308**, 359-368 (2011).
[2] Liu, C.Z., *et al*., *Nature*, 452, 311-315 (2008).
[3] Salters, V.J.M., et al., *Geochem. Geophys. Geosys*. 12, Q08001.

Integrated TIMS-TEA/LA-ICPMS constraints on pluton emplacement

K. SAMPERTON[1*], B. SCHOENE[1], J. COTTLE[2] AND J. CROWLEY[3]

[1]Princeton University, Department of Geosciences, Princeton NJ, USA, ksampert@princeton.edu (*presenting author)

[2]University of California–Santa Barbara, Department of Earth Science, Santa Barbara CA, USA, cottle@geol.ucsb.edu

[3]Boise State University, Department of Geosciences, Boise ID, USA, jimcrowley@boisestate.edu

Major conceptual and technical breakthroughs over the past decade have increased temporal and spatial resolutions for both ID-TIMS and LA-ICPMS. An outgrowth of this development is the ability to address whether zircon U-Pb ages can be assumed *a priori* to equate to the timing of pluton emplacement. We employ an integrated analytical regime coupling U-Pb TIMS-TEA with *in situ* LA-ICPMS trace element characterization in order to 1) assess intra-grain trace element zoning at the five micron scale and couple this with "bulk" geochemical and geochronological data, 2) fingerprint crystal populations within a single sample and better interpret age spread in high-precision datasets, and 3) characterize the temporal and geochemical evolution of magmas during ascent, mixing, and pluton assembly.

We apply this methodology to the 32-30 Ma Bergell Intrusion (N Italy), which preserves a spectacular 12-15 km crustal section through a single, continuous magmatic system, in addition to distinct process zones (pluton roof, floor, and feeder zone/tail). Preliminary U-Pb ID-TIMS zircon geochronology of CL-imaged grain fragments documents 400-500 kyr of zircon growth within individual hand samples ranging in composition from megacrystic granodiorite to tonalite. Precision on individual analyses of 10-20 ka (~0.05%) makes this duration easily resolveable. *In situ* trace element transects performed on the exact same minerals prior to ID-TIMS dating exhibit evolving core-to-rim REE and Hf abundances, which are interpreted to represent evolving magma composition and/or temperature. Variability in trace elements across single grains is often small compared to variation across many grains, necessitating high-precision ID-TIMS U-Pb geochronology in conjunction with the trace element data in order to evaluate long term (> tens of ka) trends in magma evolution, even in apparently autocrystic zircon populations. Geochemical transects were used to generate numerically modeled bulk trace element signatures and compared to TIMS-TEA data. The combination of these approaches produces trends strongly suggestive of closed system evolution of zircon chemistry through time for samples from ~15-20 km paleodepth.

While our data support TIMS-TEA as a viable analytical protocol, further work is required to understand the emplacement history of the Bergell. Expansion of our existing geochronologic/trace element dataset to include other dateable accessory phases indentified in Bergell samples, including monazite, allanite, and sphene, will be integrated with field observations and structural data in order to place robust constraints on such geochemical information. Our geochronological approach in the context of detailed geologic mapping will allow us to directly test competing models of Bergell emplacement (e.g., diapiric uprise vs. incremental assembly) by comparing the chronologies of different process zones (e.g., synmagmatically-deformed pluton floor vs. ballooning roof).

https://doi.org/10.1180/S0026461X00008434 Published online by Cambridge University Press

The role of fluids in the formation of REE (-Zr, Nb, Ta) deposits associated with alkaline plutons

IAIN M. SAMSON[1] AND ANTHONY E. WILLIAMS-JONES[2]

[1]University of Windsor, Department of Earth and Environmental Sciences, ims@uwindsor.ca
[2]McGill University, Department of Earth and Planetary Sciences

Mineral deposits in which a variety of rare elements, including REE, Zr, Ta, Nb, Be, and Ga, are concentrated are associated with alkaline to peralkaline plutons, typically in rift settings. Although, in general, there are common features among such deposits, the plutons can vary substantially in their internal character and structure, and their degree of Si saturation, from Si-oversaturated (e.g., Strange Lake, Quebec/Labrador) to Si-undersatured (e.g., Thor Lake, NWT, and Illimaussaq, Greenland). The former are characterized by alkaline granites and the latter by nepheline syenites. This variable magma character is reflected in a diverse primary rare element mineralogy. For example, at Strange Lake, Zr was mainly hosted by zircon and elpidite, Nb by pyrochlore and the REE by all three minerals. In contrast, in the Nechalacho deposit at Thor Lake, Zr and REE were hosted by zircon in the upper, miaiskitic, zone and by eudialyte in the lower, agpaitic, zone. Columbite is likely to have been the primary host for Nb. In both settings, the mineralization is characterized by higher HREE/LREE than other systems, such as those associated with carbonates.

The concentration of rare elements through fractional crystallization into pegmatites or by physical crystal accumulation was important in these deposits, however, hydrothermal fluids have played an important role in the subsequent transport and precipitation of rare elements. In particular, water-rock interaction and hydrothermal alteration have significantly modified the mineralogical character of the REE and Zr minerals, and this has increased the mineralogical diversity in such deposits, and resulted in upgrading and ease of beneficiation. The water-rock interaction history can be complex and multi-stage, leading to texturally and mineralogically complex assemblages in which pseudomorphing of early-formed minerals (both rare-element and non-rare element bearing) played a critical role in rare-element mineral precipitation.

The increasing availability of experimental data on the stability of aqueous rare element complexes is making modelling of the processes mentioned above easier, although a lack of data on mineral solubility remains a hindrance. Many models of deposit formation, both in silicic and carbonatitic environments, have employed fluoride complexes to facilitate element transport, with precipitation resulting from their destabilization as a consequence of the addition of Ca from host rocks or by fluid mixing, and the precipitation of fluorite. Although there is ample evidence for Ca metasomatism in the above-mentioned and other deposits, a true evaluation of this model is hindered by a lack of information on ligand concentrations, particularly fluoride. Furthermore, mineralogical and textural observations from these and other systems suggest that other complexation and precipitation models need to be considered.

Zircon, zircon everywhere: What caused the zircon superfertility of Grenville magmas?

SCOTT D. SAMSON[1]*, AARON SATKOSKI[2], DAVID MOECHER[3]

[1]Syracuse University, Earth Sciences, Syracuse, NY, USA, sdsamson@syr.edu (* presenting author)
[2]Syracuse University, Earth Sciences, Syracuse, NY, USA, amsatkos@syr.edu
[3]University of Kentucky, Earth and Environmental Sciences, Lexington, KY, USA, moker@uky.edu

A common assumption in many detrital zircon studies is that the abundance of zircon grains defining a particular age range directly corresponds to the area of exposed continental crust of that age. This is often not the case, however, as much modern alluvium and Paleozoic sandstone have large, sometimes exclusive, 1.3 – 1.0 Ga age peaks, a so-called Grenvillian signature. This is true even for sedimentary rocks very distal to exposed Grenville crust, such as Cambrian sandstone in California and clastic sediment in northwestern Canada. One of the reasons for the extreme abundance of ~ 1 Ga detrital zircon is that magmas associated with Grenville orogenic events contain unusually abundant, and often surprisingly large, zircon crystals. Large and abundant crystals will dominate the zircon budget of alluvium, particularly if sediment has been transported significant distances by major river systems.

A fundamental question about the Grenville Orogeny thus arises: what caused the magmas associated with the tectonic events to be so zirconium rich? One possibility is that the high Zr content, often > 500 ppm, is the result of a high abundance of zircon xenocrysts in the Grenvillian plutons. In this scenario the high Zr whole-rock contents would not be due to actual magmatic compositions but would reflect the total zircon crystal cargo of the intrusion. A second possibility is that the sources of Grenvillian magmas themselves were unusually Zr rich. A recent suggestion has been made that long-lived subduction beneath Laurentia may have significantly chemically enriched the Laurentian mantle lithosphere prior to Grenvillian magmatism. Furthermore, if Zr-enriched parent material was partially melted then the newly formed magma would be even higher in Zr content (assuming Zr distribution coefficients << 1). A third possibility is that unusually hot continental lithospheric conditions existed during the assembly of Rodinia. Very high temperature magmas can become very Zr-rich prior to reaching zircon saturation and thus can crystallize an abundant amount of zircon. These three, not necessarily mutually exclusive, hypotheses have yet to be thoroughly tested, despite their importance to an understanding of what might be one the most Zr-rich magmatic episodes in Earth history. But regardless of the cause, the role of zircon superfertility must be a primary consideration when using detrital zircon as a proxy for studies of continental crustal growth. Estimates of the amount of juvenile crust generated based on isotopic analysis of detrital zircon could be biased if variation in zircon fertility is not taken into consideration.

https://doi.org/10.1180/S0026461X00008434 Published online by Cambridge University Press

An experimental and field study on P, Si, As, Cr, V and Se binding to Fe- and Al-hydroxysulfates under oxic and anoxic conditions in acidic pit lakes: chemical *vs.* microbial controls

JAVIER SÁNCHEZ-ESPAÑA[1*], MARTA DIEZ ERCILLA[1], CARMEN FALAGÁN[1], IÑAKI YUSTA[2]

[1]Unidad de Mineralogía e Hidrogeoquímica Ambiental (UMHA). Instituto Geológico y Minero de España, Madrid, Spain, j.sanchez@igme.es (* presenting author)

[2] Unidad de Mineralogía e Hidrogeoquímica Ambiental (UMHA), Universidad del País Vasco (UPV-EHU), Bilbao, Spain, i.yusta@ehu.es

Introduction and scopes

The chemical composition of acidic mine pit lakes usually include trace elements which may form either oxyanions or some other anionic species, depending on pH-Eh conditions and sulfate concentration. Some elements (e.g., P, Si) are biogeochemically important, whereas others (e.g., As, Cr, V, Se) may be highly toxic to aquatic ecosystems. In the pit lakes of the Iberian Pyrite Belt (SW Spain), the fate and transport of most of these trace elements has been shown to be closely associated to the formation and (meta)stability of low-crystallinity solid phases like schwertmannite and hydrobasaluminite [1]. The present work reports recent field and experimental observations on the mobility of these elements through the water column, redoxcline and the sediment/water interfase.

Results and discussion

Schwertmannite is the most abundant mineral product of microbial Fe^{II} oxidation in the studied pit lakes (pH 2.2-3.1) [1]. Field and experimental evidence exists to support that As, Cr and P are temporaly immobilized by sorption on µm- to nm-scale schwertmannite colloids. Experimental data (including titrations under oxic and anoxic conditions) coupled to geochemical modeling, indicate that the most important retention mechanism is that of sorption of arsenate, chromate and phosphate anions to the positively charged, highly reactive schwertmannite surfaces. The process seems to be reversible, and these elements can be again released to the aqueous phase during settling to the underlying, anoxic part by either (i) microbial reductive dissolution, and/or (ii) schwertmannite aging (conversion to jarosite and/or goethite).

The behaviour of Si, V and Se appears to be more closely linked to the precipitation of hydrobasaluminite or an analogous Al phase. An evident discrepancy exists between the sorption behaviour observed under field and experimental conditions. Such discrepancy could be accounted for by recent microscopic (SEM-EDS) findings, which suggest a strong microbial control on Al precipitation and the associated sorption of Si and other elements. The role of acidophilic microbes in the Fe-Al co-precipitation at pH~4.0 represents a geochemically singular aspect which deserves further investigation.

[1] Sánchez-España, J., Yusta, I., Diez, M. (2011) *Applied Geochemistry* **26**, 1752-1774.

The density of carbonate and silicate melts in the upper mantle

CARMEN SANCHEZ-VALLE[1,*], SUJOY GHOSH[1], WIM J. MALFAIT[1], RITA SEIFERT[1], SYLVAIN PETITGIRARD[2] AND JEAN-PHILIPPE PERRILLAT[3]

[1]Institute for Geochemistry and Petrology, ETH Zurich, Zurich, Switzerland, carmen.sanchez@erdw.ethz.ch (* presenting author)

[2]ESRF, Grenoble, France.

[3]Laboratoire de Sciences de la Terre, UCB Lyon1-ENS Lyon-CNRS, Lyon, France

Although carbonate melts are volumetrically minor phases in the mantle, they may control the mobility of C and its residence time in the mantle, ultimately contributing to the gobal carbon cycle [1]. Carbonate melts are also considered as effective metasomatic agents because of their wetting properties, high migration rate and characteristic trace element enrichment [2]. The density of carbonate liquids is thus an important parameter to model their percolation through the mantle and evaluate their behavior as metasomatic agents and carbon reservoirs, but available data remains scarce at relevant P-T conditions and melt compositions [3,4].

In this contribution we report *in situ* invetigations of the density of carbonate liquids in the Mg-Fe binary and Mg-Fe-Ca ternary systems at upper mantle conditions (2 GPa and 1900 K). Density was determined from the X-ray absorption contrast between the samples and a diamond capsule used to contain the sample at high pressure and temperature conditions. Experiments were perfomed using a panoramic Paris-Edinbugh press at ID27 beamline of the ESRF. Pressure and temperature were determined from the X-ray diffaction patterns of hBN and Pt using the double-isochore method. The measurements provide preliminary constrains on the equation of state of carbonate liquids representative for natural carbonatites, including melt compositions produced by the partial melting of carbonated peridotites [5]. The results are combined with own recent data for the density of silicate melts (rhyolites and phonolites) and literature data for mantle minerals to discuss buoyancy relations in the upper mantle and their evolutions with pressure to better quantify the extraction of C-bearing liquids from residual rocks during partial melting and the ascent of melts through the mantle. Ultimately, we will discuss the role of carbonate-silicate liquids as metasomatic agents and carbon reservoirs.

[1]Dasgupta and Hirschmann (2010) *Earth Planet. Sci. Lett.* 2**98**, 1-13.
[2]Green and Wallace (1988) *Nature* **336**, 459-462.
[3]Dobson et al., (1996) *Earth Planet. Sci. Lett.* **143**, 207-215.
[4]Liu et al. (2007) *Contrib. Mineral. Petrol*. **153**, 55-66.
[5]Dasgupta and Hirschmann (2006) Nature **440**, 659-662.

https://doi.org/10.1180/S0026461X00008434 Published online by Cambridge University Press

Composition of SOM in the Canadian high Arctic

REBECCA L. SANDERS[1*], RACHEL L. SLEIGHTER[2], TULLIS C. ONSTOTT[3], LYLE G. WHYTE[4], PATRICK G. HATCHER[5], AND SATISH C. B. MYNENI[6]

[1]Princeton University, Department of Geosciences, rlsander@princeton.edu (* presenting author)
[2]Old Dominion University, Department of Chemistry and Biochemistry, rsleight@odu.edu
[3]Princeton University, Department of Geosciences, tullis@princeton.edu
[4]McGill University, Department of Natural Resoure Sciences, lyle.whyte@mcgill.ca
[5]Old Dominion University, Department of Chemistry and Biochemistry, phatcher@odu.edu
[6]Princeton University, Department of Geosciences, smyneni@princeton.edu

Permafrost underlies one fourth of the Earth's surface and contains approximately half of the global organic carbon (OC) in soils. Thawing and rapid losses of OC in the form of CO_2 and CH_4, associated with warming of arctic regions, raises serious concerns about the stability of OC in permafrost soils and its influence on the biogeochemical cycling in the surrounding Arctic Ocean. The composition of extractable OC in a soil profile collected from the McGill Arctic Research Station on Axel Heiberg Island in the Canadian high Arctic has been characterized using ultrahigh resolution mass spectrometry and nuclear magnetic resonance spectroscopy. The OC in this polar desert is oxygen-poor and highly enriched in lipids, because algae and detrital carbon from surrounding rocks are the main carbon sources. The OC is poor in lignin and protein in the high Arctic soils when compared to soils of other climates because of the lack of vascular plants. In addition, the OC composition of the whole soils was analyzed by carbon K-edge XANES, which indicated that the OC consisted of mostly aliphatic carbon as well as smaller contributions from unsaturated OC, carboxyls, and proteins. Most striking was the absence of oxygenated OC, which is often present as carbohydrates in polar region soils with more vegetation.

Such a contrasting composition of OC in Arctic soils may result in carbon losses from climate warming that may disagree with the widely-accepted models based upon the biogeochemistry of temperate soils. Heating experiments are currently underway to investigate how and to what extent the OC composition changes as a function of warming, indicative of how these soils may evolve as a result of climate change. Understanding how recalcitrant this highly aliphatic, oxygen-poor terrestrial carbon is will be critical to identifying its impact on the biogeochemical cycling in the surrounding Arctic Ocean.

Geochemistry of mercury and trace elements captured by activated carbons in a Canadian coal-fired power plant

HAMED SANEI[*1], FEIYUE WANG[2], FRANK HUGGINS[3]

[1]Geological Survey of Canada, Calgary, AB, T2L 2A7, Canada, hsanei@nrcan.gc.ca (* presenting author)
[2]Department of Chemistry, University of Manitoba
[3]Department of Chemical and Materials Engineering, University of Kentucky, Lexington, Kentucky, USA

Abstract

The coal-fired power plants in Canada are required to reduce the emission of Hg up to 80% by 2018 and beyond to meet the national and regional regulatory targets. Activated carbon (AC) is considered by industry as an efficient sorbent to capture Hg from the flue gas during the combustion process. A widespread use of AC is anticipated by the coal-fired power plants to reduce the emission of Hg and meet their regulatory obligations.

This study investigates the geochemistry of ESP fly ash and related feed coal samples during an experiment trial by a full-scale coal-fired power plant in Western Canada. Furthermore capturing efficiency and retention ability of 5 different commercial ACs were examined. While the significant amount of Hg is being captured by ACs, the ultimate fate of Hg after capture and possible environmental impacts related to handling and use of Hg-rich fly ash has been a major concern. This study investigates volatilization and leachability of Hg and other elements from the captured fly ash.

The results show that capturing ability varies depending on AC's injection rates, fly ash particle size sorting, and temperature of the flue gas. Thermal release of Hg from fly ash samples appears negligible up to a temperature of 80°C. De-volatilization of Hg begins beyond 80°C, showing a sudden increase after 120°C. The constant heating at 140°C resulted in a steady de-volatilization of Hg during the 8 hour experiment that suggests a slow release of Hg during long exposure to heat. We recommend further investigation of possible Hg de-volatilization at higher temperature with the samples being exposed for a longer period of time.

Mercury is mostly leachable under strong acid digestion suggesting strong chemical retention. However, <10% of the total captured Hg can be released under the more moderate chemical digestion. The retention ability tends to decrease significantly in fine-grained fly ashes. The fly ashes injected with high sulphur AC provided the strongest chemical retention for Hg. We conclude that the possible Hg-S binding associated with ACs not only provides the best Hg capture capacity, but also provides the strongest thermal and chemical retention ability.

https://doi.org/10.1180/S0026461X00008434 Published online by Cambridge University Press

Solid - Liquid Equilibria for the ternary $Na_2B_4O_7$ - NaBr - H_2O System at 348 K

SHIHUA SANG[1, 2]*, HUIYI NING[1], AND DAN WANG [1]

[1]College of Materials and Chemistry & Chemical Engineering, Chengdu University of Technology, Chengdu 610059, China.

* sangsh@cdut.edu.cn

[2]Mineral Resources Chemistry Key Laboratory of Sichuan Higher Education Institutions，Chengdu 610059, China

Introduction

Many salt lake brines on the Qinghai - Tibet plateau in China are well known for high concentrations of Li, K and B. Furthermore, a huge amount of underground gasfield brine was also discovered in China,such as Sichuan western basin. Sodium chloride, potassium, boron , bromine and sulfates are the major chemical component of the oilfield brine, which often accompanies Li, Sr and I. The ternary system $Na_2B_4O_7$ - NaBr - H_2O is a subsystem of the underground gasfield brines.

Results

The solid - liquid equilibria for the ternary system $Na_2B_4O_7$ - NaBr - H_2O at 348 K were measured experimentally using the method of isothermal solution saturation. On the basis of experimental data, the phase diagram of the ternary system was constructed. In the phase diagram of the ternary system $Na_2B_4O_7$ - NaBr - H_2O at 348 K(Figure 1), there are one invariant point E and two univariant curves E1E and E2E. The points E1 and E2 represent the solubility of the binary systems of $Na_2B_4O_7$- H_2O and NaBr - H_2O at 348K with mass fraction ($100w_b$) of 19.30 and 54.35, respectively. Curve E1E and E2E are the solubility isotherms of $Na_2B_4O_7 \cdot 5H_2O$ and NaBr, respectively. The invariant point E corresponds to the solution saturated with both NaBr and $Na_2B_4O_7 \cdot 5H_2O$. Phase equilibrium solids were NaBr and $Na_2B_4O_7 \cdot 5H_2O$ in the studied ternary system. The crystallization area of $Na_2B_4O_7 \cdot 5H_2O$ (E1ED field) in the phase diagram is obviously bigger than that of NaBr (E2EA field).

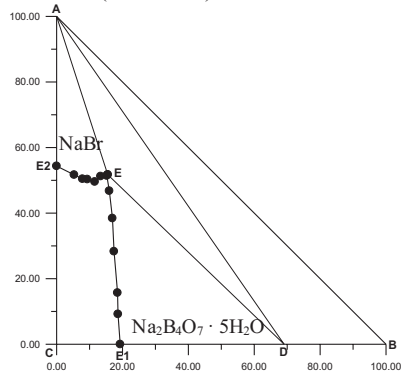

Figure 1 Phase diagram of the ternary system $Na_2B_4O_7$ - NaBr - H_2O at 348 K

Acknowledgements: This project was supported by the National Natural Science Foundation of China (No. 40973047) and the Youth Science Foundation of Sichuan Province, China (08ZQ026-017).

Use of two new Na/Li thermometric relationships for geothermal fluids in volcanic environments

BERNARD SANJUAN[1*], RAGNAR ASMUNDSSON[2], ROMAIN MILLOT[3] AND MICHEL BRACH[3]

[1] BRGM, Department of Geothermal Energy, Orléans, France, b.sanjuan@brgm.fr (* presenting author)

[2]Tiger Energy Services, Taupo, New Zealand, ragnar.asmundsson@tigerhd.com

[3]BRGM, Department of Metrology, Monitoring and Analysis, Orléans, France, r.millot@brgm.fr, m.brach@brgm.fr

Thermometers such as Silica, Na/K, Na/K/Ca, Na/K/Ca/Mg or $\delta^{18}O$ (H_2O-SO_4), based on empirical or semi-empirical laws derived from chemical equilibrium reactions between water and minerals in the deep reservoirs, are commonly used in geothermal exploration in order to estimate the reservoir temperatures. Unfortunately, these estimations are not always concordant because of processes which can perturb the chemical composition of the fluids during their ascent up to the surface (water mixing, fluid cooling, etc.). Given these discordances, auxiliary thermometers such as Na/Li, based on statistical relationships, were also developed. As Li is rather lowly reactive, the use of this thermometer can give more reliable temperature estimations. Presently, three different Na/Li relationships ([1], [2]) are mainly available according to the fluid salinity and the geological environment (volcanic/granitic and sedimentary rocks).

This study carried out in the framework of the European HITI project (HIgh Temperature Instruments for supercritical geothermal reservoir characterization and exploitation) with the collaboration of ISOR Iceland Geosurvey proposes two new Na/Li thermometric relationships. The first concerns the fluids derived from high-temperature seawater-basalt interaction processes existing in the oceanic ridges and rises as well as in the emerged rifts such as those of Iceland (Reykjanes, Svartsengi and Seltjarnarnes geothermal fields) and Djibouti (Asal-Ghoubbet and Obock geothermal areas). It can be expressed as follows:

$$\text{Log (Na/Li in mol/l)} = 920/(T°K) + 1.105 \quad (r^2 = 0.994).$$

The second relationship, developed using dilute fluids collected only from Icelandic geothermal wells in the 100-325°C range, surprisingly close to that determined by Fouillac and Michard (1981) for volcanic saline fluids at temperatures ≥ 200°C, is:

$$\text{Log (Na/Li in mol/l)} = 1786/(T°K) - 0.936 \quad (r^2 = 0.976).$$

The uncertainty on temperature estimation is ± 25°C for both relationships. These results confirm that the Na/Li ratios not only depend on temperature but also on other parameters. The nature of the reservoir rocks and fluid seems to be the most influent one. Some literature case studies and thermodynamic considerations suggest that the Na/Li ratios could be controlled by chemical equilibrium reactions involving different mineral assemblages where illite and micas would be, however, always present.

[1] Fouillac Ch. and Michard G. (1981) *Geothermics,* **10**, n°1, 55-70. [2] Kharaka and Mariner (1989) *Naeser and McCulloch Eds, Springer-Verlad, New York,* 99-117.

https://doi.org/10.1180/S0026461X00008434 Published online by Cambridge University Press

Carbonated basalts at depth: density, compression mechanisms, and potential buoyancy

C. SANLOUP[1*], C. CRÉPISSON[2], G. MORARD[3], H. BUREAU[3], G. PROUTEAU[4] AND S. PETITGIRARD[5]

[1]University of Edinburgh, Edinburgh, UK, chrystele.sanloup@ed.ac.uk (* presenting author)
[2]Ecole Normale Supérieure, Paris, France, celine.crepisson@ens.fr
[3]Université Pierre et Marie Curie – Paris 6, Paris, France
[4]ISTO, Orléans, France
[5]European Synchrotron Radiation Facility, Grenoble, France

Introduction

The alkali basalt composition was chosen as representative of two potentially relevant contexts : alkali basalts dragged in the Japanese sea have been interpreted as originating from the asthenosphere [1,2], and their high vesicularity suggested high CO_2 content in the pre-eruptive melt. Also, primitive alkali basalts are generated in subduction contexts, as the one used here (Stromboli [3]) and as such, could have contributed to the formation of cratonic roots.

Experiments

In situ density and structural measurements were collected using respectively x-ray absorption and x-ray diffraction techniques. High P-T conditions up to 7 GPa were generated using the Paris-Edinburgh press at the european synchrotron (ESRF, ID27 beamline) and the cell-assembly described in [5]. Recovered quenched samples were analyzed by EPMA and Raman spectroscopy to check for CO_2 content and speciation.

Density measurements as a function of pressure show a higher compressibility than for non-carbonated basalts. Structural data, as expressed by pair distribution function of the melt, show an increased coordination number of Al. Such effect had been proposed based on viscosity measurements at modest P [6,7], and seems emphasized at higher P.

Density of the carbonated alkali basalt is then compared to seismological and petrological values of the density for surrounding rocks to check for potential neutral buoyancy at depth.

[1] Hirano (2001) *GRL* **28**, 2719-2722. [2] Hirano (2006) *Science* **313**, 1426-1428. [3] Pichavant et al. (2009), *J. Pet*. **50**, 601-624. [4] [5] Van Kan Parker et al. (2010) *High Pressure Res*. **30**, 332-341. [6] Brearley (1989) *GCA*, **53**, 2609-2616.[7] White (1990) *JGR* **95**, 15683-15693.

Interpretation of helium isotopes in modern hydrothermal systems

Y. SANO[1] AND T. P. FISCHER[2, 3]

[1]Atmosphere and Ocean Research Institute, University of Tokyo, Kashiwanoha, Chiba 277-8564, Japan (*correspondence: ysano@aori.u-tokyo.ac.jp)
[2]Division of Earth Sciences, National Science Foundation, Arlington, VA 22230, USA
[3]Department of Earth and Planetary Sciences, University of New Mexico, Albuquerque, NM87131-1116, USA

Many reviews and textbooks on terrestrial helium isotopes have been published since the discovery of mantle helium in 1969. This work focuses on the interpretation of helium isotopes of fluid samples in modern hydrothermal systems. In hot spot regions such as Hawaii, Yellowstone and Iceland, helium isotopes of fluid samples are generally higher than MORB-type He (8.0+/-1.5) Ra where Ra is the atmospheric ratio of $1.4x10^{-6}$. Seismic tomography data of the three regions show that a continuous low-velocity anomaly is imaged from the surface to at least the surface of the lower mantle [1-3]. The plume-type He may be derived from the lower mantle. In the other hot spot regions such as Afar, Canary and Reunion, the thermal conduit associated with mantle upwelling extends to depths greater than 500 km. There is a weak positive correlation between maximum helium isotopes and the buoyance flux except for Hawaii. Graham [4] compiled 658 MORB glass data and reported that the more than 90% of helium isotopes are lying between 6.5-9.5 Ra. Hydrothermal fluids in MOR shows the helium isotopes varying from 7.2 Ra to 9.2 Ra with the average of (8.09+/-0.49) Ra, identical to that of the global average of MORB. The average ^3He/heat ratios is calculated (8.6+/-3.8) x 10^{-18} mol/J world-wide. When we take into account of a global axial heat flow in MOR [5], the total ^3He flux would become (2.8+/-1.2) atom/cm^2/s, a little smaller than the well-established value of 4 atom/cm^2/s [6]. Helium isotope data of subduction zones were compiled by Hilton et al [7]. Now additional data are available in the Kamchatka, Izu-Bonin, Ryukyu-Taiwan, Sangihe arc in Indonesia and Central American system. The cir-cum Pacific helium data are summarized as follows: (a) helium isotopes vary significantly from 0.01 Ra to 10.1 Ra and the rage is much larger than that of MOR-type He. (b) The highest value of 10.1 Ra observed in the Vanuatu islands suggests the contribution of plume-type He. (c) The second highest values (8.8-8.9) Ra are found in the Colombian Andes and Sunda arc systems, falling within the range of MOR-type He. (d) Relatively lower values (6.5–7.0) Ra are observed in the Ecuadorian, Peruvian and Chilean Andes and the eastern Sunda/Banda arc, slightly lower than that of MOR-type. There is no apparent correlation between the maximum value of arc segments and the magma production rate or the taper angle of the slab.

[1] J. Lei and D. Zhao (2006) *EPSL* **241**, 438-453. [2] H. Yuan and K. Dueker (2005) *GRL* **32**, L07304. [3] J. Ritsema and R. Allen (2003) *EPSL* **207**, 1-12. [4] D. Graham (2002) in *Noble Gases, Reviews in Mineral. Geochem.* **Vol. 47**, 247-317. [5] C.R. German and K.L. Von Damm (2004) in *Treatise Geochem.* **Vol. 6**, 181-222. [6] H. Craig et al. (1975) *EPSL* **26**, 125-132. [7] D. Hilton et al. (2002) in *Noble Gases, Reviews in Mineral. Geochem.* **Vol. 47**, 319-370.

https://doi.org/10.1180/S0026461X00008434 Published online by Cambridge University Press

Comparative study of synthetic and natural iron sulfates and oxides by Raman spectroscopy

ANTONIO SANSANO[1*], JESUS MEDINA[2], FERNANDO RULL[3], PABLO SOBRON[4]

[1]Unidad Asociada UVA-CSIC Centro de Astrobiologia, Spain, sansanoca@cab.inta-csic.es

[2] Unidad Asociada UVA-CSIC Centro de Astrobiologia, Spain, medina@fmc.uva.es

[3] Unidad Asociada UVA-CSIC Centro de Astrobiologia, Spain, rull@fmc.uva.es

[4] Space Science and Technology, Canadian Space Agency, Canada, Pablo.Sobron@asc-csa.gc.ca

The study of iron minerals, in particular, sulfates and oxides of evaporitic characteristics, has carried a great interest in the last years, not only for their direct application in the analysis of mine drainage, also in their application to the study of the mineralogy of Mars surface. The jarosite discovery[1], as well as of other hydrated sulfates[2] in the surface of the red planet carried out by MERs represent an important focus of interest for the study of the evolution and the geodynamics of the planet and their possible astrobiological implications.

The use of quick and precise techniques, susceptible of being boarded in missions to other planets, is revealed as an important aspect when carrying out so much analysis of synthetic materials as collected materials from different geologic analogs. In particular, Raman spectroscopy as part of the payload of the mission Exomars[3] and that it will be launched in the 2018 to Mars, shows up like a very powerful technique when analyzing in-situ and in a non destructive way the molecular composition of the analyzed materials, besides giving us a quite precise idea of structural aspects that could be extrapolated in reference to their possible genesis.

In this work we present the results of the application of this technique to materials synthesized in laboratory also to materials extracted in diverse campaigns to different Martian analogs as are Rio Tinto River and El Jaroso Ravine, both in Spain[4]. On one hand, the use of materials of synthetic origin provides us so much patterns for reference use and also an approach to the necessary conditions for the formation of one or another compound, in a controlled way. On the other hand, the materials picked up in the natural localizations give us a real panoramic of how they are distributed and this materials become in the geochemical conditions that surround them. This allows us to compare them among and with the synthetic ones being been able to extract conclusions about the conditions of their origin, their structural characteristics and being able to formulate hypothesis on their formation process and could be extrapolated by methods of the analysis in situ in Mars, of the materials that there are.

[1] Klingelhöfer et al. (2004), Science, 306, 1740-1745 [2] Johnson et al. (2007) JGR, V34, L13202 [3] Rull et al (2006) Spect.Now. v18, 18-21 [4] Rull et al. (2008) LPSC XXXIX, #1616.

Multiple sulphur isotope evidence for an oceanic sulphate concentration decrease in the Marinoan glaciation aftermath

P. SANSJOFRE [1*], P. CARTIGNY[1], M. ADER[1], R. TRINDADE [2] AND A. NOGUEIRA[3]

[1] Equipe de Géochimie des Isotopes Stables, Institut de Physique du Globe de Paris, Sorbonne Paris Cité, Univ Paris Diderot, UMR 7154 CNRS, F-75005 Paris, France, sansjofre@ipgp.fr (* corresponding author)

[2] Departamento de Geofisica IAG, Universidade de São Paulo, Brazil, rtrindad@iag.usp.br

[3] Instituto de Geociências, Universidade Federal do Pará, Bélem, Brazil, anogueira@ufpa.br

In order to better contrain the sulphur cycle in the aftermath of the Marinoan Glaciation, we performed sulphur isotope composition analysis ($\delta^{33}S$ - $\delta^{34}S$ - $\delta^{36}S$) of Ediacarian carbonates, on both Carbonate Associated Sulphate (CAS) and pyrite. Samples come from Carmelo quarry (Mato Grosso, Brazil) where 20m of white dolomicrite (Mirassol d'Oeste Formation) directly cover the glacial sediments related to the Marinoan glaciation (~635Ma). This dolomicrite is overlying by 150m of Guia Formation limestone's which begin with 40 meters of carbonate-rich siliciclastic material evolving to pure carbonate intercalated with thin layers of marls.

Results show an increase in both $\delta^{34}S_{pyr}$ and $\delta^{34}S_{CAS}$ upward along the section. $\delta^{34}S_{pyr}$ and $\delta^{34}S_{CAS}$ vary from -10‰ to +26‰ and from +16 to +51‰ respectively. Our $\delta^{34}S_{CAS}$ data are relatively high compared to present day oceanic sulphate value (+21‰), but they are in agreement with previous data reported for the same time period. $\Delta^{33}S$ data show values close to 0‰ (0.03 ± 0.02‰) at the base of the section and significatively higher values in the upper part, up to +0.16 ± 0.02‰.

For steady-state ocean sulphur concentration, an increase in the isotopic values can be partially explained by an increase in pyrite burial rate together with a higher $\delta^{34}S_{sulphate}$ input. However this model cannot account neither for the extremely high values of $\delta^{34}S_{CAS}$ nor for the $\Delta^{33}S$ signal. We thus developped a non steady state model in which we take into account the effect of Rayleigh distillation on $\delta^{34}S_{CAS}$, $\delta^{34}S_{pyr}$ and $\Delta^{33}S$ values. Results show that the increase in both $\delta^{34}S$ (CAS and pyrite) and $\Delta^{33}S$ are well explained by a decrease of ~50% in the oceanic sulphate concentration. We thus propose that the post-Marinoan ocean experienced a decrease in sulphate concentration which could result from an increase in sulphate consumption by BSR relative to the net riverine sulphate delivery input.

https://doi.org/10.1180/S0026461X00008434 Published online by Cambridge University Press

Membrane-dependent microbial inhibition during CO_2 sequestration: Implications for the alteration of subsurface community composition

EUGENIO-FELIPE U. SANTILLAN[1*], CHRISTOPHER R. OMELON[1], TIMOTHY M. SHANAHAN[1], AND PHILIP C. BENNETT[1]

[1]University of Texas Austin, Austin, TX, USA
efu.santillan@utexas.edu (* presenting author)

Background

When CO_2 is stored in deep saline aquifers, many geochemical changes will occur due to CO_2 dissolution [1]. High PCO_2 will also perturb the existing microbial communities that influence the geochemistry of the reservoir through their metabolic activities.

The CO_2 molecule itself is toxic to microorganisms. It is easily permeable through cell membranes changing membrane fluidity, the proton pump, and intracellular pH [2]. Adaptations that slow the diffusion of CO_2 into the cell, like biofilms and thick cell walls, will be selected for in the new environment.

In this study, we assessed the tolerance of several representative organisms to high PCO_2 based on their membrane morphologies: the Gram-negative bacterium *Shewanella oneidensis*, the Gram-positive bacterium *Bacillus subtilis* sp0A mutant, the Gram-positive endospore forming bacterium *Geobacillus stearothermophilus*, and the methanogenic archaeon *Methanothermobacter thermoautitrophicus*.

Results and Conclusions

Results show the Gram-negative organism is the most susceptible to CO_2 toxicity surviving a maximum pressure of 25 atm for 2 hours. However, when grown in the presence of a mineral, survival time increases beyond 8 hours due to biofilm formation. Archaea can withstand 50 atm of CO_2 for 8 hours and Gram-positive endospores can handle 50 atm of CO_2 for at least 24 hours potentially due to thick and rigid cell membrane or wall compositions.

Images taken by transmission electron microscopy show all experimental organisms have a threshhold tolerance to CO_2. We observed clumping of cytoplasmic contents at differing CO_2 pressures suggesting CO_2 plays an effect in altering intracellular activity. Lipid profiles of the bacteria also show a decrease in concentrations of monounsaturated or of short-chained fatty acids during CO_2 exposure indicating CO_2 causes a loss in cell viability.

Our findings suggest that during CO_2 sequestration, biofilms, Gram-positive endospores, and methanogens are organisms that will survive in the new environment. Because each organism varies in their CO_2 tolerance, regions surrounding the CO_2 plume may eventually form where different organisms are most active This in turn can have effects on mineral precipitation catalyzed on cell membranes and the geochemistry of the greater subsurface.

[1] Kharaka et al. (2006) *Geology* **34**, 577-580. [2] Hong and Pyun (1999) *Journal of Food Science* **64**, 728-733.

In situ remediation and pedogenesis in bauxite residue ('red mud')

TALITHA SANTINI[1,2*], MARTIN FEY[1], AND ANDREW RATE[1]

[1]University of Western Australia, Perth, Australia,
talitha.santini@uwa.edu.au (* presenting author)
[2]McMaster University, Hamilton, Canada

Introduction

'*In situ*' approaches to tailings management typically address unfavourable properties of the tailings after deposition in storage areas by surface application of treatments. In the case of bauxite residue, *in situ* remediation means selecting treatments that will aid in lowering pH from values of >12 to <9, lowering electrical conductivity from values of >4 dS/m to <1 dS/m, and that will stimulate biological activity in the initially sterile tailings. Treatments including sewage sludge, tillage, green waste, dredge spoil, and topsoil were applied at a bauxite residue ('red mud') storage area in Corpus Christi, Texas.

Results and discussion

Rainfall leaching (for 40 years) prior to amendment removed excess soluble salts, but not all residual sodalite ($Na_8(AlSiO_4)_6Cl_2$) and calcite ($CaCO_3$) which slowly dissolve and continue to buffer pH at values >8. Substantial replacement of Na^+ with Ca^{2+} has occurred on cation exchange sites, particularly in surface residue layers. Calcite dissolution, facilitated by rainfall leaching and organic acids and $CO_{2\,(g)}$ from plant roots, may provide Ca^{2+} for this exchange.

Bauxite residue pore water was high in Al, Ca, Fe, Na, and Si. Formation of gravel in the residue was attributed to precipitation of aluminosilicate coatings on surfaces exposed to the atmosphere during drying and cracking of residue (Figure 1). Some pores in the gravel contained nordstrandite or bayerite (both $Al(OH)_3$). Given that silicate inhibits crystallisation of aluminium hydroxides from solution [1], it appears that the aluminosilicate coatings formed first, lowering Si content of pore water, which then allowed precipitation of nordstrandite/ bayerite inside the gravel pores after further drying.

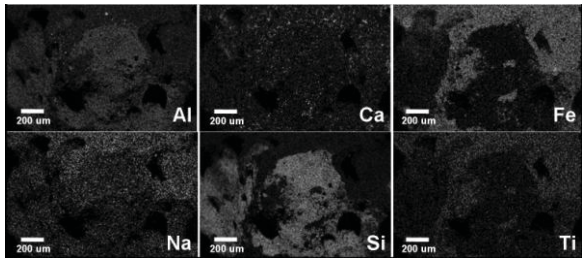

Figure 1: Element maps from gravel with aluminosilicate coating.

Sewage sludge was more effective than dredge spoil or topsoil in lowering bauxite residue pH, and increasing total N and extractable NH_4^+. Sewage sludge outperformed other treatments in terms of generating a suitable soil-like medium for plant cover, and addressing high pH and lack of plant nutrients such as organic C and N, K, Mg, and P in bauxite residue. Applied treatments can influence bauxite residue chemistry and mineralogy, and improve soil formation and *in situ* remediation.

https://doi.org/10.1180/S0026461X00008434 Published online by Cambridge University Press

Sr and Nd isotope composition of the Alcáçovas calc-alkaline rocks (Ossa-Morena Zone, Portugal)

JOSÉ F. SANTOS[1]*, PATRÍCIA MOITA[2], JONI MARQUES[1]

[1]Geobiotec / Dep. Geociências, Univ. Aveiro, Portugal, jfsantos@ua.pt*

[2]Centro de Geofísica / Dep. Geociências, Univ. Évora, Portugal

The Alcáçovas area is located in the SW sector of the Ossa-Morena Zone (OMZ), close to a major fault that separates this geotectonic unit from the South Portuguese Zone (SPZ). Along this boundary, in the OMZ, testimonies of low-K tholeiitic and calc-alkaline magmatism are common and have been interpreted as being related to the operation of a subduction zone between OMZ and SPZ during the Variscan cycle [1]. Two main igneous lithologies, both displaying calc-alkaline compositions, can be found in the studied area: gabbro-diorites and dacitic-rhyolitic porphyries [2,3]. Outcrop conditions have not yet allowed to establish unequivocally the sequence of magma emplacement. In previous geochronological studies on the porphyries, whole-rock Rb-Sr dates and K-Ar ages cluster around 320 Ma [4,5,6].

According to field observations, sometimes felsic dykes cut mafic rocks, but there are also gradual transitions from gabbroic to tonalitic compositions, within bodies mapped as gabbro-diorite, revealing that different melts coexisted.

In this study, rock samples of both gabbro-dioritic bodies and porphyries were analysed for Rb-Sr and Sm-Nd isotopes. Considering the whole set of samples, no isochron was obtained, showing that they can not be simply related by crystal fractionation processes.

Rb-Sr data of porphyries from a single quarry (at Lameira, 7 km to the SW of Alcáçovas) give 323±16 Ma (MSWD=1.9; initial $^{87}Sr/^{86}Sr$=0.7097±0.0018). Taking into account that the rocks of the Lameira outcrop show strong hydrothermal alteration, this date must be viewed as a consequence of a very efficient redistribution of mobile elements during aqueous fluid circulation and, as such, it places a minimum limit to the actual magmatic age

The plot of compositions of the gabbro-dioritic bodies, including their transitions to tonalites and the associated felsic dykes, in the ε_{Nd}-$^{87}Sr/^{86}Sr$ diagram, define an almost perfect hyperbole (from εNd_{323} = +3.9 and $^{87}Sr/^{86}Sr_{323}$ = 0.7058 to εNd_{323} = -3.8 and $^{87}Sr/^{86}Sr_{323}$ = 0.7085), as expected in a mixture between mantle-derived melts and crustal materials. In the same diagram, samples from the Lameira quarry show an almost constant εNd_{323}, between -2.4 and -2.9, and $^{87}Sr/^{86}Sr_{323}$ varying from 0.7092 to 0.7106. Therefore, the Lameira porphyries could represent a member of the same mixture, with the Sr signature modified by hydrothermal fluids with a stronger crustal component.

Funding: FCT through projects Petrochron (PTDC/CTE-GIX/112561/2009) and Geobiotec (PEst-C/CTE/UI4035/2011).

[1] Santos et al. (1990) *Comun. Serv. Geol. Portugal* **76**, 29-48.
[2] Gonçalves et al. (1992) *Not. Expl. Carta Geol. Torrão*, 86 pp.
[3] Caldeira et al (2007) *Comun. Geol. INETI* **94**, 05-28.
[4] Andrade (1974) *Mem. Not. Univ. Coimbra* **78**, 29-36.
[5] Coelho et al. (1986) *Ciências da Terra UNL* **8**, 65-72.
[6] Priem et al. (1986) *Comun. Serv. Geol. Portugal* **72**, 03-07.

Correlation of magnetic susceptibility with $\delta^{18}O$ data in magnetite- and ilmenite-type granites from Iberian massif

HELENA SANT'OVAIA[1*], HELENA MARTINS[1], JOSÉ CARRILHO LOPES[2], JOANA MACHADO[1] AND FERNANDO NORONHA[1]

[1] DGAOT, Centro de Geologia, F.C. Univ. Porto, Portugal, hsantov@fc.up.pt (* presenting author)

[2] Centro Geologia Univ. Lisboa; Dep. Geoc., E.C.T. Univ. Évora, Portugal (carrilho@uevora.pt)

The relationship between oxygen isotopic values and magnetic susceptibility composition on 11 Variscan Portuguese granites has been investigated. Whole-rock oxygen-isotope ($\delta^{18}O$) values for Vieira do Minho (VM), Vila Pouca de Aguiar (VPA), Chaves, Castelo Branco (CB), Manteigas and Serra da Estrela (SE) granitoids, were compilated from bibliography [1,2,3,4], and $\delta^{18}O$ for Santa Eulalia Plutonic Complex (SEPC) were obtained by laser fluorination at the Stable Isotopic Laboratory of Salamanca. Magnetic susceptibility (Km) values were obtained with a Kappabridge equipment from Toulouse University and Geology Centre, Porto University [2,5,6,7,8]. In this study is shown that there is a significant inverse correlation between Km and $\delta^{18}O$. *Magnetite*-type granites (Manteigas granodiorite and SEPC external facies) have Km>10^{-3} SI and low $\delta^{18}O$ values ranging from 8.9 to 10.3‰ instead those of *ilmenite*-type (all the other granites) have Km≤10^{-4} SI and are $\delta^{18}O$ enriched (9.3 to 13.5‰). The *I*-type granites (VM, VPA, Chaves, Manteigas and SEPC external facies) show lower average $\delta^{18}O$ (10.2‰) and higher Km values (100x10^{-6} SI) than the *S*-type granites (SE and CB) with $\delta^{18}O$ = 12.6‰ and Km = 65x10^{-6} SI.

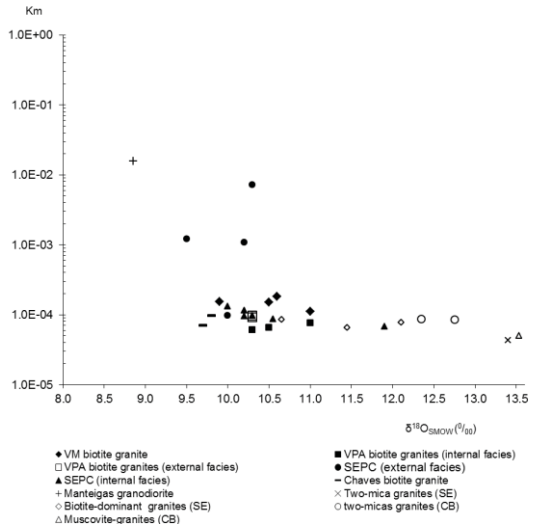

Figure 1: Semi-log plot of Km (in Si units) versus $\delta^{18}O$.

This work has been financially supported by PTDC/CTE-GIX/099447/2008 (FCT-Portugal, COMPETE/FEDER).

[1] Martins *et al.* (in prep.) [2] Martins *et al.* (2009) *Lithos* **111**, 142-155. [3] Antunes *et al.* (2008) *Lithos* **103**, 445-465. [4] Neiva *et al.* (2009) *Lithos* **111**, 186-202. [5] Sant'Ovaia *et al.* (2010) *JSG* **32**, 1450-1465. [6] Sant'Ovaia *et al.* (2000) *TRSE, ES* **91**, 123-127. [7] Sant'Ovaia *et al.* (2008) *33rd IGC* CD. [8] Sant'Ovaia *et al.* (2011) *Min. Mag.* **75**, 3, 1795.

https://doi.org/10.1180/S0026461X00008434 Published online by Cambridge University Press

Dissolved iron in the vicinity of the Kerguelen Islands, Southern Ocean, during the KEOPS 2 experiment

G. SARTHOU[1*], F. QUÉROUÉ[1,2,3], F. CHEVER[1], A.R. BOWIE[2], P. VAN DER MERWE [2], E. BUCCIARELLI[1], M. FOURQUEZ [4], S. BLAIN[4]

[1]LEMAR, UMR 6539 CNRS UBO IRD IFREMER, Place Nicolas Copernic, F-29280 Plouzané, France (* presenting author: Geraldine.Sarthou@univ-brest.fr)
[2]Antarctic Climate and Ecosystems CRC, University of Tasmania, Hobart, Tasmania, Australia
[3]Institute for Marine and Antarctic Studies, University of Tasmania, Hobart, Tasmania Australia
[4]LOMIC, UMR 7621 CNRS UPMC, avenue du Fontaulé, 66650 Banyuls sur mer, France

During KEOPS 2 (KErguelen Ocean and Plateau compared Study 2, Oct.-Nov. 2011), the distribution of dissolved Fe was investigated in the upper 1300 m in the vicinity of the Kerguelen Islands. Samples were analysed on board by flow injection analysis and chemiluminescence detection, with a detection limit of 0.02 ± 0.02 nM (n=13). A clear enrichment was observed above the Plateau. Indeed, the highest concentrations (2-4 nM) were observed at the most coastal station, east of the Kerguelen Islands. Then concentrations decreased eastward with the lowest values in an anti-cyclonic structure (0.06 nM at sea-surface and 0.3-0.4 nM at depth). A similar behaviour was observed at our reference station in the HNLC area, west of the Kerguelen Islands. In the polar front region, concentrations increased with values around 0.3-0.4 nM at sea-surface and 0.6-0.7 nM at depth. On-board incubations on natural plankton communities clearly showed a strong iron limitation at our reference station, a moderate one in the anti-cyclonic structure and no limitation above the Plateau.

Sorption of borate on calcined products of natural dolomite

Keiko Sasaki[1*], Yukiho Hosomomi[2], and Xinhong Qiu[3]
[1]Kyushu University, Earth Resources Engineering, Fukuoka, Japan, keikos@mine.kyushu-u.ac.jp (* presenting author)
[2] Kyushu University, Earth Resources Engineering, Fukuoka, Japan, y-hosomomi11@mine.kyushu-u.ac.jp
[3] Kyushu University, Earth Resources Engineering, Fukuoka, Japan, q-q11@mine.kyushu-u.ac.jp

Introduction

Boron is a dynamic trace element that can affect the metabolism or utilization of numerous substances involved in life processes, and also one of the most difficult elements to immobilize in aquatic environments [1]. Natural dolomite was modified to provide as a sorbent for borate. Calcination condition was investigated at 700 °C ~900 °C under air and reducing atmosphere.

Results and Conclusion

Calcite ($CaCO_3$) and magnesian calcite (Ca, Mg)CO_3 were included as impurities as well as dolomite ($CaMg(CO_3)_2$) in the specimen. Increasing with calcination temperature, sequential decarbonation was confirmed by XRD, that is, transformation of dolomite into magnesia and calcite at 700 °C, transformation of magnesian carbonate into magnesia and calcite at 800 °C, and transformation of calcite into lime at 900 °C. Surface molar ratio of Ca/Mg decreased from 1.6 to 0.6 independently of calcination temperatures. Sorption isotherm of borate at 25 °C was compared with calcined products under different conditions. In calcination under air, the greatest sorption density of borate was found with calcined product at 700 °C (Fig. 1). BET type of sorption isothedrm curve suggests that removal of borate is expected to occur through destructive sorption of MgO in calcined products. However, under reducing conditions the greatest sorption density was observed with calcined product at 900 °C.

Removal mechanism of borate is principally co-precipitation with $Mg(OH)_2$ in hydration nof MgO. The above result suggests the surface of magnesia (MgO) was more significantly affected by CO_2 in a process of decarbonation at higher temperature, and that higher crystalinity of MgO is more reactive in hydration.

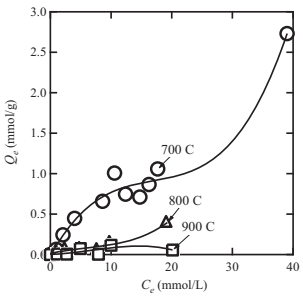

Figure 1: Sorption isotherm of borate at 25 °C on calcined products of natural dolomite at 700 °C ~900 °C under air.

[1] Sasaki *et al.* (2011) *J. Hazard. Mater.,* **185,** 1440-1447.

https://doi.org/10.1180/S0026461X00008434 Published online by Cambridge University Press

Experimental studies on carbon isotope fractionation in the deep Earth

M. SATISH-KUMAR [1*], TAKASHI YOSHINO[2], SHOGO MIZUTANI[1], HAYATO SO[3], AND MUTSUMI KATO[4]

[1]Department of Geosciences, Shizuoka University, Shizuoka, Japan smsatis@ipc.shizuoka.ac.jp
[2] ISEI, Okayama University, Misasa, Japan
[3]Asahi Diamond Industrial Co. Ltd, Mie, Japan
[4]Graduate School of Sciences, Chiba University, Chiba, Japan

Carbon is the fourth most abundant element in the solar system. It has a key role in the melting phase relations of mantle rocks [1] and metallic core [2]. Carbon further acts as an agent of mass transfer in the form of mobile carbonate-rich melts [1]. An efficient tool to understand the carbon cycle, both in the shallow and deep Earth environments, is by using carbon isotopic composition. However, our understanding of carbon isotopic composition of deep Earth is very limited. Here we present results of experimental determination of partitioning of carbon isotopes at high-pressure high-temperature conditions, in systems analogous core formation environment and carbonate melting in the mantle conditions.

High-pressure experiments were performed using a Kawai type multi-anvil high-pressure apparatus at the ISEI, Okayama University, Misasa, Japan. Two types of starting materials were used. First type is a mixture of Fe + 9.0wt% C with known carbon isotopic composition. Second set of experiments were carried out in the Mg-Si-C-O system, where San Carlos enstatite and olivine was mixed with graphite and magnesite. Experiments were carried out at a pressure of 5 and 10 GPa at temperature conditions between 1200 ºC and 2100 ºC. Carbon isotope measurements were carried out using an IRMS.

The distribution of carbon isotopes between iron carbide melt and graphite/diamond at high-pressure high-temperature conditions shows the presence of large and measurable carbon isotope fractionation in the Fe-C system. These results were also consistent with the carbon isotope distribution between graphite and cohenite (Fe_3C) in iron meteorites. A temperature-dependent fractionation of carbon isotopes between iron carbide melt and graphite/diamond, as reported in [3], is believed to have created a "^{12}C-enriched core" with a significant difference in the distribution of carbon isotopes between the carbon core and bulk silicate Earth during accretion and differentiation of early Earth. In order to further characterize the carbon movement in the mantle, the carbon isotope systematics during melting of carbonated mantle in the presence of graphite/diamond were investigated in the Mg-Si-C-O system. Preliminary results indicate that carbon isotopes show considerable partitioning between graphite/diamond and carbonate melt at temperatures and pressures corresponding to upper mantle conditions. We attempt to discuss the carbon isotope systematics in the mantle and core based on our experimental results.

[1] Dasgupta & Hirschmann (2006) *Nature*, **440**, 659-662 [2] Dasgupta & Walker (2009) *Geochimica Cosmoshim. Acta,* **72**, 4627-4641 [3] Satish-Kumar et al., (2011) *Earth Planet. Sci. Lett.* **310**, 340-348

δ^{26}Mg of brachiopod shells and the composition of past seawater

S. SAULNIER*[1], C. ROLLION-BARD[1], C. LECUYER[2], N. VIGIER[1] AND M. CHAUSSIDON[1]

[1]CRPG-CNRS, BP 20, Vandoeuvre-lès-Nancy, France, saulnier@crpg.cnrs-nancy.fr (* presenting author)
[2]Laboratoire de Géologie de Lyon, CNRS, Université Claude Bernard Lyon 1, Villeurbanne, France.

The Mg isotope composition of marine carbonates can provide information on the dynamics of the Mg cycle through geological times (e.g. [1]). Brachiopods were extensively used for tracking both physicochemical conditions and secular isotopic variations of past oceans (e.g. [2]). Articulated brachiopods shells are made of low-Mg calcite, which is relatively resistant to most diagenetic processes [3]. However, significant intravariability in oxygen and carbon isotope ratios have been shown for several species, mainly due to kinetic and metabolic effects operating during calcite formation (e.g. [4]).

Magnesium, oxygen and carbon isotopes were measured in various fragments of a fossil *Terebratula scillae* (2.1 Ma) in order to test whether brachiopod shells could constitute valuable proxies of the seawater Mg isotope composition. The external parts of the shell, including the primary layer and external contamination were physically removed before analyses. Mg isotope ratios were measured by MC-ICP-MS Neptune *Plus*, with an external 2σ error of 0.15‰. Oxygen and carbon isotope ratios were measured by IRMS, with an 2σ error of 0.04‰.

The ventral and dorsal valves have similar isotope compositions and variability: δ^{26}Mg ranges from -2.95 to -2.02 ‰, δ^{18}O ranges from 2.57 to 3.15‰ and δ^{13}C ranges from 1.12‰ to 2.00‰. No correlation is observed with Mg/Ca ratio. A negative trend can be observed between δ^{26}Mg and δ^{18}O. The lowest δ^{26}Mg values correspond to isotope equilibrium determined for inorganic calcite relative to seawater Mg (Saulnier et al., submitted), and are systematically observed in the fragments located at the outer parts of the shell. This suggests that the outermost parts of brachiopod shells can be used to track the Mg isotope composition of past seawter. This aspect will be tested by studying ancient brachiopods with geological ages spanning from 0 to 54 Ma.

[1] Higgins and Schrag (2010) *GCA* **74**, 5039-5053. [2] Veizer et al. (1999) *Chem. Geol.* **161**, 58-88. [3] Brand and Veizer (1980) *J. Sedimt Petrol.* **50**, 1219-1236. [4] Auclair et al. (2003) *Chemical Geology* **202**, 59-78

https://doi.org/10.1180/S0026461X00008434 Published online by Cambridge University Press

Diffusion chronometry and seismology: insights into eruption precursors

KATE SAUNDERS[1*], JON BLUNDY[1], RALF DOHMEN[2] AND KATHY CASHMAN[1]

[1]Department of Earth Sciences, University of Bristol, Bristol, UK, Kate.Saunders@bristol.ac.uk (* presenting author)

[2]Institut für Geologie, Mineralogie und Geophysik, Ruhr-Universtät Bochum, Germany

Timescales of magmatic processes are key to our understanding of active volcanic systems, yet remain one of the most poorly constrained variables. Today many active volcanoes are monitored through a combination of seismicity, ground deformation, gas emissions and geodetic methods. In some instances these methods can be used to track magma movement in the crust prior to eruption, but not every magma pulse of magma results in an eruption.

Petrological methods can interrogate the products of recent eruptions. Zoned volcanic crystals potentially perserve a record of magmatic processes during the lifetime of a crystal from nucleation to eruption. As the magma evolves, changes in the composition, water content, temperature or pressure will result in renewed growth of a different composition generating zoned crystals. In particular, diffusion chronology (relaxation of elements across compositional interfaces) enables us to calculate a time series, precisely dating the perturbations that occur in the magma chamber prior to eruption. These petrologically determined times series can be correlated with time series generated through geophysical techniques from the same eruption to ascertain links to pre-eruptive processes.

Mount St. Helens produced a series of well studied and characterised eruptions during 1980-86. Orthopyroxene is an ubiqitous crystal phase throughout the eruption sequence. Over 500 orthopyroxene crystals from nine of the eruptions have been investigated through a combination of back-scattered electron imaging and major element chemistry by electron probe microanalyser. This revealed multiple orthopyroxene crystal populations of both unzoned and zoned crystals. Zoned crystals populations were further sub-divided into: (1) normal zoned crystals (Fe-rich rims); (2) reversed zoned crystals (Mg-rich rims); (3) oscillatory zoned crystals. Diffusive chronometry of Mount St. Helens zoned orthopyroxene reveals that the majority of rim growth occurred within two years prior to eruption. Episodes of magma mixing identified in the petrological rocord are temporally correlated with the recorded seismicity indicating both tectonic and degassing driven seismic events occurred.

Molecular- and pore-scale response of uranium to advective geochemical gradients in heterogeneous sediments

KAYE S. SAVAGE[1*], WENYI ZHU[1], MARK O. BARNETT[2], C. TYLER WOMBLE[1] AND JAN E. PATTON[1]

[1]Wofford College Environmental Studies, Spartanburg SC, USA, savageks@wofford.edu (* presenting author), zhuw@wofford.edu, womblect@email.wofford.edu, pattonje@email.wofford.edu

[2]Dept. Civil Engineering, Auburn University, AL, USA, barnem4@auburn.edu

Experimental approach

Column experiments were devised to investigate the role of changing fluid composition on mobility of uranium through a sequence of geologic media. Fluids and media were chosen to be relevant to the ground water plume emanating from the former S-3 ponds at the Oak Ridge Integrated Field Research Challenge (ORIFC) site. Synthetic ground waters were pumped upwards at 0.05 mL/minute for 21 days through layers of quartz sand alternating with layers of uncontaminated soil, quartz sand mixed with illite, quartz sand coated with iron oxides, and another soil layer. Increases in pH or concentration of phosphate, bicarbonate, or acetate were imposed on the influent solutions after each 7 pore volumes while uranium (as uranyl) remained constant at 0.1mM. A control column maintained the original synthetic groundwater composition with 0.1mM U. Pore water solutions were extracted to assess U retention and release in relation to the advective ligand or pH gradients. Following the column experiments, subsamples from each layer were characterized using microbeam X-ray absorption spectroscopy (XANES) in conjunction with X-ray fluorescence mapping and compared to sediment core samples from the ORIFC, at SSRL Beam Line 2-3.

Results

U retention of 55 – 67 mg occurred in phosphate >pH >control >acetate >carbonate columns. The mass of U retained in the first-encountered quartz layer in all columns was highest and increased throughout the experiment. The rate of increase in acetate- and bicarbonate-bearing columns declined after ligand concentrations were raised. U also accumulated in the first soil layer; the pH-varied column retained most, followed by the increasing-bicarbonate column. The mass of U retained in the upper layers was far lower.

Speciation of U, interpreted from microbeam XANES spectra and XRF maps, varied within and among the columns. Evidence of minor reduction to U(IV) was observed in the first-encountered quartz layer in the phosphate, bicarbonate, and pH columns while only U(VI) was observed in the control and acetate columns. In the soil layer, the acetate and bicarbonate columns both indicate minor reduction to U(IV), but U(VI) predominated in all columns. In the ORIFC soils, U was consistently present as U(VI); sorption appears to be the main mechanism of association for U present with Fe and/or Mn, while U occurring with P appears in discrete particles consistent with a U mineral phase. U in soil locations with no other elemental associations shown by XRF are likely uranium oxide phases.

https://doi.org/10.1180/S0026461X00008434 Published online by Cambridge University Press

A silicon isotopic record of long term changes in continental weathering

PAUL S. SAVAGE[1,2]*, R. BASTIAN GEORG[3], HELEN M. WILLIAMS[4] & ALEX N. HALLIDAY[1]

[1]Department of Earth Sciences, University of Oxford, Oxford, UK
[2]Department of Earth and Planetary Sciences, Washington University, St. Louis, MO, USA (* presenting author; savage@levee.wustl.edu)
[3]WQC, Trent University, Peterborough, Ontario, Canada
[4]Department of Earth Sciences, Durham University, Durham, UK

High precision MC-ICP-MS analyses of a suite of globally sourced clastic sediments suggest that the Si isotope system behaves more conservatively than other stable isotope tracers (i.e. Li, Mg, O) during continental weathering. This is contrary to expectation, as previous studies have shown that Si isotopes can be significantly fractionated toward lighter compositions during formation of secondary phases [1]. Nevertheless, Si isotopes in shales do not correlate with canonical proxies for weathering. Instead, good negative correlations between δ^{30}Si values and insoluble element concentrations (Nb, Hf, TiO_2) indicate that intensive chemical weathering is required before resolvable negative Si isotopic fractionation occurs in such lithologies.

On this basis, Si isotope variations in the long-term clastic sedimentary record could be used to provide a reliable proxy for investigating long term changes in the degree of reworking of continental crust and/or the intensity of continental weathering. When there is extensive formation and exposure of continental material (the Si in which has not undergone prior weathering), erosion should produce sediment with Si isotopic compositions similar to igneous continental crust [2]. If the availability of new crustal material is reduced, then the sedimentary record will become increasingly dominated by reworking of pre-existing lithologies, which will drive the Si isotope compositions to lighter values over time.

Such a hypothesis has been tested here using the post-Archaean Australian shale (PAAS) suite [3]. These samples are ideal, as they were all sourced from the same continental mass (Australia and, before, Gondwanaland) and have a wide range of depositional ages, from 1500Ma to 200Ma. The data display an enrichment in isotopically light Si with time, which appears to relate to increasing Nd crustal residence age [4]. As such, sediment derived from sources dominated by recycling of older crustal lithologies display the lightest isotopic compositions, as predicted. There is also evidence, however, that incorporation of authigenic marine lithologies can complicate this simple relationship.

Extremely negative Si isotopic compositions in Archaean shales (also sourced from Gondwanaland) cannot be explained by long-term continental weathering, as they were deposited when new continental crust dominated the budget. This could, therefore, reflect more intense weathering, due to more aggressive climatic conditions, early in Earth history.

[1] Ziegler et al., (2005) *GCA*, **69(19)**, pp 4597–4610
[2] Savage et al., (2011) *Mineralogical Magazine,* **75(3)**, pp 1803
[3] Nance and Taylor, (1976), *GCA*, **40**, pp 1539-1551
[4] Allègre and Rousseau, (1984) *EPSL,* **67**, pp 19-34

Improved calibration technique for magnetite analysis by LA-ICP-MS

D. SAVARD[1]*, S.-J. BARNES[1], S. DARE[1], G. BEAUDOIN[2]

[1]Université du Québec à Chicoutimi, Chicoutimi (Qc), Canada, G7H 2B1 *ddsavard@uqac.ca
[2]Université Laval, Québec (Qc), Canada

Oxide minerals such as magnetite and chromite are becoming popular in the field of geochemical exploration because the wide variety of trace elements present could potentially be used in provenance studies [1]. The method of analysis used is commonly LA-ICP-MS because it provides limits of detections down to ng/g levels when the analytical parameters can be optimized. No matrix-matched reference materials (RM) are available at the moment for *in-situ* calibration. Artificial glasses could be used to calibrate but only Fe can be used as an internal standard because of the inhomogeneous distribution of most of the other elements in magnetite. [2] proposed using NIST-610 to calibrate. However, the Fe content in NIST-610 is low at c.a. 0.05% while Fe in magnetite is c.a. 72%, thus limiting the use of NIST-610 to a beam >25µm, with a maximum precision of R^2<0.85 when results are compared to EMPA analysis of natural magnetite. [3] proposed the combination of 5 iron-rich RM to cover the elements of interest. Based on the elements for which EMPA results are available this calibration is satisfactory. However, this technique is time consuming and reduces the space available in the ablation cell.

We have found that USGS glasses GSE-1g and GSD-1g provide an accurate calibration for a beam size down to 4µm. The glasses are produced from natural basaltic material, containing c.a. 10% Fe, doped with a wide variety of trace elements. Figure 1 shows a good correlation between working values and those obtained at LabMaTer (UQAC) using a 193nm Resonetics M-50 laser and Aglilent 7700X ICP-MS. GSE-1g was used to calibrate while GSD-1g was used to monitor the precision and accuracy of the calibration. A natural magnetite from the Bushveld, BC-28 [4], was used as a quality control RM. Based on EMPA data, the calibration technique is also suitable for chromites, ilmenites and other Fe-rich oxides.

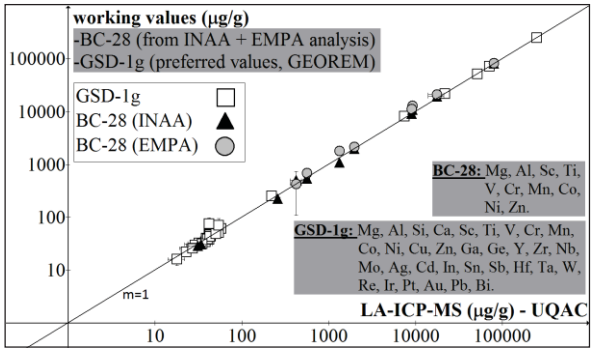

Figure (1): Accurate LA-ICP-MS calibration for magnetite analysis using GSE-1g as calibrant, GSD-1g and BC-28 as quality controls, and ^{57}Fe as internal standard.

[1] Dupuis C. and Beaudoin G. (2011) *Miner. Deposita* **46**:319-335. [2] Nadoll P. and Koenig A.E. (2011) *JAAS* **26**:1872-1877. [3] Savard *et al.* (2010) *Geoch. Cosmo. Acta* **74** (12):A914. [4] Barnes S.-J. *et al.* (2004) *Chem. Geol.* **208:**293-317.

https://doi.org/10.1180/S0026461X00008434 Published online by Cambridge University Press

How mobile is selenium in claystone? Insights given by radiochemistry and X-ray absorption spectroscopy

S. SAVOYE[1*], M.L. SCHLEGEL[1], B. FRASCA[1,2]

[1] CEA DANS/DPC, L3MR & LISL, Gif sur Yvette, France, sebastien.savoye@cea.fr (* presenting author), michel.schlegel@cea.fr

[2] University of Paris-Sud, France, benjamin_frasca@yahoo.fr

Introduction

The transport in the Callovo-Oxfordian clay formation of Se under its more oxidised forms, *i.e.* Se(IV) and Se(VI), was studied by means of batch and diffusion experiments [1], carried out at lab in N_2/CO_2 glovebox for mimicking as much as possible the physico-chemical conditions prevailing in-situ. A radiochemical approach using HTO, ^{36}Cl and ^{75}Se, as tracers, was supplemented by a non-radioactive one, for which the solid was investigated by X-Ray Absorption Spectroscopic (XAS) methods.

Results and Discussion

Results showed that Se(VI) diffused almost like ^{36}Cl, with little affinity towards clayey rocks (Rd < 0.02 mL g^{-1}). Conversely, the batch and diffusion-experiments revealed that Se(IV) exhibited a much stronger affinity towards the Callovo-Oxfordian claystone, in inverse correlation to initial Se concentration. Values of Rd were estimated, ranging from 10 to about 200 mL g^{-1} for $[Se(IV)]_{ini}$ decreasing from 10^{-3} to 10^{-6} mol L^{-1}. This behaviour could not be reproduced only with a simple model, especially for the pristine samples (diffusion experiments), since Se showed a secondary maximum ~ 2 mm under the surface, both in the radioactive and stable diffusion cells (Figure 1). The determination of the selenium oxidation state by XAS revealed that the total Se profile was clearly the sum of the contribution of (i) Se(IV), exhibiting a relative regular diffusion profile and of (ii) the more reduced selenium species (Se(red) ~ Se (0), Se(-I) and/or Se(-II)), especially located at about 2 mm from the interface (Figure 1).

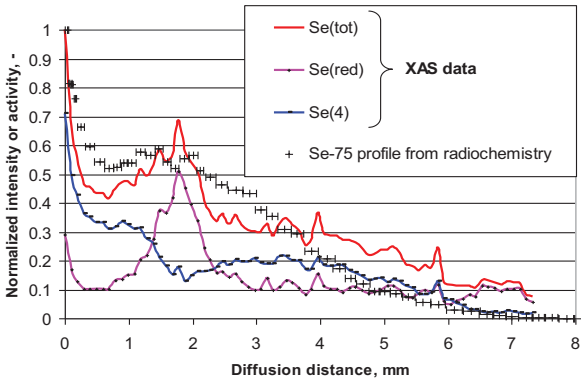

Figure 1: Distribution of the Selenium species along the rock profile obtained by XAS and comparison with radiochemistry data

The origin of the selenium distribution linked to some reduction processes was discussed regarding the mineralogy and the physico-chemical conditions prevailing in the pores.

[1] Savoye *et.al.* (2010) *Environ. Sci. Techn.* **44**, 3698-3704.

Retention of melt in granulite terrains

EDWARD SAWYER

Université du Québec à Chicoutimi, Sciences de la terre, ewsawyer@uqac.ca

Introduction

Previous work [1] showed that metagreywacke protoliths in the Ashuanipi Subprovince in northern Quebec produced approximately 600000 km^3 of granitic melt during granulite facies anatexis. Virtually all that melt was extracted from where it formed, leaving behind an Opx + Bt + Pl ± Qz residuum. What became of that melt?

Results

Fieldwork shows that very little of the anatectic melt collected into leucosomes, but a significant proportion remained in the granulite terrain as secondary diatexite migmatite. Melt accumulated in regional-scale dilatant sites. Field, geochemical and microstructural studies indicate that the secondary diatexite plays an important role in the evolution of granitic magma. Their microstructure and whole rock geochemistry indicates that a small proportion have the composition appropriate for the initial, anatectic melt. Most have compositions (supported by field relations) indicative of significant contamination by their melt-depleted wall rocks; contamination by the peritectic phase (Opx) alone is not sufficient. The microstructure (form and composition) of the feldspar-crystal framework in the diatexite reveals a wide range of responses to deformation during solidification. In places, meter-sized patches of leucocratic monzogranite occur in the diatexite and indicate local fractional crystallisation. However, most of the secondary diatexite represents an accumulation of plagioclase from which the fractionated melt has been removed. Kilometre-sized bodies of leucocratic monzogranite in the terrain represent part of the volume of fractionated melt that separated from the secondary plagioclase-rich cumulate diatexite, the balance moved to higher crustal levels.

Conclusions

Granulite terrains are much less depleted in melt than analysis of the residual rocks alone indicates. Large amounts of anatectic melt may be retained and melt from different source rocks can accumulate in the same sites. These sites represent a key reservoir in the deep crust where the composition of granite magma is established. Fractional crystallisation and general contamination exert a greater control on composition than source rock composition, or entrainment of peritectic phases.

[1] Guernina & Sawyer (2003) *Journal of Metamorphic Geology* **21**, 181-201-pp.

https://doi.org/10.1180/S0026461X00008434 Published online by Cambridge University Press

Geochemical investigations of the intrabasaltic palaeosols (bole beds) from Deccan Traps, India in deducing the palaeoclimatic conditions

MOHAMMED RAFI SAYYED [1*] AND SAJID HUNDEKARI[2]

[1]Geology Department, Poona College, Camp, Pune, India, mrgsayyed@yahoo.com (* presenting author)

[2] Geology Department, Poona College, Camp, Pune, India, sajid_hundekar@yahoo.com

Geochemical analysis of the intrabasaltic bole beds (palaeosols) occurring in the parts of Deccan Volcanic Province (India) was applied in deducing the palaeoenvironmental conditions prevailed during their formation. The bole beds the study area occur as red or green couloured clayey intercalations between the basaltic lava flows and show distinct environmental conditions during their formation when compared with the modern soils. In general red boles show higher weathering intensity, much leaching of the bases than the green boles while modern soils show moderate weathering but quite high leaching of the bases. The Weathering Potential Index (WPI) however suggests higher weathering in red boles, moderate in green boles and lesser in the modern soils. The Parkers Weathering Index (PWI) and calcination values indicate an enrichment of calcium during the formation of green boles thereby indicating aridity. Red boles were formed under higher rainfall but lesser temperature (more hydrolysis) than the green boles (less hydrolysis) while modern soils were formed under much higher rainfall and comparatively low temperature (strong hydrolysis). Iron species ratio, Product Index and FeO/Mgo values suggest that red boles were formed under strongly oxidizing but lesser acidic conditions while green boles were formed under less oxidizing but higher acidic conditions. The modern soils however indicate not much oxidizing but alkaline conditions. More retention of original mafic components in red boles and felsic components in green boles indicate selective dissolution of mafic components from green boles in more acidic fluids. Less hydrolysis and more calcination in green boles (than red boles) point towards more arid conditions during their formation than the red boles. However modern soils were formed under considerably humid conditions. The values of salinization indicate that the red boles were formed under fairly leached but relatively poorly drained conditions than the green boles while modern soils formed under quite intensely leached but poorly drained conditions. In conclusion the red boles were formed as a result of intense weathering under strongly oxidizing, acidic, more humid (more hydrolysis) environment with fairly leached but relatively poorly drained conditions than the green boles, suggestive of distinct weathering regimes. As a whole the palaeoclimates during the bole bed formation were quite different than the Holocene as the conditions were rather arid, fairly drained more acidic and strongly oxidizing with comparatively lesser rainfall but higher temperature. Although there is lack of age of control it is believed that the modern soil formation from Deccan traps represent much longer geomorphic history than the time lapsed during the formation of individual bole bed. In view of this, much intense weathering under stronger oxidizing conditions and more acidic conditions yet more aridity than the Holocene indicate catastrophic climatic conditions during the bole bed formation which can be related to the perturbations due to Deccan volcanic activity.

Inter-hemispheric patterns of Holocene Glacier and Temperature Change

JOERG M. SCHAEFER[1*], AARON PUTNAM[1,] GEORGE DENTON[2], DAVID BARRELL[3], ROBERT FINKEL[4], TOBY KOFFMAN[2], CHRISTIAN SCHLUECHTER[5], IRENE SCHIMMELPFENNIG[1], ROSEANNE SCHWARTZ[1], SUMMER RUPPER[6]

[1] Lamont-Doherty Earth Observatory, Palisades, NY-10964, USA, schaefer@ldeo.columbia.edu (* presenting author)

[2] University of Maine and Climate Change Institute, Orono, ME 04469, USA

[3] GNS Science, Dunedin, New Zealand

[4] University of California, Berkeley, USA

[5] University of Berne, Switzerland

[6] Brigham Young University, Provo, Utah, USA

Glacier and Temperature Change

Glaciers are among the most sensitive recorders of climate change, making them highly valuable as paleo-climate recorders and, at the same time, highly vulnerable to ongoing climate change.

Using independent lines of argument from glaciology, glacial geology and climate science, we make the case that glaciers in temperate climate zones are pre-dominantly driven by temperature change and, in turn, form sensitive thermometers.

Holocene Temperatures from glacier and marine records

Recent progress in the method of cosmogenic nuclide surface exposure dating now affords for precise reconstructions of glacier fluctuations throughout the Holocene and up to present day. In combination with detailed mapping of the paleo-snowline, a measure of past glacier extent, relative to today's snowline, we present comprehensive records of glacier advances in southern and northern mid-latitudes during the Holocene, and deduce regional Holocene temperatures. We compare these terrestrial temperature records with near-by and far field marine temperature estimates to better understand the inter-hemispheric patterns of Holocene temperatures.

We finally discuss implications and potential of these data sets for improving climate models.

https://doi.org/10.1180/S0026461X00008434 Published online by Cambridge University Press

Modeling of concentrations in major elements of subsurface and deep waters in the Ringelbach granitic research catchment (Vosges, France)

T. SCHAFFHAUSER[1*], F. CHABAUX[1], B. FRITZ[1], B. AMBROISE[1], A. CLEMENT[1] AND Y. LUCAS[1]

[1]LHYGES, Université de Strasbourg/EOST, CNRS, France (*correspondence: thiebaud.schaffhauser@etu.unistra.fr)

For constraining the nature of water-rock interactions occuring within granitic watersheds and exploring the potential relationships existing between subsurface and deep waters a geochemical study combined with a modeling approach has been undertaken in the small Ringelbach granitic catchment (Vosges, France). Concentrations of major elements were measured in water samples from the main springs emerging within the catchment as well as from two 150-m deep boreholes (deep waters) drilled through the whole weathering profile of the granite bedrock.

The coupled transport/reaction model KIRMAT [1] has been used in this study to discuss and constrain the main spatial and temporal geochemical variations observed in these different waters. It combines geochemical reactions, including clay precipitation [2], and 1D mass transport equations to simulate the reactive transport of a fluid through a rock along a given water pathway.

In the case of the Ringelbach watershed, we have simulated the transfer of rainwaters along different water pathways, from very permeable surficial arenic formation to almost impermeable deep fresh granite. Simulations point out that the initial chemical signature of rainwater is rapidly lost during its transfer through the substratum due to the weathering of rock-forming minerals. Furthermore, simulations indicate that the geochemical characteristics of spring waters and deep waters are mainly controlled by two different water pathways within the substratum: high-rate downslope subsurface flow for the springs, and very low flows through the whole granitic massif for borehole waters. These results suggest therefore that spring waters and deep waters are largely disconnected in the Ringelbach catchment.

[1] Gérard *et al.* (1998) Chemical Geology, **151**, 247–258.
[2] Fritz *et al.* (2009) GCA, **73**, 1340-1358.

The construction of the Alpine Adamello batholith as recorded by zircon

U. SCHALTEGGER[1*], C. BRODERICK[1], A. SKOPELITIS[1], D. FLOESS[2], A. ULIANOV[2], O. MÜNTENER[2], L. BAUMGARTNER[2], P. BRACK[3] AND P. ULMER[3]

[1]Earth and Environmental Sciences, University of Geneva, Switzerland, urs.schaltegger@unige.ch (*presenting author)
[2]Institute of Mineralogy and Geochemistry, University of Lausanne, Switzerland
[3]Institute of Geochemistry and Petrology, Swiss Federal Institute of Technology ETH, Zürich, Switzerland

Batholiths are formed by incremental melt addition over time scales spanning millions of years. They consist of composite plutons, which are formed through individual melt pulses that cool over a 10 to 100 ka timescale.

Careful laser ablation ICP-MS and CA-ID-TIMS zircon geochronology on the Adamello Batholith in Northern Italy not only reveals these different timescales, but also allows reconstruction of some of the batholith-forming processes: (a) The entire batholith grows from 43 to 33 Ma through melts derived from an increasingly crust-contaminated arc-type source; (b) single mappable plutons are compositionally more or less heterogeneous and consist of a number of melt pulses; (c) each pulse intruded and cooled as a single unit over timescales of several 10 to 100 ka; (d) the Val Fredda pluton in the southernmost Re di Castello unit shows bimodal magmatism with gabbroic melts injecting into tonalite mushes and sharing some 100 ka of crystallization and cooling; (e) the subsequent pulses of diorites and tonalites of the Lago della Vacca pluton are recognized to tap the same source mushes and continuously recycle the crystal cargo [1], while in the case of more evolved tonalites of the Central Adamello unit the pulses consist of fractionated residual melt without inheritance of crystal cargo.

Chemical-abrasion, high-precision ID-TIMS zircon dating also revealed that mapped units show a significant age spread with clear geographic trends interpreted as accretion of pulses that are not discernible in the field. The trace element and Hf isotopic composition of dated zircon is a paramount tool to trace fractionation of major and accessory minerals during zircon crystallization, mixing of melts with different source components or of mixing ante- or xenocrystic crystal cargo into a melt batch [2] In this way, zircon provides a means to trace the thermal and magmatic evolution of deeper crustal reservoirs. Additional titanite U-Pb data may help to quantify the rate of high-temperature cooling down to the solidus or, alternatively, trace prolonged heat advection followed by partial remelting and homogenization of subsequent melt batches, as seen in the Lago della Vacca unit.

[1] Schoene et al. (in press) *Earth Planet. Sci. Lett.* [2] Schoene et al. (2010) *Geochim. Cosmochim. Acta* **74**, 7144-7159.

https://doi.org/10.1180/S0026461X00008434 Published online by Cambridge University Press

Estimating isotope fractionation driven by nuclear size

E. A. SCHAUBLE[1*], S. GHOSH[2], B. A. BERGQUIST[2]

[1]UCLA, Los Angeles, CA, USA schauble@ucla.edu (* presenting author)
[2]U. Toronto, Toronto, ON, Canada

Mass-independent fractionation (MIF), where isotope abundance variations are disproportionate in mass, can have several causes. The nuclear field shift effect, proposed by Jacob Bigeleisen to explain mass independent uranium isotope signatures observed in chemical exchange experiments, stems from slight perturbations in chemical bond strengths caused by variation the volume and shape of nuclei[1]. It is unique in being a thermodynamically driven MIF mechanism that persists at conditions of equilibrium isotope exchange, and is truly independent of isotopic mass. Theoretical calculations have so far been limited to fairly small molecules, atoms and ions, in part because relativity becomes important for electrons interacting closely with nuclei, necessitating an approximate solution of the Dirac equation for electronic structure modeling. Methods for estimating isotopic fractionation factors in more complex materials are needed in order to understand recent detections of nuclear volume signatures in evaporating liquid metals, ores, and sediment, and to guide future studies. In this study we have developed procedures for cross-calibrating calculations made with relativistic electronic structure theory against less computationally intensive models.

Our initial goal was to calculate the equilibrium fractionation between liquid mercury liquid and mercury vapor to compare with experiment[2]. We observed a strong correlation ($R^2 \approx 0.9$) between a) relativistically estimated nuclear volume fractionation and b) the Mulliken population of 6s electrons in Hg-bearing species calculated with methods that incorporate relativistic effects only in the generation of a mercury pseudopotential. This is consistent with the strong correlation between atomic polar tensor charges and fractionation observed previously[3]. Based on the slope of the correlation (~1.5‰ in $^{202}Hg/^{198}Hg$ per 6s electron at 295 K), and estimated ~70-80% occupation of 6s orbitals in liquid mercury[4], we estimate 0.5-0.9‰ nuclear volume fractionation of $^{202}Hg/^{198}Hg$ between liquid and vapor, liquid being enriched in neutron-rich isotopes, and a positive $\Delta^{199}Hg$ signature of 0.1-0.2‰ in vapor. Including mass dependent fractionation effects, a total liquid-vapor $^{202}Hg/^{198}Hg$ fractionation of 0.7-1.3‰ is calculated, in good agreement with experimental results.

Plane-wave density functional theory methods, which can be applied to crystalline solids and liquids (within a periodic boundary condition approximation), appear to similarly show strong correlation with relativistic estimates of nuclear-volume fractionation. This suggests that it may be possible to estimate equilibrium MIF signatures in a wide variety of complex, geochemically interesting materials.

[1] Bigeleisen, 1996, JACS 118:3676. [2] Estrade et al. 2009, GCA 73: 2693; Ghosh et al, in press, Chem. Geol. [3] Wiederhold et al. 2010, Env. Sci. Tech. 44:4191. [4] Mattheiss et al. 1977, Phys. Rev. B 16:624.

The Rofna Porphyry Complex: Combining LA-ICPMS and CA-TIMS U-Pb ages on zircons.

THOMAS SCHEIBER[1*], BENJAMIN D. HEREDIA[1], JASPER BERNDT[2], AND O. ADRIAN PFIFFNER[1]

[1] Institute of Geological Sciences, University of Bern, Switzerland, scheiber@geo.unibe.ch, benjamin.heredia@geo.unibe.ch, pfiffner@geo.unibe.ch
[2] Institut für Mineralogie, Universität Münster, Germany jberndt@uni-muenster.de

The Rofna Porphyry Complex (RPC) in the northern part of the Suretta nappe of the Penninic zone in eastern Switzerland, is mainly composed of two different lithologies: porphyritic rock types and augengneisses (Fig. 1). The augengneisses are cross-cut by porphyritic rocks and have been traditionally interpreted as Ordovician intrusives [1] without having any radiometric age control. Our field observations indicate that (a) the augengneisses show homogenous penetrative deformation whereas the porphyritic rocks reveal variable degrees of Alpine deformation, and (b) the augengneisses occur structurally above the porphyritic rocks (Fig. 1).

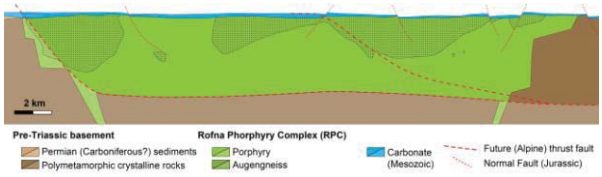

Figure 1: Restored section of the frontal part of the Suretta nappe - a feasible pre-Alpine constellation at the time of Jurassic rifting.

The magmatic event emplacing the porphyry has already been dated by ID-TIMS at 268.3 ± 0.6 Ma, which is a mean $^{206}Pb/^{238}U$ age of two nearly concordant multigrain fractions [2]. In order to constrain the age relationship between the different RPC rock types, we performed U-Pb LA-ICPMS measurements on zircons. In the augengneiss two age populations can be observed: One showing little spread at 311 Ma, and another younger one with a larger spread from 250 to 288 Ma. For the porphyritic rocks there is only one cluster of LA-ICPMS ages yielding an age range from 260 to 278 Ma.

Our new data suggest that the augengneisses are not the result of Ordovician magmatism, but may be related to the Variscian orogeny. The younger population in the augengneisses overlaps with the intrusion age of the porphyry and could either be the result of zircon neoformation or partial resetting of the U-Pb system.We therefore interpret the RPC as a composite late-Variscan and post-Variscan intrusive complex, where the pophyritic rocks followed pre-existing magma conduits, replenishing and disrupting the older augengneiss body at a shallow crustal level. High precision CA-TIMS data will provide further control of the emplacement relationships between these metamorphosed magmatic rocks.

[1] Spicher (1980) *Geological map of Switzerland,* 1:500.000. [2] Marquer, Challandes & Schaltegger (1998) *Schweiz. Mineral. Petrogr. Mitt.* **78**, 397-414.

https://doi.org/10.1180/S0026461X00008434 Published online by Cambridge University Press

Iron isotopes as a tracer in an acid-sulfate soil system

K. SCHEIDERICH[1*], J. KIRBY[1], P. SHAND[1,2]

[1]CSIRO Land and Water, Urrbrae, Australia, kate.scheiderich@csiro.au (*presenting author)
[2]Flinders University, Adelaide, Australia

Iron isotopes have been extensively studied in many systems and the fractionation factors are at least experimentally well understood for many common processes on earth's surface, including Fe-oxide mineral formation, precipitation reactions, and biological transformations such as microbially-mediated reductive dissolution of hematite. In complex environments, these well-undestood fractionations can be applied to assess the transport and speciation of Fe. However, only a few attempts have been made to understand the fractionations occuring in sulfur-rich systems, and these have been limited to acid mine drainage and hydrothermal vents. Salt marshes, tidal flats, and terrestrial floodplain environments, though well studied from the perspective of nutrients, trace metal cycling, and light stable isotopes (particularly C and S), have received little attention, yet are Fe-rich as a result of Fe monosulfide and pyrite formation.

Here we examine Fe isotope fractionation and Fe speciation in acid sulfate soil profiles and sediments from the Murray River system (South Australia), in order to gain an understanding of processes, pathways and biogeochemical cycling of Fe and associated metals through this environment. Inland acid sulfate soils are present in most fresh and saline wetland systems in the Murray-Darling Basin, largely due to the build-up of sulfide minerals during high pool levels. This situation has existed since the installation of locks in the 1930's. Prolonged recent drought led to oxidation of sulfide minerals and soil acidification with severe impacts on the local soil ecosystem. However, in the floodplain soils, desiccation of pyrite-laded, organic rich sediment allows Fe oxidation, then re-flooding events release acid to the river. Prelimary results from two oxidized soil samples of have a small range of light, near-zero δ^{57}Fe values. However, significant fractionation has been observed between primary sulfide minerals and their oxidation products in other acid sulfate soils in Australia. This is consistent with previously observed isotope fractionation between oxidized Fe minerals precipitated from Fe-rich sulfidic mine drainage [1, 2]. Additional data regarding the exact Fe mineral phases present in the soils, as well as sequential extractions of these phases and isotopic analysis of the extracts may provide additional constraints on Fe translocation in these environments.

[1] Egal, M., Elbaz-Poulichet, F., Casiot, C., Motelica-Heino, M., Négrel, P., Bruneel, O., Sarmiento, A., Nieto, J. (2008) *Chemical Geology* **253**, 162-171. [2] Herbert, R., Shippers, A. (2008) *Environ. Sci. Technol*. **42**, 1117-1122.

Coupled geochemical processes limiting phytosiderophore-promoted iron uptake from soils

W.D.C. SCHENKEVELD[1*], E. OBURGER[2], Y. SCHINDLEGGER[3], A. REGELSBERGER[3], S. HANN[3], M. PUSCHENREITER[2] AND S.M.KRAEMER[1]

[1]Universität Wien. Dept. of Environmental Geosciences, Althanstrasse 14, 1090 Wien, Austria, schenkw6@univie.ac.at (* presenting author)
[2]University of Natural Resources and Life Sciences, Dept. of Forest and Soil Sciences, Tulln, Austria
[3]University of Natural Resources and Life Sciences, Dept. of Chemistry, Wien, Austria

Graminaceous plant species (grasses) exude multidentate complexing agents called phytosiderophores (PS) for the purpose of iron aquisition, in particular under conditions of iron deficiency stress. Upon release from the root surface, the ligands diffuse into soil solution and solubilize iron from iron bearing phases in the soil, forming iron complexes which are taken up at the root surface.

Although the mechanism of action of PS has been intenisively studied, this was mostly done in hydroponics or in soil suspensions with a low soil to solution ration that did not allow to investigate coupled geochemical processes. The aim of the current project is to quantitatively understand the geochemical and geophysical processes limiting PS promoted iron uptake.

In the present work the rate of iron mobilization from various soils by the PS deoxymugineic acid (DMA) was examined in batch experiments, both with and without addition of a sterilant (sodium azide) to prevent biodegradation of the DMA ligand. Both clay and sandy soils, differing in iron availability were included.

Fe mobilization corresponded with 10 to 60% of the added DMA. The extent to which Fe was mobilized positively correlated with Fe availability parameters (e.g. DTPA-extractable Fe) and negatively correlated with the clay content of the soils. Especially in soils of low Fe availability, Fe mobilization was strongly compromised by the mobilization of competing cations like Cu, Zn, Ni and Co.

In absence of sterilant, all metal-DMA complexes were removed from solution within 4 days. Depending on the soil, Fe mobilization reached a maximum after 0.25 to 8 hours.. Except for one soil, maximum Fe mobilization was not dependent on sterilant addition. Also when sterilant was added, FeDMA concentrations eventually decreased, indicating that processes other than biodegradation significantly compromise the FeDMA concentration.

These results strongly indicate that for improving the understanding of plant iron acquisition, the kinetics and thermodynamics of coupled rhizosphere processes need to be studied coherently.

https://doi.org/10.1180/S0026461X00008434 Published online by Cambridge University Press

Fe electron transfer and atom exchange at mineral/water interfaces

M. SCHERER*[1], D. LATTA[2], T. PASAKARNIS[1], A. NEUMANN[1], M. BARGER[1], K. ROSSO[3], AND C. JOHNSON[4]

[1]Civil and Environmental Engineering, University of Iowa, Iowa City, IA 52242(*correspondence: michelle-scherer@uiowa.edu)
[2] Molecular Environmental Science Group, Biosciences Division, Argonne National Laboratory, Argonne, IL 60439, USA
[3]Chemical and Materials Science Division, Pacific Northwest National Laboratory, Richland, Washington 99352
[4]Dept. of Geoscience, University of Wisconsin-Madison, Madison WI 53706

Electron and ion exchange reactions at mineral/water interfaces influence the composition of natural waters, the biogeochemical availability of nutrients, and the environmental fate of heavy metals and contaminants. A new conceptual model is emerging to describe the reaction of aqueous Fe(II) at the mineral/water interface that couples oxidation and reduction reactions between spatially separated surface sites connected through the bulk mineral via either electrical conduction, atom diffusion, both, or some other yet unknown mechanism [1, 2]. We are collaborating to combine ^{57}Fe Mössbauer spectroscopy, Fe isotope tracer experiments, and molecular modeling to investigate Fe electron transfer at mineral surfaces and the rates and mechanism of Fe atom exchange.

We are exploring these processes in commonly occurring Fe oxides and Fe-containing clay minerals over a range of environmentally relevant conditions. Here we provide a summary of what we have learned so far, as well as present new findings investigating whether cation substitution influences the rate of atom exchange, and whether similar reactions will occur in clay minerals, as well as between aqueous Fe(III) and Fe(II) containing minerals.

[1] Gorski and Scherer (2011) *Aquatic Redox Chemistry* **1071**, 315-343.
[2] Yanina and Rosso (2008) *Science* **320**, 218-222.

Effect of Ce(III) oxidation by Mn(IV) on its use as a paleo-redox proxy

JOHAN SCHIJF[1*] AND KATHLEEN S. MARSHALL[2]

[1]University of Maryland Center for Environmental Science, Chesapeake Biological Laboratory, Solomons, MD, USA, schijf@cbl.umces.edu (* presenting author)
[2]University of Maryland Center for Environmental Science, Chesapeake Biological Laboratory, Solomons, MD, USA, marshall@cbl.umces.edu

Research outline

Marine sedimentary cerium (Ce) anomalies are due to enhanced Ce sorption with respect to the strictly trivalent REEs as it is oxidized from Ce(III) to more reactive Ce(IV). They are often interpreted as indicative of oxidizing conditions, specifically the presence of free oxygen, in the bottom water of ancient ocean basins at the time of sediment deposition. Such an interpretation could be complicated if Ce(III) were oxidized in the absence of free oxygen, as has been shown to occur on the surface of manganese oxides. We performed sorption experiments under anaerobic conditions with yttrium and the REEs in 0.5 M NaCl on pure synthetic Fe(III) and Mn(IV) oxides, plus three synthetic ferromanganese oxides containing 25, 50, and 90 mol% Mn. All precipitates were found to be X-ray amorphous and to contain Mn(IV) only.

REE sorption on the pure Fe and Mn oxides is well described with a non-electrostatic surface complexation model (SCM) that accounts for the higher acidity of hydroxyl groups on the Mn oxide, for monodentate and bidentate binding of the REEs by these groups, and for the binding of REE–hydroxide complexes at elevated pH [1,2]. REE sorption on ferromanganese oxides is moreover adequately described with a linear combination of the pure Fe and Mn oxide SCMs that reflects the proportion of each phase in the mixture. A clear presence, respectively absence, of Ce anomalies indicates that Ce(III) is oxidized on Mn oxide at all experimental pH values (4–8), but never on Fe oxide. The extent of oxidation on ferromanganese oxides is similar to that on pure Mn oxide, even at the lowest Mn content.

Below pH ~ 5.5 the Ce anomaly in pure Mn oxides is independent of pH, suggesting that the oxidation reaction involves direct transfer of an electron from Ce(III) to Mn(IV). Above pH ~ 5.5 the Ce anomaly has a linear pH dependence and the oxidation reaction may involve the species $CeOH^{2+}$, or otherwise require the presence of H_2O or OH^-.

Conclusions

Laboratory experiments of REE sorption on pure Fe and Mn oxides and on ferromanganese oxides with a wide range of Mn contents, in 0.5 M NaCl at T = 25°C, demonstrate that Ce(III) is oxidized under anaerobic conditions at the Mn oxide surface and thus probably by Mn in ferromanganese oxides, not by Fe. Hence, marine sedimentary Ce anomalies are not a reliable proxy of the presence of free oxygen in the deep paleo-ocean wherever Mn oxides abound in the watercolumn or on the seafloor. At the very least, such records should be interpreted with appropriate caution.

[1] Schijf & Marshall (2011) *Marine Chemistry* **123**, 32-43.
[2] Marshall & Schijf (2012) *Chemical Geology*, in review.

https://doi.org/10.1180/S0026461X00008434 Published online by Cambridge University Press

Microbially-mediated isotopic fractionation of selenium : Relevance for biogeochemical processes in the geological record

KATHRIN SCHILLING[1*], THOMAS M. JOHNSON[2], ROBERT SANFORD[2] AND PAUL R. D. MASON[1]

[1]Utrecht University, Utrecht, The Netherlands, k.schilling@uu.nl (* presenting author)

[2]University of Illinois at Urbana-Champaign, Urbana, IL, USA

The terrestrial and marine evolution and preservation of life are sensitive to changes in redox conditions. Selenium as an redox-sensitive element can provide information about the oxyengenation history of the ocean and atmosphere. Microbial reduction of Se-oxyanions causes isotopic fractionation, and stable Se isotope ratios can be used as a novel tool to detect biological Se cyling in the geological record. In addition, Se isotope ratios, in the geological record as well as in modern environments, may fingerprint specific metabolisms. However, our knowledge about microbially-mediated Se isotopic fractionation is limited due to lack of experimental studies under environmentally relevant Se and electron-donor concentrations. Here we determine new pure culture Se isotopic fractionation factors and investigate their dependence on experimental conditions including selenium and electron-donor concentrations. Results are given as magnitudes of isotopic fractionation, ε (ε=1000*(α-1)[‰]; α = $(^{82}Se/^{76}Se)_{Reactant}/(^{82}Se/^{76}Se)_{Product}$. We aim to investigate metabolically diverse microorganisms, including *Desulfitobacterium* st. Viet1, *Geobacter sulfurreducens* PCA, *Pseudomonas stutzeri* KC, *Aneromyxobacter dehalogenans* FRCW, and *A. dehalogenans* FRC-R5.

The pure cultre of *Desulfitobacterium* Viet1 coupled the reduction of 44µM Se(VI) with oxidation of lactate under strictly anaerobic conditions. This reduction yielded an ε Se(VI)→Se(0) = 9.4±0.3‰ (n=2) . This ε is higher than those previously reported for *Bacillus selenitireducens*, *Bacillus arsenicoselenatis* and *Sulfurospririllum barnesii* [1] and could be useful in explaining very high $\delta^{82/76}$Se values (up to −12.77‰) observed in high-selenium carbonaceous shales from Yutangba deposit, China [2]. Further experiments will determine the ε's for microbial Se reduction under electron-donor rich and electron-donor poor conditions. The results of this study will be useful in interpreting the measured Se isotope ratios in the rock record and may reflect the distribution of microorganisms in modern and ancient Earth.

[1] Herbel (2000) *Fractionation of selenium isotopes during bacterial respiratory reduction of selenium oxyanions* **64#**, 3701-3709.
[2] Wen (2007) *Large selenium isotopic variations and its implication in the Yutangba Se deposit, Hubei Province, China* **52#**, 2443-2447.

Geochemistry and thermobarometry of postglacial Llaima tephras

JULIE C. SCHINDLBECK[1] (*), ARMIN FREUNDT[1], STEFFEN KUTTEROLF[1], KAREN STREHLOW[1]

1 GEOMAR, Kiel, Germany, jschindlbeck@geomar.de(*)

Llaima is a large active stratovolcano in the Southern Volcanic Zone in Chile. Field work in 2011 revised the postglacial stratigraphy after Naranjo&Moreno (1991) and led to the subdivision into units I to V. Postglacial activity started 13.500 years ago with caldera-forming eruption of two mafic ignimbrites (unit I). These are overlain by a sequence of three basaltic-andesitic to two dacitic lapilli fallout deposits and reworked tuffaceous sediments (unit II). At ~8600 cal BC a large Plinian eruption emplaced a compositionally zoned dacitic to andesitic fallout tephra (unit III) that became capped by subsequent andesitic surge deposits (unit IV) when the eruption became unstable. The following unit V represents a time interval of ~7000 years during which at least 30 basaltic to andesitic ash and lapilli fallout deposits with intercalated tuffaceous sediments and paleosols were emplaced.

Bulk-rock, mineral and glass chemical analyses constrain the vertical compositional changes of Llaima tephras. Tephra compositions switch between a calc-alkaline differentiation trend (unit I) and a more tholeiitic trend (units II-IV), with samples of unit V varying between both trends, indicating a strong control of $f(O_2)$ (and $P(H_2O)$) on the relative timing of Fe-Ti oxide fractionation. Moreover, iron rich fayalites that are in equilibrium with the glass composition occur in units II and III with calculated T-$f(O_2)$ close to the FMQ suggesting that late-stage fayalite precipitation involved crossing of the FMQ boundary. The younger unit V tephras and historical compositions define a second differentiation trend relatively enriched in K_2O, Rb, Ba and Zr; this is not the results of changing source conditions but can be explained by a stronger early olivine fractionation in the respective magmas.

Thermobarometric calculations based on amph, cpx-liq, plag-liq, ol-liq and Fe-Ti-oxide compositions constrain changing magma chamber positions over time. Storage depths were 14 - 19 km for unit I andesite and and varied between 10 to 17 km for unit II andesites and dacites. The compositionally zoned eruption of units III and IV withdrew dacite magma from ~10 km depth but andesite from a deeper level of 13-15 km. Storage depths of unit V andesitic magmas ranged from 6 to 15 km. Based on temporally changing storage depths and differentiation paths, a 4-stage evolution of the postglacial magmatic system of the Llaima volcanic complex is proposed.

https://doi.org/10.1180/S0026461X00008434 Published online by Cambridge University Press

Characterization of U-bearing phases at a U-tailings facility in Sask. Canada

MICHAEL SCHINDLER*[1], JENNIFER DUROCHER[1] AND TOM KOTZER[2]

[1] Laurentian University, Department of Earth Sciences mschindler@laurentian.ca (*presenting author) ; jl_durocher@laurentian.ca

[2] Cameco Corporation, Senior Environmental Geochemist tom_kotzer@cameco.com

Uranium mobility around radioactive waste products such as mine tailings is a growing environmental concern. The characterization of particular U-bearing solid phases in the surface and subsurface around U-mine tailings facilities is essential in understanding and controlling the mobility of uranium [1]. The Key Lake milling facility located in Saskatchewan, Canada, has the world's largest annual U production capacity (25 million pounds U_3O_8) where it processes various grades of U-ore (maximum grade 18%, average grade 4%) from local operations [2]. In general, the ore is crushed; U is dissolved and leached using sulfuric acid and finally extracted and purified using ammonium sulfate and ammonia gas treatments [3]. Mining and milling waste products including tailings (1983-1996) and a portion of the acidic leachates and raffinates are stored in the engineered on-site Above Ground Tailings Management Facility (AGTMF) [4]. The occurrence, paragenesis and chemical composition of U-bearing phases at the AGTMF were examined, in both unconsolidated as well as epoxy impregnated samples to a maximum depth of 10 cm, using Scanning Electron Microscopy, X-ray Diffraction, Raman Spectroscopy, Laser Ablation ICP-MS, X-ray Photoelectron Spectroscopy and synchrotron-based micro-X-ray Fluorescence Spectroscopy. Uranium-bearing phases were observed as micro-sized coatings and included phases belonging to the zippeite group as well as the autunite group. Detailed mineralogical and chemical characterization of the tailings also indicated the presence of β-U_3O_8 (Fig. 1a) and U-bearing gypsum (Fig. 1b).

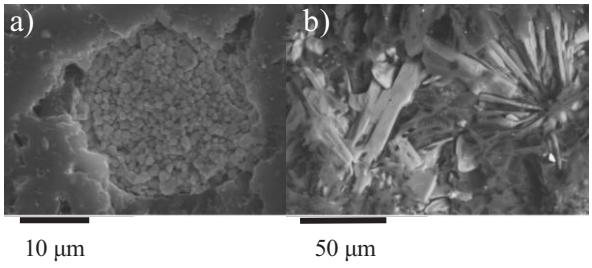

Figure 1: Backskatter electron images of (a) a cluster of β-U_3O_8 and (b) uranium-bearing gypsum.

Pb-isotope measurements and Raman spectra suggest that β-U_3O_8 is an alteration product of uraninite ore rather than a product of the milling process or bacterial reduction. LA-ICP-MS analyses of the gypsum crystals showed surprisingly high U-concentrations which were attributed to nanometre-scale intergrowths and coatings.

[1] Buck *et al.* 1996. *Environmental Science & Technology* **30,** 81. [2] Gandhi 2007. *Geological Survey of Canada,* open file **5005,** *Sask. Industry and Resources,* open file **2007-11**. [3] Cameco 2010. Key Lake Extension Project [4] Jarrell 2004. *IAEA-TECDOC-1419*. 45-74.

The Last Stages of Terrestrial Planet Formation: Dynamical Friction and the Late Veneer

H. E. SCHLICHTING[1,*], P. H. WARREN[1], Q.-Z. YIN[2]

[1]Dept. of Earth & Space Sciences, UCLA 595 Charles E. Young Drive East, Los Angeles, CA 90095 (hilke@ucla.edu) (* presenting author)

[2]Department of Geology, University of California Davis, One Shields Avenue, Davis, CA 95616 (qyin@ucdavis.edu)

The final stage of terrestrial planet formation consists of the cleanup of residual planetesimals after the giant impact phase. Dynamically, a residual planetesimal population is needed to damp the high eccentricities and inclinations of the terrestrial planets to circular and coplanar orbits after the giant impacts stage. Geochemically, highly siderophile element (HSE) abundance patterns inferred for the terrestrial planets and the Moon suggest that a total of about 0.01 $M_\oplus$ of chondritic material was delivered as 'late veneer' by planetesimals to the terrestrial planets after the end of giant impacts. Here we combine these two independent lines of evidence for a leftover population of planetesimals and show that: 1) A residual population of small planetesimals containing 0.01 $M_\oplus$ is able to damp the high eccentricities and inclinations of the terrestrial planets after giant impacts to their observed values. 2) At the same time, this planetesimal population can account for the observed relative amounts of late veneer added to the Earth, Moon and Mars provided that the majority of the accreted late veneer was delivered by small planetesimals with radii ≤10 m. These small planetesimal sizes are required to ensure efficient damping of the planetesimal's velocity dispersion by mutual collisions, which in turn ensures sufficiently low relative velocities between the terrestrial planets and the planetesimals such that the planets' accretion cross sections are significantly enhanced by gravitational focusing above their geometric values. Specifically we find, in the limit that the relative velocity between the terrestrial planets and the planetesimals is significantly less than the terrestrial planets' escape velocities, that gravitational focusing yields a mass accretion ratio Earth/Mars ~ $(\rho_\oplus/\rho_{mars})(R_\oplus/Rmars)^4$ ~17, which agrees well with the mass accretion ratio inferred from HSEs of 12-23. For the Earth-Moon system, we find a mass accretion ratio of ~ 200, which, as we show, is consistent with the mass accretion ratio inferred from HSE abundances of 150-700. We conclude that small residual planetesimals containing about ~ 1% of the mass of the Earth could provide the dynamical friction needed to relax the terrestrial planets' eccentricities and inclinations after giant impacts, and also may have been the dominant sources for the relative and absolute amounts of late veneer added to Earth, Moon and Mars. We argue that the terrestrial planets volatile elements were also delivered by the late veneer in order to account for the ~4.4Ga old terrestrial hydosphere and early felsic crust of granitoids reflected in Hadean zircons [1]. [1] Harrison (2009) *Annual Review of Earth Planet. Sci.* **37,** 479–505.

https://doi.org/10.1180/S0026461X00008434 Published online by Cambridge University Press

Nanoscale microstructure and texture patterns of bivalve nacre

W. W. Schmahl[1], E. Griesshaber[1], H. S. Ubhi[2]

[1]Department of Earth and Environmental Sciences, LMU München, Germany, wolfgang.schmahl@lrz.uni-muenchen.de

[2]Oxford Instruments, Halifax Road, High Wycombe, UK, Singh.Ubhi@oxinst.com

Biological hard tissues are hierarchical composites. EBSD is one of the best methods available for structural characterization of biological tissues, since it provides microstructure imaging and crystal orientation determination on several hierarchical levels. While the conventionally used 20 kV acceleration voltage yields EBSD with a spatial resolution in the micrometer range, high resolution, low kV (8 to 15) EBSD renders a 100-400 nm step resolution. This enables the investigation of nanostructures such as orientation patterns in the nacreous parts of biological skeletons.

We could map orientation patterns of calcite with high resolution, low kV (8 to 15) EBSD. This rendered measurements with 100-400 nm step resolution and enabled for the first time the investigation of biological nanostructures, especially orientation patterns in nacre and the nacreous parts of biological skeletons. The investigated specimens are the nacreous portions of the oyster *Crassostrea gigas* and of the bivalve *Mytilus edulis.* Further, we investigated the shells of *Elliptio crassidens*, *Cristaria plicatus* (composed entirely of nacreous aragonite) and the pearl of the freshwater mollusk *Hyriopsis cumingii*. The aragonite nanoplatelets are untwined single crystals that assemble to platelets. Stacks of almost equally oriented platelets form clusters with distinct orientations. Within a cluster the orientation goes across the platelets, while neighbouring platelets that belong to different clusters often form twin related orientations (rotation by 60 degrees around the c-axis). The normal to the platelets is the c-axis (setting: a=4.96 Å, b=7.97 Å, c=5.75 Å). The size of the correlated clusters and the abundance of twin relationships between adjacent platelets varies significantly between the investigated mollusk species.

For *Crassostrea gigas*, *Cristaria plicatus* and the pearl of *Hyriopsis cumingii* one crystal orientation dominates, such that the overall texture pattern has a 3D single crystal like appearance. For *Mytilus edulis* and *Elliptio elliptio* the three twin orientations are of similar abundance.

3D STXM tomography of Fe(II)-oxidizing bacteria

Gregor Schmid[1*], Likai Hao[1], Andreas Kappler[1], Martin Obst[1]

[1]University of Tuebingen, Germany, Center for Applied Geoscience, gregor.schmid@uni-tuebingen.de (* presenting author) likai.hao@uni-tuebingen.de, andreas.kappler@uni-tuebingen.de, martin.obst@uni-tuebingen.de

In pH-neutral environments ferrous iron can be oxidized under anoxic or microoxic conditions by Fe(II)-oxidizing bacteria. Different microbial metabolisms of Fe(II) oxidation and biomineralization of these bacteria have been identified and characterized so far. Initial Fe(III) mineral precipitation in the periplasm and subsequently cell encrustation was observed with the mixotrophic, nitrate-reducing, Fe(II)-oxidizing *Acidovorax* sp. strain BoFeN1 isolated from anoxic littoral sediments from Lake Constance, Germany [1]. Iron mineral precipitation in vicinity to the cell was shown for the phototrophic, anaerobic Fe(II)-oxidizing *Rhodobacter* sp. strain SW2 [2]. Also, under microaerophilic conditions iron minerals can be deposited within extracellular polymeric structures such as twisted stalks or sheats which are extruded by microaerophilic *Gallionella* strains [3].

To further our understanding of the different mineralization patterns and mechanisms of Fe-biomineralization, we investigated BoFeN1, SW2 and an environmental biofilm containing twisted stalks (similar to those observed for *Gallionella* strains) from an abondoned silver mine in Germany. We conducted conventional soft X-ray scanning transmission microscopy (STXM) in combination with angle-scan tomography measurements allowing for a 3D reconstruction. The advantage of STXM is the combination of high spatial resolution (≈10 nm) with the possibility of identifying and quantifying cell components such as proteins and lipids, extracellular polymeric substances (EPS) and iron minerals. Therefore, we acquired image sequences across the C1s, O1s and Fe2p absorption edges for BoFeN1, SW2 and an environmental biofilm containing twisted stalks. Compositions maps of the macromoleculars components were obtained by linear combination fits of reference spectra of proteins, lipids, polysaccharides and iron minerals. The association of the Fe-phases with the organic components of the cell-mineral aggregates was then analyzed quantitatively in 3D by correlation analysis.

Our results confirmed that iron is precipitated within the periplasm of BoFeN1, in contrast to SW2 and the environmental biofilm where the iron precipiates are closely asscociated with organic expolymers.

[1] Miot (2009) *Geochim. Cosmochim. Ac.* **73**, 696-711.
[2] Kappler (2004) *Geochim. Cosmochim. Ac.* **68**, 1217-1226.
[3] Chan (2004) *Science* **303**, 1656-1658.

https://doi.org/10.1180/S0026461X00008434 Published online by Cambridge University Press

Interpretation of Lu-Hf garnet geochronology by investigation of HREE zoning profiles

ALEXANDER SCHMIDT [1a*], MATTHIAS KONRAD-SCHMOLKE [1b]

1 Institute of Earth- & Environmental Science, University of Potsdam, Germany
[a] alexander.schmidt@geo.uni-potsdam.de (* presenting author)
[b] mkonrad@geo.uni-potsdam.de

Garnets are well suited for Lu-Hf and Sm-Nd geochronology, and a growing number of studies now focus on the Lu-Hf system for evaluating the evolution of different types of metamorphic rocks, because of the difference in the ages obtained by the two isotope systems (Lu-Hf dating early, Sm-Nd dating late growth). However, the interpretation of ages obtained for garnets by the Lu-Hf system is not always straightforward due to the ambiguity in the explanation of observed sharp Lu-peaks in garnet cores. Garnet strongly controls the Lu (and other HREE) budget of many metamorphic rocks, and also more often than not inherit information obtained during pro- and retrograde growth through enrichment of Lu & HREE in early formed cores. The mere occurrence of sharp Lu peaks in garnet cores in rocks of (ultra)high-pressure and high-temperature conditions indicates a resistance to metamorphic resetting, therefore attesting to the suitability of Lu-Hf garnet geochronology for complex metamorphic rocks.

In this study we concentrated on the Lu & HREE distribution in garnets from different metamorphic rocks to evaluate the modes of incorporation during growth and also processes of resetting of these growth profiles. We also investigated the impact of these growth profiles on the Lu and Hf isotopic composition of different garnet zones, trying to determine growth rates of garnets, and how this will affect the Lu-Hf ages obtained for bulk-garnet separates. This includes both a model approach to assess the influence of several garnet growth events on bulk garnet ages, as well as the "in-situ" (small portions of a garnet zone cut-out/drilled-out) measurement of the isotopic composition in suitable garnet grains.

As more garnets from different types of rocks are being analysed for their potential Lu growth profiles our understanding of how to interpret the obtained ages is improving, especially when we compare Lu-Hf ages with geochronology of other minerals based on other isotope systems. Hence a larger database will shed light on the discussion of e.g. which mineral best yields an age estimate for prograde, peak and retrograde conditions in a metamorphic rock.

Experimental study on the pseudobinary H_2O+$NaAlSi_3O_8$ at 600–800 °C and to 2.5 GPa

CHRISTIAN SCHMIDT[1*], ANKE WATENPHUL[2], ANKE WOHLERS[1], AND KATHARINA MARQUARDT[1]

[1] GFZ German Research Centre for Geosciences, Potsdam, Germany, christian.schmidt@gfz-potsdam.de (* presenting author), anke.wohlers@gfz-potsdam.de, katharina.marquardt@gfz-potsdam.de
[2]Hamburger Synchrotronstrahlungslabor HASYLAB at Deutsches Elektronen-Synchrotron DESY, Hamburg, Germany, anke.watenphul@desy.de

There are still uncertainties in phase relations in the high-temperature portion of P-T diagrams for H_2O+$NaAlSi_3O_8$ (e.g., [1]). Dissolution of albite in H_2O is usually considered to be congruent or nearly congruent [2], although many experiments showed formation of the aluminous solids paragonite (e.g., at 500–650 °C, 0.5–0.9 GPa [2], at 500 °C, 0.2–0.7 GPa and 600 °C, 0.4–0.8 GPa [3], and at 700°C, 1–1.5 GPa [4]) and corundum (e.g., at 800 °C, 0.7–2 GPa [4]). However, some of these P-T conditions intersect that of the critical curve [5] along which no solid phase can be present. For information to resolve this conflict, we conducted experiments on several pseudobinary mixtures between 39 and 54 wt% $NaAlSi_3O_8$, i.e., near the critical composition [5]. The system was studied by optical observation and Raman spectroscopy using a hydrothermal diamond-anvil cell [6]. Synthetic zircon was used as Raman spectroscopic pressure sensor [7].

At the start of each run, the assemblage silicate glass and aqueous fluid was heated to 600 °C. Then, the resulting melt and aqueous fluid were held at this temperature until a solid had formed. Jadeite grew rapidly at $P \geq 2$ GPa. In experiments at pressures to 1.06 GPa, albite nucleated within a minute to a few hours. Paragonite formed at 1.64 GPa in an experiment with 54 wt% $NaAlSi_3O_8$ and at 1.09 GPa at 39 wt% $NaAlSi_3O_8$. Upon heating, paragonite was still present at and above the temperature of homogenization of silicate melt and aqueous fluid to a single fluid phase, whereas albite always showed the expected melting at temperatures less than that of melt and aqueous fluid homogenization.

Our data indicate that the high-pressure portion of the critical curve [5] is a metastable extension at $T < 760$ °C, at which paragonite is stable. Furthermore, the formation of a substantial fraction of paragonite at intermediate bulk $NaAlSi_3O_8$ concentrations implies that the aqueous fluid must have a peralkaline composition, which in turn enhances the solubility of high field strength elements. The obtained data for the P-T location of the critical curve based on the determined isochores are close to or at slightly higher pressure than those reported in ref. [5].

[1] Hayden & Manning (2011) *Chem. Geol.* **284**, 74-81. [2] Shmulovich *et al.* (2001) *Contrib. Mineral. Petrol.* **141**, 95-108. [3] Davis (1972) PhD diss., Penn. State Univ. [4] Antignano & Manning (2008) *Chem. Geol.* **255**, 283-293. [5] Shen & Keppler (1997) *Nature* **385**, 710-712. [6] Bassett *et al.* (1993) *Rev. Sci. Instrum.* **64**, 2340-2345. [7] Schmidt *et al.* (2011) *Min. Mag.* **75** (3), 1819.

https://doi.org/10.1180/S0026461X00008434 Published online by Cambridge University Press

The arc delaminate: a geochemical reservoir twice the size of the continental crust

MAX W. SCHMIDT[1*]. OLIVER JAGOUTZ[2]

[1]Dep. Earth Sciences, ETH Zurich, Switzerland, max.schmidt@erdw.ethz.ch (* presenting author)
[2]Dep. Earth Atmos. Planet. Sciences, MIT, Cambrige, USA, jagoutz@mit.edu

Most primitive melts in arcs are basaltic in composition but the continental crust or arc average is andesitic. To evolve from a primitive basalt to an andesitic composition, cumulates have to be fractionated and, if gravitationally unstable, can be delaminated. Such lower crustal cumulates are exposed in the Kohistan arc (N Pakistan) in a 10 km section through dunites, wehrlites, websterites, cpx-bearing garnetites and hornblendites, and garnet gabbros. We have compiled primitive melts for nine island arcs from the literature and fitted these with the bulk Kohistan arc [1] or average bulk continental crust [2] and the Kohistan cumulates. By average, ~15 wt% wehrlite + ~20% garnet hornblendite + ~35% garnet gabbro complement ~30% arc or continental crust and explain very well (r^2~2) the evolution from a tholeiitic/calc-alkaline primitive high-Mg basalt to the continental crust. The bulk delaminate has 44-48 wt% SiO_2, total alkalis of 1.1-1.4 wt% and an X_{Mg} of 0.67-0.69. Mass fractions derived from major elements were employed to compare trace elements: cumulates+crust deviate on average only by 25-30% from primitive melts, with the biggest deviations on the subduction-added traces. Relative to the continental or arc crust, the delaminate mass results to 1.8-2.5 times that of the continental crust.

The delaminates have ρ=3.2-3.5 g/cm^3 and V_P=7.9-8.2. At the base of the crust, they are thus difficult to distinguish seismically. Once reaching a critical thickness, they may sink into the deeper mantle where they form a geochemical reservoir twice the size of the continental crust. With respect to primitive mantle, the delaminate is enriched in Ba, K, Sr, and P and REE with LREE<HREE. The delaminate reservoir would develop highly unradiogenic Pb over time and would counterbalance the radiogenic MORB and OIB reservoirs. Delamination of twice as much material as remains in the arc crust increases the flux of primitive melt in arcs threefold. This places the magma production rate at arcs (per km arc length) slightly above that at mid-ocean ridges indicating that global fluxes and magmatic heat loss need to be revised.

[1] Rudnick R.L., Gao S. (2003) *Treatise of Geochemistry* **3**, 1-64. [2] Jagoutz O. Schmidt M.W. (2012) *Chem.Geol.* doi:10.1016/j.chemgeo.2011.10.022

Structural changes on dehydration of amorphous calcium carbonate

MILLICENT P. SCHMIDT[1*], BRIAN L. PHILLIPS[1], ANDREW J. ILOTT[2], AND RICHARD J. REEDER[1]

[1]Stony Brook Unviersity, Geosciences, Stony Brook, NY USA millicentpschmidt@gmail.com (* presenting author), brian.phillips@sunysb.edu, rjreeder@stonybrook.edu
[2]Stony Brook Unviersity, Chemistry, Stony Brook, NY USA andyilott@gmail.com

Introduction and Methods

Amorphous calcium carbonate (ACC) is a common transient precursor to biogenic calcium carbonate, but the transformation and stabilization mechanisms remain unknown. Studies have shown that the calcium carbonate biomineralization pathway for two different biogenic ACC samples follows the progression of hydrated ACC ➔ anhydrous ACC ➔ calcite, aragonite and/or vaterite.[1][2] In this study, we present a structural analysis and comparison of hydrated and partially-dehydrated, synthetic ACC applying novel synthesis techniques to examine the under-studied first transformation step in the biomineralization pathway.

ACC was synthesized using three different methods and then partially-dehydrated by heating to temperatures below the crystallization temperature (ca. 185 °C or 330 °C depending on the synthesis method).[3][4] Hydrated and partially-dehydrated ACC samples were analyzed by X-ray absorption fine structure (XAFS) spectroscopy, pair distribution function (PDF) analysis from X-ray total scattering, FT-IR spectroscopy, thermal analysis, and nuclear magnetic resonance (NMR) spectroscopy.

Results and Conclusions

Thermal analysis showed total mass losses averaging 10% (46% loss of total water) with dehydration to 115 °C (16% and 75%, respectively for heating to 150 °C). XAFS and total scattering results showed no evidence of significant structural changes with heating, suggesting that the effects of dehydration relate primarily to the water component in ways that are largely insensitive to the X-ray based techniques. FT-IR spectra show a loss of structural water as evidenced by decreases in the intensity of the O-H bending and stretching bands at 1630 and 3300 cm^{-1}, respectively. The ^{1}H NMR spectra of hydrous ACC, obtained indirectly via ^{13}C-detection, contain signals from three principal hydrogen environments: a broad spinning sideband envelope from rigid structural water, a narrow peak near +5 ppm from restrictedly mobile water, and a small narrow peak at +0.2 ppm due to hydroxyl. Dehydration of ACC leads to a reduction in signal intensity from both rigid and mobile water that increases with increased dehydration temperature but with little change in their relative proportions. No significant change in the intensity of the hydroxyl peak was observed in samples heated up to 200 °C. The retention of some restrictedly mobile water and lack of change in the PDFs from X-ray total scattering in dehydrated ACC suggest that thermal dehydration does not significantly disrupt the calcium-rich framework of the ACC [5].

[1] Radha (2010) *PNAS,* **107**, 16438-16443. [2] Politi (2008) *PNAS,* **105**, 17362-17366.[3] Koga (1998) *Thermochim. A.* **318.** 239-244. [4] Faatz (2004) *Adv. Mater.* **16** 996-1000. [5] Goodwin (2010) *Chem. Mater.* **22.** 3197-3205.

https://doi.org/10.1180/S0026461X00008434 Published online by Cambridge University Press

Actinide sorption and reactivity at the muscovite-aqueous interface

M. SCHMIDT[1, 2,*], S. S. LEE[1], R. E. WILSON[1], K. E. KNOPE[1], P. FENTER[1], L. SODERHOLM[1]

[1]Chemical Sciences and Engineering Division, Argonne National Laboratory, Argonne, IL, USA

[2]Current Address: Institute for Nuclear Waste Disposal, Karlsruhe Institute for Technology, Karlsruhe, Germany, moritz.schmidt@kit.edu (* presenting author)

Introduction

We present recent findings regarding the interaction of tri- and tetravalent actinides (Th, Pu) with the charged (001) basal plane of muscovite. *In situ* crystal truncation rod measurements and resonant-anomalous x-ray reflectivity were applied to investigate structures in the near-interface region under varying solution conditions (ionic strength, actinide concentration, chemical speciation of the actinide, background electrolyte).

Results

The results show a broad variety of potential forms of interaction, that strongly depends on the actinides' aqueous chemistry. The strongly hydrated cations do not shed their hydration layers upon sorption, but remain as extended outer sphere complexes [1]. In this sorption state the cations are highly concentrated in the near-interface region, and also highly mobile which allows for subsequent reactions (e.g. polymerization) between sorbed species to occur. In the case of plutonium this interfacial reactivity has been found to dominate the sorption behavior.

The results are expected to provide valuable input to the ongoing discussion about potential nuclear waste repository strategies as well as enrich the molecular level understandifng of the actinides' environmental geochemistry in general.

[1] Lee (2010) *Langmuir* **26,** 16647-16651.

Unraveling the chemical space of extreme natural environments and chondritic organic matter

PHILIPPE SCHMITT-KOPPLIN[1*], ZELIMIR GABELICA[2], NANCY HINMANN[3], MICHAEL GONSIOR[4] , WILLIAM COOPER[5], REGIS GOUGEON[6], MOURAD HARIR[1], NORBERT HERTKORN[1]

[1]Helmholtz Zentrum Muenchen, Analytical BioGeoChemistry, Germany schmitt-kopplin@helmholtz-muenchen.de

[2] Université de Haute Alsace, Lab. GSEC, France

[3] Uniersity of Montana, Missoula, USA

[4] University of California, Irvine, USA

[4] Linköping university, Linköping, Sweden

[6] Université de Bourgogne, Institut Jules Guyot, France

Natural organic matter (NOM) occurs in soils, freshwater, marine and hydrothermal environments, in the atmosphere and represents an exceedingly complex mixture of organic compounds that collectively exhibits a nearly continuous range of properties (size-reactivity continuum). The fate NOM in the bio- and geosphere is governed according to the rather fundamental restraints of thermodynamics and kinetics. In these intricate materials, the "classical" signatures of the (geogenic or ultimately biogenic) precursor molecules, like lipids, glycans, proteins and natural products have been attenuated, often beyond recognition, during a succession of biotic and abiotic (e.g. photo- and redox chemistry) reactions. NOM incorporates the hugely disparate characteristics of abiotic and biotic complexity.

Numerous descriptions of organic molecules present in organic chondrites (COM) have improved our understanding of the early interstellar chemistry that operated at or just before the birth of our solar system. However, all molecular analyses were so far targeted toward selected classes of compounds with a particular emphasis on biologically active components in the context of prebiotic chemistry. Here we demonstrate that a non-targeted molecular analysis of the solvent-accessible organic fraction of Murchison extracted under mild conditions allows one to extend its indigenous chemical diversity to tens of thousands of different molecular compositions and likely millions of diverse structures. This molecular complexity, which provides hints on heteroatoms chronological assembly, suggests that the extraterrestrial chemodiversity is high compared to terrestrial relevant biological and biogeochemical-driven chemical space.

(ultra)High resolution analytical approaches will be presented in their application to unravel the chemical nature and organic signatures in biosystems [1], geosystems [2-4] with a focus on extreme environments such as hydrothermal and meteoritic origins [5] with a special focus on sulphur organic compounds.

[1] Rosselló-Mora et al. (2008) Nature – ISME Journal **2**, 242-253

[2] Schmitt-Kopplin *et al* (2010) Anal. Chem. **82**, 8017–8026.

[3] Gonsior et al (2011) Water Research **45(9)**, 2943-2953.

[4] Schmitt-Kopplin *et al.* (2011) Biogeosciences Discuss. **8**, 11767-11793.

[5] Schmitt-Kopplin *et al* (2010) *PNAS* **107(7)**, 2763-2768.

https://doi.org/10.1180/S0026461X00008434 Published online by Cambridge University Press

Multi-scale geochemical time series constraints on Archean lithosphere formation

BLAIR SCHOENE[1]* AND C. BRENHIN KELLER[1]

[1]Princeton University, Princeton, NJ, 08544 USA, bschoene@princeton.edu*, cbkeller@princeton.edu

Robsust comparisons of lithosphere formation processes in the Archean, Proterozoic and Phanerozoic require: 1) geochronology of adequate resolution to sequence magmatic and stuctural processes with precision relevant to tectonic processes (~1 Ma), which has been difficult in older terranes; 2) an unbiased and continuous assessment of secular change in, for example, petrologic processes through Earth history.

Recent advances in chemical abrasion ID-TIMS U-Pb geochronology permit sub-million year precision on $^{207}Pb/^{206}Pb$ dates of single closed system Archean zircons. Applied to the pristine ca. 3.2 Ga Usutu magmatic system in the eastern Kaapvaal craton, such high-precision geochronology permits evaluation of geochemical evolution during piecewise batholith construction over <20 Ma. Combined with structural data and placed into the context of the adjacent Barberton greenstone belt, these constraints are used to construct a model where regional subhorizontal contraction occurred synchronous with emplacement of an evolving magmatc system. The temporal resolution provided by this work is unprecedented in Archean systems, and allows direct comparison with Phanerozoic arc- and plume-related magmatic systems.

In order to reconstruct billion-year records of secular variation in the continental rock record, we have compiled a database of over 70,000 igneous samples from various sources, each with age, spatial coordinates, and major and trace element data. Monte Carlo simulations with weighted bootstrap resampling significantly reduces sample collection and temporal biases, and allows precise estimation of mean global igneous geochemistry for 3.8 Ga. Both low SiO_2 (basalts) and evolved high SiO_2 rocks show statistically significant trends through time, the former being consistent with decreasing mantle melt fraction in the present and the latter showing increased importance of deep crustal fractionation/partial melting and TTG production in the Archean. Mean values of many geochemical proxies from both SiO_2 ranges show step functions near 2.5 Ga. These data support a model linking high degree mantle melting and lower crustal delamination and TTG production as being more important in the Archean; this process is largely independent of driving plate tectonic models but can be used to inform them.

Our geochemical dataset can be directly linked with geophysical models estimating crustal and lithospheric thickness, heat flow, and seismic velocities. Doing so reveals correlations between, for example, mean crustal thickness and mean geochemistry of continental igneous rocks, that change through time. This secular variation can provide a connection between the formation of continental lithosphere and magma production and evolution, and be used to inform tectonic models for specific terranes. Conversely, inferences from long term average records must be consistent with detailed structural, geochronological, and geochemical studies of preserved crust.

Was more continental crust destroyed than created during Phanerozoic time?

DAVID W. SCHOLL[1*] and ROBERT J. STERN[2]

[1]University of Alaska Fairbanks, USA, dscholl@usgs.gov
[2]University of Texas, Dallas

Introduction

It is easy to study what exists but not what has disappeared, so it is generally assumed that the volume of continental crust has increased with time. Field observations can be used to estimate how much new, (juvenile) mantle-derived continental and island arc (CIA) crust is generated and how much CIA material is lost (recycled) to the mantle. Greatest additions (via arc magmatism) and losses (via sediment subduction and subduction erosion) occur at ocean-margin and crust-suturing (collisional) subduction zones (SZs). Lesser volumes are added to plate interiors at rifted margins and hotspots and removed by lower crust delamination.

Estimated Phanerozoic Gains and Losses

The best estimates for additions and losses come from geophysical, geological, and drilling studies of modern SZs and, less reliably, from fossil Cenozoic and older ones. We have estimated that long-term average gains and losses for the Phanerozoic are similar at ~3.2 km^3/yr (i.e. 3.2 AU--Armstrong Units) [1]. These estimates, which do not include a term for

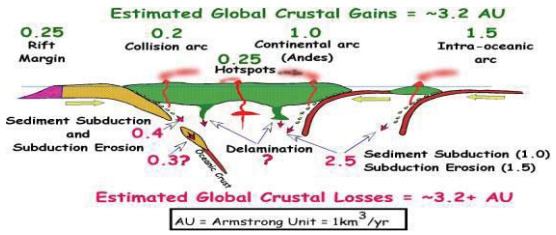

crustal foundering, are comparable to, but distinctly lower than, those of Clift et al. [2] (additions <5 AU, losses ~4.9 AU) or losses (5.25 AU) assessed by C. R. Stern [3]. The range of these estimates usefully captures our present understanding and uncertainty. Losses are least constrained for deeply subducted continental crust, for example Africa, Arabia, India, and northern Australia today, and at older collisional SZs, and by crustal delamination.

Plausible Net Phanerozoic Crustal Loss

It seems likely that at crust-suturing SZs estimated losses of deeply subducted CIA crust (based chiefly on two examples, the Paleoproterozoic Wopmay orogen of NW Canada and the Cenozoic Melanesian orogen of New Guinea), could easily be higher than our [1] estimate of 0.3 AU, and certainly a loss must be considered for our un-estimated volume of lower crust delamination. In consideration of these concerns, the uncorrected-for component of remelted older crust in continental (Andean) arc magma, and the higher volumes of recycled crust estimated by Cliff et al. [2] and C. R. Stern [3], it is plausible that during at least the Phanerozoic the net product of gains and losses has been to reduce Earth's inventory of CIA crust.

[1] Stern and Scholl (2010) Inter. Geology Rev. **52**, 1–31. [2] Cliff, Vannucchi, & Morgan (2009) Earth Sci. Rev. **97**, 80-104. [3] C.R. Stern (2011) Gondwana Research **20**, 284-308.

https://doi.org/10.1180/S0026461X00008434 Published online by Cambridge University Press

Spatial and temporal trends of iron and iron isotope cycling in the Peruvian oxygen minimum zone

FLORIAN SCHOLZ[1*], CHRISTIAN HENSEN[1], SILKE SEVERMANN[2], ANNA NOFFKE[1], BRIAN HALEY[3], JAMES MCMANUS[3], RALPH SCHNEIDER[4] AND KLAUS WALLMANN[1]

[1]Helmholtz Centre for Ocean Research Kiel (GEOMAR), Kiel, Germany, fscholz@geomar.de (* presenting author), chensen@geomar.de, anoffke@geomar.de, kwallmann@geomar.de

[2]Institute for Marine and Coastal Sciences (IMCS), Rutgers University, New Brunswick, NJ, USA, silke@marine.rutgers.edu

[3]College of Earth Ocean and Atmospheric Sciences (CEOAS), Oregon State University, Corvallis, OR, USA, bhaley@coas.oregonstate.edu, mcmanus@coas.oregonstate.edu

[4]Institute for Geosciences (IfG), Kiel University, Kiel, Gernany, schneider@gpi.uni-kiel.de

Iron (Fe) is a key element in the global ocean's biogeochemical framework because of its essential role in numerous biological processes. A poorly studied link in the oceanic Fe cycle is the reductive release of Fe from sediments in oxygen depleted ocean regions - the oxygen minimum zones (OMZs). Changing rates of Fe release from OMZ sediments may have the potential to modulate ocean fertility which has far-reaching implications considering the high amplitude oxygen fluctuations throughout earth history as well as the ongoing ocean deoxygenation projected for the near future. In order to explore spatial and temporal trends of Fe cycling in OMZs, we present here Fe isotope and speciation data for surface sediments from a transect across the Peruvian upwelling area, one of the most pronounced OMZs of the modern ocean.

Because of continuous dissimilatory Fe reduction and diffusive loss across the benthic boundary, sediments within the OMZ are strongly depleted in reactive Fe components, and the little reactive Fe left behind has a heavy isotope composition. In contrast, surface sediments below the OMZ are enriched in reactive Fe, with the majority being present as Fe oxides with comparably light isotope composition. This lateral pattern of Fe depletion and enrichment indicates that Fe released from sediments within the OMZ is reoxidized and precipitated at the oxycline. First-order calculations suggest that the amount of Fe mobilized within the OMZ and that accumulated at the boundaries are largely balanced. Therefore, benthic Fe fluxes in OMZs should be carefully evaluated prior to incorporation into global models, as much of the initially released Fe may be reprecipitated prior to vertical or offshore transport.

First XRF core scanning results for partly laminated piston cores from the OMZ boundaries reveal downcore oscillations in the content of reactive Fe and redox-sensitive trace metals that are attributed to past changes in OMZ extension. Ongoing work on these cores will focus on their dating and the downcore investigation of Fe and trace metal records in order to better understand past Fe cycling within the Peruvian OMZ and potential interactions with climate variability.

Lung Fluid-Mineral Interaction: Experimental Challenges and Outcomes

MARTIN A. SCHOONEN[1*], ANDREA HARRINGTON[1]

[1]Stony Brook University, Department of Geosciences martin.schoonen@stonybrook.edu (*presenting author) Andrea.Harrington@stonybrook.edu

Introduction

The inhalation of mineral dust can potentially lead to lung disease. Perhaps the best-known examples are exposure to asbestos, quartz, and coal, which can lead to mesothelioma, silicosis, and coal workers' pneumoconiosis, respectively. Despite clear causal evidence, the mechanisms by which mineral particles induce these diseases remain, in part, unknown. Geochemists are in a position to contribute to a better understanding of the mechanisms by which particles induce disease by conducting experimental studies to determine mineral biodurability and their ability to generate reactive oxygen species (ROS). Biodurability is an important factor as it expresses how long a particle is expected to remain in the lung after inhalation on the basis of its solubility in lung fluid. ROS are intermediate species in the reduction of molecular oxygen. Hydrogen peroxide and hydroxyl radical are the two most important ROS. Recent work shows that minerals, such as pyrite and olivine, produce hydrogen peroxide and hydroxyl radical when dispersed in water. Hydroxyl radical is particularly detrimental to human health.

While there is a wealth of data on the dissolution of minerals in water and some data is available on ROS formation in mineral slurries, few experiments have been conducted in a lung fluid proxy. A promising avenue of research is to conduct mineral dissolution experiments in Simulated Lung Fluid (SLF). There is, however, no single, standard recipe for SLF. One approach is to create a "simple" SLF solution that contains a phosphate buffer and several inorganic salts and organic acids. This formulation captures the essentials in terms of pH and ionic strength, but lacks complexity due to the absence of proteins, lipids and other macromolecules.

A comparison of pyrite dissolution rate in water and a simple SLF showed a drastic decrease in rate of dissolution in SLF. Addition of Survanta™, a bovine pulmonary surfactant, showed little or no change in rate, suggesting that the addition of the natural mixture of lipids, proteins and other biomolecules had no effect on dissolution rate. On the other hand, the addition of Survanta™ did lead to a rapid decrease of hydrogen peroxide in the slurry.

Conclusion

It is possible for Geochemists to contribute to a better understanding of lung diseases triggered by inhalation of mineral dust by conducting experiments with well-characterized minerals in SLF. While the addition of complex biomacromolecules is likely to affect the stability of hydrogen peroxide and possibly hydroxyl radical, dissolution rate data obtained in simple SLF are probably good biodurability indicators. The speciation of ROS is affected by the presence of complex biomolecules. It is possible that their presence promotes reactions that consume hydrogen peroxide and/or hydroxyl radicals.

https://doi.org/10.1180/S0026461X00008434 Published online by Cambridge University Press

Towards a consistent quantitative description of mineral precipitation and dissolution rates

J. SCHOTT[1*], E. H. OELKERS[1], P. BÉNÉZETH[1], Q. GAUTIER[1], O.S. POKROVSKY[1], G. JORDAN[2], AND G.D. SALDI[3]

[1]Université de Toulouse & CNRS, GET, Toulouse, France, jacques.schott@get.obs-mip.fr (*presenting author)
[2]Ludwig-Maximilians-Universität München, Germany
[3]Lawrence Berkeley Laboratory, Earth Science Div., Berkeley, USA.

Knowledge of the mechanisms and rates of mineral dissolution and precipitation, especially at close to equilibrium conditions, is essential for describing the temporal and spatial evolution of natural and industrial processes including weathering, diagenesis, hydrothermal deposit formation, CO_2 sequestration, and radioactive waste disposal. The Surface Complexation approach (SC) combined with Transition State Theory (TST) provides an efficient framework for describing mineral dissolution over wide ranges of solution composition, chemical affinity, and temperature. There has been a large debate for several years, however, about the comparative merits of SC/TS versus classical growth theories for describing mineral dissolution and precipitation at near to equilibrium conditions. The paucity of combined microscopic and macroscopic rate measurements on identical samples has prevented reconciliation of the surface coordination chemistry and crystal growth approaches.

This study considers recent results obtained in our laboratory on quartz, brucite, gibbsite, boehmite, kaolinite, magnesite, dolomite, and hydromagnesite dissolution and precipitation at near to equilibrium conditions via the combination of complementary techniques including batch and mixed flow reactors, hydrogen-electrode concentration cell (HECC), potentiometric titration cell, and hydrothermal atomic force microscopy (HAFM). Results show that the dissolution and precipitation of hydroxides, kaolinite and hydromagnesite powders of relatively high surface area closely follow SC/TST rate laws with a linear dependence of both dissolution and precipitation rates on fluid saturation state even at close to equilibrium ($\Delta G < 500$ J/mol) conditions. This occurs because sufficient reactive sites are available for dissolution and growth (kink, steps, edges) allowing reactions to proceed via the direct and reversible detachment/attachment of reactants at the surface. In contrast, for quartz and magnesite crystals, whose surfaces contain much fewer active sites, crystal growth (and dissolution) rates at near equilibrium conditions exhibit either a parabolic (defect assisted nucleation, spiral growth) or linear (attachment/detachment at reactive sites) dependence on saturation state depending on the treatment of the crystals before the reaction. For example, after extended dissolution (a process that creates active sites) both quartz and magnesite crystals exhibit transient linear growth rates. SC/TST rate laws can thus be applied only to those minerals that have abundant reactive sites density. It follows that determination of the active site density and origin (screw dislocations, preexisting steps…) on mineral surfaces is critical to identifying the mechanism and thus the rate equations that can describe quantitatively mineral dissolution and precipitation rates as a function of fluid composition in natural and industrial processes.

Intact polar tetraether lipids in the Arabian Sea water column and sediments: Implications for TEX_{86} paleothermometry

STEFAN SCHOUTEN[1,*], SABINE LENGGER[1], ANGELA PITCHER[1], ELLEN C. HOPMANS[1], LAURA VILLANUEVA[1] AND JAAP S. SINNINGHE DAMSTÉ[1]

[1]Royal Netherlands Institute for Sea Research, PO Box 59, Den Burg, Texel, The Netherlands. stefan.schouten@nioz.nl (* presenting author)

The TEX_{86} is an increasingly used paleotemperature proxy and relies on the fact that temperature affects the number of cyclopentane moieties in thaumarchaeal membrane lipids (glycerol dibiphytanyl glycerol tetraether lipids, GDGTs). In living Archaea, these lipids are present as intact polar lipids (IPL) with sugar- and/or phosphate-containing head groups attached to the core lipids (CL). Most studies on TEX_{86}, however, have up to now examined (fossil) CL GDGTs rather than IPL GDGTs, derived from living Archaea.

In this study, we examined the distribution and TEX_{86}-values of CL and IPL GDGTs in both the water column and sediment cores of the Arabian Sea, which contains a pronounced oxygen minimum zone. The depth profiles of crenarchaeol core lipid with a phosphohexose or dihexose head group match profiles of (expressed) genes specific for ammonia-oxidizing Thaumarchaeota. However, crenarchaeol with a hexose head group did not match the genetic depth profiles, suggesting that this IPL is partially of fossil origin. Furthermore, the concentration profiles of core lipid crenarchaeol and IPL-derived crenarchaeol showed a second peak in their abundance within the core of the OMZ which was not found in the archaeal gene concentration profiles. This representing additional evidence for a fossil contribution to the IPL pool, specifically for the glycosidic GDGTs. TEX_{86} values of both fossil core lipid and IPL-derived GDGTs increased from surface waters to the core of the OMZ, below which they decreased again, and did not correlate with *in situ* temperature. TEX_{86} values of IPL-derived GDGTs did correlate well with the relative amount of glycosidic GDGTs and were consistently higher than that those of CL GDGTs.

We subsequently isolated IPL GDGTs from Arabian Sea sediments to determine cyclopentane distributions and TEX_{86} of the individual IPL GDGTs. We observed strong differences in GDGT-composition amongst head groups: GDGT-2 and -3 (numbers indicate the number of cyclopentane moieties) are predominantly present as glycolipids, while GDGT-1 is predominantly present as phosphoglycolipid. A similar observation is made for IPL GDGTs of enriched Thaumarchaeota, i.e. GDGT-0, -1 and crenarchaeol predominantly occurring as CL of phosphoglycolipids, and GDGT-2, -3 and -4 as CLs of dihexose GDGTs [1]. As a consequence, in enrichment cultures, the TEX_{86} shows a relation with the relative amount of dihexose GDGTs, i.e. increasing TEX_{86} with increasing amount of dihexose GDGTs.

Our results thus suggests that head group composition of IPL GDGTs in Thaumarchaeota and selective preservation of glycosidic GDGTs during diagenesis may strongly impact TEX_{86} values of produced GDGTs in deep marine waters.

[1] Schouten S., et al. (2008) *Geochim Cosmochim Acta* **74**, pp. 3806 - pp. 3814.

https://doi.org/10.1180/S0026461X00008434 Published online by Cambridge University Press

Arsenic in soils from poultry litter application

MADELINE E. SCHREIBER[1]*

[1]Department of Geosciences, Virginia Tech, Blacksburg, VA 24061 USA (*presenting author, mschreib@vt.edu)

Introduction

The use of organoarsenicals in poultry feed additives has raised a concern about air, water and soil quality in regions of poultry production. This study examined the impact of poultry litter application on the distribution of As and other trace elements in soils. Soils from fields with varying litter applications in the Shenandoah Valley, Virginia, a region of intense poultry production, were collected, digested and analyzed for trace elements of interest. Data were statistically analyzed to examine relationships between litter application rates and trace element concentrations.

Methods

Sixteen cores were collected from the Frederick series, a well-drained silt loam. Sites were selected to represent soils with different histories of litter use: no litter use (control), and low, moderate and high litter use. The three litter amended sites had the following estimated litter application rates: 1.5 tons/acre/year (low), 3 tons/acre/year (moderate) and 6 tons/acre/year (high). At each site, four locations were chosen randomly for soil core collection. Soils in 15 cm increments were collected the surface to 120 cm depth. A total of 128 soil samples were collected for analysis. Soil samples were dried and ground, measured for particle size, organic matter and pH. Subsamples were digested for both Mehlich-extractable elements and acid-extractable elements (As, P, K, Ca, Mg, Zn, Cu, Fe). Statistical analysis was conducted on the dataset using several techniques, including correlation analysis, 1-way ANOVA comparison of means, and principal component analysis using JMP.

Results and Conclusions

Statistical analysis revealed that As does not concentrate in litter-amended soils, in contrast to litter-derived species P, Cu and Zn. While P, Cu, and Zn concentrations decrease with depth in the soil profile, As concentrations increase with depth in all soils and are correlated with iron and clay content, suggesting that As is adsorbed to iron oxides and clays, even in control soils that have not received litter application. At the highest litter application rate (20,000 kg/hectare/year; equivalent to 6 tons/acre/year), an As litter concentration of 40 mg/kg, a soil density of 1.6 m^3/kg, and a 30 year period of litter application, As concentrations in the top 20 cm of litter-amended soil are predicted to be only 4.5 mg/kg above background concentrations, assuming conservative behavior. This low level of As may be difficult to detect, especially in heterogeneous soils. Transport of As in due to competitive desorption by phosphate and DOC, complexation, or adsorption onto mobile particles may also contribute to the lack of observed accumulation of As in soils.

Growth of *Streptomyces mirabilis* P16B1 in heavy metal contaminated soil and impact to Soil Organic Matter formation

EILEEN SCHÜTZE(*)[1], MICHAEL KLOSE[1],DIRK MERTEN[2], SANDOR NIETZSCHE[3], MATTHIAS KÄSTNER[4], ERIKA KOTHE[1]

1 Institute for Microbiology - Microbial Phytopathology, Friedrich-Schiller-University, Neugasse 25, D-07745 Jena, Germany, (Email: eileen-schuetze@web.de)
2 Institute of Geosciences, Friedrich-Schiller-University, Burgweg 11, D-07749 Jena, Germany
3 Centre of Electron Microscopy, Friedrich-Schiller-University Jena, Ziegelmühlenweg 1, D-07740 Germany
4 Helmholtz Centre for Environmental Research - UFZ, Department of Bioremediation, Permoserstraße 15 , D-04318 Leipzig, Germany

It has been shown that streptomycetes are a dominant group of bacteria in heavy metal contaminated soil and that growth of soil bacteria had positive effects on bioremediation, on bioavailability of metals in soil and on biogeochemical cycles.

The former uranium mining site Wismut in Eastern Thuringia, Germany, shows extreme environmental conditions such as scant nutrients, intense salt load and low pH, followed by high metal content. Such habitats only can be colonized by microbes which are adequately adapted. Actinobacteria isolated from this hostile environment show high resistances against a range of heavy metals like nickel, cobalt, cadmium or zinc. Growth of *Streptomyces mirabilis* P16B1 was investigated in mesocosms of contaminated soil from the especially nickel and zinc contaminated sample sites K7 (WISMUT area Ronneburg, Germany). As control uncontaminated soil PaO (paradise parc Jena, Germany) was used. Heavy metal sensitive *S. lividans* TK24 was used as control in both types of soil as well as dead biomass from both used strains. This experiment gave insight in growth and contribution to soil organic matter (SOM) formation of the strain, as well as its impact to heavy metal availability. Scanning electron microscopy and XRD analysis were used to detect the mycelium, spore production, as well as dead bacterial biomass and its attachment to soil particles as patchy fragments. The metal content of soil from the samples was determined by SE methods and MS. Superoxide-dismutase (SOD)-production of *S. mirabilis* P16B1 under natural conditions was detected via native PAGE and qualitative SOD-staining as well as quantitative Assay with extracted protein. Auxine production and siderophore production were measure via MS.

It could be shown that inoculation with the strain has an effect of SOM formation in soil, as well as heavy metal availability in mobile and specifically adsorbed fraction. Due to Fenton reaction and elevated concentration of heavy metals SOD expression could be seen as an important resistance factor of strains. Auxine and siderophore production by streptomycetes could be shown directly in soil. Thereby application of extremely heavy metal resistant strains from WISMUT area for microbial enhanced phytoremediation could be recommended.

https://doi.org/10.1180/S0026461X00008434 Published online by Cambridge University Press

Marine terrace soils along the west coast of North America: a weathering archive?

MARJORIE SCHULZ[1*], COREY LAWRENCE[1], DAVE STONESTROM[1], TOM BULLEN[1], JENNIFER HARDEN[1], ART WHITE[1], JOHN FITZPATRICK[1] AND CARRIE MASIELLO[2]

[1]US Geological Survey, Menlo Park, California, USA, mschulz@usgs.gov (* presenting author), clawrence@usgs.gov, dastones@usgs.gov, tdbullen@usgs.gov, jharden@usgs.gov, afwhite@usgs.gov, jfitzpat@usgs.gov

[2]Rice University, Houston, Texas, USA, masiello@rice.edu

Soil chronosequences provide a framework for understanding the influence of time on soil and ecosystem properties. To simultaneously examine how landscapes of different ages will respond to future climate shifts, we can compare landscapes across age and climate. North America's west coast has a significant precipitation gradient (wet in the north, dry in the south), supporting a gradation of ecosystems from northern temperate rainforests, through mixed forests, semi-arid Mediterranean chaparral and southern desert ecosystems. Marine terraces occur up and down the west coast of North America; each flight of stair-like terraces is a chronosequence. The soils of coastal marine terraces in the west provide a "climosequence of chronosequences" ideally suited to examine the interactions of landscape age and climate on soil and ecosystem resistance and resilience to climate change.

Building on work at the Santa Cruz (CA) marine terraces, we are developing a network of terrace chronosequences along the west coast. Past work at the Santa Cruz terraces examined soil development and elemental cycling in detail. Ongoing work on these terraces includes field, laboratory, and modeling efforts to understand carbon cycling. Our future work will extend the methods we have refined at Santa Cruz to other well-established North American marine terrace chronosequences.

We hypothesize that soil properties, processes, and rates on west coast terraces might be meaningfully assigned to climate zones as well as age of soil formation. Comparison of results from different marine terrace chronosequences will require addressing several important questions linking the paleohistory of soil formation with contemporary soil properties: The central question is what memories of past climate do soils possess, and how can we measure them? This problem requires multidisciplinary discussions, inspiration, and work. Soil properties that turn out to be indicative of distinctive climate-ecosystem combinations are potentially useful as references for judging the timing and extent of change in other soils. For example, data from the Santa Cruz chronosequence suggests that the isotopic fractionation of Fe may indicate past chaparral or forested ecosystems in soils currently occupied by coastal prairies. We hope to establish which soil properties change most with climate, and by utilizing multiple time sequences of soils, to bracket the timing of the changes. In this way the potential of naturally occurring archives recorded in marine terraces along North America's west coast can be used to address questions about future effects from climate change.

The case of p-Process ^{180}W heterogeneities in Iron Meteorites

T. SCHULZ[1,3*], C. MÜNKER[1,2], S. PETERS[1,2]

[1] Institut für Geologie und Mineralogie, Universität Köln, Germany

[2] Steinmann Institut, Universität Bonn, Germany

[3] Department für Lithosphärenforschung, Universität Wien, Austria toni.schulz@univie.ac.at (* presenting author)

Introduction

For most elements, in particular for r- and s-process isotopes, the abundances of non-radiogenic isotopes appear to be fairly homogeneous in the early solar system. This is likely to reflect efficient homogenisation of materials in the protoplanetary disk. However, a notably small number of elements are reported to display distinct anomalies, interpreted as being nucleosynthetic. Due to their low abundances, only few studies so far have measured heavy p-process isotopes [e.g. 1]. The low abundances of these neutron deficient nuclides reflect their particular formation conditions [e.g. 2]. Our recently presented ^{180}W measurements in iron meteorites reported clearly resolvable anomalies of up to ~+700ppm [3], interpreted to be of nucleosynthetic origin. However, recent studies [4] argued that such non-radiogenic stable W isotope anomalies may reflect analytical artifacts, resulting from molecular interferences. We therefore conducted replicate measurements of the Cape York IIIAB iron meteorite using modified analytical protocols.

Methods

Tungsten measurements were conducted using the Neptune multicollector ICP-MS at the University Bonn that is equipped with high sensitivity 10^{12} Ohm amplifiers for measuring ^{180}W and the ^{178}Hf interference monitor. Measurements were run in low- and high resolution and by using different sampler cones, including so-called "Jet Cones" with wider aperture. About 6g of Cape York metal was dissolved and loaded onto conventional anion exchange columns. Following modified elution procedures, W was purified from the 6 g sample, and AMES standard solutions were processed as well. For multiple measurements of AMES W standard solutions we obtained external reproducibilities of ±80 ppm (2σ r.s.d). ^{178}Hf intensities were typically an order of magnitude lower than required for accurate ^{180}Hf interference corrections.

Results and Discussion

Our preliminary results confirm a clearly resolvable ^{180}W anomaly for Cape York. Using standard and Jet-cone setups we obtained ^{180}W values of about ~+350ppm and typical ^{182}W and ^{184}W signatures in low- and medium resolution. In high resolution we could reproduce the ^{180}W excess using standard cones, but an offset of as much as 4500ppm using Jet-cones, which can be attributed to anomalous mass bias behaviour potentially reflecting matrix effects. Terrestrial W isotope compositions obtained with standard cones for all AMES W solutions which were processed during column chemistries and for terrestrial metals from reduced basalts provide further support for a nucleosynthetic origin of the measured anomalies.

Conclusions

Evidence for ^{180}W heterogeneities in iron meteorites is provided from (1) systematic excesses in ^{180}W between different iron meteorite groups [3], (2) offsets from the respective group averages for long exposed meteorites due to cosmogenic burn-out of ^{180}W [3]) and (3) analytical evidences presented here. Our results call for further studies evaluating mass bias behaviour in modified ("Jet Cone") interface devices in MC-ICPMS systems.

[1] Fehr M.A. et al. (2005) **69**, 5099-51112. [2] Woosley S.E. and Howard W.M. (1978) ApJS, **36**, 285. [3] Schulz T. And Münker C. (2010), 73rd Met.Soc., #5116. [4] Holst J.C. et al. (2011), Workshop Hawaii. LPI Contr. **1639**, p. 9065.

https://doi.org/10.1180/S0026461X00008434 Published online by Cambridge University Press

Oxalate-promoted formation of saponite at 60°C and 1 atm pressure

DIRK SCHUMANN[1*], HYMAN HARTMAN[2], DENNIS D. EBERL[3], KELLY S. SEARS[4], REINHARD HESSE[1], HOJATOLLAH VALI[1,4]

[1]Earth & Planetary Sciences (McGill), Montreal, Canada, dirk.schumann@mail.mcgill.ca*

[2]Biomedical Engineering (MIT), Cambridge, USA, hymanhartman@hotmail.com

[3]USGS, Boulder, USA, ddeberl@usgs.gov

[4]FEMR (McGill), Montreal, Canada, hojatollah.vali@mcgill.ca

Introduction and Results

In carbonaceous chondrites there is a strong correlation between the occurrence of clay minerals and the presence of polar organic molecules (*e.g.* oxalic acid) [1][2]. Oxalic acid in the aqueous alteration phase of these meteorites could have enhanced the alteration of olivine and orthopyroxene to form Mg- and Fe-rich phyllosilicates [2]. It has also been proposed that clay minerals might have caused an enrichment of chiral "left"-handed amino acids like isovaline in these meteorites [3]. It is therefore important from the point of view of prebiotic chemistry whether oxalic acid might have catalyzed the formation clay minerals.

In this study we tested whether oxalate catalyses the crystallization of saponite from a silica gel powder at 60ºC and ambient pressure. For comparison in a second experiment NaOH solution was used instead of oxalate. Low magnification TEM images showed clusters of well developed globular aggregates consisting of packets of saponite crystals in the oxalate experiment and poorly crystallized saponite from the NaOH solution. High-resolution TEM lattice-fringe images of the ultrathin sections of the saponite globules treated with octadecylammonium (n_C=18) cations revealed the presence of 2:1 layer structures having variable interlayer charges: (1) short sequences of low-charge 2:1 silicate layers with an interlayer spacing of 13 to 14 Å and (2) sequences of higher charge 2:1 silicate layers having highly expanded interlayers of 25 to 33 Å. The difference in interlayer expansion results from the variation in the substitution of Al^{3+} for Si^{4+} within the tetrahedral sheets of the saponite crystallites. The Si/Al ratio seems to be passed on from layer to layer by heritage which is demonstrated by the regular interlayer expansion within the packets.

Conclusions

This study (i) showed the strong catalytic effect of oxalate on the nucleation and growth of saponite at low temperatures and pressure in contrast to NaOH, (ii) established the composition and structure of the 2:1 silicate layers of the saponite, and (iii) evaluated the replicating capability of the saponite. This study does not only offer an explanation for the formation of clay minerals in carbonaceous chondrites but may also explain the origin of clay minerals in other systems that contain oxalic acid associated with endolithic and epilithic (*e.g.* lichen) communities.

[1] Becker & Epstein (1982) *GCA* **46**, 97-103. [2] Hartman *et al.* (1993) *Origins of Life and Evolution of Biosphere* **23**, 221-227. [3] Pizzarello *et al.* (2003) *GCA* **67**, 1589-1595.

Transformations of mercury, arsenic and selenium in river sediments contaminated with coal ash: Field and laboratory studies

G. SCHWARTZ[1*], A. DEONARINE[1], L. RUHL[2], A. VENGOSH[2], G. BARTOV[3], T. JOHNSON[3], H. HSU-KIM[1]

[1]Duke University, Department of Civil and Environmental Engineering, Durham, NC, USA, grace.schwartz@duke.edu *

[2]Duke University, Division of Earth and Ocean Sciences, Durham, NC, USA

[3]University of Illinois at Urbana-Champaign, Department of Geology, Urbana, IL, USA

Coal combustion products, including coal ash, represent the largest industrial waste stream in the United States and contain elevated levels of toxic elements such as mercury (Hg), arsenic (As), and selenium (Se). Much of this waste is stored in unlined holding ponds and landfills that are not always monitored for their discharge to adjacent waters. Moreover, these holding ponds are susceptible to failures such as the disaster at the Tennessee Valley Authority (TVA) Kingston Fossil Plant in 2008 that caused more than 1 billion gallons of coal ash slurry to spill into the adjacent Emory River. In such cases, the fate of toxic elements associated with coal ash is greatly influenced by environmental conditions such as redox potential and microbial activities that induce transformations and leaching of contaminants. Here, we investigated the mobilization of coal ash contaminants in sediments through a field study of the river system surrounding the TVA coal ash spill site and also through laboratory sediment slurry experiments to understand how river conditions could facilitate mobilization of trace elements and production of methylmercury (MeHg). In the field survey, we sampled the sediments and surface water at the spill site during a two year period after the spill event. The results indicated elevated levels of MeHg in the river sediments near the spill site. The mercury originating from the coal ash demonstrated a stable Hg isotope signature that was different from the mercury originating from historical sources to this ecosystem. Thus, the isotope data suggested that the coal ash was stimulating MeHg production in the river sediments near the TVA site (either by providing Hg or other substrates for methylating bacteria). In the laboratory experiments, we cultured anaerobic sediment slurries to determine how the addition of coal ash could influence porewater chemistry and Hg speciation. The microcosms were prepared using sediment and surface water from a location several miles upstream of TVA spill site and cultured in an anaerobic chamber. A selection of the slurries was amended with coal ash obtained from the TVA Kingston Plant. Preliminary results of the sediment slurry incubations showed that the coal ash increased the amount of dissolved As and Se in the slurries at the initial time point. Over 4 days of incubation, dissolved As continued to increase while dissolved Se decreased in the slurries. These results suggested that arsenic was converting from As(V) to more soluble As(III) species in the slurries while selenium was converting from oxidized forms (e.g. selenate or selenite) to less soluble, reduced forms (e.g. elemental Se, selenide). The concentration of dissolved sulfate also decreased during the experiment, consistent with low redox potential in the slurries. While MeHg was observed in all slurry samples, the effect of coal ash on Hg speciation was mixed, with the coal ash providing a stimulating effect for MeHg production in some slurries and no effect in others. Further work will include sediment-coal ash slurries with more active microbial growth conditions. Overall, our field and laboratory studies highlight the need to consider environmental conditions in assessing the potential hazards of contaminants associated with coal ash.

https://doi.org/10.1180/S0026461X00008434 Published online by Cambridge University Press

Age of the Bushveld Complex

JAMES S. SCOATES[1*], COREY J. WALL[1], , RICHARD M. FRIEDMAN[1], JILL A. VANTONGEREN[2], AND EDMOND A. MATHEZ[2]

[1]Pacific Centre for Isotopic and Geochemical Research, Earth and Ocean Sciences, Vancouver, BC, Canada, jscoates@eos.ubc.ca, cwall@eos.ubc.ca, rfriedman@eos.ubc.ca

[2]Geology and Geophysics, Yale University, New Haven, CT, USA, jill.vantongeren@yale.edu

[3]American Museum of Natural History, New York, NY, USA, mathez@amnh.org

Determining the precise age of the Bushveld Complex, the world's largest layered intrusion located in the northern Kaapvaal craton of South Africa, has been a longstanding problem. The age and duration of magmatism associated with the complex is critical for establishing the genetic relations among its different rock units (Rustenburg Layered Suite, overlying Rooiberg Group felsic volcanic rocks, intrusive Rashoop Granophyres) and timing of formation of its world-class ore deposits (Cr-PGE-V). We report chemical abrasion ID-TIMS U-Pb zircon results (all ages reported as weighted $^{207}Pb/^{206}Pb$ averages) for 8 samples from the layered mafic rocks of the complex and the roof. These results demonstrate that the Bushveld Complex spans an ~7 million year interval from 2061 to 2054 Ma with major magma emplacement at ca. 2060 and 2055 Ma. In the mafic rocks of the Rustenburg Layered Suite, the ages overlap within analytical uncertainty at ca. 2055-2056 Ma for a diorite from the top of the Upper Zone ~50 m below the roof (2056.52 ± 0.81 Ma) and for two samples, ~300 km apart in the Western and Eastern limbs, from the PGE-rich Merensky Reef at the top of the Upper Critical Zone (2055.30 ± 0.61 Ma; 2056.13 ± 0.70 Ma, revised from [1]). These results are consistent with rapid filling, crystallization, and cooling of the upper 2/3 of the intrusion [2]. Ages for felsic rocks in the roof above the level of the Upper Zone diorite in the Eastern Limb range from 2054-2056 Ma, including a granodiorite mixed with hornfels or "leptite" (2054.83 ± 0.86 Ma), a granophyre from the Rashoop Granophyre Suite (Stavoren: 2055.70 ± 1.0 Ma), and a granite from the Nebo/Lebowa granites (2054.23 ± 0.79 Ma). These ages indicate that mafic and felsic rocks of the Bushveld Complex are broadly coeval and support the proposal that some of the original magma volume in the intrusion was expelled to form the Upper Rooiberg Group lavas or Rashoop granophyres [3]. Below the Merensky Reef, there is a shift to older ages at ca. 2060 Ma. Results for two samples at different locations of footwall pyroxenite immediately below the UG-2 chromitite (Eastern Limb), ~380 m below the Merensky Reef, are 2060.5 ± 1.4 Ma and 2059.8 ± 1.2 Ma. It has long been recognized that initial Sr isotope ratios in both plagioclase and whole rocks increase sharply at the Merensky Reef over a few metres due to the emplacement of a compositionally distinctive magma batch [4]. The U-Pb geochronological results of this study indicate an age gap of perhaps as much as 5 million years between the uppermost Upper Critical Zone (UG-2 chromitite) and the Merensky Reef and overlying Main and Upper zones. The lowermost mafic-ultramafic rocks of the Bushveld Complex (Lower Zone and Critical Zone) appear to result from an earlier phase of magmatism at ca. 2060 Ma, coeval with the nearby 2060 Ma Phalaborwa carbonatite [5]. After a hiatus, now marked by the level of the Merensky Reef, the major volume of the Bushveld Complex was emplaced at ca. 2055 Ma.

[1] Scoates & Friedman (2008) *Econ. Geol.* **103**, 465-471. [2] Cawthorn & Walraven (1998) *J. Petrol.* **39**, 1669-1687. [3] VanTongeren *et al.* (2010) *J. Petrol.* **51**, 1891-1912. [4] Kruger & Marsh (1982) *Nature* **298**, 53-55. [5] Wu *et al.* (2011) *Lithos* **127**, 309-322.

Paleoproterozoic collapse in seawater sulfate and subsequent shallowing of the methane cycle in marine sediments

C. T. SCOTT[1*], B. WING[1], A. BEKKER[2], N. PLANAVSKY[3], P. MEDVEDEV[4], S. M. BATES[3], M. YUN[2], T. W. LYONS[3]

[1]Department of Earth and Planetary Sciences, McGill University, Montreal, Canada, clinton.scott@mcgill.ca

[2] Department of Geological Sciences, University of Manitoba, Manitoba, Canada

[3]Departmet of Earth Sciences, University of California, Riverside, USA

[4] Institute of Geology, Karelian Research Center, RAS, Petrozavodsk, Russia

The initial accumulation of atmospheric oxygen, referred to as the Great Oxidation Event or GOE, is fairly well-constrained to between 2,450 and 2,320 Ma. However, the magnitude and duration of that rise in oxygen is subject to debate. It is also not clear how the dynamic oxidation of the early Paleoproterozoic transitioned into the environmental stasis of the Boring Billion. In order to examine the history of Paleoproterozoic surface oxidation, we used a combination of pyrite multiple-sulfur (^{32}S, ^{33}S and ^{34}S) and organic carbon isotopes from marine black shales. We analyzed the (1) 2,320 Ma Rooihoogte and Timeball Hill Formations, from which the GOE is dated; (2) the 2,200 to 2,100 Ma Sengoma Argillite Formation, deposited during the peak of the Lomagundi carbon isotope excursion in an open-marine setting on the Kaapvaal craton; and (3) the Upper Zaonega Formation of the Ludikovian Series, Russian Karelia, deposited in a marine basin between 2,100 and 2,000 Ma, in the immediate aftermath of the Lomagundi carbon isotope excursion.

Pyrite S isotopes display large ^{34}S-^{32}S fractionations (>30‰) relative to seawater sulfate, indicating that a large marine sulfate reservoir (2-20 mM) developed as an immediate result of the GOE and persisted for nearly 250 Ma. In the aftermath of the Lomagundi carbon isotope excursion, pyrite sulfur isotope fractionations drop to <15‰, suggesting a rapid collapse of the marine sulfate reservoir to <200 μM. These low-sulfate conditions persisted for at least 600 Ma. Thus, it appears that the high oxidation state of the atmosphere-ocean system that developed as the immediate result of the GOE was largely lost by 2,000 Ma and did not return until the Ediacaran period. Accordingly, the Boring Billion is best described as a long-lived redox regime that was intermediate between those of the Archean and the early Paleoproterozoic, rather than between the early Paleoproterozoic and the Phanerozoic.

Organic carbon isotopes record a secular shift to more negative values at ca. 2,050 Ma, which is tightly coupled to the positive excursion in pyrite S isotopes. We interpret this carbon isotope excursion as an enhancement in the biological methane cycle in marine sediments as a result of the crash in seawater sulfate. As seawater sulfate concentrations dropped, methanogenesis operated closer to the sediment-water interface, setting up conditions suitable for subsequent methanotrophy and incorporation of ^{13}C-depleted biomass into the marine sedimentary organic carbon pool.

https://doi.org/10.1180/S0026461X00008434 Published online by Cambridge University Press

Formation and evolution of cores in asteroids: clues from iron meteorites

EDWARD R. D. SCOTT

University of Hawai'i, Honolulu, HI 96821, USA, escott@hawaii.edu

In 12 out of 14 groups of iron meteorites, chemical variations are consistent with fractional crystallization of single pools of molten Fe-Ni-S (e.g., Ir is inversely correlated with Ni and varies by factors of 10^{1-4}) [1]. These irons have W isotopic compositions indicating they were isolated from Hf-bearing rock <1 Myr after CAI formation [2]. By contrast, irons in groups IAB and IIE do not show fractional crystallization trends (e.g. Ir is uniform), they contain abundant silicate inclusions including chondritic fragments, and their W isotopic compositions indicate more recent metal-silicate exchange. This suggests that most irons come from cores of asteroids that accreted <1 Myr after CAIs when ^{26}Al was abundant enough to form molten cores. Irons in groups IAB and IIE probably come from bodies that accreted later when there was insufficient ^{26}Al to allow metallic pools to form cores.

Irons from cores of differentiated asteroids should have cooled more slowly than irons from metallic pools. However, fractionally crystallized irons show fast cooling rates, e.g., 60-300 °C/Myr for IIIAB irons, 100-6600 °C/Myr for IVA irons, and 500-5000 °C/Myr for IVB irons [3-5]. These cooling rates are incompatible with cooling in cores of asteroids that were melted by ^{26}Al for two reasons. 1) Each group has a wide range of cooling rates whereas metallic cores should have cooled almost isothermally as metal conducts heat much more rapidly than silicate. 2) Bodies that were small enough to have cooled at these rates would have had radii of <10 km and could not have been melted by ^{26}Al. In addition, the 4565 Myr Pb-Pb age of a IVA iron [6] is incompatible with conventional models for fully differentiated asteroids which require cooling over tens to hundreds of Myr. The metallic cores supplying most iron meteorites must have cooled rapidly with little or no insulating mantle.

Impacts between asteroids at current impact velocities of ~5 km/s cannot efficiently remove silicate mantles from cores. However, impacts at lower speeds during accretion can disrupt projectiles impacting at grazing angles and speeds comparable to mutual escape velocities [7]. Repeated collisions under these conditions may have allowed core material to cool with little or no silicate insulation. Low-velocity collisions during accretion may also explain the presence of rock fragments in the IAB and IIE iron meteeorites.

The diversity of melted and unmelted asteroids and meteorites may result from formation of iron meteorites and achondrites from planetesimals that accreted near the terrestrial planets whereas chondrites accreted later in the asteroid belt [8]. Grazing impacts eviscerated differentiated asteroids so that fragments were lofted into the asteroid belt. Planetary accretion may have been a very inefficient process so that the differentiated asteroids represent the construction debris [7].

[1] Goldstein et al. (2009) *Chemie der Erde* **69**, 293-325. [2] Kleine et al. (2009) *GCA* **73**, 5150-5188. [3] Yang & Goldstein (2006) *GCA* **70**, 3197-3215. [4] Yang et al. (2008) *GCA* **72**, 3043-3061. [5] Yang et al. (2010) *GCA* **74**, 4493-4506. [6] Blichert-Toft et al. (2010) *EPSL* **296**, 469-480. [7] Asphaug (2010) *Chemie der Erde* **70**, 199–219. [8] Bottke et al. (2006) *Nature* **439**, 81-824.

Microscopy based detection and analysis of carbon nanocomposites in commercially available baseball bats

KEANA SCOTT[1*], CHRISTOPHER MARVEL[2], STEPHAN STRANICK[1] AND JOHN HENRY SCOTT[1]

[1]National Institute of Standards and Technology, Gaithersburg, MD, USA, keana.scott@nist.gov (* presenting author), stephan.stranick@nist.gov, johnhenry.scott@nist.gov

[2]Lehigh University, Bethlehem, PA, USA, cjm312@lehigh.edu

The number of consumer products incorporating polymer nanocomposites has rapidly increased in recent years [1]. Especially in sport equipment, the enhanced material properties such as high strength, high toughness and low density of these nanocomposites are effectively translated into a lighter equipment with improved performance characteristics. Although much work has been done in developing and characterizing these nanocomposite materials and nanofillers (nano-tubes, -particles, -fibers, etc.), characterization and lifecycle studies of nanocomposites in their product condition have been lacking. However, several recent studies have examined nanocomposite degradation and disposal products and explored their environmental impacts. Nguyen et al. have shown that surface exposure of carbon nanotube (CNT) network can result from the photodegradation of polymer matrix under UV exposure of CNT-polymer nanocomposites [2]. Wohlleben et al. have evaluated nanocomposite fragments for the nanofiller release and their in-vivo toxicity [3].

In this study, we examined two different types of commercially available baseball bats that incorporate CNT-polymer nanocomposites into their structures. Several different microscopy techniques were used to identify and analyze the CNTs in the bat and in the release fragments from two different use scenarios (normal and recycle/disposal). The normal use scenario included abrasion of the bat surface with different grades of polishing cloth and sand paper, simulating normal wear and tear. The recycle/disposal scenario included sawing and ripping the bat pieces. The cross-sectional samples of the bats were used to identify the locations of CNT nanocomposites and confirm the presence of CNTs in these materials. The bat surfaces and the release fragments from the two use scenarios are examined for the particle size distribution, release particle morphology and presence of loose or exposed CNTs. The preliminary results from the normal use scenario showed no loose or exposed CNTs in the wear particles or the abraded bat surfaces. The bulk of the release fragments from the sawing and ripping operation were mm to μm sized fragments. However, albeit in very low level, several types of nano-sized particles and fibers, including some that showed morphology consistent with polymer coated CNTs, were also detected in the release fragments. Additional work is in progress to characterize and quantify the nano-sized debris from the disposal scenario.

[1] http://www.nanotechproject.org/inventories/consumer/
[2] Nguyen et al. (2009) *Proc. Eur. Weathering Symposium* **11**, 149-161.
[3] Wohlleben et al. (2011) *Small* **7**, 2384-2395.

https://doi.org/10.1180/S0026461X00008434 Published online by Cambridge University Press

Constraining the composition of basinal brines in the Athabasca basin from individual fluid inclusion analysis in quartz overgrowths

RYAN SCOTT[1*], GUOXIANG CHI[2]

[1]University of Regina, Regina, Canada, ryan.dj.scott@gmail.com (* presenting author)
[2]University of Regina, Regina, Canada, guoxiang.chi@uregina.ca

Constraining the geochemical composition of basinal brines in the Athabasca basin is crucial in understanding the role of diagenetic fluids during the formation of high-grade unconformity-type uranium deposits. In order to characterize the diagenetic fluids before they were involved in mineralization, samples must be collected distally from mineralization or alteration zones. The Rumpel Lake drill core, which is located far away from known mineralization, is an excellent target for this type of analysis.

Isolated and clustered fluid inclusions in quartz overgrowths in the Athabasca Group sandstones (Fig. 1) were selected for analysis. Unlike minerals in veins, quartz overgrowths cannot be separated for bulk fluid inclusion analysis, therefore individual inclusions were analyzed with the heating-freezing, decrepitation SEM-EDS and cryogenic Raman spectroscopic methods [1, 2]. Ice-melting temperatures range from -37.5 to -11.0°C, suggesting that $CaCl_2$ may be present in addition to NaCl. Raman spectra obtained from frozen fluid inclusions show peaks that are comparable to published data for mixed NaCl-$CaCl_2$ systems (Fig. 1) [1]. SEM-EDS analysis shows that the decrepitates of the inclusions are composed of NaCl+KCl+$CaCl_2$±$MgCl_2$. These results are generally consistent with the proposals that the Athabasca basinal brines were derived from seawater evaporation [3], and indicate that some calcium in the basinal fluids found in uranium deposits may have been derived from fluid-rock interactions within the basin, rather than solely from the basement.

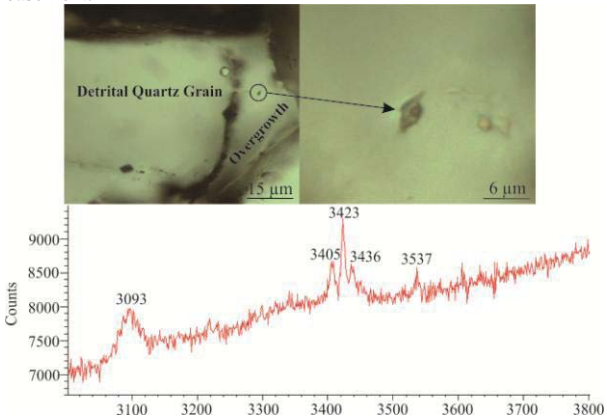

Figure 1: Upper: Isolated fluid inclusion located in the quartz overgrowth. Lower: Raman spectra of the depicted fluid inclusion homogeneously frozen to -185°C.

[1] Samson and Walker (2000) *The Canadian Mineralogist* **38**, 35-43. [2] Savard and Chi (1998) *Economic Geology* **93**, 920-931. [3] Richard *et al.* (2011) *Geochimica et Cosmochimica Acta* **75**, 2792-2810.

Vegetation collapse on Flores 69,000 years ago: A consequence of the Toba super-eruption, or a volcanic disaster closer to home?

NICK SCROXTON[1*], MICHAEL K. GAGAN[1], IAN S. WILLIAMS[1], JOHN C. HELLSTROM[2], HAI CHENG[3], LINDA K. AYLIFFE[1], GAVIN B. DUNBAR[4], WAHYOE S. HANTORO[5], HAMDI RIFAI[6], AND BAMBANG W. SUWARGADI[5]

[1]Research School of Earth Sciences, The Australian National University, Canberra, Australia, nick.scroxton@anu.edu.au (* presenting author), michael.gagan@anu.edu.au, ian.williams@anu.edu.au, linda.ayliffe@anu.edu.au,
[2]School of Earth Sciences, The University of Melbourne, Parkville, Australia, j.hellstrom@unimelb.edu.au,
[3]Institute of Global Environmental Change, Xi'an Jiatong University, Xi'an, China, cheng021@unm.edu,
[4]Antarctic Research Centre, Victoria University of Wellington, Wellington, New Zealand, gavin.dunbar@vuw.ac.nz,
[5]Research Center for Geotechnology, Indonesian Institute of Sciences, Bandung, Indonesia, whantoro@gmail.com, bambang.suwargadi@gmail.com,
[6]Department of Physics, State University of Padang, Padang, Indonesia, hamdi_unp@yahoo.com,

A large ~8‰ positive $\partial^{13}C$ excursion has been identified at 69,000 years BP in the speleothem archive from Liang Luar cave, Flores, Eastern Indonesia. The excursion, by far the largest in 92,000 years of record, begins abruptly, lasts for over 500 years, and only fully recovers to background $\partial^{13}C$ after 800 years. At its peak the excursion approaches bedrock values and we therefore interpret this event as massive vegetation destruction in western Flores followed by progressive recovery.

The excursion is coeval with the largest spike in concentration of elemental sulphur in the speleothem across this interval, measured using in situ, 30µm scale Sensitive High Resolution Ion Microprobe (SHRIMP) analysis. Atmospheric volcanic sulphate is introduced to the cave system through dissolution in rain and then groundwater. The concentration of sulphate in speleothems serves as a relatively new proxy for volcanic activity.

Taken together, the $d^{13}C$ and sulphur records indicate that this outstanding century-scale event represents massive vegetation loss in western Flores in the aftermath of a major volcanic eruption. Could the Toba super-eruption be the cause of this major event in the history of Flores? We will present $\partial^{18}O$, $\partial^{13}C$ and sulphur concentration records from Flores and nearby Sulawesi detailing the relative timings of the isotopic and concentration changes in order to separate the effects of local eruptions on Flores from the remote volcanic impact of the Toba super-eruption.

https://doi.org/10.1180/S0026461X00008434 Published online by Cambridge University Press

Proxy Recognition of Volcanic Ash and Eolian Dust: Implications for Climate Records, Tectonics, and Nutrient Cycling

RACHEL P. SCUDDER[1](*), RICHARD W. MURRAY[1], STEFFEN KUTTEROLF[2], JULIE C.SCHINDLBECK[2]

[1]Department of Earth Sciences, Boston University, Boston, MA, USA, rscudder@bu.edu (* presenting author), rickm@bu.edu
[2]GEOMAR, Kiel, Germany, skutterolf@geomar.de, jschindlbeck@geomar.de

Delivery of aluminosilicate material to the oceans in the form of eolian dust and volcanic ash is controlled by a number of geologic and climate mechanisms. This material can provide a record of physical processes (e.g., tectonics, climate, volcanology) and is also an important part of biogeochemical cycling (e.g., nutrient delivery). In the NW Pacific Ocean, large inputs of volcanic ash from convergent arc systems (e.g., Izu-Bonin, Marianas, Kamchatka) and eolian dust from China are related to the tectonic evolution of volcanic arcs and Cenozoic climate.

Differentiating eolian dust from altered and unaltered volcanic ash, and distinguishing both from primary authigenic phases, is difficult [1]. This is further complicated due to the presence of a large, relatively unrecognized component of volcanic ash that is mixed into the bulk sediment ("dispersed" ash). This dispersed ash is quantitatively significant and is an under-utilized source of critical geochemical and tectonic information [2]. For example, volcanic ash may provide as much bioavailable nutrients (e.g., Fe) to the surface water as does the eolian sources [3]. Because all these phases are aluminosilicates with a small compositional range, distinguishing between them to a precise degree is best achieved by a combination of chemical and quantitative multivariate statistical treatments [2].

We here extend our earlier study of ODP Site 1149 by presenting an enhanced data set that allows higher resolution study of volcanic input to the Izu-Bonin system. Our new expanded study confirms the presence of a significant dispersed ash component at Site 1149 [2]. The aluminosilicates are likely composed of four end members, i.e., loess and three other ash components. Geochemical signatures (e.g., K_2O, Fe_2O_3) of the dispersed ash can be exploited to provide insight into the clay mineralogy (i.e., smectite), which is involved in the hydrologic budget of subducting sediments. We will also present results from discrete ash layers as compared to the dispersed ash.

[1] Ziegler et al., (2007) *EPSL* **254,** 416-432. [2] Scudder et al., (2009) *EPSL* **284**, 639-648. [3] Olgun et al., (2001) *Global Biogeochem. Cycles* **25,** GB4001.

Hydrochemical analyses to evaluate groundwater system in Horonobe Area, Hokkaido, Japan

M. SEGUCHI [1*], M. OHOKA[1], M. NAKAMURA[1], Y. ICHIKAWA[1], R. SAKAI [2], M. MUNAKATA[2], J.-I. ISHIBASHI[3]

[1]OYO Corporation, 2-2-19 Daitakubo, Minami, Saitama, Japan (seguchi-mariko@oyonet.oyo.co.jp)
[2]Nuclear Safety Reserch Center , Japan Atomic Energy Agency, Tokai-mura, Naka-gun, Ibaraki-ken, Japan (sakai.ryutaro@jaea.go.jp)
[3] Faculty of Science, Kyushu University, Fukuoka 812-8581, Japan (ishi@geo.kyushu-u.ac.jp)

For the safety assessment of a geological disposal of radioactive waste, it is important to establish validation method for estimating regional groundwater flow system.

In this study, first we collected more than 200 data of saline waters which were analyzed by JAEA and other organizations. And in order to indicate the mixing ratio of saline waters from different origins, the multivariate analyses were carried out based on the M3 (Multivariate, Mixing and Mass-balance) model developed by SKB (Laaksoharju et al., 1999) . We analyzed on these data in three cases where chemical components combinations are different. These combinations are as follows: 1.Cl^-, δ D, δ ^{18}O (the components which are not involved in water-rock reaction) 2. Na^+, K^+, Ca^{2+}, Mg^{2+}, Cl^- (the components involved in water-rock reaction) 3. Na^+, K^+, Ca^{2+}, Mg^{2+}, Cl^-, δ D, δ ^{18}O (all components) .

We tried to construct a hydrochemical model in the region where Neogene to Quaternary marine sedimentary rocks are deposited. The Wakkanai formation and the overlying Koetoi formation which consist of siliceous and diatomaceous mud-stones are the main targets of our study.

As the result of the multivariate analyses, four types of endmembers were extracted. They are: 1. surface water , 2. Cl-poor water (HDB-5) , 3. Cl-rich saline water (HDB-7), 4. Ca-rich saline water((HOKUSHIN R-1). Spatial plotting of these endmembers shows that high concentration part of HDB-5 water is distributed in deeper region where abnormal formation pressures were measured, and HDB-7 water is more rich in western site. This result suggests that in this area, there are some types of deep groundwaters which flow in different directions.

This study is regulatory support research funded by the Nuclear and Industrial safety Agency, Ministry of Economy, Trade and Industry, Japan.

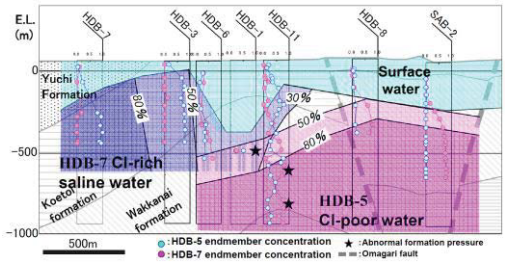

Figure 1: Projecting distribution of the endmenbers

[1] Laaksoharju et al., (1999) *Applied Geochemistry* **14#**, 861-871.

https://doi.org/10.1180/S0026461X00008434 Published online by Cambridge University Press

Interactions of U(VI) with archaea: what is different than with bacteria?

SONJA SELENSKA-POBELL[1*], THOMAS REITZ[1], AND MOHAMED MERROUN[2]

[1]Institute of Resource Ecology, HZDR, Dresden, Germany, s.selenska-pobell@hzdr.de (* presenting author)
[2]University of Granada, Granada, Spain, merroun@ugr.es

Archaea, in contrast to the diverse and dense bacterial populations, occur in uranium mining wastes in low numbers and belong mostly to particular crenarchaeal groups, some of them not yet cultured [1,2]. On the example of the termoacidophilic crenarchaeon *Sulfolobus acidocaldarius*, indigenous for many uranium contaminated wastes [3,4], we demonstrate that archaea tolerate substantially lower concentrations of U(VI) than bacteria and that they interact with this radionuclide in a significantly different way. One of the reasons for this behaviour is the unusual cell wall structure of the representatives of *Crenarchaeota* which is restricted to a single proteinaceous surface layer (S-layer), that is in contrary to the complex, rather thick, and rich on metal-binding ligands cell wall structure of bacteria. Due to the extreme acidic and mechanic stability of the *S. acidocaldarius* S-layer, it was possible to produce empty cells (ghosts) consisting only of the outermost S-layer membrane and to study their interactions with U(VI) at highly acidic (pH 1.5 and 3.0) and at moderate acidic (pH 4.5 and 6.0) conditions. Applying a set of modern spectroscopic techniques such as Time-Resolved Laser-induced Fluorescence (TRLF), X-ray Absorption, and Fourier-Transformed Infrared (FT-IR) we were able to demonstrate that at highly acidic conditions the *S. acidocaldarius* S-layer does not play any protective role against the toxic U(VI). At these conditions low amounts of uranium are bound mainly by the phosphate groups of the cytoplasma membrane [5]. This finding is in distinction to the results obtained with S-layers of the bacterial isolates recovered from uranium mining wastes. The S-layers of the latter bind significant amounts of U(VI) and strongly contribute to the remarkable uranium resistance of their hosts [6]. The high capability of the mentioned bacterial S-layers to bind U(VI) was atributed to the fact that they are phosphorylated [6]. This feature is unusual for both bacterial and archaeal S-layers and is not the case for the S-layer of *S. acidocaldarius* [6, 7]. At moderate acidic conditions (pH 4.5), typical for most uranium mining wastes, the studied archaeal S-layer ghosts, again in contrast to the bacterial ones, bind insufficient amounts of U(VI) exclusively via the carboxylic groups of their carboxylated amino acid residues [7]. At pH 6.0, which is substantially above the growth optimum of *S. acidocaldarius*, the permeability of its cells is increased due to the pH stress and possibly also to the presence of U(VI). As a result uncontrolled uptake of U(VI) as well as release of phosphorylated biomolecules and also of orthophosphate occurs. These processes result initially in formation and precipitation of mixed uranyl phosphate phases. With time most part of U(VI) is biomineralized in inorganic mineral phases. The efficacy of the biomineralization processes is, however, much lower then those published for bacteria, possibly due to the lower amount of polyphosphatic bodies in the studied archaeon [8]. We suggest that the limited presence of archaea in uranium wastes is related to their lower resistance to U(VI) which is determined by their cell wall structure and possibly also by some particular physiological and biochemical characteristics.

[1] Rastogi (2009) *Microbial Ecology* **58**, 129-139. [2] Reitz (2007) FZR-Report **459,** 42. [3] Marsh (1983) *FEMS Microb. Lett.,* **17**, 311-315. [4] Groudev (1993) FEMS Microb. Rev., **11**, 260-268. [5] Reitz (2010) *Radiochim Acta* **98**, 249-257. [6] Merroun (2005) *Appl. Environ. Microbiol.* **71**, 5532-5543. [7] Reitz (2011) *Radiochim Acta* **99,** 543-553. [8] Remonselez (2006) *Microbiology*, **152**, 59-66.

Novel Thermochronometric Techniques Applied to the Lavrion Detachment, Lavrion Peninsula, Attica, Greece

SPENCER SEMAN[1*], KONSTANTINOS SOUKIS[2], DANIEL STOCKLI[1], EMMANUEL SKOURTSOS[2], HARALAMPOS KRANIS[2]AND STYLIANOS LOZIOS[2]

[1]University of Texas at Austin, Jackson School of Geoscience, Texas, USA, spencer.seman@utexas.edu (*)
[2]National and Kapodistrian University of Athens, Athens, Greece,

The Lavrion Peninsula (SE Attica) is situated at the western boundary of the Attic-Cycladic Crystalline Complex (ACCC). The ACCC underwent blueschist to eclogite facies metamorphism during the Eocene followed by a greenschist facies overprint coincident with broad regional extension during the Miocene. This extension is generally attributed to the process of slab rollback and led to the formation of crustal scale detachments in the Aegean. In Lavrion, the dominant structure is a sub-horizontal detachment which juxtaposes lower plate rocks of the Kamariza Unit against the Lavrion Unit of the upper plate. Both units are dominated by greenschist facies calc-schists and marbles. The Lavrion Detachment (LD) is defined by a mylonitic zone which displays a top-to-SSW sense of shear. This is consistent with the overall sense of shear of the larger West Cycladic Detachment System (WCDS) exposed on the islands of Kea, Kythnos, Serifos and Makronisos directly to the east of the Lavrion Peninsula The LD, therefore, may represent the western most exposure of the larger WCDS. Exhumation of lower plate rocks along the WCDS on Kea, Kythnos, and Serifos occurred between 5-8Ma, 11-15Ma, and 5-8Ma, respectively[1]. In order to further constrain timing of movement on the LD and how it correlates to the WCDS, (U-Th)/He dating was conducted to understand the low temperature evolution of the lower plate and proximal upper plate rocks. Many upper and lower plate rocks (e.g. low grade calc-schists and marbles) of the LD are not conducive to traditional low temperature thermochronometric techniques so this study will employ titanite (U-Th)/He dating coupled with zircon and apatite (U-Th)/He where appropriate lithologies are present. Titanite is a common phase in greenschist facies calc-schists and possesses a closure temperature similar to zircon, making it an ideal chronometer for this study.[2]

[1] Grasemann (2012) *Lithosphere* **Volume 4**, 23-39.
[2] Reiners (1999) *Geochimica et Cosmochimica Acta* **Volume 63**, 3845-3859.

https://doi.org/10.1180/S0026461X00008434 Published online by Cambridge University Press

Modeling reactive transport of biogenic uraninite and its re-oxidation by Fe(III)-(hydr)oxides

S. S. ŞENGÖR[1*], J. GRESKOWIAK[2], H. PROMMER[3]

[1]Southern Methodist University, Dallas, USA, (* correspondence: sssengor@gmail.com)
[2]University of Oldenburg, Oldenburg, Germany
[3]CSIRO Land and Water, Wembley, Australia

Uranium contamination in the subsurface is a global problem in surface and groundwater, soils, sediments and related ecosystems due to its chemical and radioactive toxicity to human and ecosystem health. A promising strategy for in-situ remediation of U-contaminated subsurface is through stimulating iron and/or sulfate reducing indigenous bacterial species to catalyze the reduction of soluble U(VI) to insoluble U(IV) – uraninite (UO_2), typically accomplished by amending the groundwater with an organic electron donor. Thus, uraninite is generally regarded as the most desirable end product of this bioreductive process due to its low solubility, and hence stability under reducing conditions. However, it has recently been shown that once the electron donor is entirely consumed, the biogenic uraninite can be can be reoxidized (and remobilized) by Fe(III)-(hydr)oxides, which may potentially impede the cleanup efforts. Therefore, it is vital to understand the governing factors that control the redox behavior of the bioreduced uraninite with respect to uranium fate, transport, and long-term stability. Based on the experiments [1], a suitable biogeochemical reaction network was developed to integrate the experimental data and simulate these interactions in subsurface environments focusing on the role of sulfide, Fe(II), Fe(III) (hydr)oxides, and the effect of nanoscale particle size on the stability of biogenic uraninite and its reoxidation [2]. Model results showed that the oxidation of sulfide by Fe(III) directly competed with UO_2 reoxidation as thermodynamically, Fe(III) oxidizes sulfide preferentially to UO_2. The re-oxidation of UO_2 is thus shown to depend on the relative rates of UO_2 and sulfide oxidation by Fe(III), as well as to the activity of Fe(II) in solution [2]. The developed reaction network and the interplay that emerges between flow, physical transport and reactions has been further studied in 2-D numerical experiments that were based on the setting found at the South Oyster site, Eeastern Virgina [3]. These simulations included surface complexation of U(VI) and Fe(II) onto Fe(III) oxides, microbial sulfate reduction using acetate with reductive dissolution of ferrihydrite and considered a highly heterogeneous property distributions.

[1] Sani *et al.* (2004) *Geochim. Cosmochim. Acta* **68**, 2639–2648.
[2] Spycher *et al.* (2011) *Geochim. Cosmochim. Acta* **75**, 4426-4440 .
[3] Scheibe *et al.* (2006) *Geosphere* **2**, 220-235.

Biological productivity in the Subarctic North Pacific and Bering Sea: A proxy evaluation

SASCHA SERNO[1,2*], GISELA WINCKLER[1,3], ROBERT F. ANDERSON[1,3], CHRISTOPHER T. HAYES[1,3], HAOJIA REN[1], RAINER GERSONDE[4] AND GERALD H. HAUG[2,5]

[1]Lamont-Doherty Earth Observatory, Palisades, NY, USA, sserno@ldeo.columbia.edu (* presenting author), winckler@ldeo.columbia.edu, boba@ldeo.columbia.edu, cth@ldeo.columbia.edu, hren@ldeo.columbia.edu
[2]DFG-Leibniz Center for Surface Process and Climate Studies, Potsdam University, Potsdam-Golm, Germany
[3]Department of Earth and Environmental Sciences, Columbia University, New York, NY, USA
[4]Alfred Wegener Institute for Polar and Marine Research, Bremerhaven, Germany, Rainer.Gersonde@awi.de
[5]Geological Institute, ETH Zürich, Zürich, Switzerland, gerald.haug@erdw.ethz.ch

The Subarctic North Pacific (SNP) is one of the three principal HNLC (high nutrient low chlorophyll) regions in the modern ocean where biological production is limited. More than 20 years ago, John Martin and co-workers suggested that phytoplankton growth in the SNP is limited by iron which is mainly brought in by atmospheric eolian dust input from East Asian dust sources [1].

Productivity proxies (e.g., opal, carbonate, biogenic barium) show discrepancies in their interpretation from sediment cores in the SNP and Bering Sea for the last ~150 kyr. We will present results from a spatial survey of core-top sediments from 37 stations of the INOPEX cruise, with an extensive coverage of the whole SNP and Bering Sea. We will map and compare results from different productivity proxies (^{230}Th-normalized fluxes of opal, carbonate and biogenic barium) to evaluate the efficiency of the different proxies to reconstruct the spatial pattern in primary and export production with strong gradients across the SNP, as shown in studies of annual primary productivity estimated from the climatology of satellite ocean color observations [2] and of biological drawdown of pCO_2 [3]. Further, comparison with results from sediment trap studies will help to identify possible preservation problems for the different productivity proxies. First results indicate a good correlation between opal fluxes and published data of biological drawdown of pCO_2 in the northwestern and northeastern SNP. Results from this core-top study will be crucial for our ultimate goal to test the dust fertilization hypothesis over the last deglaciation using different dust flux and biological productivity proxies in sediment cores from the SNP.

[1] Martin and Fitzwater (1988) *Nature* **331**, 341-343. [2] Gregg et al. (2003) *GRL* **30**, 1809, doi:10.1029/2003GL016889. [3] Takahashi et al. (2002) *DRS II* **49**, 1601-1622.

https://doi.org/10.1180/S0026461X00008434 Published online by Cambridge University Press

The iron isotopic imprint of benthic iron release in suspended particles from the African oxygen minimum zone

SILKE SEVERMANN[1], DANIEL OHNEMUS[2] AND PHOEBE J. LAM[2]

[1]Institute for Marine and Coastal Sciences (IMCS), Rutgers University, New Brunswick, NJ, USA, silke@marine.rutgers.edu

[2]Woods Hole Oceanographic Insitution, 266 WOODS HOLE RD, Woods Hole, MA 02543

Continental margin sediments are increasingly being recognized as an important source of bioavailable iron to the open ocean. Benthic iron fluxes are particularly high in oxygen deficient ocean regions, such as the major Oxygen Minimum Zones (OMZs) off the African and South American west coasts. In these highly productive regions of the oceans, benthic (diagenetic) iron sources may be of similar importance to atmospheric iron sources. Iron isotopes are emerging as a powerful tool to trace the influence of reducing margins as a supply of iron to the open ocean. Redox recycling of reactive iron in the organic-rich shelf sediments imparts a characteristically light iron isotope signature on the benthic iron efflux. Aerosol iron, in contrast, typically resembles crustal material and shows no distinct isotope fractionation relative to average igneous rock. To examine the isotopic imprint of benthic iron release in oxygen deficient ocean regions we have measured the iron concentrations and isotope composition of suspended particles along two transects through the southern African OMZ at 13°S and 26°S. Dissolved and particulate iron concentrations are strongly elevated along the northern transect, which passes near the core of the OMZ. This pattern of high iron concentrations at intermediate depth suggests significant release of iron from the shelf sediments at bottom water oxyen concentrations <40μM. Despite this strong benthic release signal, iron isotope compositions of highly reactive Fe (0.5 M HCl leach at 60°C overnight) does not vary significantly from 0 ‰. At the southern sites, in contrast, overall sediment iron fluxes are smaller, but isotope compositions as low as -0.54 ‰ ($\delta^{56/54}$Fe, normalized to igneous rocks) are consistent with a diagenetic iron source from suboxic or anoxic sediments. Previous porewater studies have revealed a reversal in iron isotope fractionation during progression from suboxic/anoxic to sulfidic early diagentic reactions, potentially producing an iron efflux with isotope compositions close to 0 ‰ or even slightly positive. Consequently, rather than invoking an atmospheric signal at the northern site, we suggest a greater role for sulfides in the reduction and release of Fe^{2+} in the most oxygen-depleted regions of the OMZ. Light particulate isotope compositions at the southern site suggests that a significant proportion of dissolved Fe^{2+} is adsorbed or forms authigenic iron phases, and that particles are potentially an important vector for the transfer of reduced iron from the shelf to the open ocean. Results from this study provides a useful framework for the investigation of particles and their ispotope composition in the forthcomming GEOTRACES Pacific Section, which cosses the Peru OMZ.

Disturbance of the U/Pb and Th/Pb chronometers during low-T alteration of monazite.

A.-M. SEYDOUX-GUILLAUME[1*], J.-M. MONTEL[2], B. BINGEN[3], V. BOSSE[4], PH. DE PARSEVAL[1], J.-L. PAQUETTE[4], E. JANOTS[5] AND R. WIRTH[6]

[1] GET, UMR 5563 CNRS - Université Paul Sabatier - IRD, 14 avenue Edouard Belin, 31400 Toulouse, France. anne-magali.seydoux@get.obs-mip.fr
[2] G2R, CNRS, Ecole Nationale Supérieure de Géologie, Nancy-Université, BP 70239, 54056 Vandoeuvre-les-Nancy, France
[3] Geological Survey of Norway, 7491 Trondheim, Norway
[4] Clermont Université, CNRS UMR 6524, Université Blaise Pascal and IRD, 5 rue Kessler, 63038 Clermont-Ferrand France
[5] ISTerre BP 53, 38041 Grenoble CEDEX 9, France
[6] Helmholtz-Zentrum Potsdam, Deutsches GeoForschungsZentrum, Telegrafenberg, D-14473 Potsdam, Germany

Low-temperature alteration of monazite is documented in three centimetric monazite crystals from Norway (Arendal), Madagascar (Ambato), and Srilanka. The three crystals have different chemical compositions, especially regarding U, Th, Y and Pb contents and have ages ranging from 491 to 900 Ma. Optical and Electron microscope (SEM and TEM) images and electron microprobe analyses (EPMA) show that all of them share the same texture, suggesting an alteration reaction following which unaltered monazite (Mnz1) reacts to form a secondary, Th-U(-Y)-depleted, high-Th/U-monazite (Mnz2) associated with variable proportions of thorite ($ThSiO_4$), thorianite (ThO_2) and xenotime (YPO_4), depending on the initial composition of Mnz1. Images reveal variably intense fracturing, with cracks filled with Th-rich +/- Fe-rich phases. Monazite-xenotime thermometry demonstrates that Mnz1 interacted with a low temperature fluid. The alteration process is interpreted to follow a mechanism of fluid-present coupled dissolution-precipitation. Chemical dating with EPMA show no isochron age difference between primary and secondary monazite, except for the Ambato monazite, where altered domains are apparently older (750 Ma). U/Pb and Th/Pb isotope dating using LA-ICP-MS give dates consistent with EPMA dates, in pristine zones. However, in Mnz2, the systems are disturbed. In the case of Srilanka and Arendal, only $^{232}Th/^{208}Pb$ dates give a reasonable estimate of alteration age, respectively 450 and 864 Ma. U/Pb systems are disturbed due to common Pb contamination (up to 40%) and U fractionation relative to Th, responsible for depletion of U in altered monazites (and increase of Th/U). In contrast, for the Ambato monazite, both U/Pb and Th/Pb systems were affected and give inconsistent older dates for altered zones. This is attributed to significant common Pb contamination (up to 80%), also affecting all Pb isotopes and explained why electron probe ages were disturbed as well. Secondly disturbance results from Th-U-silicate contamination during measurement, due to the presence of high density of nano-phases and nano-fractures filled with Th-U-silicates, only visible using TEM. Finally, these results demonstrate the important role of radiation damage effects, in particular swelling-induced fracturing, and the essential role of porosity and cracks, which allow fluid (charged with elements) migration through the sample during this process.

https://doi.org/10.1180/S0026461X00008434 Published online by Cambridge University Press

Micron-scale imaging of the distribution of bio-available metals (Fe, Zn, Ni, Co) in modern and ancient microbial mats

MARIE CATHERINE SFORNA[1]*; PASCAL PHILIPPOT[1]; MARK VAN ZUILEN[1], ANDREA SOMOGYI[2], KADDA MEDJOUBI[2], PIETER VISSCHER[3] AND CHRISTOPHE DUPRAZ[3]

[1]Institut de Physique du Globe de Paris, Sorbonne Paris Cité, Paris, France; sforna@ipgp.fr (*presenting author)
[2]Synchrotron SOLEIL, Saint-Aubin, Gif sur Yvette, France
[3]Department of Marine Sciences, University of Connecticut, Groton, Connecticut, USA

Metals are essential micronutrients for all living organisms since they are used as structural elements or as catalytic centers in enzymes. Some, like Fe, are universally used, while others, such as Ni or Co, have a more limited biological function. Yet, they can be associated with enzymes that catalyze specific types of metabolism (e.g. N-assimilation). The evolution of these metalloenzymes likely reflects the variable paleogeochemistry of metals throughout Earth history. However, in addition to direct uptake for biological use, metals can be incorporated in bacterial exopolymer (EPS) constituting the biofilm matrix in microbial mats. The high chemical reactivity of such surfaces is ideal for metal cation scavenging, and thus leads to metal enrichment during diagenesis. Therefore, in order to use metals as tracers of past biological activity in the ancient rock record, knowledge of the mechanisms of metal uptake in living and diagenitically-modified microbial mats is required.

Here we present a study of the distribution of metals in modern and ancient stromatolites. These structures, ubiquitous in the rock record for the last 3.5Ga, have the potential to preserve biosignatures and are an excellent target for studies of metal tracers. We focused our study on 2.7Ga old stromatolites from the Tumbiana Formation (Western Australia) and on three modern stromatolites from the Bahamas (Storr's Lake, Big Pond and Highborne Cay).

In order to detect metal variation in the laminated organic fraction of stromatolite structures we used synchrotron-based scanning X-ray fluorescence technique. It was applied at the X-ray fluorescence microscopy line of the Australian Synchrotron. We used the Maia detector which consists of 384 detectors-elements. This permitted to perform multielemental imaging of ~cm sample areas with 2µm spatial resolution.

In modern stromatolites organic layers are enriched in metal with a general distribution of Fe, Zn >> Ni and Co. This enrichment becomes higher with increased degree of diagenesis. Indeed, the top of Big Pond's stromatolite contains high organic content linked to a low Fe content whereas the bottom shows lower organic content (diagenetic effect) and higher Fe content. Modern stromatolites, then, show clear evidence of early diagenesis where metals such as Fe, Zn display strong affinity for the organic layers. The ancient stromatolites from the Tumbiana Formation also show a strong metal enrichment in the organic fractions. In organic layers, Fe >Ni, Co > As, V, Ti > Zn are presents. Disseminated organic globules also show this general metal distribution. This could be evidence for pervasive fluid diagenesis in organic layers and of the preservation of the early diagenesis in organic globules. The high metal content in these samples confirms the strong affinity for organic fractions incorporating more and more type of metals with time.

Experimentally Determined Fe Isotope Fractionation between Metal and Silicate

ANAT SHAHAR[1*], MARY F. HORAN[2], JULIANA MESA GARCIA[1,3], TIMOTHY D. MOCK[2], VALERIE J. HILLGREN[1] AND LIWEI DENG[1]

[1]Geophysical Laboratory, Carnegie Insitution of Washington, Washington, D.C. , USA, ashahar@ciw.edu (* presenting author)
[2]Department of Terrestrial Magnestism, Carnegie Insitution of Washington, Washington, D.C., USA,
[3]EAFIT University, Medellin, Antioquia, Colombia

There has been much work done on quantifying the iron isotopic fractionation of naural samples but the mechanism(s) responsible for the measured fractionations is still largely unknown. Iron is not striaghtforward to understand because of its differing redox states and compatibility constraints. In this study we aim to understand the mechanism(s) responsible for iron isotope fractionation by performing high pressure and temperature experiments. We have varied the composition, temperature, and duration of the experiments. In particular we have examined the iron isotopic fractionation between metal and silicate with and without the influence of sulfur to represent a possible core formation model for Earth and Mars.

Experiments were conducted in a ½ inch piston cylinder apparatus at temperatures ranging from 1600°C – 1800°C at 1 GPa and for times ranging from 5 to 240 minutes. The run products were characterized, mechanically separated, dissolved and purified by anion exchange before introduction into a Nu Plasma II MC-ICPMS for isotopic analyses. It is crucial in these experiments to prove isotopic equilibrium so microprobe analyses, the three-isotope technique, and textures of run products were all utilized. Of the 50+ experiments conducted so far, fewer than 10% have passed all the requirements for isotopic equilibrium. However, in the experiments in which we are confident that equilibrium was achieved we find that there is a small but resolvable equilibrium iron isotopic fractionation factor between metal and silicate at high temperature, with the metal phase more enriched in $^{57}Fe/^{54}Fe$ than coexisting silicate.

Determining whether there is an equilibrium iron isotope fractionation between metal and silicate is central to understanding the Fe isotope signatures found within different meteorites and planetary bodies. The initial set of experiments duplicate the magnitude and direction of data from pallasite meteorites with higher $^{57}Fe/^{54}Fe$ in the metal than in coexisting olivine. And extrapolation of our results to the temperature of the Earth during core formation (~3000 K) results in an iron isotopic fractionaton of 0.08‰ between the core and mantle. By adding sulfur to the second set of experiments we can test how sensitive the iron isotopic fractionation is to a change in the surrounding ions as well as provide an analog to Mars.

https://doi.org/10.1180/S0026461X00008434 Published online by Cambridge University Press

Behavior of accessory minerals during Paleoproterozoic (1.9 Ga) weathering processes, Beaverlodge Ridge, NWT, Canada

PAUL SHAKOTKO*[1], LUKE OOTES[2] AND YUANMING PAN[1]

[1]University of Saskatchewan, Geological Sciences
phs090@mail.usask.ca
yup034@mail.usask.ca
[2] NWT Geoscience Office, Yellowknife, NT
luke_ootes@gov.nt.ca

Abstract

A well-preserved 1.9 Ga regolith that formed from a quartz-feldspar porphyry of dacitic composition at Beaverlodge Ridge, NWT, Canada, is overlain by a quartz arenite and has been overprinted by a greenschist facies regional metamorphism. Continental reconstruction placed Beaverlodge Ridge near the equator and thus tropical paleolatitude conditions at ~ 1.8 Ga [1]. The maximum AI and PIA values of 77 and 96, respectively, indicate heavy weathering during the formation of the Beaverlodge Ridge regolith. While Si, Fe, K, Ca, and Ti display an upward increase towards the unconformity, Na and Mg have been removed from the profile. Aluminum, Mn, and P remain relatively constant throughout the profile. These major element trends are inconsistent with other Paleoproterozoic regoliths (Gall, 1994; Pan and Stauffer, 2000) and are also inconsistent with a modern-day dacite weathering profile (Shangyi et al., 2007). Both of these show an upward loss in Ca. Subsequent analysis of the weathering rinds of porphyry in the quartz arenite shows a depletion in Ca relative to the altered porphyry. This suggests that the upward increase in Ca observed in the porphyry might be due to later overprinting events.

Electron microprobe analysis and back-scattered electron imaging reveal that accessory minerals such as zircon, allanite, and fluoroapatite in the Beaverlodge Ridge regolith are well preserved, whereas Fe and Ti oxides such as magnetite and rutile often display extensive weathering and show evidence of surface weathering such as etching and pitting. Zircon grains are sub- to euhedral, whereas allanite grains are anhedral. Fluoroapatite occurs in two different morphologies: 1) distinctly zoned, sub- to euhedral grains with overgrowth rims that often containing monazite inclusions within or adjacent to these overgrowths, and 2) lacking growthzones and monazite inclusions. Further morphological and compositional analyses of accessory minerals are underway to examine their roles in controlling the major and trace elements in the Beaverlodge Ridge regolith. These results are expected to shed new light on the oxic atmosphere ca. 1.9 Ga and lead to a greater understanding of GOE.

References

[1] Hou et al. (2008) Gondwana Research. **14**, 395-409.
Gall, (1994) Precambrian Research. **68**. 115-137.
Pan and Stauffer, (2000) American Mineralogist. **85**, 898-911.
Shangyi et al. (2007) Chinese Journal of Geochemistry. **26**, 4, 434-438.

OSMIUM CONTAMINATION OF SEAWATER SAMPLES STORED IN POLYETHYLENE BOTTLES

M. SHARMA[1]*, C. CHEN[1,2], T. BLAZINA[1,3] AND, K. LANDAU[1]

[1]Dept of Earth Sciences, Dartmouth College, Hanover, NH 03755 USA Mukul.Sharma@dartmouth.edu (* presenting author)
[2]Halliburton, 1805 Shea Center Dr, Suite 400 Highlands Ranch, CO 80129 USA
[3]Eawag, Überlandstrasse 133, 8600 Dübendorf, Switzerland.

A low blank-high yield procedure for the accurate determination of seawater osmium concentration and isotope composition has been developed. The resulting improvement in the detection limit reveals a subtle but significant temporal increase in the concentration of samples obtained during the GEOTRACES expeditions. This increase in Os concentration is accompanied by a decrease in the $^{187}Os/^{188}Os$ ratio of the water indicating contamination of waters from the storage bottles. These samples were stored in HDPE bottles. In comparison, analyses of another aliquot of water stored in a Teflon bottle show no Os contamination. Extending our analyses further to samples collected in LDPE bottles during SAFe expedition we find that the water has been contaminated. Additional investigations reveal that LDPE bottles could contribute large amounts of Os with an $^{187}Os/^{188}Os$ ratio that is distinctly lower than seawater. We also find that an acidified melted snow sample stored in an acid washed Teflon bottle is not contaminated after two years of storage. We conclude that the acidified seawater samples need to be stored in Teflon bottles for accurate and precise estimate of Os concentration and isotope composition. Consideration of reliable Os isotope data indicates that Os is not a conservative element and that the $^{187}Os/^{188}Os$ ratio of the surface water of the interior of the north Atlantic and north Pacific gyres is ~2-3% lower than that of the deep oceans. Additional analyses from the recently completed GEOTRACES cruise in the Atlantic are underway and will be presented.

https://doi.org/10.1180/S0026461X00008434 Published online by Cambridge University Press

Evidence of transport of Composition B colloids/nano-colloids in range soils

PRASESH SHARMA[1,*], MELANIE MAYES[1], AND GUOPING TANG[1]

[1]Oak Ridge National Lab, Subsurface Sciences Group, sharmap@ornl.gov (*presenting author), mayesma@ornl.gov and tangg@ornl.gov

Abstract

Munition constituents (explosive particles such as Composition B or simply Comp B) distributed heterogeneously at operational range sites from low-order denotations may be the source of contamination of TNT, RDX and HMX to underlying aquifers. Comp B consists of ~59% RDX, 40% TNT and 1% HMX. Mobility of these compounds in soils/groundwater may occur via dissolution of Comp B and/or via transport of Comp B particles/colloids. To determine this, we collected soils from the E horizon of Massachusetts Military Range (MMR) where RDX and TNT contamination was recently observed. Column experiments were conducted where Comp B particles (<2 μm) were applied on top of the MMR-E soil filled column and leached with background solution of 1 mM NaCl. Effluents were collected every hour and separated into two aliquots: 1) <1 μm (or total), 2) dissolved (<2nm) fractions. Each aliquot was analysed with HPLC to quantify TNT, RDX and HMX. Difference between the <1 μm and <2 nm fraction denotes the amount of TNT, RDX and HMX in the colloidal/nano-colloidal fraction.

Results showed that up to ~80% of TNT and between 40-50% of RDX and HMX in the system were transported in colloidal/nano-colloidal (>2 nm -1 μm). While comparing the breakthrough in <1 μm fractions, the breakthrough of RDX was the fastest followed by HMX and then TNT. While comparing breakthrough of dissolved vs colloidal/nano-colloidal fractions, the breakthrough of the colloidal fraction for TNT, RDX and HMX was relatively faster than the dissolved fraction. Using ATR-FTIR spectroscopy we were also able to identify Comp B colloids in column effluents.

Results conclude that: 1) Comp B particles may move as colloids/nano-colloids in soils, 2) Faster breakthrough of RDX and HMX suggests lower binding affinity whereas TNT binds more strongly to the soil matrix regardless of particle size and 3) The faster breakthrough of TNT, RDX and HMX in <1 μm fraction compared to the dissolved fraction suggests that Comp B colloids/particles may move in the subsurface with less retardation compared to dissolved TNT, RDX and HMX.

The results, for the first time, show evidence of colloidal transport of munition constituents in column systems. Transport of Comp B as colloids should thus be considered while studying contaminated field sites such as MMR. Current results will be compared with column experiments in which Comp B will be applied to intact MMR-E columns collected from the same site. Intact columns may contain fractures and macropores likely to enhance the propagation of colloidal phases.

Precise, accurate measurement of U-Th isotopes in a single solution by ICP-MS

REGINA MERTZ-KRAUS[1], KENNETH R. LUDWIG[1], AND WARREN D. SHARP[1*]

[1]Berkeley Geochronology Center, Berkeley, USA, rmertz@bgc.org, kludwig@bgc.org, wsharp@bgc.org (*presenting author)

U-series isotope measurements by ICP-MS commonly utilize separate runs for U and Th, and standard-sample bracketing to determine corrections for mass fractionation and ion counter yield. Here we present an approach where all information necessary to calculate a sample's age (aside from background/baseline levels) is determined while analyzing a single solution containing both U and Th. Such an internally calibrated procedure reduces any bias caused by distinct behavior of samples versus standards (e.g., matrix effects), eliminates drift, and offers simplicity of operation, calculation of preliminary ages in real time, and simplified analysis of errors and their sources. Hellstrom [1] developed a single-solution, internally calibrated technique for an ICP-MS with multiple ion counters (Nu Plasma), but to our knowledge such a technique has not been available previously for an ICP-MS with a single ion counter. We use a Thermo Neptune *Plus* multi-collector ICP-MS with eight movable Faraday cups and a fixed center cup/ion counter equipped with a high abundance-sensitivity filter (RPQ). We use Faraday cups to measure all masses except 230 and 234, which are generally measured on the ion counter with the RPQ detuned (i.e., set 50 volts below the acceleration voltage). Analyses are dynamic, with sequential axial masses of circa 229, 230, 233, 234, and 239. ^{238}U is maintained in cups throughout the analysis to avoid reflections and is used to normalize signal instabilities related to sample introduction. Each analysis has a three-part structure in which 1) background/baseline levels, 2) sample composition, and 3) peak-tails are sequentially measured. In step 1, multiplier dark noise/Faraday baselines plus background intensities at each mass are determined while aspirating running solution. During sample measurement in step 2, ion counter yields for Th and U are determined using signals of 300-500 kcps for ^{229}Th and ^{233}U by measuring ^{229}Th/^{238}U and ^{233}U/^{238}U ratios with the minor masses first on the ion counter and then in cups. Mass bias can be determined using the ^{233}U/^{236}U ratio of the spike, allowing the sample's ^{238}U/^{235}U ratio to be measured. In step 3, we monitor peak-tails at half-mass positions (229.5, 231.5, 234.5) and on mass 237 while aspirating sample solution. Tail measurement requires a distinct cup configuration to maintain 238 in the cups; however, no sample is consumed during automated cup reconfiguration.

We monitor the accuracy of ^{234}U/^{238}U ratios using CRM 145, which gives a weighted mean atom ratio of $(5.2899 \pm 0.0021) \times 10^{-5}$ (all errors 2 SEM), consistent with published and reference values. The reproducibility of ^{230}Th/^{238}U ratios is monitored using the Schwartzwalder Mine secular-equilibrium standard (SM). We detect no bias in ^{230}Th/^{238}U or ^{234}U/^{238}U ratios measured for SM at beam intensities ranging over a factor of four, consistent with accurate correction for IC yields. Aladdin's cave coral (AC-1), analyzed to check our method on carbonate, yields a mean age of 124.42 ± 0.37 ka, in agreement with published values. We are currently applying the method to corals, speleothems, pedogenic coatings, and tufas.

[1] Hellstrom (2003) *J. Anal. At. Spectrom.* **18**, 1346–1351.

https://doi.org/10.1180/S0026461X00008434 Published online by Cambridge University Press

Using ^{222}Rn, water isotopes and major ions to investigate a large alpine through-flow lake

GLENN D. SHAW[1*], AND ELIZABETH WHITE[1]

[1]Montana Tech of the University of Montana, Geological Engineering, Butte, MT USA, gshaw@mtech.edu (* presenting author)

Session 22a. Tracing Groundwater Variability

Geochemical and isotopic tracers in groundwater and surface water studies in montane catchments have become increasingly popular because monitoring wells are often sparse and terrain is complex (e.g. fractures and folds), which makes physical hydrogeologic methods difficult to characterize quantitatively. In this study several geochemical tracers (^{222}Rn, δ^2H, δ^{18}O, and major ions) were collected spatially in Georgetown Lake, Granite County Montana, a large montane lake with a surface area of 1489 ha. The geochemistry of nearby precipitation, surface water, and groundwater was also characterized to assess the chemistry of source waters mixing with the lake. Physical and chemical measurements were used to i) construct a water balance for the lake, ii) characterize groundwater flow locations and amounts with the lake, and iii) develop a conceptual model for geologic controls on groundwater-lake interactions. Stable isotopes were used in an endmember mixing analysis to separate the relative fractions of source waters mixing with the lake, a physical water budget was used to quantify the difference between groundwater inflows and outflows, and a radon mass balance was used to characterize the groundwater flow locations and amounts to the lake.

Results from the stable isotopes show three endmembers mix with the lake. They are precipitation (39%), groundwater (26%), and a strongly evaporated endmember (35%). The evaporated endmember is most likely groundwater and/or surface water that later evaporated after entering the lake. The physical water budget suggests little difference between groundwater inflows and outflows, but could not be used to quantify groundwater inflow or outflow amounts. The radon mass balance suggests that groundwater inflows to the lake are substantial. Based on the physical water budget, this implies that groundwater outflows are also significant and the lake is a through-flow lake. Radon measurements also show that nearly all of the groundwater inflows occur along the eastern side of the lake, which is underlain by carbonate bedrock. The western portion of the lake (~75% area) is underlain by western dipping Precambrian metasedimentary bedrock. The steep dip and limited groundwater elevations suggest that the western portion of the lake is losing. It appears that groundwater enters through fractures, caverns, and shallow alluvium from the carbonates, and groundwater exits through the western dipping bedding planes and fractures in the metasedimentary rocks.

The use of ^{222}Rn for determining groundwater discharge locations and amounts provides a simple, but crucial, method for developing the conceptual model in this study. The spatial measurements of ^{222}Rn elucidate groundwater interactions that could not be assessed by geology, water levels and physical water budgets alone. Even conservative water isotope mass balances were limited in characterizing the nature of groundwater-lake interactions.

The crystallization of Amorphous Calcium Carbonate (ACC), and the effects of magnesium and sulfate

SAM SHAW[1*], PIETER BOTS[1], JUAN-DIEGO RODRIGUEZ-BLANCO[1], CLIVE WOOD[1,2], ANDREW P. BROWN[2] AND LIANE G. BENNING[1]

[1]Earth Surface Science Institute, School of Earth and Environment, University of Leeds, Leeds, UK, s.shaw@see.leeds.ac.uk (* presenting author)

[2]Institute for Materials Research, University of Leeds, Leeds, UK

Many organisms use transient ACC during biomineralization, as a means to control the particle shape/size and structure (e.g. calcite, aragonite or vaterite) of the crystalline calcium carbonate formed. For example, sea urchin larvae produce highly elongated single crystals of calcite by the controlled deposition and transformation of ACC [1]. Organisms also adjust or control the crystallization pathway using inorganic ions, organic molecules and/or membrane structures. Resolving the mechanisms and kinetics of ACC crystallization in abiotic systems, and evaluating the role of inorganic additives (e.g. Mg and SO_4) is key to underpinning our understanding of biologically-controlled calcium carbonate formation. In particular, the pathway of crystallization from disordered hydrated ACC to fully crystalline calcite needs to be quantified.

Using *in situ* small and wide angle X-ray scattering (SAXS/WAXS) at fast time resolution (1 sec.) we studied the crystallization of ACC to vaterite/calcite in the absence and presence of variable Mg and SO_4 concentrations. We show that pure ACC crystallizes via a multi-stage process [2]. Firstly, hydrated and disordered ACC forms, then rapidly transforms to more ordered and dehydrated ACC; in conjunction with this, vaterite forms via a spherulitic growth mechanism. This is followed by Ostwald ripening of the vaterite particles, and finally transformation to calcite via a surface controlled growth mechanism. The presence of Mg in ACC significantly reduced the rate of crystallization and led to the direct formation of calcite (Mg = 10%), or various Ca-Mg-CO_3 polymorphs (Mg > 10%), including monohydrocalcite and dolomite (T>60°C) [3]. The presence of SO_4 did not alter the overall ACC crystallization mechanism, but reduced the rate of vaterite nucleation, growth and ripening due to surface adsorption [2]. Also, SO_4 dramatically increased the stability of vaterite compared to the pure system (i.e. stable for hours/days).

These results provide a comprehensive mechanistic description of the abiotic ACC crystallization pathway, with the final crystalline product being controlled by the initial ACC composition (e.g., Mg or SO_4 content). These abiotic crystallization mechanisms are similar to those observed in marine organisms [1], where it has been shown that secondary calcite nucleates within ACC, a process comparable to the secondary (vaterite) and tertiary (calcite) nucleation and growth observed in our systems.

[1] Killian *et al.* (2009) *J. Am. Chem. Soc.* **131,** 18404-18409. [2] Bots *et al* (2012) *J. Am. Chem. Soc* (Submitted). [3] Rodriguez-Blanco et al (2012a,b) *Geochim. Cosmochim. Acta*. (In Review)

https://doi.org/10.1180/S0026461X00008434 Published online by Cambridge University Press

Bioaccessibility and bioavailability of arsenic-bearing mine wastes via the inhalation pathway

SHDO, S.M.[1*], MOLINA, R.[2], BRAIN, J.[2] KIM, C.S.[1]

[1] Schmid College of Science, Chapman University, Orange, CA 92866, USA

[2]Harvard School of Public Health, Boston, MA 02114, USA

Due to extensive processing of ore from gold and silver mines in the Mojave Desert, CA, elevated concentrations of associated toxic metal(loid)s including arsenic (As) are often mobilized by the transport of mine wastes into surrounding communities. The fine-grained fraction of mine waste particles can readily become airborne and inhaled. making their bioaccesibility and bioavailibility extremely relevant.

Bulk samples were collected from a number of mines throughout the Mojave Desert and sieved to obtain fine size fractions. The size fraction was then ground using a ball mill to a size fraction (≤2.5 μm in particle diameter). The bioaccessibility of As as a function of pH was examined in phagolysosomal simulant fluid (PSF) Finally, the bioavailability of As was analyzed *in vivo* by intratracheally instilling the material.

Results from four different mine sites indicate that the mine wastes showed similar trends of arsenic dissolution within PSF, with the percent As released decreasing from pH 1.8-4.2 and then slightly increasing pH 5 (Figure 1). The As solubility at low pH is likely due to the dissolution of As-bearing mineral phases while the solubility at higher pH is likely due to the desorption of As sorbed to Fe-oxides. The *in vivo* studies will provide organ-specific bioavailability information which can be correlated with results from the PSF experiments.

This information will help to determine the operational pH for a PSF extraction that most accurately the *in vivo* outcome, with the eventual goal of developing a predictive bench-top bioaccessibility assay that can be used to estimate bioavailability of arsenic in mine wastes as introduced through the inhalation pathway.

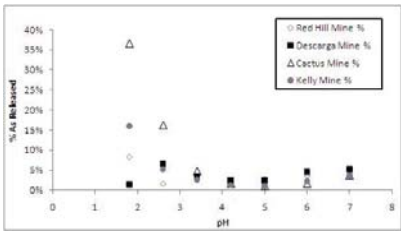

Figure 1: Percentage As released vs. pH

Extensive life on land ~1.1 Ga ago

NATHAN D. SHELDON[1*] AND MICHAEL T. HREN[2]

[1]Department of Earth and Environmental Sciences, University of Michigan, Ann Arbor, MI, USA, nsheldon@umich.edu* (presenting author)

[2]Department of Earth and Planetary Sciences, University of Tennessee, Knoxville, TN, USA, mhren@utk.edu

The precise timing of life's move onto land in the Precambrian, along with the extent of the terrestrial biosphere, is poorly constrained, with only a sparse record before the Neoproterozoic, known primarily from paleokarsts [1]. A recent study by Strother and colleagues [2] described the earliest non-marine eukaryotes from the ~1 Ga old lacustrine Diabaig Formation (Torridon Group, Scotland). Penecontemporaneous lakeshore and alluvial deposits well away from marine shorelines from Scotland also record microbially induced sedimentary structures [3]. Thus, at least locally, a significant and potentially diverse terrestrial biosphere was present, but the extent of the Mesoproterozoic terrestrial biosphere remains an open question.

Here, we present sedimentological and isotopic evidence for an extensive terrestrial biosphere preserved in sediments that are part of the ~1.1 Ga old Midcontinent Rift (MCR) of North America. The active rifting phase of the MCR was short-lived, from 1109 to 1087 Ma [4], and clastic sediments were deposited both as intrabasaltic units and as post-emplacement units. Rifting ceased due to Grenvillian compression to the East, which resulted in a partial re-closure of the rift. Penecontemporaneous intrabasaltic units from both sides of the rift in Minnesota and Michigan record a variety of sedimentary environments including paleosols [5-6], braid plains, alluvial fans, and lacustrine units; sites are currently >150 km apart, a distance that would have been significantly larger prior to the tectonic reversal caused by the Grenvillian compression. The sedimentary units have never been deeply buried or experienced any significant metasomatic alteration [5-6]. Microbially induced sedimentary structures including abraded Kinneyia, pustulose mound structures, multi-directional wave ripples, textured bedding planes, and stromatolites were recently documented [7]. Organic matter is also preserved on both sides of the rift in paleosols and microbial mat structures, as detrital carbon in laminated fluvial sediments, and occluded with the carbonate of lacustrine stromatolites in Michigan. "Clumped isotope" (Δ_{47}) analyses of stromatolitic carbonate range from 0.513–0.603 (± 0.004), which indicates carbonate formation temperatures of 35–60°C (±4°C), and that there was no significant post-burial heating of the preserved organic matter. $\delta^{13}C_{org}$ values range from -29.6 to -24.0‰, suggesting C fixation by photosynthesis. Some $\delta^{13}C_{org}$ depth profiles through paleosols indicate diffusive enrichment comparable to modern soils, which suggests that the microbial communities were present both at the soil surfaces and subsurface. Together, these various lines of evidence indicate an extensive terrestrial biosphere by ~1.1 Ga ago.

[1] Horodyski & Knauth (1994) *Science* **263**, 494-498. [2] Strother *et al*. (2011) *Nature* **473,** 505-509. [3] Prave (2002) *Geology* **30,** 811-814. [4] Ojakangas *et al*. (2001) *Sed. Geol.***141-142**, 421-442. [5] Mitchell & Sheldon (2009) *Precam. Res.* **168**, 271-283. [6] Mitchell & Sheldon (2010) *Precam. Res.* **183**, 738-748. [7] Sheldon (in press) *SEPM Special Paper*

https://doi.org/10.1180/S0026461X00008434 Published online by Cambridge University Press

Origin of the acidic rocks of the Early Permian Panjal Traps, Kashmir, India

J. GREGORY SHELLNUTT[1*], GHULAM M. BHAT[2], KUO-LUNG WANG[3], MICHAEL E. BROOKFIELD[4], JAROSLAV DOSTAL[5], AND BOR-MING JAHN[6]

[1]National Taiwan Normal University, Department of Earth Science,
jgshelln@ntnu.edu.tw (* presenting author)

[2]University of Jammu, Department of Geology
bhatgm@jugaa.com

[3]Academia Sinica Institute of Earth Sciences
kwang@earth.sinica.edu.tw

[4]Department of Environmental, Earth and Ocean Sciences University of Massachusetts at Boston
mbrookfi@hotmail.com

[5]Saint Mary's University, Department of Geology
jarda.dostal@stmarys.ca

[6]National Taiwan University, Department of Geosciences
bmjahn@ntu.edu.tw

Abstract

The Panjal Traps of northern India represent a significant outpouring of mafic and felsic volcanic rocks during the Early Permian and are synchronous with the opening of the Neotethys Ocean. Previous studies have suggested that the felsic volcanic rocks are derived by differentiation of mafic magmas. Dacites and rhyolites collected from the lower-middle portion of the volcanic pile near Pampore, Kashmir are peraluminous (ANCK > 1.0) in composition. Their whole rock I_{Sr} values are variable (I_{Sr} = 0.69307 to 0.71825) and indicate open system behavior of either Rb or Sr or both whereas their Nd isotopic compositions ($\varepsilon Nd_{(T)}$ = -8.6 to -8.9) are nearly uniform. The $\varepsilon Nd_{(T)}$ values and trace element (Th/Nb_{PM} > 4; Nb/U < 10; Th/Ta > 8) ratios suggest the rocks are derived from the crust. Major and trace elemental modeling suggest the likely source was from the middle crust rather than the lower or upper crust. Furthermore, the felsic Panjal Traps have trace element compositions similar to some felsic volcanic rocks and A-type granitic rocks from other large igneous provinces (e.g. Karoo, Parana and CAMP) and that they were likely derived by partial melting of an ancient crustal (i.e. T_{DM} = 1836 to 1937 Ma) source which experienced multiple episodes of crustal recycling. In contrast to other LIP felsic volcanic rocks, the acidic Panjal Traps are unique in that they were not derived from a mafic mantle source material. The heat required to melt the crust was likely due to the continuous injection of contemporaneous basaltic magmas which formed the majority of the mafic Panjal Traps.

Biogeochemistry Improves Prediction of Metal Bioaccessibility of Yard Soils in Tar Creek, USA

YONGMEI SHEN*, SUZIE SHDO, EMILY R. ESTES[1], AMI R. ZOTA[2], DANIEL J. BRABANDER[3], AND JAMES P. SHINE[1]

[1] Harvard School of Public Health, Boston, USA,
yshen@hsph.harvard.edu,
shdo100@mail.chapman.edu,
eestes@fas.harvard.edu,
jshine@hsph.harvard.edu

[2] University of California San Francisco, San Francisco, USA,
ZotaAR@obgyn.ucsf.edu

[3] Geosciences Department of Wellesley College, Wellesley, USA,
dbraband@wellesley.edu

Introduction

Heavy metal contamination in soils is ubiquitously observed due to mining, smelting, and industrial processes. Current approaches to determine the risk of metals via oral ingestion from soils are through operationally defined in-vivo or in-vitro tests. In addition, regulatory agencies often assume a default value as the bioavailable proportion of total metal. However, metal bioavailability in soil varies greatly based on their chemical forms, retention and releasing process, as well as exposure pathways. In order to better assess risks, it is necessary to bridge the gap between geochemistry, bioaccessibility and risk assessment of metals.

Method

In-vitro simple bioaccessibility extraction tests (SBET) and sequential extractions were conducted on yard soil samples collected from the Tar Creek Superfund Site, OK, a former lead and zinc mining area. In addition, we conducted SBET and sequential extraction on pure phase metal minerals and metal minerals spiked in a reference soil to determine the role of both speciation and soil matrix effects on metal bioaccessibility. X-ray absorption spectroscopy techniques were also used as a supplementary tool on a subset of yard soil samples. We applied statistic models to predict metal bioaccessibility in soils given metal distribution in the soil matrix.

Conclusion

Sequential extraction enables one to identify direct and potential hazardous metal fractions in soil in terms of being bioaccessible. Compared with total metal content, taking into account metal speciation in soil improves the estimation of the extent of bioaccessibility to different extents for different metals (Pb, Mn, Zn, Cd, Cu). The results help figure out the profound effects of mineralogical composition of metals, soil properties and particle size on determining metal bioaccessibility. Based on the results, site-specific metal biogeochemistry information might be able to be utilized to make metal bioavailability assessment more accurate.

https://doi.org/10.1180/S0026461X00008434 Published online by Cambridge University Press

Uranium adsorption by *Shewanella oneidensis* MR-1 in the presence of $NaHCO_3$

LING SHENG *, JEREMY B. FEIN

Civil Engineering and Geological Sciences, University of Notre Dame, Notre Dame. * lsheng@nd.edu (* presenting author)

There have been several previous studies that have measured the adsorption behavior of U(VI) onto non-metabolizing bacteria in experiments either devoid of dissolved CO2 or in systems open to the atmosphere. There is considerable evidence for extensive adsorption of U(VI) above pH 6-7 where the aqueous uranyl-tricarbonate aqueous complex dominates the aqueous budget of uranium. However, there is considerable uncertainty regarding the identity and thermodynamic stability of the bacterial surface complexes that cause this adsorption. It is particularly important to determine these parameters in order to model the effect of bacterial adsorption of U(VI) in a range of natural or engineered carbonate-bearing aqueous systems.

In order to constrain the stoichiometry and stability of the important U(VI)-bacterial surface complexes, we measured the adsorption of 60 ppm aqueous U(VI) as a function of $NaHCO_3$ concentration in solution from 0.0 to 30.0 mM. Experiments were conducted in 0.1 $NaClO_4$ to buffer ionic strength, and pH was varied from 3 to 9 in order to vary the extent of protonation of bacterial surface sites so that the sites that are important in U(VI) binding could be identified. All the experiments were conducted open to the atmosphere. The observed extents of U(VI) adsorption are independent of $NaHCO_3$ concentration in the system below pH 5. Above pH 5, the extent of adsorption decreases with increasing $NaHCO_3$ concentration, but the observed extent of adsorption in each case is greater than that predicted assuming only aqueous uranyl-carbonate complexation and neglecting ternary uranyl-carbonate-bacterial complexation.

We used a non-electrostatic surface complexation approach to model the adsorption data. The data require the existence of at least two uranyl-carbonate-bacterial surface complexes, and we use the observed adsorption measurements to constrain values for the stability constants for each of these complexes. The modeling results suggest the presence of additional uranyl-carbonate bacterial surface complexes than have been previously identified under conditions with elevated carbonate concentrations. These complexes can control the U(VI) adsorption behavior in systems with high carbonate concentrations and hence our results can be used to predict the extent of U(VI) adsorption onto bacteria in a range of natural and engineered systems.

Environmental monitoring of tungsten in Fallon, Nevada

PAUL R. SHEPPARD[1*], GARY RIDENOUR[2], AND MARK L. WITTEN[3]

[1]University of Arizona, Laboratory of Tree-Ring Research, Tucson, AZ USA, sheppard@ltrr.arizona.edu (* presenting author)
[2]Physician, Fallon, NV USA, docridenour@charter.net
[3]Odyssey Research, Tucson, AZ USA, mlwitten@yahoo.com

Environmental Monitoring in Fallon

Fallon, Nevada, USA, experienced a cluster of childhood leukemia beginning in 1997 [1]. Extensive research was conducted in Fallon by multiple entities to determine what might have caused this childhood leukemia cluster. For our part, we employed multiple techniques of environmental monitoring for metals in Fallon, including chemistry of airborne dust, lichens, surface dust, surfaces of tree leaves, and tree rings [2].

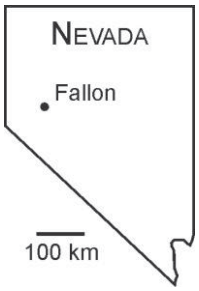

Figure 1: Map showing location of Fallon, Nevada, USA

Results

Tungsten and cobalt were elevated in airborne dust of Fallon relative to comparison towns. Tungsten and cobalt were elevated in lichen tissues within Fallon relative to desert sites outside of town. Surface dust showed tungsten and cobalt concentrations peaking just northwest of the center of Fallon relative to the outskirts of town. Leaf surfaces confirmed this spatial pattern of tungsten and cobalt peaking just northwest of the center of Fallon. Tree rings, a technique that emphasizes temporal resolvability, showed tungsten increasing in central Fallon by the mid to late 1990s, coinciding roughly with the onset of the cluster of childhood leukemia. Tree rings also showed high inter-tree variability in tungsten and cobalt across sampled trees within Fallon relative to comparison towns.

Conclusion

Fallon is distinctive by experiencing a cluster of childhood leukemia and having elevated airborne tungsten and cobalt. Linkage between a disease and an environmental condition cannot be made from environmental data alone. However, the co-occurrence in Fallon of elevated airborne tungsten and cobalt and a cluster of childhood leukemia logically should prompt biomedical research to evaluate the potential linkage between leukemia and the combined exposure to airborne tungsten and cobalt.

[1] Steinmaus et al. (2004) *Environmental Health Perspectives* **112**, pp. 766-771. [2] Sheppard, Ridenour, & Witten (2009) pp. 141-156 in *Airborne Particulates*, Cheng & Liu (Eds.), Nova Science Publishers, New York.

https://doi.org/10.1180/S0026461X00008434 Published online by Cambridge University Press

Multisite Surface-Complexation of Zn and Cu on Goethite

DAVID M SHERMAN*[1], DAVID MOORE

[3]School of Earth Sciences, University of Bristol, Bristol, BS8 1RJ, UK dave.sherman@bris.ac.uk (* presenting author)

Goethite (α-FeOOH) is the paradigm mineral for the scavenging of metals in terrestrial environments. The structure of goethite is based on edge-sharing FeO_6 octahedra which form double chains along the **b**-direction (using space-group setting Pnma); the double chains are linked to each other via corner-sharing in the **a**- and **c**-directions. At the nano-scale, goethite forms long needles along the **b**-direction with the {101} surfaces being dominant (Fig 1). The {101} surfaces have singly coordinated surface oxygens which can complex to metals via the formation of a bidentate double corner-sharing (2C) complex. However, the goethite needles are terminated by a {210} surface; on this surface, Zn and Cu could bind by forming an edge-sharing 2E complex (Fig. 2). The {210} surfaces comprise only a few per-cent of the surface area of goethite but we can infer that the {210} surfaces would be much more reactive than the {101} surfaces. We hypothesise that sorption of metals such as Zn and Cu to goethite will first take place on the more reactive {210} surface. However, since this surface only comprises a few percent of the total surface area the sorption capacity of the {210} surface will be limited to ~0.01wt % Cu or Zn.

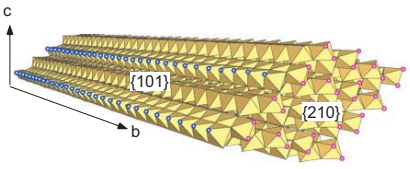

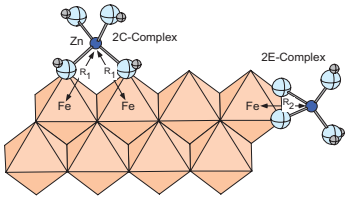

We have measured the sorption of Cu and Zn to goethite as a function of surface loading (0.008 to 0.8 wt. %). We find that our sorption edges can only be simultaneously modelled if we invoke several different surface complexes. For both Cu and Zn, the strong edge-sharing 2E complex on the {210} surface dominates at loadings < 0.01 wt. %. The weaker double corner-sharing 2C complex on the {101} surface dominates at loadings near 0.1 wt. %. Above 0.1 wt. %, both Cu and Zn form polynuclear complexes. Previous EXAFS studies of Cu [1] and Zn [2], at surface loadings > 0.1 wt %, only resolved 2C and polynuclear complexes of Zn or Cu on the {101} surface. However, at more environmentally relevant surface loadings, the 2E complexes on the {210} surface should be dominant. More powerful synchrotron sources (e.g., I20 at Diamond) will enable us to confirm the existence of the 2E complexes, at least for Zn.

[1] Peacock, L., & Sherman, D. M. (2004). *Geochimica et Cosmochimica Acta*, *68*(12), 2623-2637. [2] Trivedi, P., Axe, L., & Tyson, T. A. (2001). *Journal of Colloid and Interface Science*, *244*(2), 230-238.

Mercury in precipitation, sediments, and largemouth bass in FL: Insights using mercury stable isotopes

LAURA S. SHERMAN[1*] AND JOEL D. BLUM[2]

[1]University of Michigan, Earth and Environmental Sciences, Ann Arbor, MI, USA, lsaylors@umich.edu (*presenting author)

[2](Same as 1), jdblum@umich.edu

Mercury (Hg) concentrations in precipitation and fish are elevated across Florida (FL), U.S.A.[1] However, it is difficult to determine the specific biogeochemical pathways by which fish aquire Hg. Recent studies suggest that newly deposited Hg can be more bioavailable than Hg in sediments and that this Hg can rapidly enter aquatic food webs.[2] To gain insight into the sources of Hg to fish in FL, we analyzed Hg stable isotope ratios in precipitation, lake sediments, and largemouth bass collected across central FL.

We sampled surface sediments from freshwater lakes in central FL that are impacted by a mixutre of local and regional Hg sources. These surface sediments displayed a wide range of δ^{202}Hg values from -1.19 to -0.46‰ (mean = -0.72‰, 1 s.d. = 0.24‰, n = 18) and did not display significant mass-independent fractionation (MIF). Largemouth bass collected from a subset of these lakes displayed a range of δ^{202}Hg values and significant positive MIF (Δ^{199}Hg up to 4.43‰). We suggest that this MIF is due to photochemical degredation of methylmercury[3] prior to uptake into the food web. By using an experimentally derived fractionation relationship[3], we estimated δ^{202}Hg values of the fish methylmercury prior to photochemical processing and uptake. These δ^{202}Hg values were consistently offset from those of the corresponding sediments by 0.50‰ (1 s.d. = 0.14‰, n = 8). In addition, δ^{202}Hg values in the sediments were found to be correlated with the calculated δ^{202}Hg values for the fish methylmercury (r^2 = 0.47). These data suggest that methylmercury in the fish originates in large part from Hg in the sediments, which represents a mixture of historic Hg and modern atmospheric Hg. Prior to uptake by fish, non-photochemical processes[4, 5] cause an increase in δ^{202}Hg of ~0.50‰ and photochemical demethylation causes further increases in δ^{202}Hg values as well as large increases in Δ^{199}Hg values.

To examine the impact of a single, isolated source of Hg deposition on these relationships, we collected precipitation samples, lake sediments, and largemouth bass near a large coal-fired power plant in Crystal River, FL. These precipitation samples were uniquely characterized by large negative δ^{202}Hg values (mean = -2.56‰, 1 s.d. = 1.10‰, n = 28).[6] However, we did not observe similarly negative δ^{202}Hg values in sediments or fish collected in the area. Instead, δ^{202}Hg values of sediments and fish from the Crystal River area were comparable to those of the other lakes and were similarly offset and correlated. If emissions from the power plant have been isotopically consistent through time, this suggests that these emissions are not more rapidly bioavailable and are instead mixed with Hg in sediments prior to uptake by largemouth bass.

[1] Hand and Friedemann (1990) Florida Department of Environmental Regulation Report, 57pp. [2]Harris et al. (2007) *PNAS* **104**, 16586-16591. [3] Bergquist and Blum (2007) *Science* **318**, 417-420. [4] Rodríguez-González et al. (2009) *Environ. Sci. Technol.* **43**, 9183-9188. [5] Kritee et al. (2009) *Geo. Cosmo. Acta* **73**, 1285-1296. [6] Sherman et al (2012) *Environ. Sci. Technol* **46**, 382-390.

https://doi.org/10.1180/S0026461X00008434 Published online by Cambridge University Press

Natural Fe fertilization mechanisms in the Amundsen Sea Polynya, Antarctica

ROBERT M. SHERRELL[1,2]*, SILKE SEVERMANN[1,2], MARIA LAGERSTRÖM[1], KATHERINE ESSWEIN[1], KURIA NDUNGU[3], PER ANDERSSON[4], SHARON STAMMERJOHN[5], PATRICIA YAGER[6]

[1]Rutgers University, Institute of Marine and Coastal Sciences sherrell@marine.rutgers.edu (* presenting author) lagerstrom@marine.rutgers.edu kesswein@marine.rutgers.edu
[2]Rutgers University, Department of Earth and Planetary Sciences silke@marine.rutgers.edu
[3]Stockholm University, Applied Environmental Science kuria.ndungu@itm.su.se
[4]Swedish Museum of Natural History Per.Andersson@nrm.se
[5]INSTAAR, University of Colorado Sharon.Stammerjohn@Colorado.EDU
[6] University of Georgia, Sch. of Marine Programs pyager@uga.edu

The polynya of the Amundsen Sea, West Antarctica, is the most productive region of the Antarctic Shelf (~40 mg/m3 Chl-a in Dec. 2010), and is a test case for natural Fe fertilization, in stark contrast to the Fe-limited Antarctic Circumpolar Current (ACC) that borders this shelf region. ASPIRE (Amundsen Sea Polynya International Research Expedition, field work completed 2010-11), is an multidisciplinary study with a core emphasis on the mechanisms and pathways of bioavailable Fe delivery to the polynya euphotic zone. Candidate Fe sources include atmospheric deposition, upwelling of Modified Circumplar Deep Water, sea ice melting, glacier and iceberg melting, and inputs from shallow sediments. Samples for dissolved and particulate (>0.45um) trace metals and for Nd isotopes were collected at 35 stations in Dec. to early Jan. using a Geotraces-type CTD-rosette and in-situ pumps. Dissolved Fe (dFe) concentrations varying widely, and generally increase with depth. High values (up to 2nM) occur in near-bottom (~700m) waters of the western bathymetric trough and in the outflow from under the Dotson ice shelf (1nM at 150-600m). Lowest values (<0.1nM) are found in surface waters of the most productive central polynya region. Suspended particulate Fe (pFe), ranging 5-60nM, exceeds dissolved Fe throughout. Leachable fractions (LpFe; 25% acetic acid) range 0.2-16nM (2-35% of pFe), are lowest in the euphotic zone and highest in two important regions: at 50-600m where glacial meltwater-influenced flow emanates from under the ice shelf, and at ~300m adjacent to a drifting iceberg encountered in the southern polynya. Euphotic zone leachable Fe/P ratios are generally >10 mmol/mol, suggesting Fe-replete phytoplankton at most stations. Strikingly, Fe/P is very high (>1000 mmol/mol) and nearly identical at 50-150m in both the ice shelf and iceberg stations, suggesting that these are regions of injection of potentially bioavaible glacially-sourced LpFe into the upper water column. Dissolved Nd isotopes (<0.2um), a quasi-conservative tracer of continental sources, support the importance of glacial terrigenous inputs, with values as low as -6.0 at the ice-shelf outflow station (compare to adjacent ACC at ~ -8.0), tracing Fe inputs from radiogenic source rocks to shelf waters.

Inputs of dissolved and especially of labile particulate Fe resulting from flow under glacial ice-shelves are a major source of bioavailable Fe fueling productivity in the Amundsen Sea polynya.

Network of Terrestrial Subsurface sites in Precambrian Shields: Insights for Early Earth and Mars

B. SHERWOOD LOLLAR[1]*, T.C. ONSTOTT[2], T.L. KIEFT[3], L. LI[1], E. VAN HEERDEN[4], G.F. SLATER[5], D.P. MOSER[6], G. LACRAMPE-COULOUME[1], G. HOLLAND[7] AND C.J. BALLENTINE[7]

[1]University of Toronto, Toronto, Canada, bslollar@chem.utoronto.ca (* presenting author)
[2]Princeton University, Princeton, USA, tullis@princeton.edu
[3]New MexicoTech, Socorro, NM, USA, tkieft@nmt.edu
[4]University of Free State, Bloemfontein, South Africa, vheerde@ufs.ac.za
[5]McMaster University, Hamilton, Canada, gslater@mcmaster.ca
[6]Desert Research Institute, Las Vegas, USA, Duane.Moser@dri.edu
[7]University of Manchester, UK, chris.ballentine@manchester.ac.uk

Like the Lost City Hydrothermal Vents or Rainbow field, at depths of 2-3 km below the Earth's surface, saline fracture waters in the Precambrian Shields of Canada, Fennoscandia and South Africa are some of the most H_2 –rich on the planet and hence an important setting to investigate the planet's habitability – but significantly under investigated compared to the higher temperature hydrothermal systems and marine analog sites. The deep fracture waters host some of the deepest microbial communities yet identified on the planet: a low biomass, low biodiversity ecosystem subsisting at maintenance rates far from the photosphere – dominated by H_2-utilizing sulphate-reducing bacteria and H_2 derived from radiolysis and serpentinization [1,2]. These subsurface sites represent a critical environment in which to determine whether the types of chemolithotrophic life recognized at the vents are supported in the much larger segments of the Earth's crust where lower temperatures and hence slower rates of water-rock reaction prevail.

The tectonically quiescent, ancient fractured rock subsurface is directly relevant to single plate planets such as Mars, where surface expressions of volcanism such as hydrothermal vents are unlikely. Many of the investigated sites are located in northern regions in areas of continuous or semi-continuous permafrost, providing the opportunity to investigate psychrophilic life and hence as analogs for potential extinct or extant life on the icy planets and moons. Unlike high temperature seafloor systems like Lost City, where rapid fluid circulation and mixing means that the products of water-rock reaction such as H_2 rapidly diffuse away, the hydrogeologically isolated fracture waters in Precambrian Shield rock provide virtual "time capsules" in which, despite the slower rates of reaction, the products of water rock reaction and potential substrates for microbial life can accumulate and build up high concentration gradients over geological long time scales. The deepest and oldest fracture networks have residence time estimates derived from noble gas studies on the order of tens of millions of years [3], preserving a geochemical and microbial environment minimally impacted by hydrogeological mixing with the surface. They may provide a window into a different aspect of the Earth's biodiversity, but most significantly may preserve a more deeply branched and potentially evolutionarily older component of the Earth's life history with important implications for the origin and radiation of life on Earth. The deepest fracture water may even provide the opportunity to investigate controls on the biotic-abiotic transition and limits to life in the deep Earth.

[1] Lin et al. (2006) *Science* **314,** 479-482.
[2] Chivian et al. (2009) *Science* **322,** 275-278.
[3] Lippmann-Pipke et al. (2011) *Chemical Geology* **283,** 287-296.

https://doi.org/10.1180/S0026461X00008434 Published online by Cambridge University Press

High pressure constraints core formation from x-ray nanoscale tomography

YINGXIA SHI[1]*, WENDY L MAO[1, 2], LI ZHANG[3], WENGE YANG[4], YIJIN LIU[2], JUNYUE WANG[4]

[1]Stanford University, Stanford, USA, yingxias@stanford.edu*
[2]SLAC National Accelerator Laboratory, Menlo Park, USA
[3]Carnegie Institution of Washington, Washington, D. C., USA
[4]Argonne National Laboratory, Argonne, USA

Core-formation represents the most significant differentiation event in Earth's history. Percolation of liquid iron-rich alloy through a crystalline silicate matrix has been suggested as a possible core formation mechanism, especially for the differentiation of planetesimals during the early history of our solar system, since radioactive decay of short-lived isotopes in the small accreting bodies cannot provide enough heat to form extensive melting (i.e. magma ocean) [1-2]. Previous experimental results looking at dihedral angles in silicate metal samples synthetized at elevated pressures and temperatures suggest that percolation is unlikely to be an efficient mechanism in our planet [3-4]. However, experimental conditions in previous work have been limited in upper mantle conditions (<30GPa). Moreover the measurement of dihedral angles using transmission electron microscopy or backscattered electron microscopy may not generate satisfactory statistics. Nanoscale x-ray computed tomography (nanoXCT) has exciting potential as an accurate probe to study the 3D connectivity and permeability of core forming melts in crystalline silicates. Using a laser-heated diamond anvil cell, experimental conditions over the entire pressure-temperature range in the lower mantle can be accessed. In this study, we compressed and heated the mixture of iron-rich alloy + orthopyroxene, and then used a focused ion beam (FIB) to mill the quenched samples to extract a portion for nano-XCT. Pilot studies from our group using 3D nano XCT have demonstrated the ability to image the detailed morphology of the iron-alloy and silicates, along with details of Fe-FeS eutectic intergrowth patterns, which help to distinguish the relative Fe content in Fe and FeS. Data resulting from the combination of these techniques could improve our understanding of planetary core-forming processes.

[1] Keil *et al* (1997) *Meteoritics and Planetary Science* **32**, 349-363.

[2] Rubie, *et al* (2007) *Evolution of the Earth* **9**, 51-90.

[3] Shannon & Agee (1996) *Geophysical Research Letters* **23,** 2717-2720.

[4] Terasaki *et al* (2008) *Earth and Planetary Science Letters* **273**, 132-137.

Lead Adsorption on Iron-amended Composts

ZHENQING SHI,*[1] YEEWEI CHAN[1], AND JAMES HARSH[1]

[1]Washington State University, Pullman WA, USA, zhenqing.shi@wsu.edu (* presenting author)

Biosolids high in Fe have been shown to reduce the bioavailability of soil Pb both to plants and, when ingested or inhaled, to humans. We characterizing an Fe-rich compost that was developed to serve the same role as Fe-rich biosolids. The objectives of this work are (1) to determine the effectiveness of this material in lowering the bioavailability of Pb in soils (2) to characterize the nature of the reactive sites and their mechanism of metal sequestration. In this study, we (1) determine the capacity for Pb as a function of Fe concentration and Fe source, (2) assess the ability of Fe-compost to transform Pb in contaminated soils to highly recalcitrant states, and (3) model the distribution of Fe between organic- and Fe-sites.

Batch experiments were conducted to study the capacity of the iron-amended compost to adsorb Pb, including adsorption isotherms at various pH and adsorption edges at various initial Pb concentrations. For some selected experiments, the compost samples with varying iron contents were used to evaluate the effect of iron-amendment. Generally, the iron-amended composts showed high Pb adsorption capacity (> 3% Pb in composts), suggesting high concentrations of reactive organic matter and iron oxides in these compost samples. Lead adsorption increased with Fe concentration, suggesting that Fe sites played a role in increased adsorption.

The ability of iron-amended composts to sequester Pb in contaminated soils was investigated by incubating two contaminated soils with the compost samples at the field moisture content. We are evaluating the extractability of Pb in these treated soils with sequential extraction methods.

The preliminary modeling results with WHAM VI described the Pb adsorption results well using humic material and iron oxides as adsorbents. The modeling results also suggested that organic matter dominated adsorption at high Pb concentrations and adsorption to iron oxides was greatest at lower Pb concentrations. We are currently calibrating the model parameters with more data and comparing the performance of different speciation models, such as SHM and CD-MUSIC. We hope to acquire a quantitative understanding of the roles of both organic matter and iron minerals on Pb sequestration by the composts.

https://doi.org/10.1180/S0026461X00008434 Published online by Cambridge University Press

Uranium isotope fractionation associated with biostimulation experiments at the Old Rifle mill site

ALYSSA E. SHIEL[1]*, PARKER LAUBACH[1], THOMAS M. JOHNSON[1], CRAIG C. LUNDSTROM[1], KENNETH H. WILLIAMS[2] AND PHILIP E. LONG[2]

[1]Dept. of Geology, University of Illinois at Urbana–Champaign, Urbana, IL USA; ashiel@illinois.edu (*presenting author)
[2]Lawrence Berkeley National Laboratory, Berkeley, CA USA

Microbial and geochemical factors controlling subsurface U mobility are evaluated in the U contaminated aquifer at the former U mill site in Rifle, CO USA. Biotic reduction of U(VI) is induced by the injection of acetate (electron donor) into the contaminated aquifer and is used to immobilize U as U(IV). Experimental plots consist of monitoring wells both upgradient and downgradient of an injection gallery. The 2010–11 experiment (Plot C) was designed to isolate the impacts of reduction and sorption processes. Previous work has shown large shifts in $^{238}U/^{235}U$ (hereafter discussed as $\delta^{238}U$) accompany U(VI) bioreduction ($\Delta^{238}U = 1.05‰$) [1]. We provide the results of a more detailed study to increase confidence in the use of $\delta^{238}U$ as an indicator of U(VI) reduction and seek to apply this method to bioremediation experiments in which groundwaters are treated with acetate only or both acetate and bicarbonate (desorbs U from aquifer solids). In addition, this data set gives us, for the first time, $\delta^{238}U$ measurements during rebound of U(VI) concentrations as reduction wanes. This is particularly important as the long-term success of this remediation technique depends on the stability of sequestered U(IV).

We present groundwater U(VI) concentration and $\delta^{238}U$ results for two wells downgradient of the injection gallery; one of the wells (CD-01) was amended with acetate and the other (CD-14) with both acetate and bicarbonate. Preinjection values for the two wells are identical to those upgradient, within the uncertainties. For CD-01, the acetate injection upgradient led to a dramatic drop in [U(VI)] (from 165 to 10.6 ppb) and $\delta^{238}U$ (from 0.03 to -1.32‰), resulting from the preferential removal of ^{238}U as reduced U(IV). An excursion to greater $\delta^{238}U$ values during the period when [U(VI)] was at a minimum may be related to a contribution of relatively heavy U from nano-colloidal U(IV) in the filtered groundwater. After the amendment ceased, the groundwater [U(VI)] and $\delta^{238}U$ returned to approximately preinjection values. Lack of an increase of $\delta^{238}U$ above preinjection values is consistent with advection of U(VI) from upgradient, rather than reoxidation of U(IV), as the primary source.

For CD-14, a large increase in the [U(VI)] was induced by the bicarbonate injection (up to 415 ppb), while no change was observed in $\delta^{238}U$. This is in agreement with previous Rifle field experiments that revealed the absence of significant U isotope fractionation with adsorption–desorption of U(VI) [2]. The acetate injection led to a dramatic decrease in the [U(VI)] and $\delta^{238}U$ values (to 15 ppb and -1.19‰). The recovery of [U(VI)] and $\delta^{238}U$ is much slower for CD-14. Despite the return of [U(VI)] to preinjection values by the end of the field season, sustained U isotope fractionation (-0.43‰) is observed.

[1] Bopp *et al.* (2010) *Environ. Sci. Technol.* **44**, 5927–5933. [2] Laubach et al. (2010) *GSA Abstracts with Programs* **42**, 231.

Dissolved rhenium and molybdenum in rivers

ALAN SHILLER[1]*

[1]University of Southern Mississippi, Stennis Space Center, MS, USA, alan.shiller@usm.edu

Various workers have reported dissolved concentrations of Re and Mo in rivers and have generally concluded that sulfide weathering is the dominant source of these elements. This is based both on the well-known association of these elements with Black Shales as well as correlation with fluvial sulfate. We have examined the dissolved concentrations of Re and Mo in the Yukon River Basin in Alaska, the Loch Vale watershed, the lower Mississippi River, and the East Pearl River (Miss.). We find that fluvial sulfate correlates nearly 1:1 with estimates of non-carbonate calcium, suggesting that the fluvial Re- and Mo-sulfate correlations are not necessarily conclusive of a sulfide source. We also observe significant seasonal variability of Mo and sometimes Re in some rivers, suggestive of seasonal redox effects on element mobilization and transport.

https://doi.org/10.1180/S0026461X00008434 Published online by Cambridge University Press

Electrolyte Ion Adsorption at the Hematite/Water Interface: Cryogenic X-ray Photoelectron and Electrochemical Impedance Spectroscopic Studies

KENICHI SHIMIZU[1]*, ANDREY SHCHUKAREV[1], ANDRZEJ LASIA[2], JOSEPHINA NYSTRÖM[1], PAUL GELADI[3], BRITTA LINDHOLM-SETHSON[1], JEAN-FRANÇOIS BOILY[1]

[1]Department of Chemistry, Umeå University, Sweden, kenichi.shimizu@chem.umu.se (*presenting author)
[2]Department of Chemistry, University of Sherbrooke, Canada
[3]Unit of Biomass Technology and Chemistry, Swedish University of Agrecultural Sciences, Sweden

Hematite (α-Fe_2O_3) is a commonly occurring mineral in natural environments and its (electro)chemical attributes are of great importance to various geochemical and technological settings. A fundamental understanding of reactions taking place on hematite surfaces is particularly important in this regard. In this study, electrolyte ion adsorption and electrostatic potential development across the hematite/water interface are respectively probed by cryogenic X-ray photoelectron spectroscopy (XPS) and by electrochemical impedance spectroscopy (EIS).

Cryogenic XPS measurements are carried out on colloidal hematite particle surfaces equilibrated in 50 mM aqueous solutions of monovalent ions (Na^+, K^+, Rb^+, Cs^+, NH_4^+, F^-, Cl^-, Br^-, I^-) at pH 2-11. Results consistently reveal coexisting cations and anions both below and above the point of zero charge of hematite. Inverse correlation between pH dependent surface loadings and hydrous ionic radii is observed in both alkali metal ($Na^+ > K^+ > Rb^+ \approx Cs^+$) and halide ($F^- > Cl^- \approx I^- > Br^-$) ions. Ammonium ion sorption occurs through surface-bound NH_3 species (*e.g.* ≡Fe-OH···NH_3) shifting the protonation constant of the cation from pK = 9.3 in bulk solution to pK = 8.4 at the interface.

Hematite single crystal electrodes with various crystallographic orientations are used to obtain the pH dependence of electric surface potentials in NaCl and NH_4Cl solutions. Three distinct interfacial processes, space charging, electrical double layer, and adsorption of proton and/or electrolyte ions, are extracted by fitting experimental impedance data using an equivalent circuit model (Fig. 1). Double layer capacitance values vary with pH and exhibit a minimum at pH around 8.7, close to the point of zero charge of this mineral. This capacitance-pH behavior closely resembles that of the interfacial concentrations of electrolyte ions on colloidal hematite particles obtained by XPS. Our results reveal systematic effects of pH and electrolyte ion identity on the intrinsic activity of hematite surfaces.

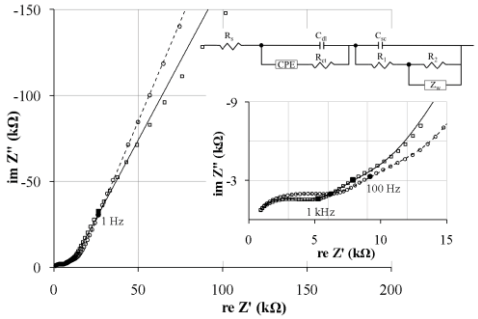

Fig. 1 *Complex plane plots of hematite in 0.1 M NaCl (pH 3.8, ○) and NH_4Cl (pH 3.5, □), including an equivalent circuit model.*

The Structure and reactivity of iron-organic matter coprecipitates

MASAYUKI SHIMIZU[1*], MARTIN OBST[2], ANDREAS KAPPLER[3], THOMAS BORCH[1,4]

[1]Department of Soil and Crop Sciences Colorado State Univervity, Fort Collins, U.S., masayuki.shimizu@colostate.edu (* presenting author)
[2]Center for Applied Geoscience Eberhard Karls University Tuebingen, Tuebingen, Germany, martin.obst@uni-tuebingen.de
[3]Center for Applied Geoscience Eberhand Karls University Tuebingen, Tuebingen, Germany, andreas.kappler@uni-tuebinge.de
[4]Department of Chemistry Colorado State University, Fort Collins, U.S., thomas.borch@colostate.edu

Introduction

Iron (Fe) (oxy)(hydr)oxides can have large specific surface areas and reactive functional groups, which make them important sorbents for soil nutrients, contaminants, and organic matter (OM). Thus, Fe oxides play a critical role in stabilizing soil organic matter. In the natural environment, pure Fe oxides, such as ferrihydrite, are rarely formed. For instance, OM can be incorporated in the ferrihydrite structure via coprecipitation, likely resulting inboth structual and reactivity changes. Despite the high natural abundance of Fe-OM coprecipitates, only few studies have attempted to determine their reactivity and characterize their chemical and physical properties. In this study, we synthesized Fe-OM coprecipitate with various methods, such as hydrolysis vs. oxidation and with different composition of OM, such as humic acid or fulvic acid. We then characterized the morphology, structure, and reactivity of these coprecipitates to gain new insight into how OM controls the biogeochemical cycling of Fe oxides.

Results and Conclusion

X-ray diffractometry (XRD) analysis indicated that coprecipitated OM did not change the crystal structure of 2-line ferrihydrite. Electrophoretic mobility (EM) analysis was conducted to study the impact of coprecipitated OM on the zeta potential of suspended Fe oxide particles between pH 5 and 9. The EM measurements clearly showed that the addition of OM resulted in more negatively charged partiles of coprecipitates compared to ferrihydrite. Particles with higher C/Fe ratios were more negatively charged than particles with lower C/Fe ratios. Scanning transmission X-ray microscopy (STXM) was used to obtain both two and three dimensional chemical maps of the Fe-OM coprecipitates as well as information about the most likely bounds formed between specific C and Fe surface functional groups. The STXM analysis indicated that Fe and C are evenly distributed within particles and that carboxylic-C may play an important role in complexation with Fe oxides. Complementary techniques, such as X-ray absorption spectroscopy, Mössbauer spectroscopy, TEM, SEM, specific surface area analysis were also conducted for the additional characterization. Our results indicate that both the ferrihydrite morphology and reactivity is strongly influenced when coprecipitated with soil organic matter.

https://doi.org/10.1180/S0026461X00008434 Published online by Cambridge University Press

Elucidating the Deep Sulfur Cycle: A Progress Report of Techniques and Findings

N. SHIMIZU*[1] AND C. W. MANDEVILLE [2]

[1] Woods Hole Oceanographic Institution, Woods Hole, USA, nshimizu@whoi.edu
[2] USGS, Reston, USA, cmandeville@usgs.gov

We have developed a SIMS method for in-situ determination of sulfur isotopic composition in silicate glasses has been developed, using a Cameca IMS 1280 ion microprobe. Calibrations were carried out for instrumental mass fractionation against well-documented natural and synthetic glasses with $\delta^{34}S$ ranging from -6 to +12‰. $\delta^{34}S$ in silicate glasses can be obtained with internal and external precisions ranging 0.4 – 0.7‰ (2σ). Accuracy is controlled by bracketing unknowns by repeated analyses of standards.

We used this method to determine ranges of natural variability in sulfur isotopic compositions in olivine-hosted melt inclusions from MORB, IAB and OIB to investigate how deep recycling of sulphur from oxidized and reduced surface reservoirs influences the sulfur isotopic compositions of mantle-derived melts. We found that (1) $\delta^{34}S$ of undegassed basalt MIs from arcs are most commonly heavy; Galunggung (Indonesia) ranging up to +10.7‰, Krakatau (Indonesia) to +8.8‰, and hydrous and highly oxidized (SO_4/total S =1) MIs from Augustine (Alaska) to +17.2‰, reflecting efficient recycling of oxidized sulfur into mantle wedge melting regions; and (2) Olivine-hosted melt inclusions from MORB and OIB display large variations in individual lavas; -10 to +10‰ for primitive FAMOUS MIs, -5 ~ +5‰ for depleted MIs from17°N (MAR), -6 ~ +2‰ for 26 – 29°N (MAR), among others, and MIs from 1960 Kilauea picrite range from -10 to -2‰. The variations are largest for MIs in Fo 90 – 91 olivines and appear to diminish as Fo decreases to Fo 82, reflecting the presence of large sulfur isotopic variability on local scales in the mantle and the effect of averaging during mixing of melt fractions prior to eruption of lavas.

It is evident that isotopic variations characterizing surface reservoirs survive during deep recycling. Elucidating co-variations with radiogenic isotopes and trace element abundance patterns will require a systematic approach to obtain sample suites that represent mantle endmember components.

U-Pb zircon ages of Early Archean gneisses from northern Labrador

M. SHIMOJO[1]*, S. YAMAMOTO[1], K. MAKI[2], T. HIRATA[2], Y. SAWAKI[3], K. AOKI[1], A. ISHIKAWA[1], Y. OKADA[4], K.D. COLLERSON[5], AND T. KOMIYA[1]

[1]Department of Earth Science and Astronomy, The University of Tokyo, Komaba, Meguro, Tokyo, 153-8902, Japan (*correspondence: shimojo@ea.c.u-tokyo.ac.jp)
[2]Laboratory for Planetary Sciences, Kyoto University, Kyoto, Japan
[3]Japan Agency for Marine-Earth Science and Technology (JAMSTEC), Kanagawa, Japan
[4]Department of Earth and Planetary Sciences, Tokyo Institute of Technology, Tokyo, Japan
[5]School of Earth Sciences, The University of Queensland, Brisbane, Qld. Australia

Early Archean crustal records are rare, but contiguous units are best preserved in N. Labrador and the NWT (Canada) and in SW Greenland. The Saglek-Hebron area (N. Labrador), located at the W. extension of the North Atlantic Craton (NAC), contains well-preserved Eo-Paleoarchean suites including pre-3.8 Ga Nanok Fe-rich monzodioritic gneiss, the Nulliak supracrustal assemblage (*ca.* 3.8 Ga), 3.7-3.6 Ga Uivak I TTG gneisses, 3.5-3.4 Ga Uivak II augen gneisses and Mesoarchean 3.2 Ga Lister gneiss [1-3]. Saglek dykes are present in the Eo and Paleoarchean gneisses, but not in the younger Lister gneisses. Despite confirmation of the antiquity of the area [3,4] a comprehensive zircon U-Pb dating with LA-ICPMS employing cathodluminescence (CL) imaging has not been undertaken for orthogneisses and supracrustal suites. CL images are essential to discuss inherited grains, pristine core and overgrowth.

We conducted LA-ICPMS U-Pb geochronological study of zircons from TTG Uivak I gneiss from the Saglek-Hebron area. The CL images of zircon grains display internal structures of oscillatory zoning and homogeneous core with overgrowth rim. Results show that samples collected as Uivak I TTG gneisses can be classified into three groups based on the distribution of zircon ages. The first group of TTGs is characterized by both presence of older zircons than 3.8 Ga, with the maximum age of 3914 ± 40 Ma in $^{207}Pb/^{206}Pb$ age, and apparent lack of 3.6 to 3.8 Ga zircons. These are obviously members of the Nanok gneiss. Based on intrusive relationships observed in the field, the Nanok gneiss is pre-date emplacement of the protoliths of the Uivak I gneisses. The second and third groups have clear peaks at 3.7-3.6 Ga and *ca.* 3.3 Ga in their age distribution of zircon cores, indicating that TTGs of the second and third groups correspond to Uivak I gneiss and the Lister gneiss, respectively. Importantly, overgrowth rims of zircons we analyzed here show *ca.* 2.7 Ga, which reflect zircon growth during late Archean thermal event in the NAC, possibly associated with assembly of different terranes within the gneiss complex. We show that the combination of *in-situ* U-Pb dating and CL imaging can reveal the tectonothermal history of early Archean from the gneisses in N. Labrador.

[1] Collerson (1983) *Lunar planet. Inst. Tech. Rep.* **83-03**, 28-33. [2] Schiøtte *et al.* (1989) *Can. J. Earth Sci.* **26**, 1533-1556. [3] Collerson *et al.* (1991) *Nature* **349**, 209-214. [4] Schoenberg *et al.* (2002) *Nature* **418**, 403-405.

https://doi.org/10.1180/S0026461X00008434 Published online by Cambridge University Press

Volatile inventory of excess degassing

HIROSHI SHINOHARA[1*]

[1]Geological Survey of Japan, AIST, Tsukuba, Japan.
shinohara-h@aist.go.jp (* presenting author)

Overview

Excess degassing is heterogeneous emission of volatiles and magma caused by gas-magma decoupling in the upper crust. There are two types of excess degassing caused by different mechanisms. Excess degassing by eruption is considered as the result of eruption of bubble accumulated magma [1] whereas excess degassing by non-erupting persistant degassing is driven by conduit magma convection [2]. Sulfur budgets of eruptions, in particular of silicic magmas at subduction zones, suggest that one to two orders of magnitude larger amount of sulfur than in the erupted magma was accumulated prior to the eruption. Composition of the accumulated gas phase can be estimated based on melt inclusion and solubility studies [1, 3], however, bulk volatile composition of the magma supplied to the shallow crust is hard to constrain based on those studies.

Persistent degassing emits about ten times larger amount of SO_2 than degassing by erutpion at subduction zone and is the major source of crustal degassing [2]. Conduit magma convection continuously transports magams stored at a deep chamber to a shallow vent and causes low-pressure degassing, resulting in almost complete magma degassing of volatiles species with low solubility, such as H_2O, CO_2 and S. Therefore, compositions of the persistent degassing would be a good approximate of bulk volatile composition of original magmas and provied important constraints to volcatile budget of the shallow crust.

Composition of Persistent Degassing

Quantitative estimates of Composition of persistent degassing became possible by application of FT-IR and Multi-GAS techniques to volcanic plume observation. Accumulation of such data for Japanese volcanoes suggests that magmas with a similar volatile comosition are supplied to different volcanoes. One of the most intensively degassed volcano in this century, is Miyakejima volcano, Japan, which emitted about 24 Mt of SO_2. The intensive degassing of started in 2000 and the SO_2 flux decreased by almost 100 times during ten years but gas compositions remained similar; H_2O/CO_2 (mol ratio) =50, CO_2/SO_2 = 0.7. Based on H_2O content of basalt melt inclusions, volatile contents in the original basaltic magma are estimated as H_2O=3.0, CO_2=0.15 and S=0.17 (wt.%) [4]. Other persistently degassing volcanoes in Japan have similar CO_2/SO_2 ratio of 0.5-2, indicating that subduction zone magmas are not always CO_2-rich. In contrast, there are some other subduction volcanoes, such as Stromboli, Masaya and Sourfiere Hills, which persistently discharge gases with larger CO_2/SO_2 ratios of 6-10. If the CO_2-rich magma is necessary to cause bubble accumilation at a deep chamber resulting in the excess degassing by erutpion, occurrece of the excess degassing might be coincident with the CO_2-rich persistent degassing. Further accumulation of the composition data of persistent degassing might reveal such coincidence, if any, and constrain the volatile budget in the upper crust.

[1] Wallace (2001) *J Volcanol Geotherm Res* **108**, pp. 85-pp. 106. [2] Shinohara (2008) *Rev Geophys* **45**, 2007RG0244. [3] Keppler (2010) *Geochim Cosmochim Acta* **74**, 646-600. [4] Saito *et al* (2010) J Geophys Res 115, doi:10.1029/2010JB007433. [5] Blundy *et al* (2010) *Earth Planet Sci Lett* **290**, 289-301.

Characteristic of the long-term accumulation of lanthanides on *Saccharomyces cerevisiae*

H. SHIOTSU[1], M. JIANG[1], Y. NAKAMATSU[1], T. OHNUKI[2] AND S. UTSUNOMIYA[1]

[1]Department of Chemistry, Kyushu University, Fukuoka 812-8581, Japan (utu@chem.rc.kyushu-u.ac.jp)
[2]Advanced Science Research Center, Japan Atomic Energy Agency, Tokai, Ibaraki 319-1195, Japan (ohnuki.toshihiko@jaea.go.jp)

Interaction between actinides and fissiogenic rare earth elements (REEs) and microorganisms have attracted increasing attention due to the ubiquitous occurrence of microorganisms in the subsurface environment and to implication to the safety assessment of nuclear waste disposal. Although the post-adsorption nanomineralization process of individual REE was proposed by a recent study [1], the contaminating fluid may contain a series of actinides and fission products. Hence, the present study has investigated the post-adsorption process on microorganisms in the system containing a series of lanthanides (Ln) to understand the effect of coexisting Ln on the adsorption and post-adsorption process.

S. cerevisiae (yeast) was harvested in a YPD (P-rich) media prior to the experiment. The yeast was then contacted with a P-free solution containing 14 lanthanide elements (La-Lu) upto 72 h, in which the concentration of individual Ln was 0.0063 mM with the total Ln concentration of 0.085 mM. The experiment was conducted at three pHs, 3, 4, and 5, and at two different temperatures, 25 and 4 ^{o}C (no metabolism). The analytical techniques include ICP-MS -AES, FESEM-EDX, and TEM.

During exposure in the solution at 25 ^{o}C, all Ln were eliminated from the solution by 24 h at pH 4 and 5, while 50 % of the initial amount remained in the solution at pH 3 after 24 h. Particle at the size of ~100 nm precipitated on the cell surfaces at pH 3, while ~30 nm-sized nanoparticles were observed at pH 4 and 5. These nanoparticles are phosphate containing a series of Ln. The nanoparticles at pH 3 had monazite strucure, while the particles formining at pH 4 and 5 were amorphous, indicating that crystallization took place only at pH 3. Deprotonation merely occurs at the funcional group at pH 3 as evidenced by the other experiments at 4 ^{o}C, and the nanocrystallites possibly nucleated from the locally saturated solution adjacent to the cell surfaces. In contrast, Ln electrostatically adsorbed to the functional group was bound to P released from inside cell at pH 4 and 5. Most likely the geometry of Ln complex formation prevented the crystallization.

As for the Ln pattern, the greater amount of light REEs was removed from the solution than that of heavy REEs. The difference between the distribution coefficient, K_d(ml/g), of LREE and of HREE increased with time increasing. At 24 h, the K_d rate Nd to Tm ($K_{d,\,Nd}/K_{d,\,Tm}$) is 1.72, 4.61, and 6.86 at pH 3, 4, and 5, respectively. The K_d ratios greater than 1 indicate the preferential uptake of LREE by the microorganisms, which may be attributed to the lower solubility products of REE phosphate [2]. The present study demonstrated that the cell surfaces play a key role on kinetics and crystal formation in the post-adsorption biomineralization.

[1] M. Jiang *et al.* (2010) Chemical Geology, 277, 61-69
[2] Z. S. Cetiner *et al*. (2005) Chemical Geology, 217, 147-169

https://doi.org/10.1180/S0026461X00008434 Published online by Cambridge University Press

Microbial Coenocline Associated with Geochemical Gradients at a Groundwater Discharge Zone

V.L. SHIROKOVA[1]* AND F.G. FERRIS[2]

[1] University of Toronto, Toronto, Canada, vshi@geology.utoronto.ca
[2] University of Toronto, Toronto, Canada, grant.ferris@utoronto.ca

Abstract

A combined metagenomic, geochemical, and statistical investigation was used to characterize a groundwater spring with a dramatic electrochemical gradient. Eh, pH, precipitated iron, and sulfate concentration increased downstream of the source. The ferrihydrite saturation index, as well as ferrous iron, ferric iron, sulfide, ammonium, and nitrite concentration decreased downstream. A total of 672 clones were compiled into a cDNA library, with taxonomic identities across 9 phyla, including *Acidobacteria, Actinobacteria, Bacteroidetes, Chlorobi, Chloroflexi, Firmicutes, Nitrospirae, Planctomycetes,* and *Proteobacteria.* The variation in the relative abundance of the OTU phyla in response to geochemical parameters was modeled using coenoclines. *Alpha-proteobacteria* were the most sensitive to geochemical change, while *Acidobacteria* were least sensitive. Spearman's rank correlation coefficients were used to evaluate the relationship between geochemical variables and relative abundance of microbial OTU. Reduction-oxidation potential appears to be an overarching parameter in the stream, controlling the distribution of redox species and leading to strong segregation of microbial functional groups. Our study of Ogilvie Creek represents one of the first to combine geochemical, metagenomic, and statistical analysis in an effort to gain insight on the interrelationships between biogeochemical processes in natural systems.

Determining reactive thiol concentration in naturally occuring organic molecules

ELIZABETH M. SHOENFELT[1], CLARESTA M. JOE-WONG[2*], NYSSA M. CROMPTON[3], EMILY A. JAYNE[3], SATISH C. B. MYNENI[3]

[1] Department of Geosciences, Princeton University, Princeton, USA, eshoenfe@princeton.edu
[2]Departments of Geosciences & Chemistry, Princeton University, Princeton, USA, cmjoe@princeton.edu (*presenting author)
[3]Departments of Geosciences & Chemistry, Princeton University, Princeton, USA

Thiols, components of soil and aquatic organic molecules, exhibit high affinity for soft Lewis acids such as Cd^{2+} and Hg^{2+} and play an important role in metal speciation in natural waters. However, thiols' low abundance, high reactivity, and structural similarity to other reduced-S ligands such as methionine make their detection difficult. We propose a novel method to measure thiol concentrations in natural systems using the water soluble, charged, thiol-sensitive fluorophore monobromo(trimethylammonio)bimane (qBBr), which fluoresces upon binding to a thiol. Once the sample's natural fluorescence is subtracted out, a solution's fluorescence intensity is proportional to the concentration of thiol-bound fluorophore. By measuring the fluorescence intensities of a series of solutions with fixed sample concentration and increasing fluorophore concentrations, the saturation point can be calculated, giving the sample's thiol concentration. This method accurately estimates thiol concentrations in pure thiol-containing solutions, dissolved organic matter (DOM), and microbial cell membranes. Moreover, the presence of other chemical species often found in natural systems does not influence this method's sensitivity.

When pure glutathione or cysteine solutions were examined, this method produced an estimated thiol concentration within 1.85% of the expected value at micromolar concentrations, and within 7.40% at nanomolar concentrations. Although species such as dissolved salts, carboxylic acids, and other organo-sulfide groups might affect the absolute fluorescence intensity of the thiol-bound fluorophore, we found that these species do not interfere with determining the thiol concentration. Testing glutathione solutions with dissolved magnesium chloride in 500-fold excess resulted in calculated saturation values accurate to 6.40%. Likewise, adding up to 15-fold excess malate, a surrogate for carboxylic acids common in DOM, does not affect accuracy. Similar tests show that qBBr does not react with other sulfur groups such as disulfides and thioesters.

Using the technique developed for model systems, thiol concentrations in the DOM pool and microbial biopolymers can be calculated. The cell membrane thiol concentrations of three model microorganisms common to natural systems—*Bacillus subtilis*, *Shewanella oneidensis*, and *Geobacter sulfurreducens*—were estimated. *G. sulfurreducens* exhibited the highest thiol concentration, and *B. subtilis* the lowest. The calculated thiol: dissolved organic carbon ratio in surface water DOM from the Pine Barrens in New Jersey is approximately 10^{-3}-10^{-4}. Estimation of thiol concentration is necessary to understand the role of thiols in contaminant and nutrient speciation and transformation, and this method offers a simple way to measure thiol concentrations in natural systems.

https://doi.org/10.1180/S0026461X00008434 Published online by Cambridge University Press

Compositional trends of Icelandic basalts: Implications for short-length scale lithological heterogeneity in mantle plumes

OLIVER SHORTTLE* AND JOHN MACLENNAN

University of Cambridge, Department of Earth Sciences, Cambridge, UK, os258@cam.ac.uk (* presenting author), jcm1004@cam.ac.uk

Lithological variations in the mantle source beneath mid-ocean ridges and ocean islands have been proposed to play a key role in controlling melt generation and basalt composition. Iceland, as an extremum of oceanic crustal thickness and positioned at the centre of a long wavelength geochemical enrichment in Mid-Atlantic Ridge basalt chemistry, is an excellent place to study the relative importance of source lithology, mantle potential temperature and mantle flow field in generating melting and compositional anomalies on the Earth.

We begin by looking specifically at the major element composition of the end-member Icelandic melts, to constrain the lithologies contributing to melting. End-member melt compositions are identified using a plot of whole rock Nb/Zr against MgO, and coloring the points by a second major element. With a large dataset, as exists for Iceland, a plot such as this allows the effect of concurrent mixing and crystallisation on basalt major element chemistry to be separated from the geochemical variability which is mantle in origin. Applying this technique we identify the enriched end-member melt on Iceland to have higher FeO (11.3 wt%) and lower CaO (11.2 wt%) than the depleted melts (9.2 wt% FeO and 12.9 wt% CaO). To relate these end-member melt characteristics to source lithology we compare their compositions to a dataset of experimental partial melt compositions from the literature, produced from melting at a range of pressures, melt fractions and of peridotitic and pyroxenitic starting lithologies. Traditionally, experimental partial melts and natural melts have been compared graphically. In contrast, we quantify the difference between the basalt compositions across the major oxides (CaO-FeO-MgO-Al_2O_3-SiO_2) and, accounting for uncertainties, identify those experimental melts most like the end-member Icelandic basalts. The key result of this analysis is that no single source lithology available in the literature can account for the major element variability observed on Iceland, with the enriched Icelandic melt compositions requiring their source to have been refertilized by addition of up to 40% mid-ocean ridge basalt.

Significant refertilization of the enriched source beneath Iceland means that it will be more fusible than a KLB1-like peridotite, and as such will be over-represented in accumulated melts compared with its abundance in the source. The likely abundance of enriched material in the Icelandic source was estimated to be ~10%, by taking this bias into account and weighting observed compositions by erupted volume. To investigate whether this fraction of enriched material can account for the high crustal thickness at Iceland (up to 35 km) we develop a bi-lithologic peridotite-pyroxenite melting model in which the latent heat of melting of both the enriched and depleted material are considered - allowing for the effect of significant amounts of fusible source material on melt production to be assessed. This modelling demonstrates that with 10% pyroxenite in the source, significant temperature anomalies (+200K) and a plume driven mantle flow field are required to generate crustal thickness as high as observed in central Iceland.

A dedicated “clean lab” sampling facility for studying the natural filtration of trace metals by soils: the artesian springs of the Elmvale Groundwater Observatory

WILLIAM SHOTYK, BOCOCK CHAIR FOR AGRICULTURE AND THE ENVIRONMENT

Department of Renewable Resources, University of Alberta, 839 General Services Building, Edmonton, Alberta T6G 2H1 shotyk@ualberta.ca

Increasing, elevated concentrations of trace metals in the surface layers of soils may result from a diverse array of anthropogenic, atmospheric sources, in addition to chemical weathering of parent material and other natural sources. There is considerable, ongoing concern about the fate and transformations of these elements, and their eventual release to surface waters and groundwaters. The first step in this process is their release to the soil solution, and the first step in beginning to understand these processes is to obtain representative water samples for testing and analysis. The Elmvale Groundwater Observatory (Springwater Township, Ontario) consists of two dedicated groundwater sampling systems designed exclusively for the analysis of trace metals. One well was constructed entirely of surgical stainless steel, the other made using acid-washed high density polyethylene (HDPE). Both wells are artesian flow systems. Using ICP-SMS and the clean lab methods developed for polar snow and ice, it is possible to measure all of the trace metals of contemporary environmental interest. Sampling the water within a laminar flow clean air cabinet helps to eliminate variability by protecting the samples from anthropogenic aerosols in ambient air. Many trace metals such as Cr and Pb are found at concentrations (1 ng/L) significantly lower than the Arctic ice from the mid-Holocene (ca. 4 K to 8 K yr BP). Groundwater quality monitoring programs undertaken in the same region typically show “concentrations” for the same trace metals which are three orders of magnitude greater (1 µg/L) because of the introduction of colloids during sampling. The purpose of our studies is analytical and academic whereas the monitoring studies are intended to ensure that metal concentrations in groundwaters do not exceed the relevant water quality guidelines. Illustrative results of the two approaches are presented and their implications compared, with a view to better understanding the mechanisms of natural filtration of water by soils as well as analytical procedures to better characterize soil water quality.

https://doi.org/10.1180/S0026461X00008434 Published online by Cambridge University Press

Reconstructing anthropogenic, atmospheric emissions of trace metals using environmental archives: comparison of polar snow and ice, ombrotrophic peat bogs, *Sphagnum* moss from herbaria, and lake sediments

WILLIAM SHOTYK, BOCOCK CHAIR FOR AGRICULTURE AND THE ENVIRONMENT
Department of Renewable Resources, University of Alberta, Edmonton, Alberta, Canada T6G 2H1
shotyk@ualberta.ca

Given the long history of mining and metallurgy, many trace elements of contemporary environmental interest have been released to the environment since Antiquity. Reconstructing anthropogenic emissions requires suitable archives to provide records extending sufficiently far back in time to allow the natural fluxes and sources to be determined, for comparison with modern values. A number of archives have been employed to reconstruct historical records of atmospheric trace elements, each with its inherent advantages and disadvantages.

Ice cores from the Arctic and peat cores from ombrotrophic bogs both receive inputs of Pb exclusively from the atmosphere. Using examples from Devon Island, Nunavut, Canada and Etang de la Gruére, Jura Mountains, Switzerland, it was found that

1) the natural ratio of Pb to Sc was effectively constant for thousands of years and comparable values were found in both archives; this supports the hypothesis that natural atmospheric Pb was effectively dominated by soil dust particles supplied by weathering of crustal rocks.

2) anthropogenic Pb inputs to the Arctic are clearly seen in ice layers ca. 3,000 years old, with pronounced Pb enrichments and declines in $^{206}Pb/^{207}Pb$ ratios in samples from the Roman and Medieval periods, supporting the hypothesis that human activities have dominated atmospheric Pb inputs for three millenia.

3) although Pb enrichments have declined during recent decades, even in the most recent snow samples, the Pb/Sc and Pb isotope data show that 90 to 95% of the Pb is still anthropogenic.

Although *Sphagnum* moss from herbaria do not extend back in time further than ca. 200 years, they received trace metals exclusively from the atmosphere, the date of sample collection is known exactly, and they are not affected by chemical diagenesis in acidic, anoxic bog waters. The isotopic composition of atmospheric Pb obtained using peat cores from Europe (dated for the past ca. 150 years using ^{210}Pb) are in excellent agreement with the records for the same interval preserved in *Sphagnum* moss from herbaria.

Comparing the isotopic composition of Pb in recent layers of lake sediments from the Kawagama Lake watershed in central Ontario with a peat core from a local bog shows that the sediments are a much less sensitive indicator of atmospheric change, largely failing to record the declines in $^{206}Pb/^{207}Pb$ ratios since the elimination of leaded gasoline, and the growing relative importance of Pb from smelters in northern Ontario and Quebec.

The *in situ* occurrence of bacteria on gold grain surfaces: Implications for bacterial contributions to gold nugget structure and chemistry

JEREMIAH SHUSTER[1*], CHAD JOHNSTON[2], NATHAN MAGARVEY[2], ROBERT GORDON[3] NEIL BANERJEE[1] AND GORDON SOUTHAM[1]

[1]Department of Earth Sciences, The University of Western Ontario, London, Canada, jshuster@uwo.ca (*presenting author)
[2]Department of Biochemistry & Biomedical Sciences/Chemistry and Chemical Biology, McMaster University, Hamilton, Canada
[3]Advanced Photon Source, Argonne National Laboratory, Lemont, USA

16a. Microbe-mineral interactions in time and space

Natural gold grains often possess secondary gold as colloidal particles, crystalline gold and bacteriomorphic structures. The latter form known as 'biogenic' gold that was first reported as structures resembling gold-encrusted microfossils on placer gold specimens [1]. Recent research suggest that Bacteria and Archaea are involved in the biogeochemical cycling of gold [2, 3, 4]. In this study gold grains from sediment sampled from Rio Saldana, Colombia were analyzed for the purpose of better understanding the formation of secondary gold in a tropical placer environment. Morphological analysis, using scanning electron microscopy, demonstrated that gold grains appeared as elongated disk shapes with articulated surfaces occurring predominantly on the perimeter. Bacteria were directly and indirectly attached as biofilms on the articulated surfaces of all gold grains. Iron oxide occurred on some grains as globular and patina coatings possessing casts of bacteria. The grains also possessed micron size secondary gold textures occuring on the outer periphery of the grains. Compositional analysis, inferred from energy dispersive spectroscopy and x-ray absorption fine structure, indicated that trace silver, mercury and copper was associated with gold. Unlike silver, mercury and copper appeared to have localized regions of heterogenous distributions throughout the gold grain. A pure bacterial culture, isolated from a single gold grain, was identified as *Nitrobacter* sp. 263 based on 16S sequencing. This *Nitrobacter* sp. removed gold from a gold (III) chloride solution within an hour. Transmission electron microscopy and scanning electron microscopy demonstrated that gold immobilization occurred as abundanct colloids and octahedral platelets less than 100 nm in diameter concentrated within the cell envelope. The occurrence of secondary gold on the surface of these grains and the ability of *Nitrobacter* to form crystalline gold suggests that this organism may contribute to the growth of gold grains in this placer environment. Gold biomineralization would be continuous if concentrations of aqueous gold input are low and bacterial metabolic growth is maintained by reproducing biomass lost to biomineralization.

[1] Watterson (1992) *Geology* **20**, 315-318. [2] Reith and McPhail (2009) *Chem. Geol.* **258**, 315-326. [3] Reith *et al.* (2011) *Geochim. Cosmochim. Acta.* **75**, 1942-1956. [4] Reith *et al.* (2010) *Geology.* **38, 843-846.**

https://doi.org/10.1180/S0026461X00008434 Published online by Cambridge University Press

Did I lose some LA-ICP-MS data somewhere?

STEPHEN SHUTTLEWORTH[1*], STUART GEORGITIS[2]

[1]Photon Machines, Redsmond, WA, USA, Shutts@photon-machines.com (* presenting author)
[2]Spectro Analytical Instruments, Mahwah, NJ, USA, Stuart.Georgitis@ametek.com

The combination of Laser Ablation (LA) and Inductively Coupled Plasma Mass Spectrometry (ICP-MS) provides an analytical tool capable of both high sensitivity elemental analysis and high precision isotopic analysis in a wide variety of matrices. Since its introduction in the mid 1980's LA-ICP-MS has been applied to a very broad range of applications across science in order to provide high spatially resolved chemical and isotopic information at the micron scale in the solid. The technique is now commonly used by researchers across the geochemical sciences.

As a destructive technique, data not captured as a consequence of detection duty cycle and dead time will be forever lost. Only now has a truly simultaneous ICP-MS been coupled to a laser thus eliminating the prior limitations that single spot analysis can only best be done with a restricted number of isotopes or a restricted section of the mass range. This paper will discuss the merits of laser ablation coupled with a truly simultaneous ICP-MS capable of analysing the entire periodic table for each indivudual laser shot. The use of a simultaneous dual detection range ICP-MS for laser ablation is investigated as a means to capture the whole ICP-MS spectrum of a single laser transient signal. The technique will be applied for both elemental mapping and isotopic analysis of mineral phases.

The Early Paleozoic of the Argentine Precordillera: C-isotope Excursions

A. N. SIAL[1*], S. PERALTA[2], C. GAUCHER[3], A.J. TOSELLI[4], V.P. FERREIRA[1], R. FREI[5], M. M. PIMENTEL[6]

[1]NEG-LABISE, Dept. Geol. UFPE, Recife, Brazil, sial@ufpe.br (* presenting author)
[2] Inst. Geología, Univ. Nac. San Juan-CONICET, Argentina
[3] Dept. Paleont., Fac. de Ciencias, 11400 Montevideo, Uruguay
[4] INSUGEO, San Miguel de Tucuman, Argentina, 4000
[5] Inst. Geogr. Geol., Geol. Section, Univ. Copenhagen, Denmark
[6] Inst. Geosc., Fed. Univ. Rio Grande do Sul, Porto Alegre, Brazil

Introduction. We have searched for the register of C-isotope excursions in the Upper Cambrian and Ordovician of the Argentine Precordillera. We report the register of the SPICE and SNICE in one same section in the Precordillera. The Darriwilian positive excursion (MDICE) and a Late Sandbian positive C-isotope excursion (GICE) have been registered in two sections. A pre-GICE positive C-isotope excursion (Sandbian S1, *N. gracilis* biozone) with $\delta^{13}C$ peak of ~ +3‰ is, perhaps, equivalent to the positive Spechts Ferry excursion of N. America. A positive $\delta^{13}C$ excursion registered at the base of the Upper Hirnantian La Chilca Fm. probably corresponds to HICE. **Causes**. These C-isotope excursions are probably related to oceanographic events: (a) sea-level rise and vigorous fluctuations in the Steptoean (SPICE), (b) sea-level fall in the Sunwaptan (SNICE), (c) important transgression in the Sandbian (pre-GICE and GICE), and (d) sea-level fall in the Late Hirnantian (HICE). In the Darriwilian and Sandbian stages, organic burial has led to a large ^{12}C sequestration in deep-ocean anoxia with saline bottom water, recorded by the graptoliferous black shales in the Gualcamayo and Los Azules formations, helped the building of the MDICE, one pre-GICE and GICE anomalies. O-isotope values for the Upper Cambrian are likely near-primary signals that point to progressive cooling from the SPICE to the SNICE, whereas for Sandbian carbonates they indicate strong T fluctuations. The $\delta^{13}C$ peaks of the GICE coincide with cooler periods with T progressively cooler towards Late Hirnantian. In the Zonda Fm., $^{87}Sr/^{86}Sr$ ratios vary from 0.7090 to 0.7109 while in Los Azules and Las Aguaditas Fms., they are ~ 0.7090. εNd values plot along the Nd isotopic evolution trend of the Iapetus Ocean.

Conclusions. The register of these excursions in the Precordillera is valuable proxy for the Early Paleozoic stratigraphy, regional/global high-resolution correlations, and sea-level change history.

https://doi.org/10.1180/S0026461X00008434 Published online by Cambridge University Press

Kinetics of phosphorus adsorption on iron oxyhydroxide residuals

PHILIP L. SIBRELL[1*]

[1]U.S. Geological Survey, Leetown Science Center, Kearneysville, West Virginia, USA, psibrell@usgs.gov (* presenting author)

Experimental Research and Findings

We have investigated the use of iron oxide media generated from mine drainage residuals for the removal of oxyanions from waste water, with a special emphasis on phosphorus (P) [1]. The use of packed column or fixed bed sorption systems allows treatment of waste water without requiring subsequent solid-liquid separation, and has been the focus of our research. In these trials we used 2.5 cm diameter glass columns packed with air-dried iron oxyhydroxides for treatment of wastewater with a variety of influent P concentrations, flow rates and media particle sizes. We then used Adsorption Design Software from the Michigan Technological University [2] to model results, estimate test parameters and to predict future outcomes. Results of several fixed bed trials are shown in Figure 1, where the effluent P concentration (normalized by the influent concentration C_i) has been plotted as a function of treatment time. It is clear that early breakthrough of the P was experienced in many of the column tests. In the most successful test (Run 7), we removed over 96% of the P from the influent waste stream over a period of 46 days of continuous operation. We have also observed that performance was strongly related to the value of the surface diffusion modulus *Ed*, enabling prediction of column performance based on test conditions.

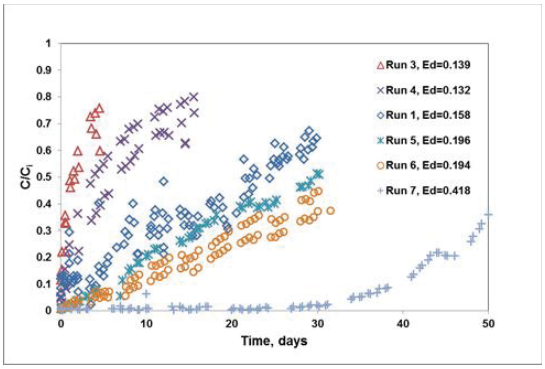

Figure 1: Fixed bed performance based on treatment time

Summary and Conclusions

Test results show that very good removal of P is possible using fixed bed columns packed with iron oxyhydroxide media. Conversion of test parameters into dimensionless forms enables prediction of the shape of the breakthrough curve based on the value of the surface diffusion modulus *Ed*. Preliminary batch tests with arsenic suggest that similar results may be possible for other metalloids as well, including arsenic and selenium.

[1] Sibrell *et al.* (2009) *Water Research*, **43(8)**, 2240-2250. [2] Mertz, K. A., *et al.* (1999) *Manual: Adsorption Design Software for Windows,* available at http://cpas.mtu.edu/etdot/

Zircon U–Pb, O and Hf isotope characteristics of granites emplaced during Cretaceous wrench to transtension in West Antarctica

CHRISTINE S. SIDDOWAY[1*], C. YAKYMCHUK[2], C. MARK FANNING[3], AND MICHAEL BROWN[2]

[1] Geology Dept., Colorado College, Colorado Springs, CO 80903, USA, csiddoway@coloradocollege.edu (*presenting author)
[2]Laboratory for Crustal Petrology, Department of Geology, University of Maryland, College Park, MD 20742, USA
[3]Research School of Earth Sciences, The Australian National University, Mills Road, Canberra, ACT 0200, Australia

The Fosdick Mountains in West Antarctica expose a migmatitic gneiss dome emplaced within a wrench setting during the Cretaceous dextral oblique convergence along the East Gondwana margin that affected both West Antarctica and once-contiguous New Zealand. Kilometer-scale, three-dimensional outcrop offers expansive views of a region of formerly melt-rich middle crust that responded to changes in strain during sequential wrench, transtension and oblique detachment [1]. Consistent with temperatures >800°C attained during metamorphism [2, 3], there is pervasive evidence for the prior presence of melt across a range of scales, including granite within foliation-parallel sheets and interboudin partitions, magmatic folds, and conjugate magmatic shear bands. Microstructures include euhedral to subhedral phases bordered by thin, delicate residual melt pseudomorph structures in interstices and on grain boundaries.

Based on SHRIMP U-Pb zircon and monazite geochronology for anatectic granites and residual migmatites, crustal melting, and melt transfer and accumulation occurred from c. 130 to 96 Ma, with the possibility that these processes were underway as early as c. 140 Ma [1, 3]. This previous work has revealed three phases of anatectic granite that occupy distinct structural settings. To evaluate whether there are distinctions in source for these three generations of granite, a Lu–Hf and O isotope study of previously dated zircon grains from 8 granite samples was undertaken. Taken together, zircons from Cretaceous granites show a comparatively large spread in εHf(t), with values from -14 to +5, and a wide range of $\delta^{18}O$ values between 6‰ and 14‰. In zircon of c. 120–99 Ma age, there is a trend toward higher $\delta^{18}O$ with greater homogeneity of zircon populations. An exception is one of the youngest granites, which has lower $\delta^{18}O$ values of 6.4 to 7.8. The isotopic characteristics of zircon from the three granite phases change with time. Zircon in c. 117–114 Ma granites, emplaced in steep foliation-parallel panels during *wrench* tectonics, has a wide range of $\delta^{18}O$ values from 6.2 to 11.6, reflecting a low degree of homogeneity of the zircon populations. Zircon in leucogranites that occur in subhorizontal sheets emplaced during *transtension* at c. 107–102 Ma, have elevated $\delta^{18}O$ values and more enriched εHf(t), attributed to a greater contribution of metasedimentary rocks in the source. Finally, zircon of c. 102 Ma age from a *detachment*-hosted granite records input from a source with more juvenile εHf(t) and $\delta^{18}O$, which may mark the availability of a less-evolved, mantle-like source due to lithosphere thinning.

[1] McFadden et al. (2010) Tectonics, 29, TC4022.
[2] Yakymchuk (2012) this volume.
[3] Korhonen et al. (2012) J Metamorphic Geology, Early View.

https://doi.org/10.1180/S0026461X00008434 Published online by Cambridge University Press

Stable isotope geochemistry of the Varuträsk rare-element pegmatite (northern Sweden)

KARIN SIEGEL[1*], THOMAS WAGNER[2], ROBERT TRUMBULL[3], ERIK JONSSON[4], CHRISTOPH A. HEINRICH[2]

[1]McGill University, Earth and Planetary Sciences, Montreal, Canada, karin.siegel@mail.mcgill.ca (* presenting author)
[2]ETH Zurich, Institute of Geochemistry and Petrology, Zurich, Switzerland, thomas.wagner@erdw.ethz.ch, heinrich@erdw.ethz.ch
[3]GFZ Potsdam, Inorganic and Isotope Geochemistry, Potsdam, Germany, bobby@gfz-potsdam.de
[4]Swedish Geological Survey, Mineral Resources, Uppsala, Sweden, erik.jonsson@sgu.se

The Varuträsk pegmatite, located in the Skellefte district in northern Sweden, is a classical representative of highly fractionated LCT-type rare-element pegmatites [1,2]. The Varuträsk pegmatite shows a typical primary zonation pattern, composed of well-developed border, wall and intermediate zones and a quartz core [3]. Major rare-element enrichment is mainly related to late-stage assemblages such as albite-lepidolite and pollucite units. Previous work [4] has focused on the major and trace element characteristics of key minerals (feldspars, micas, tourmaline, columbite-tantalite), demonstrating progressive magmatic fractionation trends in the primary pegmatite zones. Significant compositional changes observed in the late-stage mineral assemblages (reversals of magmatic fractionation trends, depletion in elements typically enriched in aqueous fluids) indicate that a magmatic fluid exsolved after the development of the primary pegmatite zonation.

The results of the present stable isotope (B, H, O) study further constrain the role of a magmatic fluid phase in formation of rare-element enrichment. Stable isotope analysis (O, H, B) has been performed on quartz, mica and tourmaline from all principal mineral assemblages in the pegmatite body. Boron isotope data of tourmalines using SIMS microanalysis are in the range between –14.6 and –6.2 ‰. The $\delta^{11}B$ data of different tourmaline types conforming to the primary pegmatite zonation show a clear magmatic fractionation trend. By contrast, tourmalines related to late-stage assemblages show a reversed fractionation that is correlated with the behavior shown by several major and minor elements in the tourmaline (Na, Fe, Mn, F). The B isotope evolution cannot be modeled by purely magmatic melt-tourmaline fractionation, but requires fluid-tourmaline partitioning to be operative for the late-stage assemblages. Hydrogen isotope data of micas indicate a substantial increase in δD from –76 to –53 ‰ from the wall to the innermost zones, requiring closed-system fractionation processes that involved melt and fluid. Taken together, the stable isotope data demonstrate that rare-element enrichment in the most fractionated assemblages is related to the transition from purely magmatic crystallization to conditions where a magmatic fluid phase was important.

[1] Cerny, P. 1991: Rare-element Granitic Pegmatites. Part I: Anatomy and internal evolution of pegmatite deposits. Geosci. Canada, 18, 49-67 [2] Cerny, P., Ercit, T.S. 2005: The classification of granitic pegmatites revisited. Can. Mineral., 43, 2005-2026 [3] Quensel, P. 1952: The Paragenesis of the Varuträsk Pegmatite. Geol. Mag., 89, 49-60 [4] Matalin, G., Wagner, T., Jonsson, E., Wälle, M., Heinrich, C.A., 2012. Evolution of the Varuträsk LCT-type rare-element pegmatite (N Sweden): mineral chemistry constraints. Contrib. Mineral. Petrol. (submitted)

Deep ocean mixing, the bipolar seesaw, and polar ocean biogeochemical change

D.M. SIGMAN [1*], A.S. STUDER[2], M. TREMBLAY[3], M. STRAUB[2], M.P. HAIN[1], G.H. HAUG[2]

[1]Department of Geosciences, Princeton University, Princeton, USA (*sigman@princeton.edu, mhain@princeton.edu)
[2]Department of Earth Sciences, ETH Zurich, Zurich, Switzerland (anja.studer@erdw.ethz.ch, marietta.straub@erdw.ethz.ch, gerald.haug@erdw.ethz.ch)
[3]Barnard College, New York, USA (mmt2130@barnard.edu)

At the scale of the global ocean, deep water formation is coupled to processes – most notably, vertical mixing and wind-driven upwelling – that reduce the density of deep water or otherwise remove dense water from the deep ocean. This formation/removal coupling may play a critical role in glacial/interglacial changes in polar ocean circulation and in atmospheric carbon dioxide. Considering the two regions of modern deep water formation, the North Atlantic and the Antarctic, if deep water formation ceases in one region but the loss of dense deep water does not decrease equivalently, then the other polar region must increase its deep water formation rate. This is one proposed physical mechanism behind the observed "bipolar seesaw" in high latitude temperatures on millennial time scales. Since deep water formation in the North Atlantic and the Antarctic have opposite effects on the efficiency of the global biological pump, any tendency for anti-correlation in their rates has a major effect on atmospheric CO_2. Accordingly, there is intense focus on an ocean seesaw mechanism for the CO_2 rises at the end of ice ages. However, there are divergent views as to the importance of deep ocean mixing *versus* the winds in driving such a North Atlantic/Antarctic seesaw. If the biogeochemical conditions of the polar ocean surface can be reconstructed back through time, we will have greater insight into how the polar regions have changed in their ventilation of the ocean interior and their impact on deep ocean carbon storage. In this talk, in addition to drawing upon numerical model experiments to lay out the arguments above, we will describe new diatom- and foraminifera-bound nitrogen isotope data from the Antarctic and the North Atlantic that support the view of seesaw-like behaviour between the two regions over major glacial/interglacial transitions and on millennial time scales. In this context, we will revisit the question of deep mixing *versus* the winds as driving this pattern.

https://doi.org/10.1180/S0026461X00008434 Published online by Cambridge University Press

Characterizing vadose zone hydrocarbon biodegradation using CO_2 effluxes, isotopes, and reactive transport modeling

NATASHA J. SIHOTA[1] AND K. ULRICH MAYER[1]*

[1]University of British Columbia, Department of Earth and Ocean Sciences, Vancouver, Canada, nsihota@eos.ubc.ca , umayer@eos.ubc.ca (* presenting author)

Introduction

Biodegradation in the vadose zone may result in substantial mass removal at hydrocarbon spill sites. At these sites, estimates of contaminant loss rates are needed to evaluate source zone longevity and long-term impact on the environment. Recently, Sihota et al. [1] showed that the measurement of CO_2 effluxes at the ground surface is a suitable method to derive depth-integrated rates of contaminant degradation. However, the accuracy of loss rate estimates obtained from CO_2 effluxes is limited by the ability to quantitatively separate CO_2 effluxes from contaminant destruction and naturally occuring soil respiration. To address this gap, measured CO_2 effluxes were complemented with detailed analysis of vadose zone gas composition, including stable and radioisotope analysis in CO_2. Results of field measurements were integrated using the reactive transport code MIN3P-DUSTY [2], which accounts for advective and multicomponent diffusive gas transport.

Results and Conclusions

Comparison of measured pore gas distributions to previous observations at the Bemijdi site [3] show biodegradation has approached a quasi steady state within the vadose zone. Radiocarbon results prove that, in the source zone, the majority of CO_2 is produced from contaminant destruction and indicate that the CO_2 efflux method provides an adequate estimate of contaminant mass loss rates.

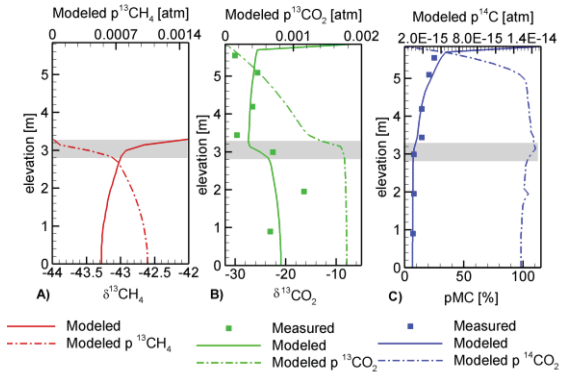

Figure 1: Comparison of measured and simulated isotopic values for a 1D vertical profile in the vadose zone at the Bemidji site.

Highly constrained simulations for a 1D vertical profile in the source zone are able to closely reproduce historical saturations, field observed fluxes, concentration profiles, and isotopic signatures. Simulation results also showcase that gas transport is diffusion-dominated and strongly affects measured isotopic signatures, in addition to effects caused by biogeochemical reactions.

[1] Sihota, Singurindy & Mayer (2011) *Environ. Sci. Tech.* **45**, 482-488. [2] Molins & Mayer (2007) *Water Resour. Res.* **43**, W05435. [6] Molins *et al.* (2010) *J. Contam. Hydrol.* **112**, 15-29.

Hand-held XRF in exploration for REE–bearing phosphate deposits.

GEORGE J. SIMANDL[1]*; SUZANNE PARADIS[2], ROBERT FAJBER[3], AND KEITH GRATTAN[4]

[1]British Columbia Geological Survey, Victoria, Canada, george.simandl@gov.bc.ca (*presenting author)
[2]Natural Resources Canada, Sidney, BC, Canada
[3]University of Victoria, Victoria, Canada
[4]Elemental Controls Limited, Mississauga, Canada

Sedimentary phosphate deposits consist of francolite [$(Ca_5(PO_4)_3(OH,F,Cl)$] and gangue minerals. They supply most of the phosphate raw materials used by the phosphate fertilizer industry and they are also considered as potential sources of F, REE, and/or U. Samples of phosphate rocks from the Fernie Formation (British Columbia) were analysed using a hand-held XRF analyser (HhXRF) and by lithium metaborate fusion–inductively coupled plasma (LMB-ICPMS) method. The results from both methods were compared; and correction factors for the HhXRF analyser were developed. HhXRFs can be used in exploration for phosphate deposits by analyzing samples directly for phosphorus (P) and if correction factors are applied for vectoring towards REE-rich zones, and/or delineating zones with high levels of deleterious elements such as U, Th, Cr, As, Hg, Cd and Se. Figures 1 illustrates two examples of relationships between hhXRF and LMB-ICPMS methods. Following a successful orientation survey, HhXRF does become fast and reliable vectoring tool that is easily incorporated into integrated exploration programs.

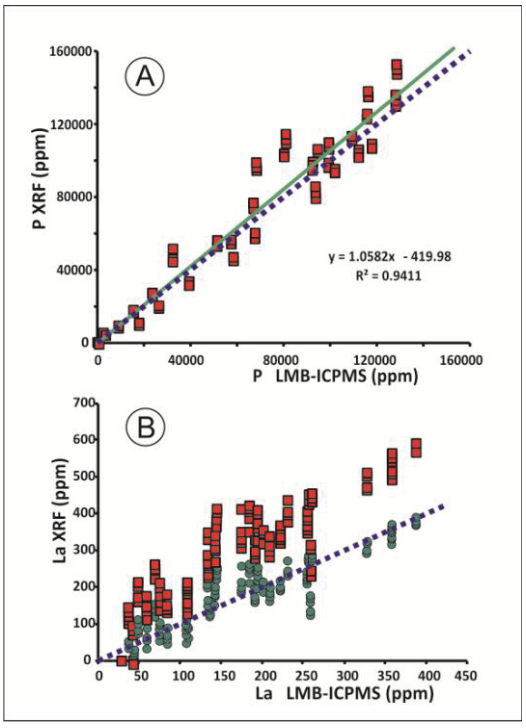

Figures 1: Comparison of the HhXRF and LMB-ICPMS for P (A) and La (B). Raw data as red squares. Corrected values as green circles. No correction was required for P.

https://doi.org/10.1180/S0026461X00008434 Published online by Cambridge University Press

Using Melt Inclusions to Constrain Magma Evolution and Pre-eruptive Plumbing System Architecture of Mutnovsky Volcano, Russia

SIMON, A. [1*], ROBERTSON, K.[1], PETTKE, T. [2], SMITH, E.[1], KIRYUKHIN, A.[3], SELYANGIN, O.[3], MULCAHY, S.[4], WALKER, J.[5]

[1]University of Nevada Las Vegas (UNLV), Las Vegas, NV, U.S.A., adam.simon@unlv.edu
[2]University of Bern, Bern Switzerland
[3]Institute of Volcanology and Seismology, Petropavlovsk-Kamchatsky, Russian Federation
[4]University of California Berkeley, Berkeley, California, U.S.A.,
[5]Universityof Kansas, Lawrence, Kansas, U.S.A.

Melt inclusions provide much more detailed samples of melt compositions than can be accessed with whole rock analyses alone. As such, melt inclusions have become an increasingly powerful tool for improving our understanding of magmatic processes owing to their ability to record discrete time steps during the polybaric and polythermal evolution of a particular magmatic system. In this study, we report and discuss melt inclusion data for samples from Mutnovsky Volcano, located on the Kamchatka island arc, that elucidate the causes for compositional diversity, and the iterative assembly of the pre-eruptive subvolcanic magma chamber.

Mutnovsky has formed a series of four stratocones over its ~100 ka history. Erupted rocks are dominantly basalt and basaltic andesite, and also include andesite, dacite and rhyodacite. We analyzed melt inclusions from all erupted compositions and eruptive centers to investigate the causes of the compositional heterogeneity, melt evolution, and pre-eruptive magma storage system. Melt inclusion compositions range from low silica (44 wt. %), hosted in olivine and clinopyroxene and plagioclase, to high silica (78 wt. %), hosted mainly in plagioclase and orthopyroxene. The melt inclusion compositions span a wider range than whole rocks. Geochemical modeling of the melt inclusion data, combined with field evidence and plagioclase phenocryst zoning, indicate that fractional crystallization and magma mixing operated in tandem to produce compositional diversity of the rocks erupted at Mutnovsky. The data are consistent with a model wherein fractional crystallization of individual aliquots of magma in an evolved subvolcanic magma chamber drove the melt(s) toward more felsic bulk compositions. Textural and compositional evidence also indicate that the subvolcanic magma chamber was effected by periodic injection and admixture of new olivine- ± clinopyroxene-saturated basaltic magma. This finding is consistent with observations from other volcanic systems.

The new twist that we employed was to calculate apparent pressures and temperatures of entrapment of orthopyroxene- and clinopyroxene-hosted melt inclusions by using the chemistry of melt inclusions and host mineral with the mineral-liquid thermobarometry equations from [1,2]. The results suggest that orthopyroxene and clinopyroxene crystallized at distinctly different levels in the magma plumbing system, which allows us to assess the variation in melt compositions as a function of vertical position in the evolving magma plumbing system. We will discuss these results, and the role that post-entrapment modification of melt inclusions may have on the model thermobarometry results, in the context of the iterative assembly and evolution of crustal magma chambers.

[1] Putirka et al. (2003) *American Mineralogist* **88**, 1542-1554. [2] Putirka (2008) *Reviews in Mineralogy and Geochemistry* **69**, 61-120.

Magnetic, mineralogical and geochemical (μXRF) properties of a central Baffin Bay sedimentary sequence spanning the last 100 ka

QUENTIN SIMON[1,*], GUILLAUME ST-ONGE[1,2], CLAUDE HILLAIRE-MARCEL[1], PIERRE FRANCUS[1,3]

[1]GEOTOP-UQAM, Montréal, Qc, Canada,
[2]Canada Research Chair in Marine Geology, ISMER-UQAR, Rimouski, Qc, Canada,
[3]INRS-ETE, Québec, Qc, Canada,
*quentin.simon@gmx.com

A terrigenous sedimentary sequence from central Baffin Bay (core HU2008-029-016PC – 70°46.14'N/-64°65.77W – 2063 m) was analyzed for its magnetic, mineralogical and geochemical (μXRF - Itrax) properties in order to 1) link the sedimentary history to ice-margin dynamics along the surrounding coastlines (W. Greenland, E. Baffin Island and N.E. Ellesmere Island), and 2) eventually associate the continental ice dynamics to specific climate events of the last glacial cycle. A chronology based on relative paleointensity (RPI) and paleomagnetic secular variation (PSV) has been set. It provides an age model for a site where current chronological approaches (^{14}C and isotope stratigraphy) failed for various reasons. This age-model indicates a mean sedimentation rate of ~6.5 cm/ka, but also illustrates increases (> 15 cm/ka) linked to major sedimentological events of local origin. The timing and properties of these sedimentological events are discussed with special emphasis on their source and mode of deposition, as well as their linkage with specific ice margin responses to climate changes along surrounding islands. On one hand, coarse-grained and rapidly-deposited detrital carbonate-rich layers seem broadly coeval with major interstadials of the GISP2 ice core record. This suggests fast retreat episodes along related ice-stream routes during major interstadials. Rock magnetic data point to coarser magnetic grain size in these layers. This is especially the case during the 11– 12 ka (~YD) and 14.8–16 ka (H1) intervals. On the other hand, feldspar-rich layers also depicting high clay and silt size material contents are characterized by a finer magnetic grain size in the pseudo single domain to single domain ranges. Magnetic grain size ratios such as k_{ARM}/k_{LF} and Fe/k_{LF} show finer magnetic grains during the locally extendedLast Glacial Maximum interval (16 – 24 cal ka BP). This suggests that, during glacial maxima, mechanical grinding of the bedrock by surrounding ice sheets (in particular along the continental shelves of Greenland and Baffin Island) released large amounts of “glacial flour” characterized by feldspar-rich and finer magnetic supplies.

https://doi.org/10.1180/S0026461X00008434 Published online by Cambridge University Press

An account of the Chernobyl Pilot Site studies: 25 years later

CAROLINE SIMONUCCI[1*], ARNAUD MARTIN-GARIN[2], NATHALIE VAN MEIR[1,3], PIERRE DICK[1], OLIVIER DIEZ[4], CELINE ROUX[1,5], DMITRI BUGAI[6] AND VALERIY KASHPAROV[7]

[1]IRSN, SRTG/LETIS, caroline.simonucci@irsn.fr (* presenting author), pierre.dick@irsn.fr
[2]IRSN, SERIS/L2BT, arnaud.martin-garin@irsn.fr
[3]IG-BAS, Geosciences, nathalie.vanmeir@irsn.fr
[4]IRSN, SRTG/LAME, olivier.diez@irsn.fr
[5]UMR 7330, Geosciences, celine.roux.1@etu.univ-cezanne.fr
[6]IGS, Geosciences, dmitri.bugay@gmail.com
[7]UIAR/NUBiP, Geosciences, vak@uiar.org.ua

Introduction

25 years have passed since the accident at the Chernobyl NPP, but up to now scientists are still working on answering the question "what are the consequences of the accident?", and in particular, can we define radionuclide (RN) migration processes today and for the future in soils, vegetation and possibly air re-suspension?. Following the Chernobyl accident (26/04/1986), the contaminated topsoil layers containing fuel particles and contaminated organic matter, coming from the Red forest, were buried in trenches only a few meters deep in the Chernobyl exclusion zone in order to prevent RN dispersion and especially to diminish the exposure dose to workers (liquidators) on site in 1987. Since 1999, the French Institute of Radioprotection and Nuclear Safety (IRSN), in collaboration with the Ukrainian Institute of Agricultural Radiology (UIAR/NUBiP) and the Ukrainian Institute of GeoSciences (IGS), has been studying the impact of the contaminated waste trench T-22, located 2.5 km South-West from Chernobyl NPP, on the aquifers below. The Chernobyl Pilot Site (CPS), which includes the trench T-22, was equipped to carry out in situ radioecological and hydrogeological investigations. The objectives of the research are devoted to the characterization of RN migration both upward into the vegetation and downward to the aquifer, in order to validate RN's transfer models in the environment.

Results and Conclusion

To this end, flow and transport mechanisms were first decoupled. Water flow only studies are still carried out in the different soil layers and in the aquifer. Soil –RN interactions are still studied first in the laboratory (especially for Cs-137 and Sr-90) and analogues were/are also studied on the field. In a second step, these processes were re-coupled by calculating, the reactive transport of RN both at the laboratory scale, under well controlled conditions, and in the CPS where the Sr-90 migration's plume is surveyed for 20 years. In connection to the dynamic of RN migration, our studies also addressed: (i) the nature of the waste material in order to better estimate the amount of the RN stock and its release properties over time; (ii) the possible evidence of enhanced transport down to the aquifer and in the saturated zone due to specific and stable aqueous species of RN and/or to the presence of colloidal substances, and (iii) the upward migration of RN due to the root system of the plants that grow mainly over the trench as such export fluxes from the trench probably constitute one of the main hazards for the near future. The future investigation at CPS and extended to the larger Chernobyl Exclusion Zone include a better understanding of the joint biogeochemical, radioecological and hydrological processes.

Local structure and crystallization pathways of amorphous calcium carbonate

JARED WESLEY SINGER[1]*, A. ÖZGÜR YAZAYDIN[2,3], GEOFFREY M. BOWERS[1,4], AND R. JAMES KIRKPATRICK[5]

[1] Department of Material Science and Engineering, New York State College of Ceramics at Alfred University, Alfred, New York, USA, jws4@alfred.edu (* presenting author)
[2] Department of Chemical Engineering, University of Surrey, Guildford, UK, a.yazaydin@surrey.ac.uk
[3]Department of Chemistry, Michigan State University, East Lansing, Michigan, USA, yazaydin@msu.edu
[4]Division of Chemistry, College of Liberal Arts & Sciences, Alfred University, Alfred, New York, USA, Bowers@alfred.edu
[5]College of Natural Science, Michigan State University, East Lansing, Michigan, USA, rjkirk@cns.msu.edu

We compare local structures of synthetic amorphous calcium carbonate (ACC) by ^{43}Ca- and ^{25}Mg-nuclear magnetic resonance (NMR) to long-range order by low-angle and conventional x-ray diffraction and to characterization by thermal gravimetric analysis, scanning electron microscopy, and energy dispersive spectroscopy. The range of parent solution compositions, temperatures, and $Na_2CO_{3(s)}$ induced precipitation yields ACC compositions of 10-40 weight percent water and 0-50% Mg. Subsequent crystallization can yield all anhydrous and hydrous polymorphs of $CaCO_3$, mixed assemblages, and dolomite. In spite of this variability, the ^{43}Ca NMR spectra of ACC collected immediately after synthesis consist of broad, featureless resonances with Gaussian line shapes (mean chemical shift = -0.4±0.5ppm, FWHH = 27.6±1ppm) that do not depend on Mg^{2+} or H_2O content. We derive indistinguishable maximum mean Ca-O bond distances of 2.45 Å for all samples and our analysis suggest that spectral widths are dominated by chemical shift dispersion that arises from local disorder. Preliminary ^{25}Mg-NMR suggests the presence of rigid and mobile ^{25}Mg populations. [Mg] of the parent solution correlates with ACC stability, though our data suggest Mg^{2+} incorporation in the solid phase is not responsible for the observed stabilization. Within experimental ranges we also observe ACC mesocrystallization, ikaite ($CaCO_3 \bullet 6H_2O$) decomposition to monohydrocalcite ($CaCO_3 \bullet H_2O$), and low-temperature proto-dolomite.

https://doi.org/10.1180/S0026461X00008434 Published online by Cambridge University Press

Extracellular *c*-Type Cytochromes from *Geobacter bemidjiensis*

CINDY J. CASTELLE[1], KELLY C. WRIGHTON[2], MICHAEL J. WILKINS[3], MARY S. LIPTON[3], JILLIAN F. BANFIELD[2], STEVEN W. SINGER[1*]

[L]Lawrence Berkeley National Laboratory, Berkeley, CA, USA; SWSinger@lbl.gov
[2]University of California-Berkeley, Berkeley, CA, USA
[3]Pacific Northwest National Laboratory, Richland, WA, USA

The subsurface clade 1 of the *Geobacteraceae* often predominates during acetate-stimulated bioremediation of uranium-contaminated sites. The metabolic activity of this clade has been linked to solid phase U(VI) and Fe(III) reduction in the subsurface. Despite its importance for subsurface metal reduction, the complement of electron transfer proteins expressed by members of this clade have not been identified. *Geobacter bemidjiensis* is a cultured representative of subsurface clade 1 and is an excellent model system to begin to understand electron transfer in the subsurface *Geobacteracae* clade 1. Inspection of the genome of *G. bemidjiensis* identified 84 proteins predicted to encode for *c*-type cytochromes. To identify the dominant *c*-type cytochromes expressed by *G. bemidjiensis*, proteomics was performed on cultures grown with fumarate as an electron acceptor. A substantial fraction of *c*-type cytochromes were localized in the extracellular medium or were easily sheared from the outer-membrane. The most abundant of these *c*-type cytochromes was a flavocytochrome that clustered with fumarate reductases from *Shewanella* species. Other abundant *c*-type cytochromes included a homolog of OmcB, a cytochrome required for optimal reduction of Fe(III) oxides in *G. sulfurreducens*, and a nonaheme cytochrome whose only homologs were found in *Geobacter* species from subsurface clade 1. Seven expressed *c*-type cytochromes were predicted to have >25 heme prosethetic groups. Peptides from the abundant *G. bemidjiensis* cytochromes were also found in proteomic measurements of groundwater from a uranium-contaminated site at Rifle, CO undergoing acetate stimulation. The extracellular *c*-type cytochromes are distinct from those cytochromes identifed for *G. sulfurreducens* and suggest that the *Geobacteraceae* from subsurface clade 1 may possess novel pathways for electron transfer.

Dissolution of uranyl precipitates in contaminated vadose zone sediments

ABHAS SINGH[1*], JOHN M. ZACHARA[1], JAMES P. MCKINLEY[1], CHONGXUAN LIU[1], MAXIM I. BOYANOV[2], KENNETH M. KEMNER[2], DEAN A. MOORE[1]

[1]Pacific Northwest National Laboratory, Richland, WA 99354 USA; abhas.singh@pnnl.gov (* presenting author), john.zachara@pnnl.gov, james.mckinley@pnnl.gov, chongxuan.liu@pnnl.gov, damoore@pnnl.gov
[2]Argonne National Laboratory, Argonne, IL 60439 USA; mboyanov@anl.gov, kemner@anl.gov

Metatorbernite, $Cu(UO_2PO_4)_2 \cdot 8H_2O_{(s)}$, was idenified as the dominant form of uranium in contaminated sediments below former nuclear waste disposal ponds in the Hanford 300-Area (Washington State) in past microscopic and synchrotron-based spectroscopic and diffraction studies [1-3]. Uranium(VI) release from these sediments to groundwater, however, could not be explained by metatorbernite solubility determined from pure mineral studies at acidic conditions [4]. This work aims to reconcile these differences between known solid-phase speciation and the aqueous phase composition generated. Carbonate and synthetic groundwater extractions on metatorbernite and variable sediment:solution ratios and sediment sizes were peformed in different experimental settings (e.g., batch, stir-flow) to quantify uranium(VI) release. Solid phase speciation before and after these extractions was investigated using scanning and transmission electron microscopy, micro X-ray diffraction and X-ray absorption techniques.

Preliminary results indicate that metatorbernite dissolution in synthetic groundwater is slow and is facilitated by secondary precipitation of an unidentified copper phase that limits the dissolved copper concentration (Figure 1). Metatorbernite in sediments may be gradually tranforming to a uranyl carbonate phase as indicated by X-ray absorption spectroscopy. These results will be combined with other solid-phase characterization results and interpreted within a reaction-based modeling framework including dissolution-precipitation and aqueous speciation reactions.

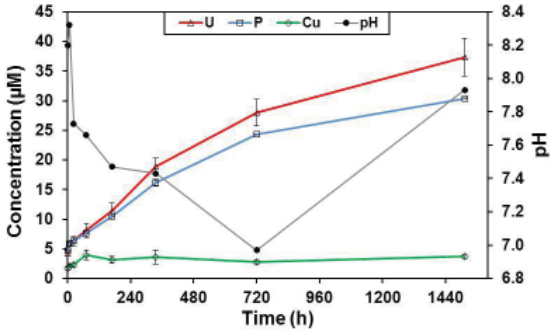

Figure 1: Measured dissolved concentrations and pH from metatorbernite dissolution in synthetic groundwater.

[1] Catalano et al. (2006) *Environmental Science & Technology* **40**, 2517-2524. [2] Arai et al. (2007) *Environmental Science & Technology* **41**, 4633-4639. [3] Stubbs et al. (2009) *Geochimica Et Cosmochimica Acta* **73**, 1563-1576. [4] Ilton et al. (2010) *Environmental Science & Technology* **44**, 7521-7526.

https://doi.org/10.1180/S0026461X00008434 Published online by Cambridge University Press

Distribution of dissolved neodymium and ε_{Nd} in the Bay of Bengal

SATINDER PAL SINGH[1] AND SUNIL KUMAR SINGH[2*]

[1]Physical Research Laboartory, Ahmedabad, India, satinder@prl.res.in
[2]Physical Research Laboartory, Ahmedabad, India, sunil@prl.res.in (* presenting author)

The concentrations and isotope composition of dissolved Nd have been measured in the water column along 87°E transect in the Bay of Bengal to investigate the impact of water mass mixing and desorption of Nd from particulates in determining their distribution in the Bay. The concentration of Nd in surface waters of the BoB shows a North-South decreasing trend (~ 46 to ~ 22 pmol/kg) with increasing salinity, whereas its depth profiles typically show a high value in surface waters, a minimum (~ 15 to ~ 23 pmol/kg) in shallow subsurface (~ 50-200 m) followed by a gradual increase with depth. The Nd concentration of the BoB waters is generally higher than that at corresponding depth in nearby oceanic basins. The ε_{Nd} of the northern BoB waters ~ -15 ± 1 overlaps with that of dissolved and particulate phases of the Ganga-Brahmaputra (G-B) Rivers, but less radiogenic than those reported for other regions of global oceans, except the Baffin Bay and the North Atlantic Subpolar Gyre. The abundance and distribution of dissolved Nd and its unradiogenic isotope composition suggests that the dominant source of Nd in the BoB is the dissolved and/or particulate phase of the G-B river system.

The ε_{Nd} values in the BoB show greater variation in the upper water column with more radiogenic values ~ -8 in surface waters of the southernmost profile (~ 6°N), which decreases to -15 in the northernmost profile (~ 20°N). This latitudinal trend is most likely a result of the variation in mixing proportion between the Indonesian Throughflow surface waters (IW) and the G-B river water. Inverse model calculations suggest that excess Nd of the order of ~1 to 65 % of measured Nd concentration is required from other source(s) in addition to various water masses. The calculations also show that ε_{Nd} of the additional source(s) has to be in the range of ~ -16 ± 2, typical of G-B river sediments. These observations coupled with the North-South distribution of dissolved Nd and ε_{Nd} indicate that this additional source is release from particulate phases supplied by the G-B river system and the continental margin sediments. This study underscores the significant role of dissolved/particulate Nd from the Ganga-Brhamputra river system in contributing to the dissolved Nd budget of the global ocean.

LA-MC-ICPMS iron isotopic measurements of zoned olivine

C.K. SIO [1*], N. DAUPHAS[1], F.Z. TENG[2], M. CHAUSSIDON[3], R.T. HELZ[4], M. ROSKOSZ[5], Y. XIAO[6], AND T. IRELAND[1]

[1] Origins Lab, Dept. of the Geophysical Sciences, the University of Chicago, USA, ksio@uchicago.edu (* presenting author)
[2]Dept. of Geosciences, the University of Arkansas, USA
[3]CRPG-CNRS, Vandoeuvre lès Nancy, France
[4]United States Geological Survey, Reston, VA, USA
[5]UMET, Université de Lille 1, France
[6]Institute of Geology and Geophysics, Chinese Academy of Sciences

Previous studies have revealed that iron and magnesium isotopes may be used to identify diffusion-driven zoning in olivine crystals [1-3]. In magmatic systems, Mg-rich olivine is an early crystallizing phase. As the melt evolves, it becomes more Fe-rich, so that in reaching equilibrium, Fe diffuses into and Mg diffuses out of the initial olivine crystal. Because light isotopes diffuse faster than heavy isotopes [4-5], such diffusion-driven mechanism is accompanied with 1) a negative correlation of Fe and Mg isotopes, and 2) a negative correlation of Fe isotopes and a postive correlation of Mg isotopes with Fo#. Teng et al. [1] showed these correlations in olivine fragments from Kilauea Iki lava lake. Sio et al. [3] used microdrilling techniques to spatially resolve the same correlations in a single olivine crystal.

Many zoned olivine crystals are smaller than or comparable to the size of a drill bit (300 μm used in [3]). Hence, it is imperative to develop *in-situ* techniques that provide better spatial resolution. Using a UP193HE laser, we conducted LA-MC-ICPMS iron isotopic measurements on the same sample analyzed in [3]. The spot sizes used in the sessions were 40-55 μm, an improvement of lateral and depth spatial resolution by approximately an order of magnitude relative to microdrilling. Smaller spot sizes may be used if ^{57}Fe is not analyzed.

Numerous tests were conducted to evaluate sample mount orientation and matrix effects. These tests suggest that the orientation effect must be carefully evaluated in order to obtain accurate data and true errors, which can be three times greater than the error taken only from measured isotopic variations on a single crystal. The typical precision is 0.2 ‰ (1 SD) based on repeat analyses of the same profile. The final iron isotopic profile agrees with the microdrilling results, with the rim at δ^{56}Fe -0.2 ‰ and the core at -1.2 ‰. A plot of δ^{56}Fe versus Fo# is also in perfect agreement with microdrilling data.

LA-MC-ICPMS provides the means to measure iron isotopic compositions with high spatial resolution in olivines. Such techniques can be employed on zoned crystals to better understand their crystallization and cooling histories. Our work establishes LA-ICPMS Fe isotopic analyses as a powerful tool of petrology in the study of igneous zoned minerals.

[1] Teng *et al.* (2011) *EPSL* **308**, 317-324. [2] Dauphas *et al.* (2010) *Geochim. Cosmochim. Acta* **74**, 3274-3291. [3] Sio *et al.* (2011) Goldschmidt Abstract 1884. [4] Richter *et al.* (2009) Geochim. Cosmochim. Acta **73**, 4250-4263. [5] Roskosz *et al.* (2010) Goldschmidt Abstract A882.

https://doi.org/10.1180/S0026461X00008434 Published online by Cambridge University Press

Effects of water on the nucleation of Li-rich granitic melts

MONA-LIZA C. SIRBESCU[1*], MAX WILKE[2], ILYA VEKSLER[2], AND ALAN G. WHITTINGTON[3]

[1]Central Michigan University, Earth and Atmospheric Sciences, Mt. Pleasant, MI, USA, sirbe1mc@cmich.edu (* presenting author)
[2]Deutsches GeoForschungsZentrum, Potsdam, Germany
[3] University of Missouri, Geological Sciences, Columbia, MO, USA

The amount of dissolved water controls the nucleation and crystallization of granitic melts by lowering their liquidus and glass transition temperature, their free energy relative to crystals, and viscosity. Although pegmatites and rhyolites are similarly affected by undercooling and cooling rate, they are at the opposite ends of the spectrum of igneous texture because pegmatite melts have incorporated and retained H_2O whereas rhyolites have lost H_2O [1].

Sixty nucleation-crystallization experiments on Li-B-haplogranite-H_2O compositions confirm that igneous texture is strongly controlled by the concentration of water. Time-series, isothermal runs (from 1 to 30 days) were performed at temperatures ranging from 400 to 700°C at 300 MPa, coresponding to variable degrees of undercooling between liquidus and glass transition. H_2O contents ranged from 2.6 to 8.3%, and kept below fluid saturation. Although metastable, mineral assemblages are reproducible. Viscosity data collected via the parallel-plate method indicate that the glass transition of both melts containing 6.5 % H_2O is just under 300°C, indicating that nucleation and crystallization took place in a liquid not in glass.

Clearly, H_2O concentration influences the time of incubation, nucleation densities, and crystal growth rates, but the effects are a nonlinear function of dissolved H_2O. For example, at 600°, nucleation delays are >5 days for a concentration of 8.3 % H_2O, decrease to a minimum of only one day for 6.5 % H_2O, and increase again to 2.5 days at 3.0 % H_2O. Growth and nucleation rates follow a similar parabolic behavior, as a consequence of the double role played by H_2O. On one hand, H_2O stimulates development of large crystals because of increased diffusion rate. On the other hand, H_2O decreases the liquidus temperature of the melt, therefore reducing the value of effective undercooling, which has the opposite effect of slowing down crystal growth. A "Goldilocks" behavior rules the development of pegmatite texture including large, skeletal crystals, graphic intergrowth, and low nucleation density. Ultimately, the value of effective undercooling has to be "just right".

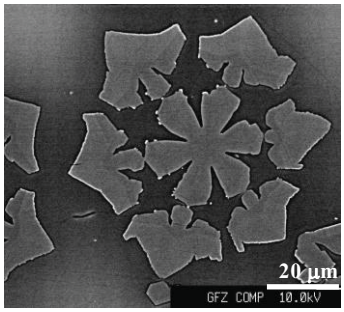

Figure 1: Skeletal "stuffed" beta-quartz produced in 30-day long run, at 500°C, in a haplogranitic melt with 3.0% (g/g) H_2O, 1% Li_2O, and 2.3 % B_2O_3

[1] Nabelek et al. (2010) *Contrib. Min. Pet.* **160**, 313-325.

Feedback effects of clay minerals formation on the kinetics and mechanisms of olivine carbonation within tholeiitic basalt

OLIVIER SISSMANN[1,2*], DAMIEN DAVAL[3], ISABELLE MARTINEZ[1], FABRICE BRUNET [4], ANNE VERLAGUET [5], YVES PINQUIER [2], FRANÇOIS GUYOT [1,6]

[1]IPGP - CNRS UMR 7154, Université Paris Diderot, Paris, France
*sissmann@ipgp.fr
[2] Laboratoire de Geologie - CNRS UMR 8538, ENS, Paris, France
[3] LHyGeS - CNRS UMR 7517, Strasbourg, France
[4] ISTerre - CNRS UMR 5275, Univ. J. Fourier, Grenoble, France
[5] ISTeP - CNRS UMR 7193, UPMC, Paris, France
[6] IMPMC - CNRS UMR 7590, UPMC, Paris, France

Geological storage of CO_2 in basic rocks relies on the dissolution of its silicate components, followed by the precipitation of carbonates. However, the slow dissolution kinetics of Mg-rich silicates has proven a critical issue. Previous batch carbonation studies on separated olivine grains[1] ($(Mg,Fe)_2SiO_4$), have emphasized the deleterious role of secondary phases, such as amorphous silica layers (SiO_2(am)) in controlling the dissolution rate of the parent mineral and the transport of reactants from and to the reactive surface.

We show here that carbonation processes and kinetics are strongly different for olivine within a tholeiitic basalt than for separated olivine. Batch experiments were conducted (at 150°C and P_{CO2} = 280 bars) on an Mg-rich (9.3 wt.% MgO and 12.2 wt.% CaO) tholeiitic basalt from Iceland, composed of olivine, Ti-magnetite, plagioclase and clinopyroxene. After 45 days of reaction, carbonation rates were quantified by CO_2 extraction with phosphoric acid, yielding up to 60 wt.% carbonation of Mg-rich phases as $MgCO_3$, but less than 0.5 wt.% of Ca-rich phases as $CaCO_3$.

Such observations diverge noticeably from those previously reported in lower T carbonation studies on Ca-rich, Mg-poor basalts[2]. In addition, X-ray diffraction analysis on the reaction products reveals a substantial decrease in olivine content, supporting the idea that magnesite formation mainly follows from olivine dissolution. Therefore, these results suggest that in our experiments, no passivating silica layer was formed on the surface of olivine. Instead, investigations by transmission electron microscopy reveal that a thin layer (~100 nm) of porous, iron-bearing, aluminous phyllosilicate has formed on the surface of the remaining primary silicates. Taken together, these observations suggest that, in an Al rich-medium, the formation of clay minerals may consume the silicon of potential silica-rich surface layers, or directly inhibit their formation. Those phyllosilicates would therefore represent the ultimate sink for Si, with lesser impact on the transport of reactants than SiO_2(am). By providing a constant driving force for Si removal, we eventually propose that such phases allow olivine to dissolve as rapidly as it is known to occur in open natural systems, and therefore to reach higher carbonation rates[3].

[1] Daval et al (2011), Chemical Geology, v.284, p.193-209
[2] Schaef et al (2010), IJGGC, v.4, p.249-261
[3] Matter and Kelemen (2010), Nature Geoscience, v.2, p.837-841

https://doi.org/10.1180/S0026461X00008434 Published online by Cambridge University Press

Nanoparticle remediation through porous media

R.L. SKUCE[1]*, D.J. TOBLER[1], M.R. LEE[1] AND V.R. PHOENIX

[1]School of Geographical and Earth Sciences, University of Glasgow, Glasgow, G12 8QQ, UK (*correspondence: r.skuce.1@research.gla.ac.uk)

The use of engineered nanoparticles continues to expand rapidly. As this intensifies, so does the environmental risk posed if they are released into the environment. This is of particular concern due to the potential toxicity of some nanoparticles. As it stands, we are poorly prepared to deal with nanoparticle pollution and thus remediation strategies must be developed Here, ureolysis-driven calcium carbonate precipitation by the urease positive bacterium *Sporosarcina pasteurii* is investigated as a means of removing nanoparticles from aquatic systems. This technology has been investigated for the solid phase capture of radionuclide and trace element contaminants in groundwater systems [1]. However its potential to capture nanoparticles has yet to be examined.

Batch experiments show the successful removal of highly stable organo-metallic nanoparticles at concentrations up to 10mg/l (the highest concentration tested thus far). Over 90% of nanoparticles where captured within 24 hours and capture efficiency appeared to be inversely proportional to calcite precipitation rate. As calcite precipitates, the nanoparticles become trapped within the growing calcite crystal. As the calcite-nanoparticle composite continues to grow, it adheres to surfaces (such as the edge of the reaction flask, or the edge of a pore space), immobilizing the nanoparticles from solution.

Following this an experiment was devised to determine the capture efficiency of nanoparticles through saturated porous media. It has been demonstrated that nanoparticles act as nucleation sites to the precipitating calcite, it is now imperative to determine whether nanoparticles are preferentially incorporated into the precipitating calcite when multiple nucleation sites are available, that is the sand grains. Breakthrough curves obtained determine the capture efficiency of nanoparticles in saturated porous media.

This technology has the potential for application in contaminated groundwater and soil as an in-situ remediation technique for nanoparticle pollutants.

[1] Warren, L.A Maurice, P.A. Ferris, N, P, F, G. (2011) *Geomicrobiology Journal* **18**, 93-115.

Bottom water redox conditions and sea level changes during Zn-Pb and phosphate mineralization, Howards Pass district, Yukon Territory

JOHN F. SLACK[1]*, HENDRIK FALCK[2], KAREN D. KELLEY[3], GABRIEL G. XUE[4]

[1]U.S. Geological Survey, MS 954, Reston, VA 20192, USA, jfslack@usgs.gov (*presenting author)
[2]NWT Geoscience Office, P.O. Box 1500, Yellowknife, NWT X1A 2R3, Canada
[3]U.S. Geological Survey, MS 973, Denver, CO 80225 USA
[4]Selwyn Resources Ltd., 509 Richards St., Vancouver, BC V6B 2Z6, Canada

Stratabound Zn-Pb sulphide deposits of the Howards Pass district occur in the Middle Ordovician-Early Silurian Duo Lake Formation (DLF). From base to top, the DLF in the district comprises four principal members: pyritic mudstone, calcareous mudstone, active (Zn-Pb), and upper siliceous mudstone. Sulphide lenses in the active member consist of layered, laminated, and massive sphalerite ± galena. Pyrite forms thin laminae of fine-grained framboids. The upper calcareous mudstone and the base of the active member locally contain apatite-rich units; the upper siliceous member has abundant apatite laminae 0.1-1.5 cm thick.

Whole-rock analyses for Zn- and Pb-poor DLF mudstones (n = 58) from three drill cores in relatively undeformed parts of the XYC and HCW deposits contain variable silica (to 90 wt % SiO_2), phosphate (to 24.7 wt % P_2O_5), and carbonaceous material (to 16.5 wt % Corg). V concentrations are highest in the calcareous mudstone member (to 3000 ppm), implying sedimentation near the suboxic-anoxic boundary; large variations in marine V/Mo ratios (0.74-209) reflect fluctuating bottom-water redox over time [1]. Re/Mo ratios [2], considered the best paleoredox proxy, record sulphidic or anoxic conditions (Re/Mo <0.001) in bottom waters during deposition of the pyritic mudstone, most of the calcareous mudstone, and active members; these conditions predominated in the basin prior to and during Zn-Pb mineralization, aiding accumulation and preservation of sulphides. In the upper siliceous member, Re/Mo ratios are mostly higher (0.004-0.013), indicating suboxic (<5 μM O_2) bottom waters. Suboxic conditions within the upper part of the calcareous mudstone and the base of the active member, and especially in the upper siliceous member, promoted deposition of abundant phosphate and correlate temporally with two periods of global sea level rise [3]; falling sea level may have facilitated the development of crucial anoxic to sulphidic bottom waters during Zn-Pb mineralization. Lithologic similarity to part of the Monterey Formation (Miocene) of coastal California suggests that the DLF and its contained Zn-Pb deposits formed in a restricted basin near a continental margin, accompanied by high productivity required for the accumulation of abundant phosphate, biogenic silica, and organic matter.

[1] Piper, D.Z., Calvert, S.E. (2009) *Earth-Sci. Reviews* **95**, 63-96.
[2] Ross, D.J.K., Bustin, R.M. (2009) *Chem. Geol.* **260**, 1-19.
[3] Munnecke, A., et al. (2010) *Palaeogeogr. Palaeoclimatol. Palaeoecol.* **296**, 389-413.

https://doi.org/10.1180/S0026461X00008434 Published online by Cambridge University Press

Exploring Water Quality and Flow Paths Using Boron Isotope Data

A.T. SLADE[1]*, N.R. WARNER[2], A. VENGOSH[2] AND B. WHITEHEAD[1]

[1] School of Environment, The University of Auckland, 23 Symonds Street, Auckland 1142, New Zealand, a.slade@auckland.ac.nz (* presenting author)

[2] Division of Earth and Ocean Sciences Nicholas School of the Environment, Duke University, Durham, NC 27708

Boron isotope data is rarely used by water quality (WQ) authorities to elucidate processes occurring in hydrologic systems in order to improve WQ management protocols. In concert with a suite of chemicals this study explores the use of boron as a tracer in a WQ study that also helps reveal potential flow paths for water in a pulp and paper waste site. The results not only provide the local WQ authorities with a tool for improving the management of their waterways, they come at a critical stage in the history of the site as the parties legally responsible for the waste and management of the site will change in December of 2012.

Study Site

A pulp and paper waste site, located on top of active geothermal features, in the Bay of Plenty region of New Zealand is at risk of having a sustained and detrimental impact on the environment given the following historical and contemporary issues: 1) the waste site floods periodically causing temporary ponding, which in the past has resulted in the banks of the adjacent Tarawera River (TR) to breach; 2) the natural underlying geologic units and waste material generated by the pulp and paper mill are highly permeable; and 3) the two shallow unconfined aquifers in and under the waste are thought to house substantial volumes of water that are connected to the TR. As such, it is important to identify the source, provenance, and chemical profile of the water as it migrates through the geologic units and waste material in an effort to assist in mitigating any future environmental impacts.

Results of Study

This study involves a comprehensive chemical evaluation of water samples collected between 2009 and 2011, from the pulp and paper waste site, with an emphasis placed on boron isotope data. The types of water sampled and their associated $\delta^{11}B$ values collected from the 1 km^2 area that encompasses the waste site were: surface water (10.1-15.4‰); groundwater (-5.0-0.0‰); leachate (-1.5-6.7‰); geothermal water (-1.2‰); natural spring water (11.9‰); and rain water (25.9-28.9‰). The collation of the data provides a final assessment of the waste site's hydrologic system through the lens of boron isotope chemistry and showcases the ability to use it to improve WQ management protocols.

Timing and carbon sources for microbial processses in the deep terrestrial carbon cycle

SLATER, G.F.*[1], MAILLOUX, B[2]., SILVERN, R.[2], LI, L[3], SHERWOOD LOLLAR B[3]., ONSTOTT T.C.[4],

[1]McMaster University, Hamilton, Canada, gslater@mcmaster.ca,
[2]Bernard College, New York, USA
[3]University of Toronto, Toronto, Canada
[4]Princeton University, USA

The presence of microbial communities living in ancient, fractured rock in deep (2-3+ km) subsurface terrestrial environments suggests that the metabolic activities of these organisms may play a role in fluxes of carbon moving into, or out of, these deep Earth environments. This study investigated the carbon source and metabolic activities in fracture water feeding an artesian borehole located 1.3 deep in the Beatrix mine, South Africa. Isotopic analysis of the ^{18}O and ^{2}H of the waters lie along the GMWL but offset from modern precipitation indicating a paleometeoric origin confirmed by noble gas derived residence times on the order of a few Ma (1).

Multiple isotope analysis of carbon isotopes (^{13}C, ^{14}C) was applied to microbial cellular components (PLFA, DNA) and potential carbon sources and/or metabolites including dissolved inorganic carbon (DIC) and CH_4. $\Delta^{14}C$ of DIC was observed to be -980 ‰, slightly enriched above expectation for geologically old carbon ($\Delta^{14}C$ = -1000 ‰). Concurrently, PLFA and DNA $\Delta^{14}C$ were -940 ‰ demonstrating microbial utilization of highly ^{14}C depleted carbon sources. This is the first study we are aware of to compare two such distinct cellular components. The close agreement of these independent measurements supports the accuracy of both approaches. The fact that these microbial cellular components were slightly isotopically enriched related to the DIC suggests inputs from a ^{14}C enriched carbon source. The potential role of methane ($\delta^{13}C$ =-52 ‰ at this site) as a C source in this ecosystem is suggested by the $\delta^{13}C$ of PLFA from these communities (-50 to -65 ‰). This hypothesis will be investigated by on-going isotopic analysis of the ^{14}C methane and ^{13}C DIC pools.

[1] Lippman et al, (2003) GCA 67: 4597-4619

https://doi.org/10.1180/S0026461X00008434 Published online by Cambridge University Press

Subduction-driven growth and modification of cratons: examples from Canada and Greenland

K. A.SMART[1, 2*], S.TAPPE[1, 2], A.SIMONETTI[1,3] AND S.KLEMME[2]

[1]University of Alberta, Edmonton, Canada
[2]WWU, Münster, Germany kasmart@uni-muenster.de (*presenting author) sebastian.tappe@uni-muenster.de, stephan.klemme@uni-muenster.de
[3]Univ. of Notre Dame, Notre Dame, USA simonetti.tony@gmail.com

Cratonic crust and underlying mantle roots are thought to have a shared history of growth and modification since the Archean. However, debate continues on whether their coupled growth was due to mantle plumes or early forms of subduction. Cratonic mantle eclogites are central to this debate and here we present evidence from two such xenolith suites from Canada and Greenland for subduction-driven growth and modification of cratonic lithosphere.

We have determined the Pb isotope compositions of clinopyroxenes from eclogite xenoliths from the northern Slave and the West Greenland North Atlantic craton (NAC). Clinopyroxenes from NAC eclogites define a secondary isochron with an age of 2.7±0.3 Ga, which intersects a terrestrial Pb isotope evolution curve at ca. 2.62 Ga. This suggests Late Archean eclogite formation via melt extraction during subduction of oceanic crust [1]. Pb isotope compositions of the Slave clinopyroxenes do not define a statistically meaningful isochron. Instead, they appear to form a mixing array extending from clinopyroxene with unradiogenic Pb ($^{206}Pb/^{204}Pb$ ~ 14.3) to the host Jurassic kimberlite ($^{206}Pb/^{204}Pb$ ~ 19.2). We believe this array was produced by mixing between kimberlitic- and eclogitic derived Pb. Hence, the least radiogenic Pb isotope composition that intersects the Stacey-Kramers evolution curve at ca. 2.2 Ga has age significance. Importantly, this model age falls within the age range of 2.3-1.8 Ga shown by other eclogites from the Slave craton [2].

Both the Slave and NAC eclogite xenoliths have geochemical signatures that indicate oceanic crust protoliths, including $\delta^{18}O$ values that range above the mantle average (5.2-6.4‰). Moreover, the eclogite ages coincide with putative subduction events in each craton. NAC eclogite formation coincides with 2.9-2.7 Ga crustal growth marked by the intrusion of TTG granitoids in West Greenland. These TTGs are interpreted as melts of subducted oceanic basalts from their complementary relationship with the refractory NAC eclogites. The Slave eclogites coincide in age with the ca. 1.9 Ga subduction event that affected the western craton margin. Unlike Greenland, this subduction event did not add significantly to the Slave cratonic crust, and instead introduced eclogitic material to the craton root [2]. Furthermore, ca. 1.9 Ga eclogitic diamonds from the Slave craton [3] suggest that this subduction event introduced appreciable amounts of carbon into the mantle lithosphere. Thus, while both eclogite suites record craton evolution events, major crustal growth was only associated with the Archean Greenland eclogites, whereas late-stage cratonic root modifcation including metasomatism and diamond growth are marked by the Paleoproterozoic Slave eclogites.

[1] Tappe *et al.* (2011) *Geology* **39** 1103-1106. [2] Schmidberger *et al.* (2005) *EPSL* **240**, 621-633.

Formation of eclogites and pyroxenites below Attawapiskat, Superior Craton (Canada)

KAREN V. SMIT*[1], THOMAS STACHEL[1], ROBERT A. CREASER[1], S. ANDREW DUFRANE[1], RYAN B. ICKERT[2], RICHARD A. STERN[2] AND MICHAEL SELLER[3]

[1] Department of Earth and Atmospheric Sciences, University of Alberta, Edmonton, Canada, kvsmit@ualberta.ca*
[2] Canadian Centre for Isotopic Microanalysis, Department of Earth and Atmospheric Sciences, University of Alberta, Edmonton, Canada
[2] De Beers Canada, Toronto, Canada

Seventeen eclogite and 16 pyroxenite xenoliths from the Victor kimberlite at Attawapiskat will be used to assess whether they show evidence for a shallow origin as oceanic crust, emplaced into the Superior SCLM by tectonic stacking. Eclogites contain omphacite + garnet, whereas the pyroxenites contain diopside + garnet ± enstatite; three broad groups (Ca, Fe or Mg-rich) are recognised through their reconstructed whole rock major and rare earth element chemistry.

The sole high-Ca kyanite-bearing eclogite is the only sample with a positive Eu anomaly and has a subchondritic REE_N pattern consistent with an oceanic crust precursor undergoing dehydration/low degree partial melting during subduction. Fe-rich eclogites have flat $MREE_N$ to $HREE_N$ –indicative of a low-pressure origin – and depleted $LREE_N$. The high Mg eclogites and pyroxenites have similar flat $MREE_N$ to $HREE_N$, but enriched $LREE_N$ indicating a shallow origin and a subsequent stage of fluid metasomatic enrichment. Reconstructed whole rock compositions for these high Mg eclogites and pyroxenites rocks overlap with orogenic pyroxenites [1], suggesting a possible primary origin as basaltic intrusives in the shallow lithosphere.

Cpx from all the compositional groups have depleted Sr isotopic compositions (0.7019-0.7039) relative to present day bulk earth (0.7045). The majority of the samples have $\delta^{18}O$ overlapping, within uncertainty, to the mantle value. Mantle-like $\delta^{18}O$ values do not rule out oceanic crust as protoliths [2,3], and therefore these data cannot be used to distinguish between a low versus a high pressure origin. Evidence for involvement of crustal components in the genesis of the Superior's lithospheric mantle are flat $MREE_N$ to $HREE_N$ patterns and a positive Eu anomaly in the kyanite-bearing eclogite. Re-Os analyses and in-situ cpx Pb-Pb dating of these eclogites and pyroxenites are currently underway.

[1] Pearson et al. (1993) *Journal of Petrology* **34,**1,125-172 [2] Hart et al. (1999) *Geochimica et Cosmochimica Acta* **63**,4059-4080 [3] Schmickler et al. (2004) *Lithos* **75**,173-207

https://doi.org/10.1180/S0026461X00008434 Published online by Cambridge University Press

Iron isotope fractionation in stromatolitic oncoidal iron formation, Mesoarchean Witwatersrand-Mozaan Basin, South Africa

ALBERTUS J.B. SMITH[1*], NICOLAS J. BEUKES[1], JENS GUTZMER[1,2], CLARK M. JOHNSON[3], AND ANREW D. CZAJA[3]

[1]PPM, Department of Geology, University of Johannesburg, Johannesburg, South Africa, bertuss@uj.ac.za (* presenting author), nbeukes@uj.ac.za

[2]Department of Mineralogy, Techische Universität Bergakademie Freiberg, Freiberg, Germany, jens.gutzmer@mineral.tu-freiberg.de

[3]Deparment of Geoscience, University of Wisconsin-Madison, Madison, Wisconsin, USA, clarkj@geology.wisc.edu, aczaja@geology.wisc.edu

Iron isotope fractionation in an Archean marine basin through biological and abiological processes is well illustrated in an iron rich unit in the Mesoarchean (2.96-2.92 Ga) Witwatersrand-Mozaan Succession [1] of South Africa and Swaziland. The unit comprises the oldest known shallow water oncoidal granular iron formation interbedded with magnetite- and stilpnomelane-rich mudstone and mixed mineralogical facies banded iron formation. The banded iron formation marks the most distal and the oncoidal iron formation the most proximal depositional settings. The oncoidal iron formation shows domal and columnar micro-stromatolite rims composed of magnetite around chert and calcite grains in a matrix of chert and minor iron-rich silicate. The more distal banded iron formations and iron-rich mudstones have δ^{56}Fe values ranging from slightly positive to strongly negative depending on the dominant iron-rich phase. The stromatolitic oncoidal iron formation has δ^{56}Fe values from zero to strongly positive. Moreover, the δ^{13}C values of the calcite in the latter are strongly negative, suggesting the carbonates formed through the oxidation of organic carbon.

The geochemical evidence along with the depositional facies reconstrution show that the mode of iron deposition varied from the distal to proximal depositional settings, and is the most dominant control on iron isotope fractionation. The limited iron source that reached the proximal setting of the stromatolitic oncoidal iron formation had zero to positive δ^{56}Fe values. Textural and geochemical evidence suggest that iron oxidizing microbes [2] living on the rims of reworked chert grains used the limited ferrous iron in the shallower part of the basin in their metabolism to precipitate ferrihydrite, which would concentrate heavy iron isotopes [3]. The ferrihydrite underwent a redox reaction with organic carbon during diagenesis to form magnetite that retains the heavy iron isotopic signature and isotopically light calcite. The lighter iron isotopes remaining in solution were incorporated into iron-rich silicates in the matrix.

[1] Beukes & Cairncross (1991) *Trans. Geol. Soc. S. Afr*. **45**, 44-69. [2] Konhauser *et al.* (2002) *Geology* **30**, 1079-1082. [3] Croal *et al.* (2004) *Geochim Cosmochim Ac* **68**, 1227-1242.

The pyroxene sponge: amphibole signatures and controls on water in arc magmas

D. J. SMITH[1*]

[1]University of Leicester, Leicester, UK, djs40@le.ac.uk (* presenting author)

Many arc magmas show evidence of amphibole fractionation, in the form of characteristic REE profiles and exhumed amphibole cumulates. However, amphibole is not always a major modal phase in the erupted suites: thus, fractionation is cryptic [1]. In water-rich (>4 wt% H_2O) magmas where amphibole fractionation is most pronounced, high Sr/Y signatures develop [2]. Elevated Sr/Y magmas have an association with porphyry mineralisation (e.g. [3]) – most likely an indicator that water-rich, amphibole stable melts are fertile for porphyry formation [4].

Clinopyroxene is an early and abundant fractionating phase in most arc magmas, and unlike amphibole is common in the erupted rocks. New data from the Solomon Islands suggest that the early-formed clinopyroxene cumulates can react with evolving magmas, forming amphibole as a secondary metasomatic phase. The "cryptic" fractionation of amphibole may in fact be clinopyroxene cumulate–melt reactions, generating REE profiles characteristic of amphibole removal without it being a major modal phase in the crystallising magma.

Furthermore, the Solomon Islands data show that these metasomatic amphibole cumulates can be contrasted with true amphibole cumulates (i.e. directly crystallised and fractionated amphibole), with only the true amphiboles generating strong Y depletion (and by extension, high Sr/Y) in the daughter magmas.

The clinopyroxene cumulates are potentially acting as a sponge, modifying the daughter magma's REE signature, and locking up water as they react to form amphibole. More hydrous magmas, able to directly crystallise amphibole and generate high Sr/Y, may only form where the sponge has been entirely metasomatised, and is no longer capable of locking up water. The clinopyroxene sponge possibly limits water content and magma fertility under normal arc-fractionation conditions. Fertile magmas are either more hydrous at source (able to directly crystallise amphibole), or only develop after repeated cycles of intrusion and cumulate–melt reaction.

References

[1] Davidson *et al.* (2007) *Geology* **35**, 787–790.
[2] Smith *et al.* (2009) *Contributions to Mineralogy & Petrology*, **158**, 785–801.
[3] Oyarzun et al. (2001) *Mineralium Deposita*, **36**, 794–798.
[4] Richards (2011) *Economic Geology* **106**, 1075-1081.

https://doi.org/10.1180/S0026461X00008434 Published online by Cambridge University Press

Enhanced multicollector ICP-MS coupled with a desolvating nebulizer system for geochronology

FRED G. SMITH[1*], VICTOR POLYAK[2]

[1]CETAC Technologies, Omaha NE USA, fsmith@cetac.com(* presenting author)
[2]University of New Mexico, Earth and Planetary Sciences, Albuquerque NM, USA, polyak@unm.edu

Abstract

Multicollector ICP-MS instruments are very specialized devices for high precision isotope ratio measurements. For accurate measurement of low abundance isotopes, signal enhancement is often required. In addition, sample preparation and/or sample aerosol desolvation may be necessary to reduce or eliminate mass spectral interferences such as oxides and hydrides.

This paper will examine the coupling of an enhanced multicollector ICP-MS instrument with a dedsolvating nebulizer system for geochronology. The hardware specification of the ICP-MS will be detailed, including a revised vacuum system and special sampler and skimmer interface cones. Important operating conditions of the desolvating nebulizer system include argon sweep gas and nitrogen addition gas flows.

Application of this coupled system to U-series dating will be described.

Mineralogy and porewater geochemistry of processed kimberlite: implications for acid rock drainage and metal releases

LIANNA J.D. SMITH[1*], MICHAEL C. MONCUR[2], DOGAN PAKTUNC[3], AND YVES THIBAULT[3]

[1]Rio Tinto - Diavik Diamond Mines, Yellowknife, YK, Canada, Lianna.smith@riotinto.com (*presenting author)
[2]Alberta Innovates-Technology Futures, Calgary, AB, Canada, michael.moncur@albertainnovates.ca
[3]CANMET Mining and Mineral Sciences Laboratory, Ottawa, ON, Canada, dpaktunc@NRCan.gc.ca, ythibaul@nrcan.gc.ca

The development of diamond mines in Canada's North emphasizes the need to assess the environmental implications of storing processed kimberlite tailings (PK) in regions with continuous permafrost. The Diavik Diamond Mine (Diavik) is located in the barren lands on an island in Lac de Gras, 300 km northeast of Yellowknife, NT, Canada. During the life of the mine, up to 42 million tonnes of PK will be produced and disposed on site for permanent storage. In 2009, a study was initiated to understand the mineralogy and evolution of porewater geochemistry in the PK tailings impoundment. Porewater was collected and analyzed from a number of core and drive-point piezometers located across an exposed PK beach and in the central pond. The core samples were analyzed and characterized in detail. The samples collected from the tailings pond are composed of Ni-bearing olivine, calcite, quartz, garnet, lizardite, biotite, albite, saponite and both framboidal and massive pyrite. Olivine and its alteration products made of lizardite, iron oxides and magnesian aluminosilicates are the dominant minerals. Neutralization potentials of the samples are between 39 to 85 kg $CaCO_3$ eq/t, far exceeding the acid generating potentials in the 5 to 12 kg $CaCO_3$ eq/t range due to the presence of pyrite. Porewater samples from the unsaturated zone of the impoundment have the lowest pH values and highest concentrations of dissolved SO_4 and metals. With depth, pH values increase and dissolved SO_4 and metals concentrations decrease towards the water table. In the saturated zone, average dissolved concentrations decrease by almost an order of magnitude compared to the unsaturated zone for SO_4, major cations and most metals (e.g SO_4: 3500 to 350 mg/L; Mg: 730 to 80 mg /L, Ni: 0.82 mg/L to 0.038 mg/L). Sulfur isotope ratios measured from the porewater are strongly depleted averaging -17.9 ‰ and show minimal fractionation from the unprocessed kimberlite, suggesting dissolved sulfate concentrations are resulting from sulfide oxidation; however, there are no apparent mineralogical features on pyrite grains indicative of oxidative dissolution. Except for a single grain of $BaSO_4$, no other sulfate minerals were identified in the PK. Porewaters from the underlying frost zone show further increases in pH and decreases in dissolved SO_4 and metal concentrations. Groundwaters collected from piezometers installed in PK stored below a water cover revealed dissolved concentrations of major ions and metals which are comparable to those measured from the frost zone. Results from this study show that subaqueous disposal and freezing of the PK material would restrict oxidation and dissolution processes and limit the release of dissolved concentrations of metals and SO_4.

https://doi.org/10.1180/S0026461X00008434 Published online by Cambridge University Press

Solubilities of arsenic oxy- and thio–compounds in calcium rich waters

MATT SMITH[1*] AND DIRK WALLSCHLÄGER[2]

[1]Trent University ENLS Graduate Program, Peterborough, Canada, mattsmith@trentu.ca (* presenting author)
[2]Trent University Department of Chemistry, Peterborough, Canada, DWallsch@trentu.ca

16l. Biogeochemistry of Oxyanion-Forming Trace Elements in the Environment

The mobilisation of arsenic by thiolation is a significant driver of As solubility in sulphidic, reducing systems and alkaline environments [1, 2]. The determination of the chemistry of arsenic thioanions requires specific analytical methods to for detection. The complex chemistries of environments containing thioarsenicals create problems with regard to preservation of *in situ* arsenic speciation. Co-precipitation of arsenic with iron[3] or other minerals salts has been shown to occur during the lag time between *in situ* sampling and laboratory analyses. Calcium (Ca) is a ubiquitous element in alkaline natural systems containing As. The insolubility of Ca-arsenate salts has been documented[4] thus quantitative losses of As from *in situ* samples containing Ca is a probable mechanism.

Interactions between Ca and arsenic oxy- and thioanions were studied under anoxic, alkaline conditions. We have studied the precipitation of Ca-thioarsenate salts, and have been able to experimentally determine the K_{SP}, $\Delta G°_f$, $\Delta H°_f$, and $\Delta S°$, for Ca-monothioarsenate, Ca-arsenite, and Ca-arsenate. Trithioarsenite, trithioarsenate and tetrathioarsenate do not form Ca-arsenic salts or absorb to Ca carbonate ($CaCO_3$), Ca hydroxide or Ca sulphate, indicating that these species are the most soluble anionic arsenic species. Dithioarsenate is more soluble than monothioarsenate and arsenate, and arsenite is the least soluble As species. The solubilities of Ca sulphate and $CaCO_3$ are less than those of the Ca-arsenic salts, thus adsorption of arsenite and arsenate to Ca sulphate and $CaCO_3$ can be a significant mechanism of removal of As oxyanions in the environment. Increasing thiolation enhances the solubility of As anions such that no chemical interaction exists between As and Ca in the environment for tri- and tetra-thiolated species.

[1] Fisher (2008) *Environ. Sci. Technol,* **42(1),** 81–85.
[2] Wallschläger (2007) *Anal. Chem,* **79,** 3873–3880.
[3] Suess (2011) *Chemosphere* **83(11),** 1524–1531.
[4] Bothe (1999) *J. Haz. Mater. B* **69,** 197–207.

Ionic force fields for electrolytes and molecular simulation of chemical potentials and aqueous solubility

WILLIAM R. SMITH[1*] AND FILIP MOUČKA,[1,2]

[1]University of Ontrio Institute of Technology, Oshawa, Canada, william.smith@uoit.ca*
[2]J.E. Purkinje University, Ústí n. Labem, Czech Republic, fmoucka@seznam.cz

We have recently [1,2] developed the Osmotic Ensemble Monte Carlo (OEMC) method for calculating the chemical potentials and solubility of aqueous electrolytes and their mixtures by molecular simulation. OEMC is a computationally efficient algorithm that uses a type of semi grand canonical ensemble, with a fixed number of water molecules at temperature T and pressure P, and electrolyte chemical potentials specified by the inter-phase equilibrium reaction involving the ions and their crystalline solid. To calculate solubility, we use accurate chemical potential data for the solid from thermochemical tables[3]. By appropriately setting the solid's chemical potential to other values, the entire chemical potential vs concentration curve of the ions in solution can be mapped out.

Although our results show good qualitative and reasonable quantitative accuracy, improvements depend on the use of more accurate ionic force fields. In this talk, we describe calculation strategies and show results for new force-field models for Na^+ and Cl^- compatible with SPC/E water. Our new force fields demonstrate good accuracy for the combined ion pair chemical potentials, the solution density, the predicted solubility and the solid chemical potential and density. Preliminary results are shown in the figure.

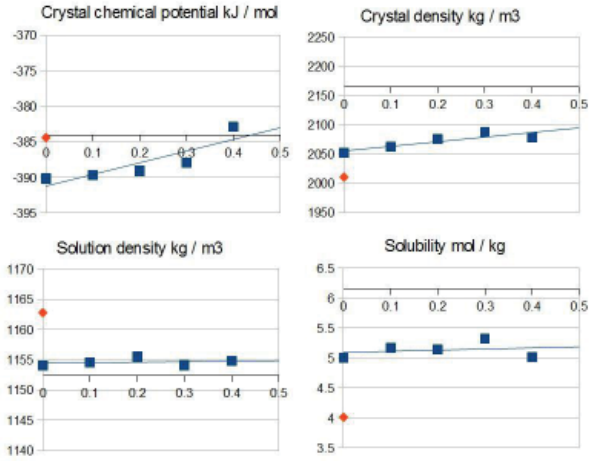

Figure: NaCl crystal and solution properties as functions of a model parameter after one iteration of the force-field adjustment strategy. Blue: our results; Orange:results using the force field of Joung and Cheatham[4]; Horizontal lines: experiment.

[1] Moučka, Lísal, Škvor, Jirsák, Nezbeda & Smith (2011) *J. Phys. Chem. B* **115**, 7849–7861.
[2] Moučka, Lísal, Smith (2012) *J. Phys. Chem. B*, submitted.
[3] Chase (1998) *J. Phys. and Chem. Reference Data Monograph No.9, Am. Chem. Society, Am. Inst Physics*.
[4] Joung, & Cheatham (2008) *J. Phys. Chem. B* **112**, 9020-9041.

https://doi.org/10.1180/S0026461X00008434 Published online by Cambridge University Press

Insights into the 2300Ma magmatic shutdown

R.G. SMITS[1*], M.HAND[1], W.J. COLLINS[2]

[1]Centre for Tectonics, Resources and Exploration, University of Adelaide, S.A. 5005, Australia, russell.smits@adelaide.edu.au (* presenting author)

[2]School of Environmental and Life Sciences, University of Newcastle, NSW 2308, Australia,

Zircon geochronology and isotope geochemistry allows insights into the temporal and geodynamic controls on tectonic events. The global record of magmatic events reflected from zircon spectra is episodic, with large widespread events in zircon geochronology occurring periodically and related to supercontinent amalgamation. Conversely large troughs in the zircon spectra have been inferred to tectonic shutdown and magmatic hiatus. A large trough in the global zircon record around 2300Ma is interpreted to reflect this phenomenon, with widespread reduction in magmatic activity beginning at 2.45Ga to 2.2Ga (Condie *et al.* 2009). Whilst no direct outcrop of 2.3Ga magmatic lithologies has been sampled, a number of detrital samples record distinct populations at 2.3Ga allowing for interrogation of this geodynamically distinct time in the Earths evolution. The detrital zircon spectra in the Warumpi Province sediment samples display peaks at 1.8Ga, 2.5Ga with minor 2.3Ga comparable to the North China Craton and to a lesser extent Antarctica. Coupled U-Pb geochronology and Hf isotopic data from detrital samples in the central Australian Warumpi Province reveals distinct populations of 2300Ma zircons and the source mantle composition. The similarities in the age distributions raise the possibilities of co-evolution between these cratons and the links to the Nuna Supercontinent formation in the Paleoproterozoic. The coupled Hf isotope and U-Pb age analysis for zircons between 2.45-2.2Ga display variable arrays and large distribution between juvenile mantle to evolved sources, with distinct clusters observed. The variable spread of the Hf isotopic data indicates there are varied geodynamic systems at large during a period of proposed tectonic quiescence.

CONDIE K. C., O'NEILL C. & ASTER R. C. 2009. Evidence and implications for a widespread magmatic shutdown for 250 My on Earth. *Earth and Planetary Science Letters* **282**, 294-298.

The U-Th-Pb allanite petrochronometer: a combined ID-TIMS and LA-ICP-MS study

A.J. SMYE [1*], N.M.W. ROBERTS[1], D.J. CONDON[1], M.S.A. HORSTWOOD[1], R.R. PARRISH[1,2]

[1]NERC Isotope Geosciences Laboratory, British Geological Survey, Keyworth, Nottingham, NG12 5GG, U.K.

[2]Department of Geology, University of Leicester, University Road, Leicester, LE1 7RH, U.K.

Abstract

Allanite ($(Ce,Ca,Y,La)_2(Al,Fe^{+3})_3(SiO^4)_3(OH)$) is important as a U-Th-Pb petrochronometer of metamorphic and igneous crustal processes. Largely, this is because of its extended *P—T—X* stability field over other U-Th-Pb mineral chronometers [1], its ubiquity in felsic to aluminous melts [2] and its ability to retain radiogenic Pb at temperatures > 650ºC [3]. Furthermore, allanite plays a key role in the transport of LREE, U, Sr and Th in subducted crust [4].

Weight % concentrations of U and Th mean that both U-Pb and Th-Pb systems can potentially be used to constrain the age of radiogenic Pb in-growth. Th/U values up to 1000 mean that the Th-Pb system is preferentially targeted. However, successful U-Th-Pb allanite geochornology is hampered by: (**i**) the propensity of allanite to sequester high levels of non-radiogenic Pb (up to 95%); (**ii**) the presence of excess-^{206}Pb arising from incorporation of ^{230}Th; (**iii**) its common lack of crystallographic integrity, and (**iv**) compositional solid-solution with the epidote group minerals. Therefore, as the use of allanite U-Th-Pb data becomes more widespread, it is vitally important to understand the limitations and strengths of allanite as a petrochronometer.

Available allanite reference materials are poorly characterised; notably, there is a dearth of accurate U-Pb, and particularly, Th-Pb ID-TIMS data. Given that allanite is most commonly dated by LA-ICP-MS and SIMS, this means that many published datasets likely conceal considerable uncertainty in the accuracy of calculated age estimates.

This contribution presents the results of a combined ID-TIMS and LA-ICP-MS U-Th-Pb study on a suite of allanite reference materials, including two of the most commonly used allanite standards: the SISS and Tara allanites [5], in addition to a new potential allanite reference material. Both ID-TIMS and LA-ICP-MS analyses have been performed on the same allanite grain fractions so as to minimise normalisation-induced uncertainty. The high spatial resolution of the LA-ICP-MS technique, together with WDS-SEM imaging and powder XRD shows that allanite retains closed-system U-Th-Pb isotope systematics despite its pervasively metamict state. Open-system behaviour is restricted to clearly-identifiable zones of fluid-mediated alteration.

[1] Spear (2010) *Chem. Geol.* **279**, 55-62.
[2] Giere *et al.* (2004) *Rev.Min. Geochem.* **56**, 431-493.
[3] Heaman *et al.* (1991) *Min. Assoc. Can.* **19**, 59-102.
[4] Hermann (2002) *Chem. Geol.* **192**, 289-306.
[5] Gregory *et al.* (2007) *Chem. Geol.* **245**, 162-182.

https://doi.org/10.1180/S0026461X00008434 Published online by Cambridge University Press

Redox conditions of Hadean magmas: Insight from Ce-in-zircon oxygen barometry

DUANE J. SMYTHE[1*] AND JAMES M. BRENAN[1]

[1]University of Toronto, Department of Geology, Toronto, Canada, smythe@geology.utoronto.ca (* presenting author), j.brenan@utoronto.ca

Positive Ce anomalies on chondrite normalized REE abundance diagrams are a nearly ubiquitous feature of zircon. This is the result of the presence of trace amounts of Ce^{4+} in natural systems and the higher compatibility of Ce^{4+} over Ce^{3+} in zircon. Using experimental determinations of the Ce^{4+}/Ce^{3+} in the melt as a function of fO_2 and melt composition, we have calibrated a Ce-in-zircon oxygen barometer independent from that of Trail et al. [1]. Our method takes the approach of Ballard et al. [2], applying the lattice strain model to measured D(zircon/melt) trace element distribution coefficients for both the REEs and a suite of 4+ cations (Zr, Hf, Th, U) which allows the estimation of the end-member D values for Ce^{3+} and Ce^{4+}. Measured "bulk" D_{Ce} values, which plot on a mixing curve between these end members, can then be related to the fraction of Ce as 4+ in the melt. Our calibration then allows for this to be linked directly to fO_2.

Evaluation of this technique has been carried out on zircons from three different lithologies whose fO_2 (expressed as Δ FMQ) has been estimated independently: rhyolite from the Bishop tuff, California (FMQ +1.1 ± 0.6), dacite from the Toba tuff, Indonesia (FMQ +0.9 ± 0.6), and monzodiorite from the Umiakovik pluton, Nain plutonic suit, Labrador (FMQ -2.4 ± 1.4). Trace element concentrations of zircon and host glass were measured by LA-ICP-MS. Values of Δ FMQ calculated by our method are +1.6 ± 0.4 (Bishop tuff), +0.8 ± 0.7 (Toba tuff) and -3.9 ± 0.5 (Umiakovik pluton), which are within error of the independent estimates.

Using D(zircon/melt) values for the REEs from Sano et al. [3] and empirical estimates for the 4+ cations, we have applied our oxygen barometer to Hadean zircons from the Jack Hills, Australia. Calculated values of Δ FMQ for zircons whose $\delta^{18}O$ is in the mantle range yield a bimodal distribution with peaks at –2.4 (n = 4) and +2.0 (n = 7). This appears to be connected to the crystal chemistry as light REE enriched samples consistently give lower estimations of fO_2. In addition to fO_2 we have also observed considerable dependence in Ce^{4+}/Ce^{3+} on melt composition. For the likely range in composition of zircon crystallizing melts this would affect the calculated fO_2 by at most 1 Δ FMQ unit. Therefore, the range in fO_2 observed is beyond that which can be explained by melt composition alone. This suggests that heterogeneities in fO_2 persisted in the source region for the zircon-producing magmas during the Hadean.

[1] Trail et al. (2011) *Nature* **480**, 79-82. [2] Ballard et al. (2002) *Contrib. Mineral. Petrol.* **144**, 347-364. [3] Sano et al. (2002) *Chem. Geol.* **184**, 217-230.

Atomic scale imaging of U, Th and radiogenic Pb in zircon

DAVID R. SNOEYENBOS[1*], DAVID REINHARD[1], AND DAVID P. OLSON[1]

[1]Cameca Instruments Inc., Madison, WI, USA David.Snoeyenbos@ametek.com (* presenting author)

Radiometric dating of a mineral depends on the assumption that the parent radionuclides and daughter radiogenic Pb have remained together within the analyzed volume. Isotopic dating techniques continue to evolve from bulk methods towards *in situ* techniques with ever smaller analyzed volumes such as afforded by LA-ICPMS and SIMS. The use of small sample volumes in zircon minimizes common Pb from microinclusions, but increases the importance of knowing if there has been any spatial redistribution of the radiogenic Pb relative to its parents.

In Atom Probe Tomography (APT) a specimen with dimensions of a few hundreds of nanometers is evaporated atomic layer by atomic layer. The original position of each atom is identified, along with its atomic species, and in most cases its isotope. The result is a reconstruction allowing quantitative three-dimensional study of the specimen at the atomic scale, with very low detection limits and high mass resolution.

A zircon specimen in garnet from recently identified possible UHP rocks from the Taconian of Western Massachusetts, USA [1] was selected for study by APT. WDS mapping and quantitative analysis by FE-EPMA had revealed high concentrations of Th and U in a submicron envelope between a resorbed zircon core, and a subsequent metamorphic overgrowth.

Guided by FE-EPMA trace-element mapping, a sample of this envelope was extracted by FIB and milled into 200nmX100nm conical tips appropriate for APT. A dataset of ~11 million atoms was obtained, revealing a 25nm wide band of zircon between core and overgrowth containing >0.25 at% each of U and Th.

Sufficient radiogenic Pb had accumulated within the specimen to be detectable by APT, consistent with the high concentrations of radionuclides and the expected 4-500my age of the specimen,. Strong spatial covariance was observed between U and 206Pb, without apparent migration or agglomeration of the radiogenic Pb atoms.

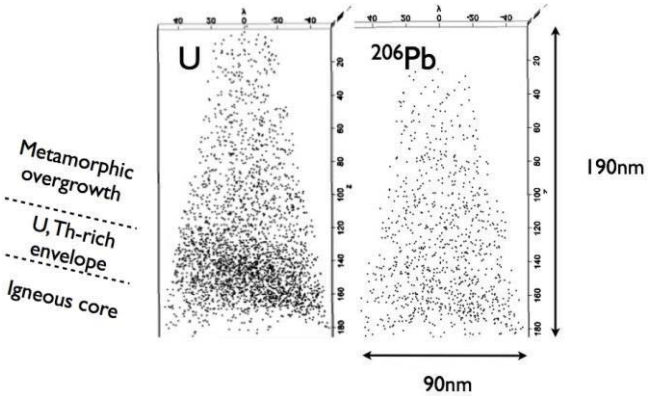

Figure 1: Ion image of U(total) and 206Pb atoms detected by APT.

[1] Snoeyenbos, Koziol, Russell, Ebel and Valley (2011) *EOS Trans. Fall meeting Suppl.* **Vol 92**, Abstract V21G-04

https://doi.org/10.1180/S0026461X00008434 Published online by Cambridge University Press

Sr, Nd, Pb and Hf isotopic constraints on mantle sources in the Payenia backarc basalts (Mendoza, Argentina)

NINA SØAGER[1*], PAUL MARTIN HOLM[1], MATTHEW F. THIRLWALL[2]

[1]University of Copenhagen, Copenhagen, Denmark, ns@geo.ku.dk (*presenting author)
[2]Royal Holloway University of London, London, UK, M.Thirlwall@rhul.ac.uk

The mainly alkaline basalts and trachybasalts from the Payenia volcanic province of southern Mendoza show a great variation in geochemistry ranging from intraplate to arc-backarc compositions. In Pb-Sr-Nd-isotopic space the retroarc and Nevado volcanic field samples form a common trend from the isotopic composition of the Andes transitional southern volcanic zone arc (TSVZ) towards a component with higher Sr and lower Nd-isotopes. This is interpreted as contamination by lithospheric mantle melts due to a sharp decrease in La/Sm, Tb/Yb and incompatible element contents (except Ti) along this trend, making upper crustal contamination unlikely.

The intraplate basalts from the Río Colorado area have lower Pb and Sr and slightly higher Nd-isotopic composition than the Nevado samples and apparently reveal the composition of an astenospheric mantle end-member. The very low Th/Nb, high U/Pb and Ce/Pb of the Río Colorado basalts precludes any significant input from the subduction zone. In Nd-Hf isotopic space they plot at negative ΔεHf along with FOZO and HIMU-type basalts but the Sr-isotopic values are slightly higher (~0.70355) than these. The Pb-isotopes and trace element patterns are comparable to EM1-type ocean island basalts (OIB) which could suggest that the Río Colorado mantle source is a mixture of FOZO and EM1 material. Even though the trace element patterns are very similar to some Somuncura basalts (another Patagonian hotspot [1, 2]), the Somuncura EM1 end-member is dissimilar in Pb-isotopic space [2]. The presence of recycled crust in the mantle source is supported by the indication that some of the Río Colorado and Payún Matrú basalts are pyroxenite melts as judged by their low Ca, Sc, Mn and MgO and high FeO_T, Ni and SiO_2 compared to peridotite melts.

The high $^{143}Nd/^{144}Nd$ Nevado and retroarc samples have similar εNd to Río Colorado samples but higher εHf and possibly trend towards South Atlantic N-MORB compositions. Furthermore, the major element composition of these lavas is akin to peridotite melts. This suggests that there are two asthenospheric mantle sources beneath the Payenia province: a South Atlantic normal upper mantle and an OIB-type mantle which dominates in the Río Colorado and Payún Matrú regions. The normal upper mantle peridotite is apparently only melted when fluids are added from the subduction zone whereas the OIB mantle melts due to a higher mantle temperature or/and a lower solidus temperature of the pyroxenite components.

[1] Remesal et al. (2002) *Rev. Asoc.Geol. Arg.* **57 (3)**, 260-270. [2] Kay et al. (2007) *Journal of Petrology* **48 (1)**, 43-77.

Melt inclusions as a source of principal geochemical information

ALEXANDER V. SOBOLEV[1,2,3]

[1] University J. Fourier, ISTerre, Grenoble, France. alexander.sobolev@ujf-grenoble.fr
[2] Max Planck Institute for Chemistry, Mainz, Germany.
[3] Vernadsky Institute of Geochemistry, RAS, Moscow, Russia.

Recent papers [1-5] on the in-situ radiogenic isotope composition of melt inclusions report controversial conclusions on the scale and origin of isotope heterogeneities. In this paper I will review these results focusing mostly on the question: whether melt inclusions can provide the new geochemical information on the origin, composition and scale of mantle heterogeneity?

The study of some 140 olivine hosted melt inclusions from a single lava of Mauna Loa volcano (Hawaii) reveals incredible Sr isotope source heterogeneity: at least 87Sr/86Sr=0.7027-0.7074 (Fig 1) [5]. Based on the 2-sigma criterion we found that 21% of inclusions fall out of the isotopic range of Mauna Loa lavas and 8% fall out of the isotopic range of all Hawaiian Lavas (Fig 1). Most compositionally distinct melts were trapped in high Mg olivine (Fo>86). We show that melt fractions with different compositions were mixed up during olivine crystallization producing typical Mauna Loa lavas. This result indicates unprecedented Sr isotope anomaly in Hawaiian mantle source caused by entrainment of Phanerozoic oceanic crust altered by seawater [5]. It also shows that bulk rocks could easily mask original source heterogeneity, which can be often deciphered ONLY by melt inclusions study.

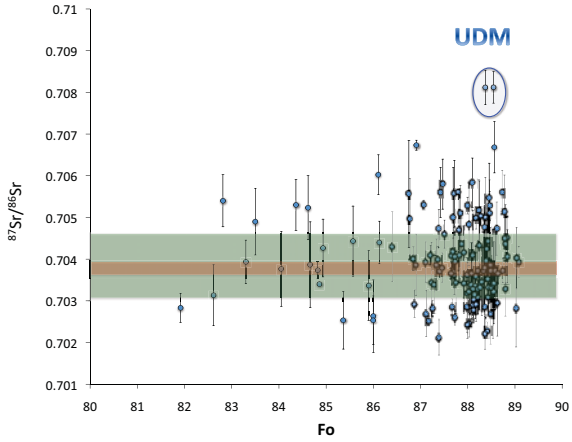

Figure 1: Isotope compositions of melt inclusions in olivine phenocrysts from a single lava sample of Mauna Loa volcano, Hawaii versus composition of host olivine [5]. Narrow (brown) and wider (green) fields manifest composition of all Mauna Loa lavas and all Hawaiian lavas respectively. Error bars: one standard error. Outlined are ultra-depleted melt inclusions (UDM).

[1] E. Saal *et al.*, (2005) *EPSL* **240**, 605-620. [2]. M. G. Jackson, S. R. Hart, (2006) *EPSL* **245**, 260-277. [3] J. Maclennan, (2008) *GCA* **72**, 4159-4176. [4] B. Paul *et al.*, (2011) *Chemical Geology* **289**, 210-223. [5] A. V. Sobolev, et al (2011), *Nature* **476**, 434-437.

https://doi.org/10.1180/S0026461X00008434 Published online by Cambridge University Press

The way to destroy thick cratonic lithosphere

STEPHAN V. SOBOLEV [1]* AND ALEXANDER V. SOBOLEV[2,3]

[1]GFZ, Geodynamic Modelling, Potsdam, Germany, stephan@gfz-potsdam.de (* presenting author)
[2]University J. Fourier, ISTerre, Grenoble, France, alexander.sobolev@ugf-grenoble.fr
[3] Vernadsky Inst. of Geochemistry, RAS, Moscow, Russia

Thick and chemically distinct cratonic lithosphere is known to be tectonically stable. However there are natural examples when large areas of such lithosphere are flooded by huge volumes of basalts comprising Large Igneous Provinces (LIPs). The examples of LIPs that were at least partially extruded at Archean or Proterozoic lithosphere since 250 Ma are numerous, i.e. Siberian Traps, Central Atlantic Province, Karoo, Parana, North-Atlantic Province etc. The outstanding example of the older (2 Ga) LIP is Bushveld Complex located at Archean craton. Thinning of lithosphere is required by any model of origin of such LIPs because only when the source ascends to shallow level can normal mantle peridotite produce a large amount of melt.

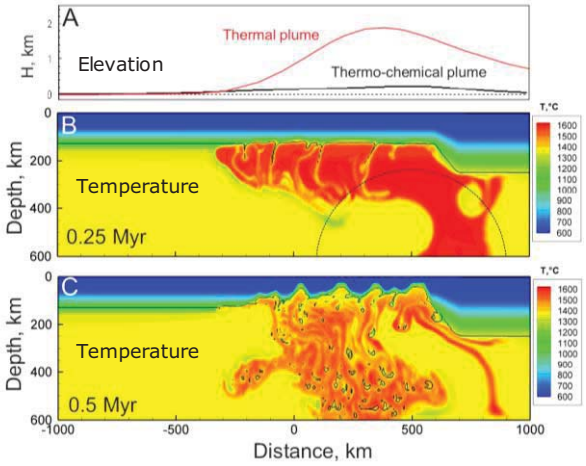

Figure 1: Model of rapid destruction of thick cratonic lithosphere by thermochemical plume without pre-magmatic surface uplift [1].

Recently, a numeric model of LIPs formation focused at Siberian LIP [1] explained rapid destruction of the cratonic lithosphere by the thermo-chemical mantle plume having potential temperature of 1600°C and containing large amount (15 Wt%) of recycled oceanic crust. The huge amount of melt generated from this plume intruded into the lithosphere and caused its delamination/foundering in less than 1 mln years (Figure 1).

In this study we explore limitations of this process. We demonstrate that realistic mantle plume with potential temperature up to 1650 °C, carrying as much recycled oceanic crust as it can remaining positively buoyant in the mantle, can significantly damage lithospheric root up to 200km thick.

[1] S.V. Sobolev et al. (2011) *Nature* **477**, 312-316.

Integrated geochemical and mineralogical investigation of lake deposits at Da Langtan (China) - implications for surface processes on Mars.

SOBRON, P.[1*], WANG, A.[2], MAYER, D.P.[3], SOBRON, F.[4], KONG, F.J.[5], ZHENG, M.P.[5]

[1]Canadian Space Agency, St. Hubert, Canada, pablo.sobron@asc-csa.gc.ca (* presenting author)
[2]Dept. of Earth and Planetary Sciences and the McDonnell Center for the Space Sciences, Washington University in St. Louis, St. Louis, USA, alianw@levee.wustl.edu
[3]Clark University, Worcester, USA, dmayer@clarku.edu
[4]Unidad Asociada UVa-CSIC, Centro de Astrobiologia (CAB-INTA), Valladolid, Spain, sobron@iq.uva.es
[5]R&D Center of Saline Lakes and Epithermal Deposits, Chinese Academy of Geological Sciences, Beijing, China, kongjie69@hotmail.com, zmp@public.bta.net.cn

The Qaidam Basin (QB)(32°-35°N/90°-100°E), located in the northern edge of the Qinghai-Tibet Plateau (China), is a high-altitude desert (aridity index ~0.04). Located at ~3000 m above sea-level, the basin features numerous dissicated evaporative lakes. Fig. 1 displays a partially eroded anticlinal structure (Xiao Liangshan (XL)) within the remains of a former lake in the Da Langtan (DL) playa region of the QB. The evaporation of the lake occurred in parallel with the rise of the anticline, thus producing the spectacular sequence of light and dark-toned rings shown in Fig. 1. This sequence depicts the multiple stages in the evolution of the lake. In-situ IR reflectance spectra were recorded along a traverse across XL, and samples were collected for subsequent laboratory analysis using Vis-NIR reflectance spectroscopy, Raman spectroscopy, and laser-induced breakdown spectroscopy (LIBS). XL was also imaged by Hyperion onboard NASA's EO-1 satellite to extract spectral endmembers from the scene and generate a mineral facies classification map. The surface mineralogy includes carbonates, gypsum, halides, hydrated Mg- and Na-sulfates, and chlorites. This mineral sequence resembles that observed at various locations on Mars, particularly at Gale crater. We have built a lake evaporation model that constrains the physico-chemistry of the DL lake's water (T, pH ...), and can help understand the occurrence of water-related mineral deposits and elucidate the geochemistry of putative former aqueous systems on Mars that resemble those we are investigating at Da Langtan.

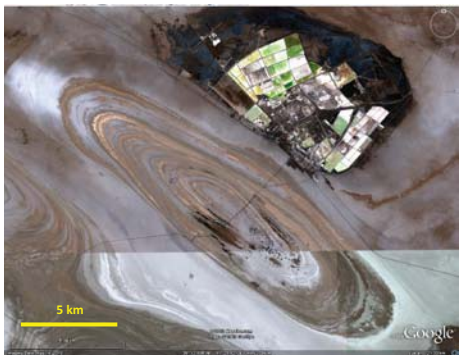

Figure 1: Xiao Liangshan image. Note the ring structure of the deposits across the anticline. Older deposits are on top.

https://doi.org/10.1180/S0026461X00008434 Published online by Cambridge University Press

Soil water vapor isotopes as a tool for understanding ecohydrological processes

K. SODERBERG*[1], S. P. GOOD[1], L. WANG[2], AND K. K. CAYLOR[1]

[1]Department of Civil and Environmental Engineering, Princeton University, Princeton, NJ, USA, soderbrg@princeton.edu (* presenting author)

[2]School of Civil and Environmental Engineering, University of New South Wales, Australia

Abstract

Soil evaporation can represent a significant loss of moisture from an ecosystem. As part of our research into evapotranspiration (ET) dynamics [1], we utilize continuous (1 Hz) measurements of water vapor isotopes to help partition ET into transpiration (T) from plants and evaporation (E) from the soil. This type of measurement is made possible through the recent development of portable, laser-based water vapor isotope analyzers. Defining the necessary isotopic endmembers is relatively straightforward in the case of δ_T using a chamber attached to leaves [2]. The δ_E isotopic signal is more difficult to characterize given that it involves both equilibrium and kinetic isotope fractionation. The liquid soil water isotope composition that gives rise to the δ_E signal can also be very heterogeneous in time and space. We have utilized both a modified Craig-Gordon (CG) modelling approach [3,4] as well as *in situ* measurement of soil water vapor isotopic composition. The CG model was designed to describe the evolution of isotopic composition during evaporation from open water, but is commonly applied to soil evaporation. We propose that soil water potential be used to adjust the normalized humidity parameter in this model, just as the activity of water is used to model evaporating brines. We present results from field measurements at our eddy covariance flux tower in central Kenya, as well as some laboratory data. The effect of this modification is variable, but appears to become significant with soil water potentials drier than around -10 MPa. The *in situ* measurements indicate that even shallow (5-10 cm) soil water vapor appears to be in isotopic equilibrium with adjacent liquid soil water. However, we are currently looking into the effects that soil matric forces can have on equilibrium isotope fractionation factors.

[1] Wang et al. (2010) *Geophysical Research Letters*. **37**, L09401
[2] Wang et al. (2012) *Agricultural and Forest Meteorology*. **154-155**, 127-135.
[3] Craig and Gordon (1965) *Stable isotopes in oceanographic studies and paleotemperatures,* pp. 9-130.
[4] Horita (2008) *Isotopes in Environmental and Health Studies*, 44, 23-49.

Stoichiometry of dissolved bioactive trace metals in the Indian Ocean

HUONG THI DIEU VU[1] AND YOSHIKI SOHRIN[2]*

[1]Institute for Chemical Research, Kyoto University, Uji, Japan, huong@inter3.kuicr.kyoto-u.ac.jp

[2] Institute for Chemical Research, Kyoto University, Uji, Japan, sohrin@scl.kyoto-u.ac.jp (* presenting author)

Introduction

GEOTRACES JAPAN has conducted a section study in the Indian Ocean during the KH-09-5 cruise of R/V Hakuho Maru from November 2009 to January 2010 (Fig. 1). Here we report the results on dissolved bioacitive trace metals (Al, Mn, Fe, Co, Ni, Cu, Zn, Cd and Pb) in seawater. This is the first simultaneous distribution of the nine metals in the Indian Ocean.

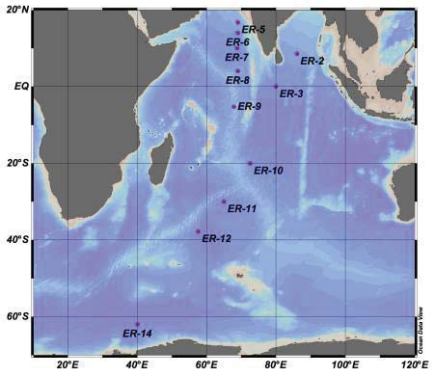

Figure 1: Sampling locations in the Indian Ocean

Methods

Seawater samples were collected using clean technique in accordance with the GEOTRACES protocol. The bioactive trace metals were preconcentrated by solid extraction using the NOBIAS CHELATE-PA1chelating resin [1] and determined by HR-ICP-MS.

Results and Conclusion

The dissolved bioactive trace metals are divided into 3 groups: (1) scavenged-type for Al, Mn, Co and Pb, (2) nutrient-type for Ni, Cu, Zn and Cd, and (3) recycled and scavenged-type for Fe. The atmospheric dust deposition and horizontal advection cause elevated concentrations of DAl, DMn, DCo, DCu and DPb in the upper water column in the Arabian Sea and the Bay of Bengal. Manganese reduction and iron reduction occur in the Oxygen Minimum Zone resulting the increase of DMn, DCo and DFe. Mid-depth enrichment of DMn and DFe above the Central Indian Ridge is influenced by hydrothermal plumes. The distribution of DNi, DCu, DZn and DCd is controlled by the biogeochemical cycle. Although DFe does not show a linear correlation with macronutrients and nutrient-type DMs, iron will be a co-limiting factor for phytoplankton production in most of the study area. The stoichiometry of DMs is generally comparable between deep waters in the northern Indian Ocean and the North Pacific Ocean, suggesting consistence of the mechanism controlling the behaviors of DMs between the Indian and Pacific Oceans.

[1] Sohrin, *et al.* (2008) *Anal. Chem.* **80**, 6267-6273.

https://doi.org/10.1180/S0026461X00008434 Published online by Cambridge University Press

Iberian paleogeography traced by U-Pb zircon ages of Ediacaran-Cambrian rocks

RITA SOLÁ[1*], FRANCISCO PEREIRA[2, 5], MARTIM CHICHORRO[3], LUÍS LOPES[2], AXEL GERDES[4] AND J.BRANDÃO SILVA[5]

[1] Laboratório Nacional de Energia e Geologia and Centro de Geociências, Portugal, rita.sola@lneg.pt (* presenting author)
[2] Dep. de Geociências, Universidade de Évora, Portugal
[3] Dep. de Ciências da Terra, Universidade Nova de Lisboa, Portugal
[4] Institut für Geowissenschaften, Frankfurt am Main, Germany
[5] Instituto Dom Luiz, Universidade de Lisboa, Portugal

The stratigraphic sequence of the Estremoz Anticline in the Ossa-Morena Zone (SW Iberia) includes: 1) an Neoproterozoic basement in the core - Série Negra Succession with greywackes, pelites and black cherts - unconformably overlain by 2) a lower Cambrian Dolomitic Formation, with arkosic sandstones and dolomitic limestones followed by 3) a Volcanic-Sedimentary Complex (VSC) with rhyolites and basalts interbedded with pelites and marbles.

The age of the VSC of the Estremoz Anticline has been a matter of debate, either due to the scarcity of fossils or to the complexity of the regional Variscan deformation. It was firstly attributed to the lower Cambrian, latter reported to the Ordovician or even to the Silurian [1]. Recently, a new interpretation attributed an upper Silurian to Devonian age to the VSC based on a lithological correlation with fossiliferous detritic carbonate rocks that outcrop in the vicinity of the Estremoz Anticline [2].

In this study we present new U-Pb ages of zircons from the Estremoz Anticline stratigraphic sequence.

The spectra of detrital zircon ages of the Ediacaran greywackes (Série Negra Succession) and lower Cambrian arkosic sandstones (Dolomitic Formation) indicates a predominance of Neoproterozoic ages (69-86%) and few Paleoproterozoic (10-16%) and Archean (2-12%) ages. The spectra of Proterozoic detrital zircon ages (with a typical gap in Mesoproterozoic ages) are similar to other peri-Gondwana correlatives with West African Craton provenance [3]. The source area is characterized by an important population of zircon ages in the range c. 850-545Ma. These Cryogenian and Ediacaran ages correspond to zircon crystallization events related to North Gondwana assembly during Pan-African/Cadomian orogenic processes.

The metarhyolites that are interbedded in the marbles of the VSC yielded a magmatic zircon crystallization age of 499.4 ± 3.3 Ma (MSWD=1.16; n=15/16; upper Cambrian). The result obtained indicates that carbonate production was episodic and occurred during lower and upper Cambrian in SW Iberia, related to North-Gondwana break-up. This new evidence should be taken into account in the reshaping of paleogeographic reconstruction models that have erroneously insisted on placing Iberia at southerly cold water higher latitudes (>60ºS) during the Furongian [4].

[1] Piçarra & Le Menn (1994) *Comunicações do Instituto Geológico e Mineiro* **80**, 15-25. [2] LNEG-LGM (2010) *Geological Map of Portugal, scale* 1:1000 000. [3] Pereira *et al* (2008) *GSL-Special Publication* **297**, 385-408. [4] Pereira *et al* (accepted) *Gondwana Research.*

The importance of a conceptual framework for interpreting tracer data

D. K. SOLOMON[1*], S. D. SMITH[1], B. J. STOLP[1], A. MASSOUDIEH[2]

[1]University of Utah, SLC, USA, kip.solomon@utah.edu (* presenting author)
[2]The Catholic University of America, Washington D.C., USA

Introduction

The interpretation of tracer data are highly dependent on the conceptual framework of the system being investigated. We describe several of our field and laboratory investigations in which the time scale of the tracer was poorly matched to the equilibration time of the system being invesitaged. Numerical modeling has been used to evaluate the extent to which a suite of tracer data can be used to uniquely characterize groundwater flow systems.

Results and Conclusions

A stream tracer test was performed by injecting NaBr for a period of about three times the the in-stream transit time, but steady was still not obtained due to long hyporheic flow paths. This led to estimates of groundwater discharge into the stream that were inflated by a factor of five. A combination of groundwater age data and major ion chemistry in both the stream and groundwater were required to develop a conceptual model that is more consistent with the injected tracer data.

At a geologic time scale we have evaluated the equilibration of helium in pore fluids with quartz grains in an attempt to use the helium content of quartz as a proxy for pore fluids [1]. While pore fluid and quartz helium values agree to within an order of magnitude, we have found differences that are best explained by transients in the groundwater flow systems that are less than the quartz equilibration time (0.01 to 2 MA). A realization of the non-steady effects resulted by applying multiple methods, each with their own time scale.

We have employed multiple tracers/techniques in an attempt to help define the conceptual framework of systems including the residence time distributions with some limited success; however, the introduction of transients as additional unknowns severly complicates obtaining a unique model from even a large suite of tracer data. Such complexities are likely to require large amounts of distributed data within a system, as well as tracer data at discharge points, to even narrow the possible range of conceptual models.

[1] Lehmann, B.W., Waber, H.N.m Tolstikhin, I, Kamensky, I., Gannibal, M., and Kalashnikov, E. (2003) *JGR* **30,** no. 3 p. 4

https://doi.org/10.1180/S0026461X00008434 Published online by Cambridge University Press

Investigations of Fe(II) sorption onto montmorillonite. A wet chemistry and XAS study

D. SOLTERMANN[1*], M. MARQUES FERNANDES[1], R. DÄHN[1], B. BAEYENS[1], AND M.H. BRADBURY[1]

[1]Laboratory for Waste Management, Paul Scherrer Institut, Villigen PSI, Switzerland, (*daniela.soltermann@psi.ch)

For some important radionuclides (RN) redox processes in high-level waste repositories play an important role in their retention. Virtually all deep underground repository concepts contain large amounts of iron, and reducing conditions will prevail in the long-term. The presence of high ferrous iron (Fe(II)) concentrations in the interstitial porewaters in the near- and far-fields could have a significant influence on the sorption behaviour of certain RNs through sorption competition effects. The best suited approach to investigate the sorption of Fe(II) on clay minerals and the influence of high aqueous Fe(II) concentrations on the RN retention is a multi-disciplinary one, consisting of macroscopic sorption experiments and advanced microscopic techniques, such as X-ray absorption spectroscopy (XAS).

Fe(II) sorption isotherms were measured on native iron containing montmorillonites (SWy with 3.4 wt.% structural Fe and STx with 0.7 wt.% Fe [1]), on a partially reduced SWy (structural Fe(III) reduced by sodium dithionite [2]) and on a synthetic iron-free montmorillonite (IFM) at pH 6.2 in 0.1 M $NaClO_4$ under anoxic conditions (O_2 < 0.1 ppm). The iron sorption on a reduced SWy and on IFM is significantly lower than that measured on native SWy and STx montmorillonites and agrees well with a calculated Fe(II) isotherm using the 2 Site Protolysis Non Electrostatic Surface Complexation and Cation Exchange (2SPNE SC/CE) sorption model [3]. The high sorption values on native iron bearing montmorillonites suggest that the sorbed Fe(II) is oxidised at the clay mineral surface to Fe(III).

XAS was employed to determine the oxidation state and the local structural environment of Fe sorbed on IFM. The results indicate that iron is predominantly present as Fe(II). Furthermore, the XAS analysis showed that Fe(II) is forming inner-sphere complexes at the IFM surface.

These findings support the hypothesis that oxidation of sorbed ferrous iron on the clay mineral surface might occur through an electron transfer to the structural ferric iron. The results of this study will help to better understand the role of Fe(II) in retention processes in radioactive waste repositories and contribute to an improved molecular interpretation of the Fe(II)-clay interaction at the solid-liquid interface under anoxic conditions.

Reference:

1. Van Olphen, H. and J.J. Fripiat, Data Handbook for Clay Materials and Other Non-metallic Minerals. 1979, New York: Pergamon.
2. Stucki, J.W., D.C. Golden, and C.B. Roth, Preparation and handling of dithionite-reduced smectite suspensions. Clays Clay Miner., 1984. **32**(3): p. 191-197.
3. Bradbury, M.H. and B. Baeyens, A mechanistic description of Ni and Zn sorption on Na-montmorillonite. 2. Modelling. J. Contam. Hydrol., 1997. **27**(3-4): p. 223-248.

Identification of Cu-Mo anomalous zones using the Thermo Scientific Niton portable XRF analyzer in the Eaglehead Cu-Mo porphyry deposit, British Columbia, Canada

ALIREZA SOMARIN[1*], AND DAVID CLIFFORD[1]

[1]Thermo Fisher Scientific, Billerica, MA 01824
alireza.somarin@thermofisher.com (* presenting author)

Introduction

The Eaglehead Cu-Mo deposit is a classic porphyry style mineralization hosted by a granite-granodiorite intrusion and felsic volcanic wall rocks in northern British Columbia, Canada. The mineralization varies from disseminated to sporadic veins and veinlets of quartz±chalcopyrite±bornite±molybdenite. To identify Cu-Mo anomalous zones and compare assay data from the Thermo Scientific Niton portable XRF analyzer with the lab data, three sets of analyses were carried out on samples from drill hole DDH-106. These assays include direct shot on the core with the analyzer, and analyses of powder samples obtained from portable mill and grinder.

Results and Conclusion

The comparative studies show that Cu correlation (R^2) increases from 0.81 in direct shot assays to 0.84 and 0.86 in powder samples from mill and grinder, respectively (Table 1). Mo correlation increases from 0.87 in direct shot analyses to 0.95 in samples obtained by grinder. Zn correlation also increases by using powder samples from mill and grinder.

Thermo Scientific Niton XRF Analyzer Method	Lab (ICP-MS)		
	Cu	Mo	Zn
Direct Shot	0.81	0.87	0.66
Grinder	0.86	0.95	0.82
Mill	0.84	NA*	0.88
* Mill material contains Mo.			

Table 1: Correlation (R^2) between Thermo Scientific Niton XRF analyzer and lab assays.

In addition, depth-metal diagrams (Figure 1) show that Cu and Mo anomalous zones can be identified by using the Thermo Scientific Niton analyzer in the field.

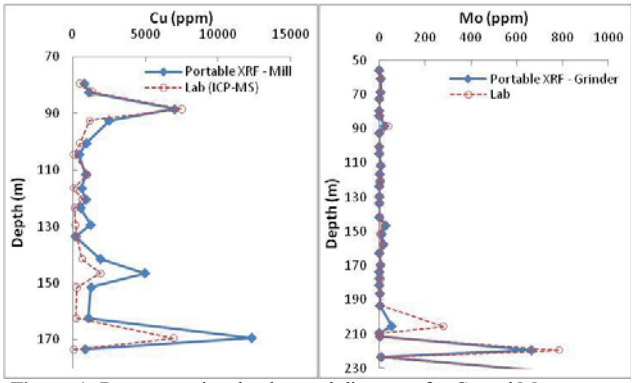

Figure 1: Representtaive depth-metal diagrams for Cu and Mo.

https://doi.org/10.1180/S0026461X00008434 Published online by Cambridge University Press

Characterization of re-suspended ash from the Eyjafjallajökull

FRANK SOMMER[1*], VOLKER DIETZE[2], BERNARD GROBÉTY[3], AND RETO GIERÉ[1]

[1] Universität Freiburg, Geowissenschaften, 79104 Freiburg, Germany (FrankSommer@t-online.de) (* presenting author)
[2] Deutscher Wetterdienst, Research Centre Human Biometeorology, Air Quality Department, 79104 Freiburg, Germany
[3] Université de Fribourg, Geosciences, 1700 Fribourg, Switzerland

The 2010 eruption of the Eyjafjalla volcano had a great impact on international air traffic as well as on the local population and illustrated the potential risks of active volcanism. The explosive reaction between magma and glacier ice produced an ash plume of up to 20 km in height in the atmosphere. The present study is focussed on re-suspended ash in ambient air samples collected near the volcano and aims to develop automated analysis techniques for airborne particles in volcanic environments.

Ambient air samples of airborne re-suspended ash were collected in winter 2010/11 with a passive sampler (Sigma-2, Deutscher Wetterdienst), positioned 12 km south of the eruption zone. In a first step, approximately 200 particles were characterized individually using an optical microscope under transmitted, polarized and cross-polarized light and an electron microprobe with BSE and EDX analysis. Subsequently, the light optical images from the same sample were processed with an automated image analysis program, which allowed for classification of the individual particles as glass, mineral, composite or agglutinated particles. Chemical compositions of individual particles were determined from EDX spectra. To gain a statistically relevant dataset for the sample and to maximize the efficiency of the analytic work, a larger area of the same sample, including the area studied manually, was examined using automatic single-particle SEM analysis (EDAX Genesis program), which resulted in characterisation of approximately 1600 particles. The results of both methods were compared against each other to evaluate the advantages and disadvantages of the different approaches and to advance this combined analytical approach. Additionally, one sample of re-suspended ash was examined using X-ray diffraction supplemented by Rietveld-refinement to determine its mineral content.

The examined particles range from 2.5-80 µm in size (equivalent diameters), and their size distribution is typical of ambient aerosol, particles, i.e., decreasing number of particles with increasing diameter. Only ~10% (surface area) of the particles consist of glassy material, i.e. most particles are crystalline. With a surface-area fraction of 63%, feldspar is the predominant mineral (plagioclase 43%, K-feldspar 20%), followed by pyroxene (18%), and quartz (12%). Minor quantities (≤1%) of olivine, ilmenite and titanite are found as well. The sample is also contaminated with salt of oceanic and/or volcanic origin. These results are consistent with the data obtained from the Rietveld-refinement.

Our study shows that a combination of automated and manual analysis is required to obtain best results. Only an automated method allows for examination of a large number of particles, but the manual control is necessary to collect more detailed information about the composition and the crystallinity of the individual particles.

Geochemical evaluation of the karstified Bangestan reservoirs in the Dezful Embayment, SW Iran

HOSSEIN RAHIMPOUR-BONAB[1], AMIN NAVIDTALAB[1], HAMZEH MEHRABI[1], ROSHANAK SONEI[1,2*]

[1]Department of Geology, College of Science, University of Tehran, Iran rahimpor@khayam.ut.ac.ir
[2]Department of Earth Sciences, University of Ottawa, Canada rsone092@uottawa.ca (* presenting author)

Geochemical composition of carbonate sediments are in equilibrium with the contemporaneous sea-water composition in absence of considerable biotic fractionation. However, in carbonate sediments, diagenetic imprints may have considerable effects on primary sediments textures, mineralogy, reservoir quality and finally geochemical characters. Depending on some factors including primary (depositional) sediments characteristics, governing climate and diagenetic history, geochemical composition of carbonates has been altered by post-depositional overprints. Stable isotopes and trace elements analyses can be used as a good tool to measure the extent of these alterations[1,2]. Coupled imprints of tropical climate and recurring emersions had considerable effects on Middle-Upper Cretaceous carbonate reservoirs of the SW Iran (Dezful Embayment) and Middle East region[3]. Petrographic studies (from core to thin section scales) and geochemical analyses (stable isotopes and trace elements) were carried out on 478 samples from five giant and supergiant oilfields in these embayment to reveal the main diagenetic alterations of these karstified carbonate sequences (Fig. 1). Variations in $\delta^{18}O$ and $\delta^{13}C$ compositions and trace elements (Mn, Fe and Sr) concentrations are useful diagenetic indicators that resulted in classification of studied intervals into four diagenetic classes according to their meteoric diagenetic features, intensities and developments.

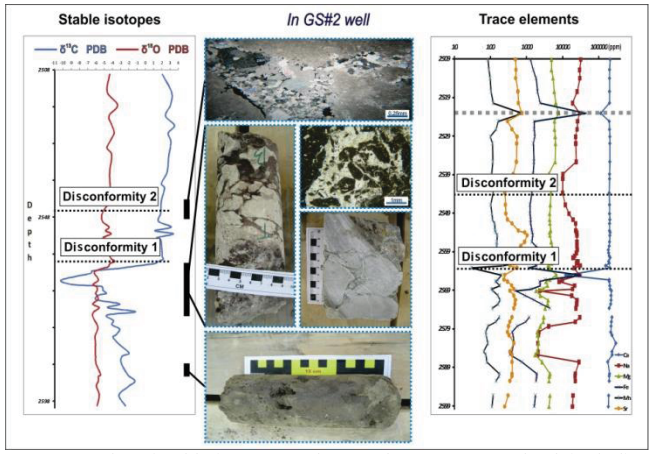

Figure 1: Plot of stable isotopes and trace elements versus depth including the petrographic evidences of karstified intervals of the Bangestan reservoir in GS-2 well.

[1] Brand, U. and Veizer, J., 1980. Chemical diagenesis of a multicomponent carbonate system-I: Trace elements. J. Sediment. Petrology 50: 1219–1236.
[2] Brand, U. and Veizer, J., 1981. Chemical diagenesis of a multicomponent carbonate system-II: stable isotopes: J. Sediment. Petrology, v. 51, p. 987-997.
[3] Hollis, C. 2011. Diagenetic controls on reservoir properties of carbonate successions within the Albian–Turonian of the Arabian Plate. Petroleum Geoscience vol. 17, 3: 223-241.

https://doi.org/10.1180/S0026461X00008434 Published online by Cambridge University Press

Silicate polymerization on crystalline and amorphous TiO_2: an ATR-IR and synchrotron XPS investigation

YANTAO SONG[1*], PETER JAMES SWEDLUND[1], JAMES METSON[1], GEOFFREY I.N. WATERHOUSE[1] AND BRUCE COWIE[2]

[1]School of Chemical Sciences, the University of Auckland, y.song@auckland.ac.nz (* presenting author)
[2]Australian Synchrotron, SoftXRay@synchrotron.org.au

Introduction

The presence of silicate at metal oxide-aqueous interfaces influences many oxide properties. Understanding the chemistry of silicate at these interfaces is important to describe the geochemistry of these metal oxides and elements associated with the oxides [1-2]. This work compares silicate sorption and polymerization on the disordered surface of an amorphous TiO_2 ($TiO_{2(am)}$) with silicate chemistry on the well defined faces of rutile TiO_2. The work used *in situ* attenuated total reflectance-infrared spectroscopy (ATR-IR) and *ex situ* synchrotron based X-ray photoelectron spectroscopy (XPS).

Results and Conclusion

The ATR-IR results show that a monomeric silicate species with a Si-O stretching mode at ≈ 950 cm^{-1} formed on all TiO_2 surfaces at low surface coverage. Linear oligomeric silicates with a Si-O IR adsorbance at ≈ 1020 cm^{-1} form when the surface coverage reaches a threshold value (Figure 1). The process of silicate oligomerization was favoured on the crystalline rutile surface compared to the amorphous TiO_2. This agrees with the XPS results and the proposed model of heterogeneous silicate polymerization which would be favoured by the arrangement of TiO_2 octahedra on the rutile (110) face (Figure 2).

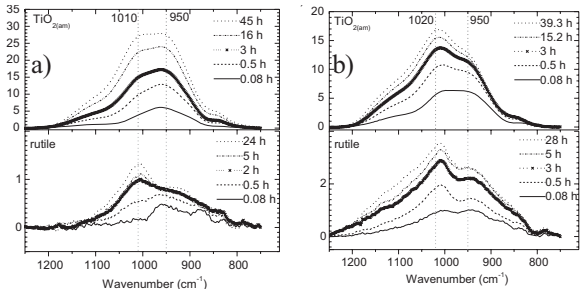

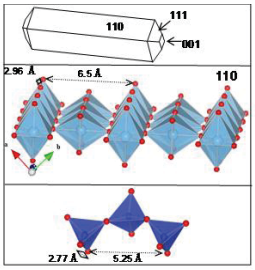

Figure 1 (above): ATR-IR spectra of H_4SiO_4 adsorbed on the surface of $TiO_{2(am)}$ and rutile at pH 9 and 0.1 M NaCl measured over time. Final concentrations of H_4SiO_4 are (a) 0.2 mM and (b) 1.5 mM.

Figure 2 (left): Rutile morphology and enclosing faces. Bottom panel shows a section of ferrosilite, a linear silicate.

[1] Swedlund *et al.* (2011) *Chem. Geol.* **285**, 62-69.
[2] Dol Hamid *et al.* (2011) *Langmuir.* **27**, 12930-12937.

Cr(VI) Reduction and Isotopic Fractionation In Bacteria: Cytoplasmic/Extracellular Reduction Rate and Diffusion Controls

ERIC SONNENTHAL[1*], JOHN N. CHRISTENSEN[1], AND RUYANG HAN[1]

[1]Earth Sciences Division, Lawrence Berkeley National Lab, Berkeley, CA, USA, elsonnenthal@lbl.gov (* presenting author)

Reduction of Cr(VI) to Cr(III) by bacteria is well documented and leads to significant Cr isotopic fractionation ($^{53}Cr/^{52}Cr$), with experimental values in abiotic systems of ~3.4‰[1] to 5‰[2], and theoretical equilibrium values of 6-7‰[3]. Biologically-mediated Cr isotopic fractionation of ~4.2‰[4] has been attributed to kinetic fractionation, with possible controls by metabolic pathways, transport, or reduction sites. In lactate-amended cell suspension experiments with *Pseudomonas stutzeri* strain RCH2, Cr isotopic fractionation was less under denitrifying vs. aerobic conditions[5], and attributed to Cr(VI) transport limitation. In this work, a reactive-transport model was developed to evaluate effects of cytoplasmic/extracellular reduction rates and transport in bacteria on Cr isotopic fractionation with comparison to experimental data.

The multicontinuum reactive-transport model is based on a simplified structure of bacterium *Pseudomonas stutzeri*, of average dimension of 2 x 0.5μm, a cell membrane thickness of 15nm, and an average bacterium spacing derived from the suspension cell density. Cr reduction in the cytoplasm is dependent on chromate diffusive transport through the outer membrane (via sulfate channels), the periplasmic space, and to reduction sites. Cell wall diffusivities were estimated from published cell wall permeabilities. Cr reduction was assumed to be thermodynamically and kinetically-controlled by $Cr(OH)_3$ precipitation using a solid solution model of $^{53}Cr(OH)_3$ and $^{52}Cr(OH)_3$. Simulations considered an aerobic case with lactate oxidation to pyruvate, and a denitrifying case forming pyruvate, as well as conditions of the experiments described in [4].

Simulations with differing cell densities using Toughreact [7] showed that it is necessary to limit diffusive transport through the cell wall by ~4 orders of magnitude to match the change in Cr isotopic fractionation from ~2‰ (aerobic) to ~0.4‰ (denitrifying). By severely limiting diffusive transport, Cr reduction rates decrease significantly, inconsistent with experimental data. In contrast, by increasing the Cr reduction rate in the cytoplasm, a large decrease in the fractionation factor is observed, without inhibiting the Cr reduction rate, capturing the observed $^{53}Cr/^{52}Cr$ and Cr reduction rates over a range of cell densities. Although it is not known where Cr reduction was localized in the cell suspension experiments[5], simulations show that Cr reduction in the extracellular medium also leads to higher Cr reduction rates and Cr isotopic ratios close to the maximum value for the reduction reaction.

[1] Ellis, Johnson & Bullen (2002) *Science* **295**, 2060–2062. [2] Zink, Schoenberg & Staubwasser (2010) *GCA* **74**, 5729–5745. [3] Schauble, Rossman & Taylor (2004) *Chem Geol* **205**, 99-114. [4] Sikora, Johnson & Bullen (2008) *GCA* **72**, 3631-3641. [5] Han *et al.* (in press) *AEM.* [6] Han *et al.* (2010) *ES&T* **44**, 7491-7497. [7] Xu *et al.* (2011) *Comp Geosc* **37**, 763-774.

https://doi.org/10.1180/S0026461X00008434 Published online by Cambridge University Press

Structural modifications in densified soda alumino silicate glasses

CAMILLE SONNEVILLE[1*], DOMINIQUE DE LIGNY[1], DANIEL R. NEUVILLE[2], PIERRE FLORIAN[3], SYLVIE LE FLOCH[4], CHARLES LE LOSQ[2] AND GRANT S. HENDERSON[5]

[1]Université de Lyon, Université Lyon 1, Laboratoire de Physico-Chimie des Matériaux Luminescents, CNRS, UMR5620, Villeurbanne, France. camille.sonneville@univ-lyon1.fr (*presenting author)

[2]CNRS-IPGP, Sorbonne Paris Cité, Paris, France

[3]CEMHTI-CNRS, Orléans, France

[4] Université de Lyon, Université Lyon 1, Laboratoire PMCN; CNRS, UMR 5586, Villeurbanne Cedex, France

[5]Dept of Geology, University of Toronto, Toronto, Canada

Summary:

The behaviour of soda aluminosilicate glasses and melts under pressure and temperature is of interest in both the materials and Earth Sciences, especially for understanding magmatic processes. Although these systems have been well studied at room pressure by several workers, their structural modifications at high pressure (HP) are less well known. Several studies have been carried out on glasses quenched from HP using both NMR and XANES. The latter have also been performed on glasses and melts at HP. All these studies revealed structural changes occurring in the glasses and/or melts with increasing pressure.

We synthesized glasses along the NS3/Albite glass join extended into the peralumimous domain. The glasses were permanently densified in a Belt press at the Lyon Plateform of High Pressure Experimentation (PLECE) (5GPa, 600°C) and in a Multi Anvil press at the University of Toronto (7GPa, 600°C). The densified samples were studied with various methods in order to follow the pressure induced structural modifications. Short range order (SRO) was investigated using ^{23}Na, ^{27}Al NMR and Si L-edge XANES. The intermediate range order (IRO) was studied by Raman spectroscopy and long range order (LRO) with Brillouin spectroscopy.

^{27}Al NMR spectra show, with increasing pressure, an increase in the Al coordination, with large amounts of ^{V}Al and ^{VI}Al appearing in glasses with low Al_2O_3 contents. Contrary to this, ^{V}Al and ^{VI}Al increase more slowly for albite and peraluminous glasses. ^{23}Na NMR spectra exhibit a decrease in the Na-O bond length with pressure.

For glasses between NS3 and albite composition, Raman experiments show an increase in Q^2 and Q^4 species with pressure and a symmetrical decrease of the Q^3 species. A strong shift of the vibrational band around 500 cm^{-1} toward higher wavenumbers is observed for albite and peraluminus glass.

The pressure induced structural modifications noted in these glasses are dependent upon composition. For compositions characteristic of depolymerized glasses Al coordination increases and further depolymerization are primarily responsible of the densification process. For compositions indicative of fully polymerized glasses densification mainly occurs as a decrease in the intertetrahedral angle T-O-T. Al *L*- edge XANES and O, Na, Al, and Si *K*-edge XANES along with *in situ* (DAC) experiments will be performed soon to complete this preliminary study.

Heterogeneous hydrous mantle in arc settings: Constraints on the genesis of silica-undersaturated arc magmas

F. SORBADERE[1,2*], E. MEDARD[1,2], D. LAPORTE[1,2], P. SCHIANO[1,2]

[1] Laboratoire Magmas et Volcans, Clermont Université, Université Blaise Pascal, BP 10448, 63000 Clermont-Ferrand, France.

[2] CNRS, UMR 6524, IRD, R 163, 5 rue Kessler, F-63038 Clermont-Ferrand Cedex.

(*F.Sorbadere@opgc.univ-bpclermont.fr)

Partial melting of a hydrous lherzolite mixed with variable amounts of amphibole-bearing clinopyroxenite (OCA2) [1] has been experimentally investigated at 1 GPa between 1150 and 1300°C (piston-cylinder, $Au_{80}Pd_{20}$ capsules) under oxidized condition (FMQ+2). Our new capsule configuration [2] allows efficient melt extraction, with melt layers more than 50 µm wide in the capsule traps.

Peridotite derived melts are hypersthene-normative while amphibole-clinopyroxenite melts are strongly Si-undersaturated (~7 % normative nepheline). Melts derived from lherzolite-clinopyroxenite mixtures containing less than 50% clinopyroxenite have identical major element compositions than melts derived from pure peridotite. Above 50% pyroxenite, the CaO content in melt increases and the SiO_2 content decreases with increasing fraction of pyroxenite in the starting mixture. The transition between Hy-normative and Ne-normative melts occurs for mixtures containing between 50 and 75 % clinopyroxenite, when orthopyroxene disappears from the residue. In contrast, minor elements (K_2O, Na_2O, TiO_2 and H_2O) show a more linear behaviour with continuous mixing trends between the two lithologies, thus highlighting the source heterogeneity. Thus the signature of mantle heterogeneities is preserved in the minor/trace elements composition of the magmas, whereas the major elements are buffered by the dominant peridotitic lithology. Forsterite content of olivines in equilibrium with the melts reaches 91.3 for peridotite and 91.8 for clinopyroxenite and/or mixed lithologies at 1300°C. High-Mg olivines can thus crystallize from non-peridotitic magmas under relatively oxidized conditions at high temperatures.

Most primitive magmas found in arc environments and preserved as melt inclusions in high-Mg olivine (Fo ≥ 88) show Si-undersaturated compositions. The involvement of a heterogeneous source containing amphibole-bearing clinopyroxenites in addition to peridotites is often mentioned to account for the Si-undersaturated character of these melt inclusions [1; 3-5]. Our experiments give further support for this hypothesis, but indicate that either the source is almost exclusively made of amphibole-bearing clinopyroxenites, or the Si-undersaturated melts issued from the clinopyroxenites do not reequilibrate with the peridotites.

[1] Médard *et al.* (2006) *J. Petrol.* **47**, 481-504. [2] Hoffer (2008) PhD thesis, Clermont-Ferrand [3] Métrich *et al.* (1999) *EPSL* **167**, 1-14. [4] Schiano *et al.* (2000) *G3* **1**, n°5, 1018. [5] Elburg *et al.* (2007) *Chem. Geol.* **240**, 260-279.

https://doi.org/10.1180/S0026461X00008434 Published online by Cambridge University Press

Transition metal stable isotopes in komatiites

PAOLO A. SOSSI[1], OLIVER NEBEL[1], HUGH ST. C. O'NEILL[1], STEPHEN M. EGGINS[1], MARTIN VAN KRANENDONK[2]

[1] Research School of Earth Sciences, Australian National University, Canberra, 0200, Australia
[2] Geological Survey of Western Australia, 100 Plain St, East Perth, WA 6004, Australia

Komatiites represent large degree partial melts of the mantle (30-50%), which segregated from their sources at high temperatures (>1500°C) and pressures (>5GPa), and are thus largely restricted to the Archaean. As the magnitude of stable isotope fractionation decays according to $1/T^2$, the difference in the stable isotope composition between komatiites and their mantle source is negligible (Dauphas et al., 2009). This permits the characterisation of the stable isotopic composition of the mantle source, provided the effects of alteration and fractional crystallisation can be accounted for.

We present high precision Cu, Zn and Fe isotope analyses for a suite of Early Archaean komatiites (3.5-3.2Ga) from the Pilbara craton, separated from a single dissolution. Fe isotopes bracket a range of compositions from δ^{57}Fe (vs. IRMM-014) of -0.17‰ to +0.17‰. Zn isotopes show a more restricted range of compositions, with δ^{66}Zn varying from -0.1‰ to -0.16‰ (vs. IRMM-3702), consistent with the smaller range hitherto observed in igneous rocks (Albarède, 2004). A well defined increase in both δ^{57}Fe and δ^{66}Zn with decreasing Cr and MgO is attributed to a strong olivine control on their stable isotope composition. Cu isotopes scatter around 0‰ (vs. SRM-976), lacking any systematic trend with indices of differentiation. Nevertheless, confirmation of δ^{65}Cu values near 0‰ in other igneous rocks (Li et al., 2009) indicates no discernible change in the Cu isotope composition of the Earth over time.

While δ^{66}Zn and δ^{65}Cu values are representative of current-day mantle, the komatiite array has δ^{57}Fe that extends to ≈-0.15‰ lighter than the contemporary mantle value. At a given stage in their differentiation, the Pilbara komatiites are also 0.1‰ lighter than komatiites from Alexo (Dauphas et al., 2010).

Compared to carbonaceous chondrites, the Zn composition of the Earth lies at the volatile-poor end of a volatile-depletion trend, where δ^{66}Zn becomes lighter with decreasing Zn/Mg. This is the opposite trend to that expected if Zn were being lost by vaporisation.

[1] Dauphas et al., (2009) *EPSL* **288**, 255-267. [2] Albarède (2004) *RiMG* **55**, 409-427 [3] Li et al., (2009) *Chem. Geol.* **258**, 38-49 [4] Dauphas et al., (2010) *GCA* **74**, 3274-3291

Use of MC-ICPMS for laser ablation U/Pb geochronology of baddeleyite

SOUDERS A.K[1*] AND SYLVESTER P.J.[1]

[1]Department of Earth Sciences, Memorial University of Newfoundland, St. John's, NL, Canada (*kate.souders@mun.ca, psylvester@mun.ca)

Microbeam analyses by laser ablation inductively coupled plasma mass spectrometry (LA-ICPMS) are increasingly used for U-Pb geochronology of zircon. LA-ICPMS is a powerful method for U-Pb geochronology because grains can be dated directly in thin section, avoiding time-consuming laboratory procedures involving heavy liquid separations and ion exchange chromatography. In many silica-poor terrestrial rocks such as mafic dikes, anorthosites, gabbros and carbonatites as well as lunar rocks and Martian meteorites, baddeleyite (ZrO_2) rather than zircon is present. Unlike zircon, the baddeleyite tends to form very small elongate grains, typically no more than 30-50 μm in the longest dimension and less than 20 μm in the smallest dimension. This makes U-Pb analyses of baddeleyite by LA-ICPMS more challenging than for zircon because smaller laser spot sizes (<20 μm) and shorter ablation times (<30 sec) are required, reducing analytical precision significantly compared to zircon analyses.

High-precision thermal ionization mass spectrometry (TIMS) is commonly used for U-Pb baddeleyite geochronology of Large Igneous Provinces (LIPs), particularly where mafic magmatic events need to be determined with a precision better than 5 Ma. In cases where ages with uncertainties of approximately 20 Ma provide useful data for LIPs, however, it would be desirable however to apply LA-ICPMS to U-Pb baddeleyite geochronology.

We report a U-Pb dating method for baddeleyite by LA-multi-collector-ICPMS using a Thermo Scientific NEPTUNE MC-ICPMS. The collector array consists of six Channeltron ion counters allowing for the simultaneous collection of ^{202}Hg, ^{204}Pb, ^{206}Pb, ^{207}Pb, ^{208}Pb and ^{235}U isotopes. The use of a collector array consisting only of ion counters eliminates the need of cross-calibration between ion counters and Faraday detectors. Standard – sample – standard bracketing is employed to correct for instrumental mass bias using Forest Center baddeleyite (FC-4b; TIMS age = 1095.42 ± 0.16 Ma) as a standard. A slow line scan ablation is used where a 4μm laser beam with an energy density of 9 J/cm^2 and a repetition rate of 5 Hz scans across the sample surface at a rate of 1 μm/sec. Using the method described, after 30 sec (150 pulses) of ablation, the ^{207}Pb/^{206}Pb age determined for the ca. 2060 Ma Phalaborwa baddeleyite is 2058.9 ± 18 Ma (2σ, n = 6) with an external precision of 0.9 % (2RSD). While this result is comparable to U-Pb zircon and analyses by single-collector LA-ICPMS, the smaller volume of material consumed and the shorter ablation time required to achieve such precision during multi-collector analyses is more suitable for, typically smaller, baddeleyites. The described method can be used as a reconnaissance tool to screen baddeleyite grains prior to physical separation for further high precision TIMS analyses, in order to identify critical samples that can be used for paleocontinental reconstruction in LIPs.

https://doi.org/10.1180/S0026461X00008434 Published online by Cambridge University Press

AMS studies in "Foz do Douro metamorphic complex" (N Portugal): preliminary insight

MÓNICA SOUSA[1*], HELENA SANT'OVAIA[1] AND FERNANDO NORONHA[1]

[1]Porto University, DGAOT, CGUP, Porto, Portugal, monica.sousa@fc.up.pt (* presenting author) hsantov@fc.up.pt fmnoronh@fc.up.pt

Introduction

The "Foz do Douro Metamorphic Complex" (FDMC) is situated on the shoreline of Porto extending along a series of small beaches between the Douro river mouth and the "S. Francisco Xavier" Fort. The geology of this zone is marked by the presence of Porto-Tomar-Fereira do Alentjo, NNW-SSE dextral, shear zone and by magnificent outcrops of a thin band of Precambrian metamorphic rocks intruded by Variscan granites [1,2]. The metamorphic band is represented by outcrops of metasedimentary rocks, spatially associated to orthogneisses of different types and ages (606±17 to 567± 6 Ma) and amphibolites that constitute the FDMC [3]. The granites belong to a late-Variscan granite group (298±11Ma) [4].

A Anisotropy of magnetic susceptibility (AMS) study is being carried out in these several types of orthogneisses. In this work we present the first data obtained with 49 samples of leucocratic gneisses, some with garnet, and augen gneisses (Group 1) and with 15 samples of biotite-rich orthogneisses (Group 2).

Results and Discussion

Magnetic susceptibility (K) ranges between 20.0 and 72.3 x 10^{-6} SI in Group 1 orthogneisses which indicates a paramagnetic behaviour of this lithology, due to ferromagnesian minerals, such as biotite. However in Group 2 orthogneisses, K presents values > 10^{-3} SI (0.12 x 10-3 SI, in average) which enhance the presence of magnetite. These two distinct behaviours indicate two different types of Precambrian magmatism: a oxidized type (magnetite type) (Group 2) and a reduced type (Group 1).

Magnetic anisotropy, expressed by the ratio Kmax/Kmin, ranges from 1.052 to 1.144 in Group 1 orthogneiss and is higher (1.204) in the Group 2 gneisses. These values are typical of deformed rocks but the high anisotropy of the Group 2 orthogneisses also reflects the presence of magnetite. In both lithologies, magnetic fabric is characterised by subvertical magnetic lineations associated to subvertical E-W to ESE-WNW and NW-SE trending magnetic foliations, related to a shear deformation.

[1] Chaminé *et al*. (2003) *Cadernos Lab. Xeolóxicos de Laxe* **28**, 37-78. [2] Ribeiro *et al.* (2009) *C. R. Geoscience* **341**, 127-139. [3] Noronha & Leterrier (2000) *Revista Real Academia Galega de Ciências* **XIX,** 21-42. [4] Martins *et al.* (2011) *C. R. Geoscience* **343**, 387-396.

Acknowledgements

Research carried out at the "Centro de Geologia UP" an R & D unit from "Fundação para a Ciência e Tecnologia" (FCT) and first author is being funded by a doctoral scholarship from FCT (SFRH/BD/47891/2008).

The Role of Metal Redox Coupling Processes in Carbon Cycling and Stabilization

DONALD L. SPARKS[*1], CHUNMEI CHEN[1], OLESYA LAZAREVA[1], JOSHUA LEMONTE[1], JAMES J. DYNES[2], JIAN WANG[2], AND TOM REGIER[2]

[1] Delaware Environmental Institute (DENIN), Newark, USA dlsparks@udel.edu* (*presenting author), cmchen@udel.edu, olazarev@udel.edu, lemonte@udel.edu

[2]Canadian Light Source, Saskatoon, Canada James.Dynes@lightsource.ca , Jian.Wang@lightsource.ca, Tom.Regier@lightsource.ca

The association of carbon with mineral phases has been increasingly recognized as a major stabilizing mechanism for protecting organic matter against microbial degradation in soils. Iron (Fe) and manganese (Mn) oxides are of particular importance because of their abundance in soils and high reactive surface area. Both Fe and Mn are susceptible to redox variability along landscape gradients. Reductive dissolution and transformation of Fe and Mn minerals governs the amount, form and transport of sequestered C. We have investigated Fe speciation as well as the composition of organic matter and its molecular interaction with soil minerals across hillslope transects within the Christina River Basin Critical Zone Observatory (CRB-CZO) to link iron-redox coupling processes with soil C cycling. Selective chemical extractions, X-ray absorption spectroscopy (XAS), micro-XAS techniques, and Mossbauer spectroscopy were employed to characterize soil Fe speciation. Applying scanning transmission X-ray microscopy (STXM) and carbon near edge X-ray absorption fine structure (CNEXAFS) spectroscopy, we mapped the spatial distribution of carbon and carbon forms, and imaged the association of organic functional groups with specific minerals in the soils. Ferrihydrite, because of its ubiquitous occurrence in the environment and its high surface area, contributes significantly to the sorption of organic matter and protects it against microbial degradation in soils and sediments. In addition, ferrihydrite often forms in the presence of dissolved organic matter in the natural environment, which leads to coprecipitation of organic matter with ferrihydrite. However, the extent and mechanisms of organic matter adsorption to or coprecipitation with ferrihydrite, and the consequences of such reactions for the properties of sorbed versus coprecipitated organic matter remain largely unknown. In this presentation, we compare adsorption and coprecipitation with dissolved organic matter from a forest litter layer. To examine the chemical fractionation of the organic matter and the mechanisms of organo-ferrihydrite complex formation associated with these two processes CNEXAFS and Fourier transform infrared (FTIR) spectroscopic techniques were employed. To study spatial distribution, macromolecular structure, and chemical composition of sorbed and coprecipitated OM at the nanometer-scale we used STXM. Data on the role of Mn in C cycling will also be presented. Such studies will enhance our understanding of OM stabilization mechanisms on soil mineral surfaces and will provide new insights on the metal-redox coupling processes affecting carbon cycling at soil/sediment-water interfaces.

https://doi.org/10.1180/S0026461X00008434 Published online by Cambridge University Press

Tectonic implications of short metamorphic episodes

FRANK S. SPEAR[1]*, KYLE T. ASHLEY[2], LAURA E. WEBB[3], AND J. B. THOMAS[1]

[1]Renssaelaer Polytechnic Institute, Troy, USA, spearf@rpi.edu (*presenting author), thomaj2@rpi.edu
[2]Virginia Tech, Blacksburg, USA, ktashley@vt.edu
[3]University of Vermont, Burlington, USA, lewebb@uvm.edu

Quartz inclusions in garnet undergo exchange of Ti with the host garnet resulting in diffusion of Ti into the quartz. Modeling of this diffusion in samples from the Barrovian terrane of eastern Vermont reveals that the entire metamorphic episode (heating from 450 C to metamorphic peak and cooling back to 450 C) has occurred in less than 1 m.y. and perhaps in as little as a few hundred thousand years, depending on the presumed peak metamorphic temperature. This terrane does not contain volumetrically significant plutons, so the only possible cause must be tectonic.

Two-dimensional thermal modeling has been used to constrain the rates of thrusting required to achieve such short-lived metamorphic episodes. Rocks heat rapidly when overthrust by hot rocks and cool rapidly when they are thrust onto cooler rocks, a process that has been modeled as a simple, mid-crustal duplex structure. A typical model involves the first thrust sheet moving up a 20 degree ramp at a rate of 10 cm/year (0.1 m/year) for 0.1-0.5 m.y. then the fault stepping out (in sequence) and a second thrust sheet moving up a similar ramp for a similar time interval. The rocks of interest are those in the horse between the two thrusts which are initially loaded quickly and subsequently heated by thermal conduction from the overlying hotter rock mass. The second thrust places these hot rocks onto cooler substrate which initiates cooling of the mass but not necessarily a change in pressure. Exhumation was likely to have been rapid following the metamorphic peak, consistent with the rapid post-peak cooling history inferred from the diffusion studies. The near isothermal loading exhibited by P-T paths of rocks from eastern Vermont also supports the hypothesis of crustal loading at rates of 5-10 cm/year.

The rate of heating and cooling depends on the thermal difference between the overthrust sheet and the rocks of interest, and the proximity of the rocks to the thrust. Models with different thrust sheet dimensions reveal that it is impossible to rapidly heat and cool the same rock if the sheet is thicker than ca 5 km. This fact raises the interesting possibility that metamorphic terranes that have experienced such rapid heating and cooling are comprised of thin thrust sheets bounded by ductile shear zones stacked together in duplex-like geometries with significant internal deformation. Such geometries might be very difficult to decipher with the limited outcrop exposure in Vermont. It is also interesting to speculate that the two major “deformations” that produce the two dominant fabrics in these rocks were caused by the initial loading and subsequent ramping of the thrust sheet, respectively. Thrust ramps also produce ramp anticlines that, in ductile terranes, will have the geometries of domes as are seen in eastern Vermont.

Such rapid tectonic juxtaposition is unresolvable by current geochronologic techniques, and is only revealed through diffusion modeling of systems with diffusivities appropriate for the metamorphic conditions.

Timing and mechanism for intratest Mg/Ca variability in living planktic foraminifera

HOWARD J. SPERO[1*], STEPHEN M. EGGINS[2], ANN D. RUSSELL[1], LAEL VETTER[1], BÄRBEL HÖNISCH[3]

[1]University of California Davis, Dept. Geology, Davis CA., USA; hjspero@ucdavis.edu (* presenting author)
[2]The Australian National University, Research School of Earth Sciences, Canberra, Australia; Stephen.Eggins@anu.edu.au
[3] Columbia University, Lamont-Doherty Earth Observatory, Palisades, NY, USA, hoenisch@ldeo.columbia.edu

Problem and Results

Recent microscale data indicate that Mg/Ca in foraminifera tests is distributed heterogeneously, thereby challenging its use as a robust tool for paleotemperature reconstructions. We present Mg/Ca and Ba/Ca data collected by laser ablation (LA) ICPMS from living *Orbulina universa*, that were grown in controlled laboratory experiments. Test calcite was labeled with Ba-spiked seawater for 12h periods during either day or night calcification, to quantify the timing of intratest Mg-banding across diurnal cycles. Results demonstrate high Mg bands are precipitated during the night, whereas low Mg bands are precipitated during the day. Similarly, the amplitude of the Mg/Ca ratios in Mg-rich bands decreases in experiments with elevated pH (and $[CO_3^{2-}]$). These results suggest that symbiont photosynthesis influences but does not fully control Mg/Ca banding. We hypothesize that mitochondrial uptake of Mg^{2+} may explain Mg-depleted calcite layers. Symbiont photosynthesis and foraminifera respiration may exert a secondary influence on shell Mg/Ca via their effect on $[H^+]$ in the microenvironment around the calcifying shell. Data obtained from specimens growing at 20º and 25ºC show that intrashell Mg/Ca ratios increase with temperature in both high and low Mg bands, such that average test Mg/Ca ratios are in excellent agreement with temperature calibrations based on bulk solution ICPMS analyses.

Conclusion

Results presented here demonstrate that Mg banding is an inherent component of the biomineralization process. However, despite intratest Mg/Ca variability, the Mg/Ca paleothermometer as measured on whole tests remains a robust tool for reconstructing past ocean temperatures from the fossil foraminifera record.

https://doi.org/10.1180/S0026461X00008434 Published online by Cambridge University Press

Ab initio vibrational properties of silica species in aqueous fluids

G. SPIEKERMANN[1*], M. STEELE-MACINNIS[2], C. SCHMIDT[1], P. M. KOWALSKI[1] AND S. JAHN[1]

[1]GFZ German Research Centre for Geosciences, Section 3.3, Telegrafenberg, 14473 Potsdam, Germany, spiek@gfz-potsdam.de (* presenting author)

[2]Department of Geosciences, Virginia Tech, Blacksburg VA 24061, USA, mjmaci@vt.edu

The solubility of minerals in aqueous fluids is an important property to understand the chemical transport of elements. On the atomic-scale the solubility is related to the solute speciation in the fluid. Vibrational spectroscopy is especially useful for probing solute speciation in aqueous fluids because vibrational frequencies depend on molecular structure. Assignment of spectroscopic features to specific structural units can be challenging, but atomic-scale modeling may provide support [1, 2].

We investigate the vibrational properties of silica species in aqueous solution at high pressures and temperatures. The investigated species include H_4SiO_4 and $H_3SiO_4^-$ monomers, $H_6Si_2O_7$ and $H_5Si_2O_7^-$ dimers, three and fourfold silica rings and higher polymers [3]. Simulations are performed at the level of density-functional theory with the PBE exchange-correlation functional. We use periodic boundary conditions and a system of 25-27 H_2O molecules at 300 K and 1000 K, at a fluid density around 1 g/cm^3.

In our approach to analyze the vibrational properties, we exploit the two facts that (1) observed Raman frequencies are equal to the real vibrational frequencies, and (2) the spectroscopically important silica vibrations are quasi-localized normal-mode-like vibrations. The concept of mode-projected velocity autocorrelation (VACF) and its Fourier transform [4] is applied to yield normal-mode-like vibrational subspectra of the vibrational density of states, e.g. from tetrahedral subunits (T_d), Si-O-Si units of bridging oxygens (C_{2v}), the dimer (C_{3d}/C_{3h}), the SiOH bending, and "breathing" of silica rings.

Our results give a comprehensive picture of the vibrational behaviour of small silica species such as monomers and dimers. New insight is given into the polymerization-driven frequency shift. Our studies help to clarify vibrational contributions of Q^1 tetrahedra, the silica dimer, Q^2 tetrahedra, and the SiOH bending motions. We demonstrate that the mode-projection technique is a powerful tool for investigation of vibrational properties of isolated and network-forming species in their environment at elevated temperatures and pressures.

[1] Zotov & Keppler (2000), *American Mineralogist*, **85**, 600-604
[2] Tossell (2005), *Geochimica et Cosmochimica Acta*, **69**, 283-291
[3] Spiekermann, Steele-MacInnis, Kowalski, Schmidt & Jahn (2012), submitted to *Journal of Chemical Physics*
[4] Pavlatou, Madden & Wilson (1997), *Journal of Chemical Physics*, **107**, 10446-10457

Lunar Lu-Hf and Sm-Nd systematics – effects of neutron capture reactions

P. SPRUNG[1*], T. KLEINE[2], AND E.E. SCHERER[3]

[1]Institute for Geochemistry and Petrology, ETH Zürich, Switzerland, sprung@erdw.ethz.ch (* presenting author)

[2]Institut für Planetologie, Westfälische Wilhelms-Universität Münster, Germany, thorsten.kleine@uni-muenster.de

[3]Institut für Mineralogie, Westfälische Wilhelms-Universität Münster, Germany, escherer@uni-muenster.de

The silicate differentiation history of planetary objects including the Moon can be constrained by combined Lu-Hf and Sm-Nd studies [1]. Previous Lu-Hf studies on lunar basalts [2-6] yielded results broadly consistent with a magma ocean history for the Moon as constrained by Sm-Nd systematics, but some inconsistencies persist: Most KREEP-rich bulk rocks have initial $^{176}Hf/^{177}Hf$ that are too radiogenic, overlapping the composition of chondrites at the same time, and are inconsistent with the unradiogenic initial $^{143}Nd/^{144}Nd$ of KREEP. This disparity in the Lu-Hf and Sm-Nd systems may reflect a non-chondritic composition of the Moon [7] but could also be due to capture of (epi)thermal neutrons (NC) during cosmic-ray exposure of the lunar surface [8]. NC reactions can induce positive shifts in measured $^{176}Hf/^{177}Hf$ [8] and negative shifts in measured $^{143}Nd/^{144}Nd$ [9]. However, none of the previous Lu-Hf studies of lunar samples accounted for NC effects. To assess the significance of NC effects on the lunar Lu-Hf and Sm-Nd systematics we obtained Lu-Hf, Sm-Nd, and Hf and Sm isotope data for a suite of lunar samples (KREEP-rich rocks and mare basalts).

The KREEP-rich samples display no NC-induced Hf or Sm anomalies and yield the lowest initial $^{176}Hf/^{177}Hf$ yet reported for any KREEP-rich rock. In contrast, most mare basalts exhibit well-resolved, NC-induced anomalies in Hf and Sm. Low-Ti mare basalts show the strongest NC effects, with $^{180}Hf/^{177}Hf$ and $^{149}Sm/^{152}Sm$ as low as ≈820 ppm and ≈72 ε-units below those of terrestrial samples, respectively. NC-induced ^{180}Hf and ^{149}Sm anomalies are well correlated, yielding distinct slopes for low- and high-Ti mare basalts. The errors in measured $^{176}Hf/^{177}Hf$ and $^{143}Nd/^{144}Nd$ induced by NC reactions are up to +12 and -0.7 ε-units, respectively.

The well-defined, distinct correlations between ^{149}Sm and ^{180}Hf anomalies in low- and high-Ti mare basalts imply almost constant neutron energy spectra for chemically similar samples. Using the respective neutron energy spectra and published ^{149}Sm data [e.g., 9], we estimate that the $^{176}Hf/^{177}Hf_{now}$ previously reported for low- and high-Ti mare basalts are too high by up to 7 and 1.7 ε-units, respectively. Published ^{149}Sm data suggest that previously reported data for KREEP-rich rocks are biased by NC reactions too, thus yielding more radiogenic initial $^{176}Hf/^{177}Hf$ values than expected for KREEP. Interpreting lunar Lu-Hf and Sm-Nd systematics without accounting for NC effects may thus yield erroneous conclusions.

[1] Patchett (1983) *GCA* **47**, 81-91. [2] Unruh et al. (1984) *J Geophys Res* **89 suppl.**, B459-B477. [3] Unruh and Tatsumoto (1984) *LPS XV,* 876-877. [4] Beard et al. (1998) *GCA* **62**, 525-544. [5] Patchett and Tatsumoto (1998) *LPS XII* , 819-821. [6] Brandon et al. (2009) *GCA* **73**, 6421-6445. [7] Caro and Bourdon (2010) *GCA* **74**, 3333-3349. [8] Sprung et al. (2010) *EPSL* **295**, 1-11. [9] Nyquist et al. (1995) *GCA* **59**, 2817-2837.

https://doi.org/10.1180/S0026461X00008434 Published online by Cambridge University Press

Integrating geochemical, reactive transport, and facies-based modeling approaches at the contaminated Savannah River F-Area

NICOLAS SPYCHER[1*], SERGIO BEA[1], HARUKO WAINWRIGHT[1], SUMIT MUKHOPADHYAY[1], JOHN N. CHRISTENSEN[1], WENMING DONG[1], SUSAN S. HUBBARD[1], JIM A. DAVIS[1], AND MILES DENHAM[2]

[1]Lawrence Berkeley National Lab., Berkeley, CA 94720, USA, nspycher@lbl.gov (* presenting author)
[2]Savannah River National Laboratory, Aiken, SC 29808, USA

Objective

This study aims at understanding key hydrogeochemical processes dictating pH behavior and U transport at the Savannah River F-Area in South Carolina, USA. A nearly 1 km long acidic plume has developed under this site from the disposal of low-level acidic radioactive waste solutions into seepage basins overlying relatively permeable, mostly sandy sediments. The impact of chemical and physical heterogeneities on contaminant mobility is of particular interest.

Approach and Results

Various geochemical, horizontal 1D, and vertical 2D reactive transport simulations are conducted, that include the effects of mineral dissolution and precipitation, as well as H+ and U(VI) sorption using surface complexation models. Simulations consider the historical 35-year discharge of U-bearing nitric acid solutions, followed by a post-discharge period of 65 years. The concept of "reactive facies", integrating sediment chemical and hydrophysical properties with geophysical signatures, is explored to spatially distribute linked physical and chemical heterogeneities at local and field scales. Results of isotopic studies are also used to constrain the modeling effort. Simulations are conducted in a step-wise manner, first considering only the saturated zone then increasing complexity by including the vadose zone and a free water table.

Simulations indicate that H^+ sorption reactions on goethite and kaolinite (the main minerals at the site besides quartz), and the precipitation of Al minerals could delay the pH rebound for decades. Such slow rebound is likely to be exacerbated by residual saturation of the plume below the discharge basins. U concentrations potentially could decrease faster than pH from dilution with clean recharge water.

Two reactive facies are identified in the main formation at the site, each with distinct effects on predicted plume migration. Heterogeneous reactive properties (i.e., surface areas) within each facies, however, do not appear to affect the simulated historical pattern of the plume, because sorption sites become quickly saturated by the massive H^+ and U influx during the discharge period. Consequently, intra-facies heterogeneities mostly affect the predicted pH and U transport at early times and at the plume edges, and are expected to become relevant over the long term only once contaminant concentrations have decreased below sorption saturation levels. Rigorous uncertainty quantification studies are underway to further evaluate the effect of key model input parameters on model predictions.

Calcite Growth from the Molecular Scale.

ANDREW G. STACK[1*], JACQUELYN N. BRACCO[2], PAOLO RAITERI[3], JULIAN D. GALE[3], MEG C. GRANTHAM[2]

[1] Chemical Sciences Division, Oak Ridge National Laboratory, Oak Ridge, TN, U.S.A., stackag@ornl.gov * presenting author
[2] School of Earth and Atmospheric Sciences, Georgia Institute of Technology, Atlanta, GA, U.S.A.
[3] Nanochemistry Research Institute, Dept. of Chemistry, Curtin University, Perth, WA, Australia

Calcite ($CaCO_3$) growth and dissolution play important roles in determining ocean and subsurface geochemistry, such as buffering pH and serving as a biomineral for a large number of organisms. An understanding of the molecular-level mechanisms by which calcite grows and dissolves may enhance our ability to understand and predict the response of calcite to changes in these environments.

While abundant measures of calcite growth and dissolution rates exist, these are often made by measuring the solution composition over time, a method which convolutes the multiple reactions that occur on the mineral surface itself and these studies therefore have limited value in understanding reaction mechanisms. Historically, most surface sensitive techniques applied to this problem have probed calcite reactivity under stoichiometric solution compositions, which also cannot distinguish between the independent reactivities of calcium and carbonate. Using *in situ* atomic force microscopy, Stack and Grantham[1] and others[2] have recently shown that the ratio of calcium-to-carbonate plays an important role in determining overall reaction rate.

Here, we will evaluate the efficacy of analytical crystal growth models applied to the advance of monomolecular steps on the calcite surface. In particular we will focus on how well they capture the response of step velocity under varying saturation index as well as aqueous calcium-to-carbonate ratio. We will use strontium and its inhibitio of growth as an indicator of how well these models are capturing the salient aspects of reactions such as the nucleation and propagation of kinks on steps. At the time of writing, no single model yet derived captures the entirety of the richness of reactivity observed.

As an alternative to pre-defined analytical models fit to experimental data, we also will show the results of rare event theory molecular dynamics simulations applied to the same kink site reactions on the calcite surface. This method was recently successfully applied to the barite ($BaSO_4$) {120} steps[3]. These have the potential to give accurate reaction rates and mechanisms independent of a crystal growth model.

This research was sponsored by the Division of Chemical Sciences, Geosciences, and Biosciences, Office of Basic Energy Sciences, U.S. Department of Energy.

[1] Stack, A. G.; Grantham, M. C. (2010) *Cryst. Growth Des.*, **44**, 1602.
[2] Perdikouri, C. et al. (2009) *Cryst. Growth Des.*, **9**, 4344.
[3] Stack, A. G.; Raiteri, P.; Gale, J. D. (2012) *J. Am. Chem. Soc.* **134**, 11.

https://doi.org/10.1180/S0026461X00008434 Published online by Cambridge University Press

Arsenic transport from former mine sites: an empirical modeling approach

DAVID H. STACK[1*], CHRISTOPHER S. KIM[2], JAMES J. RYTUBA[3]

[1]Chapman University, School of Earth and Environmental Sciences, Orange, USA, stack104@mail.chapman.edu (* presenting author)
[2]Chapman University, School of Earth and Environmental Sciences, Orange, USA, cskim@chapman.edu
[3]U.S. Geological Survey, Menlo Park, USA, jrytuba@usgs.gov

As a result of extensive gold and silver mining in California, elevated levels of naturally-occurring arsenic and other trace metals are exposed in mine wastes located in semi-arid regions (e.g. the western Mojave Desert). With extended periods of weathering and erosion, these potentially toxic elements can become mobilized and contaminate surrounding communities. Concerns over the health of individuals living in and visiting these communities have increased due to the greater awareness of this issue [1, 2]. In the past, other studies on this topic have focused on the chemical characteristics of wash sediments [3], the spatial distribution around mine sites [4], and the sources of the heavy metals [5]. While there has been some work in other semi-arid environments examining wash sediments [6], an empirical model used to reconstruct the concentration patterns observed in mining regions has not been developed.

This study sought to examine the role infrequent rain events have on the transport of mine tailings down washes and conduct a quantitative analysis of the empirical observations at multiple mine sites. Soil and sediment samples were collected from multiple mine sites in the Mojave Desert and analyzed for a suite of 49 elements. Distances between points were calculated and plotted against arsenic concentration. An empirical model was then developed and fitted to the data to explain the fluvial migration of mine wastes down washes.

The field data indicated that arsenic concentrations are highest closest to the main waste pile. Generally, as the distance from the pile increases, the arsenic concentration decreases. However, due to the complex patterns of each wash resulting from multiple source inputs and episodic movements of mine wastes, multiple power law trends were used to model the variations, and apparent pulses, of arsenic concentration. These pulses can be representative of infrequent, but intense, rainfall events occurring in the past that are characteristic to semi-arid environments. This has implications for future modeling efforts in similar environments as a potentially predictive tool for the nature of mine waste fate and transport.

[1] Eisler (2004) *Elements* **180**, 133-165. [2] Hudson-Edwards (2011) *Elements* **7**, 375-379. [3] Gonzalez-Fernandez (2011) *Environmental Earth Sciences* **63**, 1227-1237. [4] Chopin (2007) *Water Air and Soil Pollution* **182**, 245-261. [5] Wu (2011) *Environmental Earth Sciences* **64**, 1585-1592. [6] Razo (2004) *Water Air and Soil Pollution* **152**, 129-152.

Strontium-, Magnesium- , Sulfur- and Bromine-isotopes as indicators for brine origin and migration

SUSANNE STADLER[1]*, FRIEDHELM HENJES-KUNST[1], ORFAN SHOUKAR-STASH[2], DIETER BUHL[3]

[1]BGR-Federal Institute for Geosciences and Natural Resources, susanne.stadler@bgr.de (* presenting author)
[2]University of Waterloo, Canada
[3]Ruhr-University Bochum, Germany

Introduction

Causes and extents of subrosion processes following potash mining activities are still under debate for the city of Stassfurt, Germany. In our study, we investigate the role of groundwater in this context, and examined a set of environmental tracers to identify the water's origin from different aquifers (Quaternary, Triassic, caprock and the saline Zechstein formation (including flooded former mining shafts). Groundwater flow in strata covering the salt dome is well constrained: Stadler et al. [1] showed that the sampled groundwater could be related to multi-component mixing processes having occurred under three time scales: young groundwater ages were locally found (0-50 a), an old (< 40 ka) component was identified by radiocarbon data, and contact between meteoric water and Zechstein salts (naturally or anthropogenically induced) could be identified by the presence or absence of Permian crystallization water from the dissolution of e.g. Carnallite and/or Kieserite. Interactions between these components could be idenfied for the studied site. However, the origin and fate of highly saline water sampled from both the salt dome and the mining shalts remained unclear. A non-traditional isotope ($^{87}Sr/^{86}Sr$, $\delta^{26}Mg$, $\delta^{81}Br$, $\delta^{34}S$-SO_4 and $\delta^{18}O$-SO_4) study was initiated to gain insight into the brine history.

Results and Conclusion

$^{87}Sr/^{86}Sr$ of saline water samples range 0.70713 to 0.71014 with Sr concentrations varying between 0.2 and 52.3 mg/L. $\delta^{81}Br_{SMOB}$ values were found to range between 0.16‰ and 1.01‰ with Br concentrations of 6 to 3336 mg/L. $\delta^{34}S_{VCDT}$ and $\delta^{18}O_{VSMOW}$ (of SO_4) range from 0.5‰ to 15.4‰ and from 4.5‰ to 11.7‰, respectively, with SO_4 concentrations varying between 0.2 and 33 g/L. $\delta^{26}Mg_{DSM3}$ values range from -0.794‰ to 0.291‰ with Mg concentrations up to 84 g/L. Rocks from the various aquifers were also examined. Combining the isotopic results with geochemical data indicate that saline water samples from the Zechstein formation are largely unmodified residual brines formed during evaporation. The brines could be identified according to their origin (potash salt z(K2) or anhydrite z(A3) (and in few cases Leine salt residuals z(Na3)). For instance, potash salts and related brines could be linked by in part highly radiogenic $^{87}Sr/^{86}Sr$. $\delta^{26}Mg$ could not differentiate betweeen z(K2) and z(A3). Both sets of isotopes can however, clearly identify evaporitic components in fluids of cover layers.

[1] Stadler, S., Sültenfuß, J., Holländer, H., Bohn, C. Jahnke, C., Suckow, A. (2012): Isotopic and geochemical indicators for groundwater flow and multi-component mixing near disturbed salt anticlines. Chemical Geology 294-295: 226-242.

https://doi.org/10.1180/S0026461X00008434 Published online by Cambridge University Press

The stability of carbon and carbonate within eclogites

V. STAGNO[1]*, Y. FEI[1], C.A. MCCAMMON[2] AND D. J. FROST[2]

[1] Geophysical Laboratory, Carnegie Institution of Washington, Washington, DC, USA. (* presenting author)
vstagno@ciw.edu
[2] Bayerisches Geoinstitut, Universität Bayreuth, D-95440, Germany

The redox conditions at which carbon and carbonate are stable in eclogitic settings are still relatively uncertain with respect to temperature and pressure of stability for these rocks. A comparison between the oxygen fugacity defined by carbon/carbonate equilibria in peridotite [1] and eclogite assemblages [2] indicates that diamond-bearing eclogites might be stable at conditions where only carbonates would be stable in peridotite rocks. However, these conclusions are suggested by thermodynamic predictions involving possible equilibria in eclogitic rocks, while an experimentally calibrated oxybarometer is still not available.

We conducted experiments to determine the oxygen fugacity at which elemental carbon coexists with carbonate minerals and melts in synthetic eclogites representative of natural assemblages. We performed experiments at both above and below the solidus of a carbonated eclogite in the Na-Ca-Mg-Al-Si-Fe-O-C system at pressures between 3 and 25 GPa and temperature of 800-1600 °C. Iridium powder was added to the starting mixture to act as redox sensor. Experiments were run in piston cylinder and multi anvil devices. Further, we were able to measure the ferric iron of omphacite and garnet equilibrated with graphite (or diamond) and carbonate (solid or melt) in the eclogitic assemblages using Mössbauer spectroscopy. Experimental results of the oxygen fugacity at which graphite/diamond and carbonate are equilibrated within an eclogitic assemblage, were parameterized as a function of pressure and temperature.

Results from this study improve our knowledge regarding the origin of diamonds in eclogitic rocks as well as the fate of carbon when subducted back into the mantle. Further, the results allow us to determine the ferric iron contents of eclogitic minerals, such as garnet and omphacite, as a function of pressure and temperature in presence of carbon-bearing phases, and they are used to develop an oxygen thermo barometer for eclogitic rocks.

[1] Stagno, V., and D. J. Frost (2010) *Earth Planet. Sci. Lett.* **30**, 72-84. [2] Luth, R.W. (1993) *Science,* **261**, 66-68.

Carbon cycling in oil sands tailings ponds mature fine tailings under sulphate - reducing and methanogenic conditions: A microcosm study

SEBASTIAN STASIK[1]* AND KATRIN WENDT-POTTHOFF[1],

[1]UFZ Helmholtz Centre for Environmental Research,Magdeburg, Germany, sebastian.stasik@ufz.de (* presenting author)

Oil sands tailings ponds are considered as a permanent storage and remediation approach for the extraction waste of the oil sands industry in the Athabasca Basin in northeastern Alberta (Canada). The anaerobic biodegradation of organic contaminants as well as the microbially mediated methane production, which can enhance the densification of the fine tailings, have been studied for many years. Thereby the anaerobic degradation of hydrocarbons is proposed to be accomplished by a complex microbial consortium, including syntrophic and methanogenic microorganisms as well as microbes of the iron,- nitrogen- and sulphur cycle.

Using selective cultivation, we detected heterotrophic and autotrophic sulphate reducers, thiosulphate oxidisers, and iron reducers in frequencies similar to those of natural lakes. To understand the interactions of indigenous methanogenic and sulphate-reducing communities, we conducted a 6 month microcosm experiment with mature fine tailings (MFT) supplemented with different carbon sources as well as molybdate and/or BES as specific inhibitors for the processes of sulphate reduction and methanogenesis. The carbon sources comprised low molecular weight electron donors (e.g. acetate, lactate, ethanol) that are and typically generated during hydrocarbon degradation and serve as easily available carbon sources[1].

We found that sulphate reduction was more limited by the presence of sulphate than by the availability of extra carbon sources, since considerable sulphate reduction occurred in microcosms without additional organic carbon, when sulphate was available. Methanogenesis increased when microcosms were supplemented with extra carbon sources, but was completely inhibited by the addition of BES. Molybdate not only inhibited sulphate reduction, but also methanogenesis, indicating a positive relation between the two processes. The turnover of the extra carbon sources differed between microcosms treated with molybdate and BES. Acetate and propionic acid were not consumed in microcosms amended with molybdate, indicating that sulphate–reducing communities were most responsible for the metabolization of these carbon sources, and that methane was rather produced by hydrogenotrophic instead of acetoclastic methanogens. In microcosms without molybdate, concentrations of lactate, ethanol and propionic acid decreased, while acetate accumulated during the first weeks and was consumed afterwards, indicating the occurrence of both, incomplete and complete oxidizing sulphate reducers. Ethanol and lactate were consumed in microcosms even when treated with BES and molybdate together, demonstrating that other processes than methanogenesis and sulphate reduction are involved in carbon cycling in the MFT.

[1] Hulecki JC, Foght JM, Gray MR, Fedorak PM (2009) *J. Ind. Microbiol. Biotechnol.* **36**, 1499-1511.

https://doi.org/10.1180/S0026461X00008434 Published online by Cambridge University Press

Interactions between network cation coordination and oxygen speciation in oxide glasses

JONATHAN F. STEBBINS[1*], LINDA M. THOMPSON[1], JINGSHI WU[1]

[1]Dept. of Geological and Environmental Sciences, Stanford University, Stanford CA 94305 USA, stebbins@stanford.edu (* presenting author)

Recent experimental studies of aluminosilicate glasses and melts have greatly enhanced our information on the details of network structure that supersede conventional approximations, notably the presence of non-bridging oxygens (NBO) in metaluminous and even peraluminous compositions, and the widespread presence of significant concentrations of five-coordinated Al even in highly peralkaline (and peralkaline-earth) regions. Especially as Al, Si, (and B) coordination increase at high pressures, the interactions of these species become important for melt properties (e.g. density, viscosity, configurational entropy) and component activities. This interplay can sometimes be more apparent in borosilicate and germanate analog systems, even at ambient pressure, as composition and temperature have now well-known, large effects on structure. For example, the sizes and charges of the network modifier cations can have strong effects, as smaller and/or higher-charged cations often favor the formation of NBO and/or BO such as Al-O-Al linkages, both of which serve as relatively concentrated negative charge that can more effectively coordinate the modifier cations. We will compare results on such speciation reactions for a variety of oxide melt systems, note similarities and differences, and suggest important areas for future investigation.

Diffusion versus surface reaction control of mineral precipitation and dissolution kinetics at the pore scale

CARL I. STEEFEL*, DAVID TREBOTICH, SERGI MOLINS, LI YANG, CHAOPENG SHEN

Lawrence Berkeley National Laboratory, Berkeley, USA, CISteefel@lbl.gov (* presenting author)

Introduction

The rates of mineral precipitation are important as a subsurface carbon sequestration mechanism in the case of carbonates, while mineral dissolution is important as a source of both metal cations and alkalinity for precipitation. Pore scale flow and transport processes within the complex pore structure of the subsurface can lead in some cases to a complete or partial control of reaction rates by molecular diffusion. The extent to which a diffusion control develops depends on the rates of local surface reaction, but also on the pore geometry and the rate of flow, since these effects influence the width of diffusion boundary layers that develop adjacent to reactive mineral surfaces.

Approach and Results

In this study, we use Direct Numerical Simulation of pore scale reactive transport processes to investigate the effect of a complete or partial limitation of rates by molecular diffusion through a hydrodynamic boundary layer (Figure 1). We focus here on the dissolution and precipitation of carbonate phases, with rates at the mineral surface taken from experimental studies in which a complete surface reaction control can be demonstrated. The partial control of rates by molecular diffusion, which is particularly pronounced for larger grain sizes within porous subsurface materials, is investigated as a function of the saturation state of the bulk solution with respect to the carbonates, as well as temperature and pH, since these can influence both the rate of surface reaction and multicomponent diffusion. The simulations are combined with selected microfluidic reactor experiments in which hydrodynamic boundary layers and surface reaction can be rigorously quantified. The simulations demonstrate that a partial diffusion control of reaction rates in medium to coarse grained materials is much more prevalent than is commonly thought.

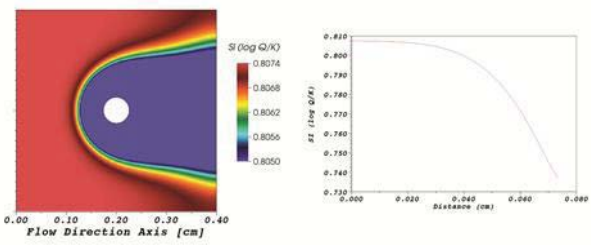

Figure 1: Left: Contour plot of calcite supersaturation surrounding a spherical calcite grain. Right: Profile of supersaturation with respect to calcite across a diffusion boundary layer, with mineral grain on the right, bulk solution on the left.

https://doi.org/10.1180/S0026461X00008434 Published online by Cambridge University Press

Quartz precipitation and fluid-inclusion characteristics in submarine hydrothermal systems

M. STEELE-MACINNIS[1*], L. HAN[1], R.P. LOWELL[1], J.D. RIMSTIDT[1] AND R.J. BODNAR[1]

[1]Department of Geosciences, Virginia Tech, Blacksburg VA 24061 USA, mjmaci@vt.edu (* presenting author)

Numerical modeling of quartz dissolution and precipitation in a sub-seafloor hydrothermal system was used to predict where in the system quartz could deposit and trap fluid inclusions. The spatial distribution of zones of quartz dissolution and precipitation is complex, owing to the many inter-related factors controlling quartz solubility, including temperature, fluid salinity and fluid immiscibility, and quartz may exhibit either prograde or retrograde solubility, depending on the *PTX* conditions [1]. Using the *PVTX* properties of H_2O-NaCl, the petrographic and microthermometric properties of fluid inclusions trapped at various locations within the hydrothermal system are predicted. Vapor-rich inclusions are trapped as a result of the retrograde temperature-dependence of quartz solubility as deep convecting fluid is heated in the vicinity of the magmatic heat source. Coexisting liquid-rich and vapor-rich inclusions are also trapped in this deep region when quartz precipitates as the convecting fluid enters the region of fluid immiscibility. Vapor generated as a result of fluid immiscibility migrates upward, entraining variable amounts of brine and/or heated seawater. During ascent, vapor condenses and mixes with seawater entrained in the upwelling plume. Fluid inclusions trapped along the upflow path in the shallower subsurface near the seafloor vents and in the underlying stockwork are liquid-rich and homogenize at 200-400 °C. Salinities of these inclusions are similar (but generally not equal) to that of seawater. Volcanogenic massive sulfide (VMS) deposits represent fossil submarine hydrothermal systems, in which mineralization commonly forms a stockwork zone beneath seafloor vents. Because the spatial variation of fluid-inclusion properties in this portion of the submarine hydrothermal system can be predicted, relationships between fluid-inclusion properties and location within the hydrothermal system can be inferred. Fluid inclusion properties can thus be used as an exploration tool for VMS deposits. Importantly, fluid inclusions can define vectors to infer the direction towards potential massive sulfide ore within fossil submarine hydrothermal systems, and can be used to determine the "up" direction within a deformed or tilted volcanic pile.

[1] Akinfiev, Diamond (2009) *Geochim. Cosmochim. Acta* **73**, 1597-1608.

Climate forcing of ice sheet dynamics in West Antarctica

ERIC J. STEIG[1]*

[1]University of Washington, Seattle, WA, USA, steig@uw.edu (* presenting author)

Recent West Antarctic Climate and Ice Sheet Change

Ice shelves and glaciers along the margin of the Antarctic ice sheet are thinning rapidly. The greatest thinning rates are in West Antarctica, where warm Circumpolar Deep Water (CDW) floods the continental shelf and melts the ice shelves from below. This region has also experienced significant climate changes in the last 30 years or more, including rising temperatures over most of continental West Antarctica and the Antarctic Peninsula, and declines in sea ice in the Amundsen-Bellingshausen Seas [1].

Climate and glaciological changes in West Antarctica are linked by changes in the regional atmospheric circulation which have caused increased poleward warm-air advection, sea ice convergence, and wind-driven inflow of CDW onto the shelf. These changes in regional atmospheric circulation are largely a response to forcing from the tropical Pacific (Figure 1). Particularly in the 1990s, strong sea surface temperature anomalies and anomalous deep convection in the central tropical Pacific caused enhanced Rossby wave activity, resulting in anomalous westerlies along the Amundsen Sea coast of West Antarctica [2].

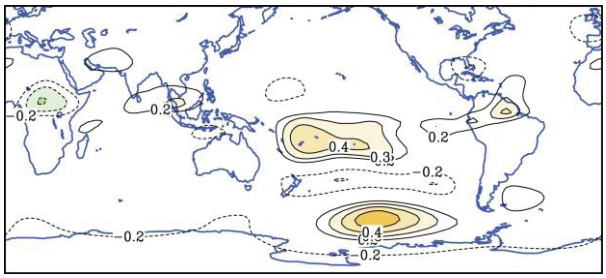

Figure 1: Correlation between the global 200 hPa stream function and the westerly wind stress over the West Antarctic shelf edge [2].

Attribution

These results imply that recent glaciological changes in West Antarctica can be attributed to anthropogenic forcing only to the extent that recent changes in the tropical Pacific can be so attributed. Paleoclimate record from corals shows that the anomalous conditions in the tropics in the last ~30 years are very likely exceptional in the last millennium. Similarly, the ice core record from West Antarctica shows that the 1990s are the most anomalous decade in at least the last 300 years. Nevertheless, attribution of tropical Pacific climate changes to anthropogenic forcing remains equivocal, largely because there is significant uncertainty in the response of the El Niño-Southern Oscillation. Uncertainty in projections of the future behavior of the West Antarctic ice sheet is further complicated by uncertainty in projections of tropical climate.

[1] Ding *et al*. (2011), *Nature Geosci.* **4,** 398-403.
[2] Steig *et al.* (2012) *Annal. Glaciol.* **62**, in press.

https://doi.org/10.1180/S0026461X00008434 Published online by Cambridge University Press

What is source rock?

H.J. STEIN[1,2] AND J.L. HANNAH[1,2]

[1] AIRIE Program, Colorado State University, Fort Collins, CO, USA
[2] Physics of Geological Processes, University of Oslo, Norway

From the perspective of a commodities expert, the likely answer will be organic-rich shales with hydrocarbon potential, or metal-bearing magmatic or sedimentary systems. You're either a petroleum geologist or an ore geologist, and the two professions typically stay on their own side of the fence. Has anyone seen a petroleum geologist regularly gobbling-up science at ore geology meetings or, even more unheard of, the reverse? And up the middle, are those studying "fluids in the crust", knowing the economic potential of their efforts but feeling uncertain how to access it – how to break into the terminology and be embraced as an outsider in resource-driven clubs. These are the statements that give us pause and discomfort.

The futures of research in both resource fields, hydrocarbons and metals, are co-dependent. The big leaps in commodity-driven science will be made by those who move unabashed between these two fields. Too many ore geologists fall back on the same tired models, never stepping outside their own sandbox to explore different ways to play. Ore deposits are formed by "deep-seated mantle-derived fluids" or by "granite-derived fluids", we are told. Who stops to consider the importance of organic complexes, or the chemical and physical consequences of hydrocarbon maturation? Similarly, how many petroleum geologists ponder the metal porphyrins that populate hydrocarbon systems, and what becomes of those metals as the organic molecules are cracked?

Modeling the mobility and concentration of both metals and hydrocarbons requires a keen understanding of fluids and volatiles in all kinds of rocks. Source rock is any rock that experiences breakdown of kerogen or undergoes oxidation thereby liberating metal from sulfide, silicate, or organic-rich material. Neither process is very interesting in the absence of water and CO_2, a pressure gradient, and space to move.

It is the fluid and volatile phases in rocks that move natural resources into place. The processes involved may be incremental to catastropic. The time scales may be instantaneous to hundreds of millions of years depending on one's perspective. But the notion that an ore deposit in the crust had a direct pipeline to the mantle should be put to rest. Rather, large scale mantle events stimulate processes in the crust over long time-scales. Source rock can be any rock implicated in the process with volatile, fluid, metal, or hydrocarbon to contribute.

Field-based examples that capture these processes are explored in this contribution. Processes that "upgrade metals" and "downgrade kerogen" are constrained in absolute time through precise Re-Os dating of sulfides and hydrocarbon.

Mantle plume chemical asymmetry - implications from geodynamic models

BERNHARD STEINBERGER[1,2*], RENÉ GASSMÖLLER[1] AND ELVIRA MULYUKOVA[1]

[1]GeoForschungsZentrum Potsdam, Potsdam, Germany, bstein@gfz-potsdam.de (* presenting author)
[2]Physics of Geological Processes, Univ. of Oslo, Oslo, Norway

Introduction

Recent results indicate that mantle plume composition systematically varies with position relative to the plume center, and that this heterogeneity could correspond to different regions where the plume material came from before rising through the plume conduit [1,2]. Here we present results of a numerical model regarding the relation of source region and location in the plume.

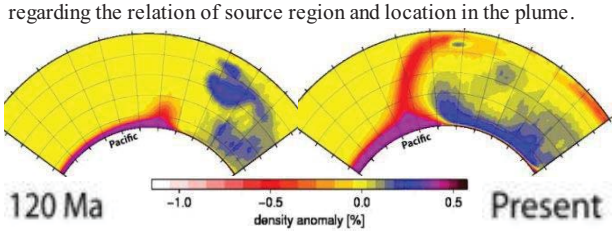

Figure 1: Cross sections for a mantle model [3]. Subducted slabs (blue) sink to the base of the mantle, and push hot material from the thermal boundary layer (red) towards the edges of thermo-chemical piles (violet) where it rises in the form of mantle plumes.

Observations and Models

Almost all Large Igneous Provinces, when reconstructed to their eruption locations, fall above the margins of either of the two Large Low Shear Velocity Provinces beneath the Pacific and Africa [4], often viewed as chemically distinct. Based on plate reconstructions since 250-300 Ma, we model a pattern of several plumes each at the edges of two thermo-chemical piles in the lowermost mantle, both with a numerical code based on spherical harmonics [5] and the finite element code CitcomS [6,7]. We develop a 2-D finite element code that allows us to accurately model entrainment of chemically distinct material in plumes.

Results and Conclusions

Model plumes often occur at locations similar to observed hotspots with conduit shapes similar to [8] where flow is based on tomography-based density models. By tracking along flow lines, both for subduction- and tomography-based flow superposed with plume influx, we map source regions onto predicted location in the plume. The mapping allows insights into the element distribution in the source region by comparing the properties of plume-related magmas. Furthermore, comparing the created models allows us to constrain under which conditions plumes entrain chemically distinct material in their source region and whether these are likely to occur on earth. Based on high-resolution 2-D results we assess entrainment and where inside the conduit chemically distinct material is expected to occur.

[1] Weis *et al.* (2011) *Nat. Geosci.* **4**, 831-838. [2] Huang, Hall & Jackson (2011) *ibid.*, 874-878. [3] Steinberger & Torsvik [2012] *G-Cubed* **13,** Q01W09. [4] Torsvik et al. [2006] *GJI* **167**, 1447-1460. [5] Hager & O'Connell [1981] *JGR* **86**, 4843-4867. [6] Zhong et al. [2000] *JGR* **105**, 11063-11082. [7] Tan et al. [2006] *G-Cubed* **7**, Q06001. [8] Steinberger & O'Connell [1998] *GJI* **132**, 412-434.

https://doi.org/10.1180/S0026461X00008434 Published online by Cambridge University Press

Compositional heterogeneity within the Yellowstone magma reservoir: Insight from zircon age, trace-element, and Hf-isotopic analyses

MARK E. STELTEN[1*], KARI M. COOPER[1], JORGE A. VAZQUEZ[2], JOSH WIMPENNY[1], GRY H. BARFOD[1], QING-ZHU YIN[1]

[1]University of California – Davis, Davis, CA, USA, mestelten@ucdavis.edu (* presenting author)
[2]U.S. Geological Survey, Menlo Park, CA, USA

Introduction

The Yellowstone Plateau (USA) hosts one of the largest Quaternary magmatic systems in the world, with caldera forming eruptions at 2.059 ± 0.004 Ma, 1.285 ± 0.004 Ma, and 0.639 ± 0.002 Ma, as well as numerous intracaldera and extracaldera eruptions between caldera-forming events [1]. The most recent eruptive episode at Yellowstone caldera produced the Central Plateau Member (CPM) of the Plateau Rhyolite, which erupted intermittently between ~170-70ka with a cumulative volume ≥600km^3, thereby approaching the ≥1000km^3 (dense rock equivalent) of rhyolite erupted during the preceding caldera forming eruption of the Lava Creek Tuff [1]. Thus, the CPM rhyolites provide snapshots of an evolving large silicic magma reservoir though time.

In this study we examine the degree of compositional heterogeneity ca. 100ka in the Yellowstone magma reservoir by comparing sub-crystal-scale SIMS age, SIMS trace-element, and LA-MC-ICPMS Hf-isotopic data from zircons hosted in three CPM rhyolites erupted at different locations within the caldera during the 100-120ka time period, as well as an ~118ka extracaldera rhyolite. Linking the age, trace-element, and Hf-isotopic compositions of zones within individual zircons provides a robust method for recognizing distinct crystal populations and magma compositions within the CPM reservoir, and monitoring the evolution of the magma reservoir over time using crystal zoning patterns. Comparing crystal populations in coeval rhyolites erupted from different parts of the caldera furthermore allows for assessment of whether the rhyolites have similar crystal populations and provides insight into the degree of compositional heterogeneity within the magma reservoir at ~100ka.

Results and Conclusions

Age, trace-element, and Hf-isotopic data for zircons from the intracaldera West Yellowstone flow, Solfatara Plateau flow, and Hayden Valley flow as well as from the extracaldera Gibbon River flow document the presence of multiple zircon populations within the CPM magma reservoir. Hf-isotopic compositions of zircons in the CPM rhyolites vary from -8.5 εHf to 1.2 εHf, with individual grains displaying large (>4 εHf) Hf-isotopic variations. These data document that the CPM reservoir experienced mixing and crystal exchange with multiple magmas prior to eruption, and place constraints on the degree of compositional heterogeneity in the Yellowstone magma reservoir ca. 100ka.

[1] Christiansen *et al.* (2007) *Geol. Sur. Open File Rep*, **1071**, 1-98.

Temporal variation of sulfur and iron metabolisms within composite tailings and overlying sand cap at Syncrude's Mildred Lake property

KATE STEPHENSON[1*], KATHRYN KENDRA[1], TARA COLENBRANDER-NELSON[1], RODERICK AMORES[1], STEVEN HOLLAND[1], TARA PENNER[2], AND LESLEY WARREN[1]

[1]McMaster University, School of Geography and Earth Sciences, Hamilton, Canada, stephk2@mcmaster.ca (* presenting author)
[2]Syncrude Environmental Research, Edmonton, Canada, penner.tara@syncrude.com

In accordance with provincial regulations, the Alberta oil sand companies must reclaim mined areas and composite tailings (CT) deposits produced as a by-product of bitumen extraction. Syncrude, the largest operator in the Alberta oil sands is currently building the first pilot fen reclamation project overtop of CT. Dewatering of CT associated with reclamation activities at Syncrude's Mildred Lake property (Fort McMurray, AB), has resulted in unexpected incidents of H_2S gas release from CT dewatering wells, identifying the need for in depth biogeochemical characterization of these materials and identification of the potential roles of microbial activity in H_2S generation. The objectives of this field and experimental research are to establish the existence of Fe- and S- respiring bacteria within CT porewaters and their potential linkages to H_2S release over seasonal and spatial scales within the CT deposit. An operationally defined sequential extraction procedure was used to quantify biologically accessible pools of amorphous Fe and S substrates within the sand cap overlying the CT, an important interface between the CT pore-water brine and the developing fen. Results show high concentrations of bioavailable Fe (124 µmol/g) and S (48 µmol/g) in the reducible ("amorphous and crystalline oxyhydroxides") and the oxidizable ("organic/sulfide") sediment fractions respectively. Porewater wells within CT and the overlying 10 m sandcap on which the fen is currently being constructed were sampled 4 times from June 2010 to October 2011. H_2S was detected in all wells and at all sampling dates, the highest concentration detected was for a well within the sandcap of 183 µmol/L. Enrichments for S and Fe oxidizing and reducing bacteria from samples collected in June and September 2010 and July 2011, have shown positive growth for S- and Fe- oxidizing and reducing bacteria in well water from the location of reported H_2S_g release, consistent with the involvement of these microbes in S- cycling and H_2S production in CT. Experimental mesocosms with targeted Fe and S metabolisms are currently being assessed for H_2S generation to identify key metabolic pathways involved. Select field and laboratory results, including 16S rRNA sequencing of environmental enrichments and the bulk well water community, along with the results of experimental mesocosms will be discussed.

https://doi.org/10.1180/S0026461X00008434 Published online by Cambridge University Press

The role of subduction erosion in the recycling of continental crust

CHARLES R STERN[1]

[1]University of Colorado, Department of Geological Sciences, Boulder, CO 80309-0399 USA, Charles.Stern@colorado.edu

Subduction erosion occurs at all convergent plate boundaries, even if they are also accretionary margins. Frontal subduction erosion results from a combination of erosion and structural collapse of the forearc wedge into the trench, and basal subduction erosion by abrasion and hydrofracturing above the subduction channel. High rates of subduction erosion are associated with relatively high convergence rates (>60 mm/yr) and low rates of sediment supply to the trench (<40 km^2/yr), implying a narrow and topographically rough subduction channel which is neither smoothed out nor lubricated by fine-grained water-rich turbidites such as are transported into the mantle below accreting plate boundaries. Rates of subduction erosion, which range up to >440 km^3/km/my, vary temporally as a function of these same factors, as well as the subduction of buoyant features such as seamount chains, submarine volcanic plateaus, island arcs and oceanic spreading ridge, due to weakening of the forearc wedge. Globally, subduction erosion is responsible for >1.7 Armstrong Units (1 AU = 1 km^3/yr) of crustal loss [1], a significant proportion of the yearly total crustal loss caused by sediment subduction, continental lower crustal delamination, crustal subduction during continental collision, and/or subduction of rock-weathering generated chemical solute that is dissolved in oceanic crust. The paucity of pre-Neoproterozoic blueschists suggests that global rates of subduction erosion were probably greater in the remote past, perhaps due to higher plate convergence rates. Subducted sediments and crust removed from the over-riding forearc wedge by subduction erosion may remain in the crust by being underplated below the wedge, or these crustal debris may be carried deeper into the source region of arc magmatism and incorporated into arc magmas by either dehydration of the subducted slab and the transport of their soluble components into the overlying mantle wedge source of arc basalts, and/or bulk melting of the subducted crust to produce adakites. In selected locations such as in Chile [2,3], Costa Rica, Japan and SW USA, strong cases can be made for the temporal and spatial correlation of distinctive crustal isotopic characteristics of arc magmas and episodes or areas of enhanced subduction erosion. Nevertheless, overall most subducted crust and sediment, >90% (>3.0 AU), is transported deeper into the mantle and neither underplated below the forearc wedge nor incorporated in arc magmas. The total current rate of return of continental crust into the deeper mantle is equal to or greater than the estimates of the rate at which the crust is being replaced by arc and plume magmatic activity, indicating that currently the continental crust is probably slowly shrinking [4,5]. However, rates of crustal growth may have been episodically more rapid in the past, most likely at times of supercontinent breakup, and conversely, rates of crustal destruction may have also been higher during times of supercontinent amalgamation. Thus the supercontinent cycle controls the relative rates of growth and/or destruction of the continental crust. Subduction erosion plays an important role in producing and maintaining this cycle by transporting radioactive elements from the crust into the mantle, perhaps as deep as the core-mantle boundary.

[1] Stern (2011) *Gondwana Research* **20,** 284-308.
[2] Stern (1991) *Geology* **19**, 78-81.
[3] Stern et al. (2011) *Andean Geology* **38**, 1-22.
[4] Stern & Scholl (2010) *International Geology Review* **52**, 1-31.
[5] Clift et al. (2009). *Earth Science Reviews* **97**, 80-104.

Stable strontium isotope behaviour in Himalayan river catchments

EMILY I. STEVENSON[1]*, KEVIN W. BURTON[2], IAN J. PARKINSON[3], CHRISTOPHER R. PEARCE[3] FATIMA. MOKADEM[1], AND RACHAEL JAMES[4]

[1]Department of Earth Sciences, Oxford University, South Parks Road, Oxford, OX1 3AN, UK. emilys@earth.ox.ac.uk (* presenting author)
[2]Department of Earth Sciences, Durham University, Durham, DH1 3LE, UK
[3]Department of Environment, Earth and Ecosystems, The Open University, Milton Keynes, MK7 6AA, UK
[4]National Oceanography Centre, European Way, Southampton, SO14 3ZH, UK

The radiogenic strontium ratio ($^{87}Sr/^{86}Sr$) is commonly used as a weathering tracer of continental sources in seawater, with carbonate and silicate based lithologies having different $^{87}Sr/^{86}Sr$ ratios. However, $^{87}Sr/^{86}Sr$ interpretations can be hindered by the difficulty of distinguishing changes in riverine flux from changes in composition. This is a particular problem for Himalayan rivers as those draining both silicate and carbonate catchments have elevated $^{87}Sr/^{86}Sr$ ratios, and there is debate as to how much of the ^{87}Sr flux is actually derived from silicate weathering [1].

Recent stable strontium isotope data suggested that carbonate weathering yields a $\delta^{88/86}Sr$ value distinct from those of both silicate weathering and seawater [2]. This difference in isotopic ratio could resolve whether inputs into rivers, and eventually the oceans, are truly dominated by either silicate or carbonate lithologies and may also be used to distinguish between flux and source.

This study presents high-precision $\delta^{88/86}Sr$ data and $^{87}Sr/^{86}Sr$ data obtained from river waters draining both silicate and carbonate dominated terrains in the Himayala. Rivers draining carbonate based terrains have an average $\delta^{88/86}Sr$ value of 0.28±0.08‰ and increase to heavier values downstream (heading towards those of the Ganges, 0.38±0.01‰ [3]), possibly because of continued carbonate precipitation through the catchment. The $\delta^{88/86}Sr$ of carbonate rivers also correlates with [Si], and other major divalent cations as well as sulphate concentration. [4] Silicate rivers are generally heavier (0.34±0.07‰), but show little systematic behaviour with other elements. These results indicate that the carbonate rivers are generally lighter than those draining silicate terrains, and also suggest that continued secondary mineral precipitation (primarily carbonates) is occuring with within those catchments.

[1] Bickle et al. (2005) *GCA* **69**, 2221-2240. [2] Krabbenhöft et al., (2010) *GCA* **74** 4097-4109. [3] Pearce et al., (2011) *AGU, Fall Meet. Abs*. B21D-0342. [4] Kisakürek et al., (2005) *EPSL* **237** 387-401.

https://doi.org/10.1180/S0026461X00008434 Published online by Cambridge University Press

Uranium association and interaction with redox boundary in Rifle surface seep sediments

BRANDY D. STEWART[1*], PETER S. NICO[2], AND BRENT M. PEYTON[1]

[1]Montana State Universiy, Bozeman, MT, USA
(* presenting author)
[2]Lawrence Berkeley National Laboratory, Berkeley, CA, USA
Brandy.stewart@erc.montana.edu
psnico@lbl..gov
bpeyton@coe.montana.edu

Owing to ecosystem and human health consequences, understanding uranium's potential for mobility in environmental settings is important. In anaerobic soils and sediments, oxidized U(VI) may be reduced through biological or chemical pathways to U(IV), forming sparingly soluble solids. However, formation of uranyl-calcium-carbonato complexes may limit reduction and authogenic UO_2 is susceptible to reoxidation. Determining reaction pathways of uranium that promote solids stable under aerobic and anaerobic conditions is critical for limiting dissolved concentrations and migration of uranium. This is of particular concern in settings near or at redox boundaries where surface and subsurface environments may be subjected to fluctuating redox conditions. We examined the nature and association of solid-phase uranium in both oxidized and reduced sediments from a hillside surface seep in Rifle, Colorado where uranium appears to be naturally attenuated in the solid phase. Visibly reduced sediments occur at the surface of the seep adjacent to (< 100cm from) pockets of freshly precipitated iron (III) phases, indicative of a redox boundary. Uranium release and solid-phase association were measured in systems containing sediment and 3 mM Fe(II) that were maintained under reducing conditions for 15 d followed by 5d of oxidation to simulate a redox cycle. Aqueous and solid-phase results show that >75% of uranium present in the sediments remains associated with the solid phase throughout the oxidation portion of the experiments.

Predicting the speciation and transport behaviour of contaminants in a wet discard dam

GIDEON STEYL[1]*, IZAK L. MARAIS[2], LORE-MARI CRUYWAGEN[2]

[1]University of the Free State, Chemistry Department, Bloemfontein, South Africa, steylg@ufs.ac.za (* presenting author)
[2]University of the Free State, Institute for Groundwater Studies, Bloemfontein, South Africa, CruywagenLM@ufs.ac.za

The burning of pulverised coal in coal-fired boilers to generate heat causes the production of fly ash. In addition water used in the process of cooling and turbine propulsion results in the production of high saline effluents. The high saline streams (ca. 20% ash) are used for the hydraulic transport of ash to the dumping sites, which results in ash dams that can act as salt sinks. The slurry that is pumped onto the wet dump area is allowed to settle. The water that has separated from the ash is skimmed off and re-circulated to transport more fly ash to the site. However a certain fraction of the water infiltrates the dam resulting in geochemical transformations.

Due to the presence of high saline water during the operational phase an extensive salt loading is observed onto the ash particles. During the decommisioning phase of the ash dam certain physical and chemical processes need to be considered to manage the produced water from the system. In particular the mechanism of leachate production needs to be considered in conjunction with the temporal and spatial extent.

The results presented will focus on the effect that disposal methods of the fly ash has on the transport of chemical species within the ash dam (Figure 1). In addition the rate of release of chemical species will also be presented as this influences the measures required to manage these facilities over an extended time period.

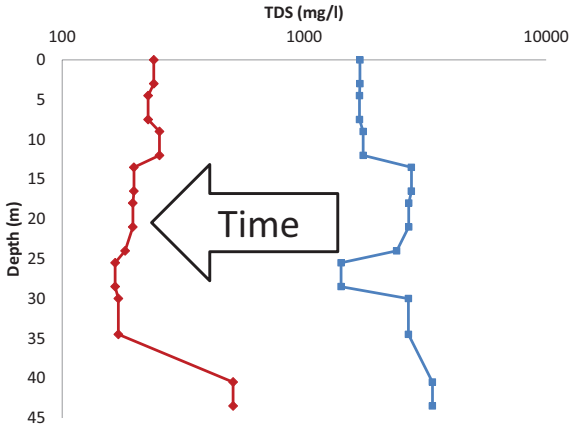

Figure 1: Diagram depicting the change in TDS values over time from a leachate analysis. The build-up of initially higher TDS values can be observed in two distinct areas (15 – 24 and 30 – 45 m).

https://doi.org/10.1180/S0026461X00008434 Published online by Cambridge University Press

When the surface is not what you think it is

STIPP S.L.S.[1], HASSENKAM T.[1], YANG M.[1], SKOVBJERG L. L.[1], SAND K.K.[1], PASARÍN I.[1], BOHR J.[2]

[1]Nano-Science Center, Department of Chemistry, University of Copenhagen, stipp@nano.ku.dk
[2]DTU Nanotech, Danish Technical University, Denmark.

More than a century ago, chemists began to explore the thermodynamic and kinetic relationships between solids and fluids in nature. Goldschmidt attempted to classsify them and Garrels, Christ, Krauskopf, Stumm, Schindler, Helgeson, Sposito and many others taught us to use thermodynamic relationships to predict natural system behaviour. When it has failed, we have often blamed kinetics.

About two decades ago, surface sensitive techniques first demonstrated that a calcite surface is not simply a termination of the bulk atomic structure. Surface atoms shift position, water delocalises charge on dangling bonds, adventitious carbon is ubiquitous and even on surfaces that appear dry, an adsorbed water film promotes recrystallisation[1]. New instruments allow us to see ever closer, giving new insights into the properties and behaviour of nano-particles and mineral-fluid interfaces so there is now little doubt. Surfaces are not simply where the bulk terminates.

Still, however, there are many cases where natural surfaces do not behave as we assume they ought to[2]. Molecular modelling, atomic force microscopy (AFM) and X-ray reflectivity show that water, structured at calcite surfaces, is displaced by ethanol and the alcohol orders itself, almost like a lipid layer. Adhesion properties change in response to ionic strength but reproducibility is elusive on ideal surfaces, whereas mineral grains plucked from sandstone, with their natural adventitious carbon, behave consistently. It is this organic "contamination" on these mineral surfaces that determines their hydrophillic properties, not the mineral beneath. Recent AFM studies have also revealed that sediment grain surfaces are frequently covered by nanocrystals of clay. These are far too thin for detection by X-ray diffraction so they have previously gone unnoticed but in some cases they cover significant portions mineral surfaces, meaning they can control water-rock properties. Finally, sea creatures produce aragonite and calcite in crystal forms tailored to their needs but these biogenic materials behave differently than inorganically produced minerals, even when organic components that remain associated with the biominerals are present only in the parts per billion range.

Materials adsorbed on mineral surfaces change properties in unexpected ways. By understanding surfaces better, we are likely to discover why large scale geological systems do not always behave as thermodynamics leads us to expect. We can hope that our new insight brings us to a point where we might have less need of the excuse "kinetically hindered".

[1] Stipp and Hochella (1991) *GCA* **55**, 1723-1736; Stipp et al. (1994) *Amer. Min.* **81**, 1-8; Stipp (1999) *GCA* **63**, 3121-3131. [2] Bohr et al. (2010) *GCA* **74**, 5985-5999; Cooke et al. (2010) *Langmuir* **26**, 14520-14529; Sand et al. (2010) *Langmuir* **26**, 15239-15247; ; Hassenkam et al. (2011) *PNAS*, 7307-7312; Hassenkam et al. (2011) *Coll. Surf. A* **390**, 179-188; Skovbjerg et al. (2012) *GCA in review*; Pasarín I.S. et al. (2012) *Langmuir in press*.

Mechanisms controlling $^{238}U/^{235}U$ isotopic fractionation in low- and high-temperature environments

C.H. STIRLING[1*], A. KALTENBACH[1] AND Y. AMELIN[2]

[1]Department of Chemistry, University of Otago, Dunedin, New Zealand, cstirling@chemistry.otago.ac.nz (* presenting author), akaltenbach@chemistry.otago.ac.nz
[2]Research School of Earth Sciences, Australian National University, Canberra ACT, Australia, yuri.amelin@anu.edu.au

Recent studies have documented sizeable, permil-level isotopic fractionation between ^{238}U and ^{235}U in low-temperature environments, facilitated by analytical advancements in multiple-collector ICP-MS (MC-ICPMS) [1,2]. Variability in $^{238}U/^{235}U$ has a direct impact on the accuracy of the U decay series chronometers, requiring the $^{238}U/^{235}U$ of every sample to be characterized, and the revision of important cosmo- and geo-chronological models. Further efforts have focussed on investigating the processes controlling $^{238}U/^{235}U$ isotope fractionation, especially during U reduction. To this end, the ^{238}U-^{235}U isotope system offers significant potential as a monitor of redox conditions in U bioremediation studies [3], and as a paleo-redox tracer of the extent of anoxia in the historic oceans [4] to complement the growing inventory of other redox-sensitive metal isotope tracers (e.g. Mo and Fe) which each have differing redox potentials and respond to anoxia at different rates. However, additional studies are required to gain an improved understanding of the mechanisms controlling ^{238}U-^{235}U isotope fractionation before these applications can be fully explored, as the available datasets show some contrasting U isotopic behaviour during U reduction.

Using MC-ICPMS, we report $^{238}U/^{235}U$ observations for samples collected from a range of low- and high-temperature environments. A ^{233}U-^{236}U double spike was employed to monitor instrumental mass fractionation, allowing variations in $^{238}U/^{235}U$ to be resolved at the 0.005 % level (2σ) on 50 ng U sample sizes, and at the 0.003 % level (2σ) on larger sample sizes by pooling the data of replicate analyses. In all of the low-temperature environments we have investigated, the magnitude and direction of the $^{238}U/^{235}U$ isotopic fractionation is consistent with the 'nuclear field shift effect' [5] as the dominant fractionation mechanism, favouring enriched $^{238}U/^{235}U$ compositions in the reduced reaction product where the electron density near the nucleus is lower. Our results for a wide range of meteorites [6,7] and volcanic terrestrial samples reveal small (0.01 % level) but resolvable variations in $^{238}U/^{235}U$ in high-temperature environments. Further efforts should focus on identifying U fractionation mechanisms in high-temperature systems by linking $^{238}U/^{235}U$ to U concentration and oxidation state. Bulk samples and mineral aggregate sub-samples spanning the primitive to differentiated meteorite classes should also be be investigated to determine the extent to which $^{238}U/^{235}U$ variations are controlled by U isotope heterogeneity or extant ^{247}Cm effects in the early solar system versus U 'stable' isotope fractionation during subsequent chemical and thermal processing.

[1] Stirling et al. (2007). *EPSL* **264**, 208-25; [2] Weyer et al. (2008). *GCA* **72**, 345-59; [3] Bopp et al. (2010). *Env. Sci. Tech*. **44**, 5927-33; [4] Montoya-Pino (2010). *Geol*. **38**, 315-18; [5] Bigeleisen (1996). *J. Am. Chem. Soc.* **118**, 3676-80; [6] Amelin et al. (2010). *EPSL*. **300**, 343-350; [7] Kaltenbach et al. (2012). *LPSC* #1691.

https://doi.org/10.1180/S0026461X00008434 Published online by Cambridge University Press

Deep water in the Upper Rhine Rift Valley, central Europe

INGRID STOBER

Institute of Geosciences. University of Freiburg. Albertstr. 23b. D-79102 Freiburg. Germany. ingrid.stober@minpet.uni-freiburg.de

Section 9f: Innovative geochemical approaches to understanding geothermal systems

Hydrochemical data from deep wells in the Upper Rhine Graben area in France and Germany were collected und examined. Primary targets were the potential geothermal reservoirs: Hauptrogenstein (Dogger). Upper Muschelkalk (middle Triassic) and Buntsandstein (lower Triasic). The data (table) were used to characterize the fluids found in the hydrogeothermal reservoirs [1. 2]. Waters at < 500 m depth are weakly mineralized. Water composition is controled by the rock. With increasing depth also TDS increases and the distinct waters of the three different aquifers all evolve to Na-Cl brines independent of the reservoir rock. Water from 3000 m depth is of very similar composition. All waters are saturated with respect to calcite and some other minerals. When thermal water is pumped to the surface and cooled, they become oversaturated with respect to a series of predictable solids including calcite, barite, celestite and others.

Table: Selected hydrochemical analyses (mg/kg):

Well	depth (m)	Na	Ca	Cl	HCO_3	SO_4
Buntsandstein						
GB1 Bruchsal	2537.	35840.	7415.	82220.	520.	384.
TB Zähringen II	843.	1115.	621.	330.	680.	3114.
Eschau 1	1619.	28307.	400.	44375.	180.	125.
GB Cronenbourg	3220.	32560.	4680.	61550.	305.	220.
Meistratzheim 2	1437.	8500.	600.	12800.	671.	2240.
Mutzenheim 1	1857.	23500.	912.	35720.	1415.	4640.
Muschelkalk						
Langenbrücken	607.	12240.	1660.	21130.	500.	1850.
Bad Schönborn	636.	9760.	1367.	16770.	571.	1942.
Bad Krozingen	591.	554.	707.	348.	1519.	1960.
TB Freiburg 1	858.	390.	632.	113.	918.	2240.
Bad Bellingen III	1194.	308.	2525.	3454.	2227.	1585.
GB 1 Riehen	1547.	4900.	805.	7270.	1012.	2550.
Eschau 1	1407.	28307.	400.	44375.	180.	125.
Staffelfelden 9	2529.	19710.	800.	30530.	950.	1900.
GB Helios	1146.	6712.	1979.	13783.	326.	960.
Hauptrogenstein						
TB 3 Freiburg	483.	59.	67.	31.	386.	98.
Georg-Quelle	487.	928.	462.	1758.	961.	291.
Blodelsheim I	1891.	7431.	1200.	13490.	1870.	1300.

Within the underlain Variscan crystalline basement the fracture porosity is filled with saline thermal water[3]. Its composition forms a continuum with the waters from the deep sedimentary aquifers. The crystalline basement in the Upper Rhine Graben is used for enhanced geothermal systems (EGS). TDS at 5000 m depth is about 100 g/kg.

[1] HE. K. & STOBER. I. & BUCHER. K. (1999): Chemical Evolution of Thermal Waters from Limestone Aquifers of the Southern Upper Rhine Valley. - Applied Geochemistry. 14. 223 – 235. Exeter/UK.
[2] STOBER. I. & JODOCY. M. (2011): Hydrochemie der Tiefenwässer im Oberrheingraben - eine Basisinformation für geothermische Nutzungssysteme. – Z. geol. Wiss.. 39. 1. S. 39 - 57.
[3] STOBER. I. & RICHTER. A. & BROST. E. & BUCHER. K. (1999): The Ohlsbach Plume: Natural release of Deep Saline Water from the Crystalline Basement of the Black Forest.- Hydrogeology Journal. vol 7 (3). pp. 273-283. Springer. Berlin/Heidelberg.

Magnetite (U-Th)/He dating– Attractive Dates in Mafic and Ultramafic Rocks

DANIEL F. STOCKLI[1], JORDAN L. TAYLOR[2*], EUGENE SZYMANSKI[2], RICHARD A. KETCHAM[1]

[1]University of Texas, Austin, USA, stockli@jsg.utexas.edu (*presenting author), ketcham@jsg.utexas.edu
[2]University of Kansas, Lawrence, USA, jordanleightaylor@gmail.com, eugene.szymanski@gmail.com

Magnetite is a common mineral phase in felsic, mafic, hydrated ultramafic igneous and metamorphic rocks. Magnetite (U-Th)/He (MHe) dating has been shown to be a reliable and powerful alternative method for obtaining absolute age constraints from mafic volcanic rocks in light of inherent difficulties in $^{40}Ar/^{39}Ar$ dating due to excess ^{40}Ar and/or recoil, susceptibility to alteration, or lack of datable mineral phases [1]. More recently, we have explored MHe as a novel and exciting geo- and thermochronometric technique for constraining the formation and thermal processes related to serpentinization and exhumation of sub-lithospheric mantle during continental break-up. While ultramafic rocks (e.g., sub-lithospheric mantle) do not commonly contain mineral phases that are datable by traditionally for geo- and thermochronometric, magnetite occurs ubiquitously as an alteration phase in serpentinized peridotites as a result of olivine breakdown. MHe Tc of ~250°C [1] can be exploited to elucidate the thermal history of exhumed mantle and formation of serpentinites. Application of MHe ages should provide critical temporal insights into continental rifting and serpentinization during break-up along magma-poor continental margins. As attractive and powerful as MHe dating is, not all magnetite samples are suitable for MHe dating due to its texture, grain size, and [U] making it prone to matrix He implantation. Detailed petrographic characterization of basaltic and ultramafic magnetite is required to determine the suitability of magnetite size and textures for MHe dating. The biggest hurdles in reliable magnetite dating, however, are grain morphology and He implantation, as matrix [U] commonly is one order of magnitude greater than magnetite (~100 ppb). While air-abrasion tends to alleviate this in large magnetite [1], irregular and complexly intergrown magnetite require careful pre-analysis screening. We have the developed the routine use of non-destructive microCT scanning for imaging of magnetite, identification of suitable magnetite, and monitoring of air-abrasion progress and high-U matrix removal. Understanding petrologic context and screening prior and during analysis are critical for deriving reliable and meaningful MHe dates.

[1] Blackburn et al. (2007) EPSL, vol. 259, p. 360–371.

https://doi.org/10.1180/S0026461X00008434 Published online by Cambridge University Press

Calcite nucleation and growth on basaltic glass and silicate minerals

GABRIELLE J. STOCKMANN[1,2*], ERIC H. OELKERS[2,3], DOMENIK WOLFF-BOENISCH[3], NICOLAS BOVET[4] AND SIGURDUR R. GISLASON[3]

[1]Nordic Volcanological Center, University of Iceland, Iceland, gjs3@hi.is (* presenting author)
[2]GET-Université de Toulouse-CNRS-IRD-OMP, France, eric.oelkers@lmtg.obs-mip.fr
[3]Institute of Earth Sciences, University of Iceland, Iceland, sigrg@raunvis.hi.is
[4]Nano-Science Center, University of Copenhagen, Denmark, bovet@nano.ku.dk

Mineral substrates and their effect on calcite nucleation and growth

Calcite was precipitated in flow-through experiments at 25 ºC from supersaturated aqueous solutions in the presence of seeds of calcite and six different silicates: augite, basaltic glass, enstatite, labradorite, olivine, and peridotite. The aim of the experiments was to determine how calcite nucleation and growth depends on the identity and structure of the growth substrate. Calcite saturation was achieved mixing a $CaCl_2$-rich solution with a $NaHCO_3$-Na_2CO_3 buffer in a mixed-flow reactor containing 0.5-2 grams of mineral grains. This led to a calcite saturation index of 0.6 and pH 9.1 for the reactive solution inside the reactor.

Although chemical conditions, flow rate and temperature were identical for all experiments, the onset of calcite nucleation and the amount of calcite being precipitated depended on the identity of the mineral substrate. With calcite as the growth substrate, new calcite crystals formed instantaneously. Calcite nucleated relatively rapidly on olivine, enstatite, and peridotite (mainly composed of Mg-olivine). Scanning Electron Microscope images showed silicate crystals to be almost completed covered with calcite coatings at the end of the experiments. Less calcite growth was found on labradorite and augite, and least on basaltic glass. In all cases, calcite precipitation occurs on the mineral substrate and not adjacent to them.

Results and Conclusion

These findings indicate that calcite nucleation and its subsequent growth depends on the crystal structure of the silicate substrate. Orthorhombic silicate minerals (olivine and enstatite) are the easiest for trigonal calcite to nucleate on. Monoclinic augite and triclinic labradorite show intermediate behavior, whereas basaltic glass with its non-ordered crystal structure is the least favorable platform for calcite growth. The results have implications for CO_2 mineralization in ultramafic and basaltic rocks [1,2] indicating that trigonal carbonates easier precipitate on crystalline rather than glassy rocks, but even glass surfaces can serve as a substrate for calcite nucleation.

[1] Oelkers *et al.* (2008) *Elements* **4**, 333-337. [2] Gislason *et al.* (2010) *Int. J. Greenhouse Gas Control* **4**, 537–545.

Smart K_d-concept based on Surface Complexation Modeling

M. STOCKMANN[1]*, V. BRENDLER[1], J. SCHIKORA[1], S. BRITZ[2], J. FLÜGGE[2], AND U. NOSECK[2]

[1]Helmholtz-Zentrum Dresden-Rossendorf, D-01328 Dresden, Germany, m.stockmann@hzdr.de (*presenting author)
[2]GRS Braunschweig, D-38122 Braunschweig, Germany

Methodology

Sorption on mineral surfaces of sediments is one important retardation process for radionuclides to be considered in long-term safety assessments for radioactive waste repositories. Previously, the K_d-concept with temporally constant values was applied to describe the radionuclide retardation in the far field of a repository.

In this study, pre-calculated distribution coefficients (K_ds) based on surface complexation models (SCM) are implemented in the existing 3D transport program r³t [1]. The so-called smart K_d-values are calculated as a function of important environmental parameters to reflect changing geochemical conditions. Respective multi-dimensional K_d-matrices are generated and stored a-priori to any r³t run. The calculations follow a bottom-up approach, i.e. the sorption of an element on each single mineral phase contributes to the distribution coefficient for a sediment.

Results

As an exemplary proof-of-concept, the Gorleben site (a potential repository site in Germany) was selected. Figure 1 shows the 3D plot for the $\log K_d$-matrix of UO_2^{2+} in the upper aquifer (UAF) at the Gorleben site as a function of pH, [Ca], and [DIC] (logarithmic scale).

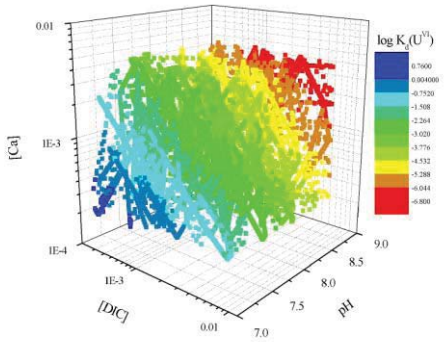

Figure 1: Multidimensional K_d-matrix for UO_2^{2+} in UAF as a function of pH, [Ca], and [DIC] (K_d in m³/kg, logarithmic scale).

These pre-calculated $\log K_d$-values vary between -6.8 and 0.75. Comparing to the temporally constant conservative $\log K_d$ of -2.7 from [2], which was previously used in r³t for the retention of UO_2^{2+} in fresh water in the upper aquifer at the Gorleben site, the resulting mean $\log K_d$ of -2.74 shows a good general agreement, but account now for geochemical variations.

[1] Fein (2004) *Report GRS-192*, *BMWi-FKZ 02E9148/2*. [2] Suter *et al.* (1998). *Proceedings DisTec 98*.

https://doi.org/10.1180/S0026461X00008434 Published online by Cambridge University Press

Measurement of intact methane isotopologues, including $^{13}CH_3D$

DANIEL A STOLPER[1], ALEX L SESSIONS[1], JOHN M EILER[1]

[1]California Institute of Technology, dstolper@caltech.edu

Methane (CH_4) is both a significant greenhouse gas and resource. Its present and past cycling can be studied through measurements of concentration and/or bulk isotopic ratios ($^{13}C/^{12}C$, D/H, and $^{14}C/^{12}C$). Currently, isotope ratios are measured by mass spectrometric analysis of H_2 and CO_2 produced from CH_4, or by spectroscopy of CH_4. However, the interpretation of bulk isotopic variations of CH_4 are often equivocal, necessitating additional tracers.

We have developed a technique for mass spectrometric analysis of several isotopologues of intact CH_4, including $^{12}CH_4$, $^{13}CH_4$, $^{12}CH_3D$, and $^{13}CH_3D$ (and the method can be extended to others). Our most novel capability is the analysis of the multiply substituted isotopologue $^{13}CH_3D$, which is expected to differ relative to a random isotopic distribution due to kinetic isotope effects, mixing processes, and as a function of temperature at equilibrium. Measurements of $^{13}CH_3D$ concentrations (along with the singly substituted species) could elucidate the formation temperatures of thermally generated CH_4, discriminate between sources of CH_4 to the atmosphere (e.g., microbial vs thermogenic gas), and help to characterize CH_4 chemistry in the atmosphere where potentially large enrichments are expected (e.g., [1], [2], [3]).

Measurement of intact CH_4 requires a mass spectrometer capable of separating CH_4 species both from water and from internal isobars (CH_4 adducts, fragments, and isotopologues). We show here the initial results and capabilities of such measurements using the MAT 253 Ultra prototype high-resolution gas-source mass spectrometer. We reproduced δD values of known samples to within 0.2 ‰ (1 s.e. = 0.1‰). In addition to demonstrating accuracy, this result reveals that the method may result in improved precision for δD measurements of CH_4 relative to conventional techniques. We have measured ratios of $^{13}CH_3D$ to mass 17 species ($^{13}CH_4$, $^{12}CDH_4$, and $^{12}CH_5$) to better than ±0.4 ‰ (1 s.e.); this value reflects counting statstics and should be improved with longer counting times. The critical enabling feature of our mass spectrometer is the ability to cleanly separate a portion of the $^{13}CH_3D^+$ peak from that of $^{13}CH_5^+$ (shown in Figure 1.)

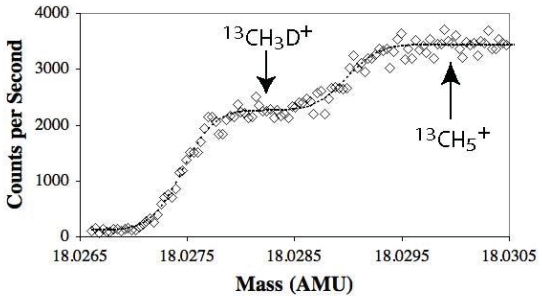

Figure 1: Peak scan of mass 18 CH_4 with a model fit through the data. Water is sufficiently resolved as to not appear at this scale.

[1]Ma et al., (2008) *GCA* **72** 5446-56. [2] Mroz et al., (1989) *GRL* **16**, 677-678. [3] Kaye and Jackman (1990) *GRL* **17**, 659-60.

The Unsaturated (Vadose) Zone—the Where of Weathering

DAVID A. STONESTROM[1*], MARJORIE S. SCHULZ[2], AND ARTHUR F. WHITE[3]

[1]US Geological Survey, Menlo Park, CA, USA, dastones@usgs.gov (*presenting author)
[2]US Geological Survey, Menlo Park, CA, USA, mschulz@usgs.gov
[3]US Geological Survey, Menlo Park, CA, USA, afwhite@usgs.gov (emeritus)

The unsaturated zone (UZ), that portion of the Earth's crust between land surface and the regional water table—the latter being defined as the surface below which pore-water pressure is persistently above atmospheric—is the vital bio-geochemical reactor that sustains the planetary critical zone. Weathering reactions in the UZ sustain life by releasing bioessential elements such as potassium, calcium, and magnesium that are mostly locked up in solid mineral phases during the bioaccessible parts of the rock cycle. The UZ sits at the intersection of the lithosphere, atmosphere, and terrestrial biosphere, acting as a highly non-linear regulator of water, carbon, and nutrient dynamics. It is the key interface controlling hydrospheric influences on land based life. UZ water is the mobile solvent that delivers aqueous reactants and removes aqueous products from the sites of weathering reactions. It also partitions the pore space within the evolving geometry of soil structure, thereby controlling crucial pore-geometric relations including proximal and long-range connectedness (topology) of gas and liquid phases. The resulting dynamics mediate residence times, redox states, complexation, and chemical activity, along with fluid permeabilities and solute dispersivities. Hysteresis in the relations between water content θ and matric pressure ψ acts to partially constrain fluxes of water (and heat) to the uppermost UZ. This provides plant-root microcosms more opportunity for water and nutrient extraction and moderates weathering reactions by controlling equilibrium versus kinetic control of chemical processes. UZs may be classified according to water-table depth, water balance, and water-flux variability in time and space. These determine whether UZs act as (1) rapid, disequilibrium pass-through conduits with little opportunity for weathering reactions, (2) equilibrium controlled static reservoirs of water and solutes where not much is happening, or (3) totally happening places essential for oxygen-intensive life.

The ideas herein stem from many fruitful discussions and collaborations with Art White, Jorie Schulz, Alex Blum, Jennifer Harden, Sue Brantley, Kate Maher, Michelle Walvood, Bridget Scanlon, Jim Constantz, John Nimmo, Dave Prudic, Amanda Garcia, Brian Andraski, Jacob Rubin, Laurie Flint, Alan Flint, and others.

Vive la Weathering. Vive l'UZ Science. Vive l'Art!

https://doi.org/10.1180/S0026461X00008434 Published online by Cambridge University Press

The Fingerprint of Geologic Carbon on Glacial/Interglacial Marine Carbonate Chemistry and Atmospheric CO_2

LOWELL STOTT[1*]

[1] University of Southern California, Earth Sciences, stott@usc.edu (* presenting author)

The rise in atmospheric pCO_2 during the last glacial termination was accompanied by a 190‰ decrease in surface ocean $\Delta^{14}C$ between 17 to 10 kyB.P., which cannot be explained without calling upon an input of ^{14}C-depleted carbon from either a formally isolated deep ocean reservoir or input of geologic carbon. There are now enough marine $\Delta^{14}C$ records spanning the deglaciation to make clear that Pacific deep water $\Delta^{14}C$ did not track the atmosphere whereas the $\Delta^{14}C$ of intermediate waters did, except in the eastern equatorial Pacific (EEP) where there were large negative excursions in $\Delta^{14}C$. To explain the contrasting deep and upper ocean deglacial $\Delta^{14}C$ histories a new hypothesis calls upon a release of ^{14}C-depleted CO_2-rich hydrothermal fluids at intermediate water depths as the ocean warmed during the deglaciation. Here we use an Earth System model of intermediate complexity (cGENIE) with new geochemical records from the tropical Pacific to test this hypothesis. We show that a total release of 1400Gt of ^{14}C-dead DIC into intermediate waters of the EEP (700Gt) and Arabian Sea (700Gt) causes $\Delta^{14}C$ changes throughout the ocean that agree with observations. The injection also causes a ~40μmol/kg drop in $[CO_3^{=}]$ of tropical surface waters. Trace metal proxies of $[CO_3^{=}]$ and carbonate preservation data are presented for the EEP that document a transient decrease in $[CO_3^{=}]$ in association with the deglacial $\Delta^{14}C$ excursions. This carbonate preservation event is associated with elevated V/Ca, Zn/Ca and Cu/Ca in planktonic foraminifera from the EEP.

Taken together, the model and geochemical data provide strong support for the hypothesis that there was a release of geologic carbon during the deglaciation that contributed as much as 60ppm to the rise in atmospheric pCO_2. If the geochemical signatures documented across glacial Termination 1 are found to occur at earlier glacial terminations as well, these findings will have profound implications for our understanding of glacial/interglacial CO_2 variability. Hydrothermal systems in the oceans may act as a CO_2 capacitor, regulating storage and release of carbon, and in doing so, affect the radiative balance that determines Earth's climate on orbital time scales.

Inter-mineral Mg isotope fractionation in mantle xenoliths

ANDREAS STRACKE[1,2*], EDWARD T. TIPPER[3,2], MICHAEL BIZIMIS[4]

[1]Westfälische Wilhelms Universität, Münster, Germany, stracke.andreas@uni-muenster.de (* presenting author)
[2]ETH Zürich, Zürich, Switzerland
[3]University of St. Andrews, St Andrews, U.K., ett@st-andrews.ac.uk
[4]University of South Carolina, Columbia, SC, U.S., mbizimis@geol.sc.edu

The bulk Mg isotope composition of the silicate Earth is homogeneous and identical within analytical error to that of chondritic meteorites [1-7]. Systematic fractionations among minerals in mantle peridotites [1,2,4,8-10] are resolvable, however, and are broadly consistent with theoretical predictions for high-T equilibrium Mg isotope fractionation [10]. Theory predicts that tetrahedral crystallographic sites have higher $^{26}Mg/^{24}Mg$ than octahedral sites; up to 0.5 – 0.8‰ for spinel – silicate pairs at 1000K [10], which is in agreement with recent data from two spinel peridotites [9].

Here we investigate the inter-mineral Mg isotope fractionation in 5 spinel peridotite and 5 garnet pyroxenite xenoliths from Salt Lake Crater, Hawaii. Calculated whole rock $\delta^{26}Mg$ compositions of both rock types are within error of those of bulk silicate Earth, suggesting that inter-mineral differences are due to equilibrium isotope fractionation. In the spinel peridotites, the $\delta^{26}Mg$ of olivine (ol), orthopyroxene (opx) and clinopyroxene (cpx) are indistinguishable. In the three measured olivine-spinel pairs, the spinels (sp) have consistently higher $\delta^{26}Mg$ values than the olivines, by 0.21 - 0.28‰. The sp-ol difference in $\delta^{26}Mg$ suggests an equilibration temperature of ca. 1700°C, considerably higher than the calculated opx-cpx mineral equilibration temperature of ca. 1100°C. The $\delta^{26}Mg$ of garnet in the garnet pyroxenites is consistently lower by 0.38 - 0.45‰ than in the coexisting cpx. Hence, the $\delta^{26}Mg$ values increase from garnet with a Mg coordination number of 8, to the octahedrally coordinated silicates (ol ≤ opx ≤ cpx) and the tetrahedrally coordinated spinels, consistent with coordination number exerting a first-order control on inter-mineral high-T equilibrium Mg isotope fractionation [10].

However, a strong positive correlation of $\delta^{26}Mg_{spinel}$ with the spinel Cr (Al) content or spinel Cr# shows that composition also influences the $\delta^{26}Mg$ values of individual minerals. The latter observation may explain the discrepancy between calculated equilibration temperatures based on mineral equilibria (opx-cpx) and Mg isotope fractionation ($\delta^{26}Mg_{ol-sp}$), and may hamper the use of spinel-silicate Mg isotope fractionation as a reliable geothermometer in magmatic rocks.

[1] Yang et al. (2009), *Earth Planet. Sci. Lett.* **288**, 475-482. [2] Handler et al. (2009) *Earth Planet. Sci. Lett.* **282**, 306-313. [3] Bourdon et al. (2010) *Geochim. Cosmochim. Acta* **74**, 5069-5083. [4] Chakrabarti & Jacobsen (2010) *Earth Planet. Sci. Lett.* **293**, 349-358. [5] Schiller et al. (2010) *Earth Planet. Sci. Lett.* **297**, 165-173. [6] Teng et al. (2010) *Geochim. Cosmochim. Acta* **74**, 4150-4166. [7] Pogge van Strandmann et al. (2011) *Geochim. Cosmochim. Acta* **75**, 5247-5268. [8] Wiechert & Halliday (2007) *Earth Planet. Sci. Lett.* **256**, 360-371. [9] Young et al. (2009) *Earth Planet. Sci. Lett.* **288**, 524-533. [10] Schauble (2011) *Geochim. Cosmochim. Acta* **75**, 844-869.

https://doi.org/10.1180/S0026461X00008434 Published online by Cambridge University Press

Tracing subduction erosion through arc chemistry in the central Mexican Volcanic Belt

SUSANNE M. STRAUB[1*], GEORG F. ZELLMER [2], ARTURO GÓMEZ-TUENA[3], YUE CAI[1], FINLAY M. STUART[4], CHARLES H. LANGMUIR[5]

[1]LDEO, Columbia University, Palisades, NY USA, smstraub@ldeo.columbia.edu (* presenting author), cai@ldeo.columbia.edu

[2]Institute for Earth Sciences, Academia Sinica, Taipei, Taiwan, gzellmer@earth.sinica.edu.tw

[3] Centro de Geociencias, UNAM, Querétaro, México, tuena@dragon.geociencias.unam.mx

[4] Isotope Geosciences Unit, SUERC, East Kilbride, UK, fin.stuart@glasgow.ac.uk

[5]EPS, Harvard University, Cambridge, MA USA, langmuir@eps.harvard.edu

Continental crust recycled via subduction erosion has been suggested to be a quantitatively important component that may overshadow the crustal contributions from subducted trench sediment to arc magmas at erosional convergent margins [1]. However, unlike the trench sediment that can be measured directly and linked to arc chemistry [2], the composition of eroded lower continental crust is essentially unknown. Hence, its identification in arc magmas poses a real challenge as signals of the eroded crust must be distinguished from those of the trench sediment and also from contamination by the overlying crust.

Here we present results of a comprehensive geochemical study from two Holocene high-Nb monogenetic arc volcanoes (Texcal Flow and V. Chichinautzin) that were erupted within ~1100 year and within only 6 km from each other. Major and trace element and Sr-Nd-Hf-Pb-He isotope systematics demonstrate that the basaltic and basaltic-andesitic magmas are mixtures of mantle and crustal materials. High $^{3}He/^{4}He$ of 6-7 R_a in equilibrium olivines, however, and high and increasing melt Nb (from 17 to 36 ppm) and Nb/Ta (from 16 to 19) with increasing melt SiO_2 preclude substantial assimiliation of the overlying crust. Combined Sr-Nd-Hf isotope data and trace elements argue against the trench sediment as an isotopic end member as this would require an unreasonably large loss of Nd (~50%) relative to Hf in the trench sediment. Alternatively, we propose that Sr-Nd-Hf-Pb isotope and trace element systematics may best be explained through melting of a subarc mantle that was infiltrated with crustal components recycled via subduction erosion from the lower Mexican forearc crust. The data suggest for this region a model in which the recycled eroded crust may dominate arc chemistry together with fluids released from the subducted igenous oceanic crust while the signals of the subducted trench sediment are largely eclipsed. This may be explained by the low volumeric flux of sediment in this region owing to the young age of the subducting plate.

[1] Clift & Vannucci (2004) *Reviews of Geophysics* **42(2)**, 1-31. [2] Plank & Langmuir (1993) *Nature* **362,** 739-743.

The diagenetic history of marine sediments as revealed by C-S-Fe systematics

HARALD STRAUSS

Westfälische Wilhelms-Universität, Münster, Germany, hstrauss@uni-muenster.de

Marine sediments archive the products of primary productivity, subsequent mineralization of the sedimentary organic matter through microbial and/or inorganic processes, the input of detrital components, and the authigenic mineral formation within the sedimentary column. The C-S-Fe system constrains respective depositional as well as diagenetic aspects within marine sediments, frequently occurring under changing redox conditions. A diverse set of petrographic, geochemical, and isotopic proxy signals has evolved during the past fifty years with an ever increasing specificity. These proxy signals allow distinguishing between local/regional phenomena and perturbations of global geochemical cycles, both in modern sediments as well as for sedimentary rocks in the geologic record. Hartmann and Nielsen [1] were among the very early researchers applying some of these proxy signals in their study of marine coastal sediments from the Kiel Bight, Baltic Sea, northern Germany.

Abundances of carbon, sulfur, and iron, organic and inorganic carbon isotopes, multiple sulfur isotopes of sulfides and sulfates, and oxygen isotopes for sulfate were measured in pore waters and sediments collected during a revisit of these Baltic Sea sediments some 45 years after the original study. Respective proxy signals reveal a complex diagenetic evolution that is largely governed by bacterial sulfate reduction. Key features include a sizeable sulfur isotopic fractionation of up to 64‰ between sulfate and sulfide. The downcore evolution towards ^{34}S-enriched sulfur isotope values for both sulfur species in the pore waters suggest the development of sulfate limiting conditions. Disproportionation of sulfur intermediates cannot be excluded and would be consistent with the observed large fractionations in $\delta^{34}S$ as well as from a combination of $\delta^{34}S$ and $\Delta^{33}S$. Conclusions derived here overall confirm interpretations made by [1]. At the same time, an expanded analytical approach allows for more detailed information about microbially driven processes in the pore water realm and the sediments.

[1] Hartmann & Nielsen (1965) *Geologische Rundschau* **58**, 621-655.

https://doi.org/10.1180/S0026461X00008434 Published online by Cambridge University Press

Microbial characterization of groundwater from boreholes at CRL

SIMCHA STROES-GASCOYNE[1*], DANIELLE BEATON[2], MARILYNE AUDETTE-STUART[2], KAREN KING-SHARP[2], AMY FESTARINI[2], CONNIE HAMON[1], STEVE ROSE[2] AND LEE BELLAN[2]

[1]Atomic Energy of Canada Limited, Whiteshell Laboratories (WL), Pinawa, MB, Canada, stroesgs@aecl.ca (* presenting author)

[2]Atomic Energy of Canada Limited, Chalk River Laboratories (CRL), Chalk River , ON, Canada

Purpose of study and methods

A microbiological characterization study was carried out on groundwater samples from various depths in older (CR9, CR18) and recently drilled boreholes (CRG-1, CRG-2, CRG-4A) at Chalk River Laboratories (CRL). This work was carried out as part of a technical feasibility study assessing the suitability of the CRL site to host a proposed Geologic Waste Management Facility for CRL's radioactive non-fuel waste.

A multi-analysis approach was used to characterize the water samples for microbial content. Analyses included: (1) Geochemical analysis for major cations, anions, pH, Eh and DOC. (2) Total (live + dead) and viable (live) cell counts using a number of different dyes and probes. (3) Phospholipid fatty acid (PLFA) analysis for viable cells and community structure. (4) Classic culturing for heterotrophic aerobic and anaerobic bacteria, nitrate-utilizing and -reducing bacteria and sulphate-reducing bacteria. (5) Identification of isolates using BIOLOG GEN III. (6) Identification of microbes using DNA extraction and (pyro-) sequencing.

Result and Conclusions

The water samples contained a total population of 10^4 to 10^5 cells/mL of which generally only < 1% could be cultured. However, a large percentage of the total population was viable and showed some signs of metabolic activity. Identification results for isolates showed a dominance of *Pseudomonas*, *Sphingomonas* and *Acidovorax* species. Identification based on DNA sequencing showed a dominance of different species. The combined microbial and geochemical results suggest an oligotrophic biogeochemical system in the CRL groundwater. The presence of a population of viable but not culturable cells implies that, given an increased source of electron donors (e.g., DOC) and electron acceptors (e.g., metals) leached from the waste, microbial activity could increase significantly in a potential GWMF. This could have both positive effects (e.g., lower Eh and radionuclide (RN) solubility) and negative effects (e.g., increased RN mobility, ^{14}C-containing gas production). Ultimately the biogeochemical system is expected to return to its original oligotrophic conditions but the rate at which this would occur is uncertain because waste leach rates and *in situ* microbial metabolic activity rates are unknown. This study illustrates that microbial effects need to be considered in the safety assessment of a deep geologic nuclear waste repository.

Biogeochemical Characterization of a Late Archean Sub-Seafloor Hydrothermal System, Dome Mine, Timmins, Ontario, Canada

JESSICA STROMBERG[1]*, NEIL BANERJEE[1], GORD SOUTHAM[1], ED CLOUTIS[2], GREG SLATER[3], ERIK BARR[4]

[1]University of Western Ontario, Earth Science, London, Canada, jstromb@uwo.ca*

[2]Univeristy of Winnipeg, Geography, Winnipeg, Canada, e.cloutis@uwinnipeg.ca

[3]McMaster University, Geography and Environmental Science, Hamilton, Canada, gslater@mcmaster.ca

[4]Goldcorp Porcupine Mine, South Porcupine, Canada, Erik.Barr@goldcorp.com

Much of our understanding of early life on Earth is dependant on the characterization of habitable environments preserved in Archean terrains. One such example can be found in the Tisdale mafic volcanics and hydrothermally altered metasediments of the Abitibi greenstone belt in Northern Ontario [1]. These late Archean volcanics host greenstone quartz-carbonate vein gold desposits, which are characterized by iron-carbonate alteration from low-salinity, CO_2-rich hydrothermal fluids, resulting in the precipitation of carbonates such as dolomite and ankerite.

Previous work has identified endogenous molecular fossils within the 2,770-2,685 Ma Tisdale assemblage, suggesting the presence of a subsurface hydrothermal biosphere [1]. This study is focused on a unique set of 2,690-2679 Ma crustiform banded ankerite veins within the Tisdale mafic volcanics at the Dome mine, in Timmins. This ankerite horizon provides an opportunity for the characterization of an ancient sub-seafloor hydrothermal system and its potential biosphere. We are using multiple biogeochemical techniques to characterize the system, to elucidate its environmental conditions, genesis and evolution, as well as biomarkers, and any associations with gold mineralization.

XRD and IR-spectroscopy have identified compositional variations in the carbonate speciation and minerology of the ankerite horizon. These datasets in combination with SEM and stable C- and O- isotope analysis are being used to determine the degree of hydrothermal alteration, the fluid composition and genesis, and provide environmental constraints for the system. Extracted biosignatures are being characterized by GC-MS, stable C-isotope, and ToF-SIMS analysis.

An understanding of early earth habitable environments, the developement of methods for their characterization, and the identification of biosignatures is a key aspect in furthering the search for evidence of habitable environments and extant life on Mars [2]. In particular, given the detection of Fe-Mg carbonates on the Martian surface [3,4]. As well, this research has potential implications for the development of paleobiological vectors for mineral exploration.

[1] Ventura et al. (2007) *PNAS* **104**, 14260-14265. [2] Summons et al. (2011) *Astrobiology* **11**, 157-181. [3] Ehlmann et al. (2008) *Science* **322**, 3671-1832. [4] Morris et al. (2010) *Science* **23**, 421-424.

https://doi.org/10.1180/S0026461X00008434 Published online by Cambridge University Press

Photochemistry of arsenite on ferrihydrite and goethite

NARAYAN BHANDARI[1], RICHARD J. REEDER[2], AND DANIEL R. STRONGIN[1,*]

[1]Department of Chemistry, Temple University, Philadelphia, PA 19122, USA (dstrongi@temple.edu)

[2]Department of Geosciences, Stony Brook University, Stony Brook, NY 11794, USA

The photochemistry of arsenite (As(III)) in the presence of the iron oxyhydroxides, ferrihydrite and goethite, has been investigated. Attenuated total reflection Fourier transform infrared spectroscopy (ATR-FTIR), X-ray absorption near edge structure (XANES), and solution phase analysis have been used to characterize the surface bound and aqueous phase species. Both ATR-FTIR and XANES show that the exposure of ferrihydrite or goethite to As(III) for up to 24 h in the dark leads to no change in the oxidation state of the adsorbed or aqeuous phase As species. Exposure of either the As(III)/ferrihydrite or As(III)/goethite system to simulated solar radiation results in the majority of the surface bound As(III) becoming oxidized to arsenate (As(V)). At a solution pH of 5, this conversion of As(III) to As(V) on ferrihydrite results in the partitioning of a stoichiometric amount of Fe(II) into the aqueous phase. The majority of the As(V) product remains bound to the ferrihdyrite surface. This chemistry on ferrihydrite is relatively similar in the absence or presence of dissolved oxygen. Also, in the ferrihydrite circumstance, the As(III) to As(V) conversion shows the characteristics of a self-terminating reaction in that there is a significant suppression of this redox chemistry before 10% of the total iron making up the ferrihydrite partitions into solution as ferrous iron. The self-terminating behavior exhibited by this photochemical As(III)/ferrihydrite system is likely due to the passivation of the ferrihydrite surface by the strongly bound As(V) product. In contrast, the As(III)/goethite system shows a different photochemical behavior in the absence or presence of dissolved oxygen. In the presence of dissolved oxygen at a solution pH of 5, results suggest that in contrast to ferrihydrite the majority of the As(V) product is in the aqueous phase and the relative amount of aqueous Fe(II) is significantly less than in the ferrihydrite circumstance. A possible reason for this experimental observation is that in the oxic environment Fe(II) on the goethite, which forms via the photoinduced oxidation of As(III), is oxidized to Fe(III) by dissolved oxygen resulting in the formation of reactive oxygen species that can lead to the further oxidation of As(III) in solution. Additional experiments suggest that this behavior is not observed on ferrihydrite at pH 5, due to the lower affinity of the surface for Fe(II), compared to goethite. Overall, the research has brought forward how differences in the surface properties of iron oxyhydroxides can result in changes in redox chemistry.

Characterisation of arsenic and trace metals in acid sulfate environments

JACQUELINE L. STROUD[1]* AND RICHARD N. COLLINS[1]

[1]School of Civil and Environmental Engineering, UNSW, Sydney, Australia, j.stroud@unsw.edu.au (* presenting author)

Contaminant mobilisation in acid sulfate environments

Disturbed acid sulfate environments pose a serious threat to water quality, ecosystem health and commercial activities. The interaction between hydro-biogeochemical factors leads to the discharge of sulfuric acid and toxic concentrations of dissolved contaminants including iron and aluminium to adjacent water bodies. Comparatively little is known about trace metals and arsenic mobilisation in these environments.

We evaluated the mobilisation of trace metals and arsenic in groundwater and adjacent drain waters during a 10-day rainfall event at our Tweed Valley field site, NSW, Australia. This site has previously been identified as a metal mobilisation hotspot. We used multi-piesometers, drain water autosamplers and Diffusive Gradients in Thin films (DGT) devices to monitor the temporal changes in contaminant mobilisation. Metal and metalloid concentrations were determined using ICP-MS, and arsenic speciation (As(III), As(V), DMA and MMA) was analysed using HPLC-ICP-MS. Changes in contaminant concentrations were compared to concomitant changes in redox potential, pH, anions and dissolved organic carbon concentrations in order to characterise mobilisation processes. Elevated concentrations of cadmium, zinc and arsenic (arsenate and arsenite) were detected, suggesting that trace metals and arsenic also contribute to the poor water quality in these environments. DGT devices were effective in metal and metalloid assessments, and we were able to measure the fluctuations in contaminant concentrations downstream from the metal mobilisation hotspot.

Outcomes

These results will help us to understand the mobilisation and transport processes of trace metals and metalloids in these environments and better predict their risk to water quality.

https://doi.org/10.1180/S0026461X00008434 Published online by Cambridge University Press

Oxidative corrosion of the uraninite (111) surface

JOANNE E. STUBBS[1]*, PETER J.ENG[1], CRAIG A. BIWER[1], ANNE M. CHAKA[2], GLENN A. WAYCHUNAS[3], AND JOHN R. BARGAR[4]

[1]Center for Advanced Radiation Sources, University of Chicago, Chicago, IL, USA, stubbs@cars.uchicago.edu (* presenting author)

[2] Physical Measurement Laboratory, National Institute of Standards and Technology, Gaithersburg, MD, USA

[3] Lawrence Berkeley National Laboratory, Berkeley, CA, USA

[4] Stanford Synchrotron Radiation Lightsource, Menlo Park, CA, USA

Uraninite (UO_2) is the most abundant uranium ore mineral, the product of proposed bioremediation strategies for uranium-contaminated soils and aquifers, and its synthetic analog is the primary constituent of most nuclear fuels (1-3). This material is known to incorporate interstitial oxygen up to a stoichiometry of $UO_{2.25}$ without disruption of the uranium lattice, but the structural details of the process are the subject of ongoing study and debate (e.g., 4-5). Because the solubility and dissolution kinetics of uraninite depend heavily on the oxidation state of uranium, understanding the mechanims of UO_2 surface oxidation and corrosion is essential to predicting its stability in the environment throughout the nuclear fuel cycle. To date, however, no study has addressed this process at the molecular scale at atmospheric pressure and room temperature.

We present results of a crystal truncation rod (CTR) x-ray diffraction study of the UO_2 (111) surface. This hard x-ray technique is ideally suited to such studies, because it can probe the structures of interfaces at atmospheric conditions and buried below liquids and solids. The single-crystal surface was prepared under anoxic conditions, measured under dry helium, then exposed to dry O_2 gas and measured at several time points over the course of two weeks. The pristine surface is characterized by minimal contraction of the uppermost atomic layers and the addition of an oxygen layer above the vacuum-terminated surface. Following exposure to dry O_2, an oxidation front proceeds into the crystal, intersitial oxygen atoms penetrate to depths of 30 Å or more, U-U layer distances contract (consistent with bulk uraninite oxidation), and an ordered superlattice, which is commensurate with the underlying bulk, forms. These results demonstrate that the solid state diffusion of oxygen into UO_2 and UO_{2+x} surfaces is facile and that ordering kinetics are relatively rapid, even at room temperature.

Ab initio thermodynamics, which combines density-functional theory calculations with macroscopic thermodynamics, provides insight into the energetics, bonding, and oxidation processes that occur as oxygen reacts with the surface and diffuses into the solid. Surface oxidation results in formation of a U^{+6} cation triply bonded to single oxygen adatoms. Subsurface oxidation is predicted to contract U-U layers consistent with experimental observations.

[1] Finch & Murakami (1999) *Rev. Mineral. Geochem.* **38**, 91-180.
[2] Bargar et al. (2008) *Elements* **4,** 407-412.
[3] Janeczek et al. (1996) *J. Nucl. Mat.* **238**, 121-130.
[4] Willis (1987) *J. Chem. Soc., Faraday Trans.* **83**, 1073-1081.
[5] Conradson et al. (2004) *Inorg. Chem*. **43**, 6922-6935.

A COMPARISON OF GLASS AND MINERAL INCLUSIONS IN QUARTZ AND ZIRCONS FROM KEWEENAWAN RHYOLITE FLOWS

JAMES STUDENT[1*] AND ALEXANDRA MASSAD[2]

[1] Central Michigan University, Mount Pleasant, MI 48859, USA stude1jj@cmich.edu (* presenting author)

[2]Department of Geological Sciences, University of Texas at El Paso, El Paso, TX 79968, USA

Melt inclusions (MI) and a wide-variety of mineral inclusions are well preserved in quartz phenocrysts and zircons from porphyritic rhyolite flows of the Midcontinent Rift System. The inclusions and their host minerals have been examined using EPMA, cathodoluminescence microscopy (CL), SEM/EDS, and LA-ICP-MS. Rhyolite from the North Shore Volcanic Group, the Porcupine Mountains, the Portage Lake Volcanics, and the Michipicoten Island Formation were utilized in this study. Inclusions hosted by quartz and zircons were studied in thin sections and grain mounts, respectively.

The MI were categorized based on their phase assemblages and preservation style [1]. CL images of the host quartz phenocrysts reveal multiple stages of growth and dissolution. Ti contents (measured by EPMA and LA-ICP-MS) in the quartz vary widely and range from <15 to 280 ppm. Using a modified TitaniQ method [2], this corresponds to a temperature change of more than 250 °C in individual samples (using $aTiO_2$=1 and isobaric conditions). Presently there are still too many variables to constrain the absolute crystallization temperatures. The MI were analysed by LA-ICP-MS for major oxides and trace elements including Zr and Ti. The ranges in zircon saturation temperatures calculated using the model described by [3] agree with the TitaniQ temperature ranges. Unfortunately, it has been difficult to confidently constrain the Ti content (for TiO_2 activity calculations) in the MI using LA-ICP-MS analyses. This is due to the complex nature of the Ti distribution in the surrounding host quartz. The occurrence and distribution of zircon as inclusions in the quartz does suggest coeval crystallization of both phases.

An examination of SEM/EDS spectra of inclusions in zircon revealed at least 18 different minerals. They include K-spar, plagioclase, pyroxene, quartz, Fe-Ti oxides, apatite, monazite, and several different sulphides. Mineral inclusion assemblages in the zircons are distinct in each of the rhyolite samples that were studied. The mineral inclusions occur as isolated grains within zircon and inside glass bearing MI in zircon. While the majority of the inclusions appear to be primary and pristine, some of mineral and MI show evidence of modification by secondary processes. Utilization of the trace element chemistry of the mineral and MI trapped in zircon can potentially be used to better constrain the activity of TiO_2 in the melt during crystallization. This approach can lead to a more accurate estimate of quartz crystallization temperatures for Keweenawan rhyolite.

[1] Student *et al.* (2006): *Eos Trans. AGU,* **87**(52), Abstract V23C-0619. [2] Thomas *et al.* (2010) *Contrib. Mineral. Petrol.* **160**, 743-759. [3] Watson & Harrison (1983) *Earth and Planet. Sci Lett.* **64**, 295-304.

https://doi.org/10.1180/S0026461X00008434 Published online by Cambridge University Press

Enhanced nutrient consumption in the glacial Antarctic

A.S. STUDER[1*], A. MARTINEZ-GARCIA[1], M. STRAUB[1], D.M. SIGMAN[2], R. GERSONDE[3], G.H. HAUG[1]

[1]Department of Earth Sciences, ETH Zurich, Zurich, Switzerland ([*]anja.studer@erdw.ethz.ch, alfredo.martinez-garcia@erdw.ethz.ch, marietta.straub@erdw.ethz.ch, gerald.haug@erdw.ethz.ch) ([*] presenting author)
[2]Department of Geosciences, Princeton University, Princeton, NJ, USA (sigman@princeton.edu)
[3]Alfred Wegener Institute, Bremerhaven, Germany (Rainer.Gersonde@awi.de)

Productivity in surface waters leads to the sequestration of carbon dioxide (CO_2) in the deep ocean, a process known as the ocean's "biological pump." The Antarctic Zone of the Southern Ocean represents the major "leak" in this pump. Nutrient- and CO_2-rich waters are brought to the surface, allowing CO_2 to outgas. The scarcity of iron and/or light reduces phytoplankton productivity, leaving some of the major nutrients (nitrate, phosphate) unused. Those "preformed" nutrients are subducted into the subsurface without re-sequestering CO_2 into the deep ocean, introducing a degree of inefficiency to the global biological pump. To explain lower glacial atmospheric CO_2, it has been suggested that there was a decrease in the exchange between polar surface water and ocean interior, described as "polar ocean stratification." This physical change would have, in itself, reduced the outgassing of CO_2, and it may have increased the fraction of nutrients utilized in Antarctic surface ocean, rendering the region a more efficient part of the global biological pump. The first efforts to reconstruct nitrate utilization in the Antarctic measured nitrogen (N) isotopes on bulk sediment, but this can be biased by diagenesis and/or allochthonous N input. Subsequent studies measured the N isotopes encapsulated in diatom frustules ($\delta^{15}N_{db}$), which carry the pristine signal, but results have varied. Here, we report a consistent increase in $\delta^{15}N_{db}$ into the last two glacial periods, with abrupt decreases during the subsequent deglaciations. In contrast, the descent from interglacial to glacial conditions was more gradual/stepwise, reminiscent of the general atmospheric CO_2 pattern. The first major $\delta^{15}N_{db}$ increase into the last ice age occurred at the MIS 5e/5d transition, coincident with the major decline in Antarctic temperature and the first 40 ppm step in ice age CO_2 decline. In addition to our analysis of the total biogenic opal <100 µm, we analyzed the $\delta^{15}N_{db}$ of two distinct diatom species assemblages. Their $\delta^{15}N_{db}$ values are offset by roughly 1‰ but show the same trends through time. This rules out the possibility that the glacial-interglacial $\delta^{15}N_{db}$ changes measured on the total diatom community are caused by changing diatom species composition, a concern that had been raised previously.

Noble gas radionuclides in Yellowstone geothermal gases

N. C. STURCHIO[1*], R. YOKOCHI[2], R. PURTSCHERT[3], W. JIANG[4], G.M. YANG[4], P. MUELLER[4], Z.T. LU[2,4], B.M. KENNEDY[5], AND Y. KHARAKA[6]

[1]University of Illinois at Chicago, Chicago, IL, USA, sturchio@uic.edu, (* presenting author)
[2]University of Chicago, Chicago, USA, yokochi@uchicago.edu
[3]University of Bern, Switzerland, purtschert@climate.unibe.ch
[4]Argonne National Laboratory, Argonne, IL, USA, wjiang@anl.gov, pmueller@anl.gov, lu@anl.gov
[5]Lawrence Berkeley National Lab., Berkeley, CA, USA, bmkennedy@lbl.gov
[6]U. S. Geol. Survey, Menlo Park, CA, USA, ykharaka@usgs.gov

We collected and analyzed noble gas radionuclides (^{39}Ar, half-life = 269 yr; ^{81}Kr, half-life = 229,000 yr; ^{85}Kr, half-life = 10.8 yr) in gases from four geothermal features at Yellowstone National Park (Beryl Spring, Frying Pan Spring, Ojo Caliente Spring, and Mud Volcano). In the field, condensation of water vapor and chemical stripping of CO_2 were done to reduce the samples to manageable volumes which were compressed into gas cylinders. Separations of Kr and Ar from gas samples were performed by existing methods [1,2]. Kr radionuclides were measured by atom-trap trace analysis at Argonne using ATTA-3 [3], and ^{39}Ar was measured by low-level counting at Bern [2].

Isotopic abundances of ^{39}Ar in all four samples were 4 to 6 times higher than atmospheric, indicating substantial contributions from subsurface nucleogenic production, as reported earlier [4]. ^{81}Kr isotopic abundances were not significantly different from atmospheric. ^{85}Kr isotopic abundances were 0.55 to 0.96 times atmospheric, possibly indicating contributions from recent groundwater recharge (≤ 10 yr) and/or contributions of both ^{39}Ar and ^{85}Kr from subsurface production at a ratio typical of that in granitic rock (see Figure).

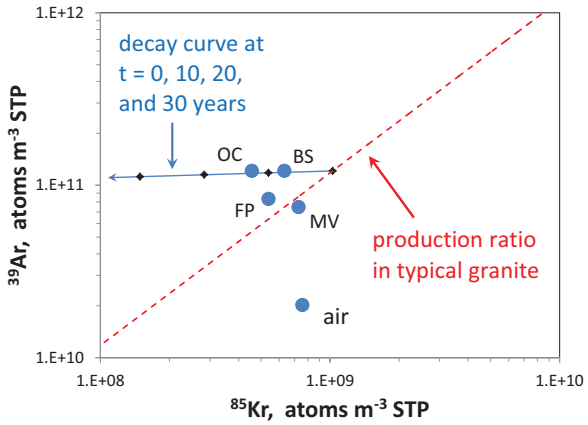

[1] Yokochi et al (2008) *Anal. Chem.* **80**, 8688-8693.
[2] Forster & Loosli (1989) In: *Isotopes of Noble Gases as Tracers in Environmental Studies*, IAEA, Vienna.
[3] Jiang et al. (2012) manuscript in review.
[4] Purtschert et al. (2009) Goldschmidt abstract, Davos.

https://doi.org/10.1180/S0026461X00008434 Published online by Cambridge University Press

Residence times of the upper low-arsenic aquifers in Bangladesh at the onset of increased abstraction

M. STUTE[1,2*]. I. MIHAJLOV[1], P. SCHLOSSER[1], K.M. AHMED[3] AND A. VAN GEEN[1]

[1]Lamont-Doherty Earth Observatory of Columbia University, Palisades, NY, USA, martins@ldeo.columbia.edu (*presenting author)

[2]Barnard College, New York, NY, USA

[3]Dhaka University, Dhaka, Bangladesh

Elevated levels of dissolved arsenic in shallow aquifers in the Bengal basin will result in increased use of deeper, currently low-arsenic aquifers. Compared to the shallow aquifers, relatively little is known about the flow dynamics of the deeper systems (>100 m depth).

Radiocarbon, ^{3}H, stable isotope, and noble gas data were obtained from both aquifer systems in our field area in Araihazar, 25 km east of Dhaka, Bangladesh. Noble gas temperatures of shallow groundwater generally reflect current water temperature at the water table despite elevated CO_2 (up to 12%) and depleted O_2 concentrations in the unsaturated zone. ^{3}H and $^{3}H/^{3}He$ data are consistent with recharge during the past 50 years. Most of the deeper groundwater (>100m depth) underlying the high-arsenic zone is ^{3}H free; and radiocarbon, stable isotope, and noble gas data indicate that recharge likely occurred at the transition between the late glacial period and the Holocene, a time of major changes in sea level, vegetation, and climate.

The relatively high residence time of water in the aquifer suggests a low recharge rate (cm's/year) until large-scale groundwater pumping for municipal supplies began in Dhaka in the 1960s.

Increased usage of this resource will result in higher recharge rates and might cause leakage from shallow high-arsenic aquifers and needs to be considered in management of water resources in Bangladesh.

Modulation of the product of U(VI) reduction by phosphate and calcium

MALGORZATA STYLO[1]*, DANIEL S. ALESSI[1], JUAN S. LEZAMA-PACHECO[2], JOHN R. BARGAR[2] AND RIZLAN BERNIER-LATMANI[1]

[1]Environmental Microbiology Laboratory, Ecole Polytechnique Federale de Lausanne, EPFL, Lausanne CH 1015, Switzerland, malgorzata.stylo@epfl.ch (*presenting author)

[2]Stanford Synchrotron Radiation Lightsource, Menlo Park, CA 94025, USA, bargar@slac.stanford.edu

One bioremediation strategy for uranium-contaminated aquifers involves the enzymatic reduction of soluble U(VI) to less mobile U(IV) species. The mineral uraninite, $UO_{2(s)}$, is considered to be the most desirable product of bioremediation due to its relative stability under reducing conditions. However, it has been shown repeatedly that uraninite is not the sole product of U(VI) reduction. Among these other U(IV) products are monomeric U(IV) species, believed to coordinate to bacterial biomass via phosphate and/or carboxylate groups and likely to be less stable than uraninite. For bioreduction to be a viable remediation strategy, it is crucial to pinpoint the factors promoting the formation of uraninite versus monomeric U(IV). Investigations to date have suggested that certain solutes, including PO_4^{3-} and Ca^{2+}, lead to preferential formation of monomeric U(IV). However, the mechanism of this process remains unknown.

In this study, we examine (1) the influence of PO_4^{3-} and Ca^{2+} on the product of U(VI) bioreduction and (2) the fate and behavior of those solutes during U(VI) reduction. Uranium L_{III} edge X-ray absorption spectroscopy and a wet chemical extraction technique were used to quantify the relative contribution of these two U(IV) species in systems in which the solute concentrations were systematically varied. We initially hypothesized that Ca^{2+} shields PO_4^{3-} from negatively charged groups and thus allows the binding of phosphate to the cell wall and the complexation of U(IV) by phosphate, leading to preferential monomeric U(IV) formation. To test this hypothesis, we measured the concentration of the two solutes during U(VI) reduction.

The results confirm that the U(IV) product of bioreduction is a mixture of uraninite and monomeric U(IV). The presence of calcium enhances the fraction of monomeric U(IV) produced. Moreover, even a low concentration of phosphate (1.9 mg/l) promotes greater formation of monomeric U(IV). However, the contribution of monomeric U(IV) does not change with increasing concentrations of this solute. The combination of calcium and phosphate results in a close to pure monomeric U(IV) product. Surprisingly, the aqueous concentrations of PO_4^{3-} or Ca^{2+} during U(VI) bioreduction are constant, suggesting little binding of these solutes to biomass. Hence, the direct association of these solutes with biomass cannot account for the observed effect. This suggests an indirect influence of phosphate and calcium on biological controls over the product of U(VI) reduction. For example, the production of bacterial extracellular polymeric substances could be limited by these solutes, restricting the number of nucleation sites for uraninite precipitation and promoting the formation of monomeric U(IV).

Our work provides a first glimpse into the complexity of the influence of geochemical factors on the biological controls of U(IV) product formation.

https://doi.org/10.1180/S0026461X00008434 Published online by Cambridge University Press

Solubility of Palladium (Pd) in Hydrocarbons: Application to Ore Genesis

ICHIKO SUGIYAMA[1]* and ANTHONY WILLIAMS-JONES[1]

[1]Department of Earth and Planetary Sciences, McGill University, Montreal, Quebec, ichiko.sugiyama@mail.mcgill.ca (*presenting author)

In natural systems, the platinum group elements (PGE) are commonly associated spatially with hydrocarbons. For example, pyrobitumen in the Kupferschiefer, Poland, has been shown to have high concentrations of Pd and Pt [1]. Black shales in South China likewise have been shown to contain elevated Pd and Pt (0.4 ppm Pd and 0.3 ppm Pt in the Zunyi deposit) [2]. These observations and preliminary experiments showing that crude oils can dissolve metals to potentially exploitable concentrations, suggest that liquid hydrocarbons could constitute important ore fluids [3]. The objective of this research is to experimentally determine the solubility of Pd in selected organic compounds known to be important constituents of natural liquid hydrocarbons, and thereby contribute to the body of knowledge on ore forming processes involving hydrocarbons. Approximately 40 to 50% of crude oil is composed of paraffins, including straight chain alkanes. In view of this and the fact that Pd is known to have a strong affinity for sulphur (some crude oils contain appreciable sulphur), we have investigated the solubility of Pd in dodecane and dodecanethiol.

Our experiments were performed in light-weight titanium autoclaves treated with nitric acid to produce an inert internal surface coated with TiO_2, and involved measuring the solubility of palladium metal in dodecane and dodecanethiol at 150 °C. The durations of the experiments ranged from 15 to 60 days. After completion of an experiment, the autoclave was quenched, and samples of the quenched solutions, and solutions used to wash the autoclaves (Pd commonly precipitated on the surface of the autoclave), were analyzed for Pd using NAA.

The concentration of Pd in dodecane was 0.33 ppm ± 0.18 ppm and in dodecanethiol was 0.90 ppm ± 0.45 ppm. These data show that that Pd is very soluble in these simple analogues of natural liquid hydrocarbons at temperatures commonly encountered in oil reservoirs, and that its solubility may be increased by complexation with thiol groups. We therefore conclude that liquid hydrocarbons could be very effective agents of Pd transport. This and the observed close spatial association of Pd with hydrocarbons in some PGE deposits suggest that liquid hydrocarbons could be important ore fluids for these deposits.

[1] Kucha, H. and Przybylowicz, W. (1999) Noble metals in organic matter and clay-organic matrices, Kupferschiefer, Poland. Economic Geology, 94,1137-1162. [2] Coveney, R.M., Nansheng, C. 1991. Ni-Mo-PGE-Au-rich ores in Chinese black shales and speculations on possible analogues in the United States. Mineralium Deposita, 26, 83-88. [3] Williams-Jones AE, Bowell RJ, Migdisov AA (2009) Gold in solution. Elements 5: 281-287.

Exploration and enhancement of Sm/Nd carbonate geochronology

N.C. SULLIVAN[1], E.F. BAXTER[1], AND K. MAHER[2]

[1]Boston University, Boston, MA, norasull@bu.edu, efb@bu.edu
[2]Stanford University, Palo Alto, CA, kmaher@stanford.edu

Carbonate mineralization occurs across a broad spectrum of Earth's environment. Direct dating of carbonate minerals has become an important goal. Prior work has used the ^{14}C, U-series, and U/Pb isotope systems, but all have limtations. The Sm-Nd system has rarely been attmepted because most carbonate has very low $^{147}Sm/^{144}Nd$ ratios (<0.2), indicating limited geochronologic potential. A handful of published studies [e.g. 1,2,3] suggest that some high (0.2 to >1.0) $^{147}Sm/^{144}Nd$ carbonates do exist and that meaningful age information can potentially be extracted. These studies use mild acids to extract multiple carbonate separates from a single vein or deposit.

Our preliminary work has focused on three samples: a metamorphic calcite vein from Vermont, a hydrothermal dolomite from an ultramafic hosted talc deposit, also from Vermont, and a siderite from the Copper Chief Mine in Arizona. All three samples were put through an 8-step sequential extraction procedure (5.0, 4.2, 3.9, 3.5pH acetic, glacial acetic, 1.5N HCl, conc. HNO_3, HF) to isolate a high $^{147}Sm/^{144}Nd$ reservoir within the carbonates. All leachates were analyzed for Sm/Nd isotopes and major and trace element concentrations. Differences in Ca, Mg, Mn, Fe, and Sr between each leachate show that they represent different reservoirs. Electron microprobe data confirms there is subtle compositional zoning within the carbonate, at the micron scale, in all three samples.

As with previous studies, there is scatter in our "isochron" data. A 9-point isochron for the Vermont calcite vein shows a $^{147}Sm/^{144}Nd$ range of 0.09884-0.21180 yielding an age of 386 ± 34 Ma (MSWD 4.7). The high MSWD implies that some leached material did not form in isotopic equilibrium with the concordant carbonate fractions and therefore does not belong on the isochron. Assuming most of the carbonate is dissolved in the pH-controlled acetic leachates, and discarding the stronger acid extractions, we calculate a 4-point isochron age of 353 ± 27 Ma (MSWD 1.17). This age agrees with a published monazite age of 352.9 ± 8.9 Ma from the same outcrop [4]. The same effect is seen with the Vermont dolomite sample: when all leachates are considered the isochron yields an age of 508 ± 93 Ma (MSWD 41), but if we eliminate the stronger acid leachates the age becomes 657 ± 62 Ma (MSWD 1.05). The low MSWD implies this is a reliable "isochron", however the age is clearly older than Taconic or Acadian metamorphism expected for this sample. The siderite sample from Arizona shows a $^{147}Sm/^{144}Nd$ range of 0.21105-0.44711 and gives a reasonable Proterozoic age.

Our data shows that there are multiple chemical and isotopic domains present within each sample and our leaching procedure has begun to successfully isolate them. To refine sample selection and improve the reliability and precision of the carbonate ages, we are combining major and trace element data with electron microprobe images to identify the origin of the compositional variations and determine which acid extractions should be included in the isochron.

[1] Henjes-Kunst *et al.* (2008) *GCA* A368. [2] Nie *et al.* (1999) *Resource Geology* **49**, 13-25. [3] Peng *et al.* (2003) *Chemical Geology* **200**, 129-136. [4] Wing *et al.* (2003) *Contrib. Mineral Petrol* **145**, 228-250.

https://doi.org/10.1180/S0026461X00008434 Published online by Cambridge University Press

Halogens and noble gases subducted into the mantle: constraints from mantle wedge peridotites and olivines in arc lavas

HIROCHIKA SUMINO[1*], LISA ABBOTT[2], AYA SHIMIZU[3], RAY BURGESS[2] AND CHRIS J. BALLENTINE[2]

[1]GCRC, University of Tokyo, Tokyo, Japan, sumino@eqchem.s.u-tokyo.ac.jp
[2]SEAES, University of Manchester, Manchester, UK, lisa.abbott@postgrad.manchester.ac.uk, ray.burgess@manchester.ac.uk, Chris.Ballentine@manchester.ac.uk
[3]Tokyo Metropolitan Industrial Technology Research Institute, Tokyo, Japan, shimizu.aya@iri-tokyo.jp

Findings of subducted halogens and noble gases with seawater and sedimentary pore-fluid signatures in exhumed mantle wedge peridotites and eclogites from the Sanbagawa-metamorphic belt, southwest Japan [1, 2], as well as that of seawater-derived heavy noble gases (Ar, Kr, Xe) in the convecting mantle [3], challenge a popular concept that the water flux into the mantle wedge is controlled only by hydrous minerals in altered oceanic crust and sediment resulting in that subduction volcanism acts as a 'subduction barrier' which efficiently recycles volatile components contained in subducted slabs back to the Earth's surface. To verify whether and how such subduction fluids modify the composition of the mantle beneath subduction zones, we determined noble gas and halogen compositions of mantle wedge peridotites and olivines in arc lavas.

MORB-like $^{3}He/^{4}He$ and halogen ratios of olivines in lavas from the northern Izu-Ogasawara arc and a peridotite from the Horoman alpine-type peridotite complex in northern Japan indicate insignificant contribution to the mantle wedge of radiogenic ^{4}He and porefluid-like halogens both observed in the subduction fluids in the Sanbagawa samples to a depth ranging from 40 to 100 km [1, 2]. A hotter mantle wedge than those of mature subduction zones is proposed for the Sanbagawa subduction system [4], in contrast the Izu subducting slab is relatively cold and would therefore lose relatively little water at equivalent depths to other slabs [5]. This implies a relatively small amount of the pore water subduction fluids would be released from the Izu slab at a sub-arc depth (150-200 km) resulting in further subduction to great depths in the mantle.

The mechanism by which the seawater-like noble gases are delivered to the convecting mantle remains to be elucidated. Serpentinized lithosphere of subducting slab is probably the best candidate, because if the hydration of the lithosphere by pore fluids is operating in a closed system, subduction of the serpentinized lithosphere can transport pore-fluid derived noble gases and halogens into the deep mantle [1, 2]. This is supported by a recent observation of noble gases and halogens in exhumed serpentinites similar to that of seawater and sedimentary pore fluids [6].

[1] Sumino *et al.* (2010) *Earth Planet. Sci. Lett.* **294**, 163-172. [2] Sumino *et al.* (2011) *Mineral. Mag.* **75**, 1963. [3] Holland & Ballentine (2006) *Nature* **441**, 186-191. [4] Mizukami & Wallis (2005) *Tectonics* **24**, TC6012. [5] van Keken *et al.* (2011) *J. Geophys. Res.* **116**, B01401. [6] Kendrick *et al.* (2011) *Nature Geosci.* **4**, 807-812.

Gold complexation within a halophilic cyanobacterium

KELLY L. SUMMERS*, JEREMIAH SHUSTER, MARTIN J. STILLMAN AND GORDON SOUTHAM

The University of Western Ontario, London, Canada
ksummer4@uwo.ca (* presenting author)

Introduction

Understanding the biogeochemical processes that transform gold are important in improving our ability to identify anomalies within dispersion halo environments, and potentially to recover trace amounts of gold [1]. Cyanobacteria have been implicated as potential gold nanofactories [2], and may contribute to gold nanoparticle formation in placer environments [3].

Octahedral platelet and nanoparticle gold precipitation has been observed after exposure of bacteria, e.g., *Plectonema boryanum* 485 [4], to $HAuCl_4$. The mechanism by which gold nanoparticles form within these cells is not well understood; however, adsorption of Au(I) to sulfur was reported following the addition of $HAuCl_4$.

Results and Discussion

X-ray analysis of near edge spectra (XANES), a synchrotron method, showed that the reaction of a halophilic *Plectonema sp*., with 0.5 mM $HAuCl_4$ reduced Au(III) to Au(I), which then formed complexes with sulfur. At higher gold concentrations (5 mM) Au(III) was reduced to elemental Au.

To investigate Au binding to known sulfur-containing proteins we probed glutathione (GSH), using Electrospray Ionization Mass Spectrometry (ESI-MS). GSH reduced Au(III) chloride to Au(I) and coordinated the Au through its cysteine residue (Figure 1). GSH binds Au as a monomer and as a dimer.

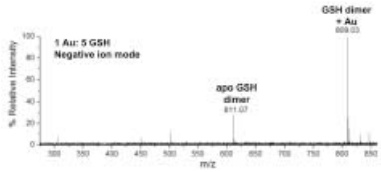

Figure 1. ESI-MS of a glutathione (GSH) complex with Au(I). $HAuCl_4$ added to 40 µM GSH for a final ratio of 1 Au: 5 GSH.

Cells reacted with 0.5 mM $HAuCl_4$ were lysed by liquid homogenization. Visualization of disrupted cells using phase contrast light microscopy revealed cell debris, and examination of whole mounts using TEM showed some cell envelope fragments. We recovered a soluble- and a cell envelope-fraction that bound Au. AAS and ESI-MS of the soluble fraction demonstrated the presence of low molecular weight Au-binding peptides. Occurrences of low molecular weight cysteine-rich metallothionein proteins in some species of marine cyanobacteria [5, 6] are targeted as possible gold-complexing organic compounds [7].

[1] Lengke et al. (2006) *Geomicrobiol. J.* **23**, 591–597.
[2] Chakraborty et al. (2009) *J. Appl. Phycol.* **21**, 145–152.
[3] Reith et al. (2010) *Geology* **38**, 843–846.
[4] Lengke et al. (2006) *Environ. Sci. Technol.* **40**, 6304–6309.
[5] Blindauer (2008) *Chem. Biodiv.* **5**, 1990–2013.
[6] Blindauer (2011) *J. Biol. Inorg. Chem.* **16**, 1011–1024.
[7] Stillman et al. (1994) *Met. Based Drugs.* **1**, 375-394.

https://doi.org/10.1180/S0026461X00008434 Published online by Cambridge University Press

Microbial siderophore effects on Pb sorption and mineral nucleation

SARA SUMMERS[1]*, GELIANG SONG[2], BRUCE BUNKER[2], AND PATRICIA MAURICE[1]

[1]University of Notre Dame, Civil Engineering & Geological Sciences, Notre Dame, IN 46556, USA ssummer1@nd.edu (* presenting author), pmaurice@nd.edu

[2]University of Notre Dame, Physics, Notre Dame, IN 46556, USA gsong@nd.edu, bunker@nd.edu

Siderophores are low molecular weight organic ligands released by many aerobic microorganisms and plants to acquire Fe. These ligands may also bind other metals such as Pb, thus affecting Pb sorption and nucleation and growth of Pb-bearing minerals. In this study, a combination of batch experiments and XAS analysis was used to determine the effects of the trihydroxamate siderophore desferrioxamine B (DFOB) on Pb sorption to montmorillonite (mmt) clay. In the absence of DFOB, Pb sorption increased with increasing pH and decreased at higher background electrolyte ($NaClO_4$) concentrations. In some instances, Pb carbonates were detected in the sorption experiments, with nucleation perhaps enhanced by the presence of the clay. DFOB was observed to have complex pH- and ionic-strength dependent effects on Pb sorption to mmt. Ternary surface complexes were observed when both Pb and DFOB were present, under pH conditions at which Pb-DFOB complexes form in solution.

In order to explore more thoroughly Pb carbonate formation, experiments were conducted in which cerussite ($PbCO_3$) and/or hydrocerussite ($Pb_3(CO_3)_2(OH)_2$) were grown in the presence and absence of DFOB. DFOB was found to strongly affect the crystal size and habit of the Pb(hydroxy)carbonate precipitates. XAS analysis of structure is ongoing.

Bacterial Necromass as a driver of bacterial weathering

STEPHEN SUMMERS*[1,2], CHARLES S. COCKELL[3] AND ANDREW S. WHITELEY[2]

[1]Department of Planetary Science, The Open University, UK, stemme@ceh.ac.uk (* presenting author)

[2]Molecular Microbial Ecology Laboratory, Centre for Ecology & Hydrology, UK, aswhi@ceh.ac.uk

[3]School of Physics and Astronomy, University of Edinburgh, UK, c.s.cockell@ed.ac.uk

Background

The rock – soil interface (critical zone) is where many crucial geochemical processes occur. This region of the Earth's crust is an important source of nutrients that are required for life; however these are locked away in minerals unavailable to most biota. Recent studies have shown that bacteria can play a pivotal role in the release of these elements in a biologically available form [1, 2]. Many bacteria that show the ability to weather minerals are known to be heterotrophic [3], yet the environments that are most significant when discussing weathering are limited in organics. We have investigated the question: can heterotrophic bacteria in the critical zone use isotopically labelled bacterial necromass as a source of carbon? Plants have been shown to actively select for bacterial communities in rhizosphere by manipulating the environment and providing nutrients [4, 5], yet where does organics originate in areas known to have significant weathering but lacking in plants.

A lake site in Skorradalur, Iceland that has been shown to have significant rates of weathering at locations in some cases devoid of plants was investigated. We show that necrotic bacterial matter is a source of carbon for the organisms in the critical zone. Some of this necromass may be accounted for by fresh bacterial input during spring snowmelt.

Results and Conclusions

Stable isotope probing was used to show that most bacteria in the critical zone are heterotrophic and able to utilize bacterial necromass to drive metabolic activity. Exceptions to this were of Nitrospirales, some of which are lithoautotrophic [6] and Rhizobiales some of which are methanotrophic and are capable of using methyl alcohol and methane as a sole carbon source.

Using flow cytometry observed cell concentrations within snow packs covering sample site were measured to be up to 4.4 $x10^5$ cells per millilitre. This is a substantial influx of fresh organic matter each spring as snow melts.

[1] Cockell, C.S., et al (2009) Geomicrobiology Journal **26**(7) p. 491-507.

[2] Cockell, C.S., et al (2009) Geobiology **7**(1) p. 50-65.

[3] Uroz, S., et al (2007) Applied and Environmental Microbiology **73**(9) p. 3019-3027.

[4] Bashan, Y., G. Holguin, and R. Lifshitz (1993) Methods in plant molecular biology and biotechnology. CRC Press, Boca Raton, Fla, p. 331-345.

[5] Calvaruso, C., M.P. Turpault, and P. Frey-Klett (2006) Applied and Environmental Microbiology **72**(2) p. 1258-1266.

[6] Lebedeva, E., et al (2008) International journal of systematic and evolutionary microbiology **58**(1) p. 242-250.

https://doi.org/10.1180/S0026461X00008434 Published online by Cambridge University Press

U-Pb ages and Sr–Nd isotopic compositions of perovskite from the Yakutian kimberlites, Siberian Craton

JING SUN[1*], FU-YUAN WU[1], CHUAN-ZHOU LIU[1]

[1]Institute of Geology and Geophysics, Chinese Academy of Sciences, sunjing@mail.iggcas.ac.cn (* Presenting author)

Perovskite in kimberlites commonly contain high contents of U, Sr and Nd, and thus could provide effective constraints on the emplacement age and Sr-Nd isotopes of kimberlitic magmas [1, 2]. In this study, perovskite have been selected from 38 kimberlites from 10 fields in the Yakutian area, Siberian Craton, and analysed in-situ by LA-MC-ICPMS method. The obtained perovskite U-Pb ages suggest that kimberlites in the Yakutian field were emplaced in four episodes, ~420 Ma, ~360 Ma, ~220 Ma and ~160 Ma. Different kimberlite pipes in the same field were emplaced at the same time. Furthermore, all the diamondiferous kimberlites in Yakutian field were erupted around 360 Ma. The perovskites display $^{87}Sr/^{86}Sr$ ratios ranging from 0.70282 to 0.70375 and $^{143}Nd/^{147}Nd$ ratios from 0.51229 to 0.51271. The Sr-Nd isotope range displayed by perovskites is much narrower than that given by the whole-rock Sr-Nd isotopic compositions, i.e., 0.70318~0.70641 and 0.51048~0.51270, respectively [3]. On one hand, this suggests that whole-rock Sr-Nd isotope compositions of kimberlites have been contaminated during erupted route to surface. On the other hand, the relatively depleted Sr-Nd isotopic compositions shown by the perovskites also indicate that the Yakutian kimberlites belong to the Group-I kimberlite, and were derived from a similarly depleted mantle source.

[1] Yang *et al*. (2009) *Chemical Geology* **264**, 24-42. [2] Wu *et al.* (2010) *Lithos* **115**, 205-222. [3] Kostrovitsky *et al.* (2007) *Russian Geology and Geophysics* **48**, 272-290.

The formation of the giant Bayan Obo REE deposit: Constraints from Mg isotopes

WEIDONG SUN[1*], MING-XING LING[2], YU-LONG LIU[1], XIAOYONG YANG[3], FANG-ZHEN TENG[4]

[1]Key Lab of Mineralogy and Metallogeny, Guangzhou Institute of Geochemistry, The Chinese Academy of Sciences, Guangzhou China, weidongsun@gig.ac.cn (* presenting author)

[2]State Key lab of Isotope Geochemistry, Guangzhou Institute of Geochemistry, The Chinese Academy of Sciences, Guangzhou China, mxling@gig.ac.cn

[3]School of Earth and Space Sciences, University of Science and Technology of China, Hefei, China, xyyang@ustc.edu.cn

[4] Isotope Laboratory, Department of Geosciences, University of Arkansas, Fayetteville, AR 72701, USA, fteng@uark.edu

The Bayan Obo REE-Nb-Th-Fe deposit, located in Inner Mongolia, North China, is the largest REE deposit and the second largest Nb deposit in the world. Its genesis is highly debated, ranging from carbonatite magmatism, alteration of sedimentary carbonate rocks, through deposition of carbonates on the sea floor accompanied by simultaneous metasomatism, to formation due to Caledonian subduction. None of the models so far proposed can fully explain all the major facts[1, 2]. The key problem is the relationship between carbonatite dykes, sedimentary dolomite, REE ore body and iron ore body. The REE ore bodies have trace element patterns and initial Nd isotope values identical to those of carbonatite dykes nearby, implying genetic links. Carbon isotopic composition of the carbonatite dyke is similar to the normal mantle $\delta^{13}C$ value of -5±2‰, but their O isotope compositions range from 13.9 to 16.4‰ for calcite, which are much higher than the mantle $\delta^{18}O$ value of 5.7±1.0‰. Consistently, the Mg isotopes of calcite carbonatite dykes range from mantle value to sedimentary values. All these indicate that the calcite carbonatite dykes have major sedimentary components, through recycling or assimilation, or a combination of both. By contrast, Mg isotopic compositions of ore bodies and dolomite carbonatite dykes are all close to mantle value, indicating major components from the mantle. The age of ore-forming monazite (330 to 760 Ma) is scattered with a main peak at about 400 Ma, roughly coincident with the evolution of the Central Asian orogenic belt nearby, but is much younger than carbonatite dykes (1300 Ma). Such large age dispersal indicates protracted mineralization driven by a persistent heat source for about 400 Ma. Considering that the host dolomite has high SiO_2 contents and carbon and oxygen isotopes distinctively different from those of carbonatite dykes, all these observations point to protracted steam-cooking of carbonatite by subduction released high-Si fluids, which leached Fe from the mantle wedge and, REE, Nb and Th from carbonatite, forming the Bayan Obo deposit in overlying sedimentary carbonate.

[1] Yang X Y, Sun W D, Zhang Y X, et al. Geochimica et Cosmochimica Acta, 2009, 73: 1417-1435

[2] Liu Y L, Williams I S, Chen J F, et al. American Journal of Science, 2008, 308: 379-397

https://doi.org/10.1180/S0026461X00008434 Published online by Cambridge University Press

Si isotope signatures preserved in BSi hold temperature information

XIAOLE SUN[1*], PER ANDERSSON[2], CHRISTOPH HUMBORG[3,4], BO GUSTAFSSON[4], DANIEL CONLEY[5], PATRICK CRILL[1], AND CARL-MAGNUS MÖRTH[1,4]

[1]Stockholm University, Geological Sciences, Stockholm, Sweden, xiaole.sun@geo.su.se (* presenting author)
[2]Swedish Museum of Natural History, Labrotary for Isotope Geology, Stockholm, Sweden
[3]Stockholm University, Applied Environmental Science, Stockholm, Sweden
[4]Stockholm Resilience Center, Baltic Nest Insititute, Stockholm, Sweden
[5]Lund University, Earth and Ecosystem Sciences, Lund, Sweden

High-latitude aquatic ecosystems of the subarctic and arctic region have been shown to be influenced by climate fluctuations on short growing seasons for diatoms[1]. In our study[2], we reconstructed diatom production in Bothnian Bay, the subarctic northern tip of the Baltic Sea, by analysing Si isotopes in biogenic silica (BSi) perserved in sediments using MC-ICP-MS. The sediment core dated by ^{210}Pb gamma-ray spectrometer covered the period of 1820 to 2000, consisting of an unperturbed period from 1820 to 1950 and a second period affected by human activities from 1950 to 2000. The Si isotope values ranging between δ^{30}Si −0.18‰ and +0.58‰ in BSi were used to infer diatom production by using the Rayleigh model for fractionation patterns (Fig. 1). This exhibited that the production was correlated with air and water temperature, which in turn were correlated with the mixed layer depth. Especially after cold winters and deep water mixing, diatom production was limited. We also observed a shift of Si isotope values in the sediments after 1950, which is most likely caused by large scale damming of rivers which was heavily carried out between 1940 and 1960. Our findings offers a new way to estimate diatom production over much longer periods of time in diatom dominated aquatic systems, i.e. a large part of the world's ocean and coastal seas.

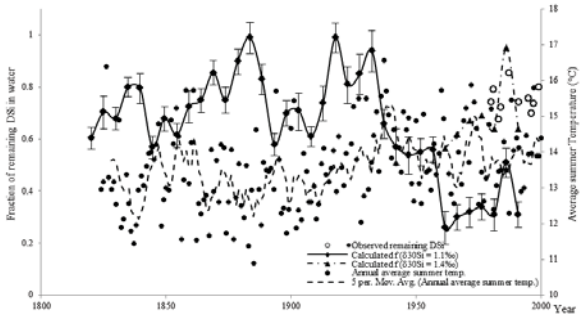

Figure 1: Fraction of the remaining DSi (f) in the water column reconstructed by the Rayleigh model, plotted with average summer air temperature through years. The inferior and superior error bars on f -values are the first quartile and third quartile for each f -value[2].

[1] Douglas & Smol (2010), The diatoms: applications for the environmental and earth sciences, *Smol J.P. & Stoermer E. F. eds, 12,* 231-248. [2] Sun et al. (2011) *Biogeosciences* **8**, 3491-3499.

EXAFS studies of Fe speciation in natural stream waters

ANNELI SUNDMAN*, TORBJÖRN KARLSSON, PER PERSSON

Umeå University, Umeå, Sweden
anneli.sundman@chem.umu.se (* presenting author)
torbjorn.karlsson@chem.umu.se
per.persson@chem.umu.se

Introduction

Fe speciation in organic rich soils and aquatic environments depends on the interactions between Fe and natural organic matter (NOM)[1]. These interactions also have a large influence on the availability of nutrients such as phosphorus and thus on biological productivity in natural environments. Accordingly, the Fe-NOM interactions are of fundamental importance but the generally low Fe concentrations in natural stream waters prevent direct spectroscopic studies. In this work we have developed a gentle and non-invasive method for concentrating stream water samples using adsorption via electrostatic forces onto permanently charged particles. The Fe speciation in these samples was subsequently analyzed by means of EXAFS spectroscopy. Stream waters were collected at the well-studied Krycklan Catchment[2], 64°, 16'N, 19°, 46E, in northern Sweden, with Fe concentrations in the range of 8-40μM.

Results

EXAFS investigations of negatively charged metal model complexes concentrated by our method showed that no significant distortions were induced as compared to the solution structures, which is in accordance with previous results[3,4]. The local structures of Fe(III) complexes in stream water samples from a forested site were investigated by applying the same technique. The EXAFS results indicated that the Fe(III) speciation was dominated by mononuclear organic chelate complexes and hydrolyzed Fe with ferrihydrite-like structures. We have also performed EXAFS studies of Fe speciation in soil solutions and groundwater, and these results will also be discussed. Finally, the method is not limited to EXAFS and we will show how it can be applied to P-NMR studies of natural waters, facilitating differentiation between inorganic and organic phosphorus species.

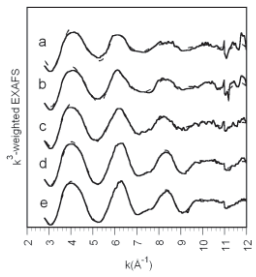

Figure 1. k^3-weighted EXAFS data from stream waters collected at the Krycklan Catchment[2], in February 2010, for a gradient series with a) 100%, b) 84%, c) 77%, d) 42% and e) 28% adsorption of Fe from the stream water. Solid lines represent experimental data and broken lines are fitted data.

[1] Rose et al. (1998) *Colloids and Surfaces A: Physicochemical and Engineering Aspects* **136**, 11-19. [2] Laudon et al. (2011) *Ecosystems* **14**, 880-893. [3] Bargar et al. (1999) *Geochimica et Cosmochimica Acta* **63**, 2957-2969 [4] Kaplun et al. (2008) *Langmuir* **24**, 483-489

https://doi.org/10.1180/S0026461X00008434 Published online by Cambridge University Press

Strontium stable isotope variations in lunar basalts

CHELSEA N. SUTCLIFFE[1*], KEVIN W. BURTON[2], IAN J. PARKINSON[3], DAVID COOK[1], BRUCE L. A. CHARLIER[3], DON PORCELLI[1], FATIMA MOKADEM[1], ALEX N. HALLIDAY[1]

[1]Department of Earth Sciences, University of Oxford, Oxford , UK chelsea.sutcliffe@st-annes.ox.ac.uk (* presenting author)
[2]Department of Earth Sciences, Durham University, Durham, UK
[3]Department of Earth and Environmental Sciences, The Open University, Milton Keynes, UK

In the terrestrial environment strontium stable isotopes may experience significant fractionation, both at low- and high-temperatures (e.g. [1,2]). Recent data for lunar basalts suggests that these rocks may possess light Sr stable isotope compositions ($\delta^{88}Sr$ = +0.16±0.07) [2] relative to mantle derived terrestrial basalts ($\delta^{88}Sr$ = +0.30±0.07) [2,3]. However, few samples have been analysed thus far, and at the ±50 ppm precision of these measurements, obtained using an MC-ICP-MS [2,3] smaller variations that may exist cannot be clearly resolved.

This study presents high-precision double spike TIMS data for $^{87}Sr/^{86}Sr$ (±5 ppm) $^{88}Sr/^{86}Sr$ (±10ppm) and $^{84}Sr/^{86}Sr$ (±20 ppm) for a suite of lunar basalts and highland rocks. These data indicate that there are significant and resolvable variations in $\delta^{88}Sr$ ranging from +0.30 for a ferroan anorthosite to +0.10 for a high-Ti Mare basalt. The lunar highland rocks (including anorthosites, troctolites and norites) possess a relatively small range of $\delta^{88}Sr$ values from +0.30 to +0.24 (0.06‰) whereas the mare basalts are distinctly lighter and encompass a larger range of $\delta^{88}Sr$ values, from +0.26 to +0.10 (0.16‰). The Mare basalts all possess negative Europium anomalies consistent with having been derived from a plagioclase depleted source, whereas the anorthosites are plagioclase rich. These observations suggest that the preferential incorporation of heavy Sr stable isotopes in plagioclase is the dominant mechanism controlling stable isotope fractionation in lunar basalts (similar to that seen in evolved terrestrial basalts [2]). Preliminary $^{84}Sr/^{86}Sr$ data suggests that the lunar rocks may possess slightly lighter compositions than terrestrial rocks, but this cannot be resolved at the present level of analytical precision. Taken together, these results clearly indicate that for the Moon primary igneous processes alone can generate significant variations in $\delta^{88}Sr$, without the biological fractionation and recycling that may occur on Earth.

[1] Fietzke & Eisenhauer (2006), *Geochem. Geophys. Geosyst.* **7**, Q08009 [2] Charlier et al. *Earth Planet. Sci. Lett*. Submitted (2011) [3] Moynier et al. (2010) *Earth Planet. Sci. Lett.* **3-4,** 359-366

Exclusive use of a soil gas hydrocarbon geochemistry to vector towards mineral deposits

DALE SUTHERLAND

Activation Laboratories Ltd., Ancaster, Ontario, Canada, dalesutherland@actlabsint.com

This Soil Gas Hydrocarbon (SGH) geochemistry has been scientifically shown to detect those hydrocarbons released from the decomposition of bacteria at the end of their life cycle. From a "you are what you eat" perspective, the 162 specific hydrocarbons in the C5 to C17 carbon series range that are able to be detected provide an information rich forensic signature of identification from the bacteria that were directly growing on specific types of mineral deposits.

The forensic signature has been tested through projects administered by the Canadian Mining Industry Research Organization (CAMIRO) as well as those conducted by the Ontario Geological Survey. The use of the hydrocarbon signature has been able to differentiate between barren and ore bearing conductors and geophysical targets of mineralization or kimberlites from naturally occurring signals such as from granite gneiss.

Although the SGH name implies the exclusive use of soils, this geochemistry is also able to use other sample media such as humus, peat, sand, till, submerged sediment, and even snow. As these hydrocarbons are relatively neutral species the state of the flow of hydrocarbons that migrate and geochromatographically disperse through the overburden can be captured by the surface area of the sample media taken in a survey. This capability is vital in areas of difficult terrain where a complete sample survey may cover swamps, lakes, peaty areas as well as high ground. This multi-media survey can be processed and mapped together without data leveling, thereby significantly reducing the bias in interpretation represented by areas where sampling was formerly not warranted.

Several independent studies have also illustrated the successful depiction of blind mineralization that is shallow or to depths in excess of 700 metres. Figure 1 illustrates additional penetrating capability of this nano-scale geochemistry at dramatically delineating gold mineralization beneath a basalt cap. Similar results have been shown over areas of permafrost.

As a forensic signature the identification and vectoring capability of SGH provides a high level of confidence. The robustness of this geochemistry has allowed it to be used to discover new resources in not only greenfield applications but has also delineated mineralized extensions in brownfield surveys.

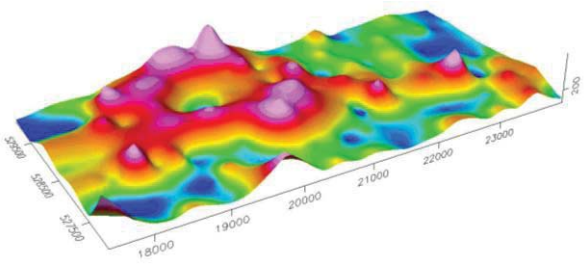

Figure 1: SGH gold anomaly below basalt cap, Mali, Africa

https://doi.org/10.1180/S0026461X00008434 Published online by Cambridge University Press

Viscosity of carbon dioxide-bearing silicate melt at high pressure

AKIO SUZUKI[1*]

[1]Department of Earth and Planetary Materials Science, Tohoku University, Sendai, Japan, a-suzuki@m.tohoku.ac.jp (* presenting author)

Knowledge of the viscosity of silicate melts at high pressure is of importance for modeling igneous processes in the Earth's interior. In natural magmas, volatiles are dissolved and affects physical properties. It has been known that volatiles reduce the viscosity of magmas. However, very few studies have been performed to investigate the effect of volatiles on the viscosity at mantle pressures. In the present study, the viscosity of carbon dioxide-bearing jadeite melt has been determined up to 4 GPa. We adopted the falling sphere method for viscometry. Experimental detail has been described elsewhere[1, 2]. X-ray radiography technique enables us to measure the falling velocity of a platinum sphere in situ. Experiments were performed at the NE7A station at the High Energy Accelerator Research Organization (KEK). We used a Kawai type multi anvil apparatus driven by a DIA type guide block installed on the MAX-III apparatus. A charge-coupled device (CCD) camera with a YAG:Ce fluorescence screen was used as an X-ray camera. The present study shows that an addition of carbon dioxide produces a viscosity decrease.

[1] Suzuki *et al*. (2002) *Phys. Chem. Miner.* **29**, 159-165. [2] Suzuki *et al*. (2011) *Phys. Chem. Miner.* **38**, 59-64.

Unveiling key players in the geological disposal environment

YOEHY SUZUKI[1*], AKARI FUKUDA[2], UTA KONNO[3], MARIKO KOUDUKA[3], HIROKI HAGIWARA[2], ANDREW MARTIN[4], NAOTO TAKENO[3], KAZUMASA ITO[3], TAKASHI MIZUNO[2]

[1]The University of Tokyo, Earth and Planetary Sciences, yohey-suzuki@eps.s.u-tokyo.ac.jp (* presenting author)
[2]Japan Atomic Energy Agency, mizuno.takashi@jaea.go.jp
[3]National Institute of Advanced Industrial Science and Technology, Institute of Geology and Geoinformation, n.takeno@aist.go.jp
[4]National Cooperative for the Disposal of Radioactive Waste, Andrew.Martin@nagra.ch

Introduction

It is well established that the speciation, distribution and transport of radionuclides is profoundly influenced by microbial activities in the shallow aquifer. However, it remains to be challenging to predict microbial influences on radionuclide migration in the deep aquifer for geological disposal of radioactive wastes. Currently, there are two major gateways to the deep biosphere through long vertical boreholes from the surface or short horizontal boreholes from the underground tunnel. Neither approach is exempt from the disturbance of the steady biogeochemical state and microbiological populations established through the long evolutionary history within the fracture networks. Despite the disturbance, it is very critical to identify indigenous microbial populations that potentially affect the long-term behavior of radionuclides (e.g. biosorption and redox transformation) and contaminant ones playing short-term roles during the recovery from the disturbance by consuming artificially introduced oxidants.

Underground research laboratories for comparison

The Grimsel Test Site (GTS), central Switzerland, has been in operation since 1984. The GTS provides 400-500-m deep granitic groundwater from boreholes that vary in age from 1 to 25 years. The Mizunami URL (MIU), which is being constructed in central Japan, provides 200-400-m deep granitic groundwater since 2007. The microbial comparison of the URLs associated with freshwater groundwater might result in the clarification of microorganisms commonly associated with the deep granitic subsurface.

Key indigenous and contaminant microbial populations

16S rRNA gene sequence analyses were conducted for groundwater samples from the GTS and the MIU. Sequences related to "*Candidatus* Magnetobacterium bavaricum" of Nitrospirae were predominant in all GTS boreholes, while β-proteobacterial sequences were only obtained from 1-2 year old GTS boreholes. Similarly, the predominance of β-proteobacterial sequences was gradually shifted to that of Nitrospirae sequences within several years after horizontal drilling at the MIU. The detection of the common microorganisms from the geographically distinct URLs suggests that these microbes are cosmopolitan in the granitic aquifer, radionuclide interactions with which should be clarified to provide general and reliable information for the safety of geological disposal in granitic repositories.

Acknowledgement

This study was supported by grants from the Nuclear and Industrial Safety Agency (NISA).

https://doi.org/10.1180/S0026461X00008434 Published online by Cambridge University Press

Cyanobacteria and photoferrotrophs: together again?

ELIZABETH D. SWANNER[1*] AND ANDREAS KAPPLER[1]

[1]University of Tübingen, Center for Applied Geoscience (ZAG), Geomicrobiology, Tübingen, Germany.
elizabeth.swanner@ifg.uni-tuebingen.de (* presenting author)

Phototrophs in a Ferrous Ocean

Anoxygenic phototrophs capable of metabolically oxidizing Fe^{2+} to Fe^{3+} are believed to be responsible for the deposition of mixed-valence Fe-containing Banded Iron Formations (BIF) in a Precambrian atmosphere of low O_2 [1]. The evolution of oxygenic photosynthesis by cyanobacteria has long been regarded as the primary mechanism for a rise in atmospheric O_2 in the Paleoproterozoic [2], and this O_2 would have further reacted with abundant aqueous Fe^{2+} to contribute to the deposition of BIF. As BIF were deposited across a wide range of Earth history and represent several distinct depositional settings, they potentially recorded changes in the makeup of the marine biosphere, particulalry among the anoxygenic photo(ferro)trophs and cyanobacteria. We ask what these changes were, and whether or not they are recorded in the style and substance of BIF deposition.

To address this, we report on our attempts to co-cultivate marine species of cyanobacteria and a photoferrotroph under conditions relevant to the hypothosized Precambrian ferrous ocean. Both strains will be independently evaluated to determine what chemical and physical factors imposed by changing ocean chemistry could have limited growth. These include light intensity, temperature and trace element availability. The results will be useful to compare with datasets reporting the calculated abundance of trace elements (e.g. Ni, Co) in the Precambrian ocean [3]. Then, the spatial distribution of trace metals and phosphorus to Fe and organic carbon from cell-mineral precipitates of Fe-containing co-culture experiments will be used for late-stage diagenesis experiments at temperature and pressure conditions observed in BIF to determine whether any trace element signatures associated with the phototrophic metabolisms in a ferrous ocean would be retained through time. A combination of fluorescence-based metal dyes in confocal microscopy and scanning transmission X-ray microscopy (STXM) will be used to assess these relationships both before and after simulated diagenesis.

Analogues for Precambrian Microbial Communities

As ferrous-rich marine environments today are scarce, analogue environments to study the phototrophic biosphere as occurred in the Precambrian and its implications for BIF are lacking. However, laboratory experiments are most useful if relevant to natural systems. Therefore we will compare the results of our data with the natural distribution of cyanobacteria and photoferrotrophs from a circumneutral Fe-rich freshwater lake. As most knowledge about photoferrotrophs is currently sourced from work with pure cultures, further molecular, chemical and cultivation-based studies of these organisms in natural environments is warranted.

[1] Kappler et al (2005) *Geology* **33**, 865-868. [2] Cloud (1968) *Science* **160**, 729-736. [3] Konhauser et al (2009) *Nature* **458**, 750-754.

An assessment of submarine groundwater discharge and its nearshore ecological impacts: Examples from the U.S. west-coast and Hawai'i

P.W. SWARZENSKI[1*], C.A. SMITH[2], P. M. GANGULI[3], J.A. IZBICKI[4] AND R.W. SHEIBLEY[5]

[1]USGS, Santa Cruz, CA (pswarzen@usgs.gov) (*presenting author)
[2]USGS, St. Petersburg, FL (cgsmith@usgs.gov)
[3]University of California, Santa Cruz, CA (pganguli@ucsc.edu)
[4]USGS, San Diego, CA (jaizbick@usgs.gov)
[5]USGS, Tacoma, WA (sheibley@usgs.gov)

The dynamic exchange of a coastal aquifer with sea water is a ubiquitous but still mostly inadequately quantified vector for nutrients and trace elements enroute to the sea. Biogeochemical reactions within this coastal aquifer/sea water mixing zone will transform many chemical species, including the redox sensitive- and microbially-mediated elements. As a result, this mixing zone can be a productive incubator zone for transformation products that rely on microbes or steep redox gradients. Geochemical and geophysical data from sites that extend from southern California to Puget Sound and Hawai'i will be used to assess submarine groundwater discharge (SGD) rates, scales, and constituent loadings. Unique geologic, climatic, and hydrologic characteristics define many west-coast U.S. and Hawaiian coastal systems. In these systems, the physical drivers and anthropogenic impacts on SGD are often unique and are assessed using a suite of naturally-occurring radionuclides (^{222}Rn and ^{223,224,226,228}Ra) and multi-channel electrical resistivity techniques. SGD is also evaluated as a sustained vector for nutrient (e.g., N and P) and trace element (e.g., Hg, U) loadings to nearshore environments and discussed in terms of ecosystem processes and impacts.

https://doi.org/10.1180/S0026461X00008434 Published online by Cambridge University Press

Coastal groundwater discharge near Kahekili Beach Park, Lahaina, Maui, Hawai'i

P.W. SWARZENSKI[1*], C.G. SMITH[2], C.D. STORLAZZI[1], L. DIAZ AND M.L. DAILER[3]

[1]USGS, Santa Cruz, CA (pswarzen@usgs.gov) (*presenting author)
[2]USGS, St. Petersburg, FL (cgsmith@usgs.gov)
[1]USGS, Santa Cruz, CA (cstorlazzi@usgs.gov)
[1]USGS, Santa Cruz, CA (ldiaz@usgs.gov)
[3]University of Hawai'i, Honolulu, HI (dailer@hawaii.edu)

This presentation describes a study conducted off Kahekili Beach Park, located just north of Lahaina on the west coast of Maui, Hawai'i, to better understand rates and drivers of coastal groundwater discharge and associated material transport into nearby coastal waters. This site has recently been well studied to examine how focused municipal wastewater plumes may be conveyed to the coastal waters by discharging groundwater [1, 2]. At this location there are multiple spring vents close to shore (water depth < 2m), where much lower salinity water can readily be observed discharging into the water column. There has also been a notable change in bottom type; this site was once dominated by corals and now is dominated by turf- or macro-algae [1]. This suggests a likely local nutrient imbalance that warrants further investigation. Previous reports have utilized dissolved nitrate - $\delta^{15}N$ records [1] as well as a suite of tell-tale organic pollutants [2] to infer focused municipal wastewater discharges at this location. Our study presents the first estimates of coastal groundwater discharge to this site based on the submarine groundwater discharge tracer, ^{222}Rn, and extends our understanding of the scales, magnitudes, and constituent loads conveyed by this submarine route.

[1] Dailer, Knox, Smith, Napier & Smith (2010) *Marine Pollution Bulletin*, **60**, 655-671. [2] Hunt & Rosa (2009) U.S.G.S. *Scientific Investigations Report*, 2009–5253, 166 p.

Pore scale CO_2-brine-mineral interactions in caprock

ALEXANDER M. SWIFT[1*], DAVID R. COLE[2], MICHAEL V. MURPHY[2], JULIA M. SHEETS[2], SUSAN A. WELCH[2]

[1] The Ohio State University, Columbus, Ohio, USA, swift.63@osu.edu (* presenting author)
[2] The Ohio State University, Columbus, Ohio, USA

Although the carbon sequestration capacity of the Mount Simon formation in western Ohio has been the subject of much published work, less is known about the ability of the overlying Eau Claire to serve as a caprock over geologic time. Predicting this involves a better understanding of how mineralogic heterogeneity controls the nature and extent of precipitation (pore-closing) and dissolution (pore-opening) in response to CO_2 perturbation. Preliminary study of select rock core indicates that the Eau Claire comprises subfacies on the scale of cm to m dominated by quartz-rich sandstone, shale and carbonate. At the pore scale (mm to microns), the relative abundance and pore-accessibility of reactive minerals such as illite, iron oxides, pyrite, and chlorite become key factors in controlling local geochemical regimes.

Results are presented here from *in situ*, temperature- and pressure-corrected kinetic models of CO_2-saturated brine in contact with rock that draw upon pore, rather than bulk, mineralogies. 2D mineral and pore scan raster maps of thin sections are obtained using a field emission gun scanning electron microscope (FEG-SEM) equipped with QEMSCAN software that compares backscattered electron (BSE) and characteristic x-ray signals against a database of standard mineral patterns. These methods permit the analysis of how micron-scale mineralogical heterogeneity varies over distances of tens of vertical meters. As quantifying the effective reactive pore surface area is a key step in improving the predictability of reactive transport models used to assess the fate of CO_2 in the subsurface, the surface area of pores down to micron scale is estimated by summing pore-non pore pixel edges. A sensitivity study is performed on parameters of particular relevance: CO_2 fugacity (8 – 32 MPa), mineral proportions (informed by sample composition), and brine chemistry (date, location, and depth-matched with rock samples).

Preliminary results indicate that, because of the relative abundance of Mg- and Fe-rich minerals at pore surfaces, CO_2-saturated brine-rock interactions exhibit greater reactivity and are more pH-fO_2-dependent than is predicted by models based on the same samples but considering only bulk mineralogy.

Work is performed by the Subsurface Energy Materials Characterization and Analysis Lab at The Ohio State University, and is sponsored by the Dept. of Energy "Nanoscale Control of Geologic CO_2" Energy Frontier Research Center. Core is provided by the Ohio Department of Natural Resources.

https://doi.org/10.1180/S0026461X00008434 Published online by Cambridge University Press

Fate of magnetite nanoparticles in leachate-impacted groundwater

A.L. SWINDLE[1*] AND A.S. MADDEN[1]

[1]University of Oklahoma, Norman, OK, USA, (aswindle@ou.edu, amadden@ou.edu)

Nano-scale iron oxides, particularly magnetite, have been suggested as potential reductants for a number of environmental contaminants such as heavy metals, radionuclides, and volatile organics. Experiments have generally shown that magnetite is a viable reductant of a number of contaminants in a laboratory setting [1], though effectivness is influenced by iron-oxide particle size and the presence of additional cationic and anionic species [2]. However, key questions remain about the fate of magnetite nanoparticles in groundwaters with complex chemistry.

Magnetite nanoparticles were synthesized in the laboratory by partial oxidation of ferrous iron sulfate in a basic medium. A combination of TEM and XRD were used to characterize the reation products. A custom-made nanoparticle holder was designed to be compatible with the existing 1" OD groundwater wells at the USGS Norman Landfill Site. By means of this nanoparticle holder, magnetite nanoparticles were deposited on TEM grids and then inserted into a groundwater monitroing well at the USGS Norman Landfill Site. The particles were reacted for 10 days, retrevied from the site, and then stored in an anearobic chamber prior to anaylsis. The reaction products were anaylzed via TEM and compared to the intial characterization. Total volumes were calculated for both the initial synthesis products and the reacted magnetite particles. These volumes were compared to determine the volume of material lost and to calculate an approximate dissolution rate.

TEM characterization of the synthesis products indicated euhedral magnetite with a size range of 250 to 11 nm, along with euhedral goethite particles. Mineralogies identified in synthesis products via TEM were confirmed by XRD analysis. TEM analysis of the reacted particles revealed that the particles were subhedral, indicating dissolution of the magnetite particles, primarily at the corners and edges. Bright field images also indicated a textured surface on the reacted magnetite surfaces, which is also indicative of dissolution of the iron oxide particles.

Experimental results indicate that the magnetite particles lost 10 to 30 percent of their total volume over the 10 day time period. Interestingly, no clear trend between particle size and total volume lost was apparent in the data. An approximate dissolution rate of 2.9 (0.9) x 10^{-9} nmol/m^2*day was obtained using the TEM images.

[1] Roh (2003) *Clay and Clay Minerals* **51**, 83-95. [2] Roonasi (2010) *Surface and Interface Analysis* **42**, 1118-1121.

Implications of noble gases in Stardust samples for the source of Earth's water

TIMOTHY D. SWINDLE

Lunar and Planetary Laboratory, University of Arizona, Tucson AZ USA, tswindle@lpl.arizona.edu

Comets as the Source of Earth's Water

Comets have long been considered a possible source of Earth's water. The compositions of comets would provide an obvious constraint, but the only compositional parameter that has been widely applied is the D/H ratio. Although most comets in which D/H have been measured have ratios a factor of two higher than Earth's oceans, a recent measurement of Comet Hartley 2 gave an Earth-like ratio [1], reviving interest in the idea of a cometary source.

Another compositional parameter that could prove powerful is the noble gas abundance in comets. Based on a spectroscopic measurement of the Ar/O in the coma of Comet Hale-Bopp [2], Swindle and Kring [3] argued that if comets had brought in the Earth's water, orders of magnitude more noble gas would be in Earth's atmosphere than there presently is. However, that measurement has not been replicated, and other measurements suggest much lower noble gas abundances in comets, giving only upper limits [4].

More recently, noble gases have been measured in samples returned from the coma of Comet Wild 2 by the Stardust mission, so it is appropriate to revisit the argument, considering only the noble gases in the dust.

Extrapolating Stardust measurements to Xe in comets

Marty et al. [5] measured He and Ne in Stardust samples, and concluded that the dust contained ~0.1 cm^3STP of Q-type ^{20}Ne per gram of dust (~9 x 10^{-5} g_{Ne}/g). If we conservatively assume that comets are 10% dust, that would mean that to bring in an amount of H_2O equivalent to the Earth's oceans, 3 x 10^{-4} of Earth's mass [6] would also bring in more than 1000 times as much Ne as is currently present in the atmosphere (~10^{-12} g_{Ne}/g). However, Ne is light enough that it is possible that it would not be retained during cometary impacts (although its molecular weight is higher than that of H_2O). If we consider Xe instead, the ^{20}Ne/^{132}Xe (molar) ratio in Q-type gas is 3.2, which would mean that an ocean's worth of cometary water would contain more than 10,000 times as much ^{132}Xe as the present atmosphere. It is difficult to envision ways to lose that amount of Xe, although the argument does depend on the identification of the Stardust Ne as Q-type. Furthermore, this argument only applies to the dust, and does not even consider the ice, which could have large amounts of noble gases as well.

Once again, noble gas abundances appear to be a problem for arguing for a cometary source for Earth's water, but more definitive measurements are clearly needed.

[1] Hartogh et al. (2011) *Nature* **478,** 218-220. [2] Stern et al. (2000) *Astrophys. J.* 544, L169-L172. [3] Swindle and Kring (2001) *11th Goldschmidt Conf.*, Abstract #3785. [4] Weaver et al. (2002) *Astrophys. J.* 576, L95-L98. [5] Marty et al. (2008) *Science* **319**, 75-78. [6] Abe et al. (2000) In *The Origin of the Earth and Moon*, 413-433.

https://doi.org/10.1180/S0026461X00008434 Published online by Cambridge University Press

Isotopic constraints on water and carbon fluxes in Langat Basin, Peninsular Malaysia: A Reconnaissance Study

MUHAMMAD.I.SYAKIR[1,2*], IAN.D.CLARK[1], JAN VEIZER[1]

[1]University of Ottawa, Dept. of Earth Sciences, Ottawa, Canada, misha104@uottawa.ca (*presenting author)
[2]Universiti Sains Malaysia, School of Industrial Technology, Penang, Malaysia

Introduction

Evapotranspiration is a nexus for planetary energy and carbon cycles, but it remains poorly constrained. Here we use stable isotopes of Oxygen and Hydrogen to partition flux of water due to plant transpiration from the direct evaporative flux from soils, water bodies and plant surfaces in the tropical watershed of Peninsular Malaysia.

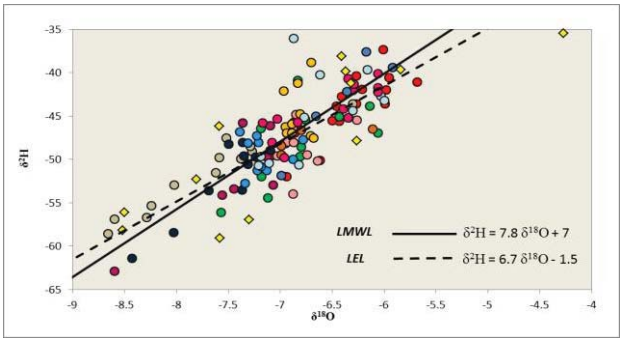

Figure 1 : Intersection of Local Meteoric Water Line (LMWL) and the Local Evaporative Line (LEL) in the Langat Basin.

Results and Conclusions

Mean annual rainfall, obtained from 30 years of hydrological data, is ~2078 mm. Tentatively, 45% of this precipitation returns to the atmosphere via transpiration (T), with 38% partitioned into discharge (R), 9% into interception (I_n), and 8% into evaporation (E_d), emphasizing the role of water cycle as a "conveyor belt" essential for nutrient transport in terrestrial ecosystems [1,2]. The flux of carbon from the atmosphere to the tropical ecosystem of the watershed, related to this transpiration water flux via water utilization factor (WUE), is about 505 g C m^{-2} yr^{-1}.

[1] Ferguson & Veizer (2007) *J.Geophys.Res.*, **122**, D24SO6
[2] Schulte et.al. (2011) *Earth-Science Review* **109**, 20-31.

Metagenomic Analysis of Inactive Hydrothermal Sulfides from Lau Basin

JASON B. SYLVAN[1*] AND KATRINA J. EDWARDS[2]

[1]University of Southern California, Los Angeles, CA, USA, jsylvan@usc.edu*

The East Lau Spreading Center (ELSC) and Valu Fa Ridge comprise a ridge segment in the southwest Pacific Ocean where rapid transitions in the underlying mantle lenses manifest themselves by gradients in seafloor rock geochemistry. At the spreading center in the north, basaltic host rock extrudes while the influence of subduction in the south creates mainly basaltic andesite host rock, with a continuous gradient between these two end members. We studied the geology and microbial diversity of seafloor silicate rock samples and inactive sulfide chimney samples collected along the ELSC and Valu Fa Ridge by X-ray diffraction, elemental analysis, thin section analysis, bacterial 16S rRNA sequencing and metagenomic analysis. Here, we discuss results from the inactive sulfides. On a chimney collected from the ABE vent field, the outside portion of the chimney was dominated by sulfur oxidizing Gammaproteobacteria in the SUP05 clade whereas the inside conduit of the same inactive chimney was dominated by the sulfate reducers in the deltaproteobacterial family Desulfobulbaceae. An inactive sulfide chimney sampled from Tui Malila vent field, where host rock is more strongly influenced by dewatering reactions from the subducting plate, hosted a starkly different bacterial community; sulfur oxidizing Epsilonproteobacteria in the genera *Sulfuromonas* and *Sulfurovum* were recovered from the same sample along with sulfate reducing Desulfobulbaceae and methane oxidizing Gammaproteobacteria in the order Methylococcales, indicating that this sample was either recently inactive or in the final stages of cessation of venting. We also present here the preliminary analysis of metagenomes sequenced from these samples using an Ion Torrent next generation sequencing machine.

https://doi.org/10.1180/S0026461X00008434 Published online by Cambridge University Press

The record of early crustal evolution preserved in detrital zircons from Mount Murchison metasedimentary rocks, Western Australia

P.J. SYLVESTER[1*], A.K. SOUDERS[1] AND J.S. MYERS[2]

[1]Department of Earth Sciences, Memorial University, St. John's, NL, Canada (*psylvester@mun.ca, kate.souders@mun.ca)
[2]Department of Applied Geology, Curtin University, Perth, WA, 6845, Australia (myersm@iinet.net.au)

The Mt. Narryer and Jack Hills metasedimentary belts of the Narryer Terrane of Western Australia have been the subject of intense study for almost thirty years because they contain ca. 4.35 Ga detrital zircons, which are the oldest minerals known on Earth. These rocks also contain numerous younger populations of Hadean and Archean detrital zircons of diverse provenance, preserving a rich archive of information on early crustal evolution. Largely ignored has been a third major sequence of metasedimentary rocks in the Narryer Terrane, located at Mt. Murchison, 27 km south-southeast of Mt. Narryer and 98 km southwest of the Jack Hills. The detrital zircon population at Mt. Murchison can provide insights into the extent of Hadean sources in the Narryer Terrane, and whether magmatic events that produced detrital zircons in this region were episodic or continuous during the Archean.

The Mt. Murchison metasedimentary belt is 5 km long and 2 km wide, and contains fuchsitic quartzite, bedded coarse-grained quartzite, glassy quartzite, and quartz pebble conglomerate that appear similar in appearance to mature clastic units at Mt. Narryer and the Jack Hills. We have determined the U-Pb ages of detrital zircons in a sample of fuchsitic quartzite from Mt. Murchison using laser ablation-inductively coupled plasma mass spectrometry. One-hundred-thirty-nine detrital zircon grains in the sample are concordant within 10%. Seventy percent of the grains have $^{207}Pb/^{206}Pb$ ages that fall within four populations: 3125 ± 40 Ma (16%), 3235 ± 40 Ma (23%), 3445 ± 40 Ma (18%) and 3540 ± 40 Ma (13%). The oldest grain has a $^{207}Pb/^{206}Pb$ age of 3955 ± 12 Ma (2s); the youngest grain is 3001 ± 20 Ma (2s).

The detrital zircon population of the Mt. Murchison sample differs from those of quartzites and conglomerates from Mt Narryer and the Jack Hills in the paucity of grains older than 3.6 Ga, and the presence of a large population of 3.1 – 3.2 Ga grains. On the other hand, the 3.4 Ga age peak in the Mt. Murchison sample is also a prominent detrital zircon age population in the Jack Hills, and 3.5 Ga sources contributed to all three metasedimentary belts. This suggests that while there was significant age heterogeneity in the detrital sources of the Narryer Terrane, there were also some common sources that linked the paleodrainage systems of the Mt. Murchison, Mt. Narryer and Jack Hills areas.

When combined, the detrital zircon age data for all three metasedimentary belts define a rather continuous record of major magmatism in the Narryer Terrane from *ca.* 3100 to 3650 Ma. This implies unusually long-lived and continuous (rather than episodic) magmatic processes for crustal growth in the early Archean. Reconstructing the record of ages of clastic sedimentary sources in ancient terranes requires analysis of multiple depositional units of paleodrainage systems.

PGE abundances in upper mantle xenoliths from the Carpathian-Pannonian Region

CSABA SZABÓ[1] KEIKO HATTORI[2], WILLIAM GRIFFIN[3] , SUE O'REILLY[3] AND LÁSZLÓ ELŐD ARADI[1]

[1]Lithosphere Fluid Research Lab, Eötvös University, Budapest, Hungary (cszabo@elte.hu)
[2]Department of Earth Sciences, University of Ottawa, Canada (khattori@uottawa.ca)
[3]GEMOC, Department of Earth and Planetary Sciences, Macquarie University, Australia

The contents of Os, Ir, Ru, Rh, Pt and Pd were determined in lherzolite xenoliths and their sulfide grains (up to 150 μm) from the Carpathian-Pannonian region (CPR) to evaluate the abundance of the highly siderophile elements in the subcontinental lithospheric mantle beneath the region of the Alpine-Mediterranean area. The studied locations include the Styrian basin (western CPR, Austria), Bakony—Balaton-Highland (central CPR, Hungary), Nógrád-Gömör (northern CPR, Hungary, Slovakia), and the East-Transylvanian basin (eastern CPR, Romania).

Total PGE contents range between 7 and 21 ppb regardless of location. Ir-type PGEs are overall high, 5-12 ppb, which confirms the residual mantle nature of the xenoliths. The ratio of Ir- and Pd-type PGEs varies between 0.83 and 2.83. Os/Ir ratios in xenoliths from Styrian and East-Tranylvanian basins are slightly below the chondritic ratio, whereas those from Bakony—Balaton-Highland are above the chondritic value. Ru/Ir is ca. 30 % higher than the chondritic value in the majority of xenoliths from Styrian and East-Transylvanian basins. In contrast, xenoliths from the Bakony—Balaton-Highland show chondritic Ru/Ir, except xenoliths most strongly depleted in Al. These PGE ratios do not show correlations with Al. Pt and Pd contents and their ratios with Ir-type PGEs correlated with Al, as expected, due to incompatible nature of Pt and Pd during partial melting in the Bakony—Balaton-Highland xenoliths, which have the widest range in Al contents. In situ PGE analyses on sulfide grains (mss, chalcopyrite and pentlandite) show positive correlations of Os, Ir, Ru and Rh, except in sulfides from the Bakony—Balaton-Highland and some sulfides from Nógrád-Gömör and East-Transylvania, whereas Pt and Pd correlate poorly with the Ir-type PGEs. The total concentrations of PGEs range between 4 and 796 ppm. The majority of the PGE patterns show high and variable abundances of Os, Ir, Ru and Rh, with decreasing abundance from Rh to Au and a strong negative Pt anomaly. Sulfides in xenoliths from the Bakony—Balaton-Highland, being basically mss, show a smooth negatively sloped PGE pattern from Os to Au.

Whole-rock and in situ sulfide grain analyses demonstrate that the upper mantle beneath the CPR shows a district-scale variation in PGE abundances. Although the xenoliths show no evidence for modal metasomatism, the variation can be explained by different degrees of partial melting and cryptic metasomatism.

https://doi.org/10.1180/S0026461X00008434 Published online by Cambridge University Press

Complex calc-alkaline volcanism recorded in Mesoarchaean supracrustal belts in SW Greenland

KRISTOFFER SZILAS[1*], J. ELIS HOFFMANN[3] AND ANDERS SCHERSTÉN[4]

[1]Geological Survey of Denmark and Greenland - GEUS, Copenhagen, Denmark ksz@geus.dk (* presenting author)
[2]Steinmann Institut, Abt. Endogene Prozesse, Universität Bonn, Germany hoffjoel@uni-bonn.de
[3]Department of Geology, Lund University, Sweden anders.schersten@geol.lu.se

Abstract

In this geochemical study we investigate the petrogenesis of three Mesoarchaean co-magmatic supracrustal belts (Ravns Storø, Bjørnesund and Perserajoorsuaq) situated in southern West Greenland. They comprise mainly amphibolites with a tholeiitic basaltic composition and leucoamphibolites with a calc-alkaline andesitic composition. Both lithological units are cut by aplite sheets of tonalite-trondhjemite-granodiorite (TTG) composition with U-Pb zircon ages of c. 2900 Ma. Lu-Hf and Sm-Nd isochrons based on whole rock samples yield ages of 2990 ±41 Ma and 3020 ±78 Ma, respectively. Leucoamphibolites from the three supracrustal belts show apparent chemical mixing trends between tholeiitic amphibolites and TTG gneisses end-members. By assimilation-fractional-crystallisation (AFC) modelling we can show that one group of leucoamphibolites can be explained by contamination of the parental melts by a TTG-like end-member and another group of high P_2O_5, La and Nb leucoamphibolites can be explained by contamination involving a hypothetical low-silica adakite (slab-melt) end-member. However, the leucoamphibolites are juvenile with $\varepsilon Nd_{(2970Ma)}$ from +2.1 to +3.5 and $\varepsilon Hf_{(2970Ma)}$ of +3.5 to +4.3. Thus, the mafic source of the felsic contaminant melts must have been derived from a depleted mantle source more or less at the same time (<60 Ma) as the volcanism took place. Contamination by older continental crust is not a viable explaining of the data.

Accordingly, our preferred interpretation of the geochemical and isotopic data is that the protoliths of the supracrustal rocks formed in an island arc setting, where early tholeiitic volcanism gave way to calc-alkaline volcanism in a maturing island arc. The apparent AFC trends are best explained by in-situ partial melting of basaltic arc crust to form juvenile TTG- and adakite-melts that mixed with mafic magmas or contaminated their mantle source to produce the calc-alkaline leucoamphibolite protolith. This model has important implications for the general interpretation of other Archaean supracrustal belts, because AFC and chemical mixing trends towards a TTG-like end-member are not uniquely diagnostic of crustal contamination, but may rather reflect processes operating at source levels in volcanic arcs such as melting-assimilation-storage-homogenisation (MASH) or slab-melt metasomatism of their mantle source. This study strongly argues for the operation of uniformitarian subduction zone processes as far back as at least 3000 Ma.

Understanding the formation and properties of Titan's aerosols with the PAMPRE laboratory experiment

C. SZOPA[1*], N. CARRASCO[1], J.J. CORREIA[1], E. HADAMCIK[1], P.R. DAHOO[1], T. GAUTIER[1], A. MAHJOUB[1], J. HE[2], A. BUCH[2], AND G. CERNOGORA[1]

[1]LATMOS, Univ. Pierre & Marie Curie Paris 6 and Univ. Versailles St Quentin, UMR CNRS 8190, IPSL, Paris, France, cyril.szopa@lamtos.ipsl.fr (* presenting author), nathalie.carrasco@lamtos.ipsl.fr, correia@lamtos.ipsl.fr, edith.hadamcik@lamtos.ipsl.fr, prd@lamtos.ipsl.fr, thomas.gautier@lamtos.ipsl.fr, ahmed.mahjoub@lamtos.ipsl.fr, guy.cernogora@lamtos.ipsl.fr
[2]Ecole Centrale Paris, Chatenay Malabry, France, arnaud.buch@ecp.fr, jing.he@ecp.fr

Type Section Heading Here [bold, 9pt font size]

In order to support the treatment and interpretation of data collected by the Cassini and Huygens instrumentation, our team developped in 2004 a laboratory experiment based on a radio-frequency reactive plasma to produce analogues of Titan's aerosols (or "tholins"). This experiment, named PAMPRE, enables to produce tholins under variable controlled conditions compatible with the present and past Titan's upper atmosphere ones. The originality of PAMPRE, compared with other experimental set-ups used to porduce tholins, comes from its capability to generate and maintain the tholins inside the plasma without any wall effects. This specificity thus allows to study the tholins production and growth directly in situ by using the appropriate analytical diagnostics.

The studies we do with PAMPRE can be shared in four distinct actions:

1. Study the physical and chemical properties of tholins. This part is originally the most important one since it is partly dedicated to produce reference data which can be compared with observational data. We also study the influence of the production conditions on the tholins properties to better understand the context in which Titan's aerosols can be produced.
2. Characterize the plasma chemistry in order to constrain the chemical pathways leading to the production of solid organic particles directly from the gaseous phase. This part is obviously correlated to the chemistry that occurs in Titan's atmosphere to generate the aerosols.
3. Characterize the physicla properties of the plasma. This original task is very important to understand the influence the context in which the tholins are produced in the experimental set-up. This makes easier the transposal of our results obtain in laboratory to the Titan's atmosphere.
4. More recently we started the study of the evolution in time of Titan's tholins we produce in the context of Titan's geological times.

The goal of this paper is to present an overview of results obtained in the different branches of study of Titan's tholins with the PAMPRE experiment, with an emphasize on the most recent ones.

https://doi.org/10.1180/S0026461X00008434 Published online by Cambridge University Press

Fluxes of sulfide-derived sulfate in the Rio Grande valley

ANNA SZYNKIEWICZ[1*], DAVID M. BORROK[1] AND DAVID VANIMAN[2]

[1]University of Texas at El Paso, Geological Sciences, El Paso TX, USA, aaszynkiewicz@utep.edu (* presenting author), dborrok@utep.edu

[2]Planetary Science Institute, Tuscon AZ, USA, dvaniman@psi.edu

Sulfide oxidation is an important weathering pathway in surface environments. However, few data are available to address the contributions and fluxes of sulfide-derived SO_4^{2-} in hydrologic systems. In order to better understand this process, we measured the seasonal fluxes of SO_4^{2-} and the $\delta^{34}S$-$\delta^{18}O$ of riverine SO_4^{2-} as well as sulfate-rich salt efflorescenses in three watersheds connected to the upper Rio Grande valley. In this region, the $\delta^{34}S$ of hydrothermal and biogenic sedimentary sulfides differ by 20-30 ‰ compared to S from evaporites. Therefore, the contribution and fluxes of sulfide-derived SO_4^{2-} can be estimated using S isotope mass balance constraints.

In the Red River, a small tributary to the Rio Grande within the Taos Plateau in northern New Mexico, sulfide-rich mineralization in the form of hydrothermal veins and disseminated pyrite undergoes oxidation in natural alteration scars and abandoned mine waste piles. In April and August of 2010, the measured $\delta^{34}S$ and $\delta^{18}O$ of riverine SO_4^{2-} varied from -2.5 to +1.3 ‰ and from -7.1 to -4.0 ‰, respectively. These variations were consistent with the previously reported $\delta^{34}S$ of pyrite (-13.6 to +2.7 %), and the $\delta^{34}S$ and $\delta^{18}O$ values of gypsum/jarosite (-12.1 to +2.6 ‰ and -9.3 to +3.1 ‰) formed by surface oxidation of hydrothermal sulfides. In the Red River valley, nearly 100 % of aqueous SO_4^{2-} appears to be sourced by sulfide oxidation. The measured flux of sulfide-derived SO_4^{2-} was higher during the snowmelt in April (19.3 tons/day) compared to baseflow conditions in August (15.2 tons/day).

In the Rio Chama and Rio Puerco, tributaries to the Rio Grande in western and central New Mexico, sulfides occur as biogenic pyrite in Cretaceous shale and coal formations. Sulfate-rich salt efflorescences are common weathering products in surface outcrops of these formations. Analysis by X-ray diffraction shows that these are largely Mg, Na, and Ca sulfates (e.g., starkeyite or hexahydrite, thenardite, and gypsum) and $\delta^{34}S$ analyses indicate that the sulfate in these phases formed by sulfide oxidation. Between 2009 and 2011, the contribution of sulfide-derived SO_4^{2-} to the total S load varied widely in the Rio Chama (from 48 to 95 %). S isotopes indicated mixing of SO_4^{2-} from the dissolution of salt efflorescence (-25.2 to -9.5 ‰) and Jurassic evaporites (+15.1 to +17.7 ‰). In the lower reaches of the Rio Chama, the fluxes of sulfide-derived SO_4^{2-} varied widely between Nov 2009 (10.5 tons/day) and Apr 2010 (134.3 tons/day). These variations, however, were to some degree controlled by water releases from upstream reservoirs. Similar contributions of sulfide-derived SO_4^{2-} were calculated for the semi-arid Rio Puerco (68 % of the total S load) during the snow melt season. Because less water is available in the Rio Puerco, the fluxes of sulfide-derived SO_4^{2-} were significantly lower (~3.8 tons/day) compared to the Rio Chama. This investigation indicates that much of the SO_4^{2-} (>50 %) in the upper Rio Grande valley is derived from sulfide oxidation in the surrounding watersheds.

https://doi.org/10.1180/S0026461X00008434 Published online by Cambridge University Press

Possible source of iron-60 in the early solar system based on recent estimates of its initial abundance

SHOGO TACHIBANA*

[1]Department of Earth and Planetary Science, The University of Tokyo, Hongo, Tokyo, Japan.
tachi@eps.s.u-tokyo.ac.jp (* presenting author)

The former presence of short-lived radionuclides (SLRs) in the early solar system (^{10}Be, ^{26}Al, ^{36}Cl, ^{41}Ca, ^{53}Mn, ^{60}Fe, ^{107}Pd, ^{129}I, and ^{182}Hf) has been inferred from excesses in the abundances of their daughter nuclides in meteorites, which are linearly correlated with the abundance of a parent element. The SLRs with half-lives ($\tau_{1/2}$) shorter than 5 million years (Myrs) could have been produced either by energetic-particle irradiation in the early solar system or by stellar nucleosynthesis just prior to or shortly after the birth of the solar system. Iron-60 ($\tau_{1/2}$=2.62 Myrs [1]) is effectively formed only by stellar nucleosynthesis, and its initial abundance in the early solar system could constrain the birth environment of the solar system. It has been found that ion microprobe studies on ^{60}Fe in the solar system [2-5] overestimated its initial abundance due to statistical bias for data reduction [6]. Recent studies using MC-ICPMS and MC-TIMS have shown that the initial abundance of ^{60}Fe in the solar system, $(^{60}Fe/^{56}Fe)_0$, could be as low as 10^{-8} [7-13], which could be comparable or lower than the galactic background. However, recent ion microprobe analyses with a proper data reduction method showed that there are chondrules with solid evidence of live ^{60}Fe and that the inferred initial ratio is in the range of $(3\text{-}5)\times10^{-7}$ [14].

These recent findings imply either that the initial abundance of ^{60}Fe in the solar system could be ~10^{-8} [10, 11] or that ^{60}Fe was heterogeneously distributed in the early solar system [9, 12, 14]. In this talk, I will discuss a possible source of ^{60}Fe in the early solar system and the birth environment of the solar system based on recent estimates of the abundance and distribution of ^{60}Fe in the solar system.

[1] Rugel G. et al. (2009) *Phys. Rev. Lett.* **103,** 072502. [2] Tachibana S. and Huss G. R. (2003) *Astrophys. J.* **588,** L41-L44. [3] Mostefaoui S. et al. (2005) *Astrophys. J.* **625,** 271-277. [4] Tachibana S. et al. (2006) *Astrophys. J.* **639,** L87-L90. [5] Mishra R. K. et al. (2010) *Astrophys, J.* **714,** L217-L221. [6] Ogliore R. C. et al. (2011) *Nucl. Instrum. Methods. Phys. Res. B* **269,** 1910-1918. [7] Regelous M. et al. *EPSL* **272,** 330-338. [8] Chen J. H. (2009) *GCA* **71,** 1461-1471. [9] Quitté G. et al. (2010) *Astrophys. J.* **720,** 1215–1224. [10] Tang H. and Dauphas N. (2011) *Workshop on Formation of the First Solids in the Solar System* #9146 (abstr.). [11] Wadhwa M. et al. (2011) *Workshop on Formation of the First Solids in the Solar System* #9132 (abstr.). [12] Quitté G. et al. (2011) *GCA* **75,** 7698-7706. [13] Moynier F. et al., *Astrophys. J.* **741,** 71-76. [14] Telus M. et al. (2011) *Workshop on Formation of the First Solids in the Solar System* #9127 (abstr.).

Distribution of neodymium in sedimentary planktonic foraminiferal tests and associated mineral phases obtained by NanoSIMS

KAZUYO TACHIKAWA[1]*, TAKASHI TOYOFUKU[2], ISABELLE BASILE-DOELSCH[1], AND THOMAS DELHAYEC[3]

[1]CEREGE, Aix-Marseille Univ, CNRS, IRD, Technopole de l'Arbois, BP 80, 13545 Aix en Provence, France (*correspondance: kazuyo@cerege.fr)

[2] Institute of Biogeosciences (BioGeos) JAMSTEC, Yokosuka, Japan

[3]Université de Rennes 1, Campus de Beaulieu, Batiment 24, Salle 006 (NB:Case 2401 pour courrier) 263 Avenue du General Leclerc CS 74205 35042 RENNES CEDEX, France

Type Section Heading Here [bold, 9pt font size]

Neodymium isotopic ratios recorded in calcareous foraminiferal tests and associated authigenic minerals have been used to trace past water masses although exact origin of preserved Nd signals is still a matter of debate [1-3]. We determined, for the first time, Nd distribution in two species of planktonic foraminifera (*Globigerinoides ruber* and *Neoquadorina dutertrei*) and coexisting authigenic minerals from a marine sediment core in the Panama Basin. Elemental mapping of Nd, Ca, Fe, Mn, and Si was performed using NanoSIMS and electron probe microanalysis (EPMA) for uncleaned tests from two selected time slices (15.6 kyr and 129 kyr) together with Scanning Electron Microprobe (SEM) imagery. EPMA and SEM images indicate the existence of Fe-rich framboidal minerals inside of test pores and inner chambers, in particular for the older samples. This phase is estimated to be pyrite. The younger sample presents also Fe and Mn-rich patches on the inner test wall that is evaluated to be Mn-Fe oxides. Neodymium intensity in Fe-Mn oxides and oxidized pyrite is much higher than in foraminiferal calcite. For all analyzed samples, Nd distribution in foraminiferal tests is randomly heterogeneous with no systematic feature such as Nd-rich layer, species-specific difference, and primary calcite and crust. Relationship between Nd and Fe, and between Nd and Mn reveals that the most efficient Nd carrier is oxidized pyrites, possibly Fe oxy-hydroxides. This suggests a central role of Fe minerals to Nd cycle during diagenesis. Since Nd related to the authigenic precipitates reflects pore water signal (a mixture of scavenged, bottom water and soluble fraction from bulk sediments), conflicting origin of Nd isotopic signals from sedimentary foraminiferal tests could be at least partly explained by contribution of pore water-derived Nd.

[1] Elmore *et al*. (2011) *Geochem. Geophys. Geosyst*. **12(9)**, Q09008. [2] Roberts *et al*. (2010) *Science* **327(5961)**, 75-78. [3] Vance *et al.* (2004) *Paleoceanography* **19(PA2009)** doi:10.1029/2003PA000957.

https://doi.org/10.1180/S0026461X00008434 Published online by Cambridge University Press

Ediacaran carbon isotope anomaly records shallow marine event, not entire ocean

MIYUKI TAHATA[1]*, YUICHIRO UENO[1], YUSUKE SAWAKI[2], RYOHEI KIKUMOTO[1], MANABU NISHIZAWA[2], TSUYOSHI KOMIYA[3], NAOHIRO YOSHIDA[4], SHIGENORI MARUYAMA[1]

[1]Tokyo Institute of Technology, Tokyo, Japan. tahata.m.aa@m.titech.ac.jp
[2]Jamstec, Kanagawa, Japan
[3]The University of Tokyo, Tokyo, Japan
[4]Tokyo Institute of Technology, Kanagawa, Japan

The Ediacaran is one of the most important periods in the history of life when multicellular animals firstly appeared on the earth. However, we still poorly understand the relationship between the abrupt biological evolution and environmental change. Ediacaran sections record the largest $d^{13}C$ arnomaly through the Earth's history, named Shuram excursion [1, 2] . The observed excursion may reflect extensive remineralization of large organic matter in the Ediacaran ocean [2, 3], or merely the result of diagenetic alteration [4]. However, marine sediments must have been globally preconditioned in a unique way, to allow ordinary and local process to produce an extraordinary and widespread response [5]. We analyzed carbon and nitrogen isotopes by using drill core samples from four different depositional settings in South China: shallow marine Three Gorges and Weng'an sections, and deeper Tianping and Shiduping sections. The new results of deeper sections show high carbon isotope ratio and no negative excursion in spites of high spacial resolution. Weng'an section in shalow shelf also shows only smaller negative excursion (>-4‰) compare to that of Three Gorges section in another shallow marine setting. Thus, the limited appearance of the negative $d^{13}C$ excursion in shallow marine settings may suggest that extensive remineralization took place only in shallow part of the organic-carbon-rich Ediacaran ocean. Alternatively, shallow section preferentially suffered from diagenetic alteration possibly in response to sea-level fall, though the regressive trend is not evident. On the other hand, $d^{15}N_{TN}$ in Three Gorges shows long-term gradual decrease from the Shuram excursion to early Cambrian, which may rather reflect change in long-term oceanic signal.

[1] Calver (2000) *Precambrian Research* **100**, 121-150. [2] Fike (2006) *Nature* **444**, 744-747. [3] Rothman (2003) *PNAS* **100**, 8124-8129. [4] Knauth (2009) *Nature* **460**, 728-732. [5] Grotzinger (1995) *Science* **270**, 598-604.

Elemental partitioning and Eu^{2+}/Eu^{3+} XANES calibration between synthetic KREEP basalt, apatite, and whitlockite vs. T and f_{O_2}

N.D. TAILBY[1,2*], D. TRAIL[1,2] AND E.B. WATSON[1,2]

[1]Department of Earth and Environmental Sciences, Rensselaer Polytechnic Institute, Troy, NY, USA.
[2]New York Center for Astrobiology, Rensselaer Polytechnic Institute, Troy, NY, USA.
*tailbn@rpi.edu (presenting author)

Apatite, a common accessory phase found in a broad range of rock types, is known to host a number of important trace elements (U, Th, REEs, Sr, etc). The purpose of this research is to synthesize and equilibrate apatite from KREEP analogue melts as a function of temperature (T) and oxygen fugacity (f_{O_2}) in order to calibrate an apatite crystallization redox sensor.

The experimental method incorporates the use of seven different solid-state media buffers (ranging from -magnetite-hematite to graphite-CO-CO_2, representing ($\Delta f_{O_2} \approx 12$ log units) contained within evacuated silica tubes to control f_{O_2}. KREEP glasses are artificially doped with P_2O_5 to ensure apatite saturation [1-2] and enriched in REE (including La, Ce, Sm, Eu, Gd and Lu) in order ensure cocentrations sufficient for x-ray analysis (including EPMA and XANES). Experiments are carried out at 1000 – 1175 ˚C, incorporating conditions ranging from subsolidus to near-liquidus. Crystalline phases co-existing with apatite include olivine, plagioglase and whitlockite.

As indicated in a number of previous works [e.g., 3-4] the spectral components comprising the Eu L_3 XANES region are sensitive to $Eu^{3+}/\Sigma Eu$. Experimental results here show systematic increases from almost no Eu^{2+} in apatite at NNO to almost 45% Eu^{2+} at the graphite-CO-CO_2 buffer. Similar changes in $Eu^{3+}/\Sigma Eu$ are seen the synthetic glasses, thus indicating that Eu valence behaviour can be used as a valence or redox sensor for basaltic source melts that exist at low f_{O_2} (relative to terrestrial environments).

REE partitioning results for apatite (and where possible, whitlockite) are similar to those previously reported within the literature [5], indicating equilibria. The combined results of partitioning and XANES provide the first experimental constraint on redox sensitive geochemical processes that control trace element systematics within phosphates.

[1] Watson (1979) *Geophys . Res. Lett.* **6**, 937-940. [2] Watson (1980) *Earth Planet. Sci. Lett.* **51**, 322-335. [3] Rakovan *et al.* (2001) *Am. Mineral.* **86**, 697-700. [4] Shearer *et al.* (2011) *Am. Mineral.* **96**, 1418-1421. [5] Watson and Green (1981) *Earth Planet. Sci. Lett.* **56**, 405-421.

https://doi.org/10.1180/S0026461X00008434 Published online by Cambridge University Press

Grain scale pressure heterogeneity produced through volume change associated with mineral reaction

TAJČMANOVÁ L.[1], POWELL R.[2], PODLADCHIKOV Y.[3], VRIJMOED J.[3] AND MOULAS E.[1]

[1]Department of Earth Sciences, ETH Zurich, Switzerland, lucataj@gmail.com (* presenting author)
[2] School of Earth Sciences, University of Melbourne, Vic. 3010, Australia
[3]Department of Earth Sciences, University of Lausanne, Switzerland

Recent work on melting, corona textures and phase precipitation developed in high metamorphic-grade rocks has focused on the chemical potential relationships that account qualitatively for the spatial and chemical relationships involved. There are two related ways in which this work can be advanced. The first involves using or devising diffusion coefficients to move towards quantitative modelling. The second, more critical step is to realize that mineral reaction cannot take place independently of the strength of its immediate environment. We will consider various aspects of this, on the basis that the diffusional relaxation modifies the elastic state of the material and affects its mechanical properties. As the induced stress may have a profound effect on diffusion in a solid, the elastic and chemical response of the material must be taken into account simultaneously. In geomaterials, only limited information exists on reactions that involve chemical transport combined with reaction-induced stress, but the mechanical feedback of volume change that is involved in chemical reaction in rocks may significantly control the progress of reaction. Pressure variations that existed at the grain scale during decompression and cooling of higher-pressure rocks are likely to have influenced the final microstructure. Our data based on numerical modelling show that pressure variations may be generated and maintained on a geological time scale as a result of the mechanical feedback of the rock during metamorphic reactions which take place in a restricted space.

Decrease of the potential of oxalic acid and other organic acid aerosols as cloud condensation nuclei by the complex formation with metal ions

YOSHIO TAKAHASHI AND TAKEMA FURUKAWA*

[1]Hiroshima University, ytakaha@hiroshima-u.ac.jp

Secondary organic aerosols (SOA) play a key role on the solar radiation balance in troposphere, since SOA can act as cloud condensation nuclei (CCN) due to its high hygroscopic nature. Oxalic acid is one of the most dominant components of SOA, which has cooling effects of the earth by acting as CCN. However, it is uncertain whether the oxalic acid can exist as free oxalic acid or metal-oxalate complexes in aerosols, even if there is a largedifference in their solubilities into water. Consequently, XAFS measurement was conducted to demonstrate the presence of metal-oxalate complexes.

Size fractionated aerosol samples were collected in Tsukuba (located at northeast about 60 km from Tokyo) using a low-volume Andersen-type air sampler. The sampler had eight stages and a back-up filter. The sampling was conducted during winter and summer in 2002.

Calcium oxalate was observed in finer particles in each period from Ca K-edge XANES, and its fractions among total Ca were approximately 20%. Similarly,, Zn oxalate was also detected in finer particles from Zn K-edge XANES and EXAFS. The [Zn-oxalate] / [Zn]total ratio in each period clearly increased with the decrease in the particle diameter. This result revealed that Zn-oxalate was formed in the aqueous phase at particle surfaces or in cloud processing. In other words, Zn-oxalate was abundant at the particle surface, resulting from the increase in the [surface]/[bulk] ratio with decreasing particle size. Based on (i) total concentrations of oxalate, Ca, and Zn determined by ion-chromatography and ICP-AES analyses and (ii) Ca- and Zn- oxalate fractions obtained by XAFS, we determined the fraction of metal-oxalate complexes among total oxalate in aerosols. In winter, Ca- and Zn- oxalate fractions reached about 60% of total oxalate in the ranges of 1.1-2.1 μm and 0.65-1.1 μm, while the value was about 60-80% in the same particle size range in summer. On the other hand, Ca- and Zn-oxalates are highly insoluble, showing that the complexes cannot act as CCN. Therefore, the ability of oxalic acid as CCN is needed to be reconsidered, because most of oxalic acid in aerosols exists as metal-oxalate complexes as shown by XAFS spectroscopy in this study. Moreover, the formation of stable metal-oxalate complexes at particle surface can inhibit the chance of the particle's activation to produce other chemical species.

References

[1] T. Furukawa and Y. Takahashi, 2011. Atom. Chem. Phys., 11, 4289-4301.

https://doi.org/10.1180/S0026461X00008434 Published online by Cambridge University Press

Primitive Submarine Basalts and Three Primary Magma Types from Pagan, Mariana arc

YOSHIHIKO TAMURA[1]*, OSAMU ISHIZUKA[2], ROBERT J. STERN[3], AKIKO NUNOKAWA[1], HIROSHI SHUKUNO[1], HIROSHI KAWABATA[1], ROBERT W. EMBLEY[4], SHERMAN BLOOMER[5], ALEX NICHOLS[1] AND YOSHIYUKI TATSUMI[1]

[1] IFREE, JAMSTEC, Yokosuka, Japan, tamuray@jamstec.go.jp (* presenting author)
[2] GSJ/AIST, Tsukuba, Japan, o-ishizuka@aist.go.jp
[3] U. Texas at Dallas, Richardson, USA, rjstern@utdallas.edu
[4] NOAA, Newport, USA, robert.w.embley@noaa.gov
[5] OSU, Corvallis, USA, Sherman.Bloomer@oregonstate.edu

Primitive Basalts from the Mariana Volcanic Front

Pagan is an active volcano located in the volcanic front of the central Island Province of the Mariana arc (18°07'N) and is one of the largest volcanoes in the Mariana arc; its main edifice rises from a base ~3,000 m below sea level and has a volume of 2,160 km^3 [1]. Tamura et al. (2011) demonstrate the existence of near-primitive, phenocryst-poor lavas at NW Rota-1 volcano in the Mariana arc, which is located about 40 km west of the volcanic front. These magnesiana basalts are petrographically distinct cpx-olivine basalt (COB) and plagioclase-olivine basalts (POB) [2].

The active Pagan volcano has erupted near-primitive lavas on its submarine flanks. The least fractionated compositions recovered from the NE flank (HPD1147) extend to higher MgO (7-11 wt %) and Mg# (60-70), than have ever been sampled from Pagan island lavas.

The Fo contents of olivine (up to Fo_{94}) and Cr-number of spinels (up to 0.8) suggest that these magmas formed from high degrees of mantle melting. There are three geochemical groups of cpx-olivine basalt (COB1, COB2 and COB3). TiO_2, Na_2O, K_2O, Rb, Nb are lowest in COB1 and highest in COB3. COB3 have steeper LREE-enriched patterns but the REE patterns of COB1 show contrasting LREE-depleted patterns, suggesting that COB1 formed from higher degrees of mantle melting. On the other hand, COB1 have the highest Ba/Th ratios and COB3 have the lowest, suggesting that a shallow subduction component is more important for COB1 than COB3, with COB2 intermediate. COB1, COB2 and COB3 show a negative trend on the Ba/Nb-Nb/Yb diagram (Fig. 1), suggesting that greater subduction components resulted in larger degrees of melting.

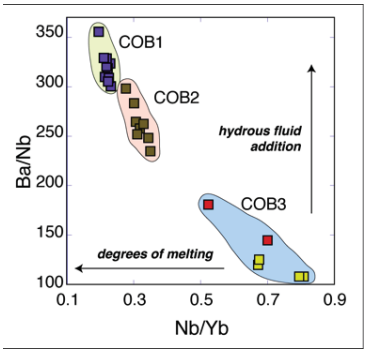

Figure 1: Ba/Nb vs Nb/Yb. The higher Ba/Nb of the COB1 indicate that the COB1 contain greater abundances of slab-derived subduction components than the COB2 and COB3. Nb/Yb suggests that the degree of melting of the COB1 source is higher than for the COB2 and COB3.

[1] Bloomer *et al.* (1989) *Bulletin of Volcanology* **51,** 210-224.
[2] Tamura *et al.* (2011) *Journal of Petrology* **52**, 1143-1183.

Modeling U(VI) reduction in a field test with Emusified Vegetable Oil (EVO) as the electron donor

G. TANG[1*], D.B. WATSON[1], W.-M. WU[2], C.W. SCHADT[1], J. C. PARKER[3], AND S.C. BROOKS[1]

[1]Environmental Sciences Division, Oak Ridge National Laboratory, Oak Ridge, TN 37831, USA, tangg@ornl.gov(*), watsondb@ornl.gov, schadtcw@ornl.gov, brookssc@ornl.gov
[2]Department of Civil and Environmental Engineering, Stanford University, Stanford, California 94305, USA, billwu@stanford.edu
[3]Department of Civil and Environmental Engineering, University of Tennessee, 62 Perkins Hall, Knoxville, Tennessee 37996, USA, jparker@utk.edu

A one-time 2-hour EVO injection in a fast flowing aquifer resulted in decreased U(VI) flux to an surface stream for over a year. A model was developed to couple EVO hydrolysis, production and oxidation of long-chain fatty acids (LCFA), glycerol, acetate and H_2, reduction of nitrate, Fe(III), U(VI) and sulfate, and methanogenesis with growth and decay of microbial functional groups. Literature values were used for U(VI) sorption and microbially-mediated reduction reactions with acetate and H_2. Microcosm test data were used to estimate hydrolysis, glycerol fermentation, and LCFA oxidation parameters. The model was implemented in PHT3D to model coupled processes in the field test.

The model approximately matched the observed aqueous acetate, nitrate, Fe, U (Figure 1), and sulfate concentrations, and decribed the trends of growth and decay of microbial functional groups. While the lab-determined parameters were generally applicable for the field-scale simulation, the hydrolysis rate constant was estimated to be an order of magnitude faster in the field than in the microcosms. Sulfate reducer biomass was predicted to accumulate near the injection wells and along the side boundaries of the treatment zone where electron donors (LCFA) and electron acceptors (sulfate) from the surrounding environment met. Consequently, biogenic U(IV) accumulation in these locations was predicted (Figure 2).

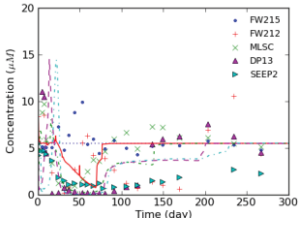

Figure 1 Observed (points) vs. calculated (curves) aqueous U(VI) concentrations

Figure 2. Predicted U(IV) distribution at 50 days

While EVO retention and hydrolysis characteristics were expected to control the treatment longevity, these modeling results indicated that electron acceptors such as sulfate not only compete for electrons but also may play a conducive role in degrading LCFA and enhancing U(VI) reduction and immobilization. The models could be useful for further research and bioremediation design.

https://doi.org/10.1180/S0026461X00008434 Published online by Cambridge University Press

Zn isotopes variation in field hyperaccumulator plant species

TANG YT.[1,2,3], CLOQUET C.[3*], STERCKEMAN T.[2], MOREL JL[2], CARIGNAN J.[4], QIU RL[1], ECHEVARRIA G[2]

[1]School of Environmental Science and Engineering, Sun Yat-sen University, Guangzhou, P.R.China, eestyt@googlemail.com
[2]LSE-INRA, Nancy, France, Thibault.Sterckeman@ensaia.inpl-nancy.fr
[3]CRPG-CNRS, Nancy, France, cloquet@crpg.cnrs-nancy.fr (* presenting author)
[4]Takuvik, CNRS-ULaval, Québec, Canada, Jean.Carignan@takuvik.ulaval.ca

Abstract

Stable Zn isotope signatures offer a potential tool to trace the mechanisms of Zn uptake and transfer within plant-soil system. In this study, we determined Zn isotopic compositions in three ecotypes of the Zn hyperaccumulator *Noccaea caerulescens* collected at a Zn-contaminated site (Viviez), a non-contaminated site (Ste Eulalie) and a serpentine site (Vosges) in France. The Zn-tolerant species *Silene vulgaris* collected from Viviez was also studied for comparison. While the δ^{66}Zn differentiated substantially among ecotypes, *N. caerulescens* exhibited a similar pattern with an enrichment in heavy Zn isotopes of 0.40–0.72‰ from soil to root, followed by a depletion in heavy Zn from root to stem (–0.05 to –0.31‰) and from stem to leaf (–0.05 to –0.22‰). The positive or negative shift of isotopes is probably attributed to the high ability of Zn accumulation and translocation in the hyperaccumulator, as δ^{66}Zn in *N. caerulescens* showed a significant and negative correlation with Zn concentration and bioconcentration factor. In *S. vulgaris*, however, the root was slightly depleted in heavy Zn with respect to soil, indicative of an ion-channel controlled diffusion into root cell under Zn excess conditions. The mass balance yields bulk Zn isotopic composition between plant and soil Zn $\Delta\delta^{66}Zn_{plant\text{-}soil}$ of –0.01‰ to 0.63‰ in *N. caerulescens* and –0.05‰ in *S. vulgaris*. We confirm that quantifying Zn stable isotopes is useful to study Zn accumulation pathways in plant and to document Zn status in media.

Cr(III) oxidation by biogenic maganese oxides

YUANZHI TANG*, COLLEEN M. HANSEL

School of Engineering and Applied Sciences, Harvard University, Cambridge, MA 02143, USA. ytang@seas.harvard.edu (*presenting author), hansel@seas.harvard.edu

Chromium (Cr) is a significant anthropogenic metal contaminant in soils and aquatic systems due to its widespread industrial applications. The toxicity and transport behavior of Cr depends strongly on its valence state. Cr(VI) compounds are typically soluble, mobile, bioaccessible, and are considered carcinogenic upon inhalation exposure. Cr(III) generally forms sparingly soluble (oxyhydr)oxides and is a essential micronutrient.

The redox transformation between Cr(III) and Cr(VI) in the environment is strongly mediated by (bio)geochemical reactions involving iron (Fe) and manganese (Mn) (oxyhydr)oxides, with Mn oxides (MnOx) being the only known natural oxidant of Cr(III). Understanding the impact of reaction conditions and MnOx structure are key for assessing the transport and fate of Cr. Given the much faster rate of microbially mediated Mn(II) oxidation as compared to solution or mineral-surface-catalyzed oxidation, MnOx are generally considered biogenic. However, most previous studies on the structural impacts of MnOx on Cr(III) oxidation were either limited because of the use of sythetic MnOx or complicated by the microbe species used, which required the presence of cells for MnOx production. Recent studies of *Roseobacter* sp. AzwK-3b, a bacterium that oxidizes Mn(II) through the production of extracellular superoxide and maintains oxidative activity in the cell-free filtrate[1,2], provides a good opportunity for studing the structure-reactivity relationship of biogenic MnOx toward Cr(III) oxidation.

In this study, we examined the roles of light, organics, pH, and structure of biogenic MnOx on Cr(III) oxidation. MnOx produced by the cell-free filtrate of *R.* AzwK-3b were aged in an organic-rich (K) medium for varied amounts of time under light or dark conditions, which induced structural change from a hexagonal birnessite phase to triclinic birnessite phase. MnOx with different structures were then reacted with Cr(III) at varied pH, concentration and time in K medium or artificial sea water (ASW) under light or dark conditions. Batch uptake results show that Cr(III) oxidation efficiency is highest at near neutral pH (7.2). With the same MnOx, under light conditions, the oxidation effiency is higher in the organic-rich medium than ASW. For fixed solution composition and varied MnOx age, a negative correlation is observed between the age of MnOx and oxidative reacitivity in the presence of organics and light, whereas no changes in reactivity is shown under ASW and dark conditions. These results strongly point to the role of photo-induced organic radicals. We propose that the Mn(II) produced from the oxidation of Cr(III) and reduction of MnOx is recycled in the system under organics and light conditions, and is responsible for the continuous oxidation of Cr(III). Ongoing structural analysis of the initial and reacted MnOx by synchrotron X-ray absorption spectrosocpy (XAS) will provide more insights on the reaction kinetics and mechanisms.

[1] Hansel (2006) *Appl. Environ. Microbiol.* **72**, 3543-3549.
[2] Learman (2011) *Nature Geoscience* **4**, 95-98.

https://doi.org/10.1180/S0026461X00008434 Published online by Cambridge University Press

Coseismic fluid-rock interaction in an active fault zone estimated from Sr speciation analysis of fault gauge

MASAHARU TANIMIZU[1,2*], TSUYOSHI ISHIKAWA[1,2], YOSHIO TAKAHASHI[2,1], WONN SOH[1], SHENG-RONG SONG[3]

[1]JAMSTEC, Nankoku, Japan, tanimizum@jamstec.go.jp
[2]Hiroshima Univ. Higashi-Hiroshima, Japan
[3]Natonal Taiwan Univ., Taipei, Taiwan

Chemical behavior of trace elements during fluid-rock interaction is generally estimated on the basis of the change in their concentration in solid or fluid phases. Changes in mineral phases associated with fluid-rock interactions are discussed based on the correlation with concentration changes of elements, but the trace element-hosting phases themselves have been identified scarcely by spectroscopic observation. This is because XRD analyses can detect only major mineral phases hosting major elements, and cannot applied to the host mineral phase estimation for trace elements.

In this presentation, we applied XAFS (X-ray Absorption Fine Structure) analysis to fault-gauge system to understand the behavior of elements related to the coseismic fluid-rock interactions. XAFS is a powerful spectroscopic tool to estimate chemical species of elements from local electron environment condition around the objective elements. The Chelungpu fault in Taiwan was selected for this purpose. The Taiwan Chelungpu-fault Drilling Project (TCDP) was undertaken after the the Chi-Chi earthquake (M7.6; 1999), and gauge samples were collected from three fault zones from 1100 m to 1300 m in depth from Hole-B core samples. Distinct changes observed in concentration for various trace elements at the center of the fault zone relative to the adjacent rocks are interpreted as a result of coseismic fluid-rock interactions at above 350 degrees centigrade [1]. For example, Sr concentration increased twice at the center of the fault zone with distinctly lowering $^{87}Sr/^{86}Sr$ ratio. The host mineral phase of Sr was estimated from XANES analysis of Sr, Ca, and S.

XANES spectra of Ca and S and literature data [2] suggested that potential host phase of Sr newly produced at the center of the fault zone is calcite, gypsum, and plagioclase. XANES spectra of Sr from the samples at the center of the fault zone were consistent with that of albite (sodic plagioclase) among the candidate minerals. The production of albite phase enriched in Sr indicates occurrence of high temperature fluid more than 250 degrees centigrade, which is consistent with the previous discussion [1] estimated from elemental concentration increase/decrease trends. Occurrence of such high-temperature fluids during the earthquake will play an important role to the fault weakening.

[1] Ishikawa (2008) *Nature Geosci.* **1**, 679-683. [2] You (1996) *Earth Planet. Sci. Lett.* **140**, 41-52.

Remediation of Heavy Metals in Nano-Materials

REBECCA TANNEY,[1*] KEON JEFFREY[1], MARIA ALFREDSSON[1]

[1]University of Kent, Canterbury, United Kingdom, rt274@kent.ac.uk

Remediation Techniques for Heavy Metals in Soil

Zeolites act as molecular sieves by crystallising in cage and channel structures. There are three proposed mechanisms that zeolites use to immobilise heavy metals; modification of the pH of the soil, sorption of metals onto mineral surfaces, and cation exchange process[1].

The aim of this project is to determine the effectiveness of zeolite-A to act as a remediation tool for lead and arsenic in contaminated soils.

Pyrite ash is a waste product from the production of sulphuric acid characterised as mostly iron oxides and silicate *nanoparticles*. The material contains high levels of arsenic and lead up to 15,000 and 24,000 mg/kg, respectively.

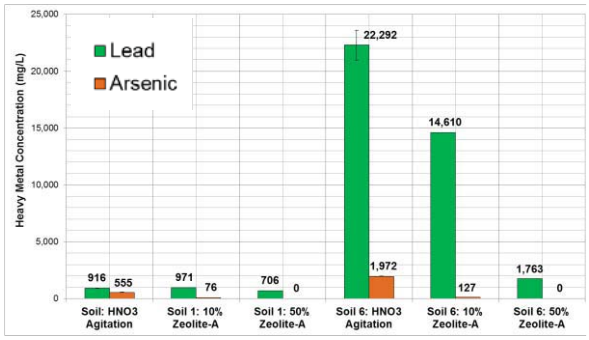

Figure 1 - Concentration of Soil Leachate following Remedial Action with Zeolite-A Additives at 10% and 50% Quantities Compared to Original Leachate Concentrations (mg/L)

Results and Conclusion

Zeolite-A has been found to give positive results as a remediation technique. Two soil samples, 1 and 6, were collected from a pyrite ash contaminated site. The particle size is around 100 nm, and the pH of the two samples are 1.8 and 5.5, respectively. It was found that zeolite-A more readily adsorbs arsenic rather than lead (see Figure 1).

A 10% weight dosage of zeolite-A successfully immobilised 86% of the arsenic in sample 1, and 93% from sample 6. A 50% dosage of zeolite-A removed 100% of the arsenic in both soil samples. Zeolite-A was found to be less efficient remediating lead, which showed using 10% zeolite-A, only 34% was removed.

Further experiments will be carried out using XRD, XRF, AAS, and SEM-EDX. We aim to fully understand the complexation and insertion mechanisms for lead and arsenic, and to determine the potential of zeolite-A as an affordable and accessible method of remediation.

[1] Shu, Shao, Li, Shao, and Du (2009) *J. Hazard. Mater.* **170**, 1-6.

https://doi.org/10.1180/S0026461X00008434 Published online by Cambridge University Press

Carbon fluxes beneath cratons: Insights from West Greenland kimberlites and carbonatites

S. TAPPE[1, 2*], K.A. SMART[2], A. STRACKE[2], R.L. ROMER[3], A. STEENFELT[4] AND K. MUEHLENBACHS[1]

[1]University of Alberta, Edmonton, Canada, tappe@ualberta.ca (*presenting author)
[2]Westfälische Wilhelms-Universität, Münster, Germany
[3]GeoForschungszentrum, Potsdam, Germany
[4]Geological Survey of Denmark and Greenland, Copenhagen, Denmark

Kimberlite and carbonatite magmas intruding cratonic lithosphere are considered the deepest probes into Earth's mantle. In this setting their co-existence is commonly interpreted to represent a primary melting sequence of carbonated peridotite at >150 km depths, possibly as deep as the transition zone. The carbon involved in this magmatism is thought to be either of primordial origin or derived from recycled subduced oceanic crust [1].

To better understand carbon fluxes beneath cratons and their role in the deep carbon cycle, we have studied kimberlite dyke swarms and associated carbonatite intrusions of the North Atlantic craton in West Greenland [2, 3]. Our new Nd-Hf-Pb isotope data suggest that both magma types were derived from a common convective upper mantle source. Moreover, the absence of hallmark recycled oceanic crust signatures such as highly radiogenic Pb and decoupled Nd-Hf isotope systematics are indicative of a primordial mantle origin of the carbon involved in Greenland kimberlite and carbonatite magmatism. Based on phase relationships and geochemistry, including carbon isotopes, we identify Greenland kimberlites as near-primary melts (-6 to -4‰ $\delta^{13}C$). The intrusive carbonatites (-4 to -2‰ $\delta^{13}C$), however, represent mixtures of cumulus crystals and liquid. The kimberlites and carbonatites appear to be linked by a two-stage fractionation process that commenced at uppermost mantle depths. First, liquidus olivine+phlogopite were removed from kimberlitic carbonate-silicate melts at high-T, leading to residual carbonate-rich melt fractions. Second, upon continued ascent into the cratonic crust and cooling, these carbonate-rich melts precipitated calcite+dolomite along with minor olivine+magnetite [2].

Rayleigh carbon isotope fractionation modelling suggests that 70-to-90 vol% of mantle-derived carbonate involved in this deep magmatism is now captured in the intrusive carbonatite bodies. Thus, it appears that CO_2 outgassing associated with kimberlite and carbonatite magmatic activity is volumetrically insignificant compared to global basaltic magmatism, and that carbonatite intrusions represent a major cache of primordial mantle carbon.

[1] Deines (2002) *Earth-Science Reviews* **58**, 247-278. [2] Tappe et al. (2009) *Lithos* **112**, 385-399. [3] Tappe et al. (2011) *EPSL* **305**, 235-248.

$^3He/^4He$ in volcanic and hydrothermal fluids of the Mexican subduction zone

YURI TARAN[1*] AND SALVATORE INGUAGGIATO[2]

[1]Institute of Geophysics, Universidad Nacional Autonoma de Mexico, taran@geofisica.unam.mx (* presenting author)
[2]INGV-Palermo, Italy, s.inguaggiato@pa.ingv.it

New and published data on $^3He/^4He$ in volcanic and hydrothermal fluids of Mexico are discussed in terms of the structure and geodynamics of the Mexican subduction zone that extends from the Gulf of California at ~ 22°N to Tacana volcano on the border with Guatemala and includes at least three apparently independent volcanic areas: a ~700 km-long Trans Mexican Volcanic Belt (TMVB), a short, ~150 km-long Chiapanecan Volcanic chain (CVC), and Tacana volcano that belongs to the Central America Volcanic Arc (CAVA). The TMVB is a volcanic front that originates from the subduction of two oceanic plates beneath the continent: a mini Rivera plate at north and the Cocos plate further to south. The subduction of the Cocos plate is also responsible for the CVC and Tacana volcanism. In spite of a complicated geometry of the TMVB, high-temperature hydrothermal fluids from deep wells and natural manifestations of four drilled geothermal fields along the TMVB (La Primavera, Los Azufres, Los Humeros and Acaculco) are characterized by high and uniform $^3He/^4He$ maximum values of 7.2Ra to 7.5Ra (Ra = $1.39x10^{-6}$, air $^3He/^4He$ ratio). Numerous thermal groundwater systems along TMVB discharge gases with a wide spectrum of $^3He/^4He$ ratios from 2 to 6Ra with higher values in the western part, close to the triple point of intersection of three rift-like structures: Chapala, Colima and Tepic-Zacoalco. El Chichon, the only active volcano of CVC is characterized by MORB-like $^3He/^4He$ values of 7.7Ra to 8.1Ra in the crater fumaroles, while in fumaroles and hot springs of the Tacana volcanic complex much lower values of <6.2Ra were measured. A high-temperature (850°C) fumarole of Colima volcano discharged gas with $^3He/^4He$ of 6.6Ra. Distribution of He isotopes adequately responses on the complex tectonic structure of the western part of TMVB together with the fore-arc area that includes Jalisco Block, a newly forming terrain originated from the present day complex tectonic mobility and bordered by Colima and Tepic-Zacoalco rifts and the Rivera plate subduction trench. He-isotopes clearly mark deep fault systems surrounding the Jalisco Block and shed light on the geometry of the Cocos-Rivera plate boundary close to the trench. $^3He/^4He$ anomalies in coastal thermal springs near Colima graben may be interpreted as being provided by a difference in the initial dip angle of the subduction and thus indicating a gap between plates and permeability for mantle He.

https://doi.org/10.1180/S0026461X00008434 Published online by Cambridge University Press

Chemical interpretation of mantle electrical heterogeneities in MORB source regions

PASCAL TARITS*[1], DAVID SIFRE[2], CECILE GRIGNE[1], MALCOLM MASSUYAU[2], LEILA HASHIM[2], SOPHIE HAUTOT[1], FABRICE GAILLARD[2]

[1] Domaines Océaniques, IUEM, Place Nicolas Copernic, F29280 Plouzané, France, tarits@univ-brest.fr (* presenting author)
[2] CNRS-INSU, Université d'Orléans, ISTO, UMR 7327, 45071, Orléans, France, gaillard@cnrs-orleans.fr

The electrical conductivity of mantle rocks being greatly affected by partial melting [1], the MELT magnetotelluric surveys have allowed major improvements in the knowledge of melt pathway, melt extraction and melt formation in MORB source regions [2]. The connection between electrical structure and melt chemistry remains however difficult to establish.

Here, analyses and interpretations of the MELT magnetotelluric data are discussed to infer the mantle structure down to the transition zone. Magnetotelluric response tensors inverted for a 3-D isotropic conductivity structure allows identification of strong electrical heterogeneities, with profils showing elevated conductivity from the transition zone up to depth where MORB are formed. Such conductive plumes are observed in the south and the north of the studied area, while the central zone is in contrast poorly conductive. The results suggest a fairly complicated scheme for melt migration under this portion of the EPR but it must reflect chemical heterogenities allowing volatile-rich low melt fractions [3] to wet peridotite grain boundaries along some profils whereas others regions remain 100% solids.

Based on new laboratory data on volatile-rich carbonated melts, we discuss these heterogeneities in terms of heterogenity in mantle redox state. Carbonated melts are stable and connected from the transition zone to the depth of MORB formation if redox conditions are sufficiently oxidizing [4]. Otherwise, diamond is stable and chemically enriched carbonated melts are not or poorly involved in MORB generation. This may generate chemical heterogenities in MORB.

[1] Caricchi *et al*. (2011) *Earth and Planetary Science Letters* **302**, 81-94. [2] Evans *et al*. (2005) Nature **437**, 249-252 [3] Gaillard *et al.* (2008) *Science* **322**, 1363-1365. [4] Stagno & Frost (2010) *Earth and Planetary Science Letters* **300**, 72-84.

Copper Partitioning in CO_2-Bearing Melt-Vapor-Brine Systems

BRIAN TATTITCH[1*], PHILIP CANDELA[1], PHILIP PICCOLI[1], ROBERT BODNAR[2], LUCA FEDELE[2]

[1]Laboratory for Mineral Deposits Research, University of Maryland, College Park, USA, bctatti@geol.umd.edu (*presenting author)
[2]Virginia Tech, Blacksburg, USA

Analysis of fluid and melt inclusions from arc-related intrusions and porphyry copper deposits (PCD) reveal that many fluid inclusions from PCD are typically characterized by $X_{CO2} < 0.10$, which is lower than that found in volatile phases exsolved from shallow (e.g., 5 to 10 km), arc magmas, in general (X_{CO2} up to order ~ 0.45). This disparity remains to be resolved.

The efficiency with which copper can be removed from arc magmas into exsolving volatile phases is a function of the competition between crystalline phases (± liquid sulphides), and the exsolving vapor ± brine. Experiments in melt-vapor-brine systems permit the investigation of the partitioning of copper between silicate melts and volatile phases under magmatic conditions. However, the effect of CO_2 on melt-volatile phase equilibria relevant to the formation of PCD has remained unconstrained. In this study, the partitioning of copper in CO_2-bearing, sulfur-free and sulfur-bearing, experiments may provide additional insights into copper partitioning and the generation of PCD.

We present results from experiments performed at 800 °C and 100 MPa in CO_2-bearing, sulfur-free and sulfur-bearing melt-vapor-brine systems with X_{CO2} (bulk vapor ± brine) = 0.10 and 0.38. The compositions of vapor and brine inclusions and run-product glasses were used as proxies for the compositions of the magmatic phases. The salinities of vapor inclusions that nucleated clathrate (CO_2 ± H_2S clathrate) upon cooling were determined via Raman analysis and microthermometry [1]. The partitioning of copper between brine and vapor ($D^{b/v}_{Cu}(\pm 2\sigma)$) increases from 25(±6) to 100 (±30) for sulfur-free experiments and from 11(±3) to 95(±23) for sulfur-bearing experiments, as X_{CO2} is increased from 0.10 to 0.38. The partitioning of copper between vapor and melt increases with the addition of sulfur at $X_{CO2} = 0.10$: ($D^{v/m}_{Cu}(\pm 2\sigma)$) = 9.6(±3.3) (sulfur-free, metaluminous melt); 18(±8) (sulfur-bearing, peralkaline melt); and 30(±11) (sulfur-bearing, metaluminous melt). These values are to be contrasted with ($D^{v/m}_{Cu}(\pm 2\sigma)$) = 2(±0.8) at $X_{CO2} = 0.38$ (the effect of sulfur cannot be distinguished at this mole fraction of CO_2). These data demonstrate that changes in the salinity of the vapor and brine, which are controlled by changes in X_{CO2}, play a major role in controlling copper partitioning in sulfur-free, CO_2-bearing systems. Sulfur-bearing experiments demonstrate that magmatic vapors are enriched in copper in the presence of sulfur at low X_{CO2}. However, the enrichment of copper in the magmatic vapor is suppressed for sulfur-bearing systems at high X_{CO2}. These data indicate that the efficient removal of copper from silicate melts into vapor ± brine is mitigated by high concentrations of CO_2. Furthermore, the poisoning effect of CO_2 is more pronounced for sulfur-bearing volatile phases. As a result, high concentrations of CO_2 may play a negative role in the formation of PCD.

[1] Fall et al. (2011) *Geochimica et Cosmochimica Acta* **75**, 951-964.

https://doi.org/10.1180/S0026461X00008434 Published online by Cambridge University Press

Variations of catchment P in stream water constrained by oxygen isotopes in phosphate

HEINRICH TAUBALD[1*], KARIN TONDERSKI[2], LOTTA ANDERSSON[3], AND RASMUS ROENNBERG[2]

[1]University of Tübingen, Isotope Geochemistry, 72074 Tübingen, Germany, taubald@uni-tuebingen.de (* presenting author)
[2]Linköping University, IFM Ecology, 58183 Linköping, Sweden, karsu@ifm.liu.se
[3]SMHI, 60176 Norrköping, Sweden, Lotta.Andersson@smhi.se

Introduction

We present oxygen isotope measurements (δ^{18}Op) on dissolved inorganic phosphate (DIP) from stream water (outflow of catchment), field drains and rural sewage/waste water to trace and quantify the contribution of different sources of P to the total P discharge from a catchment in South Sweden. Recent studies by Young et al. [1] proved that δ^{18}Op values can be an efficient tool to study sources and transport pathways for dissolved phosphate. A periodic sampling was performed between March 2009 and October 2011, sample handling, and isotope measurements were done similar to the procedures described by McLaughlin et al [2]. Due to significant concentrations of DOC activated carbon powder was added prior to filtering in order to remove organic matter (modified after Gruau et al. 2005 [3]).

Results and Conclusion

δ^{18}Op values of field drains vary from +8.0 to +15.7 ‰, sewage/waste water samples show δ^{18}Op values of +12.1 to +16.2 ‰, stream water at catchment outflow shows a seasonal variation between +10.3 and +15.8 ‰, the δ^{18}Ow of the ambient water ranges seasonally between -9.0 to -13.5 ‰, all values reported relative to V-SMOW2. δ^{18}Op values of sewage and waste waters as potential contaminants are in good agreement with recent data from Young et al [1]. A comparison of δ^{18}Op with δ^{18}Ow shows that most samples are not in oxygen isotope equilibrium, thus their δ^{18}Op probably reflects the isotope signature of the P source. Isotopic variations of field drains correlate with DIP concentrations and might reflect mixing processes with different waste and/or sewage sources. Covarations in isotopic signal and DIP concentrations in the stream water (catchment outflow) are also best explained by individual and possibly changing contributions from different P sources. Interestingly δ^{18}Op in stream water shows a seasonal signal, a phenomenon only recently observed by Angert et al. [4] for soil δ^{18}Op. Further detailed geological background informations and hydrological data in particular are necessary to fit these data into a model.

[1] Young et al. (2009) *Environ. Sci. Technol.*, **43**, 14, 5190-5196. [2] McLaughlin et al. (2004) *Limnol. Oceanogr. : Methods* **2**, 204-212. [3] Gruau et al. (2005) *Water Research*, **39**, 232-238. [4] Angert et al. (2011) *Geochimica Cosmochimica Acta*, **75**, 4216-4227.

3D Visualization of the Horne Hydrothermal System

B.E. TAYLOR[1*], E. DE KEMP[1], E. GRUNSKY[1], L. MARTIN[2], D. RIGG[3], J. GOUTIER[4], K. LAUZIÈRE[5] AND B. DUBÉ[5]

[1]Geological Survey of Canada, Ottawa, Canada, btaylor@nrcan.gc.ca (*presenting author)
[2]Xstrata Copper Canada, Timmins, Canada, Louismartin196@gmail.com
[3]Alexis Minerals, Toronto, Canada, david.rigg@alexisminerals.com
[4]Bureau de l'Exploration Géologique du Québec, Rouyn-Noranda, Canada, Jean.Goutier@mrnf.gouv.qc.ca
[5]Geological Survey of Canada, Québec, Canada, lauzier@gsc.nrcan.gc.ca, dube@gsc.nrcan.gc.ca

The hydrothermal architecture of the coeval Horne and Quemont deposits was visualized by 2D and 3D modelling using Kriging methods on a suite of whole-rock stable isotope and geochemical data. Hydro-thermal mapping integrated both surface and subsurface data: 416 δ^{18}O values (2.7 to 16.3‰), 4845 analyses of SiO_2, H_2O, MgO, Al_2O_3, S and wt.% H_2O, as well as SiO_2/Al_2O_3 ratios and REE data for intrusive and volcanic rocks. Zones of alteration about the steeply-dipping Horne deposit were mapped in 3D, to depths up to 2 km. The Quemont deposit is centered on the Powell pluton, which intruded into a volcanic-filled, caldera-type, or rift-graben structure, but the Andesite and Horne Creek Faults removed evidence of Horne-related up-flow zones and intrusions.

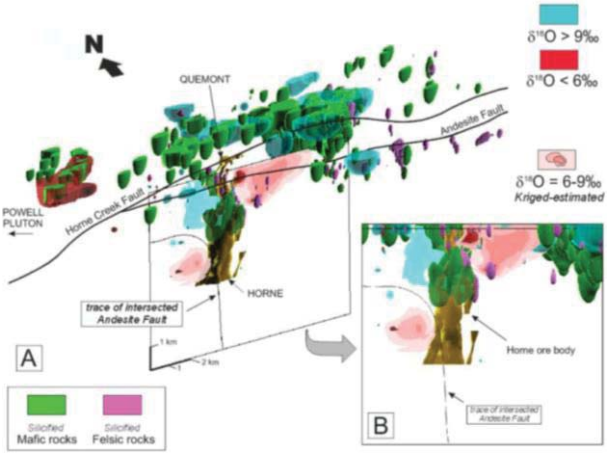

Figure 1: 3D model of the Horne hydrothermal system

Cooling of hydrothermal fluid by cold seawater in permeable rocks led to marked footwall silicification at the Horne deposit. Stratigraphic stability of the hydrothermal system may explain its large sulfide tonnage.

Separate magmatic hydrothermal systems influenced development of significant ore bodies in the area. Robust 2D and 3D data integration are needed to better understand these complex systems.

https://doi.org/10.1180/S0026461X00008434 Published online by Cambridge University Press

Microfocus X ray and laser fluorescence, analytical and mapping techniques, on heterogeneous minerals

R.P TAYLOR[1,2*], A.A. FINCH[1], J.F.W MOSSELMANS[2], P.D.QUINN[2]

[1]Dept. of Earth Sciences, St Andrews, KY16 9AL, U.K., * rpt5l@st-andrews.ac.uk

[2]Diamond Light Source, Didcot, OX11 0DE, U.K ountry, richard.taylor@diamond.ac.uk

Fluorescence is a highly sensitive phenomenon capable of detection at concentrations below PPM which is widely used. A recurring problem in mineralogical and petrological applications of fluorescence is that this sensitivity leads to the collected data representing a number of convoluted signals that make interpretation difficult. We present results from two complementary time resolved (TR) techniques Photo luminescence (PL) extensively used in biological applications as Fluorescence lifetime imaging microscopy. (FLIM) and TR X-ray Excited Optical Luminescence (XEOL) Results are presented from some obviously hetrogeneuos minerals and also examples from some with much less obvious heterogeneity. The (XEOL) is collected on the I18 microfocus beamline at the Diamond Light source. The system can be used to simutaneously collect X-ray Absorption spectra or X-ray flourescence (XRF) and simultaneuosly collect (CW) (XEOL), or (TR) (XEOL). This enables the combination of very high sensitivity with accurate quantification. Analysing the different decay lifetimes and ratios for a spatially resolved point emissions ~ 3/3 micron. Alows us to deconvolute the complex fluorescent signal. CW XEOL spectral data from 200-900nm collected from the same spatial resolution allows us to compare identified features with the literature. We also discuss mapping capabilities in both (XRF) and (CW) (XEOL) as either a function of either wavelength or incident photon energy.

Fluorescence intensity and lifetime map (figure1) collected from a Polished section of Microcline from the Derry Township Quebec The map is ~ 0.5µm square collected using a confocal (TR) multiphoton pulsed laser excitation

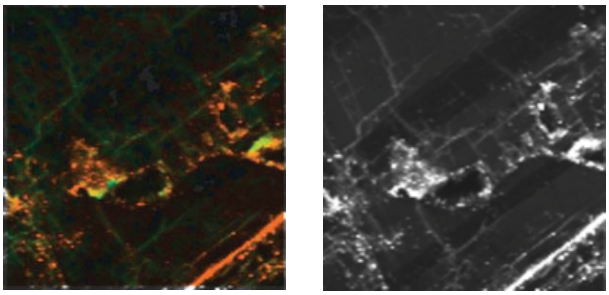

Figure 1: RHS luminesence intensity map LHS the same (TR) signal with deconvoluted lifetimes shown with false colour displaying the decay lifetime concentrations, deconvolution of complex multi component with signal red short lifetime blue long lifetime.

Accurate force fields built from ab-initio: the case of clays

SAMI TAZI*, MATHIEU SALANNE, BENJAMIN ROTENBERG AND PIERRE TURQ

UPMC Univ Paris 06, CNRS, ESPCI, UMR 7195 PECSA, F-75005 Paris, France
sami.tazi@upmc.fr (* presenting author)

Section heading

Molecular scale studies are essential for the prediction of sorption onto minerals such as clays, in particular in the context of the geological disposal of radioactive waste. The current state-of-the-art force field for clays, ClayFF [1], reproduces well several properties. However, it does not account for polarization, which is known to play an important role at solid liquid interface, in particular in influencing chemical specificity of cation sorption. We develop a polarisable force field for clays from DFT calculations, using on the one hand a force/dipole-fitting procedure, which provides a high degree of transferability [2], and on the other hand a systematic derivation using maximally localized Wannier functions [3].

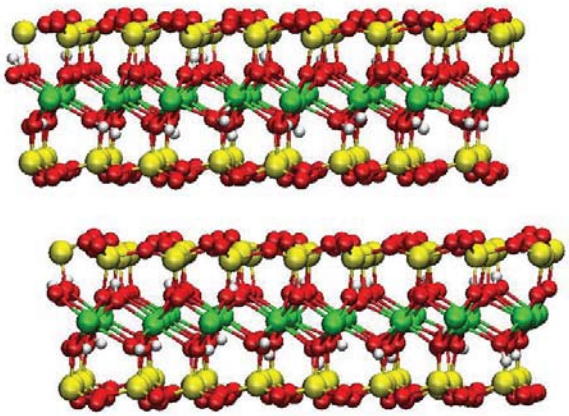

Results and conclusion

We present here how the polarisable force field is constructed. We then demonstrate its validity by comparing structural properties to experimental data and to the current state-of-the-art non-polarisable force field ClayFF [1].

Figure 1: Snapshot of the pyrophyllite simulation box

[1] Cygan *et al.*, *J. Phys. Chem. B,* 108 (2004) 1255-1266.
[2] Jahn and Madden, *Phys. Earth Planet. Inter.*, 162 (2007), 129-139.
[3] B. Rotenberg *et al.*, *Phys. Rev Lett.*, 104 (2010).

https://doi.org/10.1180/S0026461X00008434 Published online by Cambridge University Press

Pressure-induced anomalous isotopic fractionation of Li in magmatic hydrothermal systems

A. J. TEAGUE[1*], D.M. SHERMAN[1], J. D. BLUNDY[1], P. A. E. POGGE VON STRANDMANN[2]

[1]School of Earth Sciences, University of Bristol, Bristol, UK, alex.teague@bristol.ac.uk (*presenting author)

[2]Department of Eartyh Sciences, University of Oxford, Oxford, UK

Lithium has been demonstrated to undergo significant fractionations in geological environments, both elementally and isotopically. Such fractionations have been shown to occur due to various processes, with both chemical and kinetic effects contributing to the observed partitioning. Isotopic fractionation in particular, has been used to constrain processes of fluid release in the slab and mantle wedge through to the degassing of magmas and the subsequent condensation of hydrothermal fluids and fumarolic gases.

In this study, lithium isotope fractionation between synthetic granite and aqueous Cl bearing fluids was investigated experimentally. Experiments were conducted at 800°C and between 1.0-2.8 kbar, with the salinity of the fluid varying between 0, 0.1, 1 & 10 wt% NaCl. A strong systematic fractionation of ^{7}Li into the fluid of 1 - 10‰ was observed, with the strongest fractionations occurring at higher Cl concentrations. However, the most marked effect is that caused by pressure, with the fractionation doubling between 2.0 and 2.8 kbar.

Ab initio calculations of isotopic fractionation between $Li(H_2O)_4^+$ and $LiCl_n(H_2O)_{4-n}^{1-n}$ predict values of Δ^7Li ($Li(H_2O)_4^+$-$LiCl_2(H_2O)_2^-$) near +5 ‰ at 1000°C but in ideal gas at zero pressure. Accordingly, we would expect the fluid to increasingly favour the light isotope due to Cl complexation. However, we find that the fluid strongly favours the heavy isotope with increasing Cl. We attribute this to a very strong pressure effect on isotope fractionation between $Li(H_2O)_4^+$ and $LiCl_n(H_2O)_{4-n}^{1-n}$. For a 0.1*m* Cl solution Δ^7Li (fluid-glass) increases by 4‰ with a 0.8 kbar pressure increase.

In summary, Li is light enough to still undergo substantial isotopic fractionation even at magmatic hydrothermal temperatures. However, the effect of pressure is comparable, and opposite, to that of temperature and complexation by Cl. The interpretation of Li isotopes measured in natural systems must account for these competing effects. On the other hand, the isotopic composition of Li offers potential as a geobarometer at elevated T.

Petrografic and geochemical characteristic of metagreywackes (Central Portugal): implication of Zr content

MARIA RIBEIRO[1] HELENA C.B. MARTINS[1] DANIEL TEIXEIRA[1*]

[1] Centro Geologia da Universidade do Porto, DGAOT – FCUP, R. Campo Alegre, 4169-007 Porto, Portugal (*maribeir@fc.up.pt)

Introduction

Petrography and geochemistry (major, trace and rare earth elements) of two greywackes samples from the Upper Proterozoic to Lower Cambrian "Complexo Xisto-Grauváquico – CXG" (Central Portugal) have been investigated as support of subsequent mineralogical study of zircons. The two samples: Alv 51 and Alv 55 are close one to another (ca 20m), being the last near a fault zone.

Results

The petrographic and geochemical studies have shown significant differences: (i) Alv 51 is a metagreywacke in chlorite zone conditions, with a clastic texture and an anisotropic mica-quartz matrix. Anisotropy is marked by a spaced anastomosing foliation, with microlithons controlled by the size of quartz and plagioclase porphyroclasts. Detrital zircons are presents as accessory mineral with euhedral oscillatory zoning crystals (60-120 μm). (ii) Alv 55, near the fault zone, presents heterogranular granoblastic texture, with quartz, chlorite, calcite, muscovite, sphene and rutile, resulting from local hydrothermal metamorfism. Detrital zircons are not identified, but chlorite shows pleochroic haloes associated with very small zircons (1-2 μm) and abundant rutile needles.

The major elements composition of the samples is quite different: Alv 51 is richer in SiO_2 and K_2O while Alv55 present higher content in all the others major elements, especially in MgO, TiO_2, P_2O_5, but also in CaO and Na_2O. The trace elements content is also very different. Alv 55 shows an enrichment of LREE, Ba, Sr, Ni, Cr, and especially Hf, Th and U. This sample has higher Zr content (Alv 55 Zr= 376ppm; Alv 51 Zr = 275ppm). The UCC [1] normalized spider plot highlights these differences.

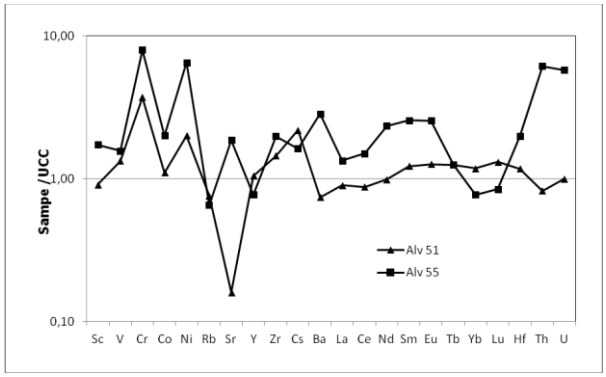

Figure 1: UCC [1] normalized spider plot.

The high content of Cr, TiO_2 LREE, Hf, Th and U and low contents of HREE in Alv55 may suggest that the Zr is partly associated with the rutile (anatase) and not only with the zircon. The incorporation of Zr in rutile, by substitution of Ti is favored by increasing temperature and is used as geothermometer [2].

This work has been supported by POCI 2010 (FCT-Portugal, COMPETE/FEDER)

[1] Taylor,McLennan (1985). The C Crust…Blackwell, 312p

[2] Zack *et al* (2004) *Contrib Mineral Petrol* ,**148:** *471-488*.

https://doi.org/10.1180/S0026461X00008434 Published online by Cambridge University Press

The importance of electron microprobe dating of monazite from some granites of northern Portugal

R. J. S. TEIXEIRA[1]*, A. M. R. NEIVA[2] AND M. E. P. GOMES[3]

[1, 3]Department of Geology, University of Trás-os-Montes e Alto Douro, Vila Real and Geosciences Centre, University of Coimbra, Portugal, rteixeir@utad.pt, mgomes@utad.pt (* presenting author)

[2]Department of Earth Sciences and Geosciences Centre, University of Coimbra, 3000-272 Coimbra, Portugal, neiva@dct.uc.pt

Ten Variscan S-type granites (G1 to G10) occur in Carrazeda de Ansiães region, northern Portugal, intruding Precambrian to Ordovician metasedimentary rocks. The U-Pb ID-TIMS data obtained in zircon and monazite from these granites yield crystallization ages comprised between 329.9 ± 0.8 Ma and 316.2 ± 0.7 Ma. The variation diagrams of these peraluminous granites and their minerals and the whole-rock REE patterns, whole-rock $\delta^{18}O$ values of 10.55 – 11.86 ‰, the different mean whole-rock values of $(^{87}Sr/^{86}Sr)_i$ and εNd_t for G1 (0.7097 ± 0.0000; -6.3), G2 (0.7149 ± 0.0008; -8.2), G4 (0.7112 ± 0.0006; -8.0), G5 (0.7124 ± 0.0007; -7.5), G7 (0.7156 ± 0.0005; -8.5) and G8 (0.7155 ± 0.0007; -8.4) point to the existence of distinct pulses of magmas, which were probably formed by the partial melting of heterogeneous metasedimentary rocks. Three differentiation series are distinguished: a) G2 and G3, b) G5 and G6 and c) G8, G9 and G10.

The zircon systematics are generally complex due to Pb loss and to the presence of inherited cores, but the latter can also affect some of the monazites. Therefore, the fast and low cost age determination on monazites, by electron microprobe, using the U-Th-Pb method [1], can be a useful tool in the interpretation of U-Pb ID-TIMS data. Its high spatial resolution can allow a detailed study of heterogeneities inside the same crystal, in areas with diameters as small as 5 µm. The monazite populations from the granites of the three differentiation series show ages similar to those from the ID-TIMS U-Pb results: 321 ± 6 Ma for G2, 318 ± 5 Ma for G3, 319 ± 7 Ma for G5, 319 ± 7 Ma for G6, 316 ± 7 Ma for G8, 315 ± 4 Ma for G9 and 315 ± 9 Ma for G10. However, in the rims of all monazite crystals and internal domains related to the rims, ages from 281 ± 8 Ma to 298 ± 9 Ma were also obtained, which should correspond to recrystallization events. On the other hand, in monazites from granites G6 and G9, inherited components were detected, presenting ages of 352 ± 7 Ma and 345 ± 5 Ma (Figure 1), which can explain the U-Pb age spreading of some concordant monazites in granite G9.

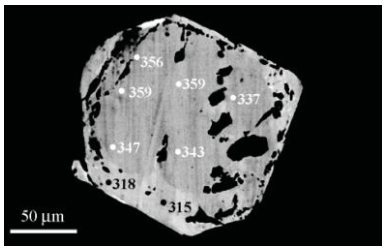

Figure 1: BSE image of a monazite from granite G9, with ages (in Ma) determined by electron microprobe.

[1] Montel (1996) Chemical Geology 131, 37-53.

Arsenic speciation and distribution controls throughout Murshidabad, West Bengal, India

KATHERINE TELFEYAN[1*], SANKAR M.S[2], SAUGATA DATTA[2], SOPHIA FORD[2], KAREN JOHANNESSON[1]

[1]Tulane University, New Orleans , LA, USA, ktelfeya@tulane.edu (* presenting author)

[1]Kansas State University, Manhattan, KS, USA, sdatta@ksu.edu

Over 2% of the world's population lives in the Bengal Delta, the world's largest fluvial-delta system. However, the rapid burial of Himalayan sediments has ultimately resulted in the release of arsenic (As) from sediment grains and tragically affected the health of millions of people [1]. In January 2012, field surveys of four blocks in the Murshidabad district of West Bengal, India were conducted, sampling tubewells, irrigation water, ponds, and sediment cores. Two sites, Beldanga and Hariharpara located east of the Ganges distributary, Bhāgirathi-Hooghly River, whereas Nabagram and Kandi are located to the west of the river. High As is associated with gray, reduced sediments, whereas low As is associated with orange-brown, oxidized sands [2]. Field test kits show total As concentrations ranging from less than 10 ppb to greater than 500 ppb. Eight groundwater samples were passed through ion exchange columns to separate As(III) from As (V) for analysis. Reductive dissolution of iron hydroxides is the primary cited cause of As mobilization. However, the source of the organic matter responsible for the reduction of iron and As is not fully understood. Previous studies have suggested human and animal waste, surface ponds, irrigation return-flow, and in situ organic matter at depth [3,4]. Analysis of dissolved organic carbon is discussed with regards to potential sources. In addition to organic matter, As concentrations are compared to those of other trace elements, such as Fe and Mn, that also vary as a function of redox conditions and pose health problems in Murshidabad.

[1] Mukherjee et al. (2009) *Journal of Asian Earth Sciences* **34** 228-244. [2] Neal (2010) *Master's Thesis Kansas State University*. [3] MacArthur et al. (2004) *Applied Geochemistry* **19** 1255-1293. [4] Harvey et al. (2006) *Chemical Geology* **228** 112-136.

https://doi.org/10.1180/S0026461X00008434 Published online by Cambridge University Press

Mesocosms as an Essential Tool to Assess the Environmental Exposure to Nanomaterials during their Life Cycle

M. TELLA[1,2], L. BROUSSET[2,3], J.Y. BOTTERO[1,2*], M. AUFFAN[1,2], B. ESPINASSE[4,5], E. ARTELLS[2,3], A. THIERRY[2,3], C. SANTAELLA[2,6], J. ROSE[1,2], A. MASION[1,2], M.R. WIESNER[4,5]

[1]CEREGE, CNRS-Aix Marseille Univ., Aix-en-Provence, France, bottero@cerege.fr (* presenting author)
[2]iCEINT, Aix-en-Provence, France.
[3]IMBE, CNRS Aix Marseille Univ., Marseille, France.
[4]Duke University, Durham NC, USA.
[5]CEINT, Durham NC, USA.
[6]LEMIRE CNRS CEA,Aix Marseille Univ, St Paul lez Durance, France.

In the past decade, there has been a growing concern about the use of nanoparticles/nanomaterials which are now present in 1000+ consumer products. There is no established current state of the art regarding the risks associated with the manufacturing and use of nano-enabled products, but rather a large collection of a somewhat contradictory literature. The vast variety of parameters and processes (physico-chemical, (micro)biological, (eco)toxicological...) is the source of a complexity level that cannot be easily resolved.

Hazard is the factor that is generally studied first but the multiplicity of experimental protocols makes it difficult to efficiently used these data. The exposure cannot be easily defined because of the complex interplay of intrinsic properties of the nanomaterial, their process dictated surface modification(s), and the evolution of their speciation during aging in regular use, accidental release or disposal scenarios.

A way to circumvent experimental artifacts in the determination of environmental exposure is to let nature have its way. Of course, for practicality, nature needs to be "harnessed", and experiment management/monitoring becomes a predominant issue. The use of mesocosms, i.e. downscaled ecosystems with in sizes ranging from a table top aquarium to backyard swimming pools, is the most promising way to achieve relevant evaluation of environmental exposure to-/ bioavailability of- nanomaterials at varying stages of their life cycle.

The current work demonstrates how such mesocosm experiments need to be implemented in terms of operational setup to be relevant for the assessment of exposure scenarios. First results provide a validation of this approach.

Magnesium isotopic composition of the lower continental crust: A xenolith perspective

FANG-ZHEN TENG[1*], WEI YANG[1,2] AND ROBERTA L. RUDNICK[3]

[1]Isotope Laboratory, Depart. of Geosciences, University of Askansas, Fayetteville, AR, USA, fteng@uark.edu (*presenting author)
[2]Institute of Geology and Geophysics, Chinese Academy of Sciences, Beijing, China, yangw@mail.iggcas.ac.cn
[3]Isotope Geochemistry Laboratory, Department of Geology, University of Maryland, College Park, MD, USA, rudnick@umd.edu

The large isotope fractionation during low-temperature water-rock interactions and limited fractionation during igneous differentiation make Mg isotopes a potentially powerful tracer of the influence of chemical weathering on the continental crust composition. Magnesium isotopic composition of the upper continental crust is highly heterogenous [1], and on avarage heavier than the mantle [e.g., 2]. By contrast, the Mg isotopic composition of the hydrosphere, as represented by seawater [e.g., 3], is very light. The distinct Mg isotopic distribution among the mantle, upper continental crust and the hydrosphere is interpreted as a result of continental weathering, during which light Mg isotopes are partitioned into the hydrosphere relative to the weathered regolith [4].

Better understanding the Mg isotopic cycling between the crust, mantle and hydrosphere requires knowledge of the bulk crustal Mg isotopic composition, which is heavily influenced by the deep crust. Here, we report Mg isotopic data for two sets of well-studied lower crustal granulite xenoliths from North Queensland, Australia (Chudleigh and McBride suites) [5, 6]. The Chudleigh granulites are a suite of cogenic crystal cumulates derived from mafic magmas that intruded and assimilated the preexisting lower crust. Their mineralogy varies from olivine-bearing assemblages to plagioclase-garnet-clinopyroxene assemblages indicating a range of equilibrium temperatures (600 to 1000 ºC) and depths (20 to >40 km). McBride granulites range from mafic to felsic bulk compositions, with most of them formed through mixing between mantle-derived basalts and preexisting crust. Overall, these two sets of granulite xenoliths match the estimated composition of the lower crust and hence are ideal for studying the average Mg isotopic composition of the lower crust.

Magnesium isotopic compositions of Chudleigh xenoliths are homogenous and mantle-like, with δ^{26}Mg varying from -0.3 to -0.2‰. By contrast, δ^{26}Mg of McBride xenoliths is highly variable from -0.7 to +0.2‰, significantly overlapping that of the upper continental crust. The contrasting behaviors of Mg isotopes between Chudleigh and McBride xenoliths mainly reflect their different proportions of mantle vs. crustal Mg. Based on these xenoliths, the lower continental crust has a heterogneous Mg isotopic composition, with a weighted average δ^{26}Mg of -0.2‰, which is similar to that of the upper crust, but slightly heavier than the mantle.

[1] Li et al. (2010) *Geochimica et Cosmochimica Acta* **74**, 6867-6884. [2] Teng et al. (2010) *Geochimica et Cosmochimica Acta* **74**, 4150-4166. [3] Ling et al. (2011) *Rapid Communications in Mass Spectrometry* **25**, 2828-2836. [4] Teng et al. (2010) *Earth and Planetary Science Letters* **300**, 63-71. [5] Rudnick et al. (1986) *Geochimica et Cosmochimica Acta* **50**, 1099-1115. [6] Rudnick and Taylor (1987) *Journal of Geophysical Research* **92**, 13981-14005.

https://doi.org/10.1180/S0026461X00008434 Published online by Cambridge University Press

Effect of water and sulfide on magnesium carbonate crystallization

H. HENRY TENG[1*], HUIFANG XU[2], FANFFU ZHANG[2], JIE XU[1]

[1]Dept. Chemistry, The George Washington University, Washington, DC, 20052, USA, hteng@gwu.edu*, jxu@email.gwu.edu

[2]Dept. Geoscience, The University of Wisconsin, Madison, WI 53706, USA, hfxu@geology.wisc.edu; fzhang9@wisc.edu

8a. Mineral growth and dissolution: modern approaches to molecular-level reaction mechanism determination with implications for toxic metal sequestration, biomineralization, and engineering

Magnesium is the second most widely occurred metal component in carbonates next only to Ca, but low temperature precipitation of anhydrous Mg-CO_3 phases has proven virtually impossible. The difficulty encountered herein is often attributed to the highly hydrated character of Mg^{2+}. The seemingly clear understanding in the role of water leads to an interesting question: will magnesite precipitate if the formation of aqueous hydration shell is breached or prevented? Meanwhile, a plethora of literature data documented the occurrence of dolomite in the presence of sulfur reducing bacteria SRB, leaving no lucid explanation for the kinetic effect of water. The ultimate goal of our research is to address these issues through experimentally testing the follwoing hypotheses: (1) weakend solvation shell around Mg^{2+} will lead to $MgCO_3$ crystallization if dehydration is the kinetic hindrance and (2) sulfide is the ultimate mediating agent for SRB facilitated dolomite formation.

Crystallization experiments were carried out in dry organic and organo-aqueous binary solvents and in the presence of sulfide ions. Experimental results indicate (1) Anhydrous $MgCO_3$ precipitates under dry conditions but appears in amophous form instead of crystalline magnesite. (2) Crysalline anhydrate only forms when both Mg and Ca are present in organic solvent. XRD identifies the occurrence of dolomite with ~37% $MgCO_3$ in solutions containing 1:1 ratio of Mg and Ca. (3) The presence of minute amount of water in organic solvents leads to the precipitation of hydrated magnesium carbonate. (4) Tri-hydrate Mg-CO_3 nesqhehonite is the dominant phase in binary solvent, similar to the result in pure aqueous environments. However, the presence of organic solvent greatly accelerate the crystallization kinteics. (5) Input of solutions with Mg/Ca = 5 instantly halts the growth on seeded calcite crystals in saturated solutions. However, in situ AFM observations on the (104) faces reveals the inhibation tackles primarily nulceation but not step flow despite the change of hillock morphology. (6) The retardation effect of Mg is greatly alleviated, if not eliminated at all, when the input solutions contains 0.5 mM sulfide. Initial effect of Mg changes the hillock from the rhombic to a tear-drop mophology, but continued growth leads to step bunching in the $< \bar{4}41 >$ directions and ultimately a return to the cleavage form.

These observations indicate that the crystallization of Mg-containing carbonate may be inhibited both kinetically and energetically. The kinetic effect is shown by the formation of metastable hydrous phases in the presence even minimal amount of water. However, the inhibition on step nucleation but not step flow, as well as the lack of crystalline $MgCO_3$ phase in dry solvents, suggest the difficulty for Mg^{2+} and CO_3^{2-} to establish ordered long-range structures.

The Leaching of Heavy Metals from Steel Slag in Panzhihua Region

YANGUO TENG[1*], JIE YANG[2], ZHENGQI XU[3]

[1] College of Water Sciences, Beijing Normal University, Beijing City, China, teng1974@163.com (* presenting author)

[2] College of Water Sciences, Beijing Normal University, Beijing City, China, yangjie8769@163.com

[3] Department of Geochemistry, Chengdu University of Technology, Chengdu City, xuzhengq@163.com

Introduction

From 1970s to nowadays, approximately 3000000 t/a steel slag were dumping in Panzhihua region. [1] Heavy metals such as V, Cr, and Ni will influence environmental quality when they leach from slag pile. [2] In order to investigate the leaching of heavy metals from steel slag, some experiments were carried out.

Material and Method

The steel slag was selected in Baguanhe slag pile in Panzhihua region, and the chemical composition was Al_2O_3 1.69%, CaO 51.2%, Cr_2O_3 0.11%, FeO 10.66%, MgO 4.55%, MnO 1.54%, P_2O_5 0.37%, SiO_2 10.05%, TiO_2 5.33%, V_2O_5 6.35%. The steel slag was grounded and seived through d<0.075 mm, then 7 steel slag samples (each sample weight was 140 g) were put into 7 beakers which were added 100 ml pH=1, 3, 5, 7, 8, 10, 12 acid or alkali solutions, respectively. After 14 days soaking and shaking, heavy metals in the solution were detected by ICP-MS.

Results and Discussion

The leaching of heavy metals from slag was shown in Figure 1. When the pH value of solution was 1, the leaching of heavy metals was highest. And when the pH value of solution was 3, 5, 7, 8, 10, and 12, the concentration of heavy metals varied not obviously. Cr and Ni in leaching solution exceeded to Identification standards for hazardous wastes - Identification for extraction toxicity (GB5085.3-2007), which threatend regional environmental safety.

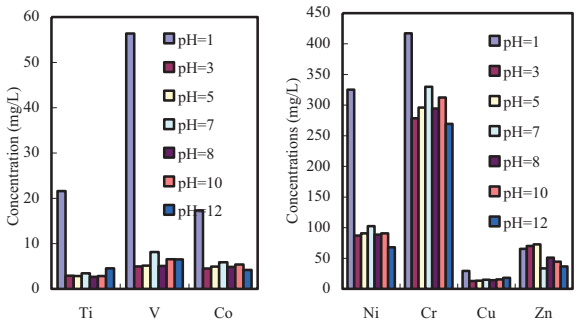

Figure 1: Heavy metas in solution after 14 days slag leaching

Conclusion

The steel slag which contained some heavy metals was hazardous waste. Heavy metals could release from the leaching of steel slag, especially, Cr and Ni would pollute water and soil.

Acknowledgement

This study is granted by NSFC project (No.41073068).

[1] Teng, et al (2006) *Chinese Journal of Geochemistry* **25(4)**, 378-384. [2] Proctor, et al (2002) *Human and Ecological Risk Assessment* **8(4)**, 681-711.

https://doi.org/10.1180/S0026461X00008434 Published online by Cambridge University Press

Ion exchange model for reversible sorption of divalent metals on calcite

EMMANUEL TERTRE[1*], CATHERINE BEAUCAIRE[2] AND JACQUES PAGE[2]

[1]Université de Poitiers - CNRS, UMR 7285 IC2MP, Poitiers, France, emmanuel.tertre@univ-poitiers.fr (* presenting author)
[2]CEA, DEN/DANS/DPC/SECR/L3MR, Gif-sur-Yvette, France, catherine.beaucaire@cea.fr; jacques.page@cea.fr

Problematic and objectives

Previous studies dealing with electrokinetic properties of the calcite/water interface have shown that Ca^{2+} and CO_3^{2-} are the main species determining the potential of the calcite surface [1 among others]. This is particular true when systems are in equilibrium with both calcite and a fixed $p_{CO2(g)}$ value, a common case of environment conditions. However, most of the thermodynamic models proposed in literature describing the surface speciation of calcite do not predict a significant contribution of sorbed Ca(II) [2 among others]. Therefore, the aims of this study are (1) to propose a model, based onto the ion exchange theory, able to describe the reversible sorption of Ca(II) at the calcite surface and (2) to apply this model to some divalent metals (*e.g.*, Zn(II), Cd(II) and Pb(II)). Note that aqueous metallic cations presented in natural waters are always in competition with Ca^{2+} and H^+ for sorption sites located on mineral surfaces. Therefore, these two latter species should be systematically included in all models predicting sorption of divalent metals on calcite.

Methodology and main results

Concentrations of Ca(II) sorbed reversibly on the calcite are obtained using a previous methodology based on isotopic measurements [3]. Data are obtained at different pH using solutions saturated with both calcite and a fixed $p_{CO2(g)}$ value (from 10^{-5} to 10^{-2} atm.). Concentration of sorbed Ca(II) is significant as suggesting by previous electrokinetic data and is practically constant in the [7 - 9.5] pH range to a value close to $1.2\pm0.4\ 10^{-3}$ eq.kg^{-1}. Such value is in agreement with total sorption site density calculated by crystallographic considerations. Experiment data are fitted to obtain a selectivity coefficient between Ca^{2+} and H^+. Using previous published experimental data [4 among others] fitted metal-protons selectivity coefficients are also proposed for reversible sorption of Zn(II), Cd(II) and Pb(II) on calcite. Finally, the model was used to calculate the contribution of calcite to the sorption of Cd(II) on a natural and complex solid (*e.g.*, calcareous aquifer sand).

[1] Cicerone *et al.* (1992) *J. Colloid Interf. Sci.* **154**, 423-433.
[2] Van Cappellen *et al.* (1993) *Geochim. Cosmochim. Acta* **57**, 3505-3518.
[3] Tertre *et al.* (2010) *J. Colloid Interf. Sci.* **347,** 120-126.
[4] Zachara *et al.* (1991) *Geochim. Cosmochim. Acta* **55**, 1549-1562.

Plio-Pleistocene evolution of water mass exchange and erosinal input in the Nordic Seas

CLAUDIA TESCHNER[1*], MARTIN FRANK[1], BRIAN A. HALEY[2], JOCHEN KNIES[3]

[1] GEOMAR | Helmholtz-Centre for Ocean Research Kiel, Wischhofstr. 1-3, Kiel, Germany, cteschner@geomar.de (* presenting author)
[2] COAS, Oregon State University, Corvallis, OR 97331-5503, USA
[3] Geological Survey of Norway, Leiv Eirikssons vei 39, NO-7491 Trondheim, Norway

The Arctic Ocean and Norwegian-Greenland Seas (NGS) are presently one of the most important areas for deep water formation in the Northern Atlantic Ocean. Therefore, it is particularly essential to better understand Plio-Pleistocene variations of the circulation in these areas. Significant climatic and oceanographic changes occurred during this period of time including the major intensification of the Northern Hemisphere Glaciation (starting at 2.82 Ma) and the Mid-Pleistocene Transition (1.5 – 0.5 Ma).

To reconstruct erosional input and water mass exchange between the NGS and the Arctic ocean we use the composition of the radiogenic isotopes neodymium (Nd), lead (Pb) and strontium (Sr). For this purpose, we leached the authigenic metal oxide phase on sediments particles [1] of different ODP Sites in the Norwegian-Greenland Seas (Site 911, 986, and 644) and in the North Atlantic Ocean (Site 982).

The first analyses were performed on sediment samples from northernmost ODP site 911 (Leg 151, in 900 m water depth) located on the southeastern slope of the Yermak Plateau in the Fram Strait. Today this location is strongly influenced by the inflow of Atlantic water from the NGS, which is supported by the core top εNd value agreeing well with Atlantic values [2]. Based on these results, downcore samples covering the past 5 million years were analysed.

The record of the Yermak Plateau shows no significant general trend with time, but a very high variability with more radiogenic Nd isotope data during glacial periods at 0.72 Ma, 1.36 Ma, 2.4 Ma, and 2.69 Ma. These shifts indicate major inflow of waters influenced by highly radiogenic source areas, either by the Icelandic basalts in the south or by the Siberian Putorana flood basalts in the hinterland of the Kara/Laptev Sea region. The εNd data suggest that mixing of water masses from the Arctic Ocean and the NGS have controlled the Nd isotope signatures of deep waters on the Yermak Plateau since the onset of the Northern Hemisphere Glaciation (NHG). In contrast, the Pb istotope data of deep waters in the Fram Strait appear to have been dominated by glacial weathering inputs from old continental landmasses, such as Greenland or parts of Svalbard since 2 Ma.

In order to better understand past water mass exchange between the Norwegian-Greenland Seas and the North Atlantic Ocean we will compare these data with isotopic records of ODP Sites 986, 644 (NGS), and 982 (North Atlantic Ocean).

[1] Gutjahr et al. (2007) *Chemical Geology* **242**, 351-370 [2] Lacan, F. and C. Jeandel (2004) *Geochem. Geophy. Geosyst.*, **5**, Q11006

https://doi.org/10.1180/S0026461X00008434 Published online by Cambridge University Press

Tracing magmatic fluid in hydrothermal deposits within subduction zone setting

S. TESSALINA

John de Laeter Centre of Isotopic Research, Curtin University, Perth, Australia, Svetlana.Tessalina@curtin.edu.au

The metals in sea-floor hydrothermal systems may arise purely from the interaction of circulating sea-water with host rocks, or there may be an admixture from the fluid escaping from magtma at depth. Here we present direct evidence for the involvement of magmatic fluid in the formation of Volcanogenic Massive Sulphide (VMS) deposits in Devonian arc rocks of the Southern Urals, Russia.

The plot of isotope data for the hydrothermal chimneys from the Yaman-Kasy VMS deposit defines the best-fit line with the age of 362±9 Ma. The molybdenite sample from the Kul-Yurt-Tau VMS deposit shows the model age of 363.4±0.5 Ma. These ages are similar to that previously reported from the Urals VMS deposits [1,2] and younger than presumed biostratigraphic ages of ore-hosting rocks. The observed ages post-date the subduction of older Proterozoic blocks from adjacent East-European continent, which was constrained at 380-372 Ma from the high-pressure metamorphic rocks in the area [3]. The subducted Proterozoic rocks have distinct low radiogenic $^{206}Pb/^{204}Pb$ isotopic signature, which was identified in VMS deposits in fore-arc and arc setting, diminishing with a distance from the subducted front and annihiliating in the back-arc setting where the magmatic contribution was not detected.

Based on presented radiogenic isotope dataset, we conclude that the VMS deposits fromation was initiated after the continent has collided with the volcanic arc. This stage of Urals development was identified as hydrous suprasubduction melting characterised by large scale granitoid magmatism [4]. The generation of volatile-rich felsic magma at shallow depth may be due to the entrance of less dense continental blocks which shallowed the angle of slub subduction. Felsic magma may be produced by melting of cumulates remaining from previous melting events. Metal-rich magmatic fluid is released from volatile-rich felsic magma, which are prelevant at convergent margin setting. Indeed, the presence of magmatic aqueous-carbonic fluid with significant contents of H_2S has been previously detcted at some of the Urals VMS deposits [5].

Based on presented data, we conclude that the arc-continent collision played a major role in Urals VMS systems formation. The similar relationship my be established for younger hydrothermal systems in Banda arc. The collided arcs host a large number of mineral deposits worldwide, but until now the role of continent in mineral deposits formation was not fully understood. Here we show that the collision event is directly responsible for mineral deposits formation within Devonian volcanic arc of Southern Urals. The tectonic processes involved in arc-continent collision could be responsible for the mineral deposits formation worldwide.

[1] Gannoun *et al*. (2003) *Chem. Geol.* **196**, 193-207. [2] Tessalina *et al*. (2008) *Ore Geol. Rev.* **33**, 70-80. [3] Beane & Connelly (2000) *Journal of Geol. Society* **157**, 811-822. [4] Fershtater *et al*. (2007) *Geotectonics* **41**, 465-486. [5] Bailly *et al*. (1999) *Stanley et al. (ed.) Balkema*, 13-16.

Stable Pb isotope ratios as mid-1800s stratigraphic markers for sediments from Eastern Canada lakes

ANDRÉ TESSIER[1*], CHARLES GOBEIL[1], AND RAOUL-MARIE COUTURE[2]

[1]Université du Québec, INRS-ETE, Québec, Canada, atessier@ete.inrs.ca and charles.gobeil@ete.inrs.ca (* presenting author)

[2]University of Waterloo, Earth and Environmental Sciences, Waterloo, Canada, raoul.couture@uwaterloo.ca

We determined the vertical distribution of Pb concentrations and stable Pb isotope ratios in ^{210}Pb-dated sediment cores from 10 headwater lakes located in various regions of Southern Québec, Eastern Canada. The depth profiles of stable Pb isotope ratios show, for the post-19th Century period, the influence of several isotopically distinct anthropogenic sources of Pb, including mainly Pb emitted from two Canadian smelters and from leaded gasoline combustion in Canada and in the United-States. A most interesting feature of the profiles, however, is the presence of sharp peaks of Pb stable isotope ratios at 1-2 cm below the depth of detectable unsupported ^{210}Pb (i.e., corresponding to mid-1800s) in sediments of most of the seasonally anoxic lakes where bioturbation is negligible. Minor amounts of Pb, whose isotopic signature was significantly different from that of Pb from local natural sources, were deposited in many lakes at an early stage of industrialisation in North America. Using a binary mixing model and assuming that natural Pb concentrations and isotopic compositions are given by the pre-industrial sediments in the cores, we find that the isotopic composition of most (>50%) of the non local Pb added to the sediments at this time period was typical to that of the Upper Mississippi Valley Pb ores. This observation is consistent with the previous work of Lima et al. (2005) [1] in laminated (varved) sediments of the Pettaquamscutt River, Rhode Island. These authors argued that, during the mid-19th Century, mining and smelting activities in the Mississipi Valley were responsible for most anthropogenic Pb emissions in North America and propose to use the chronology of these emissions as a stratigraphic marker for sediments deposited in the Northeastern USA. Our results confirm this conclusion and suggest that it can be generalized to all Eastern North America.

[1] Lima A. L. et al. (2005) Geochimica et Cosmochimica Acta, 69: 1813-1824.

https://doi.org/10.1180/S0026461X00008434 Published online by Cambridge University Press

Pyrosequencing analysis of bacterial diversity in Chernobyl contaminated trenches

N. Theodorakopoulos[4*], R. Christen[5,6], L. Piette[1,2,3], L. Fevrier[4], F. Coppin[4], A. Martin-Garin[4], C. Le Marrec[9], C. Sergeant[7,8], C. Berthomieu[1], V. Chapon[1]

[1]CEA, DSV, IBEB, SBVME, LIPM, F-13108 Saint-Paul-lez-Durance, France (virginie.chapon@cea.fr)
[2]CNRS, UMR 6191, F-13108 Saint-Paul-lez-Durance, France
[3]Université d'Aix-Marseille, F-13108 Saint-Paul-lez-Durance, France
[4]IRSN/PRP-ENV/SERIS/L2BT-Bât 186, B.P.3, Cadarache Center, F-13115 Saint-Paul-lez-Durance cedex, France (*correspondence: nicolas.theodorakopoulos@irsn.fr)
[5]Université de Nice-Sophia-Antipolis, Centre de Biochimie, Parc Valrose, F-06108 Nice, France (richard.christen@unice.fr)
[6]CNRS, UMR 6543, Centre de Biochimie, Parc Valrose, F-06108 Nice, France
[7]Univ. Bordeaux, CENBG, UMR5797, F-33170 Gradignan, France
[8]CNRS, IN2P3, CENBG, UMR5797, F-33170 Gradignan, France (sergeant@cenbg.in2p3.fr)
[9]ISVV, UMR 1219, Institut Polytechnique de Bordeaux/INRA, POB 50008, F-33882 Villenave d'Ornon, France (clehenaff@enscbp.fr)

Following the Chernobyl nuclear disaster, contaminated soils, vegetation and other radioactive debris were buried *in situ* in trenches. It is now well known that micro-organisms play an essential role in contaminant mobility in soils. In the case of radionuclides, the interactions engaged could retain or induce their transfer from the trenches. However, radionuclides might also exert toxic effects on the micro-organisms and hence reduced their role in the transfer. This study focused on the impact of a radioactive environment on bacterial community's diversity with an underlying question: did a chronic radioactive exposure lead to the extinction of bacterial diversity?

To address this issue, a pyrosequencing-based analysis of 16S rRNA genes was conducted on radionuclides contaminated and non contaminated control samples. The huge diversity obtained by this technique was illustrated by an average of 19,000 sequences per sample, with 963 genera and 39 phyla represented. The 4 most predominant phyla, detected in all samples, were *Chloroflexi*, *Proteobacteria*, *Acidobacteria*, and *Verrucomicrobia*. Some phyla, as *Thermotogae*, were clearly more represented in control samples and seemed to be sensitive to radioactivity. Those results refined the conclusions previously given based on genetic fingerprinting method (DGGE) on the same samples [1]. Results indicated that a long term exposure to radionuclides did not lead to extinction of bacterial diversity in Chernobyl T22 trenches soils. A statistical analysis (principal component analysis) of the pyrosequencing data evidenced however a clear distinction of bacterial community between contaminated and control samples.

The pyrosequencing data will permit the selection of a bacterial model among a collection of 250 heterotrophic aerobic cultivable isolates provided from these contaminated and non contaminated areas. This model strain will be further used for laboratory experiments to study interactions with some radionuclides of the trenches (^{137}Cs, U, ^{90}Sr).

[1] Chapon *et al*. (2011) *Applied Geochem* (in press).

Sr isotopes reveal new insights about the source of turquoise at the Aztec Templo Mayor

Alyson M. Thibodeau[1]*, Leonardo López Luján[2], David J. Killick[3], Joaquin Ruiz[1]

[1]Department of Geosciences, University of Arizona, Tucson, Arizona, 85721, USA
(*correspondence: amthibod@email.arizona.edu)
[2]Museo Templo Mayor/INAH, Mexico City, Mexico
[3]Department of Anthropology, University of Arizona, Tucson, Arizona, 85721, USA

Turquoise [$CuAl_6(PO_4)_4(OH)_8 \cdot 4H_2O$] was highly valued in late Postclassic Mesoamerica (900-1521 CE), especially by the Mixtecs and the Aztecs, who used it as part of elaborate mosaics and other ceremonial and status objects. Because turquoise mineralization in North America is primarily restricted to the present day southwestern United States (U.S.) and northern Mexico, archaeologists have identified these regions as likely sources of turquoise found thousands of kilometers away in archaeological sites across Mesoamerica. However, despite more than a century of speculation about acquisition of turquoise by Mesoamericans through long-distance trade networks with the Southwest U.S., no geochemical data has been published in support of this idea.

To address this question, we use Pb and Sr isotope geochemistry to investigate the geologic origin of turquoise found in multiple offerings throughout the Aztec Templo Mayor in Mexico City. We directly compare the isotopic ratios obtained for Templo Mayor turquoise to the isotopic signatures of turquoise samples from over 16 areas of turquoise mineralization in the southwestern U.S. and northern Mexico. Initial results indicate that the Sr isotopic signature of at least some of the turquoise from the Templo Mayor ($^{87}Sr/^{86}Sr < 0.706$) is distinct from the isotopic signatures of all turquoise samples (n=200) examined from the southwestern United States and northern Mexico ($^{87}Sr/^{86}Sr > 0.706$).

Turquoise is a supergene mineral that forms in the oxide zone and it acquires trace amounts of Pb and Sr through weathering processes associated with its formation. It particular, it often forms from the weathering of igneous rocks rich in copper, phosphorous, and aluminum, and is commonly precipitated in the open spaces and fractures of such rocks. We tentatively interpret the unique and relatively unradiogenic Sr isotopic signature of turquoise from the Templo Mayor to indicate the turquoise was mined from a source or sources in Mexico. This provisional interpretation is supported by (1) the empirical contrast between $^{87}Sr/^{86}Sr$ ratios of turquoise from Templo Mayor and the $^{87}Sr/^{86}Sr$ ratios of turquoise from the southwestern U.S., and (2) the existence of igenous rocks with similar Sr isotope ratios ($^{87}Sr/^{86}Sr<0.706$) within the Mexican Volcanic Belt and the Sierra Madre Occidental which could theoretically host small pockets of turquoise mineralization. This interpretation implies the Aztecs did not have to acquire turquoise through interregional trade networks with the Southwest and thus provides fundamentally new insights into the nature of proposed long distance interactions between these areas.

https://doi.org/10.1180/S0026461X00008434 Published online by Cambridge University Press

Low oxygen events in the Laurentian Channel during the Holocene

BENOIT THIBODEAU[1]*, ANNE DE VERNAL[2] AND AUDREY LIMOGES[3]

[1]AORI-University of Tokyo, Kashiwa, Japan, thibodeau@aori.u-tokyo.ac.jp (* presenting author)
[2]GEOTOP-UQAM, Montréal, Canada, devernal.anne@uqam.ca
[3]GEOTOP-UQAM, Montréal, Canada, limoges.audrey@courrier.uqam.ca

Recent warming in the Laurentian Channel bottom water has been observed in the St. Lawrence Estuary [1] and Gulf [2]. This warming might be linked to an enhanced proportion of warm Atlantic water entering the Laurentian Channel and could be the main cause of the year-round hypoxia observed during the last 30 years in bottom waters of the lower Estuary. We observed a temperature trend of similar amplitude in a low sedimentation rate box-core located in the Esquiman Channel. Warm bottom waters conditions, however, are not exclusive to the recent time interval as shown by data from the lower part of the core, which is also characterized by low $\delta^{18}O$ values in *Globobulimina auriculata* and occurrence of both *Brizalina subaenariensis* and *Oridorsalis umbonatus*. Such data suggest the existence of low-oxygen and high temperature conditions in the bottom water of the Esquiman Channel 6-4 ka ago. These conditions are likely related to the inflow of Atlantic water in the Gulf of St. Lawrence through the Cabot Strait and the Laurentian Channel, possibly linked to large scale ocean circulation changes in the northwest North Atlantic. Hence, our results highlight the sensitivity of bottom water properties in the Gulf of St. Lawrence to North Atlantic circulation patterns.

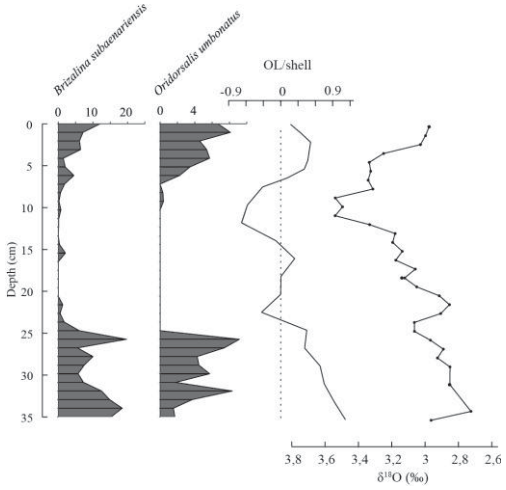

Figure 1: Abundance of *B. subaenariensis* and *O. umbonatus* (%), calcium carbonate dissolution index (logarithm of the foraminifer linings vs shells ratio) and oxygen isotope composition in *G. auriculata* against depth in core CR06-TCE.

[1] Thibodeau *et al.* (2010), Geophysical Research Letters, **37**, L17604 [2] Genovesi *et al* (2011) Limnology and Oceanography, **56**, 1319-1329.

Adding uptake kinetics and surface entrapment to geochemical models

BRUNO THIEN[1]*, DMITRII A. KULIK[1], ENZO CURTI[1]

[1]Paul Scherrer Institut, 5232 Villigen PSI, Switzerland, bruno.thien@psi.ch (* presenting author)

Experimentally measured trace element partitioning between a host mineral and the aqueous solution often depends on precipitation or recrystallization rates and is frequently irreversible, as shown by the occurrence of zoned crystals. Kinetic-dependent trace element uptake can be realistically simulated using partial-equilibrium aqueous- solid solution (sorption) thermodynamic models. This means that in a reaction-path sequence of equilibrium states, some amounts of relevant phases, end members, or sorbed species must be declared metastable according to time-dependent kinetic rate laws.

In this context, we considered three uptake kinetics models: Growth Entrapment (GE) [1], Surface Reaction (SR) [2], and Adsorption – In-Diffusion (AD) [3]. Each model predicts a final metastable solid-aqueous distribution of trace elements or isotopes. However, different mechanisms and parameters are invoked: the competition between mineral growth and near-surface diffusivity (GE); purely kinetic laws for gross forward and backward reaction rates for host and trace components (SR); or diffusion of trace component into the solid (AD). All models can adequately describe the trace element uptake (Fig.1) for single element/host mineral pairs (Sr/calcite, Ra/barite, P/goethite) under simplifying assumptions, such as the constancy of growth rate and of the aqueous composition.

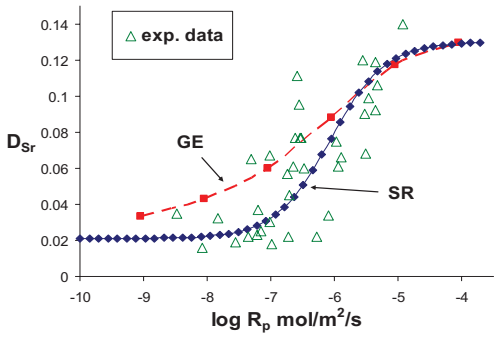

Fig 1.: Sr distribution coefficient in calcite *vs* precipitation rate.

In order to make them applicable in geochemical reactive transport simulations, these models are currently implemented in the GEM-Selektor code (http://gems.web.psi.ch) in integrated forms that control time-step-dependent metastability constraints in the Gibbs energy minimization algorithm [4]. This tool can also account for changes in solid and aqueous chemistry that may occur upon the uptake in a closed system (e.g. from pore solution), while keeping track of surface areas of minerals during growth or dissolution.

The research leading to these results has received funding from the European Atomic Energy Community's Seventh Framework Programme (FP7/2007-2011) under grant agreement n° 269688.

[1] Watson (2004) *GCA* **68**, 1473-1488. [2] DePaolo (2011) *GCA* **75**, 1039-1056. [3] Barrow (1983) *J. Soil Science* **34**, 733-750. [4] Karpov et al. (2001) *Geochem. Internat.* **39**, 1108-1119.

https://doi.org/10.1180/S0026461X00008434 Published online by Cambridge University Press

Late Cretaceous Evolution of Southern Hemisphere Seawater Neodymium Isotope Composition

DEBORAH J. THOMAS[1*], DANIEL P. MURPHY[2]

[1]Texas A&M University, College Station, TX, United States, dthomas@ocean.tamu.edu (*presenting author)
[2]University of Southampton, Southampton, United Kingdom, D.Murphy@noc.soton.ac.uk

Background

The predominant source of dissolved Nd to the oceans is the weathering and drainage of subaerially exposed terranes. Nd has become a commonly used tracer of water mass provenance (and hence deep-water circulation patterns) because water masses essentially form with the Nd isotopic signature of the weathering inputs in the region of formation. However, temporal variations in the isotopic composition of the water mass may result from changes in the composition of the weathering inputs.

Studies of modern river dissolved and particulate Nd isotopic composition indicate that fine fraction sediments record the same isotopic signature as the dissolved inventory [1]. Thus, we can reconstruct changes of Nd inputs to a given ocean basin through analysis of the detrital sediments in conjunction with the seawater composition. Here we apply this strategy to reconstruct the history of deep-water formation from 8 sites in the Indian and Atlantic sectors of the Southern Ocean during the Late Cretaceous.

Late Cretaceous Reconstructions

During the Cenomanian to early Campanian, the South Atlantic was divided into several distinct basins [2]. Previous work demonstrated that deep-water production in the Southern Ocean became the primary source of deep water in the South Atlantic during the early Campanian [2]. New seawater and detrital Nd isotope data from DSDP Sites 361, 511, 530 and 690 help constrain the timing of the subsidence of deep water gateways. By 75 Ma all sites in the South Atlantic shared a common water mass.

New data from Indian Ocean ODP Sites 763, 765, 766 and 1138 suggest that variations in the composition of weathering inputs controlled the overall evolution of proto-Indian Ocean water mass composition. Such variations were driven by the emplacement and subdidence of the Kerguelen Plateau and Broken Ridge during the Late Cretaceous. Weathering of subaerially exposed portions of these terranes caused Indian Ocean seawater Nd isotope values to increase, coincident with the peak of the mid-Cretaceous warmth. As the LIPs subsided below sea level, the input of radiogenic weathering products diminished and the isotopic composition of intermediate and deep waters in the region decreased, reflecting the weathering inputs from older terranes. The Indian Ocean sites extend the record of high-latitude deep-water formation back into the Early Cretaceous, prior to the onset of the mid-Cretaceous peak warmth. The growing body of data supports a mode of MOC in part characterized by high-latitude downwelling during the peak of greenhouse warmth of the Mesozoic.

[1] Goldstein and Jacobsen (1988) *Earth Planet. Sci. Lett.* **87**, 249-265.
[2] Robinson et al. (2010) *Geology* **38**, 871-874.

Probing the effects of organic ligands on mercury biouptake

SARA THOMAS*, TIEZHENG TONG, ISABELLE JI, AND JEAN-FRANÇOIS GAILLARD

Northwestern University, Evanston, USA, sarathomas2007@u.northwestern.edu (* presenting author)

Introduction

Methylation of mercury (Hg) only occurs afer Hg has passed through the bacterial cell membrane [1]; therefore, understanding the mechanisms of Hg biouptake is essential to gain insight into the fate of Hg in the environment. Hg has a strong affinity for organic ligands, which influence Hg speciation and subsequenly its transport across the bacterial cell membrane. The relationship between Hg complexation in aquatic systems and its biouptake remains poorly understood, partially due to the difficulty of directly measuring intracellular Hg. One approach for monitoring the biouptake of Hg is to use a luminescent whole-cell biosensor [2]. In this study, we employed a chromosomally-based biosensor to examine the effects of various organic ligands (*e.g.*, EDTA, NTA and three thiol-containing ligands) on Hg uptake by bacteria in presence of 50nM of Hg.

Main results

In the presence of EDTA and NTA, we observed a slight increase in Hg biouptake. On the other hand, we found that biouptake of Hg in the presence of cysteine was highly dependant on the concentration of the ligand, consistent with the results of Schaefer & Morel [3]. From 0.1 to 10μM of cysteine, we observed a significant increase in Hg biouptake while 100 and 1000μM of cysteine resulted in a dramatic drop in biosensor signal. Both glutathione and penicillamine enhanced Hg biouptake when they were present at low concentrations, with the lowest concentration (0.1μM) leading to the highest biosensor signal. As their concentration reached a certain threshold (10μM for glutathione and 100μM for penicillamine), Hg uptake was severely inhibited.

We calculated the chemical speciation of Hg in the exposure medium using ChemEQL with thermodynamic constants selected from the JESS database [4]. Results show that in most instances Hg was predominantly complexed by the added organic ligands, indicating that Hg-ligand complexes contribute to Hg biouptake.

Significance

This study suggests that Hg biouptake can be promoted by the presence of organic ligands in solution. Our results parallel the findings from Hg biomethylation experiments, indicating a promising application of biosensor for studying Hg biouptake.

[1] Benoit, Gilmour & Mason (1999) *Environ Sci Technol* **35**, 127-132. [2] Dahl, Sanseverino & Gaillard (2011) *Environ Chemistry* 8, 552-560. [3] Schaefer & Morel (2009) *Nat Geosci* 2, 123-126. [4] http://jess.murdoch.edu.au/jess_home.htm.

https://doi.org/10.1180/S0026461X00008434 Published online by Cambridge University Press

Fe reduction and atom exchange rates during redox oscillation of Luquillo CZO forest soils

AARON THOMPSON[1*], BRIAN GINN[1], VIKTOR TISHCHENKO[1], CHRISTOF MEILE[2], JARED WILMOTH[1], TIM PASAKARNIS[3], AND MICHELLE SCHERER[3]

[1]Univ. of Georgia, Crop & Soil Sci., Athens, USA, *AaronT@uga.edu, jwilmoth@uga.edu, tiviserg@gmail.com, bginn3@gmail.com

[2]Univ. of Georgia, Marine Sci., Athens, USA, cmeile@uga.edu

[3]Univ. of Iowa, Envron. Engin. & Sci., Iowa City, USA, timothy-pasakarnis@uiowa.edu, michelle-scherer@uiowa.edu,

The fate and bioavailability of carbon in soil undergoing frequent shifts in redox status are tightly coupled to iron cycling We examined the influence of dynamic redox conditions on soils from the Bisley Site of the Luquillo Critical Zone Observatory in Puerto Rico. These soils contained ~2 g kg^{-1} C and ~62 g kg^{-1} Fe that resides predominately in a nano-crystalline Fe^{III} oxyhydroxide phase with an ^{57}Fe Mössbauer spectra most similar to nano-goethite. We conducted eight-week incubations of triplicate soil slurries subjected to 0 - 21% O_2 redox oscillations with a ratio of time under oxic to anoxic conditions of 1:6at three frequencies (3.5-d, 7-d, and 14-d). HCl-extractable Fe^{II} was reduced to less than 30 mmol kg^{-1} soil during all oxic cycles and increased to >140 mmol kg^{-1} soil and included a significant contribution from $Fe^{2+}_{(aq)}$ during the reducing cycles. As the experiment progressed, the rate of Fe reduction increased, and the Fe^{II} concentration reached a plateau of ca. 160 mmol kg^{-1} during each reducing cycle. This coincides with the amount of Fe extractable by citrate-ascorbate and the portion of Fe^{III} that magnetically orders between 77K and 13K in the Mössbauer spectra. By the end of the experiment newly precipitated Fe could be re-reduced in less than three days. Synthesis of this experimental data within our preliminary numerical model suggests temporal dynamics of Fe(II) can be explained by minor increases in the population of Fe reducers accompanied by progressive reductive dissolution of recalcitrant Fe(III) solid phases. To further constrain the rapid turnover of iron oxides, we probed the susceptibility of soil Fe phases toward Fe^{II}-facilitated atom exchange using isotopically-labeled Fe^{2+}(aq) coupled with a numerical model. We found that aqueous Fe atoms can be exchanged with both the labile (0.5 M HCl-extractable) and bulk (7M HCl-extractable) Fe pools, with turnover times on the order of hours and months, respectively.

Quadrupolar corrections and increased accuracy for non-bridging oxygen measurements in silicate glasses using ^{17}O NMR

LINDA M. THOMPSON[1*], JONATHAN F. STEBBINS[1]

[1]Department of Geological and Environmental Science, Stanford University, Stanford, USA, lison@stanford.edu (* presenting author)

Abstract

Oxygen-17 nuclear magnetic resonance (NMR) has been used to investigate glass and melt structure, providing useful insights. In particular, ^{17}O NMR is being used to measure the non-bridging oxygen (NBO) content as a way to test structural models in a wide variety of glasses, especially metaluminous aluminosilicate glasses where NBO are present. Because of the importance of accurate measurements in these areas, we have synthesized a crystalline barium silicate, $BaSiO_3$, and a barium silicate glass, $(BaO)_{0.43}(SiO_2)_{0.57}$, in order to test the accuracy of this technique. These samples were chosen for the resolution between the NBO and BO components of the spectra, to reduce the sources of error introduced by overlapping. For the $BaSiO_3$, correcting the observed intensities for the quadrupolar effects as in Massiot et al., 1990[1], we measure an NBO content of 67.6% versus the known value of 67.7%. Applying the same correction technique to the glass gives a measured NBO content of 58.4 % ± 0.7% versus the 55.5% ± 1.6% expected from stoichiometry (based on EMPA analysis). Comparison with the frequently used technique of sideband subtraction shows that this method offers a simple and robust correction, especially in glasses where estimates must be made for the asymmetry and average quadrupolar values. By improving our knowledge of the accuracy of this technique, we should be able to provide new insight into questions such as the presence of absence of measureable amounts of free oxide ions or oxygen triclusters in both simple silicate and more complex aluminosilicate glasses.

[1] Massiot et al. (1990) Journal of Magnetic Resonance **90** 231-232

https://doi.org/10.1180/S0026461X00008434 Published online by Cambridge University Press

Evidence for the role of carbonate melts in the origin of superdeep diamond inclusions from the Juina-5 kimberlite, Brazil.

A.R. THOMSON[1*], M.J. WALTER[1], S.C. KOHN[1], B.C. RUSSELL[1], G.P. BULANOVA[1], D. ARAUJO[2] AND C.B. SMITH[1]

[1]School of Earth Sciences, University of Bristol, Bristol, BS8 1DR, UK, andrew.thomson@bristol.ac.uk (* presenting author)
[2]Instituto de Geociências, Universidade de Brasília, CEP 70910-900 Brasília, DF, Brazil

Over the past 30 years multiple studies of inclusions in naturally occurring diamonds have observed minerals which must have formed at sublithospheric depths in the earth [1]. In a recent study [2], lower mantle minerals interpreted to have formed in a basaltic protolith were found as inclusions in diamonds from the Juina-5 kimberlite, Brazil. These inclusions demonstrate subduction of ocean floor material into the lower mantle, and implicate diamond formation in the deep mantle from carbon-bearing fluids or melts.

This study reports the finding and analysis of new inclusions from the Juina-5 kimberlite. We find multiple examples, to complement those previously reported, of phases corresponding to those stable in a basaltic protolith at transition zone and lower mantle pressures. Most inclusions have undergone retrograde reactions and/or unmixing during acsent to the surface. Inclusions include several examples of unmixed NAL phase, iron-rich phases similar to TAPP, and multiple calcium- and titanium-rich phases with perovskite stoichiometry.

During the study samples have been analysed both by electron microbe and SIMS to determine major and trace element compositions. Early results show that the calcium perovskite phases are highly enriched in incompatible elements including REE and HFSE, but are depleted in LILE. The trace element enrichments and abundance patterns are very similar to Ca-Ti-perovskite inclusions found in the Collier-4 kimberlite [3], located approximately 50km from Juina-5. Consistent with previous results [3], we interpret these inclusions as crystallisation products of small degree melts from subducted carbonated basaltic crust. Melting of carbonated basalt may occur in thermalized lithosphere stranded in the transition zone or lower mantle [4]. The melt can then be reduced upon infiltration into surrounding mantle, which is reducing and likely bearing a free metal phase; the carbonate component of the melt is thus reduced and forms diamond by redox freezing [5].

[1] Harte (2010) *Min Mag.* **74**, 189-215. [2] Walter *et al.* (2011) *Science* **334**, 54-57. [3] Walter *et al.* (2008) *Nature* **454,** 622-625. [4] Litasov & Ohtani (2010) *EPSL* **295**, 115-126. [5] Rohrbach & Schmidt (2011) *Nature* **472,** 209-212

Removal of volatile groundwater contaminants in vertical soil filter systems: quantitative process analysis

MARTIN THULLNER[1*], CECILIA DE BIASE[2], ULI MAIER[3] AND SASCHA E. OSWALD[4]

[1] Department of Environmental Microbiology, Helmholtz Centre for Environmental Research - UFZ, Leipzig, Germany, martin.thullner@ufz.de (* presenting author)
[2] Department of Environmental Microbiology and Department Groundwater Remediation, Helmholtz Centre for Environmental Research - UFZ, Leipzig, Germany, cecilia.debiase@ufz.de
[3] Center for Applied Geosciences, University of Tübingen, Tübingen, Germany, uli.maier@uni-tuebingen.de
[4] Institute of Earth and Environmental Sciences, University of Potsdam, Potsdam, Germany, sascha.oswald@uni-potsdam.de

Biodegradation of groundwater contaminants is a common remediation strategy but the assessment of the remediation success is challenged by abiotic processes leading to contaminant concentration reductions without the desired destructive mass removal. In unsaturated subsurface systems volatile contaminants might enter the soil air and such volatilization might eventually be a significant contribution to contaminant mass removal and to emissions of contaminants into the atmosphere. Any assessment of the fate of volatile contaminants in such systems thus needs to distinguish between the contribution of biodegradation and of volatilization to observed contaminant removal.

The present study focuses on the processes controlling the removal of benzene and MTBE from groundwater applied to pilot scale vertical flow filter systems. The soil filter systems were intermittently irrigated by the contaminated groundwater which led to a highly transient flow and transport system. Measured contaminant concentrations indicated a high mass removal [1] but did not allow for a quantitative assessment of individual removal processes due to the high spatio-temporal dynamics of the systems. To obtain such quantitative analysis conservative solute tracer tests, stable isotope fractionation and measurements of natural radon concentration in the treated groundwater [2] were used as additional data basis for a reactive transport modeling approach. Numerical simulations using the model MIN3P considered variably saturated flow, the transport of species in the water and the gas phase as well as the biogeochemical transformation of reactive species.

The model allowed for reproducing the experimental data and the model results suggest that for the investigated volatile compounds biodegradation is the dominating mass removal process with volatilization contributing only to minor or negligible amounts. These results indicate that also gas phase gradients of volatile compounds can be affected by biodegradation suggesting the unsaturated zone to act as a biofilter for contaminants in the soil air.

[1] Van Afferden (2011) *Water Research* **45**, 5063-5074.
[2] De Biase (2011) *Ecological Engineering* **37**, 1292-1303.

https://doi.org/10.1180/S0026461X00008434 Published online by Cambridge University Press

Phosphate effects on copper and lead sorption to ferrihydrite

C. TIBERG[1*], J.P. GUSTAFSSON[2], C. SJÖSTEDT[2], I. PERSSON[3]

[1]Swedish University of Agricultural Sciences, Dep. of Soil and Environment, Uppsala, Sweden, Charlotta.Tiberg@slu.se*
[2]KTH (Royal Institute of Technology), Dep. of Land and Water Resources Engineering, Stockholm, Sweden, gustafjp@kth.se, carinsj@kth.se
[3] Swedish University of Agricultural Sciences, Dep. of Chemistry, Uppsala, Sweden, Ingmar.Persson@slu.se

Introduction

Elevated concentrations of phosphate can retard transport of copper and lead in soil. More detailed knowledge about the mechanisms behind this is of interest for example in risk assessments of contminated soils. It is well known that the mineral pyromorphite is formed at high concentrations of lead and phosphate in combination with high pH. This effect has been used to immobilize metals in remediation of contaminated soil. It has also been shown that the sorption of lead and copper to iron oxide surfaces [1, 2] may be enhanced in precence of phosphate but the details of how phosphate interacts with copper/lead and iron oxide has not yet been established, and there are seemingly contradictory results [1, 3]. This mechanism acts also at low concentrations of metal and phosphate when no precipiatates are formed.

Methods

Here, batch experiments, X-ray absorption spectroscopy (EXAFS) and surface complexation modeling with the three-plane CD-MUSIC model has been used to study the effect of phosphate on sorption of copper and lead to ferrihydrite. The aim is to investigate what surface complexes that are formed and to derive new and improved surface complexation constants.

Results and conclusions

The results show that addition of phosphate increases the sorption of copper and lead to ferrihydrite in batch experiments as compared to the same system without addition of phosphate. The effect is stronger than predicted by the CD-MUSIC model when considering electrostatic interactions only and as will be shown, the results from EXAFS analysis support this observation. The EXAFS results show, in agreement with earlier studies [4, 5], that copper and lead form bidentate mononuclear complexes on ferrihydrite in systems without phosphate. However, in the presence of phosphate, other complexes are formed. The results are being used to suggest new surface complexation constants for reactions that consider ternary interactions.

[1] Xie and Giammar (2007) In *Adsorption of metals by geomedia II* (Eds. M.O. Barnett and D.B. Kent) **7**, 349-373
[2] Lin et al (2004) *Colloids and Surfaces A: Physicochem. Eng. Aspects* **234**, 71–75
[3] Weesner and Bleam (1998) *Journal of Colloid and Interface Science* **205,** 380-389
[4] Trivedi et al (2003), *Environ. Sci. Technol.* **37,** 908-914
[5] Scheinost et al (2001), *Environ. Sci. Techno.l* **35,** 1090-1096

Carbonatite metasomatism: evidence from geochemistry and isotope composition (U-Pb, Hf, O) on zircons from two Precambrian carbonatites of the Kola Alkaline Province

MARION TICHOMIROWA[1*], MARTIN WHITEHOUSE[2], AXEL GERDES[3], JENS GÖTZE[1]

[1]TU Bergakademie Freiberg, Inst. Mineralogie, tichomir@mineral.tu-freiberg.de (* presenting author)
[2]Swedish Museum of Natural History, martin.whitehouse@nrm.se
[3]Goethe University Frankfurt,gerdes@em.uni-frankfurt.de

Zircon grains from two Precambrian carbonatites of the Kola Alkaline Province (Siilinjärvi, Tiksheozero) were studied by in situ geochemical and isotope investigations. Zircon domains which preserved the primary mantle signatures were identified by a combination of microscopic investigations of thin sections of the carbonatite rocks and separated zircon grains (optical microscopy, SE, CL, BSE images).

In case of the 2.6 Ga old Siilinjärvi carbonatite complex, the new carbonatite melt batch caused mainly solid state recrystallisation of former zircon grains. Zircon regions which preserved the primary signatures yielded high HREE/LREE ratios, undisturbed U-Pb ages, ε_{Hf} values close to CHUR (chondritic uniform reservoir), $\delta^{18}O$ values typical for the mantle, and Ti concentrations in accordance with known carbonatite melt temperatures. The solid state recrystallisation of zircon caused by carbonatite metasomatism led to (i) diffusion driven loss of HREE, Th, U, (ii) partial disturbance of the U-Pb system, (iii) a small shift of the $\delta^{18}O$ toward lower values.

In difference, in the 2.0 Ga old Tiksheozero complex the infiltration of a new carbonatitic melt led to dissolution-reprecipitation of former zircon grains. Dissolved-reprecipitated zircon grains often have a spongy texture with a lot of micro-inclusions of apatite, calcite and phlogopite. Apatite micro-inclusions seem to be most abundant according to elevated Th and U concentrations, lowered $\delta^{18}O$ values and increased Hf isotope ratios in such domains. These tiny apatite inclusions seem to be responsible for the widely occurring disturbance of the U-Pb dating system and for the unusually high Th/U ratios (>1) in many carbonatitic zircons worldwide. Hf and O isotope values varied widely even within a single zircon grain.

https://doi.org/10.1180/S0026461X00008434 Published online by Cambridge University Press

The Distribution of Gallium in the Nechalacho REE deposit, NWT, Canada

ALEXANDER TIMOFEEV* AND A.E. WILLIAMS-JONES

McGill University, Department of Earth & Planetary Sciences, alexander.timofeev@mail.mcgill.ca (* presenting author)

The layered Nechalacho Nepheline Syenite at Thor Lake, which is located within the alkaline to peralkaline Blachford Lake Complex near Yellowknife, Northwest Territories, is a potential source of exploitable gallium. It also contains large reserves of Rare Earth Elements (REE), Y, Nb, Ta and Zr, which are most enriched in the Basal Zone, an altered eudialyte cumulate layer [1]. Intense hydrothermal alteration involving replacement of primary magmatic mineral assemblages by a potassic assemblage comprising K-feldspar, biotite and magnetite, was followed by late albitisation.

Bulk-rock geochemical analyses and analyses of secondary minerals indicate that the Nechalacho Nepheline Syenite has unusually high concentrations of gallium, and that this element was both enriched and depleted by hydrothermal processes. Gallium occurs in concentrations more than a magnitude higher than its average concentration in crustal rocks. Similar enrichments are rare in nature, and the Nechalacho deposit therefore provides an excellent opportunity to identify the geochemical and mineralogical factors controlling the distribution of this element. Gallium can substitute for Al^{3+}, Fe^{3+} and other elements with similar valence and ionic radius, but is rarely found in a mineral dominated by this element.

Aluminium-bearing minerals from samples of the Nechalacho Nepheline Syenite with bulk rock Ga contents of 150 ppm or higher were analysed using the electron microprobe, following petrographic analysis. These samples are not unusually enriched in the REE. Analyses over the entire depth of a single drill hole were used to evaluate the relative importance of magmatic and hydrothermal processes to gallium enrichment.

Albite, orthoclase, biotite, chlorite, and allanite, in order of decreasing modal proportion, contain appreciable gallium. By contrast, the content of Ga in the Fe^{3+} mineral, aegirine, is below the limit of detection (≈140 ppm). Median Ga concentrations were ~ 250 ppm in albite, biotite, and chlorite and ~150 ppm in orthoclase. Variations of 200 ppm Ga or higher were observed in individual albite and orthoclase grains, and are linked to hydrothermal alteration. Fluid inclusion-rich zones in albite and orthoclase are characterised by significantly lower Ga contents than fluid inclusion-poor zones, in both albitised and non-albitised samples. Previous studies of the aqueous mobility of gallium suggest that hydroxyl and fluoride complexation may play a role in the hydrothermal mobilisation of gallium [2]. Chloritisation of biotite resulted in a Ga enrichment of ~ 150 ppm. Trends in gallium concentration for individual minerals along a single drill hole vary with the degree and nature of the alteration of the host rocks. Based on the observations presented here, albite and biotite are the principal hosts of Ga in the Nechalacho Nepheline Syenite, Ga enrichment was partially independent of REE concentration and Ga was both enriched and depleted by hydrothermal processes.

[1] Sheard *et al.* (2012) *Economic Geology* **107**, 81-104. [2] Wood & Samson (2006) *Ore Geology Reviews* **28**, 57-102.

Ten millennia of North Atlantic seasonality: evidence from stable isotope values of micromilled molluscs

SANDRA TIMSIC[1*], WILLIAM P. PATTERSON[1], BRUCE M. EGLINGTON[1], AND JOHN T. ANDREWS[2]

[1]University of Saskatchewan, Geological Sciences, sat903@mail.usask.ca (* presenting author); bill.patterson@usask.ca; bruce.eglington@usask.ca

[2]University of Colorado, Institute of Arctic and Alpine Research, John.T.Andrews@colorado.edu

Seasonality in temperature, the difference between winter low and summer high temperatures, is one of the dominant causal variables that determines the distribution of species through time. Bivalves are particularly valuable proxies of seasonality because growth bands of bivalve shells archive high-resolution records of temporally discrete environmental information, including water temperature recorded by $\delta^{18}O$ and diet/metabolism by $\delta^{13}C$ values. Here, we present a record of North Atlantic Holocene seasonality derived by computer-controlled micromilling of well-preserved mollusc shells recovered from a near shore marine core in NW Iceland. Thirty-seven aragonitic bivalve specimens retrieved from the core were sequentially micromilled concordant with growth banding to retrieve carbonate aliquots with subseasonal resolution, and then analysed for $\delta^{18}O$ and $\delta^{13}C$ values. Previous research [1] observed significant variations in seasonal temperature in this region over the period ~360 B.C to ~A.D 1660. Here, we extend this seasonality record back to ~10,650 cal years BP, thus providing the first ~10,000-year record of climatic snapshots ~1 to 9 years in duration for the North Atlantic.

Our sampling resolution (generally 30-50μm) generated subseasonal (*e.g.* weekly to bi-monthly) $\delta^{18}O_{(CaCO3)}$ and $\delta^{13}C_{(CaCO3)}$ records from molluscs that recorded ambient seafloor water temperatures during their lifetimes. Most of the molluscs were from the genera *Macoma*, *Nuculana*, and *Thyasira*, all recovered from a single core (core ID: MD99-2266). The temperature record archived as $\delta^{18}O_{(CaCO3)}$ values was calculated assuming a constant bottom water value of 0.1‰ (based on ~50 years of $\delta^{18}O$ measurements from the bottom waters of our study region) and using an aragonite temperature-fractionation relationship [2].

Our results indicate that the oldest 1/3 of the record (~10,100 – 7,600 cal yr BP) displayed maximum summer temperatures ~2°C higher than the subsequent period from ~7,000 – 4,500 cal yr BP, while the winter temperatures were similar throughout both periods. Sporadic warm periods after 4,500 cal yr BP are evident, where the maximum summer temperatures reached ~7 to 9°C at ~4,500 and ~3,400 cal yr BP. The highest reconstructed temperatures of the entire 10,000-year record occurred during the Roman Warm Period (~200 B.C. to A.D. 400), higher than modern temperatures (typically ranging between -1 to 11°C). Temperatures calculated for the Little Ice Age were similar to those from ~10,100 to 7,600 cal yr BP and 4,500 – 2,000 cal yr BP.

[1] Patterson *et al*. (2010) *PNAS* **107**, 5306-5310. [2] Patterson *et al*. (1993) *Geophysical Monograph* **78**, 191-202.

https://doi.org/10.1180/S0026461X00008434 Published online by Cambridge University Press

Arsenic association with iron-based colloids in historic gold mine tailings

KATHRYN J. TINDALE[1], PRITESH J. PATEL[2] AND DIRK WALLSCHLÄGER[3*]

[1]Trent University, Peterborough, Canada, kathryntindale@trentu.ca
[2] Trent University, Peterborough, Canada, priteshpatel@trentu.ca
[3] Trent University, Peterborough, Canada, dwallsch@trentu.ca
(* presenting author)

Background

Historic gold mining activities in Nova Scotia, Canada, have left behind large amounts of spent and weathered tailings material that usually contains very high arsenic concentrations. Several of the larger abandoned mining sites are in proximity of residential areas, raising potential concerns about arsenic export off-site via surface and/or ground water flow. Previous studies have found elevated arsenic concentrations in surface, pore and ground waters at the sites. Since physical and chemical speciation have significant impacts on arsenic mobility and toxicity, we investigated if colloidal arsenic species existed in the waters at these sites.

Methods

64 surface water, ground water and pore water samples were collected at three locations within two abandoned gold mine sites in Nova Scotia in May 2011. Samples were analyzed for colloidal arsenic, as well as other colloidal constituents, by asymmetric flow-field flow fractionation-inductively-coupled plasma-mass spectrometry (FFF-ICP-MS), for dissolved arsenic species by anion-exchange chromatography-ICP-MS, and for total dissolved arsenic by ICP-MS.

Results

Colloidal arsenic fractions were encountered only in a small number of the collected samples. In those samples, colloidal arsenic constituted < 20 % of the total dissolved arsenic. Most of the colloidal arsenic was associated with iron-based mineral particles of 6 – 9 nm mean diameter. Based on the iron/arsenic ratio of these colloids, they appeared to be either discrete iron-arsenic minerals like scorodite, or iron (oxy)hydroxide with adsorbed arsenate. In one sample, we also obtained some tentative evidence of arsenic being associated with very small (< 2 nm mean diameter) organic matter-based colloids, which also contained iron and manganese.

To our knowledge, this is one of the first reports of the existence of colloidal arsenic in ambient samples. At the studied sites, colloidal arsenic was only an infrequent and minor component of the total dissolved arsenic concentration during the conducted sampling campaign, and therefore probably not very important for the overall transport and toxicity of arsenic in these systems.

Acknowledgments

Funding for this study was provided by the National Science and Engineering Research Council of Canada (NSERC) through a Strategic Project Grant. The assistance of Mike Parsons (Natural Resources Canada), Heather Jamieson, Andrew Gault and Stephanie DeSisto (Queen's University) and Laura Tyler (Trent University) before and during the field campaign is gratefully acknowledged.

The Study of the Sequence Stratigraphy and the Sedimentary Enviroment of Ordovician in Southern Margin of Sichuan Basin

YANG WEI[1] ,ZHANG TINGSHAN[2*],LIU ZHICHENG[3] , AND MIN HUAJUN[4]

[1]State key laboratory of oil and reservoir geology and exploitation,Chengdu, China
rexswpu@163.com
[2] State key laboratory of oil and reservoir geology and exploitation,Chengdu, China
zts_3@126.com (* presenting Author)
[3] State Key Lab.of Oil&Gas Reservoir G&E Engineering,Chengdu, China,
rex_swpu2005@126.com
[4] State Key Lab.of Oil&Gas Reservoir G&E Engineering,Chengdu, China
minesky@126.com

Southern margin of Sichuan Basin contains well developed Ordovician, which carbonate rocks in this area are well developed and widely distributed except for the Wufeng Formation in upper Ordovician and the Meitan Formation in lower Ordovician, those are clastic deposition. According to the data analysis of outcrop and bore hole in the study area, the sequence stratigraphic framework of Ordovician was established using the application of theories in carbonate sequence stratigraphy, combined with petrology, paleontology, the characteristics of carbon and oxygen isotopic, six third-order sequences were developed from the Lower Ordovician to the Upper Ordovician, and each sequence can be subdivided into transgression systems tract (TST) and high systems tract (HST),but be lack of the lowstand system tract(LST) because the study area of Ordovician was mainly located on a carbonate platform. On this basis, it is shown that the broadly open sea shelf type with flat floor and the platform sediment model are well developed in the study area of Ordovician. There were two large scale sea-level rise in the Ningguo period of the Lower Ordovician and Wufeng period of the Upper Ordovician between Linxiang period. Under the effect of sea-level changes, the carbonate platform was rapid coverd by the accumulation of siliciclastic. During the period the western Yangtze plate developed a wide sea shelf and shale deposited, which occurred carbonate platform drowning incidents. The results reveal that the carbon and oxygen isotopic migration are consistent with the process of environment changes. Sea level changes were the principal factor that controlled the development of Ordovician depositional system in southern margin of Sichuan Basin of Ordovician. It is found that the carbon and oxygen isotopic change in the grain size sediment is not only closed to the sea-level changes, but better identify to the condensed section, sequence boundaries et al, which can be used as a reliable secondary sign to determine the sequence stratigraphy division and the depositional environment.

Reference:

[1]Feng Zengzhao. Lithofacies paleogeography of the Cambrian and Ordovician in China[M]. Beijing: Petroleum Industry press,2009.(Chinese with English Abstract)
[2]Wang Xunlian. The define of outcrop sequence stratigraphy and the identification of different levels standard in sedimentary sequence[J]. Science in China(Series D), 2003,33(11):1057-1068.
[3]Zhu Binquan. isotope System theory and application in earth science[M].Beijing: Sciences Publishing House,1998,247-257. (Chinese with English Abstract)

https://doi.org/10.1180/S0026461X00008434 Published online by Cambridge University Press

Mg isotopes in natural waters: what do they mean?

EDWARD T TIPPER[1]

[1]Dept. Earth Sciences, University of St Andrews, Fife KY16 9AL, UK, ett@St-Andrews.ac.uk

It has been known for decades that river water elemental or isotopic ratios are controlled by mixtures of end-members with differing compositions. The compositions of such end-members are either inherited from heterogeneity in the orginal lithological sources (e.g., carbonate, silicate and evaporite) or from process-related fractionation of elemental or isotopic ratios during weathering. Distinguishing process-related variations from lithological mixing trends is a problem fundamental to partitioning weathering fluxes between different sources, and are a fundamental problem for quantifying the carbon consumption associated with silicate weathering. In most catchments, distinguishing chemical signatures in river waters related to lithology from those related to weathering processes is complex because of heterogeneous lithology.

New isotopic tracers such as the isotope ratios of Mg therefore have the potential to help deconvolve the extent to which rivers reflect mixing, or the extent to which rivers have compositions which are chemically evolved by physicochemical processes. In a geological context this is similar to distinguishing fractionational crystallisation from magma mixing. The stable isotopes of Mg offer important advantages over more common place isotope ratios such as Sr, that have been used for decades. This is because they have the potential to trace both source and process effects of one the major cations in solution rather than just source effects of a trace cation. It is now more than a decade since Mg isotope ratios have been published on natural waters, but progress in using them to place constraints on the origin of solutes requires careful calibration before the data can be successfully applied.

Almost all published Mg isotope data on natural waters falls between the end-member δ^{26}Mg values of the carbonate and silicate rocks that are drained. This could suggest that waters simply relfect mixing between end-members, but coherent relationships with elemental ratios that have typically been used to infer mixin relationships are rare. This leads to a catch22 scenario: Is it possible to infer a mixing relationship using an X/Mg ratio when δ^{26}Mg doesn't show the same relationship?

In simple mono-lithological catchments where there is inferred to be a single source of Mg, δ^{26}Mg is apparently fractionated and co-varies with Li isotopes. The relationship between Mg and Li is complex. Li isotopes are thought to be strongly influenced by clay, but the precise relationship between Mg, Li and clay is not yet known. The mixing versus process problem will be discussed with examples, illustrating what we have learned so far from Mg isotopes in natural waters, and the many things that Mg isotopes still have to tell us about.

Immobilisation of hexavalent actinides in cementitious materials: Evidence for structural incorporation in calcium-silicate-hydrates

J. TITS[1*], N. MACÉ[1], T. STUMPF[2], C. WALTHER[2], E. WIELAND[1]

[1]Paul Scherrer Institute, Laboratory for Waste Management, CH-5232 Villigen-PSI, Switzerland

[2]Karlsruhe Institute of Technology, Institute for Nuclear Waste Disposal, D-76021, Karlsruhe, Germany

*Corresponding author: jan.tits@psi.ch

Abstract]

Cementitious materials are an important component of the multi-barrier concepts developed in many countries for the safe disposal of low and intermediate level radioactive waste in deep geological repositories. Studies of the retention of radionuclides by cementitious materials have focused predominantly on adsorption as the relevant uptake process. However, other immobilization processes, such as incorporation in the solid matrix, may take place and, thus, exert a beneficial effect on radionuclide retardation. Calcium silicate hydrates (C-S-H), the major cement constituent, are characterized by high recrystallisation rates making them an ideal system for the incorporation of radionuclides present in cement-based repositories.

In the present study, wet chemistry and luminescence spectroscopy experiments have been performed under high pH conditions, with the aim of determining the speciation of hexavalent actinides (An(VI)), U(VI) and Np(VI), in C-S-H. Batch sorption experiments have been carried out with C-S-H and titanium dioxide, a solid phase stable under high pH conditions and often used as a model material for surface complexation studies. Comparison of the sorption of U(VI) and Np(VI) on both solids allows the influence of incorporation processes on the immobilisation of hexavalent actinides by C–S–H to be determined.

The An(VI) sorption behaviour on TiO_2 and on C-S-H phases appeared to be nearly identical; R_d values were found to decrease with the increasing predominance of negatively charged species in the aqueous phase suggesting the weaker sorption of these actinyl anions. Uranyl-doped C–S–H exhibited inhomogeneously broadened luminescence bands following non-selective laser excitation at liquid helium temperature (4K). Luminescence spectra following selective resonant laser excitation showed these broad band structures to consist of a superposition of many overlapping narrower bands associated with slightly different non-interacting uranyl luminescence centers in a disordered environment indicating incorporation in the amorphous C–S–H structure. The characteristics of the luminescence spectra provided information on the local coordination geometry of the incorporated uranyl moiety leading to the conclusion that it is incorporated in the C–S–H interlayers. The study shows that, under high pH conditions, the wet chemical behaviour (pH dependence and effect of aqueous Ca concentration) is similar for An(VI) incorporated in the interlayers of C–S–H and uranyl bound on the surface of TiO_2.

https://doi.org/10.1180/S0026461X00008434 Published online by Cambridge University Press

Microbial transport through rock and its importance for microbially-induced mineral precipitation

DOMINIQUE J. TOBLER[1*], SUSITHRA LAKSHMANAN[1] AND VERNON R. PHOENIX[1]

[1]School of Geographical and Earth Sciences, University of Glasgow, Glasgow, G12 8QQ, UK (*correspondence: dominique.tobler@glasgow.ac.uk)

Emerging bio-technologies offer natural, minimally invasive and cost-effective methods for dealing with environmental remediation and engineering problems. Microbially-induced mineral precipitation could become one of these innovative technologies as it has shown great potential for soil stabilisation, solid-phase capture of pollutants and porosity sealing to control leakage at nuclear waste depository and CO_2 storage sites. Critically, deployment strategies for microbially-induced processes are heavily dependent on the movement, homogeneous distribution and viability of micro-organisms over long injection distances. Problematically, we have little understanding of how microorganisms are transported in subsurface rock environments.

Initial data on bacterial transport through sandstone clearly showed that bacteria get easily immobilised in rock compared to packed sand [1] (Figure below). This is a significant problem as most previous bacterial transport studies have been undertaken on homogeneous packed sand; data which clearly cannot be used reliably to predict bacterial transport through rock. Furthermore, the subsurface is inherently heterogeneous, leading to preferential flow paths, and this will greatly affect bacterial transport behaviour.

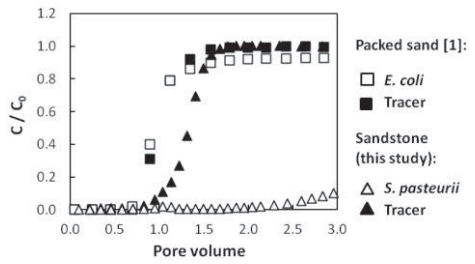

Figure: Breakthrough curves for bacteria (10^8 cells/ml) and a conservative tracer (0.3 mM NO_3).

Here, Breakthrough Curve (BTC) analyses were extended to quantify the effect of rock composition, heterogeneity and injected bacterial density on bacterial transport through porous and fractured rock. BTC data was modelled using colloidal filtration theory to obtain information about the dispersivity and sticking efficiency of injected microorganisms. This data was then used to develop and test improved injection strategies for the application of microbially-induced mineral precipitation to seal subsurface rocks. For this, different rock cores were subjected to repeated cycles of ureolysis-driven calcite precipitation until a significant decrease in permeability was measured. The spatial distribution of the produced calcite fill, and thus the effectiveness of the applied injection approach, was quantified using scanning electron microscopy.

[1] Liu et al. (2011) *EST* **45**, 3945–3951.

Involvement of recycled silica-rich pyroxenite in continental intraplate magmatism: Evidence from alkaline basalts in NW Kyushu, SW Japan

SATOSHI TOKESHI[1*], RYOJI TANAKA[1], KATSURA KOBAYASHI[1], AKIO MAKISHIMA[1] AND EIZO NAKAMURA[1]

[1]The Pheasant Memorial Labaratory for Geochemistry and Cosmochemistry, Institute for Study of the Earth's Interior (ISEI), Okayama University at Misasa, Tottori, Japan, tokeshi@misasa.okayama-u.ac.jp

Abstract

Recycled silica-rich materials such as pyroxenite (eclogite) are important sources of mantle-derived magmas not only in oceanic magmatism but also in continental intraplate magmatism [1]. Here, we show an evidence for presence of the silica-rich pyroxenite in the continental intraplate magmatism by using major and trace elements and Sr-Nd-Pb-Hf isotopes for Miocene alkaline basaltic lavas from northwestern Kyushu, SW Japan. The alkaline lavas, defined by silica versus total alkali contents, are mostly normative hypersthene. In contrast, alkali basalts with normative nepheline are scarce. Their primitive mantle-normalized trace element patterns show strong enrichment in incompatible elements and remarkable negative spikes in B, Pb and Li, and some of the alkaline lavas show slightly weak depletions in high-field strength elements (HFSE). The isotopic compositions in the alkaline lavas significantly correlate with major elements (e.g. SiO_2, MgO, CaO, Na_2O and CaO/Al_2O_3) and trace element ratios (e.g. Nb/U, Zr/Hf and Sr/Nd). These correlations cannot be explained either by shallow-level magma chamber processes such as fractional crystallization and in situ crustal assimilation, or variable degree of partial melting of a homogeneous mantle source. Instead, constraints from coupling between the major element compositions and those of partial melts of the silica-rich pyroxenites from high pressure experiments (e.g. [2] and [3]), and the negative correlation of $^{176}Hf/^{177}Hf$ versus Zr/Hf, these indicate the involvement of the recycled silica-rich pyroxenite within an asthenospheric upwelling that triggered the continental intraplate magmatism. The correlations between the isotopic compositions and trace element ratios further suggest that the recycled silica-rich pyroxenite was derived from oceanic basaltic protoliths metasomatized by overlying sediment. It is thus inferred that the recycled pyroxenite and its peridotite matrix were major sources of the normative hypersthene melts and the normative nepheline melts, respectively. Mixing between their melts derived from lithologically and chemically distinct end-members would have taken place at low pressures in melt conduits and magma chambers. The involvement of crustal recycling might be closely linked with tearing of subducted stagnant slab beneath the East Asia.

[1] Sobolev *et al.* (2007) *Science* **316**, 412-417. [2] Pertermann & Hirschmann (2003) *J. Petrol.* **44**, 2173-2201. [3] Spandler *et al.* (2008) *J. Petrol.* **49**, 771-795.

https://doi.org/10.1180/S0026461X00008434 Published online by Cambridge University Press

Temporal and depth variation of Os isotope composition in ferromanganese crusts from the Takuyo Daigo Seamount (#5 Takuyo Smt), northwestern Pacific Ocean

AYAKA TOKUMARU[1*], TATSUO NOZAKI[2], KOSUKE T. GOTO[3], YUTARO TAKAYA[4], KATSUHIKO SUZUKI[2], QING CHANG[2], YASUHIRO KATO[4], AKIRA USUI[5], AND TETSURO URABE[1]

[1]Dept. of Earth and Planet. Sci., Univ. of Tokyo, Tokyo 113-0033, Japan, tokumaru@eps.s.u-tokyo.ac.jp (* presenting author)
[2]IFREE/SRRP, JAMSTEC, Yokosuka 237-0061, Japan
[3]GSJ, AIST, Tsukuba 305-8567, Japan
[4]Dept. of Systems Innov., Univ. of Tokyo, Tokyo 113-8656, Japan
[5]Natural Sciences Cluster, Kochi Univ.,Kochi 780-8520, Japan

Introduction

Fe-Mn crusts were collected by *ROV Hyper Dolphin* / *RV Natsushima* (NT09-02 Leg.2 cruise) at the depth interval between 2,990 and 950 mbsl of the #5 Takuyo Smt directly from the outcrops using manipulator and underwater diamond saw. These samples allowed us to investigate systematically the temporal and depth variations of the geochemical compositions in the Fe-Mn crusts.

Os isotope compositions

Os isotope compositions in the surface layer (<3 mm) of the Fe-Mn crust coincide very well with those of present seawater values ($^{187}Os/^{188}Os$ ~1.06) regardless of the water depth. This result indicates that Fe-Mn crusts in the #5 Takuyo Smt are formed hydrogenetically and have a potential to provide paleoceanographic information. So, we measured Os isotope compositions perpendicular to the growth layer and applied the Os isotope stratigraphy (e.g., [1, 2]) to estimate the growth rate of the Fe-Mn crust. From the upper section of the sample, we found similar Os isotope profile with that of marine Os isotope evolution curve established from seafloor sediments. A negative Os isotope excursion ($^{187}Os/^{188}Os$ ~0.73) was also found around 36 mm depth from the surface layer. Given that this excursion reflects eruption of the Columbia River flood basalts during the middle Miocene [2], the growth rate of our Fe-Mn crust is estimated to be 3 mm/My. This is nearly consistent with the results of ^{10}Be dating method (ca. 4 mm/My). In the lower section, we found large deviation of Os isotope compositions from that of marine Os isotope evolution. This deviation can be explained either by the occurrence of growth hiatus (~34 Ma) or effects of phosphatization. Previous studies have reported hiatus [2-4]. Growth hiatus may record some global event, such as marine redox change. Alternatively, pronounce phosphatization of the older crust may cause the deviation [5]. Our result suggests that secondary phosphatization effects have to be taken into account when using the Os isotope stratigraphy.

Part of the present research is funded through TAIGA Project, a New Scientific Research on Innovative Areas, Grants-in-Aid for Scientific Research.

[1] Klemm et al. (2005) *EPSL* **238**, 42-48. [2] Klemm et al. (2008) *EPSL* **273**, 175-183. [3] Li et al. (2008) *Sci China Ser D-Earth Sci* **51(10)**, 1452-1459. [4] Meng et al. (2009) *Sci China Ser D-Earth Sci* **51(10)**, 1446-1451. [5] Koschinsky et al. (1997) *GCA* **61(19)**, 4079-4094.

Noble gases as proxies for the transport of deep pore fluids in the Lake Van (Turkey) sediments

YAMA TOMONAGA[1*], MATTHIAS S. BRENNWALD[1], ROLF KIPFER[1,2,3]

[1]Eawag, Swiss Federal Institute of Aquatic Science and Technology, Water Resources and Drinking Water, Duebendorf, Switzerland, tomonaga@eawag.ch (* presenting author)
[2]Institute of Biogeochemistry and Pollutant Dynamics, Swiss Federal Institute of Technology (ETH), Zurich, Switzerland
[3]Institute of Geochemistry and Petrology, Swiss Federal Institute of Technology (ETH), Zurich, Switzerland

The accumulation of non-atmospheric noble-gas isotopes allows tracing the geochemical origin and transport processes of the pore fluids in unconsolidated sediments [e.g. 1]. For instance, the abundance of terrigenic helium (He) isotopes reflects the residence time and transport dynamics of the dissolved species in the pore space. The $^{3}He/^{4}He$ ratio of terrigenic He can be used to constrain the geochemical origin of the pore fluids [1,2].

Lake Van (Turkey) is one of the largest terminal lakes and the largest soda lake on Earth. The lake basin is situated in a tectonically active region characterized by the presence of major faults and volcanoes and is known to accumulate mantle fluids [1,2,3]. Helium isotopes are therefore expected to yield insights into the origin and transport processes of terrigenic fluids in the sediment pore space and their release into the water body of Lake Van.

In summer 2010 the ICDP PaleoVan drilling project collected 220 m long sediment cores from Lake Van with the aim to study the past climate conditions in eastern Anatolia [4,5]. Within the frame of this deep-drilling project we collected bulk sediment samples for noble-gas analysis [6,7].

In this work we present He concentrations measured in the pore water of the ICDP PaleoVan sediment samples. These results are compared with He concentration profiles from short cores (< 2 m) taken at different sites throughout the lake basin [1] and discussed in terms the deep fluid transport in the Lake Van sediments.

[1] Tomonaga *et al.* (2011) *Geochim. Cosmochim. Acta* **75** (10), 2848–2864.
[2] Kipfer *et al.* (1994) *Earth Planet. Sci. Lett.* **125** (1-4), 357–370.
[3] Kaden *et al.* (2010) *Water Resour. Res.* **46**, W11508.
[4] Litt *et al.* (2009) *Quat. Sci. Rev.* **28** (15-16), 1555–1567.
[5] Litt *et al.* (2011) *Eos* **92** (51), 477–479.
[6] Brennwald *et al.* (2003) *Limnol. Oceanogr. Methods* **1**, 51–62.
[7] Tomonaga *et al.* (2011) *Limnol. Oceanogr. Methods* **9**, 42–49.

https://doi.org/10.1180/S0026461X00008434 Published online by Cambridge University Press

Measuring the speciation of iron in hydrothermal plume particles

BRANDY M. TONER[1*], JOHN A. BREIER, JR.[2], KATRINA J. EDWARDS[3], SIRINE C. FAKRA[4], CHRISTOPHER R. GERMAN[5], MATTHEW A. MARCUS[4], AND OLIVIER J. ROUXEL[6]

[1]Department of Soil, Water, and Climate, University of Minnesota, St. Paul, MN, USA, toner@umn.edu (* presenting author)
[2]Department of Applied Ocean Engineering, Woods Hole Oceanographic Institution, Woods Hole, MA, USA, jbreier@whoi.edu
[3]Departments of Biological Sciences and Earth Sciences, University of Southern California, Los Angeles, CA, USA, kje@usc.edu
[4]The Advanced Light Source, Lawrence Berkeley National Laboratory, Berkeley, CA, USA, sfakra@lbl.gov
[5]Department of Geology and Geophysics, Woods Hole Oceanographic Institution, Woods Hole, MA, USA, cgerman@whoi.edu
[6]Europole Mer, Universite de Bretagne Occidentale, Brest-Iroise, Plouzane, France, orouxel@univ-brest.fr

Abstract

The global mid-ocean ridge (MOR) system is a 60,000 km submarine volcanic mountain range that crosses all of the major ocean basins on Earth. Along the MOR, sub-seafloor circulation of seawater exchanges heat and elements between the ocean crust and seawater. The amount of iron (Fe) released by hydrothermal venting to the ocean per year is similar in magnitude to that of global riverine runoff. Until recently, measurement and modeling activities to understand the contribution of hydrothermal Fe to the ocean budget have been largely neglected.

The goal of the present research is to identify and quantify the forms of Fe present in hydrothermal plume particles to better understand the bioavailability, geochemical reactivity, and transport properties of hydrothermal Fe in the ocean. Direct Fe speciation data in hydrothermal plume precipitates has been reported only twice. This lack of data reflects how difficult it has been to obtain high quality samples and measure Fe speciation in the complex physical-chemical mixtures that compose hydrothermal plume particulates. These challenges have slowed our understanding of hydrothermal Fe speciation and transport, as well as the potential contribution of hydrothermal Fe to the global ocean budget.

On-going sediment trap deployments and new *in situ* filtration equipment are making it easier to obtain great samples. Improved synchrotron-radiation X-ray microprobe instruments and data analysis tools are making measurements of Fe speciation accessible and hold promise for quantitative research applications. In this contribution, the application of synchrotron-radiation X-ray microprobe to the mapping and quantification of Fe valence states and species will be discussed for hydrothermal plume particles collected by sediment trap and *in situ* filtration at the East Pacific Rise 9-10 N.

Timing and source of cold seeps at the northern slope of South China Sea: Evidence from U/Th dating and Sr isotopes

HONGPENG TONG[1], DONG FENG[2], HAI CHENG[3, 4], SHENGXIONG YANG[5], HONGBIN WANG[5], ANGELA M. MIN[4], R. LAWRENCE EDWARDS[4] AND DUOFU CHEN[1, 2 *]

[1]CAS Key Laboratory of Marginal Sea Geology, Guangzhou Institute of Geochemistry, Chinese Academy of Sciences, Guangzhou, China, cdf@gig.ac.cn
[2] CAS Key Laboratory of Marginal Sea Geology, South China Sea Institute of Oceanology, Chinese Academy of Sciences, Guangzhou, China, fd@gig.ac.cn
[3]Institute of Global Environmental Change, Xi'an Jiaotong University, Xi'an, China
[4]Department of Geology and Geophysics, University of Minnesota, Minneapolis, USA
[5]Guangzhou Marine Geological Survey, Guangzhou, China

Methane-rich fluid and gas expulsion often leads to authigenic carbonate formation close to the seafloor along continental margins. These carbonates represent excellent geochemical archives of methane emanation and possibly gas hydrate destabilization. Here, we report U/Th dating and Sr isotopes of seep carbonates from Shenhu area and Dongsha area on the northern continental slope of South China Sea. The obtained data will be used to discuss the timing of cold seep activity and potential driving processes involved and the source of fluids as well. The U/Th ages of the carbonates span a long time interval. Especially, carbonates from Shenhu area show a wide range of U/Th ages, between 152 ka and 330 ka. In contrast, carbonates from Dongsha area reveal U/Th ages between 42 ka and 77 ka. However, most of the carbonates revealed U/Th ages that point to formation during sea level lowstand. In addition, some of the studied carbonates, for example, samples from Site 3 of the NE Dongsha area have positive $\delta^{18}O$ isotopic signatures, presumably caused by gas hydrate dissociation. The results suggest that enhanced fluid flow during these time intervals closely related to sea level variations associated with glacial/interglacial cycles and possibly environmental change that affected the stability of gas hydrate reservoirs. The $^{87}Sr/^{86}Sr$ ratios of the carbonates range between 0.709025 and 0.709259. Specifically, samples from SW Dongsha display less radiogenic values, that are lower than that of modern seawater (0.709175). The carbonates must have formed either at or near the seafloor in contact with less radiogenic pore fluids, presumably deeper in the sediment. In contrast, samples from all the other areas are characterized by more radiogenic Sr values, suggesting that the seep fluids in contact with more radiogenic terrigenous material such as basinal brine and/or meteoric water.

This study was funded by the NSFC (91028012), CAS (KZCX2-YW-GJ03), and 973 Program (2009CB219508).

https://doi.org/10.1180/S0026461X00008434 Published online by Cambridge University Press

High-throughput Analysis of Eco-toxicity of Nano-TiO_2 to Model Bacteria under Simulated Environmental Conditions

TIEZHENG TONG[1]*, CHU THI THANH BINH[2], JOHN J. KELLY[2], JEAN-FRANÇOIS GAILLARD[1], AND KIMBERLY A GRAY[1]

[1] Department of Civil and Environmental Engineering, Northwestern University, Evanston, USA, tiezhengtong2014@u.northwestern.edu
[2] Department of Biology, Loyola University Chicago, Chicago, USA

Introduction

Nano-TiO_2 (n-TiO_2) is among the most common engineered nanomaterials (ENM) and is applied in a diverse array of industrial and commercial products from sunscreens and disinfectants to catalysts. Due to its extensive applications and rapid growth of production, n-TiO_2 is inevitably released into natural environment, which has led to growing concerns on its potential environmental and health consequences. However, little is known about the effects of n-TiO_2 on bacteria under environmental conditions. In this study, we tested the toxicity of four types of commercialized n-TiO_2 to model bacteria *E. coli* and *B. subtilis* under simulated environmental conditions, with the help of the high-throughput screening technique.

Experimental design and results

Water collected from Lake Michigan was used as the solution matrix and a xenon arc lamp that provides simulated sunlight was used as the light source. Cell viability was evaluated with the BacLight Kit and reactive oxyten species (ROS) production was determined with carboxy-H_2DCFDA. Results confirmed a strong dependence of n-TiO_2 toxicity on the type of n-TiO_2 and illumination conditions. With broad spectrum illumination from the xenon arc lamp, Degussa P25 and two anatase exhibited significant toxicity to both bacteria while rutile caused no obvious toxicity. Under dark condition n-TiO_2 toxicity was almost negligible. Optic filters were used to assess the effects of light wavelength on n-TiO_2 toxicity. With exposure of Degussa P25 to light of above 400 nm, the viability of bacteria was similar to that under dark conditions, while exposure to light above 320nm produced cell mortality similar to that seen with broad spectrum illumination, indicating the importance of wavelengths between 320-400nm for n-TiO_2 toxicity. Suwannee River fulvic acid (SRFA) was used to assess the effects of natural organic matter (NOM) on n-TiO_2 toxicity. In contrast with the traditional assumption that NOM would enhance n-TiO_2 toxicity by reducing the size of n-TiO_2 aggregate, SRFA was found to decrease n-TiO_2 toxicity, probably due to its absorbance of light within UV region. Our study also suggests that photocatalytic activity of n-TiO_2, which is known to produce ROS, played an important role in bacterial inactivation. A correlation was observed between the decrease of bacterial viability and the increase of ROS production.

Significance

Environmental conditions determine the transport, fate and toxicity of n-TiO_2. Therefore, the simulated environmental conditions employed in our study makes our results more representative of the real scenario in the nature environment. Our study provides critical first steps in understanding the potential ecological effects of ENM.

Provenance, weathering and comminution ages of late Quaternary Weddell Sea sediments

A. TORFSTEIN[1,*], J. MCMANUS[1,2], S. HEMMING[1,2]

[1] Lamont-Doherty Earth Observatory, Columbia University, USA, adi.torf@ldeo.columbia.edu (* presenting author)
[2] Department of Earth and Environmental Sciences, Columbia University, USA, jmcmanus@ldeo.columbia.edu, sidney@ldeo.columbia.edu

The location and geometric setting of the Weddell Sea, one of the large marginal seas of Antarctica, make it a sensitive recorder of the input of subglacial erosion products from Antarctica over glacial-interglacial time scales.

We present a study of Pb, Sr and Nd isotopic compositions, U-decay series, and trace element concentrations of siliciclastic sediments deposited over the last ~250 kyrs in the East and North Weddell Sea (EWS and NWS, respectively). Each sample was separated into three grain size fractions of carbonate free material (>20um, 20-2um, <2um).

Significant differences are observed between sediment compositions between both studied regions as well as between grain size fractions within each sample. Lead isotopic compositions show a clear distinction between both sites with $^{206}Pb/^{204}Pb$ ratios in the EWS and NWS ranging between 17.958-18.307 and 18.655-18.939, repsectively. The isotopic composition of Sr is generally similar in both sites, 0.7152-0.7231, except for <2um particles from the NWS that significantly higher values between 0.7256 and 0.7338. The latter also display the strongest ^{234}U-depletion with ($^{234}U/^{238}U$) ratios typically ranging between 0.766-0.850.

These observations imply that the clay fraction in the NWS originates from a distant region, most likely East Antarctica, and that it was exposed to more intense weathering relative to the coarser particles. Hence, secular variations in $^{87}Sr/^{86}Sr$ and ($^{234}U/^{238}U$) ratios provide a sensitive recorder of changes in the combined effect of the sediments comminution ages (i.e., their time of transport between source and sink) and the intensity of weathering processes they were exposed to. Additional acid leaching experiments provide quantitative constraints on the effects of chemical weathering compared to the preferential loss of ^{234}U through recoil and will be discussed in the context of determining the sediments' comminution ages, which are closely connected to the history of the Weddell Gyre and Antarctic glacial weathering processes.

https://doi.org/10.1180/S0026461X00008434 Published online by Cambridge University Press

Uranium isotopic variations as a tracer of environmental contamination in sediment cores

R. TORTORELLO[1*], E. WIDOM[1], AND W. RENWICK[2]

[1] Department of Geology & Environmental Earth Science, Miami University, Oxford, Ohio, USA, tortorrd@muohio.edu (*presenting author)

[2] Department of Geography, Miami University, Oxford, Ohio, USA, renwicwh@muohio.edu

This study investigates potential environmental uranium contamination from the Fernald Feed Materials Production Center (FFMPC) located in SW Ohio. In 1951, the FFMPC site was established to process high purity uranium products from natural uranium ore and recycled recoverable residues, including enriched (EU) and depleted uranium (DU). The facility is estimated to have inadvertently released 200,000 to 1 million pounds of uranium into the environment during its operation from 1952 to 1985 [1]. Previous studies conducted in proximity to the FFMPC site have found elevated uranium concentrations in sediment cores [2] and non-natural uranium isotopic signatures indicative of an anthropogenic source in local tree bark [3].

This study tests the utility of lake sediment as a proxy for the temporal and aerial extent of uranium contamination, as well as to constrain the sources of uranium. A sediment core 80 cm in length was collected from an impoundment located 6.7 km south of the FFMPC site. The core was divided into 2 cm sections, resulting in forty sediment samples. Three samples that span the length of the core (top, middle and bottom) were analyzed using gamma spectrometry to determine ^{210}Pb and ^{137}Cs ages. The relative ^{210}Pb excess and the lack of measurable ^{137}Cs in the deepest sample suggest that it dates to the early 1950's and thus may pre-date any FFMPC activity.

Forty samples representing the entire sediment core were analyzed by ICP-MS, and were found to have U concentrations ranging from 0.33 to 1.33 ppm. Most samples exhibit a strong positive correlation between U and Th concentration. However, anomalously elevated U concentrations were found in nine consecutive samples from immediately above the base of the core (62 to 78 cm depth). In order to determine whether the elevated U was due to natural or anthropogenic sources potentially related to the FFMPC, twenty-one samples were analyzed for U isotopic composition by TIMS. The deepest sample, inferred to have been deposited in the early 1950's, has a natural ^{235}U/^{238}U signature and no measurable ^{236}U, consistent with this sediment pre-dating FFMPC activity. Furthermore, the samples with anomalously high U concentrations have variable ^{235}U/^{238}U ranging from DU to EU signatures (0.00645-0.00748), and all contain measurable ^{236}U with ^{236}U/^{238}U ranging from 2.1×10^{-6}–3.6×10^{-5}. Samples in the upper 0 to 40 cm of the core display natural ^{235}U/^{238}U signatures, but measurable ^{236}U/^{238}U, suggesting a continued presence of contaminant uranium in the local environment.

[1] Makhijani (2000) Inst. Energy & Environ 5. [2] Hardesty (1991) *Miami University*. 1-70. [3] Widom (2010) *Goldschmidt Conference Abstracts*.

H_2CO_3 and its Anions and Oligomers: Updates on Experimental and Theoretical Studies

JOHN A. TOSSEL[1,*]

[1] George Washington University, Department of Chemistry, 725 21st Street, Washington, DC 20052, tossell@gwu.edu (* presenting author)

Most chemistry textbooks assert that H_2CO_3 is the dominant species in aqueous carbonic acid. Yet, geochemists know that H_2CO_3 is present at only very low concentration in aqueous solution of carbonic acid, which is instead dominated by hydrated CO_2. H_2CO_3 has recently been characterized in cryoscopic environments and a species which is probably H_2CO_3-HCO_3^- has been created and characterized in aqueous solution. The dianion $(HCO_3^-)_2$ has been characterized as an impurity in calcite. All the oligomeric carbonate species are stabilized by H-bonding. Oligomeric H_2CO_3 has been suggested as a form in which anthropogenic CO_2 can be sequestered. Recent quantum studies on the structures and properties of these species will be presented.

https://doi.org/10.1180/S0026461X00008434 Published online by Cambridge University Press

Primordial mantle heterogeneities revealed by coupled ^{182}W and ^{186,187}Os investigations

M. TOUBOUL[1*], J. G. LIU[1], J. O'NEIL[2], I. S. PUCHTEL[1] AND R. J. WALKER[1]

[1]Department of Geology, University of Maryland, College Park, MD, 20742 USA, mtouboul@umd.edu (* presenting author), gobyliu@umd.edu, ipuchtel@umd.edu, rjwalker@umd.edu

[2]Observatoire de Physique du Glode de Clermont-Ferrand, Clermont-Ferrand, France, joneil@dtm.ciw.edu

Subtle W isotope anomalies within the Earth's mantle have been recently evidenced by high-precision measurements for 3.8 Ga Isua rocks [1], and the 2.8 Ga Kostomuksha komatiites [2]. These samples have ~15 ppm ^{182}W excesses, which are similar to the isotope composition of the mantle prior to the arrival of late accreted materials, as estimated assuming that the highly siderophile elements (HSE) present in the silicate Earth today were derived entirely from this HSE-rich extraterrestrial contribution. However, the mantle source of the Kostomuksha komatiites had total HSE abundances ca. 80% of those estimated for the modern mantle. These observations are inconsistent with Kostomuksha komatiites being derived from a pre-late accretionary mantle reservoir. Instead, their mantle source, also characterized by coupled ^{186,187}Os excesses [3], must have contained a primordial component, which is argued [2] to have formed during the lifetime of ^{182}Hf (<60 Myr after Solar System formation) via either magmatic differentiation or metal-silicate equilibration. These processes were modeled [2] to have resulted in development of high Hf/W, Pt/Os, and Re/Os ratios.

Here, we report new high-precision W isotope data for ~4.3 Ga rocks from the Nuvvuaggittuq supracrustal belt (Northern Quebec, Canada). These results, coupled with Os isotope and HSE abundance data, as well as published ^{142}Nd data [4], are used to further constrain the timing and the nature of processes involved in the generation of ^{182}W heterogeneities. Four samples analyzed show ^{182}W anomalies of ca. +16 ppm, whereas the other two have W isotope compositions that cannot be resolved from that of the modern mantle. Samples with positive ^{182}W anomalies have total HSE abundances between 45 and 60% of those estimated for the modern mantle. Assuming that their HSE abundances are representative of their source HSE composition, the data would indicate that a substantial proportion of the late accreted materials were delivered to Earth prior to ~4.3 Ga. This would imply that the ^{182}W anomalies of some Nuvvuaggittuq rocks must have been produced by an early mantle differentiation process and provide further evidence that geochemical heterogeneities were created in the Earth's mantle while accretion was still ongoing, most likely prior to the giant impact and the formation of the Moon at ~4.50 Ga. These mantle domains were preserved until at least the late Archean. Preservation of early differentiation products during accretion events may suggest that the Earth's mantle has never been completely homogenized and/or entirely molten.

[1] Willbold M. et al. (2011) *Nature* 477, 195.
[2] Touboul M. et al., *Science*, in press.
[3] Puchtel et al. (2005) *EPSL* 206, 411.
[4] O'Neil J. et al. (2008) *Science* 321, 1828

MODELLING WATER/ROCK INTERACTIONS IN CLAY-ROCK FORMATIONS: A SYNTHESIS.

C. TOURNASSAT[1*], E.C. GAUCHER[1], A. VINSOT[2]., F.J. PEARSON[3], P. WERSIN[4], F. CLARET[1], S. ALTMANN[5]

[1]BRGM, Orleans, France, c.tournassat@brgm.fr (*presenting author)
[2]ANDRA, Bure, France, agnes.vinsot@andra.fr
[3]Ground Water Geochem, New Bern, USA, fjpearson@gmail.com
[4]Grüner LTD, Basel, Switzerland, paul.wersin@gruner.ch
[5]ANDRA, Châtenay-Malabris, France, scott.altmann@andra.fr

The chemistry of pore water and its controlling mechanisms are important properties of clayrocks being considered as host rocks for long-term storage of radioactive waste. Ionic strength, pH and redox potential are key parameters for assessing the speciation and thus the mobility of radionuclides under storage conditions. Porewater-controlling mechanisms must also be known to predict the evolution of the artificial and natural barriers foreseen in storage concepts. Since pore waters in clay-rich rocks cannot generally be sampled directly from rock samples, their chemistry must be estimated using geochemical modelling constrained by laboratory-measurable properties of core samples. In parallel to modelling work, considerable efforts have been made during the last ten years to obtain pore water samples from specially equipped boreholes in Underground Research Laboratories (URLs). Some of these experiments aim at obtaining water samples with minimal perturbations in order to enable comparisons with pore water geochemical modelling. Others obtain samples under disturbed conditions (e.g. bacterial, alkaline, redox, thermal perturbations) which can be used to assess the effectiveness of predicted controlling mechanisms.

Current modelling concepts of porewater composition will be reviewed together with their ability to explain key features in experimental results from the Bure (France) and Mont-Terri (Switzerland) URLs. We will show that pH and ionic strenght as well as major solutes concentrations (Na, K, Ca, Mg, Cl, SO_4, *etc.*) are adequatly predicted in undisturbed conditions, but that redox potential remains a difficult modelling issue. Controlling mechanisms for trace metal concentrations and their impact on radionuclides retention will be also discussed. Hereafter, we will show how the knowledge on solute parameters controls enables predicting the evolution of storage-material under various perturbation scenarios. Model uncertainties and limitations (*e.g.* thermodynamic database accuracy and completeness, kinetic controls, etc.) will be discussed in order to better emphasize the significance of long-term predictive modelling of storage-material evolution.

https://doi.org/10.1180/S0026461X00008434 Published online by Cambridge University Press

Stable isotopes and radiocarbon as tracers of atmospheric methane sources

AMY TOWNSEND-SMALL[1*], STANLEY C. TYLER[2], DIANE E. PATAKI[3], XIAOMEI XU[3], AND LANCE E. CHRISTENSEN[4]

[1]University of Cincinnati, Department of Geology, Cincinnati, OH, USA, amy.townsend-small@uc.edu (*presenting author)
[2]Norco College, Department of Chemistry, Norco, CA, USA, styler@uci.edu
[3]University of California, Irvine, Department of Earth System Science, Irvine, CA, USA, dpataki@uci.edu; xxu@uci.edu
[4]Jet Propulsion Laboratory, California Institute of Technology, Pasadena, CA, USA, lance.e.christensen@jpl.nasa.gov

Recent studies have suggested that CH_4 emissions in urban areas may be underestimated, probably because most regional models to estimate CH_4 fluxes are based largely on agricultural emissions factors [1]. Other studies have proposed that increased extraction and use of natural gas, specifically from shale formations, may increase total methane emissions from fossil fuel sources [2,3]. In this presentation, we will demonstrate the use of stable isotopes (^{13}C and D) and radiocarbon (^{14}C) as tracers of sources of CH_4 in Los Angeles, California [4]. As expected, measurements of the $\delta^{13}C$ and δD of CH_4 from discrete sources showed separation between fossil fuel-derived sources, such as vehicle emissions, power plants, oil refineries, landfills, and sewage treatment plants and biological sources like cows, biofuels, landfills, sewage treatment plants, and cattle feedlots. We also implemented high-altitude monitoring of well-mixed air using continuous tunable laser spectroscopy measurements of CH_4 concentration combined with isotope analyses (^{14}C, ^{13}C, and D) of discrete samples. Our data, particularly variation of δD and (to a lesser extent) $\delta^{13}C$ with CH_4 concentration, indicate that the major source of excess CH_4 in Los Angeles is leakage of fossil fuels, such as from geologic deposits, natural gas pipelines, oil refining, and/or power plants. This is in contrast to some previous studies that have shown that landfills and waste treatment are the dominant source of CH_4 in urban areas. California state inventories currently lack urban emissions factors. More research is needed to constrain fluxes of this "fugitive" CH_4 from gas distribution and refining, as this flux may increase with greater reliance on natural gas and biogas for energy needs. The combination of high-resolution tunable laser concentration measurements and precise stable isotope measurements made via mass spectrometry is a very promising and powerful tool for verifying reductions in greenhouse gas emissions and constraining regional-scale emissions inversion models.

This presentation will include an overview of methods for using isotopes for source apportionment for atmospheric methane, a discussion of previous studies that have successfully applied these methods, and potential applicability to studies of shale gas extraction.

[1] Wunch et al. (2009) *Geophys. Res. Lett.* **36**, L15810. [2] Howarth et al. (2011) *Climactic Change* **106**, 679-690. [3] Wigley (2011) *Climatic Change* **108**, 601-608. [4] Townsend-Small et al. (in review) *J. Geophys. Res. Atm.* doi:10.1029/2011JD016826.

Major element incorporation into apatite: implications for thermometery

DUSTIN TRAIL[1*], LESLIE A. HAYDEN[2], E. BRUCE WATSON[1], NICHOLAS D. TAILBY[1]

[1]Department of Earth and Environmental Sciences & New York Center for Astrobiology, Rensselaer Polytechnic Institute, Troy, NY 12180, USA.
[2]U.S. Geological Survey, Menlo Park, CA 94025, USA.
*traild@rpi.edu (presenting author).

Apatite is a ubiquitous accessory mineral that crystallizes in a wide variety of melts from basaltic to granitic. Apatite may also grow in low temperature (~40°C) aqueous solutions and during metamorphism. Crystals incorporate a variety of trace (e.g., rare earth elements [REEs], Sr, U, Th), minor (e.g., Mn) and major (e.g., Fe, Mg, Si) elements that may be used to trace the evolution of rocks, including magma volatile contents [1-4]. It is widely accepted that the incorporation of elements into minerals is at least sensitive to temperature [3]. Therefore, understanding and interpreting the chemisty of apatite crystals (e.g, REEs, U, Th, F, C, OH, Cl, S) may be extended by knowledge of the crystalization temperature.

We report synthesis experiments of apatite crystals grown in melts from 800 to 1200 °C and pressures of 1 and 2 GPa. Synthetic and natural silicate mixes (including SUNY MORB e.g., [5]) were doped with excess moles of CaO, P_2O_5, F, ±Cl, ±S to ensure apatite saturation. Major and minor element concentrations in apatites and co-existing phases (including quartz, diopside, augite, tremolite, and glass) were characterized by electron microprobe. Preliminary data suggest that some major rock forming elements (e.g. Si, Fe, Mg) correlate with temperature when a phase is present that buffers the activities of system components containing these elements. In experiments that contain only apatite and glass, major element concentrations are still demonstrably sensitive to temperature, though component activities are not well constrained.

Elements which are structurally accommodated by the apatite lattice, coupled with component activities that are 'buffered' by other assemblages – in nature and in laboratory experiments – are likely to be the most promising candidates for apatite thermometry. As an example, the activity of SiO_2 in most (silicate) melts can usually be constrained. However, application of apatite Si contents as a thermometer may be hindered because the entry of Si into the P site requires charge compensation with other elements (e.g., trivalent REEs satisfy this requirement). Other elements such as Mg and possibly Fe, for example, may be better candidates that require fewer assumptions. Nevertheless, an apatite thermometer will require an estimate of component activities for application.

[1] McCubbin *et al.* (2010) *PNAS* **107**, 11223-11228. [2] Boyce *et al.* (2010) *Nature* **466**, 466-469. [3] Watson and Green (1981) *Earth Planet. Sci. Lett.* **56**, 405-421. [4] Spear and Pyle (2002) *Rev. in Min.* **48**, 293-335. [5] Richter et al. (2003) *GCA* **67**, 3905-3923.

https://doi.org/10.1180/S0026461X00008434 Published online by Cambridge University Press

Titan aerosol analogs from aromatic precursors: Comparisons to Cassini CIRS observations in the thermal infrared

MELISSA G. TRAINER[1*], JOSHUA A. SEBREE[1], CARRIE M. ANDERSON[1], AND MARK J. LOEFFLER[1]

[1]NASA Goddard Space Flight Center, Greenbelt, MD USA, melissa.trainer@nasa.gov (* presenting author)

Background

Since Cassini's arrival at Titan, ppm levels of benzene (C_6H_6) and possibly polycyclic aromatic hydrocarbons (PAHs) have been detected in the atmosphere.[1] Aromatic molecules, photolytically active in the ultraviolet, may be important in the formation of the organic aerosol comprising the Titan haze layer even when present at low mixing ratios. Yet there have not been laboratory simulations exploring the impact of these molecules as precursors to Titan's organic aerosol.

Observations of Titan by the Cassini Composite Infrared Spectrometer (CIRS) in the far-infrared (far-IR) between 560 and 20 cm^{-1} (~18 to 500 μm) have been used to infer the vertical variations of Titan's aerosol from the surface to an altitude of 300 km.[2] Titan's aerosol has several observed emission features which cannot be reporoduced using currently available optical constants from laboratory-generated Titan aerosol analogs [2,3,4], in particular a broad far-IR feature centered approximately at 140 cm^{-1} (71 μm).

Analog Studies

There is a need to revisit the infrared spectrum of laboratory-produced aerosol, particularly in the far-IR. We speculate these features may be a blended composite of low-energy vibrations of two-dimensional lattice structures of large molecules, such as PAHs or nitrogenated aromatics. Such structures do not necessarily dominate the composition of analog materials generated from CH_4 and N_2 irradiation.

We are performing studies forming aerosol analogs via UV irradiation of several aromatic precursors – with and without nitrogen heteroatoms – to understand how the unique chemical architecture of the products influence observable aerosol characteristics. The optical and chemical properties of the aromatic analog will be compared to those formed from CH_4/N_2 mixtures [5,6], with a focus on the as-yet unidentified far- and mid-IR absorbance features. These studies show that the aerosol formed from aromatic precursors have distinct chemical composition as compared to previously studied analogs, which has implications for the optical properties of Titan's aerosol.

[1] Waite, J. H., et al. (2007) *Science* **316** 870-875.
[2] Anderson, C.M, et al. (2011) *Icarus* **212** 762-778.
[3] Khare, B.N., et al. (1984) *Icarus* **60** 127 – 137.
[4] Imanaka, H., et al. (2012) *Icarus* **218** 247 - 261.
[5] Trainer, M.G., et al. (2006) *PNAS* **103** 18035 - 18042.
[6] Trainer, M.G., et al. (2012) *Astrobiology,* in press.

Calcite farming in Florida caves: Calibrating modern calcite $\delta^{18}O$ and $\delta^{13}C$ to ventilation and *in situ* air temperature

D. M. TREMAINE[1*], B.P. KILGORE[1] AND P. N. FROELICH[2]

[1]Florida State University; NHMFL – Geochemistry; Tallahassee, FL, USA; (*presenting author: tremaine@magnet.fsu.edu)
[2]Froelich Education Services, 3402 Cameron Chase Drive, Tallahassee, FL, 32309-2898, USA, pfroelich@comcast.net

Stable isotope records ($\delta^{18}O$ and $\delta^{13}C$) in cave speleothems are typically interpreted as climate changes in rainfall amount and source, cave air temperature, atmospheric CO_2, and overlying vegetation. But these records are difficult to interpret without *in situ* calibrations between cave microclimate (e.g., ventilation) and contemporaneous calcite isotopic composition. In this study at Hollow Ridge Cave (HRC) in Marianna, Florida (USA), cave dripwater and modern calcite (farmed *in situ*) were collected in conjunction with continuous cave air pCO_2, temperature, barometric pressure, relative humidity, radon-222 activity, airflow velocity and direction, rainfall amount, and drip rate data [1, 2]. We analyzed rain and dripwater isotopes, dripwater [Ca^{2+}], pH, $\delta^{13}C$ and TCO_2, cave air pCO_2 and $\delta^{13}C$, and farmed calcite $\delta^{18}O$ and $\delta^{13}C$ to examine the relationships among rainwater isotopic composition, cave air ventilation, cave air temperature, seasonal calcite growth rate and timing, and calcite isotopic composition. Farmed calcite $\delta^{13}C$ decreases linearly with distance from the front entrance to the interior of the cave during all seasons, with a maximum ventilation-induced entrance-to-interior gradient of $\Delta\delta^{13}C$ = -7‰. Farmed calcite $\delta^{18}O$ exhibits a +0.82 ± 0.24‰ offset from values predicted by both theoretical calcite-water calculations and by laboratory-grown calcite (Figure). Unlike calcite $\delta^{13}C$, oxygen isotopes show no ventilation or evaporation effects and are a function only of temperature. Combining our data with other speleothem studies, we find a new empirical relationship for cave-specific water–calcite oxygen isotope fractionation across a range of temperatures and cave environments: **$1000\ \ln \alpha = 16.1(10^3\ T^{-1}) - 24.6$** (light blue dashed line in the Figure).

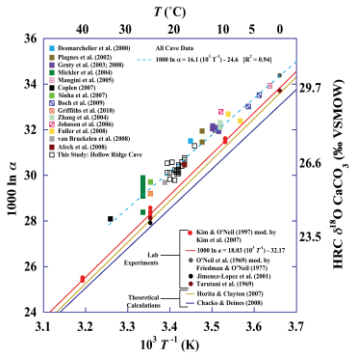

Figure: 1000 ln α vs. $10^3\ T^{-1}$ for HRC calcite (black open squares) plotted with other modern cave studies (solid & crossed squares), laboratory inorganic precipitation values (circles), and theoretical calc-ulations (solid lines). The red line is the best-fit line from [3] as modified by [4]: 1000 ln α = 18.03 ($10^3\ T^{-1}$) - 32.17.

[1] Kowalczk & Froelich (2010) *Earth Planet. Sci. Lett.* **289**, 209-291. [2] Tremaine et al. (2011) *Geochim. Cosmochim. Acta* **75**, 4929-4950. [3] Kim & O'Neil (1997) *Geochim. Cosmochim. Acta* **61**, 3461-3475. [4] Kim et al. (2007) *Chem. Geol.* **246**, 135-146.

https://doi.org/10.1180/S0026461X00008434 Published online by Cambridge University Press

Archaeo-environmental characterization of the Arvernian gold mines of Auvergne (France)

FRÉDÉRIC TRÉMENT[1*], JACQUELINE ARGANT[2], ELISE BRÉMON[1], HERVÉ CUBIZOLLE[3], BERTRAND DOUSTEYSSIER[1], JOSÉ ANTONIO LÓPEZ-SÁEZ[4], GUY MASSOUNIE[1], PIERRE RIGAUD[5] AND ALAIN VERON[6]

[1]MSH-CHEC-EA 1001, University Clermont-Ferrand, France, frederic.trement@wanadoo.fr, e_lisou@hotmail.fr, bertrand.dousteyssier@univ-bpcclermont.fr, guy.massounie@wanadoo.fr

[2]MMSH-LAMPEA-UMR 7269 CNRS, Aix-en-Provence, France, j.argant@wanadoo.fr

[3]EVS-ISTHME-UMR 5600 CNRS, Saint-Etienne, France, herve.cubizolle@univ-st-etienne.fr

[4]Laboratorio de Arqueobotánica, CEH, CSIC, Madrid, Spain, cehl149@ceh.csic.es

[5]IRAMAT-UMR 5060 CNRS, Orleans, France, rigaud@cnrs-orleans.fr

[6]CEREGE, UMR7330 CNRS, Aix en Provence, France, veron@cerege.fr

During the Iron Age, the Gaulish *Arverni* and *Lemovices* influence extended well beyond Auvergne (Central France), into the Mediterranean regions owing to extensive agricultural activities and silver mining. Recent discoveries showed that gold mining in the area of Haute-Combraille (Auvergne) may also has contributed to the wealth of these communities. Gold was possibly extracted as well during the first two centuries AD. at the onset of Roman occupation.

Our project (MINEDOR) aims to study from an interdisciplinary and diachronic point of view these ancient gold mines, traditionally attributed to the Gaulish period, discovered in large numbers at the fringes of the *Arverni* and *Lemovices* territories, in the area of Upper Combraille (Puy-de-Dôme). Our goals are 1) to accurately identify the mines through fieldwalking and aerial surveys, analysis of vertical aerial photographic coverage and localization by dual-frequency DGPS, 2) to assess their environmental impact using palaeoenvironmental (palynology, microfossils) and geochemical (heavy metals, trace elements, stable lead isotopes) analyses in wetlands, and 3) to date transient phases of exploitation.

Here we present high-resolution peat core analyses from the Haute-Combraille highlands (900-1000m) that allow to evidence gold mining operational phases since the Iron Age through vegetation cover changes and the release of lead (Pb) from mining activities. These new data highlight important features of the ancient economy of the Massif Central and the transient environmental impact of mining operation on watershed quality.

Advances in MC-TI-MS for precise and accurate Ca isotopic analysis

ANNE TRINQUIER[1*], CLAUDIA BOUMAN[1], NICHOLAS LLOYD[1], MICHAEL DEERBERG[1], AND JOHANNES SCHWIETERS[1]

[1]Thermo Fisher Scientific, Bremen, Germany, anne.trinquier@thermofisher.com (* presenting author)

Ca isotopes have proved to be powerful isotopic tracers in a number of disciplines within Geosciences, including Paleoceanography, Geochronology and Biogeochemistry, and Cosmochemistry, where minute anomalies relative to Earth are a key to deciphering the origin of Earth and the terrestrial planets. However, accurate and precise Ca isotope analysis is highly challenging, due to, both, the extreme range of relative Ca isotopic abundances - ^{40}Ca alone representing 97% of Ca isotopes - and the extreme mass dispersion of the Ca isotope array of 20%. These limiting features have prevented optimized multicollection (MC) analysis of all Ca isotopes, and introduced uncertainties due to ion beam instabilities and inferior counting statistics for the minor Ca isotopes. Precision and accuracy can be improved by optimizing sample loading and double spike techniques, but ultimately, there is a need for improved mass spectrometry performance in order to improve the state-of-the-art for Ca isotopic analysis.

The TRITON *Plus* offers new solutions to address these analytical challenges:

[1] An extended mass dispersion provides *simultaneous collection of all Ca isotopes*, without the requirement of applying a zoom to deflect the Ca ion beam. Peak-jumping mode is no longer required for Ca isotope analysis, thus saving acquisition time and limiting the potential detrimental effects of Ca ion-beam instabilities on precision and reproducibility.

[2] Different gain current amplifiers (10^{10}, 10^{11} and 10^{12} Ohm) can be combined. The 10^{12} Ohm amplifiers provide a factor of 2-3 improvement in the signal/noise ratio relative to a classical 10^{11} Ohm amplifier, and can be associated to the cup(s) collecting the minor Ca isotope(s). Additionally, a 10^{10} Ohm amplifier can be connected to the cup collecting ^{40}Ca, and hence increase the dynamic range by a factor of 100. Amplifier switching to any cup is supported by the tried and tested relay matrix already equipping TRITON instruments. The combination of these current amplifiers ultimately contributes to enhancing Ca isotope in-run precision through improved ion counting statistics and by application of more precise instrumental mass fractionation correction as the normalizing ratio ^{42}Ca/^{44}Ca can be determined at 10 times higher beam intensities.

[3] The new TRITON *Plus* Ca package consists of 2 special cups: an extended cup attached on the high mass side of the focal plane that accomodates acquisition of the heaviest Ca isotope (^{48}Ca); and an oversized cup on the low mass side of the focal plane for the high intensity ^{40}Ca beam.

https://doi.org/10.1180/S0026461X00008434 Published online by Cambridge University Press

Elevated crustal CO_2 liberation at Merapi volcano: linking rock-, mineral- and gas-geochemistry

V. R. TROLL[1*], F.M. DEEGAN[2], E. M JOLIS[1], D.R. HILTON[3], J.P. CHADWICK[4], L. S. BLYTHE[1], C. FREDA[5], L.M. SCHWARZKOPF[6], R. GERTISSER[7], M. ZIMMER[8]

[1]Dept. Earth Sciences, CEMPEG, Uppsala, Sweden (* valentin.troll@geo.uu.se)
[2]Lab. For Isotope Geology, SMNH, Stockholm, Sweden
[3]Scripps Oceanographic Institute, San Diego, USA
[4]Dept. Petrology, Vrije, Universiteit Amsterdam, Netherlands
[5]Istituto Nazionale di Geofísica e Vulcanologia, Rome, Italy
[6]GeoDoCon, Konradsreuth, Germany
[7]Dept. Earth Sciences, Keele University, UK
[8]GeoForschungsZentrum, Potsdam, Germany

Indonesia's Merapi volcano is one of the most active and dangerous on the planet, characterized by long periods of dome growth and intermittent explosive pyroclastic events. Merapi currently degasses continuously through high-T fumaroles (>200°C), and has recently erupted mainly crystal-rich basaltic-andesite that contains a large range of igneous and calc-silicate crustal inclusions. To evaluate mechanisms that trigger explosive eruptions, we sampled lavas, inclusions (xenoliths), and gas from active fumaroles. We also experimentally established a time-integrated reaction series of crustal assimilation at Merapi under magmatic conditions.

Merapi lava contains abundant, complexly zoned plagioclase crystals that show variations in anorthite (An) content between 40 and 95 mol% across resorption surfaces. A negative correlation between An content and other indicators of magmatic fractionation, such as MgO and FeO, has been observed. Moreover, *in-situ* Sr isotope analysis of discrete zones in plagioclase yields $^{87}Sr/^{86}Sr$ values that notably exceed those of the host lavas. Zones with the highest An content tend to also show the highest radiogenic Sr values, and, by contrast, low MgO, consistent with a Ca-rich, MgO-poor crustal contaminant. Abundant metamorphosed crustal limestone xenoliths contain compositionally identical feldspar to the lavas (up to An_{95}), demonstrating that magma-crust interaction is a significant process at Merapi.

Carbon isotope ratios of fumarole CO_2 sampled during quiet periods form a baseline of $\delta^{13}C_{2001\text{-}2006}$ = -4.1‰. The notable exceptions are the 2006 values, sampled during the eruption and after the 6.4 magnitude Yogyakarta earthquake, which show elevated $\delta^{13}C$ values up to -2.4‰. Notably, the rise in $\delta^{13}C$ values coincided with an increase in eruptive intensity and volcano seismicity by a factor of 3 to 5 for several weeks after the earthquake. This is consistent with a late-stage, crustal volatile component added to purely mantle and slab-derived volatile sources, arguing for extensive and ongoing magma-crust interaction beneath the volcano, especially during eruptive and/or seismic events.

High P-T experiments show that interaction between Merapi magma and limestone can rapidly liberate crustal CO_2 on a timescale of only seconds to minutes in our experiments [1]. We therefore expect vigorous CO_2 bubble nucleation and growth on a scale of perhaps hours to days in nature. Late volatile input could therefore accelerate or trigger explosive eruptions independently of magmatic recharge and fractionation by sudden over-pressurization of the upper parts of the magma system. Such an event would provide shallow seismic warning signals only and these would be temporally very close to an erratic, CO_2-driven, eruption crisis.

[1] Deegan, F. M., Troll, V. R., Freda, C., Misiti, V., Chadwick, J.P., McLeod, C.L., Davidson, J.P., (2010), *J. Petrol.*, **51**, 1027-1051.

Paleo-environmental characterization of the Pelusiac branch of the Nile (Egypt)

HERVÉ TRONCHÈRE[1*], ALAIN VÉRON[2], JEAN-PHILIPPE GOIRAN[1], IRENE FORSTNER-MULLER[3]

[1]CNRS UMR 5133 Archéorient, Maison de l'Orient et de la Méditerranée, Lyon, France, herve.tronchere@mom.fr (*presenting author), jean-philippe.goiran@mom.fr
[2]CNRS UMR 7330 CEREGE, University Aix-Marseille, Aix en Provence, France, veron@cerege.fr
[3]Austrian Archaeological Institute, Cairo, Egypt, irene.forstner_mueller@oeai.at

The paleo-Pelusiac branch of the Nile delta once housed Avaris, the capital city of the Hyksos kings during the 2nd millenia BC. The now defunct Pelusiac branch also was one of the seven largest diffluents of the Nile and therefore offers the opportunity to investigate paleo-environmental changes in the delta according to hydrological fluctuations and anthropogenic activities.

The Nile has three main affluents that connect in Sudan, the White Nile, the Blue Nile and the Atbara river, more than 2.500km south of the apex of the delta. These three rivers drain much dissimilar geological basins, from the plutonic rocks of the White Nile to the effusive rocks of the Blue Nile. The heavy metals load carried by the Nile reflects this diversity along with dust deposition from Saharan plumes and local discharge from anthropogenic activities. Lead (Pb) and its stable isotopes are known to efficiently trace the geological diversity of sediment particles and to discriminate anthropogenic sources leached into natural reservoirs thanks to the specific imprint of metallic ores [1]. Here we propose to use these isotopes measured from cores collected in the Pelusiac branch to resolve (1) changes in sediment source dynamics and (2) local human activities during the 2nd millenia BC. into the Nile delta.

Lead isotopes, luminescence datings and sediment analysis allow to correlate fluctuations of the delta hydrosystem to regional climate shifts such as the transition from late Pleistocene deposits to more recent Holocene alluvia. Pb isotopes in sediments deposited prior to the onset of the Hyksos city display non contaminated imprints spread between several natural sources. This distribution illustrates transient changes in the Nile hydrodynamics and prevailing climatic settings. Here are also presented anthropogenic signals identified during the Bronze Age in the Eastern Nile delta.

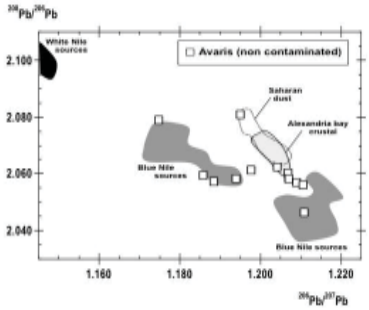

Figure 1: Distribution of the natural Pb isotope imprints at Avaris

[1] Doe, B.R. (1970) *Lead isotopes*, Springer-Verlag, Berlin, 137p.

https://doi.org/10.1180/S0026461X00008434 Published online by Cambridge University Press

Magnesium isotopic fractionation in arid Hawaiian soils

KYLE D. TROSTLE[1*], LOUIS A. DERRY[2], NATHALIE VIGIER[3], OLIVER A. CHADWICK[4]

[1]Cornell University, Ithaca, USA, kdt42@cornell.edu (* presenting author)
[2]Cornell University, Ithaca, USA, lad9@cornell.edu
[3]CRPG, Nancy, France, nvigier@crpg.cnrs-nancy.fr
[4]UC Santa Barbara, Santa Barbara, USA, oac@geog.ucsb.edu

Sampling and Methods

Soil, streamwater, and parent material samples were taken from the arid leeward coast of the Kohala Volcano on the Big Island of Hawaii to investigate the fractionation of magnesium isotopes within the weathering environment. Soil samples were taken from both the Pololu (~350 ka) and Hawi (~170 ka) lava flows, and streamwaters were taken from streams under different discharge conditions. Soils were characterized on site and with x-ray diffraction techniques in order to determine horizonation and mineralogy. These samples were then processed via a sequential extraction to isolate carbonate, exchangeable, and soil organic matter fractions, and will be further processed to isolate noncrystalline phases, poorly crystalline phases, kaolin, and residual materials. Major element chemistry of these extractions was determined, and samples were processed according to an ion exchange method developed by Bolou-Bi et al. (2009) [1] in order to isolate monoelemental solutions of magnesium from each. These were run on a Thermo-Fisher Neptune multi-collector inductively coupled plasma mass spectrometer (MCICPMS) at the Centre de Recherches Petrographiques et Geochimiques (CRPG) in Nancy, France, using standard-sample bracketing techniques to determine δ^{26}Mg with respect to the standard DSM3.

Results and Conclusions

The δ^{26}Mg isotopic composition of soil carbonates (n=7) ranged considerably from -1.05 ± 0.32 per mil to -2.31 ± 0.16 per mil, whereas the magnesium isotopic composition of the exchangeable fraction (n=7) consistently averaged -1.12 ± 0.21 per mil, in both the Pololu (~350 ka) and Hawi (~170ka) soils. The variation in carbonate magnesium isotopic composition may be due to a variety of factors, including depth, age, and phase, but with only seven carbonate samples analyzed, further work is needed to confirm trends within the data. Both of the soil carbonate and exchangeable reserviors of magnesium, in both the Pololu and Hawi soils, are isotopically lighter than the primary sources of magnesium to Hawaiian soils, which include precipitation at a value of -0.8 per mil and basalt at -0.3 per mil [1]. The streamwaters (n=5) measured fall inbetween the isotopic values of precipitation and basalt, with an average value of -0.54 ± 0.20 per mil, although this consistency in magnesium isotopic composition within the streamwaters may be the result of groundwater influence. A magnesium budget for these soils has been created to interpret these findings.

[1] Bolou-Bi, Vigier, Brenot & Poszwa (2009) *Geostandards and Geoanalytical Research* **33**, 95-109.

The effects from soil mineralogy and groundwater acidity on *Lolium multiflorum* (ryegrass)

FANNY TRUONG[1,2*], KUMARI A. BISWAS[1,3], SHAGUN SINGH[1,4], BONNIE A.B. BLACKWELL[1,5*], AND JOEL I.B. BLICKSTEIN[1]

[1] RFK Science Research Institute, Glenwood Landing, NY, 11547
[2] fannytruong4@gmail.com (* presenting author)
[3] kumari.ananna.biswas2010@gmail.com
[4] s.singh_95@yahoo.com
[5] Dept of Chemistry, Williams College, Williamstown, MA, 01267 bonnie.a.b.blackwell@williams.edu (* presenting author)

Abstract

Acid rain reduces plant diversity, growth, and population size. Anthropogenic activities that release SO_2 and NO_x produce acid precipitation, and cause to groundwater acidification. This experiment tested the ideal soil mixture for *Lolium multiflorum* (ryegrass), when exposed to low concentrations of acid rain. Using different mixtures of sphagnum peat moss, montmorillonite, and quartz sand, 21 different soils were created. For each, 48 *L. multiflorum* seeds were planted individually, and watered with an average of 10 mL/day of deionized water. Plants were grown in controled conditions under artificial light and were rotated regularly to ensure equal light intensity reaching each plant over a seven day period. On Day 19, each group was split in half, with one half continuing to receive 10 mL/d water, while the rest subsequently received 10 mL/d of 0.0001 M of H_2SO_4 at pH = 3.62. Plant heights were measured and health was monitored via leaf number and general appearance daily. After 35 days, biomass production was measured. Sprouting percentages, mean growth rates, and mean longevity were calculated for each group. In the absence of acid, the sprouting percentage is highest for soils with ≤ 20 vol% sand, ≤ 60 vol% peat moss, and ≤ 80 vol% montmorillanite, while the mean plant heights were tallest for soils with 40 vol% sand, 20 vol% peat moss, and 40 vol% montmorillanite after 35 days. If exposed to acid, the plants grew tallest in soils with 40 vol% peat moss and 60 vol% clay, but plant longevity was highest for soils with 20 vol% peat moss, 20-60 vol% sand and 20-60 vol% montmorillanite. Biomass production was highest for plants exposed to water when their soil averaged 20-40 vol% clay, but for plants exposed to acid, biomass production was highest if their soil had 40-60 vol% clay. Therefore, for ryegrass exposed to acid, growth will be improved, if clay concentrations in their soil are higher than for plants exposed to water alone. Nonetheless, pH of 3.62 did not dramatically affect potential growth for *L. multiflorum.* Thus, it might make a suitable species to use for reme-diation in areas with clay-rich soils and acidified groundwater. Future experiments will examine the ions leached from the soil under these conditions.

Figure 1. Mean plant heights on Day 35 for plants growing in the acidic groundwater (above) and in water lacking acid (below).

https://doi.org/10.1180/S0026461X00008434 Published online by Cambridge University Press

Facies architecture and Evolution of Late Permian Carbonate Platform Margin,Northeastern Sichuan,China

ZHANG TINGSHAN[1]*, ZHAO GUQAN[2], LIU ZHICHENG[3],CHEN XIAOHUI[4], YANG WE[5], MING HUAJUN[6]

[1]State Key Lab.of Oil&Gas Researvoir Geology and Exploitation Engineering,Chengdu,China
zts_3@126.com (* presenting author)
[2]State Key Lab.of Oil&Gas G&E Engineering,Chengdu,China
zhaoga@petrochina.com.cn
[3] State Key Lab.of Oil&Gas G&E Engineering,Chengdu,China
rex_swpu2005@126.com
[4] State Key Lab.of Oil&Gas G&E Engineering,Chengdu,China
zts_3@sina.com
[5] State Key Lab.of Oil&Gas G&E Engineering,Chengdu,China
rexswpu@163.com
[6] State Key Lab.of Oil&Gas G&E Engineering,Chengdu,China
minesky@126.com

Intriduction

The Lopingian of late Permian carbonate platform margin developed in Northeastern Sichuan,China,which located at the west part of Upper Yangzi Platform tectonically，that contain a peculiar and widespread microbial facies, but have received little attention. The microbial facies have been reported from PTB limestone from southeastern China and Japan and have been placed in the basal Griesbachian *Hindeodus parvus* zone (Sano et al.,1997; Kershaw et al., 2002).But the microbial structures developed below that horizon here and also influenced the evolution of carbonate platform margins. The study area in Daba mt.offers a few locations where the Late Permian carbonate platform margins can be studied along the continuous outcrops. Some very good exposured outcrops of Changxing Fm. provide detailed information on the platform margin evolution.

Facies architecture and Evolution

Three stages of the platform margin have been identified:1)ramp stage developed at the first and second member of Changxing Fm. , the thin dark micrite bed with small sponge mounds deposited with about 150 m in thickness. This stage was in the high stand system tract;2)microbial mound rimmed margin developed at the lower part of third member of Changxing Fm. with about 210 m in thickness,and the transgressive system tract developed at this time. The microbial mound shows three internal growth phases vertically including sponges-thrombolite, thrombolite-tubiphytes and thrombolite.The sponges-thrombolite developed in the lowest part of the microbial mound with lower topography and gentle slope,then,the thrombolite-tubiphytes and thrombolite， are the main contributors to mounds, developed quickly and made the rimmed margin to showing higher topography and steep slope gradually. The microbial mound structures play a key factor controlling the progradational geometry of the platform margins;3.oolitic and arenitic shoal stage ,which developed in the high stand system tract, distribute at the upper part of third member of Changxing Fm. with about 46 m in thickness. The evolution of the microbial structures as well as the final demise of late Permian reefs followed by microbial mound without true metazoan reefs may reflect the characteristics of the Late Permian biological crisis.

Conclusion

The evolution of the Late Permian platform margin here was mainly controlled by relation sea-level oscillation, microbial facies architectures, other control factors such as tectonic subsidence, synsedimentary faults may play the subordinate actions.

[1]Sano, H., and Nakashima, K., 1997, Lowermost Triassic (Griesbachian) microbial bindstone-cementstone facies, southwest Japan: Facies, v. **36**, p. 1–24.
[2]Kershaw, S., Guo, L., Swift, A., and Fan, J.S., 2002, Microbialites in the Permian-Triassic boundary interval in Central China: structure, age and distribution: Facies,v. **47**, p. 83-89

Sea floor methane emissions in high-latitude continental shelves and the role of anaerobic methane oxidation

IANA TSANDEV[1*], PIERRE REGNIER[2], ANDY W. DALE[3]

[1] Faculty of Geosciences, Utrecht University, Utrecht, the Netherlands i.tsandev@uu.nl (* presenting author)
[2] Department of Earth and Environmental Sciences, Université Libre de Bruxelles, Brussels, Belgium, pregnier@ulb.ac.be
[3] Helmholtz-Zentrum für Ozeanforschung Kiel (GEOMAR), Kiel, Germany, adale@geomar.de

The melting of submerged permafrost and increases in temperature in high latitude sediments have brought the Earth's methane gas hydrate reservoir closer to destabilisation which is a subject of great concern. Fluxes of methane from sea floor gas hydrates are a potential key forcing of Earth's climate; for example the abrupt environmental change of the Paleocene Eocene Thermal Maximum (PETM) has been linked to methane release from destabilized gas hydrates [1].

If the released methane is oxidized aerobically, such as in a ventilated water column or the surface oxidized layer of the sediment, it results in an increase in dissolved inorganic carbon (DIC), no change in alkalinity (ALK) and thus $CaCO_3$ dissolution. The effect can be opposite if anaerobic oxidation of methane takes place (eg. throughout the reduced part of the sediment column) as this process releases two equivalents of alkalinity per mole of methane oxidized and, thus, induces carbonate precipitation.

In this communication we explore the benthic geochemical dynamics following hydrate melting in high-latitude shelf environments typical of the W. Svalbard coast that are recognised areas for hydrate destabilization [2]. Benthic fluxes were calculated using the 1-D reaction-transport model, BRNS, after imposing an upward flux of methane based on hydrate dissolution estimates. Anaerobic methane oxidation (AOM) significantly reduced the efflux of methane to the overlying water and led to accumulation of DIC and ALK inventories in the sediment porewaters, favouring carbonate precipitation. This also resulted in increased effluxes of DIC and ALK to the overlying seawater.

The magnitude of AOM is, however, very sensitive to the assumed rate constant for this process. We therefore modulated the rate of AOM with microbial biomass growth dynamics [3] and observed a transient response of the microbial community to the upward methane flux. The microbial ecosystem was slow to respond to the fast methane supply leading to a transient loss of methane from the sediment into ocean waters.

[1] Dickens (2003) *EPSL* **213** , 169 – 183. [2] Biastoch et al. (2011). *Geophys. Res. Lett*. 38, doi:10.1029/2011GL047222. [3] Dale et al. (2008) *EPSL* **265**, 329 – 344.

https://doi.org/10.1180/S0026461X00008434 Published online by Cambridge University Press

Geochemical trends across the Palaeoproterozoic Kuruman and Griquatown BIFs, Transvaal Supergroup, South Africa, and implications for the GOE

HARILAOS TSIKOS*[1], LINDI FRYER[1], HELEN WILLIAMS[2], SIMON POULTON[3], AND ADRIAN BOYCE[4]

[1]Geology Department, Rhodes University, Grahamstown, South Africa h.tsikos@ru.ac.za
[2]Department of Earth Sciences, Durham University, UK
[3]Civil Engineering & Geosciences, Newcastle University, UK
[4]Scottish Universities Environmental Research Centre, UK

The Transvaal Supergroup on the Kaapvaal Craton of South Africa contains one of the thickest (up to ~1000m), most complete, and best preserved sequences of banded iron-formation (BIF) of early Palaeoproterozoic age (~2.5-2.4 Ga). The stratigraphically lower Kuruman BIF exhibits typical microbanded textures dominated by chert and magnetite, with lesser siderite and Fe silicate; it is conformably overlain, through a gradual facies transition, by the granular to microbanded, siderite-Fe silicate-rich Griquatown BIF.

We have carried out a reconnaissance (generally one sample every 10-15m) geochemical study of both the Kuruman and Griquatown BIFs. Our key objective was to test whether these BIFs stratigraphically record geochemical signals of potential relevance to the evolution of the atmosphere-ocean system leading to the Great Oxidation Event (GOE) at *ca.* 2.4Ga. Our sampling focused on two complementary drillcore intersections located approximately 60 km NW of the town of Kuruman. The two drillcores together capture the entire BIF stratigraphy, which in this specific area measures ~400m thick. The Kuruman BIF is stratigraphically underlain by the Klein Naute black shale that overlies the Campbellrand carbonate sequence at the base of the Transvaal Supergroup, whilst the Griquatown BIF is overlain conformably by the Makganyene diamictite.

Our sample suite captures essentially all major sub-lithofacies of the Transvaal BIFs as described previously [1]. Geochemical results show a number of broad stratigraphic trends: (i) bulk carbonate $\delta^{13}C$ data range between -6 and -11 per mil, and fluctuate in concert with corresponding fluctuations in the non-ferrous carbonate component of the samples; (ii) Fe and Mn speciation data record a general upward increase in the Mn:Fe ratio of carbonate (and bulk-rock); and, (iii) bulk $\delta^{57}Fe$ data range between -2.7 and 0.9 per mil, with lower values generally corresponding to samples with high modal siderite relative to magnetite, as seen particularly in the Griquatown BIF.

We regard the stratigraphic increase in the Mn:Fe ratio and attendant decrease in bulk $\delta^{57}Fe$, as possible precursor signals to the stratigraphically higher, manganiferous and ^{57}Fe-depleted Hotazel Formation, itself thought to have formed prior to the GOE in a highly evolved – chemically and isotopically – stratified marine basin. Mass balance considerations also suggest that C and Fe isotope variations in the BIFs may record primary precipitation from a chemically and isotopically stratified water column, rather than isotopic fractionation related entirely to biogeochemical redox processes during diagenesis.

[1] Beukes and Gutzmer (2008) *Reviews in Economic Geology* **15,** 5-47.

Kinetic theory of crystallization from meta-stable phases

K. TSUKIMURA[1]*, M. SUZUKI[1], Y. SUZUKI[1], T. MURAKAMI[2]

[1]AIST, Geological Survey of Japan, Tsukuba, Ibaraki 305-8567, Japan
[2]University of Tokyo, Tokyo 113-0033, Japan

Abstract

Various kinds of meta-stable phases are formed on the Earth's surface. Most of these phases are amorphous or poorly crystallized nano-particles. These phases can contain various kinds of harmful elements. When we discuss the behavior of these harmful elements contained in the meta-stable phases, we need to estimate the lifetime of the meta-stable phases because these meta-stable phases are transformed to crystalline stable phases. This paper describes a kinetic theory of the crystallization from a metastable phase [1]. The theory assumes that a crystal nucleates only on the surface of a meta-stable phase, the crystal stops growing at a certain size, and the concentration of metal ion in solution is close to the solubility of the meta-stable phase. On the basis of these assumptions, we have derived integral equations for $R(t)$ (crystal ratio as a function of time). We have solved the integral equations with a successive approximation method. When time t is less than t_{inflec} ($=r_{max}/G$, r_{max}: maximum radius of crystal, G: growth rate of crystal), $R(t)$ is close to fourth power of time; when t is larger than t_{inflec}, $R(t)$ is close to an exponential-type function. The kinetic theory has been applied successfully to the transformation of ferrihydrite nanoparticles to goethite or hematite crystals (Fig. 1), and the crystallization of TiO_2 and ZrO_2. The theory shows that the nucleation rate of crystal essentially determines the crystallization rate, and that induction period is observed when the growth of crystal is slow.

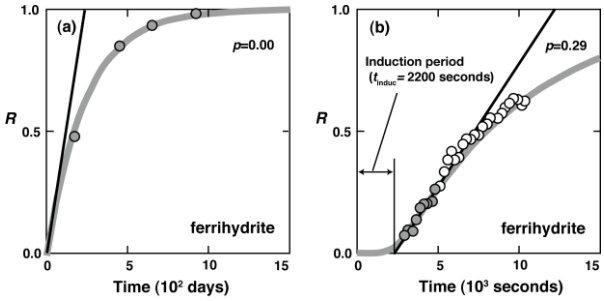

Figure1: Relation between observed and calculated values of R [1]; (a) the transformation of ferrihydrite at pH 6 and 297 K [2] and (b) the transformation of ferrihydrite at pH 10.7 and 361 K [3]. Circles denote experimental data points and solid curves calculated values based on the present theory. Data points in grey symbols were used for the determination of parameters p and t_{inflec} ($=4/3\ t_{induc}$) .

[1] Tsukimura et al. (2010) *Crystal Growth & Design* **10**, 3596-3607. [2] Schwertmann et al. (1983) *Clays Clay Mineral.* **90**, 277-1860.
[3] Shaw et al. (2005) *Am. Mineral.* **90**, 1852-1860.

https://doi.org/10.1180/S0026461X00008434 Published online by Cambridge University Press

Tailings pond mixed species biofilm gives metal precipitates

RAYMOND J. TURNER[1] *, SUSANNE R. GOLBY[1], HOWARD CERI[1]

Biofilm Research Group, Department of Biological Sciences, University of Calgary, AB, Canada, turnerr@ucalgary.ca (*presenting author)

Background

Our group has been interested in metal ion resistance and tolerance of bacteria growing as a biofilm compared to that of their free-swimming planktonic state [1]. As expected overall bacteria growing as a biofilm are more tolerant to metals. Recently we have moved from single model species to environmental community isolates. This study utilized the Calgary biofilm device (CBD) as a microscale reactor to cultivate mixed species biofilms directly from Alberta oil sands tailings pond sediments, under a variety of different culture conditions [2]. This approach revealed that the organisms within the biofilms strongly represented the indigenous population in the tailings used as the inoculum and contained over 10 different genera per biofilm including organisms belonging to *Pseudomonas, Thauera, Hydrogenophaga, Rhodoferax* and *Acidovorax* [2].

New results

Subsequently we have been challenging these organisms to salts of metals known to be present in the tailings ponds and at other mining sites including Cu, Pb, Cr, V, Ni, Zn, and Sr as well as Ag, due to its strong microbial biocidal activity. We observed that the mixed species biofilms showed higher tolearance to metal ion stress than a monospeci biofilms isolated from the community. The highest tolerance was to Pb and Sr. The metals Cu, Ag, Pb and Sr were found in deposits on, and within, the biofilms suggesting that the organisms in the biofilm community were seeding the crystal formation not seen in monospecie biofilms (example see Figure 1).

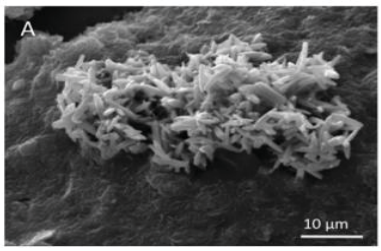

Figure 1: Scanning electron microcrosopy image of biofilm exposed to 1000 mg/L $CuSO_4$. Crystals shown to be Copper by energy dispersive spectrometry.

Summary

A process of growing mixed species biofilms directly from environmental samples has been established. This growth method demonstrated biogeochemical transformation of several metal ions to preciptiates on and within the biofilm.

[1] Harrison *et al.* (2007) *Nature Rev. Microbiology*. **5**, 928-938.
[2] Golby *et al.* (2012) *FEMS Micro. Ecol.* **79**, 240-250.

Mantle flow, slab-surface temperatures and melting dynamics in the north Tonga arc – Lau Basin

S.TURNER[1*], J. CAULFIELD[1], R. ARCULUS[2], C. DALE[3], N. KELLER[4], J. PEARCE[5] AND C. MACPHERSON[3]

[1]Department of Earth and Planetary Sciences, Macquarie University, Australia, simon.turner@mq.edu.au*
[2]Research School of Earth Sciences, ANU, Australia
[3]Department of Earth Sciences, University of Durham, UK
[4]Institute of Earth Sciences, University of Iceland, Iceland
[5]School of Earth and Ocean Sciences, Cardiff University, UK

The Fonualei Spreading Centre is a nascent series of en échelon ridges that extend north from near Fonualei volcano, on the Tonga arc front, to the Mangatolu Triple Junction in the northeastern Lau Basin. Fresh basaltic glasses dredged from these ridges afford an excellent opportunity to evaluate geochemical changes with increasing depth to the slab. Here we augment previously published major and trace element data with new Sr, Nd, Pb, Hf and U-Th-Ra isotope data for selected Fonualei Spreading Centre samples as well as present new Hf isotope data from boninites and seamounts to the north of Tonga. The Pb and Hf isotope data are used to appraise interpretations of the extent and distribution of Samoan plume mantle beneath the Lau Basin based on He and Pb isotope data. If elevated ^{208}Pb and lowered Hf isotope ratios in lavas from Niuafo'ou Island and the Mangatolu Triple Junction reflect a Samoan plume influence this is not visible in He isotopes. The boninite and seamount data indicate that the tear in the northern end of the slab may not extend east as far as the boninite locality. Mantle flow is inferred to be oriented to the southwest. In the Fonualei Spreading Centre lavas, Ce/Pb, $^{87}Sr/^{86}Sr$ and $^{208}Pb/^{204}Pb$ increase, whereas U/Th, Th/Nb and $^{143}Nd/^{144}Nd$ decrease, with increasing distance from the arc front. These changes are accompanied by increasing slab surface temperatures (725-940 ºC) as inferred from decreasing H_2O/Ce ratios. Consistent with experimental data, the geochemical trends are interpreted to reflect changes in the amount and composition of wet pelite melts and aqueous fluids derived from the slab under appropriate conditions. With one exception, all of the lavas preserve both ^{238}U excesses and ^{226}Ra excesses. Ba-Yb, Na_8-Fe_8 and U-series isotope systematics suggest that lavas from the Fonualei Spreading Centre and Valu Fa Ridge reflect fluid-fluxed melting. However, there is a change to decompression melting in lavas from the East and Central Lau Spreading Centres where slab surface temperatures reach ~ 900-1000ºC. A similar observation is found for the Manus and East Scotia back-arc basins and may reflect the absence of lawsonite in the subducted basaltic crust.

https://doi.org/10.1180/S0026461X00008434 Published online by Cambridge University Press

Evaluating permeability change due to altered pore geometry in CO_2 sequestration systems

BENJAMIN M. TUTOLO*, ANDREW J. LUHMANN, XIANG-ZHOU KONG, MARTIN O. SAAR, WILLIAM E. SEYFRIED, JR.

Department of Earth Sciences, University of Minnesota Minneapolis, MN, USA
(*presenting author: tutol001@umn.edu)

Background

Experimental, numerical, and field investigations of CO_2 injection into deep saline aquifers indicate alteration of formation mineralogy and permeability in CO_2-affected regions. Permeability typically increases in carbonate-hosted systems with the formation of preferential flow pathways and typically decreases in feldspar-rich systems due to formation of secondary clay minerals.

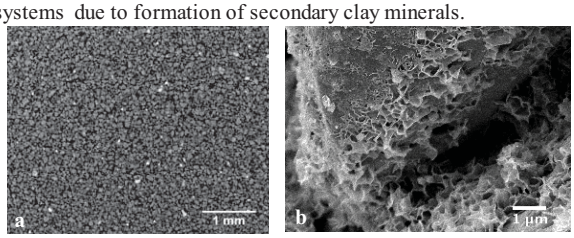

Figure 1 a: XMT image of packed arkosic sediment core
b: SEM image of alteration minerals on feldspar grain surface

Approach

With X-ray Microtomography (XMT, Fig. 1a) and Scanning Electon Microscopy (SEM, Fig. 1b) images of cores before and after they are subjected to CO_2-saturated water/brine experiments at elevated temperatures and pressures, we observe pore-scale alteration of flow path geometry. The reconstructed XMT images are thresholded to separate pore space from solids and divided into Representative Elementary Volumes (REVs, Fig. 2) to calculate permeability fields over large sections of the core with lattice-Boltzmann methods. Real-time monitoring of core permeability and geochemical modeling of core mineralogy and sampled solution chemistry yield additional, vital data to observe the rates and characteristics of mineral and permeability alteration throughout the experiment.

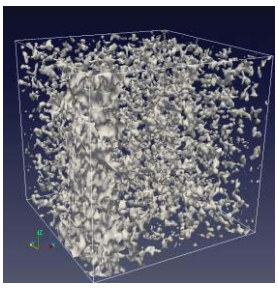

Figure 2: REV reconstructed from XMT images.

Results

This combined experimental and numerical approach is used to characterize and predict permeability modification resulting from CO_2 injection for several rock types, including arkose, dolostone, and basalt. This approach avoids bulk porosity-permeability relationships commonly used in reactive transport modeling to predict permeability changes and instead focuses on physical changes due to chemical alteration at the pore scale.

Assessing the importance of extracellular iron scavenged on phytoplankton cells with synchrotron x-ray fluorescence microscopy

BENJAMIN S. TWINING[1*]

[1]Bigelow Laboratory for Ocean Sciences, W. Boothbay Harbor, USA, btwining@bigelow.org (* presenting author)

Iron is an essential micronutrient for phytoplankton, and it has been shown to limit primary production in large swaths of the ocean with low external inputs. Dissolved iron occurs primarily as Fe(III) in the oxic surface waters of the ocean, and ferric iron is nearly insoluble under these conditions. Thus iron is prone to precipitate and scavenge onto particle surfaces. Oceanographers have long considered that a non-negligible fraction of iron associated with ocean plankton may be extracellularly adsorbed rather than associated with intracellular biological moieties. A number of studies have been conducted to investigate the behavior of this iron, and several operationally-defined chemical rinses have been developed and utilized to remove this extracellular fraction prior to elemental analyses. I have analyzed numerous plankton cells from both natural open-ocean environments and laboratory cultures with synchrotron-based hard x-ray fluorescence (SXRF) microprobes, occasionally in conjunction with the above-mentioned rinses. By and large, the spatial distributions of iron and other bioactive elements in these cells suggest that the extracellular adsorbed fraction is only a minor component of cellular iron contents. I will present data from both lab and field studies in support of this observation, discuss reasons for its occurrence, and suggest ways to reconcile these observations with geochemical evidence for Fe scavenging in the ocean.

https://doi.org/10.1180/S0026461X00008434 Published online by Cambridge University Press

Enriched mantle source for the Cretaceous alkaline lamprophyres from the Catalonian Coastal Ranges (NE Spain)

TERESA UBIDE*, CARLOS GALÉ, ENRIQUE ARRANZ, MARCELIANO LAGO, PATRICIA LARREA, PABLO TIERZ, AND TOMÁS SANZ

University of Zaragoza, Department of Earth Sciences, Spain, tubide@unizar.es (* presenting author)

During the Cretaceous, the opening of the Bay of Biscay led to a widespread alkaline magmatism in northeast Iberia [1]. This magmatism is recognised in the Pyrenees [2] and in the Catalonian Coastal Ranges [3]. In the latter sector, it is represented by lamprophyre sills, classified as camptonites. They are hypocrystalline porphyritic rocks composed of large mafic crystals (clinopyroxene, kaersutite, olivine pseudomorphs and opaque minerals) set in a fine-grained groundmass. Most of the groundmass consists of microlites of feldspars and kaersutite; apatite is a common accessory phase.

The lamprophyres are basic and ultrabasic rocks enriched in incompatible elements (10 to more than 100 times over the primitive mantle). They show a Ti/V ratio over 50, similar to OIB-type rocks. In order to obtain petrogenetic information from the incompatible trace elements, only the most primitive samples (MgO > 7 wt. %) were considered. In addition, rocks with high volume fractions of large crystals were dismissed as their composition is strongly influenced by the accumulation of the crystals [4].

The primitive mantle-normalised multi-element patterns are very similar to each other, suggesting a common magma source. $(La/Lu)_N$ values (14.9-17.3) indicate highly fractionated patterns. All the samples show positive anomalies for Nb-Ta and smaller ones for Ba; some of the samples also present a negative anomaly in Pb. These data point to an astenospheric enriched mantle source similar to EM-1 [5]. Small differences are observed for K, which correlate with the proportion of kaersutite in the samples. Slight differences in P are probably related to the presence of apatite.

The εSr values define a wide variation range (-11.7 to +14.9). Given that these variations do not correlate with the SiO_2, MgO or Sr contents, crustal contamination can be ruled out. Therefore, a heterogeneous mantle source is inferred, as previously reported for the Permian and Triassic magmatisms in the Pyrenees [6].

In contrast, the εNd values (+3.1 to +4.4) and the Pb isotopic ratios ($^{206}Pb/^{204}Pb$: 19.06–19.46; $^{207}Pb/^{204}Pb$: 15.65–15.70; $^{208}Pb/^{204}Pb$: 39.28–39.82) show small variations. The low Pb ratios discard the involvement of a HIMU-type component. The Sr-Nd-Pb isotopic values support a heterogeneous, astenospheric mantle source with the involvement of an EM-1 component [5].

The obtained T_{DM} ages are very consistent (0.55-0.60 Ga). They may reflect a Cadomian fractionation event in the mantle.

[1] Montigny *et al.* (1986) *Tectonophysics* **129**, 257-273. [2] Azambre *et al.* (1992) *Eur. J. Mineral.* **4**, 813-834. [3] Solé *et al.* (2003) *Cretaceous Res.* **24**, 135-140. [4] Ubide *et al.* (2012) *Lithos* **132-133**, 37-49. [5] Hofmann (1997) *Nature* **385**, 219-229. [6] Lago *et al.* (2004). *Geol. Soc. Sp. Publ.* **223**, 439-464.

Photodissociation origin of Archean S-MIF and dynamical sulfur cycling under highly reducing atmosphere

YUICHIRO UENO[1]*, SEBASTIAN DANIELACHE[1], YOSHIAKI ENDO[1], MATTHEW JOHNSON[2], NAOHIRO YOSHIDA[3]

[1]Department of Earth & Planetary Sciences, Tokyo Institute of Technology, Tokyo, Japan. ueno.y.ac@m.titech.ac.jp

[2]Copenhagen Center for Atmospheric Research, Department of Chemistry, University of Copenhagen, Denmark.

[3]Department of Environmental Sciences and Technology, Tokyo Institute of Technology, Yokohama, Japan.

Mass-independent fractionation of sulfur isotopes (S-MIF) demonstrated that Earth's atmosphere was virtually oxygen-free in the Archean [1], and is a key to understand chemistry of atmosphere and ocean before the rise of oxygen. However, the mechanism and factor controlling the S-MIF signal have been poorly understand yet. We newly determined higher resolution UV absorption cross sections of not only $^{32}SO_2$, $^{33}SO_2$ and $^{34}SO_2$ but also $^{36}SO_2$ within the two absorption bands: (1) 190 – 220 nm and (2) 250 – 320 nm. These data together with chemical reaction model allow us to predict isotopic compositions of photochemical product. The calculated photochemical fractionation pattern assuming broadband solar UV flux reproduce our previous work [2], though the effect of UV shielding by each atmospheric species including SO_2 itself differ from previously estimated trend. Nonetheless, almost all of the simulations result in $\Delta^{36}S/\Delta^{33}S$ ratio of -0.9 ~ -1.1, generally reproducing those observed in Archean sedimentary rocks. Thus, we conclude that photodissociation of SO_2 was a primary MIF-yielding reaction in the Archean atmosphere. Our simulation predict, however, the remaining SO_2 after UV photolysis acquires positive $\Delta^{33}S$ as opposed to widely-accepted previous model where H_2SO_4 ($-\Delta^{33}S$) and S_8 ($+\Delta^{33}S$) aerosols carried "opposite" MIF signals into ocean and sediment [4,5]. We speculate the possibility that almost Archean sulfide deposits were produced by sulfate reduction. The new model requires relatively innert reducing form of sulfur reservior. If the atmosphere was strongly reducing and contained high level of CO or CH_4, photolytically produced SO was finally transferred into OCS [2] or organo-sulfur compounds [6], respectively, which remained in the atmosphere and were not readily converted into sulfide. Occasional oxidation of the reducing sulfur pool enhanced sulfate concentration and deposited rare sulfate minerals with negative $\Delta^{33}S$. The new dynamical sulfur cycle model may explain observed heterogeniety of S-MIF records in the basin to microscopic scale. If correct, this implies more reducing Archean atmosphere than previously thought.

[1] Farquhar *et al.* (2000) *Science,* **289**, 756-758. [2] Ueno *et al.* (2009) *PNAS* **106**, 14784-14789. [3] Danielache *et al.* (2008) *J Geophys Res* **113**, D17314. [4] Pavlov & Kasting (2002) *Astrobiology* **2**, 27-41. [5] Ono *et al.* (2003) *EPSL* **213**, 15-30. [6] Domagal-Goldman *et al.* (2011) *Astrobiology* **11**, 419-441.

https://doi.org/10.1180/S0026461X00008434 Published online by Cambridge University Press

Petrological Exploration of podiform chromitite by using of detrital spinel, Sangun Zone, southwest Japan.

TOMOYUKI UMEDA[1*] AND ICHIRO MATSUMOTO[1]

[1] Department of Education, Shimane University, Matsue, Japan, umedatomoyuki@gmail.com (* presenting author) chromim@edu.shimane-u.ac.jp (second author)

Sangun zone ultramafic rocks and chromitite

Many ultramafic complexes some of which have chromitite bodies are exposed in the Sangun zone in central Chugoku district, Southwest Japan. All complexes are harzburgite-dominant, and dunite is various in amount on each complex and sometimes has small amounts of chromitite in it [1]. A chromitite pod is always enclosed by dunite envelopes and large chromitite bodies are exclusively found in relatively dunite-dominant complexes or portions [1, 2]. Largest chromite mines of Japan that are Wakamatsu and Hirose are exists in the northern part of Tari-Misaka complex.

Detrital chromian spinel as a tool for exploration of podiform chromitite

Exploration of podiform chromitite has been difficult, because its occurrence is usually very irregular in ultramafic complex. Matsumoto and Arai (1997) proposed the petrological exploration of podiform chromitite by using of spinel chemistry and morphology from the rocks from the outcrops [2, 3]. Above study is epoch-making as an investigating method for exploration of podiform chromitite. However, an investigation precision does not go up by this Method. Because it dose not have the good exposure of ultramafic rocks in the Sangun zone. In this research, we observed detrital spinel in bottom sediment of small creek in and around the ultramafic complex. By this method, there is an advantage that can analyze much spinel grain at once. Moreover, it is expected that we can evaluate a large locality (complex) with a comparatively sufficient precision.

Cr# (Cr/Cr+Al) of detrital chromian spinels from the creek around relativery dunite rich ultramafic complex varies from 0.55 to 0.65. In contract to this, from the creek around dunite free or poor ultramafic complex, Cr# of detrital chromian spinels varies from 0.40 to 0.60. And complex with relativery large chromitite show high in Cr# and Mg# (Mg / (Mg+Fe^{2+})) of chromian spinel. Above results are basically same as Matsumoto and Arai (1997). However, it is very significant results for exploration of chromitite that we have calculated the quantitive chromitite's existence rate each ultramafic complex separately. That is northern part of Tari-Misaka complex is the place where most high potenciality of chromitite deposit. This result also concordant with the idea of chromitite formation proses [4, 5].

[1] Matsumoto *et al*. (1995) *J. Japan Assoc. Minerl. Petrol. Econ. Geol.* **90**, 13-26.
[2] Matsumoto & Arai (1997) *Resource Geology* **47**, 189-199.
[3] Matsumoto & Arai (2001) *Mineralogy and Petrology* **73**, 305-323.
[4] Arai & Yurimoto (1994) *Economic Geology* **89**, 1279-1288.
[5] Zhou *et al*. (1994) *Mineral. Deposita* **29**, 98-101.

Microbial characterization at iron-clay interfaces after 10 years of interaction *in situ* in an argillaceous formation (Tournemire, France)

LAURENT URIOS[1*], FRANCOIS MARSAL[2], DELPHINE PELLEGRINI[2], MICHEL MAGOT[1]

[1]Université de Pau et des Pays de l'Adour, IPREM UMR 5254, Equipe Environnement et Microbiologie, IBEAS, F-64013 PAU, France, laurent.urios@univ-pau.fr (* presenting author)
[2]Institut de Radioprotection et de Sûreté Nucléaire (IRSN), DSU/SSIAD/BERIS, B.P. 17, 92262 Fontenay aux Roses Cedex, France, francois.marsal@irsn.fr

Introduction

Microbial activity has been proven to occur in argillaceous formations, as well as the development of exogenous microorganisms within disturbed areas [1]. In the context of a geological disposal of radioactive waste in clayey formations, the consequences of such a microbial activity are of concern regarding the corrosion of metallic materials. In particular, sulfate- or thiosulfate-reducing bacteria may influence localised corrosion processes [2], that may lead to a premature loss of watertightness of containers. Moreover, the passive film, which is formed progressively during the generalised corrosion process and induces a decrease of corrosion rates, may react with iron-reducing bacteria which could thus promote corrosion [3]. The purpose of the present work was to characterise the microbial diversity that may have impacted corrosion processes at the interface between re-compacted argillite and steel coupons after 10 years of interaction under *in situ* conditions inside the Toarcian argillite layer in Tournemire (France).

Results and Conclusion

The characterization of the microbial diversity was carried out using 16S rRNA genes cloning and culture media. More than 630 clone sequences were analyzed and 123 isolates were identified. Altogether, 19 phylotypes and 55 taxa were defined. They were affiliated to only 3 bacterial phyla: *Firmicutes*, *Actinobacteria* and *Proteobacteria*. The biodiversity identified differs depending on the steel type and the location of the sample, indicating the influence of *in situ* physico-chemical conditions. Moreover, isolates and clone sequences have revealed that sulfate-reducing bacteria, iron-reducing bacteria as well as thermotolerant strains able to grow at temperatures up to 75°C could develop in this environment. Different microbial populations can colonize the interfaces between materials in a very short period of time compared with the timescales of a geological disposal. These results should be considered to assess the consequences of microbial activities on the evolution of the metallic disposal components.

[1] Urios *et al.* (2011) *Appl. Geochem.* In press. doi:10.1016/j.apgeochem.2011.09.022. [2] Magot *et al.* (1997) *Int. J. Syst. Bacteriol.* **47,** 818-824. [3] Herrera & Videla (2009) *Int. Biodeter. Biodegrad.* **63,** 891-895.

https://doi.org/10.1180/S0026461X00008434 Published online by Cambridge University Press

Evidence from D/H and volatile abundances of impact melts for a surficial water reservoir on Mars

TOMOHIRO USUI[1, 2*], CONEL M. O'D. ALEXANDER[3], JIANHUA WANG[3], JUSTIN I. SIMON[1] AND JOHN H. JONES[1]

[1]ARES, Johnson Space Center, NASA, Houston, TX, USA. tomohiro.usui@nasa.gov (* presenting author)
[2]Lunar Planetary Institute, Houston, TX, USA.
[3]DTM, Carnegie Institute of Washington, Washington DC, USA.

Martian surface morphology implies that persistent liquid water once existed on its surface and played a significant role in the formation of weathered regolith. In order to study this surficial water we measured volatile abundances (H_2O, CO_2, S, Cl, F) and H isotopes of impact melts (IMs) and maskelynite (shocked plagioclase) in geochemically enriched (LAR 06319 [LAR06]) and intermediate (EETA79001 [EETA79]) shergottites by ion microprobe analysis. Early studies of inert gases contained in IMs from EETA79 match the relative abundances of modern Martian atmosphere.

IMs in LAR06 contain lower H_2O (~150ppm), CO_2 (~20ppm) and S (100-400ppm) but higher F (10-30ppm) and Cl (40-80ppm) than IMs in EETA79 (~300ppm H_2O, ~300ppm CO_2, 3200ppm S, <3ppm F, ~30ppm Cl). The major element compositions of IMs are probably derived by partial melting of primary plagioclase and pyroxene. Likewise, the halogen abundances could possibly reflect the incorporation of primary phosphates. On the other hand, the much higher H_2O/CO_2 ratios than that of the Martian atmosphere ($<10^{-3}$) imply the presence of another water source.

In a previous study [1] based on olivine-hosted melt inclusions we showed that the primary magma of the geochemically depleted shergottite (Yamato 980459 [Y98]) had a chondritic low-δD value of 275‰, whereas that of LAR06 had a very high-δD value of 5079‰. In contrast with such extreme δD differences, matrix phases in Y98 and LAR06 both have moderate δD values. Groundmass glasses (GGs) in Y98 exhibit a slightly greater δD variation of 200-1600‰, but still much less extreme than the range exhibited by the melt inclusions. The δD values of the Y98 GGs rise with increasing water contents, implying mixing of two components: near-surface moderate-δD and magmatic low-δD components. On the other hand, IMs and maskelynites in LAR06 exhibit lower δD values of ~1000-3000‰ than the primary LAR06 melt (5079‰), although mixing calculations suggest that these matrix δD values could have been modified by contamination of <30ppm terrestrial water (δD~-200‰). IMs in EETA79 also have a moderate δD value of ~1600‰.

This study shows that the matrix phases (GG, IM and maskelynite) in all three shergottites have a relatively limited range of δD values regardless of the distinct δD of their magmatic sources. A [δD *vs.* $1/H_2O$] mixing diagram shows a convergence among the matrix δD values, which could be attributable to the impact-induced addition of a common near-surface water with a moderate δD value (~1200-2000‰). The origin of this surficial water reservoir remains unresolved: (1) it may be derived from the Martian atmosphere, but its moderate δD values are distinctly lower than the widely-accepted atmospheric δD value of ~4000-5000‰, and/or (2) it could originate from the addition of a weathered soil/dust component enriched in volatile elements. [1] Usui *et al.* (2012) *43rd LPSC*, #1341.

Natural variations of uranium isotopes in uranium ore minerals

YULIA A. UVAROVA[1], KURT KYSER[1*], MAJDI LAHD GEAGEA[1], AND DON CHIPLEY[1]

[1]Queen's University, Kingston, Canada, kyser@geol.queensu.ca (* presenting author)

Introduction

Recent studies have shown significant variations in $^{235}U/^{238}U$ and $^{234}U/^{238}U$ ratios in geologic materials. We have investigated the uranium isotopic compositions of natural ores from various uranium deposit types with the use of MC-ICP-MS to better understand mechanisms and processes for fractionation of uranium isotopes in different geologic conditions.

Results

The $\delta^{235}U$ and $\delta^{234}U$ values of uranium minerals from various types of deposits worldwide show variations of 1.8 and 500‰, respectively, measured relative to NBL CRM 129-A. Higher $\delta^{235}U$ values are generally recorded by magmatic- or metasomatic-related U mineralization or deposits that have igneous rocks as a source of uranium (Fig. 1). High-grade unconformity type deposits have $\delta^{235}U$ values around -0.9‰. Vein-type, sandstone-hosted, most unconformity-type deposits, and uranium mineralization in the Beaverlodge area have lower $\delta^{235}U$ values (Fig. 1). $\delta^{234}U$ values for most samples analyzed are around 30‰ and record secular equilibrium. Some samples have $\delta^{234}U$ values much lower or higher than 30‰ associated with addition or removal of ^{234}U during the past 500 Ka.

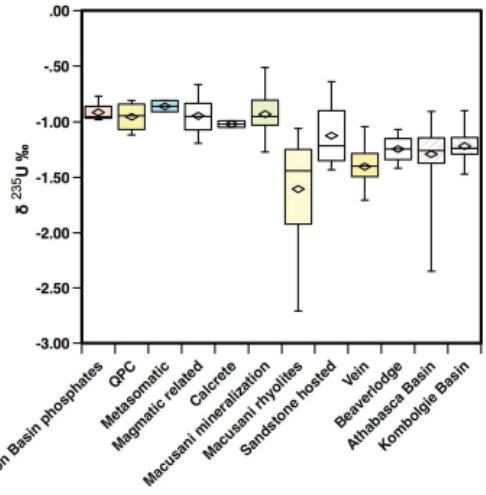

Figure 1: $\delta^{235}U$ values for studied samples

Discussion

The $\delta^{235}U$ and $\delta^{234}U$ values recorded in uranium ores from different types of deposits indicate that there are at least two different mechanisms responsible for $^{235}U/^{238}U$ and $^{234}U/^{238}U$ fractionation. $^{234}U/^{238}U$ disequilibria ratios indicate fluid alteration of the uranium minerals or rocks and postdepositional migration of ^{234}U. Fractionation of ^{235}U and ^{238}U as a result of nuclear volume effects results in enrichment of the heavy isotope in reduced insoluble species relative to oxidized mobile species. Therefore, isotopic fractionation effects should be reflected in $^{235}U/^{238}U$ ratios in U ore minerals formed either by reduction of U^{6+} to UO_2 or chemical precipitation in the form of U^{6+} minerals. $\delta^{235}U$ values of uranium ore minerals from a variety of deposits are controlled by isotopic signature of the U source, the efficiency of U precipitation, and later fluid-produced alteration of the ore.

https://doi.org/10.1180/S0026461X00008434 Published online by Cambridge University Press

Climate extremes and volcanic eruptions: Trace elements, isotopes and U-series geochronology recorded by a [1]Late Quaternary stalagmite

I. TONGUÇ UYSAL[1*], EMMA J. ST PIERRE [1], AND JIAN-XIN ZHAO[1]

[1] University of Queensland St Lucia, QLD, 4072, AUSTRALIA, t.uysal@uq.edu.au (*presenting author)

Documenting the timing of large volcanic eruptions is critical in climate change research because volcanic gas and ash spreading globally from equatorial eruptions can cause a significant change in global temperatures [*1,2,3,4*]. Cave carbonate deposits provide an unprecedented opportunity to reconstruct climate changes, volcanic eruptions, and recurrence patterns of paleo-seismic events [*5*]. Through high-precision U-series dating and micro-chemical analysis, speleothems are capable of providing tandem records of climate and environmental change, and thus can offer new insights into the complex interplay of seismic, volcanic and hydrological processes.

We investigated a stalagmite sample from a cave in a volcanically active region in Indonesia by a high-resolution micro-sampling, high-precision U-series dating combined with trace element, C, O, and Sr isotope analysis. The stalagmite contains several dark laminas that record major volcanic eruption cycles and/or episodic climatic shifts. A sharp increase in the trace element abundance, which correlates clearly with increasing $\delta^{18}O$ and $\delta^{13}C$ values and a drop in $^{87}Sr/^{86}Sr$ values, is conspicuous in the black layers. Strikingly, the pattern of $^{87}Sr/^{86}Sr$ values of the investigated stalagmite sample parallels their U/Th age spectra. Voluminous CO_2 emission due to phreatic eruptions and/or a sudden turnover to dry climate episodes are interpreted as leading to carbonate growth hiatuses before the precipitations of black layers. More future studies of millimetre to submillimetre-scale geochemical investigations and precise age dating of speleothems from volcanically active regions will provide detailed insight into interplay among volcanic cycles, fluid flow events and climate changes.

[1] Adams., et al. (2003) *Nature,* ***426***, 274-278. [2] Anchukaitis et al. (2010) *Geophysical Research Letters,* ***37***, L22703, doi:22710.21029/22010GL044843. [3] Cadle et al. (1976) *Journal of Geophysical Research*, ***81***, 3125-3132. [4] Robock et al. (2009) *Journal of Geophysical Research*, **114**, D10107, doi:10.1029/2008JD011652. [5] Tuccimei, P., et al. (2006) *Earth and Planetary Sccience Letteers* ***243***, 449-462

https://doi.org/10.1180/S0026461X00008434 Published online by Cambridge University Press

Phosphorus sorption properties of surface sediments in the northeastern Baltic Sea

ANU VAALAMA* AND KAARINA LUKKARI

Marine Research Centre/Finnish Environment Institute, Helsinki, Finland
anu.vaalama@ymparisto.fi*, kaarina.lukkari@ymparisto.fi

Introduction

Hypoxia weakens water ecosystem's health by reducing habitats for living resources and altering the biogeochemical cycle of nutrients. In the Baltic Sea, hypoxia has been present intermittently since the excistence of the sea but its spatial extent and intensity has increased due to anthropogenic nutrient loading [1]. The Gulf of Finland is one of the most eutrophied basins in the Baltic Sea and receives hypoxic near-bottom water from the Baltic Proper.

Oxygen depletion further feeds eutrophication by promoting release of phosphorus (P) from reducible iron(oxyhydr)oxides in sediments. However, P is released from sediments also in oxic conditions, for example, as a result of organic matter decomposition and bioturbation. In addition, P adsorption onto iron(oxyhydr)oxides is at least partly reversible [2,3] and can result in P release also from oxidized particle surfaces. Significant spatial variation in the sediments' P storages and their chemical composition in the Gulf of Finland [4] suggests variation also in P sorption ability of the sediments.

We investigated P sorption-desorption behaviour in occasionally hypoxic surface sediments in the open Gulf of Finland and the northern Baltic Proper by equilibrating oxidized sediments with artificial sea-water of varying P concentrations. In addition, we determined physico-chemical characteristics of the sediments, such as specific surface area, amount of organic matter, total P, as well as iron, aluminium, manganese and their (oxyhydr)oxides, to find out, whether these factors explain the P sorption behaviour.

Results and Conclusions

According to our preliminary results, P sorption behaviour varied among the study sites. P sorption was efficient in sediments with high organic matter and low ambient oxygen concentration in the bottom-water. In these sediments, iron-bound P was probably released during hypoxia but there was enough iron to regenerate good P sorption capacity when samples were oxidized again. The low concentration of easily desorbable P in these sediments and, in contrast, high easily desorbable P in sediments with poor P sorption ability, supported this conclusion.

Sorption-desorption behaviour of P at the sediment-water interface is a dynamic phenomenon. In addition to prevailing oxygen conditions, other physico-chemical characteristics describing the sorption environment are important in explaining the behaviour of P. These results suggest that the iron-rich, poorly oxygenated sediments in the open Baltic may bind P efficiently if oxic conditions return.

[1] Conley *et al.* (2009) *Environ. Sci. Technol.***43,** 3412-3420. [2] Froelich (1988) *Limnol Oceanogr* **33**, 649-668. [3] Ruttenberg & Sulak (2011) *Geochimica et Cosmochimica Acta* **75**, 4095-4112. [4] Lukkari *et al.* (2009) *Biogeochem* **96**, 25-48.

LA-ICP-MS as a tool for elemental mapping geological samples

TOMAS VACULOVIČ*[1,2], N. GARDENOVÁ[1], V. KANICKÝ[1,2], K. BREITER[3], LENKA VYSLOUŽILOVÁ[4]

[1] Department of Chemistry, Faculty of Science, Masaryk University, Brno, Czech Republic
[2] CEITEC, Masaryk University, Brno, Czech Republic (vaca_777@yahoo.com, presenting author)
[3] Institute of Geology, Academy of Science CR, Prague , Czech Republic
[4] Department of Cybernetics, Faculty of Electrical Engineering, Czech Technical University, Prague, Czech Republic

17 c. Laser ablation ICPMS for trace-element, isotope and imaging applications in geochemistry

LA-ICP-MS represents suitable analytical tools for elemental mapping minor and trace elements in geological samples. The advantages consists in low limits of detection and sufficient lateral resolution.

We present possibility of elemental mapping by means of LA-ICP-MS. The presented elemental maps were obtained by laser ablation of granitoids from Bohemian massif what represents sufficient heterogenous samples. The new lab-made software was used for creation of elemental maps (Fig.1).

The second part is focused on quantification procedures for elemental mapping – total sum of signals of isotopes and external calibration with internal standard normalization. Their advantages and drawbacks in quantification of heterogeneous samples will be discussed.

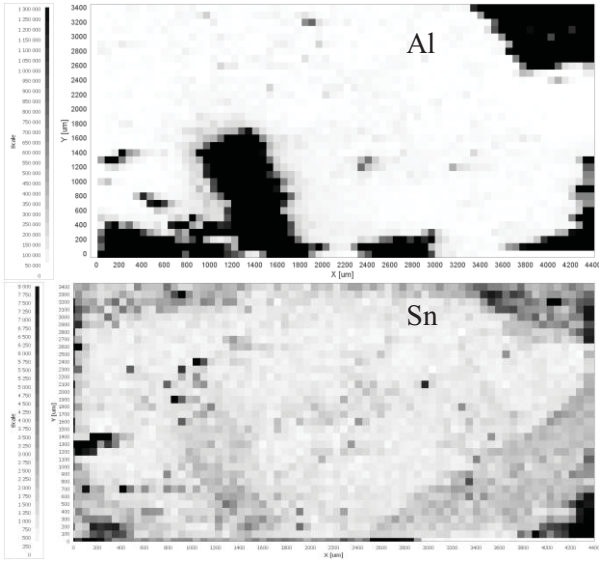

Figure 1: Elemental map of aluminium and tin in granitoid sample from Bohemian massif

Czech Science Foundation (GA P210/10/1309) and European Regional Development Fund (CEITEC – CZ.1.05/1.1.00/02.0068) are acknowledged for support.

https://doi.org/10.1180/S0026461X00008434 Published online by Cambridge University Press

Oxygen Isotope Geochemistry of Zircon

JOHN W. VALLEY [1*]

[1]Department of Geoscience, University of Wisconsin, Madison, WI 53706, USA, valley@geology.wisc.edu

In situ analysis by SIMS and LA-ICP-MS allows correlation of multiple geochemical systems within single sub-domains as small as 1 μm^3 of a zircon crystal. Such data have provided detailed records of igneous, metamorphic and sedimentary events in the crust of Earth and elsewhere.

Igneous zircons with $\delta^{18}O$ values outside of the "mantle-equilibrated" range (5.3±0.6‰ 2sd) indicate crustal input to parent magma. These values are preserved by slow diffusion rate in non-radiation-damaged zircon even through granulite metamorphism and anatexis (1). Zircon growth zoning can thus record magma contamination or mixing during sucessive tectonic events. In contrast to radiogenic isotope systems that evolve with time and trace elements that fractionate due to different degrees of incompatibility, $\delta^{18}O$ fractionates largely in response to low temperature exchange with fluids. Each system contributes complimentary information.

High values of $\delta^{18}O$ in igneous zircons (>6‰) are not in equilibrium with primitive mantle and provide a clear indication of magmas that contain a significant crustal component. This crustal signature provides a means for sorting U-Pb age and εHf data, when correlated *in situ* for sub-domains in zircon, to distinguish quantities of recycled crust and identify mantle extraction events (2).

The range of $\delta^{18}O$ in igneous zircons has increased since the end of the Archean with maximum values of 7.5‰ throughout the Archean increaseing to ~12‰ in the Phanerozoic (3). This secular trend of $\delta^{18}O_{max}$ started at ~2.5 Ga due to increased recycling of high-$\delta^{18}O$ supracrustal material into melts. Clay-rich mudstones are the largest high-$\delta^{18}O$ reservoir on Earth today, but were less common in the Archean suggesting that zircons document increased continental weathering after 2.5 Ga due to expansion of continents and epeiric seas, and oxygenation of the atmosphere.

Low $\delta^{18}O$ igneous zircons (<4.5‰) are most common in young rocks, but this has been argued to result from poor preservation of near-surface environments (3). The absence of a secular trend in minimum values of $\delta^{18}O$(Zrc) is high-lighted by zircons with $\delta^{18}O$ as low as -26‰ at 2.4 Ga (4).

In contrast to the relatively restricted variability of $\delta^{18}O_{max}$ for igneous zircons, values of $\delta^{18}O$ for metamorphic zircons are generally more variable and range up to 25.5‰ in detrital (probably Tertiary) metamorphic zircons (5) and 10.4‰ at 2.6 Ga (1). Thus higher $\delta^{18}O$ metasediments existed *locally* throughout the rock record and the apparent absence (scarcity?) of such elevated $\delta^{18}O$ igneous zircons indicates homogenization of larger *regional* domains by magmatism. Metamorphic zircons thus preserve unique evidence of smaller-scale environments that may be key to understand the larger transitions on Earth.

(1) Bowman et al. (2011) Am J Sci **311**, in press. (2) Kemp et al. (2006) Nature **439**, 580-583.(3) Valley et al. (2005) Contr Min Pet **150**, 561-580. (4) Bindeman et al. (2010) Geology **38**, 631-634. (5) Cavosie et al. (2011) Contr Min Pet **162**, 961-974.

Tracing nanoparticle interactions within living systems and in the environment: a case for the use of stable isotope labelling

EUGENIA VALSAMI-JONES*[1,2], AGNIESZKA DYBOWSKA[2], SUPERB MISRA[2], DEBORAH BERHANU[2], MARIE-NOËLE CROTEAU[3] AND SAMUEL LUOMA[4]

[1]School of Geography, Earth & Environmental Sciences, University of Birmigham, Birmingham, UK, e.valsamijones@bham.ac.uk

[2]Department of Mineralogy, Natural History Museum London, UK, a.dybowska@nhm.ac.uk, s.misra@nhm.ac.uk, d.berhanu@nhm.ac.uk

[3]USGS, Menlo Park, California, USA, mcroteau@usgs.gov

[4]University of California, Davis, USA, snluoma@ucdavis.edu

Background

Nanotechnology has the potential to revolutionise modern life, but has also been linked with concerns about the potential toxicity of newly created materials. This is because on the nanoscale, common materials can take on entirely new chemical, physical and biological properties, offering new unique technological opportunities, but also leading to unpredictable and potentially harmful biological or environmental effects. A substantial body of research now exists on the potential toxicity of nanomaterials, but many of these studies have been limited by difficulties in detecting nanoparticles in biological or envioronmental media, at appropriate concentrations. Often, the concentrations that make an experiment environmentally relevant are so low that the identification of nanoparticles containing elements already present at elevated concentrations (e.g. of Cu or Zn) in the environment and/or biota is not feasible.

.

Results and Conclusions

Here, we are reviewing the results from a number of very recent studies on isotopically modified CuO and ZnO [1,2,3] which have successfully demonstrated the application of this labelling method in *in vivo* experiments with environmental relevance. We are also considering the challenges in the synthesis of labelled particles and speculating about where the method of stable isotope modification has potential to go in the future, including in a life-cycle context. We are finally reviewing the importance of appropriately designed experiments, in which a thorough understanding of the behaviour of nanoparticles in experimental media can be established, specifically in terms of aggregation, dissolution and complexation and how labelling can also contribute to improvement of experimental designs.

References

[1] Misra *et al* (2012) *Environmental Science & Technology* **46**, 1216-1222. [2] Croteau *et al* (2011) *Nanotoxicology* **5,** 79-90. [3] Dybowska *et al* (2011) *Environmental Pollution* **159,** 266-273.

https://doi.org/10.1180/S0026461X00008434 Published online by Cambridge University Press

Rhenium-Osmium dating of black shales from the Neoproterozoic Shaler Supergroup, Victoria Island, Canada

DAVID VAN ACKEN[1*], DANIELLE THOMSON[2], ROBERT H. RAINBIRD[3], AND ROBERT A. CREASER[1]

[1]University of Alberta, Edmonton, Canada, vanacken@ualberta.ca (* presenting author), rcreaser@ualberta.ca
[2]Carleton University, Ottawa, Canada, dthomso2@connect.carleton.ca
[3]Geological Survey of Canada, Ottawa, Canada, rrainbir@nrcan.gc.ca

The Neoproterozoic Shaler Supergroup from Victoria Island, Canada, is a diverse sequence of sandstone, carbonate, evaporite and shale that was deposited in an intracontinental basin within the supercontinent Rodinia. The ~ 4km-thick succession was intruded by diabase sills and dykes of the ca. 720 Ma Franklin igneous event, which provide a minimum depositional age for the Shaler Supergroup. Its maximum depositional age, from detrital zircon geochronology, is about 1000 Ma. The Shaler Supergroup has been used as a reference section for global $^{87}Sr/^{86}Sr$, $\delta^{13}C$ and biostratigraphic correlation of Neoproterozoic sedimentary successions, notably with the Canadian Mackenzie Mountains Supergroup and the Australian Bitter Springs Formation.

Whereas global chemostratigraphic correlations are better established in the late Cryogenian and Ediacaran, precise age information for the late Tonian and early Cryogenian Periods that encompass the Shaler Supergroup is scarce. The Wynniatt Formation of the Shaler Supergroup has been correlated to the ~830 Ma Gillen Member of the Bitter Springs Formation in Australia based on lithostratigraphy and matching low $^{87}Sr/^{86}Sr$ from carbonates.

Recent advances in Re-Os geochronology allow for direct dating of black shales as a tool for chrono-stratigraphic correlation of sections where other chronostratigraphic and biostratigraphic information are lacking. In order to constrain the depositional history of the Shaler Supergroup, Re-Os analyses were obtained from core and outcrop samples of black shale from the Wynniatt and Boot Inlet formations collected from the Minto Inlier of Victoria Island.

Black shales from the Wynniatt Formation, several hundred meters below the contact with ~720Ma basalts that mark the top of the Shaler Supergroup, yield preliminary Re-Os ages around 770 – 790 Ma. Samples from the Boot Inlet Formation, about 1 km stratigraphically below the Wynniatt Formation, yield Re-Os ages around 900-920 Ma. These ages provide additional valuable anchor points for the Neoproterozoic timescale.

Old and new geochemical proxy evidence for deciphering the southern high latitude 'doubthouse'

T. VAN DE FLIERDT[1] AND EXPEDITION 318 SCIENCE PARTY

[1]Imperial College London, London, UK, tina.vandeflierdt@imperial.ac.uk

Antarctica is the least explored continent on our planet Earth, largely due to today's massive ice cover on the continent, reaching a thickness of 4500 m in places, leaving only 0.3% of the land area uncovered. This ice sheet, however, was not always in place, and its inception ~34 million years ago at the Eocene-Oligocene boundary marked one of the most fundamental climate transitions in recent Earth history: the transition from the greenhouse world of the Cretaceous and early Paleogene to the icehouse world we are currently living in.

Global climate in the greenhouse world seems to have been characterized by low latitudinal temperature gradients and subtropical temperatures at high latitudes. Atmospheric CO_2 levels were probably well in excess of 1000 ppm, and it is hypothesised that there was no or only very little ice on the poles. A range of geochemical proxies have been used over the years to characterize baseline conditions as well as rapid climate excursions during the 'doubthouse' (ca. 144 to 34 Ma).

Here I will provide a summary and critical evaluation of some of the proxies that can shed light on the interrelationship between Earth's cryosphere, ocean chemistry and temperature, and the carbon cycle. I will pay particular attention to the early Paleogene in the southern high latitudes and to evaluating the use of radiogenic isotope systems (i.e., Hf, Nd, Pb isotopes). I will furthermore highlight some of the spectacular initial results obtained from material recovered during IODP Expedition 318, which sailed in January to March 2010 to the Wilkes Land coast, East Antarctica. Seven sites were drilled along an inshore to offshore transect, yielding ~2000 m of middle Eocene to Holocene sediment. At Site U1356, a partial record of the early Paleogene was retrieved (Expedition 318 Scientists, 2011), offering the rare opportunity for detailed geochemical studies on a marine section from the southern high latitudes during this time.

[1] Expedition 318 Scientists (2011). Site U1356. *In* Escutia, C., Brinkhuis, H., Klaus, A. and the Expedition 318 Scientists, *Proc. IODP*, **318**: Tokyo (Integrated Ocean Drilling Program Management International, Inc.). doi:10.2204/iodp.proc.318.104.2011.

https://doi.org/10.1180/S0026461X00008434 Published online by Cambridge University Press

Tracing seawater-rock interaction in slow spreading oceanic crust: precise chlorine measurements in MORB by microprobe

F.M. VAN DER ZWAN[1*], J. FIETZKE[1], C.W. DEVEY[1], R.R. ALMEEV[2] AND K.M. HAASE[3]

[1]Geomar | Helmholtz Centre for Ocean Research, Kiel, Germany, fzwan@geomar.de (* presenting author)
[2]Institut für Mineralogy, Universität Hannover, Germany
[3]GeoZentrum der Friedrich-Alexander Universität Erlangen-Nürnberg, Erlangen, Germany

Chlorine is a key element in tracing present and past interaction between magmas/rocks of the oceanic crust and seawater due to the large differences in concentration between magmas derived from the asthenosphere and seawater.

Processes, such as assimilation of hydrothermally altered oceanic crust by mid ocean ridge magmas, which lead to higher magmatic chlorine concentrations, have been demonstrated for fast spreading ridges [e.g. 1, 2]. Similar features have, up to present, not been observed at slow spreading ridges, partly because their intrinsically low chlorine contents made this work analytically challenging and variations in concentrations could not be explored with conventional methods.

To change this situation we have developed a new method to measure chlorine in basaltic glass by electron microprobe. Using a combination of mapping and standard-sample bracketing techniques, chlorine can be measured at very low detection limits (10's of ppm's) with a precision of 1-2 ppm standard deviation. With this, the very low chlorine concentrations in Mid Ocean Ridge Basalts from slow spreading ridges can be explored, and the new method enables us to reveal variations that could not be observed before.

We have used this method to examine a sample set of basaltic glasses from the Southern Mid Atlantic Ridge at 7-10 °S, for which large variations in depth of last equilibration with a mafic mineral assemblage have previously been shown [3]. We find chlorine concentrations which decrease from about 200 to 60 ppm with this crystallisation depth. However, several samples,have much higher chlorine contents which are independent of depth (>300 ppm).

The chlorine variations observed may have multiple causes: 1) hydrothermal interaction, related to the present spreading, and subsequent assimilation of altered crust, 2) alteration of the rocks at the seafloor, or 3) a mantle anomaly, which potentially can be related to melting processes and/or older interaction of the ocean with the magmatic system. With the aid of other trace elements the nature of the observed chlorine enrichment will be determined and a distinction between the causes made.

[1] Michael & Schilling (1989) *Geochim. Cosmochim. Acta* **53,** 3131-3143.
[2] Gillis *et al.* (2003) *Earth Planet. Sci. Lett.* **213**, 447-462.
[3] Almeev *et al,* (2008) *J. Petrol.***49**, 25-45.

Polymict eucrite NWA 5232: composition of clasts

KATRINA VAN DRONGELEN[1,2*], KIM TAIT[1,2], MIKE GORTON[1], AND IAN NICKLIN[2]

[1]University of Toronto, Dept. of Geology, k.vandrongelen@geology.utoronto.ca (* presenting author)
[2]Royal Ontario Museum, Dept. of Natural History, ktait@rom.on.ca

Northwest Africa (NWA) 5232 is an 18.535 kg polymict eucrite, a member of the Howardite-Eucrite-Diogenite (HED) meteorite group, which are interpreted to come from the asteroid 4 Vesta [1]. NWA 5232 is comprised of four main constituents: eucrite (lithic) clasts, CM clasts, melt clasts, and matrix. A Petrographic microscope and JEOL JSM-6610LV scanning electron microscope at the University of Toronto were used to examine textures and mineral constituents of these phases. Clast sizes typically range from less than 0.5 mm to 3 cm and are variable in their distribution and angularity. The matrix is very fine- to coarse-grained, making up a significant proportion of this matrix-supported breccia. Various shock features were identified in the clasts and matrix, including bent pyroxene lamellae and pervasive fractures. The eucrite clasts show various textures, primarily subophitic, of varying coarseness and range in size from <0.5-30 mm, averaging 5 mm. Distinguishing basaltic and cumulate eucrite clasts on the basis of texture alone is problematic as both groups may be medium- to coarse-grained, have pyroxenes with exsolution lamellae, and consist of the same major mineral phases (pyroxene and plagioclase). Minor and accessory phases include SiO_2, ilmenite, chromite, Fe,Ni-metal, and troilite. A Horiba LabRAM Aramis confocal Raman spectrometer with SWIFT mapping stage at the Royal Ontario Museum was used to identify terrestrial weathering phases using the 532 nm laser. Pervasive fractures have been filled with calcite during terrestrial weathering.

Eucrite clasts were analyzed with a Cameca SX50 electron microprobe (EMP) with a 1 µm beam, an accelerating potential of 15 keV, and beam current of 15 nA at the University of Toronto. Eucrite clast pyroxenes have a Fe/Mn (afu) of 31.1 ± 2.3 n=329 (within the characteristic range of HED meteorites [2]) and of the 30 eucrite clasts analyzed with EMP, only one plotted on a pyroxene quadrilateral outside of the basaltic eucrite field as a cumulate eucrite [3]. Plagioclase compositions are within those expected for eucrites (An_{79-91}, avg $An_{87} \pm An_{1.8}$, and K (afu) = 0.003 ± 0.001 n=94) [3].

Two matrix samples and ten eucrite clasts were analyzed with INAA (Instrumental Neutron Activation Analysis) at the University of Toronto and generally show a ~5 x CI REE pattern with a LREE (La) depletion. The high $(Yb/La)_{CI}$ values (average 4.03 ± 1.24) may be due to dissolution of REE-rich phosphates during weathering [4]. The relatively high Co, Ni, and Ir contents of matrix samples (*e.g.* 27, 390, 0.032 ppm, respectively for a sample with mass of 229 mg) are consistent with the contribution of a chondritic component [4].

NWA 5232 is a polymict eucrite comprised of eucrite, CM, and melt clasts in a heterogenenous matrix. Lithic clasts are primarily basaltic eucrite clasts and no diogenite material was identified.

[1] Li *et al.* (2011) *Icarus*, **216**, 640-649. [2] Papike *et al.* (2003) *American Mineralogist*, **88**, 469-472. [3] Takeda H. (1997) *Met. & Planet. Sci.*, **32**, 841-853. [4] Mittlefehldt & Lindstrom (2003) *Geochim et Cosmochim*, **67**, 1911-1935.

https://doi.org/10.1180/S0026461X00008434 Published online by Cambridge University Press

Beyond Henry's Law: Interpreting element signatures in oxide minerals at high concentrations

VINCENT VAN HINSBERG* AND BERNARD WOOD

Earth Sciences, University of Oxford, Oxford, United Kingdom, V.J.vanHinsberg@gmx.net (* presenting author), Bernie.Wood@earth.ox.ac.uk

The compositions of minerals are frequently used to estimate the compositions of the fluids and melts from which they formed. For major elements, concentrations in a coexisting melt or aqueous solution are readily estimated from mineral solubility data, and partition coefficients enable calculation of trace element contents. Intermediate concentrations are more difficult to constrain, however, because the impact of minor elements on solubility is commonly poorly known, and such concentrations exceed Henry's Law behaviour required for a partitioning approach. This is a problem, as this concentration range is of key interest, especially in ore formation, where it traces enrichment of the ore element. Moreover, knowledge of the changing element content in the fluid can reveal clues about the mechanisms of enrichment and ore formation.

Here, we experimentally explored the distribution of a suite of trace elements between mineral and melt at increasing concentrations of a dopant. We used perovskite ($CaTiO_3$) as our model mineral and doped with either La, Nd or Yb from 500 ppm to 5 wt%. The other REE + Mg,Sr,Ba,Li and Na were added at ~100 ppm to act as passive tracers of the impact of the dopant. Experiments were run in a 1 atm furnace, cooling a Ca-Ti-Si-O melt suspended from Pt wire from 1450°C to 1370°C at 1°C/hr, followed by 80hr equilibration.

Results show an abrupt change in REE distribution behaviour as a "Henrian limit" is encountered in agreement with earlier work [1]. Below this limit, a characteristic partition coefficient (D) describes the mineral-melt REE distribution, and the mineral concentration can be directly translated to a REE content in the melt. In contrast, above this limit, the REE distribution depends on the dopant concentration, and the REE content of the melt is strongly underestimated when using the Henrian D value. This change in behaviour is due to exhausting the inherently available vacancies in the perovskite structure. The change in REE behaviour is mirrored by the 1+ trace elements, which show an *increase* in D value with increasing dopant level beyond the "Henrian limit". We link this increased incorporation of the 1+ elements in perovskite to charge compensation for 3+ dopant uptake. In contrast, the 2+ trace elements can substitute isovalently, and, as therefore expected, are unaffected by increasing dopant concentration. Moreover, the systematics in element distribution among isovalent trace elements remain unchanged.

We conclude that mineral-fluid/mineral-melt distribution of elements at elevated concentrations differs strongly from that at low concentrations, even for elements that are at trace levels, which can lead to both under- and overestimation of fluid concentrations. However, the systematics among an isovalent suite of elements, such as the REE, are preserved and minerals therefore remain an accurate tracer of the REE pattern of their host fluid.

[1] Corgne & Wood (2005) *Contrib Mineral Petrol* **149** 85-97

Speciation of Nickel in Workplace Aerosols Using X-Ray Near Edge Structure Spectroscopy

LISA L VAN LOON[1*], MIKE D DUTTON[2], CHRIS[3]

[1]Canadian Light Source Inc., Saskatoon, SK, Canada , lisa.vanloon@lightsource.ca (* presenting author)
[2]Vale Base Metals.Mississauga, ON, Canada, mike.dutton@vale.com
[3]Activation Laboratories Ltd, Ancaster, ON, Canada, chamilton@actlabs.com

Type Section Heading Here [bold, 9pt font size]

X-ray absorption near-edge structure (XANES) spectroscopy provides new interpretations of Ni speciation in sulfidic Ni processing, particularly with respect to soluble Ni in workplace aerosol samples collected at the Copper Cliff nickel smelter and refinery. Typically, Ni speciation is identified using a sequential extraction developed by the Ni industry for determining workplace exposures. However, as this technique and its variants become more widely applied, there is evidence that the method may not always accurately report soluble and metallic Ni. Because of the importance of exposure reconstruction to the determination of carcinogenicity classification of Ni compounds, we have begun to evaluate alternative speciation methodologies for Ni. Here we present the results of a study comparing Ni speciation results obtained using XANES spectroscopy and sequential extraction along with complementary SEM, EDX, and XRD results.

https://doi.org/10.1180/S0026461X00008434 Published online by Cambridge University Press

Bio-mediated ground improvement: from concept to field application

LEON A VAN PAASSEN[1*], WOUTER RL VAN DER STAR[2], GERARD VAN ZWIETEN[3],& LENNART R VAN BAALEN[4]

[1]Delft University of Technology, Department. of Geotechnology, Stevinweg 1, 2628CN Delft, The Netherlands, l.a.vanpaassen@tudelft.nl (* presenting author)

[2]Deltares, Department.of Soil & Groundwater. P.O. Box 177, 2600 MH Delft, The Netherlands

[3]Volker Staal en Funderingen, P.O. Box 54548 3008 KA Rotterdam, The Netherlands

[4]Visser & Smit Hanab, P.O. Box 305, 3350 AH, Papendrecht, The Netherlands.

Biomineralization can be used as ground improvement method, for a wide range of geo-engineering applications, like mitigation of liquefaction and associated damage, improving the stability of dikes, dams, levees and slopes, reducing the permeability of underground leaking structures or stopping or diverting subsurface transport of contaminants by forming impermeable or reactive barriers. Most studies on applied biomineralization involve the precipitation of calcium carbonate, in particular by urea hydrolysis. In this process urea hydrolyzing bacteria are introduced in the subsurface and supplied with urea and calcium chloride. By hydrolyzing urea, the bacteria produce ammonium and carbonate. The carbonate precipitates with calcium carbonate and remaining ammonium chloride is removed. The calcium carbonate crystals form a binding cement between the soil particles while (partly) filling up the pore space, which increases the strength and stiffness of the soil and reduces the permeability. Using an empirical approach the feasibility of MICP by urea hydrolysis as ground improvement method has been demonstrated at full scale using conditions and techniques as used in practice, both as single point injection or over a horizontal distance using screens of injection and extraction wells. Engineering parameters correlated well with $CaCO_3$ content or dry density [1]. At the same time, a more fundamental approach was used to improve our understanding of the MICP process that involved multiple components including bacteria and multiple chemical species that are subject to both kinetically controlled and equilibrium reactions over multiple phases, undergoing transport in porous medium with changing porosity and permeability. Understanding of these processes was required to enable control of the *in situ* distribution of bacterial activity and reagents and the resulting distribution of $CaCO_3$ and related engineering properties. The combined approach of theory, experiments, modeling and monitoring has resulted in the first field applications in which biomineralization was used to cement gravel layers in order to improve borehole stability during horizontal directional drilling [2].

[1] Van Paassen, LA, Ghose, R, Van der Linden, TJM, Van der Star, WRL and Van Loosdrecht, MCM, 2010. *ASCE Journal of Geotechnical and Geoenvironmental Engineering*, **136(12)**: 1721–1728 [2] Van der Star, WRL, van Wijngaarden-van Rossum, WK, van Paassen, LA, van Baalen, LR, van Zwieten, G, 2011, *Proceedings of the 15th European Conference on Soil Mechanics and Geotechnical Engineering*, *12 -17 Sep 2011, Athens, Greece*, 85-90.

$^{40}Ar/^{39}Ar$ cooling dates and deformation history on the southern flank of the Thor-Odin dome BC: tectonic implications of overlapping compressional and extensional regimes in the Paleocene-Eocene.

D. VAN ROOYEN[1]* AND S.D. CARR[1]

[1] Ottawa-Carleton Geoscience Centre, Dept. of Earth Sciences, Carleton University, Ottawa, ON, Canada K1S 5B6 (*dvrooyen@connect.carleton.ca)

The southern flank of the Thor-Odin dome comprises an ~12 km thick S-dipping panel of amphibolite to granulite facies rocks, the lower half of which is migmatitic. Throughout the structural section the rocks have a pervasive composite transposition foliation, with rootless folds, folded by syn- and refolded by post-metamorphic NE verging folds. Metamorphism and the youngest stages of ductile deformation are Late Cretaceous to Eocene and young progressively down section. On the basis of cross cutting granitoids dated by U-Pb studies, transposition and folding had ceased by: (i) 73 Ma at the highest structural levels (e.g. in the southern part of the study area near Whatshan Lake and west of the dome at Joss Mountain); (ii) 64 – 62 Ma (in the central section west of Arrow Park lake); (iii) ~58 Ma on the upper margin of the dome at Cariboo Alp; and, (iv) ~56 – 54 Ma within the dome. Cooling from the thermal peak of metamorphism to ~300°C occurred between 62 and 52 Ma on the basis of $^{40}Ar/^{39}Ar$ cooling dates. Thor-Odin dome and its southern flank lie in the footwall of the ~55 Ma and younger, E-dipping Columbia River normal fault. Proposed models for the exhumation of the dome and overlying rocks on the southern flank include extension, extrusion or diapirism (with an erosional contribution).

$^{40}Ar/^{39}Ar$ cooling dates on hornblende, muscovite and biotite from 80 samples at all structural levels were studied in order to place constraints on the timing of the exhumation over a temperature range of ~600 to 300°C. Hornblende $^{40}Ar/^{39}Ar$ cooling dates (calculated closure temperatures from 500 - 600°C) are ~62-58 Ma at the top of the panel, ~57-56 Ma in the middle, and ~55-53 Ma near the upper margin of the dome. Hornblende $^{40}Ar/^{39}Ar$ data from migmatites in the dome are disturbed and do not produce meaningful dates. Biotite cooling dates (280 - 350°C) are ~52-51 Ma throughout the 12 km thick structural section, including the dome. Since rocks from all different structural levels cooled through ~300°C at the same time the structural section was tilted prior to cooling or cooling rates were extraordinarily high. 51-50.5 ± 0.2 Ma muscovite dates from greenschist-facies muscovite intergrowths in extensional structures in the dome, grew below their closure temperature and date late stage extension.

The downward younging progression of deformation and the thermal history are consistent with that of a highly strained crystalline sheet that was deforming progressively as it overrode a basement ramp, the Monashee ramp imaged in Lithoprobe seismic reflection profiles 6, 7 and 8. Exhumation and cooling as a result of syn-convergent extension in the upper part of the structural section was ongoing during the last stages of transposition and folding in the dome in the Late Paleocene to Early Eocene. By ~51 Ma, extensional structures were active at all structural levels reflecting crustal scale extension and exhumation via normal faulting linked to continuing motion on the Columbia River and possibly the Okanagan Valley extensional fault systems.

https://doi.org/10.1180/S0026461X00008434 Published online by Cambridge University Press

Combining experimental and numerical studies of lunar differentiation

WIM VAN WESTRENEN[1*], JELLIE DE VRIES[1,2], MIRJAM VAN KAN PARKER[1], ELODIE J. TRONCHE[1], NACHIKETA RAI[1], ARIE VAN DEN BERG[2], CHRYSTÈLE SANLOUP[3], AND MICHEL JACOBS[4]

[1]VU University Amsterdam, Faculty of Earth and Life Sciences, Amsterdam, the Netherlands, w.van.westrenen@vu.nl (* presenting author)
[2]Utrecht University, Faculty of Geosciences, the Netherlands
[3]University of Edinburgh, UK
[4]Institut für Metallurgie, TU Clausthal, Germany

The lunar magma ocean (LMO) model [1,2] remains the starting point for most models of early lunar differentiation. Petrologists have studied LMO crystallisation sequences [3,4], and numerical thermochemical convection models have been developed to study the evolution of layered cumulate piles formed during MO crystallisation [5-7]. These models generally take into account changes during differentiation in major element composition and density of the minerals involved.

Here, we give an overview of our recent progress on combining mineral and melt density measurements [8-10], experimental studies of the distribution of trace elements during and after LMO crystallisation, and numerical models of lunar interior thermal evolution. Recent experimentally determined mineral-melt partitioning data [11,12] show that the interior distribution of the main heat-producing elements K, U and Th is highly heterogeneous in the aftermath of LMO crystallisation and differentiation. This has significant effects on the thermal evolution of the lunar interior after solidification - effects that are missed if partitioning of heat-producing elements is ignored.

In the Moon, K, U and Th are concentrated in late-crystallising, dense ilmenite/cpx-rich cumulates. Thermochemical convection models show that sinking of these cumulates towards the lunar core, and increased levels of heat production associated with their trace element chemistry lead to (a) the formation of a thermal blanket on the core which could play a role in the recently proposed extreme longevity of lunar dynamo activity [13] (b) prolonged interior mantle dynamics consistent with the young ages of some surface lava flows derived from crater density analysis [14]. These results illustrate the value of combining experimental and numerical approaches to planetary interior evolution.

[1] Smith *et al.* (1970) *GCA Suppl* **1**, 897–925. [2] Wood *et al.* (1970) *GCA Suppl* **1**, 965–988. [3] Snyder *et al.* (1992) *GCA* **56**, 3809–3823. [4] Tronche & Van Westrenen (2011) *LPSC* **42**, 1415. [5] Hess & Parmentier (1995) *EPSL* **134**, 501–514. [6] Elkins-Tanton *et al.* (2002) *EPSL* **196**, 239–249. [7] De Vries *et al.* (2010) *EPSL* **292**, 139-147. [8] Tronche *et al.* (2010) *Am Min* **95**, 1708-1716. [9] Van Kan Parker *et al.* (2012) *Nature Geoscience*, in press. [10] Van Kan Parker et al. (2011) *GCA* **75**, 1161-1172. [11] Van Kan Parker et al. (2011) *Chem. Geol.* **285**, 1-14. [12] Van Kan Parker *et al.* (2011) *GCA* **75**, 4179-4193. [13] Shea et al. (2012) *Science* **335**, 453-456. [14] Hiesinger et al. (2003) *JGR* **108**, 5065.

Isotopic tracers of metal cycling in the oceans and sediments

D. VANCE[1*], S.H. LITTLE[1], V. CAMERON[1], D. M. SHERMAN[1], S. WESTERMANN[1], A. MATTHEWS[2] AND T.W. LYONS[3]

[1]School of Earth Sciences, University of Bristol, Bristol, UK, d.vance@bristol.ac.uk (* presenting author)
[2]Institute of Earth Sciences, Hebrew University, Jerusalem, Israel, alan@vms.huji.ac.il
[3]Department of Earth Sciences, University of California, Riverside, USA, timothy.lyons@ucr.edu

The emerging isotopic systems of the transition metals potentially have much to tell us about sources of metals to the oceans, their biogeochemical cycling within the oceans, and the nature of the output processes to sediment. With respect to the latter, it has been the redox-sensitivity of the outputs, and the variability of the isotopic fractionations involved in different output pathways, that has attracted most attention. For example, the isotopic composition of Mo in marine sediments has already been used as a monitor of ancient water-column redox conditions. Here, we introduce the isotopic systems of other transition metals (Cu, Zn, Ni), systems that are much less developed, and assess their potential for providing complementary paleoceanographic information to Mo.

Isotopic data for seawater and Fe-Mn crusts reveal that the light isotope of Cu, as with Mo, is preferentially removed from the seawater solution under fully oxic conditions. In contrast, Zn isotopic compositions of Fe-Mn crusts are heavier than Zn in the dissolved phase in the deep ocean, by about 0.5 ‰ for $^{66}Zn/^{64}Zn$. Sorption experiments for Cu to Mn oxide reproduce the sense of the natural fractionation, but the magnitude of the latter is slightly greater than in the experiments. For Zn, by contrast, the fractionation seen in the Mn oxide experiments is opposite to that in nature. This could be due to complexing of Zn in the natural seawater solution, or to the superimposition of other biological effects on Zn isotopes in the oceans.

In contrast to the oxic output discussed above, and in a developing picture that looks qualitatively very similar to Mo, it appears that both Cu and Zn undergo little or no isotopic fractionation as a result of removal from seawater solution under anoxic conditions. For example, in the most euxinic sediments from the Black Sea and Cariaco Basin, enrichments of Cu and Zn are associated with isotopic compositions that are identical to (Zn) or likely very close to (Cu) the local deep ocean.

We are at an earlier stage in the development of Ni isotopes. It is clear that seawater is homogeneous at $\delta^{60/58}Ni_{SRM986}$ = 1.44±0.1 ‰. In common with both Cu and Mo this is distinctly heavier than the riverine input (at about 0.8 ‰ based on the discharge-weighted mean of 7 large and small rivers), while rivers themselves, again in common with Cu and Mo, are heavier than rocks (0.1-0.2 ‰). These observations imply fractionation of Ni isotopes in both the weathering and marine environment. In the case of Ni it appears that it is not the oxic sink that removes the light isotope to push seawater to heavy values, as analyses of Fe-Mn crusts suggest that they are significantly heavier than seawater at 1.7-1.9 ‰.

https://doi.org/10.1180/S0026461X00008434 Published online by Cambridge University Press

Zinc isotopic data from the NE Pacific reveals shallow recycling

D. VANCE[1*], YE ZHAO[1], J. CULLEN[2], AND M. LOHAN[3]

[1]School of Earth Sciences, University of Bristol, Bristol, UK, d.vance@bristol.ac.uk (* presenting author), y.zhao@bristol.ac.uk

[2]School of Earth and Ocean Sciences, University of Victoria, Victoria, Canada, jcullen@uvic.ca

[3]School of Geography, Earth and Environmental Sciences, University of Plymouth, Plymouth, UK, maeve.lohan@plymouth.ac.uk

Isotopic data for biologically-active trace metals can elcuidate their sources to seawater and their biogeochemical cycling within the oceans. Here we present new dissolved-phase Zn concentration and isotopic data for depth profiles along a transect (Line P, around 50°N) from the North American continental margin to the open ocean in the NE Pacific, with 10-25m depth resolution in the upper 100m of the water column.

Zn concentrations increase with depth, with surface or near-surface concentrations as low as 0.05 nM and concentrations at 2000m at 10-11 nM. There are two distinct differences between the new dataset and the only previous study of Zn in the NE Pacific of similar geographical scope [1]. Firstly, concentrations at 10m depth increase gradually from 0.09 nM at the marginal station to 0.65 nM at the open ocean station, a reversal of findings for samples collected in 1999, and showing a closer coupling to Si. Secondly, at some stations the shallow sub-surface (at 50-100m at the marginal station) is characterised by a distinct bulge in the concentration depth profile.

The isotopic data for the deep ocean, for Zn concentrations ≥ about 7 nM (beneath 200-600m, depending on the station), are very homogeneous, with $\delta^{66}Zn_{Lyons\text{-}JMC}$ = 0.52±0.10 ‰ (2 SD, n = 15). The upper ocean is much more variable. Firstly, the immediate sub-surface (50-100m at the marginal station) is characterised by distinctly light Zn isotopic compositions, down to $\delta^{66}Zn$ = -0.4 ‰. This feature persists along the transect but the depth range over which this light isotope value is found shallows oceanwards. Above the thin isotopically light layer, the surface ocean has heavier isotopic compositions at very low Zn concenttrations, by 0.5-0.8 ‰ and with the shift occuring over a depth range of 10m or less.

The three features described above – a homogeneous deep ocean, an isotopically light layer in the immediate sub-surface, and a return to variably heavy values in the photic zone – are proving to be common to Zn isotope depth profiles in the ocean in a small but building database. But they are particularly clear in the NE Pacific, perhaps partly because of a highly-stratified water column. Moreover, only here is the sub-surface isotopic feature associated with recognisable features in the concentration profile. The new isotopic data shed light on the biogeochemical cycling of Zn in the upper ocean that are not readily apparent from concentration data alone. In particular, the anomalously light isotopic compositions are most likely to be explained by the very shallow recyling of a pool of light Zn sequestered into phytoplankton cells [2] in the photic zone.

[1] Lohan et al. (2002) *Deep-Sea Res. II* **49**, 5793-5808. [2] John et al. (2007) *Limnol. Oceanogr.* **52**, 2710-2714.

Evaluating Changes in Sources and Pathways of Trace Metals Over Time Using Lake Sediment

VANNIER, RYAN G.[1*], LONG, DAVID T.[1], ROBINSON, AMANDA M.[1], YOHN, SHARON, S.[2]

[1]Michigan State University, East Lansing, MI, USA, milakes@msu.edu (* presenting author)

[2]Juniata College, Huntington, PA, USA, yohn@juniata.edu

Abstract

Environmental regulation has reduced the loadings of metals to the environment since the advent of the Clean Air and Water Acts in the 1970's. Reducing emissions may have changed transport pathways since this legislation targeted major sources of metals which influenced the environment on a regional scale. Watershed-scale processes may now provide the significant contribution to metals loadings. Thus, our working hypothesis is that the reduction of major emission sources has allowed local influences and watershed features to affect metal transport pathways. If true then there should be differences in watershed attributes/influences (e.g., %urban, population density) changed the pathways of metals transport of these metals. In this study we examine Pb, Cu, Zn, and Ni because these metals 1) build from previous studies, 2) exhibit similar environmental behaviour but separate pathways, 3) represent various degrees of contaminant enrichment. To test this hypothesis, sediment accumulation rates of these metals at decadal intervals were compared to selected watershed attributes. Sediment cores were collected from the deepest portion of 35 inland lakes representing diverse land uses. Cores were sectioned; microwave digested, and analyzed using mass spectrometry. Sedimentation rates, ages and sediment focusing were determined via 210Pb/137Cs/stable Pb profile analysis. Similar to the previous work, the data show regional sources of the metals studied to subside upon introduction of environmental legislation in the 1970's. However, watershed-scale sources provide a more significant portion contaminant loading in nearly all lakes studied, preventing lakes from reacquisition of reference condition values. When compared to landscape attributes, these patterns provide some insights into the causes for the continued contaminant loading. Population density and percent urban provide excellent predictors for recent metals loadings. Lead also showed excellent correlation with slope percent. Unexpectedly all metals showed a change in watershed attributes influencing accumulation rates between the two decades, even though some have not had a significant atmospheric transport pathway or contaminant loading. The reasons for this are subject to further study.

https://doi.org/10.1180/S0026461X00008434 Published online by Cambridge University Press

Sorption of cationic amines to soils and soil minerals: Role of intermolecular interactions.

DHARNI VASUDEVAN*[1], TERESAY AREY[1], MARK NEWMAN[1], TINA ZHANG[1], AND HEATHER KINNEAR[1].

[1]Bowdoin College, Department of Chemistry, Brunswick, ME, USA. dvasudev@bowdoin.edu(* presenting author)

Introduction and Project Goals

Numerous chemicals containing cationic amine functional groups, such as antibiotics, herbicides, and antidepressant drugs, have been detected in surface and ground waters, and some of these pose risks to humans and ecosystems. Understanding and predicting the extent of sorption under a wide range of environmental conditions is key to anticipating potential contamination of groundwater by these chemicals. Cation exchange, the primary mechanism for cationic amine sorption has been well studied. However, there is a lack of knowledge about potential secondary mechanisms of sorption that may result in non-linear sorption isotherms and about the soil characteristics that may facilitate secondary, intermolecular interactions between amines sorbed to the surface and adjacent amines in solution. By examining the sorption of a series of model compounds that represent important sub-structures of antibiotics and pesticides, this study addresses three significant gaps in current understanding of cationic amine fate: (i) the influence of compound structural criteria on amine cation sorption, (ii) secondary interactions mechanisms that contribute to non-linearity in sorption phenomena, and (iii) effect of soil properties on sorption linearity and non-linearity.

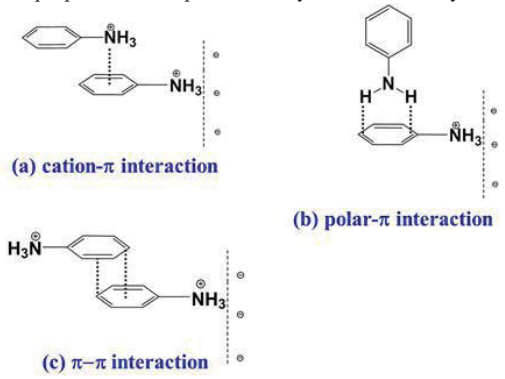

Figure 1: Hypothesized intermolecular interactions contributing to sorption isotherm non-linearities.

Results and Conclusions

On evaluating the sorption of several substituted anilines, benzylamines and cyclohexane methyl amine to Ca- and Na-montmorillonite, we established that the primary sorption mechanism, cation exchange, is influenced by the charge density on the amine moiety and compound hydrophobicity. In addition, we found that the presence of a π system, orientation of the molecule on the surface, and electron density at the center of the aromatic ring influenced the extent of intermolecular interaction between a sorbed amine and an adjacent amine. Furthermore, on evaluating cation amine sorption to a wide range of soils, we established that soils with higher density and closer proximity of negatively charged sites (i.e., soils with high cation exchange capacities) may facilitate secondary intermolecular π interactions.

Evolution of the Strange Lake pluton: Insights from melt and fluid inclusions

O.VASYUKOVA* AND A.E.WILLIAMS-JONES

Department of Earth and Planetary Sciences, McGill University, Montreal, QC, H3A 2A7, Canada, olga.vasyukova@mcgill.ca

The Mid-Proterozoic Strange Lake pluton (Québec-Labrador, Canada) hosts economic rare earth element (REE) and high field strength element (HFSE) mineralization. The richest zones are confined to the most altered areas within subsolvus granite and associated pegmatites. The main HFSE mineral, the zirconosilicate, gittinsite, is commonly accompanied by armstrongite, kainosite-(Y), bastnäsite, gagarinite-(Y), monazite, pyrochlore and gadolinite.

Previous data on fluid inclusions from quartz pseudomorphs after elpidite and narsarsukite, quartz veins and pegmatitic quartz [1] revealed the importance of late Ca-metasomatism for the REE/HFSE mineralization of the Strange Lake pluton. Two fluids were found to contribute to the mineralization, a high salinity magmatic aqueous liquid containing a reduced carbonic component [2], and a Ca-rich meteoric fluid. Fluid mixing caused oversaturation of the fluid with fluorite and its precipitation, which triggered precipitation of Zr, Y and REE minerals as a result of decreased ligand concentration.

This study reports the results of observations of fluid and melt inclusions characterising progressive stages of the melt-to-fluid evolution. Quartz phenocrysts contain melt inclusions trapped during the very early stage of formation of the Strange Lake granites and pegmatites. A later population of magmatic quartz hosts melt inclusions representing more evolved magmas. Early fluorite included in late magmatic quartz and late arfvedsonite contains two types of inclusions, devitrified melt inclusions and NaCl-and possibly $FeCl_2$-rich fluid inclusions. This association presents evidence of the timing of exsolution of fluid from the magma. The next stage of melt-to-fluid evolution is preserved in quartz from miarolitic cavities, which contains abundant aqueous inclusions of variable salinity. The final stage of hydrothermal activity, which is associated with REE/HFSE mineralization, involved Ca-rich aqueous fluids, which were trapped as primary fluid inclusions in late hydrothermal fluorite and secondary inclusions in pegmatitic quartz.

The study of melt and fluid inclusions is permitting reconstruction of the melt-to-fluid evolution of the Strange Lake pluton from the very earliest magmatic stage to the latest stage of mineralization, thereby providing a deeper understanding of the REE/HFSE mineralizing processes at Strange Lake.

[1] Salvi&Williams-Jones (1990) *Geochim. Cosmochim. Acta* **54**, 2403-2418.
[2] Salvi&Williams-Jones (2006) *Lithos* **91**, 19-34.

https://doi.org/10.1180/S0026461X00008434 Published online by Cambridge University Press

Dating groundwater in Québec using noble gases, U and stable isotopes and major elements

GENÈVIEVE VAUTOUR[1*], GUILLAUME MEYZONNAT[2], PAULINE MÉJEAN[3], DANIELE LUIGI PINTI[4], MARIE LAROCQUE[5], MARIA CLARA CASTRO[6], CHRIS M. HALL[7], JEAN-FRANÇOIS HÉLIE[8]

[1,3,4,8]GEOTOP-UQAM, Montréal, QC, Canada
[1] vautour.genevieve@courrier.uqam.ca (* presenting author)
[3] mejeanpauline@gmail.com
[4] pinti.daniele@uqam.ca
[8] helie.jean-francois@uqam.ca
[2,5]Département des Sciences de la Terre et de l'Atmosphère, UQAM, Montréal, QC, Canada
[2] meyzonnat.guillaume@courrier.uqam.ca
[5] larocque.marie@uqam.ca
[6,7]Dept. of Earth and Environmental Sciences, University of Michigan, Ann Arbor, MH, USA
[6] mccastro@umich.edu
[7] cmhall@umich.edu

The Quebec government has recently launched an ambitious program to quantify the Province's groundwater resources. In this framework, a multi-isotopic study involving noble gases, U and stable isotopes and major elements was initiated in the Bécancour River catchment basin, Central Québec, with the goal of dating groundwater and identifying flow paths. This basin is particularly interesting because this same area is a target for shale gas exploitation. This basin extends from the Appalachian Mts. down to the St. Lawrence River. Unconfined and partially confined sandy aquifers of Holocene age (Champlain sea) are mainly recharged in the mountains but also receive some local recharge in the plain.

A preliminary survey using noble gases along with stable and U isotopes was carried out along two transects, one parallel to the main flow direction, the second perpendicular to it. A plot of $^{20}Ne/^{4}He$ vs. $^{3}He/^{4}He$ ratios clearly points to the occurrence of three water bodies with distinct helium isotopic signatures.

Modern waters from shallow wells (5-7 m depth) show nearly atmospheric He and Ne concentrations ($^{20}Ne/^{4}He$ = 3.5) as well as $^{3}He/^{4}He$ ratios close to 1.1 Ra, where Ra is the atmospheric $^{3}He/^{4}He$ ratio. These waters are extremely young, with ages ≤10 years. Groundwater localized in the north-eastern border of the basin shows tritiogenic ^{3}He excesses up to $1.80x10^{-13}$ ccSTP/g. Using the Ottawa tritium decay curve from IAEA, which is valid for central Québec [1] and measured ^{3}He content in groundwater, leads to a first-order estimation age of ~19-21 yrs old.

The third water body contains large amounts of radiogenic ^{4}He, up to $4.48x10^{-5}$ ccSTP/g. These amounts are three orders of magnitude higher than the atmospheric background. A simple *in situ* U-Th-^{4}He age model [2] yields ages varying between 2 and 22 Ma, an age range that is older than the age of the aquifers themselves. The well with the highest ^{4}He content is located in the proximity of the recharge area and U and stable isotopes as well as major elements suggest freshly recharged water. A possible mechanism for water ageing is related to vertical transport of radiogenic ^{4}He by: (1) a diffusive crustal basal flux; (2) upward advection of ^{4}He-rich fossil brines from the basement through fault pathways; or (3) upward degassing of methane from the Utica shales carrying ^{4}He.

[1] Murphy et al. (2011) *Hydrogeology* **19**, 195-207. [2] Torgersen and Clarke (1985) *Geochimica Cosmochimica Acta* **49**, 1211-1218.

In situ colonization of HgS mineral by sulfur-oxidizing bacteria and the enhancement of HgS weathering

A.I. VAZQUEZ-RODRIGUEZ[1]*, C.M. SANTELLI[2], C.S. KIM[3], S.C. BROOKS[4], AND C.M. HANSEL[1]

[1]School of Engineering and Applied Sciences, Harvard University, Cambridge, MA USA, avazquez@fas.harvard.edu (*presenting author)
[2]Department of Mineral Sciences, Smithsonian Institution, Washington, DC USA, santellic@si.edu
[3]Chapman University, Orange, CA, USA, cskim@chapman.edu
[4]Environmental Sciences Division, Oak Ridge National Laboratory, Oak Ridge, TN USA, brookssc@ornl.gov

Soils and sediments, where mercury (Hg) can exist as Hg sulfide minerals (HgS), represent major reservoirs of Hg in aquatic environments. Due to their low solubility, primary and authigenic HgS (eg. cinnabar and metacinnabar) have historically been considered insignificant sources of soluble Hg(II) to the environment. Recently however, HgS solubility was shown to be greatly enhanced in the presence of a natural microbial consortium [1]. Mechanisms for this enhanced solubility have yet to be assessed. Further, bacteria capable of colonizing HgS surfaces in the environment have not been identified, yet their association with the mineral makes them likely key players in effecting chemical changes that can impact dissolution.

To this end, we assessed the microbial diversity on HgS surfaces in the Hg-contaminated sediments of the East Fork Poplar Creek (EFPC) in Oak Ridge, TN and examined the effect of these communities on HgS solubility. Mineral sections of metacinnabar, the dominant Hg species in EFPC sediments, were incubated 4 cm below the sediment surface in the creek channel and bank. Cinnabar and other metal sulfides were also incubated to distinguish mineral structure and host metal effects on the colonizing community.

Bacterial community composition and diversity were determined after 6 weeks of incubation via pyrosequencing targeting the 16S rRNA. Metacinnabar colonization was dominated by sulfur-oxidizing bacteria. Specifically, members of the genus *Thiobacillus*, *Sulfuricurvum* and *Sulfuricella* were among the most abundant community members. Members of these genera are known to use reduced sulfur compounds as electron donors during growth.

Following field incubation, oxidation rinds were observed on metacinnabar. Synchrotron-based X-ray microprobe mapping and X-ray absorption spectroscopy reveal the incubated metacinnabar interior contained pyrite inclusions, and the rind was enriched in Fe(III). Oxidation was not observed on cinnabar where, interestingly, sulfur-oxidizing bacteria were not dominant community members.

Microbial enrichments obtained from field-incubated sulfides were incubated in the presence of HgS in the lab. Both metacinnabar and cinnabar solubility were significantly enhanced in the presence of these consortia. The extent, rate, and mechanisms of HgS dissolution by the consortia and, in particular, sulfur-oxidizing bacteria are currently under investigation. The results from this study may have important implications on the role of microbial communities in the dissolution of HgS phases and hence Hg mobility in the environment.

[1] Jew *et al*. (2007) AGU Fall Meeting.

https://doi.org/10.1180/S0026461X00008434 Published online by Cambridge University Press

Abiotic U(VI) reduction by biogenic mackinawite

HARISH VEERAMANI[1*], NIKOLLA P QAFOKU[2], RAVI KUKKADAPU[2], AMY PRUDEN[1], MITSUHIRO MURAYAMA[1], NIVEN MONSEGUE[1] AND MICHAEL F HOCHELLA JR[1,2]

[1] Virginia Tech, Blacksburg, USA (* presenting author, harish@vt.edu)
[2] Pacific Northwest National Laboratory (PNNL), USA

Biostimulation of dissimilatory metal and/or sulfate reducing bacteria (DMRB and DSRB) has been extensively researched as a remediation strategy for mitigating subsurface uranium [U(VI)] contamination. These bacteria derive energy by reducing oxidized metals as terminal electron acceptors by utilizing organic substrates as electron donors. Iron [Fe(III)], an abundant subsurface element, represents a substantial sink for electrons from DMRB, and the reduction of Fe(III) leads to the presence of dissolved Fe(II) and/or reactive biogenic Fe(II)- and mixed Fe(II)/Fe(III)- mineral phases. Likewise, reduction of other electron acceptors such as sulfates by DSRB leads to the formation of sulfide-bearing minerals in subsurface environments. Thus, when evaluating the potential for *in-situ* uranium remediation in heterogeneous subsurface media, it is important to understand how the presence of alternative electron acceptors such as Fe(III) and sulfate affect U(VI) remediation and the long term behavior and reactivity of reduced uranium. Consequently, abiotic U(VI) reduction by reactive forms of biogenic Fe(II) and sulfide-bearing minerals will be a potentially important process for uranium immobilization.

In this study, amendment of Fe(III) and sulfate to a culture of *Shewanella putrefaciens* CN32 (DMRB) bacterium, resulted in the production of biogenic mackinawite, a Fe(II)-bearing sulfide mineral. This biogenic mineral was systematically characterized by X-ray powder diffraction (XRD), electron microscopy (SEM, TEM, HRTEM) and Mössbauer spectroscopy. Batch experiments involving biogenic mackinawite and U(VI) were carried out at room temperature under strict anoxic conditions. Following complete reduction of uranium (determined by ICP analysis), the biogenic mackinawite was analyzed by a suite of analytical techniques including X-ray absorption spectroscopy (XAS), SEM, HRTEM and Mössbauer spectroscopy to determine the speciation of uranium and concomitant phase transformation(s) with respect to mackinawite. SEM and selected area electon diffraction (SAED) analyses showed reduction of U(VI) to nanoparticulate UO_2 on the surface of biogenic mackinawite. These findings are consistent with XANES analysis that indicate reduction of U(VI) to U(IV) and μXRF analysis that was used to map iron and uranium in the sample. Determining the speciation of uranium is critical to success of a remediation strategy. The present work elucidates abiotic molecular scale redox interactions between biogenic mackinawite and uranium.

Extreme microbial sulfur isotope fractionation in a Mars analogue environment at Rio Tinto, SW Spain

E. VELASCO[1*], P. MASON[2], P. VROON[1], W. RÖLING[1], R. AMILS[3,4] AND G. R. DAVIES[3]

[1]Faculty of Earth and Live Sciences, VU University Amsterdam, The Netherlands, e.velascodominguez@vu.nl (* presenting author)
[2]Department of Earth Sciences, Utrecht University, Utrecht, The Netherlands
[3]Centro de Astrobiologia, Torrejon de Ardoz, Spain
[4]CBM-SO, Universidad Autonoma de Madrid, Spain

Sulfur isotopes are likely to be a key tool for the detection of past or present life on Mars, where abundandt sulfate minerals are present. To investigate the link between the activity of sulfate reducing microortanisms and sulfur isotope fractionation, we incubated sediments from a modern hyper-acidic, Fe-rich subareal environment at Rio Tinto, SW Spain.This site has frequently been used as a geochemical anologue of Mars.

Sediments were sampled from the upper part of the Rio Tinto (Marismilla) as well as the estuary (Moguer). Laboratory incubation were carried out at 30° C using an artificial input solution with sulfate in excess and following techniques developed by Stam et al. [1]. The experiments were performed with an input solution at pH 7 and pH 3 and electron donors were provided by the natural substrate. Duplicate reactors were incubated for a total of 10 weeks. Initial data indicate moderate sulfate reduction rates of between 5 and 90 nmol cm^{-3} h^{-1} in Marismilla and between 5 and 45 nmol cm^{-3} h^{-1} in Moguer, independently of the inflow solution pH. Outflow solutions showed pH close to 7, regardless of inflow pH of 3 or 7, suggesting buffering within the sediments. Sulfur isotope fractionation was extreme in the Moguer estuary, extending beyond the maximun of 47‰ as predicted by the starndard Rees model [2] of microbial sulfur isotope fractionation, suggesting that additional fractionation is possible [3] or indicating multiple cycles of reduction and oxidation of sulfate within the reactors. These data indicate that sulfur isotopes may have a potential to be sensitive indicators of biotic activity on Martian sulfate minerals.

[1] Stam (2010) *Chemical Geology* **278#**, 23-30.
[2] Rees (1973) *GCA* **37#**, 1141-1161.
[3] Brunner (2005) *GCA* **69#**, 4759-4771.

https://doi.org/10.1180/S0026461X00008434 Published online by Cambridge University Press

Potential impacts to ecosystem health and water quality from Marcellus Shale drilling

DAVID J. VELINSKY*, PAULA ZELANKO, FRANK ANDERSON, RICHARD J. HORWITZ, AND JERRY V. MEAD

Academy of Natual Sciences of Drexel University, Patrick Center for Environmental Research, Philadelphia, USA (* presenting author) velinsky@ansp.org

Pilot Study

As drilling for natural gas in the Marcellus Shale increases, so do the concerns for the welfare of the surrounding environment. In a July 2010 pilot study, biological and chemical indicators were used to assess the potential effects of gas extraction on streams in north eastern Pennsylvania. Sites ranged from streams draining areas with high well density and known violations to sites with no wells. Density of natural gas wells within a watershed was the main test variable (gradients in potential covariates such as land cover were controlled for). Stream health indicators were regressed against well density to determine possible impacts. Several stream health indicators had significant ($p<0.10$) negative (macroinvertebrates family, Shannon-Wiener diversity index of macroinvertebrates) or positive (water conductivity) correlations with well density. Multiple t-tests among groups of sites with high, low and no wells found that the correlations resulted from differences between sites with high well density and those with low density or no wells. Significant differences were not found between low density and reference sites.

Figure 1: Field team taking stream measurements (left), collecting benthic samples (middle), and collecting water (right).

Expanded Study

During summer and fall of 2011, 60 sites with varying well densities were sampled for water quality analysis. Wastewaters produced from drilling activities in the same region were also tested to identify a "produced water" signature. This signature, consisting of a particular combination of cations and anions, are being compared to samples from the 60 sites. Preliminary data, plotted as Stiff diagrams, suggests three sites have a produced water fingerprint. Two sites had documented spills, while the third site had the highest well pad density. In addition, concentrations of chloride ions increased with well density.

Future Research

Biota samples were also collected at 30 of the water quality sites. As in the pilot study, stream health analysis will be applied to this data in the near future. In 2012, previous sampling sites will be re-visited and new sites added for water quality and biota sample collection. Time transgressive sampling will provide additional information on the potential impacts of Marcellus drilling activities throughout the region.

High resolution aerosol sources and anthropogenic impacts in Central Europe during the Holocene

ALAIN VÉRON[1*], MARTIN NOVAK[2], EVA BRIZOVA[2] AND GAËL LE ROUX[3]

[1]CEREGE, CNRS UMR7330, University Aix-Marseille, Aix en Provence, France, veron@cerege.fr (* presenting author)
[2]Czech Geological Survey, Prague, Czech Rep., martin.novak@geology.cz, eva.brizova@geology.cz
[3]Ecolab, CNRS-University of Toulouse, Castenet Tolosan, France, gael.leroux@ensat.fr

Aerosol transport and deposition is a well-known indicator to assess environmental impacts due to climate changes (erosion, droughts…) and/or human activities (deforestation, quarries, mining…). In particular, sudden climate shifts have become a key issue to develop and test models dealing with recent and forthcoming climate change. Meanwhile, transient and rapid environmental fluctuations in landlocked continental regions cannot be resolved by means of the sole remote ice and marine (generally poorly discriminated at the scale of the Holocene) cores. Because ombrotrophic peatlands are fed by atmospheric deposition only they can archive a full suite of proxies (such as dust, pollens, carbon, trace elements including metals) to resolve climate uncertainties at a high temporal resolution during the Holocene [1]. They also uniquely trace human activities and its environmental effects [2].

Here we present proxy's imprints recorded from a 13,000 years old peat bog collected in Central Europe (Czech Rep.). The well-known Younger Dryas cold interval is clearly characterized with increased dust fluxes at 11.5-12.7 ky BP, a period that compares well to other continental records of this event. Another significant dust episode is identified at 9.3-8.8 ky BP while the marine 8.2 ky BP circum North Atlantic event is not detected. Other major multi-century dust episodes are recorded at 6.0 ky and 3.3-2.9 ky BP that fit cold events from Greenland ice cores and German tree rings. Pollen records are consistent with these findings and show the transition from Late Glacial to Boreal and Atlantic climate zones. In order to verify aerosol sources during these events and to better define successive identified dust peaks we have measured stable Pb isotope ratios that are key markers for the diversity of aerosol sources. We could clearly differentiate aerosol from various regions including the Gobi and Saharan deserts, the Chinese loess, the Scandinavia shield, and the local Czech Bohemian bedrock.

Pb enrichment and specific isotopic ratios could also indicate a long-range transport of pollutant Pb from the Mediterranean regions as early as 5.2 ky BP. This invasion of warmer Mediterranean airflows could explain the advent of warm deciduous species (hazel, elm, oaks) in our peat as also observed in German mires during the same climatic optimum. Mixed imprints of local bedrock and Bohemian ores are observed between 4.4 and 1.7 ky BP that demonstrate well-established regional mining activities.

https://doi.org/10.1180/S0026461X00008434 Published online by Cambridge University Press

Ore origin of Middle-Bronze Age copper artefacts from Sidon

ALAIN VÉRON[1*], GAËL LE ROUX[2], DAVID BAQUÉ[2], ANDRÉ POIRIER[3] AND CLAUDE DOUMET-SERHAL[4]

[1]CEREGE, CNRS UMR7330, University Aix-Marseille, Aix en Provence, France, veron@cerege.fr (* presenting author)
[2]Eco-Lab, ENSAT, Toulouse, France, gael.leroux@ensat.fr
[3] GEOTOP-UQAM, Science de la terre et de l'atmopshère, Earth and Planetary Sciences, Montreal, Canada, poirier.andre@uqam.ca
[4]British Museum, University College, London, England, claude.lbfnm@binternet.com

Over one hundred burials dating from the Middle Bronze Age (2000-1550BC) have been excavated in Sidon since 1998 under the direction of The British Museum and the Department of Antiquities [1]. These excavations led to the discovery of copper (Cu) artefacts (named "bronzes" according to the regional archaeological terminology) that could provide unique indication on the origin of metal used to manufacture them, and therefore help elucidate trade relations between the Levantine coast and the rest of the Mediterranean. These artefacts included weapons (daggers, knife, arrow head, spear head), jewels (torque, belt) and some miscellaneous (pin, fish hook). Our goal was to determine the geographic origin of the mines from which Cu were extracted by means of stable lead (Pb) isotopes that are efficient tracers of Cu, Pb and Ag ore sources [2] [3].

Lead isotope ratios from twenty-eight Bronzes were compared to well-known antique Cu and Pb ore body isotope signatures from Crete, Greece, Turkey, Oman, Sardinia, Spain, Italy, Cyprus, Egypt, Southern Levant, Iran-Iraq and Syria. Both Cu and Pb ore imprints from the same geographic area generally overlap except in the Taurus region and Egypt. The three most common possible geological origins for these bronzes were located in Cyprus, Crete, and, more unexpectedly, in the Cu rich Oman Gulf region. Only one artifact could be related to the abundant Southern Levant Cu mines in spite of its geographic proximity to Sidon and none to Egypt or any other location in the Western Mediterranean basin. Silver (Ag) artifacts from two burials were attributed to Turkish sources. No clear pattern between provenances, as determined by Pb isotopes, burial's chronologies and objects could be established. Trace element analyses were used to resolve source uncertainties associated with mixed/recycled ores and corrosion.

This archeometric approach confirmed archaeological findings about possible networks bewteen the Aegean, Cyprus, Turkey and Sidon more than three thousands years ago. The Gulf of Oman is less likely reliable as a trade partner, but could not be denied on the basis of Pb analyses only.

[1] Doumet-Serhal (2007) in *The Bronze Age in Lebanon*, 11-44, eds. M. Bietak and E. Czerny. [2] Gale and Stos-Gale (1982) *Science* **216**, 4541, 11-19. [3] Gale (2001) *European Journal of Archaeology* **4**, 1, 113-130.

Earthworm secreted calcium carbonate – a new palaeothermometer?

EMMA A. A. VERSTEEGH[1*], MARK E. HODSON[1] AND STUART BLACK[2]

[1]University of Reading, Soil Research Centre, Reading, UK, e.a.versteegh@reading.ac.uk (* presenting author), m.e.hodson@reading.ac.uk
[2]University of Reading, Scientific Archaeology, Reading, UK, s.black@reading.ac.uk

Oxygen and carbon isotope ratios of calcium carbonate skeletons, produced by a range of aquatic and terrestrial organisms, have often been found to be useful proxies for environmental variability [1]. Although they do not form skeletons, many earthworm species are true biomineralisers, secreting granules of intricately zoned calcite [2]. These granules are frequently found in archaeological finds and buried soils. We are currently investigating the utility of stable isotope compositions of earthworm secreted calcite granules for reconstructing past environments.

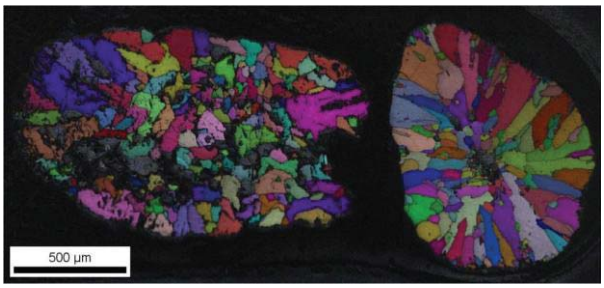

Figure 1: Electron Backscatter Diffraction (EBSD) orientation contrast maps of two Pleistocene earthworm granules highlighting their polycrystalline microstructure. Image by Martin Lee, School of Geographical and Earth Sciences, University of Glasgow.

Experiments were designed in which individual earthworms (*Lumbricus terrestris*) were kept in bags of soil for up to four months. Two different types of soil (C3 and C4 vegetation) were used, which were air-dried and then moistened with three isotopically different types of mineral water. The experiment was performed at three different temperatures. $\delta^{13}C$ and $\delta^{18}O$ values were measured for the soil organic matter, soil pore water, food (manure), soil air, earthworm tissues and $CaCO_3$ granules. Preliminary results show that the $\delta^{18}O$ values of the granules accurately reflect those of the pore water, in a similar way as for inorganically precipitated calcite. $\delta^{13}C$ values appear to reflect those of food offered to the earthworms.

In combination with U/Th dating, the stable isotope composition of earthworm secreted calcite granules can likely help in the reconstruction of past temperatures, vegetation and soil organic matter composition. As such it provides a much needed new terrestrial proxy for the reconstruction of past environments in archaeological and geological contexts.

[1] Versteegh et al. (2010) *Geochemistry, Geophysics, Geosystems* **11**, 16. [2] Lee et al. (2008) *Geology* **36**, 943-946.

https://doi.org/10.1180/S0026461X00008434 Published online by Cambridge University Press

Micron-scale intrashell $\delta^{18}O$ variation in cultured planktic foraminifers

LAEL VETTER[1*], REINHARD KOZDON[2], CLAUDIA I. MORA[3], STEPHEN M. EGGINS[4], JOHN W. VALLEY[2], BÄRBEL HÖNISCH[5], AND HOWARD J. SPERO[1]

[1]Dept. of Geology, University of California, Davis, CA, 95616, USA (*corr: lvetter@ucdavis.edu)
[2]WiscSIMS, Dept. of Geoscience, University of Wisconsin, Madison, WI, 53706, USA
[3]Los Alamos National Laboratory, Los Alamos, NM, 87544, USA
[4]Research School of Earth Sciences, The Australian National University, Canberra, ACT, Australia
[5]Lamont-Doherty Earth Observatory of Columbia University, Palisades, NY, 10964, USA

Introduction

Recent studies have used *in situ* analyses via Secondary Ion Mass Spectrometry (SIMS) to document $\delta^{18}O$ heterogeneity within the shell walls of planktic foraminifers and shell microstructures [1,2] that may result from ontogenetic, ecologic, or diagenetic controls. Here we show that the rate of precipitation of shell calcite in the extant planktic foraminifer *Orbulina universa* is sufficiently rapid that 12h calcification periods in ^{18}O-labeled seawater can be resolved and accurately measured using SIMS with a 3 µm spot. *Orbulina universa* secretes a large, spherical shell that thickens over the course of 3-5 days. Live *O. universa* were collected via scuba diving and maintained at constant temperature (22°C). These individuals calcified continuously while they were transferred every 12h between ambient seawater ($\delta^{18}O_w$ = -0.4‰ VSMOW), and seawater with enriched barium (4x ambient seawater) and $\delta^{18}O_w$ = +18.6‰ VSMOW. Transfers produced geochemically distinct layers of calcite that were enriched in both Ba and ^{18}O, separated by layers precipitated in ambient seawater. We quantified the position of the Ba-spiked calcite in the shell wall of *O. universa* specimens via laser ablation ICP-MS depth profiling of trace element ratios, and then measured intrashell $\delta^{18}O$ in the same specimens using SIMS with a 3 µm spot and an average precision of 0.6‰ (±2 SD).

Results and Conclusion

Measured $\delta^{18}O_{calcite}$ values in *O. universa* shell layers are -2.0±0.5‰ VPDB (n=5) for ambient calcite and +16.4±0.4‰ VPDB (n=3) for ^{18}O-labeled calcite. These values agree well with predicted values of -2.2‰ and +16.8‰, respectively, computed using empirical $\delta^{18}O$-temperature calibrations from live culture of *O. universa* [3]. Elemental and oxygen isotope data show that LA-ICP-MS and SIMS measurements can be cross-correlated within the spatial resolution of the two analytical techniques. Precipitation of ^{18}O and Ba seawater tracers in planktic foraminifer shell calcite appears to be synchronous, with no measurable spatial offsets. These results demonstrate the capability of SIMS to resolve diurnal growth increments in foraminiferal shells, and highlight the potential to address paleoceanographic and biomineralization questions.

[1] Kozdon *et al.* (2009) *Chemical Geology* **258**, 327-337. [2] Kozdon *et al.* (2011) *Paleoceanography* **26**, PA3206. [3] Bemis *et al.* (1998) *Paleoceanography* **13**, 150-160.

Development of the MultiGAS for determining fumarole gas chemistry in geothermal systems

VIGOUROUX, NATHALIE[1]*, WILLIAMS-JONES, GLYN[2], RODRIGUEZ, CAROLINA[1], YEHIA, RON[1], BONA, PAOLO[1], HICKSON, CATHERINE[1]

[1]Alterra Power Corp., Vancouver, Canada, nvigouroux@alterrapower.ca (* presenting author)
[2]Simon Fraser University, Burnaby, Vancouver, glynwj@sfu.ca

Geothermal exploration relies on the gas geochemistry of fumaroles, bubbling/boiling springs and steaming ground to offer insight into the nature of the fluids at depth, procceses affecting them when rising to the surface, and provide estimates of the temperature of last equilibration of the gases within the reservoir. Traditional measurements involve direct sampling of the gases in pre-evacuated Giggenbach glass bottles before being sent to the lab for chemical analysis. Gas component analysis, combined with the isotope ratios of certain components (e.g., CO_2, He), provides insight into the proportion of magmatic, crustal, meteoric and atmospheric components in the fluid, and the state of equilibrium and temperature of these fluids at depth.

The Multi-component Gas Analyzing System (MultiGAS) was developed by the volcanological community over 10 years ago as a field-portable instrument for in-situ analysis of the major volcanic gas components in diffuse and dilute gas emissions. No two instruments are identical but all consist of various sensor types now capable of simultaneously analyzing for H_2O, CO_2, CO, SO_2 and H_2S.

In high-temperature (volcanic) geothermal systems, surface manifestations are often composed of gas emissions. In some cases, low temperatures and/or low flow rates make traditional sampling of fumaroles difficult, due to rapid vapor condensation and atmospheric contamination. The MultiGAS is best suited to these types of manifestations, providing a tool that can be used at a wide variety of gas emmission styles.

The MultiGAS has been field-tested in a geothermal prospect area characterized by steaming ground and fumaroles at the boiling temperature of water. Results of the MultiGAS analysis ($H_2O/CO_2/H_2S$ ratios) are compared with the equivalent ratios obtained from traditional sampling and analytical procedures, in order to identify the advantages and disadvantages of this new technique, and allow for the characterization of the hydrothermal system from the gas phase. The MultiGAS also allows for the gas/steam ratio of fumaroles to be quickly assessed in the field, which can aid in mapping/targeting of fumaroles in a large field, and the selection of the most ideal fumaroles to sample using the traditional method.

https://doi.org/10.1180/S0026461X00008434 Published online by Cambridge University Press

Mass transport experiments in low permeability shale

PETER VILKS[1*] AND NEIL H. MILLER[2]

[1]AECL, Whiteshell Laboratories, Pinawa, Canada, vilksp@aecl.ca (* presenting author)
[2] AECL, Whiteshell Laboratories, Pinawa, Canada, millern@aecl.ca

Introduction

The process of understanding sorption and its role in the transport of radionuclides in Canadian sedimentary rocks under saline conditions requires a combination of batch sorption experiments and mass transport tests to demonstrate that sorption coefficients (K_d) can be applied to explain mass transport. Although sorption in low permeability shale is diffusion dominated, transport tests with induced hydraulic flow are performed using the High Pressure Radioisotope Migration (HPRM) apparatus [1] in an attempt to obtain transport information on a shorter time scale than possible with diffusion tests. Tests are performed on core samples by pumping fluid through the core (along the core axis) using pressures as high as 4.5 MPa. The rock matrix permeability is calculated from the measured pressure differential between the inlet and outlet side of the core, and from the flow rate determined by the volume of eluted water [1]. Mass transport tests are performed by injecting a combination of sorbing and non-sorbing tracers and monitoring their eluted concentrations.

Results and Discussion

Initial tests were performed with a core sample of Queenston Formation. First deionized water was pumped through the sample to remove existing brine from pore spaces so that Cl from the subsequent brine injection could help define porosity. The deionized water was followed by 300 g/L TDS Na-Ca-Cl brine solution, and then same brine solution with uranine dye tracer. The average flow rates of water through the rock sample varied from 0.004 to 0.05 mL/day. The permeability varied from 1.0×10^{-21} to 7.5×10^{-21} m^2 and although the viscosity in permeability calculations was not increased for higher salinity, the resulting permeability values were not significantly affected by fluid composition. The sample pore volume estimated by the initial breakthrough of Cl from the brine injection was 0.22 ± 0.03 cm^3, which is in agreement with the 7 % porosity of a 2.5 cm diameter core with a length of 0.6 cm. In the mass transport test, uranine breakthrough was slower than that of Cl (assumed to be non-sorbing), producing a retardation factor of 1.44 ± 0.31 for uranine. Using a bulk mass density of 2.66 g/cm^3 for Queenston shale, this retardation factor corresponds to a sorption coefficient (K_d) of 0.167 ± 0.036 cm^3/g. This value is in agreement with batch measurements of uranine sorption on dolomite, calcite and quartz in the presence of Dead Sea brine solution [2]. Results of ongoing migration tests in shale using a brine solution containing a mixture of conservative (Li) and sorbing (Ni, Cu, Pb, Bi, Zr, U) tracers will be reported. These tests are aimed at demonstrating the role of sorption in mass transport processes by comparing the derived K_d values to that obtained from the batch sorption tests.

[1] Vilks & Miller (2007) *Nuclear Waste Management Organization* **TR-2007-11**. [2] Magal, Weisbrod, Yakirevich & Yechieli (2008) *Journal of Hydrology* **358**, 124-133.

Geochronology and hygrochronology of metamorphic and metasomatic rocks

IGOR M. VILLA[1,2*] AND MICHAEL L. WILLIAMS[3]

[1]Institut für Geologie, Universität Bern, 3012 Bern, Switzerland igor@geo.unibe.ch (* presenting author)
[2]Università di Milano Bicocca, 20126 Milano, Italy
[3]Dept Geosciences, U of Massachusetts, Amherst, MA 01003, USA

Metamorphism, metasomatism, retrogression, and aqueous alteration are based on the same underlying mechanism at the atomic scale; their different names depend on the large-scale context. They all require recrystallization, which can be viewed as nano-scale dissolution/reprecipitation, mediated by an aqueous fluid [1].

What drives compositional or isotopic modification? Even if 19th century chemistry emphasized "diffusion", mass balance arguments made it quicky clear that changes in stoichiometry need a chemically open system, i.e. advection, rather than diffusion. Aqueous fluids are the main control on the formation of metamorphic parageneses [2], and on isotope exchange in minerals [3]. The reason is that the rate constants for fluid-mediated isotope transport are orders of magnitude larger, and activation energies much smaller, than those for diffusion. Recrystallisation is energetically less costly at almost any temperature than diffusive reequilibration [3].

In a companion abstract [4], it is argued that stepwise release and spatially resolved analyses are a decisive tool in understanding the petrologic processes controlling isotope exchange. However, unambiguous constraints can also derive from petrology alone, provided one knows what to look for. Diffusion is detectable against a background of faster transport only when water was absent and P-T-A-X calculations give an "asterisk" (an overdetermined set of independent reaction equilibria, all intersecting in one point) as proof of retrogression-free rocks.

The observations demonstrate that only in rare cases diffusion is the sole promoter of isotope resetting. Further, the observations require a major shift in perspective on the significance of mineral ages. Just as the "diffusionist" view that zircon discordance is due to thermal disturbances [5] was superseded by the petrological understanding that it is due to recrystallization [6], interpretations of intra-mineral age variations in terms of a purely thermal history neglecting the microchemical-petrogenetic context is no longer tenable.

Because fluid-mediated dissolution/reprecipitation depends mainly on water activity and only very loosely on temperature, isotope data provide a geohygrometric but not an unambiguous geothermometric datum.

[1] Putnis A (2009) *Rev Mineral Geochem* **70**, 87-124. [2] Lasaga A (1986) *Mineral Mag* **50**, 359-373. [3] Cole DR et al (1983) *Geochim Cosmochim Acta* **47**, 1681-1693. [4] Villa IM (2012) this meeting, Theme 17. [5] Steiger RH, Wasserburg GJ (1969) *Geochim Cosmochim Acta* **33**, 1213-1232. [6] Mezger K, Krogstadt EJ (1997) *J Metam Geol* **15**, 127-140.

https://doi.org/10.1180/S0026461X00008434 Published online by Cambridge University Press

Spatial resolution, stepwise release: connecting the multi-isotope record with microchemistry and petrology

IGOR M. VILLA[1,2*]

[1]Institut für Geologie, Univ. Bern, 3012 Bern, Switzerland [2]Univ. Milano Bicocca, 20126 Milano, Italy. - igor@geo.unibe.ch

Most metamorphic reactions require dissolution/reprecipitation, i.e. water activity controls petrology in metamorphic minerals, and also the isotope record, as radiogenic isotopes (except ^{4}He) do not diffuse faster than major elements forming the mineral structure [1]. Isotopic inheritance in relicts (i.e. slow diffusion) was observed in zircon, monazite, amphibole, K-feldspar, and micas. However, a priori there could be causes of isotope loss/exchange other than recrystallization. Temperature was proposed to play a role by changing diffusivity in geochronometers [2]. If diffusion has been the factor limiting isotopic (or chemical) closure, the concentration profile is bell-shaped. To ascertain if isotope transport in a sample was controlled by diffusion or recrystallization, spatial information is needed: only bell-shaped gradients are compatible with volume diffusion. So far, in-situ dating *never* described bell-shaped isotope gradients in patchily zoned minerals. On the contrary, patches are certain evidence of fluid-mediated local recrystallization, i.e. a guarantee of petrological, and therefore isotopic, disequilibrium.

The geochronology of mixed diachronous phases is managed by two complementary "SR techniques": spatially resolved analyses and stepwise release. SR techniques have shaped a better understanding of geochronology, as they reveal the elemental & isotopic compositions on the subgrain scale, and allow the recognition and the chemical/ isotopic characterization of relicts and retrogression. In SR techniques, the chemical signature is also measured in the same analysis as the age. Electron microprobe "chemical" geochronology [3] offers the most complete microchemical characterization of intra-crystalline zonations. ^{39}Ar-^{40}Ar analyses yield the concentrations of three elements (K, Ca, Cl) and their ratios to radiogenic ^{40}Ar. Why worry about the Ca/Cl ratio in a mineral, if the age is calculated from the Ar/K ratio? So as to unravel polyphase mixtures by comparing Cl/Ca/K signatures with independent microchemical data. When K-Ar ages of metamorphic minerals are older than we expect, they are brushed off as "excess Ar". Much confusion can arise if we mix up "excess Ar" (^{40}Ar gain) with "inherited Ar" (^{40}Ar loss). Inherited Ar often correlates with Ca/Cl. In addition to just K-Ar, multi-isotope geochronology (Rb-Sr, Lu-Hf, etc) should be used. If Ar and Sr correlate, it's due to Ar and Sr inheritance, not to excess Ar [4]. Overdetermined Rb-Sr isochrons [5] also can reveal inheritance.

Thanks to submicroscopic petrology, isotopic inheritance can be put into context with petrogenetic disequilibria. Analytical advances allow dating of each mineral generation. This opened up a wealth of data on the P-T-A-X-d history of rocks. In the long run, this will improve our ability to develop credible numeric models.

[1] Villa (1998) *Terra Nova* **10**, 42-47 [2] Jäger (1967) *Beitr Geol Karte Schweiz* **134**, 11-21 [3] Williams et al (2007) *Ann Rev Earth Planet Sci* **35**, 137-175 [4] Villa et al (2006) *J Volc Geoth Res* **152**, 20-50 [5] Glodny et al (2008) *Geochim Cosmoch Acta* **72**, 506

Selenate reduction rates in littoral sediments of a hypersaline lake, the Salton Sea, CA

JUAN FERNANDO VILLAROMERO[1]* AND CÉLINE PALLUD[2]

[1]PMB, University of California, Berkeley, USA;
[2]ESPM, University of California, Berkeley, USA
(*correspondence: villaromero@berkeley.edu)

The Salton Sea is California's largest lake and is located in the Salton Basin of the Colorado Desert. It supports one of the most productive fisheries of the Western hemisphere and more than 400 species of birds, including endangered migratory populations. The Alamo and New Rivers collect agricultural runoff from a 2,250 Km^2 area, and deliver 80% of the annual water inflow along with selenium (Se) and salts to the Salton Sea. Today, Se concentrations reach 10 mg Kg^{-1} in the sediments of the lake, and salinity is expected to further increase from its current value of 48. Such high selenium concentrations and increasing salinity pose a serious threat to the unique avian diversity of the Salton Sea [1]. Selenium naturally occurs in Western U.S. bedrock and can be mobilized through irrigation water as selenate (SeO_4^{2-}) and/or selenite (SeO_3^{2-}). Upon reaching anaerobic sediments in the Salton Sea, Se is microbially reduced to Se(0) and immobilized. Reduced selenium species are expected to remain sequestered in sediments as long as anaerobic conditions persist.

To identify the environmental factors that control selenate reduction rates in the Salton Sea, we measured these rates at salinity 45, along with porosity, bulk density, C:N, and the abundance of selenate-reducing bacteria (SeRB) in littoral sediment samples collected from seven sites. We also measured pH and salinity in water overlying sampling sites.

Higher selenate reduction rates (45.42 nmol h^{-1}cm^{-3}) and a higher abundance of SeRB (4×10^3 cells cm^{-3}) occurred at the site with the lowest C_{org}:N (2.7). Frequent and massive fish die-offs are commonly reported in the Salton Sea and lead to an accumulation of fish carcasses in the littoral potentially explaining such low C_{org}:N. Without nitrogen limitations, and given that selenate was the only terminal electron acceptor provided, SeRB can thus achieve higher abundances and higher selenate reduction rates.

Salinity averaged 48.41 in six out of seven sites; however, it was only 2.97 in a site mapped to the Alamo River delta. Selenate reduction rates and the abundance of SeRB were maximal in this site (223.3 nmol h^{-1}cm^{-3} and 3.5×10^3 cells cm^{-3}, respectively). The low salinity measured in this site may result from the mix between river freshwater and Salton Sea water. Interestingly, salinity is reported to negatively correlate with microbial diversity [2]; also, salinity imposes significant energetic requirements to microbial cells, especially under anaerobic conditions [3]. Finally, higher diversity results in communities more resistant to salinity stress [4]. Consequently, we hypothesize that the sediment exposed to salinity 2.97 supports a more diverse community of SeRB, and this higher diversity may facilitate a better response to salinity stress in experimental anaerobic slurries at salinity 45, detected as higher SeRB numbers and higher selenate reduction rates.

Our preliminary results show that water salinity and sediment C_{org}:N are important factors controlling selenate reduction in littoral sediments of the Salton Sea.

[1] Department of the Interior (2007) Restoration of the Salton Sea Summary Report.
[2] Parnell (2011) Aquatic Microbial Ecology **64**, 267-273
[3] Oren (1999) Microbiol. Mol. Bio. Rev. **63**, 334-348
[4] Wittebolle (2009) Nature **458**, 623-626

https://doi.org/10.1180/S0026461X00008434 Published online by Cambridge University Press

Calcium-(bi)carbonate equilibria in aqueous solutions: a high-accuracy titration-based study

A. VILLEGAS-JIMÉNEZ[1*], R. M. HAZEN,[1] AND D.A. SVERJENSKY[2]

[1]Carnegie Institution of Washington, Geophysical Laboratory, Washington, D.C. 20015, USA
adriano@gl.ciw.edu (* presenting author)

[2]Johns Hopkins University, Earth and Planetary Sciences, Baltimore, MD 21218, USA

A thorough understanding of calcium-(bi)carbonate equilibria in aqueous solutions is key for making accurate predictions of aqueous speciation in Ca-HCO_3-CO_3-H_2O-CO_2 systems and assessing the extent of precipitation (or dissolution) of $CaCO_{3(s)}$ polymorphs in environmental, biological, and industrial systems. Despite earlier determinations of the formation constants of calcium-(bi)carbonate ion pairs in aqueous and seawater-like solutions, recent studies postulating the formation of metastable [1,2] or stable prenucleation $CaCO_3$ nanoclusters [3,4] have triggered new interest on calcium-(bi)carbonate interactions, particularly at near-calcite saturation conditions. Moreover, anomalous pH values and calcium concentrations consistently observed during acidimetric titrations of aqueous calcite suspensions suggest that the chemical equilibria governing the $CaCO_3$-HCO_3-CO_3-H_2O-CO_2 system may not be fully understood [5].

In this study we perform a critical review of the available thermodynamic constants describing the formation of calcium-(bi)carbonate ion pairs and compare these values with constants extracted from new experimental data acquired over fairly broad compositional ranges. Our experimental approach consists of performing high-accuracy titrations of (bi)carbonate solutions in contact with a gas phase but completely isolated from the atmosphere. For the first time in this type of determinations, $CO_{2(g)}$ exchange across the gas-water interface is quantitatively monitored and the chemistry of the solution is fully characterized (analytically overdetermined) through a combination of pH, alkalinity, pCO_2, ΣCO_2 pCa, and ΣCa measurements at each titration point. Data fitting and parameter extraction is made stochastically following a genetic algorithm approach described earlier [6].

[1] *J. Amer. Chem. Soc.* (2008), **130**, 12342-12347.
[2] *Nanoscale* (2011), **3**, 1158-1165.
[3] *Science* (2008), **322**, 1819-1822.
[4] *Nat. Comm.* (2011), **2**, : 590 doi:10.1038/ncomms1604.
[5] *Phys. Chem. Chem. Phys.* (2009), **11**, 8895–8912.
[6] *Math. Geosci*. (2010), **42**, 101–127

Leachate analyses of volcanic ashes from Sakurajima volcano, Japan: insights into the magmatic degassing processes

NICOLAS VINET[1,*], HIROSHI SHINOHARA[2], AND ISOJI MIYAGI[3]

[1] Geological Survey of Japan, AIST, Tsukuba, Japan
vinet.nicolas@yahoo.com (* presenting author)

[2] Geological Survey of Japan, AIST, Tsukuba, Japan
shinohara-h@aist.go.jp

[3] Geological Survey of Japan, AIST, Tsukuba, Japan
miyagi.iso14000@aist.go.jp

Ash erupted from active vents acts, by adsorption onto its surface in volcanic plumes, as an efficient scavenger of volatile elements such as sulphur (as sulphate, SO_4^{2-}), halogens, and other species present as soluble salts adhering to the particle surface. Analysis of water-soluble ash leachates is a suitable supplement for remote monitoring of volcanic gases at inaccessible volcanoes. The chemical composition of ash leachates is considered as a proxy for volcanic plume chemistry (volatile ratios), and its temporal variations reflect changes in the magmatic conditions, eruptive activity, along with local conduit- and plume-related processes. The importance of ash-leachate analysis also lies in the fact that up to 30-40% of the volatile budget emitted by subduction-related volcanoes are scavenged by such adsorption processes on volcanic ash. This adsorbed component has been generally neglected, resulting in excess degassing underestimated by 30-40%.

In this study, we investigate the temporal variations of the chemical composition of water-soluble leachates from volcanic ashes emitted from Sakurajima volcano, Southern Kyushu, Japan, during the period 1981-2011 (with emphasis on 2010-2011). Pristine ash was collected on-site, ca. 3 km away from the vent, directly after an explosion occurred.

We observe a strong positive correlation between SO_4, F and Cl/SO_4 against Cl, especially in ash leachates from 2008 to 2011, corresponding to the reactivation of Showa vent. Our results also show significant long-term and short-term temporal variations in ash leachate compositions (SO_4, F, Cl, Cl/SO_4, S/F, Mg/Na), reflecting changes in the eruption rate and style. Since ash-gas interactions started at the fragmentation level within the vent, these temporal variations may also reflect changes in the fragmentation mode or the volatile accumulation (adsorption) process onto the ash within the vent. In turn, this is linked to the mean residence time of magma in the upper conduit (including the vent), as a response to magma renewal and/or convection in this part of the volcano system.

In addition to chemistry we also investigate the influence of grain size distribution and texture on ash-leachate analyses over time. This is at present time very preliminary, but if correlations are found in particular between volatile ratios in ash leachates and the grain size and/or texture, it will provide new and valuable semi-quantitative information on the degassing processes in the shallow volcanic conduit.

https://doi.org/10.1180/S0026461X00008434 Published online by Cambridge University Press

Improved carbon isotope modeling of biogenic coalbed methane systems: The nature of initial CO_2

DAVID S. VINSON[1*], JENNIFER C. MCINTOSH[1], DANIEL J. RITTER[1], NEAL E. BLAIR[2], AND ANNA M. MARTINI[3]

[1]University of Arizona, Dept. of Hydrology and Water Resources, dsvinson@email.arizona.edu (* presenting author), mcintosh@hwr.arizona.edu, dritter@email.arizona.edu

[2]Northwestern University, Depts. of Civil & Environmental Engineering and Earth & Planetary Sciences, n-blair@northwestern.edu

[3]Amherst College, Dept. of Geology, ammartini@amherst.edu

Carbon isotope signatures (e.g. $\alpha_{CO2\text{-}CH4} = (\delta^{13}C_{CO2}+1000)/(\delta^{13}C_{CH4}+1000)$) for distinguishing acetoclastic methanogenesis vs. CO_2 reduction were investigated in a biogenic coalbed methane (CBM) system, the Powder River Basin (WY/MT, USA). Past studies of this basin present inconsistent isotopic [1,2] and microbiological [3,4] evidence of methanogenic pathways.

Combined gas and groundwater analysis of monitoring and CBM production wells along a 25 km transect indicates several geochemical trends from shallow, basin-edge wells to deeper wells. Broadly, these basinward trends indicate: increasing pH (7.4-8.5), alkalinity (13-33 meq/kg), and temperature (11-28 ºC); increasing $\delta^{13}C_{CH4}$ (-78 to -56‰), $\delta^{13}C_{CO2}$ (-24.7 to 4.7‰), and $\delta^{13}C_{DIC}$ (-11.0 to 16.2‰) values; increasing calcite saturation indices (-0.71 to 0.60); increasing $\delta^{2}H$ (-164 to -129‰) and $\delta^{18}O$ (-21.2 to -17.2‰) values; and decreasing apparent inputs of sulfate from shallow formations. Across this gradient of geochemical and isotopic conditions, *apparent* values of $\alpha_{CO2\text{-}CH4}$ are characteristic of CO_2 reduction (most 1.05-1.07). Given that $\delta^{13}C$ values of residual CO_2 are distinctively >0‰ in closed CO_2-reducing systems, inputs of DIC from microbial respiration (e.g. sulfate reduction) and/or carbonate dissolution would contribute isotopically depleted CO_2 to the reactant pool. This initial CO_2 is modified by methanogenesis. The lower $\delta^{13}C_{CH4}$ and $\delta^{13}C_{CO2}$ values observed in shallower, calcite-undersaturated waters are consistent with possible inputs of alternative electron acceptors (e.g. sulfate) from shallow units. Moreover, subequent reduction of this CO_2 would represent an early stage of methanogenesis yielding depleted $\delta^{13}C_{CO2}$ and $\delta^{13}C_{CH4}$ relative to late-stage methanogenesis, in which more of the CO_2 pool has been reduced [2]. Thus, both the nature of initial CO_2 and the extent of reactant pool consumption can strongly influence observed $\delta^{13}C_{CO2}$ and $\delta^{13}C_{CH4}$.

The potential role of acetate remains undetermined. Low acetate concentrations basinwide (low µM range [3]) imply (1) a depleted acetate pool or (2) steady-state acetate production and consumption. Analysis of compound-specific and intramolecular C isotope ratios of acetate may elucidate acetate's role. The relative importance of methanogenic pathways has implications for understanding subsurface contributions to the C cycle and for the potential stimulation of sustainable gas production from CBM systems.

[1] Flores *et al.* (2008) *Int. J. Coal. Geol.* **76**, 52-75. [2] Bates *et al.* (2011) *Chem. Geol.* **284**, 45-61. [3] Ulrich & Bower (2008) *Int. J. Coal. Geol.* **76**, 25-33. [4] Green, Flanegan & Gilcrease (2008) *Int. J. Coal. Geol.* **76**, 34-45.

Chemical, Optical and Magnetic Susceptibility Characterization of Coal Fly Ash

JENNIFER N. GABLE[1], ELLEN COWAN[2], KEITH SERAMUR[3], ROCK J. VITALE[4*], ,WILLIAM J. ROGERS[5], NEIL E. CARRIKER[6], AND CAROL BABYAK[7]

[1] Environmental Standards, Inc., Valley Forge, Pennsylvania, United States, jgable@envstd.com

[2] Appalachian State University, Boone, North Carolina, United States, cowanea@appstate.edu

[3] Appalachian State University, Boone, North Carolina, United States, seramurkc@appstate.edu

[4] Environmental Standards, Inc., Valley Forge, Pennsylvania, United States, rvitale@envstd.com (* presenting author)

[5] Tennessee Valley Authority, Muscle Shoals, Alabama, United States, wjrogers@tva.gov

[6] Tennessee Valley Authority, Chattanooga, Tennessee, United States, necarriker@tva.gov

[7] Appalachian State University, Boone, North Carolina, United States, babyakcm@appstate.edu

Abstract

Following the December 2008 rupture of a coal fly ash retaining pond at the Tennessee Valley Authority (TVA) Kingston Fossil Plant near Harriman, Tennessee, a comprehensive monitoring effort was intiated to evaluate the extent of ash deposition in the terrestrial and aquatic environments directly impacted by the release. The chemical characteristics of ash and impacted sediment samples were determined through analysis for a variety of metals using inductively coupled plasma atomic emission spectroscopy (ICP-AES) and mercury using cold vapor atomic absorption spectroscopy (CVAA). In addition, polarized light microscopy (PLM) was utilized for the determination of percent ash of sediment samples. A comparison of the percent ash data to the metals and mercury concentrations revealed a strong correlation between ash content and concentration of some metals constituents (*e.g.*, arsenic, strontium, and selenium). Other metals constituents (*e.g.*, aluminum, boron, and iron) demonstrated weak or no correlation to ash content.

In addition to monitoring associated with the recovery effort, a research team from Appalachian State University evaluated the use of mass magnetic susceptibility (MS) as a potential indicator of ash content. MS was observed to correlate fairly well with ash content in the river bottom sediment samples; however, MS measurements showed a weaker correlation to some elements typically considered to be constituents of coal fly ash (*e.g.*, selenium).

Conclusion

This paper evaluates the correlations among various analytical techniques and potential uses of alternate methods as a cost-savings measure for monitoring. PLM may be useful as an alternate method for estimating metals concentrations based on ash content. In addition, MS may be useful as an alternate analytical method for estimating ash content in bottom sediments in aquatic environments.

https://doi.org/10.1180/S0026461X00008434 Published online by Cambridge University Press

Force field for oxoanions in solid state and aqueous solutions

LUKAS VLCEK[1*] AND ARIEL A. CHIALVO[2]

[1]Oak Ridge National Laboratory, Oak Ridge, TN 37631, U.S.A, vlcekl1@ornl.gov (* presenting author),
[2]Oak Ridge National Laboratory, Oak Ridge, TN 37631, U.S.A, chialvoaa@ornl.gov

A delicate balance between ion hydration and crystallization plays a crucial role in natural processes leading to dissolution and precipitation of minerals, and forms the basis of many technological applications, such as nuclear waste separation and storage. Our primary interest is to investigate salt crystallization from mixed electrolyte solutions in porous rocks, but the results also pertain to the rational design of complexation agents used in selective crystallization of homologous series of oxoanions.

A reliable description of molecular and ionic interactions is needed to understand atomic-scale mechanisms underlying the thermodynamics and dynamics of electrolyte solutions. Our goal is to develop a consistent force field for the study of oxoanions including CO_3^{2-}, NO_3^-, and those of general formula XO_4^{2-} (X=S, Se, Cr, Mo, W). While several force fields exist for the description of simple alkali metal and halide ion series [1], and isolated models for selected oxoanions have been published [2], a consistent force field for oxoions suitable for comparative studies is missing.

The choice of an appropriate potential model form is dictated by intended applications, balancing accuracy and computational efficiency. Since adsorption and salt precipitation happen over large time and length scales, the simplicity of the model is of high importance. While most of the concerned ions are highly polarizable, their mineral environment is consistently polar, justifying the use of effective pair potentials. We therefore consider pair potentials represented by a combination of point charges and Lennard-Jones interactions compatible with the SPC/E model of water [3].

The force field is optimized against experimental data including hydration free energy at infinite dilution [4], chemical potential at finite concentration obtained from Kirkwood-Buff equations [5], lattice constant and lattice energy for selected crystals, and diffusion coefficient [4]. The potential parameters (at least 5 for each oxoion) were determined using global optimization based on the coupling parameter technique [6].

[1] Joung et al (2008) *J. Phys. Chem. B* **112**(30), 9020-9041.
[2] Cannon et al. (1994) *J. Phys. Chem.* **98**(24), 6225-6230.
[3] Berendsen et al. (1987) *J. Phys. Chem.* **91**(24), 6269-6271.
[4] Marcus, Y., *Ion properties* 1997, New York: Marcel Dekker.
[5] Gee et al. (2011) *J. Chem. Theory Comput.* **7**(5), 1369-1380.
[6] Vlcek et al. (2011) *J. Phys. Chem. B* **115**(27), 8775-8784.

Acknowledgements. This work was supported as part of the "Center for Nanoscale Control of Geologic CO_2", an Energy Frontier Research Center funded by the U.S. Department of Energy, Office of Science, Office of Basic Energy Sciences, and by the Division of Chemical Sciences, Geosciences, and Biosciences, Office of Basic Energy Sciences, U.S. Department of Energy.

Dynamic precipitate formation during Fe(II) oxidation in aerated phosphate-containing water

ANDREAS VOEGELIN[*], RALF KAEGI

Eawag, Swiss Federal Institute of Aquatic Science and Technology, Dübendorf, Switzerland, andreas.voegelin@eawag.ch ([*] presenting author)

The oxidation of Fe(II) at biogeochemical redox interfaces results in the formation of nanoparticulate Fe(III)-precipitates that act either as immobilizing sorbents or colloidal carriers for contaminants and nutrients. In previous work on Fe(I) oxidation products in neutral aqueous suspensions [1, 2], we concluded that nanoparticulate amorphous Fe(III)-phosphate is the first precipitate that forms during Fe(II) oxidation in the presence of phosphate (P), with a molar P/Fe ratio of the solid of ~0.55 (in absence of Ca). At initial dissolved P/Fe ratios less than ~0.55, the formation of Fe(III)-phosphate is followed by the precipitation of amorphous to poorly crystalline Fe(III)-(hydr)oxides (depending on silicate/Fe ratio). These conclusions, however, were based on the study of precipitates collected after complete Fe oxidation and precipitation (no time-resolution) and covering a limited number of P/Fe ratios.

In onoing work, we explore the dynamics of precipitate formation during Fe(II) oxidation in aerated phosphate-containing solutions (bicarbonate-buffered to pH 7.0) time-resolved and over a larger number of initial P/Fe ratios. We monitor the decrease in filterable (<0.2 μm) element concentrations during Fe(II) oxidation and characterize precipitates collected during and after complete Fe(II) oxidation by a suite of complementary techniques, including X-ray absorption spectroscopy and transmission electron microscopy. To monitor precipitate evolution in-situ, additional experiments are performed using time-resolved UV-Vis spectroscopy.

The results from time-resolved experiments confirm the initial formation of an amorphous Fe(III)-phosphate with a P/Fe ratio of ~0.55 (at the time when dissolved P is depleted). However, our results also suggest that in systems with initial dissolved P/Fe ratios substantially below 0.55, initially formed Fe(III)-phosphate transforms or dissolves during ongoing Fe(II) oxidation in P-depleted solution, resulting in the formation of Fe(III)-(hydr)oxides with higher degree of Fe(III) polymerization to which P is sorbed. From our current results, we conclude that at initial dissolved P/Fe ratios less than ~0.17, initially formed Fe(III)-phosphate is absent in the final product of Fe(II) oxidation at near-neutral pH. These results demonstrate that Fe(III) precipitation during Fe(II) oxidation in aqueous solutions is a highly dynamic process that may involve formation of transient precipitates that are absent in the fresh precipitate after complete Fe(II) oxidation. In future work, we plan to further investigate Fe(III) precipitation dynamics during Fe(II) oxidation and the aging of fresh precipitates, also with respect to implications for the solubility and mobility of co-transformed trace elements.

[1] Voegelin *et al.* (2010) *Geochim. Cosmochim. Acta* **74**, 164-186.
[2] Kaegi *et al.* (2010) *Geochim. Cosmochim. Acta* **74**, 5798-5816.

https://doi.org/10.1180/S0026461X00008434 Published online by Cambridge University Press

Oxygen and deuterium stable isotope signals in Northeast Atlantic waters

ANTJE H. L. VOELKER[1]* AND ALBERT COLMAN[2]

[1]LNEG, Unidade Geologia Marinha, Amadora, Portugal, antje.voelker@lneg.pt (* presenting author)
[2]The University of Chicago, Dept. of Geophysical Sciences, Chicago, USA, asc25@uchicago.edu

Material and Methods

A comprehensive study of seawater stable isotope properties in the mid-latitude North Atlantic is still missing [1], especially for the intermediate and deep water masses. To fill this gap seawater samples were collected along various transects in the Northeast Atlantic. During the Atlantic Meridional Transect (AMT) 18 expedition the upper 300 m were sampled between 46.6 and 24.7°N. RV Poseidon cruises P334, P349, P377, and P383 to the Azores Front region (38.3–30°N; 22–20°W) generally yielded samples down to 2000 m. High resolution sampling over the whole water column was performed during the OVIDE 2010 (Portugal to Reykjanes ridge) and KN199-4 cruises. Cruise KN199-4 implemented the section from Lisbon to the Cape Verde Islands of the US GEOTRACES North Atlantic transect. AMT 18 and P cruise samples were analyzed for $\delta^{18}O$ using the Delta E mass spectrometer at the Leibniz Laboratory (Kiel, Germany). Analysis of $\delta^{18}O$ and dD in the OVIDE 2010 and KN199-4 samples was done at the Godwin Laboratory (Cambridge, UK) using the PICARRO L2120 water isotope analyzer. Splits of some of the KN199-4 samples were also analyzed for both isotope ratios at the University of Chicago using a GasBench II linked to a Delta V Plus mass spectrometer.

Results and Conclusions

Along the AMT 18 transect, i.e. in the central basin, a clear boundary is visible with $\delta^{18}O$ values in the upper 100 m of 0.75–1.15 permil north of 38°N and 1.3–1.5 permil south of it. The range narrows in the North Atlantic Central Water (NACW) to 0.9–1.2 permil with the stations in the subtropical gyre, as expected, showing the higher values. In the eastern basin variability in the upper mixed layer (<300 m) is much larger with values ranging from 0.4 to 1.6 permil. The high variability can be attributed to seasonal mixing processes at the Azores Front, upwelling along the Iberian margin and the influence of riverine water at KN199-4 station 1 positioned in the Setubal canyon. Below 300 m the subpolar and subtropical NACW can clearly be distinguished in the isotope profiles. Along with temperature, $\delta^{18}O$ values decrease with depth to generally less than 0.7 permil below 2000 m. Along the Iberian margin this trend is, however, interrupted between 500 and 1500 m due to the Mediterranean Outflow Water (MOW). The different cores of the MOW are clearly visible in the $\delta^{18}O$ and dD (which is highly correlated to salinity) profiles, especially those close to the Iberian margin. Results for many of the OVIDE and GEOTRACES stations are pending and when they are available it will be possible to better define the isotopic properties of the subsurface water masses, especially the North Atlantic Deep Water and the Antarctic Bottom Water.

[1] LeGrande & Schmidt (2006) *Geophys. Res. Lett.* **33**, L12604.

Carbonate diagenesis in the Pacific Equatorial Age Transect (PEAT) Sites and the preservation of geochemical signals in foraminifera

JANETT VOIGT[1]*, ED HATHORNE[1], MARTIN FRANK[1]

[1]GEOMAR | Helmholtz Centre for Ocean Research Kiel, Wischhofstr. 1-3, Kiel, Germany
jvoigt@geomar.de (* presenting author)

The calcite shells (tests) of foraminifera used for reconstructions of oceanic and climatic conditions in the past can be altered after deposition by a process where the original biogenic calcite is replaced by secondary (inorganic) calcite. It is important to quantify changes in the elemental and isotopic composition of the tests caused by this recrystallisation process and thus the reliability of the proxy data. We present initial results from a multi-component study of recrystallisation in sediments from the IODP Expedition 320/321 Pacific Equatorial Age Transect (PEAT), where sediments of similar age and initial composition have been subjected to different diagenetic histories.

$^{87}Sr/^{86}Sr$ ratios of bulk carbonate leachates and the associated pore waters generally suggest that recrystallisation occurred relatively rapidly as the values are indistinguishable (within 2σ uncertainties) from contemporaneous seawater [1]. Notable exceptions include Site U1336, where pore waters and the bulk carbonates in sediments older than 20.3 Ma have lower $^{87}Sr/^{86}Sr$ ratios than contemporaneous seawater, most likely resulting from the upward diffusion of Sr from older recrystallised carbonates.

Furthermore, the lower Sr/Ca ratios of bulk carbonates from Site U1336, compared to the other PEAT sites, suggest more extensive diagenetic alteration as less Sr is incorporated into secondary calcite. Although the recrystallisation of bulk carbonates is well documented, the fate of foraminiferal chemistry is potentially different. To investigate this, laser ablation ICP-MS element/Ca ratio depth profiles through tests of the planktonic foraminifera *G. venezuelana* from Sites U1336 and U1338 were obtained for two time intervals (13.9 Ma and 15.5 Ma). The depth profiling technique reveals heterogeneity of Mg/Ca and Mn/Ca ratios through the wall of the tests comparable to those reported for modern foraminifera from sediment traps [2]. The Sr/Ca ratios show little heterogeneity and fluctuate around 1.1-1.2 mmol/mol as also observed for modern tests. The Sr/Ca ratios exhibit no systematic difference between the sites and time intervals. Therefore, the intra-test element/Ca heterogeneity suggests that foraminifera react differently to bulk carbonates (nanno-fossils) during diagenetic recrystallisation and much of the original geochemical proxy signal may have been retained.

[1] McArthur *et al.* (2001) *The Journal of Geology* **109**, 155-170
[2] Hathorne *et al.* (2009) *Paleoceanography* **24**, PA4204

https://doi.org/10.1180/S0026461X00008434 Published online by Cambridge University Press

Boron isotopes as a proxy of primary mineral weathering mechanisms

A. VOINOT[1,2 *], D. LEMARCHAND[1], F. CHABAUX[1], AND M-P. TURPAULT[2]

[1]Laboratoire d'Hydrologie et de Géochimie de Strasbourg, EOST, Université de Strasbourg et CNRS, 1 rue Blessig, 67084 Strasbourg, France (*correspondence: alexandre.voinot@etu.unistra.fr)

[2]INRA UR 1138 Biogéochimie des Ecosystèmes Forestiers, Centre INRA de Nancy, 54280 Champenoux, France

Determining the current state of mineral weathering in soils is a key point to understand and model pedogenic processes. Nevertheless, it remains a real challenge given to the difficulty to get informations on the mineral sites actually active and the non-stoichiometric release of site-forming cations.

Boron has been demonstrated experimentaly to be located in different reactive sites of pure biotite (replacing silicon in tetrahedrons or adsorbed in interfoliar sites) with very contrasted isotopic compositions (up to 80 ‰ difference between interfoliar and lattice sites, Voinot et al., in prep). This huge isotopic partitionning between the different mineral sites allowed to distinguish between transformation and dissolution reactions with an higher sensitivity than classic chemical tracers (K and Si).

To assess the ability of boron to better characterize the current weathering state in soils, quantitative mineralogical analyses have been coupled to boron isotopes in a series of sorted minerals (< 50 µm) with varying weathering rates along an Alocrisol profile developped on a granitic bedrock (Breuil-Chenue forest, France). Distinction has been made between rather transforming (biotite, plagioclases) or dissolving minerals (muscovite, K-feldspars).

For biotite and muscovite, even though deep weathering processes lead to low dissolution and transformation rates, we observe that the bulk B chemical and isotopic compositions seem to rapidly equilibrate with the surrounding soil solution. Shallower soil layers show similar B behavior in fine grain fraction of these two minerals, whereas coarser grains tend to accumulate boron in their structure (up to 4 time the initial boron content). Plagioclases dissolve very quickly in the weathering sequence to be replaced mainly by kaolinite, with a strong concentration increase and still seem to equilibrate isotopically with the soil solution. K-feldspars show no specific weathering mechanisms other than dissolution and this is reflected by a progressive depletion with invarious isotopic composition.

In a second series of samples (from the same site but this time on total soil) we assessed the evolution of these mechanisms in presence of organic matter and close to vegetation (comparison of bulk vs rhizospheric soil subsamples in the < 2 mm fraction) in shallower horizons (0 to 23 cm) under two different tree species (beech and spruce). Very shallow processes (0-3 cm horizon) are characterized by a strong organic matter influence (in both bulk and rhizospheric soils), with contrasted boron isotopic compositions between the two tree species (about 8 ‰). In the 10-23 cm horizon, this influence is greatly disminished and lets place to a more mineralogy-controlled mechanism with similar isotopic signature under spruce and beech.

Oxic-anoxic oscillations driven by infaunal hydraulic activity

NILS VOLKENBORN[1*], LUBOS POLERECKY[2], CHRISTOF MEILE[3], DAVID S. WETHEY[1], AND SARAH A. WOODIN[1]

[1]Department of Biological Sciences, University of South Carolina, Columbia, SC 29208, USA (*presenting author: nils@biol.sc.edu)

[2] Max Planck Institute for Marine Microbiology, Bremen 28359, Germany

[3]Department of Marine Sciences, University of Georgia, Athens, GA 30602, USA

Over the last few years we have investigated some of the most important bioturbating infaunal groups with respect to their hydraulic activity and the related porewater advection and oxygen dynamics. This was done by combining time-lapse photography, porewater pressure sensing and planar optode imaging of oxygen. Despite species-specific traits, the investigated crustaceans, bivalves and polychaetes all engage in hydraulic activities that cause intermittent and bidirectional transport of water away and towards the organisms [1, 2]. As a consequence, the sediment surrounding the burrows, as well as the sediment surface, experience frequent oscillations between oxic and anoxic conditions on the scale of minutes to hours.

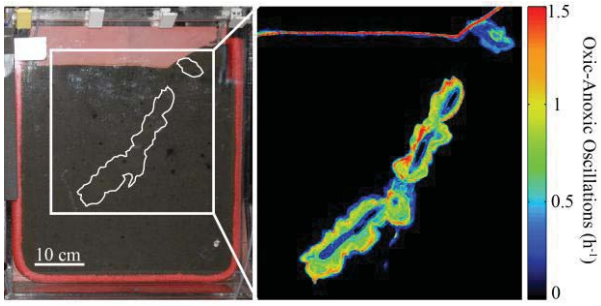

Figure 1: Two-dimensional representation of oxic-anoxic oscillations induced by hydraulic activity of the ghost shrimp *Neotrypaea californiensis*.

The sediment characterized by oscillatory conditions is limited to a thin layer around burrows in muddy environments but can be substantial in intermediate to high permeability sediments. Oscillatory conditions induced by hydraulically active organisms are expected to have significant implications for the distribution of microbial communities, with the durations of oxic and anoxic periods being a crucial determinant of biogeochemcial pathways and rates.

In this talk we will visualize the dynamic nature of geochemical conditions in the presence of hydraulically active organisms, and present quantitative data analysis and reactive-transport model simulations to explore the species- and sediment-specific oscillatory character of bioturbated sediments.

[1] Volkenborn et al. (2010) *Limnol. Oceanogr.* **55**, 1231-1247.
[2] Woodin et al. (2010) *Integr. Comp. Biol.* **50**, 176-187.

https://doi.org/10.1180/S0026461X00008434 Published online by Cambridge University Press

Marine carbonate burial rates at the Phanerozoic mass extinctions

HAUKE VOLLSTAEDT[1*], ANTON EISENHAUER[1], FLORIAN BÖHM[1], JAN FIETZKE[1], KLAUS WALLMANN[1], VOLKER LIEBETRAU[1], JURAJ FARKAŠ[2,3], ADAM TOMAŠOVÝCH[4], AND JÁN VEIZER[5]

[1] GEOMAR | Helmholtz-Zentrum für Ozeanforschung Kiel, hvollstaedt@geomar.de (* presenting author)
[2] Department of Geochemistry, Czech Geological Survey
[3] Department of Environmental Geosciences, Czech University of Life Sciences
[4] Department of Geophysical Sciences, The University of Chicago
[5] Ottawa-Carleton Geoscience Center, University of Ottawa

Several mass extinctions have disturbed the evolution of life during the Phanerozoic Eon. Information about the past environmental conditions and triggers for the extinctions can be inferred from the geological record and in particular from the analysis of different isotope systems (i.e. carbon, sulfur, and calcium) as well as the extinction selectivity [1].

To extend earlier published mass extinction scenarios we measured radiogenic ($^{87}Sr/^{86}Sr$) and stable strontium (Sr) isotope ratios ($\delta^{88/86}Sr$, [1]) simultaneously on globally distributed brachiopod and belemnite samples to constrain changes in Phanerozoic seawater chemistry. This includes quantitative information about the marine Sr output flux, primarily controlled by the burial of marine carbonates, as the precipitation of calcite and aragonite preferentially incorporates the light Sr isotope [2,3], leaving seawater isotopically heavier.

Our Phanerozoic $\delta^{88/86}Sr$ seawater record shows considerable variability from 0.25‰ to 0.60‰ suggesting major changes of the marine carbonate burial fluxes. To quantify our results we developed a numerical box model to reconstruct changes in the inventory and fluxes of seawater Sr, calcium (Ca), and total alkalinity (TA).

The model results reveal severe disturbances in the marine budgets of Sr (0-300 µmol/l), Ca (0-40 mmol/l), and TA (0-30 mmol/l) at the Phanerozoic extinction events, especially at the Permian/Triassic boundary. These changes in the marine carbonate system are explained by processes including carbonate production rates, (shelf) carbonate dissolution, ocean anoxia associated with bicarbonate production by bacterial sulfate reducers (BSR), and shifts in the dominant carbonate mineralogy (calcite/aragonite). The first time geochemical quantification of these processes is a novelty in the field of Paleocanography and will help to identify the causal processes leading to global mass extinctions in the marine realm.

[1] M. E. Clapham, J. L. Payne (2011), *Geology* **39**, 1059-1062.
[2] J. Fietzke, A. Eisenhauer (2006), *Geochem. Geophys. Geosyst.* **7**. [3] A. Krabbenhöft *et al. (2010)*, *Geochim. Cosmochim. Acta* **74**, 4097-4109.

Do mountains withdraw CO_2?

FRIEDHELM VON BLANCKENBURG*[1], JEAN L. DIXON[1]

[1]German Research Center for Geosciences GFZ, Earth Surface Geochemistry, Potsdam, Germany, fvb@gfz-potsdam.de (* presenting author)

Common gospel holds that the rise of mountains in the late Cenozoic has increased global rates of silicate weathering, and, as a consequence, increased withdrawal of atmospheric CO_2. Seawater isotope ratio curves of radiogenic Sr, radiogenic Os, and most recently, stable Li [1] supposedly testify to this change. We challenge this hypothesis on three grounds.

1) A compilation of weathering and denudation rates at both the soil scale and the river catchment scale show that "speed limits" restrict both soil formation (270 t km^2 yr^{-1}, or 0.1mm yr^{-1}) and silicate weathering (135 t km^2 yr^{-1}). Even in high, active mountains, these limits are obeyed. We use a global topographic model to show that due to the combination of weathering speed limit and the small spatial extent of active mountain belts, areas in which erosion exceeds the soil formation speed limit contribute <10% to global weathering fluxes today. In the geologic past, due to the limited range of weathering rates imposed by speed limit, large global changes in uplift and erosion would have resulted in only small changes in global weathering.

2) A reassessment of global and regional erosion rates inferred from global sedimentation rates has shown that a supposed increase in global mountain erosion rates in the late Cenozoic is only an apparent one, and that the underlying increase in sedimentation rates is due to incomplete preservation of sedimentary strata [2].

3) An increasing body of evidence shows that the seawater curves of radiogenic Sr and Os isotope ratios record provenance of these elements [3], or the increasingly glacial contribution to erosion [4] rather than weathering rates. The new stable Li isotope data [1] is intriguing, but we still lack detailed insight into these metal stable isotope systems to attribute their variability with certainty to an increase in terrigenous weathering. In contrast, the ocean $^{10}Be(meteoric)/^{9}Be$ ratio, a weathering proxy that combines an isotope of constant flux with a stable one of weathering-dependent flux, is steady over the last 10My [2]. It is therefore unlikely that changes in CO_2 withdrawal over this period were engineered by silicate weathering.

We conclude that the optimal conditions for CO_2 withdrawal are those where a large fraction of the terrestrial Earth surface is soil covered, and is eroding near soil production speed limit. At lower global denudation rate, global soils will be transport-limited. The consequence of such a low global denudation regime is that the potential for feedbacks between climate, weathering, and CO_2 withdrawal to operate is low. In such a period the Earth system could fail all climate weathering feedbacks.

[1] Misra and Froelich (2012) *Science* in press
[2] Willenbring and von Blanckenburg (2010) *Nature* 465
[3] Kashiwagi et al. (2008), *Palaeogeog Palaeocl Paleoecol* 270
[4] Clark et al. (2006) *Quat Sc. Rev*. 25

https://doi.org/10.1180/S0026461X00008434 Published online by Cambridge University Press

Development of Flow-Field Flow Fractionation based methods for the characterization of engineered nanoparticles in a complex matrix

S. LEGROS[1], F. VON DER KAMMER[1*], S. WAGNER[1], B. MEISTERJAHN[1], E. H. LARSEN[2], K. LOESCHNER[2], J. NAVRATILOVA[2] & T. HOFMANN[1]

[1]Univ. of Vienna, Dept. of Env. Geosciences, Vienna, Austria
[2]National Food Institute, Division of Food Chemistry, Technical University of Denmark, Søborg, Denmark.
(*presenting author: frank.kammer@univie.ac.at)

Engineered nanoparticles (ENPs) containing consumer products are already on the market. These may release the containing nanoparticles into the environment during their production, use and disposal/recycling. To assess the risk related to this release accurate methods for nanoparticle quantification in a wide variety of matrices are needed. These standardized methods to detect, quantify and characterize ENPs in consumer products are in fact nonexistent.

Field Flow Fractionation (FFF) coupled to specific detectors is one of the most promising techniques for these tasks. To establish robust methods for analyzing ENPs in products, biological media and the environment a systematic approach to thoroughly optimze and validate FFF for certain combinations of ENP and sample matrix is needed. Many parameters like cross flow, carrier composition, membrane type, channel height and injection procedure determine the performance of FFF. The same is true for the sample preparation and the specific particle detection following separation as e.g. by ICP-MS.

The strategy to be adopted depends strongly on the analytical information requested, the type of the ENPs and the nature of the matrix. The examples of nanoparticles of silica-NPs in a food sample (tomato soup) and silver-NPs in food and the environment will be presented.

The sample preparation was performed by several particle/matrix adapted approaches using colloidal extraction, acidic, alkaline and enzymatic attacs. Flow-FFF coupled to online UV-DAD, multi-angle light scattering, dynamic light scatering and ICP-MS were used to characterize compositions and properties of nanoparticles as a function of size. The optimization schemes aimed at maximum recovery, lowest possible influence on peak shape and position, minimum alteration of the original ENP during analytical procedure and pratical applicability (e.g. analysis time). The results show that ENPs can be analyzed in complex matricees with good recovery. Also it is evident how strong FFF results depend on the interplay of sample characteristics and run conditions.

Thoroughly adapted and optimized analytical methods, as those presented here, are essential to investigate the fate of ENPs during the entire life cycle of the consumer product.

Detrital zircon age populations and provenance of the Cape–Karoo succession in South Africa and correlatives in Argentina

CLARISA VORSTER*, JAN KRAMERS, NIC BEUKES, HERMAN VAN NIEKERK

Department of Geology, University of Johannesburg, South Africa, clarisav@uj.ac.za (* presenting author); jkramers@uj.ac.za; nbeukes@uj.ac.za; hermansvn@uj.ac.za

The similarities in litho- and biostratigraphy between the rock successions in the Paleozoic Cape-Karoo basin in Southern Africa and the Sauce Grande basin in Argentina as well as the structure of the Cape and Sierra de la Ventana folded mountain belts that deformed strata of these basins along their southern margins as part of the Gondwanide tectonic terrane, have long been recognized [1, 2]. In order to better constrain the provenance terrains for the two basins, a comparative U/Pb age study of detrital zircon populations was undertaken using LA-ICP-MS . Arenaceous samples were collected in the southwestern Cape region of South Africa, and at Mar del Plata and the Sierre de la Ventana in Argentina. Samples came from the broadly equivalent Ordovician-Silurian Table Mountain and Curamadal Groups, Devonian Bokkeveld and Ventana Groups, uppermost Carboniferous to lowermost Permian glaciogenic Dwyka and Sauce Grande diamictites and greywackes of the lower Permian Ecca and Bonete successions

Results display remarkable similarities but also important subtle diffences in detrital zircon age populations between the two basins, Most characteristic of both areas is the dominance of two major populations of zircons namely late Mesoproterozoic (1200 – 1000 Ma) and late Neoproterozoic to Cambrian (600 – 500 Ma) with perhaps a subordinate late Paleoproterozoic (1900 – 1700 Ma) population in some samples with absolute scarcity or absence of any older zircons. Apart from the glaciogenic Sauce Grande Formation in the Ventana region, all the other formations sampled in this area essentially hold only a late Neoarchean – early Phanerozoic zircon population. In contrast the samples from the western Cape in south Africa are virtually all characterized by both late Neoproterozoic – early Phanerozoic and late Mesoproterozoic age populations. Interestingly a sample of arenite from Mar del Plata along the west coast of Argentina also displays the two major zircon age populations that are characteristic of the correlative Table Mountain arenites in the western Cape. Results indicate that the successions in the Western Cape and eastern part of the Sauce Grande basin were mainly sourced from late Neoproterozoic Pan African/Brasiliano and late Mesoproterozoic Namaqua-Natal metamorphic belts. Rocks in the Ventana area, however, were essentially sourced from Brasiliano terranes. A prominent early Permian zircon population is present in the Bonete Formation of the Ventana region suggesting transport from a juvenile source to the south in the Gondwanide orogen.

[1 Du Toit (1937) *Our Wandering Continents; An Hypothesis of Continental drifting* ,Oliver & Boyd, London, UK.
[2] Milani et al (2008) *Geological Society, London, Special Publications* **294**, 319-342.

https://doi.org/10.1180/S0026461X00008434 Published online by Cambridge University Press

Prediction and observation of dissolved geochemistry of the Fraser River, British Columbia

B. M. VOSS[1,2*], B. PEUCKER-EHRENBRINK[1], T. I. EGLINTON[1,3], S. MARSH[4], S. L. GILLIES[4], G. FISKE[5], W. WOLLHEIM[6], R. STEWART[6], M. ALAMWALA[4], M. BENNETT[4], B. DOWNEY[4], J. FANSLAU[4], H. FRASER[4], J. HERBERT[4], G. MACKLAM-HARRON[4], B. WIEBE[4]

[1]Woods Hole Oceanographic Institution, Woods Hole 02543, USA ([*]bvoss@whoi.edu)
[2]Massachusetts Institute of Technology, Cambridge 02139, USA
[3]Eidgenössische Technische Hochschule, Zürich 8092, Switzerland
[4]University of the Fraser Valley, Abbotsford V2S-7M8, Canada
[5]Woods Hole Research Center, Woods Hole 02540, USA
[6]University of New Hampshire, Durham 03824, USA

The global correlation between bedrock age and the dissolved $^{87}Sr/^{86}Sr$ composition of continental runoff [1] suggests that sufficiently detailed knowledge of spatial distributions of lithological units and runoff fields may allow for more representative predictions of the geochemical nature of continental material exported to the ocean [2]. At the scale of individual drainage basins, however, variations in contributions from geochemically disparate portions of a basin over timescales of weeks to years can cause systematic shifts in the composition of dissolved material exported at different times. In such cases where variability in seasonal hydrology and geochemical "end-members" within a drainage area are significant, predicted geochemical properties must be compared with actual observations at high enough temporal frequency to determine if large-scale modeling approaches can reasonably be applied at the regional or catchment scale.

The Fraser River basin is of intermediate size (232,000 km^2) but possesses stark spatial variability in bedrock geology and precipitation patterns on account of its complex mountainous terrain. Conservative geochemical properties of dissolved constituents (including δD_{H2O} and $^{87}Sr/^{86}Sr$) measured over two years near the Fraser mouth demonstrate a stronger influence during the spring and summer from headwaters with radiogenic $^{87}Sr/^{86}Sr$ and depleted δD. $^{87}Sr/^{86}Sr$ ranges from 0.709 in late winter up to 0.714 in the summer. A mixing model is presented, in which a discharge-weighted average of tributaries is calculated to predict the values of these properties downstream. Strong agreement between the modeled and measured values suggests that such an approach adequately captures the spatial heterogeneity and temporal variability of the Fraser basin. The predicted $^{87}Sr/^{86}Sr$ based on gauging station discharge data agrees well with that based on discharge generated by a global hydrologic model [3], showing promise for extending such an approach to other river systems.

This study provides a framework for further work constraining fluxes and variability of nonconservative constituents (e.g. dissolved organic carbon, nutrients).

[1] Peucker-Ehrenbrink et al. (2010) *Geochem Geophy Geosy* **11(3)**. [2] Roelandt et al. (2010) *Global Biogeochem Cy* **24(2)**. [3] Vörösmarty et al. (1998) *J Hydrol* **207**.

In situ silicon isotope analysis of Archean cherts and BIFs by laser ablation MC-ICPMS

P.Z. VROON [1*], H. TSIKOS[2], B. VAN DER WAGT [1], M.J. VAN BERGEN[3], S. EGGINS[4], L. KINSLEY[4]

[1]Dept. of Petrology, FALW, VU University, The Netherlands, p.z.vroon@vu.nl (* presenting author), b.vander.wagt@vu.nl
[2]Dept. of Geology, Rhodes University, Grahamstown, South Africa, H.Tsikos@ru.ac.za
[3]Dept. of Earth Sciences, Utrecht University, Utrecht, The Netherlands, m.j.vanbergen@uu.nl
[4]RSES, The Australian National University, Canberra, Australia, stephen.eggins@anu.edu.au, leslie.kinsley@anu.edu.au

We present results of in situ stable Si isotope measurements on Archean Cherts and Banded Iron Formations (BIFs) from the Pilbara (Western Australia) and Barberton (South Africa) greenstone belts. Samples were obtained from outcrops and drill cores. In this study we used: (1) a Microlas Geolas Laser ablation (LA) system equipped with a 193 nm Excimer laser at the VU Amsterdam (VUA) and an inhouse built LA system with a 193 nm Excimer laser at ANU. Both LA systems were connected to a Thermo Neptune MC-ICPMS. Molecular isobaric interferences of $^{12}C^{16}O^+$, $^{14}N^{2+}$, $^{14}N^{16}O^+$ that are present on masses ^{28}Si, ^{29}Si and ^{30}Si, were resolved with the aid of the medium resolution slit (RP=4000). An ablation pit size of 49 by 300um and with a 5-10 Hz repetition rate and 5 $J.cm^{-2}$ was used on both LA systems. The LA measurements on the VUA and ANU MC-ICPMS were performed with the same setup as described by [1]. To assess precision, accuracy and matrix effects of the LA technique, chert and BIF samples were analyzed that were previously characterized for silicon isotopes by micro-drilling and subsequent liquid chromatographic purification **[1]**. A chemically homogenous chert sample that is well characterized for silicon isotopes by wet chemical techniques and has a $\delta^{30}Si$ of 0.50 ±0.20 (2sd, relative to NIST RM8546) was used as a standard at both the VUA and ANU.

LA silicon isotope results are significantly influenced by the matrix; e.g. in BIF layers with more than 50% Fe_2O_3, we observed a shift of more than 40‰ in $\delta^{30}Si$, compared to values obtained by micro drilling and chemical purification. This shift is highly dependant on the tuning conditions of lasers and MC-ICPMS. It is therefore necessary to carefully match standards and samples, and only if the chemical composition of the samples is relatively constant can accurate data be obtained.

BIFs display significant variations between iron poor and iron rich layers (maximum observed difference ~1.8‰). In all cases the iron rich layers have higher $\delta^{30}Si$ than the iron poor layers. Variations in $\delta^{30}Si$ of up to 1.2‰ were also observed within individual layers on a mm scale. Cherts display variation between black and white bands with a maximum $\delta^{30}Si$ difference of 1.2‰. The data of this study confirm that silicon isotope signatures are not altered by post depositional burial and metamorphism. Therefore, the laser ablation technique opens new possibilities to unravel the depositional mechanisms for Archean BIFs and cherts, provided samples are correctly matrix-matched with standards.

[1] Van den Boorn et al. (2006) J. Anal. At. Spectrom., 21, 734–742.

https://doi.org/10.1180/S0026461X00008434 Published online by Cambridge University Press

Thiocyanate adsorption onto ferrihydrite and its availability during the aging of ferrihydrite

H. P. VU[1]* AND J. W. MOREAU[1]

[1]University of Melbourne, Melbourne, Australia, hong.vu@unimelb.edu.au (* presenting author)

Thiocyanate (SCN^-) contamination results from many industrial sources such as coal processing and metal separation. Although SCN^- is less toxic than cyanide it is still harmful to aquatic organisms and humans [1]. The use of iron oxides to immobilise contaminants has been shown to be an effective treatment [2] but little is known about the removal of SCN^- by iron oxides.

Adsorption of SCN^- onto the surface of ferrihydrite and the availability of adsorbed SCN^- during the transformation of ferrihydrite were studied using macroscopic techniques complemented with Transmission Electron Microscopy (TEM). The preliminary results show that adsorption of SCN^- decreases as pH increases. Adsorption of SCN^- is strongly affected by the concentration of electrolyte with decrease in concentration of $NaNO_3$ leading to increase in SCN^- adsorption (Figure 1). This indicates that SCN^- adsorbs onto ferrihydrite as outer-sphere complexes.

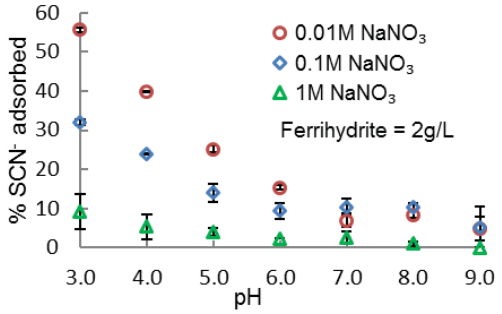

Figure 1: Macroscopic uptake of SCN^- as a function of pH and electrolyte concentration.

The adsorption isotherm reveals that adsorption capacity increases with increases in concentration of SCN^-. Within the studied range of SCN^- concentrations adsorption capacity is linearly proportional to the equilibrated concentration of SCN^- (Figure 2).

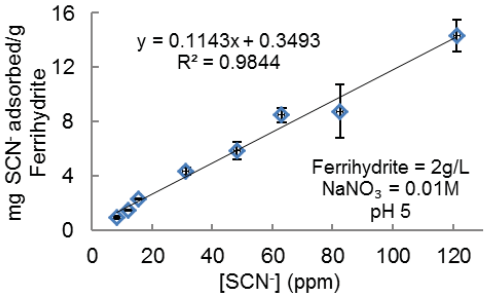

Figure 2: SCN^- adsorption isotherm.

[1] Bhunia *et al* (2000) *Bull. Environ. Contam. Toxicol.* **64**, 197-204. [2] Cundy *et al* (2008) *Sci. Total. Environ.* **400**, 42-51.

First-principle simulations of silver in hydrothermal fluids

RODOLPHE VUILLEUMIER[1*], ROMAIN JONCHIÈRE[2], GUILLAUME FERLAT[2], A. MARCO SAITTA[2], ARI P. SEITSONEN[3]

[1]UMR 8640 CNRS-ENS-UPMC, Département de Chimie, Ecole normale supérieure, 24 rue Lhomond, 75005 Paris, France, Rodolphe.Vuilleumier@ens.fr (* presenting author)

[2]IMPMC, Université Paris 6, CNRS, 4 Place Jussieu, 75005 Paris, France, Romain.Jonchiere@hotmail.fr, Guillaume.Ferlat@upmc.fr, Marco.Saitta@upmc.fr

[3]Physikalisch Chemisches Institut, Universität Zürich, Winterthurerstrasse 190, CH-8057 Zürich, Switzerland, Ari.P.Seitsonen@iki.fi

The knowledge of the speciation of coinage metals is a key element of the understanding of their transport in hydrothermal conditions and the formation of metal deposits from geological fluids. In saline brines, the main carrier of silver, solvated as silver cation Ag^+, is the chloride anion Cl^-. Extrapolations from low temperature thermodynamical data, which suggest either $AgCl_2^-$ [1] or $AgCl_4^{3-}$ [2] as the dominant species at high temperature, lead to solubilities of Ag-bearing minerals that differ by two to three orders of magnitudes at elevated temperature. Molecular modelling can help putting constrains on these models. The interaction of silver or other coinage metals with water is, however, more complex than that of simple cations like Na^+ [3]. Moreover, at elevated temperatures, the hydrogen bond network of water is largely broken and its dielectric constant much lower than at ambient conditions, which questions the validity of empirical force-fields. First-Principles Molecular Dynamics (FPMD) makes no a priori assumption about the interactions and enables the description of such complex chemical systems.

We will first briefly discuss the FPMD description of supercritical water, with particular emphasis on the role of long-range dispersion interactions [4]. We will then present results from large scale FPMD simulations of silver solvation in aqueous solutions at ambient and elevated temperature, with various Cl^- contents. Modelled EXAFS signals will be compared to recently obtained experimental data. In agreement with very recent FPMD study using smaller samples [5], we find that $AgCl_2^-$ and $AgCl_3^{2-}$ species are stable at ambient conditions. We also find the $AgCl_4^{3-}$ complex to be stable in our simulations. $AgCl_2^-$ is found to be a linear complex while $AgCl_3^{2-}$ is trigonal planar and $AgCl_4^{3-}$ a distorted square planar complex. The largest complexes are, however, not stable at high temperature where only AgCl and $AgCl_2^-$ complexes are found. These structures appear very fluxional. Transitions between these complexes at ambient temperature and chlorine exchange in $AgCl_2^-$ at high temperature occur on a time-scale of about 10 picoseconds. The role of quadrupolar polarizability of Ag^+ in the stability and dynamics of these structures will be discussed.

[1] Akinfiev N.N. and Zotov A.V. (2001) *Geochem. Intern.* **39**, 990-1006. [2] Sverjensky D.A. *et al.* (1997) *Geochim. Cosmochim. Acta* **61**, 1359-1412. [3] Vuilleumier R. and Sprik M. (2001) *J. Chem. Phys.* **115**, 3454. [4] Jonchière R. *et al.* (2011) *J. Chem. Phys.* **135**, 154503. [5] Liu X. *et al* (2012) *Chem. Geo.* **294**, 103-112.

https://doi.org/10.1180/S0026461X00008434 Published online by Cambridge University Press

Clumped isotopes applied to Silurian brachiopod shells, Gotland/Sweden

ULRIKE WACKER[1*], JENS FIEBIG[1], AXEL MUNNECKE[2], MICHAEL M. JOACHIMSKI[2] AND BERND R. SCHÖNE[3]

[1]Department of Geosciences, Goethe University Frankfurt, Germany (* U.Wacker@em.uni-frankfurt.de; Jens.Fiebig@em.uni-frankfurt.de)

[2]GeoZentrumNordbayern, FAU Erlangen-Nürnberg, Germany (axel.munnecke@pal.uni-erlangen.de; michael.joachimski@gzn.uni-erlangen.de)

[3]Institute of Earth Sciences, Johannes Gutenberg-University, Mainz, Germany (schoeneb@uni-mainz.de)

Several O and C isotope records from the Silurian sequence of Gotland/Sweden are published, which are based on brachiopod shell calcite [1,2], micritic limestones [3] and biogenic phosphates [4]. All recorded isotope curves show similar trends with pronounced shifts in $\delta^{18}O$ and $\delta^{13}C$. Besides, three C isotope excursions are measured globally. Correlation between the C and O isotope signals supports the assumption that the values are of primary origin.

We are applying the carbonate clumped isotope thermometer to brachiopod shells from Gotland to decipher both, temperature and $\delta^{18}O$ of Silurian ocean water. Based on the ordering of isotopes, i.e. on the clumping of ^{13}C-^{18}O within carbonate groups of minerals, precipitation temperatures can be estimated independently of the isotopic composition of the water from which the crystals grew. The measure of temperature is Δ_{47}, which describes the deviation of the 47/44 abundance ratios in CO_2 derived from H_3PO_4 digestions of carbonates from the corresponding stochastic 47/44 ratios.

Due to different pre-analyses of brachiopod shells from Gotland various researchers interpret most of these fossils not to be influenced by diagenesis [1,2], and stable isotope ratios are assumed to be preserved. However, temperatures between 40 and 60°C are estimated from first Δ_{47} measurements, which indicate a diagenetic overprint that affected at least ^{13}C-^{18}O clumping in carbonate groups. It needs to be proven, whether the $\delta^{18}O$ values reflect a pristine signal or had been reset at least in parts, and whether geochemical signatures of these fossils can be used for paleoreconstructions. This will be tested by a comparison of Δ_{47} and $\delta^{18}O$ values of pristin and altered shell sections which were already identified using CL and SEM. Additionally, trace element concentrations were measured.

High resolution sampling along ontogenetic transects of four brachiopods indicate variations in $\delta^{18}O$ of about 1.5‰ within the single shells expressed by a constant trend to lower values with increasing distance to the hinge, but a shift to higher values in the most anterior part. Δ_{47} analyses along growth directions of these brachiopods might provide additional information whether the O isotopic pattern reflects primary fluctuations of temperature or $\delta^{18}O$ during growth of the organisms.

[1] Samtleben et al. (1996) *IJES* **85(2)**, 278-292. [2] Wenzel and Joachimski (1996) *PPP* **122(1-4)**, 143-166. [3] Munnecke et al. (2003) *PPP* **195(1-2)**, 99-124. [4] Wenzel et al. (2000) *GCA* **64(11)**, 1859-1872.

Phosphate reaction with PbS stimulates microbial S oxidation

ALEXANDRA B. WALCZAK[1*], NATHAN YEE[2], LILY Y. YOUNG[2]

[1]Rutgers Univeristy, Microbiology and Molecular Genetics, New Brunswick, USA walczaal@eden.rutgers.edu (*presenting author)

[2]Rutgers Univeristy, Dept. of Environmental Science, New Brunswick, USA nyee@envsci.rutgers.edu, lyoung@aesop.rutgers.edu

Introduction

The reaction of lead (Pb) and phosphorus-containing compounds causes the formation of pyromorphite-type mineral phases [1]. These mineral phases have a low solubility and bioaccessibility, making their formation a viable option for stabilizing Pb contamination in soil and waste rock [1]. In cases where an insoluble mineral such as galena (PbS) is the primary form of Pb the effect of phosphorus amendment on the sulfur speciation and the microbial interactions are still poorly understood.

Methods

Pure culture experiments were set up with *Bosea* sp. str. WAO, an autotroph which is capable of growth on several reduced sulfur sources [2]. Replicate flasks containing 40 mM phosphate buffered growth medium and 2 mM PbS were amended with either live cells (active), killed cells (sterile control), or no cells (background control). Flasks were maintained aerobic by shaking and incubated at 30°C. Periodic samples were taken to measure sulfate, total dissolved sulfur, and Pb in the bulk medium and solid phase.

Results and Conclusions

The addition of phosphate to the growth medium containing powdered PbS caused the abiotic exchange of sulfide for phosphate, producing lead phosphate $Pb_9(PO_4)_6$, and was confirmed by powder XRD. The released sulfide was then available for strain WAO to use as an energy source for growth.

The microbial oxidation of the released sulfide to sulfate was compared to background and sterile controls. Active cultures containing 2 mM PbS produced ~1.7 mM sulfate as measured by IC within 9 days of incubation. No production of sulfate was measured in the background and sterile controls during the incubation period. Metal analysis by ICP-OES measured less than 0.2 mM of Pb in the bulk medium after incubation for active or control, while 2 mM was recovered after acid extraction of the precipitate.

WAO preferentially colonized the PbS mineral surface to gain access to the released sulfide as shown with epifluorescence microscopy on slide cultures of mineral powder. The biomass of strain WAO increased on the mineral surface over time and was also shown to be closely associated using confocal microscopy.

Although the phosphate amendment makes the Pb less bioavailable, it is increasing the availablity of sulfide which can stimulate the growth of sulfide oxidizing organisms and the production of sulfate. In situations where there are high concentrations of these sulfidic minerals the addition of phosphate may increase the microbial S oxidation, an important contributor to acid mine drainage.

[1] Kumpiene *et al.* (2008) *Waste Management* **28**, 215-225. [2] Rhine *et al.* (2008) *Environmental Sci. Technol* **42**, 1423-1439.

https://doi.org/10.1180/S0026461X00008434 Published online by Cambridge University Press

Combined ^{182}W, ^{186,187}Os and ^{142,143}Nd Constraints on Terrestrial Differentiation and Mantle Mixing

R. J. WALKER*, M. TOUBOUL AND I. S. PUCHTEL

Department of Geology, University of Maryland, College Park, MD 20742, USA, rjwalker@umd.edu

Collectively applied, the ^{182}Hf-^{182}W, ^{190}Pt-^{187}Re-^{186,187}Os, and ^{146,147}Sm-^{142,143}Nd radiogenic isotope systems are potentially useful for exploring early planetary processes ranging from metal-silicate segregation (via Hf-W and Re-Pt-Os), to crystal-liquid fractionation in silicate domains (via Hf-W, Pt-Re-Os and Sm-Nd). For example, study of the 2.8 Ga Kostomuksha komatiites of NW Russia revealed a mantle source that was ~15 ppm enriched in ^{182}W, relative to ambient terrestrial W [1], and also modestly enriched in ^{186}Os and ^{187}Os [2], relative to chondritic references. However, the ^{142}Nd and ^{143}Nd isotopic compositions of these rocks are generally consistent with those of the contemporary ambient mantle [3,4]. Accounting for these isotopic characteristics is challenging. The necessary magnitude of fractionations of Hf/W, Pt/Os, and Re/Os could have been generated as a result of metal-silicate segregation at high temperatures and pressures. Such process would not have affected the initial chondritic Sm/Nd. Thus, these komatiites may, in part, have tapped a mantle domain that formed within the first ~30 Myr of the Solar System history, as required by the 8.9 Myr half-life of ^{182}Hf. The Kostomuksha komatiite source, however, had abundances of highly siderophile elements (HSE) within the range of estimates for the primitive mantle, so the dominant Os isotopic signature, as well as the HSE abundances, must have been inherited from ambient mantle that had acquired its HSE budget via late accretion. It is equally plausible that the necessary fractionations occurred as a result of crystallization and overturn in transient magma oceans, although the effects of such processes on Pt/Re/Os systematics at present are poorly constrained. Further, diverse, 3.8 Ga rocks from Isua, Greenland [5] have also been shown to have comparable ^{182}W enrichments, yet are also enriched in ^{142}Nd. Consequently, it is clear that there is no single mantle domain that can account for the variations that are now known for ^{182}W, ^{186}Os, ^{187}Os, and ^{142}Nd in ancient rocks. Numerous, important implications can be drawn from these findings. For example, the requirement for very early formation of the sampled mantle domain means that the putative giant impact that led to creation of the Moon > 50 Ma following Solar System formation [6], could not have resulted in the complete melting and mixing of the mantle. In addition, long-term preservation of such early-formed mantle domains means that materials added to the mantle by late accretion might also still be preserved in the mantle and identified by diverse nucleosynthetic signatures. A new era of study of early-Earth chemical geodynamics, utilizing combined short- and long-lived radiogenic isotope systems, has begun.

[1] Touboul et al. (2012) *Science*, in revision.
[2] Puchtel et al. (2005) *EPSL* **237**, 118-134.
[3] Puchtel et al. (1998) *EPSL* **155**, 57-74.
[4] Boyet M., Carlson R.W. *EPSL* **250**, 254-268.
[5] Willbold et al. (2011) *Nature* **477**, 195-198.
[6] Touboul et al. (2007) *Nature* **450**, 1206-1209.

Assessing the Release of Bioactive Trace Elements from Coal Fly Ash into Natural Fresh Waters

C. WALL[1]*, B. SOHST[2], G. CUTTER[3], P. SEDWICK[4]

[1]Old Dominion University, Ocean Earth and Atmospheric Sciences, Norfolk, USA, cwall022@odu.edu (*presenting author)
[2]Old Dominion University, OEAS, Norfolk, USA, bsohst@odu.edu
[3]Old Dominion University, OEAS, Norfolk, USA, gcutter@odu.edu
[4]Old Dominion University, OEAS, Norfolk, USA,psedwick@odu.edu

Introduction

Each year a significant amount of coal fly ash enters the environment, where it can potentially cause adverse effects by releasing a range of bioactive trace elements. In this context, environmental studies have largely focused on the leaching of trace elements from the coal ash in landfills by rainwater and groundwater, while there has been relatively little study of the release of bioactive trace elements from coal fly ash deposited in natural fresh waters such as rivers and lakes. Furthermore, the batch leaching methods that have been used to study the interaction of rainwater and groundwater with coal ash in landfills are not readily extrapolated to rivers and lakes, where the solution to particle ratio is typically high. To address this problem, we have adapted a flow-through leaching protocol that has been used to estimate the fractional dissolution of trace elements from mineral aerosols in ocean waters. We argue that this rapid leaching technique more closely resembles the interaction of coal ash with fresh waters, thus allowing us to assess the release of coal fly ash constituents into rivers and lakes.

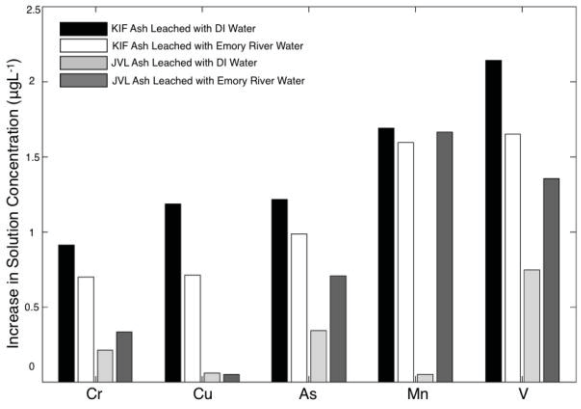

Figure 1. Increase in solution concentration of bioactive trace elements in Emory River water leach solutions.

Results

We have performed a series of flow-through leaching experiments using fresh coal ash and fresh waters collected from rivers and lakes in the southeastern U.S. A suite of bioactive trace elements have been analyzed in the resulting leach solutions and in acid digests of the bulk coal ash, using high-resolution plasma-source mass spectrometry. Our preliminary data (Fig. 1) suggest that significant fractions of a number of bioactive trace elements in coal ash are readily soluble in natural fresh waters.

https://doi.org/10.1180/S0026461X00008434 Published online by Cambridge University Press

Age of the Stillwater Complex

COREY J. WALL[1*], JAMES S. SCOATES[1], RICHARD M. FRIEDMAN[1], AND WILLIAM P. MEURER[2]

[1]Pacific Centre for Isotopic and Geochemical Research, Earth and Ocean Sciences, Vancouver, BC, Canada, cwall@eos.ubc.ca*, jscoates@eos.ubc.ca, rfriedman@eos.ubc.ca

[2]ExxonMobil Upstream Research, Houston, TX, USA, william.p.meurer@exxonmobil.com

The Archean Stillwater Complex, a large mafic-ultramafic layered intrusion in the Beartooth Mountains of Montana (USA) and host to the world-class J-M Reef platinum group element deposit [1], may represent a sub-volcanic reservoir through which a substantial quantity of magma was processed [2]. We present U-Pb ID-TIMS results for ultramafic, mafic, and felsic samples from across the exposed max. 8 km-thick intrusion to constrain the age and duration of magmatism associated with this major intrusion. The accepted age for plagioclase-rich rocks of the Banded Series is ca. 2704 Ma with older ages recorded in the basal sills and dikes (2710-2713 Ma) [3]. Our U-Pb results for three mafic samples reveal a small range of weighted $^{207}Pb/^{206}Pb$ ages at ca. 2709 Ma, which we interpret as the age of crystallization of the Banded Series: 2708.80 ± 0.75 Ma (baddeleyite) and 2709.05 ± 0.85 Ma (zircon) for a troctolite from the J-M Reef package in the Lower Banded Series, and 2708.70 ± 0.82 Ma (zircon) for an olivine gabbronorite in the OB3 Zone and 2709.82 ± 0.51 Ma (zircon) for anorthosite from the AN2 Zone of the Middle Banded Series. A preliminary age of 2710.7 ± 1.1 Ma for high Th/U (8-14) zircon from a feldspathic orthopyroxenite at the top of the Bronzitite Zone suggests that the lower Ultramafic Series could be resolvably older than the overlying Banded Series.

Small-volume granophyric and pegmatitic rocks are found throughout the Banded Series and some may represent extreme differentiates [4]. Samples studied include a pegmatitic ksp-qtz core to a gabbroic pegmatoid in the Lower Banded Series (N1 Zone), an alaskite (quartz diorite) and an amphibole-rich reaction zone between the alaskite and anorthosite (AN1 Zone) in the Middle Banded Series, and an amphibole-bearing granophyre from the Upper Banded Series (GN3 Zone). U-Pb dating of zircon from the N1 pegmatite yields a weighted $^{207}Pb/^{206}Pb$ age of 2709.65 ± 0.80 Ma, which is identical to ages from the dated mafic rocks. Zircon grains from the other three samples are strongly metamict and U-Pb results are strongly discordant (12-86%). Stepwise leaching experiments on the GN3 granophyre reveal two distinct Pb-loss events at ca. 2.0 Ga (leachates) and 2.7 Ga (residues). Titanite ages from the pegmatite and the alaskite agree with the U-Pb zircon ages from the mafic rocks (ca. 2708-2709 Ma), whereas titanite from the other two samples exhibits a wide range of discordance (1.5-61%) suggesting multiple stages of Pb-loss. The disturbed titanite U-Pb systematics and identified Pb-loss events reflect the combined thermal and alteration effects produced by a wide range of post-crystallization events, including the emplacement of a regionally extensive granitic batholith (Mouat quartz monzonite), multiple generations of mafic dike swarms, and greenschist facies metamorphism.

[1] Helz (1995) *American Mineralogist* **80**, 1343-1346; [2] McCallum (1996) *Layered Intrusions*, 441-484; [3] Premo *et al.* (1990) *Geology* **18**, 1065-1068; [4] Czamanske *et al.* (1991) *American Mineralogist* **76**, 1646-1661.

Tc(IV) complexation with organic ligands - an overview

NATHALIE A. WALL[1*], AND BAOHUA GU[2]

[1] Washington State University, Pullman, US, nawall@wsu.edu

[2] Oak Ridge National Laboratory, Oak Ridge, US, gub1@ornl.gov

Introduction

^{99}Tc represents a significant environmental contaminant because of its long half-life of $2.1 \cdot 10^5$ y, complex chemistry, and potential high mobility. Although the anionic and highly mobile Tc(VII) is stable under oxic environments, it can be reduced to the sparingly soluble Tc(IV) and reductive precipitation of Tc has been proposed as one of the promising remedial approaches to impede Tc migration offsite. However, at environmentally relevant pH Tc(IV) forms cationic and neutral species, which can complex to soluble organic ligands and induce Tc(IV) solubilization. It is therefore necessary to assess Tc(IV) complexation with relevant organic ligands, including ligands commonly found in nuclear wastes (e.g. EDTA) and those ubiquitous in the environment (e.g. humic acids).

Results and conclusions

The stability constants of Tc(IV) with acetate, citrate, EDTA, and a variety of humic acids were experimentally determined using a solvent extraction method – a summary of these stability constants is presented in **Table 1**. Additionally, the influence of selected organic ligands (EDTA and humic acids) on Tc(IV) solubity was experimentally measured [6]. The addition of 2.5 mM EDTA leads to an increase of Tc(IV) solubility by over two folds, reaching a Tc(IV) concentration of $4 \cdot 10^{-7}$ M at pH 6, in good agreement with modeling calculations performed based on the EDTA stability constants, which predicts a Tc(IV) solubility of $4.6 \cdot 10^{-7}$ M in presence of the same EDTA concentration and at same pH.

Acetate	$\log\beta^0_{1,-1,1} = 2.8 \pm 0.3$	I = 0 M	[1]
Oxalate	$\log\beta^0_{1,0,1} = 7.2 \pm 0.2$	I = 0 M	[2]
Citrate	$\log\beta^0_{1,-1,1} = 7.5 \pm 0.2$	I = 0 M	[3]
Humic acid	$\log\beta_{1,-1,1} = 6.2 \pm 0.6$	I = 0.1 M	[4]
EDTA	$\log\beta^0_{1,0,1} = 20.0 \pm 0.4$ $\log\beta^0_{1,1,1} = 25.3 \pm 0.5$	I = 0 M I = 0 M	[5]

Table 1: Stability constants of Tc(IV) complexes with different organic ligands.

Acknowledgements

This work was supported by the Office of the Biological and Environmental Research, Office of Science, U.S. Department of Energy (DOE) under the grant DE-FG02-08ER64696 with Washington State University and by the U.S. Nuclear Regulatory Commission under the grant 3808953.

[1] Boggs et al. (2010) *Radiochimica Acta* **98** 583-587.

[2] Xia, et al. (2006) *Radiochimica Acta*. **94** 137-141.

[3] Wall and Karunathilake (2011) *submitted*

[4] Boggs et al. (2011) *Environ. Sci. Technol*. **45** 2718-2724.

[5] Boggs et al. (2011) *Radiochimica Acta* Accepted.

[6] Gu et al. (2011) *Environ. Sci. Technol*. **45** 4771-4777

https://doi.org/10.1180/S0026461X00008434 Published online by Cambridge University Press

Global variations in H_2O/Ce: Relationships to arc magma geochemistry & slab surface temperatures

PAUL J. WALLACE[1*], DANIEL M. RUSCITTO[2], LAUREN B. COOPER[3], TERRY PLANK[4], ELLEN M. SYRACUSE[5], AND CRAIG E. MANNING[6]

[1]University of Oregon, Eugene, USA, pwallace@uoregon.edu (* presenting author)
[2]Rensselaer Polytechnic Institute, Troy, USA, ruscid2@rpi.edu
[3]University of Geneva, Geneva, Switz., lauren.cooper@erdw.ethz.ch
[4]Columbia University, Palisades, USA, tplank@ldeo.columbia.edu
[5]Univ. of Wisconsin, Madison, USA, syracuse@geology.wisc.edu
[6]University of California, Los Angeles, USA, manning@ess.ucla.edu

We have compiled a dataset of 114 primitive arc magma compositions from melt inclusion and whole rock analyses to compare volatile contents, slab tracers, and calculated subduction component compositions between 18 subduction zone segments spanning the global range in slab thermal structure [1]. The average primitive magma H_2O content in our dataset is 3.3 ±1.2 wt.% (1 s.d.) for melts erupted within 50 km of the volcanic front. Although there is a wide range of volatile contents in magmas within individual arcs, the highest values occur in magmas erupted from vents along the volcanic front, where the subducting slab is located 104 ±29 km (avg. ±1 s.d.) beneath the surface. This observation, coupled with positive correlations between H_2O, Cl, S, and B contents and predictions from geodynamic models, provides strong evidence for the active supply of subduction-related components from the slab beneath volcanic arcs. Furthermore, calculated subduction component compositions become increasingly solute-rich in arcs with hotter slabs (lower thermal parameter), suggesting that fluids/melts of differing compositions are added beneath different arcs.

We have also calculated slab fluid temperatures for 51 volcanoes in 10 subduction zones [2] using the newly developed H_2O/Ce thermometer. The temperatures, adjusted to *h*, the vertical depth to the slab beneath the volcanic arc, range from ~730 to 900°C, and agree well (within 30°C on average for each arc) with sub-arc slab surface temperatures predicted by recent thermal models. The coherence between slab model and surface observation implies predominantly vertical transport of fluids within the mantle wedge. Slab surface temperatures are well reconciled with the thermal parameter (the product of slab age and vertical descent rate) and *h*. Arcs with shallow *h* (80 to 90 km) yield a larger range in slab surface temperature (up to ~200°C between volcanoes) and more variable magma compositions than arcs with greater *h* (120 to 180 km). This diversity is consistent with coupling of the subducting slab and mantle wedge, and subsequent rapid slab heating, at ~80 km. Slab surface temperatures warmer than the H_2O-saturated solidus implicate ubiquitous melting at the slab surface. Our results imply that melts or solute-rich fluids, and not H_2O-rich fluids, are thus the agents of mass transport to the mantle wedge.

[1] Ruscitto *et al.* (2012) *Geochem., Geophys., Geosys.*, in press. [2] Cooper *et al.* (2012) *Geochem., Geophys., Geosys.*, in press.

Leak fluid chemistry control on ^{90}Sr sorption mechanism in sediments

S. H. WALLACE[1*], S. SHAW[1], K. MORRIS[2], J. S. SMALL[3] AND I. T. BURKE[1]

[1]School of Earth and Environment, University of Leeds, UK, *eeshw@leeds.ac.uk
[2]School of Earth, Atmospheric and Environmental Science, University of Mancherster, UK
[3]National Nuclear Laboratory, Risley, Warrington, UK

Strontium-90 is present in contaminated land at nuclear sites around the world and is also an important component of nuclear waste inventories. The mobility of ^{90}Sr in the subsurface is often controlled either by adsorption to sediment particle surfaces or incorporation reactions into secondary mineral precipitates. Here, we present an overview of a multidisciplinary study examining the behaviour of ^{90}Sr in West Cumbrian unconsolidated aquifer sediments under a range of groundwater compositions relevant to contaminated land scenarios.

Batch experiments have been used to test the influence of pH and ionic strength (IS) on the degree of adsorption to sediments. In other experiments hyperalkaline cement waters were used to investigate the effect of mineral alteration and secondary mineral precipitation on ^{90}Sr sorption. Experiments containing 20 ppm Sr^{2+} (spiked with ^{90}Sr tracer) were sampled from 2 days up to one year. Change in Sr speciation within sediments was determined using X-ray absorption spectroscopy and sequential extraction techniques. Mineral precipitates were characterised using SEM, microprobe and TEM techniques.

pH titration experiments showed the optimum pH for maximum ^{90}Sr sorption was between pH 6-8, and in experiments using low IS groundwaters ~99% of ^{90}Sr was removed from solution at circumneutral pH. In experiments with higher IS artificial waste tank leachate at pH 11 only ~80% of ^{90}Sr was removed, suggesting that higher concentration of ions in solution inhibited ^{90}Sr sorption. When both Na^+ and Ca^{2+} solutions were used as competing ions, sorption decreased markedly in experiments when IS was greater than 5 mmol L^{-1}, closely matching model fits to the data. Sr K-edge EXAFS analysis of sediment samples revealed Sr-O bond distances at 2.60 Å, indicating outer-sphere sorption. Sequential extractions found 70-85% of ^{90}Sr remained exchangeable after one year.

In contrast, experiments using high pH young cement water, found sorption to be >99% despite the extremely high IS, suggesting another mechanism of Sr removal predominated. Sequential extractions on a sediment sample aged at 70°C for a year, found that 25±6 % of ^{90}Sr was residual. Sr K-edge EXAFS analysis of a 70°C aged sample contained evidence for an additional Sr-O-Si(Al) bond distance at 3.45 Å consistent with Sr incorporation in a neoformed silicate mineral. XRD and electron microscopy analysis indicate that the neoformed mineral could be chabazite, a zeolite mineral.

These results indicate that at contaminated nuclear sites, ^{90}Sr in the environment will predominantly sorb at circumneutral pH, but can be remobilised if affected by higher IS solutions. In a high pH cementitious repository, alkali alteration of silicate minerals could provide a sink for ^{90}Sr, however even after alteration much of the ^{90}Sr may remain exchangeable with other ions in solution.

https://doi.org/10.1180/S0026461X00008434 Published online by Cambridge University Press

Geochronology and geochemistry of Precambrian basement from the Fort McMurray area, Alberta: A geothermal perspective

NATHANIEL WALSH,[1*], THOMAS CHACKO[1], LARRY M. HEAMAN[1], S. ANDREW DUFRANE[1], JOHN J.M. DUKE[2], JACEK MAJOROWICZ[3]

[1]Earth & Atmospheric Sciences, University of Alberta, Edmonton, Canada, nwalsh@ualberta.ca (*presenting author), Tom.Chacko@ualberta.ca, Larry.Heaman@ualberta.ca, dufrane@ualberta.ca
[2]SLOWPOKE Nuclear Reactor Facility, University of Alberta, Edmonton, Canada, jduke@pharmacy.ualberta.ca
[3]Department of Physics, University of Alberta, Edmonton, Canada, majorowi@ualberta.ca

To reduce energy consumption and CO_2 emissions in oil sands processing, a study was recently initiated under the auspices of the Helmholtz-Alberta Initiative to examine the possibility of a cheaper source of hot water in northeastern Alberta by geothermal methods. The particular geothermal method being considered is Engineered Geothermal Systems (EGS), which aims to extract economic quantities of heat from low permeability and porosity rocks. The present study is the geochemical/petrological component of a larger investigation into the feasibility of using EGS as a hot water source for oil sands processing in the Fort McMurray area. Specifically, our aim is to document the rock types, mineralogy, crystallization ages and heat-producing element concentrations of 37 basement drill core samples recovered in 23 petroleum exploration wells drilled into Precambrian basement within a 125 km radius of Fort McMurray.

Most of the drill core samples are part of the Taltson Magmatic Zone (TMZ), a 500 km long, Paleoproterozoic orogenic belt, more than half of which is buried beneath Phanerozoic cover rocks. The investigated samples are mostly deformed granitoids but also include two amphibolites and one sample likely of metasedimentary origin. Preliminary U-Pb isotopic age determinations conducted on thin sections of these samples by laser-ablation MC-ICP-MS yielded zircon crystallization ages ranging from 1.84 to 2.4 Ga. On the basis of these data, the samples can be divided into five age suites. The oldest suite yields relatively poorly constrained ages between 2.2 and 2.4 Ga (n=5). A second group of samples indicate ages of ~2.0 Ga (n=2). The samples from suites 3 (n=6) and 4 (n=6) record two separate periods of granitoid intrusion at 1.95-1.97 Ga and 1.925-1.935 Ga, respectively. The ages noted above correspond well with ages that have been previously reported from the exposed part of the TMZ. The 5th suite (n=1), which is from the Rimbey domain immediately to the south of the TMZ, yielded an age of ~1.84 Ga

Heat-producing element concentrations (K, U, Th) are wide ranging but on average the younger granitoid suites have higher concentrations of these elements. The youngest suite (Suite 5) has by far the highest U content (13.6 ppm) of any of the rocks analyzed in the present study. The temperature recorded at the base of the 2.36 km deep Hunt Well, which is located near the Fort McMurray town site, is ~47°C [1]. Given that the Hunt Well is drilled in the older (ca. 2.2-2.4 Ga) and less radiogenic rock suite, it seems reasonable to conclude that geothermal gradients at other locations within the study area may be at least as high as those documented at the Hunt Well.

[1] Majorowicz et al., 2011

Origin of saline aqueous fluids in the lower crust

JOHN V. WALTHER

Department of Earth Sciences, Southern Methodist University, Dallas, TX 75275, USA, (walther@smu.edu)

Low viscosity H_2O plus NaCl fluids are an important component of metamorphism in the lower crust. They contain up to 50 wt% NaCl (X_{NaCl} = 0.24) that varies widely over short distances judging from fluid inclusion observations. The origin of these fluids is still being debated. Downward circulation of salt-rich surface fluids by thermal convection has been proposed [1]. These fluids are ruled out because they are too buoyant to penetrated downward into the middle or lower crust where fluid pressure = rock pressure and buoyancy controls fluid movement. Low-density H_2O-rich fluids at these depths like magmas tend to rise but not sink.

H_2O with NaCl is given off by upper mantle and lower crustal magma during the final stages of their crystallization. By interacting with deeply buried evaporites these fluids could become even more saline [2]. The fluids could then flux upward. However, considering the dynamics of fluid flow it is likely that these fluids will coalesce into major channelways as they are transported upward. This is similar to flow in the dendritic pattern of stream flow on the earth's surface. These mantle and lower crustal fluids are then likely to be contained in widely spaced fractures and not produce the extensive metamorphism or variable salt concentration observed.

This leaves fluids produced locally during metamorphism by the destruction of hydroxyl containing minerals as they are buried. These fluids are produced at every volatile mineral that is undergoing destruction with increased pressure and temperature and therefore can be pervasive. In pelites ~2 moles of fluid per 1 kg of rock is produced to medium grades of metamorphism [3]. This process is responsible for the low salinity fluids that are a component of mid-crustal metamorphism. How can some of these fluids become more saline at lower crustal levels while others are less so?

The H_2O-bearing minerals, hornblende in mafic rocks and mica in pelites that survive to lower crustal levels have lower thermodynamic activities. This occurs because Cl^- and F^- are present in the OH^- sites in these minerals. For the activity of muscovite in mica:

$$SiO_2 + KAl_3Si_3O_{10}(OH)_2 \rightarrow KAlSi_3O_8 + Al_2SiO_5 + H_2O$$

$$\mathbf{K} = a_{ksp}a_{kyn}a_{H2O}/a_{qtz}a_{mus}$$

$$a_{mus} = (X_K)(X_{Al\sim M1})(X_{Al\sim M2})^2(X_{Si})^3O_{10}(X_{OH})^2$$

When this low activity mica finally becomes unstable, high Cl^- fluids are produced with F^- partitioning into the remaining minerals. For the same activity of the hydrous phase if the F^- changes locally the fluid produced will change its Cl^- fluid concentration. Mica and hornblende compositions whose destruction produces $X_{Cl} > 0.24$ can be present [4],[5]. Destruction of compositionally different hydrous phases, stable in the lower crustal because of their high salt content, can account for the range of salinities observed in fluid inclusions.

[1] McLelland, *et al* (2002) *J. Meta. Geol.* **20**, 175-190. [2] Yardley & Graham (2002) *Geofluids* **2**, 249-256. [3] Walther and Orville (1982) *Contrib. Min. Petrol.* **79**, 252-257. Walther (2009) Essentials of Geo-chemistry 2nd ed, 342-352. [4] Tracy (1991) *Amer. Mineral.* **76**, 1683-1693. [5] Oen & Lustenhouwer (1992) *Econ. Geol.* **87**, 1638-1648.

https://doi.org/10.1180/S0026461X00008434 Published online by Cambridge University Press

Mössbauer evidence of rapid pyrite formation during the interaction between dissolved sulfide and lepidocrocite

M. WAN[1*], C. SCHRÖDER[1,2] AND S. PEIFFER[1],

[1]Department of Hydrology, University of Bayreuth, Bayreuth Germany, moli.wan@uni-bayreuth.de (* presenting author); s.peiffer@uni-bayreuth.de

[2]Center for Applied Geoscience, Eberhard Karls University, Tübingen, Germany, christian.schroeder@ifg.uni-tuebingen.de

Mössbauer spectroscopy has been applied to study mineral transformation during the interaction between lepidocrocite and dissolved sulphide with two different initial concentration ratios. Synthetic lepidocrocite enriched with the Mössbauer sensitive isotope Fe-57 was reacted with dissolved sulphide at neutral pH in an anoxic glove box, the initial molar ratios of iron and sulphide being 3.125 and 0.5, respectively. Solid samples for Mössbauer analysis were collected by filtration at different time steps after 15 min, 2hrs, 48hrs, 72hrs and 1 week for the 3.125 iron-sulphide ratio; and after 72h and 1 week for the 0.5 iron-sulphide ratio. Dissolved and solid phase ferrous iron, dissolved sulphide and elemental sulphur were measured with wet chemistry analysis techniques in parallel runs.

Mössbauer spectra provide evidence for rapid pyrite formation within 48hrs during the reaction at an initial molar ratio of 3.125. Pyrite formation was accompanied by a decrease of elemental sulphur and mackinawite, which is the main iron intermediate product with minor pyrrhotite and magnetite. At the ratio of 3.125, excess lepidocrocite existed and dissolved sulphide was completely consumed after 15min. Acid extractable Fe(II) concentration was in excess of that of Fe(II) bonded as FeS, which has been reported before[1,2] and the difference of the two iron species was defined as excess Fe(II)[2]. In the experiment with an initial ratio of 0.5, lepidocrocite was completely transferred to mackinawite. In this system dissolved sulphide was not completely consumed even after 1 week. No pyrite could be detected. Species including elemental sulphur and mackinawite were stable in 1 week without any further transformation. The long term preservation of unstable iron sulphide minerals at a low concentration of dissolved sulphide is consistent with the observation in marine sediment [3].

These experiments show an important linkage between rapid pyrite formation and surplus lepidocrocite and/or the excess Fe(II) formed during reaction. Together with wet chemistry analysis results we propose that some of the electrons donated by sulphide oxidation are preserved temporally in the lepidocrocite bulk and lead to formation of the excess Fe(II) fraction and ultimately rapid pyrite formation.

[1] Poulton *et al.*(2004) *Geochim. Cosmochim. Act* **68**, 3703–3715.
[2] Hellige *et al.* (2011) *Geochim. Cosmochim. Acta* **81**, 69-81
[3] Gognon *et al.* (1995) *Geochim. Cosmochim. Acta* **59**, 2663-2675.

The characterization and evaluation of different biochars as reactive materials for Mercury (II) stabilization

ALANA O. WANG[1*], PENG LIU[1], CAROL J. PTACEK[1], DAVID W. BLOWES[1], RICHARD C. LANDIS[2], WILLIAM R. BERTI[2], JAMES A. DYER[2]

[1]Department of Earth and Environmental Sciences, University of Waterloo, Waterloo, Canada

***o3wang@uwaterloo.ca**

[2]E. I. du Pont de Nemours and Company, Wilmington, USA

Introduction and Objectives:

Biochars, produced through low-temperature pyrolysis of environmental biomass, have considerable potential for stabilizing heavy metal in aquatic and sediment systems through surface adsorption reactions. Recent advancements in the uses of biochars to remediate heavy metals, such as Pb, Cd, and Cu, have not been extended to Hg. The complex properties of biochars can also limit the understanding about the leaching potential for nutrients and trace elements. The objectives of this study are to characterize and evaluate different types of biochars for their potentials for Hg treatment and soluble elements releasing. In this study, three biochars produced from different raw materials were evaluated, including spent mushroom soil, pine bark, and fresh mushroom soil containing poultry manure. These biochars were first characterized by surface area, total sulphur and total carbon content, scanning electron microscope/energy dispersion X-ray spectroscopy (SEM/EDX), and Fourier transform infrared spectroscopy (FT-IR). These biochars were then evaluated through a series of laboratory batch studies using Hg-spiked river water or natural river water as the equilibrating solution witin 2 days and 14 days reaction time. Subsequent washing experiments were conducted to evaluate the sustained reactivity of biochars.

Results and Discussions:

The mushroom soil-based biochars (spent, and fresh mushroom soil) were observed to have higher surface area than the wood-based biochar, which are consistent with their irregular distorted porous structures as observed by SEM. The surfaces of all three biochars were also observed to have various functional groups as indicated through FT-IR analyses, which might stablize Hg and release nutrients and trace elements. In batch studies with all three biochars using Hg-spiked river water, greater than 80% and greater than 95% of Hg was removed from the Hg-spiked river water with an initial concentration of 8000 ηg L^{-1} within 2 days and 14 days reaction time, repectively. When compare these bacth tests, the mushroom soil-based biochars were found to reduce greater amount of Hg from the Hg-spiked river water than the wood-base biochar, indicating better surface adsorptions. In batch studies using natural river water, the alkalinity and concentrations of nutrients (NH_3-N, PO_4-P, DOC), anions (SO_4^{2-}, Cl^-), and trace elements (As, Pb, and Cu) were observed to increase especailly in the river water containing the mushroom soil-based biochars. The effective Hg removal and the soluble constituents releasing were all consistent with the presence of functional groups observed by FTIR. Step-wise washing of these biochars resulted in substantial decrease in the release of nutrients and anions with minor decrease in the Hg removal rates. In fact, greater than 85% Hg removal rates were observed in all batch equilibrating solutions after using these washed biochars. These results suggest that, of all biochars evaluated, both the unwashed biochars and the washed biochars have the potential to immobilize Hg without the addition of soluble constituents as mentioned above.

https://doi.org/10.1180/S0026461X00008434 Published online by Cambridge University Press

Ore texture and titanomagnetite composition of the Hongge Fe-Ti-V oxide deposit, SW China: implications for the origin of the deposit

CHRISTINA YAN WANG[1*], MEI-FU ZHOU[2]

[1] Key Laboratory of Mineralogy and Metallogeny, Guangzhou Institute of Geochemistry, Chinese Academy of Sciences, Guangzhou 510640, China, wang_yan@gig.ac.cn (* presenting author)

[2] Department of Earth Sciences, The University of Hong Kong, China, mfzhou@hkucc.hku.hk

9h. Trace elements in oxide minerals from ore deposits: Petrogenetic interpretation and implications for exploration

The Hongge magmatic Fe-Ti-V oxide deposit in the Panxi region, SW China, is hosted in a layered mafic-ultramafic intrusion. The 2.7-km-thick, lopolith-like intrusion consists of the Lower, Middle and Upper zones, which are mainly composed of olivine clinopyroxenite, clinopyroxenite and gabbro, respectively. Abundant oxide layers mainly occur in the Middle zone and the lower part of the Upper zone.

There are net-textured, massive and disseminated Fe-Ti oxide ores. Fe-Ti oxides include Cr-rich and Cr-poor titanomagnetites and granular ilmenite. Both Cr-rich and Cr-poor titanomagnetites contain ilmenite lamellae. Cr-rich titanomagnetite is usually enclosed in olivine and clinopyroxene of disseminated ores in the lower parts of both the Lower and Middle zones and contains 1.89 to 14.9 wt.% Cr_2O_3 and 3.20 to 16.2 wt.% TiO_2, whereas Cr-poor titanomagnetite typically occurs in net-textured and massive ores of the Middle and Upper zones and contains <0.4 wt.% Cr_2O_3 and 0.11 to 18.2 wt.% TiO_2.

Cr-rich titanomagnetite of the disseminated ores is clearly an early crystallized phase, whereas Cr-poor titanomangetite of the net-textured and massive ores crystallized later. Occurrence of Cr-poor titanomagnetite, granular ilmenite and apatite as clusters in the net-textured ores may have formed from Fe-Ti-(P) rich melts. We propose that these Fe-Ti-(P) rich melts were immiscible in silicate magmas similar to the formation of magmatic sulfide ores and that immiscibility occurred because of oversaturation of Fe, Ti and P during the crystallization of silicate minerals. The segregation of dense Fe-Ti-(P) rich melts behaved like a heavy mineral that settled downward in a silicate crystal mush to form net-textured and massive Fe-Ti oxide ores as part of the cumulate sequence.

The co-evolution of prokaryotes-eukaryotes and ocean chemistry on the North China Craton during Mesoproterozoic (1.6–1.3 Ga)

CHUNJIANG WANG*, MENG WANG, JIN XU, YONGLI LI, YAN YU, JIE BAI, TING DONG, JUN WANG, SHIPENG HUANG, XIAOYU ZHANG, LEI WANG, XIAOFENG XIONG, AND HAIFENG. GAI

State Key Laboratory of Petroleum Resources and Prospecting, China University of Petroleum, Beijing 102249, China, wchj333@126.com (* presenting author)

The North China Craton is one of the representative research regions for revealing the co-evolution of life and ocean environment during the early-middle Mesoproterozoic (1.6–1.3Ga). Here, we report the results of a comprehensive study including biomarkers, C-S-isotopic and trace elemental compositions, based on high-resolution geochemical sampling from 6 sections and 4 core-drills.

The Mesoproterozoic sedimentary successions on North China Craton record a suit of negative $\delta^{13}C_{carb}$ values, averaging from -2.4‰ to -1.7‰ for the carbonate sequences, which are more negative than the uniform $\delta^{13}C_{carb}$ values (0.0–1.0‰) of the Mesoproterozoic sedimentary successions worldwide [1]. It may suggest that the primary production and organic carbon burial in the North China Carton were extremely low during the Mesoproterozoic, which are probably the main constraints for sustaining an intermediate redox state in the oceans during the Mesoproterozoic Era. The $\delta^{13}C_{org}$ values of the three organic-rich sequences (Gaoyuzhuang, Hongshuizhuang and Xiamaling Fm) are -34.1‰, -32.7‰ and -31.5‰ in avereage, respectively. Likewise, the $\delta^{13}C_{org}$ values are highly homogeneous in each Formation, and present a well coupling with $\delta^{13}C_{carb}$ in the secular variation.

The carbonate sediments usually present eukaryotic biomarker assembly including C_{26}–C_{29} regualr steranes, 4- and 3-m-steranes as well as very lower concentrations of dinosteranes, but the shales have no detectable steranes. Our biomarker data reveal well co-evolutions of eukaryotes/prokaryotes and ocean environments on the North China Craton during the Mesoproterozoic.

Mo concentrations are 4.7, 42.1 and 17 ppm, and Mo/TOC values are 5.0, 8.9 and 5.2 (ppm/wt%) in average for Gaoyuzhuang, Hongshuizhuang and Xiamaling Fm, respectively. The Mo-lean figures are consistent with the Mo enrichment pattern in Mesoproterozoic black shales [2, 3]. The $\delta^{34}S$ values of sulfides decrease from 7.1–20.6‰ in Gaoyuzhuang Fm to -6.3–7.7‰ in Xiamaling Fm, indicating an enhanced S geochemical cycling during Xiamaling period (1.4–1.3Ga).

[1] Frank et al. (2003) *Geol. Mag*. **140**, 397–420. [2] Scott et al. (2008) *Nature* **452**, 456-459. [3] Lyons et al. (2009) *Annu Rev Earth Planet Sci* **37**: 507–534.

https://doi.org/10.1180/S0026461X00008434 Published online by Cambridge University Press

The size dependent interaction between nanoparticles and collagen: Implications for biomineralization

DONGBO WANG[1(*)], JING YE[1], STEVEN HUDSON[1], VIVEK PRAHBU[1], KEANA SCOTT[2] AND SHENG LIN-GIBSON[1]

[1]Polymers Division, National Institute of Standards and Technology, dongbo.wang@nist.gov (* presenting author)

[2]Surface and Microanalysis Division, National Institute of Standards and Technology

Collagen is the primary structural protein found in connective tissues, making up more than 25 % of the whole-body protein content. It is also the primary biological molecule responsible for the organization of mineralized tissue. Bone and teeth are surprisingly complex organic/inorganic hybrid structures mainly composed of type I collagen and the calcium phosphate mineral – hydroxyapatite (HA). These tissues are hierarchically organized from the nanometer to the meter length scales. Traditionally, collagen mineralization was thought to occur by calcium phosphate nucleation and growth processes from dissolved ions. Recently, these ideas have been challenged and the new concept of "non-classical" mineralization has emerged[1]. In biological tissues it is now proposed that the mineralization process starts with the formation of small amorphous calcium phosphate (ACP) clusters, which infiltrate collagen, and then transform to form intrafibular HA.

We begin to test this new "non-classical" understanding of collagen mineralization by studying the interaction between collagen matrices and colloidally stable/non-reactive gold nanoparticles as models for ACP. We measure *in situ* changes in collagen matrix mechanical properties after introduction of gold nanoparticles using Quartz Crystal Microbalance with Dissipation monitoring (QCM-D). The QCM-D data show a particle size dependent interaction, where 2 nm particles strongly interact with the collagen matrix and cause stiffening in the bulk. Larger particles (3 nm – 40 nm) only interact to the surface of the collagen matrix and don't penetrate into the bulk. We observe the same interaction dynamics with both positively and negatively charged nanoparticles. These results have been confirmed through imaging by AFM and FIB/STEM. However, 2 nm particles, which are comparable in dimension to ACP clusters may not fully infiltrate into collagen fibrils. Therefore size alone likely does not fully explain the ability of ACP clusters penetrate into collagen and form mineralized structures. Continuing work focuses on using QCM-D to investigate stabilized calcium phosphate nanoparticles and their interactions with collagen matrices.

[1] Gebauer and Colfen (2011) *Nano Today* **Volume 6**, 564-584.

Geochronology and tectonic nature of "Precambrian" basement in eastern Heilongjiang province, NE China: constraints from zircon U-Pb dating

F. WANG[1], F.H.GAO[1*], W.L. XU[1], W.L. HAO[1], H.H. CAO[1]

[1]College of Earth Sciences, Jilin University, Changchun 130061, China (jlu-wangfeng@sohu.com, *gaofuhong213@sina.com)

NE China is located in the eastern section of the Central Asian Orogenic Belt (CAOB) [1]. The region includes the Erguna, Xing'an, Songnen-Zhanguangcai Range, and Jiamusi massifs from west to east. Recently, with application of modern dating techniques, previously beleived Precambrian strata in the Erguna, Xing'an, and Jiamusi massifs have been almost disintegrated into sedimentary and igneous rocks with different Paleozoic ages rather than Precambrian [2-4]. Then, when did the previously determined Precambrian strata including the Dongfengshan (DG), Zhangguangcailing (ZG), and Yimianpo groups (YG) in the Songnen-Zhangguangcai Range Massif form? These Precambrian strata are composed of a set of meta-sedimentary and volcanic rocks. The dating results, together with field geology, indicate that the oldest sedimentary unit from the DG deposited later than 821 Ma, whereas the youngest sedimentary unit deposited during Early Permian (275~271 Ma), that the sedimentary rocks from the YG formed later than Late Triassic (223 Ma), whereas the volcanic rocks from the YG formed in Early Jurassic (179~189 Ma) and Early Permian (271~292 Ma), respectively, and that the oldest sedimentary rocks from the ZG formed during 450~426 Ma, whereas youngest sedimentary rocks formed during 226~211 Ma. The above dating data indicate that the ZG and YG formed from Early Paleozoic to Early Mesozoic, whereas the majority of the DG formed from Early to Late Paleozoic, some of them formed in the Neoproterozoic. Combined with field profile and dating results, we conclude that the ZG could be a tectonic mélange and the melanging could take place during Early-Middle Jurassic.

Furthermore, sediment provenance analysis indicates that nearly all the sediments of these previously beleived Precambrian strata directly sourced from the Phanerozoic intrusions in the Songnen-Zhangguangcai Range and Jiamusi massifs while widespread occurrence of the detrital zircons with ages of 0.8~0.9 Ga and 1.8 Ga as well as 2.4-2.5 Ga implies the existences of the Neoproterozoic magmatisms and remnants of an ancient Precambrian basement within the Songnen-Zhangguangcai Range Massif in eastern Heilongjiang Province, NE China.

This research was financially supported by research grants from the Natural Science Foundation of China (Grant 41072038).

[1] Sengör *et al*. (1993) *Nature* **364**, 299–307. [2] Wilde *et al*. (2003) *Precambrian Research* **122**, 311–327. [3] Miao *et al*. (2007) *Chinese Science Bulletin* **52**, 1112–1134. [4] Wu *et al*. (1993) *Island Arc* **16**, 156–172.

https://doi.org/10.1180/S0026461X00008434 Published online by Cambridge University Press

3D geochemical exploration in Luanchuan district, China

GONGWEN WANG [1*], EMMANUEL JOHN M. CARRANZA[2]

[1]China Universityof Geosciences, Beijing, China, gwwang@cugb.edu.cn (*presenting author)
[2]Faculty of Geo-Information Science and Earth Observation (ITC), University of Twente, Enschede, The Netherlands,carranza@itc.nl

The Luanchuan district in the Henan province of China is known for its large porphyry-skarn type Mo deposits and hydrothermal vein type Pb-Zn-Ag deposits. Jurassic intrusions are associated with Mo-W deposits, whereas the Luanchuan Group is associated with Pb-Zn-Ag deposits. The Pb-Zn-Ag deposits are distributed around the Jurassic porphyry-Mo intrusions and hosted in a metamorphic sedimentary formation consisting of terrigenous clastic rock and carbonatite of either Mesoproterozoic or Neoproterozoic age, which is intruded by Neoproterozoic gabbro and syenite and Jurassic acidic porphyries. The Mo and Pb-Zn-Ag deposits are controlled by Jurassic structural and magmatic activities. Anticline structure is associated with the Mo-W deposits, whereas syncline structure is associated with the Pb-Zn-Ag deposits. However, in fault and fold structrual zones, porphyry intrusions can generate complex and multiple types of mineral deposits. For example, the outcropping Yuku porphyry-type Mo-W deposit led to the discovery at depth of the hydrothermal vein-type Pb-Zn-Ag orebody in the Luanchuan Formation based on borehole data. Thus, analysis and integration of exploration data sets in three-dimension (3D) is desirable

Multiple scales and multiple types of geochemical exploration datasets were used to identify mineral potential targets in 3D. The vertical range of the datasets is less than 2.5 km. District scale (1:50,000) stream sediment multi-element geochemical were analyzed using multifractal modeling, resulting in delineation of Mo-W anomalies zones associated with intrusions and and Pb-Zn-Ag anomalies associated with the Luanchuan Formation, and NW- and NE-trending fault structures. The anomalous zones were further used to identify potential targets by integrating the information with a '2.5D' geological model (e.g., mineralized strata and Jurassic intrusions) based on 1:10,000 scale digital elevation model of the study area. Prospect scale (1:2,000) structural-lithological data and 14-element lithogeochemical data along nine exploration lines (105 km) were analyzed and integrated, resulting in delineation of Mo-W and Pb-Zn-Ag mineralized zones. The lithogeochemical data were analyzed using PCA and multifractal mapping. The delineated mineralized zones were further used in conjunction with a 3D geological model of the study area [1] to identify concealed Mo and Pb-Zn-Ag deposits. Deposit-scale borehole geological and geochemical data were used (a) to delineate probable mineralized zones by multifractal concentration-volume modeling of geochemical data and (b) and to estimate metal resources by fractal modeling based on available orebody thickness and metal grade data. The analyses resulted in identification of eight potential Mo targets and 15 potential Pb–Zn–Ag targets.

[1] Wang et al (2011) *Computers & Geosciences* **37**, 1976-1988.

Types and metallogenic age of molybdenum deposits in Eastern Jilin Province, NE China

H. WANG*, Y. S. REN, AND H. N. HOU

College of Earth Science, Jilin University, Changchun, China, wang_hui2007@ qq.com (* presenting author)

The eastern Jilin Province is an important molybdenum metallogenic centralized region, besides the Daheishan deposit (super large-scale), over ten large or medium-scale molybdenum deposits have been discovered in recent ten years, such as Fuanpu, Jidetun, Dashihe, Liushengdian and Shuangshan molybdenum deposits. The rich molybdenum resources have drawn much attentions. According to the newly research data, molybdenum deposits in this area generally belong to the porphyry type, but the mineralization types can be listed as veinlet-disseminated type and stringer-network vein type.

The Daheishan molybdenum deposit is one of typical veinlet-disseminated porphyry deposits. The molybdenum ore bodies are hosted in a complex massif which is mainly consisted of the granodiorite porphyry and biotite granodiorite, and composed of veinlet-disseminated molybdenites. The zonation of mineralization and wall-rock alteration is obvious. The granodiorite porphyry in the complex massif playing an important role in molybdenum mineralization has a zircon U-Pb age of (170±3) Ma[1], and the Re-Os isochron age of molybdenites is (168±3.2) Ma[2], which suggest that Daheishan molybdenum deposit was formed in early Yanshanian period.

Comparatively, the stringer-network molybdenum mineralization is more common and important than the veinlet-disseminated mineralization in this area. Such newly discovered deposits as Liushengdian, Dashihe and Shuangshan molybdenum deposits belong to this type. The similar characteristics of these deposits are as follows. Firstly, most molybdenum ore bodies are consisted of quartz-molybdenite veins accompanying a spot of single molybdenite veins. Secondly, the wall-rock alteration zonation is ofen weak or even lacking. Thirdly, not all the ore-bearing rock-bodies are metallogenic rock-bodies, for example, the currently discovered ore bodies of Dashihe deposit are all hosted in Neo-proterozoic strata made up of epimetamorphic rocks. The Re-Os weighted mean ages of Liushengdian, Dashihe, and Shuangshan deposits are (169.36±0.97) Ma, (186.7±5) Ma and (173.3±1.1) Ma, indicating that molybdenum mineralization took place in early Yanshanian period.

The molybdenum deposits which occurred in eastern area of Jilin Province are the products of porphyry-fluid metallogenic system and mainly formed in early Yanshanian period (metallogenic ages vary from 190Ma to 165Ma). Metallogenic process was possibly influenced by the subductin of the Pacific plate. There are two mineralization types including veinlet-disseminated type and stringer-network vein type, and most belong to the latter. The stringer-network vein is a significant prospecting indicator in this area.

[1] GE et al. (2007) *Chinese Science Bulletin*. **52**, 2407-2417. [2] WANG et al. (2009) *Rock and Mineral Analysis*. **28**, 269-273.

https://doi.org/10.1180/S0026461X00008434 Published online by Cambridge University Press

Petrogenesis of Paleogene basaltic rocks drilled from Western Taiwan: insight to rifting at the SE Asian continental margin

Kuo-Lung Wang[1]*, Sun-Lin Chung[2], Yi-Ming Lo[2], Ching-Hua Lo[2], Huai-Jen Yang[3], Ryuichi Shinjo[4], Tung-Yi Lee[5]

[1]IES, Academia Sinica, Taipei, Taiwan, kwang@earth.sinica.edu.tw
[2]Dept. of Geosci., Natl. Taiwan Univ., Taipei, Taiwan
[3]Dept. of Earth Sci., Natl. Cheng Kung Univ., Tainan, Taiwan
[4]Dept. of Physics & Earth Sci., Univ. of the Ryukyus, Okinawa, Japan
[5]Dept. of Earth Sciences, Natl. Taiwan Normal Univ., Taipei, Taiwan

Since the Cenozoic time, the SE Asian continental margin was subjected to extension, which is generally believed as a consequence of the India-Asia collision during late Cretaceous [1]. This extension led to submergence of the margin and formation of rift basins with widespread intraplate basaltic volcanism. The Paleogene volcanics occur sporadically in the rift basins, whereas only Neogene basalts are exposed on land in Penghu Islands and NW Taiwan [2, 3]. In this study, volcanic rocks recovered from the CPC deep boreholes in the SW Taiwan, in the Taiwan Strait and in Penghu Islands, and from the outcrop on Huahsu islet are studied for their ages and geochemical characteristics. $^{40}Ar/^{39}Ar$ dating results of these volcanic rocks show two episodes of volcanic activities: ~57-38 Ma (Eocene) and ~11-10 Ma (Miocene). The volcanic rocks are composed dominantly of basalts and basaltic andesites, with few dacites and rhyolites, but no andesite was found. The two episodes of basaltic rocks have distinct chemical characteristics. Some Eocene basalts belong to alkaline series, while all Miocene basalts are sub-alkaline. In comparison to the Miocene basalts, the Eocene basalts are more depleted in basaltic components such as Ca, Fe and Ti but have higher Al content. They are also more enriched in large ion lithophile elements (LILE) and light rare earth elements (LREE) and depleted in high field strength elements (HFSE). The Sr-Nd-Pb isotope compositions show the Miocene basalts are relatively homogeneous and unradiogenic ($\varepsilon Nd = 3.8 \sim 6$) similar to the depleted onland Miocene basalts [3] and the MORB-type South China Sea basalts [4], whereas the Eocene basalts have the wider range ($\varepsilon Nd = 5.6 \sim -3.2$) with more radiogenic feature towards an enriched mantle source. The overall geochemical characteristics suggest these two episodes of basalts originated from distinct mantle sources: a refractory mantle source metasomatized by subduction-related processes to generate the Eocene basalts and a fertile but isotopically depleted mantle source similar to that of MORB for the Miocene basalts. These two mantle sources most likely reside in the lithospheric mantle and asthenospheric mantle, respectively. The change of magma mantle sources with time reflects evolution of the tectonic regime from the initial rifting along the continental margin to upwelling of the asthenosphere due to thinning of lithosphere. Considering the extension regime is dominant in the Paleogene, together with lack of the intermediate andesite indicative of subduction, the subduction origin proposed for the Eocene basalts due to their HFSE depletion appears unfavorable.

[1] Tapponnier et al. (1982) Geol. 10, 611-616. [2] Chung et al. (1994) Chem Geol. 112, 1-20. [3] Chung et al. (1995) GCA 59, 549-555. [4] Tu et al. (1992) Chem. Geol. 97, 47-63.

Kinetics of calcium phosphate nucleation and growth on calcite

LIJUN WANG[1*], ENCARNACION RUIZ-AGUDO[2], CHRISTINE V. PUTNIS[3], MARTINA MENNEKEN[3], AND ANDREW PUTNIS[3]

[1]Huazhong Agricultural University, College of Resources and Environment, Wuhan, China, ljwang@mail.hzau.edu.cn (* presenting author)
[2]University of Granada, Department of Mineralogy and Petrology, Granada, Spain, encaruiz@ugr.es
[3]University of Münster, Institut für Mineralogie, Münster, Germany, putnisc@uni-muenster.de

Introduction

Calcium orthophosphate (Ca-P) is the most ubiquitous form of P among the geological phosphate-bearing minerals [1]. Unraveling the kinetics of Ca-P precipitation and dissolution is important for our understanding of the transformation and mobility of dissolved phosphate species in soils [2]. Here we use *in situ* atomic force microscopy (AFM) coupled with a fluid reaction cell to study the interaction of phosphate-bearing solutions with calcite surfaces.

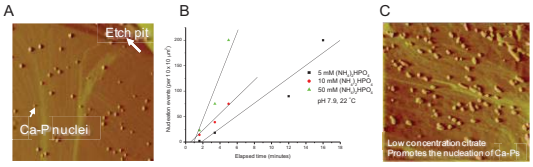

Figure 1: Kinetic analysis of surface nucleation of Ca-P phases on calcite substrates. (A) AFM image of Ca-P particles on a calcite surface during *in situ* nucleation events. Image 10 × 10 μm. (B) Plot against time of different concentrations of $(NH_4)_2HPO_4$. (C) AFM image of Ca-P phases on calcite in the presence of 1 μM citrate with 50 mM $(NH_4)_2HPO_4$ at pH 7.9. Image 10 × 10 μm.

Results and conclusion

We observe that the mineral surface-induced formation of Ca-P phases is initiated with the aggregation of clusters leading to the nucleation and subsequent growth of Ca-P phases on calcite, at various pH values and ionic strengths relevant to soil solution conditions. A significant decrease in the dissolved phosphate concentration occurs due to the promoted nucleation of Ca-P phases on calcite surfaces at elevated phosphate concentrations and more significantly at high salt concentrations. Also, kinetic data analyses show that low concentrations of citrate caused an increase in the nucleation rate of Ca-P phases. However, at higher concentrations of citrate, nucleation acceleration was reversed with much longer induction times to form Ca-P nuclei. These results demonstrate that the nucleation-modifying properties of small organic molecules may be scaled up to analyze Ca-P dissolution - precipitation processes that are mediated by a more complex soil environment. This *in situ* observation, albeit preliminary, may contribute to an improved understanding of the fate of dissolved phosphate species in diverse soil systems.

[1] Filippelli (2008) *Elements* **4**, 89-95. [2] Wang & Nancollas (2008) *Chem. Rev.* **108**, 4628-4669.

https://doi.org/10.1180/S0026461X00008434 Published online by Cambridge University Press

The ca. 90 Ma Mg-rich volcanic rocks from SE Nyima, central Tibet: Products of lithospheric delamination?

QING WANG[1,*], DI-CHENG ZHU[1,*], ZHI-DAN ZHAO[1], LI-QUAN WANG[2], XUAN-XUE MO[1]

[1]State Key Laboratory of Geological Processes and Mineral Resources, China University of Geosciences, Beijing 100083, China, qing726@126.com or dchengzhu@163.com

[2]Chengdu Institute of Geology and Mineral Resources, Chengdu 610082, China, cdwlqgys@sina.com

The Early Cretaceous tectonomagmatic events in the northern Lhasa Terrane have been associated with subduction, slab breakoff of the Bangong–Nujiang Ocean seafloor, and final Lhasa–Qiangtang amalgamation [1]. However, mantle dynamic processes involving crust-mantle interaction in the northern Lhasa Terrane during the Late Cretaceous are poorly known largely due to the limited understanding of the nature of related magmatic records. In this paper we report a dataset of bulk-rock major and trace element, Sr-Nd isotope, zircon U-Pb age, and zircon Hf isotopic data of the Zhuogapu volcanic rocks, ~50 km SE Nyima in the northern Lhasa Terrane. Zircon SHRIMP U-Pb dating reveals that the Zhuogapu volcanic rocks were emplaced at ca. 91 Ma. These rocks consist of andesites and dacites, having MgO of 2.78–5.86 wt.% and 2.30–2.61 wt.% with $Mg^{\#}$ of 54–64 and 55–58, respectively, comparable to high-Mg andesite and high-Mg dacite elsewhere [2]. Eight andesite samples have small negative $\varepsilon_{Nd}(t)$ (–3.2 to –1.7), with $(^{87}Sr/^{86}Sr)i$ of 0.7054–0.7065. Similar Sr-Nd isotopic compositions are also present in the three dacite samples [$\varepsilon_{Nd}(t)$ = –2.7 to –2.2, $(^{87}Sr/^{86}Sr)i$ = 0.7056–0.7060]. Thirteen analyses from a dacite sample give positive zircon $\varepsilon_{Hf}(t)$ (+5.6 to +8.7). Geochemical data indicate that the dacites could not have been produced by fractional crystallization (or plus assimilation) of the andesites. In combination with the other coeval magmatic rocks that show within-plate basalt [3] and adakitic affinities [4] recently reported in the northern Lhasa Terrane, the Zhuogapu Mg-rich volcanic rocks are interpreted as a result of varying extents of mixing between the juvenile lower crust-derived melts and ancient Lhasa basement-derived melts. Considering the development of the Upper Cretaceous molasse that unconformably overlies the underlying strata and the timing of lithospheric stacking or crustal thickening that occurs during the Late Cretaceous [5], we propose that the generation of the coeval 90 Ma magmatism in the northern Lhasa Terrane may be a result of lithospheric delamination. The abundant inherited zircons of ca. 90 Ma with positive zircon $\varepsilon_{Hf}(t)$ from Miocene ultrapotassic rocks in the central Lhasa Terrane (Zhidan Zhao, personal communication, 2011) suggest an extensive magma underplating at the base of the central–northern Lhasa lower crust, corroborating our lithospheric delamination model.

[1] Zhu *et al.* (2011) *EPSL* **301**, 241-255. [2] Gao *et al.* (2004) *Nature* **432**, 892-897. [3] Ma & Yue (2010) *Acta Petrologica et Mineralogica* **29,** 525-538. [4] Yu *et al.* (2011) *Acta Petrologica Sinica* **149**, 2011-2022. [5] Kapp *et al.* (2007) *GSA Bulletin* **119**, 917-932.

Breakdown of the Ostwald step rule: The precipitation of calcite and dolomite from seawater at 25° and 40°C

TINGTING WANG[1*], AND ALFONSO MUCCI[2]

[1]Department of Earth and Planetary Sciences, McGill University tingting.wang@mail.mcgill.ca (* presenting author)
[2]Department of Earth and Planetary Sciences, McGill University alfonso.mucci@mcgill.ca

The scarcity of modern dolomite contrasts strongly with its common abundance in Precambrian sedimentary rocks of marine origin, leading to the paradox commonly referred to as the "dolomite problem". Whereas dolomite can readily be precipitated from aqueous solutions above 100°C [1], many researchers have attempted unsuccessfully to synthesize dolomite at room temperature from natural seawater [2,3,4]. Nevertheless, by alternating between intervals of dissolution and precipitation in artificial brines, Deelman (1999) succeeded in synthesizing dolomite at low temperatures (between 313K and 333K) [5]. He concluded that multiple cycling of a solution between supersaturation and undersaturation with respect to calcite and/or aragonite would cause the metastable phases to dissolve, while preserving more stable nuclei (i.e. dolomite and/or low-magnesian calcite) in solution. In this study, natural seawater was equilibrated with $CaCO_3$ (mixture of calcite and aragonite) at a pCO_2 of 10%. After the solution reached equilibrium, the solid was removed by filtration and ambient air (pCO_2 ~390 ppm) was bubbled through the CO_2-charged seawater solution, leading to a highly supersaturated solution and the nucleation and precipitation of aragonite. Following the precipitation, the ambient air-equilibrated solution and the precipitate were purged with a 10% CO_2:N_2 gas mixture and most of the original precipitate was redissolved. Once equilibrium was reached with the gas phase, the solution should be undersaturated with respect to aragonite, in equilibrium with calcite, but remain supersaturated with respect to dolomite. The cycle was repeated 18 times and ultrapure N_2, instead of ambient air, was used in the last cycle, to maximize precipitate recovery. As the solution remains supersaturated with dolomite at all times, after each cycle, dolomite nuclei should be preserved and accumulate at the expense of aragonite and calcite. The experiments described above were carried out at 25° and 40°C. Preliminary results show that, whereas aragonite was obtained during the first few cycles, only calcite was detected in the last cycle of the experiments carried out at 25°C.

[1] Arvidson R.S. and Mackenzie F.T. (1999) *Am. J. Sci*., **299,** 257-288.
[2] Land L.S. (1985) *Journal of Geological Education*, **33**, 112-125.
[3] Land L.S. (1998) *Aquatic Geochemistry* **4**, 361-368.
[4] McKenzie, J.A.(1991) Controversies in modern geology: New York, Academic Press, 490.
[5] Deelman J.C. (1999) *NJb.Miner.Mh*., **7**, 289-302.

https://doi.org/10.1180/S0026461X00008434 Published online by Cambridge University Press

Natural gas accumulation characteristic of the reef-oolitic reservoir in LG area, Sichuan basin

WANG TONGSHAN[1*], LI XIA[1], AND LI QIUFEN[1]

[1] Research Institute of Petroleum Exploration & Development, PetroChina
wts2007@petrochina.com.cn (*presenting author)

Reef and oolitic gas reservoirs previously discovered in Changxing Fm.–Feixianguan Fm. of Sichuan Basin mainly are distributed in the platform margin zone near Kaijiang-Liangping Bay. This zone has high prospectivity for gas exploration at present [1]. Longgang area is located in the main body of platform margin zones on the southwestern sides of the bay. Longgang area is located in the gentle structural belt lying west of the Huayingshan fault zone.

Reef and oolitic reservoirs are controlled by the high energy facies belts on the south sides of Kaijiang-Liangping Bay, with only slight changes in width and spatial location corresponding to variations in paleoenvironment and paleotopography at different geological periods. The lithologies and spatial types of the reef and oolitic reservoirs are similar, as are their other properties such as porosity and permeability. The oolitic reservoirs of the Feixianguan Fm. in the Longgang area have a porosity of 2%–12% (5.8% on average) and a permeability of 0.06mD–223.7mD (27.7 mD on average). The gypsum rock units in the Lower Triassic Jialingjiang Fm. and Middle Triassic Leikoupo Fm. are thick (117m–557m), widely distributed, and act as the effective caprock for reef and oolitic gas accumulations. The type and salinity of formation water also support the strong preservation conditions of the reef and oolitic series of strata. The homogenization temperatures of fluid inclusions in the reef and oolitic reservoirs generally include three phases. The homogenization temperature for phase I was low (<120°C), indicating liquid hydrocarbon inclusions and early charging of liquid hydrocarbons. The homogenization temperature for phase II was 130°C–150°C, reflecting gas-liquid two-phase hydrocarbon inclusions as well as mixed charging of liquid hydrocarbons and their associated gas with gaseous hydrocarbons sourced from coal measures. The homogenization temperature for phase III was higher than 160°C, indicating brine-bearing gas hydrocarbon inclusions. In addition, the Laser Raman detection result shows H_2S-bearing high temperature gas hydrocarbon inclusions (dominated by methane) as well as liquid hydrocarbon pyrolysis and gas generation and accumulation events (Fig 1). Tectonic activities in the Himalayan period caused gas reservoirs to be destroyed or reformed. Gas reservoirs were subsequently shaped after the Himalayan period.

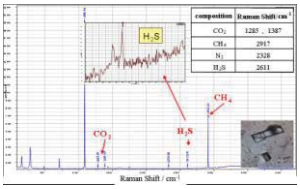

Figure1: Raman spectra of reef and oolitic reservoir fluid inclusions

This study has great significance in the promotion of research into gas accumulation and the development of gas fields in the region.

[1] Ma Y S *et al.* (2007) *AAPG 91*, 627-643.

Mapping geo-anomalies of hydrothermal mineralization in southeastern Yunnan district, China

WENLEI WANG[1*], JIE ZHAO[1], QIUMING CHENG[1,2,3] AND JIANGTAO LIU[1,3]

[1]Department of Earth and Space Science and Engineering, York University, Toronto, Canada, bznb@yorku.ca (*presenting author)
[2]Department of Geography, York University, Toronto, Canada
[3]State Key Laboratory of Geological Processes and Mineral Resource, China University of Geosciences, Wuhan and Beijing, China

Based on existing literature [1], controlling factors of hydrothermal mineralization in southeastern Yunnan district are granite intrusions, sedimentary carbonate rocks and complex structural features. Geo-anomalies associated with the superposition of these factors benefit mining activities in this area. Current research conducts an anomaly analysis by local singularity theory to characterize the influence of faults on the spatial distribution of geochemical signatures for enhancing mineral prospectivity.

Singularity theory is efficient to identify things' changing behaviors produced by geological processes, and the things can be materials, physical or chemical properties, events, and others with multifractality [2]. Discontinuously distributed geochemical signatures by tectonics are commonly used to delineate potential areas for targets of interesting. Applying singularity theory, geochemical anomalies of selected ore forming and associated elements are investigated and sorted into positive and negative, representing element accumulation and depletion properties, respectively. The positive anomalies well indicate weak local anomalies which are hidden within strong variance of background and were not properly identified by means classic methods. Moreover, selected element assemblages are integrated by Principal Component Analysis (PCA) to illustrate that the distribution of ore forming materials has undergone various geological processes. In the context of complex geologic structures, like highly faulted area, ore forming materials will have more space and time for migration and interaction with surroundings. Fault intensity defined as total length of faults per unit area is one of representatives of geologic structure complexity. By singularity theory, areas with increased intensity are identified to highlight spatial distribution properties of multi-element signatures.

For modeling mineral prospectivity, PCA is used further to integrate anomalies of element assemblages and fault intensity, patterns of which indicate both distribution of elements and migration tracks. The cross referencing of anomalies from geochemical and fault intensity efficiently characterizes the migration and sedimentation processes of ore-bearing hydrothermal solutions, and further supports researches on ore control mechanism.

[1] Zhuang et al. (1996) *Geology of Gejiu Tin-Copper Polymetallic Deposits*, 188p. [2] Cheng (2007) *Ore Geology Reviews* **32**, 314-324.

https://doi.org/10.1180/S0026461X00008434 Published online by Cambridge University Press

On the timing and mechanisms of Heinrich Stadials: a speleothem study from Southern Brazil

XIANFENG WANG[1,2,3*], ZHIGUO RAO[4], YANJUN CAI[5], XINGGONG KONG[6], AULER S. AULER[7], HAI CHENG[3,8], AND R. LAWRENCE EDWARDS[3]

[1]Earth Observatory of Singapore, Nanyang Technological University, Singapore, xianfeng.wang@ntu.edu.sg*
[2]Lamont-Doherty Earth Observatory of Columbia University, Palisades, USA
[3]Department of Earth Sciences, University of Minnesota, Minneapolis, USA, edwar01@umn.edu
[4]College of Earth & Environment Sciences, Lanzhou University, Lanzhou, China, zgrao@lzu.edu.cn
[5]Institute of Earth Environment, CAS, Xi'an, China, yanjun_cai@ieecas.cn
[6]College of Geographical Sciences, Nanjing Normal University, Nanjing, China, kongxinggong@njnu.edu.cn
[7]Instituto do Carste, Belo Horizonte, Brazil, aauler@gmail.com
[8]Institute of Global Environmental Change, Xi'an Jiaotong University, Xi'an, China, cheng021@umn.edu

Recent paleoclimate data and modelling results revitalized the debate on the cause of the extreme cold events in the North Atlantic during the last glacial period, the so-called Heinrich Stadials (HS), and their durations. We established a new speleothem $\delta^{18}O$ record from Botuvera Cave, southern Brazil, with significantly improved data resolution and U/Th chronology. The $\delta^{18}O$ profiles from multiple stalagmites show that the HS0 (YD), HS2, HS3 and HS4 are about 1,000 years long, centred approximately 12.0, 24.6, 30.0 and 39.0 kyr BP, respectively, whereas HS1 is about 3,000 years long, lasting from 17.5 to 14.5 kyr BP. Following the earlier studies, we interpret the calcite $\delta^{18}O$ as a proxy of South American Summer Monsoon (SASM) intensity in the region. The abrupt drops on calcite $\delta^{18}O$ during the HS intervals, with an amplitude of ~ 2‰ VPDB, suggest that climate change in this region is manifested as a dramatic increasing of rainfall. The one-to-one correlation with the updated Hulu Cave record confirms our previous finding that on millennial timescales, precipitation change in southern Brazil is anti-phased with that in the north, which is probably controlled by the meridional migration of the intertropical convergence zone (ITCZ). Thanks to micromill sampling techniques and high sample growth rates, we are able to characterize detail precipitation changes in southern Brazil during HS. For example, we did not observe SASM reversals in any HS except HS1 within which a minor $\delta^{18}O$ jump of ~ 0.5‰ can be identified at 15.3 kyr BP. Typically, precipitation increases abruptly in the earlier stage of HS, whereas during the later stage, precipitation decreases more gradually. This asymmetric pattern of change is different from the temperature behavior in the North Atlantic, which warms much more dramatically in the final stage of a HS than it cools in the initial phase. Such decoupling may suggest that ITCZ meridional migration is preferably controlled by the temperature gradient between the high and low latitudes in the cold hemisphere.

Isotope exchange rates and equilibrium fractionation between Cr(III) and Cr(VI)

XIANGLI WANG*, THOMAS M. JOHNSON

University of Illinois at Urbana-Champaign, Geology
wang298@illinois.edu (* presenting author)
tmjohnsn@illinois.edu

Kinetic fractionation of Cr stable isotopes resulting from reduction of mobile and toxic Cr(VI) to immobile and relatively non-toxic Cr(III) has been applied to monitoring and quantifying the extent of reduction in Cr-contaminated groundwater [1]. However, equilibrium fractionation resulting from isotope exchange between Cr(III) and Cr(VI) [2], if fast enough, can potentially overprint kinetic isotope fractionations. In this study we measured the exchange rates between solid Cr(III) and dissolved Cr(VI) at 25°C using a ^{50}Cr-enriched tracer method. We also measured the equilibrium fractionations between 0.2 M dissolved Cr(III) and 0.2 M dissolved Cr(VI) under acidic conditions at 25°C, 40°C, and 60°C.

At 60°C, the dissolved 0.2M Cr(VI) and Cr(III) reach isotopic equilibrium after ca. 39 days with $\Delta^{53}Cr_{VI\text{-}III} = 4.9 \pm 0.1$ ‰. At 40°C, the system reaches equilibrium at ca. 319 days with $\Delta^{53}Cr_{VI\text{-}III} = 5.2 \pm 0.1$ ‰. At 25 °C, the system evolved only ca. 20% toward equilibrium after 684 days of exchange.

The isotope exchange rates between solid Cr(III) (10 ppm to 100 ppm) and dissolved Cr(VI) (200 μM to 1400 μM) were measured over a range of conditions (pH 6.5 to pH8) and fit to an isotopic exchange model[3] to obtain the rate law: $R = 5.91 \times 10^{-3} \cdot [Cr(VI)]^{0.48} \cdot [Cr(III)]^{0.64} \cdot [H^+]^{0.39}$, where R gives the isotope exchange rate in mol/L/day. Using this rate law, we estimate that in an aquifer containing 20 μM Cr(VI) and 10 ppm solid Cr(III) with a pH of 7.5, it would take ca. 20 years to evolve halfway toward equilibrium.

Goethite, which we hypothesized might increase the exchange rate as a semi-conductor, actually slowed exchange somewhat, probably due to adsorption of Cr(VI). Anthraquinone-2, 6-disulfonate (AQDS), as an analog of electron shuttle molecules in natural organic matter, accelerated the exchange rate by a factor of 10.

Based on our results, we conclude: 1) higher temperatures, higher concentrations, lower pH, absence of adsorbing agents, and presence of electron shuttles contributed to faster isotope exchange rates between solid Cr(III) and dissolved Cr(VI); 2) For Cr-contaminated aquifers without organic electron shuttles and/or little exposed Cr(III), equilibrium fractionation will not overprint the kinetic-fractionation-based isotope method to monitoring remediation of Cr contamination; 3) For Cr-contaminated aquifers with abundant exposed Cr(III) and dissolved organic electron shuttles present, $^{53}Cr/^{52}Cr$ ratios of dissolved Cr(VI) may be affected by isotopic exchange over several years time or longer. This would tend to shift the ratios toward equilibrium values and away from values generated by kinetic isotope fractionation occurring during Cr(VI) reduction.

[1] Ellis *et al.* (2002) *Science* **295**, 2060-2062.
[2] Schauble *et al.* (2004) *Chem. Geol.* **205**, 99-114.
[3] Cole *et al.* (2001) *Rev. Mineral. Geochem.* **43**, 83-223.

https://doi.org/10.1180/S0026461X00008434 Published online by Cambridge University Press

Understanding the contrasting geochemical features of the crust in the Jiangnan orogen

XIAO-LEI WANG [1*], GUO-CHUN ZHAO [2], JIN-CHENG., ZHOU [1], JIN-HAI. YU [1]

[1] State Key Laboratory for Mineral Deposits Research, Department of Earth Sciences, Nanjing University, Nanjing 210093, PR China, wxl@nju.edu.cn (* presenting author)

[2] Department of Earth Sciences, The University of Hong Kong, Pokfulam Road, Hong Kong, gzhao@hkucc.hku.hk

The primary uniform South China Block (SCB) was formed due to the Neoproterozoic amalgamation between the Yangtze Block to the northwest and the Cathaysia Block to the southeast, as recorded by the Jiangnan orogen (JO) in the interior of the SCB [1]. A significant crustal heterogeneity is confirmed here by the zircon Hf and whole-rock Nd isotopes for the rocks from the western and eastern segments of the JO. The Neoproterozoic granitoids of the eastern segment have positive zircon $\varepsilon_{Hf}(t)$ and neutral whole-rock $\varepsilon_{Nd}(t)$, obviously contrasting to the rocks from the western segment that show moderate negative epsilon values. This is also consistent with the whole-rock $\varepsilon_{Nd}(t)$ results for the low-greenschist-facies metamorphosed basement sequences in the JO. U–Pb dating results for detrital zircons constrain the duration of these sequences at ca. 0.86–0.82 Ga, obviously later than the timing of arc-continent collision in the area. Hf isotopes of the detrital zircons imply consistent crustal growths at 1.00–0.85 Ga and 2.60–2.45 Ga for both segments. However, another crustal growth at 1.75–1.50 Ga is significant for detrital zircons from the western segment. This growth period is absent in the Yangtze Block, but appears in the southern part of the Cathaysia Block. These U-Pb dating and Hf isotopic results suggest that the arc-continent collisional belt may have been the dominant source for the sequences in both segments but there exists an additional source from the Cathaysia Block and its adjacent continents (India and Antarctic?) for the western segment of the JO. Moreover, the 1.9–1.7 Ga and 2.6–2.4 Ga age peaks of the JO are consistent with those of the Cathaysia Block, while the age peaks of 3.0–2.7 Ga and 2.1–1.9 Ga that are characterized for the Yangtze Block are unmatched in the JO. Therefore, the basement sequences in the JO have close affinities with the crust of (1) the arc-continent collisional belt and (2) the Cathaysia Block and its adjacent continents during early to middle Neoproterozoic. More incorporation of old recycled crusts from the Cathaysia Block led to the more unradiogenic isotopic features of the basement sequences in the western JO.

[1] Wang et al. (2007) *Precambrian Res.* **159**, 117-131.

Changes in fire regimes on Chinese Loess Plateau since the last glacial maximum and implications for linkages to paleoclimate and past human activity

XU WANG[1*], ZHONGLI DING[1], AND PING'AN PENG[2]

[1]Key Laboratory of Cenozoic Geology and Environment, Institute of Geology and Geophysics, Chinese Academy of Sciences, Beijing 100029, China, xuking@mail.iggcas.ac.cn (* presenting author)

[2]Guangzhou Institute of Geochemistry, Chinese Academy of Sciences, Guangzhou 510640, China

A high-resolution black carbon (BC) record from 27.5 kyr BP to present was reconstructed using a chemical oxidation method on loess and paleosol samples from the Lijiayuan section of the Chinese Loess Plateau. The black carbon mass sedimentation rates (BCMSR) and carbon isotopic record reveal a paleofire history and its relationship with climate and vegetation changes at the study site. The BCMSR record was decomposed into two components: background BCMSR and the BCMSR peaks. The background BCMSR represents regional fires and shows high fire activities occurred contemporaneous with the Younger Dryas, Older Dryas, Heinrich events and Greenland stadials as registered in the loess grain size record. This suggests a rapid response of regional fires on the Loess Plateau to abrupt climate changes. Spectral analysis of background BCMSR showed two meaningful periodicities of 1620 and 1040 years, close to the cyclicity of the East Asian monsoon as recorded in the stalagmite $\delta^{18}O$ record in Central China. This indicates a tight control of millennial scale wet–dry changes in the monsoonal climate on regional fires on the Loess Plateau. By contrast, the BCMSR peaks are considered to reflect local fire episodes. The occurrences of local fires were more frequent during the last glacial period, with a maximum frequency of ~6 episodes/1000 years during the Last Glacial Maximum (LGM) (22.3 to 14.6 kyr BP), when the climate was drier and more continuous grassy fuels existed on the landscape. During the last glacial–interglacial transition (LGIT) period (14.6 to 11.0 kyr BP), fire frequency was largely reduced due to an increase in precipitation and more woody vegetation. If the LGIT period is taken as an analog for the projected near future, then future global warming alone may not produce large wildfires in northwestern China. Wildfires remained infrequent during the early-to-middle Holocene. Biomass burning increased after 4.0 kyr BP, when the climate became drier and land-use was more intensive. BC carbon isotope ratios may well reflect changes in the vegetation being burnt (i.e., grasses versus trees), yielding results consistent with the associated pollen data in the region.

This work is finnacially suported by National Basic Research Program of China (973 Program) (No: 2010CB950204) and National Science Foundation of China (grant 40502019).

https://doi.org/10.1180/S0026461X00008434 Published online by Cambridge University Press

Role of iron oxides and organic matter in the accumulation of uranium in a peatbog

Y. WANG[1]*, M. FRUTSCHI[1], V. PHROMMAVANH[2], M. DESCOSTES[2] AND R. BERNIER-LATMANI[1]

[1]Ecole Polytechnique Fédérale de Lausanne (EPFL), Environmental Microbiology Laboratory (EML), Station 6, CH-1015 Lausanne, Switzerland (* presenting author: yuheng.wang@epfl.ch)

[2]AREVA - Business Group Mines, Direction R&D, BAL 3720C, Tour AREVA, 1, place Jean Millier, 92084 Paris La Défense Cedex, France

A peatbog located in central France and impacted by both historical uranium mining activities and continued uranium leaching from granite rocks harbors U-enriched zones reaching a concentration of 4,000 mg/kg [1]. The mechanism leading to this remarkable accumulation is unknown. In order to unravel it and to evaluate the impact of proposed remediation strategies, extensive depth-resolved sampling of soil and porewater was carried out at three different areas as well as at a U-free background location in July and November 2011. Extensive physicochemical and microbial characterization of the four locations was conducted.

The porewater results show decreasing dissolved oxygen (DO) and increasing Fe(II) concentrations at 15-35 cm, suggesting that a redox transition zone (RTZ) occurs at that depth. The Fe(II) and total Fe profiles overlap exactly, suggesting that there is no measurable Fe(III) in the porewater. Secondly, a strong correlation was found between the U and Fe and U and total organic carbon (TOC) profiles, suggesting that U mobility may be controlled by adsorption to Fe oxides above the RTZ and by organic matter complexation in the porewater below that zone. Chemical extraction of U from soil revealed that U is concentrated at shallow depths (above 45 cm). Moreover, soil U occurs as a mixture of U(IV) and U(VI) and the profile of the ratio of U(VI)/U_{total} displays no clear trend as a function of depth. The persistence of U(VI) in a reduced environment may be attributable to its stabilization by complexation with organic matter. Finally, a clay layer, composed mainly of muscovite and quartz and rich in U, occurs at a depth of 10-25 cm in the peat soil. This unusual occurrence may have resulted from an anthropogenic input into the peat bog. The results to date suggest the involvement of iron oxides in immobilizing U in the oxic zone and the role of organic matter in binding U below the RTZ. Further mineralogical and microbial characterizations are underway to probe that current intrepretation of the data.

[1] Moulin (2008). PhD thesis, Ecole Centrale de Paris.

Abundances of sulfur, selenium and tellurium in mantle peridotites: constraints on planetary fractionation and late accretion

ZAICONG WANG* AND HARRY BECKER

Institut für Geologische Wissenschaften, Freie Universität Berlin, Germany, zaicongwang@gmail.com (* presenting author)

The addition of a chondritic late veneer after core formation has been a popular explanation for the high abundances and mostly chondritic ratios of highly siderophile elements (HSE) in the silicate Earth. The HSE are mostly hosted by sulfides, which also control the mantle's budget of S, Se and Te [1]. S, Se and Te are moderately to highly siderophile at high P-T conditions [2], but they also are moderately volatile elements with very similar 50% condensation temperatures [3]. Thus, the detailed fractionation of these elements in the mantle, also in relation to HSE abundances, may provide insight into both the volatile element composition of a late veneer and the influence of metal-silicate partitioning on their mantle abundances. Until recently, the mantle abundances of Se and Te have not been well constrained and the influence of secondary alteration, partial melting and refertilization on S, Se and Te abundances are incompletely understood [1,4]. To address this problem, we have obtained new precise S, Se and Te data on post-Achean peridotites. Fresh samples of variable fertility were digested in a high pressure asher and S, Se and Te concentration data were obtained on the same digestion aliquot by isotope dilution ICPMS. Sulfur, Se and Te concentrations display excellent linear correlations, and decrease with decreasing Al_2O_3 contents. In spite of large concentration variations, Se/Te remains relatively constant (6.8 ± 3.1, 2sd, n=39, total range from 3.8 to 10.0) with variable fertility. S/Se in lherzolites also displays no systematic variation (2710±1580, n=27, most within 2000-4000), whereas harburgites tend to have higher values. Similar results (S/Se=3120 ± 500, Se/Te=8.6±2) have been obtained on lherzolites from Lherz (Pyrenees), which are believed to reflect melt refertilization [4]. The absence of substantial systematic variations of S/Se and Se/Te with fertility suggests that during moderate degrees of partial melting or refertilization no systematic fractionations occur between S, Se and Te. This appears to be at odds with Se and Te data on MORB [5], but the latter may have been influenced by crustal fractionation processes. We conclude that Se/Te in mantle peridotites is constant, but 20-30% lower than CI chondrite (Se/Te ≈ 9), whereas S/Se might be about 10-20% higher than in CI chondrites. If the experimental partition coefficients are valid [2], the Se and Te budget of the mantle should reflect the contribution from a late veneer, whereas the suprachondritic S/Se, possibly hints at significant residual S in the mantle after core formation. CI chondrite normalized Te/Ir_N, Se/Ir_N and S/Ir_N of the mantle are 0.5 to 0.6 and constrain the predominant composition of the late veneer. These values are consistent with slightly volatile depleted CM2 or transitional C1/C2 chondrites.

[1] Morgan (1986) *JGR* **91**:12375-12387. [2] Rose-Weston *et al.* (2009) *GCA* **73**, 4598-4615. [3] Lodders (2003) *Astrophysical Journal* **591**, 1220-1247. [4] Lorand & Alard (2010) *CG* **278**, 20-130. [5] Hertogen *et al.* (1980) *GCA* **44**, 2125-2143.

https://doi.org/10.1180/S0026461X00008434 Published online by Cambridge University Press

Study on the influence factors of oil cracking

ZHAOYUN WANG[1]*, YONGXIN LI[1], SHIZHEN TAO[1], TIANSHU ZHANG[1] AND WENZHI ZHAO[2]

[1] Research Institute of Petroleum Exploration and Development, Petrochina, Beijing, China, wzy@petrochina.com.cn (*presenting author), lyxin@petrochina.com.cn, tsz@petrochina.com.cn, zhangtianshu@ petrochina.com.cn

[2] PetroChina Exploration & Production Company, Beijing, China, zwz@petrochina.com.cn

Oil cracking gas is an important source of deep gas. The oils generated from kerogen have three kinds of existing states: dispersive liquid hydrocarbon inside of source rocks, dispersive liquid hydrocarbon outside of source rocks and concentrated liquid hydrocarbon outside of source rocks, which is paleo-oil pool.

A comparetive study on the gas generating from oil cracking and from kerogen shows that large quantities of gas are generated from oil when temperature reaches 160℃, that is the major period of gas generation from oil cracking occurs later than that from kerogen degradation, giving rise to the relay contribution of natural gas generation at different evolution stages. The above knowledge enlarges exploring field of deep gas.

The average activity energy of oil cracking methane is relevant to oil physical properties through kinetic experiments. That of light oil and heavy oil is 62.34 Kcal/mol and 68.86 Kcal/mol, respectively. Both the oil samples were selected from Lunnan area, Tarim basin in China.

In view of the overall situation, high pressure constrains the decomposition of oil to gas, but this repression is not noticeable in fast buried condition and it also has different effect at different evolution stages.

Through kinetic experiments on mixtures of oil with various minerals, using mixture with mudstone represents dispersive liquid hydrocarbon inside of source rocks while with calcareous rock and sandstone represent dispersive liquid hydrocarbon outside of source rocks, we infer that the carbonatite has the greatest influence on oil cracking and can largely reduce the activation energy of oil cracking gas, which leads to the decrease of pyrolysis temperature. The mudstone ranks the second and the sandstone the smallest. The corresponding Ro value of main gas generating period in different medium are as follows: 1.5%～3.8% with pure crude oil, 1.2%～3.2% with dispersive oil in carbonatite, 1.3%～3.4% with dispersive oil in mudstone and 1.4%～3.6% with dispersive oil in sandstone.

[1] Behar et al (1988) *Preprint of the 4th UNITAR/UNDP Conference on Heavy Crude and Tar Sand* **5**, 1-14. [2] Mango (1990c) *Nature* **352**, 146-148. [3] Mango (1997) *Geochim Cosmochim Acta* **61**, 5347-5350. [4] Vandenbroucke (1999) *Organic Geochemistry* **30**, 1105-1125. [5] Stephane (2003) *Journal of Geochemical Exploration* **26**, 421-425.

Mg isotope fractionation between aragonite and fluid

ZHENGRONG WANG[1*] SHUANG ZHANG[1] CASEY SAENGER[1] AND PING HU[1]

[1]Department of Geology and Geophysics, Yale University, New Haven, USA, zhengrong.wang@yale.edu

The detectable Mg-isotope variations in biogenic aragonite (including corals, aragonitic forams and sponges) can potentially be applied as a paleoproxy. In this study, we report the result of a set of inorganic precipitation experiments to evaluate factors that could control Mg isotope fractionation between aragonites and fluid.

These 'free drift' experiments were conducted at 23.5-55 ^{o}C in freshwater by passive degassing for 1-4 weeks, with initial Ca concentration ([Ca]) spanning 400-2000 ppm and Mg/Ca molar ratio of 5.0. The solution chemistry (including pH and alkalinity) was closely-monitored over the course of the experiments. Observations using SEM after experiments demonstrate the occurrence of aragonite as major mineral phases. Magnesium from final solution and aragonite precipitates was purified by two chromatographic columns to remove Na, Ca, Sr and Ba, and pure Mg solution (in 5% HNO_3) was analysed for $^{26}Mg/^{24}Mg$ ratio by MC-ICP-MS (Neptune) at Yale University.

Our results show the initiation of aragonite precipitation occurred at different time for experiments having various [Ca], i.e., in an experiment initially having higher [Ca] aragonite started to precipitate earlier (e.g., a couple of hours for [Ca] = 2000ppm vs. a couple of days for [Ca] = 400 ppm), with a drop in pH and alkalinity at lower pH (e.g., pH = ~ 6.5 for [Ca]=2000ppm vs. pH = ~ 8.2 for [Ca] = 400 ppm). The Mg isotope fractionation between aragonite and final solution decreases noticeably with increasing temperatures, having a temperature sensitivity of ~0.01-0.0133‰/^{o}C. This fractionation also depends on [Ca], i.e., Mg isotope fractionations in aragonites precipitated from solutions with higher [Ca] are smaller, and have smaller temperature sensitivity. These results can be understood by a kinetic model that can explain both Mg and O isotope fractionation in aragonites, and are consistent with our previous observations and models on the kinetic process of aragonite precipitation from seawater during CO_2 degassing. This temperature-dependent Mg isotope fractionation has the potential to be used as a paleo-thermometer to extract SSTs from coral skeletons, and provide constraints on biomineralization process.

https://doi.org/10.1180/S0026461X00008434 Published online by Cambridge University Press

Petrogenesis of the Guposhan granitic complex, south China

ZHIQIANG WANG[1*], BIN CHEN[1,2], AND XINGHUA MA[1]

[1]Key Laboratory of Orogenic Belts and Crustal Evolution, Peking University, Beijing 100871, China, wangzq@pku.edu.cn (*presenting author)

[2]Institute of Geology and Exploration Engineering, Xinjiang University, Urumqi 830046, China, binchen@pku.edu.cn

Most Mesozoic granitic complex from south China consists of predominant intrusions and late-stage, supplementary intrusions (volumetrically much smaller than the former). Traditionally, supplementary intrusions were considered to be residual melts through fractionation of the predominant intrusions. We choose to study a typical granite complex, the Guposhan pluton, and propose a different model for its origin. The predominant intrusions of the Guposhan complex are the Wanggao biotite monzogranite/ syenogranite, the Lisong hornblende biotite monzogranite and the Xinlu biotite monzogranite. They are intruded by the late-stage, supplementary Baishuidai syenogranite. One sample from the supplementary granite is chosen for zircon La-ICP-MS U-Pb dating, and yields a concordant age of 155.3±1.5Ma, which is significantly younger than the predominant granites (162 Ma) of the Guposhan complex. In the plots of SiO_2 versus other major oxides and trace elements, the data points of the predominant and supplementary granites show different evolutionary trends, and compositional gaps are visible between the two phases, especially in the plots of Fe_2O_3 、P_2O_5、TiO_2、Sr、Ba versus SiO_2. Trace element modeling using Rb-Ba and Sr-Ba co-variations suggests that the supplementary phase is unlikely to be the derivative from the predominant granites via fractionation. So we conclude that the supplementary granite formed through a new partial melting event related to an extensional regime. The supplementary granite is a typical A-type granite, having high SiO_2, alkaline, HFSE contents as well as high Ga/Al and Fe/Mg ratios, and is extremely depleted in Ba, Sr, P, and Ti. The predominant phases of the Guposhan complex probably have formed through a process of magma mixing between dominantly crustal melts and minor mantle-derived magmas, as is suggested by the presence of micro mafic enclaves, and by the significantly varied Nd isotopic compositions, with εNd(t)=-6.0 to -3.7 (predominant intrusions) and -5.6 to -3.4 (supplementary intrusions). The trace elements and Nd isotopic data suggest that the basement rocks (major source rocks for the Guposhan complex) should be dominated by paleoproterozoic orthometamorphic rocks. We suggest that the flat subduction of the Pacific slab and subsequent break-off and rollback have triggered the extension of the lithosphere in the mid- to late Jurassic. Asthenospheric upwelling and basaltic underplating played an important role in causing the partial melting of the basement rocks in South China.

Oxidative Dissolution of Uraninite in the Presence of Manganese Oxide

ZIMENG WANG[1*], SUNG-WOO LEE[2], BRADLEY M. TEBO[2], AND DANIEL E. GIAMMAR[1]

[1]Department of Energy, Environmental and Chemical Engineering, Washington University, St. Louis, MO, USA zimengwang@wustl.edu (*presenting author), giammar@wustl.edu

[2]Division of Environmental and Biomolecular Systems, Oregon Health & Science University, Beaverton, OR, USA lees@ebs.ogi.edu, tebo@ebs.ogi.edu

Manganese is present at appreciable concentrations at several U-contaminated sites, and coupling of the biogeochemical cycles of U and Mn may affect the fate and transport of uranium. The long-term stability of U(IV) species produced in the subsurface during *in situ* bioremediation can potenitally be limited by reoxidation to more mobile U(VI) species. Manganese oxide (MnO_2), which can be produced biologically even at low dissolved oxygen concentration, can act as a powerful oxidant that accelerates the oxidative dissolution of UO_2. Laboratory studies have been performed to investigate the physical and chemical factors controlling the interaction between UO_2 and MnO_2.

Because both MnO_2 and UO_2 are insoluble at environmentally relevant conditions, the degree to which physical contact was necessary for UO_2 oxidation was unknown. A well-mixed multi-chamber reactor with a permeable membrane was used to eliminate direct contact of the two minerals while still allowing transport of aqueous species. The oxidation of UO_2 was not significantly enhanced if MnO_2 was physically separated. Complete mixing of MnO_2 with UO_2 lead to a much greater extent and rate of U oxidation. It suggests that effective redox reactions between UO_2 and MnO_2 may require physical contact or close proximity. We hypothesize that dispersion and colloid migration of U(IV) species, and the spatial dynamics of biological Mn oxidation are critical factors in assessing the impact of coupled U-Mn biogeochemical processes on U stability in the subsurface.

Continuous stirred-tank reactors (CSTR) were used to quantitatively examine the rates of MnO_2-mediated UO_2 dissolution and the effects of chemical factors (mixing ratio and carbonate concentration). MnO_2 dramatically promoted the UO_2 dissolution at steady states, but the degree of promotion leveled off when the MnO_2:UO_2 ratio exceeded a certain value. UO_2 oxidation by MnO_2 was faster at higher carbonate concentrations. Substantial amounts of U(VI) were retained on MnO_2 surfaces through adsorption. The amounts of U(VI) adsorbed on MnO_2 were inversely related to UO_2 dissolution rates, suggesting that the U(VI) product could passivate MnO_2 surfaces. The release of Mn into the effluent was less than that of U, indicating that the fate of Mn and the changes of its oxidation states were more complex than previously anticipated. Based on the fundamental understandings of grain-to-grain contact, electron transfer, and surface speciation, a conceptual model was proposed to predict the oxidation rate of UO_2 by MnO_2. The model is applicable to broader water chemistry conditions and may be relevant to other redox processes involving two poorly soluble minerals.

https://doi.org/10.1180/S0026461X00008434 Published online by Cambridge University Press

Compositional evolution of melts during ascent through the ocean crust based on olivine-hosted melt inclusions

WANLESS, V.D.[1*], SHAW, A.M.[1], AND BEHN, M.D.[1]

[1]Woods Hole Oceanographic Institution, Woods Hole, USA, dwanless@whoi.edu (* presenting author)

Here we present volatile (CO_2, H_2O, F, S, Cl), major, and trace element data from >150 olivine-hosted, glassy, melt inclusions and glasses erupted on the fast-spreading East Pacific Rise (EPR) and intermediate-spreading Juan de Fuca Ridge (JdFR). We provide geochemical constraints on both compositional variations and depths of crystallization beneath the respective ridge axes using vapor-saturation pressures derived from volatile concentrations. Vapor-saturation pressures calculated from equilibrium CO_2-H_2O concentrations suggest crystallization occurs over a range of depths from below the crust-mantle transition to the seafloor for both the fast-spreading EPR and the intermediate-spreading JdFR. Combining these depths of crystallization with major and trace element concentrations of the melt inclusions, results in a detailed picture of how melt compositions evolve as they ascend through the ocean crust.

Major and trace element concentrations of the melt inclusions show no consistent fractional crystallization or melt-rock reaction trends with depth. For example, the most primitive melt inclusion compositions (MgO >9.5 wt%) are found at all depths within the crust, while the more evolved compositions are restricted to the shallow crust. This suggests that some melts ascend through the ocean crust with little to no differentiation, while other melts crystallize during ascent. Melt-rock reaction processes should result in a decrease in Al_2O_3 and CaO/Al_2O_3 concentrations with decreasing depth due to olivine and plagioclase assimilation and precipitation of clinopyroxene, however, this is not observed in our melt inclusions. Finally, major element and volatile concentrations from the EPR are more variable in the upper crust compared to the lower crust. For instance, Cl concentrations in EPR melt inclusions formed in the upper crust range from 10 to 66 ppm, compared to only 42 to 51 ppm in melt inclusions formed deeper in the crust. This may result from higher degrees of fractional crystallization and/or increased fluid-rock interaction in the shallow crust.

Evaluating the control on the kinetic Cr isotope fractionation factor: a reactive transport modeling approach

CHRISTOPH WANNER* AND ERIC L. SONNENTHAL

Lawrence Berkeley National Laboratory, Berkeley, CA, USA, cwanner@lbl.gov (* presenting author)

Fractionation of the four stable Cr isotopes (^{50}Cr, ^{52}Cr, ^{53}Cr and ^{54}Cr) is a well-accepted proxy for demonstrating Cr(VI) reduction occurring in geological systems [1]. Regarding Cr(VI) contaminated sites, tracking of Cr(VI) reduction is especially powerful when assessing the natural Cr(VI) reduction capacity or when performing an efficiency control of in-situ remediation measures. For typical near neutral pH-values, field scale Cr(VI) reduction efficiency has been quantified using a Rayleigh-type model assuming that the effective kinetic Cr isotope fractionation factor α_{kin} is known [2]. This requirement, however, is often very difficult to achieve. Even at the laboratory scale, published values for α_{kin} vary over a large range (0.9950-0.9985) [1, 3-4]. Most of these studies propose different Cr(VI) reduction mechanisms as being responsible for the wide range of α_{kin}. Alternatively, varying reaction rates and/or transport limitations have been suggested as the cause for the large range of α_{kin}.

To quantitatively assess the different possible contributions on α_{kin} two series of reactive transport model simulations were performed using the code Toughreact [5]. The proposed reaction network is based on a novel multi-continuum approach and the specification of a $^{53}Cr(OH)_{3(s)}$ – $^{52}Cr(OH)_{3(s)}$ solid solution forming the product of Cr(VI) reduction. In doing so, Cr(VI) reduction was considered to occur at solid surfaces and Cr isotope fractionation was modeled by defining an equilibrium fractionation factor only.

Simulating Cr(VI) reduction occurring along a 1D flow path suggested that for a given reaction mechanism α_{kin} can vary over a large range. According to our simulations, the lower range of α_{kin} (=larger fractionation) is defined by a reaction mechanism's theoretical equilibrium fractionation factor. In contrast, high reduction rates and/or transport limitations induced by Cr(VI) transport to reactive surfaces can shift α_{kin} to values close to 1 (=no fractionation). In the second series of model simulations our modeling approach was used to propose an alternative kinetic interpretation for the low α_{kin} observed in the Cr(VI) reduction experiment performed by Dossing et al. [4].

Our generic model simulations suggest that the individual contributions of reaction rates, transport limitations and reaction mechanisms should be addressed more carefully when interpreting experimentally determined kinetic Cr isotope fractionation factors and Cr isotope data derived from field sites. Reactive transport models that can treat isotopic fractionation caused by homogeneous and heterogeneous reactions coupled to transport form a unique tool for quantitative assessment of these individual contributions and for providing constraints on the field scale Cr(VI) reduction efficiency.

[1] Ellis et al. (2002) *Science* **295**, 2060-2062. [2] Wanner et al. (2011) *Appl. Geochem.* in press, doi: 10.1016/j.apgeochem.2011.11.009. [3] Zink et al. (2010) *Geochim.Cosmochim. Acta* **66**, 1095-1104. [4] Dossing et al. (2011) *Chem. Geol.* **285**, 157-166. [5] Xu et al. (2011) *Comp. & Geoscience.* **37**, 763-774.

https://doi.org/10.1180/S0026461X00008434 Published online by Cambridge University Press

Regional evaluation of catchment-scale weathering: surface-water chemical indicators of lithology, and mechanical and biological effects

WANTY, R.B.[1*], BERN, C.[1], VERPLANCK, P.L.[2], SCHMIDT, T.S.[3], TODOROV, T.[1], SANJUAN, C.[2], AND FEY, D.L.[2]

[1]U.S. Geological Survey, MS 964d Denver Fed. Ctr., Denver, CO 80225, USA rwanty@usgs.gov, cbern@usgs.gov, ttodorov@usgs.gov (* presenting author)

[2] U.S. Geological Survey, MS 973 Denver Federal Center, Denver, CO 80225, USA, plv@usgs.gov, csanjuan@usgs.gov

[3] U.S. Geological Survey, Fort Collins Science Center, 2150 Center Ave., Bldg. C. Fort Collins, CO 80526. tschmidt@usgs.gov

In central Colorado, USA, samples were collected from 227 alpine streams between 2004 and 2007 [1] to evaluate the effects of catchment lithology on stream-water chemistry, aquatic communities, and weathering mechanisms. The study area, about 55,000 km^2, includes catchments with a variety of lithologies. The area also includes zones of hydrothermal alteration which have added metals such as Zn, Pb, Cu, Cd, Au, and Ag to the rocks. Abandoned mines in some of the catchments have introduced these metals to the weathering environment.

In altered and mined catchments, rapid weathering of sulfide minerals such as pyrite dominates the aqueous geochemical signature (low pH and high metal and SO_4 concentrations). In unaltered and unmined catchments, catchment lithology determines certain aspects of stream-water quality, including pH, salinity, and relative and absolute concentrations of major and trace elements. Dissolved Ge concentrations are greater in streams draining certain lithologic groups, including the Pikes Peak Granite, although secondary chemical effects, such as the relation between Ge and F, are possible. Prior studies of Ge/Si systematics in lithologically homogeneous areas like Hawai'i [2] have traced weathering processes, but in this study lithologic effects appear to play a stronger role in Ge variations.

Average catchment slope was calculated using GIS software. Steeper slopes likely promote exposure of fresh mineral surfaces because of mechanical processes and decreased soil and vegetation. Across a wide range of lithologies, our data show a small ($r^2 = 0.08$) but significant ($p<0.01$) increase in average weathering rate with increased slope. The effect is greater in catchments with hydrothermal alteration and historical mining.

Benthic macroinvertebrates (n=153) were collected in 125 streams to evaluate effects of trace-metal concentrations on insect abundance and diversity. As metal concentrations increase, sharp drops in diversity and abundance are observed, beginning at lower metal concentrations than were previously reported [3], and likely the result of synergistic effects of several metals on stream biota.

[1] Wanty, Verplanck, SanJuan, Church, Schmidt, Fey, DeWitt, Klein (2009) *App. Geochem.* **24**, 600-610. [2] Kurtz, Derry, Chadwick (2002) *Geochim. Cosmochim. Acta* **66**, 1525-1537. [3] Schmidt, Clements, Mitchell, Church, Wanty, Fey, Verplanck, SanJuan (2010) *Env. Tox. Chem.* **29(11)**, 2432-2442.

Isotopic and geochemical evidence for the natural migration of Marcellus-like brine to shallow drinking water in northeastern Pennsylvania

NATHANIEL R WARNER[1]*, S. OSBORN[2], A. DOWN[1], K. ZHAO[1], R. JACKSON[1], A. VENGOSH[1]

[1] Division of Earth and Ocean Sciences, Nicholas School of the Environment, Duke University, Durham, NC USA, nrw@duke.edu (*presenting author), adrian.down@duke.edu, zhao.kaiguang@duke.edu, jackson@duke.edu, vengosh@duke.edu

[2] Geological Sciences Department, California State Polytechnic University Pomona, Pomona, CA USA, sgosborn@csupomona.edu

The recent increase in production of natural gas from the unconventional shales of the Appalachian Basin represents an important new energy resource. But the drilling and hydraulic fracturing processes required to obtain the gas have generated an increased concern over possible contamination of shallow drinking water resources [1]. Reports of shallow groundwater contamination caused by natural gas drilling are often dismissed based on the large vertical separation between the shallow drinking water wells and the shale-gas formations. Assessing the possible risk to shallow drinking water hinges on the hydraulic connectivity between the shale gas formations and the overlying aquifers.

In this study, we analyze the geochemistry of water samples from three principle aquifers, Catskill, Lockhaven, and Alluvium located across six counties of northeastern Pennsylvania (NE PA). We hypothesize that a detailed analysis of major (Br, Cl, Na, Ba, and Sr) and trace (Li) element geochemistry, coupled with utilization of a specific spectrum of isotopic tracers ($^{87}Sr/^{86}Sr$, $^{228}Ra/^{226}Ra$), could provide evidence of potential hydraulic connections between shallow drinking water aquifers and deep formation waters from the Marcellus or other deep formations. Findings suggest that mixing relationships between a fresh, shallow groundwater and a Marcellus-like brine could cause the groundwater salinization observed in some locations of NE PA. The occurrence of the saline water does not appear to be correlated with the location of shale-gas wells and the same water type was reported prior to the recent and rapid shale-gas development in the region [2]. However, the presence of these pathways could suggest specific areas in NE PA where shallow drinking water resources are at greater risk of contamination with deeper formation brines and gases during drilling and hydraulic fracturing of shale gas.

[1] Osborn *et al.* (2011) *PNAS* **108**, 8172-8176. [2] Williams, Taylor and Low (1998) *Pennsylvania Department of Conservation and Natural Resources* **Water Resources Report 68**, 1-89.

https://doi.org/10.1180/S0026461X00008434 Published online by Cambridge University Press

Towards determining noble gas partitioning between supercirtcial CO_2 and water

O. WARR[1*], A. MASTERS[2], C. ROCHELLE[3] C.J. BALLENTINE[1]

[1]SEAES, University of Manchester, M13 9PL, UK

oliver.warr@postgrad.manchester.ac.uk (*presenting author)

[2]CEAS, University of Manchester, M13 9PL, UK

[3]British Geological Survey, Nottingham, NG12 5GG, UK

Geological storage of carbon dioxide within deep saline aquifers remains a solution to reduce global CO_2 emmisions [1]. However significant uncertainties remain in quantifying the rates of CO_2 dissolution into the water phase, rates of reaction with the aquifer minerals, and also in identifying techniques to trace reservoir leakage. Noble gas isotopes can play a key role in quantifying all of these areas [e.g. 2,3]. Nevertheless, the partitioning of noble gases between supercritcial CO_2 and water has never been determined, with studies to date assuming that noble gas partitioning between these phases can be approximated by data existing for gas/water systems. Indeed, the effect of significant volumes of CO_2 dissolved in the water phase on noble gas solubility in water has also not been determined and is presently neglected in modeling noble gases in natural systems.

We have taken an experimental and modeling approach to resolve this lack of information. We have constructed a Gibbs-Ensemble Monte Carlo (GEMC) model for calculating noble gas partitioning by simulating the molecular configurations of both the water-rich and carbon dioxide-rich phases. This model is currently at a stage where it reproduces carbon dioxide-water binary phase equilibria for the conditions of interest (40-140 Bars, 310-340 K) [4]. The model is now ready for input of noble gas atoms to determine their theoretical distribution between phases. Experimental work equilibrates noble gases between CO_2 and water in the British Geological Survey high-PT laboratory. We extract an aliquot of each phase at equilibrium and determine the noble gas concentration of each using a quadrupole mass spectrometer system developed at the Univeristy of Manchester.

Preliminary results from the experimental program suggest that noble gas solubilities are increased in the water phase when the water contains a high dissolved CO_2 content. In a sub-critical gas/water system at 50°C supporting a 37 bar CO_2 phase, an enhancement in noble gas solubility in water can be observed for Helium and Argon respectively. Confirmation of this increase in solubility is underway with an analytical program that expands the pressure and temperature range to includes the supercritical phase.

[1] Holloway & Savage, (1993) *Energy Convers. Mgmt* **34**, 925-932. [2] Gilfillan *et al.*, *Nature* (2009) [3] Mackintosh & Ballentine, *Chemical Geology* (2012) In Press [4] Vlcek *et al.*, (2011) *J. Phys. Chem. B* **115,** 8775-8784

Characterising exhumation of mid- and lower-orogenic crust during late-stage collision: a case history from NW Bhutan

C.J. WARREN[1*], D. GRUJIC[2], D. KELLETT[3], J. COTTLE[4], R.A. JAMIESON[2]

[1]Department of Environment, Earth and Ecosystems, CEPSAR, The Open University, Walton Hall, Milton Keynes, MK7 6AA, (*c.warren@open.ac.uk)

[2]Department of Earth Sciences, Dalhousie University, Halifax, Nova Scotia, B3H 4J1, Canada.

[3]Geological Survey of Canada, 601 Booth St., Ottawa, Ontario, K1A 0E8, Canada.

[4]Department of Earth Science, Earth Research Institute, University of California Santa Barbara, CA 93106-9630, USA

Abstract

Rare mafic rocks exposed in NW Bhutan, eastern Himalaya, preserve evidence for a granulite-facies event overprinting patchy evidence for precursor eclogite-facies conditions. These rocks yield U-Pb zircon ages of 15.3 ± 0.3 to 14.4 ± 0.3 Ma, interpreted as dating the timing of eclogite-facies metamorphism due to the trace element geochemistry of the zircons [1]. Monazite U-Th-Pb ages of 13.9 ± 0.3 Ma in leucosomes within associated pelitic opx-bearing granulites suggest that granulite-facies conditions were reached rapidly after eclogite-facies conditions [2]. Furthermore, U-Pb ages of rutile in both mafic and pelitic rocks of 10.1 ± 0.4 and 10.8 ± 0.1 Ma respectively, suggest that exhumation proceeded at rates of >40°C Ma^{-1} following the initiation of cooling [3]. These high grade rocks are exposed in the hanging wall of the Kakthang thrust system which emplaced them over older (21-17 Ma, U-Pb monazite) amphibolite-facies rocks which never reached eclogite or granulite facies conditions. Finally, 14.6 ± 1.2 Ma U-Pb ages of titanite in mafic rocks in the nearby Jhomolari Massif [3], which show textural evidence for eclogite-facies overprinted by an amphibolite event, suggest a third unit of high grade metamorphic rocks in Bhutan which experienced a distinct metamorphic history.

Taken together, these data show that rocks were exhumed from distinct middle and lower orogenic crustal levels at different times during the later stages of the India-Asia collision. Their exhumation raises questions about the mechanisms by which crustal material is transported in collision belts. Lower crustal eclogites have no inherent buoyancy, and therefore require a tectonic driver coupled with a lowering of viscosity to promote their exhumation. A strong, cold Indian plate indentor may have driven this hot weak material towards the surface. Multiple pulses of exhumation from different orogenic levels at different times are predicted by this "plunger" mechanism in numerical channel-flow models e.g. [4] which also predict the different PTt paths recorded in nature.

[1] Grujic et al., (2011) *Lithosphere* **3,** 346-366. [2] Warren et al., (2011) *Tectonics* **30**, TC2004. [3] Warren et al., (in press) *J. Met. Geol.* doi:10.1111/j.1525-1314.2011.00958.x. [4] Jamieson et al., (2006) *Geol. Soc. Lond. Spec Pub.* **268,** 165-182.

https://doi.org/10.1180/S0026461X00008434 Published online by Cambridge University Press

Metamorphic rocks seek meaningful cooling rates: New views from muscovite $^{40}Ar/^{39}Ar$ dating

C.J. WARREN[1*], S.P. KELLEY[2], S.C. SHERLOCK[1]

[1]Department of Environment, Earth and Ecosystems, CEPSAR, The Open University, Walton Hall, Milton Keynes, MK7 6AA, UK. (*c.warren@open.ac.uk)

[2]Department of Physical Sciences, CEPSAR, The Open University, Walton Hall, Milton Keynes, MK7 6AA, UK.

Abstract

The cooling and exhumation rates of metamorphic terranes determined using muscovite $^{40}Ar/^{39}Ar$ chronology underpin many tectonic models. Infra-red laser single grain fusion and UV-laser spot-profiling $^{40}Ar/^{39}Ar$ muscovite data from variably overprinted high pressure terranes in Oman [1], the Alps [2] and Norway show that individual samples and even individual grains can yield age ranges which span >50 Ma. Samples analysed in this spatially detailed way commonly yield bulk average ages that are similar to ages determined by single- or multi-grain step heating techniques. This result suggests that the latter technique may commonly mask the absolute variation in $^{40}Ar/^{39}Ar$ age between and within grains. Core to rim $^{40}Ar/^{39}Ar$ age profiles within individual grains determined by UV laser ablation vary from no determinable difference across the grain to grains with older cores or even apparently older rims [1]. These data suggest heterogeneous grain boundary Ar reservoirs during metamorphic evolution. Many of the single grain fusion ages are older than the timing of peak metamorphism determined from e.g. U-Pb on zircon and are therefore attributable to "excess argon" (^{40}Ar decoupled from its parent ^{40}K). For ages which are younger than the timing of peak metamorphism, it is more difficult to assess whether any resulting ages constrain the "true" timing of cooling and exhumation due to a varying amount of excess argon contamination, inefficient Ar removal from the grain boundary or system resetting by deformation or recrystallisation. Careful evaluation of the metamorphic pressure-temperature-time history experienced since the time of mica crystalisation coupled with detailed UV-laser intra-grain age profiling and predictions from numerical diffusion modelling places constraints on data interpretation [3]. In many cases the age variability is best explained by spatial and temporal variations in grain boundary Ar concentration which act to hinder open system Ar removal. Muscovites affected in this way do not yield "true" cooling ages as suggested by the Dodson equation [4] and cooling rates based on these ages may not be tectonically reliable.

[1] Warren et al., (2011) *Contrib. Min. Pet.* **161**, 991-1009; [2] Warren et al., (2012) *J. Met. Geol.,* **30**, 63-80; [3] Warren et al., (2010) *Chem. Geol.* **291**, 79-86; [4] Dodson (1973) *Contrib. Min. Pet.* **40**, 259-274

Controls on summer deposition of atmospheric sulphate and nitrogen in alpine valleys of the Southern Canadian Rocky Mountains

VIVIAN WASIUTA[1*], MELISSA LAFRENIERE[1], KURT KYSER[2], ANN-LISE NORMAN[3], MEREDITH HASTINGS[4]

[1]Queens University, Geography, vivian.wasiuta@queensu.ca (* presenting author), melissa.lafreniere@queensu.ca

[2]Queens University, Geological Sciences and Geological Engineering, kyser@geol.queensu.ca

[3]University of Calgary, Physics and Astromony, Environmental Science, alnorman@ucalgary.ca

[4]Brown University, Geological Sciences, Meredith_Hasings@brown.edu

Introduction

Alpine ecosystems, which are generally nutrient poor and exist under extreme climatic conditions, are particularly sensitive to environmental and climatic stressors, including enhanced N and S deposition. The magnitude of regional N and S emissions in Western Canada oppose the Canadian norm and are increasing, a trend that is forecast to continue. However, evaluation of the magnitude of atmospheric deposition, and processes controlling deposition at potentially vulnerable alpine sites is lacking.

Methods

This study evaluates the controls on summer 2010 nitrogen (N) and sulphate (S) deposition to alpine valleys in the Southern Canadian Rocky Mountains. Deposition is evaluated using bulk precipitation collected from sites at three elevations, in adjacent valleys, on opposing sides of the Continental Divide. Major ion concentrations and stable isotope signals ($\delta^{18}O_{H2O}$ and $\delta^{2}H_{H2O}$, $\delta^{34}S_{SO4}$ and $\delta^{18}O_{SO4}$, $\delta^{15}N_{NO3}$ and $\delta^{18}O_{NO3}$) of the precipitation in combination with synoptic metrological conditions are evaluated.

Results

A dominant source of well mixed atmospheric sulphate is suggested by the relatively uniform precipitation $\delta^{34}S$ values (7.2 ± 3.8‰). These values are higher than commonly reported for well mixed continental sources in North America, and suggest the influence of an emission source with higher positive $\delta^{34}S$ values such as coal, oil, or sour gas. Strongly correlated $[NO_3^-]$ and $[SO_4^{2-}]_{nss}$ ($r=.88$ $p<0.1$) implies they have a common pollutant origin.

Generally, the north-west facing Robertson Valley (RB) receives lower precipitation volumes, but higher NO_3^- loads, and similar SO_4^{2-} and NH_4^+ loads, than the south-east facing Haig Valley (HG).

Precipitation accumulated over discrete intervals also shows variable trends in stable isotope signals as well as ion loads with elevation. Increasing elevation is usually associated with higher $\delta^{34}S_{SO4}$ and $\delta^{18}O_{NO3}$ and lower $\delta^{18}O_{H2O}$ and $\delta^{15}N_{NO3}$ although inverse relationships also occur. We anticipate evaluation of the synoptic metrological conditions, along with back trajectory analysis associated with each sampling interval will help elucidate the dominant controls on atmospheric N and S deposition at the field sites.

https://doi.org/10.1180/S0026461X00008434 Published online by Cambridge University Press

Trace metal isotope fractionation during adsorption to Mn oxyhydroxide: mechanisms, patterns, and further questions

LAURA E. WASYLENKI[1]*

[1]Dept. of Geological Sciences, Indiana University, Bloomington, Indiana, USA, lauraw@indiana.edu*

Adsorption to mineral surfaces is the often the first step when dissolved trace metals are removed from the water column and associated with sediment. Many factors govern the concentrations and isotopic compositions of adsorbed trace metals, and recent research has yielded some mechanistic insight into those factors. Whether the set of atoms adsorbed is the same set eventually incorporated within a mature sediment is unclear (and unlikely), and this complication demonstrates the need to better understand how adsorbed metals become more permanently incorporated in sediments.

My colleagues and I have conducted simple experiments in the past five years to quantify metal stable isotope fractionation during adsorption of several paleoceanographically important trace metals (Mo, U, Zn, Cd, Ni) to the mineral birnessite, a predominant phase in hydrogenetic ferromanganese crusts. In all of these experiments, the lighter isotopes of the metal in question have preferentially adsorbed. Our results indicate that we are measuring equilibrium, rather than kinetic, isotope effects.

In some cases (Mo and U), the fractionations we see in our experiments exactly match the fractionations observed in nature between dissolved metal in seawater and metal in young ferromanganese crusts. This strongly suggests a direct relationship between adsorption and final incorporation of these trace metals. EXAFS spectra from experimental and natural samples demonstrate that the observed isotope effects are driven by differences in coordination chemistry between dissolved and adsorbed metals.[1,2]

For Zn, Cd, and Ni, the fractionations observed in experiments do not match what is observed in nature. Chemical and mineralogical (and perhaps biological) differences between our simple experimental systems and nature may be the cause for the discrepancies. Other hypotheses involve additional reactions occurring during incorporation of metal into mineral structures or following burial that can modify the set of trace metal atoms and the metal isotope ratios initially associated with sediment. These hypotheses and their implications for isotope paleoproxies will be discussed.

[1] Wasylenki et al. (2011) *Geochim. Cosmochim. Acta* **75** 5019-5031. [2] Brennecka et al. (2010) *Env. Sci. Tech.* **45**, 1370-1375.

Anomalous Fractionations of Sulfur Isotopes during High Temperature Reactions between Solid Organic C- and Oxidized S Compounds

YUMIKO WATANABE[1*], HIROSHI HAMASAKI[1], ANDREW P. CHORNEY[1] AND HIROSHI OHMOTO[1]

[1]NASA Astrobiology Institute and Department of Geosciences, Penn State University, University Park, USA, yxw129@psu.edu; hzh114@psu.edu; apc5060@psu.edu; hqo@psu.edu

Until recently, many researchers have thought that UV-photolysis of volcanic SO_2 gas in an O_2-poor (i.e., $pO_2 < 10^{-6}$ atm) atmosphere created the anomalous isotope fractionations of sulfur isotopes (AIF-S) found in many (but not all) sedimentary rocks >2.4 Ga in age. However, we suggest that redox reactions between solid organic compounds (e.g., kerogen in sedimentary rocks) and oxidized S-bearing compounds (e.g., SO_4^{2-}, SO_2) at elevated temperatures (T > ~150°C) may have created most (if not all) AIF-S signatures in nature, based on the following discoveries: (1) SO_2 photolysis using a broad-band UV lamp, which simulates the UV spectra of the sunlight, produced the AIF-S signatures that differed significantly from those in natural rocks [1, 2]; (2) AIF-S signatures occur in some post-2.4 Ga samples, including the ~1.8 Ga black shales in Finland [3], and most interestingly in SO_4 in pollutants in the Beijin air, which were produced by the burning of pyrite-rich coals [4]; (3) Shales with large AIF-S signatures are characteristically kerogen- and pyrite-rich black shales that deposited under the influence of large-scale submarine hydrothermal activity [5]; and (4) The reduced S-bearing compounds, generated from reactions among simple amino acid crystals, sulfate crystals and H_2O at 150-200°C, possess variable AIF-S signatures ($\Delta^{33}S$ = 0.2 to +13‰; $\Delta^{36}S$ = -1.3 to +1.1‰), and most of the data ~~are~~ match with those in sedimentary rocks [6, 7]. Reactions using some complex organic compounds did not produce AIF-S. The results of these laboratory experiments, and also those of our recent study on reactions between activated carbon and SO_2(g) at 150-200°C, suggest that variable fractionations of S isotopes occur during: (i) adsorption of oxidized S-species on the surfaces of solid C-bearing compounds; (ii) series of reduction of the adsorbed S-species on/in the solid; and (iii) desorption of the reduced S-compounds. The isotope effects during (i) and (iii) are probably due to the chemisorption isotope effects proposed by Lasaga et al. (2008) [8], which may affect on one or more S isotopes, whereas those during (ii) may be caused by the magnetic isotope effects that affect only on ^{33}S.

Therefore, the AIF-S record in sedimentary rocks may indicate the evolutions of the biosphere (species and abundances) and environments (e.g., influence of submarine hydrothermal activity) rather than of the atmosphere.

[1] Naraoka and Poulson (2008) *GCA* **72**, A671; [2] Masterson et al. (2011) *EPSL.* **306**, 253-260; [3] Young et al. (2009) *GSA Ann. Mtg. Absts_165626* [4] Ding et al. *GCA* **70**, A142; [5] Kaufman et al (2007) *Science* **317**, 1900-1903; [6] Watanabe et al. (2009) *Science* **324**, 370-373; [7] Oduro et al. (2011) *PNAS.* doi: 10.1073/pnas.1108112108; [8] Lasaga et al. (2008) *EPSL.* **268**, 225-238.

https://doi.org/10.1180/S0026461X00008434 Published online by Cambridge University Press

Raman spectroscopic study on the Cr^{6+} speciation in aqueous fluids at elevated P and T

ANKE WATENPHUL[1*] AND CHRISTIAN SCHMIDT[2]

[1]Hamburger Synchrotronstrahlungslabor HASYLAB at Deutsches Elektronen-Synchrotron DESY, Hamburg, Germany, anke.watenphul@desy.de (* presenting author)
[2]GFZ German Research Centre for Geosciences, Potsdam, Germany, hokie@gfz-potsdam.de

In oxidizing environments, chromium is hexavalent. There is a considerable number of Cr^{6+} minerals, which are almost exclusively chromates. Chromium(VI) is much more mobile than Cr^{3+} due to the higher solubility of Cr^{6+} in aqueous fluids. Chromium(VI) equilibria in aqueous solutions have been studied at ambient P and T, e.g. as function of pH and total Cr^{6+} concentration [1]. Here, we report first results on changes in the aqueous Cr^{6+} speciation with pressure and temperature.

We recorded Raman spectra of an H_2O + 11.7 wt% $K_2Cr_2O_7$ fluid and a D_2O + 19 wt% $K_2Cr_2O_7$ fluid up to 1.6 GPa and 400 °C using a hydrothermal diamond-anvil cell [2] and quartz as pressure sensor [3]. The Raman spectra reflect mostly the chromate $[CrO_4]^{2-}$ – dichromate $[Cr_2O_7]^{2-}$ equilibrium. The normalized integrated intensities of the stretching bands of $[Cr_2O_7]^{2-}$ tend to decrease and that of $[CrO_4]^{2-}$ to increase slightly with pressure. The ratio of the integrated intensity of these bands does not change significantly with temperature. The formation of $[CrO_4]^{2-}$ is strongly suppressed in the D_2O fluid, but this has no effect on the observed behavior of the $[Cr_2O_7]^{2-}$ and $[CrO_4]^{2-}$ species with pressure and temperature.

In both experiments, a new band at 260–290 cm^{-1} appears in the spectra at temperatures above 200 °C. The intensity of this broad band shows no distinct dependence on pressure, but increases strongly at 300 and 400 °C, which is coupled with a decrease in the intensity of bands assigned to chromate and dichromate bending modes. This suggests the formation of another Cr-species in the fluid. In analogy to Raman bands of phosphate [4] and sulfate [5] in aqueous solutions, the new band is tentatively assigned to a restricted translation mode from Cr–O···HOH or Cr–O···DOD and may thus result from hydrated chromate or dichromate ions in the solution at elevated temperatures. This interpretation is supported by the observed band shift by about 20 cm^{-1} to lower wavenumbers in the experiment using D_2O, which indicates an involvement of hydrogen or deuterium in the species.

[1] Ramsey *et al.* (2001) *Corros Sci.* **43**, 1557-1572. [2] Bassett *et al.* (1993) *Rev. Sci. Instrum.***64**, 2340-2345. [3] Schmidt & Ziemann (2000) *Am. Mineral.* **85**, 1725-1734. [4] Rudolph & Irmer (2007) *Appl. Spectrosc.* **61**, 1312-1327. [5] Rudolph (2010) *J. Solution. Chem.* **39**, 1039-1059.

Geochemistry across the Frasnian / Famennian Boundary, Hongguleleng Formation, Xinjiang Province, China

WATERS, JOHNNY A.[1], CARMICHAEL, SARAH K. [1], DEREUIL, AUBRY A. [1], SUTTNER, THOMAS J.[2], KIDO, ERIKA[2], AND CHEN, XIUQIN[3] , TALENT, JOHN A[4], MAWSON, RUTH[4]

[1] Department of Geology, Appalachian State University, Boone, NC 28608, USA. watersja@appstate.edu*
[2] Commission for the Palaeontological and Stratigraphical Research of Austria, Austrian Academy of Sciences, Graz, 8010, Austria
[3] State Key Laboratory of Palaeobiology & Stratigraphy, Nanjing Institute of Geology & Palaeontology, Nanjing, China
[4]Department of Earth and Planetary Sciences, Macquarie University, Sydney, NSW, Australia

The Hongguleleng Formation has yielded a very diverse Famennian shallow marine community and records the rebound from the Frasnian–Famennian (F/F) extinction event in a highly fossiliferous shallow marine setting associated with a Devonian oceanic island arc complex. Faunas from the Hongguleleng demonstrate that the rebound from the F/F extinction event happened much more rapidly than previously thought and suggest that central Asia may have acted as a refugium. This study uses a multiproxy geochemical approach to put constraints on environmental changes, which occurred at the F/F boundary (Late Devonian) within the Hongguleleng Formation. Recent conodont studies place the F/F boundary approximately three meters above the base of the Hongguleleng Formation, giving us an opportunity to conduct detailed geochemical and sedimentological studies across the boundary in a unique setting (oceanic island arc complex) in a part of the world which has a paucity of data at this interval. Changes in the detrital flux were evaluated by examining variations in mineral composition and diagnostic elemental ratios. The hydrothermal and volcanic influence on sedimentation was estimated using Al/(Al+Fe+Mn) and Zr/Al_2O_3 proxies. The input of nutrients was determined by excess P_2O_5 and Ba. The degree of anoxia during deposition was constrained by the V/Cr ratio and the concentration of redox sensitive metals in the sediment.

Samples were collected from the basal six meters of shale and limestone in the Hongguleleng Formation and the upper one meter of shale and volcaniclastic sandstone in the underlying Zhulumute Formation. This interval also spans the *linguiformis* / *triangularis* conodont zone boundary which forms the F/F boundary. Although the Kellwasser event is not recognizable in outcrop by evidence of black shale, it can be recognized geochemically as series of dysoxic and anoxic events that span three meters of section below the boundary. The same interval also shows high levels of biological productivity based on excess Ba and P_2O_5 proxies. The upper limestone surfaces in this interval often have large concentrations of brachiopods. In contrast, limestones and shales in the lower Famennian show oxic to slightly dysoxic conditions. Pulses of volcaniclastic and hydrothermal components to detrital sedimentation are common throughout the interval and are recognized by mineralogy and Al/(Al+Fe+Mn) and Zr/Al_2O_3 .

The analysis of multiple geochemical proxies allows us to confirm the presence of the Kellwasser event in the open oceanic part of Paleotethys. The tectonic setting of the Hongguleleng Formation is in contrast to the sections previously studied, which were located near Laurussia, Gondwana, Siberia, and the South China plate. We plan additional studies of C, O and Sr isotopes in the near future to further refine our model of changing climatic and oceanographic conditions in the Hongguleleng Formation.

https://doi.org/10.1180/S0026461X00008434 Published online by Cambridge University Press

Resolving the effects of degassing vs. magma mingling in andesites and dacites from Medicine Lake Volcano.

LAURA E. WATERS[1*] AND REBECCA A. LANGE[1]
[1]University of Michigan, Ann Arbor, MI, USA, lewaters@umich.edu

Abstract

A detailed petrologic study is presented for seven phenocryst-poor andesites and dacites erupted from Medicine Lake Volcano, CA. This volcanic edifice has erupted phenocryst-poor liquids ranging over the complete compositional spectrum from basalt to rhyolite, often coevally (Donnelly-Nolan *et al.,* 2008), which makes it the ideal place to evaluate and resolve the effects of degassing vs. magma mingling in producing complex textures and zonation patterns in the phenocrysts of intermediate magmas. Despite having only 2 to 10% phenocrysts (+ microphenocrysts), the andesites and dacites featured in this study are each multiply saturated with six to seven mineral phases (plagioclase + orthopyroxene + clinopyroxene + ilmenite + titanomagnetite + apatite ± hornblende). Plagioclase, orthopyroxene and clinopyroxene phenocrysts often display diffusion-limited growth textures (e.g., swallow tail and hopper textures, large melt hollows, etc.). Temperatures (±1σ) were calculated with the two Fe-Ti oxide geothermometer of Ghiorso & Evans (2008) and range from 960 (±25) to 1021 (±16)°C for the andesites and from 876 (±18) to 966 (±19)°C for the dacites. Oxygen fugacities, relative to the Ni-NiO buffer (ΔNNO ± 1σ), range from -0.2 (±0.02) to 1.1 (±0.1). With temperature known, the plagioclase-liquid hygrometer of Lange *et al.* (2009) was employed to determine pre-eruptive melt water concentrations. Maximum melt water concentrations, based on the most calcic plagioclase phenocryst in each sample, range from 3.4 to 4.2 wt% H_2O for the andesites and from 4.2 to 5.8 wt% H_2O for the dacites. These results require that the magmas were fluid saturated at pressures >0.9-1.7 kbars (~3-6 km), and underwent degassing upon ascent to the surface. Plagioclase phenocrysts span a wide range in composition (20-40 mol% An). Some of this variability can be attributed to degassing, owing to the fact that dissolved water strongly affects plagioclase composition. The basis of the plagioclase-liquid hygrometer is that dissolved hydroxyl groups preferentially speciate with Na vs. Ca, thus reducing the albite component in the melt, leading to more calcic plagioclase at higher melt water concentrations. Orthopyroxene, like plagioclase, also spans a wide range in composition (≤ 27 mol% En) in the andesites and dacites, and again some of this compositional variability can be attributed to changing melt water concentration during degassing. Because hydroxyl groups preferentially speciate with Mg vs. Fe^{2+}, higher melt water contents lead to more Fe-rich orthopyroxenes. Thus, the effect of degassing is to produce more sodic plagioclases and more Mg-rich orthopyroxenes. According to calculations based on the JANAF tables, plagioclase is expected to be more sensitive than orthopyroxene to changing melt water concentrations during degassing, and the Fe-Ti oxides are expected to change little. Therefore, another diagnostic tool to resolve the effects of degassing vs. magma mingling in andesites and dacites, in addition to phase equilibrium experiments to verify phenocrystic compositions, is the observed variability of calculated temperatures from all possible pairs of ilmenite and titanomagnetite crystals.

Fire as a Gaian mechanism to regulate atmospheric oxygen: an experimental investigation

ANDREW J WATSON[1*] AND JAMES E. LOVELOCK[2]

[1] School of Environmental Sciences, University of East Anglia, Norwich, U.K., a.watson@uea.ac.uk [2]Coombe Mill Experimental Station, Devon, U.K. and Oxford University, U.K.
(* presenting author)

In his first book on Gaia, Lovelock suggested the idea that fire might be an important regulator of atmospheric oxygen. Here we describe experimental investigations undertaken in the 1970s, but not widely published then, designed to test this idea. Rate of spread and the energy required for ignition were measured in paper, as an analogue for natural fuels, and the results were mapped as functions both of the moisture content of the fuel and the atmospheric oxygen tension. These can be translated approximately into probabilities of ignition and rates of spread of wildfires under different oxygen mixing ratios, by comparison with fire danger rating indices. The results suggest that wildfire destructiveness has a rapidly increasing dependence on atmospheric oxygen at the present concentration of about 21%. Consideration of the importance of fire in limiting productivity on land today, then suggests that fire is an important factor setting the current and past atmospheric oxygen concentrations, and that this sensitivity can provide an explanation for why atmospheric oxygen is stable on geological time scales, at present levels.

https://doi.org/10.1180/S0026461X00008434 Published online by Cambridge University Press

Zircon as a Witness to Earth's First 500 Myr: an Experimentalist's View

E.B. WATSON[1]*, D.J. CHERNIAK[2], D. TRAIL[3], N.D. TAILBY[4]

[1]New York Center for Astrobiology, Rensselaer Polytechnic Institute, Troy, NY, USA, watsoe@rpi.edu (*presenting author)
[2]Department of Earth and Environmental Sciences, RPI, Troy, NY, USA, chernd@rpi.edu
[3]New York Center for Astrobiology, RPI, Troy, NY, USA, traild@rpi.edu
[4]New York Center for Astrobiology, RPI, Troy, NY, USA, tailbn@rpi.edu

The past decade has seen major advances in our understanding of the first 500 million years of Earth history. Cataclysmic events such as the formation of the core, atmosphere and Moon are understood mainly through models and isotopic systematics of large reservoirs (e.g., meteorites, Earth's mantle and/or atmosphere, Moon rocks), but when it comes to details of early-Earth conditions, we must turn to the geologic record. Ancient zircons are the most tenacious record of the early-Earth story. Even though their original host rocks are long gone, Western Australia's Hadean zircons still provide insight into not only the protolith of the magmas in which they grew but also the conditions that prevailed during early crustal magmatism.

The interpretation of chemical and isotopic signatures in natural zircons has been significantly expedited by laboratory experiments that define the high P-T equilibria and kinetic properties of this remarkable mineral. Most basic among these properties is the saturation behavior of zircon in magmas. Knowledge of zircon saturation as a function of melt composition, temperature and pressure provides broad constraints on zircon crystallization scenarios, Hadean or otherwise. In combination with analyses of ancient zircons, other experimentally determined properties shed light on petrogenetic processes and protoliths. The Ti content of zircons provides estimates of magmatic temperatures, and Ce anomalies inform us about oxygen pressures (fugacities) that prevailed during zircon crystallization (and, by inference, in Earth's early crust and mantle). Knowledge of magmatic oxygen fugacities gives us indirect insight into the nature of C-O-H-N-S molecular species in gaseous volcanic emanations. The general picture of early Earth portrayed by the oldest zircons is that the sedimentary cycle was in full swing within 150 Myr of Earth's origin, the oxygen fugacity of the mantle was similar to that of today, and volcanic inputs into the atmosphere were similarly "modern" in molecular character, and neutral—that is, mainly CO_2 and H_2O.

Information is preserved in zircons not only because the crystals themselves have survived, but also because diffusive transport of most ions in zircon is very slow. Oxygen (in H_2O-free environments), U, Th, Pb, Hf, rare earths, Ti, and have been shown to diffuse so slowly that post-crystallization re-setting is unlikely in a zircon that has not been damaged by radioactive decay. On the other hand, O (under H_2O-present conditions), Li, and H may be mobilized in ancient zircons that experience post-crystallization re-heating. Even in the case of Li and O, however, there is evidence that original abundances and/or isotope ratios have been preserved in some cases.

A summary will be provided of experiment-based knowledge of zircon properties (and limitations), followed by a general perspective on early Earth that emerges from "decoding" Hadean zircons.

Diffusion/Deposition/Remobilization of Uranium in Bioreduced Zones

DAVID WATSON[1]*, GUOPING TANG[1], JENNIFER EARLES[2], AND SCOTT BROOKS[1]

[1]Oak Ridge National Laboratory, Environmental Sciences Division, watsondb@ornl.gov (* presenting author), tangg@ornl.gov, earlesje@ornl.gov, and brookssc@ornl.gov

It is common practice to inject substrates and other reactants to reduce the mobility and/or toxicity of subsurface contaminants through bioreduction and other remediation techniques. These injections result in manipulated zones that are in a state of chemical disequilibrium. For example, bioreduction can significantly reduce the concentration of contaminants (like U) and other inorganics in groundwater but increase the concentration on the solid phase. Due to preferential transport through subsurface heterogeneities, there will be abrupt aqueous concentration gradients between well connected high permeability zones that receive a high concentration of treatment media (low U zone) and adjacent lower permeability zones that do not receive treatment media (high U zone). The objective of this study is to assess the diffusion of U into bioreduced zones from adjacent unreduced zones, deposition of the U in the bioreduced zone and remobilization of U after the bioreduction has stopped.

Laboratory bottle tests, field observations at the U.S. DOE Oak Ridge Integrated Field Research Challenge site during U bioreduction experiments and numerical modelling were employed to meet these objectives. U contaminated soils encapsulated in polyacrylamide hydrogels (Spalding and Brooks, 2005) were used in the lab and the field to determine U release and diffusion rates (Figure 1). A two site kinetic model was used to predict release and diffusion of U from unreduced zones to adjacent reduced zones.

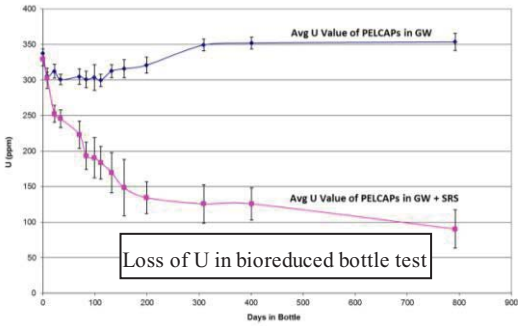

Figure 1: Loss of U from soils encapsolated in hydrogel observed for over 800 days during bioreduction of groundwater.

The results of our study suggest that U will migrate from unreduced zones into reduced zones when bioreduction is active resulting in "extra" U being deposited in high permeability transport pathways. However, if bioreduction conditions are not maintained, an unintended consequence may be an increase in the U flux (relative to pre-bioreduced conditions) as the "extra" U is released as a result of oxygenated groundwater entering the previously reduced zone.

[1] Spalding and Brooks. 2005. *Environ. Sci. Technol.* 39(22):8912-8918

https://doi.org/10.1180/S0026461X00008434 Published online by Cambridge University Press

Rapid core segregation in planetesimals: Results from in-situ X-ray microtomography

HEATHER. C. WATSON[1*], KASEY TODD[1], YANBIN WANG[2], TONY YU[2]

[1] Northern Illinois University, Dekalb, IL, USA. hwatson@niu.edu (* presenting author)
[2] Center for Advanced Radiation Sources, The University of Chicago, Chicago, IL, USA

Differentiation of the terrestrial planets into silicate mantles and metallic cores is one of the most significant events in their history. Although a magma ocean scenario is often used to explain this event for large planets such as Earth, smaller planets and planetesimals likely never achieved the high temperatures necessary for such wide scale melting. In these smaller bodies, ^{26}Al decay is thought to contribute enough heat to melt only the core forming metallic phase, and leave the silicate as a solid phase. W-Hf isotopic signatures in meteorites suggest that some planetesimals differentiated within just a few million years [1]. Achieving core segregation on this time scale by a percolative flow mechanism whereby core material drains though a solid silicate mantle via an interconnected network of melt faces two major problems: (1) in a hydrostatic situation, the *percolation threshold* is above 5 vol% melt, so the process would lead to inefficient core formation, and several vol% of core material would remain stranded in the mantle, which is not supported by observations (2) the *permeability* of fully connected melts at microstructural equilibrium is low enough that some planetesimals may still not be able to differentiate on the short time scale that is required [2]. It has been suggested that shear deformation can cause isolated melt pockets to become connected even at low melt fractions [3,4].

Here, we have measured the change in permeability of core forming melts in a silicate matrix due to deformation. Mixtures of San Carlos olivine and FeS close to the equilibrium percolation threshold (~5 vol% FeS) were pre-synthesized to achieve an equilibrium microstructure, and then loaded into the rotational Drickamer apparatus at GSE-CARS, sector 13-BMD, at the Advanced Photon Source (Argonne National Laboratory). The samples were then pressed to ~2GPa, and heated to ~1100°C. Alternating cycles of rotation to collect X-ray tomography images, and twisting to deform the sample were conducted. Qualitative and quantitative analyses were performed on the resulting 3-dimensional x-ray tomographic images to evaluate the effect of shear deformation on permeability and migration velocity. Preliminary results from Lattice-Boltzmann simulations show a marked increase in the permeability with increasing deformation, which would allow more rapid and efficient core formation in planetesimals.

[1] Kleine et al. (2002) *Nature* **418**, 952-955. [2] Watson and Roberts (2011) *Phys. Earth. Planet. Int.* **186**, 172-182. [3] Bruhn *et al.* Nature **403,** 883-886. [4] Hustoft and Kohlstedt (2006) Geochem. Geophys. Geosyst. **7,** Q02001 doi:10.1029/2005GC001048

Large-volume silicic magma genesis at Yellowstone, Heise, and Caetano: Isotope and geochronology insights from three supervolcanoes in the western U.S.A.

KATHRYN E. WATTS[1]*, JOSEPH P. COLGAN[1], DAVID A. JOHN[1], ILYA N. BINDEMAN[2], AXEL K. SCHMITT[3], CHRISTOPHER C. HENRY[4]

[1]U.S. Geological Survey, Menlo Park, CA, U.S.A., kwatts@usgs.gov (*presenting author)
[2]University of Oregon, Eugene, OR, U.S.A.
[3]University of California, Los Angeles, CA, U.S.A.
[4]Nevada Bureau of Mines and Geology, Reno, NV, U.S.A.

Large caldera "supervolcanoes" are fed by silicic magma chambers that may reach thousands of km^3 in size. We investigate the processes and time scales by which voluminous silicic magmas are generated by combining laser ablation/fluorination O isotope analyses of major phenocrysts with ion microprobe U-Pb dates and O isotope analyses of accessory zircon. We compare these for three supervolcanoes in the western U.S.A.–Yellowstone (Wyoming, 2.1-0.64 Ma), Heise (Idaho, 6.6-4.5 Ma), and Caetano (Nevada, 34 Ma). Yellowstone and Heise are multi-cyclic caldera complexes that produced large volumes of crystal-poor, anhydrous, high-silica rhyolites, many with low-δ^{18}O signatures diagnostic of remelting large volumes of hydrothermally altered rock in the shallow crust (δ^{18}Omelt=0-4‰). U-Pb ages and δ^{18}O compositions for doubly fingerprinted zircon spots reveal that caldera-wide batch assembly of heterogeneous melts with unique δ^{18}O compositions occurs over short time scales (~0.1-0.3 Ma) prior to voluminous tuff and lava eruptions at Yellowstone and Heise. Caetano is a single caldera that produced large volumes of crystal-rich, hydrous (biotite- and hornblende-bearing), low- and high-silica rhyolites with exclusively normal-high δ^{18}O signatures (δ^{18}Omelt=10-11‰). U-Pb ages of Caetano Tuff zircons range from within error of sanidine ^{40}Ar/^{39}Ar eruption ages to ~3 Ma older, indicating a prolonged period of magma assembly and growth. In addition to having different crustal sources, magma assembly time scales, and petrological characteristics, Caetano is also disparate from Yellowstone and Heise in that it has not produced any large-volume pre- or post-caldera rhyolite lavas. However, two resurgent granitic plutons intrude the intracaldera Caetano Tuff, providing clear evidence for magmatism postdating caldera collapse. U-Pb zircon ages, sanidine ^{40}Ar/^{39}Ar eruption ages, whole-rock major and trace element geochemistry, and O isotope signatures indicate a genetic connection between the Carico Lake resurgent pluton (δ^{18}Ozircon= 8.2±0.1‰) and the Caetano Tuff (δ^{18}Ozircon= 8.3±0.1‰), supporting the model of linked volcanic-plutonic components in caldera settings.

https://doi.org/10.1180/S0026461X00008434 Published online by Cambridge University Press

A bio-nanotechnological approach to the remediation of alkaline Cr(VI) containing leachate from chromite processing ore residue

MATHEW WATTS[1*], RUSSELL THOMAS[2], JONATHAN R LLOYD[1]

[1]University of Manchester, Manchester, UK, (*correspondence mathew.watts@postgrad.manchester.ac.uk)
[2]Parsons Brinckerhoff, Bristol, UK

Interactions at the microbe-mineral interface are known to produce reactive nano-scale mineral phases. These nanoparticles (NPs) can be harnessed in an innovative "bio-nanoremediation" approach to various contaminated land problems. The purpose of this study was to develop a novel treatment strategy for the redox active metal, chromium via reduction of mobile toxic Cr(VI) to the relatively insoluble and non-toxic Cr(III). Hyperalkaline (pH≈12) Cr(VI) leachates ascociated with chromite processing ore residue (COPR) have led to significant environmental Cr(VI) contamination. Over the last century up to 1.5 million m^3 of COPR were produced and landfilled in the urbanised area of Glasgow, UK, alone [1]. This has led to sustained leaching of residual Cr(VI) contaminating groundwaters and tributary streams flowing in to the River Clyde.

Cr(VI) removal from COPR related waters was assessed for a nano-engineered magnetite (BnM) biomineral. This nanoparticle, exhibiting reducing properties due to its high surface Fe(II) content, was synthesised via reduction of amorphous ferrihydrite by the Fe(III)-reducing bacterium *Geobacter sulferreducens* [2]. The biogenic magnetite was then subjected to a one-step functionalization process, to generate nanoscale Pd(0) on its surface giving a novel magnetically recoverable bio-nanocatalyst (Pd-BnM) [3]. These biogenic NPs were then compared to a synthetic alternative, nano Zero Valent Iron (nZVI), for remediation applications.

Using pure Cr(VI) solutions at environmentally relevant alkaline pH values, an approximate 50% loss in efficiency (compared to performance in acidic conditions) was observed in both the BnM and nZVI NP treatments, with the nZVI demonstrating a greater capacity for removal. The Pd-BnM performed best, with sustained Cr(VI) removal when supplied with hydrogen gas, removing 240 mg Cr(VI) per g of NP within 50 hours reaction time (reaching over 450 mg after 290 hours) in comparison to a maximum of 29 mg removal when supplied with formate as an electron donor for metal reduction. The fate of the Cr was investigated using TEM and XPS analysis.

Following application of the NP treatments to the COPR leachate slurry, complete removal of the 1.6 mM Cr(VI) in solution was achievable with comparable removals to those observed from pure Cr(VI) solutions. This study therefore demonstrates the ability of both biogenic and synthetic NPs for removal of Cr(VI) from alkaline leachates from COPR.

[1] Farmer, J.G., et al (2002) *Journal of Environmental Monitoring,* **4**, 235-243.
[2] Cutting, R. S., et al (2009) *Geochimica et Cosmochimica Acta,* **73**, 4004-4022.
[3] Coker, V. S., et al (2010) *ACS Nano,* **4,** 2577-2584.

Ethanol binding, orientation and bilayer structure on R-plane corundum surfaces

Glenn Waychunas[1*], Jaeho Sung[2] and Y. Ron Shen[2]

[1]Lawrence Berkeley National Laboratory, Earth Sciences Division, Berkeley, CA, USA , gawaychunas@lbl.gov (* presenting author)
[2]University of California, Physics Department, Berkeley, CA, USA yrshen@lbl.gov

Introduction

The interaction and binding of organic species with mineral surfaces is a large frontier in geochemistry. Mineral surfaces may sequester, sort, or contribute to breakdown reactions of organic molecules, but much of the details of these processes are poorly informed. Compared to inorganic sorbates, which interact with a surface by forming covalent and hydrogen bonds, and couple strongly to surface water molecules; organic structures may have partial or dominant hydrophobic interactions and reduced interaction with waters, multiple charges on a single molecule (e.g. zwitterion), and complex multi-site interactions with surface functional groups. In addition, a range of conformations may be possible, allowing adaptation to a surface, but differing from the solvated water-borne entity. These considerations have limited both the scope and utility of many past studies, with the vast majority involving measurement of uptake without information on the actual binding geometry or reaction mechanisms. The topic is one of profound interest given enormous numbers of industrial organic pollutants, natural biological agents, and pharmaceutical breakdown products entering the environment.

Results

We are developing a program to couple sum-frequency vibrational spectroscopy (SFVS), surface x-ray scattering methods, and computer simulations to characterize organic species interactions with well-known mineral surfaces. The first work involves ethanol as a single monolayer, and as a bulk liquid, on the corundum R-plane (1-102) surface [1]. SFVS spectra in the C-H range show that the monolayer has a well-defined anisotropic arrangement consistent with the R-plane termination. Specific molecular orientations and anisotropy can be explained by the formation of two hydrogen bonds between the ethanol molecules and the hydroxyls on the surface [2]. When bulk ethanol is present, the first layer is similarly anisotropic, but the second is apically opposite with a nearly isotropic distribution.

[1] Sung et al. (2011) *J. Phys. Chem. C* **115**, 13887-13893., Sung et al. (2011) *J. Amer. Chem. Soc.* **133**, 3846-3853. [2] Sung et al. (2011) *J. Phys. Chem. Lett.* **2**, 1831-1835.

https://doi.org/10.1180/S0026461X00008434 Published online by Cambridge University Press

Calibrating the silica-phytolith paleothermometer

ELIZABETH A. WEBB[1*], FREDERICK J. LONGSTAFFE[2], AND ZHENZHEN HUANG[3]

[1]Western University, London, Ontario, Canada, ewebb5@uwo.ca (* presenting author)
[2]Western University, London, Canada, flongsta@uwo.ca
[3]Western University, London, Canada, zhuang9@uwo.ca

Paleoclimate potential of phytolith $\delta^{18}O$ values

Plants absorb aqueous silicic acid from soils and precipitate silica phytoliths in cells along the transpiration stream. Phytoliths are composed of opal-A and can accumulate in soils when plants decay. Ancient phytoliths can provide paleoclimate information because their $\delta^{18}O$ values vary with temperature and the $\delta^{18}O$ values of plant water. However, a detailed understanding is required of how the $\delta^{18}O$ values of phytoliths vary in response to flucutations in temperature and plant water $\delta^{18}O$ values over the growing season.

Horsetail (*Equisetum hyemale*) plants were grown under constant temperatures for 6 months. The $\delta^{18}O$ values of watering-water, plant-water and atmospheric-water vapour were monitored monthly and the $\delta^{18}O$ values of phytoliths were determined after the plants reached maturity. Fluctuations in plant-water $\delta^{18}O$ values resulted from changes in the $\delta^{18}O$ values of atmospheric vapour, the maturity of the plant and related changes in transpiration. Higher plant-water $\delta^{18}O$ values occurred in the warmer growth chambers but also toward the apex each plant and these values increased over time. Phytolith $\delta^{18}O$ values increased from 35.9, 37.1, 37.5 to 43.4 ‰ in the 15, 20, 25 and 30 °C growth chambers, respectively.

Comparison to opal-A paleothermometers

Plant-water and phytolith $\delta^{18}O$ values were used to evaluate the fit of the observed phytolith oxygen-isotope fractionation to existing opal-A paleothermometer equations developed for diatoms and phytoliths grown under field conditions where temperatures were variable [1,2]. A linear relationship between $1000\ln\alpha$ and $10^6/T^2$ was not observed for the phytoliths when the plant-water $\delta^{18}O$ values were averaged over the growing season. Instead, the phytolith paleothermometer equation most closely resembles recent diatom paleothermometers [1] when plant-water $\delta^{18}O$ values from the latter half of the growing season are used for plants grown at 20-30°C and when plant-water from the mid-growing season is used to calculate $1000\ln\alpha$ for the plants grown at 15°C. These results support earlier finding [2] that the $\delta^{18}O$ values of phytoliths are dominated by phtyoliths produced later in the growing season. Horsetails grown at 15°C were unhealthy at the end of the experiment and phtyolith deposition was likely restricted after the fifth month.

This study demonstrates that the oxygen-isotope fractionation between phytoliths and water is similar to that observed for diatom opal-A. However, interpretation of a phytolith oxygen-isotope paleothermometer must consider the timing of silica deposition. Non-ideal growth conditions can limit phytolith formation, creating disequilibrium between silica and average seasonal plant water.

[1] Dodd & Sharp (2010) *Geochim. Cosmochim. Acta* **74,** 1381-1390. [2] Shahack-Gross et al. (1996) *Geochim. Cosmochim.Acta* **60,** 3949-3953.

Plankton diversity and ocean circulation regulate the ocean nitrogen reservoir

THOMAS S. WEBER[1*], CURTIS DEUTSCH[2]

[1]University of California Los Angeles, Los Angeles, USA, tweber@atmos.ucla.edu (* presenting author)
[2]University of California Los Angeles, Los Angeles, USA, cdeutsch@atmos.ucla.edu

Regulation of the ocean N reservoir

The average elemental composition of marine plankton is closely matched to the availability of the major nitrogen (N) and phosphorus (P) nutrients. This is understood to arise from biological control over the ocean's N budget, in which removal of N by denitrification selects for diazotrophic phytoplankton that add new N to the ocean when it limits the growth of other species. Current understanding of this feedback mechanism derives from box models of the ocean, which lack a realistic representation of physical mixing and the spatial heterogeneity of biological processes.

Role of plankton diversity and ocean circulation

We show that in the context of a realistic ocean circulation and a uniform 'Redfieldian' N:P ratio of plankton biomass, this feedback mechanism consistently yields too little N relative to observations. The solution lies in the large-scale variability of phytoplankton N:P ratios, which range from ~10:1 in diatom-dominated regions to >20:1 in low-diatom regions [1]. Because diazotrophs compete with high N:P subtropical plankton, the N reservoir is restored towards a higher value than in the Redfieldian case. However, low N:P communities outside the subtropics do exert some leverage over the ocean's nutrient balance, because their stoichiometric signature is transported to diazotrophic habitats through shallow pathways of ocean circulation.

Conclusions

Our study demonstrates that a combination of local ecosystem dynamics, plankton biogeography, and large-scale circulation patterns control the availability of fixed N in the ocean, and thus ocean fertility and carbon storage over millennial timescales.

[1] Weber & Deutsch (2010) *Nature* **467,** 550-554.

https://doi.org/10.1180/S0026461X00008434 Published online by Cambridge University Press

Solubilities of H-O-C-S-Cl volatiles in fluids and silicate melts and their control on magmatic processes

JAMES WEBSTER[1]*, BETH GOLDOFF[2], M. FRANCESCA SINTONI[3], BENEDETTO DE VIVO[4]

[1]American Museum of Natural History, New York, USA, jdw@amnh.org (* presenting author)
[2]American Museum of Natural History, New York, USA, bgoldoff@amnh.org
[3]University of Naples Federico II, Naples, Italy, francescasintoni@gmail.com
[4]University of Naples Federico II, Naples, Italy, bdevivo@unina.it

The fluid-driven ascent of buoyant magma, explosive volcanic eruptions, and mineralizing hydrothermal processes are controlled by the abundances and solubilities of the dominant magmatic volatile components H_2O, CO_2, $H_2S/SO_2/SO_3$, and Cl in melts and in coexisting fluids and/or sulfide liquids. The efficacy of these processes depends on the presence, quantity, and composition of fluids that are dominantly aqueous; their presence in magma is the cause of excess magmatic and volcanic degassing. The solubilities of these volatiles in melts and fluids are constrained by experimental observations and thermodynamic and empirical modelling, but until recently the experimental constraints have been largely limited to simple binary volatile systems: H_2O-CO_2, H_2O-Cl, H_2O-S.

Recent and emerging experimentally derived solubility data on H-O-C-S-Cl volatile components in basaltic to rhyolitic melts provide fundamentally important constraints and new insights on volatile behavior in complex natural systems. It is well established that trace quantities of CO_2 and/or Cl dramatically reduce the concentrations of H_2O in melt required to force exsolution of one or more fluid phases from volatile-bearing melts. Recent research further demonstrates that the addition of S reduces Cl solubility by 25-30 percent relative in rhyodacitic, trachytic, phonolitic, and a variety of basaltic melts for oxygen fugacities at and above NNO ([1]; see summary in [2]). Hence, the overall influence of adding relatively oxidizing S is to reduce Cl and H_2O solubilities in melts and to enhance the stability of fluid(s) which fosters excess magmatic degassing. Other experimental work shows reduced CO_2 solubilities in various melts and increased solubilities in coexisting fluid at shallow crustal pressures. The (fluid/melt) partition coefficient for CO_2 in haplogranitic melts increases by nearly a factor of ten with the addition of geologically relevant abundances of reduced S^{2-} to silicate melt at oxygen fugacities of NNO-0.4 to NNO+0.3 [3]. Other research [4] at more reducing conditions (NNO-1.6 to NNO-3.2) observed decreased CO_2 solubility in basaltic melt due to dilution of CO_2 in the coexisting fluid by the presence of comparatively reduced C species. Moreover, ongoing research shows that the addition of Cl to a CO_2-H_2O vapor reduces the solubility of CO_2 in a coexisting phonolitic melt by 80 relative percent; this apparently results from the condensation of saline brine from the vapor phase and the formation of two fluid phases [5]. These new experimental observations will be interpreted in light of and applied to processes of fluid exsolution and excess magmatic degassing for subduction-related and other magmas.

[1] Botcharnikov *et al.* (2004) *Chem. Geol.* **213**, 207-225. [2] Webster & Botcharnikov (2011) *Rev. Mineral. Geochem.* **73**, 247-283. [3] Webster *et al.* (2011) *Contrib. Mineral. Petrol.* **162**, 849-865. [4] Morizet *et al.* (2010) *Chem. Geol.* **279**, 1-16. [5] Webster *et al.* (in preparation).

Glacially derived iron as the key driver for biogeochemical processes in Arctic fjord sediments (West Svalbard)

L. M. WEHRMANN[1*], J. D. OWENS[1], M. J. FORMOLO[2], T. G. FERDELMAN[3] AND T. W. LYONS[1]

[1]University of California, Riverside, Riverside, CA, USA, laura.wehrmann@ucr.edu, jowens@student.ucr.edu, timothyl@ucr.edu (* presenting author)
[2]University of Tulsa, Tulsa, OK, USA, michael-formolo@utulsa.edu
[3]Max Planck Institute for Marine Microbiology, Bremen, Germany, tferdelm@mpi-bremen.de

Glaciers deliver an important fraction of bioavailable iron to the high latitude oceans. This iron is produced by mechanical and microbially enhanced chemical weathering, e.g., oxidation of iron-sulfide minerals in proglacial and supraglacial environments, and may enter the marine system in aqueous form, as (nannoparticulate) Fe-(hydr)oxides, or more stable Fe mineral phases [1]. A fraction of glacial iron is delivered directly to the open ocean by icebergs [1]. However, little is known about the fate of the large iron pool that enters high latitude coastal marine waters, particularly fjord systems, by glacial meltwater runoff.

In two comprehensive sampling campaigns along the Western Svalbard coast in 2010 and 2011, sediment cores were collected at Smeerenburgfjorden, Kongsfjorden, and Van Keulenfjorden along transects from the mouth of the fjords to the tidewater glaciers at the terminal end of the fjords. Results of pore water and solid phase analyses show that the input of glacially derived iron plays an important role in biogochemical processes in the fjord sediments by controlling the cycling of sulfur and manganese and by providing a large Fe-oxide pool for dissimilatory iron reducers. High solid phase reactive iron concentrations and high dissolved Fe concentrations in the pore water prevail in Kongsfjorden and Van Keulenfjorden, and suggest a benthic flux of dissolved iron from the sediment to the water column. Correspondingly, the concentration and sulfur isotope composition of chromium reducible sulfur (CRS) in the iron-dominated fjord sediments largely reflect the delivery rate and isotope composition of detrital pyrite originating from the adjacent glaciers. These values deviate strongly from the sulfur isotope composition of sedimentary acid volatile sulfur (AVS), which presumably formed from hydrogen sulfide production during organoclastic sulfate reduction, although nearly constant pore water sulfate concentrations with depth in Kongsfjorden and Van Keulenfjorden sediments argue for low production.

Overall, our data point to extensive benthic iron cycling in Svalbard fjord sediments, probably coupled to considerable oxidative sulfur cycling promoted by sediment bioirrigation by the benthic macrofauna. Our findings contribute to the hypothesis that benthic recycling of glacially derived iron in high latitude fjord sediments facilitates the transport of this micronutrient across the fjords while maintaining its bioavailability for fertilization of primary productivity on the adjacent continental shelf.

[1] Raiswell (2011) *Elements* **7**, 101-106.

https://doi.org/10.1180/S0026461X00008434 Published online by Cambridge University Press

What do post-shield and rejuvenated lavas tell us about the source of the Hawaiian mantle plume?

DOMINIQUE WEIS[1*], DIANE HANANO[1], MICHAEL O. GARCIA[2] AND DENNIS GEIST[3]

[1]Pacific Centre for Isotopic and Geochemical Research, Earth & Ocean Sciences, Univ. of British Columbia, Vancouver, BC V6T1Z4, Canada, dweis@eos.ubc.ca, dhanano@eos.ubc.ca

[2]Department. of Geology and Geophysics, Univ. Hawai'i, Honolulu, HI 96822, USA, mogarcia@hawaii.edu

[3]Department of Geological Sciences, Univ. of Idaho, Moscow, ID, 83844-3022, USA, dgeist@uidaho.edu

On Hawai'i, volcanoes lie on two geographical trends (Loa and Kea). Their shield lavas define two clear geochemical trends over ~5 Myr, distinct in Pb, Nd, Sr and Hf isotopes [1,2] and in elemental concentrations [3], that reflect the sampling of different components in the deep source of the mantle plume, at the core-mantle boundary.

Hawaiian volcanoes also include post-shield and rejuvenated lavas, alkalic in composition, that occur just after the shield phase or after an eruptive hiatus of variable duration (~0.5-2 Myr), respectively. These magmas correspond to smaller degrees of partial melting and provide finer resolution of compositional variation in the plume source. We compiled all recent high-precision literature data on late-stage lavas (130 samples for Pb and 103 for Sr, Nd and Hf isotopes), and added new data for Kaula and Middle Bank volcanoes (32 samples). Except Hualalai, which is characterized by a very distinct Loa signature [4] of very low $^{206}Pb/^{204}Pb$ ratios (<18.02) and light $\delta^{7}Li$ (down to 0.75 ‰), most post-shield lavas plot on the Kea side of the Pb-Pb boundary of [2]. Two groups appear: 1) post-shield lavas from the Big Island and Maui Nui (<1.7 Ma) with isotopic compositions partly overlapping those of the shield lavas from their respective volcanoes, and 2) post-shield lavas from Oahu and Kauai (>3.6 Ma) with more distinct isotopic signatures than their respective shield, and more depleted isotopic compositions (lower $^{206}Pb/^{204}Pb$, $^{87}Sr/^{86}Sr$ and higher ε_{Nd}, ε_{Hf}). These latter compositions overlap with the homogeneous field defined by rejuvenated lavas, mostly from the same volcanoes, but significantly younger (<2.5 Ma). Rejuvenated lavas and >3.6 Ma post-shield lavas define mixing trends subparallel to those of the shield lavas in all binary isotope diagrams. Middle Bank post-shield lavas (6.4 Ma) are the only known exception, with Pb ratios overlapping those of Mauna Kea post-shield lavas.

Most post-shield and rejuvenated lavas on Hawai'i are devoid of the enriched signatures present on Loa trend volcanoes that have been related to sampling of the Pacific ultra-low-velocity-zone [1]. This implies either that this enriched material is not sampled by lower degrees of partial melting, or that the late-stage lavas only derive from the northeast part of the plume, which is more homogeneous and controlled by the Kea component. In contrast to shield lavas, there is also no systematic isotopic variation with time for the post-shield and rejuvenated lavas, therefore providing further insight into the source heterogeneity of the Hawaiian mantle plume.

[1] Weis et al. (2011) *Nature Geosciences* **4**, 831-838. [2] Abouchami et al (2005) *Nature* **434**, 851-856. [3] Hauri (1996) *Nature* **382**, 415-419. [4] Hanano et al. (2010) *G-cubed* doi:10.1029/2009GC002782.

Evolutionary pathways of biomineralization explored using transformed *Dictyostelium*

I.M. WEISS[1*], M. EDER[1], E. WEBER[1] AND V. SCHÖNITZER[2]

[1] INM – Leibniz Institute for New Materials, D-66123 Saarbruecken, Germany, ingrid.weiss@inm-gmbh.de (* presenting author)

[2] LMU – Clinical Center University of Munich, Department of Surgery, Experimental Surgery and Regenerative Medicine, D-80336 Muenchen, Germany

The biological control mechanisms for forming functional mineralized hard materials have developed over long periods of time during evolution. In some way, evolution went hand in hand with the transition from unicellular to multicellular organisms. Our research team takes advantage of a non-mineralizing model organism with uni- and multicellular stages as part of its life cycle: The slime mold *Dictyostelium discoideum*. We recently achieved transgenic expression of a mollusc myosin chitin synthase in *Dictyostelium* and observed that this complex enzyme involved in shell biomineralization is enzymatically active in our cellular model system [1,2]. Clearly, this is only one side of the coin. There are a number of other biomineralization proteins on the other side, which interact with either chitin or mineral phases, or both. The fact that the native extracellular matrix of *Dictyostelium*, in principle, inhibits mineral precipitation can be exploited to match certain environmental conditions with heterologously expressed biomineralization genes, which then favor mineralization with increasing levels of control. Our transgenic approach might be suitable to identify key molecules in the evolutionary pathway of biomineralization inspired from contemporary organisms with some impact for today's environmental challenges such as climate change.

[1] Schönitzer V., Eichner N., Clausen-Schaumann H., Weiss I.M. (2011) *Biochemical and Biophysical Research Communications* **415**, 586-590.
[2] Kaufmann K., Weiss I.M., Eckstein V., Tanaka M. (2012) *Biochemical and Biophysical Research Communications*, in press.

https://doi.org/10.1180/S0026461X00008434 Published online by Cambridge University Press

Seasonal variability in B speciation and B/Ca in planktonic foraminifera from the Cariaco Basin, Venezuela

KATHERINE E. WEJNERT[1*], ROBERT C. THUNELL[1,2], MICHAEL BIZIMIS[2], PERRY PELLECHIA[3], AND YRENE ASTOR[4]

[1]Marine Science Program, University of South Carolina, Columbia, SC 29208, kwejnert@geol.sc.edu (* presenting author)
[2]Department of Earth and Ocean Sciences, University of South Carolina, Columbia, SC 29208
[3]Department of Chemistry and Biochemistry, University of South Carolina, Columbia, SC 29208
[4]Estacion de Investigaciones de Margarita, Fundacion La Salle de Ciencias Naturales, Porlamar 6301, Venezuela

We determined B/Ca on four planktonic foraminiferal species (*Globigerinoides ruber, Globigerinoides sacculifer, Orbulina universa,* and *Globorotalia menardii*) on a Thermo Element 2 high resolution ICP-MS. The material is from biweekly sediment trap samples collected in Cariaco Basin, Venezuela (10°30' N, 65°31' W) over a three year period between May 2003 and May 2006. The data are compared to local hydrography and water column chemistry to evaluate environmental controls on B incorporation into foraminiferal calcite. In addition, seasonal variability of B speciation in the foraminiferal calcite is assessed using ^{11}B magic angle spinning (MAS) nuclear magnetic resonance (NMR) on samples of *O. universa* from January, February, and April 2007 and of *G. menardii* from December 2006. The B/Ca (μmol/mol) data displays clear depth stratification with the surface dwelling *G. ruber* having the highest B/Ca, followed by *G. sacculifer* and the deeper dwelling *G. menardii* and *O. universa* having the lowest, consistent with a decrease in pH with depth. The data also show a repeatable seasonal pattern with the highest values occurring when the water column is stratified in June and July and the lowest occurring during upwelling in December and January. However, none of the environmental variables have a strong correlation with B/Ca. The ^{11}B MAS NMR *O. universa* data show a seasonal change in the speciation of B within the foraminiferal calcite. During January the boron is almost entirely incorporated (~ 90%) in a previously unrecognized trigonal form. However, in April only ~75% of the boron is in this trigonal form, whereas the rest of the boron is divided evenly between borate and boric acid. The observed trigonal form has a C_q of 3.0, which is similar to the theoretical value of 3.15 [1] for the corner-sharing borate carbonate complex, $B(OH_2)CO_3^-$. It is hypothesized that during calcification boron is converted to a borate carbonate complex, which is ultimately converted to either borate or boric acid with each equally likely [1, 2]. Our results support this hypothesis except that most of the boron does not complete this reaction, but remains in the intermediate borate carbonate complex form.

[1] Tossel (2006) *Geochimica et Cosmochimica Acta* **70**, 5089-5103. [2] Klochko et al. (2009) *Geochimica et Cosmochimica Acta* **73**, 1890-1900.

Natural sources of uranium in shallow groundwater in Northeastern Alberta

B. WELSH[1*], M.C. MONCUR[2], D. PAKTUNC[3], Y. THIBAULT[3], S.J. BIRKS[2], M. WIESER[4] AND B. MCKIERNAN[4]

[1]Alberta Environment and Water, Edmonton, AB, Canada, brent.welsh@gov.ab.ca (*presenting author)
[2]Alberta Innovates-Technology Futures, Calgary, AB, Canada, michael.moncur@albertainnovates.ca, jean.birks@albertainnovates.ca
[3]CANMET Mining and Mineral Sciences Laboratory, Ottawa, ON, Canada, dpaktunc@NRCan.gc.ca, ythibaul@nrcan.gc.ca
[4]University of Calgary, Calgary, AB, Canada, mwieser@ucalgary.ca, bmckiern@ucalgary.ca

Elevated dissolved uranium (U) concentrations up to 170 μg L^{-1} were measured in shallow (<25 m depth) domestic water wells near Bonnyville, Alberta. This area of Alberta is covered in glacial till deposits up to 200 m thick with several regional interglacial sand and gravel aquifers. Sediment coring for mineralogical analyses and installation and monitoring of nested piezometers were conducted at two sites to determine the source of U in shallow aquifers in the area. Field observations indicated that the till at both sites showed signs of oxidation at depths down to 6 m, suggesting that the primary source of U in the shallowest underlying aquifer may be from weathering and leaching of overlying U-bearing minerals. Speciation modelling showed that porewater was undersaturated with respect to secondary U minerals in the vadose zone, but that groundwater became saturated with respect to secondary U-hydroxide minerals with depth as conditions became more reducing. The dominant U complexes in groundwater were found to be U-hydroxides for U(IV) species and uranyl carbonates for U(VI) species.

The quantitative mineralogical study included analyses of the oxidized and unoxidized till, aquifer sediments and secondary precipitate samples. No major mineralogical differences were observed between the till and sand sediments other than a higher proportions of dolomite and clay minerals present in the till samples. The major U carrier for both sediments was zircon. Two types of U-bearing zircons were observed, with the highest U concentrations up to 4500 ppm coming from the samples showing characteristics of metamict zircon, possibly altered at near-surface conditions in the oxidized till. The other type was a near-end-member zircon, which was observed more frequently in the unoxidized clay-till. A secondary precipitate collected from a plumbing fixture at one site exhibited elevated concentrations of U consisting of Ca-rich carbonates such as monohydrocalcite, which was likely acting as a sink for U. XANES characterization indicated that U is present as U(VI) coprecipitated with carbonate minerals. $^{234}U/^{238}U$ isotope ratios measured in groundwaters showed minimal variability between the two sites despite variations in U concentration and with depth suggesting a regional source rather than a point source. The combined results did not show any evidence of an anthropogenic source of U, but suggest that alteration of metamict zircon naturally present in near-surface environments (at near neutral pH and low temperatures) could result in the release of dissolved U, leading to elevated U concentrations observed in local groundwater.

https://doi.org/10.1180/S0026461X00008434 Published online by Cambridge University Press

The evolution of magmas at a large stratocone volcano, Mount Shasta, N. California

ALLISON M.WENDE[1*],TIMOTHY A. ZEICHERT[1], CLARK M. JOHNSON[1], BRIAN L. BEARD[1], ROBERT L. CHRISTIANSEN[2], ANDREW T. CALVERT[2]

[1]University of Wisconsin-Madison, Madison, USA, wende@wisc.edu (* presenting author) clarkj@geology.wisc.edu, beardb@geology.wisc.edu

[2]U.S. Geological Survey, Menlo Park, USA, rchris@usgs.gov, acalvert@usgs.gov

Mount Shasta, the largest stratovolcano in the Cascade volcanic arc, has been rebuilt since a major sector collapse in at least four major cone-building stages since ~300 ka [1,2]. In conjunction with earlier elemental and isotopic studies [3,4,5,6,7], new Sr, Nd, and Pb isotope data reported here, as well as in-progress U-Th isotope studies, document mantle and crustal contributions to magmas at Mt. Shasta.

The dominantly andesitic Mt. Shasta lavas are characterized by Sr, Ba, Th, Rb and Pb enrichment, depletions in Nb, Ta and HREE, and MORB-like Sr isotopic ratios. Major element modelling is consistent with fractional crystallization of an arc basalt type parent. However, incompatible element enrichments in the lavas 2–3 times higher than predicted by this model preclude magmatic evolution by fractional crystallization alone. Elevated Rb and Ba in other southern Cascade volcanoes are attributed to crustal contamination [6], which may also account for similar enrichments in the Shasta lavas. U-Th isotope data indicate Th enrichment [8] that may be explained by production of garnet in the lower crust via dehydration melting of amphibole.

Sr, Nd, and Pb isotopes indicate a blend of crust and mantle components. $^{87}Sr/^{86}Sr$ ratios vary from 0.7027 to 0.7035 and ε_{Nd} values range from +4 to +6. These compositions are more mantle-like than at Lassen Peak, although they extend to more crust-like compositions than primitive central Cascade lavas. $^{206}Pb/^{204}Pb$-$^{207}Pb/^{204}Pb$ variations form a tight linear array between Juan de Fuca/Gorda Ridge MORB and Cascade region upper crust, a trend that could reflect a subduction component or interaction with the crust. Upper crustal assimilation, however, fails to account adequately for all trace element and isotopic data, providing support for an important lower-crustal role. Evidence for a significant slab contribution comes from trace-element and isotopic variations: high $(Sr/P)_n$ lavas have Sr and Pb enrichments, large Nb and Ta depletions, and Juan de Fuca MORB or slab-like Sr and Pb isotopic ratios; low $(Sr/P)_n$ lavas have more radiogenic Sr and Pb isotopic ratios and lower $^{143}Nd/^{144}Nd$ ratios, similar to OIB, or a mantle like component [6]. Thus, magmatic evolution at Mt. Shasta involves fractional crystallization of an arc basalt type parent, variable slab-fluid influence, and potential assimilation of lower crust, but relatively little upper crustal assimilation. Many of the older lavas have more radiogenic Sr and Pb but non-radiogenic Nd, suggesting greater crustal assimilation in the early history Mount Shasta, reflecting evolution of the conduit system.

[1] Christiansen *et al.* (1977) US Geol Surv, 77-250. [2] Calvert and Christiansen (2010) AGU Abstract. [3] Baker (1988) PhD Thesis [4] Baker *et al.* (1994) *Cont Min Pet* **118**, 111-129. [5] Grove *et al.* (2002) *Cont Min Pet* **142**, 375-396. [6] Borg *et al.* (1997) *Can Mineral* **35**, 425-452. [7] Bacon *et al.* (1997) *Can Mineral* **35**, 397-423. [8] Newman *et al.* (1986) *Cont Min Pet* **93**, 195-206.

Tire-wear particles and their impact on human lung cells

MELANIE WENZEL[1*], SANDRA EBELING[2], IRMGARD MERFORT[2], VOLKER DIETZE[3], AND RETO GIERÉ[1*]

[1] Universität Freiburg, Geowissenschaften, 79104 Freiburg, Germany, melanie.wenzel@venus.uni-freiburg.de

[2] Universität Freiburg, Chair for Biology and Biotechnology, Dept of Pharmaceutical Sciences, 79104 Freiburg, Germany

[3] Deutscher Wetterdienst, Research Center Human Biometeorology, Air Quality Department, 79104 Freiburg, Germany

In the recent literature, there has been a debate about the real properties of tire-wear particles, especially concerning their size and chemical composition but also with respect to their effects on human health. The aims of this study, therefore, were to characterize tire-wear particles using geochemical and mineralogical techniques and to evaluate the toxicological properties of these particles. Another important goal was to develop standard experimental procedures, which lead to representative results.

Samples of tire-wear particles were produced in a standardized tire-test rig, which allowed for collection of particles from three different types of car tires. In addition, one pure-tire sample was obtained by grinding shredded scrap car tires. These four samples were characterized by using scanning electron microscopy (SEM) and optical microscopy with an associated image analysis system (IAS) in order to determine size distribution, chemical composition, particle structure, and optical properties. The investigations of the different samples indicated that a large fraction of particles have equivalent diameters <10 µm with distinct size distributions for the different samples. All samples contained particles smaller 5 µm. IAS showed that all samples contained both opaque and transparent particles. Usually only the opaque particles are regarded as tire material, whereas the transparent particles are assumed to originate from the pavement material. The amount of transparent particles can be used to trace impurities in the tire samples but a certain fraction also seems to originate from the tires themselves.

Subsequently, the tire-wear and tire particles were investigated in terms of their toxicity and their inflammatory effects on human lung cells (from the commonly used lung cell line A549). The experiments have shown that the lung cells, which were exposed for up to 8 h to various concentrations of particles in suspension between 5 and 50 µg/cm², did not show any increase in NF-κB-DNA binding activity. An exception is one sample, for which an 8 h exposure to 50 µg/cm² sample material, led to a stronger increase in NF-κB-DNA binding activity as measured by electrophoretic mobility shift assays (EMSA). The activation of the transcription factor NF-κB in cells is closely linked to inflammatory processes. The cytotoxicity tests revealed an increased cytotoxic potential for all samples from the tire-test rig but not for the pure-tire material. The extent of cytotoxicity, as measured by MTT-tests, varies with concentration. Whereas cytotoxicity was only slight for various particle concentrations, one sample induces cytotoxicity up to about 50%.
The question of the critical role played by size rather than chemical composition of the tire particles will be studied further.

https://doi.org/10.1180/S0026461X00008434 Published online by Cambridge University Press

Temperature, charge and radius dependence of multivalent cation adsorption on rutile (α-TiO_2) in aqueous 1:1 electrolytes

DAVID J. WESOLOWSKI[1], MICHAEL L. MACHESKY[2], MOIRA K. RIDLEY[3] AND MILAN PŘEDOTA[4]

[1]Oak Ridge National Laboratory, Oak Ridge, TN, USA wesolowskid@ornl.gov (*presenting author)
[2]Illinois State Water Survey, Champaign, IL, USA machesky@sws.uiuc.edu
[3]Texas Tech University, Lubbock,TX, USA Moira.Ridley@ttu.edu
[4]University of South Bohemia, Ceske Budejovice, Czech Republic predota@prf.jcu.cz

Sorption isotherms – percent adsorption of trace amounts (typically 10^{-3} molal) of multivalent cations (Ca^{2+}, Sr^{2+}, Co^{2+}, Ni^{2+}, Zn^{2+}, Nd^{3+}, Y^{3+}) in 0.03 to 0.3 molal aqueous, non-complexing 1:1 electrolytes (NaCl, RbCl, NaTrifluormethanesulfonate) – on (Tioxide Corp.) rutile submicron powder suspensions were collected at approximately constant solution/solid ratio (~50 g solution/1 g of 15 m^2/g rutile). The pH at temperature was measured using a hydrogen-electrode concentration cell, and samples were taken through an *in situ*, submicron filter for analysis of unadsorbed cation concentration by ICP-AES. Under these conditions, the pH of 50% adsorption, readily extracted from the sigmoidal sorption isotherms, represents a model-independent measure of the relative sorption affinity of the multivalent cations, which are shown in the figure below to be remarkably systematic and increase strongly (lower $pH_{50\%}$) with increasing cation charge and temperature (linear with inverse temperature) and decreasing ionic radius. Alkaline earth cations sorb weakly and show ionic strength dependence, while smaller divalent transition metals and especially trivalent rare earths sorb much more strongly and do not exhibit significant ionic strength dependence. Multiplication of the $pH_{50\%}$ sorption value by $(Z^2/R)^{1/2}$, (Z=cation charge; R=bare cation radius in pm), greatly reduces the total variance at a given temperature. This behavior is also found for uraninite (UO_2) and may be typical of multivalent ion sorption on high-bulk-dielectric solids that exhibit inner-sphere cation sorption, as we have demonstrated for rutile by combined X-ray reflectivity and molecular modeling studies. The results have important implications for contaminant migration in subsurface environments and suggest a simple approach for recovery of rare earth elements from phosphate production waste streams, and separation from actinides.

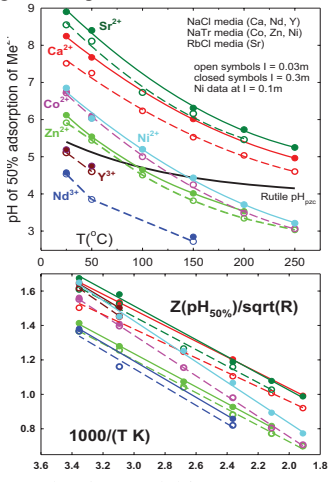

Research sponsored by the Division of Chemical Sciences, Geosciences and Biosciences, Office of Basic Energy Sciences, U.S. Department of Energy.

VARIATION IN THICKNESS OF THE CHEMICAL WEATHERING ZONE AND IMPLICATIONS FOR EROSIONAL AND CLIMATIC CONTROLS ON EARTH'S GLOBAL WEATHERING THERMOSTAT

A. JOSHUA WEST[1*]

[1]University of Southern California, Department of Earth Sciences, Los Angeles, CA, USA, joshwest@usc.edu (* presenting author)

The variability of weathering fluxes on the modern Earth surface provides key information about how associated CO_2 consumption may have varied in Earth's geologic past. Understanding the functioning of the planet's thermostat rests on unravelling the range of parameters that are empirically observed to influence weathering. This has not proved to be an easy task, partly because little is known about where the most important weathering reactions take place. Indeed, the locus of weathering, and the depth at which weathering reactions take place, is difficult to measure directly. In this work, a new approach is used to try to infer how the thickness of the weathering zone varies, and how this influences variability in weathering and CO_2 drawdown.

The approach taken in this work centers on inverse analysis of a parametric model describing weathering, with respect to previously compiled data on weathering fluxes derived from the solute load of headwater catchments draining felsic bedrock [1]. Though there are significant uncertainties inherent in this approach, the results provide first-order constraints on the variability in the depth over which weathering takes place. Results suggest that the effective weathering thickness varies relatively little across several orders of magnitude of denudation rate. At low to moderate erosion rates, reactions in the soil zone dominate weathering fluxes at the catchment scale, but the contribution from soil weathering decreases significantly at higher erosion rates. Continually increasing silicate weathering fluxes at higher denudation rates are sustained by progressively greater contributions from weathering in bedrock.

These results have important implications for understanding the climatic and erosional forcing of weathering fluxes, with broad repercussions for models of carbon cycle evolution. Broadly speaking, increases in erosion lead to increases in weathering, but this effect becomes progressively less significant at the highest denudation rates. The weathering model used here implies that the effect of climate (temperature and runoff) on weathering fluxes is appreciably weaker at relatively low denudation rates on the modern Earth (the supply limited case), such that erosion is critical to maintaining climate-stabilizing feedbacks in the global carbon cycle. Whether these feedbacks continue to strengthen as denudation rates increase is not completely clear, because of the changing locus of reaction. In rapidly eroding settings, bedrock weathering at depth appears to become dominant, and the effect on climate-weathering feedbacks may be more complicated in this case, since it is not known how weathering at depth may respond to changes in climate at the Earth's surface. This question demands further attention.

[1] West et al. (2005) *Earth Plan. Sci. Lett.* **235**, 211-218.

https://doi.org/10.1180/S0026461X00008434 Published online by Cambridge University Press

Observational constraints on the Titan haze from Cassini/Huygens

ROBERT A. WEST[1]

[1]Jet Propulsion Laboratory, California Institute of Technology, Pasadena, CA, USA, Robert.A.West@JPL.NASA.gov

Overview

Prior to the Cassini/Huygens mission, observations from the ground, from the Hubble Space Telescope, and from the Pioneer and Voyager missions established the general properties of Titan's haze. The haze is optically thick at visible wavelengths, it shows subtle hemispheric contrast with seasonal reversals, it shows unique structure in the winter polar region, it contains solids with organic composition, it has a 'detached' layer, and the particles in the main haze layer are aggregates of much smaller 'monomers'[1-3]. The Huygens mission put a probe into Titan's atmosphere in January, 2005 and the Cassini mission has made many remote sensing measurements from orbit beginning in 2004.

Findings of the DISR instrument on the Huygens Probe

The Descent Imager and Spectral Radiometer (DISR) instrument on the Huygens Probe is a composite instrument containing seven sub-assemblies. The solar aureole camera, in particular, sampled within a few degrees of the sun and measured polarization at two wavelengths. These measurements, combined with DISR spectrometer data from the blue to near-IR wavelengths provided the following picture of the haze at the probe landing site [4]. The main haze below 145 km altitude is composed of, on the average, aggregates of 4000 monomers whose radius is 40 nm. The haze density follows an exponential fall-off with a scale height of about 65 km above 80 km altitude. Between 80 km and 30 km the density is constant, and below 30 km it is again constant but with a different value. Particles are less absorbing below 80 km indicating condensation by one or more of several possible condensates.

Findings from the Cassini Orbiter

The Cassini orbiter carried, among other instruments, four optical sensing cameras and spectrometers covering the range from EUV to far-infrared. These instruments provided new detail at wavelengths, locations and times not available to the DISR and these together form a more complete picture of the haze. Highlights from these investigations [5] include (1) an axial tilt of the haze, temperature and wind fields, (2) a near-equatorial band, (3) compositional signatures in the spectra, (4) haze extincition profiles to nearly 1000 km altitude and observations of heavy ion precursors near 1000 km, and (5) large-amplitude seasonal variations in the altitude of the detached haze. The orbiter is expected to provide additional critical observations of the seasonal behavior of the haze until end of mission at solstice in 2017.

[1] Sromovsky et al. (1981) Nature 292, 698-702. [2] West and Smith (1991) Icarus 90, 330-333. [3] Samuelson and Mayo (1991) Icarus 91, 207-219. [4] Tomasko et al. (2008) Planet. Space Sci., 56, 669-707. [5] West et al. (in press, 2012) Titan Haze in Titan: Surface, Atmosphere and Magnetosphere, Mueller-Wodarg et al., Eds., Cambridge Univ. Press.

Fluctuations in ocean anoxia: Evidence from Cretaceous OAEs

S. WESTERMANN[1*], D. VANCE[1], C. ARCHER[1] AND S. A. ROBINSON[2]

[1]Bristol Isotope Group, School of Earth Sciences, University of Bristol, UK

[2]Department of Earth Sciences, University College London, Gower Street, London, UK

(* correspondence: stephane.westermann@bristol.ac.uk)

In sedimentary rocks, especially organic-rich deposits, redox-sensitive trace metal (RSTM) distrubutions have the potential to track change in the oxygenation state of the ocean over geological time. Oceanic anoxic events (OAEs) correspond to periods of profound and rapid environmental change, which have lead to both the widespread deposition of black shales and development of widespread anoxia in the ocean. Understanding the variations of redox conditions during these events is of primary importance, since recent observations and modelling have shown that processes invoked to explain the origin of OAEs are being observed today as a consequence of anthropogenic change.

Here, we compare RSTM distrubtion and molybdenum (Mo) isotope variations during two major Cretaceous OAEs (OAE 1a, Selli event & OAE 2, Bonarelli event). Whereas RSTM have the potential to provide insights regading the depositional conditions and processes in paleoceanographic systems, Mo-isotope data can, under certain circumstances, provide quantitative estimates of how the extent of seawater anoxia may have fluctuated in the past.

For OAE 1a, the RSTM contents in the samples of Gorgo a Cebara (Italy) indicate more reducing conditions, with evidence of watermass restriction within the Selli interval. The Mo isotopes show surprisingly negative values through the section. Before the Selli interval, an increasing trend in $\delta^{98/95}$Mo is observed with values ranging from -0.89 up to 0.08 ‰. Within the Selli level, $\delta^{98/95}$Mo values show a progressive shift towards more negative values. This trend is interrupted by a positive peak to 0.13 ‰, corresponding to samples with the highest Mo content (up to 94 ppm).

For OAE 2, the preliminary results on the samples from the sections of Bottacione and Monte Petrano (Italy) suggest fluctuations in the degree of anoxia during the Bonarelli event, reaching from suboxic to euxinic conditions in an unrestricted watermass system.

During both time intervals, the studied samples show variations in the oxygenation state of the western Tethys, reaching anoxic/euxinic conditions. However, the light $\delta^{98/95}$Mo values suggest that the redox conditions may not have been fully euxinic during OAE 1a. Our preliminary results on OAE 2 samples suggest a different paleoceanographic regime and more reducing conditions. Futher Mo-isotope measurement will be preformed on these samples in order to test ideas on the timing, extent and duration of one of the most pronounced OAEs.

https://doi.org/10.1180/S0026461X00008434 Published online by Cambridge University Press

What controls silicon isotope fractionation during dissolution of biogenic silica?

FLORIAN WETZEL[1*], BEN C. REYNOLDS[1], GERALD HAUG[2],

[1]Institute of Geochemistry and Petrology, Department of Earth Sciences, ETH Zurich, Switzerland, wetzel@erdw.ethz.ch (* presenting author)

[2]Geological Institute, Department of Earth Sciences, ETH Zurich, Switzerland

How nutrients are distributed and cycled in the oceanic water column determines what the net effect of biological activity on ocean-atmosphere ΔpCO_2 is. Paleoceanographers and paleoclimatologists are therefore interested in the past nutrient state of the sunlit surface ocean. Biological matter production and recycling involves isotope fractionation which enables the characterization and quantification of nutrient dynamics. Isotope studies of nutrients (carbon and nitrogen) have been used to characterize the nutrient state of the surface Southern Ocean over glacial-interglacial time scales, and recent advances in analytical techniques enabled the inclusion of silicon isotopes. The marine silicon dynamics, distribution and isotopic composition has been established. In the Southern Ocean diatoms are the dominating phytoplankton species essentially controlling silicon cycling by utilizing silicon to build their opaline frustules and remineralizing after death. While the isotope fractionation associated with silicon uptake by diatoms has been found to be essentially constant, the reverse effect, remineralization, could cause diatoms to not preserve their silicon isotope fingerprint from the surface ocean.

In our study we try to assess if isotope fractionation is involved in diatom dissolution and if so, what causes the effect and what are potential implications for silicon isotopes as a tracer for the biological pump. In all experiments we used 5 mM NaOH to start diatom dissolution. To terminate dissolution diatoms were either separated from NaOH by filtering or the unfiltered solution was directly loaded onto the cation exchange resin. Temperature, amount of opal, opal grain size fraction and community structure were varied.

We find that no analytically resolvable isotope effect during dissolution is observed for all filtered samples for the grain size fraction <20 µm, independent of temperature, amount of opal and community structure. Unreproducable isotope fractionation relative to the bulk sample was associated with dissolution of the 20-63 µm grain size fractions that have a heterogeneous community structure (e.g. radiolaria included). All non-filtered samples were found to react with the cation exchange resin and produced significant isotope fractionation. In our presentation we discuss the potential causes for the variability of isotope fractionation and are able to conclude that carefully cleaned and purified diatom material with a grain size of <20 µm reliably preserves the silicon isotope composition attained in the surface ocean.

Contrasting plateau- and intra-oceanic arc (IOA)-related plagiogranites, Nicoya and Santa Elena complexes, Costa Rica

SCOTT A. WHATTAM[1*] AND ESTEBAN GAZEL[2]

[1]Department of Earth and Environmental Sciences, Korea University, Seoul 136-701, Republic of Korea (*correspondence: whattam@korea.ac.kr)

[2]Department of Geosciences, Virginia Tech, Blacksburg, Virginia 24061, USA

Oceanic tonalite-trondhjemite-granodiorite (TTG) suites (i.e., oceanic plagiogranites) [1] are common in oceanic basins, subvolcanic regions of island arc systems and ophiolites. However, to our knowledge, plagiogranites are exceedingly rare in oceanic plateaus. Here, we present geochemical evidence from Costa Rica oceanic complexes for the existence of both plateau- and arc-related plagiogranites. The plateau-derived Nicoya Complex [e.g., 2] preserves low-Al (mean 12.22 wt.% Al_2O_3) plagiogranites whereby the arc-related Santa Elena Complex [3] encompasses high-Al (mean 17.96 wt.% Al_2O_3) plagiogranites.

In contrast to granites and continental trondhjemites, oceanic plagiogranites are characterized by very low K_2O (<0.5 wt.%). On a plot of SiO_2 vs. K_2O [4], all six Nicoya samples of granodioritic or granitic composition (i.e. with >63 wt.% SiO_2) and the single Santa Elena sample of granodioritic composition plot completely within the field of oceanic plagiogranite; four of five samples with 57-63 wt.% SiO_2 also fall within the field of oceanic plagiogranite. On various granite discrimination plots [5], Nicoya plagiogranites generally fall within the field of ocean ridge granite whereby Santa Elena plagiogranites consistently plot within the field of volcanic arc granites. This is consistent with the interpretation of Nicoya and Santa Elena mafic rocks as plateau/MOR and volcanic arc-related products, respectively. On the basis of chondrite-normalized REE plots, both the Nicoya and Santa Elena plagiogranites are consistent as localized, late-stage felsic differentiates of tholeiitic magma.

U-Pb SHRIMP (zircon) dating at the SHRIMP facility, Korea Basic Science Institute (KBSI) is currently underway on these Nicoya and Santa Elena plagiogranites. The geochemical data suggests that plagiogranites from each complex represent magmas which fractionated from a hydrous gabbroic source and are not the result of other mechanisms sometimes invoked for plagiogranite petrogenesis, e.g., anatexis of mafic crust. If this is accurate, Nicoya plagiogranites should be ~95-85 Ma, an interval of which corresponds to the most voluminous pulse of magmatism related to Galapagos plume activity. On the other hand, Santa Elena plagiogranites should be of the order of ~ 120 Ma, an age of which was obtained on associated gabbros via $^{40}Ar/^{39}Ar$ dating [3]. We integrate the new U-Pb ages with the aforementioned chemical evidence to constrain the petrogeneses of Nicoya and Santa Elena plagiogranites.

[1] Coleman and Peterman (1975) *J. Geophys. Res.* **80**, 1099-1108. [2] Sinton et al. (1997) *J. Geophys. Res.* **102**, 15507-15520. [3] Hauff et al. (2000) *G*^{3} **1**, doi 10.1029/1999-GC000020. [4] Coleman and Donato (1979), In: Barker (Ed.) *Trondhjemites, dacites and related rocks*, 149-167. [5] Pearce et al. (1984) *J. Pet.* **25**, 956-983.

https://doi.org/10.1180/S0026461X00008434 Published online by Cambridge University Press

Can Experimental Dissolution Studies Reproduce Natural Weathering Rates?

A . F. WHITE[1*], D. V. VIVIT[2] AND M. S. SCHULZ[3]

[1*]U. S. Geo. Survey, Menlo Park, CA, USA, afwhite@usgs.gov.
[2] U. S. Geo. Survey, Menlo Park, CA, USA (deceased).
[3] U. S. Geo. Survey, Menlo Park, CA, USA msschultz@usgs.gov.

Introduction

Chemical weathering rates are controlled both by intrinistic mineralogic properities (e.g., defects and surface areas) and extrinistic effects (e.g., solution compositions and saturation states)[1]. During natural weathering, these properities are expected to evolve over geologic time scales which are not reproducable under laboratory conditions. A long term (12 years) experimental column study characterizes the changes of both the relative importance of individual mineral phases and their kinetic reaction rates for 4 pairs of crushed fresh and weathered granite rocks obtained from well-characterized watersheds.

Results

Effluents from the fresh granites indicated a progression in mineral reactivity, dominated initially by defect-dominated plagioclase surfaces (< 1 week), followed by the successive contributions from trace amounts of disseminated calcite (< 1 year) and the oxidation of biotite (<2 years) and finally, by the end of 12 years, by the stoichiometric dissolution of plagioclase. For weathered granites, accessory phases are absent or already oxidized, and effluents are dominated by bulk plagioclase dissolution throughout the experiments.

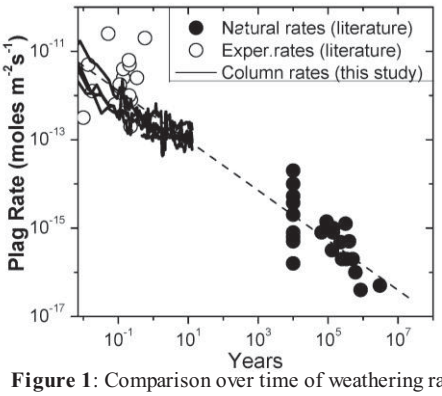

Figure 1: Comparison over time of weathering rates of plagioclase from this study and literature experimental and natural rates.

While initial plagioclase rates for the fresh granites, normalized against BET surfaces, were significantly faster than for weathered granites, the rates converged by the end of 12 years, indicating that extrinsic effects were removed during the course of the experiments. However both sets of rates, while less than those reported for previous experimental studies, remained 1 to 3 orders of magnitude faster than natural rates (Fig, 1). Calculations indicate that while effluents were saturated with respect to gibbsite and kaolinite, they remained significantly undersaturated with plagioclase due to fluid flow rates faster than for most natural conditions.

[1] White & Brantley (2005) Chem. Geol. **202** 479-506.

Updated and extended activity–composition models for thermodynamic calculations in metapelitic systems

WHITE RW[1*], POWELL R[2], JOHNSON TE[1] AND HOLLAND TJB[3]

[1]Institute for Geosciences, University of Mainz, Mainz, Germany, rwhite@uni-mainz.de (* presenting author) [8pt font size]
[2]School of Earth Sciences, University of Melbourne, Melbourne, Australia, powell@unimelb.edu.au
[3]Department of Earth Sciences, University of Cambridge, Cambridge, United Kingdom, tjbh@cam.ac.uk

The direct application of calculated phase diagrams to metamorphic rocks is dependent on the availability of sophisticated activity–compositional (a–x) models in large chemical systems. While the development of such models has advanced considerably in the last decade, existing models span a range of approaches and degrees of sophistication. The development of a new internally-consistent thermodynamic dataset [1] necessitates the modification of these models to be consistent with the dataset. However, this also provides the opportunity to undertake a thorough expansion, and modernisation of the models.

Updated models for chlorite, cordierite, biotite, staurolite, chloritoid, ilmenite-hematite and melt are presented. Key changes include consideration of ferric iron in chlorite & staurolite, with the additional inclusion of titanium in staurolite, a non-ideal model for cordierite and Fe-Mg order-disorder in chlorite. Calibration of the models has been undertaken in the NCKFMASHTO system utilising a large dataset of coexisting mineral pairs from experimental studies and rocks and via comparison with observed phase relationships in experimental studies and rocks. By developing all the models at the same time, each of the models utilises a consistent approach to formulation, order-disorder and the size of the mixing parameters (W). Thus, many of the inconsistencies between earlier models, which were developed at different times, are eliminated. Diagrams calculated with the new models compare favourably with previous diagrams, with some notable improvements. Extension of the models to include Mn is currently underway.

[1] Holland & Powell (2011) *Journal of Metamorphic Geology* **29**, 333-383.

https://doi.org/10.1180/S0026461X00008434 Published online by Cambridge University Press

Implications of unsupported radiogenic Pb in ancient zircon

M.J. WHITEHOUSE[1*], M.A.KUSIAK[1,2] AND A.A.NEMCHIN[2]

[1]Swedish Museum of Natural History, Stockholm, Sweden, martin.whitehouse@nrm.se

[2]Dept. of Applied Geology, Curtin University, Perth, Australia, mkusiak@twarda.pan.pl, a.nemchin@curtin.edu.au

The complexity of zircon U-Th-Pb systematics from strongly layered early-Archean ortho- and paragneisses at Mount Sones and Gage Ridge (Napier Complex, Antarctica) was reported in some of the earliest SIMS zircon studies [1,2]. We report here new SIMS analyses untaken to further investigate this complexity. Notably brown/black coloured, non-cathodo-luminescent, relatively low-U (few 100's ppm) zircons from orthogneisses show a wide range in isotopic composition and exhibit a characteristic reverse discordance pattern. Analyses are distributed broadly along a discordia line (lower intercept ca. 2.5 Ga) that crosses concordia at ca. 3.3 Ga and extends to strongly reverse discordant compositions. As also noted in previous studies [1,2], inspection of the internal peak-hopping signal traces reveal spikes in Pb without corresponding spikes in U. The relatively low U content of the analysed grains as well as the distribution along a well-defined discordia line argues against operation of the well-documented matrix effect seen in SIMS analysis of high U zircon. Instead this effect appears to be related to redistribution of radiogenic Pb within the zircon, with both Pb-loss and Pb-gain (U migration is a less likely mechanism).

To further investigate and constrain the processes responsible for this phenomenon, we have undertaken two types of multicollector Pb isotope analysis in the same grains. Spot analyses exhibit a strong within-run correlation between the Pb count rate and the $^{207}Pb/^{206}Pb$ ratio/age, demonstrating Pb components (sometimes more than one in the same analysis) up to ca. 3.9 Ga. Scanning ion image analysis with a 2 μm spot size rastered over 70 x 70 μm reveal patchy variations of Pb within the zircon (Fig. 1) and in many cases "hot-spots" with $^{207}Pb/^{206}Pb$ ratio/ages up to ~4.2 Ga. These data are consistent with previous suggestions of radiogenic Pb redistribution and suggest that geochronology of ancient zircons such as the ≤ 4.4 Ga Jack Hills detrital zircon suite, which primarily utilises $^{207}Pb/^{206}Pb$ ages, may need to be treated with caution.

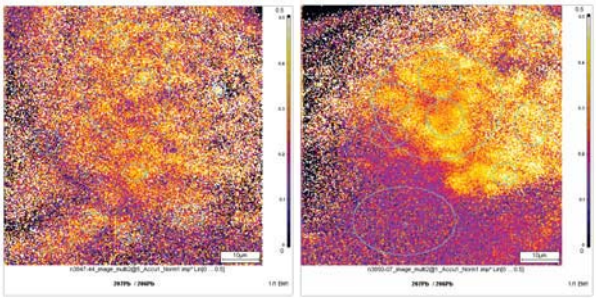

Figure 1: Scanning ion image of the $^{207}Pb/^{206}Pb$ ratio in zircons from Mt Sones and Gage Ridge.

What can zircon really tell us about Earth's earliest crustal evolution?

MARTIN J. WHITEHOUSE [1*] AND ALEXANDER A. NEMCHIN

[1] Swedish Museum of Natural History, Stockholm, Sweden, martin.whitehouse@nrm.se (* presenting author)

[2] Department of Applied Geology, Curtin University of Technology, Perth , Australia, a.nemchin@curtin.edu.au

High-spatial resolution studies of ancient (<4.4 Ga) detrital zircon from the Jack Hills, Western Australia, have yielded invaluable geochemical and isotopic data that are relevant to the evolution of the Earth's earliest crust. While zircon does indeed provide a unique "time capsule" from this period, its use in isolation can however lead to models for early crustal evolution that are at odds with other constraints.

Several lines of evidence from the Jack Hills detrital zircon suite appear to support the existence of modern-style plate tectonics, subduction and well-developed continental (-type) crust on the Earth as early as 4.4 - 4.5 Ga. These include: (1) stable isotope evidence for transfer of surface material to zircon crystallisation depths [1, 2]; (2) inclusion assemblages suggesting relatively high P-T conditions [3]; (3) Ti-in-zircon temperature and REE signatures suggesting crystallisation from evolved melts [4].

In contrast, observations both from zircon and post-Hadean isotopic reservoirs require several 100 Ma isolation of Hadean "proto-crust" and are therefore inconsistent with modern-style plate tectonics. These include: (1) Lu-Hf systematics of the Jack Hills zircons which show no significant input of juvenile material into their source region [5]; (2) unusually radiogenic initial Pb-isotope compositions of some early Archaean rocks requiring long-term high-μ source isolation [6]; (3) solar-like isotopic compositions of rare gases in modern plumes requiring ancient, long-term surface regolith accumulation and subsequent transfer to deep mantle [7]; (4) Th/Nb systematics of post-Hadean mantle-derived rocks recording progressive development of the crust-mantle system [8]; (5) graphite and diamond inclusions in some Jack Hills zircons which are inconsistent with a granite source [9]. These observations have been used to propose an alternative view of the Hadean Earth characterised by a less differentiated basaltic crust (or "stable lid") and the absence of modern style plate tectonics [10].

This apparent dichotomy of evidence needs to be addressed in formulating fully consistent models of the Hadean Earth. Specifically, proponents of plate-tectonic models need to explain the long term isolation of Hadean crust while proponents of models that exclude plate tectonics need to propose mechanisms that can deliver surface-derived materials to middle- lower-low crustal levels.

[1] Wilde, S.A. et al (2001) *Nature* **409**, 175-178; [2] Mojzsis, S.J. et al (2001) *Nature* **409**, 178-181; [3] Hopkins, M. et al. (2008) *Nature* **456**, 493-496; [4] Watson, E.B. & Harrison, T.M. (2005) *Science* **308**, 841-844; [5] Kemp, A.I.S. et al (2010) *EPSL* **296**, 45-56; [6] Kamber, B.S. et al (2003) *Contrib Mineral Petr* **145**, 25-46; [7] Tolstikhin, I. & Hofmann, A.W. (2005) *Phys. Earth Planet Interiors* **148**, 109-130; [8] Collerson, K. D. & Kamber, B. S. (1999) *Science* **283**, 1519-1522, [9] Menneken, M. et al. (2007) *Nature* **448**, 917-915; [10] Kramers, J.D. (2007) *J Geol Soc London* **164**, 3-17.

https://doi.org/10.1180/S0026461X00008434 Published online by Cambridge University Press

Ocean deoxygenation and nutrient redistribution: subarctic Pacific perspective

FRANK A WHITNEY[1]*, STEVEN BOGRAD[2] AND TSUNEO ONO[3]

[1] Institute of Ocean Sciences, Fisheries and Oceans Canada, Sidney, B.C., Canada, whitneyf@shaw.ca (* presenting author)
[2]Environmental Research Division, Southwest Fisheries Science Center, NOAA, Pacific Grove, CA, USA, steven.bograd@noaa.gov
[3]Subarctic Oceanography Division, Hokkaido National Fisheries Research Institute, Fisheries Research Agency, Kushiro 085-0802, Japan, tono@fra.affrc.go.jp

Abstract

Large regions of the global ocean are losing oxygen at rates dependent on processes governing their ventilation (gas exchange with the atmosphere). The most rapid losses are being observed in the Subarctic Pacific, a basin in which oxygen transport into its pycnocline (~100-500 m depth) occurs in localized regions undergoing changes in ice cover (Okhotsk Sea) or upper ocean stratification (Russian coast). Circulation of these waters brings them into contact with the atmosphere every few decades, then isolates them below a fresh surface layer where remineralization processes remove oxygen and regenerate nutrients.

Within the pycnocline, time-series measurements record nutrient increases matching oxygen losses. The enrichment of these waters immediately below the winter mixed layer appears to be counteracting an increasing buoyancy of surface waters, keeping nutrient supply stable over the past several decades. This trend has yet to be realized in models attempting to estimate impacts of global warming on ocean productivity.

Denitrification is a common sink for nitrate along continental margins throughout the North Pacific. As oxygen levels decline, an expansion of oxygen minimum zones (OMZ) is predicted to increase rates of nitrate loss and nitrous oxide production. In addition, warming oceans could release methane stored in frozen hydrates, placing new demands on oxygen.

Some biological consequences

Primary productivity in the SAP has not been impacted by increased upper ocean stratification. Our initial understanding of processes allowing the pelagic community to adapt to change suggests a successful future adaptation to climate changes. However, increased storage of nutrients in the upper ocean comes at a cost. Presently, we can only suggest a reduced export either to the subtropics or deep ocean is occurring. Satellite chlorophyll indicates an expansion of the low chlorophyll biome northward, an expected outcome of changing wind patterns.

Also, expanding OMZs are predicted to compress habitat, making some species more vulnerable to predation. In coastal waters of the SAP, oxygen levels sharply define habitat for complex assemblages, placing pressure on fish communities including those presently harvested. Habitat loss will compound stresses on these fish and their habitat. Realistic projections of oxygen losses in coastal waters are needed to provide sensible management options.

Mass dependent stable isotopic fractionation ($\delta^{88/86}$Sr) during the precipitation of barite, Zodletone Spring, Oklahoma

WIDANAGAMAGE, I.H.[1*], SCHER, H.D.,[2], SENKO, J.M.[3] AND GRIFFITIH, E.M.[1]

[1] Kent State University, Kent, U.S.A., iwidanag@kent.edu, egriffi9@kent.edu
[2] Universtiy of South Carolina, Columbia, U.S.A. hscher@geol.sc.edu
[3] The University of Akron, Akron, U.S.A. senko@uakron.edu

Barite precipitation in a continental setting occurs at Zodletone Spring, Slick Hills, southwestern Oklahoma and shows mass dependent stable $\delta^{88/86}$ Sr isotopic fractionation, exhibiting lower values in the mineral barite relative to the solution from which it precipitated as expected. [1] The possibility of using stable Sr isotopic fractionation in barite as a bio-signature could be useful in understanding ancient and extraterrestrial samples. Zodletone Spring flows into a stream which merges into the southern bank of Saddle Mountain Creek. The precipitation of barite on the crust encircling the spring and along the stream is suggested to be microbially mediated. [2] Anaerobic, anoxygenic bacteria oxidize sulfide to sulfate in the system inducing barite precipitation in the barium-enriched water (Ba, 0.4-0.01 mM, Sr, 0.2-0.3 mM). $^{87}Sr/^{86}Sr$ for the spring (0.7103) and the creek (0.7102) were identical in both barite and the waters. Thus barite records the value of the water in which it precipitated. These values are more radiogenic than the underlying carbonates suggesting a deep source of Sr to the spring (~1500 m) from an intrusive rhyolite. Barite is saturated in both the spring and creek. The saturation index of barite for the spring is 1.5 at 20.5^{o}C and 1.9 in the creek at 33.6^{o}C. Different morphologies of barite from the sites were seen. Barite crystals from the crust on the spring are 10-50 μm in diameter and form rosettes which are likely biogenic barite. Rosettes and diamond shape barite at the end of the stream are 10-20 μm, and probably have both biotic and abiotic origins. Barite crystals from the creek show rosettes, diamond and tabular shapes with diameters varying 5-30 μm. This is also probably a mixture of biogenic and abiotic barite. Barite crystals precipitated at the left bank of the creek are 6-10 μm and rosettes (~10%) and ellipsoidal crystals (~80%) indicating that the dominant type is likely abiotically precipitated barite (i.e. ellipsoidal). Preliminary data show the stable isotope fractionation during precipitation ($\Delta^{88/86}Sr_{\text{barite-water}}$) ranges from -0.25‰ to -0.33‰ in the spring and the creek. Given the uncertainty of the isotopic measurements (approximately 0.05‰) the stable isotopic fractionation does not appear to be significantly affected by processes resulting in the varied morphologies (abiotic or biotic) at this site.

[1] Schauble and Griffith (2011) EOS Trans.AGU, PP41E-01.
[2] Senko et al (2004) Geochim.Cosmochim.Acta **68**, 773-780.

https://doi.org/10.1180/S0026461X00008434 Published online by Cambridge University Press

Can Li isotopes help detect leakage in future CCS sites? The example of a natural analogue in France

WIDORY DAVID[1*], MILLOT ROMAIN[1]

[1]BRGM, Orléans, France, d.widory@brgm.fr

Introduction

Natural analogue sites where geologic CO_2 is leaking to the surface provide excellent opportunities to test approaches suitable for monitoring potential CO_2 leakage at carbon capture and storage sites. We tested here the possibility of completing the classical CO_2 chemical/isotope monitoring approach with the study of the Li isotope systematic, at a CO_2 analogue site near Sainte-Marguerite in the Massif Central (France).

Study site

The Sainte-Marguerite area is located in the southern part of the Limagne graben (French Massif Central). The basement, composed of highly fractured granite, outcrops toward the west of the study area, notably around the Saladis spring. An intercalated arkosic permeable interval between fractured granite and Oligocene marls and limestones acts as a stratiform drain for fluid migration while the overlying thick Oligocene interval is impermeable and acts as a seal. The Allier river bed is located near the contact between the basement and the sedimentary rocks. Deep CO_2-ladden fluids migrate through the arkose interval toward the Sainte-Marguerite area and sustain a number of local springs (Figure 1). The Sainte-Marguerite area is known for the travertine deposits associated with the CO_2-rich natural springs

Results

The previous characterisation of $\delta^{13}C$ and $\delta^{18}O$ from dissolved CO_2[1] indicated some water samples are in isotope equilibrium with degassing mantle CO_2 while other are not. The study of the corresponding δ^7Li isotope compositions (Figure 1) confirm that Li is explained by a binary mixing relationship between a ^7Li-depleted endmember originating from a deep thermal source, and Li originating from the Allier river.

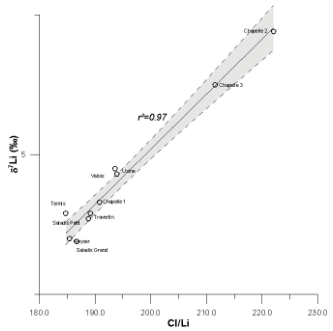

Figure 1: Li concentrations and isotope compositions covariations.

[1] Widory *et al.* (2011) *AGU Fall Meeting*, **H23B-1251**.

ZIRCON AS A PROBE OF PLANETARY IMPACT HISTORY

MATTHEW M. WIELICKI[1], T. MARK HARRISON[1], PATRICK BOEHNKE[1] AND OLEG ABRAMOV[2]

[1]Department of Earth and Space Sciences, University of California, Los Angeles, 595 Charles E. Young Drive East, Los Angeles, CA 90095

[2]U.S. Geological Survey, Astrogeology Science Center, 2255 N. Gemini Drive, Flagstaff, AZ 86001

The impact history of the early solar system remains controversial. The longstanding paradigm of a Late Heavy Bombardment (LHB) at 3.8-4.0 Ga that largely resurfaced the Moon (and by implication, ~30% of Earth) is to a significant degree supported by highly problematic interpretations of $^{40}Ar/^{39}Ar$ ages. Recent studies indicate that zircon has the potential to preserve evidence of impact events on Earth and possibly other solar system bodies. For example, LHB-era Jack Hills zircon grains and epitaxial rims grown between 3.85-3.95 Ga both show evidence of temperature excursions possibly due to impacts. Lunar zircons have also been interpreted to result from large-scale impacts on the Moon. However the geochemical signatures of zircons produced within impact events are poorly understood and caution must be used when assigning an impact as opposed to igneous origin. Ion microprobe U-Pb ages, Ti-in-zircon thermometry and trace element geochemistry of impact-produced zircon obtained from four preserved terrestrial craters reveal broadly similar thermal conditions of formation and provide a basis of comparison with which to distinguish zircon crystallized within an impact event from grains that formed by endogenic igneous processes. A zircon saturation model of hypothetical target rock compositions undergoing thermal excursions associated with the LHB was developed to predict the Ti-in-zircon temperature spectra expected from impacts. Modeled impact zircon production is a function of ambient temperature, Zr content, target composition, and impact energy. Impacts need to be sufficiently large to permit decompression melting of uplifted middle to upper crust (i.e., low energy bolides will not produce melt sheets and thus impact zircon). Target compositions were estimated from large geochemical databases (including meteorites for other solar system bodies such as the Moon and Mars) and selected through a Monte Carlo process allowing a spectrum of compositions to be randomly accessed. Model results for impact produced zircon yield a zircon crystallization temperature distribution significantly higher than that, for example, from Hadean Jack Hills zircons, but considerably lower than the temperature spectrum of lunar zircons. For modern terrestrial crustal target compositions, modeled results yield zircon formation temperatures remarkably similar to Ti-in-zircon crystallization temperatures for recent, large terrestrial impacts. Importantly, the model predicts that zircon growth in response to impacts form in dominantly felsic melts, with little to no zircon formed in mafic melts. This result appears to rule out most lunar zircons documented for both U-Pb age and [Ti] as having formed in response to impact melting and provides an explanation for the apparent absence of impact zircon from Mars samples.

https://doi.org/10.1180/S0026461X00008434 Published online by Cambridge University Press

Evidence of Bacterial Molybdenum Isotope Fractionation

MICHAEL WIESER[1*], BERNADETTE PROEMSE[2], RAYMOND TURNER[3], HALI MORRISON[1] AND ADAM MAYER[1]

[1]Department of Physics and Astronomy, University of Calgary, 2500 University Drive NW, Calgary, AB, T2N 1N4, Canada, mwieser@ucalgary.ca (*presenting author)
[2]Department of Geoscience, University of Calgary
[3]Department of Biological Sciences, University of Calgary

Although the trace metal molybdenum (Mo) is not very abundant, its occurrence is manifold. Molybdenum cofactors play key roles for many enzymes [1, 2, 3] during nitrogen fixation [4], nitrogen reduction, and other processes [5]. Enzymes use trace metals to catalyze chemical reactions by taking advantage of different oxidation states. Molybdenum is available to organisms as molybdate (MoO^{2-}) and varies in oxidation states between +IV, +V and +VI, hence mobilizing two electrons [1]. We have investigated Mo concentrations and the Mo isotopic composition ($\delta^{98/95}$Mo) of cell fractions of the bacterial strain Escherichia coli MC4100. Differential centrifugation was used to separate cytosol, cell membrane and LSP ("low speed pellet"). The cytosol, the intracellular fluid, had the lowest Mo concentrations, and the cell membrane itself the highest Mo concentration. First Mo isotope abundance results suggest that the incorporation of Mo into the cell is associated with isotopic fractionation during production of membrane-anchored Mo-containing proteins and the water-soluble Mo-containing proteins found in the periplasm.

[1] Schwarz et al. (2009) *Nature* **Volume 460**, 839-847. [2] Schneider et al. (1991) *Analytical Biochemistry* **Volume 193**, 292-298. [3] Blaschke et al. (1991) *Archives of Microbiology* **Volume 155**, 164-169. [4] Zerkle et al. (2011) *Geobiology* **Volume 9**, 94-106. [5] Magalon et al. (2011) *Coordination Chemistry Reviews* **Volume 255**, 1159-1178.

High pressure experimental constraints on majorite transformation of chromium-rich garnets

C.H. WIJBRANS[1*], S. KLEMME[1], A. ROHRBACH[1]

[1]Institut für Mineralogie, Westfälische Wilhelms-Universität Münster, Germany, ineke.wijbrans@uni-muenster.de*

Garnet-Majorite transformation

Garnet is an important constituent of the upper mantle, as is evidenced by its frequent occurrence in mantle xenoliths and as inclusions in diamonds. With increasing pressure silica is incorporated into the octahedral site of garnet resulting in a majorite component [1]. The transformation of garnet to majorite is reported to depend on a number of factors besides pressure, such as bulk compositions and presence of other Al bearing phases (such as cpx) or melt [2]. Furthermore, the presence of the minor element chromium has been suggested to decrease the majorite stability with increasing pressure [3].

If true, the effect of chromium on majorite transformation has implications for the interpretation of the formation depth of diamond inclusions as the Cr/(Cr+Al) ratio is much higher in depleted lithospheric mantle compared to fertile mantle [4].

Experimental methods

To investigate this further, we performed sub-solidus high-pressure high-temperature experiments in a Walker-type multi anvil press (Bristol design) at pressures of 6, 9 and 12 GPa, and a range of temperatures. The starting materials consist of silicate glasses in the system Cr_2O_3-CaO-MgO-Al_2O_3-SiO_2, with varying $Cr_2O_3/(Al_2O_3+Cr_2O_3)$. Electron microprobe is used to determine the concentration of major and minor elements in the different phases.

Results

All experiments yielded garnet, opx, olivine and (minor) cpx as stable phases. Preliminary results indicate that for constant pressures and temperatures, the majorite component in garnet decreases with increasing Cr/(Cr+Al) of the bulk composition. There also appears to be a small temperature effect on the stability of the majorite component in garnet but more experiments are needed to confirm this.

[1] Akaogi and Akimoto (1977) *Physics of the Earth and Planetary Interiors* **15**, 90-106. [2] Draper et al (2003) *Physics of the Earth and Planetary Interiors* **139**, 149-169. [3] Klemme (2004) *Lithos* **77** 639-646. [4] Stachel (2001) *European Journal of Mineralogy* **13**, 883-892.

https://doi.org/10.1180/S0026461X00008434 Published online by Cambridge University Press

Mineral and chemical composition of the biomass ash

WANDA WILCZYŃSKA-MICHALIK[1*], RENATA GASEK[1], MAREK MICHALIK[2]

[1]Institute of Geography, Pedagogical University, Kraków, Poland, wmichali@up.krakow.pl (* presenting author), rgasek@ap.krakow.pl

[2]Institute of Geological Sciences, Jagiellonian University, Kraków, Poland, marek.michalik@uj.edu.pl

Biomass is considered as important non-fossil renewable energy source. Its share in co-combustion with hard coal in power plants in Poland increases. Addition of biomass significantly modifies the composition and properties of fly ash and influences possiblilities of its application. The study is based on mineralogical and chemical analysis of ash obtained at temperature ca 470°C from various types of biomass.

Content of elements in ashes varies within broad range, e.g. Ca from below 2 (corn bran) to >16 wt% (sawdust); P from below 0.5 (beech bark) to >5 wt% (corn bran and palm kernels); Mg from 0.6 (beech bark) to 6.3 wt% (corn bran); K from 2.3 (beech bark) to >10 wt% (corn bran, sunflower, sawdust, olive residue, straw, palm kernels); S from 0.5 (beech bark, corn bran) to >3 wt% (sunflower).

Mineral composition of ash is variable. Beech bark ash is composed of quartz, calcite, fairchildite, lime, mica and barite and aluminosilicate spheres as minor components; olive residue ash contains quartz, arcanite, talc, kutnahorite and Fe oxides, and Zn sulphide as minor components; sunflower ash – fairchildite, arcanite, quartz ; straw ash – quartz, calcite, bustamite; palm kernel ash – quartz, calcite, bayerite, cristobalite, and Mg, K, Ca phosphates; sawdust ash – calcite, fairchildite, quartz, gatehauseite (?), and barite, zincite, lime, K and Mg phosphates as minor componets; corn bran ash – tephroite, quartz, corundum, and K and Mg phosphate aggregates composed of very small spheres (ca 1 μm in size).

Very small grains are abundant in the studied ash samples. For example, sunflower ash is composed of very fine carbonate and sulphate particles, straw ash is rich in small rods and prisms of quartz and carbonates.

Mineral and chemical composition of ash is related partly to the composition of plants but content and composition of detrital components (derived from soil, atmospheric dust particles deposited during cultivation or storage) is also important. Relatively big angular or rounded quartz grains of detrital origin are present in several samples (abundant in sawdust and beech bark ash). K-feldspar grains (up to 0.2 mm in size) are present in beech bark ash. Aggregates composed of kaolinite in iron oxides matrix (probably derived from soil) are present in palm kernels ash. Small detrital grains are probably also present but their identification is dubious.

Significant variation in mineral and chemical composition of biomass ash suggests that usage of various types of biomass in co-combustion with coal can result in strong variation of fly ash composition.

Study was supported by NCN grant No. 0579/B/P01/2011/40.

Pre-Late Heavy Bombardment terrestrial crust: review of the zircon evidence for its nature and origin

SIMON A. WILDE[1]*

[1] The Institute for Geoscience Research, Curtin University, GPO Box U1987, Perth, Western Australia 6845, s.wilde@curtin.edu.au (* presenting author)

Distribution

Evidence of pre-Late Heavy Bombardment (LHB) [1] crust on Earth is hampered by the myriad of subsequent geologic processes that could potentially destroy it. However, zircons pre-dating the LHB at 3.85-3.95 Ga are widely distributed on Earth. Locations include the Slave Craton of Canada [2], the Yilgarn Craton of Western Australia [3], Enderby Land in Antarctica [4], and the North [5] and South [6] China cratons, as well as in Tibet [7].

This distribution in four continents and in a variety of hosts that include igneous, metamorphic and sedimentary rocks – and with an age range for the hosts from 4.03 Ga to 0.05 Ga – establishes both the wide distribution and the long-term survival of the ancient grains, and potentially portions of ancient crust.

Origin

The question remains as to the origin and source of these ancient zircon crystals. Models for the site of generation include a solidified magma ocean, oceanic islands or extensive continental crust with oceans; driven by either modern-style plate tectonics or processes possibly unique to the early Earth. Intriguingly, zircon hafnium model ages indicate a dichotomy in the 3.95-4.4 Ga population: some extend back to 4.4-4.5 Ga, whereas others are younger and within error of the U-Pb crystallization age. Similarly, in the oldest rocks that just post-date the LHB, zircon hafnium model ages rarely extend back much beyond 4.0 Ga: what is the significance of this? In terms of preservation, evidence from the Yilgarn Craton indicates that ancient zircon was present in the mid/lower crust in the late Archean, becoming incorporated in granitoid magma at that time. However, in the North and South China cratons, the depository was tapped in the Phanerozoic. In the North China Craton, this occurred in the Ordovician, whereas in the South China Craton, ancient zircon was incorporated in Cenozoic volcanic rocks. So what are the controls on this distribution and how do they relate to continental formation, destruction and amalgamation? A variety of scenarios will be examined in an attempt to explain these features.

[1] Tera et al (1974) *EPSL* **22**, 1-21.
[2] Bowring and Williams (1999) *CMP* **134**, 3-16.
[3] Wilde and Spaggiari (2007) Elsevier *Developments in Precambrian Geology* **15**, 275-304.
[4] Black et al (1986) *CMP* **94**, 427-437.
[5] Diwu et al 2010 *Acta Petrol Sinica* **25**, 1171-1174.
[6] Zheng et al (2011) *GCA* **75**, 242-255.
[7] Duo et al (2007) *Chin Sci Bull* **52**, 23-26.

https://doi.org/10.1180/S0026461X00008434 Published online by Cambridge University Press

On the interaction of minerals and brine with pure / impure CO_2

FRANZISKA D.H. WILKE[1,2]*, JÖRG ERZINGER[1,2], MÓNICA VÁSQUEZ[2], THOMAS WIERSBERG[1] AND RUDOLF NAUMANN[1]

[1]German Research Centre for Geosciences, Potsdam, Germany, fwilke@gfz-potsdam.de (* presenting author)
[2]University of Potsdam, Potsdam, Germany

Objectives

The aim of this study is the investigation of the long term behavior of mineral phases and fluids in systems convenient for CO_2 injection and storage like saline aquifers or hydrate bearing sediments.

Introduction and Settings

Batch experiments were conducted to investigate the interactions of supercritical CO_2 (>7.4 MPa/ >31°C), brine and rock-forming mineral concentrates (albite, microcline, kaolinite, bentonite, biotite, muscovite, calcite, dolomite, and anhydrite) using a newly developed experimental set-up. The solid to fluid ratio was about 1:50. Experiments with mixtures of supercritical CO_2 (99.5 vol.%) and SO_2 or NO_2 impurities (0.5 vol.%) take into account the incomplete purification of industrial captured CO_2 using the oxyfuel technology. In addition, the vessels were not evacuated before the experiments and therefore contained oxygen (ca. 10 cm^3 per experiment), which is also expected in industrially captured CO_2. Before, during and after the experiments approximately 3 ml of fluids were sampled every time and analyzed for pH instantaneously and for dissolved constituents using ICP-MS and IC. After up to 1000h lasting experiments the dissolution and solution characteristics of the solids were examined by XRD, XRF, SEM and EDS, respectively.

Results

Our results suggest the formation of sulfuric acid and nitric acid, reflected in pH values between 1 to 4 for experiments with silicates and anhydrite and between 5 to 6 for experiments with carbonates. These acids should be responsible for the general larger amount of cations dissolved from the mineral phases compared to experiments using pure CO_2. For pure CO_2 a pH of around 4 was obtained using silicates and anhydrite, and 7 to 8 for carbonates.

Silicates do not exhibit visible alterations during all experiments but released an increasing amount of cations in the reaction fluid during experiments with impure CO_2. Si was obtained in ascending concentrations during experiments with silicates whereas Al and Fe exhibited increasing concentrations only during the beginning of the experiments but were variable towards the end. The amounts of Mg and K in the fluids increased or kept constant during all experiments. Ca behaved variable. Nonetheless, precipitated secondary carbonates could not be identified.

Dissolution of carbonates was observed after both pure and impure CO_2 experiments. The total amount of dissolved constituents in the reaction fluid is at least twice as high for carbonates and anhydrite than for silicates. Anhydrite was corroded by approximately 50 wt.% and gypsum precipitated during experiments with supercritical CO_2+NO_2.

Degassing a rhyolite: are the old Ar-Ar ages real, inherited or excess?

WILKINSON, C. M. [1*], KELLEY, S. P. [1], SHERLOCK, S. C. [1], WILSON, C. J. N.[2], CHARLIER, B. L. A. [1]

[1]Department of Environment, Earth & Ecosystems, The Open University, Milton Keynes, MK7 6AA, UK (*presenting author: c.m.wilkinson@open.ac.uk)
[2] SGEES, Victoria University, PO Box 600, Wellington 6040

The aim of this project is to test the resolution of Ar-Ar dating and understand some of the minor anomalies that can affect the fidelity of resulting eruption ages. Few reliable age data exist for post-caldera rhyolitic lavas and domes of the Snake River Plain, USA. The Sheridan Reservoir dome (SRD) has previously been dated by U-Pb geochronology and the published age (~2.07 Ma [1]) overlaps with the generally accepted age of the Huckleberry Ridge Tuff (HRT) (~2.05 Ma [2]). New $^{40}Ar/^{39}Ar$ age data has uncovered possible contamination and higher than expected Ar-Ar apparent ages in feldspar crystals. The SRD post-dates the HRT (C. Wilson, 2011 pers. comm.), but new Ar-Ar ages are older than both the existing U-Pb age for the dome and the generally accepted Ar-Ar age of the HRT.

Extraneous argon, artificially elevating ages may either reflect **1.** excess argon ($^{40}Ar_E$) incorporated into a mineral during crystallization (via diffusion into the mineral lattice or hosted within inclusions) or **2.** inherited radiogenic argon (sourced from a component older than the age of eruption) [3].

To further our understanding of extraneous argon contamination of the SRD phenocrysts, we carried out $^{40}Ar/^{39}Ar$ single-grain fusion dating of feldspar and rhyolitic groundmass. Here we present new age data, where initial results show feldspar ages to be variable and too old, whereas $^{40}Ar/^{39}Ar$ ages obtained from the groundmass are less affected. Diffusion modelling (using DIFFARG [4]) has been carried out to show that these older ages are a consequence of radiogenic argon residing in incompletely outgassed feldspar xenocrysts caught up in the SRD eruption..

[1] Bindeman *et al*., (2007) *Geology* **35,** 1019-1022.
[2] Christiansen, R. (2001) *USGS Special Publication*.
[3] Kelley, S. (2002) *Chemical Geology* **188,** 1-22.
[4] Wheeler, J. (1996) *Computers & Geoscience* **22,** 919 – 929.

https://doi.org/10.1180/S0026461X00008434 Published online by Cambridge University Press

Mass-dependent molybdenum isotope variations in ocean island basalts

MATTHIAS WILLBOLD*, TIM ELLIOTT, AND COREY ARCHER

University of Bristol, School of Earth Sciences, Bristol, United Kingdom, M.Willbold@bristol.ac.uk (* presenting author)

Systematic differences in the mass-dependent molybdenum (Mo) isotopic composition of chemical sediments have recently been used to infer the oxygenation state of past and present oceans [1-4]. Sediments deposited under oxic conditions (i.e. Fe-Mn-oxides) are marked by overall light isotopic compositions (δ^{98}Mo<0.5‰ [1,3]), whereas sediments deposited in euxinic environments (i.e. black shales) have heavier isotopic compositions (δ^{98}Mo >0.5‰ [1,5]) relative to the convecting mantle value (δ^{98}Mo ~ 0; [1-3]). In contrast, it is generally accepted that magmatic processes do not induce any mass-dependent Mo isotope fractionation [6].

Here we investigate the use of mass-dependent Mo isotope data as a tracer for recycled crustal components in the source of ocean island basalts. The Mo isotopic compositions of samples from the ocean islands of La Palma, Hawaii, Iceland, Tubuaii, and Mangaia were determined by MC-ICPMS using a double spike (^{97}Mo-^{100}Mo) approach. Repeated measurements of the USGS basaltic reference material BHVO-2 over a period of two years yielded a δ^{98}Mo reproducibility of ca. 0.06‰ (2σ; N=62).

Samples from Iceland, Tubuaii, and Mangaia have similar values with δ^{98}Mo = -0.02 to +0.07‰. In contrast, samples from La Palma show an offset to more negative values in δ^{98}Mo (0.00 to -0.25‰), whereas samples from Hawaii display a much larger spread in δ^{98}Mo extending from -0.25 to +0.18‰ with the majority of data ranging between δ^{98}Mo -0.04 to +0.18‰.

Thus ocean island basalts record significant mass-dependent Mo isotopic heterogeneity in the Earth's mantle. We interpret the Mo isotopic variability as reflecting different contributions of crustal-derived components that have recycled into the mantle, although further work is required in more precisely constraining the Mo isotope composition of different deep subducted protoliths. However, it appears that mass-dependent Mo isotopic compositions of oceanic basalts can be used as a sensitive tracer of recycled component in the convecting mantle.

References

[1] Barling, J. (2001) Earth and Planetary Science Letters **193**, 447-457. [2] McManus (2002) Geochemistry Geophysics Geosystems **3**, doi: 10.1029/2002GC000356. [3] Siebert (2003) Earth and Planetary Science Letters **211**, 159-171. [4] Archer (2008) Nature Geoscience **1**, 597-600. [5] Arnold (2004) Science **304**, 87-90. [6] Anbar (2004) Reviews in Mineralogy and Geochemistry **55**, 429-454.

Fractionation of iron stable isotopes by magmatic processes: progress and potential

HELEN M. WILLIAMS[1]*, MICHAEL BIZIMIS[2], STEPHEN MOORBATH[3] & KATRINA E. J. HIBBERT[4]

[1]Department of Earth Sciences, Durham University, Durham, UK (* presenting author; h.m.williams2@durham.ac.uk)

[2]Department of Earth and Ocean Sciences, University of South Carolina, Columbia, USA

[3]Department of Earth Sciences, University of Oxford, Oxford, UK

[4]Bristol Isotope Group, Department of Earth Sciences, University of Bristol, Bristol, UK

The last five years have seen unprecedented advances in the measurement and application of non-traditional stable isotope systems, including the transition metals and elements such as Li, Mg, Si, Tl and U. Improvements in analytical precision have facilitated the application of these isotope systems to magmatic processes, where the magnitudes of stable isotope fractionation ($\propto 1/T^2$) are expected to be small. Previous studies have shown that Fe stable isotopes in igneous rocks are a potential tracer of changes in mantle oxidation state [1, 2]. Variations in the Fe isotope composition of the mantle may, therefore, provide an independent means of monitoring secular variations in mantle oxygen fugacity (fO_2) complimenting information from other tracers, such as V/Sc ratios [3], V partitioning data [4], and Fe^{3+}bearing mineral equilibria. However, it has also been shown that Fe isotopes are fractionated by processes such as metasomatism [5] and magma differentiation [6, 7] and it is important to be able to distinguish these effects from fractionation induced by melting and variations in fO_2. In order to investigate this further, a series of highly characterised peridotite xenoliths from Salt Lake Crater, Oahu, Hawai'i [8], which display extreme variations in fO_2 [9], were analysed for their Fe isotope compositions. The Fe isotope compositions of both separated minerals and bulk samples display striking negative correlations with indicators of melt extraction such as Mg/Mg+Fe as well as Hf isotope compositions. No correlation exists between Fe isotopes and fO_2, Sr or Nd isotopes or highly incompatible elements such as the LREE, which are all considered to have been reset by metasomatic processes. Iron stable isotopes therefore have the potential to "see through" metasomatic events and record primary melt extraction processes.

The Fe isotope compositions of metabasalts and ultramafic rocks from Isua (3.6 Ga) and komatiites from Belingwe (2.7 Ga), Vetreny (2.4 Ga) and Gorgona (0.089 Ga) define clear arrays with Mg/Mg+Fe and redox-sensitive trace element ratios such as V/Sc [10, 11]. These data provide evidence for the fractionation of Fe isotopes during melting, with the partitioning of Fe^{3+} and isotopically heavy Fe into the melt phase and, critically, demonstrate that the nature of this fractionation appears has remained more or less constant over the last 3.6 Ga. This observation implies that the Earth's mantle has been oxidised since the Archean, in agreement with other studies.

[1] Williams et al., 2004 *Science* **304,** 1656–1659; [2] Dauphas et al., 2009, *EPSL* **288,** 255-267; [3] Lee et al., 2005, *J. Pet*, **46,** 2313-2336; [4] Canil, 1999, *GCA* **63** 557-572 [5] Weyer and Ionov, 2007, *EPSL* **259,** 119–133 [6] Teng et al., 2008, *Science* **320,** 1620-1622; [7] Schuessler, 2009, *Chem Geol* **258,** 78-91; [8] Bizimis et al., 2003, *EPSL*, **217**, 43-58; [9] Tibbetts et al., 2010, *GCA* **74** Suppl 1 A1045; [10] Hibbert et al., 2012, *EPSL,* in press; [11] Williams and Moorbath, 2012, *in prep*.

https://doi.org/10.1180/S0026461X00008434 Published online by Cambridge University Press

Iron isotope variations in Icelandic soil profiles and fractionation of Fe isotopes during weathering

HELEN M. WILLIAMS[1]*, SOPHIE OPFERGELT[2,3], CHRISTOPHER SIEBERT[3], REBECCA NEELY[3] & KEVIN W. BURTON[1]

[1]Department of Earth Sciences, Durham University, Durham, UK (* presenting author; h.m.williams2@durham.ac.uk)

[2]Earth and Life Institute, Université catholique de Louvain, Louvain-la-Neuve, Belgium

[3]Department of Earth Sciences, University of Oxford, Oxford, UK

Iron stable isotopes have considerable potential as a new geochemical tool that can be used to address the bioavailability and biogeochemical cycling of Fe in soils and the behaviour of Fe during weathering processes. The degree to which Fe isotopes may be fractionated during pedogenic and weathering processes is, however, controversial [e.g. 1-4]. This study investigates the distribution of Fe stable isotopes in four typical Icelandic soil profiles from a basaltic catchment (Borgarfjördur): Histic Andosol (HA), Histosol (H), Gleyic Andosol (GA), Brown andosol (BA). Among the soil profiles, the weathering degree increases following the sequence BA<GA<H<HA, as supported by a decreasing Total Reserve in Bases (TRB, the total content in Ca+Na+Mg+K) or an increasing content in crystalline Fe-oxides with increasing weathering. These soil profiles are all derived from the same parental basalt and hence provide an ideal opportunity to investigate the response of Fe stable isotopes to pedogenic and weathering processes. Bulk soil samples, pore waters, oxalate extracts (Fe_O, specific for short range ordered Fe-oxide and humus-bound Fe) and dithionite–citrate–bicarbonate extracts (Fe_d, including Fe_O and crystalline Fe oxides, thus excluding Fe bound in silicates) were analysed for their Fe isotope compositions by MC-ICP-MS (Thermo Neptune) at Durham University using standard Fe purication and mass spectrometry procedures (long-term reproducibility: 0.03‰/amu 2 S.D.; blanks < 1ng Fe) [5]. Bulk soil Fe isotope compositions (δ^{57}Fe, relative to the IRMM014 Fe standard) are correlated with the TRB weathering index: the most weathered soil profiles (e.g. HA) display isotopically light and variable Fe isotope compositions (-0.55 ± 0.08‰ to 0.20 ± 0.04‰ 2 S. D.) relative to the parental Icelandic basalt (0.07 ± 0.08‰), providing direct evidence for the fractionation of Fe isotopes during weathering to progressively lighter values. In contrast, poorly weathered soils (e.g. BA) display relatively invariant Fe isotope compositions (0.01 ± 0.07‰ to 0.20 ± 0.06‰) within error of the δ^{57}Fe value of the parental basalt. In these poorly weathered soil profiles, pore waters, Fe_O and Fe_d also show minimal deviations in δ^{57}Fe value with respect to the parental basalt, whereas in the highly weathered HA soil profile the Fe isotope compositions of pore waters, Fe_O and Fe_d are highly fractionated. In HA, the Fe isotope compositions of Fe_d are extremely similar to those of the bulk soils, reflecting the large proportion of crystalline Fe oxides in this soil profile. In contrast, Fe_O from the near-surface horizons in HA (0.34 ± 0.08‰ to 0.66 ± 0.06‰) are heavier than the bulk soil and become increasingly lighter than the bulk soil with depth. This pattern is also displayed by the soil pore waters, which suggests that the cristallinity of Fe-oxides in soils partly controls the fractionation of Fe isotopes in dissolved Fe in pore waters.

[1] Guelke et al., (2010) *Chemical Geology,* 277, **3–4**, pp 269-280; [2] Poitrasson et al., (2008) *Chemical Geology,* 253, **1–2**, pp 54-63; [3] Emmanuel et al., (2005) *Chemical Geology,* 222, **1–2**, pp 23-34; [4] Wiederhold et al., (2007) *GCA,* 73, **23**, pp 5821-5833; [5] Williams et al., (2012) *EPSL,* in press

Accounting for post-depositional effects of a neo-Tethyan Permian-Triassic Section in the Himalayan Mountains.

JEREMY C. WILLIAMS[1*], ROBYN HANNIGAN[1], ASISH BASU[2], NILOTPAL GHOSH[2], AND MICHAEL BROOKFIELD[1]

[1] University of Massachusetts Boston, Department of Environmental, Earth, and Ocean Sciences, Boston, MA USA 02125

Jeremy.Williams002@umb.edu (* presenting author)

[2] Univeristy of Rochester, Department of Earth and Environmental Science, Rochester, NY USA 14627

The Permian-Triassic Boundary (PTB) extinction is considered the largest extinction in earth's history. However interpreting paleo-environmental conditions from sedimentary records may prove difficult due to the occurrence and preservation of PTB sections. The PTB sediments of the Spiti Valley (Himchal Pradesh, Himalaya, India) have been subjected to diagenesis and low-grade metamorphism. These two processes potentially alter the original geochemical signatures. In Spiti Valley, PTB sections consist of Permian Gungri Formation (Kuling Group) black shale unconformably overlain by an iron-rich pebbly layer ("ferruginous layer") which marks the PTB. Overlying the ferruginous layer is the Triassic Mikin Formation, a limestone inter-bedded with calcareous and black shales. In this study we assessed the post-depositional overprint on the geochemistry of Spiti Valley Muth PTB section using methods geochemical and chemometric approaches to identify original signatures preserved in this section. The results show that the section does preserve original signatures useable for paleoenvironmental reconstruction. More importantly we show evidence of depositional events preceding the Neo-Tethyan main regression associated with the timing of the extinction.

https://doi.org/10.1180/S0026461X00008434 Published online by Cambridge University Press

Microbial reduction of U(VI) at alkaline pH relevant to geological disposal

ADAM J. WILLIAMSON,[1*] KATHERINE MORRIS,[1] GARETH T. W. LAW,[2] SAMUEL SHAW,[3] AND JONATHAN R. LLOYD[1]

[1] Research Centre for Radwaste and Decommissioning and Williamson Research Centre, School of Earth, Atmospheric and Environmental Sciences, The University of Manchester, adam.williamson-2@postgrad.manchester.ac.uk (* presenting author), katherine.morris@manchester.ac.uk, and jon.lloyd@manchester.ac.uk

[2] Research Centre for Radwaste and Decommissioning and Centre for Radiochemistry Research, School of Chemistry, The University of Manchester, gareth.law@manchester.ac.uk

[3] School of Earth Sciences, University of Leeds, s.shaw@see.leeds.ac.uk

The UK's intermediate level radioactive wastes (ILW) will be disposed of in a deep geological disposal facility (GDF) [1]. Here, one likely scenario for disposal in the UK GDF is mixing ILW with cement, grouting into stainless steel canisters followed by further backfilling with cement. Post-closure, re-saturation of the cementitious GDF over time will form a hyperalkaline chemically disturbed zone (CDZ) within the host rock.

Microbial processes, especially Fe(III) reduction, may immobilise redox active radioactive contaminants in the waste either through direct enzymatic reduction or via interactions with biogenic Fe(II) [2]. Here, we explore the extent of microbiologically-mediated U(VI) reduction under GDF relevant alkaline conditions. Microcosms were set up using sediments taken from legacy lime works, adjusted to pH 10, augmented with electron donor (organic acids with yeast extract) and systems were run with and without added Fe(III) oxyhydroxides. Systems were established with lower (20 ppm) and higher (100 ppm) concentrations of UO_2^{2+} and allowed to progress through a series of redox processes, potentially including metal reduction, and to assess sorption of U(VI), uranium biotransformations and to prepare samples for XAS analysis.

A cascade of microbial redox processes occurred at high pH in all microbially active systems with U(VI)-removal occurring in sediments with and without added Fe(III) oxyhydroxides. In Fe(III) augmented systems, which displayed high levels of Fe(III)-reduction, magnetite was the dominant Fe(II) bearing bio-mineral product. XANES analyses of all microbially active sediment end-members confirmed reduction of U(VI) to U(IV). Interestingly, controls using pre-reduced, autoclaved sediments showed no sign of U(VI) reduction, suggesting that U(VI) reduction in these systems is predominantly enzymatic. Overall, these results show that microbial metal reduction can occur in a high pH environment analogous to that of an evolved GDF and demonstrates the reductive removal of U(VI) from solution in such systems is likely mediated by direct enzymatic processes.

[1] Morris, K. Law, G.T. & Bryan, N.D. (2011). *Issues in Environmental Science and Technology* **32,** 129-151.
[2] Lloyd, J.R. (2003). *FEMS Microbiology Reviews* **27,** 411-425.

SIMS carbon isotope analysis of Proterozoic microfossils

KENNETH H. WILLIFORD[1*], TAKAYUKI USHIKUBO[1], J. WILLIAM SCHOPF[2], KEVIN LEPOT[1], KOUKI KITAJIMA[1], JOHN W. VALLEY[1]

[1]WiscSIMS, NASA Astrobiology Institute, Dept of Geoscience, University of Wisconsin, Madison, WI, USA, kwilliford@geology.wisc.edu (* presenting author)

[2]Dept of Earth and Space Sciences, University of California, Los Angeles, CA, schopf@ess.ucla.edu

We present new in situ carbon isotope ($\delta^{13}C$) data from permineralized microfossils in the stromatolitic cherts of the Gunflint (~1880 Ma), Bitter Springs (~830 Ma), Chichkan (~775 Ma), and Min'yar (~740 Ma) Formations. Specimens were selected for their excellent preservation and analyzed in thin section with a reproducibility of 1–2‰ (2 SD) using secondary ion mass spectrometry (SIMS). The range of $\delta^{13}C$ values (–34.6 to –22.1‰ VPDB) exhibited among the 46 specimens is consistent with photoautotrophic carbon fixation by ribulose bisphosphate carboxylase (RuBisCO), the acetyl-CoA pathway, or heterotrophic assimilation. In light of the morphologies, however, the $\delta^{13}C$ values support taxonomic assignments of these specimens as photoautotrophs using RuBisCO. Fossil cyanobacteria from the Gunflint, Bitter Springs, and Min'yar Formations, for which available carbonate $\delta^{13}C$ data can be used to estimate $\delta^{13}C$ of dissolved organic carbon (DIC), exhibit a consistent ~20‰ total fractionation ($\delta^{13}C_{DIC} - \delta^{13}C_{org}$) similar to that observed in living cyanobacteria. Morphologically diverse microfossils in a ~1 mm^2 part of a microbial mat from the Min'yar Formation exhibit $\delta^{13}C$ values that correlate with morphology-based taxonomy and cellular anatomy, suggesting that isotopic signatures of their original biosynthetic processes are preserved. Carbon isotopic compositions consistent with the different fractionations observed in modern cyanobacterial and eukaryotic RuBisCO are preserved in a colonial cyanobacterium and a phytoplanktonic protistan acritarch situated < 1 cm apart in in the stromatolitic Chichkan chert.

Due to the low total organic carbon (TOC) of permineralized microfossils, analyses were conducted using a relatively large (15 µm) spot, high (2.5 nA) intensity primary beam, an electron multiplier to collect ^{13}C, and standardized with a low TOC carbonaceous chert PPRG 215-1 [1,2]. This is distinct from our technique for $\delta^{13}C$ analysis of high TOC materials (e.g., kerogen in shales) which employs a 6 µm spot, two faraday cup collectors, an anthracite coal standard, and has a reproducibility of 0.4‰ (2 SD) [3]. Standardization of microfossils with kerogen in a low TOC carbonaceous chert avoids potential barriers to accuracy (different instrumental bias) presented by standardization with crystalline materials that have a high C content (e.g., graphite), and along with analyses of microfossils from the Gunflint and Bitter Springs Formations, the PPRG 215-1 standard enables a direct interlaboratory comparison with the first study of this kind [2].

Results from these exceptionally well-preserved Proterozoic microfossil specimens provide a baseline for a more extensive study of the effect of organic matter preservation on carbon isotope composition in a large suite of Proterozoic microfossils [4], and they demonstrate that it is possible to distinguish subtle differences between metabolic (e.g., eukaryotic vs. bacterial RuBisCO) and biosynthetic (e.g., peptidoglycan vs. lipid synthesis) pathways in individual ancient microbial fossils [5].

[1] Walter et al. (1983) *Earth's Earliest Biosphere: It's Origin and Evolution*. Princeton Univ. Press, 385–413. [2] House et al. (2000) *Geology* **28**, 707-710. [3] Williford et al. (2011) AGU Fall Meeting Abs. B21E-0323 [4] Schopf et al. (2005) *Astrobiology* 5, 333-371. [5] Williford et al. (in review) *EPSL*.

https://doi.org/10.1180/S0026461X00008434 Published online by Cambridge University Press

Anaerobic methanotrophy in Cretaceous methane seep deposits, Canadian High Arctic

K.WILLISCROFT[1*], B. BEAUCHAMP[2], S. GRASBY[3], D. BIRGEL[4]

[1]University of Calgary, Calgary, Canada, krwillis@ucalgary.ca (* presenting author)
[2]University of Calgary, Calgary, Canada, bbeaucha@ucalgary.ca
[3]Geological Survey of Canada, Calgary, Canada, steve.grasby@nrcan.gc.ca
[4]University of Vienna, Vienna, Austria, daniel.birgel@univie.ac.at

Over 120 ancient methane seep deposits have been found on Ellef Ringnes Island, Canadian high Arctic, within the Early Cretaceous marine shale of the Christopher Fm. The seep deposits range in size from less than 0.3 m to over 7 m height and are composed of varying proportions of background sediment and authigenic calcite. Many mounds are highly fossiliferous, including abundant bivalves, ammonites and tubeworms.

The $\delta^{13}C_{carbonate}$ values range from -55‰ to -30‰, implying an origin through oxidation of methane and subsequent carbonate deposition. The seep mounds are largely confined to one stratigraphic horizon indicating a major methane flux from the basin occurred at that time. This timing is consistent with the basin burial history and onset of thermogenic methane production, suggesting gas migration to the sea floor was synchronous with methane generation.

Mo/Al ratios of the seep deposits, in comparison to the surrounding Christopher shale host, suggests seep deposits formed in an isolated anoxic setting in an otherwise oxic environment. Biomarker analysis is consistent with this model and suggests anaerobic oxidation of methane (AOM) was most likely carried out by both ANME -1 and -2 archaea, which may represent various consortia active either temporarily or spatially. The low contents of SRB-derived biomarkers may point to a predominance of ANME-1, which are not closely tied to sulphate reducing bacteria (SRB).

Due to the local anoxic conditions during deposition, many early diagenetic carbonate phases preserve organic matter, with the exception of high magnesium botryoidal calcite, which is completely devoid of organic material. There are no hopanoids or steroids preserved in any of the methane seep deposit phases to support aerobic methanotrophy, indicating that these cements do not represent a switch to more oxic conditions as originally interpreted. Instead it is proposed that the waxing and waning of methane/nutrient flux and its ability to move through the sediment is controlling the precipitation of the two cement phases. Alternatively, it is also possible the rate of microbial growth and methanotrophy during cementation effects the formation of the two cements.

Imposed redox frequency and amplitude flux in the study of iron biogeochemical dynamics

JARED WILMOTH[1*], CHRISTOF MEILE[2], BRIAN GINN[1], TIM PASAKARNIS[3], STEVEN HALL[4], MICHELLE SCHERER[3] AND AARON THOMPSON[1]

[1]University of Georgia, Crop and Soil Sciences, Athens, USA, jwilmoth@uga.edu, AaronT@uga.edu
[2]University of Georgia, Dept. of Marine Sciences, Athens, USA, cmeile@uga.edu
[3]University of Iowa, Environmental Engineering and Science, Iowa City, USA, timothy-pasakarnis@uiowa.edu, michelle-scherer@uiowa.edu
[4]University of California Berkeley, Environmental Science, Berkeley, USA, stevenhall@berkeley.edu

The chemical stability and microbial bioavailability of iron (Fe) oxides in soils, and the coupling between carbon (C), Fe and phosphorous (P) cycles, depends on biogeochemical conditions and their temporal variability. To assess the impact of periodic redox fluctuations commonly found in variably saturated soils, a custom bioreactor system was developed in which redox fluctuations (i.e. Eh frequency and amplitude) were imposed via N_2 and O_2 gas exchange with Bisley, Puerto Rico, (CZO) soil suspensions while allowing for sub-sampling of Fe, P, CO_2 and microbial DNA. Characterization of Bisley site soils included variable temperature ^{57}Fe-Mössbauer spectroscopy (at 298, 140, 70, and 15K), X-ray diffraction (XRD) and chemical extractions of operationally defined Fe pools to evaluate Fe phase heterogeneity. Extraction data show that 20% of the total Fe oxide pool is associated with the dithionite-citrate-bicarbonate (DCB) fraction, of which half is associated with the citrate-ascorbic acid (CA) fraction. Mössbauer spectra show quadrapole distribution sites for Fe^{II}/Fe^{III} in clay and a hyperfine distribution site (sextet) that closely resembles that of nano-goethite. The difference between averaged sextet spectral areas at 70 and 15K (11.7% relative abundance) may correlate with the % abundance of CA extracted Fe. Currently, microbial fingerprinting techniques (i.e. denaturing gradient gel electrophoresis (DGGE) and ribosomal intergenic transcribed spacer analysis (RISA)) are being used to characterize changes in bacterial community composition in response to bioreactor redox oscillations. Finally, process-based kinetic model simulations have been used to describe and test mechanisms of Fe reduction, abiotic transformations, phase partitioning, and microbial population growth in the Bisley (CZO) soils. Preliminary simulations show that Fe concentrations can be reproduced closely by adjusting the time period in oxic and anoxic cycles in accord with experimental conditions.

https://doi.org/10.1180/S0026461X00008434 Published online by Cambridge University Press

Atmospheric dust input to the Subarctic North Pacific

GISELA WINCKLER[1,2*], SASCHA SERNO[1,3], ROBERT F. ANDERSON[1,2], CHRIS T. HAYES[1,2], HAOJIA REN[1], RAINER GERSONDE[4], GERALD H. HAUG[5]

[1]Lamont-Doherty Earth Observatory, Columbia University, Palisades, NY, USA, winckler@ldeo.columbia.edu (* presenting author)
[2]Department of Earth and Environmental Sciences, Columbia University, New York, NY, USA
[3]DFG-Leibniz Center for Surface Process and Climate Studies, Potsdam University, Potsdam-Golm, Germany
[4]Alfred Wegener Institute for Polar and Marine Research, Bremerhaven, Germany
[5]Geological Institute, Climate Geology, ETH Zürich, Zürich, Switzerland

The Subarctic North Pacific is one of the three primary high-nutrient-low chlorophyll regions of the modern ocean, where the biological pump is relatively inefficient at transferring carbon from the atmosphere to the deep sea. The system is thought to be iron-limited. Atmospheric dust is an important source of iron and other trace elements that are essential for the health of marine ecosystems and potentially a controlling factor of the high-nutrient-low chlorophyll status of the Subarctic North Pacific. However, spatial patterns of dust fluxes in the present and in the past are poorly known for this region.

We trace and quantify the supply of sedimentary phases across surface sediments from 37 multi-core core-top sediments from the Subarctic North Pacific, obtained during the SO202/INOPEX cruise in 2009, in order to obtain a robust representation of the spatial pattern in the supply of dust. To this end, we map the spatial patterns of Th/U isotopes, helium isotopes and rare earth elements in. In order to deconvolve the detrital endmembers in regions of the North Pacific affected by volcanic material, IRD and hemipelagic input, we use a combination of trace elements with distinct characteristics in the different endmembers. This approach allows us to calculate the relative eolian fraction, and in combination with ^{230}Th-normalized mass flux data, to quantify the dust supply.

We compare the spatial patterns of the reconstructed dust fluxes to results of published reconstructions of modern dust trajectories, model output and water column based estimates. The results from this study will be used for future research focusing on dust flux and productivity changes during the abrupt climate change sequence of the last deglaciation: the sequence from the cold and dusty Heinrich Stadial 1, through the dust-poor Bølling-Allerød warm period and a return to the near-glacial conditions of the Younger Dryas stadial. Ultimately, our results will allows us test the traditional hypothesis of eolian iron input primarily controlling the biological productivity in the Subarctic North Pacific and to evaluate how the Subarctic North Pacific's ecosystem mediates climate change.

Origin and evolution of Red Sea brines - Insights from noble gases

GISELA WINCKLER[1,2*], WERNER AESCHBACH-HERTIG[3], ROLF KIPFER[4], REINER BOTZ[5], MARK SCHMIDT[6] AND ENRICO BONATTI[1]

[1]Lamont-Doherty Earth Observatory, Columbia University, Palisades, NY, USA, winckler@ldeo.columbia.edu (* presenting author)
[2]Department of Earth and Environmental Sciences, Columbia University, New York, NY, USA
[3]Institute of Environmental Physics, University of Heidelberg, Germany
[4]EAWAG, Dep. Water Resources and Drinking Water, Duebendorf, Switzerland
[5]Institute of Geosciences, University of Kiel, Germany
[6]GEOMAR Helmholtz Center for Ocean Research Kiel, Germany

The Red Sea represents a unique setting where an oceanic basin is actively forming and, thus, is an ideal natural laboratory to study young rifiting processes and to test models of hydrothermal circulation. The central rift zone of the Red Sea is known to contain more than twenty morphological depressions filled by highly saline brines. Historically, one of these deeps, the Atlantis II brine, provided the first geochemical evidence for the existence of hydrothermal vents on the ocean floor [1].

Due to their conservative nature, noble gases represent powerful tools to study the dynamics of fluid systems. They have proven to be useful to decode the complex geochemical processes underlying the origin and formation of the Red Sea brines and their relation to the tectonic setting of the Red Sea. Atmospheric noble gas data are used to reconstruct dynamic processes such as bubble formation and degassing within the brine layer and at the brine/seawater interface or boiling. Non-atmospheric noble gas isotope data, i.e. helium and argon isotopes, are applied to interpret the origin of the brines in the tectonic context of the Red Sea.

Here, we present a compilation of atmospheric and non-atmospheric noble gas data from several brine basins, the Kebrit, Discovery and Atlantis II Deep [2,3] as well as new noble gas data from the Shaban Deep, the northernmost Deep of the Red Sea [4]. The noble gas data provide unique insights into the development of sea floor spreading in this active region. Placing the new data in the context of the previous studies, the Shaban Deep appears to be an isolated seafloor spreading cell similar to, but less developed than the Atlantis II Deep.

[1] Degens and Ross (1969) Hot Brines and Heavy Metal Deposits in the Red Sea. *Springer, New York*. [2] Winckler et al. (2000) *Geochimica et Cosmochimica Acta* **64 (9)**, 1567-1575. [3] Winckler et al. (2001) *Earth and Planetary Science Letters* **184**, 671-68, [4] Aeschbach-Hertig et al. (2012), in prep.

https://doi.org/10.1180/S0026461X00008434 Published online by Cambridge University Press

Geochemical and bacterial evidence for 9800 years of meromixis and euxinia in alpine Lake Cadagno

S.B. WIRTH[1*], A. GILLI[1], T.W. DAHL[2], H. NIEMANN[3], D. RAVASI[4], M.F. LEHMANN[3], R. PEDUZZI[4], S. PEDUZZI[4,5], M. TONOLLA[4,5,6] & F.S. ANSELMETTI[7]

[1]Geological Institute, ETH Zürich, Zürich, Switzerland
[2]Institute of Biology and NordCEE, University of Southern Denmark, Odense, Denmark
[3]Department of Environmental Sciences, University of Basel, Basel, Switzerland
[4]Alpine Biology Centre Foundation, Piora, Switzerland
[5]Cantonal Institute of Microbiology, Bellinzona, Switzerland
[6]Microbiology Unit, Department of Botany and Plant Biology, University of Geneva, Geneva, Switzerland
[7]Eawag, Swiss Federal Institute of Aquatic Science and Technology, Dübendorf, Switzerland

Lake Cadagno is a meromictic high-alpine lake in the southern Alps of Switzerland (1921 m asl, 0.26 km^2, max. water depth 21 m). The inflow of sulfate-rich waters from subaquatic springs located in dolomitic bedrock results in a permanent chemocline at 10 to 13 m water depth with sulfidic conditions in the hypolimnion [1]. As yet, it is unknown how far back in time euxinia has prevailed in the Lake Cadagno water column, maintaining a diverse anaerobic community of bacteria at and below the redox-transition zone.

Here, we present results documenting the lake's redox-state evolution through the Holocene period using sediment cores (10.5 m) that cover the past ~12,000 years and applying sedimentological, geochemical and molecular analyses.

Trace metal analysis by XRF core scanning and ICP-MS measurements documents the transition from oxic conditions after the lake formation (~12,000 cal yr BP) to sulfidic conditions at 9800 cal yr BP. Part of this transition is a ~1000-year period with enhanced accumulation of Mn (up to 5.9 wt% of Mn) in the sediments, indicating an intermediate oxygenation state with fluctuating redox conditions. We propose that the high Mn concentrations are the result of Mn^{2+} leaching from the sediments during reducing conditions and subsequent rapid precipitation of Mn-oxide minerals during episodic and short-term mixing events. Thereafter, a stable chemocline formed and sulfidic conditions, documented in the sediments by high Mo burial rates (Mo concentrations of up to 470 ppm) [2], prevailed until modern times without any lasting hypolimnetic oxygenation. The onset of euxinia probably corresponds in time to the actuation of the subaquatic springs after the last glacial termination.

The evidence of a stable and persistent chemocline over ~10 kyr in Lake Cadagno offers the framework to study the evolution of anaerobic bacterial communities in an extreme lacustrine environment that could serve as an equivalent for conditions in ancient oceans.

[1] Del Don *et al.* (2001) *Aquat. Sci.* **63**, 70-90. [2] Dahl *et al.* (2010) *Geochim. Cosmochim. Acta* **74**, 144-163.

A general quasi-chemical solution model for ordered many-component systems

AARON S. WOLF[1*], PAUL ASIMOW[1], AND RAZVAN CARACAS[2]

[1]California Institute of Technology, Geological and Planetary Sciences, Pasadena, USA, awolf@caltech.edu (* presenting)
[2]Ecole Normale Superieure de Lyon, Laboratoire de Sciences de la Terre, Lyon, France

As first principles quantum mechanical techniques have developed to take advantage of increasing computational power, theoretical mineral physicists have begun to turn their attention toward more realistic systems with greater compositional complexity. While it is now possible to use density functional theory to calculate Gibbs energies of both crystal and liquid solutions composed of many compositional end-members, we will forever be limited by the exponential growth of the parameter space with each added component. Resigned to only sparsely sampling such large many-dimensional composition spaces, we must therefore rely on accurate, and ideally predictive, solution models to interpolate into the large intervening spaces between data points.

In this talk, we will present a new quasi-chemical model that can be used to accurately describe the Gibbs energy surface for many component solutions in addition to providing a physically-based method for projecting into the interior of the many-component space. Our model is a union and extension of the work presented on the polynomial solution model in Saulov (2006) and on the modified associates model in Saulov (2009) [1, 2]. In particular, we have adapted this quasi-chemical model, which is carefully constructed to avoid violating entropy constraints, and applied it to describe the locally ordered regions of solutions. By fitting the model to data along the bounding binaries of the system, we can estimate the non-ideal Gibbs energy cost associated with having local n-body regions in the solution of mixed composition. We have further developed and fully generalized a probabilistic projection method, extending Saulov (2006) to many dimensional systems with Gibbs energy surfaces of realistic complexity, which uses the derived set of binary models to project inside the ternary, quaternary, or higher dimensional space. Because the model is physical rather than merely geometric, it has considerably more predictive power than other commonly used projection methods like the Kohler or Muggianu models [3]. Also, we incorporate a statistically rigorous probability weighting scheme, which straightforwardly produces error estimates on the resulting Gibbs energy surface while enabling mixed compositional data to be incorporated and later used to update model parameters.

We will also discuss the strengths and limitations of the model, by applying it to a number of example solid and liquid solutions. For the liquid solutions, we discuss the difficulties posed with deciding what to choose as the basic "atomic unit" of mixing. For the more straightforward case of solid solutions, we will apply the model to our own DFT calculations and use it to understand the role of spin state in iron-bearing magnesium silicate perovskite.

[1] D. Saulov, (2006) *Calphad.* [2] D. Saulov et al., (2009) *Journal of Alloys and Compounds.* [3] M. Hillert, (1998) *Cambridge University Press*.

https://doi.org/10.1180/S0026461X00008434 Published online by Cambridge University Press

Fluorite (U-Th)/He thermochronology

R. WOLFF[1*], I. DUNKL[2], H.V. EYNATTEN[3]

[1]University of Göttingen, GZG-Sedimentology, Göttingen, Germany, rwolff@gwdg.de
[2]University of Göttingen, GZG-Sedimentology, Göttingen, Germany, idunkl@gwdg.de
[3]University of Göttingen, GZG-Sedimentology, Göttingen, Germany, heynatt@gwdg.de

Why fluorite?

The (U-Th)/He method is a low-temperature thermochronometer dating single crystals. It uses the ^{4}He accumulation from the radioactive decay of U, Th and Sm. The most used U and Th bearing accessory minerals are apatite and zircon with closure temperatures of 60 - 70 and ~180 °C. However, more minerals are suited for (U-Th)/He chronology. Fluorite is one of these because it is quite common all over the world, occurs in high- and low-temperature felsic hosted hydrothermal veins and Mississippi Valley Type (MVT) ore deposits. Moreover, its geochemistry is well studied. Consequently, fluorite (U-Th)/He chronology is promising for dating hydrothermal events, secondary fluorite formation in limestones, or regional cooling events.

First results indicate the potential of this method [1,2,3,4,5]. However, the reported diffusion parameters and closure temperatures differ greatly. According to [3] the parameters are E_a = 30.5 ± 3.9 kcal/mol, $\log(D_o/r^2)$ = 4.9 ± 0.6 s^{-1} and T_c = 90 ± 10 °C (10°C/Ma, 1 - 3 mm) but [4] reports a closure temperature of T_c = 200 °C. Thus we decided to follow a two-fold strategy.

Approach and Results

On the one hand we perform a regional study in the Erzgebirge, Germany, that combines analysis of fluorite with the thermal history of the study area constrained by well established thermochronometers. The comparision of the results will indicate the closure temperature of fluorites for this case study. Diffusion experiments on the other hand give laboratory based information on the closure temperature and the diffusion parameters.

Our fluorite (U-Th)/He data fit well into the independently measured Upper Cretaceous to Paleocene regional cooling history of the Erzgebirge and the diffusion experiments suggest a behaviour of fluorite similar to Durango apatite.

Conclusions and Outlook

The results show that fluorite is suitable for low-temperature thermochronology. This opens a window into the chronology of hydrothermal systems, limestones and MVT ore deposites. Additional attention has to be turned on fluorite because it occurs in a variety of colors (colorless, yellow, pink, brown, green, blue, black, fetid fluorite). Due to changes in chemistry and REE patterns they may show also changes in diffusion kinetics.

[1] Evans (2002) *Geochim Cosmochim Acta* **66** (15A suppl 1), A219. [2] Evans (2005) *Journal of Analytical Chemistry* **60** (12), 1159–1165. [3] Evans (2005) *Applied Geochemistry* **20** (6), 1099–1105. [4] Pi (2005) *Mineralium Deposita* **39** (8), 976–982. [5] Siebel (2009) *International Journal of Earth Science* **99** (6), 1187-1197.

Calcite growth kinetics and solution stoichiometry

M. WOLTHERS[1,2*], G. NEHRKE[3], P. VAN CAPPELLEN[4]

[1]Department of Earth Sciences, Utrecht University, Utrecht, The Netherlands, m.wolthers@uu.nl (* presenting author)
[2]Department of Chemistry, University College London, London, United Kingdom.
[3]Alfred Wegener Institute for Polar and Marine Research, Bremerhaven, Germany, Gernot.Nehrke@awi.de
[4]Department of Earth and Environmental Sciences, University of Waterloo, Waterloo, Canada, pvc@uwaterloo.ca

The influence of solution stoichiometry on calcite crystal growth kinetics has recently attracted increasing attention. Here we present a process-based calcite growth model (Figure, adapted from [1]) that is founded in a surface structural model for the calcite–aqueous solution interface [2] and extends the growth model for binary symmetrical electrolyte crystals [3]. The model combines kinetic descriptions of the incorporation of calcium, carbonate and bicarbonate ions at kink sites along step edges, with equilibrium calculations of the surface chemical structure of the calcite–aqueous solution interface under variable chemical conditions. Key model parameters are calibrated by fitting the model to a selected set of step velocities on calcite surfaces measured by Atomic Force Microscopy [4-5]. Without any further adjustment of the parameter values, the model reproduces the observed dependence of the macroscopic growth rate of single calcite crystals on the solution activity ratio of calcium and carbonate ions under alkaline conditions. A variable surface roughness factor is introduced in order to reconcile the new process-based growth model with bulk precipitation rates measured in seeded calcite growth experiments. For practical applications, we further present empirical parabolic rate equations fitted to bulk growth rates of calcite in common background electrolytes and in artificial seawater-type solutions. Both the process-based and empirical growth rate equations agree with measured calcite growth rates over broad ranges of ionic strength, pH, solution stoichiometry and degree of supersaturation.

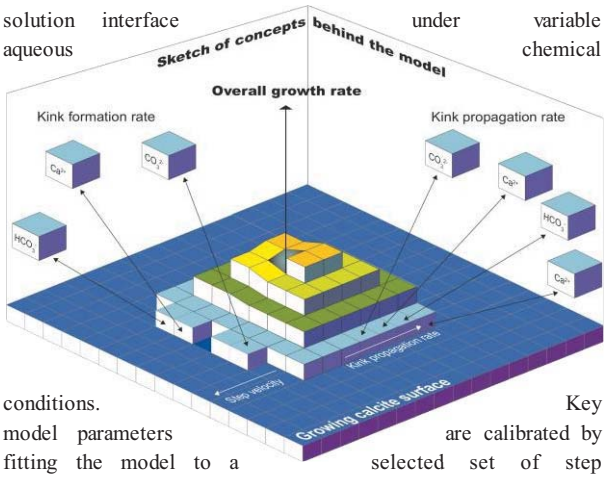

[1] Wolthers et al. (2012). *Geochim. Cosmochim. Acta* **77**, 121–134. [2] Wolthers et al. (2008) *Am. J. Sci*. **308**, 905–941. [3] Zhang and Nancollas (1998) *J. Colloid Interf. Sci*. **200**, 131–145. [4] Teng et al., (2000) *Geochim. Cosmochim. Acta* **64**, 2255–2266. [5] Stack and Grantham (2010) *Cryst. Growth Des*. **10**, 1414–1418.

https://doi.org/10.1180/S0026461X00008434 Published online by Cambridge University Press

Experimental investigation of mass-(in)dependent cadmium isotope fractionation during evaporation

FRANK WOMBACHER[1]*, VICTORIA KREMSER[1], WERNER ERTEL-INGRISCH[2], DON B. DINGWELL[2], CARSTEN MÜNKER[1], AND ALEXANDER HEUSER[3].

[1]Universität zu Köln, Institut für Geologie und Mineralogie, 50674 Köln, Germany, fwombach@uni-koeln.de (* presenting author).
[2]Ludwig Maximilians Universität, Department für Geo- und Umweltwissenschaften, 80333 München, Germany.
[3]Rheinische Friedrich-Wilhelms-Universität Bonn, Steinmann Institut, 53115 Bonn, Germany.

Evaporation experiments for volatile elements provide insight into stable isotope fractionation mechanisms and therefore aid in interpreting results from e.g. volcanic or meteorite samples.

We present data from two types of experiments: i) evaporation of molten Cd into vacuum at 10^{-4} mbar and ~180°C [1] ii) evaporation of Cd and other volatile elements from silicate melts at ~1300°C, atmospheric pressure and variable logfO2 using a mechanically assisted equilibration technique [2].

Cadmium stable isotope data were obtained using a Neptune MC-ICP-MS. To resolve small mass-independent anomalies, residual Cd metal samples were analysed at high ion beam intensities (typically > 20V for ^{114}Cd) and long analysis times (30 minutes). Loss of volatile elements from the silicate samples has been quantified using an ElementXR SF-ICP-MS and external calibration.

Residual Cd metal samples from vacuum evaporation experiments are well described by Rayleigh destillation with a vapor-residue fractionation factor $\alpha = 0.9900$ for ^{114}Cd/^{110}Cd (i.e. -10.0 ‰) [1]. This fractionation is much less than predicted from kinetic theory (α_{kin} = (mass ^{110}Cd / mass ^{114}Cd)$^{0.5}$ = 0.9829; i.e. -17.7 ‰), a mismatch that is frequently observed, e.g. [3]. In contrast, α for the high temperature evaportion from silicates under atmospheric pressure is much lower and corresponds to -1.6 and -0.3 ‰ respectively. The supressed Cd isotope fractionation may in part relate to back reaction.

The accurate quantification of mass-independent fractionation (MIF) in residual Cd metals required that the large mass-dependend fractionation is accurately corrected. This is facilitated using the generalized power law and normalization to ^{110}Cd/^{114}Cd of the starting material [1]. After correction, deficits ranging from 8 to 28 ppm were well resolved for ^{111,113,116}Cd/^{114}Cd. This pattern is in accord with predictions from nuclear charge radii and thus constrain nuclear volume effects. The preferential evaporation of ^{111}Cd, ^{113}Cd and ^{116}Cd may result from their more tightly bond 5s electrons and hence weaker metallic bonds in the liquid as previously suggested for Hg [4,5], another group 12 element. The observation of nuclear volume effects thus suggests that (metallic) bonding in the melt results in reduced fractionation factors.

[1] Wombacher *et al.* (2004) *GCA* **68**, 2349–2357. [2] Ertel-Ingrisch & Dingwell (2010) *AGU Fall meeting*, Abstract 966650. [3] Richter et al. (2009) *Chem. Geol.* **258**, 92–103 [4] Estrade *et al.* (2009) *GCA* **73**, 2693–2711. [5] Gosh *et al.* (*in press*) *Chem. Geol.*.

Metal-silicate partitioning of Mo and W: evidence for late S accretion

B. J. WOOD* AND J. WADE

University of Oxford, UK; berniew@earth.ox.ac.uk

Abstract

We have performed experiments to determine the partitioning of Mo and W between liquid Fe-rich metal and liquid silicate at pressures of 1.5-24 GPa and temperatures of 1803-2723K. Experiments performed in MgO capsules at 1.5 GPa/1923 K indicate that Mo is in the +4 oxidation state in the silicate at oxygen fugacities >2 log units below the IW (Fe-FeO) buffer. In contrast W^{6+} is the dominant tungsten oxidation state in the silicate at 1.5 GPa/1923 K and 1.8-3.3 log units below the IW buffer. We find no evidence that W changes oxidation state in the pressure range to 24 GPa.Metal-silicate partitioning of both Mo and W shows strong dependence on silicate melt composition with both elements becoming more siderophile as the melt becomes more SiO2-rich. When our results are considered in terms of a continuous accretion model consistent with the silicate Earth contents of Ni, Co, V, Cr and Nb, W should partition twice as strongly into the core as Mo. This is in stark contrast to the estimated core-mantle partition coefficients of ~40 for W and 90-140 for Mo. Neither changes to the accretionary path nor the assumption of partial disequilibrium alters the result. The cause is one of the light elements in the core.

The calculated Si content of the core (~4%) comes directly from the metal-silicate partitioning behaviour of Si (Tuff et al., 2011) and the P-T- oxidation state path of accretion defined by the refractory elements. This is not the cause of the discrepancy noted above. We therefore investigated the effect of S on our accretionary model by adding 2% of this element (consistent with cosmochemical estimates) to the core. If S is added at constant S/Fe ratio throughout accretion the net effect is negligible. If, however, S is added exclusively during the last 10-20% of accretion DMo and DW become consistent with the silicate Earth contents of these elements. We conclude that the Mo and W contents of the silicate Earth indicate that S (and other moderately volatile elements) was added to the Earth during core formation but only during the last ~20% of accretion. This conclusion is the same as that reached by (Schönbächler et al., 2010) from the Ag isotopic composition of silicate Earth.

Schönbächler, M., R. W. Carlson, M. F. Horan, T. D. Mock, and E H. Hauri, 2010, Science, v. 328, p. 884-887.

Tuff, J., B. J. Wood, and J. Wade, 2011, Geochimica Et Cosmochimica Acta, v. 75, p. 673-690.

https://doi.org/10.1180/S0026461X00008434 Published online by Cambridge University Press

Speciation of lead in aqueous solutions

RYAN J. WOOSLEY[1]* AND FRANK J. MILLERO [1]

[1]Rosenstiel School of Marine and Atmospheric Science, University of Miami, Miami, FL, USA rwoosley@rsmas.miami.edu (*Presenting author)
fmillero@rsmas.miami.edu

Introduction

Lead (Pb^{2+}) has been widely studied because of its toxicity to organisms. Since it is the chemical form that is important, rather than the total concentration, in determining the bioavailablity, behavoir and fate of the metal in natural waters, an accurate knowledge of speciation is required. Speciation is determined by complexation with organic and inorganic ligands, which is a function of temperature, inonic strength, and media; therefore reliable formation constants over a range of temperature, ionic strangth, and media are essential. In most natural waters, the inorganic speciation of lead is dominated by chloride and carbonate complexes. To date only a limited number of lead formation constatnts (β_i) have been made due to difficulty in their determination as a result of the limited solubitlity of lead. Instead, formation constants have often been estimated from correlations with other metals; direct measurements are limited. Recently serveral studies of lead chloride and lead carbonate complexation have been done over a large range of ionic strength and in several different media [1,2]. We've combined these previous measurements of lead chloride complexes in various media and lead carbonate complexes in $NaClO_4^-$ with new measurements of $PbCO_3$ in NaCl to model the speciation of lead in natural waters using a Pitzer model.

Pitzer Model

The formation constant of $PbCO_3$ in NaCl was measured using a spectrophotometric method since $PbCO_3$ is known to absorb in the ultraviolet, with a peak in the ultraviolet wavelengths. Measurments were made from 0.001-6 m NaCl at various [CO_3^{2-}]. The β_{PbCO3} was determined through nonlinear least-squares regressions using the global curve-fitting function in OrginPro 8.6. These formation constants were combined with earlier measurements of PbCl complexation (critically reviewed by [1]) and recent measurements of $PbCO_3$ in $NaClO_4^-$ [2] into a Pitzer model. These Pitzer coefficients allow for the inorganic speciation of lead to be determined in many natural waters including brines and seawater.

[1] Powell et al. (2009) Pure Appl. Chem. **81**(12) 2425-2476.
[2] Easley and Byrne (2011) Geochim. et Cosmochim. Acta **75**(19) 5638-5647.

Magnesium isotope cycling within *Acer saccharum* (sugar maple)

S. WORSHAM[1*], C. HOLMDEN[1], AND N. BÉLANGER[2]

[1]Saskatchewan Isotope Laboratory, University of Saskatchewan, Saskatoon, Canada (*correspondence: srw039@mail.usask.ca, ceh933@mail.usask.ca)
[2]Université du Québec à Montréal, Montréal, Canada (belanger.nicolas@teluq.uqam.ca)

Magnesium (Mg) serves as an important macronutrient for plants being involved with metabolic functions, respiration and most importantly, photosynthesis. Previous studies have demonstrated mass dependent fractionation of Mg within laboratory grown vegetation [1,2] while there has been only one confirmed case of plant fractionation in the field [3]. This study builds on previous work by coupling laboratory and field based investigations of Mg isotope fractionation within *Acer saccharum* (sugar maple) plants. Our main objective is to determine whether Mg isotopes might serve as useful tracer of a forest Mg-cycle.

The study site consists of a sugar maple stand within a first-order catchment located in southern Québec, Canada. Significant Mg isotope fractionation has been established between different tree tissues such as roots, stemwood, and leaves (both senescent and photosynthesizing) as well as other reservoirs including soil waters, precipitation, throughfall, and stream water. The total range of $\delta^{26}Mg$ ($^{26}Mg/^{24}Mg$) values within the study plot is $1.37‰_{DSM3}$ (approximately 30% of reported terrestrial variation).

Earlier laboratory based studies of potted plants have demonstrated a light isotope enrichment of Mg in the soil pool, complementing heavy isotope uptake and incorporation into plant material [1,2]. In contrast to these reported data trends, we do not see light isotope enrichment within the soil pool in nature when whole seedlings are analyzed as analogues of adult trees. We are conducting our own pot experiment with sugar maple to investigate this effect, which will guide our interpretations of this field study. Full results will be presented and discussed in detail regarding factors influencing Mg isotope cycling within a sugar maple dominated catchment.

[1] Black et al. (2008) Environ. Sci. Technol. **42**, 7831-7836. [2] Bolou-Bi et al. (2010) Geochim. Cosmochim. Acta **74**, 2523-2537. [3] Tipper et al. (2010) Geochim. Cosmochim. Acta **74**, 3883-3896.

https://doi.org/10.1180/S0026461X00008434 Published online by Cambridge University Press

Insights into zircon U-Pb systematics from intercalibration with astronomical time

JÖRN-FREDERIK WOTZLAW[1*], URS SCHALTEGGER[1], SILJA K. HÜSING[2] AND FREDERIK J. HILGEN[3]

[1]Earth and Environmental Sciences, University of Geneva, Geneva, Switzerland joern.wotzlaw@unige.ch (* presenting author)
[2]Paleomagnetic Lab., Department of Earth Sciences, Utrecht University, Utrecht, Netherlands
[3]Stratigraphy and Paleontology, Department of Earth Sciences, Utrecht University, Utrecht, Netherlands

High-precision U-Pb geochronology of accessory minerals is an integral part of various Earth Science disciplines. Recent advances in U-Pb geochronology by isotope dilution – thermal ionization mass spectrometry (ID-TIMS) allow dating of high uranium accessory minerals (most commonly zircon) at permil precision and external reproducibility. Such high temporal resolution may result in complex zircon age populations, reflecting prolonged growth, magma residence and/or zircon recycling, previously only resolvable by in-situ U-Th dating in Pleistocene magmatic systems. This allows to track the evolution of Cenozoic magmatic systems at unprecedented resolution and to add absolute time constraints to thermal and petrogenetic models. However, these complexities have also been considered to systematically bias zircon U-Pb derived eruption ages, to compromise chronostratigraphic applications of high-precision zircon U-Pb geochronology and to contribute to systematic offsets between the K-Ar and U-Pb systems [1,2].

Orbitally tuned Miocene sedimentary sequences around the Mediterranean contain abundant intercalated zircon-bearing ash beds. These sequences provide the rare opportunity to compare ash-bed zircon U-Pb dates with independent and accurate deposition ages derived from orbital tuning. This allows us to evaluate effects of prolonged crystallization and zircon recycling on zircon U-Pb derived ash bed deposition ages. We present a large data set (*N=18, n>200*) of high precision zircon U-Pb dates for ash beds from an almost continuous Messinian to Langhian (6.2-15.4 Ma) sedimentary sequence near Ancona, Italy [3, 4]. The majority of ash beds contain abundant zircons that predate eruption by several 10s to 100s of ka. However, considering only the youngest single zircon dates to interpret ash bed deposition, results in stratigraphycally consistent deposition ages that, for most of the section, agree with the astrochronologic age model. In the upper part of the section, we find an increasing offset between zircon U-Pb dates and astrochronologic age model within an ~8 m thick ash-rich interval. This may suggest that prolonged zircon growth and zircon recycling is more likely to bias U-Pb dates over short, ash-rich intervals where ash beds are likely derived from a repeatedly tapped, common magmatic source.

[1] Simon et al. (2008) *EPSL* **266**, 182-194. [2] Renne et al. (2010) *GCA* **74**, 5349-5367. [3] Hüsing et al. (2009) EPSL **282**, 140-157. [4] Hüsing et al. (2010) *EPSL* **290**, 254-269.

Temperature dependent structural changes in aluminoborosilicate melts with different modifier cations (Na, Ba, Ca)

JINGSHI WU[1*], JONATHAN F. STEBBINS[1]

[1]Stanford University, Department of Geological & Environmental Sciences, Stanford, California, USA, jswu@stanford.edu (* presenting author), stebbins@stanford.edu

Introduction

Borosilicate glasses and melts are critical in technology. Because of the ease of transition among three- and four-coordinated boron with composition, temperature and pressure, they may also serve as analog system for silicates at high pressure. The effect of temperature on the structure of aluminoborosilicate liquids has been studied by ^{11}B, ^{17}O and ^{27}Al MAS NMR spectroscopy using glass samples prepared with different cooling rates and thus different fictive temperatures (T_f). The abundances of BO_3 groups and of non-bridging oxygens (NBO) increase with increasing T_f, indicating that the reaction $BO_4 \leftrightarrow BO_3$+NBO shifts to the right at a higher T. The modifier cation with higher cation field strength (Valence/square of ionic radius) promotes formation of BO_3 and NBO.

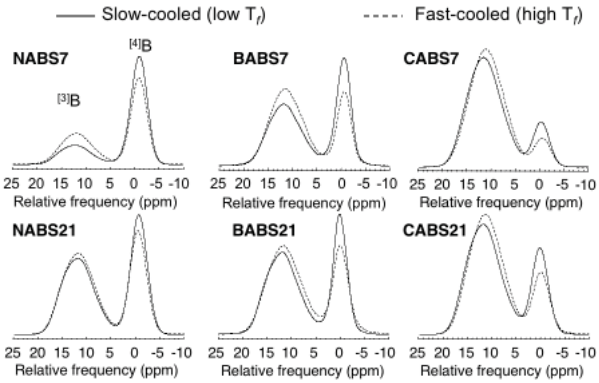

Figure 1: ^{11}B MAS NMR spectra at 14.1 Tesla. Dashed lines are samples with higher cooling rates. Solid lines are samples with low cooling rate. The peak centred around 12ppm is 3-coordinated boron, and the one centred around 0 ppm is 4-coordinated boron. The peak heights are normalized to constant total peak areas. The peak intensities are obtained by peak area integration. All the samples have 20 mol% of modifier cations (N for Na_2O, B for BaO, C for CaO), 8 mol% of Al_2O_3. The samples in first row have 7 mol% of B_2O_3, and 65 mol% of SiO_2; in the second row have 21 mol% of B_2O_3, and 51 mol% of SiO_2.

Conclusion

The observed T dependence of BO_4 species abundance allows us to estimate the enthalpy (ΔH) of the reaction $BO_4 \leftrightarrow BO_3$+NBO to be 20 to 50 kJ/mol in different glass compositions and closely related with the amount of NBOs in the glass. The ΔH is lower for the higher field strength network modifier cations ($Ca^{2+} > Ba^{2+} > Na^{+}$). This observation suggests that the divalent cations promote the formation of NBO much more effectively (lowers their enthalpy and thus free energy), which in turn helps to stabilize the modifier cation in the melt networks.

https://doi.org/10.1180/S0026461X00008434 Published online by Cambridge University Press

Stable iron isotope fractionation between aquoeus Fe(II) and smectite

LINGLING WU[1,2,3*], BRIAN L. BEARD[1,2], ANKE NEUMANN[4], MICHELLE M. SCHERER[4], ERIC E. RODEN[1,2], AND CLARK M. JOHNSON[1,2]

[1]University of Wisconsin-Madison, Madison, USA, lwu@geology.wisc.edu (* presenting author)
[2]NASA Astrobiology Institute, Madison, USA
[3]University of Waterloo, Waterloo, Canada
[4]University of Iowa, Iowa City, USA

Redox transformations of Fe-bearing phyllosilicate minerals play an important role in Fe cycle in the subsurface environments. This experimental study determined the stable Fe isotopic exchange and fractionation factor between a ^{57}Fe-enriched aqueous Fe(II) and an isotopically "normal" smectite SWa-1 (iron oxide impurities stripped off by purification) using a three-isotope method. Leaching of solid with 0.5 M HCl for 0.5 hr, following separation with aqueous Fe(II) at different time points, yielded mostly Fe(II) in extract 1 and subsequent leaching with 0.5 M HCl for 24 hrs yielded mostly Fe(III) in extract 2.

Isotopic exchange between different components was monitored by changes in their $\delta^{57/56}$Fe values. Isotopic exchange was limited between aqueous Fe(II) and bulk smectite. When excluding bulk smectite from the system, however, about 90% of exchange was achieved between aqueous Fe(II) and extract 1 (a weakly sorbed component) in the beginning of the experiments and leveled off with time, suggesting a steady-state condition was reached early on in the experiments between aqueous Fe and extract 1. Fraction of isotopic exchange (F) reached ~50% between aqueous Fe(II) and extract 2. The equilibrium fractionation factor betweem aquoues Fe(II) and extract 2 has been determined to be ~ –2.4‰ (below figure represents one of the duplicate experiments). Extract 2 could be an iron oxide phase as observed during eletron transfer between aqueous Fe(II) and smectite [1] and the mineralogy nature of extract 2 will be further identified using Mössbauer spectra. Nevertheless, the equilibrium Fe isotope fractionation between aqueous Fe(II) and smectite, driven by redox changes, has important implications for understanding redox processes in subsurface environments that is enriched in ferrous iron and clay minerals.

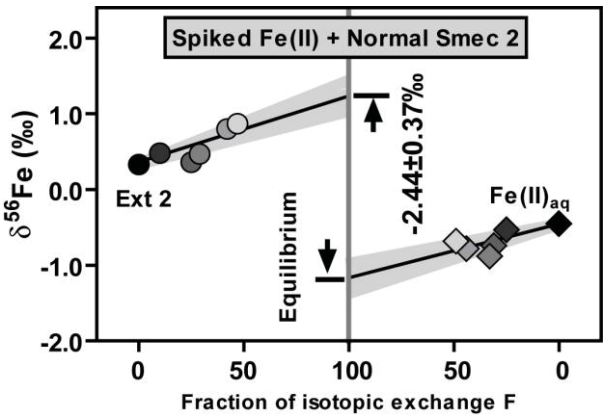

[1] Schaefer et al. (2011) *Environ. Sci. Technol*. **45**, 540-545

Multiple sulfur isotopic composition of carbonate associated sulfate in Carboniferous brachiopods: oceanic sulfur cycling and its implications

NANPING WU[1*], JAMES FARQUHAR[1, 2], HARALD STRAUSS[3]

[1]Deparment of Geology, University of Maryland, College Park, Maryland, USA, 20740 (*Correspondence: npwu@umd.edu)
[2]Earth System Science Interdisciplinary Center, University of Maryland, College Park, Maryland, USA, 20740
[3]Institut für Geologie und Paläontologie, Westfälische Wilhelms-Universität Münster, Germany

We present multiple sulfur isotopic records of carbonate associated sulfate from Carboniferous rocks in the Ukraine, Belgium and Moscow Basin [1, 2]. The most significant feature of this data is that the values of δ^{34}S change from higher values (18.4±3.5‰) in the early Carboniferous to lower values (12.6±1.8‰) in the late Carboniferous. In contrast, Δ^{33}S remains similar throughout the early and late Carboniferous (-0.003±0.028‰ and -0.006±0.027‰, respectively). These sulfur isotope records also show evidence for shorter timescale variations that are superimposed on the first order observations in δ^{34}S and Δ^{33}S.

The decline in δ^{34}S is concurrent with a 3‰ increase in δ^{13}C observed in Carboniferous brachiopod shells of the Russian platform [3]. This negative correlation between δ^{34}S and δ^{13}C is similar to the long term linkage between the carbon and sulfur cycles throughout the Phanerozoic. The favored interpretation of carbonate δ^{13}C is that higher δ^{13}C reflects an increasing fraction of organic matter burial. In line with this, we hypothesize that the perturbation of the terrestrial organic carbon cycle plays a more prominent role in the global carbon cycle, based on the observation of significant coal deposits in the late Carboniferous. In this context, the shift in δ^{34}S may reflect the decreasing burial of marine organic matter and reduced burial of pyrite and/or a change in the quality of organic matter that can be used for sulfate reduction because of an increasing fraction of terrestrial organic carbon in the marine sediments, and/or enhanced delivery of sulfate with low δ^{34}S to the late Carboniferous oceans coupled to increasing sulfate levels.

The relatively constant Δ^{33}S record, in conjunction with falling δ^{34}S, may be attributed to a decrease in the sulfur isotope fractionation between sulfate and pyrite with a constant fraction of pyrite burial, and no change in the parameter λ that relates ^{34}S/^{32}S to ^{33}S/^{32}S. Alternatively, it could implicate a change in λ but with constant ^{34}S/^{32}S fractionation associated with pyrite burial to compensate for an increasing influx of sulfur to oceans. The changes in λ would imply that sulfide re-oxidation played a smaller role in the sulfur cycle. Ongoing work will further explore the implications of the high-order variation in these sulfur isotopic records.

[1] Kampschulte et al., (2001) *Chem Geol* **175**, 145-173.
[2] Kampschulte and Strauss, (2004) *Chem Geol* **204**, 255-286.
[3] Mii et al., (2001) *Chem Geol* **175**, 133-147.

https://doi.org/10.1180/S0026461X00008434 Published online by Cambridge University Press

Chemical weathering of large river catchments in China and the global carbon cycle

WEIHUA WU [1*], HONGBO ZHENG [1], JIEDONG YANG [2] AND CHAO LUO [1]

[1] Institute of Surficial Geochemistry, School of Earth Sciences and Engineering, Nanjing University, Nanjing 210093, China. wuwh@nju.edu.cn (* presenting author)

[2] Center of Modern Analysis, Nanjing University, Nanjing 210093, China.

Analyzing chemical compositions of river waters, rain waters, sediments, and rocks of large river catchments in China and combining with hydrological information, we use the forward model to generally assess the chemical weathering rates and capacity and mechanism of the atmospheric CO_2 consumption, and discuss the variation trend of chemical weathering and their controlling factors in different environments of climate, lithology, topography, and vegetation. The atmospheric CO_2 consumptions derived from silicate and carbonate weathering are 421~ 627×10^9 mol/y and 1323×10^9~ 2025×10^9 mol/y, which accounts for about 4.8 ~ 7.1 % and 11.1 ~ 16.1 % of the total consumption from the global rivers, respectively. The results show that China as a country of karst wide distribution, the influence of carbonate weathering on the global carbon cycle is more important. The atmospheric CO_2 consumptions from silicate and carbonate weathering in the Yangtze River, Yellow River, and Pearl River catchments account for about 2/3 and 90 % of river catchments in China.

By comparing the characteristics of chemical weathering in some small river catchments draining the typical silicate rock regions, the Nandujiang River flowing on basalt formations in tropical climate zone has the highest silicate weathering rates (7.2×10^5 mol/km^{2}a), and followed by the Beijiang River (6.99×10^5 mol/km^{2}a) and Dongjiang River (5.39×10^5 mol/km^{2}a) flowing on granite formations in tropical climate zone, which close to those rivers in New Guinea near the equator. Under similar lithology conditions, atmospheric CO_2 consumption rates have positive correlation with temperature and rainfall and negative correlation with elevation.

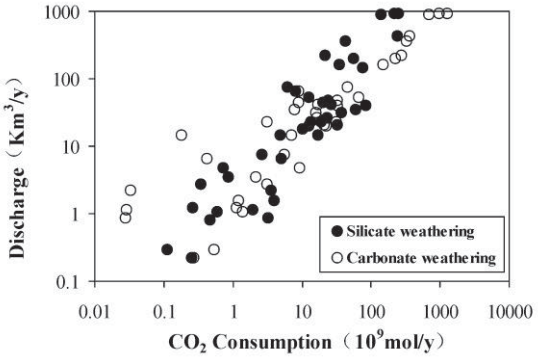

Figure 1: Scatter plots of atmospheric CO_2 consumptions resulted from silicate and carbonate weathering vs. water discharge. Good positive correlation indicates that discharge is an important factor affecting CO_2 consumption flux.

Biomineralization of deep-sea iron reducing bacteria *Shewanella piezotolerans* WP3

WENFANG WU[1,2*], YONGXIN PAN[1,2]

[1]Key Laboratory of the Earth's Deep Interior, Institute of Geology and Geophysics, Chinese Academy of Sciences, Beijing 100029, China

[2]Franco-Chinese Biomineralization and Nano-Structures Laboratory, Chinese Academy of Sciences, Beijing 100029, China wuwenfang@mail.iggcas.ac.cn(* presenting author) yxpan@mail.iggcas.ac.cn

Introduction

Iron reducing bacteria (IRB) that can utilize Fe(III) as its terminal electron acceptor are ubiquitously distributed on earth surface and subsurface. They are of great significance in iron biogeochemical cycling, environmental bio-remediation and magnetic nanoparticle bio-synthesis. However, the biomineralization of deep-sea IRB is rarely studied, whereas the deep-sea environment is quite different, for example, dark, microaerobic or anaerobic, oligotrophic. Besides, bacteria live in deep sea often tolerate great high hydrostatic pressure and quite low temperature, which can exert great influence on microbes.

Here we investigated the laboratory iron reduction and biomineralization behavior of a deep-sea IRB *Shewanella piezotolerans* WP3 under various hydrostatic pressures (0.1, 5, 10, 20 and 50 MPa) at 4°C and 20°C, in the aim of understanding pressure and temperature effects on microbial mineralization.

Results and Conclusion

S. piezotolerans WP3 was isolated from West Pacific deep-sea sediments at a water depth of ~1,914 m. It is a Gram-negative, facultative anaerobic psychrotolerant and piezotolerant bacterium, highly adaptive to dynamic environments. Ferrihydrite was quickly reduced by *S. piezotolerans* WP3 with an initial iron reduction rate of 175 μM/h at 20°C and 0.1 MPa. During iron bio-reduction, the pH increased while the Eh (redox potential) decreased greatly, which were favorable for magnetite formation and precipitation. During biomineralization, room-temp and low-temp magnetic parameters (e.g., M_s, M_{rs}, B_{cr}, B_c and T_p) of the bio-products changed systematically, corresponding to the mineral transformation from ferrihydrite to magnetite. The final bio-products are well crystalline superparamagnetic magnetite nanoparticles (<10 nm) [1].

Under all the tested pressures *S. piezotolerans* WP3 can reduce ferrihydrite and induce magnetite biomineralization. A slower iron reduction and magnetite formation accompany with diminished cell growth were observed at elevated pressures. Under the same pressure, it was slower at 4°C for the iron bio-reduction and mineralization as well as the cell growth than that at 20°C. Low-temp magnetic characterization showed a smaller average particle size for the magnetite biominerals at either higher pressure or lower temperature.

As *S. piezotolerans* WP3 can reduce Fe(III) and mediated magnetite biomineralization at high hydrostatic pressure and low temperature, this study suggests that IRB like WP3 can play an important role in deep-sea iron cycling and sedimentary magnetism that we might have previously overlooked.

[1] Wu et al. (2011) *J. Geophys. Res.* **116**, G04034.

https://doi.org/10.1180/S0026461X00008434 Published online by Cambridge University Press

Cr(VI) Adsorption on organic rich soil from Kleinstuck Marsh, Kalamazoo, MI

Davina Wyman[1*], Carla M. Koretsky[2], and Michelle L. Barger[3]

[1]Western Michigan University, Geosciences Department, davina.a.wyman@wmich.edu (* presenting author)

[2]WMU, Geosciences Dept., carla.koretsky@wmich.edu

[3]University of Iowa, IIHR-Hydroscience & Engineering, michelle-barger@uiowa.edu

Abstract

Chromium is a highly toxic chemical species that has leaked into natural systems via many industrial processes. There is much about Cr(VI) biovailability and mobility that remains poorly understood, but past studies have demonstrated that Cr(VI) is typically mobile in the environment. Cr(VI) mobility can be diminished via adsorption onto sediments, especially sediments containing reduced organic matter, iron (FeII) or manganese (MnII) because these can reduce Cr(VI) to Cr(III) which is more readily sorbed. The objective of this study is to measure the adsorption of Cr(VI) onto organic-rich sediment as a function of pH, time and after step-wise removal of operationally defined sediment fractions.

Sediment cores (10 replicates) were collected to a depth of 50 cm with a Russian peat corer from Kleinstuck Marsh, a minerotrophic fen in Kalamazoo, MI. The upper 10 cm and the lower 10 cm of each core was separated and combined with the same depth interval from the other cores, homogenized in ziplock bags, and promptly freeze-dried. A 4-step sequential extractions procedure [1] was used to selectively remove exchangeable, carbonate, reducible, and oxidizable fractions. Supernatants from each extraction step were analyzed for a suite of metals via ICP-OES. The bulk sediment, together with sediment remaining after each progressive sequential extraction were used to measure Cr(VI) adsorption as a function of pH and time. Adsorption was tested using kinetic edge experiments in which 1 g/L sediment, 10^{-5} M Cr(VI), and 0.01 M $NaNO_3$ were combined in 15 mL plastic centrifuge tubes. Each tube was titrated to a particular pH (spanning 3-10) and placed on a shaker. After 24 hr, 48 hr, 1 week, and 2 weeks, pH was retested in each tube and subsamples (~15 mL) were removed, centrifuged, syringe-filtered (0.2 μm) and the supernatant tested for Cr(VI) and total Cr, using the colorimetric diphenylcarbazide procedure and ICP-OES, respectively. For all sediments except those with the oxidizable fraction removed, Cr(VI) sorption edges are very similar, with nearly 100% sorbed below pH 4, decreasing to less than 5% sorbed above pH 7. In contrast, adsorption is greatly diminished with removal of the oxidizable fraction: after 2 weeks, a maximum of 50% Cr(VI) is sorbed at pH 3, with <20% sorbed between pH 4 and 7. This suggests that much of the Cr(VI) binds to organic matter or other reduced fractions of the soil (e.g. Fe(II)-bearing clays). For all experiments, sorption increased significantly for the first week, with much smaller increases beween 1 and 2 weeks. For pH 3-6.5, agreement between colorimetric and ICP data suggests that Cr in solution was primarily Cr(VI). Above pH 6.5, however, there is an increasing divergence between ICP and colorimetric data, demonstrating that up to 40% of the Cr at alkaline pH is reduced to Cr(III) and released into solution. These data will be used to develop surface complexation models, based on both the component additivity and composite sediment approaches.

[1] Tessier, Campbell and Bisson (1979) *Analytical Chemistry* **51**, 844-851.

https://doi.org/10.1180/S0026461X00008434 Published online by Cambridge University Press

Evolution and Depositing Response During the Mesozoic and Cenozoic in Dunhua Basin,Northeastern China

CHEN XIAO-HUI[1]*, ZHANG TING-SHAN[2], LIU ZHICHENG[3],

[1]State Key Lab.of Oil&Gas G&E Engineering,Chengdu,China zts_3@sina.com(* presenting author)

[2]State Key Lab.of Oil&Gas G&E Engineering,Chengdu,China zts_3@126.com

[3]State Key Lab.of Oil&Gas G&E Engineering,Chengdu,China rex_swpu2005@126.com

Dunhua Basin is located in the middle of Dunhua Mishan Graben in Northeastern China. And it is a rift-fault depression superposed basin which is controlled by the Dunhua Mishan fracture zone. A series of tectonic system transitions happens during the Mesozoic and Cenozoic period in the Dunhua Mishan fracture zone （Zhang et al.,1994; Yin ,1993; Li,1994）.The transitions starts in the Late Triassic. In the Late Jurassic, it is compressional; during the Cretaceous–Paleogene, it has a left-lateral displacement and a certain scale of extension; there is a compression in the late Paleogene, which then turns into the extension state again after Neogene. The evolution of Dunhua Mishan fracture zone plays a controlling role in the generation,development and evolution of the Dunhua basin. The evolution of the Dunhua Basin in the Mesozoic–Cenozoic period is: the compressional orogeny, strike slip & pull-apart and the initial rifting stage in Late Jurassic–Early Cretaceous (rift development stage); the inversion, uplifting and exhumation stage in Late Cretaceous-Paleocene;rift basin development stages in the Eocene–Oligocene period and Depression and basalt eruption stage after the Neogene. Different evolution stages have different deposition response characteristics.

[1]Zhang Z M,Liou J G,Coleman R G(1984).Geological Society of America Bulletin，1984，**Volume** 95：2952–3120.

[2]Yin A,Nie S Y(1993).Tectonics，1993，**Volume12**：801–813.

[3]Li ZX(1994) .Geology，1994，**Volume** 22：739–742.

ANAMMOX ACTIVITY IN CONTAMINATED GROUNDWATER HAVING HIGH AMMONIUM AND NITRATE CONCENTRATIONS

YANGPING XING[1]*, ELIF TEKIN[1], DANIELLE FORTIN[1], ROBERT TIMLIN[2], IAN D CLARK[1]

[1]University of Ottawa, Department of Earth Sciences, Ottawa, Canada, yxing@uottawa.ca (* presenting author)

[2]SNC-Lavalin Environment, Ottawa, Canada, robert.timlin@snclavalin.com

Abstract

Anaerobic ammonium oxidation (anammox) has been recognized as a critical process for removing nitrogen components in marine and surface aquatic systems, and recent studies suggest that anammox appears to be ubiquitous in natural and engineered environments. However, the activity and reaction rates of anammox in contaminated groundwater environments have never been directly quantified and their relative importance is still unknown. In our study, microcosm tracer incubation experiments with $^{15}N\text{-}NH_4^+$, $^{15}N\text{-}NO_3^-$, and $^{15}N\text{-}NO_2^-$ were performed with groundwater and sediment samples from a contaminated aquitard near Elmira, Ontario, Canada, in order to measure the potential reaction rates and assess the respective contribution of anammox and denitrification activities. The tracer experiments showed that the potential anammox reaction rates ranged from 71.5 to 148.1 nmole N_2 L^{-1} d^{-1} which are very comparable to those reported in freshwater lakes. A comprehensive mathematical calculation suggested that 32 to 48% of N_2 production was attributed to anammox at the Elmira site.The measurements of NH_4^+ and NO_3^- before and after incubation and elevated $\delta^{15}N\text{-}NO_3^-$ indicated a complex and interactive ammonium attenuation mechanism including anammox and both microaerobic and anaerobic ammonium oxidation. Together with fluorescence *in situ* hybridization (FISH) results, our study points to anammox as an active process in the highly contaminated Elmira groundwater and to the fact that anammox organisms show a strong adaptability to heavy total nitrogen loads up to 46.5 mmol L^{-1} and relatively high dissolved oxygen concentrations up to 65.3 µmol L^{-1}.

https://doi.org/10.1180/S0026461X00008434 Published online by Cambridge University Press

Pairing Re-Os systematics with geochemical proxies – environmental conditions and seawater chemistry

G. XU[1,2*], J. L. HANNAH[1,2,3], B. BINGEN[2] AND H. J. STEIN[1,2,3]

[1]AIRIE Program, Department of Geosciences, Colorado State University, Fort Collins, CO 80523-1482 USA (*presenting author: Guangping.Xu@colostate.edu)
[2]Geological Survey of Norway, 7491 Trondheim, Norway
[3]Physics of Geological Processes, University of Oslo, 0316 Oslo, Norway

Re-Os systematics of black shales provide depositional ages and syndepositional seawater $^{187}Os/^{188}Os$ ratios. The seawater Os-isotope record is a proxy for short-term changes in continental weathering rates. Additionally, both Re and Os are redox sensitive elements, and can be used with other redox sensitive trace metals to infer depositional conditions and seawater chemistry. Here we report Re-Os data, trace metal concentrations and sizes of pyrite framboids for Triassic black shale from Svalbard, Svalis Dome and Kong Karls Land across the Barents Shelf, spanning the Olenekian to early Carnian stages. Using these data, we discuss the evolution of Triassic environmental conditions.

Seawater $^{187}Os/^{188}Os$ ratios in the Barents Sea region decrease from ca 0.85 in the Olenekian to 0.65 in the late Ladinian and then increase to 0.73 in the early Carnian. These variations are synchronous with the decrease of $^{87}Sr/^{86}Sr$ ratios through the middle Triassic and a subsequent increase in the Carnian [1]. Decreasing Os and Sr isotope ratios reflect decreasing global continental weathering rates from Olenekian to late Ladinian.

Olenekian black shales from Svalbard and Svalis Dome have higher Mo contents for a given TOC content than younger late Anisian black shales. The decrease in [Mo]/TOC ratios suggests increasing restriction as the Panthalassa ocean retreated from Svalbard and Svalis Dome [2]. Olenekian black shales from Svalbard and Svalis Dome also have low Re/Mo and V/Mo ratios and small pyrite framboids, indicating euxinic conditions, whereas early Carnian shales from Kong Karls Land have low Mo contents and high Re/Mo and V/Mo ratios suggesting suboxic – oxic conditions.

In summary, from the Olenekian to the latest Ladinian in the Barents Sea region, continental input to the oceans decreased, and the depositional environment on the Barents shelf changed progressively from euxinic, deep, open marine to a shallow, water-restricted anoxic embayment.

This work was funded by Petromaks - NFR 180015/S30

[1] Korte et al. (2003) *GCA* **177**, 47-62.
[2] Xu et al. (2009) *EPSL* **288**, 581-587.

Sweet Spot for the Formation of Sedimentary Dolomite

HUIFANG XU*

NASA Astrobiology Institute, Department of Geoscience, The University of Wisconsin, Madison, WI 53706, USA, hfxu@geology.wisc.edu

8i. Interactions at the interface between organic components and minerals

The roles of organic matters in dolomitization were considered important, although their precise functions remain unclear. There are four proposed mechanisms for explaining the roles of organics and microbes in dolomitization: (1) Organic bounded Mg was released during decay of the organics; (2) extracellular polymeric substance may serve as nucleation sites; (3) Removal of sulphate (believed to be an inhibitor) through sulphate-reducing bacteria promotes dolomite crystallization, and (4) Oxidation of organics and proteins increases pH and alkalinity. However, laboratory experiments based on the proposed mechanisms failed to synthesize dolomite inorganically at room temperature. Mg^{2+} ions, which form one of the strongest bonds with water molecules among the divalent ions may only be partially dehydrated when incorporated into a growing nucleus of calcite or dolomite. The residual hydration sphere of the incorporated Mg^{2+} ions would then inhibit the further growth of the crystal. Dolomite crystals preferentially associated with organic rich layers / lamina in some partially dolomitized limestone and stromatolites. Early formed Mg-calcite or calcite crystals served nucleation sites for the dolomite. Synthesis experiments indicate polysaccharides in extracellular polymeric substance (EPS) of certain anaerobic bacteria can promote dolomite nucleation and growth. The polysaccharides adsorbed on surfaces of calcite or dolomite through hydrogen bonding with surface carbonate anions will lower the kinetic energy barrier for dehydration of metal complexes between H_2O and surface Mg^{2+}. Author acknowledges supports from NSF and NASA Astrobiology Institute.

https://doi.org/10.1180/S0026461X00008434 Published online by Cambridge University Press

CO_2-rich fluids in lode gold deposits at the Sarekoubu- Qiaxia area, southern Altaides, China

XU JIUHUA*, LIN LONGHUA, XIAO XING, AND YANG RUI

Resource Engineering Department, University of Science and Technology Beijing, Beijing 100083, China
jiuhuaxu@ces.ustb.edu.cn (* presenting author)

Geological Setting

The Sarekoubu and Qiaxia lode gold deposits, located in the southern margin of Altaides, occur in metamorphic volcano clastic rocks of the lower Devonian Kangbutiebao Formation ($D_1k_2^2$) [1]. There are two groups of gold(copper)-bearing quartz veins(Fig.1): 1) lentoid or streaked quartz veins (QI) which are parallel to the foliated structure of the biotite-chlorite or garnet-chlorite schist; 2) sulfide quartz veins (QII) cutting across chlorite mica schist .

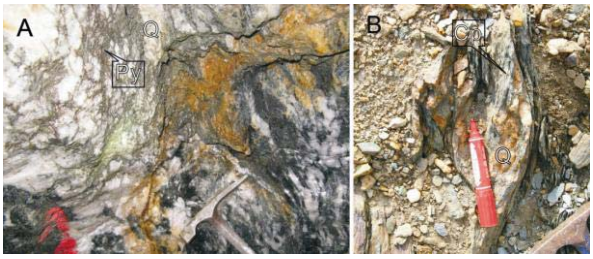

Figure 1: Au-Cu-quartz veins in the Sarekoubu and Qiaxia area

Fluid Inclusion Study

Carbonic fluid inclusions that are free of water are often found in the Sarekoubu deposit. They are of primary origin in QII veins, while a large number of these inclusions are of secondary origin in QI. There are two instances for $T_{m,CO2}$ and $T_{h,CO2}$: 1) $T_{m,CO2}$ = -60℃ ~-56.5℃ and $T_{h,CO2}$ =-23℃~+31℃; 2) $T_{m,CO2}$ <-57℃, to a minimum of -78.1℃, and $T_{h,CO2}$ =-33.7℃~-17.7℃. The $T_{h,TOT}$ of CO_2-H_2O fluid inclusions in vein quartz of the Sarekoubu deposit are 227~374 ℃(QI) and 205~370℃(QII). In this situation the lowest trapping pressures of CO_2–rich fluids can be estimated to be 110~ 300MPa based on CO_2 densities and CO_2 phase diagram at high *P-T* of Van den Kerkhof [2]. The ^{18}O delta values of fluid inclusions in quartz are 7.54~11.84‰ (QI) and 3.82~7.82‰ (QII), whereas the D delta values are -84.7~-98.2 ‰ (QI) and -75.8~-108.8 ‰ (QII) respectively.

CO_2-H_2O fluid inclusions composed of a liquid CO_2 phase and a H_2O phase are commomly observed in the Qiaxia deposit. The melting temperatures of frozen CO_2 ($T_{m,CO2}$) range from -63~ -56.6 ℃ for QI, and from -62.6~-58.6℃ for QII; the homogenization temperatures of CO_2 ($T_{h,CO2}$)= 19.6~28.9℃ for QI, and 25.2~27.9℃ for QII. The final homogenization temperatures ($T_{h,TOT}$) of these inclusions are mostly 180~380℃ (QI) and 180~360 ℃ (QII).

Conclusions

Gold and copper mineralization in the Sarekoubu and the Qiaxia area has a close relationship with CO_2-rich fluids and belongs to orogenic. The source of ore-forming fluids is related with regional metamorphism and associated magmatism.

[1] Xu *et al.* (2011) *Economic Geology* **106,** 145-158. [2] Van den Kerkhof & Thiéry (2001), *Lithos* **55,** 49-68.

Geochemical Characteristics of Heavy Metals in Water-Sediment Media in Panzhihua V-Ti-Magnetite Zone，China

ZHENGQI XU[1,2*], SHIJUN NI[1], YANGUO TENG[2], CHENGJIANG ZHANG[1]

[1]Chengdu University of Technology, Chengdu, China , xuzhengq@163.com (* presenting author)
[2]Beijing Normal University, Beijing, China,xuzhengqi@cdut.cn

Sulphide mines have always been the concerns of people because of their various forms and the resultant environmental problems, whereas oxide mines are paid less attention and not studied much because they do not cause obvious environmental problems such as acid mining drainage（AMD）. However, the potential environmental problems caused by oxide mines can not be ignored.

The author chooses Panzhihua V-Ti-Magnetite, a famous oxide mine in China, as the subject of research. In this thesis, the geochemical characteristics of heavy metals in water-sediment environmental media in the zone during the process of mining are systematically studied by using those media as research carriers and employing the analyzing methods of ICP-MS and ICP-OES. The research results are shown below:

The research on the geochemical characteristics of heavy metals in the system of water-suspended solid-sediment in the mining zone show that: the contents of heavy metals in water are very low, while those in suspended solids and sediments are relatively higher; the contents of Cu, Zn, Co, Ni, Fe and As in suspended solids are higher than those in sediments; the contents of Pb, V, Ti and Cr in sediments are higher than those in suspended solids. The partition coefficients show that: Hg is most active, As and Ni are less active, and Ti is least active. The morphological analyzing results of sediments show that in the sediments in Panzhihua Mining Zone, Ti is most stable, V, Cu and Cr are relatively stable, and Zn, Mn, Co and Ni are more active. The index evaluation on potential ecological risk shows that most heavy metal elements in the sediments are contaminated, whether heavily or in a medium degree, in which Cu, Co, V and Ti are contaminated heavily or even more severely. The potential ecological risk index shows that all places are in light ecological risk and generally the potential ecological risk of heavy metals in the sediments are not high and they have limited influence on environment.

https://doi.org/10.1180/S0026461X00008434 Published online by Cambridge University Press

Coupled-Process Modeling of a Uranium Bioremediation Field Experiment

STEVEN B. YABUSAKI [1*], YILIN FANG [1], MICHAEL J. WILKINS[1], AND PHILIP E. LONG[2]

[1]Pacific Northwest National Laboratory, Richland, Washington, USA
yabusaki@pnnl.gov,yilin.fang@pnnl.gov, michael.wilkins@pnnl.gov
[2]Lawrence Berkeley National Laboratory, Berkeley, California, USA
pelong@lbl.gov

Field biostimulation experiments at a former uranium mill tailings site are being used to better understand the processes, properties, and conditions controlling engineered bioremediation of uranium contaminated groundwater. A key component of the research is the development of a mathematical model that incorporates three-dimensional variably saturated flow through physically and chemically heterogeneous sediments, as well as the interaction of biologically-mediated reaction products with the subsurface geochemical environment. We present the modeling of the 2008 uranium bioremediation field experiment, in which pulsed acetate groundwater amendment was used to stimulate indigenous metal-reducing bacteria to transform aqueous U(VI) to immobile solid-associated U(IV).

Uranium mobility is sensitive to pH, Eh, alkalinity, calcium, and reactive surface area, as well as aqueous uranium concentrations. In the model, these geochemical conditions are impacted directly by the terminal electron accepting process (TEAP) reactions and indirectly by subsidiary reactions induced by the biologically-mediated reaction products. For example, uranium surface complexation is directly affected by the large amount of bicarbonate produced by the acetate-oxidizing microorganisms but also indirectly by changes in the pH from mineral reactions induced by sulfide. The modeling also addresses site-specific issues such as the continuous influx of actionable levels of U(VI) into the treatment zone, seasonal water table variation, spatially variable physical (hydraulic conductivity, porosity) and geochemical (reactive surface area) material properties, and competition for the acetate electron donor by sulfate reducing bacteria.

Findings include: 1) uranium bioreduction is most effective when acetate concentrations are engineered to exceed the sulfate-reducing bacteria demand; 2) biogenic sulfide promotes the dissolution of Fe(III) minerals leading to an abiotic but biologically mediated Fe(II) source; 3) falling water table sequesters residual reactants and products in the newly unsaturated pores; 4) preferential flow paths for acetate delivery create local zones of enhanced TEAP reactivity and subsidiary reaction; and 5) predicted central metabolic pathway reaction fluxes from a genome-scale metabolic ("*in silico*") model of *Geobacter metallireducens,* correlate well with proteomics data from the field experiment.

The eSTOMP subsurface simulator was used to exploit the large memory and high-performance of massively parallel computers needed to address the high spatial and temporal resolution, large number of reactive species and minerals, and detailed process models.

Cretaceous *P–T–t* evolution of the Fosdick migmatite–granite complex, West Antarctica: orogenic collapse along the East Gondwana margin

CHRIS YAKYMCHUK[1*], FAWNA J. KORHONEN[2], MICHAEL BROWN[1], PHILIP M. PICCOLI[1] AND CHRISTINE S. SIDDOWAY[3]

[1]Laboratory for Crustal Petrology, Department of Geology, University of Maryland, College Park, MD 20742, USA, cyak@umd.edu (* presenting author)
[2]Geological Survey of Western Australia, Department of Mines and Petroleum, East Perth, Australia
[3]Department of Geology, The Colorado College, Colorado Springs, CO 80903, USA

The Fosdick migmatite–granite complex in West Antarctica represents a rare exposure of the anatectic middle crust from along the former active margin of East Gondwana. The complex preserves a polyphase metamorphic history and contains a detailed record of crustal differentiation during a Cretaceous transition from oblique tectonic convergence to divergence across the most long-lived and extensive active plate margin in the Phanerozoic. Migmatites that crop out in the complex preserve evidence of Lower Cretaceous high–*T* metamorphism and anatexis, and subsequent retrograde decompression inferred to record orogenic collapse early during the Upper Cretaceous breakup of the East Gondwana margin. Migmatites collected from the eastern and western extents of the complex contain peak metamorphic assemblages that include garnet, garnet + cordierite or cordierite associated with leucosomes. Sillimanite is preserved as inclusions in garnet, cordierite, and biotite. Phase equilibria modelling constrains prograde heating into the sillimanite + garnet + liquid stability field at temperatures of 850–900°C and pressures of 0.7–1.1 GPa, which was followed by decompression into a cordierite + liquid stability field immediately above an elevated solidus at conditions of metamorphism of temperatures of 850–880°C and pressures of 0.6–0.7 GPa. Melt reintegration along a model isobaric heating path at 0.7 GPa suggests that the metasedimentary protoliths could have produced up to 24 mol.% melt, most of which must have been extracted in order to preserve the garnet– and cordierite–bearing mineral assemblages. This melt was emplaced at higher crustal levels, as represented by Cretaceous peraluminous granites exposed in the periphery of the Fosdick complex—a process that contributed to the differentiation and ultimate stabilization of the East Gondwana active margin now exposed in West Antarctica.

In situ SHRIMP U–Pb isotope analysis of monazite from stromatic metatexite migmatites yield dominantly Cretaceous ages of c. 111–96 Ma. Individual Cretaceous monazite grains show variable zoning patterns in Y and Th, but most contain low-Y cores and high-Y rims. This is consistent with progressive monazite growth associated with garnet breakdown during near-isothermal decompression. These data suggest orogenic collapse and exhumation of the Fosdick complex as a gneiss dome was underway by c. 111 Ma, which supports geophysical studies in West Antarctica and regional studies in the outboard part of the once contiguous margin of East Gondwana that suggest breakup had begun by c. 110–100 Ma.

https://doi.org/10.1180/S0026461X00008434 Published online by Cambridge University Press

Pu isotopes in water columns of the northern North Pacific

MASATOSHI YAMADA[1*], JIAN ZHENG[2]

[1]Department of Radiation Chemistry,Institute of Radiation Emergency Medicine, Hirosaki University, Hirosaki, Japan, myamada@cc.hirosaki-u.ac.jp (* presenting author)

[2]Research Center for Radiation Protection, National Institute of Radiological Sciences, Chiba, Japan, jzheng@nirs.go.jp

Introduction

Anthropogenic radionuclides such as ^{239}Pu (half-life: 24,100 yr), ^{240}Pu (half-life: 6,560 yr) and ^{241}Pu (half-life: 14.325 yr) mainly have been released into the environment as the result of atmospheric nuclear weapons testing. In the North Pacific Ocean, two distinct sources of Pu isotopes can be identified; i.e., the global stratospheric fallout and close-in tropospheric fallout from nuclear weapons testing at the Pacific Proving Grounds in the Marshall Islands.[1] The objectives of this study are to measure the ^{240}Pu/^{239}Pu atom ratios in seawater from the northern North Pacific Ocean and to discuss the transport processes of Pu.

Materials and methods

Seawater samples were collected at Stn. DR-10 in the northern North Pacific and Stn. DR-13 in the Bering Sea with a double barrel PVC large-volume sampler.[2] The ^{240}Pu/^{239}Pu atom ratios were measured with a double-focusing SF-ICP-MS, which was equipped with a guard electrode to eliminate secondary discharge in the plasma and to enhance overall sensitivity. [3]

Results and discussion

The total (water + sediment) inventory of 53.8 Bq m^{-2} at Stn. DR-10 in the northern North Pacific was mostly the same as that (58.1 Bq m^{-2}) of the expected cumulative deposition density of atmospheric global fallout at the latitude of 40 – 50°N. The atom ratio of ^{240}Pu/^{239}Pu showed no notable variation from subsurface water of 100 m depth to deep water of 2000 m depth, then increased with depth to 0.255 at the bottom layer. The atom ratios in water column of the northern North Pacific were significantly higher than the mean global fallout ratio of 0.18.[4] High atom ratios of ^{240}Pu/^{239}Pu in the northern North Pacific prove the presence of close-in tropospheric fallout from nuclear weapons testing at the Pacific Proving Grounds.

[1] Yamada & Zheng (2010) *Sci. Total Environ.* **408**, 5951-5957. [2] Nagaya & Nakamura (1993) *Deep Ocean Circulation, Physics and Chemical Aspects*. *Elsevier,* 157-167. [3] Zheng & Yamada (2007) *Anal. Sci.* **23**, 611-615. [4] Kelley et al. (1999) *Sci. Total Environ.* **237/238**, 483-500.

Negative growth of the continental crust at present: Significance of arc subduction

S. YAMAMOTO[1]*, S. MARUYAMA[2]

[1]Department of Earth Science and Astronomy, The University of Tokyo, Komaba, Meguro, Tokyo, 153-8902, Japan (*correspondence: syamamot@ea.c.u-tokyo.ac.jp)

[2]Department of Earth and Planetary Sciences, Tokyo Institute of Technology, Tokyo, Japan

Subduction and recycling of differentiated material into the mantle are of significance not only for continental growth but also for creating mantle heterogeneities. Continental crust is predominantly created by arc magmatism and returned to the mantle via sediment subduction, subduction erosion and continental subduction [1]. Oceanic arcs, primary form of continental crust, have been thought to be entirely accreted during arc-collision due to its buoyant nature. Modern oceanic arcs are, however, mostly subducted into the mantle. The best examples of arc subduction are observed around the Japan islands [2,3]. Among the more than 15 examples of arc–arc collision in the western Pacific, arc–arc amalgamation is possible only in the case of parallel collision [2,4]. Parallel collision of two arcs is rather rare case, compared to the normal arc–arc collision, therefore these observation imply that the predominant subduction of arc crust is in general and that a majority of the intra-oceanic arc in the Earth history must have been subducted into the mantle.

Geophysical and geological studies document that sediment subduction and subduction erosion move large volumes of continental material toward the mantle, and comprehensive studies for the rate of continental reduction versus production suggest a balance, resulting in no growth of continental crust at present [5,6]. However, these estimates do not take into account the concept of arc subduction. Considering direct subduction of oceanic arcs into the mantle, we conclude negative growth of the continental crust on the Earth at present.

[1] Scholl & von Huene (2010) *Can. J. Earth Sci*. **47**, 633-654. [2] Yamamoto *et al*. (2009a) *Gondwana Res*. **15**, 443-453. [3] Yamamoto *et al*. (2009b) *Gondwana Res*. **16**, 572–580. [4] Santosh *et al*. (2009) *Gondwana Res*. **15**, 324-341. [5] Clift *et al*. (2009) *Earth Sci. Rev*. **97**, 80-104. [6] Stern & Scholl (2009) *Int. Geol. Rev.* **52**, 1-31 (2009).

https://doi.org/10.1180/S0026461X00008434 Published online by Cambridge University Press

Geochemical and carbon isotopic study in a karst groundwater system on Miyakojima Island, Japan

MASARU YAMANAKA

Nihon University, Department of Geosystem Sciences, Tokyo, Japan, yamanaka@chs.nihon-u.ac.jp

Groundwater $\delta^{13}C$ values and chemical compositions were employed to quantitatively evaluate the controlling processes and sources of dissolved inorganic carbon in a karst aquifer system on Miyakojima Island (MI), southwestern Japan. Most MI groundwater is Ca-HCO_3 type water. The groundwater Ca/HCO_3 ratio was relatively constant, as predicted by the dissolution processes of calcite and of CO_2 in the groundwater. WATEQ4F and PHREEQC calculations demonstrated that all groundwater samples, not only Ca-HCO_3 type groundwater but also groundwater of other types, were strongly influenced by dissolution of calcite and of soil CO_2 in this karst aquifer system. The system was open with respect to CO_2 with mostly around 10–50 matm as gas pressure, and most groundwater was saturated with respect to calcite. Detailed comparison of measured values and PHREEQC calculations for MI groundwater revealed that oxidation of ammonium sulfate (applied as fertilizer) played a key role in the groundwater chemistry by adding H^+, which caused surplus calcite dissolution. Model calculations using the $\delta^{13}C$ values and pH of the groundwater samples with PHREEQC were used to determine the mass fractions of DIC initially from calcite dissolution and from C3 and C4 organic materials, the origin of the soil CO_2. On average, the contributions of calcite and C3 and C4 organic materials were estimated to be 46.4%, 18.5% and 35.1%, respectively. Of these, contribution of calcite was relatively constant in any groundwater, indicating easily occurrence of this process at anywhere in karst aquifer systems. The calculated mixing ratios of C3 and C4 organic materials, which explained the contribution of each to the DIC in the groundwater, were concordant with the land use on MI, that is, the distributions of forest and sugarcane fields. This fact indicates that the calculated mixing ratios from the model can be reasonably used to constrain groundwater information, such as its recharge area and flowpahts, in a specific study area where the distributions of organic materials in soil initially from C3 and C4 plants are clear.

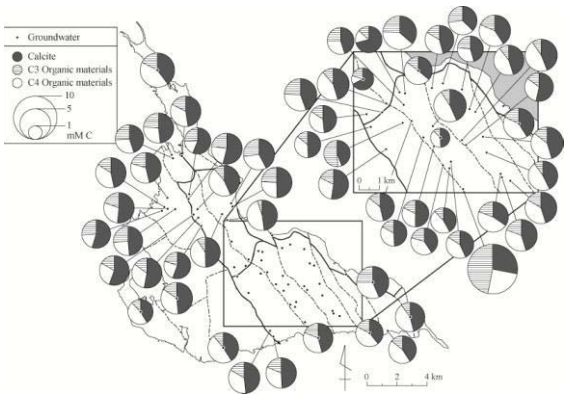

Fig.1: The mass fractions initially from calcite and C3 and C4 organic materials by pie charts within the bubbles, expressing DIC contents in the MI groundwater.

New time constraints on brittle faulting in the Toki Granite, central Japan

S. YAMASAKI [1*], H. ZWINGMANN[2], K. YAMADA[1], K. UMEDA[1] AND T. TAGAMI[3]

[1]JAEA TGC, Gifu, Japan, yamasaki.seiko@jaea.go.jp (* presenting author)
[2]CSIRO ESRE, Perth, Australia, horst.zwingmann@csiro.au
[1]JAEA TGC, Gifu, Japan, yamada.kunimi@jaea.go.jp
[1]JAEA TGC, Gifu, Japan, umeda.koji@jaea.go.jp
[3]KUEPS Kyoto University, Kyoto, Japan, tagami@kueps.kyoto-u.ac.jp

Numerous studies [e.g. [1]] have highlighted the potential for determining the timing of near-surface brittle deformation using isotopic dating of authigenic illites in fault gouge. In recent years, precise size separation combined with mineral characterization of gouge samples has demonstrated the suitability of illite K-Ar dating for constraining the timing of brittle deformation [e.g. [2]], despite analytical difficulties such as contamination.

We discuss new K-Ar and fission-track age data from gouge samples collected from a fault in the Cretaceous Toki granite, central Japan. The fault occurs sub-vertically along the wall of a shaft exposing granite host rock. The minimum age of the fault deformation is estimated to be older than 20 Ma, as the Miocene sedimentary formation is not displaced by the fault. The gouge samples were separated into five grain-size fractions (<0.1, <0.4, <2, 2-6, 6-10 μm) and characterized by laser particle analyses, XRD, SEM, and TEM.

The fine fractions provide younger K-Ar ages, suggesting enrichment in more recently grown authigenic illites. The finest fractions (<0.1 μm) give ages of 46 ±1 and 43 ±1 Ma (±2 sigma). The K-Ar ages of the fractions with no detectable contamination from detrital K-bearing minerals on XRD analysis, range from 53 to 43 Ma. The obtained illite age range is consistent with the stability field of illite and the main temperature field of brittle deformation within the cooling history of the host granite body of the fault, which was evaluated by apatite and zircon fission-track and K-Ar biotite ages from the host rock.

The internal consistency of the ages obtained from K-Ar dating of the two subsurface fault gouges, as well as their consistency with constraints from existing geochronological data demonstrate the potential of gouge dating in providing new data to constrain timing of brittle deformation in the Toki granite.

[1] Lyons and Snellenburg (1979), Geol. Soc. Amer. Bull. **82**, 1749-1752. [2] Zwingmann et al. (2010) Chem. Geol. **275**, 176-185.

https://doi.org/10.1180/S0026461X00008434 Published online by Cambridge University Press

Oxidation of pyrite in anoxic aquifers in the presence of nitrate

R. YAN[1*], A. KAPPLER[2], H. H. RICHNOW[3], M. HORN[4], S. PEIFFER[1]

[1] Department of Hydrology, University of Bayreuth, 95440 Bayreuth, Germany
[2] Geomicrobiology Group, Center for Applied Geosciences, Eberhard-Karls-University Tuebingen, Germany
[3] Department of Isotope Biogeochemistry, Helmholtz Centre for Environmental Research, 04318 Leipzig, Germany
[4] Department of Ecological Microbiology, University of Bayreuth, 95440 Bayreuth, Germany
[*]corresponding author: ruiwen.yan@uni-bayreuth.de, 0049 (0)921/55-2191

Denitrification coupled to pyrite oxidation has been observed in many groundwater aquifers, although a direct reaction between nitrate and pyrite can not be detected [1, 2]. Our understanding of the mechanisms of this redox process is, however, still limited. Since Fe(III) is detected as a well-known oxidant for pyrite in the presence of oxygen even at neutral pH [3], we postulate that electron transfer is being mediated through this reaction also in the presence of nitrate as terminal electron acceptor. Microbial catalysis by bacteria, such as Fe(II) oxidizing or sulfide reducing bacteria, is considered to affect the denitrification and pyrite oxidation rates significantly. Therefore, bacteria are supposed to mediate the electron transfer from pyrite to nitrate.

The goal of the work is to understand the mechanism of the anaerobic oxidation of pyrite coupled to nitrate reduction in anoxic groundwater sediments. To this end batch experiments have been set up in which synthesized pyrite is exposed to nitrate-dependent Fe(II)-oxidizer strain ***BoFeN1*** [4] and nitrate-reducing Fe(II)- and sulfide-oxidizing bacteria--***Thiobacillus denitrificans*** [5] testing kinetics of this process--the effect of initial concentration of pyrite and nitrate.

Results

Pyrite was oxidized with nitrate by ***Thiobacillus denitrificans***, but not by ***BoFeN1***. The reaction rate is dependent on the initial conc. of nitrate, in contrast, the initial conc. of pyrite did not show any effect of the rate.

[1] Joergensen C. J., Jacobsen O. S.; Elberling B.; Aamand J. (2009) Environmental Science & Technology 43(13): 4851-4857.
[2] Schippers A. & Joergensen B. B. (2001) Geochimica Et Cosmochimica Acta 65(6): 915-922.
[3] Peiffer S. & Stubert I. (1999) Geochimica Et Cosmochimica Acta 63(19-20): 3171-3182.
[4] Kappler et al. (2005) Geobiology 3(4): 235-245.
[5] Beller, H. R., P. S. G. Chain, et al. (2006). Journal of Bacteriology 188(4): 1473-1488.

Petrogenesis of the Mesozoic intermediate intrusive rocks in the central North China Craton: Constraints from zircon U–Pb chronology and geochemistry

D.B. YANG, W.L. XU, F.P. PEI, AND D.Y. WANG

College of Earth Sciences, Jilin University, Changchun 130061, China (yangdb@jlu.edu.cn, xuwl@jlu.edu.cn, peifp@jlu.edu.cn, wangdy@jlu.edu.cn)

The nature of the Mesozoic lithospheric mantle in the central North China Craton (NCC) is the key for us to reveal the mechanism of the NCC destruction [1]. However, LA–ICP–MS zircon U–Pb ages and whole rock geochemical data of the Mesozoic alkaline intrusive rocks, including quartz syenite and quartz monzonite, from the Shuiye, Huyanshan, Wanrong, and Erfengshan intrusions in the Shanxi and Henan provinces, central North China, provide insights for the nature of the Mesozoic lithospheric mantle beneath the central NCC.

The analyzed zircons show typical oscillatory growth zoning and striped absorption in CL images, indicating a magmatic origin. LA–ICP–MS zircon U–Pb dating results indicate that the Shuiye, Huyanshan, Wanrong, and Erfengshan quartz syenitie – quartz monzonite intrusions formed in the Early Cretaceous [2], i.e., their weighted mean $^{206}Pb/^{238}U$ ages being 130±5 Ma, 130±3 Ma, 125±2 Ma, and 127±2 Ma, respectively. Several inherited zircon cores yield Paleoproterozoic to Neoarchean ages of 1791 Ma, 2088 Ma, 2208 Ma, 2339 Ma, and 2559 Ma, indicating the presence of Paleoproterozoic and Neoarchean lower crustal basement rocks of the NCC.

These quartz syenite – quartz monzonite, together with the contemporaneous Huanglongnao nepheline syenite and Taershan quartz syenite [3], have SiO_2 = 59.42 ~ 64.98 wt%, MgO = 0.21 ~ 1.38 wt% ($Mg^{\#}$ = 21 ~ 45), and (Na_2O+K_2O) = 7.45 ~ 14.38 wt%. They are enriched in large ion lithophile elements (e.g., Rb, Ba, Sr, and K) and light rare earth elements, depleted in high field strength elements (e.g., Nb, Ta, Zr, Hf, and Ti) and heavy rare earth elements, and display prominent positive Pb anomalies. The initial $^{87}Sr/^{86}Sr$ ratios and ε_{Nd} (130 Ma) values of the Mesozoic intermediate intrusive rocks in the central NCC range from 0.7031 ~ 0.7062 and –13.3 ~ –20.0, respectively.

Based on the presence of the Paleoproterozoic and Neoarchean inherited zircons, whole rock Sr–Nd isotopic compositions, and their prominent positive Pb anomalies, we propose that the primary magma for these Mesozoic intermediate intrusive rocks could been mainly derived from partial melting of an enriched lithospheric mantle modified by the delaminated NCC lower crust. The Early Cretaceous quartz syenite – quartz monzonite intrusions in the Shanxi and Henan provinces could form under an extensional environment related to the subduction of the Paleo-Pacific plate beneath the Eurasian continent.

This research was financially supported by the NSFC (90814003 and 41002018).

[1] Xu et al. (2010) *Chem. Geol.* **270**, 257-273. [2] Ying et al. (2011) *Lithos* **125**, 449-462. [3] Xu et al. (2004) *Geochimica* **33**, 221-231.

https://doi.org/10.1180/S0026461X00008434 Published online by Cambridge University Press

Geochronology and kinetics of the Shapinggou porphyry Mo deposit in Jinzhai, eastern Qinling-Dabie orogenic belt

LI YANG [1, 2], FUKUN CHEN [2], YUE QI [2], XI-YAN ZHU [1]

[1] Institute of Geology and Geophysics, Chinese Academy of Sciences, Beijing 100029, China

[2] CAS Key Laboratory of Crust-Mantle Materials and Environments, School of Earth and Space Sciences, University of Science and Technology of China, Hefei, 230026, China

The east-west trending Qinling-Dabie orogenic belt formed through the collision of the North China craton and the Yangtze block in early Mesozoic. This belt holds the world's most significant Mo ore province that is mainly situated along the southern margin of the North China craton, including the Jinduicheng, Nannihu-Sandaozhuang, Shangfanggou and Donggou super-large Mo deposits mainly of late Mesozoic in age. Several Mo deposits have been also discovered recently in northern Dabie terrain. This terrain is bordered by the Luanchuan-Gushi fault to the north and by the Xiangfan-Guangji fault in the south. The Shapinggou Mo deposit, being estimated as the largest Mo deposit in China, is one of several newly found Mo deposits in the Dabie region. All the Mo deposits in the Qinling and Dabie areas are directly related to Mesozoic magmatic rocks of different compositions.

In the field observation, we can find that the Mo mineralization occurs in veins and stockworks and is hosted both in granite porphyry and quartz syenite porphyry. Model ages achieved by the Re-Os isotopic analysis on molybdenite and U-Pb ages of zircons from the granite porphyry and quartz syenite porphyry, obtained from the LA-ICP-MS technique, demonstrate that the Mo mineralization is almost simultaneous with the formation of the ore-bearing porphyry, which is consistent with the early to middle Cretaceous Mo mineralization in the eastern part of the Qinling orogenic belt. During this time, the eastern China was characterized by rapid extension, lithospheric thinning, and asthenospheric upwelling. These tectonic activities possibly triggered partial melting of the crust. The Mo mineralization in northern Dabie, represented by the Shapinggou porphyry Mo deposit, likely occurred in such a geodynamic setting. This study is supported by the NSFC grant (No. 41090372).

Global impacts of the Antarctic Circumpolar Current appearance on nutrient distributions and biogeochemistry

SIMON YANG[1]*, ERIC GALBRAITH[2]

[1] McGill University, Montreal, Canada, simon.yang@mail.mcgill.ca (* presenting author)

[2]McGill University, Montreal, Canada, eric.galbraith@mcgill.ca

Abstract

At present, the Southern Ocean is the global nexus for upwelling of deep, nutrient rich waters, and provides the primary supply of nutrients to low latitudes. However, this was not always the case. Prior to the opening of the Drake Passage (DP) ~30 Ma, there was no Circumpolar Current, necessitating a very different return pathway for nutrients from the deep ocean to the surface. Paleo-records therefore provide an opportunity to better understand the global implications of the circumpolar current. However, understanding paleo-records spanning this transition are complicated by the closing of the Panama Isthmus (PI), which appears to have occurred sometime later. Here, we investigate the interactions between these two events, and the implications for marine biogeochemistry, using CM2Mc, a lower resolution version of the standard Geophysical Fluid Dynamics Laboratory (GFDL) fully coupled earth system model, with the BLING biogeochemical module. We carry out four runs : closed PI / opened DP, opened PI / opened DP, opened PI / closed DP, closed PI / shallow DP. The gateways have large impacts on the upwelling flux of nutrients to the Southern Ocean, and their redistribution to low latitudes (as shown in figure 1). They also impact the ventilation of the deep ocean, with implications for re-mineralized nutrients and therefore atmospheric pCO2.

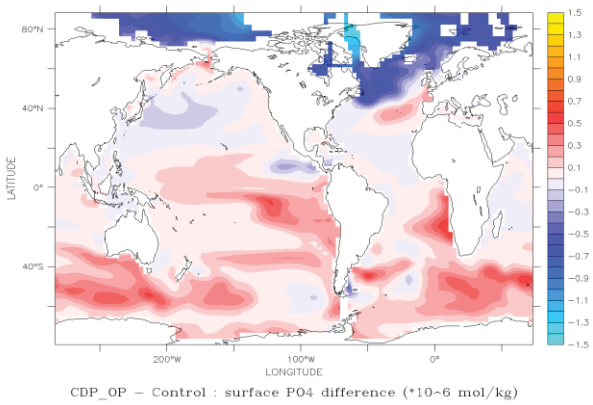

Figure 1: Difference in surface phosphate upon closing the drake passage.

https://doi.org/10.1180/S0026461X00008434 Published online by Cambridge University Press

Geochemistry and petrogenesis of dolostone from the Paleogene Shahejie Formation in Qikou depression, Bohaiwan basin, China

Y. YANG[1], F.H. GAO[1*], AND X.G. PU[2]

[1]College of Earth Sciences, Jilin University, Changchun 130061, China (yy_11@mails.jlu.edu.cn, *gaofh@jlu.edu.cn)

[2]Research Institute of Exploration and Development, Dagang Oilfield Company, CNPC, Tianjin 300280, China (puxgang@petrochina.com.cn)

Petrogenesis of dolostones from the Paleogene Shahejie Formation, Qikou depression, Bohaiwan basin, China has been a controversial. This paper reports carbon-oxygen isotopic and, trace element compositions of the dolostones from the Paleogene Shahejie Formation, Qikou depression, Bohaiwan basin, with the aim of revealing petrogenesis of dolostone.

Two major types of dolostones can be recognized as dolomicrite and grainy dolostone in the study area. The $\delta^{13}C$ and $\delta^{18}O$ values from 24 selected samples in the 2th section of the Paleogene Shahejie Formation range from -1.2‰ to 2.4‰ (V-PDB, averaging 0.7‰) and -6.8‰ to -3.9‰ (V-PDB, averaging -5.5‰), respectively. There is a positive relation between their $\delta^{13}C$ and $\delta^{18}O$ values, indicating a closed environment. Based on their minor correlation coefficient (<0.7), it is suggested that an external fluid might have been involved in their formation. Their total rare earth element abundance vary from 45.41 to 151.89 ppm (averaging 83.56 ppm), being higher than those of the marine carbonate. Additionally, their Y/Ho ratios are between 27.7 and 30.7 (averaging 29.7), similar to the average value of the upper crust (27.5). Their Sr/Ca ratios range from 0.0125 to 0.034, yielding an average value of 0.0180, which is located within those of the fresh water. The above results indicate that dolomitization could take place in the continental environment.

Nevertheless, their $^{87}Sr/^{86}Sr$ ratios (0.7092 to 0.7099, averaging 0.7095) are lower than that of fresh water (0.7119) [1] and higher than the average value (0.7080) of the sea-water in the Paleogene [2], indicating that the marine transgression might be the most important factor during formation of the Paleogene dolostones. Based on the empirical formula of Keith and Weber [3], we calculate that Z values (121.7~129.7) of the dolostones are more than 120, similar to ones of the marine carbonates. Combined with their buried depths (from 454m to 903m), we propose that that these Paleogene dolostones could form in a shallow buried diagenetic environment with the high salinity, which is also supported by their positive Gd anomaly showing a seawater source during the dolomitization.

In summary, we conclude that the Paleogene dolostone in the study area formed under a shallow burial condition, which had been influenced by the Rupelian transgression in the Paleogene.

[1] Palmer M.R. and Edmond J. M. (1989) *Earth Planet. Sci. Lett.* **92**, 11-26. [2] McArthur J. M. (2001) *J. Geol.***109**, 155-170.[3] Keith M.L. and Weber J.N. (1964) *Geochim. Cosmochim. Acta* **28**, 1787-1816.

Study on distribution regularities of the soil radionuclide contents in China

Y.X. YANG*, Y. ZHANG, L.S.CAO, Y.M.ZHENG AND X.M.WU

State Key Laboratory Breeding Base of Nuclear Resources and Environment, East China Institute of Technology, Nanchang 330013, Jiangxi, P. R. China, yxyang@ecit.cn(* presenting author)

Radionuclide content in soil is an important component to study the environment natural radioactivity level. It provides a reference for timely detection of radioactive contamination of the environment and has significance for an accurate assessment of environmental radioactive contamination. Therefor, it's necessary to research the contents of ^{238}U, ^{226}Ra, ^{232}Th and ^{40}K by combining with the distribution of uranium resources in China and the geological background of the provinces.

Through this survey, the area-weighted content average values of radionuclides ^{238}U, ^{226}Ra, ^{232}Th and ^{40}K in 28 provinces and cities in China were 39.5, 36.5, 49.1 and 580.0 Bq/kg respectively. The results approximated to the national average. The content of ^{238}U was slightly higher, and the contents of ^{226}Ra, ^{232}Th and ^{40}K were slightly lower. At the same time, the results were higher than the world average values of ^{238}U, ^{226}Ra, ^{232}Th and ^{40}K, but they belonged to the normal background level of the world[1].

By analyzing the changes of the soil radionuclide contents in 28 provinces along with the provinces, it could be seen that the contents of soil ^{238}U, ^{226}Ra and ^{232}Th were basically the same trend, namely one nuclide content in a province was high, the other two nuclide contents were also high, but the content of ^{40}K did not have this trend, which was influenced by human factors, such as burning straw and sowing the potash to the soil.

Through the survey, the contents of soil ^{238}U, ^{226}Ra and ^{232}Th in Fujian, Guangdong, Guangxi, Hunan, Jiangxi, Tibet, Yunnan and Zhejiang provinces were the top eight. In the eight provinces, the soil mother rocks of Fujian, Guangdong, Jiangxi, and Hunan mainly were granite, that of Tibet mainly were sediment and granite, and that of Zhejiang mainly were the quaternary and clay. Thus when soil mother rock was the granite, the contents of natural radionuclides in the soil were relatively high. The extensive granite was one of the reasons for higher levels of radionuclide contents in the soil in China.

By the end of 2008, more than 340 uranium deposits had been proved up. The resources were occupied 90 percents by 10 provinces which were Jiangxi, Inner Mongolia, Guangdong, Xinjiang, Hunan, Guangxi, Hebei, Liaoning, Yunnan and Zhejiang. In the top 8 provinces whose soil radionuclide contents were high, the uranium resources of six provinces were in the top ten. It was obvious that the uranium resources were relative with the soil radionuclide contents.

This study was granted by the project （2009BHA16100）of Jiangxi Province Department of Science and Technology, China

[1] Zhang et al. (2008), *Chinese Journal of Occupational Health and Damage* **Volume 23**, 339-341.

https://doi.org/10.1180/S0026461X00008434 Published online by Cambridge University Press

Geochemistry and geochronology of Cu-bearing adakitic rocks in the Edong-Jiurui area, eastern China

YI-ZENG YANG, FUKUN CHEN, QUN LONG, TING CHENG, YUE QI, JIA-DE WU

CAS Key Laboratory of Crust-Mantle Materials and Environments, School of Earth and Space Sciences, University of Science and Technology of China, Hefei, 230026, China

The middle-lower Yangtze River belt in eastern China is characterized by metallization with numerous copper, gold and iron deposits related to the Mesozoic magmatism distributed along this belt. The host magmatic rocks are commonly granodiorites, quartz-diorites and partly granites. However, genesis of the magmatic rocks and the related mineralization is still fully debated. Here we present geochronological and geochemical data of Cu-bearing magmatic rocks exposed in the eastern Hubei and northern Jiangxi area (the Edong-Jiurui area) to understand the origin of the Mesozoic magmatism in the middle-lower Yangtze River belt.

Zircon U-Pb dating using the LA-ICP-MS technique on the copper mineralization-related magmatic rocks yields variable ages ranging from about 152 Ma to 139 Ma, suggesting the earliest magmatic activity in Mesozoic related to metallic mineralization in this belt. These magmatic rocks are characterized by high Sr/Y and La/Yb ratios with high SiO_2, Al_2O_3 contents and are enriched in Sr- and Na_2O contents, light REEs and LILEs, depleted in Nb-, Ta-, Ti-contents. These features are comparable with those of the high-SiO_2 adakitic rocks. Pb isotopic composition of the whole-rocks exhibits feature of the mixture of mid ocean ridge basalts and sediments. Their $^{206}Pb/^{204}Pb$ ratios range 17.75 to 18.17, $^{207}Pb/^{204}Pb$ ratios from 15.51 to 15.63, and $^{208}Pb/^{204}Pb$ ratios from 38.03 to 38.44. Initial ε_{Nd} values of these magmatic rocks vary from -3.4 to -8.5. They have high Th/Yb and low Pb/Ce ratios. These adakitic rocks are further characterized specially by Mg# of 32-60, low Cr- and Ni-contents (<50 ppm and <35 ppm), implying that the magmas underwent quick reaction with peridotites in mantle during the magma ascending. They are enriched in Ba-content, coupled with high Sr/Nd and Ba/La ratios and low K/Rb ratio, indicating existence of slab-derived fluid during the magma formation. From the view of geochemical characteristics of the adakitic rocks in the Edong-Jiurui area, it can be proposed that the origin of the Mesozoic magmatic rocks, including granodiorites, diorites and partly granites, most likely originated from the slab melting with a significant addition of sediments. This study is supported by the NSFC grant (No. 41090372).

Ecological Risk Assessment of Soil Heavy Metals in Fruit Producing Area

Y. Y.YANG[1*], D.Y.WANG[1], Y.F.LI[1], Q. FU[1] AND D.Y.GUO[1]

[1] Jilin University, College of Earth Sciences, Changchun, China, yangyuan52415241@163.com*, wang_dy@jlu.edu.cn, yfli@jlu.edu.cn, fly19881118@yahoo.com.cn, jluguodongyan@163.com

Introduction

With the global agricultural products polluted by heavy metals more seriously, people put more emphasis on the monitoring and evaluation of green food and non-polluted fruit producing soil environment quality.

Material, Method, Results and Discussion

In this paper, the concentrations of 8 heavy metals (As, Hg, Cr, Cu, Ni, Pb, Zn and Cd), collected from 120 surface soil samples of apple-pear main production areas in Longjing-Yanji (LJ-YJ), Sanhe (SH), Tumen (TM), Hunchun (HC)—Yanbian area (in eastern Jilin Province, NE China) are analyzed by means of statistical analysis, the single factor indices, Nemerow soil pollution indices and Hakanson potential ecological risk assessment indices. The results indicate that the accumulations of 8 heavy metals in study area are regionally different and heavy metals are mainly accumulated in SH and TM. The most metal concentrations in SH, in different degrees, do appear higher than soil background values and drastically elevated concentration of As is found in TM contrast with background levels (the ratio of As content and Jilin soil background value is up to 2.64). The metal concentrations in LJ-YJ and HC are not significantly increased compared with background values. The spatial variability of 8 heavy metals is quiet different and the order of metals variability is As > Hg > Cd > Ni > Cr > Cu > Zn > Pb. According to the National Environmental Quality Standard for Soils in China (GB 15618-1995), single factor indexes of 8 heavy metals in Yanbian area are all less than 1, respectively, indicating that soil environment quality is judged as clean and free from pollution and heavy metal concentrations are completely in accordance with the soil quality requirements of nuisanceless agro-food production. Additionally, soil potential ecological risk is mild while it reaches the most serious in SH. The order of average ecological risk indices of 8 heavy metals is Cd>Hg>As>Ni>Cr>Cu>Pb>Zn.

Conclusion

Taken together, we conclude that ecological risk assessment of soil heavy metals could provide the scientific basis data of soil quality in land utilization to get high quality agricultural products and safeguard human health.

[1] Garcia-Salgado *et al.*(2012) Water Air and Soil Pollution **223**, 559-572. [2] Wan, Zhou&Zhao (2005) Scientia Geographica Sinica **25**, 329-334.

https://doi.org/10.1180/S0026461X00008434 Published online by Cambridge University Press

Simultaneous precise and accurate measurement of $^{147}Sm/^{144}Nd$ and $^{143}Nd/^{144}Nd$ isotopic ratios in natrual geological samples by MC-ICP-MS without Sm and Nd separation and use of costly spike

Y.-H. YANG*, F.-Y. WU, Z.-Y. CHU, L.-W. XIE AND J.-H. YANG

State Key Laboratory of Lithospheric Evolution, Institute of Geology and Geophysics, Chinese Academy of Sciences, P. O. Box 9825, Beijing 100029, P. R. China, e-mail:yangyueheng@mail.iggcas.ac.cn (* presenting author)

It's well-known in applications of radiogenic isotopes in the fields of geochemistry and cosmochemistry, not only the determination of isotope ratios of radiogenic daughter elements is needed but also the ratios of parent to daughter elements. In terms of Sm-Nd isotopic system, the precise and accurate determination of $^{147}Sm/^{144}Nd$ and $^{143}Nd/^{144}Nd$ isotope ratios in rocks and minerals is essential in applications of geochemical tracer and geochronology in the geological and planetary sciences. Generally, $^{147}Sm/^{144}Nd$ ratio can be determined by isotope dilution (ID) analysis, which is, without doubt, a well-known technique for its excellent precision and accuracy when properly used. This technique requires the use of artificial and costly enriched spikes (*e.g.,* commonly-used ^{149}Sm and ^{150}Nd spike). This is usually done in two steps: (1) the determination of total concentration of Sm and Nd by ID method; and (2) calculation of the concentration of isotope to evaluate $^{147}Sm/^{144}Nd$ ratios from their isotopic abundances. As for $^{143}Nd/^{144}Nd$ ratio measurements, owing to its inherent high precision, classic TIMS is still regarded as the benchmark technique for Nd isotope analysis. Recently, MC-ICP-MS has become a competitive technique for $^{143}Nd/^{144}Nd$ ratio measurements with high sample throughput and comparable precision to classic TIMS since its commercial advent in the mid 1990s.

MC-ICP-MS has the potential for directly measuring isotope ratios of different elements contained in single solution. The main objective of our work is attempted to study the performance of MC-ICP-MS for simultaneous measurement $^{147}Sm/^{144}Nd$ and $^{143}Nd/^{144}Nd$ ratios after one-step chemical purification. Up to now, this is the first report of simultaneous measurement $^{147}Sm/^{144}Nd$ and $^{143}Nd/^{144}Nd$ ratios of real geological sample without used costly spikes. Then we carried out present protocol on several international standard solution and certified reference materials encompassing a wide range of silicate rock type. The results are compared well with those obtained by the conventional approach involving ID methods. Therefore, the Nd and Sm separation and costly spike is unnecessary, allowing for a simple and rapid sample preparation and the high analytical throughput inherent to the MC-ICP-MS can be fully exploited for classic Sm-Nd isotope analyses.

References

[1] Yang, Y. H. *et al*., (2010) *Anal. Lett.* **43**, 142–150. [2] Fisher, C. M. *et al*., (2011). *Chem. Geol.*. **284**, 1–20.

Magma mixing as trigger for sulfide saturation in the UG2 chromitite (Bushveld, South Africa): Evidence from recrystallized silicate and sulfide melt inclusions in chromite

MEIJUAN YAO[1, 2] AND PEDRO J. JUGO[1]*

[1]Laurentian University, Sudbury, Canada,
[2]China University of Geosciences, Beijing, China,
yaomeijuan@cugb.edu.cn, yaomeijuan1016@126.com
pjugo@laurentian.ca (*presenting author)

Abstract

Mineral assemblages enclosed in chromite grains from the UG2 chromitite reef (Bushveld Igneous Complex, South Africa) were analyzed to understand the genesis of sulfides in this reef and in chromitite seams elsewhere. Two distinct types of assemblages were found. The first type consists of assemblages containing only sulfides. These range from complex assemblages containing pyrrhotite, chalcopyrite, pentlandite, and pyrite (up to ~60 micrometers in diameter and with roughly circular sections) to chalcopyrite-pentlandite pairs to small and isolated crystals of chalcopyrite or pentlandite (of less than 5 micrometers diameter). The more complex assemblages were likely trapped as an immiscible sulfide melt that produced the sulfide assemblages on cooling. The origin of the isolated sulfides grains in chromite is less certain. They could be the only exposed phase of multi-phase assemblages (with other phases hidden within the grain or removed during polishing) but could be interpreted also as crystalline sulfides that co-precipitated with chromite. The second type consists of assemblages containing quartz, Na-rich plagioclase (An_8 to An_{21}), pyroxene, biotite, zircon, rutile, chalcopyrite, and pentlandite. These silicate-oxide-sulfide assemblages are also interpreted as the result of slow cooling of immiscible melts trapped during chromite growth. However, the proportion of sulfide to non-sulfide phases observed in section is variable and the apparent volume of sulfides to silicates is too large to be explained solely by sulfide saturation from a S-bearing silicate melt. Thus, these assemblages likely represent simultaneous trapping of two immiscible liquids (a sulfide melt and a silicate melt) in variable proportions. The chromitites also contain interstitial (intercumulus) pyroxene, Ca-rich plagioclase (An_{61} to An_{76}), and minor sulfides (mostly chalcopyrite, pentlandite, and pyrite; but no pyrrhotite). The presence of quartz and zircon in the enclosed assemblages and the sharp contrast in composition between interstitial plagioclase (An_{61} to An_{76}) end enclosed plagioclase (An_8 to An_{21}) is consistent with the existence of a felsic silicate melt during chromite crystallization and, therefore, consistent with models proposing felsic-mafic magma mixing as the trigger for chromite and sulfide saturation. Similar features have been documented in the Merensky reef of the Bushveld Igneous Complex[1]. Thus, felsic-mafic magma mixing events could have been a recurrent feature during the crystallization of the Bushveld Igneous Complex.

[1] Li et al. (2005) *Contrib Mineral Petrol* **v. 150**, 119-130.

https://doi.org/10.1180/S0026461X00008434 Published online by Cambridge University Press

Segregation Processes in Metamorphism: the Role of Nucleation

B. W. D. YARDLEY[1]* G. SCHETTLER[2] AND W. HEINRICH[2]

[1]University of Leeds, Leeds, U K, b.w.d.yardley@leeds.ac.uk (*presenting author)

[2] GFZ, Potsdam, Germany, georg.schettler@gfz-potsdam.de whsati@gfz-potsdam.de

The composition of veins is often assumed to reflect the composition of the fluids from which they form, but where veins form by segregation from the surrounding rocks, it may be that the nature of the minerals that nucleate in the vein actually determines the composition, and hence dictates what segregates. Pelitic schists in eastern Connemara, Ireland, experienced low-P, high-T regional metamorphism and exhibit a progression from staurolite zone to andalusite-staurolite assemblages. However andalusite appears in schist-hosted veins at slightly lower grades than in the schist itself, often forming veins that are over 75% andalusite, with quartz and minor muscovite. Andalusite veins are only present in staurolite schists but the wall rocks are not immediately depleted in Al-silicate. One interpretation of the veins is that they arise through selective nucleation of andalusite in fracture walls when the staurolite – muscovite breakdown reaction is first overstepped. This nucleation pattern in turn drives progressive concentration of Al-silicate into the fracture to form a vein.

We have carried out hydrothermal experiments which appear to mimic the effect of nucleation-controlled segregation in a closed system. Small cylinders of fine grained honfels, with a central hole drilled out for part of their length, were loaded in gold capsules with water or NaCl solution and run for periods of up to 3 months, generally at 400°C and 3kbar. Two starting rocks were used: a cordierite – K-feldspar hornfels and a two-pyroxene basaltic hornfels.

At the end of the experiments the basaltic hornfels cores were coated with fine-grained, honeycomb-textured saponite, but coarser saponite lined the central cavity, and was particularly well-developed in the experiment with 3M NaCl fluid. Orthopyroxene in the rock core was partially replaced by saponite but also developed secondary porosity. Pelitic hornfels with 3M NaCl developed albite overgrowths on K-feldspar which grew into the central cavity, while an experiment at 500°C with pure water developed euhedral quatz crystals in the central cavity, which was lined with new mica growths.

The experiments all took place in closed systems and resulted in segregation of material into the central cavity provided, and to a lesser extent to space between core and capsule. Analyses of water extracted from runs with basaltic hornfels show that Na, K and Ca concentrations were much greater than those of Mg and Al, whereas the saponite is near to the Mg-end member with several percent Al.

We conclude that the composition of the material that segregated was dictated by the composition of the phases that nucleated, and was not closely related to the composition of the fluid. These results emphasise the difficulty in identifying the role of segregation in forming veins from consideration of mass transfer distances, since the transport step is not initially rate-limiting.

Sulfur and Lead Isotopic compositions of Hetaoping Pb-Zn Deposit, Baoshan, China

LIN YE[1*], YULONG YANG[1,2], TAN BAO[1,2]

[1] State Key Laboratory of Ore Deposit Geochemistry, Institute of Geochemistry, Chinese Academy of Sciences, Guiyang, China yelin@vip.gyig.ac.cn

[2] Graduate School of Chinese Academy of Sciences, Beijing, China

Located in the northern of Baoshan block, the Hetaoping Pb-Zn deposit is one of the most important types of Pb-Zn deposit at the northern-middle section of Lancangjiang tectonic-metallogenic belt in Western Yunnan Province. Strata exposed in the ore area range from Upper Sinian to Cambrian in age. The deposit consists of five sectors with a total reserve of over 2.0 million tons of Pb+Zn. Its orebody is vein in shape and hosted in skarn and marbleized limestone of the Upper Cambrian Hetaoping Formation, and controlled by Baichonghe anticline and SN-trending compresso-tensional interstratal faults. Skarnized, silicification, marbleization and pyritization is dominant wall-rock alteration.

Systematic studies on the sulfur and lead isotope compositions of sulfide minerals, ore and regional strata shows that: (1) the sulfur isotopic compositions of most sulfide minerals are characterized by relatively lower positive values with a narrow variation range (0.95‰~7.20‰, mean value=4.88‰), which is consistent with that of hydrothermal type deposits related to the intermediate-acid granitic intrusion in Baoshan region, but different from that of sulfate in Cambrian oceans. Moreover, some sulfide minerals interfused by reductive sulfur of strata also show higher sulfur isotopic compositions, relative to that of magmatic sulfur. It is suggested that the sulfur in the ore-forming fluids of the deposit deived mainly from deep magma chamber and partly from the Cambrian submarine sulfates. Normally, the sulfur isotope compositions of different sulfide minerals display the trend of $\delta^{34}S_{sphalerite} > \delta^{34}S_{chalcopyrite} > \delta^{34}S_{galena}$, implying the sulfur in the ore-forming fluids of the ore field had already reached isotopic equilibrium. The results of sulfur isotopic geothermometer show there is a relatively high temperature(415~488°C) mineralizing stage in this deposit; (2) The consistent lead isotopic compositions in galena and sphalerite are characterized by the the feature of the upper crustal lead with high μ value (>9.58) and low radiogenic lead isotopic composition, which are different from that of Cambrian strata, but and similar to that of Yanshanian - Himalayan crust type granites in Baoshan region, indicate that the ore lead of this deposit probably came from the upper crustal rocks with high concentration of U and Th. The concealed intermediate-acid intrusive rocks may be the important source of lead, while the strata (e.g. Hetaoping Formation) also contribute some lead to the deposit.

It is suggested that the Hetaoping deposit belong to middle-high temperature skarn type Pb-Zn deposit related to concealed intermediate-acid crust type intrusive rocks, the magmatic hydrothermal might play an important role during the mineralization process.

Acknowledgements: This research project was jointly supported by the National Natural Science Foundation of China (No.41173063) and Chinese National '973 Project' (No.2009CB421003).

https://doi.org/10.1180/S0026461X00008434 Published online by Cambridge University Press

The impact of gas on flow of DNAPL in porous media

SHUJUN YE[1*], JING YANG[1] AND JICHUN WU[1]

[1]Department of Hydrosciences, Nanjing University, Nanjing, China, sjye@nju.edu.cn

In order to investigate the multiphase flow and migrate of dense non-aqueous phase liquid (DNAPL) in a gas/water two phase system in porous media, two DNAPL infiltration experiments were conducted in a two-dimensional sand-filled cell (55 cm wide x 45 cm high x 1.28 cm thick). TCE was selected as DNAPL. In the first experiment, TCE was injected to the cell under water saturated condition. About 213ml of TCE was injected. In the second experiment, after 223 ml of air displacing water, TCE was added to the cell under gas/water two phase condition. About 194 ml of TCE was added. Light Transmission Method was applied to monitor the DNAPL flow process [1] and quantify DNAPL saturation. Comparing the results of the two experiments, the gas phase hindered the horizontal movement of TCE, shown as Fig.1 and Fig2. The volume of TCE calculated by its saturation obtained from the light transmission method agreed with that recorded injection volume under water saturated condition and gas/water two phase condition, and the migration process of TCE was clearly demonstrated by dynamic variations of the light intensity.

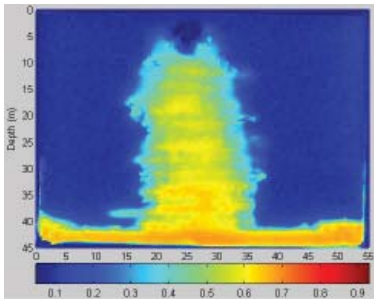

Figure 1: The distribution of TCE saturation in the flow cell in NAPL/water two phase system

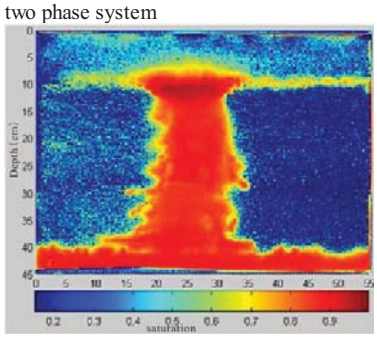

Figure 2: The distribution of TCE saturation in the flow cell in NAPL/water/gas three phase system

Acknowledgements

Funding for this research from 973 Program No. 2010CB428803, and from NSFC No. 40872155, 40725010 and 41030746 is gratefully acknowledged.

[1] Niemet & Selker (2001) Adv. Water Res. **24**, 651-666.

Genome-enabled study of alternate respiratory pathways in a novel As(V)-respiring bacterium

INES RAUSCHENBACH[1], ELISABETTA BINI[1], MAX M. HÄGGBLOM[1], NATHAN YEE[1*]

[1]Rutgers University, New Brunswick NJ, USA nyee@envsci.rutgers.edu (* presenting author)

Background

A redox hierarchy based on thermodynamics is frequently invoked to explain the microbial utilization of electron acceptors in which the substrate that provides the most energy for cell growth is preferentially reduced. However, recent experimental and modeling studies have suggested that a thermodynamic ladder of electron accepting processes does not always develop in anaerobic microbial systems. From a physiological perspective, microbes may have evolved growth and respiratory mechanisms that do not follow the electron tower paradigm.

Desulfurispirillum indicum strain S5 is an obligate anaerobic bacterium belonging to the phylum *Chrysiogenetes*. This organism is able to grow by respiring arsenate to arsenite, nitrate to ammonium, as well as selenate and selenite to elemental selenium. From genome analysis, the genes encoding for respiratory arsenate reductase (Arr), periplasmic nitrate reductase (Nap) and the membrane-bound nitrate reductase (Nar) have been identified. Using this genomic information, we carried out gene expression and growth experiments to test the redox hierarchy hypothesis in strain S5.

Materials and Methods

Strain S5was grown anaerobically in a mineral salts medium containing nitrate and/or arsenate as the electron acceptor. Growth was monitored by measuring the optical density and direct cell counts. The loss of arsenate and nitrate from the culture medium was monitored using ion chromatography. Gene expression of *D. indicum* growing under arsenate and nitrate reducing conditions was examined using qRT-PCR. Primer pairs were used for the specific detection of *arrA*, *narG*, and *napA* genes. After RNA extraction and DNAse treatment, qRT-PCR reactions were carried out using the iScript One-Step qRT-PCR with SYBR Green Kit.

Results and Discussion

Consistent with thermodynamic predictions, the experimental results showed that the reduction of nitrate to ammonium yielded higher cell densities than the reduction arsenate to arsenite. However, S5 grew considerably faster by respiration on arsenate compared to nitrate, with doubling times of 4.3 ± 0.2 h and 19.2 ± 2.0 h respectively. S5 growing on both electron acceptors exhibited the preferential utilization of arsenate before nitrate. The expression of the arsenate reductase gene *arrA* was up-regulated approximately 100-fold during arsenate reduction, as determined by qRT-PCR. Conversely, the nitrate reductase genes *narG* and *napA* were constitutively expressed under the conditions tested. The results of this study suggest that physiology, rather than thermodynamics, controls the growth rates and hierarchy of electron acceptor utilization in *D. indicum* strain S5.

https://doi.org/10.1180/S0026461X00008434 Published online by Cambridge University Press

$^{18}O^{18}O$ and $^{17}O^{18}O$ in the atmosphere

LAURENCE Y. YEUNG*, EDWARD D. YOUNG, AND EDWIN A. SCHAUBLE

University of California-Los Angeles, Los Angeles, CA, USA
lyyeung@ucla.edu (* presenting author)

The isotopic composition of atmospheric O_2 reflects the balance between photosynthesis, respiration, and the hydrologic cycle over millennial timescales. The Quaternary oxygen-isotope budget in atmospheric O_2, however, is under-constrained, and measurements of the $^{18}O^{18}O$ and $^{17}O^{18}O$ content in the atmosphere will provide additional information.

For instance, the tendency for ^{18}O-^{18}O and ^{17}O-^{18}O bonds to form upon photosynthesis is expected to be insensitive to the isotopic composition of the source water, as C-O bond ordering in carbonates has been shown to be independent of the isotopic composition of carbonate source water [1]; water has no O-O bonds to pass on, so photosynthetic O_2 cannot inherit a bond-ordering signature from its source water.

Oxygen consumption via respiration, in contrast, is expected to alter the bond ordering in O_2. Microbial respiration and photorespiration fractionate oxygen isotopologues in a manner similar to Knudsen diffusion, leaving the residue between +14-30‰ and +7-15‰ enriched in $\delta^{18}O$ and $\delta^{17}O$, respectively [2,3] resulting in the well-known atmospheric Dole effect. If the mass dependence of respiration mimics that of diffusion, then $^{18}O^{18}O$ and $^{17}O^{18}O$ in the fractionated residue should be depleted relative to the stochastic distribution [1]. Thus, the Dole effect may manifest itself as a depletion in $^{18}O^{18}O$ and $^{17}O^{18}O$ relative to the stochastic distribution in atmospheric O_2.

We examined the exceedingly rare $^{18}O^{18}O$ and $^{17}O^{18}O$ isotopic variants of O_2 in tropospheric air. We find that these species are enriched relative to the stochastic distribution of isotopes – opposite in sign from signatures predicted to be imposed by the biosphere. We demonstrate, with laboratory experiments, that bond ordering in atmospheric O_2 is likely governed by autocatalytic $O(^3P)$ + O_2 isotope-exchange reactions that cycle through the atmospheric O_2 reservoir on decadal timescales. Our analysis of the atmospheric budget suggests that trends in O-O bond ordering over geologic time may be sensitive to tropospheric $O(^3P)$ concentrations, tropopause temperature, and stratosphere-troposphere exchange flux, offering constraints on the abundance of short-lived trace gases and the strength of circulation in the ancient atmosphere.

[1] Eiler, J. M. (2007) *Earth Planet. Sci. Lett.***262**, 309-327.
[2] Guy, R. D. *et al.* (1989) *Planta* **177**, 483-491.
[3] Kiddon, J., *et al.* (1993) *Global Biogeochem. Cycles* **7**, 679-694.

Characterizing the dissolved organic composition of water in the oilsands region via FT-ICR MS

Y. YI[1,2*+], J. HAN[3+], S.J. BIRKS[1], J.J. GIBSON[1,2], C. BORCHERS[3]

[1]Integrated Water Management, Alberta Innovates-Technology Futures
[2]Department of Geography, University of Victoria
[3]University of Victoria - Genome BC, Proteomics Centre
yiyi@uvic.ca (*presenting author, + equal contribution to the research)

Introduction

Ultrahigh-resolution FT-ICR MS (Fourier Transform – Ion Cyclotron Resonance) is an emerging technique to characterize complex compositions of thousands of organic compounds dissolved in water and provide the potential to help identify impacts of oilsands development on aquatic environments. Here, we present a case study demonstrating the distinct compositional differences in the organic profiles of various water types collected in the region, which highlights the potential of FT-ICR MS in characterizing and profiling water for environmental monitoring and water resources management.

Results and Discussion

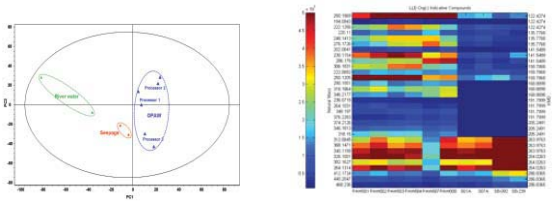

Figure 1: a) the score plot of PCA of FT-ICRMS results acquired in negative mode demonstrating distinctions and differences among various types of water. **b) heatmap** showing proposed key indicative compounds for each water type.

The FT-ICR MS analyses after Liquid-Liquid Extraction of oil sands process affected waters (OPAW) and river water lead to the successful detection of up to 7,300 compounds in water samples. The organic-rich OPAW and seepage samples analyzed in this study showed a wide range of organic compositions. Distinct patterns of mass distribution and elemental composition can be linked to the type of water. Principle Component Analysis (PCA) showed clear separation trends and groupings among various water types (Figure 1a). Further statistical analysis via Partial Least Square Discrimination Analysis (PLS-DA) proposed a series of homologues indicative of each water type (Figure 1b). The distinctive organic profile of industrially processed water as compared to background organics suggests great potential in applying FT-ICR MS in water resources management and aquatic environmental monitoring.

https://doi.org/10.1180/S0026461X00008434 Published online by Cambridge University Press

Reactive transport modeling of Sr-90 sorption in reactive sandpacks

Jun Yin[1,*], K. Ulrich Mayer[2], and Sung-Wook Jeen[3]

1. University of British Columbia, Earth and Ocean Sciences, jyin@eos.ubc.ca (* presenting author)
2. University of British Columbia, Earth and Ocean Sciences, umayer@eos.ubc.ca
3. Atomic Energy of Canada Limited, Chalk River Laboratories, jeens@aecl.ca

Granular clinoptilolite was shown to be an effective material to treat groundwater contaminated with the radionuclide Sr-90, as proven in a permeable reactive barrier (PRB) at the Chalk River site, Ontario, Canada [1]. A large number of pore volumes can be treated, because clinoptilolite is characterized by a high sorption potential with effective distribution coefficients (K_d) exceeding 6900 cm^3/g [2]. Recently, an alternative treatment technology has been proposed, using the same reactive material as an in-situ reactive sandpack to reduce contaminant levels in extracted groundwater. Reactive sandpacks can be installed around the well during construction and contaminated water is treated in the direct vicinity of the extraction well [2].

A proof-of-concept study was initiated by conducting a series of in-well column experiments to test adsorption behaviour for Sr-90 and contaminant treatment for flow conditions representative to those near a well screen [2]. Fitted distribution coefficients were strongly correlated to flow rates, indicating that Sr-90 adsorption cannot be described by an equilibrium sorption model [2]. In addition, a reduction in flow rates was observed over time, which was attributed to iron oxide precipitation in the treatment material [2], potentially also causing a reduction in clinoptilolite reactivity.

To further interpret the observed data, the reactive transport model MIN3P was used to simulate the experimental results in an attempt to better understand the sorption mechanisms. Transient boundary conditions were accounted for by varying flow rates and aqueous Sr-90 concentrations. Preliminary results confirm that the distribution coefficient (K_d) varies as a function of flow rates and breakthrough occurs earlier than predicted based on the equilibrium model. Therefore, in addition to transient boundary conditions, a kinetically-controlled linear adsorption model is used to reproduce observation data.

In addition, we evaluate whether a cation exchange model coupled with multi-rate mass transfer processes provides a more adequate description of Sr-90 attenuation. Building on the work of Jeen et al. [3], a formulation that simultaneously considers the reduction of hydraulic conductivity and decrease of reactivity as a function of mineral precipitation will be presented. This new formulation will allow to carry out long-term simulations constrained by experimental data, accounting for iron oxide precipitation as observed in the sectioned solid samples.

[1] Lee & Hartwig (2005) In *Canadian Nuclear Society Waste Management, Decommissioning and Environmental Restoration for Canada's Nuclear Activities: Current Practices and Future Needs, Ottawa, Ontario, Canada, May 8-11, 2005*
[2] Jeen (2011) In *Proceedings of Canadian Nuclear Society's Waste Management, Decommissioning and Environmental Restoration for Canada's Nuclear Activities, Toronto, Ontario, Canada, September 11-14, 2011.*
[3] Jeen *et al.* (2007) *Environ. Sci. Technol*. **41,** 1432-1438.

Multi-episodic modification of the lower crust beneath the North China block: responses to the Phanerozoic decratonization

JI-FENG YING*, HONG-FU ZHANG, YAN-JIE TANG, BEN-XUN SU, XIN-HUA ZHOU

Institute of Geology and Geophysics, Chinese Academy of Sciences, Beijing, China, jfying@mail.iggcas.ac.cn (* presenting author)

It has been generally accepted that the North China craton has considerably lost its continental lithospheric root in the Phanerozoic on the basis of multidisciplinary studies on the lithosphric evolution over the past decade. The formerly existed thick, cold Archean lithospheric mantle has been severely thinned, destructed and replaced by relatively hot and young mantle with oceanic affinity. It is worth noting, however, that the previous investigations regarding to the lithospheric evolution were mainly focued on the mantle lithosphere, how does the lower crust, namely, the other part of the lithosphere respond to such tremendous change in lithospheric structure is another important issue to be addressed.

With the outcrops of crustal materials as old as 3.8 Ga, the North China craton is one of the oldest cratons in the world. The widely distributed 2.5 Ga basement, on the one hand confirmed the existence of ancient lower crust, and on the other hand suggested that the North China was cratonized at that time. Our latest geochronological and geochemical studies on a suite of lower crustal granulite xenoliths entrapped in the Mesozoic volcanic rocks, along with the results of granulite and pyroxenite xeoliths from the other localities on the craton have shed light on the evolution of the lower crust. Zircon U-Pb age analyses revealed that, besides the ubiquitous Archean age population (predominantly 2.5 Ga), there are also Phanerozoic age populations ranging from Permian to Paleogene, varying from different localities. The Archean age population implies the existence of the ancient lower crust throughout the North China craton, while the Phanerozoic age populations imply that the ancient lower crust has been modified, most possibly through multi-episodic magmatic underplating. Zircons of different age populations also show varied Hf isotopic compositions, suggesting that the underplating magmas were from different sources. In addition to the compositional modification, the depth that the lower crust extended at different time was also changed remarkably, similar to the thinning mantle lithosphere during the Phanerozoic, the thickness of lower crust has also been thinned since the early Mesozoic.

This study was financially supported by the NSFC grant (40973027) and the Chinese Academy of Sciences (KZCX2-YW-Q08-3-1, KZCX2-EW-QN106) .

https://doi.org/10.1180/S0026461X00008434 Published online by Cambridge University Press

Drying behavior of a rock and its implication to weathering

TADASHI YOKOYAMA[1*], NAOKI NISHIYAMA[1]

[1]Department of Earth and Space Science, Osaka University
tadashi@ess.sci.osaka-u.ac.jp (* presenting author),
nnishiyama@ess.sci.osaka-u.ac.jp

Rocks near the ground surface undergo cyclic wetting and drying. Dynamic movement of pore water and significant change of chemical composition are induced by drying. Knowledge on these processes is important for considering weathering of rocks. We studied the way pore water moves and solute concentration changes during drying. A core of porous rhyolite from Kozushima, Japan [1], main pore diameter ranging from 0.1 μm to 260 μm, was used in the experiment. The core was saturated with deionized water, dried at 20°C and weight loss was monitored. Figure 1 shows the change in water-saturation (water volume per total pore volume) with elapsed time of drying. Drying rate was relatively constant for the initial 5 hours (constant-rate stage [2]) and then decreased (falling-rate stage [2]). In order to evaluate the size and chemical composition of pore water under different degrees of drying, we employed centrifugation. It is known that water is progressively extracted from water-bearing rock in order of large to small pores as centrifugal speed increases [3]. Therefore, by extracting pore water with increasing centrifugal speed in incremental steps, we can know the changes in the size of pore water and the solute concentration with progress of drying. The result of the stepwise centrifugation (Figure 2) demonstrates that as drying advances, first larger pores and subsequently smaller pores lose water. Also, solute concentration significantly changed with the progress of drying. Based on the results, we discuss how drying affects dissolution of primary minerals and precipitation of secondary products.

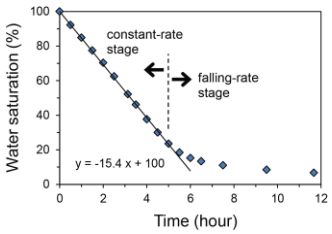

Figure 1: Change in water-saturation with elapsed time of drying

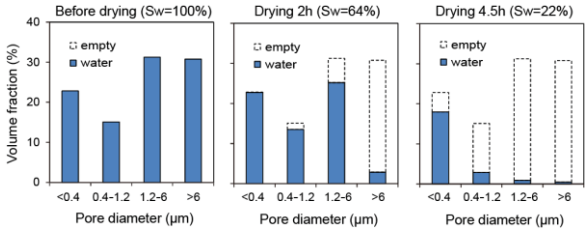

Figure 2: Change in size distribution of pore water with progress of drying (Sw: water saturation)

[1] Yokoyama & Banfield (2002) *GCA* **66**, 2665-2681. [2] Jury & Horton (2004) *Soil Physics* 370 pp. [3] Yokoyama *et al*. (2011) *Appl. Geochem.* **26**, 1524-1534.

Sr isotope anomalies in chondritic acid leachates

TETSUYA YOKOYAMA[1*], NOBUAKI ITO[1], YUSUKE FUKAMI[1] AND WATARU OKUI[1]

[1] Deptartment of Earth and Planetary Sciences, Tokyo Institute of Technology, Tokyo, Japan. (*: tetsuya.yoko@geo.titech.ac.jp)

A variety of nucleosynthetic isotope anomalies for heavy elements are documented in bulk chondrites and their components. Such data point to the existence of isotope heterogeneity in the protosolar nebula [1-2], although the mechanism that preserved nebular spatial heterogeneity at the time of planetary formation is not totally understood. In this study, we investigated stable Sr isotopic anomalies in carbonaceous chondrites. Strontium has four isotopes produced by the stellar nucleosynthesis of s-process (^{86}Sr, ^{87}Sr and ^{88}Sr), r-process (^{87}Sr and ^{88}Sr), and p-process (^{84}Sr). Radioactive decay of ^{87}Rb ($T_{1/2}$ = 48.8 Gyr) also contributes to ^{87}Sr. Recently, high precision TIMS analysis revealed both mineral and planetary scale Sr isotope anomalies in various meteorites [3]. Large ^{84}Sr excesses (>100 ppm) were also found in CAIs [3,4].

To better understand the isotopically anomalous carriers for Sr in chondrites, we examined the sequential acid leaching for bulk rocks of two chondrites, Allende (CV3) and Tagish Lake (C2-ung), and analyzed Sr isotopes by TIMS. We followed the leaching procedure of [5], in which powdered chondrites were successively leached from weak to harsh acids in six steps; AcOH (20°C) – HNO_3 (20°C) – HCl (75°C) – HF+HCl (75°C) – HF+HCl (150°C) – HNO_3+HF (120°C). The ^{84}Sr/^{86}Sr ratios are reported in μ^{84}Sr units, which represent 10^6 relative deviations from NIST987 Sr. Most of the Allende leachates have positive μ^{84}Sr that are close to the bulk Allende (+75 ppm). For Tagish Lake, the μ^{84}Sr gradually decrease from leachate #1 (+40 ppm) to #5 (-16 ppm), and an extremely large negative anomaly (-326 ppm) is observed in leachate #6. Bulk Tagish Lake has a marginally positive μ^{84}Sr (+16 ppm) that is apparently lower than that of bulk Allende.

The positive μ^{84}Sr represents the existence of materials enriched in Sr synthesized by the p- and/or r-process, while the enrichment of s-process Sr makes a negative μ^{84}Sr. Most of the presolar phases in Allende has been destroyed via thermal metamorphism on the parent body. Thus, the anomalies in Allende leachates are presumed to be dominated by CAI components. We found no FUN-like CAI signature which has a drastically low μ^{84}Sr (-4200 ppm, [6]). The μ^{84}Sr in Tagish Lake leachates suggest that leachates 1 and 2 contain presolar grains rich in p- and/or r-process Sr, while leachate 6 contains presolar grains rich in s-process Sr. This means that Tagish Lake has at least two different presolar phases produced in different stellar environment. The easily leachable presolar phase(s) in leachates #1 and #2 is not yet identified, but presumably consists of minerals produced by supernovae. The acid resistant phase in leachate #6 is most likely presolar SiC synthesized in AGB stars.

[1] Trinquier, A. et al. (2009) *Science* **324**, 374–376. [2] Burkhardt, C. et al. (2011) *EPSL* **312**, 390–400. [3] Moynier, F. et al. (2011) *LPSC* **XLII**, 1239. [4] Hans, U. et al. (2011) *LPSC* **XLII**, 2672. [5] Reisberg, L. et al. (2009) *EPSL* **277**, 334–344. [6] Papanastassiou, D. A. and Wasserburg, G. J. (1978) *GRL* **5**, 595-598.

https://doi.org/10.1180/S0026461X00008434 Published online by Cambridge University Press

Spectroscopic and Quantum Chemical Investigation of Selective Incorporation of Arsenate and Selenite into Calcite

YUKA YOKOYAMA*, YOSHIO TAKAHASHI, AND MASATO TANAKA

Hiroshima University, Hiroshima, Japan
yoshiyuka@hiroshima-u.ac.jp (* presenting author)

Calcite ($CaCO_3$) is known as a mineral which can play a role as an effective scavenger of toxic elements in the surface environment. This study focused on the interactions of arsenic (As) and selenium (Se) oxyanions with calcite. The contamination of natural water with them is occurring in various areas in the world. Especially, migration of ^{79}Se from nuclear wastes to biosphere will pose a serious problem for the safe geological disposal of nuclear wastes.

Our coprecipitation experiments and XANES measurements revealed that calcite selectively incorporated arsenate rather than arsenite [1], and selenite was selectively incorporated rather than selenate. Although molecular geometries of dissolved selenite and selenate are similar to those of arsenite and arsenate, respectively, there is no relationship between their molecular geometries and incorporation behavior into calcite. EXAFS analyses using FEFF shows that these oxyanions are incorporated into calcite through substitution with carbonate ion, which indicated that these impurities are combined with Ca^{2+} ion when they deposit on the calcite surface. In order to determine the factor controlling the preferences of arsenate and selinite for the incorporation of As and Se, respectively, into calcite, their affinities to Ca^{2+} ion, which reflect their reactivities with calcite at the calcite-water interface, were evaluated based on the quantum chemical calculation (QCC).

Estimation of intermolecular binding energies between each oxyanion and Ca^{2+} ion by QCC shows that the affinity orders for Ca^{2+} ion are arsenite > arsenate and selenite > selenate. The preference of selenite for incorporation into calcite is related to its higher affinity to Ca^{2+} ion than selenate. On the other hand, though QCC shows that arsenite has higher affinity for Ca^{2+} ion than arsenate, arsenite is hardly incorporated into calcite as shown experimentally [1]. This preference can be attributed to the difficulty of arsenite deprotonation as shown in its large dissociation constant (p*K*a = 9.3). Other oxyanions (arsenate, selenite, and selenate) dissociate into their anionic forms and can interact with Ca^{2+} ion under pH conditions where calcite can precipitate, whereas neutrally charged arsenite cannot display its high affinity for Ca^{2+} ion except for under high alkaline condition. Hence, the factors controlling their preferences for the incorporation into calcite are different between As and Se; for As, the charge of the aqueous species is important, whereas affinity to Ca^{2+} ion is important for Se. Additional QCC of the interactions between the oxyanions and calcite surface with the cluster models mimicking calcite-water mineral interface is expected to contribute to further investigation at the molecuar-scale. The present findings should provide some insights into natural behavior of As and Se, because their oxidation states are variable in subsurface environment.

[1] Yokoyama *et al.* (2009) *Chem. Lett.* **38**, 910-911.

Pore-scale evaluation of calcium carbonate precipitation and dissolution kinetics in a microfluidic pore network

HONGKYU YOON[1*], THOMAS DEWERS[1], ALBERT J. VALOCCHI[2], AND CHARLES J. WERTH[2]

[1] Geomechanics, Sandia National Laboratories, Albuquerque, USA, hyoon@sandia.gov (* presenting author), tdewers@sandia.gov
[2] Civil and Environmental Engineering, University of Illinois, Urbana, IL, USA, valocchi@illinois.edu, werth@illinois.edu

Introduction and background

Dissolved CO_2 during geological CO_2 storage may react with minerals in fractured rocks or confined aquifers resulting in mineral precipitation and dissolution. The overall rate of reaction can be affected by coupled processes among hydrodynamics, transport, and reactions at the (sub) pore-scale. Pore-scale models of coupled fluid flow, reactive transport, and heterogeneous reaction at mineral surfaces developed in our previous work [1] are applied to account for transient experimental results of calcium carbonate precipitation and dissolution in a microfluidic pore network [2]. In the micromodel, precipitation is induced by transverse mixing along the centerline in pore bodies. Pore-scale modeling is used as a basis for understanding the significance of pore-scale processes that may accoutn for large-scale phenomena involving geochemical reactions.

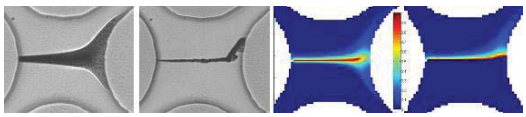

Figure 1: Experimental images (left) and simulated results (right) of $CaCO_3$ precipitates at 13 min and 118 min in the micromodel

The model is used to test the influence of different reaction rate laws on spatial and temporal reaction patterns. These include elementary reaction-based, affinity-based, and nano-scale in-situ measurement-based rate laws in the literature. The sensitivity of diffusion coefficient, reactive surface area, and rate constant on precipitate morphology, reaction rate, and amount of precipitates are evaluated in order to evaluate the governing physics of sub-micron scale reactions. Implications for evaluating mineral precipitation patterns observed in natural analogues for CO_2 storage and leakage are discussed to link pore-scale models to domains of relevance for geological CO_2 storage.

Hongkyu Yoon and Thomas Dewers were supported as part of the Center for Frontiers of Subsurface Energy Security, an Energy Frontier Research Center funded by the U.S. Department of Energy, Office of Science, Office of Basic Energy Sciences under Award Number DE-SC0001114. Sandia National Laboratories is a multi-program laboratory managed and operated by Sandia Corporation, a wholly owned subsidiary of Lockheed Martin Corporation, for the U.S. Department of Energy's National Nuclear Security Administration under contract DE-AC04-94AL85000.

[1] Yoon et al. (2012) Water Resour. Res. (In press). [2] Zhang et al. (2010) ES&T 44(20), 7833–7838.

https://doi.org/10.1180/S0026461X00008434 Published online by Cambridge University Press

Carbon sequestration using asbestos-containing slate waste: detoxification of asbestos and carbonate mineralization

SUNGJUN YOON* AND YUL ROH-
Chonnam National University, Gwangju, Korea, rohy@jnu.ac.kr

Introduction

One of the representative asbestos-containing waste materials is a slate used as a roofing material. Asbestos-containing slate waste consists of chrysotile asbestos (10~20%) and cement (80~90%). As time goes by, calcium hydroxide which forms a constituent part of cement dissolves in water and chrysotile asbestos harmfully remain in the environment. Generally, asbestos-containing slate waste is dumped in controlled waste sites in Korea. However, this cannot be regarded as an ultimate solution because dispersion of asbestos fibers in the air is an intrinsic risk during dumping operations and in the long term management. An alternative solution is thermal transformation of asbestos-containing material into non-hazardous phase [1, 2]. Also, chrysotile is one of the raw materials to form carbonate mineral for CO_2 sequestration in previous studies [3, 4]. Therefore, the aims of the study were to detoxify chrysotile asbestos in slate waste via heat treatment and to sequester CO_2 using asbestos-containing slate waste via carbonate mineralization.

Materials and Methods

Two steps of experiments were designed: (1) transformation of fibrous asbestos into non-fibrous material through heat treatment after pulvering the slate waste and (2) synthesis of carbonate mineral, calcite ($CaCO_3$), via the physicochemical reactions of heat treated slate waste with CO_2. Chemicophysical properties of slate wastes before and after the treatment were investigated by TG-DTA and XRF analyses. And mineralogical characteristics of the slate waste and byproducts after treatments were examined by PLM, XRD, SEM, TEM and EDS analyses.

Results and Conclusion

Mineral characterization showed minerals such as chrysotile [$Mg_3Si_2O_5(OH)_4$], calcium hydroxide [$Ca(OH)_2$] and calcite ($CaCO_3$) in the slate waste were transformed to magnesite ($MgCO_3$), fosterite (Mg_2SiO_4), and calcium oxide (CaO) by heat treatment. PLM, SEM and TEM analyses showed that chrysotile fibers were transformed into rod-shaped forsterite. Calcite ($CaCO_3$) was formed after reaction of heat treated slate with CO_2. These results indicate that thermal treatment of asbestos-containing slate combined with physicochemical reactions with CO_2 can detoxify chrysotile asbestos in slate waste and sequester CO_2 by forming carbonate mineral.

[1] Zaremba & Peszko (2008) *J. Therm. Anal. Calorim* **92**, 873-877.
[2] Leoneli *et al.* (2006) *J. Hazard. Mater* **135**, 149-155.
[3] Oelkers *et al.* (2008) *Elements* **4,** 333-337.
[4] Gerdemann *et al.* (2007) *Environ. Sci. & Technol.* **41**, 2587-2593.

Geological Environmental assessment of Lakes Shinji-ko and Nakaumi by stream sediment, Shimane Prefecture, Japan.

KEISUKE YOSHIDA[1*] AND ICHIRO MATSUMOTO[1]

[1] Department of Education, Shimane University, Matsue, Japan,
keisuke0406@gmail.com (* presenting author)
chromim@edu.shimane-u.ac.jp (second author)

Lakes Shinji-ko and Nakaumi

Lakes Shinji-ko and Nakaumi are the continuous brackish water lakes representing Japan, located Japan seacoast side over Shimane and Tottori prefectures. These lakes had many brackish resources and sightseeing, and many researches have mainly been done water quality or an ecosystem. It is because declining of water quality and the influence on brackish products are becoming serious by human life in recent years [1]. In this research, we investigated the sediment from the river, which flows into lakes. It is because sediment is an basically very important for the ecosystem of the bottom of a lakes. Moreover, it is expected that the rate of an influence to a lakes will be estimatable.

Results and discussion

In this research, we observed the mineral composition of sediment by using of XRD-method and mode counting of minerals and rock fragments under the microscope. All sediment mainly consists of Quartz, feldspars and rock fragment, and accompany with hornblende, biotite, pyroxene, olivine and magnetite. There are no difference between Lakes Shinji-ko and Nakaumi. However, rivers which flow in from south of lakes show high ratio in “granite origin-mineral and fragment”. This result is concordant with geological feather surrounding the lakes. That is Thertiary sandstone and mudstone is mainly consisting of Shimane peninsula, which closes the north of a lakes. The granite is widely distributed to the south of lakes. That is, it became clear that the chemical influence according to the geology of the basin is brought to a lake through each river. Importance of this is that the rate of the chemical influence in natural became calculable with the basin area of each river.

It makes clear that Hii river has most affected the lakes Shinji-ko and Nakaumi, as a preliminary report. And Iinashi river has also large affected the lake Nakaumi as well as Hii river. Matsumoto (2009) has reported the same result using a heavy metal element concentration [2, 3, 4]. Our preliminary report is concordant with the result and idea of Matsumoto (2009). In addition, Matsumoto (2009) show only Hii and Iinashi rivers, however we can show the almost all river surrounding the lakes. We are going to study these results in details further and to perform the environmental impact assessment to the lakes Shinji-ko and Nakaumi from viewpoints of a nature and a human life.

[1] Takayasu, K (2001)*: Tatara-syobou (press),* pp184.
[2] Matsumoto, I (2009): *Laguna,* **16**, 53-62.
[3] Matsumoto, Komatsu and Kamei et al. (2008): *Memories of Faculty of Education, Shimane Univ*, **42**, 97-105.
[4] Matsumoto, I., Hoffman D., Wolfe J. and Ishiga H. (2010): *Texas Journal of science*, **62,** 223-236.

https://doi.org/10.1180/S0026461X00008434 Published online by Cambridge University Press

Sr isotopic composition of pore water of shelf cores from IODP Expedition 317: Canterbury Basin, New Zealand

TOSHIHIRO YOSHIMURA[1]*, HODAKA KAWAHATA[1], MASAHARU TANIMIZU[2], SIMON C. GEORGE[3], JULIUS S. LIPP[4], AND GEORGE E. CLAYPOOL[5]

[1] Atmosphere and Ocean Research Insttitute, The University of Tokyo, yoshimura@aori.u-tokyo.ac.jp (* presenting author)
[2] Kochi Institute for Core Sample Research, JAMSTEC
[3]Department of Earth and Planetary Sciences, Macquarie University
[4] MARUM, University of Bremen
[5]8910 West 2nd Avenue, Lakewood, CO, USA

We used Sr isotope ratios to investigate diagenetic and sedimentary controls on the chemical composition of pore water in shelf sediments of deep-penetration (>300 m) cores recovered by Integrated Ocean Drilling Program Expedition 317 at three sites on a landward-to-basinward transect in the Canterbury Basin off New Zealand (sites U1353, U1354, and U1351, Fig. 1).

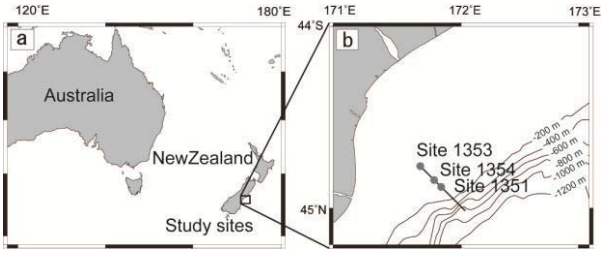

Figure 1: Map showing the locations of drilling sites of IODP Expedition 317: Canterbury Basin, New Zealand.

In general, the pore-water Sr concentration increased as $^{87}Sr/^{86}Sr$ values decreased in the shelf environment. Such Sr enrichment accompanied by rapid decreases of $^{87}Sr/^{86}Sr$ reflect the diagenetic release of Sr from reactive minerals such as biogenic carbonate and silicate minerals (e.g., plagioclase, mica). The degree of Sr enrichment was less and $^{87}Sr/^{86}Sr$ was higher in the pore water of the core from the most nearshore site (U1353) compared with the other two cores. Moreover, molar ratios of major cations remained constant throughout most of the U1353 core. These results suggest that the site U1353 sediments underwent less diagenesis. In addition, a less saline lens was observed in the uppermost 150 m only at site U1353. $^{87}Sr/^{86}Sr$ values in the less saline lens were uniform, and the plot of $^{87}Sr/^{86}Sr$ versus 1/Sr showed no significant mixing trend related to salinity changes. The $^{87}Sr/^{86}Sr$ data suggest that the less saline lens can be explained by the introduction of freshwater in the past in association with sea-level fluctuations. The repeated freshwater intrusion during periods of emergence followed by seawater replenishment after submergence that probably accompanied Pleistocene to Holocene sea-level changes would have homogenized $^{87}Sr/^{86}Sr$ values and caused some pore water to be discharged into the ocean. Moreover, no hydrocarbons were detected at site U1353 and sulfate concentrations were close to the seawater value. We propose that during sea-level lowstands, climate-driven flushing of pore water was accompanied by the inhibition of methane generation in the fine-grained sediments.

Fate of nitrogen during oxic submarine groundwater discharge into Stony Brook Harbor, New York

CAITLIN YOUNG[1*], GILBERT N HANSON[2]

[1]Stony Brook University, Stony Brook,NY,11794, USA, (correspondence: cryoung@ic.sunysb.edu)
[2]Stony Brook University, Stony Brook,NY,11794, USA, (ghanson@notes.cc.sunysb.edu)

A combination of electrical resistivity surveys, porewater sampling and ultrasonic seepage meter measurements were used to investigate nitrogen attenuation in a subterranean estuary STE in Stony Brook Harbour, an embayment with direct connection to Long Island Sound. Nitrogen loading calculations for Long Island Sound assume conservative transport of nitrogen during submarine groundwater discharge through the subterranean estuary (STE) [1]. However, the STE is increasingly recognized as a potential nitrogen sink due to rapidly changing redox conditions at the freshwater/saltwater interface. To minimize cesspool and lawn fertilizer derived nitrogen inputs to coastal waters, municipal land planners require better estimates of nitrogen attenuation in the STE.

Coupled land-sea electrical resistivity profiles show distinct shallow saline tidal recirculation cells overlying a 9m thick freshwater zone in the coastal aquifer. STE porewater was sampled in two perpendicular to shore piezometer transects 75m apart. Each transect consisted of 5 piezometer wells, sampled at intervals of 0.5m to a maximum depth of 7.6m. Ultrasonic seepage meters were placed offshore to record discharge during STE porewater sampling. A combination of N_2/Ar and $\delta^{15}N\text{-}NO_3^-$ are used to determine extent of denitrification in the shallow saline transition zone. This approach is used in traditional groundwater denitrification studies[2] but this study is the first to employ this method in a STE.

The shallow saline transition zone, where salt water from tidal oscillations penetrates into discharging fresh water, is the most geochemically active portion of this STE. Dissolved oxygen concentrations were above 70% saturation throughout the freshwater portion of the STE. Where dissolved oxygen concentrations were less than 2mg L^{-1}, nitrate concentrations were less than 50μM L^{-1} and salinity was 20ppt or greater, but no NH_4^+ is present. Along one transect, NO_3^- concentrations decreased seaward to 5 mg L^{-1} over a distance of 26 meters. Anammox, coupled nitrification-denitrification or dilution of nitrate in the shallow saline zone may account for this removal of nitrogen.

In STEs where groundwater is oxic, nitrate concentrations remain high but may be diluted during transport, as evidenced by silica and sulfate porewater distributions. Nitrogen attenuation occurs in the shallow saline transition zone, where saltwater derived dissolved organic carbon drives microbial reactions. Combined N_2/Ar and $^{15}N\text{-}NO_3^-$ elucidate attenuation mechanisms in the shallow saline transition zone.

[1] Scorca, M and Monti, J (2001) *U.S. Geological Survey Water-Resources Investigations Report* **00-4196**, 29 [2] Singleton et al (2007) *Environmental Science and Technology* **41 (3)**, 759-765

https://doi.org/10.1180/S0026461X00008434 Published online by Cambridge University Press

Chondrite Chronology, Planetesimal Accretion, and Implications for Water Delivery to Earth

EDWARD D. YOUNG[1*], HILKE E. SCHLICHTING[1,2]

[1]Department of Earth and Space Sciences, UCLA 595 Charles E. Young Drive East, Los Angeles, CA, eyoung@ess.ucla.edu (* presenting author)

[2]Hubble Fellow, hilke.schlichting@gmail.com

Two advances in the fields of cosmochemistry and solar system dynamics are raising new questions about the materials from which Earth and the other terrestrial planets were made. One is a change in our understanding of the relative antiquity of differentiated and undifferentiated planetesimals in the early solar system and the other is the recognition that planetesimals were widely scattered as a consequence of giant planet migration. We address the potential implications of these advances here.

High-precision chronometers based on short-lived radionuclides and their decay products (e.g., ^{182}Hf/^{182}W, ^{26}Al/^{26}Mg) reveal that bodies that differentiated into a rocky mantle and metallic core formed very rapidly, often with metal-silicate separation ages nearly indistinguishable from calcium-aluminum-rich inclusion (CAI) formation. Similarly, it is now well known that chondrules comprising chondrites formed several million years after CAIs. For example, new Mg isotope data from this lab for CV and LL3 chondrites show a single initial ^{26}Al/^{27}Al of 1.25x10^{-5}, corresponding to a crystallization age of 1.5 Myr after closure of the solar system based on $\Delta t = -1 / \lambda \ln\left(\left(^{26}\mathrm{Al}/^{27}\mathrm{Al}\right) / \left(^{26}\mathrm{Al}/^{27}\mathrm{Al}\right)_{\odot}\right)$. These data and other published data analogous to these in turn are suggesting that chondrites themselves accreted as late as ~ 3 and possibly even 4 Myr post CAI. Ordinary chondrites, representing the inner asteroid belt (S-type asteroids), and carbonaceous chondrites, representative of the central asteroid belt (C-type asteroids), both exhibit late chondrule formation (> 1 Myr). Therefore, the idea that heliocentric gradations in the distribution of asteroid types is the consequence of a sharp gradient in accretion time seems less likely now.

A simple order-of-magnitude calculation suggests that the growth timescale for a planetesimal of radius R, in the absence of gravitational focusing, is given by $\tau \sim \rho R / (\sigma\Omega)$ where ρ is the density of the coagulating planetesimals, σ is the mass surface density of solids and Ω is the Keplerian angular frequency around the sun. This implies a growth timescale for a 10km sized planetesimal at 3 AU of $\tau \sim 1.3\ (a / 3\mathrm{AU})^{3}$ Myr where we used $\rho \sim 3\mathrm{g/cm}^3$ and assumed a minimum mass solar nebular with a surface density profile $\sigma \propto r^{-1.5}$ (r = heliocentric distance). The scaling with semi-major axis, a, suggests a delayed growth of ~3Mys, as indicated by chondrule chronology data, can be achieved by forming planetesimals at 4AU (i.e., beyond the asteroid belt). Formation *in situ* in the asteroid belt would suggest accretion within ~ 0.4 to 1.5 Myr.

Recent models for giant planet migration allow for populating the asteroid belt and the terrestrial planet region with small bodies from distal regions of the early solar system. We suggest that combining the detailed chronology of chondrites with a better understanding of planetesimal growth timescales can be used to test these models.

Responses of deep-sea carbonate system to carbon reorganization and sea level changes

JIMIN YU[1,2*], WALLY BROECKER[1], ZHANGDONG JIN[3], JAMES RAE[4], AND ROBERT ANDERSON[1]

[1]*Lamont-Doherty Earth Observatory of Columbia University, Palisades, NY, USA.*
(* correspondence: jiminyu@ldeo.columbia.edu)

[2]Lawrence Livermore National Laboratory, Livermore, CA, USA

[3]*State Key Laboratory of Loess and Quaternary Geology, Institute of Earth Environment, Chinese Academy of Sciences, Xi'an, China*

[4]*Department of Earth Sciences, University of Bristol, Bristol, UK*

It is widely accepted that lower atmospheric CO_2 during glacials is caused by a greater sequestration of carbon in deep oceans. However, specific mechanisms causing such changes remain elusive despite intensive studies in the past decades. Transferring carbon into and out of the deep ocean would inevitably affect deep ocean carbonate chemistry such as deep water carbonate ion concentration and carbon isotopes (*1*). The associated deep ocean carbonate compensation and ocean alkalinity changes serve as important feedbacks to further affect atmospheric CO_2. As a step forward to understand the deep ocean carbonate system, we quantify deep-sea carbonate ion concentration using benthic foraminiferal B/Ca (*2*) and δ^{11}B (*3*) ratios for a few cores from the equatorial Pacific Ocean at various water depths over the last glacial-interglacial cycle. Combined with carbon isotopes, these results provide insights into the carbon cycle in the atmosphere-ocean-terrestrial biosphere system in the past. We explore responses of deep-sea carbonate chemistry to ocean circulation changes, the carbon reorganization within the ocean, and the shelf-basin carbonate fractionation associated with sea level changes. Our data allow us to evaluate past ocean alkalinity changes and their impacts on atmospheric CO_2. The reconstructed deep-sea carbonate ion also places constraints on what controlled the deep ocean carbonate preservation in the past (*4*).

1. J. Yu *et al.*, *Science* **330**, 1084 (2010).
2. J. M. Yu, H. Elderfield, *Earth Planet. Sci. Lett.* **258**, 73 (2007).
3. J. W. B. Rae *et al.*, *Earth Planet. Sci. Lett.* **302**, 403 (2011).
4. R. F. Anderson *et al.*, *Deep-Sea Res.*, doi:10.1016/j.marchem.2007.11.011 (2008).

https://doi.org/10.1180/S0026461X00008434 Published online by Cambridge University Press

Transformation and interaction of trace elements in soil-plant system under waterlogged and dry cultivation, southeastern China

XUYIN YUAN[1,2]*, TIANYUAN LI[2], AND JIZHOU LI[1,2]

[1]Key Laboratory of Integrated Regulation and Resource Development on Shallow Lakes, MOE, Nanjing, China, *yxy_hjy@hhu.edu.cn (* presenting author)
[2] Hohai University, College of Environment, Nanjing, China

Introduction

The yellow brown soil is a primary soil in the southeast China, which is cultivated for crop planting. The cultivation in waterlogged and dry fields is common manner in the study area. Trace elements of corps (rice and rape) and soils in two cultivated conditions were investigated to expound their transformation and interaction in soil-plant system. It is beneficial for risk assessment of trace metals in different land uses.

Results

The ratio of trace element concentration in crop shoot to that in soil is defined as an translocation coefficient (T), and the ratio of trace element concentration in grain to that in shoot as a allocation coefficient (A). These coefficients were researched in two soil-crop systems (rice-waterlogged field and rape-dry field). The results displayed T >1 for Cd and Mo, 0.44 < T < 0.86 for As, Hg, Se, Zn and Cu, T < 1 for Pb and Cr in soil- rice system. But the allocation coefficients for all trace elements in rice were less than 1. It showed A> 0.5 for Mo, 0.1< A < 0.5 for Hg, Se, Cu, Zn, Cd and Cr, A <0.1 for As and Pb. In the dry field, it showed that the translocation coefficients of rape were larger than 1 for Cd, 0.14< T<0.55 for Zn, Cu, Mo, Se and Hg, T< 0.1 for Pb and As. Meanwhile, the allocation coefficients of Zn and Mo were larger than 1, and those of other elements were between 0.01 and 0.57.

Based on correlation analyses, the significant affecting factors for metal translocation of rice were sulphur and pH value, and $CaCO_3$ showed a weak effect. Sulphur was also in the primary factor influencing the elemental allocation from shoot to grain, P and B were the secondary factors. Fe oxides took a important role in promoting translocation of trace elements, TOC and $CaCO_3$ also showed obviously effects on metal translocation of rape. The allocation coefficients of rape were significantly affected by iron. The other affecting factors included P, S, K and Na. It is indicated the nutrient elements are important for allocation of metals in crop[1].

Conclusions

Overall, the crop under waterlogged field shows high translocation ratios of trace elements, but trace elements under dry field are more easy to transport for shoot to grain. Relatively, the crop translocation and allocation show more affecting factors under dry field, which may due to redox and elemental characteristicss of soils[2].

[1] Lin et al (2010) *J. Hazard Mater1***74**, 202-208. [2] Gupta et al. (2008) *Environ Geol* **55**, 731-739.

Transformation of marine wood-falls into anoxic-sulfidic environments: Voltammetric time series and kinetic modeling

MUSTAFA YUCEL[1*], LEONARDO CONTREIRA[2], PIERRE E. GALAND[3], SONJA FAGERVOLD[4] AND NADINE LE BRIS[5]

UPMC, Univ Paris 06, Observatoire Océanologique and CNRS, FRE 3350 Laboratoire d'Ecogéochimie des Environnements Benthiques / Benthic Ecogeochemistry Laboratory (LECOB), 66650 Banyuls-sur-mer, France
[1]yucel@obs-banyuls.fr (* presenting author)
[2]conteira@obs-banyuls.fr, [3]galand@obs-banyuls.fr,
[4]fagervold@obs-banyuls.fr, [5]lebris@obs-banyuls.fr

Seafloor wood-falls were recently found to support chemosynthetic communities, pointing to the development of reducing conditions and redox interfaces in these organic falls over time. This discovery was in contrast with the presumed sluggish degradation of woody substrates containing such recalcitrant organic polymers. Two major questions arise in this context: How and when wood-falls transform into anoxic-sulfidic environments and what biotic and abiotic processes regulate the concentrations of redox sensitive degradation products, particularly reduced sulfur, on wood-falls? In this communication we describe a 200-day chemical dynamics of redox species on the surface and the interior of a simulated marine wood-fall using continuous multi-analyte voltammetry with Au/Hg microelectrodes, and discuss the combined microbial and abiotic kinetics of possible sulfur transformations during marine wood-fall degradation. Our voltammetry results showed that after a 5-week suboxic period, the wood interior became sulfidic, and after 8 weeks, sulfide was detected at the surface for the first time. Steady-state sulfidic conditions in the wood interior were observed after about 13 weeks, following an unsteady period where sulfide concentration fluctuated between 1 mM and several µM. Sulfide oxidation seems to play an important part in the wood-fall sulfur cycle as evidenced by the surface biofilm bacterial composition and the relatively lower concentrations of sulfide on the wood surface. The succession of transient dynamic states, in otherwise physically and chemically stable experimental conditions, suggests a complex dynamic system linking microbial communities producing and consuming sulfide with the reactivity of wood components towards sulfide. These findings shed light on the dynamics of the transformation of wood-falls into anoxic-sulfidic environments and have implications for the fate of land-derived coarse woody debris in the marine environment.

https://doi.org/10.1180/S0026461X00008434 Published online by Cambridge University Press

Mobilization of exchangeable aluminum in acid sulfate soils (ASS)

YLIANE YVANES-GIULIANI[1,2*], DAVID FINK[3], JÉRÔME ROSE[2], T. DAVID WAITE [1], RICHARD N. COLLINS[1,3]

[1]School of Civil and Environmental Engineering, The University of New South Wales, Sydney, Australia, d.waite@unsw.edu.au; y.yvanes-giuliani@student.unsw.edu.au (* presenting author)

[2]CEREGE, Université Paul Cézanne Aix/Marseille III, Aix en Provence, France, rose@cerege.fr

[3]Institute for Environmental Research, Australian Nuclear Science and Technology Organisation, Lucas Heights, Australia, fink@ansto.gov.au; richard.collins@unsw.edu.au

The conversion of coastal lowland sulfidic sediments for agricultural activities has been a common practice and has caused substantial acidification and degradation of adjacent estuarine water quality and ecosystems in Eastern Australia, and other areas worldwide [1].

The geochemistry of Al in acid sulfate soils (ASS) has rarely been the focus of research that has been published to date despite the abundance of this metal in released waters. Reactive, or, exchangeable Al can easily be sorbed/desorbed from soil mineral surfaces. Hence, the study of this pool of Al represents an opportunity to identify some release mechanisms and a more appropriate method to estimate Al likely to be released from ASS.

Extractants were chosen to isolate the exchangeable pool of Al in 30 soil samples from the Tweed Shire in north-eastern NSW, Australia: 1M KCl ($Al_{KCl\ ext}$), 0.2 M $CuCl_2$ ($Al_{CuCl2\ ext}$) and isotope exchange using ^{26}Al as a tracer (Al_{exch}) with analysis via Accelerator Mass Spectrometry (AMS). 1M KCl extraction is a standard method to determine the 'exchangeable' pool of Al and other metals [2 - 6] and is currently the recommended method for ASS. $CuCl_2$ was used for its high affinity for organic ligands [2, 3, 7] while ^{26}Al isotope exchange is a novel method than can be used to study the complex processes of aluminum storage and release [7, 8].

The results showed that the pool of Al extracted by 1M KCl was significantly lower than the isotopically exchangeable Al, especially in NOM-rich soils. Al_{CuCl2} was higher than $Al_{KCl\ ext}$ in all soils and was up to 8-fold higher in high NOM content soils, suggesting significant complexation of Al by NOM.

Therefore, the data obtained from current methods of estimation of exchangeable Al in ASS containing large amounts of NOM should be used cautiously as they will not be representative of the reactive Al likely to be released into solution and to contribute to acid generation.

[1] Johnston *et al.* (2009) *Estuar. Coast. Shelf Sci.,* **81**, 257-266. [2] Hargrove & Thomas (1981) *Soil Sci. Soc. Am. J,* **45**, *151-153*. [3] Garcia-Rodeja *et al.* (2004) *Catena,* **56**, 155-183. [4] Matús *et al.* (2006) *Talanta*, **70**, 996-1005. [5] Soon (1993) *Comm. Soil Sci. Plant Anal.,* **24**, 1683-1708. [6] Walna *et al.* (2005) *J. Inorg. Biochem.,* **99**, 11807-1816. [7] Kleja *et al.* (2005) *GCA,* **69**, 5263-5277. [8] Collins *et al.* (2009) *16th AINSE Conference on Nuclear Complementary Techniques of Analysis 2009*.

https://doi.org/10.1180/S0026461X00008434 Published online by Cambridge University Press

Glacial-interglacial paleotemeperatures and paleohydrology in the Jourdan River Valley from clumped isotopes in fresh water snails.

SHIKMA ZAARUR[1*], MORDECHAI STEIN[2], HAGIT AFFEK[1]

[1]Yale University, Geology and Geophysics , New Haven, USA shikma.zaarur@yale.edu (* presenting author), hagit.affek@yale.edu

[2]Geological Survey of Israel, Jerusalem, Israel, motistein@gsi.gov.il

Oxygen isotope composition of carbonate minerals is the most popular proxy in paleo-climate research and is especially common in the marine environment; however, since implementation of $\delta^{18}O$ records for reconstruction of environmental temperatures requires an independent estimate of paleo-water composition, it is difficult to interpret this proxy in terrestrial records. Carbonate clumped isotopes thermometry is based on the relationship of ^{13}C-^{18}O bond abundance in the carbonate lattice (measured as Δ_{47}) with the carbonate formation temperature. Most marine biogenic carbonates are consistent with the laboratory precipitation experiments that are used as calibration for the clumped isotopes thermometer.

We examine Δ_{47} in fresh water snails, focusing on *Melanopsis* snails that were collected in various water-bodies along the Jordan Rift Valley (Israel). The modern samples cover a range of ~10°C. As in marine biogenic carbonates, the temperatures derived from clumped isotopes in these modern shells are consistent with the water temperatures. Measured oxygen isotopic compositions of sampled water-bodies broadly agrees with $\delta^{18}O_{water}$ values calculated from clumped isotope temperatures and living-shell $\delta^{18}O$. This suggests that clumped isotopes in *Melanopsis* shells, as in marine organisms, reflect isotopic equilibrium and agree with the same clumped isotopes thermometer calibration.

We further analysed fossil *Melanopsis* snails collected in the Northern Jordan Valley and at sites near the modern-day northern and the southern banks of the Sea of Galilee. Our samples ages range from MIS 3 to Late-Holocene. We find fairly constant temperatures during the glacial period with low temperatures and $\delta^{18}O_{water}$. Post-glacial temperature increase to a peak in Mid-Holocene, followed by a decrease to intermediate modern values. River and lake water temperatures are generally warmer than estimated Mediterranean Sea surface temperatures [1]. Mid-Holocene Jordan River and northern Sea of Galilee water are ^{18}O-enriched by ~2‰ relative to both the LGM and modern values, and southern Sea of Galilee waters are highly enriched.

This enrichment is opposite to the depletion glacial-interglacial trend observed in other regional records such as Dead Sea sediments, Soreq cave speleothems, and Mediterranean Sea foraminifera. It is likely to reflect a change in the hydrological balance, mainly in the contribution of snow-melt to the Jordan River. The difference between the northern and southern Sea of Galilee sites are likely to reflect a change in lake evaporation following the partitioning of the glacial Lake Lisan into 2 basins with the difference observed between Southern Sea of Galilee and Northern Jordan River Valley reflecting the hydrological evolution of the northern basin through the Holocene.

[1] Almogi-Labin et al. (2009) *Quaternary Science Reviews* **28**, 2882-2896.

Silica-stabilized actinide(IV) colloids at near-neutral pH

H. ZÄNKER[1*], S. WEISS[1], C. HENNIG[1], I. DREISSIG[1]

[1]Helmholtz-Zentrum Dressden-Rossendorf, Institute of Resource Ecology, P.O. Box 51 01 19, D-1314 Dresden, Germany (*presenting author, h.zaenker@hzdr.de)

Due to their low solubility, tetravalent actinides, An(IV), are usually assumed to be immobile in natural waters. However, it is also well known that insoluble precipitation products can be mobile if they occur as colloids. For An(IV) oxyhydroxides this phenomenon has thoroughly been studied [1]. Here we describe the formation of a new type of An(IV) colloids [2].

Evidence is provided that uranium(IV) and Th(IV) can form silicate-containing colloids in near-neutral solutions containing background chemicals of geogenic nature (carbonate, silicate, sodium ions). These particles remain stable in aqueous suspension over years. A concentration of up to 10^{-3} M of colloid-borne An(IV) was observed which is a concentration significantly higher than the concentrations of truly dissolved or colloidally suspended waterborne An(IV) species hitherto reported for the near-neutral pH range. The prevailing size of the particles is below 20 nm. The higher the silicate concentration and the pH, the smaller (and obviously the more stable) are the particles that are formed (however, silicate at the concentrations tested does not form particles in the absence of the actinides). Electrostatic repulsion due to a negative zeta potential caused by the silicate stabilizes the nanoparticles. The isoelectric point of the nanoparticles is shifted toward lower pH values by the silicate. The mechanism of colloidal stabilization can be regarded as "sequestration" by silicate, a phenomenon well known from trivalent heavy metal ions such as iron(III) [3] or curium(III) [4], but never reported for tetravalent actinides so far. U-O-Si bonds, which increasingly replace the U-O-U bonds of the amorphous uranium(IV) oxyhydroxide with increasing silicate concentrations, make up the internal structure of the colloids. The next-neighbor coordination of U(IV) in the U(IV)-silica colloids is comparable with that of coffinite, $USiO_4$.

The assessment of actinide behavior in the aquatic environment should take the possible existence of An(IV)-silica colloids into consideration. Their occurrence might influence actinide migration in anoxic waters.

[1] Altmaier *et al.* (2004) *Radiochim. Acta* **92**, 537-543. [2] Dreissig *et al.* (2011) *Geochim. Cosmochim. Acta* **75**, 352-367. [3] Robinson *et al.* (1992) *J. Am. Water Works Assn.* **84**, 77-82. [4] Panak *et al.* (2005) *Radiochim. Acta* **93**, 133-139.

https://doi.org/10.1180/S0026461X00008434 Published online by Cambridge University Press

Weathering of granular basalt on a volcanic crater slope: an electron microprobe and synchrotron-XRD approach

DRAGOS G. ZAHARESCU[1*], KATERINA DONTSOVA[1], NICOLAS PERDRIAL[2], CARMEN BURGHELEA[1], JON CHOROVER[2], JULIA PERDRIAL[2], RAINA MAIER[2], TRAVIS HUXMAN[1]

[1]University of Arizona, Biosphere-2, Tucson, Arizona, U.S.A., zaharescu@email.arizona.edu (* presenting author), dontsova@email.arizona.edu, huxman@ email.arizona.edu

[2] University of Arizona, Soil Water and Environmental Science chorover@cals.arizona.edu, perdrial@email.arizona.edu, jnperdri@email.arizona.edu, rmaier@ag.arizona.edu

Weathering of rock primary minerals is among the first biogeochemical events that dictates the availability of major and micro elements for wider ecosystem and ultimately shapes landscape structure and its evolution [1]. This is also the focus of two multi-annual, different scale experiments initiated at Biosphere-2, University of Arizona, i.e. 'Bio-weathering experiment' and 'Landscape Evolution Observatory'. Basalt, one of the major crustal renewal rocks on Earth, has been chosen as test rock in both studies.

In order to predict incipient mineralogical changes and element cycling during the experiments, and hence provide a link to natural setting, we examined basalt weathering progression at microscale from a total of 20 surface and subsurface samples collected on the external slopes of Merriam volcano at Flagstaff, N. Arizona. Samples representing both, unweathered and weathered granular basalt were subjected to electron microprobe and synchrotron-based XRD.

The analyses discriminated two major mineral transformation events. The presence of a weathering front inside grain structure

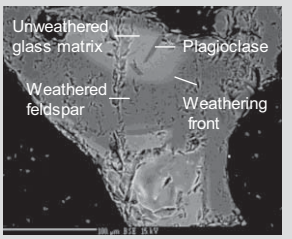

A

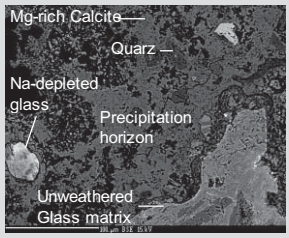

B

Figure 1: Microprobe results showing (A) weathering front and (B) surface grain precipitation in Flagstaff basalt

(Fig. 1A) is indicative of preferential weathering and shows loss of primary ions of Ca, Na, Mg and P from both, amorphous glass matrix and embeded crystaline minerals.

Secondly, there is evidence of low-temperature secondary phase precipitation onto primary mineral surfaces with major elements incorporating into various hydrous minerals including Mg-Al silicates, Mg and Mg-P rich calcites, Si-P calcite and quartz (Fig. 1B). The results and field assessment are consistent with large scale dissolution of glass and feldspars starting at crater top, followed by reprecipitation as Ca and Si-rich phases (often evaporites) in areas where subsurface flow at mountain base is shallow.

The effects of magma composition on the genesis of magmatic-hydrothermal ore deposits

ZOLTAN ZAJACZ[1*], PHILIP CANDELA[2], PHILIP PICCOLI[2] AND CARMEN-SANCHEZ VALLE[1]

[1]ETH Zürich, Zürich, Switzerland, zoltan.zajacz@erdw.ethz.ch (* presenting author)

[2]University of Maryland, College Park, USA, candela@umd.edu

The composition of magmas significantly affects the likelyhood of the formation of various magmatic-hydrothermal ore deposits. Understanding the distribution of economically important metals and their key ligands (S and Cl) between the liquid, solid and volatile phases in the system is of prime importance for the prediction of the efficiency of their sequestration from evolving magmas.

We conducted experiments to investigate the solubilities and partitioning of Au, Cu, Mo, S and Cl as a function of silicate melt composition, oxygen fugacity and temperature. Gold shows the lowest affinity to dissolve in oxide matrices and its solubility is primarily controlled by reduced S-species both in magmatic volatiles and silicate melts. The efficiency of the complexation of Au by S in the latter phases is furhter increased by increasing alkali metal and chloride activities. Estimated volatile/melt partition coefficients of Au suggest that it can be extracted efficiently by magmatic volatiles from mafic to intermediate magmas in early stages of magmatic evolution.

Copper shows a much lower affinity to complex with sulfur both in the volatile phase and the silicate melt. In most magmatic volatiles, Cu-chloride complexes are predicted to be dominant, with the exception of sulfur-rich alkaline magmas. In silicate melts, Cu dissolves into the oxide matrix and its solubility is only moderately increased by the presence of S and Cl in concentrations typical of natural systems. Both increasing degree of polymerization, and decreasing temperature reduce Cu solubilities in silicate melts; however, the effect of temperature is greater. As temperature shows the opposite effect on Cu solubility in magmatic volatiles and pyrrhotite relative to the melt, it is likely that the Cu budget of evolving magmas shifts in favour of these phases. The extraction of Cu by magmatic volatiles may be prevented if the magma evolves in the sulfide stability field ($\log f O_2 < NNO+0.5$) and the sulfides get entrapped in crystallizing minerals, or are otherwise left at deeper levels, preventing their later resorption due to S loss from the system during degassing. As opposed to Au, the extraction of Cu by exsolving volatiles will only be efficient from evolved magmas. Thus, input of volatiles originating from mafic magmas into the hydrothermal fluids will only promote porphyry Cu deposit formation through addition of S. Such volatiles will increase the Au/Cu ratio of the forming ore deposit in relatively reduced systems ($\log f O_2 < NNO+0.5$).

Molybdenum dissolves as an oxide species, and partitions in favor of andesite melts independent of S and Cl concentrations in the volatile phase within the compositional range realistic for natural systems. It is likely that higher volatile/melt partition coefficents of Mo previously observed in felsic systems is due to the reduced solubility of Mo in polymerized melts. Therefore, efficient Mo extraction is most likely from highly evolved felsic magmas.

https://doi.org/10.1180/S0026461X00008434 Published online by Cambridge University Press

Methods for quantifying methane fluxes during shale hydraulic fracturing

RASA ZALAKEVICIUTE[1], JED P. SPARKS[1*], ROBERT HOWARTH[1], ANTHONY INGRAFFEA[1], ROXANNE MARINO[1]

[1]Cornell University, Ithaca, NY, U.S.A., jps66@cornel.edu*

The U.S. Department of Energy currently predicts an increase of ~75% by 2035 of the total domestic production of natural gas from unconventional sources [1]. One of the unconventional methods used to an ever-increasing degree is shale gas extraction, using hydraulic fracturing and vertical drilling. However, this process is highly uncertain in terms of the magnitude of methane loss to the atmosphere during well production, storage, and transport. Methane has a significant global warming potential and a need exists to quantify the amount of fugitive gas loss during the lifetime of well operation.

We outline the current measurement techniques that could be employed to assess methane fluxes associated with hydraulic fracturing. These techniques include ground-based eddy covariance (EC) flux systems (e.g., the LI-COR 7700 open-path methane gas analyzer). EC is a continuous, fast in situ measurement technique, providing net flux of an atmospheric component at thirty-minute resolution. It can be used from a variety of platforms including tall towers and tethered balloons offering variable flux footprints depending upon implementation. Other methods include airborne platforms using small to medium size aircraft providing very large footprint and robust flux measurements. Advantages and drawbacks exist for each method depending upon the scale of measurement. Identification of methane sources is usually not possible from most flux measurements unless isotopic measurements are made in parallel. Advances in cavity ring-down spectroscopy have made isotopic measurements fast and reliable and reasonably deployable on multiple platforms including aircraft. Here we present recommendations for future measurement and assessment of fugitive methane associated with hydraulic fracturing of shale.

[1] Annual Energy Outlook 2011 Early Release Overview. DOE/EIA-0383ER(2011). Energy Information Agency, U.S. Department of Energy.

Non-traditional isotope variations at Cedar Butte volcano; insight into magmatic differentiation

T. ZAMBARDI[1*], X.-X. LI[1], C.C. LUNDSTROM[1]

C. HOLMDEN[2] AND M. MCCURRY[3]

[1]Dpt. of Geology, Univ. of Illinois Urbana-Champaign, IL, USA.
[2]Dpt. of Geological Sciences, Univ. of Saskatchewan, Canada.
[3]Dpt. Of Geology, Univ. of Idaho, ID, USA.

Cedar Butte (ID, USA) is a silicic volcano in the mainly basaltic Eastern Snake River Plain that produced a compositionally zoned rhyolite to basaltic andesite eruption sequence at ~400 ka. This study aims to investigate the stable isotopic compositions of Ca and Fe for selected samples from the Cedar Butte magmatic suite. Previous work shows the suite follows expectations of fractional crystallization. Despite the limited isotopic fractionations expected from non-traditional stable isotope systems in high-temperature contexts, current mass-spectrometry methods allows us to resolve significant, albeit small, isotopic variations. These tools should help us to both track and better understand differentiation mechanisms related to rock petrogenesis.

Fe isotope ratios were measured using a Nu plasma HR MC-ICP-MS (Nu Instrument, Inc.) in dry plasma mode using the sample-standard bracketing method. Results are expressed as permil δ^{57}Fe values relative to the IRMM-14 isotopic reference material. Ca isotope ratios were measured using a double spike method on a TIMS (Finnigan Triton). Calcium data are expressed as δ^{44}Ca relative to SRM915a reference material. Long-term external reproducibilities are 0.1‰ and 0.07‰ (2SD) for δ^{57}Fe and δ^{44}Ca, respectively.

Total δ^{57}Fe variations in this study range from 0.10‰ to 0.62‰, and correlate with SiO_2 content as observed previously [e.g., 1, 2, 3]. Samples from basaltic to andesitic compositions do not exhibit significant δ^{57}Fe variations (from 0.10‰ to 0.19‰), whereas samples from andesitic to rhyolitic compositions show a positive correlation leading to a 0.5‰ increase of δ^{57}Fe in the most differentiated materials. Ca isotopes do not display as clear a correlation as Fe, although the most differentiated samples also tend to enrich in heavy isotopes. Total δ^{44}Ca variations range from -1.41‰ to -0.86‰, with the exception of one Ca-rich rhyolite that displays an extremely negative – and reproducible – δ^{44}Ca = -2.5‰. This sample however did not yield a comparably shifted δ^{57}Fe value. These results thus underline the ability of multiple stable isotope data to identify multiple sources and selective processes affecting the overall differentiation process. Additional information may be provided by measurements of other stable isotopes systems such as Si and Mg.

We assess 4 possible processes for explaining the isotope-differentiation relationship: 1) fractional crystallization [2]; 2) thermal migration [4]; fluid/rock interactions [1, 3], and/or partial melting/assimilation of preexisting crustal materials.

[1] Poitrasson & Freydier (2005) *Chem. Geol.* **222**, 132-147. [2] Schuessler et al. (2008) *Chem. Geol.* **258**, 71-91 [3] Heimann et al. (2008) *Geochim. Cosmochim. Acta* **72**, 4379-4396 [4] Huang et al. (2009) *Geochim. Cosmochim. Acta* **73**, 729-749.

https://doi.org/10.1180/S0026461X00008434 Published online by Cambridge University Press

First-Principles Studies of Dissolution Reactions OF Orthoclase

HAIYING HE[1], XIN TAN[1], PAUL FENTER[2], NEIL STURCHIO[3], PETER ZAPOL[1,2]*

[1]Argonne National Laboratory, Materials Science, Argonne, USA, zapol@anl.gov (* presenting author)

[2]Argonne National Laboratory, Chemical Sciences and Engineering, Argonne, USA

[3]University of Illinois at Chicago, Chicago USA.

Introduction

Subcontinuum approaches based on first-principles theory have been successfully applied to a variety of condensed matter problems in the past, including reactivity of glass and mineral surfaces with water, to develop understanding of reaction mechanisms at the atomic scale and provide estimates of reaction rates. To develop atomistic-informed constitutive models for the dissolution rate, we chose to study a well-characterized crystalline aluminosilicate – orthoclase - as initial model system. Time resolved X-ray reflectivity was previously used to obtain the face-specific dissolution rates of orthoclase (001) surfaces under a wide range of pH and temperature conditions.[1] By studying elementary reactions of water and ions on orthoclase using first-principles methods, and combining these studies with Kinetic Monte Carlo (KMC) simulations, our goal is to develop fundamental models to understand the observed experimental dependence of dissolution rates on pH and temperature.

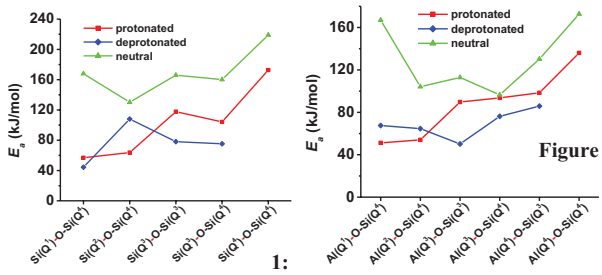

Figure 1: Calculated activation energies for different sites on the orthoclase (001) surface.

Results and Conclusion

We have performed first-principles-based modelling of surface site distribution as a function of pH and temperature on orthoclase surfaces of two different orientations (001) and (010). Differences in the surface species distribution are found for the two surfaces, suggesting different initial dissolution behavior. To evaluate reaction pathways, we have performed first-principles calculations of reaction barriers for water reactions with neutral, protonated and deprotonated sites of constituting network formers Si and Al (Fig. 1). The calculated reaction barriers together with the surface site distribution model are used to estimate the overall dissolution rates and compare with experimental values.[1] Kinetic Monte Carlo studies were used to validate a phenomenological constitutive model. This work is aimed at better understanding of the dissolution behavior and development of predictive models for dissolution rates.

1. P. Fenter, L. Cheng, C. Park, Z. Zhang, N. C. Sturchio, Geochim. Cosmochim. Acta, **67**, 197 (2003)

In situ monitoring of lepidocrocite bio-reduction and magnetite formation by backscattering Mössbauer spectroscopy

ZEGEYE ASFAW*, ABDELMOULA MUSTAPHA, AND RUBY CHRISTIAN.

University of Lorraine LCPME UMR 7564 CNRS –, Jean Barriol Institute, 405 rue de Vandoeuvre, 54600 Villers-lès-Nancy, France (*correspondence: asfaw.zegeye@lcpme.cnrs-nancy.fr)

Magnetite, a mixed valence Fe(II-III) oxide ($Fe_{3-\delta}O_4$), is a commonly occurring mineral on Earth usually found in soils and sediments. Depending on the geochemical environments in which Fe(III) bio-reduction takes place, dissimilatory iron reducing bacteria (DIRB) activity can lead to diverse biogenic minerals such as magnetite. Consequently, the discovery of magnetite at depth of 6.7 km in subsurface has been used as a marker of DIRB activity [1-2]. Moreover, the quantity of extracellular magnetite induced by DIRB could be several thousand times more than magnetotactic bacteria do per unit of biomass [3-4]. Whereas, many reports have focused on magnetite precipitated by magnetotactic bacteria, very few studies have been able to demonstrate the unequivocal existence of extracellularly precipitated magnetite. This discrepancy could be explained by the higher reactivity of magnetite formed by DIRB [5]. Indeed, the reactivity and stability of magnetite is dictated partly by its stoichiometry. It was shown that stoichiometric magnetite had the lowest reduction potential in comparison with a non-stoichiometric magnetite, consistent with higher reactivity toward pollutants such as nitrobenzene compounds [6].

The miniaturized Mössbauer spectrometer (MIMOS II) was used to monitor *in situ* the mineralogical transformation of lepidocrocite (γ-FeOOH) in *Shewanella putrefaciens* CIP 8040 culture under anaerobic condition using methanoate as the electron source. Magnetite ($Fe_{3-\delta}O_4$) was the only biogenic mineral formed during the course of the incubation. The analysis of the biogenic mineral by transmission electron microscopy (TEM) revealed cube-shaped crystals with a relatively homogeneous grain size of about 50 nm. After one day of incubation, the departure from stoichiometry δ of the biogenerated magnetite was very low (δ ~ 0.025) and rapidly reached values close to zero indicating the precipitation of a stoichiometric magnetite. The experimental setup used in this study could be replicated in field experiments when assessing the formation of magnetite in modern geological settings when its formation is suspected to be caused by a strong bacterial activity.

[1] Lovlet et al., (1987) *Nature* **330**, 252-254 [2] Gold (1992) *Science* **89**, 6045-6049 [3] Frankel (1987) *Nature* **330**, 208-208 [4] Lovley (1991) Iron Biominerals *R.B. Frankel, and R.P. Blakemore, Eds.,* 155-166 [5] Li et al., (2009) *Geobilogy* **7**, 25-34 [6] Gorski et al., *Environmental Science and Technology* **43**, 3675-3680.

https://doi.org/10.1180/S0026461X00008434 Published online by Cambridge University Press

Zircon alteration in Archean orthogneisses: Insights from U-Pb-Hf-O isotopes and trace elements

ARMIN ZEH[1], AXEL GERDES[1], AND RICHARD STERN[2]

[1] Goethe University Frankfurt am Main, Mineralogy
a.zeh@em.uni-frankfurt.de, (* presenting author)
gerdes@em.uni-frankfurt.de

[2] University of Alberta, Canadian Centre for Isotopic Microanalysis
rstern@ualberta.ca

In this study we present new results of detailed investigation on zircon populations from several granitoids of Swaziland, which comprises the oldest crust of the Kaapvaal Craton with intrusion ages between 3.66 and 2.70 Ga. Zircons from all granitoids show significant internal variations with respect to their U-Pb ages, REE patterns, and $\delta^{18}O$ (VSMOW) – far beyond analytical uncertainties, but show within error identical initial $^{176}Hf/^{177}Hf$ isotope compositions. These patterns are most pronounced for the oldest granitoids from Swaziland, comprising the 3.66 Ga TTG gneisses from Piggs peak. CL/BSE images reveal clear core-rim relationships for most zircons, but also zircons with complex zoning related to several stages of alteration. Pb-Pb ages of the "magmatic" zircon cores scatter between 3.65 to 3.26 Ga, Th/U = 0.32 to 1.12, $\delta^{18}O$ = 5.4 to 3.4‰. Furthermore, they show steep to moderate chondrite normalized LREE-patterns with a positive slope (La/Sm_N=0.002 to 0.09). In contrast, the "metamorphic" rims commonly show diffuse zoning patterns in CL, and lower Pb-Pb ages (3.28 to 3.20 Ga), Th/U (0.01 to 0.3) and $\delta^{18}O$ (1.3 to 1.7‰), and a negative slopes in LREE patterns (La/Sm_N = 2.8-3.5). Despite these differences, the analyses of all domains yielded identical initial $^{176}Hf/^{177}Hf$ of 0.28040 ± 0.00004 (2 SD). This indicates that all zircon domains (core, rims, alteration zones) were initially formed during magma crystallisation at ca. 3.66 Ga, and that the different domains were differently affected by subsequent alteration processes, causing a reset of the U-Th-Pb system, and dramatic changes of the REE patterns and $\delta^{18}O$, but left the hafnium isotope system unaffected. The low $\delta^{18}O$ of the zircon rims + altered domains (1.5‰) indicate that they probably formed by interaction with hot meteoric water. This interpretation is consistent with the strongly elevated LREE contents. These hydrothermal fluids obviously also altered some of the magmatic cores (5.3-4.1‰), even such which still look pristine in CL images and with concordant U-Pb ages! This observation has clear consequences for the interpretation of the Hadean/Early Archean detrital zircons.

The role of water in the petrogenesis of arc magmas from SW Japan

GEORG F. ZELLMER[1*], NAOYA SAKAMOTO[2], YOSHIYUKI IIZUKA[1], MASAYA MIYOSHI[3], YOSHIHIKO TAMURA[4] AND HISAYOSHI YURIMOTO[2]

[1] Academia Sinica, IES, Taipei, Taiwan, gzellmer@earth.sinica.edu.tw (* presenting author)
[2] Hokkaido University, IIL, Sapporo, Japan, naoya@ep.sci.hokudai.ac.jp
[3] University of Fukui, Dept. of Education and Regional Studies, Fukui City, Japan, miyoshi@eri.u-tokyo.ac.jp
[4] JAMSTEC, Institute for Research on Earth Evolution, Japan, tamuray@jamstec.go.jp

Thermometry and hygrometry in SW Japan arc volcanics

We have studied mafic melts from the volcanic centres of Kirishima, Aso, Kuju, Yufu, and Oninomi in Kyushu, and Abu, Menkame, Daisen and Kannabe in Western Honshu. We present results from pyroxene thermometry, 2-pyroxene thermobarometry, and plagioclase hygrometry, extending our published dataset from this region [1]. We show that initial magma water contents vary coherently along the arc, dropping from about 5wt% in Kyushu to about 2wt% in Western Honshu. Water appears to control (a) the average ponding depth of magmas at a given temperature, (b) the equilibrium phase assembleage during lower crustal differentiation and therefore the geochemical evolution of mafic melts towards intermediate (andesitic and adakitic) compositions [1].

SIMS determination of hydrogen in volcanic olivines

To determine H_2O variations directly, we have attempted to measure hydrogen in olivine by SIMS, because melt inclusions in magnesian olivines from this area are generally too small for analysis. Hydrogen concentrations are ubiquitously low (typically < 20 ppm), and in contrast to plagioclase hygrometry data do not vary coherently along the SW Japan arc (Fig. 1). Crystallization modeling suggests that olivine only becomes stable at upper crustal pressures (< 5 kbar) in these magmas, which at that stage all may already have experienced some degassing. We conclude that plagioclase is more suitable than olivine in determining the H_2O content of parental arc magmas, even if olivine melt inclusions are available.

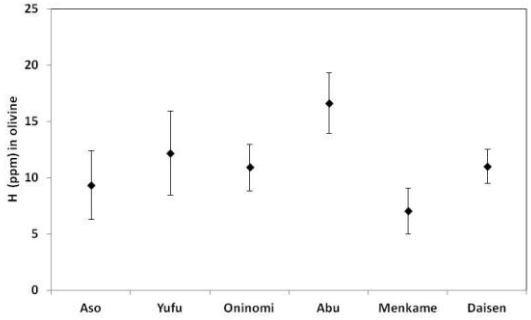

Figure 1: Summary of hydrogen concentrations in volcanic olivines from SW Japan, n ~ 10 for each center.

[1] Zellmer *et al.* (2012) *Geology,* DOI: 10.1130/G32912.1

https://doi.org/10.1180/S0026461X00008434 Published online by Cambridge University Press

Metastable Phase Equilibria for the Marine Sedimentary Deep Brine Enriched with Potassium

Y. ZENG[1,2,3*], X. D. YU[1]

[1]College of Materials and Chemistry & Chemical Engineering, Chengdu University of Technology, Chengdu, 610059, P. R. China
[2]Mineral Resources Chemistry Key Laboratory of Sichuan Higher Education Institutions, Chengdu, 610059, P. R. China
[3]Development & Comprehensive Utilization of Marine Sedimentary Brine Sichuan Provincial Key Laboratory, Chengdu, 611530, P. R. China
(* correspondence: zengyster@gmail.com)

Besides salt lake brine, underground brine is another kind of important liquid mineral resource. Pingluoba underground brine, located in the west of Sichuan basin, is famous for its high concentration of sodium, potassium, lithium, borate, and rubidium. The potassium reserves of Pingluoba underground brine is about 4.55 million ton. The exploitation of this brine can reduce the burden of potassium requirement in China.

The Pingluoba underground brine belongs to a marine sedimentary deep brine, with distinguishing features of deep buried depth (over 4500 m), high pressure (about 97 MPa), high temperature (about 393 K), and high salinity (over 420 g/L). [1] The hydrochemistry of Pingluoba underground brine is a chloride type and the main component of the brine can be simplified as the complex system $Li^+ + K^+ + Rb^+ + Mg^{2+} + Cl^- +$ borate $+ H_2O$. In this six-component system, magnesium chloride can form various hydrate salts and a solid solution can be easily formed between potassium and rubidium in chloride solution.

To exploit brine resources, the studies on the phase equilibria about the water-salt system at multi-temperature are necessary. Up to now, a series of researches about the metastable phase equilibria of the salt – water system enriched with potassium focused on Pingluoba underground brine have been done at 298 K, 323 K, 348 K by our research group.[2-6] These research results give us good information about the crystalloid forms, crystallization zones, and crystallization order of different salts, which are useful for the exploiting of brine. Neverless, most of the exiting research focused on the ternary and quaternary subsystems, the results are not enough for the comprehensive utilization of the brine, the investigation about the more complex system are necessary.

The authors acknowledge the support of the National Natural Science Foundation of China(41173071), the Project of the China Geological Survey(1212011085523) and the Research Fund for the Doctoral Program of Higher Education from the Ministry of Education of China (20115122110001).

[1] Zheng (2010) *Acta Geologica Sinica.* **Volume 84**, 1523-1553.
[2] Zeng (2011) *Miner. Mag.*. **Volume 75**, 2246.
[3] Zeng (2011) *Adv. Mater. Res.* **Volume 233-235**, 1619-1622.
[4] Yu (2010) *J.Chem.Eng.Data.* **Volume 55**, 5771-5776.
[5] Yu (2011) *J.Chem.Eng.Data.* **Volume 56**, 3384-33912.
[6] Yu (2012) *J.Chem.Eng.Data.* **Volume 57**, 127-132.

Remains of ancient precursor of perennial springs in the High Arctic

MARCOS ZENTILLI[1*], CHRISTOPHER R. OMELON[2], JACOB HANLEY[3], DARREN LEFORT[3], DALE T. ANDERSEN[4], WAYNE H. POLLARD[5]

[1]Department of Earth Sciences, Dalhousie University, Halifax, Nova Scotia, Canada, marcos.zentilli@dal.ca (*presenting author)
[2]Department of Geological Sciences, The University of Texas at Austin, Austin, Texas, USA, omelon@jsg.utexas.edu
[3]Department of Geology, St. Mary's University, Halifax, Nova Scotia, Canada, Jacob.Hanley@smu.ca; darrenlefort@gmail.com
[4]Carl Sagan Center for the Study of Life in the Universe, SETI Institute, Mountain View, California, USA, dandersen@seti.org
[5]Department of Geography, McGill University, Montréal, Québec, Canada, wayne.pollard@mcgill.ca

Saline springs in the Canadian high Arctic where water flows perennially at constant temperatures, despite the presence of deep (>400 m) permafrost, are being studied as possible environments for the development of bacterial life as an analogue for similar situations in other planets. Most documented spring activity occurs marginal to large evaporite diapirs (e.g. salt domes), and have been interpreted to represent recent phenomena related to deglaciation [1].

A relict of an ancient precursor of the active springs was found in 2005 on a steep west flank eroded by White Glacier (WG) at Expedition Fiord, Axel Heiberg Island (79.44˚N; 90.70˚W; 350 m.a.s.l.). A network of veins, mineralized fractures, layered masses and breccias is exposed across an area of ca. 350 x 50 m, where the host rock is brecciated dolomitic limestone and sandstone, anhydrite-gypsum, and intrusive igneous rocks (altered basalt). Mineralization consists of calcite in acicular, radial aggregates lining fractures and cavities, with textures wholly reminiscent of brownish calcite in active springs at Colour Peak, only 13.7 km southwest of this site. Iceland spar calcite fills the centre of larger cavities. Abundant crystalline Fe sulfides (FeS_2 marcasite, pyrite) occur in the veins and as alteration of basalt. Quartz occurs in some veins, and epidote and chlorite rim some veins where the host rock is igneous.

Fluid inclusions in calcite (5-10 μm) have salinities that fall into two distinct groups: one very low, ca. 1.5 and another ca. 16 NaCl wt% equivalent. Inclusions that occupy growth zones in some of the coarser acicular calcite crystals and deemed primary, have T_h ranging from 100˚C to 300˚C (n = 26, average 207˚C; independent of salinity), hence orders of magnitude higher than the average ca. 6˚C [2] of the brines in the active springs. Despite the similarities of the WG site with perennial springs at nearby Colour Peak [2], these results cannot be explained by models invoking shallow circulation of fluids related to deglaciation [e.g. 1]. We propose a model by which deeply-circulating hot basinal fluids associated with evaporite structures mixed with low-salinity surficial waters, in recurrent pulses. Low-temperature thermochronology (apatite fission tracks) indicates that the rocks now exposed at the surface at WG were at several km depth and temperatures of ca. 100°C until ca. 10 Ma, thus compatible with long-lasting circulation of warm fluids well before the Quaternary and ample opportunity for microbial colonization.

[1] Andersen, Pollard, MacKay, Heldmann (2002) J. Geophys. Research (Planets), **107** (E3), 5015, 7p.
[2] Omelon, Pollard, Andersen (2006) Applied Geochem. , **21**, 1–15.

https://doi.org/10.1180/S0026461X00008434 Published online by Cambridge University Press

Periodic formation of organic haze in the Neoarchean atmosphere

AUBREY L. ZERKLE[1*], MARK W. CLAIRE[2], SHAWN D. DOMAGAL-GOLDMAN[3], JAMES FARQUHAR[4] AND SIMON W. POULTON[1]

[1]School of Civil Engineering and Geosciences, Newcastle University, Newcastle upon Tyne, England, UK, aubrey.zerkle@ncl.ac.uk (*presenting author)

[2]School of Environmental Sciences, University of East Anglia, Norwich, England, UK

[3]Fellow of the NASA Postdoctoral Program, administered by Oak Ridge Associate Universities, in residence at NASA Headquarters, Washington, D.C., USA

[4]Department of Geology and ESSIC, University of Maryland, College Park, MD, USA

Photochemical models of the evolution of atmospheric redox on the early Earth suggest that a collapse in reductants (e.g., methane) was equally important to (if not required for) the rise in O_2 associated with the GOE [e.g., 1]. We present geochemical records directly linking changes in atmospheric chemistry with periodic increases in methane concentrations in the Neoarchean atmosphere. We have generated a multi-proxy dataset of ocean and atmospheric redox from sediments deposited on the Campbellrand-Malmani platform of South Africa from ~2.65-2.5 Ga, on the run-up to the GOE. Trends in Fe speciation and major sulfur isotope ratios ($\delta^{34}S_{pyrite}$) provide evidence for oxygen production in microbial mats and localized oxygenation of surface waters. At the same time, minor sulfur isotope values ($\Delta^{33}S$ and $\Delta^{36}S$) preserve mass-independent fractionations (S-MIF) indicative of a reducing atmosphere. Most significantly, changes in the character of S-MIF signals occur in several distinct sedimentary intervals correlated with areas of highly ^{13}C-depleted organic matter. These correlations extend to other datasets, implying a global trend between methane in the biosphere and variations in atmospheric S-MIF signals. We hypothesize that these signals record the periodic formation of a hydrocarbon haze at high CH_4:CO_2 ratios [e.g., 2], which could have altered S-MIF signals, either through shielding or by changing the redox chemistry of S species in the atmosphere. These results suggest that carbon-bearing compounds played an important role in regulating the redox state of the Neoarchean atmosphere, and support arguments that the GOE would have required (and/or could have been caused by) a concommital decrease in the biological flux of methane.

[1] Zahnle et al. (2006) *Geobiology* **4**, 271-283. [2] Domagal-Goldman et al. (2008) *Earth and Planetary Science Letters* **269**, 29-40.

Volumetric properties of KCl-NaCl and $CaCl_2$-NaCl binary aqueous solutions at elevated temperatures and pressures

D. ZEZIN*, T. DRIESNER, AND C. SANCHEZ-VALLE

Institute of Geochemistry and Petrology, ETH Zurich, Clausiusstrasse 25, 8092 Zurich, Switzerland denis.zezin@erdw.ethz.ch (*presenting author), thomas.driesner@erdw.ethz.ch, carmen.sanchez@erdw.ethz.ch

Modeling and understanding of geochemical processes involving aqueous fluids requires knowledge of thermodynamic properties of such solutions. Aqueous solutions in the upper crust are typically mixtures of electrolytes, thus the properties of an aqueous fluid cannot be approximated by a single-electrolyte model (e.g., NaCl-H_2O) accurately. The properties of multi-electrolyte mixtures are largely unstudied at elevated temperatures, and at pressures above the vapour pressure saturation curve. Namely, data on volumetric properties that would characterize the pressure-dependencies are essentially inexistent. These data are of particular importance in hydrothermal and geothermal fluid-related modeling, petroleum and geothermal reservoir engineering, processing and utilization of industrial brines and CO_2. We have undertaken a detailed study of the volumetric properties of multicomponent electrolyte solutions over a wide range of temperatures, pressures, and compositions.

This experimental study provides the volumetric properties of KCl-NaCl and $CaCl_2$-NaCl aqueous electrolyte solutions at temperatures up to 300 °C and pressures up to 400 bar for ionic strengths up5.8 and 12 m, respectively. A vibrating-tube densimeter was used to measure the relative density of aqueous solutions containing mixtures of alkali and alkali earth chlorides. Pressure, temperature and composition dependence of the density of binary mixtures were constrained. Mean apparent molar volume of the electrolyte solutions were calculated from the experimental data. A model based on a Pitzer-type equation was used to approximate the apparent molar volume of solutions and evaluate the partial molar volumes of dissolved components. The latter were compared to other mixing models predicting the properties of mixture of electrolytes from the properties of pure end-member electrolyte solutions.

The pressure- and concentration- dependence of the apparent molar volume may also provide important information about the structure of a solution and ionic interactions occurring in aqueous liquids. The pressure dependence of activity coefficients of dissolved components can be revealed from the variable pressure series of density measurements. Ultimately, the results of this study will permit a quantitative modeling of the properties of complex aqueous solutions and simulation of fluid-rock interaction processes occurring in geochemically relevant systems.

https://doi.org/10.1180/S0026461X00008434 Published online by Cambridge University Press

Kinetics of phosphate adsorption on goethite in seawater

JIA-ZHONG ZHANG *, AND CHARLES FISCHER

Ocean Chemistry Division, Atlantic Oceanographic and Meteorological Laboratory, National Oceanic and Atmospheric Administration, Miami, Florida 33149, USA
jia-zhong.zhang@noaa.gov (* presenting author)

The adsorption kinetics of phosphate on goethite was studied at low concentrations of both adsorbent and adsorbate to adequately measure the initial rate of decreasing phosphate concentration in solution. Phosphate sortion desplayed a two-step process. A rapid decrease in phosphate concentration was observed during the first few minutes, which was followed by a slow decrease over hours and days. Batch experimental data were fitted with a model of film-diffusion at particle-water interface for the fast process and a intra-particle/pore diffusion model for the slow process.

Batch adsorption experiments were performed at different concentrations of goethite and phosphate, as well as a range of temperatures and salinities in pH 7.9 seawater. The rate of adsorption increased with increasing concentrations of either goethite or initial phosphate concentration. At a given goethite and phosphate concentrations, the rate of adsorption increased linearly with increasing temperature from 5 to 45°C. The rate of adsorption also increased with decreasing salinity from 36 to 18 A more rapid increase was observed at salinities below 18.

Phosphate adsorption rates were similar both in seawater and artificial seawater. Comparison of rates in different seasalt solutions was used to reveal the effect of individual ions on the adsorption rate. The rate decreased exponentially with an increasing bicarbonate concentration at a constant pH 7.9. At seawater pH and total dissolved inorganic carbon concentration (2mM), the rates were constant in NaCl solution with concentrations ranging from 0.1-0.7M. This suggests that the initial rate is independent of ionic strength. The addition of SO_4^{2-} to the NaCl solution decreased the rate. In contrast, the rate was increased with the addition of Ca^{2+} or Mg^{2+} to the NaCl solution. Adding Ca^{2+}, Mg^{2+} and SO_4^{2-} together at the seawater ratio diminished the acceleration effects of Ca^{2+} or Mg^{2+}. This is likely due to the formation of ion pairs of $CaSO_4$ and $MgSO_4$ which reduced the free ion concentrations. For anions in seawater, the capacity for rate reduction was in an order of $HCO_3^- > SO_4^{2-} > Cl^-$. For cations, the order for capacity of rate acceleration was $Ca^{2+} > Mg^{2+} > Na^+$.

In-situ determination of crystal structure of $(Mg,Fe)SiO_3$

LI ZHANG[1*], WENGE YANG[2], YUE MENG[3], LIN WANG[2], QIAO-SHI ZENG[4], WENDY L. MAO[4,5] AND HO-KWANG MAO[1]

[1]Geophysical Laboratory, Carnegie Institution of Washington, Washington DC, USA, lzhang@ciw.edu
[2]High Pressure Synergetic Consortium, Geophysical Laboratory, Carnegie Institution of Washington, Argonne IL, USA
[3]High Pressure Collaborative Access Team, Geophysical Laboratory, Carnegie Institution of Washington, Argonne IL, USA
[4]Geological and Environmental Sciences, Stanford University, Stanford CA, USA
[5]Photon Science and Stanford Institute for Materials and Energy Sciences, SLAC National Accelerator Laboratory, Menlo Park, USA

$(Mg,Fe)SiO_3$ silicate is believed to be the principal mineral in Earth's lower mantle. Precise measurements of structural transitions and associated changes in composition of $(Mg,Fe)SiO_3$ at the high pressure (P) and temperature (T) conditions within Earth's lower mantle are required to interpret the seismic observations.

The $(Mg_{1-x},Fe_x)SiO_3$ (x=0.15 and 0.4) orthopyroxene starting materials were compressed to 60-130 GPa in separate symmetric diamond anvil cells and heated by the double-sided YLF laser system at the beamline 16 ID-B of the Advanced Photon Source (APS), Argonne National Laboratory (ANL). The crystal structure of the $(Mg_{1-x},Fe_x)SiO_3$ phase was studied as a function of pressure and temperature, in comparison with the known *Pbnm* orthorhombic structure. The structural details of the micron-size $(Mg,Fe)SiO_3$ crystals at high pressure were determined by the combined *in-situ* powder X-ray diffraction (XRD) and single-crystal XRD techniques. The unit-cell parameters were obtained from powder XRD measurements. The orientation matrix of individual micron-size crystal was determined in a polycrystalline sample with a focused 5×10 μm monochromatic X-ray beam. All possible reflections were then predicted with tuning diffraction angle and intensity of each reflection was measured for structure solution.

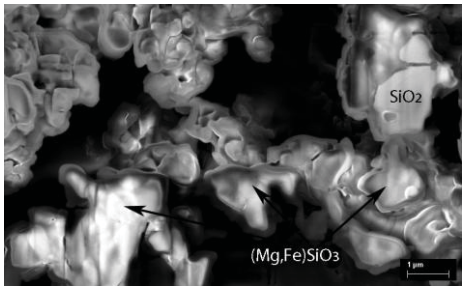

Figure 1: Cross-section of recovered $(Mg,Fe)SiO_3$ and SiO_2 in $(Mg_{0.6},Fe_{0.4})SiO_3$ from 85 GPa and 2500 K in Neon media.

The recovered samples were prepared by FIB (focused ion beam) for chemical analysis. $(Mg,Fe)SiO_3$, (Mg,Fe)O, SiO_2 and metallic Fe were selectively present in the recovered product, depending on temperature profile and starting composition.

The structural information of $(Mg,Fe)SiO_3$ silicate and associated changes in chemical composition at high *P-T* conditions is used to build a reliable mineralogical model for the lower mantle in consistent with the seismic observations.

https://doi.org/10.1180/S0026461X00008434 Published online by Cambridge University Press

Smart surfaces with switchable superoleophilicity and superoleophobicity in aqueous media: toward controllable oil/water separation

LIANBIN ZHANG[1], ZHONGHAI ZHANG[1], PEN GWANG[1,*]

[1]Chemical and Life Sciences and Engineering Division, Water Desalination and Reuse Center (WDRC), King Abdullah University of Science and Technology (KAUST), Thuwal 23955-6900, Saudi Arabia, lianbin.zhang@kaust.edu.sa, zhonghai.zhang@kaust.edu.sa, peng.wang@kaust.edu.sa (* presenting author)

Abstract

Advanced materials with surfaces that have controllable oil wettability when submerged in aqueous media have great potential for various underwater applications. Here, we have developed smart surfaces on commonly used materials, including non-woven textiles and polyurethane sponges, that are able to switch between superoleophilicity and superoleophobicity in aqueous media. The smart surfaces are obtained by grafting a block copolymer comprising blocks of pH-responsive poly(2-vinylpyridine) and oleophilic/hydrophobic polydimethylsiloxane (i.e., P2VP-*b*-PDMS) on these materials. The P2VP block can alter its wettability and its conformation via protonation and deprotonation in response to the pH of aqueous media, which provides controllable and switchable access of oil by the PDMS block, resulting in the switchable surface oil wettability in aqueous media. On the other hand, the high flexibility of the PDMS block facilitates the reversible switching of the surface oil wettability. As a proof of concept, we also demonstrate that materials functionalized with our smart surfaces can be used for highly controllable oil/water separation processes.

Figure: Graphic abstract

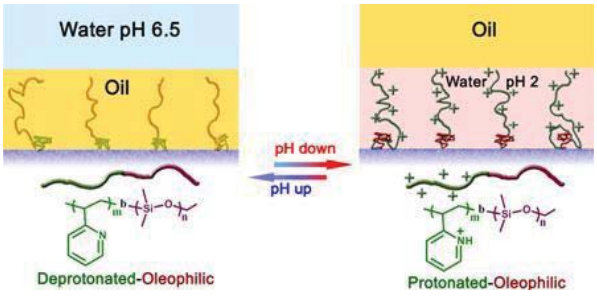

Schematics showing the switchable oil wettability of the P2VP-b-PDMSgrafted surface in aqueous media with different pH.

[1] Zhang, LB., Zhang, Z.H., Wang, P. 2012, *NPG Asia Materials* (DOI: *doi:10.1038/am.2012.14*).

Formation and evolution of Precambrian crust in South China: insights from the Dongling complex

SHAO-BING ZHANG, QIANG HE, YONG-FEI ZHENG

School of Earth and Space Sciences, University of Science and Technology of China, Hefei 230026, China (sbzhang@ustc.edu.cn)

To understand the early history of Precambrian crust in South China, a combined study of isotope geochronology and geochemistry was carried out for a Precambrian complex at Dongling, which was traditonally viewed as one of the most anicent basements in South China. The Dongling Complex is exposed at Anqing in the interior of South China and mainly composed of schist and gneiss. It is intruded by a Mesozoic granite pluton and covered by Phanerozoic strata. We analyzed whole-rock major and trace elements, zircon U-Pb and Lu-Hf isotopes, and mineral oxygen isotopes in schist and gneiss from the Dongling complex. The results provide not only temporal constraints on the deposition and metamorphism of metasedimentary protolith, but also insights into the formation and evolusuion of Precambrian crust in South China.

The whole-rock REE and trace elements in the Dongling complex show similar patterns in the spidergram to PAAS and upper continental crust. Mineral O isotope analyses obtained that most zircon $\delta^{18}O$ values are higher than 6‰ and most quartze $\delta^{18}O$ values are higher than 10‰, suggesting that their sources experienced low-temperature supracrustal recycling. Zircon U-Pb dating gave three groups of Precambrian ages. The first group of ages are older than 2.4 Ga, as high as 2.8 Ga. Some of them were obtained from inherited zircon cores and others are from the detrital zircon of Archean age. The second group is about 2.0 Ga, mainly obtained from zircon without oscillatory zone. The third group is about 800 Ma and can be categorized into two subgroups at 730-780 Ma and 800-830 Ma. This group of zircon have typical oscillatory zones of magmatic origin. Zircon grains with different U-Pb ages have similar REE partition patterns but variable total REE concentrations, indicating diversity of their sources. Zircon Lu-Hf isotope compositions vary significantly for three groups of zircons. The first group has variably negative $\varepsilon_{Hf}(t)$ values. The ~2.0 Ga zircon grains have variable $\varepsilon_{Hf}(t)$ values from -19.8 to -5.6 and two-stage Hf model ages (T_{DM2}) from 2.99 to 3.81 Ga, suggesting reworking of Archaen rocks in the middle Palaeproterozoic. The ~800 Ma zircon grains have variable $\varepsilon_{Hf}(t)$ values from -24.8 to 4.9 and T_{DM2} from 1.39 to 3.18 Ga, suggesting reworking of both ancient and juvenile crustal rocks in the middle Neoproterozoic. There is a lack of positive $\varepsilon_{Hf}(t)$ values close to the depleted mantle value, suggesting that the growth of juvenile crust is not recorded in these zircon grains.

In conclusion, premetamorphic protolith of the Dongling complex was probably deposited at middle Neoproterozoic. It contains crustal relicts of Late Archean, Paleoproterozoic and Neoproterozoic, suggests crustal reworking at these times in South China.

https://doi.org/10.1180/S0026461X00008434 Published online by Cambridge University Press

Chlorite Dissolution Rates in scCO$_2$-Saturated Saline Water at 100°C and 100 bar

SHUO ZHANG[1,2*], LI YANG[2], DONALD J. DEPAOLO[2], AND CARL STEEFEL[2]

[1]University of California Berkeley, Earth and Planetary Science, shuozhang@berkeley.edu (* presenting author)
[2]Lawrence Berkeley National Laboratory, Earth Sciences, lyang@lbl.gov , djdepaolo@lbl.gov , cisteefel@lbl.gov

Mineralogical trapping is one of several trapping mechanisms of CO_2 for geological carbon sequestration, and presents the most secure form of CO_2 storage over millenia. Mineralization of CO_2 requires release of cations from dissolution of divalent cation-bearing silicate minerals, so the extent and timing of CO_2 mineralization depends on the mineralogy and dissolution kinetics of the sandstone reservoir rocks. There are currently few experiments that measure the coupled dissolution and precipitation rates of reactions of multi-mineral systems under the conditions of sequestration. We have experimentally measured the rate of chlorite dissolution in saline water saturated with supercritical CO_2 (pCO_2 = 100 bar) at 100ºC using a mixed flow reactor. This experiment simulates the reactive front of supercritical CO_2 and aquifer water.

Chlorite is mechanically broken to pieces in the cm-range and then ground to millimetre size. Particles from 100 to 150 micron are sieved (surface area = 4.872 m^2 g^{-1}) and washed. 1 gram of chlorite particles is used for the experiment. The reactor is filled with saline water (0.01 mol/L NaCl), and brought to experimental run temperature. Supercritical CO_2 is pumped into the reactor to 100 bar and then equilibrated with saline water at this temperature and pressure. Saline water fills 260 ml of the 300 ml reactor and forms a 40 ml CO_2 cushion above the water surface to ensure that brine is always saturated with CO_2. The reactor containing chlorite is stirred as saline water is continually pumped through.

The measured release rate of Fe and Mg is 1-2 picomole/m^2/sec, which is not far from typical silicate dissolution rates under standard laboratory conditions. Nevertheless, this rate, especially when considered in the light of relatively high surface area for chlorite, is sufficient to allow substantial CO_2 mineralization in chlorite-bearing sands on a timescale of 1000 years.

Lattice Boltzmann modelling of Stellate Plagioclase, central layered series of Isle of Rum, Scotland

STEVEN ERGONG ZHANG[1]*, ANTHONY FOWLER[1], IVAN L'HEUREUX[1]

[1]University of Ottawa, Ottawa, Canada, ezhan053@uottawa.ca*, afowler@uottawa.ca, ilheureu@uottawa.ca

Abstract

We propose a model for the formation of branching plagioclase textures visible at both macroscopic (~cm to m) and microscopic scale within melagabbro, Isle of Rum Scotland. The plagioclase crystals are typically linked as twins and form meshes of planar stellate structures (m-scale) with a large range in geometrical organization from patchy to radiating. Evidence of macroscopic crystal aggregation and alignment is attributed to interfacial free energy minimization at the microscopic scale during growth. Accordingly, a binary immiscible Lattice Boltzmann model was developed to simulate diffusion of simplified plagioclase in the melt phase. Isothermal phase transitions modelled via first order chemical reactions are subsequently coupled with stochastic dynamics at the crystal growth front to simulate energy minimization processes including twinning during crystallization in an igneous environment. A flexible coupling of the solid phase with respect to the melt phase sets the overall ratio between the rate of diffusion and chemical enrichment in the liquid state and the rate of crystallization. Results are in reasonable agreement with observations. Aspects of the model and current progress will be presented.

https://doi.org/10.1180/S0026461X00008434 Published online by Cambridge University Press

New Understanding of Changxing Formation reefs in Permian in eastern Sichuan area, China

Liu Zhicheng[1], Zhang Tingshan[1]*, Yang Wei[1], Ming Huajun[1], Dang Lurui[2], Zheng Chao[2],Yang Yang[3]

[1]State Key Lab. of Oil & Gas Reservoir Geology and Exploitation Engineering, Chengdu, China, zts_3@126.com (* presenting author)

[2]Chongqing Gas District of SW Oil & Gas Co., Ltd., CNPC, Chongqing, China, zhengchao@petrochina.com.cn

[3] Shunan Gas District of SW Oil & Gas Co., Ltd., CNPC, Luzhou, China, jerp@qq.com

Reefs have been reported in Changxing formation within the eastern Sichuan area, are important gas reservoirs.[1] They have been characterized by coralline sponges, including the sphinctozoans and inozoans as their framebuilder.[2] These reefs are mainly divided into platform marginal reef and patch reef in platform, with obvious different characteristics. The platform marginal reef is characterized by large scale, integrate facies belt of reef combination, strong water energy, controlled by paleogeographic location and paleogeomorphic environment, and fasciculate distribution mainly on both sides of the oceanic trough. In contrast, the patch reef in platform is characterized by small scale, weak water energy, a few reef -forming organism individual, no deposition of reef front or reef back, more cycles of the reef, development of thrombolite, inexplicit distribution regularity, controlled by paleogeomorphology, and random distribution along local highland in the platform(Figture1). Samples of reefs rock and host rock were examined using thin sections，casting sections and scanning electron microscope experiments. and the application of various analytical techniques including analysis to reservoir properties - pore structure parameters curve and pattern analysis of pore structure, reservoir characteristics of reef have been thoroughly investigated. The results revealed a very close relationship between the reservoir and reefs. The reservoir were be strictly controlled by both sedimentary microfacies and lithology. The favorable facies belt includes framework reef and bonding reef. The rock types of reservoir mainly are dolomite particles, micrite particles and the bioclastic. The reef has complex types of pores, and the reservoir space of reef including intergranular dissolution pore, large dissolution pore, dissolution pore, intragranular dissolved pore and large cavity pore. The formation of the pores are mainly affected by the cementation and dissolution with few primary pores, however, the secondary pores are abundant and form excellent reservoir for gas.

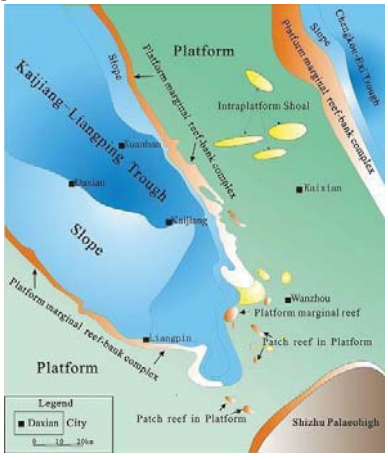

Figture1:Map of Sedimentary Facies and Its Distribution in Changxing Formation, Eastern Sichuan Area

[1]Zhang Tingshan, Jiang Zhaoyong, Chen Xiao-hui(2008)Characteristics and controlling factors of development of Paleozoic reef-banks in the Sichuan basin[J]. *Geology in China*,**35(5)**:1017-1030.

[2]Yang Wanrong, Li Xun(1995)Permian reef types and controlling factors of reef formation in south china[J].*Acta Palaeontologica Sinica*, **34(1)**:67-77.

Re-Os isotopes of Chaihe mantle xenoliths constrain the age of the subcontinental lithospheric mantle in Inner Mongolia Province, China

YAN-LONG ZHANG[1,*], WEN-CHUN GE[1], CHUAN-ZHOU LIU[2]

[1] College of Earth Sciences, Jilin university, Changchun, China, zhangyanlong@jlu.edu.cn (* Presenting author)

[2] Institute of Geology and Geophysics, Chinese Academy of Sciences, Beijing, China, chzliu@mail.iggcas.ac.cn

Nearly 30 Cenozoic volcanoes that were erupted during the Pleistocene-Holocene have been discovered in Chaihe area, mid-Great Xing'an Range. The Holocene alkaline basalts contain abundant mantle xenoliths. The 27 samples selected in this study are composed of 11 spinel lherzolites, 8 spinel harzburgites，7 garnet lherzolites and one garnet harzburgite. The garnet is commonly kelyphited. The spinel lherzolites contain 1.36-3.52 wt.% Al_2O_3 and 1.55-3.84 wt.% CaO, whereas the harzburgites have lower contents of both Al_2O_3 and CaO, i.e. ~0.46-1.69 wt.% and ~0.36-1.32 wt.%, respectively. Clinopyroxene in the harzburgites is enriched in LREE, and displays negative Ba, Nb, Zr, Hf and Ti anomalies. Clinopyroxene in the lherzolites show variable REE patterns, such as LREE-enriched, LREE-depleted and MREE-enriched patterns. The Chaihe xenoliths have $^{187}Os/^{188}Os$ ratios ranging from 0.1106 to 0.1276. The most refractory spinel harzburgite (03Ch-10), with an olivine Fo value of 92.1, has the lowest $^{187}Os/^{188}Os$ ratios of 0.1106, which gives a rehenium depletion age (T_{RD}) of 2.6 Ga relative to the primitive upper mantle (PUM). Sr-Nd-Hf isotopes ($^{87}Sr/^{86}Sr$= 0.70665, $^{143}Nd/^{144}Nd$=0.51289, $^{176}Hf/^{177}Hf$=0.282805) of clinopyroxene in this sample is slightly more enriched than that in other samples ($^{87}Sr/^{86}Sr$= 0.70252-0.70504, $^{143}Nd/^{144}Nd$=0.51289-0.51366, $^{176}Hf/^{177}Hf$=0.283125-0.284552). This indicates the existence of ancient lithospheric mantle relics in the Chaihe region. On the other hand, the $^{187}Os/^{188}Os$ ratios are 0.12066-0.12755 in spinel lherzolites, 0.12278-0.12716 in garnet lherzolites, 0.11214-0.12359 in spinel harzburgites (except 03Ch-10), and 0.11453 in garnet harzburgite. Most of xenoliths have $^{187}Os/^{188}Os$ ratios indistinguishable from the modern convecting upper mantle [1], and their clinopyroxenes also have depleted Sr-Nd-Hf isotope compositions. Therefore, lithospheric mantle in the Chaihe region is mainly composed of juvenile mantle accreted from the asthenosphere, but with minor ancient mantle relics.

[1] Liu *et al.* (2008) *Nature* **452**, 311-316.

https://doi.org/10.1180/S0026461X00008434 Published online by Cambridge University Press

Ring Index: Towards quality-controls for the TEX_{86} paleothermometer

YI GE ZHANG* AND MARK PAGANI

Department of Geology and Geophysics, Yale University, New Haven, CT 06511, yige.zhang@yale.edu (*presenting author)

The ocean temperature proxy TEX_{86} is founded on the distribution of cyclopentane rings associated with the archaeal membrane lipids, glycerol dialkyl glycerol tetraethers (GDGTs). Because GDGTs are ubiquitous in marine sediments, TEX_{86} temperatures have been increasingly applied to a variety of marine settings from the Cretaceous through the Cenozoic. However, some TEX_{86}-derived paleotemperatures are known to substantially deviate from other proxy-based temeprature records, and appear to challenge our physical understanding of the climate system. These issues could be due, in part, to incomplete knowledge of GDGT production, transportation and preservation, or evolutionary effects that cause the TEX_{86} temperature calibration to deviate from modern relationships. Presently, there is no established criteria to determine the quality or veracity of TEX_{86} paleotemperatures.

Here we report a potential method to assess the veracity of TEX_{86} temperatures using the close relationship between Ring Index (RI, weighted average number of cyclopentane rings in GDGTs) and TEX_{86} in the modern ocean, computed from surface sediment dataset published by Kim et al., (2010) and Ho et al., (2011) [1, 2]. Correlation between RI and TEX_{86} is no surprise because TEX_{86} is based on the observation that the average number of cyclopentane rings in the GDGT pool increases with growth temperature [3]. In other words, RI and TEX_{86} will always closely correlate if the GDGT distribution is temperature dependent, although RI represents the total weighted ring average while TEX_{86} represents a subset of GDGTs using four compounds. When RI and TEX_{86} values are decoupled, it suggests that environmental signals other than temperature influence the relative adundance of GDGTs. Indeed, the modern ocean RI-TEX_{86} correlation disappears from samples associated with gas hydrates where GDGTs are derived from methanotrophic archaea [4]. Alternatively, when RI and TEX_{86} are related but their relationship deviates from the correlation expressed by modern ocean GDGT distribution, it likely implies that TEX_{86} is still reflecting temperature, but application of the modern calibration is no longer warranted and the precision of the TEX_{86} temperature is compromised.

We evaluated the RI-TEX_{86} relationship using published and unpublished data from the Cretaceous to Cenozoic and demonstrate that in sample sets where the RI-TEX_{86} relationship resembles the modern calibration, TEX_{86} appears to produce temperature estimates that are more consistent, and in better agreements with other temperature proxies. In constrast, TEX_{86}-derived temperatures often lack consistency and are less comparable to other available temperature proxies (e.g. $U^{k'}_{37}$, Mg/Ca) when the modern RI-TEX_{86} correlation fails.

[1] Kim et al., (2010) *Geochim. Cosmochim. Acta* **74**, 4639-4654.
[2] Ho et al., (2011) *Org. Geochem.* **42**, 94-99.
[3] Schouten et al., (2002) *Earth Planet. Sci. Lett.* **204**, 265-274.
[4] Zhang et al., (2011) *Earth Planet. Sci. Lett.* **307**, 525-534.

Light Elements in the Core and Equilibration Degree with Silicate Mantle: Perspective from First-Principles Molecular Dynamics

YIGANG ZHANG[1], QING-ZHU YIN[2*]

[1]Institute of Geology and Geophysics, Chinese Academy of Sciences, Beijing, 100029, China, zhangyg@mail.iggcas.ac.cn

[2]Department of Geology, University of California, Davis, One Shields Avenue, Davis, CA 95616, USA (*presenting author) qyin@ucdavis.edu

The degree of chemical equilibration (hereafter as *Ke*), defined as the cumulative mass fraction of the metalic core in equilibrium with the silicate mantle during the Earth accretion processes, greatly influences determination of the timing of the Earth core formation [1]. If *Ke* is larger than ~0.4, Hf-W chronology implies a fast accretion in less than 30 Myr for the Earth. Otherwise, Hf-W data can only be used to constrain the *Ke* instead of timing [1]. Here we use the two-phase first-principles molecular dynamics (FPMD) [2] to constrain the solubility of light elements in liquid iron in equilibration with silicate melt at temperatures from 2500 to 4200 K, pressures from 20 to 120 GPa, and two compositions simplified from the "O-bearing" and "Si-bearing" bulk Earth model compositions of McDonough [3]. The solubility data are then used in the simulations of the many possible accretion scenarios of the Earth as outlined in [4], considering magma ocean depth, homogeneous vs heterogeneous accretion etc. For each accretion route, we calculate the effective core-mantle equilibration degree (*Ke*),

$$K_e = \sum_{i}^{N} Ke_i \times W_i$$

where Ke_i *and* W_i are the core-mantle equilibration degree and the accreted mass fraction of the i^{th} step, respectively. The successful *Ke* are selected based on the criterion that the resulting Earth's core must meet the required density deficit [5]. The *Ke* in those successful simulations are all found to be larger than 0.57, implying that the core-mantle differentiation has to occur early [1], within 30 millions years from the beginning of the solar system as originally stated [6].

Additional simulations (all at 3200 K and 40 GPa) are also made to calculate the partition coefficients of several other light elements. Combined with the bulk Earth compositions of these elements [3], it is found Si, O, and S are the major light elements in the core while C, P, Mg, H, N, and He are the minor elements in the core. We show [7] that FPMD calculations lend strong support to the classical geochemical mass balance approach in accessing light elements in the core [3]. The impact of lower carbon content to the siderophile and chalcophile element distribution in the Earth's core and mantle (e.g. core pumping of Pb) will need to be critically evaluated. And the helium partition coefficient of $\sim 10^{-2}$ makes the core a plausible source of primordial helium alternative to the undifferentiated lower mantle [8].

[1] Rudge et al. (2010) *Nature Geosci* **3**, 439. [2] Zhang & Guo (2009) *GRL* **36**, L18305. [3] McDonough (2003) *Treatise Geochem* **2**, 547. [4] Rubie et al. (2011) *EPSL* **2**, 301. [5] Birch (1952) *JGR*, **57**, 227. [6] Yin et al (2002) *Nature* **418**, 949. [7] Zhang and Yin (2012) *Nature Comm.* submitted. [8] Jephcoat et al. (2008) *Phil Trans R Soc A* **366**, 4295.

https://doi.org/10.1180/S0026461X00008434 Published online by Cambridge University Press

On diffusion in heterogeneous media

YOUXUE ZHANG[1]*, LIPING LIU[2]

[1]Dept of Earth and Environ. Sciences, Univ of Michigan, Ann Arbor, MI 48109, USA, youxue@umich.edu (* presenting author)

[2]Dept. of Mechanical & Aerospace Engineering, Dept. of Mathematics, Rutgers Univ, Piscataway, NJ 08554, USA, liu.liping@rutgers.edu

Diffusion in heterogeneous media has been investigated for over forty years. However, the derived equations for bulk (effective) diffusivity in multi-phase systems were mostly incorrect because of the use of an inappropriate similarity between diffusion and other physical properties such as thermal conductivity. The mistake has permeated through the literature and textbooks. Specifically, the role of concentration partitioning between different phases in diffusion was not considered in such similarity relations. In this work, we present the correct method to derive such relations in heterogeneous media.

Barrer [1] used the similarity between diffusivity and thermal conductivity to derive the relation between the bulk (effective) diffusivity and the individual-phase diffusivities. The approach was followed by many others [2-4]. Unfortunately the similarity approach by Barrer [1] is incorrect because there is also dissimilarity. The key difference is that, even though heat conduction and mass diffusion are characterized by a similar flux equation ($\mathbf{J}_{\text{heat}} = -k\nabla T$ for heat conduction and $\mathbf{J}_{\text{mass}} = -D\nabla C$ for diffusion), in heat conduction, T is continuous across phase boundaries, whereas in diffusion, C is usually not continuous across phase boundaries. The concentration in each phase plays a major role in controlling the contribution by the phase to the bulk diffusive flux and hence the bulk diffusivity. For example, if the concentration of a component in a phase is very low, even if the diffusivity in the phase is high, the contribution of diffusion in that phase to the bulk diffusion flux can still be negligible. Hence, previous models for diffusivity in composite materials or multi-mineral rocks, no matter how sophisticated, are fundamentally wrong because the foundation is a mistake.

Correcting the mistake is straightforward. Write the mass flux in terms of chemical potential and mobility [5]:

$$\mathbf{J}_{\text{mass}} = -M\nabla\frac{\mu}{RT},$$

where M is mobility, μ is chemical potential, R is the universal gas constant, and T is absolute temperature. Because $\mu/(RT)$ is continuous across phase boundaries, the relation between bulk mobility and individual-phase mobilities is the same as that between bulk heat conductivity and individual-phase heat conductivities. That is, all previous relations for diffusion cannot be directly applied to diffusivities, but can be applied to mobilities. Then, from the relation between diffusivity and mobility: $D_i = M_i/C_i$ (ignoring nonideality, [5,6]), where C is concentration and subscript i indicates the phase or the bulk system, the correct relations can be obtained, which will be presented.

[1] Barrer (1968) *Diffusion in Polymers*, Academic Press, 165. [2] Crank (1975) The Mathematics of Diffusion, Clarendon Press. [3] Brady (1983) *Am. J. Sci.* **283A**, 181. [4] Torquato et al. (1999) *J. Appl. Phys.* **85**, 1560. [5] Lesher (1994) *J Geophys. Res.* **99**, 9585. [6] Zhang (1993) *J Geophys. Res.* **98**, 11901.

Probing quartz (101) surface structure in water with X-ray scattering method

Z. ZHANG*[1], P. FENTER[2], AND D. J. WESOLOWSKI[3]

[1] X-ray Science Division, Argonne National Laboratory, Argonne, IL, 60439 (*correspondence: zhanzhang@anl.gov,)

[2] Chemical Sciences and Engineering, Argonne National Laboratory, Argonne, IL 60439 (fenter@anl.gov)

[3] Chemical Science Division, Oak Ridge National Laboratory, Oak Ridge, TN 37831 (wesolowskid@ornl.gov)

Knowledge of the atomic level structures at the quartz water inteface will be a crutial component for understanding the behavior of such surface during the dissolution/precipitation processes. An earlier study probed the interfacial structure of quartz (101) and (100) surface in water along the surface normal direction [1]. Our prevoius work revealed the 3D interfacial structures at the single crystal quartz (101)–deionized water interface, including the relaxations of the atoms in the near surface region and the distribution of the interfacial water molecules [2]. In this study, a different interfacial structure was observed at the quartz (101)-water interface with high resolution surface X-ray scattering method (i.e., crystal truncation rod). This might indicate a different terminations of the surface when in contact with water. The detail structure information of quartz surface in water would be an important first step in revealing the reaction paths of the dissolution/precipitation processes when exposed to aqueous solutions at various conditions.

[1]. Schlegel, M.L., et al., (2002) Geochimica Cosmochimica Acta, **66,** 3037-3054.

[2]. Zhang, Z., et al., (2010) Geochimica Cosmochimica Acta, **74**, A1218.

https://doi.org/10.1180/S0026461X00008434 Published online by Cambridge University Press

Mapping target area of magnetite deposits by integrating aeromagnetic data and Fe_2O_3 geochemical data

JIE ZHAO[1*], WENLEI WANG[1], QIUMING CHENG[1,2,3] AND JIANGTAO LIU[1,3]

[1]Department of Earth and Space Science and Engineering, York University, Toronto, Canada, zhaojie@yorku.ca (*presenting author)

[2]Department of Geography, York University, Toronto, Canada

[3]State Key Laboratory of Geological Processes and Mineral Resource, China University of Geosciences, Wuhan and Beijing, China

Magnetite deposit is one of the most productive iron mineralization types in Eastern Tianshan mining zone, China. Previous work on exploring magnetite deposits were mainly consulting with the aeromagnetic survey data and Fe_2O_3 concentration in stream sediment geochemical data. The former is a direct physical indicator of magnetite as well as geologic bodies with extraordinary magnetism. The later is corresponding with existence of assorted iron enrichment (e.g. hematite, magnetite, iron-polymetallic mineralization, etc.). However it is difficult to identify magnetite mineralization when relying on only one of these two datasets because none of the anomalies of these two datasets can be interpreted as unique geological event. The objective of this research is to map the potential area of magnetite deposits by integrating the aeromagnetic survey data and Fe_2O_3 geochemical data with the method of Geographically Weighted Regression (GWR).

Compared to linear regression models, GWR is more realistic to explore the non-stationarity of the coefficients across an area by assigning the independent parameters for each location in space different weights [1]. In this research the singularity [2] of aeromagnetic data and singularity of Fe_2O_3 concentration are assigned as the dependent variable and independent variable, respectively, because the lower values ($\alpha < 2$) in singularity map of Fe_2O_3 and aeromagnetic data can delineate corresponding local accumulation of iron oxide and positive aeromagnetic anomalies.

The regression result of GWR is much more convincing than of the Ordinary Least Square (OLS) by examining the R-squared values. All 3 magnetite deposits in the study area are situated within high value range of coefficient map, which is consistent with the reality that both variables present lower singularity value on the areas of magnetite deposits. However, 14 out of 15 other types of iron deposits are located in the middle and lower coefficient value ranges, which is also proved by the fact that the aeromagnetic data does not present positive anomalies of magnetism around other types of iron deposits. In conclusion, the geographically non-stationary coefficient map produced by GWR can not only differentiate magnetite deposits from other types of iron mineralization, but also delineate target areas with higher potential of magnetite mineralization.

[1] Brunsdon et al. (1996) *Geographical Analysis* **28**, 281-298. [2] Cheng (2007) *Ore Geology Reviews* **32**, 314-324.

Thermodynamic and Kinetic Effect of Organic Solvent on the Nucleation of Nesquehonite

LIANG ZHAO[1*], CHEN ZHU[1], JUNFENG JI[1], JUN CHEN[1], H. HENRY TENG[1,2]

[1]School of Earth Sciences and Engineering, Nanjing University, Nanjing, PRC, zhaoliang@nju.edu.cn (* presenting author)

[2]Department of Chemistry, the George Washington University, Washington, USA

Introduction

Magnesium carbonate has a number of naturally occurring forms. Of the half dozen phases, nesquehonite is the most commonly observed near ambient conditions while various basic species appear more often at elevated (> ~ 40 ^{o}C) temperature with low pCO_2. Despite its frequent occurrence in nature, nequehonite has not attracted significant attention from scientific communities until recently due to the potential of magnesium in sequestering anthropogenic CO_2. The working principle in the approach of magnesium carbonation can be described in theory by the following reaction:

$$MgO + CO_2 = MgCO_3 \qquad (1)$$

This is a thermodynamically favored reaction not only because it is exothermic (ΔG = -48.31 kJ/mol, 25 ^{o}C) but because the product is also the most stable magnesium carbonate mineral form of all. In reality, however, the formation of anhydrous $MgCO_3$ through this route proves virtually impossible at ambient environments; instead, the tri-hydrate (i.e. nesquehonite) often turns out to be the most common product. Therefore, we should study the crystallization process of nesquehonite to avoid the limit to our understanding of magnesium carbonation reaction and its application to carbon sequestration.

Results and Conclusion

Nesquehonite crystallization experiments were conducted in H_2O and water/dimethylformamide (DMF) mixture to examine solvent effect on the nucleation kinetics. Results show a reduction of nucleation induction time in the presence of DMF and a positive correlation between nucleation rate and DMF concentration. Analysis in the context of the classic nucleation theory reveals an unexpected increase in the surface energy of nesquehonite upon the solvent change, implying that kinetic factors, rather than surface energetics, is the driving force behind the resultant enhancement in nucleation rate. Further analyses suggest that kinetic acceleration under higher surface energy conditions is possible if nucleation proceeds through a cluster aggregation mechanism instead of critical nucleus formation. Fitting the Smoluchowski's coagulation theory to the experimental data seems to provide support to the operation of the non-classic nucleation mechanism as it shows that the cluster association rate is independent of the sizes of the precursors but positively correlated to the DMF concentration, consistent with the scenario of growing population of sub-critical nuclei and ensuing higher probability of cluster collision/aggregation leading to an accelerated nucleation.

https://doi.org/10.1180/S0026461X00008434 Published online by Cambridge University Press

Origin of the ~1.74 Ga, Anorthosite-hosted Damiao Fe-Ti-P Ore Deposit, North China

TAI-PING ZHAO[1*], WEI TERRY CHEN[2] AND MEI-FU ZHOU[2]

[1]Guangzhou Institute of Geochemistry, Chinese Academy of Sciences, Guangzhou, China, tpzhao@gig.ac.cn

[2]Department of Earth Sciences, University of Hong Kong, Pokfulam Road, Hong Kong, China, chenweifly1@163.com (W.T.Chen), meifuzhou@hotmail (M.F.Zhou)

The Damiao deposit is hosted in the ~1.74 Ga Damiao anorthosite complex, the only known massif-type anorthosite in China. It has been mined for several decades at an annual production of 2 million tons ore, and has long been an important source of Fe, Ti, P and V in China.[1] The deposit contains hundreds of ore bodies occurring as irregular lenses, veins or pods intruding hosting anorthosite. These discordant oxide ores contain abundant but variable apatite, and are classfied into Fe-Ti ore, nelsonitic ore and oxide-apatite gabbronorite on the basis of apatite contents and ore structures.

Combined with detailed field investigations, bulk ore major and mineral EPMA major and LA-ICPMS trace elemental analyses were conducted to understand the origin of the Damiao deposit. Intrusive feature of nelsonitic ores and contrast densities between Fe-Ti oxides and apatite suggest that the nelsonitic ores have crystallized from an immiscible nelsonitic melt. Fe-Ti ores displaying similar compositional range of Fe-Ti oxides and silicate minerals are interpreted to have also crystallized from the immiscible nelsonitic melt, which is further supported by the spatially close association of Fe-Ti and nelsonitic ore bodies and their comparable mineral assemblages of plagioclase, pyroxene, Fe-Ti oxides and apatite. This interpretation that fractional crystallization of the immiscible nelsonitic melt forming both Fe-Ti and nelsonitic ores is well consistent with linear variations of Sr, Y, Th, U and REE contents of apatite and the parallel chondrite-normalized REE patterns.

Oxide-apatite gabbronorite display relatively larger variable but more evolved compositions of silicate minerals than nelsonitic ores (and Fe-Ti ores), pointing to a separate origin in each case. Apatite of oxide-apatite gabbronorite contains lower Sr and MgO but higher REE contents and Y than those of nelsonitic ores, further indicating that nelsonitic ores are relatively more primitive [2], excluding the possibility that they have formed by immiscible segaration from oxide-apatite gabbronorite, as previously proposed. Based on their dissminated texture and continuous chemical variation, we considered that oxide-apatite gabbronorite may have formed by normal fraction crystallization process through a trend of iron enrichment in residual liquids, different from the immiscible origin for nelsonitic ores. Oxygen fagacity (fO_2) might be one of the important factors resulting in different forming processes for nelsonitic ores and oxide-apatite gabbronorite, because liquid immiscibility field expands generally with increasing fO_2. Higher fO_2 for nelsonitic ores is well indicated by their smaller negative Eu anomalies of apatite, because apatite readily accepts the Eu^{3+} into its structure but excludes the larger Eu^{2+}.

[1] Ye DH, Yang QW, Xing JR (1996) *The 30th International Geological Congress, China*.

[2] Dymek RF, Owens BE (2001) *Economic Geology* 96: 797–815

Geochemistry and tectonic settings of Carboniferous volcanic rocks in the Junggar basin of China

ZHAO XIA[1]*, WEI YANZHAO[1], YANG JUN[2],LIU JIANGLIN[3], ZHANG JIANBIN[3]

[1]Research Institute of Petroleum Exploration & Development, Petrochina, Beijing, China.
(*correspondence: zhaox601@petrochina.com.cn)

[2]Chang'an University, Xi'an, China.

[3]Fengcheng Oil Feild, Xinjiang Oilfield Company, Petrochina, Xinjiang, China.

Intruduction

The Junggar basin, an important part of central Asia orogenic belt, is a Mesozoic and Cenozoic sedimentary basin developing upon Precambrian crystalline basement and Palaeozoic fold basement. The basement of the Junggar basin is a part of Kazakhstan plate, and interspersed in the Tarim plate and the Siberia plate. The Carboniferous volcanic rocks in the Junggar basin consisting of volcanic lava and volcaniclastic rock are most widely developed. Furthermore, oil and gas reservoirs have found in it. The geochemistry and tectonic settings of Carboniferous volcanic rocks in the Junggar basin are studied in this article. And the research about the tectonic setting of volcanic rocks of the basin has important significance on volcanic rock oil and gas exploration[1].

Method and Resolut

The volcanic lava in this area has characteristics of low K_2O, high Na_2O, high TiO_2 and high ΣREE. The REE distribution plots show the volcanic rocks are enriched in LREE and LILE, and depleted in Nb and Ta. In addition, the plots also reveal the characteristic of LREE and HREE differentiation. The ratios of Th/Nb and Nb/Zr as well as the tectonic setting discrimination diagrams show that the volcanic rock main body is characterized by intraplata volcanic rock, and formed under the tectonic setting of intraplata extension. The lava of this area with low Th/Nb, low La/Nb, slightly elevated LREE, as well as Nb/La-Th/Nb and La/Ba-La/Nb discrimination diagrams, show that depleting of Nb and Ta relative to Th is the result of subtractive component adding to volcanic source[2].

Conclusion

According to geochemical analyses, the lava with charcaterisctics is similar with "post collision arc volcanic rock"[3]. It is generated in an extensional setting of the late stage of orogenesis, and the magma source may be influenced by earlier oceanic plate subduction. Combining with the regional geologic characteristic, Carboniferous volcanic rocks in the Junggar basin were formed in an extensional rifting setting of the late stage of orogenesis, which is consistent with the region rifting function of large scale. The conclusions of this research make a significant improvement for the study of volcanic reservior distribution.

[1]Kang (2008) *Petroleum geology&experiment***30**,321-307. [2] Saunders, Storey&Kent(1992)*Geol.Soc.Spec***68**,41-60. [3]Mo (2001) *Acta petrologica et mineralogica***20**,360-366.

https://doi.org/10.1180/S0026461X00008434 Published online by Cambridge University Press

Syn-exhumation magmatism during continental collision: Evidence from alkaline intrusives of Triassic age in the Sulu orogen

ZI-FU ZHAO*, AND YONG-FEI ZHENG

CAS Key Laboratory of Crust-Mantle Materials and Environments, School of Earth and Space Sciences, University of Science and Technology of China, Hefei 230026, China, zfzhao@ustc.edu.cn

While oceanic subduction zones are characterized by syn-subduction arc magmatism, continental subduction zones are characterized by syn-exhumation alkaline magmatism. The latter is illustrated by alkaline intrusive rocks (including gabbro, syenite and granite) in the Sulu orogen, eastern China. In order to decipher the crust-mantle interaction in the continental subduction zone and subsequent decompression melting of ultrahigh-pressure (UHP) metamorphic rocks, we carried out a combined study of zircon U-Pb ages and Lu-Hf isotopes, mineral O isotopes, whole-rock major-trace elements and Sr-Nd isotopes. SIMS and LA-ICPMS zircon U-Pb dating yields Late Triassic ages of 201±2 to 212±1 Ma for their crystallization. These ages are younger than Middle Triassic ages for UHP metamorphism of country rocks, corresponding to the syn-exhumation magmatism during continental collision. The alkaline rocks are characterized by the arc-like patterns of trace element distribution, with relative enrichment of LILE and LREE but relative depletion of HFSE. They have high initial $^{87}Sr/^{86}Sr$ ratios of 0.7064 to 0.7114 and highly negative $\varepsilon_{Nd}(t)$ values of -16.4 to -13.8 with two-stage Nd model ages of 2.11 to 2.33 Ga for whole-rock. Zircon Lu-Hf isotope analyses also show highly negative $\varepsilon_{Hf}(t)$ values of -20.9±0.5 to -14.1±0.9, with two-stage Hf model ages of 2.10±0.06 to 2.56±0.03 Ga. The zircon exhibits relatively consistent $\delta^{18}O$ values of 5.6 to 6.2‰, slightly higher than normal mantle values. The enrichment of radiogenic Sr-Nd-Hf isotopes in the gabbro indicates its origination from an isotopically enriched mantle source, whereas the arc-like pattern of trace element distribution for it suggests a fertile mantle source with enrichment of LILE and LREE. Thus, it is part of the orogenic lithospheric mantle that would be generated by underplate reaction of the subcontinental lithospheric mantle-wedge peridotite with hydrous felsic melts derived from the subducted continental crust during the Triassic continental collision. On the other hand, there are general similarities in trace element and radiogenic isotope characteristics between the syenite-granite and UHP metaigneous rocks in the Dabie-Sulu orogenic belt, suggesting its genetic link to the subducted continental crust itself. Therefore, the alkaline intrusives are derived from partial melting of the orogenic lithospheric mantle and the subducted continental crust in the stage of exhumation. They provide a petrological record of recycling the subducted continental crust into mantle depths with the crust–mantle interaction in the continental subduction channel.

Hydrocarbon generation kinetics of oil cracking in different reaction system

ZHENG HONGJU[1*], WANG ZECHENG[1], AND WANG TONGSHAN[1]

[1] Research Institute of Petroleum Exploration & Development, PetroChina

hjzheng@petrochina.com.cn (*presenting author)

Pyrolysis experiment of crude oil with 3 reaction systems ($MgSO_4+H_2O$+crude oil, $CaSO_4+H_2O$+crude oil, crude oil) are carried out to simulate the gas generation characteristic when H_2O and ions such as SO_4^{2+}, Mg^{2+}, Ca^{2+} participate in the oil cracking, and discuss the generating mechanism of natural gas containing H_2S, and quantitatively calculate the deplete of hydrocarbons and their carbon isotope by TSR.

.The experiment results show that the TSR reaction did not occur under the system of "$CaSO_4+H_2O$+crude oil", oppositely, TSR obviously occurred under the system of "$MgSO_4+H_2O$+crude oil" and the yield rate of H_2S reach up to 60~80ml/g. Hydrocarbon yield rates under the reaction system with TSR occurred are significantly lower than that in the reaction system without TSR occurred (Fig 1), indicating the deplete of gaseous hydrocarbons by TSR [1]. In addition, TSR also had a significant effect on the carbon isotope fractionation of hydrocarbons, so that methane, ethane, propane carbon isotope weight gain with a range of 3~6‰ (Table 1).The activation energy distribution show that, the activation energy of gas generation under the system of "$MgSO_4+H_2O$+crude oil" lower than that in the system of "$CaSO_4+H_2O$+crude oil", the former is 48~60KJ/mol, while the latter is 62~74KJ/mol. It could indicate that participation of Mg^{2+} make a low activation energy of hydrocarbon generation and oil cracking reaction easier.

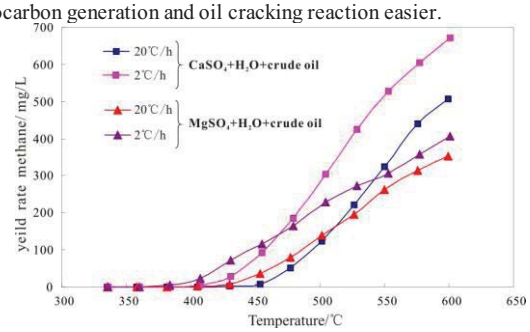

Figure 1: Yield rate of the methane generated in different system

Recent research show that adding buffer such as NaCl into the system of "$CaSO_4+H_2O$+crude oil" could help to TSR, indicating that only SO_4^{2+}-hydrocarbon molecules is not enough in TSR, and the catalyst of metal ions (e.g. Mg^{2+}, Na^{+}) is very important.

Temperature /℃	$MgSO_4+H_2O$+crude oil		$CaSO_4+H_2O$+crude oil	
	Methane	Ethane	Methane	Ethane
453.7	-45.19	-41.73	-54.08	-43.09
501.8	-45.79	-36.74	-49.35	-37.55
550.0	-39.90	-24.66	-43.89	-31.04

Table 1: Carbon isotope of hydrocarbons generated in different system (‰)

[1] Cai C F, *et al.* (2003) *Chemical Geology* **202**, 39-57.

https://doi.org/10.1180/S0026461X00008434 Published online by Cambridge University Press

Tracing metal inputs and cycles in the South Atlantic with rare earth elements

XIN-YUAN ZHENG[1*], ABIGAIL NOBLE[2], MAK SAITO[2], MATTHEW POINTING[1], PHILIP HOLDSHIP[1], AND GIDEON HENDERSON[1]

[1]University of Oxford, Department of Earth Sciences, Oxford, UK OX1 3AN, xinyuan.zheng@earth.ox.ac.uk (* presenting author)
[2]Woods Hole Oceanographic Institution, Woods Hole, Massachusetts 02543, UAS

Rare earth element (REE) concentrations in seawater are not only controlled by external inputs such as dusts and rivers, but also fractionated by oceanic processes including scavenging and redox [1]. The characteristic REE patterns imposed by different inputs and processes may provide powerful tools with which to improve understanding of the sources and cycles of biolimiting trace metals such as Fe and Zn. REEs and their isotopes, especially Nd isotopes, are also commonly employed as paleoceanographic tracers to infer the status of the ocean in the past, but there is some controversy about the processes controlling their oceanic distribution.

Despite their potential utility, and their relative ease of measurements, high-quality seawater REE data are usually limited to a few single stations, and remain sparse for much of the modern ocean. This limits our ability to fully understand the cycling of REEs in seawater, or their use to trace micronutrient cycles.

In this study, we use isotope-dilution MC-ICP-MS analysis on ~100ml, and a relatively high sample throughput, to report the first full-depth zonal sections of REE-concentrations in South Atlantic along ~11^{o}S collected by the CoFeMUG cruise, and along 40^{o}S in the Cape Basin collected by UK-GEOTRACES GA10 cruise.

Secondary maxima in REE concentrations at ~1000m observed in these sections are consistent with the presence of UCDW at the same depth, and higher REE concentrations at bottom waters in the western basin than those at Angola Basin conforms to the absence of AABW in Angola Basin which is blocked by Walvis Ridge in the South. Both evidence suggests ocean circulation controlled REE-distribution at ~11^{o}S.

Ce anomalies are used to trace redox-related addition/removal of REEs. Two prominent plumes with elevated Ce-anomaly values and Ce concetrations occur nearshore in Angola Basin in the CoFeMUG section at ~500m and ~1500m respectively, indicating the addition of REEs possibly from reducing shelf sediments. An additional source of REEs is supported by more negative seawater ε_{Nd} than typical for the Angola Basin [2]. Inter-element comparison with Fe and Mn demonstrates elevated Ce anomalies associated with Fe on the east of the basin, but this is not accompanied by increased Mn concentrations, indicating unusual decoupled cycling of Ce and Mn.

[1] Elderfield (1988) *Phil. Trans. Roy. Soc. London A* **325**, 105-126.
[2] Rickli (2009) *EPSL* **280**, 118-127.

The preliminary study on prospecting uranium mine in radioactively physical geography using factor analysis method

Y. ZHENG, XIN-MIN WU*, Y. ZHANG, AND Y.X. YANG

Engineering Research Center of Nuclear Technology Application, East China Institute of Technology, Ministry of Education, Nanchang , Jiangxi Province, China, 330013, ymzheng@ecit.cn (* presenting author)

In natural radioactive energy spectrum measurement, to explain radioactive anomalies an distinguish the type of some soil and rock on the basis of three combination factors of uranium, thorium and potassium were more reasonable and accurate than a single radioactive element [1]. So the original data, based on the collection original data of reconnaissance ground energy spectrum measurement of uranium district in Yanzhuang, Wengyuan County, Guangdong Province, were processed by the method of R type factor analysis. The KMO test value of the Yanzhuang mining area was 0.68 by the calculation, greater than 0.6,and Bartlett's significant parameter was less than 0.05,which reached a significant level, showing that the variables were suitable for principal components analysis .Then the model of factor analysis was established, seen the formula (1), (2).

The first principal component is:

$$y1 = 0.71std.U - 0.03std.Th + 0.70std.K \quad (1)$$

The second principal component is:

$$y2 = -0.19std.U + 0.96std.Th + 0.22std.K \quad (2)$$

Collect original data into the model to calculate the abnormal lower limit for mining area: y1 = 1.793935, y2 = 1.537696. The y1, y2 anomalies delineated figure made by MAPGIS showed that the delimitation from the working drawing of abnormal and practical exploration was unified, which indicated that factor analysis could be a good combination of several factors to form a single measurement for radioactive exploration data interpretation.

This study was granted by open education fund (HJSJYB2010-14) of Engineering Research Center of Nuclear Technology Application, East China Institute of Technology, Ministry of Education, China.

[1] Zheng et al. (2009) *Chinese Journal of Uranium Mining and Metallurgy* **28**, 220-224.

https://doi.org/10.1180/S0026461X00008434 Published online by Cambridge University Press

Formation of amorphous silica with distinct morphologies and implication for biosilification

JIA-YUAN SHI[1], QI-ZHI YAO[2], GEN-TAO ZHOU[1*], SHENG-QUAN FU[3]

[1]School of Earth and Space Sciences, University of Science and Technology of China, Hefei 230026, P. R. China, gtzhou@ustc.edu.cn(* presenting author)

[2]School of Chemstry and Materials, University of Science and Technology of China, Hefei 230026, P. R. China

[3] Hefei National Laboratory for Physical Sciences at Microscale, University of Science and Technology of China, Hefei 230026, P. R. China

Biosilica displays many kinds of intricate patterns that are constructed on a nanometer-to-micrometer scale. At the nanoscale, for example, it involves the polymerization products of silica apparently mediated by the interactions between different biomolecules with special functional groups. An emerging consensus is that organic amines (e.g., long chain polyamines), proteins, and polysaccharides are general organic components in diatom's cell walls, and are responsible for the formation of hierarchical silicious structures. Another basic fact in biosilicification is that the silica formation occurs within a specialized compartment known as the silica deposition vesicle (SDV), whose membrane, called the silicalemma, consists of a typical lipid bilayer. Several researches have revealed that the membrane-bound SDV could provide not only spatial constraints but also possibly distinct chemical influences for the polymerization and morphogenesis of the silica. Nevertheless, there are few publications illuminating the interactions between amines and lipids in biosilicification. Herein, dodecylamine (DA) and phospholipid (PL) were selected as model organic additives to influence the precipitation of silica in biomimetic silicification. The results show that increasing PL concentrations leads to the formation of siliceous elongated structures, and the localized enlargement is also clearly observed during the further growth of the elongated structures, displaying some features of silica biomineralization at the earliest recognizable stage of biosilica development in diatom. Moreover, a series of NH_3-PL experiments reveal that no elongated structures can be obtained in the presence of PL, suggesting that the cooperative interactions between PL and DA molecules cause the silica structures to be elongated. Based on the special importance of both organic amines and phospholipid membranes (e.g., silicalemma) for biosilicification, our results may provide a novel pathway towards a deeper insight into the biosilicification mechanism.

Source characteristics of a high-K to ultrapotassic volcanic rock zone in NE China:A typical EMI signature from an orogenic belt

XIN-HUA ZHOU[1] *, JI-AN SHAO[2], JI-FENG YING[1], BEN-XUN SU[1]

[1] State Key Lab of Lithosphere Evolution, Institute of Geology and Geophysics, Chinese Academy of Sciences, Beijing, China, xhzhou@mail.iggcas.ac.cn, (* presenting author)

[2] College of Earth & Space Sciences, Peking University, wangcc@mail.tsinghua.edu.cn

As a common sense by previous global study, the enriched mantle end-member, i.e. EMI in continental region has been always attributed to craton-related subcontinental lithosphere (eg. Zindler and Hart, 1982, Hofmann, 2003). Based on updated isotopic geochemical survey, we report a case study on high-potassic to ultra-potassic volcanic rock zone in NE China, which shows a typical EMI source geochemical characteristics and located near the east end of East-Central Asian orogenic belt.

The systematic Sr-Nd-Pb-Hf isotopic composition, along with REE and spider diagram patterns of ultra-potassic volcanic rocks, mostly are leucitite, do show a typical EMI end-member signature, not only for entire Phanerozoic mantle-derived rocks in eastern China, but also on global scale, such as compare with those from Lucite Hill and Smoky Butte, North America, and lamproites in Aldan Shield, Far East Russia (eg. Davies et al., 2006). In addition, a sires of metasomatic minerals, such as phlogopite, apatite and so on have been recognized from mantle-derived xenoliths of these host rocks. Detailed mineralogical and geochemical studies have demonstrated the multiple and distinct mantle metasomatism, occurred in different geological time, from ancient one (Archearn) to recent one. Furthmore, the regular geological occurance, NW trending, of these potassic volcanic rocks, accompanied with tectonic rifting, seismic activities and geothermal anomaly would provide severe and further geological and geophysical constraints on the origin of such enriched mantle source beneath an orogenic belt.

This work is supported by NSFC (grant 41173045 and 41172196).

[1] Zindler and Hart, 1986, *Annu. Rev. Earth Planet. Sci. Letters*, **14**:493-571.

[2] Hofmann, 2003, *Treatise of Geochemistry*, **2**:61-101.

[3] Davies et al., 2006, *J. Petrology*, **47**:1119-1146.

https://doi.org/10.1180/S0026461X00008434 Published online by Cambridge University Press

A microscopic view of nucleation in the anatase-to-rutile transformation

YA ZHOU [1*] AND KRISTEN A. FICHTHORN [2]

[1]Department of Chemical Engineering,The Pennsylvania State University, University Park, USA zhou@engr.psu.edu (* presenting author)

[2] Department of Chemical Engineering and Department of Physics, The Pennsylvania State University, University Park, USA fichthorn@psu.edu

We use molecular simulation techniques to investigate the anatase-to-rutile transformation in Titania nanocrystals. A thermodynamic analysis indicates that edge and corner atoms significantly influence the critical size at which rutile nanocrystals become energetically preferred over anatase. Using molecular dynamics simulations, we probe kinetics of the transformation in individual anatase nanocrystals and in nanocrystal aggregates. We follow structural evolution using simulated X-ray diffraction. Additionally, we develop a local order parameter to distinguish individual Ti ions as anatase, rutile, or anatase {112} twin-like. We apply our local order parameter to track the formation and growth of rutile nuclei. Anatase {112} twins form easily at surfaces and interfaces of nanocrystal aggregates and rutile nucleates among the twins. Stable rutile nuclei maintain {101} facets during growth, as a result of nucleation from layers of alternating anatase {112} twins. Our results are in agreement with experiment and indicate the central role of {112} twin-like anatase in the transformation.

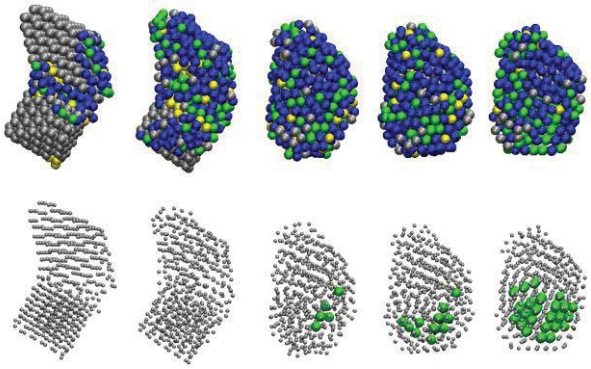

Figure 1: Structural evolution of an aggregate during transformation at 1473 K. Upper row: only Ti ions in the aggregate are shown, with anatase ions in silver, anatase {112} twins in blue, rutile in green, and undefined ions in yellow. Lower row: Ti ions in the stable rutile nuclei are in green and magnified, all other Ti ions are shown in silver.

Temporal changes in magma geochemistry in the northern Lhasa Terrane, Tibet: Response to the Lhasa–Qiangtang collision

DI-CHENG ZHU[1],*, ZHI-DAN ZHAO[1], YAOLING NIU[2,3], YILDIRIM DILEK[1,4], QING WANG[1], XUAN-XUE MO[1]

[1]State Key Laboratory of Geological Processes and Mineral Resources, China University of Geosciences, Beijing 100083, China, (dchengzhu@163.com); [2]School of Earth Sciences, Lanzhou University, Lanzhou 730000, China (niu.yaoling@yahoo.co.uk); [3]Department of Earth Sciences, Durham University, Durham DH1 3LE, UK (niu.yaoling@yahoo.co.uk); [4]Department of Geology, Miami University, Oxford, OH 45056, USA (dileky@muohio.edu)

Magma generation and evolution is a natural consequence of mantle dynamics and crust-mantle interaction. As a result, magma compositional variation in time and space can be used, in turn, to infer these deep processes. Indeed, the Baingoin Batholith, the largest batholith in the northern Lhasa Terrane, manifests this efficacy. This batholith was emplaced in response to the Lhasa–Qiangtang continental collision (ca. 140–110 Ma). Our data indicate that it was emplaced in three distinct pulses (i.e., 132 ± 2, 121 ± 3, and 113 ± 3 Ma) rather than in a single phase (ca. 121 Ma), as previously thought, and that its magma chemistry changed through time (Figure 1). The 132 ± 2 Ma samples are silica-rich and have small whole-rock ε_{Nd} (t) (–2.7 to –2.4), positive zircon ε_{Hf}(t) (+2.3 to +11.0), low zircon $\delta^{18}O$ (5.81–7.16 ‰) values, and low Ti-in-zircon temperatures (T_{Ti}^{zir} = 630–660°C). The 121 ± 3 Ma samples are compositionally diverse and show varying ε_{Nd}(t) (–10.0 to –4.8), decreased zircon ε_{Hf}(t) [–8.5 to +5.9], increased zircon $\delta^{18}O$ (7.42–9.52 ‰), and increased T_{Ti}^{zir} (ca. 650–750°C) relative to the 132 ± 2 Ma rocks. The 113 ± 3 Ma samples have similar ε_{Nd}(t) (–9.5 to –4.8) and T_{Ti}^{zir} (ca. 680–750°C) but slightly increased zircon ε_{Hf}(t) (–7.1 to +6.4) with varying zircon $\delta^{18}O$ (6.25–11.12 ‰) relative to the 121 ± 3 Ma rocks. Similar changes of magma geochemistry are also present in the coeval magmatic rocks from Yanhu (Figure 1). It is evident that the parental magmas of the 132 ± 2 Ma rocks originated from hydrous partial melting of juvenile crust. Progressive incorporation of ancient crustal material into the source region of the 121 ± 3 Ma rocks coincided with the involvement of the subducting Qiangtang continental crust or the contamination of the Lhasa basement-derived melts during the Lhasa–Qiangtang collision. The significant input of mantle-derived component in the 113 ± 3 Ma rocks may have resulted from slab breakoff-induced magmatism and related mantle melting events, following the final Qiangtang–Lhasa amalgamation.

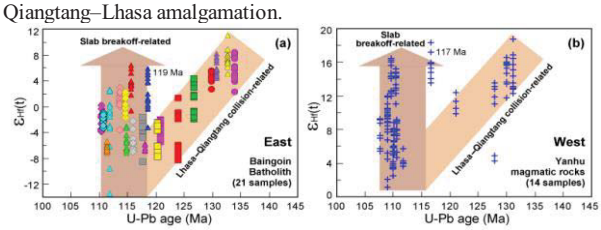

Figure 1: Space-time variations of zircon ε_{Hf}(t) of Early Cretaceous magmatic rocks from the northern Lhasa Terrane, central Tibet

https://doi.org/10.1180/S0026461X00008434 Published online by Cambridge University Press

Isotopic fractionation of selenium in higher plants

JIAN-MING ZHU[1,2*], THOMAS M. JOHNSON[2*], HAI-BO QIN[1], XIANG-LI WANG[2] AND YONG-QIANG YUAN[1]

[1]State Key Lab. of Environmental Geochemistry, Inst. of Geochemistry, CAS, Guiyang, 550002, China. zhujianming@vip.gyig.ac.cn (*present author)

[2]Department of Geology, University of Illinois at Urbana-Champaign, Urbana, 61801, USA. tmjohnsn@illinois.edu

The extent of isotopic fractionation of selenium in plants is poorly understood, but potentially is important to understand and quantify the fractionation processes involved in Se biogeochemical cycling in surface environments[1]. Here, by ^{74}Se-^{77}Se double spike technique with high presion developed on HG (hydride generator)-MC-ICP-MS[2], we determined Se isotopic compostion of different plant components including roots, stems, leaves and seeds of rice (*oryza sativa L.*) and corn (*zea mays L.*), and the Se accumulaing herb booor's mustard (*thlaspi arvense L.*). The $\delta^{82/76}$Se values ranged from -1.41‰ to -0.24‰ in rice, from -3.56‰ to -1.80 ‰ in corn, and from -0.62 ‰ to 2.21‰ in mustard herb. The overall range of $\delta^{82/76}$Se was 5.77‰, indicating Se isotopic variation can occur in plants to a small extent.

For all three species, roots are shifted isotopically relative to total Se in the soils they grew in, but not in any systematic way. This probably reflects Se isotopic fractionation among the various Se species in the soils, which is expected to result from redox cycling. Since Se is taken up mainly as selenate, selenite and certain organic compounds, the roots' isotopic composition may differ from the total soil, and is expected to depend on several variables[3].

A slight systematic enrichment in heavy Se isotopes in shoots (above ground) relative to roots occurred in corn and mustard herb with up to 0.22 ‰ in $\Delta\delta^{82/76}Se_{shoot\text{-}root}$, but not in rice. This shows the transport of Se in plants from root to shoot does not induce obvious fractionation. In contrast, $\Delta\delta^{82/76}Se_{leave\text{-}root}$ and $\Delta\delta^{82/76}Se_{leave\text{-}shoot}$ in all three plants show the obvious heavy isotope enrichment in leaves of at least 0.35‰ (the maximum is 1.85‰), indicating there are at least two different types of mechanism to explain Se isotopic variations. One is transport from rhizome to stems which involves no or smaller fractionation; another is from stem to leaves and/or leaves to atmosphere which cause significant fractionation. In the latter case, we envision Se methylation and loss of this volatile species from leaves during growth could induce heavy Se isotope enrichment in leaves, particular in Se accumulated plants such as *thlaspi arvense L.*

The work was supported by the National Natural Science Foundation of China (41073017, 40973085) and the Knowledge Innovation Program of the Chinese Academy of Sciences (KZCX2-YW-JC101).

[1] Johnson (2004) *Chem Geol* 201-214. [2]Zhu et al. (2008) *Chinese J Anal Chem* **36, 1385-1390**. [3] Sors et al. (2005) *Photosynthesis Rev.* **86, 373-389**.

Peraluminous rare metal granites in South China

JINCHU ZHU[1]*, RUCHENG WANG[2], JIANJUN LU[3], AND LEI XIE[4]

[1]Nanjing University, Nanjing, China. jczhu@nju.edu.cn (*Presenting author)

[2]Nanjing University, Nanjing, China. rcwang@nju.edu.cn.

[3]Nanjing University, Nanjing, China. lujj@nju.edu.cn.

[4]Nanjing University, Nanjing, China. xielei@nju.edu.cn.

There exist many alumina-saturated Sn-W-Ta-Nb bearing granites in South China, including the Yichun Li-Ta-Nb granite in Jiangxi Province, the Limu Ta-Nb-Sn granite in Guangxi Province, the Xianghualing Ta-Nb-W-Sn granite in Hunan Province, etc. They are usually stocks in occurrence, ultra-acidic in chemistry, rich in Al, Na, Li, Rb, Ta, Nb, Sn, W, F etc. elements, mostly P-rich, but in some cases P-barren.

One of the most fundamental features for these granites is well developed vertical zonation. From the upper contact downwards to the deeper levels the following zones are usually successively observed: the pegmatoid stockscheider (pegmatite, aplite and massive quartz assemblage), the greisen zone, the lepidolite-topaz-albite granite zone, the Li-muscovite granite zone, the two-mica granite zone, and the protolithionite granite zone. Along with the direction from protolithionite granite upwards, Li, Rb, F and rare-metal contents gradually increase, but Zr and REE concentrations gradually decrease. Geological, textural, geochemical evidences and coexisting coeval subvolcanic-volcanic rare metal bearing dykes suggest that this kind of vertical zonation and rare metal mineralization were caused by fractional crystallization and magmatic-hydrothermai differentiation of rare metal-rich parental magmas. This evolutionary process led to gradual depletion of Zr and REE, and gradual enrichment of Li, Rb, Ta, Nb, Sn, W etc. rare metals and F etc. volatiles in the apical parts of the stocks.

The original rocks of the peraluminous rare metal granites in South China are considered to be of S-type derived from the crustal materials, especially for the P-rich ones. However, the aluminous A-type granites are also should be considered, especially for the P-barren ones. For example, the protolithionite granite in the deeper part of the Xianghualing granite has high contents of REE, Y, Zr, Nb, Th, U etc. HFSEs, relatively higher zircon ε_{Hf} values (from -5.9 to -1.9, averaging -4.2) and relatively lower two stage Hf model ages (T_{DM} values from 1.32 Ga to 1.58 Ga, averaging 1.47 Ga), which evidently indicate that this granite belongs to the aluminous A-type and was derived from the crust-mantle mixed sources.

https://doi.org/10.1180/S0026461X00008434 Published online by Cambridge University Press

Early-stage phase transformation and growth of iron oxyhydroxides during neutralization of simulated acid mine drainage

MENGQIANG ZHU[1*], BENJAMIN LEGG[2], HENGZHONG ZHANG[2], BENJAMIN GILBERT[1], YANG REN[3], JILLIAN F. BANFIELD[1,2] AND GLENN A. WAYCHUNAS[1]

[1]Lawrence Berkeley National Laboratory, Earth Sciences Division, Berkeley, CA, USA, mzhu@lbl.gov (* presenting author)
[2]University of California, Earth and Planetary Science, Berkeley, CA, USA, jbanfield@berkeley.edu;
[3]Argonne National Laboratory, Advanced Photon Source, Argonne, IL, USA, ren@aps.anl.gov

Metal and coal mines produce iron-rich sulfuric acid solutions that contain a broad range of toxic elements [1]. These solutions, referred to as acid mine drainage (AMD), adversely affect environmental quality. When AMD mixes with neutral water bodies, such as in rivers or during wetland treatment, interacts with rock surfaces, or reacts with lime during remediation, neutralization occurs. As a result, ferric iron (Fe^{3+}) hydrolyzes and precipitates as Fe oxyhydroxide nanoparticles, such as ferrihydrite and schwertmannite. However, the formation pathways of these nanoparticles are relatively unknown largely due to their rapid formation rates and low abundances of initially-formed species. In this study, we used *in situ* time-resolved synchrotron radiation X-ray diffraction (XRD), quick-scanning extended X-ray absorption fine structure (QEXAFs) and UV-Vis spectroscopic techniques to study the products formed initially ($2 < t < 60$ minutes) when ferric iron sulfate solutions ($[Fe^{3+}] = 0.2$ M) are partially neutralized ($[HCO_3^-]/[Fe^{3+}] < 3$) by addition of $NaHCO_3$.

When $[HCO_3^-]/[Fe^{3+}] = 0.6$ (initial pH ~ 2.2), the only particles formed were ferrihydrite-like clusters that were stable throughout the duration of the experiment. When $[HCO_3^-]/[Fe^{3+}] = 1$ (initial pH ~ 2.5), the ferrihydrite-like molecular clusters formed initially but mostly disappeared and were replaced by schwertmannite. Schwertmannite and larger ferrihydrite particles formed immediately when $[HCO_3^-]/[Fe^{3+}] = 2$ (initial pH ~ 2.7), but the ferrihydrite particles completely disappeared and were replaced by schwertmannite. The schwertmannite particle size increased with reaction time, and extensive particle aggregation occurred.

The ferrihydrite-like cluster is very intriguing and its structure deserves further characterization. The data are consistent with Fe_{13} having Baker-Figgis δ-keggin structure, i.e., the motif in the ferrihydrite structure proposed by Michel et al. [2]. The existence of the cluster may result from sulfate binding on its surface, preventing the cluster from growing into larger ferrihydrite particles.

In conclusion, the results suggest that particular molecular clusters and small nanoparticles may be important, early-formed components of natural acidic solutions.

[1] Evangelou & Zhang (1995) *Crit. Rev. Environ. Sci. Technol.* **25**, 141-199.
[2] Michel et al. (2007) *Science* **316**, 1726-1728.

XPS study of bioleached arsenopyrite by *Acidithiobacillus ferrooxidans*

TINGTING ZHU[1*], XIANCAI LU[1], RUCHENG WANG[1], AND JIANJUN LU[1]

[1]School of Earth Sciences and Engineering, Nanjing University, Nanjing, China, ttzhu.nju@gmail.com (* presenting author)

Arsenopyrite (FeAsS) is a commonly discarded sulfide mineral in mining wastes. The arsenic release from it due to oxidation can cause serious environment contamination in mines. It has been well proved previously that microorganisms can remarkably accelerate the oxidation of arsenopyrite. However, the detailed oxidation mechanism is still unclear. This study on surface chemistry of bioleached arsenopyrite may cast insights into it.

In our experiments, the arsenopyrite obtained from a W-Sn deposit and a strain of *Acidithiobacillus ferrooxidans* isolated from the acid mine drainage in Tongling, eastern China, were used. The sterilized 9K culture with an adjusted Fe^{2+} concentration of 16 mM was poured into 6 flasks and then divided into two groups. Three flasks were inoculated with *Acidithiobacillus ferrooxidans* and the other three were only abiotic. Arsenopyrite particles were dropped into flasks simultaneously, and then extracted after 4 days, 7 days and 10 days, respectively. The reacted samples were freeze-dried in vacuum and ready for SEM observation and XPS analysis.

Several types of secondary mineral, such as elemental sulfur and scorodite, can be observed on the surface of 4 days-biooxidized arsenopyrite. However, native sulfur diminished gradually as bio-oxidation continuing and finally disappeared on the 10 days-biooxidized surface. The XPS depth profiles show that the altered layer of biooxidized arsenopyrite is much thicker than that of abiotic case. In addition, the contents of Fe(III), As(V) and sulfate in surface layer of bio-oxidized arsenopyrite are all higher than those of abiotically oxidized sample. The oxidation progress varies with the elements in both experimental systems. In the biotic system, the oxidized sequence is in the order of As, S, and then Fe, whereas in the abiotic system Fe is preferentially oxidized than As and S. In the depth profile of altered layer of each systems, a transition depth can be identified, where the contents of As, S and Fe change sharply. This depth of bio-oxidized arsenopyrite is about 450 nm, and that of abiotically oxidized one is around 30 nm. The change of Fe speciation in depth profile reveals that *A. ferrooxidans* initially breaks Fe(II)-AsS to form Fe(III)-AsS and a small quantity of Fe(III)-OH, and at a very late stage a trace fraction transform into Fe(III)-SO. For As-oxide, As(III)-O dominates on the bio-oxidized surface while As(I)-O prevails on the abiotically oxidized one. The contents of S^0 and S_n^{2-} of abioticaly oxidized surface keep stable as depth increase, while those of bio-oxidized surface show a significant increase from 500 nm to 1000 nm, which is consistent to the observed emergence and dis-appearance of native sulfur. It is proposed that native sulfur is only an intermediate product during microbial oxidation.

Acknowledgement: We appreciate the support from the National Science Foundation of China (40930742 and 10979018).

https://doi.org/10.1180/S0026461X00008434 Published online by Cambridge University Press

Kinetic and Thermodynamics Studies of Cadmium Adsorption Behavior on Montmorillonite

XIAPING ZHU[1*] HUI LIU[2] NIANNIAN XIANG[3] YINGFENG TIAN[4]
[1234]Institute of Material and Chemistry & Chemical Engineering, Mineral Resources Chemistry Key Laboratory of Sichuan Higher Education Institutions,Chengdu University of Technology, Chengdu, China
[1]zhuxiaping@cdut.edu.cn (* presenting author)
[2] 271212495@qq.com
[3] 841945777@qq.com
[4] 742911585 @qq.com

Montmorillonite is the most important clay minerals in soils. It has good cation exchange and adsorption capacity. Montmorillonite was a major factor for cadmium retention in soils due to electrostatic attraction, ion exchange, complexation, and precipitation[1]. The sample was collected from Sihui, Guangdong, China. Its physical and chemical properties had been measured, meanwhile, infrared spectroscopy, X-diffraction analysis, and simultaneous thermal analysis had been conducted, then cadmium adsorption behavior on montmorillonite had been studied. The cadmium adsorption on montmorillonite was fit to Langmuir model and Freudlich model, the latter was better. Adsorption of cadmium on montmorillonite was severely affected by ionic strength, the saturated adsorption capacity of cadmium calculated by the Langmuir model had a good negative correlation to ionic strength, the correlation coefficient was 0.9987. The adsorption index (1 / n) concluded by the Freudlich models were smaller, indicating that the montmorillonite was prone to adsorbing Cd^{2+}. The adsorption volume of cadmium on montmorillonite exhibited a process of rise-fall-rise-balance with the time delay at different temperature. The adsorption of cadmium on montmorillonite met the Lagergren second-order kinetic equation well, the correlation coefficients were 0.9999,1,0.9999 at 303, 313, 323 K, respectively. The false thermodynamic parameters were calculated through adsorption kinetics data of cadmium at the different temperature[2], the adsorption enthalpy（ΔH）was 23.31 kJ / mol, it showed that the adsorption process was an endothermic process, and it was the physical adsorption, the free energy of adsorption(ΔG) at different temperature were less than zero, indicating that the adsorption was spontaneous. The absolute value of ΔG increased and the driving force became larger with the temperature increase, the temperature was benefit to the adsorption. The entropy (ΔS) was greater than zero, the degree of disorder increased after Cd adsorbed to the montmorillonite. Cadmium replaced the more lively metal ions (Ca, Na, Mg, etc.) or the hydrogen ion in the interbedded area of montmorillonite, 1mol of cadmium ion could exchange 2mol of hydrogen or sodium ion, which induced the entropy increase more than the entropy decrease caused by ion adsorption [3].The results reported in the present study will benefit environmental contamination applications concerning cadmium mobility, cadmium transformation, and other possible applications in various fields (e.g. soil decontamination, agriculture irrigation and water treatment).

[1] Xiaping Zhu(2008) *Doctor paper of Chengdu university of technology*,106
[2] A. Agrawal, K.K. Sahu(2006) *Journal of Hazardous Materials*, 137, 915-924.
[3] Enjun Song Dong Zhang Liangzi Xu Guangjun Ren(2010) *Ion exchange and adsorption*, 26, 16 ~ 23

Filamentous microorganisms interacting with sheet silicates

W. ZIDAN[1*], S. NIETZSCHE[2], C. FISCHER[3], E. KOTHE[4], R. GAUPP[1]

[1]Institute of Geosciences, Jena, Germany, wafaa.zidan@uni-jena.de (* presenting author), reinhard.gaupp@uni-jena.de
[2] Center for Electron Microscopy, University Hospital Jena, Germany, sandor.nietzsche@uni-jena.de
[3] Georg-August-Universität Göttingen, Göttingen, Germany, cornelius.fischer@geo.uni-goettingen.de
[4]Institute of Phytopathology, Jena, Germany, erika.kothe@ uni-jena.de

Aim of the work

The goal of our work is to study the effect of two filamentous microorganisms (the fungus *Schizophyllum commune* and the actinobacterium *Streptomyces acidescabies E13*) on mineral dissolution and surface alteration when incubated with three different sheet silicates; the nontronites (Nau1, Nau2) and ripidolite (clinochlore). Incubation without iron added to the minimal media was performed in order to induce mineral dissolution by microorganisms for nutrient acquisition.

Results and conclusion

While the actinobacterium *S. acidescabies E13* has formed microbial pellets with the three sheet silicates, the fungus *S.* commune hasn't formed any microbial pellets with any of the sheet silicates. The Streptomycete's pellets formed with nontronite were regular, round (Fig. 1A) and there were not too many mineral flakes left as they were dissolved to a large extent, but the hyphae were encrusted. Streptomycete's pellets formed with ripidolite, in contrast to nontronite were irregular (Fig. 1B), many mineral flakes were preserved and the hyphae were smooth. Our interpretation is that the higher Fe concentration of nontronite is responsible for this contrasting behavior in terms of pellet's shape and hyphae's encrustation.

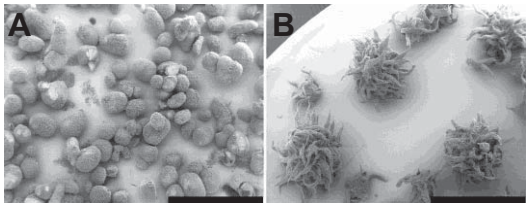

Figure 1: SEM images of Streptomycete's pellets with nontronite (A) and with ripidolite (B). Scale bar: 2 mm.

Furthermore, the *S. acidscabies E13* had decreased the pH from 6 to 4, and once again increased to pH 7 in case of interacting with clinochlore, while with nontronite the pH decreased and stayed constant at pH 4. This suggests that acidification might be a mechanism for mineral dissolution by the actinobacterium. However, this is not the case for the fungus *S. commune,* where the pH stayed neutral. The fungus excreted more protein when interacting with Nau2 as compared to Nau1 and clinochlore. Incubation of *S. commune.* with polished clinochlore samples caused an evolution of deep pits upon interaction as shown by vertical scanning interferometry (VSI). Data were used to analyze reaction kinetics as a function of crystallographic orientation. Our experiments showed different sheet silicate dissolution by filamentous bacterial and fungal microorganisms.

https://doi.org/10.1180/S0026461X00008434 Published online by Cambridge University Press

Silicon and oxygen isotopes during diagenesis of the Monterey chert

K. ZIEGLER[1,2,*], J. MARIN-CARBONNE[1,3]

[1]Department of Earth and Space Sciences, University of California, Los Angeles, CA 90095, USA.
[2]current address: Institute of Meteoritics, University of New Mexico, Albuquerque, NM 87131, USA. (kziegler@unm.edu) ([*]presenting author)
[3]current address: Institut de Physique du Globe, Geobiosphere actuelle et primitive, Paris, France. (jmarincarbonne@gmail.com)

An important aspect for the evaluation of the use of (Archean) cherts as proxies for environmental conditions at their formation, is the fidelity of δ^{30}Si and δ^{18}O ratios of cherts during their diagenetic transitions from their precursor material (biogenic opal).

The Miocene Monterey Formation (California) is an exemplary location for the study of chert diagenesis. The Monterey Formation contains a diagenetic silicate sequence from marine biogenic opal-A to opal-CT to cristobalitic chert. This precursor-to-chert transition is due to dissolution-precipitation processes related to interactions of the opal with later diagenetic water [1, 2].

We analyzed δ^{30}Si values by MC-ICPMS (Neptune™), and δ^{18}O values of cherts by ion microprobe (Cameca 1270) at UCLA. Due to ionprobe matrix effects in opal, their δ^{18}O values were taken from literature [1, 3].

The δ^{18}O values of the Monterey opal (37‰) and chert (28-34‰) suggest formation temperatures of 15°C and 48±8°C, respectively [1]. The opal has a δ^{30}Si value of 1.4‰, and the chert has a more negative value of 0.0‰. Diatomaceous opal formed in highly productive oceans is expected to have high δ^{30}Si values, wheras diagenetic fluids expelled from the Monterey Shales during burial are expected to have more negative δ^{30}Si values [4].

The chertification process of the Monterey opal has imprinted δ^{30}Si and δ^{18}O ratios onto Monterey cherts that are different from the initial isotopic values of the biogenic opal. This example illustrates that isotope values of cherts are not necessarily indicative for the environmental conditions that prevailed during intial marine silica deposition.

If the precursor-chert transformation was associated with an external fluid, the isotope ratios of the chert reflect the conditions of this chertification event rather than that of the silica deposition. Such proceses will have to be understood and assessed when using O and Si isotopes of cherts for paleoclimate reconstructions.

We thank Jim Boles (UCSB) for providing the samples.

[1] Murata *et al.* (1977), *AJS* **277**, 259-272. [2] Pisciotto (1981), *Sedimentology* **28**, 547-571. [3] O'Neil & Hay (1973), *EPSL* **19**, 257-266. [4] Ziegler *et al.* (2005), *GCA* **69,** 4597-4610.

The distribution of neodymium isotopes and REE patterns in the water column of the tropical Atlantic Ocean

M. ZIERINGER[1], M. FRANK[1]* AND E. HATHORNE[1]

[1]GEOMAR | Helmholtz Centre for Ocean Research, Wischhofstrasse 1-3, 24148 Kiel, Germany (* mfrank@geomar.de)

Neodymium (Nd) isotopes and rare earth element (REE) patterns are used as tracers to fingerprint source provenances of water masses. We present full water column Nd isotopic compositions and dissolved REE distributions in seawater of the tropical Atlantic Ocean. Samples were collected during GEOTRACES expedition A11 (R/V Meteor) from Las Palmas (Canary Islands) to Port of Spain (Trinidad and Tobago).

Highly variable REE concentrations and characteristic REE patterns in surface waters can be grouped into different oceanic provinces and reflect prominent local source provenances, such as volcanic islands and dust particles of continental origin. Generally, concentrations in the eastern basin, especially in the vicinity of the Canary Islands and off the coast of NW Africa, are higher than in the western basin. In the area of the Canary Islands shale-normalized REE patterns are characterized by pronounced heavy REE enrichments originating from weathering of the volcanics while further south REE patterns are almost flat as a consequence of Saharan dust inputs.

Nd concentrations in surface waters range from a minimum of 14 pmol/kg in surface waters with reduced salinities (< 33.6 psu) due to freshwater input by the Amazon river to maxima off NW Africa originating from partial dissolution of Saharan dust and ocean island wheathering. This is also reflected in the surface water Nd isotopic compositions, which range from ε_{Nd} = - 12.7 to - 8.8. The most radiogenic values are measured between Tenerife and Grand Canary while the Nd isotope composition is least radiogenic in the open ocean surface waters.

In addition to the surface waters we present full water column profiles of Nd isotope compositions and REE patterns including samples from all major water masses of the Atlantic Meriodional Overturning Circulation in the western and eastern Atlantic basins.

https://doi.org/10.1180/S0026461X00008434 Published online by Cambridge University Press

On the Interpretation of Zircon U-Pb ages from (U)HP Host Gneisses in the Woodlark Rift of Papua New Guinea

N. Alex Zirakparvar[1*], Suzanne L. Baldwin[1], Axel K. Schmitt[2] , Paul G. Fitzgerald[1]

[1]Syracuse University Department of Earth Science, Syracuse, New York, USA, nazirakp@syr.edu (* presenting author)

[2]University of California Los Angeles, California, USA, axel@oro.ess.ucla.edu

Abstract

Conventional analysis of accessory minerals in 'spot-mode' in polished sections samples crystal volumes, that even in high-sensitivity secondary ionization mass spectrometry (SIMS), have diameters of ~10-20 μm. These 'spot mode' analyses can reveal the ages and trace element compositions of crystal domains if the domains are larger than the lateral beam dimensions. They cannot, however, be used to characterize variations that occur over smaller dimension, or that occur at sharp boundaries between discrete domains often observed in cathodoluminescence (CL) images. Because of this spatial limitation, conventional spot analysis cannot be used to investigate processes operative at scales <10 μm, and the relationship between the U-Pb isotopic and trace element records in the same crystal volume.

In this study SIMS depth-profiling was used to characterize zircons from felsic and intermediate gneisses that host the world's youngest (U)HP eclogites in southeastern Papua New Guinea. Many zircon CL images show cores overgrown by dark CL rims. SIMS depth profiling perpendicular to unpolished zircon surfaces, and penetrating to a depth of ~15 μm, effectively measured the U-Pb isotopic and trace element composition at a depth resolution of <1 μm. Crystal domains up-to and across the sharp transition from overgrowth into inherited core were investigated. These depth profiles are augmented by U-Pb data collected in 'spot mode' on 1) polished cross sections, and 2) external (i.e., unpolished) surfaces.

The U-Pb results reveal zircon grew in the Pliocene as individual crystals, and as overgrowths on Late Jurassic to Cretaceous cores. Zircons lacking Cretaceous cores and with uniformly Pliocene ages also displayed complex internal zoning patterns under CL. The Pliocene zircons are within error of $^{40}Ar/^{39}Ar$ mineral ages on the (U)HP host gneisses and indicate zircon crystallization during (U)HP exhumation. The U-Pb zircon systematics in the host gneisses provide information about the protolith age followed by zircon growth at temperatures of ~590 to 690 °C based on Ti-in-zircon thermometry. Small scale geochemical disequilibrium within the host gneisses at the time of zircon crystallization is indicated by contrasting trace element compositions for different zircons that crystallized simultaneously under similar conditions. The fact that zircons of uniform age display complex CL zoning patterns indicates that the zoning observed in CL images is not a function of growth rate, but instead may be related to changes in trace element concentration at the zircon-matrix interface during zircon growth.

Temporal resolution of LA-ICPMS analyses of fish hard parts

Andreas Zitek[*], Johanna Irrgeher[a], Stefanie Kappel, Florian Kendlbacher and Thomas Prohaska

[1]University of Natural Resources and Life Sciences, Department of Chemistry, Division of Analytical Chemistry, VIRIS Laboratory, A-3430 Tulln, Austria, andreas.zitek@boku.ac.at (* presenting author)

[a]Recipient of a DOC-fFORTE-fellowship of the Austrian Academy of Sciences

As far as elemental and isotopic distributions vary locally in natural ecosystems, they are also taken up by living organisms and consequently incorporated in time resolved manner in incrementally growing tissues. Increasingly, this phenomenon is also used to answer key questions in fish ecology, such as seasonal habitat use, migration and dispersal.

Unfortunately, basic hydrobiological processes are increasingly disturbed by human activities in river systems all over the world. Understanding the spatio-temporal behaviour of fish and their connectivity needs is crucial for e.g. coordinated river rehabilitation and management.

Beside the local differences in the elemental distributions the naturally varying Sr isotopic composition of river water, derived from geological differences within the river catchment, provides the basic prerequisite for studying these phenomena based on the microchemical analyses of different fish hard parts.

In order for the elemental and isotopic signature of water getting unambigously reflected in hard parts of fish (like otoliths, scales, vertebrae or fin rays), fish have to stay a certain time in an habitat for equilibration and sufficent uptake of the environmental information. However, the time needed for equilibration and for incorporating a unique signal is unknown and differs between species and life stage.

Laser ablation coupled to multi-collector inductively coupled plasma mass spectrometry (LA-(MC)-ICPMS) was used for the determination of elemental concentrations and Sr isotope ratios in fish hard parts for studying the potential reflection of short term migrations and habitat changes. Much effort has been made with respect to the optimization of laser parameters in order to achieve best spatial resolution on different hard parts of fish while keeping uncertainties as low as possible. Fish from different sources (natural, aquaculture) and the related water chemistry were investigated. In addition, a caging experiment was conducted to study the uptake of environmental information into fish hard parts under semi-controlled conditions. European chub, *Squalius cephalus* (L.), for example, were moved between rivers with contrasting water chemistries and exposed in cages for three and six months. The main aim was to determine the required time of residence of a fish in a certain habitat to create a unique signal matchting the river environment when LA-(MC)-ICPMS is used for the determination of both elemental concentrations and Sr isotope ratios. The major focus was set on the analyses of otoliths, vertebrae, scales and fin rays, with the latter two options representing important non-lethal sampling alternatives.

Herein, we present our latest results on on different fish hard parts measurements using LA-ICMPS, including a discussion about the implications of the results for an application of this technology to fish ecological questions.

https://doi.org/10.1180/S0026461X00008434 Published online by Cambridge University Press

Thermodynamic properties of antlerite, brochantite, and posnjakite

A. H. ZITTLAU[1*] AND J. MAJZLAN[1]

[1*]Institute of Geosciences, Friedrich-Schiller University, Jena, Germany, (*correspondence: Arne.Zittlau@uni-jena.de)

Weathering of primary copper minerals (e.g., chalcopyrite, bornite) leads to the formation of secondary copper sulfates, phosphates, and arsenates. In this work, we focused on Cu sulfate-hydroxide minerals antlerite ($Cu_3SO_4(OH)_4$), brochantite ($Cu_4SO_4(OH)_6$) and posnjakite ($Cu_4SO_4(OH)_6 \cdot H_2O$). We synthesized these phases in the laboratory and measured their thermodynamic properties.

The synthesis procedure was a titration of a 0.1 M sodium hydroxide solution into a 0.001 M solution of copper sulfate. The temperature of the $CuSO_4$ solution ranged from 25 to 80 °C and the end-point pH was set between 6 and 11. By variations of temperature and the end-point pH, the precipitates contained brochantite, posnjakite, and tenorite (CuO). We were able to determine systematic variations of the nature of the precipitated product with temperature and pH. Antlerite was synthesized as described in [1]. All these samples were characterized by X-ray diffraction (XRD). Subsequently, the best samples were analyzed by scanning electron microscopy (SEM) for phase purity and prepared for calorimetric measurements.

The calorimetric measurements were carried out by an acid-solution calorimeter at T = 298 K in 5 N HCl as the solvent, using CuO, $CuSO_4 \cdot 5H_2O$, and KCl as the reference compounds. For all measurements, appropriate thermochemical cycles were constructed. The formation enthalpies ($\Delta_f H^0$) of antlerite, brochantite and posnjakite are -1734.9±4.0 kJ/mol, -2157.8±7.0 kJ/mol, and -2457.1±7.0 kJ/mol, respectively.

The results presented here will be soon augmented by heat capacity measurements and standard entropy calculations. Once the data are complete, we will calculate phase diagrams and compare them to the synthesis results described above. Our ultimate goal is a comprehensive model of Cu- and sulfate-rich fluids present in oxidation zones of ore deposits and tailings of Cu ores.

[1] Lin'ko et al. (2001) *Russ J Inorg Chem+* **46**, 298-301.

The initial stage of mica weathering

P. ZUDDAS[1*], K. PACHANA[1], P. CENSI[2]

1. Université P.et M. Curie - Paris Sorbonne, ISTEP, Paris, France.

pierpaolo.zuddas@upmc.fr (*presenting author)

biotite59@hotmail.com

2. Dipartimento di DiSTeM, Università di Palermo, Palermo, Italy.

19c. Kinetics of interfacial geochemical processes

We investigated the early stage of muscovite alteration combining chemical analysis of the interacting solution with *in situ* Atomic Force Microscopy determinations of the reacting mineral surface. Experiments were carried out using a liquid cell of an Atomic Force Microscopy determining simultaneously the evolution of the reacting fluids and the nanometers size details of the mineral surface. The state of the muscovite monocrystal's pristine (001) surface after cleavage was observed to be perfectly flat, with no apparent evidence of defect points or dislocations. The surface's molecular periodicity resolution showed the hexagonal-like formations typical of the nanoscale occurrence of Si-centered tetrahedral arrangements along muscovite sheets. However, when a solution was introduced in the liquid cell by way of a peristaltic pump, pits appeared rapidly displaying a stair-shape pattern consistent with the mineral structure of a T-O-T periodicity. This early stage evolution is responsible for the stoichiometric Al/Si ratio in solutions. Our nanometer scale determinations allowed us to estimate the anisotropic loss of matter generated by the step movement. We found the directional lateral velocity $\mathbf{V}_{(hk0)}$ to be 3 fold higher than the basal velocity $\mathbf{V}_{(00l)}$, demonstrating the higher reactivity of the lateral compared to basal surfaces during the dissolution process. The directional velocity of dissolution at the lateral face decreased by more then one order of magnitude for a 5-fold increase in pH, while velocity at the basal face did not change significantly as a function of pH. We observed also the formation of new phases of nanometer size that coating the dissolving mineral surface inhibits the step movement with consequence loss in congruency. Coatings that initially form at the lateral higher reactive faces control the overall dissolution process. Coat formation and growth depends on both aqueous solution composition and dissolving mineral structure.

https://doi.org/10.1180/S0026461X00008434 Published online by Cambridge University Press

Cadmium isotopes in northeast Pacific Ocean seawater

C.M. ZURBRICK[1,*], D. BILLER[2], C. HARRIS[3], M. REHKÄMPER[4], K.W. BRULAND[2,5], A.R. FLEGAL[1,5]

[1]Department of Microbiology and Environmental Toxicology, UC Santa Cruz, Santa Cruz, USA, CZurbric@ucsc.edu (* presenting author)
[2]Department of Ocean Sciences, UC Santa Cruz, Santa Cruz, USA, DBiller@ucsc.edu, Bruland@ucsc.edu
[3]Stanford University, Palo Alto, USA, CHarris2@stanford.edu
[4]Imperial College, London, United Kingdom, MarkRehk@imperial.ac.uk
[5]Institute of Marine Sciences, UC Santa Cruz, Santa Cruz, USA, Flegal@ucsc.edu

Background

Seawater was collected from the California Current Upwelling Zone in the northeast Pacific to investigate factors influencing cadmium concentrations and isotopic compositions in that dynamic region. As expected, cadmium and nutrient (phosphate, nitrate) concentrations were highly correlated both (i) in the cores of intense upwelling eddies and (ii) in relaxed and downwelling eddies [1]. Cadmium isotopic composition of those waters and associated plankton were then compared to test the hypothesis that primary productivity accounts for the relative depletion of lighter cadmium isotopes in surface seawater [2]. Cadmium isotopes in seawater were also compared with iron and zinc concentration data to further resolve factors contributing to the cadmium isotope depletion in surface waters.

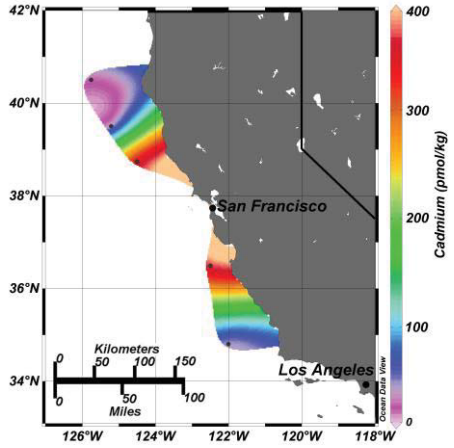

Figure 1: Cadmium concentration (pmol/kg) in the surface waters of the California Current Upwelling Zone.

Preliminary Results

Preliminary results show that freshly upwelled waters have similar cadmium isotopic signatures as deep waters. Nutrient rich waters that had large phytoplankton blooms with subsequent nutrient drawdown showed isotopic fractionation consistent with previous hypotheses [2, 3] and correlate with Fe and Zn data.

[1] Bruland *et al.* (1978) *Limnol. Oceanogr.* **23**, 618-625.
[2] Ripperger *et al.* (2007) *EPSL* **261**, 670-684.
[3] Abouchami *et al.* (2011) *EPSL* **305**, 83-91.

Brittle fault dating from the Mesoproterozoic to the Neogene

HORST ZWINGMANN[1]*, NEIL MANCKTELOW[2], GIULIO VIOLA[3] JAN PLEUGER[2], SEIKO YAMASAKI[4] AND TAKAHIRO TAGAMI[5]

[1]CSIRO ESRE, Perth, Australia, horst.zwingmann@csiro.au (* presenting author)
[2]ETH Zuerich, Switzerland, neil.mancktelow@erdw.ethz.ch
[3]NGU, Trondheim, Norway, giulio.viola@ngu.no
[2]ETH Zuerich, Switzerland, jan.pleuger@erdw.ethz.ch
[4]JAEA, Gifu, Japan, yamasaki.seiko@jaea.go.jp
[5]KUEPS Kyoto University, Japan, tagami@kueps.kyoto-u.ac.jp

Over the last decade constraining the timeframe of brittle faulting has been applied successfully in many case studies. We present fault gouge illite age data from several studies in the European Alps, Finland and Japan. All studies deal with igneous or metamorphic rocks collected from tunnel or drill core samples, which offer a unique advantage as no detrital illite is present in the host rock, thus reducing potential contamination and weathering sources. The age data were obtained using a simplified and standarized method described by Zwingmann et al. (2010). Illite ages range from the Mesoproterozoic (1240±26 Ma) for the Finland samples to the Neogene (6.0±2.1 Ma) for the European Alps study.

For the European Alps study, samples were collected from the AlpTransit tunnel and the K-Ar ages for illite fractions range between 9.5 and 3.9 Ma.

The remarkable dating of Mesoproterozoic and Neoproterozoic ages for the Finnish brittle faults proves the potential of the technique also in the case of extremely old cratonic terranes and their faulting histories. In addition, the preservation of both Meso- and Neoproterozoic isotopic signatures within one single fault core and the geologically meaningful dating of two coexisting but texturally different gouges of different age document a rare case of age determination of a faulting episode and of a subsequent reactivation in the brittle realm.

Within the Japan case study, gouge samples were investigated from a subsurface fault collected within a shaft in the Cretaceous Toki granite. The K-Ar ages of the fractions with no detectable contamination from detrital K-bearing minerals range from 53 to 43 Ma.

In all case studies the illite ages generally decrease with grain size, and they are consistent with the cooling history of the host rocks as bracketed by AFTA and ZFTA ages. The data indicate that that the fault-rock samples formed within the stability field of illite and the main temperature field of brittle deformation (<300°C). The internal consistency of the K-Ar ages of fault gouges from both surface and subsurface samples, as well as their consistency with constraints from field relationships and existing geochronological data demonstrate the potential of this simplified method for providing new data to constraint absolute timing of brittle deformation.

[1] Zwingmann et al. (2010) *Geology* 38, 6, 487-490; doi10.1130/G30785.1

https://doi.org/10.1180/S0026461X00008434 Published online by Cambridge University Press

-A-

https://doi.org/10.1180/S0026461X00008434 Published online by Cambridge University Press

-B-

https://doi.org/10.1180/S0026461X00008434 Published online by Cambridge University Press

https://doi.org/10.1180/S0026461X00008434 Published online by Cambridge University Press

-C-

https://doi.org/10.1180/S0026461X00008434 Published online by Cambridge University Press

https://doi.org/10.1180/S0026461X00008434 Published online by Cambridge University Press

-D-

https://doi.org/10.1180/S0026461X00008434 Published online by Cambridge University Press

https://doi.org/10.1180/S0026461X00008434 Published online by Cambridge University Press

-E-

-F-

https://doi.org/10.1180/S0026461X00008434 Published online by Cambridge University Press

https://doi.org/10.1180/S0026461X00008434 Published online by Cambridge University Press

-G-

https://doi.org/10.1180/S0026461X00008434 Published online by Cambridge University Press

-H-

https://doi.org/10.1180/S0026461X00008434 Published online by Cambridge University Press

https://doi.org/10.1180/S0026461X00008434 Published online by Cambridge University Press

-I-

https://doi.org/10.1180/S0026461X00008434 Published online by Cambridge University Press

-J-

-K-

https://doi.org/10.1180/S0026461X00008434 Published online by Cambridge University Press

https://doi.org/10.1180/S0026461X00008434 Published online by Cambridge University Press

-L-

https://doi.org/10.1180/S0026461X00008434 Published online by Cambridge University Press

https://doi.org/10.1180/S0026461X00008434 Published online by Cambridge University Press

-M-

https://doi.org/10.1180/S0026461X00008434 Published online by Cambridge University Press

https://doi.org/10.1180/S0026461X00008434 Published online by Cambridge University Press

https://doi.org/10.1180/S0026461X00008434 Published online by Cambridge University Press

-N-

https://doi.org/10.1180/S0026461X00008434 Published online by Cambridge University Press

-O-

-P-

https://doi.org/10.1180/S0026461X00008434 Published online by Cambridge University Press

https://doi.org/10.1180/S0026461X00008434 Published online by Cambridge University Press

-Q-

-R-

https://doi.org/10.1180/S0026461X00008434 Published online by Cambridge University Press

-S-

https://doi.org/10.1180/S0026461X00008434 Published online by Cambridge University Press

https://doi.org/10.1180/S0026461X00008434 Published online by Cambridge University Press

https://doi.org/10.1180/S0026461X00008434 Published online by Cambridge University Press

-T-

https://doi.org/10.1180/S0026461X00008434 Published online by Cambridge University Press

https://doi.org/10.1180/S0026461X00008434 Published online by Cambridge University Press

-U-

-V-

-W-

https://doi.org/10.1180/S0026461X00008434 Published online by Cambridge University Press

https://doi.org/10.1180/S0026461X00008434 Published online by Cambridge University Press

-X-

-Y-

https://doi.org/10.1180/S0026461X00008434 Published online by Cambridge University Press

-Z-

https://doi.org/10.1180/S0026461X00008434 Published online by Cambridge University Press